

Annual Cumulated Index

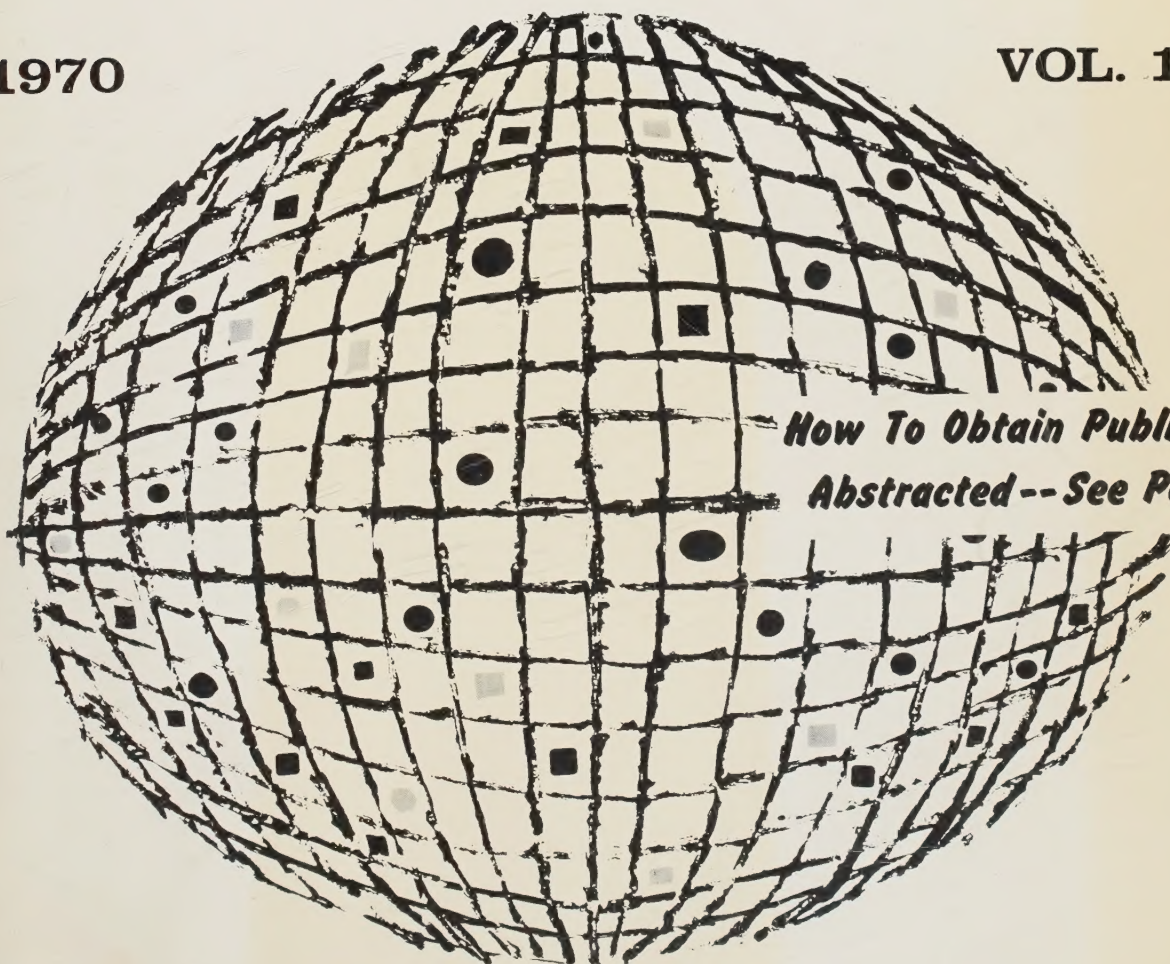
ACCESSION NOS. A70-10001 to A70-46414

INTERNATIONAL AEROSPACE ABSTRACTS

PART 1, PERIODICALS SCANNED, SUBJECT INDEX, A - L

1970

VOL. 10



*How To Obtain Publications
Abstracted -- See Page IV*

PUBLISHED BY THE TECHNICAL INFORMATION SERVICE
AMERICAN INSTITUTE OF AERONAUTICS AND ASTRONAUTICS



Digitized by the Internet Archive
in 2023

INTERNATIONAL AEROSPACE ABSTRACTS

ANNUAL CUMULATED INDEX

PART 1

PERIODICALS SCANNED, SUBJECT INDEX, A – L

VOLUME 10

JANUARY – DECEMBER

1970

ACCESSION NUMBERS A70-10001 to A70-46414

INTERNATIONAL AEROSPACE ABSTRACTS is prepared and published semimonthly (except June and December, which have three issues) by the Technical Information Service, American Institute of Aeronautics and Astronautics, Inc., for the Institute and the National Aeronautics and Space Administration under Contract No. NASW-1949. Editorial and Subscription Offices: 750 Third Avenue, New York, N. Y. 10017. Copyright © 1970 by the American Institute of Aeronautics and Astronautics, Inc. (The indexes, however, may be reproduced for any bibliographic purpose.)

Telephone: 212 TN-7-8300

TWX: 212 867-7265

SUBSCRIPTION INFORMATION. Semimonthly issues: United States and Possessions, 1 year, \$75 postpaid; Foreign Countries, 1 year, \$90 postpaid. Cumulated Index Volumes: United States and Possessions, 1 year, \$30 postpaid; Foreign Countries, 1 year, \$35 postpaid. Second-class postage paid at Phillipsburg, N. J.

CONTENTS

PART 1

INTRODUCTION	iii
HOW TO OBTAIN PUBLICATIONS ABSTRACTED	iv
CROSS REFERENCES	iv
PERIODICALS SCANNED	v – xxvii
SUBJECT INDEX, A – L	A1 – A1018

PART 2

INTRODUCTION	iii
HOW TO OBTAIN PUBLICATIONS ABSTRACTED	iv
CROSS REFERENCES	iv
SUBJECT INDEX, M – Z	A1019 – 2064

PART 3

INTRODUCTION	iii
HOW TO OBTAIN PUBLICATIONS ABSTRACTED	iv
PERSONAL AUTHOR INDEX	B1 – B848
CONTRACT NUMBER INDEX	C1 – C47
MEETING PAPER & REPORT NUMBER INDEX	D1 – D30
ACCESSION NUMBER INDEX	E1 – E163

STAFF, AIAA

Administrator—Technical Information Programs, Robert R. Dexter

STAFF, TECHNICAL INFORMATION SERVICE

Director, John J. Glennon

Associate Director—Administrative, Thomas J. Meskel

Associate Director—Technical, Irene W. Bogolubsky

Abstracts Editor, Nanu Davis

Index Editor, Angelica Mihalakos

Chief Librarian, Patricia M. Marshall

INTRODUCTION

INTERNATIONAL AEROSPACE ABSTRACTS (IAA) is an abstracting and indexing service covering the world's published literature in the field of aeronautics and space science and technology. IAA is issued semimonthly, on the 1st and 15th of each month.

Coverage of Published Literature

The following types of publications are covered in IAA:

- Periodicals (including government-sponsored journals) and books.
- Meeting papers and conference proceedings issued by professional societies and academic organizations.
- Translations of journals and journal articles.

Coverage of Reports ("Unpublished" Literature)

Abstracts and indexes of report literature are issued in SCIENTIFIC AND TECHNICAL AEROSPACE REPORTS (STAR), which is published by the Scientific and Technical Information Division, National Aeronautics and Space Administration.

By special arrangement between NASA and the American Institute of Aeronautics and Astronautics, IAA is issued in coordination with the twice-monthly schedule of STAR, which appears on the 8th and 23rd of each month.

IAA and STAR both utilize identical subject categories and indexes, which are described below.

Thus the two services provide comprehensive access to the national and international unclassified report and published literature of current significance to aerospace science and technology.

Arrangement of the Semimonthly Issues

IAA is arranged in two major sections:

- (1) Abstracts Section. This section contains complete bibliographic citations with informative abstracts, arranged by appropriate subject categories to facilitate scanning. The subject categories are numbered from 01 to 34, and the scope of each category is outlined in the Table of Contents and again at the beginning of each category in the Abstracts Section. Each abstract is prefixed by the IAA accession number.
- (2) Index Section. Five indexes are contained in this section: Subject, Personal Author, Contract Number, Meeting Paper and Report Number, and Accession Number. Each index is prefaced by explanatory notes to guide the user to the desired abstract.

Cumulated Indexes

The semi-annual cumulated index is issued promptly at the end of the first six months and the annual cumulated index is issued promptly at the end of the twelve-month period.

Each cumulated index contains the following sections: A—Subject Index, B—Personal Author Index, C—Contract Number Index, D—Meeting Paper and Report Number Index, and E—Accession Number Index.

Indexing Vocabulary

The Preliminary Edition of the NASA THESAURUS (December 1967) (NASA SP-7030) is the authority for the indexing vocabulary that appears in the subject indexes to STAR and IAA. The NASA Thesaurus should be consulted for a total picture of the current indexing vocabulary and associated cross-reference structure. Copies of the NASA Thesaurus may be obtained from the National Technical Information Service or the U.S. Government Printing Office at a price of \$8.50 for the three-volume set.

how to obtain publications abstracted

Documents abstracted are available from the AIAA Technical Information Service as follows:

- Paper copies of accessions announced in IAA and STAR and of other documents in the TIS library are available at \$5.00 per document up to a maximum of 20 pages. The charge for each additional page is \$0.25.
- Microfiche of documents announced in IAA are available at the rate of \$1.00 per microfiche on demand. Documents available in this manner are identified by the symbol # following the accession number in the Abstracts Section and in the Meeting Paper and Report Number and the Accession Number Indexes.
- Minimum air-mail postage to foreign countries is \$1.00.
- A number of publications, because of their special characteristics, are available only for reference in the library.

Address all inquiries and requests to:

Technical Information Service
American Institute of Aeronautics
and Astronautics, Inc.
750 Third Avenue, New York, N. Y. 10017

Telephone: 212 TN-7-8300
TWX: 212 867-7265

**PLEASE REFER TO THE ACCESSION NUMBER WHEN
REQUESTING PUBLICATIONS**

CROSS REFERENCES

The subject index includes two types of cross references to aid the user of the index in locating the material being sought:

1. "USE" references (U) direct the user to alternate headings under which material on the subject will be found, for example

COLUMBIUM
U NIOBIUM

2. "NARROWER TERM" references (NT) refer the user to more specific headings in the same subject area for example

LUMINESCENCE
NT ELECTROLUMINESCENCE

The periodicals listed in this section were scanned during the preparation of *International Aerospace Abstracts* for 1970. The periodicals were received regularly in all but a few instances. In the case of titles preceded by an asterisk, only the articles abstracted in *International Aerospace Abstracts* are available. All abstracted articles can be obtained from the AIAA Technical Information Service.

BM — Bimonthly
BW — Biweekly
Irreg. — Irregular
M — Monthly

Q — Quarterly
SA — Semiannual
SM — Semimonthly
W — Weekly

Aachen, Aerodynamisches Institut, Abhandlungen. Rheinische-Westfälische Technische Hochschule, Aachen, West Germany. Irreg.

Abastumanskaia Astrofizicheskaiia Observatoriia, Biulleten'. Akademiia Nauk Gruzinskoi SSR, Tbilisi. Irreg.

Académie des Sciences (Paris), Comptes Rendus, Série A — Sciences Mathématiques, Série B — Sciences Physiques. Académie des Sciences; Gauthier-Villars, Paris. W

Académie des Sciences (Paris), Comptes Rendus, Série C — Sciences Chimiques. Académie des Sciences; Gauthier-Villars, Paris. W

Académie des Sciences (Paris), Comptes Rendus, Série D — Sciences Naturelles. Académie des Sciences; Gauthier-Villars, Paris. W

Académie Polonaise des Sciences, Bulletin, Série des Sciences Mathématiques, Astronomiques et Physiques. Académie Polonaise des Sciences; Państwowe Wydawnictwo Naukowe, Warsaw. M

Académie Polonaise des Sciences, Bulletin, Série des Sciences Techniques. Académie Polonaise des Sciences; Państwowe Wydawnictwo Naukowe, Warsaw. M

Académie Royale de Belgique, Classe des Sciences, Bulletin. Académie Royale de Belgique; Office International de Librairie, Brussels. M

**Académie Royale de Belgique, Classe des Sciences, Mémoires.* Académie Royale de Belgique, Brussels.

Academy of Management Journal. Academy of Management, University of Washington, Graduate School of Business Administration, Seattle. Q

Academy of Sciences, USSR, Izvestiya, Atmospheric and Oceanic Physics (Akademiia Nauk SSSR, Izvestiia, Fizika Atmosfery i Okeana). American Geophysical Union, Washington, D.C. M

Accademia di Scienze e Lettere, Istituto Lombardo, Rendiconti, Serie della Classe di Scienze Matematiche e Naturali, Sezione A — Scienze Matematiche, Fisiche, Chimiche e Geologiche. Istituto Lombardo di Scienze e Lettere, Milan. Irreg.

Accademia Nazionale dei Lincei, Atti, Rendiconti — Classe di Scienze Fisiche, Matematiche e Naturali. Accademia Nazionale dei Lincei, Rome. BM

**Accounts of Chemical Research.* American Chemical Society, Washington, D.C. M

ACM, Communications. Association for Computing Machinery, Baltimore, Md. M

Acoustical Society of America, Journal. Acoustical Society of America; American Institute of Physics, Inc., New York. M

Acta Astronomica. Polska Akademia Nauk; Państwowe Wydawnictwo Naukowe, Warsaw. Q

Acta Biologica et Medica Germanica. Akademie-Verlag GmbH, Berlin. M

Acta Cardiologica. Editions Acta Medica Belgica, Brussels. BM

**Acta Crystallographica.* Munksgaard International Booksellers & Publishers, Copenhagen. BM

Acta Electronica. Laboratoires d'Electronique et de Physique Appliquée, Limeil-Brévannes (Val de Marne), France. Q

Acta Geophysica Polonica. Polska Akademia Nauk; Państwowe Wydawnictwo Naukowe, Warsaw. Q

Acta Mechanica. Springer Verlag, Vienna. 8 issues per year

Acta Metallurgica. Pergamon Press, Inc., Elmsford, N.Y. M

Acta Physica. Akadémiai Kiadó, Budapest. BM

Acta Physica Austriaca. Österreichische Akademie der Wissenschaften; Springer Verlag, Vienna. Q

Acta Physica Polonica, Seria A. Polska Akademia Nauk, Instytut Fizyki and Polskie Towarzystwo Fizyczne, Warsaw.

Acta Physica Polonica, Seria B. Polska Akademia Nauk, Instytut Fizyki and Polskie Towarzystwo Fizyczne, Warsaw.

Acta Physiologica Polonica. Polska Akademia Nauk; Państwowy Zakład Wydawnictw Lekarskich, Warsaw. BM

Acta Polytechnica Scandinavica, Civil Engineering and Building Construction Series. Scandinavian Council for Applied Research; Stockholm. Irreg.

Acta Polytechnica Scandinavica, Electrical Engineering Series. Scandinavian Council for Applied Research, Stockholm. Irreg.

Acta Polytechnica Scandinavica, Mathematics and Computing Machinery Series. Scandinavian Council

INTERNATIONAL AEROSPACE ABSTRACTS

- for Applied Research, Stockholm. Irreg.
- Acta Polytechnica Scandinavica, Mechanical Engineering Series.* Scandinavian Council for Applied Research, Stockholm. Irreg.
- Acta Technica.* Akadémiai Kiadó, Budapest. 4 vols. per year
- Acta Technica ČSAV.* Československá Akademie Věd, Prague. BM
- Acta Universitatis Wratislaviensis, Seria Matematyka, Fizyka, Astronomia.* Wydawnictwa Uniwersytetu Wrocławskiego, Wrocław. Irreg.
- Acustica.* S. Hirzel Verlag, KG, Stuttgart, West Germany. Irreg.
- Administrative Science Quarterly.* Cornell University, Graduate School of Business and Public Administration, Ithaca, N.Y. Q
- Advances in Physics.* Taylor & Francis, Ltd., London. BM
- *Advances in Polymer Science.* Springer Verlag, Berlin. Irreg.
- AEG-Telefunken, Technische Mitteilungen* (formerly *Technische Mitteilungen AEG-Telefunken*). AEG-Telefunken, Berlin. BM
- Aequationes Mathematicae.* University of Waterloo, Ontario, Canada; Birkhäuser Verlag, Basel. 3 issues per year
- Aero Medical Society of India, Journal.* Institute of Aviation Medicine, Bangalore.
- Aero-Revue.* Aero-Club der Schweiz and OSTIV; National-Zeitung AG, Basel. M
- Aerodinamika Razrezhennykh Gazov.* Izdatel'stvo Leningradskogo Universiteta, Leningrad. Irreg.
- Aeronautical Journal.* Royal Aeronautical Society, London. M
- Aeronautical Quarterly.* Royal Aeronautical Society, London. Q
- Aeronautical Society of India, Journal.* Aeronautical Society of India, New Delhi. Q
- L'Aéronautique et l'Astronautique.* Association Française des Ingénieurs et Techniciens de l'Aéronautique et de l'Espace and Société Française de l'Astronautique; Editions Air & Cosmos, Paris. M
- Aerospace Management.* General Electric Co., Aerospace Group, Philadelphia, Pa. Q
- Aerospace Medicine.* Aerospace Medical Association, Washington, D.C. M
- L'Aerotecnica.* Associazione Italiana di Aerotecnica, Rome. BM
- AFEDES, Cahiers.* Editions Européennes Thermique et Industrie, Paris.
- AIAA Journal.* American Institute of Aeronautics and Astronautics, Inc., New York. M
- AIAA Student Journal.* American Institute of Aeronautics and Astronautics, Inc., New York. Q
- AIChE Journal.* American Institute of Chemical Engineers, New York. BM
- Air et Cosmos.* Paris. W
- Air Line Pilot.* Air Line Pilots Association/International, Washington, D.C. M
- Air University Review.* Aerospace Studies Institute, Maxwell Air Force Base, Ala. BM
- Aircraft Engineering.* Bunhill Publications, Ltd., London. M
- Airline Management and Marketing Including American Aviation.* Ziff-Davis Publishing Co., New York. M
- Akademiia Nauk Armianskoi SSR, Biurakanskaia Observatoriia, Soobshcheniia.* Akademiia Nauk Armianskoi SSR, Yerevan. Irreg.
- Akademiia Nauk Armianskoi SSR, Doklady.* Akademiia Nauk Armianskoi SSR, Yerevan. 10 issues per year
- Akademiia Nauk Armianskoi SSR, Izvestiia, Fizika.* Akademiia Nauk Armianskoi SSR, Yerevan. BM
- Akademiia Nauk Armianskoi SSR, Izvestiia, Mekhanika.* Akademiia Nauk Armianskoi SSR, Yerevan. BM
- Akademiia Nauk Armianskoi SSR, Izvestiia, Seria Tekhnicheskikh Nauk.* Akademiia Nauk Armianskoi SSR, Yerevan. BM
- Akademiia Nauk Azerbaidzhanskoi SSR, Doklady.* Akademiia Nauk Azerbaidzhanskoi SSR; Izdatel'stvo Elm, Baku. M
- Akademiia Nauk Azerbaidzhanskoi SSR, Izvestiia, Seria Fiziko-Tekhnicheskikh i Matematicheskikh Nauk.* Akademiia Nauk Azerbaidzhanskoi SSR; Izdatel'stvo Elm, Baku. BM
- Akademiia Nauk BSSR, Doklady.* Akademiia Nauk Belorusskoi SSR, Minsk. M
- Akademiia Nauk Gruzinskoi SSR, Soobshcheniia.* Akademiia Nauk Gruzinskoi SSR, Tiflis. M
- Akademiia Nauk Kazakhskoi SSR, Izvestiia, Seria Fiziko-Matematicheskaiia.* Akademiia Nauk Kazakhskoi SSR, Alma Ata. BM
- Akademiia Nauk Kazakhskoi SSR, Vestnik.* Akademiia Nauk Kazakhskoi SSR; Izdatel'stvo Nauka, Alma Ata. M
- Akademiia Nauk Latviiskoi SSR, Izvestiia, Seria Fizicheskikh i Tekhnicheskikh Nauk.* Akademiia Nauk Latviiskoi SSR, Riga. BM
- Akademiia Nauk SSSR, Doklady.* Akademiia Nauk SSSR; Izdatel'stvo Nauka, Moscow. 36 issues per year
- Akademiia Nauk SSSR, Izvestiia, Energetika i Transport.* Akademiia Nauk SSSR; Izdatel'stvo Nauka, Moscow. BM
- Akademiia Nauk SSSR, Izvestiia, Fizika Atmosfery i Okeana.* Akademiia Nauk SSSR; Izdatel'stvo Nauka, Moscow. M
- Akademiia Nauk SSSR, Izvestiia, Mekhanika Tverdogo Tela.* Akademiia Nauk SSSR; Izdatel'stvo Nauka, Moscow. BM
- Akademiia Nauk SSSR, Izvestiia, Mekhanika Zhidkosti i Gaza.* Akademiia Nauk SSSR; Izdatel'stvo Nauka, Moscow. BM
- Akademiia Nauk SSSR, Izvestiia, Metally.* Akademiia Nauk SSSR; Izdatel'stvo Nauka, Moscow. BM
- Akademiia Nauk SSSR, Izvestiia, Neorganicheskie Materialy.* Akademiia Nauk SSSR, Moscow. M
- Akademiia Nauk SSSR, Izvestiia, Seria Biologicheskaiia.* Akademiia Nauk SSSR; Izdatel'stvo Nauka, Moscow. BM
- Akademiia Nauk SSSR, Izvestiia, Seria Fizicheskaiia.* Akademiia Nauk SSSR; Izdatel'stvo Nauka, Moscow. M
- Akademiia Nauk SSSR, Izvestiia, Seria Matematicheskaiia.* Akademiia Nauk SSSR; Izdatel'stvo Nauka, Moscow. BM
- Akademiia Nauk SSSR, Izvestiia, Tekhnicheskaiia Kibernetika.* Akademiia Nauk SSSR; Izdatel'stvo Nauka, Moscow. BM
- Akademiia Nauk SSSR, Sibirskoe Otdelenie, Izvestiia,*

- Seriia Tekhnicheskikh Nauk.* Akademiia Nauk SSSR, Sibirskoe Otdelenie; Izdatel'stvo Nauka, Novosibirsk. 3 issues per year
- Akademiia Nauk SSSR, Vestnik.* Akademiia Nauk SSSR; Izdatel'stvo Nauka, Moscow. M
- Akademiia Nauk Tadzhikskoi SSR, Doklady.* Akademiia Nauk Tadzhikskoi SSR; Izdatel'stvo Donish, Dushanbe. M
- Akademiia Nauk Tadzhikskoi SSR, Institut Astrofiziki, Biulleten'.* Akademiia Nauk Tadzhikskoi SSR; Izdatel'stvo Donish, Dushanbe. Irreg.
- Akademiia Nauk Tadzhikskoi SSR, Otdelenie Fiziko-Matematicheskikh i Geologo-Khimicheskikh Nauk, Izvestiia.* Akademiia Nauk Tadzhikskoi SSR; Izdatel'stvo Donish, Dushanbe. Q
- Akademiia Nauk Turkmenskoi SSR, Izvestiia, Seriia Fiziko-Tekhnicheskikh, Khimicheskikh i Geologicheskikh Nauk.* Akademiia Nauk Turkmenskoi SSR; Izdatel'stvo Ylym, Ashkhabad. BM
- Akademiia Nauk Ukrains'koi RSR, Dopovidi, Seriia A – Fiziko-Tekhnichni i Matematichni Nauki.* Akademiia Nauk Ukrains'koi RSR; Izdatel'stvo Naukova Dumka, Kiev. M
- Akademiia Nauk Ukrains'koi RSR, Dopovidi, Seriia B – Geologii, Geofizika, Khimii i Biologii.* Akademiia Nauk Ukrains'koi RSR; Izdatel'stvo Naukova Dumka, Kiev. M
- Akademiia Nauk Ukrains'koi RSR, Visnik.* Akademiia Nauk Ukrains'koi RSR; Izdatel'stvo Naukova Dumka, Kiev.
- Akademiia Nauk Uzbekskoi SSR, Doklady.* Akademiia Nauk Uzbekskoi SSR, Tashkent. M
- Akademiia Nauk Uzbekskoi SSR, Izvestiia, Seriia Fiziko-Matematicheskikh Nauk.* Akademiia Nauk Uzbekskoi SSR, Tashkent. BM
- Akademiia Nauk Uzbekskoi SSR, Izvestiia, Seriia Tekhnicheskikh Nauk.* Akademiia Nauk Uzbekskoi SSR, Tashkent. BM
- Akademiia Navuk BSSR, Vestsi, Seryia Fizika-Tekhnichnykh Navuk.* Akademiia Navuk Belaruskai SSR, Minsk. Q
- Akusticheskii Zhurnal.* Akademiia Nauk SSSR; Izdatel'stvo Nauka, Moscow. Q
- *Alabama Academy of Science, Journal.* Auburn University, Auburn, Ala. Q
- Alata Internazionale.* Etas Kompass, Milan. M
- Alta Frequenza.* Associazione Elettrotecnica ed Elettronica Italiana, Milan. M
- Alta Frequenza (English Edition).* Associazione Elettrotecnica ed Elettronica Italiana, Milan. M
- Alta Frequenza, Supplemento.* Associazione Elettrotecnica ed Elettronica Italiana, Milan.
- Aluminium.* Aluminium-Zentrale e.V.; Aluminium-Verlag GmbH, Düsseldorf. M
- American Ceramic Society Bulletin.* American Ceramic Society, Inc., Columbus, Ohio. M
- American Ceramic Society, Journal.* American Ceramic Society, Inc., Columbus, Ohio. M
- American Chemical Society, Journal.* American Chemical Society, Washington, D.C. BW
- *American Dietetic Association, Journal.* American Dietetic Association, Chicago. M
- American Heart Journal.* C. V. Mosby Co., St. Louis, Mo. M
- American Helicopter Society, Journal.* American Helicopter Society, Inc., New York. Q
- American Industrial Hygiene Association Journal.* American Industrial Hygiene Association, Southfield, Mich. BM
- *American Journal of Botany.* Botanical Society of America, Inc., New York. 10 issues per year
- American Journal of Cardiology.* American College of Cardiology; Reuben H. Donnelley Corp., New York. M
- *American Journal of Clinical Nutrition.* American Society of Clinical Nutrition, Inc., Bethesda, Md. M
- *American Journal of Ophthalmology.* Ophthalmic Publishing Co., Chicago. M
- American Journal of Optometry and Archives of American Academy of Optometry.* Minneapolis, Minn. M
- American Journal of Physics.* American Association of Physics Teachers; American Institute of Physics, Inc., New York. M
- American Journal of Physiology.* American Physiological Society, Bethesda, Md. M
- *American Journal of Psychology.* University of Illinois Press, Urbana, Ill. Q
- *American Journal of Roentgenology, Radium Therapy and Nuclear Medicine.* American Roentgen Ray Society; American Radium Society, Springfield, Ill. M
- *American Journal of Science.* Yale University, Kline Geology Laboratory, New Haven, Conn. M
- *American Journal of the Medical Sciences.* Ed. Russell S. Weiser, Lea & Febiger, Philadelphia, Pa. M
- *American Mathematical Society, Proceedings.* American Mathematical Society, Providence, R.I. M
- American Mathematical Society, Transactions.* American Mathematical Society, Providence, R.I. M
- American Meteorological Society, Bulletin.* American Meteorological Society, Boston. M
- *American Mineralogist.* Mineralogical Society of America, Washington, D.C. BM
- *American Philosophical Society, Proceedings.* American Philosophical Society, Philadelphia, Pa. BM
- *American Psychologist.* American Psychological Association, Washington, D.C. M
- American Society of Civil Engineers, Engineering Mechanics Division, Journal.* American Society of Civil Engineers, New York. BM
- American Society of Civil Engineers, Structural Division, Journal.* American Society of Civil Engineers, New York. M
- *American Statistical Association, Journal.* American Statistical Association, Washington, D.C. Q
- *American Veterinary Medical Association, Journal.* Ed. Dr. A. Freeman, Chicago. SM
- *Analytica Chimica Acta.* Elsevier Publishing Co., Amsterdam. M
- *Analytical Biochemistry.* Academic Press, Inc., New York. M
- *Analytical Chemistry.* American Chemical Society, Washington, D.C. M
- Annalen der Physik.* Johann Ambrosius Barth Verlag, Leipzig, East Germany. Irreg.
- Annales de Géophysique.* Centre National de la Recherche Scientifique, Paris. Q
- Annales de Physique.* Centre National de la Recherche

- Scientifique; Masson & Cie., Paris. BM
- Annales des Télécommunications*. Centre National d'Etudes des Télécommunications, Issy-les-Moulineaux (Seine), France. BM
- Annali di Geofisica*. Istituto Nazionale de Geofisica, Rome. Q
- Annals of Physics*. Academic Press, Inc., New York. M
- Annual Review of Physical Chemistry*. Annual Reviews, Inc., Palo Alto, Calif. Annual
- **Annual Review of Plant Physiology*. Annual Reviews, Inc., Palo Alto, Calif. Annual
- Aplikace Matematiky*. Československá Akademie Věd, Matematický Ústav, Prague. BM
- Apparecchiature Idrauliche e Pneumatiche*. Etas Kompass, Milan. BM
- Applied Electrical Phenomena (Elektronnaia Obrabotka Materialov)*. Consultants Bureau, New York. BM
- Applied Mechanics Reviews*. American Society of Mechanical Engineers, New York. M
- Applied Microbiology*. American Society for Microbiology, Bethesda, Md. M
- Applied Optics*. Optical Society of America; American Institute of Physics, Inc., New York. M
- Applied Physics Letters*. American Institute of Physics, Inc., New York. SM
- Applied Polymer Symposia*. Interscience Publishers, New York.
- Applied Scientific Research*. Martinus Nijhoff, The Hague. Irreg.
- Applied Spectroscopy*. Society for Applied Spectroscopy, Boston College, Mass.; American Institute of Physics, Inc., New York. BM
- **Arbeit und Leistung*. Bartmann Verlag, Cologne. M
- **Arbeitsmedizin, Sozialmedizin, Arbeitshygiene*. Gentner-Verlag, KG, Stuttgart, West Germany. M
- Archiv der elektrischen Übertragung*. S. Hirzel Verlag, KG, Stuttgart, West Germany. M
- Archiv für Elektrotechnik*. Springer Verlag, Berlin. BM
- Archiv für Meteorologie, Geophysik und Bioklimatologie, Serie A – Meteorologie und Geophysik*. Springer Verlag, Vienna. Irreg.
- Archiv für Meteorologie, Geophysik und Bioklimatologie, Serie B – Klimatologie, Bioklimatologie, Strahlungsforschung*. Springer Verlag, Vienna. Irreg.
- **Archiv für Mikrobiologie*. Springer Verlag, Berlin. 4 vols. per year
- Archiv für technisches Messen und industrielle Messtechnik*. Verlag R. Oldenbourg, Munich. M
- Archive for Rational Mechanics and Analysis*. Springer Verlag, Berlin. Irreg.
- Archives des Sciences*. Société de Physique et d'Histoire Naturelle de Genève, Geneva. 3 issues per year
- **Archives of Biochemistry and Biophysics*. Academic Press, Inc., New York. M
- Archives of Environmental Health*. American Medical Association, Chicago. M
- **Archives of Neurology*. American Neurological Association; American Medical Association, Chicago. M
- Archiwum Automatyki i Telemekhaniki*. Polska Akademia Nauk; Państwowe Wydawnictwo Naukowe, Warsaw. Q
- Archiwum Budowy Maszyn*. Polska Akademia Nauk, Komitet Budowy Maszyn; Państwowe Wydawnictwo Naukowe, Warsaw. Q
- Archiwum Elektrotechniki*. Polska Akademia Nauk; Państwowe Wydawnictwo Naukowe, Warsaw. Q
- Archiwum Mechaniki Stosowanej*. Polska Akademia Nauk, Instytut Podstawowych Problemów Techniki; Państwowe Wydawnictwo Naukowe, Warsaw. BM
- Arkiv för Astronomi*. Kungliga Svenska Vetenskapsakademien; Almqvist & Wiksells Boktryckeri AB, Stockholm. Irreg.
- Arkiv för Fysik (see Physica Scripta)*.
- Arkiv för Geofysik*. Kungliga Svenska Vetenskapsakademien; Almqvist & Wiksells Boktryckeri AB, Stockholm. Irreg.
- Artificial Satellites*. Polish Academy of Sciences, Warsaw. Q
- ASCE, Transportation Engineering Journal*. American Society of Civil Engineers, New York. Q
- ASHRAE Journal*. American Society of Heating, Refrigerating and Air-Conditioning Engineers, Inc., New York. M
- ASLE Transactions*. American Society of Lubrication Engineers; Academic Press, Inc., New York. M
- ASM Transactions Quarterly (see Metallurgical Transactions)*.
- ASME, Transactions, Series A – Journal of Engineering for Power*. American Society of Mechanical Engineers, New York. Q
- ASME, Transactions, Series B – Journal of Engineering for Industry*. American Society of Mechanical Engineers, New York. Q
- ASME, Transactions, Series C – Journal of Heat Transfer*. American Society of Mechanical Engineers, New York. Q
- ASME, Transactions, Series D – Journal of Basic Engineering*. American Society of Mechanical Engineers, New York. Q
- ASME, Transactions, Series E – Journal of Applied Mechanics*. American Society of Mechanical Engineers, New York. Q
- ASME, Transactions, Series F – Journal of Lubrication Technology*. American Society of Mechanical Engineers, New York. Q
- Association for Computing Machinery, Journal*. Association for Computing Machinery, Inc., New York. Q
- Association Technique Maritime et Aéronautique, Bulletin*. Association Technique Maritime et Aéronautique, Paris. Annual
- **ASTM Special Technical Publication*. American Society for Testing and Materials, Philadelphia, Pa. Irreg.
- Astrofizika*. Akademiia Nauk Armianskoi SSR, Yerevan. Q
- Astronautica Acta*. International Academy of Astronautics; Pergamon Press, Ltd., Oxford. BM
- Astronautical Society of the Republic of China, Transactions*. Astronautical Society of the Republic of China, Taiwan. Annual
- Astronautics and Aeronautics*. American Institute of Aeronautics and Astronautics, Inc., New York. M
- Astronautik*. Hermann Oberth-Gesellschaft, e.V., Hannover, West Germany. Q
- Astronautyka*. Polskie Towarzystwo Astronautyczne, Warsaw. Q
- Astronomical Institutes of Czechoslovakia, Bulletin*. Československá Akademie Věd, Prague. BM
- Astronomical Institutes of the Netherlands, Bulletin*.

- Supplement Series.** Astronomical Institutes of the Netherlands; North-Holland Publishing Co., Amsterdam. Irreg.
- Astronomical Journal.** American Astronomical Society; American Institute of Physics, Inc., New York. 10 issues per year
- Astronomical Society of Australia, Proceedings.** Astronomical Society of Australia; Sydney University Press, Sydney. SA
- Astronomical Society of Japan, Publications.** Astronomical Society of Japan, c/o Tokyo Astronomical Observatory, Mitaka, Tokyo. Q
- Astronomical Society of the Pacific, Publications.** Astronomical Society of the Pacific, San Francisco. BM
- Astronomicheskii Vestnik.** Vsesoiuznoe Astronomo-Geodezicheskoe Obshchestvo; Izdatel'stvo Nauka, Moscow. Q
- Astronomicheskii Zhurnal.** Akademiia Nauk SSSR; Izdatel'stvo Nauka, Moscow. BM
- L'Astronomie.** Société Astronomique de France, Paris. BM
- Astronomie und Raumfahrt.** Deutsche Astronautische Gesellschaft, Berlin. BM
- Astronomisch Bulletin.** Koninklijke Sterrewacht van België, Belgium.
- Astronomische Gesellschaft, Mitteilungen.** Astronomische Gesellschaft, Hamburg; G. Braun GmbH, Karlsruhe, West Germany. Irreg.
- Astronomische Nachrichten.** Akademie-Verlag GmbH, Berlin. Irreg.
- Astronomy and Astrophysics.** Springer Verlag, Berlin. M
- Astronomy and Astrophysics Supplement Series.** Leiden Observatory, Leiden. M
- Astronomy Today.** Planet Publications, London. Q
- Astrophysical Journal.** American Astronomical Society; University of Chicago Press, Chicago. M
- Astrophysical Journal Supplement Series.** American Astronomical Society; University of Chicago Press, Chicago. M
- Astrophysical Letters.** Gordon & Breach Science Publishers, Ltd., London. M
- Astrophysics and Space Science.** D. Reidel Publishing Co., Dordrecht, Netherlands. M
- Atmospheric Environment.** Pergamon Press, Ltd., Oxford. BM
- *Australian Journal of Chemistry.** Commonwealth Scientific and Industrial Research Organization, Melbourne. M
- Australian Journal of Physics.** Commonwealth Scientific and Industrial Research Organization, Melbourne. BM
- Australian Journal of Physics, Astrophysical Supplement.** Commonwealth Scientific and Industrial Research Organization, Melbourne. BM
- Australian Mathematical Society, Journal.** Australian Mathematical Society; Wolters-Noordhoff N. V., Groningen, Netherlands. BM
- Australian Meteorological Magazine.** Bureau of Meteorology, Melbourne. Q
- Automatic Welding (Avtomaticheskaiia Svarka).** The Welding Institute, Cambridge. M
- Automatica.** Pergamon Press, Ltd., Oxford. BM
- Automation and Remote Control (Avtomatika i Telemekhanika).** Consultants Bureau, New York. M
- Automatisme.** Association Française pour la Cybernétique Economique et Technique; Dunod Editeur, Paris. BM
- Automatizace.** Ministerstvo Průmyslu; Nakladatelství Technické Literatury, Prague. M
- Aviation Review.** Smiths Industries, Ltd., Aviation Div., Wembley, Middx., England. Irreg.
- Aviation Week and Space Technology.** McGraw-Hill, Inc., New York. W
- Aviatsiia i Kosmonavtika.** Voenizdat, Moscow. M
- Aviatsionnaia Tekhnika.** Ministerstvo Vysshego i Srednego Spetsial'nogo Obrazovaniia SSSR; Izdanie Kazanskogo Aviatsionnogo Instituta, Kazan. Q
- Aviazione di Linea — Aeronautica e Spazio.** Publitecno International, Rome. M
- Avtomatika.** Akademiia Nauk Ukrainskoi SSR; Izdatel'stvo Naukova Dumka, Kiev. BM
- Avtomatika i Telemekhanika.** Akademiia Nauk SSSR; Izdatel'stvo Nauka, Moscow. M
- Avtomatika i Vychislitel'naia Tekhnika.** Akademiia Nauk Latvinskoi SSR; Izdatel'stvo Zinatne, Riga. BM
- Babeş-Bolyai, Universitas, Studia, Series Physica.** Babeş-Bolyai, Universitas, Cluj, Rumania. SA
- Battelle Information.** Battelle-Institut, Frankfurt/Main. Irreg.
- Battelle Research Outlook.** Battelle Memorial Institute, Columbus Laboratories, Columbus, Ohio. Q
- Bayerische Akademie der Wissenschaften, mathematisch-naturwissenschaftliche Klasse, Sitzungsberichte.** Bayerische Akademie der Wissenschaften, Munich. Irreg.
- Bee-Hive.** United Aircraft Corp., East Hartford, Conn. Q
- *Behavior Research Methods and Instrumentation.** Psychonomic Journals, Inc., University of Wisconsin, Madison, Wis. BM
- Behavioral Science.** Mental Health Research Institute, University of Michigan, Ann Arbor. BM
- Beiträge aus der Plasmaphysik.** Akademie-Verlag GmbH, Berlin.
- Beiträge zur Physik der Atmosphäre.** Friedr. Vieweg & Sohn GmbH, Braunschweig. Q
- Beiträge zur Radioastronomie.** Max-Planck-Institut für Radioastronomie; Ferd. Dümmlers Verlag, Bonn. Q
- Bell Laboratories Record.** Bell Telephone Laboratories, Inc., Murray Hill, N.J. M
- Bell System Technical Journal.** American Telephone & Telegraph Co., New York. 10 issues per year
- Bendix Technical Journal.** Bendix Corp., Southfield, Mich. 3 issues per year
- Bildmessung und Luftbildwesen.** Deutsche Gesellschaft für Photogrammetrie; Herbert Wichmann Verlag, Karlsruhe, West Germany. Q
- Bio-Medical Engineering.** United Trade Press, Ltd., London. M
- Biochemical and Biophysical Research Communications.** Academic Press, Inc., New York. SM
- *Biochemical Genetics.** Plenum Publishing Corp., New York. BM
- *Biochemistry.** American Chemical Society, Washington, D.C. M
- *Biochimica et Biophysica Acta.** Elsevier Publishing Co., Amsterdam. W

- *Biological Conservation.* Elsevier Publishing Co., Ltd., Barking, Essex, England. Q
- *Biological Psychiatry.* Society of Biological Psychiatry; Plenum Publishing Corp., New York. Q
- Biophysical Journal.* Biophysical Society; Rockefeller University Press, New York. M
- *Biophysik.* Springer Verlag, Berlin.
- BioScience.* American Institute of Biological Sciences, Washington, D.C. M
- Biotechnology and Bioengineering.* Interscience Publishers, New York. BM
- Biulleten' Eksperimental'noi Biologii i Meditsiny.* Akademiia Meditsinskikh Nauk SSSR; Izdatel'stvo Meditsina, Moscow. M
- B'lgarska Akademiia na Naukite, Fizicheski Institut s ANEB, Izvestiia.* B'lgarska Akademiia na Naukite, Otdelenie za Matematicheski i Fizicheski Nauki, Sofia. Irreg.
- B'lgarska Akademiia na Naukite, Geofizichni Institut, Izvestiia.* B'lgarska Akademiia na Naukite, Sofia. Irreg.
- B'lgarska Akademiia na Naukite, Institut po Elektronika, Izvestiia.* B'lgarska Akademiia na Naukite, Otdelenie za Matematicheski i Fizicheski Nauki, Sofia. Irreg.
- B'lgarska Akademiia na Naukite, Institut po Khidrologiia i Meteorologiia, Izvestiia.* B'lgarska Akademiia na Naukite, Otdelenie za Matematicheski i Fizicheski Nauki, Sofia. Irreg.
- B'lgarska Akademiia na Naukite, Institut po Tekhnicheska Kibernetika, Izvestiia.* B'lgarska Akademiia na Naukite, Otdelenie za Tekhnicheski Nauki, Sofia. Irreg.
- B'lgarska Akademiia na Naukite, Institut po Tekhnicheska Mekhanika, Izvestiia.* B'lgarska Akademiia na Naukite, Otdelenie za Tekhnicheski Nauki, Sofia. Irreg.
- B'lgarska Akademiia na Naukite, Izvestiia na Geofizichni Institut (see B'lgarska Akademiia na Naukite, Geofizichni Institut, Izvestiia).*
- B'lgarska Akademiia na Naukite, Matematicheski Institut, Izvestiia.* B'lgarska Akademiia na Naukite, Otdelenie za Matematicheski i Fizicheski Nauki, Sofia. Irreg.
- B'lgarska Akademiia na Naukite, Sektsiia po Astronomiia, Izvestiia.* B'lgarska Akademiia na Naukite, Otdelenie za Matematicheski i Fizicheski Nauki, Sofia. Irreg.
- B'lgarska Akademiia na Naukite, Tsentralna Laboratoriia po Geodeziia, Izvestiia.* B'lgarska Akademiia na Naukite, Otdelenie za Matematicheski i Fizicheski Nauki, Sofia. Irreg.
- Bolgarskaia Akademiia Nauk, Doklady.* B'lgarska Akademiia na Naukite, Sofia. M
- Bosch Technische Berichte.* Robert Bosch GmbH, Stuttgart, West Germany. Irreg.
- Boundary-Layer Meteorology.* D. Reidel Publishing Co., Dordrecht, Netherlands. Q
- *Brain Research.* Elsevier Publishing Co., Amsterdam. M
- Brennstoff-Chemie.* Verlag W. Girardet, Essen, West Germany. M
- British Astronomical Association, Journal.* British Astronomical Association, Hounslow West, Middx., England. BM
- British Interplanetary Society, Journal.* British Interplanetary Society, London. M
- *British Journal of Pharmacology.* British Pharmacological Society; Macmillan (Journals), Ltd., London. 9 issues per year
- Bucuresti, Institutul Politehnic Gheorghe Gheorghiu-Dej, Buletinul.* Institutul Politehnic Gheorghe Gheorghiu-Dej, Bucharest. BM
- Bucuresti, Universitatea, Anale, Seria Stiintele Naturii - Matematica, Mecanica.* Bucuresti, Universitatea, Bucharest. Irreg.
- *Building Science.* Pergamon Press, Ltd., Oxford. Q
- Bulletin Astronomique.* Centre National de la Recherche Scientifique, Paris. Q
- Bulletin d'Informations Scientifiques et Techniques.* Commissariat à l'Energie Atomique; Dunod Editeur, Paris. M
- Bulletin Géodésique.* Association Internationale de Géodésie, Paris. Q
- Bulletin Mathématique.* Societatea de Stiinte Matematice, Bucharest. Q
- Bulletin of Mathematical Biophysics.* MIT Press, Cambridge, Mass. Q
- Bulletin of the Atomic Scientists.* Educational Foundation for Nuclear Science, Chicago. 10 issues per year
- Business and Commercial Aviation.* Ziff-Davis Publishing Co., New York. M
- California Management Review.* University of California, Graduate School of Business Administration, Berkeley. Q
- Cambridge Philosophical Society, Proceedings.* Cambridge University Press, London. BM
- Canada, National Research Council, Division of Mechanical Engineering and National Aeronautical Establishment, Quarterly Bulletin.* National Research Council of Canada, Ottawa. Q
- Canada, National Research Council, Radio and Electrical Engineering Division, Bulletin.* National Research Council of Canada, Ottawa.
- Canadian Aeronautics and Space Journal.* Canadian Aeronautics and Space Institute, Ottawa. M
- *Canadian Journal of Mathematics.* University of Toronto Press, Toronto. BM
- *Canadian Journal of Microbiology.* National Research Council of Canada, Ottawa. BM
- Canadian Journal of Physics.* National Research Council of Canada, Ottawa. SM
- *Canadian Journal of Physiology and Pharmacology.* National Research Council of Canada, Ottawa. M
- *Canadian Journal of Psychology.* Canadian Psychological Association; University of Toronto Press, Toronto. Q
- Canadian Metallurgical Quarterly.* Canadian Institute of Mining and Metallurgy, Metallurgical Society, Ottawa. Q
- Canadian Operational Research Society, Journal.* Canadian Operational Research Society, Ottawa. 3 issues per year
- *Carbon.* Pergamon Press, Ltd., Oxford. BM
- Cardiovascular Research.* British Cardiac Society; British Medical Association, London. Q
- CASI Transactions.* Canadian Aeronautics and Space Institute, Ottawa. SA
- Celestial Mechanics.* D. Reidel Publishing Co., Dordrecht, Netherlands. Q
- Československý Časopis pro Fysiku, Sekce A.* Českoslo-

- venská Akademie Věd, Prague. BM
- Chartered Mechanical Engineer.* Institution of Mechanical Engineers, London. M
- Chemical and Engineering News.* American Chemical Society, Washington, D.C. W
- **Chemical Communications.* Chemical Society, London. SM
- Chemical Engineering Progress.* American Institute of Chemical Engineers, New York. M
- Chemical Engineering Progress, Symposium Series.* American Institute of Chemical Engineers, New York. M
- Chemical Physics Letters.* North-Holland Publishing Co., Amsterdam. BW
- **Chemical Society, Journal, Section C – Organic Chemistry.* London. M
- **Chemical Society of Japan, Bulletin.* Chemical Society of Japan, Tokyo. M
- Chemie-Ingenieur-Technik.* Gesellschaft Deutscher Chemiker; Verlag Chemie GmbH, Weinheim, West Germany. M
- **Chemistry in Britain.* Royal Institute of Chemistry, London. M
- Chubu Institute of Technology, Memoirs.* Chubu Institute of Technology, Nagoya. Irreg.
- Ciel et Terre.* Société Belge d'Astronomie, de Météorologie et de Physique du Globe, Brussels. BM
- Circulation.* American Heart Association, Inc., New York. M
- Circulation Research.* American Heart Association, New York. M
- **Clinical Orthopaedics.* J. B. Lippincott Co., Philadelphia, Pa. BM
- Cobalt.* Centre d'Information du Cobalt, Brussels. Q
- Combustion and Flame.* Combustion Institute; American Elsevier Publishing Co., Inc., New York. BM
- Combustion, Explosion, and Shock Waves (Fizika Goreniia i Vzryva).* The Faraday Press, Inc., New York. Q
- Combustion Science and Technology.* Gordon & Breach Science Publishers, Ltd., London. BM
- Comments on Astrophysics and Space Physics.* Gordon & Breach Science Publishers, Ltd., London. BM
- Communications in Mathematical Physics.* Springer Verlag, Berlin. Irreg.
- Communications on Pure and Applied Mathematics.* New York University, Courant Institute of Mathematical Sciences; Interscience Publishers, New York. BM
- **Comparative Biochemistry and Physiology.* Pergamon Press, Ltd., Oxford. M
- Composites.* Iliffe Science and Technology Publications, Ltd., Guildford, Surrey, England. Q
- **Computers and Biomedical Research.* Academic Press, Inc., New York. Q
- Computing.* Springer Verlag, Vienna. Q
- Contamination Control.* American Association for Contamination Control; Blackwell Publishing Co., Inc., Los Angeles. BM
- Contemporary Physics.* Taylor & Francis, Ltd., London. BM
- **Contributions to Mineralogy and Petrology.* Springer Verlag, Berlin. 3 vols per year
- Control Engineering.* Reuben H. Donnelley Corp., New York. M
- Coopération Méditerranéenne pour l'Energie Solaire, Bulletin.* Coopération Méditerranéenne pour l'Energie Solaire (COMPLES), Marseilles. SA
- Corrosion.* National Association of Corrosion Engineers, Inc., Houston, Tex. M
- Cosmic Electrodynamics.* D. Reidel Publishing Co., Dordrecht, Netherlands. Q
- Cosmic Research (Kosmicheskie Issledovaniia).* Consultants Bureau, New York. BM
- **Cryobiology.* Society for Cryobiology, Rockville, Md. BM
- Cryogenic Technology.* Cryogenic Society of America; Value Engineering Publications, Inc., Los Angeles. BM
- Cryogenics.* Iliffe Science & Technology Publications, Ltd., London. BM
- **Crystal Lattice Defects.* Gordon & Breach Science Publishers, Ltd., London. Q
- Current Science.* Current Science Association, Bangalore, India. SM
- Czechoslovak Journal of Physics, Section B.* Československá Akademie Věd, Prague. M
- Czechoslovak Mathematical Journal.* Československá Akademie Věd, Prague. Q
- **Deep-Sea Research and Oceanographic Abstracts.* Pergamon Press, Ltd., Oxford. BM
- Defence Science Journal.* Indian Ministry of Defence, New Delhi. Q
- Defense Management Journal.* Directorate for Management Improvement Programs, Office of the Assistant Secretary of Defense; Supt. of Documents, Washington, D.C. Q
- Demonstratio Mathematica.* Politechnika Warszawska, Instytut Matematyki, Warsaw.
- Deutscher Aerokurier.* Deutscher Aero Club, e.V., Frankfurt/Main. M
- **Developmental Psychobiology.* Interscience Publishers, New York. Q
- DGLR Mitteilungen.* Deutsche Gesellschaft für Luft- und Raumfahrt, e.V., Cologne. Q
- Differentsial'nye Uravneniia.* Izdatel'stvo Nauka i Tekhnika, Minsk. M
- Dinamika i Prochnost' Mashin.* Izdatel'stvo Khar'kovskogo Gosudarstvennogo Universiteta, Kharkov. Irreg.
- Dominion Observatory, Publications.* Canada, Department of Energy, Mines and Resources, Observatories Branch, Ottawa. Irreg.
- Dornier-Post* (English Edition). Dornier AG, Munich. Q
- Earth and Extraterrestrial Sciences.* Gordon & Breach Science Publishers, Ltd., London. Irreg.
- Earth and Planetary Science Letters.* North-Holland Publishing Co., Amsterdam. M
- **Earth Science Reviews.* Elsevier Publishing Co., Amsterdam. Q
- L'Echo des Recherches.* Centre National d'Etudes des Télécommunications, Issy-les-Moulineaux, France. Q
- Eesti NSV Teaduste Akadeemia, Toimetised,*

INTERNATIONAL AEROSPACE ABSTRACTS

- Füüsika-Matemaatika.* Izdatel'stvo Periodika, Tallin. Q
- Electrical Communication.* International Telephone and Telegraph Corp., New York. Q
- Electrical Communication Laboratory, Review.* Nippon Telegraph & Telephone Public Corp., Tokyo. BM
- Electrical Engineering in Japan (Denki Gakkai Zasshi).* Institute of Electrical Engineers of Japan; Institute of Electrical and Electronics Engineers, Inc., New York. M
- Electro-Technology.* Industrial Research, Inc., Beverly Shores, Ind. M
- Electrochemical Society, Journal.* Electrochemical Society, Inc., New York. M
- Electroencephalography and Clinical Neurophysiology.* International Federation of Societies for Electroencephalography and Clinical Neurophysiology; Elsevier Publishing Co., Amsterdam. M
- Electron Technology.* Polish Academy of Sciences, Institute of Electron Technology; Państwowe Wydawnictwo Naukowe, Warsaw. Irreg.
- Electronic Design.* Hayden Publishing Co., Inc., New York. BW
- Electronic Engineering.* Morgan-Grampian (Publishers), Ltd., London. M
- Electronic Packaging and Production.* Milton S. Kiver Publications, Inc., Chicago. M
- Electronic Progress.* Raytheon Co., Lexington, Mass. Q
- Electronics.* McGraw-Hill, Inc., New York. BW
- Electronics and Communications in Japan (Denshi Tsushin Gakkai Ronbunshi).* Institute of Electronics and Communications Engineers of Japan; Institute of Electrical and Electronics Engineers, Inc., New York. M
- Electronics and Power.* Institution of Electrical Engineers, London. M
- Electronics Letters.* Institution of Electrical Engineers, London. BW
- Elektromekhanika.* Ministerstvo Vysshego i Srednego Spetsial'nogo Obrazovaniia SSSR, Novocherkassk. M
- Elektronik.* Franzis-Verlag, Munich. M
- Elektronika* (formerly *Przegląd Elektroniki*). Wydawnictwa Czasopism Technicznych NOT, Warsaw. M
- Elektronische Datenverarbeitung.* Friedr. Vieweg & Sohn GmbH, Braunschweig. M
- Elektronische Rechenanlagen.* Verlag R. Oldenbourg, Munich. BM
- Elektrosviaz'.* Ministerstvo Sviazi SSSR and Tekhnicheskoe Obshchestvo Radiotekhniki, Elektroniki i Sviazi; Izdatel'stvo Sviaz', Moscow. M
- Elementarnye Chastitsy i Kosmicheskie Luchi.* Ministerstvo Vysshego i Srednego Spetsial'nogo Obrazovaniia SSSR; Moskovskii Inzhenerno-Fizicheskii Institut; Atomizdat, Moscow. Irreg.
- *Endocrinology.* Endocrine Society; J. B. Lippincott Co., Philadelphia, Pa. M
- Energomashinostroenie.* Ministerstvo Tiazhelogo, Energeticheskogo i Transportnogo Mashinostroeniia SSSR and Nauchno-Tekhnicheskoe Obshchestvo Mashinostroitel'noi Promyshlennosti; Izdatel'stvo Mashinostroenie, Leningrad. M
- Energy Conversion.* Pergamon Press, Ltd., Oxford. Q
- Engelhard Industries Technical Bulletin.* Engelhard Minerals & Chemicals Corp., Newark, N.J. Q
- The Engineer.* Morgan-Grampian (Publishers), Ltd., London. W
- Engineering Bulletin.* Motorola, Inc., Government Electronics Div., Scottsdale, Ariz. Irreg.
- Engineering Cybernetics (Akademiia Nauk SSSR, Izvestiia, Tekhnicheskaja Kibernetika).* Scripta Publishing Corp., Washington, D.C. BM
- Engineering Fracture Mechanics.* Pergamon Press, Ltd., Oxford. Q
- Entropie.* Editions Barthélemy & Cie., Paris. BM
- Environmental Engineering.* Society of Environmental Engineers, London; Kenneth Mason, Havant, Hants., England. BM
- Environmental Quarterly.* Little Neck, N.Y. Q
- Environmental Research.* Academic Press, Inc., New York. BM
- Environmental Space Sciences (Kosmicheskaja Biologiya i Meditsina).* Consultants Bureau, New York. BM
- EOS.* American Geophysical Union, Washington, D.C. M
- Ergonomics.* Ergonomics Research Society, Nederlandse Vereniging voor Ergonomie, International Ergonomics Association; Taylor & Francis, Ltd., London. Q
- Ericsson Technics.* Telefonaktiebolaget LM Ericsson, Stockholm. Q
- ESRO/ELDO Bulletin.* European Space Research Organization and European Space Vehicle Launcher Development Organization, Neuilly-sur-Seine, France. Q
- ESSO Air World.* ESSO International, Inc., New York. BM
- Eurocontrol.* Eurocontrol, Public Relations Div., Brussels. SA
- Evaluation Engineering.* A. Verner Nelson Associates, Highland Park, Ill. BM
- Experientia.* Birkhäuser Verlag, Basel. M
- Experimental Brain Research.* Springer Verlag, Berlin. Irreg.
- *Experimental Cell Research.* International Society for Cell Biology; Academic Press, Inc., New York. M
- Experimental Mechanics.* Society for Experimental Stress Analysis, Westport, Conn. M
- *Experimental Neurology.* Academic Press, Inc., New York. M
- Explosivstoffe.* Erwin Barth Verlag, KG, Mannheim, West Germany. M
- Facilities for Atmospheric Research.* National Center for Atmospheric Research, Boulder, Colo. Q
- *Federation Proceedings.* Federation of American Societies for Experimental Biology, Washington, D.C. Q
- Finommechanika.* Lapkiadó Vállalat, Budapest. M
- Fizika.* Ministerstvo Vysshego i Srednego Spetsial'nogo Obrazovaniia SSSR; Izdatel'stvo Tomskogo Universiteta, Tomsk. M
- Fizika Aerodispersnykh Sistem.* Izdatel'stvo Kievskogo Universiteta, Kiev. Irreg.
- Fizika Goreniia i Vzryva.* Akademiia Nauk SSSR, Sibirskoe Otdelenie; Izdatel'stvo Nauka, Novosibirsk. Q
- Fizika i Tekhnika Poluprovodnikov.* Akademiia Nauk SSSR; Izdatel'stvo Nauka, Leningrad. M
- Fizika Metallov i Metallovedenie.* Akademiia Nauk SSSR; Izdatel'stvo Nauka, Sverdlovsk. M

- Fizika Tverdogo Tela.* Akademiia Nauk SSSR; Izdatel'stvo Nauka, Leningrad. M
- Fiziko-Khimicheskaia Mekhanika Materialov.* Akademiia Nauk Ukrainskoi SSR; Izdatel'stvo Naukova Dumka, Kiev. BM
- Fiziologicheskii Zhurnal SSSR.* Akademiia Nauk SSSR; Izdatel'stvo Nauka, Leningrad. M
- Fiziologichnii Zhurnal.* Akademiia Nauk Ukrainskoi SSR, Institut Fiziologii; Izdatel'stvo Naukova Dumka, Kiev. BM
- Der Flieger.* Luftfahrt-Verlag Walter Zuerl, Steinbach-Wörthsee, West Germany. M
- Flight International.* Royal Aero Club; IPC Business Press, Ltd., London. W
- Flight Safety.* Pergamon Press, Ltd., Oxford. Q
- Flugrevue/Flugwelt International.* Club der Luftfahrt von Deutschland, e.V., Bonn; Vereinigte Motor-Verlage GmbH, Stuttgart, West Germany. M
- Fluid Dynamics (Akademiia Nauk SSSR, Izvestiia, Mekhanika Zhidkosti i Gaza).* The Faraday Press, Inc., New York. BM
- Fluidics Quarterly.* Ann Arbor, Mich. Q
- FOA Reports.* Försvarets Forskningsanstalt, Stockholm. Irreg.
- Forces Aériennes Françaises.* Comité d'Etudes Aéronautiques Militaires, Paris. M
- Forschung im Ingenieurwesen.* Verein Deutscher Ingenieure; VDI-Verlag GmbH, Düsseldorf. BM
- Fortschritte der Physik.* Physikalische Gesellschaft; Akademie-Verlag GmbH, Berlin. M
- Fortune.* Time, Inc., Chicago. M
- France, Ministère de l'Air, Publications Scientifiques et Techniques.* Centre de Documentation de l'Armement, Paris. Irreg.
- France, Ministère de l'Air, Publications Scientifiques et Techniques, Notes Techniques.* Centre de Documentation de l'Armement, Paris. Irreg.
- Franklin Institute, Journal.* Franklin Institute, Philadelphia, Pa.; Pergamon Press, Ltd., Oxford. M
- Frequency Technology.* Stillman Publications, Inc., Norwood, Mass. M
- Frequenz.* Fachverlag Schiele & Schön, Berlin. M
- Frontier.* IIT Research Institute, Chicago. SA
- Fujitsu Scientific and Technical Journal.* Fujitsu, Ltd., Kanagawa, Japan. Q
- Fyzikálny Časopis.* Slovenská Akademia Vied, Bratislava. Q
- Geliotekhnika.* Akademiia Nauk Uzbekskoi SSR, Tashkent. BM
- *General and Comparative Endocrinology.* Academic Press, Inc., New York. BM
- Génie Biologique et Médical.* Nancy, France. Q
- Geochimica et Cosmochimica Acta.* Geochemical Society and Meteoritical Society; Pergamon Press, Ltd., Oxford. M
- Geodeziia i Aerofotos'emka.* Ministerstvo Vysshego i Srednego Spetsial'nogo Obrazovaniia SSSR; Izdatel'stvo Moskovskogo Instituta Inzhenerov Geodezii, Aerofotos'emki i Kartografii, Moscow. BM
- Geodeziia i Kartografiia.* Glavnoe Upravlenie Geodezii i Kartografii pri Sovete Ministrov SSSR; Izdatel'stvo Nedra, Moscow. M
- Geodeziia, Kartografiia i Aerofotos'emka.* Izdatel'stvo L'vovskogo Universiteta, Lvov. Irreg.
- Geodezja i Kartografia.* Polska Akademia Nauk, Komitet Geodezji; Państwowe Wydawnictwo Naukowe, Warsaw. Q
- Geofisica e Meteorologia.* Società Italiana di Geofisica e Meteorologia, Genoa. 3 issues per year
- Geofisica Internacional.* Unión Geofísica Mexicana, Ciudad Universitaria, Mexico. Q
- Geofysiske Publikasjoner (Geophysica Norvegica).* Norsk Videnskaps-Akademi, Oslo. Irreg.
- *Geological Society of America, Bulletin.* Geological Society of America, Boulder, Colo. M
- *Geologische Rundschau.* Geologische Vereinigung; Ferdinand Enke Verlag, Stuttgart, West Germany. Irreg.
- Geomagnetism and Aeronomy (Geomagnetizm i Aeronomiia).* American Geophysical Union, Washington, D.C. BM
- Geomagnetizm i Aeronomiia.* Akademiia Nauk SSSR; Izdatel'stvo Nauka, Moscow. BM
- Geomagnitnye Issledovaniia.* Izdatel'stvo Nauka, Moscow. Irreg.
- Geophysical Fluid Dynamics.* Gordon & Breach Science Publishers, Ltd., London. M
- *Geophysics.* Society of Exploration Geophysicists, Tulsa, Okla. BM
- Gerlands Beiträge zur Geophysik.* Akademische Verlagsgesellschaft Geest & Portig, KG, Leipzig, East Germany. BM
- Gidroaeromekhanika i Teoriia Uprugosti.* Izdatel'stvo Khar'kovskogo Universiteta, Kharkov. Irreg.
- Gidromekhanika.* Akademiia Nauk Ukrainskoi SSR; Izdatel'stvo Naukova Dumka, Kiev. Irreg.
- Göttingen, Akademie der Wissenschaften, Nachrichten, Mathematisch-physikalische Klasse.* Vandenhoeck & Ruprecht, Göttingen. Irreg.
- Harvard Business Review.* Harvard University, Graduate School of Business Administration, Cambridge, Mass. BM
- Heat Transfer — Soviet Research.* American Society of Mechanical Engineers, New York. BM
- Helvetica Physica Acta.* Societas Physicae Helveticae; Birkhäuser Verlag, Basel. Irreg.
- High Temperature (Teplofizika Vysokikh Temperatur).* Consultants Bureau, New York. BM
- *High Temperature Science.* Academic Press, Inc., New York. Q
- High Temperatures — High Pressures.* Pion, Ltd., London. BM
- *Histochemie.* Springer Verlag, Berlin.
- Hochfrequenztechnik und Elektroakustik.* Akademische Verlagsgesellschaft Geest & Portig, KG, Leipzig, East Germany. BM
- Hovering Craft and Hydrofoil.* Kalerghi Publications, London. M
- Human Factors.* Human Factors Society, Inc., Santa Monica, Calif.; The Johns Hopkins Press, Baltimore, Md. M
- Hydraulics and Pneumatics.* Industrial Publishing Corp., Cleveland, Ohio. M

INTERNATIONAL AEROSPACE ABSTRACTS

**Hydrocarbon Processing*. Gulf Publishing Co., Houston, Tex. M

I & EC - Industrial and Engineering Chemistry. American Chemical Society, Washington, D.C. M

I & EC - Industrial and Engineering Chemistry, Fundamentals. American Chemical Society, Washington, D.C. Q

I & EC - Industrial and Engineering Chemistry, Process Design and Development. American Chemical Society, Washington, D.C. Q

I & EC - Industrial and Engineering Chemistry, Product Research and Development. American Chemical Society, Washington, D.C. Q

Iași, Institutul Politehnic, Buletinul. Iași, Institutul Politehnic, Iași, Rumania. SA

IBM Journal of Research and Development. International Business Machines Corp., Armonk, N.Y. BM

IBM Systems Journal. International Business Machines Corp., Armonk, N.Y. Q

Icarus. Academic Press, Inc., New York. BM

IEE Reviews. Institution of Electrical Engineers, London. Annual

IEEE, Proceedings. Institute of Electrical and Electronics Engineers, Inc., New York. M

IEEE Journal of Quantum Electronics. Institute of Electrical and Electronics Engineers, Inc., New York. M

IEEE Journal of Solid-State Circuits. Institute of Electrical and Electronics Engineers, Inc., New York. BM

IEEE Spectrum. Institute of Electrical and Electronics Engineers, Inc., New York. M

IEEE Transactions on Aerospace and Electronic Systems. Institute of Electrical and Electronics Engineers, Inc., New York. BM

IEEE Transactions on Antennas and Propagation. Institute of Electrical and Electronics Engineers, Inc., New York. BM

IEEE Transactions on Audio and Electroacoustics. Institute of Electrical and Electronics Engineers, Inc., New York. Q

IEEE Transactions on Automatic Control. Institute of Electrical and Electronics Engineers, Inc., New York. BM

IEEE Transactions on Bio-Medical Engineering. Institute of Electrical and Electronics Engineers, Inc., New York. Q

IEEE Transactions on Broadcasting. Institute of Electrical and Electronics Engineers, Inc., New York. Q

IEEE Transactions on Circuit Theory. Institute of Electrical and Electronics Engineers, Inc., New York. Q

IEEE Transactions on Communication Technology. Institute of Electrical and Electronics Engineers, Inc., New York. BM

IEEE Transactions on Computers. Institute of Electrical and Electronics Engineers, Inc., New York. M

IEEE Transactions on Education. Institute of Electrical and Electronics Engineers, Inc., New York. Q

IEEE Transactions on Electrical Insulation. Institute of Electrical and Electronics Engineers, Inc., New York. Q

IEEE Transactions on Electromagnetic Compatibility.

Institute of Electrical and Electronics Engineers, Inc., New York. Q

IEEE Transactions on Electron Devices. Institute of Electrical and Electronics Engineers, Inc., New York. M

IEEE Transactions on Engineering Management. Institute of Electrical and Electronics Engineers, Inc., New York. Q

IEEE Transactions on Engineering Writing and Speech. Institute of Electrical and Electronics Engineers, Inc., New York.

IEEE Transactions on Geoscience Electronics. Institute of Electrical and Electronics Engineers, Inc., New York. Q

IEEE Transactions on Industrial Electronics and Control Instrumentation. Institute of Electrical and Electronics Engineers, Inc., New York. Q

IEEE Transactions on Information Theory. Institute of Electrical and Electronics Engineers, Inc., New York. BM

IEEE Transactions on Instrumentation and Measurement. Institute of Electrical and Electronics Engineers, Inc., New York. Q

IEEE Transactions on Magnetics. Institute of Electrical and Electronics Engineers, Inc., New York. Q

IEEE Transactions on Man-Machine Systems. Institute of Electrical and Electronics Engineers, Inc., New York. Q

IEEE Transactions on Microwave Theory and Techniques. Institute of Electrical and Electronics Engineers, Inc., New York. M

IEEE Transactions on Nuclear Science. Institute of Electrical and Electronics Engineers, Inc., New York. BM

IEEE Transactions on Parts, Materials and Packaging. Institute of Electrical and Electronics Engineers, Inc., New York. Q

IEEE Transactions on Reliability. Institute of Electrical and Electronics Engineers, Inc., New York. Q

IEEE Transactions on Sonics and Ultrasonics. Institute of Electrical and Electronics Engineers, Inc., New York. Q

IEEE Transactions on Systems Science and Cybernetics. Institute of Electrical and Electronics Engineers, Inc., New York. Q

Impact of Science on Society. UNESCO, Paris. Q

Indian Academy of Sciences, Proceedings, Section A. Indian Academy of Sciences, Bangalore. M

Indian Institute of Science, Journal. Indian Institute of Science, Bangalore. Q

Indian Journal of Mathematics. Allahabad Mathematical Society, Allahabad. 3 issues per year

Indian Journal of Pure and Applied Physics. Council of Scientific and Industrial Research, New Delhi. M

Indian Journal of Technology. Council of Scientific and Industrial Research, New Delhi. M

Indiana University Mathematics Journal (formerly Journal of Mathematics and Mechanics). Indiana University, Dept. of Mathematics, Bloomington, Ind. M

Industrial Laboratory (Zavodskaja Laboratoriia). Consultants Bureau, New York. M

Industrial Management Review. Industrial Management Review Association; Massachusetts Institute of Technology, Cambridge, Mass. 3 issues per year

- Information and Control*. Academic Press, Inc., New York. M
- Information Display*. Society for Information Display; Information Display Publications, Inc., Los Angeles. BM
- Infrared Physics*. Pergamon Press, Ltd., Oxford. Q
- Ingegneria*. Editore Ulrico Hoepli, Milan. M
- Ingegneria Meccanica*. Etas Kompass, Milan. M
- Ingeniería Aeronáutica y Astronáutica*. Asociación de Ingenieros Aeronáuticos, Madrid. BM
- De Ingenieur*. Koninklijk Instituut van Ingenieurs; A. Oosthoek Publishing Co., Utrecht, Netherlands. W
- Ingenieur-Archiv*. Springer Verlag, Berlin. BM
- Innovation*. Technology Communication, Inc., New York. M
- **Inorganic Chemistry*. American Chemical Society, Washington, D.C. M
- Institut Fourier, Annales*. Centre National de la Recherche Scientifique, Paris; Institut de Mathématiques Pures, Saint-Martin-d'Hères, France.
- Institut Teoreticheskoi Astronomii, Trudy*. Akademiia Nauk SSSR, Institut Teoreticheskoi Astronomii; Izdatel'stvo Nauka, Leningrad. Irreg.
- Institute of Mathematics and Its Applications, Journal*. Academic Press, Inc. (London), Ltd., London. Q
- Institute of Navigation, Journal*. Institute of Navigation; John Murray (Publishers), Ltd., London. Q
- Institute of Physical and Chemical Research, Scientific Papers*. Institute of Physical and Chemical Research, Saitama, Japan. Q
- Institution of Electrical Engineers, Proceedings*. Institution of Electrical Engineers, London. M
- Institution of Engineers (Australia), Mechanical and Chemical Engineering Transactions*. Institution of Engineers, Sydney. SA
- Institution of Engineers (India), Journal, Electronics and Telecommunication Engineering Division*. Institution of Engineers, Calcutta. 3 issues per year
- Institution of Engineers (India), Journal, Mechanical Engineering Division*. Institution of Engineers, Calcutta. BM
- Institution of Mechanical Engineers, Proceedings*. Institution of Mechanical Engineers, London. Irreg.
- **Institution of Radio and Electronics Engineers (Australia), Proceedings*. Institution of Radio and Electronics Engineers, Sydney. M
- Institution of Telecommunication Engineers, Journal*. Institution of Telecommunication Engineers, New Delhi. M
- Instruments and Control Systems*. Chilton Co., Philadelphia, Pa. M
- Instruments and Experimental Techniques (Pribory i Tekhnika Eksperimenta)*. Instrument Society of America, Pittsburgh, Pa., Consultants Bureau, New York. BM
- Instytut Lotnictwa, Biuletyn Informacyjny*. Instytut Lotnictwa, Warsaw. BM
- Instytut Lotnictwa, Prace*. Instytut Lotnictwa; Wydawnictwo Naukowo-Techniczne, Warsaw. Irreg.
- Instytut Maszyn Przepływowych, Prace*. Polska Akademia Nauk, Instytut Maszyn Przepływowych, Gdansk; Państwowe Wydawnictwo Naukowe, Warsaw. Irreg.
- Inter-Electronique*. Compagnie Française d'Éditions Paris. M
- Interavia*. Interavia S.A., Geneva. M
- International Journal for Numerical Methods in Engineering*. John Wiley & Sons, Ltd., Chichester, Sussex, England. Q
- International Journal of Biometeorology*. International Society of Biometeorology; Swets & Zeitlinger, Amsterdam. 3 issues per year
- International Journal of Control, First Series*. Taylor & Francis, Ltd., London. M
- International Journal of Electronics, First Series*. Taylor & Francis, Ltd., London. M
- International Journal of Engineering Science*. Pergamon Press, Ltd., Oxford. M
- International Journal of Fracture Mechanics*. Wolters-Noordhoff Publishing, Groningen, Netherlands. Q
- International Journal of Heat and Mass Transfer*. Pergamon Press, Ltd., Oxford. M
- International Journal of Man-Machine Studies*. Academic Press, Inc. (London), Ltd., London. Q
- International Journal of Mechanical Sciences*. Pergamon Press, Ltd., Oxford. M
- International Journal of Nondestructive Testing*. Gordon & Breach Science Publishers, London.
- International Journal of Non-Linear Mechanics*. Pergamon Press, Ltd., Oxford. Q
- International Journal of Powder Metallurgy*. American Powder Metallurgy Institute, New York. Q
- **International Journal of Quantum Chemistry*. Interscience Scientific Journals, John Wiley & Sons, Inc., New York. BM
- **International Journal of Radiation Biology*. Taylor & Francis, Ltd., London. M
- International Journal of Solids and Structures*. Pergamon Press, Ltd., Oxford. M
- **International Journal of Theoretical Physics*. Plenum Publishing Co., Ltd., London. Q
- Internationale Elektronische Rundschau*. Verlag für Radio-Foto-Kinotechnik GmbH, Berlin. M
- **Internationale Zeitschrift für angewandte Physiologie einschliesslich Arbeitsphysiologie*. Springer Verlag, Berlin. Q
- Inzhenerno-Fizicheskii Zhurnal*. Akademiia Nauk Belorusskoi SSR; Izdatel'stvo Nauka i Tekhnika, Minsk. M
- Irish Astronomical Journal*. Observatory, Armagh, Northern Ireland. Q
- ISA Transactions*. Instrument Society of America, Pittsburgh, Pa. Q
- Ishikawajima-Harima Engineering Review*. Ishikawajima-Harima Heavy Industries Co., Ltd., Tokyo. BM
- Isotopes and Radiation Technology*. U. S. Atomic Energy Commission, Oak Ridge, Tenn. Q
- **Israel Journal of Chemistry*. Weizmann Science Press of Israel, Jerusalem. BM
- Israel Journal of Mathematics*. Weizmann Science Press of Israel, Jerusalem. Q
- Israel Journal of Technology*. Weizmann Science Press of Israel, Jerusalem. BM
- Issledovaniia po Uprugosti i Plastichnosti*. Izdatel'stvo Leningradskogo Universiteta, Leningrad. Irreg.
- İstanbul Teknik Üniversitesi Bülteni*. İstanbul Teknik Üniversitesi, İstanbul. Annual
- ITU Telecommunication Journal*. International Telecommunication Union, Geneva. M

INTERNATIONAL AEROSPACE ABSTRACTS

Japan, Defense Academy, Memoirs. Defense Academy, Yokosuka, Japan. Irreg.

Japan Air Self Defence Force, Aeromedical Laboratory, Reports. Aeromedical Laboratory, Tachikawa, Japan. Q

**Japan Academy, Proceedings.* Tokyo. M

Japan Institute of Light Metals, Journal. Japan Institute of Light Metals, Tokyo. BM

Japan Institute of Metals, Journal (Nippon Kinzoku Gakkai-shi). Japan Institute of Metals, Sendai. M

Japan Institute of Metals, Transactions. Japan Institute of Metals, Sendai. BM

Japan Society for Aeronautical and Space Sciences, Journal. Japan Society for Aeronautical and Space Sciences, Tokyo. M

Japan Society for Aeronautical and Space Sciences, Transactions. Japan Society for Aeronautical and Space Sciences, Tokyo. Irreg.

Japan Society of Lubrication Engineers, Journal. Japan Society of Lubrication Engineers, Tokyo. M

Japan Society of Materials Science, Journal. Society of Materials Science, Kyoto. M

Japanese Journal of Applied Physics. Physical Society of Japan and Japan Society of Applied Physics, Tokyo. M

Jemná Mechanika a Optika. Ministerstvo Průmyslu; Státní Nakladatelství Technické Literatury, Prague. BM

Jena Review. VEB Verlag Technik, Berlin. BM

JETP Letters (ZHETF Pis'ma v Redaktsiiu). American Institute of Physics, Inc., New York. SM

Journal de Mathématiques Pures et Appliquées. Gauthier-Villars, Paris. Q

Journal de Mécanique. Gauthier-Villars, Paris. Q

Journal de Physique. Société Française de Physique, Paris. M

Journal de Recherches Atmosphériques. Universités de Clermont-Ferrand et de Toulouse, Observatoire du Puy de Dôme, Clermont-Ferrand, France. Q

**Journal of Adhesion.* Technomic Publishing Co., Inc., Stamford, Conn. Q

Journal of Air Law and Commerce. Southern Methodist University, School of Law, Dallas. Q

Journal of Air Traffic Control. Air Traffic Control Association, Inc., Washington, D.C. BM

Journal of Aircraft. American Institute of Aeronautics and Astronautics, Inc., New York. BM

Journal of Applied Meteorology. American Meteorological Society, Boston. BM

Journal of Applied Physics. American Institute of Physics, Inc., New York. 13 issues per year

Journal of Applied Physiology. American Physiological Society, Washington, D.C. M

**Journal of Applied Polymer Science.* Interscience Publishers, New York. M

Journal of Applied Psychology. American Psychological Association, Washington, D.C. BM

Journal of Atmospheric and Terrestrial Physics. Pergamon Press, Ltd., Oxford. M

Journal of Bacteriology. American Society for Microbiology, Bethesda, Md. M

Journal of Biological Chemistry. American Society of Biological Chemists, Inc., Baltimore, Md. M

Journal of Biomechanics. Pergamon Press, Ltd., Oxford. Q

Journal of Business. University of Chicago Press, Chicago. Q

**Journal of Catalysis.* Academic Press, Inc., New York. BM

**Journal of Chemical Education.* American Chemical Society, Div. of Chemical Education, New York. M

Journal of Chemical Physics. American Institute of Physics, Inc., New York. SM

**Journal of Chromatographic Science.* Preston Technical Abstracts Co., Evanston, Ill. M

**Journal of Chromatography.* Elsevier Publishing Co., Amsterdam. M

**Journal of Clinical Endocrinology and Metabolism.* Endocrine Society; J. B. Lippincott Co., Publishers, Philadelphia, Pa. M

Journal of Clinical Investigation. American Society for Clinical Investigation, Inc., New York. M

**Journal of Colloid and Interface Science.* Academic Press, Inc., New York. M

**Journal of Comparative and Physiological Psychology.* American Psychological Association, Inc., Washington, D.C. M

Journal of Composite Materials. Technomic Publishing Co., Inc., Stamford, Conn. BM

Journal of Computational Physics. Academic Press, Inc., New York. Q

Journal of Computer and System Sciences. Academic Press, Inc., New York. BM

**Journal of Crystal Growth.* North-Holland Publishing Co., Amsterdam. BM

Journal of Differential Equations. Academic Press, Inc., New York. BM

Journal of Engineering Mathematics. Wolters-Noordhoff Publishing, Groningen, Netherlands. Q

**Journal of Environmental Health.* National Association of Sanitarians, Denver, Colo. BM

Journal of Environmental Sciences. Institute of Environmental Sciences, Mt. Prospect, Ill. BM

**Journal of Experimental Psychology.* American Psychological Association, Inc., Washington, D.C. M

Journal of Experimental Psychology (Monograph) (see *Journal of Experimental Psychology, Monograph Supplement*).

Journal of Experimental Psychology, Monograph Supplement. American Psychological Association, Inc., Washington, D.C. Q

Journal of Fire and Flammability. Technomic Publishing Co., Inc., Stamford, Conn. Q

Journal of Fluid Mechanics. Cambridge University Press, London. 20 issues per year

**Journal of Geology.* University of Chicago Press, Chicago. BM

Journal of Geomagnetism and Geoelectricity. Society of Terrestrial Magnetism and Electricity, Kyoto, Japan. Q

Journal of Geophysical Research. American Geophysical Union, Washington, D.C. 36 issues per year

**Journal of Gerontology.* Gerontological Society, St. Louis, Mo. Q

**Journal of Heterocyclic Chemistry.* Albuquerque, N.M. BM

Journal of Hydronautics. American Institute of Aeronautics and Astronautics, Inc., New York. Q

Journal of Interdisciplinary Cycle Research. International

- Institute for Interdisciplinary Cycle Research, Leiden; Swets & Zeitlinger, N.V., Amsterdam.
- **Journal of Macromolecular Science, Series A – Chemistry*. Marcel Dekker, New York. Q
- Journal of Materials*. American Society for Testing and Materials, Philadelphia, Pa. Q
- Journal of Materials Science*. Chapman & Hall, Ltd., London. M
- Journal of Mathematical Analysis and Applications*. Academic Press, Inc., New York. M
- Journal of Mathematical and Physical Sciences*. Indian Institute of Technology, Madras, India.
- Journal of Mathematical Physics*. American Institute of Physics, Inc., New York. M
- **Journal of Mathematical Psychology*. Academic Press, Inc., New York. 3 issues per year
- Journal of Mathematics and Mechanics* (see *Indiana University Mathematical Journal*).
- Journal of Mechanical Engineering Science*. Institution of Mechanical Engineers, London. Q
- Journal of Metals*. American Institute of Mining, Metallurgical and Petroleum Engineers, Inc., New York. M
- Journal of Microwave Power*. International Microwave Power Institute, Ltd., Edmonton, Alberta, Canada. Q
- **Journal of Molecular Biology*. Academic Press, Ltd., London. BW
- **Journal of Molecular Spectroscopy*. Academic Press, Inc., New York. M
- **Journal of Morphology*. Wistar Institute Press, Philadelphia, Pa. M
- **Journal of Neuro-Visceral Relations*. Springer Verlag, Vienna.
- **Journal of Nutrition*. American Institute of Nutrition, Bethesda, Md. M
- Journal of Occupational Medicine*. Industrial Medical Association; Charles B. Slack, Inc., Thorofare, N.J. M
- Journal of Optimization Theory and Applications*. Plenum Publishing Corp., New York. M
- **Journal of Organic Chemistry*. American Chemical Society, Washington, D.C. M
- **Journal of Pharmacology and Experimental Therapeutics*. American Society of Pharmacology and Experimental Therapeutics, Inc.; Williams & Wilkins Co., Baltimore, Md. M
- Journal of Photographic Science*. Royal Photographic Society of Great Britain, London. M
- Journal of Physical Chemistry*. American Chemical Society, Washington, D.C. BW
- Journal of Physical Oceanography*. American Meteorological Society, Boston. Q
- Journal of Physics, Part A – General Physics*. Institute of Physics and The Physical Society, London. BM
- Journal of Physics, Part B – Atomic and Molecular Physics*. Institute of Physics and The Physical Society, London. M
- Journal of Physics, Part C – Solid State Physics*. Institute of Physics and The Physical Society, London. M
- Journal of Physics, Part D – Applied Physics* (formerly *Journal of Physics, Part D – British Journal of Applied Physics*). Institute of Physics and The Physical Society, London. M
- Journal of Physics, Part D – British Journal of Applied Physics* (see *Journal of Physics, Part D – Applied Physics*).
- Journal of Physics, Part E – Journal of Scientific Instruments* (see *Journal of Physics, Part E – Scientific Instruments*).
- Journal of Physics, Part E – Scientific Instruments*. Institute of Physics and The Physical Society, London. M
- **Journal of Physics and Chemistry of Solids*. Pergamon Press, Ltd., Oxford. M
- Journal of Physiology*. Physiological Society; Cambridge University Press, London. M
- Journal of Plasma Physics*. Cambridge University Press, London. Q
- **Journal of Polymer Science, Part A*. Interscience Publishers, Inc., New York. M
- **Journal of Polymer Science, Part B – Polymer Letters*. Interscience Publishers, Inc., New York. M
- Journal of Quality Technology*. American Society for Quality Control, Inc., Milwaukee, Wis. Q
- Journal of Quantitative Spectroscopy and Radiative Transfer*. Pergamon Press, Ltd., Oxford. M
- **Journal of Radioanalytical Chemistry*. Elsevier Publishing Co., Amsterdam. BM
- Journal of Research, Section A – Physics and Chemistry*. National Bureau of Standards; Supt. of Documents, Washington, D.C. BM
- Journal of Research, Section B – Mathematical Sciences*. National Bureau of Standards; Supt. of Documents, Washington, D.C. Q
- Journal of Research, Section C – Engineering and Instrumentation*. National Bureau of Standards; Supt. of Documents, Washington, D.C. Q
- Journal of Science and Engineering Research*. Indian Institute of Technology, Kharagpur, West Bengal, India. SA
- Journal of Science and Technology*. The General Electric and English Electric Companies Limited, London. Q
- Journal of Scientific and Industrial Research*. Council of Scientific and Industrial Research, New Delhi. M
- Journal of Sound and Vibration*. British Acoustical Society; Academic Press, Inc. (London), Ltd., London. BM
- Journal of Spacecraft and Rockets*. American Institute of Aeronautics and Astronautics, Inc., New York. M
- **Journal of Statistical Physics*. Plenum Publishing Corp., New York.
- Journal of Strain Analysis*. Joint British Committee for Stress Analysis; Institution of Mechanical Engineers, London. Q
- Journal of Systems Engineering*. Tinnon-Brown, Inc., Book Publishers, Los Angeles. Q
- Journal of the Astronautical Sciences*. American Astronautical Society, Inc., Washington, D.C. BM
- Journal of the Atmospheric Sciences*. American Meteorological Society, Boston. BM
- **Journal of the Experimental Analysis of Behavior*. Society for the Experimental Analysis of Behavior, Inc., Indiana University, Bloomington, Ind. BM
- Journal of the Less-Common Metals*. Elsevier Sequoia S.A., Lausanne. M
- Journal of the Mechanics and Physics of Solids*. Pergamon Press, Ltd., Oxford. BM
- Journal of Vacuum Science and Technology*. American

Vacuum Society; American Institute of Physics, Inc., New York. BM
JSME, Bulletin. Japan Society of Mechanical Engineers, Tokyo. BM

Kazanskii Aviatsonnyi Institut, Trudy, Seriya Aviatsonnaia Tekhnologiya i Organizatsiya Proizvodstva. Kazanskii Aviatsonnyi Institut, Kazan. Irreg.

Kazanskii Aviatsonnyi Institut, Trudy, Seriya Aviatsonnye Dvigateli. Kazanskii Aviatsonnyi Institut, Kazan. Irreg.

Kazanskii Aviatsonnyi Institut, Trudy, Seriya Prikladnaia Mekhanika. Kazanskii Aviatsonnyi Institut, Kazan. Irreg.

Khimiia i Tekhnologiya Topliv i Masel. Ministerstvo Neftepererabatyvaiushchei i Neftekhimicheskoi Promyshlennosti SSSR, Akademiia Nauk SSSR, and Nauchno-Tekhnicheskoe Obshchestvo Neftianoi i Gazovoi Promyshlennosti; Izdatel'stvo Khimiia, Moscow. M

Khimiko-Termicheskaya Obrabotka Stali i Splavov. Nauchno-Tekhnicheskoe Obshchestvo Mashinostroitel'noi Promyshlennosti; Izdatel'stvo Mashinostroenie, Moscow. Irreg.

Kleinheubacher Berichte. Fernmeldetechnisches Zentralamt, Darmstadt, West Germany. Irreg.

**Kolloid-Zeitschrift und Zeitschrift für Polymere.* Dietrich Steinkopff Verlagbuchhandlung, Darmstadt, West Germany. M

Komety i Meteory. Akademiia Nauk Tadzhikskoi SSR; Izdatel'stvo Donish, Dushanbe. Irreg.

Koninklijke Nederlandse Akademie van Wetenschappen, Proceedings, Series B — Physical Sciences. North-Holland Publishing Co., Amsterdam. 5 issues per year

Kontrol'no-Izmeritel'naia Tekhnika. Izdatel'stvo Lvovskogo Universiteta, Lvov. Irreg.

Kosmicheskaya Biologiya i Meditsina. Ministerstvo Zdravookhraneniia SSSR; Izdatel'stvo Meditsina, Moscow. BM

Kosmicheskii Issledovaniia. Akademiia Nauk SSSR; Izdatel'stvo Nauka, Moscow. BM

Kosmicheskii Luch. Izdatel'stvo Nauka, Moscow. Irreg.

Kovové Materiály. Slovenská Akadémia Vied, Bratislava. BM

Kristallografiia. Akademiia Nauk SSSR; Izdatel'stvo Nauka, Moscow. BM

Krymskaya Astrofizicheskaya Observatoriia, Izvestiia. Akademiia Nauk SSSR; Izdatel'stvo Nauka, Moscow. BM

Kvantovaya Elektronika. Akademiia Nauk Ukrainskoi SSR, Institut Poluprovodnikov; Izdatel'stvo Naukova Dumka, Kiev. Irreg.

Kybernetika. Československá Akademie Věd, Prague. BM

Kyoto University, Faculty of Engineering, Memoirs. Kyoto University, Kyoto. Q

Kyoto University, Faculty of Science, Memoirs, Series — Physics, Astrophysics, Geophysics and Chemistry. Kyoto University, Kyoto. Irreg.

Kyushu University, Faculty of Engineering, Memoirs. Kyushu University, Fukuoka, Japan. Q

Kyushu University, Research Institute for Applied Mechanics, Reports. Kyushu University, Fukuoka, Japan. Irreg.

**The Laryngoscope.* American Laryngological, Rhinological and Otolological Society; Laryngoscope Co., Collinsville, Ill. M

Laser. Fachschriftenverlag Aargauer Tagblatt AG, Aarau, Switzerland. Q

Laser Journal. Laser Industry Association; A. Z. Publishing Corp., Los Angeles. BM

Leningradskii Gosudarstvennyi Universitet, Astronomicheskaya Observatoriia, Trudy. Izdatel'stvo Leningradskogo Gosudarstvennogo Universiteta, Leningrad. Irreg.

Leningradskii Universitet, Vestnik, Matematika, Mekhanika, Astronomiya. Izdatel'stvo Leningradskogo Universiteta, Leningrad. Q

Lietuvos Fizikos Rinkiny. Akademiia Nauk Litovskoi SSR; Izdatel'stvo Mintis, Vilnius. Q

Lietuvos Matematikos Rinkiny. Akademiia Nauk Litovskoi SSR; Izdatel'stvo Mintis, Vilnius. Q

Life Sciences, Part I — Physiology and Pharmacology. Pergamon Press, Ltd., Oxford. SM

Life Sciences, Part II — Biochemistry, General and Molecular Biology. Pergamon Press, Ltd., Oxford. SM

Lockheed-Georgia Quarterly. Lockheed-Georgia Co., Marietta, Ga. Q

Lockheed Horizons. Lockheed-California Co., Burbank, Calif.

Logistics Spectrum. Society of Logistics Engineers, Los Angeles. Q

**London Mathematical Society, Journal.* London Mathematical Society; C. F. Hodgson & Son, Ltd., London. Q

Lubrication Engineering. American Society of Lubrication Engineers, Park Ridge, Ill. M

Luftfahrttechnik Raumfahrttechnik. Verein Deutscher Ingenieure; VDI-Verlag GmbH, Düsseldorf. M

Machine Design. Penton Publishing Co., Cleveland, Ohio. 31 issues per year

Magnitnaia Gidrodinamika. Akademiia Nauk Latvinskoi SSR; Izdatel'stvo Zinatne, Riga. Q

Manufacturing Engineering and Management. Society of Manufacturing Engineers, Dearborn, Mich. M

Marconi Review. Marconi Co., Ltd., Chelmsford, Essex, England. Q

**Marine Technology Society Journal.* Marine Technology Society, Washington, D.C. SA

Mashinostroenie. Ministerstvo Vysshego i Srednego Spetsial'nogo Obrazovaniia SSSR; Izdanie Moskovskogo Vysshego Tekhnicheskogo Uchilishcha imeni N. E. Baubana, Moscow. M

Matematicheskaya Fizika. Akademiia Nauk Ukrainskoi SSR; Izdatel'stvo Naukova Dumka, Kiev. Irreg.

Matematicheskii Sbornik. Akademiia Nauk SSSR and Moskovskoe Matematicheskoe Obshchestvo; Izdatel'stvo Nauka, Moscow. M

Matematichki Vesnik. Drushtvo Matematichara, Fizichara

- i Astronoma SRS and Matematichki Institut, Belgrade. Q
- Matematika.** Ministerstvo Vysshego i Srednego Spetsial'nogo Obrazovaniia SSSR; Izdatel'stvo Kazanskogo Universiteta, Kazan. M
- Materials Evaluation.** American Society for Nondestructive Testing, Inc., Evanston, Ill. M
- Materials Journal.** Society of Aerospace Material and Process Engineers, Azusa, Calif. Q
- Materials Protection.** National Association of Corrosion Engineers, Inc., Houston, Tex. M
- Materials Protection and Performance.** National Association of Corrosion Engineers, Houston, Tex. M
- Materials Research and Standards.** American Society for Testing and Materials, Philadelphia, Pa. M
- Materials Science and Engineering.** American Society for Metals, Metals Park, Ohio; Elsevier Sequoia S.A., Lausanne. BM
- *Mathematical Biosciences.** American Elsevier Publishing Co., Inc., New York. Q
- Mathematics of Computation.** American Mathematical Society, Providence, R.I. Q
- Mathematika.** University College, Dept. of Mathematics, London. SA
- Max-Planck-Institut für Aeronomie, Mitteilungen.** Springer Verlag, Berlin. Irreg.
- Meccanica.** Italian Association of Theoretical and Applied Mechanics; Tamburini Editore, Milan. Q
- Mechanical Engineering.** American Society of Mechanical Engineers, New York. M
- Mechanika Teoretyczna i Stosowana.** Polskie Towarzystwo Mechaniki Teoretycznej i Stosowanej; Państwowe Wydawnictwo Naukowe, Warsaw. Q
- Medical and Biological Engineering.** International Federation for Medical and Biological Engineering; Pergamon Press, Ltd., Oxford. BM
- Medical Research Engineering.** Medical-Research-Technology, Little Falls, N.J. BM
- Mekhanika Polimerov.** Akademiia Nauk Latviiskoi SSR; Izdatel'stvo Zinatne, Riga. BM
- Mekhanika Tverdogo Tela.** Akademiia Nauk SSSR; Izdatel'stvo Nauka, Moscow. Irreg.
- Mémoires Scientifiques de la Revue de Métallurgie.** Paris. M
- Mérés és Automatika.** Lapkiadó Vállalat, Budapest. M
- Messerschmitt-Bölkow-Blohm, Mitteilungen.** Messerschmitt-Bölkow-Blohm GmbH, Munich. M
- Messtechnik.** Friedr. Vieweg & Sohn GmbH, Braunschweig. M
- Metal Construction and British Welding Journal.** The Welding Institute, London. M
- Metal Progress.** American Society for Metals, Metals Park, Ohio. M
- Metal Science and Heat Treatment (Metallovedenie i Termicheskaiia Obrabotka Metallov).** Consultants Bureau, New York. BM
- Metal Science Journal.** Institute of Metals and Institution of Metallurgists, London. BM
- Metallovedenie i Termicheskaiia Obrabotka Metallov.** Ministerstvo Stankostroitel'noi i Instrumental'noi Promyshlennosti SSSR and Nauchno-Tekhnicheskoe Obshchestvo Mashinostroitel'noi Promyshlennosti; Izdatel'stvo Mashinostroenie, Moscow. M
- Metallurgical Society of AIME, Transactions** (see *Metallurgical Transactions*).
- Metallurgical Transactions** (formerly *ASM Transactions Quarterly*; *Metallurgical Society of AIME, Transactions*). Metallurgical Society of the American Institute of Mining, Metallurgical and Petroleum Engineers, Inc., New York; American Society for Metals, Metals Park, Ohio. M
- Metals Engineering Quarterly.** American Society for Metals, Metals Park, Ohio. Q
- Meteor-Forschungsergebnisse, Reihe B – Meteorologie und Aeronomie.** Gebrüder Borntraeger, Berlin. Irreg.
- Meteoritics.** Meteoritical Society and Arizona State University Bureau of Publications, Tempe, Ariz. Q
- Meteornoe Rasprostranenie Radiovoln.** Izdatel'stvo Kazanskogo Universiteta, Kazan. Irreg.
- Meteorological Magazine.** Meteorological Office; Her Majesty's Stationery Office, London. M
- Meteorological Society of Japan, Journal.** Meteorological Society of Japan, c/o Japan Meteorological Agency, Tokyo. BM
- Meteorologiya i Gidrologiya.** Glavnoe Upravlenie Gidrometeorologicheskoi Sluzhby SSSR; Gidrometeoizdat, Moscow. M
- Meteorologische Anhandlungen.** Freie Universität Berlin, Institut für Meteorologie und Geophysik; Verlag Dietrich Reimer, Berlin. Q
- Meteorologische Rundschau.** Verband Deutscher Meteorologischer Gesellschaften; Springer Verlag, Berlin. BM
- *Microbios.** Faculty Press, Cambridge. 5 issues per year
- Microelectronics and Reliability.** Pergamon Press, Ltd., Oxford. BM
- Microwave Journal.** Horizon House, Inc., Dedham, Mass. M
- MicroWaves.** Hayden Microwaves Corp., New York. M
- Middle East Technical University Journal of Pure and Applied Sciences.** Middle East Technical University, Ankara. 3 issues per year
- Milano, Seminario Matematico e Fisico, Rendiconti.** Milano, Università, Milan. Annual
- Missili e Spazio.** Associazione Italiana Razzi, Rome. BM
- Mitsubishi Heavy Industries Technical Review.** Mitsubishi Heavy Industries, Ltd., Tokyo. BM
- Mitsubishi Technical Bulletin.** Mitsubishi Heavy Industries, Ltd., Tokyo. Irreg.
- *MNASSA.** Astronomical Society of Southern Africa; Royal Observatory, Cape Province, South Africa. M
- *Modern Geology.** Gordon & Breach Science Publishers, Ltd., London. Q
- *Molecular Crystals and Liquid Crystals.** Gordon & Breach Science Publishers, Inc., New York. Q
- Monthly Weather Review.** U. S. Weather Bureau; Supt. of Documents, Washington, D.C. M
- The Moon.** D. Reidel Publishing Co., Dordrecht, Netherlands. Q
- Moskovskii Universitet, Vestnik, Seriya I – Matematika, Mekhanika.** Izdatel'stvo Moskovskogo Universiteta, Moscow. BM
- Moskovskii Universitet, Vestnik, Seriya III – Fizika, Astronomiya.** Izdatel'stvo Moskovskogo Universiteta, Moscow. BM

INTERNATIONAL AEROSPACE ABSTRACTS

Nachrichtentechnische Zeitschrift. Nachrichtentechnische Gesellschaft; VDE-Verlag GmbH, Berlin. M

Nagoya University, Faculty of Engineering, Memoirs. Nagoya University, Nagoya. Irreg.

Nagoya University, Institute of Plasma Physics, Annual Review. Nagoya University, Nagoya. Annual

Nagoya University, Research Institute of Atmospheric, Proceedings. Research Institute of Atmospheric, Toyokawa-Shi, Aichi-Ken, Japan. Irreg.

National Academy of Sciences, Proceedings. National Academy of Sciences, Washington, D.C. M

National Contract Management Journal. National Contract Management Association, Inglewood, Calif. SA

National Institute of Sciences of India, Proceedings, Part A - Physical Sciences. National Institute of Sciences of India, New Delhi. BM

Nature. Macmillan (Journals), Ltd., London. W

**Naturwissenschaften.* Max-Planck-Gesellschaft zur Förderung der Wissenschaften; Springer Verlag, Berlin. SM

Naturwissenschaftliche Rundschau. Wissenschaftliche Verlagsgesellschaft mbH, Stuttgart, West Germany. M

Naval Research Logistics Quarterly. U. S. Navy, Office of Naval Research; Supt. of Documents, Washington, D.C. Q

Naval Research Reviews. U. S. Navy, Office of Naval Research; Supt. of Documents, Washington, D.C. M

Navigation Institute of Navigation, Washington, D.C. Q

Navigation (Paris). Institut Français de Navigation, Paris. Q

NEC Research and Development. Nippon Electric Co., Ltd., Tokyo. Q

**Neues Jahrbuch für Mineralogie, Abhandlungen.* Schweizerbart'sche Verlagsbuchhandlung, Stuttgart, West Germany. M

**Neurology.* American Academy of Neurology, Minneapolis, Minn. M

**New Jersey Academy of Science, Bulletin.* Ed. M. Lelyn Brawin, Summit, N.J. SA

New Scientist. New Science Publications, Ltd., London. W

New York Academy of Sciences, Annals. New York Academy of Sciences, New York. Irreg.

New York Academy of Sciences, Transactions, Series 2. New York Academy of Sciences, New York. 8 issues per year

New York State Journal of Medicine. Medical Society of the State of New York, New York. SM

New Zealand Journal of Science. Department of Scientific and Industrial Research, Wellington, New Zealand. Q

Non-Ionizing Radiation. Iliffe Science & Technology Publications, Ltd., Guildford, Surrey, England. Q

**Nordisk Tidsskrift for Informationsbehandling.* Regnecentralen, Copenhagen. Q

Nordrhein-Westfalen, Forschungsberichte. Westdeutscher Verlag, Cologne. Irreg.

Nouvelle Revue d'Optique Appliquée (formerly Revue d'Optique). Masson & Cie., Editeurs, Paris. BM

Nova Acta Leopoldina. Deutsche Akademie der Naturforscher Leopoldina; Johann Ambrosius Barth Verlag, Leipzig, East Germany. Irreg.

Nuclear Applications and Technology. American Nuclear Society, Inc., Hinsdale, Ill. M

Nuclear Engineering and Design. North-Holland Publishing Co., Amsterdam. M

Nuclear Fusion. International Atomic Energy Agency, Vienna. Q

**Nuclear Instruments and Methods.* North-Holland Publishing Co., Amsterdam. BW

**Nuclear Physics.* North-Holland Publishing Co., Amsterdam. W

Nuclear Science and Engineering. American Nuclear Society, Inc., Hinsdale, Ill. M

Numerische Mathematik. Springer Verlag, Berlin. Irreg.

Nuovo Cimento. Società Italiana di Fisica, Bologna. 36 issues per year

Nuovo Cimento, Lettere. Società Italiana di Fisica, Bologna. 36 issues per year

Nuovo Cimento, Rivista. Società Italiana di Fisica, Bologna. Q

Observatorio de Madrid, Boletín Astronómico. Instituto Geográfico y Catastral, Madrid.

The Observatory. Royal Greenwich Observatory, Hailsham, Sussex, England. M

Obzornik za Matematiko in Fiziko. Izdaja Društvo Matematikov, Fizikov in Astronomov SR Slovenije, Ljubljana, Yugoslavia. Q

L'Onde Electrique. Société Française des Electroniciens et des Radioélectriciens; Editions Chiron S.A., Paris. M

ONERA, TP. Office National d'Etudes et de Recherches Aéropatiales, Chatillon-sous-Bagneux (Seine), France. Irreg.

Operational Research Quarterly. Operational Research Society, Ltd., London; Pergamon Press, Ltd., Oxford. Q

Operations Research. Operations Research Society of America, Baltimore, Md. BM

**Operations Research Society of Japan, Journal.* Operations Research Society of Japan, Tokyo. Q

Ophthalmic Research. S. Karger AG, Basel. BM

Optica Acta. Taylor & Francis, Ltd., London. M

Optical Society of America, Journal. Optical Society of America, Inc., Washington, D.C.; American Institute of Physics, Inc., New York. M

Optical Spectra. Optical Publishing Co., Inc., Pittsfield, Mass. M

Optics and Laser Technology (formerly Optics Technology). Iliffe Science & Technology Publications, Ltd., Guildford, Surrey, England. Q

Optics Communications. North-Holland Publishing Co., Amsterdam. M

Optics Technology (see Optics and Laser Technology).

Optika i Spektroskopiia. Akademiia Nauk SSSR; Izdatel'stvo Nauka, Leningrad. M

**Organic Mass Spectrometry.* Heyden & Son, Ltd., London. BM

**Organic Preparations and Procedures.* Marcel Dekker, Inc., New York. Q

Osaka Prefecture, University, Bulletin, Series A - Engineering and Natural Sciences. Osaka Prefecture, University, Osaka. Irreg.

Osaka University, Technology Reports. Osaka University, Osaka. SA

Österreichische Akademie der Wissenschaften, Mathema-

- tisch-naturwissenschaftliche Klasse, Sitzungsberichte, Abteilung 2.* Österreichische Akademie der Wissenschaften; Springer Verlag, Vienna. Irreg.
- Otbor i Peredacha Informatsii.* Akademiia Nauk Ukrain-skoi SSR; Izdatel'stvo Naukova Dumka, Kiev. Irreg.
- Oxidation of Metals.* Plenum Publishing Corp., New York. Q
- The Pacer.* International Correspondence Schools, Scranton, Pa. BM
- Pacific Journal of Mathematics.* Berkeley, Calif. M
- Papers in Meteorology and Geophysics.* Meteorological Research Institute, Tokyo. Q
- *Perception and Psychophysics.* Psychonomic Journals, Inc., Austin, Tex. M
- Perceptual and Motor Skills.* Missoula, Mont. BM
- Periodica Polytechnica, Electrical Engineering.* Budapest, Technical University, Budapest. Q
- Periodica Polytechnica, Electrical Engineering Series* (see *Periodica Polytechnica, Electrical Engineering*).
- Periodica Polytechnica, Mechanical Engineering.* Budapest, Technical University, Budapest. Q
- Periodica Polytechnica, Mechanical Engineering – Mashinostroenie* (see *Periodica Polytechnica, Mechanical Engineering*).
- Perspective.* Cornell Aeronautical Laboratory, Inc., Buffalo, N.Y. Q
- Pflügers Archiv.* Springer Verlag, Berlin.
- Philips Research Reports.* N. V. Philips' Gloeilampenfabrieken, Research Laboratories, Eindhoven. BM
- Philips Research Reports Supplements.* N. V. Philips' Gloeilampenfabrieken, Research Laboratories, Eindhoven. Irreg.
- Philips Technical Review.* N. V. Philips' Gloeilampenfabrieken, Research Laboratories, Eindhoven. M
- Philips Telecommunication Review.* N. V. Philips' Telecommunicatie Industrie, Hilversum. Q
- Philosophical Magazine, 8th Series.* Taylor & Francis, Ltd., London. M
- Photochemistry* (see *Phytochemistry*).
- Photogrammetria.* International Society of Photogrammetry; Elsevier Publishing Co., Amsterdam. BM
- Photogrammetric Engineering.* American Society of Photogrammetry, Falls Church, Va. M
- Photographic Applications in Science, Technology and Medicine.* Photographic Applications in Science and Technology, Inc., New York. BM
- Photographic Science and Engineering.* Society of Photographic Scientists and Engineers, Washington, D.C. BM
- Physica.* Physica Foundation; North-Holland Publishing Co., Amsterdam. Irreg.
- Physica Scripta* (formerly *Arkiv för Fysik*). Royal Swedish Academy of Sciences; Almqvist & Wiksell Periodical Co., Stockholm. M
- Physica Status Solidi.* Akademie-Verlag GmbH, Berlin; Academic Press, Inc. (London), Ltd., London. M
- Physica Status Solidi (A) – Applied Research.* Akademie-Verlag GmbH, Berlin; Academic Press, Inc., New York. 3 issues per year
- Physical Review, 2nd Series.* American Physical Society; American Institute of Physics, Inc., New York. 72 issues per year
- Physical Review A – General Physics, 3rd Series.* American Physical Society; American Institute of Physics, Inc., New York. M
- Physical Review B – Solid State, 3rd Series.* American Physical Society; American Institute of Physics, Inc., New York. SM
- Physical Review C – Nuclear Physics, 3rd Series.* American Physical Society; American Institute of Physics, Inc., New York. M
- Physical Review D – Particles and Fields, 3rd Series.* American Physical Society; American Institute of Physics, Inc., New York. SM
- Physical Review Letters.* American Physical Society, Inc., New York. W
- Physical Society of Japan, Journal.* Physical Society of Japan, Tokyo. M
- Physics in Medicine and Biology.* Hospital Physicists' Association; Taylor & Francis, Ltd., London. Q
- Physics Letters.* North-Holland Publishing Co., Amsterdam. W
- Physics of Fluids.* American Institute of Physics, Inc., New York. M
- Physics of the Earth and Planetary Interiors.* North-Holland Publishing Co., Amsterdam. BM
- Physics Today.* American Institute of Physics, Inc., New York. M
- *Physiologia Plantarum.* Scandinavian Society for Plant Physiology, Copenhagen. 4 vols. per year
- *Physiological Reviews.* American Physiological Society, Bethesda, Md. Q
- *Physiology and Behavior.* Pergamon Press, Ltd., Oxford. Q
- *Phytochemistry.* Pergamon Press, Ltd., Oxford. M
- Pisa, Scuola Normale Superiore, Annali, Scienze Fisiche e Matematiche.* Pisa, Scuola Normale Superiore, Pisa. Q
- Planetary and Space Science.* Pergamon Press, Ltd., Oxford. M
- Planseeberichte für Pulvermetallurgie.* Metallwerk Plansee Aktiengesellschaft, Reutte, Austria. 3 issues per year
- *Plant Physiology.* American Society of Plant Physiologists, Washington, D.C. M
- *Planta.* Springer Verlag, Berlin. Q
- Plasma Physics.* Pergamon Press, Ltd., Oxford. M
- PMM – Journal of Applied Mathematics and Mechanics (Prikladnaia Matematika i Mekhanika).* Pergamon Press, Ltd., Oxford. BM
- PMTF – Zhurnal Prikladnoi Mekhaniki i Tekhnicheskoi Fiziki.* Akademiia Nauk SSSR, Sibirskoe Otdelenie; Izdatel'stvo Nauka, Novosibirsk. BM
- Polish Medical Journal (Polski Tygodnik Lekarski).* Państwowy Zakład Wydawnictw Lekarskich, Warsaw; National Technical Information Service, Springfield, Va. Irreg.
- Polish Review of Radiology and Nuclear Medicine (Polski Przegląd Radiologii i Medycyny Nuklearnej).* Państwowy Zakład Wydawnictw Lekarskich, Warsaw; National Technical Information Service, Springfield, Va. Irreg.
- Politechnika Częstochowska, Zeszyty Naukowe, Nauki Techniczne – Mechanika.* Politechnika Częstochowska, Częstochowa, Poland. Irreg.

- Politechnika Śląska, Zeszyty Naukowe, Matematyka — Fizyka.* Politechnika Śląska, Gliwice. Irreg.
- Politechnika Śląska, Zeszyty Naukowe, Mechanika.* Politechnika Śląska, Gliwice, Poland. Irreg.
- Polska Akademia Nauk, Instytut Automatyki, Prace.* Polska Akademia Nauk, Warsaw. Irreg.
- Poluprovodnikovaia Tekhnika i Mikroelektronika.* Akademia Nauk Ukrainsoi SSR; Izdatel'stvo Naukova Dumka, Kiev. Irreg.
- Poluprovodnikovye Pribory i ikh Primenenie.* Izdatel'stvo Sovetskoe Radio, Moscow. Irreg.
- Polymer Engineering and Science.* Society of Plastics Engineers, Inc., Greenwich, Conn. BM
- Pomiary, Automatyka, Kontrola.* Naczelna Organizacja Techniczna, Warsaw. M
- Poroshkovaia Metallurgii.* Akademia Nauk Ukrainsoi SSR; Izdatel'stvo Naukova Dumka, Kiev. M
- Postępy Astronautyki.* Polskie Towarzystwo Astronautyczne, Lodz. Q
- Postępy Astronomii.* Polskie Towarzystwo Astronomiczne; Państwowe Wydawnictwo Naukowe, Warsaw. Q
- Postępy Fizyki.* Polskie Towarzystwo Fizyczne; Państwowe Wydawnictwo Naukowe, Warsaw. BM
- Priborostroenie.* Ministerstvo Vysshego i Srednego Spetsial'nogo Obrazovaniia SSSR; Izdatel'stvo Leningradskogo Instituta Tochnoi Mekhaniki i Optiki, Leningrad. M
- Priborostroenie (Kiev).* Ministerstvo Vysshego i Srednego Spetsial'nogo Obrazovaniia SSSR; Izdatel'stvo Tekhnika, Kiev. Irreg.
- Pribory i Sistemy Avtomatiki.* Izdatel'stvo Khar'kovskogo Gosudarstvennogo Universiteta, Kharkov. Irreg.
- Pribory i Tekhnika Eksperimenta.* Akademia Nauk SSSR; Izdatel'stvo Nauka, Moscow. BM
- Prikladnaia Matematika i Mekhanika.* Akademia Nauk SSSR; Izdatel'stvo Nauka, Moscow. BM
- Prikladnaia Mekhanika.* Akademia Nauk Ukrainsoi SSR, Otdelenie Matematiki, Mekhaniki i Kibernetiki; Izdatel'stvo Naukova Dumka, Kiev. M
- Priroda.* Akademia Nauk SSSR; Izdatel'stvo Nauka, Moscow. M
- Problemy Difraksii i Rasprostraneniia Voln.* Izdatel'stvo Leningradskogo Universiteta, Leningrad. Irreg.
- Problemy Fiziki Atmosfery.* Izdatel'stvo Leningradskogo Universiteta, Leningrad. Irreg.
- Problemy Kosmicheskoi Fiziki.* Izdatel'stvo Kievskogo Universiteta, Kiev. Irreg.
- Problemy Peredachi Informatsii.* Akademia Nauk SSSR; Izdatel'stvo Nauka, Moscow. Q
- Problemy Prochnosti.* Akademia Nauk Ukrainsoi SSR, Institut Problem Prochnosti; Izdatel'stvo Naukova Dumka, Kiev. M
- Problemy Tekhnicheskoi Elektrodinamiki.* Akademia Nauk Ukrainsoi SSR; Izdatel'stvo Naukova Dumka, Kiev. Irreg.
- Proceedings of Vibration Problems.* Polska Akademia Nauk; Państwowe Wydawnictwo Naukowe, Warsaw. Q
- Prochnost' i Dinamika Aviatsionnykh Dvigatelei.* Izdatel'stvo Mashinostroenie, Moscow. Irreg.
- Progress of Theoretical Physics.* Research Institute for Fundamental Physics and The Physical Society of Japan; Kyoto University, Kyoto. M

Przegląd Elektroniki (see Elektronika).

- *Psychiatrya, Neurologia, Neurochirurgia.* Netherlands Society of Psychiatry and Neurology; Elsevier Publishing Co., Amsterdam. BM
- *Psychological Review.* American Psychological Association, Inc., Washington, D.C. BM
- Psychonomic Science.* Psychonomic Journals, Inc., Austin, Tex. SM
- *Psychophysiology.* Society for Psychophysiological Research, Detroit, Mich. BM
- Pure and Applied Geophysics.* Birkhäuser Verlag, Basel. BM
- Quality Progress.* American Society for Quality Control, Inc., Milwaukee, Wis. M
- Quarterly Journal of Mechanics and Applied Mathematics.* Oxford University Press, London. Q
- Quarterly of Applied Mathematics.* Brown University, Providence, R.I. Q
- *Radiation Research.* Academic Press, Inc., New York. M
- Radio and Electronic Engineer.* Institution of Electronic and Radio Engineers, London. M
- Radio Engineering and Electronic Physics (Radiotekhnika i Elektronika).* Scripta Publishing Corp., Washington, D.C. M
- Radio Research Laboratories, Journal.* Ministry of Posts and Telecommunications, Radio Research Laboratories, Tokyo. BM
- Radio Research Laboratories, Review.* Ministry of Posts and Telecommunications, Radio Research Laboratories, Tokyo. Q
- Radio Science.* American Geophysical Union, Washington, D.C. M
- Radiobiologia — Radiotherapia.* VEB Verlag Volk und Gesundheit, Berlin. BM
- *Radiochemical and Radioanalytical Letters.* Elsevier Sequoia S.A., Lausanne. M
- *Radiochimica Acta.* Akademische Verlagsgesellschaft, Frankfurt/Main. Q
- Radiotekhnika.* Ministerstvo Vysshego i Srednego Spetsial'nogo Obrazovaniia SSSR; Izdatel'stvo Kievskogo Politekhnikeskogo Instituta, Kiev. M
- Radiofizika.* Ministerstvo Vysshego i Srednego Spetsial'nogo Obrazovaniia SSSR; Izdanie Gor'kovskogo Universiteta, Gorki. M
- Radioizluchenie Solntsa.* Izdatel'stvo Leningradskogo Universiteta, Leningrad. Irreg.
- *Radiology.* Radiological Society of North America, Inc., Syracuse, N.Y. M
- Radiotekhnika.* Nauchno-Tekhnicheskoe Obshchestvo Radiotekhniki i Elektrosviazi; Izdatel'stvo Sviaz', Moscow. M
- Radiotekhnika (Kharkov).* Izdatel'stvo Khar'kovskogo Gosudarstvennogo Universiteta, Kharkov. Irreg.
- Radiotekhnika i Elektronika.* Akademia Nauk SSSR; Izdatel'stvo Nauka, Moscow. M
- Raumfahrtforschung.* Deutsche Gesellschaft für Luft- und Raumfahrt, e.V., Stuttgart, West Germany. BM
- RCA Review.* RCA Research and Engineering, Princeton,

N.J. Q

Reactor Materials. U. S. Atomic Energy Commission, Oak Ridge, Tenn. Q

**Real Academia de Ciencias Exactas, Físicas y Naturales, Revista.* Madrid. Q

La Recherche Aéronautique. Office National d'Etudes et de Recherches Aéronautiques, Chatillon-sous-Bagneux (Seine), France. BM

La Recherche Spatiale. Centre National d'Etudes Spatiales; Dunod Editeur, Paris. M

Remote Sensing of Environment. American Elsevier Publishing Co., Inc., New York. Q

Report of Ionosphere and Space Research in Japan. Science Council of Japan, Ionosphere Research Committee, Tokyo. Q

Reports on Progress in Physics. Institute of Physics and The Physical Society, London. BM

Research/Development. Technical Publishing Co., Thompson Div., Barrington, Ill. M

Research Management. Industrial Research Institute, Inc.; Interscience Publishers, New York. BM

Research Trends. Cornell Aeronautical Laboratory, Inc., Buffalo, N.Y. Q

Respiration Physiology. North-Holland Publishing Co., Amsterdam. BM

Review of Scientific Instruments. American Institute of Physics, Inc., New York. M

Reviews of Geophysics (see *Reviews of Geophysics and Space Physics*).

Reviews of Geophysics and Space Physics (formerly *Reviews of Geophysics*). American Geophysical Union, Washington, D.C. Q

Revista de Aeronáutica y Astronáutica. Ministerio del Aire, Madrid. M

Revista Transporturilor. Ministerul Transporturilor; Consiliul Național al Inginerilor și Technicienilor, Bucharest. M

Revue de Médecine Aéronautique et Spatiale. Société Française de Physiologie et de Médecine Aéronautique et Cosmonautique; Masson & Cie., Paris. Q

Revue de Métallurgie. Paris. M

Revue de Physique Appliquée. Société Française de Physique, Paris. M

Revue des Corps de Santé des Armées. Centre de Recherches du Service de Santé des Armées, Paris. BM

Revue d'Optique (see *Nouvelle Revue d'Optique Appliquée*).

Revue Energie Primaire. Union des Ingénieurs de Louvain, Brussels. Q

Revue Française de Droit Aérien. Société Française de Droit Aérien et Spatial, Paris. Q

Revue Française de Mécanique. Société Française des Mécaniciens, Paris. Q

Revue Générale de l'Air et de l'Espace. Editions Internationales, Paris. Q

Revue Générale de l'Electricité. Société Française des Electriciens, Paris. M

Revue Générale de Thermique. Institut Français des Combustibles et de l'Energie; Société Française des Thermiciens, Paris. M

Revue Internationale des Hautes Températures et des Réfractaires. Société Nationale Française des Hautes Températures et des Réfractaires; Masson & Cie.,

Paris. Q

Revue mble. Société Anonyme MBLÉ, Brussels. Q

Revue Roumaine de Mathématiques Pures et Appliquées. Académie de la République Socialiste Roumaine, Bucharest. 10 issues per year

Revue Roumaine de Physique. Académie de la République Socialiste Roumaine, Bucharest. BM

Revue Roumaine des Sciences Techniques, Série de Mécanique Appliquée. Académie de la République Socialiste Roumaine, Bucharest. BM

Revue Scientifique et Technique CECLES/CERS (formerly *Revue Technique CECLES/CERS*). Gauthier-Villars, Paris. Q

Revue Technique CECLES/CERS (see *Revue Scientifique et Technique CECLES/CERS*).

Revue Technique Thomson — CSF (formerly *Annales de Radioélectricité*). Thomson — CSF, Service de Documentation Technique; Masson & Cie., Paris. Q

Ricerca Scientifica. Consiglio Nazionale delle Ricerche, Rome. BM

Rivista Aeronautica. Rome. M

Rivista di Medicina Aeronautica e Spaziale. Servizio Sanitario dell'Aeronautica Militare, Rome. Q

Rivista di Meteorologia Aeronautica. Servizio Meteorologico dell'Aeronautica, Rome. Q

Rolls-Royce Journal. Rolls-Royce, Ltd., Bristol.

Royal Astronomical Society, Memoirs. Royal Astronomical Society, London; Blackwell Scientific Publications, Oxford. Irreg.

Royal Astronomical Society, Monthly Notices. Royal Astronomical Society, London; Blackwell Scientific Publications, Oxford. M

Royal Astronomical Society, Quarterly Journal. Royal Astronomical Society, London; Blackwell Scientific Publications, Oxford. Q

Royal Astronomical Society of Canada, Journal. Royal Astronomical Society of Canada, Toronto. BM

Royal Institution of Great Britain, Proceedings. Royal Institution of Great Britain; Elsevier Publishing Co., Barking, Essex, England. 3 issues per year

Royal Meteorological Society, Quarterly Journal. Royal Meteorological Society, London. Q

Royal Society (Edinburgh), Proceedings, Section A. Royal Society of Edinburgh, Edinburgh. Irreg.

Royal Society (London), Philosophical Transactions, Series A. Royal Society, London. Irreg.

Royal Society (London), Proceedings, Series A. Royal Society, London. Irreg.

Rozprawy Inżynierskie. Polska Akademia Nauk, Instytut Podstawowych Problemów Techniki; Państwowe Wydawnictwo Naukowe, Warsaw. Q

Ruimtevaart. Nederlandse Vereniging voor Ruimtevaart, The Hague. Q

Russian Engineering Journal (Vestnik Mashinostroeniia). Production Engineering Research Association of Great Britain, Melton Mowbray, Leics., England. M

Russian Journal of Physical Chemistry (Zhurnal Fizicheskoi Khimii). Chemical Society, London. M

SAE Aerospace Information Report. Society of Automotive Engineers, Inc., New York. Irreg.

SAE Aerospace Recommended Practice. Society of Auto

INTERNATIONAL AEROSPACE ABSTRACTS

- motive Engineers, Inc., New York. Irreg.
- SAE Aerospace Standards.** Society of Automotive Engineers, Inc., New York. Irreg.
- SAE Journal.** Society of Automotive Engineers, Inc., New York. M
- SAE Journal of Automotive Engineering.** Society of Automotive Engineers, Inc., New York. M
- Safe Engineering.** Survival and Flight Equipment Association; Value Engineering Publications, Inc., Los Angeles. BM
- SAIT Electronics Review.** SAIT Electronics, Brussels. Q
- Samoletostroenie i Tekhnika Vozdushnogo Flota.** Izdanie Khar'kovskogo Gosudarstvennogo Universiteta, Khar'kov. Irreg.
- SAMPE Journal.** Society of Aerospace Material and Process Engineers; SAMPE Publications, Inc., Los Angeles. BM
- SAMPE Quarterly.** Society of Aerospace Material and Process Engineers, Azusa, Calif. Q
- Schweizer Archiv** (see *Schweizer Archiv für angewandte Wissenschaft und Technik*).
- Schweizer Archiv für angewandte Wissenschaft und Technik.** Schweizer Verband für die Materialprüfungen und Schweizerische Gesellschaft für Vakuumphysik und Technik; Verlag Vogt-Schild AG, Solothurn, Switzerland. M
- Schweizerische Technische Zeitschrift.** Schweizer Technischer Verband, Zurich. M
- Science.** American Association for the Advancement of Science, Washington, D.C. W
- Science Dimension.** National Research Council of Canada, Ottawa. BM
- Science Journal.** IPC Business Press, Ltd., London. M
- Science Progrès Découverte.** Société des Ingénieurs Civils de France; Dunod Editeur, Paris. M
- Science Progress.** Blackwell Scientific Publications, Ltd., Oxford. Q
- Sciences et Industries Spatiales.** SADESI — Société Anonyme d'Editions Scientifiques et Industrielles, Geneva. BM
- Sciences et Techniques.** Société des Ingénieurs Civils de France, Paris. M
- Scientific American.** Scientific American, Inc., New York. M
- Scripta Metallurgica.** Pergamon Press, Inc., New York. M
- Secrétariat Général à l'Aviation Civile, Revue.** Secrétariat Général à l'Aviation Civile, Paris. Irreg.
- Seismological Society of America, Bulletin.** Seismological Society of America; Waverly Press, Inc., Baltimore, Md. BM
- *Separation Science.** Marcel Dekker, Inc., New York. BM
- SERL Technical Journal.** Services Electronics Research Laboratory, Baldock, Herts., England.
- Shell Aviation News.** Shell Oil Co., London. M
- SIAM Journal on Applied Mathematics.** Society for Industrial and Applied Mathematics, Philadelphia, Pa. 8 issues per year
- SIAM Journal on Control.** Society for Industrial and Applied Mathematics, Philadelphia, Pa. Q
- SIAM Journal on Mathematical Analysis.** Society for Industrial and Applied Mathematics, Philadelphia, Pa. Q
- SIAM Journal on Numerical Analysis.** Society for Industrial and Applied Mathematics, Philadelphia, Pa. Q
- SIAM Review.** Society for Industrial and Applied Mathematics, Philadelphia, Pa. Q
- Sibirskii Matematicheskii Zhurnal.** Akademiia Nauk SSSR, Sibirskoe Otdelenie; Izdatel'stvo Nauka, Novosibirsk. BM
- Siemens Review.** Siemens Aktiengesellschaft, Erlangen, West Germany. M
- Signal.** Armed Forces Communications and Electronics Association, Washington, D.C. M
- Simulation.** Simulation Councils, Inc., La Jolla, Calif. M
- Sky and Telescope.** Sky Publishing Corp., Cambridge, Mass. M
- Skyline.** North American Rockwell Corp., El Segundo, Calif. Q
- Slaboproudý Obzor.** Státní Nakladatelství Technické Literatury, Prague. M
- SMPTe, Journal.** Society of Motion Picture and Television Engineers, Inc., New York. M
- Società Astronomica Italiana, Memorie.** Gia Società degli Spettroscopisti Italiani, Milan. Q
- Società degli Ingegneri e degli Architetti in Torino, Atti e Rassegna Tecnica.** Turin. Irreg.
- Société Royale des Sciences de Liège, Bulletin.** Société Royale des Sciences de Liège; Université de Liège, Liège. Irreg.
- Société Royale des Sciences de Liège, Mémoires.** Société Royale des Sciences de Liège; Université de Liège, Liège. Q
- Society for Experimental Biology and Medicine, Proceedings.** Society for Experimental Biology and Medicine, New York. 11 issues per year
- Society for Information Display, Proceedings.** Society for Information Display; Western Periodicals Co., North Hollywood, Calif. Q
- Society of Experimental Test Pilots, Technical Review.** Society of Experimental Test Pilots, Lancaster, Calif. SA
- Society of Instrument and Control Engineers, Transactions.** Society of Instrument and Control Engineers, Tokyo. M
- *Society of Rheology, Transactions.** Interscience Publishers, New York. SA
- *Soil Biology and Biochemistry.** Pergamon Press, Ltd., Oxford.
- *Soil Science.** Williams & Wilkins Co., Baltimore, Md. M
- *Soil Science Society of America, Proceedings.** Soil Science Society of America, Madison, Wis. BM
- Solar Energy.** Solar Energy Society, Arizona State University, Tempe; Pergamon Press, Ltd., Oxford. Q
- Solar Physics.** D. Reidel Publishing Co., Dordrecht, Netherlands. M
- Solar System Research (Astronomicheskii Vestnik).** Consultants Bureau, New York. Q
- *Solid-State Communications.** Pergamon Press, Ltd., Oxford. M
- Solid-State Electronics.** Pergamon Press, Ltd., Oxford. M
- Solid State Technology.** Cowan Publishing Corp., New York. M
- Soprotivlenie Materialov i Teoriia Sooruzhenii.** Izdatel'stvo Budivel'nik, Kiev. Irreg.
- Sound and Vibration.** Acoustical Publications, Inc., Cleveland, Ohio. M
- *Southeastern Geology.** Ed. S. Duncan Heron, College Station, Durham, N.C. Q

- Soviet Astronomy (Astronomicheskii Zhurnal)*. American Institute of Physics, Inc., New York. BM
- Soviet Journal of Nondestructive Testing (Defektoskopiia)*. Consultants Bureau, New York. BM
- Soviet Journal of Optical Technology (Optiko-Mekhanicheskaiia Promyshlennost')*. Optical Society of America, Inc., Washington, D.C.; American Institute of Physics, Inc., New York. M
- Soviet Physics — Doklady (Akademiia Nauk SSSR, Doklady)*. American Institute of Physics, Inc., New York. M
- Soviet Physics — JETP (Zhurnal Eksperimental'noi i Teoreticheskoi Fiziki)*. American Institute of Physics, Inc., New York. M
- Soviet Physics — Technical Physics (Zhurnal Tekhnicheskoi Fiziki)*. American Institute of Physics, Inc., New York. M
- Soviet Physics — Uspekhi (Uspekhi Fizicheskikh Nauk)*. American Institute of Physics, Inc., New York. BM
- Soviet Plastics (Plasticheskie Massy)*. Rubber and Plastics Research Association of Great Britain; Rubber & Technical Press, Ltd., London. M
- Soviet Powder Metallurgy and Metal Ceramics (Poroshkovaia Metallurgiiia)*. Consultants Bureau, New York. M
- Space/Aeronautics*. Ziff-Davis Publishing Co., New York. M
- Space Life Sciences*. D. Reidel Publishing Co., Dordrecht, Netherlands. Q
- Space Science Reviews*. D. Reidel Publishing Co., Dordrecht, Netherlands. 9 issues per year
- Spaceflight*. British Interplanetary Society, London. M
- SPARMO Bulletin*. Solar Particles and Radiation Monitoring Organization, Meudon, France. Irreg.
- SPE Journal*. Society of Plastics Engineers, Inc., Greenwich, Conn. M
- *Spectrochimica Acta*. Pergamon Press, Ltd., Oxford. M
- Sperry Rand Engineering Review*. Sperry Rand Corp., Great Neck, N.Y. Q
- SPIE Journal*. Society of Photo-Optical Instrumentation Engineers, Redondo Beach, Calif. BM
- Srpska Akademija Nauka i Umetnosti, Glas, Odeljenje Tehnichkikh Nauka*. Srpska Akademija Nauka i Umetnosti; Nauchno Delo, Belgrade. Irreg.
- Stantsii Opticheskogo Nabludeniia Iskusstvennykh Sputnikov Zemli, Biulleten'*. Astronomicheskii Sovet Akademii Nauk SSSR, Moscow. Irreg.
- Sterne und Weltraum*. Verlag Bibliographisches Institut AG, Mannheim, West Germany. M
- STP Notes*. IUCSTP Secretariat, c/o National Academy of Sciences, Washington, D.C. M
- Strain*. British Society for Strain Measurement, London. Q
- Strength of Materials (Problemy Prochnosti)*. Consultants Bureau, New York. Q
- Studia Geophysica et Geodaetica*. Československá Akademie Věd, Prague. Q
- Studia Scientiarum Mathematicarum Hungarica*. Hungarian Academy of Sciences, Budapest. SA
- Studies in Applied Mathematics*. MIT Press, Cambridge, Mass. Q
- Studii și Cercetări de Astronomie*. Academia Republicii Socialiste Române, Bucharest. SA
- Studii și Cercetări de Fizică*. Academia Republicii Socialiste Române, Bucharest. 10 issues per year

- Studii și Cercetări de Mecanică Aplicată*. Academia Republicii Socialiste Române, Bucharest. BM
- Studii și Cercetări Matematice*. Academia Republicii Socialiste Române, Bucharest. 10 issues per year
- Surface Science*. North-Holland Publishing Co., Amsterdam. M
- Tech Air*. Society of Licensed Aircraft Engineers and Technologists, Kingston-upon-Thames, England. M
- Technika Lotnicza i Astronautyczna*. Stowarzyszenie Inżynierów i Techników Mechaników Polskich, Sekcja Lotnicza; Naczelna Organizacja Techniczna, Warsaw. M
- Technische Mitteilungen AEG-Telefunken (see AEG-Telefunken, Technische Mitteilungen)*.
- Technology Review*. Massachusetts Institute of Technology, Cambridge, Mass. 9 issues per year
- *Technometrics*. American Statistical Association, Washington, D.C. Q
- Tecnica Italiana*. Trieste. M
- Tehran University, Institute of Geophysics, Publication*. Tehran University Press, Amirabad, Tehran. Irreg.
- Teknisk Tidskrift*. Svenska Teknologföreningen, Stockholm. 20 issues per year
- Telecommunications*. Horizon House, Dedham, Mass. M
- Telecommunications and Radio Engineering. Part I — Telecommunications, Part II — Radio Engineering (Elektrosviaz', Radiotekhnika)*. Scripta Publishing Corp., Washington, D.C. M
- Telemetry Journal*. International Foundation for Telemetering; Value Engineering Publications, Inc., Los Angeles. BM
- Tellus*. Svenska Geofysiska Föreningen, Stockholm; Almqvist & Wiksells Boktryckeri AB, Uppsala. BM
- Telonde*. Thomson-CSF, Paris. Q
- Teoreticheskaiia Elektrotekhnika*. Izdatel'stvo L'vovskogo Universiteta, Lvov. Irreg.
- Teoreticheskaiia i Matematicheskaiia Fizika*. Akademiia Nauk SSSR; Izdatel'stvo Nauka, Moscow. M
- Teoriia Funktsii, Funktsional'nyi Analiz i ikh Prilozheniia*. Izdatel'stvo Khar'kovskogo Gosudarstvennogo Universiteta, Kharkov. Irreg.
- Teoriia i Raschet Impul'snykh i Usilitel'nykh Skhem na Poluprovodnikovyykh Priborakh*. Moskovskii Inzhenerno-Fizicheskii Institut; Atomizdat, Moscow. Irreg.
- Teoriia Veroiatnostei i ee Primeneniia*. Akademiia Nauk SSSR; Izdatel'stvo Nauka, Moscow. Q
- Teplotfizika i Teplotekhnika*. Akademiia Nauk Ukrainskoi SSR; Izdatel'stvo Naukova Dumka, Kiev. Irreg.
- Teplotfizika Vysokikh Temperatur*. Akademiia Nauk SSSR; Izdatel'stvo Nauka, Moscow. BM
- Teplovye Napriazheniia v Elementakh Konstruktsii*. Akademiia Nauk Ukrainskoi SSR, Institut Mekhaniki; Izdatel'stvo Naukova Dumka, Kiev. Irreg.
- *La Termotecnica*. Associazione Termotecnica Italiana, Milan. M
- *Tetrahedron*. Pergamon Press, Ltd., Oxford. SM
- *Tetrahedron Letters*. Pergamon Press, Ltd., Oxford. W
- Thermochimica Acta*. Elsevier Publishing Co., Amsterdam. BM
- Thin Solid Films*. Elsevier Sequoia S.A., Lausanne. M

Tohoku University, Institute of High Speed Mechanics, Reports. Tohoku University, Sendai. Irreg.
Tohoku University, Research Institute for Strength and Fracture of Materials, Reports. Tohoku University, Sendai. Irreg.

Tokyo, University, Institute of Space and Aeronautical Science, Bulletin. Tokyo, University, Institute of Space and Aeronautical Science, Tokyo. Q

Tokyo, University, Institute of Space and Aeronautical Science, Report. Tokyo, University, Institute of Space and Aeronautical Science, Tokyo. Irreg.

Tokyo, University, Tokyo Astronomical Observatory, Annals, Second Series. Tokyo, University, Tokyo.

Tokyo Astronomical Observatory, Tokyo Astronomical Bulletin, Second Series. Tokyo Astronomical Observatory, Tokyo. Q

Tokyo Institute of Technology, Bulletin. Tokyo Institute of Technology, Tokyo. Irreg.

Tool and Manufacturing Engineer. American Society of Tool and Manufacturing Engineers, Dearborn, Mich. M

Torino, Accademia delle Scienze, Classe di Scienze Fisiche, Matematiche e Naturali, Atti. Torino, Accademia delle Scienze, Turin. Irreg.

Toshiba Review. Tokyo Shibaura Electric Co., Ltd., Tokyo. BM

Trend in Engineering. University of Washington, Office of Engineering Research, Seattle. Q

TRW Space Log. TRW Systems Group, Redondo Beach, Calif. Q

Tsvetnaia Metallurgii. Ministerstvo Vysshego i Srednego Spetsial'nogo Obrazovaniia SSSR; Izdanie Severokavkazskogo Gornometallurgicheskogo Instituta, Ordzhonikidze. BM

Ukrains'kii Fizichnii Zhurnal. Akademiia Nauk Ukrain's'koi RSR, Kiev. M

Ukrainskii Matematicheskii Zhurnal. Akademiia Nauk Ukrainskoi SSR; Izdatel'stvo Naukova Dumka, Kiev. BM

Ultrasonics. Iliffe Science & Technology Publications, Ltd., Guildford, Surrey, England. Q

Unione Matematica Italiana, Bollettino. Nicola Zanichelli Editore, Bologna. BM

Universitas Comeniana, Acta Facultatis Rerum Naturalium — Physica. Slovenské Pedagogické Nakladatelstvo, Bratislava. Irreg.

URSI Bulletin d'Information. URSI, Secrétaire Général, Brussels. BM

U. S. Naval Institute Proceedings. U. S. Naval Institute, Annapolis, Md. M

Uspekhi Fizicheskikh Nauk. Akademiia Nauk SSSR; Izdatel'stvo Nauka, Moscow. M

Uspekhi Fiziologicheskikh Nauk. Akademiia Nauk SSSR; Izdatel'stvo Nauka, Moscow. Q

USSR Computational Mathematics and Mathematical Physics (Zhurnal Vychislitel'noi Matematiki i Matematicheskoi Fiziki). Pergamon Press, Ltd., Oxford. BM

Uzbekskii Biologicheskii Zhurnal. Akademiia Nauk Uzbekskoi SSR, Tashkent. BM

VDI-Forschungsheft. Verein Deutscher Ingenieure; VDI-Verlag GmbH, Düsseldorf. BM

VDI-Z. Verein Deutscher Ingenieure; VDI-Verlag GmbH, Düsseldorf. SM

VDI-Z Fortschritt-Berichte, Reihe 4 — Bauingenieurwesen. Verein Deutscher Ingenieure; VDI-Verlag GmbH, Düsseldorf. Irreg.

VDI-Z Fortschritt-Berichte, Reihe 7 — Strömungstechnik. Verein Deutscher Ingenieure; VDI-Verlag GmbH, Düsseldorf. Irreg.

VDI-Z Fortschritt-Berichte, Reihe 11 — Schwingungstechnik, Lärmbekämpfung. Verein Deutscher Ingenieure; VDI-Verlag GmbH, Düsseldorf. Irreg.

VDI-Z Fortschritt-Berichte, Reihe 12 — Verkehrstechnik. Verein Deutscher Ingenieure; VDI-Verlag GmbH, Düsseldorf. Irreg.

Verkehrsmedizin und ihre Grenzgebiete. Transpress VEB Verlag für Verkehrswesen, Berlin. M

Vertical World. Vertical World, Inc., Evanston, Ill. BM

VertiFlite. American Helicopter Society, Inc., New York. M

Vibrotehnika. Izdatel'stvo Mintis, Vilnius. Irreg.

Le Vide. Société Française des Ingénieurs et Techniciens du Vide, Paris. BM

Vilnius, Astronomijos Observatorijos, Biuletenis. Vilnius. Irreg.

**Virology.* Academic Press, Inc., New York. M

Vision Research. Pergamon Press, Ltd., Oxford. M

Voenno-Meditsinskii Zhurnal. Tsentral'noe Voenno-Meditsinskoe Upravlenie Ministerstva Oborony SSSR; Izdatel'stvo Krasnaia Zvezda, Moscow. M

Voprosy Dinamiki i Prochnosti. Rizhskii Politekhnicheskii Institut; Izdatel'stvo Zinatne, Riga. Irreg.

Vychislitel'naia i Prikladnaia Matematika. Izdatel'stvo Kievskogo Universiteta, Kiev. Irreg.

Vychislitel'nye Metody i Programirovanie. Izdatel'stvo Moskovskogo Universiteta, Moscow. Irreg.

Wärme- und Stoffübertragung. Springer Verlag, Berlin. Q

Wear. Elsevier Sequoia S.A., Lausanne. M

**Wehrkunde.* Verlag Europäische Wehrkunde, Munich. M
Wehrmedizinische Monatsschrift. J. F. Lehmanns Verlag, Munich. M

Welding Journal. American Welding Society, New York. M

Welding Production (Svarochnoe Proizvodstvo). Welding Institute, Cambridge. M

Weltraumfahrt Raketentechnik. Umschau Verlag, Frankfurt/Main. BM

**Western Pharmacology Society, Proceedings.* Ed. James M. Dille, University of Washington, Seattle.

Westinghouse Engineer. Westinghouse Electric Corp., Pittsburgh, Pa. BM

Wetter und Leben. Österreichische Gesellschaft für Meteorologie; Verlag Wetter & Leben, Vienna. BM

Wissenschaftliche Berichte AEG-Telefunken. AEG-Telefunken, Berlin. Q

Wissenschaftliche Zeitschrift. Dresden, Technische Universität, Dresden, East Germany. BM

World Health. World Health Organization, Geneva. M

WRC Bulletin. Welding Research Council, New York. 10 issues per year

Yamagata University, Bulletin (Engineering). Yamagata University, Yamagata, Japan.

Zagadnienia Drgań Nieliniowych. Polska Akademia Nauk, Instytut Podstawowych Problemów Techniki; Państwowe Wydawnictwo Naukowe, Warsaw. Irreg.

Zashchitnye Pokrytiia na Metallakh. Akademiia Nauk Ukrainsoi SSR, Institut Problem Materialovedeniia; Izdatel'stvo Naukova Dumka, Kiev. Irreg.

Zastosowania Matematyki. Polska Akademia Nauk, Instytut Matematyczny; Państwowe Wydawnictwo Naukowe, Warsaw. 3 issues per year

Zeitschrift für angewandte Mathematik und Mechanik. Akademie-Verlag GmbH, Berlin. M

Zeitschrift für angewandte Mathematik und Physik. Birkhäuser Verlag, Basel. BM

Zeitschrift für angewandte Physik. Deutsche Physikalische Gesellschaft, e.V.; Springer Verlag, Berlin. M

Zeitschrift für experimentelle und angewandte Psychologie. Deutsche Gesellschaft für Psychologie; Verlag für Psychologie, Göttingen. Q

Zeitschrift für Flugwissenschaften. Deutsche Gesellschaft für Luft- und Raumfahrt, e.V., and Deutsche Forschungs- und Versuchsanstalt für Luft- und Raumfahrt, e.V.; Friedr. Vieweg & Sohn GmbH, Braunschweig. M

Zeitschrift für Geophysik. Deutsche geophysikalische Gesellschaft, Hamburg; Physica-Verlag, Würzburg. BM

Zeitschrift für Luftrecht und Weltraumrechtsfragen. Köln, Universität, Institut für Luftrecht und Weltraumrechtsfragen; Carl Heymanns Verlag, KG, Cologne. Q

Zeitschrift für Metallkunde. Deutsche Gesellschaft für Metallkunde, e.V.; Riederer-Verlag GmbH, Stuttgart, West Germany. M

Zeitschrift für Meteorologie. Meteorologische Gesellschaft; Akademie-Verlag GmbH, Berlin. Irreg.

Zeitschrift für Naturforschung, Teil a. Verlag der Zeitschrift für Naturforschung, Tübingen. M

Zeitschrift für Naturforschung, Teil b. Verlag der Zeitschrift für Naturforschung, Tübingen. M

Zeitschrift für Physik. Deutsche physikalische Gesellschaft; Springer Verlag, Berlin. Irreg.

Zeitschrift für Vermessungswesen. Deutscher Verein für Vermessungswesen; Verlag Konrad Wittwer, Stuttgart, West Germany. M

Zemlia i Vselennaia. Akademiia Nauk SSSR; Izdatel'stvo Nauka, Moscow. BM

Zentralblatt für Verkehrs-Medizin, Verkehrs-Psychologie, Luft- und Raumfahrt-Medizin. Deutsche Gesellschaft für Luft- und Raumfahrt-Medizin and Deutsche Gesellschaft für Verkehrs-Medizin; J. F. Lehmanns Verlag, Munich. Irreg.

Zhurnal Eksperimental'noi i Teoreticheskoi Fiziki. Akademiia Nauk SSSR; Izdatel'stvo Nauka, Moscow. M

Zhurnal Nauchnoi i Prikladnoi Fotografii i Kinematografii. Akademiia Nauk SSSR; Izdatel'stvo Nauka, Moscow. BM

Zhurnal Prikladnoi Spektroskopii. Izdatel'stvo Nauka i Tekhnika, Minsk. M

Zhurnal Tekhnicheskoi Fiziki. Akademiia Nauk SSSR; Izdatel'stvo Nauka, Leningrad. M

Zhurnal Vychislitel'noi Matematiki i Matematicheskoi Fiziki. Akademiia Nauk SSSR; Izdatel'stvo Nauka, Moscow. BM

Zhurnal Vysshei Nervnoi Deiatel'nosti. Akademiia Nauk SSSR; Izdatel'stvo Nauka, Moscow. BM

Zpráva VZLÚ. Výzkumný a Zkušební Letecký Ústav, Prague. Irreg.

Zpravodaj VZLÚ. Výzkumný a Zkušební Letecký Ústav, Prague. BM

A Notation of Content, rather than the title of the publication, appears under each subject heading; it is listed under several subject headings which provide multiple access to the subject content of each accession. The IAA accession number is located under and to the right of the Notation of Content. It is preceded by numbers identifying the issue and page of *International Aerospace Abstracts* where the abstract is located.

To illustrate:

Issue Number	Page Number	Accession Number
01	p0196	A70-10845

A

A STARS

A-type supergiants microturbulence, determining atmospheric small scale velocity fields

14 p2641 A70-30885

Ap star kappa Cancr model atmosphere analysis based on observed energy distribution and hydrogen line profiles

14 p2652 A70-31381

Near Galactic plane condensations of spectral A stars in HD catalog, investigating by Monte Carlo method and Poisson formula

15 p2797 A70-31616

Observational evidence concerning validity of Saha and Boltzmann laws in O, B and A stellar atmospheres

17 p3170 A70-35387

Am and Ap stars metallic absorption lines, determining photometrical indices correction

19 p3523 A70-38689

Single normal main sequence stars rotational velocities compared with giant, supergiant, Be, A and metallic line stars and Population II objects

23 p4248 A70-44802

Rotating stellar atmospheric models for middle and late A star masses, emphasizing Altair observed and predicted energy distribution

23 p4250 A70-44812

Stellar rotational velocities in open star clusters, noting evolutionary expansion, tidal coupling in binaries and Ap stars magnetic braking

23 p4251 A70-44820

A type stars rotation, examining UVB color and rotational velocity relationship, spectral classification and spectroscopic binaries

23 p4251 A70-44822

Deutsch period vs line width relation for periodic Ap stars, determining rotational velocities with rigid rotator model

23 p4251 A70-44825

Heavy elements diffusive separation as explanation of metallic and magnetic A stars abundance anomalies at outer convective envelope bases

24 p4410 A70-45775

A-7 AIRCRAFT

A-7 aircraft TF-41 engine tolerance to steam ingestion, discussing test program and results and engine modifications

01 p0165 A70-10700

A-11 SATELLITE

U ECHO 1 SATELLITE

A-12 SATELLITE

U ECHO 2 SATELLITE

A-300 AIRCRAFT

Seat capacity effect on operational costs of short/medium range high capacity A 300 B aircraft

02 p0402 A70-12368

A-300B twin engine short haul giant transport aircraft, discussing engines, aircraft performance and systems reliability

[RAES PAPER 11] 03 p0411 A70-13543

European A-300-B Airbus program, discussing technical and economical aspects

18 p3213 A70-36509

AAP

U APOLLO APPLICATIONS PROGRAM

ABBREVIATIONS

U SYMBOLS

ABDOMEN

Chest, abdominal wall and diaphragm displacements of rabbits during partial and whole body exposure to shock waves produced by hexotol charges

02 p0331 A70-11704

Mechanical behavior of anesthetized dog abdominal vena cava from pressure wave transmission characteristics, discussing chemical and electrical stimuli

04 p0630 A70-14630

Force input and thoraco-abdominal strain due to sinusoidal motion of electrohydraulic shake table over 2-14 Hz range imposed on human body

13 p2359 A70-29438

Morphology of adult mammalian thoracic and abdominal aortic segments indicating deviation from medial lamellar architecture

24 p4298 A70-45801

ABEL FUNCTION

Hilbert space stability theory over locally compact Abelian groups developed to obtain spectral theory and positivity conditions

03 p0461 A70-14169

Zeta-Kleinian functions derived from Abelian functions

[ONERA-TP-800] 09 p1712 A70-22837

Fourier transform calculations on finite Abelian groups

12 p2261 A70-27423

Tensor and torsion functors on Abelian semigroups

13 p2440 A70-29076

ABERRATION

Danjon astrolabe for star position and aberration constant determination with improved accuracy, discussing Mars observation

05 p0912 A70-16453

Objective lens systems with high chromatic aberration correction for visible spectral region

08 p1494 A70-20834

Chromatic aberrations of Pottava observatory AVR-2 refractor

08 p1496 A70-21161

Mirror-grating system optical properties emphasizing coma-type aberration elimination

09 p1729 A70-23528

Lens aberrations compensations in partially coherent image holography

10 p1891 A70-24838

Angular aberrations produced by airborne radomes calculated by computer, allowing optimal parameters selection and knowledge of radio properties

12 p2195 A70-27274

Field distribution determination in holographic image space, obtaining ideal image and aberration terms

13 p2405 A70-28826

Fourth order aberration in gas lens used as focusing element in light beam waveguide systems

15 p2697 A70-31829

Dipole antenna arrays feeds design and performance for spherical aberration correction, discussing polarization mismatch

16 p2871 A70-32955

ABIOGENESIS

Porphyrin in Fig Tree shale and Onverwacht chert from Swaziland System sediments, noting age of three billion years and importance in abiogenesis research

01 p0070 A70-10327

Book on chemical evolution of life covering molecular paleontology, prebiotic chemistry, membrane structures, molecular evolution and structure, etc

02 p0230 A70-11685

Organic compounds synthesis by electric discharges

in simulated primitive atmosphere, considering mechanism for biologically significant molecules formation

07 p1225 A70-19104

Peptide formation by stepwise tetramer-mediated condensation of alpha-amino acid as possible prebiotic process

07 p1204 A70-19202

Conditions for life in universe, analyzing evolutionary stages of matter to determine steps producing complex organic compounds

09 p1762 A70-23121

Peptide formation during glycine reaction with linear polyphosphates and cyclic metaphosphates, considering prebiotic synthesis

09 p1630 A70-23395

Electric discharge reactions in mixtures of phosphine with methane, ammonia and water, obtaining biologically significant inorganic and organic phosphorus compounds

09 p1630 A70-23396

Adenosine phosphates hydrolysis in solutions containing Ca ions and in synthetic seawater, investigating living systems energy transfer and prebiological evolution

11 p1986 A70-25702

Primitive earth prebiological organic synthesis via amino acids shock heating in atmosphere-simulating gas mixture, suggesting energy sources from atmospheric entry

12 p2167 A70-27269

Replicating molecules on primordial earth, suggesting chemical evolution on Jupiter via demonstrable alpha-aminonitriles synthesis

14 p2536 A70-30364

Atmospheric oxygen history, using primeval anoxic terrestrial atmosphere simulation to show organic molecule formation by abiogenic process

16 p2898 A70-33990

Optically active organic compounds origin on primordial earth, emphasizing role of asymmetric catalysis

17 p3024 A70-34700

Book on biochemical predestination covering life origin, biomonomer synthesis, polymerization, colloidal systems, etc

17 p3025 A70-34925

Cells chemical origin, discussing terrestrial fractionation, amino acids, macromolecules, metabolism, etc

20 p3569 A70-38992

Bibliographical guide for literature concerning chemical evolution and origin of life

23 p4148 A70-44842

Abiotic synthesis of meteoritic aliphatic hydrocarbons produced by open flow Fischer-Tropsch processes for hydrogen and Co interactions

24 p4402 A70-45377

ABLATION

Ablation effects on transition Reynolds number of hypersonic boundary layer on slender cones

03 p0465 A70-12945

Parietal ablation in phenolic resins using chemical kinetics

[ONERA-TP-734] 03 p0606 A70-13634

Acoustic technique for flow transition detection on hypersonic ablating reentry vehicles, presenting supersonic wind tunnel test results

04 p0620 A70-15531

Particle removal in ablation of artificial graphite linked to oxidation, using high speed motion pictures in analysis

04 p0787 A70-15610

Ablative cooling mechanisms and applications, discussing environmental effects on material performance, pyrolyzed and graphitized plastics, phenolic ablators, etc

05 p0856 A70-16617

Reusable booster rocket heat protection system design, discussing ablation and insulation methods

05 p0958 A70-16635

Dynamic stability loss on ablating vehicles ascribed to boundary layer transition effect from turbulent aft body heating

[AIAA PAPER 69-106] 06 p0961 A70-17166

Melting ablation for two dimensional and axisymmetric blunt bodies with body force, predicting gas-liquid interface temperature for free stream conditions

06 p1176 A70-17690

Laminar ablation testing under turbulent boundary layer heating conditions, obtaining recession rate and heat of ablation for turbulent ablation of Teflon [AIAA PAPER 70-226] 06 p1179 A70-18071

Viscous radiating flowfield coupled with ablation for computations on blunt body entering earth atmosphere at interplanetary return velocities [AIAA PAPER 70-128] 06 p0970 A70-18090

Ablation of heat shielding materials subjected to superorbital reentry conditions, noting dependence on heating rate to surface [AIAA PAPER 70-202] 06 p0970 A70-18100

Graphite microstructure effect on ablation performance, discussing grain size, porosity and degree of graphitization [AIAA PAPER 70-155] 06 p1092 A70-18147

Faint meteor ablation processes, presenting evidence of solid consistency prior to atmospheric entry, vaporization, wake blending and trails 06 p1151 A70-18481

Pressure effects in predicting ablation velocities for gas-solid systems, assuming reactions and gaseous products reversible adsorption on solid surfaces 07 p1422 A70-19373

Streamwise directed vortices and crosshatched surface roles in heat transfer and ablation processes of reentry vehicles 07 p1394 A70-19729

Ablation products and high temperature boundary layer chemistry of polytetrafluoroethylene (Teflon) in arc jet streams using mass spectrometer 07 p1319 A70-19886

Meteor ablation, investigating removal rate of molten film and droplet evaporation 09 p1754 A70-22476

Current sheet velocity in coaxial plasma accelerator, noting drag due to insulator ablation and degassing [AIAA PAPER 69-265] 09 p1736 A70-23202

Cross hatching on surface of ablating bodies exposed to supersonic turbulent boundary layer flow using mathematical model 09 p1605 A70-23232

Book on quasi-linearization and nonlinear fluid and orbital mechanics covering ablating wall, electrostatic probe, laminar boundary stability, pipe flow and optimum bang-bang transfer 11 p2072 A70-26225

Ablation and temperature effects in hollow viscoelastic cylinder 13 p2508 A70-28487

Hypersonic wind tunnel testing of Plexiglas and nylon hemispheres instrumented with strain gages and thermocouples, comparing with calculated strain, temperature and ablation 13 p2520 A70-28727

Ablation test facilities capability extension by surrounding high enthalpy flow with coaxial cold air jet [AIAA PAPER 70-588] 13 p2522 A70-29883

Liquid rocket engine combustion analysis, discussing bipropellant spray mass distribution, drop size and velocity, spray evaporation interphase drag and ablative chambers [AIAA PAPER 70-622] 16 p2997 A70-33527

Static aerodynamic characteristics of slender ablating reentry vehicle, discussing coupling between flow field and thermochemical analyses of heat shield materials response [AIAA PAPER 70-826] 16 p3001 A70-33939

Visual cortical anomalous response to paired photic stimulus in rabbits with ablations in rostral part of brain stem 18 p3221 A70-37214

Carbons and graphites ablation tests for predicting performance under reentry conditions, considering microstructure effects 20 p3735 A70-39214

Heat shield analysis covering high temperature ablation interactions in conical anisotropic structure immersed in hypersonic environment 20 p3738 A70-40054

Bilateral cortical cerebellar hemispheric ablations effect on feline light-dark discrimination learning 21 p3762 A70-41142

Ablative response predictions analytical tools, discussing boundary layer edge conditions definition, atmospheric entry, rocket propulsion, etc 21 p3952 A70-42055

Laser and flash X ray shadowgraph techniques in hypervelocity ablation/erosion investigations in hypervelocity range [SMPT PREPRINT 28] 22 p4034 A70-43047

Ablative heat transfer to nonstagnation surfaces of high speed rocket vehicle in continuum atmosphere, using finite difference theory 22 p4125 A70-43433

Cracked Teflon heat shields ablative behavior for laminar and turbulent boundary layers in supersonic flow, describing heat transfer to substructure 23 p4282 A70-44585

ABLATIVE MATERIALS

Polyethyl methacrylate fuel for hypersonic air breathing propulsion systems, studying ablation, mixing and combustion processes 03 p0603 A70-12942

Ablative throat nozzle performance, plotting change in thrust, exit pressure and Mach number as function of ablated to initial area ratio 03 p0410 A70-14336

Stress analysis for nonlinear viscoelastic cylinder with ablating moving inner surface used to investigate propellant grain in solid fuel rocket under firing condition [ASME PAPER 69-WA/APM-14] 04 p0771 A70-14914

Nozzle throat ablative materials for controlled high regression rates in tactical rocket motors, primarily nylon reinforced thermosetting resins [AIAA PAPER 69-423] 04 p0713 A70-15428

Photographic pyrometry for surface temperature measurements on ablation models, discussing technique accuracy and limitations 04 p0694 A70-15536

Ablation chars, carbon and graphite spectral emittance and reflectance as function of wavelength and temperature, noting applications to atmospheric entry heat shielding 04 p0787 A70-15590

Surface recession of low density phenolic nylon in arc heated air using stagnation point models, noting char removal processes 04 p0787 A70-15602

Preimpregnated materials processing, discussing molding, resin-reinforcement, unidirectional materials, ablative applications, mechanical data and air-frame uses 05 p0874 A70-16614

Ablative cooling mechanisms and applications, discussing environmental effects on material performance, pyrolyzed and graphitized plastics, phenolic ablators, etc 05 p0856 A70-16617

Elastomeric silicone ablator reinforced by carbon cloth or fibers for Venus entry heat protection [AIAA PAPER 70-201] 06 p1157 A70-18086

Ablation of heat shielding materials subjected to superorbital reentry conditions, noting dependence on heating rate to surface [AIAA PAPER 70-202] 06 p0970 A70-18100

Full scale R/V flight test base pressure data for slender cones with ablative heat shields, considering mass flow and addition effects [AIAA PAPER 70-109] 06 p0973 A70-18148

Plasma arc tests to simulate stagnation reentry heating on spherical subized models of nuclear heat source to investigate heat shield materials ablation characteristics [AIAA PAPER 70-200] 06 p0974 A70-18172

Phenolic nylon ablative thermal effectiveness in arc heated nitrogen, air and nitrogen-carbon dioxide streams [AIAA PAPER 70-154] 06 p1183 A70-18233

Convective and radiative heat fluxes measurement on charring ablative materials surface in rocket nozzle environment 06 p1070 A70-18444

Ablative materials for thermal protection at low convective heating rates, comparing foam and state-of-art materials performance 07 p1316 A70-18927

Reentry thermal protection materials technology, discussing thermophysical, thermomechanical and kinetic effects, noting interdisciplinary approach 07 p1319 A70-19878

Radiative heating rates and gas environments effects on ablative material performance from tests at arc image facility 07 p1319 A70-19888

Electrically conductive ablative materials rapidly heated to 7000 F in test facility, discussing heating method and high strain rate testing 07 p1250 A70-20042

Refurbishable ablative thermal protection for reusable lifting reentry vehicles [AIAA PAPER 70-277] 07 p1397 A70-20386

Structural analysis of Titan 3 Stage 2 ablative nozzle extension made of composite material 08 p1595 A70-21910

Thermal protection polymers ablator efficiency evaluation using high vacuum DTA cell coupled to high resolution mass spectrometer 11 p2070 A70-25813

Insulators, ablators, reflectors and computer analyses for aerodynamic and engine heat for aerospace thermal design 11 p1980 A70-25874

Ballistic range tests to study ablation effects on aerodynamic characteristics of ablating and nonablating slender cones [AIAA PAPER 69-179] 11 p2148 A70-25976

Line source technique for ablative heat shield materials thermal conductivity measurements, comparing vacuum and atmospheric test results [AIAA PAPER 69-1013] 11 p2051 A70-26142

Quasi-steady analysis of material under ablation-erosion heat transfer for hypersonic vehicles 11 p2149 A70-26144

Radiation profiles in ablating flat plate air-Teflon laminar boundary layer, discussing viscosity, UV and IR wavelengths 12 p2211 A70-27803

Charring ablative plastic thermal properties simultaneous measurement using modified heat transfer model and nonlinear regression analysis 12 p2333 A70-28111

Liquid film steady motion on ablating body surface allowing for radiative heat transfer from interior 12 p2334 A70-28244

Cone roll dynamics-ablation patterns coupling in hypersonic wind tunnels [AIAA PAPER 70-562] 13 p2340 A70-29025

Differential thermal analyzer coupled to mass spectrometer for kinetics of reactions giving volatile products at high temperature, considering ablative materials 14 p2664 A70-30292

Apollo thermal protection system noting low density ablation, flight and ground tests [AIAA PAPER 68-1142] 15 p2813 A70-32514

Ablative composites containing in situ reaction formed refractory metal carbides 16 p2937 A70-33371

Unequal diffusion film coefficient formulation based on transfer coefficient approach for ablative material coupled multicomponent boundary layer problems 16 p2998 A70-33879

Ablative materials performance in high radiative heat flux environments produced by CW carbon dioxide laser [AIAA PAPER 70-864] 16 p2939 A70-33907

Gas phase chemical reactions effect on heat transfer to charring ablator, deriving numerical solution for multicomponent stagnation point flow [AIAA PAPER 70-869] 16 p2999 A70-33912

Mechanical erosion concomitant with thermochemical erosion in mass and energy transfer at interface of boundary layer and ablating nylon-silica-phenol material [AIAA PAPER 70-824] 16 p2941 A70-33942

High pressure ablation of plastic composites and graphites in arc heater, measuring erosion rate, shape change, surface roughness and physical characterization [AIAA PAPER 70-770] 17 p3193 A70-34482

Teflon crosshatched ablation patterns elimination by grooving or glass filler addition [AIAA PAPER 70-769] 17 p3193 A70-34483

Probstein-Gold model for ablating materials crosshatching patterns, using interaction between inelastic deformable surface and supersonic turbulent boundary layer [AIAA PAPER 70-768] 17 p3009 A70-34504

Reinforced plastic composites thermal protection and ablative performance in high temperature environments for reentry vehicle applications 20 p3656 A70-40029

Charring ablators transient heat transfer model, calculating surface temperature and recession and pyrolysis mass loss [AIAA PAPER 70-1143] 20 p3738 A70-40280

Convective and radiative heat flux measurement incident on ablative surface in solid rocket nozzles 21 p3824 A70-40858

Full scale R/V flight test base pressure data for slender cones with ablative heat shields, considering mass flow and addition effects [AIAA PAPER 70-109] 21 p3745 A70-41753

Surface ablation patterns in sublimating materials tested in high temperature structures tunnel 21 p3951 A70-41755

Gases interaction with ablator and components during thermal conductivity, measuring nitrogen, helium, carbon dioxide and water sorption 21 p3951 A70-41873

Thermocouple transient response characteristics in deflagrating and ablative low conductivity materials with high temperature gradients [ASME PAPER 70-HT-7] 22 p4122 A70-42440

Charring ablative composites pyrolysis products composition determination, comparing chemical analysis techniques 23 p4158 A70-44519

Phenolic nylon ablative thermal effectiveness in arc heated nitrogen, air and nitrogen-carbon dioxide streams [AIAA PAPER 70-154] 23 p4282 A70-44520

ABLATIVE NOSE CONES

Diffusive transport term in hydrodynamic equations describing flow over strongly ablating entry objects, discussing charge separation and pressure diffusion 03 p0405 A70-12926

Three dimensional ablation calculated for reentry sphere-cone taking into account shape changes and internal heat conduction [AIAA PAPER 70-199] 06 p1181 A70-18150

Nonsimilar ablation of graphite sphere cones under ballistic entry conditions, predicting steady state rate and surface temperature 13 p2523 A70-29975

- Nonpenetrative reentry vehicle nose thickness ablation sensor using gamma radiation backscatter
17 p3094 A70-35519
- Ablating nose equilibrium shape in laminar hypersonic flow during reentry
18 p3208 A70-36707
- Ballistic reentry vehicle roll-pitch coupling, showing influence of nose asymmetries
[ALAA PAPER 69-101]
21 p3930 A70-41736
- ## ABNORMALITIES
- NT GEOMAGNETIC HOLLOW
- NT MAGNETIC ANOMALIES
- NT NEUROSES
- NT PHOBIAS
- NT PSYCHOTIC DEPRESSION
- Global diurnal variations in F 2 layer seasonal anomaly during high and low solar activity, noting corpuscular radiation role
19 p3491 A70-37326
- ## ABORT APPARATUS
- Space shuttle atmospheric maneuvers, examining booster and orbiter entry, flyback and abort
[AAS PAPER 70-047]
17 p3175 A70-34787
- Apollo Lunar Module strapdown Abort Guidance system, correlating performance prediction with flight test results
[ALAA PAPER 70-1028]
20 p3666 A70-39509
- Apollo spacecraft pyrotechnic systems and devices functions during lunar exploration mission and in aborts
[SAE PAPER 700833]
24 p4416 A70-45888
- ## ABORT TRAJECTORIES
- Abort and staging separation maneuvers of two equal size reusable lifting entry vehicles in wind tunnel tests
[ALAA PAPER 70-260]
07 p1397 A70-20389
- ## ABORTED MISSIONS
- Return to earth abort capability for Apollo missions for various mission phases
[ALAA PAPER 70-94]
06 p1156 A70-18035
- Manned spacecraft abort guidance and control problems, discussing various modes and emergency conditions
24 p4374 A70-46210
- ## ABRASION
- Hydrogen effects on ELI Ti-Al-Sn alloy, conducting tensile, fretting and abrasion tests on stressed and thermal cycled specimens
[ALAA PAPER 69-585]
07 p1309 A70-19710
- Abrasive wear of polymers subject to plastic and elastic deformation, considering papers, metal gauze and rough metal surfaces
07 p1296 A70-20003
- Lubricating fluids effects on three-body abrasion wear rates, considering roles of viscosity and abrasive type
13 p2419 A70-28896
- Material thickness tolerances control for weight minimization of aerospace vehicles by abrasive metal grinding, improving surface quality
[SAE PAPER 827]
20 p3638 A70-40358
- ## ABRASION RESISTANCE
- Carbide rupture energy in wear resistant alloys during abrasion, considering metallographic data and energy parameters
04 p0707 A70-15212
- Metals and hard materials sliding wear due to granular abrasives in heated vacuum chamber
17 p3100 A70-34646
- Wear resistant titanium carbide based cermet material production by impregnation techniques, discussing grain size and heat treatment effects
19 p3450 A70-37453
- ## ABRASIVES
- Tangential cutting force measurements during Ti grinding by microtools, noting properties of W, aluminum boride and zirconium carbide
04 p0697 A70-14466
- Wear intensity of abrasives during fine grinding of Armc Fe, Ti and Ti alloys, comparing friction and chemical composition effects
15 p2743 A70-31640
- Erosion by solid particles, discussing impacting velocity effects, natural sand quartz particle size distribution and composition, artificial industrial abrasives, etc
17 p3126 A70-35600
- Molybdenum disulfide abrasiveness on test rings coated with bonded solid lubricant
[ASLE PREPRINT 70AM 5A-1]
19 p3439 A70-38811
- Pt and Ag surface effects on LOX nucleate boiling heat transfer, considering embedded abrasives relationship to hysteresis
21 p3947 A70-41056
- Grinding by abrasive tape, superimposing transverse vibrations to improve performance and life
22 p4046 A70-42816
- ## ABSCISSAS
- ## U COORDINATES
- ## ABSOLUTE TEMPERATURE SCALES
- ## U TEMPERATURE SCALES
- ## ABSORBENTS
- Granular amine used as regenerable absorbent in cycling two bed system for carbon dioxide removal
01 p0038 A70-10972
- Time dependent transmission of carbon dioxide in air flowing through molecular sieve adsorber beds, developing and programming weighted least squares analysis
04 p0786 A70-15315
- ## ABSORBERS [EQUIPMENT]
- Nonlinear acoustic absorbers behavior analysis, discussing spectral and temporal computation methods
20 p3672 A70-39237
- Spectral and real time computation for acoustic absorbers with nonlinear material characteristics
23 p4219 A70-44393
- ## ABSORBERS [MATERIALS]
- ## NT SOLAR ENERGY ABSORBERS
- Laser mode locking due to saturable absorbers taking into account dispersive property of active material, expanding electric field within cavity
01 p0109 A70-10428
- Frequency spectrum, Q factor and single mode selectivity of two mirror laser resonator with absorbing thin metallic films, showing agreement for Ag and Ni
03 p0500 A70-13459
- Chlorotrifluoroethylene and difluorodichloromethane saturable absorbers for wavelength extensions of passively Q switched carbon dioxide lasers
03 p0502 A70-13816
- Radiation transfer in scattering medium with nonuniform density distribution of absorbing matter expressed in terms of photon distribution
09 p1666 A70-22178
- Panel sound absorber acoustic impedance variation with frequency predicted taking into account panel mass, stiffness and internal damping
09 p1770 A70-22390
- Radiant heat exchange local and angular coefficients determined allowing for absorbing and scattering medium between bodies
10 p1969 A70-25141
- Layered electromagnetic absorbers performance analysis by variable metric optimization method, handling functions defined over polyhedral region of real space
11 p2019 A70-26713
- Carbon dioxide laser passive Q switching, using ethylene and methanol as saturable absorbers
18 p3270 A70-36749
- Nuclear-electromagnetic cascades longitudinal development in glass, Fe and W absorbers, presenting Monte Carlo simulation
18 p3293 A70-36895
- Q switching of nitrous oxide laser with Freon 12 and sulfurhexafluoride absorbers, comparing wavelengths with carbon dioxide laser outputs
21 p3834 A70-40567
- Thermal blooming of 10.6 micron laser beam in carbon dioxide absorption cell
22 p4049 A70-42335
- Passive Q switching and mode locking of carbon dioxide laser with saturable absorbers and buffer gases, using electric pulse excitation
22 p4050 A70-43023
- ## ABSORPTANCE
- Fluorel spectral reflectance, transmittance and absorbance under monochromatic irradiation, considering thermal analysis and surface finish
09 p1710 A70-22794
- ## ABSORPTION
- Reduced Nd ion absorption in matrices of fluorides, fluoride mixtures or oxygen-containing compounds with various ion concentrations, analyzing optical centers statistical properties
01 p0107 A70-10210
- W oxidation kinetics as function of ribbon temperature and absorption time using flash technique with sweep pulse mass spectrometer
07 p1306 A70-19275
- Inert gas absorption from tissue cavities in body, using models with different wall distribution patterns of capillaries and diffusion resistance
12 p2171 A70-28025
- Surface adsorbed and absorbed radioactive Kr 85 gas for displaying surface microdefects in materials
20 p3638 A70-39950
- ## ABSORPTION BANDS
- ## U ABSORPTION SPECTRA
- ## ABSORPTION COEFFICIENT
- ## U ABSORPTIVITY
- ## ABSORPTION CROSS SECTIONS
- Inelastic muon-nucleon scattering implications on cosmic rays, studying equation validity for absorption cross section
02 p0359 A70-12702
- Inelastic He atom-ion collisions provide understanding of capture and excitation cross sections
05 p0885 A70-16555
- Absorption cross sections for single and double molecules of oxygen and in UV region noting disagreement with Beer law
06 p1114 A70-18632
- Nitrogen molecule photoabsorption and photoionization cross sections determination, discussing ionization probability variations and radiationless transitions
07 p1347 A70-20358
- Uranyl ion luminescence and absorption cross section in silicate glass excited by high power light beam, considering Q switching action of ion
08 p1510 A70-20516
- UV absorption cross sections of CO, HCl and ICN, analyzing reactions causing various spectral features
08 p1455 A70-21340
- Photon capture cross sections for surface silicon electronic states using IR photoconductivity measurements
17 p3144 A70-35707
- Ion-polar molecule collision time history plots and computer movies, calculating capture cross sections for mass spectrometry
18 p3292 A70-36561
- Solar B8-Be decay neutrinos energy spectrum and absorption cross sections calculation
20 p3698 A70-39307
- Autoionization spectral lines growth curves analysis, applying to 3s-4p transition in Ar at 466 A with specified absorption cross section
21 p3781 A70-41931
- Negative hydrogen ion forbidden bound-free continuum absorption cross section recalculation, deriving 10 to 8th power smaller than previous value
24 p4404 A70-45410
- ## ABSORPTION SPECTRA
- ## NT FRAUNHOFER LINES
- ## NT HERZBERG BANDS
- ## NT TELLURIC LINES
- Natural absorption band absorption coefficient frequency and temperature dependences in doped n-InSb
01 p0154 A70-10100
- Ruby green /U/ absorption band magnetic circular dichroism calculations in linear approximation, considering spin-orbital interaction constant and magnetic field strength
01 p0156 A70-10188
- Quasars variability, distribution, absorption line characteristics, red shift peaks, physical models, cosmological problems, etc
01 p0177 A70-10341
- IR reflectance studies of lunar surface composition, showing absorption spectra suggestive of ferrous iron, olivines and orthopyroxenes
01 p0182 A70-10721
- IR spectrometer on Mariner 7 Mars flyby recording sharp absorption near 3 microns at Martian southern polar cap
01 p0182 A70-10823
- Quasars emission and absorption red shifts distribution analysis suggesting cluster interpretation
01 p0183 A70-10895
- Spectrometer scanning .20-15 microns in 3 sec, measuring absorption and emission spectra of hot samples alternately, discussing resolutions at various bands
01 p0091 A70-10914
- Luminescence quantum yield in neodymium glass, noting independence to stimulating light frequency
01 p0114 A70-11595
- Absorption band observation near 0.43 mu in solar spectra and scattered radiation of sky, determining nontelluric origin
01 p0084 A70-11613
- Lorentz absorption line shape computations in radiation scattered by homogeneous planetary atmosphere compared with results for isotropic scattering by van de Hulst similarity relations
02 p0364 A70-11792
- Hydrogen pressure-induced IR absorption spectra, noting applications to planetary atmosphere studies
02 p0341 A70-11805
- Methane and ammonia absorption bands and possible structure of Jupiter and Saturn cloud layers by spectrophotoelectric observations
02 p0366 A70-11807
- Variable distribution of ammonia absorption on Jupiter deduced from IR spectra, indicating scattering in cloud layer
02 p0366 A70-11810
- Absorption spectra computation for model planetary atmosphere using Neumann series for solving seminfinitesimal radiative transfer equation
02 p0342 A70-11826
- Excitation, reemission and absorption spectra of Cr activated powdery Mg titanate prepared, using MgO and Ti dioxide with LiCl as flux
02 p0350 A70-11848
- Photoelectric line photometry used to study H beta/gamma and He I 4471 absorption line intensities of early B stars, determining projected rotational velocity
02 p0369 A70-12072

Jupiter Red Spot continuous spectrum intensity distribution and methane/ammonia absorption between 3300-6500 Å

02 p0374 A70-12427

Ammonia absorption band at 6450 Å in Jovian atmosphere, clarifying controversial absorption time variations

02 p0375 A70-12428

Crossed Fabry-Perot etalons and spectrographs for studying atmospheric solar absorption spectra

02 p0299 A70-12438

Variable atmospheric attenuation of 5 mm wavelength band, considering oxygen absorption spectrum and attenuation for reference atmosphere

02 p0260 A70-12570

Eta Carinae IR region emission and absorption spectra characteristics in tabular form

03 p0565 A70-13269

Quasar spectra interpretation, analyzing observational data and absorption lines correspondence to different red shifts

03 p0570 A70-13484

Zeeman-split Fraunhofer line profiles for pure absorption lines determined taking into account solar atmosphere elliptical birefringence

03 p0570 A70-13595

Interband transitions and optical absorption edge analysis in indium telluride using dependence on photon energy

03 p0541 A70-13725

Cloud layer multiple scattering in Jovian atmosphere, discussing influence on Lorentzian contour of planetary absorption lines

03 p0574 A70-13882

Absorption line identification in sunspot spectra by calculating Zeeman patterns, using Zeeman splitting for magnetic field measurement

03 p0574 A70-13934

AD Herculis components as Algol system with gas flow based on observed absorption effects

03 p0577 A70-14100

L-alpha absorption equivalent width measurements in UV spectra of beta-one, delta and pi Scorpii for interstellar hydrogen densities

04 p0748 A70-14586

Depth and shape of 0.94 micron water vapor absorption band for clear and cloudy skies, noting radiation distortion for dark dense clouds

04 p0690 A70-15024

Statistical model of ozone absorption bands for calculating intensity, rotational line position and transmission functions of complex spectral regions

04 p0680 A70-15252

Spectral absorption and transparency of water vapor, carbon dioxide, carbon monoxide, methane and nitrous oxide bands in IR region

04 p0715 A70-15255

Opacity-probability distributions for CO, computing theoretical spectra of line absorption coefficient, discussing effects of temperature and/or turbulent velocity

05 p0919 A70-16938

Methane abundance in Jovian atmosphere deduced from line equivalent widths, obtaining line intensity for J manifolds

05 p0919 A70-16940

Nomograms for spectral transparency of atmosphere at 2.8-5.6 microns

06 p1053 A70-17208

Carbon dioxide-nitrogen laser emission absorption in atmospheric surface layer by wings of distant strong lines investigated statistically

06 p1082 A70-17807

Spectral broadening mechanisms for trivalent Eu ions in glass, considering fluorescence and absorption spectra measurements

06 p1127 A70-18640

Absorption spectra of single crystals TbAlG and DyAlG garnets, investigating Verdet constant dependence on ion concentration

07 p1355 A70-18705

Absorption lines in quasars spectra indicating line formation close to quasar nucleus

07 p1383 A70-19402

N-type InAs single crystals optical properties with various carrier concentrations at 1-6 mu wavelengths and 300-78 K temperatures, studying absorption spectra

08 p1555 A70-20512

Magnetic field effects on ruby absorption in R-line region

08 p1555 A70-20543

Titanium monoxide absorption bands in class M stars spectra, estimating band head intensities

08 p1569 A70-20829

Solar magnetic field strength determination from various absorption lines, considering Rowland intensity, line lower level excitation potential, optical depth, etc

08 p1569 A70-20836

Effective depths of formation of absorption lines in solar atmosphere used for magnetic field recording

08 p1570 A70-20842

Absorption lines in hazy planetary atmosphere with isotropic scattering, examining phase variations of equivalent width

08 p1571 A70-20910

Venus clouds absorption spectra correlation with carbon suboxide frost reflection spectra, suggesting absence of carbon suboxide in atmosphere

08 p1571 A70-20911

Molecular oxygen concentration determined by absorption spectroscopy of solar hydrogen Lyman alpha line

08 p1490 A70-21390

IR spectral absorption coefficients determined for water vapor at high temperatures, describing experimental details including data acquisition and reduction

09 p1725 A70-22069

IR absorption spectral curve interpretation using computer program for iterative solution

09 p1726 A70-22138

Temperature effects on IR absorption by water and carbon dioxide vapors measured in narrow spectral intervals

09 p1666 A70-22180

Electron paramagnetic resonance absorption curve influence on power transfer characteristics and maximum passband of multicavity maser

09 p1695 A70-22278

Photochromism of dihydroquinoline compounds and absorption spectra of color forms, noting color development upon UV light irradiation and thermal eradication

09 p1629 A70-22334

Saturn ring atmosphere absorption spectrum observation during earth passage through ring plane

09 p1754 A70-22497

Absorption spectra of n-type GaAs before and after proton irradiation, discussing dependence on wavelength

09 p1739 A70-22753

Ni L alpha X ray emission line shape and position as function of bombarding electron energy, observing differential self absorption in anode

09 p1731 A70-22777

Binary collision-induced rotational far IR spectrum of tetrahedral molecular gas, using induced absorption theory

09 p1732 A70-22905

GaAs-Ge platelet laser output, observing absorption edge dynamic Burstein shift

09 p1697 A70-22920

Spectroscopic technique measuring OH concentrations behind shock waves by measuring absorption of OH lines, using water cooled RF powered lamp

09 p1683 A70-23512

Radiative transport in nongray cylindrical medium using total band absorbance

09 p1790 A70-23553

Formaldehyde absorption profile in direction of Milky Way center observed using lunar occultation

10 p1936 A70-23905

Sagittarius sources A and B2 O18H absorption lines measured at microwave frequencies, determining oxygen isotopes abundance ratios

10 p1936 A70-23907

Equivalent widths for rotational lines to detect interstellar hydrogen gas, discussing absorption line

10 p1937 A70-23947

Galactic radio source W 31 distance from sun determined from measurements of OH, H I and formaldehyde absorption lines

10 p1937 A70-23949

Quadratic Stark shifts of absorption lines hyperfine components in cesium atom beam measured using optical spectroscopy

10 p1887 A70-24033

Oscillator strengths relative values determined from flame atom absorption line sensitivity measurements

10 p1828 A70-24259

Absorption strengths of j-manifolds in R branch of Jupiter atmosphere methane band, discussing fine structure blending

10 p1919 A70-24473

Emission and absorption by nonhomogeneous gases with vibration-rotation bands determined by scaling approximation

10 p1968 A70-24474

Quasar spectra searched for intergalactic absorption lines, discussing red shift

10 p1947 A70-24998

Q switched ruby laser light effect on absorption spectra of NaCl crystals

10 p1902 A70-25221

Sun effect on anomalous frequency shift in 21 cm absorption spectrum in Taurus A

11 p2108 A70-25659

Solar boron abundance from BH, BN and BO absorption bands in sunspot spectra, noting no traces in solar atmosphere

11 p2108 A70-25738

Excess color method for photometric and spectral studies of interstellar absorption in cluster NGC 6913

11 p2116 A70-26585

Excess color method for studying interstellar absorption around cluster NGC 6823

11 p2116 A70-26586

Densities and extents of absorbing clouds in open cluster NGC 7086 determined from photometry and spectral classifications of stars

11 p2116 A70-26587

Spectral absorption characteristics for C atom radiative processes in carbon dioxide-nitrogen mixtures at high temperatures corresponding to Venusian atmosphere

12 p2275 A70-27317

Absorption spectra of seminsulating gallium arsenide in IR region, investigating transmittance and absorption coefficient at room and low temperatures

12 p2287 A70-27492

IR absorption in ozone band, including atmospheric inhomogeneity effects on accuracy of transmittance calculations

12 p2223 A70-27515

Maser amplifier with nonoriented Fe-doped rutile powder as active material, observing broad absorption bands under magnetic field

12 p2249 A70-27649

Nova Delphini brightness variations, observing absorption lines shift toward violet

12 p2306 A70-27860

Elsasser and statistical band models in single parameter functions representing mean absorption in given spectral range

12 p2191 A70-28295

Sterically hindered aryldiazonium salts absorption spectra and quantum yield data interpretation, considering photochemical properties

12 p2182 A70-28300

Spectrographic measurements of Jovian Red Spot and Southern Tropical Zone molecular absorption bands related to cloud cover density and depth

12 p2311 A70-28305

Nonoriented cadmium silicon arsenide single crystals optical properties, determining spectral distribution of IR absorptivity for various photon energies

13 p2470 A70-28883

Homogeneous absorption line and peak power widths relationship in high resolution gas laser with internal absorbing cell

13 p2428 A70-29365

Molongolo pulsars H line absorption and dispersion in interstellar medium

13 p2495 A70-29788

Tunable diode laser for high resolution IR spectroscopy of sulfur hexafluoride absorption near carbon dioxide laser lines

13 p2430 A70-29832

Synthetic autoclave grown quartz crystals with W and Ga impurities, discussing spectral properties and weak absorption bands after irradiation

14 p2625 A70-30154

Forbidden lines of OI, NI, CI, Fe II, Ni II, Si I, Si and Ca II in solar absorption, investigating effects on element abundance and gaps in thermodynamic equilibrium

14 p2637 A70-30339

Atmospheric molecular oxygen photometric absorption spectral bands, calculating growth curves

14 p2572 A70-30403

Water vapor absorption bands in solar IR spectrum, considering earth curvature and atmospheric inhomogeneity and refraction

14 p2572 A70-30404

Ca atom-graphite grain model for interstellar absorption at 4430 Å, calculating resonant line shift and width as functions of atom-surface distance

14 p2639 A70-30729

Venus carbon dioxide absorption bands determining atmospheric scattering model suitability for all data

14 p2642 A70-30889

Absorption spectrum of terrestrial atmosphere with sun as source, obtaining formaldehyde line with rotating grid spectrometer

14 p2579 A70-31256

Vibration-rotation band absorbance for nonisothermal gaseous radiation in terms of parameters describing isothermal gas

15 p2825 A70-31816

Solar disk 10830 Å He absorption line, attributing depression at blue wing to triplet

15 p2802 A70-32488

Absorption bands in reflection spectra of various asteroids, comparing Vesta composition to meteorites and Apollo 11 samples

16 p2972 A70-32987

Book on stellar spectra theory covering line absorption coefficient expressions, radiative transfer, line source function, line broadening, etc

16 p2974 A70-33270

Defect F centers formation in MgO, discussing optical absorption bands, oscillator strengths, luminescence band, impurity centers, etc

16 p2940 A70-33938

Nitric oxide gas IR radiation properties at high temperatures, determining spectral mean fine structure and total band absorbance correlations

16 p3003 A70-34253

Spectrum of bright IR object VY Canis Majoris, noting absorption feature attributed to SiO molecules in stellar atmosphere

17 p3154 A70-34540

- Interstellar silicate absorption in IR spectra, discussing existing observations 17 p3157 A70-34840
- Quasar and radio galaxies, observing absorptions at red shifts close to emission line 17 p3157 A70-34846
- Red giant star chromospheric activity, discussing Balmer absorption lines and emission lines 17 p3161 A70-34889
- High resolution solar spectrum at 2000-2200 Å from sunpointing Skylark rocket flight, noting detectable absorption lines 17 p3162 A70-34896
- UV absorption lines in H I regions heated by cosmic rays, discussing possible detection by rocket or satellite spectroscopic observations 17 p3152 A70-35748
- Water vapor pure rotational absorption spectrum compared with calculated far and near IR spectra 18 p3244 A70-35949
- Optical system of absorption tubes for planetary atmosphere spectra simulation 18 p3314 A70-36408
- Mars UV reflectivity, examining spectrum, absorption features, planet albedo and ozone content by rocket-borne instruments and atmospheric models 18 p3317 A70-37011
- Na I 5889 Å pressure broadening by high temperature neutral He, allowing damping constant direct measurements 18 p3318 A70-37013
- Hydrogen line absorption at 21 cm from Centaurus A (NGC 5128) radio galaxy 18 p3318 A70-37017
- Spectrophotometry of methane and ammonia absorption bands indicating decrease toward Jupiter disk edge 18 p3323 A70-37140
- Trichroic IR absorption lines of triglycine selenate, computing optical and dielectric constants from transmission and reflection data 19 p3470 A70-37366
- Atmospheric humidity measuring equipment and procedures for high altitudes, considering hygrometers, mass spectrometers, sondes, absorption spectra, etc 19 p3461 A70-37635
- Pulsar AP 2015 21cm line absorption profile, indicating uniform density and temperature neutral H model invalid 19 p3518 A70-38026
- Radio polarization of quasars with and without absorption line spectra 19 p3523 A70-38605
- Am and Ap stars metallic absorption lines, determining photometrical indices correction 19 p3523 A70-38689
- Electronic absorption spectra of single crystal praseodymium acetate tetrahydrate in natural and polarized light 19 p3488 A70-38742
- Interstellar molecular H Lyman resonance-absorption bands in far UV spectrum using rocket observation 20 p3701 A70-39002
- Quasars PHL 5200 and RS 23 spectra absorption lines, examining resonance line transfer of radiation through differentially expanding atmosphere 20 p3701 A70-39006
- Multiphoton absorption coefficient for semiconductors, using interband absorption method 20 p3687 A70-40020
- Interstellar silicate absorption bands four color photometric observations in galactic direction, using metal mirror telescope 20 p3713 A70-40431
- Carbon dioxide and CO IR vibration-rotation spectral absorption coefficients, noting harmonic oscillator approximation 21 p3851 A70-40589
- Solar photosphere absorption line weakened region, examining temperature increase effects on neutral and ionized lines 21 p3885 A70-40953
- Southern objective prism plates B stars with strong neutral He I absorption lines 21 p3890 A70-41160
- Absorption diffuse band systems of diatomic argon molecule in vacuum UV region 21 p3853 A70-41395
- Atomic Ar absorption spectrum in vacuum UV region, observing Rydberg series interactions as perturbations and autoionizations 21 p3781 A70-41933
- Spectral absorption characteristics for c atom radiative processes in carbon dioxide-nitrogen mixtures at high temperatures corresponding to Venusian atmosphere 21 p3854 A70-42058
- X ray K and L emission bands and absorption spectra from TiO, TiN and TiC compared with density of states histograms, considering electronic band structure 22 p4086 A70-43003
- Saturated absorption spectroscopy of various molecules using emission spectra of carbon dioxide and nitrous oxide lasers 22 p4050 A70-43239
- Chandrasekhar H function approximation for isotropic scattering, calculating absorption line contours 22 p4109 A70-43750
- Solar disk 10830 Å He absorption line, attributing depression at blue wing to triplet 23 p4240 A70-43911
- N-type GaAs samples doped with Ag, Se and Te respectively, measuring absorption coefficients spectral dependences at room temperature 23 p4229 A70-43928
- IR absorption bands absolute intensities determination method, giving special consideration to absorption band wings and precision 23 p4217 A70-44203
- IR absorption spectra of high-cis forms of deuterated polyisoprenes 23 p4157 A70-44274
- Spectral absorption of 2.7 micron water vapor band under various high temperature and pressure conditions, using black body radiation 23 p4220 A70-44444
- Absorption line multiple scattering in thick planetary atmosphere, using successive scattering method for single-scattering phase function based on line profile and equivalent width 23 p4222 A70-44550
- WC radiation damage by resonant absorption following Coulomb excitation observed from gamma ray spectra 23 p4231 A70-44888
- Narrow resonances in saturated absorption at molecular vibrational-rotational transitions in carbon dioxide laser 23 p4202 A70-45059
- Intraband absorption in p-type GaAs associated with carrier transitions between heavy and light hole in valence band 23 p4232 A70-45066
- Doubly excited antiferroelectrics absorption spectrum band and bound states, discussing zero approximation 0-0 transitions of alpha oxygen molecules and permeability tensor 24 p4392 A70-46362
- ABSORPTION SPECTROSCOPY**
- Satellite probing method for transmission absorption spectroscopy of planetary atmospheres 14 p2650 A70-31230
- Time controllable continuous photon emission from plasma produced by pulsed laser vacuum spark applied to absorption spectroscopy in vacuum UV 15 p2734 A70-31757
- ABSORPTIVE INDEX**
- U ABSORPTIVITY**
- ABSORPTIVITY**
- He camera with reduced linear absorption coefficient for contact microradiography, relating exposure, X ray wavelength and atmosphere 01 p0084 A70-10013
- Natural absorption band absorption coefficient frequency and temperature dependences in doped n-InSb 01 p0154 A70-10100
- Carbon dioxide lasers passive Q switching by gaseous methyl fluoride and phosphorus pentafluoride, presenting absorption coefficients 01 p0110 A70-10561
- Semiconductors as optical limiters for Q switched lasers, reporting temperature values for nonlinear absorption coefficients of Si, CdSe, CdTe and GaAs 01 p0158 A70-10563
- Plane and spherical albedos of planet surrounded by infinite optical thickness atmosphere, with application to Venusian atmosphere 01 p0193 A70-11591
- Rotation-vibration matrix elements of quadrupole moments and absorption coefficients of ground electronic states of hydrogen, HD and deuterium 02 p0342 A70-11823
- He-Ne multimode laser radiation peak as function of pressure in methane-containing absorption cell installed in resonator 03 p0502 A70-13750
- Diffusivities of argon, krypton and xenon determined in olive oil by curve-fitting analysis of sorption curves 03 p0429 A70-14159
- Far IR spectra of liquid hydrogen at para concentrations, noting absorption coefficient variation consistent with composition 04 p0718 A70-14696
- Absorption coefficient 5-step model applied to shock tube measurements of end wall radiative heat transfer behind reflected shock waves in air 04 p0787 A70-15606
- Electron bremsstrahlung in intense magnetic fields calculated for emission rate and absorption coefficient in large quantum number limits 06 p1104 A70-17182
- Moisture absorptivity and hydrolytic stability effects on operational parameters of gas turbine engine lubricants 06 p1075 A70-17222
- Yttrium-iron garnet optical properties at various wavelengths and temperatures, noting absorptivity decrease in IR region 06 p1126 A70-17767
- Uranium plasma design and characteristics, measuring emission and absorption coefficients as function of temperature and pressure [AIAA PAPER 70-43] 06 p1122 A70-18084
- Probability of three photon band-band excitation of electron in semiconductors using S-matrix formalism, calculating absorption coefficient for two band approximation 07 p1356 A70-19795
- Laser pulse power effect on edge absorption of glass filter used for Q switching applications 07 p1299 A70-19855
- Plasma discharge absorption coefficients measurement using Q switched ruby laser 09 p1694 A70-22139
- Thermal radiation absorption in hemispherical cavity, determining apparent absorptivity for diffuse and parallel irradiation 09 p1790 A70-23565
- Bremsstrahlung radiation in intense magnetic field proposed as emission mechanism from pulsars, discussing absorption coefficient 11 p2104 A70-25697
- CO vibration-rotation bands, calculating high resolution and temperature steradiance and spectral absorption coefficient 12 p2275 A70-27171
- Materials absorption coefficients determination at high temperatures based on spectrophotometric analysis of emission from samples of different thicknesses 12 p3331 A70-27305
- Light absorption coefficient frequency dependence related to interband transitions in highly doped semiconductors 12 p2287 A70-27487
- Magnetically sensitive Fe lines usefulness to solar polarimetry, observing absorption coefficient dependence on temperature variations 12 p2303 A70-27706
- He-Ne laser radiation absorption in dense Li plasma, calculating absorptivity for bremsstrahlung and photoionization 13 p2465 A70-29710
- Convergence corrections for absorption coefficient measurements by far IR Michelson interferometer 14 p2586 A70-30988
- Hydrogen plasma refractive index and absorption constant for laser radiation frequencies as functions of electron temperature and atomic density 16 p2959 A70-34338
- Absorption coefficient of n-type indium arsenide single crystals with varying electron and doping concentrations, investigating spectral dependence 17 p3144 A70-35705
- Oxygen absorption coefficients at Lyman alpha line and other transmission windows, verifying dependence on pressure source line width and doublet separation 18 p3293 A70-36753
- Spectrophotometric solar brightness temperature measurements in far IR, discussing collision type spectral variation of absorption coefficient 18 p3319 A70-37056
- Milky Way appearance and galactic spiral structure, using models with variable and different absorption values of arms 18 p3329 A70-37181
- IR absorption by water vapor in transmittance windows, considering continuous absorption coefficient dependence on window width 19 p3461 A70-37425
- Radial profiles of emission and absorption coefficients and temperatures in cylindrically symmetric plasmas 19 p3475 A70-37551
- Tables on thermal radiative properties of heated air covering absorption coefficients for wide range of photon energies and temperatures 19 p3552 A70-38009
- Posterior electrode structural modification for reducing silicon photovoltaic cells absorptivity and operating temperature 19 p3358 A70-38492
- Gaseous media absorption coefficient and refractive index in field of two nonmonochromatic radiation streams quasi-resonant with neighboring atoms and molecules transitions 19 p3448 A70-38740
- Formaldehyde absorption coefficients measured photoelectrically in vacuum UV range 20 p3703 A70-39165
- Multiphoton absorption coefficient for semiconductors, using interband absorption method 20 p3687 A70-40020

Plasma nonequilibrium state formation and light absorptivity variation under high power laser pulsed radiation
20 p3684 A70-40387

Absorptivity, transition probability and collision broadening frequency of dimethylether at 3.51 micron He-Xe laser wavelength, noting pressure dependence, transition lifetime and saturation intensity
21 p3853 A70-40573

Integrating cavity spectroscopy for measuring absorption coefficient of material
21 p3822 A70-40817

Surfaces separated by radiatively nonparticipating medium, determining absorptivities and heat transfer boundary conditions in gray surface problems by irradiation factor method
21 p3953 A70-42085

Uranium plasma diagnostics, measuring emission and absorption coefficients as function of pressure and temperature
22 p4069 A70-42361

Particle size, shape and absorptivity effects on inclusion damage of Nd-doped barium crown laser glass
22 p4050 A70-43007

Weak EM transmission through resonant medium of two-level atoms in presence of intense monochromatic wave, obtaining absorption coefficient and refractive index
22 p4075 A70-43473

Ultrasound inductive absorption coefficient of metals in quantized magnetic field
22 p4075 A70-43473

N-type GaAs samples doped with Ag, Se and Te respectively, measuring absorption coefficients spectral dependences at room temperature
23 p4229 A70-43928

Vibrational relaxation measurements of specific carbon dioxide vibrational-rotational states from tunable carbon dioxide laser beam absorption
23 p4421 A70-44011

Ionospheric radio wave absorption above polar aurorae during solar activity minimum, discussing diurnal and annual behavior
23 p4162 A70-44058

Monochromator design for UV and visible wavenumbers linear output, noting application to absorption coefficient measurement
24 p4336 A70-45669

ABSTRACTS

Abstracts with references to literature sources on oceanography from space and aircraft
09 p1665 A70-22014

ABUNDANCE

Iron group nuclei abundance relative to oxygen determined for solar cosmic ray event of 2 September 1966
01 p0167 A70-10042

Photospheric Fe I abundance variation with excitation potential
01 p0175 A70-10239

Primary cosmic ray nitrogen nuclei intensity and spectrum measured by balloons and Pioneer 8 space probe, obtaining abundance difference from solar atmosphere
01 p0169 A70-10319

Nitrogen abundances measured in enstatite chondrites by inert carrier gas fusion extraction technique, noting agglomeration of chondrules
01 p0179 A70-10475

Extreme UV spectral line intensity enhancement during class 3 flare related to abundance of radiating element
02 p0358 A70-12205

Cosmic ray origin in high energy H and He isotopic abundances and energy spectra observed by IMP 4 satellite during solar quiet times
02 p0358 A70-12250

Martian topographic contours determined from detected carbon dioxide abundances indicating large scale differences from previous data
02 p0373 A70-12390

NH bands in stellar spectra by visual inspection of spectrograms, noting abundance of N in normal and strong CN stars
02 p0379 A70-12708

Solar photospheric Fe abundance determined from IR supermultiplet line spectra, considering LTE effects
04 p0749 A70-14597

Solar core opacity influence on revised photospheric iron abundances, discussing neutrino flux prediction doubling in solar models
05 p0905 A70-16985

Globular clusters in M31, discussing metallicity and heavy element enrichment in Andromeda
06 p1138 A70-17306

Solar Cd abundance, using spectrograph and synthetic spectral line computer program
06 p1143 A70-17995

Uranium abundance in hypersthene chondrites determined by homogenized fission track analysis, comparing age estimation with iron meteorite event occurrence
07 p1391 A70-20354

Fe abundance in solar photosphere, evaluating various determination methods
09 p1753 A70-22382

Sigma Orionis E hydrogen-deficient atmosphere, using grid of constant-flux model atmospheres to determine abundances of five elements
09 p1755 A70-22504

Metal-poor stars evolution during hydrogen and helium burning from main sequence to giant branch, estimating relative cluster ages
09 p1755 A70-22507

Solar wind properties and helium abundance determined from satellite-borne electrostatic analyzers
09 p1746 A70-23482

Rare gases abundance patterns on earth and in chondrites, proposing chemical adsorption mechanism at planetesimal stage during accretion
09 p1764 A70-23610

Solar boron abundance from BH, BN and BO absorption bands in sunspot spectra, noting no traces in solar atmosphere
11 p2108 A70-25738

Star eta Arietis spectra analyzed for Fe and V abundance
13 p2487 A70-28715

Arcturus atmosphere Mg abundances from rotational lines noting terrestrial proportions
14 p2637 A70-30540

Hydrogen abundance in Jupiter atmosphere quadrupole line used in comparing jupiter and solar atmosphere C/H ratios
14 p2650 A70-31221

Relativistic cosmic rays primordial chemical composition above atmosphere from abundance data obtained with satellite-borne nuclear emulsion detector
15 p2793 A70-31735

Galactic abundances and cosmic ray spectra by IMP-4 satellite, obtaining He ratio
15 p2793 A70-31794

Ionization potentials of elemental abundances in lunar rocks compared with earth crust and class I carbonaceous chondrites, showing lunar materials differentiation
15 p2801 A70-32463

Hydrogen abundance in white dwarfs, discussing inconsistencies in mass and bolometric magnitude models for Sirius and Eri B
17 p3170 A70-35389

Jupiter atmosphere ammonia abundance from laboratory curves of growth analysis for ammonia bands
18 p3310 A70-35937

Solar Ga abundance from spectral synthesis of region around 4172 A line
18 p3316 A70-36894

Helium abundance in unevolved main sequence eclipsing binaries by comparing to homogeneous models in mass luminosity plane
18 p3318 A70-37023

Submarine basalt sea water alteration effects, examining Sr and rare earth concentrations, Ba enrichments or depletions and trace element data
19 p3413 A70-38015

Allende Type III carbonaceous chondrite, examining rare earth and other elemental abundances
19 p3519 A70-38028

Heavy cosmic ray abundance attributed to thermal nucleosynthesis during silicon burning at high temperature and density
19 p3507 A70-38132

Highly charged cosmic ray heavy nuclei primaries, examining charge spectra and solar elements abundances
19 p3508 A70-38136

Relativistic cosmic rays nuclei abundances from Gemini 11 flight
19 p3509 A70-38144

Cosmic ray elements abundance at sources relative to carbon, comparing near-earth composition and solar photosphere
19 p3509 A70-38147

Solar chromospheric Fe abundance, considering f-value effects
19 p3524 A70-38697

Stellar interiors and cosmic He abundance observations, discussing B stars, sun galactic and globular clusters, planetary nebulae, interstellar medium, novae, etc
20 p3706 A70-39931

Lunar elemental abundances examined by Surveyor project, discussing albedo contrasts, surface rock density, bulk composition, thermal regime and chondritic meteorites
20 p3707 A70-39957

Solar photospheric spectrum Ni II forbidden lines analysis, determining abundance of Ni for comparison with coronal and meteoritic data
20 p3711 A70-40405

Sodium behavior in young and old late type stars, examining relation to iron abundance in F, G and K dwarf and giant stars
21 p3887 A70-41114

Solar iron abundance from forbidden Fe II magnetic dipole transition probabilities
21 p3888 A70-41118

Globular cluster color-magnitude diagram parameters, examining giant branch and metal content
21 p3889 A70-41153

Apollo 11 lunar rocks, breccias and fines age and chemistry, major element, trace element and rare earth abundances, texture, crystallization and meteoritic effects
21 p3906 A70-41563

Apollo 11 lunar fines trapped noble gas elemental and isotopic abundances, suggesting solar wind origin
21 p3906 A70-41565

Lunar rock composition difference from meteorites and terrestrial basalts, indicating complexities in solar abundances and initial earth and moon compositions
21 p3906 A70-41567

Apollo 11 lunar material actinide element abundance and isotopic composition, examining Th, U and transuranium elements by mass spectrometric and radiometric techniques
21 p3774 A70-41569

Apollo 11 lunar rocks elemental abundances determination by instrumental activation techniques
21 p3775 A70-41574

Apollo 11 sample elemental abundances, investigating environmental, paragenetic and petrogenetic problems and moon evolution
21 p3907 A70-41575

Rare earth and trace element abundances for Apollo 11 lunar samples by neutron activation, comparing with Bruderheim chondrite and submarine basalts
21 p3907 A70-41578

Apollo 11 lunar rock and soil elemental abundances, discussing composition, volatile element depletion, rare earths, basalt and geochemical processes
21 p3909 A70-41593

Apollo 11 lunar rock and fines primordial radionuclide abundances and concentration gradients by gamma ray spectrometry at Lunar Receiving Laboratory
21 p3776 A70-41595

Apollo 11 lunar rock K, Rb, Sr, Ba and rare earth element concentrations, examining relationship to terrestrial and chondritic levels
21 p3776 A70-41600

Elemental abundances of Apollo 11 lunar rocks and soils, using activation analysis or mass spectrometric isotope dilution
21 p3909 A70-41606

Solar chromosphere elements abundances methods, suggesting Fe differences origin in Fe I and Fe II inconsistencies
21 p3925 A70-42194

Solar coronal and photospheric iron abundances from absorption forbidden lines, discussing discrepancy with permitted lines
21 p3925 A70-42195

Abundance ratios of metallic line star 15 UMa, using absorption spectrophotometric observations
21 p3909 A70-42270

Mars atmospheric nitrogen abundance relative to carbon from spacecraft UV spectrometer data
23 p4238 A70-43805

Stellar abundance determination, considering rapid uniform rotation effects on equivalent spectral line widths
23 p4250 A70-44811

Nitrogen abundance of subgiant nu Indi from observed and computed stellar spectra of CN violet bands
24 p4404 A70-45411

Relativistic cosmic ray LH nuclei abundance via Cerenkov scintillator telescope on polar orbiting OV1-10 satellite
24 p4397 A70-45522

Heavy elements diffusive separation as explanation of metallic and magnetic A stars abundance anomalies at outer convective envelope bases
24 p4410 A70-45775

Murchison and Lost City chondrites element abundance analysis by thermal neutron activation and wet chemical techniques, noting low oxygen content
24 p4411 A70-45790

Stellar surface and solar system light element abundances, explaining formation by energetic proton flux nucleosynthetic effect
24 p4398 A70-46163

AC [CURRENT]

U ALTERNATING CURRENT

AC GENERATORS

Homopolar Inductor Alternators of minimum weight and maximum efficiency for aerospace power supplies
15 p2710 A70-32587

High speed homopolar inductor alternators with minimum leakage reactance, using geometric programming for objective function optimization
16 p2879 A70-34059

High speed aerospace homopolar alternator, calculating end zone three dimensional magnetic flux distribution and leakage reactance
22 p3999 A70-43585

ACCELERATED LIFE TESTS

Turboprop aircraft engine service life extension, correcting deficiencies via accelerated tests based on relation between failure rate and usage
15 p2787 A70-31535

Aluminum alloys endurance limit determination by accelerated methods, evaluating errors by comparison with conventional tests

15 p2755 A70-31539

Passenger aircraft structures accelerated testing for safety and fatigue durability under operational conditions, describing tests planning and evaluation

15 p2673 A70-31541

Accelerated vacuum testing of ball bearings and slippers at 30-130 F, considering dry lubricated brush/slipping material combinations

17 p3101 A70-34762

Accelerated life testing, discussing accumulated damage for graphical procedure in normal conditions [ASME PAPER 70-PROD-10]

21 p3832 A70-40871

Accelerated failure tests of ammonia-Al-stainless steel heat pipes for fluid loss or energy transport degradation

21 p3947 A70-41049

Accelerated vibration equipment testing for reducing test time, discussing vibration environment simulation

23 p4269 A70-44336

ACCELERATION [PHYSICS]

NT ANGULAR ACCELERATION

NT DECELERATION

NT HIGH ACCELERATION

NT IMPACT ACCELERATION

NT PARTICLE ACCELERATION

NT PLASMA ACCELERATION

NT SPIN REDUCTION

NT TRANSVERSE ACCELERATION

Transport aircraft takeoff length reduction by applying various runway inclinations with respect to takeoff accelerations

02 p0275 A70-12223

Acceleration and regulating system of free turbine turboprop engines studied by graph-analytical method used for nonlinear circuit analysis

03 p0552 A70-13927

Phobos motion observational results compared with Sharpless determination of secular acceleration

04 p0743 A70-14399

Nonexistence of large mascons at Mare Marginis and Mare Orientale deduced from residual acceleration analysis of Lunar Orbiter Doppler tracking data

04 p0743 A70-14424

Material flow acceleration in jet propulsion systems, discussing acceleration by gravitational field, thermodynamic nozzle expansion, electrostatic forces and Lorentz force

04 p0671 A70-15090

Prediction errors lower bound for accuracy in predicting future position of randomly accelerating target

04 p0652 A70-15342

Rotation effects of two point scatterer on radar measurements of coherent acceleration

04 p0652 A70-15348

Incompressible laminar Falkner-Skan boundary layer suffering sudden acceleration by moving belt, noting boundary layer separation [AIAA PAPER 69-40]

04 p0674 A70-15534

Hot star photogravitational acceleration determined from difference between apex and antipeak brightness, noting constant magnitude and direction of principal component of apex force

05 p0918 A70-16914

Tangential thrust, constant acceleration trajectories for close solar probe missions using low thrust electric engines

06 p1137 A70-17177

Aluminized solid propellant transient burning rate augmentation during acceleration loads [AIAA PAPER 70-126]

06 p1129 A70-18047

Force-acceleration product method for controlling input vibratory motion to vibration test specimen based on specimen dynamics

06 p1069 A70-18437

Inertial acceleration in relative motion of two bodies subjected to external forces, basing equations of motion on rotating coordinates

07 p1375 A70-18890

Pursuit games theory with bounded accelerations, using differential equations

07 p1323 A70-18947

Photoelastic stress analysis of composite structures subjected to gravitational forces using immersion analogy, considering constant acceleration stresses

07 p1413 A70-20038

Two degrees of freedom assemblies transient motions using computer, solving acceleration and deceleration problems in mechanical systems

08 p1502 A70-20699

Boundary layer development on body accelerating in viscous incompressible fluid, using straight lines approximation and asymptotic expansions

08 p1485 A70-21631

Shock absorbing forces for absorber with one degree of freedom optimized for given acceleration during periodic disturbances by variational method

09 p1727 A70-22537

Projectile acceleration under gas explosion calculated for velocity

09 p1777 A70-22723

F-8D aircraft transonic flight and wind tunnel tests for buffet onset prediction, considering effects of g level and fluctuation amplitude and frequency [AIAA PAPER 70-341]

09 p1611 A70-23020

Taylor instability of vertically accelerated horizontal two dimensional interface between liquid and air solved by method of strained coordinates

09 p1661 A70-23071

Optimal acceleration from earth orbit to hyperbolic velocities of low thrust space vehicle, constructing asymptotic expansions near and far from central field

10 p1940 A70-24305

Stress, strain and acceleration spatial variation in plate structures under broad frequency band excitation using statistical energy method

10 p1962 A70-25065

Solid body acceleration by ideally conducting gas in constant gravity field under magnetic field, considering rarefaction, reflected waves, motion equation, wall pressure, etc

11 p2082 A70-25389

Subsonic, transonic and supersonic laminar boundary layers acceleration and cooling effects, discussing heat transfer and gas enthalpy

12 p2211 A70-27830

Unsteady fluid flow around circular cylinder with sudden acceleration using flow pattern photographs

13 p2387 A70-29056

Acceleration influence on radar signal reception during range and velocity measurements

13 p2366 A70-29301

Rigid cylinder acceleration within elastic shell-core structure under pressure pulse distribution over shell semicircumference

13 p2518 A70-29984

Mesoscale slope limits in constant pressure surfaces relation to g-forces on aircraft at SST altitude, using radiosonde measurements

14 p2530 A70-30607

Heat transfer from acceleration induced boundary layer reverse transition, considering free stream turbulence effects

14 p2667 A70-31169

Heating and g forces on rockets and space vehicles in descent trajectories as function of reentry velocity, achieving control by attack angle variation

15 p2812 A70-32361

Burning rate increase of nonmetalized composite propellants in acceleration field, assuming surface retention of ammonium perchlorate particles

16 p2963 A70-33861

Acceleration effects on burning rates of double base propellants with and without Al additive

16 p2963 A70-33883

Stress, strain and acceleration spatial variation in structures subject to broad frequency band vibration excitation, considering simply supported flat plate

16 p2992 A70-34017

Rarefied binary gas mixture transient Couette flow, considering nonlinear case of plate with equal temperature accelerated impulsively

17 p3067 A70-34546

Forced convective heat transfer in annular passage with axially varying cross section, noting role of acceleration parameter

17 p3195 A70-34999

Solid propellant combustion, observing burning rate in spin acceleration environments

17 p3145 A70-35209

Wave-periodic acceleration feedback during vibrational flame propagation in tubes, testing carbon monoxide-air mixture

17 p3196 A70-35350

Lunar longitude secular acceleration from occultation observations

17 p3171 A70-35444

Time of acceleration to rated speed for three-phase asynchronous gyroengine rotor

19 p3420 A70-37259

Power law fluid flow past suddenly accelerated wall, applying group theory to similarity solutions

19 p3406 A70-38444

Full scale aircraft spinning motion, computing static, damping, cross and acceleration aerodynamic characteristics for antispin devices

20 p3561 A70-39581

Solar chromosphere spicules acceleration via super-sonic jet formed by magnetic field under gravity and Melon seed effect

21 p3925 A70-42192

Accelerated supersonic motion of plate with attached shock wave at finite angle of attack in ideal gas, using perturbed nonstationary motion equations

21 p3748 A70-42209

Balloon satellites orbital accelerations, considering effects due to air drag, solar radiation pressure and spin

24 p4409 A70-45557

Atmospheric pressure surface sharp slopes at SST altitudes producing vertical acceleration based on temperature gradients inspection

24 p4372 A70-46050

ACCELERATION PROTECTION

Antihypoxic preparations protective effect on white mice and rats subjected to gravitational accelerations

03 p0425 A70-13890

ACCELERATION STRESSES [PHYSIOLOGY]

NT CENTRIFUGING STRESS

Arterial pressure pulse waves mathematical analysis applied to variations in stroke volume in anesthetized dogs subjected to spine-to-breast accelerations

01 p0012 A70-10125

Mathematical model for vestibular nystagmus adaptation to subjective sensation of rotation, noting time constants

01 p0032 A70-10362

Space or atmospheric flight caused or aggravated ophthalmic lesions, noting retinal and conjunctival hemorrhages from barometric pressure fall and rapid acceleration and deceleration

01 p0022 A70-10858

Chicken body mass and percentage body fat following 24 weeks chronic acceleration determined from fatty acid metabolism, liver citrate cleavage and malic enzyme activities

02 p0233 A70-11720

Atmospheric turbulence effects on accelerations experienced by passengers in supersonic and subsonic transport aircraft compared

02 p0325 A70-12219

Tegmental nucleus neurons of cats cerebellum, considering responses to acceleration changes and natural stimulation of vestibular apparatus

03 p0421 A70-13510

Human motion coordination under acceleration followed by weightlessness during jet flights along Keplerian orbits, discussing initial disturbance and subsequent subsiding

03 p0425 A70-13897

Mice and hamster infection resistance following short term acceleration stress, eliminating low hydrocortisone level as protective agent

03 p0428 A70-14067

Acceleration component in pelvis to head direction found influencing hyperemia of brain at various g forces

04 p0630 A70-14579

Physiological and physiopathological effects of transverse accelerations on spacecraft crews, discussing cardiovascular and respiratory systems

05 p0799 A70-15763

Electrocardiographic changes during positive headward acceleration of normal human subjects after oxygen breathing and propanolol administration

05 p0808 A70-16675

Cerebellar cortex reactions to sciatic nerve stimulation in rats under transverse accelerations in centrifuge

05 p0804 A70-17116

Human heart chronotropic reactions during centrifuge acceleration tests up to tolerance limit, establishing sinus tachycardia in various degrees

05 p0804 A70-17120

Physiological reactions of living organisms to aircraft and spacecraft acceleration, discussing physical, pharmacological and training methods to increase tolerance

07 p1200 A70-18785

Tolerance level to z axis acceleration from centrifuge techniques, noting irreplacability of intermittent stepwise increasing accelerations tests

07 p1201 A70-18790

Acceleration effects on chest organs by X ray studies noting heart shape changes, pulmonary areas, diaphragm position, etc

07 p1201 A70-18791

Vestibular semicircular canal excitation thresholds of experienced and candidate pilots for imposed angular accelerations

07 p1201 A70-18795

Rat body fluids displacement during positive centripetal accelerations by radioisotope tracer compounds, freezing rats in liquid nitrogen to fix hemodynamic changes

07 p1202 A70-18796

Acceleration and weightlessness effects on efficiency, reliability and capacity in pilots and astronauts muscular system

07 p1202 A70-18797

Z axis acceleration and high temperature effects on guinea pig carbohydrate metabolism, discussing blood and muscle tissues composition

07 p1202 A70-18798

Intracerebral, peripheral and central blood circulation relationship in humans during transverse accelerations

07 p1209 A70-19520

Acceleration environment duplication difficulties, considering human physiological responses dependence on centrifuges performance characteristics and geometries

07 p1222 A70-19927

Quantification of subjective estimates of well-being during onset and remission of motion sickness symptomatology in slow rotation room

08 p1448 A70-21941

- Human sensory-motor adaptation and aftereffects of exposure to accelerative forces using hand-eye coordination measurements 09 p1628 A70-23466
- Physiopathologic effects on organs of longitudinal and tangential accelerations, decelerations, vibrations and weightlessness 11 p1986 A70-25821
- Tilting rotating chair producing vestibular stimulus via linear rotating acceleration to study motion sickness 11 p1988 A70-26515
- Acceleration effects on mental working capacity of fighter pilots, discussing attention shift and stability, operational memory, sensorimotor reactions 13 p2351 A70-29337
- Acceleration effects on Na, K, and pH in rabbits cerebrospinal fluid and cerebral blood 13 p2352 A70-29347
- Suprathreshold angular acceleration effects on ocu-logryal illusion, obtaining magnitude estimates during and after acceleration 14 p2543 A70-30897
- Vestibular threshold dependence on gravity, considering linear accelerations effect on canals sensitivity 14 p2539 A70-30916
- Fluid analog for lung tissue response to gravitational acceleration, examining lung density, transpulmonary pressure, expansion, etc 16 p2850 A70-34257
- Vestibular stimulation by square wave acceleration, evaluating Ewald laws for nystagmus behavior 17 p3037 A70-35127
- Complex accelerations effects on vestibular apparatus from physical and mathematical viewpoint 17 p3037 A70-35128
- Intrapulmonary distribution of gases inhaled during positive and transverse accelerations 17 p3037 A70-35130
- Acceleration measurements on switchback cars, revolving cabins and oscillating attractions in amusement parks, noting motion sickness rarity 17 p3037 A70-35136
- Human water-salt metabolism following exposure to transverse accelerations, discussing diuresis and Cl-K excretion 17 p3038 A70-35364
- Soviet book on peripheral vestibular apparatus and higher nervous system roles in motion sickness covering Coriolis acceleration tests, pilot training and selection, drugs, etc 19 p3359 A70-37406
- Frank orthogonal vectorcardiograms on humans during acceleration, using beat-by-beat real time analog-digital computer technique 20 p3572 A70-39435
- Human gluco-regulatory hormone reserve depressions following acute and chronic acceleration exposure 20 p3572 A70-39436
- Antimotion sickness drugs evaluated for effectiveness under standardized stress conditions in slow rotation room 20 p3572 A70-39439
- Prolonged transverse acceleration effects on rats kidney and posterior hypophysis neurosecretions 20 p3575 A70-40188
- Lung alveolar and capillary wall structure in mammals under normal conditions, transverse acceleration and mechanically changed pulmonary circulation 20 p3575 A70-40190
- Left ventricular surface electrocardiogram T-wave amplitude and circumflex coronary artery blood flow during headward acceleration in unanesthetized dogs, observing velocity decrease 21 p3764 A70-41481
- Activation energies of acceleration and hypoxia stress in man and rats, noting brain function survival 21 p3764 A70-41484
- Jet pilot EEG radio telemetry showing psychomotor stresses during takeoff and acceleration 22 p3978 A70-42877
- Glucose metabolism in chickens under chronic centrifugal acceleration, meeting increased energy requirements 23 p4147 A70-44786
- Sea sickness symptoms in relation to reduced minute blood volumes in human after Coriolis acceleration 23 p4149 A70-45079
- Pitch illusion in flight personnel under centripetal acceleration 24 p4306 A70-45330
- Pulmonary blood flow and ventilation distribution during forward acceleration by xenon 133 and lung scanning 24 p4302 A70-46105

ACCELERATION TOLERANCE

- Spine acceleration tolerance after prolonged human exposure to weightlessness, noting osseous apparatus tissue decalcination 03 p0423 A70-13712

- Antihypoxic preparations protective effect on white mice and rats subjected to gravitational accelerations 03 p0425 A70-13890
- Physiological and physiopathological effects of transverse accelerations on spacecraft crews, discussing cardiovascular and respiratory systems 05 p0799 A70-15763
- Physiological reactions of living organisms to aircraft and spacecraft acceleration, discussing physical, pharmacological and training methods to increase tolerance 07 p1200 A70-18785
- Centripetal acceleration tolerance level correlated with circulatory system functional tests and physical exercises, discussing strength and speed endurance 07 p1201 A70-18787
- Surface and underwater swimming tests for statistical correlation to linear maximum accelerations effects 07 p1201 A70-18788
- Circulatory system tests during linear, intermittent and continuous accelerations on centrifuge, noting lack of statistical correlation between centrifuge tests and functional tests 07 p1201 A70-18789
- Tolerance level to z axis acceleration from centrifuge techniques, noting irreplacability of intermittent stepwise increasing accelerations tests 07 p1201 A70-18790
- Emotional stability relationship to pilot acceleration tolerance tested on centrifuge, confirming instability correlation to poor resistance 07 p1201 A70-18793
- Vital capacity measurements made preflight and postflight on jet fighter aircrew breathing pure oxygen at various G forces 07 p1222 A70-19934
- Adaptation to Coriolis accelerations associated adaptation schedule to with 1-rpm increments developed for preventing motion sickness in slow rotating environment 07 p1223 A70-19938
- Rotating circular disk under angular acceleration, analyzing stress and deformation distributions 08 p1596 A70-21980
- Acceleration training schedules performed with animals and test subjects, assessing schedules effectiveness in increasing tolerances to transverse acceleration 09 p1623 A70-22086
- Human tolerance to short duration high acceleration in centrifuge concerning peripheral or central vision trouble or syncope 09 p1626 A70-23112
- Amphetamine, caffeine and secunine effects on hypodynamic syndrome in subjects during orthostatic tests and transverse G-forces under prolonged hypokinesia 10 p1817 A70-24690
- Transverse g-force tolerance and stability after prolonged hypodynamia in bed rest, noting effects of pharmaceuticals, physical exercise and prophylactic measures 10 p1817 A70-24695
- Spine acceleration tolerance after prolonged human exposure to weightlessness, noting osseous apparatus tissue decalcination 11 p1985 A70-25512
- Centrifuging acceleration tolerance of various animals, relating physiological and morphological effects 12 p2174 A70-28361
- Acceleration and hypoxia resistance of mice and rats after injections of phenamine, sidnocarb, strychnine, secunine, araleside, trioxazine, banactisine and chlordiazepoxide 13 p2358 A70-29344
- Somatotropic hormone and esculamine injection effects on rat survival rates under acceleration, noting sex linked differences 13 p2352 A70-29345
- Pattern center hypothesis for habituation to centrifugal and linear accelerations in man, investigating aftereffects by nystagmography 14 p2538 A70-30913
- Unanesthetized dogs renal hemodynamic response to negative centrifugal acceleration 15 p2681 A70-31883
- Blind persons susceptibility to acute motion sickness during stressful Coriolis acceleration 15 p2689 A70-31887
- Radial acceleration effects on tissue carbohydrate in starved female rats, observing blood glucose increase and muscle glycogen levels decrease 15 p2684 A70-32536
- Acceleration training schedules performed with animals and test subjects, assessing schedules effectiveness in increasing tolerances to transverse acceleration 15 p2693 A70-32682
- Centrophenoxine effects on rabbits centrifugal acceleration resistance 17 p3025 A70-35131

Dehydration effects on rabbits acceleration resistance 17 p3025 A70-35134

Human acceleration resistance and psychomotor behavior under emergency flight conditions, including high temperature exposure and remaining in clinostatic position 17 p3037 A70-35135

Hypoglycemia role in air sickness, aggravating effects of hypoxia and acceleration 17 p3040 A70-35914

Human cardiac flow during acceleration as function of time with and without anti-g suit, using electric plethysmograph 17 p3040 A70-35915

Mathematical model for short term adaptation effects in human semicircular canal response to rotation, discussing nystagmus 18 p3216 A70-35940

Hypokinesia and reduced diet effects on human tolerance to static loads, discussing acceleration tolerance prediction 20 p3576 A70-40198

Renal hemodynamic response of unanesthetized dogs to positive accelerations within physiological tolerance range, measuring pressure and blood flow velocity 20 p3577 A70-40332

Space travel genetic effects, discussing radiation, weightlessness, vibration and acceleration 21 p3761 A70-40842

Lateral and angular acceleration effects on blood and urine contents in specific metabolic indices of healthy young men 22 p3971 A70-43136

Acceleration effects on human organisms, describing centrifuge, rocket sleds and catapult simulators 22 p3979 A70-43528

Optimum acceleration profile for minimum severity index in injuries sustained by human subject 23 p4150 A70-44376

ACCELEROMETERS

NT STRAIN GAGE ACCELEROMETERS

Floated single degree of freedom gyroscope and pendulous integrating gyroscope accelerometer, discussing design features as inertial sensors for future space missions 01 p0086 A70-10313

Optimal control algorithm for spacecraft descent in atmosphere based on nominal trajectory and acceleration measurements 01 p0197 A70-11499

Semistatic acceleration sensor, using ferrite rod magnetostriiction effects to convert acceleration stress to microwave resonant frequency shift 03 p0495 A70-14191

Pendulous integrating gyro accelerometer gas bearing wheel characteristics at high slew rates monitored by differential varmeter 04 p0698 A70-14770

Self acting, hydrostatic and squeeze-film gas lubricated bearings applications to gyroscopes, accelerometers, torque testers, etc 05 p0855 A70-16446

Fluidic accelerometer utilizing seismic mass nulled by feedback loop and independent of supply pressure variations 06 p1068 A70-18429

Subminiature sensor element integrated with silicon semiconductor strain gages for simultaneous three dimensional measurement of acceleration components 06 p1069 A70-18434

Piezoelectric accelerometer transverse sensitivity calibration using reference accelerometer comparison technique 06 p1073 A70-18599

Model of ideal accelerometer in form of mass point suspended within body of accelerometer mounted in spatial elastic weightlessness suspension on moving object 07 p1288 A70-20178

Mechanical shock accelerometer calibration by light frequency Doppler shift measurement using laser interferometer and single sideband carrier insertion circuit 08 p1493 A70-20602

FM telemetry channel noise effects on digital and analog accelerometer outputs accuracy, suggesting mean square error reduction methods 10 p1893 A70-25318

Rocket-borne flight testing of sensitive accelerometer developed to measure small forces applied to satellite or space probe surface 13 p2403 A70-28433

Air-damped capacitance accelerometers and velocimeters in data acquisition systems using signal processing 13 p2405 A70-28813

Combined neutron and gamma ray irradiation effects on piezoresistive accelerometers 13 p2405 A70-28814

Pendulous integrating gyro accelerometer float excursions minimization in random vibration environment /Saturn 5 launch/ by statistical technique 14 p2589 A70-31344

- Flight testing of high sensitivity Cactus accelerometer, measuring deceleration components due to sphere drag
15 p2735 A70-31813
- Hypervelocity gas, electromagnetic, explosive drive and exploding wire accelerometers and high explosive, shaped charge, plasma drag and electrostatic accelerators for projectile impact studies
15 p2718 A70-32783
- HF shaker for accelerometer calibration and resonance evaluation, discussing construction materials, accuracy and test results
16 p2889 A70-34021
- Laser interferometry for accelerometer and dynamic pressure transducer calibration and vibration measurement
17 p3089 A70-35124
- Acceleration measurements on switchback cars, revolving cabins and oscillating attractions in amusement parks, noting motion sickness rarity
17 p3037 A70-35136
- Piezoelectric accelerometer reference systems calibration by function separation
17 p3089 A70-35173
- Accelerometer installation resonant frequency, discussing mounting methods, structure material, geometry and total mass
17 p3089 A70-35174
- Subminiature solid state piezoresistive accelerometer using diffused four arm Wheatstone bridge sensor
17 p3094 A70-35522
- Pendulous integrating gyro accelerometer gas bearing wheel characteristics at high slew rates monitored by differential varmeter
[ASME PAPER 69-WA/LUB-3] 19 p3436 A70-37618
- Sensing elements piezoresistive Si and indium antimonide film sensing elements for high sensitivity pressure transducers and accelerometers, discussing airborne telemetry applications
19 p3431 A70-38538
- Multiaxis clusters of single axis pendulous accelerometers with coincident centers of angular motion insensitivity
19 p3431 A70-38539
- Seismic fluid suspended triaxial angular accelerometer for high performance aerospace vehicle flight test application
19 p3431 A70-38540
- ONERA accelerometer flight test of performance in zero gravity environment, using Vesta sounding rocket for simulation
19 p3431 A70-38541
- Accelerometer calibration in low g range by mass attraction as equivalent acceleration input
[AIAA PAPER 70-1030] 20 p3631 A70-39507
- Hollow test platform for gyros and accelerometers used in inertial navigation
[AIAA PAPER 70-952] 20 p3606 A70-39577
- Moving object coordinates autonomous determination errors in accelerometers with dry friction, investigating inertial navigation system with integral horizon correction
23 p4193 A70-43981
- Point accelerations on semirigid body spacecraft from accelerometer data with structural vibration noise at landing
23 p4200 A70-44387
- Cactus high sensitivity accelerometer flight tests, discussing operation and experimental conditions
[ONERA-TP-875] 23 p4198 A70-44660
- Orbiting spacecraft angular velocities via inertial sensing platform consisting of linear accelerometers
24 p4372 A70-45475
- ACCEPTABILITY**
Risk interpretation of prior distributions in acceptance sampling by Bayesian analysis
19 p3440 A70-38817
- ACCEPTANCE**
U ACCEPTABILITY
ACCEPTOR MATERIALS
Frequency dependent negative resistance of n-type semiconductor doped at acceptor level near valence band top
10 p1927 A70-24273
- Negative resistance and cut-off voltage of doped Si p-i-n diodes subject to deep acceptor levels
10 p1849 A70-24274
- Acceptor level formation kinetics from measuring Hall constant as function of temperature after diffusion of copper into n-type GaAs
15 p2782 A70-31633
- Shallow acceptor level in Au-doped n-type GaAs, using photoconductivity temperature dependence
17 p3143 A70-35702
- Solubility isotherms of alloying elements in Ge-Al-P semiconductor-acceptor-donor system at high temperatures
24 p4391 A70-46143
- ACCESS TIME**
Time division multiple access (TDMA) system for Symphonic communication satellite using PCM phase shift keyed RF carrier
10 p1837 A70-24353
- Bit clock synchronous system for communications satellites TDMA
10 p1839 A70-24368
- Time allocation with sampling interpolation (ATIC) for TDMA satellite telephone communications, considering auxiliary circuits, transmission quality, bit rates, demand assignment, etc
10 p1840 A70-24370
- Controlled digital data relay satellite system to provide multiple access between central station and user terminals, noting computer time sharing operation
11 p2008 A70-26230
- ACCIDENT INVESTIGATION**
NT AIRCRAFT ACCIDENT INVESTIGATION
Radiation dose estimates by biological and physical methods after radiation accident, discussing chromosome aberration counting
17 p3034 A70-35761
- ACCIDENT PREVENTION**
Forced cooling water flow temporary loss accident at Plum Brook Reactor, discussing inspection and corrective action
01 p0140 A70-10323
- Aircraft systems safety analysis, discussing accident causes and prevention, risk allocation, safety equipment, etc
02 p0225 A70-12263
- Bioelectronic equipment shock hazards reduction by current limiting diodes use in signal and ground leads
06 p0998 A70-17285
- Preventive measures against fire and blast hazards in high oxygen concentration chambers
08 p1599 A70-21795
- Decompressed crewmember rescue onboard spacecraft and aircraft by compartmentalization combined with air locks
08 p1454 A70-21938
- Human factors responsibility for aircraft accidents, discussing cooperation between air safety service and flight surgeons
09 p1626 A70-23016
- Airport runway slipperiness rating, predicting and alleviating to reduce aircraft accidents
[SAE PAPER 700265] 12 p2206 A70-27434
- Accident prevention in laser operation emphasizing eye protection
13 p2361 A70-30018
- Safety characteristics of potassium chloratellactose mixtures as standard for comparing dangerousness of pyrotechnical compositions
15 p2786 A70-31848
- Systems approach to flight accident prevention and inquiry management
15 p2674 A70-32207
- Flight safety standards, criteria and requirements, stressing accident prevention shift from accident investigation
15 p2831 A70-32212
- Aircraft accident prevention via reduction of pilot attention distractions
15 p2692 A70-32226
- Corporate aircraft accident statistics, causes and prevention, noting pilot errors, mechanical failures, etc
16 p2842 A70-33814
- Book on air safety and commercial aviation accidents
16 p2842 A70-33964
- Aircraft accident prevention and investigation, noting economic factors as deterrent to safety measures implementation
17 p3022 A70-35860
- Flight recorder role in aircraft accident investigation and prevention, noting audio instruments and data recovery
19 p3356 A70-38613
- U.S. Army rotary wing mishap experience for product assurance and accident prevention
19 p3356 A70-38825
- Human error as factor in aircraft accidents, considering man machine incompatibility and prevention measures
21 p3771 A70-41723
- Apollo spacecraft program evolution, discussing Apollo 13 accident, command and service module modifications, oxygen tank design, mission objectives, etc
23 p4245 A70-44640
- Helicopter hazards elimination measures, considering crash resistant fuel systems, flotation devices, redesigned seats, in-flight escape, etc
24 p4292 A70-46383
- ACCIDENT PRONESS**
Flying accident liability predictions reliability from pilot trainee aptitude test performance at selection, discounting accident proneness theory
12 p2178 A70-27048
- Medical and professional disadaptation in fighter pilots, considering fatigue, digestive disorders, anxiety, absenteeism, efficiency loss and accident proneness
16 p2850 A70-34347
- ACCIDENTS**
NT AIRCRAFT ACCIDENTS
- Vital function telemetry system specifications, design and application to highway accident victims
02 p0243 A70-12096
- ACCLIMATIZATION**
NT ALTITUDE ACCLIMATIZATION
NT COLD ACCLIMATIZATION
Cross adaptation criteria and modifications in physiologic and biochemical processes in man and mammals, demonstrating positive cross acclimation between hypertension and hypoxia exposure
02 p0242 A70-12825
- Physiological reactions of humans to orthostatic heat tolerance and natural acclimatization in summer and winter using tilt-table test and bicycle ergometer
12 p2169 A70-27656
- Biophysical model of heat transfer from organism, describing adaptation to ambient temperature
18 p3218 A70-36531
- Gas exchange adaptation to heat and cold in rats with different ecological backgrounds
18 p3218 A70-36533
- Varying thermoregulatory responses of different rodent species to long term heat and cold
18 p3218 A70-36534
- Gas metabolism in passerine birds adaptation to ambient temperature
18 p3219 A70-36536
- ACCOMMODATION**
NT VISUAL ACCOMMODATION
ACCOMMODATION COEFFICIENT
GeTe thermoelectric power, electrical/thermal conductivity and expansion coefficient measured at 20-600 K, determining suitability as thermoelectric material
01 p0158 A70-10755
- Energy accommodation coefficients for He-3 and He-4, comparing results with classical gas-solid interaction theory
04 p0721 A70-14388
- Accommodation coefficients ratio of He 4 to He 3 measured on W and K clean surfaces
06 p1183 A70-18257
- Electromagnetic torsion balance measurement of forces exerted on clean Au surfaces by monoenergetic steady state Ar and Kr beams, calculating thermal accommodation coefficients
06 p1066 A70-18258
- Nitrogen molecule-tungsten surface interactions, computing trajectories and accommodation coefficients for various temperatures by equations of motion
06 p1110 A70-18262
- Velocity distributions of incident and reflected Ar beams, determining partial energy accommodation coefficients for reflection from copper and carbon dioxide deposited surfaces
06 p1111 A70-18264
- Rarefied gas flows and heat transfer between parallel plates, concentric cylinders and spheres in presence of fractionally accommodating boundaries
06 p1049 A70-18330
- Thermal accommodation coefficients of Ar atomic beams scattered from nominal plane of Ag crystal measured by time of flight techniques
07 p1343 A70-20125
- Surface parameters influence on energy transfer to arc jet anode, discussing work function, accommodation coefficient and diffuse reflection coefficient of electrons
[AIAA PAPER 69-107] 12 p2281 A70-27809
- Hypersonic near free molecule flow over flat plate with sharp leading edge, using linearized kinetic B-K-G equation for small thermal accommodation coefficient
15 p2673 A70-32796
- High temperature aluminum species in vapor over solid alumina, determining thermodynamic properties, composition and accommodation coefficient by Knudsen effusion and mass spectroscopy
23 p4281 A70-44451
- ACCRETION**
U DEPOSITION
ACCUMULATORS
NT ACCUMULATORS [COMPUTERS]
NT DUST COLLECTORS
NT SOLAR COLLECTORS
NT SOLAR REFLECTORS
Accumulator model for psychophysical discrimination, discussing stimulus presentation and sampling, parameter values estimation, response latencies, etc
10 p1827 A70-24767
- Space collector ring systems surface physics, discussing dry thin film lubricants, smoothness, service life, etc
16 p2917 A70-33485
- ACCUMULATORS [COMPUTERS]**
Thyristor circuit for storing or generating digital control signals, considering reliability at high noise levels
19 p3385 A70-37377
- ACCURACY**
Third order accuracy for nonlinear hyperbolic system of partial differential equations extended to equations with independent variables
17 p3131 A70-35891

- Missile systems accuracy determination, analyzing pertinent errors statistical properties [AIAA PAPER 70-1007] 20 p3657 A70-39525
- Small angle of rotation measurement of coherent radiation polarization plane, discussing technique for increasing sensitivity and accuracy 20 p3643 A70-39759
- Measuring and test equipment economic approach to quality levels and accuracy ratios, deriving cost tradeoffs in optimum inspection fidelity 20 p3634 A70-40453
- Interpolation method for nonlinear automatic control systems accuracy, discussing numerical integration optimal step and node number selection 22 p4003 A70-42886
- Unguided rockets dispersion firing pattern and accuracy, discussing aerodynamic forces and ballistic coefficients 22 p4110 A70-43156
- ACETALDEHYDE**
- Charge, hydrogen atom and ion transfer in collisions involving deuterium-labeled methanol- acetaldehyde system and molecular ions 14 p2543 A70-30110
- ACETATES**
- Thermal decomposition of acetate ion in potassium halide matrices, using IR spectroscopy 22 p3981 A70-42453
- ACETAZOLAMIDE**
- Hypoxia and acetazolamide effects on color sensitivity zones in visual field 15 p2684 A70-32533
- ACETIC ACID**
- Prolonged hypokinesia effect on dynamics of 5-oxindoleacetic acid elimination in rat urine, showing occurrence of shifts in serotonin metabolism 09 p1615 A70-22092
- Prolonged hypokinesia effect on dynamics of 5-oxindoleacetic acid elimination in rat urine, showing occurrence of shifts in serotonin metabolism 15 p2685 A70-32688
- Resinous compounds content determination in jet fuels using ice cold acetic acid for desorbent to improve accuracy 16 p2961 A70-33203
- Serotonin, 5-hydroxyindoleacetic acid /5-HIAA/ and monoamine oxidase in bovine pituitary organ and median eminence 21 p3761 A70-40850
- ACETONE**
- Red bicyclic condensation product from reaction of acetone with sym-trinitrobenzene and diethylamine 02 p0251 A70-12278
- Photodecomposition of 1,4-dichlorobutane sensitized by n, pi singlet state of acetone as chemical process 04 p0646 A70-15319
- Acetone formation mechanisms during neopentane oxidation when added to slowly reacting molecular hydrogen and oxygen 11 p1995 A70-26379
- ACETYL COMPOUNDS**
- Acetylferrocene preparation by reacting ferrocene with acetic anhydride in phosphoric acid and reducing acetylferrocene to alpha-hydroxyethyl ferrocene by potassium borohydride in methanol 02 p0249 A70-11678
- Coenzyme A and acetyl CoA in tissue extracts determined for concentrations by recycling CoA through coupled enzyme system 04 p0640 A70-15754
- Sleep-wakefulness cycle regulation role of serotonin, noradrenalin and acetylcholine in CNS of animals 15 p2680 A70-31745
- Assay procedures for extraction and determination of N-acetylglucosamine in soil 18 p3226 A70-36959
- Peroxyacetyl nitrate decomposition products under continued and discontinued irradiations determined by IR spectral analysis 22 p3983 A70-42944
- ACETYLENE**
- Reaction analysis of acetylene-oxygen flames with known concentrations and temperature profiles, integrating one dimensional flame equations numerically 02 p0251 A70-12035
- Ethylene and ethylene-acetylene mixtures ion-molecule reaction product distributions calculation using quasi-equilibrium theory of unimolecular reactions 16 p2858 A70-34012
- Electric field control of oscillatory acetylene flame combustion for chemical rocket engines 21 p3942 A70-40885
- Ion-molecule reactions in mixtures of hydrogen sulfide with ethylene and acetylene from deuterium labeling studies via ion cyclotron resonance spectroscopy 21 p3773 A70-41200
- ACHONDRISES**
- NT KAPOETA ACHONDRISE
- NT NORTON COUNTY ACHONDRISE
- Ca-rich basalt achondrites cosmogenic isotopes characteristics, discussing lunar or cosmic origin 01 p0174 A70-10136

- Chemical abundance data of lunar surface rocks, suggesting basaltic achondrites and eucrites origin from moon 06 p1137 A70-17196
- Ti demonstrated as predominantly chalcophilic in highly reduced enstatite chondrites and achondrites 07 p1391 A70-20352
- Enstatite chondrites and achondrites electron microprobe analysis for Si, P and Ni in metal grains and associated schreibersite and pyrrhotite 10 p1935 A70-23849
- U and Th abundances correlation in tektites and achondrites based on oxygen isotopic composition of lunar rock specimens 13 p2488 A70-28720
- Chondritic and achondritic meteorites Zr and Hf abundances, distributions and ratios, using thermal and neutron activation analyses 18 p3310 A70-35968
- Carbon and nitrogen abundances in Apollo 11 rocks, basaltic achondrites and terrestrial basalts, using meteorite analytical techniques 21 p3776 A70-41592
- Chemical analysis for Li, Na, K, Rb, Cs, Ca, Sr and Ba in achondrites and Apollo 11 lunar rocks, breccia and soil samples 21 p3910 A70-41611
- ACID BASE EQUILIBRIUM**
- Acid base responses of arterial plasma of anesthetized man during acute carbon dioxide partial pressure changes, discussing anesthesia effects 01 p0020 A70-10651
- Human sea-level natives physiological changes during high altitude physical exercise, considering carbon dioxide arterial pressure, plasma cortisol, adrenal function indexes, etc 08 p1453 A70-21873
- Oxygen uptake capacity, ventilation, heart rate and acid base values during bicycle ergometer exercise 17 p3036 A70-34594
- Ganglione and quaterone cholinolytic agents effects on arterial blood acid-base balance indicators in cats 24 p4298 A70-45633
- ACIDOSIS**
- Acidosis effects on anoxic rat heart cardiac performance and anaerobic energy generation 04 p0635 A70-15461
- Hypoxemia and acidosis avoidance during respiration cessation in halothane anesthesia 10 p1822 A70-25086
- Hypoxia effects on cerebral blood flow in anesthetized dogs, considering acidosis and vasodilation 20 p3577 A70-40330
- ACIDS**
- NT ACETIC ACID
- NT AMINO ACIDS
- NT AMOBARBITAL
- NT ASCORBIC ACID
- NT ASPARTIC ACID
- NT BORIC ACIDS
- NT BUTYRIC ACID
- NT CITRIC ACID
- NT CYSTEINE
- NT DEOXYRIBONUCLEIC ACID
- NT FATTY ACIDS
- NT FOLIC ACID
- NT GLUTAMIC ACID
- NT GLUTAMINE
- NT GLYCINE
- NT HEXOGENES [TRADEMARK]
- NT HISTIDINE
- NT HYDROCHLORIC ACID
- NT HYDROFLUORIC ACID
- NT LACTIC ACID
- NT LEUCINE
- NT LYSINE
- NT METHIONINE
- NT NITRIC ACID
- NT NUCLEIC ACIDS
- NT OLEIC ACID
- NT OXIDASE
- NT PERCHLORIC ACID
- NT PHENYLALANINE
- NT PYRIDINE NUCLEOTIDES
- NT RIBONUCLEIC ACIDS
- NT SULFURIC ACID
- NT THYMIDINE
- NT THYMINE
- NT THYROXINE
- NT TRYPTOPHAN
- NT URIC ACID
- Gas chromatographic-mass spectrometric identification of aliphatic hydroxy acids in plants and sediments 02 p0252 A70-12521
- Molecular interactions, surface pressures and potentials of mixed monolayers of stearic acid and stearyl alcohol with inorganic substructures 15 p2695 A70-32547
- ACOUSTIC ATTENUATION**
- NT SHOCK WAVE ATTENUATION

- Sound attenuation rate of rectangular flat steel plates contact and branch point relation to velocity difference and absorption length 03 p0526 A70-14353
- Sound attenuation in acoustically lined turbomachinery ducts with no air flow, indicating spinning lobes and generation frequency effect on liner material performance [ASME PAPER 69-WA/GT-11] 04 p0734 A70-14885
- Contralateral remote masking /CRM/ increase of LF tone burst produced by middle ear muscle contractions 04 p0632 A70-15082
- Atmospheric absorption of noise investigated for characteristics based on aircraft flyby tests 05 p0795 A70-16786
- Broadband sound attenuation in soft walled /low acoustic impedance/ circular ducts found dependent on frequency 05 p0883 A70-16787
- Sound wave velocity and damping in liquid N measured along saturated vapor line using thermal Brillouin scattering techniques 06 p1105 A70-17491
- Sonic speed and damping in two phase potassium flow, discussing linear equations and propagation velocity 09 p1725 A70-22036
- Panel sound absorber acoustic impedance variation with frequency predicted taking into account panel mass, stiffness and internal damping 09 p1770 A70-22390
- Resonant absorption in ruby crystal under combined acoustic and laser pulses, noting use for laser intensity measurements 12 p2251 A70-28331
- Perturbation method to obtain analytical expressions for attenuation of plane wave sound propagation in lined ducts 17 p3136 A70-34523
- Sound wave radiation and excitation in plane infinite plate by vortices 19 p3354 A70-38722
- Acoustic pulse transmission through plane vortex sheet, examining zone of silence, geometrical acoustics and sound radiation 21 p3849 A70-41243
- Ultrasonic absorption in gaseous molecular relaxation processes, considering error due to neglecting thermal conductivity effect on frequency dependence 22 p4073 A70-42649
- Spectral and real time computation for acoustic absorbers with nonlinear material characteristics 23 p4219 A70-44393
- ACOUSTIC COMBUSTION**
- U COMBUSTION STABILITY
- ACOUSTIC DELAY LINES**
- Solid state microwave acoustic variable delay devices for radar, fuses, repeaters, altimeters, etc, emphasizing magnetoelastic wave method 06 p1018 A70-17356
- Microwave acoustic delay lines design and fabrication for UHF to X band frequency ranges 11 p2005 A70-26163
- Surface acoustic wave delay lines using interdigital transducers based on piezoelectrics with applications in VHF and UHF signal processing 11 p2005 A70-26165
- Microwave surface acoustic delay lines properties, advantages, electron beam fabrication, optical probing for propagation loss measurement, etc 11 p2005 A70-26166
- X band acoustic delay lines using thin film piezoelectric transducers 16 p2874 A70-33391
- Nonlinear effects of harmonic generation and mixing in lithium niobate microwave acoustic surface wave delay lines measured using laser light deflection 19 p3485 A70-37698
- ACOUSTIC DUCTS**
- Sound attenuation in acoustically lined turbomachinery ducts with no air flow, indicating spinning lobes and generation frequency effect on liner material performance [ASME PAPER 69-WA/GT-11] 04 p0734 A70-14885
- Broadband sound attenuation in soft walled /low acoustic impedance/ circular ducts found dependent on frequency 05 p0883 A70-16787
- Aircraft fan and turbine noise reduction, discussing blade wake interaction, jet mixing and duct acoustic linings 16 p2963 A70-32946
- Mach number effect on sound propagation in tuning acoustically lined rectangular duct with uniform flow 20 p3673 A70-39709
- Aircraft acoustical duct treatments - ASA Conference, Philadelphia, April 1969 22 p4089 A70-42528
- NASA acoustically treated nacelle program reducing noise under commercial transport flight path near airports 22 p4089 A70-42529

Acoustic lining technology and materials for turbofan engine ducts, considering environmental factors and noise spectra

22 p4089 A70-42530

Structural and environmental design criteria for acoustical duct-lining materials in turbofan noise suppression

22 p4089 A70-42531

Duct lining parameters effects on engine inlet and fan discharge noise reduction during fan jet landing

22 p4090 A70-42532

Acoustically treated inlet and fan exhaust duct configurations for JT3D turbofan engine on DC 8 aircraft

22 p4090 A70-42533

COUSTIC EXCITATION

Acoustic transients in mammalian eye induced by normal and Q switched laser pulse absorption

02 p0313 A70-12325

Piezovibrator operation with two side acoustical loading in pulse mode

02 p0301 A70-12482

Acoustic wave excitation and damping in cryogenic He plasma produced by HF pulse discharge, considering nonadiabatic heating and dissipation during reflection

03 p0529 A70-13056

Discrete frequency noise generation associated with wakes due to fluid flow over turbomachine blades, supporting spokes, flat plates, etc

[ASME PAPER 69-WA/GT-13] 04 p0733 A70-14883

Minute volume changes under acoustic excitation of mice for assessing respiratory process without strain on organs

07 p1214 A70-19824

Dynamic response of infinite cylindrical shell subjected to arbitrary time and space dependent forcing function in acoustic medium

08 p1593 A70-21621

Acoustic fluidic amplifiers, considering receiver, transmitter and operating mode

09 p1672 A70-22012

Turbulent combustion stability in chamber, taking into account boundary effects due to acoustic perturbations reflection

09 p1786 A70-22106

Sound energy transmission and radiation into room by flexible structural panels subjected to acoustic excitation using wave equations

10 p1964 A70-25224

Coupled panel-cavity vibrations analysis, emphasizing sonic boom excitation of large window-room combinations

11 p2133 A70-25728

Sound transmission properties in terms of medium excitation by primary and secondary sound sources

11 p2083 A70-25730

Crack propagation in tensioned plates subjected to sonically induced vibrations

11 p2133 A70-25731

Aerodynamic sound emission from compact eddy region by singular perturbation approach, discussing Lighthill and Ribner theories

11 p1977 A70-26687

Cylindrical shell response to random acoustic excitation, considering single point transfer functions and equivalent force power spectral densities

12 p2317 A70-27125

Double acoustical resonators transient response to excitation by single sine wave, presenting pressure magnification factors as function of frequencies

17 p3135 A70-34521

Sound wave radiation and excitation in plane infinite plate by vortices

19 p3354 A70-38722

Magnetoacoustic waves in MHD channels, investigating excitation, damping and effects on mean current density and Hall field strength

22 p4081 A70-42822

COUSTIC FATIGUE

Concorde aircraft structural acoustics and design problems, discussing noise, fatigue and testing techniques and facilities

01 p0199 A70-10288

Fatigue life of stiffened skin panels under acoustic loading of wideband frequencies to achieve structural resistance optimization

[DGLR-69-63] 04 p0774 A70-15140

Laboratory electronics role in Concorde aircraft structural and acoustical fatigue analysis, flight simulation and flight studies

07 p1250 A70-19745

Etiopathogenesis of auditory disorders in flying personnel and aircraft engineers resulting from exposure to acoustic stresses

17 p3034 A70-35677

Honeycomb panels with fiber reinforced facings, obtaining acoustic fatigue design criteria

[AIAA PAPER 70-897] 17 p3064 A70-35814

Aircraft structures acoustic fatigue testing, discussing test facilities, environment simulation, etc

23 p4269 A70-44329

COUSTIC GENERATORS

U SOUND GENERATORS

ACOUSTIC IMPEDANCE

Broadband sound attenuation in soft walled /low acoustic impedance/ circular ducts found dependent on frequency

05 p0883 A70-16787

Acoustic impedances of periodically compressed thin fluid layers, discussing effect of mass, viscosity, elasticity and compressibility of medium

06 p1107 A70-18475

Acoustic impedance method for nondestructive testing exploiting phase defect of signal from piezoelectric transducer

06 p1074 A70-18629

Acoustic conductivity of burning solid propellant surface calculated, showing positive values or possible amplification at LF

09 p1741 A70-22113

Panel sound absorber acoustic impedance variation with frequency predicted taking into account panel mass, stiffness and internal damping

09 p1770 A70-22390

Shock impedance definition consistent with acoustic limit, considering use of impedance mismatch to reduce sonic boom overpressure

10 p1805 A70-24522

Electroacoustic transducer driven by acoustic pressure and electronic generator, describing electrical properties for functioning as characteristic impedance of acoustic transmission line

19 p3422 A70-37701

ACOUSTIC INSTABILITY

Constant flux gas core nuclear rocket acoustic instabilities, presenting idealized physical model with gas dynamic field perturbed by wave phenomena

09 p1725 A70-23227

Acoustic wave propagation in continuum of inviscid compressible heat conducting fluid, determining stability criteria

22 p4073 A70-42571

Thermal-acoustic oscillations in forced convection, giving time delay analog for perturbation feedback

23 p4280 A70-44369

ACOUSTIC MEASUREMENTS

Rolls-Royce RB 211 three shaft turbofan engines development and tests, noting preparation, building, cradle installment, open air facilities and noise measurements

01 p0161 A70-10079

Acoustic emission analysis for material evaluation and polymorphic phase transformations characterization for metals and alloys, discussing electronic instrumentation and experimental techniques

02 p0276 A70-12551

Sound attenuation rate of rectangular flat steel plates contact and branch point relation to velocity difference and absorption length

03 p0526 A70-14353

Rotating acoustic modes generated at blade passing frequencies in inlet duct of axial flow fan or compressor measured

04 p0691 A70-15079

Plume-induced X band radar attenuation, AM and PM noise measured in aluminumized solid propellant motor firings

04 p0736 A70-15409

Acoustic technique for flow transition detection on hypersonic ablating reentry vehicles, presenting supersonic wind tunnel test results

04 p0620 A70-15531

Subjective measurement of sound level of impulses and pulses, investigating 1 kHz tone and selection of time length between sound events

05 p0882 A70-16344

Sound levels and frequency spectra of noises measured in AN-24 and IL-18 turboprop aircraft cockpits

05 p0796 A70-16925

Hearing threshold and ear canal pressure levels, using circumaural enclosure with varying acoustic field

06 p0994 A70-17598

Automatic formant-frequency extraction using vowel-type spectrum, inverse filtering, moment calculation and evaluation by synthesized speech

06 p1009 A70-17909

Interacting coaxial supersonic jet flows noise reduction based on noise distribution characteristics measurement in anechoic chamber

[AIAA PAPER 70-236] 06 p1040 A70-18112

Computer operated digital system for controlling acoustic test environment and dynamic test data acquisition

06 p1030 A70-18432

Perceived aircraft noise level based on objective acoustic measurements related to subjective response, tabulating noys as function of sound pressure

[SAE-ARP-865A] 07 p1190 A70-18803

Turbulence measurement by piezoceramic acoustic sensors, considering capacitance

07 p1284 A70-19829

Turbulent atmosphere circulation measurement over centimeter scale using acoustical transducers

07 p1285 A70-19836

Directional dependence of broadband artificial ear signal spectrum and correlation functions using dummy head

09 p1624 A70-22761

Subjective and objective measurement of sound impulses, pauses and intervals duration sensation, showing adjustment accuracy

09 p1618 A70-22763

Quantizing noise measured for single integration delta modulation coders using unequal positive and negative integrator step sizes

09 p1638 A70-23368

Ultrasonic pulse technique for measuring fiber reinforced composites elastic constants

11 p2052 A70-26341

Heart dimension measurement by miniature implantable ultrasonic sonomicrometer, describing system design and operation

12 p2174 A70-26897

Engine firing rate measurement from acoustic waveform autocorrelation analysis

12 p2290 A70-27161

Noise characteristics and measurement, discussing aircraft noise generation and reduction

13 p2473 A70-28443

Thermal porous bronze screened microphones for noise measurements in medium under large heat flow

14 p2555 A70-30298

Computerized statistical analysis programs finding plastic stress and acoustic emission as predictors of annealed steel fatigue life

15 p2760 A70-32326

Ground test noise measurements accuracy and repeatability on JT8D turbojet engine

17 p3060 A70-35183

Acoustic measurement of surface pressure fluctuations in supersonic transitional boundary layers

17 p3092 A70-35482

Acoustic measurement for transition localization on reentry vehicles, describing apparatus and techniques

17 p3093 A70-35483

Digital data acquisition and control system for acoustic testing of large spacecraft

17 p3062 A70-35506

Sound measurement, discussing impulse level meters, noise exposure index, sound level recorder and classification, frequency analysis and filters

17 p3097 A70-35925

Localization of lunar acoustic energy, discussing long reverberation time measured at Apollo 12 site after module explosion

18 p3319 A70-37053

Acoustical holography forming optical wavefield analog for nondestructive testing, medical diagnosis, underwater and seismic imaging

19 p3425 A70-37887

Critical review of aircraft noise characteristics measurement and analysis techniques, noting nonuniformity problems control through standards

19 p3396 A70-37907

Automatic sound monitoring system for measuring aircraft noise in airport vicinity

19 p3397 A70-37908

Computer controlled aircraft noise monitoring system at Stuttgart airport

19 p3397 A70-37909

RMS spectrum analysis system for wideband acoustic data processing, using analog method with digital output

19 p3397 A70-37910

Clear lower atmosphere meteorological parameters remote sensing for weather forecasting, comparing optical, radio and acoustic radar techniques

21 p3785 A70-40802

Acoustic interferometer for speed of sound measurement in pure gases, determining second virial coefficient for Ar and N

21 p3828 A70-41766

Hypersonic sound speeds measured in methane at moderate pressures by spontaneous Brillouin light scattering experiments

21 p3830 A70-41938

Acoustic emissions method for monitoring structural stability of solid materials assemblies via crack formation and movement detection

22 p4027 A70-42582

Microplasma and burst noise measurements on discrete silicon planar transistors indicating origin at emitter-base junction

22 p3998 A70-43331

Ultrasonic measurements of flow velocity and fluid rate, using high speed switching and synchronous demodulator

22 p4041 A70-43619

Aircraft noise sources, examining compressors with dynamic pressure devices and jets with turbulence investigations

[ICAS PAPER 70-22] 23 p4232 A70-44111

Fatigue crack growth detection by acoustic emission techniques

23 p4194 A70-44214

High bypass model jet noise study, describing test setup and noise measurement results as function of secondary/primary flow velocity ratio

23 p4233 A70-44394

Single component fluid behavior in liquid-vapor critical point vicinity, using LF acoustic resonant cavity technique for isochoric measurements 23 p4222 A70-44432

ACOUSTIC PROPAGATION

Acoustic emission to monitor metal structures, pipes, pressure vessels and graphite shapes to detect structural deterioration before failure, emphasizing nuclear reactor pressure systems 01 p0054 A70-10015

Ultrasonic methods for materials evaluation, discussing goniometry, measuring techniques and acoustic wave propagation in various materials 01 p0104 A70-10878

Sonic boom theory of geometric acoustics with non-linear effects modification, emphasizing horizontally stratified atmospheric propagation, discussing failure near caustic 05 p0796 A70-16794

Acoustic wave propagation in partially ionized gas in external electric field, solving differential equations by Laplace transformation 08 p1552 A70-21503

Acoustic wave transmission and reflection through blade row in axial flow compressor analysis based on semiactuator disk theory and acceleration potential method 11 p2103 A70-26705

Acoustic energy backscattered from vertically directed beam of sound by lower troposphere density structure inhomogeneities 12 p2262 A70-26953

One dimensional radiatively driven acoustic waves analysis by approximation for radiative heat addition, achieving better accuracy than substitute-kernel method 13 p2520 A70-28633

Transient signal generation during large amplitude ultrasonic pulse propagation through carbon tetrachloride 16 p2952 A70-34097

Ionospheric acoustic wave propagation from seismic waves of Kurile Islands earthquake on 11 Aug 1969 17 p3075 A70-34569

Acoustic wave propagation through positive column of glow discharge of three component plasma, noting amplitudes dependence on excitation wave amplitude 17 p3140 A70-34872

Sound passage through rigid screen of arbitrary wave thickness with apertures, using linear algebraic equations 18 p3291 A70-36306

Acoustic propagation from spherical source into surrounding medium, using Laplace transform of function with simple discontinuities 21 p3850 A70-41423

Acoustic wave propagation in continuum of inviscid compressible heat conducting fluid, determining stability criteria 22 p4073 A70-42571

Pressure and temperature effects on large amplitude acoustic pulses propagating in stratified atmosphere 22 p4010 A70-42689

ACOUSTIC PROPERTIES

NT ACOUSTIC IMPEDANCE
NT ACOUSTIC INSTABILITY
NT ACOUSTIC SCATTERING
NT ACOUSTIC VELOCITY
NT REVERBERATION
NT SOUND INTENSITY
NT ZERO SOUND

Coherent light beams scanning and propagation direction control by acoustooptical method for laser applications 09 p1695 A70-22315

Rigid rectangular box with supported flexible wall analyzed for internal acoustostructural mode coupling factors and corresponding modal average radiation efficiency 09 p1770 A70-22393

Acoustic and gas dynamic characteristics of jet noise muffler using adapters at outlet section of exhaust nozzle 12 p2160 A70-27295

Acoustooptics materials selection guidelines, estimating lead molybdate figure of merit on basis of chemical composition and density 13 p2469 A70-28796

Acoustic conductivity of burning solid propellant surface, discussing critical conditions and variable surface measurement methods 13 p2522 A70-29421

Wave scattering by acoustically soft, hard and perfectly conducting spheres 15 p2700 A70-32410

Wave scattering by acoustically soft and hard prolate spheroids 15 p2700 A70-32411

High velocity center to center collision of two absolutely elastic rods in acoustic medium in terms of Einstein nonclassical mechanics 15 p2775 A70-32890

F-1 rocket engine acoustic liner, reevaluating damping data for combustion stability improvement 16 p2968 A70-33588

Aerodynamic and acoustic characteristics of subsonic and supersonic jets from convergent nozzles with room temperature air supply 17 p3005 A70-34460

Acoustic fields of circular, rectangular and line focused ultrasonic emitters for small defect detection 22 p4048 A70-43618

ACOUSTIC RADIATION

U SOUND WAVES

ACOUSTIC SCATTERING

NT REVERBERATION

Immittance, transfer and scattering characteristics for interdigital acoustic surface wave transducers, using linear equivalent circuit model 06 p1062 A70-17478

Acoustic scattering parameters for interdigital transducer as function of electrical loading and frequency using equivalent circuit model 06 p1062 A70-17485

Plane acoustic wave steady state scattering at circular cylinder in semibounded region 07 p1334 A70-19089

Piezoelectric scattering effects on electron temperature and mobility in IIB-VIA semiconductor compounds with nonparabolic conduction band 13 p2471 A70-29373

Collection of papers on electromagnetic and acoustic scattering by simple shapes 15 p2699 A70-32401

EM and acoustic scattering by simple shapes covering Maxwell equations, boundary and radiation conditions, radar cross sections, EM potentials, etc 15 p2700 A70-32402

Acoustic and EM scattering by hyperbolic cylinder, considering plane wave incidence and line sources 15 p2700 A70-32406

Hyperboloid of revolution acoustic scattering, using Bloom-type method for hard hyperbolic cylinder 15 p2701 A70-32416

Cone geometry for electromagnetic and acoustic scattering 15 p2701 A70-32417

Acoustic field scattering from multipole point sources by solid spherical surface 22 p4010 A70-42693

Aerodynamic noise scattering by semiinfinite compliant plate in turbulent flow, using Lighthill theory and Wiener-Hopf technique 23 p4179 A70-43968

ACOUSTIC SIMULATION

Sonic bang simulation by linearly distributed explosives, creating blast waves with wide range of shapes and durations 05 p0796 A70-16796

Shallow water waves simulation method for studying aerodynamic noise of free jet emitted from nozzle with variable wall roughness 08 p1485 A70-21608

ACOUSTIC STABILITY

U FREQUENCY STABILITY

ACOUSTIC STREAMING

Frequency dependent effects of applied acoustic fields on attached jet flows for Reynolds numbers over curved surfaces [ASME PAPER 70-FLCS-1] 22 p4008 A70-42430

ACOUSTIC VELOCITY

Emission from broadband impulsive point source refracted by spherical interface between fluids with different acoustic velocities, showing emitted and inverse waveform disturbances 01 p0046 A70-11190

Weak shock waves relaxation time and amplitude and acoustic velocity as functions of thermorelaxing media 01 p0068 A70-11588

Sonic throat formation from two dimensional viscous layer interaction with supersonic inviscid outer stream, using boundary layer equations 04 p0665 A70-14452

LF sound velocity measurement in carbon dioxide near critical point, noting existence of logarithmic divergence 04 p0718 A70-14685

Sound wave propagation in liquid containing gas bubbles allowing for relative motion of bubbles and liquid, deriving steady shock wave structure 04 p0671 A70-14991

Sonic waves induced by shock of laser produced brass and graphite vapor in air at atmospheric pressure using high speed shadowgraphs 05 p0857 A70-15802

Sonic speed and damping in two phase potassium flow, discussing linear equations and propagation velocity 09 p1725 A70-22036

Heat treatment effects on hardened steels acoustic constants, calculating sound velocity in liquid metals 09 p1692 A70-22643

Acoustic velocity in rarefied argon and nitrogen using Brillouin scatter and Burnett equations 09 p1698 A70-23314

Sound speed and horizontal wind velocity components determined in upper atmosphere from measured data of Rocket Grenade Experiment 11 p2121 A70-25678

Compressible fluids steady state equations invariant transformation, establishing sound speed-Mach number relation 13 p2389 A70-29458

Sound velocity relation with specific heat at constant volume at liquid-gas equilibrium critical point 15 p2826 A70-30222

Sound velocity differences related to composition of lunar and terrestrial rocks 16 p2978 A70-33973

Acoustic turbulence spectrum in compressible fluid with potential motion, using complex traveling wave amplitudes in hydrodynamic equations 18 p3242 A70-36637

Sound velocity in isotropic nonlinear elastic Cosserat continuum with constrained particle rotation, analyzing uniaxial and hydrostatic compression 20 p3734 A70-40434

Acoustic interferometer for speed of sound measurement in pure gases, determining second virial coefficient for Ar and N 21 p3828 A70-41766

Hypersonic sound speeds measured in methane at moderate pressures by spontaneous Brillouin light scattering experiments 21 p3830 A70-41938

One dimensional sound propagation in reacting gas mixture near equilibrium, obtaining equilibrium and frozen sound speed 22 p4074 A70-42752

Equilibrium sonic velocity in reacting gas mixture in nozzle flow for unlimited species and independent chemical reactions 22 p4074 A70-42753

Sound velocity in isotropic nonlinearly elastic continuum with microstructure, showing dispersion coincident with Cosserat constant 22 p4120 A70-43713

Sintered material density-sound velocity relation, deriving ultrasonic wave propagation time dependence 24 p4360 A70-45731

ACOUSTIC VIBRATIONS

U SOUND WAVES

ACOUSTICS

NT BIOACOUSTICS

NT MAGNETOACOUSTICS

NT PSYCHOACOUSTICS

NT UNDERWATER ACOUSTICS

Book on technical acoustics physics covering propagation, dissipation, reflection, field perturbation in real solids, liquids and gases, lumped constants, resonators, etc 01 p0144 A70-11328

Acoustooptical processing for amplification of weak radar echoes, describing design and operation of modulators, correlators, filters, etc 02 p0266 A70-12630

Sonic boom theory of geometric acoustics with non-linear effects modification, emphasizing horizontally stratified atmospheric propagation, discussing failure near caustic 05 p0796 A70-16794

Acoustic turbulence generated noise intensity and spectrum using statistical thermodynamics 07 p1194 A70-19618

Monograph on acoustic theory for determining frictional pressure drop effect on gas state behind reflected wave in shock tube 12 p2209 A70-27000

Ferrous and ferric ions properties in corundum from observing acoustic paramagnetic resonance 15 p2784 A70-32397

Acoustic cavities use in suppressing acoustic modes of combustion instability demonstrated on LM ascent engine [AIAA PAPER 70-618] 16 p2998 A70-33614

Optimum receiver for acoustical holography using discrete transducers arrays for image conversion 17 p3088 A70-35029

Acoustical holography with single stationary point detector noting reciprocity between detector and point source illuminator 17 p3088 A70-35030

Acoustic/microwave/ holography for large masses by crossed linear array of microphones, discussing computer simulation of virtual holograms and image reconstruction 21 p3822 A70-40715

LF acoustic disturbances effect on root portion of turbulent jet from conical nozzle 21 p3954 A70-42223

Acoustic Bragg diffraction for laser light deflection, solving high speed photography and holography motion problems [SMPT PREPRINT 5] 22 p4035 A70-43055

Acoustic and scanned holography for nondestructive testing, showing defects in metal samples 22 p4041 A70-43620

Acoustic holographic system producing two dimensional picture in real time, using stationary linear transducer arrays 24 p4339 A70-46080

ACQUISITION

NT DATA ACQUISITION

NT TARGET ACQUISITION

Weapon systems acquisition projects, studying procurement decisions interactions
[ASME PAPER 69-WA/MGT-6] 04 p0788 A70-14833

Project acquisition based on consideration of logistic effects /ABLE/ for tool measuring logistic consequences of reliability and maintainability
15 p2832 A70-32634

ACROBATICS

Loading conditions measured during aerobatic maneuvers in flight test to determine structural design requirements for aerobatic-type aircraft
[SAE PAPER 700222] 11 p1980 A70-25894

Heterochromism of coordinated cophasal flexor and extensor movements during acrobatic leap in human subjects
12 p2168 A70-27344

Acrobatic pilots equilibrium behavior in vestibular training, discussing labyrinth reactions and fluid intake role
17 p3041 A70-35919

MBB Bo-209 Monsun travel, commuter and acrobatics aircraft, discussing configurations, specifications, structure and handling characteristics
19 p3355 A70-37388

ACROLEINS

Acrolein photoisomerization in lower excited states, determining fluorescence and phosphorescence quantum yields
15 p2694 A70-31730

ACRYLATES

Cyanoacrylate and anarobic polymer single component adhesives performance
22 p4046 A70-43120

ACRYLIC RESINS

Laser velocimeter measurements on drag reducing polyacrylamide solution compared to water
03 p0502 A70-13821

Processing temperature effects on breaking strength-modulus relation for carbonized acrylic fibers
10 p1907 A70-24533

Lattice resolution of layer planes in polyacrylonitrile based carbon fibers ground and dispersed by ultrasonic irradiation
14 p2598 A70-30793

Graphite fibers made from polyacrylonitrile yarn examining density-Young modulus relationship
17 p3127 A70-35149

ACTH

U ADRENOCORTICOTROPIN [ACTH]

ACTINIDE SERIES

NT PLUTONIUM ISOTOPES
NT THORIUM
NT THORIUM ISOTOPES
NT URANIUM
NT URANIUM ISOTOPES
NT URANIUM 233
NT URANIUM 238

Apollo 11 lunar material actinide element abundance and isotopic composition, examining Th, U and transuranium elements by mass spectrometric and radiometric techniques
21 p3774 A70-41569

ACTINIDE SERIES COMPOUNDS

NT THORIUM OXIDES
NT URANIUM OXIDES

ACTINOGRAPHS

U ACTINOMETERS

ACTINOMETERS

NT DICKE RADIOMETERS
NT INFRARED DETECTORS
NT INFRARED SCANNERS
NT MICROWAVE RADIOMETERS
NT PYRANOMETERS
NT RADIOMETERS
NT SOLAR SPECTROMETERS
NT SPECTRORADIOMETERS

Atmospheric radiation and heat fluxes calculations comparison with satellite and ground station actinometric measurements
15 p2770 A70-32067

Soviet papers on actinometry, atmospheric optics and ozonometry
20 p3624 A70-39026

Angular and geometric properties of actinometers, pyrohelimeters and photometers, measuring direct and scattered circumsolar radiation
20 p3625 A70-39028

Correction procedures for measurement errors in actinometers and pyrohelimeters caused by circumsolar radiation
20 p3625 A70-39029

Phytoactinometers and phytopyranometer graduating methods, discussing measurement of photosynthetically active radiation
20 p3626 A70-39035

Armored actinometer with electroplated thermopile, describing construction and performance
24 p4333 A70-45137

ACTIVATION [BIOLOGY]

Appetitive behavior of rats following cessation of hypothalamic stimulation, observing eating and drinking inhibition
01 p0027 A70-11275

Controlled premature atrial stimulation effects on atrioventricular conduction in man, using electrode

catheter technique to record electrical activity of specialized conducting fibers
03 p0415 A70-12886

Aplysias periodic spontaneous gill movements controlled by central neuron activity in abdominal ganglion
04 p0629 A70-14425

Mathematical model for computer simulation of homogeneous neuron nets with recurrent inhibition control, considering activated and inactivated states
04 p0640 A70-14553

QRS and ST-T areas in multiple bipolar chest leads during normal and abnormal activation in patient measured for checking ventricular gradient concept
04 p0632 A70-15307

Lipoprotein lipase activation on emulsified triglycerides by specific glycopeptides of human serum lipoproteins
24 p4298 A70-45802

Alpha and beta reciprocal hunger regulating systems localized in rats hypothalamus areas by varying injection sites of alpha and beta adrenergic drugs
24 p4304 A70-46233

ACTIVATION ANALYSIS

NT NEUTRON ACTIVATION ANALYSIS

Ni effect on nitrogen activity in Fe-Ni-N austenite between 600-1200 C using Strohlein analyzer
06 p1088 A70-17612

Apollo 11 lunar rocks elemental abundances determination by instrumental activation techniques
21 p3775 A70-41574

Sequential instrumental activation analysis for trace elements in rocks and stony meteorites, comparing with silicate method
24 p4310 A70-46407

ACTIVATION ENERGY

Alloying additions effect on plastic deformation anisotropy in GaAs single crystals, determining dislocation activation energies from creep tests
01 p0160 A70-11606

Impurity diffusion in Ni using diffusion theory, considering activation energies for Mo and W
02 p3317 A70-12396

Bimolecular transfer reactions activation energies for multivalent gaseous compounds estimated by bond energy method avoiding use of adjustable parameters
03 p0441 A70-14045

Activation energy measurement using stress relaxation for plastic flow in commercially pure Al compared with creep and tensile method
04 p0777 A70-15495

Creep in single crystal and polycrystalline Nb between 1300-1900 C under stresses, showing stress independent activation energy
05 p0862 A70-16202

Radioactive sodium and potassium diffusion in single crystal and polycrystalline Mo and Nb at various temperatures, calculating activation energies and coefficients
06 p1089 A70-17745

Meyer-Neldel rule interpretation of distribution width parameter dependence on activation energy annealing of defects in irradiated Si
06 p1106 A70-17925

Hydrogenated Ni activation energy difference for lower and higher critical temperatures due to hydride dislocations binding energy
08 p1522 A70-21705

Austenitic Fe-Cr-Ni-Ti alloys at high temperature to determine activation energy for nitrogen diffusion, noting oxygen role
08 p1522 A70-21707

Hydrides precipitation in Ti-Al-Mo-V alloys using transmission electron microscopy, discussing crystal structure, activation energy, hydride-matrix phase interface, etc
08 p1525 A70-21964

Crab Nebula continuing energetic activity study indicating origin in nebula center and association with supernova remnant
09 p1750 A70-22000

Excitation energy transfer processes in oxide glasses containing trivalent Tb ions in combination with other rare earth activators
09 p1738 A70-22137

Creep behavior transition analysis, considering activation energies and creep rate dependence on temperature, stress and grain size
09 p1704 A70-22720

Porous Ti powder sintering process activation energy determination, noting influence of oxides solution in surface layer of Ti particles
12 p2254 A70-27283

Compacted titanium carbide powder coarsening recrystallization within homogeneous region, determining relation between initial activation energy and carbide composition
12 p2254 A70-27284

Semiconductor diamond films electrical conductivity obtained by injecting various ions during isochronal stepwise annealing, studying activation energy values
12 p2286 A70-27479

Fe and Ni doped GaAs photoconductivity at various temperatures, determining activation energy level
12 p2287 A70-27489

Al-aluminum oxide composite steady state creep due to grain boundary sliding, accounting for activation energy level
12 p2258 A70-28348

Toroidal solar field emergence to surface forming magnetic field of active region
13 p2493 A70-29392

Kinetics for two free radical conversion processes in electron irradiated D, L-valine, measuring activation energies by electron spin spectroscopy
14 p2544 A70-30111

Stress relaxation of Mo under plastic deformation controlled by diffusion of interstitial atoms and dislocations, determining activation energy
15 p2758 A70-32124

Heterodiffusion coefficients and activation energy for Cu, Ag and Au impurities in Al, using gamma spectrometry and X ray emission microanalysis
16 p2930 A70-33081

Mo powder compacting by hot pressing, determining activation energy
16 p2931 A70-33222

Activation energy for creep at intermediate temperatures, allowing for elastic modulus change
16 p2991 A70-33790

Reaction rate kinetics characteristics from isothermal data, investigating relationship to activation energy distribution
17 p3042 A70-35330

Alumina effects on Nb creep activation energy at elevated temperatures, noting independence from chemical composition and creep stresses
19 p3453 A70-38710

Argon hydrostatic pressure effect on self diffusion coefficients and activation energy of Al and Be single crystals
20 p3644 A70-38961

Dislocation network recovery kinetics of cold worked undoped powder metallurgical W wires by electrical resistivity measurements, determining activation energy
21 p3839 A70-40797

Activation energies of acceleration and hypoxia stress in man and rats, noting brain function survival
21 p3764 A70-41484

MOS field effect transistor, measuring electrons and holes thermal emission rates and activation energies at gold contacts in Si
22 p3997 A70-43016

Bcc Fe base alloys volume diffusion measurements, determining activation energy and frequency factor dependence on solute content
24 p4357 A70-45232

Chemical diffusion kinetics of zirconium silicates formation during sintering under pressure, noting activation energy estimation
24 p4367 A70-45479

ACTIVE SATELLITES

NT EARLY BIRD SATELLITES
NT SYNCOM SATELLITES

Passive and active satellite systems for point-to-point communication network with multiple access capacity, comparing technical and economic competitiveness
11 p2011 A70-26335

ACTIVITY [BIOLOGY]

Artificial hypobiosis state maintenance in animals exposed to cooling after administering lytic mixtures for suppressing oxidation
01 p0029 A70-11464

Neurons tracing activity and cellular memory mechanisms in cortical projection region of cutaneous analyzer of immobilized rats following electric acoustic stimuli
01 p0030 A70-11468

Early and late response component of associative cortical area in cerebral hemispheres of cats connected with mono and polysensory neuron activity
03 p0421 A70-13688

Origin and functional designation of associative evoked potentials in orbital cortex of cats, showing phases connected with neuron activity and excitation
03 p0422 A70-13689

Collection of Soviet papers on physiological foundation of activity regimes covering human cerebral cortex, skin and muscles responses to stimuli, etc
04 p0638 A70-15501

Canines conditioned reflex activity as function of cortex sections following head exposure to X ray irradiation
07 p1199 A70-18729

External environment changes effect on animal activity, considering reactions on molecular, physiological and behavioral levels
07 p1199 A70-18782

Guinea pigs visual analyzer during stimulations by diffuse light, nonspecific thalamic nuclei and microelectrodes polarization, determining A- neuron activity
07 p1213 A70-19788

Midbrain reticular neurons activity in cats during response to individual and coincident cortical and hypothalamic stimulations
07 p1213 A70-19789

- Symmetrical motor centers inequality significance in humans during interaction under conditions of successive innervations during exercise
07 p1213 A70-19790
- Simultaneous recording of fast and slow precision manual movements with electroencephalogram and electromyogram
08 p1452 A70-21438
- Dogs spinal cord bioelectric activity monitoring by implanted electrodes, noting interelectrode resistances after prolonged operation
09 p1615 A70-22091
- Mars biological activity suggested from metabolic energy cycle based on oxidation of carbon monoxide [NGL-07-004-043]
09 p1765 A70-23798
- Biologically active fragments formation and functions in organism following liberation from inactive proteins via limited proteolysis
10 p1811 A70-24390
- Neuron activity of cortical motor and visual regions and corpus geniculatum laterale in cats during diffuse thalamic electrostimulation combined with light signals
12 p2173 A70-28355
- Actoballistocardiography based on piezoelectricity for biorythmic activity, respiratory movements and heart rate of small animals
14 p2543 A70-31321
- Dogs spinal cord bioelectric activity monitoring by implanted electrodes, noting interelectrode resistances after prolonged operation
15 p2685 A70-32687
- Transport processes in chemical reactions and biological functions of living systems, using nonequilibrium thermodynamics approach
17 p3032 A70-35539
- Human brain LF activity in visual evoked response, determining relationship to stimulation
19 p3360 A70-37846
- Muscular activity in regulation of organism functions during aging, considering hypokinesia effects
22 p3968 A70-42894
- Muscular activity influence on energetic processes and functions in aging organism, relating oxygen consumption to aerobic metabolism
22 p3968 A70-42895
- Bioelectric activity changes in rats lumbar neurons, membrane and postsynaptic potential and discharge frequency during and after asphyxiation
22 p3971 A70-43404
- Spinal cord thermal stimulation effects on regional sympathetic activity in rabbits and cats determined from integrated sympathetic efferents discharges
22 p3971 A70-43406
- ACTIVITY CYCLES (BIOLOGY)**
- Metabolism and biological activity of urea, citrulline, arginosuccinic acid in organism ornithine cycle, discussing role in brain and liver
01 p0019 A70-10513
- Periodic components distribution of human cardiac activity rhythm noting slow waves
07 p1210 A70-19556
- Circadian rhythmical changes in biological organisms by earth rotation, emphasizing diurnal variations role in sleep-wakefulness rhythm
15 p2680 A70-31742
- Mechanisms responsible for sleep-wakefulness rhythm, investigating effect of lesions in CNS, electrical excitation of brain, neurons activity, etc
15 p2680 A70-31744
- Sleep-wakefulness cycle regulation role of serotonin, noradrenalin and acetylcholine in CNS of animals
15 p2680 A70-31745
- Human and animal adaptation and responses to time intervals and temporal activity cycles, discussing conditioned reflexes in terms of physiological factors
15 p2687 A70-32869
- Circadian and seasonal adaptive function rhythms in animals, discussing terrestrial environment and thermoregulation
19 p3365 A70-38409
- Photoperiod effects on rats food and water intake, noting endogenous feeding rhythm correlation with activity patterns
24 p4296 A70-45332
- ACTUATOR DISKS**
- Large-tilt-angle lifting surface theory for V/STOL aircraft based on inclined actuator disk analysis
04 p0619 A70-15377
- Compressible fluid flow velocity profile in turbine stage evaluated by streamline correlation and actuator disk method
06 p0967 A70-17469
- Wing lifting surface theory for V/STOL aircraft based on inclined actuator disk theory to predict span loading and downwash angle
07 p1190 A70-20408
- Acoustic wave transmission and reflection through blade row in axial flow compressor analysis based on semiactuator disk theory and acceleration potential method
11 p2103 A70-26705

F-111 aircraft wings unstable fore and aft oscillations in swept forward position ascribed to actuator motor drive rate variations
12 p2160 A70-27112

ACTUATORS

- Servoactuator simulating vertical acceleration in F-104 simulator, duplicating other forces conventionally
02 p0229 A70-12864
- Nonlinear characteristics of electromagnet actuating mechanism induced by magnetic field of coil
07 p1281 A70-19529
- Soviet book on pneumatic actuators theory and design, using digital computers to solve dynamic equations and to obtain diagrams and nomograms
08 p1440 A70-20752
- Hydraulic regenerative servoamplifier system for electrohydraulic actuator design, discussing specifications and test results
09 p1614 A70-23686
- Dynamic stability of multipoint servocontrol system actuating thin deformable primary mirror of orbiting telescope
12 p2203 A70-27413
- Parameters optimization of nonlinear electric servo actuator on basis of statistical criteria
14 p2559 A70-30157
- Electropneumatic actuation systems for rocket engines in extreme environment applications involving high nuclear radiation levels and high and cryogenic temperatures
14 p2535 A70-31343
- Electromechanical servopump for positioning and handling of objects in weightless environment, discussing design and operations
16 p2919 A70-33720
- Mariner 4 scan platform structure and actuator design, development and performance
16 p2845 A70-34106
- Scan platform servomechanical actuator for Mariner Mars 1969 spacecraft, emphasizing gear arrangement and train dynamics
16 p2845 A70-34108
- Tactical missiles electromechanical control actuator with reduced size and weight, describing mathematical model for analog simulation
16 p2845 A70-34111
- Explosively actuated /pyromechanical/, devices for spacecraft, discussing guidelines for design, testing, application and cost efficiency
16 p2963 A70-34125
- Nonmagnetic lightweight oscillating actuator for multiple indexing of spacecraft magnetometer
16 p2845 A70-34128
- Fluid thermal actuator for temperature control of ITOS /Improved Tiros Operational System/ meteorological satellite, discussing design and performance
16 p2846 A70-34129
- Solar power panel orientation servomechanism using passive elements without power consumption
16 p2846 A70-34130
- Lightweight spiral wound bimetallic actuators for active spacecraft thermal control systems
17 p3022 A70-34755
- Mariner Mars 1971 gimbal actuator design and life test for autopilot system using hypergolic bipropellant rocket engine
17 p3022 A70-34758
- Automatic control system stability, allowing for position and velocity loads and compressibility of fluid in force cylinder of hydraulic actuating mechanism
17 p3024 A70-35367
- Servoactuator for stick force augmentation on light turboprop STOL aircraft at high angles of attack [AIAA PAPER 70-909]
17 p3019 A70-35821
- Boeing 2707 SST horizontal tail multiple channel actuation system features
17 p3020 A70-35827
- Supply valve influence on dynamic characteristics of volumetric hydraulic actuator
18 p3215 A70-36126
- Logarithmic amplitude characteristic of automatic rate stabilization systems for controlled electric actuators systems
18 p3215 A70-36296
- Three digit hydromechanical step type actuator drives with slide valve assembly for computer data sampling systems
18 p3216 A70-37071
- Vacuum brazed stainless steel hot gas actuators for guided weapons
18 p3265 A70-37202
- Aircraft auxiliary systems and spacecraft power supplies, considering fly-by-wire control actuators, pyrotechnics and stowable solar array
20 p3564 A70-39669
- Prototype synchronizing valves for maintaining identical flow velocities of two hydraulic actuating elements, noting unbalanced hydrodynamic forces and orifices asymmetry effects
20 p3564 A70-39717
- Pneumatic actuator control system improvement, using invariance theory to compensate load variability and dynamic response of medium
20 p3564 A70-39848

Liquid metal hydraulic servoactuation packages for flight control in high temperature environments without coolant systems
21 p3750 A70-40785

Hydraulic synchronizers for motors and actuators speed equalization, describing operation and technical specifications
21 p3756 A70-40800

Energy methods for stability of linear inflatable pouch actuator based on energy change in pouch deflection
21 p3760 A70-41966

Harmonic linearization method for automatic control systems having hydraulic or pneumatic actuating device with two nonlinear elements
22 p4002 A70-42841

ACUITY

NT VISUAL ACUITY
AD-A SATELLITE
U EXPLORER 19 SATELLITE

ADAPTATION

- NT ACCLIMATIZATION
NT ALTITUDE ACCLIMATIZATION
NT COLD ACCLIMATIZATION
NT DARK ADAPTATION
NT DESERT ADAPTATION
NT LIGHT ADAPTATION
NT RETINAL ADAPTATION
- Rodents hypoxia tolerance following adaptation to hypercapnia by recording time of useful consciousness /TUC/ in repeated sloped surface clinging tests
01 p0026 A70-11249
- Receptive fields in visual systems, discussing characteristics, size, geometry, adaptation effects, sensory interactions, etc
02 p0236 A70-12304
- Diurnal rhythms of physiological functions and human adaptation to shifted sleep-wakefulness schedule on healthy pilots subjected to solitary confinement
03 p0423 A70-13711
- Resistance to decompression sickness increased and mortality rate decreased in mice after adaptation to hypoxia at normal barometric pressure
07 p1206 A70-19469
- Human sensory-motor adaptation and aftereffects of exposure to accelerative forces using hand-eye coordination measurements
09 p1628 A70-23466
- Diurnal rhythms of physiological functions and human adaptation to shifted sleep-wakefulness schedule on healthy pilots subjected to solitary confinement
11 p1985 A70-25511
- Vestibular adaptation to heat and rotary stimulation in animals and men
11 p1986 A70-25822
- Human and animal adaptation and responses to time intervals and temporal activity cycles, discussing conditioned reflexes in terms of physiological factors
15 p2687 A70-32869
- Medicopsychological and labyrinthine exploration of flight crew candidates aeronautical adaptation, using electronystagmographic method of swinging chair
17 p3041 A70-35918
- Adaptation to extreme stimulation in machine-organism system
18 p3224 A70-36529
- Gas metabolism, chemical thermoregulation, body temperature and weight of rats during adaptation to repeated high temperature exposure
18 p3219 A70-36538
- Adaptive recession of gas metabolism in rats during multiple high temperature exposures
18 p3220 A70-36545
- White rats adaptation to multiple high temperature exposures, examining oxygen tension in skeletal muscles
18 p3220 A70-36549
- Iterative adaptation algorithms, using automatic search techniques for single and multiparameter systems
19 p3394 A70-38163
- Circadian and seasonal adaptive function rhythms in animals, discussing terrestrial environment and thermoregulation
19 p3365 A70-38409
- Adaptation of cardiovascular system in aging and old individuals under muscular activity
22 p3968 A70-42896
- Astronaut work capacity and adaptation during long term flight of space vehicle Soyuz-9
23 p4154 A70-44651
- ADAPTERS**
- AI-B composite missile adapter design for aerospace structures
02 p3006 A70-11951
- Automatic test equipment for electronic devices, discussing computerized design of interface adapters for unit under test
08 p1470 A70-20657
- ADAPTIVE CONTROL**
- NT LEARNING MACHINES
NT SELF ADAPTIVE CONTROL SYSTEMS

Digital adaptive-element building blocks in monolithic Si structures for MOS large scale integration, considering serial/parallel multiplier and shift register chips
01 p0047 A70-10458

Adaptive man machine systems, display design - IEEE/ERS Conference, Cambridge, England September 1969, Volume 4
02 p0245 A70-12147

Adaptive man machine system for automated training of pilot dynamic control skills /decision and motion/, describing synthesis procedure
02 p0246 A70-12148

Adaptive training concepts, methods, implementation and comparison of characteristics with fixed trainers
05 p0805 A70-16004

Time constant of man machine system as adaptive variable in training devices derived from combined vehicle properties and human control characteristics
05 p0805 A70-16005

Adaptive multiparameter experiment for iterative minimization of investigated data points, based on human response pattern to psychophysical inputs
05 p0805 A70-16006

Adaptive training applied to simulated pilot training system, discussing methods for variables selection, error measurement, trainee feedback, etc
05 p0805 A70-16007

Adaptive frequency selection of optimum channels for radio communication on noninterference basis, discussing implementation and compatibility problems with nonadaptive systems
05 p0814 A70-16347

Identification experiments and computational algorithms allowing synthesis of adaptive optimization process for real dynamic plants
06 p1023 A70-17634

Adaptive control algorithm for parameter adjustment of unknown dynamic characteristics of linear systems
06 p1025 A70-17956

Control system employing adaptive modeler to estimate state, dynamics and future trajectory of unknown plant through performance index minimization
06 p1025 A70-17965

Hyperstability conditions of model reference adaptive control systems, noting applications
06 p1026 A70-17966

Decision algorithms simulating human controller adaptive behavior in controlling VTOL aircraft in hover following stability augmentation system failure
07 p1216 A70-18860

Adaptive control function technique for lateral stability augmentation system design for manned lifting body entry vehicle
07 p1247 A70-20404

Adjustment process dynamics in digital adaptive system with task of ensuring minimum quadratic criterion for parameters using gradient search technique
08 p1480 A70-21017

Adaptive equalizer consisting of canonical link structure with minimum number of delay elements applied to fast data transmission
09 p1640 A70-22039

Readjustment algorithm for auto-oscillatory adaptive control system with variable structure, using harmonic linearization
11 p2022 A70-25343

Control theory, Volume 1, covering linear, nonlinear, stochastic, optimal, adaptive and learning systems, sensitivity analysis, etc
11 p2023 A70-25771

Gain determination from dynamic /on line/ solutions to Riccati equation for model reference adaptive control applicable to multiple input/ output or stochastic systems
11 p2029 A70-26339

Nonlinear time-varying multivariable adaptive control system design using signal synthesis technique
12 p2203 A70-27415

Self organization and adaptive routing communication system for military network, describing routing algorithm and entropy organization measure based on stochastic switching matrices
12 p2187 A70-27934

Adaptive flight control systems utilization to compensate for variations in aerospace vehicle rigid body dynamics, noting control system performance requirements
[AIAA PAPER 68-970]
12 p2204 A70-28076

Adaptive variable-parameter spacecraft trajectory control, discussing loop synthesis and model reference system stability and dynamic accuracy
13 p2380 A70-28383

Stochastic adaptation process, investigating asymptotic properties based on concept of random system with complete connections
13 p2383 A70-29490

Adaptive optimization methods involving minimization of unknown function, determining new input location via sequential search
13 p2383 A70-29583

Nonlinear optimal filtration and adaptive quasi-coherent reception of Markov signals on white noise background
13 p2369 A70-29731

Mathematical models for human adaptive and optimizing characteristics in manual control systems regarding behavior phase
13 p2360 A70-29780

Adaptive extremal control systems operational stability, defining optimal convergence coefficient values for identifier and perceptron
14 p2559 A70-30175

Adaptive hydraulic servomechanism control systems synthesis by Liapunov direct method, noting parameter compensation effect on state error reduction
14 p2534 A70-30621

Optimum adaptive reception for binary sequences, using posteriori probability density function computing device synthesized from correlator, instantaneous nonlinearity and multiplier
14 p2552 A70-31188

Discrete approximation of differential game of navigation, considering control of object transfer to given set by finite time
15 p2775 A70-32472

Stable adaptive control design for linear time-invariant system with same number of inputs as outputs, considering disturbance effect
16 p2881 A70-33035

Optimal adaptive digital autopilot design for reentry vehicle flight path control
16 p2946 A70-33307

Steerable microwave circular array to provide 360 deg electronic beam steering with computerized adaptive amplitude and phase control
16 p2874 A70-33392

Adaptive radar beacon forming, using conjugate reflections for propagation path errors compensation
16 p2865 A70-34061

Continuous time nonlinear feedback control systems, using modified gradient procedure for parameters adaptation
17 p3056 A70-34952

Adaptive system synthesized to compensate stochastic feedback or external disturbance, obtaining quasi-optimal compensation algorithms
17 p3056 A70-35368

Identification-adaptive control algorithm for quadratic cost control of discrete linear systems
17 p3057 A70-35558

Adaptive control systems stability treatment by Liapunov direct method
18 p3279 A70-36060

Discrete automatic control theories, including linear, nonlinear, feedback, optimal and adaptive systems and bibliographies
18 p3235 A70-36626

Analytical adaptation algorithms for PID controllers operation
19 p3394 A70-38162

Nonlinear adaptive reaction jet attitude control for long life space vehicles, providing optimal performance over bias acceleration disturbances
[AIAA PAPER 69-945]
20 p3716 A70-39680

Identification adaptive quadratic cost linear system control by mean and covariance correction algorithm
21 p3801 A70-40741

Adaptive AC null detector with tuned compression amplifier used for oscilloscope display drive
21 p3828 A70-41469

Adaptive pattern recognition systems design based on notions of convergence and feedforward interconnection of two systems
21 p3794 A70-41499

Recurrent adaptive methods for verification of multialternative hypotheses in stepwise signal processing
22 p3993 A70-42565

Phased array radar for missile defense, discussing development trends toward adaptive system logic control and microwave digital circuitry for signal processing
23 p4172 A70-44012

Optimal adaptive digital autopilot design and operation, discussing linear differential equations of motion, algorithms, etc
23 p4215 A70-44504

State-space method of parameter tracking for adaptive control, using Riccati equation and Kalman filtering
23 p4177 A70-44675

Adaptive time optimum inertial satellite attitude control using air jet
23 p4265 A70-45048

ADAPTIVE CONTROL SYSTEMS
U ADAPTIVE CONTROL
ADAPTIVE FILTERS
Special purpose computer organized as time-shared digital filter for real time applications with adaptable coefficients, programming and multiplexing scheme
05 p0818 A70-16415

Solid state resonant bandpass electronic filter composed of ferroelectric dielectric capacitors with adaptable voltage gain
09 p1653 A70-33801

Adaptive Kalman filtering with unknown process and measurement noise covariance matrices
16 p2880 A70-32983

Adaptive tracking filter for bending mode stabilization of large flexible boosters
[AIAA PAPER 69-874]
20 p3716 A70-39682

Adaptive channel equalization approach leading to adaptive detector for slowly time varying channel
22 p3989 A70-43172

ADDITION
Algorithm for Fast Two Dimensional Fourier Transform requiring logarithm additions and multiplication
11 p2073 A70-26250

Small digital computer arithmetic unit design, discussing number representation, addition and subtraction methods for performance and cost
21 p3793 A70-40757

ADDITION RESINS
NT ACRYLIC RESINS
ADDITION THEOREM
Addition theorems for cylindrical functions, discussing applications to shell stress analysis and three dimensional elasticity theory
15 p2819 A70-32187

ADDITIVES
NT ADMIXTURES
NT ANTIFREEZES
NT ANTICorrosion ADDITIVES
NT ANTIOXIDANTS
NT OIL ADDITIVES
NT PROPELLANT ADDITIVES
NT PROPELLANT BINDERS
NT SOLID ROCKET BINDERS
Second phase formation in Czochralski grown Cr-doped GaAs crystals by metallography, radioactive indicators and X ray analysis
01 p0156 A70-10189

Gallium found suitable for doping cadmium/tin arsenide semiconductor, exhibiting hole-type conductivity
01 p0156 A70-10214

Alloying additions effect on plastic deformation anisotropy in GaAs single crystals, determining dislocation activation energies from creep tests
01 p0160 A70-11606

Chemical additives effect on H- Cl-N mixtures burning velocity in air and nitrogen
02 p0398 A70-12031

Grain refining of continuously cast Al by additions of B and Ti
02 p0309 A70-12299

Temperature dependence of magnetic susceptibility in liquid and solid states of binary Al-Mn alloys with additions of Cr, V and Ti
02 p0316 A70-12300

Al and Ti single additions effects on recrystallization of Ni-Cr alloys, noting phase transformation and hardness variations
03 p0513 A70-14300

High energy dopant ion implants into silicon, discussing implantation profiles and electrical conductivity for use in type conversion and electrical junctions
04 p0730 A70-14727

Chromium doping effect on ionizing radiation damage in MOS field effect transistors
04 p0658 A70-14744

Ni addition effects on Mg-Nd and Mg-Nd-Mn alloys structure and heat resistance
04 p0706 A70-15189

Photostability of Nd-activated glass elements as function of dopant concentration and laser mode operation
05 p0858 A70-16266

N-substituted tetrabromophthalimides prepared as fire retardant additives to PVC, polyester and epoxy resins
05 p0811 A70-16585

Long chain molecule additive effect on drag reduction in turbulent flow of aqueous polymeric solutions
[AIAA PAPER 70-56]
06 p1037 A70-18030

Alloying elements effects on vanadium alloys case hardening by boronizing
07 p1303 A70-18742

Doped semiconductor unsteady stimulated emission, solving kinetic reactions in multimodal approximation
07 p1357 A70-19862

Bonds strength involving metallic, organic and ceramic adhesives at various temperatures, considering metallic additives effect
08 p1504 A70-20891

Carbon-bearing materials for modification of Mg-Al-Zn-Mn alloys filtration processes
08 p1505 A70-21132

GaAs solar cells performance as function of doping levels, ascribing poor efficiencies to surface recombinations
08 p1557 A70-21721

Alloying Ni, Cu and Nb effects on grain and strengthening of low carbon precipitation-hardenable ferritic steels
09 p1705 A70-22804

Ion accelerator for doping semiconductors, discussing electronic bombardment of low pressure

vapors, electrostatic extraction, focusing and mass spectrometer

09 p1649 A70-23325

Epitaxial surface morphology layer electrical properties and autoping at GaAs-Ge heterojunctions as function of substrate temperature, orientation and HCl concentration

11 p2098 A70-26392

Dopant effect on dislocation mobility in elastically loaded silicon crystal using internal friction and modulus defect measurements

11 p2099 A70-26394

Doped semiconductors electronic state density in forbidden band, assuming fluctuations in impurities in form of homogeneous spheres with varying charges and radii

12 p2286 A70-27363

Chromium doped GaAs photoconductivity spectral distribution at various temperatures, determining temperature dependence of impurity maximum

12 p2286 A70-27366

Electrostatic charging hazard and flight evaluation of aviation fuels with static dissipative additive [SAE PAPER 700278]

12 p2289 A70-27439

Fe and Ni doped GaAs photoconductivity at various temperatures, determining activation energy level

12 p2287 A70-27489

Li and Cr additives effects on Al-Zn-Mg stress corrosion resistance, considering cracking, precipitation hardening and intercrystalline corrosion

13 p2433 A70-28844

Interband Faraday effect in doped semiconductors by quasi-classical approximation

13 p2469 A70-28878

Metal-Ge n-type semiconductor tunnel junctions, discussing Sb and As doped units and conductance and barrier heights air cleavage effects

14 p2626 A70-30482

B, In or Ga doped Si photosensitivity dependence on sample temperature, supply voltage and illumination intensity, determining optimal operating conditions

15 p2782 A70-31631

Ge and Si hemispherical emittance, showing doping and temperature effects

15 p2784 A70-32055

Ion implantation doping for MOS devices, discussing improved HF performance, integrated circuitry and threshold voltage selection

16 p2872 A70-33054

Thickners and low shrink additives for premix and sheet molding compounds (SMC)

16 p2936 A70-33363

Ti binary alloys beta phase continuous cooling transformation, investigating additives effects

17 p3118 A70-34408

Long chain molecule additive effect on drag reduction in turbulent flow of aqueous polymeric solutions

17 p3066 A70-34525

Shallow acceptor level in Au-doped n-type GaAs, using photoconductivity temperature dependence

17 p3143 A70-35702

Absorption coefficient of n-type indium arsenide single crystals with varying electron and doping concentrations, investigating spectral dependence

17 p3144 A70-35705

MIS structures with silicon nitride film deposited by RF glow discharge, observing doping increase in epitaxial substrate

17 p3055 A70-35873

Ti, Nb and Mo solubility during surface doping in Al melts containing various metals, discussing metal lattice structure effects

18 p3276 A70-36208

B and P ions bombardment techniques for Si doping of multilayered transistor structures

19 p3385 A70-37268

Dispersion hardened Co strength and plasticity temperature dependence, determining Ti and Nb carbides additives effects

19 p3450 A70-37350

Iron cyanide surface additives effect on photodamage to ZnO powder, using ESR method

19 p3372 A70-37543

Interactions between moving alkali-metal seeded dense plasma and metallic thermionically emitting electrode with surface properties influenced by seed particle absorption

20 p3681 A70-40007

Sn and tetraethylammonium ions effects on Zn electrodeposition on Zn single crystals in aqueous KOH, using scanning electron microscopy

21 p3772 A70-40726

Cycloaliphatic epoxy resins toughness improvement by modification with elastomers, maintaining high heat distortion temperature

21 p3842 A70-40733

Hybrid ion implanted diffused emitter n-p-n transistor two dimensional doping profiles, considering emitter oxide window edge shape effect

22 p3997 A70-42924

Addition effects on lattice and electrophysical properties of trititanate prepared by Ba, Pb, Ca and Ti precipitation

22 p4087 A70-43134

Rb and Cs ions implanted Si analyzed by Hall effect and sheet resistivity measurements and channeling techniques

22 p4087 A70-43143

Electrode and electrolyte additives effect on corrosion and polarization of alkaline zinc electrode

22 p3965 A70-43417

N-type GaAs samples doped with Ag, Se and Te respectively, measuring absorption coefficients spectral dependences at room temperature

23 p4229 A70-43928

Maraging steels hardening mechanisms, discussing dislocations density and distribution and Ni, Mo and Co additives effects

23 p4208 A70-44919

Cu and Ni doped n-p and p-n silicon solar cells, examining radiation damage and isochronal annealing properties

24 p4294 A70-45810

ADDRESSING

Digital computers structural and operational address format dependence on number of storage readouts expressible with aid of linear function

05 p0818 A70-17004

Modular plated-wire digital associative processor with content addressable memory, distributed arithmetic and I/O capability at each word

22 p3994 A70-43104

ADDUCTS

Isolation and structural characterization of adduct formed from propionaldehyde, sym-trinitrobenzene and triethylamine

02 p0251 A70-12275

ADENOSINE DIPHOSPHATE [ADP]

Indirect ADP deamination and reamination of corresponding deamino form of inosine diphosphate in rabbit brain tissue

01 p0018 A70-10506

Platelet aggregation in whole blood, basing measurement method on filtration pressure with added adenosine diphosphate /ADP/

07 p1210 A70-19591

Adenosine phosphates hydrolysis in solutions containing Ca ions and in synthetic seawater, investigating living systems energy transfer and prebiological evolution

11 p1986 A70-25702

ADP-ATP catalyzed exchange reaction in turtle bladder microsomes, using chromatographic measurements of conversion rates

17 p3034 A70-35900

ADENOSINE TRIPHOSPHATE [ATP]

Positive Na and K ion effects on mitochondrial respiratory control, O₂ uptake and adenosine triphosphate activity in rat liver

01 p0026 A70-11063

Adenosine phosphates hydrolysis in solutions containing Ca ions and in synthetic seawater, investigating living systems energy transfer and prebiological evolution

11 p1986 A70-25702

Molar growth yields from chemostat cultures of Hydrogenomonas eutropha on succinate and on fumarate, noting equivalence to ATP via oxidation

13 p2350 A70-29113

ADP-ATP catalyzed exchange reaction in turtle bladder microsomes, using chromatographic measurements of conversion rates

17 p3034 A70-35900

Intermediary complexes between Na-K ion stimulated ATPase /adenosine triphosphate/ and microsomal proteins of turtle bladder epithelial cells

18 p3225 A70-36233

ADENOSINES

NT ADENOSINE DIPHOSPHATE [ADP]

NT ADENOSINE TRIPHOSPHATE [ATP]

Dogs coronary vasodilator responses to hypoxia and induced tachycardia before and after lidoflazine and adenosine

02 p0230 A70-11702

ADHEROMETERS

U ADHESION TESTS

ADHESION

Sliding friction and adhesion mechanisms theories based on thermodynamics, noting frictional heat and adhesive joints

[ASME PAPER 69-LUB-4]

Plane two body contact creep problem in presence of adhesive forces reduced to solving coupled integral equations with complex valued kernels

04 p0766 A70-14421

Adhesive rocking and parallel translation contact for circular cylindrical punch indenting elastic half space solved using simultaneous equations

05 p0932 A70-16139

Fcc metals surface changes following adhesion using low energy electron diffraction /LEED/, relating intersurface metal transfer to applied adhesive force

07 p1305 A70-18920

Metallic adhesion produced by surfaces compression, discussing asperities plastic deformation and macrodeformation caused by contact area growth

07 p1292 A70-18939

Contact resistance measurements used in contaminant removal and metallic adhesion on iron surfaces

07 p1293 A70-18940

Metal surface adhesion to materials, examining structure and energy with allowance for environmental effect

08 p1503 A70-20878

Elastic contact between bodies in presence of friction or adhesion by reducing singular integral equations to Fredholm equation

08 p1585 A70-20958

Adhesive bonding of aircraft components, describing autoclave environmental control for curing adhesives, parts prefabricating, core fitting and quality control

09 p1690 A70-22022

Strain gages for static deformation measurement of fiberglass reinforced plastics at room and higher temperatures, discussing error sources and gage-specimen adhesive bonding

09 p1780 A70-23107

Thermal control pressure sensitive adhesive tapes for spacecraft applications, discussing properties degradation due to simulated terrestrial and space environments

11 p2067 A70-26366

Sliding rigid conical indenter friction experiments over work hardenable metal flats in high adhesion conditions, observing forces, stresses and deformation modes

13 p2421 A70-29548

Aircraft tires tread design for improved adhesion under wet runway conditions

14 p2532 A70-31336

Radioisotopic and complementary surface chemical analysis of coupling agent films on glass surfaces

16 p2917 A70-33375

Polymeric binders adhesion to glass fibers as function of type and chemical structure

16 p2938 A70-33379

Elastic contact between bodies in presence of friction or adhesion by reducing singular integral equations to Fredholm equation

20 p3719 A70-39381

Joint designs, attachment methods and load introduction in composite structures, suggesting adhesive bonding

20 p3730 A70-40041

Time dependent adhesion in ultrahigh vacuum of Apollo 11 lunar soil sample 10065-33, considering microchemical and microphysical properties

21 p3915 A70-41658

Intermaterial adhesion relation to association contact resistance-tension characteristics based on electric potential barrier model for Maxwell-Wagner effect

24 p4379 A70-45617

ADHESION TESTS

Cu, W and oxidized W adhesion to Ni surface, examining before and after adhesion contact with low energy electron diffraction

[ASLE PREPRINT 69-LC-13]

Metal fabrication shop environment contamination effect on bond strength of various adhesive system tested by humidity and salt spraying exposures

02 p0310 A70-12664

Solid lubricant films adhesion to metallic surfaces measured using pivot-twist technique

03 p0485 A70-13485

Bond quality and strength of high temperature adhesive films for titanium

[DGLR-69-56]

Silicate enamel coating formulas for application on titanium exhibiting adequate adhesion

05 p0872 A70-16599

Thermoplastic polymers adhesion to glass fibers determined by measuring force necessary to pull fiber from flat film of polymer

06 p1091 A70-17317

Adhesive joint failure, studying adhesive, cohesive and adherend ruptures by evaporative rate analysis

07 p1292 A70-18931

Metal adhesive joints peeling and stripping strength determinations, describing static and dynamic tests

08 p1503 A70-20884

Metal adhesive joints nondestructive tests involving acoustic and supersonic, X ray and heat flow characteristics methods

08 p1503 A70-20885

Metal adhesive joints behavior under prolonged static stresses, showing time dependence of tensile strength

08 p1504 A70-20887

Adhesive bonds strength in metal joints under stress cycling, examining effects of temperature and cycles frequency

08 p1504 A70-20888

Metal adhesive joints under cyclic stresses, studying stress distribution and fracture occurrence by high speed cameras

08 p1504 A70-20889

Metal adhesive joints permanence under various environmental conditions, considering surface properties effect

08 p1504 A70-20890

Bonds strength involving metallic, organic and ceramic adhesives at various temperatures, considering metallic additives effect

08 p1504 A70-20891

Adhesion characteristics in composites, investigating correlation between short beam and torsion shear tests in glass and graphite reinforced epoxy materials 08 p1531 A70-21892

Nondestructive test procedures development and implementation for bond strength of honeycomb sandwich and metal-metal adhesive bonded structures of F-5 and T-38 aircraft 09 p1692 A70-22798

Electrical conductance test for composite materials adhesive bond degradation by liquids 11 p2071 A70-26345

Adhesive bonds strength parameters, discussing substrate type, surface preparation, etc [ASME PAPER 70-DE-33] 16 p2939 A70-33504

Adhesive bond between steel wire and epoxy resin, investigating hydrostatic pressure effect on shear strength 17 p3123 A70-34623

Adhesive debonding in case-bonded solid propellant rocket motors, describing stress analysis and interfacial surface energy measurement 17 p3146 A70-35222

Graphite fiber reinforced polycarbonate composites interfacial adhesion improvement by controlled thermal treatment 20 p3652 A70-39168

Clean iron /011/ surfaces, determining sulfur, oxygen and hydrogen sulfide films effects on adhesion behavior 21 p3831 A70-40748

Strain rate sensitivity and stress waves effects on dynamic response and adhesion failures of rain erosion resistant coatings 22 p4059 A70-43102

Thermal IR nondestructive testing of adhesively bonded boron composite/Al honeycomb structures, discussing surface, cross section and instrumentation sensitivity effects 24 p4341 A70-45570

Holographic interferometry for NDT inspection of adhesive bonded honeycomb sandwich aerospace structures 24 p4338 A70-45754

ADHESIVES

NT GLUES

NT PASTES

Metal fabrication shop environment contamination effect on bond strength of various adhesive system tested by humidity and salt spraying exposures 02 p0310 A70-12664

Solder mechanical contact strength to CdS insulating crystal platelets tested in liquid N, noting Ag epoxy 02 p0319 A70-12738

Interactions between adhesive polymers and fillers, emphasizing reinforced plastics composites properties [ONERA-TP-733] 03 p0516 A70-13644

Forces at boundary surface in solid phase in solids and adhesive film interactions, considering boundary surface energy 08 p1503 A70-20879

Adhesives chemistry, discussing ionic, covalent and intermolecular bonds allowing for chemical and physical properties 08 p1455 A70-20880

Organic adhesives preparation and application to metal surface for bonding, examining time, pressure and temperature effects on curing 08 p1503 A70-20881

Adhesive metal bonding, considering methods for application of pressure and heat 08 p1503 A70-20882

Ceramic adhesives with glassy matrix for metal bonding, describing chemical reactions in interface, adhesive processing and application 08 p1526 A70-20883

Metal adhesive joints strength under tensile and torsional stresses, considering effects of dimensions, metal type and surface finishing 08 p1504 A70-20886

Shear stress distribution in metal adhesive joints, discussing methods for calculating 08 p1504 A70-20892

Metal adhesive joints strength and suitable dimensions determination, presenting parameter relations for design 08 p1584 A70-20893

Adhesive joints design, considering layer type, pipe connections and honeycomb structures for application in aircraft and automotive industries 08 p1585 A70-20894

Composite materials application to structural members, considering bond or adhesive shear strength 08 p1594 A70-21855

Adhesive bonding of aircraft components, describing autoclave environmental control for curing adhesives, parts prefitting, core fitting and quality control 09 p1690 A70-22022

Titanium and titanium alloys bonding, discussing pretreatment, adhesives and assessment of temperature, environment and nuclear radiations 09 p1704 A70-22750

Adhesive bond stress of aircraft structural joints between metal plates of variable cross section designed for shear 10 p1957 A70-24296

Monograph on adhesive materials covering selection criteria tables, mechanical properties, specifications, surface preparation and joint strength 10 p1908 A70-25225

Adhesive bonding for structural efficiency, lower weight, reduced production costs and improved appearance in general aviation industry [SAE PAPER 700221] 11 p2134 A70-25893

Bonding and sealing of fluid amplifiers with epoxy resin dry-film adhesive, noting low rejects rate 12 p2164 A70-27075

Polymer-metal adhesive joints rupture characteristics, considering polymer in solid or structurally fluid/elastic/ state during tests 12 p2244 A70-28341

Organic adhesives for bonding continuous surface and core-to-face joints, discussing strength, environmental resistance, producibility and reproducibility 13 p2419 A70-29118

Free radical coupling of silyl peroxides in reinforced plastics, laminates and adhesives 16 p2937 A70-33377

Adhesives selection based on bond performance requirements, considering joint design, stress distribution, temperature effects, etc [ASME PAPER 70-DE-69] 16 p2939 A70-33519

Energy balance criterion for continuum mechanics analysis of fracture threshold for blistered adhesive elastic layer between elastic material and rigid substrate 19 p3536 A70-37774

Adhesive bonded aircraft structures, discussing methods and requirements for establishment and control of manufacturing procedures 19 p3438 A70-38594

Book on adhesives for metals covering cleanliness, surface treatment, joint designs, sealants, etc 20 p3652 A70-39194

Synthetic resin adhesives for aircraft components fabrication 20 p3657 A70-40532

Epoxy and polyurethane adhesives stress-strain behavior in lap joints, examining bond thickness and cryogenic temperature effects 21 p3844 A70-42139

Polyurethane adhesives differential thermal analysis, rebound resilience and tensile properties at cryogenic temperatures 21 p3844 A70-42141

Polymers as cryogenic adhesives, evaluating role of chain structure below glass transition temperature 21 p3783 A70-42142

Cyanoacrylate and anarobic polymer single component adhesives performance 22 p4046 A70-43120

Nondestructive testing of adhesively bonded metal assemblies 22 p4047 A70-43523

Resilience and tensile properties of polyurethane adhesive at cryogenic temperatures measured by differential thermal analysis 23 p4209 A70-44275

Airframe skin panels adhesive bonding in wide-bodied jet transports, emphasizing fuselage fatigue and corrosion resistance [SAE PAPER 700863] 24 p4349 A70-45875

ADIABATIC CONDITIONS

Adiabatic invariance of action integral for motion in nonregular fields, explaining charged particles motion through magnetic shock front in interplanetary space 02 p0359 A70-12788

Adiabatic disturbances propagating as transverse waves in inviscid fluid rotating as Rankine vortex about cylindrical container axis, discussing harmonics 03 p0467 A70-13779

Viscous compressible heat conducting laminar perfect gas flow in slender axisymmetric channels with adiabatic walls, using equations of motion 03 p0471 A70-14383

Matrix elements of nonadiabatic perturbation emphasized in semiempirical theory for evaluating polyatomic molecules radiationless rate constants in terms of electronic-vibrational state 04 p0722 A70-14699

Adiabatic calorimeter for exothermic chemical reactions determining heats of polymerization, curing rate and thermal decomposition rates as temperature function for high energy propellants 04 p0688 A70-14711

Solar protons captured in earth dipole trap, discussing conditions for nonadiabatic escape 07 p1374 A70-20442

Chemiluminescence from NO adiabatically expanded against supersonic H atoms stream in inert carrier 10 p1831 A70-24566

Real gas adiabatic lapse rate applied to Venus atmosphere assumed to consist of pure carbon dioxide 11 p2107 A70-25646

Combustion gases compositions and adiabatic flame temperatures of potassium seeded propane-air mixtures calculated at various equivalence ratios and temperatures assuming thermal equilibrium 12 p2330 A70-27227

Electrostatic wave modes in inhomogeneous adiabatic plasma, discussing waves with gamma-fold ion and electron drift velocity 12 p2280 A70-27783

Air masses nonadiabatic ascent under elevated temperature inversion in atmosphere, assuming three layer model with linear profiles 12 p2265 A70-28335

Adiabatic index effect on shock waves reflection, emphasizing critical angle dependence on incident wave intensity 13 p2388 A70-29416

Boundary layer transition at high Mach numbers on adiabatic wall, showing effects of wind tunnel size, surface roughness and freestream disturbances [ALAA PAPER 70-586] 13 p2342 A70-29884

Adiabatic relation between initial plasma density perturbations and radiation temperature fluctuations during galaxies formation, discussing relic radiation fluctuations 14 p2632 A70-31286

Intergalactic medium lukewarm models, considering physical state, cosmic photon spectrum and isothermal and adiabatic expansion 14 p2651 A70-31291

Plasma containment in adiabatic magnetic traps, discussing particles, Coulomb collisions, instabilities, cyclotron resonance masers, Van Allen belts, etc 16 p2958 A70-33232

Adiabatic calorimeter for heat flux sensor contact calibration, describing operational principles and design 18 p3257 A70-36115

Conical shock wave-turbulent boundary layer interaction data obtained for adiabatic wall conditions at supersonic free stream Mach numbers, including suction effects 18 p3241 A70-36448

Umbral flash as magnetoacoustic wave, examining Ca II K line variations formation during adiabatic compression 21 p3885 A70-40958

Adiabatic-transition state theory of chemical reactions in dilute gases with separate binary collisions, considering Morokuma, Eu and Karplus results 21 p3773 A70-41396

Vibrationally adiabatic model for reaction dynamics of atomic and molecular hydrogen systems, using zero point energy path 21 p3773 A70-41397

Thermoelectricity theory concerning Navier-Stokes-Fourier type fluid universal motion characterization in absence of body forces and external heat supply 22 p4010 A70-42637

Particle motions in magnetic field, demonstrating existence of adiabatic region in particle phase space for Van Allen belt region 23 p4238 A70-44898

Molecular jet velocity distribution, investigating adiabatic focalization conditions 24 p4351 A70-45370

ADIABATIC EQUATIONS

Release adiabats and recentered Hugoniot curves determination by shock reverberation techniques for compressible nonlinear materials, presenting results for epoxy resin and porous tuff 01 p0198 A70-10106

Coupled Schroedinger equations for diatomic molecules internal motion solved using best adiabatic approximation to obtain energy correction to Born-Oppenheimer method 08 p1548 A70-21522

Adiabatic corrections to long range Born-Oppenheimer interatomic potentials from rotationally coupled Schroedinger equations 17 p3138 A70-35199

Adiabatic invariant of nonlinear periodic wave described by partial differential equations in weakly inhomogeneous medium 18 p3291 A70-36642

ADIABATIC FLOW

Nitrogen hypersonic transitional flow at adiabatic sharp flat plate leading edge, presenting density, flow-field shape and local rotational temperature for various regions 06 p0982 A70-18361

Geometric, cinematic and dynamic conditions of ideal fluid adiabatic nonstationary movement expressed by differential external system /s/ 09 p1659 A70-22254

Velocity distribution along cylindrical pipe in adiabatic flow with friction and known inlet parameters 09 p1607 A70-23616

Adiabatic flow coefficient in supersonic nozzle with choked flow conducted over throat Reynolds number range 11 p1976 A70-25999

Turbulent base flowfields in multinozzle configurations, considering adiabatic flow and determining base pressure distribution from reverse jet impingement [AIAA PAPER 69-570] 13 p2338 A70-28511
Comparative sets of higher order adiabatic motion equations for plasmas in electric and magnetic fields with slow variations 14 p2624 A70-31043

Reinforced shells of revolution carrying capacity upper limit subjected to internal adiabatic ideal gas flow 15 p2814 A70-31534

Aerodynamic pressures dependence on angle of incidence for profiles in adiabatic compressible flow 16 p2833 A70-33074

Adiabatic and chemically inactive hypersonic continuum flow around blunt body, analyzing flow field 17 p3010 A70-35036

Transient heat and mass transfer in adiabatic regenerator, solving mathematical model in terms of Green functions 17 p3197 A70-35542

Ideal relativistic fluids adiabatic flow, investigating heat exchange effects within framework of special relativity 18 p3347 A70-36554

ADIPOSE TISSUES

Brown fat thermoregulatory function and physiological control in mammals, discussing heat production and biochemical stimulation 02 p0230 A70-11683

Altitude changes effect on brown fat content and metabolism in deer mice, noting oxygen consumption and heat production limitation by hypoxia 02 p0242 A70-12865

Temperature and morphological changes of animals adipose tissue under various nutrition conditions, based on measurements by thermocouples implanted in fat deposits 04 p0640 A70-15514

Norepinephrine-induced depolarization effects on brown fat thermogenesis in cold-acclimated rats determined from in vivo measurement of intracellular potentials 05 p0799 A70-16020

ADJOINTS

Solutions existence for differential, integral and integrodifferential equations proved by variational imbedding of nonlocal linear Euler-Lagrange operator functioning as automatic adjoint calculator 05 p0881 A70-16060

Self adjoint boundary value problems with interior point boundary conditions using differential operator in Hilbert space 05 p0876 A70-16423

Adjointness in nonadjoint boundary value problems, extending Neuberger symmetry study to obtain expansion theorem for nonself adjoint p-point problems 10 p1910 A70-24606

ADJUSTING

Readjustment of aircraft navigation systems based on inertial platforms, discussing errors, corrections and damping stressing single platform 02 p0336 A70-12608

Roller machine adjustment parameters determination by analytical relations allowing for intermediary zone 07 p1292 A70-18837

Adjustment process dynamics in digital adaptive system with task of ensuring minimum quadratic criterion for parameters using gradient search technique 08 p1480 A70-21017

Liapunov direct method for synthesizing self adaptive model reference control system with simultaneously used passive/signal/ and active/parameter/ adjustment loops 08 p1480 A70-21018

Electrical axis adjustment of east-west antenna array of crossed radio telescope by statistical processing of discrete sources observations 08 p1473 A70-21067

Optimal adjusting of laser with instantaneously increasing Q without pumping and relaxation effects during pulse, using nonlinear differential equation 09 p1695 A70-22412

Readjustment algorithm for auto-oscillatory adaptive control system with variable structure, using harmonic linearization 11 p2022 A70-25343

Single beam grazing incidence spectrophotometer with concave diffraction grating for far UV region, emphasizing instrument adjustment 16 p2915 A70-34218

Adjustment program for aerial block triangulation with independent models, using planimetry-height iterations 18 p3248 A70-36779

Electric resistance adjustment of thick and thin film resistors on ceramic substrate, using laser for material evaporation 20 p3640 A70-39416

ADJUSTMENT
U ADJUSTING

ADMINISTRATION

U MANAGEMENT

ADMITTANCE

U ELECTRICAL IMPEDANCE

ADMIXTURES

Admixtures effect of chloroform, diethyl ether and acetone vapors on carbon dioxide laser output power 04 p0702 A70-15202

ADRENAL GLAND

Phospholipid metabolism intensity in brains of adrenalectomized and pseudo operated rats under hypoxia 01 p0012 A70-10054

Flight fatigue syndrome origin, therapy and prevention, noting cortical adrenal hormones tests 01 p0031 A70-10234

Adrenocortical responses of military recruits to subtropical climate, making serum and urinary 17-OHCS measurements on subjects fasting, inactive and at thermoneutrality 01 p0032 A70-10359

Adrenal function in patients with acute myocardial infarction correlated with prognosis 01 p0029 A70-11405

Blood pH effects on adrenomedullary response to hemorrhage, studying catecholamines release in anesthetized dogs 02 p0235 A70-11733

High altitude environmental effects on adrenal glands and hypothalamic neurosecretion in rats 04 p0629 A70-14568

Sinusoidal vertical vibration effect on adrenocortical function in guinea pigs 06 p0992 A70-17424

Glutethimide and aminoglutethimide reversible inhibitory effect on rat pituitary adrenal system in response to stress 07 p1203 A70-18902

Parathyroidectomy effects on high altitude adaptation and adrenal cortex activity in rats exposed to chronic hypoxia 08 p1442 A70-20719

Hypoxia biphasic effect on adrenal catecholamine content of guinea pigs and rats during short and prolonged periods 11 p1989 A70-26665

Circadian variation of pituitary-adrenal steroid levels, noting light role 14 p2540 A70-31430

Positive pressure breathing effects on cerebral blood pressure and catecholamine content of hypothalamus and adrenal glands in dogs 16 p2849 A70-33997

Sympathetic-adrenal system activity of trained organism during muscular work and emotional excitation 24 p4300 A70-45841

ADRENAL METABOLISM

Human sea-level natives physiological changes during high altitude physical exercise, considering carbon dioxide arterial pressure, plasma cortisol, adrenal function indexes, etc 08 p1453 A70-21873

Hormones excreted by adrenal cortex function in rhesus monkeys pathogenesis after irradiation by sublethal dose 09 p1620 A70-22822

Dietary intake and adrenal cortex effects on diurnal rhythm of hepatic tyrosine transaminase activity and adrenal corticosterone content in rats 09 p1621 A70-23437

Sympathoadrenals activity in pilots during supersonic flight, investigating urinary catecholamine output 15 p2690 A70-31891

Human cortisol intermittent secretion during early morning sleep and sleep-wake cycle, examining adrenal activity 24 p4305 A70-46410

ADRENALINE

U EPINEPHRINE

ADRENERGICS

Beta-adrenergic blockade effect on abnormal R-ST segment and T-wave changes, showing propranolol use in stress catecholamine and organic cardiovascular diagnosis 08 p1449 A70-21945

Neurogenically maintained blood pressure component, discussing autonomic nervous system activity in hypertension and normotension, sympathetic agents effectiveness in hypertensive treatment, etc 24 p4299 A70-45805

Alpha and beta reciprocal hunger regulating systems localized in rats hypothalamus areas by varying injection sites of alpha and beta adrenergic drugs 24 p4304 A70-46233

ADRENOCORTICOTROPIN [ACTH]

Pituitary hormone ACTH stimulatory effect on steroid hormone cortisol secretion by canine adrenal cortex, constructing seventh order state variable model 10 p1819 A70-24868

Ionizing radiation effects on endocrine system, studying ACTH metabolism in rats under X ray irradiation 19 p3372 A70-38723

Adrenocorticotrophic hormone effect on oxygen tension in rabbit kidney 24 p4301 A70-45845

Brain cortex protein metabolism alterations induced by anticipation stress and ACTH in rats 24 p4301 A70-45999

ADSORBENTS

Molecular sieve mixed gas adsorption and vacuum desorption of carbon dioxide in Apollo spacecraft cabin 01 p0040 A70-11450

Cyclic changes in concentration produced in fluid flowing through fixed bed of solid adsorbent, governing separation by beds waste propagation properties 04 p0780 A70-14712

Breakthrough curve shape prediction during adsorption from gas stream in fixed bed adsorbents for trace contaminant control applied to activated charcoal 04 p0786 A70-15317

ADSORPTION

NT CHEMISORPTION

Chemical and physical adsorption of gaseous oxygen contaminants to maintain purity for respiratory purposes, noting trichlorethylene and carbon tetrachloride 01 p0031 A70-10236

Interfacial equilibrium free surface energies between glass fibers, coupling agent and resin matrix, considering wetting, absorption and bonding 01 p0128 A70-10486

Adsorption properties of pulverized silica gel, quartz, C and graphite under electron bombardment from low temperature plasma, showing surface and physicochemical influence 03 p0516 A70-13468

Anions adsorption at platinum determined by ellipsometry, finding perchlorate and fluoride ions adsorption below detection limit 03 p0441 A70-14043

Equations and techniques to analyze transient heat and mass transfer characteristics of packed adsorption beds for spacecraft life support systems 04 p0786 A70-15316

Work function measurement for adsorption of diatomic I, Br and Cl on W crystal using electron beam retarding potential method 05 p0891 A70-15973

He and Ne adsorption and desorption on field ion microscope tip, determining minimum required field strengths of gas films at different temperatures 05 p0891 A70-15975

Al alloys crack growth effects due to gaseous environment and fatigue frequencies, suggesting role of gas adsorption 05 p0938 A70-16478

Pressure effects in predicting ablation velocities for gas-solid systems, assuming reactions and gaseous products reversible adsorption on solid surfaces 07 p1422 A70-19373

Carbon dioxide adsorption and desorption in Martian bright areas, discussing assumptions relative to temperature, pressure and dust adsorption 08 p1579 A70-21566

Lennard-Jones atom interaction potential, calculating adsorption energy of atom onto surface structure of fcc substrate, tabulating adsorption and surface diffusion activation energies 10 p1927 A70-24078

Nuclear converter with porous metal adsorption reservoir working with or without liquid cesium 10 p1915 A70-25039

Seeded dense plasma-electrode system behavior, studying effect of adsorption and emission from boundary surfaces 11 p2090 A70-25952

Oxygen adsorption on W(110)/ surface determined for coverage as function of exposure by Auger electron spectroscopy 12 p2180 A70-27253

Polycrystalline molybdenum desorption of adsorbed hydrogen, oxygen and water by electron impact 12 p2182 A70-27679

CO adsorption on smooth polycrystalline platinum and rhodium electrodes at various potentials 12 p2182 A70-27761

Outgassing pressure variation with time near perigee in satellite-borne pressure gages, using Langmuir model of surface adsorption 13 p2408 A70-29202

Gases adsorption on water snows in cometary nucleus, noting sublimation rate role as regulating mechanism in gas production 14 p2650 A70-31244

Adsorption influence on electrical and photoelectrical properties of CdSe thin films 17 p3143 A70-35674

Light gas atoms adsorption on solid surfaces, calculating wave function, energy, mobility, sticking coefficient, etc 18 p3225 A70-36186

Physisorption isotherms for nitrogen on stainless steel at various temperatures and very low pressures 18 p3226 A70-36322

- Electronegative adsorbate effect on work function of Ba-W system 18 p3298 A70-37111
- Clean Ru/0001/ and Rh/111/ surface properties by LEED and Auger electron spectroscopy, discussing gas adsorption 19 p3483 A70-37546
- Critique of paper on electron diffraction study of Ce adsorption on W surface, discussing electron work function changes and data discrepancies 19 p3473 A70-37548
- Surface adsorbed and absorbed radioactive Kr 85 gas for displaying surface microdefects in materials 20 p3638 A70-39950
- Hydrogen adsorption and coadsorption with oxygen on W single crystal surface measured by mass spectroscopy and low energy electron diffraction method 21 p3862 A70-41887
- Tungsten adatoms migration and binding energies on W surfaces, taking relaxation effects into account 21 p3862 A70-41888
- Room temperature oxygen adsorption on tungsten surfaces 22 p4087 A70-43235
- Oxygen and nitrogen adsorption on thin tantalum films, measuring pressure, electrical resistivity and temperature 24 p4363 A70-46219
- ADSORPTIVITY**
- Oxygen sticking coefficients and desorption kinetics on tungsten crystal by step desorption/ reflection technique, postulating formation and decomposition of surface oxide phases 10 p1832 A70-25147
- ADVECTION**
- Omega equation interpretation showing vertical motion related to advection of vorticity in upper troposphere and to warm advection in lower troposphere 05 p0838 A70-16154
- AE-A SATELLITE**
- U EXPLORER 17 SATELLITE
- AE-B SATELLITE**
- U EXPLORER 32 SATELLITE
- AEOLOTROPISM**
- Perturbation effects on elastic material deformation due to nonorthogonality of curves defining curvilinear aeolotropy, with application to circular cylindrical tube 05 p0929 A70-16065
- Disturbances in infinite aeolotropic inhomogeneous medium due to transient forces and twists on elastic cylindrical source surface 07 p1407 A70-19382
- Stress distribution in aeolotropic cylindrical shell due to shearing force varying linearly and quadratically with depth on inner boundary 14 p2658 A70-30994
- Displacements and stresses in freely vibrating aeolotropic deep spherical shells, including effects of shear deformation, rotary inertia and transverse normal strain 16 p2993 A70-34091
- AERIAL EXPLOSIONS**
- Chest, abdominal wall and diaphragm displacements of rabbits during partial and whole body exposure to shock waves produced by hexolot charges 02 p0231 A70-11704
- Hazards model for probabilistic prediction of casualties by exploding solid propellant rockets, deriving casualty expectation equation [AIAA PAPER 69-461] 06 p1154 A70-17169
- Similarity model for spherically symmetrical flow following explosion in rarefied atmosphere satisfying hydrodynamic energy conservation equation 07 p1260 A70-19981
- Strong point explosion in atmosphere with density dependent on height, obtaining numerical solutions for exact gas dynamic equations 09 p1658 A70-22112
- Computerized numerical integration of nonlinear partial differential equations describing blast wave in ionosphere with finite electric conductivity under uniform magnetic field 12 p2227 A70-28212
- AERIAL PHOTOGRAPHY**
- Photogeological mapping at medium to small scales, comparing satellite transparencies with aerial photographs 02 p0298 A70-12202
- Stereocomparator and electronic computer used to determine aerial photographs relative orientation elements, discussing measurement error elimination 03 p0482 A70-13108
- Stereoscopic device for photogrammetric points selection and marking on aerial photographs 03 p0482 A70-13109
- Photometry as aid for aerial photography, discussing resolution, mapping, etc 03 p0486 A70-13554
- Geodetic air mapping and surveying system, describing cartographic camera and system operation 03 p0489 A70-13655
- Royal Air Force air reconnaissance function, discussing cameras, films, processing and printing, photointerpretation, etc 03 p0495 A70-14144
- Multiband photographic system for automatic earth resources aerial sensing and lunar orbital mapping with manual override provisions [AAS PAPER 69-582] 04 p0687 A70-14657
- Automatic exposure control system for airborne cameras, providing iris and shutter control through taking lens for sudden light changes 05 p0844 A70-15771
- Aerial color IR photography for crop disease identification by tonal and geographic patterns, discussing cameras, films, filters and exposure procedures 05 p0837 A70-16144
- Remote sensing aerial and space surveys application to agriculture, forestry and water resources, discussing imaging systems and information acquisition and analysis techniques 05 p0838 A70-16164
- Earth resources remote sensing investigations from spacecraft and aircraft, noting Gemini and Apollo photography, hydrological surveys and radar techniques 05 p0849 A70-16450
- Geological interpretation of aerial photographs, discussing picture quality, scale, film material and applications 05 p0840 A70-16499
- Optimal scale selection for aerial surveys by analyzing aerial photography data 07 p1278 A70-18690
- Photogrammetric processing of aerial photographs using setting values of phototriangulation by stereocomparator and electronic computer 07 p1278 A70-18691
- Threefold reduction of aerial negatives facilitating microfilming without impairing accuracy and clearness of image details 07 p1278 A70-18692
- Remote sensors application to direct and indirect fish detection in fishery research, using aerial and Gemini photography 07 p1262 A70-18957
- Visual and quantitative image definition, evaluating microdetail clarity in panchromatic, IR, color and color IR aerial photographs 07 p1281 A70-19369
- Aircraft range-only radar trial applications in stereotopographic surveys of difficult-access areas, discussing organizational problems 07 p1282 A70-19632
- Minimum altitudes for illumination levels of aerial color photographic film calculated for different landscapes 07 p1283 A70-19633
- Visual perception of black-and-white photo in aerial photographic interpretation, examining processes in human brain 07 p1221 A70-19777
- Aerial photographs interpretation methodology based on soil sciences taking into consideration reference level of photointerpreter 07 p1284 A70-19778
- Mathematical models for photogrammetric disposition in aerial photography 07 p1284 A70-19780
- Geology from air covering aerial and space photography, nonvisible spectrum utilization, photograph transmission from Mars and moon, balloon flights, etc 07 p1272 A70-20225
- Aircraft mounting plate for 70-mm multispectral mapping quadricamera assembly to photograph wildland and agricultural resources 08 p1497 A70-21542
- Aerial color photography, considering lens types, exposure, filters, films, etc 08 p1498 A70-21543
- Abstracts with references to literature sources on oceanography from space and aircraft 09 p1665 A70-22014
- Photographic emulsions design for increased water depth penetration during aerial multispectral recording of light absorption and scattering in water masses 09 p1674 A70-22261
- Airborne real time IR imagery of thermal anomalies for geophysical exploration of water resources 09 p1674 A70-22262
- Automated crop surveys from integrating observations made at different times/ time dimensioning/ during growing season, noting earth resources satellites role 09 p1666 A70-22263
- Remote sensing systems for vegetation analysis, discussing machine-aided photointerpretation methods for data analysis [AIAA PAPER 70-308] 09 p1678 A70-22879
- Coastal areas remote sensing instrumentation and techniques, discussing data handling and analysis and ground verification of color and multispectral imagery [AIAA PAPER 70-299] 09 p1669 A70-22885
- EROS program earth imaging models characteristics, describing airborne and spaceborne film return and global and geosynchronous space data transmission [AIAA PAPER 70-294] 09 p1678 A70-22889
- Errors in aerial stereo photogrammetry, deriving equation to account for lens distortion and internal orientation 09 p1682 A70-23394
- Multipurpose multiband photographic system used for aerial remote sensing of earth resources 09 p1686 A70-23755
- Airborne camera resolution degradations /window losses/ introduced by multigazing wedge, irregularity and structural deformation 09 p1687 A70-23767
- Analytical aerial triangulation iterative solution mathematical convergence parameters tests, considering photogrammetric relations for standard conditions in variable size block 10 p1878 A70-24729
- MUSAT program and AN/USQ-28 SHIRAN controlled aerial photographs photogrammetric evaluation by U.S. Army Topographic Command, indicating bias in nadir positions 10 p1890 A70-24730
- Photogrammetric three dimensional control extension investigated by plotter and method of Independent Model Aerotriangulation 10 p1890 A70-24731
- Inter census population estimate by air photos, topographic maps and local and state census of population and housing 10 p1878 A70-24737
- Aerial photographic surveys of urban land use and natural resources, considering data analysis, display, computer compilation, updating and remote sensing 10 p1891 A70-24738
- Orthophoto Attachment for A8 autograph to produce black and white and color aerial photographs on negative film 10 p1891 A70-24739
- Oil pollution remote sensing by aircraft, utilizing 9-14 micron IR mapper, 19.35 GHz microwave radiometer, aerial cameras and multiband video system 10 p1878 A70-24740
- Aerial photography applications to timber management programs of forest industries 10 p1879 A70-24746
- Coastal erosion survey by aerial photography, measuring change in beach locations over period of time lapse by corresponding reference points on photograph 10 p1879 A70-24748
- Wastes dispersion discharged into sea analyzed by aerial photography, measuring diffusion 10 p1879 A70-24749
- Aerial photography analysis of drainage basin discharge properties, discussing surface runoff, subsurface flow and underground water movement 10 p1879 A70-24750
- Color and color IR aerial photography, discussing effects of solar spectrum, films, filters, etc, in connection with terrain analysis 10 p1880 A70-24751
- Radar flight configuration parameters effect on visual stereo model, expressing equivalent camera locations in terms of radar beams depression angles 10 p1841 A70-24752
- Forest inventory data collection by 70 mm photography, creating correction surface over model area of large scale pair 10 p1880 A70-24754
- Polluted air mass concentration determined by photogrammetry, producing topographic type map with respect to vertical and oblique aerial photographs 10 p1880 A70-24755
- Aerial super wide angle photography for mapping, discussing cost reduction, accuracy requirements and photographic techniques 10 p1891 A70-24756
- Slope failure erosional and mass wastage forms identification, characteristics and distribution based on large scale aerial photography depicted by remote sensor returns 12 p2217 A70-26913
- Aerial oceanographic photographic image enhancement by including blue spectral region, presenting Apollo 9 space photographs 12 p2217 A70-26917
- Aerial IR film optical density related to preharvest crop yield indicators in micro experiments with remote sensors 12 p2217 A70-26918
- Plant leaves discrimination by multispectral reflectance indicated in transmittance measurements via remote sensing from aircraft and spacecraft 12 p2218 A70-26920
- Multispectral color aerial photography, describing instrumentation, oceanographic and agricultural applications, atmospheric effects on images, etc 12 p2220 A70-26937

Photography for geological interpretation, comparing color, color IR, and black-and-white photographs from spacecraft and aircraft

12 p2221 A70-26956

Airborne geological mapping by IR emission spectroscopy, describing instrumentation, materials discrimination capability, data processing, etc

12 p2230 A70-26957

Landscape structure interpreting from aerial photos taken vertically from overflying aircraft

12 p2231 A70-27237

Photoelectric receiver and light beam alignment in gas laser aerial photography, considering directrix rectilinearity verification

12 p2247 A70-27476

Aerial reconnaissance of soils, rocks, vegetation and streams, comparing color, IR color, and black-and-white photography

12 p2236 A70-27873

Optimum image scale and longitudinal overlap in continuous orthophoto map production regarding sheet dimensions, instrumental ranges, flight path tolerances and ground relief

13 p2407 A70-29165

Spatial filters for ratio W/H measurement in aerial mapping

14 p2581 A70-30144

Air photographs or imagery linear features, assessing sensors performance and developing interpretation criteria in photogeological research

14 p2573 A70-30641

Airphoto interpretation, discussing descriptive, digital and photographic methods of representing recognition process results

14 p2585 A70-30642

Census analysis and population data acquisition using aerial photography

14 p2576 A70-30978

Soil characteristics determination from black and white, color and IR aerial photographs

14 p2577 A70-30980

Mixed hardwoods and pine area forest cover types identification by aerial photography

14 p2577 A70-30981

Reflectance of single leaves and field plots of cotton, determining Cycocel treatment effects on aerial IR photography

14 p2577 A70-31233

Remote sensors applied to classification of aerial data concerning housing quality at different scales, using variables observation

14 p2577 A70-31234

Auxiliary minus-visual filters in high altitude IR aerial color photography, suggesting tests for film sensitometric properties

14 p2588 A70-31235

Aerospectrometric camera facilitating spectral brightness coefficients determination for object identification

16 p2908 A70-33227

Optical filtering applied to aerial photointerpretation of oceanographic, archeologic and town planning data

17 p3081 A70-34620

False color aerial photography with IR film for distinguishing vegetation types and assessing plant vigor based on leaf reflectance

17 p3078 A70-35613

Large scale aerial color photography over spruce fir stands during 10 year period for assessing damage caused by budworm epidemic

17 p3078 A70-35614

Remote sensing experiment demonstrating utility of multispectral color aerial photography for detection of differences among vegetative species

17 p3095 A70-35615

Remote multispectral sensing of environmental and vegetative gradients in Yellowstone National Park by intercomparison of thermal IR and visible band imagery

17 p3079 A70-35617

Shallow water bottom biota, sediments and morphology determination by aerial and satellite photography

17 p3079 A70-35620

Aerial IR surveys of surface temperature patterns of Hudson Bay during ice free seasons

17 p3079 A70-35621

Optimum developer for aerial photofilms processing, relating light sensitivity and information capacity

18 p3258 A70-36283

Computer programs for photogrammetric aerial triangulation with independent models

18 p3248 A70-36778

Adjustment program for aerial block triangulation with independent models, using planimetry-height iterations

18 p3248 A70-36779

Instrumental measurement of projection center coordinates for aerial triangulation with independent models

18 p3248 A70-36780

Soviet book on aerial photo plotting of aerogeophysical routes and anomalies covering techniques, equipment, low altitude surveys, etc

19 p3410 A70-37408

Meteor spectro-sensitometric properties of panchromatic plates and films for aerial photos, investigating parametric conditions effect on image quality

19 p3422 A70-37653

Geological and cartographical data acquisition and processing, considering aircraft and satellite-borne photography of earth surface

20 p3616 A70-39061

Aerial cameras for topographic mapping, emphasizing geometrical image accuracy, optical picture quality and shutter performance

21 p3826 A70-41268

Natural and cultural landscape pattern classification in aerial photointerpretation using land-system concept

21 p3826 A70-41401

Soil science and climatology in Central Europe archeological site location by aerial photography

21 p3826 A70-41402

Internal and integral photointerpretation in aerial photography, discussing landscape information reliability increase by interdisciplinary method

21 p3826 A70-41403

EROS program earth imaging models characteristics, describing airborne and spaceborne film return and global and geosynchronous space data transmission

[AIAA PAPER 70-294]

21 p3829 A70-41871

Spatial aerotriangulation by analytical method based on independent models matched with geodesic grid

22 p4013 A70-42597

Aerial terrain analysis by color and color IR photography, analyzing physical factors affecting final image

22 p4018 A70-42963

Horizontal passpoint error in block analytic aerotriangulations with dense perimeter ground control

22 p4031 A70-42964

Optimal timing for aerial photographic mapping of landscape types including tundra, forest, steppe, meadow, desert and mountain areas

24 p4328 A70-45196

Earth curvature effects on position of terrain points on planar aerial photographs for various survey altitudes

24 p4333 A70-45197

Internal and external orientation elements of aerial cameras from star photographs on clear dark sky

24 p4333 A70-45198

Optical properties of terrain for optimal time charting of aerial mapping, considering seasonal variations and atmospheric transmittance

24 p4333 A70-45199

Vibration transfer coefficient of aerial camera-photographic assembly system for shock absorption during surveys

24 p4333 A70-45200

Flood plain boundaries delineation by panchromatic and color airphoto interpretation

24 p4329 A70-45362

Aerial survey cameras exposure time automatic control circuits for high quality photographs with constant integral density

24 p4334 A70-45497

Field control method for aerial photograph planar tying-in, applying to cartographic reference point coordinate determination in triangulation

24 p4334 A70-45499

AERIAL RECONNAISSANCE

Aircraft multispectral IR scanning systems for earth resources remote sensing, discussing capabilities

03 p0491 A70-13670

Royal Air Force air reconnaissance function, discussing cameras, films, processing and printing, photointerpretation, etc

03 p0495 A70-14144

Aerial remote sensing package for Earth Resources Program

09 p1687 A70-23761

Photointerpretation applications to kaolin deposit detection, railway tunnel collapse analysis and highway drainage

10 p1873 A70-24075

AERIAL RUDDERS

Rudder control of aircraft nullifying yawing and sideslip angles, analyzing rolling response to proportional control by ailerons

13 p2348 A70-29450

AEROBEE ROCKET VEHICLE

Auroral pulsation observed by Aerobee rocket instruments and ground multichannel photometer indicating primarily temporal fluctuation

09 p1671 A70-23497

Gyroless attitude control system for pointing Aerobee sounding rocket payload at sun using solar sensors

13 p2501 A70-28422

AEROBES

Continuous *Chlorella* production as function of total illumination in high intensity light system incorporating aerobic fermenter for heterotrophic cells

04 p0645 A70-15454

Aerobic metabolism of heart muscle cells and oxygen utilization of coronary artery blood

10 p01821 A70-25081

AEROBIOLOGY

Airborne bacteria and fungi in atmosphere of Tekute I underwater habitat

15 p2681 A70-31880

AERODONTALGIA

U TOOTH DISEASES

AERODYNAMIC AXIS

U AERODYNAMIC BALANCE

AERODYNAMIC BALANCE

Swept wings aerodynamic center and span load distributions with respect to quarter-chord line

04 p0156 A70-15393

Air floated skin friction balance adaptable for cylindrical and plane surfaces

06 p1076 A70-17625

Ballistic reentry vehicle roll related to trim angles caused by inertia asymmetries

[AIAA PAPER 70-204]

L-1011 onboard system for gross weight and center of gravity determination, describing transducers placement, computer design and display panel

[SAWE PAPER 837]

Concorde loadability, with comparison of flight balance situation for supersonic and subsonic aircraft, describing fuel system

[SAWE PAPER 835]

Fighter aircraft configuration design balancing, comparing weight penalties

[SAWE PAPER 840]

Trim changes definition, discussing exact meaning

24 p4289 A70-45436

AERODYNAMIC BRAKES

NT BALLUTES

NT DRAG CHUTES

NT TRAILING-EDGE FLAPS

NT WING FLAPS

Parachute design for decelerating upper atmosphere rocket probes at high altitudes, using high drag coefficients in Stokes flow regime

[AIAA PAPER 68-949]

Tail screens and spoiler rings aerodynamic braking effect in hypersonic range, discussing separated boundary layer periodic unsteady flow

06 p0965 A70-17247

Mars lander atmospheric entry digital simulation for deceleration system design, discussing ballistic coefficient, aeroshell diameter, parachute size and deployment altitude, etc

08 p1582 A70-20932

Reentry vehicle recovery deployment initiation, comparing performances of conical wake drogue and body attached spoilers hypersonic deceleration devices

[AIAA PAPER 70-1207]

Ballistic trajectory, packageability, deployment and flight stability of attached ram air inflatable decelerator for high speed/low altitude store delivery

[AIAA PAPER 70-1199]

Basket weave fabrics for gliding descent decelerators with polyurethane and nylon coatings for tearing strength and pressure packing

[AIAA PAPER 70-1180]

Decelerator fabric elastic constants for structural analyses using generalized Hooke's law

[AIAA PAPER 70-1179]

Drag prediction for Ballute and parachute trailing decelerators at supersonic speed and zero angle of attack, using flow field computations

[AIAA PAPER 70-1177]

Nonuniform free stream supersonic flow past aerodynamic decelerators, calculating inviscid flow fields by method of characteristics

[AIAA PAPER 70-1176]

Hypersonic aerodynamic deceleration devices for axisymmetrical bodies with cylindrical main sections and various front sections, using gun tunnel techniques

[AIAA PAPER 70-1174]

Snatch force during lines-first deployment of aerodynamic decelerator, including effects of canopy skirt acceleration and suspension wave propagation characteristics

[AIAA PAPER 70-1171]

Attached Inflatable Decelerator for planetary atmospheric entry, discussing mission applications and wind tunnel models performance

[AIAA PAPER 70-1163]

Aerodynamic braking for returning high speed recoverable space tug to low earth orbit

23 p4259 A70-44611

AERODYNAMIC BUZZ

U FLUTTER

AERODYNAMIC CENTER

U AERODYNAMIC BALANCE

AERODYNAMIC CHARACTERISTICS

NT AERODYNAMIC BALANCE

NT AERODYNAMIC DRAG

NT AERODYNAMIC STABILITY

NT INTERFERENCE LIFT

NT JET LIFT

NT LIFT

NT ROTOR LIFT

NT STATIC AERODYNAMIC CHARAC-
TERISTICS
NT SUPERSONIC DRAG
Supersonic flow around thin warped delta wing, taking into account current separation at subsonic leading edges for pressure distribution and aerodynamic characteristics
01 p0002 A70-10546
Linearized potential theory application in aerodynamic design and analysis of supersonic aircraft emphasizing far field viewpoint
[AIAA PAPER 69-1132] 01 p0002 A70-10608
Unmixed gases diffusion burning calculations, discussing turbulent flame burning aerodynamics in jet flows
01 p0217 A70-11007
Aerodynamic performance of cascade of porous gas turbine blades with cooling air effusion compared with solid noneffusing blades
02 p0355 A70-12311
Automatic flight control systems with aerodynamic characteristic and control parameters deviation from nominal values, discussing mathematical model describing aerodynamic characteristics behavior
02 p0381 A70-12408
Circumferential contour shape influence on three dimensional flow pattern of fan shaped annular turbine stages
03 p0407 A70-13417
Air cooling with radial and jet blowing on gas turbine stage, discussing influence on aerodynamic characteristics
03 p0551 A70-13486
Ground proximity effect on rectangular wing, studying lift and pitching coefficients dependence on angle of attack
03 p0407 A70-13493
Axisymmetric incompressible fluid flow aerodynamic properties in flat vortex chamber, studying core and boundary layer interactions and velocity fields
03 p0551 A70-13731
Flexible flight vehicles longitudinal stability with tandem lifting surfaces, studying aerodynamic time delay effects by root locus technique
03 p0408 A70-13802
Subsonic lifting surface theory including leading edge, discussing singularities in solution of integral equation for determination of aerodynamic properties
[AIAA PAPER 69-37] 04 p0619 A70-15387
Reusable lifting entry vehicle flight tests, investigating handling qualities and subsonic-transonic aerodynamics of M2-F2/M2-F3/, HL-10 and X-24A
[SAE PAPER 690662] 05 p0792 A70-15840
Aerodynamic characteristics, stability and controllability of swept wing and delta wing supersonic aircraft at subsonic velocities
05 p0796 A70-16966
Slender wing with blunted leading edge to reduce thermal stresses at supersonic speed studied for aerodynamic characteristics in hypersonic flow
05 p0791 A70-17001
Aerodynamic flight characteristics of lifting reentry bodies in subsonic to hypersonic range in wind tunnel tests
06 p1154 A70-17249
Upper surface suction effect on thin plate aerodynamic characteristics, considering relations for lift and pitching moment coefficients
06 p0968 A70-17851
Ram wing vehicles aerodynamics application to high speed ground transportation, studying effect on passenger ride quality
[AIAA PAPER 70-142] 06 p0973 A70-18145
Slender body theory for steady state aerodynamic characteristics of high speed ground vehicles with arbitrary cross sections, discussing side wind
[AIAA PAPER 70-139] 06 p0973 A70-18155
Retrorocket effects on aerodynamic stability and drag of conical aeroshell planetary entry vehicles, discussing supersonic wind tunnel tests and jet shock interaction
[AIAA PAPER 70-219] 06 p0974 A70-18166
Dynamic characteristics of systems consisting of train and air in tunnel using one dimensional incompressible fluid description
[AIAA PAPER 70-141] 06 p1042 A70-18216
Turbine blade tip clearance effect on aerodynamic characteristics in nonuniform flow
07 p1187 A70-18980
Wind tunnel tests for aerodynamic and thermal environment of hypersonic glider VERAS (Vehicle for Experimentation and Research in Aerothermodynamics and Structures/
[DGLR-69-042] 07 p1187 A70-18981
Reusable lifting reentry bodies subsonic and hypersonic aerodynamic characteristics, considering viscosity effects
[DGLR-69-038] 07 p1392 A70-18984
Supersonic aircraft aerodynamic properties and control systems performance, considering piloting of delta wing fighters
07 p1194 A70-19640

Aerodynamic characteristics of rotating transverse cylinder in subsonic normal flow from analysis of cylinder vortex system, discussing friction drag coefficient
08 p1431 A70-20720
Flow turbulence in wind tunnel model tests, observing generation methods effect on aerodynamic flow characteristics distribution
08 p1483 A70-21074
Aerodynamic characteristics of nonconvex bodies in free molecular flow of monoatomic gas
08 p1547 A70-21081
Aerodynamic characteristics of cylinder with wings in free molecular hypersonic flow of monoatomic gas at various angles of attack and slip
08 p1432 A70-21083
Aerodynamic characteristics of bodies in rarefied gases calculated using surface momentum flow dependence on local angle of attack
08 p1432 A70-21091
Airfoil cascade flow deflection angle using linearized jet flap theory
08 p1433 A70-21323
Aerodynamic characteristics of plane straight walled diffusers initial and stabilized flow segments, assuming incompressible fluid and turbulent boundary layer
09 p1659 A70-22430
Numerical solutions of variational problems concerning symmetrical wings with minimum drag and optimal aerodynamic efficiency in hypersonic flow
09 p1603 A70-22433
Aerodynamic characteristics of cooled blunt spherical bodies in low density hypersonic gas flow, discussing heat flux representation for different body surface temperatures
09 p1604 A70-22447
Hypersonic wind tunnel for erosion test of multiple particle impacts, considering dust on cork, carborazole and silicone rubber
[AIAA PAPER 69-341] 09 p1656 A70-23240
Air compressibility effects on aerodynamic characteristics of slender rectangular wings moving at subsonic speed near earth surface approximated by lifting surface theory
10 p1801 A70-24276
Molecular reflection effects on aerodynamic characteristics of rarefied gas flow past plate
11 p1973 A70-25386
Circular cascade design from rectangular cascade flow data using conformal transformation, considering aerodynamic properties
11 p1974 A70-25786
Ballistic range tests to study ablation effects on aerodynamic characteristics of ablating and nonablating slender cones
[AIAA PAPER 69-179] 11 p2148 A70-25976
Proton 2 satellite orientation and motion about center of mass determined from telemetric data analysis under aerodynamic moment
11 p2128 A70-26783
Satellite aerodynamic characteristics, considering orbital position and attitude of cylindrical body and separate plate
11 p2128 A70-26795
Adaptive flight control systems utilization to compensate for variations in aerospace vehicle rigid body dynamics, noting control system performance requirements
[AIAA PAPER 68-970] 12 p2204 A70-28076
Rotorcraft design and aerodynamics, discussing structural vibrations and all-weather operation
13 p2344 A70-28545
Soviet book on aerodynamics of Tu 134 aircraft, covering 30 turbojet engines, flight characteristics, etc
13 p2344 A70-28875
Finned configurations with nonlinear aerodynamic properties, obtaining solutions for angular motion at and near resonance
[AIAA PAPER 70-535] 13 p2506 A70-29026
Aerodynamic characteristics of supercavitating airfoil, investigating effect of free surface of unsteady fluid flow with stream separation, solving boundary value problem
13 p2391 A70-29650
Missile aerodynamic characteristics investigation in subsonic low turbulence wind tunnel with three degrees of freedom angular motions
[AIAA PAPER 70-578] 13 p2342 A70-29891
Low aspect ratio wing aerodynamic characteristics in shear flow, noting forces dependence on flow velocity gradients
14 p2529 A70-31274
Aerodynamic characteristics of wing with tip clearance within uniform flow, investigating main stream flow pattern effect
14 p2529 A70-31331
Deformable and rigid wings aerodynamic characteristics with subsonic leading and trailing edges, calculating action of gust
15 p2671 A70-31486
Surface temperature color contour maps of objects undergoing aerodynamic testing, utilizing electro-optical and computer techniques
16 p2905 A70-33169

Two dimensional film cooled turbine blade aerodynamics, investigating massive blowing effect through discrete holes in single blade test facility
[AIAA PAPER 70-713] 16 p2834 A70-33537
Aerodynamic performance of axisymmetric body traveling at transonic Mach numbers for predicting installed nozzle flow fields and efficiency
[AIAA PAPER 70-700] 16 p2835 A70-33562
Space shuttle aerodynamic studies including staging, launching, entry and booster cruise
16 p2981 A70-33702
Hypersonic glider VERAS aerodynamic and thermal environments, noting wind tunnel tests by thermosensitive paint method
16 p2837 A70-33765
Longshot free piston gun tunnel for high Reynolds number hypersonic flow tests
16 p2889 A70-33855
Transpiration and film cooling effects on aerodynamic characteristics of slender cone in hypersonic flow tested in hypervelocity wind tunnel using mass injection
16 p2837 A70-33857
Static aerodynamic characteristics of slender ablating reentry vehicle, discussing coupling between flow field and thermochemical analyses of heat shield materials response
[AIAA PAPER 70-826] 16 p3001 A70-33939
Aerodynamic and acoustic characteristics of subsonic and supersonic jets from convergent nozzles with room temperature air supply
17 p3005 A70-34460
Compressor erosion correlation with aerodynamic parameters in gas turbine engines
17 p3147 A70-34711
Aerodynamic and structural considerations in prop/rotor design for tilt-rotor aircraft, discussing blade twist effect on cruise efficiency and figure of merit
17 p3014 A70-34719
Forcing time functions prediction for structures under shock tube test, relating aerodynamic parameters to mechanics terminology
17 p3060 A70-35180
Aerodynamic characteristics of transonic and supersonic blunt vehicles, reviewing numerical methods
17 p3012 A70-35895
High temperature radial turbine design for small gas turbine engines, discussing aerodynamic, structure and thermal analyses
18 p3301 A70-36450
Longitudinal dynamics of VTOL aircraft during hover-forward flight transition, using multiple time scale analysis
[AIAA PAPER 69-130] 18 p3213 A70-36681
Transpiration cooling for high temperature gas turbines, investigating effects on aerodynamic and thermodynamic performance
[ASME PAPER 70-GT-56] 18 p3303 A70-36839
Plane and annular cascade facilities data application to aerodynamic design of axial flow compressors
[ASME PAPER 70-GT-106] 18 p3303 A70-36845
Lifting reentry vehicles control surface aerodynamics, considering boundary layer separation, shock interference, unsteady flow, etc
18 p3333 A70-36958
Soviet book on wing structures analytical design methods covering thin supersonic wings, mass distribution, aerodynamic characteristics, etc
18 p3344 A70-37025
Soviet book on helicopter aerodynamics covering main rotor operation, types classification and various flight characteristics
19 p3355 A70-37390
High angle of attack aerodynamic characteristics of swept wing navy aircraft designs improved via leading edge modifications
[AIAA PAPER 70-904] 19 p3355 A70-37392
Aerodynamic characteristics of thick sharp edged cropped delta and gothic wings, giving low lift-dependent drag
19 p3353 A70-38615
Hypersonic aerodynamic characteristics of sharp slender right circular cones at angles of attack, using Newtonian impact theory modified for flow separation effects
[AIAA PAPER 70-979] 20 p3558 A70-39550
Turbofan engine aerodynamic interactions, cryogenic space storable propellants, space station attitude control biowaste resistojel and long burning time solid propellants
20 p3688 A70-39667
Reentry bodies of revolution subsonic and supersonic aerodynamic characteristics
20 p3558 A70-39704
Merit factor for evaluation of aircraft types and missions, matching aircraft characteristics to mission load, range and speed
[SAWE PAPER 842] 20 p3562 A70-40360
Aerodynamic parameters of ionized Ar supersonic steady one dimensional nonviscous flow in thermodynamic equilibrium and subjected to Laplace accelerating forces
21 p3858 A70-41444

All-flexible parawings aerodynamic performance prediction based on slender wing theory and circular arc approximations for canopy shape
[AIAA PAPER 70-1188] 21 p3754 A70-41827

Transonic wind tunnel porous walls, investigating interference effects and aerodynamic characteristics
22 p3958 A70-42337

Aerodynamic characteristics of elliptical airfoils with jet circulation control for VTOL rotors including dual jets and cyclic results
[AIAA PAPER 69-741] 22 p3959 A70-42705

Horizontal flight speed effects on aerodynamic characteristics of air cushion vehicles with elliptical planform
22 p3959 A70-42801

Aircraft control surface aerodynamic characteristics, considering low aspect ratio wing elevons with variable sweep leading edge as longitudinal and lateral controls
[ICAS PAPER 70-26] 23 p4131 A70-44107

Stationary elliptic cylinders in subcritical flow, determining Strouhal number, pressure fluctuations and wake geometry as functions of angle of attack
[AIAA PAPER 69-745] 23 p4134 A70-44564

Wave rider aerodynamic properties at small Reynolds numbers, using non-Weiler wing for flow field, pressure and force measurements at rarefied flow conditions
[AVA-FB-7029] 23 p4135 A70-44668

Propeller blade aerodynamic characteristics at zero advance ratio, reducing singular integral equation to nonsingular form for computer solution
23 p4136 A70-44993

Space transportation system concept and operational objectives, discussing configurational aspects, aerodynamic complexity propulsion systems, payloads, performance and aerothermodynamic constraints, etc
[AIAA PAPER 70-1249] 24 p4418 A70-45965

AERODYNAMIC CHORDS
U AIRFOIL PROFILES
AERODYNAMIC COEFFICIENTS

Aerodynamics of conventional aircraft high lift devices, considering effect of leading edge geometry on lift coefficient at stall of plain and flapped airfoils
01 p0001 A70-10046

Minimum drag hypersonic delta wing, analyzing shape for given planform, lift, pitching moment and volume using correction for pressure coefficient
01 p0002 A70-10557

Aircraft lift, thrust and drag coefficients inaccuracies expressed as errors in measured flight performance characteristics
04 p0624 A70-15386

Free stream turbulence effect on drag coefficient of bluff sharp edged cylinders with small square section
05 p0789 A70-15923

Estimated aerodynamic coefficients of reentry body compared with coefficients derived from Antares and Berenice flights
06 p0966 A70-17248

Aircraft wing load calculations using aerodynamic influence coefficients based on linear subsonic or supersonic flow theory
06 p0967 A70-17255

One dimensional compressible flow analysis for near field aerodynamics of tube-vehicles, showing drag coefficient dependence
[AIAA PAPER 70-140] 06 p1038 A70-18077

Nonlinear aerodynamic moments for arbitrary motions of bodies of revolution in free flight
[AIAA PAPER 70-205] 06 p0971 A70-18102

Drag coefficients of sharp and blunt cones in rarefied supersonic flow for bluntness ratios and angles of attack
06 p0981 A70-18360

Dynamic simulation parameters for sphere drag coefficient data correlation in near free molecular flow
06 p0983 A70-18374

Free flight ballistic range method for measuring average drag coefficients for microscopic spherical iron particles in free molecular flow
06 p0983 A70-18378

Lifting reentry compact body aerodynamic coefficients, comparing calculated and experimental values for subsonic, supersonic and hypersonic flows
[DGLR-69-036] 07 p1392 A70-18982

Transverse free molecular flow past broken plate of infinite span, determining aerodynamic coefficients
08 p1432 A70-21082

Aerodynamic coefficients of nonconvex bodies in free molecular flow of monatomic gases based on delta representation of flow velocity distribution function
08 p1432 A70-21084

Rarefied plasma flow past bodies, considering determination of aerodynamic coefficients, charged states, electric and magnetic fields and plasma parameters
08 p1432 A70-21087

Aerodynamic drag coefficients and moments for axisymmetric bodies of revolution in rarefied plasma derived for limiting case of delta flux
08 p1432 A70-21088

Aerodynamic coefficients for axisymmetric bodies moving in rarefied plasma, calculating corrections for thermal velocities
08 p1432 A70-21089

Aerodynamic coefficients for blunt cones in rarefied gas calculated as functions of angle of attack using empirical formulas
08 p1432 A70-21092

Aerodynamic forces acting on circular plates in rarefied gases, calculating coefficients as functions of angle of attack
08 p1433 A70-21093

Variations after one revolution in semimajor axis, period and eccentricity computed for orbit using variable drag coefficient involving satellite and air thermal speeds
10 p1951 A70-24824

Shear flow near walls through cascade of untwisted blades, observing variation in lift coefficient across span
11 p1975 A70-25788

Aerodynamic coefficients from observed motion of body in flight, eliminating need for closed form solutions by employing numerical solutions to equations of motion
[AIAA PAPER 69-134] 12 p2156 A70-27824

Nondimensional aerodynamic forces and moments coefficients independent of air density and acting on satellites in low orbits
13 p2500 A70-28403

Atmospheric density variations and functional dependence of aerodynamic moment coefficient on incident angle from Saturn Workshop flight experiment
14 p2528 A70-30559

Hypersonic low density transitional flow over slender conical vehicle, calculating drag coefficient and density profiles
14 p2529 A70-31365

Real time analog simulation of helicopter rotor, calculating lift and drag coefficients along blade
15 p2672 A70-31775

Forced vortex impeller in axial flow fan without inlet vanes, presenting lift and drag coefficients of blade sections, loss of head, etc
19 p3352 A70-38222

Monoeenergetic nitrogen free molecule beam impingement on solid surface, calculating satellite drag coefficients from momentum transfer measurements
21 p3745 A70-41743

Surface pressure coefficient dependence on specific heat ratio for yawed conical lifting bodies in supersonic streams
21 p3747 A70-41877

Aerodynamic lift, drag and momentum coefficients in supersonic regime for rectangular and trapezoidal wings with spanwise variable profile
22 p3958 A70-42615

Nonlinear equations of motion approximate solution, determining ordnance weapons aerodynamic stability coefficients from angle of attack
[AIAA PAPER 69-135] 23 p4133 A70-44515

Missiles aerodynamic coefficients parameter sensitivity from test data, using least squares analysis
23 p4133 A70-44525

Bodies of revolution optimal configuration, considering minimum head drag coefficient and low heat transfer at hypersonic speeds, using modified Newtonian and hypersonic flow theories
23 p4136 A70-45021

German monograph on airfoil and wings aerodynamic coefficients calculations, showing advantages of analog computers based on singularity theory and distance functions
24 p4287 A70-45097

Kinematically unsteady aerodynamic coefficients consistent with stiffness and inertia properties of lifting surface in supersonic flow by finite element method
24 p4287 A70-45154

AERODYNAMIC CONFIGURATIONS

Man-computer graphic systems utilization for wing/body aerodynamic design and analysis concept for subsonic vehicles
[AIAA PAPER 69-1130] 01 p0002 A70-10610

Modified tailored delta configuration selection for U.S. SST, discussing power plant installation choice
[RAES PAPER 17] 03 p0411 A70-13544

Slender bodies optimum aerodynamic shape for supersonic velocities, discussing minimum wave drag and total drag two step analysis using calculus of variations
03 p0408 A70-13801

Two dimensional cascade tests of turbine blade airfoil plotted by Legendre hodograph method, discussing pressure distribution measurements
03 p0410 A70-14272

Trailing edge flow of slender aerodynamic shapes terminating in cusp or wedge, analyzing boundary layer reactions
04 p0613 A70-14457

Turbine blade designs considered for increasing load capacity covering tandem, jet-blade and base plain blade configurations and test results
[ASME PAPER 69-WA/GT-1] 04 p0734 A70-14894

Slender wings and fuselages resistance at zero lift in supersonic flow, using Karman and Moore linear theory
[DGLR-69-28] 04 p0616 A70-15154

Aerobell extendible nozzle rocket engine design and performance, cold flow and simulated hot flow test results
[AIAA PAPER 69-4] 06 p1129 A70-17168

Monatomic gas flow past moderate curvature body, obtaining approximate solutions to Boltzmann equation under form of matched asymptotic expansions
06 p0979 A70-18316

Aerodynamic characteristics of bodies in rarefied gases calculated using surface momentum flow dependence on local angle of attack
08 p1432 A70-21091

Aerodynamics role in large commercial aircraft design, noting mathematics models problem in high speed wing design
09 p1609 A70-22024

Drop sondes dynamic and aerodynamic design for lower Venus atmosphere based on solution for free fall of body in atmosphere with constant temperature gradient
09 p1766 A70-22935

Aerodynamic forces and moments effect of VTOL aircraft lift fan configurations on flow past wing
10 p1798 A70-24047

Shape of minimum drag slender body of revolution in Newtonian flow for given volume, length and maximum cross section determined by stochastic optimality principle
10 p1802 A70-24278

Second order conical flows around wing-fuselage system, deriving expressions for axial perturbation velocity for various attack geometries
10 p1804 A70-24972

Tapered resonance tubes matching supersonic air jet geometries considered for explosion hazards created by pneumatic system seals failure
11 p2035 A70-25981

Powered nacelles simulating exhaust flow for propulsion and airframe problems in subsonic flow
[AIAA PAPER 70-636] 16 p2888 A70-33594

Internal efficiency of turbine stages with long twist-varying blades
19 p3490 A70-37250

Digitally controlled milling machine for complex aerodynamic profiles and prismatic blades
22 p4046 A70-43117

Lifting reentry flight test vehicle aerodynamic configuration development, emphasizing lateral stability and maneuverability
[ICAS PAPER 70-02] 23 p4257 A70-44118

Axisymmetrical nozzle aerodynamic shape design for conical to axially uniform flow conversion, using method of characteristics
23 p4136 A70-44991

Bodies of revolution optimal configuration, considering minimum head drag coefficient and low heat transfer at hypersonic speeds, using modified Newtonian and hypersonic flow theories
23 p4136 A70-45021

AERODYNAMIC DRAG
NT SUPERSONIC DRAG

Canilevered and doubly supported structures calculated for critical aeroelastic divergence speed resulting from lift and drag
01 p0200 A70-10551

Leading edge suction analogy for predicting low speed lift and drag-due-to-lift characteristics of sharp edge delta and related wing planforms
[AIAA PAPER 69-1133] 01 p0002 A70-10607

Parachute inflation dispersion studied by plotting dimensionless products characterizing incompressible flow process
01 p0006 A70-10849

Ionosphere atmospheric densities from Explorer 32 drag data including semiannual variations
01 p0077 A70-11206

Monograph on aircraft aerodynamic nozzle asymmetry effects for pressure drag reduction in critical conditions
03 p0465 A70-13003

Aerodynamic roughness length estimation and site roughness increase due to micrometeorological equipment
03 p0483 A70-13166

Circular cylinder drag in hypersonic transverse flows between continuum and free molecular flow, measuring drag and pressure distribution
04 p0615 A70-15089

Supersonic missile drag reduction through wake heating assuming conical shaped missile tail and flow nonseparation
[DFVLR-SONDDR-36] 04 p0616 A70-15165

Atmospheric turbulence characteristics related to drag loads of tail spacecraft structures by boundary layer wind model
06 p1160 A70-17165

Lift and vortex drag due to flaps on thin sweptback tapered wings in inviscid incompressible flow, obtaining spanwise loadings
06 p0967 A70-17256

Induced drag dependence on Reynolds number for wings without camber and warping
06 p0967 A70-17257

Hyperboloids and paraboloids in flow of Reynolds number 22-55000 and Mach number 10, discussing viscous interactions effects on pressure, drag and skin friction
[AIAA PAPER 70-182] 06 p0976 A70-18240

Knudsen iteration for predicting cooled blunt body near free molecular drag in hypersonic stream, using BGK model for collisions
06 p0979 A70-18313

Sphere drag in near free supersonic molecular flow
06 p0983 A70-18377

First collision Monte Carlo method for calculating aerodynamic drag on hard sphere and Maxwell molecular models in near-free molecular flow
06 p0983 A70-18379

Level flight optimization in horizontal wind varying with altitude, using glider concept and induced drag correction
[ONERA-TP-700] 07 p1193 A70-19131

Meteoroids atmospheric drag and heat transfer coefficients, considering weak shielding by repelled and vaporized molecules
08 p1572 A70-20945

Drag on sharp cones in hypersonic flow, studying effects of intense transverse mass injection through porous walls
09 p1603 A70-22441

Optimal deformation and minimum wave drag for wings with supersonic leading and straight trailing edge, solving variational problem by Ritz method
09 p1604 A70-22444

Drag on cylinder in transverse rarefied gas flow varying from free molecular to almost continuum
09 p1604 A70-22448

Lift and drag characteristics of flexible parawings at subsonic speeds, predicting angle of attack for trailing edge flutter commencement
12 p2157 A70-28079

Gas temperature effects on aerodynamic drag of carbon particles burning during nonisothermal motion
13 p2520 A70-28582

Cylinders and airfoils drag tests and simulation in two dimensional sheared flow, considering shapes optimization
[AIAA PAPER 70-576] 13 p2342 A70-29893

Single and twin jet afterbody configuration models, describing drag and interference characteristics at subsonic speeds
14 p2528 A70-30862

Wing section pressure distributions, lift and drag in transonic mixed flow, considering prediction methods
14 p2529 A70-30866

Flight testing of high sensitivity Cactus accelerometer, measuring deceleration components due to sphere drag
15 p2735 A70-31813

Meteoroids atmospheric drag and heat transfer coefficients, considering weak shielding by repelled and vaporized molecules
15 p2806 A70-32757

Book on aerodynamics of bodies of revolution covering hypersonic flow parameters effects, method of characteristics, slender body drag, blunt bodies, rarefied gas aerodynamics, etc
16 p2834 A70-33271

Aerodynamic drag coefficients of micron size particle clouds in compressible transonic flow, using light extinction method
16 p2894 A70-33882

High speed ground tube vehicle transportation system aerodynamics, presenting drag coefficients and static wall pressure measurements
16 p2839 A70-34264

Base flow component of total drag for axisymmetric supersonic afterbody with single exhaust jet, considering turbulent mixing
17 p3011 A70-35656

Aft tail and canard configurations trim drag considerations for maneuvering aircraft
[AIAA PAPER 70-932] 17 p3021 A70-35842

Close-spaced nozzles twin jet configuration, achieving low nozzle and total afterbody drag
[AIAA PAPER 70-934] 17 p3149 A70-35844

One dimensional channel flow theory for ram wings, deriving lift and drag laws for comparison with wind tunnel and free flight tests results
[AIAA PAPER 70-971] 20 p3558 A70-39558

Streamers /drag devices/ tests at subsonic speeds, measuring drag dependence on size, weight, shape and velocity
20 p3559 A70-40282

Low drag supersonic compressors for aircraft engines, calculating start and cruise conditions of quasi-isentropic flow cascades
21 p3745 A70-41405

Dust content effect on hypersonic wind tunnel flow test results, noting drag force on slender and blunt nosed models
21 p3749 A70-42224

Drag estimation for circular cylinders at subcritical Reynolds numbers and subsonic speeds, using Kármán vortex street theory for wake
23 p4131 A70-43894

Low speed airfoil two dimensional testing in wind tunnel with slotted wall, examining lift, drag and pitching moments
[ICAS PAPER 70-08] 23 p4132 A70-44119

Strike fighter aircraft fuselage side air intakes, measuring external drag as function of design at subsonic and supersonic speeds
[ICAS PAPER 70-49] 23 p4133 A70-44146

Aerodynamic drag and local convective heat transfer on smooth plate for various flow velocities, determining effects of turbulator in boundary layer transition region
23 p4283 A70-44733

Thermal flux surface distribution lifting bodies, discussing aerodynamic efficiency dependence on drag and zero angle of attack Mach number
23 p4136 A70-45019

AERODYNAMIC FORCES

NT AERODYNAMIC DRAG

NT AERODYNAMIC LOADS

NT BLAST LOADS

NT GUST LOADS

NT HYPERSONIC FORCES

NT INTERFERENCE LIFT

NT JET LIFT

NT LIFT

NT ROTOR LIFT

NT SUPERSONIC DRAG

NT WING LOADING

Blade forces of helicopter rotor in forward flight calculated by unsteady lifting-line theory
01 p0004 A70-11366

Aerodynamic velocity field induced by plate in motion correlated with ideal gas flow at specific Reynolds number, discussing wake formation
03 p0410 A70-14270

Wind tunnel testing technique innovations, reducing time and cost for low drag aircraft configurations by simultaneous force and pressure model transonic testing
[SAE PAPER 690677] 05 p0825 A70-15868

Normal force component distribution and aerodynamic pressure position on rocket bodies at supersonic and hypersonic velocities
06 p0964 A70-17238

Matrix method for calculating aerodynamic loads, shearing forces, bending moments, torques, etc, in hinged main rotor helicopter blades during hover and vertical flight
06 p1167 A70-17914

Aerodynamic forces for boundary layer profiles of flexible plate under transient motion in shear flow using computer programs
[AIAA PAPER 70-76] 06 p0972 A70-18122

Stochastic Liapunov stability of satellite motion influenced by aerodynamic and gravity gradient torques, considering atmospheric density uncertainty
[AIAA PAPER 70-37] 06 p1159 A70-18185

Tangent plane method and polar coordinates for lifting surfaces, calculating normal velocity at field point on surface carrying doublet distribution for incompressible flow
[AIAA PAPER 70-78] 06 p0975 A70-18195

Lift and drag forces measured on metal surfaces inclined to Ar ion stream above and below earth-satellite speeds in free molecular flow
06 p1111 A70-18269

Aerodynamic forces and heat transfer on shielded flat plates in free molecular flow calculated by Monte Carlo technique
06 p0981 A70-18358

Atomic and molecular beams produced by nozzle beams aerodynamic acceleration, discussing condensation effects, internal energy, scattering cross sections, etc
07 p1341 A70-20102

Soviet book on motion of guided rockets in space covering aerodynamic and structural aspects, stabilized and disturbed rocket motion, etc
08 p1582 A70-20756

Aerodynamic forces acting on circular plates in rarefied gases, calculating coefficients as functions of angle of attack
08 p1433 A70-21093

Unsteady aerodynamic forces on helicopter rotors using pressure measurements and wind tunnel visualizations of smoke emission
[ONERA-TP-777] 08 p1434 A70-21847

Illusory visual signals experienced by pilots ascribed to aerodynamic forces interference with normal functional relationships between sensory systems
09 p1627 A70-23131

Mathematical model with straight wake airfoil to determine aerodynamic forces on oscillating rotor blades in hovering flight
09 p1605 A70-23222

Resultant of elementary aerodynamic pressures on profile with angular point of attachment
10 p1797 A70-23874

Aerodynamic forces and moments effect of VTOL aircraft lift fan configurations on flow past wing
10 p1798 A70-24047

Triangular conical wing with supersonic leading edges analyzed for aerodynamic forces in supersonic flow
10 p1798 A70-24121

Spanwise distribution of aerodynamic torsion on sailplane wings in vertical dive, discussing wing twist and lift effects
12 p2156 A70-27721

Nondimensional aerodynamic forces and moments coefficients independent of air density and acting on satellites in low orbits
13 p2500 A70-28403

Booster control system reducing maximal wind-induced bending torques, examining booster response to aerodynamic forces
13 p2500 A70-28413

Flapping wing unsteady periodic motion relationship to forces effect on wing profile and vortex street in wake, determining propeller thrust by potential theory
13 p2337 A70-28479

Stability and wind response determining spacecraft structure forces and bending moments
[AGARDOGRAPH-115] 13 p2504 A70-28754

Airframe-propulsion system integration for Mach 6 transport and Mach 12 research airplane, examining off-design operation effects and interaction of aerodynamic forces
[AIAA PAPER 70-542] 13 p2345 A70-29009

Propeller in axial motion through homogeneous turbulence, studying forces and moments by statistical analysis
[AIAA PAPER 70-549] 13 p2339 A70-29014

VTOL aircraft multiple and nonuniform jets aerodynamics, considering induced field and secondary flows
14 p2528 A70-30851

Unsteady aerodynamic forces on oscillating circular cylinder, using wind tunnel two dimensional dynamic model
14 p2529 A70-31050

Equilibrium configurations, considering aerodynamic forces for axisymmetric satellites attitude stability using infinitesimal analysis and Liapunov method
15 p2809 A70-31779

Aerodynamic pressures dependence on angle of incidence for profiles in adiabatic compressible flow
16 p2833 A70-33074

Aerodynamic forces exerted by compressible fluid on airfoil cascade in subsonic potential flow
16 p2833 A70-33075

Perturbation complex potential and aerodynamic forces determined for rectilinear profile motion under free surface, using linear theory
16 p2837 A70-33848

Forces on two dimensional oscillating airfoil in subsonic compressible wind tunnel flow, solving partial differential equation for pressure potential by integral transform technique
16 p2839 A70-34248

Parameter model of VTOL airplane in transition, considering aerodynamic forces and moments and digital simulation
17 p3015 A70-34724

Unsteady aerodynamics prediction of supersonic elastic aircraft, discussing aerodynamics influence coefficients /AIC/ method refinement
[AIAA PAPER 70-944] 20 p3558 A70-39583

Asymmetric rotating bodies mass properties measurement on Dynamic Balancing Machine, taking into account aerodynamic forces
[SAWE PAPER 818] 20 p3634 A70-40351

Parachute canopy surfaces transient aerodynamic pressures during unsteady processes, using piston theory
[AIAA PAPER 70-1175] 21 p3754 A70-41838

Aerodynamic forces on flexible launch vehicles and missiles in supersonic flight based on first order method, solving boundary value problem for surface velocities
21 p3746 A70-41853

Unsteady aerodynamic forces at stall flutter, applying vortex sheet theory to separated flow field around thin airfoil at high angle of attack
22 p3957 A70-42284

Harmonically oscillating wing linearized motion in subsonic flow, calculating generalized aerodynamic forces
22 p4105 A70-43118

Liquid droplet breakup by aerodynamic forces, obtaining solutions for fluid flow inside droplet and in coupled liquid-gaseous boundary layer
22 p4012 A70-43741

Glauert equations applied to trailing wire shape for steady state aerodynamic forces on aircraft and trailing antennas, discussing computer solutions
23 p4131 A70-43893

Pressure distribution, force and heat transfer measurements on varied-configurations of lifting reentry vehicles in hypersonic flow
[ICAS PAPER 70-03] 23 p4132 A70-44117

Wave-riders aerodynamics and heat transfer, investigating lift to drag ratios for supersonic and hypersonic vehicles

[ICAS PAPER 70-18] 23 p4276 A70-44129

Aerodynamic and gravitational torque effects on orbiting satellites attitude stability, applying Liapunov direct method in case of conservative aerodynamic torque

[ALAA PAPER 69-832] 23 p4258 A70-44559

Aerodynamic forces and torque on airfoil in potential jet from boundary asymptotes position, determining flow characteristics by electrical analogy

24 p4288 A70-45438

Turbine blades aerodynamic forces theoretical and experimental investigation, noting cascade series interaction induced pressure pulsations

24 p4288 A70-45504

Turbine blades deformation by centrifugal and aerodynamic forces, discussing theory for bending stress free blade design

24 p4288 A70-45505

AERODYNAMIC HEAT TRANSFER

NT HYPERSONIC HEAT TRANSFER

NT SUPERSONIC HEAT TRANSFER

Heat transfer in turbulent boundary layer of airflow injected on smooth plate from nozzle in subsonic stepwise heated wind tunnel

01 p0216 A70-11001

Heat transfer on supersonic sweptback wing for case of laminar boundary layer with vortex distribution

07 p1187 A70-18921

Meteoroids atmospheric drag and heat transfer coefficients, considering weak shielding by repelled and vaporized molecules

08 p1572 A70-20945

Surface pressure and heat transfer over blunt conical body in hypersonic flow with uniform mass addition of various gases

[ALAA PAPER 69-716] 13 p2523 A70-29977

Meteoroids atmospheric drag and heat transfer coefficients, considering weak shielding by repelled and vaporized molecules

15 p2806 A70-32757

Stagnation point heat transfer coefficient to elliptical model taking into account pressure, model blunting and diameter, Mach number, etc

20 p3737 A70-39699

Charring ablators transient heat transfer model, calculating surface temperature and recession and pyrolysis mass loss

[ALAA PAPER 70-1143] 20 p3738 A70-40280

AERODYNAMIC HEATING

NT SHOCK HEATING

Radiant heat transfer in hypersonic aerodynamic heating, discussing radiant flux and carbon dioxide concentration in reentry problems

01 p0219 A70-11625

Supersonic missile drag reduction through wake heating assuming conical shaped missile tail and flow nonseparation

[DFVLR-SONDDR-36] 04 p0616 A70-15165

Reentry body aerodynamic heating and thermal insulation system design, discussing analytical procedure taking into account complex geometrical configurations

04 p0616 A70-15186

Thermal stresses in transversely isotropic hollow circular cylinder, applying formulas derived to reentry vehicles aerodynamic heating

04 p0779 A70-15608

Dynamic stability loss on ablating vehicles ascribed to boundary layer transition effect from turbulent aft body heating

[ALAA PAPER 69-106] 06 p0961 A70-17166

Soviet book on guided ballistic missiles design and construction employing liquid and solid propellant engines with emphasis on aerodynamic heating

06 p1155 A70-17410

Aerodynamic heating of blunt-nosed reentry bodies noting effects of angles of attack

[DGLR-69-4401] 07 p1392 A70-18983

Aerodynamic heating of blunt bodies, investigating dependence of hypersonic limit distribution on Mach number

09 p1603 A70-22419

Large amplitude free vibration of rectangular plates subjected to aerodynamic heating with different boundaries and temperature distribution, deriving Duffing nonlinear differential equation

10 p1957 A70-24417

Large amplitude free vibration of heated circular plates, analyzing energy equations by successive approximation method and elliptic integrals

10 p1957 A70-24480

Compression process in turbulent boundary layer on control surface at hypersonic speeds, noting influence on surface effectiveness and heating

[ONERA-TP-814] 11 p1979 A70-25815

Off-centerline heating on lee surface of supersonic delta wing with separation and vortex initiation at leading edge

11 p1976 A70-25996

Staging along reentry trajectory in atmosphere, discussing parent body and separation point influence on aerodynamic loading and heating of ejected body

11 p2124 A70-26151

Reentry vehicles development, discussing systems analysis and design, vehicle aerodynamics, aerodynamic heating and shielding, and flight mechanics and control

13 p2506 A70-29055

Upper stratosphere-mesosphere monthly-mean charts from reentry heating and atmospheric model based on hydrodynamics

14 p2608 A70-30590

Heating and g forces on rockets and space vehicles in descent trajectories as function of reentry velocity, achieving control by attack angle variation

15 p2812 A70-32361

Scaling relations showing effects of ballistic coefficient, flight path angle and inverse atmospheric scale height on heating of ballistic entry bodies

17 p3012 A70-35667

Two-layer slab under aeroheating, solving bondline temperature graphically

20 p3737 A70-39693

Laminar heating in hypersonic vehicles interior corners, analyzing helium tunnel heat transfer data for various intersecting wedge corners

20 p3737 A70-39700

Aerodynamic heating prediction methods for delta body space shuttle orbiter, comparing with wind tunnel test data

21 p3744 A70-41016

Aerodynamic heating constraints on space shuttle design, discussing prediction uncertainties for boundary layer transition, laminar, turbulent heating, etc

21 p3744 A70-41017

Ablative heat transfer to nonstagnation surfaces of high speed rocket vehicle in continuum atmosphere, using finite difference theory

22 p4125 A70-43433

Lifting entry vehicles turbulent boundary layer aerodynamic heating, comparing heat transfer prediction methods

23 p4258 A70-44530

Thermal flux surface distribution lifting bodies, discussing aerodynamic efficiency dependence on drag and zero angle of attack Mach number

23 p4136 A70-45019

AERODYNAMIC LIFT

U LIFT

AERODYNAMIC LOADS

NT BLAST LOADS

NT GUST LOADS

NT WING LOADING

Aerodynamic load distribution due to wind action on elastic structures, calculating various ratios between wind and critical divergence velocity

02 p0385 A70-11913

Tangential jet, tandem, jet flap and vortex generator blade concepts investigated for turbine blade loading efficiency

[ASME PAPER 69-WA/GT-5] 04 p0734 A70-14890

Turbine blade designs considered for increasing load capacity covering tandem, jet-blade and base plain blade configurations and test results

[ASME PAPER 69-WA/GT-1] 04 p0734 A70-14894

Tektite size restricted by thermal stress limit on diameter and aerodynamic load limit on length

05 p0916 A70-16831

Electric propulsion system and initial gross weights estimation for manned Mars missions

05 p0924 A70-17093

Meteorites explosive fragmentation under aerodynamic loads simulated by steel balls shot into increasing-density target, discussing parameters

08 p1572 A70-20947

Vertical air motions rate from aerodynamic loads on aircraft and pitch angle and center of mass vertical velocity fluctuations

08 p1538 A70-21113

Supersonic jet force acting on target investigated for air and argon using dimensional analysis

10 p1804 A70-25122

Loading conditions measured during aerobatic maneuvers in flight test to determine structural design requirements for aerobatic-type aircraft

[SAE PAPER 700222] 11 p1980 A70-25894

Light aircraft lateral and longitudinal response to atmospheric turbulence, presenting equations and charts for design load calculations

[SAE PAPER 700239] 11 p1981 A70-25908

Staging along reentry trajectory in atmosphere, discussing parent body and separation point influence on aerodynamic loading and heating of ejected body

11 p2124 A70-26151

Aerodynamic loadings on planar wings in oscillatory subsonic flow determined by collocation for performing Gaussian quadrature integration of pressure and kernel functions

12 p2155 A70-27102

Nonlinear panel flutter for random excitation and linear/nonlinear aerodynamic loading, using Rayleigh-Ritz approximation to Hamilton variational principle

12 p2316 A70-27105

Wind load aerodynamics effects on launch vehicle flight control systems design

[AGARDOGRAPH-115] 13 p2504 A70-28753

Wind-launch vehicle interaction in flight, using equations of motion for aerodynamic loads

[AGARDOGRAPH-115] 13 p2504 A70-28756

Slender bodies surface pressure distribution under various aerodynamic loads, discussing cruciform wing, circular body-slender wing configuration, etc

13 p2341 A70-29749

Unsteady nonlinear aerodynamic loads measurements in wind tunnel, using linearized mathematical analog

[ALAA PAPER 70-573] 13 p2343 A70-29896

Aerodynamic and structural configuration effects on spacecraft inflight wind load calculations, showing Apollo interface lateral bending

14 p2653 A70-30585

Atmospheric wind profiles and boundary layer turbulence power spectra for calculation of wind loads on space vehicles during prelaunch and launch

14 p2653 A70-30600

Airframe critical part structural reliability on basis of ultimate static strength test data and extreme gust spectrum and maneuver loads

14 p2658 A70-30852

Meteorites explosive fragmentation under aerodynamic loads simulated by steel balls shot into increasing-density target, discussing parameters

15 p2806 A70-32759

Aerodynamic admittance of paraboloid dish aerial in scaled atmospheric turbulent boundary shear layer simulated in wind tunnel by vortex generators

16 p2878 A70-33766

Subsonic and supersonic aircraft dynamic loads under conditions of variable atmospheric density

17 p3013 A70-34685

Helicopter rotor blade differential pressure and structural load characteristics in transient and steady state maneuvers

17 p3016 A70-34739

Wind tunnel balance for measuring small aerodynamic loads on scale models, describing three component construction

17 p3062 A70-35490

Flight loads data extraction and analysis from damaged magnetic tapes after aircraft crash

17 p3094 A70-35518

Flight loads spectrum data for army CH-47A, UB-1B and CH-54A helicopters components compared with fatigue life spectra

18 p3210 A70-35955

Water ballast effect on glider loads, using concept of characteristic velocities

18 p3213 A70-36253

Structural reliability testing methods and loads prediction for rotary wing vehicle components, considering AH-56A compound helicopter

19 p3356 A70-38612

Concorde loadability, with comparison of flight balance situation for supersonic and subsonic aircraft, describing fuel system

[SAWE PAPER 835] 20 p3563 A70-40365

Supersonic jet force acting on target investigated for air and argon using dimensional analysis

20 p3560 A70-40515

Oscillating wing aerodynamic load boundary value problem reduction to sequence of steady lifting-surface problems

22 p3959 A70-42715

Parachute trajectory and opening load prediction based on inflation process and added mass, determining drag area as function of distance

[ALAA PAPER 70-1168] 23 p4137 A70-43993

Parachute opening load amplification due to suspension line elasticity, using two-body spring-mass model

23 p4142 A70-44531

Short-term creep and erosion resistance testing of Ti alloy in high speed air flows under aerodynamic vibrations

24 p4360 A70-45826

AERODYNAMIC MOMENTS

U STABILITY DERIVATIVES

AERODYNAMIC NOISE

Aerodynamic sound generation by subsonic jet engines noting jet thrust relation to emitted acoustic power

03 p0552 A70-13926

Fan rotors aerodynamic noise tonal annoyance reduction by blade unequal circumferential spacing, noting sound-pressure wave shape determination

[ASME PAPER 69-WA/FE-23] 04 p0614 A70-14776

Theoretical model of fan/compressor noise blade passing frequency generation and transmission, noting duct length and configuration in engine operation

04 p0734 A70-14886

Noise radiated from VTOL lifting fan in wing inlet under static inflow conditions, attributing discrete tones to spacing between rotor and stator blades

[ASME PAPER 69-WA/GT-6] 04 p0734 A70-14889

Rotating acoustic modes generated at blade passing frequencies in inlet duct of axial flow fan or compressor measured

04 p0691 A70-15079

Aerodynamic noise - Conference, University of Toronto, May 1968
05 p0795 A70-16776
Engineering methods developed for controlling boundary layer, jet and compressor noise, discussing theoretical formulations usefulness
05 p0896 A70-16778
Subsonic circular jet noise radiation intensity and directional distribution, based on effects of refraction and Lighthill quadrupole model for aerodynamic noise
05 p0834 A70-16780
Experimental and analytical work on structural panels vibratory response and acoustic radiation excited by turbulent boundary pressure fluctuations, evaluating applicability to noise research
05 p0835 A70-16789
Acoustic power output from supersonic jets, considering aerodynamic and acoustic characteristics for supersonic exhaust velocities
[AIAA PAPER 70-237] 06 p1132 A70-18115
Shallow water waves simulation method for studying aerodynamic noise of free jet emitted from nozzle with variable wall roughness
08 p1485 A70-21608
Low Mach number aerodynamic sound generation by turbulent flow at sharp edged thin scattering half plane solved with Green function
10 p1802 A70-24521
Coaxial fluid streams mixing within finite length tube based on dimensional analysis of aerodynamic noise generation, discussing subsonic and supersonic flows within ejector
13 p2474 A70-29080
Laminar boundary layer transition on sharp cone at zero yaw in supersonic wind tunnels, correlating aerodynamic noise disturbances with transition Reynolds numbers
[AIAA PAPER 70-799] 17 p3006 A70-34462
Collection of papers on aerodynamic noise covering noise generation, solid boundaries effect, strength distribution, jet noise, perturbation theory, etc
17 p3071 A70-35448
Buzz-saw noise of transonic compressor due to rotating pressure field at supersonic blade tip speeds
[ASME PAPER 70-GT-54] 18 p3303 A70-36838
High intensity noise testing of missile and spacecraft structures, simulating acoustically induced vibrations due to aerodynamic turbulence
19 p3531 A70-37697
Flow noise mechanisms, considering discharge, propeller, ventilator, jet engine, boundary layer, water pipe and supersonic aircraft sources
19 p3406 A70-38474
Soviet papers on physics of aerodynamic noise covering axial compressors noise spectra, air intake wall design effects, surface roughness effects, air jets, etc
19 p3353 A70-38651
Discrete components formation in noise spectra of axial turbocompressor intake, considering relationship between blades and rotor disk
19 p3353 A70-38652
Rod surface roughness effect on eddy sound frequency and intensity and on aerodynamic resistance
19 p3353 A70-38654
Supersonic air jet noise spectrum analysis at various pressures
19 p3354 A70-38659
Boundary layer transition application to space shuttle design, relating aerodynamic noise to turbulent boundary layers
21 p3744 A70-41015
Supersonic air intake unsteady buzz phenomenon, examining shear layer under cowl and boundary layer detachment at shock wave base for design improvement
21 p3744 A70-41262
Sound generation by fluctuating subsonic jet flow, considering field directional characteristics and sound pressure variations with Mach number
21 p3850 A70-41422
Aerodynamic noise scattering by semiinfinite compliant plate in turbulent flow, using Lighthill theory and Wiener-Hopf technique
23 p4179 A70-43968
Lighthill aerodynamic noise theory fundamental equation for acoustic field density distribution, determining flow fields for surfaces in uniform translational motion
24 p4324 A70-45268

AERODYNAMIC STABILITY
Roll acceleration influence on angle of attack convergence and windward meridian rotation rate of rolling reentry vehicles
[AIAA PAPER 69-100] 04 p0764 A70-15546
Aerodynamic damping measured for parabolic satellite communication antenna with pronounced flexibility in azimuth drive, simulating by scaled wind tunnel models
05 p0938 A70-16455
Viscous damping effect on aeroelastic stability of thin plate in inviscid compressible airstream, observing instability in subsonic and supersonic flow
05 p0941 A70-16517

Hypersonic aerodynamic measurements on cone, investigating effects of oscillatory mass addition on stability
[AIAA PAPER 70-217] 06 p0974 A70-18171
Unstable spiral precursor to jet upset /Mach tucks/ in executive jet transports
06 p0987 A70-18248
Soviet book on aerodynamic, stability and controllability characteristics of variable geometry wing aircraft
13 p2344 A70-28648
Helical engraving influence on aerodynamic stability of bullets at long range, discussing wind tunnel tests
[AIAA PAPER 70-557] 13 p2340 A70-29022
Subcaliber cylindrical boom at base of spin stabilized projectile shown to produce aerodynamic changes in static and Magnus moments
[AIAA PAPER 70-558] 13 p2340 A70-29023
Flutter analysis, criteria and experiments emphasizing aircraft applications
15 p2815 A70-31798
Aerodynamic stability of branched diffuser systems used in annular combustors of gas turbine engines
[ASME PAPER 70-GT-27] 18 p3209 A70-36868
Thin plates and thin walled cylinders aeroelastic stability in fluid flow, analyzing panel flutter
19 p3546 A70-38342
Spike effect on nose drag and static stability of blunt bodies, estimating optimum length for drag reduction at zero angle of attack
20 p3558 A70-39702
Nonlinear equations of motion approximate solution, determining ordnance weapons aerodynamic stability coefficients from angle of attack
[AIAA PAPER 69-135] 23 p4133 A70-44515
Aeroelastic and aerothermoelastic development of winged interorbital space shuttle concerning panel flutter, stability and nonstationary lifting surface theory
23 p4273 A70-44760
Aeroelastic stability for circular cylindrical structures under periodic Karman vortex excitation
23 p4274 A70-44764
Aerodynamic interferences of lifting surfaces harmonically vibrating in subsonic flow
23 p4136 A70-44765

AERODYNAMIC STALLING
Aerodynamics of conventional aircraft high lift devices, considering effect of leading edge geometry on lift coefficient at stall of plain and flapped airfoils
01 p0001 A70-10046
Spread fin design as antisuperstall and antispin auxiliary device, discussing wind tunnel and simulation tests
06 p0967 A70-17258
Unsteady airfoil stall in incompressible flow, including pitch rate induced accelerated flow effect on leading edge and trailing edge stall
[AIAA PAPER 70-77] 06 p0976 A70-18237
Stage matching under local stall conditions for multistage axial flow compressor off-design and surge initiation characteristics
09 p1608 A70-23741
Space shuttle structural dynamic problems, discussing stall flutter due to transition from high angle of attack to normal aircraft flying attitude
[AIAA PAPER 70-740] 12 p2312 A70-27150
Helicopter blade sections dynamic stall characteristics, considering accelerated flow generation by nonzero pitch rate
17 p3014 A70-34718
Helicopter rotor blade stall flutter response prediction based on NACA 0012 airfoil aerodynamic data
17 p3009 A70-34734
Airfoil trailing edge stall in laminar flow, investigating circulation around flat plate
18 p3205 A70-36194
Dynamic airfoil stall simulation in wind tunnels, considering pitch rate, Reynolds number, oscillation and test equipment effects
[AIAA PAPER 70-945] 20 p3558 A70-39582
Unsteady aerodynamic forces at stall flutter, applying vortex sheet theory to separated flow field around thin airfoil at high angle of attack
22 p3957 A70-42284

AERODYNAMIC VEHICLES
U AIRCRAFT
AERODYNAMICS
NT **AEROTHERMODYNAMICS**
NT **HYPERSONICS**
NT **ROTOR AERODYNAMICS**
Aircraft aerodynamics, Volume II, covering profile and wing theory at subsonic and supersonic speeds, fuselage, wing-fuselage and tail assembly, etc
03 p0407 A70-13350
Transonic wind tunnel of aerodynamic research station in Goettingen, Germany, taking into account fixed nozzle replacement by flexible nozzle
03 p0463 A70-13799
Ionospheric aerodynamics concerning plasma flow and stability, ion motion, radio wave scattering, etc
03 p0479 A70-14386
Flow phenomena about beating plates, fins and wings, discussing biological and engineering applications
05 p0790 A70-16155

Aerodynamics - Conference, Berlin, October 1968
06 p0961 A70-17226
Helicopter dynamics structural model extended to LF longitudinal motions by including stabilizing feedback loop representing forward velocity influence on main rotor
06 p0987 A70-17910
Gaussian quadrature integration technique developed for collocation approach for integral equation of steady subsonic lifting surface theory
[AIAA PAPER 70-191] 06 p0970 A70-18097
Test facilities and procedures for obtaining aerodynamic data required for studying vehicle-in-tube transportation systems
[AIAA PAPER 70-225] 06 p1030 A70-18221
Holography for visualization and analysis of aerodynamic flow fields in wind tunnel experiments, recreating events in space and time
08 p1493 A70-20650
Soviet handbook on practical aerodynamics of aircraft with turboactive engines covering flight stability, aircraft controllability, etc
08 p1435 A70-20760
Soviet book on practical aerodynamics and flight vehicles covering supersonic aircraft, sweptback wings, military aviation and satellites
08 p1435 A70-20765
Computers impact on engineering science and design, detailing digital computers use in aerodynamics, structures and aeroelasticity
08 p1466 A70-21030
Dynamic behavior of subcritical fluid flow past airfoils, expanding flow potential to obtain formulas for velocities, local Mach numbers and pressure
08 p1433 A70-21173
Axial compressor aerodynamics and efficiency in aircraft turbine engines
[ONERA-TP-767] 09 p1604 A70-22656
Potential flow and boundary layer theory application as design tools in aerodynamics, basing calculations on digital computer methods
09 p1605 A70-22947
Nonlinear flutter of three dimensional simply supported curved plates, employing quasi-steady supersonic aerodynamic theory
09 p1780 A70-23212
Photo-optical processes and optical measuring techniques in research programs at Ames Research Center for aerodynamics, life sciences and space sciences
09 p1657 A70-23501
Quasi-one dimensional motion of perfect compressible flow through pipe, considering one dimensional schemes in aerodynamics
10 p1865 A70-24102
Transonic aerodynamics problems concerning plane and spatial rotational flows of perfect gas, discussing analytical and numerical methods
10 p1800 A70-24132
Aerodynamic sound emission from compact edge region by singular perturbation approach, discussing Lighthill and Ribner theories
11 p1977 A70-26687
Free fall vehicle dynamics for wind tunnel measurements of research shapes used in computer simulation of vehicle trajectories
[AIAA PAPER 69-229] 12 p2157 A70-28081
Book on aerodynamics covering flow theory, boundary layers, shock waves, wing design, etc
12 p2157 A70-28148
Volterra method applied to solution of mixed boundary value problems for wave equation
12 p2159 A70-28243
Shock patterns for simple caret wings generating specific flow patterns
13 p2509 A70-28542
Aerodynamic effects of bluntness on slender cones in free flight tests at Mach 17
[AIAA PAPER 70-554] 13 p2340 A70-29019
Book on aerodynamics and flight mechanics, discussing aircraft parts, subsonic, transonic and supersonic flows, level ascending and descending flights, landing and takeoff, etc
15 p2672 A70-32075
Book on aerodynamics for engineering students covering hydro- and aerostatics, flow theory, propulsion principles, aerofoil theories, aircraft performance and stability, etc
16 p2838 A70-33953
External aerodynamics role in handling qualities of amphibious hovercraft, discussing tests of hull shape, air cushion efflux and hollow models
17 p3017 A70-34919
Aerodynamics theory for separated flow effects on helicopter lift-drag capability, taking into account three dimensional flow and blade aeroelasticity
18 p3205 A70-35956
Significant terms in equations of motion for parachutes inflating in free air and in wind tunnel experiments
[AIAA PAPER 68-924] 18 p3213 A70-36449
Soviet book on passenger aircraft aerodynamics covering motions of gases and immersed bodies, similarity laws, boundary layer theory, finite span wing, etc
18 p3208 A70-36507

Thin airfoil theory in magnetoaerodynamics, considering steady two dimensional flow of compressible perfectly conducting inviscid fluid in presence of uniform magnetic field

19 p3351 A70-37597

Soviet papers on kinetics and aerodynamics of fuel combustion processes covering supersonic flow, flame stabilization, fluid atomization, nonequilibrium recombination, etc

20 p3736 A70-39265

Liquid jets aerodynamic atomization at orifice exit in reentry vehicle into gaseous crossflow, investigating critical Weber number variation with Knudsen number

20 p3610 A70-39701

Aerodynamics of steady, inviscid transonic flows around slender bodies and wing-body combinations at free stream Mach number one

[AIAA PAPER 70-798]

20 p3559 A70-39900

Large MHD generator channel aerodynamics, discussing pressure distributions to stall and stagnation pressure loss

20 p3612 A70-40002

Newtonian hypersonic aerodynamic theory for arbitrary bodies, discussing computational difficulty for shadowed areas

21 p3747 A70-41866

Supersonic aerodynamic design tools, discussing technological application of high speed computer and limitations

[AIAA PAPER 68-1018]

22 p3958 A70-42701

European wind tunnels suitable for Post Apollo Program aerodynamic testing, presenting detailed tabulated information on available facilities

22 p4007 A70-43503

European hypersonic aerodynamic research activities, describing Eurohyp program

22 p4127 A70-43507

Aerodynamic theory of pressure fluid induced on lifting surface by isotropic atmospheric turbulence, considering transfer function of Concorde aircraft

[ICAS PAPER 70-30]

23 p4138 A70-44104

Aerodynamic problems due to mixed subsonic and supersonic/ transonic flows on swept wings, nacelle lips and helicopter rotor blades

[ICAS PAPER 70-14]

23 p4132 A70-44125

AEROELASTICITY

NT AEROTHERMOELASTICITY

Cantilevered and doubly supported structures calculated for critical aeroelastic divergence speed resulting from lift and drag

01 p0200 A70-10551

Aircraft structural weight optimization for given fundamental vibration frequency obtained by aeroelastic constraints

03 p0598 A70-14231

Longitudinal stability derivatives prediction for rigid and elastic airplanes, using influence coefficient method

[AIAA PAPER 69-131]

04 p0624 A70-15383

Viscous damping effect on aeroelastic stability of thin plate in inviscid compressible airstream, observing instability in subsonic and supersonic flow

05 p0941 A70-16517

Dynamic stability of complex aeroelastic structures including V/STOL aircraft using simplified technique, noting application to tilt rotor aircraft design

[AIAA PAPER 70-22]

06 p1170 A70-18119

Variable sweep aircraft aeroelastic stability, considering wing-tail interaction flutter

[AIAA PAPER 70-80]

06 p1170 A70-18162

Soviet book on unsteady attached turbulent flow in turbine lattices, studying blade aeroelastic vibrations onset and attenuation in compressible and incompressible fluids

07 p1189 A70-19602

Computers impact on engineering science and design, detailing digital computers use in aerodynamics, structures and aeroelasticity

08 p1466 A70-21030

Optimal control conditions for elastic aircraft motion with delayed wing downwash determined by hyperbolic partial differential equations with delay

08 p1480 A70-21178

Aeroelasticity problems, discussing unrestrained flexible structures design, nonconservative systems stability, biomechanics, etc

09 p1777 A70-22972

Panel flutter theory applied to aeroelastic stability of flat unloaded plates and cylindrical shells

11 p2134 A70-25951

Aeroelastic test equipment for Concorde, describing operating principles, installation, test results, etc

15 p2717 A70-31810

Combined internal pressure and axial loading influence on aeroelastic stability of thin walled cylindrical shell in supersonic flow field

16 p2991 A70-33851

Aeroelastic test equipment for Concorde SST using harmonic method and electromagnetic shakers

19 p3402 A70-38548

Unsteady aerodynamics prediction of supersonic elastic aircraft, discussing aerodynamics influence coefficients /AIC/ method refinement

[AIAA PAPER 70-944]

20 p3558 A70-39583

Potential flow around oscillating shell-plate structure subjected to supersonic gas flow at zero angle of attack, solving nonlinear aeroelasticity problem

22 p4117 A70-43362

Elastic fuselage flight vehicle dynamic stability at supersonic speeds, using automatic pilot stabilization

23 p4139 A70-44157

Dynamic systems stability with periodically varying parameters analyzed by Hill type infinite determinant, exemplifying helicopter rotor aeroelastic stability in forward flight

23 p4220 A70-44556

ONERA calculations in aeroelasticity including lifting surface optimization, control surface vibration, pressure fields, aircraft transfer functions and panel flutter

23 p4274 A70-44762

Aeroelastic stability for circular cylindrical structures under periodic Karman vortex excitation

23 p4274 A70-44764

Orthogonality of eigenmodes of aircraft vibrations based on F-104G ground measurements

23 p4274 A70-44766

Elastic coupling and dynamic equations for flight elastomechanical vibration systems, including tiptanks on aircraft wings

23 p4274 A70-44767

Stationary aeroelastic cases studied in subsonic flow range, providing criteria for aircraft design with required flight characteristics

24 p4422 A70-45443

AEROEMBOLISM

Platelet and lipid changes in thrombocytopenic and control rats subjected to bends producing technique in aeroembolism

01 p0015 A70-10364

Histopathological evidence for pulmonary emboli in experimental decompression sickness in dogs detected by radioisotopic lung scanning

06 p0991 A70-17295

Decompression disorders after exposures to safe pressure or altitude in cats, noting potential embolia from nongradual high-to-normal pressure passage

23 p4157 A70-45080

AEROLOGY

Aerological radio thermometers random and systematic errors compared to network radio probe

05 p0848 A70-16206

Meteorological rocket probing, noting 100 and 170 km range probes in U.S.S.R., thermobaric maps and aerological stations for high altitude aviation

15 p2771 A70-32108

Volcanic blankets aerological investigation by polarization and spectral techniques, determining brightness distribution of reflected solar light

15 p2803 A70-32495

AEROMAGNETISM

U GEOMAGNETISM

AEROMAGNETO FLUTTER

U FLUTTER

AERONAUTICAL ENGINEERING

UK aeronautics R and D, attributing competitive technology lag in military and subsonic civil fields to failure in aims and targets and program cost justification

02 p0402 A70-12306

Soviet book on assembly, control and testing of aeronautical devices covering theory, technology, quality control, accuracy, industrial cleanliness, vacuum and gas filling, etc

03 p0479 A70-12870

Czechoslovakian Aeronautical Research and Test Institute history, organization, activities, equipment and achievements

03 p0464 A70-13925

Airline aircraft finishes for protection against corrosion, air pollution, discussing paint application and polyurethane technology

03 p0497 A70-14053

Computer-aided design using third generation computers and interactive graphic systems applied to transonic aerodynamics problems

05 p0816 A70-16122

L band transponder design for aeronautical satellite, giving block diagrams

07 p1234 A70-19292

German Research Establishment for Air and Space Navigation covering aerodynamics, aircraft design, flight mechanics, guidance and jet propulsion

07 p1249 A70-19671

Airline industry, considering expected increases in traffic, aircraft development and interface problems

08 p1600 A70-20588

Aircraft development for subsonic and transonic flight dependent on methods using blowing and boundary layer control and Coanda and Magnus effect

09 p1610 A70-22220

Ground and flight tests in aeronautical system development process as transfer of basic technology into cost effective operational systems

[AIAA PAPER 70-381]

10 p1857 A70-24172

Italian aviation and space industry development for local and sectional character and participation in European production

10 p1971 A70-24663

BAC 111 short/medium range jet airliner family status report on program activity

10 p1806 A70-24846

Aviation and astronautics - Conference, Tel Aviv and Haifa, March 1970

11 p1978 A70-25676

Aviation future development based on airplane evolution, considering aircraft configurations, flight problems, nuclear propulsion, jet propelled aircraft

12 p2161 A70-27523

Book on aerodynamics covering flow theory, boundary layers, shock waves, wing design, etc

12 p2157 A70-28148

Probabilistic methods in aeronautical research and development

14 p2563 A70-31393

Book on aerodynamics for engineering students covering hydro- and aerostatics, flow theory, propulsion principles, aerofoil theories, aircraft performance and stability, etc

16 p2838 A70-33953

Polish Institute of Aviation, describing facilities and current test programs

21 p3804 A70-40799

Airframe and systems design optimization for aeronautical communications systems, considering airplane configurations, structural and electronics technology

21 p3750 A70-41349

Rumanian book on methods, equipment and facilities for aeromechanical measurements covering fluid flow, wind and shock tunnels, flow measurements, etc

23 p4199 A70-45000

AERONAUTICS

Soviet book on aeronautical astronomy covering reference stars, time and natural illumination measurements, aircraft course determination, position fixing, etc

02 p0329 A70-11695

German society of aeronautics and astronautics, yearbook 1968

03 p0411 A70-13789

Maritime and aeronautics technology - Conference, Paris, May 1969

07 p1192 A70-19126

Space systems for communications, surveillance and navigation needs of international aviation, discussing service requirements, spectrum utilization, technology limitations and terminal design

07 p1330 A70-19290

Soviet book on meteorological conditions analysis and prediction for aviation covering fog, storms, showers, stratospheric turbulence studies, etc

08 p1535 A70-20772

Clear air turbulence significance in aviation and atmospheric science, noting Kelvin-Helmholtz model

08 p1539 A70-21559

Bibliographies for AIAA technical disciplines

09 p1792 A70-22344

Aviation and space industry metallic and nonmetallic materials testing, discussing corrosion and ultimate fatigue due to impurities

10 p1861 A70-24664

Radio Technical Commission for Aeronautics - Conference, Washington, D.C., November 1969

11 p2078 A70-25719

Aeronautics and astronautics bibliographies for college students

12 p2336 A70-27666

AERONOMY

Aeronomy of Jovian upper atmosphere at pressures below 25 mb, discussing stratospheric heat sources, thermal emissivity, photochemistry of methane, ammonia, etc

02 p0366 A70-11804

Vertical ion concentration profile in troposphere and stratosphere from ozone distribution satellite measurements using aeronomical reactions

02 p0291 A70-12389

Carbon dioxide electron impact cross sections, analyzing discrete excitation, autoionization, direct and dissociative ionization and use to aeronomy

04 p0722 A70-15121

AEROS satellite A2 launching to investigate aeronomic processes in outer atmospheric layers, discussing scientific research program, mission data, satellite and ground station equipment

[DGLR-69-050]

07 p1393 A70-19149

Aeronomic neutral reaction rates, describing ozone excited state photochemistry

10 p1872 A70-23824

Upper atmosphere electromagnetic probing theory and techniques, noting applications to aeronomic problems

12 p2223 A70-27726

Aeros aeronomic satellite mission, orbit and design for upper atmosphere observations, noting braking field analyzer for ion and electron speed measurement

13 p2505 A70-28767

Ground sounding of ionization variations and vertical distribution using model, integral and normal laminar methods

15 p2729 A70-32078

AEROPHYSICS

U ATMOSPHERIC PHYSICS

AEROS SATELLITE

Aeros satellite active magnetic position control system of axis and spin noting design and operation [DGLR-69-056] 07 p1393 A70-19148

AEROS satellite A2 launching to investigate aeronomic processes in outer atmospheric layers, discussing scientific research program, mission data, satellite and ground station equipment [DGLR-69-050] 07 p1393 A70-19149

Aeros aeronomic satellite mission, orbit and design for upper atmosphere observations, noting braking field analyzer for ion and electron speed measurement 13 p2505 A70-28767

AEROSOLS

NT FOG

Aerosol particles Brownian motion under inertial forces in absence/presence of obstacle 01 p0143 A70-10997

Aerosol size distribution from data on atmospheric spectral transmittance and solar corona brightness spectral and angular variations 02 p0292 A70-12434

Sky brightness distribution data to determine shape of aerosols scattering as function of wavelength 02 p0292 A70-12435

Intermediate air layer optical properties explained by assuming presence of small and large size aerosol particles 02 p0328 A70-12436

Aerosol induced light scattering optical properties in atmospheric boundary layer measured with three photometer setup with He-Ne laser 02 p0328 A70-12437

Vertical concentration and size distribution determinations for aerosols in stratosphere, suggesting volcanic origin 02 p0294 A70-12842

Charged aerosol charge/mass ratio measurement and colloidal propulsion system thrust, efficiency and exhaust velocity determinations 03 p0551 A70-12936

Aerosols size distribution and chemical composition and carbon monoxide, nitrous oxide and sulfur dioxide concentrations measured in pure atmosphere 03 p0521 A70-14289

Mie scattering and polarization functions of atmospheric aerosols determined on basis of logarithmic Gaussian distributions 05 p0879 A70-16664

Twilight atmospheric brightness calculation for models of vertical distribution of aerosol scattering coefficient, using numerical data 06 p1056 A70-17828

Polarization level of outgoing short wave radiation calculated along solar vertical in aerosol containing multiply scattering atmosphere 06 p1097 A70-17829

Spectral transparency inversion of aerosol-containing atmosphere 06 p1098 A70-17832

Haze model atmospheres scattering characteristics by computer simulation concerning optical contrast reduction by aerosols for direct and diffuse radiation [AIAA PAPER 70-194] 06 p1057 A70-18156

Chemical composition effects on Zr-Ti, Zr-Si, Ni-Al and Ni-Ti alloy aerosols combustion temperature 07 p1419 A70-18755

Visibility, atmospheric light scattering coefficient and aerosol mass concentration related by integrating nephelometer measurements 07 p1328 A70-18923

Vertical temperature profile diurnal variations of Mars atmosphere using models, noting aerosol influence 07 p1385 A70-19422

Precondensation visibility dependence on aerosol particle swelling due to increasing humidity 08 p1539 A70-21921

Soviet monograph on growth rate of coagulating and condensing aerosol particles, considering kinetic theory 09 p1713 A70-22205

Upper atmosphere aerosols and cosmic dust properties investigation by laser beam scattering measurements using photoelectron counters for weak signal detection 10 p1898 A70-23818

Polydisperse dielectric system distribution parameters determined from hard monochromatic polarized radiation scatter by artificial aerosols 10 p1916 A70-24500

Polarization of solar scattered radiation measured by radio probes for aerosol particle concentration and size distribution as function of altitude 10 p1884 A70-25253

Deposition zone on sphere and aerosol particles flux onto sphere as functions of flow Reynolds and Stokes numbers, discussing drop deformation effects 12 p2263 A70-27513

Inhalation in functional respiratory exploration, describing equipment for aerosol volume measurement in contact with bronchopulmonary effectors 14 p2541 A70-30377

Cloud droplets coagulation growth, calculating aerosols inertial capture coefficient by fine jet method 14 p2602 A70-30390

Droplets collision and coagulation for processes in aqueous aerosols, discussing interaction with collectors 14 p2603 A70-30391

Detonation process one dimensional stability in combustible aerosol, considering gas dynamic disturbances effect 14 p2665 A70-30397

Atmospheric optical thickness in visual spectrum region relationship to meteorological characteristics, plotting vertical profiles of humidity and aerosol attenuation coefficient 14 p2603 A70-30407

Atmospheric optical aerosol model based on vertical attenuation profile, particle concentration and size distribution and air conductivity 14 p2603 A70-30410

Laser radar measurements for atmospheric scattering properties, observing aerosol content, atmospheric density and composition 14 p2550 A70-30746

Aerosol particle convective diffusion from gas medium into obstacle, solving Fokker-Planck equation for particle distribution 15 p2774 A70-31493

Bistatic lidar /laser radar/ detection of atmospheric aerosol size distribution, using angular scattering measurements of polarization parameters 15 p2704 A70-32609

Atmospheric structure studies using lidar method to detect particulate content in clear air 16 p2862 A70-33014

Cloud droplet agglomeration by weak shock waves, discussing growth mechanism 17 p3067 A70-34549

Thermophoresis of aerosol particles in nearly free molecular nonuniformly heated gas, using linearized Boltzmann equation 18 p3292 A70-36254

Atmospheric aerosols, fog and rain effects on signal transmittance and backscatter at 3400-10600 A 18 p3248 A70-36751

Atmospheric particle distribution spectrum by optical methods, estimating aerosol concentration from scattering coefficient 18 p3251 A70-36980

Earth aerosol layer formation mechanism, giving atmospheric brightness measurements in terms of dust particles density and size 18 p3251 A70-36981

Atmospheric aerosols vertical distribution from aerostat measurements, considering particle size distribution 19 p3461 A70-37636

Atmospheric aerosols optical and microphysical measurements comparison, evaluating sample collection equipment, errors, etc 19 p3421 A70-37637

Aerosol correction for atmospheric ozone content measurements using direct sunlight 20 p3615 A70-39032

Surface haze and vertical aerosol attenuation for various meteorological ranges within 1.2-15 km, tabulating for UV, visible and IR wavelengths 20 p3661 A70-39082

Book on molecular and aerosol backscatter measurement from stratosphere by means of ground based laser beams 20 p3623 A70-39925

Aerosol IR emission, discussing relative humidity, water droplet size and temperature effects on atmospheric radiance levels 21 p3846 A70-40804

Polarization of radiation reflected and transmitted by earth atmosphere, calculating scattering matrix for aerosol size distribution model 21 p3820 A70-41725

Spectral radiation extinction at atmospheric aerosol particles, discussing particles complex refractive indices and size distributions 22 p4065 A70-43171

Planetary albedo changes due to pollution aerosols, showing absorption-to-backscattering ratio function in atmospheric heating or cooling 22 p4096 A70-43419

Aerosol impact traps for ground and airborne water vapor condensation studies 23 p4195 A70-44272

Optical laser radar for upper atmospheric density and aerosol concentration measurements 24 p4353 A70-45561

AEROSPACE ENGINEERING

NT AERONAUTICAL ENGINEERING

Systems design experience derived from Mercury, Gemini and Apollo projects, discussing thermal protection, launch propulsion, life support, etc [AIAA PAPER 69-1077] 01 p0193 A70-10604

Manned reusable space transportation system technology requirements and vehicle types [AIAA PAPER 69-1116] 01 p0194 A70-10613

Manned space station system analysis for identifying control subsystem functions /weight penalties/ and system characteristics to minimize penalties [AIAA PAPER 69-1078] 01 p0194 A70-10628

Aircraft/aerospace fluid systems flexible hose and rigid tube assemblies fire resistance and test requirements 01 p0011 A70-11459

Aerospace structures design - Conference, Seattle, Washington, August 1969 02 p0385 A70-11931

Carbon materials manufacture, properties and applications in space technology, discussing carbon fibers, textiles, graphite, pyrolytic carbon, composites and vitreous carbon 03 p0516 A70-13618

Linear separation systems for aerospace applications covering mild detonating fuse and cord flexible linear shaped charge, SUPER ZIP concepts, etc 03 p0546 A70-14103

Aerospace laboratories organization concepts, discussing dependence on product, size, location and technological trends 03 p0612 A70-14313

X-15 aircraft project experiments utilized in space research including IR and UV spectrometer, horizontal scanning, stellar photography, micrometeorite and solar energy studies, etc 04 p0622 A70-14673

Soviet engineering reference book on space flight technology covering astronomical and geophysical data, flight mechanics, vehicles and systems 04 p0761 A70-14703

Space projects quality assurance with allowance for technological trends, discussing product and system oriented organizational requirements, failure potentials, contractor performance, etc 04 p0699 A70-15138

Ti alloys, high strength steels and plastics for aircraft and spacecraft constructions, including aging behavior of lap joints and prepreg laminates in vacuum [DGLR-69-58] 04 p0699 A70-15162

High temperature coatings in industrial, military and space applications, noting use in metal melting and working, furnace protection, propulsion systems, rocket engines, etc 04 p0709 A70-15630

Soviet aerospace manufacturing technologies development, considering forging, extrusion, metal working and joining, etc [SAE PAPER 690701] 05 p0853 A70-15826

German research institutes activities in fluid mechanics, structural materials, propulsion, flight control and electronics, space physics and medicine 05 p0829 A70-16374

Welding of satellite and spacecraft segments in space, discussing arc, electron beam, resistance, vacuum diffusion, cold pressure and brazing techniques 05 p0855 A70-16375

Plastics applications in aircraft, missile systems, satellites, sounding rockets and manned spacecraft, discussing reinforced plastics and structural laminates 05 p0874 A70-16623

Radio astronomy spacecraft /RAS/ engineering design, technology and flight results 06 p1153 A70-17151

Life styles of engineering, comparing U.S. and European attitudes to aircraft development and design 06 p1184 A70-17198

Biomedical concepts for aerospace engineering, discussing human body as self regulating system /homeostasis/ and physiological time regulator /circadian/ 06 p0992 A70-17315

Space programs and future missions assessment based on technical feasibility, considering effects of economic and social factors 06 p1185 A70-17644

Spectroscopic quantitative diagnostics of high density plasma sources encountered in aerospace applications and chemistry 06 p1063 A70-17729

Propellant transfer unit for weapon or space vehicle systems, specifying aerospace ground equipment criteria [SAE-AIR-1129] 07 p1248 A70-18806

Fluids for aerospace power technology, tabulating properties of hydraulic, damper and heat transfer fluids, fuels, oils, etc 07 p1316 A70-18807

Aerospace technology contributions to oceanography, discussing lightweight structures, electronics, automatic systems and submarine laboratory application 07 p1263 A70-19135

German Research Establishment for Air and Space Navigation covering aerodynamics, aircraft design, flight mechanics, guidance and jet propulsion 07 p1249 A70-19671

Space shuttle program from technological and budgetary objections viewpoint, evaluating risks against program options [AIAA PAPER 70-264] 07 p1398 A70-20394

Soviet book on liquid rocket engines dynamics, emphasizing computational engineering methods and engines automatic control

08 p1558 A70-20757

Collection of papers on aerospace technology covering Fokker F-28 aircraft design, airfoil computer graphics, helicopter rotor tuft analysis, aircraft fatigue, launch vehicle guidance, etc

08 p1438 A70-21863

Seadrome advantages and structural design concepts, describing floating runways, breakwaters, noise reduction, building costs, etc

09 p1655 A70-22243

Quality planning for Japanese solid propellant sounding rocket motor production, discussing documentation, design, development and process controls, inspection and tests, etc

09 p1691 A70-22570

Test-aided aerospace design, noting design engineer attitude and software problems

09 p1766 A70-22678

Apollo command and service modules from metallurgical viewpoint

09 p1766 A70-22792

Materials and processing technology roles in NASA programs involving manned space stations, service spacecraft and unmanned space exploration

10 p1902 A70-23855

Space engineering, flight instrumentation features and spacecraft subsystems integration problems

10 p1950 A70-24610

Aviation and space industry metallic and nonmetallic materials testing, discussing corrosion and ultimate fatigue due to impurities

10 p1861 A70-24664

Thermal conductivity, electrical resistivity, Lorentz ratio and thermopower of aerospace alloys in 4-300 K range, separating electronic and lattice contributions

11 p2065 A70-25758

Insulators, ablaters, reflectors and computer analyses for aerodynamic and engine heat for aerospace thermal design

11 p1980 A70-25874

Cylindrical shell segments supersonic flutter boundaries engineering estimates related to Saturn 5 booster, obtaining thickness requirement as function of panel geometry

[AIAA PAPER 68-284]

11 p2134 A70-25959

Nuclear propulsion systems types, discussing relative capabilities and future roles in aerospace applications

11 p2082 A70-26055

Space engineering - Conference, Venice, May 1969

11 p2124 A70-26276

Dynamic measurements of aerospace mechanical quantities covering tensometry, vibration, torque, angular velocity, pressure, telemetry and data processing

11 p2057 A70-26750

SAE aerospace applied thermodynamics manual covering aerodynamics, fluid dynamics, heat transfer, materials properties, aerospace application engineering, etc

12 p2329 A70-26872

Computer applications in aerospace research involving flutter, supersonic flow, unsteady wing flow, etc

12 p2191 A70-27025

Diffusion bonding processes for Ti aerospace structural elements, describing electric blanket, roll and press bondings

[SME PAPER AD-70-736]

12 p2242 A70-27089

Stress analysis experimental techniques in aerospace engineering including strain gages, deformation methods, photoelasticity, etc

12 p2205 A70-27127

Adaptive flight control systems utilization to compensate for variations in aerospace vehicle rigid body dynamics, noting control system performance requirements

[AIAA PAPER 68-970]

12 p2204 A70-28076

Europa 3 satellite carrier system configurations, discussing rocket design, propellant composition, etc

13 p2502 A70-28445

Reentry vehicles development, discussing systems analysis and design, vehicle aerodynamics, aerodynamic heating and shielding, and flight mechanics and control

13 p2506 A70-29055

Engineering design and drafting techniques in aerospace industry, emphasizing cost reduction

13 p2423 A70-29820

Space design, considering problems due to weightlessness, vacuum, thermal effects, micrometeorite, cosmic forces, etc

14 p2656 A70-30301

Aerospace technology and system analysis application possibilities to urban social and economic planning problems

14 p2670 A70-31191

Collection of papers on space science and technology covering lunar and planetary explorations, trans-tellar navigation, Trojan Relay satellite communication, utility, etc

15 p2800 A70-32057

Workmen as environmental variables in design, introducing Human Factors Report during spacecraft components manufacture and testing

15 p2693 A70-32636

Aerospace electronics - IEEE Conference, Dayton, May 1970

16 p2908 A70-33426

Collection of papers on aerospace mechanisms, Part A, covering scanning, separation, thermal and stabilization devices, booms, cameras, etc

16 p2983 A70-34101

Aerospace mechanisms design attitudes effects on cost and success of space mission

16 p2985 A70-34102

Aerospace mechanism design from test laboratory viewpoint, balancing technical, cost and schedule factors with mission objective

16 p2921 A70-34103

Swinging gear drive, breather cartridge and hypocy-cloid timer mechanisms for reliable aerospace applications

16 p2921 A70-34104

Mariner 4 scan platform structure and actuator design, development and performance

16 p2845 A70-34106

Gemini/Agna docking mechanism design and function, describing latch and rigidizing devices

16 p2986 A70-34151

Collection of papers on aerospace mechanisms, Part B, Bearings and suspensions

16 p2922 A70-34154

Lubrication role in aerospace engineering, discussing lubricant and component selection, environmental factors, etc

16 p2923 A70-34155

Flexural pivots for space structures, describing design, fabrication and applications

16 p2924 A70-34170

Space shuttle systems structural design and thermal protection technology, stressing hardware reliability and reusability

16 p2986 A70-34227

Aerospace thermophysics considerations in spacecraft and hypervelocity vehicles systems thermal design, discussing thermal control and control coatings optical and radiative properties

[AIAA PAPER 70-812]

17 p3194 A70-34509

Aerospace technology applications to air pollution problems, including turbojet aircraft sources, rocket emissions, etc

[AIAA PAPER 70-815]

17 p3200 A70-35194

Apollo ordnance systems design and reliability, stressing redundant components role

17 p3179 A70-35263

Systems design experience derived from Mercury Gemini and Apollo projects, discussing thermal protection, launch propulsion, life support, etc

[AIAA PAPER 69-1077]

17 p3180 A70-35644

Engineering for 1970s - IEEE Conference, Huntsville, Alabama, November 1969

19 p3392 A70-37842

Aerospace instrumentation - Conference, Cranfield Institute of Technology, England, March 1970

19 p3428 A70-38514

Fiber reinforced plastics (FRP) composites applications in Japanese aircraft production and aerospace industries

20 p3657 A70-40057

Material thickness tolerances control for weight minimization of aerospace vehicles by abrasive metal grinding, improving surface quality

[SAWE PAPER 827]

20 p3638 A70-40358

Space technology and heat transfer - ASME Conference, Los Angeles, June 1970, Part 1

21 p3927 A70-40976

Space systems and thermal technology - ASME Conference, Los Angeles, June 1970, Part 2

21 p3942 A70-41014

Aerospace nuclear applications - Conference, Huntsville, Alabama, April 1970

22 p4069 A70-43177

Bonded honeycomb sandwich structure fastening techniques in aerospace design, noting application to aircraft and spacecraft structures

[SAE PAPER 700850]

24 p4425 A70-45882

Aerospace pyrotechnics applications, considering pressure controlled propellant actuated device for escape systems

[SAE PAPER 700831]

24 p4295 A70-45889

AEROSPACE ENVIRONMENTS

NT CISLUNAR SPACE

NT DEEP SPACE

NT INTERPLANETARY SPACE

NT INTERSTELLAR SPACE

Impingement pressure analysis associated with two phase cryogenic propellant venting to space environment

[AIAA PAPER 69-571]

01 p0196 A70-10845

Soviet book on physico-technological basis of space research covering near earth and interplanetary environmental factors and effects on spacecraft designs and materials

02 p0360 A70-11693

Space environment and radiation on Biosatellite 2 enhancing radiation effects in developing flour beetle Tribolium confusum

02 p0238 A70-12517

Gear materials evaluation program for space environment application with unlubricated or solid film lubricated operation mode

[ASLE PREPRINT 69-LC-6]

02 p0309 A70-12539

Biological rhythm disturbances of astronauts during air and space travel, discussing sleeping habits, alertness under weightlessness conditions, etc

02 p0241 A70-12763

Surface coating optical and thermal properties investigated in preparation for HELIOS solar probe

[DGLR-69-46]

04 p0762 A70-15163

Collection of articles on space environment covering planetary atmospheres, temperature in space, meteoroid hazard, radiation and protection, etc

05 p0913 A70-16626

Radiation environment in space and effect on man, discussing particulate and high energy electromagnetic radiation components

05 p0903 A70-16630

Matrix optimization of boron filament reinforced polymers for short duration high temperature aerospace applications

08 p1530 A70-21891

Venous pressure of man in space, investigating return to heart in absence of gravity and distention by hydraulic pressure

08 p1448 A70-21943

Thermal controls for spacecraft in space and planetary atmospheres, including heat inputs by solar radiation and planetary albedos

09 p1789 A70-23130

Solid radiating sphere cooling in space, determining transient temperature distribution by finite difference computing techniques

09 p1790 A70-23562

Gear materials evaluation program for space environment application with unlubricated or solid film lubricated operation mode

10 p1893 A70-23837

Si-Ge air-vacuum thermocouples for thermoelectric conversion, describing construction materials, mechanical and electrical properties, radiative heat transfer operation, etc

10 p1807 A70-24896

Mercury bombardment ion thruster life test in space environment onboard space electric rocket test (SERT) satellite, describing passive satellite thermal control system design

11 p2127 A70-26606

Thermal coated extendable boom for space applications, describing construction and vacuum metallizing technique

12 p2242 A70-27266

Space design, considering problems due to weightlessness, vacuum, thermal effects, micrometeorite, cosmic forces, etc

14 p2656 A70-30301

Aerospace meteorology - AMS-AIAA Conference, Las Vegas, May 1970

14 p2604 A70-30551

Aerospace environment models development by NASA for engineering use in Space Vehicle Design Criteria program

14 p2637 A70-30554

Wind profiles derivation for environmental influence upon missile systems design, limiting bulky input into computer programs

14 p2608 A70-30586

Solar furnaces in space for treatment of high purity products in space vacuum, discussing design and operational problems

15 p2717 A70-31802

Passive optical crossed beam detection systems monitoring meteorological parameters in rocket or aircraft environments, noting real time display

15 p2736 A70-32032

Atomic clock for climatic and mechanical conditions of aerospace environment, using optically pumped rubidium cell

15 p2740 A70-32366

Space manufacturing in weightless environment, discussing unique processes, potential materials, product groups, planned experiments for Skylab Orbital Workshop mission, etc

16 p2888 A70-33716

Materials preparation processes and improvements in space weightless environment, considering metals and ceramics melting, solidification, electromagnetic process control, etc

16 p2919 A70-33717

Orbital zero and low g environment utilization for space manufacturing processes and related operational and tooling requirements

16 p2919 A70-33718

Sliding electrical contacts in vacuum and space - Conference, Virginia Polytechnic Institute, September-October 1969

16 p2919 A70-33805

Ruggedized spacecraft mechanisms for severe shock environments

16 p2922 A70-34121

Spacecraft boom selection, discussing parameters, intended use, environment and effect on vehicle 16 p2986 A70-34140

Bearings for nuclear reactor control components in space environment, discussing sliding friction, compatibility and prototype assemblies tests 16 p2923 A70-34162

SNAP reactor control system mechanisms development for operation in space environment 16 p2951 A70-34163

Conical pivot bearings for impact accelerations tolerance in space environments, discussing optimum dimensions and minimal torque design 16 p2923 A70-34164

Ball bearing materials for ultrahigh vacuum space environments, determining frictional and wear behavior 17 p3099 A70-34573

Microelectronics in space environment, discussing circuit reliability, radiation effects, etc 17 p3053 A70-35269

Laminar heat transfer in circular tube under solar radiation in space 18 p3347 A70-36503

Arc welding in space under high vacuum weightless conditions, describing equipment design and Soyuz 6 experiments 19 p3436 A70-37803

Computer aided laboratory testing of flight vehicles in real environmental conditions, illustrating vertical stabilizer subject to gust loads 19 p3396 A70-37874

Space processing under zero gravity conditions, discussing crystal growth, metal glass and ceramic melting and casting and biological product centrifugation and electrophoresis 19 p3436 A70-37926

Magnetomotive tools and power systems for maintenance, repair and assembly in space weightless environment 19 p3436 A70-37949

Space environment physical properties near earth, discussing neutral atmosphere, solar radiation, ionosphere, electric and magnetic fields and radiation belts 19 p3520 A70-38277

Apollo spacecraft tests in Space Environment Simulation Laboratory, discussing thermal data, astronaut training, extravehicular activity, reaction control system, etc 21 p3805 A70-41271

Thermoelectric outer planet spacecraft (TOPS/flight environment, systems design and Titan 3D/Centaur launch vehicle with Burner II upper stage 21 p3930 A70-41795

Skylab Orbital Workshop fabrication experiments under space environment conditions, discussing weightlessness and vacuum effects on various manufacturing techniques 22 p4046 A70-43075

Apollo program medical data contribution to knowledge of human response to space environment 22 p3980 A70-43651

Environmental engineering - Conference, Delft University, Netherlands, April 1970 23 p4268 A70-44326

Materials problems in space and spacecraft environments, discussing particle density, composition and UV radiation, spacecraft structure, payloads, vibration, etc 23 p4209 A70-44328

Temperature measurement on thin steel shield subjected to hydrogen peroxide motor exhaust heating at cryogenic temperatures in space 23 p4280 A70-44389

AEROSPACE INDUSTRY

NT AIRCRAFT INDUSTRY

Technology transfer between large company aerospace group and commercial products group 02 p0403 A70-12636

Technology transfer experience in terms of aerospace company policies and technical management mechanics 02 p0389 A70-12638

German society of aeronautics and astronautics, yearbook 1968 03 p0411 A70-13789

Aeronautics and astronautics sociopolitical aspects, discussing German scientific and industrial organization, American-European technology gap, taxation for research, etc 04 p0788 A70-15181

Polycrystalline metals strength factors in aircraft and aerospace construction as relation between rupture time and embrittled grain boundary at high temperatures 04 p0779 A70-15671

Filament winding methods of aerospace industry based on motor case winding, emphasizing reinforcing materials, winding geometry and finished composite evaluation methods 05 p0856 A70-16615

Solid film lubricants pretreatment and applications in aircraft and aerospace industries 06 p1075 A70-17341

Quality control manager role in aerospace company overall cost reduction 06 p1185 A70-17987

Aerospace scientific and engineering work force movement between geographical areas and resource location 07 p1426 A70-18799

Aerospace ground air conditioning design, discussing ground support equipment, manuals, manufacturer catalogs, etc [SAE-AIR-992] 07 p1248 A70-18808

Static electricity hazards and problems in electronics and aerospace industries 07 p1333 A70-18930

Italian aviation and space industry development for local and sectional character and participation in European production 10 p1971 A70-24663

Aviation and space industry metallic and nonmetallic materials testing, discussing corrosion and ultimate fatigue due to impurities 10 p1861 A70-24664

Industry role in sounding rocket program, highlighting activities in various areas 13 p2523 A70-28679

HF resistance welding and roll diffusion bonding fabrication of thin complex structures from Ti alloys in aerospace industry 13 p2418 A70-28828

Engineering design and drafting techniques in aerospace industry, emphasizing cost reduction 13 p2423 A70-29820

Program risk analysis by aerospace industry pursuant to Federal Government procurement requirements 16 p3003 A70-33427

Titanium electron beam welding in aerospace industry, discussing alloy properties and strength behavior 16 p2919 A70-33683

Aircraft interiors products and services supplied by British firms 16 p2841 A70-33768

Mono Graf casting process for Ti alloy aerospace applications, utilizing high strength/weight ratio and corrosion resistance 17 p3097 A70-34361

Aerospace industry instrumentation - Conference, Las Vegas, May 1969, Volume 15 17 p3091 A70-35476

Instrumentation in aerospace industry - Conference, Seattle, May 1970 19 p3423 A70-37873

Space environment simulation installations design, discussing aerospace industry requirements 19 p3554 A70-38278

Aerospace industry in Europe, discussing role in electronics, international cooperation and projects allocation 19 p3554 A70-38493

Instrumentation magnetic recorders in aerospace industry in relation to new components and techniques development, investigating airborne recorder as flight test tool 19 p3429 A70-38516

Value engineering for British aerospace industry management planning 19 p3555 A70-38619

British government technological partnership with domestic industry and other countries 21 p3956 A70-41892

Magnesium Al and Ti alloys electron beam welding for aerospace industry, discussing material requirements, weld quality and optimum conditions 22 p4042 A70-42338

Book on guide to aerospace defense contracts covering purchase control, marketing solicitation, project management, reports, logistics etc 22 p4126 A70-42723

U.S. aerospace industry participation in European Application Satellites Program 22 p4127 A70-43506

Industry-university interaction in competitive teaching of spacecraft design 23 p4285 A70-44643

Sandwich structures in aerospace hardware, considering joining methods, materials and geometries [SAE PAPER 700859] 24 p4425 A70-45879

AEROSPACE MEDICINE

Medico-engineering experiment in partially closed ecological system for long term manned space missions 01 p0032 A70-10363

Syncope occurrence among flight crews 01 p0033 A70-10371

Aerospace technology application to biomedical problems in astronautics 01 p0027 A70-11256

French book on aeronautical and astronautical physiopathology and pathology covering stress factors of flying, high speed and altitude including hypoxia, atmospheric vacuum, etc 01 p0029 A70-11380

Interview with Yegorov, discussing ECG, EEG, muscular effort, eyeball movement, blood pressure changes and vision changes during space flight 02 p0230 A70-11675

Respiratory and cardiac activities, body weight variations, blood and urine electrolytic composition of astronauts during Soyuz orbital flights from medical tests 03 p0423 A70-13709

Pharmacology for long term manned space 04 p0629 A70-14566

Crew requirements influence on systems design and operations criteria for long duration biomedical and behavioral measurement program in earth orbiting space laboratory [ASME PAPER 69-WA/BHF-17] 04 p0643 A70-14858

Physician-monitored central control facility communicating with remote site facilities staffed by paramedical personnel for public health care, based on aerospace experience 04 p0644 A70-15357

Radiography of spine in seated position, discussing aircraft seats, aeronautical ergonomics, etc 05 p0804 A70-15765

German research institutes activities in fluid mechanics, structural materials, propulsion, flight control and electronics, space physics and medicine 05 p0829 A70-16374

Flying disability period due to coccidioidomycosis in southwestern U.S., giving recommendations for earlier return to flying duty 06 p1000 A70-17300

Pilots temporal lobe epilepsy case history and diagnosis 06 p1000 A70-17301

Biomedical concepts for aerospace engineering, discussing human body as self regulating system /homeostasis/ and physiological time regulator /cyclostasis/ 06 p0992 A70-17315

Automatic control of continuous medical monitoring in manned space flight 07 p1220 A70-19512

Asymptomatic pilot with idiopathic paralysis of hemidiaphragm, discussing clinical picture and aeromedical significance 07 p1215 A70-19942

Aviation medicine, discussing pilots physical fitness and training, spatial orientation, ground crew, data flow, etc 08 p1451 A70-20977

Cardiovascular aging and aeromedical maintenance programs for selecting test pilots 08 p1453 A70-21739

Soviet bibliography on aviation, high altitude and space biology and medicine 09 p1615 A70-22204

German collection of papers on flight stress and medicine 09 p1624 A70-23002

Aeromedical Evacuation System in overall treatment process for seriously ill patient 09 p1628 A70-23467

Respiratory and cardiac activities, body weight variations, blood and urine electrolytic composition of astronauts during Soyuz orbital flights from medical tests 11 p1985 A70-25509

Automatic control of continuous medical monitoring in manned space flight 11 p1991 A70-26111

Report to COSPAR on space exploration research in Poland including satellite tracking, geodesy, meteorology and aerospace medicine 15 p2830 A70-31721

Soviet monograph on gas laws in aviation medicine for reduced oxygen pressure pathology, discussing kinetic theory, temperature effects, solubility, diffusion, etc 15 p2682 A70-31925

Space research cost effectiveness in weather forecasting, TV broadcasting, space biology and medicine, geodesy, aerial and maritime navigation, earth resources, etc 15 p2811 A70-32283

Air sickness frequency, pathogenesis and prevention, discussing cadet selection 17 p3037 A70-35129

Aerospace Medical Association Conference, St. Louis, April 1970 17 p3026 A70-35326

In-flight coronary occlusions role in aircraft accidents, discussing need for full autopsies, Double Masters ECG and full medical histories 17 p3033 A70-35570

Medicobiological approach to living conditions for sustained residence and human activity during prolonged space flights, describing sealed chamber experiment 19 p3367 A70-37525

Medical support for long space missions based on space crews morbidity prediction, discussing onboard equipment and astronaut training 20 p3575 A70-40194

- Astronauts medical examination, using thermal load as functional and diagnostic test 20 p3575 A70-40195
- Neurotic syndromes in aviation medicine, discussing acute reactions, anxiety, depressions, structured syndromes and psychosomatic disorders 21 p3771 A70-41490
- Flight crews with aortic insufficiency, observing hemodynamically insignificant valvular defect 21 p3771 A70-41492
- Apollo program medical data contribution to knowledge of human response to space environment 22 p3980 A70-43651
- Aerospace medicine - Conference, Amsterdam, September 1969 22 p3973 A70-43690
- Cardiological examination of flying personnel, taking ECG anomalies and artery wall elasticity into account 22 p3981 A70-43694
- Aerospace medicine approach to medical investigation training for aircraft accidents, noting flight surgeon role as life support specialists chief 23 p4152 A70-44454
- Aviation psychiatry role in pilots selection and treatment 24 p4296 A70-45124
- Occipital migraine in flying personnel, discussing diagnosis and flight status disposition 24 p4297 A70-45344
- AEROSPACE SCIENCES**
- X ray spectrometer for space science and laboratory research, presenting CrK spectrum and fine structure 01 p0092 A70-11172
- IR systems in military intelligence and space research including aerospace and planetary investigations, discussing IR detection and IR and earth radiation 01 p0144 A70-11255
- Soviet book on physicochemical basis of space research covering near earth and interplanetary environmental factors and effects on spacecraft designs and materials 02 p0360 A70-11693
- ESRO aims, structure and achievements in space technology improvement by research involving satellites, interplanetary probes and sounding rockets 06 p1185 A70-18395
- Space research in terms of earth environment in space, discussing near-earth spacecraft role in solar, magnetospheric and ionospheric studies 08 p1488 A70-21344
- Large scale aerospace data acquisition, processing, handling and dissemination systems analysis and design [AIAA PAPER 70-322] 09 p1641 A70-22865
- Data management functions of National Space Science Data Center /NSSDC/, discussing data processing and information system for secondary usage [AIAA PAPER 70-320] 09 p1641 A70-22866
- Photo-optical processes and optical measuring techniques in research programs at Ames Research Center for aerodynamics, life sciences and space sciences 09 p1657 A70-23501
- Collection of papers on analytical chemistry in space covering solar system history, atmospheres, composition, lunar and planetary surface analysis, mass spectroscopy, etc 10 p1941 A70-24608
- Book on space physics covering earth radiation belts, atmosphere, ionosphere, and magnetosphere, solar structure and composition, interplanetary space, etc 12 p2309 A70-27973
- Weak magnetic fields in geo- and space physics - Conference, Paris, May 1969 13 p2413 A70-30026
- Applied sciences research and utilization of lunar resources - Conference, New York, October 1968 14 p2633 A70-30192
- Collection of papers on space science and technology covering lunar and planetary explorations, trans-tellar navigation, Trojan Relay satellite communication, utility, etc 15 p2800 A70-32057
- Space technology and science - Conference, Tokyo, August 1969 17 p3164 A70-35201
- Space orientation vs geocentrism in science and philosophy 19 p3553 A70-37397
- Space technology spin-off benefits to mankind, considering medical and industrial applications 19 p3554 A70-38609
- Orbital international laboratory and space sciences - Conference, Cloudcroft, New Mexico, September 1969 22 p4107 A70-43626
- Space and astronomic methods applied to solid earth and ocean physics 22 p4025 A70-43669
- Data management functions of National Space Science Data Center /NSSDC/, discussing data processing and information system for secondary usage [AIAA PAPER 70-320] 23 p4285 A70-44514
- Experimental astronomy and role of space technology, discussing artificial satellites, extraterrestrial life, moon, Mars and Venus exploration, etc 23 p4247 A70-44775
- Satellite data acquisition and dissemination functions of National Space Science Data Center /NSSDC/ 24 p3422 A70-45615
- AEROSPACE SYSTEMS**
- Computer program for automatically selecting redundant parts and redundancy types for various aerospace systems characteristics 01 p0103 A70-10488
- Quick-disconnect couplings selection guide for aerospace fluid systems, emphasizing functional and weight considerations [SAE-AIR-1047A] 01 p0197 A70-11461
- NASA aerospace system safety program implementation and supporting organization with emphasis on background, concepts, constraints, methods and results [SAE PAPER 690710] 05 p0792 A70-15856
- Electronics and Aerospace Systems - IEEE Conference, Washington, D.C., October 1969 12 p2185 A70-27901
- Collection of papers on space science and technology covering lunar and planetary explorations, trans-tellar navigation, Trojan Relay satellite communication, utility, etc 15 p2800 A70-32057
- Astronautics utility in astronomy, physics, earth observation, communication, commercial, military, navigational, meteorological, social applications, considering present and future possibilities 15 p2831 A70-32062
- Technical methods defining, monitoring and controlling life limited aerospace components during storage 19 p3441 A70-38831
- Aerospace methods for revealing and evaluating earth resources - Conference, Princeton University, September 1969 20 p3615 A70-39051
- Space systems and thermal technology - ASME Conference, Los Angeles, June 1970, Part 2 21 p3942 A70-41014
- Aerospace digital computers impact on aerospace systems design 21 p3794 A70-41685
- Computerized aerospace systems man machine interface mechanization for performance optimization, emphasizing integrated approach to avionic displays 21 p3795 A70-41689
- Aerospace system design, considering use of microprogram-controlled digital computers 21 p3795 A70-41690
- High speed aerospace homopolar alternator, calculating end zone three dimensional magnetic flux distribution and leakage reactance 22 p3999 A70-43585
- Space systems supporting international air transportation growth, discussing UHF satellite R and D programs on beam antennas [SAE PAPER 700760] 24 p4372 A70-45870
- Space transportation system concept and operational objectives, discussing configurational aspects, aerodynamic complexity, propulsion systems, payloads, performance and aerothermodynamic constraints, etc [AIAA PAPER 70-1249] 24 p4418 A70-45965
- AEROSPACE VEHICLES**
- Aerospace vehicles testing cost and technical analysis, discussing component failure, motivation effects, test design optimization, flight simulation, etc [AIAA PAPER 70-239] 07 p3196 A70-20379
- Global distribution and intensity of solar radiation, determining radiation of satellites and other high altitude devices 11 p2105 A70-26010
- Statistical analysis of photogrammetrically surveyed three dimensional space points sets for aerospace vehicles and projectiles position location 15 p2733 A70-31550
- Neighboring optimum feedback control scheme for aerospace vehicles to handle small disturbances from nominal trajectory with unspecified final time 16 p2887 A70-33438
- Composite materials in aerospace vehicle design, discussing mechanical behavior, applications and characteristics 17 p3127 A70-34674
- Seismic fluid suspended triaxial angular accelerometer for high performance aerospace vehicle flight test application 19 p3431 A70-38540
- Papers on aerospace vehicle flight control systems covering controller design, flow difference sensors, etc 21 p3926 A70-40780
- Aerospace vehicles testing cost and technical analysis, discussing component failure, motivation effects, test design optimization, flight simulation, etc [AIAA PAPER 70-239] 21 p3931 A70-41876
- AEROSTATS**
- U AIRSHIPS**
- AEROTHERMOCHEMISTRY**
- Aerothermochemistry of two phase flow in gaseous media of solid or liquid particles or spherical gas pockets [ONERA-TP-691] 08 p1600 A70-21848
- Space vehicle reentry hypersonic boundary layer characteristics, considering air components chemical reactions due to excessive heat 18 p3346 A70-36384
- AEROTHERMODYNAMICS**
- Turbulent heat transfer on heated horizontal circular cylinder rotating freely in space, discussing dimensionless numbers relations and frictional heating 01 p0215 A70-10926
- Aerodynamics, heat and mass transfer in vapor condensation from humid air on flat plate in longitudinal flow in asymmetrically cooled slot 01 p0004 A70-11178
- Wind tunnel tests for aerodynamic and thermal environment of hypersonic glider VERAS /Vehicle for Experimentation and Research in Aerothermodynamics and Structures/ [DGLR-69-042] 07 p1187 A70-18981
- Quasi-steady analysis of material under ablation-erosion heat transfer for hypersonic vehicles 11 p2149 A70-26144
- Aerothermopressor experiment in subsonic and supersonic gas flow compared with numerical solutions of equations 15 p2720 A70-31900
- Hypersonic glider VERAS aerodynamic and thermal environments, noting wind tunnel tests by thermosensitive paint method 16 p2837 A70-33765
- Aerospace thermophysics considerations in spacecraft and hypervelocity vehicles systems thermal design, discussing thermal control and control coatings optical and radiative properties [AIAA PAPER 70-812] 17 p3194 A70-34509
- Soviet papers on aerothermodynamics covering turbulent and laminar boundary layers, heat and mass transfer, etc 20 p3610 A70-39801
- Thermal and aerodynamic interactions between wires of velocity sensitive anemometric crossed-wire probe, showing reduction by correction of measurements and minimal gap 22 p4038 A70-43242
- Space transportation system concept and operational objectives, discussing configurational aspects, aerodynamic complexity, propulsion systems, payloads, performance and aerothermodynamic constraints, etc [AIAA PAPER 70-1249] 24 p4418 A70-45965
- AEROTHERMOELASTICITY**
- Aeroelastic and aerothermoelastic development of winged interorbital space shuttle concerning panel flutter, stability and nonstationary lifting surface theory 23 p4273 A70-44760
- AEROZINE**
- Water or bromotrifluoromethane content required in propellant Aerozine-50 /A-50/ spill to inert against ignition in air, considering fire extinguishment 04 p0732 A70-15408
- Aerozine-50 toxicity therapeutic treatment by pyridoxine and phenobarbital resulting in 100 percent survival of mice 07 p1222 A70-19926
- AFC [CONTROL]**
- U AUTOMATIC FREQUENCY CONTROL**
- AFCS [CONTROL SYSTEM]**
- U AUTOMATIC FLIGHT CONTROL**
- AFFERENT NERVOUS SYSTEMS**
- Relationships between frog vestibular afferents, cerebellum and efferent vestibular system, using electron microscopy and Nauta degeneration technique 01 p0014 A70-10351
- Termination mode of primary and secondary vestibular fibers in cerebellar cortex of frog and cat, measuring evoked field and unitary potentials 01 p0014 A70-10353
- Evoked potentials arising in entorhinal cortex of rabbits in response to stimulation of somatic nerves, light and sound 03 p0417 A70-13070
- Skin sensitivity representation in cats cerebellar cortex during electrocutaneous stimulation in chronic experiment, providing information on afferent system 03 p0417 A70-13216
- Thalamic N.VPL role in distributing afferent flux in anesthetized cats cortex, using stimulating contralateral sciatic nerve 07 p1199 A70-18723
- Efferent and afferent fibers presence in optic nerves determined by unilateral and bilateral enucleation of dogs and cats 07 p1207 A70-19476
- Light sensitivity restoration in humans exposed to bright flashes, studying photonic afferent system braking effect on scotopic system 08 p1450 A70-20747

- Anterior lobe role of brain limbic region in analysis of afferent pulses arising in receptors of respiratory system
11 p1987 A70-25942
- Mammalian ultricular macula design, considering microelectrode data and information from light and electron microscopy, behavioral experiments and computer simulation
11 p1988 A70-26231
- Evoked cerebellar potentials time characteristics during spinal cord stimulation in cats, investigating cerebellar intercentral connections effect
13 p2353 A70-29357
- Skin receptors afferent discharge characteristics during vibrotactile stimulation
13 p2354 A70-29594
- Human cerebral cortex intercentral relations during repose and afferent stimulation, using electroencephalogram cross correlation
15 p2687 A70-32868
- AFFINITY**
Mass spectrometric determination of proton affinities of simple molecules determined from proton transfer and ion-molecule reactions
05 p0885 A70-17081
- Hydrogen ion-molecule reactions analysis by flowing afterglow technique, noting application to proton affinity measurement
16 p2857 A70-34005
- AFRICA**
Air cargo transport routes and geographical distribution, examining development in African countries
02 p0402 A70-12225
- Ocean floor-spreading tectonic effects, considering Arabian Shield separation from African continent
24 p4332 A70-46408
- AFTERBODIES**
Drag reduction on blunt-based body of revolution with boat-tailed afterbodies in low speed flow
05 p0790 A70-16501
- Cylindrical afterbody drag reduction in transonic flow by combined gas ejection and boat-tailing
11 p1976 A70-25991
- Turbulent base pressure on conical afterbodies in supersonic axisymmetric flow, including initial direction effect
[AIAA PAPER 70-555] 13 p2340 A70-29020
- Pressure distribution and drag for inviscid flow past slender sharp-nosed fuselages and afterbodies at arbitrary transonic Mach numbers
[AIAA PAPER 70-556] 13 p2340 A70-29021
- Subcylindrical boom at base of spin stabilized projectile shown to produce aerodynamic changes in static and Magnus moments
[AIAA PAPER 70-558] 13 p2340 A70-29023
- Single and twin jet afterbody configuration models, describing drag and interference characteristics at subsonic speeds
14 p2528 A70-30862
- Close-spaced nozzles twin jet configuration, achieving low nozzle and total afterbody drag
[AIAA PAPER 70-934] 17 p3149 A70-35844
- Drag optimal stem section of plane body at supersonic flow, allowing for friction forces
18 p3206 A70-36261
- Cylindrical afterbodies base pressure drag under powered supersonic flight, modifying Korst flow model recompression criterion
22 p3959 A70-42713
- AFTERBURNERS**
U AFTERBURNING
AFTERBURNING
Stable two phase water flow system for transpiration cooling in thermal protection of SST noise suppressor situated in afterburning engine exhaust gas stream
[AIAA PAPER 70-151] 06 p1181 A70-18146
- Main stream interaction with flame stabilizing jets in combustion chambers and afterburners using gas dynamic models
07 p1419 A70-18754
- Mixture composition and airflow rate dependence of combustion efficiency in turboprop afterburner chamber with air-fuel flame stabilizer
10 p1929 A70-24282
- Chemical kinetic and turbulent transport coefficients effects on afterburning rocket exhaust plumes and sea level transverse radar attenuations
[AIAA PAPER 70-733] 17 p3194 A70-34513
- Turboprop engines afterburner flame stabilization at low inlet temperature, noting flame holder geometry role
22 p4088 A70-42336
- Allison/Rolls-Royce TF41 turboprop engine improved power and reduced weight versions, comparing afterburning Model 912-B23 to nonafterburning TF41-A-2
23 p4234 A70-44596
- AFTERGLOWS**
NT HELIUM AFTERGLOW
NT OXYGEN AFTERGLOW
Negative ion reactions relevant to D region measured in ESSA flowing afterglow system as function of temperature
01 p0070 A70-10406
- Atomic O, H and D and molecular oxygen, deuterium and sulfur hexafluoride effects on nitrogen vibrational population distribution in nitrogen afterglow
01 p0148 A70-11356
- Microwave cavity perturbation measurements of electron densities at electroacoustic resonances excited in afterglow plasma
04 p0728 A70-15004
- Stationary nitric oxide afterglow, studying molecular ionic species by time resolved mass spectrometry
06 p1114 A70-18635
- Production rate constants for hydrated positive ions in photoionized nitric oxide-water afterglows
07 p1346 A70-20245
- Coupled differential rate equations governing growth and decay of positive and negative ion and electron concentrations in afterglow with ambipolar diffusion and electron attachment
11 p2088 A70-25703
- Artificial aurora generated by Starfish in northern conjugate region and afterglow spectra
14 p2578 A70-31245
- Nitrogen dioxide continuum in green-white afterglow of molecular oxygen and nitrogen, using spectrometry and photometry
14 p2579 A70-31254
- Atomic emission in water vapor afterglow, revealing presence of Balmer series of H atom with sodium D line
14 p2579 A70-31255
- Rare gas diatomic ions reactions with molecules and rare gas atoms, measuring rate coefficients and product channels by flowing afterglow technique
15 p2776 A70-31726
- Ni particles induced quenching measured by probes in afterglow plasma of pulsed linear discharge, determining deionization rate
16 p2958 A70-33687
- Cold nonuniform plasma slab model for afterglow echoes at upper hybrid resonance in uniform magnetic field
20 p3679 A70-39664
- Lunar postsunset horizon afterglow observed by Surveyor 7, discussing small particle diffraction on surface
20 p3708 A70-39960
- Carbon dioxide-He-nitrogen gas mixture pulsed discharge system afterglow gain measurements up to one atmosphere, using CW laser
21 p3837 A70-41719
- LF self excited oscillations in inhomogeneous afterglow magnetoplasma measured by Langmuir probe, noting dissipative drift instabilities
22 p4079 A70-42372
- Pulsating light source afterglow increasing high speed film information content, discussing streak image, tearing process and impact stress tests
[SMPT PREPRINT 66] 22 p4032 A70-43036
- AFTERIMAGES**
Human size-selective neurons indicated by aftereffect from successive viewing of striped patterns with different spatial frequencies
01 p0035 A70-10724
- Rod aftereffect relationship to percent rhodopsin bleached in S potentials from cat retina
05 p0801 A70-16381
- Perceptual suppression of retinal emissive afterimages by rapid eye movements
23 p4147 A70-44780
- AGC [CONTROL]**
U AUTOMATIC GAIN CONTROL
AGE DETERMINATION
U CHRONOLOGY
AGE FACTOR
Visual faculties testing to improve performances in visual inspection tasks, considering threshold line concept and visual performance relation to age
01 p0023 A70-10862
- Hemoglobin concentration in red blood cells in men of various ages as function of altitude, discussing correlations with body weight and plasma protein
01 p0024 A70-10978
- Age correlations with ballistocardiogram amplitudes and waveform grades in test pilots
02 p0240 A70-12683
- Red blood cell mechanical fragility independence from cell age in rats
06 p0989 A70-17221
- Static tensibility and vital capacity of lungs statistically analyzed in relation to sex and age
07 p1210 A70-19524
- Vectorcardiogram variations of clinically normal individuals over forty compared with young adults
08 p1452 A70-21264
- Human movement speed and accuracy as function of age in pencil tapping between paper-drawn targets
10 p1817 A70-24711
- Zero age intermediate and low mass stellar models and evaluation of physical parameters for population I and II chemical compositions
10 p1944 A70-24955
- Aged pilots hearing acuity using speech audiometry, noting discrimination loss for HF verbal sounds
11 p1990 A70-25669
- Age and retinal illumination influence on human pupillary near reflex investigated by photographic measurements
12 p2171 A70-28036
- Maximal oxygen intake, pulse heart rate and lactate levels variations with physical activity in middle aged man free of cardiovascular disease
13 p2356 A70-29826
- Lunar maria absolute age from lunar craters rim height changes via isostatic settling and small craters quantity
14 p2649 A70-31213
- Intrinsic heart rate /IHR/ range and variability in healthy subjects measured showing age as important determinant in absence of heart disease
15 p2678 A70-31433
- Excitation conduction velocity maximum along motor fibers of peripheral nerves as function of age in healthy subjects
15 p2679 A70-31602
- Pulmonary vital capacity measurements in young recruits for respiratory function, considering relationship to body weight and height
16 p2850 A70-34348
- O-B5 stars mean ages estimation by hyperbolic approximation based on distribution in stellar associations
19 p3524 A70-38762
- Thermally prepared poly-alpha-amino acids catalytic activity after long term dry state storage, suggesting enzyme activity role in biological evolution
21 p3772 A70-40713
- Age, grade, educational institution and attitude effects on pilot personality test performance
22 p3977 A70-42870
- Age determined hemodynamic reactions in men and women performing walking motions in lying position
22 p3970 A70-42908
- Time constant loci and theoretical luminosity functions for various compositions and ages of metal poor globular clusters
22 p4108 A70-43735
- Inherited hypertension genetic and autonomic factors, discussing rats crossbreeding for genetic contribution ratio in males vs females, age effects, etc
24 p4299 A70-45806
- AGE HARDENING**
U PRECIPITATION HARDENING
AGENA D ROCKET VEHICLE
Agena D vehicle self destruct charge ordnance component, discussing design, performance and tests
16 p2963 A70-34126
- AGENA ROCKET VEHICLES**
NT AGENA D ROCKET VEHICLE
Agena propulsion system performance model for predicting propellant flow rate, mixture ratio, thrust time and specific impulse
[AIAA PAPER 69-453] 14 p2629 A70-30754
- AGGLOMERATION**
Teflon-bonded gas diffusion electrode flooded agglomerate model, determining porosity, surface area, IR drop, etc
10 p1829 A70-24455
- AGGREGATES**
Stellar rings and galactic structure, examining prolate ellipsoidal star aggregate diameter constancy
18 p3330 A70-37187
- AGING**
Solid propellant mechanical properties tests, failure and physical deterioration /aging/
07 p1361 A70-19913
- Minuteman 3 Reentry System real time laboratory aging and surveillance test program to evaluate long-term storage effects on equipment behavior
[AIAA PAPER 70-395] 10 p1952 A70-24910
- AGING [BIOLOGY]**
Diffusion phenomenon in cross linkage theory of biological aging formulated as model in differential equation form, obtaining solution and applications
01 p0028 A70-11374
- Chronological age correlations with ballistocardiographic modalities /stroke volume and minute volume indices/ for patients with no cardiovascular disease
02 p0248 A70-12682
- Collection of papers on physical activity and aging, discussing physiology, biochemistry, coronary patients cardiovascular performance, electrocardiography, pathology, epidemiology, etc
07 p1211 A70-19689
- Physical training effects on factors in cardiovascular system influenced by age
07 p1212 A70-19691
- Cardiovascular aging and aeromedical maintenance programs for selecting test pilots
08 p1453 A70-21739
- Cotton leaf light reflectance and transmittance changes with maturity
12 p2218 A70-26919
- Human lung closing and subdivision volume relationship to age and body position
12 p2169 A70-27657
- Motor reactions and neural negative induction duration in male and female human subjects of different ages
12 p2174 A70-28356

- Maximum oxygen uptake correlation to age of subjects performing physical and sedentary work
13 p2350 A70-29112
- Maximal oxygen intake, pulse heart rate and lactate levels variations with physical activity in middle aged man free of cardiovascular disease
13 p2356 A70-29826
- Senescent *Drosophila melanogaster* flight muscle electron microscopic examination showing mitochondria in stages of degeneration
20 p3574 A70-40075
- Jet pilot aging effects on physical functions based on medical examinations during six years, noting visual accommodation changes
22 p3978 A70-42878
- Motor activity and aging - Conference, Kiev, April 1968
22 p3967 A70-42893
- Muscular activity in regulation of organism functions during aging, considering hypokinesia effects
22 p3968 A70-42894
- Muscular activity influence on energetic processes and functions in aging organism, relating oxygen consumption to aerobic metabolism
22 p3968 A70-42895
- Adaptation of cardiovascular system in aging and old individuals under muscular activity
22 p3968 A70-42896
- Active recreation in motor function regulation in aging individuals
22 p3968 A70-42897
- Aged conditioned changes in muscular working capacity, relating developments in functionally labile nerve centers
22 p3969 A70-42898
- Body oxygen control under muscular activity in aging individuals
22 p3969 A70-42899
- Anaerobic carbohydrate metabolism in aging individuals under physical loads
22 p3969 A70-42900
- Mathematical model of heart beat control during muscular activity in aging individuals, reflecting neural and hormonal control circuits
22 p3969 A70-42901
- Kinesophilia mechanisms of motor-visceral integration in aging organism
22 p3969 A70-42902
- Occupational and age composition of working population of U.S.S.R., comparing cardiovascular and respiratory systems
22 p3969 A70-42904
- Physical training effects on blood circulation, respiratory and muscular functions in aging persons
22 p3970 A70-42905
- Hemodynamic indices of aged individuals engaging in physical exercises over long period of time
22 p3970 A70-42906
- Contractive function of myocardium in middle and advanced age individuals under high physical loads during prolonged periods
22 p3970 A70-42907
- Coronary heart disease prediction based on clinical suspicion, age, total cholesterol and triglyceride, using relationships established by cinearteriographic studies
23 p4145 A70-43947
- Cardiovascular dimensions changes and heart volume in physically trained young men, comparing with response in old age
24 p4303 A70-46109
- AGING [METALLURGY]**
- Combined aging and plastic deformation treatment effects on breaking point, yield stress, elongation and contraction of austenitic Fe-Ni-Ti alloy
01 p0115 A70-10064
- Ni-Cb intermetallics phase precipitation during aging of Inconel alloy 718, composition, stability and structure
01 p0116 A70-10093
- Dielectric layers electrical conductivity in ceramics containing Ti during aging, observing different characteristics ascribed to nonequilibrium current carriers injection
01 p0156 A70-10221
- Critical current density enhancement in Ta-rich Zr alloys in magnetic fields at low temperature after aging
01 p0122 A70-11238
- Ternary Al-Zn-Mg alloys stress corrosion cracking properties, showing effects of aging temperature and prestrain
01 p0123 A70-11387
- Ti-Mn alloy quenched in brine and aged at high temperature studied for structural transformations using electron microscope
01 p0125 A70-11640
- Calorimetric analysis and hardness test to investigate low temperature aging behavior of maraging stainless steels
01 p0125 A70-11642
- Strain hardening on single crystals of aging Ni-based alloys with ordered separated phase
03 p0505 A70-13104
- Intermediate aging influence on Bauschinger effect in low carbon steel at 270 C and 2 hr holding time
04 p0776 A70-15266
- Maraging steel mechanical properties as function of aging temperature and time
05 p0865 A70-16873
- Recrystallization behavior of Al alloy containing Mg and Si subjected to maximum aging before cold working
06 p1085 A70-17418
- Alloy specimen shortening due to aging during stress relaxation under vibration
07 p1304 A70-18820
- Interstitial atoms effect on dislocation relaxation and aging of Mo and Nb single crystals
07 p1309 A70-19638
- Al-Mg alloys mechanical properties and corrosion resistance during aging, noting Zr and Mo additives effects
08 p1517 A70-21129
- Yield strength of cold worked MP Co-Ni alloys during aging at elevated temperatures, noting behavior in overaged condition
08 p1525 A70-21960
- Aged Al-Cu alloys hardness test data normalized and correlated for interpretation in terms of physical metallurgy
08 p1525 A70-21967
- Growth kinetics of gamma prime precipitate in Ni-Ti alloy noting Ti content variation as function of aging
09 p1706 A70-22812
- Lattice defects in Al-Zn alloy due to fatigue investigated for mechanism and effect on aging kinetics by resistivity measurement
09 p1707 A70-23326
- Isomorphous beta type Ti-Mo alloy omega phase transformations and morphology by electron microscopy, relating hardness to aging
10 p1902 A70-23817
- Duplex aging treatment effect on Ni-Co-Mo-Ti maraging steels mechanical properties
10 p1905 A70-25171
- Zone and phase aging of aluminum alloys, discussing structural and property characteristics of solid solution decomposition
11 p2066 A70-25912
- Ti-8Al alloy embrittlement from ordered phase precipitation during aging using tensile, impact and hardness tests, optical and electron transmission microscopies
13 p2436 A70-29624
- Al-Zn-Mg alloys aging kinetics and rupture mechanism, discussing stress corrosion, welded structures stability, activation energy, etc
14 p2597 A70-30965
- Plastic deformation and aging effects on fatigue characteristics of steels until rupture under cyclic loads
15 p2755 A70-31540
- Omega phase embrittlement in aged Ti-V alloys, discussing precipitation effect on tensile properties
15 p2756 A70-31570
- Phase transformations in beta isomorphous Ti alloys, discussing effects on omega and alpha phases during quenching and aging and on martensite under stress
15 p2763 A70-32807
- Preprecipitation and reversion stages in Ni-Co-Mo steel, observing dislocation nucleated phase growth initiation by aging
16 p2929 A70-33047
- Weld cracks in welded joints of Ni-Cr base alloys due to residual stresses during aging, recommending annealing for prevention
16 p2930 A70-33051
- Metastable beta phase decomposition in Ti alloy during mechanothermal treatment and aging, determining correspondence to alpha phase segregations via electron microscopy
16 p2931 A70-33207
- Gamma phase particle distribution changes in homogeneous segregation in Co-Ti alloy attributed to elastic interaction during aging temperature changes
16 p2931 A70-33208
- Metastable ageable beta Ti-Mo-V-Fe-Al alloy, discussing plate, sheet and forgings producibility, metallurgical characteristics and structural properties
17 p3121 A70-34435
- Omega transformation in Hf-Nb alloys, investigating aging at various temperatures
18 p3273 A70-36044
- Carbide precipitation and grain boundary migration in solution annealed duplex stainless steel as function of aging time
18 p3274 A70-36050
- High temperature reaging in Ni-Cr-Ti austenitic steel following reversion and interrupted quenching
18 p3274 A70-36054
- Ti-Al alloys room temperature mechanical properties after age hardening
18 p3274 A70-36055
- Automatic dilatometers for volume variations in steel and Co-W alloy during aging and heat treatment, noting microstructural changes
18 p3257 A70-36202
- Internal residual stress relaxation theory in dielectric aging in tetragonal solid solutions of calcium titanate in barium titanate
19 p3486 A70-37776
- Ternary Al-Cu-Mg alloys, considering aged structure relationship to fatigue strength
19 p3454 A70-38955
- Ni-Cr heat resistant alloys structural transformation kinetics under aging, creep and operational conditions, discussing solid solution decomposition, hardening phases coagulation and dissolution, etc
20 p3645 A70-39037
- Microstructure and phase distribution in maraging steels subjected to austenization and subsequent aging in reversible transformation temperature range
20 p3645 A70-39038
- Beta Ti alloy decomposition study during aging by diffraction electron microscopy, forming finely dispersed coherent precipitates
20 p3645 A70-39041
- Two stage aging effects on stress corrosion cracking of Al-Zn-Mg alloys, discussing precipitated particles size, surface roughness change and temperature effects
22 p4052 A70-42306
- Low alloy Mo sheet recovery and aging characteristics studied by X ray scattering
22 p4055 A70-43124
- Al-Be-Mg alloys under solution treatment, noting aging and prolonged heating effects on mechanical properties from solid solution decomposition diagram
22 p4056 A70-43127
- Alloy aging process after plastic deformation, examining relationship of phase distribution and mechanical and physical properties
22 p4056 A70-43340
- Al-Zn-Mg alloy prolonged aging behavior, examining Gp and intermediate zones, equilibrium phases, maximum strength and serrated stress strain curve
24 p4362 A70-46189
- Zn-Al alloy high velocity deformation characteristics, examining ductility and aging at various temperatures and heat treatments
24 p4363 A70-46194
- AGITATION**
- NT ULTRASONIC AGITATION**
- AGRICULTURAL AIRCRAFT**
- U UTILITY AIRCRAFT**
- AGRICULTURE**
- Earth resources satellites use in agriculture, considering materials reflectance and emittance, electromagnetic spectrum wavelengths identification and data accuracy standards
01 p0220 A70-10624
- Carrot plants growing during 374 days in conveyor type aeroponic assembly, noting yield and morphological features
03 p0436 A70-13902
- Multispectral scanner for Earth Resources Technology Satellite, discussing agriculture applications and advantages over return beam vidicon
03 p0493 A70-13957
- Remote sensing application to agriculture, forestry and range resources in terms of human priority over monetary benefits, noting high altitude aircraft use
04 p0788 A70-14638
- Remote sensing data applications to agricultural statistics, discussing policy and standards for aggregate data release, confidentiality, error analysis, etc
09 p1793 A70-22868
- Agricultural pilots fatigue based on flight and environmental effects
11 p1993 A70-26522
- Data acquisition by earth resources technology satellite (ERTS) for user needs in forestry and agriculture
20 p3616 A70-39062
- Aircraft/spacecraft assisted agricultural resource information system design concerning nongovernmental user and remote sensing needs
20 p3740 A70-39067
- Agricultural crop identification, using optical Stokes parameters such as wavelength, geometry, and bidirectional photometric and polarization factors
22 p4014 A70-42769
- AILERONS**
- Aircraft roll rate response and aileron step input matching in terms of modal parameters with flight test records by analog computer program
08 p1465 A70-20781
- Fokker F-28 wing flap, lift dumpers and aileron development, including wind tunnel and flight tests
08 p1438 A70-21864
- Rudder control of aircraft nullifying yawing and sideslip angles, analyzing rolling response to proportional control by ailerons
13 p2348 A70-29450
- Nonlinear balance mass solutions for tab-aileron flutter free operation of jet trainer for arbitrary store configuration
17 p3185 A70-34923
- AIR**
- NT ALVEOLAR AIR**
- NT COMPRESSED AIR**

Aircraft air conditioning, discussing temperature and humidity control, cooling systems, etc
19 p3358 A70-37975

Air conditioning in piston-powered light general aviation aircraft, comparing vapor cycle and cryogenic systems
19 p3359 A70-38500

AIR CONDUCTIVITY
Electrical conductivity of air behind incident and reflected shock wave fronts as function of temperature and Mach numbers measured by electrode method
01 p0095 A70-11622

Pure-tone air conduction audiogram for diagnosis of patients exposed to intense noise indicating conductive or sensorineural origin of loss
09 p1621 A70-23457

AIR COOLING
Aircraft piston engines air cooling analysis, discussing forced cooling for high altitude aircraft and helicopters
02 p0355 A70-12224

Aerodynamic performance of cascade of porous gas turbine blades with cooling air effusion compared with solid noneffusing blades
02 p0355 A70-12311

Air cooling with radial and jet blowing on gas turbine stage, discussing influence on aerodynamic characteristics
03 p0551 A70-13486

Internally air cooled turbine blades and vanes emphasizing coolant aerodynamics, heat transfer and blade life, high temperature in jet engines, etc [AIAA PAPER 22]
03 p0551 A70-13545

Physical theory of ball lightning based on cooling air spheres models, calculating equilibrium composition, temperature profiles, output radiation and mass density
05 p0843 A70-17102

Turbine blade and vane air cooling need established by advantages of operating aircraft turbines at high turbine entry temperatures [AGARDGRAPH-120]
08 p1559 A70-21931

Altitude influence on forced ventilation of cooled electronic apparatus, analyzing flow change and temperature roles
09 p1643 A70-22040

Thermal stresses in gas turbine blade calculated, showing role of initial temperature increase of blade cooling air
09 p1775 A70-22596

Air ventilated cassette-type electronic equipment steady thermal regime, measuring local excess temperatures relative to ambient temperature
11 p2017 A70-25583

Gas turbine shrouded rotating disk system with radial outflow of air coolant, investigating fluid dynamics, pressure distribution and frictional moment [ASME PAPER 70-GT-6]
18 p3208 A70-36862

Powdered flat steel plates cooling by air blown through pores, determining internal heat exchange coefficients
23 p4283 A70-44731

Heat transfer at air cooled gas turbine blade trailing edges at various wall temperatures and Reynolds numbers
23 p4283 A70-44737

Temperature distribution in cylinders of aircraft internal combustion rotary piston engine under air cooling
23 p4234 A70-44742

Avionic components reliability, determining non-steady cooling air environment effects
23 p4175 A70-44744

AIR CURRENTS
NT JET STREAMS [METEOROLOGY]
NT MERIDIONAL FLOW
NT VERTICAL AIR CURRENTS
Air current in upper atmosphere meteor zone above equator, noting diurnal and semidiurnal harmonics in wind velocity components
23 p4188 A70-44049

AIR CUSHION VEHICLES
U GROUND EFFECT MACHINES
AIR DEFENSE
NT ANTIMISSILE DEFENSE
Systems concepts in design of computer operated display systems in air defense and air traffic control systems, discussing alphanumeric display, panoramic display, etc
05 p0827 A70-16183

STRIDA II consoles operation for treating air defense data, discussing data display system, work positions organization and console construction method
05 p0828 A70-16192

Future U.S. aerospace power in terms of military technology and defense policies and attitudes
05 p0960 A70-16633

Tactical air defense multiple site tracking data correlation equation to select gate sizes
11 p2009 A70-26263

Analog-digital real time data automatic acquisition and radar tracking system for air defense and air traffic control
11 p2014 A70-26313

Field maintenance interface between human engineering and maintainability, discussing air defense system malfunction and troubleshooting deficiencies
16 p2852 A70-33665

Displayed cursor velocity effect on radar target acquisition time for subjects in simulated air defense environment
16 p2853 A70-33670

Harrier aircraft in Marine Corps close air support role [AIAA PAPER 70-885]
17 p3018 A70-35804

AIR DENSITY EXPLORER A
U EXPLORER 19 SATELLITE
AIR DUCTS
Boundary layer separation in divergent portion of conical ducts in overrelaxed supersonic regime in air and water, showing influence of medium, pressure and thrust
03 p0467 A70-13682

Air deflection and modulation /ADAM/ turbofan propulsive wing V/STOL design [AIAA PAPER 69-201]
12 p2162 A70-28087

AIR FILTERS
Boeing inertial separator system for eliminating air dust taken by CH-46 helicopter engines during takeoff and landing on unprepared areas
01 p0162 A70-10677

Particle removal efficiency of engine inlet separator-filter devices evaluated at Naval inlet test facility for simulated engine airflows, scavenging conditions, etc
01 p0163 A70-10679

T-63 gas turbine engine air induction system protection for OH-58A light observation helicopter against debris with minimum power loss and intake air distortion
01 p0164 A70-10681

Inertial particle separator-type turbine engine air cleaner for OH-6A light observation helicopter, describing evolution
01 p0164 A70-10682

Powered centrifugal separator for inlet filtering of rotary wing aircraft turbine engines, discussing efficiency and feasibility
01 p0164 A70-10683

CH-54A engine air particle separator /EAPS/ field experience, discussing engine removal times due to erosion, environment evaluation and design improvements
01 p0164 A70-10684

CH-54A helicopter gas turbine engine air particle separator /EAPS/ field service in Vietnam, noting time before engine removal for erosion [ASME PAPER 70-GT-97]
18 p3303 A70-36844

Gas turbines, dust and air cleaners interrelationship in preventing failure due to air contaminants [ASME PAPER 70-GT-104]
18 p3305 A70-36890

Helicopter gas turbine engine protection against sand and dust erosion using particle separators, screens and coatings [SAE PAPER 700705]
22 p4090 A70-42671

AIR FLOW
NT AIR CURRENTS
NT JET STREAMS [METEOROLOGY]
NT MERIDIONAL FLOW
NT VERTICAL AIR CURRENTS
Air flow density measurements with interferometer in supersonic square Laval nozzle, showing flow core motion and wave structure
01 p0064 A70-11000

Velocity and density profiles obtained from mass diffusivity time measurements in axisymmetric turbulent air pipe flow over specific Reynolds number range
02 p0295 A70-11853

Combustion instability in gas turbine main combustors, noting heat release and inlet air flow rates coupling
02 p0353 A70-12012

Hot-wire and hot-film anemometry in two phase air-water and steam-water flow, discussing bubble passage, signal processing and measurements
02 p0305 A70-12836

Stratified air flow above relief in baroclinic atmosphere, considering plane nonlinear and three dimensional linearized flow models
03 p0521 A70-13270

Graphite sphere mass erosion in low temperature hypersonic air plasma shock flow, determining breakdown temperature and mass entrainment rates
03 p0517 A70-13741

Air-glass particle suspensions flows in shock tubes, deriving effective drag coefficients from simultaneous particle concentration and pressure measurements [ASME PAPER 69-WA/FE-21]
04 p0667 A70-14778

Multiple array critical flow venturi air flow metering system constructed for gas turbine engines, developing pressure control valve [ASME PAPER 69-WA/FM-5]
04 p0688 A70-14838

Settling length for turbulent air flow velocity profile in smooth concentric annuli with square-edged and bellmouth entrances [ASME PAPER 69-WA/APM-24]
04 p0669 A70-14908

Schlieren recorder and Erdmann field absorption methods applied to qualitative and quantitative flow process studies in high velocity wind tunnel
04 p0689 A70-14925

Sound propagation along cylindrical duct of wind tunnel, discussing fluid flow effect on modal cut-off frequencies
04 p0719 A70-15078

Electron quench additives electrophilic effects in high temperature air plasma flow, simulating reentry flight conditions
04 p0664 A70-15561

State and velocity distribution measurements for air in counterflow vortex tube to determine axial variation of flow quantities
05 p0831 A70-15884

Viscous damping effect on aeroelastic stability of thin plate in inviscid compressible airstream, observing instability in subsonic and supersonic flow
05 p0941 A70-16517

Air leakage between contacting surfaces assuming surface irregularities as microscopic truncated cones with ideally plastic or elastic mechanical properties
06 p1031 A70-17133

Air backflow in nuclear exhaust system duct for ground testing of NERVA engines, noting overpressure effect [AIAA PAPER 69-325]
06 p1027 A70-17174

Breathing valve with reduced air resistances based on aerodynamic principles
06 p1000 A70-17433

Lift forces and pressure on vibrating cylinders in plane perpendicular to air flow measured in wind tunnel
06 p0968 A70-17545

Combustion and flow characteristics associated with direct injection of liquid hydrocarbons into high speed air stream [AIAA PAPER 70-88]
06 p1182 A70-18198

Water droplets and air supersonic mixing, determining droplets size and optical properties [AIAA PAPER 70-90]
06 p0975 A70-18199

Dynamic characteristics of systems consisting of train and air in tunnel using one dimensional incompressible fluid description [AIAA PAPER 70-141]
06 p1042 A70-18216

Electron beam fluorescence in rarefied air flow at low static temperature used to study influence of secondary electron emission on rotational temperature measurements
06 p1123 A70-18300

Air flow in updraft through and around cloud region containing precipitation particles using numerical model, computing horizontal divergence
06 p1100 A70-18572

Numerical model of thunderstorm cold air outflow, providing horizontal flow as function of height from computer program using vertical velocity and storm motion
06 p1100 A70-18574

Thunderstorm cold air outflow leading edge structure recorded by NASA meteorological tower at Kennedy Space Center
06 p1100 A70-18575

Inviscid hypersonic flow analysis for chemically relaxing air about wedges and pointed circular cones using Dorodnitsyn integral method [DGLR-69-037]
07 p1188 A70-18986

Heat transfer at inlet edge of turbine blade based on wind tunnel study of cylinder in air flow
07 p1362 A70-19061

Heat transfer in Ni wires in laminar air flow from wind tunnel investigation
07 p1420 A70-19064

Wind tunnel study of heat transfer on smooth plate surfaces in longitudinal air flow using intermittently insulated calorimeter
07 p1279 A70-19065

Heat protection effectiveness of rectangular channel plane wall with flow by air injection through aperture on wall
07 p1420 A70-19066

Microphone output level in airstream relation to sound pressure and pressure fluctuations caused by turbulent flow
07 p1334 A70-19372

Disturbances of air flow originating from small scale mountains using numerical model
07 p1330 A70-19799

Air flow disturbances over mountains in terms of turbulent boundary layer separation dissolution
07 p1330 A70-19800

Spectral functions of airflow velocity pulsations in circular pipe at various Reynolds numbers, considering laminar, transition and turbulent regimes
07 p1259 A70-19826

Turbulent energy and velocity spectra of air flow at atmospheric boundary layer over water analyzed statistically, assuming rippling surface activity
07 p1259 A70-19838

Temperature gradients, viscosity and conduction measurements in air stream between parallel plates, investigating limiting value of total Prandtl number

07 p1260 A70-19999

Transverse curvature effects on turbulent boundary layer thickness and velocity profiles on circular cylinders in water and air

07 p1261 A70-20301

Turbulent Prandtl number and eddy viscosity distribution in thermally stratified turbulent boundary layer of air shear flow dependent on wall distance and thermal stability

08 p1599 A70-21581

Human nostril airflow resistance during supported sitting and lateral recumbency and crutch pressure, discussing ipsilateral nasal congestion mechanisms

08 p1448 A70-21874

Natural heat convection in vertical annular space taking into account variations of volumetric mass, viscosity and thermal conductivity of air with temperature

09 p1786 A70-22047

Air flow turbulence intensity and plug effect influence on local heat exchange on cylinder surface

10 p1797 A70-24028

Velocity and concentration profiles for mixing of two dimensional foreign gas jet injected into parallel air mainstream, emphasizing film cooling applications

10 p1801 A70-24155

Air compressibility effects on aerodynamic characteristics of slender rectangular wings moving at subsonic speed near earth surface approximated by lifting surface theory

10 p1801 A70-24276

Carbon oxyfluoride IR radiation from boundary layer formed by arc-heated air passing over Teflon surface

10 p1968 A70-24475

Heat transfer at inlet edge of turbine blade based on wind tunnel study of cylinder in air flow

10 p1930 A70-25212

Heat transfer in Ni wires in laminar air flow from wind tunnel investigation

10 p1970 A70-25215

Wind tunnel study of heat transfer on smooth plate surfaces in longitudinal air flow using intermittently insulated calorimeter

10 p1970 A70-25216

Heat protection effectiveness of rectangular channel plane wall with flow by air injection through aperture on wall

10 p1970 A70-25217

Film cooling effectiveness measured following air injection through discrete holes into turbulent boundary layer of air on flat plate

11 p2146 A70-25690

Secondary peripheral air injection effects on subsonic airflow through slotted tube, discussing primary flow, flow separation, static and stagnation pressures and temperature changes

11 p2036 A70-26140

Hydrogen-air turbulent diffusion flame structure at differing air and hydrogen velocities

11 p2151 A70-26387

DC air flow plasmatron arc chamber operation with metal surfaces used for charge stabilization, obtaining I-V characteristics and gas flow parameters in quasi-limiting region

11 p1984 A70-26738

Interaction between turbulent air flow and water surface based on Fourier analysis of finite intervals of field

11 p2042 A70-26775

Laminar boundary layer and heat flux at forward stagnation point of indestructible body in partially ionized air flow calculated as function of enthalpy

12 p2156 A70-27287

Turbulent heat diffusion coefficients in air and water tube flow calculated from statistical characteristics, extending method to boundary layers

12 p2210 A70-27322

Nonisothermal burn-up rates of graphite surfaces in turbulent air flow under neutral gas shield estimated by measuring channel diameter

12 p2331 A70-27323

Human lung and upper airway pressure drop and fluid flow regime of inspired air

12 p2170 A70-27660

Turbulent Prandtl number values for air with injection and suction obtained from velocity and temperature profile data

12 p2210 A70-27699

Vibrational dissociation relaxation effects on chemical reactions, molecular energy and thermal quanta in air flow behind direct shock wave

12 p2213 A70-28232

Turbulent diffusion coefficients and time dependent velocity pulsations in air flow, considering relation between Eulerian and Lagrangian turbulence characteristics

12 p2213 A70-28235

Radiant shock layer in hypersonic air flow past blunt bodies, showing effects on temperature field and density

12 p2159 A70-28245

Mesoscale waves in jet stream flow within Coriolis force over rotating earth by amplitude functions and phase velocities asymptotic series representation

12 p2265 A70-28334

Air velocities measurement with heated thermistors probe, discussing calibration and reliability dependence on flow velocity range

13 p2405 A70-28841

Heat transfer in Z shaped regenerative heat exchangers with/without air mixing, determining parameters defining thermal efficiency

13 p2520 A70-28857

Circulated air natural and technical impurities effects on gas turbine time dependent performance emphasizing erosion, deposits and overheating

13 p2475 A70-29713

Plane stationary nonlinear problem of air flow over earth surface roughnesses, using three layer atmospheric model

14 p2602 A70-30160

Wind velocity components on nonuniformly heated plane slope with linear periodic temperature function

14 p2602 A70-30165

Short term creep of Ni in vacuum, stationary air and high speed air flow at various temperatures and loads

14 p1594 A70-30167

Multiband radiative cooling effect on enthalpy distribution behind incident wave in cylindrical shock tube for air, using differential approximation

14 p2663 A70-30268

Atmospheric airflow model above changes in surface roughness, temperature and heat flux, using boundary layer approximations and Businger-Dyer and mixing length hypotheses

14 p2602 A70-30368

Methane and propane flames in rotating air flow fields generated by cylindrical rotating wire mesh screen, discussing flame lengths and blowoff velocities

14 p2666 A70-31090

Radiation effects on large scale atmospheric air flows, accounting for role in global circulation by parameterization techniques

15 p2771 A70-32109

Mixed forced and natural convection with low speed air flow over horizontal electrically heated cylinders

15 p2740 A70-32373

Boron particles ignition and combustion in supersonic air stream, emphasizing axial and lateral two phase flow injection

16 p2856 A70-33496

Stable operating range of supersonic mixed compression inlet increase by air flow removal via throat bleed system

16 p2967 A70-33585

Turboramjet powered hypersonic aircraft axisymmetric inlet systems using forward translating cowl and centerbody for various air flow characteristics

16 p2835 A70-33586

Far wake properties of reentry body in hypersonic air flow calculated with or without chemical kinetics, using finite difference method

16 p2836 A70-33753

Flow structure in wake of blunt bodies placed perpendicular in parallel airstream determined from hot-wire anemometry

16 p2838 A70-33876

Interface stability of thin liquid film adjacent to supersonic air flow, using sphere-cone and blunt wedge test configurations

17 p3005 A70-34461

Supersonic air flow control by electrostatic discharges tested by Mach 3 wind tunnels, using schlieren system for bow shock wave

17 p3008 A70-34492

Plane turbulent jet expansion from linear wedge apex, allowing for ejected air axial velocity attenuation and static pressure variation

17 p3011 A70-35349

German monograph on gas turbine combustion chambers part-load behavior improvement by load controlled change of flame tube air cross section

17 p3148 A70-35373

Free convection in air and water above horizontal wire heated by DC current, measuring flame temperature distribution by diffraction interferometer

17 p3198 A70-35743

Sonic boom minimization through airstream alteration by force or heat fields and aircraft body shaping

17 p3019 A70-35817

Wall cooling effects on turbulent boundary layer in low speed air flow, using smooth tube and thermocouple measurements

18 p3347 A70-36505

Turbulent air flow in vertical square duct, investigating local heat transfer and friction coefficients

18 p3347 A70-36506

Steady state nonlinear dynamics of low latitude atmospheric global boundary layer, indicating inverse relation between air flow vertical velocity and distance from equator

19 p3460 A70-37417

Diaphragmatic muscle reactions and pneumogram changes in rats immediately after air passage obstruction

19 p3360 A70-37804

Probe connected to microphone membrane chamber by transmission tube for fluctuating pressure measurement at discrete point in air flow

20 p3635 A70-40509

Subsonic air flow around airflow in wind tunnel, detecting density gradients by pulsed ruby laser holographic visualization

21 p3822 A70-40809

Supersonic air intake unsteady buzz phenomenon, examining shear layer under cowl and boundary layer detachment at shock wave base for design improvement

21 p3744 A70-41262

Calibration data correlation for constant temperature hot film anemometer for low speed nonisothermal laminar air flow, using modified King law

21 p3828 A70-41475

Turbulence measurements in ducted coaxial air flow with faster outer stream pertinent to gas core nuclear rocket feasibility

21 p3809 A70-41748

Turbulent heat diffusion coefficients in air and water tube flow calculated from statistical characteristics, extending method to boundary layers

21 p3811 A70-42063

Nonisothermal burn-up rates of graphite surfaces in turbulent air flow under neutral gas shield estimated by measuring channel diameter

21 p3952 A70-42064

Turbulent air flow measurements through heated pipe, determining local heat flux from simultaneous velocity and temperature fluctuation

21 p3811 A70-42091

Relaxation behind shock waves in air, calculating radiation spectral distribution for comparison with shock tube experimental data

21 p3812 A70-42219

Supersonic air flow interaction with transverse gas jet from plate orifice

21 p3749 A70-42222

Two dimensional turbine cascade air flow, examining boundary layer regime, thickness, velocity and pressure coefficient at any point by Mach-Zehnder interferometer

22 p4026 A70-42344

Liquid jet breakup in supersonic airstream, using high speed photographic techniques

22 p4036 A70-43063

Nickel surface layer fine structure changes in supersonic air flows at various temperatures and times

22 p4056 A70-43341

Radiative cooling of shock heated air in cylindrical shock tubes, calculating enthalpy profiles for nonadiabatic air flow

23 p4282 A70-44586

Strong shocks propagation in atmosphere of variable density at rest, obtaining numerical solution of similarity flow behind shocks

23 p4182 A70-44599

Transition zone heat exchange during air mixed flow in pipes with conical duct or Vitoshinski nozzle inlets

23 p4283 A70-44729

Turbulent heat exchange coefficient and Prandtl number in turbulent air flow through heated pipe with constant heat flux

23 p4183 A70-44740

Air circulation around radial flow machine rotor blades calculated without velocity distribution factor

23 p4183 A70-44774

Average isobaric air flow field divergence calculation of vertical motion by two dimensional Gaussian integral theorem

24 p4371 A70-45134

Neutral air winds in ionospheric F region for asymmetric global pressure system, including ion velocity correction

24 p4329 A70-45356

Jet engine combustion chamber pressure loss, flow velocity through flare tube holes and air supply calculation, noting adaptation for computer use

24 p4393 A70-45446

Laser light scattering by moist air flows with condensed droplets of water vapor

24 p4353 A70-45565

Short-term creep and erosion resistance testing of Ti alloy in high speed air flows under aerodynamic vibrations

24 p4360 A70-45826

Two dimensional incompressible air flow past circular cylindrical body, investigating separation point control by suction and jet injection

24 p4288 A70-46010

Resistance to two phase gas-liquid flow in airways simulating human bronchial tree

24 p4303 A70-46111

AIR FREIGHT

U AIR CARGO

AIR INLETS

U AIR INTAKES

AIR INTAKES

NT ENGINE INLETS

AIR JETS

NT HYPERSONIC INLETS
NT SUPERSONIC INLETS
T-63 gas turbine engine air induction system protection for OH-58A light observation helicopter against debris with minimum power loss and intake air distortion
01 p0164 A70-10681
Concorde engine and air intake electronic controls
02 p0353 A70-11837
Flow development in conical diffusers, delaying stall with high velocity air injection through annular slot at diffuser inlet predicted by finite difference method
02 p0224 A70-12866
Air inlet and exhaust nozzle form and location effect in afterburning turbofan engines, discussing stalling, afterburner blowouts and thrust losses prevention
05 p0895 A70-15807
Ramjet engines combustion chamber and air intake design for velocities between Mach 2 to 7
06 p1130 A70-17932
Undried atmospheric air humidity effect on pressure and water vapor supercooling in supersonic wind tunnel nozzles
09 p1606 A70-23613
Condensation start dependence on air humidity at inlet and nozzle geometry applied to supersonic wind tunnel using undried atmospheric air
09 p1606 A70-23614
Free jet test facility for supersonic engine/ intake combination testing, discussing benefits to aircraft flying hours, development costs and safety
11 p2101 A70-25854
Concorde Olympus 593 power plants air intake and engine control system design for rapid servicing, discussing fault diagnosis and checkout
14 p2535 A70-31337
Air intake distortions effect on compressor performance, discussing radial and peripheral gradients
15 p2787 A70-32248
F-111A airplane in-flight inlet pressure fluctuations for engine compressor surge, discussing average turbulence factor
[AIAA PAPER 70-624] 16 p2840 A70-33543
F-14A engine air inlet control, describing variable geometry system open loop design
[AIAA PAPER 70-697] 16 p2841 A70-33560
Axial compressor air intake wall design influence on sound propagation
19 p3353 A70-38653
Strike fighter aircraft fuselage side air intakes, measuring external drag as function of design at subsonic and supersonic speeds
[ICAS PAPER 70-49] 23 p4133 A70-44146

AIR JETS
Fuel injections into supersonic air stream through isolated normal ports and porous wall, using interferometry, schlieren and high speed photography
02 p0354 A70-12044
Air plasma pulsed discharge jets erosive effects on metals, semiconductors and dielectrics, noting role of thermal effect
03 p0532 A70-13742
Structural characteristics of supersonic twisting underexpanded air jet, using filming and schlieren photography
04 p0618 A70-15246
Discrete components in noise spectrum of heated and unheated supersonic air jets, using axisymmetric and conical nozzles
04 p0618 A70-15247
Near noise fields of choked axisymmetric air jet, discussing sound pressure levels surrounding jet
05 p0834 A70-16783
IR crossed beam system for direct density turbulence measurements in mixing region of subsonic air jet
[AIAA PAPER 70-235] 06 p1065 A70-18091
Heat transfer during plane air jet impact into concave surface with parabolic profile, determining specific thermal fluxes by electrocalorimetry
07 p1189 A70-19810
Pressure recovery for stagnation of underexpanded sonic air jet in chamber having transparent walls and containing nozzle and diffuser in coaxial positions
07 p1189 A70-19811
Supersonic air jet structure in central shock wave region affected by both Mach number and flow rarefaction
09 p1734 A70-22185
Nozzle fuel and air system geometrical parameters to determine mean diameter of fuel droplets, dispersion angle and spectrum and flame jet shape
10 p1930 A70-24295
Flat plate normal to two dimensional impinging air jet, investigating heat/mass/transfer structure using naphthalene method
11 p1977 A70-26411
Bistable fluidic thrusters and circular sonic control jets interaction with airstream surrounding tactical missile configuration, investigating effect on amplification factors
[AIAA PAPER 70-583] 13 p2391 A70-29887

Ventilating flowmeter tests with jet deflection for respiration measurement in patient
14 p2541 A70-30380
Surface heat transfer coefficients under perforated plate of multiple square array round impinging air jets
[ASME PAPER 69-GT-4] 14 p2666 A70-31025
High velocity gas jet injection into subsonic and supersonic air streams from wall injectors
[AIAA PAPER 70-714] 16 p2834 A70-33538
Air jets from sonic orifice, investigating three zones of isochor families by visualization and density measurement
17 p3070 A70-35046
Turbulent mixing of axisymmetrical supersonic air jet into hot air, investigating Mach number and temperature difference effects on axial decay of velocity
17 p3072 A70-35546
Supersonic air jet noise spectrum analysis at various pressures
19 p3354 A70-38659
Heat transfer during plane air jet impact into concave surface with parabolic profile, determining specific thermal fluxes by electrocalorimetry
20 p3736 A70-39260
Rocket course correction by lateral air expulsion /ram air control/, deriving model for performance prediction
[AIAA PAPER 70-90] 20 p3715 A70-39559
Interaction zone between gas flow and injected air jets, measuring turbulence characteristics by thermomometer
21 p3809 A70-41773
Moist air expansion through supersonic nozzle, investigating small ions role in water condensation
22 p4011 A70-42774
Adaptive time optimum inertial satellite attitude control using air jet
23 p4265 A70-45048
Jet momentum for flow separation control of air past circular cylindrical surface
24 p4288 A70-46011

AIR LAUNCHING
Ground environmental simulation test for captive carrying cycling of air launched missiles
17 p3060 A70-35182
Digital computer six degree of freedom wind tunnel separation simulator for air launched missile trajectory analysis
17 p3063 A70-35509

AIR LOCKS
Decompressed crewmember rescue onboard spacecraft and aircraft by compartmentalization combined with air locks
08 p1454 A70-21938
Expandable and modular structures technology for manned and unmanned space missions, discussing expandable air lock experiment
17 p3177 A70-35230

AIR MASSES
Favorable air mass type and season for long cross country soaring flights over eastern U.S. determined from record analysis
09 p1718 A70-23062
Atmospheric ray paths calculations applied to determination of optical air mass and twilight ray paths in earth atmosphere
10 p1873 A70-23830
Thermodynamic properties of periodically variable air volume in pneumatic pressure generator of pressure sensor calibration bench
10 p1863 A70-24027
Polluted air mass concentration determined by photogrammetry, producing topographic type map with respect to vertical and oblique aerial photographs
10 p1880 A70-24755
Air masses nonadiabatic ascent under elevated temperature inversion in atmosphere, assuming three layer model with linear profiles
12 p2265 A70-28335
Troposphere and lower stratosphere trace element concentration measurements, establishing origin, history and movement of various air masses
15 p2728 A70-31996
Air mass climatology in terms of pressure temperature and moisture content
15 p2772 A70-32457

AIR NAVIGATION
NT ALL-WEATHER AIR NAVIGATION
Thermal preconditioning using radioisotope heat source to eliminate inertial sensor warmup time by maintaining aircraft navigation system at constant temperature
01 p0140 A70-10310
Aeronautical satellites for monitoring positions of many commercial aircraft simultaneously crossing North Atlantic, discussing navigational error correction and atmospheric
01 p0178 A70-10454
Area navigation and automatic data communications in air traffic control proposed for New York area STOL aircraft operations and Boeing 747 aircraft
[AIAA PAPER 69-1054] 01 p0138 A70-10640

Minimum operational characteristics /MOC/ for vertical guidance in airborne area navigation systems, including VOR-DME accuracy criteria
01 p0138 A70-11049
Automatic IR control and tracking systems for aviation, space flights and military use, discussing sensor elements
01 p0139 A70-11262
Satellite navigation efficiency compared with inertial and Omega navigation techniques
01 p0139 A70-11263
Moving map displays applications in marine and air navigation, discussing human factors and impact on ATC
01 p0139 A70-11284
Statistical decision problem of Brownian motion with moving boundaries in automatic daylight star tracker design for aircraft navigation solved by image method
01 p0139 A70-11635
Three dimensional navigation and guidance system for transport aircraft to alleviate operational problems, noting application to STOL aircraft
02 p0334 A70-11983
Aircraft navigation systems performance, discussing navigation aid integration by digital management computer coupling navigation sensors to display and control devices
02 p0334 A70-11984
Air traffic congestion alleviation by applying general purpose computers for navigation in civil transport aircraft
02 p0334 A70-11985
Airborne computer civil navigation system designed for output coordination from navigation sensors
02 p0334 A70-11986
Polar diagrams control for distributed radiating systems, generating localizer planes for high flying aircraft navigation aids
05 p0812 A70-16150
Commercial navigation systems for long range subsonic transports, discussing accuracy, avionics hardware and crew responsibility optimization
06 p1102 A70-17638
Soviet book on air navigation covering civil navigator training, geographic concepts, navigation means, flight and meteorological conditions, instrument errors, etc
06 p1103 A70-17642
Optimum filter for aircraft inertial navigator and radio position fix data mixing using mathematical model of error propagation
[AIAA PAPER 70-35] 06 p1103 A70-18184
Aeronautical satellites application to supersonic air transportation economy, discussing navigational information relay between aircraft and control center
07 p1191 A70-18988
Space systems for communications, surveillance and navigation needs of international aviation, discussing service requirements, spectrum utilization, technology limitations and terminal design
07 p1350 A70-19290
Spot III satellite-supported system for transoceanic aircraft navigation, traffic control, voice and data communication, etc
07 p1331 A70-19291
European air transport navigation, discussing air traffic control and planned VHF omnirange/distance measuring equipment network /VOR/DME/
07 p1332 A70-20226
Radio air navigation systems by time separation signals with reference to anticollisional methods and ATC
08 p1541 A70-21019
Loran and Decca hyperbolic navigation systems
08 p1541 A70-21022
Airborne sidescan radar for fix-point navigation at low flight altitudes involving computerized sensing evaluated for operator performance
08 p1541 A70-21563
Loran in range-range mode for computing user position based on remote clock synchronization, evaluating accuracy
09 p1719 A70-22192
Air safety and navigation systems data transmission, discussing analog to digital conversion and modulation
09 p1720 A70-22550
Ring array synthesis for prescribed radiation pattern by sampling theory, considering application for aircraft navigation
09 p1646 A70-22702
Long range navigational aids requirements for airlines, discussing self contained navigation systems capabilities
09 p1722 A70-23028
Primary long range navigation system for SST, considering operational goals, Doppler radar systems, navigation aids, inertial systems, etc
09 p1722 A70-23029
Hybrid long range en route navigation system extended to short range role meeting ATC and terrain problems
09 p1722 A70-23032

- Commercial aircraft inertial navigation, examining gyroscope, accelerometer and electronic computer and gyroscopic stabilization 10 p1914 A70-23848
- Seasonal variations in radio signal propagation from aircraft navigation system antenna located in dense forest, solving problem with Doppler-VOR installation 10 p1854 A70-25254
- VHF aerosat antenna design and system interactions, analyzing impact of spacecraft dynamics, control system, power supply and propulsion [AIAA PAPER 70-486] 11 p2120 A70-25439
- Air transportation and air traffic control factors relating to satellites applications to surveillance, navigation and communication over contiguous U.S. [AIAA PAPER 70-488] 11 p2077 A70-25443
- VHF aeronautical communication satellites extended for use in aircraft position determination and surveillance, discussing accuracy and error source reduction [AIAA PAPER 70-490] 11 p2002 A70-25487
- Self optimizing Kalman filter for hybrid inertial air navigation systems, noting implementation on airborne digital computer 11 p2078 A70-25682
- ATC procedures based on system error and aircraft accident probabilities, traffic flow and navigation control and controller manpower 11 p2078 A70-25721
- Area navigation system advantages for pilots, flight control systems and improved accuracy through rejection of VOR course scalloping [SAE PAPER 700214] 11 p2079 A70-25885
- Aircraft control through airspace from takeoff to landing, discussing role of Department of Transportation Air Traffic Control Advisory Committee 11 p2080 A70-26256
- Remote area terminal system providing navigation and guidance signals for aircraft landing 11 p2081 A70-26509
- Soviet book on air navigation covering position determination methods, wind measurement, equipment design and use, etc 12 p2266 A70-26875
- Sea roughness effect on bandwidth of radar backscatter, analyzing Doppler signals of eight millimeter aircraft navigation system 12 p2228 A70-26906
- Area navigation for reducing cockpit navigation workload, permitting aircraft operations on desired course and enhancing pilot response to ATC instructions [SAE PAPER 700283] 12 p2266 A70-27426
- Short distance VHF omnirange navigation and distance measuring equipment considered for performance improvements feasibility to meet civil air traffic demands through 1980 12 p2268 A70-27643
- VORTAC system providing navigation service to civil and military air traffic on worldwide basis 12 p2269 A70-27919
- Low altitude satellite system for aircraft navigation, considering cost factors, military applications, traffic control capabilities, etc 12 p2270 A70-27922
- Midaltitude satellite system for continuous three dimensional navigation, considering elevation angles, constellations and orbits 12 p2270 A70-27923
- Multiple user satellite system for air navigation and traffic control, presenting comparative error analyses for position determination by spherical and hyperbolic ranging 12 p2270 A70-27925
- Satellite system for air traffic control providing data links for aircraft position determination for U.S. in 1990s using 24-hour inclined elliptical orbits 12 p2270 A70-27926
- Computerized aircraft navigation utilizing Doppler dead reckoning system and Tacan integration with least square adjustment method 13 p2447 A70-28550
- Aircraft and ship navigation using precision time measurement signals transmitted between vehicles and earth satellites 13 p2448 A70-28748
- Aeronautical navigation under various wind velocity conditions, studying flight times for closed flight paths 13 p2448 A70-28750
- Multifunctional multimode avionics design integrating communications, navigations and identification subsystems [JCN1] 13 p2368 A70-29619
- Doppler radar aircraft navigation system with gyroscopic reference platform and computer, showing error propagation dependence on velocity and latitude 13 p2449 A70-29621
- Air traffic control, reviewing air navigation, communication systems and radar techniques 13 p2450 A70-29998
- Air traffic, navigation and community - Conference, London, May 1970 14 p2611 A70-30101
- Air navigation and control systems cost-benefit analysis including ground services, safety and R and D 14 p2667 A70-30103
- Land and airspace demands in navigation, surveillance and traffic control, discussing application of current techniques 14 p2611 A70-30105
- Loran C coordinates bias function determination by regression analysis using observed time differences 14 p2615 A70-31195
- Optimum carrier phase delay estimation for one way ranging aircraft navigation, investigating receiver signal processing 16 p2947 A70-33449
- Short range VOR/DME area navigation techniques in U.S. National Airspace System 16 p2948 A70-33470
- Time ordered system for air traffic control providing data link, collision avoidance and navigation data through single channel 16 p2948 A70-33476
- Aircraft/ship navigation system using three synchronous satellites positioned over equator for Pacific applications 17 p3134 A70-35302
- Doppler radar frequency tracker with servomechanism applicable to velocity computation of aircraft for self contained navigation 18 p3226 A70-36063
- Commercial aircraft strapdown inertial navigation systems, examining initial self alignment techniques 18 p3289 A70-36442
- Inertial navigation platform system for long range flights, passing command through computer to automatic pilot 18 p3290 A70-36950
- Area navigation system charting, discussing effect on flight information publications 19 p3465 A70-38231
- Military Airlift Command jet aircraft computerized area navigation system operational procedures 19 p3465 A70-38232
- Airline area navigation in national airspace system, emphasizing moving map display for navigation charting 19 p3465 A70-38233
- Pictorial display methods for pilot error reduction in area navigation via guidance control and capability beyond visual field 19 p3465 A70-38234
- Time-synchronized approach control, combining aircraft precision navigation and guidance with ATC equipment 19 p3466 A70-38237
- Ground and cockpit initiated collision avoidance commands system based on satellites surveillance of aircraft position and velocity data 19 p3466 A70-38242
- Self navigation feasibility in future mass air traffic flow control 19 p3469 A70-38643
- V/STOL aircraft automatic flight control, guidance and navigation by onboard computer, discussing mathematical model and simulation results [AIAA PAPER 70-1035] 20 p3665 A70-39502
- Aircraft trajectory postflight reconstruction involving photographic starfield and landmark referenced to inertial navigator output, discussing optimal data smoothing technique [AIAA PAPER 70-1022] 20 p3666 A70-39512
- Aircraft and rocket guidance systems navigation error analysis, discussing numerical integration techniques and computer program [AIAA PAPER 70-1004] 20 p3667 A70-39527
- Airborne integrated computerized ASW system, describing navigation, flight control, display and sensor subsystems 21 p3821 A70-40575
- Sea and air navigation in U.S. with satellites, considering cost estimates 21 p3848 A70-41130
- Integrated communication, navigation and identification for worldwide needs of military aircraft 21 p3786 A70-41132
- Air navigation Dioscures project satellites, discussing spin or three axis stabilization, system replenishment strategies and subsystem reliability 21 p3929 A70-41259
- Airborne three dimensional area navigation equipment for reducing mid-air collision exposure and for raising landing safety in terminal areas 22 p4066 A70-42296
- General aviation traffic control, discussing limitations of present system and improvements of position information and area navigation approach procedures 22 p4066 A70-42385
- Air traffic safety problems, discussing satellite radiobeacons applications to aerial navigation 22 p4066 A70-42652
- Integrated air navigation by least square adjustment, analyzing Doppler navigation errors 22 p4067 A70-42655
- Dioscures satellite navigation system for aircraft and ships, discussing coverage, radio links, project costs, etc 22 p4067 A70-42657
- Area navigation for aircraft guidance with radio aids, discussing advantages, airborne equipment, Dynamic Map Displays, etc 22 p4067 A70-42658
- Concorde SST horizontal navigation, discussing data sources, equipment specifications, flight rules, man-machine interaction, etc 22 p4067 A70-42660
- Radio navigation system using multiple satellite beacons /NAVSTAR/ for large area air and sea coverage 22 p4067 A70-42662
- Limiting effects of topographic quasi-optical radar propagation above 100 MHz in radar aircraft navigation, clear air disturbances detection and IR warning technique 23 p4163 A70-44230
- Worldwide common satellite network for sea and air navigation, discussing cost estimate and economics 23 p4216 A70-44608
- Pilot navigation efficiency in low altitude terrain following flight, using synchronized TV and simulator with inertial guidance 24 p3407 A70-45506
- General aviation aircraft influences on federal airways systems, considering area and Omega navigation examples [AIAA PAPER 70-1314] 24 p4373 A70-45929
- Satellite based navigation/air traffic control information systems for short range STOL air carrier aircraft [AIAA PAPER 70-1338] 24 p4373 A70-45930
- Pilot interface with area navigation system, describing control and display unit for navigation situation, flight plan and system status [AIAA PAPER 70-1335] 24 p4373 A70-45933
- STOL aircraft guidance and control, discussing area navigation utilization, multiple airways, data links and ground ATC computers [AIAA PAPER 70-1334] 24 p4373 A70-45934
- ATC, air navigation facilities and airport design requirements for short haul transportation system [AIAA PAPER 70-1288] 24 p4323 A70-45973
- AIR PIRACY**
- Air piracy, maritime law applicability, definition, international laws and French law 05 p0960 A70-16538
- Illegal aircraft route diversion by unauthorized persons, discussing air piracy suppression efforts of various international bodies 05 p0960 A70-16539
- Aircraft hijacking epidemiology from preventive viewpoint 22 p3981 A70-43698
- Air hijacking as aviation safety problem, discussing history, prevention and detection methods and equipment, law enforcement, etc 23 p4285 A70-44496
- AIR POLLUTION**
- Turbojet engines air pollution emissions processes resulting from combustor primary and secondary zone conditions, discussing engine design modifications [AIAA PAPER 69-1040] 01 p0162 A70-10602
- Aircraft engine exhaust emissions air pollution role in air terminal area and adjacent communities [ASME PAPER 69-WA/APC-4] 04 p0733 A70-14788
- Meteorological parameters influence on diurnal variations of radionuclide activity and resulting global air pollution 05 p0903 A70-16662
- Vitiated contamination effect on airbreathing engine ground testing, considering equilibrium, vibrational and chemical relaxation, condensation, combustion, mixing and engine performance [AIAA PAPER 69-456] 06 p1172 A70-17172
- Collection of papers on air pollution aerophysics covering eddy diffusion, aerosol particle size, Los Angeles smog, etc 06 p1096 A70-17321
- Jet aircraft air pollutant production and dispersion of nitric oxide and soot, discussing mixing process [AIAA PAPER 70-115] 06 p1131 A70-18070
- Atmospheric contamination due to Be solid propellant exhaust products, discussing pollution levels, governmental restrictions on testing, etc 06 p0997 A70-18085
- Electrostatic methods considered for using earth electric field in smog dispersion in polluted areas and for airport fog clearing [AIAA PAPER 70-118] 06 p1058 A70-18217
- Radiobiological and radioecological aspects of radioactive pollution of earth atmosphere, considering international cooperation for preventive measures 07 p1199 A70-18781
- Gas turbine engines contribution to air pollution, using model combustor to study burned gas composition, emphasizing nitric oxide concentration 08 p1559 A70-21481
- Satellite monitoring of air pollution, discussing sulfur dioxide measurement in UV, optical correlation

techniques, IR and visible spectra, stratospheric balloon tests, etc
[AIAA PAPER 70-305] 09 p1668 A70-22875

Reflected solar radiation polarization over land, sea and cloud surfaces to determine atmospheric pollution
09 p1747 A70-23603

Polluted air mass concentration determined by photogrammetry, producing topographic type map with respect to vertical and oblique aerial photographs
10 p1880 A70-24755

Ultraclean technology to eliminate pollution traces present in laboratories, discussing turbulent flow and horizontal and vertical laminar flow rooms
10 p1828 A70-25240

Water vapor pollution of stratosphere by supersonic transports, considering effects on temperature, cloudiness, albedo, etc
11 p2077 A70-26618

Air pollution measured from high altitude balloons and satellites by remote sensing of diffused atmospheric gases, using solar illumination
12 p2221 A70-26950

Aircraft turbine engines gaseous emission measurements, discussing instrumentation for continuous pollutant concentration monitoring
[SAE PAPER 700249] 12 p2290 A70-27428

Standard method for aircraft engine exhaust smoke measurement for air pollution control
[SAE PAPER 700250] 12 p2290 A70-27429

Jet engine pollution reduction for airport areas, discussing chemical equilibrium failure in exhaust gases and combustor design
12 p2291 A70-27993

IR spectroscopy and lasers for analysis of atmosphere in air pollution research and monitoring
13 p2407 A70-29106

SST aircraft fuels and lubricants, discussing fire hazard and pollution minimization
13 p2473 A70-29999

Aircraft smoke emission reduction and elimination by engine modifications
14 p2628 A70-30190

Meteorological effects on air and noise pollution at U.S. airports
14 p2530 A70-30610

Air pollution by turbojets and gas turbines, discussing control of carbon particles and nitrogen oxides
16 p2963 A70-32922

Remote Raman spectroscopy of air contaminants, considering electro-optical technology and data processing
16 p2900 A70-33018

Atmospheric contaminants dispersion simulation in meteorological wind tunnel with capability to simulate thermally stratified boundary layers
17 p3065 A70-34496

Community air pollution from airports, discussing exhaust emissions, pollutant dispersion, etc
17 p3200 A70-35177

Aerospace technology applications to air pollution problems, including turbojet aircraft sources, rocket emissions, etc
[AIAA PAPER 70-815] 17 p3200 A70-35194

Ozone concentration in San Francisco Bay Area, discussing temperature inversion, air pollution, destruction rate and distribution patterns of oxidants
18 p3284 A70-35945

Gas turbine emissions analysis for air pollutants, determining species distribution and concentration
[ASME PAPER 70-GT-81] 18 p3226 A70-36883

Transport ratio for I-131 air to milk concentrations, determining mean value and statistical variation from Project Rover data
19 p3361 A70-38012

Correlation spectrometry for earth resources, considering sulfur dioxide, nitrogen oxide and iodine pollution
20 p3626 A70-39055

Raman spectroscopy with lidar for remote mapping of air pollutants and concentrations
20 p3627 A70-39126

Pulsed laser lidar measurements of atmospheric turbidity, diffusion, pollution, visibility and cloud physics
20 p3584 A70-39127

Spectroscopic detection of sulfur dioxide and carbon dioxide molecules and concentrations in polluted atmosphere by laser-Raman radar technique
20 p3640 A70-39389

Air polluting sulfur dioxide and nitrogen dioxide remote sensing based on radiation molecular absorption using long line correlation spectrometer
20 p3633 A70-39793

Aerodynamic holder stabilized smoke flames to avoid intermittent flaming and thick puffs for incinerator air pollution reduction
21 p3942 A70-40887

Planetary albedo changes due to pollution aerosols, showing absorption-to-backscattering ratio function in atmospheric heating or cooling
22 p4096 A70-43419

Jet engine air pollution in U.S., discussing fuel types, additives and burner design for smoke emission reduction
23 p4233 A70-44200

Reduced smoke combustion chambers for jet aircraft engines tested in full scale JT8D engine
24 p4396 A70-46387

AIR PURIFICATION

Space stations life support systems for air purification, water reclamation and oxygen recovery
08 p1449 A70-20630

Air revitalization chemicals reactions with water vapor and gaseous carbon dioxide, describing apparatus for kinetic studies
24 p4307 A70-45348

AIR SAMPLING

Air sample removal from hermetically sealed cavities during studies of toxic gas emanations from polymeric materials
07 p1221 A70-19516

Portable unit for collection and analysis of toxic gas contaminants in enclosed aircraft and spacecraft cabin atmospheres
07 p1224 A70-20222

Rocketborne cryogenic sampler using shock diffuser inlet for air collection at supersonic speeds during rocket ascent
10 p1949 A70-23937

Air sample removal from hermetically sealed cavities during studies of toxic gas emanations from polymeric materials
11 p1991 A70-26115

Aerobee rocket-borne cryogenic air samplers heat exchanger design by mathematical model and computer solution
23 p4280 A70-44365

AIR TO AIR MISSILES

Air to air missile guidance to moving target via optimal feedback strategies
11 p2080 A70-26244

Fighter-missile launch and control using direct radar information for guidance to reduce computation time and computer storage space
11 p2015 A70-26332

Air to air armament selection effect on aircraft configuration
[AIAA PAPER 70-939] 17 p3021 A70-35848

Air to air missile launch range maximization for plane trajectories and nonmaneuvering targets, discussing optimal fuel burning rate
[AIAA PAPER 70-980] 20 p3668 A70-39549

AIR TO AIR REFUELING

Flight evaluation of direct lift control (DLC) on modified B-52 aircraft, noting controllability improvement during ILS approaches and aerial refueling
[SAE PAPER 690406] 03 p0411 A70-12896

AIR TO AIR ROCKETS

U AIR TO AIR MISSILES

AIR TO SURFACE MISSILES

Fluidic inertial platform feasibility model for air to surface missile line-of-sight guidance, noting cost, reliability and environmental advantages
[AIAA PAPER 70-1009] 20 p3667 A70-39523

Kalman filter sizing for air-launched tactical missile via covariance sensitivity matrix
[AIAA PAPER 70-954] 20 p3601 A70-39574

AIR TRAFFIC

Air traffic problems connected with Boeing 747 introduction, discussing cargo/passenger handling, fueling and maintenance procedures
02 p0227 A70-12620

Flights best day part and weekly leg schedules concept based on decision making model for traffic volume estimation in airline operations
02 p0403 A70-12787

Illegal aircraft seizures inspired by political motives, discussing suppression, air traffic volume effects, Tokyo Convention juridical decisions, etc
05 p0960 A70-16537

Inclusive Tour /IT/ Charter definition within framework of commercial air traffic, discussing concepts of scheduled and nonscheduled air services
07 p1427 A70-18885

International air traffic jurisdictional area of German aeronautical law regarding aircraft equipment regulations and residents
07 p1427 A70-18886

Monograph on HFB 600 V/STOL transport for civil and military air traffic, discussing intercity travel, military dispersal requirements, systems performance, cockpit layout, etc
07 p1194 A70-19605

Civil air transportation in India, using mathematical models to estimate optimal development and efficiency of future air traffic potential
08 p1601 A70-21544

Air traffic vibration effects on human organs and sensations, considering blood circulation, lungs, eyes and muscles
09 p1625 A70-23007

Regional air traffic in Germany, discussing aircraft, airports, growth rate and control
10 p1970 A70-24199

Air transportation demand growth forecast in terms of flights, airport operations and airborne aircraft at peak periods
12 p2336 A70-27626

Aircraft noise reduction effects on airport capacity and community exposure levels
12 p2207 A70-27628

Midair collisions incidence correlated with traffic factor proportional to square of number of operations
12 p2269 A70-27912

Pilot landing aids for increasing air traffic, discussing Integrated Communication Navigation Identification
13 p2449 A70-29053

Air traffic, navigation and community - Conference, London, May 1970
14 p2611 A70-30101

Air traffic in 1980s in UK, considering domestic services, V/STOL operation and private and executive aviation
14 p2667 A70-30102

Large scale V/STOL service introduction for decongesting short haul routes between major cities of Northeast Corridors
14 p2615 A70-31276

Air traffic - Conference, Versailles, June 1970
18 p3288 A70-36389

Aircraft traffic on ground at airports by digital simulation, investigating influence of constraint represented by infrastructure of taxi tracks
18 p3236 A70-36390

Avionics role in STOL air transportation operational capabilities in congested air traffic environment
19 p3466 A70-38238

Airport capacity and layout, considering air traffic increase, runway occupancy, taxiway and computer simulation
19 p3468 A70-38636

Air cargo traffic problems, discussing mechanized terminals, automatic handling equipment, direct container delivery, mass traffic and large freighter aircraft
22 p4126 A70-43268

STOL system traffic analysis simulation model for interurban transportation system as tool for flight hardware evaluation
22 p4007 A70-43731

Contrail effects on atmospheric thermal radiation budget in heavy jet traffic regions from airborne IR and solar radiometric observations
23 p4214 A70-44033

Goals oriented airport planning and design approach, considering air traffic growth, capacity, environment and aircraft noise problems
[AIAA PAPER 70-1264] 24 p4431 A70-45924

AIR TRAFFIC CONTROL

Monograph on future air traffic control concerning radio navigation, color display and computer determined flight paths
01 p0136 A70-10090

Inertial navigation techniques application to commercial air traffic control, indicating decreased dependence on external navigation aids in oceanic operations
01 p0136 A70-10304

Omega position location experiment applied to ship navigation, air traffic control and moving vehicle surveillance, noting daytime and night fixing accuracy
01 p0136 A70-10307

National air traffic control system modernization based on Department of Defense military experience to achieve safe and efficient air space utilization
[AIAA PAPER 69-1113] 01 p0137 A70-10616

Airport surface traffic system analysis, discussing control and guidance isolation, information acquisition/processing and response actions
[AIAA PAPER 69-1086] 01 p0137 A70-10630

Air traffic control system automation, anticipated benefits to users and operators and potential pitfalls associated with implementation
[AIAA PAPER 69-1057] 01 p0137 A70-10638

V/STOL air traffic control and equipment considerations for increased demand, suggesting time/velocity separation system using direct routing, positive and automated control
[AIAA PAPER 69-1055] 01 p0137 A70-10639

Area navigation and automatic data communications in air traffic control proposed for New York area STOL aircraft operations and Boeing 747 aircraft
[AIAA PAPER 69-1054] 01 p0138 A70-10640

Air traffic control inadequacy and restrictive regulations influence on aviation growth, implying need of airport-airways system improvements
[AIAA PAPER 69-1052] 01 p0138 A70-10642

Air traffic control development covering control methods, regulatory procedures, equipment and navigational systems
[AIAA PAPER 69-1051] 01 p0138 A70-10643

Airborne DME minimum operational characteristics for air traffic control navigation and communication systems including equipment specifications, environmental conditions, accuracy and range
[DO-141] 01 p0138 A70-11050

- ATC terminal displays procurement and use, discussing effects of traffic growth and FAA automation program 01 p0139 A70-11285
- Air traffic control methods for transport aircraft delay elimination 01 p0139 A70-11367
- Civil aviation electronics - Conferences, London, September 1969, Part 3, Air traffic control 02 p0330 A70-11956
- Secondary surveillance radar to operate autonomously with digital techniques and digital handling systems, discussing design and ATC applications 02 p0266 A70-11957
- ATC surveillance radar for high density traffic, discussing optimum electronic scanning rates, 3D radar and MTI 02 p0330 A70-11958
- Electronic scanning role in ATC radar, discussing combined search and track radar with elevation and azimuth scanning 02 p0331 A70-11959
- Digital computers in air traffic control, discussing reliability, automated area choice, controller tasks, planning, etc 02 p0331 A70-11960
- Cost effective phased buildup of computerized ATC systems 02 p0401 A70-11961
- ATC display devices, discussing digital systems requirements, data storage, etc 02 p0331 A70-11962
- Secondary surveillance radar /SSR/ automatic pilot extractors and display processors for providing information on aircraft height and identity for air traffic control 02 p0256 A70-11963
- Secondary surveillance radar and interferometry techniques to determine aircraft positions in real time and all weathers for air terminal approach control 02 p0331 A70-11965
- Three dimensional radar system for automatic tracking all aircraft in terminal area to increase air traffic control system safety and capacity 02 p0332 A70-11967
- Computer simulation of automated ATC systems, discussing operational gaming and mathematical models 02 p0274 A70-11968
- Air traffic control radar velocity resolution for eliminating ground, rain and angel clutter by optimizing wavelengths, pulse length and beam width 02 p0332 A70-11969
- Radar system for air traffic control using twin beam antenna to improve performance with respect to ground and angel clutter 02 p0332 A70-11970
- Mathematical models construction for predicting and measuring air traffic controller workload, using synthetic and analytic methods 02 p0332 A70-11972
- Digital real time simulation for training and evaluating ATC controllers, discussing system hardware, software, design and implementation 02 p0274 A70-11977
- Computerized navigation system for controlling aircraft movement on airports under zero visibility conditions 02 p0274 A70-11978
- Air traffic congestion alleviation by applying general purpose computers for navigation in civil transport aircraft 02 p0334 A70-11985
- Computer simulation of automated air traffic control concepts, formulating and implementing generalized model of automated transition/terminal area systems 02 p0335 A70-12133
- Air traffic control system for intercity and metropolitan VTOL airway reducing pilot and air traffic controller workloads 02 p0335 A70-12135
- Transistorized lightning protected VHF ground antenna for air traffic communication providing high operational safety standards 03 p0459 A70-14297
- Management role in air traffic controllers stress reduction, considering human factors affecting ATC system capacity 03 p0439 A70-14316
- Human controller decision in air traffic control, discussing manpower, on-line computer use and maximized systems [ASME PAPER 69-WA/AV-1] 04 p0643 A70-14903
- Physiological limitations of air traffic controllers, considering stress factors connected with workload 04 p0716 A70-15314
- Air traffic control problems in avoiding midair collisions, satellite utilization in transatlantic flight control and anticollision devices and procedures 04 p0623 A70-15350
- Correlation protected instrument landing system proposed for international consideration to meet future aircraft traffic density 05 p0880 A70-16107
- Operational/technical system improving air traffic control services efficiency by increased utilization of automation, displaying radar information and synthetic air situation presentations 05 p0827 A70-16179
- Systems concepts in design of computer operated display systems in air defense and air traffic control systems, discussing alphanumeric display, panoramic display, etc 05 p0827 A70-16183
- Airborne digital letdown computer to guide VTOL aircraft flying complex trajectories to relieve airport congestion 05 p0880 A70-16416
- Instrument landing system techniques based on hyperbolic geometry and correlation detection for terminal area traffic control, discussing applications 06 p1102 A70-17637
- Runway acceptance rate improvements to alleviate air traffic congestion metroplex areas, using approach and landing sequence model for conventional jet aircraft [AIAA PAPER 70-74] 06 p1029 A70-18078
- Aeronautical satellites application to supersonic air transportation economy, discussing navigational information relay between aircraft and control center 07 p1191 A70-18988
- Spot III satellite-supported system for transoceanic aircraft navigation, traffic control, voice and data communication, etc 07 p1331 A70-19291
- Encounter statistics and operational environment of aircraft collision-hazard warning systems in terminal area 07 p1331 A70-20060
- European air transport navigation, discussing air traffic control and planned VHF omnirange/distance measuring equipment network /VOR/DME/ 07 p1332 A70-20226
- ATC real time simulation exercises in Brussels Upper Information Region 07 p1250 A70-20227
- Airline industry, considering expected increases in traffic, aircraft development and interface problems 08 p1600 A70-20588
- V/STOL Do 231 design, discussing propulsion, control, safety, traffic control and economic factors 08 p1435 A70-20640
- Terminal air traffic control automation, discussing Advanced Radar Traffic Control System /ARTS/ and control tower data transfer aspects 08 p1540 A70-20678
- Linear programming for aircraft takeoff and landing schedules for traffic control on airport runway, using simplex technique for proposed algorithm 08 p1540 A70-20872
- Functions generation to determine probabilistic parameters of automatic air traffic control system 08 p1541 A70-20873
- Radio air navigation systems by time separation signals with reference to anticollisional methods and ATC 08 p1541 A70-21019
- Secondary radar application to assist ATC achieving air to ground communications reduction 08 p1541 A70-21020
- General aviation urban airport capacity problem, suggesting diversion of training portion of peak-hour traffic 08 p1481 A70-21306
- Real time simulation of air traffic control problems in Brussels upper information region /UIR/ 08 p1541 A70-21361
- Omega Position Location Experiment with synchronous satellite /ATS-3/ as radio relay for merchant shipping, air traffic control and moving vehicle location and communication 09 p1720 A70-22193
- ATC and SST operations in terminal area simulation study involving airline crews and controllers in real time traffic situation 09 p1721 A70-22946
- Satellite potential for long range air traffic control, discussing airline navigation requirements and ATC requirements for position determination 09 p1722 A70-23027
- Hybrid long range en route navigation system extended to short range role meeting ATC and terrain problems 09 p1722 A70-23032
- Aeronautical satellite system for North Atlantic air traffic position monitoring, discussing simultaneous position display 09 p1723 A70-23040
- Aircraft and ship position surveillance by satellites system with independent capability and undelayed voice and digital communication 09 p1723 A70-23043
- Compound helicopter in civil aviation to alleviate air traffic congestion, discussing design and operative capacities of S-65-200 10 p1804 A70-24046
- Regional air traffic in Germany, discussing aircraft, airports, growth rate and control 10 p1970 A70-24199
- Beacon identification-friend-foe/selective- identification-feature code-validation schemes for ATC, deriving expression for cumulative probability of validation on or within N interrogations 10 p1914 A70-24446
- Boeing 747 aircraft impact on air transportation passenger and freight rates and traffic congestion reduction 10 p1806 A70-24765
- Microwave pencil triodes and cavities of miniature design for Air Traffic Control Beacon Systems 10 p1852 A70-24886
- Air traffic control system using ground controlled satellite-borne phased array antenna to overcome UHF downlink phase loss [AIAA PAPER 70-497] 11 p2077 A70-25421
- Air transportation and air traffic control factors relating to satellites applications to surveillance, navigation and communication over contiguous U.S. [AIAA PAPER 70-488] 11 p2077 A70-25443
- Navigation-traffic control satellite system application to transoceanic traffic surveillance [AIAA PAPER 70-487] 11 p2000 A70-25462
- Optimal two level air traffic control avoiding conflict on runway and in flight and minimizing landing time deviations 11 p2077 A70-25603
- Optimal operational control of aircraft takeoff and landing times using stochastic programming 11 p2077 A70-25608
- Radio Technical Commission for Aeronautics - Conference, Washington, D.C., November 1969 11 p2078 A70-25719
- Air traffic control procedures pertaining to personnel, hardware and regulations 11 p2078 A70-25720
- ATC procedures based on system error and aircraft accident probabilities, traffic flow and navigation control and controller manpower 11 p2078 A70-25721
- ATC ground hardware technology implementation, considering national air space system, airports, cost estimates and capacity increase 11 p2078 A70-25722
- Ground ATC facilities, discussing landing, automation, surveillance, communication and navigation 11 p2079 A70-25723
- ATC airborne hardware covering transponders, area navigation, DME, course directors and approach couplers 11 p2079 A70-25724
- Aircraft control through airspace from takeoff to landing, discussing role of Department of Transportation Air Traffic Control Advisory Committee 11 p2080 A70-26256
- Analog-digital real time data automatic acquisition and radar tracking system for air defense and air traffic control 11 p2014 A70-26313
- Bayesian probabilistic information processing in psychological decision making in air traffic control, discussing bookbag and poker-chip applications 12 p2178 A70-27047
- Area navigation for reducing cockpit navigation workload, permitting aircraft operations on desired course and enhancing pilot response to ATC instructions [SAE PAPER 700283] 12 p2266 A70-27426
- Terminal automation system /ARTS/ digital computerized beacon tracking for future ATC facilities, noting add-on packages to increase system reliability [SAE PAPER 700282] 12 p2206 A70-27441
- Air Traffic Control Advisory Committee recommendations for improving future ATC [SAE PAPER 700293] 12 p2266 A70-27445
- Airborne equipment for Air Traffic Control System, improving pilot/controller cooperation [SAE PAPER 700300] 12 p2266 A70-27448
- Continental air traffic control design, discussing systems analysis approach advantages in terms of capacity 12 p2267 A70-27598
- Urban airport runway capacity increase via reduced aircraft separation, additional parallels and improved terminal traffic control, discussing design for acceptable safety levels 12 p2207 A70-27627
- Midair collisions between controlled and uncontrolled traffic in terminal areas associated with aircraft operations and airport density 12 p2267 A70-27632
- Aircraft separation standards in air traffic control system design regarding collision hazards, noting beacon system role 12 p2267 A70-27635
- Midair collision frequency under VFR as function of aircraft density derived, noting ATC role in safe separation 12 p2267 A70-27636
- Air controllers traffic capacity using automation, discussing airspace loading effect, area navigation and rerouting 12 p2267 A70-27637

ATC data processing requirements for higher automation level in terms of computer instruction rate and storage 12 p2267 A70-27638

ATC radar beacon system, discussing interacting factors lowering reply reliability from transponder 12 p2267 A70-27639

Radar beacon target processing system providing ATC information, noting target detecting and locating ability in noisy environment 12 p2268 A70-27640

ATC radar beacon system, discussing narrow interrogator beams, siting and beam shaping, interrogation environment control, data link transmissions and message content 12 p2268 A70-27641

Multipath tolerant ranging and data acquisition for air-ground-air links in ATC based on mathematical scattering theory 12 p2268 A70-27642

Air traffic control surveillance and data system using synchronous satellites in inclined elliptical orbits for communications and aircraft position determination 12 p2268 A70-27644

North Atlantic air traffic control system using aeronautical satellites, discussing flight levels, surveillance and positioning, terminals, etc 12 p2268 A70-27645

ATC data processing requirements based on projected traffic growth 12 p2268 A70-27910

Second generation radar beacon system for ATC using discrete address roll call 12 p2268 A70-27911

Airport capacity increase via electronic aids enhancing guidance, flight control, reduced aircraft separation, ATC automation and runway configurations 12 p2208 A70-27914

Position location and aircraft communication equipment concept and Experimental PLACE System providing ATC two-way voice and digital data communications via geostationary satellites 12 p2269 A70-27921

Multiple user satellite system for air navigation and traffic control, presenting comparative error analyses for position determination by spherical and hyperbolic ranging 12 p2270 A70-27925

Satellite system for air traffic control providing data links for aircraft position determination for U.S. in 1990s using 24-hour inclined elliptical orbits 12 p2270 A70-27926

Pictorial display area navigation system for air traffic control in terms of cockpit utilization, interface with ground navigation aids, parallel multiple routes, etc [AIAA PAPER 69-798] 13 p2449 A70-29171

Wet runway operations in air traffic control, discussing viscous, reverted rubber and dynamic hydroplaning 13 p2348 A70-29779

Air traffic control, reviewing air navigation, communication systems and radar techniques 13 p2450 A70-29998

Land and airspace demands in navigation, surveillance and traffic control, discussing application of current techniques 14 p2611 A70-30105

Air traffic control and customer cooperation, considering pilots, gliders, private, business, military and ultralight aircraft and air taxis 14 p2611 A70-30106

Avionics technology application to air traffic, discussing airborne computers use in navigation and control, secondary radar and correlation protected ILS 14 p2611 A70-30107

Aircraft characteristics effects on traffic control and community, considering passengers and freight 14 p2612 A70-30108

Ground and air based avionics for traffic control 14 p2612 A70-30109

Nationwide automated ground based air traffic control system for increased flight operations 15 p2772 A70-31962

Automatic ground based aircraft collision avoidance using combined associative processor-sequential computers 16 p2948 A70-33468

General aviation growth forecast during next decade, considering economic importance, air traffic control, collision avoidance, etc 16 p3003 A70-33469

Time ordered system for air traffic control providing data link, collision avoidance and navigation data through single channel 16 p2948 A70-33476

Time frequency concept application to air traffic control and collision avoidance systems 16 p2948 A70-33477

Time-frequency national airspace system, using distributed sensors and closed loop control to meet safety and traffic handling requirements 16 p2948 A70-33478

Satellite communication/navigation/surveillance systems for domestic and transoceanic ATC 16 p2949 A70-33479

Air traffic control, discussing precision instrument landing, approach lighting, collision avoidance, navigation aids, etc 17 p3133 A70-35185

ATC lag due to air transport growth and associated aircraft design and operations advances, discussing automation, noise abatement effects, etc 17 p3133 A70-35857

Nationwide air traffic control, using radar network and real time computer flight information centers for air safety 17 p3135 A70-35880

Heavy jet effect on airport acceptance rates, discussing various sequencing strategies 18 p3212 A70-36209

Associative processor concept for air traffic control, discussing tracking and correlation problem 18 p3288 A70-36392

Automated radar terminal system, ARTS-III Beacon Tracking Level for continuous aircraft identification on controllers radar display 18 p3288 A70-36393

Statistical properties of civil ATC system based on central processor, discussing system informational congestion 18 p3288 A70-36394

Data processing system for automatic air traffic control, describing hardware and software 18 p3288 A70-36395

Air traffic control - Conference, Versailles, June 1970 18 p3289 A70-36396

Central passenger traffic schedule role in air traffic control, discussing computer solutions, aircraft optimal use, etc 18 p3289 A70-36397

Computerized simulation role in air traffic control 18 p3236 A70-36398

National airspace system /NAS/, describing en route stage A automated air traffic control 18 p3289 A70-36399

Air traffic control system for continental U.S.A. in 1980s, discussing ATC Advisory Committee recommendations 18 p3349 A70-36400

Optimum approach and departure paths for VTOL aircraft simulated by hybrid computer under constraints [AIAA PAPER 69-209] 18 p3213 A70-36452

Terminal airspace utilization from ATC viewpoint, discussing airport capacity, data acquisition, weather, etc [SAE PAPER 700281] 18 p3237 A70-36809

STOL systems 1975 technical and economic characteristics in terms of passenger market, aircraft design, terminal facilities and ATC capability [SAE PAPER 700311] 18 p3350 A70-36812

Airport planning and design, discussing role of computers in capacity and site analysis, wind data processing, passenger and baggage flows analysis, etc 19 p3396 A70-37749

National Airspace System air traffic control automation program for en route and terminal facilities 19 p3464 A70-37914

Automatic ATC with feedback, describing information processing and flight plan algorithm 19 p3464 A70-38161

Air traffic control - Conference, St. Louis, April 1970 19 p3464 A70-38226

Air traffic control third generation system upgrading programs increasing airport, en route and terminal airspace capacities 19 p3464 A70-38227

ATC systems safety, capacity and delay, discussing terminal operations, runway capacity and aircraft spacing 19 p3465 A70-38228

USAF operations integration into ATC system 19 p3465 A70-38229

Helicopter operations integration into civil air traffic system, noting special requirements for mixed fixed and rotary wing terminal environments 19 p3465 A70-38230

Maximum throughput-rate capacity for runway and final approach path airspace involving multiple IFR landings 19 p3465 A70-38235

Airport capacity analysis for terminal areas, using simulation for alternatives to parallel runway operation 19 p3397 A70-38236

Time-synchronized approach control, combining aircraft precision navigation and guidance with ATC equipment 19 p3466 A70-38237

ATC airborne surveillance, communication and control system functioning as CAS after error or failure, discussing minimum parallel runway separation 19 p3466 A70-38241

Air traffic control - Conference, Stockholm, March 1969 19 p3466 A70-38629

IATA policy on future ATC development, discussing controlled airspace, communications and radar requirements 19 p3555 A70-38630

ATC and general aviation growth, considering airport capacity, radars, navigation, National Airspace System, etc 19 p3467 A70-38631

IFALPA views on ATC services, emphasizing aircraft approach spacing in North Atlantic airways 19 p3467 A70-38632

ATC integration of SST, discussing en route and terminal projects of national airspace system, modular automation, instrument flight rules, etc 19 p3467 A70-38633

UK organization of ATC services, considering responsibilities, facilities and personnel recruitment 19 p3467 A70-38634

ATC automation in France, applying method of filters for controller feed, radar and accident avoidance 19 p3468 A70-38635

Operational analysis and real time computer simulation models in ATC development 19 p3468 A70-38637

ATC simulation at EUROCONTROL Experimental Center, discussing dynamic simulator, data processor and display 19 p3468 A70-38638

System design and development of EUROCONTROL Center for optimum upper airspace in Benelux-FRG region 19 p3468 A70-38639

Airborne navigation systems operational aspects in ATC, discussing sensors, digital computer, cockpit displays, etc 19 p3468 A70-38640

Eurocontrol evaluation of navigational aid systems air traffic control, examining HARCO and VORDAC systems 19 p3468 A70-38641

Navigation errors and time delays in prediction techniques for air traffic control 19 p3468 A70-38642

Self navigation feasibility in future mass air traffic flow control 19 p3469 A70-38643

Digital extraction of primary and secondary radar data for air traffic control 19 p3469 A70-38644

Air traffic control CRT plan position indicators, considering alphanumeric symbols strokes design 19 p3469 A70-38645

Signal automatic air traffic control system /SATCO/ for flight plan processing, using multi-processing real time computer, electronic displays and software facilities 19 p3469 A70-38646

Air traffic controller stress reduction, discussing work-rest intervals and various management and human factors 19 p3371 A70-38647

Human factors in ATC, discussing simulation trials and impending problems 19 p3371 A70-38648

Air traffic controller role in future air traffic system, considering automation in operations 19 p3371 A70-38649

ATC personnel training at International ATC Academy, discussing objectives and syllabus 19 p3372 A70-38650

Airborne electronic equipment, collision avoidance systems, displays, instrumentation, human response and ground based control in air traffic control 20 p3665 A70-39198

Telecommunication, ATC and navigation satellite systems, examining economic bases for aeronautical and maritime space systems 20 p3740 A70-39407

ATC by scanning beam ILS and onboard control systems, increasing airport capacity and terminal area safety [AIAA PAPER 70-1033] 20 p3666 A70-39504

Satellite-based air traffic control system for North Atlantic, applying stochastic optimal control theory [AIAA PAPER 70-966] 20 p3669 A70-39563

Aerospace electronics covering fly-by-wire aircraft flight control, ATC, star trackers for spacecraft attitude control, etc 20 p3669 A70-39668

Italian automated ATC system /ATCAS/, discussing subsystem functions, display devices, data acquisition, information distribution, etc 21 p3847 A70-40911

Dioscures project for ATC over Atlantic Ocean, describing distance measurement by simultaneous use of two geostationary satellites 21 p3848 A70-41258

Automated airline communications system for collecting, analyzing, storing, transmitting, receiving and presenting information required by ATC and advisory services 21 p3789 A70-41347

- ATC data link communications system speeding information flow between controller and pilot
21 p3789 A70-41348
- General aviation traffic control, discussing limitations of present system and improvements of position information and area navigation approach procedures
22 p4066 A70-42385
- Air traffic safety problems, discussing satellite radio beacons applications to aerial navigation
22 p4066 A70-42652
- Inertial navigation system application to air transportation, discussing system mechanization and compatibility with ATC requirements
22 p4066 A70-42654
- Correlation detection methods providing information for ILS in terminal area congestion, discussing role in aircrew-ATC cooperation
22 p4068 A70-42667
- Airport and air route radar surveillance, beacon systems, microwave links and instrument landing systems, discussing transmission and reception problems
22 p4068 A70-43486
- Satellite technology application to aeronautics, predicting synchronous satellites communication for transoceanic and overland ATC
22 p4111 A70-43512
- Automatic conflict detection and resolution in ATC planning, discussing flight paths, zones of protection, etc.
[ICAS PAPER 70-58] 23 p4215 A70-44154
- V/STOL guidance and control system with bad weather landing capability, requirements for V/STOL integration into overall air traffic, terminal area guidance procedures, etc
23 p4216 A70-44843
- Automatic Data Processing and Display System for ATC over Belgium, Holland and Germany, relieving traffic controller routine tasks
23 p4216 A70-44860
- ATC radar data processing and display systems equipment and operation, emphasizing economy
23 p4216 A70-45044
- Satellite technology applications to ATC, including communications, navigation, surveillance over water and data acquisition
[AIAA PAPER 70-1301] 24 p4373 A70-45922
- Satellite based navigation/air traffic control information systems for short range STOL air carrier aircraft
[AIAA PAPER 70-1338] 24 p4373 A70-45930
- Air traffic flow digital computer simulation model including departure, enroute and arrival phases for collision avoidance, weather effects and control constraints
[AIAA PAPER 70-1316] 24 p4373 A70-45945
- FAA airport and airway capacity improvement program, considering runway-taxiway configurations, surface guidance and control, terminal design, takeoff, approach and landing systems, etc
[AIAA PAPER 70-1315] 24 p4431 A70-45946
- Air traffic control, future national airspace system improvements in view of air transportation growth, computerized automation technology, etc
[AIAA PAPER 70-1263] 24 p4374 A70-45969
- ATC, air navigation facilities and airport design requirements for short haul transportation system
[AIAA PAPER 70-1288] 24 p4323 A70-45973
- Upper Air Space Control Center Automatic Data Processing and Display System for air traffic control
24 p4323 A70-46238
- Aircraft climb and descent trajectories approximation compatible with air traffic control operation, noting parameters effects
24 p4375 A70-46239
- AIR TRANSPORTATION**
- Air traffic control inadequacy and restrictive regulations influence on aviation growth, implying need of airport-airways system improvements
[AIAA PAPER 69-1052] 01 p0138 A70-10642
- Interurban air transportation network structure contribution to airport and airways congestion, considering addition of nonstop links
[AIAA PAPER 69-1037] 01 p0005 A70-10647
- Party autonomy application to standardized international air transport contracts, discussing international treaties, law court judgments and literature
02 p0402 A70-12267
- Great Britain air transport industry manpower recruitment and training, technology changes effects and costs
02 p0402 A70-12307
- Seat capacity effect on operational costs of short/medium range high capacity A 300 B aircraft
02 p0402 A70-12368
- STOL in northeast corridor, discussing technology applications, economics, requirements for progress, industry, government regulations and decision making
[SAE PAPER 690418] 03 p0608 A70-12897
- Helicopters for injured or sick persons transportation as compared with ambulance use based on West Germany experience
03 p0436 A70-13822
- Health conditions and operational efficiency of Italian military paratroopers during air transportation analyzed from questionnaire data
05 p0807 A70-16494
- California future transport complex, considering STOL and ESTOL /extremely short takeoff landing aircraft/ design requirements
06 p0985 A70-17197
- Civil air transport passenger escape devices design and installation criteria
[SAE-ARP-495A] 07 p1191 A70-18805
- Twinjet helicopter design for business transport, emphasizing redundant systems for safety and bad weather flight capability
07 p1191 A70-18844
- European air transport navigation, discussing air traffic control and planned VHF omnirange/distance measuring equipment network /VOR/DME/
07 p1332 A70-20226
- VSTOL and STOL transport development concerning aircraft types, air traffic control and navigation, airports, etc
07 p1194 A70-20250
- Airline industry, considering expected increases in traffic, aircraft development and interface problems
08 p1600 A70-20588
- V/STOL intercity airliner potential and development noting benefits of noise reduction, ground space economy, etc
08 p1434 A70-20619
- Air transport facilities planning in Canada, describing systems planning approach and major influencing factors
08 p1481 A70-20621
- SOAR /Simulation of Airlift Resources/ model for stochastic productivity variations of strategic airlift systems
08 p1466 A70-20930
- Civil engineering research needs in air transportation, discussing information sources and processing and industry estimates of manpower, facilities and funding
08 p1481 A70-21305
- Jet lift passenger aircraft considered better suited for medium stage routes than rotor/ propeller designs for VTOL transport
08 p1436 A70-21347
- Civil air transportation in India, using mathematical models to estimate optimal development and efficiency of future air traffic potential
08 p1601 A70-21544
- Circadian rhythm of pilot efficiency and multiple time zone travel effects
[DFVLR-SONDDR-29] 08 p1453 A70-21935
- Air freight transportation economics, rate reductions and comparison with passenger aircraft
09 p1792 A70-22244
- World air transport system in 1970s, analyzing industry economic performance, discussing fares, rates, technological developments, passenger and air freight increases, etc
09 p1792 A70-22332
- VTOL aircraft applications to intercity traffic compared to competing transportation methods, discussing possible transportation time reductions
[DGLR-70-005] 10 p1970 A70-24045
- Civil jet VTOL transportation based on Do 31, discussing market, passenger requirements, noise, flight safety and economic factors
[AIAA PAPER 70-001] 10 p1805 A70-24051
- Boeing 747 aircraft impact on air transportation passenger and freight rates and traffic congestion reduction
10 p1806 A70-24765
- Air transportation and air traffic control factors relating to satellites applications to surveillance, navigation and communication over contiguous U.S.
[AIAA PAPER 70-488] 11 p2077 A70-25443
- Licensing aspects of Edwards Report, criticizing Air Transport Licensing Board /ATLB/ organization
11 p2153 A70-25856
- Criticism of public administration aspect of Edwards Report, noting parliamentary and constitutional difficulties in some proposals
11 p2153 A70-25857
- Edwards Report consideration of economic and investment opportunities in civil aviation, discussing denationalizing airways corporations
11 p2153 A70-25859
- British air transport from aircraft manufacturing industry viewpoint, discussing governmental organization of air industries and aircraft design negotiation atmosphere
11 p2153 A70-25861
- FAA recommendations on general aviation airports and heliport design standards, explaining standards establishment or modification procedures
[SAE PAPER 700231] 11 p2031 A70-25900
- Aircraft interior design styling and material selection, discussing industrial design department function and organization, styling as marketing tool, etc
[SAE PAPER 700233] 11 p1980 A70-25902
- Air transport and European cooperation involving supersonic transports, jumbo jets and STOL aircraft
12 p2334 A70-26966
- Automatic air transportation passenger handling and postflight financial and statistical data processing
12 p2335 A70-27016
- Crane helicopters characteristics, history and projected applications to petrochemical, shipping, construction and power transmission industries
[SAE PAPER 700284] 12 p2160 A70-27427
- Total community annoyance measurement /TACM/ applied to urban VTOL port planning for aircraft noise
[SAE PAPER 700286] 12 p2161 A70-27442
- V/STOL aircraft approaches to air passenger surface travel time reduction, emphasizing Manhattan-to-airport transportation problems
[SAE PAPER 700287] 12 p2335 A70-27443
- General aviation requirements for national aviation system of 1970s including use of airspace and airports under all conditions
[SAE PAPER 700296] 12 p2335 A70-27446
- VTOL profitability in Northeast Corridor, discussing city center ports accessibility for S-65-200 short hauls and economic and ground acreage advantages
[SAE PAPER 700310] 12 p2335 A70-27452
- V/STOL air transportation systems for short haul traffic, considering vehicle guidelines, ground facilities and operational requirements
[SAE PAPER 700312] 12 p2161 A70-27453
- Economic factors in developing STOL and VTOL metrolift service, proposing evolutionary process beginning with short term demonstration
[SAE PAPER 700313] 12 p2335 A70-27454
- American Airlines-McDonnell Douglas intermetropolitan STOL evaluation tests, noting microwave landing guidance system
[SAE PAPER 700336] 12 p2161 A70-27464
- Helicopters for short haul intercity transport, discussing power failure safety, weather factors and costs
12 p2161 A70-27596
- Continental air traffic control design, discussing systems analysis approach advantages in terms of capacity
12 p2267 A70-27598
- Air transportation demand growth forecast in terms of flights, airport operations and airborne aircraft at peak periods
12 p2336 A70-27626
- Antiair sickness medications effectiveness and secondary effects during low altitude transport of troops, observing sleepiness but no impairment of physical capacity
12 p2179 A70-28038
- Air transport of cardiac patients with auriculoventricular blocks, noting feasibility due to portable surveillance and treatment apparatus
12 p2172 A70-28041
- Long air voyage after exteriorization of Wallenberg syndrome, discussing case history of subject with cerebral vascular accident
12 p2172 A70-28044
- Article 9 of 1944 Chicago treaty in view of prohibited air navigation area established by Spain around Gibraltar 11 April 1967
13 p2523 A70-28824
- Patients emergency transportation by helicopter, discussing vehicle types and onboard medical treatment
14 p2540 A70-30191
- Large scale V/STOL service introduction for decongesting short haul routes between major cities of Northeast Corridors
14 p2615 A70-31276
- Rest periods assignment on long distance air travel of passengers based on physiological stress factor
15 p2690 A70-31892
- Air transport safety, applying experience from space programs
15 p2692 A70-32227
- Power plants development for air transport propulsion system economics, noting engine reliability, traffic delays, etc
16 p2841 A70-33770
- Computerized air transportation service including passenger name record, fare quotation, ticketing, etc
17 p3199 A70-34688
- Polish Lot airline long haul air transportation cost analysis
17 p3199 A70-34689
- Long haul air transportation profitability based on Polish Lot airline ton passenger-km computation comparison
17 p3199 A70-34691
- Computerized metropolitan air transit system, discussing system redundancy for safety level maintenance and all-weather dependability
17 p3199 A70-34730
- Power plant efficiency, size, maintenance and operating economics of propulsion systems for air transport
17 p3200 A70-34917
- Commercial air transport mission payload and range capability analysis, noting on-line flight planning computers
[AIAA PAPER 70-899] 17 p3204 A70-35815

Air transportation growth with regularity and safety - Conference, London, November 1969

17 p3021 A70-35851

Air transport operations and economics in 1970 decade, taking into account cost-revenue ratio and cost effectiveness of various aircraft

17 p3204 A70-35852

Air cargo transport growth, considering deterrents of high freight rates, ground movement time and customs clearance

17 p3204 A70-35853

ATC lag due to air transport growth and associated aircraft design and operations advances, discussing automation, noise abatement effects, etc

17 p3350 A70-35857

Mass air transportation, discussing aircraft characteristics, traffic growth, scheduling, passenger and cargo handling, etc

18 p3350 A70-36656

Legal aspects of suborbital space transports based on air transportation concepts

18 p3350 A70-36661

National air transportation systems approach, emphasizing data acquisition, methodology, planning and policy making [SAE PAPER 700337]

18 p3237 A70-36796

Corporate-executive market for helicopters related to fixed wing business air transportation problems [SAE PAPER 700285]

18 p3350 A70-36814

V/STOL short haul air transportation program in western U.S., assessing public acceptance and economic viability [AIAA PAPER 70-888]

19 p3552 A70-37394

Air freight carrier liabilities in passenger transportation international regulations, noting conflicting interpretations

19 p3553 A70-37562

International civil aviation, discussing ICAO functions, airports and terminal facilities problems

19 p3553 A70-37748

Air transportation of respiratory failure patients, considering medical equipment adaptation for aircraft use

20 p3580 A70-39440

International transportation regional hub airport planning with spin-off parking, circular terminal facilities and high speed interterminal passenger and baggage controls

20 p3606 A70-39673

Aviation in 1970s, discussing traffic increase, airport planning, aircraft design, ballistic transport, noise factors, etc

20 p3741 A70-40157

Air transport regulatory system, considering operational, technological and economic factors

21 p3954 A70-40579

Metropolitan air transit system design, considering compound helicopters, automatic control by central computer, onboard avionics system and terminal facilities

21 p3956 A70-41250

Inertial navigation system application to air transportation, discussing system mechanization and compatibility with ATC requirements

22 p4066 A70-42654

Air transport system technical and operational functions optimization

22 p3962 A70-43532

Long range air transport routes, predicting equipment and expenditures modifications

22 p4128 A70-43533

Passengers physiological and medical problems on subsonic and supersonic aircraft

23 p4150 A70-44223

Space systems supporting international air transportation growth, discussing UHF satellite R and D programs on beam antennas [SAE PAPER 700760]

24 p4372 A70-45870

Short haul intercity center facilities air transportation traffic alleviation by VTOL aircraft, emphasizing performance, ground facilities, system operation and economics [AIAA PAPER 70-1243]

24 p4290 A70-45914

U.S. western region short haul air transportation, discussing demand, modal split, STOL and VTOL aircraft, avionics and ground systems [AIAA PAPER 70-1284]

24 p4322 A70-45915

Air transportation beyond 1970, discussing general aviation, short haul systems, STOL, helicopter, V/STOL, subsonic, supersonic and hypersonic aircraft [AIAA PAPER 70-1262]

24 p4291 A70-45918

Planning criteria for optimum metropolitan airport system considering operational, physical, social and economic factors [AIAA PAPER 70-1266]

24 p4430 A70-45921

Airport planning for air transportation in underdeveloped nations, discussing economic, financial, technical and operational factors [AIAA PAPER 70-1268]

24 p4323 A70-45926

Short haul metropolitan air transportation, considering systems engineering as unifying technology [AIAA PAPER 70-1281]

24 p4373 A70-45927

FAA airport and airway capacity improvement program, considering runway-taxiway configurations, surface guidance and control, terminal design, takeoff, approach and landing systems, etc [AIAA PAPER 70-1315]

24 p4431 A70-45946

Demand analysis data generation for V/STOL systems suitable for New York-Philadelphia-Washington business travel market, applying model to selected designs [AIAA PAPER 70-1241]

24 p4374 A70-45961

Air traffic control, future national airspace system improvements in view of air transportation growth, computerized automation technology, etc [AIAA PAPER 70-1263]

24 p4374 A70-45969

STOL aircraft operational constraints, considering economics, short haul market characteristics, community acceptance, speed, propulsion system, takeoff/landing performance and maneuverability [AIAA PAPER 70-1283]

24 p4374 A70-45972

AIRBORNE EQUIPMENT

NT AIRBORNE/SPACEBORNE COMPUTERS

Airborne aeromagnetic gradiometer theory and design, using superconducting thin film tunneling junctions

01 p0085 A70-10289

Mark III airborne Omega system designed as receiver-computer to demonstrate real time operation, discussing flight test results

01 p0136 A70-10302

Airborne sensor simulator using recorded imagery for target detection and recognition problems, discussing closed circuit TV

01 p0088 A70-10810

Minimum operational characteristics /MOC/ for vertical guidance in airborne area navigation systems, including VOR-DME accuracy criteria

01 p0138 A70-11049

Airborne DME minimum operational characteristics for air traffic control navigation and communication systems including equipment specifications, environmental conditions, accuracy and range [DO-141]

01 p0138 A70-11050

Airborne SHF communication system for operation with passive satellites installed in C-121 aircraft

01 p0045 A70-11122

Cost effectiveness analysis applicable to DOD military system selection and acquisition, using model to study airborne electronics subsystem

02 p0401 A70-11673

In-flight data acquisition systems to overcome manual methods limitations, discussing applications and system configuration

02 p0224 A70-11839

Airborne instrument landing systems and ground facilities analysis and specifications, examining future use of microwave frequencies

02 p0333 A70-11982

Airborne secondary surveillance radar transponders performance and system optimization for automatic altitude reporting, separation standards maintenance and automatic plot extraction

02 p0267 A70-11990

Airborne UHF transmitters, discussing data on designs, performance, packaging and limiting factors of solid state devices for RF utilization

02 p0267 A70-12183

Venusian atmosphere water content determined by airborne interferometer

02 p0377 A70-12554

Channel constraints on multiple access systems obtained from airborne propagation tests via satellites, studying disparities in received signal strength

02 p0260 A70-12569

Synthetic aperture airborne side-looking radar using coherent optical data processor, discussing system configuration and operation

02 p0263 A70-12632

Airborne optics control subsystem /AOCS/ in optical measurement program for radiation originating in reentry events in project PRESS /Pacific range electromagnetic signature study/

03 p0489 A70-13652

Airborne multispectral sensing based on modified AN/AAS-5/XE-2 scanners mounted in C47 aircraft, discussing applications

03 p0491 A70-13669

Polarization diversity provided to parallel plate antennas in airborne radar applications by orthogonal vector processing

03 p0452 A70-13967

X-15 aircraft project experiments utilized in space research including IR and UV spectrometer, horizontal scanning, stellar photography, micrometeorite and solar energy studies, etc

04 p0622 A70-14673

Feedback technique for frequency stability requirements of airborne radar systems, discussing non-coherent radar applications and cost comparison to power-amplifier approach

04 p0656 A70-14708

Amplitude scanning, multiple beam and dual baseline phase comparison direction finding receivers for installation in aircraft to locate and analyze radar signatures

04 p0653 A70-15657

Airborne system for calibrating remote precision clocks using two way radio transmitter, measuring error by system similar to radar beacon transponder system

05 p0844 A70-15773

Proximity Warning System /Pilot Warning Indicator/ for helicopters, discussing applications to fixed wing aircraft

06 p0985 A70-17710

Physiological and environmental factors influencing oxygen breathing system design and use for passengers and aircrews of high flying aircraft

06 p1003 A70-17716

Cool gas inflation systems for evacuation equipment on large aircraft with size and weight fitting into aircraft doors

06 p0986 A70-17721

Far IR measurement of solar minimum temperature with Michelson interferometer carried on NASA research aircraft

06 p1143 A70-17997

Airborne and ground based radar data on thunderstorm echoes compared within framework of storm reflectivity model and radar theory

06 p1010 A70-18246

Book on space observatories covering rocket mounted telescopes for atmospheric structure, opaque wall, air diffusion, clouds and refraction, particle bombardment, meteorite melting, etc

07 p1379 A70-19099

Distributed ground clutter effects computation in airborne pulse Doppler radars, describing high PRF radar

07 p1236 A70-20063

Flight test evaluation program for airborne multisensor electro-optical display systems performance in TV mode under variety of optical conditions

07 p1289 A70-20403

Geomagnetic field total vector modulus secular variations from airborne measurements

07 p1278 A70-20461

Forward looking airborne radar /FLAR/ moving target indicator for military helicopter mounting

08 p1462 A70-21358

Aircraft mounting plate for 70-mm multispectral mapping quadricamera assembly to photograph wildland and agricultural resources

08 p1497 A70-21542

Airborne sidescan radar for fix-point navigation at low flight altitudes involving computerized sensing evaluated for operator performance

08 p1541 A70-21563

Airborne EROS collision avoidance system, discussing flight performance, range and closing rate measurements

09 p1720 A70-22241

Cryostat design and performance for use with optical telescopes in high altitude balloons

09 p1674 A70-22294

Sector Tactical Air Navigation System to supply onboard information on bearings, slant range and elevation and computer input signals

09 p1720 A70-22491

NASA operation of Convair 990 jet transport as airborne scientific research platform for optical observations

09 p1682 A70-23504

Airborne monochromator and photoelectric filter radiometer for solar spectral irradiance measurements, estimating instrument errors

09 p1683 A70-23515

Far IR airborne spectroscopy for measuring solar brightness temperature, emphasizing scanning Michelson interferometer and radiometric calibration

09 p1683 A70-23525

Airborne IR line scanning systems for forest fire surveillance, determining size and characteristics during smoke or darkness

09 p1686 A70-23753

Aircraft surface temperature measured with airborne IR TV system

09 p1686 A70-23754

Airborne pyrotechnic cloud seeding system development, testing and application, comparing rainfall from test and control clouds

10 p1886 A70-23931

Airborne precipitation drop sampler imprint size relationship to water drop diameter

10 p1857 A70-23932

Airborne simulator program for evaluation of motion and visual cue effects on pilot performance in roll, using compensatory tracking tasks [AIAA PAPER 70-351]

10 p1857 A70-24202

Ground-based and in-flight simulation using variable stability aircraft, investigating pilot rating [AIAA PAPER 70-354]

10 p1858 A70-24209

Swedish real time IR imaging system, discussing airborne applications in locating fresh water springs and defining irrigation patterns

10 p1879 A70-24743

Airborne side-looking radar antenna optimal directional characteristics analysis from viewpoint of maximum surveillance range

10 p1843 A70-25139

ACME hybrid airborne satellite TV and communications system for India, using airborne TV transmitters [AIAA PAPER 70-472] 11 p1998 A70-25418

ATC airborne hardware covering transponders, area navigation, DME, course directors and approach couplers 11 p2079 A70-25724

Design criteria for minimizing EMC problems confronting engineers of aircraft electrical and electronic equipment [SAE PAPER 700215] 11 p1980 A70-25887

Gravity waves structure simultaneous determination from airborne ozone and temperature sensors and satellite observations data 11 p2076 A70-26072

Atmospheric temperature and pressure profiles remote measurement using airborne microwave radiometer 11 p2056 A70-26502

Remote sensing from aircraft and satellites of chlorophyll concentrations for monitoring of biological productivity of sea 12 p2217 A70-26915

Multistage sampling of space and aircraft remote sensor imagery for forest inventory 12 p2228 A70-26921

Clear air turbulence detection by radar equipped aircraft, considering reflection from refractive inhomogeneities 12 p2262 A70-26952

Angular aberrations produced by airborne radomes calculated by computer, allowing optimal parameters selection and knowledge of radio properties 12 p2195 A70-27274

Airborne equipment for Air Traffic Control System, improving pilot/controller cooperation [SAE PAPER 700300] 12 p2266 A70-27448

Solid state power controllers for aircraft electrical power systems [SAE PAPER 700304] 12 p2195 A70-27450

Semiconductor power controllers for switching aircraft electrical power supplies [SAE PAPER 700308] 12 p2195 A70-27451

Laser profilometer for airborne ocean wave profile measurement 12 p2249 A70-28003

Aircrew equipment assemblies taking into account altitude, flight acceleration, environment, escape and survival 13 p2345 A70-28971

Minimum performance standards for airborne radio receiving and direction finding equipment covering normal and environmental test procedures 13 p2365 A70-29000

Tactical aid displays /TAD/ for lightweight multisensor airborne ASW localization missions, discussing mission planning, avionics design, operator direction airborne tactical decision structures, etc [AIAA PAPER 70-517] 13 p2407 A70-29036

Airborne equipment microelectronics technology application to interrogators, transponders and UHF/VHF transceivers 14 p2558 A70-31294

Airborne electro-optical array system design and performance for particle size measurement 16 p2906 A70-33175

Phased arrays, discussing ground based, shipboard and airborne research programs for military 16 p2863 A70-33264

MHD power sources for onboard military aircraft electrical application 16 p2964 A70-33474

High voltage DC electric power systems design for aircraft, considering filtering, transmission and loads interaction 16 p2844 A70-33475

Airborne flight test data acquisition and ground based automatic bulk data processing system for helicopter test and development programs 17 p3014 A70-34713

Millimeter wave radar for high resolution aircraft landing aid, describing experiments to obtain backscatter data from airborne platform 17 p3133 A70-34721

Airborne multispectral sensing, describing multichannel scanners, pattern recognition techniques and equipment, etc 17 p3083 A70-34874

Airborne illumination using argon vortex-stabilized arc lamp, noting applicability in near IR spectral range 17 p3023 A70-35152

Humidity resistance test method involving flight simulation for airborne equipment in tropical environment 17 p3058 A70-35159

Hypsometer design for accurate pressure measurements at high balloon altitudes 17 p3090 A70-35313

DC-10 airborne flight test PCM data system, discussing capability, onboard operating characteristics and test results 17 p3093 A70-35498

Airborne data acquisition and flight recorder systems, comparing civil and military aircraft requirements 17 p3094 A70-35515

Airborne IR scanner as geophysical research tool depicting surface emission and heat mass transfer 18 p3259 A70-36558

S band CW power amplifier and varactor doubler module for airborne phased arrays 18 p3231 A70-36674

Aircraft-borne spectrometer for atmospheric IR spectral transparency 18 p3260 A70-36972

ATC airborne surveillance, communication and control system functioning as CAS after error or failure, discussing minimum parallel runway separation 19 p3466 A70-38241

Instrumentation magnetic recorders in aerospace industry in relation to new components and techniques development, investigating airborne recorder as flight test tool 19 p3429 A70-38516

Flight test and airborne data recovery and processing, discussing data format, recorder characteristics, ground equipment and time requirement 19 p3429 A70-38517

Boeing 747 transport airplane flight test data system, discussing recording media, major PCM and FM tape systems, etc 19 p3431 A70-38531

Magnetic tape instrumentation system installed aboard Hawker Siddeley Harrier for flight development, discussing digital format recording system 19 p3384 A70-38549

Airborne navigation systems operational aspects in ATC, discussing sensors, digital computer, cockpit displays, etc 19 p3468 A70-38640

Airborne electronic equipment guarantees, discussing USAF experience with full life, maximum failure rate and failure free plans 19 p3391 A70-38843

Airborne electronic equipment, collision avoidance systems, displays, instrumentation, human response and ground based control in air traffic control 20 p3665 A70-39198

Airborne atmospheric turbulent flux measurement system with fast response wind velocity, temperature, humidity and aircraft motion sensors, discussing performance and data reduction 20 p3665 A70-40109

Axial mode helical antenna design with built-in impedance transformer for airborne applications 21 p3796 A70-40758

Aircraft electronics and instrumentation history, discussing anemometer, barometric altimeter, radar, communications systems, computers, flying control and various flight conditions 21 p3826 A70-41257

Aircraft-borne and descent systems performance and weight optimized for midair retrieval [AIAA PAPER 70-1201] 21 p3751 A70-41805

Magnetic recording in airborne systems, discussing printed motor-optical tachometer design for transport accuracy and ferrite spin-alloy heads 21 p3829 A70-41921

Airborne data acquisition equipment for accident flight path and engine performance recording 21 p3796 A70-41922

Airborne three dimensional area navigation equipment for reducing mid-air collision exposure and for raising landing safety in terminal areas 22 p4066 A70-42296

Airborne optical scanning gyro for measuring sea surface radiation emission 22 p4039 A70-43558

Aircraft electronics and instrumentation history, discussing anemometer, barometric altimeter, radar, communications systems, computers, flying control and various flight conditions 23 p4193 A70-43888

Survival and flight equipment - Conference, Las Vegas, September-October 1970, Volume 2 23 p4152 A70-44479

Battery operated electronic servo governed photoelectric polarimeter for airborne measurements of skylight polarization, discussing design and operation principles 23 p4199 A70-45006

Microwave radiometric airborne measurement of salinity of Mississippi River outflow, using P3A aircraft 24 p4330 A70-45979

Airborne radiometer slim multibeam millimetric antenna, describing design, construction and performance 24 p4316 A70-46320

AIRBORNE INFECTION

Airborne bacteria and fungi in atmosphere of Tektite I underwater habitat 15 p2681 A70-31880

AIRBORNE TERRAIN ANALYSIS
U TERRAIN ANALYSIS

AIRBORNE/SPACEBORNE COMPUTERS

Mark III airborne Omega system designed as receiver-computer to demonstrate real time operation, discussing flight test results 01 p0136 A70-10302

Aerospace digital computer design development, proposing data processing system with improved flexibility by making subassemblies more independent with multiplexed interface 01 p0047 A70-10305

Airborne DME minimum operational characteristics for air traffic control navigation and communication systems including equipment specifications, environmental conditions, accuracy and range [DO-141] 01 p0138 A70-11050

Aerospace computers stringent design requirements and applications in spacecraft, ballistic missiles and integrated avionic systems 02 p0264 A70-11688

Aircraft navigation systems performance, discussing navigation aid integration by digital management computer coupling navigation sensors to display and control devices 02 p0334 A70-11984

Air traffic congestion alleviation by applying general purpose computers for navigation in civil transport aircraft 02 p0334 A70-11985

Airborne computer civil navigation system designed for output coordination from navigation sensors 02 p0334 A70-11986

Cosmic X ray astronomy, discussing existing techniques, limitations, use of onboard computers and future requirements 02 p0304 A70-12795

Spaceborne computer system for manned space station to perform functions in addition to guidance and navigation including processing [AAS PAPER 69-581] 04 p0654 A70-14651

Airborne digital leaddown computer to guide VTOL aircraft flying complex trajectories to relieve airport congestion 05 p0880 A70-16416

Computational algorithms transformation to forms convenient for aircraft computer adaptation for reducing digital network length with small accuracy penalty 05 p0818 A70-17005

Onboard computer requirements for inertial navigation of spinning and maneuvering vehicle, determining design parameters [AIAA PAPER 68-839] 06 p1013 A70-17161

Federated and integrated computer systems for aerospace applications, discussing system dependent variables 06 p1013 A70-17352

Complex integrated avionics computer system design for navigation, guidance and control of rotary wing aircraft, emphasizing microelectronic modular assembly 06 p1014 A70-17353

Avionic and space electronic equipment converging design, considering chip computer 06 p1017 A70-17354

Aircraft computer design performing basic arithmetic operations by sampling method noting speed increase 06 p1014 A70-17859

Airborne computer system program for antisubmarine warfare enhancing human element in man machine system 06 p1185 A70-17974

Flight software for onboard Apollo Primary Guidance, Navigation and Control System flight qualification by digital simulation, including software diagnostics [AIAA PAPER 70-173] 06 p1029 A70-18060

Apollo onboard computers tracking data state-vector corrections covariance matrix, considering initial estimate, noise and tracking geometry errors [AIAA PAPER 70-162] 06 p1015 A70-18072

Space vehicle digital control system attitude computations using quaternion matrix algebra to simplify control equations [AIAA PAPER 68-825] 07 p1393 A70-19302

Onboard modular computer research in strapdown guidance technology for computational ability and long term reliability of unmanned missions 07 p1238 A70-20062

Distributed ground clutter effects computation in airborne pulse Doppler radars, describing high PRF radar 07 p1236 A70-20063

Prototype Onboard Processor /OBP/ designed for high reliability, low power dissipation, small size and low weight, discussing attitude control signal processing 08 p1464 A70-20609

Aerospace digital computers automatic checkout, considering computers functional and mechanical properties and test equipment configuration and operation 08 p1469 A70-20653

Workload relieving displays and controls for general aviation, discussing feasibility of digital computer driven integrated displays 08 p1601 A70-21679

LSI Mark 3 airborne Omega system with computerized signal processing for navigation parameters, discussing system features and flight test results
09 p1719 A70-22190

Apollo mission simulation, discussing Command Module Simulator (CMS), onboard computer system and dynamic visual presentation via infinity-optics display [SMPT PAPER 105-74]
09 p1655 A70-22226

Thermoelectric outer planet spacecraft (TOPS)/project incorporating adaptable data handling system and self testing and repairing computer with triple redundancy subsystems
11 p1996 A70-25368

Self optimizing Kalman filter for hybrid inertial air navigation systems, noting implementation on airborne digital computer
11 p2078 A70-25682

Fighter-missile launch and control using direct radar information for guidance to reduce computation time and computer storage space
11 p2015 A70-26332

Digital air data system vibrating diaphragm pressure sensor
11 p1983 A70-26508

Airborne computer design for short range attack missile (SRAM) to perform aircraft navigation and missile fire control
12 p2192 A70-27800

Apollo Guidance Computer operations and functions during lunar orbit rendezvous
13 p2446 A70-28390

Minimum-time thrust vector control law in Apollo lunar module computerized autopilot
13 p2499 A70-28399

Spaceborne information processing for manned missions, describing layered system with fault tolerance and onboard checkout
13 p2372 A70-28415

Onboard satellite information processing systems for bandwidth compression using digital filters and error correcting coding
13 p2381 A70-28431

Onboard computers automatic reliability control with implementation of self repair, modeling by Markov processes nonhomogeneous in time
13 p2372 A70-28438

Digital computers for interplanetary spacecraft, comparing centralized and decentralized approaches for implementing onboard functions [AIAA PAPER 68-840]
14 p2554 A70-30757

Spacecraft onboard computer for prelaunch targeting constants verification through checksum equation and error detection scheme, using generated number sequence [AIAA PAPER 69-946]
14 p2599 A70-30769

Digital guidance and control system, discussing communication device providing data transfer between airborne digital computer and control device [AIAA PAPER 69-988]
14 p2615 A70-30771

Digital computers in aircraft, discussing automatic control systems, components and advantages over analog systems
15 p2705 A70-32299

Avionics computers field repair method permitting removal and replacement of flat packs and discrete components on multilayer interconnection boards
15 p2706 A70-32655

Optimal adaptive digital autopilot design for reentry vehicle flight path control
16 p2946 A70-33307

Optimal interceptor-target allocation and guidance for linear interception and rendezvous using real time and storage computer
16 p2947 A70-33311

Cost effectiveness of higher order language /HOL/ for airborne computers
16 p3003 A70-33428

Space programming language SPL/36 replacing machine language programming in flight software capable of expressing complex vector mathematics and decision control
16 p2868 A70-33429

Common high order programming language and program debugging in aerospace software
16 p2868 A70-33430

Aerospace compiler design for software cost reduction without affecting reliability, describing input language
16 p2868 A70-33432

X band airborne antenna phased array, describing phase shifter, radiation pattern, associated computer, etc
16 p2864 A70-33454

Airborne multiprocessor building blocks, discussing central processor, input/output controller and interface, memory unit and power supply
16 p2869 A70-33465

General purpose parallel processor design for avionics, considering radar signal processing
16 p2910 A70-33467

Aircraft electronic propulsion control system using flight type computers and analog to digital conversion equipment [AIAA PAPER 70-693]
16 p2966 A70-33556

Airborne vertical glide path guidance computer for aircraft landing, using barometric altitude and DME data
16 p2871 A70-34053

Military aircraft avionics central digital computers, discussing memory capacity, computational speed requirements, cost and tradeoffs
17 p3049 A70-34673

Digital computer technology impact on advanced aircraft design, discussing airborne computers, distributed and lumped computer systems, outer loop control, engine control and system integrity
17 p3049 A70-34993

Real time computers design tradeoffs in avionics systems
17 p3050 A70-35510

Integrated flight management system for commercial aircraft pilot using computer [AIAA PAPER 70-908]
17 p3134 A70-35820

STOL navigation systems, evaluating Vector Analog Computer, Decca Omnitrac IIB and inertial system
18 p3289 A70-36513

Aero gas turbine engines digital computer control, discussing special properties, design and safety problems [ASME PAPER 70-GT-40]
18 p3304 A70-36870

Meteorological satellites, discussing observation continuity, orbital characteristics onboard memory capacity and sensing methods
19 p3460 A70-37386

Computerized airborne integrated data acquisition and analysis system, discussing hardware, software and airborne-ground elements interfaces [AIAA PAPER 70-935]
19 p3382 A70-37393

ESRO applied research program, discussing IR technology, onboard computers, electric propulsion, etc
19 p3553 A70-37870

Economic payback of AIDS /Aircraft Integrated Data System/ recording for operational performance monitoring and engine analysis
19 p3382 A70-37894

Airborne integrated data system /AIDS/ for accepting, processing, recording and displaying aircraft systems data, describing installation and design criteria
19 p3382 A70-37895

Logic, arithmetic, control and instruction capacities of dedicated onboard telemetry preprocessor
19 p3383 A70-37904

Military Airlift Command jet aircraft computerized area navigation system operational procedures
19 p3465 A70-38232

Piezoresistive Si pressure transducer design for Digital Air Data Computers, achieving optimum resistor matching and long term stability
19 p3430 A70-38521

Jaguar flight test data processing system, discussing airborne digital computer
19 p3384 A70-38536

Emmanual magnetic recording system used with airborne digital computers for aircraft in-flight tests
19 p3432 A70-38547

N body numerical integrator using virtual mass technique for computing trajectories with speed and accuracy suitable for spacecraft onboard computer applications [AIAA PAPER 70-1057]
19 p3528 A70-38872

V/STOL aircraft automatic flight control, guidance and navigation by onboard computer, discussing mathematical model and simulation results [AIAA PAPER 70-1035]
20 p3665 A70-39502

Digital fail-operative flight control computers for automatic landings, describing system requirements and problems and flight test program [AIAA PAPER 70-1032]
20 p3591 A70-39505

Pilot/vehicle feedback systems with flight director computer for transport aircraft longitudinal control during landing, discussing design by manual control displays theory [AIAA PAPER 70-1001]
20 p3560 A70-39530

Recursive digital filters for flight control system and airborne computer, considering quantization effects and eigenvalue sensitivity [AIAA PAPER 70-953]
20 p3601 A70-39575

High performance aircraft self adaptive feedback control system, using airborne digital computer with inputs of elevator deflection and pitch rate for effectiveness identification
20 p3605 A70-40119

Airborne integrated computerized ASW system, describing navigation, flight control, display and sensor subsystems
21 p3821 A70-40575

Soyuz and Apollo spacecraft on board computers, discussing design, guidance, navigation and requirements
21 p3793 A70-41071

Communications satellite carrier instrumentation, using computer controlled frequency shift radiometer for power monitoring
21 p3826 A70-41345

Papers on air and spaceborne computers covering devices and systems technologies, man computer relationship optimization, impact on aerospace systems design
21 p3794 A70-41684

Aerospace digital computers impact on aerospace systems design
21 p3794 A70-41685

Aerospace computers design, considering real time operation and reliability requirements
21 p3794 A70-41686

Aerospace digital computer family structural commonality, considering architecture, hardware and support software
21 p3794 A70-41687

Aerospace digital computer and avionics systems man machine relationship optimization, considering human information and control response requirements
21 p3794 A70-41688

Computerized aerospace systems man machine interface mechanization for performance optimization, emphasizing integrated approach to avionic displays
21 p3795 A70-41689

Aerospace system design, considering use of microprogram-controlled digital computers
21 p3795 A70-41690

Modular aerospace digital computer system architecture using off-shelf components for rapid avionic computing system realization
21 p3795 A70-41691

Semiconductor circuits large scale integration for aerospace computers, discussing fabrication and design
21 p3799 A70-41692

Aerospace microelectronic digital computer design, discussing optimal packaging by use of integrated circuits
21 p3795 A70-41694

Ultrasurvivable and maintainable computer design involving redundant spare modules and own tester for aerospace applications
21 p3795 A70-41695

Programming and checkout of computer for ELDO inertial guidance system, including flight simulation and autopilot tests [AIAA PAPER 69-961]
21 p3795 A70-41862

Airborne digital computers in aircraft systems, discussing optimization, design and economic effectiveness
21 p3796 A70-41920

Airborne test computer for in-flight radar checkout featuring tape storage of computer program and cockpit mounted optical readout
22 p3993 A70-42320

Airborne computerized time frequency systems for aircraft range and velocity determination, using stable clocks with ambiguity resolution
22 p4067 A70-42659

Avionics digital computer system using associative memory for executive control functions implementation to mechanize task assignment algorithm
22 p3994 A70-43105

Manned spacecraft onboard data management systems, discussing information transfer, processing, control, display and man machine interface
23 p4167 A70-44647

Integrated data processor-operation controller for stellar TV photometer systems in spaceborne observatory, considering limited channel transmission capacity
23 p4167 A70-44649

Onboard digital information processing, discussing applications to tactical missile guidance and manned vehicles [AIAA PAPER 70-1230]
24 p4317 A70-45976

Unmanned Luna 16 landing mission, discussing launching and automatic mission control via onboard computer and earth-radioed data
24 p4412 A70-45982

AIRCRAFT
Maximum likelihood methods for aircraft identification problems, considering model types, flight disturbances and available data
16 p2885 A70-33326

Aircraft, helicopters and rockets aviation systems design and components service life problems, emphasizing maintenance intervals
17 p3100 A70-34686

Aircraft capabilities as scientific observation platform in astronomy and geophysics, including instrument adaptation and IR absorber problems
22 p4019 A70-43146

AIRCRAFT ACCIDENT INVESTIGATION
Helmet loss and failure role in major and fatal head injuries of USAF ejections
01 p0032 A70-10370

Safety analysis of VTOL aircraft for passenger transport based on accidental failures caused by technical defects, human error, weather, sabotage, etc
05 p0794 A70-16348

Victim examination, human factors and forensic problems in flight accident investigations
05 p0807 A70-16497

- Book on human factor in aircraft accidents covering desire to please, fatigue, diurnal rhythm, psychology, etc
06 p0987 A70-18249
- Aircraft accidents victims identification, considering use of specialized laboratories
09 p1626 A70-23018
- Pathogenic mechanisms of fatal injuries during supersonic ejection determinable by radiography
09 p1627 A70-23114
- Pilot disorientation in dark night takeoff accident type, presenting illusory angular displacement of vertical, flight paths and sequential accelerations
13 p2359 A70-29441
- Systems approach to flight accident prevention and inquiry management
15 p2674 A70-32207
- Aircraft accident investigation, discussing interrelations between official investigator and manufacturers coordinator
15 p2675 A70-32217
- Book on air safety and commercial aviation accidents
16 p2842 A70-33964
- Flight loads data extraction and analysis from damaged magnetic tapes after aircraft crash
17 p3094 A70-35518
- Fatal general aviation accidents examined by pathologists, determining pilot incapacity, accident sequence, aircraft design modification and crash protection performance
17 p3033 A70-35567
- General aviation aircraft accident investigation toxicological findings, describing methods of examination for drugs and toxic agents
17 p3033 A70-35569
- Focal myocarditis associated with aircraft accidents, discussing difficulties in diagnosis and assessment
17 p3033 A70-35571
- Aircraft passenger tie-down failure, comparing injury patterns in various accidents to aid reconstruction
17 p3039 A70-35572
- Aircraft accident injuries possible misinterpretation
17 p3039 A70-35575
- General aviation aircraft accident post mortem findings, emphasizing standardization of format and terminology
17 p3040 A70-35579
- Aircraft accident prevention and investigation, noting economic factors as deterrent to safety measures implementation
17 p3022 A70-35860
- Flight data recording systems for accident investigation and operational purposes, discussing U.S., British and French regulations
18 p3258 A70-36341
- Flight/accident data recorders and associated equipment for civil and military aircraft requirements
18 p3258 A70-36342
- Airborne crash recorders objectives, design and features ensuring crash survival of recordings
19 p3429 A70-38518
- Flight recorder role in aircraft accident investigation and prevention, noting audio instruments and data recovery
19 p3356 A70-38613
- Aircraft nighttime and daytime accident rate comparison, considering darkness, flight phase, etc
21 p3751 A70-41489
- Aircraft accident filing system data analysis using Fortran programs
22 p3962 A70-42880
- Aerospace medicine approach to medical investigation training for aircraft accidents, noting flight surgeon role as life support specialists chief
23 p4152 A70-44454
- Over water aircraft accident investigation aids for greater survival, improved location searches and faster recovery of essential parts
23 p4153 A70-44498
- Soviet civil aircraft-bird collisions, stressing hazard forecast and prevention by bird identification and migration patterns
24 p4289 A70-45644
- AIRCRAFT ACCIDENTS**
Ground and ditching emergency evacuation tests of C-9A aeromedical aircraft under worst possible simulated crash conditions
01 p0035 A70-10716
- Beacon equipment as means of crashed or forced-landed aircraft locator to increase survival possibilities and reduce search cost
01 p0035 A70-10719
- Scientifically oriented pilot selection objectives criteria taking into account data concerning accident causes
02 p0242 A70-11684 [DVL-892]
- Aircraft systems safety analysis, discussing accident causes and prevention, risk allocation, safety equipment, etc
02 p0225 A70-12263
- Biphasic nature of pilot error in gliding, suggesting means of reducing aircraft accidents
03 p0433 A70-13261
- Pilot visual information display systems influence on flight safety, discussing aircraft accidents and human error factors
04 p0691 A70-15143
- Heat exchanges between man and environment due to incidents or accidents during aircraft operation evaluated by combined heat transfer coefficient
05 p0799 A70-15764
- British military and civilian aircraft and flying between World War I and II, discussing weapons systems and accidents
05 p0794 A70-16113
- DC-8 aircraft ditching in San Francisco Bay on 22 November 1968, discussing accident sequence, evacuation operations, life raft stowage and deployment, etc
06 p0985 A70-17705
- Crash control for reduction of operational hazards and flight accidents to survivable level, discussing pilot training for emergencies
07 p1191 A70-19008
- Emergency equipment for aircraft accidents with dual channel radio beacons installed on life rafts, noting electronically conducted search
07 p1191 A70-19011
- Survival psychology for civil aviation, discussing irrational behavior after forced landings resulting from exhaustion of mental resources and inappropriate activity
07 p1204 A70-19018
- Visual aspects of collision avoidance, describing prudent mid-air maneuvers
08 p1449 A70-20481
- Survival on sea following air accident, based on medical and technical considerations, emphasizing life jackets
09 p1625 A70-23008
- Human factors responsibility for aircraft accidents, discussing cooperation between air safety service and flight surgeons
09 p1626 A70-23016
- Human psychophysiological inability to avoid mid-air collisions investigated for aviation safety
09 p1611 A70-23465
- Commercial aviation safety on basis of aircraft accidents relationship to distance covered, considering clear air turbulence and cosmic radiation dangers
10 p1804 A70-24050
- Short range aircraft collision pilot warning indicator for low altitude and closure speeds
11 p2078 A70-25706
- Flight safety evaluation based on ICAC and German flight accident data indicating pilot role and tabulating statistical analysis
11 p1981 A70-25948
- Aircraft impact against nuclear containment vessel and associated structures for dangers in aircraft-nuclear power station collisions
11 p2144 A70-26683
- Flying accident liability predictions reliability from pilot trainee aptitude test performance at selection, discounting accident proneness theory
12 p2178 A70-27048
- Psychological tests of pilot adaptation to accident situation using photo display assessment
12 p2179 A70-27052
- Gelled and emulsified fuels for jet transport aircraft, testing rheological and physical properties regarding fire hazard reduction in crashes
12 p2160 A70-27430 [SAE PAPER 700251]
- Aircraft crash fire fighting equipment and tactics for future airport needs
12 p2160 A70-27433 [SAE PAPER 700262]
- Airport runway slipperiness rating, predicting and alleviating to reduce aircraft accidents
12 p2206 A70-27434 [SAE PAPER 700265]
- Collision and missed approach risks in high capacity airport landing operations, discussing parallel runways spacing and aircraft longitudinal separation
12 p2207 A70-27629
- Midair collisions between controlled and uncontrolled traffic in terminal areas associated with aircraft operations and airport density
12 p2267 A70-27632
- Visual aircraft-to-aircraft detection effectiveness in collision avoidance as function of pilot performance and closing speed
12 p2267 A70-27633
- Midair collision frequency under VFR as function of aircraft density derived, noting ATC role in safe separation
12 p2267 A70-27636
- Midair collisions incidence correlated with traffic factor proportional to square of number of operations
12 p2269 A70-27912
- Intermittent positive control (IPC) role in midair collision avoidance, using mathematical model to determine command frequency and implementation
12 p2269 A70-27913
- Fatal accidents involving airline aircraft/1968-69/
15 p2674 A70-32208
- Accident/incident information exchange in aviation community, noting Flight Safety Foundation
15 p2674 A70-32209
- Aircraft accidents during descent, approach and landing, discussing B 747, C5A and SST
15 p2675 A70-32216
- Human survival problems of transport aircraft in various airport ground-air situations and environmental conditions
15 p2676 A70-32224
- Aircraft accident prevention via reduction of pilot attention distractions
15 p2692 A70-32226
- Human factors in aircraft accidents, noting cockpit crew members overconfidence and carelessness
15 p2692 A70-32228
- Corporate aircraft accident statistics, causes and prevention, noting pilot errors, mechanical failures, etc
16 p2842 A70-33814
- European requirements for aircraft accident and maintenance recording systems
17 p3094 A70-35517
- Carboxyhemoglobin saturation in post mortem examination of aircraft accident victims, discussing errors in methodology
17 p3033 A70-35568
- In-flight coronary occlusions role in aircraft accidents, discussing need for full autopsies, Double Masters ECG and full medical histories
17 p3033 A70-35570
- Characteristic injuries from aircraft controls inflicted in fatal accidents, showing pilot position and hand location upon impact
17 p3039 A70-35573
- USAF aviation accidents diagnostic patterns of injury and death, noting increase in fire and/or associated complications
17 p3039 A70-35574
- Lumbar vertebrae transverse processes fractures in air crashes, considering factors involved, incidence and pathogenesis
17 p3033 A70-35578
- Bird strikes in U.S.S.R., discussing frequency, damage, etc
18 p3212 A70-35986
- Birdstrikes as aircraft hazard, discussing structural damage, engine ingestion and various countermeasures
18 p3213 A70-36319
- Aircraft in-flight and post crash fire protection developments, considering controlled flammability fuel systems and fire fighting methods
18 p3215 A70-36847 [ASME PAPER 70-GT-109]
- Flight data recording system /FDRS/ for crashes expanded to aircraft integrated data system /AIDS/ for airlines
19 p3426 A70-37893
- ATA Collision Avoidance System based on time and frequency synchronization via ground stations or other aircraft
19 p3466 A70-38239
- U.S. Army rotary wing mishap experience for product assurance and accident prevention
19 p3356 A70-38825
- Aircraft systems safety requirements, consisting of accident probability, confidence level and demonstration test period
19 p3442 A70-38840
- Human error as factor in aircraft accidents, considering man machine incompatibility and prevention measures
21 p3771 A70-41723
- Airborne data acquisition equipment for accident flight path and engine performance recording
21 p3796 A70-41922
- Soviet monograph on collision hazards between aircraft and birds covering accidents, damage and preventive measures
23 p4137 A70-44099
- Aircraft crash protection with preinflated air bag added to conventional seat/lap belt tested with human sled subjects
23 p4140 A70-44456
- In-flight escape systems and survival equipment reliability in U.S. Navy ejections
23 p4143 A70-44460
- Nonflammable fibrous textile materials for injury and personnel loss prevention in fires by aircraft accidents
23 p4153 A70-44481
- AIRCRAFT ANTENNAS**
UHF shallow-cavity crossed-slot aircraft antenna for satellite to air communications
02 p0269 A70-12585
- Computer predicted horn antenna radiation patterns through aircraft radome compared with measured values
09 p1645 A70-22689
- Concorde aircraft radar signal transmission, describing modified Flexwell waveguide
13 p2379 A70-29561
- X band airborne antenna phased array, describing phase shifter, radiation pattern, associated computer, etc
16 p2864 A70-33454

Antenna design for single engine light general aviation aircraft weather radar, reviewing attenuation and terrain return problems 16 p2864 A70-33471

X band aircraft antennas selection and design for defense communications satellite systems, emphasizing steerable phased array 16 p2865 A70-33712

Glauret equations applied to trailing wire shape for steady state aerodynamic forces on aircraft and trailing antennas, discussing computer solutions 23 p4131 A70-43893

AIRCRAFT APPROACH INSTRUMENTS

U APPROACH INDICATORS

AIRCRAFT APPROACH SPACING

Pattern recognition concepts applied to synthesis of aircraft approach progress monitor as adjunct to pilot decision process, discussing feasibility experiments [SRCC-106] 02 p0335 A70-12138

Control system, operational procedures, aircraft guidance and runway design for increasing runway capacity, noting roles of automation and reduced separation [SAE PAPER 700280] 12 p2206 A70-27440

Urban airport runway capacity increase via reduced aircraft separation, additional parallels and improved terminal traffic control, discussing design for acceptable safety levels 12 p2207 A70-27627

Collision and missed approach risks in high capacity airport landing operations, discussing parallel runways spacing and aircraft longitudinal separation 12 p2207 A70-27629

Aircraft separation standards in air traffic control system design regarding collision hazards, noting beacon system role 12 p2267 A70-27635

Midair collision frequency under VFR as function of aircraft density derived, noting ATC role in safe separation 12 p2267 A70-27636

Airport capacity increase via electronic aids enhancing guidance, flight control, reduced aircraft separation, ATC automation and runway configurations 12 p2208 A70-27914

Heavy jet effect on airport acceptance rates, discussing various sequencing strategies 18 p3212 A70-36209

Maximum throughput-rate capacity for runway and final approach path airspace involving multiple IFR landings 19 p3465 A70-38235

Airport capacity analysis for terminal areas, using simulation for alternatives to parallel runway operation 19 p3397 A70-38236

ATC airborne surveillance, communication and control system functioning as CAS after error or failure, discussing minimum parallel runway separation 19 p3466 A70-38241

IFALPA views on ATC services, emphasizing aircraft approach spacing in North Atlantic airways 19 p3467 A70-38632

AIRCRAFT BASES

U MILITARY AIR FACILITIES

AIRCRAFT BRAKES

NT TRAILING-EDGE FLAPS

NT WING FLAPS

Recommended design practices to assure good brake system performance with compatibility for skid control equipped aircraft 01 p0007 A70-11457

Commercial aircraft brake temperatures under HF landing conditions, using energy input and heat transfer computer programs 14 p2532 A70-31341

SST electrohydraulic primary and standby brake control systems, discussing design and advantages [AIAA PAPER 70-913] 17 p3024 A70-35825

Attached inflated BALLUTE /balloon-parachute/ for stabilization and retardation of aircraft stores, high altitude descent devices and planetary entry vehicles [AIAA PAPER 70-1200] 21 p3752 A70-41816

Drag prediction for Ballute and parachute trailing decelerators at supersonic speed and zero angle of attack, using flow field computations [AIAA PAPER 70-1177] 21 p3746 A70-41836

Snatch force during lines-first deployment of aerodynamic decelerator, including effects of canopy skirt acceleration and suspension wave propagation characteristics [AIAA PAPER 70-1171] 21 p3754 A70-41842

AIRCRAFT BREATHING APPARATUS

U BREATHING APPARATUS

AIRCRAFT CABINS

U AIRCRAFT COMPARTMENTS

AIRCRAFT CARRIERS

Navy/pilot aircraft control performance during day and night final approach to landing on carriers for empirical performance criteria 02 p0243 A70-12131

Carrier-based attack aircraft avionics, describing optimal large scale analysis procedure for flight control, communications and radar subsystems 08 p1470 A70-20660

General purpose support system /GPSS/ simulation for carrier operations and avionic maintenance, considering attack aircraft operations, spare parts, personnel requirements, etc 08 p1470 A70-20661

Versatile avionics shop test /VAST/ Implementation Study recommendations on project management for automatic test equipment support system aboard attack aircraft carriers 08 p1601 A70-20663

Holographic dynamic head-up display system for aircraft carrier deck landings in low visibility 12 p2232 A70-27371

S-3A carrier based ASW weapons system, discussing onboard equipment, navigation, avionics integration, etc [AIAA PAPER 70-882] 17 p3018 A70-35802

Versatile Avionic Shop Test maintenance system supporting avionic equipment aboard aircraft carriers 21 p3804 A70-40772

AIRCRAFT COMMUNICATION

Airborne SHF communication system for operation with passive satellites installed in C-121 aircraft 01 p0045 A70-11122

Multipath spectral and statistical characteristics in VHF satellite-aircraft link, discussing geometric considerations and reflection from Gaussian surfaces 02 p0259 A70-12565

UHF shallow-cavity crossed-slot aircraft antenna for satellite to air communications 02 p0269 A70-12585

Cockpit information transfer between pilot and flight control information displays improved by on-board data processing system 03 p0436 A70-14021

Electronic search and rescue system developed for West German Air Force, consisting of personal transceiver and automatic distress signal transmitter unit, etc 05 p0793 A70-15904

Space systems for communications, surveillance and navigation needs of international aviation, discussing service requirements, spectrum utilization, technology limitations and terminal design 07 p1330 A70-19290

Carrier-based attack aircraft avionics, describing optimal large scale analysis procedure for flight control, communications and radar subsystems 08 p1470 A70-20660

Signal properties of VHF satellite-to-aircraft communications link, discussing results of ATS tests 08 p1463 A70-21779

Beacon identification-friend-foe-selective-identification-feature code-validation schemes for ATC, deriving expression for cumulative probability of validation on or within N interrogations 10 p1914 A70-24446

Harrier communications and radio navigation aid VLF/UHF and TAC/VHF equipment 10 p1841 A70-24849

Air transportation and air traffic control factors relating to satellites applications to surveillance, navigation and communication over contiguous U.S. [AIAA PAPER 70-488] 11 p2077 A70-25443

Ground ATC facilities, discussing landing, automation, surveillance, communication and navigation 11 p2079 A70-25723

Integral relay operations effectiveness based on random spatial distribution of aircraft under control of Army flight operations center 11 p2080 A70-26265

Position location and aircraft communication equipment concept and Experimental PLACE System providing ATC two-way voice and digital data communications via geostationary satellites 12 p2269 A70-27921

Air traffic control, reviewing air navigation, communication systems and radar techniques 13 p2450 A70-29998

Equipment and subsystems application to flight management avionics in military and commercial aircraft, noting role of ground-air information transfer 16 p2878 A70-33724

Aircraft digital interior communication systems, combining multiplexing techniques with solid state integrated circuits technology and systems integration [SAE PAPER 700302] 18 p3216 A70-36813

Aircraft streamer /spark/ discharges formation, waveforms and RF noise levels, using mathematical model for electric field strength 19 p3380 A70-38179

IATA policy on future ATC development, discussing controlled airspace, communications and radar requirements 19 p3555 A70-38630

Electromagnetic interference in aircraft communication due to jet engine charging, considering various prevention measures 20 p3561 A70-39724

Integrated communication, navigation and identification for worldwide needs of military aircraft 21 p3786 A70-41132

Automated airline communications system for collecting, analyzing, storing, transmitting, receiving and presenting information required by ATC and advisory services 21 p3789 A70-41347

Airframe and systems design optimization for aeronautical communications systems, considering airplane configurations, structural and electronics technology 21 p3750 A70-41349

Airport and air route radar surveillance, beacon systems, microwave links and instrument landing systems, discussing transmission and reception problems 22 p4068 A70-43486

Satellite technology applications to ATC, including communications, navigation, surveillance over water and data acquisition [AIAA PAPER 70-1301] 24 p4373 A70-45922

AIRCRAFT COMPARTMENTS

Cabin interior materials studied and tested for greater fire resistance, lower smoke and toxic gas by-products and flash fire possibility lessening 03 p0437 A70-14057

Human reactions to confined interiors design, examining human-environment interactions present in aircraft [SAE PAPER 700234] 11 p1990 A70-25903

Falcon 10 economical executive aircraft development involving dimensions of cabin, powerplant and range 12 p2162 A70-28027

Transport aircraft interior design based on anthropological, architectural and engineering factors 16 p2841 A70-33767

Aircraft interiors products and services supplied by British firms 16 p2841 A70-33768

Loudspeaker optimal arrangement for speech intelligibility in aircraft crew compartments, discussing apparent SNR improvement 17 p3039 A70-35564

Hypoxia warning systems using polarographic sensor and miniaturized electronics for face-mask and cabin installation for aircraft and spacecraft 20 p3579 A70-39429

Automatic air conditioning systems for hermetically sealed aircraft cabins, deriving control laws for air pressure, temperature and humidity 20 p3564 A70-39843

Flame resistant nonmetallic materials for manned spacecraft and aircraft interiors, considering fibers, polymers, paper and composites 22 p4058 A70-42295

AIRCRAFT CONFIGURATIONS

STOL aircraft configurations optimization including cost effectiveness, considering propulsive lift systems [AIAA PAPER 69-1131] 01 p0162 A70-10609

CL-84 tilt wing V/STOL program to develop best configuration for ground support operations 01 p0007 A70-11317

Helicopter engineering covering structure, rotor systems, aerodynamics, vibration and applicability to fixed wing aircraft 02 p0225 A70-12309

Wing and body design for upgrading transonic aircraft performance, discussing blending, spanwise sweep variation, curved leading edge and aspect ratio 04 p0613 A70-14504

Three dimensional flow separations on upswept rear fuselages, using flow visualization and pressure measurement 05 p0790 A70-16097

L-1011 TriStar design for transcontinental airline requirements, discussing propulsion, noise suppression, configuration, passenger comfort, etc 05 p0793 A70-16098

Aircraft configurations designed for eliminating sonic boom due to lift 05 p0791 A70-16798

Stability derivatives from flight data of fixed-wing aircraft determined by modified Newton-Raphson method 07 p1194 A70-19272

Tuft position on rotating helicopter blade in hovering and forward flight, calculating tip path plane and tuftlines 08 p1438 A70-21868

Fixed wing aircraft and associated subsystems simulation by digital computer, having full FORTRAN capability [AIAA PAPER 70-572] 13 p2385 A70-29897

Single and twin jet afterbody configuration models, describing drag and interference characteristics at subsonic speeds 14 p2528 A70-30862

Tailless delta Avro Vulcan aircraft design, hardware and flight results 14 p2532 A70-31391

Sonic boom causes and nature, considering aircraft configuration and attitude and minimizing effects 15 p2673 A70-31852

Structural weight reduction and increased aerodynamic efficiency in aircraft design by including flight control technology early in configuration development phase
[AIAA PAPER 70-874] 17 p3017 A70-34817

Sonic boom minimization through airstream alteration by force or heat fields and aircraft body shaping
[AIAA PAPER 70-903] 17 p3019 A70-35817

Air to air armament selection effect on aircraft configuration
[AIAA PAPER 70-939] 17 p3021 A70-35848

Lower bounds for sonic boom, considering negative overpressure region in configuration tailoring
18 p3241 A70-36456

MBB Bo-209 Monsun travel, commuter and acrobatics aircraft, discussing configurations, specifications, structure and handling characteristics
19 p3355 A70-37388

Aircraft stretch efficiency factor as function of productivity and payload growth
[SAWE PAPER 838] 20 p3563 A70-40369

Airframe and systems design optimization for aeronautical communications systems, considering airplane configurations, structural and electronics technology
21 p3750 A70-41349

SST configurations minimizing sonic booms obtainable for given length and weight
[ICAS PAPER 70-23] 23 p4138 A70-44110

Aircraft geometry effects on longitudinal flight characteristics calculations, noting wing aspect ratio and horizontal tail changes
24 p4289 A70-45437

Noise reduction regulations effects on subsonic transport design and configuration
[SAE PAPER 700806] 24 p4290 A70-45876

All-body configuration hypersonic transport aircraft performance by computer synthesis, considering sonic boom constraint, maximum payload ratio and optimal cruise speed
[AIAA PAPER 70-1224] 24 p4291 A70-45957

AIRCRAFT CONSTRUCTION

U AIRCRAFT STRUCTURES

AIRCRAFT CONTROL

NT HELICOPTER CONTROL

TV system for controlling QF-9 drone aircraft landing, takeoff and BQM-34A target drone in-flight test operations
01 p0058 A70-10815

Aircraft optimal spin recovery by aileron, elevator and rudder control calculated using Pontryagin principle to minimize altitude loss
01 p0006 A70-10924

Electronic displays role in pilot-aircraft interaction, considering flight safety, cost effectiveness, onboard data input, etc
01 p0039 A70-11260

Recommended design practices to assure good brake system performance with compatibility for skid control equipped aircraft
01 p0007 A70-11457

Electrical signaling civil aircraft systems, discussing design and integrated maneuver demand controls
02 p0224 A70-11835

Navy/pilot aircraft control performance during day and night final approach to landing on carriers for empirical performance criteria
02 p0243 A70-12131

Optimal control of aircraft angle of attack based on minimum terminal velocity during passive flight in spherical nonrotating earth atmosphere
02 p0227 A70-12409

Aircraft controls response critical speed as function of transmission lag and transfer function of control link elements
02 p0227 A70-12410

Flight evaluation of direct lift control /DLC/ on modified B-52 aircraft, noting controllability improvement during ILS approaches and aerial refueling
[SAE PAPER 690406] 03 p0411 A70-12896

Airplane stability and control technology, considering flight research, flying qualities, compressibility and aeroelastic phenomena
[AIAA PAPER 69-1137] 03 p0411 A70-13636

Man machine interface in VTOL aircraft control and stabilization systems adaptation during manually controlled hovering flight
03 p0414 A70-14094

Human functional changes in controlling C-8 trainer measured by flicker value, pulse rate, reaction time and instrument and control error before and after flight
04 p0643 A70-14976

Unsteady flows effects on aircraft longitudinal motion, flight stability and control, discussing horizontal and vertical effects of rough air
04 p0623 A70-15172

Flight tests with mounted and unmounted SG 1262 hovering test rig in Germany to determine optimal control and stability characteristics for VTOL VAK 191B
04 p0624 A70-15704

Forward air control and light attack aircraft survivability design
[SAE PAPER 690707] 05 p0791 A70-15829

Emergency auxiliary hydraulic and electric power for commercial and military aircraft control, proposing self contained monofueled turbine system
[SAE PAPER 690658] 05 p0797 A70-15838

Drift error of correctable three degree of freedom free-floating astatic gyrocompass mounted on aircraft flying straight course at uniform speed
05 p0848 A70-16224

Computational algorithms transformation to forms convenient for aircraft computer adaptation for reducing digital network length with small accuracy penalty
05 p0818 A70-17005

Supersonic aircraft control and stability at low speeds, discussing sweepback angle, low aspect ratio, lift, etc
05 p0797 A70-17088

VTOL aircraft control and stability with emphasis on flight characteristics and man machine interaction
05 p0809 A70-17089

Flight deck displays based on digital computer providing signals for CRT and instrumentation
06 p1061 A70-17319

Cooper aircraft handling rating scale on basis of test pilot experience
06 p1003 A70-18018

Stability derivatives from flight data of fixed-wing aircraft determined by modified Newton-Raphson method
07 p1194 A70-19272

Supersonic aircraft aerodynamic properties and control systems performance, considering piloting of delta wing fighters
07 p1194 A70-19640

Concorde simulator for determining aircraft control responses and integrating pilot function into problem
07 p1249 A70-19743

Quasi-optimum design of aircraft landing control system, performing worst case simulation for jet transport
07 p1195 A70-20405

Electronic displays and flight control system of Multi-Role Combat Aircraft developed by Germany, Italy and UK
08 p1493 A70-20631

V/STOL Do 231 design, discussing propulsion, control, safety, traffic control and economic factors
08 p1435 A70-20640

State observers /filters/ construction in multivariable control systems using phase transformation
08 p1478 A70-20778

Aircraft roll rate response and aileron step input matching in terms of modal parameters with flight test records by analog computer program
08 p1465 A70-20781

Kalman filtering techniques to identify aircraft lateral motion data
08 p1478 A70-20782

Differential correction algorithm for identifying airplane parameters from flight test data, assuming differential equations
08 p1465 A70-20783

Quasi-linearization technique in computer program for aircraft parameters identification featuring efficient search for optimal parameters in algebraic or differential equations
08 p1465 A70-20784

Optimal control conditions for elastic aircraft motion with delayed wing downwash determined by hyperbolic partial differential equations with delay
08 p1480 A70-21178

Workload relieving displays and controls for general aviation, discussing feasibility of digital computer driven integrated displays
08 p1601 A70-21679

Flight tests to investigate external munitions carriage effect on aircraft stability and control
08 p1437 A70-21733

Pilot systems for controlling aircraft in flight, considering direct lift control, displays, simulators, tests, etc
08 p1437 A70-21734

In-flight investigation to determine effect of variations in bank angle control parameters on cruise flight handling qualities
08 p1437 A70-21738

Onboard measurements of single engine propeller-driven aircraft performance, stability and control in nonsteady symmetric flight
08 p1438 A70-21869

Soviet book on flight dynamics in turbulent atmosphere covering air motion, aircraft lateral and longitudinal motion, gust loads, autopilot flight, takeoff and landing
09 p1610 A70-22598

Linear high order aircraft and missile control systems design using Horowitz frequency response method
09 p1654 A70-22835

Fighter aircraft inflight thrust control using thrust reverser technology to improve operational capability
[AIAA PAPER 70-513] 09 p1610 A70-23019

Swept and delta wing supersonic military aircraft stability and controllability, discussing variation in maximum lift coefficient as function of Mach number
09 p1611 A70-23129

Soviet book on aircraft control systems design covering optimal functional or function parameters, circuits controlling pitch, roll, yaw motions, human operator systems, etc
09 p1725 A70-23472

Visual threshold effect on closed loop control of aircraft of poor resolution studied by flight simulation of approach and flare, showing degraded control accuracy
[AIAA PAPER 70-357] 10 p1858 A70-24206

Root loci construction for differential equations with quadratic free parameters applied to aircraft motion with roll control
11 p2071 A70-25393

Performance, stability and control improvements of light aircraft, applying computerized parametric analysis
[SAE PAPER 700240] 11 p1981 A70-25909

Aircraft control through airspace from takeoff to landing, discussing role of Department of Transportation Air Traffic Control Advisory Committee
11 p2080 A70-26256

Control system, operational procedures, aircraft guidance and runway design for increasing runway capacity, noting roles of automation and reduced separation
[SAE PAPER 700280] 12 p2206 A70-27440

Midair collisions between controlled and uncontrolled traffic in terminal areas associated with aircraft operations and airport density
12 p2267 A70-27632

Intermittent positive control system for issuing commands to normally uncontrolled aircraft for midair collision avoidance, discussing aircraft and conflict detection
12 p2267 A70-27634

Glider longitudinal stability and control in symmetrical flight positions, determining flight characteristics
12 p2161 A70-27723

Optimal and suboptimal aircraft lateral directional stability augmentation applying optimal control and model-following techniques
12 p2162 A70-27812

Harrier fighter aircraft hydraulic systems and flying controls
12 p2166 A70-27889

Soviet book on aerodynamic, stability and controllability characteristics of variable geometry wing aircraft
13 p2344 A70-28648

X-22A ducted propeller V/STOL research aircraft handling characteristics and design
13 p2345 A70-28972

Frequency and amplitude during longitudinal control surface pumping by pilots in precise flight path handling for aircraft design
[AIAA PAPER 70-567] 13 p2346 A70-29032

Pilot-aircraft closed-loop characteristics, using pilot transfer functions for handling qualities prediction
[AIAA PAPER 70-568] 13 p2346 A70-29033

Longitudinal short-period flying qualities as closed-loop pilot-airplane system, noting acceptance values
[AIAA PAPER 70-569] 13 p2346 A70-29034

Hypokinesia effects on working capacity of subjects performing manual aircraft control assignments during bed rest
13 p2352 A70-29340

Rudder control of aircraft nullifying yawing and sideslip angles, analyzing rolling response to proportional control by ailerons
13 p2348 A70-29450

Air navigation and control systems cost-benefit analysis including ground services, safety and R and D
14 p2667 A70-30103

DC-9 aircraft instrument subsystems and operating procedures of KLM, discussing series 15 and 30 aircraft
14 p2530 A70-30416

VTOL aircraft stability augmentation system design based on control theory state variable methods, using minimum power levels
14 p2531 A70-30856

V/STOL control systems design for aircraft stabilization and pilot workload reduction
14 p2615 A70-31278

Aircraft optimal roll stabilization control system design using performance index with weighting matrix
14 p2552 A70-31395

Rumanian book on flight stability and control covering Liapunov general stability theory, control systems, stability models, etc
15 p2673 A70-31695

Digital computers in aircraft, discussing automatic control systems, components and advantages over analog systems
15 p2705 A70-32299

Aircraft vertical channel landing condition autopilot using state variable feedback control techniques
15 p2773 A70-32553

Supersonic aircraft stability and controllability during turns about longitudinal and vertical axes
16 p2840 A70-33204

Dynamic systems control and guidance by man in light of anthropotechnics, treating approaches to man machine systems optimization
16 p2850 A70-33263

Optimal control surface location for flexible aircraft determined by matrix minimum principle and calculus of variations

16 p2840 A70-33316

Emergency auxiliary hydraulic and electric power for commercial and military aircraft control, proposing self contained monofueled turbine system

[AIAA PAPER 70-651] 16 p2970 A70-33616

Aerodynamic causes for aircraft spinning, discussing initiation and termination

16 p2842 A70-34173

DC 8 Super 63 aircraft direct lift control flight evaluation

17 p3018 A70-35496

Servoactuator for stick force augmentation on light turboprop STOL aircraft at high angles of attack

[AIAA PAPER 70-909] 17 p3019 A70-35821

C-5A aircraft six wheel main landing gear bogie pitching control, emphasizing braking torque compensating mechanism design

[AIAA PAPER 70-914] 17 p3020 A70-35826

Concorde aircraft man machine simulation and handling using fixed cabin, variable stability and ground based simulators

[AIAA PAPER 70-923] 17 p3064 A70-35834

In-flight evaluation of selected aircraft pilots controllers, noting role in design

[AIAA PAPER 70-925] 17 p3020 A70-35836

Aft tail and canard configurations trim drag considerations for maneuvering aircraft

[AIAA PAPER 70-932] 17 p3021 A70-35842

Optokinetic and vestibular effects on human operator reliability in aircraft control systems

18 p3223 A70-36184

Airplane stability and control technology, considering flight research, flying qualities, compressibility and aerodynamic phenomena

18 p3213 A70-36441

Necessary and sufficient conditions for optimal control law existence for model following system, discussing applications to aircraft control

18 p3235 A70-36443

Soviet book on man in aircraft control system covering engineering psychology, complex flight problems, human factors and instrument panels

19 p3367 A70-37236

Soviet book on statistical calculation methods for linear and nonlinear automatic aircraft control systems design, using correlation theory of stochastic processes

19 p3463 A70-37403

Fixed wing and VTOL aircraft all-weather landing guidance and control philosophy

19 p3466 A70-38365

Self navigation feasibility in future mass air traffic flow control

19 p3469 A70-38643

Bobweights effects on pilot induced oscillations, noting role in flying qualities and control system design

[AIAA PAPER 70-1002] 20 p3560 A70-39529

Turbulence effects on lateral directional flying qualities, examining pilot task performance, control workload and compensatory behavior

[AIAA PAPER 70-998] 20 p3560 A70-39533

Sensitivity optimization for linear optimal control systems design, describing aircraft lateral-directional control case study

[AIAA PAPER 70-962] 20 p3600 A70-39567

Free wing aircraft dynamic characteristics, discussing gust alleviation and handling qualities

[AIAA PAPER 70-947] 20 p3561 A70-39580

Aircraft auxiliary systems and spacecraft power supplies, considering fly-by-wire control actuators, pyrotechnics and stowable solar array

20 p3564 A70-39669

VTOL aircraft longitudinal motion automatic stabilization in presence of turbulence and internal disturbances, using rotors and jet engines

20 p3561 A70-39838

Automatic aircraft lateral motion stabilization during flight in perturbed atmosphere by HF invariant systems

20 p3670 A70-39839

Invariant autopilot control system during flight in turbulent atmosphere, allowing for aircraft elastic properties and invariance of coordinates

20 p3561 A70-39845

High performance aircraft self adaptive feedback control system, using airborne digital computer with inputs of elevator deflection and pitch rate for effectiveness identification

20 p3605 A70-40119

Variable wing sweep aircraft angular motion mathematical model, analyzing inertial moments influence on control dynamics

20 p3562 A70-40182

Aircraft flying at constant speed in circular orbits, calculating flight path under effect of uniform velocity wind

21 p3750 A70-40920

Fighter aircraft higher order control system dynamics effects on longitudinal handling qualities evaluated by in-flight simulator for role of pilot induced oscillations tendencies

[AIAA PAPER 69-768] 22 p3961 A70-42711

Low and medium power turboprop engines for V/STOL aircraft, discussing development trends concerning operational control

22 p4091 A70-43081

Aircraft control, considering wind gradient effects on takeoff, ascent and overflight conditions

22 p3962 A70-43082

Aircraft control surface aerodynamic characteristics, considering low aspect ratio wing elevons with variable sweep leading edge as longitudinal and lateral controls

[ICAS PAPER 70-26] 23 p4131 A70-44107

Stability augmentation in aircraft design for handling and operation benefits, discussing control techniques, autopilot modes and load limitations

[ICAS PAPER 70-24] 23 p4138 A70-44109

Aircraft handling qualities specifications and definitions evolution based on test pilot rating correlation with engineering data and piloting ease evaluation with transfer functions

[ICAS PAPER 70-19] 23 p4138 A70-44114

Hypersonic aircraft stability and control problems, discussing bulky engines and air intake and exhaust geometry

[ICAS PAPER 70-17] 23 p4138 A70-44128

Fluidically augmented artificial feel system for fighter and attack aircraft control, discussing improved handling qualities

[SAE PAPER 700785] 24 p4294 A70-45859

Turbojet and turbofan engine control evolution, noting increased complexity and adoption of hybrid fluidics and computer technologies

[SAE PAPER 700825] 24 p4394 A70-45894

STOL aircraft guidance and control, discussing area navigation utilization, multiple airways, data links and ground ATC computers

[AIAA PAPER 70-1334] 24 p4373 A70-45934

STOL aircraft field length, terminal area performance and minimum handling qualities requirements for safe and efficient operations

[AIAA PAPER 70-1240] 24 p4292 A70-45960

Aircraft navigation control system by digital computer combined with inertial platform, considering emergency backup, slow drift and system malfunctions

24 p4374 A70-46092

Maneuver demand control using electric signalling feedback technique in Avro 707C and Hunter Mk 12 aircraft

24 p4374 A70-46203

AIRCRAFT DESIGN

NT HELICOPTER DESIGN

Concorde aircraft structural acoustics and design problems, discussing noise, fatigue and testing techniques and facilities

01 p0199 A70-10288

Linearized potential theory application in aerodynamic design and analysis of supersonic aircraft emphasizing far field viewpoint

[AIAA PAPER 69-1132] 01 p0002 A70-10608

Economic tradeoffs in airport and commercial aircraft design, considering traffic growth, increased weight impact minimization and costs

[AIAA PAPER 69-1087] 01 p0056 A70-10623

Turbofan VTOL or STOL intercity transports noting lift engines, noise, aircraft design and interior

[AIAA PAPER 69-1039] 01 p0005 A70-10645

Noise reduction for V/STOL aircraft operation by introducing quiet propellers, discussing variable camber propellers, propeller aerodynamics, etc

[AIAA PAPER 69-1058] 01 p0005 A70-10646

Bird impact damage effect on aircraft structural design, considering forward facing areas and minimum weight

01 p0200 A70-10687

Inertia cross coupling during aircraft design stage allowing later flight testing, discussing analysis complexity and sensitivity to aerodynamic data change

01 p0007 A70-11315

Recommended design practices to assure good brake system performance with compatibility for skid control equipped aircraft

01 p0007 A70-11457

Air cargo transport development and organization trends, considering cost and aircraft types

02 p4041 A70-11736

SST Ti body frame optimum design for high temperature environment and economical and fatigue resistance requirements

02 p0386 A70-11937

Aircraft structural damage due to high speed hail-stone impact, considering aircraft design modifications

02 p0386 A70-11938

Commercial aircraft design, considering structural allowables effect on economics, using shear web analysis program as example

02 p0225 A70-11947

Cargo transport aircraft design and operation, discussing costs, cargo density, runway strength, gear design, customer service, etc

02 p0225 A70-12262

Harrier close-support fighter aircraft with short or zero takeoff run capability, discussing design, cruise

efficiency, maneuverability and navigation- attack system

02 p0225 A70-12310

V/STOL fatigue design parameters, balancing fail-safe and safe-life design procedures

[AHS PAPER 376] 02 p0228 A70-12764

Deviation angle optimization for cruising hypersonic jet aircraft, noting effect of rotation losses on design

03 p0406 A70-13019

Aircraft ground support system analysis from airplane designers viewpoint

[SAE PAPER 690561] 03 p0463 A70-13265

Aircraft aerodynamics, Volume II, covering profile and wing theory at subsonic and supersonic speeds, fuselage, wing-fuselage and tail assembly, etc

03 p0407 A70-13350

A-300B twin engine short haul giant transport aircraft, discussing engines, aircraft performance and systems reliability

[RAES PAPER 11] 03 p0411 A70-13543

Collection of papers on jet transport design covering subsonic zero lift drag rise properties, performance characteristics, supersonic aircraft design, etc

03 p0414 A70-14018

Growth test vehicle /GTV/ flight test program for development of hypersonic flight to orbital speeds, discussing design, costs, capabilities, etc

03 p0582 A70-14188

Aircraft structural weight optimization for given fundamental vibration frequency obtained by aeroelastic constraints

03 p0598 A70-14231

Blended wing-body design concept for F-15 air superiority fighter, providing fixed wing planform for maneuverability at transonic speed

04 p0622 A70-14395

Wing and body design for upgrading transonic aircraft performance, discussing blending, spanwise sweep variation, curved leading edge and aspect ratio

04 p0613 A70-14504

Sigma glider design for high cruising speed, using extensible wing to double area in flight

04 p0622 A70-14625

German VTOL transport aircraft projects, discussing Dornier 231 /lift by turbojets/ and Bolkow 140 /swiveling wing with gas turbine propellers/

04 p0623 A70-14955

Design and economic concepts of Lockheed L-1011 wide body trijets, discussing airport and airway congestion alleviation, passenger appeal, etc

04 p0623 A70-15044

Mounted-above-wing jet engine effect on wing pressure distribution and elevator unit, using fluid mechanical model

04 p0735 A70-15146

German transport VTOL projects, discussing VC-500 swiveling wings with turbine powered propellers and HFB-600 blade cascade flow deflectors for vertical takeoff

04 p0623 A70-15349

Boeing 747 aircraft family design options related to utilization, performance and economics, discussing development through large turbofan engine availability

[AIAA PAPER 68-1020] 04 p0624 A70-15382

Aircraft design in commercial air transport safety, discussing turbine blade oxidation and crack prevention, engine cooling, fuels, lightning protection, etc

04 p0624 A70-15644

Protection methods for increasing ground fire survivability of military aircraft hydraulic systems classified by cost, system and component design criteria

05 p0797 A70-15777

Forward air control and light attack aircraft survivability design

[SAE PAPER 690707] 05 p0791 A70-15829

Aircraft food service and galley integration considered joint responsibility shared between airframe manufacturer and air carrier

[SAE PAPER 690671] 05 p0791 A70-15834

Design safety requirement and philosophy differences distinguishing commercial from military aircraft programs

05 p0792 A70-15855

VTOL fixed wing aircraft design parameters evaluation by digital variable stability system

[SAE PAPER 690696] 05 p0792 A70-15859

DO-231 fixed wing V/STOL airliner project based on DO-31 development, construction and flight tests, considering design problems, controls, safety, performance targets, etc

05 p0793 A70-15901

Fighter aircraft design combining optimal qualities with economy

05 p0793 A70-15902

Schleicher AS-W15 glider wing span, weight, wing loading capacity and speed range, noting performance in international competition

05 p0793 A70-15905

Engine development for 3 and 4 engine large capacity jet aircraft, discussing fan cowl size and weight, installational drag effects, etc

05 p0895 A70-15928

- L-1011 TriStar design for trancontinental airline requirements, discussing propulsion, noise suppression, configuration, passenger comfort, etc 05 p0793 A70-16098
- Trident passenger aircraft development, discussing airframe changes, engine development, weight and drag reduction, etc 05 p0794 A70-16112
- Two place sport gliders development, design reliability and competition requirements 05 p0794 A70-16352
- VTOL technical problems relating to military and civil transport applications, discussing sensitivity to mission requirement variations including design costs, noise levels, etc 05 p0797 A70-17077
- Orbit-shuttle and SST craft hypersonic flight vehicles design, discussing aerodynamic heating, shock stresses and propulsion system requirements 05 p0797 A70-17087
- Harrier G.R. Mk 1 VTOL vectored thrust aircraft for attacking targets at conventional strike aircraft speed, discussing design and combat effectiveness 06 p0985 A70-17157
- California future transport complex, considering STOL and ESTOL /extremely short takeoff landing aircraft/ design requirements 06 p0985 A70-17197
- Life styles of engineering, comparing U.S. and European attitudes to aircraft development and design 06 p1184 A70-17198
- Aircraft wing load calculations using aerodynamic influence coefficients based on linear subsonic or supersonic flow theory 06 p0967 A70-17255
- RAPIDJET escape, recovery and survival system providing rapid escape for large aircrew complement by manual bailout system utilizing semiautomatic escape slide 06 p0986 A70-17719
- Severe storm research importance to aircraft design and operating efficiencies improvement by identifying meteorological alternatives for operations in and near adverse environments 06 p1102 A70-18587
- Aircraft design formulas for equivalent gust velocity compared with vertical acceleration form, discussing design problems for large jets and T-tailed configurations 06 p0988 A70-18589
- Aircraft transport tariffs used to determine economic approach to design 07 p1426 A70-18841
- Hansa 330 fan jet design for executive and commuter market, discussing forward-swept wing concept and standardized structures and systems 07 p1194 A70-19619
- VSTOL and STOL transport development concerning aircraft types, air traffic control and navigation, airports, etc 07 p1194 A70-20250
- Concorde aerodynamic design compromise between high and low speed requirements, kinetic heat problems and materials selection [AIAA PAPER 69-759] 07 p1195 A70-20399
- Damage tolerance as design consideration for aircraft safety and reliability, discussing application of failed single principal member concept to airframe construction [AIAA PAPER 69-212] 07 p1417 A70-20401
- Quasi-optimum design of aircraft landing control system, performing worst case simulation for jet transport 07 p1195 A70-20405
- V/STOL concepts for short haul commercial aircraft compared for gross weight, operating cost, gust sensitivity and noise levels [AIAA PAPER 67-938] 07 p1195 A70-20409
- Hawker Siddeley Harrier structural design, power plant, rear fuselage, wing tail unit structures, undercarriage features, weight control, fatigue testing, etc 08 p1435 A70-20620
- STOL touring aircraft propeller design and aerodynamics, discussing takeoff runs, landing runs, high lift, downwash, ground effects, etc 08 p1435 A70-20628
- V/STOL transport aircraft design in Germany, analyzing demands in military and civil sectors 08 p1435 A70-20639
- V/STOL Do 231 design, discussing propulsion, control, safety, traffic control and economic factors 08 p1435 A70-20640
- Jet lift passenger aircraft considered better suited for medium stage routes than rotor/ propeller designs for VTOL transport 08 p1436 A70-21347
- Collection of papers on aerospace technology covering Fokker F-28 aircraft design, airfoil computer graphics, helicopter rotor tuft analysis, aircraft fatigue, launch vehicle guidance, etc 08 p1438 A70-21863
- Fokker F-28 wing flap, lift dumpers and aileron development, including wind tunnel and flight tests 08 p1438 A70-21864
- Airfoil analysis and synthesis, discussing computer graphics application to low speed shape and improved pressure distribution 08 p1594 A70-21867
- Fibrous reinforced composites influence in aircraft structural design based on DOD- industry development programs, investigating interlaminar shear 08 p1595 A70-21899
- C-5 Galaxy airlifter design, delivery capacity, aerodynamics and flight test program 09 p1609 A70-22020
- C-5 design features for entire environment assuring human integration as crew member or troop passenger 09 p1609 A70-22021
- Aerodynamics role in large commercial aircraft design, noting mathematics models problem in high speed wing design 09 p1609 A70-22024
- Aircraft development for subsonic and transonic flight dependent on methods using blowing and boundary layer control and Coanda and Magnus effect 09 p1610 A70-22220
- Acoustic noise control on Boeing aircraft electromagnetic components, noting iron-core magnetostriiction demanding transformer redesign 09 p1647 A70-22764
- Potential flow and boundary layer theory application as design tools in aerodynamics, basing calculations on digital computer methods 09 p1605 A70-22947
- Sailplane design standards concerning retractable undercarriage and trailing-edge flaps revised to achieve better performance 09 p1612 A70-23575
- V/STOL transport aircraft cockpit design in terms of size, geometry and equipment accommodation 10 p1804 A70-24048
- Fiat G-222 aircraft featuring high wing twin engine retractable landing gear for military cargo transport 10 p1805 A70-24381
- Concorde SST aerodynamic, structural and thermal analysis and simulation using computers 10 p1849 A70-24382
- Canard and variable geometry aircraft designs noting SAAB 37 Viggen performance 10 p1805 A70-24764
- Harrier armament system design for ordnance carriage to full combat load factors, describing Weapon Control Panel 10 p1807 A70-24848
- VFW 614 nose-contoured cockpit panes, discussing structural weight and strength, vision and window frame fabrication 10 p1806 A70-24866
- Book on aircraft environmental control covering design, construction and operation of various systems 10 p1809 A70-25203
- British air transport from aircraft manufacturing industry viewpoint, discussing governmental organization of air industries and aircraft design negotiation atmosphere 11 p2153 A70-25861
- Computerized design of aircraft contours, determining three dimensional surface by second degree equation [SAE PAPER 700202] 11 p2013 A70-25876
- Aircraft design structural development and substantiation utilizing computer analysis and testing [SAE PAPER 700216] 11 p2134 A70-25888
- Loading conditions measured during aerobatic maneuvers in flight test to determine structural design requirements for aerobatic-type aircraft [SAE PAPER 700222] 11 p1980 A70-25894
- General aviation aircraft styling and interior developments, describing seat construction role in personalized aircraft production costs [SAE PAPER 700232] 11 p1980 A70-25901
- Aircraft interior design styling and material selection, discussing industrial design department function and organization, styling as marketing tool, etc [SAE PAPER 700233] 11 p1980 A70-25902
- Human reactions to confined interiors design, examining human-environment interactions present in aircraft [SAE PAPER 700234] 11 p1990 A70-25903
- Cessna CITATION aircraft design, considering engineering, marketing and corporate cooperation [SAE PAPER 700241] 11 p1981 A70-25910
- Circumplanetary aircraft design for solo nonstop great circle around world flight without refueling, noting application to sport, transportation, surveillance, photography, etc 11 p1981 A70-26046
- Experimental stress analyses for aircraft design enhancing structural fatigue strength, using S-N diagrams and photoelastic models 12 p2318 A70-27128
- Reinforced epoxy models as precursor to prototype design and analysis of aircraft structures, discussing stress analysis methods 12 p2318 A70-27129
- Jet powered Ultra STOL aircraft engine selection, considering effects of engine size, wing loading, thrust loading, etc [SAE PAPER 700266] 12 p2161 A70-27435
- Reliability and maintainability from airline standpoint, discussing concepts, language and standards for aircraft design [SAE PAPER 700326] 12 p2335 A70-27460
- Complex airframe design for economic and safe operation and long life using fatigue and fracture mechanics [AIAA PAPER 70-512] 12 p2324 A70-27466
- Aviation future development based on airplane evolution, considering aircraft configurations, flight problems, nuclear propulsion, jet propelled aircraft 12 p2161 A70-27523
- Harrier short takeoff fighter aircraft cockpit design, describing layout, lighting, warning and escape systems, etc 12 p2162 A70-27888
- Twin turbofan executive aircraft /Falcon/ development, describing modifications and antinoise features 12 p2162 A70-28026
- Falcon 10 simplified airliner-type equipment for operation under Category 2 weather conditions 12 p2167 A70-28028
- Air deflection and modulation /ADAM/ turbofan propulsive wing V/STOL design [AIAA PAPER 69-201] 12 p2162 A70-28087
- Collection of papers on aircraft design and structural research 13 p2337 A70-28476
- In-flight thrust measurement via internal gas generator and external traverse methods, discussing accuracy requirements, errors and aircraft design role 13 p2474 A70-28539
- VTOL and STOL design and operation, discussing noise and vibration reduction 13 p2344 A70-28544
- Harrier V/STOL trainer aircraft design features including fuselage, cockpit, power plant, etc 13 p2345 A70-28923
- Aircraft escape systems, discussing F-111 system capabilities and development 13 p2345 A70-28969
- Cockpit data monitor allowing pilot selection of instrumentation parameter readout 13 p2345 A70-28970
- X-22A ducted propeller V/STOL research aircraft handling characteristics and design 13 p2345 A70-28972
- Airframe-propulsion system integration for Mach 6 transport and Mach 12 research airplane, examining off-design operation effects and interaction of aerodynamic forces [AIAA PAPER 70-542] 13 p2345 A70-29009
- Tactical fighter requirements and designs, considering operational environment and weapon characteristics with emphasis on turning performance [AIAA PAPER 70-516] 13 p2346 A70-29035
- European Panavia 100/200 two engine variable wing military aircraft, noting prototype design, use and production sharing 13 p2347 A70-29051
- Aircraft design analysis with reference to terminal maneuvering area, cruise and climb performance and noise and flight deck layout, discussing airborne equipment 14 p2530 A70-30104
- Preliminary aircraft wing design for gusts or landing impacts inducing vibrations, inertia effects and dynamic overloads 14 p2655 A70-30177
- Tensile tests on wings and wing components of plastic engine-driven aircraft, discussing design, configurations and mechanical properties 14 p2656 A70-30250
- Jet thrust reversers mechanical design limits, objectives and materials 14 p2628 A70-30500
- Noise of large commercial V/STOL aircraft and effect on design and operation, predicting acoustic signatures 14 p2531 A70-30854
- Helicopter gust response at high forward speed for various rotor loads noting effects of gust shape, gradual penetration, nonsteady aerodynamics and blade aeroelasticity [AIAA PAPER 68-981] 14 p2531 A70-30855
- Man powered aircraft /MPA/ designs, considering bird flight aerodynamic characteristics 14 p2531 A70-30859
- Civil aircraft design optimization, considering operating and seat mile costs, speed, wing and fuselage, engine location, etc 14 p2531 A70-30941
- Designer and operator influence on total aircraft operating costs 14 p2669 A70-30942
- R and D impact on transport aircraft design economics 14 p2669 A70-30945
- BAC 111 commercial aircraft family development, discussing program management 14 p2532 A70-31334
- Airliner fuselage shape design and effect on manufacturing and flight operation economics 14 p2532 A70-31369

Commercial aircraft design evolution and trends concerning performance and operating cost reduction
14 p2532 A70-31370

Short haul Mercure airliner weight saving design and manufacture
14 p2593 A70-31371

Aircraft design optimization by multisearch programs, considering mathematical model role
14 p2532 A70-31400

Supersonic aircraft lateral stability and controllability design, discussing directional and weathercock stabilities
15 p2673 A70-31625

L-1011 aircraft payload, range, configuration, engine selection, design features, equipment systems, flight characteristics, internal arrangement, maintenance and performance
15 p2673 A70-31947

Soviet book on gas turbine engines for helicopters covering aircraft design and flight dynamics
15 p2787 A70-32199

Hazard analyses of Concorde aircraft design, noting engine control failures and emergency equipment use probabilities
15 p2675 A70-32213

Airplane design safety considerations covering turbine cooling, liquid methane fuel, turbine wheel burst damage and lightning hazards
15 p2676 A70-32230

Mercure passenger aircraft development schedule, cost, delivery and features, emphasizing weight balance and convenience
15 p2676 A70-32365

Weight-dimensions correlation for gas turbine engine/airplane optimization analyses, determining tradeoffs among performance, noise, drag characteristics, etc
16 p2967 A70-33575

Transport aircraft interior design based on anthropological, architectural and engineering factors
16 p2841 A70-33767

Aircraft design, construction, operation and maintenance improvement efforts by FAA, discussing airworthiness requirements, audit team visits to factories, etc
16 p2842 A70-33824

Flight deck design since 1920, discussing ergonomics and avionic aspects
16 p2913 A70-34048

Design modifications for BAC Vanguard 953 aircraft conversion to palletized all-cargo service, discussing interior layout, cargo door, air conditioning and weight
16 p2842 A70-34049

Aerodynamic and structural considerations in prop/rotor design for tilt-rotor aircraft, discussing blade twist effect on cruise efficiency and figure of merit
17 p3014 A70-34719

Manpowered aircraft, considering possibility as future flying sport vehicles
17 p3016 A70-34809

High lift flaps for sailplane cross country speed improvement by cruise-climb tradeoffs
17 p3016 A70-34814

Airplane performance improvement by flight control system design, discussing ride quality, flutter margin, maneuver load, etc
17 p3017 A70-34816

Structural weight reduction and increased aerodynamic efficiency in aircraft design by including flight control technology early in configuration development phase
17 p3017 A70-34817

Variable sweep high thrust-weight ratio multirole combat aircraft /MRCAL/, discussing British-French cooperation, development programs and requirements
17 p3017 A70-34916

Digital computer technology impact on advanced aircraft design, discussing airborne computers, distributed and lumped computer systems, outer loop control, engine control and system integrity
17 p3049 A70-34993

Aircraft onboard maintenance recording system, discussing design and effectiveness
17 p3094 A70-35516

F-111 high strength steel design experience concerning wing, fuselage and empennage support structure
17 p3018 A70-35803

System engineering process for survival enhancement of military aircraft to meet stringent requirements of general nuclear war
17 p3019 A70-35810

Wide body commercial jet transport structural design considerations applied to DC 10 aircraft
17 p3193 A70-35812

Composite wing section design and fabrication utilizing unidirectional glass reinforcement
17 p3193 A70-35813

Safety in airline operations, discussing roles of aircraft designer and pilot
17 p3019 A70-35819

Extensible wing flap system for cargo aircraft, discussing structural design details and advantages
17 p3020 A70-35823

Boeing 737 aircraft nose gear gravel deflector and engine vortex dissipator
17 p3020 A70-35824

Flying qualities criterion for fighter flight control systems design
17 p3020 A70-35837

Fighter aircraft design for spin resistance and recovery using analytical approach, wind tunnel and flight tests
17 p3020 A70-35838

Air superiority fighter design philosophy, including tradeoffs between armament, detection capability, thrust, speed and load factor
17 p3021 A70-35840

Aft tail and canard configurations trim drag considerations for maneuvering aircraft
17 p3021 A70-35842

Airframe-inlet integration for supersonic tactical fighters, testing wind tunnel models
17 p3149 A70-35843

Subsonic aircraft size effect in conventional design, discussing increased weight increments and economic gain rate
17 p3021 A70-35849

Subsonic and supersonic transport aircraft design, discussing supercritical wing concept, fuel consumption reduction, composite aircraft structures, short haul transports, etc
17 p3022 A70-35854

Aircraft designer role in reducing departure delay due to equipment malfunction
17 p3022 A70-35858

Aircraft damage from bird impact and alleviating measures, taking into account windshield and intake guard designs, microwave beams for protection and chemical agents as repellent
18 p3212 A70-35987

Aircraft design minimizing damage by bird strikes to gas turbine engine components, discussing service experience, airworthiness demonstration tests and research programs
18 p3300 A70-35994

YF-12A interceptor aircraft development and testing, discussing titanium alloys application, aerodynamics and thermodynamics, escape systems for high speed and altitude tests
18 p3213 A70-36451

Mass air transportation, discussing aircraft characteristics, traffic growth, scheduling, passenger and cargo handling, etc
18 p3350 A70-36656

Concorde design limitations for commercial success in civil airlines
18 p3350 A70-36665

Solid state multiplexed electrical power distribution system for future generation military and commercial airplanes
18 p3216 A70-36803

Aircraft electrical system multiplexing, discussing design features and advantages over conventional hard wired systems
18 p3216 A70-36811

STOL systems 1975 technical and economic characteristics in terms of passenger market, aircraft design, terminal facilities and ATC capability
18 p3350 A70-36812

Propulsion system impact on military/commercial STOL transport aircraft commonality, taking into account augmented jet flap and externally blown flap powered lift wing concepts
18 p3214 A70-36819

Military and commercial transports turbofan propulsion systems impact on future aircraft design and development
18 p3214 A70-36820

V/STOL attitude control system as integral propulsion system part, analyzing design and weight tradeoffs
18 p3214 A70-36832

Soviet book on wing structures analytical design methods covering thin supersonic wings, mass distribution, aerodynamic characteristics, etc
18 p3344 A70-37025

Soviet book on VTOL design covering aerodynamic and weight characteristics, turboprop and turbojet engines, flight regimes, etc
19 p3354 A70-37233

Four-seat two-engined STOL propeller passenger and sport aircraft design and performance
19 p3355 A70-37371

High angle of attack aerodynamic characteristics of swept wing navy aircraft designs improved via leading edge modifications
19 p3355 A70-37392

Static stability requirements relaxation and wing control devices additions for alleviating wing root bending moments in controls configured vehicle /CCV/ design concepts
19 p3355 A70-37395

Slender hypersonic airfoil shape optimization for maximum lift to drag ratio for given profile area, chord and free stream conditions
19 p3352 A70-38304

S-65-200 Commercial Compound Aircraft design for dispatch reliability and maintenance
19 p3356 A70-38823

European airbuses designs, considering potential market and financial problems
19 p3357 A70-38952

Composite technology effects on engineering design, emphasizing carbon-carbon materials for aircraft structural weight reduction, performance improvement and high temperature applications
20 p3653 A70-39202

Alloys for aircraft structures design, considering materials strength, corrosion resistance, producibility and cost
20 p3648 A70-39414

Aircraft stability design by parameter plane technique, using for YO-3A aircraft
20 p3560 A70-39546

Aircraft design fatigue life and cumulation damage problems, discussing information value of programmed load and random tests
20 p3720 A70-39622

Air cargo container system impact on aircraft requirements, discussing intermodal capability achievement
20 p3607 A70-40128

Aircraft engine design combining turbojet and ramjet features to ensure optimum performance
20 p3690 A70-40148

Weight growth factor in aircraft design, discussing fixed and variable weight, payload, performance, flight quality, structural criteria and life expectancy
20 p3562 A70-40363

Aircraft loadability design by computerized loading program using graphic plotter
20 p3562 A70-40364

Aircraft stretch efficiency factor as function of productivity and payload growth
20 p3563 A70-40369

Fuselage frames minimum weight analysis by automatic iterative method
20 p3733 A70-40370

Aircraft manufacturing cost estimation in conceptual design phase, using structural synthesis program for cost buildup simulation
20 p3741 A70-40371

Fighter aircraft configuration design balancing, comparing weight penalties
20 p3563 A70-40380

Skew panels supersonic flutter and vibration calculated by matrix displacement method
21 p3933 A70-40586

F-14 carrier based fighter development program requirements, inherent difficulties and variable geometry configuration
21 p3750 A70-41264

Yak-40 business jet design and flight characteristics
21 p3755 A70-42174

SN 600 Corvette business jet design and performance
21 p3755 A70-42175

Supersonic aerodynamic design tools, discussing technological application of high speed computer and limitations
21 p3958 A70-42701

Low and medium power turbojet engines for V/STOL aircraft, discussing development trends concerning operational control
22 p4091 A70-43081

Canadair CL-84 V/STOL aircraft flight characteristics and structural design
23 p4137 A70-44017

Short haul jet transport aircraft design, discussing Computer Aid Design, Airline System Simulator and Traffic Demand Predictor computer programs
23 p4284 A70-44105

Computer-aided aircraft design, discussing parts geometry data bank, visual display, etc
23 p4200 A70-44106

Stability augmentation in aircraft design for handling and operation benefits, discussing control techniques, autopilot modes and load limitations
23 p4138 A70-44109

Hypersonic airbreathers aerodynamic, structural and propulsive system interactions, discussing hydrogen fuel heat sink, airframe and engine cooling and airframe materials
23 p4138 A70-44127

Pilot influence on dynamic aircraft design, taking into account physiological state during various operational tasks
23 p4138 A70-44134

Flight simulation as aircraft design tool, discussing ground and inflight simulation techniques
23 p4178 A70-44139

Strike fighter aircraft fuselage side air intakes, measuring external drag as function of design at subsonic and supersonic speeds
23 p4133 A70-44146

Harrier aircraft development history, discussing V/STOL constraints on transonic flight properties
23 p4139 A70-44148

Mathematical modeling of atmospheric gusts in stratosphere, mountain wave and thunderstorm conditions relevant to aircraft design
24 p4371 A70-45420

Optimal propeller selection for given aircraft and engine designs, considering aerodynamic and acoustic characteristics 24 p4393 A70-45441

Stationary aeroelastic cases studied in subsonic flow range, providing criteria for aircraft design with required flight characteristics 24 p4422 A70-45443

Noise reduction regulations effects on subsonic transport design and configuration [SAE PAPER 700806] 24 p4290 A70-45876

OV-10A forward air control and light attack aircraft design, specifications and performance [SAE PAPER 700837] 24 p4290 A70-45883

Boeing 2707 SST design for low community noise, discussing engine-airframe matching effect [SAE PAPER 700808] 24 p4290 A70-45906

Quiet V/STOL transport aircraft from DC-9-10 modification, discussing flying qualities, propulsion and control system interfaces, configurations, etc [AIAA PAPER 70-1409] 24 p4291 A70-45916

Aircraft design for low weight, discussing structural failures [AIAA PAPER 70-1232] 24 p4425 A70-45917

SST sonic boom noise level reduction by thermal simulation of long body aircraft, considering thermal spike or keel [AIAA PAPER 70-1323] 24 p4291 A70-45942

AIRCRAFT DETECTION

Automatic aircraft tracking by returns from secondary surveillance radars, noting correlation of plots with track 02 p0332 A70-11966

Monograph on probability of aircraft detection by ground visual observation using mathematical model based on Poisson process, considering laws of ocular physiology 05 p0794 A70-16558

Computational load reduction in aircraft tracking, comparing sensitivity and Hilbert norm methods 11 p2025 A70-26212

Aircraft clear line of sight probability data for various altitudes and view angles 14 p2608 A70-30595

Satellite based systems for aircraft surveillance, discussing satellite power and bandwidth conservation, pulse techniques and interrogators 18 p3288 A70-36391

Erroneous line of sight rates generation by radar radome refraction errors in aircraft tracking 18 p3231 A70-36457

Ultrasonic sensor for detecting altitude and vertical velocity of aircraft near ground, applying to helicopter hovering flight or conventional airplane takeoff and landing [AIAA PAPER 70-1031] 20 p3631 A70-39506

AIRCRAFT ENGINES

Optimum R and D organization in aircraft engine production illustrated on turbofan engine 01 p0161 A70-10080

Defects development in cermet materials sealing elements in high O content gas flows of turboprop and turbojet engines 01 p0161 A70-10160

Environmental effects on aircraft and propulsion systems - Conference, Bordentown, N.J., October 1969 01 p0162 A70-10678

Particle removal efficiency of engine inlet separator-filter devices evaluated at Naval inlet test facility for simulated engine airflows, scavenging conditions, etc 01 p0163 A70-10679

Concorde power plant tests using supersonic free jet altitude test facility with Olympus 593 engine 01 p0165 A70-10701

High pressure tests of primary zone flame radiation, flame and tube metal temperatures in aircraft combustion chambers, including oxygen and vitiated inlet air effects 02 p0355 A70-12051

Aircraft piston engines air cooling analysis, discussing forced cooling for high altitude aircraft and helicopters 02 p0355 A70-12224

Single stage experimental front fan designed for aircraft engines, measuring overall and blade element performances 02 p0355 A70-12258

RB.211 aircraft engine control, describing fuel and electronic control systems design and operation [SAE PAPER 690404] 03 p0551 A70-12895

Modified tailed delta configuration selection for U.S. SST, discussing power plant installation choice [RAES PAPER 17] 03 p0411 A70-13544

R and D effect on aircraft engine business, considering aircraft operating cost, funds allocation, etc 04 p0787 A70-14390

Aircraft engine exhaust emissions air pollution role in air terminal area and adjacent communities [ASME PAPER 69-WA/APC-4] 04 p0733 A70-14788

Aircraft power plant technology trends, discussing noise and installation, rear fan engine layout, anticipated bypass and compressor pressure ratios and fuel consumption 04 p0735 A70-15043

Aircraft engine support system dynamic loads induced by fan unbalance analyzed by coupling pylon and engine vibration modes [SAE PAPER 690613] 05 p0895 A70-15850

Aircraft engine prospects in terms of power and thermal efficiency, pressure ratio and turbine entry temperature, materials and fuel cooling improvement, etc 05 p0896 A70-16111

Aircraft power plant development, discussing thrust, specific weight, speed, jet engine and noise suppression efforts 05 p0896 A70-16346

Rolls-Royce boost engine fitted to Trident 3B for improving takeoff and climb performance, discussing mounting and effect on aircraft structure and passenger capacity 06 p0985 A70-17156

Filamentary composite materials for commercial aircraft and engine construction noting boron, graphite and glass reinforcement 07 p1316 A70-18950

Soviet papers on vibrations, strength and structure of aircraft engine elements 07 p1363 A70-19109

Aircraft engine vibrational overload reducible by elastic bearings having controllable elastic characteristics 07 p1364 A70-19113

Soviet book on aircraft engines automated production including plant and machine automatic control, technical and economical factors, etc 08 p1502 A70-20767

Aircraft power plant development, discussing thrust, specific weight speed, jet engine and noise suppression efforts 08 p1558 A70-21029

Aircraft engines development and reliability, discussing rejection causes, data retrieval, repair and salvage techniques 08 p1558 A70-21031

Soviet helicopter and aircraft engines characteristics covering designer, power, rpm limits, fuel consumption, weight, geometry and applications 08 p1559 A70-21366

Supersonic compressor applications for airborne vehicles propulsion systems, discussing axial flow compressors, three dimensional design methods, supersonic radial machines, etc [AGARDOGRAPH-120] 08 p1434 A70-21929

Turbine blade and vane air cooling need established by advantages of operating aircraft turbines at high turbine entry temperatures [AGARDOGRAPH-120] 08 p1559 A70-21931

Air breathing engines for long range Mach 4 transport, discussing engine mission profile- engine configuration interface [AGARDOGRAPH-120] 08 p1560 A70-21934

International aircraft engine industry management in Europe, discussing cooperation, corporations, U.S. competition and structural changes 09 p1792 A70-22339

Aircraft turbine engines strength and gas dynamic characteristics improved by vibration decrease using elastic elements 09 p1742 A70-22471

Harrier engine nozzle actuation system role in short ground takeoff run facility, discussing pneumatic system, air motor servo unit and pilot control 09 p1610 A70-22606

Axial compressor aerodynamics and efficiency in aircraft turbine engines [ONERA-TP-767] 09 p1604 A70-22656

Ultrasonic testing of hydraulic liquids and aircraft and engine lubricating oils resistance to viscosity decrease, analyzing large molecule compounds disintegration 09 p1693 A70-23405

Soviet book on jet engine construction and operation, discussing turboprop, turbojet, direct flow, gas turbine and bypass engines, thermodynamic cycles, etc 09 p1744 A70-23474

Equivalent test results, studying damaging factors in aircraft engine compared with regular tests 10 p1929 A70-24241

Structural reliability of missile and aircraft solid propellant engines, estimating effect of loads variance, geometrical dimensions and mechanical strength 10 p1930 A70-24294

Shrouded aircraft engine turbine blades vibration stresses found minimum by setting up paired blades with fixed tension along shroud 10 p1964 A70-25288

Aircraft turbine engines structural materials and design concepts, describing fiber reinforced materials, oxide dispersion hardened alloys and integral and honeycomb structures 11 p2101 A70-25625

Small turboprop engine development, flight tests, performance and weight reduction [SAE PAPER 700206] 11 p2102 A70-25878

Operating characteristics and performance of business aircraft jet engines compared with piston engine handling [SAE PAPER 700209] 11 p2102 A70-25880

Engine design for future small passenger and sports aircraft, discussing piston, shaft turbine, Wankel and bypass engines and synthetic materials application 11 p1981 A70-25949

Technological feasibility, economical and operational compatibility of subsonic aircraft nuclear propulsion /ANP/ compared with conventional propulsion systems 11 p2081 A70-26050

Aircraft turbine engines gaseous emission measurements, discussing instrumentation for continuous pollutant concentration monitoring [SAE PAPER 700249] 12 p2290 A70-27428

Standard method for aircraft engine exhaust smoke measurement for air pollution control [SAE PAPER 700250] 12 p2290 A70-27429

Aircraft turbofan and turbojet engines military-commercial interrelationships [SAE PAPER 700268] 12 p2290 A70-27436

CF6 engine experience effects on current engine manufacturing, servicing and support in airline service, discussing maintainability, component repair and reliability, etc [SAE PAPER 700289] 12 p2290 A70-27444

Maintenance trends for transport aircraft jet engine, considering engine and component pooling, inspection accessibility, monitoring, etc [SAE PAPER 700316] 12 p2290 A70-27455

Automatic engine maintenance recording system on air transport aircraft noting data reduction [SAE PAPER 700317] 12 p2335 A70-27456

Falcon 10 economical executive aircraft development involving dimensions of cabin, powerplant and range 12 p2162 A70-28027

Altitude Test Facility in air breathing aircraft engine design, discussing plant, test cells design and flight representation and systems accuracy 13 p2473 A70-28538

Jet engines for civil and military aircraft, discussing turbine designs and noise reduction 13 p2474 A70-28546

Aircraft turbojet engine/inlet compatibility, using data system for acquisition, identification and analysis of critical time variant pressure parameters [AIAA PAPER 70-594] 13 p2375 A70-29877

Random data analysis application to aircraft inlet diagnostics [AIAA PAPER 70-597] 13 p2375 A70-29878

DC-10 aircraft wing engine calibration, isolated- and wing-nacelle testings using air-driven engine simulator [AIAA PAPER 70-590] 13 p2342 A70-29881

Aircraft smoke emission reduction and elimination by engine modifications 14 p2628 A70-30190

Design costs for large subsonic transport engines in terms of size, engine ratings and community noise 14 p2629 A70-30944

V/STOL propulsion for commercial needs, considering best tradeoff between propulsion size, weight, noise generation and fuel consumption 14 p2629 A70-31277

Concorde Olympus 593 power plants air intake and engine control system design for rapid servicing, discussing fault diagnosis and checkout 14 p2535 A70-31337

Turboprop aircraft engine service life extension, correcting deficiencies via accelerated tests based on relation between failure rate and usage 15 p2787 A70-31535

Jet engine technology, discussing thrust/weight ratio, compressors, fans, combustors, turbines, materials, manufacturing, maintainability and noise 15 p2787 A70-31698

Rolls-Royce RB 211 turbofan engine, discussing fuel consumption, specific weight, noise and smoke level, reliability and maintainability 15 p2787 A70-31948

Rolls-Royce RB 211 three shaft turbofan engine, discussing centrifugal compressor, tubular combustion chambers and single stage turbine 15 p2787 A70-31949

Non-French jet aircraft engines 15 p2788 A70-32250

Aircraft turbine engine components vibrational testing by holographic interferometry methods 16 p2903 A70-33134

Inlet-engine compatibility testing for aircraft system development program [AIAA PAPER 70-941] 16 p2965 A70-33534

Fighter engine capabilities in Mach 3 to 7 speed range, discussing propulsion system configurations [AIAA PAPER 70-943] 16 p2965 A70-33542

Aircraft electronic propulsion control system using flight type computers and analog to digital conversion equipment [AIAA PAPER 70-693] 16 p2966 A70-33556

Aircraft propulsion control system accommodating transients and yielding higher steady state performance 16 p2966 A70-33557

Power plants development for air transport propulsion system economics, noting engine reliability, traffic delays, etc 16 p2841 A70-33770

High strength Ti alloys for aircraft gas turbine engines, determining critical properties for compressor fan blades 17 p3122 A70-34436

Ti alloys use in Olympus 593 engine for Concorde SST, discussing weight saving, mechanical properties and manipulation characteristics 17 p3146 A70-34449

Ti fabrications in aircraft engines, discussing alloys properties, sheet deformation, fusion welding, porosity, etc 17 p3099 A70-34450

Rotary piston engine for powered gliders and light aircraft power source by modifying industrial Wankel engine 17 p3147 A70-34690

V/STOL 5000 hp engine design optimization, considering component arrangements, rotor design, blade cooling method and fuel control 17 p3147 A70-34709

Convertible fan-shaft engine for V/STOL tactical and transport aircraft, discussing design and performance 17 p3147 A70-34710

Aircraft gas turbine propulsion, discussing engine performance characteristics, thermodynamics, noise and installation [AIAA PAPER 70-873] 17 p3147 A70-34810

Aircraft engine failures advanced detection by spectrometric lubricating oil analysis 17 p3061 A70-35481

C-5A propulsion system onboard monitoring for malfunction detection, analysis and subsystem recording 17 p3148 A70-35497

Boeing 747 aircraft JT9D engine deflections and removals during early service experience and maintenance [AIAA PAPER 70-890] 17 p3019 A70-35807

Cooperative airline program for aircraft turbofan engine parts aging and performance deterioration evaluations [SAE PAPER 700329] 18 p3301 A70-36798

High speed and long life bearings and dampers for future jet engines, considering design factors [SAE PAPER 700318] 18 p3263 A70-36800

Jet transport aircraft turbine engine performance monitoring by flight data, discussing historical highlights and future prospects [SAE PAPER 700314] 18 p3301 A70-36801

High bypass turbofan engine design concepts and development program for airline operation [SAE PAPER 700292] 18 p3302 A70-36804

Olympus 593 engine for Concorde aircraft, describing design and test procedures [SAE PAPER 700291] 18 p3302 A70-36805

High bypass ratio aircraft turbofan engines, discussing program of factory, flight and operational suitability testing [SAE PAPER 700290] 18 p3302 A70-36806

JT9D engine design and performance, describing operational problems [SAE PAPER 700288] 18 p3302 A70-36807

Aircraft turbine engines emission sampling, handling and measurement, evaluating various instruments and techniques [SAE PAPER 700338] 18 p3226 A70-36810

Military aircraft engines performance increase and cost reduction [SAE PAPER 700722] 18 p3302 A70-36817

Aircraft engine production cost estimating techniques, discussing physical, thermodynamic and metallurgical characteristics [SAE PAPER 700271] 18 p3350 A70-36818

Lightweight lift jet engine design, testing and performance for V/STOL aircraft [ASME PAPER 70-GT-32] 18 p3302 A70-36833

Critical aviation gas turbine rotating component life limit determination, describing statistical, maintenance, inspection and life evaluation computer program [SMILE] [ASME PAPER 70-GT-66] 18 p3303 A70-36841

Concorde aircraft powerplant design using fire tunnel test [ASME PAPER 70-GT-128] 18 p3238 A70-36854

Electronic gas turbine diagnostic systems, discussing engine parameters and analysis system [ASME PAPER 70-GT-131] 18 p3259 A70-36857

Control system considerations for small shaft-type aircraft gas turbines providing torque, temperature, load sharing and overspeed limiting functions [ASME PAPER 70-GT-132] 18 p3304 A70-36858

Aero gas turbine engines digital computer control, discussing special properties, design and safety problems [ASME PAPER 70-GT-40] 18 p3304 A70-36870

Soviet book on vibrations in flight vehicle engines covering linear and nonlinear systems, computer methods, etc 18 p3305 A70-37229

Soviet book on vibration and balancing of aircraft engine rotors covering structural deformation and dynamics of turbine engines and compressors 19 p3489 A70-37237

Aircraft gas turbine engine development, considering gas dynamic and structural parameters 19 p3489 A70-37238

Normalization of mechanical properties of aircraft engine components, increasing weight efficiency and reliability 19 p3490 A70-37254

Exhaust gas ingestion suppression model tests for VTOL lift engines, measuring inlet thermal environment [AIAA PAPER 70-905] 19 p3490 A70-37396

Future aircraft with increased comfort, speed and economy, noting power plant development 19 p3355 A70-38249

Ultraminiature pressure transducer for airplane model and inlet/engine subsystem in wind tunnel tests, considering design, calibration, environments, etc 19 p3430 A70-38523

High temperature transducer for engine vibration measurement, discussing piezoelectric accelerometers mechanical design, jet engines material evaluation, crystallographic considerations, etc 19 p3430 A70-38527

Gaseous radioactive penetrant inspections for early low cycle fatigue in aircraft engine materials, discussing impact on maintainability 19 p3441 A70-38828

Jumbo jets turbofan engines design, considering fuel consumption, maintenance, reliability, noise reduction, etc 19 p3491 A70-38953

Aircraft gas turbine engine smoke emission measurement, discussing test equipment and procedure standardization 20 p3689 A70-39720

Fuel consumption related to aircraft performance and engine type 22 p4090 A70-42602

Aircraft engine diagnostics and defectoscopy, considering radioactive isotopes testing for component wear and performance 22 p4046 A70-43083

Fuel delivery and speed control systems for aircraft gas turbine engines, discussing control circuit transfers and block diagrams 22 p4091 A70-43116

Aircraft turbine engines durability estimated from rotor blade minimum tip clearance measurements 22 p4092 A70-43529

Aircraft flight propulsion systems performance improvement via materials technology for gas turbine engine components 22 p4057 A70-43573

Aircraft propulsion system test facilities, discussing altitude simulation, large subsonic and supersonic engines and component development [ICAS PAPER 70-45] 23 p4178 A70-44143

NASA research in turbojet aircraft propulsion noting inlet, compressor, combustor, turbine and nozzle component technology [ICAS PAPER 70-46] 23 p4233 A70-44144

Temperature distribution in cylinders of aircraft internal combustion rotary piston engine under air cooling 23 p4234 A70-44742

Aircraft engine manufacturing technology, discussing metal cutting and forming, bonding, electrochemical machining and electron beam welding 24 p4341 A70-45298

Computer-aided production engineering involving numerically controlled machines for Rolls-Royce aircraft engines manufacture 24 p4341 A70-45299

Optimal propeller selection for given aircraft and engine designs, considering aerodynamic and acoustic characteristics 24 p4393 A70-45441

High temperature gas turbine aircraft engine control system requirements, noting stoichiometric fuel-air ratio [SAE PAPER 700823] 24 p4394 A70-45895

Propulsion control integration for aircraft power management [SAE PAPER 700818] 24 p4394 A70-45899

TSCP700 aircraft auxiliary power unit design, fuel consumption and maintainability [SAE PAPER 700815] 24 p4395 A70-45902

Commercial STOL aircraft propulsion systems from airline viewpoint, emphasizing subsystem design, engine selection, thrust deterioration and maintainability [SAE PAPER 700810] 24 p4395 A70-45904

V/STOL powerplant development, discussion airframe and engine design, application to large aircraft and planned evolutionary process [SAE PAPER 700809] 24 p4395 A70-45905

German book on aircraft thermal propulsion systems calculation, design and evaluation, covering thermodynamic principles and atmospheric composition and properties 24 p4396 A70-46150

Turbofan, turbojet and turboprop engine development in aircraft gas turbine evolution, discussing VTOL propulsion, centrifugal and axial compressor engines 24 p4396 A70-46251

AIRCRAFT EQUIPMENT

University/industry team project Bonanza conducting aircraft flight over Colorado to investigate earth resources remote sensing techniques [AAS PAPER 69-574] 04 p0788 A70-14637

International air traffic jurisdictional area of German aeronautical law regarding aircraft equipment regulations and residents 07 p1427 A70-18886

Harrier communications and radio navigation aid VLF/UHF and TAC/VHF equipment 10 p1841 A70-24849

Vehicle System Simulator (VSS) test program for L-1011 Tristar encompassing primary and secondary flight controls, avionics, hydraulics and landing gear systems [AIAA PAPER 70-388] 10 p1861 A70-24917

Electrothermal helicopter rotor blade deicing system, discussing design, operation and solutions for mechanical and reliability problems 13 p2348 A70-29552

Aircraft equipment automatic test methods, comparing in-flight, on ground and second line testings 13 p2348 A70-29681

Aeroelastic test equipment for Concorde, describing operating principles, installation, test results, etc 15 p2717 A70-31810

Variable speed constant frequency (VSCF) generators for avionics systems, discussing power, weight, volume, cost and reliability 16 p2910 A70-33486

Aircraft electric power generators performance, discussing transients, modulation and regulation of voltage and frequency 16 p2844 A70-33487

Avionics problems in future Army aviation, discussing communications, navigation, instrumentation, automatic flight control, electronic countermeasures, fire control, etc 17 p3051 A70-34725

Minimum Equipment List from aircraft manufacturer and airline operations viewpoint [AIAA PAPER 70-900] 17 p3019 A70-35816

Aircraft electronic equipment cooling techniques, discussing natural and forced convection, phase change and heat pipes 18 p3232 A70-36763

Computerized airborne integrated data acquisition and analysis system, discussing hardware, software and airborne-ground elements interfaces [AIAA PAPER 70-935] 19 p3382 A70-37393

Soviet book on aircraft electrical and radio systems manufacturing, assembling and testing methods, considering effectiveness and standardization 19 p3357 A70-37405

Aircraft air conditioning, discussing temperature and humidity control, cooling systems, etc 19 p3358 A70-37975

L-1011 onboard system for gross weight and center of gravity determination, describing transducers placement, computer design and display panel [SAE PAPER 837] 20 p3562 A70-40359

Long range air transport routes, predicting equipment and expenditures modifications 22 p4128 A70-43533

Airline selection of Auxiliary Power Unit (APU) for transport aircraft, noting benefits of air conditioning during ground operation [SAE PAPER 700816] 24 p4394 A70-45901

Automatic control system for Boeing SST engine air intakes, optimizing engine performance and controlling noise propagation 24 p4396 A70-46214

AIRCRAFT EXHAUST

U EXHAUST GASES

AIRCRAFT FUEL SYSTEMS

Optimal fuel consumption for climbing, cruising and landing flight conditions for medium range subsonic, high supersonic and hypersonic aircraft 02 p0227 A70-12404

Methane fuel systems for high Mach number supersonic transport aircraft on basis of minimum weight [SAE PAPER 690668] 05 p0894 A70-15835

Jet aircraft fuel systems icing prevention, considering fuel filters 05 p0796 A70-17020

Business aircraft fuel management system using capacitance and mass flow rate measurements, displaying fuel quantity and flow rate and flight time remaining [SAE PAPER 700225] 11 p1983 A70-25896

SST inlet steady state pressure defects and random pressure fluctuations determining TF30 engine/inlet compatibility [AIAA PAPER 70-632] 16 p2834 A70-33530

Negative g Drone aircraft surface tension fuel system preventing air inclusion in turbojet engine fuel by tank filters /screens [AIAA PAPER 70-910] 17 p3019 A70-35822

- Boeing 747 aircraft pressure fueling system, describing tanks, feed system, refueling and electrostatic charge minimization [SAE PAPER 700276] 18 p3214 A70-36816
- Aircraft and engine fuel systems deposit formation and microstructure in various test rigs, using electron microscopy [SAE PAPER 700258] 18 p3214 A70-36823
- Jet fuel system deposits measurement, noting reliability of oxygen combustion and beta ray backscattering techniques [SAE PAPER 700257] 18 p3214 A70-36824
- Jet A kerosene deposit accumulation problem and proposed SST fuel tank design [SAE PAPER 700256] 18 p3214 A70-36825
- Catalytic combustion fuel tank inerting techniques for fire protection in military and civilian aircraft 23 p4141 A70-44485
- Fluidically controlled aircraft fuel transfer system three-tank model construction, noting maintenance and fail safe operation [SAE PAPER 700786] 24 p4294 A70-45858
- ### AIRCRAFT FUELS
- Tetrafluorodibromoethane combustion inhibitor effects on aircraft hydrocarbon fuels flame propagation rate and explosion pressure 01 p0160 A70-11011
- Liquefied natural gas or liquefied methane as burning propulsion system for SST, examining storage volume, fuel-tank insulation and implosion danger 03 p0543 A70-12998
- Supercritical demands on airport fuel handling facilities [SAE PAPER 690559] 03 p0463 A70-13263
- Fuel requirements for supersonic aircraft, discussing operational conditions and fuel quality problems 03 p0544 A70-14032
- Aviation kerosene pipeline column separation after valve closure, solving differential equations for transient pressures propagation to predict vapor cavities duration 09 p1665 A70-23744
- Lightning protection development programs application to light aircraft plastic components, emphasizing structure and fuel systems designers awareness [SAE PAPER 700220] 11 p1980 A70-25892
- Commercial aviation gasoline inspection data tabulated and compared for 1969 and 1964 [SAE PAPER 700228] 11 p2099 A70-25897
- Electrostatic charging hazard and flight evaluation of aviation fuels with static dissipator additive [SAE PAPER 700278] 12 p2289 A70-27439
- SST aircraft fuels and lubricants, discussing fire hazard and pollution minimization 13 p2473 A70-29999
- Preignition and combustion kinetics in airstream of Mg and Al suspensions in aviation kerosene and gasoline 14 p2664 A70-30395
- Static charge reducer for aircraft fuels handling safety, discussing performance factors [SAE PAPER 700277] 18 p3263 A70-36808
- Aircraft in-flight and post crash fire protection developments, considering controlled flammability fuel systems and fire fighting methods [ASME PAPER 70-GT-109] 18 p3215 A70-36847
- Concorde loadability, with comparison of flight balance situation for supersonic and subsonic aircraft, describing fuel system [SAE PAPER 835] 20 p3563 A70-40365
- ### AIRCRAFT GUIDANCE
- Conventional inertial gyro modified to provide specification performance for aircraft environments 01 p0086 A70-10312
- Airport surface traffic system analysis, discussing control and guidance isolation, information acquisition/processing and response actions [AIAA PAPER 69-1086] 01 p0137 A70-10630
- Minimum operational characteristics /MOC/ for vertical guidance in airborne area navigation systems, including VOR-DME accuracy criteria 01 p0138 A70-11049
- Electronic displays role in pilot-aircraft interaction, considering flight safety, cost effectiveness, onboard data input, etc 01 p0039 A70-11260
- Soviet book on aeronautical astronomy covering reference stars, time and natural illumination measurements, aircraft course determination, position fixing, etc 02 p0329 A70-11695
- Aircraft approach and guidance system radio components including localizer, glide path and marker systems and radio altimeters, discussing signal interference 02 p0333 A70-11980
- Three dimensional navigation and guidance system for transport aircraft to alleviate operational problems, noting application to STOL aircraft 02 p0334 A70-11983
- Lateral separations using navigation error analysis, showing values for aircraft with or without Discreurs and inertial control under North Atlantic conditions 02 p0336 A70-12607
- Readjustment of aircraft navigation systems based on inertial platforms, discussing errors, corrections and damping stressing single platform 02 p0336 A70-12608
- Tactical landing approach radar /TALAR/ guidance system for V/STOL aircraft steep angle approach and landing 02 p0336 A70-12767
- Range positioning system as automatic indicator in oceanography, aboard land vehicles and aircraft 08 p1541 A70-21360
- Integrated glide path localizer system for landing, takeoff and enroute guidance through rugged country, minimizing spurious reflection, required information bits, etc 09 p1720 A70-22222
- Nuclear landing roll aid based on gamma radiation field built along approach line, runway and taxiways 09 p1721 A70-22662
- SPOT navigation satellite system for near instantaneous fixes or continuous tracks providing height, velocity and automatic guidance and control signals 09 p1723 A70-23041
- Remote area terminal system providing navigation and guidance signals for aircraft landing 11 p2081 A70-26509
- Reference systems for two dimensional visual indications as correction device for pilot guidance errors associated with rotation effects 12 p2177 A70-27036
- American Airlines-McDonnell Douglas inter-metropolitan STOL evaluation tests, noting microwave landing guidance system [SAE PAPER 700336] 12 p2161 A70-27464
- Microwave scanning beam landing system providing aircraft radio approach guidance 12 p2269 A70-27918
- Visual display and automatic taxi guidance system testing for improved aircraft docking accuracy [AIAA PAPER 70-916] 17 p3064 A70-35828
- Commercial aircraft strapdown inertial navigation systems, examining initial self alignment techniques 18 p3289 A70-36442
- Pictorial display methods for pilot error reduction in area navigation via guidance control and capability beyond visual field 19 p3465 A70-38234
- Time-synchronized approach control, combining aircraft precision navigation and guidance with ATC equipment 19 p3466 A70-38237
- Avionics role in STOL air transportation operational capabilities in congested air traffic environment 19 p3466 A70-38238
- Fixed wing and VTOL aircraft all-weather landing guidance and control philosophy 19 p3466 A70-38365
- V/STOL aircraft automatic flight control, guidance and navigation by onboard computer, discussing mathematical model and simulation results [AIAA PAPER 70-1035] 20 p3665 A70-39502
- Aircraft and rocket guidance systems navigation error analysis, discussing numerical integration techniques and computer program [AIAA PAPER 70-1004] 20 p3667 A70-39527
- V/STOL guidance and control system with bad weather landing capability, requirements for V/STOL integration into overall air traffic, terminal area guidance procedures, etc 23 p4216 A70-44843
- STOL aircraft guidance and control, discussing area navigation utilization, multiple airways, data links and ground ATC computers [AIAA PAPER 70-1334] 24 p4373 A70-45934
- ### AIRCRAFT HAZARDS
- Atmospheric effects on SST, discussing turbulence, temperature, wind, cloud cover, hail, toxic gases, etc 02 p0325 A70-12218
- Bird strikes on aircraft, discussing airport control and environment alteration, radar tracking and link between migratory flights and weather conditions 03 p0411 A70-13075
- Icing, bird collisions and static charge problems for jet aircraft, discussing protective devices 03 p0413 A70-13792
- Aircraft wake turbulence effects, using hot film anemometry from nearby towers and penetration by instrumented aircraft 05 p0794 A70-16300
- Illegal in-flight route diversions of aircraft, discussing international juridical means of relief 05 p0960 A70-16535
- Aircraft piracy definition by 1958 U.S. Federal Aviation Act, discussing smuggling, escape of prisoners and clandestine airports 05 p0960 A70-16536
- Illegal aircraft seizures inspired by political motives, discussing suppression, air traffic volume effects, Tokyo Convention juridical decisions, etc 05 p0960 A70-16537
- Air piracy, maritime law applicability, definition, internal laws and French law 05 p0960 A70-16538
- Illegal aircraft route diversion by unauthorized persons, discussing air piracy suppression efforts of various international bodies 05 p0960 A70-16539
- Unstable spiral precursor to jet upset /Mach tucks/ in executive jet transports 06 p0987 A70-18248
- DC-8 jet transport encounter with tornado aloft on 9 November 1963 06 p0987 A70-18586
- Aircraft icing effects on conventional and jet aircraft and helicopters, discussing seasonal variations for main climatic regions 07 p1329 A70-18926
- Encounter statistics and operational environment of aircraft collision-hazard warning systems in terminal area 07 p1331 A70-20060
- Aircraft skin heating by lightning, discussing possibility of exceeding jet fuel vapor ignition temperature 07 p1195 A70-20402
- Accelerate-stop distance problem in takeoff refusal due to critical engine failure, emphasizing runway limited length hazards 08 p1436 A70-21270
- Slush and water hazards on runways, discussing investigation and amelioration methods 11 p2030 A70-25356
- Electrostatic charging hazard and flight evaluation of aviation fuels with static dissipator additive [SAE PAPER 700278] 12 p2289 A70-27439
- Wing tip trailing vortices hazard reduction on closely spaced parallel runways by suction application, discussing power requirements 12 p2207 A70-27631
- Aircraft separation standards in air traffic control system design regarding collision hazards, noting beacon system role 12 p2267 A70-27635
- Delta wing low aspect ratio aircraft vorticity generating effects, discussing wind tunnel tests for hazardous effects 12 p2156 A70-27692
- Jet transport wakes resulting from high engine thrusts considered hazardous to following aircraft, discussing multiple-instrumented runways for measuring visibility 12 p2162 A70-27995
- Hazard analyses of Concorde aircraft design, noting engine control failures and emergency equipment use probabilities 15 p2675 A70-32213
- Airplane design safety considerations covering turbine cooling, liquid methane fuel, turbine wheel burst damage and lightning hazards 15 p2676 A70-32230
- Bird hazards to aircraft - Conference, Queens University, Canada, September 1969 18 p3210 A70-35976
- Netherlands Air Force bird strike problem and warning system 18 p3211 A70-35977
- RAF aircraft damage due to bird strikes in U.K., discussing preventive measures at airfields 18 p3211 A70-35978
- German Air Force aircraft bird strikes statistics 18 p3211 A70-35979
- West German aircraft bird hazards problems, discussing research activities and recommendations for strike avoidance 18 p3349 A70-35982
- Statistical measurement of bird hazards to aircraft in terms of strike rates at airports, considering international strike rate standard 18 p3212 A70-35983
- FAA research activities on eliminating birds at airports and improving aircraft components resistance to impact, including interagency committee functions on hazard problems 18 p3212 A70-35984
- Bird hazards at Hong Kong airport, considering environmental and ecological problems 18 p3222 A70-35985
- U.S. Air Force bird-aircraft collisions problem and bird control research 18 p3211 A70-35984
- Aircraft bird hazards in New Zealand, discussing ecological research techniques and preventive measures 18 p3212 A70-35985
- Bird strikes in U.S.S.R., discussing frequency, damage, etc 18 p3212 A70-35986
- Aircraft damage from bird impact and alleviating measures, taking into account windshield and intake guard designs, microwave beams for protection and chemical agents as repellent 18 p3212 A70-35987
- Military airlift command bird hazard minimization near airfields by environmental control, including uses of scare devices, chemicals, trapping, etc 18 p3212 A70-35988

Canadian civil aircraft bird hazards problem and alleviating measures including airport surrounding lands control

18 p3212 A70-35989

Bird scaring from airfields based on ecological research

18 p3222 A70-35990

Aircraft bird hazards minimization by planning airport location and surroundings

18 p3236 A70-35991

Bird dispersal techniques in use or under study in Britain, including neurophysiological and bioacoustic systems to minimize hazards on airfields

18 p3222 A70-35992

Bird dispersal measure at airports, using behavioral and electrophysiological effects of high power microwave radiation

18 p3222 A70-35993

Aircraft design minimizing damage by bird strikes to gas turbine engine components, discussing service experience, airworthiness demonstration tests and research programs

18 p3300 A70-35994

Gas turbine aero engines damage due to bird strikes, emphasizing rig testing and simulation at first stage rotor blading

18 p3236 A70-35995

Prototype grill device for turboprop aircraft engine inlet protection against bird ingestion, discussing performance tests

18 p3212 A70-35996

International Civil Aviation Organization (ICAO) work on bird hazard reduction, including aircraft airworthiness specifications, bird data dissemination, etc

18 p3349 A70-35997

Airport bird detection equipment (ABDE) radar to display airfield map for presence and magnitude of bird groups and vegetation on runway

18 p3226 A70-35998

Birdstrikes as aircraft hazard, discussing structural damage, engine ingestion and various countermeasures

18 p3213 A70-36319

Soviet book on aircraft electrification in clouds and precipitation during subsonic flight covering atmospheric electrical properties, flight dynamics modification, communications interference, etc

19 p3356 A70-38800

Airport fog layers repetition frequency after low visibility periods

22 p4065 A70-43246

Soviet civil aircraft-bird collisions, stressing hazard forecast and prevention by bird identification and migration patterns

24 p4289 A70-45644

Helicopter hazards elimination measures, considering crash resistant fuel systems, flotation devices, redesigned seats, in-flight escape, etc

24 p4292 A70-46383

Birdproofing aircraft research program using pneumatic cannon firing real and simulated bird carcasses

24 p4292 A70-46398

AIRCRAFT HYDRAULIC SYSTEMS

Purity requirements for oil in hydraulic systems of modern aircraft, discussing filtering devices and Swedish Air Force and SAAB specifications

01 p0130 A70-11359

Hydraulic fluid cleanliness requirements for aircraft systems, filtering, servovalve life, solid particles effects on friction, etc

03 p0414 A70-12999

Allowable leakage guidelines for in-service aircraft hydraulic components, discussing causes and measurements, tabulating rates for static and dynamic seals

05 p0797 A70-15776

Protection methods for increasing ground fire survivability of military aircraft hydraulic systems classified by cost, system and component design criteria

05 p0797 A70-15777

Working pressure effects on size and weight of aircraft hydraulic systems components, allowing for fluid properties change

11 p1982 A70-25865

Harrier fighter aircraft hydraulic systems and flying controls

12 p2166 A70-27889

Hydraulic systems for Boeing 747 aircraft flight control

12 p2167 A70-28019

Automated aircraft flight safety, concerning probabilities and onboard elimination of servomotor failures in hydraulic system due to fuel contamination

22 p3961 A70-42804

Power loss reduction from disk friction and gas leakage through rotor seals of low speed centrifugal pumps in aircraft hydraulic systems and liquid propellant rocket engines

22 p4091 A70-42806

Plunger pump for aircraft hydraulic systems, measuring working fluid temperature effect on cavitation

22 p3965 A70-42817

Tubing, fitting and flexible line designs and testing for production aircraft hydraulic distribution systems [SAE PAPER 700789]

24 p4294 A70-45856

Fluidics for aircraft high pressure hydraulic systems, discussing circuit breaker, fuel computer and landing gear sequencing circuit

[SAE PAPER 700784] 24 p4295 A70-45860

AIRCRAFT INDUSTRY

STOL in northeast corridor, discussing technology applications, economics, requirements for progress, industry, government regulations and decision making

[SAE PAPER 690418] 03 p0608 A70-12897

German light aircraft construction industry situation and prospects regarding manufacture of gliders, sport- and touring aircraft and motor gliders

03 p0413 A70-13791

Rotor propelled aircraft development in West Germany, analyzing military and civil demand for rotor aircraft, light helicopters and V/STOL transports

03 p0413 A70-13793

R and D effect on aircraft engine business, considering aircraft operating cost, funds allocation, etc

04 p0787 A70-14390

Product assurance and large aircraft prototype testing in aircraft industry, discussing reliability testing

[DGLR-69-031] 04 p0699 A70-15139

Composite materials use in nonload bearing and heavily stressed materials, considering applications in aircraft industry and high strength fibers role

05 p0870 A70-16576

Solid film lubricants pretreatment and applications in aircraft and aerospace industries

06 p1075 A70-17341

Airline industry, considering expected increases in traffic, aircraft development and interface problems

08 p1600 A70-20588

Decision making leading to aircraft selection and buying by airline, evaluating traffic and technological aspects

08 p1601 A70-21866

International aircraft engine industry management in Europe, discussing cooperation, corporations, U.S. competition and structural changes

09 p1792 A70-22339

Aeronautical construction complexes in France

10 p1895 A70-24862

British air transport from aircraft manufacturing industry viewpoint, discussing governmental organization of air industries and aircraft design negotiation atmosphere

11 p2153 A70-25861

Commercial aircraft manufacturing industry in UK, discussing SST, wide cabin aircraft, turboprop replacement, engine influence on airframe industry, etc

14 p2668 A70-30936

Aircraft manufacturing market research including cost compatibility with resources and capabilities

14 p2668 A70-30937

Military aviation economics in UK emphasizing aircraft industry and government cooperation in meeting RAF requirements

14 p2668 A70-30938

Passenger awareness of airline industry problems, discussing safety, traffic control, convenience, etc

15 p2831 A70-32225

Aircraft design, development and production illustrating systems engineering functions, discussing control process model

16 p3004 A70-33676

Electronic data processing by aircraft manufacturer, handling structural and performance problems

16 p2843 A70-34350

Cost and time optimization for complex aircraft development projects via network planning

20 p3740 A70-39644

Aircraft engine manufacturing technology, discussing metal cutting and forming, bonding, electrochemical machining and electron beam welding

24 p4341 A70-45298

AIRCRAFT INSTRUMENTS

NT ALTIMETERS

NT ANEMOMETERS

NT APPROACH INDICATORS

NT ATTITUDE INDICATORS

NT AUTOMATIC PILOTS

NT FLIGHT RECORDERS

NT GYRO HORIZONS

NT GYROCOMPASSES

NT HOT-WIRE ANEMOMETERS

NT PLAN POSITION INDICATORS

NT POSITION INDICATORS

NT RADIO ALTIMETERS

NT RADIO DIRECTION FINDERS

NT SONIC ANEMOMETERS

NT SPACECRAFT POSITION INDICATORS

NT SPEED INDICATORS

NT TACHOMETERS

V/STOL air traffic control and equipment considerations for increased demand, suggesting time/velocity separation system using direct routing, positive and automated control

[AIAA PAPER 69-1055] 01 p0137 A70-10639

Factors in icing mechanism and principal features of various ice detectors for aircraft and helicopters

01 p0056 A70-10692

Single axis gyrostabilizer drifting motion mounted on aircraft subjected simultaneously to roll, pitch and yaw, deriving motion equations

01 p0091 A70-10986

Airborne cartographic azimuthal instrument with reflecting prism type optomechanical assembly and trihedral pyramid gyroscope for stabilization

01 p0093 A70-11269

Automatic flight control and instrumentation in civil helicopters, examining military developments and Ferranti automatic stabilization system

02 p0329 A70-11834

Electrical signaling civil aircraft systems, discussing design and integrated maneuver demand controls

02 p0224 A70-11835

Electronic head-up display experience in transport aircraft flight tests including human factor, installation, operational applications, etc

02 p0224 A70-11836

Comparator design for triplicated attitude indicator instrumentation system in aircraft to achieve reliability, discussing system failure characteristics

02 p0224 A70-11844

Aircraft multispectral IR scanning systems for earth resources remote sensing, discussing capabilities

03 p0491 A70-13670

X-15 aircraft project experiments utilized in space research including IR and UV spectrometer, horizontal scanning, stellar photography, micrometeorite and solar energy studies, etc

04 p0622 A70-14673

Correlation protected instrument landing system proposed for international consideration to meet future aircraft traffic density

05 p0880 A70-16107

Aircraft visual flight control displays development, considering liquid crystals in alpha numeric data output devices and holograms for three dimensional structures reproduction

05 p0853 A70-17090

Precession of aircraft mounted astatic gyroscope under constant and periodic moments of external forces, discussing roll angle and rotor axis deviations from inertia axes

07 p1282 A70-19533

Aircraft range-only radar trial applications in stereotopographic surveys of difficult-access areas, discussing organizational problems

07 p1282 A70-19632

Collision avoidance system (CAS) cockpit display equipment design and operation

08 p1492 A70-20480

Onboard integrated maintenance system for aircraft avionics in-flight subsystems monitoring

08 p1471 A70-20669

Built-in test equipment for automatic flight control systems, discussing testing programs and fail safe hybrid circuitry

08 p1471 A70-20670

Aircraft gas discharge displays, discussing segmented alphanumeric annunciator devices with field effect electroluminescent elements and incandescent lamps

08 p1493 A70-20671

Attack aircraft cockpit displays, discussing design requirements and pilot ability as controller

08 p1435 A70-20674

IR technology in aircraft, satellite and rocket electronics, discussing photography, scanners, search and pursuit devices, guided rockets, pilot warning devices, etc

08 p1494 A70-20687

Ilyushin 62 aircraft geometry, propulsion, structure, onboard equipment and performance

08 p1436 A70-21365

Computer managed display system using CRT and appropriate solid state displays providing flight crew with automatically sequenced time varying information

08 p1498 A70-21677

Visual display media requirements of future high performance vehicles, considering spacecraft and aircraft

08 p1499 A70-21691

Aircraft electronic attitude display indicators using symbology generation to combine several flight monitors indications

08 p1500 A70-21737

Integrated display for crowded tactical aircraft cockpits, presenting multisensor information for weapons and fire control systems

08 p1500 A70-21760

Aircraft instrumentation in automatic flight control, discussing inertial platform, sensors, information transmission and display and digital technology

09 p1676 A70-22607

Earth resources sensor integration into satellite or aircraft, discussing cost effectiveness

[AIAA PAPER 70-316] 09 p1677 A70-22871

Two rotor gyrocompass unperturbed motion nonasymptotic stability as function of vessel speed and cruising latitudes

09 p1681 A70-23299

Commercial aircraft inertial navigation, examining gyroscope, accelerometer and electronic computer and gyroscopic stabilization 10 p1914 A70-23848

Aircraft flight displays, simulating low altitude high speed mission by four degree of freedom Dynamic Flight Simulator [AIAA PAPER 70-343] 10 p1859 A70-24216

Book on aircraft flight and engine instruments covering fuel gages, altitude and speed indicators, altimeters, magnetic compasses, gyroscopes, tachometers, pressure, gages, flowmeters etc 11 p2048 A70-25574

ATC airborne hardware covering transponders, area navigation, DME, course directors and approach couplers 11 p2079 A70-25724

Systems engineering study of sensors in fighter aircraft avionics 11 p2081 A70-26501

Soviet book on air navigation covering position determination methods, wind measurement, equipment design and use, etc 12 p2266 A70-26875

Sea and sea ice remote sensing by four-frequency radar /4FR/ system in EC-121 aircraft 12 p2215 A70-26904

IR sensor for detecting clear air turbulence, discussing design, installation, supporting equipment and inflight test results 12 p2229 A70-26946

IR remote temperature gradient sensor as clear air turbulence detector, presenting inflight test results 12 p2229 A70-26947

Pilot midair collision warning instrument based on optical radar MTI, discussing target cross section enhancement by passive retroreflector 12 p2234 A70-27646

Aircraft instrument landing system replacement requirements in terms of airports, aircraft, approach and landing paths, service classes, etc 12 p2269 A70-27917

Course deviation indicator /CDI/ display applicability to tracking Omega lines of position, providing reduction in weight, volume, cost and complexity 12 p2269 A70-27920

Falcon 10 simplified airliner-type equipment for operation under Category 2 weather conditions 12 p2167 A70-28028

Aircraft ice crystal counter for real-time measurement in cirriform clouds, using contact electrification detection 12 p2264 A70-28091

Cockpit data monitor allowing pilot selection of instrumentation parameter readout 13 p2345 A70-28970

Low cost VHF and UHF navigation aids IFR procedures for low density airports [SAE PAPER 700230] 13 p2385 A70-29607

AC and DC driven gas discharge aircraft displays, discussing capabilities and applications 13 p2412 A70-29875

DC-9 aircraft instrument subsystems and operating procedures of KLM, discussing series 15 and 30 aircraft 14 p2530 A70-30416

General aviation demands on Pilot Warning Indicator systems for collision avoidance 14 p2615 A70-31176

Avionics and instrumentation, discussing digital techniques application to engine control, electronic head-up and head-down displays, radiation pyrometry, etc 14 p2589 A70-31338

Cloud formation and structure determination using aircraft-borne IR stereo imagery 15 p2769 A70-31687

Automatic flight control and instrumentation in civil helicopters, examining military developments and Ferranti automatic stabilization system 15 p2772 A70-31771

Atomic clock for climatic and mechanical conditions of aerospace environment, using optically pumped rubidium cell 15 p2740 A70-32366

Airborne electro-optical imaging sensor subsystems performance optimization, comparing mathematical and graphical methods for providing maximum SNR 16 p2906 A70-33172

Solid state electroluminescent phosphor displays for aircraft/spacecraft instrument panels 16 p2906 A70-33178

Low cost headup displays /HUD/ for pilot error reduction during takeoff, approach and landing, discussing displayed functions vs cost tradeoffs 16 p2911 A70-33818

CH-47 cruise guide indicator for displaying fatigue loading to pilots, discussing design and operation 17 p3082 A70-34705

Heavy lift helicopters cockpit display problems, describing photographic flight research program for data acquisition 17 p3082 A70-34731

Airborne data acquisition on high density computer tape for aircraft handling and flight dynamics research 17 p3049 A70-35499

Fluidic parallel flow low airspeed indicator for V/STOL instrumentation tested in wind tunnel [AIAA PAPER 70-906] 17 p3096 A70-35818

Aircraft perspective display as independent landing monitor based on electronic runway lights, discussing simulator development and flight validation [AIAA PAPER 70-924] 17 p3064 A70-35835

Air safety research effects on operations, training procedures and materials, discussing gust loads, on-board data recording devices, human error, etc 17 p3022 A70-35859

Heat-up display /HUD/ system, discussing development, production, commercial aircraft applications and flight sequences uses 18 p3223 A70-36210

Air total temperature measurement for jet powered aircraft, discussing subsonic and supersonic wind tunnel data for sensor thermal recovery characteristics 19 p3425 A70-37882

Mass flow ion drift anemometer applicable to aircraft speed measurement including V/STOL 19 p3425 A70-37885

Economic payback of AIDS /Aircraft Integrated Data System/ recording for operational performance monitoring and engine analysis 19 p3382 A70-37894

Engine vibration monitoring system for Boeing 747 aircraft, including piezoelectric transducer, transmission assembly and differential charge converter 19 p3426 A70-37898

Electronic attitude director indicator /EADI/ for supersonic transport, employing CRT display, head down TV and microvision sensors 19 p3463 A70-37911

Aerospace instrumentation - Conference, Cranfield Institute of Technology, England, March 1970 19 p3428 A70-38514

Aircraft compressor and turbine vibration monitor, using velocity coil or piezoelectric transducers 19 p3430 A70-38525

Airborne magnetic recording flight test instrumentation of Anglo-French Jaguar aircraft 19 p3431 A70-38535

Emmanuel magnetic recording system used with airborne digital computers for aircraft in-flight tests 19 p3432 A70-38547

Airborne electronic equipment, collision avoidance systems, displays, instrumentation, human response and ground based control in air traffic control 20 p3665 A70-39198

Aircraft vertical gyro with hydraulic damping device, calculating ballistic deviations limitation conditions 20 p3632 A70-39733

Airborne atmospheric turbulent flux measurement system with fast response wind velocity, temperature, humidity and aircraft motion sensors, discussing performance and data reduction 20 p3665 A70-40109

Aircraft capacitive fuel gage improvement by integration with flowmeter system, DC torquer display and digital techniques, considering other measurement principles 21 p3821 A70-40619

Flow difference sensor for aircraft hydraulic systems damage vulnerability reduction, discussing design, operation and flight tests results 21 p3750 A70-40786

Aircraft electronics and instrumentation history, discussing anemometer, barometric altimeter, radar, communications systems, computers, flying control and various flight conditions 21 p3826 A70-41257

Low cost and weight reliable microminiaturized IC automatic cockpit checklist systems for aircraft pilots 22 p3977 A70-42298

Area navigation for aircraft guidance with radio aids, discussing advantages, airborne equipment, Dynamic Map Displays, etc 22 p4067 A70-42658

Airborne computerized time frequency systems for aircraft range and velocity determination, using stable clocks with ambiguity resolution 22 p4067 A70-42659

Thunderstorm development processes investigated by aircraft measurements of electrical structure in cumulonimbus clouds, noting lightning probability dependence on turbulence within cloud 22 p4064 A70-42775

DR-S Raydist radio location system in fixed wing aircraft for dynamic gravimetry 22 p4068 A70-43661

Gravity measurement errors in high speed aircraft parallel to undulating geoid attributed to associated vertical accelerations 22 p4025 A70-43662

Integrated helicopter gravity measuring system for various terrains, describing instrumentation and recording monitors 22 p4042 A70-43663

Stochastic processes for probabilistic error analysis in airborne gravimetry, using gravity sensing instruments 22 p4025 A70-43666

Aircraft electronics and instrumentation history, discussing anemometer, barometric altimeter, radar, communications systems, computers, flying control and various flight conditions 23 p4193 A70-43888

U.S. SST flight deck instrumentation and cockpit displays during flight, discussing economic analysis of operations [ICAS PAPER 70-59] 23 p4139 A70-44155

Aircraft binocular head-up display, discussing system operation, history and potential applications 24 p4372 A70-45349

VTOL aircraft instrument flight in terminal area, defining requirements and operating characteristics for vertical and low speed capabilities [AIAA PAPER 70-1333] 24 p4291 A70-45935

Aircraft Doppler VHF omnidirectional radio range /DVOR/ performance test, noting improvement over VOR system 24 p4375 A70-46240

AIRCRAFT LANDING

NT CRASH LANDING

NT DITCHING [LANDING]

NT SKID LANDINGS

Microwave ILS for difficult sites or conditions, detailing capabilities and operation principles 01 p0136 A70-10301

Onboard radar self contained all-weather landing and taxiing /SALT/ system, discussing concept, requirements and results 01 p0138 A70-10641

STOL ports in city environments, discussing elevated building design, assisted takeoff and landing equipment and Navy operational safety potential 01 p0057 A70-10715

TV system for controlling QF-9 drone aircraft landing, takeoff and BQM-34A target drone in-flight test operations 01 p0058 A70-10815

Aircraft pilot-autopilot task division during automatic landing, analyzing man machine interaction in aircraft approach guidance 01 p0139 A70-11258

Head-up display for horizon, desired and actual approach paths information to assist pilot during approach, landing and overshoot 02 p0330 A70-11842

Aircraft landing measurement system /ALMS/ designed to provide computer analysis of all traffic landing at airport 02 p0331 A70-11964

Terminal area approach control sequencing, using digital computer to allocate identification mode and landing time slot 02 p0332 A70-11971

Navy/pilot aircraft control performance during day and night final approach to landing on carriers for empirical performance criteria 02 p0243 A70-12131

Lift-dump system for Hawker Siddeley DH 125, combining aerodynamic drag increase with lift reduction to improve deceleration 02 p0225 A70-12266

Simplified aircraft instrument landing system /SAILS/ employing lightweight helicopter-borne radar for tracking radio beacon at touchdown point 02 p0337 A70-12768

Ground-airborne steep descent VTOL automatic flight control and vertical path selection using hover augmentation system /HAS/ and remote area terminal system /RATS/ 02 p0337 A70-12769

Load analysis for aircraft landing gear during touchdown and braking operations 03 p0596 A70-14093

Man-machine systems design emphasizing impedance matching exemplified by visual approach landing [ASME PAPER 69-WA/GT-15] 04 p0642 A70-14856

Runway acceptance rate improvements to alleviate air traffic congestion metropolplex areas, using approach and landing sequence model for conventional jet aircraft [AIAA PAPER 70-74] 06 p1029 A70-18078

Quasi-optimum design of aircraft landing control system, performing worst case simulation for jet transport 07 p1195 A70-20405

Convergence role in distance perception during aircraft landing, testing subjects with normal binocular vision, emmetropic refraction and visual acuity 08 p1450 A70-20744

Pilot and copilot task distribution schedules adopted by European civil aviation for landing approaches under poor weather conditions 08 p1542 A70-21850

Sector Tactical Air Navigation System to supply on-board information on bearings, slant range and elevation and computer input signals 09 p1720 A70-22491

Optimal two level air traffic control avoiding conflict on runway and in flight and minimizing landing time deviations

11 p2077 A70-25603

Optimal operational control of aircraft takeoff and landing times using stochastic programming

11 p2077 A70-25608

Japanese jet aircraft pilots instrument reading and checking procedures during landing operation under contact flight rules

11 p2078 A70-25667

Ground ATC facilities, discussing landing, automation, surveillance, communication and navigation

11 p2079 A70-25723

Remote area terminal system providing navigation and guidance signals for aircraft landing

11 p2081 A70-26509

Short duration high workload effects in pilot rr interval and finger tremor during Boeing 747 aircraft let-down, approach and landing

11 p1993 A70-26521

Holographic dynamic head-up display system for aircraft carrier deck landings in low visibility

12 p2232 A70-27371

Collision and missed approach risks in high capacity airport landing operations, discussing parallel runways spacing and aircraft longitudinal separation

12 p2207 A70-27629

Wing tip trailing vortices hazard reduction on closely spaced parallel runways by suction application, discussing power requirements

12 p2207 A70-27631

Aircraft instrument landing system replacement requirements in terms of airports, aircraft, approach and landing paths, service classes, etc

12 p2269 A70-27917

Longer runways for increased airport safety indicated from data concerning overruns, undershoots and veering, discussing certification testing during takeoff and landing

12 p2208 A70-27994

Ground effect for increasing lift during aircraft landing

13 p2345 A70-28973

XB-70 aircraft flight tests in cruise and landing approach to evaluate handling qualities criteria

13 p2346 A70-29031

Pilot landing aids for increasing air traffic, discussing Integrated Communication Navigation Identification

13 p2449 A70-29053

All-weather landing aids, discussing Scan Beam and Multilateration systems including ILS, TACAN, etc

13 p2449 A70-29054

Psychophysiological characteristics of pilot activity during various landing approaches with different instrumentation levels, studying heart and respiratory rates

13 p2358 A70-29297

Terminal area guidance for unpowered aircraft instrument approach relevant to manned space shuttle effort

14 p2614 A70-30465

Space shuttle automatic landing system based on aircraft low visibility landing, considering economy and safety

14 p2614 A70-30466

Forced vibration in taxiing aircraft interaction with ground structure

14 p2563 A70-30699

Commercial aircraft brake temperatures under HF landing conditions, using energy input and heat transfer computer programs

14 p2532 A70-31341

All-weather automatic landing in blind conditions, considering Trident system

14 p2615 A70-31392

Aircraft landing and takeoff difficulties and dangers due to mud and water on runways, discussing coping methods

17 p3057 A70-34692

Low visibility aircraft landing problem concerning pilot instrument and visual cue and federal regulations governing operational approval

17 p3134 A70-35845

Precision approach and landing guidance system selection by RTCA committee, discussing aircraft antennas, scan rates, international cooperation, etc

17 p3134 A70-35846

Stochastic processes with linear dynamics and quadratic control cost, considering application to aircraft landing approach path optimization

18 p3279 A70-35973

SATRAM, multiple trajectory landing system for aircraft position indication within large airspace

18 p3289 A70-36948

Maximum throughput-rate capacity for runway and final approach path airspace involving multiple IFR landings

19 p3465 A70-38235

Fixed wing and VTOL aircraft all-weather landing guidance and control philosophy

19 p3466 A70-38365

TV display simulation of instrument and visual aircraft landing approaches, investigating color, collimation and resolution effects on pilot evaluations

20 p3578 A70-39172

Aircraft landing maneuver optimization by in-flight monitoring of approach and landing phases, furnishing decision making display

[AIAA PAPER 70-1000]

20 p3560 A70-39531

Boeing 747 pilot transition training, discussing takeoff, landing, eyelevel, flareout taxi speeds, inertial navigation and electrical, fuel and hydraulic systems

20 p3562 A70-40083

Ground Effect Takeoff and Landing /GETOL/ aircraft, evaluating energy absorption capability of air cushion landing gear in touch-down condition

22 p3961 A70-42282

Duct lining parameters effects on engine inlet and fan discharge noise reduction during fan jet landing

22 p4090 A70-42532

V/STOL aircraft landing performance, discussing relationships between approach speeds, rates of descent, structural criteria and weight penalties

[ICAS PAPER 70-53]

23 p4139 A70-44149

V/STOL guidance and control system with bad weather landing capability, requirements for V/STOL integration into overall air traffic, terminal area guidance procedures, etc

23 p4216 A70-44843

Aircraft longitudinal motion during takeoff and landing due to loss of lift after boundary layer control system failure

24 p4372 A70-45448

Aircraft onboard radar system with landing monitor perspective display of runway operating independently of ground based electronic equipment

[AIAA PAPER 70-1336]

24 p4373 A70-45932

Aircraft accessibility role in planning V/STOL aircraft landing facilities

[AIAA PAPER 70-1311]

24 p4323 A70-45947

Commercial STOL aircraft takeoff and landing physical parameters relationships based on wind tunnel and flight tests

24 p4292 A70-45959

[AIAA PAPER 70-1238]

AIRCRAFT LANDING INSTRUMENTS

U LANDING INSTRUMENTS

AIRCRAFT LAUNCHING DEVICES

Commercial aircraft launching and arresting systems for airport runway length reduction, discussing safety factors

[SAE PAPER 700264]

18 p3237 A70-36821

AIRCRAFT LIGHTS

Aircraft navigation light visibility, discussing visual threshold, source intensity, atmospheric transmissivity, color, background luminance, etc

20 p3564 A70-39719

AIRCRAFT MAINTENANCE

NDT used in airline and aircraft maintenance emphasizing practicability, reliability and costs

01 p0098 A70-10027

NDT peculiar to airline maintenance, emphasizing inspection of complex parts hidden within assembly

01 p0099 A70-10028

Soviet book on operational maintenance of flight vehicles /civilian/, emphasizing maintenance under various climatic conditions

01 p0004 A70-10502

CH-54A engine air particle separator /EAPS/ field experience, discussing engine removal times due to erosion, environment evaluation and design improvements

01 p0164 A70-10684

Commercial transport aircraft landing gear electrical circuitry dispatch reliability improvement, considering components causing flight delays due to maintenance problems

01 p0006 A70-10703

Spares management of large aircraft contract in relationship to total integrated logistics support systems management

02 p0401 A70-11672

Nondestructive inspection program for DC 10 aircraft maintenance

02 p0308 A70-12273

Large aircraft servicing, describing equipment and procedures

02 p0276 A70-12762

Centralized maintenance system organization, describing centralized system used by Spanish Air Force units

06 p1184 A70-12724

Selection criteria for nonlubricated air or liquid cooled reciprocating type prime movers used in aircraft ground support equipment

[SAE-ARP-1052]

07 p1248 A70-18801

Isochronal maintenance inspection management of Military Airlift Command /MAC/, noting C-141 utilization rate

07 p1428 A70-19673

MADAR onboard maintenance system designed for C-5 aircraft monitoring line replaceable units in electrical, avionics, environmental, mechanical and propulsion systems

[AIAA PAPER 70-243]

07 p1195 A70-20375

Onboard integrated maintenance system for aircraft avionics in-flight subsystems monitoring

08 p1471 A70-20669

Alternative equipment maintenance procedures costs by combined discrete event and continuous system simulation, discussing additional model applications

08 p1466 A70-20927

Aircraft engines development and reliability, discussing rejection causes, data retrieval, repair and salvage techniques

08 p1558 A70-21031

Aviation maintenance in Britain, discussing continuing airworthiness techniques, development and international aspects

08 p1436 A70-21256

Aircraft maintenance operations planning based on mathematical mass maintenance theory /queueing theory/

08 p1507 A70-21367

Aircraft maintenance, discussing trend toward increased use of quantified methods, failures reclassification, control techniques and check frequencies

09 p1693 A70-23371

Automatic test equipment for different type of planes and relation to self organizing systems, considering airport implantation

10 p1970 A70-24476

Harrier maintainability for reliability with minimum down-time and man hours, discussing servicing, turnaround, role change, inspection and engine changes

10 p1806 A70-24850

Nonavionics Aircraft Integrated Data System configurations evaluation by computer model, showing cost effectiveness data in terms of aircraft maintenance and availability

10 p1808 A70-24909

Transport aircraft flight recorders for parameters essential for operation and aircraft maintenance

11 p2050 A70-25818

Automatic maintenance testing of avionics systems, discussing tape controlled equipment and program preparation

11 p2017 A70-25837

Three spool turbofan engine design regarding maintainability, noting on-condition module removal and overhaul

[SAE PAPER 700204]

11 p2101 A70-25877

Nickel cadmium battery for aircraft jet engine starting, discussing selection for optimum service life and reliability under maintenance and environmental conditions

[SAE PAPER 700211]

11 p1980 A70-25883

Spectrometric oil analysis program /SOAP/ for engine and transmission components damage detection and preventive maintenance in military aircraft

12 p2240 A70-27017

CF6 engine experience effects on current engine manufacturing, servicing and support in airline service, discussing maintainability, component repair and reliability, etc

[SAE PAPER 700289]

12 p2290 A70-27444

Solid state proximity switches, sensors, logic and self test circuits for aircraft electrical applications to improve reliability and maintainability over mechanical switches

[SAE PAPER 700305]

12 p2195 A70-27449

Reliability and maintainability from airline standpoint, discussing concepts, language and standards for aircraft design

[SAE PAPER 700326]

12 p2335 A70-27460

Tradeoff decision processes scheduling maintenance frequencies for commercial transport aircraft

[SAE PAPER 700328]

12 p2243 A70-27461

Protective diffusion coatings for jet engine gas path parts, discussing repair procedures

[SAE PAPER 700332]

12 p2254 A70-27463

Cost effective spares provisioning models for airline operations, minimizing availability-cost ratio for line replaceable unit and total fleet

13 p2525 A70-29571

Relative cost benefits estimation of manual and automatic test systems for avionics in maintenance organization, proposing integrated maintenance and ATC data system

13 p2525 A70-29579

Minimum cost systems engineering in aviation equipment maintenance and reliability

14 p2669 A70-30943

Concorde Olympus 593 power plants air intake and engine control system design for rapid servicing, discussing fault diagnosis and checkout

14 p2535 A70-31337

Rolls-Royce RB 211 turbofan engine, discussing fuel consumption, specific weight, noise and smoke level, reliability and maintainability

15 p2787 A70-31948

Aircraft ground damage during maintenance and servicing

15 p2675 A70-32210

Avionics computers field repair method permitting removal and replacement of flat packs and discrete components on multilayer interconnection boards

15 p2706 A70-32655

Boeing 707 and 727 aircraft components on condition maintenance program based on statistical analysis and performance monitoring for replacing scheduled overhauls

15 p2748 A70-32656

Reliability maintenance problems in corporate aircraft operations, discussing equipment calibration, aircraft systems analysis and repair facility selection

16 p2921 A70-33821

Aircraft utilization rate vs invested money as factor determining financial justification of corporate aircraft operations, discussing maintenance engineering

16 p2921 A70-33822

Airline pitot and static altimeter systems and undercarriage maintenance and checkup, discussing water in systems, case leaks, trash, dirt, inoperative heaters, etc

16 p2842 A70-33823

Aircraft design, construction, operation and maintenance improvement efforts by FAA, discussing airworthiness requirements, audit team visits to factories, etc

16 p2842 A70-33824

Power plant efficiency, size, maintenance and operating economics of propulsion systems for air transport

17 p3200 A70-34917

Aircraft onboard maintenance recording system, discussing design and effectiveness

17 p3094 A70-35516

European requirements for aircraft accident and maintenance recording systems

17 p3094 A70-35517

Boeing 747 maintenance and inspection program, discussing condition monitoring, test methods, etc

[AIAA PAPER 70-889] 17 p3019 A70-35806

Boeing 747 aircraft JT9D engine deflections and removals during early service experience and maintenance

[AIAA PAPER 70-890] 17 p3019 A70-35807

Fastener standardization for airline maintenance requirements

[AIAA PAPER 70-894] 17 p3102 A70-35811

Airline maintenance department assurance of air service regularity, stressing management role

17 p3065 A70-35855

Aircraft designer role in reducing departure delay due to equipment malfunction

17 p3022 A70-35858

Cooperative airline program for aircraft turbofan engine parts aging and performance deterioration evaluations

[SAE PAPER 700329] 18 p3301 A70-36798

Airlines data reduction using electronic engine maintenance recorders

[ASME PAPER 70-GT-127] 18 p3259 A70-36853

Aircraft nonavionic systems performance condition and minimum maintenance duties diagnosis by integrated data system, discussing engine monitoring instruments

19 p3426 A70-37891

Avionics maintenance effectiveness logistics, discussing symptom pattern observation technique (SPOT) for in-flight data

19 p3554 A70-38399

S-65-200 Commercial Compound Aircraft design for dispatch reliability and maintenance

19 p3356 A70-38823

Helicopter cost reduction by transmission overhaul frequency reduction, discussing savings with on-condition maintenance

19 p3441 A70-38824

RAMMIT /reliability and maintainability management improvement techniques/ for processing maintenance data relevant to Army aircraft operations and support

19 p3441 A70-38826

U.S. Army UH-1/AH-1 helicopter maintainability and reliability field program, including statistical data

19 p3356 A70-38827

Condition Monitored Maintenance program for turbine engines eliminating total overhauls at specified time, using NDT

19 p3441 A70-38830

Airfreighters maintenance and reliability simulation, modeling specific aircraft designs via input data selection

19 p3357 A70-38835

Comparative demand forecasting for military helicopter spare parts, stressing exponential smoothing model

20 p3740 A70-39643

Integrated data systems for aircraft maintenance, noting information retrieval role in maintenance management for cost reduction and safety

20 p3740 A70-39647

Military and commercial aircraft maintenance costs reduction, discussing labor/material ratio, spare parts use, diagnostic systems, etc

21 p3749 A70-40750

Nondestructive testing for aircraft maintenance, considering economics

24 p4342 A70-45677

Nondestructive testing technology impact on military aircraft maintenance, discussing training, applications and advantages

24 p4342 A70-45678

C5 Malfunction Detection Analysis and Recording (MADAR) subsystem for onboard fault isolation including engines

[SAE PAPER 700820] 24 p4349 A70-45898

Aircraft maintenance cost statistical analysis recursive regression model for aircraft failure and manhour cost data

24 p4292 A70-46125

AIRCRAFT MODELS

Air combat model (AIRCOM) to evaluate close-in air-to-air fighter aircraft combat capability, determining relative changes in kill probability per firing pass

03 p0413 A70-13958

Three dimensional photoelastic model for structural analysis of aircraft bulkhead to improve fatigue life

05 p0937 A70-16376

Helicopter dynamics structural model extended to LF longitudinal motions by including stabilizing feedback loop representing forward velocity influence on main rotor

06 p0987 A70-17910

Laboratory Electronic Servo Controller for structural fatigue tests, aircraft material tests, model position and velocity control in wind tunnels

06 p0989 A70-18606

DC-10 aircraft wing engine calibration, isolated- and wing-nacelle testings using air-driven engine simulator [AIAA PAPER 70-590] 13 p2342 A70-29881

Ground effect visualization at low speed flow around aircraft models, discussing airbus, VTOL aircraft and Concorde

14 p2528 A70-30291

Parameter model of VTOL airplane in transition, considering aerodynamic forces and moments and digital simulation

17 p3015 A70-34724

Ultraminiature pressure transducer for airplane model and inlet/engine subsystem in wind tunnel tests, considering design, calibration, environments, etc

19 p3430 A70-38523

Model testing for helicopters, considering scaling, ditching and rotor performance

19 p3402 A70-38610

Airfreighters maintenance and reliability simulation, modeling specific aircraft designs via input data selection

19 p3357 A70-38835

AIRCRAFT NOISE

NT JET AIRCRAFT NOISE

NT SONIC BOOMS

Concorde aircraft structural acoustics and design problems, discussing noise, fatigue and testing techniques and facilities

01 p0199 A70-10288

Audiograms for aviators unexposed and exposed to high intensity LF noise of maritime patrol aircraft indicating no permanent effects

01 p0032 A70-10365

Turbofan VTOL or STOL integrity transports noting lift engines, noise, aircraft design and interior [AIAA PAPER 69-1039] 01 p0005 A70-10645

Noise reduction for V/STOL aircraft operation by introducing quiet propellers, discussing variable camber propellers, propeller aerodynamics, etc

[AIAA PAPER 69-1038] 01 p0005 A70-10646

Turbine noise significance in civil aircraft noise problem

[ASME PAPER 69-WA/GT-12] 04 p0734 A70-14884

Residential structures vibration response to aircraft flyover noise, discussing noise transmission, rattle phenomenon, spectra, etc

[ASME PAPER 69-WA/GT-8] 04 p0770 A70-14887

Optimum low speed ducted fan design for minimum noise generation

[ASME PAPER 69-WA/GT-4] 04 p0734 A70-14891

Rotor noise reduction in helicopter design for increased blade loadings and higher tip speed [SAE PAPER 690684] 05 p0792 A70-15865

Airport noise silencers for aircraft engines, discussing design, operation and damping efficiency

05 p0829 A70-16353

Atmospheric absorption of noise investigated for characteristics based on aircraft flyby tests

05 p0795 A70-16786

Sound radiated by fluctuating forces on helicopter rotor analyzed, predicting noise output variation as function of helicopter design parameters

05 p0796 A70-16792

Propeller noise research for achieving noise reductions in future propeller design

05 p0796 A70-16793

Sound levels and frequency spectra of noises measured in AN-24 and IL-18 turboprop aircraft cockpits

05 p0796 A70-16925

Perceived aircraft noise level based on objective acoustic measurements related to subjective response, tabulating noys as function of sound pressure [SAE-ARP-865A] 07 p1190 A70-18803

Aircraft noise reduction certifications program by tripartite draft plan

07 p1426 A70-18876

Legal aspects of liability for aircraft noise by German laws, discussing property owners obligation to permit flights over properties and admissible claims for compensation

07 p1427 A70-18884

Takeoff noise minimization by prescribing optimum takeoff trajectories, considering aircraft parameters influencing noise intensity at takeoff

11 p1979 A70-25814

Inflight aircraft cockpit noise levels effect on pilot hearing sensitivity

11 p1990 A70-25875

Commercial aircraft peak cockpit noise level during cruise and high speed descent, discussing damage risk criteria and interplot speech interference

11 p1991 A70-26275

Total community annoyance measurement (TACM) applied to urban VTOL port planning for aircraft noise [SAE PAPER 700286] 12 p2161 A70-27442

STOL aircraft noise level certification based on aircraft type, landing and takeoff paths and airports [SAE PAPER 700325] 12 p2161 A70-27459

Aircraft noise reduction effects on airport capacity and community exposure levels

12 p2207 A70-27628

Transportation vehicle noise control measures and acceptability, discussing physical and operational source modifications using aircraft noise examples

12 p2336 A70-27849

SST feasibility for U.S., considering program costs, financing, investment return and airport and community noise aspects

12 p2162 A70-27991

Noise characteristics and measurement, discussing aircraft noise generation and reduction

13 p2473 A70-28443

Meteorological problems associated with proposed tests for aircraft noise certification, discussing airport near-surface environments

14 p2610 A70-30612

Noise of large commercial V/STOL aircraft and effect on design and operation, predicting acoustic signatures

14 p2531 A70-30854

Design costs for large subsonic transport engines in terms of size, engine ratings and community noise

14 p2629 A70-30944

Vortex visualization applications in helicopter noise research, using smoke generator in rotor blade tip

17 p3057 A70-34712

Helicopter rotors noise intensity prediction for high tip Mach number, including compressibility and thickness effects

17 p3015 A70-34729

Collection of papers on aerodynamic noise covering noise generation, solid boundaries effect, strength distribution, jet noise, perturbation theory, etc

17 p3071 A70-35448

Metropolitan airports environmental considerations, noting aircraft noise role in planning [SAE PAPER 700253] 18 p3237 A70-36826

Critical review of aircraft noise characteristics measurement and analysis techniques, noting nonuniformity problems control through standards

19 p3396 A70-37907

Automatic sound monitoring system for measuring aircraft noise in airport vicinity

19 p3397 A70-37908

Computer controlled aircraft noise monitoring system at Stuttgart airport

19 p3397 A70-37909

Flow noise mechanisms, considering discharge, propeller, ventilator, jet engine, boundary layer, water pipe and supersonic aircraft sources

19 p3406 A70-38474

Temporal and spectra combination effects on aircraft sound judged noisiness, using human subjects in anechoic chamber

20 p3580 A70-39712

Transport aircraft noise at three major airports by noise exposure forecast (NEF) contours methodology

21 p3750 A70-40896

Aircraft acoustical duct treatments - ASA Conference, Philadelphia, April 1969

22 p4089 A70-42528

NASA acoustically treated nacelle program reducing noise under commercial transport flight path near airports

22 p4089 A70-42529

Aircraft noise reduction, discussing generation sources in propulsion system, noise levels and subjective responses

23 p4140 A70-44395

Boeing 2707 SST design for low community noise, discussing engine-airframe matching effect [SAE PAPER 700808] 24 p4290 A70-45906

AIRCRAFT PARTS Surface work hardening effects on steels resistance to low cycle fatigue with stress concentration, applying results to aircraft parts

06 p1085 A70-17403

Analytical structural design reliability, discussing static test failures of wings, fuselage, horizontal and vertical stabilizer and landing gear

07 p1417 A70-20400

Critical radii of curvature in elastoplastic bending of rib-reinforced aircraft components from wafer panels determined using strain energy method
08 p1506 A70-21183

Transverse and shear strengths of Al-B composite materials used in F-111 aircraft components, investigating cold work, thermal treatments and steel wire addition effects
08 p1509 A70-21857

Adhesive bonding of aircraft components, describing autoclave environmental control for curing adhesives, parts prefabrication, core fitting and quality control
09 p1690 A70-22022

Creep forming application in producing aircraft parts from metal sheets, plates and extrusions, discussing blank forming and drawing
10 p1893 A70-23854

Metal working technology of Ti and alloys for structural parts fabrication for Concorde aircraft, describing laser cutting, electron beam welding, explosive forming, etc
10 p1895 A70-24594

Low temperature tempering effects on steel transformations and axial rigidity of radial thrust ball bearings in aircraft
12 p2243 A70-27568

Computerized control of aircraft spare parts inventories, using optimization method maximizing aircraft availability and minimizing handling costs
13 p2524 A70-28836

Borsic-aluminum composite materials fabrication, properties and applications to aircraft parts
13 p2420 A70-29246

Minimum cost systems engineering in aviation equipment maintenance and reliability
14 p2669 A70-30943

Ti alloy aircraft parts heavy press forging, considering mechanical properties, temperature effects, cost factors, etc
17 p3097 A70-34360

High strength Ti alloys depth hardenability, discussing mechanical properties and use in aircraft components
17 p3121 A70-34434

Boeing 737 aircraft nose gear gravel deflector and engine vortex dissipator
[AIAA PAPER 70-912] 17 p3020 A70-35824

Flight loads spectrum data for army CH-47A, UB-1B and CH-54A helicopters components compared with fatigue life spectra
18 p3210 A70-35955

Structural reliability testing methods and loads prediction for rotary wing vehicle components, considering AH-56A compound helicopter
19 p3356 A70-38612

Reinforced plastic for aircraft parts, investigating low viscosity polyester resins of styrene crosslinking type
20 p3656 A70-40028

Synthetic resin adhesives for aircraft components fabrication
20 p3657 A70-40532

Glass plastic composite electrically heated windshield for aircraft, discussing design, fabrication, qualification testing and service experience
21 p3750 A70-41137

Load cycle sequences for full scale aircraft structures and components fatigue testing
[ICAS PAPER 70-32] 23 p4266 A70-44101

Computer-aided aircraft design, discussing parts geometry data bank, visual display, etc
[ICAS PAPER 70-27] 23 p4200 A70-44106

AIRCRAFT PERFORMANCE

NT HELICOPTER PERFORMANCE

Research program to improve performance of high lift devices on wings having small sweepback and high aspect ratio
01 p0001 A70-10047

Differences in aircraft operating costs, performance characteristics and demand for aircraft by domestic trunk airlines (1932-1965)
[AIAA PAPER 69-1059] 01 p0005 A70-10637

Turbojet aircraft engine performance correlation with relative humidity, noting air density effect on rotor performance resulting from moisture content
01 p0165 A70-10689

Harrier close-support fighter aircraft with short or zero takeoff run capability, discussing design, cruise efficiency, maneuverability and navigation-attack system
02 p0225 A70-12310

Wind tunnel comparative performance tests of glider laminar wing profile with fixed and flexible trailing-edge flap
02 p0304 A70-12800

Turbojet performance magnitude data represented by components nondimensional characteristic curves
03 p0551 A70-13021

Boeing 707 aircraft operational efficiency optimization by modification program to extend wing life
03 p0497 A70-14052

Wing and body design for upgrading transonic aircraft performance, discussing blending, spanwise sweep variation, curved leading edge and aspect ratio
04 p0613 A70-14504

Slender delta wing aircraft dynamic behavior under vertical and lateral gusts, particularly during landing approach
[DGLR-69-52] 04 p0623 A70-15145

Energy state approximation for supersonic aircraft performance optimization with extension to maximum range problems, noting comparison with complex dynamic models
[AIAA PAPER 68-877] 04 p0623 A70-15376

Boeing 747 aircraft family design options related to utilization, performance and economics, discussing development through large turbofan engine availability
[AIAA PAPER 68-1020] 04 p0624 A70-15382

Aircraft lift, thrust and drag coefficients inaccuracies expressed as errors in measured flight performance characteristics
04 p0624 A70-15386

Hypersonic glider performance in mesosphere entry using models located in rarefied gas flow at Mach 8
05 p0789 A70-15811

Fighter aircraft design combining optimal qualities with economy
05 p0793 A70-15902

Schleicher AS-W15 glider wing span, weight, wing loading capacity and speed range, noting performance in international competition
05 p0793 A70-15905

Rolls-Royce boost engine fitted to Trident 3B for improving takeoff and climb performance, discussing mounting and effect on aircraft structure and passenger capacity
06 p0985 A70-17156

Lift fan V/STOL tactical aircraft performance capabilities determination, using digital computer program
07 p1191 A70-18975

Asymptotic expansions and energy methods applied to three dimensional aircraft maneuvers involving energy climbs and turns
07 p1190 A70-20416

Ilyushin 62 aircraft geometry, propulsion, structure, onboard equipment and performance
08 p1436 A70-21365

Concorde flight testing program, discussing results on prototype, preproduction and production aircraft
08 p1436 A70-21727

Concorde aircraft test flight results, considering ground handling, takeoff, approach and landing, low speed flight, aeroelasticity, stability, power plant, etc
08 p1437 A70-21728

C-5A aircraft testing program covering ground handling, towing, cargo handling, takeoff and landing, cold weather testing, etc
08 p1437 A70-21729

Aircraft flight testing techniques modification to cover maximum performance values
08 p1437 A70-21735

In-flight investigation to determine effect of variations in bank angle control parameters on cruise flight handling qualities
08 p1437 A70-21738

Onboard measurements of single engine propeller-driven aircraft performance, stability and control in nonsteady symmetric flight
08 p1438 A70-21869

C-5 Galaxy airlifter design, delivery capacity, aerodynamics and flight test program
09 p1609 A70-22020

Dual inertial navigation transponder flight to North Pole aboard KC-135 airplane, discussing performance, installation, etc
09 p1719 A70-22189

Sailplane design standards concerning retractable undercarriage and trailing-edge flaps revised to achieve better performance
09 p1612 A70-23575

Amplitude and Rotational 3-Axis Flight Simulators for handling qualities research, outlining physical constraints and methodology for driving visual display and motion systems
[AIAA PAPER 70-353] 10 p1858 A70-24210

Civil VTOL transport aircraft handling and performance qualities using fixed base simulator with electronically generated display
[AIAA PAPER 70-345] 10 p1859 A70-24214

BAC 111 short/medium range jet airliner family status report on program activity
10 p1806 A70-24846

Airspace and airport use at terminals, discussing segregation of aircraft by performance categories
[SAE PAPER 700229] 11 p2153 A70-25899

Aircraft performance, stability and control testing from nonsteady flight measurements, ascertaining repeatability of results
[SAE PAPER 700236] 11 p1980 A70-25905

Small scale and full scale wind tunnel and flight test data correlated for Lear jet aircraft
[SAE PAPER 700237] 11 p1981 A70-25906

Performance, stability and control improvements of light aircraft, applying computerized parametric analysis
[SAE PAPER 700240] 11 p1981 A70-25909

Circumplanetary aircraft design for solo nonstop great circle around world flight without refueling, not-

ing application to sport, transportation, surveillance, photography, etc

11 p1981 A70-26046

Kalman filtering and differential correction techniques applied to T-33 flight test data for aircraft system parameters identification
11 p1982 A70-26323

Aircraft flight characteristics simulated on trainer with automatic control system and measuring system
11 p2056 A70-26455

Aviation equipment and systems operational durability, formulating physical model to construct functions for analysis
12 p2240 A70-27015

Aircraft all-movable stabilator computer aided design for optimized structural weight and performance
12 p2319 A70-27137

Aircraft turbojet and turbofan engines cost correlation to performance statistically analyzed in terms of various parameters
[SAE PAPER 700270] 12 p2335 A70-27437

Harrier aircraft flight test program considering instrumentation, data acquisition, airframe, avionics, systems engineering, etc
13 p2344 A70-28922

Aircraft dynamic response to homogeneous isotropic atmospheric turbulence analyzed for power spectral density, taking into account spacewise variations in airframe loading
[AIAA PAPER 70-544] 13 p2345 A70-29010

Tactical fighter requirements and designs, considering operational environment and weapon characteristics with emphasis on turning performance
[AIAA PAPER 70-516] 13 p2346 A70-29035

Aircraft turbulence penetration performance numerical rating, applying concept to large subsonic jet transports
[AIAA PAPER 70-543] 13 p2347 A70-29074

State of sea definition for hovercraft performance purposes, recommending Hovercraft Coastal Wind Wave Code
13 p2347 A70-29126

SA-330 Puma tactical support helicopter design and performance
14 p2530 A70-30286

Commercial aircraft design evolution and trends concerning performance and operating cost reduction
14 p2532 A70-31370

L-1011 aircraft payload, range, configuration, engine selection, design features, equipment systems, flight characteristics, internal arrangement, maintenance and performance
15 p2673 A70-31947

Book on aerodynamics for engineering students covering hydro- and aerostatics, flow theory, propulsion principles, aerofluid theories, aircraft performance and stability, etc
16 p2838 A70-33953

Optimal distance flight, discussing glider performance data
16 p2842 A70-34174

Electronic data processing by aircraft manufacturer, handling structural and performance problems
16 p2843 A70-34350

Tactical aircraft performance, discussing electro-optical devices, weaponry, communication and navigational networks, information displays and real time remotely manned control systems
17 p3013 A70-34672

SST flight efficiency trends, discussing breakthrough and development method and Concorde aerodynamic, propulsion and structural history
[AIAA PAPER 70-871] 17 p3016 A70-34811

Aircraft optimal operating procedure development by integral-variational performance analysis methods, discussing flight paths, fuel consumption, mission requirements, etc
[AIAA PAPER 70-876] 17 p3016 A70-34812

Maneuver load alleviation (MLA) configurations for wing bending load relief on transport aircraft, showing improved payload and span performance
[AIAA PAPER 70-877] 17 p3016 A70-34813

Airplane performance improvement by flight control system design, discussing ride quality, flutter margin, maneuver load, etc
[AIAA PAPER 70-875] 17 p3017 A70-34816

Airborne data acquisition on high density computer tape for aircraft handling and flight dynamics research
17 p3049 A70-35499

Boeing 747 aircraft operation in first three months of service, discussing crew training, instrumentation, navigation system improvement, etc
[AIAA PAPER 70-891] 17 p3019 A70-35805

Four-seat two-engined STOL propeller passenger and sport aircraft design and performance
19 p3355 A70-37371

Aircraft nonavionics systems performance condition and minimum maintenance duties diagnosis by integrated data system, discussing engine monitoring instruments
19 p3426 A70-37891

Future aircraft with increased comfort, speed and economy, noting power plant development
19 p3355 A70-38249

- Optimal longitudinal takeoff trajectories, formulating obstacle clearance criterion function based on aircraft design parameters effects
[AIAA PAPER 70-963] 20 p3560 A70-39566
- Merit factor for evaluation of aircraft types and missions, matching aircraft characteristics to mission load, range and speed
[SAWE PAPER 842] 20 p3562 A70-40360
- Weight growth factor in aircraft design, discussing fixed and variable weight, payload, performance, flight quality, structural criteria and life expectancy
[SAWE PAPER 839] 20 p3562 A70-40363
- Disposable load drop effect on aircraft range, using Breguet equations for graphic determination of bombing range
21 p3750 A70-40868
- Glide and landing performance of twin-keel parawings, discussing wind tunnel, radio flight and simulator tests
[AIAA PAPER 70-1186] 21 p3754 A70-41829
- Fuel consumption related to aircraft performance and engine type
22 p4090 A70-42602
- High temperature liquid metal cooled nuclear reactor for military aircraft with long flight endurance and range
22 p4071 A70-43188
- Escape and survivability rates in various aircraft flight envelope regimes, using existing escape statistics and mission profiles
23 p4141 A70-44492
- OV-10A forward air control and light attack aircraft design, specifications and performance
[SAE PAPER 700837] 24 p4290 A70-45883
- Short haul intercity center facilities air transportation traffic alleviation by VTOL aircraft, emphasizing performance, ground facilities, system operation and economics
[AIAA PAPER 70-1243] 24 p4290 A70-45914
- All-body configuration hypersonic transport aircraft performance by computer synthesis, considering sonic boom constraint, maximum payload ratio and optimal cruise speed
[AIAA PAPER 70-1224] 24 p4291 A70-45957
- STOL aircraft field length, terminal area performance and minimum handling qualities requirements for safe and efficient operations
[AIAA PAPER 70-1240] 24 p4292 A70-45960
- AIRCRAFT PILOTS**
- NT TEST PILOTS**
- Audiograms for aviators unexposed and exposed to high intensity LF noise of maritime patrol aircraft indicating no permanent effects
01 p0032 A70-10365
- Scandinavian Airlines system of pilot selection, considering personality traits, behavior characteristics, clinical examination, etc
03 p0433 A70-13260
- Commercial pilots susceptibility to emphysema and respiratory impairment in hypobaric environment, discussing flying disability implications
03 p0438 A70-14068
- Cockpit display system to reduce aircraft pilot workload and aid judgment making during critical operations
[ASME PAPER 69-WA/BHF-12] 04 p0642 A70-14854
- Aircraft pilots vertigo during flight using questionnaire and interviews, emphasizing bank directional disorientation
04 p0643 A70-14979
- Professional personality formation and organization of aviator, discussing infancy motivation, identification with instructor during training, emotional life, etc
05 p0799 A70-15767
- Physiological pilot training program of FAA, discussing slides on Aeronautical Center and Civil Aeromedical Institute
07 p1218 A70-19012
- Syncope proneness correlation with episodes of impaired consciousness in pilots during flight using physiological tests
07 p1223 A70-19944
- Jet pilot trainee qualification requirements, training process methods and equipment, considering German-French joint trainer aircraft program
08 p1452 A70-21348
- Pilot systems for controlling aircraft in flight, considering direct lift control, displays, simulators, tests, etc
08 p1437 A70-21734
- Psychic stress causing factors and reactions in aircraft pilots on duty, analyzing harmful effects on organism
09 p1620 A70-23012
- Aircraft pilots physical exercise program to maintain optimal state of fitness, discussing harmful effects caused by nervous and psychic strains
09 p1626 A70-23014
- Metabolic and heart rates determined in experienced and inexperienced pilots during Hiller 12-E and 12-EL helicopters flight through standard maneuvers
09 p1627 A70-23455
- Near visual acuity requirements in flight deck from examination of presbyopic pilots, discussing instrument panel visibility
09 p1628 A70-23469
- Aircraft pilot and captain selection system on basis of STANINE /standard nine/ method of psychological assessment
10 p1825 A70-24504
- Pilots personality studies, considering roles of defense mechanisms, Oedipus complex, infant sexuality, Icarus complex, etc
10 p1825 A70-24660
- Commercial aircraft peak cockpit noise level during cruise and high speed descent, discussing damage risk criteria and interplot speech interference
11 p1991 A70-26275
- Civil airlines training captains heart rate response to simulator stress, base conversion and line training
11 p1992 A70-26519
- Aircraft pilot ability tests validity, applying correction methods in decision making regarding applicant acceptance
[DFVLR-SONDDR-32] 12 p2176 A70-27031
- Aircraft pilot candidates reactions under simulated flight conditions tested using precision coordination analyzer /PCA II/ and instrument coordination analyzer /ICA/
12 p2176 A70-27034
- Airline flight crews training need, emphasizing pilot flight maneuver capabilities for emergencies
13 p2345 A70-28974
- USAF undergraduate pilot trainees responses in prototype spatial orientation trainer
13 p2359 A70-29439
- Multiple emergency noncombat ejections by USAF aircraft pilots, investigating success rates on second ejection relation to injuries on first
13 p2359 A70-29444
- Air traffic control and customer cooperation, considering pilots, gliders, private, business, military and ultralight aircraft and air taxis
14 p2611 A70-30106
- DC-9 aircraft pilot training including jet introduction, DC-9 conversion and route training
14 p2542 A70-30417
- Pilots energy expenditure during jet, propeller and helicopter cargo aircraft flight, using expired air samples
15 p2689 A70-31876
- Airline pilots sleep patterns during worldwide east-west routes, considering modification by irregular duty periods and time zone adaptation
15 p2689 A70-31882
- Predicting retention rate of naval pilots and flight officers beyond initial obligated duty tour based on training performance
15 p2690 A70-31888
- Asymptotic myocardial infarction in USAF flyers detected by annual electrocardiograms
15 p2690 A70-31889
- French airline pilots training program at Montpellier and St-Yan, considering selection, licensing and simulators
16 p2853 A70-33675
- Medical and professional disadaptation in fighter pilots, considering fatigue, digestive disorders, anxiety, absenteeism, efficiency loss and accident proneness
16 p2850 A70-34347
- In-flight evaluation of selected aircraft pilots controllers, noting role in design
[AIAA PAPER 70-925] 17 p3020 A70-35836
- Acrobatic pilots equilibrium behavior in vestibular training, discussing labyrinth reactions and fluid intake role
17 p3041 A70-35919
- Aeroatelectosis and pneumothorax in fighter pilot postflight chest pains, noting decompression role
17 p3041 A70-35920
- Jet pilots psychological survey on troubles, frustrations and personality trends by questionnaire
22 p3978 A70-42876
- Jet pilot EEG radio telemetry showing psychomotor stresses during takeoff and acceleration
22 p3978 A70-42877
- Jet pilot aging effects on physical functions based on medical examinations during six years, noting visual accommodation changes
22 p3978 A70-42878
- Aircraft crew and pilot in-flight workload measurement and simulator
[ICAS PAPER 70-43] 23 p4138 A70-44141
- AIRCRAFT POWER SOURCES**
- U AIRCRAFT ENGINES**
- AIRCRAFT PRODUCTION**
- UK aeronautics R and D, attributing competitive technology lag in military and subsonic civil fields to failure in aims and targets and program cost justification
02 p0402 A70-12306
- Airframe production factors involving choice of materials and fabrication methods, emphasizing weight reduction to increase payload
05 p0854 A70-15925
- Paint technology findings and recommendations for airline aircraft surface finishes emphasizing use of polyurethanes
05 p0869 A70-16106
- Hydraulic jacks for Boeing 747 support during assembly, discussing operation, console, pressure system and safety features
05 p0798 A70-16422
- TU-134 aircraft accessories assembly using fitting and aligning holes drilled into joined elements
05 p0857 A70-17019
- Procurement problems for U.S. Defense Department taking into account fighter F-15 development for USAF
07 p1428 A70-19672
- Soviet book on aircraft engines automated production including plant and machine automatic control, technical and economical factors, etc
08 p1502 A70-20767
- Machine tools used in production of Hawker Siddeley Buccaneer low level strike and reconnaissance aircraft
09 p1691 A70-22608
- Aircraft manufacturing market research including cost compatibility with resources and capabilities
14 p2668 A70-30937
- Quality control role in configuration management, considering quality assurance organization of aircraft manufacturer
14 p2669 A70-31104
- Alloy applications to Boeing supersonic transport airframe and components, discussing materials characteristics and manufacturing processes
17 p3099 A70-34451
- Investment risks and technical impact on aircraft development, world aviation growth and airline costs
17 p3200 A70-34915
- Project management in aircraft manufacturing related to weapon system
17 p3200 A70-34918
- Minimum Equipment List from aircraft manufacturer and airline operations viewpoint
[AIAA PAPER 70-900] 17 p3019 A70-35816
- European A-300-B Airbus program, discussing technical and economical aspects
18 p3213 A70-36509
- Fiber reinforced plastics /FRP/ composites applications in Japanese aircraft production and aerospace industries
20 p3657 A70-40057
- Nondestructive tests for flaw detection during various aircraft production and operation phases
22 p0407 A70-43531
- AIRCRAFT PROTUBERANCES**
- U PROTUBERANCES**
- AIRCRAFT RELIABILITY**
- NDT used in airline and aircraft maintenance emphasizing practicability, reliability and costs
01 p0098 A70-10027
- Aircraft nondestructive testing, discussing radiography requirements, ultrasonic bond testing technique, etc
01 p0104 A70-11319
- FAA engineering approach to SST certification involving airworthiness standards development and coordination with industry and foreign governments
03 p0437 A70-14060
- Product assurance and large aircraft prototype testing in aircraft industry, discussing reliability testing
[DGLR-69-031] 04 p0699 A70-15139
- Forward air control and light attack aircraft survivability design
[SAE PAPER 690707] 05 p0791 A70-15829
- Two place sport gliders development, design reliability and competition requirements
05 p0794 A70-16352
- Aviation maintenance in Britain, discussing continuing airworthiness techniques, development and international aspects
08 p1436 A70-21256
- Airplane dependability on basis of improvements in jet engine, avionics, pilot seat cushions and flight control systems
09 p1611 A70-23453
- Harrier maintainability for reliability with minimum down-time and man hours, discussing servicing, turnaround, role change, inspection and engine changes
10 p1806 A70-24850
- Supersonic transport airworthiness criteria tentatively applied to road characteristics of automobiles
11 p1979 A70-25816
- Reliability and maintainability from airline standpoint, discussing concepts, language and standards for aircraft design
[SAE PAPER 700326] 12 p2335 A70-27460
- International safety standards for SST airworthiness
12 p2161 A70-27599
- Light twin engined aircraft airframe fatigue evaluation program
[SAE PAPER 700219] 13 p2348 A70-29606
- F-111A reliability levels achieved via high reliable hardware and redundancy and alternate mode capability requirements in contract
15 p2676 A70-32638

- Reliability maintenance problems in corporate aircraft operations, discussing equipment calibration, aircraft systems analysis and repair facility selection
16 p2921 A70-33821
- Aircraft design, construction, operation and maintenance improvement efforts by FAA, discussing airworthiness requirements, audit team visits to factories, etc
16 p2842 A70-33824
- System engineering process for survival enhancement of military aircraft to meet stringent requirements of general nuclear war
[AIAA PAPER 70-893] 17 p3019 A70-35810
- FAA research activities on eliminating birds at airports and improving aircraft components resistance to impact, including interagency committee functions on hazard problems
18 p3349 A70-35982
- Aircraft damage from bird impact and alleviating measures, taking into account windshield and intake guard designs, microwave beams for protection and chemical agents as repellent
18 p3212 A70-35987
- S-65-200 Commercial Compound Aircraft design for dispatch reliability and maintenance
19 p3356 A70-38823
- U.S. Army UH-1/AH-1 helicopter maintainability and reliability field program, including statistical data
19 p3356 A70-38827
- Airfreighters maintenance and reliability simulation, modeling specific aircraft designs via input data selection
19 p3357 A70-38835
- Aircraft systems safety requirements, consisting of accident probability, confidence level and demonstration test period
19 p3442 A70-38840
- Flow difference sensor for aircraft hydraulic systems damage vulnerability reduction, discussing design, operation and flight tests results
21 p3750 A70-40786
- NDT for aircraft service life extension, discussing fatigue tests and crack detection
24 p4346 A70-45719
- STOL aircraft FAA airworthiness standards and certification rules, examining noise, control systems, all weather operation, fire protection, handling qualities and performance
[AIAA PAPER 70-1331] 24 p4291 A70-45937
- ### AIRCRAFT SAFETY
- Judicial measures against air piracy, discussing civil aviation legislation, unlawful acts aboard aircraft and international agreements
01 p0220 A70-10374
- National air traffic control system modernization based on Department of Defense military experience to achieve safe and efficient air space utilization
[AIAA PAPER 69-1113] 01 p0137 A70-10616
- CAT remote sensing for advance aircraft warning, using IR instrument to detect turbulence-associated temperature preceding aircraft
01 p0087 A70-10697
- STOL ports in city environments, discussing elevated building design, assisted takeoff and landing equipment and Navy operational safety potential
01 p0057 A70-10715
- Aircraft seat ejection systems using SCID/small column insulated delay/distribution system taking advantage of standard end devices
01 p0035 A70-10718
- Marine safety aspects of helicopters with flotation equipment, considering effects of severe winds and waves, aircraft abandonment procedure, etc
01 p0007 A70-11316
- Aircraft/aerospace fluid systems flexible hose and rigid tube assemblies fire resistance and test requirements
01 p0011 A70-11459
- Three dimensional radar system for automatic tracking all aircraft in terminal area to increase air traffic control system safety and capacity
02 p0332 A70-11967
- Aircraft systems safety analysis, discussing accident causes and prevention, risk allocation, safety equipment, etc
02 p0225 A70-12263
- Flight data recorders, examining present systems and planned improvements
02 p0302 A70-12621
- Radar visual indicator used with scan converter and as synthetic indicator with computer controlled flight safety system
02 p0263 A70-12700
- Fire and explosion suppression technology for aircraft and hypobaric and hyperbaric oxygen-rich atmospheres, discussing time available for suppression action
03 p0437 A70-14056
- Cabin interior materials studied and tested for greater fire resistance, lower smoke and toxic gas by-products and flash fire possibility lessening
03 p0437 A70-14057
- Forward and rearward facing passenger seats effects in postdecompression emergency descent of high speed high altitude aircraft
03 p0437 A70-14061
- Air traffic control problems in avoiding midair collisions, satellite utilization in transatlantic flight control and anticollision devices and procedures
04 p0623 A70-15350
- Aircraft design in commercial air transport safety, discussing turbine blade oxidation and crack prevention, engine cooling, fuels, lightning protection, etc
04 p0624 A70-15644
- Protection methods for increasing ground fire survivability of military aircraft hydraulic systems classified by cost, system and component design criteria
05 p0797 A70-15777
- Emergency auxiliary hydraulic and electric power for commercial and military aircraft control, proposing self contained monofueled turbine system
[SAE PAPER 690658] 05 p0797 A70-15838
- Design safety requirement and philosophy differences distinguishing commercial from military aircraft programs
05 p0792 A70-15855
- Aircraft life support systems and equipment evaluated in Vietnam combat environment, discussing combat ejection conditions, injuries cause and severity, fatalities, etc
05 p0806 A70-16298
- Aircraft wake turbulence effects, using hot film anemometry from nearby towers and penetration by instrumented aircraft
05 p0794 A70-16300
- Safety analysis of VTOL aircraft for passenger transport based on accidental failures caused by technical defects, human error, weather, sabotage, etc
05 p0794 A70-16348
- Aircraft piracy definition by 1958 U.S. Federal Aviation Act, discussing smuggling, escape of prisoners and clandestine airports
05 p0960 A70-16536
- Air piracy, maritime law applicability, definition, internal laws and French law
05 p0960 A70-16538
- Illegal aircraft route diversion by unauthorized persons, discussing air piracy suppression efforts of various international bodies
05 p0960 A70-16539
- Meteorological conditions effects on SST aircraft flight safety and economics, emphasizing stratospheric information for forecasting
06 p1095 A70-17193
- Collision safety standards in helicopter services for shore-to-ship transportation of pilots, stores and spares
06 p1103 A70-17639
- Commercial flight crew oxygen system using mask mounted diluter demand regulator
06 p1002 A70-17715
- Luminescence materials providing primary, secondary and emergency illumination for aircraft safety, discussing application to dials, pannels and anticollision measures
06 p0986 A70-17718
- Emergency in-flight evacuation concepts adapted from military experience considered for application to commercial aircraft
06 p0986 A70-17722
- Damage tolerance as design consideration for aircraft safety and reliability, discussing application of failed single principal member concept to airframe construction
[AIAA PAPER 69-212] 07 p1417 A70-20401
- Air safety and navigation systems data transmission, discussing analog to digital conversion and modulation
09 p1720 A70-22550
- Aircraft certification of supersonic and jumbo jet transports assuring acceptable safety level
09 p1610 A70-22948
- Certification process for supersonic transports taking into account safety and economic considerations
09 p1610 A70-22949
- Fighter flight control design criteria for providing maximum combat effectiveness, safety and survivability without excessive cost or risk
[AIAA PAPER 70-515] 09 p1611 A70-23021
- Human psychophysiological inability to avoid mid-air collisions investigated for aviation safety
09 p1611 A70-23465
- Commercial aviation safety on basis of aircraft accidents relationship to distance covered, considering clear air turbulence and cosmic radiation dangers
10 p1804 A70-24050
- Video role in air transport safety, describing runway visual range (RVR) measurement using TV camera and spaced lights
10 p1889 A70-24507
- Aircraft ground and flight tests effectiveness planning, preparation and conduct for operational safety, noting Flight Controls Development Test Stand
[AIAA PAPER 70-371] 10 p1806 A70-24843
- Flammability resistance and smoke emission characteristics of aircraft interior fire retardant materials under ambient and increased temperature and zero ventilation conditions
[AIAA PAPER 70-400] 10 p1908 A70-24905
- Slush and water hazards on runways, discussing investigation and amelioration methods
11 p2030 A70-25356
- Life support systems general inspection procedures, personal and survival equipment and accessories
11 p1990 A70-25673
- Short range aircraft collision pilot warning indicator for low altitude and closure speeds
11 p2078 A70-25706
- ATC procedures based on system error and aircraft accident probabilities, traffic flow and navigation control and controller manpower
11 p2078 A70-25721
- Transport aircraft flight recorders for parameters essential for operation and aircraft maintenance
11 p2050 A70-25818
- Edwards Committee visualization of insurance as air safety aid, discussing insurer specifications and policy conditions
11 p2153 A70-25858
- Light aircraft-airliner collision avoidance, discussing Time-Frequency Collision Avoidance System cost restriction, Pilot Warning Instruments, etc
11 p2079 A70-25872
- Aircraft control through airspace from takeoff to landing, discussing role of Department of Transportation Air Traffic Control Advisory Committee
11 p2080 A70-26256
- International safety standards for SST airworthiness
12 p2161 A70-27599
- Stacked, vertically polarized collinear arrays of independently fed omnidirectional antennas for flight testing Doppler radar aircraft warning system
12 p2199 A70-27968
- Longer runways for increased airport safety indicated from data concerning overruns, undershoots and veering, discussing certification testing during takeoff and landing
12 p2208 A70-27994
- Civil aircraft weather radar for ground collision hazard warning
13 p2447 A70-28548
- Aircraft escape systems, discussing F-111 system capabilities and development
13 p2345 A70-28969
- Aircrew equipment assemblies taking into account altitude, flight acceleration, environment, escape and survival
13 p2345 A70-28971
- Airline flight crews training need, emphasizing pilot flight maneuver capabilities for emergencies
13 p2345 A70-28974
- Multiple emergency noncombat ejections by USAF aircraft pilots, investigating success rates on second ejection relation to injuries on first
13 p2359 A70-29444
- Climatology of safe threshold Mach number and airplane ground speed for boomless supersonic cruise, considering San Francisco-New York route
14 p2530 A70-30606
- Passenger aircraft structures accelerated testing for safety and fatigue durability under operational conditions, describing tests planning and evaluation
15 p2673 A70-31541
- SST system safety program, discussing federal office structure, planning and control, design support, integration and evaluation, requirement analysis and failure recurrence control
15 p2675 A70-32214
- C-5 aircraft failures and system safety program, noting landing gear, pressure equalization, visor nose, crosswind computer, nacelle separation and propulsion design
15 p2675 A70-32215
- Air transport safety, applying experience from space programs
15 p2692 A70-32227
- Airport safety standards for overall system including aircraft, ATC, navigation, runways, etc
15 p2717 A70-32229
- Quality assurance R and D for product design and operational integrity in manned space flight, noting space developments application to aircraft safety
15 p2676 A70-32231
- Flight Impact Simulator for simulating bird strikes and bird-proofing of aircraft
16 p2888 A70-33290
- Emergency auxiliary hydraulic and electric power for commercial and military aircraft control, proposing self contained monofueled turbine system
[AIAA PAPER 70-651] 16 p2970 A70-33616
- Air safety R and D and future safety standards
16 p2842 A70-33816
- Book on air safety and commercial aviation accidents
16 p2842 A70-33964
- Blinking warning lights for air navigation, signaling of obstacles and glider onboard marker lights
16 p2889 A70-34302
- High powered high speed helicopters autorotation entry characteristics, noting capability of meeting control time delay requirement
17 p3014 A70-34715

Fatal general aviation accidents examined by pathologists, determining pilot incapacity, accident sequence, aircraft design modification and crash protection performance

17 p3033 A70-35567

Safety in airline operations, discussing roles of aircraft designer and pilot
[AIAA PAPER 70-907]

17 p3019 A70-35819

Automatic landing system assurance of DH 121 aircraft schedule all-weather regularity through high safety level via redundancy

17 p3022 A70-35856

Air safety research effects on operations, training procedures and materials, discussing gust loads, on-board data recording devices, human error, etc

17 p3022 A70-35859

Nationwide air traffic control, using radar network and real time computer flight information centers for air safety

17 p3135 A70-35880

Data acquisition system applications philosophy, discussing data integrity, expansion facility, flight safety, etc

18 p3258 A70-36339

Optimum approach and departure paths for VTOL aircraft simulated by hybrid computer under constraints
[AIAA PAPER 69-209]

18 p3213 A70-36452

Airport capacity and terminal area safety increase by scanning beam instrument landing system, discussing automatic guidance trajectory example

19 p3464 A70-37913

Aircraft systems safety requirements, consisting of accident probability, confidence level and demonstration test period

19 p3442 A70-38840

ATC by scanning beam ILS and onboard control systems, increasing airport capacity and terminal area safety
[AIAA PAPER 70-1033]

20 p3666 A70-39504

Human error as factor in aircraft accidents, considering man machine incompatibility and prevention measures

21 p3771 A70-41723

Airborne three dimensional area navigation equipment for reducing mid-air collision exposure and for raising landing safety in terminal areas

22 p4066 A70-42296

Air traffic safety problems, discussing satellite radio beacons applications to aerial navigation

22 p4066 A70-42652

Aircraft hijacking epidemiology from preventive viewpoint

22 p3981 A70-43698

Collision Avoidance System /CAS/ and Proximity Warning Indicator /PWI/ for preventing midair aircraft collisions

23 p4194 A70-44175

Flotation device for infants and small children incorporating life support and survival capabilities for aviation and marine applications

23 p4153 A70-44480

Air hijacking as aviation safety problem, discussing history, prevention and detection methods and equipment, law enforcement, etc

23 p4285 A70-44496

General aviation expansion and competitive position dependence on safety and utility improvements and simultaneous cost reductions
[AIAA PAPER 70-1220]

24 p4291 A70-45953

STOL aircraft field length, terminal area performance and minimum handling qualities requirements for safe and efficient operations
[AIAA PAPER 70-1240]

24 p4292 A70-45960

Helicopter hazards elimination measures, considering crash resistant fuel systems, flotation devices, redesigned seats, in-flight escape, etc

24 p4292 A70-46383

AIRCRAFT SPECIFICATIONS

Conventional inertial gyro modified to provide specification performance for aircraft environments
[AIAA PAPER 70-10312]

01 p0086 A70-10312

Design specifications for low noise turbofan engine used on long range subsonic transport aircraft
[ASME PAPER 69-WA/GT-7]

04 p0734 A70-14888

Boeing 747 aircraft family design options related to utilization, performance and economics, discussing development through large turbofan engine availability

04 p0624 A70-15382

Civil air transport passenger escape devices design and installation criteria
[SAE-ARP-495A]

07 p1191 A70-18805

ICAO Juridical Council criteria for nonnational aircraft registration, discussing international airlines recourse to Article 77 of Chicago Convention

07 p1428 A70-19105

Military specification revision of Flying Qualities of Piloted Airplanes evaluated by flight test including Flight Path Stability and Roll Rate Oscillation techniques
[AIAA PAPER 70-372]

10 p1806 A70-24930

Airspace and airport use at terminals, discussing segregation of aircraft by performance categories
[SAE PAPER 700229]

11 p2153 A70-25899

International Civil Aviation Organization /ICAO/ work on bird hazard reduction, including aircraft airworthiness specifications, bird data dissemination, etc

18 p3349 A70-35997

Aircraft handling qualities specifications and definitions evolution based on test pilot rating correlation with engineering data and piloting ease evaluation with transfer functions
[ICAS PAPER 70-19]

23 p4138 A70-44114

OV-10A forward air control and light attack aircraft design, specifications and performance
[SAE PAPER 700837]

24 p4290 A70-45883

AIRCRAFT STABILITY

NT HOVERING STABILITY

Aerodynamic derivatives in equations of motion governing aircraft longitudinal short period motion estimated using least squares methods

02 p0224 A70-11866

Wing-fuselage interference influence in aircraft dihedral effect, discussing role of velocity direction on wing

03 p0406 A70-13020

Dynamic stability of flexible aircraft fuselage in controlled supersonic flight at zero angle of attack, basing analysis on elastic oscillation equations
[AIAA PAPER 69-1137]

03 p0579 A70-13418

Airplane stability and control technology, considering flight research, flying qualities, compressibility and aeroelastic phenomena
[AIAA PAPER 69-1137]

03 p0411 A70-13636

Orthogonality of aircraft natural vibration modes by calculating complete matrix of generalized masses
[DGLR-69-59]

04 p0774 A70-15150

Stability characteristics from flight test results using regression analysis

04 p0623 A70-15155

Pilot response to stability augmentation system failures and design implications
[AIAA PAPER 68-819]

04 p0624 A70-15379

Flying qualities criteria and piloted simulator studies during development and flight testing of stability augmentation system for B-52 aircraft
[AIAA PAPER 68-1066]

04 p0624 A70-15380

Longitudinal stability derivatives prediction for rigid and elastic airplanes, using influence coefficient method
[AIAA PAPER 69-131]

04 p0624 A70-15383

Aerodynamic characteristics, stability and controllability of swept wing and delta wing supersonic aircraft at subsonic velocities

05 p0796 A70-16966

Supersonic aircraft control and stability at low speeds, discussing sweepback angle, low aspect ratio, lift, etc

05 p0797 A70-17088

VTOL aircraft control and stability with emphasis on flight characteristics and man machine interaction
[ONERA-TP-786]

05 p0809 A70-17089

Variable sweep aircraft aeroelastic stability, considering wing-tail interaction flutter
[AIAA PAPER 70-80]

06 p1170 A70-18162

Incompressible flow past airfoils with oscillating jet flaps used as rapid lift and momentum generators in aircraft gust load alleviation and mode stabilization
[AIAA PAPER 70-79]

06 p0975 A70-18196

Aircraft flutter equations solution by reduced frequency scanning method
[ONERA-TP-786]

06 p1171 A70-18470

Longitudinal stability of V/STOL aircraft at low speeds, discussing three tilt wings and quad ducted propeller configurations
[AIAA PAPER 69-194]

07 p1195 A70-20410

State observers /filters/ construction in multivariable control systems using phase transformation
[ONERA-TP-786]

08 p1478 A70-20778

Flight tests to investigate external munitions carriage effect on aircraft stability and control

08 p1437 A70-21733

Air transport total in-flight simulator /AT/TIFS/ equipped with six degree of freedom variable stability system for aircraft development and pilot training
[ONERA-TP-786]

08 p1437 A70-21736

In-flight investigation to determine effect of variations in bank angle control parameters on cruise flight handling qualities
[ONERA-TP-786]

08 p1437 A70-21738

Swept and delta wing supersonic military aircraft stability and controllability, discussing variation in maximum lift coefficient as function of Mach number
[ONERA-TP-786]

09 p1611 A70-23129

Clear air turbulence effect on supersonic aircraft safety and comfort, noting shallow zones and effects of topography and thunderstorms

10 p1912 A70-24506

Helicopter blade flapping torsion flutter behavior analysis showing stabilization effect in forward flight
[ONERA-TP-786]

10 p1958 A70-24559

Statistical methods for flying quality research concerning sailplane dynamic stability, maneuverability, sensitivity, rolling and pilot induced oscillations
[ONERA-TP-786]

10 p1805 A70-24582

Aircraft performance, stability and control testing from nonsteady flight measurements, ascertaining repeatability of results
[SAE PAPER 700236]

11 p1980 A70-25905

Static longitudinal stick free and stick fixed aircraft stability equations for several configurations and power effects
[SAE PAPER 700238]

11 p1981 A70-25907

Light aircraft lateral and longitudinal response to atmospheric turbulence, presenting equations and charts for design load calculations
[SAE PAPER 700239]

11 p1981 A70-25908

Performance, stability and control improvements of light aircraft, applying computerized parametric analysis
[SAE PAPER 700240]

11 p1981 A70-25909

Aircraft all-movable stabilator computer aided design for optimized structural weight and performance

12 p2319 A70-27137

Aircraft lateral and longitudinal motion stability in steady rolling, deriving inertia cross coupled stability criterion

13 p2347 A70-29445

Wind tunnel and flight test methods for determining transonic buffet characteristics on model F-4 aircraft
[AIAA PAPER 70-584]

13 p2348 A70-29886

VTOL aircraft stability augmentation system design based on control theory state variable methods, using minimum power levels

14 p2531 A70-30856

V/STOL control systems design for aircraft stabilization and pilot workload reduction

14 p2615 A70-31278

Supersonic aircraft lateral stability and controllability design, discussing directional and weathercock stabilities

15 p2673 A70-31625

Rumanian book on flight stability and control covering Liapunov general stability theory, control systems, stability models, etc

15 p2673 A70-31695

Supersonic aircraft stability and controllability during turns about longitudinal and vertical axes

16 p2840 A70-33204

Aircraft stability augmentation systems design by parameter optimization techniques and feedback selection

16 p2840 A70-33342

Nonlinear digital programming techniques for airplane stability augmentation systems design
[ONERA-TP-786]

16 p2840 A70-33343

SST inlet steady state pressure defects and random pressure fluctuations determining TF30 engine/inlet compatibility
[AIAA PAPER 70-632]

16 p2834 A70-33530

In-flight thrust reverser for tactical/attack aircraft, discussing system influence on airplane stability and control
[AIAA PAPER 70-699]

16 p2841 A70-33561

Book on aerodynamics for engineering students covering hydro- and aerostatics, flow theory, propulsion principles, aerofoil theories, aircraft performance and stability, etc

16 p2838 A70-33953

Airplane stability and control technology, considering flight research, flying qualities, compressibility and aeroelastic phenomena

18 p3213 A70-36441

Pilot induced oscillation rating regression analysis, examining time delay, slope after and time to first peak and stick force per g

18 p3213 A70-36444

Ground vibration testing for aircraft and missile flutter prevention
[ONERA-TP-816]

18 p3339 A70-36508

Static stability requirements relaxation and wing control devices additions for alleviating wing root bending moments in controls configured vehicle /CCV/ design concepts

19 p3355 A70-37395

Helicopter stabilization systems design, synthesizing controllers by modal control theory
[AIAA PAPER 70-1036]

20 p3560 A70-39501

Aircraft stability design by parameter plane technique, using for YO-3A aircraft
[AIAA PAPER 70-983]

20 p3560 A70-39546

Full scale aircraft spinning motion, computing static, damping, cross and acceleration aerodynamic characteristics for antispin devices
[AIAA PAPER 70-946]

20 p3561 A70-39581

VTOL aircraft longitudinal motion automatic stabilization in presence of turbulence and internal disturbances, using rotors and jet engines

20 p3561 A70-39838

Automatic aircraft lateral motion stabilization during flight in perturbed atmosphere by HF invariant systems

20 p3670 A70-39839

Automatic control systems for aircraft approach to landing path and subsequent stabilization on trajectory, compensating for cross wind action and radio noise disturbances

20 p3561 A70-39842

Aircraft rolling motion /eigenmotion/ in flight at small angle of attack following initial disturbance, discussing response to control action

22 p3961 A70-42515

- Fighter aircraft higher order control system dynamics effects on longitudinal handling qualities evaluated by inflight simulator for role of pilot induced oscillations tendencies 22 p3961 A70-42711 [AIAA PAPER 69-768]
- Small airplane unsteady motion downwash angle at low speeds, comparing results from rectilinear steady flights 23 p4138 A70-44108 [ICAS PAPER 70-25]
- Hypersonic aircraft stability and control problems, discussing bulky engines and air intake and exhaust geometry 23 p4138 A70-44128 [ICAS PAPER 70-17]
- Elastic fuselage flight vehicle dynamic stability at supersonic speeds, using automatic pilot stabilization 23 p4139 A70-44157
- ONERA calculations in aeroelasticity including lifting surface optimization, control surface vibration, pressure fields, aircraft transfer functions and panel flutter 23 p4274 A70-44762
- Fluidics in naval avionics, discussing CH-46A helicopter stability augmentation and approach power compensator for carrier-based aircraft 24 p4293 A70-45428
- Hybrid fluidic damper control for yaw axis stability augmentation of commercial jet aircraft 24 p4294 A70-45853 [SAE PAPER 70-794]
- Hydrofluidics flight controls for aircraft stability augmentation systems, noting component performance, transfer functions and operation 24 p4294 A70-45854 [SAE PAPER 70-793]
- AIRCRAFT STRUCTURES**
- NT AIRFRAMES**
- NT FUSELAGES**
- NT PLASTIC AIRCRAFT STRUCTURES**
- Transfer matrix method analysis of dynamic behavior of beam structures applied to single rows of aircraft panels 01 p0209 A70-11200
- HF endurance tests of Al sheet alloy used in welded aircraft structural components, plotting curves for heat treated and untreated specimens 02 p0315 A70-11658
- Brazed plate-fin superalloy panels suitable for hydrogen-cooled structures, discussing fabrication techniques, performance tests and pressure containment and fatigue characteristics 02 p0306 A70-11930
- Aircraft structural damage due to high speed hail-stone impact, considering aircraft design modifications 02 p0386 A70-11938
- Automated structural design program to treat stress, displacement, gauge and cross sectional constraints, discussing applications to aircraft structures 02 p0386 A70-11944
- Commercial aircraft design, considering structural allowances effect on economics, using shear web analysis program as example 02 p0225 A70-11947
- Harmonic vibration testing of aircraft structural nonlinearities caused by dry friction, describing pitch control system 02 p0387 A70-12215
- U.S. rotorcraft research regarding materials and engine technologies of conventional and compounded helicopters 02 p0226 A70-12314
- Aircraft structures service life estimation, comparing results of serviceability tests, solo flight tests, programmed random load tests and linear defect buildup hypothesis 02 p0391 A70-12854
- Structural aluminum alloy developed for Concorde Mach 2.2 flight, discussing cold mechanical properties, zero creep and fatigue resistance 04 p0706 A70-15041
- Three dimensional photoelastic model for structural analysis of aircraft bulkhead to improve fatigue life 05 p0937 A70-16376
- Dynamic stability of complex aeroelastic structures including V/STOL aircraft using simplified technique, noting application to tilt rotor aircraft design 06 p1170 A70-18119 [AIAA PAPER 70-22]
- Band polishing machines slave mechanisms and programmed controllers, describing helicopter longrons finishing process 07 p1291 A70-18829
- Laboratory electronics role in Concorde aircraft structural and acoustical fatigue analysis, flight simulation and flight studies 07 p1250 A70-19745
- Natural frequencies and modes of tapered swept back rudder fin of aircraft using vibration analysis 07 p1417 A70-20417
- Aircraft wing ribs tangents plotting procedure using Monge diagram 08 p1507 A70-21197
- Nondestructive process control analyzer for spot welds in aircraft structural components, monitoring expansion, current and spotweld properties 08 p1507 A70-21486
- Fiber composites-Ti alloy adhesive, rivet and combined joints for aircraft applications, noting fiber orientation role in joint tensile strength 08 p1509 A70-21905
- Nondestructive test procedures development and implementation for bond strength of honeycomb sandwich and metal-metal adhesive bonded structures of F-5 and T-38 aircraft 09 p1692 A70-22798
- Aircraft surface temperature measured with airborne IR TV system 09 p1686 A70-23754
- Adhesive bond stress of aircraft structural joints between metal plates of variable cross section designed for shear 10 p1957 A70-24296
- Metal working technology of Ti and alloys for structural parts fabrication for Concorde aircraft, describing laser cutting, electron beam welding, explosive forming, etc 10 p1895 A70-24594
- Vibration behavior theory for elastomechanical systems applied to aircraft and space constructions 10 p1961 A70-25054
- Aircraft arresting hook response to impact regarding beam flexibility and internal damping using numerical wave propagation methods 10 p1963 A70-25069
- Aircraft structures fatigue durability estimations, studying crack propagation rates under cyclic loadings by fail-safe method 11 p2132 A70-25624
- Aircraft structures fatigue, discussing prediction of response to fatigue environment, load distribution, fatigue life, crack propagation rates and residual strength 11 p2132 A70-25677
- ARAVA aircraft free-free vibrational characteristics evaluation by integral-aircraft lumped mass analytical method verified by ground resonance test 11 p1979 A70-25688
- Aircraft multicell structures venting problem and pressure calculation 11 p2134 A70-25863
- Adhesive bonding for structural efficiency, lower weight, reduced production costs and improved appearance in general aviation industry 11 p2134 A70-25893 [SAE PAPER 70-221]
- Solid state diffusion bonding techniques for aerospace Ti structural components 12 p2242 A70-27093
- Experimental stress analyses for aircraft design enhancing structural fatigue strength, using S-N diagrams and photoelastic models 12 p2318 A70-27128
- Wing and empennage structures automated fully stressed design procedures, discussing application to supersonic aircraft stabilizer 12 p2319 A70-27136
- Collection of papers on aircraft design and structural research 13 p2337 A70-28476
- Aircraft structure fabrication combining unidirectional strength and stiffness of B composite with metal, including test and weight/cost data 13 p2418 A70-28777
- Aluminum-boron composites for aircraft adapter fabrication 13 p2435 A70-29247
- Turbulent boundary layer loading function for use with finite element structural analysis system applied to elastic aircraft structures random vibration 14 p2658 A70-30853 [AIAA PAPER 69-20]
- Corrosion resistant paint systems for aircraft structural parts under severe environmental conditions simulated in carrier test stand 14 p2598 A70-31292
- Passenger aircraft structures accelerated testing for safety and fatigue durability under operational conditions, describing tests planning and evaluation 15 p2673 A70-31541
- Sonic boom variation with aircraft geometry, volume, weight, weather and environment conditions, noting effects on structures and people 16 p2840 A70-32947
- Fixed and variable sweep wing structure computerized design optimization 16 p2869 A70-33506 [ASME PAPER 70-DE-41]
- Reinforced polymer composites design for aircraft structures 16 p2939 A70-33518 [ASME PAPER 70-DE-67]
- Co base superalloys for aircraft structures and parts, discussing temperature stability, corrosion resistance, creep, fatigue and strength 16 p2932 A70-33705
- Electronic data processing by aircraft manufacturer, handling structural and performance problems 16 p2843 A70-34350
- Ti alloy forgings for aircraft industry, utilizing high strength/weight ratio 17 p3097 A70-34357
- Ti hot forming, discussing sheet use as aircraft structural material 17 p3098 A70-34444
- Aircraft structural materials, considering high strength steels Al and Ti alloys 17 p3124 A70-34675
- Materials selection for cost effectiveness in 1980s airframe applications 17 p3199 A70-34819 [AIAA PAPER 70-870]
- Crack propagation, fatigue damage and interaction effects in aircraft structures and materials under flight simulation loading 17 p3185 A70-34924
- F-111 high strength steel design experience concerning wing, fuselage and empennage support structure 17 p3018 A70-35803 [AIAA PAPER 70-884]
- Thermal effects on aircraft elastic vibration mode shapes, recommending investigation to develop analysis and design tools 18 p3213 A70-36459
- HF endurance tests of Al sheet alloy used in welded aircraft structural components, plotting curves for heat treated and untreated specimens 19 p3452 A70-38431
- Adhesive bonded aircraft structures, discussing methods and requirements for establishment and control of manufacturing procedures 19 p3438 A70-38594
- Alloys for aircraft structures design, considering materials strength, corrosion resistance, producibility and cost 20 p3648 A70-39414
- Hydraulic load loops with random force signal for aircraft structures endurance testing 20 p3593 A70-39913
- Beta III Ti alloy for aircraft fasteners, describing microstructure and mechanical properties 20 p3650 A70-39966
- Finite element stiffness matrix technique for composite structures, discussing airplane component design program 20 p3730 A70-40040
- Aircraft, rocket or other rigid or flexible structure, computing inertial constants based on measurements of generalized masses of natural modes 21 p3935 A70-41408
- High strength glass for aircraft structures, discussing applications to passenger cabin windows 21 p3843 A70-41891
- Optimum light construction design of glider wings, considering spar weight, aluminum honeycomb structure and repair 22 p3962 A70-42961
- Load cycle sequences for full scale aircraft structures and components fatigue testing 23 p4266 A70-44101 [ICAS PAPER 70-32]
- Aircraft structure fatigue load monitoring, discussing strain gage installation in critical areas 23 p4267 A70-44102 [ICAS PAPER 70-31]
- Aircraft wing box beams bending tests to failure loads, considering crushing pressure, bulkhead flexural deformations, structure initial imperfections and instability phenomena 23 p4267 A70-44103 [ICAS PAPER 70-33]
- Fatigue strength of stiffened aircraft panels subjected to repeated buckling by compression loads 23 p4267 A70-44132 [ICAS PAPER 70-35]
- Aircraft structures acoustic fatigue testing, discussing test facilities, environment simulation, etc 23 p4269 A70-44329
- Elastic coupling and dynamic equations for flight elastomechanical vibration systems, including tip tanks on aircraft wings 23 p4274 A70-44767
- Aircraft structures service life estimation, using Ir-192 and Tm-170 gamma ray radiography 24 p4346 A70-45725
- Aircraft design for low weight, discussing structural failures 24 p4425 A70-45917 [AIAA PAPER 70-1232]
- AIRCRAFT TIRES**
- Aircraft tires tread design for improved adhesion under wet runway conditions 14 p2532 A70-31336
- Large wheel and tire imperfection effects on nosegear parametric shimmy instability, using Mathieu equation 18 p3213 A70-36455
- AIRCRAFT WAKES**
- NT HELICOPTER WAKES**
- NT SLIPSTREAMS**
- Aircraft wake turbulence effects, using hot film anemometry from nearby towers and penetration by instrumented aircraft 05 p0794 A70-16300
- Carbon dioxide CW laser-Doppler velocimeter for detecting aircraft wing tip trailing vortices by measuring atmospheric aerosols backscatter 12 p2249 A70-27630
- Jet transport wakes resulting from high engine thrusts considered hazardous to following aircraft, discussing multiple-instrumented runways for measuring visibility 12 p2162 A70-27995

AIRFIELD SURFACE MOVEMENTS

- Airport surface traffic system analysis, discussing control and guidance isolation, information acquisition/processing and response actions [AIAA PAPER 69-1086] 01 p0137 A70-10630
- Computerized navigation system for controlling aircraft movement on airports under zero visibility conditions 02 p0274 A70-11978
- Instrument landing system techniques based on hyperbolic geometry and correlation detection for terminal area traffic control, discussing applications 06 p1102 A70-17637
- GPSS simulation for airport capacity, analyzing aircraft ground traffic flow characteristics and developing expansion schemes minimizing investment 08 p1481 A70-20929
- Control system, operational procedures, aircraft guidance and runway design for increasing runway capacity, noting roles of automation and reduced separation [SAE PAPER 700280] 12 p2206 A70-27440
- Forced vibration in taxiing aircraft interaction with ground structure 14 p2563 A70-30699
- Visual display and automatic taxi guidance system testing for improved aircraft docking accuracy [AIAA PAPER 70-916] 17 p3064 A70-35828
- Airport capacity and layout, considering air traffic increase, runway occupancy, taxiway and computer simulation 19 p3468 A70-38636

AIRFOIL CHARACTERISTICS

- U AIRFOILS**
- AIRFOIL FENCES**
- Potential flow past plane theoretical airfoil lattices 03 p0407 A70-13448

AIRFOIL PROFILES

- NT WING PROFILES**
- NT WING SPAN**
- Airfoil cascade blade design by iteration method equating normal velocity distribution about contour with imposed tangential velocity 01 p0001 A70-10263
- Schlieren system converted into Kraushaar diffraction grating interferometer with isolated optical platform, considering applications to supersonic flow over airfoil shapes 04 p0689 A70-15016
- Computer program to calculate ideal rotating fluid flow in arbitrary airfoil lattice on axisymmetric stream surface in variable thickness layer 04 p0617 A70-15239
- Closed form solution of modified inviscid transonic equation embodying character of viscous- transonic equation applied to shockless transonic airfoils [AIAA PAPER 70-187] 06 p0970 A70-18096
- Electret microphones application for pressure fluctuations measurements on thin aerodynamic profiles noting operation, vibration insensitivity, robustness and cost 06 p1071 A70-18473
- Pressure distribution measurement over profile by means of pneumatically activated inductive sensor 07 p1188 A70-19084
- Plane rigid airfoil frequency response in incompressible potential flow using simple equivalent oscillator based on Theodorsen function 07 p1404 A70-19232
- Velocity distribution around isolated and cascaded airfoils in plane potential flows of incompressible fluid determined by use of nonsingular integrals 11 p1974 A70-25781
- Singularity carrier auxiliary curves for design calculation of airfoil cascades, discussing existence theorems and case of thin profiles 11 p1974 A70-25783
- Singularity carrier auxiliary curves for design calculation of airfoil cascades, discussing profiles with small and large arcs 11 p1974 A70-25784
- Velocity distribution of plane airfoil cascade given by geometry, using method of least squares 11 p1974 A70-25785
- Airfoil cascades flow for given profile shape by singularity method, obtaining velocities 11 p1975 A70-25790
- Pressure distribution in two dimensional incompressible potential flow on Joukowski airfoils with normal upper surface spoilers, emphasizing potential flow theory [AIAA PAPER 67-737] 12 p2155 A70-27193
- Numerical solutions of thick cambered jet flap in ground effect for flat plate and diamond shaped airfoil [AIAA PAPER 69-738] 12 p2155 A70-27199
- Airfoil sections in transonic flow, discussing wind tunnel tests on mixed flows and shock waves [ONERA TP-815] 13 p2341 A70-29139
- Blockage ratio effect on supersonic zone with shock layer interaction on nonlifting circular arc airfoils at transonic speeds in wind tunnels 16 p2835 A70-33674
- Plane diffuser grid profiles for subcritical velocities of oncoming flow, using wind tunnel test data 18 p3205 A70-36129

- Perfect and dissociating gas nonstationary supersonic flow around sharp profile of finite thickness analyzed by linearization and method of characteristics 19 p3351 A70-37242
- Thin airfoil theory in magnetoaerodynamics, considering steady two dimensional flow of compressible perfectly conducting inviscid fluid in presence of uniform magnetic field 19 p3351 A70-37597
- Slender hypersonic airfoil shape optimization for maximum lift to drag ratio for given profile area, chord and free stream conditions 19 p3352 A70-38304
- Turbulent near wake of symmetrical airfoil, determining universal constant in mixing length formula for inner wake 20 p3559 A70-40276
- Optimum pressure distribution and airfoil profiles for maximum lift without separation in incompressible flow determined by second order theory [AIAA PAPER 69-739] 22 p3959 A70-42704
- Aerodynamic characteristics of elliptical airfoils with jet circulation control for VTOL rotors including dual jets and cyclic results [AIAA PAPER 69-741] 22 p3959 A70-42705
- Lifting quasi-elliptical airfoils with supercritical shock free flow, discussing Nieuwland hodograph theory to compute profile number [ICAS PAPER 70-15] 23 p4132 A70-44126
- Lift determination of slender curved periodically recurring airfoils array in plane potential flow of inviscid incompressible fluid 23 p4133 A70-44158

AIRFOIL SECTIONS

- U AIRFOIL PROFILES**
- AIRFOIL THICKNESS**
- U AIRFOIL PROFILES**
- AIRFOILS**
- NT AERIAL RUDDERS**
- NTAILERONS**
- NT AIRFOIL FENCES**
- NT CAMBERED WINGS**
- NT CARET WINGS**
- NT CRUCIFORM WINGS**
- NT DELTA WINGS**
- NT ELEVATORS [CONTROL SURFACES]**
- NT ELEVONS**
- NT FIXED WINGS**
- NT FLAPS [CONTROL SURFACES]**
- NT FLEXIBLE WINGS**
- NT HORIZONTAL TAIL SURFACES**
- NT JET FLAPS**
- NT LAMINAR FLOW AIRFOILS**
- NT LIFTING ROTORS**
- NT LOW ASPECT RATIO WINGS**
- NT PARAWINGS**
- NT PROPELLER BLADES**
- NT RECTANGULAR WINGS**
- NT RIGID ROTORS**
- NT RIGID WINGS**
- NT ROTARY WINGS**
- NT SLENDER WINGS**
- NT SPOILERS**
- NT SUPERSONIC AIRFOILS**
- NT SWEEP WINGS**
- NT SWEEPBACK WINGS**
- NT TABS [CONTROL SURFACES]**
- NT THIN AIRFOILS**
- NT THIN WINGS**
- NT TILTING ROTORS**
- NT TIP DRIVEN ROTORS**
- NT TRAILING-EDGE FLAPS**
- NT TRAPEZOIDAL WINGS**
- NT TWISTED WINGS**
- NT VARIABLE SWEEP WINGS**
- NT WING FLAPS**
- NT WINGS**
- Aerodynamics of conventional aircraft high lift devices, considering effect of leading edge geometry on lift coefficient at stall of plain and flapped airfoils 01 p0001 A70-10046
- Sound radiation from airfoil in turbulent jet flow, discussing direct correlation of fluctuating lift 01 p0004 A70-11192
- Electronic gauging machine for multipoint measurement at preselected points around turbine blade airfoil produced by electrochemical machining 01 p0105 A70-11397
- Two dimensional cascade tests of turbine blade airfoil plotted by Legendre hodograph method, discussing pressure distribution measurements 03 p0410 A70-14272
- Transient plane disturbance of stream angular to applied magnetic field, discussing relationship to airfoil and Alfvén waves 04 p0615 A70-15093
- Inviscid flow through staggered airfoil cascades in oscillatory and distorted flow simulating axial flow compressor [AIAA PAPER 70-131] 06 p0969 A70-18049
- Incompressible flow past airfoils with oscillating jet flaps used as rapid lift and momentum generators in aircraft gust load alleviation and mode stabilization [AIAA PAPER 70-79] 06 p0975 A70-18196

- Unsteady airfoil stall in incompressible flow, including pitch rate induced accelerated flow effect on leading edge and trailing edge stall [AIAA PAPER 70-77] 06 p0976 A70-18237
- Dynamic behavior of subcritical fluid flow past airfoils, expanding flow potential to obtain formulas for velocities, local Mach numbers and pressure 08 p1433 A70-21173
- Airfoil research in S-10 French wind tunnel for two dimensional flow, noting Reynolds and Mach number ranges [ONERA-TP-766] 08 p1433 A70-21843
- Airfoil analysis and synthesis, discussing computer graphics application to low speed shape and improved pressure distribution 08 p1594 A70-21867
- Inviscid hypersonic small disturbance theory applied to flow behind concave and convex exponential shock waves, determining supporting two dimensional airfoil surfaces 09 p1605 A70-23220
- Symmetrical, asymmetrical and three dimensional sonic flows past finite obstacle, investigating regions upstream and downstream from shock waves for airfoil 10 p1800 A70-24134
- Steady two dimensional cavity flow past sharp-edged airfoil and blunt nosed obstacle, using linearization hypothesis 10 p1801 A70-24193
- Flow characteristics of airfoil rotating cascades in variable width channel in incompressible liquid 11 p1975 A70-25789
- Parafail models development, comparing characteristics to kites and round and kite balloons 11 p1981 A70-26045
- Flat-top airfoil determined for lower surface shape to maximize lift drag ratio at hypersonic speeds using calculus of variations 11 p1977 A70-26397
- Aerofoil free vibrations with fixed center of gravity in incompressible potential flow under representative previous histories effect 12 p2328 A70-28214
- Heaving airfoil wakes visualization with jet flap augmented lift, measuring vortex street parameters 13 p2338 A70-28821
- Two dimensional unsteady incompressible fluid flow through airfoil lattice 13 p2389 A70-29491
- Aerodynamic characteristics of supercavitating airfoil, investigating effect of free surface of unsteady fluid flow with stream separation, solving boundary value problem 13 p2391 A70-29650
- Cylinders and airfoils drag tests and simulation in two dimensional sheared flow, considering shapes optimization [AIAA PAPER 70-576] 13 p2342 A70-29893
- Integral equation for transonic small disturbance flow applied to plane flows over lifting airfoils 15 p2673 A70-32768
- Aerodynamic forces exerted by compressible fluid on airfoil cascade in subsonic potential flow 16 p2833 A70-33075
- Book on aerodynamics for engineering students covering hydro- and aerostatics, flow theory, propulsion principles, aerofoil theories, aircraft performance and stability, etc 16 p2838 A70-33953
- Moving skin boundary layer control on airfoil achieved by moving wetted surface in streamwise direction [AIAA PAPER 70-881] 17 p3010 A70-34808
- Aerofoil section characteristics in shear flows of arbitrary velocity profile calculated by Glauert image method 18 p3205 A70-35957
- Airfoil trailing edge stall in laminar flow, investigating circulation around flat plate 18 p3205 A70-36194
- Dynamic airfoil stall simulation in wind tunnels, considering pitch rate, Reynolds number, oscillation and test equipment effects [AIAA PAPER 70-945] 20 p3558 A70-39582
- Equations system for determining constants in Sedov integral for conformal mapping of polygonal airfoil lattice onto Riemann surface 20 p3658 A70-39767
- Subsonic air flow around airfoil in wind tunnel, detecting density gradients by pulsed ruby laser holographic visualization 21 p3822 A70-40809
- Subcritical viscous flow around arbitrary airfoils, calculating boundary layer effect on pressure distribution from inviscid flow approximation 21 p3744 A70-40924
- Flat plate airfoil unsteady lift due to chordwise velocity perturbations, using Horlock frozen gust pattern theory 22 p3957 A70-42303
- Low speed airfoil two dimensional testing in wind tunnel with slotted wall, examining lift, drag and pitching moments [ICAS PAPER 70-08] 23 p4132 A70-44119

- Plane transonic flow around airfoils, using hodograph based methods for shock free flow and finite difference methods for flow with shock waves [ICAS PAPER 70-12] 23 p4132 A70-44123
- German monograph on airfoil and wings aerodynamic coefficients calculations, showing advantages of analog computers based on singularity theory and distance functions 24 p4287 A70-45097
- Aerodynamic forces and torque on airfoil in potential jet from boundary asymptotes position, determining flow characteristics by electrical analogy 24 p4288 A70-45438

AIRFRAME MATERIALS

- Airframe production factors involving choice of materials and fabrication methods, emphasizing weight reduction to increase payload 05 p0854 A70-15925
- Preimpregnated materials processing, discussing molding, resin-reinforcement, unidirectional materials, ablative applications, mechanical data and airframe uses 05 p0874 A70-16614
- Micro and macromechanics for design and mechanical properties prediction of laminated fibrous composites for airframes and space structures 05 p0941 A70-16619
- Fatigue defects accumulation in aluminum alloy under impact tensile loads programmed to simulate loads encountered by aircraft in practice 05 p0947 A70-17009
- Graphite fiber/resin matrix composites for airframe structures, studying tensile, compressive and in-plane shear strengths 08 p1532 A70-21901
- C-5A airframe composite materials fabrication, tooling, processing, quality assurance and nondestructive test methods 11 p2058 A70-25572
- Flash, gas-pressure and electron-beam welding of airframe steels [ASTME PAPER MR-69-712] 12 p2239 A70-26987
- Aircraft structural materials, considering high strength steels Al and Ti alloys 17 p3124 A70-34675
- Materials selection for cost effectiveness in 1980s airframe applications [AIAA PAPER 70-870] 17 p3199 A70-34819
- Air safety research effects on operations, training procedures and materials, discussing gust loads, on-board data recording devices, human error, etc 17 p3022 A70-35859
- Boron composites development for aircraft structures compared with titanium [ASME PAPER 70-GT-120] 18 p3344 A70-36851
- Armor airframed helicopter for aerial armored reconnaissance vehicle, noting design, fabrication and weight 23 p4137 A70-44095
- Hypersonic airbreathers aerodynamic, structural and propulsive system interactions, discussing hydrogen fuel heat sink, airframe and engine cooling and airframe materials [ICAS PAPER 70-16] 23 p4138 A70-44127
- Fireproof nonmetallic materials for spacecraft and aircraft, discussing functional utility, durability and aesthetic requirements relative to environmental conditions 23 p4210 A70-44610
- AIRFRAMES**
- Airframe flow field effects on propulsion system performance in transonic flight, studying case of underwing aft mounted turbojet engine nacelles 01 p0004 A70-10321
- SST Ti body frame optimum design for high temperature environment and economical and fatigue resistance requirements 02 p0386 A70-11937
- Aircraft food service and galley integration considered joint responsibility shared between airframe manufacturer and air carrier [SAE PAPER 690671] 05 p0791 A70-15834
- Airframes dynamic response during simulated launchings of externally carried missile measured in laboratory, describing dynamic load simulation and structural analysis 06 p1159 A70-18439
- F-106B aircraft in-flight study of airframes installation effects on propulsion system performance at transonic speeds 08 p1437 A70-21732
- Airframe structures fatigue crack propagation with and without strain hardening during variable amplitude loading 12 p2315 A70-27014
- Airframe structural tests in elevated temperature environment by applied load ratios and room temperature static results 12 p2205 A70-27134
- Complex airframe design for economic and safe operation and long life using fatigue and fracture mechanics [AIAA PAPER 70-512] 12 p2324 A70-27466
- Airframe-propulsion system integration for Mach 6 transport and Mach 12 research airplane, examining

- off-design operation effects and interaction of aerodynamic forces [AIAA PAPER 70-542] 13 p2345 A70-29009
- Light twin engine aircraft airframe fatigue evaluation program [SAE PAPER 700219] 13 p2348 A70-29606
- Airframe critical part structural reliability on basis of ultimate static strength test data and extreme gust spectrum and maneuver loads 14 p2658 A70-30852
- Analog/digital system for full scale airframe fatigue amplitude and phase signature measurements on CH-46D tandem rotor helicopter 15 p2739 A70-32323
- Twin jet light transport Corvette airframe, discussing flight characteristics and economical aspects 15 p2676 A70-32793
- Alloy applications to Boeing supersonic transport airframe and components, discussing materials characteristics and manufacturing processes 17 p3099 A70-34451
- Airframe-inlet integration for supersonic tactical fighters, testing wind tunnel models [AIAA PAPER 70-933] 17 p3149 A70-35843
- Airframe and systems design optimization for aeronautical communications systems, considering airplane configurations, structural and electronics technology 21 p3750 A70-41349
- Exhaust nozzle/airframe interference test evaluation for twin engine supersonic fighter [AIAA PAPER 69-430] 22 p3958 A70-42702
- Airframe installation effects at transonic speeds on underwing supersonic cruise exhaust nozzles, using flight and wind tunnel tests 22 p3960 A70-43274
- Airframe skin panels adhesive bonding in wide-bodied jet transports, emphasizing fuselage fatigue and corrosion resistance [SAE PAPER 700863] 24 p4349 A70-45875
- Direct drive turbine engine control components and airframe accessories, noting weight and frontal area reduction [SAE PAPER 700821] 24 p4394 A70-45896
- V/STOL powerplant development, discussion airframe and engine design, application to large aircraft and planned evolutionary process [SAE PAPER 700809] 24 p4395 A70-45905
- AIRGLOW**
- NT GEOCORONAL EMISSIONS
- NT NIGHTGLOW
- NT TWILIGHT GLOW
- Double beam Michelson interferometer for middle IR with moving mirrors operating in constant velocity mode, applying method to atmospheric emission spectra 01 p0091 A70-10909
- Predawn O I 6300 A airglow enhancement, observing time variations and suggesting mechanism 02 p0289 A70-12120
- Night airglow emission intensities during IQSY concerning Na, OH and H alpha lines compared with intensities during IGY 02 p0292 A70-12433
- Satellite multispectral photometry data in airglow bands correlated with cloud characteristics and surface albedo variations 04 p0715 A70-15522
- In-flight radiometric calibration of low brightness OGO 4 airglow photometer 04 p0696 A70-15645
- Compact and fully automatic fixed photometer for zenith measurements of night airglow intensities, calibrating sky observation through filter by constant intensity light source 05 p0845 A70-15821
- Night airglow variations observed during Cosmos satellite orbits, determining atmospheric albedo wavelength dependence for solid and medium cloudiness and clear skies 05 p0841 A70-16728
- Spectral intensity distribution of night airglow noting visual spectra distribution difference from G2 stars 07 p1277 A70-20457
- OI 6300 A airglow intensity decrease at dawn ascribed to scattered solar radiation 08 p1492 A70-21720
- Airglow hydroxyl emissions diurnal variations as function of height, using digital computer for time dependent solution of equations for oxygen-hydrogen atmosphere 10 p1872 A70-23826
- Sodium night airglow analyzed by Chapman mechanism, considering nocturnal intensity seasonal behavior and location in upper atmosphere 10 p1873 A70-23829
- Predawn enhancement morphology and variations of 6300 A airglow, discussing solar declination and activity effect 10 p1873 A70-23831
- Annular current effect on auroral oval location during morning and evening hours, noting airglow region shift toward equator and expansion 11 p2044 A70-25555

- Brightness temperature of earth atmospheric emission in submillimeter band at 35 km, describing airborne radiometer 12 p2265 A70-28171
- Predawn forbidden OI 6300 A airglow seasonal variations by isophoto maps, discussing photoelectron precipitation 13 p2395 A70-28944
- Postdusk and predawn seasonal variations of forbidden OI 6300 A airglow, discussing photoelectron precipitation 13 p2395 A70-28945
- 5577 A /OI/ airglow emission diurnal variations during IGY by normalization method, observing seasonal effects 14 p2578 A70-31239
- Molecular oxygen emissions in airglow, inverting calculation to determine ozone distribution from observed altitude profiles 14 p2580 A70-31265
- Night airglow space and time variations from jet aircraft observations, measuring conjugate enhancements 14 p2580 A70-31266
- Molecular nitrogen excitation under electron bombardment at auroral and airglow impact levels, using computerized Monte Carlo method 14 p2620 A70-31269
- OGO-4 observations of hydrogen Lyman-alpha airglow surrounding earth, measuring dependence on solar zenith angle 17 p3080 A70-35764
- Spectrophotometric airglow intensity measurements of OH, O I 6300, hydrogen H alpha and oxygen Herzberg I bands by airborne laboratory 17 p3080 A70-35769
- Vertical distribution of upper atmospheric 7600 A oxygen glow, discussing 8645 A band and nitric oxide data 18 p3251 A70-36977
- Night airglow hydroxyl rotational brightness temperature determined from emission spectra 19 p3412 A70-37777
- Night airglow oxygen red lines predawn enhancement calculations, confirming role of photoelectrons from magnetic conjugate ionospheric 19 p3414 A70-38380
- Hydroxyl atmospheric airglow secondary production processes, discussing vibrationally excited oxygen molecules and rapid quenching by atomic O and HO sub 2 21 p3816 A70-41068
- Annular current effect on auroral oval location during morning and evening hours, noting airglow region shift toward equator and expansion 21 p3819 A70-41305
- Predawn enhancement of O I 6300 A line, considering magnetically conjugate photoelectrons effects on atomic oxygen excitation 22 p4095 A70-43113
- Magnetosphere storm diagnostics from geomagnetic, auroral and airglow parameters, discussing calibration via satellite observations 22 p4022 A70-43289
- Sodium D lines airglow nocturnal and seasonal variations in upper atmosphere 22 p4023 A70-43295
- Airglow hydroxyl emission altitude profile observations by rocket-borne photometer 23 p4191 A70-44407
- AIRLINE OPERATIONS**
- NDT used in airline and aircraft maintenance emphasizing practicability, reliability and costs 01 p0098 A70-10027
- NDT peculiar to airline maintenance, emphasizing inspection of complex parts hidden within assembly 01 p0099 A70-10028
- Airport planning and design, considering congestion, noise, cost and necessity to work with governmental units and automation [AIAA PAPER 69-1093] 01 p0055 A70-10621
- Differences in aircraft operating costs, performance characteristics and demand for aircraft by domestic trunk airlines /1932-1965/ [AIAA PAPER 69-1059] 01 p0005 A70-10637
- Interurban air transportation network structure contribution to airport and airways congestion, considering addition of nonstop links [AIAA PAPER 69-1037] 01 p0005 A70-10647
- Air traffic control methods for transport aircraft delay elimination 01 p0139 A70-11367
- Operations research in fleet planning, discussing forecasting, frequency planning, operation simulation, traffic and revenue forecasting, etc 02 p0401 A70-11745
- TV raster scan display using CRT and beam steering scan systems, comparing alphanumeric capability for airport information and control problems 02 p0274 A70-11976
- Meteorological data provision for supersonic civil transport operations, considering various flight phases 02 p0325 A70-12221

- Party autonomy application to standardized international air transport contracts, discussing international treaties, law court judgments and literature
02 p0402 A70-12267
- Seat capacity effect on operational costs of short/medium range high capacity A 300 B aircraft
02 p0402 A70-12368
- Air traffic problems connected with Boeing 747 introduction, discussing cargo/passenger handling, fueling and maintenance procedures
02 p0227 A70-12620
- Flights best day pair and weekly leg schedules concept based on decision making model for traffic volume estimation in airline operations
02 p0403 A70-12787
- Computerized airline fleet planning methods for aircraft economics and airline operations
[SAE PAPER 690415] 03 p0609 A70-12898
- Incremental profit and total airline profit model programs for air cargo systems
[SAE PAPER 690413] 03 p0411 A70-12899
- Scandinavian Airlines system of pilot selection, considering personality traits, behavior characteristics, clinical examination, etc
03 p0433 A70-13260
- SAS pilot selection system, discussing assessment variables, physiological examinations, psychological tests, recruiting procedure, etc
03 p0433 A70-13262
- Ground support and service features present facilities to handle B-747 and DC-10 aircraft
[SAE PAPER 690560] 03 p0463 A70-13264
- R and D effect on aircraft engine business, considering aircraft operating cost, funds allocation, etc
04 p0787 A70-14390
- Airline passenger food service, discussing public health measures, low temperature and cryogenic galley cooling
[SAE PAPER 690674] 05 p0804 A70-15833
- Aircraft food service and galley integration considered joint responsibility shared between airframe manufacturer and air carrier
[SAE PAPER 690671] 05 p0791 A70-15834
- L-1011 TriStar design for transcontinental airline requirements, discussing propulsion, noise suppression, configuration, passenger comfort, etc
05 p0793 A70-16098
- Optimality criteria for selecting flight conditions for civil aviation helicopters, considering scheduled speed and efficiency, commercial load factor, wind rose, vertical separation, etc
06 p1185 A70-17874
- Severe storm research importance to aircraft design and operating efficiencies improvement by identifying meteorological alternatives for operations in and near adverse environments
06 p1102 A70-18587
- Worldwide door-to-door cargo shipping by airline, considering marketing systems approach
07 p1426 A70-18875
- Montreal agreement of 1966 approved by CAB, considering air carrier liability
07 p1426 A70-18878
- Legal and national justification for limitation in air freight carrier liability taking into consideration Warsaw convention and legal decisions
07 p1426 A70-18880
- Air carriers legal liability, considering case decided in London involving Warsaw convention text
07 p1426 A70-18881
- Questions concerning Warsaw convention and supplementary agreements signing, considering membership eligibility and factors for general international laws evolution
07 p1427 A70-18883
- Legal aspects of liability for aircraft noise by German laws, discussing property owners obligation to permit flights over properties and admissible claims for compensation
07 p1427 A70-18884
- Inclusive Tour /IT/ Charter definition within framework of commercial air traffic, discussing concepts of scheduled and nonscheduled air services
07 p1427 A70-18885
- Airfreight carriers secondary services from legal viewpoint
07 p1427 A70-18889
- ICAO Juridical Council criteria for nonnational aircraft registration, discussing international airlines recourse to Article 77 of Chicago Convention
07 p1428 A70-19105
- U.S. Civil Aeronautics Board policy in cooperative agreements involving foreign airlines, highlighting significant cases
08 p1600 A70-20578
- Stochastic programming models for flight scheduling within airlift system accounting for cargo uncertainties, using convex programming, linear programming codes, etc
08 p1600 A70-20605
- Decision making leading to aircraft selection and buying by airline, evaluating traffic and technological aspects
08 p1601 A70-21866
- World air transport system in 1970s, analyzing industry economic performance, discussing fares, rates, technological developments, passenger and air freight increases, etc
09 p1792 A70-22332
- Satellite potential for long range air traffic control, discussing airline navigation requirements and ATC requirements for position determination
09 p1722 A70-23027
- Long range navigational aids requirements for airlines, discussing self contained navigation systems capabilities
09 p1722 A70-23028
- Stable moored ocean platforms providing reliable VHF communications and secondary surveillance radar facilities for civil aviation operations over North Atlantic
09 p1723 A70-23035
- Boeing 747 aircraft impact on air transportation passenger and freight rates and traffic congestion reduction
10 p1806 A70-24765
- AIRLORD system consisting of central data processing and I/O units for predeparture handling of passengers and freight at airports
11 p2013 A70-25365
- Edwards Inquiry Report into British Civil Air Transport based on cost effective economic study, involving airlines and regulatory system
11 p2153 A70-25855
- Edwards Report on UK domestic air services, considering unprofitability, trunk route competition and V/STOL development exploitation
11 p2153 A70-25860
- Dynamic programming successive approximation method application to airline scheduling, reviewing real time dispatching, operations, schedule and fleet planning
11 p2013 A70-26209
- Automatic air transportation passenger handling and postflight financial and statistical data processing
12 p2335 A70-27016
- Ab initio pilots selection and training in Swissair, describing preselection, in-flight and final selection tests and interviews
12 p2176 A70-27033
- V/TOL aircraft approaches to air passenger surface travel time reduction, emphasizing Manhattan-to-airport transportation problems
[SAE PAPER 700287] 12 p2335 A70-27443
- CF6 engine experience effects on current engine manufacturing, servicing and support in airline service, discussing maintainability, component repair and reliability, etc
[SAE PAPER 700289] 12 p2290 A70-27444
- Avionics technology cost effectiveness effect on airlines and industry, considering systems engineering and specifications
[SAE PAPER 700299] 12 p2335 A70-27447
- Reliability and maintainability from airline standpoint, discussing concepts, language and standards for aircraft design
[SAE PAPER 700326] 12 p2335 A70-27460
- Tradeoff decision processes scheduling maintenance frequencies for commercial transport aircraft
[SAE PAPER 700328] 12 p2243 A70-27461
- Age discrimination in employment policies of air carriers, discussing legislative measures, hiring practices and retirement rules concerning stewardesses and FAA pilots
12 p2336 A70-27772
- Weather forecasting for SST operations, discussing wind, temperature, turbulence, clouds, etc
13 p2445 A70-29494
- Cost effective spares provisioning models for airline operations, minimizing availability-cost ratio for line replaceable unit and total fleet
13 p2525 A70-29571
- Aircraft design analysis with reference to terminal maneuvering area, cruise and climb performance and noise and flight deck layout, discussing airborne equipment
14 p2530 A70-30104
- Aircraft characteristics effects on traffic control and community, considering passengers and freight
14 p2612 A70-30108
- DC-9 aircraft instrument subsystems and operating procedures of KLM, discussing series 15 and 30 aircraft
14 p2530 A70-30416
- International airline collaboration in engineering and maintenance for savings in initial and operational costs of aircraft fleets
14 p2669 A70-30940
- Civil aircraft design optimization, considering operating and seat mile costs, speed, wing and fuselage, engine location, etc
14 p2531 A70-30941
- Designer and operator influence on total aircraft operating costs
14 p2669 A70-30942
- Airliner fuselage shape design and effect on manufacturing and flight operation economics
14 p2532 A70-31369
- Commercial aircraft design evolution and trends concerning performance and operating cost reduction
14 p2532 A70-31370
- Scandinavian airlines /SAS/ pilot selection system validity based on scores
15 p2689 A70-31772
- Nationwide automated ground based air traffic control system for increased flight operations
15 p2772 A70-31962
- Fatal accidents involving airline aircraft /1968-69/
15 p2674 A70-32208
- Aircraft ground damage during maintenance and servicing
15 p2675 A70-32210
- Fatigue and aircraft environment effects on physical and mental state of airline flight attendants during prolonged cruises
15 p2692 A70-32211
- Management role in flight operations safety, stressing need for confidence and discipline
15 p2831 A70-32218
- Passenger awareness of airline industry problems, discussing safety, traffic control, convenience, etc
15 p2831 A70-32225
- Airline pitot and static altimeter systems and undercarriage maintenance and checkup, discussing water in systems, case leaks, trash, dirt, inoperative heaters, etc
16 p2842 A70-33823
- Computerized air transportation service including passenger name record, fare quotation, ticketing, etc
17 p3199 A70-34688
- Polish Lot airline long haul air transportation cost analysis
17 p3199 A70-34689
- Long haul air transportation profitability based on Polish Lot airline ton passenger-km computation comparison
17 p3199 A70-34691
- Investment risks and technical impact on aircraft development, world aviation growth and airline costs
17 p3200 A70-34915
- Boeing 747 aircraft operation in first three months of service, discussing crew training, instrumentation, navigation system improvement, etc
[AIAA PAPER 70-891] 17 p3019 A70-35805
- Boeing 747 ground operations and airport services, discussing computerized check-in, baggage handling equipment, etc
[AIAA PAPER 70-892] 17 p3019 A70-35808
- Fastener standardization for airline maintenance requirements
[AIAA PAPER 70-894] 17 p3102 A70-35811
- Minimum Equipment List from aircraft manufacturer and airline operations viewpoint
[AIAA PAPER 70-900] 17 p3019 A70-35816
- Safety in airline operations, discussing roles of aircraft designer and pilot
[AIAA PAPER 70-907] 17 p3019 A70-35819
- Large capacity transports influence on air cargo operations, and joint use cargo terminal planning
[AIAA PAPER 70-920] 17 p3204 A70-35832
- Air transport operations and economics in 1970 decade, taking into account cost-revenue ratio and cost effectiveness of various aircraft
17 p3204 A70-35852
- Airline maintenance department assurance of air service regularity, stressing management role
17 p3065 A70-35855
- Aircraft designer role in reducing departure delay due to equipment malfunction
17 p3022 A70-35858
- Air safety research effects on operations, training procedures and materials, discussing gust loads, on-board data recording devices, human error, etc
17 p3022 A70-35859
- Concorde design limitations for commercial success in civil airlines
18 p3350 A70-36665
- Cooperative airline program for aircraft turbofan engine parts aging and performance deterioration evaluations
[SAE PAPER 700329] 18 p3301 A70-36798
- High bypass turbofan engine design concepts and development program for airline operation
[SAE PAPER 700292] 18 p3302 A70-36804
- Commercial aircraft launching and arresting systems for airport runway length reduction, discussing safety factors
[SAE PAPER 700264] 18 p3237 A70-36821
- Airlines data reduction using electronic engine maintenance recorders
[ASME PAPER 70-GT-127] 18 p3259 A70-36853
- Air freight carrier liabilities in passenger transportation international regulations, noting conflicting interpretations
19 p3553 A70-37562
- Flight data recording system /FDRS/ for crashes expanded to aircraft integrated data system /AIDS/ for airlines
19 p3426 A70-37893
- Airline area navigation in national airspace system, emphasizing moving map display for navigation charting
19 p3465 A70-38233

Collision avoidance system flight test and evaluation program for airline industry CAS specification 19 p3466 A70-38240

Future aircraft with increased comfort, speed and economy, noting power plant development 19 p3355 A70-38249

Boeing 747, L-1011 and DC-10 introduction costs, profits and terminal facilities 19 p3357 A70-38951

International transportation regional hub airport planning with spin-off parking, circular terminal facilities and high speed interterminal passenger and baggage controls 20 p3606 A70-39673

Air cargo terminal operations analysis, discussing manpower cost reduction 20 p3607 A70-40127

Air transport regulatory system, considering operational, technological and economic factors 21 p3954 A70-50579

Boeing 747 aircraft early operations experience covering airframe, engines and parts, performance, pilot and engineer training, maintenance, etc. [AIAA PAPER 70-886] 21 p3749 A70-40740

Military and commercial aircraft maintenance costs reduction, discussing labor/material ratio, spare parts use, diagnostic systems, etc 21 p3749 A70-40750

Automated airline communications system for collecting, analyzing, storing, transmitting, receiving and presenting information required by ATC and advisory services 21 p3789 A70-41347

Statistical data on waivers granted to airline flight crew members by French Civil Aviation Medical Board based on ICAO medical standards 21 p3771 A70-41491

Air cargo management problems, discussing economics, ground handling, Jumbo jets, terminal facilities, mechanization, document handling, information flow, data systems, etc 22 p4006 A70-43269

Air passenger legal rights and obligations, discussing contracting states, formalities, hygiene, inoculation and decontamination 22 p4127 A70-43500

Air transport system technical and operational functions optimization 22 p3962 A70-43532

Airline transport pilots selection based on psychiatric and psychological testing 22 p3981 A70-43697

Airline selection of Auxiliary Power Unit (APU) for transport aircraft, noting benefits of air conditioning during ground operation [SAE PAPER 700816] 24 p4394 A70-45901

Commercial STOL aircraft propulsion systems from airline viewpoint, emphasizing subsystem design, engine selection, thrust deterioration and maintainability [SAE PAPER 700810] 24 p4395 A70-45904

Goals oriented airport planning and design approach, considering air traffic growth, capacity, environment and aircraft noise problems [AIAA PAPER 70-1264] 24 p4431 A70-45924

Short haul metropolitan air transportation, considering systems engineering as unifying technology [AIAA PAPER 70-1281] 24 p4373 A70-45927

Satellite based navigation/air traffic control information systems for short range STOL air carrier aircraft [AIAA PAPER 70-1338] 24 p4373 A70-45930

STOL aircraft field length, terminal area performance and minimum handling qualities requirements for safe and efficient operations [AIAA PAPER 70-1240] 24 p4292 A70-45960

AIRLINERS

U COMMERCIAL AIRCRAFT

U PASSENGER AIRCRAFT

AIRLOCK MODULES

Solar cell array peak power tracker and battery charger for Airlock Vehicle coupling Apollo spacecraft and Saturn IVB stage to form manned orbiting workshop 21 p3759 A70-41221

AIRPLANE PRODUCTION COSTS

Air cargo transport development and organization trends, considering cost and aircraft types 02 p0401 A70-11736

Design and economic concepts of Lockheed L-1011 wide body trijets, discussing airport and airway congestion alleviation, passenger appeal, etc [RAES PAPER 15] 04 p0623 A70-15044

Adhesive bonding for structural efficiency, lower weight, reduced production costs and improved appearance in general aviation industry [SAE PAPER 700221] 11 p2134 A70-25893

General aviation aircraft styling and interior developments, describing seat construction role in personalized aircraft production costs [SAE PAPER 700232] 11 p1980 A70-25901

Light general aviation aircraft production cost reduction, considering adhesive bonding, production certification, etc [SAE PAPER 700242] 11 p1981 A70-25911

Deterministic model for cost effectiveness of avionics support programs based on subsystems support ability, test philosophy and test equipment design and manufacture [AIAA PAPER 69-305] 14 p2563 A70-30857

Aircraft manufacturing market research including cost compatibility with resources and capabilities 14 p2668 A70-30937

International cooperation in military aviation emphasizing cost effectiveness in R and D, production and export prospects 14 p2669 A70-30939

Mercure passenger aircraft development schedule, cost, delivery and features, emphasizing weight balance and convenience 15 p2676 A70-32365

Power plant efficiency, size, maintenance and operating economics of propulsion systems for air transport 17 p3200 A70-34917

Military aircraft engines performance increase and cost reduction [SAE PAPER 700272] 18 p3302 A70-36817

Aircraft manufacturing cost estimation in conceptual design phase, using structural synthesis program for cost buildup simulation [SAE PAPER 865] 20 p3741 A70-40371

General aviation expansion and competitive position dependence on safety and utility improvements and simultaneous cost reductions [AIAA PAPER 70-1220] 24 p4291 A70-45953

AIRPORT BEACONS

Liverpool airport lighting emphasizing beacons, approach, runway and taxiway high intensity lighting installations 10 p1857 A70-24000

AIRPORT LIGHTS

NT RUNWAY LIGHTS

Power supply equipment with automatic control for category 2 airport lighting, discussing reliability and economic efficiency 01 p0055 A70-10300

Stand-by power supply for emergency lighting of Hamburg airport, discussing circuit connections for generators 08 p1482 A70-21371

Liverpool airport lighting emphasizing beacons, approach, runway and taxiway high intensity lighting installations 10 p1857 A70-24000

Air traffic control, discussing precision instrument landing, approach lighting, collision avoidance, navigation aids, etc 17 p3133 A70-35185

AIRPORT MOBILE LOUNGES

U MOBILE LOUNGES

AIRPORT PLANNING

Systems engineering applied to airborne, airport and community socioeconomic structure in determining air freight and passenger demand impact on airport location and configuration [AIAA PAPER 69-1091] 01 p0055 A70-10605

Airport planning and design, considering congestion, noise, cost and necessity to work with governmental units and automation [AIAA PAPER 69-1093] 01 p0055 A70-10621

Airport terminal configurations payload flow-through characteristics and space allocations, discussing passenger processing, baggage systems, etc [AIAA PAPER 69-1088] 01 p0000 A70-10622

Economic tradeoffs in airport and commercial aircraft design, considering traffic growth, increased weight impact minimization and costs [AIAA PAPER 69-1087] 01 p0056 A70-10623

Air traffic control inadequacy and restrictive regulations influence on aviation growth, implying need of airport-airways system improvements [AIAA PAPER 69-1052] 01 p0138 A70-10642

Interurban air transportation network structure contribution to airport and airways congestion, considering addition of nonstop links [AIAA PAPER 69-1037] 01 p0005 A70-10647

STOL ports in city environments, discussing elevated building design, assisted takeoff and landing equipment and Navy operational safety potential 01 p0057 A70-10715

Bird strikes on aircraft, discussing airport control and environment alteration, radar tracking and link between migratory flights and weather conditions 03 p0411 A70-13075

Flexible pavements for commercial jet planes representative of current and future aircraft 03 p0462 A70-13173

Superjets demands on airport fuel handling facilities [SAE PAPER 690559] 03 p0463 A70-13263

Ground support and service features present facilities to handle B-747 and DC-10 aircraft [SAE PAPER 690560] 03 p0463 A70-13264

Aviation environment master plan concerning public relations problems confronted by USAF bases with adjoining communities 05 p0960 A70-16634

STOL/VTOL airports design, location and complementary ground access transport 06 p1028 A70-17324

Crash fire protection at Los Angeles International Airport, discussing protein foam and light water usage 06 p1028 A70-17707

Airline industry, considering expected increases in traffic, aircraft development and interface problems 08 p1600 A70-20588

Air transport facilities planning in Canada, describing systems planning approach and major influencing factors 08 p1481 A70-20621

GPSS simulation for airport capacity, analyzing aircraft ground traffic flow characteristics and developing expansion schemes minimizing investment 08 p1481 A70-20929

Civil engineering research needs in air transportation, discussing information sources and processing and industry estimates of manpower, facilities and funding 08 p1481 A70-21305

General aviation urban airport capacity problem, suggesting diversion of training portion of peak-hour traffic 08 p1481 A70-21306

Seadrome advantages and structural design concepts, describing floating runways, breakwaters, noise reduction, building costs, etc 09 p1655 A70-22243

Regional air traffic in Germany, discussing aircraft, airports, growth rate and control 10 p1970 A70-24199

ATC ground hardware technology implementation, considering national air space system, airports, cost estimates and capacity increase 11 p2078 A70-25722

Airspace and airport use at terminals, discussing segregation of aircraft by performance categories [SAE PAPER 700229] 11 p2153 A70-25899

FAA recommendations on general aviation airports and heliport design standards, explaining standards establishment or modification procedures [SAE PAPER 700231] 11 p2031 A70-25900

Air terminal design, describing mechanical systems for moving people, baggage and cargo [SAE PAPER 700259] 12 p2206 A70-27431

Performance standards for intra-airport batch type people-moving systems, discussing seating requirements, platforms and stations, communications and power systems, etc [SAE PAPER 700260] 12 p2206 A70-27432

Aircraft crash fire fighting equipment and tactics for future airport needs [SAE PAPER 700262] 12 p2160 A70-27433

Airport runway slipperiness rating, predicting and alleviating to reduce aircraft accidents [SAE PAPER 700265] 12 p2206 A70-27434

Control system, operational procedures, aircraft guidance and runway design for increasing runway capacity, noting roles of automation and reduced separation [SAE PAPER 700280] 12 p2206 A70-27440

Total community annoyance measurement (TACM) applied to urban VTOL port planning for aircraft noise [SAE PAPER 700286] 12 p2161 A70-27442

General aviation requirements for national aviation system of 1970s including use of airspace and airports under all conditions [SAE PAPER 700296] 12 p2335 A70-27446

VTOL profitability in Northeast Corridor, discussing city center ports accessibility for S-65-200 short hauls and economic and ground acreage advantages [SAE PAPER 700310] 12 p2335 A70-27452

Air transportation demand growth forecast in terms of flights, airport operations and airborne aircraft at peak periods 12 p2336 A70-27626

Urban airport runway capacity increase via reduced aircraft separation, additional parallels and improved terminal traffic control, discussing design for acceptable safety levels 12 p2207 A70-27627

Aircraft noise reduction effects on airport capacity and community exposure levels 12 p2207 A70-27628

Airport capacity increase via electronic aids enhancing guidance, flight control, reduced aircraft separation, ATC automation and runway configurations 12 p2208 A70-27914

Air terminal and ground transfer design to provide improved access to aircraft and total transportation time reduction 12 p2208 A70-27992

Longer runways for increased airport safety indicated from data concerning overruns, undershoots and veering, discussing certification testing during takeoff and landing 12 p2208 A70-27994

Low cost VHF and UHF navigation aids IFR procedures for low density airports [SAE PAPER 700230] 13 p2385 A70-29607

Meteorological effects on air and noise pollution at U.S. airports 14 p2530 A70-30610

Airport safety standards for overall system including aircraft, ATC, navigation, runways, etc 15 p2717 A70-32229

Aircraft landing and takeoff difficulties and dangers due to mud and water on runways, discussing coping methods 17 p3057 A70-34692

Mobile lounges and airport productivity concepts for optimal handling of passengers at airport terminal [AIAA PAPER 70-918] 17 p3064 A70-35830

Large capacity transports influence on air cargo operations, and joint use cargo terminal planning [AIAA PAPER 70-920] 17 p3204 A70-35832

RAF aircraft damage due to bird strikes in U.K., discussing preventive measures at airfields 18 p3211 A70-35978

FAA research activities on eliminating birds at airports and improving aircraft components resistance to impact, including interagency committee functions on hazard problems 18 p3349 A70-35982

Military airlift command bird hazard minimization near airfields by environmental control, including uses of scare devices, chemicals, trapping, etc 18 p3212 A70-35988

Canadian civil aircraft bird hazards problem and alleviating measures including airport surrounding lands control 18 p3212 A70-35989

Aircraft bird hazards minimization by planning airport location and surroundings 18 p3236 A70-35991

Bird dispersal techniques in use or under study in Britain, including neurophysiological and bioacoustic systems to minimize hazards on airfields 18 p3222 A70-35992

Bird dispersal measure at airports, using behavioral and electrophysiological effects of high power microwave radiation 18 p3222 A70-35993

Commercial aircraft launching and arresting systems for airport runway length reduction, discussing safety factors [SAE PAPER 700264] 18 p3237 A70-36821

Airport terminal design, describing electromechanical baggage handling and sorting systems [SAE PAPER 700261] 18 p3237 A70-36822

Metropolitan airports environmental considerations, noting aircraft noise role in planning [SAE PAPER 700253] 18 p3237 A70-36826

International civil aviation, discussing ICAO functions, airports and terminal facilities problems 19 p3553 A70-37748

Airport planning and design, discussing role of computers in capacity and site analysis, wind data processing, passenger and baggage flows analysis, etc 19 p3396 A70-37749

Hamburg airport terminal design including circular planets system for large aircraft, efficient intermodal transfer facilities, etc 19 p3396 A70-37750

Air traffic control third generation system upgrading programs increasing airport, en route and terminal airspace capacities 19 p3464 A70-38227

Airport capacity analysis for terminal areas, using simulation for alternatives to parallel runway operation 19 p3397 A70-38236

ATC and general aviation growth, considering airport capacity, radars, navigation, National Airspace System, etc 19 p3467 A70-38631

Airport capacity and layout, considering air traffic increase, runway occupancy, taxiway and computer simulation 19 p3468 A70-38636

ATC by scanning beam ILS and onboard control systems, increasing airport capacity and terminal area safety [AIAA PAPER 70-1033] 20 p3666 A70-39504

International transportation regional hub airport planning with spin-off parking, circular terminal facilities and high speed interterminal passenger and baggage controls 20 p3606 A70-39673

Aviation in 1970s, discussing traffic increase, airport planning, aircraft design, ballistic transport, noise factors, etc 20 p3741 A70-40157

Transport aircraft noise at three major airports by noise exposure forecast (NEF) contours methodology 21 p3750 A70-40896

Centralized terminal air cargo handling capacity, discussing Jumbo aircraft, airside ramp system, container movement, computer control and automation 22 p4006 A70-43270

STOL operations from city centers, discussing safety requirements, navigation and guidance systems, airport criteria, etc 23 p4140 A70-44174

Financing methods for airport redevelopment and expansion, discussing economic and political framework of operations [AIAA PAPER 70-1267] 24 p4430 A70-45920

Planning criteria for optimum metropolitan airport system considering operational, physical, social and economic factors [AIAA PAPER 70-1266] 24 p4430 A70-45921

Goals oriented airport planning and design approach, considering air traffic growth, capacity, environment and aircraft noise problems [AIAA PAPER 70-1264] 24 p4431 A70-45924

Airport planning for air transportation in underdeveloped nations, discussing economic, financial, technical and operational factors [AIAA PAPER 70-1268] 24 p4323 A70-45926

FAA airport and airway capacity improvement program, considering runway-taxiway configurations, surface guidance and control, terminal design, takeoff, approach and landing systems, etc [AIAA PAPER 70-1315] 24 p4431 A70-45946

Airport accessibility role in planning V/STOL aircraft landing facilities [AIAA PAPER 70-1311] 24 p4323 A70-45947

STOL aircraft field length, terminal area performance and minimum handling qualities requirements for safe and efficient operations [AIAA PAPER 70-1240] 24 p4292 A70-45960

Wide-bodied and SST aircraft impact on airport design based on economic, social and environmental considerations [AIAA PAPER 70-1269] 24 p4323 A70-45970

ATC, air navigation facilities and airport design requirements for short haul transportation system [AIAA PAPER 70-1288] 24 p4323 A70-45973

AIRPORTS

Visibility improvement in fog at airports, discussing fog-seeding and warm fog modification operations 01 p0135 A70-11320

TV raster scan display using CRT and beam steering scan systems, comparing alphanumeric capability for airport information and control problems 02 p0274 A70-11976

Structural reinforcement for existing airport pavements, discussing construction procedures 03 p0462 A70-13174

Airport fog attenuation systems design and operation consisting of power and communication cables linking diffusers to central control and command 05 p0830 A70-17092

Automatic test equipment for different type of planes and relation to self organizing systems, considering airport implantation 10 p1970 A70-24476

Meteorological problems associated with proposed tests for aircraft noise certification, discussing airport near-surface environments 14 p2610 A70-30612

Community air pollution from airports, discussing exhaust emissions, pollutant dispersion, etc 17 p3200 A70-35177

Heavy jet effect on airport acceptance rates, discussing various sequencing strategies 18 p3212 A70-36209

Aircraft traffic on ground at airports by digital simulation, investigating influence of constraint represented by infrastructure of taxi tracks 18 p3236 A70-36390

Airport operations effects on total environment, considering jet aircraft noise pollution [AIAA PAPER 70-887] 19 p3395 A70-37391

Automatic sound monitoring system for measuring aircraft noise in airport vicinity 19 p3397 A70-37908

Computer controlled aircraft noise monitoring system at Stuttgart airport 19 p3397 A70-37909

Airport capacity and terminal area safety increase by scanning beam instrument landing system, discussing automatic guidance trajectory example 19 p3464 A70-37913

Runway low visibility and ceilings frequency and duration at German airports, using 1949-1967 statistical data 19 p3462 A70-37925

Airport fog layers repetition frequency after low visibility periods 22 p4065 A70-43246

Air cargo traffic problems, discussing mechanized terminals, automatic handling equipment, direct container delivery, mass traffic and large freighter aircraft 22 p4126 A70-43268

AIRSHIPS

Atmospheric aerosols vertical distribution from aerostat measurements, considering particle size distribution 19 p3461 A70-37636

AIRSPACE

Line of demarcation of national sovereignty between air space and free space 12 p2334 A70-27009

Air controllers traffic capacity using automation, discussing airspace loading effect, area navigation and rerouting 12 p2267 A70-27637

Land and airspace demands in navigation, surveillance and traffic control, discussing application of current techniques 14 p2611 A70-30105

Terminal airspace utilization from ATC viewpoint, discussing airport capacity, data acquisition, weather, etc [SAE PAPER 700281] 18 p3237 A70-36809

Air traffic control third generation system upgrading programs increasing airport, en route and terminal airspace capacities 19 p3464 A70-38227

IATA policy on future ATC development, discussing controlled airspace, communications and radar requirements 19 p3555 A70-38630

AIRSPEED

Airborne pulse Doppler radar for tactical aircraft velocity vector measurement, improving navigation system performance 16 p2840 A70-33448

Fluidic parallel flow low airspeed indicator for V/STOL instrumentation tested in wind tunnel [AIAA PAPER 70-906] 17 p3096 A70-35818

High speed civil and commercial transport aircraft, discussing jet-orbital flight 18 p3343 A70-36664

Mass flow ion drift anemometer applicable to aircraft speed measurement including V/STOL 19 p3425 A70-37885

AIRWORTHINESS

U AIRCRAFT RELIABILITY

AIRWORTHINESS REQUIREMENTS

U AIRCRAFT RELIABILITY

AIRY FUNCTION

Incomplete Airy functions application to wave diffraction problems as canonical functions 01 p0144 A70-11090

Plane elasticity problem for Cosserat medium rectangular region with parallel boundaries free of force and moment stresses solved by Airy and Mindlin stress functions 07 p1400 A70-18668

ALARMS

U WARNING SYSTEMS

ALASKA

Seismic refraction profiles of ash flow in Valley of Ten Thousand Smokes, Alaska, obtaining P wave velocities 14 p2573 A70-30493

ALBEDO

NT COSMIC RAY ALBEDO

NT EARTH ALBEDO

Plane and spherical albedos of planet surrounded by infinite optical thickness atmosphere, with application to Venusian atmosphere 01 p0193 A70-11591

Albedo variations for single scattering in atmosphere of arbitrary optical thickness by linearizing transfer equations with perturbation technique 02 p0338 A70-11790

Venus and Jupiter Aerobee rocket photoelectric UV spectra, determining geometric albedos using reflecting layer and cloud models 02 p0367 A70-11812

Jovian cloud layer light and dark matter albedo determination, applying photographic equidensitometry 02 p0375 A70-12431

Global cloud cover and earth atmosphere heat budget measured from weather satellites, discussing Tiros pictures, radiation charts and albedo 03 p0479 A70-14348

Normal albedo of Apollo 11 landing site and intrinsic dispersion in lunar Heiligenschein determined from Apollo and earth based photographic photometry 04 p0747 A70-14549

Bolometric albedo of main sequence stars with deep convective envelopes in close binary systems derived as function of photometric proximity using entropy invariance 05 p0914 A70-16694

Rayleigh phase matrix solutions and albedo values for imperfect Rayleigh scattering in semiinfinite planetary atmosphere 06 p1149 A70-18460

Lunar surface reflectivity determined by measuring reflected cosmic noise, determining dielectric constant and surface material properties 06 p1151 A70-18488

Charged particle albedo latitude dependence estimated from balloon-borne Geiger telescopes 09 p1746 A70-23481

Multichannel IR spectrophotometer to obtain albedo curves of Martian surface 12 p2229 A70-26927

Pulverization effects on lunar rocks albedo under full moon conditions for different grain sizes, noting inverse relation to absorption coefficient 14 p2649 A70-31214

Vesta diameter and albedo determination by IR emission measurements, allowing for roughness and rotation 17 p3173 A70-35758

Mars UV reflectivity, examining spectrum, absorption features, planet albedo and ozone content by rocket-borne instruments and atmospheric models 18 p3317 A70-37011

Apollo 11 rocks spectral reflectance and albedo before/after proton irradiation and vitrification, investigating color differences for lunar surface dark and bright areas 21 p3913 A70-41645

Lunar topography from UVRI photometry, determining albedos for mountains, dark and light maria and cratered terrae

23 p4247 A70-44769
Ashen light origin, considering atmospheric refraction of sunlight illuminating dark side of planet

24 p4399 A70-45113
Pluto albedo at various wavelengths from spectrophotometric measurements

24 p4399 A70-45129
Albedo and thermal emission of Jovian satellites I-IV at 3 to 12 micron wavelengths

24 p4413 A70-46171

ALBUMINS

Separate gamma irradiation effect of enzyme and hemoglobin-albumin-globulin substrates on proteolysis dynamics

03 p0419 A70-13308
Albumin and IgG degradation, studying high altitude effect on hepatic function in man

15 p2683 A70-32532
Thermal-chemical damage to carbon particles in egg albumin under ruby laser irradiation, using chemical rate equations for protein denaturation

17 p3035 A70-34577

ALCOHOLS

NT ETHYL ALCOHOL

NT FURFURYL ALCOHOL

NT GLYCOLS

NT METHYL ALCOHOLS

NT PHENOLS

Weightlessness effects on butyl alcohol diffusion flames, studying flame damping mechanism

01 p0217 A70-11012

Charge, hydrogen atom and ion transfer in collisions involving deuterium-labeled methanol-acetaldehyde system and molecular ions

14 p2543 A70-30110

Ag species paramagnetic relaxation in gamma-irradiated frozen aqueous solutions and in frozen methanol, relating spin-lattice relaxation to isotropic coupling

14 p2544 A70-30117

Molecular interactions, surface pressures and potentials of mixed monolayers of stearic acid and stearyl alcohol with inorganic subsolutions

15 p2695 A70-32547

Cetyl alcohol and water vapor growth by absorption and condensation on hygroscopic nuclei population in atmosphere under cooling

20 p3664 A70-40066

Altitude and alcohol intake effects on blood alcohol concentrations

24 p4306 A70-45329

Alcohol effects on human short term memory, discussing pathological intoxication from flying safety viewpoint

24 p4307 A70-45345

ALDEHYDES

NT ACETALDEHYDE

NT ACROLEINS

NT FORMALDEHYDE

Isolation and structural characterization of adduct formed from propionaldehyde, sym-trinitrobenzene and triethylamine

02 p0251 A70-12275

Phenolic aldehydes generated from lignin in fossil woods and carbonaceous sediments by oxidative degradation

13 p2361 A70-28911

ALDOSTERONE

Aldosterone effects on hemodynamics of dogs under restricted motor activity, observing cardiac activity stimulation

17 p3030 A70-35358

ALERTNESS

Vestibular habituation acquisition, retention and transfer correlation with stimulation, discussing alertness and arousal effects

14 p2539 A70-30915

Human vigilance paradigm and physiology, discussing relationships between vigilance, signal detection and animal discrimination

19 p3364 A70-38324

ALFVEN WAVES

U MAGNETOHYDRODYNAMIC WAVES

ALGAE

NT BLUE GREEN ALGAE

NT CHLORELLA

NT NOSTOC

NT SCENESMUS

Hydrocarbon content of coorongite derived from algae analyzed by IR spectrometry, gas chromatography and mass spectrometry, discussing alkanes and alkenes occurrence

01 p0041 A70-10037

Hydrocarbon fraction examination of Botryococcus braunii growing in natural environment, discussing unsaturated isomeric hydrocarbons

02 p0249 A70-11679

Hydrocarbon distribution of various algae and bacteria, discussing hydrocarbons diagenesis and biological transformations in sediments

06 p0997 A70-18401

Unicellular algae protein diet effects on animal and human enteric microflora composition

09 p1615 A70-22087

Chimkurgan reservoir algae life and physicochemical characteristics

09 p1627 A70-23148

Steady state EPR signal I kinetic behavior in wild type Chlamydomonas reinhardtii and in mutant strain AC-206 lacking cytochrome 53

12 p2168 A70-27468

Unicellular algae protein diet effects on animal and human enteric microflora composition

15 p2685 A70-32683

Manganese deficiency effect on chlorophyll fluorescence in algae adapted to hydrogen, determining electron transport mechanism

16 p2848 A70-33291

Optimum algae cultivator construction for life support system, using Chlorella culture model

17 p3026 A70-35320

Anomalous substrate oxidizing specificities among red brown and green algal peroxidases and land plants

19 p3360 A70-37773

Unicellular hot spring acidophilic alga Cyanidium cadarium cultured in pure carbon dioxide, examining packed cell volume, oxygen production and growth rate

20 p3572 A70-39492

Venus vegetative life suggested from algae growth under pure carbon dioxide in hot acid media at high pressures

23 p4253 A70-44836

Closed loop life support system employing algae and bacteria cultures to recycle water in addition to atmospheric regeneration

23 p4156 A70-45024

Biological life support system based on mutual equilibration of human metabolism and technically controlled algae culture, discussing experimental evaluation

23 p4156 A70-45026

ALGEBRA

NT ADJOINTS

NT BANACH SPACE

NT BINOMIAL THEOREM

NT CANONICAL FORMS

NT CUBIC EQUATIONS

NT DETERMINANTS

NT DUFFING DIFFERENTIAL EQUATION

NT DYADICS

NT EIGENVALUES

NT EIGENVECTORS

NT GROUP THEORY

NT HERMITIAN POLYNOMIAL

NT HILBERT SPACE

NT HOMOMORPHISMS

NT JORDAN FORM

NT LIE GROUPS

NT LINEAR EQUATIONS

NT LINEAR TRANSFORMATIONS

NT MATRICES [MATHEMATICS]

NT MONGE-AMPERE EQUATION

NT NONLINEAR EQUATIONS

NT POLYNOMIALS

NT QUADRATIC EQUATIONS

NT SPINOR GROUPS

NT STATE VECTORS

NT STOKES THEOREM [VECTOR CALCULUS]

NT STRESS TENSORS

NT TENSORS

NT VECTOR SPACES

NT VECTORS [MATHEMATICS]

NT VORTICITY

Numerically stable solutions existence for one dimensional monochromatic radiative transfer, using linear algebra including vector and matrix norms, convergence, etc

02 p0340 A70-12643

First and second boundary value problems of steady vibrations of viscoelastic bodies reduced to algebraic equations

03 p0589 A70-13345

Causality and analyticity related for case of separable complex Hilbert space, using algebra characterization of causal maps

03 p0461 A70-14168

Linear system theory in abstract algebraic framework applied to nonlinear machines in automata theory, discussing Ho algorithm, convolution and Kalman module theory

03 p0520 A70-14273

Algebraic properties of indefinite Riemann in integral useful in computer programming, emphasizing invariant algebras

04 p0654 A70-14683

Mechanized Algebraic Operations software package for manipulation on computer Poisson series, noting application to celestial and nonlinear mechanics and astrodynamics

10 p1845 A70-24179

Algebraic method for role of part inversion in fluid structure problems with mixed variables

11 p2135 A70-25979

Computer techniques for rounding error analysis, stability in linear algebra, matrices factorization, Jacobi rotation method and iteration procedures

13 p2443 A70-29768

Computer oriented algebraic method for duplicator control systems applied to loop network, lag, feedback, phase lead and phase lag compensator design

14 p2560 A70-30620

First and second boundary value problems of steady vibrations of viscoelastic bodies reduced to algebraic equations

14 p2657 A70-30720

Numerical method for roots of algebraic equations, computing continuous beam lateral vibrations natural frequencies

14 p2600 A70-31330

Graph theory in Soviet literature, applications and bibliographies

14 p2600 A70-31421

Algebraic aspects of generalized Riemann invariants method of integration of quasi-linear partial differential equations

16 p2944 A70-34329

Multiple head shaker systems theory as application of linear algebra, noting open loop control system with computer control of frequency, amplitude and phase

17 p3059 A70-35167

Vector and tensor calculus features, examining contravariance and covariance with bra and ket algebra and absolute differential

18 p3281 A70-36354

Linear algebraic system stability and monotony, investigating plane structures by finite element method

23 p4213 A70-44996

ALGOL

ALGOL Dynamic Display System for debugging and optimizing computer source language program, providing real time portrayal of static and dynamic block structure, etc

02 p0264 A70-12128

ALGOL program modification for Fast Fourier Transform to eliminate computation time difference with Fortran

07 p1238 A70-19677

Lumped element microwave Y circulator, describing device performance and ALGOL program for potentials calculation

07 p1241 A70-19751

Integrated switching circuits design optimization by ALGOL program, analyzing circuits transient behavior

07 p1242 A70-19752

ALGOL algorithm for Runge-Kutta type numerical integration of simultaneous differential equations, using Merson method for step length determination

10 p1845 A70-24405

ALGOL modified Gaussian algorithm for geodetic calculations, combining matrices for storage place economy

11 p2013 A70-25797

ALGOL algorithms for solving sum and bottleneck assignment problems

12 p2192 A70-27767

Computer language related to ALGOL 60 for handling nonnumerical problems of mechanics

18 p3283 A70-36367

Kahan Babuska summation method variant in Triplex-ALGOL 60 for reducing roundoff errors in finite series calculation

19 p3385 A70-38678

Hydrometeorological information processing using ALGOL-60 translator language

19 p3463 A70-38759

ALGORITHMS

Trench algorithm for Toeplitz matrix inversion, presenting proof for nonHermitian matrices case

01 p0131 A70-10456

Algorithm for L-shaped linear programs in optimal control problems and stochastic programming, outlining cutting hyperplane

01 p0047 A70-11069

Square root filters algorithms based on covariance and invariance matrices extended to include process noise effects

01 p0144 A70-11193

Accelerated memory gradient method for minimization of functions with unconstrained variables, investigating generalization of Fletcher-Reeves algorithm

01 p0132 A70-11194

Algorithm for determining readings dispersion during cosmic rays variability, statistical nature and instrument errors

01 p0172 A70-11526

Nonlinear boundary value problem algorithm in shell theory

01 p0212 A70-11566

Algorithm for solving Dirichlet problem of nonlinear elliptical differential equations representing atmospheric dynamics balance equation

01 p0134 A70-11609

Axisymmetrical stress-strain state of body of revolution with complex cross sectional geometry

under surface loads, deriving computer algorithm for numerical analysis

02 p0384 A70-11665

Noniterative algorithm for generalized inverse of arbitrary rectangular matrix computation

02 p0387 A70-11996

Algorithms for automatic control of machine elements fabrication

02 p0308 A70-12227

Algorithm for algebraic matrix Riccati equation, using Fletcher-Powell reformulation of Davidson function minimization

02 p0324 A70-12604

Algorithm for fixed time minimum energy discrete optimal control problems of linear plants with convex constraints imposed on terminal state

02 p0273 A70-12731

Signal waveform algorithmic construction with optimal autocovariance properties, using isosum integer partitions, applied to clustered multipath distribution measurement

02 p0263 A70-12773

Sensitivity analysis of discrete filtering and smoothing algorithms, noting in-track motion of circular orbit satellite and marine inertial navigation [AIAA PAPER 68-824]

03 p0459 A70-12913

Turbine disk strength calculations, obtaining matrix expressions and optimum algorithm for arbitrary disk shapes

03 p0588 A70-13242

Algorithm for optimal controls maximizing probability of linear time dependent control processes entering target manifold under random disturbances

03 p0460 A70-13580

Linear system theory in abstract algebraic framework applied to nonlinear machines in automata theory, discussing Ho algorithm, convolution and Kalman module theory

03 p0520 A70-14273

Dual type method solving discrete optimal control problems with linear plants, convex cost and constraint taking into account dynamic structure

03 p0461 A70-14274

Shell theory resolving equations transformation to second order partial differential equations suited for solution by numerical algorithms of network method

04 p0767 A70-14495

Automatic control algorithms for subsystem malfunction identification in multisubsystem plants, analyzing conditions for diagnostic tests existence

04 p0661 A70-14554

Shooting method for real time optimization of multiple burn rocket flights, presenting analysis, algorithm and test results

04 p0761 A70-14932

Algorithm for optimal decoding of convolutional codes confirmed using error probability upper bound

04 p0654 A70-15067

Packaging and placement algorithms for modules in automated design of microelectron equipment

04 p0659 A70-15193

Step system of automatic extremal control algorithms for inertial plant in presence of noise

04 p0661 A70-15194

Algorithmic and digital computer method for approximating irrational transfer functions by rational functions in control systems

04 p0662 A70-15336

Matrix algorithm from parallel element method derived for reducing computer time required in structural modification analysis

04 p0779 A70-15589

Nonlocal variational mechanics with one field variable, developing algorithm for Euler-Lagrange operator calculation

05 p0882 A70-16137

Mathematical and numerical least squares solution of linear equations, using Householder algorithm [JPL-TR-32-1431]

05 p0876 A70-16311

Algorithm for factorizing polynomials over finite fields usable with computer

05 p0876 A70-16312

Predictor-corrector algorithm for continuing analytically families of periodic orbits beyond collision trajectories in restricted three bodies problem

05 p0908 A70-16333

Algorithm for constrained optimization problems providing rapid convergence

05 p0877 A70-16714

Brightness distribution over source, discussing regularization algorithms for radio astronomical data reduction from crossed telescope

05 p0917 A70-16902

Computational algorithms transformation to forms convenient for aircraft computer adaptation for reducing digital network length with small accuracy penalty

05 p0818 A70-17005

Computational algorithm for fast Hadamard matrix transform of order 12 via factorization

06 p1093 A70-17314

Image recognition problem analyzed by deterministic approach yielding criteria for operation of recognition algorithm

06 p1014 A70-17633

Identification experiments and computational algorithms allowing synthesis of adaptive optimization process for real dynamic plants

06 p1023 A70-17634

Monograph on computation of density functions of parameters in stochastic systems, giving algorithms involving only matrix computations of fixed dimensionality

06 p1093 A70-17730

Boltzmann equation direct numerical integration using successive iterations algorithm

06 p1036 A70-17755

Time optimal control of nonlinear systems with distributed parameters, proposing approximate algorithm

06 p1024 A70-17814

Uncoupled quasi-static boundary value problem for linear viscoelastic solids undergoing thermal and mechanical deformation solved by computational algorithm

06 p1168 A70-17937

Numerical method for field problems analysis using algorithm based on generalized Betti-Maxwell theorem

06 p1094 A70-17942

Adaptive control algorithm for parameter adjustment of unknown dynamic characteristics of linear systems

06 p1025 A70-17956

M measurement optimal feedback control algorithm for stochastic discrete time systems, considering nonlinear plant, constrained controls, nonquadratic cost and simulations

06 p1025 A70-17962

Identification algorithm for estimating parameters in constant coefficient linear system independent of prior estimates [AIAA PAPER 70-34]

06 p1015 A70-18164

Earth oblateness effects on lunar and interplanetary trajectories, using algorithm based on orbital elements variations [AIAA PAPER 70-97]

06 p1146 A70-18203

State transition matrix computation method with efficient algorithm for orbit prediction in n-body gravitational field

06 p1095 A70-18497

Algorithm applied to specific classes of random processes for calculating minimum channel capacity required by transmission system for sources in each class

06 p1012 A70-18621

Optimum compression ratio defined for Markov sources for compression algorithm efficiency and data compression schemes

06 p1013 A70-18624

Loops and paths in Mason signal flow graph of linear systems using algorithm with remote time shared digital computation

07 p1238 A70-18842

Decision algorithms simulating human controller adaptive behavior in controlling VTOL aircraft in hover following stability augmentation system failure

07 p1216 A70-18860

Suboptimal computational algorithm for terminal control of random linear dynamical system, noting increasing optimality with random variations degeneration to deterministic quantities

07 p1324 A70-19091

Primal-dual algorithm for optimal control with fixed or free terminal time

07 p1238 A70-19269

Primal and dual algorithms for discrete optimal control incorporating antijamming procedures

07 p1245 A70-19271

Sequential gradient-restoration algorithm for minimization of function subject to constraint

07 p1325 A70-19355

Control algorithm for vehicle descent after reentry based on descent range prediction by integrating motion equations allowing for motion three dimensionality

07 p1393 A70-19482

Multidimensional Kiefer-Wolfowitz stochastic approximation algorithm modified to locate regression function minimum

07 p1247 A70-20028

Time optimal control for rotation of solid supporting body with aid of pendulum, obtaining motion equations by algorithm

07 p1337 A70-20299

Differential correction algorithm for identifying airplane parameters from flight test data, assuming differential equations

08 p1465 A70-20783

Stefan problem involving mass transport and phase transformations, presenting solution algorithm

08 p1596 A70-20852

Genetic theory application to selection of partial descriptions for algorithms group handling

08 p1466 A70-20875

Variable time optimal control problem computational algorithm using only zero Hamiltonian condition, noting variable time local maximum as well as local minimum

08 p1534 A70-21459

Algorithm for evaluating nth order partial derivatives of network functions and corresponding sensitivity functions

08 p1467 A70-21643

Turbine disk strength calculations, obtaining matrix expressions and optimum algorithm for arbitrary disk shapes

08 p1580 A70-21657

Consistent and inconsistent linear inequalities evaluating speed and efficiency of algorithm for pattern recognition problems

08 p1467 A70-21782

Algorithms based on continuous-group pattern recognition, distinguishing human faces, speech and handwritten characters

09 p1640 A70-22143

Algorithm for controlled plant parameters determination based on sensitivity function calculation

09 p1653 A70-22145

Quasi-linear estimator algorithms to achieve both optimal nonlinear filtration and signal interpolation resulting in significant gain of estimate accuracy

09 p1633 A70-22408

Nonlinear complexing problem in measuring random signal, proposing optimal data processing algorithm with minimum error variance criterion

09 p1654 A70-22542

Numerical algorithms for solving Liapunov matrix equation in nonlinear stability analysis and optimal systems design

09 p1641 A70-22959

Algorithm for stress-strain state calculation of nonuniformly heated cylinder weakened by star-shaped cavity

09 p1779 A70-23094

Algorithm for inversion of geomagnetic induction problem, determining earth radial conductivity distribution

09 p1669 A70-23305

Analytical phototriangulation block equalization by two stage polygon method, discussing computer algorithm for problem solution

09 p1681 A70-23344

Three stage variable shift iteration algorithm for calculating zeros of polynomial with complex coefficients

09 p1712 A70-23419

Planar restricted three body problem in Thiele coordinates, developing recurrence formulas for coefficients in Taylor series expansions of solution

10 p1938 A70-24178

Analytical algorithm for tan-chord angle tangent determination, assuming undevelopable ruled wing surface defined by three cross sections

10 p1802 A70-24292

Demand assignment /DAMA/ and preassignment /PAMA/ Multiple Access Systems mix for cost minimization, developing algorithm for satellite high usage groups and overflow facilities

10 p1838 A70-24357

Narrow throat problems of linear dynamic programming concerning maximum linear functional determination in set of vector functions, giving algorithm for solution

10 p1855 A70-24393

ALGOL algorithm for Runge-Kutta type numerical integration of simultaneous differential equations, using Merson method for step length determination

10 p1845 A70-24405

Computer-aided class C amplifier design, discussing algorithm and computer program

10 p1849 A70-24447

Algorithm for transfer matrix Heaviside expansion, using Krylov and Vandermonde transformations for multiple eigenvalue case

10 p1910 A70-24705

Algorithm for propellant flow rate increase of nuclear rocket in minimum time without exceeding maximum allowable stress in reactor core

10 p1914 A70-24870

Iterative algorithms for numerical solution for time optimal control problems

10 p1856 A70-25232

Algorithm developed for constructing first approximation system from Cauchy matrix for Liapunov stability problem solution

10 p1917 A70-25302

Readjustment algorithm for auto-oscillatory adaptive control system with variable structure, using harmonic linearization

11 p2022 A70-25343

Digital simulation of complex dynamic systems using homing missile as example, basing algorithm on 1 transforms for linear systems

11 p2013 A70-25692

ALGOL modified Gaussian algorithm for geodetic calculations, combining matrices for storage place economy

11 p2013 A70-25797

Algorithm for selective quadrupole parameter tolerance calculation, combining random search method with statistical testing

11 p2018 A70-25923

Time-invariant linear dynamical systems transfer equivalence leading to algorithm for minimal realizations of transfer function matrices

11 p2072 A70-26161

Algorithms for transforming coordinates from photographic plate system to equatorial coordinates, noting applicability with unknown optical center position in plate system

11 p2007 A70-26188

Generalized inverse algorithm for solving linear inequalities from Ho-Kashyap algorithm

11 p2013 A70-26207

Error analysis algorithms for reducing computational load in stochastic estimation and control problems in hybrid navigation systems

11 p2025 A70-26208

Algorithm for infinite dimensional optimal control problems associated with maximum deviation cost functionals distributed systems

11 p2073 A70-26234

Feedback controller specific suboptimal estimation and control parameters determination using stochastic approximation algorithms

11 p2026 A70-26236

Telemetry decommutation algorithm for applying Bayesian decisions to demodulated received bits data

11 p2008 A70-26238

Algorithm for Fast Two Dimensional Fourier Transform requiring logarithm additions and multiplication

11 p2073 A70-26250

Routing algorithm for computer controlled unmanned autonomous roving vehicle on Martian surface

11 p2081 A70-26317

Track-while-scan algorithm, considering probabilistic interpretation of linear recursive least squares filter for velocity variations

11 p2029 A70-26319

Automatic input data generation for finite element method using algorithm based on complex geometrical configurations topological classification in terms of natural coordinates

[JPL-TR-32-1486]

11 p2144 A70-26678

Nonlinear equations systems iterative solution convergence by extending classical algorithm with optimization process

11 p2074 A70-26850

Automated optimum structural design by variable step direct search algorithm, noting application to stiffened cylindrical shells

12 p2319 A70-27138

Discrete sequential algorithms for bit synchronization implemented with digital computer for optimum data detection

12 p2184 A70-27249

Suboptimal control of discrete input system with bounded state and control variables, developing algorithm for on-line computation

12 p2203 A70-27409

Nonlinear estimation with quantized measurements, applying algorithms to PCM, predictive quantization and data compression

12 p2192 A70-27420

Iterative algorithm for synthesis of discrete minimum time and amplitude controls for linear systems, noting guaranteed convergence

12 p2204 A70-27667

ALGOL algorithms for solving sum and bottleneck assignment problems

12 p2192 A70-27767

Multiterminal electronic networks computerized fault detection based on linearized Taylor expansion algorithm

12 p2197 A70-27932

Self organization and adaptive routing communication system for military network, describing routing algorithm and entropy organization measure based on stochastic switching matrices

12 p2187 A70-27934

Algorithm based on component reliability used to determine complex systems reliability

12 p2192 A70-28009

Closed product form and simplified algorithm for efficient operation of generalized Kronecker matrices, considering role in spectral analysis

12 p2193 A70-28029

Algorithm for integrating ordinary differential equations system determined for stability condition by trial-and-error procedure programmed on computer

12 p2262 A70-28030

Liapunov functions construction through conversion of differential equation with polynomial nonlinearities into auxiliary exact differential equation using algorithm

12 p2262 A70-28070

Algorithm for feature extraction in pattern recognition, using internal and universal criterion in computerized process

12 p2193 A70-28103

Spacecraft autonomous control algorithm to ensure geographically specified landing accuracy without considering atmospheric density distribution

12 p2270 A70-28251

Reentry control algorithm for prescribed landing point of space vehicle entering earth atmosphere at parabolic velocity, discussing double-dip reentry and digital simulation

13 p2499 A70-28376

Spacecraft rendezvous control at minimal propellant consumption, deriving algorithm

13 p2499 A70-28400

Gauss-Newton nonlinear programming algorithm applications to optimization of optimal control law parameters and closed loop control system synthesis

13 p2381 A70-28435

Automatic control systems for scientific experiments, considering algorithms, mathematical models and system designs

13 p2524 A70-28887

Newton-Raphson method analog accelerating convergence of multidimensional stochastic approximation algorithm to local minimum for attitude controller design

13 p2382 A70-29069

Variable mesh multistep predictor-corrector method for iterative solution of ordinary differential equations, considering numerical stability and algorithm efficiency

13 p2440 A70-29087

Algorithms based on Newton formula for polynomial interpolation and numerical differentiation

13 p2441 A70-29100

Penalty function algorithm for linear/nonlinear programming optimization problems subject to equality/inequality constraints, discussing feasibility determination capability

13 p2373 A70-29462

Error correcting algorithms for pattern classification, finding optimal approximation to unknown optimal decision function

13 p2374 A70-29579

Training algorithms in designing multilevel quasi-optimal controllers for dynamic processes, using pattern recognition methods

13 p2383 A70-29581

Gradient algorithm for sequential identification of features in dynamic linear systems

13 p2383 A70-29582

Asymptotically optimal signal detection algorithms for statistical systems synthesis

13 p2369 A70-29726

Discrete time systems, deriving algorithm for testing decomposition property as necessary condition for linearity

13 p2375 A70-29939

Radio wave reflection from ionized meteor trails, calculating propagation parameters by computer algorithm based on cylindrical approximation method

14 p2636 A70-30327

Algorithm for Fredholm integral equation in inverse problems of satellite meteorology

14 p2603 A70-30405

Complex error function computation using approximation method with single algorithm

14 p2599 A70-30648

Sequential gradient restoration algorithm for optimal control requiring state, control and parameter to satisfy vector differential equation, initial and final conditions

14 p2561 A70-31099

Dual mode algorithm for routing unmanned autonomous roving vehicle around obstacles on planets, using dynamic programming and terrain information

14 p2655 A70-31183

Algorithm for improving approximate quadratic factor of polynomial with real coefficients using iterative method

14 p2600 A70-31227

Dynamic nonlinear estimation, deriving general algorithms for filtering, smoothing and prediction for continuous and discrete systems

14 p2562 A70-31366

Finite difference algorithm for supersonic three dimensional steady flow past blunt bodies with generating line bends, allowing for gas equilibrium and frozen states

15 p2671 A70-31495

Multiple wiring algorithm for automatic pattern design for AI interconnections and printed wiring in integrated circuits

15 p2715 A70-31842

Optimal search algorithm for stationary object hidden in one of N regions with a priori probability

15 p2767 A70-31843

Shallow shells of revolution under axisymmetrical loads, analyzing plasticity and creep by integral equations algorithm

15 p2817 A70-32164

SIRIO mission algorithm and computer program, determining spacecraft position, ground trace and tracking station visibility

15 p2811 A70-32286

Learning control systems design, deriving general learning algorithms

15 p2705 A70-32448

Optimal questionnaires characteristics and design algorithms

15 p2705 A70-32450

Optimum decision rule /likelihood ratio/ algorithm for random signals detection in Gaussian noise, using pseudo Bayes approach

15 p2703 A70-32560

Sequential and combined gradient restoration algorithms for functional minimization in control theory

15 p2716 A70-32574

Real time computer algorithm for achieving optimal position of tracking antenna with nonlinear control system

15 p2703 A70-32575

Algorithm for inverse Laplace transformation of irrational transfer function via fast Fourier transform

15 p2768 A70-32577

Sequential circuit specification in terms of input/output pair strings, allowing programmed translation algorithm for automation of flow table construction

15 p2711 A70-32605

Control algorithm for vehicle descent after reentry based on descent range prediction by integrating motion equations allowing for motion three dimensionality

15 p2813 A70-32727

Algorithm for fourth order stability equation

16 p2867 A70-32925

Feedback gains for repeated eigenvalues in Simon-Mitter pole allocation algorithm

16 p2941 A70-32986

Finite settling response for single input/output feedback control system obtained by dual rate sampled data control algorithm

16 p2882 A70-33037

Regularization techniques for optimal control problems in polynomial algorithms of data handling by groups

16 p2867 A70-33236

State estimation for nonlinear discrete time systems with quantized measurements, obtaining recursive algorithm through boundary value problem linearization

16 p2867 A70-33305

Algorithm for implementing learning controller based on subgoal concept applicable to linear stationary system

16 p2868 A70-33312

Parameter identification algorithm for nonlinear equations describing VTOL aircraft longitudinal response

16 p2942 A70-33327

X-22 VTOL aircraft initial parameter, state and covariance matrix estimates by Kalman filter and smoothing algorithms

16 p2885 A70-33329

Linear systems approximate minimum energy controller, suggesting algorithm for mathematical model evaluation

16 p2886 A70-33344

Generalized iterative inverse algorithm for linear inequalities set involved in pattern recognition and threshold logic requiring decision functions determination

16 p2870 A70-33739

Nondiverging filter with single additional multiplication by fixed scalar s at each observation time, proposing algorithm

16 p2887 A70-33872

Automatic stabilization and control of computerized nonlinear processes, proposing algorithm for stability criteria

17 p3049 A70-34640

Program for function computation replaced by notion of flow algorithm

17 p3130 A70-35140

Iterative algorithm for free terminal time control in trajectory optimization

17 p3168 A70-35290

Adaptive system synthesized to compensate stochastic feedback or external disturbance, obtaining quasi-optimal compensation algorithms

17 p3056 A70-35368

Linear time invariant plant driven by scalar control, deriving second variation algorithm for minimum fuel problems

17 p3057 A70-35555

Identification-adaptive control algorithm for quadratic cost control of discrete linear systems

17 p3057 A70-35558

Two dimensional free boundary problems approximate solution by finite difference method, deriving algorithms for computer program implementation

18 p3230 A70-35941

Human vision inertia and irradiation algorithm, satisfying Talbot law

18 p3217 A70-36082

Recording instrumental noise resolution of standard algorithm for cosmic ray stations

18 p3307 A70-36100

Self adaptation algorithm of optimally fast acting system for variable parameter plant control

18 p3234 A70-36120

Hypotheses concerning optimal methods of solving mathematical physics problems, choosing algorithms employable in digital computers

18 p3291 A70-36284

One dimensional steady gas flow, deriving algorithm for iterative solution of Boltzmann kinetic equation by statistical approach 18 p3241 A70-36285

Pivot search at Gaussian algorithm, investigating Hilbert matrix approach 18 p3283 A70-36364

Linear multistep algorithms in discretization of non-linear initial value problems of ordinary differential equations 18 p3283 A70-36366

Shallow spherical shell dynamics nonlinear problems solution with algorithm permitting use of straight lines method 18 p3341 A70-36590

Algorithm for dynamic processes in unsteady linear automatic control system during finite time interval 19 p3470 A70-37256

Algorithm for steady state oscillations in irregular waveguide structures with conducting walls 19 p3470 A70-37427

Plane EM wave diffraction by conducting strip, using algorithm for reducing integral to linear algebraic equations 19 p3376 A70-37433

Regularizing algorithm for Fredholm integral equation used in diffraction by ideally conducting strip 19 p3376 A70-37434

Forecasted algorithms to predict random processes, using mathematical statistics 19 p3382 A70-37450

Coupled open plane resonators system self oscillation intrinsic frequencies solution by numerical method, obtaining algorithm for characteristic equation roots 19 p3387 A70-37737

Fast Fourier transformation algorithm for Fourier series rapid computation 19 p3383 A70-38039

Spectra and cross-spectra estimation by fast Fourier transform algorithm 19 p3384 A70-38040

Automatic ATC with feedback, describing information processing and flight plan algorithm 19 p3464 A70-38161

Analytical adaptation algorithms for PID controllers operation 19 p3394 A70-38162

Iterative adaptation algorithms, using automatic search techniques for single and multiparameter systems 19 p3394 A70-38163

Quadratically convergent algorithms for function minimization, discussing unified method and applications to quadratic and nonquadratic functions 19 p3458 A70-38302

Axissymmetrical stress-strain state of body of revolution with complex cross sectional geometry under surface loads, deriving computer algorithm for numerical analysis 19 p3547 A70-38439

Turbine disk strength calculations, obtaining matrix expressions and optimum algorithm for arbitrary disk shapes 19 p3548 A70-38460

Algorithm for radio telescope antenna pattern reconstruction from solar transit and radiation distribution data 19 p3390 A70-38561

Satellite TV cloud picture digital representation, deriving algorithms for statistical analysis of geometrical features 19 p3463 A70-38755

Soviet book on statistical algorithms for reliability covering repairable and first failure systems with ideal and imperfect switching 19 p3395 A70-38798

Feedback regulator synthesis for linear time invariant dynamic system with quadratic performance index, using computer algorithm for algebraic Riccati matrix equation 19 p3395 A70-38937

Algorithms for processing of cosmic ray data monitored by space station with multichannels for neutron and meson components recordings 20 p3698 A70-39309

Booster parameterized guidance algorithms investigated on basis of steering forms validity, discussing exoatmospheric ascent applications [AIAA PAPER 70-1006] 20 p3669 A70-39584

Thin shells of revolution static and dynamic stability under symmetric loads, presenting eigenvalue algorithm for boundary value problems 20 p3725 A70-39863

Soviet book on flight vehicle optimal design algorithms, covering mathematical theory of variational method, multistage spacecraft, etc 20 p3716 A70-39898

Dynamic plants optimal control, deriving algorithm for determining a posteriori probability density of generalized state vector 20 p3604 A70-39907

Stochastic approximation iterative algorithms for multivariable plants mathematical models, including steepest descent method 20 p3593 A70-39910

Small hybrid computer design, describing algorithms and subsystems for statistical studies 20 p3593 A70-39914

Image detection in pattern recognition through bipolar correlation, discussing reference generating algorithms and digital simulation results 20 p3633 A70-39972

Computer program for systems reliability approximation, giving algorithm for cut and tie sets identification 20 p3594 A70-40060

Polynomials with interval coefficients, presenting Newton Raphson algorithm for real roots error bounds 20 p3659 A70-40133

Algorithm for trajectory analysis in closed loop terminal guidance of solar electrically thrusted interplanetary spacecraft [AIAA PAPER 70-1152] 20 p3670 A70-40203

Pursuit evasion game with uncertain state-dependent measurements, modifying Brown-Robinson algorithm for behavior strategies computation 20 p3660 A70-40384

Symmetric two-step algorithms for differential equations 21 p3845 A70-40735

Identification adaptive quadratic cost linear system control by mean and covariance correction algorithm 21 p3801 A70-40741

Computer algorithm for optimal linear impulse corrections to satellite orbit under inequality type constraints 21 p3801 A70-40828

Algorithm for cardiovascular force computation from phasic regional blood flow and mass motion, interpreting Bcg 21 p3763 A70-41238

Two dimensional data array contour tracing algorithm for reduction of image coding bits number 21 p3786 A70-41327

Digital radar receiver based on pseudo Bayes likelihood ratio algorithms 21 p3789 A70-41353

OP-EX, optimal explicit guidance algorithm for powered flight outside atmosphere [AIAA PAPER 68-869] 21 p3848 A70-41734

Differential dynamic programming algorithm for discrete time orbit transfer optimization 21 p3919 A70-41737

Algorithm for spacecraft rotational maneuver control based on single turn around specific axis, using onboard computer 21 p3849 A70-42236

Natural language a priori description and linguistic algorithms construction, using statistical phrase contraction with Hoffman codes 22 p3993 A70-42492

Fluctuating light pulse packet detection by inertial-less photodetector, deriving optimal algorithm 22 p3987 A70-42554

Steady random process intensity estimation, using iterative probability algorithm 22 p3987 A70-42559

Algorithms for analog wideband signals optimal reception in presence of strong Gaussian noise 22 p3988 A70-42568

Light signals detection on noise background, comparing algorithms based on nonparametric statistics 22 p3989 A70-42569

Nesbet algorithm modified for iterative evaluation of eigenvalues and corresponding eigenvectors for large matrices 22 p4062 A70-42749

Rational polynomial matrices inversion by automatic computational procedures, considering Gaussian elimination and Faddeev algorithm 22 p4062 A70-42926

Linear distributed parameter systems state estimation from noisy measurements, developing sequential algorithms for prediction, filtering and smoothing 22 p4063 A70-43026

Algorithm for fast digital computer recursive estimation of mean of random variable 22 p3993 A70-43074

Linear reinforcement learning technique for accelerating convergence of successive approximation algorithms 22 p3994 A70-43491

Discrete decision variable models formulated as linear integer programs, deriving shrinking boundary algorithm for optimization 22 p3994 A70-43497

Optimal two-way communication system with feedback and decision constraint, developing algorithm for random code reliability lower bounds 23 p4159 A70-43754

Algorithm for communication network synthesis from limited elements selection, considering fixed reliability requirements 23 p4160 A70-43763

Digital computer algorithm for automatic electronic circuit design using design engineer experience 23 p4171 A70-43953

Linear phased arrays computer aided design, discussing search algorithms in multivariable optimization program 23 p4172 A70-44015

Algorithm for moment problems in Chebyshev system with applications to numerical integration, series summation and function approximation 23 p4211 A70-44244

Optimal algorithm for searching extremum of single variable unimodal function satisfying Lipschitz condition based on maximum possible error criteria 23 p4177 A70-44305

Computerized algorithm facilitating automatic synthesis of time invariant linear compensation for highly complex multiloop control systems [AIAA PAPER 69-941] 23 p4177 A70-44561

Scientific satellite reentry guidance algorithms for inertial system, discussing controllability, onboard computer, gyros, accelerometers, jet actuators, terminal guidance, glide trajectory, etc 23 p4216 A70-44667

Algorithm for space trajectories optimization with delta velocity constraints 23 p4245 A70-44683

Pattern recognition system design, discussing criteria and algorithm for grouping multivariate data without supervision 24 p4316 A70-45103

Graph theoretical cluster technique for producing index terms thesaurus for information retrieval system, discussing algorithms 24 p4316 A70-45161

Plate overlap algorithm for photographic star catalog reduction 24 p4404 A70-45413

Closed loop synthesis algorithm and comparison to sensitivity of open loop system, noting applicability to optimal control 24 p4322 A70-46013

Algorithm for Chebyshev solution of n plus 1 inconsistent linear equations in n unknowns, using minimax technique 24 p4370 A70-46241

ALIGNMENT

NT SELF ALIGNMENT

Hologram image resolution, finding angular alignment of reconstruction wavefront as limiting factor 02 p0297 A70-11923

Mechanized glycerine process for fibers and whiskers alignment on large scale at low cost 05 p0855 A70-16580

Divided photoelectric cell position sensitive detectors in laser alignment systems, obtaining independent signals for displacements in orthogonal directions 06 p1081 A70-17624

Laser alignment sensors for measurement and control of five degrees of freedom with increased sensitivity, faster recording and remote meter readout 06 p1083 A70-18591

Pulsar model assuming magnetic dipole radiation by spinning neutron star interacting with nearby plasma 09 p1756 A70-22517

Photoelectric receiver and light beam alignment in gas laser aerial photography, considering directrice rectilinearity verification 12 p2247 A70-27476

Pulsed laser alignment using pentaprism-directed continuous laser light beam 15 p2752 A70-32047

Single mode gas laser with large saturation and dispersion effects, discussing resonator alignment to spectral line frequency 15 p2752 A70-32196

Disturbances rotational alignment in variable galaxies nuclei, using interstellar gas motions model 17 p3153 A70-34527

Solar alignment, control, intensity scanner and data collection for large Space Environmental Simulator 17 p3058 A70-35155

Laser beam alignment system for monitoring dielectric film evaporation 19 p3445 A70-37686

Gas laser iterative alignment of Mach-Zehnder interferometer for monochromatic and white light fringes 19 p3424 A70-37880

Thrust vector measuring device using floating suspension system for ion engines, detecting vertical tilt and horizontal drifts of floating platform [AIAA PAPER 70-1104] 21 p3805 A70-41789

Laser sensors as alignment instrument for control and measurement of five degrees of freedom 24 p4351 A70-45383

ALIPHATIC COMPOUNDS

NT ACETALDEHYDE

NT ACETIC ACID

NT ACETONE

NT ACETYL COMPOUNDS

NT ACETYLENE

NT ACROLEINS

NT ACRYLATES

NT ADENOSINE DIPHOSPHATE [ADP]

- NT ADENOSINE TRIPHOSPHATE [ATP]
 NT ADENOSINES
 NT ALKANES
 NT ALKENES
 NT ALKYL COMPOUNDS
 NT ALLYL COMPOUNDS
 NT ANTHRACENE
 NT BUTADIENE
 NT BUTANES
 NT CARBON TETRACHLORIDE
 NT CELLULOSE
 NT CETYL COMPOUNDS
 NT CHOLINE
 NT CITRIC ACID
 NT CYANOGEN
 NT CYCLIC HYDROCARBONS
 NT CYCLOBUTANE
 NT CYCLOPROPANE
 NT CYSTEINE
 NT DIMETHYLHYDRAZINES
 NT ETHANE
 NT ETHYL ALCOHOL
 NT ETHYLENE
 NT GALACTOSE
 NT GLUCOSE
 NT GLUCOSIDES
 NT GLUTAMATES
 NT GLUTAMIC ACID
 NT GLUTAMINE
 NT GLYCERIDES
 NT GLYCEROLS
 NT GLYCOGENS
 NT GLYCOLS
 NT GUANIDINES
 NT HEPTANES
 NT HEXENES
 NT HEXOGENES [TRADEMARK]
 NT HYDRAZINES
 NT KETENES
 NT KETONES
 NT LACTATES
 NT LACTIC ACID
 NT LACTOSE
 NT METHANE
 NT METHYL ALCOHOLS
 NT METHYL COMPOUNDS
 NT METHYLHYDRAZINE
 NT MONOSACCHARIDES
 NT NEOPENTANE
 NT NUCLEOSIDES
 NT OLEIC ACID
 NT PARAFFINS
 NT PHOSGENE
 NT POLYSACCHARIDES
 NT PROPANE
 NT PROPYL COMPOUNDS
 NT PROPYLENE
 NT SUGARS
 NT THIOLS
 NT TRIMETHYL COMPOUNDS
 NT URETHANES
 Gas chromatographic-mass spectrometric identification of aliphatic hydroxy acids in plants and sediments 02 p0252 A70-12521
 Linear aliphatic polyesters unit cell dimensions and crystalline densities 03 p0517 A70-13808
 Fatty acids and aliphatic hydrocarbons in 3.4 billion year old metamorphosed sediment, suggesting biological origin 03 p0475 A70-13820
 Aliphatic ethers low resolution mass spectra interpretation using computer program heuristic DENDRAL 09 p1631 A70-23400
 Aliphatic diesters as high temperature lubricants, discussing viscosity range extension, oxidation inhibition and thermal stability 13 p2438 A70-29125
 Cycloaliphatic epoxy resins toughness improvement by modification with elastomers, maintaining high heat distortion temperature 21 p3842 A70-40733
 Solid propellant binders of saturated aliphatic hydrocarbons, describing microstructure, performance contribution, etc 21 p3865 A70-42143
 Linear aliphatic polyesters, calculating conformational contribution to heats and entropies of fusion 22 p3981 A70-42501
 Linear aliphatic polyesters melting point, fusion heat and entropy correlations to molecular parameters 22 p3982 A70-42502
 Abiotic synthesis of meteoritic aliphatic hydrocarbons produced by open flow Fischer-Tropsch processes for hydrogen and Co interactions 24 p4402 A70-45377
- ALKALI HALIDES**
 NT SODIUM CHLORIDES
 NT SODIUM IODIDES
ALKALI METAL COMPOUNDS
 Alkali-alkaline earth niobates phase equilibrium study revealing tetragonal tungsten bronze-type solid solutions existence range 09 p1740 A70-22983

- ALKALI METALS**
 NT CESIUM
 NT CESIUM VAPOR
 NT LIQUID POTASSIUM
 NT LIQUID SODIUM
 NT LITHIUM
 NT LITHIUM ISOTOPES
 NT POTASSIUM
 NT RUBIDIUM
 NT RUBIDIUM ISOTOPES
 NT RUBIDIUM 86
 NT SODIUM
 NT SODIUM ISOTOPES
 NT SODIUM VAPOR
 NT SODIUM 22
 NT SODIUM 24
 Thermodynamic and transport properties of Na, K, Rb and Cs vapors to 3000 K, for use in liquid metal coolant and power systems 01 p0214 A70-10299
 Positive Na and K ion effects on mitochondrial respiratory control, O uptake and adenosine triphosphate activity in rat liver 01 p0026 A70-11063
 Chemiluminescence in alkali metals and halogenated methanes diffusion flames, studying diatomic Cs spectral bands 02 p0250 A70-12018
 Transverse Kelvin-Helmholtz instability in rotating thermally ionized alkali metal plasmas /Q machines/, analyzing LF drift wave edge oscillation using dispersion equation 02 p0348 A70-12239
 Threshold oxygen concentration for corrosion determined for Ta specimens subjected to low pressure contamination in NaK 04 p0709 A70-15628
 Refluxing capsule tests of refractory metal alloys-boiling alkali metals corrosion compatibility, noting role of capsule geometry 06 p1087 A70-17510
 Radioactive sodium and potassium diffusion in single crystal and polycrystalline Mo and Nb at various temperatures, calculating activation energies and coefficients 06 p1089 A70-17745
 Alkali seeded plasma electron density and temperature enhancement by laser resonance pumping 08 p1552 A70-21576
 Variational model of collisional-radiative recombination of atomic ions in hydrogen and alkali plasmas 09 p1735 A70-22828
 Tuned laser radiation to diagnose and enhance local conditions in alkali metal plasma 12 p2281 A70-27793
 Parametric resonances at zero field crossing levels of optically pumped atoms on alkali vapors, noting applications to weak magnetic measurements 13 p2456 A70-30034
 Soviet collection of papers on equipment working with alkali metals covering turbines, level meters, hydraulic coupling, etc 14 p2534 A70-31007
 Optimum alkali metal vapor humidity for turbine equipment estimated from energy output 14 p2535 A70-31008
 Humidity measurement for alkali metal vapor in turbines by electric calorimeter with two heaters 14 p2587 A70-31009
 Liquid metal level indicators and resistance type level meters for turbines using alkali metal as working media 14 p2587 A70-31010
 Refractory metals penetration by liquid alkali metals along grain boundaries and crystallographic planes, considering threshold oxygen concentration 16 p2932 A70-34203
 Monoatomic inert gas molecules interaction with continuous elastic solid of alkaline and nonalkaline metals, calculating energy exchange 19 p3373 A70-37816
 Alkali metal vapors diffusion coefficients in inert gases, determining atomic interaction parameters 19 p3473 A70-38190
 Interactions between moving alkali-metal seeded dense plasma and metallic thermionically emitting electrode with surface properties influenced by seed particle absorption 20 p3681 A70-40007
 Alkali metals ionization by photons and atomic projectiles, discussing results in first Born approximation 20 p3676 A70-40153
 Boiling point method for alkali metals vapor pressure at high temperatures, estimating data accuracy 23 p4281 A70-44448
- ALKALIES**
 NT LITHIUM HYDROXIDES
 NT POTASSIUM HYDROXIDES
 Caustic surface of spherical resonator with external mirrors used to calculate light angular divergence and spectral properties 07 p1299 A70-19859
 Ion production cross sections determined for alkali atoms and bromine molecules collisions, noting charge transfer 07 p1345 A70-20138

ALKALINE BATTERIES

- Book on alkaline storage batteries, design, manufacture, performance characteristics, charging and maintenance, electrochemical and thermodynamical background of alkaline systems, electrode kinetics, etc 09 p1612 A70-22638
 Silver/polytetrafluoroethylene water-repellant air-breathing cathodes for fuel cells with alkaline electrolytes, discussing pressure compatibility 10 p1829 A70-24454
 Fuel cells with alkaline electrolyte consuming H and O and operating near ambient temperature, discussing electrodes composition and performance 12 p2163 A70-26993
 Propylene carbonate, dimethyl formamide, acetonitrile and methyl formate diffusion coefficients measurement for estimating nonaqueous Li batteries transport limitations 15 p2766 A70-32528
 Electrode and electrolyte additives effect on corrosion and polarization of alkaline zinc electrode 22 p3965 A70-43417
- ALKALINE EARTH COMPOUNDS**
 Alkali-alkaline earth niobates phase equilibrium study revealing tetragonal tungsten bronze-type solid solutions existence range 09 p1740 A70-22983
 Thermal decomposition mechanism of inorganic oxidizers, discussing reactivity of alkali and alkali earth salts 18 p3299 A70-36240
 Effective dissociation potential measurement for alkali compound seed in MHD generator working fluid 20 p3682 A70-40159
- ALKALINE EARTH OXIDES**
 NT BARIUM OXIDES
 NT BERYLLIUM OXIDES
 NT CALCIUM OXIDES
 NT MAGNESIUM OXIDES
- ALKALOIDS**
 NT ATROPINE
 NT MORPHINE
 NT NICOTINAMIDE
- ALKANES**
 NT BUTANES
 NT ETHANE
 NT HEPTANES
 NT HEXENES
 NT METHANE
 NT NEOPENTANE
 NT PARAFFINS
 NT PROPANE
 Hydrocarbon contents of two sediments from Scottish Carboniferous Formation, examining isoprenoid alkanes abiogenesis 01 p0041 A70-10038
 Steranes and triterpanes identification from Green River shale by capillary gas liquid chromatography and mass spectrometry 02 p0252 A70-12514
 Ionene polymers, investigating cyclic and linear compounds and reaction products from tetramethyldiaminoalkanes and dibromoalkanes using NMR, IR and mass spectroscopy 06 p1004 A70-17511
 Apollo 11 lunar fines chemical analysis for alkanes of 15-30 carbon atom length, obtaining negative results 21 p3779 A70-41630
 Carbonaceous chondrites isomeric alkanes identification by mass spectrometry and gas chromatography 24 p4402 A70-45378
 Iron meteorites graphite-troilite nodules isomeric alkane composition, using gas chromatography and mass spectrometry 24 p4402 A70-45379
- ALKENES**
 NT BUTADIENE
 NT ETHYLENE
 NT HEXENES
 NT PROPYLENE
 Cycloheptane and mixture of exo- and endo-cycloheptene heats of combustion and formation, isomerization and hydrogenation 01 p0213 A70-10134
 Hydrocarbon fraction examination of Botryococcus braunii growing in natural environment, discussing unsaturated isomeric hydrocarbons 02 p0249 A70-11679
 Protonation mechanism in acid catalyzed cyclization reactions of 2-acetamido 3-methylbicyclo-heptene 02 p0253 A70-12523
 Inductive effect in C-Cl chemical bonds in chloroalkenes, using nuclear quadrupole resonance frequencies shifts 09 p1630 A70-22903
 Isomeric 1-phenylheptenes mass spectra, investigating electron impact induced rearrangements of double bond 09 p1631 A70-23401
- ALKYL COMPOUNDS**
 NT CETYL COMPOUNDS
 NT TRIMETHYL COMPOUNDS

Dialkyl ketone ion in double McLafferty rearrangement, applying ion cyclotron resonance to structural study

08 p1454 A70-20525

Evidence against electron impact induced alkyl shifts in mass spectra of alpha-hydroxy-ketones, showing thermal rearrangements

13 p2363 A70-29803

Optical charge transfer transitions in N-alkyl iodide salts, examining transient absorptions due to flash photolysis

18 p3226 A70-36765

Polyvinyl alkyl ethers multiple transitions at low temperatures, using linear variable differential transformer

21 p3844 A70-42137

ALKYNES

NT ACETYLENE

ALL-WEATHER AIR NAVIGATION

Onboard radar self contained all-weather landing and taxiing /SALT/ system, discussing concept, requirements and results

[AIAA PAPER 69-1053] 01 p0138 A70-10641

Electronics in all-weather operations systems concerned with approach, landing and takeoff, considering components of airborne, ground and supporting systems

02 p0401 A70-11832

Pilot and copilot task distribution schedules adopted by European civil aviation for landing approaches under poor weather conditions

08 p1542 A70-21850

Trident aircraft automatic landing in nearly blind conditions in regular commercial service

11 p2079 A70-25851

All-weather landing aids, discussing Scan Beam and Multilateration systems including ILS, TACAN, etc

13 p2449 A70-29054

All-weather automatic landing in blind conditions, considering Trident system

14 p2615 A70-31392

Fixed wing and VTOL aircraft all-weather landing guidance and control philosophy

19 p3466 A70-38365

All-weather Autoland control system using inertial smoothing, discussing required redundancy, fault detection, ground beam anomalies compensation, etc

19 p3469 A70-38821

V/STOL guidance and control system with bad weather landing capability, requirements for V/STOL integration into overall air traffic, terminal area guidance procedures, etc

23 p4216 A70-44843

ALLOCATIONS

Assignment problem for finite set elements pairing, discussing probabilistic formulations and applications to satellite communications problems

05 p0815 A70-16716

R and D resources allocation model based on correlated Navy technological forecast (NTF) and exploratory development goals /EDG/

09 p1794 A70-23412

Resource allocation model with cost-effectiveness relationship for Army long range R and D

09 p1795 A70-23417

ALGOL algorithms for solving sum and bottleneck assignment problems

12 p2192 A70-27767

Optimum attention allocation, discussing distraction resistance and multiple task performance

19 p3362 A70-38316

ALLOTROPY

Fiber composites dimensional changes, stresses and plastic flow during component allotropic transformation, studying temperature variations effects

03 p0585 A70-12973

Binary Co-Cr alloy open circuit potential and microstructure, examining effects of composition, heat treatment, allotropic transformation and precipitation

18 p3271 A70-35966

Cobalt binary alloys allotropic transformation and thermal expansion at various temperatures

18 p3271 A70-35967

Allotropic transformation points and linear thermal expansion coefficients of Co-base binary alloy terminal solutions, using dilatometric method

23 p4203 A70-43864

ALLOYS

NT ALUMINUM ALLOYS

NT ANTIMONY ALLOYS

NT AUSTENITIC STAINLESS STEELS

NT BAINITIC STEEL

NT BARIUM ALLOYS

NT BEARING ALLOYS

NT BERYLLIUM ALLOYS

NT BINARY ALLOYS

NT BISMUTH ALLOYS

NT BORON ALLOYS

NT BRASSES

NT BRONZES

NT CADMIUM ALLOYS

NT CARBON STEELS

NT CHROMIUM ALLOYS

NT CHROMIUM STEELS

NT COBALT ALLOYS

NT COPPER ALLOYS

NT EUTECTIC ALLOYS

NT GERMANIUM ALLOYS

NT GOLD ALLOYS

NT HAFNIUM ALLOYS

NT HASTELLOY [TRADEMARK]

NT HEAT RESISTANT ALLOYS

NT HIGH STRENGTH ALLOYS

NT HIGH STRENGTH STEELS

NT INCONEL [TRADEMARK]

NT INDIUM ALLOYS

NT IRON ALLOYS

NT KAMACITE

NT LANTHANUM ALLOYS

NT LEAD ALLOYS

NT LITHIUM ALLOYS

NT MAGNESIUM ALLOYS

NT MANGANESE ALLOYS

NT MANGANIN [TRADEMARK]

NT MARAGING STEELS

NT MARTENSITIC STAINLESS STEELS

NT MOLYBDENUM ALLOYS

NT NEODYMIUM ALLOYS

NT NICHROME [TRADEMARK]

NT NICKEL ALLOYS

NT NICKEL STEELS

NT NIMONIC ALLOYS

NT NIOBIUM ALLOYS

NT PALLADIUM ALLOYS

NT PERMALLOYS [TRADEMARK]

NT PLATINUM ALLOYS

NT QUATERNARY ALLOYS

NT REFRACTORY METAL ALLOYS

NT RENE 41

NT RHENIUM ALLOYS

NT RHODIUM ALLOYS

NT RUTHENIUM ALLOYS

NT SILICON ALLOYS

NT SILVER ALLOYS

NT SODIUM ALLOYS

NT SOLDERES

NT STAINLESS STEELS

NT STEELS

NT TANTALUM ALLOYS

NT TELLURIUM ALLOYS

NT TERNARY ALLOYS

NT TIN ALLOYS

NT TITANIUM ALLOYS

NT TUNGSTEN ALLOYS

NT UDIMET ALLOYS

NT URANIUM ALLOYS

NT VANADIUM ALLOYS

NT WASPALOY

NT WROUGHT ALLOYS

NT YTTRIUM ALLOYS

NT ZINC ALLOYS

NT ZIRCALOYS [TRADEMARK]

NT ZIRCONIUM ALLOYS

Metal and alloys micro and macro stress-strain behavior data correlated for linear differential transformers, strain gages, longitudinal resonance waves and X ray diffraction

01 p0092 A70-11248

Acoustic emission analysis for material evaluation and polymorphic phase transformations characterization for metals and alloys, discussing electronic instrumentation and experimental techniques

02 p0276 A70-12551

Atom ordering and effects on alloy properties - Conference, Kiev, Ukrainian SSR, 1969

03 p0505 A70-13101

Interstitial atoms ordering effects on low and high temperature phase transformations in alloys with bcc lattice

03 p0505 A70-13102

Neutron bombardment effect on ordering and disordering state of alloys phase diagrams, noting temperature dependence

03 p0506 A70-13107

Light alloys cold hardening effect and fatigue strength estimation, considering residual stress variability with time

03 p0587 A70-13239

Extrusion forces required for metals and alloys determined by mathematical equations correlating extrusion pressures with process variables, discussing lubrication systems effectiveness

[ASME PAPER 69-WA/LUB-6] 04 p0697 A70-14767

Filamentary casting technique for nonequilibrium alloy structures to produce continuous specimens by rapid solidification

04 p0698 A70-15135

Carbide rupture energy in wear resistant alloys during abrasion, considering metallographic data and energy parameters

04 p0707 A70-15212

Induction furnace for thermal treatments and melting of solid and liquid metals, alloys and sintering and degassing ceramic and metallic systems in vacuum

04 p0664 A70-15371

Alloy EI 602 ingots low ductility during forging ascribed to nonferrous metal atoms, decreasing iron diffusion and forming brittle nitride and carbide compounds

05 p0863 A70-16545

Mechanical properties of cast light alloys at low temperatures, showing satisfactory plasticity and insensitivity to stress raisers

05 p0864 A70-16868

Laser induced alloys erosion under various focusing conditions, determining optimal conditions for spectral studies

06 p1089 A70-17762

Alloy specimen shortening due to aging during stress relaxation under vibration

07 p1304 A70-18820

Mechanical and electrochemical polishing effect on turbine blade alloy fatigue strength, discussing surface strain hardening as function of temperature in mechanical polishing

07 p1304 A70-18838

Hard alloy mixture shaping by free vibrational compacting of powders

07 p1296 A70-19801

Softening of cold worked alloy by high speed electrical heating, noting supersaturation before natural aging

08 p1520 A70-21496

Transition metal alloys electronic effect on solubility of interstitials

08 p1521 A70-21695

Two stage electropolishing technique for preparation of multiphase alloys for transmission electron microscopy

08 p1510 A70-21966

Alloy equivalent susceptibility to damage at intermediary service periods and different stress levels under creep conditions at 750 C

09 p1701 A70-22470

Metallic solutions formation dependence on alloying elements electron structure assumed by atoms in solvent lattice

09 p1702 A70-22560

Melting diagram for five element Mo-W-Nb-Ta-V system constructed by optimal projections from known composition-property relations for corresponding ternary systems with common components

09 p1702 A70-22561

Metal and alloys hardness measuring devices at high temperatures in ultrahigh vacuum based on use of synthetic sapphire pyramidal indenter

09 p1675 A70-22566

Noble metals band structure effects on shielding cloud around impurity and alloys electronic properties in weak scattering limit

09 p1740 A70-22953

Sigma phase occurrence in transition/nontransition elements alloys, discussing solid solubility limits

09 p1708 A70-23424

Fiber-reinforced composite alloys prepared by controlled dissociation of Au-Ni and Al-Zn solid solutions

10 p1902 A70-23814

Metals, alloys and galvanic couples corrosion rates in synthetic seawater measured by polarization technique

10 p1887 A70-24044

Energy dissipation-fatigue strength relationships during vibrations for prestrained metals and alloys

10 p1956 A70-24244

Thermal conductivity, electrical resistivity, Lorentz ratio and thermopower of aerospace alloys in 4-300 K range, separating electronic and lattice contributions

11 p2065 A70-25758

Thermal conductivity coefficient of metals and alloys above 1000 C by longitudinal heat flow method

11 p2065 A70-25761

Thermal conductivity of metals and alloys, separating electronic and lattice contributions

11 p2098 A70-25762

Diffusion processes rate changes in metals and alloys resulting from radioactive emission, noting role in stress rupture strength mechanisms

11 p2068 A70-26595

Metals and metal alloys ductility development, discussing plastic flow problem in metal working

12 p2327 A70-28144

Spectral characteristics of secondary emission alloys for photocathodes in extra atmospheric radiation open-type detectors in UV range

14 p2582 A70-30166

Kovpak method for estimating and extrapolating heat resistance characteristics, considering alloy long term strength

15 p2755 A70-31528

Alloy high temperature creep and long term strength, determining exponential relations between stress, strain rate and durability

15 p2755 A70-31529

Alloys resistance against erosion-corrosion attack via abrasive slurries in corrosive media in pulp and paper industry

15 p2763 A70-32774

Lateral pressure bulging of superplastic alloy sheet, considering flat circular sheet and bulging into V grooves

16 p2916 A70-32918

Heat resistance evaluation of Zr Se-K alloy subjected to multicomponents surface diffusion

17 p3125 A70-35407

Alloy hardening statistical theory, applying flow stress to second phase randomly dispersed particles 17 p3191 A70-35458

Soft metal and dilute alloy dynamic yielding, describing high dislocation mobility effects on mechanical properties 17 p3191 A70-35459

Plastic deformation of two phase alloy with small nondeformable particles in ductile matrix, discussing cross slip, yield and flow stress, work hardening etc 17 p3126 A70-35460

Soviet papers on phase transformations of Fe, Ni, Co and Al alloys 18 p3275 A70-36201

Mechanical stresses effect on Vicalloy rotor packets magnetic properties 19 p3357 A70-37265

Combined mechanical and cyclic thermal stresses effect on plastic deformation buildup in E1435 alloy preceding breakdown 19 p3449 A70-37349

Extrusion forces required for metals and alloys determined by mathematical equations correlating extrusion pressures with process variables, discussing lubrication systems effectiveness [ASME PAPER 69-WA/LUB-6] 19 p3435 A70-37604

Low temperature electrical resistivities of Al, Ni, Cu, Ti and Fe alloys for different heat treated conditions 19 p3452 A70-37825

Light alloys cold hardening effect and fatigue strength estimation, considering residual stress variability with time 19 p3548 A70-38457

Metallic surfaces vacuum electric spark alloying, investigating pressure effects on coating layer thickness and area 20 p3636 A70-39195

Alloys for aircraft structures design, considering materials strength, corrosion resistance, producibility and cost 20 p3648 A70-39414

Hydrogen emanation and distribution in metals and alloys by Nd hydrogen metal detection method 20 p3651 A70-40071

Alloys stacking faults thermodynamics based on Gibbs treatment of interfacial free energy 22 p4124 A70-42726

Phase analysis for individual multicomponent alloys, discussing chemical composition in case of invariant equilibria and electron beam microprobe 22 p4053 A70-42734

Neutron irradiation effect on elevated temperature fracture of various fcc alloys 22 p4054 A70-42957

Alloy aging process after plastic deformation, examining relationship of phase distribution and mechanical and physical properties 22 p4056 A70-43340

Electrochemical corrosion of metals, discussing passivity and passivating techniques, inhibitors and resistant alloys 24 p4361 A70-46142

Surface alloying of alloy with three elements /Al, Si and Cr or Zr/, investigating coating stability in weight, microstructure and microhardness 24 p4364 A70-46340

ALLYL COMPOUNDS

Cyclization of N-allylamides to disubstituted-2-oxazolines, giving melting points, yields, picrate melting points and NMR spectra 02 p0249 A70-11681

ALMUCANTAR

U ELEVATION ANGLE

ALOUETTE HELICOPTERS

NT SA-330 HELICOPTER

ALOUETTE SATELLITES

NT ALOUETTE 1 SATELLITE

NT ALOUETTE 2 SATELLITE

Solar radiation influence on Aouette satellite spin behavior, with long flexible antennae, taking into account sunlight/shadow history and solar vector inclination 02 p0380 A70-11852

Aouette satellite antennas and receivers for detecting plasma resonances and VLF signals, noting ground station telemetry link 13 p2380 A70-29902

Aouette plasma resonance stimulated perpendicularly to magnetic field by planar dipole charge sheet and permeable grids 13 p2467 A70-29907

Report to COSPAR on space research in Canada, covering Aouette satellites, ISIS I, international cooperation, etc 15 p2829 A70-31708

Aouette and ISIS experiments programs and design 17 p3180 A70-35305

ALOUETTE 1 SATELLITE

Aouette 1 plasma resonance observations, analyzing electron density measurements in sheath region and cyclotron harmonic resonant frequencies 13 p2466 A70-29903

Daytime seasonal anomaly in electron density of topside F 2 region near sunspot minimum, using Aouette 1 data 15 p2726 A70-31863

ALOUETTE 2 SATELLITE

Ionogram conjugate echoes observed at Singapore longitudes by Aouette 2 topside sounder, attributing sequential occurrence to field-aligned irregularities in magnetosphere 03 p0477 A70-13986

Aouette 2 Langmuir probe measurements analyzed for size and amplitude of electron concentration fine structure irregularities in topside ionosphere, discussing F spread 04 p0679 A70-15111

Upper ionospheric electron density variations at low magnetic activity times observed with Aouette 2 satellite 05 p0901 A70-16307

Delayed ionospheric resonance echoes radiated from topside plasma after pulse sequence stimulation by Aouette 2 satellite 13 p2370 A70-29904

Floating resonance spike on Aouette 2 ionograms after sounder pulse transmission at half upper hybrid frequency, noting harmonic excitation role 13 p2370 A70-29905

Diffuse plasma resonance sequence observed on Aouette 2 ionograms, showing pattern similar to spread echo 20 p3620 A70-39335

ALPHA DECAY

Alpha particle emissivity measurement of moon by Explorer 35 spacecraft for U 238 abundance in outer crust 01 p0181 A70-10573

ALPHA PARTICLES

Ferritic stainless steel embrittlement caused by He injected into tensile samples by alpha particle cyclotron irradiation tested at elevated temperatures 01 p0122 A70-11235

Balloon measurements of cosmic ray alpha particle flux in upper atmosphere over Japan to obtain solar modulation effects data 02 p0357 A70-12122

Radioactive nuclei alpha radiation investigation methods, discussing nuclear emulsions, scintillation spectrometry, ionization chambers, semiconductor counters and magnetic spectrographs 03 p0485 A70-13479

Gas flow proportional counter for measuring high emission rates of alpha particles, discussing design and operation 04 p0695 A70-15570

Satellite HEOS-1 S 73 experiment launched during solar maximum to determine flux and energy distribution of solar wind positive component 05 p0900 A70-16077

Solar flare alpha to proton flux ratios on 23 May 1967 observed following interplanetary disturbances, suggesting electric fields as cause of modulations 05 p0902 A70-16444

Cosine dependence of F 1 critical characteristics on solar zenith angle discriminating alpha neutralization and mixed alpha-beta deionization 06 p1057 A70-17841

Alpha irradiation effect on *Chlorella* survival, cell division and mutation 07 p1208 A70-19507

Highly variable component protons and alpha particles identified in low energy cosmic rays by IMP 4 07 p1369 A70-20199

Energy distribution of solar wind alpha particles in magnetosheath observed by Heos A satellite 09 p1744 A70-22305

Oxygen enhancement ratio and relative biological effectiveness of accelerated helium nuclei on mouse tumor cells, discussing applicability in radiation therapy 09 p1617 A70-22336

Cross sections of fragments emitted in spallation reactions of carbon and nitrogen nuclei emulsion with alpha particles 09 p1733 A70-23549

Lunar surface alpha radioactivity at Surveyor 5, 6 and 7 landing sites 11 p2104 A70-25658

Alpha irradiation effect on *Chlorella* survival, cell division and mutation 11 p1987 A70-26106

Tungsten crystalline structure defects caused by alpha particles bombardment using helium ion projector at 78 K 12 p2255 A70-27544

Primary cosmic ray proton and alpha particle spectral measurements by balloon flights 12 p2293 A70-27586

Satellite observation of alpha particles trapped geomagnetically in radiation belts, including Injun 5 results 13 p2484 A70-30092

Trapped alpha particle and proton spectra from satellite measurements, considering magnetosphere injection 13 p2484 A70-30093

Alpha particles radiation damage effects in silicon surface barrier detector 14 p2584 A70-30511

Quiet time proton and alpha particle flux and differential energy spectra measured by cosmic ray detectors on OGO 3 satellite 15 p2793 A70-31795

Temporal and spectral changes in solar protons and alpha particles access to synchronous altitude in magnetosphere 19 p3494 A70-37485

Protons and alpha particles energy spectra during 25 February 1969 solar event from Centaur rocket measurements 19 p3496 A70-37509

Protons and alpha particles energy spectra following solar flares of 24-25 February 1969 from rocket measurements, estimating proton mean free path 19 p3496 A70-37510

Primary cosmic ray proton and alpha particle spectra measurements by balloon-borne equipment 19 p3505 A70-38118

High energy alpha particle beam exposed to plastic scintillators, determining spallation cross section for C12/alpha, alpha n/C11 21 p3852 A70-41138

Apollo 11 lunar rock samples alpha activity in polished thin sections, using autoradiography and electron microprobe 21 p3901 A70-41546

Differential elastic cross sections of 42 MeV alpha particles scattering from He 3, using optical model with spin-orbit potential 22 p4076 A70-42722

Auger spectra characteristics obtained with X rays and electrons from radioactive alpha sources 23 p4222 A70-44421

ALPHA RADIATION

U ALPHA PARTICLES

ALPHABETS

Automatic alphabetic characters classification model based on cross correlation and discrete Walsh-Fourier transforms, using computerized simulation 16 p2851 A70-33460

ALPHANUMERIC CHARACTERS

NT BINARY DIGITS

Alphanumeric label and vector scan converted bright display operation, characteristics and equipment, discussing line scanning method, visual storage, display phosphor problems, etc 02 p0256 A70-11974

TV raster scan display using CRT and beam steering scan systems, comparing alphanumeric capability for airport information and control problems 02 p0274 A70-11976

Alphanumeric and graphic computer driven CRT displays, discussing systems and component selection 08 p1465 A70-20672

Alphanumeric solid state displays with vertically stacked character rows for text format reading, using injection electroluminescence technology 10 p1846 A70-23882

Semiconductor alphanumeric multicolored displays, discussing phosphor coating of GaAs diodes 13 p2408 A70-29217

Computerized control for beam scanning and optical data processing concerning symbols, letters and photographic images 14 p2553 A70-30424

Air traffic control CRT plan position indicators, considering alphanumeric symbols strokes design 19 p3469 A70-38645

ALTERNATING CURRENT

Digital microcircuits for one kva three phase DC-AC inverter control to generate sinusoidal 400 Hz output using HF bridge chopper techniques 04 p0628 A70-15340

Colloid engine efficiency operating with pulsed positive voltages and square wave and sinusoidal voltages [ALAA PAPER 70-178] 06 p1132 A70-18158

Hall voltage and electric conductivity measurements in alternating magnetic field and current by narrow band amplifier with synchronous detector 07 p1279 A70-18944

AC to DC converter design for transforming average AC values into DC voltage 08 p1438 A70-20601

Monolithic zero crossing AC trigger IC for thyristor power control systems operating in on-off mode 08 p1478 A70-20786

Photoemission energy distribution curves measuring circuit using AC retarding potential method, offering improved noise performance 09 p1679 A70-22996

Alternating electric field effect on weakly ionized gases, analyzing electronic temperature and harmonics generation 13 p2458 A70-28560

Wheatstone structure impedance bridges, describing balancing method in sinusoidal alternating regime 16 p2872 A70-33106

Multibandswitch AC Wheatstone bridge design with large circuit factor 17 p3051 A70-34616

Fluidic networks nonlinear component AC and DC behavior, discussing Bernoulli equation, nonlinear resistances, transmission lines and various flows
23 p4142 A70-44296

ALTERNATING CURRENT GENERATORS
U AC GENERATORS
ALTERNATORS [GENERATORS]
U AC GENERATORS

ALTIMETERS
NT LASER ALTIMETERS
NT RADIO ALTIMETERS
Aircraft approach and guidance system radio components including localizer, glide path and marker systems and radio altimeters, discussing signal interference
02 p0333 A70-11980
Tradeoff methodology establishing evaluation criteria for comparing radar and laser systems to meet geodetic satellite altimeter performance requirements. [AAS PAPER 69-604] 04 p0686 A70-14648
Specification of minimum performance standards and test procedures for automatic pressure altitude digitizer equipment [SAE-A8-855] 07 p1279 A70-18901
Aircraft altimeter measurement for vertical separation based on atmospheric pressure unit changes /Cayleys/ compared with linear measurements in meters and feet
13 p2411 A70-29778
Civil aircraft altitude display design, anticipating application to supersonic transport
14 p2582 A70-30287
Airline pitot and static altimeter systems and undercarriage maintenance and checkup, discussing water in systems, case leaks, trash, dirt, inoperative heaters, etc
16 p2842 A70-33823

ALTITUDE
NT FLIGHT ALTITUDE
NT HIGH ALTITUDE
NT LOW ALTITUDE
NT SIMULATED ALTITUDE
Altitude dependence of low latitude cosmic ray diurnal variations from cosmic ray neutron data
13 p2479 A70-29792
Equations for converting satellite geodetic latitude and altitude into geocentric Cartesian system
20 p3669 A70-39691
Optimum altitudes for passive ranging satellite navigation systems, using electronic clocks in satellite and navigator receiver
21 p3883 A70-40724
Solar spectral irradiance measurements at different altitudes, using multichannel radiometers
22 p4013 A70-42599

ALTITUDE ACCLIMATIZATION
Book on subatmospheric decompression sickness in man, covering raised intrapulmonary pressure effects and compensating pressure applications [AGARDGRAPH-125] 01 p0019 A70-10514
Hemoglobin concentration in red blood cells in men of various ages as function of altitude, discussing correlations with body weight and plasma protein
01 p0024 A70-10978
Man and animals physiological adaptation and behavior under conditions of polar regions, highland and arid areas
01 p0030 A70-11465
Fructose metabolism in liver and extrahepatic tissues of sea level and high altitude natives, noting lactate and pyruvate accumulation in blood
02 p0233 A70-11722
Cross adaptations of physiological functions, discussing results for heat, altitude and cold adapted animals
02 p0242 A70-12824
Altitude changes effect on brown fat content and metabolism in deer mice, noting oxygen consumption and heat production limitation by hypoxia
02 p0242 A70-12865
High altitude acclimatization effects on cardiovascular system, external respiration, blood composition, optical and vestibular analyzers in human subjected to various stresses
04 p0630 A70-14576
Physiological load of exercise at altitude evaluated by heart rate and recovery rate measurements
04 p0631 A70-14984
Standardized bicycle ergometer training effects at sea level and simulated altitudes, indicating hypoxia potentiating role
05 p0807 A70-16674
Blood volume and circulation rate in dogs subjected to traumatic shock and hemorrhage under high mountain conditions
07 p1198 A70-18708
High altitude and sea level erythropoietic and somatic development in chick embryos indicating optimal physiological adaptation with prolonged exposure
07 p1202 A70-18864
Thorax potential resistivity at sea and high altitude levels measured in children and adults inferring relation to ECG differences
07 p1206 A70-19296

Nucleic acid and protein synthesis dynamics in rat brain and heart during adaptation to high altitude hypoxia
07 p1209 A70-19518
Physiology of high altitude, studying animal and man adaptation and changes in body processes due to life stresses and hypoxia
08 p1441 A70-20469
Parathyroidectomy effects on high altitude adaptation and adrenal cortex activity in rats exposed to chronic hypoxia
08 p1442 A70-20719
Acute oxygen deficiency effects on blood electrolyte concentrations in altitude-adapted and nonadapted humans
09 p1616 A70-22217
Human pulmonary ventilation during exercise in high altitude and sea level acclimated subjects
10 p1819 A70-24774
Human cardiovascular system function during adaptation at various high altitudes using simultaneous EKG and phono-KG recordings
10 p1823 A70-25179
High altitude acclimatization effect on tissue capillarity, investigating physiological evidence in rats by tissue diffusing capacity measurement
10 p1823 A70-25220
Hematologic responses of mice subjected to continuous hypoxia in subatmospheric pressure
11 p1989 A70-26666
Glycolysis and glycolytic enzymes activity increase in tissues observed during training of rats to hypoxia, discussing adaptive reactions at cellular level
12 p2167 A70-26975
Altitude acclimatization protection against lung damage from exposure to oxygen at high partial pressures experimented on rats
12 p2170 A70-27659
Cerebral circulatory reactions of smokers and non-smokers exposed to altitude, measuring vasomotor, blood flow and cardiac frequency indexes using scalp electrodes
12 p2172 A70-28042
Hematology of sea level and high altitude native Sonoran deer mice, correlating hemoglobin electrophoretic patterns with oxygen affinity
15 p2686 A70-32835
Altitude hypoxia adaptation effects on brain protein and RNA synthesis in rats, noting increase in memory resistance to environmental stress effects
17 p3030 A70-35359
Mountain climbing effects on urinary excretion of vanillylmandelic and homovanillic acids, discussing circulatory system acclimatization
17 p3039 A70-35425
Lung diffusing capacity for CO in Caucasians native to 3100 m noting membrane diffusing capacity, lung capillary volume and age effects
17 p3031 A70-35427
Spinal reflex activity in normal and altitude exposed cats before, during and after acute hypoxia
17 p3031 A70-35430
Myocardial contractile function in rats under acute overstrain, evaluating role of preliminary training to altitude hypoxia
19 p3360 A70-37805
Hemodynamic changes in Andean native after two years at sea level, measuring intravascular pressures, cardiac output, heart rate and stroke index
20 p3571 A70-39427
Oxygen breathing effects in exercise on respiration, circulation and metabolism during high altitude acclimatization
24 p4303 A70-46110

ALTITUDE CONTROL
Aircraft optimal spin recovery by aileron, elevator and rudder control calculated using Pontryagin principle to minimize altitude loss
01 p0006 A70-10924
Aircraft altimeter measurement for vertical separation based on atmospheric pressure unit changes /Cayleys/ compared with linear measurements in meters and feet
13 p2411 A70-29778
Supersonic flight altitude stability, studying effects of velocity, lift-drag ratio, thrust law, wind direction, engine unstarts, etc [AIAA PAPER 69-813] 22 p3961 A70-42712

ALTITUDE SICKNESS
Headache and personality traits related to visual acuity and brightness sensitivity increases from sea level to high altitude
04 p0633 A70-15444
Antisickness medications effectiveness and secondary effects during low altitude transport of troops, observing sleepiness but no impairment of physical capacity
12 p2179 A70-28038
Acute mountain sickness symptomatology and cognitive performance, using standardized General High Altitude Questionnaire
20 p3581 A70-40025

Decompression disorders after exposures to safe pressure or altitude in cats, noting potential embolism from nongradual high-to-normal pressure passage
23 p4157 A70-45080

ALTITUDE SIMULATION
High altitude simulation installations design for rocket motors starting tests under long term high vacuum exposure
04 p0736 A70-15179
Altitude simulation equipment for third stage Europa I booster rocket
04 p0664 A70-15302
Mathematical model for oxygen tension changes in dogs brain tissues under hypoxia during altitude simulation
07 p1208 A70-19505
Automatic control theory found effective in studying arterial blood saturation with oxygen during ascent to 4000 m in pressure chamber
07 p1210 A70-19523
Mathematical model for oxygen tension changes in dogs brain tissues under hypoxia during altitude simulation
11 p1987 A70-26104
Altitude Test Facility in air breathing aircraft engine design, discussing plant, test cells design and flight representation and systems accuracy
13 p2473 A70-28538
Turbofan engine gross thrust dependence on nozzle pressure ratio and simulated flight Mach number, considering altitude chamber test data [AIAA PAPER 70-612] 16 p2969 A70-33608
Mice immunobiological reactivity at simulated high altitude
20 p3575 A70-40189
Aircraft propulsion system test facilities, discussing altitude simulation, large subsonic and supersonic engines and component development [ICAS PAPER 70-45] 23 p4178 A70-44143
Bends incidence in altitude training, examining denitrogenation role
24 p4307 A70-45339

ALTITUDE TESTS
NT HIGH ALTITUDE TESTS
Altitude effects on Borkenstein Breathalyzer accuracy determined from alveolar ethanol analysis
06 p1000 A70-17303
Thorax potential resistivity at sea and high altitude levels measured in children and adults inferring relation to ECG differences
07 p1206 A70-19296
Drug-alcohol and hypoxia effects on multiple task operator performance tested at altitude and pressure chamber treatments
08 p1448 A70-21939
Altitude influence on forced ventilation of cooled electronic apparatus, analyzing flow change and temperature roles
09 p1643 A70-22040
Rats heart rate change during running at simulated altitude, discussing respiratory-circulatory training effect
11 p1985 A70-25671
Altitude and alcohol intake effects on blood alcohol concentrations
24 p4306 A70-45329

ALTITUDE TOLERANCE
High altitude environmental effects on adrenal glands and hypothalamic neurosecretion in rats
04 p0629 A70-14568
Motivation changes in rabbits exposed to increasing hypoxia in pressure chamber altitude simulation
07 p1208 A70-19506
Rats acute hypoxia and altitude tolerances after prolonged exposure to hyperoxic atmospheres
08 p1446 A70-21437
Human sea-level natives physiological changes during high altitude physical exercise, considering carbon dioxide arterial pressure, plasma cortisol, adrenal function indexes, etc
08 p1453 A70-21873
Decompression rates effect on altitude tolerance of white rats, discussing hypoxia influence on cardiovascular, respiratory, circulatory, thermal control and central nervous systems
09 p1614 A70-22084
Motivation changes in rabbits exposed to increasing hypoxia in pressure chamber altitude simulation
11 p1987 A70-26105
High altitude effects on total protein content and composition in rats blood serum
13 p2352 A70-29346
Hypoxia tolerance in white rats after exposure in hypercapnic medium
13 p2355 A70-29757
High altitude liver function and blood flow, determining bromsulphthalein transport maximum and storage capacity and galactose elimination
15 p2683 A70-32531
Decompression rates effect on altitude tolerance of white rats, discussing hypoxia influence on cardiovascular, respiratory, circulatory, thermal control and central nervous systems
15 p2685 A70-32680

Hypoxia and high ambient temperature effects on altitude tolerance in animals 20 p3575 A70-40186

ALU [COMPUTER COMPONENTS]

U ARITHMETIC AND LOGIC UNITS

ALUMINA

U ALUMINUM OXIDES

ALUMINATES

Fuel cells phase equilibria between carbonate melt and Li, Na and K solid aluminate electrolytes, analyzing thermal and electrical conductances 10 p1830 A70-24458

ALUMINIZING

U ALUMINUM COATINGS

ALUMINUM

NT ALUMINUM ISOTOPES

NT ALUMINUM 26

NT ALUMINUM 27

NT POWDERED ALUMINUM

NT SINTERED ALUMINUM POWDER

Ultrasonic detection of service induced cracks near tenon base region of second stage Al compressor disks 01 p0096 A70-10003

Fiber breakage during powder metallurgy fabrication of compact Al-B composites as function of density 01 p0104 A70-10741

Creep propagation determination in pure Al for microscopic and macroscopic continuum points used for determining stiffness and strain time history 01 p0121 A70-11156

Al double crystals mechanical properties improvement after shock loading, studying surface and dislocation structures and active slip planes number 01 p0124 A70-11449

Al-B composite missile adapter design for aerospace structures 02 p0306 A70-11951

Aluminum additives effects on stoichiometric ammonium perchlorate/polyformaldehyde mixtures deflagration, determining temperature distribution, burning rate dependence on pressure and heat flow due to radiation 02 p0351 A70-12004

Effects of solidification conditions and gas content in melt on continuously cast Al ingots as-cast structure 02 p0316 A70-12297

Al solidification in direct chilling molds effect on as-cast structure, analyzing heat removal, casting rate and application of water to outgoing ingot 02 p0316 A70-12298

Grain refining of continuously cast Al by additions of B and Ti 02 p0309 A70-12299

Fracture surface topography variation with specimen thickness, studying fatigue crack propagation in Al 02 p0317 A70-12317

Magnetic flux trapping experiment with Al conductor, showing decay time constant connection with sunspot theory 02 p0299 A70-12393

Out-of-phase or nonsynchronous biaxial straining effects on low cycle fatigue observed on Al specimen by cycling tension-compression and cyclic torsion 03 p0481 A70-12955

Stress distribution along stud hole threads in Al case, investigating stud design effect using strain gauge on models 03 p0585 A70-12962

Mechanical properties of Al composites reinforced with alpha-silicon carbide sintered whiskers, discussing voids, fiber breakage and orientation effects 03 p0506 A70-13113

Modified explosive bonding process for welding wire reinforced Al composite materials 03 p0497 A70-13120

Al extrusions, discussing tooling, controls, indirect extrusion, drawn tubing and painted extrusions 03 p0512 A70-13777

Al and Sn composites reinforced by E glass and silicon dioxide glass fibers compared for tensile strength, noting difference due to resistivity 03 p0514 A70-14314

Ni-Cr alloy oxidation resistance dependence on small amount of Al at high temperatures, noting role of protective oxide layer 03 p0514 A70-14315

Al fasteners design guidelines including material forming capabilities, cost consideration, applications, etc 04 p0697 A70-14722

Activation energy measurement using stress relaxation for plastic flow in commercially pure Al compared with creep and tensile method 04 p0777 A70-15495

Sliding wear of bearing Al lubricated with polyphenyl ethers in boundary region tested by pin and cylinder wear machine producing continuous record 05 p0854 A70-15910

Al foil exposed to solar wind on moon during Apollo 11 mission examined for helium particles, finding lunar solar wind albedo 05 p0900 A70-16093

Reflectance of clean and fluoride coated aluminum surfaces in vacuum UV 05 p0883 A70-16590

Structural changes in polycrystalline Al subjected to HF fatigue, using transmission electron microscopy 06 p1084 A70-17127

Cold reduction effects on press formability of pure Al sheet with allowance for tensile properties and crystallographic orientation 06 p1075 A70-17145

Cold reduction and annealing temperature effects on Al sheet ductility noting roles of hardness, crystallographic orientation and microscopic structure 06 p1075 A70-17146

Creep deformation resistance decrease in pure Al tubular specimens at high temperatures under multiple stress reversals 06 p1087 A70-17456

Sapphire whisker-Al composites fabrication methods using air elutriation techniques and semiautomatic methods for fiber alignment, discussing elastic modulus, tensile strength, etc 07 p1314 A70-19956

Deformation amplitude effects on dislocation structure and strengthening mechanism of fcc aluminum under cyclic loading 08 p1516 A70-20985

Graphite shell molds for Al castings mass production 08 p1505 A70-21135

Porosity formation in Al ingots made by semicontinuous casting, considering metal grade and purity, gas content and homogenization conditions 08 p1505 A70-21136

Al weld metal compositions and hydrogen content effects on weld porosity, locating hydrogen in weld by radioactive tracers 08 p1507 A70-21485

Compression test data of Al-B composites used for predicting structural element failure 08 p1523 A70-21886

Fractography of Al-B metal matrix composites to study micromechanical behavior, using scanning electron microscopy 08 p1524 A70-21913

Al n-type Si Schottky barrier diode characteristics, discussing I-V, barrier height, temperature dependence, photoemission, LF noise, etc 09 p1644 A70-22210

Cubic texture components preferred orientation shares into rolling texture during cold rolling of aluminum sheets determined quantitatively 09 p1690 A70-22255

Al-B composites mechanical properties, using heat treatments and transverse steel wires to increase matrix shear and transverse tensile strengths 09 p1701 A70-22551

Limit and shakedown loads in creep range investigated on sheet rolled aluminum at room temperature for structural design applications 09 p1775 A70-22591

Earing during rolling of high purity aluminum on broad hot-strip mill, investigating thickness, temperature and composition relationship 09 p1692 A70-22641

Laser-produced Al plasmas linear and nonlinear behavior, using framing camera and energy absorption measurements to study outermost ion energy increase and luminous front expansion 09 p1736 A70-23187

Silicon oxide films coated satellite aluminum surfaces solar absorptivity and thermal emissivity, noting suitability as temperature control coatings 09 p1613 A70-23514

Al and B particles combustion in methane-oxygen system, considering reaction zone models, energy release rate, particle kinetics, instabilities, etc 11 p2149 A70-26284

Aluminum sheets anomalous plastic behavior under balanced biaxial and uniaxial tensions 12 p2324 A70-27398

Aluminum-boron composite material applications to structural components of F-106 aircraft, noting weight saving and mechanical properties [AIAA PAPER 68-975] 12 p2257 A70-28082

Aluminum oxide composite steady state creep due to grain boundary sliding, accounting for activation energy level 12 p2258 A70-28348

Tensile prestrain effect on yield locus of thin walled Al tubes from stress tests in torsion-tension space 13 p2431 A70-28536

Ductile fracture in Al matrix composite reinforced with unidirectional stainless steel fibers described by critical crack tip displacement and fracture strain criteria 13 p2512 A70-28917

Weld quality relationship to aluminum surface contamination by hydrogen-containing compounds 13 p2407 A70-29108

Solid state welding processes for space, nuclear and deep submergence technologies, discussing diffusion bonding of Al and stainless steels 13 p2419 A70-29117

Borsic-aluminum composite materials fabrication, properties and applications to aircraft parts 13 p2420 A70-29246

Aluminum-boron composites for aircraft adapter fabrication 13 p2435 A70-29247

Polycrystalline Al microstrain distribution nonuniformity under creep and static tension 14 p2595 A70-30173

Preignition and combustion kinetics in airstream of Mg and Al suspensions in aviation kerosene and gasoline 14 p2664 A70-30395

Convective heat transfer from rotating Al spheres in air at rest, investigating structure and boundary layer changes by schlieren method 14 p2665 A70-30398

High temperature elastic moduli of slender polycrystalline aluminum rods with elastic waves generated by Q switched laser energy 14 p2595 A70-30638

Lubricant ingredients and additives properties effect on surface quality of cold rolled semifinished Al products 14 p2590 A70-30837

In-place gas tungsten arc fusion welding for joining small diameter precipitation hardenable aluminum tubing 14 p2590 A70-30930

Al and Be single particles combustion in various oxidizers, using pulsed Nd-glass laser and Xe flash heating device and scanning electron microscope 14 p2628 A70-30949

Uniaxial yielding correlation with substructure in Al-stainless steel metal matrix composites, using compressive loading test 15 p2756 A70-31565

Photoemission of electrons and holes from Al into aluminum oxide, giving approximate energy band diagram of Al-aluminum oxide interface 15 p2783 A70-31759

Beryllium fibers and Al matrix interactions at high temperatures and various durations, investigating diffusion by X ray diffraction, electron microscope and microprobe analysis 15 p2757 A70-31812

Torsional vibrations amplitude effect on polycrystalline Al stress-strain curve during uniaxial tensile test 15 p2758 A70-32125

Spectral emission in trivalent Ho doped Yb-Al garnet single crystals grown by optical zone melting 15 p2784 A70-32198

High temperature elastic moduli in polycrystalline Al rods from propagation velocity of elastic waves generated by Q switched laser [SESA PAPER 1641] 15 p2759 A70-32304

Al-B composites forming and machining, discussing tooling, methods and filament orientation [ASM PAPER W70-5.2] 15 p2744 A70-32334

Ultrasonic Al wire bonding for microelectronic applications, discussing tensile strength dependence on machine parameters and aging 15 p2747 A70-32647

Metastability effects on plastically deformed Al, showing superplastic flow 15 p2764 A70-32902

Super plasticity in plastically deformed pure Al related to recrystallization 15 p2764 A70-32903

Heterodiffusion coefficients and activation energy for Cu, Ag and Au impurities in Al, using gamma spectrometry and X ray emission microanalysis 16 p2930 A70-33081

Spall nucleating mechanism for Al, noting microcracks in embedded particles 16 p2991 A70-33894

Surface interaction between Al single crystals in ultrahigh vacuum, investigating galling, distortion and adhesion 16 p2924 A70-34168

Al pressure-welded joints strength, investigating surface treatment role 16 p2924 A70-34340

Al, Ga and In effects on creep and rupture stress of Ti at 500 C 17 p3120 A70-34425

Shock propagation in Al fiber-poly(methyl methacrylate) composite, calculating pressure, densities, internal energies and particle velocities 17 p3182 A70-34556

Al single crystals hardening under low temperature reactor irradiation, emphasizing yield phenomenon associated with Luders bands 17 p3123 A70-34647

Temperature and strain rate effects on polycrystalline Al strength 17 p3124 A70-34655

Aluminum spherical particles nonautonomous and autonomous combustion in O with N or Ar initiated by HF induction heating 17 p3145 A70-35042

Aluminum particle combustibility in deflagration zone of ammonium perchlorate pellets, measuring combustion rate and pyrolytic behavior 17 p3145 A70-35208

Lithium-like line spectra in Mg, Al and Si observed with grazing incidence spectrometer and low inductance microfarad spark source 17 p3138 A70-35270

Rolled fine grained aluminum-alumina particles composites, determining creep strength dependence on temperature and tensile stress axis orientation 18 p3274 A70-36051

Al particles fusion during combustion of stoichiometric mixtures of ammonium and potassium perchlorate and polyformaldehyde 18 p3299 A70-36246

Al spheres hypervelocity impact against dry quartz sand targets in light gas gun facility, discussing energy partitioning 18 p3344 A70-36769

Welded Al plates high temperature bend tests, describing materials and procedures 18 p3278 A70-37115

Deformed single crystals of high purity Al of different orientation with respect to growth during recrystallization 19 p3450 A70-37373

Longitudinal and transverse tensile strengths of Al sheet reinforced with continuous oriented steel wire of various cross sectional shapes 19 p3541 A70-38047

Clamped circular shallow Al arches stability under impulsive loading, obtaining deflection time history by high speed photography and computerized data reduction 20 p3732 A70-40265

Surface films effect on thermal contact conductance of aluminum surfaces contacting in high vacuum environment 21 p3944 A70-41024

Accelerated failure tests of ammonia-Al-stainless steel heat pipes for fluid loss or energy transport degradation 21 p3947 A70-41049

Creep and stability of microstructural Al elements under varying temperatures, noting grain boundary migration 21 p3839 A70-41429

Al yield surfaces in stress space at elevated temperatures for virgin and prestressed material in torsion 21 p3840 A70-41436

Apollo 11 lunar rocks and fines oxygen, Si and Al content determination by neutron activation analysis 21 p3774 A70-41566

Forces acting at thrust termination time with aluminum solid propellant rocket fuel, predicting thrust reversal ratio under vacuum conditions 21 p3869 A70-41869

Butt joined epoxy Al plates tensile strength, observing fracture strength dependence on stress concentration at bond edges below characteristic crack length 21 p3939 A70-42032

Thin film granular aluminum superconductors as sensitive thermometers 22 p4031 A70-43009

Copper and Al polycrystalline single crystal substructure changes, examining high temperature, unsteady and diffusion creep 22 p4056 A70-43342

Tubular Al creep resistance increase by temperature jumps during steady phase of creep 22 p4056 A70-43344

Silicon precipitation in nonrefined annealed Al, examining heat treatment effects 22 p4057 A70-43550

Boron-Al composite filament fracture behavior and postimpact tensile strength, examining shock loading and impact velocity effects 22 p4060 A70-43682

Thin metal matrix composite rods elastic properties, examining Al-W system by Young and shear modulus measurements 22 p4061 A70-43687

Book on fatigue crack propagation in pure Al covering tension and compression tests, single and polycrystalline materials, elastic stress, notched and smooth specimens, etc 22 p4057 A70-43740

Al and W specific heat and Al heat of fusion by quasi-adiabatic calorimetry, estimating anharmonic lattice vibrations role via atomic thermodynamic analysis 23 p4208 A70-44931

Pure Al thermal cycling tests, investigating effect of minimizing thermal stress during quenching on behavior of dislocations 24 p4360 A70-45518

Al and liquid Al-Mg alloys oxidation at high temperatures, noting Mg content effect 24 p4361 A70-46174

Cyclic loaded high purity Al samples, noting substructure around fatigue cracks 24 p4362 A70-46185

Thin Al foil subjected to cyclic bending stresses, investigating substructures and strain regions around fatigue crack 24 p4362 A70-46186

Al purification by subhalide reaction, discussing contamination sources and thermodynamics 24 p4349 A70-46187

ALUMINUM ALLOYS

Gamma ray beam inspection of opposed arc weld with nugget penetration in Al-Cu alloy, including averaging circuit reducing counting statistics variation 01 p0054 A70-10020

Inconel 718 and Al 2219 alloys surface flawed specimens fracture toughness and flaw growth comparison for high pressure hydrogen vessel 01 p0114 A70-10029

Loading frequency effects on Duralumin endurance limit in air and in water, noting stress level role 01 p0115 A70-10070

Stress criterion for unstable crack propagation from Al alloy sheet tests, examining fracture data for vessels of various geometries and materials [ASME PAPER 69-SESA-2] 01 p0117 A70-10451

High speed hail impact damage on flat Al alloy plates observed for effects of impact angle and velocity, plate material properties and thickness 01 p0056 A70-10690

Stress corrosion cracking in Cu-Al alloys shown dependent on alloy and Cu ion content, solution pH and stress level, discussing tarnish film formation role 01 p0119 A70-10734

Offset yield strengths of TD-Ni and Al- aluminum oxide SAP type two phase alloys in tension and compression 01 p0119 A70-10736

Aluminum alloys fatigue properties tested at ultrasonic frequencies 01 p0120 A70-10879

Ternary chemical element additions (O, Sn, Zr, Pb, Mo, V) effects on solubility range of primary alpha region of Ti-Al base alloys 01 p0122 A70-11239

Semicoherent interface dislocations in directionally solidified Ni-Al-Cr eutectic, discussing lattice mismatch 01 p0123 A70-11247

Ternary Al-Zn-Mg alloys stress corrosion cracking properties, showing effects of aging temperature and prestrain 01 p0123 A70-11387

Metal fatigue in Al alloys subjected to stress cycles, determining macrocracks propagation stages 01 p0122 A70-11607

Ti-Al-Co alloys melting points and cast structures, discussing reactions with melt 01 p0125 A70-11644

HF endurance tests of Al sheet alloy used in welded aircraft structural components, plotting curves for heat treated and untreated specimens 02 p0315 A70-11658

Al alloys strips weakened by holes, analyzing limiting tensile load-carrying capacity 02 p0384 A70-11741

Temperature dependence of magnetic susceptibility in liquid and solid states of binary Al-Mn alloys with additions of Cr, V and Ti 02 p0316 A70-12300

Mechanical strength and breakdown metallography of plate shaped structural steel and Al alloy specimen under various HF elastic vibrations 02 p0318 A70-12398

Al alloy rectangular beam stress corrosion crack initiation and propagation measurement using ultrasonic techniques, showing relationship between crack velocity and initial stress 03 p0481 A70-12958

[SESA PAPER 1564] Galvanic cell using liquid Mg chloride or Mg chloride-Ca chloride mixtures as electrolyte used to determine activities in Mg-Al liquid alloys 03 p0507 A70-13138

Al-Ni intermetallic whisker-reinforced Al microstructure and mechanical properties, studying effects of cold rolling 03 p0508 A70-13142

Al alloy and structural steel fatigue strength under superelastic cyclic axial stresses, describing observed plastic deformation patterns 03 p0509 A70-13271

Prolonged temperature exposures with applied tensile stress found to increase tensile strength and yield point of aluminum alloy subjected to artificial agings 03 p0511 A70-13354

Al-Zn-Mg-Cu alloy corrosion cracking, studying effects of heat treatment, strain percent, blank parameters and grain size 03 p0512 A70-13734

Cyclic hysteresis-loop stress-strain behavior of 1100 aluminum, deriving power function [ASME PAPER 69-WA/MET-1] 04 p0705 A70-14764

Notch-bend strength of titanium, aluminum and copper base alloys, noting geometrical size effect [ASME PAPER 69-MET-D] 04 p0705 A70-14878

Crack propagation rate in aluminum alloy plates under cyclic tensile and transverse shear loadings, noting sliding mode increasing effect [ASME PAPER 69-MET-1] 04 p0705 A70-14881

Structural aluminum alloy developed for Concorde Mach 2.2 flight, discussing cold mechanical properties, zero creep and fatigue resistance 04 p0706 A70-15041

Supersaturated Al alloy with Zr addition at high temperatures, showing tetragonal equilibrium phase and intermediate phase with cubic structure 04 p0708 A70-15369

Heat treatment produced semicoherent and incoherent precipitations diminished susceptibility to stress corrosion cracking of aluminum binary and ternary alloys 04 p0708 A70-15370

Aluminum alloys intergranular and stress corrosion, noting electron microscopy application for alloys performance improvement 04 p0710 A70-15680

Divergences in tension textures and values of anisotropy coefficients ascribed to imperfections in cubic texture of aluminum sheet deformed by straining 05 p0927 A70-15995

Brittleness of joints using Ga solders prevention by high temperature annealing noting application to aluminum alloys 05 p0855 A70-16199

Al alloys crack growth effects due to gaseous environment and fatigue frequencies, suggesting role of gas adsorption 05 p0938 A70-16478

Binary Al-Y system thermal and microstructural analyses at room temperature and 200 C, obtaining partial diagram and mechanical properties 05 p0864 A70-16546

Fatigue defects accumulation in aluminum alloy under impact tensile loads programmed to simulate loads encountered by aircraft in practice 05 p0947 A70-17009

Vibration damping properties of steels and Ti- and Al-based alloys at various temperatures under tensile and compression loads 05 p0868 A70-17048

Recrystallization behavior of Al alloy containing Mg and Si subjected to maximum aging before cold working 06 p1085 A70-17418

Al casting design considering alloy materials selection and casting methods 06 p1076 A70-17602

Thin walled tubular aluminum specimens hardening by temporary reduction of temperature during creep under torsion 06 p1089 A70-17795

Al-Zn-Mg alloys anodic corrosion behavior under various heat treatment regimes using potentiostatic method 06 p1090 A70-17922

Vibrational creep curves of Al alloy under uniaxial stress level and amplitude, noting influence of small vibrations 06 p1168 A70-17930

Vibration frequency influence on vibrational creep of Al-Mg-Si alloy, describing mechanism in terms of strain hardening, additional slip and dislocation movements 06 p1168 A70-17931

Al alloys flash welding for rings used in Poseidon program 06 p1078 A70-18502

Joint design for braze bonding and joining of Al-B composites using Borsic tape backed with alloy brazing foil 07 p1293 A70-18994

Crack behavior of Al alloy as cryogenic tankage material, establishing relationship of temperature effects and basic crack size to failure stress 07 p1279 A70-18997

Heat transfer effects during solidification on mechanical properties of Al alloy castings compared with sand castings [ASM PAPER W9-7.2] 07 p1293 A70-18998

Chemical composition and heat treatment effects on deformation resistance of nonaging aluminum alloys during hot working, noting quenching effect on recrystallization 07 p1294 A70-19388

Interrelation of precipitation state, mechanical properties and electrical conductivity of wrought aluminum age hardened alloy under varied heat treatment conditions 07 p1294 A70-19389

Ternary Al-Mn alloys precipitation hardening with Cr, V and Ti, investigating ferro and ferrimagnetic phases 07 p1307 A70-19390

Stress and intercrystalline corrosion causes and sensitivity in supersaturated Al alloys 07 p1307 A70-19391

Microbiological corrosion effects on aluminum alloy fatigue properties inducing further microbiological corrosion compared to chemical corrosion effects 07 p1310 A70-19735

Duraluminum sheets fatigue life and corrosion fatigue strength decrease with corrosion damage area increase

08 p1515 A70-20921

Creep strain effect on cyclic fatigue life of duraluminum at room temperature

08 p1516 A70-20988

Soviet papers on casting of aluminum, magnesium and titanium alloys

08 p1504 A70-21126

Rare earth elements effects on microstructures and mechanical properties of cast Al, Al-Si and Al-Si-Mg alloys

08 p1516 A70-21127

Al-Cr-Zr alloy ingots microstructural inhomogeneities, studying roles of casting rate and additives in intermetallics primary crystallization

08 p1517 A70-21128

Al-Mg alloys mechanical properties and corrosion resistance during aging, noting Zr and Mo additives effects

08 p1517 A70-21129

Al-Mg oxidation resistance and kinetics, studying Zr, Ce and Be additives effects on oxide films mechanical properties

08 p1517 A70-21130

Al alloys melting in flame furnaces, studying oxidation and various sources of metal losses

08 p1505 A70-21131

Molten Al alloys flow rate and behavior in various casting systems, considering gate geometry and casting temperature effects

08 p1505 A70-21133

Mold canting effects on nonporosity of Al alloys flat castings noting decreased metal losses

08 p1517 A70-21134

Optimum composition of sand-bentonite materials for aluminum alloy casting in molds compacted by high pressure

08 p1506 A70-21137

Aluminum-base reinforced material synthesis by liquid impregnation, investigating transition layer dependence on holding time and fiber/matrix microhardness

08 p1520 A70-21500

Thermal and athermal components of flow stress and deformation dynamics in Ti-Al alloy

08 p1521 A70-21578

Axial constant load creep and strength rupture measurements of B-coated and silicon carbide-coated B filament reinforced Al alloys

08 p1521 A70-21702

Wrought aluminum based high strength alloys structure and mechanical properties

08 p1522 A70-21708

Projectile penetration of Al alloys, noting melting during intense shear band formation

08 p1522 A70-21710

Al alloy matrix composites with beta-SiC whiskers reinforcement, evaluating tensile and fatigue properties

08 p1523 A70-21856

Transverse and shear strengths of Al-B composite materials used in F-111 aircraft components, investigating cold work, thermal treatments and steel wire addition effects

08 p1509 A70-21857

Fatigue testing and thermal mechanical treatment effects on uni- and biaxial Al alloy-B composites tensile strength at room and elevated temperatures

08 p1523 A70-21893

Tensile, fatigue, creep and stress-rupture behavior of unidirectional, unidirectional off-axis and cross-ply composites of B filaments in Al alloy matrix

08 p1531 A70-21896

Stainless steel wire-reinforced Al alloy diffusion bonded scarf joints, considering aluminum oxide coating and bonding times effects

08 p1509 A70-21906

Aged Al-Cu alloys hardness test data normalized and correlated for interpretation in terms of physical metallurgy

08 p1525 A70-21967

Al alloys fatigue cracks propagation rate using electron microfractography

09 p1701 A70-22223

High strength stress corrosion resistant aluminum alloy die forgings, evaluating tensile, tensile fatigue and fracture toughness properties

09 p1702 A70-22556

Stress concentration effect on fatigue strength of Al- and Mg-base structural alloy specimens of different sizes analyzed statistically

09 p1703 A70-22617

Fatigue limit and rupture stress distribution patterns of Al- and Mg-base structural alloys using accelerated Prot and Enomoto methods

09 p1703 A70-22621

Cold and hot work deformation of aluminum alloys, discussing flow-stress dependence on strain rate, temperature and composition

09 p1692 A70-22642

Al and Ti alloys residual stress determination by X ray diffraction

09 p1704 A70-22796

Fracture mechanics model for stress corrosion cracking of Al alloys, discussing bond strength lessening by adsorption of damaging species

09 p1706 A70-22941

Additive elements effect on structure and properties of sintered powdery Al-Cr and Al-Fe alloys obtained by atomization method, analyzing homogeneity

09 p1707 A70-23124

Gamma prime phase structure ordering effect on critical shear stresses of aging Ni-Al alloys and nimonic

09 p1707 A70-23195

Al alloys fatigue properties dependence on surface oxide cracking in moist and dry air, investigating oxidation and kerosene processing

09 p1707 A70-23206

Lattice defects in Al-Zn alloy due to fatigue investigated for mechanism and effect on aging kinetics by resistivity measurement

09 p1707 A70-23326

Failure compression tests of flat rectangular Al alloy panels presented in unitary form, adopting structural load index for solution from weight standpoint

09 p1782 A70-23376

Annealing effect on stress-strain curves of overaged and cold-rolled Al-Li alloy, observing yield drop

09 p1708 A70-23727

Phase diagram of rapidly crystallized Al-Cu-Mn alloys, observing ternary solid solutions formation during high cooling rate of melt

09 p1709 A70-23786

Phase equilibrium diagram and heat resistance of Ti-Al-Nb alloys along radial section by thermal and microstructural analysis

09 p1709 A70-23789

Aluminum and aluminum-copper alloys dislocation damping at high strain rates using impact shear tests

10 p1903 A70-23983

Al-Si and Cu-Ti eutectic alloys showing good ohmic contacts to SiC

10 p1927 A70-23990

Thickness effects on elongation of sheet type Al alloys, tabulating tensile test results

10 p1887 A70-24043

Aluminum alloy deformations and rupture strength under complex stress at low temperatures, observing anisotropy decrease with temperature

10 p1903 A70-24243

Raney alloy catalyst activity and stability in fuel cell anodes, noting properties of ternary phases of nickel, aluminum and iron, molybdenum or titanium

10 p1831 A70-24466

Rapid expansion of thin walled aluminum alloy cylinders under pulsed magnetic field pressure using high speed streak camera oscillography

10 p1964 A70-25120

Aluminum alloys hot cracking during welding, ascribing failure to combination of strain and susceptible microstructure

10 p1897 A70-25313

Hypercritical crack growth resistance and notch toughness of aluminum alloys derived from fracture tests

11 p2064 A70-25331

Sinusoidal and random loading response of age hardening aluminum alloy determined by fatigue testing

11 p2133 A70-25732

Zone and phase aging of aluminum alloys, discussing structural and property characteristics of solid solution decomposition

11 p2066 A70-25912

Tensile strength of nitrided boron-aluminum alloy composite modules, noting effect of Ti cladding on panel surfaces

11 p2066 A70-26085

Stress ratio effects on Al alloy during crack propagation and fatigue, introducing notch stress and strain approximations

11 p2066 A70-26089

Prestrain and mean stress effects on fatigue life using cumulative damage procedure based on Al alloy and aircraft quality steel tests

11 p2137 A70-26092

Stress level, block size and constant and variable loading sequence effect on fatigue life of Al alloy box beams

11 p2138 A70-26094

Fatigue life tests of Al alloy under narrow and broad band random loads based on number of peaks to failure

11 p2066 A70-26095

Surface sliding friction interactions in aluminum alloys friction welding

12 p2239 A70-26855

Fiber reinforced Al alloys fabrication by thin sheet metallurgy techniques

12 p2252 A70-26887

Spacecraft propellant tank development from Al alloy providing excellent weldability, propellant compatibility and strength to weight ratio

12 p2242 A70-27108

Decomposition of supersaturated solid solutions in granulated Al alloys with Mn, Cr, Zr, Ti, V and Mo, studying microhardness and electrical resistivity

12 p2258 A70-28274

Fatigue crack propagation dependence on environment and load frequency in Al alloys, correlating data by stress-intensity factor

13 p2431 A70-28603

Fatigue crack growth dependence on load profile, temperature, test frequency and environment and stress in high strength Al and Ti alloys and steels

13 p2431 A70-28604

Large deflections in impulsively loaded clamped circular Al alloy and steel viscoplastic plates

13 p2511 A70-28736

Inhibitive elastomeric sealing compounds and coating systems preventing aluminum alloy corrosion in aircraft

13 p2433 A70-28778

Li and Cr additives effects on Al-Zn-Mg stress corrosion resistance, considering cracking, precipitation hardening and intercrystalline corrosion

13 p2433 A70-28844

Thermodynamic data for chemical reactions of Ti alloys formation with Al obtained by measuring galvanic cells emf with solid electrolytes at elevated temperatures

13 p2434 A70-28889

Vibrocreep effect on Al-Mg-Si alloy vibration frequency and mean and maximum stress at constant temperature

13 p2512 A70-28980

Structural Al-Zn-Mg alloys strain hardening effect on mechanical and corrosion properties, noting relationship between stress corrosion cracking and shear cracks

13 p2434 A70-29155

Thin walled duralumin cylinders catastrophic fracture analysis by linear elastic fracture mechanics noting fatigue crack propagation

13 p2434 A70-29173

Quality control technique for predicting exfoliation and stress corrosion resistance of Al alloy sheet and plate

13 p2435 A70-29175

Ti-8Al alloy embrittlement from ordered phase precipitation during aging using tensile, impact and hardness tests, optical and electron transmission microscopies

13 p2436 A70-29624

Hot torsion test for Al alloys workability assessment, noting test temperature and specimen geometry effects on fracture strain values

13 p2436 A70-29816

Growth kinetics of strengthening phase during aging of Ni-Cr-W-Mo-Al-Ti alloys, considering gamma prime particles at different Al/Ti ratios

14 p1594 A70-30169

Particles shape and phase composition in combustion products of dispersed Al-Mg alloy powders by electron diffraction and X ray analysis

14 p2664 A70-30396

Be-Al-Ti system liquidus surfaces and invariant equilibria by chemical, thermal, X ray and microscopic methods, discussing phase diagrams

14 p2595 A70-30839

Soviet collection of papers on Al weldable alloy including sheets, heat treatment, aging, mechanical properties, etc

14 p2596 A70-30960

Al heat treatable alloys for welded structures, considering stress corrosion resistance, aging effects, brittle and delayed rupture resistance, etc

14 p2596 A70-30961

Al-Mg alloy sheets work hardened plastic properties, tensile strength and elongation

14 p2597 A70-30962

Work hardening and tempering effects on Al-Mg alloy stress corrosion and mechanical properties

14 p2597 A70-30963

Al-Zn-Mg weldable alloy composition, mechanical properties, heat treatment, aging effects, etc

14 p2597 A70-30964

Al-Zn-Mg alloys aging kinetics and rupture mechanism, discussing stress corrosion, welded structures stability, activation energy, etc

14 p2597 A70-30965

Al-Mg-Zn alloy composition, mechanical properties and structure for various heat treatments, discussing welded structures stability, stress relief, corrosion resistance and tensile strength

14 p2597 A70-30966

Al alloy welded sheets strength and plasticity under biaxial tension, examining excess elastic energy effects on strain kinetics and rupture

14 p2597 A70-30967

Al weldable alloys for cryogenic applications, considering plasticity, brittleness and tensile and yield strengths at low temperatures

14 p2597 A70-30968

Al alloy welded joints delayed rupture tendency, describing constant load test method

14 p2591 A70-30969

- Al-Zn-Mg alloy welds delayed rupture under constant uniaxial load in distilled water or aqueous salt solution 14 p2591 A70-30970
- Al-Zn-Mg high strength weldable alloys rupture characteristics, analyzing crack distribution, stress raisers and weld defects 14 p2591 A70-30971
- Al-Mg, Al-Zn-Mg, Al-Cu and Al-Cu-Mg welded alloys corrosion cracking resistance as function of composition and fabrication techniques 14 p2597 A70-30972
- Al-Mg alloy nonpropagating fatigue cracks at roots of sharp notches, discussing cyclic strain hardening 14 p2598 A70-31299
- Aluminum alloys endurance limit determination by accelerated methods, evaluating errors by comparison with conventional tests 15 p2755 A70-31539
- Al-Zn eutectoid alloys defect structures and interactions in superplastic deformation process 15 p2756 A70-31567
- Residual stress measurement in anodic film on duraluminum as function of film thickness and cyclic loadings in air and corrosive media 15 p2757 A70-31635
- Biaxial stress effect on fatigue crack propagation in Al alloy plate under reversed bending 15 p2821 A70-32324
- Environmental fatigue crack propagation in Al alloys at low cyclic stress intensity levels 15 p2762 A70-32390
- Al-Mg alloys creep characteristics dependence on Ag, Si and Zn additions during aging heat treatments, establishing activation energy and stress exponents 16 p2930 A70-33086
- Ti-Al alloy crystallographic structure, observing hexagonality for alpha phase 17 p3114 A70-34377
- Metastable Ti alloys beta-omega-alpha decomposition and Ti-8Al alpha-ordered alpha transformation, using automatic measuring apparatus 17 p3118 A70-34409
- Aircraft structural materials, considering high strength steels Al and Ti alloys 17 p3124 A70-34675
- Neutron irradiation effects on stress corrosion susceptibility of Al alloy 17 p3124 A70-34822
- Surface alloying of high melting points in Al melts, noting prior oxidation enhancement and simplifying of calorizing techniques 17 p3102 A70-35406
- Grain boundary allotriomorphs growth mechanisms in Al-Cu alloy at high temperatures, indicating interfacial and direct volume diffusion 18 p3271 A70-36027
- Corrosion and stress corrosion behavior comparison of aged Al-Zn-Mg alloy in aqueous chloride solution, discussing pH variation effect 18 p3271 A70-36028
- Deformation behavior of continuous W and B fibers reinforced Al alloy matrix composites, monitoring stress-strain characteristics by X ray diffraction 18 p3272 A70-36036
- Ti-Al alloys room temperature mechanical properties after age hardening 18 p3274 A70-36055
- Deformable Al alloys hardening, emphasizing heat treatment in solid state 18 p3276 A70-36308
- Critical loads for notched square Al alloy rods under tension 18 p3343 A70-36718
- Close-confinement LPE /AlGa/As junction laser properties, examining range of alloy direct bandgap transition 18 p3268 A70-36727
- Al alloy matrix-boron fiber-stainless steel wire composites fabrication into various shapes with desired mechanical properties for aerospace structural components applications 18 p3263 A70-36837
- Al alloys missile splice rings fabrication, discussing extrusion, draw forming, flash butt welding and stretch sizing 18 p3264 A70-37112
- Al-Si welding rods tests with various surface finishes, considering oxide coatings effect on gas tungsten arc weld quality 18 p3264 A70-37113
- Porosity effects on mechanical properties of high strength Al alloy weldments 18 p3265 A70-37204
- Porosity effects on mechanical properties of Al alloy gas tungsten arc welds, noting strength loss proportional to cross sectional area loss 18 p3265 A70-37205
- Al-Mg alloys recrystallization, investigating heating rate and annealing time effects on sheet grain size 19 p3450 A70-37372
- Pre-corrosion effects on strained Al alloy electrochemical response, examining strain test results graphically 19 p3451 A70-37780
- Phase equilibrium of Fe-rich Fe-Al alloys using single crystal X ray diffraction 19 p3452 A70-37838
- Fe rich Fe-Al alloys single crystals, determining three dimensional order and atomic displacements coefficients by X ray diffuse scattering 19 p3452 A70-37839
- HF endurance tests of Al sheet alloy used in welded aircraft structural components, plotting curves for heat treated and untreated specimens 19 p3452 A70-38431
- Ternary Al-Cu-Mg alloys, considering aged structure relationship to fatigue strength 19 p3454 A70-38955
- Cooling rate effect on Al-Mg equilibrium state during heat treatment after annealing 20 p3644 A70-38959
- Cu and Ag low alloying effect on Al single crystals elastic limits and first deformation stages 20 p3644 A70-38960
- Al-Zn-Mg alloys structural transformations by diffraction electron microscopy, investigating grain boundary and dislocation structure as function of heat treatment and chemical composition 20 p3646 A70-39044
- Duraluminum dislocation structure dependence on deformation temperature by electron microscopy, discussing subgrain boundaries 20 p3646 A70-39045
- Temperature effect on radiation characteristics and cryogenic tensile properties of irradiated Be, Ti and Al alloys 20 p3647 A70-39111
- Large deflection of simply supported aluminum alloy annular plate with nonlinear stress-strain curve, considering compressibility effects and membrane force 20 p3718 A70-39138
- Aluminum alloys subjected to random loading, comparing fatigue life with predictions based on linear accumulation of damage hypothesis 20 p3647 A70-39157
- Aluminum alloy corrosion stimulation and inhibition effects of cathodic polarization 20 p3647 A70-39244
- Steady state and transient fatigue behavior of stainless steel wire-Al alloy composite subjected to push-pull and pull-release frequency tests 20 p3649 A70-39946
- Al alloy products heat treatment, using synthetic quenchant for distortion control 20 p3650 A70-39967
- Ti sandwich structures low temperature brazing with Al alloy, describing fabrication process and mechanical properties 20 p3638 A70-39969
- Al alloy stress corrosion susceptibility, examining grain size and anisotropy role 20 p3651 A70-40070
- Al alloys and stainless steels tensile properties and application in lightweight cryogenic propellant tank structures, discussing Ti alloys and reinforced composite materials tests 20 p3651 A70-40123
- Rapid expansion of thin walled aluminum alloy cylinders under pulsed magnetic field pressure using high speed streak camera oscillography 20 p3735 A70-40513
- Fatigue crack growth tests on Al alloy sheets under variable amplitude loading 21 p3831 A70-40749
- Notched polycrystalline Al-Mg alloy dislocation structure near propagating fatigue crack at various stress levels 21 p3839 A70-40925
- Duralumin constant speed tensile strength tests at 200 C, discussing creep thresholds statistical distribution in elongations interval 21 p3840 A70-41432
- Al alloys heat treatment methods and equipment, discussing quenching, stress relief, incubation, postquench working and aging 21 p3834 A70-41722
- Stress concentration effect on perforated Al alloy panel fatigue, using theory for material critical thickness near notch 21 p3938 A70-41955
- Two stage aging effects on stress corrosion cracking of Al-Zn-Mg alloys, discussing precipitated particles size, surface roughness change and temperature effects 22 p4052 A70-42306
- Atmospheric environment effect on residual shear stress corrosion cracking of commercial Al-Zn-Mg alloys subjected to heat treatment regimes 22 p4052 A70-42307
- Magnesium Al and Ti alloys electron beam welding for aerospace industry, discussing material requirements, weld quality and optimum conditions 22 p4042 A70-42338
- Ti and Al alloy weldments plane strain fracture toughness and mechanical properties for cryogenic applications, using gas metal arc and gas tungsten arc welding [ASME PAPER 70-MET-4] 22 p4043 A70-42423
- Direct gap conduction band and alloy composition monitoring InAlP, using electron microprobe cathodoluminescence and X ray emission 22 p4086 A70-43019
- Recrystallized and overrecrystallized Al alloys, investigating factors controlling anisotropy of mechanical properties 22 p4056 A70-43126
- Al-Be-Mg alloys under solution treatment, noting aging and prolonged heating effects on mechanical properties from solid solution decomposition diagram 22 p4056 A70-43127
- Pulsed spray welding electrode melting rates for Al alloy, mild steel and stainless steel electrodes over range of pulse current levels 22 p4046 A70-43147
- Light rare earth metals improving Mg alloys, Al alloys, Cu alloys and superalloys 22 p4057 A70-43575
- Scale factor effect on brittle fracture resistance for Ti and Al alloys and high strength steels 23 p265 A70-43936
- Self flammability temperature of binary alloy Al-Si powders in aerosol state as function of chemical and phase compositions 23 p2405 A70-44046
- Double linear damage rule applicability to dual type alloys from two-stress level rotating bending and axial fatigue tests [ICAS PAPER 70-39] 23 p2467 A70-44137
- Papers on plane strain fracture toughness testing covering metallic materials, steels and aluminum alloys 23 p2405 A70-44189
- Low energy fracture of high strength Al alloys with void nucleating particles, using microprobe fractography 23 p2406 A70-44194
- High strength Al alloys plate and welds, comparing tear notch tests at cryogenic and room temperatures 23 p2406 A70-44352
- Aluminum, duraluminum and stainless steel tensile strength tests at cryogenic temperatures 23 p2406 A70-44353
- Al-Be eutectic alloys structure, using laue X ray method and electron microscopy in studying fibrous morphology due to unidirectional solidification 24 p3456 A70-45143
- Al-Mg alloys solid phases free energy, entropies and formation heats determination by electromotive force measurement 24 p3457 A70-45230
- Cross slip between screw dislocations coplanar arrays in Ti-Al alloy, noting fringe pattern and bowing absence 24 p3459 A70-45248
- Steel and duralumin strips with circular holes tested under axial tension, determining relationship between strength weakening and ultimate stress 24 p4420 A70-45272
- Magnetostrictive Ni-Mn-Co ferrites and Al-Fe alloys, measuring magnetic field effect on piezomagnetic coefficients at room temperature 24 p3489 A70-45400
- Al alloy sheets with multicolor protective coatings, measuring surface temperature under solar radiation 24 p4428 A70-45434
- Nondestructive tests of work-hardening Al alloy structural deterioration due to overheating, using eddy current conductivity techniques 24 p3445 A70-45703
- Crack detection in cyclic strained steel and Al alloys, using ultrasonic Rayleigh and longitudinal waves 24 p4424 A70-45718
- Al alloys structural analysis using electron diffraction pattern techniques 24 p3460 A70-45737
- Notch sensitivity dependence on plastic strain in Al alloy, heat resistant steels and Ni alloys under tensile tests at room temperature 24 p3460 A70-45827
- Nonequilibrium solidification and metastable-stable phase transformation during heating of Al-Mo and Al-Cr alloys 24 p3460 A70-45829
- Phase equilibria, hardness and electroresistivity of Ti-Al-V alloys at solid compound section for reinforced metal composites 24 p3461 A70-45831
- Al and liquid Al-Mg alloys oxidation at high temperatures, noting Mg content effect 24 p3461 A70-46174
- Al-Cu alloy unidirectional solidification, investigating interfacial transition from plane to cellular structure and segregation pattern 24 p3462 A70-46179
- Cellular breakdown in binary Al-Cu alloys in unidirectional solidification, observing small pit stability on solid-liquid interface 24 p3462 A70-46180
- Eutectic and hypereutectic Al-Si alloy quench modification by rapid solidification, investigating microstructure and mechanical properties 24 p3462 A70-46183

Al-Zn-Mg alloy prolonged aging behavior, examining Gp and intermediate zones, equilibrium phases, maximum strength and serrated stress strain curve 24 p4362 A70-46189

Zn-Al alloy high velocity deformation characteristics, examining ductility and aging at various temperatures and heat treatments 24 p4363 A70-46194

Drilling machinability of wrought Al alloys, relating tool force to hardness, feeding and cutting speed 24 p4349 A70-46195

Mg addition effects on impact strength and micro structure of Al-Si-Cu alloys, using Charpy test and metallographic methods 24 p4363 A70-46196

Grain growth abnormality in Al-Mg ingots with small amounts of Mn and Cr during secondary recrystallization 24 p4363 A70-46197

Si content and chip treatment effects on drilling machinability of Al-Si alloys 24 p4349 A70-46199

Al and Al alloys cold extrusion, discussing die entry angle, lubrication control, ingot preparation, etc 24 p4349 A70-46217

Gamma ray inspection of opposed-arc weld-nugget penetration in Al-Cu alloy 24 p4350 A70-46384

ALUMINUM CHLORIDES

Sulfur trichloride-Al tetrachloride complex ionic structure from Raman spectra and nuclear quadrupole resonance data 21 p3772 A70-40912

ALUMINUM COATINGS

Dielectric overcoatings effect on Al interconnections electromigration in IC metallization, noting longer intervals between failures 01 p0153 A70-10083

High reflectivity mirror construction for H Lyman alpha line using vacuum deposited Al layer coated by magnesium fluoride 02 p0299 A70-12367

Aluminized composite solid propellants burning rates in acceleration fields noting time dependent increase [AIAA PAPER 68-529] 04 p0709 A70-15581

High temperature properties mechanisms in alumina coated vacuum cast nickel base superalloys 04 p0711 A70-15705

Oxidation, hot corrosion resistance and mechanical properties of aluminate coated superalloys, discussing failure analysis instruments and methods 07 p1305 A70-18969

Embossed/crinkled aluminized film multilayer insulation blankets with joints performance variation with temperature predicted by radiation heat transfer correlation 11 p2150 A70-26365

Diffusion layer microprobe analysis during chromaluminization of Inconel turbine blade 14 p2595 A70-30293

Al effects on B and Cr diffusion in protective coating on Cr-Ni heat resistance alloy, noting thermochemical kinetics for homogeneous layers 17 p3125 A70-35405

Surface alloying of high melting points in Al melts, noting prior oxidation enhancement and simplifying of calorizing techniques 17 p3102 A70-35406

Aluminized Armco iron and steel diffusion layers phase composition and microstructure 24 p4350 A70-46337

Metal layer and absorbed oxygen quantities in reactive oxidation deposition of aluminum 24 p4365 A70-46354

ALUMINUM COMPOUNDS

NT ALUMINATES

NT ALUMINUM CHLORIDES

NT ALUMINUM NITRIDES

NT ALUMINUM OXIDES

NT ALUMINUM SILICATES

NT FELDSPARS

NT KAOLINITE

NT MUSCOVITE

NT ORGANIC ALUMINUM COMPOUNDS

NT SAPPHIRE

Titanium aluminate-Mo system hardness, electrical conductivity and density as function of chemical composition, presenting creep test results 03 p0510 A70-13353

Absorption spectra of single crystals TbAlG and DyAlG garnets, investigating Verdet constant dependence on ion concentration 07 p1355 A70-18705

Electroluminescence recombination emission spectra during avalanche breakdown in AlGaAs n-p and p-n heterojunctions 12 p2286 A70-27367

Crack initiation and breakdown under thermal stresses of boron nitride containing aluminosilicate 15 p2764 A70-31532

Visible light-emitting p-n junctions formed in AlAs via Zn diffusion into single crystal n-type vapor grown AlAs layers 18 p3297 A70-36316

Gallium aluminum arsenide-GaAs laser diodes properties and applications for CW operation, discussing p-GaAs layer thickness effects 19 p3447 A70-38454

Lattice parameter and thermal expansion of AlAs as function of temperature, indicating lattice match at 900 C with GaAs 22 p4086 A70-43004

ALUMINUM ISOTOPES

NT ALUMINUM 26

NT ALUMINUM 27

Dating method for stone meteorites feldspar phase based on time interval between solar nebula Al 26 production and decay into Mg 26 06 p1150 A70-18479

ALUMINUM NITRIDES

AlN deposition rate from gaseous phase on Mo substrate as function of temperature 07 p1357 A70-20311

Aluminum nitride morphology in structural Cr-Ni-Mo steel, discussing dependence on austenitization temperature and cooling conditions 08 p1519 A70-21435

ALUMINUM OXIDES

NT SAPPHIRE

Aluminum oxide whiskers/metal matrix composites, discussing metallic coatings effects on filament wetting, bonding and surface protection 01 p0117 A70-10480

Aluminum oxide solid state reaction with Ta at high temperatures using chemical analysis 03 p0511 A70-13487

Oxide layers on metal substrate noting emittance dependence on thickness in aluminum-aluminum oxide and Cu-CuO systems [ASME PAPER 69-WA/HT-4] 04 p0705 A70-14825

Vapor-liquid-solid nucleation mechanism of alpha-aluminum oxide filamentary single crystal growth, suggesting combination with suboxide condensation and disproportionation mechanism 07 p1313 A70-19890

Iron ions EPR lines widening in corundum crystals due to lattice defects, estimating mosaic blocks disorientation parameter and point defects density 08 p1556 A70-21122

Kinematic viscosity of molten steel containing corundum inclusions as function of temperature 10 p1904 A70-24271

Silicon and alpha-alumina support interface reactions during nucleation-coalescence and after epitaxial growth, investigating electrical properties 13 p2470 A70-28958

IR reflection spectrum of corundum compared for heating by reflecting furnace and laser radiation, discussing phonons statistical distribution 13 p2429 A70-29639

Book on high temperature, transition and hydrated ceramics covering nomenclature, natural occurrence, mechanical, thermal, sonic, electrical, magnetic and chemical properties 13 p2436 A70-29781

Photoemission of electrons and holes from Al into aluminum oxide, giving approximate energy band diagram of Al-aluminum oxide interface 15 p2783 A70-31759

Alumina particles marker transport in Ag wires during early sintering as function of plastic deformation by slip 15 p2745 A70-32392

Ferrous and ferric ions properties in corundum from observing acoustic paramagnetic resonance 15 p2784 A70-32397

Gaseous Al oxide bond bending frequency in Ne and Ar matrices at liquid He temperatures, investigating IR spectrum 15 p2695 A70-32830

Solid state dipole antenna array miniaturization by etching microstrip components on alumina substrate having high dielectric constant 16 p2876 A70-33409

Rolled fine grained aluminum-alumina particles composites, determining creep strength dependence on temperature and tensile stress axis orientation 18 p3274 A70-36051

Al-Si welding rods tests with various surface finishes, considering oxide coatings effect on gas tungsten arc weld quality 18 p3264 A70-37113

Ar ion laser gas discharge tube construction, using anodically oxidized directly cooled aluminum segments 19 p3444 A70-37567

Alumina effects on Nb creep activation energy at elevated temperatures, noting independence from chemical composition and creep stresses 19 p3453 A70-38710

Oscillator strengths for aluminum oxide molecular electronic sigma band system from intensity measurements in cyanogen-oxygen flame system 20 p3676 A70-40474

Decomposition kinetics of alumina particles injected into thermal argon induction plasmas 21 p3855 A70-40878

Tank collection and spectrophotometric tests in determining aluminum oxide particle size produced by small rocket engine [AIAA PAPER 69-146] 21 p3867 A70-41727

Ultrasonic and electron paramagnetic double resonance in Fe-doped corundum 22 p4074 A70-43010

Polycrystalline aluminas under thermal shock, investigating strength decrease and subcritical crack formation 22 p4059 A70-43413

High temperature aluminum species in vapor over solid alumina, determining thermodynamic properties, composition and accommodation coefficient by Knudsen effusion and mass spectroscopy 23 p4281 A70-44451

Aluminum oxide growth rate in molybdenum cermet after high temperature annealing 24 p4359 A70-45478

Colloidal alumina non-Newtonian suspension in propylene glycol, examining thixotropic behavior at various structural levels 24 p4310 A70-45625

Molybdenum disilicate and aluminum oxide coating sealing heat resistance tests 24 p4364 A70-46341

ALUMINUM SILICATES

NT KAOLINITE

Aluminosilicate glass physical properties and chemical stability in water, alkaline and acidic agents, studying titanium oxides additions effect 05 p0871 A70-16596

Curve characteristics of differential thermalgram of high alumina allophane, observing endothermal peak for water loss 06 p1004 A70-17225

Aluminosilicate coatings for increased Ni-Cr alloys heat resistance due to silicon properties 06 p1089 A70-17743

Plant cultivation in closed biobiotic cycles by hydroponic method using keramzit/alumoferrisilicate/substrate 13 p2358 A70-29328

Sodiumalumoborosilicate fiber formation and extraction by leaching, obtaining high aluminate content temperature resistant porous fiber and insulation material 24 p4367 A70-45480

ALUMINUM 26

Apollo 11 lunar surface fine material and rocks cosmogenic radio nuclides Al 26 and Na 22 concentrations determination by gamma ray spectroscopy 21 p3910 A70-41618

ALUMINUM 27

Al-27 NMR saturation effects on ruby electron cross relaxation and inversion 23 p4230 A70-43932

ALVEOLAR AIR

Human pulmonary gas mixing between large airways and alveolar spaces, using argon bolus inhalation 01 p0024 A70-10976

Human alveolar-arterial oxygen differences during rest, sleep and exercise in initial hypoxia induced by simulated high altitude exposure 03 p0429 A70-14161

Inhaled air intrapulmonary distribution uniformity and alveolar N concentration using single breath method 05 p0802 A70-16496

Altitude effects on Borkenstein Breathalyzer accuracy determined from alveolar ethanol analysis 06 p1000 A70-17303

Alveolar ventilation and pulmonary circulation during application of negative pressure to lower part of human body 09 p1615 A70-22090

Modified apparatus for volumetric determination of alveolar carbon dioxide as indicator of pilot hypernea 10 p1825 A70-24503

Gravity dependent lung region emptying sequence effects on alveolar Xe 133 and nitrogen plateaus in pivoted subjects 13 p2356 A70-29944

Stress distribution and pressure distending air spaces in lungs, using mechanical pulmonary elasticity model 13 p2356 A70-29945

Alveolar ventilation and pulmonary circulation during application of negative pressure to lower part of human body 15 p2685 A70-32686

Exhaled alveolar air data acquisition using mass spectrometer and multichannel analyzer 19 p3367 A70-37356

Topography of pleural surface pressure and vertical gradient of transpulmonary pressure above resting volume in relaxed animals as function of alveolar pressure 21 p3766 A70-42154

Altered respiratory pattern effect on alveolar gas exchange in mechanically ventilated dogs after introducing end-inspiratory pause 21 p3766 A70-42156

ALVEOLI
Vascular resistance and constriction and muscle mass related in pulmonary arteries of mice subjected to alveolar hypoxia

04 p0630 A70-14679
Alveolar ventilation difference in nasal and oral breathing in hyperventilation due to work
05 p0802 A70-16492
Lung alveolar and capillary wall structure in mammals under normal conditions, transverse acceleration and mechanically changed pulmonary circulation
20 p3575 A70-40190
Oxygen uptake at alveolar capillary membrane, investigating ventilation variability at exercise onset
20 p3577 A70-40331
Food-water deprivation influence on alveolar surface activity of rat lungs
24 p4303 A70-46115

AMBIENT TEMPERATURE
Comfort and thermal sensations and associated physiological responses during exercise at various ambient temperatures, noting effects on sensory estimates

01 p0031 A70-11648
Combined hypoxic hypoxia and high ambient temperature found relieving strain on humans by increasing heat release by evaporation
04 p0630 A70-14581
Ti-hydrogen reaction at ambient temperatures, investigating factors favoring reaction and preventive measures
05 p0863 A70-16524
Oxygen content influence on Nb-Mo alloy mechanical properties at ambient temperature in air and hydrogen
07 p1307 A70-19374
Ambient temperature measurement by constant level balloon mounted thermistors, discussing errors from differential heating of thermistor support by solar radiation
10 p1886 A70-23935
Air ventilated cassette-type electronic equipment steady thermal regime, measuring local excess temperatures relative to ambient temperature
11 p2017 A70-25583
Fuel cells with alkaline electrolyte consuming H and O and operating near ambient temperature, discussing electrodes composition and performance
12 p2163 A70-26993
Thermostability and survival rates of white mice in ambient medium with temperature variations
13 p2351 A70-29330
Ti-Al-Mo-V alloy stress corrosion cracking, investigating correlation between dislocation substructure and ambient temperature corrosion susceptibility
17 p3113 A70-34371
Ambient temperature effects on venous reactivity to hydrostatic stress, discussing posture changes and lower body negative pressure effects on index of compliance
17 p3031 A70-35426
Biophysical model of heat transfer from organism, describing adaptation to ambient temperature
18 p3218 A70-36531
Gas exchange adaptation to heat and cold in rats with different ecological backgrounds
18 p3218 A70-36533
Thermoregulation processes in oxygen consumption, blood and body temperatures and skeletal muscles in adult nutria and muskrats in air and water
18 p3218 A70-36535
Gas metabolism in passerine birds adaptation to ambient temperature
18 p3219 A70-36536
Human sweating transient state characterized by time constant following abrupt ambient temperature rise
21 p3761 A70-41140

AMINES
NT AMPHETAMINES
NT ANILINE
NT CATECHOLAMINE
NT CYSTEAMINE
NT DIAMINES
NT DIMETHYLHYDRAZINES
NT GUANIDINES
NT HISTIDINE
NT TRYPTAMINES

Nicotinamide adenine dinucleotide /NAD/ deamination and role of nicotinamide hypoxanthine dinucleotide /deamino-NAD/ in forming ammonia from amino acids in rats/rabbits brain and liver tissue
01 p0018 A70-10505
Indirect ADP deamination and reamination of corresponding deamino form of ionosine diphosphate in rabbit brain tissue
01 p0018 A70-10506
Granular amine used as regenerative absorbent in cycling two bed system for carbon dioxide removal
01 p0038 A70-10972
Isolation and structural characterization of adduct formed from propionaldehyde, sym-trinitrobenzene and triethylamine
02 p0251 A70-12275
Red bicyclic condensation product from reaction of acetone with sym-trinitrobenzene and diethylamine
02 p0251 A70-12278
Alpha-methyl-DOPA inhibitor effect on catecholamines and cardiac spontaneous activity in pacemaker fibers in rabbits
06 p0992 A70-17422
Methylamine crystals lattice vibrations IR spectra recordings, making spectral band assignments according to translational and librational motions
07 p1356 A70-18958
Vegetative cardiovascular, motor and electrophysiological reactions to electrical stimulation of limbic and reticular formations in cerebrum after adrenalin and aminazine injections
13 p2352 A70-29352
Pressure dependence and high pressure limiting values of rate constants of gas phase reaction of monomethylamine and trimethylamine with boron trifluoride
19 p3373 A70-37775
Simultaneous mass spectrometric differential thermal analysis of low pressure decompositions of nitrate salts of monomethylhydrazine and methylamine
20 p3688 A70-40475
Serotonin, 5-hydroxyindoleacetic acid /5-HIAA/ and monoamine oxidase in pineal pituitary organ and median eminence
21 p3761 A70-40850

AMBIGUITY
Optimal synthesis of filters maximizing peak-sidelobe ratio of arbitrary zone of mutual ambiguity function
13 p2369 A70-29734

AMBIPOLAR DIFFUSION
Coupled differential rate equations governing growth and decay of positive and negative ion and electron concentrations in afterglow with ambipolar diffusion and electron attachment
11 p2088 A70-25703
Monograph on ambipolar diffusion and motion instability of satellite produced artificial barium ion clouds in ionosphere and magnetosphere
11 p2048 A70-26825
Surface type airborne electrostatic probes in ambipolar diffusion flux measuring ion saturation current, discussing electrode contamination and temperature and ablation tests
13 p2412 A70-29967
Electron-ion gas ionization, neutralization and ambipolar diffusion effects on F region vertical profile
15 p2730 A70-32090
Collision dominated plasma column radial structure including ambipolar diffusion region obtained from

constant mean free time and path approximate formulas
16 p2959 A70-34311
Low pressure Hg vapor arc with remote wall, investigating magnetic self striction by ambipolar diffusion in fields
20 p3685 A70-40503
Ion and electron ambipolar velocity distribution near plasma sheath boundary in collisional positive column
22 p4080 A70-42542
Quasi-ambipolar diffusion in arc discharges in magnetic field, calculating ions and electrons density distributions between anode and cathode sheaths
24 p4384 A70-45148

AMBIT U FIELD THEORY [PHYSICS]
AMBULANCES
Air crash rescue operations by helicopter ambulances of U.S. Army Medical Department, discussing postcrash fire suppression and injured personnel removal, emergency treatment and evacuation
06 p1002 A70-17714

AMIDES
NT ACETAZOLAMIDE
NT NICOTINAMIDE
NT POLYIMIDES
NT UREAS
Cyclization of N-allylamides to disubstituted-2-oxazolines, giving melting points, yields, picrate melting points and NMR spectra
02 p0249 A70-11681
Protonation mechanism in acid catalyzed cyclization reactions of 2-acetamido 3-methylbicyclo-heptene
02 p0253 A70-12523
Polyamide and secondary amide model compounds stress cracking by metal halides using IR and nuclear magnetic resonance techniques
10 p1907 A70-24299
Refutation of Sylvén-Snellman report of catalysis of benzoylarginine beta-naphthylamide and leucine beta-naphthylamide hydrolysis by beef spleen cathepsin B
10 p1812 A70-24534

AMINO ACIDS
NT ASPARTIC ACID
NT CYSTEINE
NT FOLIC ACID
NT GLUTAMIC ACID
NT GLUTAMINE
NT GLYCINE
NT HISTIDINE
NT LEUCINE
NT LYSINE
NT METHIONINE
NT PHENYLALANINE
NT PYRIDINE NUCLEOTIDES
NT THYROXINE
NT TRYPTOPHAN
Gamma-aminobutyric acid effect on oxidative phosphorylation of rabbit and rat brain mitochondria, noting dependence on ionic concentration, temperature and amount of additions
01 p0019 A70-10509
Gamma-aminobutyric acid influence on 5-hydroxytryptamine in rat brain after intraperitoneal administration
01 p0019 A70-10510
Human capacity to discriminate between poorly and well balanced diets and liability to select amino acid imbalanced mixtures for deficient nutrient
01 p0028 A70-11314
Diet and feeding method effects on food intake and plasma amino acid concentrations of rats fed low protein diet with amino acid imbalance
02 p0231 A70-11707
Alpha-aminoisobutyric acid accumulation by soleus and plantaris muscles of rat in vivo during work induced growth, showing amino acid transport variation with work level
02 p0232 A70-11711
Rats decreased muscular work and denervation effects on alpha-aminoisobutyric acid uptake by skeletal muscle
02 p0232 A70-11712
Starvation effect on intestinal amino acid absorption of rats, noting protein synthesis reduction
02 p0234 A70-11731
Chlorobium thiosulfatophilum sulfur bacteria growth on media with/without ammonium chloride exposed to illumination, noting various amino acids effects
02 p0241 A70-12797
Amino acid stability in pyrolyzed Pleistocene Mercenaria shells, comparing decomposition rates for aqueous solution
03 p0472 A70-13150
Noble gases breathing effects on free amino acid pool increase in rat brains, considering O mixtures with He, Ar and Ne
04 p0632 A70-15086
Amino acid composition and terminal sequences of ferredoxins from photosynthetic green bacteria
06 p0994 A70-17616
Gas-liquid chromatographic separation applied in derivatization chemistry of protein amino acids as N-trimethylsilyl/TMS/ esters
09 p1629 A70-22337
Amino acid metabolism time dependent variations, studying tyrosine transaminase rhythm in rat liver
09 p1618 A70-22525
Fasting and postprandial serum amino acid patterns of human males fed protein-free or protein-sufficient diets
09 p1621 A70-23399
Butyl esters separation from protein amino acids, using acid washed Chromosorb W of various mesh sizes
10 p1828 A70-24397
Primitive earth prebiological organic synthesis via amino acids shock heating in atmosphere: simulating gas mixture, suggesting energy sources from atmospheric entry
12 p2167 A70-27269
Amino acid sequence of Chromatium ferredoxin molecule compared with other ferredoxins concerning structural, functional and evolutionary relationships
13 p2361 A70-28921
Kinetics for two free radical conversion processes in electron irradiated D, L-valine, measuring activation energies by electron spin spectroscopy
14 p2544 A70-30111
Amino acid composition of protein in blue green algae Stratonostoc Linckia
14 p2540 A70-30158
Pure oxygen effect on amino acids uptake and metabolism of Pseudomonas saccharophila stationary cells
14 p2536 A70-30343
Amino acids changes distribution in specificity regions of light polypeptide chains of immunoglobulins showing correspondence with Poisson distribution
14 p2536 A70-30349
Taro ferredoxin amino acid sequence determined from chymotryptic and thermolysin peptides sequence
14 p2544 A70-30351
Daily rhythm in accumulation of rat brain catecholamines synthesized from circulating tritiated tyrosine
16 p2848 A70-33096
Dietary amino acids combination allowing maximum growth in rat
16 p2850 A70-34320
Optically active amino acids synthesis by reduction of Schiff bases with sodium borohydride
17 p3041 A70-34748

- Optically active alpha-amino acids synthesis from esters of alpha-keto acids by hydrogenolytic asymmetric transamination
17 p3041 A70-34749
- Protein synthesis, dialysis and Mg ion concentration effects on chemical condensation of mixed amino acid adenylates
17 p3042 A70-35146
- Amino acids asymmetric polymerization on clay minerals, discussing aspartic acid and kaolinite experiments
19 p3455 A70-38030
- Tyrosine content and utilization in mouse liver, showing daily rhythm in composite metabolism rate
20 p3568 A70-38976
- Thermally prepared poly-alpha-amino acids catalytic activity after long term dry state storage, suggesting enzyme activity role in biological evolution
21 p3772 A70-40713
- Amino acids analysis of Apollo 11 lunar fines by hydrolysis of aqueous extracts
21 p3778 A70-41623
- Amino acid racemization as enantiomers in core sediment samples
21 p3781 A70-41896
- Octadecanonic anhydropolymers of amino acids, describing production by thermal condensation, heteropolymerization and panpolymerization
22 p3983 A70-42875
- Gas-liquid chromatography studies of direct esterification of protein amino acids to n-butyl esters
22 p3984 A70-43525
- Prolonged REM sleep deprivation effect on gamma-aminobutyric acid concentration in mice
23 p4146 A70-44658
- Extreme environmental temperature effects on hepatic amino acid catabolism in rats attributed to caloric deficiency
23 p4148 A70-44790
- Amino acids L-glutamate and gamma-aminobutyric acid as communication agents in brain
23 p4148 A70-44864
- Catalytic activities of thermal polyanhydro-alpha-amino acids for modeling enzymes and prebiotic protein
24 p4310 A70-45346
- AMMONIA**
NT LIQUID AMMONIA
Nicotinamide adenine dinucleotide (NAD)/deamination and role of nicotinamide hypoxanthine dinucleotide/deamino-NAD in forming ammonia from amino acids in rats/rabbits brain and liver tissue
01 p0018 A70-10505
- Structure and composition of clouds of ammonia and water bearing condensates, investigating compositional models of Jupiter atmosphere, considering ammonium hydrosulfide cloud layer
01 p0179 A70-10527
- Renal and hepatic glutamine synthetase distribution in mammals, studying relation between glutaminase and urinary activities/ammonia metabolism/
02 p0232 A70-11710
- Variable distribution of ammonia absorption on Jupiter deduced from IR spectra, indicating scattering in cloud layer
02 p0366 A70-11810
- Ammonia spectral lines positions, intensities and half widths under Jovian conditions calculated, including ground state rotation and rotation inversion bands
02 p0368 A70-11820
- Ammonia red and green bands measured line positions, strengths and half widths applied to Jupiter atmospheric pressure determination
02 p0368 A70-11821
- Ammonia absorption band at 6450 Å in Jovian atmosphere, clarifying controversial absorption time variations
02 p0375 A70-12428
- Ammonia/chlorine dioxide and ammonia/chlorine dioxide/methane flames burner stabilization and burst velocities
02 p0400 A70-12670
- Ammonia maser transient spiking effects under periodic oscillation condition modulation, noting frequency sweep width role
07 p1299 A70-19685
- Ammonia micropropulsion for geostationary satellites stabilization, discussing principle and working mode of thrusters
09 p1743 A70-22660
- Satellite attitude and orbit control systems based on electrically heated ammonia or hydrazine
09 p1767 A70-23432
- Saturn ring IR spectrum, discussing resemblance and discrepancies of ammonia and water frost spectra
10 p1935 A70-23813
- Ammonia-chlorine dioxide flame stabilization for simulating ammonium perchlorate combustion at high pressures
11 p2099 A70-25994
- Ammonium ions elimination from atmospheric moisture condensates by treatment with metal-exchange resins, discussing volume sorption capacity
13 p2362 A70-29339

- Self diffusion coefficient for gaseous ammonia at specific temperature range, applying polar gases theory
13 p2453 A70-29800
- Nitrous oxide and carbon dioxide laser Q switching by ammonia Stark effect
13 p2431 A70-29835
- Ammonia incorporation in chemolithotroph Hydrogenomonas eutropha, investigating responsible enzyme
15 p2682 A70-32000
- Jupiter atmosphere ammonia abundance from laboratory curves of growth analysis for ammonia bands
18 p3310 A70-35937
- Equivalent radioelectric plan of ammoniac maser marginal type oscillator
18 p3265 A70-35946
- Spectrophotometry of methane and ammonia absorption bands indicating decrease toward Jupiter disk edge
18 p3323 A70-37140
- Ca ion reversible effects of hydrochloric acid and ammonia water on betacyanin leakage from beetroot sections
19 p3365 A70-38375
- Upper atmosphere ammonia release experiments testing hypothetical mechanisms of radicals and ions formation in comets
20 p3708 A70-39962
- Accelerated failure tests of ammonia-Al-stainless steel heat pipes for fluid loss or energy transport degradation
21 p3947 A70-41049
- Heat pipe performance map with ammonia as working fluid, comparing thermal transport efficiency with water pipe
21 p3947 A70-41050
- IR microwave double resonance signals in systems of ammonia with nitrogen isotopes, using nitrous oxide laser
21 p3836 A70-41707
- Cotton leaves ammonia induced discoloration spectrophotometric examination, discussing light reflectance, transmittance and absorbance
22 p4014 A70-42771
- Ammonia gas phase IR intensity measurements for hydrogen bonding energy and related parameters
23 p4158 A70-44783
- Argon matrix isolated ammonia, examining IR spectra by carbon dioxide laser irradiation
24 p4354 A70-45648
- AMMONIUM CHLORIDES**
Chlorobium thiosulfatophilum sulfur bacteria growth on media with/without ammonium chloride exposed to illumination, noting various amino acids effects
02 p0241 A70-12797
- AMMONIUM COMPOUNDS**
NT AMMONIUM CHLORIDES
NT AMMONIUM NITRATES
NT AMMONIUM PERCHLORATES
NT AMMONIUM PHOSPHATES
Nitrification reactions in soil with constant ammonium solution entry rate and nitrifying organisms, considering ion concentrations as functions of time and distance
02 p0252 A70-12518
- External optical phonon modes in ammonium and deuterioammonium halides phase transitions as function of temperature, using IR and Raman spectra
04 p0646 A70-14695
- Ammonium chlorate thermal decomposition products as function of temperature using mass spectrometry
05 p0895 A70-17082
- Second and third harmonic simultaneous generation in ammonium oxalate crystals achieved by three frequency interactions
10 p1901 A70-25159
- Sn and tetraethylammonium ions effects on Zn electrodeposition on Zn single crystals in aqueous KOH, using scanning electron microscopy
21 p3772 A70-40726
- AMMONIUM NITRATES**
Hybrid rocket motor with solid oxidizer in ammonium nitrate additive, determining stable combustion conditions
15 p2790 A70-32274
- AMMONIUM PERCHLORATES**
Aluminum additives effects on stoichiometric ammonium perchlorate/polyformaldehyde mixtures deflagration, determining temperature distribution, burning rate dependence on pressure and heat flow due to radiation
02 p0351 A70-12004
- Copper chromite catalyst effects on sublimated ammonium perchlorate dissociation products, noting applications to solid propellants
03 p0544 A70-13923
- Equilibrium existing at gaseous-condensed phases interface inferred as mechanism for dissociative sublimation of ammonium perchlorate
05 p0894 A70-17079

- Ammonium perchlorate deflagrations, determining intrinsic stability of one dimensional burning configuration based on flame structure modeling
06 p1128 A70-18044 [AIAA PAPER 70-123]
- Potassium permanganate catalytic effects on ammonium perchlorate deflagration, studying catalyst dispersion degree role
07 p1358 A70-19329
- Ammonium perchlorate decomposition, deflagration, sublimation, crystal growth and surface properties, using scanning electron microscope
07 p1358 A70-19576
- Gas phase thermal decomposition of ammonium perchlorate at elevated temperatures using mass spectrometer
07 p1362 A70-20009
- Ammonium perchlorate combustion catalysis, studying preflame heating and mixing effects on gas phase flame burning velocity
07 p1425 A70-20010
- Detonation mechanism in ammonium perchlorate ascribed to mechanical breakdown of charge occurring at pressure equal or above critical deformation of explosive
09 p1741 A70-22102
- Combustion rates and temperature distribution in condensed and gaseous phases of ammonium perchlorate sandwich with synthetic resin middle layer
09 p1741 A70-22105
- Ammonium perchlorate-polymer mixtures combustion rates with/without cobalt oxide additions, studying ignition temperatures of stable flameless burning
09 p1787 A70-22108
- Thermal decomposition of ammonium perchlorate and polymethylmethacrylate mixture thin layer between Ti plates in vacuum
09 p1741 A70-22109
- Polybutadiene-ammonium perchlorate solid propellant microscopic failure analysis under uniaxial tension
09 p1741 A70-22424
- Polybutadiene-ammonium perchlorate solid propellant BPT-1 mechanical properties viscoelastic analysis under constant strain rate tension
09 p1742 A70-22425
- Burning solid ammonium perchlorate composite propellants surface structure observation to assess heterogeneous or subsurface reactions, using scanning electron microscope
09 p1742 A70-23234
- Ammonia-chlorine dioxide flame stabilization for simulating ammonium perchlorate combustion at high pressures
11 p2099 A70-25994
- Styrene-oxygen copolymer preparation methods, discussing burning rates for rocket solid propellants mixtures with ammonium perchlorate
11 p2100 A70-26146
- Stannic oxide-chromium oxide catalyst effects on thermal decomposition and ignition of ammonium perchlorate (AP), calculating activation energy
11 p2100 A70-26281
- Gamma irradiation effects on thermal stability and decomposition of ammonium perchlorate
12 p2289 A70-26870
- Pure ammonium perchlorate single crystal self deflagration, determining energy transfer mechanisms from pressure effects, combustion characteristics and subsurface profile
13 p2473 A70-29956 [AIAA PAPER 69-142]
- Hybrid rocket engine with solid ammonium perchlorate oxidizer, discussing equilibrium conditions and engine performance
15 p2786 A70-32272
- Extinction pressures of polyurethane propellants increased by presence of AP, AP coated with silane and KP
16 p2963 A70-33619 [AIAA PAPER 70-657]
- Burning rate increase of nonmetalized composite propellants in acceleration field, assuming surface retention of ammonium perchlorate particles
16 p2963 A70-33861
- Ammonium perchlorate pyrolysis, investigating exothermic surface reactions and gasification rates
16 p2963 A70-33873
- Pressure and grain size effect on burnout velocity and combustion capacity of ammonium perchlorate
17 p3145 A70-34639
- Aluminum particle combustibility in deflagration zone of ammonium perchlorate pellets, measuring combustion rate and pyrolytic behavior
17 p3145 A70-35208
- Ammonium perchlorate filler fraction effect on viscoelastic behavior, relaxation modulus and failure mechanisms of solid composite propellants
17 p3145 A70-35216
- Combustion rates acceleration of ammonium perchlorate mixtures with polystyrene and polymethyl methacrylate by KCl and LiF additions, forming molten layer on charge surface
18 p3299 A70-36248

Combustion rates and self ignition vs pressure and activity in ammonium perchlorate mixtures with Al and Mg powders compressed to maximum densities 18 p3299 A70-36249

Premature exothermic decomposition suppression in propellant grade ammonium perchlorate, using differential thermal analysis 18 p3300 A70-36699

Nucleation processes associated with thermal decomposition sites formation in ammonium perchlorate single crystals, using optical and electron microscopy 20 p3582 A70-39494

Ammonium perchlorate composite solid propellant pressure vs burning rate at various temperatures, discussing granular diffusion flame theory 20 p3694 A70-40266

Ammonium and magnesium perchlorate mixture thermal stability study with differential scanning calorimetry, noting exothermic decomposition of AP 20 p3688 A70-40272

Deflagration rate measurements by high speed cinematography of ammonium perchlorate single crystals under various ambient temperature and pressure conditions 20 p3688 A70-40468

Proton transfer mechanism for thermal decomposition of ammonium perchlorate, discussing dissociation energy and decomposition products 21 p3864 A70-40883

Pulsed ruby laser mass spectrometry technique for flash pyrolysis of ammonium perchlorate-catalyst mixtures [AIAA PAPER 68-149] 21 p3781 A70-41729

Isomorphous mixed ammonium perchlorate and potassium perchlorate crystals structural homogeneity by X ray diffraction and differential thermal and thermogravimetric analyses 21 p3784 A70-42262

AMMONIUM PHOSPHATES

One piece KDP and ADP reflector shutters used as laser Q switches, discussing compensation for working surfaces temperature displacement 01 p0106 A70-10060

Optical third harmonic generation in ADP crystals using mode locked and nonmode locked lasers 06 p1082 A70-17943

AMOBARBITAL

Hypotensive effects of chlorthalidoxepoxide, amobarbital and chlorthalidoxepoxide on behaviorally induced elevated arterial blood pressure in squirrel monkey 24 p4298 A70-45620

AMOEBAS

Cytoplasm, nucleus and membrane combination techniques for reassembly to form viable amoebae 11 p1986 A70-25849

AMORPHOUS MATERIALS

Sputtering yield of amorphous and polycrystalline targets bombarded by energetic ions or recoil atoms calculated by integrodifferential equations derived from Boltzmann transport equation 02 p0343 A70-11885

Phenomenology theory on conduction and switching behavior of amorphous semiconductor diodes 05 p0891 A70-16021

Threshold switching and thermal filaments in thick specimen of amorphous semiconductors using IR spectrum viewer 08 p1477 A70-21540

Te nuclear magnetic resonance in amorphous semiconducting sample cycled between conducting and nonconducting states 08 p1557 A70-21697

Electron tunneling into amorphous Ge films using Al-aluminum sesquioxide-germanium tunnel junctions, observing conductance dependence on bias voltage 09 p1739 A70-22918

Electronic switching effects in amorphous semiconductors emphasizing mass memory for computers based on thin films of chalcogenides 11 p2017 A70-25524

Second quantization exciton theory in amorphous disordered materials, discussing hamiltonian, boson annihilation operators and electronic polarization 14 p2627 A70-30693

Amorphous boron arsenide films deposited on Si substrates, measuring current voltage characteristics 15 p2785 A70-32584

Band model of switching effects between conducting and high resistance states of amorphous semiconductors 18 p3297 A70-35952

Amorphous film formation and crystallization, discussing thermal stability 18 p3297 A70-36320

Optical properties of amorphous polymers, considering one state calculations for flexible polypeptides in solution and disordered regions of films or proteins 21 p3780 A70-41702

Reprogrammable read-mostly memory /RMM/ using integrated circuit array of amorphous and

crystalline semiconductor devices, discussing design and applications 22 p3996 A70-42772

Amorphous semiconductors optical absorption, thermoelectric effects and switching mechanisms characterized by energy band structure model 22 p4086 A70-42773

Amorphous semiconductor alloys in As-Se system, measuring DC and AC electrical conductivity dependence on temperature 24 p4390 A70-45657

AMORPHOUSNESS

U CRYSTALLINITY

AMPERAGE

U ELECTRIC CURRENT

AMPHETAMINES

Amphetamine effects on observing and monitoring performance in squirrel monkeys, investigating lever and key responses using food reinforcements 05 p0806 A70-16128

Mild temperature and dehydration effects on toxicity of caffeine and dextroamphetamine in mice 09 p1616 A70-22329

Amphetamine, caffeine and secunarine effects on hypokinetic syndrome in subjects during orthostatic tests and transverse G-forces under prolonged hypokinesia 10 p1817 A70-24690

AMPHIBIA

NT FROGS

AMPHIBIOUS AIRCRAFT

NT SEAPLANES

AMPHIBIOUS VEHICLE

NT SEAPLANES

AMPHIBIOUS VEHICLES

External aerodynamics role in handling qualities of amphibious hovercraft, discussing tests of hull shape, air cushion efflux and hollow models 17 p3017 A70-34919

Hovercraft operational advantages and legal status 22 p4127 A70-43499

AMPLIFICATION

NT POWER GAIN

NT SOUND AMPLIFICATION

UHF signal amplification by electron beam-plasma interaction, defining amplification frequency ranges 01 p0043 A70-10658

Resonance amplification theory of standing interfacial gravity waves in viscous fluids applied to obtain wavelengths prediction of atmospheric bow waves 01 p0081 A70-11299

He-Ne laser amplifier photon density, bandwidth and gain as functions of inversion and excited Ne atoms density 01 p0114 A70-11357

Amplification cross section of 1.06 micron transition of trivalent Nd ion in alkaline silicate glass host material, based on three level energy level diagram 02 p0312 A70-12111

Gain interaction among oscillating modes of gas laser analyzed from rate equations viewpoint 03 p0503 A70-14208

Electromagnetic waves amplification in semiconductor plasma with high electron concentration, analyzing equations describing waves drift instability 04 p0731 A70-15216

Gain measurement in He-Ne laser based on small modulation of discharge current 05 p0859 A70-16267

Geomagnetic field amplification near gamma radiation steady source, describing field displacement 07 p1367 A70-19446

Neodymium-doped glass bars laser amplification efficiency increased by using conical bar and divergent beam 07 p1302 A70-20096

Interferograms taken by phase difference amplification technique with nonlinear hologram, considering amplified image accuracy 08 p1500 A70-21788

Semiconductor injection laser, analyzing light absorption by free carriers and gain characteristics 09 p1694 A70-22133

Organic dyes investigated for amplification characteristics of Raman emission stimulated by Q switched ruby laser 09 p1694 A70-22134

Self focusing antennas directive gain losses reduction for wave with jagged phase front impinging on linear array having passed through inhomogeneous atmosphere 09 p1648 A70-23163

Coherent radiation amplification factor for 0.63 micron wavelength in He-Ne mixture, noting dependence on discharge current for various pressures 09 p1698 A70-23304

Fatigue effects of incident illumination on area sensitivity, dynode gain stability and anode output for end-on photomultipliers 09 p1683 A70-23511

Solid state resonant bandpass electronic filter composed of ferroelectric dielectric capacitors with adaptable voltage gain 09 p1653 A70-23801

Channel electron multipliers design and operation, investigating parameters influencing amplification, resolving power and response probability 10 p1888 A70-24484

Lead type channel electron multipliers gain degradation in ultrahigh vacuum 10 p1849 A70-24557

Wave amplification in semiconductors relationship to coupling between space charge wave and circuit wave based on coupled-mode theory 10 p1927 A70-24619

Fields in wave interaction region during spatial trapping of parametrically amplified waves by radiation of pumping, using Laplace transformation 10 p1844 A70-25157

Gain determination from dynamic /on line/ solutions to Riccati equation for model reference adaptive control applicable to multiple input/ output or stochastic systems 11 p2029 A70-26339

Gain-stabilization of SHF traveling wave maser radiometer, using thermal noise from neon discharge tube 12 p2228 A70-26881

Electron amplification and phase velocity of plane harmonic Rayleigh wave in gallium arsenide crystals under constant electric field 12 p2285 A70-27294

Resonant nonmonochromatic radiation effects on quantum system, deriving expressions for active medium nonlinear polarization, susceptibility and gain 12 p2245 A70-27304

Active RC bandpass filter with independent linear control of Q peak gain and frequency 13 p2376 A70-28801

Gain of optimal filter and predictor, using recursive estimation in discrete linear systems 13 p2381 A70-29063

Radio wave propagation obstacle gain changes with varying distance between obstacle and path terminal 14 p2549 A70-30514

Alloy junction transistors with emitter larger than collector, analyzing minority carrier distribution in base region and effect on current amplification 15 p2714 A70-32703

Microwave parametric amplifiers with nonideal circulators, deriving gain via scattering matrix theory and signal flow graphs 16 p2874 A70-33389

Geomagnetic field amplification near gamma radiation steady source, describing field displacement 18 p3309 A70-36920

Ultrasonic surface waves amplification in piezoelectric crystal-Si semiconductor system, observing dependence on permittivity 19 p3488 A70-38675

Microwave emission from GaAs due to EM wave amplification within biased sample 20 p3686 A70-39397

Dielectric rod and Yagi antennas radiation mechanism, determining pattern, gain and effective aperture 20 p3585 A70-39398

Uniformly and nonuniformly spaced microwave antenna arrays, investigating directivity function and gain characteristics dependence on spacing 20 p3599 A70-40313

Alfven waves amplification propagating along sinusoidally perturbed magnetic field in argon plasma, noting parametric excitation 21 p3855 A70-40947

Antennas with controlled current distribution in medium wavelength range for optimal radiation pattern over desired area, discussing maximum gain tuning for daytime and nighttime operation 22 p3995 A70-42521

Parachute opening load amplification due to suspension line elasticity, using two-body spring-mass model 23 p4142 A70-44531

Feed voltages and directional gain maximization for loaded long thin-wire antennas with multiple excitations, using matrix methods 23 p4176 A70-44972

Amplification factor time dependence of dye lasing under rectangular pumping pulse, noting threshold conditions and burnout time relation to material parameters and resonator 24 p4352 A70-45473

LF plasma waves amplification by beam-plasma interaction, considering electron and ion temperatures effects 24 p4387 A70-45797

Spin waves amplification in ferromagnetic conductor crystals, taking into account arbitrary external electric field and propagation vector orientations and space charge 24 p4392 A70-46363

AMPLIFICATION FACTOR

U AMPLIFICATION

AMPLIFIER DESIGN

Wideband HF amplifier development for ionospheric radio sounding, describing various stages 02 p0255 A70-11895

Supersonic fluid amplifier performance and design for use as power amplifier and high outlet leg differentials in vacuum environments
[ASME PAPER 69-WA/FLCS-7]

04 p0626 A70-14846

Delay characteristics of narrow band double bridge amplifier used as inertial component of photoelectric star transit recorder

04 p0693 A70-15489

Transistorized wideband amplifiers synthesis by combining dynamic parameters method with poles and zeros method

05 p0819 A70-16249

Microwave transistor amplifier design and specifications, discussing applications and economy in design, production and use

06 p1018 A70-17358

Traveling wave maser with increased linear gain obtained by slow wave structure through asymmetrical positioning of dielectric

06 p1082 A70-17778

Balanced ELF chemotron tetrode amplifiers with series-fed output circuits, showing characteristics calculations and use in pyrometric assembly

06 p1022 A70-17782

Amplifier design effects on device reliability, considering sudden and gradual system failures

07 p1246 A70-19635

Response characteristics of negative feedback galvanometer amplifier with inductive source impedance for geomagnetic micropulsation detection

07 p1242 A70-19998

Transistor RF and IF amplifiers designed for 210-ft antenna of Australian National Radio Astronomy Observatory

07 p1243 A70-20350

Input conductance variation for common-emitter triode distributed-gain wideband amplifier, deriving energy equations improving tube characteristics

08 p1472 A70-20862

Noise and gain formulas for wideband distributed-gain amplifiers using quadrupole elements and transmission line configurations

08 p1472 A70-20863

Multipole coupling circuits for wideband radio amplifiers

08 p1474 A70-21225

Multistage microwave transistor amplifiers design for 4 GHz band, describing poor input/output impedance matching solution

08 p1475 A70-21279

TWT amplifiers for 4-8 GHz frequency range exhibiting decreased weight and volume and increased efficiency

08 p1477 A70-21370

Fluidic devices and applications to gas turbine control, discussing beam deflection amplifiers design parameters

08 p1559 A70-21933

Nonlinear circuits reducing nonlinear distortions in amplifiers, discussing wideband nonlinear distortion compensating circuits

09 p1643 A70-22131

Broadbanding method for microwave reflection type amplifiers using additional resonators

09 p1645 A70-22604

Low noise nonreciprocal microwave parametric amplifier with up-and-down converter and idlers in cascade

09 p1647 A70-22850

Nonresonant multipath carbon dioxide laser amplifier small signal gain of 39 dB utilizing White optical reflector design

09 p1699 A70-23365

Fluidic operational amplifier design and applications

09 p1614 A70-23687

Fluidic digital position sensor consisting of fluidic monostable amplifier, analyzing operation by characteristics method

09 p1614 A70-23689

Integrated CW UHF power amplifier modules using thin film lumped elements and UHF power transistor chips

10 p1846 A70-23884

S band CW high power broadband power source consisting of transistor amplifier-driven varactor doubler chains in hybrid integrated form

10 p1846 A70-23885

Solid state multistage high power avalanche amplifier at X band

10 p1847 A70-23890

Computer-aided class C amplifier design, discussing algorithm and computer program

10 p1849 A70-24447

Low noise wideband uncooled preamplifier for small unattended satellite communication terminals, discussing theory, design and performance

11 p2016 A70-25485

Varactor diode equivalent circuit determination for application to cooled parametric amplifiers design

11 p2017 A70-25573

Microwave amplifiers based on interaction between piezoelectric acoustic waves and collinearly drifting carriers, analyzing gain, frequency response, etc

11 p2018 A70-26164

Wideband transistorized DC amplifier circuit and operation for outputs of tensometers, thermoelectric, electrodynamic and resistance sensors

11 p2019 A70-26435

RF amplifier design procedure for maximum stable gain with minimum noise figure

11 p2019 A70-26715

Soviet book on radio frequency amplifiers covering vacuum tubes, transistors, tunnel diodes, TWT and low noise quantum paramagnetic and parametric devices

12 p2194 A70-26867

Proportional fluid amplifiers noise and instability sources related to geometry and power jet flow, considering noise reduction methods

12 p2164 A70-27071

Transient processes in n-stage aperiodic amplifier during instantaneous change in phase and amplitude of emf at input

12 p2195 A70-27536

Single and multistage parametric amplifiers for broadband communications, noting nonideal circular characteristics by scattering parameter and signal flow graph

12 p2197 A70-27933

Wideband high power output transistor amplifier design features and operational characteristics

12 p2199 A70-27980

Triple passage crystal amplifier of single frequency ruby laser emission, noting radiation structure and coherence

12 p2250 A70-28183

Operational amplifier with Darlingon circuit for high output current

13 p2377 A70-29114

Parametric amplifier as preamplifier for microwave receivers in space probes, presenting block diagrams and test results

13 p2379 A70-29559

Wideband microwave transistor IF amplifier for mm wave communication system

14 p2555 A70-30283

Computerized design of transistorized UHF wideband amplifier, using successive approximations for optimum circuit automatic selection

14 p2556 A70-30668

Amplifiers with selective feedback and clamping circuits for electrocardiology and electroencephalography

15 p2691 A70-31924

Redundant amplifier /RAMP/ for reliability improvement

15 p2708 A70-31961

Integrated tunnel diode amplifiers design using hybrid technique for communications satellites, noting stability and noise performance

15 p2710 A70-32469

Low noise wideband amplifier design for Intelsat 3 satellite ground stations

16 p2877 A70-33415

Gas tube isolator circuit for arcing amplifier in phased arrays, using programmed charge of capacitance bank during interpulse

16 p2879 A70-34072

Operational amplifier with high output current for use as thermostatic regulator, power supply unit, AC/DC converter, etc

16 p2880 A70-34100

Wideband microwave IC tunnel diode amplifier /TDA/ for artificial satellites, discussing noise, size and weight reduction

17 p3053 A70-35277

SHF traveling wave tube amplifier design and characteristics

17 p3054 A70-35413

Ferrite reactive modulation amplifier design, using yttrium garnet for noise reduction

19 p3386 A70-37629

Mechanical parametric amplification, improving SNR of acoustic systems in hostile environments

19 p3422 A70-37695

Automatic gain ranging amplifier for high speed digital computer controlled data acquisition system used to process input data levels

19 p3383 A70-37919

Four-terminal p-n-p-n small signal semiconductor tetrode amplifier operation principle and linear circuit applications

19 p3390 A70-38305

Selective inductorless amplifier design with four layered distributed RGC line in feedback loop, obtaining high Q factors in transfer function

19 p3390 A70-38674

Transistor amplifier with back coupled emitter and parallel inductive correction, calculating optimal frequency and phase characteristics under complex load

20 p3598 A70-39790

Adaptive AC null detector with tuned compression amplifier used for oscilloscope display drive

21 p3828 A70-41469

Mechanical passive cone angle amplifier for spinning sounding rockets for IR sky scanning, solving equations of motion for system

21 p3931 A70-41905

Jet-deflection proportional amplifier design and performance, discussing pressure and momentum control, static and dynamic characteristics aspect ratio, geometry effects, etc

22 p3963 A70-42410

Impact configuration fluidic amplifier, investigating modulation of power jet formed by impacting plane wall jets in bounded region

22 p3963 A70-42413

Oscillatory stability of selective RF transistor amplifiers, using stage dimensioning and gain graphs

22 p3996 A70-42818

Linear IC for RF applications including multistage amplifiers, simulating by actual units

22 p3999 A70-42821

Tunnel diode amplifier design, using gain-bandwidth nomograph

22 p3999 A70-43487

Design tolerances and compensating networks for microwave transistor amplifier, using synthesis search and trial calculation by computer

23 p4168 A70-43780

Ferromagnetic microwave amplifiers operation, describing longitudinal pumping amplifier using YIG

23 p4170 A70-43825

Fluidic amplifiers in measurement technology including turbulence, pulse, Coanda, induction, vortex, arc and focusing amplifiers

23 p4142 A70-44246

Computerized design of broadband microwave amplifiers with complex terminations, using transfer scattering parameters for analysis and optimization

24 p4316 A70-45211

Two-cascade amplifying circuits with current and voltage feedback for semiconductor precision devices

24 p4321 A70-46394

LF narrow band-pass amplifiers with distributed RC structures

24 p4321 A70-46397

AMPLIFIERS

NT BEAM PLASMA AMPLIFIERS
NT BROADBAND AMPLIFIERS
NT CROSSED FIELD AMPLIFIERS
NT CURRENT AMPLIFIERS
NT DIFFERENTIAL AMPLIFIERS
NT DISTRIBUTED AMPLIFIERS
NT FEEDBACK AMPLIFIERS
NT FLUID AMPLIFIERS
NT INTERMEDIATE FREQUENCY AMPLIFIERS
NT JET AMPLIFIERS
NT LIGHT AMPLIFIERS
NT LINEAR AMPLIFIERS
NT MICROWAVE AMPLIFIERS
NT PARAMETRIC AMPLIFIERS
NT PHOTOMULTIPLIER TUBES
NT POWER AMPLIFIERS
NT PREAMPLIFIERS
NT SERVOAMPLIFIERS
NT TRANSISTOR AMPLIFIERS
NT TRAVELING WAVE AMPLIFIERS
NT VOLTAGE AMPLIFIERS

Amplification and contactless recording device with ferroresonant servomotor controlled by low DC signals

05 p0848 A70-16364

Hall voltage and electric conductivity measurements in alternating magnetic field and current by narrow band amplifier with synchronous detector

07 p1279 A70-18944

Distributed gain amplifier circuits with K-type filters, deriving analytical relations for pulsed and transient characteristics

10 p1853 A70-25131

Active antennas definition with integrated, amplifying electronic components based on designations in two port theory

13 p2376 A70-28897

Maximum frequency response of reactive modulation amplifier using parametrically excited oscillator circuit

13 p2377 A70-29304

Noise sources and identification in low noise RF amplifiers via noise temperature or factors

15 p2708 A70-31952

Magnetically focused two and four stage cascade picture amplifiers for astronomy and nuclear physics applications

20 p3630 A70-39426

Active bandpass filter configurations with operational amplifiers, noting resonance frequency and Q factor variation relationship to amplifier gain-bandwidth product

21 p3796 A70-40561

Carbon dioxide-helium laser hollow cathode negative glow discharge amplifier, discussing construction and advantages compared to other excitation media and discharge structures

21 p3834 A70-40568

Photon-coupled biomedical amplifier for measuring and recording physiological signals

23 p4155 A70-44848

AMPLITUDE DISTRIBUTION ANALYSIS

Envelope delay and amplitude characteristics measurement of modulated carrier wave channel in radio relay link 02 p0258 A70-12475

Light-gathering amplitude and intrinsic resolution of large-area flat scintillation detectors used for cosmic rays-nuclear interaction experiments at high energies 03 p0484 A70-13466

Limits on signal amplitude, spectrum, derivatives and modulus of variations 03 p0453 A70-14283

Periodic drag of vibrating cylinders as function of excitation amplitude and frequency, noting similarity to nonlinear oscillator subjected to forced vibration 04 p0691 A70-15148

Phase and amplitude level of plane light wave propagation in medium with randomly discontinuous refractive index, discussing wave phase dependence on dielectric constant 04 p0650 A70-15288

Spatial distribution of field intensities of resonators, using diffraction gratings and prisms 04 p0651 A70-15289

Ionospheric probe for simultaneous measurement of radio signal reflection coefficient and amplitude-frequency characteristics 04 p0684 A70-15746

Radar signal amplitude fluctuations reflected from disturbed sea water surface, noting wind induced waving stochastic nature influence 05 p0812 A70-16246

Inhomogeneity and water vapor absorption influence on frequency spectrum of amplitude fluctuations of plane wave propagating in turbulent atmosphere 05 p0813 A70-16252

Fourier spectra of Pi 1 pulsations during magnetic field sudden disturbances derived from amplitude analysis 05 p0840 A70-16641

Nose bluntness, angle of attack and oscillation amplitude effect on hypersonic unsteady aerodynamics of slender cones [AIAA PAPER 70-216] 06 p0969 A70-18059

Latitudinal dependence of period and amplitude of steady Pc 3-4 pulsations observed at group of widely spaced stations 07 p1268 A70-19464

Spectral amplitude distribution of lightning spherics predicted over VLF-SHF range using theoretical analysis of lightning streamers 07 p1272 A70-20215

Turbulent thermal flux in Venus atmosphere estimated from amplitude fluctuation dispersion of Venera 4 and Mariner 5 radio signals 07 p1390 A70-20305

Finite amplitude effects on MHD thermal convection in rotating layer of conducting fluid, discussing subcritical instability 08 p1563 A70-20472

Nonenergetic parameter estimation of signal during optimal reception with random amplitude fluctuation in normal background noise using maximum probability function 08 p1461 A70-20868

Periodic and almost periodic solutions to vibrations of quasi-linear nonautonomous systems in presence of resonance, determining principal amplitudes 08 p1544 A70-20966

Amplitude-frequency characteristics of arbitrary elastic system performing flexural vibrations determined using computer 08 p1588 A70-21184

Vibration decrement of nonlinear elastic system from resonance peak width of displacement amplitude curve of perturbing force 09 p1782 A70-23295

Expansion bellows fatigue strength based on load and displacement measurements performed during low cycle model tests 10 p1965 A70-25299

Signal amplitude and intensity fluctuations after laser amplification, considering P representation for density operator 11 p2063 A70-25867

Vibrational motion sensors amplitude-frequency characteristics correction by passive electrical filters, deriving spectral transmittances 11 p2055 A70-26444

Photomultipliers single electron response by measuring electron pulse height distribution 12 p2236 A70-27850

Frequency spectra of log amplitude fluctuations of electromagnetic wave propagating in turbulent atmosphere, using geometrical optics approximation 12 p2190 A70-28173

Meteor radio reflections time-amplitude characteristics, discussing dependence on mirror point position in trail, wavelength, diffusion factor and initial radius 14 p2636 A70-30324

Ionospheric probe for simultaneous measurement of radio signal reflection coefficient and amplitude-frequency characteristics 14 p2576 A70-30830

Field amplitude distribution parameter in long distance tropospheric communications based on fading depth 15 p2696 A70-31512

Radar echo signal amplitude probability distribution during fully polarizational reception 15 p2696 A70-31517

Low amplitude waves and substantial frequencies interaction by averaging method for hydrodynamics of waves in collisionless plasmas 15 p2720 A70-32114

Holographic stereo model, comparing stereoscopic perception of phase and amplitude to model consisting of overlapping photos 16 p2908 A70-33228

Amplitude distribution selection in antenna aperture in presence of phase amplitude errors from relation between sidelobe level probabilistic and phase amplitude errors characteristics 16 p2873 A70-33241

Sky wave amplitudes analysis recorded at D region height by loop and short whip antennas during 7 March 1970 solar eclipse 16 p2898 A70-33833

Electrocardiograms amplitude probability densities, noting variations for different heart diseases 17 p3034 A70-35877

Interferometric holograms of vibrating body via numerical analysis of oscillations amplitude and phases 18 p3258 A70-36303

Latitudinal dependence of period and amplitude of steady Pc 3-4 pulsations observed at group of widely spaced stations 18 p3250 A70-36938

Wolf numbers monthly fluctuations, giving histogram of fluctuation amplitude distribution 18 p3323 A70-37137

Bounded electromagnetic wave propagation in randomly inhomogeneous medium, calculating correlation in amplitude and phase fluctuations 19 p3375 A70-37282

Merlons amplitude optimal value for open loop part characteristics in control systems design, obtaining global extremum of stipulation numbers 19 p3392 A70-37448

Holographic interferometry measurements of surface amplitudes distribution under periodic mechanical vibration 21 p3824 A70-40864

ULF ballistocardiogram amplitudes relationship to blood flow velocity for cardiovascular disease diagnosis 21 p3763 A70-41234

Comprehensive amplitude probability distribution for atmospheric radio noise, noting role in evaluating antenna size and matching 21 p3788 A70-41341

Amplitude and phase frequency characteristics of open and closed multiloop nonlinear automatic control systems by graphical methods 22 p4000 A70-42830

Pulse height distributions due to terrestrial gamma rays, using NaI/Tl scintillation counter 23 p4187 A70-43899

Harmonic oscillations recurrence in linear systems with lumped and distributed parameters, obtaining amplitudes by least squares estimator 24 p4379 A70-45483

AMPLITUDE MODULATION

Amplitude modulated pearl type geomagnetic micropulsations connected with auroral X ray emission variations 01 p0171 A70-11228

Wave front reconstruction for perfectly bleached holograms not achievable by simple coherent illumination due to remaining amplitude variation 04 p0691 A70-15033

AM baseband telemetry system for wideband signal transmission emphasizing SSB, DSB and quadrature multiplexed DSB modulation techniques 06 p1007 A70-17435

Amplitude and frequency characteristics of gas ring laser with optical feedback between oppositely moving waves amplified by reflecting mirrors 06 p1081 A70-17497

Analytical expressions for amplitude and frequency modulation characteristics of bias modulated tunnel diode oscillator on steady state mode 06 p1022 A70-17836

Phase and amplitude modulated signals transmission over band limited channel disturbed by additive white Gaussian noise 07 p1237 A70-20195

Time-frequency correlation function for fading communication channel between transmitter and receiver sites, using AM transmissions as probing signals 08 p1458 A70-20796

AM electromagnetic wave self modulation in magnetoplasma, considering self and mutual interaction of ordinary and extraordinary propagation modes 08 p1552 A70-21527

Correlation function of oscillation modulated in amplitude, phase and frequency by random processes causing spectral density maximum shift away from carrier frequency 09 p1633 A70-22409

Optimal amplitude modulated radio signal reception on white and narrow band background noise, using nonlinear filtration and phase locked control 09 p1633 A70-22416

X band Gunn oscillators amplitude modulation by pulse signals from another Gunn diode 09 p1646 A70-22707

Amplitude modulation of microwave signals propagated through periodically varying plasma 09 p1639 A70-23673

Atmospheric modulation transfer function measuring instrument based on Lindberg principle, discussing optical and mechanical design features and applications 09 p1688 A70-23769

AM and FM CW Doppler radar by combined AM-FM waveform, noting automatic track while scan radar application 10 p1840 A70-24445

Microwave devices excess AM and FM noise levels measurement by carrier suppression methods 10 p1841 A70-24579

Frequency sharing between satellite-transmitted FM TV signals and terrestrially transmitted AM-VSB TV signals [AIAA PAPER 70-438] 11 p2001 A70-25467

Spatial and amplitude modulators for laser-photographic display system producing real time TV pictures or images 11 p2062 A70-25734

Parametric effect maser developed by maintaining self oscillations in static amplitude modulated magnetic field, noting application as magnetometer 11 p2063 A70-25947

Power spectral density and autocorrelation functions of sinusoidal carrier amplitude modulated by split phase PCM and PSK 11 p2008 A70-26203

Time constant, steady state and tracking error of AGC loops at input/output of FM link in AM-FM telemetry system 12 p2184 A70-27250

Transient processes in n-stage aperiodic amplifier during instantaneous change in phase and amplitude of emf at input 12 p2195 A70-27536

Amplitude and phase fluctuations in laser with nonlinear absorption due to spontaneous emission, studying lasing instability near hysteresis threshold 12 p2248 A70-27548

High speed linear phase and amplitude modulation of X band Gunn oscillators 12 p2199 A70-28016

Laser field structure effect on spectrum of Q switched laser nonmonochromatic emission after amplitude modulation 13 p2426 A70-28872

Electro-optical light modulators representation by two port matrices, deriving amplitude modulation methods 13 p2427 A70-28924

Maximum frequency response of reactive modulation amplifier using parametrically excited oscillator circuit 13 p2377 A70-29304

Amplitude and phase modulation of laser beams by tetragonal crystal cuts 13 p2429 A70-29533

AM signal reception on strong AM noise background, describing theoretical receiver design 13 p2370 A70-29740

Amplitude modulation of ruby and neodymium-doped glass lasers via ultrasonic acoustic wave injection 16 p2926 A70-33162

Carbon dioxide laser producing nearly 100 percent amplitude modulation of output by intracavity polarization modulation technique 18 p3270 A70-36747

Two dimensional phase distribution function of mixture of Gaussian noise with amplitude modulated signal 18 p3229 A70-37110

IMPATT diode microwave oscillator with modulated bias current, discussing amplitude and frequency modulation sensitivity, thermal effects and load parameters 19 p3390 A70-38363

Cosmic ray anisotropy sidereal-diurnal effects isolation by solving simultaneous amplitude and phase modulation problem 20 p3696 A70-39282

Solar cosmic rays diurnal and semidiurnal variations modulation by noncoincidence between earth rotation axis and normal to ecliptic plane 20 p3697 A70-39289

Amplitude modulated optical band signal detection, comparing optimal direct photodetection and super-heterodyne receivers sensitivities 21 p3785 A70-40633

Wideband high speed PCM/AM optical communication system using mode locked He-Ne laser, noting simultaneous signal transmission and bit rate 21 p3789 A70-41354

Pulse angle modulation and PTM-AM equivalence, examining noise effect on conversion 22 p3989 A70-42570

Linear differential equation solution associated with FM signal generation, presenting analytical methods for FM and AM components 22 p4063 A70-43209

Bunched ion bursts amplitude modulation effects on nonlinear ion acoustic waves in grid plasma system 23 p4229 A70-44989

Carrier frequency transfer of amplitude modulated signal at two coupled transitions in traveling wave gas laser 23 p4202 A70-45055

Multidegrees of freedom electronic cabinets dynamic response to AM fast sine sweep [SAE PAPER 700846] 24 p4380 A70-45884

AMPLITUDE PROBABILITY ANALYSIS

U AMPLITUDE DISTRIBUTION ANALYSIS

AMPLITUDES

NT PULSE AMPLITUDE

NT SCATTERING AMPLITUDE

Spontaneous echoes amplitude resulting from damped electronic plasma plane wave excitation in collisionless plasma 09 p1735 A70-22843

Obliquely incident spherical wave amplitude and phase fluctuations, deriving formulae to compare variances behavior for refractive index fluctuation autocorrelation functions 14 p2574 A70-30750

Amplitude and intensity interference relations from pseudothermal light sources, noting applicability to stellar interferometry 16 p2900 A70-32999

Heterodyne conversion transducer large signal internal parameters dependence on heterodyne, signal amplitudes and intermediate voltage 16 p2873 A70-33240

Logarithmic amplitude characteristic of automatic rate stabilization systems for controlled electric actuator systems 18 p3215 A70-36296

Plane EM wave diffraction by ribbon periodic grating, determining diffraction spectrum wave amplitudes 19 p3377 A70-37718

ANALOG CIRCUITS

Feedback time sharing analog electronic multiplier for two quantities, noting linearity, accuracy and stability of measurements 02 p0268 A70-12422

Integrated analog voltage regulator sensitivity to small signal transient radiation, discussing circuit hardening by diode compensation 04 p0658 A70-14742

Discrete analog filters circuits for optimal non-coherent processing of phase manipulated signals 08 p1456 A70-20571

Precision frequency analog converter using crystal oscillator and transistor switch reducing errors 09 p1653 A70-23698

Analog fluidic elements /operational amplifiers/ with beam deflector proportional amplifiers incorporated into close coupled circuit 12 p2164 A70-27072

Signal-arrival-time invariance and SNR resolution of discretely analog filters matched to complex radio signals 13 p2380 A70-29736

Algorithmic random process pseudorandom number generator composed of analog computer elements, evaluating stability 20 p3594 A70-39918

Analog three dimensional electrical signal multiplier circuit based on Hall effect, considering division and square root extraction 24 p4319 A70-45484

Maximum-likelihood decoding in analog form of linear convolutional codes with respect to constraint length by one-step threshold method 24 p4313 A70-46059

ANALOG COMPUTERS

Analog, analog/digital, digital and hybrid computer simulation current advances, emphasizing physiological problems and optimum solution 02 p0264 A70-11687

Analog computer model of human cardiovascular control system to reproduce subject response to sub-maximal workload 03 p0438 A70-14081

Analog computer schemes for solving dynamic plants identification reducible to optimizing parametric problem of many variables function 04 p0654 A70-15435

Stability and limiting frequency of analog computer solutions of differential equations with root shifts caused by resolver imperfection 07 p1321 A70-18689

On-line computer for heart rate, isovolumetric contraction time, ejection time, stroke volume and cardiac output using vibrophonocardiogram signals 07 p1224 A70-20196

Repetitive electronic differential analyzer with transistorized operational amplifiers for iterated solutions of differential equations 08 p1478 A70-21836

Postcaloric nystagmus clinical evaluation by analog computer measuring fast-phase eye displacement in Vestibular Function laboratory 08 p1448 A70-21942

Digital and analog computers applicability to graphic arts noting lack of aesthetic theories 10 p1845 A70-24235

Circuit for analog computing system to determine function extremum of many variables in presence of constraints 11 p2023 A70-25927

Analog computer methods applied to aerospace dynamic test data analysis and high speed screening [AIAA PAPER 70-595] 13 p2375 A70-29880

Real time analog simulation of helicopter rotor, calculating lift and drag coefficients along blade 15 p2672 A70-31775

Nonlinear systems absolute stability by graphic methods, noting use of Nichol chart and analog computer 15 p2715 A70-31974

Analog computer for continuous recording of oxygen consumption of muscular area in canine foot via blood flow rate and oxygen saturation 19 p3367 A70-37354

Data management methodology for test facilities, considering on-line analog/digital computers 19 p3383 A70-37922

Digital differential analyzers one step integration method with iteration procedure truncation to single step 22 p3996 A70-42921

Flight simulation in SAAB AJ37 aircraft development, describing analog and digital computers, cockpit simulators, automatic pilots, control and display devices [ICAS PAPER 70-42] 23 p4178 A70-44140

German monograph on airfoil and wings aerodynamic coefficients calculations, showing advantages of analog computers based on singularity theory and distance functions 24 p4287 A70-45097

ANALOG DATA

Digital and analog large system data displays, considering CRT, laser, hybrid types, contrast control, etc 06 p1061 A70-17348

Waveform estimation by adaptive combination of analog and hardlimited sensor signals 12 p1287 A70-27906

Analog information transmission device using He-Ne laser radiation, discussing optical telemetry channel transfer characteristics for pulsed nanosecond analog signals 12 p2250 A70-28184

Analog data transmission over PCM telemetry link, comparing noncoherent FSK vs PSK reception performance for waveform error 14 p2552 A70-31187

Wideband pulse signal synthesis and optimal filtration by dispersive ultrasonic delay lines, estimating potential noise stability for analog data transmission 15 p2696 A70-31502

Sampled analog waveforms transmission, deriving optimum pre- and postfilters 15 p2703 A70-32557

Monograph on state variable approach to continuous estimation of random processes with applications to analog communication theory 17 p3045 A70-35189

Wideband analog signal data transmission, evaluating messages accuracy in terms of error probability 18 p3228 A70-36623

Analog shift register for use as delay line and digital filter, discussing applications to radio astronomy 18 p3261 A70-37088

Real time analog display inputs for electronic computers and tracking in physiological control circuits, describing various manual controls 19 p3367 A70-37564

Data processing systems functions and composition for random data reduction during aircraft flight tests based on analog and digital techniques 19 p3430 A70-38524

Portable catapult and arresting gear analog instrumentation data acquisition system testing aboard aircraft carriers and at land-based facilities 19 p3384 A70-38533

Sideband frequency disturbances at analog data magnetic storage using frequency modulation 20 p3586 A70-39706

Random values analog sensors classification based on physical, algorithmic and data reproduction techniques 20 p3593 A70-39917

Analog communication optimal nonlinear modulation scheme design for large SNR through transformation into inner product functions 20 p3587 A70-39973

Oscilloscope polar coordinate displays for multidimensional analog signals, noting human detection capability 21 p3823 A70-40853

Discretization interval in discrete analog filters for optimal processing of complex radar signals, estimating systematic errors 22 p3984 A70-42393

Algorithms for analog wideband signals optimal reception in presence of strong Gaussian noise 22 p3988 A70-42568

Multiplicative noise reduction during transmission of analog signals over tropospheric microwave relay links 23 p4162 A70-44090

Analog and digital low pass filters for radiometric postdetector filtering 24 p4321 A70-45622

ANALOG SIMULATION

Electrical analog simulation of cardiovascular system, determining blood flow rate and pressure in aorta and peripheral vessels 03 p0420 A70-13490

Analog computer cardiovascular system model to simulate pressure and flow events in veins including effects of gravity, collapse, breathing and venous valves action 04 p0641 A70-14632

Control system response improvement by state variable feedback illustrated by frequency and transient response tests data from analog model 04 p0662 A70-15331

Book on digital simulation of continuous systems covering programming, engineering and mathematical applications, equipment logic and construction, etc 06 p1014 A70-17475

Electrical network models simulating initial and boundary value problems of applied mechanics, exemplifying with string free vibrations and thin plate bending 06 p1094 A70-17928

Axisymmetric motion of viscous heat conducting gas by constructing indirect analog of Poiseuille gas flow, applying results to slip flow regime 06 p1048 A70-18325

Electronic analog model for simulating convective mass transport in system with stationary and dynamic phases 07 p1423 A70-19740

Human color vision simulation by mathematical and electronic analogs for photoelectric color measurement and eye resolution 08 p1450 A70-20727

Ordinary differential and algebraic equations correct analog model, noting residual system stability role 09 p1642 A70-22973

Direct digital control valves in fluid flow process evaluated for performance by analog computer simulation 09 p1613 A70-23684

Unsteady heat transfer on electronic analog model, using installation prescribing variable boundary conditions of third kind 10 p1966 A70-23872

Combined discrete event and continuous systems simulation language, discussing mathematical modeling and various applications 10 p1860 A70-24652

Digital control systems simulation on analog computer with digital logic, using conventional analog amplifiers and integrators 10 p1860 A70-24655

Human finger tips skin temperature periodical variations process and influencing factors using electronic analog model 10 p1823 A70-25306

Cardiovascular model for closed loop analog simulation of congenital heart defects hemodynamics 11 p1990 A70-25705

General aviation aircraft fixed-base engineering flight simulator involving use of analog computer, discussing equations of motion and aircraft cockpit [SAE PAPER 700235] 11 p2031 A70-25904

Automatic computation at SNECMA for turbomachines R and D, emphasizing digital computer for scientific calculation and analog simulator for engine regulation 12 p2193 A70-28073

Analog computer simulation of command signal detectors for reconstruction of transmitted binary character from noisy binary coded signal 13 p2385 A70-29560

Stochastic analog approximation method minimizing criterion functions and for recovering functions from noisy measurements of values in learning systems 13 p2442 A70-29585

Electronic simulation of neuronic membrane demonstrating nervous impulses generation and propagation behavior
14 p2542 A70-30387

Faraday type MHD generators, investigating gas velocity and temperature profiles effect on electrical performance by equivalent circuits simulation
14 p2534 A70-30537

Gas turbine performance dynamic modeling by analog and digital computer simulation providing clear picture of transient behavior
14 p2629 A70-30991

Real time analog simulation of helicopter rotor, calculating lift and drag coefficients along blade
15 p2672 A70-31775

Analog simulation of frequency multipliers and dividers with step recovery diodes
15 p2709 A70-32467

Second order hyperbolic partial differential equations analog solution based on method of characteristics, showing advantage over digital computer solution
15 p2768 A70-32819

Muscular behavior analog simulation model from generalization of laws governing viscoelastic behavior of polymeric materials
15 p2693 A70-32820

Gas turbine engine dynamic performance simulation, using analog and digital techniques
[ASME PAPER 70-GT-23] 18 p3237 A70-36830

Jupiter decametric radio emission modulation by Io simulated by DC circuit model
18 p3321 A70-37120

Elastoplastic deformation in strip with symmetrical semicircular notches simulating stress strain-state on cellular models by polarization-optical method
20 p3720 A70-39735

Analog computer for one dimensional antenna array simulation, discussing radiation pattern calculation and display
21 p3796 A70-40621

Computer program for nonlinear differential equations related to nonlinear boundary value problems based on Newtonian iteration process difference analog of linearization method
23 p4212 A70-44338

Blood circulatory system and hemodynamic interdependencies simulation by analog computer, using Warner model
23 p4155 A70-44862

Two shaft bypass jet engine analog simulation, determining angular acceleration dependence on angular velocity and fuel consumption
24 p4393 A70-45442

ANALOG TO DIGITAL CONVERTERS

Soviet book on pulse code telemetry systems covering analog-digital conversion, data transmission in communication channels, noise problem, code selection, etc
04 p0648 A70-14953

Digital computer interface for ELDO launcher inertial guidance system linking with platform, autopilots, telemetry equipment and rocket sequencers
05 p0818 A70-16572

Specification of minimum performance standards and test procedures for automatic pressure altitude digitizer equipment
[SAE-AS-855] 07 p1279 A70-18901

Electromechanical graph digital reader for records of cardiovascular studies
07 p1224 A70-20197

Air safety and navigation systems data transmission, discussing analog to digital conversion and modulation
09 p1720 A70-22550

THEMIS source encoding systems research program to investigate inherent quantizing noise and degradation of analog to digital conversion
11 p2014 A70-26255

Physical signals continuous to discrete transformation by analog to digital conversion, considering coding process and transfer functions
14 p2554 A70-30679

Aircraft electronic propulsion control system using flight time computers and analog to digital conversion equipment
[AIAA PAPER 70-693] 16 p2966 A70-33556

Digital readout test equipment characteristics and parameters for electrical properties measurement, proposing pulse counting analog-digital conversion technique
19 p3432 A70-38701

Mathematically defined curve incremental generation by computer, discussing parametric and non-parametric representations and digital differential analyzer technique
22 p3993 A70-43072

ANALOGIES

NT HYDRAULIC ANALOGIES

Electrical analogs for optical systems in communication problem of optimum filtering to improve SNR
04 p0633 A70-15660

Electrical analogs for optical systems based on linear system concepts and communication theory analysis
10 p1854 A70-25246

Composite reinforced materials similarity criteria to relate static and dynamic fields of various physical parameters, outlining mathematical simulation
12 p2259 A70-27526

Analog methods of weather forecasting involving map matching, discussing weather modification
14 p2610 A70-31141

Mechanical-stereomechanical analogy of two index Lagrange equations of second kind
17 p3130 A70-35192

Infinite elastic beams system supported on two parameter elastic foundation solved by analogy to single beam lying on one-parameter elastic foundation
17 p3189 A70-35229

Nonlinear resistance element with square law I-V characteristics for electrical analogs of hydraulic systems
19 p3359 A70-38707

Mechanical analogies of magnetodynamic oscillations in homogeneous density column subject to material body impact, relating to earth magnetic field
21 p3854 A70-40593

Krylov and Bogoliubov perturbation method extension to difference equations based on analogy between differential and difference equations
24 p4370 A70-46027

ANALYSIS [MATHEMATICS]

NT ABEL FUNCTION

NT AIRY FUNCTION

NT ANALYTIC FUNCTIONS

NT APERIODIC FUNCTIONS

NT ASYMPTOTES

NT ASYMPTOTIC SERIES

NT BANACH SPACE

NT BESSEL FUNCTIONS

NT BETHE-SALPETER EQUATION

NT BIHARMONIC EQUATIONS

NT BLASIUS EQUATION

NT BURGER EQUATION

NT CALCULUS

NT CALCULUS OF VARIATIONS

NT CAUCHY INTEGRAL FORMULA

NT CAUCHY-RIEMANN EQUATIONS

NT CHANDRASEKHAR EQUATION

NT COMPLEX VARIABLES

NT CONFORMAL MAPPING

NT CONJUGATES

NT CONTINUITY [MATHEMATICS]

NT CONVOLUTION INTEGRALS

NT COPLANARITY

NT CUBIC EQUATIONS

NT DELTA FUNCTION

NT DEPENDENT VARIABLES

NT DIFFERENTIAL CALCULUS

NT DIFFERENTIAL EQUATIONS

NT DUFFING DIFFERENTIAL EQUATION

NT EINSTEIN EQUATIONS

NT ELLIPTIC DIFFERENTIAL EQUATIONS

NT ELLIPTIC FUNCTIONS

NT ENTIRE FUNCTIONS

NT EXISTENCE THEOREMS

NT EXPONENTIAL FUNCTIONS

NT EXTREMUM VALUES

NT FALKNER-SKAN EQUATION

NT FOKKER-PLANCK EQUATION

NT FOURIER ANALYSIS

NT FOURIER SERIES

NT FOURIER TRANSFORMATION

NT FREDHOLM EQUATIONS

NT FUNCTION SPACE

NT FUNCTIONAL ANALYSIS

NT FUNCTIONAL INTEGRATION

NT GAUSS EQUATION

NT GREEN FUNCTION

NT HALF PLANES

NT HALF SPACES

NT HANKEL FUNCTIONS

NT HARMONIC ANALYSIS

NT HARMONIC FUNCTIONS

NT HELMHOLTZ VORTICITY EQUATION

NT HILBERT SPACE

NT HILBERT TRANSFORMATION

NT HILL DETERMINANT

NT HYPERBOLIC FUNCTIONS

NT HYPERGEOMETRIC FUNCTIONS

NT HYPERPLANES

NT INTEGRAL CALCULUS

NT INTEGRAL EQUATIONS

NT INTEGRAL TRANSFORMATIONS

NT JACOBI INTEGRAL

NT KERNEL FUNCTIONS

NT LAGUERRE FUNCTIONS

NT LAME WAVE EQUATIONS

NT LAPLACE TRANSFORMATION

NT LEGENDRE FUNCTIONS

NT LIAPUNOV FUNCTIONS

NT LIMITS [MATHEMATICS]

NT LINEAR EQUATIONS

NT LIOUVILLE EQUATIONS

NT LIPSCHITZ CONDITION

NT LOGARITHMS

NT MACLAURIN SERIES

NT MATHIEU FUNCTION

NT MAXIMA

NT MEASURE AND INTEGRATION

NT MEROMORPHIC FUNCTIONS

ANALYTIC GEOMETRY

NT MINIMA

NT MONGE-AMPERE EQUATION

NT NEUMANN PROBLEM

NT NONLINEAR EQUATIONS

NT NUMERICAL INTEGRATION

NT ORTHOGONAL FUNCTIONS

NT PARABOLIC DIFFERENTIAL EQUATIONS

NT PARTIAL DIFFERENTIAL EQUATIONS

NT PERIODIC FUNCTIONS

NT PHASE-SPACE INTEGRAL

NT POISSON EQUATION

NT POWER SERIES

NT QUADRATIC EQUATIONS

NT RATIONAL FUNCTIONS

NT REAL VARIABLES

NT RUNGE-KUTTA METHOD

NT SCHWARZ-CHRISTOFFEL TRANSFORMATION

NT SERIES [MATHEMATICS]

NT SINGULAR INTEGRAL EQUATIONS

NT SINGULARITY [MATHEMATICS]

NT SPHERICAL HARMONICS

NT STIELTJES INTEGRAL

NT STURM-LIOUVILLE THEORY

NT TANGENTS

NT TAYLOR SERIES

NT TESSERAR HARMONICS

NT TRIGONOMETRIC FUNCTIONS

NT VECTOR ANALYSIS

NT VLASOV EQUATIONS

NT VOLTERRA EQUATIONS

NT VORTICITY

NT WEIGHTING FUNCTIONS

NT WHITTAKER FUNCTIONS

NT WIENER HOPF EQUATIONS

NT ZONAL HARMONICS

ANALYTIC FUNCTIONS

NT ENTIRE FUNCTIONS

Error estimation during application of Cauchy approximate integral formulas to numerical differentiation of analytic functions by quadrature
01 p0131 A70-10543

Axisymmetric elasticity theory problem of stressed state of space weakened by concentric circular cracks solved using p-analytic functions to generate boundary value problems
03 p0586 A70-13077

Analytic solution for computerized vibration analysis of high speed tension test
08 p1590 A70-21332

Mathematical programming and conditional extremum problems solution in analytic functions based on Chebyshev function systems and Stieltjes moments
08 p1534 A70-21451

Zeta-Kleinian functions derived from Abelian functions
[ONERA-TP-800] 09 p1712 A70-22837

Analytic systems theory using Volterra calculus of functionals applied to nonlinear differential equations
10 p1908 A70-23845

Lagrangian nonenergetic and unconstrained systems introduced in describing Birkhoff classical dynamics, considering space of motions states as connected analytic manifold
10 p1909 A70-24190

Analytic function integration optimal rate, discussing weighting function
10 p1909 A70-24509

Metric analyticity around each point of C cubed static vacuum space-time for Einstein equations
11 p2084 A70-26553

N-locus controllability of two dimensional holomorphic systems with permissible controls
15 p2715 A70-31641

Generalized Carleman boundary value problem, discussing analytical function in simply connected region on Liapunov contour
18 p3280 A70-36159

Numerical differentiation of analytic functions involving Cauchy formula and error estimation
18 p3282 A70-36362

Hilbert type nonlinear boundary value problem, determining conditions for analytical function solutions based on algebraic isotherms theory
20 p3659 A70-40169

Confluent hypergeometric functions indefinite integrals analytic expressions and reduction formulas
22 p4062 A70-42572

Dirichlet problem with singularities for plane with cutouts along circumference, determining analytical function
23 p4211 A70-44239

Second dual space of E sub 0 /Banach space of analytic functions/ identifiable with subspace of L super infinity
24 p4370 A70-46175

ANALYTIC GEOMETRY

NT CATENARIES

NT CONICS

NT HYPERBOLAS

NT LOCI

NT OBLATE SPHEROIDS

NT PARABOLAS

NT PROLATE SPHEROIDS

NT SPHEROIDS

NT TANGENTS

NT TORUSES
 NT TRIGONOMETRY
ANALYTICAL CHEMISTRY
 Collection of papers on analytical chemistry in space covering solar system history, atmospheres, composition, lunar and planetary surface analysis, mass spectroscopy, etc
 10 p1941 A70-24608

ANALYZERS

NT ENGINE ANALYZERS
 NT SIGNAL ANALYZERS
 Microprobe analyzer for light elements using electronic optics probe, sample visualization devices and equipment for X photon detection and measurement [ONERA-TP-774]
 02 p0275 A70-12210

Broad bandwidth electronic analysis of high resolution photographic film using flying spot CRT or rotating mirror devices
 02 p0302 A70-12613

Spherical cylindrical and toroidal electrostatic analyzers with symmetrical angular characteristics for solar wind investigations
 06 p1135 A70-17896

Nondestructive process control analyzer for spot welds in aircraft structural components, monitoring expansion, current and spotweld properties
 08 p1507 A70-21486

Photoemission analyzer with finite emitter in spherically symmetric retarding field with magnetic field present, analyzing energy resolution
 09 p1679 A70-22988

Electrostatic analyzer without fringe field effects for measuring low energy particles on spacecraft
 15 p2740 A70-32432

ANALYZING

NT PREDICTION ANALYSIS TECHNIQUES

ANATOMY

NT ADRENAL GLAND
 NT AORTA
 NT ARM [ANATOMY]
 NT ARTERIES
 NT BARORECEPTORS
 NT BLADDER
 NT BLOOD VESSELS
 NT BONES
 NT BRAIN
 NT BRAIN STEM
 NT BRONCHI
 NT BRONCHIAL TUBE
 NT CAPILLARIES [ANATOMY]
 NT CARDIAC AURICLES
 NT CARDIAC VENTRICLES
 NT CARDIOVASCULAR SYSTEM
 NT CARTILAGE
 NT CEREBELLUM
 NT CEREBRAL CORTEX
 NT CEREBRUM
 NT CHEST
 NT CHOROID MEMBRANES
 NT CIRCULATORY SYSTEM
 NT COCHLEA
 NT CONNECTIVE TISSUE
 NT CONSTRICTORS
 NT CORNEA
 NT CORTI ORGAN
 NT CRANIUM
 NT DIAPHRAGM [ANATOMY]
 NT DIASTOLE
 NT EAR
 NT EARDRUMS
 NT ENDOCRINE GLANDS
 NT EOSINOPHILS
 NT EPICARDIUM
 NT ERYTHROCYTES
 NT ESOPHAGUS
 NT EYE [ANATOMY]
 NT FEMUR
 NT FINGERS
 NT FLEXORS
 NT FOREARM
 NT FOVEA
 NT GONADS
 NT HAND [ANATOMY]
 NT HEAD [ANATOMY]
 NT HEART
 NT HEMATOPOIESIS
 NT HEMATOPOIETIC SYSTEM
 NT HIPPOCAMPUS
 NT HUMAN BODY
 NT JOINTS [ANATOMY]
 NT KIDNEYS
 NT KNEE [ANATOMY]
 NT LABYRINTH
 NT LEG [ANATOMY]
 NT LEUKOCYTES
 NT LIMBS [ANATOMY]
 NT LIVER
 NT LUNGS
 NT LYMPHOCYTES
 NT MARROW
 NT MIDDLE EAR
 NT MUSCULOSKELETAL SYSTEM
 NT MYOCARDIUM
 NT NOSE [ANATOMY]
 NT OCCIPITAL LOBES
 NT OCULOMOTOR NERVES

NT ORGANS
 NT OTOLITH ORGANS
 NT OVARIES
 NT PARATHYROID GLAND
 NT PHARYNX
 NT PHOTORECEPTORS
 NT PINEAL GLAND
 NT PITUITARY GLAND
 NT PUPILS
 NT RESPIRATORY SYSTEM
 NT RETINA
 NT SALIVARY GLANDS
 NT SCIATIC REGION
 NT SEMICIRCULAR CANALS
 NT SKULL
 NT SPLEEN
 NT STOMACH
 NT SYSTOLE
 NT TESTES
 NT THERMORECEPTORS
 NT THIGH
 NT THYMUS GLAND
 NT THYROID GLAND
 NT TORSO
 NT TRACHEA
 NT ULNA
 NT VASCULAR SYSTEM
 NT VEINS
 NT VERTEBRAE
 NT VERTEBRAL COLUMN
 NT VESTIBULES

Mammalian ultraviolet macula design, considering microelectrode data and information from light and electron microscopy, behavioral experiments and computer simulation
 11 p1988 A70-26231

ANDROMEDA GALAXIES

BV photometry of Population I Cepheids in Magellanic Clouds, Galaxy and M31
 03 p0578 A70-14287

Globular clusters in M31, discussing metallicity and heavy element enrichment in Andromeda
 06 p1138 A70-17306

M31 continuum radio emission produced by magnetic field aligned along arms, discussing field turbulence effects
 14 p2642 A70-30891

Andromeda Galaxy M31 hydrodynamic model based on given mass distribution, determining kinematic functions
 15 p2808 A70-32884

M-31 galaxy OB /outermost border/ stars
 18 p3326 A70-37156

ANEOCHOIC CHAMBERS

Interacting coaxial supersonic jet flows noise reduction based on noise distribution characteristics measurement in anechoic chamber
 [AIAA PAPER 70-236]
 06 p1040 A70-18112

Anechoic chambers and test equipment for microwave antenna pattern measurements, discussing electromagnetic shielding and construction
 14 p2557 A70-31180

Temporal and spectra combination effects on aircraft sound judged noisiness, using human subjects in anechoic chamber
 20 p3580 A70-39712

ANELASTICITY

Dual model for describing brittleness and plasticity of solid elastic deformable body, formulating criteria for passage into inelastic state
 06 p1166 A70-17656

Lunar seismogram response behavior in terms of power law model of sedimentary earth rock anelasticity
 13 p2497 A70-29856

Anelasticity in lunar seismology, discussing low Q regolith layer model from Apollo 12 LP seismogram
 13 p2497 A70-29857

Filled elastomers elastic and anelastic behavior, investigating strain dependence
 13 p2440 A70-29964

ANEMOMETERS

NT HOT-WIRE ANEMOMETERS

NT SONIC ANEMOMETERS

Ar laser as suitable source for LF heterodyne anemometry experiments through noise spectrum suppression under optimum conditions
 04 p0702 A70-15569

Aircraft wake turbulence effects, using hot film anemometry from nearby towers and penetration by instrumented aircraft
 05 p0794 A70-16300

Dynamic response of constant resistance anemometers, investigating unsteady probe thermal equilibrium, inductance and feedback equations
 06 p1063 A70-17620

HF arc anemometer for subsonic and supersonic gas flow turbulence measurement
 07 p1285 A70-19837

WINDAV anemometer used as low power wind direction and velocity transducer for tethered balloon
 08 p1494 A70-20822

Cup and vane anemometers theory, determining overestimation errors of differential equation for mean values in sinusoidally fluctuating winds
 08 p1501 A70-21975

Laser anemometer for fluid flow measurements, noting sample size restraint, frequency response and velocity range
 16 p2926 A70-33141

Mass flow ion drift anemometer applicable to aircraft speed measurement including V/STOL
 19 p3425 A70-37885

Thermoanemometric velocity measurements in non-stationary MHD Hg flows by insulated Pt sensors
 21 p3831 A70-42229

Remote digital mean wind speed indicator with numerical display, using photoanemometer for airport application
 21 p3831 A70-42247

Wind velocity derivative statistical characteristics in atmospheric surface layer, using thermoanemometer, functional converter, differentiating circuit and loop oscillograph
 24 p4371 A70-45194

ANEMOMETRY

U VELOCITY MEASUREMENT

ANESTHESIA

Hypoxemia and acidosis avoidance during respiration cessation in halothane anesthesia
 10 p1822 A70-25086

ANESTHETICS

NT CYCLOPROPANE

ANGLES

Radar system for air traffic control using twin beam antenna to improve performance with respect to ground and angel clutter
 02 p0332 A70-11970

ANGLE OF ATTACK

NT ZERO ANGLE OF ATTACK

Banked position and angle of attack changes in fighter aircraft sighting and attacking target, determining spatial zone of possible attack
 02 p0227 A70-12406

Optimum angle of attack control for multistage rocket as function of phase coordinates and time by solving functional equation with finite difference method
 02 p0381 A70-12407

Optimal control of aircraft angle of attack based on minimum terminal velocity during passive flight in spherical nonrotating earth atmosphere
 02 p0227 A70-12409

Liquid film stability relation to angle of attack oscillations during reentry body deceleration
 03 p0406 A70-12939

Hypersonic flow characteristics on yawed circular cone surface at moderate angle of attack, applying results to inviscid and boundary layer flow computations
 03 p0406 A70-12944

Rectangular clamped panel flutter characteristics at various oncoming flow angles of attack
 03 p0590 A70-13382

Ground proximity effect on rectangular wing, studying lift and pitching coefficients dependence on angle of attack
 03 p0407 A70-13493

Approximate solution for hypersonic inviscid flow around spherically blunted bodies at small angle of attack, noting stagnation problems
 03 p0407 A70-13547

Integral method for studying wall heat transfer influence on compressible boundary layer on cone at angle of attack in supersonic flow
 03 p0409 A70-13593

Convective heat transfer rates measured on cooled sharp leading edge flat plates at various angles of attack in hypersonic merged flow
 [ASME PAPER 69-WA/HT-21]
 04 p0614 A70-14813

Pitching moment coefficient changes due to ground effect in fixed wing aircraft flight test method, considering constant angle of attack approach
 04 p0619 A70-15394

Anomalous roll behavior of spinning ballistic reentry vehicles with compound aerodynamic asymmetry consisting of lateral offset combined with trim angle of attack
 [AIAA PAPER 69-103]
 04 p0763 A70-15411

Roll acceleration influence on angle of attack convergence and windward meridian rotation rate of rolling reentry vehicles
 [AIAA PAPER 69-100]
 04 p0764 A70-15546

Multiple time scaling analysis of reentry roll rate and angle of attack for missiles with center of gravity and aerodynamic trim asymmetries
 04 p0764 A70-15597

Nose bluntness, angle of attack and oscillation amplitude effect on hypersonic unsteady aerodynamics of slender cones
 [AIAA PAPER 70-216]
 06 p0969 A70-18059

Pressure distributions prediction on blunt bodies at angle of attack, considering bodies of revolution and large angle cones
 [AIAA PAPER 70-208]
 06 p0971 A70-18104

Dynamic instability of finned missiles occurring as angle of attack undamping and caused by differential lift from windward and leeward fins
 [AIAA PAPER 70-206]
 06 p1158 A70-18178

- Drag on infinite cylinder in hypersonic nearly free molecular flow for various angles of attack, using kinetic approach 06 p0983 A70-18380
- Aerodynamic heating of blunt-nosed reentry bodies noting effects of angles of attack [DGLR-69-0401] 07 p1392 A70-18983
- Hypersonic orbital glider range maximization, analyzing optimal angle of attack by use of rectangular velocity components 07 p1393 A70-19341
- Aerodynamic characteristics of bodies in rarefied gases calculated using surface momentum flow dependence on local angle of attack 08 p1432 A70-21091
- Aerodynamic coefficients for blunt cones in rarefied gas calculated as functions of angle of attack using empirical formulas 08 p1432 A70-21092
- Aerodynamic forces acting on circular plates in rarefied gases, calculating coefficients as functions of angle of attack 08 p1433 A70-21093
- Infinitely wide plate bending at small angle of attack in supersonic gas flow, obtaining critical flow rate equal to divergence rate 08 p1588 A70-21175
- Vibration of thin bodies subjected to large angle attack in hypersonic flow, discussing curved bodies method to reduce problem to steady state flows 09 p1771 A70-22445
- Laminar boundary layer in symmetry plane of cone of revolution at angle of attack calculated by finite difference method 10 p1802 A70-24706
- Three dimensional hypersonic steady flow around blunt and pointed cones at nonzero angles of attack calculated by method of characteristics [AIAA PAPER 69-187] 11 p1975 A70-25969
- Perfect gas supersonic flow with constant velocity, pressure and density around finite nonaxisymmetric body at small angles of attack 12 p2158 A70-28197
- Three dimensional laminar boundary layer equations for body of revolution at angle of attack in supersonic gas flow derived for equations 12 p2158 A70-28198
- Supersonic and hypersonic motion past circular cone at angle of attack, analyzing for velocity and pressure distributions by linearizing conical motion equations 12 p2158 A70-28213
- Nonlinear rolling motion of four-finned missile, investigating function of angle of attack and cubic damping 13 p2503 A70-28531
- Missile impact and trajectory for water entry with zero angle of attack, including deceleration measuring instrumentation [AIAA PAPER 70-531] 13 p2387 A70-29039
- Rolling reentry body velocity as function of roll, pitch, yaw rates and angle of attack 13 p2343 A70-29991
- Angle of attack for nearly circular reentry motion, deriving expression for lateral rates frequencies 14 p2654 A70-30779
- Nonequilibrium dissociation effect on supersonic oxygen flow past inverted blunted cones at angle of attack, considering thermal fluxes and aerodynamic forces 15 p2671 A70-31496
- Hypersonic gas flow characteristics incident on elliptic paraboloid and triaxial ellipsoid at arbitrary angles of attack 15 p2672 A70-31647
- Aerodynamic pressures dependence on angle of incidence for profiles in adiabatic compressible flow 16 p2833 A70-33074
- Turbulent boundary layer growth and thickness on yawed cones, discussing angle of attack effect along windward and leeward rays 16 p2838 A70-33875
- Initial reentry body motion effects on angle of attack envelope value throughout trajectory, including altitude of maximum transient amplification 16 p2982 A70-33892
- Yawed two dimensional wedges in hypersonic stream, including leading edge bluntness, viscous interaction and angle of attack effects [AIAA PAPER 70-783] 17 p3009 A70-34503
- Dihedra placed at angle of attack in hypersonic rarefied gas flow, investigating base flow and near wakes 17 p3010 A70-35047
- Shock layer and combustion in supersonic flows about conical bodies at various angles of attack 17 p3012 A70-35894
- Hypersonic gas flow around blown plane of segmentally blunted cones at large angle of attack, using two dimensional model 18 p3206 A70-36258
- Flow field about leading edges of tapered wings set at incident angle of attack, using gas dynamic and Monge equations 18 p3207 A70-36376
- Two dimensional time dependent solution for impulsive motion of circular cylinder involving viscous cross flow at moderate angles of attack 18 p3207 A70-36454
- High angle of attack aerodynamic characteristics of swept wing navy aircraft designs improved via leading edge modifications [AIAA PAPER 70-904] 19 p3355 A70-37392
- Optimal angle of attack transition trajectories for space shuttle from atmospheric entry to cruising flight for conventional airport landing 20 p3713 A70-39515
- Spinning blunt entry vehicles dynamic stability tests in terminal regime, discussing dependence on angle of attack [AIAA PAPER 70-988] 20 p3714 A70-39541
- Static longitudinal aerodynamic characteristics predictions for missile configurations at various angles of attack, using digital computer [AIAA PAPER 70-981] 20 p3558 A70-39550
- Hypersonic aerodynamic characteristics of sharp slender right circular cones at angles of attack, using Newtonian impact theory modified for flow separation effects [AIAA PAPER 70-979] 20 p3558 A70-39550
- Automatic calculations for fuel volume mass properties in tanks at various angles of attack, considering total weight, gravity center moment and inertia product [SAWE PAPER 850] 20 p3563 A70-40376
- Steady viscous flow past oblique flat plate at high Reynolds number, using Oseen linearized approximation 21 p3809 A70-41714
- Accelerated supersonic motion of plate with attached shock wave at finite angle of attack in ideal gas, using perturbed nonstationary motion equations 21 p3748 A70-42209
- Aircraft rolling motion /eigenmotion/ in flight at small angle of attack following initial disturbance, discussing response to control action 22 p3961 A70-42515
- Perfect gas supersonic flow with constant velocity, pressure and density around finite nonaxisymmetric body at small angles of attack 22 p3960 A70-43322
- Three dimensional laminar boundary layer equations for body of revolution at angle of attack in supersonic gas flow derived for equations 22 p3960 A70-43323
- Stationary elliptic cylinders in subcritical flow, determining Strouhal number, pressure fluctuations and wake geometry as functions of angle of attack [AIAA PAPER 69-745] 23 p4134 A70-44564
- ANGLES [GEOMETRY]**
- NT ANGLE OF ATTACK
- NT BRAGG ANGLE
- NT BREWSTER ANGLE
- NT DIHEDRAL ANGLE
- NT ELEVATION ANGLE
- NT SWEEP ANGLE
- Angle of incidence effect on oblique impact crater formed by high speed solid spherical particles colliding with massive lead targets 03 p0592 A70-13449
- Precision and accuracy evaluation of convergence angles for measuring vertical and horizontal components of space position applicable to geodesy and flight measurement [AAS PAPER 69-605] 04 p0676 A70-14634
- Optimum impulsive velocity calculation for three dimensional deorbit from elliptical orbits to achieve specified reentry angle 06 p1152 A70-18496
- Angular size measurement for galactic X ray sources in Sagittarius region using modulation collimator aboard sounding rocket 09 p1744 A70-22521
- Functional visual field selective process, studying performance as function of display angle 10 p1827 A70-24769
- Small angle light scattering indicatrices in ruby crystals approximated by Gauss type function 13 p2431 A70-29869
- Sonic boom incident and ground reflected waves action on exterior wall, calculating arrival time as functions of aircraft speed and altitude and wall slope 14 p2566 A70-30861
- ANGULAR ACCELERATION**
- Vestibular analyzer stimulation effects on cerebral blood circulation in humans during angular acceleration using rheoencephalography 03 p0422 A70-13692
- Human oculogyral illusion thresholds determined on Ames Man-Carrying Rotation Device to establish stimulus duration effect on angular acceleration thresholds 03 p0424 A70-13765
- Vestibular semicircular canal excitation thresholds of experienced and candidate pilots for imposed angular accelerations 07 p1201 A70-18795
- Rotating circular disk under angular acceleration, analyzing stress and deformation 08 p1596 A70-21980
- Human response to angular acceleration, discussing implications for motion capability in flight simulator [AIAA PAPER 70-350] 10 p1824 A70-24212
- Pilots with high vestibular stability studied for spatial orientation, noting activity impairment due to alternating angular acceleration and optokinetic stimuli 10 p1828 A70-25180
- Oculogyral illusion provoked by angular accelerations during flying stationary and spiral turns in jet aircraft, considering semicircular canals stimulation 11 p1992 A70-26512
- Suprathreshold angular acceleration effects on oculogyral illusion, obtaining magnitude estimates during and after acceleration 14 p2543 A70-30897
- Hypoxia and parotid secretion in humans exposed to angular accelerations 17 p3038 A70-35137
- Seismic fluid suspended triaxial angular accelerometer for high performance aerospace vehicle flight test application 19 p3431 A70-38540
- Semicircular canals dynamic cross coupled responses to rotational movement, discussing mechanical model applicability 22 p3981 A70-43703
- Equatorial acceleration of sun, considering rotation and turbulent energy transport in convective zone 23 p4252 A70-44830
- Two shaft bypass jet engine analog simulation, determining angular acceleration dependence on angular velocity and fuel consumption 24 p4393 A70-45442
- ANGULAR CORRELATION**
- Angular dependence of one dimensional first and second index matching for optical parametric mixing of laser and SRS Stokes beams for tunable laser source 03 p0498 A70-13157
- Metastable He ion two photon decay, observing photon coincidence angular correlation in spectral distribution 13 p2456 A70-29811
- ANGULAR DISTRIBUTION**
- Angular distribution of muon poor extensive air showers flatter than normal showers, discussing initiation by passive particles produced by cosmic ray-atmospheric nuclei 02 p0357 A70-12079
- Cosmic ray neutrons energy spectrum and angular distribution at sea level based on measurement results 03 p0556 A70-13046
- Excess electron and combined electron-positron angular distributions compared in electron photon cascade showers, considering Coulomb scattering 03 p0556 A70-13048
- Electron multiple scattering theory graphic approximation showing angular distribution in electron beam 03 p0527 A70-13053
- Angular distribution measurements of visible and near IR radiation reflected from carbon dioxide cryodeposits formed on liquid nitrogen cooled surface in vacuum [AIAA PAPER 69-63] 04 p0720 A70-15538
- Angular distribution and production probability of secondary shower particles produced by high energy cosmic ray muons using scintillation counter facility 05 p0899 A70-15957
- Angular distribution of particles in electron photon showers without recourse to Landau approximation 05 p0899 A70-15960
- Cosmic ray angular distribution spectrum and interplanetary magnetic field properties determined from semidiurnal cosmic ray variations data 05 p0903 A70-16732
- Vertical profile of angular mass distribution of atmospheric water vapor and ozone as gas proportion function 06 p1097 A70-17794
- Angular distributions of fast scattered particles resulting from noble gases collision with metal surfaces 06 p1112 A70-18271
- Angular distribution of nonreactively scattered molecules in reactive collision, analyzing relation to reaction probability using gray sphere optical model 07 p1225 A70-18903
- Resonator aberrations and active element imperfections effect on formation of spatial and angular structures of solid state laser modes 07 p1299 A70-19854
- Angular and energy distributions of hyperthermal K atoms scattered and ionized by W surface measured as function of beam particle energy 07 p1342 A70-20115
- Low energy ions incidence angle effects on secondary electron emission from molybdenum cylinders in low pressure plasma, noting role of Langmuir sheath around target 07 p1355 A70-20356
- Laser radiation angular distribution determination by self calibrating method based on dividing light beam into spatially similar beams of various intensities 08 p1510 A70-20515

Anisotropic angular distribution of electrons and ions emitted from W targets irradiated by ruby laser pulses

08 p1512 A70-21211

Auroral electrons and photoelectrons spatial, energy and angular distributions measurements using low energy electron spectrometer onboard satellite Cosmos-261

08 p1500 A70-21797

Electron flux independence of pitch angle distribution (0-90 degrees) observed from sounding rocket measurements in auroral arc

10 p1932 A70-24492

Directional particle flux dependence on probe orientation with respect to external magnetic field, determining pitch angle distribution from count rates

10 p1932 A70-24497

Vertical profile of angular mass distribution of atmospheric water vapor and ozone as gas proportion function

10 p1913 A70-25025

Solar corpuscular fluxes angular characteristics, derived from observational data analysis, showing circular or elliptical transverse cross sections

11 p2104 A70-25545

Angular aberrations produced by airborne radomes calculated by computer, allowing optimal parameters selection and knowledge of radio properties

12 p2195 A70-27274

Population inversion effect on angular divergence of neodymium glass laser radiation, observing energy independence for refractive index of medium surrounding active rod

12 p2250 A70-28154

Cosmic ray muons energy spectra and zenith angle distributions by analyzing tracks recorded in high field heavy liquid bubble chamber

13 p2476 A70-28934

Energy spectrum and equatorial pitch angle distribution of charged particles trapped in magnetosphere resulting from inward diffusion due to third adiabatic invariant violation

13 p2476 A70-28942

Rotovolve induced flow angle variations associated with data repeatability and scatter in blow down wind tunnels at transonic speed

13 p2385 A70-29888

Angular distribution of diffusely reflected solar rays over spherical shell planetary atmosphere, determining halo brightness

14 p2632 A70-31222

Papers on chemical physics covering photoelectron angular distribution, molecular orbital theories, electron impact spectrometry, resonant electron scattering, etc

16 p2857 A70-33796

Monochromatic radiation angular distribution surface reflectance measurement using photographic reflectometer

16 p2912 A70-33904

Super and subresidual maxima in angular distribution of polarized radiation reflected from roughened dielectric surfaces

16 p2999 A70-33906

Thick plane fog layers reflection and transmission properties, using emerging light angular distribution for Milne problem

18 p3284 A70-35944

Diffuse cosmic X ray background galactic component, using model to predict angular spread

18 p3308 A70-36484

Angular structure of outgoing short wave radiation field measured from Cosmos satellite for clear and cloudy skies and various sun heights

18 p3286 A70-36965

Ascending long wave radiation brightness from aircraft measurements, observing angular distribution dependence on atmospheric stratification

18 p3287 A70-36970

Solar particle observations over polar caps, considering spatial and angular distribution measurements

19 p3494 A70-37484

Long wave outgoing radiation angular distributions based on effective mass and Curtis-Godson methods of accounting for absorption pressure dependence

19 p3461 A70-37634

Optimal reception points for radar ranging measurement of angular coordinates of meteor trails, using central transmitter

19 p3515 A70-37665

Radio source 3C 161 scintillating component angular dimensions and flux density at 60 MHz

19 p3524 A70-38760

Mirror deformation effect on laser emission angular distribution, estimating output parameters by geometric optics

20 p3642 A70-39741

Solar corpuscular fluxes angular characteristics derived from observational data analysis, showing circular or elliptical transverse cross sections

21 p3882 A70-41295

Angular distribution of thick target bremsstrahlung produced by electron bombardment of Be, Sn and Au surfaces

21 p3854 A70-42020

Monochromatic radiant flux angular distribution reflected from water and carbon dioxide cryodeposits, discussing incidence, deposit thickness and wavelengths

[ASME PAPER 70-HT-34] 22 p4122 A70-42433

Ultrasonic transducer diffraction fields in highly anisotropic crystals obtained by plane waves angular spectrum

22 p4029 A70-42643

Proton energy angular distribution measurement by OV2-5 research satellite confirming model of shell splitting in geomagnetic field

23 p4236 A70-43832

High altitude outer radiation zone boundary region electron energy measurement by satellite Injun 3, noting angular distribution dependence on local time, latitude, etc

23 p4236 A70-43833

Pitch-angle distribution of electron fluxes in auroral zone as function of geomagnetic latitude

23 p4192 A70-44878

Cosmic ray events angular distribution from scaling hypothesis

23 p4238 A70-44894

Energy dependence of equatorial pitch angle distribution for protons trapped in radiation belt, based on adiabatic theory and observational data

23 p4192 A70-44923

Discontinuity in solar wind energy and angular distribution from 2 January 1970 ESO satellite HEOS-1 observation

24 p4396 A70-45326

ANGULAR MOMENTUM

Angular momentum conservations for solar gas confined by closed field lines or outflowing along open magnetic field lines

01 p0176 A70-10251

Precession motions of rigid body with variable mass, considering angular momentum and rotation stability

01 p0141 A70-10283

Monograph on angular momentum effects on swirling flames stability, considering premixed and unpremixed flames with and without baffle barriers

01 p0214 A70-10309

Icarus asteroidal nature and fragmentation origin suggested from inclusion in angular momentum density-mass diagram

01 p0180 A70-10538

Thermal energies and angular momenta of Hubble galactic sequence using differential rotation and decreasing density stellar system model to test stellar evolution theories

02 p0376 A70-12447

Shear-free gravitational radiation described by Einstein equations, analyzing physical properties including energy, angular momentum, radiation flux and trapped surfaces

06 p1104 A70-17185

Momentum vector and spin tensor definitions for extended body moving in arbitrary gravitational and electromagnetic fields, considering test body in de Sitter universe

08 p1545 A70-21352

Spin angular momentum of planets based on particle accretion, discussing particles cloud condensation

08 p1576 A70-21400

Tidal friction induced secular changes in earth-moon system near minimum of angular momentum of moon orbit, including temporal changes in moments of inertia

08 p1579 A70-21570

General relativistic expressions for angular momentum and rotational kinetic energy of slowly rotating stars

09 p1764 A70-23608

Momentum-energy tensor and angular momentum for hydrodynamic and electrodynamic fields determined in transformations of m-parametric Lie group

10 p1922 A70-24098

Viscous fluids nonlinearized thermodynamical description with equilibrium state defined by two parameters, expressing angular momentum density by momentum density

10 p1967 A70-24153

Type I comet tails orientations dispersion attributed to nonradial plasma waves and discontinuities in interplanetary gas, calculating solar angular momentum loss rate

10 p1947 A70-24987

Pressure anisotropies contribution to solar wind corotation, discussing angular momentum and magnetic field

10 p1935 A70-25285

F-type close stars residual spatial motions and rotational velocity relationship, discussing angular momentum loss

13 p2498 A70-30015

Orbiting gyrostats equilibrium orientations under gravitational torques, considering internal angular momentum effects

14 p2655 A70-31364

Gravity stabilized gyrostat satellites internal angular momentum effect on nonlinear resonant attitude motions

15 p2810 A70-31785

Optimal desaturation of angular momentum exchange controllers in spacecraft attitude control systems, using natural environmental torques

16 p2947 A70-33345

Vortex core diameters calculation methods for axisymmetric angular momentum flows

17 p3074 A70-35750

Circular orbit stability in stationary axisymmetric space-times dependence on angular momentum per unit mass increases outward from symmetry axis

18 p3317 A70-37004

Meridional transport of angular momentum in various wavenumber-frequency domains, discussing linear and nonlinear contributions

19 p3462 A70-38258

Small low angular momentum /SLAM/ gyro for inertial guidance systems, discussing drift performance, float suspension, signal generator, flex leads, etc

[AIAA PAPER 70-1011] 20 p3631 A70-39522

Gravitational radiation scattering by Schwarzschild horizon, discussing odd parity waves of angular momentum

21 p3878 A70-40731

Stellar evolution, rotation and atmospheric motion, discussing gravity darkening, spectral lines, angular momentum, braking mechanisms and late stars

22 p4102 A70-42970

Optimal control of magnetic torque for bias momentum removal from attitude controller, discussing applications to Skylab

23 p4258 A70-44503

Stellar rotation effect on internal structures, discussing angular momentum steady state distribution for main sequence stars

23 p4249 A70-44803

Stellar rotation angular momentum loss in premain sequence convective phase, discussing polytropic structure, formation time and velocity changes

23 p4249 A70-44809

Binary star axial rotational correlation, determining coupling between components spin angular momenta

23 p4250 A70-44817

Eclipsing binary stars minima variations related to orbit perturbations and rotational angular momentum of component interiors

23 p4251 A70-44819

Solar spin down procedure simulated via Boussinesq fluid spin down in circular cylinder

23 p4252 A70-44832

ANGULAR MOTION

U ANGULAR VELOCITY

ANGULAR RESOLUTION

Spatial resolution analyses of vorticity meter and hot wire arrays for measuring velocity derivatives in isotropic turbulence

03 p0492 A70-13760

Angular resolution dependence on bearing ambiguities in radio direction finders based on interference measurement, using digital logic circuits

04 p0659 A70-15335

Scaling and angular resolution for sequential type holographic stereogram, comparing results with conventional hologram

04 p0695 A70-15574

Angular tolerance on IR radiation for phase matched image up-conversion in material with nonlinear susceptibility

04 p0703 A70-15621

Angular diameter data from Cambridge radio telescope for sources with different flux densities for cosmological models red shift tests

04 p0757 A70-15691

Electro-optical autocollimating focus sensor for optical systems of high angular resolution, analyzing defocus detection and errors

09 p1687 A70-23764

Laser radar tracking systems, calculating atmospheric turbulence effects on angular errors

19 p3379 A70-37857

Phase meter for measuring angular coordinates of reflecting meteor trails

19 p3526 A70-38777

Ultrasonic Rayleigh critical angle reflectivity of liquid-solid interface energy, detecting near-surface properties changes

22 p4027 A70-42585

Monopulse radar excited by Gaussian signal and thermal noise in multiple targets, calculating angle error output probability density function for predicting tracking performance

22 p3992 A70-43593

Products integration of unit vector components over all solid angles

24 p4370 A70-46029

Semiramis IR angular deviation measuring unit, discussing operation theory and performance characteristics

24 p4339 A70-46322

ANGULAR VELOCITY

Mathematical model for studying three dimensional whirling shaft stability as function of angular to critical velocity ratio, using Liapunov method for equations of motion

01 p0143 A70-10889

- Rotating compressor vanes vibration frequencies and modes using shell theory, considering Coriolis forces and rotation rates effects 01 p0211 A70-11427
- Symmetrical body rotational motion with asymmetrical mass distribution about center of mass, determining minimum initial value of angular velocity 01 p0192 A70-11482
- Thin liquid film equilibrium on rotating sphere, determining conditions for detachment as function of angular velocity 01 p0068 A70-11578
- Photoelectric line photometry used to study H beta/gamma and He I 4471 absorption line intensities of early B stars, determining projected rotational velocity 02 p0369 A70-12072
- Sinusoidal test for measuring knee moment increase required to flex and extend for various conditions of knee angle, angular velocity and steady knee moment 02 p0238 A70-12546
- Geomagnetic field influence on satellite motion for various angles between field vector and satellite angular velocity vector 03 p0563 A70-13180
- Human eye image accumulation effect and meteor brightness estimation dependence on angular velocity based on visual and telescopic observations 03 p0569 A70-13358
- Rats ability to discriminate slow rotation speeds, suggesting otolith organs and proprioceptors sensitivity role in discrimination 03 p0439 A70-14296
- Artificial gravitation parameters for manned compartments of spacecraft, analyzing permissible angular velocity and rotation radius regarding vestibular-vegetative disorders 04 p0760 A70-14446
- Yo-Yo system for satellite Azur to reduce payload angular velocity after separation from booster, analyzing final spin error [DGLR-69-43] 04 p0762 A70-15152
- Thermoelastic stresses in rotating circular cylinder, analyzing temperature effect on angular velocity for neo-Hookean material using finite deformation theory 05 p0930 A70-16080
- Free molecular flow through long circular tube rotating with constant angular velocity about axis, discussing rotation speed effect on mass flow 05 p0836 A70-16994
- Suboptimal stabilization of axially symmetric satellite angular velocity, using ionic propulsion system as control torque 06 p1155 A70-17554
- Angular velocities and equilibrium of rotating neutron stars compared with white dwarfs 07 p1376 A70-18911
- Visual tracking of horizontally moving object, noting acuity dependence on target angular velocity and observation time 08 p1444 A70-20745
- Propulsive and lifting motions of pointed profile in ideal incompressible fluid related to alternate vortices emission 08 p1433 A70-21234
- Yo-Yo system for satellite Azur to reduce payload angular velocity after separation from booster, analyzing final spin error 09 p1767 A70-23430
- Angular motion of deformable earth satellite as solid-elastic system with distributed masses, applying automatic control transfer function 10 p1914 A70-24308
- Solid body control moments ensuring braking from rotational motion, finite orientation and angular velocity under minimum energy constraint 11 p2023 A70-25609
- Axial flow compressor blade rings interaction effect on angular speed of rotating stall zones 11 p1974 A70-25780
- Rockets angular motion due to thrust with ramp input, presenting graphs for different inputs and inertia ratios 11 p2123 A70-26125
- Human eye image accumulation effect and meteor brightness estimation dependence on angular velocity based on visual and telescopic observations 11 p2118 A70-26723
- Liquids relative rotary motion in vertical rotating cylinders under large amplitude axial vibrations and angular velocities 12 p2209 A70-27213
- Monograph on critical speeds of nonzero mass shaft supported at both ends by bearings with nonlinear elastic displacements 13 p2416 A70-28373
- Artificial gravitation parameters for manned compartments of spacecraft, analyzing permissible angular velocity and rotation radius regarding vestibular-vegetative disorders 13 p2503 A70-28471
- Upper atmosphere superrotation velocity based on satellite polar orbit calculation of 1968-59A, correcting for lunisolar perturbations 13 p2394 A70-28895
- Asymmetric missile nonlinear angular motion, describing quasi-linear relations for frequencies, damping rates and swerving motion amplitude [AIAA PAPER 70-534] 13 p2506 A70-29002
- Asymmetrical slender planetary entry vehicle roll dynamics, analyzing steady state angular motion [AIAA PAPER 70-560] 13 p2339 A70-29003
- Finned configurations with nonlinear aerodynamic properties, obtaining solutions for angular motion at and near resonance [AIAA PAPER 70-535] 13 p2506 A70-29026
- Radar and optical meteor observations comparison, discussing luminosity function and angular velocity 13 p2490 A70-29042
- Bounds in magnetofluidynamics for angular velocity of rotating fluid mass in relative equilibrium noting generalization of Poincare theorem 13 p2463 A70-29153
- Galaxies rotation, applying optical and radio data to statistical analysis of angular velocities and periods 13 p2492 A70-29386
- Solar differential rotation measurement by spectral line shift data analysis, noting angular velocity-heliographic latitude relationship 13 p2496 A70-29840
- Mercury rotational angular velocity fluctuation in terms of orbital mean motion at different orbit positions 14 p2639 A70-30708
- Frequency locked noise effect on beat frequency measurement of angular velocity with ring laser, comparing gyroscope and phase methods 15 p2749 A70-31551
- Two body torque free gyrostat equations of rotational motion, relating rotational, spin and precession angular velocities 16 p2912 A70-33877
- Gyroscopic drifts associated with angular support motions 17 p3133 A70-34960
- Multiaxis clusters of single axis pendulous accelerometers with coincident centers of angular motion insensitivity 19 p3431 A70-38539
- B stars kinematic parameters determination from radial and tangential velocities 19 p3525 A70-38775
- Jacobi ellipsoid quasi-static evolution by gravitational radiation, discussing direction of increasing angular velocity toward nonradiating state at bifurcation point with Maclaurin sequence 20 p3702 A70-39018
- Ring lasers design and performance, measuring angular velocity by interferometry 20 p3641 A70-39418
- Ring laser gyro angular rate sensor for strapdown inertial systems [AIAA PAPER 70-1025] 20 p3631 A70-39510
- Spinning missile gravity induced angular motion for various trajectory portions, considering quasi-steady state assumption validity [AIAA PAPER 70-968] 20 p3715 A70-39561
- Kinematic interpretation of body motion in Hess solution, discussing axoid vector rolling without slip 21 p3849 A70-40617
- Relativistic observer in rotational motion relative to inertial observer, imposing velocity onto perfect relativistic fluid 21 p3851 A70-42096
- Accelerated supersonic motion of plate with attached shock wave at finite angle of attack in ideal gas, using perturbed nonstationary motion equations 21 p3748 A70-42209
- Lense-Thirring effect in test masses approaching in same orbit around rotating body, noting correction dependence on central body geometry and angular velocity 21 p3926 A70-42240
- Multipurpose transistorized tachometer for rotating body speed measurement, control and recording, using electronic integrator and magnet pickup 21 p3831 A70-42245
- Viscous flow field in pneumatic vortex rate sensor, discussing boundary layer parameters, velocity profiles and swirling flow theory [ASME PAPER 70-FLCS-16] 22 p4007 A70-42411
- Rotational velocities for main sequence stars from spectral type A5 to F9, supporting solid body rotation hypothesis 23 p4249 A70-44806
- Close binary star components axial rotation, considering synchronism, angular velocity and mass exchange 23 p4250 A70-44814
- Algol type semidetached eclipsing binaries main sequence components rotational velocities, determining deviations from synchronism 23 p4251 A70-44818
- Stellar rotational velocities in open star clusters, noting evolutionary expansion, tidal coupling in binaries and Ap stars magnetic braking 23 p4251 A70-44820
- Spectral line width distributions in main sequence stars, emphasizing B2 to A2 range rotational velocities with Maxwellian distribution 23 p4251 A70-44821
- A type stars rotation, examining UVB color and rotational velocity relationship, spectral classification and spectroscopic binaries 23 p4251 A70-44822
- Stellar axial rotational velocity statistical analysis to break-up limit, obtaining velocity distribution approximation from observed histogram 23 p4251 A70-44823
- UV Cet type flare star rotational velocity upper limits from H alpha emission line width in chromospheres 23 p4251 A70-44824
- Deutsch period vs line width relation for periodic Ap stars, determining rotational velocities with rigid rotator model 23 p4251 A70-44825
- Solar interior differential rotation, developing angular velocity distribution equilibrium model 23 p4252 A70-44834
- Head movement role in motion sickness as function of angular velocity, discussing prediction of human tolerance in space station 24 p4297 A70-45341
- Upper atmosphere average rotation speed and height variation, presenting atmospheric and earth angular velocity ratio from satellite orbit inclinations 24 p4328 A70-45353
- Orbiting spacecraft angular velocities via inertial sensing platform consisting of linear accelerometers 24 p4372 A70-45475
- ANHYDRIDES**
- Tetrabromophthalic anhydride (TBPA) in polyester and epoxy resins, studying fire retardant capabilities by comparative combustion tests 05 p0811 A70-16584
- Octadecatic anhydropolymers of amino acids, describing production by thermal condensation, heteropolymerization and panpolymerization 22 p3983 A70-42875
- ANILINE**
- Organic semiconductor electrodes for electrochemical generators, discussing redox association with ion and electron conductivity in polyanilines 10 p1830 A70-24463
- Aniline and o-anisidine production by photoelimination of nitrogen from fused ring triazoles 17 p3042 A70-34821
- ANIMALS**
- NT AMOEBA
- NT BEETLES
- NT BIRDS
- NT CATS
- NT CATTLE
- NT CEPHALOPODS
- NT CHICKENS
- NT CHIMPANZEES
- NT DOGS
- NT DROSOPHILA
- NT FISHES
- NT FROGS
- NT GOATS
- NT GROUND SQUIRRELS
- NT GUINEA PIGS
- NT HAMSTERS
- NT HUMAN BEINGS
- NT INSECTS
- NT INVERTEBRATES
- NT MAMMALS
- NT MICE
- NT MOLLUSKS
- NT MONKEYS
- NT MOTHS
- NT PIGEONS
- NT PRIMATES
- NT PROTOZOA
- NT RABBITS
- NT RATS
- NT RODENTS
- NT SHEEP
- NT SPORES
- NT SWINE
- NT TURTLES
- NT VERTEBRATES
- Hypoxic stimulation effect on erythropoiesis in vivo bone marrow 01 p0017 A70-10464
- Book on dynamics of complex systems represented by control and human operators and animals behavioral activities models 01 p0034 A70-10501
- Man and animals physiological adaptation and behavior under conditions of polar regions, highland and arid areas 01 p0030 A70-11465
- Left ventricular function during paired pulse and single pulse stimulation in dogs, sheep, goats and calves before and after induced heart failure 02 p0233 A70-11719
- Cross adaptations of physiological functions, discussing results for heat, altitude and cold adapted animals 02 p0242 A70-12824
- Pulsatile flows in living animals and model arteries, discussing flow profiles, instability and wall shear 03 p0430 A70-14244

- Ground-based biological experiments on insects and frog eggs to investigate effects of space flight weightlessness and radiation on mitosis and meiosis
04 p0631 A70-14942
- External environment changes effect on animal activity, considering reactions on molecular, physiological and behavioral levels
07 p1199 A70-18782
- Viscous fluid dynamics for reducing hydrodynamic resistance, discussing aquatic animals speeds, vortex flows, etc
10 p1871 A70-25193

ANIMATION
U MOTION

ANIONS

- Negative ion reactions relevant to D region measured in ESSA flowing afterglow system as function of temperature
01 p0070 A70-10406
- Book on negative ions and magnetron covering electron affinities determination, gases adsorption, rate processes, stability problems, etc
03 p0526 A70-12901
- Negative O, NO and nitrous oxide ions formation by electron impact on nitrous oxide as function of pressure
03 p0441 A70-14007
- Potential energy surface shapes for lowest states of temporary negative ions of nitrous oxide and carbon dioxide
03 p0441 A70-14008
- Anions adsorption at platinum determined by ellipsometry, finding perchlorate and fluoride ions adsorption below detection limit
03 p0441 A70-14043
- Charge transfer reactions of negative ions with oxygen investigated for energy dependence, yielding evidence on oxygen electron affinity
10 p1919 A70-24402
- Tropospheric negative small ions formation reaction scheme, considering hydration degree
11 p2046 A70-26390
- Negative hydrogen ion balance in high intensity plasma source, measuring flux as function of discharge current
15 p2780 A70-32195
- Electron collisional detachment from negative fluorine ions in shock tube following nonequilibrium ion overshoot in CsF dissociation in argon, noting correlation with temperature
21 p3853 A70-41705

ANISOTROPIC FLUIDS

- Turbulent fluid flow analysis described by Navier-Stokes equations, introducing asymmetric tensors for anisotropic cases
01 p0068 A70-11605
- Self similar problems of anisotropic fluid boundary layer involving infinite disk rotation and fluid flow near stagnation point
05 p0835 A70-16857
- Steady state boundary layer of anisotropic Ericksen fluid incident obliquely on infinite cylinder, obtaining differential equations for dynamic behavior
05 p0835 A70-16860
- Langmuir HF turbulence effect on anisotropic plasma oscillation spectra, determining instability conditions
08 p1554 A70-21809
- Incompressible anisotropic fluid flow around semiinfinite plate at large Reynolds numbers, using interlocked asymptotic expansions and deformed coordinates to obtain boundary layer equations
09 p1663 A70-23390
- Anisotropic multifluid cosmological models with orthogonal velocity fields
17 p3157 A70-34839
- Semiempirical theory of anisotropic turbulent transport, deriving closed system of flow equations
17 p3073 A70-35736
- Newtonian hydrodynamic analogies for homogeneous anisotropic models in general relativity
22 p4075 A70-43472

ANISOTROPIC MEDIA

NT ANISOTROPIC FLUIDS

- One dimensional nonlinear model of anisotropic plasma instability with respect to Alfvén waves growth, noting applicability to solar wind processes
01 p0153 A70-11597
- Quasi-optic electromagnetic beams slow spreading in anisotropic media due to propagation in unusual directions
03 p0447 A70-13288
- Wave numbers determined in waveguide formed by laminar inhomogeneous medium enclosed between homogeneous dielectric media, taking into account radiation losses through wall
03 p0447 A70-13290
- Stress distribution in half space of inhomogeneous media, studying scale and edge effects relation for elastic and ideally plastic media
03 p0590 A70-13376
- Rectangular anisotropic beam torsion using Green function combined with wide step network method
03 p0593 A70-13471

- Three dimensional Gaussian light beam propagation in anisotropic inhomogeneous media with dielectric constant decreasing from energy flow direction
03 p0525 A70-13533
- Variational stress solutions for static case of bounded bodies in Cosserat continuum theory, assuming anisotropic inhomogeneous material and defining boundary value problem solution
03 p0596 A70-13973
- Axisymmetric problem analysis for cylindrically anisotropic elastic bodies with restricted orthotropy based on Love-Lekhnitsky stress function generalization
03 p0601 A70-14327
- Integrodifferential equation solved for plane wave reflection and transmission by random medium assuming homogeneous background refractive index
04 p0649 A70-14970
- Electrostatic field effects of electromagnetic wave propagation in anisotropic plasma
04 p0728 A70-15002
- Nonlinear stress-strain laws and yield conditions derived for anisotropic materials on basis of one, two and three invariants
05 p0926 A70-15914
- Eigenvalues upper and lower bounds of vibrating anisotropic material with multiple elastic constants, predicting free vibration frequencies by bounding isotropic moduli
05 p0937 A70-16408
- Heat conduction in anisotropic materials to measure thermophysical parameters, using pulsed point or line heat source
05 p0957 A70-16457
- Strain hardening equation for anisotropic medium under creep
05 p0952 A70-17035
- Anisotropic plasma instability in nonlinear stage, studying turbulent relaxation of ion distribution by quasi-linear theory
06 p1119 A70-17501
- Cerenkov radiation in infinite anisotropic electron plasma linearly polarized in magnetic field having linear electron distribution moving with uniform velocity
06 p1120 A70-17538
- Variational ray path calculation method for HF electromagnetic wave in anisotropic inhomogeneous lossless ionospheric plasma
06 p1055 A70-17592
- Stress-strain state of curved rod made of anisotropic material under bending loads applied to end face cross sections
07 p1399 A70-18661
- Plane electromagnetic wave reflection from laminar anisotropic medium, analyzing piecewise-constant permittivity tensor as boundary value problem
07 p1235 A70-19448
- Laser-forced medium anisotropy effects on nonlinear optical frequency mixing and combined forced scattering
07 p1335 A70-19863
- Radio wave propagation in anisotropic plasma consisting of oxygen ions and protons, deriving expressions for radio wave refractive index
07 p1355 A70-20452
- Failure criteria application to quasi-homogeneous anisotropic materials, discussing material constants
08 p1595 A70-21890
- Variable modular elasticity theory demonstrated for anisotropic body subjected to plane stressed state, deriving expression for potential energy of deformation
09 p1769 A70-22152
- Thermal radiative transfer in nonuniform anisotropic magnetoactive plasma, correcting term of Zheleznyakov equation
09 p1734 A70-22514
- Thermal contact resistance of anisotropic materials using mathematical geometric transformation [ASME PAPER 69-HT-47]
09 p1790 A70-23552
- Wave propagation in bounded homogeneous elastic anisotropic media solved as sum of eigenvalue and static problems without transform calculus
10 p1915 A70-24058
- Stress distribution in anisotropic disk shaped into wedge loaded at vertex by concentrated moment determined by complex potentials method
10 p1956 A70-24084
- Nonlinear spin wave theory for anisotropic antiferromagnetism, solving sublattice magnetization by thermodynamic Green function for temperature dependence
11 p2097 A70-25617
- Resonant oscillations of passive Fabry-Perot resonator in optically anisotropic medium, using parabolic equations for wave vector amplitudes polarized components
11 p2063 A70-25869
- Refractive index profiles method for vertically polarized electromagnetic waves in horizontally stratified magneto-plasma extended to anisotropic media, noting relevance to ionospheric propagation
11 p2011 A70-26555

- Excitation of surface waves on impedance plane in collisionless cold anisotropic plasma with external magnetic field coinciding with source direction
12 p2278 A70-27538
- Electromagnetic pulse distortion with Gaussian envelope in longitudinally inhomogeneous anisotropic ionized media to investigate radio wave communication with ionospheric propagation
12 p2189 A70-27962
- Electric dipole radiation field in homogeneous anisotropic compressible plasma, obtaining asymptotic expressions by saddle point integration method
12 p2282 A70-27970
- Electromagnetic waves emission and propagation in chaotically inhomogeneous media, analyzing mean field and permittivity tensor for isotropic and anisotropic media
12 p2190 A70-28170
- Linear theory of homogeneous and anisotropic elastic media with microstructure, establishing reciprocity and variational theorems
13 p2512 A70-28951
- Elastic anisotropic body analysis, formulating boundary value problem solutions
13 p2516 A70-29525
- Dipole antenna current distribution in ionized homogeneous anisotropic medium, using dielectric permittivity tensor
13 p2371 A70-29923
- Electromagnetic wave propagation in cylindrical guide containing anisotropic sheets, observing TE and TM modes existence
15 p2774 A70-31946
- Stationary gas flows continuous to rarefied transition analysis based on mean free path anisotropy
15 p2721 A70-32139
- Plane deformation of anisotropic plastic nonstrain-hardenable material, analyzing state equations for stresses and strain rates
15 p2818 A70-32184
- Milne problem for anisotropic atmospheric scattering, determining radiation transmission at particular angle with arbitrary scattering indicatrices and particle albedo
15 p2801 A70-32477
- Isotropic composite materials with anisotropic components, determining microconstants for heat conduction, elasticity and thermoelasticity problems
15 p2766 A70-32896
- Anisotropic glass fiber reinforced plastics strength and deformability under cyclic axial loads
15 p2766 A70-32897
- Elastic waves on isotropic and anisotropic surfaces, discussing excitation methods, surface probing, propagation characteristics, etc
17 p3136 A70-34650
- Anisotropic temperature plasma susceptibility calculation based on velocity moment equations and circular polarized coordinates, compared to Vlasov equation solution
17 p3140 A70-34929
- Transient wave propagation in homogeneous anisotropic media, using hyperbolic equations and unitary operator
17 p3137 A70-35607
- Structural members of isotropic and anisotropic polymers, investigating creep behavior under simple stressed state
17 p3192 A70-35740
- Radiation condition for unbounded anisotropic dispersive magnetoplasma
18 p3295 A70-36492
- Symmetric functions of second rank tensors with syngonies in elastic anisotropic media
18 p3340 A70-36576
- Anisotropic composite materials comprised of B and graphite fibers in polymer matrix, discussing precision molding technologies [ASME PAPER 70-GT-126]
18 p3264 A70-36852
- Plane electromagnetic wave reflection from laminar anisotropic medium, piecewise-constant permittivity tensor as boundary value problem
18 p3229 A70-36922
- Electromagnetic wave diffraction by inhomogeneous anisotropic body, applying Fredholm integral equations
19 p3376 A70-37436
- Thermoelastic stresses in infinite anisotropic slab due to temperature field variations along thickness and length
19 p3539 A70-37872
- Safety factor limit analysis for anisotropic nonhomogeneous solids by variational method, exemplifying by four layer rectangular beam
19 p3547 A70-38355
- Hexagonal crystal dislocations treatment based on anisotropic elasticity theory, obtaining formulas for displacement and stress fields
19 p3454 A70-38954
- Anisotropic elastic solids linear dynamic theory, discussing uniqueness theorem, reciprocal identity and far elastodynamic field quiescence
20 p3718 A70-39231

- Electromagnetic wave propagation in inhomogeneous anisotropic linear media, discussing ray tracing, permittivity and relativistic electrodynamics 21 p3785 A70-40798
 - Jump relations for shocks in anisotropic collisionless magnetized plasma 21 p3856 A70-41267
 - Anisotropic material two dimensional crack propagation under deforming stress at infinity, examining fracture criterion, dislocation distributions and crack nucleation 21 p3936 A70-41413
 - Anisotropic elastic solid body thermal stresses, investigating static plain strain problem in thermoelastic linear theory 21 p3936 A70-41414
 - Acoustic surface waves phase velocity on lithium niobate with gold layer for propagation modes, predicting LF cut-off by substrate anisotropy 21 p3863 A70-42001
 - Ultrasonic transducer diffraction fields in highly anisotropic crystals obtained by plane waves angular spectrum 22 p4029 A70-42643
 - F 2 region anisotropic response to individual internal gravity waves as function of propagation azimuth 23 p4185 A70-43844
 - Milne problem for anisotropic atmospheric scattering, determining radiation transmission at particular angle with arbitrary scattering indicatrices and particle albedo 23 p4239 A70-43902
 - Anisotropic media weakened by elliptical holes, using doubly periodic solution for stress concentration 23 p4266 A70-43986
 - Anisotropic turbulent plasma EM emission due to density fluctuations, noting relationship to turbulence spectrum 24 p4384 A70-45256
- ANISOTROPIC PLATES**
- Anisotropic shells and plates dynamic field equations derived, taking into account mechanical forces and nonuniform temperature field 01 p0200 A70-10553
 - Thin anisotropic elliptical plate elastic equilibrium weakened by hole and under concentrated loads 01 p0211 A70-11445
 - Rational design of structurally anisotropic plane multilayer plates with weak binder, suggesting strengthening fibers orientation in internal stresses direction 03 p0516 A70-13379
 - Stress distribution in anisotropic half plane with reinforced circular hole under external loads applied at plane infinity and ring edge 04 p0765 A70-14417
 - Divergences in tension textures and values of anisotropy coefficients ascribed to imperfections in cubic texture of aluminum sheet deformed by straining 05 p0927 A70-15995
 - Soviet book on anisotropic plates theory, strength, stability and oscillations including corrections to classical theory 05 p0928 A70-16016
 - Galerkin method to formulate buckling problem of homogeneous and fiber reinforced anisotropic plates simply supported under uniform membrane loads 06 p1160 A70-17313
 - Rectangular and nonrectangular anisotropic plate bending and stability analysis by difference-differential technique, allowing for combined freely supported and clamped end conditions 06 p1167 A70-17864
 - Governing equations solution for simply supported laminated anisotropic rectangular plate using Fourier series method 07 p1406 A70-19305
 - Unsteady temperature field and thermal stresses in reinforced anisotropic plate strengthened at rim by thin isotropic rod 07 p1408 A70-19543
 - Plane anisotropic elastic bodies stress determination using Somigliana type integral formula to relate elastic displacement field to boundary traction and displacement vectors 07 p1412 A70-19953
 - Yield criterion for plastic bending of transversely anisotropic circular plates under plane stress 08 p1589 A70-21250
 - Laminated anisotropic rectangular plates of boron-epoxy composite material, studying shear stability by potential energy and Ritz method 08 p1595 A70-21903
 - Rigid/plastic or rigid/perfectly plastic anisotropic plate under uniform bending, analyzing stress distribution 10 p1964 A70-25092
 - Classical and elastically restrained boundary conditions requirements for anisotropic plates Ritz solution 11 p2135 A70-26076
 - Pinhole expansion in anisotropic plastic disks determined by obtaining solutions for Tresca and Mises yield functions, assuming plane stressed state 11 p2138 A70-26171
- Anisotropy effect on stress distribution at crack apex in elastic plate 12 p2329 A70-28322
 - Operator representing anisotropic element in gas laser resonator, considering phase crystalline and rotating plates 13 p2424 A70-28593
 - Annular lasers energy, polarization, radiation loss and frequency characteristics dependence on phase shift due to anisotropic plate introduction 15 p2753 A70-32860
 - Elastic constants for plates of unidirectional fiber reinforced anisotropic composite material determined by ultrasonic wave propagation 16 p2991 A70-33847
 - Anisotropic disk compressed by isotropic ring of smaller radius, considering elastic equilibrium 18 p3336 A70-36134
 - Inhomogeneous anisotropic elastic plates large deflection, using asymptotic integration of nonlinear elasticity equations to obtain successive field equations systems 24 p4423 A70-45580
 - Anisotropic bodies elastic properties, obtaining solutions for nonorthotropic beams under randomly distributed normal loads and for various plates and strips 24 p4424 A70-45589
- ANISOTROPIC SHELLS**
- Anisotropic shells and plates dynamic field equations derived, taking into account mechanical forces and nonuniform temperature field 01 p0200 A70-10553
 - Axial stress pulse induced elastic waves propagation in thin anisotropic circular cylindrical shell of helical wrap construction allowing for shear coupling 03 p0587 A70-13118
 - Carrying capacity and deformation susceptibility of anisotropic fiberglass reinforced conical and cylindrical plastic shells under axial compression 05 p0933 A70-16209
 - Geometrically linear anisotropic shell deformation under transverse shear applied to stability analysis of orthotropic shells of revolution sustaining axisymmetric stresses 05 p0933 A70-16212
 - Uniaxial and multiaxial stiffness and property characterization of anisotropic composite materials formed as thin walled cylinders 08 p1529 A70-21880
 - Thermal stresses in temperature dependent multilayered cylindrically anisotropic hollow cylinders 12 p2321 A70-27203
 - Zero moment /membrane/ theory for anisotropic thin walled shells, deriving expressions for stress-strain states and displacements under torsion 15 p2824 A70-32894
 - Stability analysis of anisotropic cylindrical shells under combined loadings using inverse operators 16 p2994 A70-34246
 - Anisotropic and laminated cylindrical shells geometric design for reduction of elastic stress gradients to predetermined limit 17 p3182 A70-34559
 - Solid or hollow anisotropic elastic cylinders rotating with variable angular velocity, determining dynamic response by Hankel and Laplace transforms 18 p3338 A70-36433
 - Zero moment theory for stress-strain state of thin walled anisotropic shells with nonuniform moduli under simultaneous torsion and tension 18 p3340 A70-36578
 - Anisotropic axisymmetric elastic shell theory including transverse stress effects, with application to orthotropic cylinder 19 p3545 A70-38337
- ANISOTROPY**
- NT ELASTIC ANISOTROPY**
- NT PLASTIC ANISOTROPY**
- Radio waves scattering in ionosphere, analyzing dependence on latitude, altitude, azimuth and polarization angle, considering anisotropy due to geomagnetic field 01 p0046 A70-11452
 - Solar /stellar/ wind solutions asymptotic behavior at large distances from central star for equations including effects of rotation and anisotropy 02 p0358 A70-12253
 - Viscosity anisotropy in fluid matrix suspensions of parallel rigid flakes as function of flake content and width-to-thickness ratio 03 p0515 A70-13122
 - Forbush decrease recorded on 26-27 January 1968 showing large anisotropies in cosmic ray flux after SC magnetic storm 03 p0560 A70-13979
 - Charged primary cosmic rays sidereal anisotropy generated diurnal/semidiurnal variations phase characteristics, using energy meson telescopes 04 p0738 A70-14513
 - Young modulus anisotropy and recrystallization texture during annealing in cold rolled TI sheets using Fourier analysis 05 p0862 A70-16200
- Pitch angle anisotropy instabilities of electromagnetic waves in space, discussing warm plasma, solar wind and Van Allen belts 06 p1118 A70-17380
 - V and Cr single crystals microhardness anisotropy and causes, noting similarity with W, Nb and silicon ferrite 06 p1088 A70-17613
 - Ni maraging steel sheets tensile strength and elongation anisotropy, studying effects of directional cold work, aging and annealing 07 p1306 A70-19072
 - Torsional vibrations of nonhomogeneous anisotropic finite circular tube, computing natural frequencies for various parameters 07 p1414 A70-20173
 - Pyrolytic C-TiC alloys obtained by precipitation from gaseous phase, discussing microstructural properties anisotropy 08 p1517 A70-21146
 - Anisotropic turbulent energy spectral distribution approximated assuming homogeneous and axisymmetric turbulence with vertical axis of symmetry 09 p1717 A70-22374
 - Neutrinos kinetic theory for anisotropic cosmological models 09 p1753 A70-22453
 - Temperature and strain dependence of strain anisotropy in Ti tested on longitudinal and transverse tensile specimens 09 p1705 A70-22807
 - Cosmic ray diurnal anisotropy, demonstrating two-solar-cycle variations for nucleonic component 09 p1746 A70-23478
 - Reflection patterns of solar radiation from cloud, water and land surfaces measured by airborne radiometer, observing anisotropy 09 p1671 A70-23523
 - Magneto-optical birefringence anisotropy and light propagation in terbium ferrite garnet in presence of Faraday and Cotton-Mouton effects 11 p2097 A70-25377
 - Gravitational field and ellipsoidal gravitational waves anisotropy, deriving gravistatics results from electrostatics 11 p2083 A70-25944
 - Anisotropic fiber reinforced composites elastic moduli determined by analytical matrix method 11 p2141 A70-26488
 - Interplanetary medium kinetic equations to limit ion temperature anisotropies in solar wind, discussing Coulomb collisions and ion-cyclotron instability effects 11 p2105 A70-26561
 - Solar photospheric turbulence from observing TI I line profiles at different center to limb distances, showing anisotropy 11 p2116 A70-26591
 - Normal and unconstrained vacuum-deposited Permalloy films composition dependence of magnetization-induced uniaxial anisotropy, noting agreement with magnetostrictive constraint theory 12 p2284 A70-27244
 - Cosmic rays components fluxes, interactions, lifetimes and anisotropy in statistical discrete source model, tabulating and graphing results 12 p2295 A70-27996
 - Anisotropic two phase plates gas laser resonator spectrum, analyzing zero or 90 degree angles between plates 13 p2424 A70-28594
 - Cosmic radiation yearly semidiurnal anisotropy characteristics based on worldwide neutron monitor stations data analysis 13 p2477 A70-29177
 - Flat emission spectra of quasars in 3CP catalog attributed to anisotropic relativistic electron fluxes 13 p2493 A70-29387
 - Cosmic ray transport in solar wind generalized with anisotropic diffusion approximation 14 p2632 A70-30887
 - Shock waves structure in radiating gases at high temperatures, taking into account radiation anisotropy in shock front 15 p2720 A70-31645
 - Correlated daily variations of ionospheric drift and anisotropy parameters in E and F regions at Thumba, India 15 p2725 A70-31858
 - Solar flare particle flux equilibrium anisotropy and convection in solar wind 15 p2793 A70-31901
 - Cosmic ray radial gradients and anisotropies, describing behavior in interplanetary medium 15 p2795 A70-32623
 - Anisotropic solar cosmic rays in inhomogeneous medium, investigating shell effect on propagation by one dimensional model 15 p2795 A70-32624
 - Beryllium mirrors optical performance, describing causes and effects of anisotropy and dimensional instability 16 p2904 A70-33146

Anisotropy and variable thickness effects on elastic stress distribution in rotating disks, discussing limiting cases

17 p3185 A70-34912

Hologram interferometry for measuring surface deformation under force and anisotropy in transparent objects

17 p3085 A70-35009

Large anisotropy observed for gravitational radiation detector intensity as function of sidereal time, suggesting source from galactic center

17 p3137 A70-35725

Ionospheric electric field formation from polarization of electron density inhomogeneities under anisotropic conditions

18 p3252 A70-36988

Multivalley semiconductors electrical conductivity anisotropy, discussing redistribution and electron transfer under strong electric field

19 p3483 A70-37294

High energy primary cosmic ray muons arrival directions examined for anisotropies underground

19 p3508 A70-38141

High energy cosmic rays sidereal and solar anisotropy, using airborne Cerenkov telescope

19 p3510 A70-38151

Galactic cosmic ray anisotropy, discussing amplitude and phase values of daily sidereal variation

19 p3510 A70-38152

Moon deficient showers intensity distribution as function of sidereal time, obtaining anisotropy upper limit by statistical analysis and Monte Carlo method

19 p3511 A70-38483

Thermotropic quasi-geostrophic atmospheric model, deriving linear and quadratic integral invariants

19 p3463 A70-38754

MHD instability of homogeneous inviscid plasma with finite electrical conductivity and anisotropic pressure, obtaining dispersion equation for mode

20 p3677 A70-39048

Cosmic ray anisotropy 27 day and seasonal variations, considering neutron component data and sunspot magnetic field strength

20 p3696 A70-39277

Cosmic ray anisotropy sidereal-diurnal effects isolation by solving simultaneous amplitude and phase modulation problem

20 p3696 A70-39282

Diurnal anisotropy variations of cosmic ray intensity, taking into account neutron monitors data

20 p3699 A70-39346

Al alloy stress corrosion susceptibility, examining grain size and anisotropy role

20 p3651 A70-40070

Uniaxial magnetic anisotropy in electrodeposited Permalloy films in terms of magnetostrictive mechanism

20 p3687 A70-40160

Closed circular cylindrical shell nonlinear problem solvability extended to anisotropic sandwich shell, using mean deflection theory

21 p3933 A70-40601

Viscous fluid motion equations through anisotropic nonrigid porous solid, discussing blood flow in capillary vessels and extracellular fluid through interstitial space

21 p3768 A70-40776

Cosmic ray signal anisotropy around 0900 h sidereal time and 30-60 degree declination, investigating muon events in liquid scintillator

21 p3882 A70-41994

Recrystallized and overrecrystallized Al alloys, investigating factors controlling anisotropy of mechanical properties

22 p4056 A70-43126

N type GaAs doped with Si, conductivity anisotropy observed from measurement and explanation in terms of electron distribution

23 p4231 A70-44890

Graphite dielectric constant as function of frequency, considering electron energy loss anisotropy in UV

24 p4380 A70-45668

ANNEALING

NT PULSE HEATING

Annealing effects on cold rolled titanium sheets, noting changes in Young modulus and characteristics of recrystallized titanium

01 p0124 A70-11620

KCl F centers isothermal annealing kinetics using EPR, considering electron irradiation levels effects

02 p0350 A70-12719

Mechanical properties of ordered Ni-Cr alloys, establishing hardening effect of annealing

03 p0505 A70-13105

Steel crystal lattice fine structure and mechanical properties during annealing using X rays as function of temperature

03 p0511 A70-13422

Young modulus anisotropy and recrystallization texture during annealing in cold rolled Ti sheets using Fourier analysis

05 p0862 A70-16200

Recrystallization annealing third stage of cold worked polycrystalline niobium by measuring electrical resistance at liquid nitrogen temperature

05 p0863 A70-16204

Cold reduction and annealing temperature effects on Al sheet ductility noting roles of hardness, crystallographic orientation and microscopic structure

06 p1075 A70-17146

Meyer-Neldel rule interpretation of distribution width parameter dependence on activation energy annealing of defects in irradiated Si

06 p1106 A70-17925

Neutron irradiation and annealing effects on lattice constants of titanium and chromium carbides analyzed for X ray diffractions

07 p1303 A70-18702

Annealing atmosphere effect on permeability of Mo Permalloy [AIME PAPER F-69-7]

07 p1304 A70-18814

Mo sheet longitudinal and transverse mechanical properties and microstructure after annealing

08 p1517 A70-21199

Annealing effect on stress-strain curves of overaged and cold-rolled Al-Li alloy, observing yield drop

09 p1708 A70-23727

Ion-implanted GaAs junction diodes anneal behavior and defect nature

11 p2098 A70-26391

Anomalous grain growth kinetics and recrystallization in electron beam annealed nickel determined by microstructural and radiographic study, noting annealing time dependence

11 p2068 A70-26596

Iron-nickel alloy phase and diffusion relationships, composition gradients and hardness variations involving long time metallic meteorite anneals

12 p2252 A70-26964

Vacuum annealing treatments effect on oxidation rate of Co-Cr alloy at high temperatures

12 p2257 A70-28007

Residual gas effects on critical load and brittleness of pure and molybdenum-coated niobium bars after annealing in vacuum

12 p2258 A70-28324

Au-Pd films boundary structure during diffusion annealing, noting polymerized oil vapor effect originating from vacuum pump

15 p2758 A70-32121

Polygonized and cellular Be structures formation, examining temperature, strain, annealing and material purity effects

15 p2758 A70-32122

Constant grain size cast Mo ductile-brittle transition temperature dependence on annealing temperature using tensile test

16 p2933 A70-34274

Ti alloys crack formation during oxidation under stress, considering annealing and recrystallizing effects

17 p3114 A70-34374

Titanium alloys quench hardenabilities, determining variations with distance from end of Jominy bars after annealing

17 p3119 A70-34415

Gas bubbles thermal rejection and formation in Ni electrodeposit during annealing over 200-1000 C range

18 p3272 A70-36039

Al-Mg alloys recrystallization, investigating heating rate and annealing time effects on sheet grain size

19 p3450 A70-37372

Electron radiation damage and stage 3 annealing effects on polycrystalline Mo properties

19 p3451 A70-37570

Two phase Ti alloy subjected to quenching and annealing studied by diffraction electron microscope, discussing needles complex fine structure

20 p3645 A70-39043

Niobium suboxide formation in Nb-O system from supersaturated solution of oxygen in niobium after annealing

20 p3648 A70-39630

Annealing properties of radiation damage in lithium-diffused silicon, formulating kinetic equation to describe processes associated with recovery and instability

20 p3687 A70-40165

Annealing temperature effect on creep rupture strength of Ta-W-Hf alloy

22 p4054 A70-42741

Radiation-produced defects in silicon semiconductor devices, annealing gamma ray, electron and fast neutron damages

22 p4087 A70-43328

Annealing response of explosively shock loaded Ni, thorium-Ni, Chromel-A, Inconel 600 and thorium-Chrome, noting activation temperature inverse relation with stacking fault free energy

23 p4204 A70-43883

Electron radiation damaged Si, investigating p type defect concentration effect on isochronal temperature in annealing by fractionation experiment

23 p4231 A70-44887

Aluminum oxide growth rate in molybdenum cermet after high temperature annealing

24 p4359 A70-45478

Crystal growth in polycrystalline Au, Ag and Au-Ag thin films annealing, observing by electron microscopy and electron diffraction

24 p4391 A70-45672

Chromium ions isothermal annealing kinetics in X ray irradiated ruby crystals, using EPR method

24 p4382 A70-46253

Cold reduction, refrigeration and annealing effects on stress corrosion cracking of austenitic stainless steels

24 p4365 A70-46389

ANNIHILATION REACTIONS

Very high energy cosmic rays disintegration and energy degradation by intense blue shifted photon fields of supernovae quasars and pulsar models

04 p0742 A70-15300

Photon scattering in inhomogeneous medium, deriving expressions for mean number of photons escaping or annihilated in medium

07 p1376 A70-18910

Hot universe model for determining magnitude constraints on Dirac monopole annihilation cross section and mass in cosmic rays

07 p1371 A70-20330

LEED pattern and germanium surface conductivity during oxidation indicating electron states annihilation

09 p1738 A70-22215

Antimatter motion in solar system and earth atmosphere, discussing vaporization and annihilation energy in collisions with interplanetary gas atoms

11 p2119 A70-26793

Second quantization exciton theory in amorphous disordered materials, discussing hamiltonian, boson annihilation operators and electronic polarization

14 p2627 A70-30693

Photon pair annihilation process in graviton pair, examining IR emission in two scalar particle collision

19 p3472 A70-38172

Antimatter detection and interaction with matter on moon, discussing radiation from electron-positron annihilation processes

19 p3521 A70-38482

Collapsing or neutronizing stars detection by recording neutrino and antineutrino flux, calculating antineutrino-deuteron interaction cross section and positron energy and angular distribution

20 p3698 A70-39302

ANNUAL VARIATIONS

Seasonal, solar diurnal and semidiurnal variations of cosmic ray soft component observed at sea over seven year period

01 p0170 A70-10467

Jacchia 1965 model discrepancies in solar and geomagnetic activity and semiannual effects observed in satellite drag measurements at 150-200 km and 700-1500 km

01 p0077 A70-11204

Satellite observations of semiannual density variations in upper atmosphere

01 p0077 A70-11205

Ionosphere atmospheric densities from Explorer 32 drag data including semiannual variations

01 p0077 A70-11206

Exospheric temperature variations by Thompson scatter technique, considering solar and geomagnetic activity effects

01 p0078 A70-11209

Seasonal phase changes of semidiurnal tidal wind components in lower ionosphere demonstrated from ionospheric drift measurements

01 p0078 A70-11212

Ionosphere total electron content diurnal and seasonal variations at midlatitudes, based on data analysis from Explorer 22 in polar orbit

01 p0080 A70-11223

Secular variations distribution on earth surface, plotting isopore charts from mean annual values of magnetic elements /1960-1965/

01 p0083 A70-11540

Seasonal effect on F region midlatitude slab thickness diurnal variations during magnetic disturbances using monitoring VHF signals from geostationary satellites

02 p0290 A70-12160

Mean and extreme atmospheric ozone concentration calculated as function of altitude and seasons in Northern Hemisphere

03 p0474 A70-13294

Seasonal variations of sporadic E virtual height at middle latitudes attributed to homospheric expansion depending on ozone amount

03 p0476 A70-13907

Seasonal and monthly mean charts forecasting method based on variation of annual difference in atmospheric circulation

04 p0715 A70-15294

Earth rotational velocity irregularities and horizontal motions of continental blocks at expense of oceanic hemisphere, noting seasonal distance changes

04 p0681 A70-15477

Earth rotation seasonal fluctuations analyzed from astronomical observations using frequency markers and quartz clocks

04 p0681 A70-15478

Electromagnetic structure of interplanetary space on basis of secondary cosmic ray intensity gradient annual variations as function of earth heliographic latitude
05 p0900 A70-15970

Meteor rate data tabulated from controlled parameter radar survey of Southern Hemisphere activity, noting diurnal and annual variations
05 p0907 A70-16001

Diurnal and seasonal variations of mortality due to cardiac and circulatory failure using model representing daylight regulation of human organism
05 p0802 A70-16663

Seasonal variation in ionospheric radiation absorption related to time variation between sunrise and constant angle attainment of sun
05 p0842 A70-16758

Electron density distributions relation to D region diurnal and seasonal variations in radiowave absorption in terms of transport processes near mesopause
06 p1054 A70-17589

Seasonal variations of maximum electron concentration in stratified E-F region, including E 2 layer recombination coefficient and F layer characteristics probability
06 p1057 A70-17842

Seasonal variation of F 1 region ion composition measured by rocket-borne mass spectrometer, noting altitude dependence of electron and ion temperatures
06 p1059 A70-18540

Atmospheric zonal circulation index annual variations calculation in latitude and time terms, using vertical vorticity component equation
07 p1328 A70-18650

Soviet book on nonperiodic processes in Northern Hemisphere stratosphere, discussing seasonal temperature fields, geopotential and circulation formation
07 p1261 A70-18733

Aircraft icing effects on conventional and jet aircraft and helicopters, discussing seasonal variations for main climatic regions
07 p1329 A70-18926

Ionospheric absorption diurnal and seasonal variations determined from field strength recordings
07 p1263 A70-19154

Effective LUF fade-out and fade-in times seasonal and diurnal variations for oblique ionospheric propagation paths, noting sunspot number effects
07 p1233 A70-19180

Quasi-biennial, annual and semiannual zonal wind and temperature harmonic amplitudes and phases in tropical and extratropical latitudes in stratosphere and low mesosphere
07 p1269 A70-19949

Polar cap magnetic field micropulsations simultaneous recordings at Greenland, Alaska, and Finland, noting seasonal variations
07 p1270 A70-20152

Yearly fluctuations of Seyfert galaxy 3C 120 light curve, discussing effects of ambient temperature
08 p1563 A70-20498

Atmospheric ground pressure seasonal changes after corpuscular flux arrival shown for Northern Hemisphere
08 p1487 A70-20554

Thermal structure transition of mesosphere at high altitudes from persistent summertime to dynamic wintertime case
08 p1539 A70-21649

Interhemispheric mass exchange as function of eddy transfer and meridional circulation
08 p1539 A70-21922

Horizontal ionospheric drift rates and traveling wave disturbances, showing differences between winter and summer
09 p1667 A70-22493

Atmospheric density in thermosphere observed by satellites, noting daily and semiannual variations related to solar and geomagnetic activities
09 p1667 A70-22626

Regular yearly pattern variations of zonal circulation index and temperature solved in Legendre polynomials
09 p1718 A70-23330

Mean zonal and meridional circulations during winter and summer, finding evidence for tropical Hadley cell
09 p1719 A70-23604

Geomagnetic field secular variation and cyclic components amplitudes separation by digital filters, observing seasonal and solar activity effects
10 p1880 A70-24808

Seasonal changes in thermospheric composition in middle latitudes, investigating molecular oxygen density and solar activity effects
10 p1881 A70-24817

Seasonal variation of spread F near magnetic equator, showing relationship with solar cycle at different geographic locations
10 p1881 A70-24818

Stratospheric equatorial wind period phases correlation with central European westerlies frequency, intensity and persistency, noting seasonal differences
10 p1913 A70-24950

Seasonal variations in radio signal propagation from aircraft navigation system antenna located in dense forest, solving problem with Doppler-VOR installation
10 p1854 A70-25254

Sunspot cycle and ionospheric D and E layers daily radio wave absorption correlation, observing seasonal variation effect
10 p1885 A70-25267

F 2 layer midday ionization level annual variation gradient, noting gradient latitudinal distribution dependence on solar activity level
11 p2042 A70-25532

Geomagnetic variations dominant polarization direction seasonal dependence based on magnetotelluric field observations, discussing micropulsations and LF cases
11 p2044 A70-25557

Radio wave absorption at 2.2 MHz measured by vertical incidence pulse method, observing maxima in February and in September-October due to auroral activity
11 p2006 A70-26176

Earth IR horizon seasonal and longer variations for horizon sensing instruments design
12 p2226 A70-27931

Long term ionospheric absorption measurements in Japan from IGY through IQSY using A1 method, discussing annual and diurnal variations correlation with solar activity
12 p2226 A70-28059

Long term ionospheric absorption measurements in Northern Hemisphere from IGY through IQSY, discussing annual and diurnal variations correlation with solar activity
12 p2226 A70-28060

Semiannual variation of geomagnetic activity related to incident solar wind, considering Manner 2 measurements
13 p2475 A70-28573

Seasonal measurements of ionospheric absorption during sunrise in D region at medium sunspot numbers, noting disagreement with rocket observation
13 p2392 A70-28574

Predawn forbidden OI 6300 A airglow seasonal variations by isophoto maps, discussing photoelectron precipitation
13 p2395 A70-28944

Postdusk and predawn seasonal variations of forbidden OI 6300 A airglow, discussing photoelectron precipitation
13 p2395 A70-28945

Horizontal geomagnetic force variations, considering ionospheric wind effects on ions in transition layer
13 p2402 A70-30057

Diurnal and seasonal variations of sporadic E layer observed at ionospheric station
14 p2568 A70-30134

Circannual rhythm in levels, amplitudes and acrophases of serum corticosterone in mice compared with phase shift after change of lighting regime
14 p2537 A70-30725

Neutral winds effect on F region vertical ion drifts derived from continuity equation, noting diurnal and seasonal variations
14 p2574 A70-30738

Lower ionosphere electron densities seasonal variations relationship to atmospheric circulation
14 p2574 A70-30742

Lunar tide in ionospheric D region absorption near magnetic equator, noting annual variation relationship to sunspots
14 p2574 A70-30747

Incoherent scatter observations of atmospheric density and temperature in lower thermosphere, observing seasonal variations
14 p2578 A70-31246

Sodium dayglow seasonal and diurnal variations observed with Zeeman cell photometer
14 p2579 A70-31253

Sodium and potassium dayglow seasonal and diurnal variations using resonance cell technique and sky polarization effect
14 p2580 A70-31263

Troposphere-stratosphere kinetic energy transfer /1964-1968/, annual variations and vertical flux correlation to circulation pattern
15 p2722 A70-31441

Daytime seasonal anomaly in electron density of topside F 2 region near sunspot minimum, using Alouette 1 data
15 p2726 A70-31863

Diurnal, seasonal and latitudinal variations of maximum electron concentration in F 2 region, using global network observations
15 p2729 A70-32077

Atmospheric ground pressure seasonal changes after corpuscular flux arrival shown for Northern Hemisphere
15 p2732 A70-32709

Annual variations of monthly mean meridional circulation, discussing observations, zonal asymmetries, accuracy and transports of angular momentum and energy
16 p2945 A70-33249

Telluric lines seasonal variations, discussing oxygen and water vapor photoelectric recordings in solar spectrum
16 p0000 A70-34185

Ionospheric cosmic noise absorption diurnal and seasonal variations at Alma-Ata during IQSY, noting chromospheric flares effects
18 p3306 A70-36089

Short wave propagation above F2 maximum usable frequency, observing field intensity and SNR seasonal and diurnal variations
18 p3226 A70-36092

Ionospheric radio wave absorption measurements, noting winter anomaly during maximum solar activity year
18 p3227 A70-36101

Ionization-recombination parameters variation as function of season and solar activity, using diurnal changes of F 2 layer maximum electron concentration
18 p3254 A70-37034

Semiannual oscillation and fine structure of earth magnetic field horizontal intensity during March and September
19 p3413 A70-38004

Annual temperature variation in low stratosphere based on harmonic analyses at 100 mb
19 p3462 A70-38263

Upper atmosphere semiannual variations dependence on lower thermosphere dynamic properties seasonal variations, using steady state models
19 p3415 A70-38384

Sporadic E layer occurrence probability over Dushanbe from ionospheric station data, discussing curves for diurnal and annual PE variations
19 p3417 A70-38785

Lunar tidal components in atmospheric pressure for various observatories, discussing seasonal variations
20 p3661 A70-39142

Radar angels activity seasonal variation and height distribution statistical relationship to meteorological parameters
20 p3661 A70-39169

H sub 500 field features during natural synoptic seasons in Northern Hemisphere, including circulation characteristics
20 p3663 A70-39271

Cosmic ray anisotropy 27 day and seasonal variations, considering neutron component data and sunspot magnetic field strength
20 p3696 A70-39277

Atmospheric dynamic effect on cosmic ray intensity, showing extremum and seasonal variation at midlatitudes
20 p3697 A70-39291

Morning and evening current reversals in equatorial electrojet, discussing seasonal variation data for refining models
20 p3621 A70-39352

Neutral atmosphere continuity equation of ionization and equation of motion in F 2 region for different seasons in various solar activity epochs
20 p3623 A70-40478

Solar activity effects on ionospheric total electron content seasonal variations over Tortosa, using BE-B satellite data
20 p3624 A70-40482

Anomalous nighttime ionospheric total electron content increases seasonal and solar cycle dependencies attributed to ionization sources due to electrodynamic drifts
21 p3815 A70-41061

Pc 1 geomagnetic micropulsation statistics for middle latitudes, discussing solar cycle and annual variations in occurrence rates
21 p3817 A70-41088

F 2 layer midday ionization level annual variation gradient, noting gradient latitudinal distribution dependence on solar activity level
21 p3819 A70-41282

Geomagnetic variations dominant polarization direction seasonal dependence based on magnetotelluric field observations, discussing micropulsations and LF cases
21 p3820 A70-41307

Stratosphere annual temperature cycle amplitude, using biannual daily temperatures over Northern Hemisphere from IQSY data
22 p4018 A70-42913

Sodium D lines airglow nocturnal and seasonal variations in upper atmosphere
22 p4023 A70-43295

Air circulation spring restructuring in Northern Hemisphere upper stratosphere, investigating summer stratospheric anticyclone evolution
22 p4066 A70-43378

Global geomagnetic field fluctuations of internal and external origins, analyzing HF spectrum based on monthly mean plots
23 p4187 A70-43861

Anomalous seasonal variation in worldwide ozone above 40 km from Umkehr measurement, considering turbidity effects
23 p4187 A70-44037

Ionosphere seasonal changes from three-point system for observing traveling ionospheric disturbances

23 p4192 A70-44868

Monthly and annual root-mean-square deviations of ionosphere radio wave absorption

24 p4312 A70-45485

ANNULAR FLOW

Heat transfer in steady state flow of electrically conducting incompressible viscous fluid in annular channel between coaxial circular cylinders under magnetic field

03 p0608 A70-14335

MHD flow velocity and current density distributions in annular duct with radial magnetic field

04 p0725 A70-14531

Electron temperature and particle density measurements in annular MHD duct, demonstrating Hall effect existence

04 p0725 A70-14532

Settling length for turbulent air flow velocity profile in smooth concentric annuli with square-edged and bellmouth entrances
[ASME PAPER 69-WA/APM-24]

04 p0669 A70-14908

Acoustic radiation from underexpanded supersonic main jet flow from nozzle impinged upon by annular jet

05 p0835 A70-16784

Repetitive scanner for wave velocity measurements in annular two phase gas or liquid flow using pivoted mirror

06 p1062 A70-17618

Viscous fluid flow calculations in fine clearance eccentric annuli allowing for pressure losses in laminar or turbulent flows

07 p1293 A70-19120

Natural heat convection measurements in vertical annular spaces, noting importance of local density and velocity product

08 p1433 A70-21671

Natural heat convection in vertical annular space taking into account variations of volumetric mass, viscosity and thermal conductivity of air with temperature

09 p1786 A70-22047

Turbulent flow downstream from abrupt widening of circular jet, using flow and momentum equations

10 p1870 A70-24782

Annular current effect on auroral oval location during morning and evening hours, noting airglow region shift toward equator and expansion

11 p2044 A70-25555

Annulus wall boundary layer effect on spatial flow in subsonic axial compressors by shearing stresses concept between stream surfaces

11 p1974 A70-25777

Homogeneous viscous fluid steady state parallel Stokes flow in annular region between concentric cylinders at low Reynolds numbers

11 p2038 A70-26478

Stability of MHD dissipative circular flow of viscous electrically conducting fluid between concentric stationary cylinders impressed with axial magnetic and radial electric fields

12 p2277 A70-27195

Flow stability of electrically conducting inviscid fluid in coaxial cylindrical annular space under influence of axial magnetic field

12 p2210 A70-27799

Turbulent heat transfer in concentric annuli entrance region with uniform wall heat flux

12 p2333 A70-28117

Supersonic flow in inner and outer regions of annular wings by method of singularities, obtaining Abel type integral equations for every step
[DFVLR-SONDDR-37]

12 p2158 A70-28207

Swirling flow between concentric cylinders, studying helical instability modes

13 p2386 A70-28805

Compressor cascade flutter phenomenon, investigating factors affecting aerodynamic damping force on annular cascade blades

13 p2341 A70-29447

Viscoelastic flow in Couette flow between coaxial cylinders and fluid between fixed plane and rotating cone

14 p2567 A70-31358

Annular turbulent flow between coaxial rotating cylinders, analyzing energy balance of averaged and pulsating motions

15 p2721 A70-32138

Annular fluids hydrodynamic mass and damping effects on long rotating cylinders vibrations, discussing theory of fluid friction and forces, vortex and turbulent flows, etc
[ASME PAPER 70-FE-30]

16 p2892 A70-33636

Annular fluids hydrodynamic mass and damping effects on long rotating cylinders vibrations, analyzing test results
[ASME PAPER 70-FE-31]

16 p2892 A70-33637

Forced convective heat transfer in annular passage with axially varying cross section, noting role of acceleration parameter

17 p3195 A70-34999

Laminar flow heat transfer in annuli, discussing correlation of local Nusselt numbers

17 p3197 A70-35545

Critical heat flux density during annular channel internal heating, examining transfer crisis under forced motion of unheated water

18 p3345 A70-36111

Colloid annular thruster performance, using low mass flow rate data and space charge formulas
[AIAA PAPER 70-1113]

20 p3692 A70-40230

Viscous magnetofluid dynamic one dimensional annular flow, reducing three dimensional field equation to coupled linear partial differential equations

21 p3855 A70-40889

Annular current effect on auroral oval location during morning and evening hours, noting airglow region shift toward equator and expansion

21 p3819 A70-41305

Earth magnetosphere LF wave annular trap, examining high energy particle interaction with magnetosonic waves

22 p4013 A70-42300

Newtonian fluid turbulent flow development characteristics in inlet region of smooth concentric annulus from momentum integral equations

22 p3957 A70-42304

Stable ellipsoidal plasma configurations in alternating electrode annular system, considering longitudinal magnetic field strength, electrode voltage and gas discharge chamber pressure

24 p4385 A70-45456

ANNULAR JETS

U ANNULAR FLOW

U JET FLOW

ANNULAR NOZZLES

Annular nozzle shapes established via method of straight line characteristics, noting flow patterns at various regions

03 p0409 A70-13872

Nonself similar problem of plane submerged fluid jet expelled from annular nozzle, obtaining asymptotic expansion for stream function

15 p2719 A70-31485

ANNULAR PLATES

Elastic ring reinforced annular plate of uniform thickness, heated nonuniformly along radius, discussing axisymmetric and asymmetric stability losses

01 p0210 A70-11415

Stability and critical loads of transversally isotropic reinforced plastic annular plates with weak shear resistance under axisymmetrical buckling

05 p0933 A70-16213

Finite bending elements for static deflections of annular and circular plates loaded by concentrated forces, calculating free vibrations

08 p1588 A70-21243

One dimensional numerical solution for steady state thermal behavior of trapezoidal profile annular fins transferring heat by conduction and radiation
[ASME PAPER 69-HT-6]

09 p1790 A70-23557

Limiting load for annular plates made of material having different yield points in tension and compression

11 p2129 A70-25560

Deflection function for annular plate simply supported and loaded with eccentric concentrated force

13 p2518 A70-29981

Nonhomogeneous Helmholtz vibration equation for sectorial-annular membranes and plates under arbitrary load, using Fourier method

19 p3535 A70-37343

Large deflection of simply supported aluminum alloy annular plate with nonlinear stress-strain curve, considering compressibility effects and membrane force

20 p3718 A70-39138

ANNULI

Dynamic response to step transverse loads of viscoelastic annulus of constant Poisson ratio in plane strain, analyzing work and spring-dashpot model
[ASME PAPER 69-LUB-23]

01 p0101 A70-10384

Squeeze film investigation between rotating plane annuli, considering inertia due to centrifugal effect
[ASME PAPER 69-LUB-6]

01 p0102 A70-10396

Dynamic response to step transverse loads of viscoelastic annulus of constant Poisson ratio in plane strain, analyzing work and spring-dash model
[ASME PAPER 69-LUB-23]

19 p3435 A70-37607

Squeeze film investigation between rotating plane annuli, considering inertia due to centrifugal effect
[ASME PAPER 69-LUB-6]

19 p3435 A70-37608

Turbulent hydrodynamic and thermal boundary layer development in internally heated annulus
[ASME PAPER 70-HT-9]

22 p4008 A70-42438

ANODES

NT CELL ANODES

DC electric arc with superimposed axial subsonic gas flow breakdown voltage and anode heat transfer using high speed photography

06 p1177 A70-17697

Anodic electric layer in self sustaining discharge in transverse magnetic field with neutral gas burnout, studying neutral atom ionization probability

09 p1734 A70-22110

Anode energy transfer model for measurement of circumferential current and heat flux distributions of MPD arc thruster

09 p1736 A70-23203

Segmented anode current and heat distribution in MPD engine measured with current shunts and calorimetric methods
[AIAA PAPER 69-244]

09 p1613 A70-23238

Mode transition characteristics of free burning argon electric arc with transpiration cooled anode, noting current blowing parameter
[AIAA PAPER 69-696]

12 p2281 A70-27806

Anodic temperature effect on Cs thermionic converter operation under arc regime, obtaining potential jump electron temperature relation near anode

15 p2677 A70-32119

Electrochemical oxidation of p-type boron anode in aqueous solutions, using galvanostatic technique

17 p3041 A70-34514

Anodes heat transfer in xenon short arc lamps

17 p3023 A70-35154

Spatial stability of transferred arc anode spots during cutting with plasma jets, noting currents associated with microspots

22 p4043 A70-42380

ANODIC COATINGS

Residual stress measurement in anodic film on duraluminum as function of film thickness and cyclic loadings in air and corrosive media

15 p2757 A70-31635

Anodic breakdown characteristics of Ti alloys as function of metal surface condition

17 p3113 A70-34366

Ar ion laser gas discharge tube construction, using anodically oxidized directly cooled aluminum segments

19 p3444 A70-37567

ANODIZING

Ti equipment anodizing methods, observing corrosion resistance reduction and embrittlement hydriding due to Fe contamination

17 p3098 A70-34363

Ni/sulfuric acid AC voltage polarization curves for anodic dissolution region

24 p4364 A70-46220

ANOMALIES

U ABNORMALITIES

ANORTHOSITE

Surveyor 5 lunar rock data from Mare Tranquilitatis compared with pyroxene gabbros, indicating gabbro or gabbroic anorthosite classification

01 p0181 A70-10575

Lherzolite, anorthosite, Gabbro and basalt dredged from Mid-Indian Ocean Ridge noting geological and geophysical features

04 p0675 A70-14422

Lunar-earth early crust anorthosites comparison, including occurrence sites, physical and chemical properties, etc

13 p2486 A70-28616

Lunar anorthosites Ni-Fe grains from Mare Tranquilitatis, discussing contamination by meteoritic metal, magnetic fractionation and fractional crystallization

19 p3519 A70-38032

Apollo 11 lunar anorthosites properties and characteristics, discussing grain size, Na content, color, density, chemical composition and geomorphic effects

21 p3903 A70-41559

ANOXIA

Acidosis effects on anoxic rat heart cardiac performance and anaerobic energy generation

04 p0635 A70-15461

Anoxia effects on biochemical processes in human body, comparing chemical energy balances under aerobic and anaerobic conditions

10 p1821 A70-25082

Rats myocardial contractility depression by free fatty acids during hypoxia or anoxia, noting mechanical performance improvement by glucose

12 p2170 A70-27898

ANTARCTIC REGIONS

Antarctic twilight observation by photoelectric scanning spectrometer in search for metallic emission lines in upper atmosphere

01 p0081 A70-11231

Thin, fat and average men responses to cold during one year period in Antarctica, measuring metabolic rates, skin and rectal temperatures

03 p0429 A70-14163

Anomalous ionization variations of F 2 layer at northern geomagnetic pole during winter coincident with decrease in solar plasma density

04 p0682 A70-15726

Magnetic activity in Antarctica during IQSY, plotting space-time characteristics of perturbations

07 p1268 A70-19462

Anomalous ionization variations of F 2 layer at northern geomagnetic pole during winter coincident with decrease in solar plasma density

14 p2575 A70-30810

Magnetic activity in Antarctica during IQSY, plotting space-time characteristics of perturbations

18 p3250 A70-36936

Auroral proton precipitation oval in antarctic winter based on H Balmer line radiation 21 p3882 A70-41091

Universal time control of south polar F layer during IGY attributed to low energy electron precipitation, comparing IGY and recent satellite data 21 p3818 A70-41101

Arctic and antarctic atmospheric circulation differences, discussing circumpolar vortices and isobaric surfaces altitude changes 22 p4065 A70-43168

ANTARCTICA

U ANTARCTIC REGIONS

ANTARES ROCKET VEHICLE

Estimated aerodynamic coefficients of reentry body compared with coefficients derived from Antares and Berenice flights 06 p0966 A70-17248

ANTENNA ARRAYS

NT ENDFIRE ARRAYS

NT LINEAR ARRAYS

NT STEERABLE ANTENNAS

NT YAGI ANTENNAS

Phased array antennas bandwidth and range resolution, discussing delay elements and antenna size affecting radiation patterns 01 p0042 A70-10262

Multielement active/passive antenna systems maximum SNR value obtained by determining conditions satisfied by parameters 03 p0456 A70-13092

Axial emission impedance antenna converting strongly delayed surface wave into weakly delayed wave forming cophased front at antenna end 03 p0456 A70-13199

Unstable problems stabilization in antenna synthesis from Fredholm equations solution, using least squares method and Chebyshev polynomials 03 p0456 A70-13452

Rapid fading intensity distribution formula for analysis of aperture phase and amplitude errors influence on antenna arrays directional characteristics 03 p0456 A70-13463

Low loss low sidelobe N-way microwave optical power divider for single plane electronically steerable Ku band phased array antenna 04 p0655 A70-14624

Surface waves excited by horn above dielectric disk backed by metallic disk, formulating characteristic wave equations and solving for attenuation and propagation constants 04 p0659 A70-15305

Rectennas design, construction and power output 04 p0660 A70-15649

Second antenna at Pleumeur-Bodou /France/ for satellite transmissions reception in Intelsat network program 05 p0826 A70-15981

Electrical and mechanical characteristics and specifications of second parabolic reflector antenna at Pleumeur-Bodou space communications center 05 p0819 A70-15982

Electrical and hydraulic units controlling second antenna at Pleumeur-Bodou space communication center 05 p0819 A70-15984

Antenna-central building connecting equipment at Pleumeur-Bodou space telecommunication center, discussing frequency compression demodulators 05 p0819 A70-15985

Artemis I and II telemetering antennas at Guiana Space Center for spacecraft tracking 05 p0819 A70-15987

Diagram compression by spatiotemporal coding of antenna array fitted with phase shifters 05 p0811 A70-15989

Cartographic radiation patterns far field characteristics of aperture antenna arrays obtained by optical simulation method 05 p0820 A70-16254

Polarization loss for elliptically polarized antennas, using curves based on Hatkin equation 06 p1019 A70-17504

Polarization insensitive phase shifter for phased array antennas, discussing limitations, design optimization and experimental results 06 p1019 A70-17508

Interdigital-line radiator /interdigital array antenna/ with broadside or endfire radiation characteristics obtained by rearranging feed point 06 p1020 A70-17569

Element pattern derived for circular arrays of axial slits on large perfectly conducting cylinders, comparing properties with planar arrays 06 p1021 A70-17571

Excitation coefficients for arrays with shaped beam patterns by perturbation of roots which lie off unit circle 06 p1021 A70-17572

Wideband cophased horizontal antennas with active dipole reflector arrays, describing feeder arrangements involving use of resistors 06 p1021 A70-17673

Circular antenna arrays synthesis, minimizing peak sidelobe level by dynamic programming 06 p1022 A70-18021

High gain paraboloidal reflector antenna with horn feed for satellite and terrestrial microwave links 06 p1022 A70-18022

Radio astronomical antenna structure synthesis based on excitation of unshaded mirror surfaces with symmetrical caustics and virtual sources outside of focal axis 07 p1239 A70-18758

Field strength prediction for vertical horizontal broadside and horizontal end-on HF antennas, noting necessary polarization corrections 07 p1232 A70-19177

Size reduction and low noise temperature in receiving antennas obtained by transistor integration and resonance frequency modulation 07 p1241 A70-19353

Signal processor with ratio-squared prediction combining for adaptive antenna array, discussing radiation patterns for coherent and incoherent signal and noise sources 07 p1242 A70-20066

Far field synthesis for calculating exciting excitation pattern of waveguide-excited aperture antenna arrays 07 p1243 A70-20325

Parallel wire antenna arrays analysis and design, emphasizing directive power gain maximization and sidelobe reduction 08 p1471 A70-20789

Operational figure of merit of high performance antennas in communication satellite earth stations as function of design 08 p1471 A70-20825

Electrical axis adjustment of east-west antenna array of crossed radio telescope by statistical processing of discrete sources observations 08 p1473 A70-21067

Antenna exciter of crossed radio telescope, discussing design, performance and increased wide band sensitivity 08 p1473 A70-21069

Antenna arrays phase synthesis method based on properties of fast fluctuating phase distribution 09 p1645 A70-22414

Standing wave measurements on radiating traveling wave dipole arrays with glide symmetric excitation, showing multimode propagation and effect on log periodic balancing 09 p1633 A70-22688

Mutual coupling in arrays of log periodic dipole antennas in terms of impedance and admittance matrices 09 p1645 A70-22690

Aberration-correcting line source feed for spherical reflector using linearly polarized flat waveguide array 09 p1646 A70-22694

Square Van Atta reflector with/without conducting plate used for mounting antenna half wave dipoles, considering scattering cross sections 09 p1646 A70-22695

Elevation patterns of vertically polarized elements above circular finite ground screens directly on soil, discussing steering illumination 09 p1634 A70-22700

Phase interpolation circuits for scanning phased array antennas, using doublers and frequency multipliers 09 p1646 A70-22701

Ring array synthesis for prescribed radiation pattern by sampling theory, considering application for aircraft navigation 09 p1646 A70-22702

Optical processing of signals from circular aerial arrays involving use of spatial filter 09 p1678 A70-22970

Error functional minimization in class of current distribution relay functions noting applications to linear antennas and FM signals synthesis 09 p1637 A70-23154

Autocollimation method for variable profile antenna adjustment and control, describing antenna-mirror array 09 p1648 A70-23155

Dispersion equation harmonic analysis for three dimensional periodic structure 09 p1637 A70-23156

Reflector focus location for variable profile antenna of radio telescope determined by modified Hartmann method in optics field 09 p1648 A70-23164

Antenna-duplexer assembly comprising log periodic antennas, power divider and hybrid loop 09 p1649 A70-23324

Antenna array circular polarization adjustment using reflections from horn radiator and mirror 09 p1650 A70-23633

Step-Track automatic angle tracking technique for communication satellites, seeking peak of antenna single beam [AIAA PAPER 70-416] 11 p1999 A70-25454

Telemetry tracking and command antenna array of Central German Ground Station for satellite communication [DFVLR-SONDDR-52] 11 p2017 A70-25800

Pleumeur-Bodou satellite telecommunications center, discussing antennas 11 p2031 A70-26009

Line source antenna arrays containing random dissimilarities in waveguide cross section analyzed for phase errors to determine sidelobe deterioration 11 p2018 A70-26177

System configuration requirements and detectability performance characteristics analysis for optimizing array reception of multipath 11 p2018 A70-26264

Phase velocity and direction estimation of unknown signal propagating across two dimensional array in dispersive waveguide, showing dependence on SNR 11 p2018 A70-26274

Aperture synthesis and spectral antenna characteristics in radio astronomy, considering Ryle systems, Mills-Christiansen crosses and variable interferometers 11 p2019 A70-26801

Spatial-temporal distribution of wind swell HF components measured by two dimensional antenna array fed by DC signals 12 p2263 A70-27516

Superwideband dipole antenna array reproducing radiation patterns in horizontal plane for signal polarization 12 p2196 A70-27539

Spacecraft high efficiency phased arrays with deployable helix radiating elements, considering gain and weight factors 12 p2197 A70-27930

Stacked, vertically polarized collinear arrays of independently fed omnidirectional antennas for flight testing Doppler radar aircraft warning system 12 p2199 A70-27968

Statistical design of density tapered planar circular and elliptical arrays for radiation patterns with good sidelobe behavior 12 p2199 A70-27987

Radiation pattern theory for primary aperture antenna with two secondary radiators 13 p2378 A70-29547

Grid assemblies as electrostatic plasma wave antennas, computing driving point and transimpedances for approximating single pole impedance in heavy Landau damping regime 13 p2371 A70-29918

Asymmetrical element spacings in thinned antenna arrays, obtaining symmetrical radiation patterns with low sidelobe levels 14 p2556 A70-30689

Aperture antennas planar finite array, calculating excitation pattern for prescribed surface current distribution 14 p2557 A70-31160

Antenna research, discussing efficiency and design considerations in phased and strip line arrays and conical scan telemetry antennas 14 p2559 A70-31375

Axisymmetric multibeam annular antenna array with interacting radiating elements synthesized by partial radiation patterns 15 p2707 A70-31513

Synthesis of vertically polarized omnidirectional pattern with cascade dipole antennas on conducting cylinder 15 p2697 A70-31832

Plane wave random signals arrival angle maximum likelihood estimation for multiple antenna systems 15 p2704 A70-32594

Medium wave thin cylindrical dipole antenna arrays design, discussing operating impedance determination 15 p2714 A70-32816

HF electrical communication based on Kelvin transmission line and Maxwell field theories, noting linear arrays 16 p2860 A70-32951

Multihorn array antenna performance improvement by shaping beam for optimum earth coverage from stabilized synchronous satellites 16 p2860 A70-32952

Antenna array system for surface target detection in receiver noise and heavy clutter by space-time decision theory 16 p2860 A70-32954

Dipole antenna arrays feeds design and performance for spherical aberration correction, discussing polarization mismatch 16 p2871 A70-32955

Mutual and self admittances for array with two monopoles, solving integral equations for current distributions 16 p2860 A70-32957

Nonuniform parallel element dipole array field patterns and synthesis by three term theory, taking into account current distribution effects 16 p2872 A70-32972

Electromagnetic field intensity measurements in focal region of wide angle spherical reflector antenna illuminated by polarized plane wave 16 p2872 A70-32976

Antenna system with linear polarization direction electronically changeable in microseconds 16 p2873 A70-33265

Steerable microwave circular array to provide 360 deg electronic beam steering with computerized adaptive amplitude and phase control 16 p2874 A70-33392

Microwave circular array with electronic beam rotation of patterns by applying linear phase tapers to Butler matrix feed 16 p2874 A70-33393

Steerable C band waveguide arrays design for forming monopulse cluster of sum and difference beams 16 p2875 A70-33395

Compact integrated microwave antenna of composite structure involving slotted waveguide planar array capable of operating in three frequency bands 16 p2876 A70-33406

Solid state dipole antenna array miniaturization by etching microstrip components on alumina substrate having high dielectric constant 16 p2876 A70-33409

Sandwich wire planar antenna array design, noting electrical performance, ruggedness, volume and weight 16 p2877 A70-33416

Multiple sensor arrays phase difference estimation, assuming Gaussian signal and noise statistics 16 p2866 A70-34064

Radio astronomy explorer (RAE) satellite main antenna array, describing elements, dispenser and take-up mechanisms, construction materials, etc 16 p2896 A70-34144

Electronic narrow sweep antenna array active element number reduction, discussing optical considerations 16 p2866 A70-34266

Antenna reflectors of evolution and double curvature optimization by iteration method 16 p2866 A70-34267

Dipole antenna finite three dimensional array, calculating excitation patterns 17 p3042 A70-34589

Ionospheric drift measurement by 89 antennas array, testing validity of methods using three antennas 17 p3076 A70-34939

Uniformly spaced antenna arrays along curve, determining far field as product of element and array factors 17 p3044 A70-35055

Antenna arrays with nonuniform spacings, synthesizing radiation patterns by deterministic and statistical density taper methods 17 p3044 A70-35056

Continuous line source, array or aperture antennas of linear rectangular or circular shape, discussing radiation patterns synthesis methods 17 p3044 A70-35057

Cylindrical antennas and arrays for transmission or reception, determining radiation patterns 17 p3051 A70-35059

Boundary value problems for symmetrically excited biconical antennas surrounded by free space, treating spherical and thin wire antennas 17 p3044 A70-35062

Radiation patterns and impedance properties of slot antenna in ground plane, slot on cylinder and sphere and waveguide slot arrays 17 p3051 A70-35064

Collection of papers on antenna theory covering reflector, lens, traveling wave, leaky wave, surface wave, log periodic antennas, etc 17 p3051 A70-35066

Log periodic antennas, discussing dipole array and planar sheath spiral structures, base current and far field pattern calculations, etc 17 p3052 A70-35073

Spatial filter properties of antennas, discussing system performance optimization and incoherent source transfer functions 17 p3045 A70-35077

Signal processing antennas, discussing synthetic and multiplicative arrays for coherent radar airborne mapping 17 p3052 A70-35078

Physical and electrical sizes in large antennas, discussing paraboloid reflectors, arrays, slot antennas, etc 17 p3053 A70-35079

Multiple narrow beam antenna system with plasma column and electromagnetic wave ring source, discussing radiation pattern and electronic scannability 18 p3294 A70-36346

Pencil beam synthesis for large circular array with arbitrary number of directive elements, determining optimum excitations 18 p3227 A70-36476

Radio astronomical antenna structure synthesis based on excitation of unshaded mirror surfaces with symmetrical caustics and virtual sources outside of focal axis 18 p3233 A70-37102

Traveling wave antenna array single lobe design using mode charts to reduce errors 19 p3376 A70-37688

Ferrite phase shifter for array antennas, discussing design trends, production, performance characteristics and future developments 19 p3388 A70-37864

Wire antennas array analysis and beam pattern synthesis by method of moments, considering application to electromagnetic compatibility 19 p3380 A70-38178

Canadian HF T array radio telescope at Dominion Radio Astrophysical Laboratory, discussing design and performance 19 p3397 A70-38275

Antenna systems with minimum angular resolving power for solar limb radio sources recording, using data from solar meridian passage 19 p3522 A70-38563

Directivity characteristics of planar antenna arrays with discrete identical elements and uniform phase progression 20 p3597 A70-39458

Traveling wave antenna arrays with resistance elements for coupling, measuring noise elimination capabilities 20 p3598 A70-40146

Uniformly and nonuniformly spaced microwave antenna arrays, investigating directivity function and gain characteristics dependence on spacing 20 p3599 A70-40313

T, Y and ring microwave antenna array configurations for radio astronomy, comparing baseline distributions 20 p3599 A70-40317

Amplitude-phase data from gathering receiving antenna array, obtaining Doppler frequency spectrum as arrival angle function 20 p3599 A70-40319

Analog computer for one dimensional antenna array simulation, discussing radiation pattern calculation and display 21 p3796 A70-40621

Strip array excitation by field with large phase shift per period, deriving approximate solution from averaged boundary conditions 21 p3784 A70-40627

Circular array radar antenna, describing feed systems, scanning switches and radiation patterns 21 p3799 A70-41360

Periodically modulated corrugated surface array for application as phase-frequency scanning aerial, deriving design equations for comparison with radiation characteristics measurements 21 p3800 A70-41944

Microwave antenna array irregularly location from hologram by optical signal processing, using far field spatial filter 21 p3792 A70-42048

Quasi-equispaced traveling wave slot arrays with below sidelobe crosspolarization, considering computer designed X band prototype 21 p3800 A70-42050

One, two and three dimensional array receiving systems, determining signal detectability characteristics by spatial filtering variation 22 p3986 A70-42527

Log periodic dipole antenna arrays, calculating HF performance and patterns in presence of ground 22 p3997 A70-43176

Full-scanning random arrays with high resolution for space exploration, radio astronomy and long range radar 23 p4160 A70-43770

Step-scanned circular array radar antenna for operation over 20 percent bandwidth, discussing design, radiation patterns and performance advantages 23 p4175 A70-44951

N-arm spiral or conical antennas radiation patterns calculation for sigma and delta excitations, using bicomplex functions 23 p4176 A70-44965

Octave bandwidth unidirectional circularly polarized reflector antenna, using crossed conical dipoles near second resonance 23 p4176 A70-44970

Aperture synthesis and spectral antenna characteristics in radio astronomy, considering Ryle systems, Mills-Christiansen crosses and variable interferometers 24 p4311 A70-45176

ANTENNA COUPLERS

NT COUPLING CIRCUITS

Plasma density and electroacoustic resonance effects on coupled cylindrical antennas self and mutual impedances measured in Hg-arc discharge 01 p0050 A70-10461

Mutual impedance coupling among minimum scattering antennas with electromagnetic properties expressed in terms of radiation patterns 12 p2198 A70-27956

Mutual impedance between coplanar skew dipoles with arbitrary lengths and terminal positions, noting convenience for computer programming 16 p2861 A70-32970

Traveling wave antenna arrays with resistance elements for coupling, measuring noise elimination capabilities 20 p3598 A70-40146

ANTENNA FEEDS

Radiometric method for calibrating loss of multimode antenna-feed components with linear or circular polarization, deriving calibration and error analysis equations 01 p0050 A70-10711

Antenna noise temperature of large aperture reflectors from feed system RF characteristics, discussing spillover and blockage factors 06 p1008 A70-17506

Phase center position of field scattered from hyperboloid subreflector in asymmetric Cassegrain antenna feed system 06 p1019 A70-17557

Deep reflector antennas mode composition by graphic computer techniques for maximum efficiency feed matches 06 p1021 A70-17575

Wideband cophasd horizontal antennas with active dipole reflector arrays, describing feeder arrangements involving use of resistors 06 p1021 A70-17673

Design features and experimental results of E-fed cavity type suppressed omnidirectional antenna for VHF operation 06 p1022 A70-18020

Parasitic effects due to coupling of wideband regenerative amplifier with nonideal ferrite circulators to antenna feeder duct 08 p1468 A70-20575

Discrete diode phase inverter for meter wavelengths providing north-south antenna control of radio telescope by diffraction method 08 p1473 A70-21064

Thin linear antennas in plasma analyzed for radiation characteristics by linearized hydrodynamic theory, showing effect of feed points displacement 09 p1643 A70-22207

Parabolic reflectors profile error compensation by means of multielement feed array with controllable phasing 09 p1644 A70-22236

Aberration-correcting line source feed for spherical reflector using linearly polarized flat waveguide array 09 p1646 A70-22694

Parabolic antenna for automatic tracking compared for characteristics between multimode and four horn feed systems 10 p1847 A70-23920

Multiple feed waveguide lens in variable coverage communications antenna for geostationary LES-7 satellite [AIAA PAPER 70-423] 11 p2016 A70-25461

Corrugated waveguide structures for aperture type feeds for spherical and paraboloidal reflector antennas, discussing experiments on 2-hybrid mode horn 11 p2018 A70-26024

Cassegrain antenna feed system for satellite communication earth stations, noting low noise characteristics 11 p2011 A70-26716

Spherical reflector antenna with Gregorian correctors, calculating gain, far field radiation pattern and efficiency as functions of subreflector and feed positions 12 p2200 A70-28052

Dipole antenna arrays feeds design and performance for spherical aberration correction, discussing polarization mismatch 16 p2871 A70-32955

Paraboloidal reflectors aperture fields from stereographic mapping of feed polarization pattern, illustrating electric and magnetic dipoles and Huygens sources 16 p2871 A70-32962

Admittance measurements of rectangular or circular waveguide fed aperture antennas illuminating displaced metal plate 16 p2872 A70-32963

Current distribution on isolated thin cylindrical center-fed dipole antenna, calculating axial electric fields and radiating properties 16 p2861 A70-32964

Illumination efficiency in shaped two reflector Cassegrain antenna system related to feed pattern deviation 16 p2861 A70-32968

Feed and terminal radiation patterns of surface wave antennas measured separately 16 p2861 A70-32973

Microwave circular array with electronic beam rotation of patterns by applying linear phase tapers to Butler matrix feed 16 p2874 A70-33393

Geodesic Luneberg lens Q band antenna design, construction and evaluation, noting point feeding and energy collimation 16 p2876 A70-33408

Attenuation characteristics for dominant hybrid mode in corrugated circular waveguide for antenna feed 16 p2879 A70-34041

Prime focus feeds performance for radiotelescopes, using one- or two-hybrid modes in circumferentially corrugated waveguides 19 p3388 A70-37967

Transmitter-antenna matching, using Pi-filter for resonance transformation 19 p3389 A70-38071

Parabolic antenna properties generated by dual band circularly polarized focused two channel monopole feed system, discussing tracking data from helicopter, Apollo 8 and Cassiopeia A 20 p3589 A70-40323

Circular array radar antenna, describing feed systems, scanning switches and radiation patterns 21 p3799 A70-41360

Parabolic reflector microwave antenna flared horn primary feeds design for maximum aperture efficiency based on electric field matching 21 p3800 A70-41946

Celestial radio source angle tracking techniques using monopole antenna receiving system applied to angle tracking radar 22 p3991 A70-43582

Dielectric filled tubular monopole antenna driven by coaxial line with TEM mode, calculating current distribution from integral equation 23 p4175 A70-44953

Annular aperture /slot/ antenna driven by coaxial line, calculating input admittance and complete near field radiation distribution 23 p4176 A70-44954

Monopulse tracking antenna beam broadening by feed displacement defocusing in parabolic reflector 23 p4165 A70-44956

Feed voltages and directional gain maximization for loaded long thin-wire antennas with multiple excitations, using matrix methods 23 p4176 A70-44972

Optimum performance of corrugated waveguide feed horns for paraboloidal reflector antennas via radiation pattern shaping with digital computer 24 p4320 A70-46222

Dual channel circularly polarized feed of monopulse tracking antenna system, noting axial ratio and gain and open loop mode autotracking 24 p4321 A70-46259

ANTENNA FIELDS

U ANTENNA RADIATION PATTERNS

ANTENNA RADIATION PATTERNS

NT SIDELOBES

Phased array antennas bandwidth and range resolution, discussing delay elements and antenna size affecting radiation patterns 01 p0042 A70-10262

Radiation patterns containing multiple beams generated by aperture phase control 01 p0050 A70-10462

Multimode excitation of large aperture horn antennas to produce electronic deflections of directional pattern 01 p0046 A70-11454

Binary digital radar signal detectors optimization for radiation pattern of sin x/x radar antenna and for non-fluctuating target 02 p0255 A70-11899

Far field radiation pattern determination particularly suitable for large parabolic antennas, detailing measurement errors 02 p0267 A70-12399

Compact range techniques using collimator for radar reflectivity and microwave antenna gain and pattern measurements 02 p0269 A70-12586

Equatorial patterns measurement of plasma covered axially slotted cylindrical antenna, describing discharge tube, facility and Langmuir probe survey of tube electron density 02 p0269 A70-12590

Numerical integration methods in electromagnetic theory, discussing scattering and radiation from thin wire structures 02 p0262 A70-12600

Radiation enhancement from spherical antenna by overdense plasma coating, noting use for reentry vehicle blackout prevention 02 p0262 A70-12601

Shaped-reflector Cassegrainian antenna characteristics calculation, using current distribution method to derive subreflector radiation pattern 02 p0270 A70-12617

Field patterns of thin resonant and nonresonant antennas in warm plasma, using digital computer to evaluate propagation constant for current distribution 02 p0263 A70-12655

E plane radiation patterns of E plane sectoral horns enhanced by metallic grills arranged in optimum positions 02 p0270 A70-12734

Normal mode helical antennas performance in medium and short wave regions, discussing advantage over log periodic antennas and maximum radiation angle achieved by phase shift 02 p0270 A70-12735

Multimirror illumination system for radio telescope antenna with reduced noise temperature, narrow

radiation pattern and optimal specular cross section, noting sensitivity 03 p0455 A70-13082

Polarization diversity provided to parallel plate antennas in airborne radar applications by orthogonal vector processing 03 p0452 A70-13967

Subcritical wavelengths processing of solar radio emission, allowing for antenna radiation pattern distortion due to surface defects 04 p0745 A70-14498

Helicone antenna /axial mode helix combined with conical horn/ compared to conical horn in pattern and polarization characteristics [AAS PAPER 69-623] 04 p0655 A70-14662

Radiation pattern computation for lens corrected conical scalar horn, comparing patterns and beam-widths with uncorrected horn and waveguide 04 p0656 A70-14721

Aperture electric field bounds presented for TE, TM and TE/TM excitation over azimuthally symmetric slotted cylinder subject to constraint of specified radiated power 04 p0649 A70-14969

Directional pattern of waveguide radiators using Kirchhoff boundary values of electric, magnetic or electric and magnetic fields, discussing aperture reflection coefficient 04 p0653 A70-15397

Polar diagrams control for distributed radiating systems, generating localizer planes for high flying aircraft navigation aids 05 p0812 A70-16150

Parasitic cross polarization lobe elimination in radiation patterns of variable profile antennas by curved conductors, including confirmation for large radio telescope 05 p0820 A70-16253

Cartographic radiation patterns far field characteristics of aperture antenna arrays obtained by optical simulation method 05 p0820 A70-16254

Statistical characteristics of field of linear antenna with square phase characteristics, deriving formulas for presence of amplitude phase errors 05 p0820 A70-16255

Antenna far field noise effect on monopulse type and conical scanning radar angle meters performance 05 p0813 A70-16256

Radiation patterns of scanning antenna using digital phase shifters to obtain suitable phase distribution to move sidelobes into invisible region 05 p0822 A70-16676

Impedance and radiation pattern of quarter wave monopole and half wave dipole antennas in isotropic plasma, considering plasma density role 06 p1117 A70-17372

S-band omnidirectional antenna patterns measurement procedure and results for Apollo spacecraft configurations, tabulating measure gains 06 p1019 A70-17507

Phase center position of field scattered from hyperboloid subreflector in asymmetric Cassegrain antenna feed system 06 p1019 A70-17557

Antenna reactive energies and modal quality factors by compact expressions given in terms of polynomials with positive coefficients not involving spherical Bessel functions 06 p1020 A70-17560

Reflection coefficients, radiation patterns and surface wave excitation calculated from aperture electric field obtained for waveguide radiating through dielectric slab 06 p1020 A70-17561

Electromagnetic radiation patterns from aperture in conducting cylinder coated with moving isotropic plasma sheath, noting sheath velocity and plasma frequency influence 06 p1020 A70-17564

Interdigital-line radiator /interdigital array antenna/ with broadside or endfire radiation characteristics obtained by rearranging feed point 06 p1020 A70-17569

Parallel plate TEM waveguides radiation pattern slope diffraction analysis 06 p1021 A70-17570

Element pattern derived for circular arrays of axial slits on large perfectly conducting cylinders, comparing properties with planar arrays 06 p1021 A70-17571

Excitation coefficients for arrays with shaped beam patterns by perturbation of roots which lie off unit circle 06 p1021 A70-17572

Vertical electric dipole transient response over circular ground screen, studying low angle radiation patterns 06 p1021 A70-17573

Two port isotropic antenna excited by independent noise sources for uniform power radiation in all directions and polarizations 06 p1021 A70-17574

Wave focusing along static magnetic field from radiating VLF source immersed in cold magnetoplasma 06 p1120 A70-17577

Design features and experimental results of E-fed cavity type suppressed omnidirectional antenna for VHF operation 06 p1022 A70-18020

Geometrical and electrical characteristics of two mirror parabolic antenna for tropospheric radio relay communications lines in centimeter band, analyzing radiation patterns 07 p1240 A70-19125

Ray theory for determining short term and averaged characteristics of nonreciprocal HF ionospheric propagation paths for single magnetoionic waves transmitted between antennas 07 p1231 A70-19171

Signal processor with ratio-squared predetection combining for adaptive antenna array, discussing radiation patterns for coherent and incoherent signal and noise sources 07 p1242 A70-20066

Spherical hybrid modes in corrugated antenna conical horns, obtaining radiation pattern and gain with small flare angle 07 p1243 A70-20284

Far field synthesis for calculating excitation pattern of waveguide-excited aperture antenna arrays 07 p1243 A70-20325

Field strength determination at reception point for long range short wave paths, taking into account multiple ray paths and antenna radiation patterns 07 p1237 A70-20435

Parallel wire antenna arrays analysis and design, emphasizing directive power gain maximization and sidelobe reduction 08 p1471 A70-20789

Gain-to-noise temperature ratio /G/T/ optimization by dish antenna shaping for nonuniform aperture field distribution 08 p1471 A70-20790

Impedance radiation pattern and actual height of receiving dipole antenna in magnetoactive plasma calculated by electrodynamic reciprocity theorem 08 p1472 A70-20970

Optical information processing in noncoherent light, considering applicability to simulating antenna radiation patterns using field distribution in aperture obtained by Fourier transformation 08 p1494 A70-20971

Optimal linear antenna synthesis, determining current distribution resulting in specified radiation pattern for superdirective antennas 08 p1472 A70-20972

Matrix method for maximizing radar antenna directive gain and simultaneously placing nulls in far field radiation patterns 08 p1477 A70-21758

Electro-optical analogies application to sidelobe reduction of radar antenna illumination patterns and optics far field diffraction patterns in terrain image formation 09 p1631 A70-22009

Thin linear antennas in plasma analyzed for radiation characteristics by linearized hydrodynamic theory, showing effect of feed points displacement 09 p1643 A70-22207

Linear antenna array synthesis by variational calculus, minimizing sidelobe level for fixed input powers and field strengths 09 p1644 A70-22404

Standing wave measurements on radiating traveling wave dipole arrays with glide symmetric excitation, showing multimode propagation and effect on log periodic balancing 09 p1633 A70-22688

Computer predicted horn antenna radiation patterns through aircraft radome compared with measured values 09 p1645 A70-22689

Parasitic loop counterpoise antenna radiation patterns, considering application to VOR systems 09 p1646 A70-22693

Bounds on near electric field outside rectangular slot in conducting ground plane applied to microwave breakdown limitation 09 p1646 A70-22696

Elevation patterns of vertically polarized elements above circular finite ground screens directly on soil, discussing steering illumination 09 p1634 A70-22700

Ring array synthesis for prescribed radiation pattern by sampling theory, considering application for aircraft navigation 09 p1646 A70-22702

Electric dipole emission near ideally conducting screen with variable surface impedance parallel strips, analyzing radiation pattern 09 p1636 A70-23140

Interference proof characteristics and shielding capability of mirror antennas improved by peripheral sheet metal or wire screens, reducing rear lobe level 09 p1648 A70-23151

Vertical Hertzian doublet with large circular screen placed above earth, calculating radiation pattern, directive gain, efficiency and radiation resistance
09 p1637 A70-23152

Polygonal-aperture antennas side radiation distribution
09 p1648 A70-23153

Dispersion equation harmonic analysis for three dimensional periodic structure
09 p1637 A70-23156

Reactive portion of mutual impedance of arbitrary antennas calculated from radiation patterns by interpolation method
09 p1648 A70-23162

Parameter optimization of V and rhombic antennas with sloped wires, determining radiation angle from radiation pattern
09 p1649 A70-23336

Radiation field of electric and magnetic dipole in double layer medium, solving Sommerfeld integrals
09 p1650 A70-23550

Stripline elements centimeter wavelength emission level determination by comparison with reference antenna radiation patterns
09 p1652 A70-23650

Antenna with 3-db slotted waveguide bridge to produce near circular polarization emission field
09 p1652 A70-23651

Waveguide slot antenna with electrical control of field polarization from linear to circular and beam scanning over wide sector
09 p1652 A70-23652

Integral equation for radiation patterns from vertical antenna over variable impedance surface
[AFCL-69-0315] 09 p1639 A70-23670

Parabolic antenna for automatic tracking compared for characteristics between multimode and four horn feed systems
10 p1847 A70-23920

Antenna characteristics and parameters as function of position and orientation in radome by automatic system consisting of electromechanical and programming device
10 p1848 A70-23971

Wave propagation in homogeneous cone region of broadband radiator, calculating field distribution by retarded potentials method
10 p1848 A70-24222

Antenna arrays elements mutual coupling effects on pattern and impedance characteristics
10 p1849 A70-24536

Antenna pattern synthesis with circular distributed current source, analyzing directivity characteristics through Fourier series nth order mode concept
10 p1849 A70-24616

Parabolic antenna radiation pattern synthesis under laboratory conditions with space limitations obtainable by defocused antenna method
10 p1853 A70-25132

Radiation patterns widened from plane and circular waveguide ends closed by planoconcave homogeneous dielectric lens
10 p1843 A70-25135

Two dimensional impedance horn antennas synthesis by aperture field distribution and radiation pattern configuration relationship, deriving energy balance equation
11 p2015 A70-25348

Earth station antenna radiation diagrams with respect to interference isolation capability
[AIAA PAPER 70-418] 11 p2015 A70-25414

Analog integrating moving window detector performance analysis for use with scanning pulse radar allowing for antenna radiation pattern and detection process dynamic characteristics
11 p2009 A70-26262

Far field radiation patterns of Cassegrain, offset paraboloid and horn reflector antennas by stationary phase approximation method
11 p2019 A70-26659

Pencil-beam antenna idealized patterns derived from maximum gains and operating wavelengths, discussing sidelobes
12 p2195 A70-27247

Superwideband dipole antenna array reproducing radiation patterns in horizontal plane for signal polarization
12 p2196 A70-27539

Radiating objects localization and tracking by radiometer equipped with two antennas having slightly divergent beams
12 p2185 A70-27689

Radiation characteristics of ion acoustic waves from monopole and dipole antennas, observing patterns of longitudinal wave in isotropic plasma
12 p2279 A70-27778

Satellite pencil and shaped beam antennas, considering maximum gain conditions for various angles
12 p2197 A70-27929

Optimum distribution over circular aperture in ground plane for best mean square approximation to specified radiation pattern
12 p2197 A70-27952

Log-periodic dipole /LPD/ antennas compressed along transmission-line axis, considering frequency dependent behavior in narrow bands and radiation pattern
12 p2198 A70-27955

Mutual impedance coupling among minimum scattering antennas with electromagnetic properties expressed in terms of radiation patterns
12 p2198 A70-27956

Optimum scattering from linear array of half-wave dipoles at bistatic angle, employing coupled impedance loading network
12 p2198 A70-27958

Thin cylindrical DC pulse driven antenna radiation fields time variation as function of angle
12 p2198 A70-27964

Circular loop antenna with traveling wave current distribution, considering phase change effects on radiation pattern and gain
12 p2198 A70-27965

Waveguide slot array operation in different frequency bands generating independent radiation patterns, utilizing orthogonal dominant modes propagation
12 p2199 A70-27967

Simulated isotropic lossless plasma radiating apertures located on nonplanar models, relating results to antenna radiation patterns
12 p2282 A70-27969

Dipole and monopole antenna radiation patterns, considering effects of soil conductivity and elevation above ground
12 p2199 A70-27979

Statistical design of density tapered planar circular and elliptical arrays for radiation patterns with good sidelobe behavior
12 p2199 A70-27987

Linearly tapered zigzag antenna of constant pitch angle observed for radiation and impedance characteristics
12 p2199 A70-27988

Surface wave antenna radiation pattern from finite aperture of corrugated horn antenna
12 p2199 A70-28017

Spherical reflector antenna with Gregorian correctors, calculating gain, far field radiation pattern and efficiency as functions of subreflector and feed positions
12 p2200 A70-28052

Leaky waveguide radiation patterns with periodic loading slots along axis
13 p2377 A70-29105

Radiation patterns of slots in flat and curved screens using open waveguide emission theory
13 p2378 A70-29305

Plane multiclement antenna field statistics as function of correlated phase-amplitude aperture errors
13 p2378 A70-29306

Radiation pattern theory for primary aperture antenna with two secondary radiators
13 p2378 A70-29547

Radiation patterns of phased array scanning antenna using digital phase shifter, reducing peak sidelobe level
13 p2380 A70-29785

Radiation characteristics of horn antennas loaded with curved transverse dielectric slabs and radial dielectric strips, discussing axial directivity and half-power beamwidth
13 p2370 A70-29836

Alouette spikes decrease with time equivalent to antenna transient response during hot plasma immersion
13 p2371 A70-29921

Microwave axicon with dielectric cone at aperture of focused antenna to reduce far-field radiation pattern beamwidth
14 p2549 A70-30512

Asymmetrical element spacings in thinned antenna arrays, obtaining symmetrical radiation patterns with low sidelobe levels
14 p2556 A70-30689

Aperture antennas planar finite array, calculating excitation pattern for prescribed surface current distribution
14 p2557 A70-31160

Anechoic chambers and test equipment for microwave antenna pattern measurements, discussing electromagnetic shielding and construction
14 p2557 A70-31180

Auroral echoes polarization with horizontal and vertical Yagis, discussing aerial patterns
14 p2578 A70-31240

Axisymmetric multibeam annular antenna array with interacting radiating elements synthesized by partial radiation patterns
15 p2707 A70-31513

Cophased two dimensional antennas fields asymptotic expansions in near and far zones with generalization to three dimensional case
15 p2707 A70-31514

Synthesis of vertically polarized omnidirectional pattern with cascade dipole antennas on conducting cylinder
15 p2697 A70-31832

Loop antenna current distribution source from radiation pattern synthesis, using Fourier series
15 p2698 A70-31837

Correction method for near field antenna measurements made with measuring antenna of arbitrary but known characteristics
15 p2698 A70-31954

On-axis pattern vector and power gain measurements by two identical antennas
15 p2698 A70-31955

Antenna pattern and power gain determination from near field measurements on electrically large horn lens, standard gain horn and measuring antenna duplicate
15 p2698 A70-31956

Convex infinite paraboloid of revolution, describing geometry and applications to electromagnetic wave scattering and antennas
15 p2701 A70-32415

Search radar antennas for monopulse direction finding with radiation pattern for sum and difference operation
15 p2704 A70-32674

Asymmetric phase error in antenna circular apertures, emphasizing beam squint resulting from distortion of paraboloidal reflector
16 p2859 A70-32942

Multihorn array antenna performance improvement by shaping beam for optimum earth coverage from stabilized synchronous satellites
16 p2860 A70-32952

Radiation pattern of radial infinitesimal current elements near or on finite length conducting cylinders, using image and geometrical theory of diffraction techniques
16 p2860 A70-32956

Backfire antennas allowing for mutual impedance between dipole elements, determining radiated field from surface current distribution
16 p2861 A70-32958

Pulse characteristics received by loop antenna in field of second antenna excited with step functions, calculating radiation characteristics
16 p2871 A70-32961

Paraboloidal reflectors aperture fields from stereographic mapping of feed polarization pattern, illustrating electric and magnetic dipoles and Huygens sources
16 p2871 A70-32962

Current distribution on isolated thin cylindrical center-fed dipole antenna, calculating axial electric fields and radiating properties
16 p2861 A70-32964

Wedge diffraction analyses of TE sub 10 mode slot radiation characteristics on circular and elliptical cylinder, considering boundary value solutions existence
16 p2861 A70-32965

Antenna gain, efficiency, half power bandwidth, sidelobe level and focal length for circularly polarized metallic lens antenna at X band frequencies
16 p2872 A70-32969

Loaded resonant circular loop radiation field patterns table, determining load impedance for antenna design
16 p2872 A70-32971

Nonuniform parallel element dipole array field patterns and synthesis by three term theory, taking into account current distribution effects
16 p2872 A70-32972

Feed and terminal radiation patterns of surface wave antennas measured separately
16 p2861 A70-32973

Excited circular cylindrical dielectric rod antenna radiation patterns derivation by Schelkunoff equivalence principle
16 p2872 A70-33121

Microwave circular array with electronic beam rotation of patterns by applying linear phase tapers to Butler matrix feed
16 p2874 A70-33393

High speed millimetric horn antenna with small azimuth and elevation beamwidths for airfield radar
16 p2876 A70-33407

X band airborne antenna phased array, describing phase shifter, radiation pattern, associated computer, etc
16 p2864 A70-33454

Lens antennas design for communication satellites, discussing power gain, beam width, sidelobe level, temperature distribution, etc
16 p2982 A70-33772

Adaptive radar beacon forming, using conjugate reflections for propagation path errors compensation
16 p2865 A70-34061

Scanning radar with feedback integration, calculating detection probabilities from antenna beam shape factor
16 p2888 A70-34063

Far field antenna patterns synthesis and steering for optical heterodyne receivers
16 p2866 A70-34261

Rod antenna radiation representation by instantaneous pictures of electric field lines, considering wave detachment mechanism
17 p3050 A70-34575

- Dipole antenna finite three dimensional array, calculating excitation patterns 17 p3042 A70-34589
- Radiation from simple slots in moving dispersionless dielectric, using Minkowski electrodynamics 17 p3043 A70-34984
- Simple antenna sources, deriving far zone radiation field from arbitrary current distribution 17 p3043 A70-35052
- Microwave antenna with aperture in infinite conducting plane, analyzing radiation patterns, scattering and diffraction 17 p3043 A70-35053
- Uniformly spaced antenna arrays along curve, determining far field as product of element and array factors 17 p3044 A70-35055
- Antenna arrays with nonuniform spacings, synthesizing radiation patterns by deterministic and statistical density taper methods 17 p3044 A70-35056
- Continuous line source, array or aperture antennas of linear rectangular or circular shape, discussing radiation patterns synthesis methods 17 p3044 A70-35057
- Cylindrical antennas and arrays for transmission or reception, determining radiation patterns 17 p3051 A70-35059
- Thin long dipole antenna, determining input admittances, current and charge distributions and field patterns by Wiener Hopf technique 17 p3051 A70-35060
- Circular loop antenna for transmission and reception, determining current distribution, admittance and radiation field by integral equation 17 p3051 A70-35061
- Boundary value problems for symmetrically excited biconical antennas surrounded by free space, treating spherical and thin wire antennas 17 p3044 A70-35062
- Prolate and oblate wave functions for EM radiation from spheroidal antenna in surrounding inhomogeneous medium 17 p3044 A70-35063
- Radiation patterns and impedance properties of slot antenna in ground plane, slot on cylinder and sphere and waveguide slot arrays 17 p3051 A70-35064
- Open waveguides and small horns theory, using Wiener Hopf method for radiation calculation 17 p3051 A70-35065
- Collection of papers on antenna theory covering reflector, lens, traveling wave, leaky wave, surface wave, log periodic antennas, etc 17 p3051 A70-35066
- Traveling wave antennas, analyzing modal characteristics of various waveguiding structures 17 p3052 A70-35070
- Leaky wave antennas, deriving radiation field distribution in terms of power leakage from interior by Sommerfeld integral and Kirchhoff-Huygens integration 17 p3052 A70-35071
- Surface wave antennas, operated on guided wave mode parallel to interface and with radiation at discontinuities, calculating excitation and radiation characteristics 17 p3052 A70-35072
- Log periodic antennas, discussing dipole array and planar sheath spiral structures, base current and far field pattern calculations, etc 17 p3052 A70-35073
- Boundary value problem of Hertzian dipole antenna in presence of conducting half space, analyzing lossy earth effects on input impedance and radiation pattern 17 p3044 A70-35074
- Infinitesimal electric and magnetic dipoles embedded in lossy media, investigating earth effect on electromagnetic field 17 p3045 A70-35075
- Antennas in plasma, investigating electromagnetic and electroacoustic waves and boundary value approach 17 p3045 A70-35076
- Flush mounted lightweight antennas for rockets, discussing construction radiation patterns, input impedance, etc 17 p3053 A70-35273
- Highly directive radio telescope antenna parameters in near zone, using focusing at minimum distance 17 p3055 A70-35679
- Linear phased antenna arrays, calculating influence of interaction between radiating elements on radiation pattern 17 p3048 A70-35686
- Statistical directivity, radiation pattern, drift and dispersion of segmented traveling wave antennas 17 p3055 A70-35687
- Multiple narrow beam antenna system with plasma column and electromagnetic wave ring source, discussing radiation pattern and electronic scannability 18 p3294 A70-36346
- Pencil beam synthesis for large circular array with arbitrary number of directive elements, determining optimum excitations 18 p3227 A70-36476
- Funnel shaped vector radiation pattern realized by synthesizing axisymmetric distribution of elliptically polarized currents on body of revolution 19 p3392 A70-37277
- Linear and circular apertures sum and difference radiation patterns for minimum sidelobes power 19 p3375 A70-37280
- Current distribution method for inverse problem of antenna theory, producing radiation pattern 19 p3385 A70-37437
- Radiation patterns Hilbert spaces for solving inverse problem of antenna theory 19 p3386 A70-37438
- Antenna radiation patterns dependence on functional spaces in inverse problem of linear antenna theory, using calculus of variations 19 p3386 A70-37439
- Traveling wave antenna array single lobe design using mode charts to reduce errors 19 p3376 A70-37688
- Power flow patterns of near to far field transition of scalar wave pencil beam without reference to specific radiating structure 19 p3536 A70-37703
- Rectangular waveguide EM radiation into plane parallel region through asymmetrical longitudinal slot 19 p3386 A70-37727
- Impedance measurements on microwave tripole antenna for circular polarization, including expressions for radiation pattern 19 p3388 A70-37868
- Center fed cylindrical half wavelength dipole antenna, computing radiation pattern by trigonometric expansion approximation for current distribution 19 p3388 A70-37869
- Experimental model for random phase errors caused by surface irregularities in paraboloid reflector antennas 19 p3388 A70-37927
- Far field diffraction, radiation and gain of wide flare angle corrugated conical horns 19 p3389 A70-37970
- Wire antennas array analysis and beam pattern synthesis by method of moments, considering application to electromagnetism compatibility 19 p3380 A70-38178
- Dipole antenna radiation in compressible anisotropic electron plasma overlying imperfectly conducting half space, solving for lunar environment 19 p3381 A70-38407
- Dipole antenna radiation in compressible anisotropic electron plasma overlying imperfectly conducting half space, evaluating Fourier-Bessel integrals for lunar environment 19 p3381 A70-38408
- Sun role in radio telescope radiation patterns analysis and adjustment, allowing for solar radio source finite dimensions and nonuniform brightness 19 p3390 A70-38560
- Algorithm for radio telescope antenna pattern reconstruction from solar transit and radiation distribution data 19 p3390 A70-38561
- Dielectric rod and Yagi antennas radiation mechanism, determining pattern, gain and effective aperture 20 p3585 A70-39398
- X band electromagnetic horn antennas, measuring triangular shape dielectrics effects on radiation pattern 20 p3599 A70-40312
- Microwave aperture antenna in finite size ground plane, calculating radiation pattern distortion by superposition of boundary value and wedge diffraction solutions 20 p3599 A70-40314
- Dolph-Pritchard technique limitations for transformation of array factor into Chebyshev polynomial as related to element spacing for single lobe endfire arrays 20 p3599 A70-40315
- Short cylindrical microwave antenna radiation directivity enhancement by optimum double impedance loading 20 p3599 A70-40318
- Two dimensional impedance horn antennas synthesis by aperture field distribution and radiation pattern configuration relationship, deriving energy balance equation 20 p3600 A70-40460
- Microwave antenna near field patterns analysis by spherical harmonic expansion, discussing validity conditions and convergence 21 p3796 A70-40556
- Aperture antenna pattern beamwidth decrease in near field with increasing scan angle 21 p3796 A70-40559
- Antenna radiation pattern analysis by application of Kirchhoff and Weber integrals, noting choice of complex radial wavenumber consistent with radial field decay 21 p3796 A70-40560
- Analog computer for one dimensional antenna array simulation, discussing radiation pattern calculation and display 21 p3796 A70-40621
- Multiple beam antenna system for regional communications satellite directing high radiated power toward specific earth areas 21 p3790 A70-41358
- Circular array radar antenna, describing feed systems, scanning switches and radiation patterns 21 p3799 A70-41360
- Periodically modulated corrugated surface array for application as phase-frequency scanning aerial, deriving design equations for comparison with radiation characteristics measurements 21 p3800 A70-41944
- Unidirectional tear drop radiation Archimedean spiral broad band frequency independent antenna using printed circuit with cavity 21 p3801 A70-42246
- Linear antenna radiation pattern broadening due to atmospheric turbulence 22 p3995 A70-42386
- Antennas with controlled current distribution in medium wavelength range for optimal radiation pattern over desired area, discussing maximum gain tuning for daytime and nighttime operation 22 p3995 A70-42521
- Cylindrical slot antennas radiation patterns in plane perpendicular to axis, discussing field emission and angular position of each slot for phase multiplier 22 p3997 A70-43131
- Log periodic dipole antenna arrays, calculating HF performance and patterns in presence of ground 22 p3997 A70-43176
- Antenna polarization and terrain depolarization effects on radar ground return, calculating echo pulse from smooth and rough terrains 22 p3990 A70-43327
- Current distribution and near field of cylindrical antennas loaded with built-in lumped elements 22 p3998 A70-43422
- Resolution limits and corresponding linear antenna apertures in presence of propagation phase errors, considering pattern angle 22 p3991 A70-43581
- Antenna far/near field correlation, noting measurement accuracy role 23 p4160 A70-43769
- Secondary source distribution of EM field induced on ground-air interface by antenna 23 p4161 A70-43773
- Antenna radiation pattern modeling by power optimization under constraints 23 p4175 A70-44800
- Step-scanned circular array radar antenna for operation over 20 percent bandwidth, discussing design, radiation patterns and performance advantages 23 p4175 A70-44951
- Annular aperture /slot/ antenna driven by coaxial line, calculating input admittance and complete near field radiation distribution 23 p4176 A70-44954
- Broadside-endfire array of cylindrical dipoles and monopoles driven by interconnecting transmission lines, calculating admittance and field patterns 23 p4176 A70-44955
- Monopulse tracking antenna beam broadening by feed displacement defocusing in parabolic reflector 23 p4165 A70-44956
- N-arm spiral or conical antenna radiation patterns calculation for sigma and delta excitations, using bicomplex functions 23 p4176 A70-44965
- Two monopole antennas on perfectly conducting sphere, calculating radiation pattern by numerical technique 23 p4165 A70-44968
- Planar conducting screen with periodic rectangular perforations, determining transmission and reflection coefficients and aperture field distribution 24 p4311 A70-45219
- Elevated horizontal and vertical electric dipole VLF fields, discussing ionospheric TE and TM mode coupling, nighttime variations and amplitude fluctuation 24 p4314 A70-46131
- Optimum performance of corrugated waveguide feed horns for paraboloid reflector antennas via radiation pattern shaping with digital computer 24 p4320 A70-46222

ANTENNAS

- NT AIRCRAFT ANTENNAS
- NT CASSEGRAIN ANTENNAS
- NT CYLINDRICAL ANTENNAS
- NT DIPOLE ANTENNAS
- NT DIRECTIONAL ANTENNAS
- NT HELICAL ANTENNAS
- NT HORN ANTENNAS
- NT LENS ANTENNAS
- NT LOG PERIODIC ANTENNAS
- NT LOOP ANTENNAS
- NT MICROWAVE ANTENNAS
- NT MISSILE ANTENNAS
- NT MONOPOLE ANTENNAS
- NT MONOPULSE ANTENNAS

NT MULTIPLE BEAM INTERVAL SCANNERS
 NT OMNIDIRECTIONAL ANTENNAS
 NT PARABOLIC ANTENNAS
 NT RADAR ANTENNAS
 NT RADIO ANTENNAS
 NT RHOMBIC ANTENNAS
 NT SATELLITE ANTENNAS
 NT SLOT ANTENNAS
 NT SPACECRAFT ANTENNAS
 NT SPIRAL ANTENNAS
 NT STEERABLE ANTENNAS
 NT TWO REFLECTOR ANTENNAS
 NT WAVEGUIDE ANTENNAS
 NT YAGI ANTENNAS

Transistorized lightning protected VHF ground antenna for air traffic communication providing high operational safety standards

03 p0459 A70-14297
 Direction finding characteristics of nonlinear antenna, including current determination and optimal angle for sidelevel level

06 p1023 A70-18561
 Short wave signal field strength measurement errors by frame antenna, outlining correction procedure

11 p2303 A70-25552
 Book on antennas and waves covering EM radiation, configurations, insulation, dissipative media, coupling, transmission lines, etc

12 p2194 A70-27095
 Active antennas definition with integrated, amplifying electronic components based on designations in two port theory

13 p2376 A70-28897
 Shot noise effect in antennas to measure electric charge density fluctuations in plasma, noting thermal equilibrium with Maxwellian distribution function

13 p2371 A70-29920
 Laser mode matching to obscured circular aperture of optical telescope system in terms of antenna gain

16 p2929 A70-33982
 Collection of papers on antenna theory, part I covering EM fields, radiation sources and patterns, etc

17 p3043 A70-35051
 Collection of papers on antenna theory covering reflector, lens, traveling wave, leaky wave, surface wave, log periodic antennas, etc

17 p3051 A70-35066
 Antennas in plasma, investigating electromagnetic and electroacoustic waves and boundary value approach

17 p3045 A70-35076
 Antennas impedances in warm isotropic plasma, using hydrodynamic and kinetic /Vlasov/ equations

19 p3380 A70-38406
 Source antenna range length and aperture diameter, discussing length, frequency, aperture size and free space conditions

21 p3784 A70-40563
 Short wave signal field strength measurement errors by frame antenna, outlining correction procedure

21 p3786 A70-41302
 Asymptotic solution for thick linear antenna admittance

23 p4171 A70-43882
 Equation for antenna noise temperature calculation

23 p4165 A70-44967

ANTHRACENE

Anthracene, polystyrene and stilbene for scintillation counters measuring cosmic ray protons, analyzing dosimetric properties

17 p3151 A70-35352

ANTHROPOMETRY

Somatometry development, concepts and practice, discussing landmarks search and anthropometric instruments

04 p0643 A70-14980
 Differential sphygmogram of young men, determining lean body mass on basis of anthropometrical data

21 p3763 A70-41229
 Body composition and weight changes estimation after physical exercise by prediction equations based on skinfold and girth measurements

21 p3766 A70-42155

ANTIRCRAFT MISSILES

Approximate time solutions to light antiaircraft projectiles velocity, altitude angles, gravity drop and downrange, reducing differential equations of motion to dimensionless forms

04 p0764 A70-15592
 Guided weapons management techniques applied to Rapier light weight antiaircraft weapon system

08 p1601 A70-21037

ANTIBIOTICS

NT STREPTOMYCIN

ANTIBODIES

NT GAMMA GLOBULIN

Autoimmunity to heart tissues in cardiac diseases, reviewing immune mechanisms in rheumatic fever, postcardiomy and postinfarction syndromes

01 p0016 A70-10438
 Local stress effect on immunocompetent cells differentiation in guinea pigs lymphatic ganglia, noting increase in number of antibody producing cells

05 p0803 A70-17114

Hypokinesia effects on cellular and humoral indices of antibody formation in rats, noting exposure time role

07 p1208 A70-19509

Hypokinesia effects on cellular and humoral indices of antibody formation in rats, noting exposure time role

11 p1988 A70-26108

ANTICOAGULANTS

Heparin role in anticoagulant therapy for myocardial infarction based on proved application to other venous thrombotic diseases, noting hemorrhagic complications controllability

04 p0636 A70-15465

ANTICYCLONES

Atmospheric circulation two level quasi-geostrophic model, examining dynamic large scale features of baroclinic wave blocking by high latitude cold anticyclonic cells

20 p3621 A70-39372

Air circulation upper stratosphere, investigating summer stratospheric anticyclone evolution

22 p4066 A70-43378

VHF and UHF radio field strength changes due to tropospheric reflecting layers disintegration during anticyclonic weather, using ray tracing technique

24 p4315 A70-46153

ANTIDIURETICS

Vasopressin antidiuretic hormone effects on evaporative body weight loss during heat exposure

01 p0020 A70-10516

Antidiuresis associated with oral cavity stimulation during food ingestion by rats

13 p2355 A70-29813

ANTIDOTES

Antihypoxic preparations protective effect on white mice and rats subjected to gravitational accelerations

03 p0425 A70-13890

ANTIFERROELECTRICITY

Doubly excited antiferroelectrics absorption spectrum band and bound states, discussing zero approximation 0-0 transitions of alpha oxygen molecules and permeability tensor

24 p4392 A70-46362

ANTIFERROMAGNETISM

Magnon energy theory for temperature dependence of ferrous and magnesium fluorides antiferromagnetic- resonance frequency, sublattice magnetization and magnetic specific heat

09 p1739 A70-22324

Shift in nuclear magnetic resonance, investigating transferred hyperfine coupling near Neel temperature for magnetic and nonmagnetic systems

10 p1928 A70-24827

Nonlinear spin wave theory for anisotropic antiferromagnetism, solving sublattice magnetization by thermodynamic Green function for temperature dependence

11 p2097 A70-25617

Antiferromagnetic resonance measurement in manganese difluoride as function of microwave frequency, sample size and shape

21 p3850 A70-41908

Anisotropic Heisenberg antiferromagnet theory, developing nonlinear spin-wave approximation

24 p4388 A70-45131

Antiferromagnetic and ferrimagnetic resonance frequencies, determining temperature dependence by spin wave theory

24 p4388 A70-45132

ANTIFREEZES

Fuel filter icing prevention by injecting antifreeze into filter instead of fuel

06 p0988 A70-17873

ANTIFRICTION BEARINGS

NT BALL BEARINGS

NT ROLLER BEARINGS

Material evaluation and selection for compact nuclear reactor control bearings operating at high temperature in vacuum

[ASME PAPER 69-WA/LUB-11]

Calculus of variations used for determining optimum one dimensional MHD slider bearing with bounded control variables

[ASME PAPER 69-WA/LUB-2] 04 p0698 A70-14771

Optimum one dimensional Rayleigh gas slider bearing, calculating step location, pressure and load capacity for range of bearing numbers

[ASME PAPER 69-WA/LUB-1] 04 p0698 A70-14772

Bearing capacity increase due to large viscoelastic or normal stress effects in lubricants, obtaining exact results for noncavitating plane slider bearings

08 p1507 A70-21476

Soviet book on bearing capacity of turbomachine rotor elements covering testing methods, stress analysis, design factors on stability, etc

14 p2658 A70-30958

Computerized design of multipad and multirecess incompressible fluid film bearings

15 p2744 A70-31958

High speed and long life bearings and dampers for future jet engines, considering design factors

[SAE PAPER 700318] 18 p3263 A70-36800

Optimum one dimensional Rayleigh gas slider bearing, calculating step location, pressure and load capacity for range of bearing numbers

[ASME PAPER 69-WA/LUB-1] 19 p3436 A70-37617

Calculus of variations used for determining optimum one dimensional MHD slider bearing with bounded control variables

[ASME PAPER 69-WA/LUB-2] 19 p3436 A70-37620

Dual spin spacecraft bearing assembly flexibility effects on attitude stability

[AIAA PAPER 70-1043] 19 p3533 A70-38858

Parallel circular squeeze film bearing, calculating Newtonian fluid inertia effect on lubrication by perturbation solution

[ASME PAPER 70-LUBS-9] 22 p4045 A70-42451

ANTIGENS

Postnatal increase of immunologic competence to sheep RBC antigen in germ free and conventionally reared mice

01 p0000 A70-11310

Antigens existence shared by human blood serum and proteins of erythrocyte stroma established through RAHS absorption by stroma and subsequent microimmunoelectrophoresis of serum

15 p2687 A70-32900

Antigens immunological response during myocardial infarction

20 p3570 A70-39151

Biochemistry of blood group antigens involved in agglutination reactions, discussing effect of proteolytic enzymes on cell membrane structure

21 p3764 A70-41447

ANTIGRAVITY

Antigravitation suit effects on rheoencephalography changes during Valsalva maneuver and horizontal-passive orthostatism transition in humans

07 p1212 A70-19738

G suit application to clinical therapeutics, noting intraabdominal bleeding control

21 p3767 A70-40737

ANTIHYPERTENSIVE AGENTS

Hypotensive effects of chlorthalidopoxide, amobarbital and chlorpromazine on behaviorally induced elevated arterial blood pressure in squirrel monkey

24 p4298 A70-45620

ANTICING ADDITIVES

Flight tests conducted in artificial and natural icing conditions, using CH-3C helicopter with rotor blades equipped with polyethylene anticling tape

01 p0006 A70-10695

Fuel filter icing prevention by injecting antifreeze into filter instead of fuel

06 p0988 A70-17873

ANTIMATTER

NT ANTINEUTRINOS

NT ANTIPARTICLES

NT POSITRONS

Symmetric cosmologies within gamma ray measurement context showing antimatter limits in Milky Way and metagalaxy

02 p0371 A70-12196

Correlation between atmospheric meteor entry and gamma and neutron radiation intensity verifying micrometeor antimatter hypothesis

03 p0454 A70-13528

Satellite recording of electron-positron annihilation gamma emission on Cosmos 135 artificial earth satellite relating to meteors antimatter nature

07 p1371 A70-20334

Antimatter motion in solar system and earth atmosphere, discussing vaporization and annihilation energy in collisions with interplanetary gas atoms

11 p2119 A70-26793

Quantum electronic space vehicle, discussing time reversing motor or inverse /anti-/ atomic engine

17 p3148 A70-35213

Antimatter distribution in universe, investigating mass lower limit

19 p3518 A70-38025

Antimatter detection and interaction with matter on moon, discussing radiation from electron- positron annihilation processes

19 p3521 A70-38482

ANTIMISSILE DEFENSE

SAFEGUARD ballistic missile defense radars, discussing terminal defense concept, data processing system and microwave components

11 p2005 A70-26162

Safeguard defense system against strategic ballistic missiles, discussing Nike X program, PAR and MSR radars and Spartan and Sprint system

15 p2810 A70-32247

ANTIMISSILE MISSILES

U.S. Safeguard plan suitability as hardpoint missile defense system, discussing technical controversy over Sentinel components

04 p0760 A70-14502

ANTIMONIDES

NT CADMIUM ANTIMONIDES

NT CESIUM ANTIMONIDES

NT GALLIUM ANTIMONIDES

NT INDIUM ANTIMONIDES

Thin film BiSb-oxide-BiSb tunneling junction I-V characteristics anomalies as function of temperature, magnetic field and bias voltage

24 p4390 A70-45662

ANTIMONY ALLOYS

- Bi-Sb alloys, discussing structural data, crystal preparation, band structure, pressure, nonohmic conductivity, thermoelectric, thermomagnetic and magnetothermal effects 14 p2625 A70-30332
- Cooled antimony-cesium film photoelectric effect for weak luminous flux, examining electronic camera reciprocity 19 p3427 A70-38175

ANTIMONY COMPOUNDS

- NT ANTIMONIDES
- NT CADMIUM ANTIMONIDES
- NT CESIUM ANTIMONIDES
- NT GALLIUM ANTIMONIDES
- NT INDIUM ANTIMONIDES
- Glass formation region of chalcogenide semiconductor arsenic triselenide-antimony triselenide system and vitreous-crystalline transformation, investigating electrical and optical properties 01 p0153 A70-10085
- Vapor composition and condensed phase structure of As and Sb compounds with group VIa elements analyzed by laser mass spectrometer 08 p1455 A70-21339

ANTINEUTRINOS

- Experimental observations of neutrino in collapsing stars in Galaxy, showing detector capability of recording positrons or electrons from antineutrino-neutrino flux induced reactions 05 p0900 A70-15966
- Earth central region chemical exploration using antineutrino flux produced by natural radioactive isotopes 09 p1761 A70-22985
- Collapsing or neutronizing stars detection by recording neutrino and antineutrino flux, calculating antineutrino-deuteron interaction cross section and positron energy and angular distribution 20 p3698 A70-39302
- Scale invariance models correlation with cosmic ray data, comparing neutrino- and antineutrino- nucleon scattering 23 p4210 A70-43800

ANTIOXIDANTS

- Radioprotective action of pyridine derivatives in monkey heart and human epithelium cells exposed to gamma radiation evaluated by dioxyphenyl alpha-alanine oxidation 03 p0418 A70-13303

ANTIPARTICLES

- NT ANTINEUTRINOS
- NT POSITRONS
- Particle-antiparticle creation in galactic nuclei, expelling particles while retaining antiparticles 02 p0371 A70-12195

ANTIPODES

- HF radio waves propagation between antipodal transmitter and receiver, discussing diurnal variations and reception over polar caps and water 01 p0045 A70-11103
- Einstein-Friedman cosmology of vanishing constants assumed in deducing relations between antipodal radio sources red shifts and universe parameters 01 p0187 A70-11274
- Lowest useful frequency /LUF/ prediction on long distance quasi-antipodal circuit, considering E layer blanketing 07 p1232 A70-19178

ANTIRADIATION DRUGS

- Topically administered vitamin A radioprotective effect on postradiation skin reactions 01 p0029 A70-11402
- Radiation protective action of aminoalkylthiols, aminoalkyl disulfides, isothioureas, thiazolidine, etc, in mouse tissues, erythrocytes and yeast cells exposed to X ray doses 03 p0419 A70-13307
- Radiation protective action of cystamin, cysteamine and aminoethyl in mice, noting equal decreases in redox potential 03 p0419 A70-13310
- Dithiols protective effect against ionizing radiation in mice, noting oxygen pressure drop role 03 p0420 A70-13311
- Antiradiation chemical substances for modifying radiation damage in peas during seed irradiation with fast neutrons 07 p1208 A70-19510
- Thymidine tracer distribution in bone marrow chromosomes of rats and mice treated with radioprotectors, noting cell metabolic activity reduction by sulphydryl-type radioprotectors 09 p1619 A70-22818
- Cholinegous muscarine-mechanism participation in radioprotective effect after cholinomimetics administration, reducing protective reactions against tissue irradiation and increasing mice survival rate 09 p1624 A70-22820
- Antiradiation chemical substances for modifying radiation damage in peas during seed irradiation with fast neutrons 11 p1988 A70-26109

ANTISERUMS

- Anticerebral cytotoxic serum effect on white rats conditioned reflex activity 07 p1199 A70-18727

ANTISUBMARINE WARFARE

- Airborne computer system program for antisubmarine warfare enhancing human element in man machine system 06 p1185 A70-17974
- Tactical aid displays /TAD/ for lightweight multisensor airborne ASW localization missions, discussing mission planning, avionics design, operator direction airborne tactical decision structures, etc [AIAA PAPER 70-517] 13 p2407 A70-29036
- Airborne integrated computerized ASW system, describing navigation, flight control, display and sensor subsystems 21 p3821 A70-40575
- NT CL-84 AIRCRAFT
- S-3A carrier based ASW weapons system, discussing onboard equipment, navigation, avionics integration, etc [AIAA PAPER 70-882] 17 p3018 A70-35802
- ANTISYMMETRY
- Supersonic flow separation at antisymmetrical delta wing edges, noting eddy layer and vertical velocity fields effects on aerodynamic characteristics 02 p0224 A70-12625
- Integral equations for antisymmetric shallow shell stress-strain state with crack, obtaining asymptotic solution in form of power series 03 p0591 A70-13420

ANTITANK MISSILES

- Antitank guided missiles guidance and control systems using optical tracking 01 p0139 A70-11261
- ACRA supersonic antitank missile with IR laser beam guidance system 22 p4110 A70-43212

ANXIETY

- NT FEAR OF FLYING
- Interindividual reaction time using target speed anticipation test and relationship with manifest anxiety scale 04 p0643 A70-14978
- Anxiety-stress effects on pilot performance in execution of acquisition tracking task minimized by training 06 p1003 A70-18016
- Pilots anxiety in military milieu during interviews and questionnaires noting effect on proficiency 12 p2179 A70-27051

AORTA

- Aortic distensibility and instantaneous left ventricular volume estimation in living man based on elastic reservoir theory and circulatory system model 01 p0040 A70-11372
- Canine aortic flow as function of simultaneous mean aortic and mean right atrial pressures 02 p0233 A70-11723
- Valvular aortic stenosis severity estimation using digital computer program and tape recorder for determining valve area 02 p0243 A70-12094
- Doppler flowmeter-catheter system to record aortic flow velocity in man during cardiac arrhythmias, considering atrial fibrillation, heart block, etc 02 p0241 A70-12697
- Hemodynamic determinants of gallop sounds in patients with aortic valve disease based on clinical, hemodynamic and angiographic observations 04 p0633 A70-15308
- Posthypoxic vasodilation in extremities of anesthetized dogs preserved after carotid and aortic reflexogenic zones exclusion 07 p1204 A70-19139
- Normal and stenosed aortic valve closure wing measurements in model valve in pulsatile water tunnel showing turbulence generation 07 p1220 A70-19249
- Traumatic rupture of aortic arch and descending thoracic aorta resulting from abrupt linear body deceleration 07 p1206 A70-19295
- Phasic aortic blood flow and left ventricular pressure measured at constant heart rates during pulsus alternans, discussing ejection duration and peak flow rate 07 p1210 A70-19588
- Diastolic and equivocal fluttering of mitral valve in aortic insufficiency by echocardiography 09 p1615 A70-22209
- Shock waves in unsteady aortic blood flow at systole beginning, considering aorta elastic properties and shock formation distances 11 p1992 A70-26479

- Blood velocity in ascending aorta in man by transcutaneous ultrasonic Doppler technique, investigating heart hemodynamic performance and systemic perfusion 21 p3770 A70-41235
- Flight crews with aortic insufficiency, observing hemodynamically insignificant valvular defect 21 p3771 A70-41492

- Aortic regurgitated flow estimation by dye injection technique, noting correlation with cineangiocardiology method 22 p3977 A70-42301
- Morphology of adult mammalian thoracic and abdominal aortic segments indicating deviation from medial lamellar architecture 24 p4298 A70-45801

APACHE ROCKET VEHICLE

- Magnus effects on Apache sounding rocket at supersonic speeds, discussing spinning model and static tests [AIAA PAPER 70-207] 06 p1157 A70-18103

APATITES

- U CALCIUM PHOSPHATES
- U MINERALS

APERIODIC FUNCTIONS

- Liapunov functions synthesis for aperiodic linear systems by inspecting traces of state matrix and products 17 p3129 A70-34955

APERTURES

- NT IRISES [MECHANICAL APERTURES]
- Radiation patterns containing multiple beams generated by aperture phase control 01 p0050 A70-10462
- Focal length-to-aperture ratio for maximizing collection of scattered light at right angles to illuminating laser beam used in Raman spectroscopy 02 p0311 A70-11888
- Maximum power transfer theorem, discussing rotation symmetry with respect to optic axis and confocal optical resonators 02 p0339 A70-12454
- Electromagnetic plane wave diffraction by slit and circular apertures in nonplanar conducting screens, presenting equiradiance contour maps 02 p0340 A70-12455
- Target velocity effects on resolution of synthetic aperture side-looking radar 02 p0268 A70-12582
- Synthetic aperture airborne side-looking radar using coherent optical data processor, discussing system configuration and operation 02 p0263 A70-12632
- Rapid fading intensity distribution formula for analysis of aperture phase and amplitude errors influence on antenna arrays directional characteristics 03 p0456 A70-13463
- Circular cylindrical shell stressed state with rectangular opening under compressed torsion, noting opening effect on loads nonuniform distribution 03 p0593 A70-13501
- Aperture electric field bounds presented for TE, TM and TE/TM excitation over azimuthally symmetric slotted cylinder subject to constraint of specified radiated power 04 p0649 A70-14969
- Aperture dissection scheme to reduce transit time of Bragg angle acousto-optical scanning of laser beam 05 p0860 A70-16657
- Variational principle used in microwave breakdown predictions for rectangular aperture antenna 05 p0824 A70-16988
- Cylindrical confocal laser resonator with circular coupling aperture in center of mirror calculated for diffraction losses by numerical iteration 06 p1079 A70-17187
- Electromagnetic radiation patterns from aperture in conducting cylinder coated with moving isotropic plasma sheath, noting sheath velocity and plasma frequency influence 06 p1020 A70-17564
- Telescope resolution limit dependence on refractive index mean square fluctuation and effective aperture in turbulent medium 06 p1067 A70-18396
- Stellar scintillation saturation at large zenith angles interpreted in terms of combined dispersion and aperture filtering 09 p1726 A70-22073
- Electrical and magnetic polarizability coefficients in theory of diffraction at small apertures by formulating bilateral variational principles 09 p1631 A70-22150
- Polygonal-aperture antennas side radiation distribution 09 p1648 A70-23153
- Diffraction effects for bilinear screen with irregular apertures determined using correction weighting function for solution 09 p1639 A70-23668
- Circular confocal laser with coupling aperture in mirror for maximum power output in specified mode, calculating field distributions and diffraction losses at reflectors 10 p1900 A70-24941
- Corrugated waveguide structures for aperture type feeds for spherical and paraboloidal reflector antennas, discussing experiments on 2-hybrid mode horn 11 p2018 A70-26024
- Microwave illuminated aperture near radiation field mapped and processed for microwave hologram suitable for optical imaging for far field pattern simulation 11 p2051 A70-26025

- Aperture synthesis and spectral antenna characteristics in radio astronomy, considering Ryle systems, Mills-Christiansen crosses and variable interferometers 11 p2019 A70-26801
- Nonlinear synthesis for direction-finding plane antenna aperture 11 p2020 A70-26814
- Plane wave three dimensional diffraction through circular aperture in infinite screen computed for normal incidence, using Babinet principle 12 p2197 A70-27951
- Optimum distribution over circular aperture in ground plane for best mean square approximation to specified radiation pattern 12 p2197 A70-27952
- Simulated isotropic lossless plasma radiating apertures located on nonplanar models, relating results to antenna radiation patterns 12 p2282 A70-27969
- Aperture field modal decomposition of optical system in terms of integral equation eigenfunctions during detection and estimation of incoherent objects 12 p2273 A70-28121
- Microwave transmission through thin film screens with apertures placed in transverse plane of X band rectangular guides 12 p2202 A70-28164
- Plane multielement antenna field statistics as function of correlated phase-amplitude aperture errors 13 p2378 A70-29306
- Book on synthetic aperture radar imaging systems theory and design covering SNR, optical data processing, phase and motion errors, ambiguity function, etc 13 p2368 A70-29603
- Stress concentration around oblique circular cylindrical apertures in steel plates [SESA PAPER 1533] 15 p2820 A70-32306
- Asymmetric phase error in antenna circular apertures, emphasizing beam squint resulting from distortion of paraboloidal reflector 16 p2859 A70-32942
- Paraboloidal reflectors aperture fields from stereographic mapping of feed polarization pattern, illustrating electric and magnetic dipoles and Huygens sources 16 p2871 A70-32962
- Phased arrays universal figure of merit, including aperture efficiency, sidelobe level, scanning frequency and noise temperature 16 p2864 A70-33482
- Laser mode matching to obscured circular aperture of optical telescope system in terms of antenna gain 16 p2929 A70-33982
- Aperture size effect on frequency shift and frequency width variation of beat signals observed with laser Doppler velocity meter 19 p3428 A70-38502
- Diffraction effects on radiometer field of view with rectangular primary and secondary apertures and field stop 20 p3627 A70-39087
- Optical aperture tapering for attenuating sidelobe impairing LF signals detection 20 p3639 A70-39089
- Dielectric rod and Yagi antennas radiation mechanism, determining pattern, gain and effective aperture 20 p3585 A70-39398
- Radiation divergence from gas laser resonator with coupling aperture 20 p3642 A70-39752
- Quantitative measurement of solar limb image motion and blurring, noting role of telescope aperture 20 p3634 A70-40424
- Resolution limits and corresponding linear antenna apertures in presence of propagation phase errors, considering pattern angle 22 p3991 A70-43581
- Aperture synthesis and spectral antenna characteristics in radio astronomy, considering Ryle systems, Mills-Christiansen crosses and variable interferometers 24 p4311 A70-45176
- Nonlinear synthesis for direction-finding plane antenna aperture 24 p4311 A70-45186
- Highspeed raster motion picture cameras with high aperture ratios 24 p4335 A70-45651
- APNEA**
- U RESPIRATION**
- APOGEES**
- Moon perigees and apogees for years 1-3000, tabulating parameters for calculations 08 p1568 A70-20635
- ELGO launcher system with apogee booster for placing payload in geostationary orbit 13 p2505 A70-28768
- Gyroscopically stabilized solid propellant apogee motor for experimental satellite of CECLES/ELDO Europa 2 program 23 p4235 A70-45018

APOLLO APPLICATIONS PROGRAM**NT APOLLO TELESCOPE MOUNT**

- Earth resources applications of Apollo 6 photography, describing camera system and photographic coverage 03 p0474 A70-13672
- Apollo Telescope Mount Extra Vehicular Activity system for Apollo Applications Program [ASME PAPER 69-WA/BHF-16] 04 p0761 A70-14857
- Environmental control of Apollo applications program orbital assembly, analyzing thermal and life support systems [SAE PAPER 690622] 05 p0922 A70-15847
- Apollo 11 laser ranging retro reflector measurements from McDonald Observatory confirming thermal design analysis performance prediction 06 p1011 A70-18482
- Human factors data standardization in NASA Apollo Applications Program for computer data processing 09 p1623 A70-22295
- Apollo Applications Program command and service module test requirements to achieve reliable hardware for extended missions [AIAA PAPER 70-378] 10 p1952 A70-24925
- Spent Saturn S-4B stage conversion into orbital workshop in Apollo Applications Program 11 p2122 A70-26044
- Solar X rays observation from manned orbiting workshop of Apollo Applications Program, describing telescope/camera assembly and X ray event analyzer 11 p2057 A70-26506
- Apollo program and outline of objectives of applications program 17 p3167 A70-35202
- Earth resources data from man operated airborne/spaceborne sensors and data handling systems, examining Apollo Applications Program 20 p3616 A70-39056
- Orbital photography interpretation from test rockets and Apollo-Gemini spacecraft, considering environmental applications 20 p3634 A70-40321
- European avionics role in Post Apollo program, noting space shuttles, space tugs, space stations and modules 22 p3999 A70-43501
- European wind tunnels suitable for Post Apollo Program aerodynamic testing, presenting detailed tabulated information on available facilities 22 p4007 A70-43503
- APOLLO FLIGHTS**
- NT APOLLO 6 FLIGHT
- NT APOLLO 7 FLIGHT
- NT APOLLO 8 FLIGHT
- NT APOLLO 9 FLIGHT
- NT APOLLO 10 FLIGHT
- NT APOLLO 11 FLIGHT
- NT APOLLO 12 FLIGHT
- NT APOLLO 13 FLIGHT
- Human response in Apollo flights emphasizing astronauts food, water, waste management, physical examination, preventive medicine problems, etc 02 p0239 A70-12669
- Secondary electron conduction TV camera tube with three color filter wheel for Apollo missions 03 p0493 A70-14025
- Relative reflectivity of lunar landing site Apollo 7 compared to site Apollo 2, showing compositional and mineralogical differences 04 p0751 A70-15059
- Apollo translunar and transearth orbit determination and navigation using ground and onboard systems [AIAA PAPER 70-27] 06 p1103 A70-18124
- Reentry targeting philosophy for Apollo missions emphasizing premission planning activities and real time targeting decisions, discussing Apollo 10 post-flight results [AIAA PAPER 70-28] 06 p1158 A70-18149
- Transposition and lunar docking simulation tests for Apollo 9 and subsequent missions using test vehicles equipped with flight type hardware [AIAA PAPER 70-170] 06 p1030 A70-18209
- Spacecraft reentry trajectory reconstruction using accelerometer and onboard navigation data from Apollo flights 13 p2485 A70-28378
- Human response in Apollo flights emphasizing astronauts food, water, waste management, physical examination, preventive medicine problems, etc 13 p2353 A70-29434
- Mission simulation testing in thermal vacuum environment for Apollo Lunar Module, noting conformal skin heaters [AIAA PAPER 69-991] 15 p2718 A70-32515
- Flight performance of Apollo LM descent-ascent propulsion systems, considering telemetry data, prediction correlation and modifications [AIAA PAPER 70-673] 16 p2967 A70-33577

- Lunar cratering rates from Apollo flights data on solidification ages for Mare Tranquillitatis 16 p2979 A70-34037
- Portable contingency transfer life support system for crewman of Apollo missions providing oxygen and cooling 20 p3580 A70-39441
- Transposition and lunar docking simulation tests for Apollo 9 and subsequent missions using test vehicles equipped with flight type hardware 20 p3606 A70-39685
- Mission Control Center and Apollo flight controller team, discussing personnel qualifications, equipment and individual evaluation 21 p3805 A70-41197
- Computer real time Apollo simulation, checkout and training system duplicating actual mission for flight controllers in Mission Control Center 21 p3805 A70-41198
- Decompression sickness relationship to physical exercise during simulated Apollo flight 24 p4307 A70-45336
- Light flashes observed by Apollo astronauts, proposing Cerenkov radiation or direct excitation of eye retina by cosmic rays 24 p4307 A70-45403
- APOLLO LUNAR EXPERIMENT MODULE**
- Localization of lunar acoustic energy, discussing long reverberation time measured at Apollo 12 site after module explosion 18 p3319 A70-37053
- Real time kalman filtering of Apollo LM/AGS rendezvous radar data [AIAA PAPER 70-957] 20 p3600 A70-39572
- APOLLO LUNAR SURFACE EXPERIMENTS PACKAGE**
- Apollo extravehicular mobility unit (EMU)/ system developed from Gemini EVA system with improved thermal control and mobility to support contingency extravehicular transfer in emergency 04 p0645 A70-15665
- Swiss Solar Wind Composition Experiment, analyzing trapped particles characteristics of Apollo 11 and 12 lunar exposed aluminum foil 11 p2105 A70-25950
- Apollo 13 lunar surface heat flow experiment to measure vertical temperature gradients as function of time and soil thermal conductivity 11 p2118 A70-26747
- Materials/design optimization of antenna-aiming mechanism deployed on moon by Apollo 12 astronauts to transmit ALSEP experiments data to earth stations 12 p2231 A70-27130
- ALSEP component configuration and deployment environment, describing passive thermal control system for data processing equipment 14 p2651 A70-31340
- ALSEP magnetometer mission and environmental requirements and mechanical design 16 p2914 A70-34152
- Mechanical design and mounting technique of Apollo 11 fused silica laser ranging retroreflector array at Tranquility Base 17 p3082 A70-34763
- Lunar surface local magnetic field measurement, describing Apollo 12 magnetometer 20 p3709 A70-40087
- Reflected ruby, laser pulses from Apollo 11 laser ranging retro-reflector /LRRR/ with telescope, measuring round trip travel time of light 21 p3912 A70-41638
- Apollo 11 passive seismic experiment package, discussing design, performance and various received signals 21 p3917 A70-41669
- Apollo lunar surface experiment package-SNAP 27 program, discussing mission profile, design and performance characteristics 22 p4071 A70-43194
- SNAP 27 thermoelectric generator for Apollo Lunar Surface Experiments Package /ALSEP/ 24 p4377 A70-46385
- APOLLO PROJECT**
- Apollo program navigation processing using Kalman optimal linear computer, emphasizing position vector and error matrix and command and lunar landing extrapolation module navigation 03 p0522 A70-13604
- Orbiter imagery analysis program for Apollo landing site selection, using photographic interpretive techniques 03 p0571 A70-13660
- Nonflammable material development program for Apollo spacecraft, noting requirements imposed by high oxygen environments, toxic offgassing and temperature range 03 p0436 A70-14055
- Materials selection and Apollo command module atmosphere design considerations, discussing fire extinguisher system, equipment design changes, etc 03 p0437 A70-14058
- Apollo/Saturn 5 Kennedy Launch Complex 39 /LC-39/ physical characteristics emphasizing high launch

rate capability, economy of operation and superior flexibility
[SAE PAPER 690714] 05 p0825 A70-15853

Spacecraft telecommunication and tracking systems in Gemini, Mercury and Apollo programs, emphasizing Apollo command and lunar modules equipment and mission ground stations
05 p0813 A70-16326

Apollo 10 and 11 photographs revealing probable igneous intrusions on lunar farside crater
06 p1137 A70-17195

Worldwide Apollo data transmission network emphasizing computer operations for message collection and distribution, command and telemetry processing, etc
06 p1005 A70-17310

Apollo reliability and quality requirements, reviewing changes due to cost reductions in space program
06 p1065 A70-17988

Return to earth abort capability for Apollo missions for various mission phases
[AIAA PAPER 70-94] 06 p1156 A70-18035

Apollo-Saturn Launch Vehicle Targeting Program for Lunar Landing Missions, describing functions of integrated digital computer programs
[AIAA PAPER 70-172] 06 p1145 A70-18093

Apollo 7 and 8 command modules TV camera systems design, considering additional function of public information
07 p1280 A70-19229

Apollo program low cost factors including engineering, management quality, reliability and inspection
[AIAA PAPER 70-241] 07 p1429 A70-20377

Thermocouple vacuum gauge joined to Apollo lunar sample return containers (JALSRC), describing two step welding procedure with transition cylinder
08 p1507 A70-21483

Apollo mission simulation, discussing Command Module Simulator (CMS/), onboard computer system and dynamic visual presentation via infinity- optics display
[SMPT PAPER 105-74] 09 p1655 A70-22226

Apollo lunar landing sites geological configuration and composition
09 p1759 A70-22772

Manned Spacecraft Center spacecraft development, mission design and planning, flight crew operations for Apollo, discussing spacecraft design principles
09 p1767 A70-23703

Apollo project hardware design and evaluation principles coupling simple design practice with stringent technical and administrative discipline
09 p1768 A70-23704

Qualification and testing procedures for Apollo Spacecraft Program components and systems, discussing vibration tests
09 p1693 A70-23705

Apollo crew procedures, simulation and flight planning, discussing navigation, guidance and control procedures
09 p1657 A70-23706

Apollo Program flight control operations personnel premission planning and training, discussing presolution of launch problems and emergencies
09 p1768 A70-23707

Apollo Program mission evaluation and flight anomalies team to identify and understand unforeseen peculiarities and systems problems during spacecraft mission
09 p1768 A70-23708

Spacecraft mission planning for trajectory control after establishing mission objectives, trajectory plan and crew timeline for Apollo flights
09 p1725 A70-23709

Apollo mission planning process, discussing flight schedule evolution from panels, meetings and working groups
09 p1768 A70-23710

Selenodetic control system, considering photogrammetric networks, Apollo landing site, topographical maps, lunar photographs, etc
10 p1890 A70-24732

Apollo lunar roving vehicles for manned exploration, discussing design proposals
12 p2208 A70-27943

Weather forecasting for manned space flights, emphasizing Apollo flights and operational decisions due to forecasts
14 p2606 A70-30557

Apollo Guidance, Navigation and Control system prelaunch checkup, flight experience and error analysis
[AIAA PAPER 69-891] 14 p2615 A70-30758

Apollo project overview and quality-cost effectiveness assurance requirements for future space programs
14 p2654 A70-31103

Evolution and current status of Apollo crew safety, discussing hazard aspects, program approach and measures and activities incorporated in project
[AAS PAPER 70-051] 17 p3176 A70-34790

Apollo program and outline of objectives of applications program
17 p3167 A70-35202

Small rocket systems research programs, discussing Apollo-Pacemaker and planetary entry parachute flight tests
17 p3177 A70-35203

Apollo lunar landing flight control functions, organization, disciplines and activities at Mission Control Center
17 p3134 A70-35292

Real time computer complex (RTCC/ supporting role in Project Apollo, describing mission control center data interfaces, equipment configuration, software, etc
17 p3060 A70-35295

Space vehicle and mission control center telecommunications networks for Apollo lunar landing program, considering NASCOM relay system
17 p3047 A70-35585

Apollo program navigation processing using Kalman optimal linear computer, emphasizing position vector and error matrix and command and lunar landing extrapolation module navigation
21 p3848 A70-41127

Book on decision making in U.S. manned lunar landing commitment covering space policy, technical planning, national interests, Apollo experience, etc
22 p4126 A70-42314

Apollo project technology for future space missions, discussing space shuttles, management, material procurement, test programs and computer utilization
22 p4128 A70-43513

Apollo program medical data contribution to knowledge of human response to space environment
22 p3980 A70-43651

Apollo spacecraft program evolution, discussing Apollo 13 accident, command and service module modifications, oxygen tank design, mission objectives, etc
23 p4245 A70-44640

Apollo and Skylab photographic systems, describing equipment and missions
24 p4333 A70-45360

Book on lunar rocks covering pre-Apollo lunar scientific knowledge, Apollo and future lunar mission planning, lunar mineralogy, petrology and geochemistry, etc
24 p4412 A70-46025

APOLLO SPACECRAFT

Nondestructive testing for Apollo Command and Service Module, describing requirements added to quality control scope
01 p0098 A70-10026

Apollo space cabin atmospheres, evaluating diluent N effect on decompression sickness in intermittently exercising men
01 p0032 A70-10368

Apollo/Saturn 5 space vehicle supporting and restraining mechanisms design and operation, discussing holddown assemblies
01 p0055 A70-10468

Apollo spacecraft hardware, command, service and lunar modules, discussing design factors and tests contributing to spacecraft reliability
[AIAA PAPER 69-1095] 01 p0194 A70-10618

Apollo spacecraft contamination control program, considering NASA role in management, contractor controls, criteria establishment and enforcement, etc
01 p0220 A70-11076

Apollo spacecraft contamination control, discussing Boeing responsibility for engineering, facilities, materials, etc, for Saturn rocket
01 p0058 A70-11077

Apollo spacecraft contamination control, describing Rocketdyne programs for rocket engines
01 p0059 A70-11078

Apollo spacecraft contamination control, describing McDonnell Douglas role in S-4B stage production
01 p0059 A70-11079

Apollo spacecraft contamination control, describing organization and operation of Grumman Contamination Control Committee
01 p0059 A70-11080

Apollo 11 electronics, discussing inertial measurement unit, optical navigation system, command module computer, communication network, TV and experimental packages
02 p0270 A70-12633

Apollo spacecraft pyrotechnics on lunar landing mission, considering standard initiator, modular cartridges, noninterchangeability of special purpose devices, postmanufacture indexing and data system
03 p0582 A70-14102

Computerized thermal model simulating environment control system, crew and vehicle structure in performance prediction for Apollo lunar module
[SAE PAPER 690621] 05 p0922 A70-15848

Apollo spacecraft propulsion systems design and operational requirements, emphasizing use of redundant components and system backups to achieve reliability
[SAE PAPER 690704] 05 p0923 A70-15858

S-band omnidirectional antenna patterns measurement procedure and results for Apollo spacecraft configurations, tabulating measure gains
06 p0109 A70-17507

Flight software for onboard Apollo Primary Guidance, Navigation and Control System flight qualification by digital simulation, including software diagnostics
[AIAA PAPER 70-173] 06 p1029 A70-18060

Apollo lunar orbit irregularities attributed to mascons beneath lunar surface, using short arc perturbation method
[AIAA PAPER 70-163] 06 p1145 A70-18068

Apollo onboard computers tracking data state-vector corrections covariance matrix, considering initial estimate, noise and tracking geometry errors
[AIAA PAPER 70-162] 06 p1015 A70-18072

Three dimensional latching dynamics and loads induced during Apollo spacecraft docking, using linear stiffness or flexibility matrices for structural elasticity
[AIAA PAPER 70-21] 06 p1158 A70-18181

Translunar Apollo orbit analysis from elementary equations relating to elliptical and hyperbolic orbits in inverse square force field
06 p1148 A70-18397

Apollo 8 mission, spacecraft and booster details, calculating earth-moon flight parameters based on laws of mechanics
07 p1375 A70-18776

Shock tunnel preflight assessment of Apollo Block 2 command module base heating
07 p1394 A70-19722

Fuel cell assemblies as primary electrical source for Apollo command and service modules, discussing heat removal, water vapor control and transient performance
08 p1439 A70-20702

Apollo space vehicles guidance and navigation using data obtained onboard, discussing inertial platforms, accelerometers and trajectory calculations
08 p1541 A70-21023

Apollo command and service modules from metallurgical viewpoint
09 p1766 A70-22792

Qualification and testing procedures for Apollo Spacecraft Program components and systems, discussing vibration tests
09 p1693 A70-23705

High speed instrumentation camera system for recording rapid motions during Apollo landing impact
09 p1688 A70-23770

Apollo lunar module manned testing in thermal vacuum, emphasizing safety aspects of hardware, procedures and training
10 p1859 A70-24389

Apollo lunar module mechanical acceptance tests evaluation based on reported flight anomalies review
[AIAA PAPER 70-401] 10 p1951 A70-24904

Apollo Spacecraft Certification Test Program at replaceable hardware assembly level noting future manned spacecraft applications
[AIAA PAPER 70-375] 10 p1952 A70-24928

Apollo Lunar Module Test Program Management, discussing test requirements optimization, control, planning, etc
[AIAA PAPER 70-368] 10 p1952 A70-24932

Spacecraft window cleaning with methyl alcohol and low pressure nitrogen providing filming control for Apollo optical experiments
11 p2051 A70-26143

Apollo service module engine design for maximum pilot safety, noting components redundancy
11 p2103 A70-26289

Apollo lunar module structural integrity for lunar landing verified by Monte Carlo dynamic analysis
12 p2312 A70-27114

Apollo Command Module inverter experience for post-Apollo spacecraft applications, discussing phase loads and control logic circuits
12 p2165 A70-27693

Apollo command and service modules environmental control system, discussing redesign of faulty hardware
[SAE PAPER 690618] 12 p2167 A70-27948

Apollo man-machine control design, discussing communication, integration, lunar landing, attitude control, CMC and LGC programs
13 p2357 A70-28379

Apollo Guidance Computer operations and functions during lunar orbit rendezvous
13 p2446 A70-28390

Trajectory predictive lunar return atmospheric reentry guidance of roll-controlled Apollo-type vehicle, using variable integration steps
13 p2446 A70-28396

Minimum-time thrust vector control law in Apollo lunar module computerized autopilot
13 p2499 A70-28399

Photographic apparatus for lunar orbiters and Apollo spacecraft, describing lunar surface closeup camera for astronauts, launch photographing, etc
13 p2406 A70-28926

NDT techniques in manufacturing of Apollo command and service modules
13 p2420 A70-29243

Landing point redesignation during Apollo lunar module descent terminal portion, defining information and control system
14 p2613 A70-30454

Aerodynamic and structural configuration effects on spacecraft inflight wind load calculations, showing Apollo interface lateral bending

14 p2653 A70-30585

Apollo Guidance, Navigation and Control system prelaunch checkout, flight experience and error analysis

[AIAA PAPER 69-891] 14 p2615 A70-30758

Real time Apollo PCM telemetry data compression and transmission using zero order predictor

14 p2550 A70-30768

Real time Apollo lunar module thermal mission data analysis using computer programs

14 p2653 A70-30774

Apollo navigation methods and data analysis covering inertial guidance with gyro-stabilized platforms, acceleration sensors, sextants and telescopes, ergodicity, filtering, etc

15 p2772 A70-31549

Apollo thermal protection system noting low density ablation, flight and ground tests

[AIAA PAPER 68-1142] 15 p2813 A70-32514

Apollo lunar module rendezvous radar redundant gyro system for reliability enhancement, discussing principles and logic

16 p2983 A70-34066

Apollo lunar module alightment system, discussing design, performance and reliability

16 p2985 A70-34122

Side access hatch system for Apollo command module

16 p2986 A70-34153

Stress corrosion cracking of Ti alloys in nitrogen tetroxide and methyl alcohol environments in Apollo spacecraft pressure vessels

17 p3199 A70-34453

Apollo docking system for CSM-LM connection and disconnection during lunar landing mission, discussing flight hardware

17 p3175 A70-34768

R-4D multiapplication rocket engine for Apollo spacecraft reaction control, discussing design, performance, quality assurance and tests

17 p3178 A70-35259

Apollo docking system design considerations and preliminary models evaluation for best choice to meet requirements

17 p3179 A70-35262

Apollo ordnance systems design and reliability, stressing redundant components role

17 p3179 A70-35263

Apollo lunar landing guidance, navigation and control, discussing inertial and optical measurements, computer, digital autopilots, rendezvous and mid-course navigation

17 p3134 A70-35288

Radiation measurements inside Apollo 4 and 6 command modules during passage through trapped radiation belts

17 p3040 A70-35645

LM-Apollo rendezvous radar and transponder electronic assemblies packaging and mechanical design

18 p3232 A70-36762

Apollo spacecraft parts environmental simulation and testing, using real time computer generated graphic display

19 p3532 A70-37918

Apollo service module retrograde motion due to propellants reorientation after reentry jetison predicted by digital simulation

[AIAA PAPER 70-1047] 19 p3534 A70-38862

Apollo digital Range Safety Command System for signal-crowded communications channels

20 p3605 A70-39497

Apollo 12 lunar module impact laboratory simulation, investigating possible downrange ballistic effects and cratering process

20 p3709 A70-39976

Apollo Command and Service Modules for lunar orbital science missions, discussing spacecraft-experiment integration

21 p3928 A70-40978

Pin fin coldplate heat exchanger for cooling Apollo spacecraft electronic equipment, calculating forced convection heat transfer and fluid pressure drop

21 p3797 A70-41025

Soyuz and Apollo spacecraft on board computers, discussing design, guidance, navigation and requirements

21 p3793 A70-41071

Command module simulators for Apollo astronaut training in moon landing, using computer, exterior visual scenes and spacecraft interior replica

21 p3804 A70-41195

Lunar module simulator for Apollo flight training using computers, digital conversion, cockpit replica, infinity-optics display and instructor control

21 p3805 A70-41196

Apollo spacecraft tests in Space Environment Simulation Laboratory, discussing thermal data, astronaut training, extravehicular activity, reaction control system, etc

21 p3805 A70-41271

Apollo command module land impact capability, discussing impact dynamics, possible landing area, spacecraft structure, crew couch and strut attenuation system, etc

[AIAA PAPER 70-1165] 21 p3930 A70-41847

Apollo TV cameras, detailing general characteristics, principal features, optical systems and operational requirements

23 p4195 A70-44382

Apollo command service module nondispersive X ray detection system for lunar composition map compilation, discussing design and performance

23 p4196 A70-44417

Space shuttle electronics requirements, considering systems in Mercury and Gemini spacecraft and Apollo lunar and command service modules

23 p4259 A70-44612

Apollo spacecraft program evolution, discussing Apollo 13 accident, command and service module modifications, oxygen tank design, mission objectives, etc

23 p4245 A70-44640

Apollo spacecraft pyrotechnic systems and devices functions during lunar exploration mission and in aborts

[SAE PAPER 700833] 24 p4416 A70-45888

Saturn 5 Apollo booster stages oscillations induced by coupling between vehicle structure and engine thrust corrected within existing systems

[AIAA PAPER 70-1236] 24 p4417 A70-45954

APOLLO TELESCOPE MOUNT

Bit-slippage errors due to onboard tape recording of PCM/FM telemetry data for Apollo Telescope Mount, noting roles of S/N ratio, data characteristics, etc

01 p0044 A70-10940

Display system for Apollo Telescope Mount designed for unoccluded sun view by orbiting astronaut-scientists, discussing human factors, film budgeting, etc

02 p0298 A70-12151

Apollo Telescope Mount Extra Vehicular Activity system for Apollo Applications Program

[ASME PAPER 69-WA/BHF-16] 04 p0761 A70-14857

Monitor for linearizing nonlinear characteristics of thermistors used for temperature sensors in Apollo Telescope Mount, optimizing circuit values with FORTRAN IV computer program

05 p0851 A70-16692

Systems engineering aspects of Apollo Telescope Mount spacecraft, considering design and manned space flight role

06 p1061 A70-17312

Solar activity model for simulating scheduling of observation experiments for Apollo Telescope Mount missions

[AIAA PAPER 70-32] 06 p1145 A70-18121

Temperature sensors for Apollo Telescope Mount experiments, comparing quartz, Pt wire and Si resistance sensors, thermistors and thermocouples

06 p1073 A70-18598

Computer scheduling model and timeline plot for Apollo Telescope Mount /ATM/ experiments using orbital trajectory simulation

07 p1394 A70-19572

Marshall Space Flight Center optical research programs technology base for launch vehicle development support, discussing Apollo Telescope Mount

09 p1657 A70-23518

Apollo telescope mount postmanufacturing checkout under simulated mission environment, ensuring flight readiness

16 p2889 A70-33723

Scanning mirror system for Apollo telescope mount UV spectroheliometer, describing design, fabrication and testing

17 p3083 A70-34764

APOLLO 6 FLIGHT

Microbial contamination levels on Apollo 6 spacecraft, discussing intramural environments for assembly and testing

16 p2849 A70-33995

APOLLO 7 FLIGHT

Ocean swell wavelength and propagation direction measurements, using Fourier optical analysis of Apollo 7 space photography

22 p4029 A70-42766

APOLLO 8 FLIGHT

Lunar surface far side stereoscopic photography by Apollo 8 mission considered for lunar control

04 p0686 A70-14618

Apollo 8 mission, spacecraft and booster details, calculating earth-moon flight parameters based on laws of mechanics

07 p1375 A70-18776

Remote sensing of lunar photometric function at small phase angles by Apollo 8 command service module

12 p2297 A70-26926

Xenon arc lamp searchlight performance and application during Apollo 8 launch

12 p2207 A70-27662

Lunar far side features position from Apollo 8 data, evaluating Apollo navigation system accuracy

12 p2309 A70-27949

APOLLO 9 FLIGHT

Apollo 9 space photography of earth surface and use for quantitative analysis of earth resources, including supporting aircraft photography

[AAS PAPER 69-572] 04 p0687 A70-14650

Microbial contamination levels and types detected on Apollo 9 spacecraft and related effects of various test and assembly environments

05 p0809 A70-16711

Apollo 9 scientific multispectral photography mission, discussing meteorological support aspect of real time planning

14 p2610 A70-30614

APOLLO 10 FLIGHT

RF EMI propagation between manned spaceflight network and Apollo 10 launch vehicle in translunar mission, considering cochannel interference possibilities

12 p2189 A70-28137

Apollo 10 color TV camera for real time scenes, describing configuration performance and total system operation

16 p2907 A70-33187

APOLLO 11 FLIGHT

Apollo 11 lunar module gravity measurement on lunar surface with pulsed integrating pendulous accelerometer to compute anomaly and radius at landing site

01 p0181 A70-10574

Apollo 11 electronics, discussing inertial measurement unit, optical navigation system, command module computer, communication network, TV and experimental packages

02 p0270 A70-12633

Normal albedo of Apollo 11 landing site and intrinsic dispersion in lunar Heiligenschein determined from Apollo and earth based photographic photometry

04 p0747 A70-14549

Optical facilities of Apollo 11 mission and NASA Manned Spacecraft Center noting Fاذow telescopes, lunar cartography, photometric surface analysis, etc

04 p0687 A70-14690

Black and white and color Apollo 11 secondary electron conduction TV cameras, discussing characteristics and mission requirements

04 p0688 A70-14692

Apollo lunar mission optics concerning liftoff alignment theodolites, spacecraft atmosphere electro-optical sensor, helmet optical coating and laser experiment

04 p0688 A70-14693

Hydrophobic-hydrophilic zero gravity liquid-gas phase separator for Apollo 11 flight life support system

[SAE PAPER 690638] 05 p0804 A70-15844

Al foil exposed to solar wind on moon during Apollo 11 mission examined for helium particles, finding lunar solar wind albedo

05 p0900 A70-16093

Apollo 11 lunar landing mission planning, control and evaluation of launch window and translunar, lunar parking orbit and transearth trajectories

[AIAA PAPER 70-24] 06 p1158 A70-18168

Apollo 11 premission planning, real time situation and postflight analysis for lunar descent and ascent phases, providing navigation correction capability for Apollo 12

[AIAA PAPER 70-25] 06 p1159 A70-18227

Apollo 11 laser ranging retro reflector measurements from McDonald Observatory confirming thermal design analysis performance prediction

06 p1011 A70-18482

Cooperation of NASA and DOD Quality Assurance personnel concerning Apollo 11, considering personnel training

07 p1428 A70-19674

Apollo 11 lunar material X ray diffraction and microscope studies, noting chemical composition agreement with Surveyor 7 data

09 p1752 A70-22245

Gaseous species in equilibrium with Apollo 11 holocrystalline rocks during crystallization

09 p1758 A70-22744

Carbon compounds composition and origin in Apollo 11 lunar samples using pyrolytic chromatography and microscopy at elevated temperature

10 p1941 A70-24531

Apollo 11 mission crew observation of operational and scientific phenomena associated with lunar landings, discussing preflight geologic training and briefings

11 p2109 A70-25847

Space navigation for Apollo 11 mission, emphasizing ground and onboard systems, interfaces with guidance and use in phases of lunar landing

13 p2447 A70-28547

Apollo lunar laser ranging experiment /LURE/ for range measurements from earth to lunar surface

15 p2750 A70-31675

Apollo 11 lunar mission results, discussing surface, seismology, laser ranging retroreflector, solar wind and rock samples

15 p2800 A70-32073

Legal problems arising from Apollo 11 lunar landing with respect to Space Treaty, discussing lunar soil removal, flag planting, Luna 15 flight, etc

17 p3203 A70-35791

Lunar surface erosion due to Apollo 11 descent engine 18 p3316 A70-36960

Apollo 11 lunar rocks mineralogy and petrology, noting anorthosite in powder and breccia 18 p3320 A70-37081

Apollo 11 lunar rocks and dust from Tranquility Sea measured for age by Rb-Sr and K-Ar methods 18 p3320 A70-37082

Apollo 11 and 12 results tabulated for soil packing characteristics, composition and rare gas analysis data 18 p3332 A70-37223

Biological tests of fish and invertebrates exposed to Apollo 11 lunar surface material, noting absence of pathological effects 19 p3513 A70-37409

Moon origin, surface, exploration, Apollo 11 landing, subsidence/uplift crater formation and Transient Lunar Phenomena 20 p3701 A70-38977

Apollo 11 lunar science - NASA Conference, Houston, January 1970, Volume 1, Mineralogy and petrology 21 p3893 A70-41501

Apollo 11 mafic crystalline rocks and mineral assemblages, discussing collection, classification and sample environments 21 p3894 A70-41502

Apollo 11 magnesium-rich opaque oxide armalcolite mineral from Tranquility Base noting relation to pseudobrookite series 21 p3895 A70-41503

Calcium-bearing iron silicate /pyroxferroite/ from Apollo 11 lunar Tranquility Base samples, discussing petrographic environment, physical and optical properties 21 p3895 A70-41504

Titanian and aluminian chromites and chromian ulvöspinel in Apollo 11 fines, microbreccias and basaltic type igneous rocks 21 p3895 A70-41505

Electron microprobe and petrographic analyses of crystalline rock and separates from Apollo 11 lunar soil samples 21 p3895 A70-41506

Apollo 11 lunar rock and fines chemistry, mineralogy and petrology, discussing composition, igneous rocks, microbreccias, glasses and pyroxene relations 21 p3895 A70-41507

Mineralogy and chemistry of Apollo 11 lunar soil samples, using three-channel electron microprobe analyzer 21 p3896 A70-41509

Trace elements in Apollo 11 lunar glass clinopyroxene, plagioclase and ilmenite, using ion microprobe mass analyzer 21 p3896 A70-41510

Apollo 11 lunar rocks, breccias, dust and chip mineralogy and petrology, examining composition, texture, grain size and morphologies 21 p3896 A70-41511

Apollo 11 lunar igneous rocks mineralogical, chemical and petrological features by optical and electron microscopy and X ray spectrometry 21 p3896 A70-41512

Opaque minerals in Apollo 11 lunar igneous and fragmental rocks, using reflecting microscope and electron microprobe 21 p3896 A70-41513

Apollo 11 lunar soil volcanic rock samples, mineralogical and petrological description and surface features 21 p3896 A70-41514

Apollo 11 lunar crystalline rock samples petrology, discussing shock and other metamorphic effects on mineral structure 21 p3897 A70-41516

Petrology, mineralogy and deformation of Apollo 11 rock samples using microscopic, X ray and electron microprobe methods 21 p3897 A70-41517

Trace phyllosilicates in Apollo 11 soil sample and rock, using electron microscopy and diffraction studies 21 p3897 A70-41518

Tranquility Base lunar soil origin, establishing component nature, size distribution, density, mineralogy, constructional or destructional history 21 p3897 A70-41519

Apollo 11 lunar soil and breccia shock metamorphism, examining plastic deformation structures in plagioclase, pyroxene and olivine 21 p3897 A70-41520

Petrologic analyses of minerals and glass spherules in Apollo 11 lunar rocks, indicating little fractionation and shallow-level differentiation 21 p3897 A70-41521

Apollo 11 lunar rock pyroxenes, examining band structure and magnetic ordering by high voltage electron microscopy and electron diffraction 21 p3898 A70-41523

Petrography and shock vaporization origin of Apollo 11 lunar breccias and glasses compared to terrestrial impactites and chondrites 21 p3898 A70-41524

Apollo 11 lunar rock mineralogy, examining petrographic and chemical features by light microscopy, electron microprobe microanalysis and detector system 21 p3898 A70-41525

Bulk chemical compositions, mineral and glass analyses, X ray data and physical properties of Apollo 11 lunar fines and rocks 21 p3898 A70-41526

Apollo 11 lunar rock fluorapatite and trace minerals, examining pressure and oxidizing conditions of formation, grain and crystallization 21 p3898 A70-41527

Apollo 11 lunar rock lavas and breccias, examining opaque minerals and olivine by reflection microscopy, electron probe and optical absorption measurements 21 p3899 A70-41530

Compositional zoning in pyroxenes from grained Apollo 11 microgabbros, implying supercooled magma origin 21 p3899 A70-41532

Apollo 11 lunar samples mineralogical and compositional studies concerning lunar origin hypothesis 21 p3899 A70-41534

Shock metamorphic granular mafic holocrystalline lithic fragments, microbreccia, glass and anorthosite from Apollo 11 lunar surface material at Tranquility Base 21 p3900 A70-41535

Petrology, crystallization and magma origin of lunar clinopyroxene, ilmenite-rich dolerite and microgabbro from Apollo 11 samples 21 p3900 A70-41536

Fission track uranium distribution studies of Apollo 11 lunar volcanic rocks, using Lexan plastic print method 21 p3900 A70-41537

Apollo 11 lunar igneous rocks minerals and glassy phases characteristics, using electron probe microanalysis 21 p3900 A70-41538

Apollo 11 samples compared to stony meteorites and terrestrial basalt, discussing lunar rock formation processes 21 p3900 A70-41540

Glass spherule lunar particles and breccia from Apollo 11 site, showing passage through impact generated cloud of hot fragmental material 21 p3901 A70-41541

Lunar sea, mascon and interior composition, discussing crystallization of Apollo 11 Tranquility samples and synthetic analogs at high pressure 21 p3901 A70-41542

Apollo 11 lunar rock clinopyroxene, plagioclase and ilmenite internal substructure, using high voltage transmission electron microscopy 21 p3901 A70-41544

Mineral chemistry of Apollo 11 igneous rocks, soil and breccia samples, comparing with meteorites 21 p3901 A70-41545

Apollo 11 lunar rock samples alpha particle activity in polished thin sections, using autoradiography and electron microprobe 21 p3901 A70-41546

Apollo 11 lunar basalt petrogenesis, examining internal constitution and origin by high pressure 21 p3901 A70-41547

Apollo 11 lunar rocks and fines, examining clinopyroxenes augite and pigeonite by single crystal X ray diffraction microprobe optical and electron optical techniques 21 p3902 A70-41549

Apollo 11 lunar rock and fines shock induced and melting microstructural mineral damage, discussing meteorite bombardment, phases without melting and microbreccia 21 p3902 A70-41550

Quantitative optical and electron probe studies of opaque phases in Apollo 11 lunar rocks 21 p3902 A70-41552

Apollo 11 lunar rock plagioclases crystallography, obtaining single crystal X ray diffraction patterns by Buerger precession method 21 p3903 A70-41555

Apollo 11 lunar igneous rock mineralogy and petrology, emphasizing ferrobasalt minerals microanalysis electron probe 21 p3903 A70-41557

Microprobe analysis of glassy spherules from Apollo 11 lunar regolith, discussing zoning, composition and hypervelocity impact formation 21 p3903 A70-41558

Apollo 11 lunar anorthosites properties and characteristics, discussing grain size, Na content, color, density, chemical composition and geomorphic effects 21 p3903 A70-41559

Apollo 11 lunar science - Conference, Houston, January 1970, Volume 2, Chemical and isotope analyses 21 p3903 A70-41560

Apollo 11 lunar rock trace elements, examining basalt, gabbroic igneous rocks, breccias and fines by DC arc emission spectroscopy 21 p3774 A70-41561

Apollo 11 lunar rocks and fines cosmic ray produced radioisotopes, considering surface exposure to high energy component flux 21 p3906 A70-41562

Apollo 11 lunar rocks, breccias and fines age and chemistry, major element, trace element and rare earth abundances, texture, crystallization and meteoritic effects 21 p3906 A70-41563

Tritium and Ar radioactivities attributable to galactic and solar cosmic ray interactions in Apollo 11 lunar rocks and soil 21 p3906 A70-41564

Apollo 11 lunar fines trapped noble gas elemental and isotopic abundances, suggesting solar wind origin 21 p3906 A70-41565

Apollo 11 lunar rocks and fines oxygen, Si and Al content determination by neutron activation analysis 21 p3774 A70-41566

Apollo 11 lunar rocks and soil hydrogen, C and Si concentration and isotopic composition 21 p3774 A70-41568

Apollo 11 lunar material actinide element abundance and isotopic composition, examining Th, U and transuranium elements by mass spectrometric and radiometric techniques 21 p3774 A70-41569

Apollo 11 lunar material water content and H and C isotope abundance, examining changes in deuterium and O by solar winds 21 p3774 A70-41570

Rare gas analysis of Apollo 11 lunar soil and breccia for surface layer history 21 p3906 A70-41571

Apollo 11 lunar material trace elements, examining chemical processes during and after formation and meteoritic matter influx rate 21 p3907 A70-41572

Apollo 11 lunar basalt chemical composition and petrogenesis, using stable isotope dilution method 21 p3907 A70-41573

Apollo 11 lunar rocks elemental abundances determination by instrumental activation techniques 21 p3775 A70-41574

Apollo 11 sample elemental abundances, investigating environmental, paragenetic and petrogenetic problems and moon evolution 21 p3907 A70-41575

Apollo 11 lunar material isotopic age determination, discussing rock crystallization, radiogenic dust, lead isotope data and moon origin 21 p3907 A70-41576

Apollo 11 fines gas evolution and physical changes via heat treatment, discussing Ar 40 anomaly, lava structure origin and oxidation rate 21 p3907 A70-41577

Rare earth and trace element abundances for Apollo 11 lunar samples by neutron activation, comparing with Bruderheim chondrite and submarine basalts 21 p3907 A70-41578

Apollo 11 lunar dust examination by neutron activation analysis, determining spallogenic manganese 53 21 p3908 A70-41579

Apollo 11 lunar samples composition for Na 22, Al 26, Th and U, investigating positron activities 21 p3775 A70-41580

Radiogenic and cosmogenic inert gases and isotopic ratios in Tranquility Base fines indicating solar wind saturation 21 p3775 A70-41581

Surface correlation of excess Ar 40 in lunar fines from Apollo 11 21 p3908 A70-41582

Apollo 11 lunar matter rare gas, H and N concentrations and isotopic abundances, discussing solar wind, gas diffusion loss from silicates and spallation component 21 p3908 A70-41583

Trapped and cosmogenic rare gases from stepwise heated Apollo 11 lunar dust and crystalline rocks, using mass spectrometry 21 p3908 A70-41584

Apollo 11 lunar rock Rb-Sr isotopic age relationships, discussing magmatic fractionation of Rb relative to Sr in moon primordial material 21 p3908 A70-41585

Carbon and sulfur concentration and isotopic variations in Apollo 11 fines, breccias and fine-grained basalts 21 p3775 A70-41586

Lead and thallium isotopic compositions of Apollo 11 fines compared with meteorites and earth for lunar surface age determination 21 p3775 A70-41588

Neutron activation analysis for Re and Os in Apollo 11 volcanic rocks, discussing possible meteoritic contamination of secondary rocks and fines 21 p3775 A70-41589

Apollo 11 lunar soil irradiation history from solar wind rare gas abundances and cosmic ray spallation products 21 p3908 A70-41590

Apollo 11 lunar rocks and soil chemical composition, examining major, minor and trace elements 21 p3776 A70-41591

Carbon and nitrogen abundances in Apollo 11 rocks, basaltic achondrites and terrestrial basalts, using meteorite analytical techniques

21 p3776 A70-41592

Apollo 11 lunar rock and soil elemental abundances, discussing composition, volatile element depletion, rare earths, basalt and geochemical processes

21 p3909 A70-41593

Trace elements K, Rb, Sr and Ba distributions and Rb-Sr isotopic relations in Apollo 11 lunar breccia and fine soil samples

21 p3909 A70-41594

Apollo 11 lunar rock and fines primordial radionuclide abundances and concentration gradients by gamma ray spectrometry at Lunar Receiving Laboratory

21 p3776 A70-41595

Apollo 11 lunar rocks oxygen isotope ratios, examining relationship to terrestrial basalts

21 p3776 A70-41596

Oxygen isotope fractionation and formation temperature of minerals from Apollo 11 rocks, including plagioclase-clinopyroxene-magnetite concordancy diagram

21 p3776 A70-41597

Apollo 11 lunar fines, breccia and crystalline rocks rare gas data, emphasizing trapped and spallation Ne, Kr and Xe isotopic compositions

21 p3909 A70-41598

Cosmogenic and primordial radionuclides in Apollo 11 lunar soil and rocks, using nondestructive gamma ray spectral measurements

21 p3776 A70-41599

Apollo 11 lunar rock K, Rb, Sr, Ba and rare earth element concentrations, examining relationship to terrestrial and chondritic levels

21 p3776 A70-41600

Halogens, mercury, lithium and osmium concentration measurements in Apollo 11 samples, using neutron and photon activation

21 p3777 A70-41601

Chemical composition and reducing capacity of Apollo 11 igneous rocks, breccia and soil fines, using semimicro X ray fluorescence

21 p3777 A70-41602

Uranium and Th isotopic composition in Apollo 11 samples compared to earth, using mass and alpha spectrometries

21 p3777 A70-41603

Apollo 11 lunar rock and soil bombardment produced radionuclide patterns, discussing solar flare protons and alphas, age determination and astronomical models

21 p3777 A70-41604

Apollo 11 lunar rocks, breccia and fines U, Th and Pb isotopes systematics, considering implications for lunar history

21 p3909 A70-41605

Elemental abundances of Apollo 11 lunar rocks and soils, using activation analysis or mass spectrometric isotope dilution

21 p3909 A70-41606

Lunar surface material age and post-crystallization from isotopic investigation of Apollo 11 samples of U-Th-Pb systematics

21 p3909 A70-41608

Apollo 11 lunar rocks and minerals oxygen 18-oxygen 16 ratios

21 p3777 A70-41609

Chemical analysis methods for Apollo 11 lunar rocks, discussing calibration standards, spectral lines and Apollo 12 data

21 p3777 A70-41610

Chemical analysis for Li, Na, K, Rb, Cs, Ca, Sr and Ba in achondrites and Apollo 11 lunar rocks, breccia and soil samples

21 p3910 A70-41611

Apollo 11 lunar rocks and soil chemical elements analysis by neutron activation scheme

21 p3777 A70-41612

Apollo 11 crystalline rocks chemical analysis by argon 40/argon 39 dating techniques

21 p3778 A70-41613

Apollo 11 lunar rocks, soil and core samples major, minor and trace elements abundance by radiochemical and instrumental activation analyses

21 p3910 A70-41614

Apollo 11 fines and rocks major and trace elements data obtained by combined instrumental and neutron activation analysis

21 p3910 A70-41615

Age determination of Apollo 11 samples from isotopic composition measurements by isotope dilution techniques, comparing to terrestrial and meteoritic values

21 p3778 A70-41616

Apollo 11 lunar, terrestrial and meteoritic basalts relationships, examining Ga, Ge, In, Ir and Au concentrations by neutron activation analyses

21 p3778 A70-41617

Apollo 11 lunar surface fine material and rocks cosmogenic radio nuclides Al 26 and Na 22 concentrations determination by gamma ray spectroscopy

21 p3910 A70-41618

Apollo 11 lunar fines examined for organic compounds via solvent extraction, vacuum crushing, programmed heating and hydrofluoric acid etching

21 p3778 A70-41619

Apollo 11 lunar dust and microbreccia micropaleontological examination, discussing biological morphology

21 p3778 A70-41620

Apollo 11 lunar fines carbon level, finding largest component carbon monoxide in complex form

21 p3778 A70-41621

Apollo 11 lunar dust and breccia micromorphology and surface characteristics implying weathering processes

21 p3910 A70-41622

Amino acids analysis of Apollo 11 lunar fines by hydrolysis of aqueous extracts

21 p3778 A70-41623

Apollo 11 lunar samples organic carbon content analysis by pyrolysis hydrogen flame ionization detection

21 p3779 A70-41624

Apollo 11 lunar fines carbon compounds, examining chemical state of porphyrins, fatty and amino acids, purines, pyrimidines and carbohydrates, etc

21 p3779 A70-41625

Apollo 11 lunar fines porphyrin-like pigments content demonstrated by fluorescence spectrometry and analytical demetallation, suggesting rocket exhaust source

21 p3910 A70-41626

Apollo 11 lunar samples organic compounds analysis by mass spectrometry, gas and liquid chromatography and nuclear magnetic resonance

21 p3779 A70-41629

Apollo 11 lunar fines chemical analysis for alkanes of 15-30 carbon atom length, obtaining negative results

21 p3779 A70-41630

Apollo 11 fines and rocks analysis by chromatography, mass spectrometry and light and scanning electron microscopy

21 p3779 A70-41631

Apollo 11 lunar fines organic compounds detection and identification by mass spectrometry

21 p3780 A70-41632

Viable organisms in Apollo 11 lunar fines, discussing tests, laboratory and sterile biological barrier system

21 p3911 A70-41634

Organic solvent extracts of Apollo 11 bulk fine sample examined for porphyrins using spectrophotometry

21 p3780 A70-41635

Apollo 11 lunar science - Conference, Houston, January 1970, Volume 3, Physical properties

21 p3911 A70-41636

Magnetic monopoles electromagnetic search in Apollo 11 rock samples

21 p3912 A70-41639

Apollo 11 rocks IR absorption properties, specific heat and thermal conductivity, discussing heat flow in surface layer

21 p3913 A70-41642

Apollo 11 rocks red luminescence and blue thermoluminescence under proton bombardment, discussing energy efficiency

21 p3913 A70-41644

Apollo 11 rocks spectral reflectance and albedo before/after proton irradiation and vitrification, investigating color differences for lunar surface dark and bright areas

21 p3913 A70-41645

Apollo 11 lunar rock and soil mechanical behavior and physical characteristics, discussing color, specific gravity, density, shapes and adhesive and cohesive properties

21 p3913 A70-41646

Apollo 11 fines thermal conductivity under vacuum, using line heat source technique

21 p3913 A70-41647

Nuclear particle tracks in Apollo 11 samples due to galactic cosmic rays and solar flares relationship to dynamic surface processes

21 p3914 A70-41648

Apollo 11 fines, breccias and crystalline rocks thermoluminescence, observing temperature dependence of glow curve peaks

21 p3914 A70-41649

Apollo 11 rocks natural remanence and induced magnetism by triaxial magnetic gradiometer at Lunar Receiving Laboratory

21 p3914 A70-41650

Apollo 11 type C breccia sample remanent magnetism, observing viscous component with several hours time constant

21 p3914 A70-41651

Rock particle tracks of primary cosmic rays, spallation recoil nuclei, nuclear fission and solar wind ions, observing time scale multiple soil orientation

21 p3914 A70-41652

Apollo 11 drive-tube core samples from Tranquility Base, expressing lunar surface environmental processes

21 p3914 A70-41653

Apollo 11 lunar fines, rocks and breccias luminescence, electron paramagnetic resonance and op-

tical properties, discussing reflection spectra, heating effects and dipole resonance

21 p3914 A70-41654

Apollo 11 lunar powder optical and HF electrical properties, discussing reflectivity, polarization, absorption, differential mass spectrum and albedo

21 p3915 A70-41655

Luminescence efficiencies of Apollo 11 lunar and terrestrial rocks and minerals, using UV excitation

21 p3915 A70-41656

Mossbauer spectra of Apollo 11 lunar fines and microbreccia, showing iron oxidation, site symmetry and magnetic state

21 p3915 A70-41657

Time dependent adhesion in ultrahigh vacuum of Apollo 11 lunar soil sample 10065-33, considering microchemical and microphysical properties

21 p3915 A70-41658

Apollo 11 lunar fines, investigating solar radiation effects on optical properties by standing and heating

21 p3915 A70-41660

Apollo 11 lunar rock and dust samples thermomagnetic properties, Curie points, magnetization and demagnetization characteristics

21 p3915 A70-41661

Mossbauer effect spectrometry application to Apollo 11 lunar rocks composition, using nuclear gamma resonance measurements for nuclide Fe 57

21 p3916 A70-41662

Apollo 11 lunar specimen thermal diffusivity, conductivity and inertia in breccias and crystalline igneous rocks measured over wide temperature range

21 p3916 A70-41663

Apollo 11 lunar dust, breccia and igneous rocks, using Mossbauer spectroscopy and petrographic techniques

21 p3916 A70-41664

Thermoluminescence, X ray and stored energy measurements of Apollo 11 samples, comparing surface outputs to interior

21 p3916 A70-41665

Apollo 11 lunar sample elastic wave velocities at high pressures, examining P and S waves, Q value and geophysical implications

21 p3916 A70-41666

Apollo 11 bulk and core tube fines and rock cosmic ray tracks, discussing material history and corpuscular radiation flux and energy spectra near moon

21 p3916 A70-41667

Magnetic properties of Apollo 11 lunar breccia samples, determining natural remanent magnetization and susceptibility via paleomagnetism instruments and methods

21 p3916 A70-41668

Apollo 11 passive seismic experiment package, discussing design, performance and various received signals

21 p3917 A70-41669

Apollo 11 rock and fines magnetic resonance, examining line shapes, temperature dependences and electron spin

21 p3917 A70-41670

Proton and UV excited luminescence of Apollo 11 Tranquility rocks and fines, indicating solar wind impingement

21 p3917 A70-41672

Fe-group cosmic ray exposure tracks in Apollo 11 lunar rock interior, erosion rate and solar flare paleontology

21 p3917 A70-41673

Apollo 11 sample specific heats at 90-350 K, using adiabatic calorimeter

21 p3917 A70-41674

Apollo 11 lunar rock and fines magnetic properties, associating remanent magnetization with lunar magnetic field

21 p3917 A70-41675

Apollo 11 lunar dust hysteresis curves and thermomagnetic curves, discussing metallic Fe abundance, susceptibility, alpha-gamma transition, etc

21 p3918 A70-41676

Tranquility Base regolith origin, examining thickness exposure histories, crater distribution and composition

21 p3918 A70-41677

Apollo 11 lunar crystalline rock and breccias petrography and luminescent properties, spectral analysis, color, emission bands and shock effects

21 p3918 A70-41678

Apollo 11 lunar crystalline rock, microbreccia and fines compressibilities at room temperature, loading-unloading and pressure volume curves

21 p3918 A70-41679

Apollo 11 lunar breccia and fines magnetic properties, examining remanence, composition, oxidation, volcanic activity and stoichiometry

21 p3918 A70-41680

Apollo 11 lunar fines glass spherules magnetic properties, considering soft and hard ferromagnetic components

21 p3918 A70-41681

Apollo 11 lunar dust small glassy spherules and cylinders examination by interferometry, discussing

specular reflection, microcracking, chipping and origin 21 p3919 A70-41682

Apollo 11 lunar samples spectral analysis, discussing Fe and Mn electron paramagnetic resonance and A127 nuclear magnetic resonance spectra 21 p3919 A70-41683

Apollo 11 data for lunar formation by earth breakup, discussing moon heating phase and correlation with planetary evolution 22 p4098 A70-42549

Apollo 11 lunar rock samples examined for clues to moon life 22 p3972 A70-43425

International space program cooperation, discussing NASA projects, Apollo 11 flight and European and Soviet programs 22 p4129 A70-43655

Apollo 11 ilmenite basalts petrology from regolith samples 23 p4239 A70-43898

Apollo 11 and 12 lunar landing sites surface properties from returned rocks chemical, physical and mineralogical analysis 23 p4241 A70-44221

Apollo 11 and 12 close-up lunar surface photography, describing specially designed camera 23 p4194 A70-44255

Apollo 11 lunar fine thermal conductivity measurement under vacuum conditions and lunar temperature range, using line heat source method 23 p4243 A70-44442

Apollo 11 and 12 results concerning lunar geology and physical features, discussing impact generated long duration seismic signals and solar wind isotopic composition experiment 23 p4244 A70-44613

Apollo 11 lunar fines glassy particles, investigating morphology, optical properties and chemical composition 24 p4403 A70-45401

APOLLO 12 FLIGHT

Physical, chemical, mineralogical and biological analysis of Apollo 12 lunar samples compared to Apollo 11 rocks, discussing landing site geologic setting 10 p1935 A70-23811

Materials/design optimization of antenna-aiming mechanism deployed on moon by Apollo 12 astronauts to transmit ALSEP experiments data to earth stations 12 p2231 A70-27130

Lunar gravity correlation with large craters indicated from negative accelerations recorded in Apollo 12 lunar module Doppler radio tracking data 12 p2298 A70-27270

Seismic echo produced by jettisoned Apollo 12 S-4B stage impact at lunar surface analyzed by multiscatter scattering theory 12 p2298 A70-27280

Conditions leading to lightning as triggered by Apollo 12 and suggestions for minimizing such hazards 13 p2394 A70-28838

Apollo 12 navigation for pinpoint lunar landing, correcting errors in downtrack position in guidance computer near powered descent initiation time 14 p2613 A70-30456

French photographic observations of Apollo 12 translunar trajectory 15 p2697 A70-31676

Rb-Sr internal isochron ages from Ocean of Storms, discussing analytical results of two texturally and mineralogically distinct crystalline rocks from Apollo 12 16 p2975 A70-33659

Luminous emissions related to Apollo 12 mission observed in Belgium, discussing flight chronology, gas ejection, stage separation, etc 16 p2981 A70-34318

Apollo 12 rock and dust analyses, discussing modifications to conclusions from Apollo 11 samples with reference to rare gas concentrations 18 p3321 A70-37085

Apollo 11 and 12 results tabulated for soil packing characteristics, composition and rare gas analysis data 18 p3332 A70-37223

Clinopyroxenes from Apollo 12 rocks studied by X ray diffraction and electron microprobe methods, noting phenocrysts, chemical composition and crystallization 19 p3519 A70-38033

Ground based radar tracking data processing method for real time information concerning lunar module (LM) position and velocity during Apollo 12 flight [AIAA PAPER 70-1020] 20 p3591 A70-39514

Apollo 12 lunar module impact laboratory simulation, investigating possible downrange ballistic effects and cratering process 20 p3709 A70-39976

Metallic Fe grains in Apollo 12 igneous rocks, discussing Ni and Co abundances 21 p3920 A70-41881

Seismic signal by Apollo 12 lunar module impact indicating deep layer of powder by signal propagation 21 p3920 A70-41894

Tektite glass absence in Apollo 12 lunar sample 23 p4238 A70-43806

Apollo 11 and 12 lunar landing sites surface properties from returned rocks chemical, physical and mineralogical analysis 23 p4241 A70-44221

Apollo 11 and 12 close-up lunar surface photography, describing specially designed camera 23 p4194 A70-44255

Apollo 11 and 12 results concerning lunar geology and physical features, discussing impact generated long duration seismic signals and solar wind isotopic composition experiment 23 p4244 A70-44613

APOLLO 13 FLIGHT

Apollo 13 flight rescue operation as function of flight crew performance and Mission Control Center [AIAA PAPER 70-1260] 24 p4412 A70-45968

APPARATUS

U EQUIPMENT

APPENDAGES

NT ARM [ANATOMY]

NT FOREARM

NT HAND [ANATOMY]

NT KNEE [ANATOMY]

NT LEG [ANATOMY]

APPLICATIONS OF MATHEMATICS

Textbook on applied numerical methods covering interpolation, approximation, integration, matrices, etc, with emphasis on digital computer algorithms 01 p0132 A70-11306

Differential equations and applications - Conference, Bratislava, Czechoslovakia, September 1966 05 p0876 A70-16560

Mathematical techniques for selenodesy computer simulation program, solving problems arising from infinite series of spherical harmonics for lunar gravitational potential 06 p1152 A70-18498

Book on mathematical bases of industrial reliability covering components, parts stocking, Poisson distribution, redundancy, etc 07 p1290 A70-18700

Numerical calculation and applied mathematics - Conference, Tours, France, July 1965 07 p1326 A70-19781

Book on statistical methods in structural mechanics covering design, fracture, stability, random loads, damage accumulation, reliability, etc 07 p1441 A70-19849

Soviet collection of papers on mathematical physics covering natural oscillation frequencies, particles periodic motion, dynamic stability of pendulum, gyro drift during perturbations, etc 08 p1542 A70-20483

Soviet book on mathematical physics covering equilibrium equations of vibration, thermal conductance and diffusion with emphasis on Laplace equations 08 p1544 A70-20763

Integral equation perturbation technique, discussing applications to electrostatics, hydrodynamics, MHD, heat and mass transfer, etc 09 p1711 A70-22350

Soviet monograph on method of functional equations for solving boundary value problems, discussing computer programs and various applications 09 p1712 A70-23548

Book on liquid masses ellipsoidal figures of equilibrium extended into coherent mathematical theory, discussing virial equations, potentials of homogeneous and heterogeneous ellipsoids, etc 10 p1917 A70-24701

One dimensional wave processes in distributed nonlinear systems, surveying mathematical methods 10 p1843 A70-25151

Finite element method application, origin, development and relation to other mathematical methods, comparing with finite difference discretization processes 12 p2315 A70-26965

Mathematical cartography, discussing uses of electronic computers in network design 13 p2395 A70-28925

Book on light and matter covering mathematical laser theory 13 p2429 A70-29574

Graph theory in Soviet literature, applications and bibliographies 14 p2600 A70-31421

Soviet book on mathematical theory of linear and nonlinear control systems covering differential and difference equations, calculus variations, etc 15 p2715 A70-32200

Book on stochastic tools in turbulence covering generalized functions, probability, moments, characteristic functions, Gaussian distribution, random functions and multidimensional fields 17 p3128 A70-34601

Applied mathematics and mechanics - Conference, Aachen, Germany, April 1969 18 p3280 A70-36351

Mathematical solutions validity in determining constant interface friction factor from ring compression tests [ASME PAPER 69-WA/LUB-8] 19 p3434 A70-37603

Book on guided EM wave theory covering mathematical methods transmission lines cavity resonators, perturbation theory, electrostatics, electric and magnetic fields, propagation, etc 23 p4172 A70-44242

Algorithm for moment problems in Chebyshev system with applications to numerical integration, series summation and function approximation 23 p4211 A70-44244

APPLICATIONS TECHNOLOGY SATELLITES

NT ATS 1

NT ATS 3

NT ATS 5

European application satellite systems operation by administrative organizations dealing with communications, earth resources determination and industry participation 03 p0609 A70-13839

TIROS, Nimbus, ESSA and ATS weather satellites configurations, onboard equipment and cloud photographs 09 p1765 A70-22227

ATS-3 hydrazine orbit control system efficiency evaluation statistical method, considering stationkeeping maneuvers 11 p2121 A70-25464

European company for providing and operating European application satellite systems /EUROSAT/, discussing organization, tasks and financial structure 12 p2335 A70-27469

Gravity gradient ATS program experiments including spin scan cloud cover and stabilization research 14 p2654 A70-31145

Two stage yo-yo with nutation damper for despinning ATS synchronous satellites, describing mechanical and thermal design, lubrication, assembly, testing, etc 16 p2985 A70-34115

ATS attitude stabilization boom packages, describing torque transmission, drum synchronization, electrical isolation, lubrication, etc 16 p2846 A70-34145

Application satellites, discussing uses in communications, meteorology, earth survey and navigation 18 p3333 A70-36348

Geomagnetic storms at ATS 1 in 1967, discussing storm-time disturbance field and associated pulsations 19 p3410 A70-37488

Optimum launch trajectories for ATS-E mission with noncircular parking orbits, considering apogee motor size, perigee radius and duration constraints [AIAA PAPER 70-1051] 19 p3528 A70-38866

One millipound cesium ion thruster for synchronous ATS-F satellite, describing power conditioning and control logic subsystems [AIAA PAPER 70-1149] 20 p3690 A70-40205

Multiple channel VHF testing on ATS 1 and 3, describing transponder intermodulation and compression corrections 21 p3791 A70-41366

Management organization of European operational application satellite systems, concerning interurban telecommunication and air traffic control 22 p4127 A70-43502

U.S. aerospace industry participation in European Application Satellites Program 22 p4127 A70-43506

Tracking and data relay satellite system performance by ATS and Nimbus spacecraft for range and range rate tracking and command and data transmission [AIAA PAPER 70-1306] 24 p4374 A70-45949

Electronic data handling and CRT display of ATS satellite cloud pictures 24 p4371 A70-46048

APPROACH

NT INSTRUMENT APPROACH

APPROACH CONTROL

NT RADAR APPROACH CONTROL

Head-up display for horizon, desired and actual approach paths information to assist pilot during approach, landing and overshoot 02 p0330 A70-11842

Secondary surveillance radar and interferometry techniques to determine aircraft positions in real time and all weathers for air terminal approach control 02 p0331 A70-11965

Terminal area approach control sequencing, using digital computer to allocate identification mode and landing time slot 02 p0332 A70-11971

Aircraft approach and guidance system radio components including localizer, glide path and marker systems and radio altimeters, discussing signal interference 02 p0333 A70-11980

Scanning beam radio guidance system for VTOL approach and landing 02 p0336 A70-12766

Tactical landing approach radar /TALAR/ guidance system for V/STOL aircraft steep angle approach and landing 02 p0336 A70-12767

Thrust control unit in Lufthansa Boeing 707 aircraft designed to maintain landing approach speed by adjusting throttle setting and landing flap position
05 p0845 A70-15903

Runway acceptance rate improvements to alleviate air traffic congestion metroplex areas, using approach and landing sequence model for conventional jet aircraft
[AIAA PAPER 70-74] 06 p1029 A70-18078

Sector Tactical Air Navigation System to supply on-board information on bearings, slant range and elevation and computer input signals
09 p1720 A70-22491

Nuclear landing roll aid based on gamma radiation field built along approach line, runway and taxiways
09 p1721 A70-22662

Sector-TACAN /SETAC/ system suitable for mobile approach and landing aid due to high accuracy and small dimensions
09 p1721 A70-22663

Subsonic glide landing approach guidance for unpowered lifting vehicles, using perturbation feedback and approximation of heading and position coordinates
[AIAA PAPER 69-865] 09 p1725 A70-23253

Visual threshold effect on closed loop control of aircraft of poor resolution studied by flight simulation of approach and flare, showing degraded control accuracy
[AIAA PAPER 70-357] 10 p1858 A70-24206

Hybrid simulation, determining vehicle and performance parameters on longitudinal flying qualities of STOL transport in power approach configuration
[AIAA PAPER 70-387] 10 p1806 A70-24918

V/STOL aircraft ground guidance systems using microwave instruments for approach and landing
[SAE PAPER 700322] 12 p2266 A70-27458

Microwave scanning beam landing system providing aircraft radio approach guidance
12 p2269 A70-27918

Terminal constraints affecting matrices comprising linear impulsive guidance law for earth approach, discussing Mars mission
13 p2447 A70-28516

Precision approach and landing guidance system selection by RTCA committee, discussing aircraft antennas, scan rates, international cooperation, etc
[AIAA PAPER 70-937] 17 p3134 A70-35846

Stochastic processes with linear dynamics and quadratic control cost, considering application to aircraft landing approach path optimization
18 p3279 A70-35973

Time-synchronized approach control, combining aircraft precision navigation and guidance with ATC equipment
19 p3466 A70-38237

Avionics role in STOL air transportation operational capabilities in congested air traffic environment
19 p3466 A70-38238

Category II longitudinal approach system model taking into account inputs, gusts, ILS beam noise, man machine interaction, etc
[AIAA PAPER 70-1034] 20 p3665 A70-39503

Pilot/vehicle feedback systems with flight director computer for transport aircraft longitudinal control during landing, discussing design by manual control displays theory
[AIAA PAPER 70-1001] 20 p3560 A70-39530

Aircraft landing maneuver optimization by in-flight monitoring of approach and landing phases, furnishing decision making display
[AIAA PAPER 70-1000] 20 p3560 A70-39531

Automatic control systems for aircraft approach to landing path and subsequent stabilization on trajectory, compensating for cross wind action and radio noise disturbances
20 p3561 A70-39842

General aviation traffic control, discussing limitations of present system and improvements of position information and area navigation approach procedures
22 p4066 A70-42385

Wheel force and roll moment nonlinearities effect on light STOL aircraft handling qualities during approach
[ICAS PAPER 70-55] 23 p4139 A70-44151

Helicopter automatic approach and hover coupler systems, discussing cockpit display devices, handling qualities, pilot workload and fatigue and external load stabilization
23 p4140 A70-44464

Fluidics in naval avionics, discussing CH-46A helicopter stability augmentation and approach power compensator for carrier-based aircraft
24 p4293 A70-45428

High energy close approach trajectories within planar free fall three body problem, using perturbation theory
24 p4412 A70-45984

APPROACH INDICATORS

Aircraft approach and guidance system radio components including localizer, glide path and marker systems and radio altimeters, discussing signal interference
02 p0333 A70-11980

Pattern recognition concepts applied to synthesis of aircraft approach progress monitor as adjunct to pilot decision process, discussing feasibility experiments [SRCC-106] 02 p0335 A70-12138

APPROXIMATION

NT BORN APPROXIMATION
NT BORN-OPPENHEIMER APPROXIMATION
NT CHEBYSHEV APPROXIMATION
NT EDDINGTON APPROXIMATION
NT FINITE DIFFERENCE THEORY
NT FINITE ELEMENT METHOD
NT HARTREE APPROXIMATION
NT LEAST SQUARES METHOD
NT MILNE METHOD
NT NEWTON-RAPHSON METHOD
NT OSEEN APPROXIMATION
NT RAYLEIGH-RITZ METHOD
NT RELAXATION METHOD [MATHEMATICS]
NT RITZ AVERAGING METHOD
NT SCHWARTZ METHOD
NT SOMMERFELD APPROXIMATION

Chapman-Enskog expansion for Boltzmann equation solution, using PLK method to obtain higher approximations for shock wave structure
01 p0063 A70-10923

Parametric approximation method extended to incompressible laminar boundary layers with surface suction or injection
02 p0277 A70-11857

Generalized multiple scales method for solving linear differential equations with variable coefficients applied to Liouville-Green approximation
03 p0518 A70-12994

Approximate solution for hypersonic inviscid flow around spherically blunted bodies at small angle of attack, noting stagnation problems
03 p0407 A70-13547

Approximate solutions to Cauchy problem describing controlled pursuit using approximate method of integrating Bellman equation
04 p0713 A70-14602

Transport theory application to differential approximations for radiative transfer problems
[ASME PAPER 69-WA/HT-45] 04 p0781 A70-14801

Governing equations of plane elasticity to define suitable approximate theories for structural analysis
[ASME PAPER 69-WA/APM-22] 04 p0771 A70-14909

Waveform-shaping transfer function rational polynomial approximation method with application to network problem in PCM communications
06 p1007 A70-17459

Weinstein approximation and iteration by digital computer for calculating disturbed Fabry-Perot laser resonator modes
06 p1081 A70-17546

Multidimensional stochastic approximation theorems useful for infinite-dimensional Hilbert space or Banach space
07 p1324 A70-19029

Approximation for axisymmetric hodograph equation for nozzle calculation
07 p1188 A70-19347

Approximate method for celestial mechanics problems, considering particle motion under gravitation from central body in cylindrical coordinate system
07 p1387 A70-19626

Dynamic characteristics approximation in transfer functions class with singularity at infinity
07 p1327 A70-19806

Laminar boundary layer equations solution by approximation compared with results from finite difference method
08 p1483 A70-21033

Navier-Stokes equation approximation for nonhomogeneous case obtained by relating Burgers equation to Riccati equation through similarity transformation
09 p1711 A70-22613

Nonlinear differential equations approximate periodic solutions generation by finding equivalent system in sense of minimum mean square difference
09 p1712 A70-22666

Laminar boundary layer in adverse pressure gradient calculated for momentum thickness from approximate equation, analyzing error
09 p1660 A70-22832

Chaplygin function approximation in subsonic steady gas flow analysis
10 p1909 A70-24293

Simultaneous singular integral equations approximate solution in orthogonal polynomials
10 p1909 A70-24603

Approximations implicit in Cayrel statistical equilibrium or non-LTE analysis of ionic hydrogen bound free continuum in sun
10 p1947 A70-24989

Algorithm developed for constructing first approximation system from Cauchy matrix for Liapunov stability problem solution
10 p1917 A70-25302

Monograph on conditions for stabilization of oscillatory systems with random parametric excitations

covering approximate calculations, stability concept definition, etc
11 p2129 A70-25496

Dynamic programming successive approximation method application to airline scheduling, reviewing real time dispatching, operations, schedule and fleet planning
11 p2013 A70-26209

Feedback controller specific suboptimal estimation and control parameters determination using stochastic approximation algorithms
11 p2026 A70-26236

Time-convergent approximations to statistical turbulence functions constructed starting with functions expansion as Taylor series in time
11 p2074 A70-26534

Markov nonlinear optimal filtration theory exact equations replaced by finite system of approximate differential equations
11 p2012 A70-26805

Book on successive approximation methods in control and oscillation theory covering two point boundary value problems iterative solutions, orbital transfer, etc
12 p2260 A70-26852

Vlasov equation approximate solution by minimum energy principle, deriving equilibrium equation for stellar gas
13 p2457 A70-28552

One dimensional radiatively driven acoustic waves analysis by approximation for radiative heat addition, achieving better accuracy than substitute-kernel method
13 p2520 A70-28633

Chaplygin approximate hodograph method variants diagrams and tables with numerical values for proper application
13 p2442 A70-29486

Complex error function computation using approximation method with single algorithm
14 p2599 A70-30648

Lambert problem solution for moderate timespan arcs by approximation, offering concise formula without iteration
14 p2639 A70-30705

Optimal trajectory and control approximate solution by asymptotic expansion, considering Mayer variational problem solution
16 p2943 A70-33897

Boundary value problem approximation method for large numbers, using projective method applicable to linear integral, integrodifferential and differential equations
18 p3282 A70-36360

Nonlinear approximation under auxiliary conditions in normed space involving minimum solution
18 p3282 A70-36363

Eigenvalues and errors in asymptotic approximation of ordinary differential equations of second and fourth order
18 p3283 A70-36365

Equivalent bodies of revolution method extension for use in semiempirical approximation technique, calculating pressure distribution of nonaxisymmetric blunt bodies
18 p3208 A70-36569

Atmospheric inhomogeneity, comparing effective mass and Curtis-Godson approximation methods for transfer function of absorbing gas distribution
19 p3461 A70-37632

Ordinary differential equations piecewise polynomial approximation using subpartitioning to liquidate residuals
19 p3458 A70-38356

High order servosystems approximation characterized by gain, time constant and dead time, discussing application to response prediction
19 p3394 A70-38503

Nonlinear discrete uniform approximation of real valued functions by gradient method
19 p3459 A70-38677

Simultaneous approximation of function and product with given operator, applying to boundary value problems of partial differential equations
19 p3459 A70-38682

Differential equations approximate solution by interval differential equations, obtaining graphs with analog computer
19 p3459 A70-38931

Orthotropic shells under arbitrary loads, deriving approximation equations
20 p3734 A70-40436

Chandrasekhar H function approximation for isotropic scattering, calculating absorption line contours
22 p4109 A70-43750

Minimal deviation estimates for linear approximations by seminorms for space defined by differential equations
23 p4210 A70-44018

Convex programming solution using quadratic approximation method with objective function
23 p4211 A70-44027

- Vertical velocity effects on ionospheric horizontal wind magnitude and direction, solving integral equations system by successive approximations
23 p4188 A70-44057
- Approximations by spline functions and polynomials, discussing modulus of continuity
24 p4369 A70-45126
- ## APPROXIMATION METHODS
- ### U APPROXIMATION
- ## APSIDAL ANGLES
- ### U ANGLES [GEOMETRY]
- ### U APSIDES
- ## APSIDES
- NT APOGEES
NT PERIGEEES
NT PERIHELIONS
- Secondary minimums role in studying eclipsing variable stars, correlating observability with detection of line of apsides motion
08 p1581 A70-21759
- ## APT [PICTURE TRANSMISSION]
- ### U AUTOMATIC PICTURE TRANSMISSION
- ## APTITUDE
- Flying accident liability predictions reliability from pilot trainee aptitude test performance at selection, discounting accident proneness theory
12 p2178 A70-27048
- Aptitude test validity taking into account selection board subjective decisions on pilot applicant acceptance
19 p3371 A70-38507
- ## AQUEOUS SOLUTIONS
- Quartz and alkaline glasses fracture stability in water vapor and aqueous solutions with enhanced surface activity as function of time
11 p2068 A70-25379
- Rhyolitic obsidian glass devitrification rate in water and alkali solutions, noting increase in Na or K rich solutions
11 p2070 A70-26003
- Oxygen and hydrogen diffusion coefficients in aqueous potassium hydroxide electrolyte solutions at various temperatures and concentrations
12 p2181 A70-27575
- Ag species paramagnetic relaxation in gamma-irradiated frozen aqueous solutions and in frozen methanol, relating spin-lattice relaxation to isotropic coupling
14 p2544 A70-30117
- Electrochemical processes associated with stress corrosion cracking of Ti-Al-Mo-V alloy in aqueous environments
15 p2755 A70-31474
- Diffusion coefficient of dissolved oxygen in blood proteins aqueous solutions
15 p2686 A70-32848
- Backscattered radiation depolarization during illumination of aqueous medium by linearly polarized laser beam
15 p2753 A70-32861
- Electrochemical oxidation of p-type boron anode in aqueous solutions, using galvanostatic technique
17 p3041 A70-34514
- Corrosion and stress corrosion behavior comparison of aged Al-Zn-Mg alloy in aqueous chloride solution, discussing pH variation effect
18 p3271 A70-36028
- ESR intensities and line widths at X and Q bands of Cr and Fe molecular ions in water/glycerol mixtures
24 p4310 A70-46045
- Laser gain coefficient increased via organic compounds addition to rhodamine 6G aqueous solution
24 p4356 A70-46273
- ## ARC CHAMBERS
- Hotshot wind tunnel performance improvement by coating arc chamber with silastane to retard heat loss and metal pollution
17 p3057 A70-34774
- ## ARC DISCHARGES
- Disturbances effect in Langmuir layer at cathode on ionization rate in arc discharge, estimating ion density and width of nonequilibrium ionization region
01 p0150 A70-10171
- Negative resistance I-V characteristics of low voltage arc discharge in Cs plasma
01 p0150 A70-10172
- Low voltage arc discharge in thermionic converter at low Ce pressures measured for current-voltage characteristics, showing degree of ionization
01 p0150 A70-10173
- Arc phenomena for producing interaction effects, discussing reflected shocks rarefaction waves and gas dynamics
02 p0345 A70-11863
- Nonequilibrium cesium plasma of low voltage arc discharge, measuring electron temperature and distribution function and diffuse-series excited level populations
03 p0532 A70-13740
- Molecular cesium ion production by arc discharge in inhomogeneous cesium plasma, describing probable reaction mechanism
08 p1551 A70-20849
- Disturbances effect in Langmuir layer at cathode on ionization rate in arc discharge, estimating ion density and width of nonequilibrium ionization region
10 p1925 A70-25017
- Low voltage arc discharge in thermionic converter at low Ce pressures measured for current-voltage characteristics, showing degree of ionization
10 p1925 A70-25018
- Electrode erosion or entrainment in MPD arcs due to excess current density, considering inner cathode and outer ring anode with axial magnetic field
10 p1925 A70-25040
- Vacuum arc discharge phases before total breakdown, studying high combustion voltage relation to interplasma double layer potential difference
10 p1969 A70-25115
- Gas jet bounding of Ar arc column, providing high power/intensity light source
12 p2237 A70-28159
- Magnetically constrained steady state plasma production by hot cathode DC arc discharge in He
13 p2465 A70-29819
- Coupled temperature and electric potential distribution in finite rotational symmetric hydrogen arc column in axial magnetic field
14 p2621 A70-30656
- Radial ion temperature distribution in hydrogen arc within axial magnetic field measured spectroscopically by thermal Doppler effect
14 p2621 A70-30657
- Coaxial electrode arc discharge plasma accelerators at reduced pressure under crossed fields, employing Hall effect
15 p2779 A70-32104
- Ar arc discharge magnetically induced retrograde rotation dynamics, using high speed photography
19 p3475 A70-37533
- Microwave diagnostics of plasma temperature and conductivity in streaming nitrogen arc with skin effect under atmospheric pressure
19 p3476 A70-37554
- Acceleration processes in MPD arc jet in Ar for symmetric discharge layer and rotating spoke types
20 p3680 A70-39992
- Arc luminosity in cathode region of quasi-steady MPD arc jet, using high speed photography and electric and magnetic field probes
20 p3683 A70-40242
- Nonequilibrium flow adjacent to cooling tube wall confining cascade arc plasma electrical discharge
21 p3805 A70-41763
- Arc ignition and cathode spot movement dynamics of thermionically emitting cathode surfaces in heat feedback plasma
21 p3859 A70-41903
- Constricted arc characteristics in air and nitrogen at various pressures, considering spectral lines radiation transfer and electron, atom and ion temperature difference effects
22 p4079 A70-42369
- Electric field radial distribution measured for stationary hydrogen arc with axial magnetic field
23 p4227 A70-44933
- Quasi-ambipolar diffusion in arc discharges in magnetic field, calculating ions and electrons density distributions between anode and cathode sheaths
24 p4384 A70-45148
- ## ARC GENERATORS
- Constricted DC Ar arc with N or O additions calibrated as vacuum UV radiation standard for photon flux measurements
02 p0343 A70-11905
- Equilibrium model of laminar arc constrictor plasma generator, correlating heat transfer, wall shear stress, friction factor and development length
03 p0533 A70-13952
- Transpiration-cooled constricted arc for plasma generation, considering transport properties, LTE assumptions and porous tube flow characteristics
07 p1351 A70-19898
- Wall stabilized arc source for spectroscopic measurements of isothermal plasma at various pressures
14 p2584 A70-30505
- Electrical and thermal characteristics of DC magnetic annular arc operating continuously at atmospheric pressure
21 p3805 A70-41758
- ## ARC HEATING
- Gas-stabilized electric arc heater electrical and gas dynamic parameters, studying velocity and enthalpy radial distributions and IV characteristics
03 p0531 A70-13386
- Spectrally and spatially resolved measurements on arc heated Ar plasma radiation for eliminating discrepancies in transition probabilities
06 p1122 A70-18187
- Phenolic nylon ablative thermal effectiveness in arc heated nitrogen, air and nitrogen-carbon dioxide streams
06 p1183 A70-18233
- Time of flight spectroscopic measurements in arc heated supersonic molecular beam using algebraic relations, sensing modulated beam by Orbitron type detector
06 p1111 A70-18266
- Electrical and thermal characteristics of stabilized gas heating by electric arc at high pressures calculated by successive approximation
07 p1350 A70-19840
- Binary mixture molecular beam apparatus combining aerodynamic acceleration and arc heating techniques, discussing particle energy and density
07 p1341 A70-20106
- Gas flow in arc heaters, discussing dissociation, ionization, swirl flow, arc discharge, gas temperature/pressure ratio, gas composition, etc
08 p1554 A70-21925
- Arc driven shock tunnel operation with expansive area change at main diaphragm, evaluating flow characteristics
09 p1657 A70-23279
- Carbon oxyfluoride IR radiation from boundary layer formed by arc-heated air passing over Teflon surface
10 p1968 A70-24475
- Austenitic stainless steels high temperature machining with W arc heating, considering constant pressure feeding and chip breaking method
20 p3638 A70-39943
- Langley 20 megawatt plasma accelerator design and operation, describing arc heater modifications, exit parameters, electrical properties, etc
20 p3606 A70-40010
- Hypersonic test flow in arc heated wind tunnel, measuring freestream Pitot pressure, mass flux, stagnation point heat transfer rate and wall pressure
20 p3607 A70-40270
- Dissociated and ionized hypersonic flows of hydrogen heated by electric arc techniques, investigating flows in wind tunnel nozzles
22 p4011 A70-42759
- Planar resonance probe in free molecular arc heated flowing plasma, examining shift nature in measured frequency position of minimum drawn current
22 p4081 A70-43013
- Phenolic nylon ablative thermal effectiveness in arc heated nitrogen, air and nitrogen-carbon dioxide streams
23 p4282 A70-44520
- ## ARC JET ENGINES
- Spectral line widths in MPD arc jet measured to determine plasma electron density and heavy particle temperature
03 p0536 A70-14371
- Entrainment rate of ambient medium by MPD arc jet, discussing flow field in and around jet and pressure distribution along vacuum tank wall
03 p0553 A70-14373
- Pulsed MPD arc jet electric propulsion system requirements, examining physical constraints, pulse duration, duty cycle, power network structural details, etc
04 p0737 A70-15424
- Dynamic I-V characteristics of megawatt pulsed MPD-ARC plasma thruster under various axial magnetic fields given for Ar and hydrogen propellants
06 p1131 A70-18092
- Pulsed plasma vacuum-arc thruster system incorporating throttle and thrust vector controls for long life satellite control applications
06 p1133 A70-18232
- Anode energy transfer model for measurement of circumferential current and heat flux distributions of MPD arc thruster
09 p1736 A70-23203
- Surface parameters influence on energy transfer to arc jet anode, discussing work function, accommodation coefficient and diffuse reflection coefficient of electrons
12 p2281 A70-27809
- Thrust measurements on pulsed vacuum-arc thruster, comparing specific impulse and efficiency with exhaust velocity measurements by ion collecting double probes
20 p3567 A70-40207
- Low power MPD arc thruster performance with downstream cathode, using Xe propellant
20 p3693 A70-40251
- Cathode geometry effect on performance of radiation cooled MPD arc thruster in continuous mode
20 p3693 A70-40252
- Electrolytic capacitor current pulse networks for quasi-steady MPD arc thrusters, determining series resistance effects on energy transfer
20 p3568 A70-40253
- Exhaust velocity, electron density and temperature of pulsed megawatt nitrogen MPD-ARC thruster, using Thomson scattering of pulsed laser light
20 p3694 A70-40254
- Quasi-steady MPD arc thruster average thrust measurements, considering time-of-flight velocity determination by ion collecting probes
20 p3694 A70-40255
- High temperature acceleration of propellants in electrothermal thrusters including resistojets, arcjet, thermionic and plasma configurations
22 p4091 A70-42763
- ## ARC LAMPS
- Xenon arc lamp searchlight performance and application during Apollo 8 launch
12 p2207 A70-27662

- Xenon high wattage short arc lamps for space/solar simulators, describing seals, electrodes shapes and cooling, operating characteristics, etc
[AIAA PAPER 69-998] 13 p2384 A70-28520
- Operation characteristics of flash, arc, incandescent and explosion type laser pump lamps
13 p2431 A70-29874
- Airborne illumination using argon vortex-stabilized arc lamp, noting applicability in near IR spectral range
17 p3023 A70-35152
- Anodes heat transfer in xenon short arc lamps
17 p3023 A70-35154
- Solar simulators using water cooled 30 kw Xe arc lamps
17 p3060 A70-35248

ARC MELTING

- Heat exchange coefficient during Ti melting in lined arc furnace, determining relation between heat flows to side walls and bottom of graphite crucible
08 p1506 A70-21140
- Ti alloy ingot chemical macrohomogeneity, investigating elimination by vacuum arc melting
17 p3112 A70-34355
- Electroslag melted titanium wrought shapes mechanical properties, comparing with double vacuum arc melted material properties
17 p3112 A70-34356

ARC SPRAYING

- Pulsed spray welding electrode melting rates for Al alloy, mild steel and stainless steel electrodes over range of pulse current levels
22 p4046 A70-43147

ARC WELDING

- NT GAS TUNGSTEN ARC WELDING
- NT PLASMA ARC WELDING
- Gamma ray beam inspection of opposed arc weld with nugget penetration in Al-Cu alloy, including averaging circuit reducing counting statistics variation
01 p0054 A70-10020
- Hydrogen, oxygen and nitrogen effects on gas shielded arc weld porosity of Ni, comparing MIG and TIG processes
02 p0310 A70-12543
- Joining small components made of difficult to weld materials by percussive welding consisting of stationary and moving electrode actuated by pretensioned spring
10 p1894 A70-24298

- DC arc facing welding device using vacuum to minimize pores, slag inclusions, cracks and defects
13 p2384 A70-28867

- Magnesium pulse arc welding, describing procedure, techniques testing and advantages
17 p3100 A70-34635

- Arc welding in space under high vacuum weightless conditions, describing equipment design and Soyuz 6 experiments
19 p3436 A70-37803

- Arc welding, discussing use of magnetic fields for improving quality
22 p4042 A70-42375

- Temperature, metal vapor density and energy balance in Ar shielded welding arc with Fe electrodes
22 p4043 A70-42381

- Pressure role in inert gas shielded metal arc welding, discussing voltage-pressure relation, weld head profile, metal transfer, etc
22 p4043 A70-42383

- Pulsed spray welding electrode melting rates for Al alloy, mild steel and stainless steel electrodes over range of pulse current levels
22 p4046 A70-43147

- High speed radiographic observation of electric arc movement and metal transfer during submerged arc welding
24 p4322 A70-45724

- Gamma ray inspection of opposed-arc weld-nugget penetration in Al-Cu alloy
24 p4350 A70-46384

ARCAS ROCKET VEHICLES

- ARCAS meteorological rocket system designed for upper atmospheric soundings to provide thermodynamic and wind data, discussing payloads
07 p1395 A70-20256

- Arcas rocket-borne chemiluminescent ozonesonde for measuring ozone concentration after deployment above stratopause level
07 p1396 A70-20263

ARCHES

- Snap-through dynamic instability of clamped shallow arches subjected to timewise step loads, establishing stability and instability conditions
03 p0583 A70-12919

- Inextensional nonlinear theory of arches applied to analysis of hinged-hinged circular arches subjected to downward point load, calculating critical load value
07 p1408 A70-19561

- Optimal inextensional buckling of uniformly loaded simply supported arches with large opening angle
08 p1589 A70-21310

- Elastic-plastic work hardening sandwich arch under given loading rate analyzed for stress rates using integral equation
[ASME PAPER 69-APM-21] 08 p1593 A70-21616

- Finite deflections theory applied to elastic-plastic arches, introducing coefficients depending on shape and degree of yielding of cross section
10 p1955 A70-24080

- Circular arch finite element solutions compared for convergence rates
12 p2327 A70-27838

- Circular sandwich arch subject to central concentrated load and symmetrically applied edge couple, obtaining shakedown interaction curve
19 p3546 A70-38354

- Clamped circular shallow Al arches stability under impulsive loading, obtaining deflection time history by high speed photography and computerized data reduction
20 p3732 A70-40265

- Elastic circular sandwich beams optimal design for minimum compliance and given weight, considering rings and semicircular arches
24 p4420 A70-45276

- Shallow arch clamped at ends and subjected to uniform lateral load, deriving nonunique equilibrium stability states
24 p4426 A70-46038

ARCS

- Critical slope load calculation for circular elastic embedded and supported arcs under radial and variable force
07 p1404 A70-19136

- Curve arc approximation by circular arc using Chebyshev modulus-minimax principle
13 p2442 A70-29743

ARCTIC REGIONS

- Explosive and diffuse stratospheric warmings over Arctic attributed to solar activity and stratospheric circulation
20 p3618 A70-39184

- Synoptic processes in Arctic tropospheric and lower stratospheric warming correlated with atmospheric circulation transformations
20 p3619 A70-39186

- Arctic and antarctic atmospheric circulation differences, discussing circumpolar vortices and isobaric surfaces altitude changes
22 p4065 A70-43168

ARGENTINA

- Report to COSPAR on Argentine Space Research Commission covering sounding rockets, cameras, launching bases, research, balloon flight, etc
15 p2829 A70-31701

ARGON

NT ARGON ISOTOPES

- Ar ion laser with high discharge current density observed for working level populations by simultaneously measuring power gain and spontaneous emission lines intensity
01 p0106 A70-10063

- Human pulmonary gas mixing between large airways and alveolar spaces, using argon bolus inhalation
01 p0024 A70-10976

- Vibrational relaxation times in carbon dioxide and carbon dioxide-argon mixtures at 360-3000 K, using shock tube and laser schlieren method
01 p0148 A70-11355

- Ionizing shock wave propagation into magnetic field from Ar gas flow characteristics in electromagnetic shock tube
03 p0532 A70-13548

- Ar X and Ar XIV identification in solar corona and unidentified coronal lines origin, discussing Fe and Ni transitions from metastable levels
03 p0571 A70-13598

- Production rates determination for Na 24 and Mg 28 isotopes in Ar exposed to cosmic rays
03 p0561 A70-14092

- Electron beam technique to measure density profiles of strong shock waves in argon
04 p0692 A70-15325

- Ar laser as suitable source for LF heterodyne anemometry experiments through noise spectrum suppression under optimum conditions
04 p0702 A70-15569

- High temperature thermal transport and ionization relaxation in Ar from measurements by thin film surface thermometer in high pressure shock tube end wall
04 p0787 A70-15607

- Pulsed Ar ion lasers at high currents, measuring plasma parameters, electrical conductivity, electron temperature and density for inversion mechanism
04 p0703 A70-15617

- Response variation and detection efficiency of funnelled channel electron multipliers for low energy protons and Ar ions
06 p1021 A70-17623

- High energy Ar atomic beams scattering from single crystal face of W measured for distribution pattern
06 p1112 A70-18270

- Ar beam scattering and UV radiation from glass target surface with adsorbed gas layer
06 p1112 A70-18274

- Diatomic Br molecular vibration-rotation coupling effects on energy transfer during Br-Ar collisions, determining probability distributions
07 p1339 A70-20054

- Energy distribution of positive Ar ions scattered from thermal diatomic D noting inelastic collisions
07 p1339 A70-20056

- Thermal accommodation coefficients of Ar atomic beams scattered from nominal plane of Ag crystal measured by time of flight techniques
07 p1343 A70-20125

- Ar-Kr integral collision cross sections based on density measurements of Ar beam passed through liquid nitrogen cooled Kr filled scattering chamber
07 p1344 A70-20135

- Anodic precursors of convergent cylindrical shock wave of z-pinch discharges in He and Ar
07 p1261 A70-20357

- Shock ionized Ar flow properties estimation using alignment charts
08 p1551 A70-21324

- Weld porosity in TIG welding of technical Ni in ternary mixtures of Ar with H, O and N
08 p1518 A70-21345

- Photon scattering by Ar in vacuum UV measured for cross sections
09 p1730 A70-22071

- Vacuum UV photons production during ground state neutral argon atomic collisions, measuring relative cross sections energy dependence
09 p1731 A70-22333

- Fast argon beam scattering by gas molecules measured to study atomic and molecular two body systems involving nitrogen and oxygen atoms
09 p1732 A70-22902

- Ar and nitric oxide free jets clumber and cluster abundance dependence on nozzle diameter and reservoir temperature and pressure
09 p1733 A70-22907

- Fast electrons spatial distribution for multiple scattering in nitrogen and argon, noting target thickness and incident energy
09 p1735 A70-23179

- Acoustic velocity in rarefied argon and nitrogen using Brillouin scatter and Burnett equations
09 p1698 A70-23314

- Wave number, intensity and half width of vibrational-rotational lines pertaining to transition of carbon monoxide perturbed by argon
09 p1733 A70-23316

- Thermal conductivity coefficients of argon in 25-700 C range and up to 1200 bars pressure, using vertical concentric cylinder apparatus
11 p2147 A70-25754

- Chemical kinetic model for photoexcitation and photoionization of cold argon ahead of strong shock wave, predicting electron and excited atom concentrations
11 p2090 A70-25953

- Energy dependence and threshold behavior of ion Ar lines excited in low-energy He ion-Ar collisions
11 p2087 A70-26402

- Ar ions excitations by low energy electron collisions, noting excitation functions and cross sections of lines and levels by optical methods
12 p2278 A70-27501

- Mode transition characteristics of free burning argon electric arc with transpiration cooled anode, noting current blowing parameter
12 p2281 A70-27806

- Ionization and metastable excitation in low energy collisions of ground state argon atoms formed by charge transfer
14 p2618 A70-30121

- Closed loop MHD test facility ARGAS I, describing engineering performance and test measurements
14 p2533 A70-30532

- Penning pump argon stability, noting influence of pressure and ion incidence angle on cathode surface
15 p2744 A70-31847

- Scattering cross sections for monoenergetic Ar beams on epitaxial Ag films
16 p2956 A70-34013

- Cyclopropane-argon mixtures translational and vibrational energies exchange efficiencies analysis based on intermolecular potential
16 p2956 A70-34083

- Excitation cross sections for Ar I and He I spectral lines in low energy He ion-Ar collisions
17 p1318 A70-34642

- Radionuclides production rates in stratosphere from spallation reactions of cosmic rays with Ar
17 p1312 A70-35759

- Argon and helium breakdown induced by ruby laser 50-picosec pulse at various pressures
18 p3267 A70-36616

- Ionized argon supersonic flow velocity and local electron density by optical methods
19 p3480 A70-38173

- Thermal release profiles and retention coefficients of injected argon ions for silicates and iron simulating meteoritic materials
19 p3474 A70-38601

- Stagnation point heat transfer of spherical cylinder in argon and air, developing electrically insulated calorimeter gage theory
21 p3941 A70-40774

- Absorption diffuse band systems of diatomic argon molecule in vacuum UV region 21 p3853 A70-41395
- Aerodynamic parameters of ionized Ar supersonic steady one dimensional nonviscous flow in thermodynamic equilibrium and subjected to Laplace accelerating forces 21 p3858 A70-41444
- Autoionization spectral lines growth curves analysis, applying to 3s-4p transition in Ar at 466 Å with specified absorption cross section 21 p3781 A70-41931
- Atomic Ar absorption spectrum in vacuum UV region, observing Rydberg series interactions as perturbations and autoionizations 21 p3781 A70-41933
- Temperature, metal vapor density and energy balance in Ar shielded welding arc with Fe electrodes 22 p4043 A70-42381
- Three body recombination and dissociation rate coefficients of nitrogen in Ar atoms heat bath, using modified phase-space theory 23 p4221 A70-44008
- CO vibrational relaxation measurements in shock tube expansion wave generated in argon heat bath 23 p4180 A70-44009
- Cryogenic fluids nitrogen, argon and carbon monoxide nucleate boiling from atmospheric to near critical pressure 23 p4279 A70-44359
- Partially ionized Ar transport properties, computing electron velocity distribution function as perturbation for Lorentzian mixture 23 p4220 A70-44437
- Argon matrix isolated ammonia, examining IR spectra by carbon dioxide laser irradiation 24 p4354 A70-45648
- ARGON ISOTOPES**
- He 4 and Ar 40 abundance in lower Venus atmosphere, underlining He 4 dominance in upper atmosphere 03 p0575 A70-13982
- Miniaturized proportional counter to measure radioactive Ar 37 ultramicroquantities, assessing errors 05 p0898 A70-15930
- Block diagrams of three stage device for extracting radioactive Ar from perchloroethylene considered for solar nucleus studies 05 p0845 A70-15933
- Ar 37 and Ar 39 isotopes in recently fallen iron-astatite and stony meteorites, discussing relevance to cosmic ray variations in space 12 p2309 A70-27950
- Lunar atmosphere as source of Ar 40 and other elements in surface materials, discussing implantation by photoionization and subsequent interaction with solar wind fields 17 p3172 A70-35624
- Tritium and Ar radioactivities attributable to galactic and solar cosmic ray interactions in Apollo 11 lunar rocks and soil 21 p3906 A70-41564
- Surface correlation of excess Ar 40 in lunar fines from Apollo 11 21 p3908 A70-41582
- Cosmic ray exposure age of lunar surface material by radioactive isotopes Ar 37 and 39 measurement, investigating temperature dependence 21 p3909 A70-41607
- Apollo 11 crystalline rocks chemical analysis by argon 40/argon 39 dating techniques 21 p3778 A70-41613
- Chondritic meteorite thermal histories based on K-Ar dating using Ar 39/40 method 21 p3921 A70-41974
- ARGON LASERS**
- Argon CW lasers stationary thermal self focusing in various absorbing crystals and glasses 01 p0107 A70-10207
- Real time recording and permanent display, using high power energy density focused Ar laser beam for ink transfer 01 p0111 A70-10782
- Matrix method applied to achromatic linear phase plates design for polychromatic Ar lasers half wave phase shift 01 p0113 A70-10988
- Ionized Ar laboratory laser development using Fabry-Perot etalon cavity and amplifying plasma obtained by electric current passage under pressure 02 p0311 A70-11869
- Rapid photoprocesses decay kinetics, using CW Ar ion laser beam interrupted periodically by electro-optical shutter 02 p0314 A70-12742
- Mode selection in Ar ion laser by plane resonator mirror with hole, plotting output power vs L/R parameters 03 p0500 A70-13458
- Longitudinal magnetic field effect on output power and emission polarization of CW Ar laser employing Brewster windows 03 p0500 A70-13529
- Argon ion CW lasers, discussing design, inverse population, plasma, radiative transition probabilities, pumping, frequency spectra and active medium 07 p1298 A70-19642
- Holograms produced with pulsed argon-ion lasers operating in singly oscillating transverse modes 07 p1287 A70-20088
- Argon ion laser output powers dependence on discharge tube design and mirror reflection coefficient in emission line 08 p1511 A70-20541
- Emission saturation in Ar CW laser at high discharge current densities under different pressures and tube channel parameters 08 p1511 A70-20542
- Time delay between pulses of discharge current and ionized argon laser power as function of current and discharge pressure 09 p1697 A70-22847
- Ar ion laser performance improvement by using beryllia for sealed-off discharge tube 09 p1699 A70-23443
- Microscopic behavior and excitation processes found similar in argon ion lasers with hollow cathode or conventional heated oxide cathode discharge 11 p2063 A70-26370
- Argon laser upper levels population measured as function of current strength at constant atom density in capillary 12 p2247 A70-27506
- Argon CW laser blue beam self focusing in methylene iodide, iodine and liquids under steady state conditions 12 p2248 A70-27545
- Ar ion lasers investigated for effect of added He on pulse output intensity 13 p2426 A70-28809
- CW argon lasers simultaneous mode selection and phase locking by electro-optic KDP crystals 15 p2753 A70-32610
- Transverse magnetic field effect on CW argon laser operation with linearly polarized radiation 15 p2754 A70-32866
- Single frequency Ar ion laser, discussing power and frequency stability 17 p3105 A70-35095
- Time resolved measurements of ion and electron temperature in pulsed Ar ion laser discharge, observing heating 17 p3108 A70-35907
- Ar ion laser gas discharge tube construction, using anodically oxidized directly cooled aluminum segments 19 p3444 A70-37567
- Argon ion laser inversion saturation at large current densities due to upper working levels depletion 19 p3449 A70-38744
- Pulsed argon ion laser output properties from electron temperatures and densities produced by He-Ar gas mixture 20 p3640 A70-39137
- Argon laser for long pulse low duty cycle operation, discussing construction and performance 22 p4052 A70-43602
- Ionized Ar laser developments, considering power output and radiation spectrum 24 p4356 A70-46324
- ARGON PLASMA**
- Constricted DC Ar arc with N or O additions calibrated as vacuum UV radiation standard for photon flux measurements 02 p0343 A70-11905
- Nonequilibrium potassium seeded Ar plasma electrical conductivity at atmospheric pressure, noting current density role 02 p0347 A70-12232
- Laser emission action at 4880 Å in plasma discharge from injecting electron beam into Ar at different pressures 03 p0530 A70-13063
- Electron relaxation in shock heated Ar plasma estimated by measuring radiation intensity at various frequencies 03 p0535 A70-14363
- Ar plasma interaction with concentric cool hydrogen sheath for simulation study for gaseous core nuclear space propulsion system 03 p0536 A70-14375
- Electric discharges in low pressure Ar in external magnetic fields, studying charge in transport coefficients and drift due to MHD forces 04 p0724 A70-14529
- Striated plasma flow in MHD duct of conducting rings using Ar with K vapor detected by high speed camera 04 p0725 A70-14533
- Discharges in Ar flow in membrane shock tube at Mach 5, discussing plasma compression, shock wave position and effect on electrode region 04 p0725 A70-14534
- Heat transfer in partially ionized argon plasma flowing in water cooled circular tube as function of temperature, Reynolds number and tube entrance diameters [ASME PAPER 69-WA/HT-54] 04 p0780 A70-14795
- Stability and shape of magnetically balanced atmospheric cross-flow arcs in Ar noting balanced modes 04 p0729 A70-15549
- Diagnostic methods for field-free plasmas with medium dispersed optical-spectrographic and source monitoring equipment 06 p1063 A70-17728
- Spectrally and spatially resolved measurements on arc heated Ar plasma radiation for eliminating discrepancies in transition probabilities 06 p1122 A70-18187
- Single and double cylindrical Langmuir probe responses in highly expanded low density flowing Ar plasma [AIAA PAPER 70-85] 06 p1066 A70-18207
- Molybdenum single crystals orientation effect on thermal resistance to argon plasma flow 07 p1309 A70-19614
- Relative transition probabilities of Si I and II determined from emission spectra obtained by injecting SiC14 vapor into argon plasma jet 09 p1737 A70-23315
- Argon plasma interaction with RF electromagnetic field using MGD model, noting plasma-field coupling and plasma temperature exhibition of skin effect 09 p1737 A70-23433
- Plasma instability in RF discharge in Ar in magnetic field 10 p1840 A70-24540
- Electron temperature and concentration in decaying He and Ar plasmas with cesium vapor addition 11 p2092 A70-26733
- Current density distributions in Ar-K plasma streams through channel with segmented electrode array, measuring electron temperatures 13 p2461 A70-28732
- Shock waves in partially ionized gas discharge argon plasma, recording potential jump at wavefront 13 p2388 A70-29419
- Induction plasmas in thermal equilibrium dominated by radial conduction losses, discussing energy balance equation and Ar plasmas at atmospheric pressure 13 p2465 A70-29701
- Thermal induction plasma discharge characteristics, considering radiation and conduction losses 13 p2465 A70-29702
- High argon plasma temperatures via pulsing constricted electric arc 14 p2621 A70-30504
- Gas kinetic pressure profile and mass density of propagating current sheet in argon pinch discharge, using piezoelectric transducer 14 p2624 A70-31041
- Neutral particle temperature, pressure and velocity measurements in argon plasma jet, using refraction index 14 p2625 A70-31350
- Transport properties of partially ionized argon based on electron velocity distribution function, comparing to Chapman-Enskog calculations 15 p2774 A70-31799
- Gas pressure effects on visible and UV laser action in small argon Z-pinch plasma discharge, using streak photographs 15 p2750 A70-31968
- Argon II line transition probabilities, observing UV spectral region, upper energy levels and temperature differences 16 p2956 A70-34251
- Transverse magnetic field effects on Ar cross flow arc temperature distribution, cross section shape and profile, discussing forced convection effects [AIAA PAPER 70-777] 17 p3138 A70-34477
- Argon plasma viscosity measurements at one atmosphere and 10-13,000 K, using discharge with laminar flow as plasma source [AIAA PAPER 70-775] 17 p3139 A70-34479
- Oxygen, nitrogen and argon plasma total radiation measurement at various wavelengths and temperatures 17 p3139 A70-34547
- Magnetic fields effect on probe measurements in weakly ionized Ar plasma flow at atmospheric pressure 17 p3139 A70-34693
- Electron emission effects on ion sheath and probe characteristics in continuum argon plasma 17 p3083 A70-34994
- Time dependent characteristics of dense argon plasma formed by pulsed lasers, measuring shock wave front velocity with streak camera 17 p3104 A70-35083
- Ar plasma generation by focused Q switched ruby laser beam, measuring density and temperature by electro-optical spectroscopy 17 p3107 A70-35111
- Ar arc discharge magnetically induced retrograde rotation dynamics, using high speed photography 19 p3475 A70-37533
- Ionization relaxation behind reflected luminous shock front in argon plasma flow interaction with magnetic fields, using spectroscopic and streak interferometric observations 19 p3479 A70-37814

Equilibrium compositions of helium-nitrogen, argon-nitrogen and xenon-nitrogen plasmas at atmospheric pressure between 5000 and 35,000 K
19 p3552 A70-37831

DC plasma generator with Ar stabilized arc, investigating heat and mass transfer in jet discharge channel
19 p3481 A70-38189

Energy distribution of ions transversal to magnetic field in argon plasma source with oscillating electrons, showing dependence on induction and discharge current
19 p3482 A70-38956

Laser interferometry with unstable external resonator, determining radial electron density distributions during implosion phase of linear z-pinch discharge in argon
20 p3630 A70-39420

Preionization in Cs seeded Ar nonequilibrium plasma for MHD generators, examining discharge characteristics, recombination reactions, etc
20 p3680 A70-39991

Acceleration processes in MPD arc jet in Ar for symmetric discharge layer and rotating spoke types
20 p3680 A70-39992

Supersonic weakly ionized plasma jet in argon, investigating axial and radial temperature profiles by electrical probe techniques and spectroscopic and photographic methods
20 p3685 A70-40463

LTE verification for argon plasma generated in free burning arc by measuring atomic line transition probability at various pressures
21 p3854 A70-40588

Decomposition kinetics of alumina particles injected into thermal argon induction plasmas
21 p3855 A70-40878

Alfven waves amplification propagating along sinusoidally perturbed magnetic field in argon plasma, noting parametric excitation
21 p3855 A70-40947

Wall heat transfer for partially ionized argon laminar flow within square channel conducting walls with and without transverse magnetic field
21 p3856 A70-41032

Extended homogeneous stationary field-free spherical plasma source, including radial density measurement with Langmuir probe in argon
21 p3805 A70-41463

Electron-ion recombination in Ar plasma, discussing transition from collisional-radiative to dissociative process as function of electron density and temperature
21 p3858 A70-41711

Numerical analysis of inductive electrodeless discharge of thermal Ar plasma column heated by RF axial magnetic field
21 p3859 A70-41902

Maintenance voltage of RF argon thermal induction plasma at atmospheric pressure as function of ring probe
21 p3859 A70-41904

Cs seeded Ar discharges electron energy distribution, discussing drift velocities, electrons elastic and inelastic collisions with ions and molecules, etc
22 p4081 A70-43198

Gas transport properties at high temperatures and pressures, discussing Ar plasma arc characteristics
23 p4226 A70-44433

Partially ionized gas electron-ion recombination rate coefficients calculation methods compared with Ar plasma data
23 p4226 A70-44436

Temperature distribution and thermal conductivity determination in Ar plasma cascade arc
23 p4226 A70-44438

Atmospheric pressure Ar plasma viscosity measured over heavy particle temperature range 3500-8500 K, using DC wall stabilized cylindrical arc
23 p4229 A70-44983

Clean shock tube maintaining high gas purity level for Ar plasma spectroscopy
24 p4388 A70-46271

ARGON 36

U ARGON ISOTOPES

ARGON 40

U ARGON ISOTOPES

ARGUMENTS [MATHEMATICS]

U INDEPENDENT VARIABLES

ARIEL SATELLITES

NT ARIEL 3 SATELLITE

UK space program, describing scientific satellites, Black Arrow launch vehicle and sounding rockets
17 p3167 A70-35206

ARIEL 3 SATELLITE

Square loop antenna radiation resistance in warm plasma, comparing theoretical results with measured values from Arie 3 satellite antenna
21 p3796 A70-40562

Global thunderstorm activity experiment by Arie 3 satellite, investigating lightning discharge number and noise power
22 p4015 A70-42778

ARIES CONSTELLATION

X ray source GX341-6 with soft spectrum detected in Aries constellation by Aerobee rocket, including neighboring X ray sources in determining galactic coordinates, positions and fluxes
02 p0372 A70-12249

ARIP [IMPACT PREDICTION]

U COMPUTERIZED SIMULATION

U IMPACT PREDICTION

ARITHMETIC

NT FLOATING POINT ARITHMETIC

Aircraft computer design performing basic arithmetic operations by sampling method noting speed increase
06 p1014 A70-17859

Trachtenberg rapid calculation methods for multiplication, describing triangular or double product method and general algebraic theory
07 p1327 A70-19785

Arithmetic codes rate upper bound derived by combinatorial analysis, discussing decoding method for multiple error correction
08 p1465 A70-20792

Digital coding systems operational capabilities, discussing arithmetic procedures and equipment types
14 p2554 A70-30678

ARITHMETIC AND LOGIC UNITS

Small digital computer arithmetic unit design, discussing number representation, addition and subtraction methods for performance and cost
21 p3793 A70-40757

ARM [ANATOMY]

NT FOREARM

Training effect on strength per unit cross sectional area of arm muscle, using ultrasonic measurement
17 p3024 A70-34592

ARMATURES

Temperature field in thermally stressed electric machine rotor obtained by solving Poisson and Laplace equations with digital computer, using network method
03 p0414 A70-13517

Capacitive pressure transducer with linearly coupled armatures for aerospace use
11 p2051 A70-26294

ARMED FORCES

NT ARMED FORCES [FOREIGN]

NT ARMED FORCES [UNITED STATES]

NT NAVY

ARMED FORCES [FOREIGN]

Royal Air Force air reconnaissance function, discussing cameras, films, processing and printing, photointerpretation, etc
03 p0495 A70-14144

Health conditions and operational efficiency of Italian military paratroopers during air transportation analyzed from questionnaire data
05 p0807 A70-16494

Centralized maintenance system organization, describing centralized system used by Spanish Air Force units
06 p1184 A70-17274

ARMED FORCES [UNITED STATES]

R and D laboratories quality and performance evaluation techniques, describing Apstein-modified Pelz technique
06 p1185 A70-17603

Procurement problems for U.S. Defense Department taking into account fighter F-15 development for USAF
07 p1428 A70-19672

Long range army budget forecasting model based on research projects cost distributions and parameters, describing computer program
09 p1794 A70-23415

Automatic base communication system /ABCS/ to handle USAF worldwide base record communications centered on electronic store and forward message switch, utilizing stored programs
11 p2009 A70-26266

Army aviation requirements in high intensity conflicts, discussing transportation, communications, intelligence acquisition, organization and suitable aircraft types
23 p4142 A70-44855

Harrier aircraft operation in Marine Corps for fast reaction close support based near maneuver units [SAE PAPER 700835]
24 p4290 A70-45887

ARMOR

Transparent ceramic armor fabrication using dense polycrystalline magnesia
19 p3437 A70-38422

Armor airframed helicopter for aerial armored reconnaissance vehicle, noting design, fabrication and weight
23 p4137 A70-44095

AROMATIC COMPOUNDS

Photochromic aminotriarylmethane filter solutions for flash blindness protection, noting stability against xenon flash UV exposure
04 p0690 A70-15028

Polymers with high temperature oxidation resistance, discussing problems caused by aromatic heterocyclic structures and manufacturing methods
05 p0873 A70-16604

Sterically hindered aryldiazonium salts absorption spectra and quantum yield data interpretation, considering photochemical properties
12 p2182 A70-28300

High temperature aromatic polyester Ekonol, discussing fabrication, properties and potential applications
21 p3842 A70-41136

Aromatic polymers synthesis for good thermal stability, describing single and double stranded chains
21 p3782 A70-42127

Aromatic polysulfone thermomechanical behavior by torsional braid analysis, discussing structure, synthesis, thermal stability, radiation effects, etc
21 p3783 A70-42134

AROUSAL

Arousal effects on vestibular nystagmus in man, discussing forced alertness in mental arithmetics form
14 p2538 A70-30911

Vestibular habituation acquisition, retention and transfer correlation with stimulation, discussing alertness and arousal effects
14 p2539 A70-30915

Noise effects on arousal level in auditory vigilance from EEG parameters
19 p3364 A70-38325

Norepinephrine synthesis inhibition effect on arousal triggering and maintenance in hibernating golden hamsters, examining sympathetic activity
23 p4148 A70-44874

ARRAYS

NT ANTENNA ARRAYS

NT ENDFIRE ARRAYS

NT LINEAR ARRAYS

NT PHASED ARRAYS

NT STEERABLE ANTENNAS

NT SYNTHETIC ARRAYS

NT YAGI ANTENNAS

Solar cell array fabrication methods extending operating temperature by pulsed spot welding techniques and deletion of adhesives
02 p0228 A70-12080

TEM wave reflection incident on conducting thin strips semiinfinite array in free space not accompanied by emission
05 p0812 A70-16243

Natural convection flow interactions from individual surfaces in closely spaced array of heated elements, discussing effect on heat transfer, induced flow and temperature field
07 p1418 A70-18644

Optical signal processing using circular array and spatial frequency filtering to yield azimuthal distribution of sources
09 p1678 A70-22969

Optimal pulse allocation for radar array in simultaneous tracking of multiple targets, suggesting algorithms
13 p2365 A70-29068

Combinational logic cells cellular arrays synthesis, considering truth table and transition matrix
15 p2712 A70-32606

Finite parallel plate waveguide arrays edge effects, comparing element radiation patterns and reflection coefficients vs scan
16 p2860 A70-32953

Mechanical design and mounting technique of Apollo 11 fused silica laser ranging retroreflector array at Tranquility Base
17 p3082 A70-34763

Optimum receiver for acoustical holography using discrete transducers arrays for image conversion
17 p3088 A70-35029

Incompressible fluid flow past array of arbitrary profiles vibrating with arbitrary phase shift, taking into account blade displacement and vortex wake effect
18 p3206 A70-36277

Plane wave diffraction by periodic array at boundary between two media, discussing asymptotic behavior of reflection and transmission coefficients
21 p3806 A70-40614

Electromagnetic scattering by two dimensional periodic arrays of conducting thin plates, calculating induced current and near field radiation distribution
23 p4165 A70-44961

ARRESTERS

Aircraft arresting hook response to impact regarding beam flexibility and internal damping using numerical wave propagation methods
10 p1963 A70-25069

ARRESTING GEAR

Commercial aircraft launching and arresting systems for airport runway length reduction, discussing safety factors [SAE PAPER 700264]
18 p2327 A70-36821

Portable catapult and arresting gear analog instrumentation data acquisition system testing aboard aircraft carriers and at land-based facilities
19 p3384 A70-38533

ARRHYTHMIA

Arrhythmia resembling atrial flutter simulated in dogs by coronary sinus and left atrial pacing and in man by coronary sinus pacing
02 p0240 A70-12696

Doppler flowmeter-catheter system to record aortic flow velocity in man during cardiac arrhythmias, considering atrial fibrillation, heart block, etc
02 p0241 A70-12697

Human atrial flutter studies using electrocardiographic electrodes placed within esophagus and right atrium
03 p0424 A70-13773

Evidence supporting concept of His bundle and not A-V node as pacemaker site in nodal rhythms using electrode catheter technique
03 p0424 A70-13774

Psychosocial factors in myocardial infarction and sudden death, considering possible causes of fatal cardiac arrhythmia
04 p0635 A70-15462

Ventricular ectopic beats and bradyarrhythmia associated with myocardial infarction, discussing enhanced automaticity, reentry activity, drugs and heart pacing
06 p0998 A70-18407

Bradycardic rhythms in acute myocardial infarction, investigating pathophysiologic, hemodynamic and electrophysiologic aspects and ECG interpretation
06 p0998 A70-18408

Arrhythmia monitor for cardiac distress prediction, using small hybrid computer for detection of abnormal rhythm and ECG complex comparison
07 p1221 A70-19604

Heart rhythm disorders among flying personnel, noting occurrence frequency of sinus bradycardia and arrhythmia
12 p2180 A70-28362

Multifocal atrial tachycardia, discussing arrhythmia progression to atrial fibrillation and association with acute and chronic diseases
21 p3761 A70-41134

ARSENIC ALLOYS
Amorphous semiconductor alloys in As-Se system, measuring DC and AC electrical conductivity dependence on temperature
24 p4390 A70-45657

ARSENIC COMPOUNDS
NT ARSENIDES
NT GALLIUM ARSENIDES
NT INDIUM ARSENIDES
Glass formation region of chalcogenide semiconductor arsenic triselenide-antimony triselenide system and vitreous-crystalline transformation, investigating electrical and optical properties
01 p0153 A70-10085

Vapor composition and condensed phase structure of As and Sb compounds with group VIA elements analyzed by laser mass spectrometer
08 p1455 A70-21339

ARSENIDES
NT GALLIUM ARSENIDES
NT INDIUM ARSENIDES
Gallium found suitable for doping cadmium/tin arsenide semiconductor, exhibiting hole-type conductivity
01 p0156 A70-10214

Hall effect and electric conductivity of cadmium arsenide at high temperatures as function of carrier concentration dependence on temperature and phase transformation
07 p1357 A70-20314

Magnesium arsenide phosphide crystal and magnetic structure using X ray and neutron diffraction
12 p2283 A70-27240

Amorphous boron arsenide films deposited on Si substrates, measuring current voltage characteristics
15 p2785 A70-32584

Visible light-emitting p-n junctions formed in AlAs via Zn diffusion into single crystal n-type vapor grown AlAs layers
18 p3297 A70-36316

ARTERIES
NT AORTA
Coronary arteries collateral circulation in man using angiographic technique
01 p0016 A70-10439

NN dimethylguanidine for prevention of arterial lesions induced by cholesterol in rabbits
01 p0020 A70-10707

Transcutaneous Doppler-shift flowmeter for arterial blood velocity measurement by ultrasound
01 p0037 A70-10880

Arterial model with effects of thick walls, linear viscoelasticity and wall tethering for studying arterial mechanics
02 p0247 A70-12550

Norepinephrine release associated with vasoconstrictor response during selective activation of arterial and venous sympathetic nerves in dog hindpaw
03 p0416 A70-13012

Postmortem coronary angiographies showing role of arterial hypertension in coronary pathology
03 p0426 A70-13939

Pulsatile flows in living animals and model arteries, discussing flow profiles, instability and wall shear
03 p0430 A70-14244

Vascular resistance and constriction and muscle mass related in pulmonary arteries of mice subjected to alveolar hypoxia
04 p0630 A70-14679

Ejection click of valvular pulmonic stenosis by external phonocardiograms and intracardiac pressure recordings during successive respiratory cycles
04 p0633 A70-15440

Primary and secondary pathological changes in small coronary arteries and role in acute myocardial infarction development, discussing coronary arteries distribution
04 p0635 A70-15457

Platelet function in coronary artery disease and myocardial infarction, considering thrombosis, atherosclerosis, emboli in microcirculation, etc
04 p0635 A70-15458

Clinicopathological studies of coronary artery occlusion and acute myocardial infarction, discussing coronary thrombosis
04 p0635 A70-15459

Coronary atheroma in hyperlipemic dog occurring in arterial tree at most intense physical stress exposure point, discussing interfacial tissue permeation
04 p0635 A70-15460

Familial aggregation for coronary artery disease and familial similarities in coronary anatomy, considering possible genetic analysis of myocardial infarction
04 p0636 A70-15467

Acute coronary occlusion effects on adjacent unoccluded artery resistance, discussing responsible mechanisms in ischemic heart
04 p0637 A70-15473

Hybrid computer simulation of small nonlinearities effects in human arterial system, using perturbation techniques
05 p0805 A70-16045

Arterial pressure and supranal blood flow in dogs under basal conditions and nerve stimulation by stochastic method using analog correlator
05 p0806 A70-16400

Peripheral arterial piezography for cardiologic screening tests and checkups of flying personnel
05 p0807 A70-16495

Blood-endothelial surface shear stress in artery inlet, considering asymmetric and radially symmetric plugging effects
07 p1220 A70-19248

Automatic control theory found effective in studying arterial blood saturation with oxygen during ascent to 4000 m in pressure chamber
07 p1210 A70-19523

Atmospheric pressure-diameter relationship of common carotid artery in head and neck region of conscious men
08 p1447 A70-21508

Cholinergic nervous mechanism of autoregulatory dilatation of pial arteries under decreased blood supply to cerebral cortex in rabbits
09 p1622 A70-23583

Arterial oscillograms, pressure and heart beat rate during prolonged hypodynamia, noting neurocirculatory dystonia
10 p1817 A70-24693

Left ventricular volumes, pressure and heart rate in patients and dogs after diagnostic coronary arteriography
10 p1820 A70-24939

Arteriographic determination of severe coronary artery disease in presence of normal resting electrocardiogram
12 p2170 A70-27775

Autonomic effects on heart rate, portal, renal, cutaneous and muscle blood flows during arterial hypoxia in unanesthetized sham operated thalamic and pontine rabbits
12 p2170 A70-27899

Intraarterial hot film constant temperature anemometry for point blood velocity measurements, detecting flow reversal
15 p2688 A70-31435

Wave propagation through Newtonian fluid in compressible thick walled viscoelastic tube, considering blood flow in arteries
15 p2691 A70-31938

Comparative arterial pressure pulse transmission velocity in dogs, relating wall elasticity with vascular disease
15 p2682 A70-31939

Phase errors of hydraulic input impedance of arterial bed due to proximal or distal pressure measurements
15 p2682 A70-31940

Mechanical model of arterial viscoelasticity effect on input impedance and wave travel in systematic tree
15 p2691 A70-31941

Arterial wall nonlinear distensibility effects on blood flow velocity profiles, considering various mathematical and physical artery models
17 p3035 A70-34468

Mathematical model of pulsatile viscous entrance flow in thick walled elastic tube, investigating flow development effects in large arteries
17 p3035 A70-34471

Arterial pH change effects on circulation and oxygen consumption in dogs, discussing respiratory acidosis heart rate, cardiac output and arterial blood pressure
17 p3024 A70-34593

Centrifugation effects on human peripheral arterial pulse behavior
17 p3037 A70-35126

Arterial blood carbon dioxide tension effects on rhythmic volley activity of respiratory medulla oblongata neurons in cats
17 p3030 A70-35354

Intact femoral artery pressure-diameter relationship in man, discussing noradrenaline infusions effects
18 p3222 A70-37222

Arterial pressure measurement by automatic control system based on external compression pressure for maximum amplitude intraarterial pressure pulse oscillations
19 p3370 A70-38215

Human body elastic properties effects on arterial pressure measurement by sphygmomanometer
20 p3581 A70-39879

Human arterial hypertension, correlating ECG changes with systemic hemodynamics
20 p3573 A70-40069

Body position effect on oxygen saturation of regional pulmonary venous blood and arterial-venous shunts in intact dogs
21 p3766 A70-42153

Cardiological examination of flying personnel, taking ECG anomalies and artery wall elasticity into account
22 p3981 A70-43694

Atherosclerosis and latent coronary insufficiency diagnosis in flight crews, evaluating various tests
22 p3975 A70-43696

Systolic and diastolic pressure in central artery of retina in deep-sea divers during oxygen inhalation at atmospheric pressure
23 p4150 A70-45081

Ganglerone and quaterone cholinolytic agents effects on arterial blood acid-base balance indicators in cats
24 p4298 A70-45633

Conduit arteries viscoelastic properties in normal and hypertensive dogs from recorded pressure and diameter waves
24 p4299 A70-45808

Arterial hemodynamics in hypertension, discussing pulse changes mechanism as consequence of decreased arterial distensibility via disturbed relationship between ventricular ejection wave and impedance characteristics
24 p4299 A70-45809

Oxygen transport, arterial resistance and consumption in normovolemic and hypovolemic dogs in hemorrhagic shock
24 p4302 A70-46106

Vagus nerve blockage effect on arterial carbon dioxide tension and breathing regulation in dogs
24 p4303 A70-46112

HF sinusoidal fluid pressure generators driven by electromagnetic vibrators for arterial applications
24 p4309 A70-46118

ARTERIOSCLEROSIS
Nutrition and atherosclerosis - Conference, Bad Ragaz, Switzerland, October 1968
03 p0430 A70-14276

Statistical data to demonstrate atherosclerotic diseases affected by cholesterol and saturated fatty acids in foods
03 p0430 A70-14277

Biochemical, electron microscopy and experimental medicine data indicating pathogenetic mechanism responsible for arteriosclerosis
03 p0431 A70-14278

Simplified laboratory test program yielding serviceable information for possible direct laboratory diagnosis of risk factors affecting atherosclerosis
03 p0431 A70-14279

Interactions between nutrition, blood coagulation and atherosclerosis by Duguid theory, emphasizing fibrinolysis, thrombosis and alimentary lipids
03 p0431 A70-14280

Cardiology role in aviation medicine, evaluating jumbo jet and SST flight stress effects on pilots and passengers in age factor study of arteriosclerosis
05 p0803 A70-16721

Frequency analysis of arterial sounds used in studying atherosclerosis, correlating spectra with jet flow turbulence past occlusion
06 p1003 A70-18220

[AIAA PAPER 70-144]
Cinecoronary arteriographic investigation of chest pain patients, establishing correlations of clinical symptoms, coronary artery narrowing, arterial lesions, serum cholesterol levels, etc
23 p4145 A70-43948

Morphology of adult mammalian thoracic and abdominal aortic segments indicating deviation from medial lamellar architecture
24 p4298 A70-45801

ARTHROPODS
NT BEETLES
NT CEPHALOPODS
NT DROSOPHILA
NT INSECTS
NT MOLLUSKS
NT MOTHS

ARTICULATION

Speech intelligibility tested using Modified Rhyme Test and air traffic control and civil disaster vocabularies, noting Articulation Index for signal-noise conditions

02 p0246 A70-12150

Asynchronous delta modulation channels with RLC integrators in feedback circuit, measuring articulation in presence and absence of noise

20 p3587 A70-40144

ARTIFACTS

Indirect blood pressure measurements using motion artifact suppression circuit based on K-sound electrocardiography

24 p4296 A70-45335

ARTIFICIAL CLOUDS

Needle-shaped filament artificial ion cloud drift and diffusion in F1 region plasma in presence of neutral wind and uniform electric field

01 p0070 A70-10401

Near IR reflection spectra of artificial cumulus clouds with progressive droplet sizes

01 p0076 A70-10911

Test program preceding first German satellite experiment using HEOS satellite for Ba ion cloud injection into deep space

02 p0380 A70-12081

Atmospheric density in meteor region and atmospheric wind conditions determined from meteor trail drifting and artificial noctilucent clouds

03 p0563 A70-13178

Cloud chamber investigation of artificial cloud of water droplets in electrostatic field, discussing cloud precipitation, collection efficiency and fog dissipation

05 p0879 A70-16689

Atmospheric density determined by using diffusion coefficients obtained from artificial luminous clouds observations

06 p1096 A70-17785

Large scale artificial plasma cloud experiments for magnetosphere, solar wind and cometary physics, discussing Ba ion and ice clouds released by satellites [AIAA PAPER 70-33]

06 p1145 A70-18183

Barium ion artificial clouds motions and striations due to cloud-ionsphere coupling, studying electron density variations below cloud in E layer

07 p1271 A70-20155

Expansion and deceleration of rocket-released artificial ion cloud in terms of snowplow expansion model and drag deceleration

07 p1271 A70-20159

Wind velocity and direction and diffusion coefficients measurements by artificial luminous clouds, injecting appropriate reagents from rockets

11 p2075 A70-25918

Monograph on ambipolar diffusion and motion instability of satellite produced artificial barium ion clouds in ionosphere and magnetosphere

11 p2048 A70-26825

Plasma experiments in space including electric fields measurement, collisionless plasma studies and artificial Ba cloud generation

12 p2214 A70-26868

Comet tail simulation by using fast acting gas valve to produce gas cloud for interaction with plasma stream

12 p2298 A70-27190

Signal decoder for barium USA Germany /BUG/ project command reception system, discussing Ba ion cloud propagation and expansion along geomagnetic field

13 p2367 A70-29557

Ba ion cloud motions agreeing with electric field data from balloon measurement in ionosphere and magnetosphere

13 p2402 A70-30079

Spherical ionized cloud movement in ionosphere uniform anisotropic plasma as function of electric field applied to rocket released ion clouds

15 p2726 A70-31867

Barium ion clouds striation formation above E layer ascribed to LF gradient drift instability

15 p2727 A70-31908

Upper atmospheric atomic nitrogen reaction with carbon tetrachloride, estimating radiation intensity and brightness of artificial luminescent cloud

18 p3252 A70-36989

Emission spectral distribution of atomic nitrogen reaction with carbon tetrachloride for artificial luminescent clouds

18 p3293 A70-36990

Wind velocity and direction determination from artificial luminescent clouds photographs, calculating topocentric coordinates

18 p3252 A70-36991

Upper atmospheric wind velocity and diffusion coefficient measurement by radar observation of artificial electron cloud from atomic K ejection

18 p3253 A70-36993

Artificial ion clouds motion in magnetosphere, using MHD model

19 p3414 A70-38378

Striation formation in artificial ion clouds aligned with local geomagnetic fields, considering visual indi-

cation of ionospheric electric field transferal along magnetic field

19 p3415 A70-38387

Luminous intensity profile of optically thick Sr artificial clouds in upper atmosphere, using Monte Carlo calculations

19 p3415 A70-38388

Upper atmosphere and magnetosphere DC electric field measurement using artificial clouds

22 p4017 A70-42791

ARTIFICIAL EARS

Directional dependence of broadband artificial ear signal spectrum and correlation functions using dummy head

09 p1624 A70-22761

ARTIFICIAL GRAVITY

Artificial gravitation parameters for manned compartments of spacecraft, analyzing permissible angular velocity and rotation radius regarding vestibular-vegetative disorders

04 p0760 A70-14446

Manned space stations development, objectives, supply, storage and waste disposal, launching and artificial gravity

05 p0923 A70-16042

Physiopathological effects of weightlessness, showing desirability of partial gravity for long voyages via spacecraft rotation

09 p1621 A70-23439

Artificial gravitation parameters for manned compartments of spacecraft, analyzing permissible angular velocity and rotation radius regarding vestibular-vegetative disorders

13 p2503 A70-28471

Energy consumption in male subjects during walking and running in erect and supine position under simulated gravity

13 p2351 A70-29335

Acceleration measurements on switchback cars, revolving cabins and oscillating attractions in amusement parks, noting motion sickness rarity

17 p3037 A70-35136

Vibration effects on vestibular components, noting applications to spacecraft artificial gravity

17 p3038 A70-35322

Attitude control of artificial gravity mass-unbalanced axisymmetric orbital space stations

23 p4258 A70-44502

Rotating flexible cable-connected space station dynamic scale model, describing suspension system and artificial gravity generation

23 p4258 A70-44528

Reflex vestibular disturbances and motion sickness prevention in artificial gravity of rotating space base, by incremental adaptation tests and drugs

23 p4154 A70-44625

Artificial gravity simulation effects on human performance in space base [AIAA PAPER 70-1329]

24 p4417 A70-45938

ARTIFICIAL INTELLIGENCE

Machine design similar to human brain for recognition and classification of information

09 p1641 A70-22708

Aliphatic ethers low resolution mass spectra interpretation using computer program heuristic

09 p1631 A70-23400

Heuristic programs and approaches in artificial intelligence

15 p2706 A70-32565

Computerized automatic ground equipment /CAGE/ as intelligence system for checkout and control of launch vehicles and spacecraft

19 p3397 A70-37915

Soviet book on computer design and construction covering man machine interfaces, internal languages, interpretation systems, memory distribution, solution processes, etc

19 p3385 A70-38794

ARTIFICIAL RADIATION BELTS

Artificial injection of trapped electrons into geomagnetic field by low altitude nuclear explosions, examining electron flux and energy

21 p3816 A70-41086

ARTIFICIAL RESPIRATION

U RESUSCITATION

ARTIFICIAL SATELLITES

NT ACTIVE SATELLITES

NT AEROS SATELLITE

NT ALOUETTE SATELLITES

NT ALOUETTE 1 SATELLITE

NT ALOUETTE 2 SATELLITE

NT APPLICATIONS TECHNOLOGY SATELLITES

NT ARIEL SATELLITES

NT ARIEL 3 SATELLITE

NT ATS 1

NT ATS 3

NT ATS 5

NT BEACON SATELLITES

NT BIOSATELLITE 3

NT BIOSATELLITES

NT COMMUNICATION SATELLITES

NT COSMOS SATELLITES

NT COSMOS 5 SATELLITE

NT COSMOS 44 SATELLITE

NT COSMOS 110 SATELLITE

NT COSMOS 149 SATELLITE

NT D-1 SATELLITE

NT DIADEME SATELLITE

NT DODGE SATELLITE

NT EARLY BIRD SATELLITES

NT EARTH RESOURCES TECHNOLOGY SATELLITES

NT ECHO SATELLITES

NT ECHO 1 SATELLITE

NT ECHO 2 SATELLITE

NT ELEKTRON 2 SATELLITE

NT ELEKTRON 4 SATELLITE

NT ENVIRONMENTAL RESEARCH SATELLITES

NT EOS

NT ESRO SATELLITES

NT ESRO 1 SATELLITE

NT ESRO 2 SATELLITE

NT ESSA SATELLITES

NT ESSA 9 SATELLITE

NT EXPLORER 1 SATELLITE

NT EXPLORER 4 SATELLITE

NT EXPLORER 17 SATELLITE

NT EXPLORER 19 SATELLITE

NT EXPLORER 20 SATELLITE

NT EXPLORER 22 SATELLITE

NT EXPLORER 31 SATELLITE

NT EXPLORER 32 SATELLITE

NT EXPLORER 33 SATELLITE

NT EXPLORER 38 SATELLITE

NT EXPLORER 40 SATELLITE

NT GEODETIC SATELLITES

NT GEOPHYSICAL SATELLITES

NT GEOS 1 SATELLITE

NT GEOS 2 SATELLITE

NT GRAVITY GRADIENT SATELLITES

NT HEOS A SATELLITE

NT HEOS SATELLITES

NT IMP

NT INTELAT SATELLITES

NT ISIS SATELLITES

NT ISIS-A

NT LINCOLN EXPERIMENTAL SATELLITES

NT LUNAR ORBITER

NT LUNAR SATELLITES

NT METEOROLOGICAL SATELLITES

NT MIDAS 4 SATELLITE

NT MOLNIYA SATELLITES

NT NAVIGATION SATELLITES

NT NIMBUS SATELLITES

NT NIMBUS 2 SATELLITE

NT NIMBUS 3 SATELLITE

NT NIMBUS 4 SATELLITE

NT OAO

NT OGO

NT OGO-A

NT OGO-B

NT OGO-D

NT OGO-E

NT OGO-F

NT ORBIS CAL SATELLITE

NT ORBITAL WORKSHOPS

NT OSO

NT OSO-B

NT OSO-1

NT OUTER PLANETS EXPLORERS

NT PAGEOS SATELLITE

NT PASSIVE SATELLITES

NT PROTON SATELLITES

NT PROTON 2 SATELLITE

NT PROTON 4 SATELLITE

NT RADIO ASTRONOMY EXPLORER SATELLITE

NT RELAY SATELLITES

NT SAN MARCO SATELLITE

NT SAN MARCO 2 SATELLITE

NT SYNCHRONOUS SATELLITES

NT SYNCOM SATELLITES

NT TIROS SATELLITES

NT TRANSIT SATELLITES

NT VELA SATELLITES

NT VENERA SATELLITES

Algorithm for solving autonomous artificial satellite orbital elements, using successive approximations

01 p0139 A70-11503

Artificial satellite rotation study on basis of SPIN program photometric data - Conference, Kishinev, Moldavian SSR, September 1968

03 p0443 A70-13176

Artificial satellites in short period highly eccentric solar orbits of arbitrary inclination for solar gravitational quadrupole moment measurement to test general relativity

06 p1139 A70-17552

Artificial earth satellites photographic observation without chronometric recording aids, determining location and time by single indicator

09 p1635 A70-23055

Satellite coordinates estimation precision by comparing artificial satellite positions obtained simultaneously by photographic cameras

11 p2008 A70-26199

- Artificial earth satellites orientation determined by onboard telemetric measurements, constructing model for rotational motion around center of mass
12 p2314 A70-28255
- Artificial planetary satellites long term orbital evolution under strong perturbations, considering solar and lunar gravitational effects
[AAS PAPER 70-038] 17 p3155 A70-34779
- Dynamic flexible artificial earth satellites with mass distribution, considering control systems design principles
17 p3180 A70-35294
- Planar Tethered Orbiting Interferometer satellite for long wavelength solar and planetary radio astronomy, discussing deployment control and libration damping
18 p3333 A70-36230
- Artificial satellite theory main problem for small and moderate eccentricities, using perturbation techniques based on Lie transforms for computer programming
18 p3334 A70-37062
- Artificial satellite orbital motion numerical integration, computing spherical harmonic terms for earth gravitational potential
18 p3334 A70-37063
- Space environment simulator for thermal vacuum performance of artificial satellites and components
19 p3401 A70-38308
- Artificial satellites photographic observation by camera, describing sighting system, tracking adjustments and shutter controls
19 p3433 A70-38793
- Artificial satellite position visual estimates based on geometric relationship to reference stars pair accuracy
19 p3531 A70-38946
- Artificial liquid satellite orbited to verify tidal theory
23 p4183 A70-44659
- Launch optimization of artificial satellites for minimizing thermal radiative heat input during low altitude orbit
23 p4264 A70-45047
- Artificial satellite motion theory, discussing gravitational and nongravitational force effects
24 p4406 A70-45527
- Radiation pressure effects on artificial satellite motion, including earth shadow perturbation
24 p4408 A70-45554
- ARTILLERY**
Artillery type projectiles field photography in flight in connection with service integrity evaluation of weapon components under real environment conditions
03 p0490 A70-13658
- Photographic techniques for artillery projectile flight evaluation, emphasizing high speed range and drum film image synchronized cameras
13 p2407 A70-29159
- ARYL COMPOUNDS**
U AROMATIC COMPOUNDS
- ASBESTOS**
Mechanical properties of asbestos as reinforcing material for fiber filled thermoplastics compared with glass fiber
02 p0320 A70-11677
- Chrysotile-type asbestos reinforcing fiber properties and applications, tabulating asbestos fiber types for commercial reinforced plastics
05 p0873 A70-16607
- Fibrillated asbestos dispersed in thermoplastic ionomer lattices, precipitated, dried and compression molded into bars, testing for flexural modulus, flexural stress and Vicat softening temperature
10 p1906 A70-24024
- Thermoplastics reinforcement with glass and asbestos fibers taking into account fiber properties
11 p2070 A70-25825
- ASCENT**
NT CLIMBING FLIGHT
Limb-SD type ascending prominences direction and velocity correlated to flares and solar radio emission
12 p2303 A70-27707
- ASCENT PROPULSION SYSTEMS**
Flight performance of Apollo LM descent-ascent propulsion systems, considering telemetry data, prediction correlation and modifications
[AIAA PAPER 70-673] 16 p2967 A70-33577
- ASCENT TRAJECTORIES**
Multistage rocket optimum ascent regime obtained by height function of engine gas outlet velocity
06 p1155 A70-17585
- Lunar module motion during optimal ascent from moon surface into circular orbit of command module, noting descent maneuver similarity
06 p1155 A70-17881
- Apollo 11 premission planning, real time situation and postflight analysis for lunar descent and ascent phases, providing navigation correction capability for Apollo 12
[AIAA PAPER 70-25] 06 p1159 A70-18227
- STOL aircraft noise level certification based on aircraft type, landing and takeoff paths and airports
[SAE PAPER 700325] 12 p2161 A70-27459
- Atmospheric ascent optimal trajectories for medium to high lift drag ratio space shuttle type rocket vehicles
[AIAA PAPER 70-978] 20 p3714 A70-39551
- Aircraft climb and descent trajectories approximation compatible with air traffic control operation, noting parameters effects
24 p4375 A70-46239
- ASCORBIC ACID**
Histochemical detection of L-gulonolactone-phenazine methosulfate oxidoreductase activity in mammals with emphasis on vitamin C synthesis in primates
04 p0647 A70-15753
- ASIA**
Asian zone solar daily and storm time ionospheric disturbance variations synoptic study during IGY-IGC period
10 p1872 A70-23822
- ASPARTIC ACID**
Glutamic and aspartic acid concentrations in brain tissue and incubation medium after adding gamma-aminobutyric acid
01 p0018 A70-10507
- Glutamine deamidation enhancement by N-acetyl-L-aspartic acid addition to mitochondrial preparations of rabbit brain incubated in Tris buffer
01 p0018 A70-10508
- Chemostat culture method for studying control mechanisms during utilization of glucose/lactose and glucose/L-aspartic acid by populations of *Escherichia coli*
01 p0021 A70-10787
- ASPECT RATIO**
NT HIGH ASPECT RATIO
NT LOW ASPECT RATIO
Boron fiber reinforced epoxy fatigue life dependence on reinforcing fibers aspect ratio
01 p0129 A70-11082
- Stiffness and expansion properties of oriented short fiber composites, discussing longitudinal modulus and expansion strain dependence on aspect ratio
03 p0587 A70-13129
- Bulk and wall temperature measurements for natural fluid convection in container with and without baffles for various heat flux and aspect ratios
06 p1175 A70-17684
- Aspect sensitivity of HF backscatter auroral echoes in F layer, utilizing F supported ground scatter echo to account for ionospheric refraction
06 p1012 A70-18541
- Straight-walled two dimensional diffusers with incompressible steady flow, noting effects of inlet blockage and aspect ratio on performance
08 p1433 A70-21322
- Tungsten fiber reinforced aluminum composites tensile strength aspect ratio using foil metallurgy technique
09 p1703 A70-22627
- Axial flow fans performance dependence on aspect ratio from empirical relationships, plotting various component losses and stage efficiency
14 p2529 A70-31418
- MAGFET devices for integrated circuits, calculating magnetic sensitivity as function of channel aspect ratio and Hall electrode position
15 p2710 A70-32572
- Ackeret theory for infinite aspect ratio, rectangular and trapezoidal constant cord wings with arbitrary spanwise variation of profile in supersonic flow
16 p2836 A70-33748
- Boron-epoxy composites rectangular reinforcing arrays spacing aspect ratios, considering matrix stress concentrations and stiffness estimates
22 p4119 A70-43688
- ASPHERICITY**
Complex profile aspherical mirrors used in He-Ne gas laser to obtain single mode emission
03 p0500 A70-13465
- Real time hologram-interferometry application to optical aspheric surfaces testing explained by geometrical optics
09 p1676 A70-22717
- Errors estimation arising in inertial navigation equations solution while neglecting terms dependent on earth asphericity and gravitational field
11 p2077 A70-25558
- Moments equations for electrostatic gyroscope drift caused by rotor asphericity
11 p2048 A70-25559
- Crab pulsar /neutron star NP 0532/ possible spherical asymmetry indicated by pulse arrival time anomalies
13 p2486 A70-28618
- ASPHYXIA**
Metabolism in left ventricular myocardium of rabbits after asphyxiations and during postasphyxial recovery
12 p2168 A70-27624
- Ambient temperature effects on rats and white mice tolerance to hypoxia, asphyxia and hypercapnia in nitrogen-oxygen and He-oxygen atmospheres
17 p3030 A70-35353
- Extracellular spontaneous sequences of action potentials of thalamic neurons during asphyxia in rats under artificial respiration
19 p3361 A70-38306
- ASPIRATION**
U VACUUM
- ASSAULTING**
U ATTACKING [ASSAULTING]
- ASSAYING**
Assay procedures for extraction and determination of N-acetylglucosamine in soil
18 p3226 A70-36959
- ASSEMBLIES**
Two degrees of freedom assemblies transient motions using computer, solving acceleration and deceleration problems in mechanical systems
08 p1502 A70-20699
- Acoustic emissions method for monitoring structural stability of solid materials assemblies via crack formation and movement detection
22 p4027 A70-42582
- ASSEMBLING**
NT ORBITAL ASSEMBLY
Automatic test equipment for assembly shops, considering skilled personnel shortage, units complexity and repeatable test and repair
13 p2423 A70-29699
- ASSEMBLY**
Turbine rotor and stator blades twist inaccuracies in assembly due to shroud induced stresses and blade root mountings clearances
07 p1291 A70-18827
- ASSIGNMENT**
U ALLOCATIONS
- ASSIMILATION**
Hydrocarbon assimilating bacteria cultures selection, considering highest specific growth rate and maximum productivity
11 p1991 A70-25939
- ASSOCIATIONS**
U ORGANIZATIONS
- ASSURANCE**
Quality assurance of automatic testing in military or industrial equipment, including acceptance criteria and statistical proving
13 p2423 A70-29694
- ASTEROIDS**
NT ICARUS ASTEROID
NT VESTA ASTEROID
Io and Europa mass and density anomalies, indicating asteroid capture by Jupiter as comet origin theory
01 p0182 A70-10671
- Cometary and asteroidal meteors discriminated by orbital elements in region of Jovian comet family adjoining asteroidal belt
02 p0373 A70-12371
- Solar photoelectric power ion propelled probe of asteroid region, describing design and mission planning
[AIAA PAPER 69-1105] 02 p0382 A70-12529
- Manned or unmanned missions to asteroids close to earth as intermediate stage in planets formation
06 p1139 A70-17551
- Asteroid families and jet streams, searching for regularities and resonances in mean family elements
06 p1151 A70-18491
- Resonance in restricted three body problem applied to asteroidal motion in asteroid-Jupiter-sun system
06 p1152 A70-18492
- Small planets observation methods, classification and designation, discussing asteroid belt origin
08 p1572 A70-20939
- Asteroids uniaxial rotation as evidence against origin by collisional fragmentation of larger bodies
08 p1581 A70-21951
- Minor planets orbits coordinates and velocities data at osculation time
09 p1756 A70-22654
- Asteroid vs planet for manned landing site, considering Martian moons mission
11 p2108 A70-25660
- Comet-asteroid evolutionary relationship based on Hidalgo orbital analysis
11 p2114 A70-26472
- Soviet monograph on minor planets origin and physical nature, considering orbits, investigative techniques, etc
13 p2488 A70-28800
- Tabulation of minor planets positions observed by photographic equatorial at Bordeaux observatory
14 p2649 A70-31124
- Tabulations of minor planets positions photographed at Besancon observatory
14 p2649 A70-31125
- Restricted three body problem taken for intermediate orbit in constructing analytical trigonometric motion theory for resonance asteroids, calculating perturbations by Bogoliubov method
15 p2803 A70-32498
- Small planets observation methods, classification and designation, discussing asteroid belt origin
15 p2805 A70-32751
- Absorption bands in reflection spectra of various asteroids, comparing Vesta composition to meteorites and Apollo 11 samples
16 p2972 A70-32987
- Asteroid identification during different oppositions, using numbered planetoids and node catalog
16 p2974 A70-33657

Trojan asteroids in sun-Jupiter system, determining density near preceding Lagrangian point
17 p3171 A70-35445

1620 Geographos observations using Ritchey-Chretien reflector and Curtis Schmidt telescope
17 p3171 A70-35446

Asteroidal parent bodies heating by electrical induction during early solar evolution
18 p3310 A70-35938

Mathematical model of asteroidal evolution and meteoritic mass distributions under collisional fragmentation using power law
18 p3312 A70-36213

Depth distribution of radioactive nuclei generated by cosmic rays in asteroidal sized bodies, calculating primary and secondary surface layer particle fluxes
20 p3698 A70-39295

Optimized trajectories and spacecraft for solar-electric missions to asteroids, using chemical booster for injection
20 p3710 A70-40223

Solar electric propulsion unmanned asteroid belt probe, discussing propulsion system, flux data acquisition, etc
20 p3717 A70-40525

Vertical force exertion on mass at ends of elongated rotating nonspherical asteroids calculated for man safety and mobility
23 p4239 A70-43849

Restricted three body problem taken for intermediate orbit in constructing analytical trigonometric motion theory for resonance asteroids, calculating perturbations by Bogoliubov method
23 p4240 A70-43919

Minor planets, comets and natural satellites positions and motions, discussing orbit and ephemerides calculation, Icarus asteroid, etc
23 p4256 A70-45038

ASTIGMATISM

Confocal parameters, spot sizes, waist positions and stability conditions of astigmatic Gaussian beams formed by spherical mirror laser cavity resonators
01 p0108 A70-10426

Two mirror astigmatic resonator mode fields and stability determined by writing Fredholm equation suitable to geometrical optics approximation
13 p2424 A70-28596

On-line reduction of nystagmic data during vestibular bithermal caloric testing by analog technique
15 p2685 A70-32570

ASTRONICS

Evaluation technique for astronics subsystems in automated spacecraft designed for interplanetary missions, considering operation times, navigation updating and midcourse correction
11 p2079 A70-26118

Soviet book on space electronics fundamentals covering equipment problems, energy requirements, communication, features, radio remote control and correction, radio astronomy, etc
19 p3375 A70-37400

Astrodynamics and astronics - Conference, New York, October 1968, Volume 2
23 p4254 A70-45013

ASTROBIOLOGY

U EXOBIOLOGY

ASTRODYNAMICS

Vlasov equations and irreversibility in plasma physics and stellar dynamics, calculating statistical entropy and relaxation time
08 p1550 A70-20556

Mechanized Algebraic Operations software package for manipulation on computer Poisson series, noting application to celestial and nonlinear mechanics and astrodynamics
10 p1845 A70-24179

Mars imaging mission and astrodynamics interaction, discussing arrival geometry and orbit size effects
11 p2112 A70-26130

Stellar hydrodynamic equations for thin disk galaxy derived from collisionless Boltzmann equation moments
11 p2117 A70-26688

Closed universe classical and quantum dynamics by ADM Hamiltonian treatment of Einstein equations for homogeneous cosmological models
13 p2495 A70-29812

Vlasov equations and irreversibility in plasma physics and stellar dynamics, calculating statistical entropy and relaxation time
15 p2781 A70-32711

Astrodynamics and astronics - Conference, New York, October 1968, Volume 2
23 p4254 A70-45013

ASTROMETRY

Earth rotation seasonal fluctuations analyzed from astronomical observations using frequency markers and quartz clocks
04 p0681 A70-15478

Time measurement errors from astronomical observations resulting from thermal and refractive effects on instrument
04 p0756 A70-15482

Transit instrument suspension improvement by isolating unloading mechanism from horizontal axis, reducing external observation errors
04 p0693 A70-15483

Transit instrument azimuthal stability, investigating horizontal axis support, screw controls and tube position during star observations
04 p0693 A70-15484

Prismatic astrolabe errors, analyzing focal plane displacement due to temperature, micrometer motor adjustment, instrument and personal errors
04 p0693 A70-15485

Time determination at astronomical observatories using transit instrument observations concerning stellar distributions and magnitudes
04 p0756 A70-15486

Triaxial universal astrometric instrument for tracking artificial satellite path with eyepiece cross-wire, considering instrument errors
05 p0851 A70-16698

Soviet collection of papers on astrometric observations including error analysis
08 p1573 A70-21151

Instantaneous latitudes observations during stellar transit at Poltava, describing error correction procedure
08 p1488 A70-21153

Lunar occultation photoelectric measurement covering star angular diameters and diffraction patterns, ephemeris theory, astrometry close double star detection, etc
17 p3170 A70-35440

ASTRONAUT LOCOMOTION

Crew locomotion effect on spacecraft attitude control using space cabin simulator tests
01 p0036 A70-10853

Reduced gravity simulators for studies of human mobility in space and lunar missions
01 p0037 A70-10958

Prototype lunar gravity simulator for studies of reduced gravity effects on human self locomotive capability, using magnetic air bearings and body support system
01 p0037 A70-10960

Weightless astronaut self rotation by limb maneuvers producing pitch and yaw motion
07 p1219 A70-19245

Astronaut maneuvering research vehicle /AMRV/ subsystems, including automatic stabilization, attitude control, propulsion and displays
16 p2853 A70-33707

Extravehicular activity maneuvering devices, describing design and performance of Gemini project unit
21 p3929 A70-41075

Partial gravity simulators at Manned Spacecraft Center for astronaut acquaintance with dynamics of moon walking
21 p3804 A70-41192

ASTRONAUT PERFORMANCE

NT BLACKOUT PREVENTION

Soviet book on survival in space covering astronauts training, behavior, impressions, performance, etc, with historical considerations
01 p0033 A70-10493

Simulated lunar environmental facility to investigate effects of high risk vacuum, lunar gravity and terrain characteristics and spacesuit encumbrances on astronaut performance
01 p0037 A70-10961

Water immersion technique to simulate zero and partial gravity conditions for investigation of astronaut capability to execute extravehicular work procedures
01 p0038 A70-10963

Simulated zero gravity tests of force application by subjects in Apollo suits, varying worksite geometry, personnel restraints and force type and direction
01 p0038 A70-10964

Life support system model using heart rate to monitor man doing physical work in space suits under simulated space environment
02 p0245 A70-12146

Biological rhythm disturbances of astronauts during air and space travel, discussing sleeping habits, alertness under weightlessness conditions, etc
02 p0241 A70-12763

Circadian rhythms characteristics in humans, animals and plants, noting possible effects of rhythm disturbances on astronauts
04 p0629 A70-14567

Biological rhythm perturbations effect on astronauts, emphasizing waking-sleeping rhythm during space flights
04 p0630 A70-14610

Wake-sleep rhythm of spacecrews for operational capacity to maintain constant watch of spacecraft, suggesting recreation of terrestrial time cycle in space
05 p0799 A70-15766

Biological model describing spacecraft operator sensorimotor activity in response to various spacecraft control stimuli, outlining computer algorithm
05 p0810 A70-17118

Acceleration and weightlessness effects on efficiency, reliability and capacity in pilots and astronauts muscular system
07 p1202 A70-18797

Astronauts visual performance during space flight, studying reduction of visual disturbances from various physiological flight factors
08 p1444 A70-20741

Water cooled space suits automatic control based on physiological changes in astronaut during hard work
09 p1627 A70-23458

Cooling system control system for astronaut thermal equilibrium and work output maximization during extravehicular space missions
13 p2357 A70-28526

High intensity noise effects on auditory thresholds, blood pressure and time response to light stimuli, showing permissible levels during space flights
13 p2358 A70-29334

Twilight sky color visual estimation from Soyuz 5 spacecraft noting cloudiness effects
15 p2723 A70-31597

Spacecrew candidates leisure time preferences, discussing off-duty concepts for long space missions
16 p2853 A70-33709

Astronaut scientific observation capabilities, discussing flexibility and instrumental design
17 p3199 A70-34776

Visual effects in astronauts and pilots, discussing optical illusions and distance estimation errors due to accelerations, runway factors, lack of oxygen, etc
18 p3225 A70-36777

Astronauts medical examination, using thermal load as functional and diagnostic test
20 p3575 A70-40195

Space station mission and configuration concepts, discussing experimental/operational capability, crew assignments, accommodation and module sizing
22 p4111 A70-43517

Astronaut distance judgement enhancement in space by combining stereoptics effect with apparent movement phenomenon
23 p4150 A70-43965

Astronaut work capacity and adaptation during long term flight of space vehicle Soyuz-9
23 p4154 A70-44651

Apollo 13 flight rescue operation as function of flight crew performance and Mission Control Center
24 p4412 A70-45968

ASTRONAUT TRAINING

Soviet book on survival in space covering astronauts training, behavior, impressions, performance, etc, with historical considerations
01 p0033 A70-10493

Astronauts physical training for space flight requirements
04 p0629 A70-14564

Psychological factors in training and education of pilots and astronauts for optimal matching between human operator and vehicle control system
05 p0809 A70-16967

Emergency ejection from lunar landing training vehicles, describing working sequence and experimental results on astronaut and test pilot
06 p1003 A70-17717

Space flight candidate selection and physical training, comparing American and Soviet training programs for efficiency and physical requirements
07 p1216 A70-18792

Astronauts celestial training, using Mercury capsule simulator and Zeiss planetarium projector for flight simulation
08 p1481 A70-21275

Apollo crew procedures, simulation and flight planning, discussing navigation, guidance and control procedures
09 p1657 A70-23706

Apollo 11 mission crew observation of operational and scientific phenomena associated with lunar landings, discussing preflight geologic training and briefings
11 p2109 A70-25847

Medical support for long space missions based on space crews morbidity prediction, discussing onboard equipment and astronaut training
20 p3575 A70-40194

Lunar and earth surfaces imaging for astronaut training in LEM simulator
20 p3607 A70-40320

Water immersion facility training for extravehicular activities and man physical movements in spacecraft, utilizing buoyancy-gravitation balance
21 p3804 A70-41191

Lunar landing training vehicle using Lunar Module free flight simulator for earth practicing of final descent handling
21 p3750 A70-41193

Translation and docking simulator for Gemini support modified for Apollo LM active lunar orbital docking with CSM
21 p3804 A70-41194

Command module simulators for Apollo astronaut training in moon landing, using computer, exterior visual scenes and spacecraft interior replica
21 p3804 A70-41195

Lunar module simulator for Apollo flight training using computers, digital conversion, cockpit replica, infinity-optics display and instructor control
21 p3805 A70-41196

ASTRONAUTICS

IR systems in military intelligence and space research including aerospace and planetary investigations, discussing IR detection and IR and earth radiation
01 p0144 A70-11255

German society of aeronautics and astronautics, yearbook 1968
03 p0411 A70-13789

Modern astronautics, discussing postwar rocket motors and ballistic missiles construction, ELDO program, moon and planetary photographs and space walk, etc
05 p0960 A70-16627

Bibliographies for AIAA technical disciplines
09 p1792 A70-22344

Aviation and astronautics - Conference, Tel Aviv and Haifa, March 1970
11 p1978 A70-25676

Aeronautics and astronautics bibliographies for college students
12 p2336 A70-27666

Astronautics utility in astronomy, physics, earth observation, communication, commercial, military, navigational, meteorological, social applications, considering present and future possibilities
15 p2831 A70-32062

Astronautics enhancement of technical progress, discussing agricultural, geological, oceanographical, meteorological, communication, electronics, materials and medical applications
16 p3004 A70-34345

Soviet book on cosmonautics covering gravitation, engine types, spacecraft facilities, planetary exploration, etc
22 p0499 A70-42675

Astronautics - IAF Conference, New York, October 1968, Volume 1, Spacecraft systems
23 p4262 A70-45001

Astronautics - IAF Conference, New York, October 1968, Volume 4, Bioastronautics
23 p4155 A70-45022

ASTRONAUTS

NT ORBITAL WORKERS

Experiments on frozen dogs to determine localized shielding effectiveness in astronauts protection from radiation
03 p0423 A70-13710

Astronaut rescue and return of objects launched into space, discussing U.S.S.R. and U.S. proposals
03 p0612 A70-14263

Space rescue requirements for earth-returning astronauts recovery under emergency conditions, discussing recovery zones determination by space flight mission control
04 p0761 A70-14929

Experiments on frozen dogs to determine localized shielding effectiveness in astronauts protection from radiation
11 p1985 A70-25510

Evolution and current status of Apollo crew safety, discussing hazard aspects, program approach and measures and activities incorporated in project [AAS PAPER 70-051]
17 p3176 A70-34790

Astronaut weight loss relation to flight duration during manned space missions
20 p3574 A70-40125

Light flashes observed by Apollo astronauts, proposing Cerenkov radiation or direct excitation of eye retina by cosmic rays
24 p4307 A70-45403

ASTRONAVIGATION

Spacecraft orientation from onboard stellar photographs, calculating absolute and relative elements, accuracy and camera parameters
01 p0198 A70-11512

Soviet book on aeronautical astronomy covering reference stars, time and natural illumination measurements, aircraft course determination, position fixing, etc
02 p0329 A70-11695

ASTRID two axis stabilization system for rocket payloads, aligning optical axis of experiment with star [DGLR-69-42]
04 p0762 A70-15161

Transstellar space navigation, discussing system concepts, measured observables during flight, instrumentation, etc
15 p2773 A70-32060

ASTRONOMICAL CATALOGS

Solar activity [1967]/ catalog containing tabulated spot area, Wolf numbers, 1966 spot groups, etc
10 p1935 A70-23838

Systematic errors of reference star catalogs in satellite geodesy, discussing influence on orbit predictability
11 p2045 A70-26180

Near Galactic plane condensations of spectral A stars in HD catalog, investigating by Monte Carlo method and Poisson formula
15 p2797 A70-31616

Asteroid identification during different oppositions, using numbered planetoids and node catalog
16 p2974 A70-33657

Moon Surface Basic Points catalogs differences, estimating position dispersion by residuals of transformations
18 p3323 A70-37143

Stellar magnitude equation from corrected catalog data to determine absolute proper motions relative to galaxies
18 p3323 A70-37145

Uranus and Mars satellite relative measures, tabulating observations
19 p3516 A70-37932

Solar flares catalog with patrol time given on graphs, tabulating principal characteristics
20 p3700 A70-39467

Radio source master catalog giving name, coordinates, flux density and frequency of observation
20 p3713 A70-40539

OPL astrolabe catalog corrections, discussing Dan-jon prototype, color-magnitude effect, time and latitude values
21 p3887 A70-41111

Catalog 4C radio sources optical identification, determining distribution, coordinates and radio luminosity
21 p3922 A70-41978

FK4 catalog system equinox and equator point corrections from lunar transit circle observations, discussing validity of moon for orientation
21 p3922 A70-41985

Plate overlap algorithm for photographic star catalog reduction
24 p4404 A70-45413

ASTRONOMICAL COORDINATES

Fourth Cambridge catalogue radio sources observed for right ascensions using east-west arm of Molonglo radio telescope, presenting data analysis procedures
01 p0191 A70-11362

Space triangulation equations based on simultaneous measurements of satellite topocentric coordinates and distances between tracking station and satellite
02 p0254 A70-11753

Stellar objects position accuracy with respect to reference stars improved by applying differential corrections methods to optical center coordinates of stellar photographs
02 p0362 A70-11759

Satellite surveys and astronomic-geodetic nets for joint terrestrial, space triangulation and gravimetric measurements, including laser distance determination
03 p0445 A70-13191

Ts1 catalog of right ascensions of stars based on photoelectric observations, including clock corrections
04 p0756 A70-15480

Catalog of right ascensions of stars obtained from photoelectric observations, comparing equatorial and zenith region with F6 catalog
04 p0756 A70-15481

Lunar ephemeris, lunar theory constants and coordinate system corrections based on conditional equations formulated by analytical partial derivatives
05 p0908 A70-16334

Coordinate system for synthesizing previous work on multifluid cosmologies, investigating noninteracting mixtures of multicomponent fluids
05 p0919 A70-16933

Eccentric and inclined motions of satellite of spherical planet in planet centered coordinate system, applying formulas to Jupiter motion
07 p1374 A70-18693

Astronomical and physical geodesy, discussing geometrical methods involving triangulation and trilateration and geocentric coordinates method in navigation
07 p1265 A70-19370

Selenocentric coordinate system originating at center of mass, determining lunar figure center from photographs with reference stars
08 p1572 A70-20942

Lunar photographs on star-calibrated plates for lunar features coordinates or physical libration determination, outlining photographic technique and computer program
09 p1674 A70-22308

Planet Saturn right ascensions tabulation /1967, 1968/
09 p1756 A70-22651

Minor planets orbits coordinates and velocities data at osculation time
09 p1756 A70-22654

Oscillations stability along symmetrical axis in galaxies analyzed by Jacobi and Lagrange equations, obtaining cylindrical coordinates upper and lower limits
09 p1761 A70-23052

Plate coordinate measurements obtained with Zeiss precision monocomparator at satellite observation station
10 p1889 A70-24501

Extraterrestrial photogrammetry role in lunar photographs analysis, considering landing site triangulation and selection, coordinate system improvement, etc
10 p1948 A70-25046

Celestial object position determination, computing local errors for coordinate improvement
11 p2113 A70-26189

Passive satellite coordinates correlations to instants of observation in U.S.S.R. ground stations, reducing quasi-synchronous observations by interpolation
11 p2007 A70-26192

Photographic reduction techniques at Meudon Observatory, discussing computation of standard and measured coordinates
11 p2007 A70-26197

Satellites photographic positions accuracy compared with stars based on stellar coordinates, investigating causes of difference
11 p2008 A70-26198

Satellite coordinates estimation precision by comparing artificial satellite positions obtained simultaneously by photographic cameras
11 p2008 A70-26199

Ring micrometer radius determination and application to right ascension changes in determining positions of comets, planets and planetary moons
11 p2057 A70-26675

Intra- and extragalactic distance indicators and Hubble constant calibration
12 p2301 A70-27581

Galactic hydroxyl emission sources right ascensions, presenting coordinates and antenna temperature measurements
15 p2796 A70-31594

Book on celestial mechanics covering perturbation methods, two body problems, astronomical coordinates, orbital mechanics, satellite rotation, gravitational effects, etc
15 p2799 A70-31998

Selenocentric coordinate system originating at center of mass, determining lunar figure center from photographs with reference stars
15 p2806 A70-32754

Astronomically determined latitude longitude and azimuth reduction to common epoch, discussing secular nonperiodic pole motion due to crust drift
18 p3323 A70-37144

Radio sources right ascension and flux densities at 60 MHz
19 p3524 A70-38761

Phase meter for measuring angular coordinates of reflecting meteor trails
19 p3526 A70-38777

Optical identification of Parkes Catalog radio sources at declinations below minus 45 degrees, using Cordoba Observatory photographs
20 p3704 A70-39476

Radio source master catalog giving name, coordinates, flux density and frequency of observation
20 p3713 A70-40539

Galactic hydroxyl emission sources right ascensions, presenting coordinates and antenna temperature measurements
23 p4242 A70-44277

ASTRONOMICAL MAPS

Mars surface features, describing diagonal and meridian-latitude grid systems, continental blocks and continental drift
01 p0183 A70-10869

Smithsonian Astrophysical Observatory /SAO/ Star Atlas of reference stars and nonstellar objects
04 p0749 A70-14676

Contour maps of radio sources structure in 3C catalog from radio telescope observations
04 p0758 A70-15698

Cambridge one mile radio telescope observations of weak sources, extending radio source luminosity function and tabulating, graphing and mapping results
08 p1578 A70-21546

Solar mapping using millimeter wave radio telescope, comparing results with H alpha photographs and magnetograms
10 p1945 A70-24963

Solar radio emission maps at 8.6 mm using parabolic antenna and TV camera for optical control
12 p2293 A70-27591

Cassiopeia A high resolution map at UHF revealing main source physical characteristics and enhanced emission compact components
12 p2309 A70-27976

Multispectral UV sky mapping and heavenly body intensity measurement onboard OAO 2 satellite
17 p3179 A70-35264

High velocity neutral hydrogen cloud observations, presenting tabulated characteristics and maps
17 p3170 A70-35439

Mercury drawings from refractor observations during 1964-1967
18 p3315 A70-36611

Neutral H spiral structure in Milky Way galaxy, discussing map derivation, pattern interpretation, arm characteristics and kinematics
18 p3327 A70-37161

- Galactic 21 cm line emission motion picture film, discussing contour maps on neutral hydrogen distribution 18 p3327 A70-37163
- Martian photographic map during 1967 opposition in red and near IR range 19 p3516 A70-37935
- Butterfly diagram showing time dependent distribution of sunspots across heliographic latitudes 20 p3704 A70-39473
- Carina nebula NGC 3372 continuum map at 5 GHz compared to optical photographs, discussing H alpha lines 21 p3887 A70-41109
- Galactic plane continuum surveys at 8000 MHz, presenting radio contour map and sources list 22 p4109 A70-43747
- Quiet sun and new moon brightness temperature measurements at 3.3 and 5.7 mm wavelengths, giving radiometric maps 23 p4241 A70-44254
- Solar radio maps compared with H alpha pictures, correlating bright and dark features 24 p4401 A70-45317

ASTRONOMICAL MODELS

- Stellar systems models numerical construction, using data on star cluster density distribution, centroid velocity, potential distribution, etc 01 p0174 A70-10200
- Coronal gas pressure boundary conditions on model upper chromosphere, determining temperature and hydrogen density assuming hydrostatic equilibrium 01 p0175 A70-10243
- Internal structure models of Mercury, Mars and Venus based on radar measurements of radius and mass, discussing two and three zone models [JPL-TR-32-1439] 01 p0176 A70-10315
- Nonthermal convection permissible models in planetary mantles, using self gravitating homogeneous nonrotating sphere containing core and overlying viscous mantle 01 p0176 A70-10317
- Pulsating very dense white dwarfs models noting general relativity 01 p0176 A70-10320
- Quasars variability, distribution, absorption line characteristics, red shift peaks, physical models, cosmological problems, etc 01 p0177 A70-10341
- Einstein equations for Bianchi type IX universe model suitable for numerical solution and application to cosmology with pure fluid stress tensor 01 p0142 A70-10522
- Pulsar synchrotron emission model, discussing elliptic polarization, pulse shape, duration and negative absorption /wave amplification/ 01 p0183 A70-10897
- DC dynamo models for planetary electromagnetic conditions, considering nonrotationally symmetric turbulence induction actions and critical values for field maintenance 01 p0185 A70-10956
- Computer model for evolution investigation of disks of stars, discussing methods to obtain gravitational potential 01 p0185 A70-11065
- Model explaining background X radiation spectral properties, assuming production by Compton scattering of radio, IR and optical quanta by relativistic electrons 01 p0171 A70-11124
- Coriolis effects in spherical Einstein universe perturbed by rigid body rotation of shell with finite thickness 01 p0186 A70-11272
- Convective red dwarfs Kr 60 A and 60 B structure and stability taking into account electrostatic interactions between gas particles 01 p0188 A70-11337
- Cool dwarf stars atmospheric models including IR opacity due to water vapor and pressure induced dipole of molecular hydrogen 01 p0190 A70-11347
- High temperature atmospheric models for red dwarf stars and sun to determine convection effect on atmospheric surface layers and emitted flux 01 p0190 A70-11349
- Nongray and constant radiative flux model at atmosphere for K dwarf stars with 4000 K effective temperature and 4.5 log surface gravity 01 p0191 A70-11350
- Finite rotating universe model construction not possessing Goedel cosmos pathological properties, discussing relation to Mach principle 01 p0191 A70-11358
- Steady state spherically symmetric model for solar plasma acceleration with distance, showing essential role of viscosity 01 p0172 A70-11519
- Ionized meteor trails initial radii statistical characteristics determined for two models 01 p0192 A70-11537

- Diffused X ray background in isotropic world models in terms of Compton radiation from cosmic ray electrons in intergalactic space 02 p0356 A70-11743
- Heavy nuclei survival in cosmic rays Colgate supernova acceleration model, assuming plasma wave instability in shock wave 02 p0357 A70-11788
- Jovian decimeter radiation polarization during 1966-1967 apparition compared with cyclotron model predictions 02 p0364 A70-11793
- Universe oscillating closed model dynamics emphasizing conditions of collapse by contraction in terms of relativity theory 02 p0370 A70-12114
- Symmetric cosmologies within gamma ray measurement context showing antimatter limits in Milky Way and metagalaxy 02 p0371 A70-12196
- Radio source ghost images in Lemaitre cosmological models, deriving luminosity functions and radio source ages 02 p0371 A70-12198
- Blast wave model for galaxy M82 explosion using Sedov self similar solutions, indicating line excitation mechanism origin in shock wave heating and compression 02 p0372 A70-12247
- Radiative energy transport in sunspot region via model computations, obtaining reduced subphotospheric flux estimates for given magnetic field 02 p0372 A70-12254
- Joule dissipation model for sunspot magnetic field, discussing field fine structure and lifetime 02 p0373 A70-12374
- Discrete statistical stellar system relation existence with continuous model proved by introducing unique volume concept for discrete systems 02 p0376 A70-12443
- Thermal energies and angular momenta of Hubble galactic sequence using differential rotation and decreasing density stellar system model to test stellar evolution theories 02 p0376 A70-12447
- Free oscillations and surface wave dispersions from lunar models based on Orbiter data and corresponding pressure region of earth crust 02 p0379 A70-12777
- Galaxy model formulated in cylindrical coordinate system using Fokker-Planck equation for cosmic radiation particles propagation, discussing trajectories of high energy particles 03 p0553 A70-12880
- Magnetic cosmological nonuniformity hypothesis leading to galaxies and clusters isolation 03 p0564 A70-13224
- UV Ceti type flare stars observational and theoretical results related to nebular or chromospheric flare models 03 p0566 A70-13316
- Binary system Nova WZ Sge model with nonnegligible secondary component contribution to total light explaining W UMa type light curve 03 p0568 A70-13324
- Energy analysis of unstable gravitational oscillations in galaxies, using two component model for normal spiral galaxies 03 p0570 A70-13532
- Solar photosphere temperature fluctuations from model consistent with convection hypothesis agreeing with limb darkening data 03 p0570 A70-13591
- Coarse structure of solar atmosphere from observations of quiet sun, discussing contradictions with existing models 03 p0570 A70-13592
- Hydrostatic models of sunspot penumbra and umbra, analyzing spot transparency influence on Wilson effect 03 p0571 A70-13596
- Rotational properties of neutron star models for Crab Nebula energy source, using expressions for angular momentum and rotational kinetic energy 03 p0571 A70-13817
- Magnetosphere dynamic morphology model, including qualitative phenomena 03 p0475 A70-13850
- Geomagnetic field representation in terms of spherical harmonics, analyzing data for spherical and oblate models of earth 03 p0476 A70-13906
- Stellar model surface convective zone using diffusion equation taking into account transport due to gravitational separation, noting role of turbulent diffusion 03 p0574 A70-13932
- Pulsars observed properties and interpretation based on oblique rotator model for neutron stars 03 p0577 A70-14099
- Convective nongray stellar atmospheres construction for stellar stability studies, accounting for convective flow nonlocality and nongray radiative transfer 04 p0745 A70-14472

- Models of partially relaxed stellar disks in galaxies, discussing gravitational instability and stellar velocities 04 p0748 A70-14588
- Galactic cosmic ray origins, discussing supernovae and galactic nucleus cosmic ray production 04 p0740 A70-15071
- Stellar systems dynamics, discussing dynamic interactions of point masses, forces in gravitational field, galactic model construction, etc 04 p0754 A70-15353
- Solar cosmic ray dose rate and total dose magnitude predictions based on Epeak and isotropic diffusion models [AIAA PAPER 69-14] 04 p0742 A70-15584
- Angular diameter data from Cambridge radio telescope for sources with different flux densities for cosmological models red shift tests 04 p0757 A70-15691
- Prescribed circulations within conducting spheres effect on initially prescribed magnetic fields, discussing magnetic field structure in uniformly rotating stars 04 p0758 A70-15694
- Neutral H study of binary galaxies showing departures from circular symmetry, suggesting model involving hydromagnetic interaction 04 p0759 A70-15709
- Solar structure models for neutrino flux prediction compared with solar structure, suggesting modification in solar and stellar evolution calculations 05 p0906 A70-15895
- Nonequilibrium processes and initial conditions in early universe, discussing neutrino viscosity efficiency at removing shear anisotropy and Misner model 05 p0907 A70-16002
- Rubattal of criticisms on resonant structure hypothesis, giving probability value for chance stellar system formation similar to solar system 05 p0910 A70-16396
- Monte Carlo radiative transfer techniques applied to develop height dependent spicule model, computing contrast curves of model against chromospheric background 05 p0911 A70-16431
- Magnetized solar wind steady state inviscid single fluid model developed using MHD, including heat equation with thermal conduction 05 p0902 A70-16445
- Local theory alternative to cosmological quasars origin theories, considering red shifts properties 05 p0913 A70-16473
- Earth model based on free air gravity anomaly with condensed topography for eliminating gravity reduction difficulties, noting use in Vening-Meins formula 05 p0840 A70-16640
- Particle acceleration during 1966-1967 radio burst of 3C 273, indicating breaking down of model of expanding source emitting synchrotron radiation 05 p0918 A70-16927
- Density wave theory and Schmidt model applied to Milky Way spiral structure, considering systematic motion of interstellar neutral hydrogen 05 p0918 A70-16928
- Coordinate system for synthesizing previous work on multifluid cosmologies, investigating noninteracting mixtures of multicomponent fluids 05 p0919 A70-16933
- Models constructed for advanced evolution phases in massive convective red supergiants, considering carbon, Ne and oxygen burning in stellar core 05 p0919 A70-16935
- Solar corona at sunspot maximum observed during 22 September 1968 total solar eclipse, noting coronal streams unpredicted by magnetostatic model 06 p1138 A70-17278
- Proton satellites measurements reconciliation with diurnal stellar variation data and cosmic rays origin models 06 p1135 A70-17885
- Sunspot umbral dot models characteristics based on three dimensional radiative transfer analysis 06 p1144 A70-18003
- Solar activity model for simulating scheduling of observation experiments for Apollo Telescope Mount missions [AIAA PAPER 70-32] 06 p1145 A70-18121
- Lunar mascons formation by isostatic and volcanic processes, using normal density lunar crust and mantle model 06 p1150 A70-18476
- Unified model for pulsars involving electron population inversion and laser type transition 07 p1375 A70-18893
- Distance between objects in Friedmann cosmological model determined on basis of red shift, determining relationship between observed and emitted wavelengths 07 p1377 A70-18945
- Lunar surface magnetometer data interpretation by analysis of moon motion relative to interplanetary magnetic field spatial irregularities, using lunar electrical conductivity models 07 p1378 A70-18974

Steady spherical plasma flow from sun analyzed by equations of solar corona hydrodynamical model
07 p1378 A70-19033

Carbon particles formation and growth model for cool variable carbon star atmosphere with sinusoidal carbon star atmosphere with sinusoidal temperature variations
07 p1380 A70-19260

Dense pulsating stellar core structure model for pulsars, discussing catastrophic collapse mechanism
07 p1380 A70-19278

Hypothesis concerning initial spectrum of metric perturbations in Friedman model, discussing long wavelength gravitational waves energy
07 p1383 A70-19406

Observational extragalactic dependences obtained within framework of Friedman universe model with matter and neutrino background
07 p1383 A70-19407

Radiation catastrophe in universe in terms of cosmological models
07 p1368 A70-19628

Hamiltonian methods applied to homogeneous cosmological models, obtaining Einstein equations, passing to quantum theory by imposing canonical commutation relations
07 p1336 A70-19921

Pulsar slowdown by radiation field torques indicated by alignment torque in magnetized oblique sphere rotating in vacuum
07 p1389 A70-20220

Model for gaseous proto-galaxy collapse and formation of spherical galaxy
07 p1390 A70-20287

Interstellar gas clouds collapse using finite difference numerical methods in solving hydrodynamic equations involving gravitation
07 p1390 A70-20288

Interstellar cloud models to investigate heating, cooling and density distribution effects on collapse and to suggest theory of stellar evolution
07 p1390 A70-20292

Hydromagnetic self gravitating galactic slab embedded in halo, deriving stability criteria using models of magnetic field
07 p1390 A70-20293

Hot universe model for determining magnitude constraints on Dirac monopole annihilation cross section and mass in cosmic rays
07 p1371 A70-20330

Pulsar magnetorelativistic model assuming neutron star with magnetic field
08 p1563 A70-20478

Ultrahigh energy primary cosmic rays model, considering galactic origin and energy spectrum
08 p1560 A70-20479

Cosmological gravitation theory for uniformly expanding universe model providing fundamental reference frame and acceleration field
08 p1563 A70-20497

Figure of gravitating inhomogeneous rotating liquid, applying results to Jupiter and Saturn model construction
08 p1564 A70-20558

Inhomogeneous model of upper lunar surface layer assuming temperature dependent heat conductivity and capacity, showing agreement with IR measurements
08 p1564 A70-20559

Historical survey of celestial mechanics including three body problem and solar system dynamic model construction
08 p1565 A70-20561

Radio wave reflection coefficient power spectra for three layer lunar surface models consistent with radar spectrum, calculating porous layer thickness
08 p1565 A70-20566

Solar modulation of low energy galactic cosmic ray protons, proposing diffusion-convection model with time dependent diffusion coefficient
08 p1561 A70-20906

F corona heliocentric dust cloud model to account for temperature variations with particle size and optical properties, computing thermal emission
08 p1571 A70-20907

Stellar gas ejection processes in corona-interplanetary plasma system, proposing hydrodynamic model with frequent collision region having finite radius
08 p1573 A70-21060

Nonthermal mechanism for high energy radiation and particle emission from X-stars and pulsars
08 p1575 A70-21364

Planetary nebula formation mechanism based on slow mass loss due to radiation pressure on grains
08 p1575 A70-21374

Magnetosphere model for quasi-circular precipitation zones of energetic particles based on geomagnetic activity distribution patterns
08 p1489 A70-21385

Stellar formation and explosions in compact gas clouds to explain quasar phenomenon, discussing temporary star concept
08 p1578 A70-21548

Hubble expansion constant and expansion deceleration value roles in cosmological model testing
08 p1581 A70-21752

Solar and stellar convection regions and coronas using photospheric models, taking into account molecule formation
08 p1581 A70-21953

Late stage stellar evolution association with supernovae in terms of gravitational collapse and exploding light emission using evolutionary model
09 p1749 A70-21993

Supernova fluorescent light excited by radiation impingement on material surrounding explosion site, assuming explosion time and UV energy
09 p1749 A70-21997

Cosmic ray origin models, considering universal and local metagalactic models and halo and disk galactic models
09 p1744 A70-22057

Observational verification of cosmological models by examination of red shift discretization in quasars
09 p1750 A70-22098

Gravitational collapse models with magnetic dipole and gravitational quadrupole, treating asymmetries as small perturbations
09 p1752 A70-22274

Moon gravity field model derived from long-arc analysis of Lunar Orbiters tracking data, considering lunar mass distribution role
09 p1752 A70-22309

Pulsar mathematical model accounting for pulse width, polarization and spectrum of emitted radiation
09 p1753 A70-22383

Neutrinos kinetic theory for anisotropic cosmological models
09 p1753 A70-22453

M87 jet, using theoretical model and observed emission lines for heating, cooling, ionization, cosmic ray proton regeneration of optical electrons, X radiation, etc
09 p1754 A70-22501

Uniformly rotating gas disk large scale spiral structure analysis, studying density waves due to gravitational disturbance by supersonic particle
09 p1755 A70-22503

Pulsar model assuming magnetic dipole radiation by spinning neutron star interacting with nearby plasma
09 p1756 A70-22517

Homogeneous model solar photosphere in strict radiative equilibrium with depth-dependent line blanketing by neutral and ionized metals
09 p1757 A70-22728

Solar equatorial XUV limb brightening for resonance lines of Li-like ions from OSO-4 observations interpreted by coronal model
09 p1757 A70-22732

Magnetic fields model for quiescent solar prominences with helical structure
09 p1757 A70-22734

Twelffold solar mass star evolution computed using chemically homogeneous model showing faster evolution rate
09 p1758 A70-22746

Static gravitation field of spherical mass immersed in cosmological gas, using combined model of Einstein and de Sitter static universes and Schwarzschild solutions
09 p1763 A70-23312

Neutron star models based on equation of state for cold degenerate matter, taking into account nuclear forces and clustering
09 p1764 A70-23607

Instability of Godel rotating universe, discussing stability to perturbations in rotation plane and unstable density perturbations along rotation axis
10 p1937 A70-23973

Einstein theory applied to sample modeling of planetary orbits and light beams touching sun in solar gravitational field
10 p1939 A70-24268

Solar wind model with electrons, protons and alpha particles coupled by electric field and expanding due to pressure gradient and solar gravitation
10 p1931 A70-24433

Cosmic ray electrons during propagation in interstellar space analyzed for energy spectrum modulation
10 p1816 A70-24633

Simple layer model of geopotential from satellite-borne Baker-Nunn camera observations
10 p1876 A70-24645

Zero age intermediate and low mass stellar models and evaluation of physical parameters for population I and II chemical compositions
10 p1944 A70-24955

Dynamic orbital mixing in self gravitating spherical stellar system using water bag model
10 p1945 A70-24965

Low mass star evolution from helium burning to white dwarf, describing red giant and mass loss stages in model
10 p1946 A70-24982

IR luminosity of galactic nucleus from far IR observations, noting considerations favoring nonthermal model consisting of multiple sources
10 p1947 A70-24996

Solar XUV lines photon flux based on one dimensional model of chromosphere-corona transition region
10 p1949 A70-25271

Homogeneous open anisotropic relativistic world model with negative space curvature, observing shear decrease with time and magnitude reciprocal variation with function R/t
11 p2109 A70-25866

Hyperbolic velocity space physical significance based on cosmological model of light propagation associated with uniformly expanding universe
11 p2114 A70-26551

Model for FU Orion irregular variable to determine turbulent convection characteristics in atmosphere at optical transparency level
11 p2115 A70-26580

Stellar atmosphere and shell models in spectral range AO-G5 for studying stellar structures dependence on chemical composition
11 p2115 A70-26582

Evolutionary cosmological models for radio sources at large red shifts, considering source counts, luminosity functions, etc
11 p2117 A70-26655

Linearized perturbation theory for quasi-static equilibrium stellar interior models, obtaining correction through bidirectional quadrature
11 p2118 A70-26709

IR radiation intensity distribution in solar neighborhood from grain models of dirty ice, graphite and graphite core-dirty ice mantle
11 p2106 A70-26710

Extragalactic radio sources evolution, discussing energy requirements of hollow-shell models
12 p2299 A70-27377

Quasar optical properties, red shift and models
12 p2299 A70-27379

Quasar model based on supermassive stars relaxation oscillations, considering energy requirements
12 p2300 A70-27380

Singular and nonsingular cosmological models validity for general relativity allowing for cosmic dust
12 p2300 A70-27394

Pulsar properties association with neutron star rotation energy, discussing alternate pulsar theories
12 p2301 A70-27579

Coronal structure prediction for 7 March 1970 solar eclipse, using model for 22 September 1968 eclipse
12 p2304 A70-27718

Stellar atmosphere model for multilevel spectral line emission, assuming semiinfinite hydrogen atmosphere with sequence of plane parallel zones
12 p2306 A70-27856

Cosmic rays origin, discussing choice between galactic halo and radio disk models for trapping region
12 p2295 A70-27883

Pulsar theory of rotating and precessing neutron stars, rejecting relevance of forced precession to behavior
12 p2308 A70-27884

Cosmic rays components fluxes, interactions, lifetimes and anisotropy in statistical discrete source model, tabulating and graphing results
12 p2295 A70-27996

Pulsars starquakes frequency relationship to solid crust shear strength based on Ruderman model, considering Crab Nebula
12 p2310 A70-27998

Dissipation mechanism and period rate increase in neutron star pulsar model with neutrino emission for damping
12 p2312 A70-28368

Cosmic rays emission by dipole magnetosphere, applying model to neutron star particle belts
13 p2476 A70-28893

Grains impurities effect on interstellar extinction curve from graphite grain model, discussing dirty ice coatings
13 p2489 A70-28915

Cosmological constant role in closed universes with matter and radiation
13 p2490 A70-28936

Steady state symmetrical model for solar wind near equatorial plane, investigating effects of magnetic forces, viscosity and anisotropic pressure on azimuthal motion
13 p2477 A70-29179

Rotating stellar configurations structure consisting of degenerate matter or density dependent temperature describing boundary value problem reduction for Cauchy problem
13 p2494 A70-29518

Cosmic microwave radiation origin based on discrete source models
13 p2479 A70-29787

Solar thermal convection model, examining effects of rotation about vertical axis
13 p2496 A70-29839

Stellar evolution numerical model for point masses constant with time in absence of external field

13 p2498 A70-30011

Self gravitating three dimensional particles system evolution using water bag model

13 p2498 A70-30012

Hydromagnetic fluid model of solar wind for interpreting discontinuities in plasma and magnetic field, interaction with atmosphere, heating mechanism and chemical composition

13 p2481 A70-30067

Solar wind interaction with moon, constructing mathematical model based on MHD equations and Explorer 35 data

14 p2630 A70-30356

Bow shock associated hydromagnetic waves generation in upstream interplanetary medium, constructing model in terms of ion cyclotron resonance

14 p2631 A70-30359

Lunar surface erosion model by small projectiles impact for analytic representation of crater shape change as function of time

14 p2637 A70-30494

Diffusion loss model for cosmic ray electron propagation in galaxy, considering direct and radio observations

14 p2631 A70-30538

Aerospace environment models development by NASA for engineering use in Space Vehicle Design Criteria program

14 p2637 A70-30554

Pulsar radiation emission by electrons and protons in close orbit taking into account density, energy and correlation in plasma

14 p2638 A70-30617

Body waves in lunar models, calculating travel times and amplitudes

14 p2638 A70-30674

Narrow band photometry calibration, using model stellar atmospheres and laboratory data for high resolution synthetic spectra of G and K giant stars

14 p2639 A70-30728

Ca atom-graphite grain model for interstellar absorption at 4430 Å, calculating resonant line shift and width as functions of atom-surface distance

14 p2639 A70-30729

Gas injection model in galactic nuclei from evolving stars, producing high temperature, low density, thermally unstable medium

14 p2639 A70-30730

Interstellar grains potential model, discussing plane electromagnetic waves scattering by infinite concentric homogeneous circular cylinders at oblique incidence

14 p2639 A70-30732

Galactic formation by spinning core theory, determining core properties by mass, energy and spin fluctuation parameters

14 p2640 A70-30734

Anisotropic plasma turbulence produced by two stream instability onset near light cylinder of rotating magnetic star for pulsar model

14 p2640 A70-30788

Nuclear reactions and elementary particle reactions in Friedman universe with positive lepton abundance and degenerate electrons, discussing prestellar helium synthesis

14 p2620 A70-30877

Long term effects model evaluation of meteoritic impact against lunar surface compared with analyses of Lunar Orbiter photographs

14 p2645 A70-31062

Synchrotron model involving electron trapping in dipolar magnetic field for Jupiter decimetric radiation

14 p2649 A70-31089

Hot universe model for demonstrating distortions in Rayleigh-Jeans region of microwave relic radiation spectrum by primeval plasma heating before recombination epoch

14 p2632 A70-31287

Third integral of stellar dynamics, considering Contopoulos galactic system model separability

14 p2651 A70-31288

Red giant model, investigating inclusion of semirelativistic partially degenerate gas characteristics by perturbatory technique

14 p2651 A70-31290

Intergalactic medium lukewarm models, considering physical state, cosmic photon spectrum and isothermal and adiabatic expansion

14 p2651 A70-31291

B3V stars atmospheres by LTE model and spectroscopic techniques

14 p2652 A70-31384

Overstable convection formation of semiconvective zones in massive stars, noting Schwarzschild and Harm models

14 p2652 A70-31386

Dynamic spectrum of density fluctuations and galaxy clustering in Einstein universe, considering self gravitation of medium

14 p2652 A70-31389

Normal logarithmic spiral model of radius vector-tangent characteristic angles for multiarm galaxies

15 p2797 A70-31617

Galactic cosmic rays origin in terms of statistical mechanical model of supernova explosions

15 p2799 A70-31793

Numerical model of diurnal variations of minor neutral constituents in mesosphere and lower atmosphere including molecular and eddy diffusion

15 p2727 A70-31909

Solar wind models based on exospheric theory assuming collisionless particles

15 p2794 A70-32613

Solar coronal streamers, considering disk locations, evolution, classification and morphological model

15 p2804 A70-32621

Anisotropic solar cosmic rays in inhomogeneous medium, investigating shell effect on propagation by one dimensional model

15 p2795 A70-32624

Coherent radio emission mechanisms of white dwarfs and neutron stars as magnetic pulsar models, discussing polarization

15 p2804 A70-32698

Figure of gravitating inhomogeneous rotating liquid, applying results to Jupiter and Saturn model construction

15 p2805 A70-32713

Inhomogeneous model of upper lunar surface layer assuming temperature dependent heat conductivity and capacity, showing agreement with IR measurements

15 p2805 A70-32714

Historical survey of celestial mechanics including three body problem and solar system dynamic model construction

15 p2805 A70-32716

Radio wave reflection coefficient power spectra for three layer lunar surface models consistent with radar spectrum, calculating porous layer thickness

15 p2805 A70-32721

Electrodynamic-gravitational model of radio galaxies and quasars accounting for complex field, particle acceleration, angular momentum, luminosity and line emission

15 p2807 A70-32811

Two dimensional hydromagnetic turbulence model for maintained seed field amplification, noting applications to star formation, stellar convection and gas cloud motions

15 p2781 A70-32813

Collisionless shock waves model in solar wind plasma, discussing instability and energy dissipation

15 p2795 A70-32825

Andromeda Galaxy M31 hydrodynamic model based on given mass distribution, determining kinematic functions

15 p2808 A70-32884

Planetary origin theories, discussing lunar probes and manned landings data, accretion and fission formation models, etc

16 p2973 A70-33115

Venus retrograde axial period contradiction between radar echoes and violet-UV photographic and interferometric spectroscopic methods explained by theory using strong magnetic dipole

16 p2973 A70-33116

Quarks properties and observation methods, discussing reaction models with Coulomb potential barrier for energy due to participation in quasar dynamics

16 p2973 A70-33119

Model classification for relativistic universes containing noninteracting matter and radiation by cosmological constant and density parameters

16 p2979 A70-34190

Solar disk center to limb variation of Fraunhofer lines, comparing measurements to predictions by BCA, Elste and Holwegger models

16 p2980 A70-34307

Compact ionized hydrogen components inside galactic H II regions of lower electron density, explaining existence and evolution by various models

16 p2980 A70-34308

Disturbances rotational alignment in variable galaxies nuclei, using interstellar gas motions model

17 p3153 A70-34527

Nucleosynthesis in supernova models based on neutrino energy transport

17 p3153 A70-34529

Relativistic solutions to model stellar wind, discussing equation of radial momentum

17 p3153 A70-34530

Pulsar observations based on magnetic dipole model, discussing turnoff time, emission characteristics, birth rate and scale height

17 p3153 A70-34531

Pulse structure, polarization, time varying features and tight beam emission by pulsar model using finite thickness interfaces

17 p3153 A70-34532

Spectrum of bright IR object VY Canis Majoris, noting absorption feature attributed to SiO molecules in stellar atmosphere

17 p3154 A70-34540

Horizontal gravity gradient components in outer space from Stokes function expansion, using sphere as model

17 p3154 A70-34682

Maxwell equations and equations of massive vector-meson fields in spatially homogeneous Bianchi cosmologies, obtaining formula for homogeneous EM field

17 p3156 A70-34827

Anisotropic multifluid cosmological models with orthogonal velocity fields

17 p3157 A70-34839

Pulsars MP 0031 and CP 1919 periodic variations in pulse intensity, considering radio emission models with plasma waves

17 p3157 A70-34843

Neutron core star models based on realistic nuclear matter calculations and hyperons equation of state

17 p3157 A70-34844

Solar rotation effects on velocity field in nonspherical solar wind, using axisymmetric wind model

17 p3151 A70-34861

Dielectric models of interstellar grains from calculations for smooth particles of homogeneous materials

17 p3159 A70-34879

Stellar UV and visual continuum observations, discussing recalibration of absolute energy distribution of alpha Lyr to improve model atmospheres

17 p3160 A70-34881

UV solar opacity observations, comparing solar model predictions

17 p3160 A70-34884

Early-type star spectral scan analysis from OAO observation, comparing model atmosphere calculations

17 p3161 A70-34887

Supergiant alpha Car UV spectrophotometry from Gemini 11, comparing with model atmosphere

17 p3161 A70-34888

Lyman alpha radiation from gaseous hydrogen nebula model, taking into account absorption by dust and interstellar neutral hydrogen

17 p3163 A70-34904

Pulsars theories review, discussing geometrical model picturing pulsar as rotating neutron star with high magnetic field

17 p3164 A70-35117

Temperature distribution of solar atmosphere, discussing solar models

17 p3169 A70-35382

Solar chromosphere model evaluation using sensitivity of flux emission in Lyman continuum

17 p3170 A70-35386

Globular cluster stars, discussing cosmological importance, stellar development models, main sequence stars, red giant models, He content, age computation, etc

17 p3171 A70-35447

Pulsar models distinguishing by Huygens principle in flat space-time, describing electromagnetic propagation in Riemann space

17 p3173 A70-35757

Solar atmosphere shock waves frequency and strength, computing radiative energy losses of chromospheric models

17 p3174 A70-35865

Uniform model universes containing gaseous matter and background blackbody radiation, solving Einstein equations without zero pressure assumption

18 p3313 A70-36215

Cyclic models of evolving universe corresponding to positive, negative or zero cosmological constant

18 p3314 A70-36421

Vacuum-like state of physical medium as initial state of Friedmann cosmology, noting fluctuation instability for conversion into ordinary matter

18 p3315 A70-36643

Extragalactic radio sources polarization variations at 8 GHz based on expanding source type model, noting synchrotron self absorption depolarization

18 p3317 A70-37002

Initial horizontal branch metal poor star models, examining opacities, luminosity and cluster ages of RR Lyrae stars

18 p3317 A70-37006

Helium abundance in unevolved main sequence eclipsing binaries by comparing to homogeneous models in mass luminosity plane

18 p3318 A70-37023

Synchrotron model limitation for nonthermal spectra, demonstrating restriction to small pitch angles and strong fields

18 p3318 A70-37024

Pulsars pulsation mechanism, using neutron star model with oblique rotation axis

18 p3319 A70-37048

Physical model of lunar soil prior to Apollo 11 landing, discussing meteoritic shock formation of powdery soil

18 p3320 A70-37080

Planetary interior density depth relationship, using modified Emden equation

18 p3321 A70-37122

Galactic spiral structure model, examining nonlinear stellar density waves in plasma cylinder

18 p3322 A70-37131

Cosmological models with matter and radiation for evolution of universe

18 p3322 A70-37132

Milky Way appearance and galactic spiral structure, using models with variable and different absorption values of arms
18 p3329 A70-37181

Flat model galaxy stability, examining unstable two armed density wave by numerical methods
18 p3330 A70-37190

Late-type barred spiral galaxies structure and dynamics with asymmetric mass distribution, using model consisting of small prolate spheroid displaced from disk center
18 p3331 A70-37194

Stellar isolated disks spiral structure, examining large numbers of point masses self consistent motion in galactic plane
18 p3331 A70-37195

Neutral hydrogen observations in Sagittarius and Scutum spiral arms, examining circular galactic rotation by density wave theory kinematic models
18 p3331 A70-37197

Galactic spiral arm helical magnetic fields related to interstellar gas flow, using magnetohydrodynamic models
18 p3331 A70-37200

Pulsar AP 2015 21cm line absorption profile, indicating uniform density and temperature neutral H model invalid
19 p3518 A70-38026

Crab Nebula electromagnetic spectrum models, considering uniform magnetic field over whole volume and strong fields in small regions
19 p3505 A70-38114

High energy galactic gamma rays photons, suggesting two-component cosmic ray source model
19 p3505 A70-38115

Galactic disk model for confinement of cosmic ray electrons, assuming isotropic background radiation
19 p3510 A70-38156

Cosmic rays propagation and production in Milky Way galaxy, using equilibrium model
19 p3510 A70-38157

Energetic cosmic ray particles transfer through interstellar space based on galactic disk model
19 p3511 A70-38158

Einstein theory applied to sample modeling of planetary orbits and light beams touching sun in solar gravitational field
19 p3520 A70-38393

Expansion motions in inner Galaxy, discussing lower velocity absorption features, mass estimation method and model
19 p3522 A70-38602

Solar envelope unstable gravitational mode model, considering spherical harmonics by numerical integration and asymptotic representation
19 p3523 A70-38688

Galaxies systems dynamic evolution and instability in terms of nuclei division process model, comparing with observational data
19 p3525 A70-38765

Pulsars CP 0834, AP 1237 and CP 1919 radiation intensity periodic variations, discussing power spectra fluctuations in circulating plasma model
20 p3701 A70-39007

Stellar matter density and composition in proton-proton cycle, applying results to real solar model
20 p3698 A70-39308

Interplanetary magnetic field structure, using solar wind model accounting for solar rotation
20 p3704 A70-39474

Neutron stars, discussing equations of state and stellar interiors, models, atmosphere, cooling, vibration, rotation and magnetic fields
20 p3706 A70-39932

Time travel and cosmological model based on Einstein relativity theory, considering hypothetical motor design, energy supply, tachyons and four dimensional orbits implications
20 p3710 A70-40132

Photospheric pore magnetic field model, investigating pore-sunspot distinctions
20 p3711 A70-40411

Neutron star superfluid turbulent state, applying dynamic model to conditions in pulsars
20 p3713 A70-40429

Rotating neutron stars, pulsars and cosmic X ray sources relationship, discussing stellar model with mass loss in presence of magnetic field
21 p3874 A70-40678

X ray emission mechanisms in galactic sources, considering black body, supernova remnants, synchrotron radiation, etc
21 p3874 A70-40679

Discrete X ray and gamma ray sources theories, considering binary and gas stream models
21 p3874 A70-40680

Sco X-1 radio emission models, considering possible binary nature and thermal bremsstrahlung
21 p3875 A70-40685

Extragalactic cosmic X ray background source models for intensity and energy spectrum, noting Compton scattering of black body photons by relativistic electrons
21 p3877 A70-40699

Galactic gamma ray sources model with magnetic fields concentration in expanding shell, suggesting production by neutral pion decays in supernova remnants
21 p3877 A70-40701

Diffuse X rays from nonthermal intergalactic bremsstrahlung, discussing cosmic ray injection models
21 p3878 A70-40705

Solar wind X ray emission, investigating diffused cosmic ray origin and flow pattern models
21 p3878 A70-40708

Close binary stars evolution, discussing initial parameters effects on mass exchange and orbital period model
21 p3884 A70-40872

Universe homogeneous isotropic model with thermal radiation at outset, considering nucleons and antineutrons interactions
21 p3884 A70-40910

Spinning cylindrical spicule model with radial and axial gradients in electron number and temperature forming Ca II K line
21 p3879 A70-40955

Pulsar research review, discussing characteristics, neutron star theory and galactic origin
21 p3886 A70-41072

Galactic evolution and secular variations of cosmic rays, magnetic fields and turbulence, assuming stellar birth rate dependence on gas density and temperature
21 p3919 A70-41700

Extragalactic radio source count interpretation of cosmological model and evolution, discussing luminosity, electron scattering and red shifts effects
21 p3923 A70-42105

Stellar envelope physical structure studied to solve equilibrium equation, applying results to stellar model
22 p4097 A70-42545

Planetary unipolar electric generator system theoretical model based on polarization charges deposition by solar wind
22 p4100 A70-42790

Galactic rotation model derived from radial velocities and spectrophotometric distances of H II regions
22 p4101 A70-42864

B-V and U-B colors and B and V polarization calculation in single scattering for slab model reflection nebulae with dielectric or graphite grains
22 p4103 A70-42984

Polytropic pre-main-sequence evolutionary tracks and main sequence models of solar composition low mass stars
22 p4104 A70-42993

De Sitter nonempty static cosmological model, examining possibility by comparing integral luminosity function for cosmic radio sources to radio galaxies statistics
22 p4106 A70-43258

Metric evolution in oscillatory mode of approach to singularity in homogeneous cosmological models in asymptotic region, showing Kasner epoch dependence on perturbation
22 p4075 A70-43478

Friedman-Lemaître model role in big bang cosmology
23 p4238 A70-43812

Interplanetary magnetic field and plasma structure observed with Mariners magnetometer, noting 27-day deviations from Parker spiral model
23 p4239 A70-43827

Circumstellar dust cloud model of spectral distribution and anomalous excess emissions in IR T Tauri and red giant stars coincident with photometric measurements
23 p4239 A70-43868

Jupiter model thermal profiles, examining metallic core and molecular envelope in convective equilibrium
23 p4241 A70-44251

Saturn ring radial structure, discussing dynamic model, gravitational forces and perturbation of planetary satellites
23 p4241 A70-44253

Einstein field equations for spatially homogeneous spaces, considering rotating matter model in regularized Euler-Lagrange form
23 p4219 A70-44406

Nonspherical stellar internal structure, developing method for models with rotational and tidal distortion
23 p4249 A70-44804

Rapidly rotating B and Be stars interior evolution models, considering mass and radiation pressure
23 p4249 A70-44808

Stellar rotation effects on atmospheres of early type main sequence stars, using models for surface gravity and temperature variations
23 p4249 A70-44810

Rotating stellar atmospheric models for middle and late A star masses, emphasizing Altair observed and predicted energy distribution
23 p4250 A70-44812

Deutsch period vs line width relation for periodic Ap stars, determining rotational velocities with rigid rotator model
23 p4251 A70-44825

Rotating magnetic star dynamic evolution, discussing magnetic and rotation axes inclinations for oblique rotator model
23 p4252 A70-44827

Nonspherical stars thermal stability, considering solar rotational models and oblateness problem
23 p4252 A70-44833

Solar interior differential rotation, developing angular velocity distribution equilibrium model
23 p4252 A70-44834

German monograph on Milky Way spiral structure, describing elliptic orbit model
24 p4399 A70-45100

Red supergiants location in H-R diagram, discussing significance of mass loss, rotational mixing and neutrino emission as stellar model mechanisms
24 p4403 A70-45393

Nonlinear Lagrangians in relativistic cosmology of open oscillating world model
24 p4404 A70-45409

Gamma Cas star time and spectra observations, examining emission line profile variations and envelope and stellar model
24 p4404 A70-45415

Pulsar intensity variations, showing fine frequency structure by interstellar scintillation model
24 p4404 A70-45416

Cluster evolution model for stars with equal masses, calculating density and velocity distribution for various cluster types
24 p4404 A70-45417

Planetary nebulae NGC 7662 and NGC 7009 axially symmetric models from density distributions, H continuum threshold optical depths and central star temperatures
24 p4409 A70-45757

Galactic evolutionary models using disklike Riemann ellipsoids with internal motions and gravitational gas equilibria
24 p4410 A70-45759

Cool star atmospheric structure, discussing models with and without graphite particle inclusion opacity
24 p4410 A70-45765

Solar wind two fluid model with boundary conditions describing electron and proton behavior in expanding corona
24 p4397 A70-45770

Pulsars correlation with stellar evolution using model, discussing distribution and formation rate in Milky Way galaxy
24 p4412 A70-45981

Stellar structure in advanced phases of evolution, considering mixing between hydrogen-rich envelope and core through surface convection zone
24 p4412 A70-46102

Corotating magnetic field model of pulsar, using electromagnetic field equations of dipole radiation in low density plasma
24 p4413 A70-46137

Main sequence and giant stars atmospheric structure models, noting metal deficiency effects
24 p4413 A70-46159

ASTRONOMICAL OBSERVATORIES

NT OAO
NT OSO
NT OSO-B
NT OSO-1

Lowell Observatory Northern Hemisphere proper motion survey, analyzing preliminary data for low luminosity stars
01 p0187 A70-11332

Reflector radio telescope of Pulkovo Astronomical Observatory noting high resolution
01 p0094 A70-11585

Lund astronomical observatory, describing Cassegrain-Nasmyth reflector and attached electrophotometer for stellar measurements
02 p0275 A70-12061

Support facilities requirements and goals for manned and unmanned solar and stellar orbital astronomy [MDAC-WD-1258]
05 p0847 A70-16074

Tabulated corrections of data concerning reduction of photographs of small planets obtained at Bucharest Astronomical Observatory
06 p1139 A70-17549

Max Planck Institute of Astronomy /Germany/ installations and equipment planned
06 p1029 A70-18024

Book on space observatories covering rocket mounted telescopes for atmospheric structure, opaque wall, air diffusion, clouds and refraction, particle bombardment, meteorite melting, etc
07 p1379 A70-19099

Transistor RF and IF amplifiers designed for 210-ft antenna of Australian National Radio Astronomy Observatory
07 p1243 A70-20350

Instantaneous latitudes observations during stellar transit at Poltava, describing error correction procedure
08 p1488 A70-21153

- Poltava observatory zenith telescope characteristics, including scale division and ocular micrometer screw revolutions 08 p1496 A70-21157
- Odessa observatory meridian circle pivots wear determined during observations of eclipsing variables 08 p1574 A70-21160
- Chromatic aberrations of Poltava observatory AVR-2 refractor 08 p1496 A70-21161
- Latitude observations at Pulkovo, considering star declinations and proper motions 08 p1574 A70-21162
- Spaceborne long wavelength radio astronomy, proposing lunar orbit and beyond Pluto observatories to reduce magnetospheric and interplanetary plasma effects 09 p1754 A70-22495
- Bright star weak longitudinal magnetic fields from telescope spectrograph 09 p1755 A70-22515
- Wide field stellar astronomical ESRO project, reviewing application of earth orbiting spin stabilized satellites and OAO 09 p1767 A70-23435
- Astronomic observation balloon Thisbe, discussing telescope, stabilization, basket control, data processing and objectives including zodiacal light and night sky brightness measurements 10 p1804 A70-23915
- TRW space program to 1978, discussing lunar optical observatory, orbital radio astronomical observatory, satellite applications, planetary exploration spacecraft, etc 10 p1951 A70-24875
- Meteor observation station design and operation, describing calibration difficulties and reflecting points coordinates determination 14 p2583 A70-30331
- Two dimensional quantitative spectral classification of F-G stars, using meniscus telescope with preobjective prism at Abastuman observatory 15 p2797 A70-31613
- Astronomical observations, discussing advantages of human operators on interplanetary spacecraft or Mars 15 p2810 A70-31853
- Shemakha observatory telescope main mirror spherical aberration, coma, astigmatism and light concentration, describing support system and adjustment and control mechanisms 15 p2738 A70-32203
- Spectral transmittance coefficients at Naugazran astronomical station, using Bouguer method 15 p2809 A70-32909
- Variable baseline interferometer installation for radio astronomy observatory, describing components and performance 20 p3605 A70-39240
- Aircraft capabilities as scientific observation platform in astronomy and geophysics, including instrument adaptation and IR absorber problems 22 p4019 A70-43146
- High Energy Astronomy Observatory for space X rays, gamma and cosmic rays research via unmanned spacecraft 23 p4261 A70-44680
- Manned earth orbital space astronomy instruments, facilities and research objectives 24 p4415 A70-45825
- ASTRONOMICAL PHOTOGRAPHY**
- Photography and photometry of solar corona during 25 February 1952 and 22 September 1968 eclipses, discussing photographic weighting techniques 01 p0181 A70-10576
- Atmospheric density on basis of photographic observations of meteors, comparing vertical profile with CIRA profile 01 p0084 A70-11556
- Stellar objects position accuracy with respect to reference stars improved by applying differential corrections methods to optical center coordinates of stellar photographs 02 p0362 A70-11759
- Galactic interstellar absorption lower limit in selected Area 19 determined from Stellar spectra densities, using Schmidt camera 02 p0370 A70-12073
- Venus photographs taken by 82-inch telescope /1950-1956/, tabulating data 02 p0378 A70-12556
- Multicolor Venus photography, discussing anomalous markings association with anomalous UV polarization 02 p0378 A70-12557
- Venus photography in UV by 61-inch telescope, discussing low contrast clouds recognition technique 02 p0378 A70-12558
- Interference filter for photography of comet heads, tabulating filter characteristics 02 p0303 A70-12707
- Ranger, Surveyor and Lunar Orbiter televised and reconstructed picture quality, suggesting improvements in existing photographic systems 03 p0490 A70-13656
- Variable object BL Lacertae flux measurements using Schmidt telescope photography and radio study, comparing results with quasar 04 p0759 A70-15711
- Chromospheric fine structure photographed at H alpha line center, discussing size, lifetimes and relationship between dark and bright mottles 05 p0910 A70-16428
- Photographic photometry of Jupiter belts and zones at reflector Newtonian focus, presenting diagram showing intensity time variation 05 p0914 A70-16650
- Cameras photogrammetric parameters determined from stellar photographs, considering distortion components, reference points, etc 05 p0852 A70-16921
- Solar photographs taken with motion picture cameras in integral light 05 p0920 A70-16974
- Tabulated corrections of data concerning reduction of photographs of small planets obtained at Bucharest Astronomical Observatory 06 p1139 A70-17549
- Sunspot temperature and pressure gradients from blue, red and IR photographs, deriving umbral depression and density scale height 06 p1143 A70-18000
- Solar flare H alpha brightness measurement from photograph taken through birefringent filter, deriving flare morphological changes from isophotes 06 p1135 A70-18004
- Photographic emulsions used for astronomical photography in U.S., discussing hypersensitization, exposure, processing and image evaluation methods 06 p1071 A70-18516
- Barred galaxies colorimetric data to study relative intensities and mean surface brightnesses as function of color 07 p1376 A70-18905
- Optical density vs illumination amount characteristic curve determined for photometric calibration of astronomical photographs of celestial bodies 07 p1279 A70-19046
- Fourth Saturn ring detection equipment and procedures, discussing negatives revealing small weak zones near globe equatorial east and west edges 08 p1567 A70-20600
- Meteor flare photographs statistical analysis, noting duration and weight distribution dependence on meteor velocity 08 p1574 A70-21214
- Crab Nebula activity from telescopic plates, illustrating polarization structure on composite plate 09 p1750 A70-21999
- Stars photographic position determination errors with NAFA-3C/25 camera, comparing films and plates 09 p1673 A70-22164
- Aerophoto film emulsion layer and backing deformation magnitude and direction, suggesting use of photoplates for astrophotography 09 p1673 A70-22166
- Lunar photographs on star-calibrated plates for lunar features coordinates or physical libration determination, outlining photographic technique and computer program 09 p1674 A70-22308
- Meteorological observations of Mars polar regions, surface activity and atmosphere with astronomical telescopes during Mariner 6 and 7 flyby 09 p1754 A70-22500
- Solar chromosphere dark and bright mottles mean lifetime from photographs, identifying with spicules 09 p1757 A70-22733
- Radio galaxy 3C 371 compact companions, studying luminous isophotes and red shift by long exposure plates with 200 inch telescope 10 p1936 A70-23908
- Weak phase objects detection based on interferential and streak photography methods, noting fringe deformation role 10 p1916 A70-24587
- Bright rims in North America Nebula, measuring electron temperature to derive profile characteristics 10 p1944 A70-24956
- Photographic films for astronomy and spectroscopy, discussing resolving power, light sensitivity, antihalo lacquer and emulsions 10 p1892 A70-25129
- Faint violet stars in southern galactic latitudes found during scanning of two color plates including halo stars, subdwarfs, white dwarfs and quasi-stellar galaxies 10 p1949 A70-25248
- Supergranules/convective cells/ development shown in quiet sun filtergrams of H alpha chromospheric network taken above Arctic Circle 11 p2109 A70-25741
- Stars identification on photographic plates and position computation in FORTRAN, using CONTROL DATA 6600 and IBM 1130 computers 11 p2113 A70-26183
- Classical astronomical photographic methods for reducing satellite photographs taking into account linear and nonlinear methods, analyzing random errors 11 p2006 A70-26184
- Saturn observation by astronomers of various countries during earth passage through plane of rings, measuring rings thickness 12 p2298 A70-27279
- Venus photographs analysis during synoptic periods, noting inconclusive results on cloud layer and planetary surface structures 12 p2311 A70-28311
- Quantitative analytic composite photography, performing image density point-to-point subtraction of two negatives 13 p2406 A70-28905
- Southern and Northern hemispheric comet observations 13 p2494 A70-29483
- Sunspot minimum intensity dependence on area, including correction for blurring or image motion, scattered light and line absorption 13 p2496 A70-29846
- Herschel effect in UV solar photography in developing autotensive photographic film for bright photospheric recording 13 p2497 A70-29853
- Stellar observations in near UV by camera having two color photometric slides, discussing atmospheric models 13 p2498 A70-30013
- Chilled emulsion photography for astronomy and spectrography, reducing long exposures with chilled plates 14 p2585 A70-30649
- Tabulation of minor planets positions observed by photographic equatorial at Bordeaux observatory 14 p2649 A70-31124
- Tabulations of minor planets positions photographed at Besancon observatory 14 p2649 A70-31125
- Comet tail structures in inner coma region using photographic observations 14 p2650 A70-31220
- Solar proton flare of 2 September 1966, discussing Abastuman observatory photographic observations and radio noise emission changes 15 p2792 A70-31618
- Churimov-Gerasimenko 1969h comet photographs and preliminary orbital characteristics 15 p2800 A70-32146
- Transistor densitometer used for variable star interpretation by amateur photographers 15 p2740 A70-32348
- Orion Nebula photographed at H alpha line with half angstrom filter 15 p2807 A70-32805
- Ground based photographic experiments using portable equipment during 7 March 1970 solar eclipse in North Carolina 16 p2977 A70-33840
- Martian blue clearing during 1967 apparition photographic observational patrol tabulated and summarized 16 p2979 A70-34035
- TV photograph image instability of stars, developing discontinuity and variability criteria as elementary approximate method for comparing nonuniformities 16 p2979 A70-34177
- H alpha filtergrams of sun during solar eclipse of 7 March 1970, showing bright plage area 16 p2980 A70-34226
- Planetary and lunar photography at French observatory, discussing Pic du Midi facilities and various photographic emulsions 17 p3082 A70-34676
- Mars 1969 planetary surface drawing and photograph evaluation, noting dark spot east of Nodus Lacoontis 17 p3154 A70-34677
- Optical study of Crab Nebula linear expansion and filamentary proper motions, considering line emission 17 p3164 A70-35113
- Large photographic telescope characteristics for stellar and planetary observations, noting differential refraction influence on plate scale factors 18 p3259 A70-36608
- Geometric relations for contact moments of solar eclipse, using crescent cord photographic measurements 18 p3315 A70-36610
- Astrophotograph optical center coordinates and camera focal length calculations 18 p3260 A70-36992
- Solar eclipse of 7 March 1970 in Mexico, discussing characteristics, research program, equipment and photographs 18 p3318 A70-37046
- Triple polarization astrophot observations of comet 1968 c Honda, noting dust component- Wolf number agreement 19 p3515 A70-37658
- Color film /XRC/ application in Mexico during solar eclipse of 7 March 1970, showing little color and tone distortion 19 p3423 A70-37751
- Martian photographic map during 1967 opposition in red and near IR range 19 p3516 A70-37935

- Cepheids periodic variations photographic analysis 19 p3525 A70-38769
- Orbital elements of photographic meteors brighter than first magnitude, tabulating dates, solar longitudes, corrected radiants, velocities, major axis, etc 19 p3526 A70-38787
- Solar atmosphere vortex ring observation in H alpha light /2 December 1969/ 20 p3703 A70-39022
- Optical identification of Parkes Catalog radio sources at declinations below minus 45 degrees, using Cordoba Observatory photographs 20 p3704 A70-39476
- Uranus and Saturn reciprocal mass determination based on astronomical observations of Saturn and Jupiter respectively 20 p3705 A70-39477
- Jupiter Red Spot 1968-1969 photographic observations, discussing area darkness, longitude oscillation and acceleration 20 p3708 A70-39963
- Sun photographs with violet interference filter, determining photospheric magnetic fields position by cospatial network 20 p3634 A70-40410
- Image orthon in high precision astronomical camera, evaluating geometric accuracy and stability by distortion measurement 21 p3822 A70-40819
- Carina nebula NGC 3372 continuum map at 5 GHz compared to optical photographs, discussing H alpha lines 21 p3887 A70-41109
- X ray source population type optical observations, discussing interstellar matter and H II regions 21 p3882 A70-41117
- Sirius components relative photographic positions and magnitude difference, discussing color effect, grating image separations and emulsion contraction 21 p3922 A70-41984
- Instrumental and atmospheric observational problems regarding dark mottles, fibrils and H alpha solar limb photographic interpretations 21 p3926 A70-42199
- International photographic planetary patrol network, discussing filmstrips of Mars and Jupiter using blue, green and red filters 23 p4242 A70-44262
- Astronomical color photography, discussing films and filters for exact reproduction 23 p4198 A70-44903
- Photographic photometry in astronomy, considering Becker method and UVB system 24 p4333 A70-45145
- Solar limb photographic, isodensity and isophotal data for eclipse of 7 March 1970 from coronagraph observations, noting coronal green line and prominence activity 24 p4402 A70-45389
- Plate overlap algorithm for photographic star catalog reduction 24 p4404 A70-45413
- Planetary nebula NGC 3242 monochromatic photographs and isophotic contours 24 p4411 A70-45788
- ASTRONOMICAL PHOTOMETRY**
- NT STELLAR SPECTROPHOTOMETRY**
- Photography and photometry of solar corona during 25 February 1952 and 22 September 1968 eclipses, discussing photographic weighting techniques 01 p0181 A70-10576
- Light curve and relative dimensions of eclipsing system V338 Herculis, from photoelectric measurements, discussing component stars 01 p0184 A70-10951
- Light curves of Algol eclipsing variable AD Herculis and semidetached system relative dimensions from BV photoelectric observations 01 p0184 A70-10952
- Visual observations of bright comets, deriving photometric parameters from comet head total magnitude 01 p0184 A70-10953
- Comet observations analysis, tabulating total head magnitude, photometric parameters, nucleus magnitude, coma diameter, tail type and direction and magnitude correlation with solar activity 01 p0184 A70-10954
- Near limb solar IR brightness distribution observed during total solar eclipse of 12 November 1966 in Argentina by sounding rocket photometers 01 p0186 A70-11271
- Solar brightness variations observed photometrically, discussing periodicity, sunspot locations, photosphere and subsurface rotations, etc 01 p0186 A70-11273
- Photometric results on beta Lyrae from various observatories during 1959 international campaign with data reduced to BV system, showing reddening at primary eclipse 02 p0369 A70-12064
- Photometric measurements in Cygnus, analyzing formulas used for conversion to standard UVB system for Javan reflector /Sweden/ 02 p0297 A70-12065
- Coronal emission lines wide slit photometry systematic error analysis and suggested error elimination by varying observation method 02 p0373 A70-12375
- Stellar system DQ Herculis photometry by synchronous signal averaging, indicating sinusoidal light curve with increasing binary period 02 p0373 A70-12392
- Jovian atmosphere photometric activity determination, showing time variation and difference in strength between Northern and Southern Hemisphere 02 p0375 A70-12430
- Jovian cloud layer light and dark matter albedo determination, applying photographic equidensitometry 02 p0375 A70-12431
- Mars multicolor filter photometry showing variation in whole-disk reflectivity 02 p0378 A70-12560
- UV photometry from OAO, observing planets, gaseous nebulae, X ray source, quasars, Crab Nebula, extragalactic nebulae, etc 02 p0303 A70-12705
- Photometric reduction of Lunar Orbiter video magnetic tapes for generation of topographic information of proposed Apollo landing sites 03 p0490 A70-13661
- BV photometry of Population I Cepheids in Magellanic Clouds, Galaxy and M31 03 p0578 A70-14287
- Normal albedo of Apollo 11 landing site and intrinsic dispersion in lunar Heiligenschein determined from Apollo and earth based photographic photometry 04 p0747 A70-14549
- Cepheid variable 1 Carinae light curve from photoelectric observations, calculating periodicities from best fitting Fourier series 04 p0759 A70-15708
- Compact and fully automatic fixed photometer for zenith measurements of night airglow intensities, calibrating sky observation through filter by constant intensity light source 05 p0845 A70-15821
- High resolution photometry near planetary limb yielding scale height and optical depth applied to Mariner 4 Mars observations 05 p0909 A70-16387
- Photographic photometry of Jupiter belts and zones at reflector Newtonian focus, presenting diagram showing intensity time variation 05 p0914 A70-16650
- Photoelectric photometry of comets to obtain principal data and to classify comets by employing same filters and stellar photometric standards 06 p1140 A70-17731
- Photoelectric multislit micrometer for astronomical purposes, presenting stochastic variables mean error difference formula for arbitrary power spectrum 06 p1071 A70-18458
- Single parameter photometric analysis for density distribution of matter in comets atmospheres 07 p1374 A70-18707
- Catalog of lunar features brightness interpreted in terms of photometric function uniformity of lunar surface, considering second order light scattering 07 p1377 A70-18971
- Photometric investigation of lunar crater rays of Tycho, Copernicus, Kepler and Aristarchus compared with terrestrial explosion craters 07 p1377 A70-18972
- Penumbra during lunar eclipses analyzed photometrically, considering effects of earth upper atmosphere and lunar luminescence 07 p1377 A70-18973
- Surface brightness distribution in comet head investigated photometrically 07 p1379 A70-19038
- Photometric observations of Ikeya-Seki comet 1965f by equidensity method, observing CN emission in head 07 p1379 A70-19043
- Optical density vs illumination amount characteristic curve determined for photometric calibration of astronomical photographs of celestial bodies 07 p1279 A70-19046
- Optimal photometric data processing for planetary characteristics and surface details, considering errors due to image blurring in telescope 07 p1384 A70-19419
- Photometric masses of bodies producing bright meteors, considering emission efficiency dependence on velocity, mass and composition 08 p1573 A70-20948
- Atmospheric extinction observed photometrically in South Africa and southern France in narrow bands and astronomical UVB bands 08 p1490 A70-21647
- Fabry-Perot interferometer application to photometric analysis of solar line profiles 09 p1756 A70-22652
- Solar eclipse coronal polarization and intensity measurements, discussing equipment, calibration, photometric reduction and results 09 p1757 A70-22736
- Photoelectric measurements of dust and CN/C2 molecular emission in atmosphere of Comet Ikeya-Seki 09 p1761 A70-23058
- Wide angle electronic camera for astronomical photometry designed to seek photometric standard stars remote from nebular regions 09 p1681 A70-23313
- Compact galaxies, discussing distribution, integral photometry and isophotometry, brightness outbursts, etc 09 p1763 A70-23373
- Photoelectric photometer for astronomic observations, discussing design and performance 10 p1886 A70-23917
- Auroral pulsations photometric observation data, noting magnetic activity effects 11 p2043 A70-25540
- Solar moustaches /transient emissions/ far wing asymmetry studied photometrically 11 p2109 A70-25745
- Iconoclastic cosmology and remote sensing of universe, discussing cosmic scale photometry and extra-galactic red shift spectroscopy 12 p2296 A70-26924
- Spectrophotometry of comet Honda 1968c, showing free cation and radical emissions and head asymmetry 14 p2635 A70-30304
- Comet Bennett 1969i photometric observations, showing blackbody-like continuum at short wavelengths with sharp peak due to silicate grains 14 p2642 A70-30895
- Size and cost of Al mirror IR photometric telescopes optimized for scientific information acquisition 14 p2586 A70-30896
- Lunar soil and rocks photometric and polarimetric properties from high resolution Surveyor pictures 14 p2644 A70-31054
- Shilts method applicability to electronic camera for stellar magnitude photometry, studying instrument limitations and errors 14 p2589 A70-31379
- Binary AX Monocerotis brightness variations in UV from photoelectric UVB observations 15 p2796 A70-31610
- Saturn rings observations during earth passage through ring plane by Abastumam observatory telescope, describing photometric processing and data reduction 15 p2797 A70-31619
- Atmospheric optical properties at various altitudes, using lunar disk photometric observations at different wavelengths during eclipse 15 p2801 A70-32476
- Photometric masses of bodies producing bright meteors, considering emission efficiency dependence on velocity, mass and composition 15 p2806 A70-32760
- Lunar occultation photoelectric measurement covering star angular diameters and diffraction patterns, ephemeris theory, astrometry close double star detection, etc 17 p3170 A70-35440
- High speed photoelectric measurements of lunar occultation using computer and nuclear physics instrumentation 17 p3171 A70-35441
- Lunar occultation photoelectric measurements, investigating irregularities of occulted stars 17 p3171 A70-35442
- Mercury photometric measurement, examining surface brightness for photometric function 18 p3319 A70-37052
- Peripheral umbra photometric analysis during lunar eclipses based on homogeneous observational material, revealing luminescence excited by solar corpuscular radiation 18 p3319 A70-37055
- Galaxies and globular clusters, obtaining data by measurements with intermediate bandpass photometry 18 p3321 A70-37121
- Photometric maps of reverse side lunar surface from AIM Zond-3 material 18 p3323 A70-37142
- Young cepheids galactic distribution determined by photometric method, showing correlation with spiral arms 18 p3330 A70-37184
- Association Carina OB 2 photometric investigation of mean distances 18 p3330 A70-37186
- Photoelectric and polarimetric observations of comet 1968 c Honda in BV system, noting dust scattering role in emission 19 p3515 A70-37657
- Photometric reduction of meteor luminosity to photovisual /international/ system 19 p3515 A70-37662
- Neptune position errors by meridian observations compared with photoelectric observation of stellar occultation 19 p3518 A70-38008

Am and Ap stars metallic absorption lines, determining photometric indices correction

19 p3523 A70-38689

Photometric cometary parameters from Van Biesbroeck data, using least squares method to compare naked eye, field glasses and small telescope observations

19 p3526 A70-38783

UV photometry from OAO-2, describing Wisconsin instrumentation and equipment

20 p3624 A70-39009

Ikeya-Seki /1967n/, Thomas /1968b/ and Honda /1968c/ comet photoelectric spectrum, examining swan bands, continuum and reflected scattered light

20 p3703 A70-39024

Image tube observations of Large and Small Magellanic Clouds and southern planetary nebulae at Cerro Tololo Observatory

20 p3705 A70-39480

Extraterrestrial planets photometric observations by telescopic mirror system on moon far side

20 p3710 A70-40131

Interstellar silicate absorption bands four color photometric observations in galactic direction, using metal mirror telescope

20 p3713 A70-40431

Optical photometric observations of nonsolar gamma and X ray sources WX Cen, NGC 5189 and GX3 plus 1

21 p3873 A70-40669

X ray source optical identification, discussing reflector optics, photometry and spectrography

21 p3873 A70-40671

Saturn ring photometric properties, discussing multiple scattering and Seeliger principal photometric theory deviation

21 p3885 A70-40932

Stellar ring 373, comparing color-magnitude and color-color diagrams to adjacent star fields

21 p3888 A70-41121

Nova HR Delphini 1967 UVB photoelectric photometry, examining absolute magnitude, distance, response curves and spectra

21 p3889 A70-41154

Eclipsing binary with very hot white dwarf, discussing effective temperature and photometric observations

21 p3889 A70-41158

IR star types T-Tauri, B-emission and M supergiants observations using UBVRI photometry

21 p3890 A70-41163

Auroral pulsations photometric observation data, noting magnetic activity effects

21 p3819 A70-41290

Lunar crater Plato optical reflectance photoelectric measurements, discussing absorption and luminescent features, radiance factors, phase angles color variations and brightness

21 p3922 A70-41983

Color-magnitude diagram of star cluster Kron 3 in Small Magellanic Cloud, using electronographic photometry

22 p4102 A70-42978

Atmospheric optical properties at various altitudes, using lunar disk photometric observation at different wavelengths during eclipse

23 p4239 A70-43901

Lunar topography from UBVRI photometry, determining albedos for mountains, dark and light maria and cratered terrae

23 p4247 A70-44769

Photographic photometry in astronomy, considering Becker method and UVB system

24 p4333 A70-45145

High resolution upper photosphere images obtained by slow raster scanning device and germanium bolometer, noting points around sunspots

24 p4400 A70-45307

High luminosity M type star photometry, determining supergiant intrinsic properties, interstellar extinction mean law and galactic evolution

24 p4410 A70-45764

Solar XUV and soft X ray photometry, describing sounding rocket and satellite grazing incidence spectrometers

24 p4339 A70-45822

ASTRONOMICAL SPECTROSCOPY

Martian carbon dioxide band observations using multislit spectrophotometer, indicating surface height variations near Syrtis Major

01 p0182 A70-10723

Quasar B264 observed with multichannel spectrometer attached to 200 inch telescope, comparing to N-type and Seyfert galaxies and other quasars

02 p0371 A70-12243

Quasar spectra interpretation, analyzing observational data and absorption lines correspondence to different red shifts

03 p0570 A70-13484

Stellar atmosphere high dispersion spectroscopy, discussing limitations for stars over 17,000 K

04 p0746 A70-14508

IR spectra of M stars and alpha Tau obtained with Michelson interferometer, observing molecular features and water vapor absorption

04 p0747 A70-14548

Intensity and spectral distribution measurement techniques for nonvisible extraterrestrial radiation, discussing rocket spectroscopy results

04 p0757 A70-15648

IR solar spectrum including water vapor, carbon dioxide and methane bands

05 p0913 A70-16566

Soviet book on celestial bodies radiation transfer and spectra covering light scattering, radiation fields, absorption, etc

08 p1568 A70-20768

Jupiter atmospheric properties on basis of spectrograms analysis

08 p1569 A70-20833

Book on stellar spectroscopy, covering stellar atmospheric models, rotation, evolution, etc

09 p1756 A70-22640

Stellar optical spectral power measurement by electronic spectroscopic technique using lasers

09 p1696 A70-22785

Bowen levels of O III radiative lifetimes and transition probabilities measurements by beam-foil spectroscopy

10 p1936 A70-23909

Eclipsing binary beta Aurigae effective temperature and surface gravity determination from photoelectric spectrum and abundance analyses

10 p1938 A70-24100

Spectroscopy in astrophysical research, discussing solar corona chemical elements, forbidden lines and temperature determination

10 p1948 A70-25181

Celestial sources energy spectrum and absolute flux by rocket flights, attributing short lived outbursts to shock wave from nova expanding into circumstellar medium

11 p2113 A70-26297

Iconoclastic cosmology and remote sensing of universe, discussing cosmic scale photometry and extra-galactic red shift spectroscopy

12 p2296 A70-26924

Electronic heterodyne astronomical spectroscopy, using lasers for absolute monochromatic flux and polarization measurements on star-like objects

13 p2408 A70-29473

Water sources associated with W3, Orion Nebula, W49 and VY Canis Majoris observed with coherent interferometers having long baseline

14 p2642 A70-30892

Total Absorption Shower Cascade /TASC/ detector for gamma ray astronomy space, discussing energy and angular resolution

14 p2587 A70-31004

B3V stars atmospheres by LTE model and spectroscopic techniques

14 p2652 A70-31384

Papers on spectroscopic astrophysics covering stellar spectral classification, growth curves, hydrogen lines, stellar spectra, interstellar space, stellar rotation, binary stars, etc

15 p2796 A70-31499

Spectral transmittance coefficients at Naugazran astronomical station, using Bouguer method

15 p2809 A70-32909

Orbit and component velocities of double line spectroscopic binary HR4072 on high dispersion spectrograms, noting mass ratio close to Guthrie relation

16 p2976 A70-33786

H-R diagram stellar spectra interpretation using model atmospheres describing temperature, gravity and chemical composition

17 p3169 A70-35381

Jupiter atmosphere ammonia abundance from laboratory curves of growth analysis for ammonia bands

18 p3310 A70-35937

Optical system of absorption tubes for planetary atmosphere spectra simulation

18 p3314 A70-36408

Astronomical Fourier spectroscopy, discussing techniques, improvements, advantages and mode of use

20 p3706 A70-39933

Venus atmosphere and water vapor, finding ice clouds by spectrum analysis

20 p3708 A70-39961

Lunar surface spectral reflectivity measured with ground based telescopes for remote mineralogical analysis

20 p3709 A70-39977

Gamma ray astronomical point sources by balloon flight and satellite observation, discussing detector system and telescope for flux and energy spectrum

21 p3821 A70-40694

Planetary nebulae radial velocities using prime focus or coude spectra

21 p3889 A70-41157

Orion nebula H alpha/forbidden N II ratio measurement using wide field multislit spectrograph

22 p4101 A70-42857

Orion Nebula and 32 other planetary nebulae spectra in yellow-green obtained with electronic camera, discussing forbidden N I and II lines

22 p4103 A70-42983

ASTRONOMICAL TELESCOPES

NT APOLLO TELESCOPE MOUNT

NT PYROHELIOMETERS

NT SPECTROSCOPIC TELESCOPES

NT X RAY TELESCOPES

Solar magnetic field investigated with parallel beam from coelostat mounting falling on magnetograph slit of solar telescope, noting field polarity change periodicity

01 p0177 A70-10347

Right ascension screw error effects on observations of stellar image passage through meridian, evaluating effect

01 p0181 A70-10662

Reflector radio telescope of Pulkovo Astronomical Observatory noting high resolution

01 p0094 A70-11585

Cassegrain telescopes lens corrector systems, critically examining various published articles

02 p0297 A70-11927

Display system for Apollo Telescope Mount designed for unclouded sun view by orbiting astronaut-scientists, discussing human factors, film budgeting, etc

02 p0298 A70-12151

UV photometry of stars and galaxies from OAO-2, discussing instruments and observational results

02 p0378 A70-12580

Optical facilities of Apollo 11 mission and NASA Manned Spacecraft Center noting Faddow telescopes, lunar cartography, photometric surface analysis, etc

04 p0687 A70-14690

Far IR extrinsic photoconductive detectors for rocket-borne liquid He-cooled IR telescope, discussing limiting noise factor

04 p0689 A70-15018

Sacramento Peak Observatory vacuum tower solar telescope and auxiliary instrumentation, providing flexibility in data collection and system adjustment by computer control

04 p0663 A70-15273

Stellar systems observations using photometers with long narrow slits in identical telescopes

05 p0852 A70-16922

Astronomical telescope performance at transfer process from object to image using optical transfer function and brightness standards

08 p1493 A70-20685

Poltava observatory zenith telescope characteristics, including scale division and ocular micrometer screw revolutions

08 p1496 A70-21157

Chromatic aberrations of Poltava observatory AVR-2 refractor

08 p1496 A70-21161

Astronomical high power telescopes construction, discussing rough casting, forming, precision polishing, Foucaultage principle for spherical mirrors, thermal effects, etc

09 p1674 A70-22218

Rapid guiding system for high resolution astronomical observations using thermal expansion of electrically conducting wires

09 p1721 A70-22741

Large optical telescopes design, discussing field correction at prime focus, low expansion materials, drive and control systems, on-line computers, etc

10 p1860 A70-24554

Temperature insensitive telescope with metallic mirror at Milan-Merate Observatory

10 p1889 A70-24584

Thermal control design for diffraction limited large diameter Cassegrainian telescope systems in orbital conditions, using computer and scale model testing

11 p2052 A70-26356

Solar horizontal telescope performance improvement by adding birefringent monochromator and diffraction grating

11 p2057 A70-26590

Big Bear Solar Observatory, discussing site selection, observatory construction and telescope optical system

12 p2205 A70-26864

Telescope servocontrol system with low pointing error and drift rate, permitting extended time exposure photography of star or deep space probe

12 p2202 A70-26869

Modal expansion method applied to thin deformable primary mirror surface control for orbiting astronomical observatory

13 p2403 A70-28427

Meteors position angles determination during telescopic observations, discussing error due to angle reversion

13 p2491 A70-29043

Universal triaxial instrument with AT-1 telescope for visual observation of satellites, discussing applications and accuracy

13 p2408 A70-29274

- Astronomical telescope system design and construction, considering optical configurations, components, mounting, atmospheric limitations, etc
15 p2736 A70-31950
- Glancing incidence extreme UV telescopes optical design in solar physics applications, employing surfaces of revolution
15 p2736 A70-32029
- Shemakha observatory telescope main mirror spherical aberration, coma, astigmatism and light concentration, describing support system and adjustment and control mechanisms
15 p2738 A70-32203
- Atmospheric ground layer temperature variations effect on astronomical telescope observations, discussing image motion character and origin
15 p2772 A70-32462
- Attitude sensing and target pointing instrumentation in earth orbiting stellar telescopes in inertial space
16 p2905 A70-33155
- Real time angular readout system for declination axis of U.S. Naval Observatory six inch transit circle, using Inductosyn as basic transducer
16 p2906 A70-33176
- Orbiting solar telescope design for solar disturbances location and monitoring in H alpha line
16 p2907 A70-33188
- Automatic active optic control of alignment and figure of primary mirror of spacecraft-borne telescope with response time stability
16 p2907 A70-33189
- Steerable 100 meter radio telescope, discussing foundations, azimuth towers, reflector, assembly, electric motors, steering and receivers
16 p2888 A70-33656
- Solar spar telescope of Lockheed Solar Observatory with closed tube protection from dust and wind
16 p2911 A70-33794
- Primary mirror development problems for large orbiting telescopes
17 p3083 A70-34873
- 1620 Geographos observations using Ritchey-Chretien reflector and Curtis Schmidt telescope
17 p3171 A70-35446
- Large photographic telescope characteristics for stellar and planetary observations, noting differential refraction influence on plate scale factors
18 p3259 A70-36608
- H 2 region and neutral gas spiral structure and radial distribution, using optical observations and radio continuum surveys
18 p3327 A70-37162
- Lens systems configuration and aberration, determining suitability for wide angle oculars of Galilean telescopes
19 p3420 A70-37262
- Portable telescope for river and ocean vessels, discussing design and operation thermal stability and hermetization
20 p3629 A70-39311
- Five-channel azimuthal underground cosmic ray telescope using proportional counters suitable for continuous recording
20 p3629 A70-39312
- Quantitative measurement of solar limb image motion and blurring, noting role of telescope aperture
20 p3634 A70-40424
- Double resonator ruby maser for observing transitions of interstellar hydroxyl, noting incorporation in modulation radiometer of astronomical telescope
21 p3835 A70-40641
- Tilted-component corrected off-axis telescope design based on third-order aberration theory
21 p3822 A70-40818
- Pointing systems for balloon-borne telescopes in astronomical investigations
22 p4041 A70-43649
- ASTRONOMY**
Book on classical astronomy and astrophysical problems covering time and longitude determination, calendar, precession, planetary motion, eclipses, gravitation, double stars, etc
01 p0191 A70-11376
- Soviet book on aeronautical astronomy covering reference stars, time and natural illumination measurements, aircraft course determination, position fixing, etc
02 p0329 A70-11695
- Astronomical and space research methods probing fundamental questions concerning universe unsolvable by classical astronomy, discussing solar wind and stellar formation and evolution
03 p0571 A70-13790
- Astronomy - Conference, Hobart, Australia, May 1969
04 p0746 A70-14506
- Book on methods of geodetic astronomy for inter-tropical zone covering azimuth, latitude and time determination, spherical geometry and geographical coordinate reduction
04 p0677 A70-14750
- Z term from astronomical latitude data compared with catalog error corrections, showing nearness to absolute star system
05 p0907 A70-16030
- General relativity taking into account astronomical and laboratory tests, cosmology and theoretical studies /1967 to 1969/
07 p1334 A70-19102
- Astronomical sounding balloon to study interplanetary scattered light, discussing actuating and control, structure, onboard and ground electronics
08 p1497 A70-21349
- German bibliography on astronomy for 1968 covering astrophysics, astronomical instruments, position determination, solar, terrestrial, planetary and lunar and stellar astronomy, etc
08 p1580 A70-21700
- Moon observation in megalithic times by means of menhirs
09 p1751 A70-22194
- Astronomy role in physical science and space exploration
10 p1940 A70-24373
- Manned space flight role in earth orbital space astronomy, examining long range program
12 p2297 A70-26997
- Collection of papers on quasars and high energy astronomy covering radio galaxies, cosmic rays, gamma rays, galactic clusters, neutrino astronomy, gravitational collapse, etc
12 p2299 A70-27376
- Astronomy - Conference, Mannheim, Germany, September 1969
12 p2300 A70-27576
- Transmission diffraction grating for astronomical applications constructed holographically with laser light and photoresist films
12 p2234 A70-27589
- Gyrostabilized platforms for astronomical observations, minimizing position errors
13 p2403 A70-28441
- Neutrino astronomy for processes in stellar interiors, emphasizing thermonuclear reactions in sun and main sequence stars
13 p2490 A70-28947
- Power spectrum analysis of division errors of graduated circles associated with meridian astronomy
19 p3523 A70-38686
- Papers on astronomy and astrophysics, discussing pulsars, solar internal rotation, nuclei of galaxies, Fourier spectroscopy, solar magnetic fields, stellar winds, etc
20 p3705 A70-39926
- Astronomical events observed in 1970 by amateur astronomers, discussing sun and moon eclipses and planets visibility
21 p3886 A70-41074
- Astronomy - Conference, Canberra, Australia, December 1969
21 p3890 A70-41176
- Earth orbital experiments synthesis in space programs methodology, discussing examples in astronomy, biology and oceanography research
22 p4097 A70-42500
- Space and astronomic methods applied to solid earth and ocean physics
22 p4025 A70-43669
- Experimental astronomy and role of space technology, discussing artificial satellites, extraterrestrial life, moon, Mars and Venus exploration, etc
23 p4247 A70-44775
- Collection of papers on astronomy covering celestial mechanics, instrumentation, solar activity, planetology, meteors and meteorites, galaxies, radio astronomy, etc
23 p4255 A70-45031
- Astronomical instrumentation and methods in different nations, emphasizing photoelectric image receivers
23 p4199 A70-45033
- Extragalactic astronomy research covering quasars, Seyfert and related galaxies, cosmology, Magellanic Clouds, supernovae, etc
23 p4256 A70-45040
- Manned earth orbital space astronomy instruments, facilities and research objectives
24 p4415 A70-45825
- ASTROPHYSICS**
Book on classical astronomy and astrophysical problems covering time and longitude determination, calendar, precession, planetary motion, eclipses, gravitation, double stars, etc
01 p0191 A70-11376
- Collective interactions effect on electron scattering opacity in stellar interiors, using Debye-Huckel radial distribution function and neglecting collisions
02 p0364 A70-11789
- Atomic configurations population inversions of astrophysical interest, assuming excitation by electron collisions, solving rate equations for level populations by computer
02 p0341 A70-11794
- Nonperiodic phenomena in variable stars by statistical and physical analysis, noting role of magnetic fields
03 p0566 A70-13313
- Physical conditions of stars in presupernova stage for type II supernovae with outburst expected due to Fe-He transition in core, confirming lower mass limit
03 p0566 A70-13314
- Smithsonian Astrophysical Observatory /SAO/ Star Atlas of reference stars and nonstellar objects
04 p0749 A70-14676
- Empirical astrophysical damping constants derived for neutral Fe lines using solar spectra, applying constants to abundances and surface gravity determination
05 p0919 A70-16939
- Stellar configurations of cold static neutral plasma consisting of nuclei and degenerate electron gas, calculating integral parameters by Newton gravitation theory
07 p1376 A70-18912
- Effective, brilliance, color and gradient temperature measurements in astrophysics, considering observer bond and thermodynamic nonequilibrium of stars
07 p1386 A70-19597
- Book on nuclear and astrophysical aspects of cosmic rays covering kinematics in collisions and decays, cascade theory, high energy interactions, origin, etc
07 p1368 A70-19666
- Lepton charge and neutrino astrophysics, discussing oscillations role in solar neutrino detection difficulties
07 p1371 A70-20329
- Book on physics of stellar interiors covering radiant energy, mechanical equilibrium, mass density distribution, nuclear reactions, etc
08 p1568 A70-20758
- German bibliography on astronomy for 1968 covering astrophysics, astronomical instruments, position determination, solar, terrestrial, planetary and lunar and stellar astronomy, etc
08 p1580 A70-21700
- Stellar evolution computations numerical instability due to coupling between hydrostatic equilibrium and thermal processes
09 p1755 A70-22508
- CH, CD and CH ion excited states decay rates determined from phase shift and frequency data, discussing implications for astrophysics
09 p1731 A70-22513
- Free radicals role in astrophysics, considering diatomic or triatomic radicals in atmospheres of earth, sun, planets, comets, stars and interstellar space
10 p1943 A70-24839
- Spectroscopy in astrophysical research, discussing solar corona chemical elements, forbidden lines and temperature determination
10 p1948 A70-25181
- Thermodynamics and statistical mechanics taking into account irreversibility, arrow of time and astrophysical schemes
11 p2146 A70-25695
- Soviet collection of papers on solar and stellar physics covering degenerate gases, variable stars, energy sources, stellar atmospheric and shell models, star clusters, etc
11 p2114 A70-26576
- Collapsed spherical bodies equilibrium structure, considering density-pressure state equations for cold neutron gas and gas-radiation mixture
12 p2300 A70-27395
- Continuity equation plasma oscillation, discussing ion current waveform flowing from discharge and implications for periodic astrophysical phenomena
14 p2638 A70-30618
- Papers on spectroscopic astrophysics covering stellar spectral classification, growth curves, hydrogen lines, stellar spectra, interstellar space, stellar rotation, binary stars, etc
15 p2796 A70-31499
- Book on interpretation of spectra and atmospheric structure of cool stars covering line identification, dissociative equilibrium, opacity, chemical composition, carbon stars, etc
16 p2978 A70-33962
- Papers on astronomy and astrophysics, discussing pulsars, solar internal rotation, nuclei of galaxies, Fourier spectroscopy, solar magnetic fields, stellar winds, etc
20 p3705 A70-39926
- Book on astrophysics and stellar structure covering physical characteristics, atmospheres, interiors and evolution
21 p3919 A70-41792
- Astrophysics and general relativity - Waltham, Mass., June-July 1968, Volume 1
22 p4098 A70-42576
- Gravitational collapse for astrophysical matter distributions, discussing differential geometry, relativity, Schwarzschild metric, static equilibrium and space-time geometries
22 p4098 A70-42579
- Astrophysical hypothesis of vorticity expulsion from strong turbulence regions, indicating mechanism of thermally driven circulation currents
22 p4010 A70-42690
- Collisionless plasma shock wave structures from geophysical and astrophysical phenomena standpoint, describing tarantula experiment
23 p4225 A70-44184

Plasma physics and MHD in astrophysics of sun and stars, discussing stellar magnetism origin and evolution, solar and stellar atmospheres, pulsars, etc
23 p4256 A70-45042

ASYMMETRY

Asymmetric thermoelasticity derived for constitutive equations based on thermodynamics of irreversible processes, formulating variational and reciprocity theorems
01 p0209 A70-11384

Stress concentrations and load cycle asymmetry effect on materials stress and breakdown behavior under various load cycles
02 p0383 A70-11656

Monograph on aircraft aerodynamic nozzle asymmetry effects for pressure drag reduction in critical conditions
03 p0465 A70-13003

Wave functions of asymmetric gyroscope in rotating coordinate system, presenting quantum equation of motion solution
06 p1105 A70-17500

Solar asymmetries associated with sun motion toward apex related to formation of N-S asymmetries of geomagnetic storms
06 p1144 A70-18011

East-west dissymmetry in solar activity center births for solar cycles XII-XIX, noting independence of latitude and invariance throughout last eight cycles
08 p1567 A70-20599

Gravitational collapse models with magnetic dipole and gravitational quadrupole, treating asymmetries as small perturbations
09 p1752 A70-22274

Asymmetry and vorticity effects on linear instability of channel flow with one parameter velocities and inflection points, proving wave speed theorem
10 p1862 A70-23951

Asymmetric missile nonlinear angular motion, describing quasi-linear relations for frequencies, damping rates and swerving motion amplitude
[AIAA PAPER 70-534] 13 p2506 A70-29002

Asymmetrical slender planetary entry vehicle roll dynamics, analyzing steady state angular motion
[AIAA PAPER 70-560] 13 p2339 A70-29003

Asymmetrical element spacings in thinned antenna arrays, obtaining symmetrical radiation patterns with low sidelobe levels
14 p2556 A70-30689

Cylindrical conical shell junction asymmetric bending, using numerical method and exact solution
15 p2822 A70-32360

Stress measurements in rotating plane disks with notched disturbed symmetry, using stroboscopic photoelasticity and numerical methods
[ASME PAPER 70-GT-26] 18 p3344 A70-36867

Stress concentrations and load cycle asymmetry effect on materials stress and breakdown behavior under various load cycles
19 p3547 A70-38429

Longitudinal and vertical wind components turbulent fluctuations distribution skewness relationship to atmospheric stability and height, noting effect on diffusion
20 p3664 A70-40064

ASYMPTOTES

Stability and asymptotic stability criteria for attraction sets in dispersed dynamic systems obtained in terms of Liapunov function
01 p0141 A70-10152

Asymptotic and approximate wave construction for system of first order quasi-linear partial differential equations
01 p0131 A70-10800

Radiative energy transfer from single small sphere to quiescent nonconducting gas with constant volumetric absorption coefficient, using method of matched asymptotic expansions
02 p0400 A70-12861

Monograph on generalized transforms properties and asymptotic behavior, discussing kernel functions, Bessel functions, Laplace transforms, Hankel transforms, etc
03 p0519 A70-13650

Helicoid precession in reentry problem found unstable in sense of Liapunov and Lagrange and asymptotically stable in sense of Poincare
04 p0765 A70-15666

Electron distribution functions in weakly ionized plasmas by asymptotic analysis of boundary layer near wall
06 p1121 A70-17903

Asymptotically periodic solution of nonlinear differential equations, discussing digital or analog computer utilization
07 p1326 A70-19782

Nonorthotropic pinched plates deflections solution, demonstrating asymptotic convergence of small parameter method
09 p1769 A70-22151

Asymptotic behavior in cold plasma model of magnetopause, describing boundary layer between plasma stream and vacuum magnetic field
10 p1921 A70-23835

Asymptotic method for aeromagnetic flutter of plane MGD nozzle, discussing conditions of MGD nozzle stability
10 p1800 A70-24129

Independent identically distributed random variables sequence, obtaining asymptotic expansion for large deviations of distribution function
10 p1910 A70-24799

Asymptotics of linear diffusion processes altered by weak nonlinear effects, discussing deterministic and statistical initial value problems
11 p2074 A70-26686

Stochastic adaptation process, investigating asymptotic properties based on concept of random system with complete connections
13 p2383 A70-29490

Criteria for estimating errors in quadratic approximations to asymptotic stability involving Popov condition based on existence of quadratic Liapunov functions
16 p2941 A70-33045

Quadratures asymptotic properties and convergence for continuous functions and function with singularity
19 p3456 A70-37415

Asymptotic behavior of boundary layer equations solution for viscous incompressible flow past curvilinear obstacle
21 p3806 A70-40613

Coherent behavior associated with thermodynamic description projected from dynamical behavior of many body system, using relation between asymptotic operators
22 p4062 A70-42547

Asymptotic properties of integral equations solutions for boundary value problems in theory of elasticity and mathematical physics
24 p4422 A70-45490

ASYMPTOTIC METHODS

Existence theorem used for proof of asymptotic methods in nonlinear stability of laminar flow
[ONERA-TP-750] 01 p0061 A70-10298

Two variable expansion method applied to ordinary differential equation and two wave propagation problems, comparing results with matched asymptotic expansions and coordinate stretching methods
01 p0132 A70-11072

Asymptotic method based on Landahl small perturbation theory applied to perturbation velocity potential for oscillating delta wing in transonic flow
02 p0223 A70-11775

Solar/stellar/wind solutions asymptotic behavior at large distances from central star for equations including effects of rotation and anisotropy
02 p0358 A70-12253

Asymptotic behavior at infinity of mixed boundary value problem analyzed for Sobolev equation involving operator
03 p0518 A70-13433

Viscous supersonic flow near wall with large local curvature, using asymptotic solutions to Navier-Stokes equations
03 p0468 A70-13867

Asymptotic solutions of paraboloidal boundary layer system for thermally driven convective flows governed by nonlinear Boussinesq equations
03 p0519 A70-14077

Sturm-Liouville problem associated with Falkner-Skan equation, obtaining asymptotic solutions
03 p0520 A70-14080

Asymptotic form of axisymmetric solution with Dirichlet integral for Navier-Stokes equations applied to flow past bodies of revolution with smooth surfaces
03 p0471 A70-14303

Asymptotic expansion method to analyze laminar boundary layers with zero wall shear, large suction and adverse pressure gradients
04 p0674 A70-15563

Finite difference wave equation to obtain asymptotic estimate for magnitude of precursor effects
05 p0875 A70-16310

Meksyn asymptotic method of integrating boundary layer equations applied to ordinary differential equations for slip flow past semiminfinite flat plate
06 p0979 A70-18348

Asymptotic behavior of approximate solutions of nonlinear differential equations
07 p1322 A70-18891

Asymptotic behavior of inviscid radiating gas flow near stagnation point of blunt body
07 p1188 A70-19315

Electrical and thermal characteristics of stabilized gas heating by electric arc at high pressures calculated by successive approximation
07 p1350 A70-19840

Viscous hypersonic flow past sphere in presence of strong injection through front surface at large Reynolds numbers using asymptotic method
07 p1189 A70-20146

Asymptotic method for Vlasov equation formulated for weakly Landau damped monochromatic plasma wave in collisionless electron plasma
07 p1353 A70-20231

Asymptotic method for Vlasov equation of plasma wave reformulated in Eulerian representation
07 p1354 A70-20232

Asymptotic expansions and energy methods applied to three dimensional aircraft maneuvers involving energy climbs and turns
07 p1190 A70-20416

Single frequency oscillations of variable cross section rods with random perturbations using asymptotic methods of nonlinear mechanics, discussing wedge oscillations
08 p1583 A70-20487

Circular dielectric waveguide modes self consistent description by asymptotic method, obtaining eigenvalues and eigenfunctions
08 p1476 A70-21288

Asymptotic analysis for axisymmetric buckling of axially compressed short cylindrical shells with free edges, using Batterman method
08 p1593 A70-21620

Oscillations of highly viscous incompressible fluid in partially filled cavity of body moving about fixed point, solving Navier-Stokes equations by asymptotic method
08 p1485 A70-21632

Blast wave eigenvalues in asymptotic expansions approximation for hypersonic flows past blunt bodies
10 p1797 A70-23953

Asymptotic eigensolutions for equations governing flow between oppositely rotating infinite plane disks in inviscid limit
10 p1870 A70-24607

Dynamic programming successive approximations optimization technique involving system state variables reduction with convergence proofs
10 p1845 A70-24871

Necessary and sufficient conditions for absolute stability of nonstationary nonlinear system, showing equivalency to asymptotic instability in small position equilibrium piecewise linear systems
11 p2021 A70-25337

Three dimensional periodic boundary layer flow noting successive approximations method, noting steady streaming in first order cross flow
11 p2037 A70-26296

Uniform asymptotic theory of diffraction by edge of three dimensional body, obtained boundary layer solution applied to scattering by circular cylinder
11 p2084 A70-26422

Asymptotic model for stationary radiative stationary transitions using Newman-Penrose spin coefficient approach to gravitational radiation for Riemann spacetime
11 p2084 A70-26547

Asymptotic properties of Cauchy problem solution for heat conduction equation
12 p2331 A70-27300

Infinitesimal dipole moving through hot uniform electron plasma in magnetic field, investigating asymptotic time behavior of plasma resonance
13 p2467 A70-29912

Radiative heat transfer in optically thick gas between concentric spheres treated by matched asymptotic expansions, comparing results with Rosseland approximation and numerical solution
14 p2663 A70-30266

Eigenvalues of membranes and plates, comparing asymptotic and numerical values
14 p2600 A70-31223

Orr-Sommerfeld equation asymptotic solution corresponding to boundary layer velocity distribution
15 p2721 A70-32357

Oscillatory and wave processes in nonlinear distributed systems by asymptotic method analogous to Bogoliubov concentrated systems
16 p2951 A70-33252

Time asymptotic solutions for hypervelocity blunt body flow field with coupled nongray radiation, treating shock as discrete surface
[AIAA PAPER 70-865] 16 p2999 A70-33908

Asymptotic analysis of wave propagation modes in circular solid elastic cylinder, obtaining displacement components and frequencies as dimensionless wave number power series
16 p2993 A70-34085

Nonlinear partial differential equations initial value problems asymptotic solution using two time method
16 p2943 A70-34245

Kinetic synthesis for multivariable system by asymptotic equivalence method
16 p2944 A70-34279

Nonlinear dynamic systems described by matrix equation, formulating asymptotically stable conditions, discussing motion equations of two degree of freedom system
16 p2995 A70-34281

Singular perturbations of boundary value problems, investigating asymptotic solutions to finite difference equations
17 p3128 A70-34613

Adaptive linear estimator for stationary time series, evaluating asymptotic mean square error bound
17 p3128 A70-34852

Unsymmetric vibrations of cylindrical shells, analyzing stress states by asymptotic method
18 p3335 A70-36059

Shadow current method for asymptotic solution to two dimensional problem of electromagnetic wave far

- diffraction field on ideally conducting plane with infinite rectilinear slot
 - 18 p3227 A70-36142
 - Plane wave diffraction by periodic grating reduced to waveguide problem, determining asymptotic behavior of integral solution
 - 18 p3291 A70-36286
 - Eigenvalues and errors in asymptotic approximation of ordinary differential equations of second and fourth order
 - 18 p3283 A70-36365
 - Asymptotic, averaging and Ritz methods for steady state periodic vibrations of nonlinear systems with many degrees of freedom
 - 18 p3338 A70-36437
 - Schwarzschild exterior metric stability against perturbations from asymptotic behavior of Einstein field equations solution in Kruskal coordinates
 - 18 p3291 A70-36650
 - Uniform asymptotic solutions of second order linear differential equations with arbitrarily many turning points or Stokes lines
 - 19 p3457 A70-37681
 - Asymptotic expansion methods for solving wave propagation and diffraction problems via localization principle
 - 20 p3657 A70-39219
 - Relativistic high temperature gas asymptotic solutions with or without body force, comparing flow field with photon gas
 - 20 p3673 A70-39654
 - Gas lubrication with injection at large compressibility numbers, deriving asymptotic solution
 - 20 p3637 A70-39817
 - Asymptotic equivalent functions for integral Laplace transformation transition to original in continuous media mechanics
 - 20 p3726 A70-39873
 - Thin plane bars elasticity theory, constructing integrals of equations by asymptotic series expansion
 - 20 p3726 A70-39881
 - Asymptotic buckling analyses of imperfect columns on nonlinear elastic foundations by perturbation expansions, equivalent linearization and truncated hierarchy approximations
 - 21 p3934 A70-40777
 - Heat conduction into semiinfinite homogeneous solid with thermal conductivity dependence on temperature, noting temperature profile asymptotic behavior for similarity solution
 - 22 p4123 A70-42641
 - Asymptotic method for nonlinear automatic control systems involving differential equations in Cauchy form with nonlinearities
 - 22 p4001 A70-42834
 - Irrational incompressible free falling jet, using asymptotic expansion solution for mixed boundary value potential problems
 - 22 p4012 A70-42938
 - Asymptotic solution for thick linear antenna admittance
 - 23 p4171 A70-43882
 - Linear stability of fluid flow, proving equivalence of slow and rapid asymptotic solutions of Orr-Sommerfeld equations
 - 23 p4180 A70-43994
 - Asymptotic and computer methods interaction in thin walled shells structural analysis and design, considering pressure vessels, cone vibration and dynamic loads
 - 23 p4271 A70-44703
 - Quantum mechanics classical equations for complex velocity variable, obtaining asymptotic series solution by applying modified WKB method
 - 24 p4378 A70-45274
 - Asymptotic small-parameter solution of boundary value problem for second-order elliptic equations with variable coefficients in thin regions
 - 24 p4424 A70-45635
 - Plane wave diffraction by infinite strips and slitted planes, obtaining asymptotic expansions valid for HF
 - 24 p4426 A70-46019
 - Differential equations with integrable coefficients, proposing asymptotic integration for second order system
 - 24 p4370 A70-46031
- ASYMPTOTIC SERIES**
- Singular perturbation problem solution asymptotic expansions applied to linearized theory of elasticity equilibrium problem with stress couples
 - 02 p0389 A70-12685
 - Boundary layer development on body accelerating in viscous incompressible fluid, using straight lines approximation and asymptotic expansions
 - 08 p1485 A70-21631
 - Lifting surface problem for finite span wing in ground effect using matched asymptotic expansions method
 - 14 p2527 A70-30280
 - Cophased two dimensional antennas fields asymptotic expansions in near and far zones with generalization to three dimensional case
 - 15 p2707 A70-31514
- Asymptotic expansion of contour integrals involving analytic functions of complex variable, using steepest descent method
 - 15 p2767 A70-31696
 - Boundary layer problems with resonance solved by matched asymptotic expansions and WKBJ method
 - 23 p4179 A70-43945
- ATAXITE**
- Petrological, X ray and chemical analyses of Muz-zaffarup Ni-rich ataxite, showing kamacite, taenite and minor schreibersite composition
 - 01 p0177 A70-10328
- ATELECTASIS**
- Aeroatelectosis and pneumothorax in fighter pilot postflight chest pains, noting decompression role
 - 17 p3041 A70-35920
- ATHLETES**
- Radio telemetry of athlete hearts, noting strenuous physical stress induction of transient serum potassium increase, metabolic acidosis, T-wave amplitudes, etc
 - 02 p0230 A70-11694
 - Muscle temperature variations and respiratory activity of athletes under various exercise regimens, outlining optimal weight lifting training programs
 - 04 p0639 A70-15507
 - Initial period of muscular energy expenditure in athletes performing exercises on veloergometer, considering oxygen consumption
 - 12 p2172 A70-28313
 - Athletes ventilation and heart rate dynamic responses to supine leg exercise with sinusoidal work load
 - 20 p3576 A70-40329
- ATHODYDS**
- U RAMJET ENGINES**
- ATLANTIC OCEAN**
- Aeronautical satellites for monitoring positions of many commercial aircraft simultaneously crossing North Atlantic, discussing navigational error correction and atmospherics
 - 01 p0178 A70-10454
 - Stable moored ocean platforms providing reliable VHF communications and secondary surveillance radar facilities for civil aviation operations over North Atlantic
 - 09 p1723 A70-23035
 - Aeronautical satellite system for North Atlantic air traffic position monitoring, discussing simultaneous position display
 - 09 p1723 A70-23040
 - Forecasting air temperature over North Atlantic, analyzing atmospheric parameters informativeness
 - 20 p3663 A70-39274
 - Satellite-based air traffic control system for North Atlantic, applying stochastic optimal control theory [AIAA PAPER 70-966]
 - 20 p3669 A70-39563
- ATLAS CENTAUR LAUNCH VEHICLE**
- Solar powered electric propulsion systems for automated missions throughout solar system by extending range of Atlas Centaur-Titan 3-C launch vehicles [AIAA PAPER 68-1120]
 - 04 p0736 A70-15401
- ATLAS LAUNCH VEHICLES**
- NT ATLAS CENTAUR LAUNCH VEHICLE**
- Atlas/Centaur and Titan/Centaur launching of Intelsat 4 communication satellites, discussing booster, stage characteristics and payload [AIAA PAPER 70-483]
 - 11 p2127 A70-26605
- ATMOSPHERE EXPLORER A**
- U EXPLORER 17 SATELLITE**
- ATMOSPHERE EXPLORER B**
- U EXPLORER 32 SATELLITE**
- ATMOSPHERIC ABSORPTION**
- U ATMOSPHERIC ATTENUATION**
- ATMOSPHERIC ATTENUATION**
- NT AURORAL ABSORPTION**
- Cosmic ray survey measurements during IQSY reduced to common atmospheric depth, determining attenuation coefficients of neutron and muon monitors
 - 01 p0167 A70-10230
 - Jovian polar zones enhanced optical transparency causes, discussing thin clouds and difference in molecular optical depth between north and south poles
 - 01 p0180 A70-10531
 - Spectral distribution of X ray atmospheric absorption used to determine high energy photoelectrons spectrum
 - 01 p0172 A70-11494
 - Albedo variations for single scattering in atmosphere of arbitrary optical thickness by linearizing transfer equations with perturbation technique
 - 02 p0338 A70-11790
 - Lorentz absorption line shape computations in radiation scattered by homogeneous planetary atmosphere compared with results for isotropic scattering by van de Hulst similarity relations
 - 02 p0364 A70-11792
 - Absorption of EUV sunlight by Jupiter upper atmosphere, discussing photoelectron energy loss, thermal equilibrium and heating efficiencies
 - 02 p0367 A70-11816
 - Atmospheric transmittance line by line calculations along variable pressure and mixing ratio paths from 1.7-20 microns [AFCLR-70-0061]
 - 02 p0289 A70-11908
- Atmospheric IR radiation transmittance in 590 to 750 per cm interval, using balloon-borne spectrometer
 - 02 p0256 A70-11928
 - Laser position finding of satellites fitted with corner reflectors, discussing atmospheric attenuation and applications to global triangulation and gravitational field measurements
 - 02 p0256 A70-12083
 - Atmospheric penetration of UV and visible solar radiation during twilight, oxygen and ozone absorption, Rayleigh scattering and atmosphere refraction
 - 02 p0357 A70-12155
 - Aerosol size distribution from data on atmospheric spectral transmittance and solar corona brightness spectral and angular variations
 - 02 p0292 A70-12434
 - Crossed Fabry-Perot etalons and spectrographs for studying atmospheric solar absorption spectra
 - 02 p0299 A70-12438
 - Variable atmospheric attenuation of 5 mm wavelength band, considering oxygen absorption spectrum and attenuation for reference atmosphere
 - 02 p0260 A70-12570
 - Wideband satellites bandwidth and aperture limits direct measurement based on ground monitoring of CW signals, taking into account ionospheric dispersion
 - 02 p0261 A70-12577
 - Troposphere microwave transmission factor determined from dispersion and attenuation caused by water vapor isolated molecular resonance
 - 02 p0261 A70-12593
 - Atmospheric absorption anomalies of UV sunlight near 50 km altitude in rocket-borne radiometer determination of ozone distribution
 - 03 p0478 A70-14197
 - Solar and sky far IR radiation in upper atmosphere, estimating precipitable water quantities and low absorption regions
 - 04 p0681 A70-15521
 - Atmospheric absorption of noise investigated for characteristics based on aircraft flyby tests
 - 05 p0795 A70-16786
 - Carbon dioxide-nitrogen laser emission absorption in atmospheric surface layer by wings of distant strong lines investigated statistically
 - 06 p1082 A70-17807
 - Atmospheric difficulties in earth surface remote sensing by satellites, describing absorption, emission and scattering as wavelength functions [AIAA PAPER 70-193]
 - 06 p1057 A70-18083
 - Passive microwave observation from space of sea surface degraded by atmosphere [AIAA PAPER 70-197]
 - 06 p1010 A70-18087
 - Atmospheric effects on passive microwave sensing in EHF region under all-weather conditions on global scale using satellites [AIAA PAPER 70-198]
 - 06 p1010 A70-18099
 - Haze model atmospheres scattering characteristics by computer simulation concerning optical contrast reduction by aerosols for direct and diffuse radiation [AIAA PAPER 70-194]
 - 06 p1057 A70-18156
 - Polarization and absorption of radio waves in ionosphere using Appleton-Hartree equations, calculating LUF as function of sunspot number
 - 07 p1229 A70-19160
 - Ray tracing in ionospheric HF communications, describing computational method for ray paths and ionospheric absorption
 - 07 p1230 A70-19166
 - Oblique incidence absorption measurements by pulse or CW signal strength observations or LOF data, comparing LUF to LOF
 - 07 p1231 A70-19173
 - Radio wave absorption in Venusian ionosphere, estimating effective collision number
 - 07 p1235 A70-19491
 - Ionospheric absorption of hydromagnetic waves propagated normal to magnetic field, comparing daytime to nighttime absorption [AFCLR-70-0133]
 - 07 p1270 A70-20031
 - Daylight ionospheric scatter propagation and absorption during energetic electron precipitation event in auroral zone using bremsstrahlung observations at balloon altitude
 - 07 p1271 A70-20154
 - Simultaneous riometer and ionosonde measurements at high latitude suggesting absorption events due to cosmic noise scattering by auroral sporadic E
 - 07 p1271 A70-20165
 - Pulsed radio signals time delay due to molecular microwave resonance in earth atmosphere and interstellar medium
 - 08 p1461 A70-20915
 - Solar heating determination by using transmission factors derived for atmospheric constituents together with spectral irradiance curves outside atmosphere
 - 08 p1573 A70-21032
 - Optimal atmospheric transmittance windows for underlying surface and cloud temperature determination from satellites
 - 08 p1538 A70-21426

Atmospheric extinction observed photometrically in South Africa and southern France in narrow bands and astronomical UVB bands

08 p1490 A70-21647

Stationary phase for beam of radio waves propagating in absorptive ionosphere as function of mean directions of real and imaginary parts of wave vector

09 p1665 A70-22049

Seasonal measurements of atmospheric transmittance spectra for horizontal near-earth paths in IR region under haze and clear weather

09 p1666 A70-22179

Atmospheric limitations on remote sensors using visible sunlight, noting applications to Earth Resources Technology Satellite and human vision

09 p1718 A70-22893

Excessive absorption in night E layer with and without geomagnetic disturbances for almost complete solar cycle, discussing winter increases/anomalies/

09 p1669 A70-23170

Terrestrial surface radiometric imaging by sensing thermal radiation at centimeter wavelengths to reduce atmospheric scattering attenuation

09 p1687 A70-23763

Ozone measurement from satellite by direct beam and scattered light methods employing UV sunlight attenuation

10 p1890 A70-24639

Millimeter wave transmission, discussing atmospheric effects, system components and applications in terrestrial communication networks, synchronous satellites, etc

10 p1842 A70-24883

Light scattering, turbulent disturbances and absorption by binary oxygen complexes in atmospheric layers

10 p1843 A70-25126

Satellite distribution of TV signal over earth surface as alternative to terrestrial linkups, overcoming rain attenuation by high power spot beam

11 p1997 A70-25410

Italian SIRIO SHF experiment for study of atmospheric effects on satellite link, discussing system design and performance

11 p1999 A70-25442

Atmospheric absorption by ozone of solar radiation measured by balloon-borne spectrometer in 9-10 micron region

11 p2045 A70-25627

Holographic compensation for atmospherically induced phase distortion of IR laser beam

11 p2049 A70-25638

Solar radiation transmitted and reflected by earth atmosphere, solving absorption and scattering by computer programs

12 p2262 A70-26951

Absorption at solar H Lyman alpha line by earth hydrogen atmosphere measured as function of altitude from Aerobee flight spectrograms

12 p2222 A70-27182

Low noise temperature radiometer to study solar radio emission, measuring atmospheric absorption

12 p2184 A70-27235

Ionospheric absorption measurements by HF and VHF techniques, discussing electron density profiles, collision frequencies, anomalies and aeronomic and ionospheric implications

12 p2224 A70-27735

Long term ionospheric absorption measurements in Japan from IGY through IQSY using A1 method, discussing annual and diurnal variations correlation with solar activity

12 p2226 A70-28059

Long term ionospheric absorption measurements in Northern Hemisphere from IGY through IQSY, discussing annual and diurnal variations correlation with solar activity

12 p2226 A70-28060

Submillimeter astronomy, discussing atmospheric absorption difficulties and principal areas of application

12 p2311 A70-28271

Ruby and He-Ne laser radiation attenuation found due to scattering by gas molecules and aerosols from atmospheric spectral transparency fine structure studies

12 p2191 A70-28294

Precipitation energetic electrons attenuation and impact ionization in ionosphere, determining vertical energy distribution profile

13 p2476 A70-28722

Atmospheric water effect on satellite communications in UHF region and above, discussing signal attenuation

13 p2364 A70-28782

Electromagnetic radiation attenuation in rain at cm and mm wavelengths, determining rainfall rates and drop size distribution

13 p2364 A70-28783

Spectroscopic parameters for attenuation and dispersion caused by 22 GHz water vapor line, using differential microwave refractometer

13 p2393 A70-28784

He-Ne laser beam transmission through atmosphere, investigating intensity, spot size, polarization and power spectrum fluctuations

13 p2427 A70-29103

Millimeter and submillimeter radio waves propagation, outlining molecular and aerosol attenuation in real atmosphere together with transmitters and receivers

13 p2366 A70-29401

Atmospheric optical thickness from radio telescopic measurements of wave absorption at millimeter wavelengths, showing dependence on lower atmospheric moisture content

14 p2546 A70-30127

Si solar cell power output and spectral response as function of angle illumination, eliminating atmospheric influence

14 p2533 A70-30337

Atmospheric absorption, scattering and turbulence effect on visible and IR radiation propagation, discussing optical systems performance

14 p2583 A70-30399

Space-surface path loss due to atmospheric gases, rain and clouds, considering military ground site location for space communication

14 p2608 A70-30596

Nonhomogeneous atmosphere with absorbing gas of constant mixing ratio, deriving transmission along isothermal and nonisothermal paths

14 p2617 A70-31304

Low altitude atmospheric effects on IR beam horizon sensors in carbon dioxide band, noting corrections for spacecraft attitude measurement

15 p2735 A70-31792

Automatic audio frequency spectrometer for ELF and VLF amplitude spectrum of atmospherics, discussing attenuation band near 3 KHz

15 p2725 A70-31856

Diurnal variations in attenuation of ELF atmospherics over different propagation paths from recordings at distant ground stations

15 p2728 A70-31994

Ionospheric structure characteristics in D, intermediate D-E and E-F 2 regions using deflecting and nondeflecting radiation absorption measurements

15 p2730 A70-32085

Sirio satellite SHF transponder for experiments in atmospheric propagation and communication between ground stations

15 p2709 A70-32285

Atmospheric transmission variability related to solar constant variations

15 p2801 A70-32371

Radio wave absorption in Venusian ionosphere, estimating effective collision number

15 p2705 A70-32736

Point to point and radar return attenuation measurements at SHF through clear air and rain

16 p2858 A70-32928

Earth-space path attenuation measurements by 8-14 micrometer telescope appended to sun tracker

16 p2861 A70-32989

Illumination level and contrast loss distribution in atmosphere to evaluate passive night vision equipment with image intensifier tubes

16 p2907 A70-33184

Solar limb image vibrations, establishing quantitative comparisons between statistical characteristics of fluctuations and weather conditions on propagation path

16 p2979 A70-34179

Atmospheric optical inhomogeneity effect on image quality, investigating deflection angles for spherical light wave passage at various altitudes

16 p2915 A70-34215

Lower ionosphere electron density and winter anomaly in HF absorption

17 p3077 A70-34948

Meteorological laser radar, discussing basis and techniques determining atmospheric radiation attenuation constant

17 p3045 A70-35106

Ionospheric radio wave absorption measurements, noting winter anomaly during maximum solar activity year

18 p3227 A70-36101

Atmospheric aerosols, fog and rain effects on signal transmittance and backscatter at 3400-10600 A

18 p3248 A70-36751

Atmospheric layer attenuation of thermal radiation from water surface by airborne radiation thermometer measurements

18 p3260 A70-36969

Aircraft-borne spectrometer for atmospheric IR spectral transparency

18 p3260 A70-36972

Radio wave absorption dependence on ionospheric sounding frequency at vertical incidence, using pulse method

18 p3255 A70-37038

Balloon-borne spectrophotometer with diffraction grating for upper atmospheric solar radiation attenuation measurement

19 p3422 A70-37639

Light characteristics and geometry of photoelectric photometer system measuring light attenuated by atmosphere, discussing error sources

20 p3625 A70-39030

Optical properties of system measuring atmospheric transmittance by recording light backscattered from atmospheric layers

20 p3660 A70-39033

Surface haze and vertical aerosol attenuation for various meteorological ranges within 1.2-15 km, tabulating for UV, visible and IR wavelengths

20 p3661 A70-39082

Atmospheric effects on passive microwave sensing in EHF region under all-weather conditions on global scale using satellites

20 p3586 A70-39703

Millimeter waves atmospheric attenuation vs frequency and altitude due to oxygen absorption, tabulating for graphical and seasonal model atmospheres

20 p3588 A70-40302

Millimeter and decimeter waves atmospheric absorption as function of pressure, temperature and water vapor density

20 p3588 A70-40303

Millimeter wave observation of sun, deriving empirical relationships between atmospheric attenuation, emission and water vapor

20 p3623 A70-40304

Heterodyne millimeter wave radiometric system for observing atmospheric attenuation due to water vapor, discussing design, development and initial measurements

20 p3588 A70-40308

Millimeter wave propagation measurements by ATS-5 satellite, observing attenuation dependence on meteorological parameters for communication data link performance prediction

20 p3589 A70-40311

X ray intensity sudden changes in 29.9-52.3 keV range from Sco X-1, correcting for atmospheric attenuation

21 p3872 A70-40661

Atmospheric communication channel modeling for laser wavelengths, considering point, area, heterodyne and direct detection receivers, nonplanar and infinite plane wave propagations, etc

21 p3793 A70-42179

ELF and VLF waves in waveguide propagation mode, calculating lower ionosphere effect on attenuation and phase velocity

22 p3989 A70-42960

Spectral radiation extinction at atmospheric aerosol particles, discussing particles complex refractive indices and size distributions

22 p4065 A70-43171

Solar L alpha absorption in upper atmosphere, using rocket-borne ionization chamber

23 p4191 A70-44270

Strong shocks propagation in atmosphere of variable density at rest, obtaining numerical solution of similarity flow behind shocks

23 p4182 A70-44599

Scattered photon effects on cosmic diffuse X ray spectrum at balloon altitude, noting overcorrection for absorption of primary X rays

23 p4237 A70-44794

Monthly and annual root-mean-square deviations of ionosphere radio wave absorption

24 p4312 A70-45485

Planetary atmosphere diffuse radiative transfer reflection and transmission, deriving reciprocity relations from integrodifferential equations

24 p4409 A70-45756

Millimeter wave solar radiation atmospheric absorption examined at sea level with Michelson interferometer

24 p4398 A70-45785

Mm wavelength radiometer for recording solar activity and radiation attenuation in atmosphere as function of time

24 p4315 A70-46236

ATMOSPHERIC CHEMISTRY

Lower atmospheric photochemistry, discussing tropospheric, stratospheric, mesospheric and polluted atmospheric chemical and photochemical reactions

06 p1058 A70-18485

Aeronomic neutral reaction rates, describing ozone excited state photochemistry

10 p1872 A70-23824

Auroral ion composition and chemistry from rocket-borne mass spectrometer measurements, investigating oxygen density and green line excitation

10 p1874 A70-24431

Diurnal variations of concentrations of ions and neutral components of NO, O and N in E region from analysis of chemical and photochemical processes

10 p1881 A70-24809

Tropospheric negative small ions formation reaction scheme, considering hydration degree

11 p2046 A70-26390

E and F layer ion chemistry dependence on ion-neutral reactions and dissociative recombination

12 p2223 A70-27220

- H and He intraatmospheric migration and dissipation, considering MHD waves, ionospheric plasma motions, chemical reactions, etc 14 p2569 A70-30211
 - Book on ionospheric chemistry, covering chemical and photochemical reactions above 60 km and ionization processes 18 p3247 A70-36212
 - Upper atmospheric atomic nitrogen reaction with carbon tetrachloride, estimating radiation intensity and brightness of artificial luminescent cloud 18 p3252 A70-36989
 - Indeterminacy interval reduction for ionospheric reaction rate constants by imposing supplementary condition on NO/oxygen molecular ion concentrations ratio 19 p3408 A70-37309
 - Nitric oxide and atomic nitrogen in mesosphere and stratosphere, discussing photochemical equilibrium 19 p3415 A70-38389
 - Chemical reactions of ions and neutral particles in D region, discussing photochemistry of atomic oxygen and ozone and reaction rate constants 19 p3418 A70-38905
 - D region water vapor chemistry effects on measurements of radio propagation, ionospheric temperature and seasonal changes 21 p3814 A70-40936
 - Midlatitude F 2 layer electron density structure using theoretical model, accounting for atmospheric physical and chemical processes 21 p3815 A70-41062
 - Reacting planetary carbon dioxide-nitrogen at mesospheric high temperature equilibrium thermodynamic and transport properties 21 p3950 A70-41747
 - Thermosphere, stratosphere and mesosphere reactions involving water, hydrogen, methane, ozone, nitric oxide and nitrogen peroxide 22 p4023 A70-43298
 - D region ion chemistry, discussing three body reactions, water cluster ion production, reaction rates and binary collisions 22 p4023 A70-43304
 - Venusian and Martian upper atmosphere chemistry, emphasizing ionization height distribution 22 p4106 A70-43312
 - H and He intraatmospheric migration and dissipation, considering MHD waves, ionospheric plasma motions, chemical reactions, etc 24 p4331 A70-46286
- ATMOSPHERIC CIRCULATION**
- Book on atmospheric circulation systems structures and physical interpretation, concentrating on lower atmosphere and North America 01 p0069 A70-10126
 - Atmospheric dynamics nonlinear equations reduction to spectral form using generalized spherical functions series 01 p0135 A70-10203
 - Stratospheric circulation and temperature variations periodicity, discussing midwinter warmings, polar vortex breakdown and relations to D region anomalies and solar events 01 p0072 A70-10580
 - Hydrodynamic explanation of upper atmosphere perturbation effects on tropospheric circulation, discussing experiments for solar activity effects on atmospheric dynamics 01 p0073 A70-10582
 - F region ionized and neutral atmospheric movements interactions, discussing ion drag forces, electromagnetic drift, wind effects, etc 01 p0074 A70-10587
 - Rotation periods of Jovian atmospheric currents showing zonal wind velocity variations with latitude 02 p0369 A70-11829
 - Stratospheric circulation model developed from radioactive element measurements, discussing large scale processes, seasonal variations, etc 02 p0291 A70-12291
 - Incomplete historical data to infer state of atmosphere based on global circulation model, noting tradeoff of temperature for wind and time for space 02 p0291 A70-12296
 - Invariant group study of free atmospheric convection equations at combination of Grashof numbers, Prandtl numbers and boundary conditions, noting infinite flux velocity 02 p0328 A70-12387
 - Zonal circulation model of atmosphere below altitude of 200 km using rocket, meteor and ionospheric drift observations 02 p0328 A70-12388
 - Stratospheric air intrusion into troposphere calculated for speed and frequency of occurrence, considering mass and energy transfer 02 p0329 A70-12690
 - Superpressure balloon flight trajectories for dynamics of tropical stratosphere, revealing distinctive circulation features 02 p0228 A70-12694
 - Atmospheric density in meteor region and atmospheric wind conditions determined from meteor trail drifting and artificial noctilucent clouds 03 p0563 A70-13178
 - Tropospheric circulation transformation from meridional to zonal forms due to macrostructure activity of solar wind, considering magnetosphere perturbations 03 p0559 A70-13757
 - Tropopause role in stratospheric-tropospheric exchange processes for radioactive debris transport 03 p0476 A70-13908
 - Clear air turbulence and mesoscale structure subsynoptic air motion experiments for numerical weather prediction 04 p0714 A70-14394
 - Weather prediction technique based on hydrodynamical equations, outlining atmospheric circulation models [AAS PAPER 69-619] 04 p0714 A70-14646
 - Seasonal and monthly mean charts forecasting method based on variation of annual difference in atmospheric circulation 04 p0715 A70-15294
 - Earth surface hydrology effect incorporated into atmospheric circulation mathematical model for climate, considering ocean as atmospheric moisture reservoir 04 p0680 A70-15296
 - Circulation model of joint ocean-atmosphere system constructed with ocean and atmospheric models, discussing heat transfer by ocean currents 04 p0680 A70-15297
 - Two level model for planetary atmospheres adapted to simulate atmospheric circulation and climate of Mars 04 p0756 A70-15515
 - Steady circulation and temperature perturbations in stratified nonrotating ideal gas atmosphere with viscosity and heat conduction 04 p0681 A70-15517
 - Vorticity entrainment effects in zonal jet flows, considering Long asymptotic series, shear enhancement, etc 04 p0715 A70-15519
 - Daily variations of winter stratospheric zonal wind and planetary waves based on synoptic charts from balloon observation 05 p0878 A70-16148
 - Pressure changes associated with surface friction and geostrophic drag coefficient related, discussing mass inflow and outflow 05 p0837 A70-16151
 - Omega equation interpretation showing vertical motion related to advection of vorticity in upper troposphere and to warm advection in lower troposphere 05 p0838 A70-16154
 - Vertically propagating waves in viscous isothermal atmosphere taking into account reflection due to nonlinearities and time dependence 05 p0833 A70-16679
 - Sonic boom theory of geometric acoustics with nonlinear effects modification, emphasizing horizontally stratified atmospheric propagation, discussing failure near caustic 05 p0796 A70-16794
 - Atmospheric circulation in tropics using weather satellite data 06 p1095 A70-17220
 - Atmospheric zonal circulation index annual variations calculation in latitude and time terms, using vertical vorticity component equation 07 p1328 A70-18650
 - Soviet book on nonperiodic processes in Northern Hemisphere stratosphere, discussing seasonal temperature fields, geopotential and circulation formation 07 p1261 A70-18733
 - Disturbances of air flow originating from small scale mountains using numerical model 07 p1330 A70-19799
 - Air flow disturbances over mountains in terms of turbulent boundary layer separation dissolution 07 p1330 A70-19800
 - Turbulent atmosphere circulation measurement over centimeter scale using acoustical transducers 07 p1285 A70-19836
 - Dust devil wind velocity relationship to environmental parameters including atmospheric temperature, wind direction and vorticity, etc 07 p1269 A70-19948
 - Collection of papers on stratospheric circulation covering rocket sounding, upper atmospheric clouds, climatology, etc 07 p1272 A70-20251
 - Meteorological Rocket Network for limited synoptic inspection of stratospheric circulation 07 p1273 A70-20252
 - PWN-8B meteorological rocket system for synoptic investigation of stratospheric circulation, describing sensor system deployment for descent measurements of wind and temperature 07 p1395 A70-20255
 - Kookaburra meteorological rocket system for sounding stratospheric circulation, describing instrument payload deployment for descending wind and temperature measurements 07 p1395 A70-20257
 - Temperature measurement in stratospheric circulation by meteorological rocketsonde wire sensor, presenting error correction technique 07 p1289 A70-20264
 - Meteorological rocket sounding data for Eurasia in mean profiles, time and lateral cross sections, discussing temperature and wind variations 07 p1274 A70-20270
 - Stratosphere-ionosphere coupling, dynamo theory on geomagnetic Sq variation and ionosphere radio wave absorption and reflection 07 p1274 A70-20271
 - Planetary scale disturbances in winter stratospheric circulation during sudden warming using rocket observations 07 p1274 A70-20272
 - Stratospheric and mesospheric circulation during winter, investigating wind fluctuations using meteorological rocket observations 07 p1274 A70-20274
 - Meteorological rockets fired in Spain, obtaining stratospheric wind and circulation data 07 p1396 A70-20278
 - Meteorological guns for synoptic sounding of stratospheric circulation, discussing system characteristics and operations 07 p1250 A70-20280
 - Short lived cosmic ray produced nuclides as lower atmospheric motion tracers, studying Na 24 characteristics and activity in rain water 07 p1373 A70-20355
 - E layer atmospheric circulation model for meteor zone, noting solar thermal radiation role 08 p1575 A70-21215
 - Jupiter geostrophy indicated by circulation, vorticity and Rossby number determined from Great Red Spot observations 08 p1580 A70-21573
 - Interhemispheric mass exchange as function of eddy transfer and meridional circulation 08 p1539 A70-21922
 - Diabatic mean profile forms in atmospheric surface layer, establishing profile relationships based on logarithmic analysis 08 p1540 A70-21973
 - Telemetry data processing of Eole scientific weather forecasting program, discussing mathematical model simulating atmospheric circulation in Southern Hemisphere 09 p1674 A70-22200
 - Global real data numerical forecasting with two layer NCAR /National Center for Atmospheric Research/ general circulation model, testing different data initialization schemes 09 p1713 A70-22303
 - Intermittency characteristics associated with fine scale structure and motion of atmosphere from data pertaining to various atmospheric layers 09 p1717 A70-22375
 - Atmospheric model for flow crossing ground obstacle using nonlinear differential equation 09 p1718 A70-22848
 - Classical model regarding general tropospheric circulation, exploring momentum, heat and moisture exchange 09 p1718 A70-23050
 - Regular yearly pattern variations of zonal circulation index and temperature solved in Legendre polynomials 09 p1718 A70-23330
 - Mean zonal and meridional circulations during winter and summer, finding evidence for tropical Hadley cell 09 p1719 A70-23604
 - Upper atmospheric waves nonlinear interactions based on tides and gravity waves propagation, taking into account terrestrial rotation 10 p1872 A70-23820
 - Intertropical convergence zone (ITCZ) movements, analyzing data obtained by ship and ESSA satellite cloud photography 10 p1912 A70-23939
 - Similarity and dimensionality theory applied to large scale motions in atmospheric circulation of Mars and Venus 10 p1939 A70-24269
 - Neutral and ionized atmosphere parameter variations and circulation during magnetic storms observed at various heights 10 p1873 A70-24310
 - Stratospheric equatorial wind period phases correlation with central European westerlies frequency, intensity and persistency, noting seasonal differences 10 p1913 A70-24950
 - Magnetosphere large-scale motions dependence on earth magnetic axis inclination against rotational axis 10 p1885 A70-25279
 - Earth atmosphere circulation mechanisms, discussing zonal and meridional components and eddy motions 11 p2075 A70-26030

Geostrophic wind vector rotation correlated with precipitation and circulation in vertical solenoid field
11 p2076 A70-26074

Radial velocity data monitored during Venera 4 descent used for determining vertical and horizontal atmospheric flows velocities
11 p2118 A70-26792

Atmospheric hemispheric general circulation model numerical time integration with moist processes and uniform earth surface
12 p2262 A70-26882

Lee wave flow disturbances due to mountains by midtroposphere balloon and aircraft observation, noting flow features nonstationarity
12 p2262 A70-26883

Short wave radiation fluxes inclusion in hydrodynamic model of general atmospheric circulation based on aircraft sounding data and aerostatic observations
12 p2263 A70-27512

Nonlinear orographic waves in atmosphere, investigating influence of meteorological parameters, temperature jump, incident flow and ridge geometry on flow patterns
12 p2263 A70-27517

Rotation law and circulation velocities in solar hydrogen convection zone under anisotropic turbulent velocity
12 p2302 A70-27588

Upper atmosphere superrotation velocity based on satellite polar orbit calculation of 1968-59A, correcting for lunisolar perturbations
13 p2394 A70-28895

Magnetospheric convection models and effects on charged particle populations
13 p2402 A70-30064

Middle stratospheric circulation in Southern Hemisphere, associating temperature changes and ozone content with planetary wave passage in Antarctic polar vortex
14 p2568 A70-30123

H and He intraatmospheric migration and dissipation, considering MHD waves, ionospheric plasma motions, chemical reactions, etc
14 p2569 A70-30211

Similarity and scaling between atmospheric and wind tunnel simulated shear flows near earth surface
14 p2602 A70-30369

Three camera method for studying upper atmosphere winds via smoke trails providing wind velocity, earth coordinate data and error indication
14 p2607 A70-30572

Lower ionosphere electron densities seasonal variations relationship to atmospheric circulation
14 p2574 A70-30742

GHOST free floating balloon system for global atmospheric circulation data acquisition in World Weather Watch
14 p2610 A70-31153

Troposphere-stratosphere kinetic energy transfer /1964-1968/, annual variations and vertical flux correlation to circulation pattern
15 p2722 A70-31441

Vertical temperature profiles and global circulation patterns in stratosphere and mesosphere, discussing Northern Hemisphere seasonal, latitudinal and longitudinal variations
15 p2724 A70-31665

Upper stratosphere and mesosphere structure and circulation in Southern Hemisphere, using meteorological rockets and radiosonde data
15 p2724 A70-31683

Atomic hydrogen escape effects on altitude distribution, discussing lateral flow limitations on thermospheric diurnal variation
15 p2725 A70-31796

Atmospheric cellular convection, reducing hydrodynamic equations to amplitude equations for vertical velocity
15 p2770 A70-32064

Radiation effects on large scale atmospheric air flows, accounting for role in global circulation by parameterization techniques
15 p2771 A70-32109

Redundant variable errors in weather prediction, specifying initial conditions for time integration of hydrothermodynamic equations for atmospheric motion
15 p2771 A70-32368

LF oscillatory convection characteristics in polytropic atmosphere in strong magnetic field based on sunspot theory
15 p2802 A70-32487

H alpha and Fe I lines, calculating velocity effects on profiles for differentially moving atmosphere
15 p2804 A70-32616

Gravitational atmosphere thermally driven motions, noting expansion towards lower density regions in solar chromosphere
15 p2804 A70-32619

Upper atmospheric unsteady horizontal wind flow from differential equations unstable solution
15 p2772 A70-32889

Annual variations of monthly mean meridional circulation, discussing observations, zonal asymmetries, accuracy and transports of angular momentum and energy
16 p2945 A70-33249

Winter stratospheric circulation quasi-geostrophic model based on joint radiative-photochemical equilibrium, investigating ozone cycle and warming
16 p2945 A70-33250

Numerical simulation of large scale atmospheric motions, considering pressure distribution, vorticity, kinetic energy, etc
16 p2946 A70-33625

Solstitial solar quiet currents along magnetic lines of force in magnetosphere, discussing ionospheric wind asymmetry effects
17 p3077 A70-34949

Solar activity sudden perturbations effect on earth pressure field and atmospheric circulation
19 p3460 A70-37315

Steady state nonlinear dynamics of low latitude atmospheric global boundary layer, indicating inverse relation between air flow vertical velocity and distance from equator
19 p3460 A70-37417

Venus cloud displacement, measuring formations longitudes and latitudes for evidence of cytherean upper atmosphere rapid bulk motion
19 p3518 A70-38027

Periodic thermal forcing role in Venus atmosphere dynamics, investigating momentum transport to support mean shear for channel flow
19 p3519 A70-38251

Venus atmospheric visible clouds circulation, determining zonal flow induced by moving heat sources
19 p3519 A70-38252

Tropical circulation structure and energetics from numerical time integration of global atmospheric model with realistic orography
19 p3462 A70-38257

Meridional transport of angular momentum in various wavenumber-frequency domains, discussing linear and nonlinear contributions
19 p3462 A70-38258

Atmospheric energy flow cycle involving large scale circulation components measured by wave number around latitude circles, using equations for closed global system
19 p3415 A70-38416

Solar atmospheric hydrodynamic response to stationary random forces homogeneous over horizontal planes, discussing common energy argument, various models and photospheric oscillation
19 p3523 A70-38690

Global scale atmospheric circulation processes numerical simulation leading to long range weather forecasts for Northern Hemisphere
19 p3462 A70-38753

Wind motions from meteor trails observation during IQSY, tabulating amplitudes and phases of constant, diurnal, semidiurnal and 8-hr components
19 p3526 A70-38788

Atmospheric zonal kinetic energy balance for Northern Hemisphere, assuming frictional destruction due to stresses across horizontal surfaces
20 p3661 A70-39145

Planetary scale unsteady atmospheric motions nonlinear problem, considering two level solenoidal model
20 p3662 A70-39177

Planetary wind field from observed pressure field by linearized balance equation, assuming solenoidal air motion
20 p3662 A70-39178

Atmospheric circulation indices in Northern Hemisphere on isobaric surfaces, comparing mean diurnal, monthly and climatic values
20 p3662 A70-39180

Stratospheric perturbation sources from atmospheric circulation as function of season, geographic latitude and altitude, suggesting high energy protons in atmosphere
20 p3618 A70-39183

Explosive and diffuse stratospheric warmings over Arctic attributed to solar activity and stratospheric circulation
20 p3618 A70-39184

Synoptic processes in Arctic tropospheric and lower stratospheric warming correlated with atmospheric circulation transformations
20 p3619 A70-39186

Solar activity effects on mean anomalies in repeatability of types of atmospheric circulation epochs and stages
20 p3662 A70-39190

Troposphere and lower stratosphere circulation during natural synoptic autumn seasons in Northern Hemisphere, noting temperature role
20 p3663 A70-39273

Atmospheric circulation two level quasi-geostrophic model, examining dynamic large scale features of baroclinic wave blocking by high latitude cold anticyclonic cells
20 p3621 A70-39372

Upper atmospheric wind currents differential equations, obtaining physical data in terms of asymptotic expansion of Gaussian error functions
20 p3622 A70-39763

Soviet book on physical atmospheric parameters covering model, solar and earth radiation fluxes and spectral energy distribution
20 p3664 A70-39799

Mode-generated average variables of atmospheric horizontal heat flux by transient cyclonic eddies used in mean motion circulation model
20 p3664 A70-40063

Simulated neutral atmospheric boundary layer measurements in wind tunnel, extending power spectral and correlation determinations
20 p3613 A70-40139

Nonlinear orographic waves in atmosphere, investigating influence of meteorological parameters, temperature jump, incident flow and ridge geometry on flow patterns
21 p3846 A70-41165

January climatology simulation experiment based on two layer version of global circulation model, comparing computed and observed results
21 p3847 A70-42120

Midwinter warming period upper stratospheric vertical motion fields, obtaining 2-mb charts
21 p3847 A70-42123

Atmospheric vorticity and dust devil rotation direction relationship, suggesting shear in horizontal flows associated with convective activity in unstable atmosphere
22 p4065 A70-42912

Arctic and antarctic atmospheric circulation differences, discussing circumpolar vortices and isobaric surfaces altitude changes
22 p4065 A70-43168

Wind directions in free atmosphere and on ground, discussing deflections by orographical factors in Upper Rhine plain
22 p4065 A70-43245

Large scale axisymmetric atmospheric vortex wind velocity determination, using statistical cloud data from meteorological satellites
22 p4065 A70-43376

Air circulation spring restructuring in Northern Hemisphere upper stratosphere, investigating summer stratospheric anticyclone evolution
22 p4066 A70-43378

Statistical-dynamical atmosphere model for global circulation simulation, taking into account meteorological variables of velocity, temperature, pressure and eddy statistics
23 p4213 A70-44029

Stationary disturbances in winter Northern Hemisphere stratosphere considered as upward propagating Rossby waves, assuming zonal winds profile
23 p4213 A70-44030

Global upper atmosphere circulation pattern by daytime tracking of high altitude rocket vapor trail, using differential radiometer
23 p4214 A70-44039

Earth atmospheric boundary layer wind velocity, temperature gradients and specific humidity differences, calculating climatic correlations from mathematical circulation model
23 p4214 A70-44264

Upper atmosphere tidal pressure and wind variations from meteor trail drift data
23 p4215 A70-44266

Tornadic vortex motion equation derivation based on kinematical modification of Kelvin theorem
23 p4215 A70-44547

Average isobaric air flow field divergence calculation of vertical motion by two dimensional Gaussian integral theorem
24 p4371 A70-45134

Vertical supergranular motions in solar atmosphere from multichannel magnetograph observations
24 p4400 A70-45306

Upper atmosphere average rotation speed and height variation, presenting atmospheric and earth angular velocity ratio from satellite orbit inclinations
24 p4328 A70-45353

H and He intraatmospheric migration and dissipation, considering MHD waves, ionospheric plasma motions, chemical reactions, etc
24 p4331 A70-46286

ATMOSPHERIC COMPOSITION

NT ATMOSPHERIC MOISTURE

NT IONOSPHERIC COMPOSITION

Jupiter and Saturn near IR spectra for relative abundances of atmospheric constituents and distribution with altitude, noting rough solar composition
01 p0179 A70-10526

Structure and composition of clouds of ammonia and water bearing condensates, investigating compositional models of Jupiter atmosphere, considering ammonium hydrosulfide cloud layer
01 p0179 A70-10527

Upper atmosphere structure and energy budget based on IGY/IQSY spectroscopic observations of temperature distribution and stratosphere-mesosphere composition
01 p0072 A70-10578

Upper atmospheric atomic H and He concentration height distribution, considering L alpha and H alpha emissions, He emission, light components and direct measurements

01 p0074 A70-10589

Jupiter chemical composition and atmosphere, considering space probe experiments

01 p0185 A70-11047

Thermospheric structure and variations obtained from satellite drag data analysis, discussing gas density, temperature and atmospheric composition

01 p0077 A70-11203

Interstellar neutral hydrogen flux effects on atmospheric hydrogen density, considering annual and semiannual density variations

01 p0186 A70-11207

Solar Lyman alpha line profile and atomic hydrogen vertical distribution measurement method for terrestrial atmosphere in 200-500 km range

01 p0078 A70-11208

Lunar atmosphere molecule and atom concentration from isotropic and uniform surface evaporation due to micrometeorite impact

01 p0192 A70-11541

Homogeneous scattering model for line formation applied to composition of Jupiter atmosphere

02 p0365 A70-11802

Structure and composition of Jovian atmosphere, discussing hydrogen helium ratio, cloud colors, etc

02 p0367 A70-11811

Methane photochemistry in Jupiter atmosphere, investigating acetylene, ethylene and ethane photolysis

02 p0367 A70-11815

Diurnal variations of intensity and height profile of diametric O concentration from photometric rocket measurements compared with balloon data

02 p0297 A70-12066

Static atmosphere model above 120 km, assuming oxygen atoms and molecules and nitrogen molecules presence to determine diffusion velocity and recombination coefficient

02 p0327 A70-12385

Martian topographic contours determined from detected carbon dioxide abundances indicating large scale differences from previous data

02 p0373 A70-12390

Molybdenum disulfide surface and bulk properties, comparing endurance of fractions and grades with synthetic chalcogenides at same layer thickness in dry atmospheres

[ASLE PREPRINT 69-LC-7]

02 p0322 A70-12538

IR spectrum of Jupiter with calibrations from laboratory studies of methane and ammonia bands

02 p0378 A70-12559

Neutron star atmospheric composition as function of time, including effects of diffusion, cooling and nucleosynthesis

02 p0378 A70-12698

Mean and extreme atmospheric ozone concentration calculated as function of altitude and seasons in Northern Hemisphere

03 p0474 A70-13294

Temporal autocorrelation functions of ozone content and concentration from data of Soviet and U.S. stations, obtaining statistical stability

03 p0474 A70-13295

Photosynthesis and respiration rate in vegetables in controlled temperature, humidity, illumination levels, carbon dioxide and oxygen contents

03 p0425 A70-13892

He 4 and Ar 40 abundance in lower Venus atmosphere, underlining He 4 dominance in upper atmosphere

03 p0575 A70-13982

Aerosols size distribution and chemical composition and carbon monoxide, nitrous oxide and sulfur dioxide concentrations measured in pure atmosphere

03 p0521 A70-14289

Rocket-borne cryogenic sampler for stratospheric composition measurement by mass spectrometer analysis for computing radiation balance in stratosphere

[AAS PAPER 69-569]

04 p0687 A70-14661

Excited oxygen molecules chemical composition in upper atmosphere calculated, considering deactivation during interactions in various energy states

04 p0684 A70-15750

Antarctic twilight Na emission abundance and concentration in lower E region, discussing meteor ablation models

05 p0836 A70-15819

Na abundance in terrestrial upper atmosphere, solving steady state continuity and momentum equations for Na atoms and ions

05 p0840 A70-16475

Mie scattering and polarization functions of atmospheric aerosols determined on basis of logarithmic Gaussian distributions

05 p0879 A70-16664

Time and altitude induced variations in daytime NO and molecular and atomic oxygen ions

05 p0841 A70-16736

Spectral transparency inversion of aerosol-containing atmosphere

06 p1098 A70-17832

Atmospheric characteristics of thermally and chemically stratified layers, discussing ionospheric ion and electron concentrations, radio wave propagation and solar activity and density correlation

07 p1262 A70-18780

Carbon particles formation and growth in Mira variables atmospheres, considering extinction effects on stellar structure and appearance

07 p1380 A70-19261

Atmospheric gases atomic and molecular binary short range repulsive forces, determining interaction potentials from elastic scattering cross sections

07 p1345 A70-20141

Arcas rocket-borne chemiluminescent ozonesonde for measuring ozone concentration after deployment above stratopause level

07 p1396 A70-20263

Photochemical calculations on mesospheric ozone for oxygen only, oxygen-hydrogen and oxygen-hydrogen-nitrogen atmospheres

07 p1273 A70-20268

Vertical eddy diffusion effect on chemical composition of mesosphere and lower thermosphere using photochemical model containing oxygen and hydrogen

07 p1274 A70-20269

Spectral band transmission functions of atmospheric water vapor, nitrogen, ozone, nitrous oxide and methane in IR region

07 p1330 A70-20306

Atmospheric ozone content and mass effect on solar radiation flux measured during total solar eclipse of 22 September 1968

07 p1275 A70-20310

Descending and albedo electron fluxes at specific geomagnetic latitude and various atmospheric depths, obtaining electron energy spectrum vertical profiles

07 p1372 A70-20335

Hydrogen supply rate by solar wind found comparable to hydrogen losses from earth by diffusion into space

08 p1487 A70-20637

Venus clouds absorption spectra correlation with carbon suboxide frost reflection spectra, suggesting absence of carbon suboxide in atmosphere

08 p1571 A70-20911

Solar heating determination by using transmission factors derived for atmospheric constituents together with spectral irradiance curves outside atmosphere

08 p1573 A70-21032

Nitrogen dioxide presence in solar atmosphere from balloon-borne spectrometer observations, presenting graph of sunset solar spectrum

08 p1575 A70-21262

Altitude profiles and absolute intensities of far UV emission features in aurora measured by filterwheel photometer in Aerobee rocket, determining molecular oxygen densities

08 p1489 A70-21384

Rats acute hypoxia and altitude tolerances after prolonged exposure to hyperoxic atmospheres

08 p1446 A70-21437

Seasonal variation of vertical profiles of atmospheric radioactivity concentration between stratosphere and troposphere due to meridional zonal wind distribution caused by eddy diffusion

08 p1539 A70-21923

Venus ionosphere, discussing day and night electron density profiles, carbon dioxide presence, plasma interaction model, etc

09 p1750 A70-22058

Atmospheric carbon dioxide and oxygen concentrations effects on white mice low temperature tolerance

09 p1614 A70-22082

Sigma Orionis E hydrogen-deficient atmosphere, using grid of constant-flux model atmospheres to determine abundances of five elements

09 p1755 A70-22504

Ion mobility estimates for air constituents, considering ion-neutral elastic and resonant charge exchange collisions

10 p1919 A70-24427

Seasonal changes in thermospheric composition in middle latitudes, investigating molecular oxygen density and solar activity effects

10 p1881 A70-24817

Jupiter atmospheric composition, gas and dust cloud formation as clues to origin and evolution of solar system

11 p2108 A70-25654

Balloon-borne device for analyzing atmospheric carbon dioxide, moisture and methane, using cyclic analysis by gas chromatography

11 p2052 A70-26371

Atmospheric hydrogen content continuous recording method based on absorption line analysis of mercury vapor from mercuric oxide reduction

11 p2052 A70-26389

Upper atmosphere probing based on light scattering from laser radar beam by atmospheric constituents

12 p1815 A70-27740

Stellar atmosphere model for multilevel spectral line emission, assuming semiinfinite hydrogen atmosphere with sequence of plane parallel zones

12 p2306 A70-27856

Raman scattering by oxygen and nitrogen in atmosphere observed by using pulsed nitrogen UV laser

12 p2189 A70-28093

Upper atmospheric composition by nitrogen molecules radiative transition analysis, using laser resonance backscattering effect

12 p2227 A70-28267

Induced nuclear processes role in radiogenic Ne-21 production in earth atmosphere

12 p2227 A70-28367

IR spectroscopy and lasers for analysis of atmosphere in air pollution research and monitoring

13 p2407 A70-29106

Atmospheric sodium concentration in twilight and daytime sky from D1 and D2 line intensities in twilight

13 p2399 A70-29239

Lower stratosphere ozone formation, suggesting origin in cosmic rays absorption

13 p2400 A70-29472

Venus atmosphere physicochemical characteristics and composition from automatic onboard Venera measurements

13 p2495 A70-29759

NO and nitrogen dioxide influence on ozone concentration and production rate in stratosphere

14 p2568 A70-30125

Atmospheric dust natural radioactivity effect on tropospheric Pb 210 mean residence time determination for Pb210 and Ra226 fallout in rain near Moscow

14 p2630 A70-30131

Thermospheric heating and conversion efficiency of short wave radiation as functions of solar radiation spectral flux, atmospheric components concentration and elementary processes cross sections

14 p2569 A70-30212

Earth atmosphere formation and oxygen-carbon dioxide balance mechanisms, including water vapor photodissociation, photosynthesis, fossil fuel burning, etc

14 p2572 A70-30350

Atmospheric ozone vertical distribution measurement based on luminescence of solid organic substances, noting chemical and optical methods

14 p2573 A70-30409

Arcturus atmosphere Mg abundances from rotational lines noting terrestrial proportions

14 p2637 A70-30540

Static diffusion model of thermosphere with allowance for temperature and chemical composition and not limited by constant 120 km boundary conditions

14 p2606 A70-30560

Laser radar measurements for atmospheric scattering properties, observing aerosol content, atmospheric density and composition

14 p2550 A70-30746

Excited oxygen molecules concentration in upper atmosphere calculated, considering deactivation during interactions in various energy states

14 p2576 A70-30834

Neptune data from photoelectric observations of 7 April 1968 occultation of BD-17 deg 4388, determining hydrogen dominance and molecular density

14 p2642 A70-30890

Spacecraft measurements revealing hot dense Venusian and cold thin Martian carbon dioxide atmospheres

14 p2646 A70-31066

Venus atmosphere data from Venera 4, 5 and 6 and Mariner 5 missions covering chemical composition, density, pressure, temperature gradients, etc

14 p2646 A70-31067

Ap star kappa Cancr model atmosphere analysis based on observed energy distribution and hydrogen line profiles

14 p2652 A70-31381

Exospheric density at opposite hemispheres, showing variations from winter helium bulge

15 p2724 A70-31679

Numerical model of diurnal variations of minor neutral constituents in mesosphere and lower atmosphere including molecular and eddy diffusion

15 p2727 A70-31909

Molecular hydrogen, methane, water vapor and tritium concentrations near stratopause from air samples collected on Aerobee flight with liquid hydrogen cooled cryocondenser

15 p2728 A70-31995

Troposphere and lower stratosphere trace element concentration measurements, establishing origin, history and movement of various air masses

15 p2728 A70-31996

Atmospheric carbon dioxide and oxygen concentrations effects on white mice low temperature tolerance

15 p2685 A70-32678

Atmospheric structure studies using lidar method to detect particulate content in clear air

16 p2862 A70-33014

Atmospheric oxygen history, using primeval anoxic terrestrial atmosphere simulation to show organic molecule formation by abiogenic process

16 p2898 A70-33990

Scanning UV spectrometer for Mariner Mars 1971 orbital mission, investigating atmospheric composition for biological activity

16 p2978 A70-34030

Venus upper atmosphere carbon atoms detection based on low resolution spectra analysis of solar illuminated atmosphere

16 p2979 A70-34036

Twilight sky brightness measurements at 5200 Å for estimating upper atmospheric dust component, discussing error rates

16 p2899 A70-34184

Atmospheric radon concentration ratios diurnal and vertical variations used for turbulent exchange and washout study

17 p3132 A70-34611

Ozone content effect on presunrise fall in LF radio waves amplitude from Radio Tashkent to Delhi, noting UV light role

17 p3077 A70-34947

Combustion efficiency and rate in oxygen enriched spacecraft atmosphere

17 p3177 A70-35210

Ambient temperature effects on rats and white mice tolerance to hypoxia, asphyxia and hypercapnia in nitrogen-oxygen and He-oxygen atmospheres

17 p3030 A70-35353

Mean molecular mass determination method for upper atmosphere based on Nicolet equation for scale height, using satellite orbit and spin decay data

17 p3138 A70-35773

Jupiter atmosphere ammonia abundance from laboratory curves of growth analysis for ammonia bands

18 p3310 A70-35937

Nimbus 3 satellite-borne Michelson interferometer IR spectrometer for spectrum measurement, obtaining temperature, water vapor and ozone vertical distribution

18 p3257 A70-36175

Upper atmospheric ion composition during Orionid meteor shower activity by rocket-borne RF mass spectrometer

18 p3247 A70-36183

Space vehicle reentry hypersonic boundary layer characteristics, considering air components chemical reactions due to excessive heat

18 p3346 A70-36384

Upper atmospheric dust composition and optical properties by crepuscular technique, using photometric measurements in 5200 Å region

18 p3251 A70-36978

Upper atmospheric layers neutral composition by rocket-borne mass spectrometers, indicating gravitational separation of argon from molecular nitrogen

18 p3252 A70-36984

Optimal separation height of instrument container in atmospheric gas composition mass spectrometric studies

18 p3260 A70-36996

Atmospheric ozone longitudinal variation in lower middle latitudes of Southern Hemisphere

18 p3256 A70-37117

Venus lower atmosphere structure and brightness temperature spectrum analysis for composition, temperature and pressure profiles

18 p3323 A70-37139

Spectrophotometry of methane and ammonia absorption bands indicating decrease toward Jupiter disk edge

18 p3323 A70-37140

Atmospheric aerosols vertical distribution from aerostat measurements, considering particle size distribution

19 p3461 A70-37636

Atmospheric aerosols optical and microphysical measurements comparison, evaluating sample collection equipment, errors, etc

19 p3421 A70-37637

Rhodamine C chemiluminescent material for atmospheric ozone measurements, describing preparation and luminescence spectrum

19 p3373 A70-37638

Atmospheric free Na atoms layer measurement during twilight and throughout night by laser radar

19 p3413 A70-37999

Atmospheric ozone remote sensing by high resolution IR interferometer spectrometer /IRIS/ aboard Nimbus 3 satellite

19 p3414 A70-38262

Venus atmosphere physicochemical characteristics and composition from automatic onboard Venera measurements

19 p3520 A70-38391

K and M star molecular constituent density calculations using model atmospheres and observations

20 p3702 A70-39015

Atmospheric ozone content during May 1966 solar eclipse, noting solar disk darkening effect on measurements

20 p3615 A70-39031

Aerosol correction for atmospheric ozone content measurements using direct sunlight

20 p3615 A70-39032

Raman spectroscopy with lidar for remote mapping of air pollutants and concentrations

20 p3627 A70-39126

Atmospheric composition cyclic changes effects on human basal metabolism under hypokinesia

20 p3576 A70-40197

Venusian atmosphere carbon dioxide, water, molecular oxygen and nitrogen contents from Venera 5 and 6 data

21 p3883 A70-40837

Vertical atmospheric ozone distribution according to direct solar radiation received on ground, using UV and IR observations

22 p4023 A70-43296

Mars atmospheric nitrogen abundance relative to carbon from spacecraft UV spectrometer data

23 p4238 A70-43805

Neutral air density and composition at 150 km, comparing satellite drag data to rocket measurements results

23 p4185 A70-43843

Anomalous seasonal variation in worldwide ozone above 40 km from Umkehr measurement, considering turbidity effects

23 p4187 A70-44037

Diurnal variation symmetry of upper atmosphere molecular oxygen concentration in terms of ozone photodissociation

23 p4190 A70-44083

Venus polywater hydrosphere, discussing vapor phase, surface temperature, evolution, observations and model data

23 p4242 A70-44260

Venus atmospheric speculations compared to Soviet and American probe findings, discussing composition, evolution cloud layer and ionosphere

23 p4253 A70-44863

Solar atmosphere radiation and structure, discussing continuum and line spectra, solar rotation, chromosphere, spicules, etc

23 p4256 A70-45035

Atomic oxygen height profile measurements in upper atmosphere by sensor consisting of thin silver film on small pyrex rod permitting molecular transport

24 p4329 A70-45359

D2A satellite optical experiments, examining atmospheric atomic H and solar and extraterrestrial 1216 Å emission

24 p4339 A70-46094

German book on aircraft thermal propulsion systems calculation, design and evaluation, covering thermodynamic principles and atmospheric composition and properties

24 p4396 A70-46150

Atmospheric composition of cool stars in relation to nucleosynthesis and galactic evolution

24 p4414 A70-46227

Thermospheric heating and conversion efficiency of short wave radiation as functions of solar radiation spectral flux, atmospheric components concentration and elementary processes cross sections

24 p4331 A70-46287

ATMOSPHERIC CONDITIONS

U METEOROLOGY

ATMOSPHERIC CONDUCTIVITY

NT IONOSPHERIC CONDUCTIVITY

Stratospheric electric field and conductivity measurements using balloon-borne electrometer tube circuit

22 p4018 A70-42799

Atmospheric electrical conductivity examination by balloon-borne instruments, discussing temperature and ion mobility height distribution profiles

22 p4018 A70-42800

ATMOSPHERIC DENSITY

Thermospheric neutral density amplitudes and phases using one dimensional model of geomagnetic activity effect, 27 day variation and semiannual variation

01 p0070 A70-10402

Atmospheric density variations during solar maximum and minimum, discussing solar corpuscular stream and EUV radiation

01 p0075 A70-10594

Turbojet aircraft engine performance correlation with relative humidity, noting air density effect on rotor performance resulting from moisture content

01 p0165 A70-10689

Atmospheric density variations in thermosphere determined from braking satellite data, discussing correlation with solar activity and temperature variations

01 p0077 A70-11202

Satellite observations of semiannual density variations in upper atmosphere

01 p0077 A70-11205

Ionosphere atmospheric densities from Explorer 32 drag data including semiannual variations

01 p0077 A70-11206

Thermospheric horizontal winds diurnal bulge, discussing maximum density-maximum temperature phase relationship

01 p0078 A70-11210

Atmospheric density profiles based on laser radar return from ruby laser detected by photomultiplier

01 p0079 A70-11220

Atmospheric density on basis of photographic observations of meteors, comparing vertical profile with CIRA profile

01 p0084 A70-11556

Solar activity indices and upper atmospheric density interrelationship from Explorer 1 satellite observations, showing statistical variations

02 p0356 A70-11762

Air density variations calculated by visual satellite observations processing, comparing results of IN-TEROBS and average anomalies methods

02 p0288 A70-11766

Model construction for structure of planetary atmospheres, particularly Jupiter, discussing gas pressure, density and temperature relationships

02 p0366 A70-11803

Atmospheric density in meteor region and atmospheric wind conditions determined from meteor trail drifting and artificial noctilucent clouds

03 p0563 A70-13178

Parachute-borne densitometer using forward scattering of low energy beta particles for direct measurement of atmospheric density at 30-60 km [AAS PAPER 69-570]

04 p0687 A70-14654

Atmospheric density measurements from Explorer 17 satellite by density gage and drag techniques resolved for difference by calibration and systematic errors considerations

04 p0691 A70-15120

Optimal lift control of hypersonic lifting body during planetary entry, assuming exponential variation of atmospheric density

04 p0620 A70-15532

Ionospheric air density profiles revision based on satellite orbits analysis

05 p0839 A70-16287

Stellar light absorption in optically dense cometary atmospheres

06 p1141 A70-17738

Atmospheric density determined by using diffusion coefficients obtained from artificial luminous clouds observations

06 p1096 A70-17785

Vertical air density profile from satellite measurements of atmospheric oxygen radio emission at 40-70 km altitudes

06 p1056 A70-17788

Stochastic Liapunov stability of satellite motion influenced by aerodynamic and gravity gradient torques, considering atmospheric density uncertainty [AIAA PAPER 70-37]

06 p1159 A70-18185

ROBIN superpressure mylar spherical falling balloon deployed from sounding rocket apogee for density and wind measurements via radar tracking

07 p1194 A70-20260

Derived winds, wind shears and densities accuracies obtained by radar meteor trail technique

07 p1237 A70-20281

Strong point explosion in atmosphere with density dependent on height, obtaining numerical solutions for exact gas dynamic equations

09 p1658 A70-22112

Atmospheric density in thermosphere observed by satellites, noting daily and semiannual variations related to solar and geomagnetic activities

09 p1667 A70-22626

Visual observations of Molniya satellite during low perigee, determining air density

10 p1875 A70-24443

Vertical air density profile from satellite measurements of atmospheric oxygen radio emission at 40-70 km altitudes

10 p1882 A70-25020

Mars upper atmosphere semiempirical model, reducing density uncertainties by allowing for solar cyclic variations

11 p2111 A70-26031

On-line parameter updating for relationship between Martian atmospheric density and height above surface during spacecraft descent based on least squares approach

11 p2113 A70-26318

Exospheric density from Echo 2 orbit, observing 27 day variations associated with sun rotation and correlation with geomagnetic disturbances

11 p2046 A70-26566

Acoustic energy backscattered from vertically directed beam of sound by lower troposphere density structure inhomogeneities

12 p2262 A70-26953

Air pressure, air density and gravity tables, including corrections for mercury barometer measurements

12 p2222 A70-27008

Low latitude atmospheric vertical density variations, comparing solar and geomagnetic activities effects

12 p2227 A70-28264

Atmospheric density estimation from observation of satellite drag-induced energy dissipation

13 p2400 A70-29530

Atmospheric density variations and functional dependence of aerodynamic moment coefficient on incident angle from Saturn Workshop flight experiment

14 p2528 A70-30559

Atmospheric density effect on satellite lifetime and position prediction, utilizing data from Cannon Ball and SPADES low altitude density research satellites 14 p2653 A70-30562

Pitot probe for high altitude atmospheric density measurements integrated with telemetry system mounted on two stage Super Loki sounding rocket 14 p2585 A70-30576

Upper stratosphere-mesosphere monthly-mean charts from reentry heating and atmospheric model based on hydrodynamics 14 p2608 A70-30590

Temperature, pressure and density extremes between 30 and 80 km, extrapolating estimates to all latitudes 14 p2608 A70-30591

Stratospheric warmings effect on atmospheric density field variations 14 p2608 A70-30592

Laser radar measurements for atmospheric scattering properties, observing aerosol content, atmospheric density and composition 14 p2550 A70-30746

Neptune data from photoelectric observations of 7 April 1968 occultation of BD-17 deg 4388, determining hydrogen dominance and molecular density 14 p2642 A70-30890

Venus atmosphere data from Venera 4, 5 and 6 and Mariner 5 missions covering chemical composition, density, pressure, temperature gradients, etc 14 p2646 A70-31067

Incoherent scatter observations of atmospheric density and temperature in lower thermosphere, observing seasonal variations 14 p2578 A70-31246

Earth satellite motion about center of mass, examining effects of random variations in atmospheric density, geomagnetic intensity and solar radiation 15 p2809 A70-31650

Temperature and density extreme variations at various levels in stratosphere and mesosphere, analyzing sounding rocket data 15 p2723 A70-31661

Upper atmosphere density and temperature height profiles perturbations in falling sphere probe 15 p2723 A70-31663

Exospheric density at opposite hemispheres, showing variations from winter helium bulge 15 p2724 A70-31679

Atmospheric density near 180 km /1968-1969/ from orbit of satellite 1967-31A /ATS 2/, noting weak dependence on solar activity and correlations to geomagnetic disturbances 15 p2724 A70-31680

Ionospheric density profiles measurement by accelerometers on SPADES and Cannon Ball 1 satellites, comparing results with prediction from atmospheric model 15 p2724 A70-31686

Atmospheric density and temperature measurements by satellite- and rocket-borne pressure gages and mass spectrometers, considering error sources 15 p2731 A70-32092

Equatorial atmospheric density during geomagnetic storm and quiet days by satellite observation 15 p2811 A70-32284

S band occultation experiment for Mariner Mars 1971 orbiters, measuring atmospheric density and ionospheric electron density profiles 16 p2978 A70-34032

Subsonic and supersonic aircraft dynamic loads under conditions of variable atmospheric density 17 p3013 A70-34685

Atmospheric density from radar observations of meteor trails drift, using wind velocity semidiurnal components amplitudes 18 p3253 A70-36994

Venus atmospheric temperature, pressure and density measurements by Venera 5 and 6 space probes, developing model 19 p3520 A70-38255

Upper atmospheric density and temperature diurnal phase and amplitude discrepancy reconciled by dynamic diffusion model 19 p3414 A70-38381

K and M star molecular constituent density calculations using model atmospheres and observations 20 p3702 A70-39015

High energy radiation belt proton flux time dependence at low altitudes, examining atmospheric density influence 20 p3620 A70-39340

German monograph on satellite orbit synergetic plane change maneuver optimal control by entry into denser atmosphere 20 p3705 A70-39924

Midlatitude stratosphere and lower ionosphere density model, discussing vertical, diurnal and seasonal variations effects on spacecraft trajectories 21 p3813 A70-40830

Altitude spectrum of ion formation in interaction of proton flux with atmosphere, using Bragg dissipation function 21 p3878 A70-40846

Parachutes for low density atmospheres, describing low and high altitude test results [AIAA PAPER 70-1164] 21 p3755 A70-41846

Wollaston prism schlieren interferometer for quantitative density gradient measurements in air [SMPT PREPRINT 25] 22 p4034 A70-43050

Thermospheric density variations as equivalent oscillator circuit system, applying to atmospheric tides 22 p4023 A70-43297

Diurnal atmospheric density variations latitude dependence from satellite data 23 p4185 A70-43842

Neutral air density and composition at 150 km, comparing satellite drag data to rocket measurements results 23 p4185 A70-43843

Phase delay between thermospheric neutral temperature and neutral density, considering frequency dependent time response to solar heat input 23 p4187 A70-43858

Strong shocks propagation in atmosphere of variable density at rest, obtaining numerical solution of similarity flow behind shocks 23 p4182 A70-44599

Air densities from polar satellites orbit analysis 24 p4329 A70-45550

Geophysical parameters from artificial earth satellite orbital elements evolution data, discussing atmospheric density and zonal harmonics 24 p4330 A70-45551

Echo 1 satellite orbital acceleration correlated with solar activity, determining atmospheric density from drag observations using PERLO computer program 24 p4408 A70-45552

Upper atmosphere diurnal, annual and solar activity induced density variations effects on satellite orbits 24 p4408 A70-45553

Optical laser radar for upper atmospheric density and aerosol concentration measurements 24 p4353 A70-45561

ATMOSPHERIC DIFFUSION

Microwave dispersion caused by atmospheric gases at water vapor line, using microwave spectrometer based on dispersion detection in refraction spectrum 02 p0260 A70-12571

Diffusion categories and propagation of radioactive elements in lower atmosphere determined with respect to measured radiation balance, temperature gradient and wind 03 p0521 A70-14290

Von Karman theory of vortex trails and vorticity diffusion applied to atmospheric mesoscale eddy patterns to calculate viscosities, ages, radii, tangential velocities, etc 06 p1098 A70-18242

Dew-point temperature of lower troposphere by diffusion equation, noting use for fog and strati forecasting 09 p1717 A70-22655

Static diffusion model of thermosphere with allowance for temperature and chemical composition and not limited by constant 120 km boundary conditions 14 p2606 A70-30560

Toxicity and downwind diffusion of Be rocket exhaust product measurements, using ADOBE experiment and AFRPL micromet meteorological data system 14 p2628 A70-30611

Upper atmospheric wind velocity and diffusion coefficient measurement by radar observation of artificial electron cloud from atomic K ejection 18 p3253 A70-36993

Longitudinal and vertical wind components turbulent fluctuations distribution skewness relationship to atmospheric stability and height, noting effect on diffusion 20 p3664 A70-40064

Diffusion effect on hydrogen and oxygen constituents height distributions in atmosphere and lower thermosphere, solving diffusion and continuity equations 22 p4020 A70-43160

ATMOSPHERIC ELECTRICITY

NT AURORAL ELECTROJETS

NT ELECTROJETS

NT EQUATORIAL ELECTROJET

NT IONOSPHERIC CURRENTS

Atmospheric space charge magnitude and polarity below 50 km based on rocket probes 04 p0675 A70-14437

Atmospheric electricity phenomena connected with micro, macro and global processes, discussing electrical generation by convective clouds and earth-atmosphere system electrical balance 07 p1262 A70-18896

Magnetic field variation rates characteristics during magnetic storms investigated for longitudinal dependence and influence of equatorial electric current 07 p1276 A70-20437

Soviet collection of papers on atmospheric electricity covering electromagnetic waves phase velocity, satellite observation of thunderstorms activity, etc 08 p1487 A70-20773

Chapman-Vestine and Birkeland-Alfven electric current systems equivalence in ground geomagnetic effect explained for polar magnetic storms 08 p1491 A70-21719

Potential gradient radiosonde field distortion formula, deriving form factors 09 p1671 A70-23602

Electrohydrodynamics of charged water drop pairs disintegration in electric field concerning warm cloud electrification 10 p1912 A70-24806

Atmospheric space charge magnitude and polarity below 50 km based on rocket probes 13 p2392 A70-28462

Ionospheric electric fields variations in ELF-VLF, confirming OV-1 satellite measurements withOGO 6 data 13 p2403 A70-30082

Thunderstorm detection and warning system, measuring vertical potential gradient and changes caused by lightning discharges 14 p2607 A70-30574

Electric space charge pulse density measurements near ground in sunny weather related to free convection 15 p2726 A70-31868

Space charge sign distribution sounding in atmosphere by electrode potential difference measurement 18 p3246 A70-36180

Air surface layer stationary electric field, considering ionization balance equation, turbulent diffusion coefficient, ion concentration vertical distribution, etc 18 p3247 A70-36520

High latitudes magnetospheric electric field structure, using electrostatic probes and artificial clouds 19 p3410 A70-37489

Geomagnetic activity effect on potential gradient and air-earth conduction current density 19 p3413 A70-38000

Ozone effect on stratospheric electricity based on numerical calculations of ion densities 19 p3413 A70-38005

Soviet book on aircraft electrification in clouds and precipitation during subsonic flight covering atmospheric electrical properties, flight dynamics modification, communications interference, etc 19 p3356 A70-38800

Thunderclouds electric fields and conductivities measurement by differential rotating mill, noting insensitivity to space charge and frictional charging 20 p3661 A70-39146

Ionospheric conductivity effects on plasma convective flow in determining magnetospheric electric fields distribution 21 p3816 A70-41084

Thunderstorm development processes investigated by aircraft measurements of electrical structure in cumulonimbus clouds, noting lightning probability dependence on turbulence within cloud 22 p4064 A70-42775

Planetary electrodynamics - Conference, Tokyo, May 1968, Volume 2 22 p4014 A70-42776

Global thunderstorm activity experiment by Ariel 3 satellite, investigating lightning discharge number and noise power 22 p4015 A70-42778

Ball lightning model assuming radiation field within plasma dielectric region resonant at higher than collision frequency 22 p4016 A70-42780

Global atmospheric electrical structure, considering emf from thermally driven tidal motions in lower atmosphere 22 p4016 A70-42783

Earth atmospheric electricity problems formulated as continuous macroscopic electrohydrodynamic model 22 p4016 A70-42784

Ionospheric electric field origin theory in terms of charge separation due to neutral wind drag 22 p4016 A70-42785

Collisionless magnetospheric plasma turbulent conductivities for weak and strong electric fields parallel to magnetic field 22 p4016 A70-42787

Upper atmosphere electric field nature, considering solar radiation as major source of ionization 22 p4017 A70-42788

Upper atmosphere and magnetosphere DC electric field measurement using artificial clouds 22 p4017 A70-42791

Lower atmosphere electric field vertical distribution measurement by combined balloon and rocket soundings 22 p4017 A70-42797

Air-earth current density time variation in stratosphere by high altitude balloon, comparing with potential gradient diurnal variation over ocean 22 p4017 A70-42798

Earth surface magnetic field variations due to magnetopause current system 24 p4329 A70-45355

Computerized simulation of raindrop effects on initiation of cloud-to-ground lightning strokes
24 p4371 A70-45978

ATMOSPHERIC EMISSION

U AIRGLOW

ATMOSPHERIC ENTRY

NT HYPERSONIC REENTRY

NT MANNED REENTRY

NT SPACECRAFT REENTRY

Blunt and conical body optimum heat shield shapes for Jupiter atmospheric entry, noting shallow flight path
[AIAA PAPER 68-1150] 01 p0195 A70-10827

Entry and terminal deceleration systems for unmanned Martian landers, discussing parachute landing and lifting entry vehicles
[AIAA PAPER 68-1147] 01 p0195 A70-10828

Reentry trajectory dispersions due to atmospheric uncertainties determined using continuous differential equations based on atmospheric random processes method
01 p0183 A70-10846

Coordination technique for pressure, density and temperature measurements by probes during parachute reentry into planetary atmospheres, taking into account reentry dynamics
01 p0197 A70-11495

Spacecraft longitudinal control during reentry of Lunar Orbiter into atmosphere, analyzing final range prediction, trajectory tracking and accelerometers performance
01 p0197 A70-11497

Spacecraft range control algorithm during reentry at parabolic velocity into atmosphere with varying parameter distributions
01 p0197 A70-11498

Optimal control algorithm for spacecraft descent in atmosphere based on nominal trajectory and acceleration measurements
01 p0197 A70-11499

Polymers development for ablative heat shields, aeroshell structures, antennas, insulators, electronic packaging, etc., to meet Mars and Venus atmospheric entry requirements
02 p0382 A70-12525

Diffusive transport term in hydrodynamic equations describing flow over strongly ablating entry objects, discussing charge separation and pressure diffusion
03 p0405 A70-12926

Venus probe high level entry deceleration simulation, discussing test program, equipment and results
03 p0463 A70-13541

Optimal descent maneuver from planetary orbit for fixed atmospheric reentry angle, considering minimum impulse/fuel consumption/
04 p0745 A70-14496

Optimal lift control of hypersonic lifting body during planetary entry, assuming exponential variation of atmospheric density
04 p0620 A70-15532

Distance of spacecraft descending on parachute through planetary atmosphere measured from center of planetary mass using onboard instrument data
06 p1155 A70-17897

Elastomeric silicone ablator reinforced by carbon cloth or fibers for Venus entry heat protection
[AIAA PAPER 70-201] 06 p1157 A70-18086

Retrorocket effects on aerodynamic stability and drag of conical aeroshell planetary entry vehicles, discussing supersonic wind tunnel tests and jet shock interaction
[AIAA PAPER 70-219] 06 p0974 A70-18166

Faint meteor ablation processes, presenting evidence of solid consistency prior to atmospheric entry, vaporization, wake blending and trails
06 p1151 A70-18481

Planetary atmospheric entry optimal three dimensional glide paths, considering polar curve altitude dependence, flight path changes, braking maneuvers, etc.
07 p1378 A70-18985

Compact reentry flight test body construction featuring extended permissible entry corridor by means of generated lift
[DGLR-69-035] 07 p1392 A70-18987

Mars lander atmospheric entry digital simulation for deceleration system design, discussing ballistic coefficient, aeroshell diameter, parachute size and deployment altitude, etc.
08 p1582 A70-20932

Meteoroids atmospheric drag and heat transfer coefficients, considering weak shielding by repelled and vaporized molecules
08 p1572 A70-20945

Staging along reentry trajectory in atmosphere, discussing parent body and separation point influence on aerodynamic loading and heating of ejected body
11 p2124 A70-26151

Laminar multicomponent boundary layer for large injection and heat transfer, with particular reference to vehicle entry into planetary atmosphere
12 p2159 A70-28234

Spacecraft optimal impulsive braking by onboard engine to ensure maximum angle of atmospheric reentry
12 p2310 A70-28253

Trajectory predictive lunar return atmospheric reentry guidance of roll-controlled Apollo-type vehicle, using variable integration steps
13 p2446 A70-28396

Asymmetrical slender planetary entry vehicle roll dynamics, analyzing steady state angular motion
[AIAA PAPER 70-560] 13 p2339 A70-29003

Blunt planetary entry body free fall drop tests determining low speed stability and base pressure characteristics
[AIAA PAPER 70-577] 13 p2342 A70-29892

Nonsimilar ablation of graphite sphere cones under ballistic entry conditions, predicting steady state rate and surface temperature
13 p2523 A70-29975

Meteoroids atmospheric drag and heat transfer coefficients, considering weak shielding by repelled and vaporized molecules
15 p2806 A70-32757

Planetary atmospheric entry optimal three dimensional glide paths, considering polar curve altitude dependence, flight path changes, braking maneuvers, etc.
[DFVLR-SONDDR-49] 16 p2982 A70-33771

Electron concentration profiles in blunt nose vehicle shock layer during atmospheric near orbital entry at high altitudes, using finite rate chemistry
16 p2837 A70-33865

Near equilibrium shock layers nonequilibrium radiant emission calculation, noting application to Mars entry conditions
[AIAA PAPER 70-773] 17 p3007 A70-34481

Atmospheric reentry nosetip shape changes supersonic flow, considering rough surface effects on heat transfer
[AIAA PAPER 70-827] 17 p3196 A70-35193

Small rocket systems research programs, discussing Apollo-Pacemaker and planetary entry parachute flight tests
17 p3177 A70-35203

Scaling relations showing effects of ballistic coefficient, flight path angle and inverse atmospheric scale height on heating of ballistic entry bodies
17 p3012 A70-35667

Optimal angle of attack transition trajectories for space shuttle from atmospheric entry to cruising flight for conventional airport landing
[AIAA PAPER 70-1018] 20 p3713 A70-39515

German monograph on satellite orbit synergetic plane change maneuver optimal control by entry into denser atmosphere
20 p3705 A70-39924

Attached inflated BALLUTE /balloon-parachute/ for stabilization and retardation of aircraft stores, high altitude descent devices and planetary entry vehicles
[AIAA PAPER 70-1200] 21 p3752 A70-41816

Attached Inflatable Decelerator for planetary atmospheric entry, discussing mission applications and wind tunnel models performance
[AIAA PAPER 70-1163] 21 p3931 A70-41848

Ablative response predictions analytical tools, discussing boundary layer edge conditions definition, atmospheric entry, rocket propulsion, etc.
21 p3952 A70-42055

Ames Hypervelocity Free Flight Facility, discussing aerodynamic tunnel, radiation tunnel and light gas gun for reentry simulation
22 p4006 A70-42764

Nonrigidly supported ballast effects on dynamic characteristics of slender body during atmospheric entry
23 p4258 A70-44594

Venus atmosphere flight vehicle configuration, discussing payload capacity, range, velocity, flight altitude and aerostatic aerodynamic, ground effect and underwater capabilities
23 p4260 A70-44627

Environmental heat shielding for various sized Jupiter atmospheric entry probes
[AIAA PAPER 70-1324] 24 p4429 A70-45941

Venus atmosphere exploration by multiple entry probe, describing spacecraft system design, launch and earth-Venus transfer trajectory, approach and entry sequence, etc.
[AIAA PAPER 70-1245] 24 p4417 A70-45963

ATMOSPHERIC ENTRY SIMULATION

Hypersonic glider performance in mesosphere entry using models located in rarefied gas flow at Mach 8
05 p0789 A70-15811

Plasma arc tests to simulate stagnation reentry heating on spherical subized models of nuclear heat source to investigate heat shield materials ablation characteristics
[AIAA PAPER 70-200] 06 p0974 A70-18172

Meteorites explosive fragmentation under aerodynamic loads simulated by steel balls shot into increasing-density target, discussing parameters
08 p1572 A70-20947

Photo-optical instrumentation for temperature estimates of nose cone in simulated reentries, using rocket monorail sleds and artificial rainfields for rain erosion effects
09 p1688 A70-23778

Meteorites explosive fragmentation under aerodynamic loads simulated by steel balls shot into increasing-density target, discussing parameters
15 p2806 A70-32759

Shock tube facility with high explosive driver for reentry flow conditions simulation of manned planetary flights
21 p3804 A70-40849

ATMOSPHERIC HEAT BUDGET

Diurnal variation for structure and energy balance of thermosphere, noting effect of global wind pattern
01 p0074 A70-10592

Global cloud cover and earth atmosphere heat budget measured from weather satellites, discussing Tiros pictures, radiation charts and albedo
03 p0479 A70-14348

Photographic detection of thin cirrus clouds effect on earth heat budget
04 p0696 A70-15575

Atmospheric long wave radiation fluxes and energy balance and daytime radiative temperature variations calculated and compared with thermocell measurements
06 p1098 A70-17831

Earth radiation balance climatological characteristics based on satellite and published data, analyzing earth-atmosphere albedo on global scale
14 p2603 A70-30402

Contrail effects on atmospheric thermal radiation budget in heavy jet traffic regions from airborne IR and solar radiometric observations
23 p4214 A70-44033

Diurnal variations of photoelectron heat fluxes and energy production by thermal coupling between upper F 2 region and magnetosphere
24 p4328 A70-45354

ATMOSPHERIC HEATING

Nonlinear flow conductance and convective terms effects on planetary thermospheres heating diurnal variations, emphasizing solar EUV heating
01 p0178 A70-10413

Stratospheric circulation and temperature variations periodicity, discussing midwinter warmings, polar vortex breakdown and relations to D region anomalies and solar events
01 p0072 A70-10580

Ionospheric absorption associated with sudden stratospheric warmings following geomagnetic disturbances in 1958 and 1963
02 p0290 A70-12159

Lower atmosphere VLF heat turbulence as function of precipitation, indicating atmospheric layers existence for different weather situations
05 p0879 A70-16315

Planetary scale disturbances in winter stratospheric circulation during sudden warming using rocket observations
07 p1274 A70-20272

Solar heating determination by using transmission factors derived for atmospheric constituents together with spectral irradiance curves outside atmosphere
08 p1573 A70-21032

Gravity waves generated by heating in auroral regions and propagating toward lower latitudes possibly causing thermospheric heating
08 p1491 A70-21675

Stratosphere-mesosphere coupling phenomena during sudden stratospheric warmings, considering ozone and ionospheric drift measurements
10 p1913 A70-24948

Ozonosphere heating between 20-60 km during high solar activity, determining positive heating rate gradient directions and maximum heating altitude
12 p2223 A70-27514

Vertical propagation of short acoustic waves from harmonic source in inhomogeneous atmosphere, calculating shock front width and heating rate
12 p2264 A70-27519

Plasmopause and polar wind, considering density discontinuity due to outer magnetosphere heating during magnetic storms
13 p2491 A70-29059

Equatorial electrojet Lorentz coupling to neutral atmosphere as source of long period traveling ionospheric disturbances
13 p2399 A70-29235

Thermospheric heating and conversion efficiency of short wave radiation as functions of solar radiation spectral flux, atmospheric components concentration and elementary processes cross sections
14 p2569 A70-30212

Stratospheric warmings effect on atmospheric density field variations
14 p2608 A70-30592

Atmospheric radiation and heat fluxes calculations comparison with satellite and ground station actinometric measurements
15 p2770 A70-32067

Winter stratospheric circulation quasi-geostrophic model based on joint radiative-photochemical equilibrium, investigating ozone cycle and warming
16 p2945 A70-33250

Stellar mass loss, considering radiation field momentum transfer or coronal heating as mechanism
17 p1572 A70-34841

Explosive and diffuse stratospheric warmings over Arctic attributed to solar activity and stratospheric circulation
20 p3618 A70-39184

Polar stratospheric winter explosive warmings correlated with solar high energy charged particles injections

20 p3618 A70-39185

Synoptic processes in Arctic tropospheric and lower stratospheric warming correlated with atmospheric circulation transformations

20 p3619 A70-39186

Trace constituent changes effects on stratospheric properties after volcanic eruption, showing prolonged atmospheric temperature increase

20 p3622 A70-39490

Vertical propagation of short acoustic waves from harmonic source in inhomogeneous atmosphere, calculating shock front width and heating rate

21 p3818 A70-41167

Midwinter warming period upper stratospheric vertical motion fields, obtaining 2-mb charts

21 p3847 A70-42123

Shock waves strength and frequency in solar atmosphere heating deduced by empirical model, integrating radiative losses over height

21 p3925 A70-42188

Heating and extension of solar chromosphere and corona via shock waves generated by piston below convection zone surface

21 p3925 A70-42189

Fluid dynamics nonlinear equations for thermally driven motions in compressible, isothermal gravitational solar atmosphere, considering flow discontinuities and heat conduction

21 p3925 A70-42191

Lower chromosphere shock wave heating, analyzing density scale height effects

22 p4105 A70-43001

Planetary albedo changes due to pollution aerosols, showing absorption-to-backscattering ratio function in atmospheric heating or cooling

22 p4096 A70-43419

Thermospheric heating by solar radiation in Schumann-Runge continuum, taking height and atmospheric components distribution into account

23 p4188 A70-44060

Thermosphere diurnal thermal influx theory, allowing for heat conductivity

23 p4214 A70-44265

Atmospheric response to heating in stable auroral red arc by two dimensional steady state dynamic model of neutral thermosphere

24 p4329 A70-45357

Thermospheric heating and conversion efficiency of short wave radiation as functions of solar radiation spectral flux, atmospheric components concentration and elementary processes cross sections

24 p4331 A70-46287

ATMOSPHERIC IMPURITIES

U AIR POLLUTION

ATMOSPHERIC IONIZATION

NT AURORAL IONIZATION

Corpuscular radiation contributions to D layer ionization determined from intensity measurements

01 p0172 A70-11490

Atmospheric humidity effects on ionization and positive corona-current pulses development, discussing radar interference

02 p0258 A70-12425

Radar pulse scattering from ionized media including nuclear explosion fireballs and high speed reentry vehicle wakes, analyzing to retrieve backscattered pulse signal envelope

02 p0262 A70-12602

Spatial distribution of cascade shower particles in atmosphere described by integrodifferential equations system, considering medium ionization

03 p0557 A70-13049

Global satellite VLF propagation system for investigating mesospheric ionization

03 p0475 A70-13827

Electron temperature anisotropy in ionospheric plasma for case of ionizing sunlight propagating along geomagnetic field

03 p0479 A70-14376

Secular variation in F region ionization response to sunspot number, noting dominant component as cosine term equal to four sunspot cycles

04 p0678 A70-14972

Hysteresis effect on cosmic ray modulation and gradient ionization near solar minimum from measurements made near earth withOGO 1 and 3 ion chambers

04 p0740 A70-15106

Atmospheric ionization by beta particles due to fission product decay, showing diagram for magnetic shell parameters and postfission periods

04 p0743 A70-15739

Dissociative recombination coefficient ratio between O ion and nitrogen oxide ion in ionosphere using rocket data

04 p0683 A70-15743

Ionospheric reaction coefficients estimate to correlate equatorial electron density profile and Jacchia model of neutral atmosphere

04 p0683 A70-15744

Topside ionosphere ionization compared during magnetic storms with steep onset, smooth variation and sudden commencement

05 p0838 A70-16283

Corpuscular radiation as F region ionization source, solving time dependent ionospheric continuity equation

06 p1054 A70-17588

Night lower ionosphere at midlatitudes additional ionization ascribed to solar corpuscular fluxes

06 p1135 A70-17839

Electron production rate enhancement by solar cosmic rays in lower ionosphere, considering particle distribution and polar cap absorption

07 p1369 A70-20153

Winter anomaly ionization in lower ionosphere at medium latitudes from radio propagation observations, comparing wave absorption and phase height measurements

07 p1274 A70-20273

Interkosmos-1 satellite for studying solar radiation and effects on ionization and molecular dissociation in atmosphere, weather and radio signals reception

08 p1582 A70-20714

Atmospheric particle interaction layer in front of meteor body, discussing ionization, diffusion, excitation, recombination, heat generation and luminosity

09 p1761 A70-23059

Hydronium ion formation mechanism for D region, obtaining experimental support from mass spectrometer observation of ion production in oxygen glow discharge

09 p1671 A70-23500

Nighttime D region ionization irregularities deduced from vertically incident VLF radio wave

09 p1671 A70-23663

Ionospheric photoelectrons resulting from solar UV radiation interaction with atmospheric gases, obtaining escape fluxes using Monte Carlo method

09 p1747 A70-23667

Blanketing type sporadic E layer associated with equatorial electrojet as thin layer of enhanced ionization

10 p1880 A70-24801

Solar cosmic ray ionization of upper atmosphere, calculating electron production rate distribution

10 p1934 A70-25199

F 2 layer midday ionization level annual variation gradient, noting gradient latitudinal distribution dependence on solar activity level

11 p2042 A70-25532

F 2 layer midday ionization equatorial anomaly during summer and winter solstices, using calculated mean critical frequencies

11 p2042 A70-25533

Delayed ionization effects in midlatitude nighttime ionosphere after geomagnetic storms, noting time lag vertical distribution

12 p2227 A70-28365

Precipitated energetic electrons attenuation and impact ionization in ionosphere, determining vertical energy distribution profile

13 p2476 A70-28722

F 2 layer ionization asymmetry for Northern and Southern Hemispheres during solstice periods due to electron density variations and aeronomic conditions

14 p2569 A70-30206

Solar activity variations effects on equation parameters, describing noontime F2 ionization levels dependence on geographical latitude

14 p2570 A70-30224

Geomagnetic field influence on annual F 2 layer longitudinal ionization at midlatitudes, relating solar activity level

14 p2570 A70-30225

Altitude distribution of radar-signal-reflecting points and ionization in meteor trails

14 p2635 A70-30308

Atmospheric ionization by beta particles due to fission product decay, showing diagram for magnetic shell parameters and postfission periods

14 p2632 A70-30823

Dissociative recombination coefficient ratio between O ion and nitrogen oxide ion in ionosphere using rocket data

14 p2576 A70-30827

Ionospheric reaction coefficients estimate to correlate equatorial electron density profile and Jacchia model of neutral atmosphere

14 p2576 A70-30828

Quiettime cosmic ray ionization altitude dependence over polar regions from measurements by integrating ionization chamber onOGO-2

15 p2793 A70-31902

Ground sounding of ionization variations and vertical distribution using model, integral and normal laminar methods

15 p2729 A70-32078

Ionization-neutralization processes and recombination coefficient in F and E regions, using radiophysical measurements

15 p2730 A70-32083

F 2 layer afternoon and evening ionization maxima dependence on season, zenith angle and solar activity

15 p2730 A70-32084

Bounded ionospheric layers gradient instability, discussing perturbation growth and lifetime

17 p3076 A70-34944

Absolute cosmic ray ionization in lower atmosphere, using air-filled ionization chamber

18 p3305 A70-36001

Venus daytime upper ionosphere observations by mariner 5 in terms of ionization sources and sinks, ambipolar diffusion and model atmospheres

18 p3311 A70-36002

F region small scale ionization discontinuities parameters observational data concerning anisotropy, dimensions, velocity and lifetime

18 p3246 A70-36088

Book on ionospheric chemistry, covering chemical and photochemical reactions above 60 km and ionization processes

18 p3247 A70-36212

Atmospheric ions interaction with rocket exhaust gas water molecules, using sounding rocket mass spectrometric data

18 p3293 A70-36982

F region photoionization rate vs height twin peak profile in presence of temperature maximum, taking into account ionization of atmospheric gases by quasis-monochromatic radiation

18 p3254 A70-37031

Ionization-recombination parameters based on diurnal variations of electron concentration in F 2 layer maximum, discussing latitudinal variations

18 p3254 A70-37033

Ionization-recombination parameters variation as function of season and solar activity, using diurnal changes of F 2 layer maximum electron concentration

18 p3254 A70-37034

F 2 layer maximum electron concentration diurnal variations dependence on ionization intensity and dissociative recombination and ion-molecular reactions rate coefficients

18 p3255 A70-37039

Ionization in ionospheric E and upper D regions, considering solar short wave radiation, small components, atmospheric dynamics and vertical mass transport

19 p3407 A70-37301

E layer electron concentrations, effective recombination coefficient and ionization sources during solar eclipse, noting soft X radiation intensity

19 p3408 A70-37310

Ionization rate experimental profiles during maximum solar activity compared with calculations, showing additional source of ionization in E region

19 p3409 A70-37322

Nitrogen dioxide and molecular oxygen ions densities in lower ionosphere as function of solar corpuscular radiation

19 p3409 A70-37325

Sporadic ionization occurrences nighttime observation in auroral E region, describing vertical electron concentration profile

19 p3410 A70-37331

Traveling horizontal ionospheric waves relationship to magnetic storm onset, showing ionization displacement occurrence

19 p3413 A70-38029

Ionization degree in moving stellar envelopes with large optical thickness

19 p3525 A70-38763

Solar UV radiation contributing to ionization in higher ionospheric layer over Dushanbe during partial solar eclipse of 20 May 1966

19 p3417 A70-38786

Ionospheric ionization minimum delay and F region alpha variation during solar eclipse

19 p3419 A70-38919

Ionized magnetospheric tubes electron content, determining ionization interchange between F region and protonosphere by whistler observations

20 p3584 A70-39332

Lower atmosphere cosmic ray ionization calculation, using high energy transport code

20 p3699 A70-39348

Neutral atmosphere continuity equation of ionization and equation of motion in F 2 region for different seasons in various solar activity epochs

20 p3623 A70-40478

Sporadic E layer ionization correlated with geomagnetic disturbances in northern auroral and polar regions

21 p3812 A70-40592

Altitude spectrum of ion formation in interaction of proton flux with atmosphere, using Bragg dissipation function

21 p3878 A70-40846

F 2 layer midday ionization level annual variation gradient, noting gradient latitudinal distribution dependence on solar activity level

21 p3819 A70-41282

F 2 layer midday ionization equatorial anomaly during summer and winter solstices, using calculated mean critical frequencies

21 p3819 A70-41283

Upper atmosphere electric field nature, considering solar radiation as major source of ionization

22 p4017 A70-42788

- Atmospheric positive ion composition measurements in D region by rocket-borne mass spectrometers, considering water cluster ions formation
22 p4017 A70-42796
- Neutral interplanetary particle impact ionization of atmosphere, discussing density of neutral interstellar media near solar system
22 p4106 A70-43291
- Upper atmosphere photoionization by extreme UV solar radiation compared with ionization by charged particles collisions
22 p4096 A70-43302
- Electron density profiles calculation from model at atmosphere, deriving F 2 layer ionization vertical distribution
22 p4023 A70-43303
- Upper atmosphere ionization balance, examining metastable species in E and F regions
22 p4106 A70-43306
- Polar cap ionization processes in F region, discussing effects of particle precipitation, solar radiation, electromagnetic field drifts, atmospheric winds and magnetospheric tail distortion
22 p4024 A70-43309
- Lower ionosphere ionization anomalies, discussing sunrise seasonal change effects in VLF-LF propagation, winter radio wave absorption and geomagnetic storm after-effects
22 p4024 A70-43311
- Venusian and Martian upper atmosphere chemistry, emphasizing ionization height distribution
22 p4106 A70-43312
- D region ionization budget, evaluating short wavelength X rays role
23 p4236 A70-43860
- F 2 layer nighttime ionization at mid-latitudes, investigating conjugate point effects on observation point
23 p4188 A70-44055
- E region additional ionization source during solar activity maximum, analyzing ion production function and electron concentration
23 p4190 A70-44077
- Lower ionosphere electron concentration space-time variations relation to ionization source intensity fluctuations based on rocket observations and ground sounding data
23 p4190 A70-44079
- Meteor trails isotropic diffusion in presence of moving point source of ionization with variable intensity, calculating plasma density on and near trajectory
23 p4240 A70-44084
- Solar L alpha absorption in upper atmosphere, using rocket-borne ionization chamber
23 p4191 A70-44270
- F 2 layer ionization asymmetry for Northern and Southern Hemispheres during solstice periods due to electron density variations and aeronomic conditions
24 p4330 A70-46281
- Solar activity variations effects on equation parameters, describing nighttime F 2 ionization levels dependence on geographical latitude
24 p4331 A70-46299
- Geomagnetic field influence on annual F 2 layer longitudinal ionization at midlatitudes, relating solar activity level
24 p4331 A70-46300
- ATMOSPHERIC MODELS**
NT DYNAMIC MODELS
NT REFERENCE ATMOSPHERES
- VLF wave propagation across sunrise line analysis based on idealized model for earth-ionosphere waveguide
01 p0042 A70-10048
- MHD model for microwave solar circular polarization bursts interpretation, suggesting Alfvén wave disturbances in solar atmosphere
01 p0168 A70-10254
- Thermospheric neutral density amplitudes and phases using one dimensional model of geomagnetic activity effect, 27 day variation and semiannual variation
01 p0070 A70-10402
- Focusing factor dependence on range in spherically stratified medium with linearly varying refractive index profile, including earth atmosphere
01 p0142 A70-10490
- Structure and composition of clouds of ammonia and water bearing condensates, investigating compositional models of Jupiter atmosphere, considering ammonium hydrosulfide cloud layer
01 p0179 A70-10527
- Spectroscopically active compounds observability in Jupiter atmosphere using solar composition adiabatic equilibrium model
01 p0180 A70-10530
- Atmospheric models of deep atmosphere thermal emission and ionosphere free-free emission used for studying Saturn microwave spectrum
01 p0180 A70-10533
- Mercury atmospheric models for preliminary environmental criteria to be used in spacecraft design and engineering tradeoff studies [AIAA PAPER 69-54]
01 p0183 A70-10838
- Jacchia 1965 model discrepancies in solar and geomagnetic activity and semiannual effects observed in satellite drag measurements at 150-200 km and 700-1500 km
01 p0077 A70-11204
- Cool dwarf stars atmospheric models including IR opacity due to water vapor and pressure induced dipole of molecular hydrogen
01 p0190 A70-11347
- M dwarf stars model atmosphere construction taking into account molecular opacities in cool stellar atmospheres
01 p0190 A70-11348
- High temperature atmospheric models for red dwarf stars and sun to determine convection effect on atmospheric surface layers and emitted flux
01 p0190 A70-11349
- Nongray and constant radiative flux model at atmosphere for K dwarf stars with 4000 K effective temperature and 4.5 log surface gravity
01 p0191 A70-11350
- Venusian atmospheric model based on Venera 4 measurements, calculating probe distance travel, temperature, density and pressure profiles
01 p0192 A70-11504
- Venus atmosphere optical properties on basis of Venera 4 data, proposing models for measured rotational temperature and subcloud atmosphere radiative equilibrium
01 p0192 A70-11507
- Magnetospheric ring current model from ground stations data to interpret observed magnetic field disturbances
01 p0082 A70-11515
- Dipole magnetosphere model with cylindrical or spherical forbidden band for studying plasma motion in quasi-hydrodynamic approximation
01 p0082 A70-11521
- Conductivity and permittivity for ion and electron resonance region of ionospheric plasma model calculated in quasi-hydrodynamic approximation
01 p0082 A70-11528
- Perturbation method developed for linearizing nonlinear singular equation for inhomogeneous stratified atmosphere H-function in theory of radiative transfer
02 p0338 A70-11791
- Homogeneous scattering model for line formation applied to composition of Jupiter atmosphere
02 p0365 A70-11802
- Model construction for structure of planetary atmospheres, particularly Jupiter, discussing gas pressure, density and temperature relationships
02 p0366 A70-11803
- Two layer model of Jovian clouds including clear space, showing computed and measured equivalent widths of H quadrupole lines
02 p0367 A70-11813
- Radiative transfer in plane parallel atmospheres computed by discrete space techniques based on invariance concept for application to planetary atmospheres
02 p0338 A70-11825
- Stratospheric circulation model developed from radioactive element measurements, discussing large scale processes, seasonal variations, etc
02 p0291 A70-12291
- Incomplete historical data to infer state of atmosphere based on global circulation model, noting tradeoff of temperature for wind and time for space
02 p0291 A70-12296
- Static thermosphere model using hydrodynamic equations, assuming uniform temperature and nonexistent Coriolis forces, viscous stresses, horizontal velocity vector and thermal fluxes
02 p0327 A70-12384
- Static atmosphere model above 120 km, assuming oxygen atoms and molecules and nitrogen molecules presence to determine diffusion velocity and recombination coefficient
02 p0327 A70-12385
- Zonal circulation model of atmosphere below altitude of 200 km using rocket, meteor and ionospheric drift observations
02 p0328 A70-12388
- VLF energy propagation using ceramic dielectric model of earth-ionosphere waveguide
02 p0269 A70-12592
- Sonic boom wave shapes and amplitudes determination in still stratified atmosphere, comparing U.S. standard atmosphere results to various atmospheric models
03 p0411 A70-12927
- Extensive air shower models, noting role of nuclear active component energy decay rate
03 p0556 A70-13038
- Aerohydrodynamic model of relief waves in baroclinic atmosphere based on convection theory, analyzing strong turbulent vortex regime responsible for CAT [ONERA-TP-727]
03 p0408 A70-13638
- Thermal model for Venus ionosphere, considering photoionization and solar wind influx for possible heat sources
03 p0575 A70-13981
- Cyclone waves development during stationary low wave basic state two dimensional quasi-geostrophic two layer model
03 p0521 A70-14288
- Convective nongray stellar atmospheres construction for stellar stability studies, accounting for convective flow nonlocality and nongray radiative transfer
04 p0745 A70-14472
- Weather prediction technique based on hydrodynamical equations, outlining atmospheric circulation models [AAS PAPER 69-619]
04 p0714 A70-14646
- Prediction accuracies of atmospheric models investigated for medium altitude satellites during disturbed geomagnetic conditions, discussing solar flux and geomagnetic indices as input data [AAS PAPER 69-617]
04 p0677 A70-14647
- Electromagnetic drifts and neutral air winds effects on F 2 region derived from electron continuity equation, using Jacchia model atmosphere
04 p0677 A70-14966
- Earth surface hydrology effect incorporated into atmospheric circulation mathematical model for climate, considering ocean as atmospheric moisture reservoir
04 p0680 A70-15296
- Two level model for planetary atmospheres adapted to simulate atmospheric circulation and climate of Mars
04 p0756 A70-15515
- Radiative-convective equilibrium model to investigate photodissociation of water in Venus atmosphere, considering greenhouse effect
04 p0757 A70-15516
- Statistical ionospheric model of sporadic E layer frequency characteristics dependence on equipment parameters, determining permissible variation of transmitter power and receiver gain
04 p0682 A70-15727
- Ionospheric reaction coefficients estimate to correlate equatorial electron density profile and Jacchia model of neutral atmosphere
04 p0683 A70-15744
- Transmission and reflection coefficients of propagating whistler modes for model ionosphere
05 p0837 A70-15880
- K line profiles of Ca II for two component chromosphere, obtaining line source function and optical depth from steady state and radiative transfer equations
05 p0911 A70-16430
- Plane magnetopause models assuming ionospheric electrons ability to short circuit electric fields, constructing distribution functions by Vlasov theory
05 p0840 A70-16568
- Spiral cloud vortex model in occluded extratropical cyclone constructed using atmospheric dynamics equations and satellite photographs
05 p0879 A70-16642
- Low energy charged particle motion parallel with magnetic force lines analyzed in magnetosphere model with constant electric field
05 p0903 A70-16726
- Physical theory of ball lightning based on cooling air spheres models, calculating equilibrium composition, temperature profiles, output radiation and mass density
05 p0843 A70-17102
- Atmospheric turbulence characteristics related to drag loads of tall spacecraft structures by boundary layer wind model
06 p1160 A70-17165
- Shear generated atmospheric clear air turbulence growth and dependence on atmospheric instabilities calculated numerically by invariant model [AIAA PAPER 70-55]
06 p1098 A70-18031
- Haze model atmospheres scattering characteristics by computer simulation concerning optical contrast reduction by aerosols for direct and diffuse radiation [AIAA PAPER 70-194]
06 p1057 A70-18156
- Solar radiation flux observation-prediction discrepancies due to Fraunhofer line absorption, studying Balmer continuum as atmospheric model criterion
06 p1148 A70-18451
- Stellar atmospheric models thermal conductivity coefficient computation for various temperatures and pressures neglecting magnetic field
06 p1150 A70-18464
- Three dimensional model current system with magnetospheric and ionospheric sections connected by currents flowing along geomagnetic field lines proposed for polar magnetic substorms
06 p1059 A70-18535
- One dimensional cumulus convection model modified by incorporating rain evaporation rate and temperature changes from downdrafts
06 p1099 A70-18568
- Model for thunderstorm downdrafts induced by rain evaporation based on one dimensional steady state formulation, deriving vertical velocity profiles
06 p1100 A70-18573
- Numerical model of thunderstorm cold air outflow, providing horizontal flow as function of height from computer program using vertical velocity and storm motion
06 p1100 A70-18574

Nonlinear planetary long range weather forecasting problems analytical solutions, describing quasi-sole-noidal atmospheric motions model

07 p1328 A70-18649

Pulse amplitudes and delays measured for oblique absorption values during IGY over 1000 km transmission path for correlation with lower ionosphere model

07 p1228 A70-19155

CO vertical distribution near tropopause from photochemical atmospheric model with CO recombination with OH for stratospheric sink

07 p1265 A70-19282

Vertical temperature profile diurnal variations of Mars atmosphere using models, noting aerosol influence

07 p1385 A70-19422

Winds above 200 km measured from vapor trail observations compared to winds deduced from satellite orbital changes and theoretical models

07 p1269 A70-19950

Similarity model for spherically symmetrical flow following explosion in rarefied atmosphere satisfying hydrodynamic energy conservation equation

07 p1260 A70-19981

Line profiles in expanding and rotating atmospheres via Monte Carlo techniques, considering noncoherent scattering, atomic levels and atmospheric characteristics

07 p1339 A70-20057

Nonlinear integral equations for inhomogeneous atmospheres derived from radiative transfer equations global form, noting relations to Ueno and Chandrasekhar equations

07 p1336 A70-20059

Polar ion-exosphere model with open geomagnetic field lines, calculating electrostatic field for region

07 p1270 A70-20077

Plasma flow structure near frontal point in earth magnetosphere, using quasi-hydrodynamic two dimensional model to obtain power series solution

07 p1391 A70-20419

Plasma concentration in nondipole magnetosphere model from Pc 5 pulsations periods for high geomagnetic latitudes, noting solar winds effect

07 p1277 A70-20443

Solar radiation reflection function for plane-parallel atmosphere with isotropic phase function calculated by successive scattering method, noting application to planetary atmospheres

08 p1571 A70-20909

Vertical plane and axis symmetrical numerical models for cumulus convection of moist atmosphere, discussing initial conditions

08 p1536 A70-21025

Short wave radiation model of single layer stratus and stratocumulus cloud based on actinometric soundings of lower troposphere

08 p1537 A70-21104

E layer atmospheric circulation model for meteor zone, noting solar thermal radiation role

08 p1575 A70-21215

Electron, oxygen and NO molecular ions concentrations for E region from computer calculations of diurnal model compared to observations

08 p1490 A70-21391

Venus surface temperature calculations with non-gray radiation balance model and Mariner 5 and Venera 4 vertical temperature profile data

08 p1579 A70-21568

Global atmospheric research program data requirements analysis based on two level numerical model

08 p1539 A70-21650

Lee wave theory for two dimensional stratified atmospheric models, noting local intense vertical beam into high stratosphere

08 p1540 A70-21972

Global real data numerical forecasting with two layer NCAR /National Center for Atmospheric Research/ general circulation model, testing different data initialization schemes

09 p1713 A70-22303

Linear nonstationary quasi-geostrophic model with external and internal heating and forcing for dynamics of ultralong waves in troposphere and lower stratosphere

09 p1713 A70-22304

Radiation effects on polytropic atmosphere convective instability using method of disturbances

09 p1753 A70-22456

Sigma Orionis E hydrogen-deficient atmosphere, using grid of constant-flux model atmospheres to determine abundances of five elements

09 p1755 A70-22504

Homogeneous model solar photosphere in strict radiative equilibrium with depth-dependent line blanketing by neutral and ionized metals

09 p1757 A70-22728

Atmospheric model for flow crossing ground obstacle using nonlinear differential equation

09 p1718 A70-22848

Classical model regarding general tropospheric circulation, exploring momentum, heat and moisture exchange

09 p1718 A70-23050

Electron precipitation modulation exponential dependence on micropulsation amplitude derived from idealized model

09 p1747 A70-23492

Acoustic gravity waves horizontal ducting in atmosphere with spatially periodic wind shears

09 p1671 A70-23498

Stellar wind theory based on spherically symmetric isothermal and stationary stellar atmosphere with negligible gravitational potential

09 p1747 A70-23605

Airglow hydroxyl emissions diurnal variations as function of height, using digital computer for time dependent solution of equations for oxygen-hydrogen atmosphere

10 p1872 A70-23826

Boundary layer atmospheric turbulence at Kennedy Space Center obtained for engineering spectral model, discussing energy balance

10 p1911 A70-23926

Atomic oxygen IR emission in earth atmospheric models, using reduction factor for comparison with optically thin atmosphere

10 p1875 A70-24439

Geomagnetic pulsations /pc 4/ characteristics from analyzing magnetosphere model yielding plasma densities consistent with experimental data

10 p1875 A70-24483

Shock propagation from point explosion energy source into cold exponential atmosphere with radiative heat transfer in rear of shock front

10 p1869 A70-24525

F region irregularity model to include field-aligned columns and sheets and frontal irregularity shapes effect on radio star and satellite scintillations

10 p1841 A70-24805

D region electron ion recombination analyzed by two-ion model

10 p1881 A70-24812

Ionospheric loss rates from rocket observation during auroral absorption interpreted by two ion model of recombination

10 p1881 A70-24813

Field-aligned plasma velocity dependence on plasma diffusion and wind velocity illustrated with model of night F 2 layer

10 p1881 A70-24814

Equivalent angles of slope calculations based on rotary oblique probing data for spherical models of earth and ionosphere, deriving minimum equivalent beam path

11 p2043 A70-25539

Linear heat propagation in rarefied and non-homogeneous atmospheres, considering Green function behavior and various boundary and initial value problems

11 p2107 A70-25542

Charged particle motion in steady and perturbed dipole fields using laboratory earth magnetosphere plasma model

11 p2104 A70-25546

Venus clouds self consistent radiative-convective model with sun as heat source

11 p2107 A70-25647

Cumulus convection one dimensional time dependent numerical model, considering horizontal mixing, evaporation, precipitation generation and freezing and thermodynamic processes

11 p2075 A70-25648

Mars upper atmosphere semiempirical model, reducing density uncertainties by allowing for solar cyclic variations

11 p2111 A70-26031

Martian atmospheric models for lander and simulator design, obtaining effective sky temperatures, surface pressures and temperatures, atmospheric compositions, etc

11 p2112 A70-26141

Ionic composition of Class I auroras based on 1965 CIRA atmospheric model atomic/molecular oxygen ratios, noting ion loss rates

11 p2046 A70-26565

Comet model atmospheres for head theoretical spectra computation, considering collisional effects through total gas density distribution

11 p2116 A70-26647

Neutral helium line profiles for line-blanketed model atmospheres grid

11 p2117 A70-26660

Atmospheric hemispheric general circulation model numerical time integration with moist processes and uniform earth surface

12 p2262 A70-26882

Short wave radiation fluxes inclusion in hydrodynamic model of general atmospheric circulation based on aircraft sounding data and aerostatic observations

12 p2263 A70-27512

Stellar atmosphere model for multilevel spectral line emission, assuming semiinfinite hydrogen atmosphere with sequence of plane parallel zones

12 p2306 A70-27856

Magnetic field effect on frequency spectrum of vertically propagating magnetoacoustic waves and reflection conditions in inhomogeneous isothermal atmosphere

12 p2227 A70-28226

Air masses nonadiabatic ascent under elevated temperature inversion in atmosphere, assuming three layer model with linear profiles

12 p2265 A70-28335

Wind field statistical properties using model incorporating quasi-steady state speed, shear, gusts and small scale motions

Wind field statistical properties using model incorporating quasi-steady state speed, shear, gusts and small scale motions

12 p2444 A70-28752

Magnetopause model, discussing equilibrium layer between magnetic field and cold plasma field-free stream

13 p2396 A70-29181

Radio sounding of Van Allen inner belt from Antarctica, comparing American and Soviet deductions about magnetosphere structure

13 p2399 A70-29273

Collision effect on phenomena associated with ion cyclotron whistler formation, considering ionospheric day time model

13 p2468 A70-29933

Stellar observations in near UV by camera having two color photometric slides, discussing atmospheric models

13 p2498 A70-30013

Solar cosmic rays entry into magnetosphere, showing entrance on smoothly connected field lines

13 p2480 A70-30059

Geomagnetic tail formation, cross section and length and auroral irradiation, discussing observations, models, vacuum magnetic merging and field aligned currents processes

13 p2402 A70-30060

Model current system for magnetospheric substorm accounting for distribution of geomagnetic disturbance field vectors on earth surface and auroral electrons and protons

13 p2481 A70-30062

Magnetospheric convection models and effects on charged particle populations

13 p2402 A70-30064

Model for droplet size spectrum in cloud with spatial inhomogeneity of nuclei concentration, determining characteristic size dependence on altitude

14 p2601 A70-30129

Plane stationary nonlinear problem of air flow over earth surface roughnesses, using three layer atmospheric model

14 p2602 A70-30160

Atmospheric airflow model above changes in surface roughness, temperature and heat flux, using boundary layer approximations and Businger-Dyer and mixing length hypotheses

14 p2602 A70-30368

Radiant heat flux for standard model, dry and humid atmosphere, calculating temperature variations with altitude for entire IR spectrum

14 p2603 A70-30401

Atmospheric optical aerosol model based on vertical attenuation profile, particle concentration and size distribution and air conductivity

14 p2603 A70-30410

Aerospace environment models development by NASA for engineering use in Space Vehicle Design Criteria program

14 p2637 A70-30554

Static diffusion model of thermosphere with allowance for temperature and chemical composition and not limited by constant 120 km boundary conditions

14 p2606 A70-30560

Global atmospheric models computations based on treating molecular and eddy diffusion as dynamic processes

14 p2606 A70-30561

Martian atmosphere modeling for obtaining Viking lander spacecraft design margins by Monte Carlo method

14 p2637 A70-30564

Solar activity predictions for earth upper atmosphere models emphasizing linear regression method

14 p2638 A70-30565

Thunderstorm bottom wind profile model, analyzing flow distribution, isotach, isogon and isotherm characteristics

14 p2607 A70-30584

Statistical mesosphere temperature, density and wind profiles models based on rocket soundings

14 p2608 A70-30593

Cloud model development and computer simulation uses, noting applications to aerospace experiment design

14 p2608 A70-30597

Stratospheric CAT-internal wave relationship, using aircraft and radiosonde HICAT measurements

14 p2609 A70-30603

Mathematical model for interaction of solar wind with geomagnetic field, predicting magnetosphere shape

14 p2574 A70-30736

Earth-ionosphere waveguide electric field strength calculation based on nighttime ionospheric models, comparing results to measurements

14 p2574 A70-30748

Statistical ionospheric model of sporadic E layer frequency characteristics dependence on equipment parameters, determining permissible variation of transmitter power and receiver gain

14 p2575 A70-30811

Ionospheric reaction coefficients estimate to correlate equatorial electron density profile and Jacchia model of neutral atmosphere

14 p2576 A70-30828

Earth atmosphere model for global forecasting using space technology, noting Global Atmospheric Research Project /GARP/

14 p2576 A70-30973

Self similar one dimensional flow behind plane shock propagating in exponentially decreasing atmosphere, considering radiation mean free paths and radiative heat transfer

14 p2567 A70-31032

Numerical modeling for earth atmosphere in terms of six pressure levels using digital computers

14 p2577 A70-31151

Numerical weather prediction requirements for global satellite observing systems using atmospheric models

14 p2610 A70-31152

Ap star kappa Cancri model atmosphere analysis based on observed energy distribution and hydrogen line profiles

14 p2652 A70-31381

Ionospheric and ground level pressure fluctuations correlation from atmospheric models, suggesting ionospheric disturbance measurement from microbarographs on land surface

15 p2769 A70-31446

Venus lower atmosphere models, discussing pressure, temperature and water vapor abundance based on radio and radar astronomy and spacecraft measurements

15 p2798 A70-31684

Ionospheric density profiles measurement by accelerometers on SPADES and Cannon Ball 1 satellites, comparing results with prediction from atmospheric model

15 p2724 A70-31686

Electromagnetic ELF radiation model for multiple return strokes of cloud to ground lightning discharges, considering channel length

15 p2726 A70-31864

Radiative transfer in spherical stellar atmosphere, considering free electrons density gradient and thermal motions, atmospheric layer curvature, optical thickness, etc

15 p2732 A70-32905

Wave propagation and group velocity in warm magnetoplasma, using adiabatic theory for ionosphere and far magnetosphere models

16 p2859 A70-32937

Maximum up- and downdrafts altitude, using two dimensional model of lee wave disturbances for post-frontal subsidence modification

16 p2945 A70-32948

Spectrophotometric and visual observations of twilight glow from Soyuz 5, comparing vertical monochromatic brightness profiles with calculations for Elterman aerosol model

16 p2896 A70-33218

Winter stratospheric circulation quasi-geostrophic model based on joint radiative-photochemical equilibrium, investigating ozone cycle and warming

16 p2945 A70-33250

Numerical simulation of large scale atmospheric motions, considering pressure distribution, vorticity, kinetic energy, etc

16 p2946 A70-33625

Atmospheric boundary layer model, considering air-surface interaction, heat and humidity exchange, wind, temperature and humidity profiles, etc

17 p1332 A70-34667

Weather prediction models, describing equation systems, roles of friction and heating, meteorological data analysis, fronts, convection, etc

17 p1332 A70-34668

Stellar UV spectral line profiles interpretation, using atmospheric models and line formation theory

17 p1361 A70-34890

H-R diagram stellar spectra interpretation using model atmospheres describing temperature, gravity and chemical composition

17 p3169 A70-35381

IR balloon observations of absolute solar brightness and stratosphere transparency, discussing BCA and HSRA models

17 p3078 A70-35580

Integral equation for three dimensional Fourier transform applied to isotropic scattering of radiation from point source in finite spheroidal atmosphere

17 p1317 A70-35599

Model calculations of Martian upper atmosphere expanding above mesopause, taking into account effects

of molecular and eddy diffusion and chemical reactions

17 p3172 A70-35643

Ballistical transport in collisionless exosphere, discussing heat flux of ballistical oxygen and model temperatures for day and night conditions

17 p3080 A70-35765

Hydrodynamic wave propagation compared in magnetospheres of plane and cylindrical geometries

18 p3311 A70-36011

High latitude magnetosphere structure, using two dipole model

18 p3312 A70-36168

Upper atmosphere IR emission model with reference to thermal excitation, chemical reactions and electron excitation

18 p3246 A70-36173

Dynamic numerical weather forecasting based on balanced model consisting of closed system of equations

18 p3284 A70-36232

Supersonic boom intensity calculation on ground, assuming isobaric inhomogeneous atmosphere and weak shock wave

18 p3213 A70-36380

Simulation studies for first GARP global experiment, discussing data redundancy, measured and derived data, sampling, etc

18 p3285 A70-36785

Ionospheric inhomogeneities electrodynamic decay rate, using ellipsoidal model with sharp boundary for irregularity

18 p3252 A70-36986

Radiative transfer equation for spectral line formed in multidimensional atmosphere, solving for two dimensional atmospheric model

18 p3317 A70-37008

Electron temperature in 500-1000 km range during minimum solar activity based on Alouette satellite data and atmospheric model, observing latitudinal variation

18 p3254 A70-37029

F 1 region unsteady model, examining vertical distribution profile of electron concentration on summer day

19 p3409 A70-37323

Light propagation in plane parallel layer of scattering medium containing absorbing substance with random density distribution

19 p3461 A70-37422

Steady symmetric flow model for Jupiter cloud banded structure, representing variable concentration of condensing constituents with latitude

19 p3519 A70-38254

Venus atmospheric temperature, pressure and density measurements by Venera 5 and 6 space probes, developing model

19 p3520 A70-38255

Venus atmosphere heat transfer processes from Venera 4, 5 and 6 probes data, evaluating radiative and convective motions model

19 p3520 A70-38256

Tropical circulation structure and energetics from numerical time integration of global atmospheric model with realistic orography

19 p3462 A70-38257

Artificial ion clouds motion in magnetosphere, using MHD model

19 p3414 A70-38378

Upper atmospheric density and temperature diurnal phase and amplitude discrepancy reconciled by dynamic diffusion model

19 p3414 A70-38381

Upper atmosphere semiannual variations dependence on lower thermosphere dynamic properties seasonal variations, using steady state models

19 p3415 A70-38384

Ionospheric electric current distribution response to horizontal wind induced emf, using lunar tidal wind models

19 p3415 A70-38386

Planetary atmospheres energy balance, considering models in terms of radiative control or large scale fluid motions

19 p3521 A70-38499

Solar atmospheric hydrodynamic response to stationary random forces homogeneous over horizontal planes, discussing common energy argument, various models and photospheric oscillation

19 p3523 A70-38690

Thermotropic quasi-geostrophic atmospheric model, deriving linear and quadratic integral invariants

19 p3463 A70-38754

Non-LTE line blanketed solar model atmospheres with various temperature distributions

20 p3703 A70-39020

Planetary scale unsteady atmospheric motions nonlinear problem, considering two level solenoidal model

20 p3662 A70-39177

Geopotential fields forecasting on isobaric surfaces over Northern Hemisphere by linear four level nonadiabatic model, discussing eddy transport and heat flux equations

20 p3662 A70-39179

Geomagnetic field configuration and magnetic drift envelopes of particles with various pitch angles at equator calculated from two-dipole model of magnetosphere

20 p3619 A70-39299

Inner magnetosphere magnetic field mapping, deriving Pogo model

20 p3621 A70-39349

Morning and evening current reversals in equatorial electrojet, discussing seasonal variation data for refining models

20 p3621 A70-39352

Atmospheric circulation two level quasi-geostrophic model, examining dynamic large scale features of baroclinic wave blocking by high latitude cold anticyclonic cells

20 p3621 A70-39372

ELF and VLF propagation for perturbed ionosphere models, discussing effects of ion collision frequencies and molecular weights

20 p3585 A70-39454

Satellite-borne conical IR scanner flight data hybrid simulation and error analysis, suggesting carbon dioxide horizon noise model

20 p3631 A70-39513

Soviet book on physical atmospheric parameters covering model, solar and earth radiation fluxes and spectral energy distribution

20 p3664 A70-39799

Mode-generated average variables of atmospheric horizontal heat flux by transient cyclonic eddies used in mean motion circulation model

20 p3664 A70-40063

Radio aurora model based on two stream, ion acoustic wave instability, investigating radar backscatter

20 p3623 A70-40465

Gust field in lowest atmospheric layer over homogeneous terrain, deriving statistical models and simulating effects on XV-5 V/STOL aircraft

21 p3750 A70-40784

Cloudy planetary atmospheres model, assessing nonlocal thermodynamic equilibrium role

21 p3813 A70-40903

Secondary flow model for planetary boundary layer, considering flow as finite perturbation

21 p3813 A70-40904

Thermal plasma model along magnetic field lines outside plasmasphere with sharp density gradient in equatorial plane, using OGO-4 ion composition measurements

21 p3815 A70-41057

Midlatitude F 2 layer electron density structure using theoretical model, accounting for atmospheric physical and chemical processes

21 p3815 A70-41062

Auroral arcs formation model based on dynamic magnetosphere-ionosphere interaction

21 p3817 A70-41089

Equivalent angles of slope calculations based on rotary oblique probing data for spherical models of earth and ionosphere, deriving minimum equivalent beam path

21 p3819 A70-41289

Linear heat propagation in rarefied and non-homogeneous atmospheres, considering Green function behavior and various boundary and initial value problems

21 p3892 A70-41292

Charged particle motion in steady and perturbed dipole fields using laboratory earth magnetosphere plasma model

21 p3882 A70-41296

Polarization of radiation reflected and transmitted by earth atmosphere, calculating scattering matrix for aerosol size distribution model

21 p3820 A70-41725

January climatology simulation experiment based on two layer version of global circulation model, comparing computed and observed results

21 p3847 A70-42120

Transition region structure between chromosphere and corona, discussing temperature, theoretical models, energy balance and magnetic fields from far UV data

21 p3924 A70-42183

Chromosphere-corona transition region model from limb-disk optically thin line intensities

21 p3924 A70-42184

Solar far UV limb brightening of C III, N III, N IV, O III, O IV and Si IV lines in chromospheric-corona transition region, correcting coronal model for spicule effects

21 p3925 A70-42186

Internal gravity waves mathematical model for atmosphere with arbitrary distributions of temperature, molecular weight, viscosity and conductivity, deriving wave propagation into thermosphere

21 p3821 A70-42257

Venus spectrum from high resolution Michelson interferometers with Fourier transform and digital computation, discussing Venus atmospheric models

22 p4099 A70-42721

Earth atmospheric electricity problems formulated as continuous macroscopic electrohydrodynamic model

22 p4016 A70-42784

Ionospheric current theoretical model and balloon measurement of ionospheric electric field

22 p4017 A70-42795

Magnetospheric tail magnetic field and particle motion calculation, assuming constant radius cylinder with current sheet bisecting center

22 p4019 A70-43111

Recombination model of diurnal variation of electron density in midlatitude D region, assuming NO ionization by solar Lyman-alpha radiation

22 p4020 A70-43158

Radio wave reflection properties in 16-3000 kHz range calculated from D and E region models for comparison with measurement

22 p3989 A70-43164

Water vapor emission computation from statistical band model, investigating accuracy limitations

22 p4065 A70-43169

Transmission calculations for homogeneous and nonhomogeneous water vapor atmospheres, evaluating various methods

22 p4065 A70-43170

Electron density profiles calculation from model atmosphere, deriving F 2 layer ionization vertical distribution

22 p4023 A70-43303

Proton energy angular distribution measurement by OV2-5 research satellite confirming model of shell splitting in geomagnetic field

23 p4236 A70-43832

Magnetospheric substorms model modification for growth phase inclusion prior to explosive expansion phase

23 p4186 A70-43853

Tropical cyclone development model for axisymmetric vortex and quasi-balanced conditions, considering vertical heat distribution, rate of intensification and energy budget

23 p4213 A70-43896

Statistical-dynamical atmosphere model for global circulation simulation, taking into account meteorological variables of velocity, temperature, pressure and eddy statistics

23 p4213 A70-44029

Noctilucent clouds blue color and rocket sounding results explained by ozone model of mesospheric clouds formation

23 p4188 A70-44048

F 2 layer critical frequency and maximum electron concentration statistical characteristics for predicting SW propagation conditions

23 p4188 A70-44056

Radar echo superrefraction and subrefraction concepts used with atmospheric waveguide model explaining extremal behavior and relations to atmospheric stratification

23 p4163 A70-44233

Thermosphere diurnal thermal influx theory, allowing for heat conductivity

23 p4214 A70-44265

Rotating stellar atmospheric models for middle and late A star masses, emphasizing Altair observed and predicted energy distribution

23 p4250 A70-44812

Spectrophotometric and visual observations of twilight glow from Soyuz 5, comparing vertical monochromatic brightness profiles with calculations for Elterman aerosol model

24 p4328 A70-45193

Solar chromosphere model convective instability, considering temperature and magnetic field effects

24 p4399 A70-45303

Atmospheric response to heating in stable auroral red arc by two dimensional steady state dynamic model of neutral thermosphere

24 p4329 A70-45357

Ionospheric wave propagation, using medium model, perturbation theory for vertical variation and computer eigenvalues of matrix system

24 p4314 A70-46132

ATMOSPHERIC MOISTURE

Vertical atmospheric vapor distribution from measuring microwave radiation of earth/atmosphere system at several wavelengths

01 p0135 A70-10202

Satellite and rocket probe measurements of water vapor in mesosphere

01 p0082 A70-11510

Atmospheric water vapor effect on contrast between natural target and sky via spectrophotometric method, exploring target visibility and contrast relations

02 p0325 A70-11873

Atmospheric humidity effects on ionization and positive corona-current pulses development, discussing radio interference

02 p0258 A70-12425

Venusian atmosphere water content determined by airborne interferometer

02 p0377 A70-12554

Linear regression equations to relate atmospheric precipitable water to surface dew point, sky cover and weather

03 p0520 A70-13163

Corrosion resistance of Ti-based alloys in humid subtropical climate, discussing sea and rain water effects

03 p0510 A70-13281

Raman backscatter of frequency doubled ruby laser beam by water vapor in atmosphere observed by optical radar, calculating water vapor mixing ratio profile

04 p0677 A70-14950

Depth and shape of 0.94 micron water vapor absorption band for clear and cloudy skies, noting radiation distortion for dark dense clouds

04 p0690 A70-15024

Vertical profile of angular mass distribution of atmospheric water vapor and ozone as gas proportion function

06 p1097 A70-17794

Dry regions in cumulus cloud near environment interpreted as evidence of compensating motion in environment

06 p1101 A70-18577

Atmospheric integral moisture content determination from thermal radio emission measurements by Cosmos 243 satellite

07 p1329 A70-19649

Ice crystal density in Martian atmosphere from brightness of Martian parhelic halo

08 p1564 A70-20547

Time dependent height of lower boundary of subinversion stratus clouds using atmospheric moisture and heat transport equations

08 p1537 A70-21102

Vertical motions and turbulent exchange influence on height variation of stratus clouds based on atmospheric moisture and heat transport equations

08 p1537 A70-21103

Upper surface roughness of internal st-sc clouds as function of vertical temperature and moisture in overlying inversion layers

08 p1537 A70-21106

Vertical water vapor profile in strato-, meso- and thermospheres measured in rocket and satellite experiments by mass spectroscopy, spectral analysis and thermal sensometry

09 p1666 A70-22187

Soviet monograph on growth rate of coagulating and condensing aerosol particles, considering kinetic theory

09 p1713 A70-22205

Heat, moisture and momentum fluxes measurement in atmospheric boundary layer, discussing instrumental accuracy necessary for various measuring techniques

09 p1717 A70-22379

Al alloys fatigue properties dependence on surface oxide cracking in moist and dry air, investigating oxidation and kerosene processing

09 p1707 A70-23206

Condensation start dependence on air humidity at inlet and nozzle geometry applied to supersonic wind tunnel using undried atmospheric air

09 p1606 A70-23614

Atmospheric water vapor profiles remote measurements using Raman component of high powered Q switched laser backscatter

10 p1886 A70-23938

Vertical profile of angular mass distribution of atmospheric water vapor and ozone as gas proportion function

10 p1913 A70-25025

Water vapor pollution of stratosphere by supersonic transports, considering effects on temperature, cloudiness, albedo, etc

11 p2077 A70-26618

Stratospheric water vapor measurement by submillimeter wave sounding, considering signal fluctuations due to scattering by high cirrus clouds

11 p2077 A70-26619

Satellite measurement of water vapor height profiles using outgoing thermal radiation and solar radiation atmospheric absorption techniques

13 p2392 A70-28571

Atmospheric water effects on electromagnetic wave propagation - NATO Conference, University of Western Ontario, August-September 1969

13 p2393 A70-28781

Atmospheric water effect on satellite communications in UHF region and above, discussing signal attenuation

13 p2364 A70-28782

Millimeter-wave probing for vertical distribution of atmospheric water vapor, comparing ground, balloon and satellite observation techniques

13 p2394 A70-28785

Ammonium ions elimination from atmospheric moisture condensates by treatment with metal-exchange resins, discussing volume sorption capacity

13 p2362 A70-29339

Solar observations in intermediate IR, measuring continuum intensity of disk center in atmospheric water vapor window

13 p2498 A70-30006

Atmospheric moisture balance solution for altitude dependent vertical velocity and turbulence coefficient, considering cloud water content and boundaries height calculation

14 p2601 A70-30137

Water vapor absorption bands in solar IR spectrum, considering earth curvature and atmospheric inhomogeneity and refraction

14 p2572 A70-30404

Atmospheric optical thickness in visual spectrum region relationship to meteorological characteristics, plotting vertical profiles of humidity and aerosol attenuation coefficient

14 p2603 A70-30407

Water vapor abundance in Mars atmosphere from high resolution spectroscopy

14 p2649 A70-31211

Liquid water occurrence on Mars surface, considering ice melting, evaporative cooling, atmospheric moisture content, etc

14 p2651 A70-31298

Growing ice crystals surface electric potentials during various stages of water vapor condensation

15 p2769 A70-31444

Ice crystal density in Martian atmosphere from brightness of Martian parhelic halo

15 p2796 A70-31456

Venus lower atmosphere models, discussing pressure, temperature and water vapor abundance based on radio and radar astronomy and spacecraft measurements

15 p2798 A70-31684

Sea surface temperature and atmospheric moisture determination from satellite measurements of atmospheric thermal radio emission on quiet and cloudy windy days

15 p2770 A70-32069

Atmospheric humidity determination from satellite radio emission measurements at SHF

15 p2771 A70-32071

Air mass climatology in terms of pressure temperature and moisture content

15 p2772 A70-32457

Microwave propagation refractive index over India, showing influence of humidity and vapor pressure

15 p2701 A70-32470

Phase stability measurements at 2695 MHz with radio link interferometer, discussing atmospheric water content effect

16 p2861 A70-32959

Water vapor pure rotational absorption spectrum compared with calculated far and near IR spectra

18 p3244 A70-35949

Atmospheric water vapor distribution by intensity measurements of outgoing radiation from satellites in carbon dioxide and water vapor spectral bands

18 p2827 A70-36971

Venus atmosphere water content, discussing chemical reactions, temperature, dehydrogenation, etc

18 p3320 A70-37075

Atmospheric moisture content vertical profile from terrestrial radiation measurements, using statistical regularization procedure

19 p3460 A70-37418

High altitude humidity from millimeter-band water vapor lines, using EHF atmospheric spectral transparency calculation

19 p3461 A70-37633

Atmospheric humidity measuring equipment and procedures for high altitudes, considering hygrometers, mass spectrometers, sondes, absorption spectra, etc

19 p3461 A70-37635

Optical hydrometer measuring water vapor content in vertical atmosphere column, using interference filters and thermoelectric sensitive element

20 p3625 A70-39027

Venus atmosphere and water vapor, finding ice clouds by spectrum analysis

20 p3708 A70-39961

Millimeter wave observation of sun, deriving empirical relationships between atmospheric attenuation, emission and water vapor

20 p3623 A70-40304

Millimeter wave and optical astronomical refraction differential measurements, showing dependence on atmospheric water vapor

20 p3588 A70-40305

Heterodyne millimeter wave radiometric system for observing atmospheric attenuation due to water vapor, discussing design, development and initial measurements

20 p3588 A70-40308

Atmospheric temperature and water vapor profiles from iterative solution of radiative transfer equation for comparison with spectral radiance observation from Nimbus satellites

21 p3846 A70-40803

Venusian atmosphere carbon dioxide, water, molecular oxygen and nitrogen contents from Venera 5 and 6 data

21 p3883 A70-40837

Cloud structure, atmospheric water vapor and liquid water contents from passive ground based microwave spectrum measurements

21 p3846 A70-40906

- Psychrometric chart for physiological research involving moist air thermodynamic properties
24 p4304 A70-46275
- Ruby laser application to air humidity measurement via hygrometric method
24 p4356 A70-46401
- ATMOSPHERIC NEUTRON FLUX DENSITY**
U **ATMOSPHERIC RADIATION**
U **NEUTRON FLUX DENSITY**
U **ATMOSPHERIC NOISE**
U **ATMOSPHERICS**
U **ATMOSPHERIC PHYSICS**
NT **CLOUD PHYSICS**
- Book on atmospheric circulation systems structures and physical interpretation, concentrating on lower atmosphere and North America
01 p0069 A70-10126
- Thermospheric neutral density amplitudes and phases using one dimensional model of geomagnetic activity effect, 27 day variation and semiannual variation
01 p0070 A70-10402
- Organic synthesis by electrical discharge in simulated Jovian atmosphere, noting appearance of orange-red cyanogen-ammonia polymer nonvolatile fraction
01 p0179 A70-10529
- Upper atmosphere structure and energy budget based on IGY/IQSY spectroscopic observations of temperature distribution and stratosphere-mesosphere composition
01 p0072 A70-10578
- Upper atmosphere-lower atmosphere interactions, middle atmospheric physics and dynamics and mesospheric seasonal and large scale zonal and meridional behavior
01 p0073 A70-10581
- F region ionized and neutral atmospheric movements interactions, discussing ion drag forces, electromagnetic drift, wind effects, etc
01 p0074 A70-10587
- Venus atmosphere ionization distribution, temperature and pressure profiles determined from amplitudes and differential Doppler of radio signals to Mariner 5 during occultation
01 p0186 A70-11084
- Tropospheric parameters determination using combinations of measurement and transhorizon radio signals propagation techniques
01 p0044 A70-11086
- Remote sensors to determine atmospheric characteristics and underlying earth surface structure, using electromagnetic and acoustic waves as signal carriers
01 p0093 A70-11266
- Algorithm for solving Dirichlet problem of nonlinear elliptical differential equations representing atmospheric dynamics balance equation
01 p0134 A70-11609
- Planetary atmospheres dynamics, discussing rotational and MHD effects, energy sources, etc
02 p0366 A70-11806
- Structure and composition of Jovian atmosphere, discussing hydrogen helium ratio, cloud colors, etc
02 p0367 A70-11811
- Ionospheric phenomenon, discussing experimental techniques, physical properties and chemical composition, regular and irregular variations, sporadic E ionization, etc
02 p0289 A70-12071
- Soviet collection of papers on theoretical problems of upper atmosphere physics, discussing various models, atmospheric composition, etc
02 p0327 A70-12383
- Static thermosphere model using hydrodynamic equations, assuming uniform temperature and nonexistent Coriolis forces, viscous stresses, horizontal velocity vector and thermal fluxes
02 p0327 A70-12384
- Hydrostatic equation nonequilibrium terms role in single and multicomponent atmospheres, deriving solutions to Boltzmann equation
02 p0328 A70-12386
- Invariant group study of free atmospheric convection equations at combination of Grashof numbers, Prandtl numbers and boundary conditions, noting infinite flux velocity
02 p0328 A70-12387
- Application of atmospheric studies to satellite transmissions - Conference, Bedford, Mass., September 1969
02 p0259 A70-12564
- Soviet monograph on weather forecasting covering hydrodynamic principles, atmospheric physics, short and long range forecasting, temperature, pressure fields, etc
03 p0520 A70-12873
- Coarse structure of solar atmosphere from observations of quiet sun, discussing contradictions with existing models
03 p0570 A70-13592
- Tropospheric fine structure influence on radio wave propagation, including atmospheric gases and precipitation effects and radar, navigation and TV applications
03 p0449 A70-13612
- Lidar and IR radiometer mobile laboratory for atmospheric optics research, including construction details and support equipment
03 p0463 A70-13677
- Ionospheric aerodynamics concerning plasma flow and stability, ion motion, radio wave scattering, etc
03 p0479 A70-14386
- Earth, Venus and Mars atmospheric structure, discussing gases escape, temperature, density, IR radiation and solar radiation absorption
05 p0914 A70-16628
- Electron flux-atmosphere interaction solved by numerical integration on computer, discussing auroral ionosphere
05 p0842 A70-16755
- Dispersion and correlation function for atmospheric transparency due to water vapor, from statistical model of absorption bands and effective mass
06 p0153 A70-17204
- Nomograms for spectral transparency of atmosphere at 2.8-5.6 microns
06 p0153 A70-17208
- Collection of papers on air pollution aerophysics covering eddy diffusion, aerosol particle size, Los Angeles smog, etc
06 p0106 A70-17321
- Surface-particle interaction and atmospheric parameters measurements by paddlewheel satellites, discussing angular distribution of re-emitted molecules and accommodation coefficients
06 p1067 A70-18287
- Atmospheric thermodynamic properties determined from radar studies of detonation waves from cesium-seeded explosive bursts in lower ionosphere
06 p1012 A70-18542
- Earth magnetosphere physics, considering solar plasma flow, ring currents, charged particles during magnetic storms, solar wind energy transfer, etc
06 p1060 A70-18552
- Tornado producing thunderstorms, using conventional surface and upper air data combined with ATS-III data, discussing mesoscale disturbances and momentum exchange
06 p1102 A70-18583
- Artificial effects on atmosphere and near-earth space caused by human activity, discussing occurrence altitude, means of action and consequences
07 p1262 A70-18778
- Atmospheric characteristics of thermally and chemically stratified layers, discussing ionospheric ion and electron concentrations, radio wave propagation and solar activity and density correlation
07 p1262 A70-18780
- Book on ionospheric physics covering neutral atmosphere, ionospheric measurements, photochemical processes, morphology, phenomena, geomagnetism, storms, etc
07 p1262 A70-18856
- Upper atmospheric horizontal sounding, discussing satellites uses in atmospheric structure studies
07 p1268 A70-19603
- Dust devil wind velocity relationship to environmental parameters including atmospheric temperature, wind direction and vorticity, etc
07 p1269 A70-19948
- Topside ionosphere morphology during IQSY, emphasizing plasma scale height diurnal and latitudinal variations role in satellite data interpretation
07 p1270 A70-20073
- ARCAS meteorological rocket system designed for upper atmospheric soundings to provide thermodynamic and wind data, discussing payloads
07 p1395 A70-20256
- Irreversible phase transition analysis of atmospheric condensation-crystallization processes
08 p1538 A70-21427
- Atmospheric regions interactions concerning stratosphere, mesosphere, troposphere, etc, noting solar activity effects
08 p1490 A70-21428
- Clear air turbulence significance in aviation and atmospheric science, noting Kelvin-Helmholtz model
08 p1539 A70-21559
- Photometric profiles of Jupiter shadows cast by large natural satellites used as upper atmosphere probes
08 p1579 A70-21571
- Atmospheric extinction observed photometrically in South Africa and southern France in narrow bands and astronomical UVB bands
08 p1490 A70-21647
- Global atmospheric research program data requirements analysis based on two level numerical model
08 p1539 A70-21650
- Atmospheric boundary layer wind and temperature analysis according to similarity scheme for mathematical modeling of atmosphere
08 p1540 A70-21974
- Soviet monograph on growth rate of coagulating and condensing aerosol particles, considering kinetic theory
09 p1713 A70-22205
- Free atmosphere clear air turbulence, discussing velocity and temperature spectra, Kelvin-Helmholtz instability, isentropic cross sections, energy budget, etc
09 p1714 A70-22354
- Atmospheric structure and turbulence relations to radar backscattering from clear air refractive index irregularities
09 p1715 A70-22361
- Atmospheric fine-scale structure determination from forward scatter radio wave propagation, considering refractive index role
09 p1715 A70-22362
- Dynamics dominant on different scales in atmosphere by spectral analysis, showing marked gap under most synoptic conditions
09 p1717 A70-22376
- Laminar-turbulent regions boundary, discussing convective layer form and FM-CW microwave and acoustic radar measurement techniques
09 p1717 A70-22378
- Atmospheric condensation nuclei activity with rough surface with decreasing spherical hollows
09 p1718 A70-23172
- Friction and orography influence on wave motions in real atmosphere, discussing planetary boundary layer and propagation in free atmosphere
09 p1718 A70-23331
- Management planning for global atmospheric research program /GARP/ applied to climatology and weather forecasting
09 p1795 A70-23545
- Similarity and dimensionality theory applied to large scale motions in atmospheric circulation of Mars and Venus
10 p1939 A70-24269
- Soviet book on physics of atmosphere covering composition, structure, circulation, cloud formation, precipitation, boundary layer kinematics, etc
10 p1912 A70-24377
- Ion mobility estimates for air constituents, considering ion-neutral elastic and resonant charge exchange collisions
10 p1919 A70-24427
- Solar and solar system planetary atmospheres including interplanetary space filled with solar wind
10 p1942 A70-24611
- Radiative transfer in inhomogeneous atmospheres using simplified matrix equations in perturbation method
10 p1933 A70-24984
- Air and solar activity electrical parameters relationship, observing ionizing radiation increase in upper atmosphere during solar activity
10 p1885 A70-25268
- Earth atmosphere circulation mechanisms, discussing zonal and meridional components and eddy motions
11 p2075 A70-26030
- Pressure gradient, wind structure and shearing stress in atmospheric boundary layer related by formulation based on quasi-parallelism and boundary condition at Ekman layer top
11 p2076 A70-26071
- Stochastic dynamic prediction assuming deterministic laws for atmospheric behavior while seeking solutions corresponding to probabilistic statements of initial conditions
11 p2076 A70-26497
- Atmospheric stability sensing by millimeter wave radiometry, discussing thermal radiation emitted and absorbed by oxygen molecules
12 p2263 A70-26955
- Book on space physics covering earth radiation belts, atmosphere, ionosphere, and magnetosphere, solar structure and composition, interplanetary space, etc
12 p2309 A70-27973
- Atmospheric activity centers movements dependence on latitudinal variation of deformation force horizontal component, noting earth poles motion
12 p2265 A70-28224
- Laser radar systems for atmospheric structure, conditions and processes, discussing clouds delineation, thermal stratification and smoke diffusion and transport
13 p2425 A70-28787
- Stable auroral red /SAR/ arc alignment-movement relationship, suggesting dominant local time control
13 p2397 A70-29193
- Precision radiometry of electromagnetic energy transfer in atmospheric and space physics emphasizing solar and terrestrial radiative fluxes measurements
13 p2409 A70-29652
- H and He intraatmospheric migration and dissipation, considering MHD waves, ionospheric plasma motions, chemical reactions, etc
14 p2569 A70-30211
- Magnetospheric dynamic processes leading to energetic and thermal auroras in middle latitudes
14 p2581 A70-31267
- Ionospheric structure characteristics in D, intermediate D-E and E-F 2 regions using deflecting and nondeflecting radiation absorption measurements
15 p2730 A70-32085

- Planetary atmospheres parameters use in spacecraft guidance 15 p2773 A70-32267
- Atmospheric structure studies using lidar method to detect particulate content in clear air 16 p2862 A70-33014
- Laser Raman scatter process applied to atmospheric probing 16 p2925 A70-33017
- Soviet collection of papers on atmospheric optics covering transmittance, sky brightness, dust component, etc 16 p2899 A70-34176
- Atmospheric optical properties stability determination for various optical densities, assuming horizontally homogeneous medium with properties constant during observation 16 p2899 A70-34181
- Automatic spectroelectrophotometer for measuring sky spectrum brightness at 6910-4040 Å, determining point of minimum brightness 16 p2899 A70-34182
- Long and short period internal gravity waves in atmosphere observed by high resolution radar, investigating generation mechanisms 17 p3075 A70-34609
- Charge source density during interaction between atmosphere and electron/proton fluxes at prescribed boundary parameters 18 p3307 A70-36178
- Unperturbed atmospheric parameters calculation from surface measurements of blunt body at hypersonic speeds under various aerodynamic conditions 18 p3247 A70-36181
- Optical observation of structure, composition, thermal spectra and aerosol layers of giant planet atmospheres 18 p3315 A70-36601
- Soviet papers on physical processes in earth upper atmosphere covering emissions, dust, particle distribution, Rayleigh scattering, temperature, inhomogeneities, etc 18 p3250 A70-36976
- Time and altitude dependences between 340-1000 km of delta parameter for height scale ratio of neutral and electron-ion gases, discussing diffusion coefficient 18 p3254 A70-37030
- Atmospheric Coulomb interaction influence on longitude dependence of electron intensity in anomaly region 19 p3491 A70-37305
- Atmospheric inhomogeneity, comparing effective mass and Curtis-Godson approximation methods for transfer function of absorbing gas distribution 19 p3461 A70-37632
- Upper atmosphere wind, density, temperature and pressure from Soviet meteor data 19 p3412 A70-37651
- Atmospheric energy flow cycle involving large scale circulation components measured by wave number around latitude circles, using equations for closed global system 19 p3415 A70-38416
- Soviet papers on actinometry, atmospheric optics and ozonometry 20 p3624 A70-39026
- Lidar technique for remote detection and mapping of atmosphere based on weather radar and optical scattering concepts 20 p3660 A70-39079
- Soviet papers on planetary atmosphere dynamics and hydrodynamic long range weather forecasting covering atmospheric motions, wind field, model, etc 20 p3661 A70-39176
- Soviet book on ionospheric interlayer formations covering electron concentration distribution, E-2 layer occurrence frequency, recombination coefficient, etc 20 p3622 A70-39823
- Atmospheric studies application to satellite transmissions - USAF Conference, Boston, September 1969 20 p3589 A70-40476
- Remote sensing of atmosphere with emphasis on earth orbiting operational and research satellites 21 p3785 A70-40801
- Cloudy planetary atmospheres model, assessing nonlocal thermodynamic equilibrium role 21 p3813 A70-40903
- Lower thermosphere minor gaseous constituents vertical transport by nonlinear gravity wave process, showing density scale height decrease from diffusive equilibrium 21 p3818 A70-41098
- Global atmospheric electrical structure, considering emf from thermally driven tidal motions in lower atmosphere 22 p4016 A70-42783
- Plasma vortices during electrodynamic distortion of curved copper wire exploding in atmospheric air, using shadowgraphs 22 p4081 A70-42807
- Winter predawn enhancement of 6300 Å airglow at higher midlatitudes, considering roles of oxygen dissociative recombination and photoelectrons production at magnetically conjugate point 22 p4019 A70-43110
- Predawn enhancement of O I 6300 Å line, considering magnetically conjugate photoelectrons effects on atomic oxygen excitation 22 p4095 A70-43113
- Plastic balloon platforms for atmospheric research and engineering applications, discussing design and use of unreinforced polyethylene and reinforced Mylar types 22 p3962 A70-43650
- Relaxation method for inverse radiative transfer equation solution, determining temperature profiles and atmospheric parameters 23 p4214 A70-44036
- Venus atmospheric parameters from microwave spectrum, discussing brightness temperature, carbon dioxide content, opacity, water vapor, dust and models 23 p4241 A70-44256
- Perfect gas statistical relations by perturbation form of state equation for atmosphere 24 p4372 A70-46071
- VHF and UHF radio field strength changes due to tropospheric reflecting layers disintegration during anticyclonic weather, using ray tracing technique 24 p4315 A70-46153
- H and He intraatmospheric migration and dissipation, considering MHD waves, ionospheric plasma motions, chemical reactions, etc 24 p4331 A70-46286
- ATMOSPHERIC PRESSURE**
- Book on subatmospheric decompression sickness in man, covering raised intrapulmonary pressure effects and compensating pressure applications [AGARDOGRAPH-125] 01 p0019 A70-10514
- Microbarographic oscillations associated with geomagnetic activity during observation of infrasonic waves on geomagnetically disturbed days 01 p0081 A70-11298
- Venusian atmospheric pressure and temperature measurements by Venera 4 probe, noting agreement with Mariner 5 observations 01 p0192 A70-11505
- Aeronomy of Jovian upper atmosphere at pressures below 25 mb, discussing stratospheric heat sources, thermal emissivity, photochemistry of methane, ammonia, etc 02 p0366 A70-11804
- Pressure and line width estimate from high resolution image tube spectra of Jupiter at 11,000 Å 02 p0366 A70-11808
- Ammonia red and green bands measured line positions, strengths and half widths applied to Jupiter atmospheric pressure determination 02 p0368 A70-11821
- Nonequilibrium potassium seeded Ar plasma electrical conductivity at atmospheric pressure, noting current density role 02 p0347 A70-12232
- Pressure changes in troposphere and lower stratosphere after strong solar flares analyzed statistically for Northern Hemisphere 03 p0476 A70-13909
- Tropospheric periodic responses to chromospheric flares, analyzing stations atmospheric pressure power spectra 04 p0742 A70-15524
- Periodic observation errors in air temperature, relative humidity, vapor and air pressure 05 p0879 A70-16665
- Solar daily atmospheric oscillations from pressure, wind and temperature recordings at ground level, discussing seasonal and worldwide variations of daily component 06 p1053 A70-17307
- Atmospheric pressure measuring device based on hypsometer and mercury barometer principles for automatic weather stations or remote readout 06 p1066 A70-18247
- Atmospheric pressure, optical thickness and Young particle size distribution of Mars atmosphere determined from polarization observations 07 p1385 A70-19421
- Barometric and atmospheric temperature corrections of cosmic ray neutron component intensity fluctuations obtained statistically from monitor recording 07 p1366 A70-19430
- Combustion of pure crystalline boron single particles injected into hot oxidizing gases streams at atmospheric pressure 07 p1359 A70-19583
- Temperature dependence of viscosity coefficient determined for hydrogen, helium, argon and nitrogen at atmospheric pressure using capillary viscometry 07 p1424 A70-19980
- Atmospheric ground pressure seasonal changes after corpuscular flux arrival shown for Northern Hemisphere 08 p1487 A70-20554
- Thermal conductivity for organic compound gases at atmospheric pressure 08 p1597 A70-21026
- Atmospheric pressure-diameter relationship of common carotid artery in head and neck region of conscious men 08 p1447 A70-21508
- Atmospheric pressure waves generated by high energy disturbance in South Pacific, using ionospheric Doppler signals correlated with ground-level pressure signals 08 p1490 A70-21646
- Physiological mechanism and differentiation of altobaric vertigo in flyers 08 p1449 A70-21947
- State equation for entropy of dissociated air with enthalpy and pressure as independent variables for calculating gas dynamic processes on computers 10 p1966 A70-23839
- Neutron monitor air pressure attenuation coefficient dependent on neutron energy being recorded 10 p1889 A70-24491
- Field strength correlation with micropressure variations caused by internal gravity waves propagating in lower troposphere 10 p1883 A70-25252
- Extraterrestrial electrical and magnetic fields effect on meteorological observations, noting relationship between atmospheric pressure distribution and ionospheric developments 10 p1913 A70-25269
- Lunar semidiurnal tidal oscillations of surface pressure in atmosphere, observing constant amplitude with maximum and minimum phase lag variations 11 p2045 A70-25645
- Atmospheric pressure variations as function of vertical movements caused by friction and orography, considering numerical forecasting 11 p2076 A70-26073
- Atmospheric temperature and pressure profiles remote measurement using airborne microwave radiometer 11 p2056 A70-26502
- Hematologic responses of mice subjected to continuous hypoxia in subatmospheric pressure 11 p1989 A70-26666
- Air pressure, air density and gravity tables, including corrections for mercury barometer measurements 12 p2222 A70-27008
- Shape and location error separation in deterministic predictions of meteorological scalar fields, considering air pressure system forecasting 13 p2445 A70-28995
- Human respiratory responses to gas mixtures with different oxygen content under rarefied atmospheric conditions 13 p2353 A70-29521
- Monograph on troposphere pressure, temperature and humidity and satellite TV photographs interpretation 13 p2446 A70-29786
- Temperature, pressure and density extremes between 30 and 80 km, extrapolating estimates to all latitudes 14 p2608 A70-30591
- Mesoscale slope limits in constant pressure surfaces relation to g-forces on aircraft at SST altitude, using radiosonde measurements 14 p2530 A70-30607
- Venus atmosphere data from Venera 4, 5 and 6 and Mariner 5 missions covering chemical composition, density, pressure, temperature gradients, etc 14 p2646 A70-31067
- Mariner 6 radio signals frequency changes analysis during occultation measurement for determining Mars surface pressure and temperature 14 p2646 A70-31071
- Numerical modeling for earth atmosphere in terms of six pressure levels using digital computers 14 p2577 A70-31151
- Mars carbon dioxide abundance and surface pressure from growth curve based on high resolution spectra 14 p2650 A70-31218
- Stabilized balloon flights during weak winds in stratosphere, discussing pressure vs time curves 14 p2531 A70-31311
- Ionospheric and ground level pressure fluctuations correlation from atmospheric models, suggesting ionospheric disturbance measurement from microbarographs on land surface 15 p2769 A70-31446
- Mariner 6/7 S band radio occultation probe of Mars atmosphere concerning surface pressure, temperature and existence of ionosphere 15 p2798 A70-31681
- Venus lower atmosphere models, discussing pressure, temperature and water vapor abundance based on radio and radar astronomy and spacecraft measurements 15 p2798 A70-31684
- Hematologic changes in mice associated with meningovirus infection and hypobaric hypoxia during barometric pressure changes 15 p2681 A70-31878
- Air mass climatology in terms of pressure temperature and moisture content 15 p2772 A70-32457

Upper troposphere pressure variations through 20 km separation layer, noting interdiurnal temperature changes

15 p2772 A70-32458

Lunar atmospheric pressure based on twilight horizon photographic data from Surveyor 7

15 p2803 A70-32500

Atmospheric ground pressure seasonal changes after corpuscular flux arrival shown for Northern Hemisphere

15 p2732 A70-32709

Carbon dioxide laser action at 10.6 micrometers at pressures up to atmospheric by transverse electrical discharges

16 p2928 A70-33643

Nongray radiant heat transfer corrections to thermal conductivity measurements for water vapor at atmospheric pressure

16 p3003 A70-34200

Zero pressure balloon as base for stratopause pressure and temperature measurements, analyzing winds and balloon trajectory and dynamics

17 p3075 A70-34608

Magnetic fields effect on probe measurements in weakly ionized Ar plasma flow at atmospheric pressure

17 p3139 A70-34693

Barometric pressure reduction effect on gaseous and volatile metabolic products elimination in men wearing oxygen-supplied rubberized suits

17 p3038 A70-35363

Barometric and atmospheric temperature corrections of cosmic ray neutron component intensity fluctuations obtained statistically from monitor recording

18 p3309 A70-36904

Venus lower atmosphere structure and brightness temperature spectrum analysis for composition, temperature and pressure profiles

18 p3323 A70-37139

Mars surface smoothness from photometric and space probe data for atmospheric optical thickness and surface barometric pressure

19 p3512 A70-37300

Solar activity sudden perturbations effect on earth pressure field and atmospheric circulation

19 p3460 A70-37315

Venus atmospheric temperature, pressure and density measurements by Venera 5 and 6 space probes, developing model

19 p3520 A70-38255

Lunar tidal components in atmospheric pressure for various observatories, discussing seasonal variations

20 p3661 A70-39142

Earth surface pressure changes related to PCA of high energy protons

20 p3695 A70-39187

Twenty two year solar activity cycle effect on earth climate, plotting odd and even 11 year cycle curves for pressure and temperature

20 p3662 A70-39189

Curvilinear motion centrifugal force compared with barometric gradient force in symmetrical cyclone, establishing clockwise direction motion possibility

20 p3663 A70-39275

Cosmic ray neutron component differential and integral barometric coefficients, showing dependence on geomagnetic cutoff rigidity and atmospheric depth

20 p3697 A70-39290

Cosmic ray beta neutron component barometric coefficients planetary distribution during IQSY, establishing latitude dependence for mountain and sea level equations

20 p3697 A70-39292

Sinusoidal vibrations effects on rats at different air pressures, discussing human vibration tolerances and resonant frequencies of thoraco-abdominal system

20 p3572 A70-39434

Lunar atmospheric pressure based on twilight horizon photographic data from Surveyor 7

23 p4240 A70-43921

Upper atmosphere tidal pressure and wind variations from meteor trail drift data

23 p4215 A70-44266

Human body heat production and transfer through convection, radiation and evaporation under normal and reduced atmospheric pressure

23 p4154 A70-44654

Atmospheric pressure Ar plasma viscosity measured over heavy particle temperature range 3500-8500 K, using DC wall stabilized cylindrical arc

23 p4229 A70-44983

Orography and friction effects on numerical forecast of atmospheric pressure variation

24 p4370 A70-45112

Neutral air winds in ionospheric F region for asymmetric global pressure system, including ion velocity correction

24 p4329 A70-45356

Radioonde errors in temperature and pressure height determination using paired AN/GMD-1 probe flights

24 p4371 A70-46047

Atmospheric pressure surface sharp slopes at SST altitudes producing vertical acceleration based on temperature gradients inspection

24 p4372 A70-46050

Circuit design providing thermal compensation for atmospheric pressure sensor, using mercury barometer

24 p4340 A70-46403

ATMOSPHERIC RADIATION

NT AIRGLOW

NT AURORAL ARCS

NT AURORAS

NT DAWN CHORUS

NT DAYGLOW

NT GEOCORONAL EMISSIONS

NT IONOSPHERIC NOISE

NT NIGHTGLOW

NT RADIO AURORAS

NT RED ARCS

NT SKY RADIATION

NT STRATOSPHERIC RADIATION

NT TROPOSPHERIC RADIATION

NT TWILIGHT GLOW

NT WHISTLERS

Characteristic X radiation intensity in atmosphere calculated using irradiating electrons spatial and energy distribution data

02 p0358 A70-12156

VLF observations of auroral beams for auroral V-emissions source and characteristics, explaining spectral shape

02 p0291 A70-12204

Jovian atmosphere photometric activity determination, showing time variation and difference in strength between Northern and Southern Hemisphere

02 p0375 A70-12430

Health hazards and physiological effects of atmospheric infrasonic waves, discussing sources, ear protecting devices and electrochemical detectors

02 p0247 A70-12467

Diffraction correction of terrestrial, atmospheric and cosmic background radiation at aperture and disk determined by artificial moon method

03 p0442 A70-13084

Soviet collection of papers on radiation fluxes and ozone in atmosphere covering concentration, UV radiation scattering, etc

03 p0473 A70-13293

D-2 experiments measuring atomic oxygen emission from terrestrial atmosphere and polarization rate and emission intensity from geocoronal hydrogen

03 p0559 A70-13828

Diffusion categories and propagation of radioactive elements in lower atmosphere determined with respect to measured radiation balance, temperature gradient and wind

03 p0521 A70-14290

Rocket-borne cryogenic sampler for stratospheric composition measurement by mass spectrometer analysis for computing radiation balance in stratosphere [AAS PAPER 69-569]

04 p0687 A70-14661

Fast neutron spectrum produced by galactic cosmic ray protons in atmosphere, presenting Monte Carlo transport calculation results

04 p0742 A70-15130

Polarimeter for atmospheric radiation with three optical channels enabling precision measurement of polarization

04 p0695 A70-15573

Line transfer with scattering described by redistribution function numerically solved, using discrete ordinate method

04 p0720 A70-15701

Satellite determination of underlying surface temperature by IR spectroscopy, measuring emitted radiation in atmospheric windows

06 p1061 A70-17205

Heat radiation effect on set-up and scale of cellular convection in atmosphere

06 p1097 A70-17789

Radiating gas flows during hypersonic planetary reentry, discussing atmospheric composition, shock layer characteristics, nonequilibrium flows, etc

06 p0985 A70-18558

Geophysical parameters of atmosphere and underlying surfaces from outgoing thermal radio emission measurements on Cosmos 243 satellite

07 p1261 A70-18724

Cerenkov generation of VLF waves in inner magnetosphere at low latitudes

07 p1265 A70-19281

Atmospheric X ray photons measured regularly by sounding balloons in U.S.S.R., discussing X ray photon flux relation to charged particle fluxes

07 p1367 A70-19445

Radiant energy transport in plane semiinfinite atmosphere with scattering indicatrix and quantum survival probability as arbitrary functions of optical depth

08 p1564 A70-20348

Jupiter atmospheric properties on basis of spectrograms analysis

08 p1569 A70-20833

Thermally emitted photons of atmospheric molecules and aerosols and planetary surface followed

by Monte Carlo method, using anisotropic single scattering functions

09 p1719 A70-23524

High energy electron and gamma quanta flux measurement in atmosphere at different heights by high altitude balloons

09 p1747 A70-23728

Atmospheric ray paths calculations applied to determination of optical air mass and twilight ray paths in earth atmosphere

10 p1873 A70-23830

Atomic oxygen IR emission in earth atmospheric models, using reduction factor for comparison with optically thin atmosphere

10 p1875 A70-24439

Night time upper atmosphere light phenomena and Tungusk meteorite observed on 30 June 1908

10 p1876 A70-24499

IR oxygen emission transmission characteristics in atmosphere compared with ground-based observation

10 p1876 A70-24538

Polarized radiation transfer through inhomogeneous semiinfinite atmosphere by matrix perturbation method, giving nonlinear singular integral equation

10 p1933 A70-24985

Heat radiation effect on set-up and scale of cellular convection in atmosphere

10 p1882 A70-25021

Vertical profiles of daytime and nighttime long wave radiation fluxes in atmosphere under stratus cloud conditions

12 p2264 A70-27521

Nonlinear integral equations of radiation transfer of stellar and planetary atmospheres

12 p2305 A70-27852

Clouds upper height boundary relation with radiation temperature field from satellite data, noting cirrus clouds influence

13 p2444 A70-28589

Auroral currents as source of atmospheric gravity waves and associated traveling ionospheric disturbances

13 p2399 A70-29234

Solar and terrestrial radiation measurements and computations in meteorology, considering diffuse radiation and radiative transfer in atmosphere

13 p2410 A70-29661

Lower and upper atmospheric IR fluxes and equivalent radiation temperatures measurements, describing two- and four-sphere mean radiation temperature /MRT/ meter

13 p2410 A70-29662

Thermal longwave radiation measurement applications to atmospheric radiation transfer and weather processes

13 p2411 A70-29663

Spectral characteristics of secondary emission alloys for photocathodes in extra atmospheric radiation open-type detectors in UV range

14 p2582 A70-30166

Atmospheric molecular oxygen photometric absorption spectral bands, calculating growth curves

14 p2572 A70-30403

Spectrometer model for short wave radiation in atmosphere, measuring sky brightness, polarization and total solar flux

14 p2583 A70-30413

Spectropolarimeter for measurements of polarization characteristics of atmospheric radiation in nanometer range

14 p2583 A70-30414

Night sky atmospheric continuum, zodiacal light and OI line observations with photoelectric color telescope

14 p2581 A70-31268

Radiant energy transport in plane semiinfinite atmosphere with scattering indicatrix and quantum survival probability as arbitrary functions of optical depth

15 p2796 A70-31457

Solar Monitoring Experiment program, observing solar activity relation to large enhancements of lower stratosphere secondary radiation

15 p2792 A70-31656

Plasma temperatures of X ray flux from laser induced breakdown plasmas in air, using absorption spectrometer

15 p2750 A70-31753

Atmospheric radiation and heat fluxes calculations comparison with satellite and ground station actinometric measurements

15 p2770 A70-32067

Spectral line formation in Mars and Venus atmospheres, discussing Lorentz and Doppler broadening

16 p2976 A70-33793

Scattered radiation from plane parallel Mie atmosphere containing spherical particles by Fourier transform method

16 p2952 A70-33983

Meteorological laser radar, discussing basis and techniques determining atmospheric radiation attenuation constant

17 p3045 A70-35106

Upper atmosphere IR emission model with reference to thermal excitation, chemical reactions and electron excitation

18 p3246 A70-36173

Atmospheric X ray photons measured regularly by sounding balloons in U.S.S.R., discussing X ray photon flux relation to charged particle fluxes

18 p3309 A70-36919

Soviet papers on atmospheric radiation processes and satellite meteorology

18 p3285 A70-36962

Simultaneous measurements of earth atmosphere radiation, comparing short and long wave data consistencies at various altitudes

18 p3286 A70-36963

Atmospheric fluorescence observation of supernova energetic photon short pulse burst, using photomultiplier

19 p3500 A70-38079

Soviet book on atmosphere and earth surface radiation characteristics covering absorption, scattering, spectral and angular distributions, radiation field, spatial structure, etc

20 p3661 A70-39171

Atmospheric gamma rays vertical intensity dependence on spectrum and altitude from high altitude balloon studies

20 p3697 A70-39286

Millimeter wave observation of sun, deriving empirical relationships between atmospheric attenuation, emission and water vapor

20 p3623 A70-40304

Spurious photomultiplier response to short intense overexposure of atmospheric return using optical radar

21 p3828 A70-41474

Atmospheric global observation for long term weather forecasts, obtaining cloud photographs and radiation data from satellites

21 p3847 A70-42255

High energy neutrinos generated by cosmic ray interactions with earth atmosphere, discussing detection, plotted energy spectrum and underground muons

22 p4093 A70-42310

Atmospheric scattering governed by Rayleigh phase function with absorption, calculating radiative transfer by numerical solution of Chandrasekhar integral equations

22 p4072 A70-42340

Planetary atmospheres X ray fluorescence, calculating Mercury, Venus, earth, Mars and Jupiter emissions

22 p4105 A70-43230

Earth and atmosphere thermal emission spectra via Nimbus 4 Michelson interferometer, obtaining atmospheric temperature, humidity and ozone profiles

23 p4192 A70-44866

Thermal emission spectra of earth and atmosphere from IR Michelson interferometer onboard Nimbus 3 satellite

24 p4330 A70-45977

ATMOSPHERIC REFRACTION

NT RADIO WAVE REFRACTION

Superrefractive layer development at 3000 ft during radio refractive index profile measurements by microwave refractometer carried on aircraft, producing enhanced signals

02 p0261 A70-12591

Helmholtz integral for radio waves scattering from surfaces expanded for reflection from terrain or atmospheric layers

04 p0648 A70-14964

Large scale ionospheric inhomogeneities anisotropy, dimensions and drift velocities from simultaneously measured irregular refraction

05 p0841 A70-16739

Light refraction in Venusian atmosphere from Venera 4 probe measured data, noting horizontal rays traversing planet along circumference at 8.3 km height

06 p1142 A70-17889

Tropospheric refractive index homogeneity from beam-swinging experiments, noting relationship to meteorological parameters and height

09 p1715 A70-22363

Potential refractive index mean vertical gradients role in turbulent mixing, noting applications to radar detection of CAT

09 p1716 A70-22365

Radar backscattering relationship to refractive index microstructure in turbulent clear atmosphere

09 p1716 A70-22366

Fossil turbulence / three dimensional quasi-isotropic refractive index microstructure left behind during turbulence patch decay/ effects on radio wave propagation

09 p1717 A70-22377

Atmospheric turbulence regarding refractive index fluctuations over UK measured by radio telescope, discussing effects on satellite communication

09 p1667 A70-22384

Geodetic satellite positional problems taking into account parallax refraction

09 p1765 A70-22653

Tropospheric electrical path length estimated by microwave radiometry using atmospheric models

09 p1640 A70-23806

Atmospheric refractive corrections in high accuracy radio interferometry

10 p1890 A70-24649

Atmospheric refractivity role in range errors from ground station to stationary satellite and in range rate measurement

12 p2189 A70-28058

Balloon-borne measurement of troposphere refractive index vertical distribution using spaced-cavity refractometer

13 p2394 A70-28789

Atmospheric difference measurements interpretation in terms of radio refractive index spectra at single point based on corresponding frequency component ratio

13 p2394 A70-28790

Range of ground station to stationary satellite and range rate measurement errors induced by atmospheric refractive index fluctuation

13 p2365 A70-29095

Refraction errors and anomalies effects on satellite observation, using atmospheric model

13 p2449 A70-29275

Balloon-borne optical dew point hygrometer and radiosonde measurements of atmospheric range refractive index

14 p2585 A70-30573

Mars upper atmosphere refractivity, free electron number density and plasma temperature altitude profiles from Mariner 1969 radio occultation measurements

14 p2646 A70-31072

Nonhomogeneous atmosphere with absorbing gas of constant mixing ratio, deriving transmission along isothermal and nonisothermal paths

14 p2617 A70-31304

Methods and equipments for light dispersion measurements for determining atmospheric refraction in terrestrial angle and electrooptical distance measurements

16 p2911 A70-33523

Coherent light propagation through turbulent atmosphere observed by applying He-Ne lasers to simultaneous measurements of scintillation effects over homogeneous optical paths

17 p3108 A70-35721

Atmospheric turbulence effects on light propagation, measuring refractive index variations by high speed temperature sensors

18 p3285 A70-36961

Lower atmosphere refractive index vertical distribution and fluctuations, using airborne refractometer

20 p3619 A70-39191

Millimeter wave and optical astronomical refraction differential measurements, showing dependence on atmospheric water vapor

20 p3588 A70-40305

Coherent beam propagation through turbulent atmosphere, discussing limiting resolving power due to random fluctuations of refractive index

22 p4072 A70-42290

Radar echo superrefraction and subrefraction concepts used with atmospheric waveguide model explaining extremal behavior and relations to atmospheric stratification

23 p4163 A70-44233

Far field power of coherent Cerenkov radio emission from cosmic ray showers in turbulent atmosphere, using radio telescopes

23 p4247 A70-44791

Ashen light origin, considering atmospheric refraction of sunlight illuminating dark side of planet

24 p4399 A70-45113

ATMOSPHERIC SCATTERING

NT TROPOSPHERIC SCATTERING

Book on ionospheric scattering effects on long distance radio communication, considering Arctic ionosphere, scatter propagation, modulation, sporadic E, etc

01 p0046 A70-11305

Lorentz absorption line shape computations in radiation scattered by homogeneous planetary atmosphere compared with results for isotropic scattering by van de Hulst similarity relations

02 p0364 A70-11792

Visible radiation reflection, transmission and inside intensities of terrestrial clouds calculated by Monte Carlo program utilizing scattering phase function

02 p0326 A70-12286

Sky brightness distribution data to determine shape of aerosols scattering as function of wavelength

02 p0292 A70-12435

Cloud layer multiple scattering in Jovian atmosphere, discussing influence on Lorentzian contour of planetary absorption lines

03 p0574 A70-13882

Laser beam broadening in atmospheric propagation from Born approximation and Gaussian model, showing no contribution by second scattered field

04 p0701 A70-14963

Atmospheric distortion effect on short laser pulses attributed to aerosols, using real time pulse comparison methods

04 p0701 A70-15020

Signal amplitude and Doppler shift statistical characteristics calculated from sounding data on scattering at lower ionospheric discontinuities

04 p0650 A70-15284

Line transfer with scattering described by redistribution function numerically solved, using discrete ordinate method

04 p0720 A70-15701

Laser atmospheric backscatter measurements using frequency shifted Raman scatter and Rayleigh components for separating returns due to gaseous and aerosol components

05 p0859 A70-16476

Radiation scattering during upper cloud altitude determination by satellite

06 p1097 A70-17790

Polarization level of outgoing short wave radiation calculated along solar vertical in aerosol containing multiply scattering atmosphere

06 p1097 A70-17829

Atmospheric difficulties in earth surface remote sensing by satellites, describing absorption, emission and scattering as wavelength functions [AIAA PAPER 70-193]

06 p1057 A70-18083

Rayleigh phase matrix solutions and albedo values for imperfect Rayleigh scattering in semiinfinite planetary atmosphere

06 p1149 A70-18460

Visibility, atmospheric light scattering coefficient and aerosol mass concentration related by integrating nephelometer measurements

07 p1328 A70-18923

Diffuse radiation intensity determination in finite optical thickness atmosphere illuminated by parallel light beams

07 p1389 A70-20204

Radiant energy transport in plane semiinfinite atmosphere with scattering indicatrix and quantum survival probability as arbitrary functions of optical depth

08 p1564 A70-20548

Solar radiation reflection function for plane-parallel atmosphere with isotropic phase function calculated by successive scattering method, noting application to planetary atmospheres

08 p1571 A70-20909

Absorption lines in hazy planetary atmosphere with isotropic scattering, examining phase variations of equivalent width

08 p1571 A70-20910

OI 6300 A airglow intensity decrease at dawn ascribed to scattered solar radiation

08 p1492 A70-21720

Atmospheric water vapor profiles remote measurements using Raman component of high powered Q switched laser backscatter

10 p1886 A70-23938

Polydisperse dielectric system distribution parameters determined from hard monochromatic polarized radiation scatter by artificial aerosols

10 p1916 A70-24500

Radiation scattering during upper cloud altitude determination by satellite

10 p1913 A70-25022

Light scattering, turbulent disturbances and absorption by binary oxygen complexes in atmospheric layers

10 p1843 A70-25126

Digital computer simulation of Bake concept as related to tropospheric CW signal scatter measurement

11 p2009 A70-26240

Radio wave scattering cross section in wake of body moving in ionosphere, using simplified procedure with asymptotic expressions

11 p2012 A70-26787

Solar radiation transmitted and reflected by earth atmosphere, solving absorption and scattering by computer programs

12 p2262 A70-26951

Scattering particle distribution relation to halo formation in polydisperse clouds, using Kirchhoff approximation for halos theory construction

12 p2264 A70-27522

Ionospheric parameters measurements by incoherent RF scattering, discussing current status of theory and observations

12 p2225 A70-27738

Electromagnetic wave scattering from atmospheric ellipsoidal plasma formations, using arbitrary permittivity and magnetic permeability tensors

13 p2366 A70-29376

Circumsolar sky radiation effect on pyrheliometric measurements, considering atmospheric scattering and turbidity

13 p2400 A70-29660

Atmospheric absorption, scattering and turbulence effect on visible and IR radiation propagation, discussing optical systems performance

14 p2583 A70-30399

Field characteristics of solar radiation reflected and scattered into outer space by earth atmosphere,

discussing brightness and angular distribution of outgoing component

14 p2603 A70-30406

Side scattered light effects on atmospheric transmittance measurements, showing influence on total receiver illumination

14 p2603 A70-30411

Laser radar measurements for atmospheric scattering properties, observing aerosol content, atmospheric density and composition

14 p2550 A70-30746

Venus carbon dioxide absorption bands determining atmospheric scattering model suitability for all data

14 p2642 A70-30889

Polarization role in radiation scattering by planetary atmosphere, considering luminance variation and Rayleigh scattering

14 p2651 A70-31302

Diffusely transmitted and reflected radiation fields for planetary isotropically scattering atmosphere bounded by Lambert law reflector

14 p2617 A70-31305

Radiant energy transport in plane semiinfinite atmosphere with scattering indicatrix and quantum survival probability as arbitrary functions of optical depth

15 p2796 A70-31457

Milne problem for anisotropic atmospheric scattering, determining radiation transmission at particular angle with arbitrary scattering indicatrices and particle albedo

15 p2801 A70-32477

Bistatic lidar /laser radar/ detection of atmospheric aerosol size distribution, using angular scattering measurements of polarization parameters

15 p2704 A70-32609

Twilight colorimetry from horizon spectra obtained by Soyuz 5, computing chromaticity coefficients for purely scattering molecular atmosphere

16 p2896 A70-33260

Isotropic scattering of radiation from asymmetric spherical source in finite atmosphere

17 p3136 A70-35598

Integral equation for three dimensional Fourier transform applied to isotropic scattering of radiation from point source in finite spheroidal atmosphere

17 p3137 A70-35599

Solar and IR radiation distribution in multiple scattering and absorbing ground fog, obtaining intensities, fluxes and vertical divergence

18 p3284 A70-35943

Sky brightness scattering indicatrix in effective atmospheric layer free from underlying surface multiple scattering and reflection distortions

18 p3248 A70-36634

Rayleigh scattering in atmosphere, determining brightness dependence on altitude, latitude and season

18 p3251 A70-36979

Atmospheric particle distribution spectrum by optical methods, estimating aerosol concentration from scattering coefficient

18 p3251 A70-36980

Magnetosphere dynamics relationship with inhomogeneous electron density formation in F region, discussing scattering diurnal variations and intensity in magnetically conjugate points

18 p3255 A70-37035

F layer scattering and earth electromagnetic field short period oscillations, relating electron density with pearl micropulsations amplitude and occurrence

18 p3255 A70-37036

Atmospheric scattering indicatrices from daytime sky brightness balloon measurements in presence of cloud cover

19 p3460 A70-37420

Optical properties of system measuring atmospheric transmittance by recording light backscattered from atmospheric layers

20 p3660 A70-39033

Book on molecular and aerosol backscatter measurement from stratosphere by means of ground based laser beams

20 p3623 A70-39925

Atmospheric scattering governed by Rayleigh phase function with absorption, calculating radiative transfer by numerical solution of Chandrasekhar integral equations

22 p4072 A70-42340

Milne problem for anisotropic atmospheric scattering, determining radiation transmission at particular angle with arbitrary scattering indicatrices and particle albedo

23 p4239 A70-43902

Daytime near horizon atmospheric luminescence measurement by Cosmos 224 satellite, discussing contributions of nitrogen and aerosol and Rayleigh scatterings

23 p4188 A70-44061

Radiative transfer equation solution for polarized light in Rayleigh scattering atmosphere with absorption, using singular eigenfunction expansion technique

23 p4219 A70-44402

Absorption line multiple scattering in thick planetary atmosphere, using successive scattering method for

single-scattering phase function based on line profile and equivalent width

23 p4222 A70-44550

Linear polarization of sunlight scattered by Venus atmosphere, giving data for integrated disk and equatorial region

23 p4246 A70-44756

Laser light pulse reflection by atmospheric boundary layer calculated on computer by Monte Carlo method, comparing results with full scale measurement

23 p4166 A70-45072

ATMOSPHERIC SHELLS

U ATMOSPHERIC STRATIFICATION

Clear air layer type radar echoes intensities compared with refractive index variations in troposphere

01 p0043 A70-10331

Focusing factor dependence on range in spherically stratified medium with linearly varying refractive index profile, including earth atmosphere

01 p0142 A70-10490

Turbulence and temperature fluctuations spectral characteristics in thermally stratified atmosphere determined for various wave numbers, using energy and mass transfer functions

01 p0136 A70-11610

Perturbation method developed for linearizing nonlinear singular equation for inhomogeneous stratified atmosphere H-function in theory of radiative transfer

02 p0338 A70-11791

Intermediate air layer optical properties explained by assuming presence of small and large size aerosol particles

02 p0328 A70-12436

Aerosol induced light scattering optical properties in atmospheric boundary layer measured with three photometer setup with He-Ne laser

02 p0328 A70-12437

Uniform stratified layers in equatorial E region determined from Centaur rocket capacitance probe electron density observations, suggesting internal atmospheric gravity waves mechanism

03 p0478 A70-14222

Intermediate ionospheric layer at high latitudes, discussing relationship to geomagnetic and auroral activity and F region continuity

04 p0678 A70-14974

Steady circulation and temperature perturbations in stratified nonrotating ideal gas atmosphere with viscosity and heat conduction

04 p0681 A70-15517

Forbidden Fe II lines and AIO band intensities in long period variable stars confirming stratified models of emitting layers

05 p0907 A70-16031

UV radiation propagation in atmospheric boundary layer, analyzing solar UV background and UV signal attenuation along horizontal path

05 p0882 A70-16241

Lower atmosphere VLF heat turbulence as function of precipitation, indicating atmospheric layers existence for different weather situations

05 p0879 A70-16315

Sonic boom overpressures generated by aircraft level rectilinear flight at supersonic speed in temperature and wind stratified atmosphere, calculating atmospheric correction factor

05 p0794 A70-16411

Optimum rocket climbing regime in dense atmospheric layers, including gravitational acceleration investigation in outside layers

06 p1155 A70-17626

Atmospheric characteristics of thermally and chemically stratified layers, discussing ionospheric ion and electron concentrations, radio wave propagation and solar activity and density correlation

07 p1262 A70-18780

Planetary boundary layer thickness estimation, considering geostrophic wind speed and potential temperature average vertical gradient

07 p1377 A70-18922

Atmospheric regions interactions concerning stratosphere, mesosphere, troposphere, etc, noting solar activity effects

08 p1490 A70-21428

Lee wave theory for two dimensional stratified atmospheric models, noting local intense vertical beam into high stratosphere

08 p1540 A70-21973

Diabatic mean profile forms in atmospheric surface layer, establishing profile relationships based on logarithmic analysis

08 p1540 A70-21973

Matrix multidimensional singular linear integral equation applied to electromagnetic radiation transfer through stratified atmosphere

09 p1711 A70-22349

Tropospheric elevated layers fine structure characteristics by balloon-borne spaced cavity refractometer

09 p1714 A70-22353

Vertical wind profiles, deriving wind shear-layer thickness exponential relationship

09 p1715 A70-22356

Stratified atmosphere boundary layer motions, studying turbulence and internal gravity waves characteristics

09 p1716 A70-22369

Turbulence and internal waves in stably stratified atmosphere and ocean, proposing velocity and temperature spectral behavior model

09 p1716 A70-22370

Intermittency characteristics associated with fine scale structure and motion of atmosphere from data pertaining to various atmospheric layers

09 p1717 A70-22375

Plane acoustic shock wave vertical propagation in gravity-stratified atmosphere with temperature gradient, using homogeneous perturbation velocity [DFVLR-SONDDR-35]

12 p2212 A70-28209

Laser radar systems for atmospheric structure, conditions and processes, discussing clouds delineation, thermal stratification and smoke diffusion and transport

13 p2425 A70-28787

Plane stationary nonlinear problem of air flow over earth surface roughnesses, using three layer atmospheric model

14 p2602 A70-30160

Numerical modeling for earth atmosphere in terms of six pressure levels using digital computers

14 p2577 A70-31151

F I layer formation and ion production rates related to F layer stratification, atomic oxygen, zenith angle and solar activity periods

15 p2730 A70-32086

Tropospheric inhomogeneities properties and wind conditions in relation to lunar limb image deformations

16 p2979 A70-34178

Atmospheric contaminants dispersion simulation in meteorological wind tunnel with capability to simulate thermally stratified boundary layers

17 p3065 A70-34496

Atmospheric boundary layer model, considering air-surface interaction, heat and humidity exchange, wind, temperature and humidity profiles, etc

17 p3132 A70-34667

Empirical autocorrelation functions describing statistical properties of vertical temperature gradients in troposphere and lower stratosphere

17 p3132 A70-35337

Turbulent energy dissipation in lower atmospheric layer on meteorological mast during various temperature stratifications

18 p3247 A70-36627

Ascending long wave radiation brightness from aircraft measurements, observing angular distribution dependence on atmospheric stratification

18 p3287 A70-36970

Wind speed pulsations measurement at atmospheric boundary layer and different heights, analyzing turbulent energy intensity

19 p3463 A70-38757

Meteorological observation on atmospheric boundary layer during winter, determining width and inclination of frontal zones

19 p3463 A70-38758

Secondary flow model for planetary boundary layer, considering flow as finite perturbation

21 p3813 A70-40904

Pressure and temperature effects on large amplitude acoustic pulses propagating in stratified atmosphere

22 p4010 A70-42689

Radar echo superrefraction and subrefraction concepts used with atmospheric waveguide model explaining extremal behavior and relations to atmospheric stratification

23 p4163 A70-44233

Atmospheric horizontal stratification and UV transmittance by signal reflection from satellites

23 p4191 A70-44268

ATMOSPHERIC TEMPERATURE

NT IONOSPHERIC TEMPERATURE

Upper atmosphere temperature lag behind solar decimeter flux 27 day variation maximum attributed to varying solar EUV heating

01 p0070 A70-10404

Stratospheric circulation and temperature variations periodicity, discussing midwinter warmings, polar vortex breakdown and relations to D region anomalies and solar events

01 p0072 A70-10580

Stratospheric temperature changes connection with winter D region absorption changes

01 p0073 A70-10583

Venus upper atmosphere average rotational temperature determined from high dispersion spectroscopic observations of 7883 A carbon dioxide band

01 p0184 A70-10912

Thermospheric structure and variations obtained from satellite drag data analysis, discussing gas density, temperature and atmospheric composition

01 p0077 A70-11203

Exospheric temperature variations by Thompson scatter technique, considering solar and geomagnetic activity effects

01 p0078 A70-11209

- Thermospheric horizontal winds diurnal bulge, discussing maximum density-maximum temperature phase relationship 01 p0078 A70-11210
- Nighttime F layer thickness relations to atmospheric temperature 01 p0078 A70-11211
- Venusian atmospheric pressure and temperature measurements by Venera 4 probe, noting agreement with Mariner 5 observations 01 p0192 A70-11505
- Turbulence and temperature fluctuations spectral characteristics in thermally stratified atmosphere determined for various wave numbers, using energy and mass transfer functions 01 p0136 A70-11610
- Upper atmospheric thermal fluctuations study based on correlation characteristics of rapid thermal perturbations, using linear differential equations 02 p0288 A70-11761
- Model construction for structure of planetary atmospheres, particularly Jupiter, discussing gas pressure, density and temperature relationships 02 p0366 A70-11803
- Jupiter atmosphere temperature and density profiles determined from thermal models based on thermal structure above dense cloud level 02 p0367 A70-11814
- Satellite measurement of mean temperature in atmospheric layers to determine vertical temperature distribution 02 p0291 A70-12279
- Incomplete historical data to infer state of atmosphere based on global circulation model, noting tradeoff of temperature for wind and time for space 02 p0291 A70-12296
- Jovian atmosphere convective energy magnitude determination for various atmospheric thicknesses and temperature gradients 02 p0375 A70-12432
- Statistical analysis of satellite drag data for characteristic time of thermal fluctuations in upper atmosphere caused by soft solar X-rays 03 p0472 A70-13179
- Thermal balance of radiosonde thermometric elements and radiation errors in atmospheric temperature measurements using spectra of radiation fluxes reflected from cloud cover 03 p0557 A70-13297
- Nimbus 3 satellite carrying IR spectrometer to measure spectral radiances and retrieve atmospheric temperature profiles 04 p0675 A70-14393
- Corrections to observed thermistor temperature profiles presented for spherical bead thermistors with long lead or thin film mounting [AAS PAPER 69-568] 04 p0687 A70-14664
- Steady circulation and temperature perturbations in viscosity nonrotating ideal gas atmosphere with viscosity and heat conduction 04 p0681 A70-15517
- Atmospheric temperature gradients above 30 km near sunrise using earth spectral radiance measurements by balloon 04 p0694 A70-15523
- Sonic boom propagation in still atmosphere with vertical temperature gradient, using graphical method of determining rays for aircraft motion 05 p0791 A70-15786
- Isothermal atmospheric temperature effects on extensive air shower characteristics and muon numbers computed at various temperature and observation levels 05 p0898 A70-15945
- Periodic observation errors in air temperature, relative humidity, vapor and air pressure 05 p0879 A70-16665
- Solar daily atmospheric oscillations from pressure, wind and temperature recordings at ground level, discussing seasonal and worldwide variations of daily component 06 p1053 A70-17307
- Thermal sounding of atmosphere from satellites under cloudy conditions, plotting temperature profiles 06 p1097 A70-17787
- Atmospheric temperature vertical profile reconstruction from ascending radiation observations using data regularization 06 p1097 A70-17793
- Wind speed and potential temperature vertical profile in day/night planetary atmospheres estimated by similarity theory of boundary layer parameters 06 p1141 A70-17827
- Thermometric convection coefficients used in automatic meteorological data correction program 06 p1183 A70-18288
- Soviet book on nonperiodic processes in Northern Hemisphere stratosphere, discussing seasonal temperature fields, geopotential and circulation formation 07 p1261 A70-18733
- Atmospheric characteristics of thermally and chemically stratified layers, discussing ionospheric ion and electron concentrations, radio wave propagation and solar activity and density correlation 07 p1262 A70-18780
- Carbon particles formation and growth model for cool variable carbon star atmosphere with sinusoidal carbon star atmosphere with sinusoidal temperature variations 07 p1380 A70-19260
- Short coherent laser radar detection of backscattered signal in measuring Doppler shift due to atmospheric temperature 07 p1297 A70-19368
- Vertical temperature profile diurnal variations of Mars atmosphere using models, noting aerosol influence 07 p1385 A70-19422
- Barometric and atmospheric temperature corrections of cosmic ray neutron component intensity fluctuations obtained statistically from monitor recording 07 p1366 A70-19430
- Height scale of loss coefficient in F 2 region under geomagnetic perturbation at midnight based on electron number profiles, estimating thermosphere temperature 07 p1265 A70-19433
- Atmospheric wind velocity and temperature oscillations measurement using acoustic anemometer, resistance thermometer and multichannel signal spectrum analyzer 07 p1284 A70-19833
- Rocket sounding to obtain thermistor temperature profiles of 30-65 km atmospheric region, discussing error correction equation 07 p1288 A70-20261
- Meteorological rocket sounding data for Eurasia in mean profiles, time and lateral cross sections, discussing temperature and wind variations 07 p1274 A70-20270
- Synoptic changes associated with midwinter 1967-1968 major stratospheric warming, including pressure and wind distributions and temperature maps 07 p1275 A70-20277
- Turbulent thermal flux in Venus atmosphere estimated from amplitude fluctuation dispersion of Venera 4 and Mariner 5 radio signals 07 p1390 A70-20305
- Omegatron mass spectrometer for rocket measurements of molecular nitrogen density and temperature in middle thermosphere 07 p1289 A70-20308
- Cosmic rays effect on atmospheric temperature and wind, discussing planetary distribution of neutron component of radiation intensity 07 p1373 A70-20346
- Kinetic temperature estimate for solar corona based on time profile of type 3 bursts 08 p1565 A70-20565
- Atmospheric temperature measurement by microwave radiometry, considering instrument design for measurements at various barometric levels 08 p1495 A70-21041
- Upper surface roughness of internal st-sc clouds as function of vertical temperature and moisture in overlying inversion layers 08 p1537 A70-21106
- Thermal structure transition of mesosphere at high altitudes from persistent summertime to dynamic wintertime case 08 p1539 A70-21649
- Solar radiation variations effect on earth climate, noting atmospheric transparency role in glaciation on thermal regime 08 p1539 A70-21919
- Troposphere-stratosphere kinetic energy transfer during 1967-1968 midwinter warming, comparing calculation by pressure interaction term with direct calculation of vertical velocity fields 08 p1540 A70-21969
- Atmospheric variables /velocity, temperature, energy, etc/ spectra in lowest few hundred meters 09 p1714 A70-22352
- Atmospheric temperature spectra at low elevation showing consistency with Monin-Obukhov scaling 09 p1715 A70-22358
- Dew-point temperature of lower troposphere by diffusion equation, noting use for fog and strati forecasting 09 p1717 A70-22655
- Drop sondes dynamic and aerodynamic design for lower Venus atmosphere based on solution for free fall of body in atmosphere with constant temperature gradient 09 p1766 A70-22935
- Wind and atmospheric temperature variations on Mars, Venus and Mercury interpreted from observational data in terms of earth atmospheric processes 09 p1762 A70-23127
- Regular yearly pattern variations of zonal circulation index and temperature solved in Legendre polynomials 09 p1718 A70-23330
- Simultaneous Thomson scatter measurements for middle and low latitudes, comparing electron density and temperature and exospheric and global temperature distributions 10 p1872 A70-23821
- Spectroscopic instruments for atmospheric temperature measurements classified in terms of filtering, modulating and multiplexing systems 10 p1873 A70-23828
- Ambient temperature measurement by constant level balloon mounted thermistors, discussing errors from differential heating of thermistor support by solar radiation 10 p1886 A70-23935
- Atmospheric temperature vertical profile reconstruction from ascending radiation observations using data regularization 10 p1913 A70-25024
- Meteorological Nimbus 3 satellite and aircraft observations of thermal radiation for vertical atmospheric temperature profile measurement 11 p2075 A70-25921
- Atmospheric temperature and pressure profiles remote measurement using airborne microwave radiometer 11 p2056 A70-26502
- Remote measurement of CAT associated temperature gradients, comparing monochromatic and finite bandpass models 12 p2262 A70-26949
- Atmospheric temperature determination by satellite IR spectrometer /SIRS-A/, describing data analysis and instrument design, calibration and performance 12 p2263 A70-26954
- Thermal shock waves structure and effective temperature in stellar atmospheres taking into account absorption effects and possible isothermicity 12 p2306 A70-27861
- Statistical analysis of atmospheric wind and temperature variables relationships to high altitude clear air turbulence observed by U-2 flights 12 p2264 A70-28092
- Temperature prediction accuracy over 24-hr period for supersonic transport flight operations 13 p2443 A70-28549
- Lower atmospheric layer temperature and wind vertical distribution effect on wind velocity ratio to geostrophic wind at earth surface 13 p2444 A70-28586
- CAT parameters sensitivity to horizontal wind and temperature distribution 13 p2444 A70-28587
- Oxygen 18 concentration in Greenland ice core correlation to solar activity index, indicating earth temperature control by solar activity 13 p2489 A70-28909
- Stellar upper atmospheric shock wave motion, discussing emission spectra interpretation and temperature gradients 13 p2493 A70-29395
- Upper atmospheric temperature-gravitational potential relationship for sun, earth and several planets 13 p2495 A70-29765
- Monograph on troposphere pressure, temperature and humidity and satellite TV photographs interpretation 13 p2446 A70-29786
- Lower stratosphere temperature and wind periodic variations associated with shear flow gravity waves 14 p2601 A70-30124
- Vertical flux densities of momentum and sensible heat dependence on displacement height and surface roughness 14 p2602 A70-30371
- Static diffusion model of thermosphere with allowance for temperature and chemical composition and not limited by constant 120 km boundary conditions 14 p2606 A70-30560
- Balloon flight measurements clarifying Arcasonde sensor bias over radiosonde atmospheric temperature data 14 p2585 A70-30570
- Fine scale temperature variability along flight path during smooth and turbulent conditions 14 p2609 A70-30605
- Northern Hemisphere temperature atlas for SST cruise altitudes, estimating probabilities of enroute temperatures and risk increase 14 p2609 A70-30609
- Venus atmosphere data from Venera 4, 5 and 6 and Mariner 5 missions covering chemical composition, density, pressure, temperature gradients, etc 14 p2646 A70-31067
- Remote atmospheric temperature profile measurements, analyzing physical processes for radiation detection by earth pointing satellite-borne sensor 14 p2611 A70-31156
- Incoherent scatter observations of atmospheric density and temperature in lower thermosphere, observing seasonal variations 14 p2578 A70-31246
- Temperature and density extreme variations at various levels in stratosphere and mesosphere, analyzing sounding rocket data 15 p2723 A70-31661
- Upper atmosphere density and temperature height profiles perturbations in falling sphere probe 15 p2723 A70-31663

Vertical temperature profiles and global circulation patterns in stratosphere and mesosphere, discussing Northern Hemispheric seasonal, latitudinal and longitudinal variations

15 p2724 A70-31665

Venus lower atmosphere models, discussing pressure, temperature and water vapor abundance based on radio and radar astronomy and spacecraft measurements

15 p2798 A70-31684

Atmospheric vertical temperature sounding from geosynchronous satellite, discussing instrumentation, cloud cover and wind effects, etc

15 p2809 A70-31690

Atmospheric temperature vertical distribution measurement using sounding balloon and Skylark rocket

15 p2725 A70-31846

Rocket and satellite data on upper atmospheric neutral/charged particles, short wave solar radiation, temperature and photochemical reactions

15 p2730 A70-32089

Atmospheric density and temperature measurements by satellite- and rocket-borne pressure gages and mass spectrometers, considering error sources

15 p2731 A70-32092

Air mass climatology in terms of pressure temperature and moisture content

15 p2772 A70-32457

Atmospheric ground layer temperature variations effect on astronomical telescope observations, discussing image motion character and origin

15 p2772 A70-32462

Atmospheric temperature fluctuation spectrum determination by energy budget solution, considering spectral density dependence on Richardson number

15 p2732 A70-32542

Kinetic temperature estimate for solar corona based on time profile of type 3 bursts

15 p2805 A70-32720

Thermal atmospheric sounding from satellites based on Fredholm integral equations, obtaining vertical temperature profiles

16 p2896 A70-33257

Atmospheric temperature and wind data before, during and after solar eclipse of 7 March 1970, using ARCAS meteorological rockets

16 p2977 A70-33828

Zero pressure balloon as base for stratosphere pressure and temperature measurements, analyzing winds and balloon trajectory and dynamics

17 p3075 A70-34608

Upper atmosphere temperatures from vapor cloud diffusion, eliminating errors from bright sky background at twilight

17 p3076 A70-34940

Empirical autocorrelation functions describing statistical properties of vertical temperature gradients in troposphere and lower stratosphere

17 p3132 A70-35337

Satellite-borne instruments for thermal sounding of troposphere, noting information limitation due to atmospheric effects

17 p3132 A70-35338

Ballistical transport in collisionless exosphere, discussing heat flux of ballistical oxygen and model temperatures for day and night conditions

17 p3080 A70-35765

Nimbus 3 satellite-borne Michelson interferometer IR spectrometer for spectrum measurement, obtaining temperature, water vapor and ozone vertical distribution

18 p3257 A70-36175

Earth radiation measurement at 10-12 microns by Cosmos 243 satellite-borne radiometer, comparing temperatures for boundary air layers in cloudless conditions

18 p3247 A70-36630

Barometric and atmospheric temperature corrections of cosmic ray neutron component intensity fluctuations obtained statistically from monitor recording

18 p3309 A70-36904

Height scale of loss coefficient in F2 region under geomagnetic perturbation at midnight based on electron number profiles, estimating thermosphere temperature

18 p3249 A70-36907

Upper atmospheric neutral components temperature determination by rocket-borne mass spectrometers

18 p3252 A70-36983

Atmospheric temperatures from thin walled ballistic rocket surface measurements with high sensitivity photometer

18 p3261 A70-36997

Venus lower atmosphere structure and brightness temperature spectrum analysis for composition, temperature and pressure profiles

18 p3323 A70-37139

Air total temperature measurement for jet powered aircraft, discussing subsonic and supersonic wind tunnel data for sensor thermal recovery characteristics

19 p3425 A70-37882

Venus atmospheric temperature, pressure and density measurements by Venera 5 and 6 space probes, developing model

19 p3520 A70-38255

Annual temperature variation in low stratosphere based on harmonic analyses at 100 mb

19 p3462 A70-38263

Upper atmospheric density and temperature diurnal phase and amplitude discrepancy reconciled by dynamic diffusion model

19 p3414 A70-38381

Free air temperature by onboard satellite IR spectrometer (SIRS), measuring earth spectral radiance in carbon dioxide 15 micrometer band

20 p3660 A70-39077

Solar activity effects on Northern Hemisphere atmospheric temperature, mapping gradients for 11 year solar cycle

20 p3662 A70-39188

Twenty two year solar activity cycle effect on earth climate, plotting odd and even 11 year cycle curves for pressure and temperature

20 p3662 A70-39189

Synoptic processes in troposphere and stratosphere with large air temperature anomalies during early summer in U.S.S.R.

20 p3663 A70-39272

Troposphere and lower stratosphere circulation during natural synoptic autumn seasons in Northern Hemisphere, noting temperature role

20 p3663 A70-39273

Forecasting air temperature over North Atlantic, analyzing atmospheric parameters informativeness

20 p3663 A70-39274

Maximum to minimum exospheric temperature ratio determination, concluding solar wind dependence of diurnal variation in thermosphere

20 p3621 A70-39345

Trace constituent changes effects on stratospheric properties after volcanic eruption, showing prolonged atmospheric temperature increase

20 p3622 A70-39490

Upper atmospheric temperature-gravitational potential relationship for sun, earth and several planets

20 p3710 A70-40090

Atmospheric temperature and water vapor profiles from iterative solution of radiative transfer equation for comparison with spectral radiance observation from Nimbus satellites

21 p3846 A70-40803

Aerosol IR emission, discussing relative humidity, water droplet size and temperature effects on atmospheric radiance levels

21 p3846 A70-40804

Atmospheric temperature profiles from terrestrial IR spectral radiances measured by balloon-borne grating spectrometer, discussing surface temperature variations

21 p3813 A70-40905

Soft X-ray enhancement during solar flares due to coronal condensation temperature increase

21 p3880 A70-40969

Real time global temperature and geopotential height profiles acquisition from satellite spectrometer measurements by least squares regression method

21 p3820 A70-42121

Atmospheric inhomogeneity and temperature gradient effects on sonic booms, discussing displacement, growth rate and shock wave radii refraction

22 p3961 A70-42311

Wind temperature measurement, taking Bernoulli effect and kinetic theory into account

22 p4009 A70-42525

Temperature and height data for synoptic stratospheric evaluation, using Nimbus 3 satellite IR spectrometer

22 p4064 A70-42618

Stratospheric clear air turbulence probability based on vertical temperature gradients and rawinsonde ascensional rates

22 p4064 A70-42619

Convective heat transport role in determining rotating planets climatic temperature zones

22 p4099 A70-42626

Hot air temperature decay, discussing relaxation process of lightning channel behavior

22 p4016 A70-42781

Stratosphere annual temperature cycle amplitude, using biannual daily temperatures over Northern Hemisphere from IQSY data

22 p4018 A70-42913

Lower atmosphere gravity wave motions due to cooling by solar eclipse shadow

23 p4185 A70-43845

Exospheric neutral hydrogen temperature diurnal variation from satellite resonance filter data, suggesting Lyman alpha source external to geocorona

23 p4186 A70-43852

Phase delay between thermospheric neutral temperature and neutral density, considering frequency dependent time response to solar heat input

23 p4187 A70-43858

Atmospheric temperature profiles using Nimbus 4 selective chopper radiometer

23 p4192 A70-44865

Temperature and gust velocity turbulence at tropopause level over hurricane Beulah by instrumented U-2 aircraft

24 p4371 A70-45422

Radiosonde errors in temperature and pressure height determination using paired AN/GMD-1 probe flights

24 p4371 A70-46047

Stratosphere radiation measurements by Nimbus 3 infrared spectrometer for 15 micron frequency, considering temperature variations

24 p4330 A70-46074

Meteorological wind and temperature distributions on selected routes at Concorde cruising level, noting computer use for flight planning

24 p4374 A70-46204

ATMOSPHERIC TIDES

Wind oscillations in stratosphere, lower mesosphere and meteor heights noting periodicities

01 p0074 A70-10591

Seasonal phase changes of semidiurnal tidal wind components in lower ionosphere demonstrated from ionospheric drift measurements

01 p0078 A70-11212

Lunar atmospheric tidal wind semidiurnal variations from Hong Kong and Uppsala data, discussing agreement with theory

02 p0325 A70-12217

Hydromagnetic forces effects on tidal period hydrodynamic waves, explaining ionospheric tidal motion behavior

03 p0478 A70-13995

Lunar tide in E region phase height from measurements of diurnal phase path change for continuous wave

04 p0678 A70-14973

Upper atmosphere wind and semidiurnal and diurnal tide interactions observed by meteor radar, noting relation to gravity waves

05 p0878 A70-15818

Solar daily atmospheric oscillations from pressure, wind and temperature recordings at ground level, discussing seasonal and worldwide variations of daily component

06 p1053 A70-17307

Atmospheric tides influence on meteors characteristics from processing observation data

06 p1140 A70-17736

Atmospheric gravity wave generation, propagation and dissipation, considering stratospheric tides

07 p1275 A70-20276

Lunar semidiurnal tidal oscillations of surface pressure in atmosphere, observing constant amplitude with maximum and minimum phase lag variations

11 p2045 A70-25645

High altitude meteor winds, investigating atmospheric tides and short term wind oscillations, wind shears and drift nature

14 p2601 A70-30122

Tidal forces effect on wind system in lower ionosphere, using Navier-Stokes equation for lower layer and Euler equations for upper layer

14 p2571 A70-30323

Book on thermal and gravitational atmospheric tides covering solar oscillations, lunar air tides, upper air data, ozone radiation absorption, etc

14 p2573 A70-30633

Venus spin-orbit resonance resulting in consistent inferior conjunction with earth, suggesting solar atmosphere tidal influence

14 p2650 A70-31216

Nonlinear diurnal tide and gravity wave interactions at meteor heights below mesopause

14 p2579 A70-31251

Constant altitude helium filled zero pressure polyethylene balloon for stratospheric meteorological data and atmospheric tides studies

17 p3075 A70-34607

Terrestrial atmospheric tidal theory applicability to Venus and Mars, considering dependence on parameters variation among planets

19 p3519 A70-38253

Ionospheric electric current distribution response to horizontal wind induced emf, using lunar tidal wind models

19 p3415 A70-38386

Global atmospheric electrical structure, considering emf from thermally driven tidal motions in lower atmosphere

22 p4016 A70-42783

Upper atmosphere tidal pressure and wind variations from meteor trail drift data

23 p4215 A70-44266

Hough eigenfunctions of lunar diurnal and semidiurnal atmospheric oscillations using matrix and group methods

24 p4328 A70-45351

Tidal forces effect on wind system in lower ionosphere, using Navier-Stokes equation for lower layer and Euler equations for upper layer

24 p4331 A70-46307

ATMOSPHERIC TURBULENCE

NT CLEAR AIR TURBULENCE

NT GUSTS

NT LOW LEVEL TURBULENCE

Vertical wind observations during lower ionosphere wind measurements by Na release method, discussing gravity effects and standing waves

01 p0078 A70-1213

Turbulence and temperature fluctuations spectral characteristics in thermally stratified atmosphere determined for various wave numbers, using energy and mass transfer functions

01 p0136 A70-11610

Atmospheric effects on SST, discussing turbulence, temperature, wind, cloud cover, hail, toxic gases, etc

02 p0325 A70-12218

Atmospheric turbulence effects on accelerations experienced by passengers in supersonic and subsonic transport aircraft compared

02 p0325 A70-12219

Doppler spectrum and radio troposcatter beam swinging in thin homogeneous turbulent scatter layer as function of height, crosswind speed and refractivity

02 p0326 A70-12288

Specular reflections influence on bistatic tropospheric radio scatter from turbulent perturbations in refractivity

02 p0326 A70-12289

Interferential picture visibility in turbulent atmosphere measured at large path differences with Michelson-Twyman-Green interferometer using He-Ne laser radiation source

03 p0498 A70-12869

Lower E region turbulence interpretation based on high resolution photographs of artificial sodium vapor trails

03 p0476 A70-13913

Cyclone waves development during stationary long wave basic state two dimensional quasi-geostrophic two layer model

03 p0521 A70-14288

Unsteady flows effects on aircraft longitudinal motion, flight stability and control, discussing horizontal and vertical effects of rough air

04 p0623 A70-15172

Wind velocity longitudinal profile measurements in atmospheric boundary layer over rough sea surface using floating beacon and statistical analysis of airflow perturbations

04 p0715 A70-15253

Hydromagnetodynamic equations of two dimensional unsteady geostrophic wind field in turbulent ionosphere

04 p0680 A70-15254

Lifting rotor blades flapping response to atmospheric turbulence, discussing time averaging and perturbation schemes

[AIAA PAPER 69-206] 04 p0624 A70-15378

Power spectral density functions of vertical gust velocities, comparing theoretical results and C-141A flight test measurements

04 p0624 A70-15384

Critique of theory of electromagnetic wave transmission in turbulent atmosphere, considering effects of approximation

05 p0811 A70-16044

Karman formula generalization for turbulent motion in atmospheric boundary layer, including improved variant for thermally stable and unstable conditions

05 p0878 A70-16205

Inhomogeneity and water vapor absorption influence on frequency spectrum of amplitude fluctuations of plane wave propagating in turbulent atmosphere

05 p0813 A70-16252

Lower atmosphere VLF heat turbulence as function of precipitation, indicating atmospheric layers existence for different weather situations

05 p0879 A70-16315

Atmospheric turbulence characteristics related to drag loads of tall spacecraft structures by boundary layer wind model

06 p1160 A70-17165

Turbulence characteristic scale for atmospheric boundary layer, using wind profile data

06 p1096 A70-17466

Electromagnetic-acoustic probe for remote wind velocity sensing and radar range performance

06 p1071 A70-18509

Remote sensing of winds and atmospheric turbulence by cross correlation of passive optical signals, discussing results for power spectrum of fluctuations and winds

06 p1072 A70-18553

Sonic boom focalization, considering linear propagation for real atmosphere with wind and Jericho experiments

07 p1193 A70-19130

Turbulent air flow velocities determined in meteor zone of atmosphere

07 p1386 A70-19461

Acoustic piezoceramic anemometer for steady state measurements of wind turbulence on meteorological tower

07 p1285 A70-19835

Turbulent atmosphere circulation measurement over centimeter scale using acoustical transducers

07 p1285 A70-19836

Turbulent energy and velocity spectra of air flow at atmospheric boundary layer over water analyzed statistically, assuming rippling surface activity

07 p1259 A70-19838

Photographic film imagery, degraded by long term artificial atmospheric turbulence, restored by spatial filters placed in Fourier transform plane

07 p1336 A70-20090

Atmospheric turbulence parameters in meteor zone determined from simultaneous photographic and radar observations, determining turbulent diffusion coefficient dependence on height

08 p1563 A70-20546

Turbulence in quiescent prominences relationship to shock waves in upper atmosphere

08 p1570 A70-20840

Vertical motions and turbulent exchange influence on height variation of stratus clouds based on atmospheric moisture and heat transport equations

08 p1537 A70-21103

Turbulence coefficient and profile in atmospheric boundary layer from wind and temperature distribution, obtaining formulas from model approximating coefficient by altitude function

08 p1538 A70-21112

Atmospheric pressure waves generated by high energy disturbance in South Pacific, using ionospheric Doppler signals correlated with ground-level pressure signals

08 p1490 A70-21646

Turbulent transfer mechanism in atmospheric surface layer, analyzing micrometeorological data for flux-gradient relationships, relating turbulent scale to eddy diffusivities

09 p1712 A70-22051

Wind HF inclination variations in lower atmosphere, considering turbulent kinetic energy dissipation and buoyancy production

09 p1714 A70-22355

Turbulent energy spectra in stably stratified atmospheric boundary layer flow

09 p1715 A70-22360

Lower atmosphere turbulence under convective conditions, comparing Doppler radar and instrumented aircraft wind speed fluctuation measurements

09 p1716 A70-22367

Stratified atmosphere boundary layer motions, studying turbulence and internal gravity waves characteristics

09 p1716 A70-22369

Turbulence and internal waves in stably stratified atmosphere and ocean, proposing velocity and temperature spectral behavior model

09 p1716 A70-22370

Stably stratified atmospheric turbulent shear flow governing spectral equations asymptotic solutions for buoyancy subrange

09 p1659 A70-22372

Self similarity concept relevance to atmospheric turbulence demonstrated from ground and airborne observational data

09 p1717 A70-22373

Anisotropic turbulent energy spectral distribution approximated assuming homogeneous and axisymmetric turbulence with vertical axis of symmetry

09 p1717 A70-22374

Atmospheric turbulence regarding refractive index fluctuations over UK measured by radio telescope, discussing effects on satellite communication

09 p1667 A70-22384

Soviet book on flight dynamics in turbulent atmosphere covering air motion, aircraft lateral and longitudinal motion, gust loads, autopilot flight, takeoff and landing

09 p1610 A70-22598

Laser measurements of permittivity fluctuations spectrum of turbulent atmosphere, noting proportionality to temperature spectra at optical frequencies

09 p1635 A70-22962

Coherent optical beam propagation measurement of fine scale turbulent atmosphere structure, inferring microscale size and permittivity spectra

09 p1635 A70-22963

Pulsed laser beams intensity fluctuations correlation functions dependence on propagation distance in turbulent atmosphere

09 p1636 A70-23135

Amplitude measurement of plane light wave propagating in turbulent atmosphere, giving log amplitude dependence on dispersion of logarithm fluctuations

09 p1636 A70-23136

Axial mode gas laser radiation intensity fluctuations for plane and spherical light waves in turbulent atmosphere

09 p1636 A70-23137

Amplitude and phase correlations of spherical waves propagating in turbulent atmosphere using smooth perturbation method

09 p1636 A70-23139

Laser beam intensity fluctuations during propagation through turbulent atmosphere

09 p1637 A70-23142

Microwave signal fading in Venus atmosphere due to turbulence, discussing atmospheric dielectric permittivity variance

09 p1764 A70-23484

Roof prism reversing-front Michelson interferometer for phase correlation measurements in turbulent atmosphere

09 p1684 A70-23535

Atmospheric modulation transfer function measuring instrument based on Lindberg principle, discussing optical and mechanical design features and applications

09 p1688 A70-23769

Boundary layer atmospheric turbulence at Kennedy Space Center obtained for engineering spectral model, discussing energy balance

10 p1911 A70-23926

Vertical wind components from balloon ascent observations, considering drag, atmospheric density, wind velocity, etc

10 p1911 A70-23927

Hot-film anemometers for measuring storm turbulence in presence of heavy rain

10 p1887 A70-23940

Cascade theory of turbulence, applying cascade decomposition resulting from Navier-Stokes application to hydrodynamic turbulence to Riemann equation for atmospheric and plasma turbulence

10 p1868 A70-24167

Focal plane intensity of focused laser beam passed through turbulent atmospheric layer

10 p1901 A70-25160

Geometrical light depolarization in randomly inhomogeneous medium, discussing light propagation in turbulent atmosphere and ionospheric radio propagation

10 p1844 A70-25162

Light aircraft lateral and longitudinal response to atmospheric turbulence, presenting equations and charts for design load calculations

[SAE PAPER 700239] 11 p1981 A70-25908

Large scale atmospheric turbulence using wave number frequency Fourier analysis of velocity distributions on latitude circles

11 p2076 A70-26498

Atmospheric turbulence, discussing transfer of heat, momentum and water vapor from sea and mixture length for analogy theory between molecular and turbulent transfer

11 p2038 A70-26527

Atmospheric turbulent boundary layer velocity signals correlation with lognormal distribution

11 p2076 A70-26531

Solar photospheric turbulence from observing Ti I line profiles at different center to limb distances, showing anisotropy

11 p2116 A70-26591

Atmospheric turbulence effects on line-of-sight electromagnetic wave propagation, deriving signal statistics for nonvalid weak scattering situations case

11 p2012 A70-26764

Remote monitoring of atmospheric wind and turbulence by cross correlation passive techniques, measuring heat and humidity fluxes

12 p2230 A70-26948

Computer plotting of flow patterns and orographic cloud over/in lee wave flow, including rotors, blocking and high level turbulence

12 p2264 A70-27722

Radiation transfer models for diffuse reflection of quanta from turbulent medium applied to electromagnetic wave propagation in turbulent atmosphere

12 p2306 A70-27855

Microwave signals covariance and spectra calculation for amplitude and phase fluctuations propagated over line-of-sight path through turbulent atmosphere

12 p1819 A70-27963

Frequency spectra of log amplitude fluctuations of electromagnetic wave propagating in turbulent atmosphere, using geometrical optics approximation

12 p190 A70-28173

Collection of papers on wind effects on launch vehicles covering aerodynamics, airframes, guidance and control, wind-vehicle interactions, atmospheric turbulence, etc

[AGARDOGRAPH-115] 13 p2504 A70-28751

Spacecraft parameters role in response to atmospheric disturbances, considering model design and control systems effects

[AGARDOGRAPH-115] 13 p2504 A70-28757

Atmospheric turbulence and irregularities, examining classical exchange coefficient and statistical theories

13 p2445 A70-28788

Aircraft dynamic response to homogeneous isotropic atmospheric turbulence analyzed for power spectral density, taking into account spacewise variations in airframe loading

[AIAA PAPER 70-544] 13 p2345 A70-29010

Aircraft turbulence penetration performance numerical rating, applying concept to large subsonic jet transports

[AIAA PAPER 70-543] 13 p2347 A70-29074

Coherence degradation of collimated and focused Gaussian beams in turbulent atmosphere, using small perturbation method

13 p2453 A70-29824

Interferometric measurement of spatial correlation function of optical radiation fields propagating through turbulent atmosphere

13 p2454 A70-29825

High altitude meteor winds, investigating atmospheric tides and short term wind oscillations, wind shears and drift nature

14 p2601 A70-30122

Transverse structural function of velocity field of turbulent motion in upper atmosphere, using meteor speed radio observations

14 p2635 A70-30312

Forward and backscattering meteor radio echo intensity variations during decay under molecular and turbulent diffusion, recombination and trapping

14 p2635 A70-30313

Correlation characteristics of turbulent motions in atmospheric meteor region, discussing diversity and single point reception methods

14 p2572 A70-30329

Variangular wind spirals for vertical wind and shear profile estimation in atmospheric boundary layer

14 p2602 A70-30370

Atmospheric absorption, scattering and turbulence effect on visible and IR radiation propagation, discussing optical systems performance

14 p2583 A70-30399

Mesoscale stratospheric turbulence recording using even activated memory recorder

14 p2573 A70-30578

Atmospheric wind profiles and boundary layer turbulence power spectra for calculation of wind loads on space vehicles during prelaunch and launch

14 p2653 A70-30600

Fine scale temperature variability along flight path during smooth and turbulent conditions

14 p2609 A70-30605

A-type supergiants microturbulence, determining atmospheric small scale velocity fields

14 p2641 A70-30885

Atmospheric turbulence effects on acoustic-gravity waves propagation, deriving dispersion relation for phase velocity and propagation constants

14 p2579 A70-31252

Ionospheric investigation techniques, considering ionization balance, winds and turbulence

14 p2580 A70-31259

Atmospheric turbulence parameters in meteor zone determined from simultaneous photographic and radar observations, determining turbulent diffusion coefficient dependence on height

15 p2796 A70-31455

Upper atmosphere turbulence spectra of passive contaminants deposited by rockets from radiometrically calibrated photographs of chemical trails

15 p2725 A70-31688

Kinetic energy turbulence spectrum in free atmosphere from rawinsonde and aircraft data

15 p0000 A70-32369

Atmospheric turbulence effects on optical communication systems in geosciences

16 p2900 A70-33019

Aerodynamic admittance of paraboloid dish aerial in scaled atmospheric turbulent boundary shear layer simulated in wind tunnel by vortex generators

16 p2878 A70-33766

German monograph on atmospheric turbulence by Rn 220 as tracer, relating concentration to various meteorological parameters

16 p2946 A70-34080

Atmospheric optical inhomogeneity effect on image quality, investigating deflection angles for spherical light wave passage at various altitudes

16 p2915 A70-34215

Richardson turbulence criterion computation from measurements during and after winter anomaly

17 p3077 A70-34945

Coherent light propagation through turbulent atmosphere observed by applying He-Ne lasers to simultaneous measurements of scintillation effects over homogeneous optical paths

17 p3108 A70-35721

Turbulent energy dissipation in lower atmospheric layer on meteorological mast during various temperature stratifications

18 p3247 A70-36627

Turbulent air flow velocities determined in meteor zone of atmosphere

18 p3316 A70-36935

Atmospheric turbulence effects on light propagation, measuring refractive index variations by high speed temperature sensors

18 p3285 A70-36961

Lagrange time scale of air turbulence from photographic measurements of smoke aerosol particle dispersion in horizontal direction across mean wind

19 p3460 A70-37416

Free atmosphere turbulent diffusion coefficient determination, releasing dipole reflectors from helicopter for radio echo observation

19 p3461 A70-37423

Atmospheric turbulence vertical component spectral density observation by aircraft in steady flight, considering transfer function computation methods

19 p3351 A70-37646

Atmospheric turbulence scale and dissipation from 80 to 120 km, using photographic observations of Leonid meteor trails

19 p3515 A70-37663

Laser radar tracking systems, calculating atmospheric turbulence effects on angular errors

19 p3379 A70-37857

Wind speed pulsations measurement at atmospheric boundary layer and different heights, analyzing turbulent energy intensity

19 p3463 A70-38757

Characteristic dimensions of large and small scale atmospheric turbulence by meteor trails photographic observations, determining energy dissipation

19 p3526 A70-38790

Pulsed laser lidar measurements of atmospheric turbidity, diffusion, pollution, visibility and cloud physics

20 p3584 A70-39127

Probability densities and distributions, moments and spectra from time derivatives of streamwise velocity fluctuation in curved mixing layer, measuring small scale turbulence structure

20 p3609 A70-39652

Invariant autopilot control system during flight in turbulent atmosphere, allowing for aircraft elastic properties and invariance of coordinates

20 p3561 A70-39845

Longitudinal and vertical wind components turbulent fluctuations distribution skewness relationship to atmospheric stability and height, noting effect on diffusion

20 p3664 A70-40064

Airborne atmospheric turbulent flux measurement system with fast response wind velocity, temperature, humidity and aircraft motion sensors, discussing performance and data reduction

20 p3665 A70-40109

Atmospheric turbulence and wind velocity remote probing by millimeter waves, comparing results with conventional anemometer measurement

20 p3665 A70-40306

Acoustic piezoceramic anemometer for steady state measurements of wind turbulence on meteorological tower

20 p3634 A70-40342

Spontaneous and induced Cerenkov emission by charged particle in turbulent medium, discussing random fluctuations effect on radiation spectra

21 p3879 A70-40928

Magnetosheath turbulence generation by hydromagnetic waves amplification carried by solar wind through earth bowshock, computing refracted and incident energy fluxes ratio

21 p3815 A70-41059

Coherent beam propagation through turbulent atmosphere, discussing limiting resolving power due to random fluctuations of refractive index

22 p4072 A70-42290

Atmospheric inhomogeneity and temperature gradient effects on sonic booms, discussing displacement, growth rate and shock wave radii refraction

22 p3961 A70-42311

Linear antenna radiation pattern broadening due to atmospheric turbulence

22 p3995 A70-42386

Light rigid civil aircraft response to continuous atmospheric turbulence estimated using two rigid body degrees of freedom method for vertical and lateral gusts

[AIAA PAPER 69-766]

22 p3961 A70-42703

Computerized integral treatment of turbulent constant pressure mixing of two dimensional gas jet with atmosphere having different temperature and composition

22 p4011 A70-42755

Perturbation method with small parameter applied to turbulent transfer equation in lower atmosphere, solving longitudinal diffusion effect on evaporation

22 p4065 A70-42911

Isotopic decay rates, solving time dependent atmospheric turbulent dispersion from steady state measurements

22 p4093 A70-42915

Synthetic aperture terrain-imaging radar systems, calculating tropospheric turbulence induced phase errors for comparison with microwave propagation experiment

22 p3991 A70-43579

Aerodynamic theory of pressure field induced on lifting surface by isotropic atmospheric turbulence, considering transfer function of Concorde aircraft

[ICAS PAPER 70-30]

23 p4138 A70-44104

Universal constant measurement methods in Kolmogoroff third hypothesis for high Reynolds number turbulence in wind over open ocean

23 p4184 A70-44980

Mathematical modeling of atmospheric gusts in stratosphere, mountain wave and thunderstorm conditions relevant to aircraft design

24 p4371 A70-45420

Temperature and gust velocity turbulence at tropopause level over hurricane Beulah by instrumented U-2 aircraft

24 p4371 A70-45422

Monin-Obukhov function and nondimensional transfer coefficients variation, discussing turbulent motion decay in lower atmosphere

24 p4372 A70-46072

Optical wave propagation through random atmospheric turbulence, deriving wave equation power series solution for homogeneous random refractive index field

24 p4314 A70-46126

ATMOSPHERICS

NT DAWN CHORUS

NT HISS

NT IONOSPHERICS

NT SUDDEN ENHANCEMENT OF ATMOSPHERICS

NT WHISTLERS

Electromagnetic energy spectra of lightning expressed as function of electric field spectral density of atmospheric

05 p0843 A70-16762

Time block pooling of atmospheric noise data, basing randomness conclusion on observations correlation

07 p1236 A70-20161

Spectral amplitude distribution of lightning spherics predicted over VLF-SHF range using theoretical analysis of lightning streamers

07 p1272 A70-20215

Recording apparatus design and operation for characteristics of electromagnetic waves generated by weather discharges, discussing electromagnetic perturbations propagation

08 p1468 A70-20467

Soviet collection of papers on atmospheric electricity covering electromagnetic waves phase velocity, satellite observation of thunderstorms activity, etc

08 p1487 A70-20773

Magnetic equator ELF noise examined with OGO 3 magnetometer, indicating unique signals in plasma-sphere

08 p1488 A70-21380

Narrow band atmospheric noise peak field strength measurement, describing design and calibration of noise meter output unit

10 p1832 A70-23998

Coulomb collisions effect on electrostatic lower hybrid resonance waves propagation in ionosphere, noting noise bands cut-off shift

10 p1874 A70-24429

VLF radio noise statistical parameters observed as functions of azimuth, considering atmospheric distribution and parameters correlations

10 p1884 A70-25259

Group delay time differences of spectral groups of VLF atmospherics respecting day and night variation for thunderstorms, determining distance dependence

10 p1884 A70-25260

Broadband and highpass LF noise in distant magnetosphere detected by VLF/LF experiment on OGO 1 satellite

12 p2222 A70-27183

Ionospheric lowest regions and magnetosphere probing based on atmospheric observations, detecting disturbed conditions

12 p2224 A70-27734

Geomagnetic noise constraints on weak field measurements in upper magnetosphere

13 p2401 A70-30056

Entire functions for analysis and representation of distant atmospherics, using concentrated spectrum and zero coordinate readings

14 p2569 A70-30210

Statistical variation of number of VLF atmospherics per unit time above given vertical electric field strength threshold

14 p2550 A70-30515

Automatic audio frequency spectrometer for ELF and VLF amplitude spectrum of atmospherics, discussing attenuation band near 3 kHz

15 p2725 A70-31856

Transient excitation of Schumann earth-ionosphere cavity resonances by large ELF atmospherics, using propagation model

15 p2726 A70-31865

Lightning discharge slow tail atmospherics relation to return stroke, using VLF spectra and frequency analysis

15 p2727 A70-31871

Diurnal variations in attenuation of ELF atmospherics over different propagation paths from recordings at distant ground stations

15 p2728 A70-31994

Slow tail atmospherics and VLF pulse measurements at close-to-thunderstorm fields, indicating return stroke origin

17 p3046 A70-35395

Atmospheric noise statistical parameters analysis on digital computer designed to measure short duration atmospheric radio noise

17 p3170 A70-35396

Tweak atmospheric occurrence frequency and directions for VLF band reflecting layer study
17 p3047 A70-35401

Signal spectral parameters for reducing VLF atmospheric data from analyzer observations
19 p3412 A70-37998

VLF wave propagation in earth atmosphere waveguide, calculating various atmospheric types from waveguide field dependence on frequencies
19 p3416 A70-38566

Close range atmospheric shape classification, using image recognition theory concepts
19 p3416 A70-38572

Terrestrial atmospheric structure, determining zero and extremum point positions and amplitudes to obtain information of VLF wave propagation path
19 p3416 A70-38574

Comprehensive amplitude probability distribution for atmospheric radio noise, noting role in evaluating antenna size and matching
21 p3788 A70-41341

Lightning discharge characteristics contributing to electromagnetic background noise at ELF determined from slow tail waveform measurements
22 p4015 A70-42777

Global thunderstorm activity location found by measuring differences between time of arrival of electromagnetic energy at three satellites
22 p4016 A70-42779

Plasma-TEM wave nonlinear interactions in magnetosphere, discussing atmospheric occurrence
22 p4021 A70-43276

Magnetosphere Alfvén velocity profile relation to ELF chorus and hiss, indicating unstable wave generation by cyclotron resonance
23 p4186 A70-43851

Threshold distribution of time intervals between atmospheric contradicting Poisson law
23 p4190 A70-44082

Earth-ionosphere cavity ELF electromagnetic pulse propagation from atmospheric source, considering transient field as frequency and time functions
24 p4314 A70-46130

Entire functions for analysis and representation of distant atmospheric, using concentrated spectrum and zero coordinate readings
24 p4330 A70-46285

ATOM CONCENTRATION

Diurnal variations of intensity and height profile of diatomic O concentration from photometric rocket measurements compared with balloon data
02 p0297 A70-12066

Ionospheric inhomogeneities motion and vertical profile of atomic oxygen concentration associated with solar particle absorption in upper layer
04 p0681 A70-15724

PdH system electrical resistivity, studying hydrogen concentration role
12 p2282 A70-26900

Argon laser upper levels population measured as function of current strength at constant atom density in capillary
12 p2247 A70-27506

Interstitial atoms arrangement in binary alloys with body centered lattice, describing pressure effects by statistical theory
13 p2435 A70-29321

Ionospheric inhomogeneities motion and vertical profile of atomic oxygen concentration associated with solar particle absorption in upper layer
14 p2575 A70-30808

Concentrations model of metallic atoms and ions in upper atmosphere with deposition from meteors, using diffusion equation
14 p2580 A70-31262

Diurnal variations of thermospheric atomic hydrogen, investigating lateral flow effects on global distribution
19 p3415 A70-38419

ATOMIC BATTERIES

U RADIOISOTOPE BATTERIES

ATOMIC BEAMS

Electromagnetic torsion balance measurement of forces exerted on clean Au surfaces by monoenergetic steady state Ar and Kr beams, calculating thermal accommodation coefficients
06 p1066 A70-18258

High energy Ar atomic beams scattering from single crystal face of W measured for distribution pattern
06 p1112 A70-18270

Atomic and molecular beams produced by nozzle beams aerodynamic acceleration, discussing condensation effects, internal energy, scattering cross sections, etc
07 p1341 A70-20102

Angular and energy distributions of hyperthermal K atoms scattered and ionized by W surface measured as function of beam particle energy
07 p1342 A70-20115

Reactive scattering from solid surfaces, discussing atom beam reaction of O with heated Ge and Si single crystals
07 p1342 A70-20117

Thermal accommodation coefficients of Ar atomic beams scattered from nominal plane of Ag crystal measured by time of flight techniques
07 p1343 A70-20125

Intermolecular potential of atoms and/or molecules determined from scattering cross sections of supersonic He and/or Ar atomic beams
07 p1344 A70-20132

Scattering cross sections of K atoms on bromine molecules determined as function of particle energy using supersonic atomic beams
07 p1344 A70-20133

Ar-Kr integral collision cross sections based on density measurements of Ar beam passed through liquid nitrogen cooled Kr filled scattering chamber
07 p1344 A70-20135

Ionizer design for hydrogen atom beam ensuring storage of polarized protons, using electron beam for ionization
09 p1732 A70-22846

Quadratic Stark shifts of absorption lines hyperfine components in cesium atom beam measured using optical spectroscopy
10 p1887 A70-24033

Luminescence of powdered silica and basalt bombarded by atomic hydrogen, relating spectral distributions dependence on ion energy to lunar luminescence
10 p1942 A70-24647

Deuterium atom reaction with hydrogen molecule yielding HD and H using modulated crossed beams, plotting angular distributions and reaction velocities
10 p1920 A70-25148

Atomic oxygen beams interaction with various surfaces at low pressure, discussing reflection probability and recombination reactions
18 p3225 A70-36187

ATOMIC CLOCKS

One way radio range measurements for surveying and navigation emphasizing McDonnell collision avoidance and geophysical surveying systems, using Rb atomic clocks
01 p0136 A70-10306

Atomic clock reproducibility short and long term stability, weight and power consumption characteristics, noting Rb gas cell for collision avoidance systems
04 p0688 A70-14724

Frequency shift in Rb-87 atomic frequency standards dependence on filter temperature interpreted for optical pumping radiation improvement
05 p0859 A70-16269

Cesium clocks at fixed locations compared for precision and accuracy, noting influence of radio frequency diurnal variations
06 p1139 A70-17474

Pulsars pulse arrival time measured using cesium clock during weekly observations
08 p1570 A70-20899

Phase comparisons between commercial cesium beam frequency standards and NASA experimental hydrogen maser NX-1
08 p1513 A70-21592

Orbiting clock experiment for measuring gravitational red shift of earth by comparing ground based and satellite-borne hydrogen maser clocks
08 p1501 A70-21950

Atomic clock applications to trajectory, discussing experimental single channel equipment for space vehicle location and results of Rb vapor clocks
09 p1722 A70-23034

Atomic frequency standards for phase calibration of large aerial arrays applied to radiotelemetry
11 p2019 A70-26300

One way radio range measurements for surveying and navigation emphasizing McDonnell collision avoidance and geophysical surveying systems, using Rb atomic clocks
13 p2449 A70-29620

Atomic clock for climatic and mechanical conditions of aerospace environment, using optically pumped rubidium cell
15 p2740 A70-32366

Stable clock precision timing systems, discussing quartz crystal, rubidium, cesium and hydrogen oscillators
23 p4195 A70-44289

ATOMIC COLLISIONS

Adiabatic and distortion approximations to two state treatment of ground state H atoms collisions at low energies
01 p1146 A70-10284

Oscillations and decomposition of diatomic gas molecules at high temperatures during atom-molecule collisions, deriving kinetic equations for energy level changes
01 p0148 A70-11630

Oxygen molecules dissociation by molecular and atomic collisions in shock tube from measuring molecular O concentration behind shock wave front
01 p0149 A70-11632

Cross section calculation for spin change in H atoms pair collision, discussing wave number and temperature effects
02 p0341 A70-11796

Electron loss in heavy body collisions from free scattering model and Born approximation
02 p0342 A70-11879

Hydrogen-hydrogen double excitation collision cross sections computed by impact parameter method, using Born and two state approximations
02 p0342 A70-11881

Rotational compound state resonances in subthreshold atom-diatom scattering determined for lowest state molecular hydrogen and deuterium model systems scattered by Xe
03 p0526 A70-13006

Electron-electron and electron-atom bremsstrahlung, giving graphical expressions for one and two electron atoms cross sections
04 p0721 A70-14667

Spin exchange theory for collisions between atoms extended to include target polarization
04 p0722 A70-14672

Hydrogen atoms van der Waal dispersion interaction effects on H lines broadening in neutral medium, taking into account resonance interaction
04 p0723 A70-15714

Vibrational energy transfer in oriented nonlinear collisions between diatomic molecule and atom, considering molecular vibration excitation
05 p0885 A70-17080

Mathematical models describing interactions between rarefied gas atoms and solid surfaces
06 p1036 A70-17759

Three dimensional model for high energy scattering of inert gas atoms from solid surfaces, calculating trapping, accommodation and flux and velocity distributions
06 p1110 A70-18261

Inert gases scattering from Ni $\{111\}$ plane as function of beam temperature and angle of incidence compared to Au and Ag
06 p1110 A70-18263

Hydrogen atoms collisional excitation cross section expressed in terms of quantum numbers of levels and ratio of colliding electron energy to transition energy
07 p1338 A70-19410

Resonant and foreign gas broadening using Schroedinger equations for collision problems
07 p1346 A70-20244

Fast electron ionization losses due to multiple scattering with atoms during passage through thin layer, calculating spatial energy distribution function
08 p1547 A70-20989

Atomic gas particles interactions with self and solid surfaces based on rarefied gas dynamics and classical mechanics
08 p1547 A70-21077

Electron ion recombination role in atomic collision process in rare gases ionization path, considering scintillation mechanism
08 p1549 A70-21815

Three body atomic systems with He atom and H negative ion on basis of scattering experiments dealing with resonance and threshold behavior
09 p1731 A70-22247

Collision effects on saturation of He line transition in He-Ne laser, determining power output dependence on cavity tuning and gas pressure
09 p1695 A70-22322

Vacuum UV photons production during ground state neutral argon atomic collisions, measuring relative cross sections energy dependence
09 p1731 A70-22333

Variational model of collisional-radiative recombination of atomic ions in hydrogen and alkali plasmas
09 p1735 A70-22828

Meteor ionized trails initial expansion and diffusion resulting in dissociation and ionization of air molecules through collision, using electromagnetic wave scattering
09 p1762 A70-23177

Quadrupole coupling between single and double excitation channels in hydrogen-hydrogen collisions found ineffective due to energy defect between channels
09 p1733 A70-23268

Charge exchange probability in proton-hydrogen atom collisions computed with two state atomic orbital expansion
09 p1733 A70-23270

Associative and collisional detachment in H atom and negative ion collisions based on complex adiabatic potential
09 p1733 A70-23431

Resonance energy calculation and transmission coefficient estimate for quantum mechanical model of reactive scattering of three atoms in line
10 p1920 A70-25145

Antimatter motion in solar system and earth atmosphere, discussing vaporization and annihilation energy in collisions with interplanetary gas atoms
11 p2119 A70-26793

Electron-atom collisions, treating elastic and Mott scatterings, Born approximation and ionization
12 p2274 A70-27062

Vibrational relaxation time and transition probability in bromine collisions with He, Ne, Ar, Xe atoms determined by shock wave method

12 p2275 A70-27353

Hydrogen and inert gas atoms collisional excitation cross sections calculated by multistate impact parameter approximation

12 p2276 A70-27378

CH molecule line formation mechanism for 4300 Å transition in solar photosphere, noting collisions with hydrogen atoms

12 p2311 A70-28309

Ionization and metastable excitation in low energy collisions of ground state argon atoms formed by charge transfer

14 p2618 A70-30121

Molecular gases ionization and dissociation by low energy atoms, using mass spectroscopy on secondary ion products of collisions

14 p2619 A70-30723

Atomic oxygen 1D excitation state obtained by metastable He atoms collision with ground state oxygen molecules in O-He discharge

14 p2579 A70-31248

Atomic collision effect on frequency range of opposing traveling wave modes in gas ring laser, using density matrix equation

15 p2749 A70-31553

Intensity and velocity distributions of thermal energy argon atoms scattered from silver (111) face, using time of flight methods

16 p2953 A70-33007

Ce atom collision with excited Hg atom, measuring ionization cross section

18 p3292 A70-36154

Bremsstrahlung from weakly ionized plasma, discussing emission and absorption characteristics, electron-atom collisions and dispersive effects

18 p3294 A70-36347

Atomic H electron transition induced by H atom collisional-excitation rates at various thermal energies, explaining anomalous recombination lines in H I regions

18 p3253 A70-37021

CW HCl chemical laser action via chlorine atoms reaction with hydrogen iodide in fast flowing mixing device

19 p3444 A70-37542

Surface atom bonding configuration energy in two-center theory of large surface unit cells on semiconductors

19 p3483 A70-37544

Positive ion and electron production in H atom collisions with atomic and molecular gases, deriving ionization cross sections

20 p3675 A70-39605

Metastable excitation levels in np⁴/ configuration for population inversion, discussing free electron collisions, forbidden line intensity and flow density pressure

20 p3642 A70-39751

Book on atomic collision physics covering slow ions transport properties and reactions in gases, alkali metals photoionization, charged particle beams, coincidence measurements, etc

20 p3675 A70-40151

Alkali metals ionization by photons and atomic projectiles, discussing results in first Born approximation

20 p3676 A70-40153

Hydrogen ionization and second quantum level excitation by collision with H atoms in ground state

21 p3852 A70-40596

Ionization cross sections for excited H atom-ground state H atom collisions, using Born approximation

21 p3852 A70-40719

Vibrationally adiabatic model for reaction dynamics of atomic and molecular hydrogen systems, using zero point energy path

21 p3773 A70-41397

Hydrogen maser frequency shift due to atomic collisions with deformable storage bulb surface

21 p3836 A70-41453

Silicon line collisional broadening by electrons and hydrogen atoms, discussing Stark effect and van der Waal interactions

22 p4076 A70-42861

Axial modes interaction in He-Ne laser with atomic prominences in active medium, computing intensities and emission frequencies

23 p4202 A70-45053

Heitler-London curves calculation for electron exchange in H-H collisions as function of internuclear distance and velocity

24 p4381 A70-45252

Electronic energy collisional transfer between atomic and molecular hydrogen, measuring excited molecule vibrational distribution

24 p4381 A70-45650

Low energy proton-hydrogen collisions, computing differential cross sections for direct elastic scattering, resonant charge exchange and direct and exchange excitation

24 p4382 A70-46226

ATOMIC ENERGY

U NUCLEAR ENERGY

ATOMIC ENERGY LEVELS

Adiabatic and distortion approximations to two state treatment of ground state H atoms collisions at low energies

01 p1146 A70-10284

Atomic configurations population inversions of astrophysical interest, assuming excitation by electron collisions, solving rate equations for level populations by computer

02 p0341 A70-11794

Lifetimes of upper levels of N II and N III UV multiplets determined from radiative deexcitation of excited ions

03 p0527 A70-13074

Mean lives measurement for excited levels in singlet system of neutral He using beam foil technique

07 p1338 A70-19821

Relaxation time calculation for ground and excited states of H atoms and H-like ions in optically thin and thick plasmas, considering electron density role

07 p1353 A70-20058

Fine structure of excited P states of Li measured for magnetic fields in proton NMR frequency using level crossing and Zeeman effect

07 p1346 A70-20239

Low field and high field hyperfine structure and lifetimes of excited P states of Li using level crossing spectroscopy

07 p1346 A70-20240

Population of P level He excitation in solar prominences in H luminescence regions, noting ionization-recombination mechanism by UV radiation

08 p1564 A70-20555

Coupled Boltzmann and rate equations for free electron distribution function and level populations in monatomic partially ionized gas including nonelastic collisions

10 p1918 A70-23958

Light scattering by atom generalized for multilevel system, showing additional coherent spontaneous scattering and incoherent stimulated combination scattering

12 p2272 A70-27549

Integral Hellman-Feynman formula applied to binding energy of molecular H and LiH, using SCF wavefunctions for atomic states

12 p2276 A70-27570

Resonance radiation transport in optically thick plane gas layer with two-level atoms

12 p2305 A70-27853

Helium excitation from ground to excited state by electron impact, determining differential and integral scattering cross sections

12 p2276 A70-27879

Hanle effect in single mode He-Ne laser, observing spontaneous emission on different spectral lines and estimating lifetimes of Ne excited states

13 p2424 A70-28598

Gas laser active medium nonlinear polarizability calculations with allowance for resonance emission capture effect on atomic velocity and population distributions

13 p2427 A70-29284

Rare earth energy band structure effect on RKKY magnetic interaction between atomic spins

13 p2472 A70-29799

Parametric resonances at zero field crossing levels of optically pumped atoms on alkali vapors, noting applications to weak magnetic measurements

13 p2456 A70-30034

Atomic Russell-Saunders coupling states classification from equivalent electrons configurations, using Young diagrams method

14 p2618 A70-30450

Atom excited state mean lifetime measurement, using correlated cascade photons method

14 p2620 A70-31378

Triply ionized oxygen atom spectrum between 500-8000 Å, determining energy levels and ionization limit

15 p2777 A70-32428

Line formation in solar magnetic fields with allowance for absorption emission and scattering processes, discussing Hanle effect and atomic level polarization

15 p2804 A70-32617

Population of P level He excitation in solar prominences in H luminescence regions, noting ionization-recombination mechanism by UV radiation

15 p2805 A70-32710

Carbon ground state correlation energy calculation, emphasizing assessment of truncation error sources

16 p2954 A70-33277

Hydrogen atom excitation at various energy levels by electron impact, applying Glauber theory

16 p2954 A70-33287

Sr 83, 85 and 87 level structure and mass defect, using stripping and pickup reactions

17 p3138 A70-34625

Light propagation-shift relationships in optically pumped atomic vapors, discussing susceptibilities, birefringence, conversion efficiencies, coupling, etc

17 p3103 A70-35000

Three level gas laser amplifier theory, considering quantum mechanical atomic system in interaction with two monochromatic EM waves

19 p3446 A70-37829

Radiation transfer in plane parallel layers consisting of two atomic energy levels, assuming free electrons Maxwellian energy distribution

19 p3525 A70-38764

M sub L alignment creation due to beam foil excitation process demonstrated with zero field quantum beats in He and H emission spectra

20 p3674 A70-39148

RF spectral recombination lines from atomic level transitions, discussing populations, H lines, electron temperature, density and emission and formation

20 p3706 A70-39934

Atomic hydrogen 2s and 2p excitations by proton and He ion impact, considering ion-multipole interactions effect

21 p3852 A70-40598

Rhodamine 6G triplet lifetime under continuous pumping by Ar laser

22 p4050 A70-43225

Weak EM transmission through resonant medium of two-level atoms in presence of intense monochromatic wave, obtaining absorption coefficient and refractive index

22 p4075 A70-43473

Atomic levels occupation numbers and ionization degree for optically thin hydrogen plasma with self consistent electron velocity distribution

23 p4227 A70-44932

ATOMIC EXCITATIONS

Rotational excitation and scattering of diatomic molecules by structureless atoms, comparing approximation methods

01 p0147 A70-10470

He-Ne laser amplifier photon density, bandwidth and gain as functions of inversion and excited Ne atoms density

01 p0114 A70-11357

Atomic configurations population inversions of astrophysical interest, assuming excitation by electron collisions, solving rate equations for level populations by computer

02 p0341 A70-11794

Coherent light scattering disturbance in level-crossing signals of Rb 85 and Rb 87 second excited state by noble gas atoms

02 p0311 A70-11851

Differential elastic and rotational excitation cross sections for electron-hydrogen scattering in close coupling approximation with electron exchange neglected

02 p0342 A70-11880

Hydrogen-hydrogen double excitation collision cross sections computed by impact parameter method, using Born and two state approximations

02 p0342 A70-11881

Direct interaction between hydrogen atom and positive ion with one electron, using Born and two and four state impact parameter treatments

02 p0344 A70-12703

Temperature dependence of luminescence quantum yields and lifetimes in transitions during excitation of ruby crystal atoms

03 p0538 A70-13059

Lifetimes of upper levels of N II and N III UV multiplets determined from radiative deexcitation of excited ions

03 p0527 A70-13074

Fe I line enhancement in flare of 7 August 1958 interpreted as selective excitation effect, discussing similarity to late type dwarf stars observations

04 p0739 A70-14598

Excitation of H-alpha and H-beta lines in night sky, calculating solar L radiations variation with altitude

04 p0679 A70-15075

Solar helium-like ion line intensities, determining electron densities and excitation rate ratios

04 p0758 A70-15696

Radiative excitation in planetary and Orion nebulae by solving transfer equations for Lyman line and continuum radiation, using normalized on-the-spot/NOS approximation

04 p0758 A70-15700

Laser radiation coherence origin explainable by mechanism consisting of many photon emission process by many atoms

05 p0883 A70-16500

Inelastic He atom-ion collisions provide understanding of capture and excitation cross sections

05 p0885 A70-16555

He excitation by low energy He ions giving support for Rosenthal-Foley postcollision-interaction model, testing model predictions

05 p0885 A70-16556

Electrically discharged O effect on N first positive band emission in surface catalyzed excitation

06 p1109 A70-17489

Nonequilibrium excitation in recombining N plasma nozzle flows

06 p1122 A70-18061

Velocity distribution of atoms evaporating from superfluid He II at low temperatures, noting roton shifting and multixcitation processes

06 p1108 A70-18639
Time of flight resolution of fast excited atoms from thermal molecular beam

07 p1341 A70-20108
Fine structure of excited P states of Li measured for magnetic fields in proton NMR frequency using level crossing and Zeeman effect

07 p1346 A70-20239
Low field and high field hyperfine structure and lifetimes of excited P states of Li using level crossing spectroscopy

07 p1346 A70-20240
Born wave for atom-atom inelastic cross sections, calculating He excitation from ground state to higher states by H atom collision

07 p1346 A70-20241
Time dependent matrix elements for multistate impact-parameter calculations for atom-atom inelastic cross sections

07 p1346 A70-20242
Population of P level He excitation in solar prominences in H luminescence regions, noting ionization-recombination mechanism by UV radiation

08 p1564 A70-20555
Excitation and layers heights for 5577 Å and O₂ bands of atmospheric and Herzberg systems in night airflow estimated, suggesting Chapman reaction for emission

08 p1492 A70-21755
Excitation cross sections for bound-bound transitions in optical levels in hydrogenlike atoms induced by fast charged particles

09 p1730 A70-22230
Excitation equilibrium relative populations calculations for Fe, Ni and Ca ions under solar coronal conditions

09 p1757 A70-22735
Quadrupole coupling between single and double excitation channels in hydrogen-hydrogen collisions found ineffective due to energy defect between channels

09 p1733 A70-23268
Power spectrum of light scattered by two level atom driven by monochromatic electric field obtained from atomic dipole moment correlation function

10 p1920 A70-24632
Cs atoms excitation and ionization in Cs diode interelectrode space under Knudsen conditions, considering luminescence and electron energy distribution

10 p1926 A70-25116
Electron and proton impact excitations of He using Born two and four state versions of impact parameter treatment

11 p2086 A70-25834
Population densities of levels of excited atoms and ions in nonthermal plasma including hydrogen-like ion partition function

11 p2086 A70-25835
Ionization equilibrium of atoms and hydrogen-like ions in nonthermal plasma, transforming into Saha formula for high electron densities

11 p2086 A70-25836
Hydrogen and inert gas atoms collisional excitation cross sections calculated by multistate impact parameter approximation

12 p2276 A70-27878
Helium excitation from ground to excited state by electron impact, determining differential and integral scattering cross sections

12 p2276 A70-27879
Coherence brightened /superradiance/ laser, discussing conditions for atomic energy single pulse radiation

12 p2251 A70-28369
Quantum mechanical Boltzmann equation for atomic gas of composite particles, considering excited level degeneracy

14 p2619 A70-30651
Excitation and radiative transport of 1304 Å triplet of atomic oxygen for dayglow and aurora

14 p2578 A70-31241
Atomic oxygen ID excitation state obtained by metastable He atoms collision with ground state oxygen molecules in O-He discharge

14 p2579 A70-31248
Atom excited state mean lifetime measurement, using correlated cascade photons method

14 p2620 A70-31378
Population of P level He excitation in solar prominences in H luminescence regions, noting ionization-recombination mechanism by UV radiation

15 p2805 A70-32710
Hydrogen atom excitation at various energy levels by electron impact, applying Glauber theory

16 p2954 A70-33287
Low energy electron impact spectrometry, discussing apparatus, procedures, electronic excitation of gas molecules, etc

16 p2857 A70-33797
Excitation cross sections for Ar I and He I spectral lines in low energy He ion-Ar collisions

17 p3138 A70-34642

Excited atoms transfer mechanism in helium plasma, using He-Ne laser

17 p3106 A70-35102

Excitation transfer by spontaneous emission in atomic gas, investigating static magnetic field effect on radioactive cascade

19 p3443 A70-37363

Helium to electron excitation ratios for population inversion in helium-neon laser

19 p3445 A70-37758

Book on thermal radiative properties of air, Volume 2, covering reaction rates, photons and charged particles interactions with air molecules, secondary air excitation, etc

19 p3552 A70-38010

M sub L alignment creation due to beam foil excitation process demonstrated with zero field quantum beats in He and H emission spectra

20 p3674 A70-39148

Muonic atoms nuclear excitation in Zn 66 and 68

20 p3674 A70-39221

Time and power dependent Lamb shift resonance shapes measurement with circular polarized RF field in beam foil excited H atoms

20 p3675 A70-39498

Hydrogen ionization and second quantum level excitation by collision with H atoms in ground state

21 p3852 A70-40596

Atomic hydrogen 2s and 2p excitations by proton and He ion impact, considering ion-multipole interactions effect

21 p3852 A70-40598

Atomic hydrogen emissions in dayglow, considering excitation by resonance absorption of solar radiation

21 p3812 A70-40728

Nightglow Na D line excitation rate in winter and summer

21 p3814 A70-40934

Electron excitation cross sections for light atoms using Slater wave functions and Born-Bethe approximations

21 p3853 A70-41393

Quantum theory of inhomogeneously broadened laser, considering atomic motion-electromagnetic field interactions and detuning effects

22 p4048 A70-42293

Forbidden iron emission lines excitation in Seyfert galaxies, discussing various mechanisms

22 p4102 A70-42977

Photoionization cross sections for atoms and ions of carbon, nitrogen, oxygen and neon as function of wavelength for H II regions and planetary nebulae

22 p4104 A70-42997

Predawn enhancement of O I 6300 Å line, considering magnetically conjugate photoelectrons effects on atomic oxygen excitation

22 p4095 A70-43113

Nightglow Na-D lines excitation, attributing emission to Chapman mechanism

22 p4023 A70-43294

Charge transfer of protons at electron capture in excited states, using proton beam and various target gases

23 p4221 A70-44209

Strong coupled rotational excitation problem in atom-diatom molecule scattering system, discussing transition probability matrices statistical analysis

23 p4212 A70-44600

Laser excited atoms quenching by iodine molecules from light pulse induced photodissociation of perfluoropropyl iodide active media

24 p4352 A70-45467

ATOMIC EXPLOSIONS

U NUCLEAR EXPLOSIONS

ATOMIC GASES

U MONATOMIC GASES

ATOMIC PHYSICS

Dipole shielding tensor of atom in arbitrary time dependent field, giving conditions for general variational calculations yielding results

04 p0721 A70-14389

H-function integrals for noncoherent isotropic scattering for two level atom, tabulating numerical values for Lorentz scattering profile

09 p1727 A70-22506

Electronic wave functions for atoms from atomic configuration-interaction/CI/ expansion for open shell states

18 p3292 A70-36185

Atomic physics of lasers and active materials, noting multiplet spectra of atoms, molecular spectroscopy, energy level population distribution and amplification

[AIAA PAPER 69-63]

18 p3316 A70-36700

Book on atomic collision physics covering slow ions transport properties and reactions in gases, alkali metals photoionization, charged particle beams, coincidence measurements, etc

20 p3675 A70-40151

Electron energies correlation in relativistic theory of atoms applied to multielectron atoms energy levels

22 p4076 A70-43470

ATOMIC RECOMBINATION

NT OXYGEN RECOMBINATION

N atom recombination rate coefficient in static system pressure dependent at low pressure

01 p0147 A70-10450

Nonequilibrium excitation in recombining N plasma nozzle flows

[AIAA PAPER 70-44]

06 p1122 A70-18061

Anomalous microwave recombination line at 11 cm detected in NGC 2024, Orion A, and IC 1795, discussing peak antenna temperature

08 p1576 A70-21399

Thermonuclear rate constant for deuterium atom recombination, using orbiting resonance theory

21 p3781 A70-41886

ATOMIC SPECTRA

Spectral line shapes determination for radiating atoms immersed in plasma developed without neglecting ion-electron interaction and static-ion assumption

07 p1346 A70-20247

Ti I spectrum oscillator strengths, determining formula for relative-absolute values transition

08 p1569 A70-20832

Oscillator strengths relative values determined from flame atom absorption line sensitivity measurements

10 p1828 A70-24259

Inhomogeneous interatomic magnetic field effects on spectral line widening and shifts of emitting atoms in low temperature plasma

12 p2278 A70-27318

Stark-broadened neutral atomic line widths and shifts, determining electron densities from H beta profiles and pressure-temperature data

13 p2455 A70-29220

Atomic spectroscopy of IR laser transitions in gases excited by HF pulsed discharges

17 p3105 A70-35093

Galactic spiral structure from atomic hydrogen line intensity longitudinal distribution

18 p3328 A70-37168

Sodium line in meteor spectrum, determining electron temperature and number of atoms as velocity and height function

19 p3514 A70-37600

Solar search for neutral rhenium lines using low noise, high resolution photometric tracings of Fraunhofer spectrum

20 p3711 A70-40406

Atomic Ar absorption spectrum in vacuum UV region, observing Rydberg series interactions as perturbations and autoionizations

21 p3781 A70-41933

Inhomogeneous interatomic magnetic field effects on spectral line widening and shifts of emitting atoms in low temperature plasma

21 p3860 A70-42059

ATOMIC STRUCTURE

Atomic and electron densities measurements in shock wave interactions with magnetic fields, using interferometric and spectroscopic method

03 p0529 A70-12876

Electron thermal capacity of d-transition metals for stable configurations determined by X ray spectral analysis

04 p0721 A70-14408

Lunar density gradient, free oscillation and tides study inferring lunar atomic number similarity to Si and earth mantle

05 p0908 A70-16316

Disordered ferromagnetic binary alloys of transition metals magnetic moment distributions based on thermal neutron scattering experiments

05 p0893 A70-16950

Liquid metal alloys surface composition and electronic structure roles in electrocatalysis evaluated by studying hydrogen-ion discharge reaction and electrical double layer

06 p1005 A70-18392

Liquid metals atomic structure, discussing X ray and neutron diffraction measurements

07 p1338 A70-19575

Metallic solutions formation dependence on alloying elements electron structure assumed by atoms in solvent lattice

09 p1702 A70-22560

Polywater electronic structure model, proposing hydrogen bonds resembling short strong bonds in HFH₂/ions

11 p1994 A70-25656

Concentrated Fe-Co alloys, effects of local atomic configurational changes on hyperfine interaction using Mossbauer spectroscopy

12 p2284 A70-27245

Recrystallization effect on 3-D graphite orientation in carbon fibers under high temperature heat treatment

12 p2259 A70-27720

Asymptotic relation between Thomas-Fermi-Dirac and Thomas-Fermi atom models for pressure with and without exchange, considering Coulomb contribution to energy

16 p2953 A70-33004

Sr 83, 85 and 87 level structure and mass defect, using stripping and pickup reactions

17 p3138 A70-34625

Neutron diffraction of ordered atomic oxygen structures in titanium suboxides, noting compositional dependence of physical properties 22 p4053 A70-42735

Atomic and molecular spin in cosmic medium 22 p4107 A70-43460

ATOMIC THEORY

NT HEISENBERG THEORY

Two phase transitions existence in Hubbard model of interacting electrons using one particle Green function solution 05 p0884 A70-16099

First order wave functions orbital correlation energies and electron affinities of first row atoms for low lying electronic states of B, C, N, O, F and Ne 06 p1108 A70-17333

Projection operators in dissociative attachment theory, considering use of truncated diagonalization method 07 p1347 A70-20248

Inner-shell ionizations by proton impact calculated for cross section using impulse approximation model, comparing results with Born approximations 09 p1732 A70-22781

Resonant electron scattering processes in atoms and molecules, discussing mechanistic models and use in interpretation of experiments 16 p2955 A70-33798

ATOMIZATION

U ATOMIZING

ATOMIZERS

Centrifugal atomizer mean drop size dependence on geometry, fluid properties and discharge velocity 18 p3300 A70-36274

ATOMIZING

Combustion chamber design for engines, considering atomization by rotating disk vs nozzle atomization 03 p0552 A70-14031

Propellant sprays behavior in high pressure combustors, calculating jet breakup or atomization length 07 p1257 A70-19331

Additive elements effect on structure and properties of sintered powdery Al-Cr and Al-Fe alloys obtained by atomization method, analyzing homogeneity 09 p1707 A70-23124

Liquid metallic particles fragmentation in two phase flow injected into vacuum, noting atomization enhancement by sodium nitrate 13 p2391 A70-29994

Two phase flows and atomization jet during fluid injection into supersonic flow, determining vaporization range 20 p3736 A70-39268

Liquid jets aerodynamic atomization at orifice exit in reentry vehicle into gaseous crossflow, investigating critical Weber number variation with Knudsen number 20 p3610 A70-39701

Fuel atomization drop size calculation for mechanical swirl injectors with and without air input 21 p3867 A70-41770

21 p3867 A70-41770

21 p3867 A70-41770

21 p3867 A70-41770

21 p3867 A70-41770

21 p3867 A70-41770

21 p3867 A70-41770

21 p3867 A70-41770

21 p3867 A70-41770

21 p3867 A70-41770

21 p3867 A70-41770

21 p3867 A70-41770

21 p3867 A70-41770

21 p3867 A70-41770

21 p3867 A70-41770

21 p3867 A70-41770

21 p3867 A70-41770

21 p3867 A70-41770

21 p3867 A70-41770

21 p3867 A70-41770

21 p3867 A70-41770

21 p3867 A70-41770

21 p3867 A70-41770

21 p3867 A70-41770

21 p3867 A70-41770

21 p3867 A70-41770

21 p3867 A70-41770

21 p3867 A70-41770

21 p3867 A70-41770

21 p3867 A70-41770

21 p3867 A70-41770

21 p3867 A70-41770

21 p3867 A70-41770

21 p3867 A70-41770

21 p3867 A70-41770

21 p3867 A70-41770

21 p3867 A70-41770

21 p3867 A70-41770

21 p3867 A70-41770

21 p3867 A70-41770

21 p3867 A70-41770

21 p3867 A70-41770

21 p3867 A70-41770

21 p3867 A70-41770

21 p3867 A70-41770

21 p3867 A70-41770

21 p3867 A70-41770

21 p3867 A70-41770

Position experiments for navigation satellite parameters system using ATS-3 distance measurements 24 p4374 A70-46201

ATS 5

ATS-5 spacecraft L band propagation performance, describing up and downlink test methods 21 p3790 A70-41363

ATS 6

ATS 6 and 7 satellite design features, operational characteristics and experiments objectives [AIAA PAPER 70-1307] 24 p4415 A70-45375

ATS 7

ATS 6 and 7 satellite design features, operational characteristics and experiments objectives [AIAA PAPER 70-1307] 24 p4415 A70-45375

ATTACHMENT

Dichlorodifluoromethane ionization and attachment coefficients for wide pressure range 22 p4076 A70-42373

ATTACK AIRCRAFT

NT A-7 AIRCRAFT
NT BUCCANEER AIRCRAFT
NT JAGUAR AIRCRAFT

Forward air control and light attack aircraft survivability design [SAE PAPER 690707] 05 p0791 A70-15829

Oxygen equipment design for USN patrol and attack aircraft, considering masks, regulators, helmets and hoses 07 p1191 A70-19005

Carrier-based attack aircraft avionics, describing optimal large scale analysis procedure for flight control, communications and radar subsystems 08 p1470 A70-20660

General purpose support system/GPSS/ simulation for carrier operations and avionic maintenance, considering attack aircraft operations, spare parts, personnel requirements, etc 08 p1470 A70-20661

Attack aircraft cockpit displays, discussing design requirements and pilot ability as controller 08 p1435 A70-20674

Harrier navigation/attack system to provide successful single pass attack for close support and strike roles, noting target finding optimization 10 p1914 A70-24847

Mirage F1 fighter aircraft, describing aerodynamic characteristics, fuselage construction, wing edges, etc 10 p1807 A70-24975

In-flight thrust reverser for tactical/attack aircraft, discussing system influence on airplane stability and control [AIAA PAPER 70-699] 16 p2841 A70-33561

Attack helicopter fire control system with day and night detection, recognition and kill capabilities, discussing system components, operation and reliability 17 p3043 A70-34732

17 p3043 A70-34732

17 p3043 A70-34732

17 p3043 A70-34732

17 p3043 A70-34732

17 p3043 A70-34732

17 p3043 A70-34732

17 p3043 A70-34732

17 p3043 A70-34732

17 p3043 A70-34732

17 p3043 A70-34732

17 p3043 A70-34732

17 p3043 A70-34732

17 p3043 A70-34732

17 p3043 A70-34732

17 p3043 A70-34732

17 p3043 A70-34732

17 p3043 A70-34732

17 p3043 A70-34732

17 p3043 A70-34732

17 p3043 A70-34732

17 p3043 A70-34732

17 p3043 A70-34732

17 p3043 A70-34732

17 p3043 A70-34732

17 p3043 A70-34732

17 p3043 A70-34732

17 p3043 A70-34732

17 p3043 A70-34732

17 p3043 A70-34732

17 p3043 A70-34732

17 p3043 A70-34732

17 p3043 A70-34732

17 p3043 A70-34732

17 p3043 A70-34732

17 p3043 A70-34732

17 p3043 A70-34732

17 p3043 A70-34732

17 p3043 A70-34732

17 p3043 A70-34732

17 p3043 A70-34732

17 p3043 A70-34732

17 p3043 A70-34732

17 p3043 A70-34732

17 p3043 A70-34732

17 p3043 A70-34732

17 p3043 A70-34732

17 p3043 A70-34732

17 p3043 A70-34732

17 p3043 A70-34732

17 p3043 A70-34732

17 p3043 A70-34732

17 p3043 A70-34732

Attention direction role in auditory recognition, testing unwanted inputs attenuation hypothesis 19 p3362 A70-38317

Enhanced evoked potentials sited by auditory stimuli in complex task, considering EEG and neurophysiological basis of selective attention 19 p3363 A70-38318

Human memory information structure, discussing pattern recognition, simultaneous attention, problem solving and logic 19 p3363 A70-38322

Human vigilance paradigm and physiology, discussing relationships between vigilance, signal detection and animal discrimination 19 p3364 A70-38324

Noise effects on arousal level in auditory vigilance from EEG parameters 19 p3364 A70-38325

19 p3364 A70-38325

19 p3364 A70-38325

19 p3364 A70-38325

19 p3364 A70-38325

19 p3364 A70-38325

19 p3364 A70-38325

19 p3364 A70-38325

19 p3364 A70-38325

19 p3364 A70-38325

19 p3364 A70-38325

19 p3364 A70-38325

19 p3364 A70-38325

19 p3364 A70-38325

19 p3364 A70-38325

19 p3364 A70-38325

19 p3364 A70-38325

19 p3364 A70-38325

19 p3364 A70-38325

19 p3364 A70-38325

19 p3364 A70-38325

19 p3364 A70-38325

19 p3364 A70-38325

19 p3364 A70-38325

19 p3364 A70-38325

19 p3364 A70-38325

19 p3364 A70-38325

19 p3364 A70-38325

19 p3364 A70-38325

19 p3364 A70-38325

19 p3364 A70-38325

19 p3364 A70-38325

19 p3364 A70-38325

19 p3364 A70-38325

19 p3364 A70-38325

19 p3364 A70-38325

19 p3364 A70-38325

19 p3364 A70-38325

19 p3364 A70-38325

19 p3364 A70-38325

19 p3364 A70-38325

19 p3364 A70-38325

19 p3364 A70-38325

19 p3364 A70-38325

19 p3364 A70-38325

19 p3364 A70-38325

19 p3364 A70-38325

19 p3364 A70-38325

19 p3364 A70-38325

19 p3364 A70-38325

19 p3364 A70-38325

19 p3364 A70-38325

19 p3364 A70-38325

19 p3364 A70-38325

19 p3364 A70-38325

19 p3364 A70-38325

19 p3364 A70-38325

19 p3364 A70-38325

19 p3364 A70-38325

19 p3364 A70-38325

19 p3364 A70-38325

19 p3364 A70-38325

19 p3364 A70-38325

19 p3364 A70-38325

19 p3364 A70-38325

19 p3364 A70-38325

19 p3364 A70-38325

19 p3364 A70-38325

19 p3364 A70-38325

19 p3364 A70-38325

19 p3364 A70-38325

19 p3364 A70-38325

19 p3364 A70-38325

19 p3364 A70-38325

19 p3364 A70-38325

19 p3364 A70-38325

19 p3364 A70-38325

Pilots with high vestibular stability studied for spatial orientation, noting activity impairment due to alternating angular acceleration and optokinetic stimuli
10 p1828 A70-25180

Vertical tilt and horizontal position of antenna rotating device in radio astronomy and radar observations using photogrammetric methods
12 p2195 A70-27478

Optimal orientation of axisymmetric spin stabilized rigid bodies as function of moments of inertia ratios, using single jet for alignment
[DFVLR-SONDDR-50] 16 p2976 A70-33773

Line tilting aftereffects on central and peripheral vision following spatial coincidence of inspection and test contours
21 p3767 A70-40752

Preferential galactic orientation based on inclination statistics of predominantly elliptical clustered nebula
22 p4099 A70-42627

Quaternion scheme for rigid body attitude determination, using Euler axis and angle
23 p4215 A70-44523

ATTITUDE CONTROL

NT DIRECTIONAL CONTROL

NT LATERAL CONTROL

NT LONGITUDINAL CONTROL

NT SATELLITE ATTITUDE CONTROL

NT THRUST VECTOR CONTROL

Crew locomotion effect on spacecraft attitude control using space cabin simulator tests
01 p0036 A70-10853

Rotational motion of self excited symmetric gyroscopes applied to attitude control and nutation damping of space vehicles
01 p0143 A70-10929

Minimum fuel consumption criteria applied to design of manned spacecraft attitude control system, using reaction jets for lateral and directional controls
01 p0196 A70-10950

In-flight compensation for space probe trajectory deviations, discussing attitude determination and control of triaxial and spin stabilized space probes
01 p0186 A70-11265

Gyro-stabilized attitude reference platform for high altitude rotating research rocket payload alignment with preselected star
03 p0579 A70-13606

Flight test results of attitude control device for TACITE rocket probe to explore solar disk and neighborhood
[ONERA-TP-762] 03 p0523 A70-13626

Time optimal attitude control for alignment of spin stabilized sounding rocket, discussing feedback control system
03 p0580 A70-13805

Fluoric altitude insensitive thruster based on two way gas flow diversion valve developed for VTOL aircraft and missile hot gas attitude control systems
[ASME PAPER 69-WA/FLCS-10] 04 p0626 A70-14843

Fluidic sun sensor design and breadboard test for spacecraft and missile attitude control systems
04 p0716 A70-15415

Wing vibration problems associated with roll attitude control in hovering autostabilized VTOL transport aircraft with wing-mounted jet lift engines
05 p0794 A70-16116

Installed thrust vector for scarf attitude control nozzles flush mounted with spacecraft cylindrical surface, predicting pressure distributions for internal thrust
06 p1154 A70-17167

Space vehicle digital control system attitude computations using quaternion matrix algebra to simplify control equations
[AIAA PAPER 68-825] 07 p1393 A70-19302

Contaminants formation during pulse mode operation of liquid bipropellant attitude control rocket engine, discussing exhaust plume effects
[AIAA PAPER 69-574] 07 p1394 A70-19708

Pilot/vehicle dynamics from flight test records, discussing close-loop attitude control tasks
10 p1824 A70-23897

Space vehicle attitude stabilization by passive control moment gyros, discussing viscous and Coulomb friction effects
10 p1950 A70-24054

Large angle suboptimal attitude control of rigid spinning spacecraft
10 p1856 A70-25236

Fuel suboptimal attitude control of spin stabilized axisymmetric spacecraft
10 p1953 A70-25237

Three axis motion simulator for in-orbit spacecraft attitude control evaluation using earth, sun and star sensor references
[AIAA PAPER 69-1029] 11 p2031 A70-26147

Initial parameter conditions influence on sustained unstable oscillations of attitude control system for large space vehicle, calculating stable region by nonlinear method
11 p2124 A70-26149

Digital guidance computer compatibility with analog attitude control loop in Digital Inertial Guidance System used in ELDO launch vehicle
11 p2080 A70-26280

Electromagnetic control system for spin rate and axis orientation of ISIS ionospheric research satellites, describing design parameters
13 p2501 A70-28414

Attitude control system for pointing rocket nose cone at sun examined by digital computer simulation
13 p2501 A70-28419

Gyroless attitude control system for pointing Aerobee sounding rocket payload at sun using solar sensors
13 p2501 A70-28422

Stochastic processes optimal control theory application to launcher attitude control under wind disturbance
13 p2501 A70-28428

Upper atmospheric sounding rocket Skylark engine, attitude control and payload components modifications for increasing versatility and performance
13 p2503 A70-28678

Skylark sounding rocket telemetry data reduction system providing attitude analysis
13 p2363 A70-28680

Three axis star pointing attitude control system for stabilized Skylark sounding rocket program
13 p2447 A70-28687

Attitude control system of three axis stabilized payload for spectral survey of comet head light
13 p2505 A70-28770

Nonlinear filtering methods for attitude computation in strapdown inertial navigation system
13 p2382 A70-29067

Newton-Raphson method analog accelerating convergence of multidimensional stochastic approximation algorithm to local minimum for attitude controller design
13 p2382 A70-29069

Low altitude atmospheric effects on IR beam horizon sensors in carbon dioxide band, noting corrections for spacecraft attitude measurement
15 p2735 A70-31792

Parameter plane method of stability analysis applied to spacecraft attitude control system with two nonlinearities related by nonlinear differential equation
16 p2881 A70-33032

Digital computer generation of system stability Liapunov functions for ninth order spacecraft attitude control
16 p2867 A70-33043

Optimal desaturation of angular momentum exchange controllers in spacecraft attitude control systems, using natural environmental torques
16 p2947 A70-33345

Fluidic attitude control for boost phase of tactical surface to surface missile
16 p2844 A70-33447

Waste hydrogen utilization in microthrusters for spacecraft attitude control involving mass expulsion of cold gas
[AIAA PAPER 70-613] 16 p2969 A70-33609

Spacecraft attitude control microthrusters utilizing catalytically reactive gas mixtures during pulse mode and steady state operation
[AIAA PAPER 70-614] 16 p2969 A70-33611

Flexible space vehicles dynamics and control covering free vibration analysis, thermal flutter and structural deflection effect on attitude control
17 p3177 A70-35233

Balloon gondola azimuthal angle control by twisting suspension rope
17 p3090 A70-35315

Reaction jet azimuth control system for balloon-borne gondola
17 p3018 A70-35316

High response thrust measurement system for pulsed attitude control rocket engines
17 p3061 A70-35479

Gyro test package, dynamic test facility and real time attitude algorithm to investigate operational capabilities of strapdown inertial attitude package
17 p3134 A70-35652

Receiving antenna for ionospheric scatter lines, calculating input power versus height and energy flux density spreading for position optimization
18 p3230 A70-36094

V/STOL attitude control system as integral propulsion system part, analyzing design and weight tradeoffs
[ASME PAPER 70-GT-31] 18 p3214 A70-36832

Control moment gyro /CMG/ for spacecraft attitude control, determining optimal gimbal angle rate for desired torque
[AIAA PAPER 70-1042] 19 p3433 A70-38857

Three axis large angle attitude control system global analysis, determining system stability, responsiveness and sensitivity to disturbances
[AIAA PAPER 70-996] 20 p3668 A70-39534

Spacecraft pulse width modulated attitude control system stability, using state space method
[AIAA PAPER 70-984] 20 p3714 A70-39545

Control moment gyro /CMG/ spacecraft attitude control systems, discussing selection and design criteria
[AIAA PAPER 70-976] 20 p3668 A70-39553

Magnetic three degree of freedom attitude control system for axisymmetric spinning spacecraft, using Kalman filter
[AIAA PAPER 70-974] 20 p3668 A70-39555

Rocket attitude stabilization using exhaust gas flow spinning plug nozzle as gyroscopic mass
[AIAA PAPER 70-67] 20 p3715 A70-39562

Aerospace electronics covering fly-by-wire aircraft flight control, ATC, star trackers for spacecraft attitude control, etc
20 p3669 A70-39668

Direction cosine attitude control logic for spin stabilized axisymmetric spacecraft, using control torques generated by reaction jet system
20 p3669 A70-39679

Nonlinear adaptive reaction jet attitude control for long life space vehicles, providing optimal performance over bias acceleration disturbances
[AIAA PAPER 69-945] 20 p3716 A70-39680

Manual attitude control for Lunar Module employing directional stability, coordinated turn and attitude command
20 p3716 A70-39683

Solar panel flexibility effect on attitude control of solar electric spacecraft for deep space mission
[AIAA PAPER 70-1140] 20 p3716 A70-40209

Large earth orbiting spacecraft minimum time attitude maneuvers with control moment gyroscopes, discussing torque calculation and gimbal angle rates
20 p3670 A70-40284

Trajectory correction propulsion subsystem /TCPS/, attitude propulsion subsystem /APS/ and pyrotechnic subsystem of thermoelectric outer planet spacecraft /TOPS/
21 p3868 A70-41800

Thermoelectric outer planets spacecraft /TOPS/ attitude control subsystem providing accurate antenna pointing and trajectory correction engine thrust vector orientation
21 p3930 A70-41801

Orientation system for pointing balloon-borne X ray detector using flux gate magnetometer, DC amplifier and motor control relay circuit
21 p3831 A70-42429

Space vehicle self oscillatory pulsed relay attitude control system with jet nozzles, determining angular motion
22 p4001 A70-42838

Space vehicle attitude control by cold gas jets, examining principles of operation, optimal conditions for gas consumption and gravitational and gyroscopic effects
[MBB-UR-37-70-0] 23 p4261 A70-44662

Warm gas reaction control thrusters via solid propellant exhaust products for ballistic missiles attitude control
[SAE PAPER 700780] 24 p4295 A70-45863

Single stage warm gas directed jet valve for missile attitude control, noting servovalve and auxiliary power unit control applications
[SAE PAPER 700778] 24 p4295 A70-45864

ATTITUDE GYROS

NT GYRO HORIZONS

Space vehicle attitude stabilization by passive control moment gyros, discussing viscous and Coulomb friction effects
10 p1950 A70-24054

Attitude and heading reference system consisting of five-gimbal platform with two degree of freedom directional gyroscope
11 p2057 A70-26503

Probe rocket Tacite 02 head attitude gyrorestoration for IR horizon analysis, using stellar sensor and signal measurements
13 p2500 A70-28408

Magnetic compensation for attitude control of gravity gradient stabilized satellite using environmental torques and moment gyro damping
[AIAA PAPER 70-993] 20 p3668 A70-39537

Aircraft vertical gyro with hydraulic damping device, calculating ballistic deviations limitation conditions
20 p3632 A70-39733

Gyro misalignment and encoder quantization effects for strapdown attitude error sources
22 p4040 A70-43588

Optimal control of magnetic torque for bias momentum removal from attitude controller, discussing applications to Skylab
23 p4258 A70-44503

ATTITUDE INCLINATION

NT PITCH [INCLINATION]

NT YAW

ATTITUDE INDICATORS

NT GYRO HORIZONS

Graphical method for determining sounding rocket attitudes from optical sensor and flux gate magnetometer data
01 p0196 A70-10841

Comparator design for triplicated attitude indicator instrumentation system in aircraft to achieve reliability, discussing system failure characteristics
02 p0224 A70-11844

- Synchronous satellite attitude measurement during early flight and operating conditions, describing PAS satellite attitude sensor configurations
03 p0581 A70-13844
- Aircraft electronic attitude display indicators using symbology generation to combine several flight monitors indications
08 p1500 A70-21737
- Star field pattern recognition methods for spacecraft attitude determination without a priori knowledge of star position-vehicle attitude relationship
09 p1725 A70-23516
- CRT displays for business aircraft emphasizing EADI/electronic attitude director indicator/
[SAE PAPER 700210]
11 p2079 A70-25882
- Kalman filter modifications for spinning satellite attitude determination in elliptical orbit prior to apogee maneuver, using sun and IR earth sensors
11 p2028 A70-26304
- Holographic device for satellite attitude determination, providing three axis reference information in analog or digital form from single star field sampling
16 p2946 A70-33158
- Scanning celestial attitude determination system /SCADS/, providing triaxial information for earth stabilized satellites
16 p2946 A70-33159
- Electronic attitude director indicator /EADI/ integrated vertical situation display, noting information volume and TV format flexibility
16 p2911 A70-33817
- Continuous time nonlinear filter for space vehicle attitude determination, using estimation theory
17 p3130 A70-35291
- Electronic attitude director indicator /EADI/ for supersonic transport, employing CRT display, head down TV and microvision sensors
19 p3463 A70-37911
- Strapdown inertial attitude indication, describing static and dynamic tests, error propagation profiles, performance prediction, etc
22 p4068 A70-42668
- ATTITUDE STABILITY**
NT DIRECTIONAL STABILITY
NT GYROSCOPIC STABILITY
NT LATERAL STABILITY
NT LONGITUDINAL STABILITY
- Satellite attitude control, discussing passive, active and hybrid stabilization methods including spin, gravity gradient and magnetic stabilization
01 p0197 A70-11264
- Magnetic torquers consisting of permanent magnets or coils for attitude stabilization of earth satellites in geomagnetic field
[IEEE PAPER 27.1]
05 p0924 A70-17000
- Liquid filled dampers for nutation damping of spacecraft with momentum wheel for attitude stabilization
06 p1154 A70-17163
- Nonspinning satellite orbit eccentricity effect on attitude stability
09 p1766 A70-23229
- Ionosphere sounding satellite attitude variation dependence on transverse moments of inertia
10 p1949 A70-23918
- Star tracker linear and nonlinear model selection influence on satellite attitude stability
10 p1953 A70-25231
- Attitude stabilization of synchronous communications satellites employing multiple narrow beam antennas
[AIAA PAPER 70-457]
11 p2119 A70-25422
- ESRO-I satellite attitude stabilization and thermal balance
13 p2505 A70-28842
- Nonspin stabilized satellite attitude reconstitution using least squares estimate
14 p2654 A70-30775
- Equilibrium configurations, considering aerodynamic forces for axisymmetric satellites attitude stability using infinitesimal analysis and Liapunov method
15 p2809 A70-31779
- Attitude sensing and target pointing instrumentation in earth orbiting stellar telescopes in inertial space
16 p2905 A70-33155
- Bearing assembly energy dissipation effects on dual spin spacecraft attitude stability, explaining satellite motion anomalies
17 p3100 A70-34756
- Rocket vehicle flight optimization for model including rigid body degrees of freedom in boundary layer approximation to attitude transients
17 p3180 A70-35664
- Gravity stabilized gyrostatt satellite attitude motion stability, using three dimensional diagram and Liapunov functions
18 p3334 A70-37061
- Magnetic perturbations effect neutralization for satellite attitude stabilization by real time simulation of satellite angular motion in magnetic field
19 p3399 A70-38286

- Nonspinning symmetrical satellite in circular orbit, analyzing laterally oriented rotor effect on attitude stability
19 p3533 A70-38340
- Dual spin spacecraft bearing assembly flexibility effects on attitude stability
[AIAA PAPER 70-1043]
19 p3533 A70-38858
- Dual spin spacecraft, considering nonlinear damping effect on attitude stability
[AIAA PAPER 70-1044]
19 p3533 A70-38859
- Gravity stabilized drag free satellites attitude instabilities due to coupling between attitude and translational motions
[AIAA PAPER 70-995]
20 p3714 A70-39535
- Digital orbital clock and telemetry adapter for TDIA satellite attitude stabilization, describing mechanical structure
21 p3798 A70-41272
- Earth gravity effect on spin vector attitude stability of flexible crossed dipole satellite configuration
22 p4110 A70-43435
- Radiation forces on flat plate in ecliptic earth orbit applicable to satellite attitude dynamics during pitching libration
22 p4125 A70-43437
- Aerodynamic and gravitational torque effects on orbiting satellites attitude stability, applying Liapunov direct method in case of conservative aerodynamic torque
[AIAA PAPER 69-832]
23 p4258 A70-44559
- ATTRIBUTES**
U PROPERTIES
AUDIO EQUIPMENT
NT LOUDSPEAKERS
NT MICROPHONES
AUDIO FREQUENCIES
Elastic bars self excited oscillations at audible frequencies, determining natural frequencies from analyzing sound
07 p1401 A70-18847
- Complex modulus measurement for rigid linear viscoelastic materials over audio frequency spectrum by harmonic end displacement ratio method
07 p1413 A70-20044
- Audio signals frequency and time resolution, discussing discretizing action of masking effect for higher information rate of spectrally encoded messages
13 p2450 A70-28647
- Automatic audio frequency spectrometer for ELF and VLF amplitude spectrum of atmospheres, discussing attenuation band near 3 kHz
15 p2725 A70-31856
- AUDIOLOGY**
Collection of papers on human hearing, source book in psychoacoustics
06 p0995 A70-17822
- Corpus callosum role in auditory information transmission between hemispheres in intact dogs
18 p3221 A70-37215
- AUDIOMETRY**
Pilots hearing level based on pure tone threshold audiograms compared with personnel not exposed to job noise
04 p0631 A70-14982
- Pure-tone air conduction audiogram for diagnosis of patients exposed to intense noise indicating conductive or sensorineural origin of loss
09 p1621 A70-23457
- Aged pilots hearing acuity using speech audiometry, noting discrimination loss for HF verbal sounds
11 p1990 A70-25669
- Pulse duration dependent threshold intensity difference for sine tones related to dynamic properties of hearing
23 p4155 A70-44699
- AUDITORY DEFECTS**
Temporary and permanent threshold shifts in hearing of guinea pigs exposed to intense rocket booster engine noise
07 p1214 A70-19931
- Pure-tone air conduction audiogram for diagnosis of patients exposed to intense noise indicating conductive or sensorineural origin of loss
09 p1621 A70-23457
- Aged pilots hearing acuity using speech audiometry, noting discrimination loss for HF verbal sounds
11 p1990 A70-25669
- Hearing loss thresholds and spontaneous and caloric nystagmus relationship in test pilots
15 p2690 A70-31893
- Sonic boom effects on guinea pigs Corti organ, comparing auditory damage in cochlea with hair cell damage
24 p4305 A70-46374
- AUDITORY PERCEPTION**
Audiograms for aviators unexposed and exposed to high intensity LF noise of maritime patrol aircraft indicating no permanent effects
01 p0032 A70-10365
- Pilots hearing level based on pure tone threshold audiograms compared with personnel not exposed to job noise
04 p0631 A70-14982

- Retroactive interference stimuli effects on pitch discrimination in short term recognition memory task
07 p2125 A70-20046
- Cortical induction phases estimated by retinal mobility index concerning activity of acoustic, olfactory and cutaneous analysors
08 p1443 A70-20735
- Subjective and objective measurement of sound impulses, pauses and intervals duration sensation, showing adjustment accuracy
09 p1618 A70-22763
- Visual restriction effects on critical flicker fusion threshold, loudness and pitch discrimination determined using reticular activating system
09 p1622 A70-23576
- Inflight aircraft cockpit noise levels effect on pilot hearing sensitivity
11 p1990 A70-25875
- Cochlear microphonics in guinea pigs using analog equivalent electrical circuit
11 p1992 A70-26494
- Forward and backward enhancement of auditory system sensitivity as function of short acoustic stimuli
11 p2084 A70-26495
- High intensity noise effects on auditory thresholds, blood pressure and time response to light stimuli, showing permissible levels during space flights
13 p2358 A70-29334
- Monaural detection and filtering of sinusoidal signals in noise, using amplitude model
17 p3033 A70-35610
- Attention direction role in auditory recognition, testing unwanted inputs attenuation hypothesis
19 p3362 A70-38317
- Auditory direction finding ability, discussing experimental arrangement, white noise production, test conduction and statistical evaluation
20 p3582 A70-40538
- Auditory perception by neuroelectrical tests based on logic coincidence among several detectors, discussing bullfrog inner ear
21 p3765 A70-41991
- Preperceptual auditory image demonstration experiments by acoustic test tone pitch identification
22 p3971 A70-43402
- AUDITORY SENSATION AREAS**
Morphological analysis of connections between auditory cortex zone and claustrum in anesthetized cats, establishing efferent nerve fibers presence
01 p0025 A70-11039
- Electrical polarization effects on discharges in individual auditory nerve fibers following current application to cochlear partition
17 p3033 A70-35609
- Corpus callosum role in auditory information transmission between hemispheres in intact dogs
18 p3221 A70-37215
- Auditory cortex projections to caudate nucleus and functions of associative subcortical area in cats
24 p4300 A70-45838
- Bilateral oligosynaptic interaction between posterior lateral thalamic nucleus and afferent systems in visual and acoustic cortical areas in cats
24 p4300 A70-45840
- AUDITORY SIGNALS**
Auditory and visual ready signal intensity effects on reaction time, considering roles of practice and individual differences
03 p0436 A70-13772
- Classical human reaction time as function of high and low auditory signal rates in vigilance setting, supporting inhibition theory of vigilance decrement
04 p0640 A70-15646
- Directional dependence of broadband artificial ear signal spectrum and correlation functions using dummy head
09 p1624 A70-22761
- Frequency function of sound localization in median plane measured psychoacoustically at both ears with narrow band signals
09 p1624 A70-22762
- Threshold excitation of cutaneous analyzer in man under vascular conditioned reflexes in response to acoustic signals with shock
12 p2173 A70-28353
- Loudness lateralization of acoustic signals in right and left ear during binaural interaction
12 p2174 A70-28357
- Audio signals frequency and time resolution, discussing discretizing action of masking effect for higher information rate of spectrally encoded messages
13 p2450 A70-28647
- Real time sonic information input/output computer system for acoustic signals and speech synthesis, concerning man machine communication
14 p2553 A70-30425
- Loud and soft signal recognition task under information feedback of presentation schedules and sequence probabilities
16 p2854 A70-33974
- Information theory of hearing, considering subjective properties of nonsteady sound signals and discernibility relations
23 p4155 A70-44700

AUDITORY STIMULI

Microelectrophysiological study of cerebellar neuron responses to stimulation of vestibular apparatus by vertical rocking performed on anesthetized adult cats

01 p0012 A70-10124

Jet aircraft flyovers annoyance relationship to physical parameters of sound evaluated, using psychophysical method of constant stimulus differences

01 p0006 A70-11199

Neurons tracing activity and cellular memory mechanisms in cortical projection region of cutaneous analyzer of immobilized rats following electric acoustic stimuli

01 p0030 A70-11468

Rabbits and cats cortical neurons responses to light and acoustic signals, using microelectrodes inserted at different depths into cortex

01 p0030 A70-11469

Human EEG relationship to verbal behavior, discussing separation of stressful from nonstressful verbal stimuli, semantics and question-answer sequences

02 p0236 A70-12119

Human perceptual and response biases in choice reaction time tasks involving visual and auditory stimuli

02 p0239 A70-12624

Pulsed noise biological effects on human organism, showing stimulation of auditory duct and baric and mechanical reception system causing neural functional shift

03 p0433 A70-13476

Reaction time task to examine relationship between preparatory intervals and auditory stimulus intensity in experimental designs

03 p0424 A70-13764

Visual, motion and auditory stimuli role in enhancing aircraft pilot training simulators realism, considering motion perception research

04 p0642 A70-14853

Classical human reaction time as function of high and low auditory signal rates in vigilance setting, supporting inhibition theory of vigilance decrement

04 p0640 A70-15646

Subjective measurement of sound level of impulses and pulses, investigating 1 kHz tone and selection of time length between sound events

05 p0882 A70-16344

Retroactive interference stimuli effects on pitch discrimination in short term recognition memory task

07 p1215 A70-20046

Ego strength relationship to respiration in response to sound and light stimulation tested in subjects balanced for alertness-drowsiness by EEG criteria

09 p1616 A70-22331

Startle auditory stimuli effects on motor performance and recovery characteristics from heart rate and skin conductance recordings

09 p1628 A70-23577

Reaction time dependence on sound signal probability determined by temporal structure of signal presentation

10 p1818 A70-24713

Auditory and visual warning signals effects as reaction stimulus in time-uncertainty situation

10 p1826 A70-24719

Forward and backward enhancement of auditory system sensitivity as function of short acoustic stimuli

11 p2084 A70-26495

Pro- and anticoagulants dynamics in rats blood during early phases of prolonged sound effect

12 p2168 A70-27347

Auditory and cutaneous sound localization acuity

13 p2354 A70-29597

Vestibular nystagmus evocation by conditioned reflexes technique after pure tone stimulation

14 p2538 A70-30910

Sensory function in multimodal signal detection forced choice experiment involving auditory, visual and auditory-visual stimuli

14 p2539 A70-31167

Electrical potentials in response to auditory stimuli recorded in cat brains by averaging computer

15 p2685 A70-32831

Noise bursts response of positive and inhibitory conditioned eyelid reflexes in cats brain, discussing auditory system function

15 p2687 A70-32871

Loudspeaker optimal arrangement for speech intelligibility in aircraft crew compartments, discussing apparent SNR improvement

17 p3039 A70-35564

Etiopathogenesis of auditory disorders in flying personnel and aircraft engineers resulting from exposure to acoustic stresses

17 p3034 A70-35677

Latent period of human motor reflex in telegraph key press testing in response to oral command

18 p3222 A70-37218

Human response time to visual stimulus preceding or following auditory stimulus as function of interstimulus interval

19 p3362 A70-38311

Enhanced evoked potentials sited by auditory stimuli in complex task, considering EEG and neurophysiological basis of selective attention

19 p3363 A70-38318

Noise effects on arousal level in auditory vigilance from EEG parameters

19 p3364 A70-38325

Rat neuron impulsive reactions and frequency response differences to varying sound signals, discussing time constant, signal intensity and frequencies

20 p3574 A70-40172

Click-evoked potentials in rat auditory cortex, medial geniculate body, reticulate formation and hippocampus during natural sleep and waking

21 p3761 A70-40917

Mammal and human acoustic reflex for impulsive sound, investigating immunization effectiveness

24 p4297 A70-45373

AUDITORY TASKS

Intermittent vs continuous noise effects on signal detection measures during audio visual checking task performance

01 p0039 A70-11167

Auditory averaged evoked potentials to clicks in man subjected to selective listening task, comparing effect on attended and rejected ear

07 p1215 A70-20213

Visual and auditory reactions in dogs to alimentary stimuli before and after partial removal of cerebellum, noting complete recovery within month

15 p2687 A70-32892

Loud and soft signal recognition task under information feedback of presentation schedules and sequence probabilities

16 p2854 A70-33974

AUGER EFFECT

Si cleaved crystal nature on basis of Auger spectra, discussing impurity stabilization

01 p0159 A70-11175

Nitrogen K-L-L Auger spectrum high energy lines measurement by high resolution electron spectrometer

14 p2620 A70-31301

Multichannel monitor for repetitive short scan Auger electron spectroscopy for surface composition changes, using low energy electron diffraction

21 p3827 A70-41467

Intergranular brittleness in powder metallurgy W by Auger Electron Emission Spectroscopy for fracture surfaces chemical analysis

22 p4053 A70-42733

Auger spectra characteristics obtained with X rays and electrons from radioactive alpha sources

23 p4222 A70-44421

AUGMENTATION

NT THRUST AUGMENTATION

AURIGA CONSTELLATION

Three color photometry of RW Auriga stars, discussing UVB curves, H-R diagram and UV emission excess

15 p2797 A70-31612

AURORAL ABSORPTION

Auroral breakup effects on sporadic E via comparison between sequential ionograms and riometer absorption data indicating transient effect in D/E regions

02 p0288 A70-11744

Postbreakup pulsating aurora association with conjugate absorption bays, indicating hard electron precipitation source location

02 p0290 A70-12161

Interplanetary field influence on auroral radio absorption, considering sector structure of solar wind

03 p0476 A70-13915

Spatial and temporal relations between auroral emission at green line 5577 and cosmic noise absorption studied to determine energy spectra and particles distribution

05 p0907 A70-16281

Large scale horizontal gradients in auroral radio absorption and effects on absorption height measurement by multifrequency riometry

06 p1055 A70-17595

HF signals propagation through auroral curtain investigated for scattering or blanketing effects, discussing ground scatter echo cut-off caused by sporadic E layer

06 p1011 A70-18538

Ionospheric radio wave /auroral/ absorption during substorm investigated for longitudinal and latitudinal variations by multistation riometer measurements, inferring electron precipitation characteristics

07 p1269 A70-20030

Ionospheric auroral anomalous radio wave absorption frequency dependence index determined from cosmic radio emission intensity data

07 p1276 A70-20433

Auroral absorption longitudinal motion from riometer recordings, showing movement from midnight meridian simultaneously eastward and westward along auroral zone

07 p1276 A70-20434

Auroral motions determined by absorption onsets pattern and infrasonic wave morphology

10 p1880 A70-24803

Ionospheric loss rates from rocket observation during auroral absorption interpreted by two ion model of recombination

10 p1881 A70-24813

Ionospheric magnetic activity effects on cosmic radio noise absorption diurnal and seasonal variations in auroral zone, noting K index and lowest reflection frequency roles

11 p2043 A70-25536

Auroral radio wave absorption in ionosphere at longitudinally opposite stations compared for appearance probability and variational properties

11 p2043 A70-25537

Auroral absorption bays meridional motion, observing absorption onset systematic lag at various ground stations

14 p2570 A70-30216

Auroral cosmic noise absorption, discussing east-west motion, conjugate magnitudes and breakdown

16 p2899 A70-34191

Cosmic noise absorption diurnal variations at auroral zone conjugate areas during geomagnetically disturbed periods

19 p3414 A70-38379

Auroral physics, discussing visibility, relations to geomagnetism and sunspots spectrum, morphology, optical emissions and particles in magnetosphere

20 p3623 A70-39929

Ionospheric magnetic activity effects on cosmic radio noise absorption diurnal and seasonal variations in auroral zone, noting K index and lowest reflection frequency roles

21 p3819 A70-41286

Auroral radio wave absorption in ionosphere at longitudinally opposite stations compared for appearance probability and variational properties

21 p3819 A70-41287

Nighttime and daytime midlatitude magnetic bays statistical correlations with riometer-auroral absorption, suggesting precipitating particles role

22 p4018 A70-43107

Ionospheric radio wave absorption above polar aurorae during solar activity minimum, discussing diurnal and annual behavior

23 p4162 A70-44058

Auroral absorption bays meridional motion, observing absorption onset systematic lag at various ground stations

24 p4331 A70-46291

AURORAL ACTIVITY

U AURORAS

AURORAL ARCS

NT RED ARCS

Directional and spectral characteristics of bremsstrahlung X rays from auroral arc in low energy range during cosmic rays sounding rocket measurements

02 p0357 A70-12069

Relationship between 6300 A monochromatic auroral arc and visible aurora during magnetic storm, determining directional speeds

03 p0478 A70-14000

Band shaped polar auroras widths from photographs analysis, noting wider bands for midnight hours and winter solstice

04 p0682 A70-15732

Auroral arcs far UV observations by OGO 4, discussing luminosity, morphology, position, etc

09 p1670 A70-23493

Electron flux independence of pitch angle distribution /0-90 degrees/ observed from sounding rocket measurements in auroral arc

10 p1932 A70-24492

Vector magnetic field and energetic particle flux profiles, indicating geomagnetically aligned currents associated with visible auroral arc

13 p3297 A70-29197

Band shaped polar aurorae widths from photographs analysis, noting wider bands for midnight hours and winter solstice

14 p2575 A70-30815

Auroral orientation curves evaluation, testing parameters by numerical integration and revised geomagnetic coordinate system

14 p2576 A70-30918

Auroral arcs formation model based on dynamic magnetosphere-ionosphere interaction

21 p3817 A70-41089

Auroral electrojet, arcs, electric and magnetic fields relationship investigated by rocket-borne magnetometers and photometers

23 p4184 A70-43835

Atmospheric response to heating in stable auroral red arc by two dimensional steady state dynamic model of neutral thermosphere

24 p4329 A70-45357

AURORAL ECHOES

Polarization nature and changes evaluation of radio echo signals reflected from polar auroras

04 p0682 A70-15730

Correlation function of auroral reflection radio signals with allowance for polar ionospheric scattering and pulse signal transmission and reception

05 p0841 A70-16741

HF signals propagation through auroral curtain investigated for scattering or blanketing effects,

discussing ground scatter echo cut-off caused by sporadic E layer 06 p1011 A70-18538

Aspect sensitivity of HF backscatter auroral echoes in F layer, utilizing F supported ground scatter echo to account for ionospheric refraction 06 p1012 A70-18541

Statistical analysis of aurora backscatter VHF measurements, discussing related stream plasma instability theory and diurnal variation 10 p1885 A70-25263

Simultaneous magnetic, photometric and backscatter radio measurement of auroral and ionospheric echoes during geomagnetic storm, confirming electrojet theory 13 p2392 A70-28575

Polarization nature and changes evaluation of radio echo signals reflected from polar auroras 14 p2575 A70-30814

Auroral echoes polarization with horizontal and vertical Yagis, discussing aerial patterns 14 p2578 A70-31240

AURORAL ELECTROJETS

High latitude capture region boundary for electrons in upper radiation belt determined relative to current electrojets in ionosphere from satellite observations 01 p0172 A70-11516

Evening time latitudinal distribution of polar magnetic field perturbations compared with nighttime distribution, indicating evening electrojets 04 p0684 A70-15751

Stably trapped magnetospheric plasma distribution determined from Pi2 micropulsations and auroral electrojet index AE 05 p0839 A70-16285

Auroral zone electrojets spatial structure and dynamic behavior based on IGY and IQSY geomagnetic data 08 p1491 A70-21717

Auroral zone electrojet return current spatial distribution using idealized models for stationary state 08 p1491 A70-21718

Auroral currents as source of atmospheric gravity waves and associated traveling ionospheric disturbances 13 p2399 A70-29234

Infrasonic waves generated by pulsating aurora, using Joule heating and Lorentz force coupling 13 p2399 A70-29236

Infrasonic waves generation by supersonic translation of auroral electrojet currents 13 p2399 A70-29237

Model current system for magnetospheric substorm accounting for distribution of geomagnetic disturbance field vectors on earth surface and auroral electrons and protons 13 p2481 A70-30062

Ba ion cloud motions agreeing with electric field data from balloon measurement in ionosphere and magnetosphere 13 p2402 A70-30079

Polar cap elementary magnetic disturbance relationship to auroral electrojet 14 p2570 A70-30215

Aurora band theory based on three dimensional current system during magnetic substorms, discussing field aligned sheet current instability 14 p2573 A70-30671

Evening time latitudinal distribution of polar magnetic field perturbations compared with nighttime distribution, indicating evening electrojets 14 p2576 A70-30835

Polar electrojet and VHF auroral radio wave backscattering correlation, discussing geomagnetic disturbances effect 19 p3376 A70-37498

Auroral electrojet, arcs, electric and magnetic fields relationship investigated by rocket-borne magnetometers and photometers 23 p4184 A70-43835

Auroral electrojet return current spatial extent from model ionospheric current distribution and geomagnetic variations 23 p4192 A70-44922

Polar cap elementary magnetic disturbance relationship to auroral electrojet 24 p4331 A70-46290

AURORAL EMISSION

U AURORAS

U LIGHT EMISSION

AURORAL IONIZATION

Horizontal electric fields relations to charged particle fluxes in polar auroral ionosphere 05 p0842 A70-16756

Auroral electron energy distribution and ionization rates characteristics based on satellite and rocket measurements 08 p1487 A70-20642

Auroral ion composition and chemistry from rocket-borne mass spectrometer measurements, investigating oxygen density and green line excitation 10 p1874 A70-24431

Ionic composition of Class I auroras based on 1965 CIRA atmospheric model atomic/molecular oxygen ratios, noting ion loss rates 11 p2046 A70-26565

Radiation belt and auroral primary ions, comparing origin possibilities of ionosphere and solar wind 13 p2481 A70-30063

Ionization rate and electron density height profiles for typical auroral proton energy spectrum, noting radio noise absorption, sporadic E and auroral aurora 22 p4024 A70-43307

Ionization rates in auroras detected by atomic oxygen and nitrogen lines 22 p4024 A70-43308

AURORAL IRRADIATION

Geomagnetic tail formation, cross section and length and auroral irradiation, discussing observations, models, vacuum magnetic merging and field aligned currents processes 13 p2402 A70-30060

Molecular nitrogen excitation under electron bombardment at auroral and airglow impact levels, using computerized Monte Carlo method 14 p2620 A70-31269

Spatial distribution of energy deposited by auroral electrons in upper atmosphere, using Monte Carlo method 15 p2725 A70-31860

Polar peak F layer electron density around magnetic noon related to dayside aurora flux, comparing with soft particle precipitation 15 p2727 A70-31872

AURORAL SPECTROSCOPY

Hydroxyl emission during auroras, noting absence of correlation with O I brightness fluctuations for IBC II-III aurora of 1 November 1968 09 p1671 A70-23496

Neutral atomic oxygen auroral and nebular emissions in twilight airglow, suggesting photodissociation of molecules by sunlight 10 p1873 A70-23832

Photometric and interferometric observations of midlatitude stable auroral red arc, determining structure, intensity and position 11 p2047 A70-26570

Auroral green line decay of atomic oxygen measured photometrically from multiple exposure spectra of meteor wakes 12 p2304 A70-27713

Excitation and radiative transport of 1304 A triplet of atomic oxygen for dayglow and aurora 14 p2578 A70-31241

Artificial aurora generated by Starfish in northern conjugate region and afterglow spectra 14 p2578 A70-31245

Nitrogen deactivation by ground state atomic oxygen resulting in metastable oxygen atom as auroral green line source 17 p3080 A70-35770

Auroral protons and resonant concept of substorm, eliminating discrepancy between hydrogen emission spectroscopic and direct measurements 18 p3307 A70-36177

Auroral UV night airglow radiation distribution over latitude range, using scanning spectrometer onboard Convair 990 aircraft 21 p3818 A70-41106

NO molecule gamma system in emission spectra of polar auroras in far UV by monochromator aboard Skylark rocket 21 p3821 A70-42261

Auroral spectrophotometer measurements from 1968 NASA airborne expedition, discussing oxygen and nitrogen spectral lines 23 p4186 A70-43855

Auroral molecular nitrogen bands tentative identification based on rocket-borne spectrometer results 23 p4186 A70-43856

AURORAL ZONES

Electrical phenomena in upper atmosphere and solar wind may control geomagnetic disturbances and aurorae 01 p0082 A70-11523

VLF observations of auroral beams for auroral V-emissions source and characteristics, explaining spectral shape 02 p0291 A70-12204

Azur satellite launching project by NASA and Germany, describing orbit for investigating earth inner radiation belt, auroral zone and solar flares 03 p0580 A70-13797

Satellite measurement of auroral particles and particles trapped in Van Allen belts 03 p0559 A70-13852

Polar cap absorption midday recovery phenomenon analysis in northern and southern polar auroral regions showing increase in ionizing flux rigidity 04 p0682 A70-15729

Magnetic disturbances and corpuscular intrusions in auroral zone, discussing daytime and nighttime magnetic activity of electron fluxes 04 p0684 A70-15752

Auroral radio reflections using two coherent bistatic radio systems, discussing ionoacoustic waves in auroral plasma 05 p0837 A70-16072

Polar auroral region displacement ascribed to distant magnetic field disturbances, proposing calculation method 05 p0842 A70-16745

Rocket measurement techniques for electron density profiles in D region, giving results from auroral zone disturbed and midlatitude quiet D region 07 p1263 A70-19152

Daylight ionospheric scatter propagation and absorption during energetic electron precipitation event in auroral zone using bremsstrahlung observations at balloon altitude 07 p1271 A70-20154

Auroral absorption longitudinal motion from riometer recordings, showing movement from midnight meridian simultaneously eastward and westward along auroral zone 07 p1276 A70-20434

Frequency spectra of Pi 2 geomagnetic field pulsations, noting effects of aural zone location, configuration and structure 07 p1277 A70-20438

Altitude asymmetry of instantaneous auroral oval plotted for geomagnetic pole and earth surface 07 p1277 A70-20456

Electron and proton precipitation measurements in auroral zone by soft particle spectrometer in ISIS-1 satellite 08 p1560 A70-20501

Altitude profiles and absolute intensities of far UV emission features in aurora measured by filterwheel photometer in Aerobee rocket, determining molecular oxygen densities 08 p1489 A70-21384

Gravity waves generated by heating in auroral regions and propagating toward lower latitudes possibly causing thermospheric heating 08 p1491 A70-21675

Low energy ion spectrum and spatial distribution measurements in auroral zones by Cosmos-261 satellite spectrometer 08 p1492 A70-21798

Rocket-borne spectrometer for measuring I-13 kev electron fluxes in auroral zone, describing design, operation and calibration 10 p1889 A70-24493

Pi2-type pulsations in and near auroral zone observed for amplitude variation dependence on geomagnetic latitude and local time 10 p1885 A70-25280

Motion of incidence regions of X ray radiation in auroral zone using simultaneous balloon measurements 10 p1935 A70-25283

Annular current effect on auroral oval location during morning and evening hours, noting airglow region shift toward equator and expansion 11 p2044 A70-25555

Latitudinal ionospheric electron density and temperature variations at 1000 km within and near auroral zone 12 p2222 A70-27186

Northern auroral regions low energy electron fluxes survey by Injun 4 satellite during minimum solar activity 13 p2477 A70-29184

Stable auroral red/SAR/ arcs, discussing radiation, orientation, etc 13 p2397 A70-29188

Auroral zone rapid motions associated with electron precipitation, discussing balloon flight data 13 p2478 A70-29198

VLF auroral and low latitude emissions along N-S chain of stations, discussing daytime and nighttime observations 13 p2371 A70-29925

Auroral and polar cap ionospheric electric fields and tensor conductivity elements using ion clouds data of Ba release experiment 13 p2402 A70-30080

Lower ionospheric drift motions observed from VHF radio signal, relating to three paths near auroral zone during dark hours 14 p2574 A70-30749

Polar cap absorption midday recovery phenomenon analysis in northern and southern polar auroral regions showing increase in ionizing flux rigidity 14 p2575 A70-30813

Magnetic disturbances and corpuscular intrusions in auroral zone, discussing daytime and nighttime magnetic activity of electron fluxes 14 p2576 A70-30836

Daytime auroral zone electron precipitation energy spectrum from atmospheric bremsstrahlung X ray balloon data 14 p2580 A70-31257

Auroral zone X rays balloon-borne conjugate recordings from Iceland and Antarctica 14 p2632 A70-31306

- Geomagnetic micropulsations horizontal polarization characteristics relationship between stations in southern and northern auroral zones
15 p2725 A70-31859
- Electric field component of waves in auroral ionosphere measured by double Langmuir probe field detectors, discussing wave-particle interactions and turbulence
17 p3096 A70-35767
- Vertical profile of electron collisions effective frequencies in auroral ionosphere E region
19 p3409 A70-37330
- Low energy electron and proton measurements by ESRO 1 satellite, discussing electron spectra, auroral zones and proton precipitation
19 p3412 A70-37516
- ESRO 1 satellite and ground observations of energetic auroral electrons angular distribution during solar event, using Geiger counters
19 p3412 A70-37519
- Temperate equatorial and auroral zones sporadic E observations and formation theories survey for prediction
19 p3416 A70-38441
- D region free electron temperatures at northern auroral zone by dual polarized antenna, observing incident noise radio fluxes
20 p3622 A70-39452
- Sporadic E layer ionization correlated with geomagnetic disturbances in northern auroral and polar regions
21 p3812 A70-40592
- Ionospheric transition and ozone correction from D region sunrise auroral rocket flight
21 p3814 A70-40935
- Electron precipitation at geomagnetic storm sudden commencement in auroral zone from X ray balloon observations
21 p3814 A70-40937
- Annular current effect on auroral oval location during morning and evening hours, noting airglow region shift toward equator and expansion
21 p3819 A70-41305
- Auroral zone electric field measurements from rocket-borne instruments
22 p4017 A70-42794
- Lower E region recombination coefficients from electron density and flux measurements in glow aurora by Nike-Apache rocket
22 p4020 A70-43163
- Geomagnetic daily variations analysis in terms of universal time components, considering solar wind-magnetosphere interactions, auroral zone effects, etc
22 p4021 A70-43278
- Pi 2 type geomagnetic pulsations relationship to auroral zone morphological features
23 p4190 A70-44085
- Pitch-angle distribution of electron fluxes in auroral zone as function of geomagnetic latitude
23 p4192 A70-44878
- AURORAS**
- NT AURORAL ARCS
NT RADIO AURORAS
NT RED ARCS
- Two station simultaneous observations of auroral infrasonic wave substorms morphologies
01 p0071 A70-10411
- Auroral light emission and electron density simultaneous measurements by rocket flights into auroral glow, deriving recombination rates
01 p0171 A70-10872
- Rotational temperature of molecular nitrogen Vegard-Kaplan bands determined from auroral spectra, including variations in vibrational levels populations
01 p0076 A70-10873
- Amplitude modulated pearl type geomagnetic micropulsations connected with auroral X ray emission variations
01 p0171 A70-11228
- Auroral electron energy diurnal variation, noting ground observations of polar auroras, riometric absorption, vertical changes in ionization layer maximum position, etc
01 p0083 A70-11535
- Nitrogen, oxygen and air luminescence spectra excited by fast electrons at low gas pressures in IR spectral region compared with polar auroral spectra
01 p0083 A70-11536
- Intermediate ionospheric layer at high latitudes, discussing relationship to geomagnetic and auroral activity and F region continuity
04 p0678 A70-14974
- Lyman alpha auroral emissions observations made with narrow band sky scanning photometer mounted on earth-oriented polar orbiting satellite
04 p0741 A70-15107
- Hard electron bremsstrahlung measurement during intense polar aurorae in January and February 1968, determining electron flux penetration region
04 p0682 A70-15731
- Fragmentary arc and band-shaped polar aurora configurations associated with corpuscular rays penetration into upper atmosphere
04 p0684 A70-15749
- Transient emissions on He I wavelength during breakup phase of auroral events, discussing observational interference by OH bands
05 p0907 A70-16277
- Spatial and temporal relations between auroral emission at green line 5577 and cosmic noise absorption studied to determine energy spectra and particles distribution
05 p0907 A70-16281
- Polar aurora rays mean length diurnal variations determined from photographic and visual observations in Tiksi bay
05 p0843 A70-16763
- UV rocket-borne up-down photometer measuring zenith and nadir intensities for auroral profile studies
06 p1072 A70-18518
- Temporal behavior of energetic particle precipitation during auroral substorm, discussing electron energy spectra and pitch angle distributions
06 p1059 A70-18536
- Energetic particle intensity fluctuations during bright aurora, using rocket-borne measurements
06 p1060 A70-18548
- VLF and LF auroral or polar hiss as generated by incoherent Cerenkov radiation from high energy electrons
07 p1264 A70-19190
- Sporadic E layers structure and dynamic characteristics during polar aurorae, determining critical frequencies
07 p1267 A70-19455
- Intensity and altitude profile of H beta light emission and energetic hydrogen fluxes during auroral breakup using rocket soundings
08 p1489 A70-21383
- Auroral pulsation observed by Aerobee rocket instruments and ground multichannel photometer indicating primarily temporal fluctuation
09 p1671 A70-23497
- Auroral green line rocket measurements, showing roles of atomic and molecular oxygen dissociative recombinations
10 p1874 A70-24432
- Auroral motions determined by absorption onsets pattern and infrasonic wave morphology
10 p1880 A70-24803
- Predicted Jupiter visual auroras investigated with high sensitivity spectrograph
10 p1947 A70-24993
- IGY and IQSY aurora observations, discussing geographic distribution of observations, diurnal variation of aurora frequency, solar activity effects, etc
10 p1884 A70-25261
- Auroral pulsations photometric observation data, noting magnetic activity effects
11 p2043 A70-25540
- Aurorae and magnetic storms theory, considering ion production, motions and interactions
11 p2044 A70-25621
- Radio wave absorption at 2.2 MHz measured by vertical incidence pulse method, observing maxima in February and in September-October due to auroral activity
11 p2006 A70-26176
- Auroral orientation curves and auroral oval, determining largest difference between locations
11 p2046 A70-26500
- Drift instability of Alfvén waves at electron plasma sheet edge as source of auroral micropulsation instability
12 p2222 A70-27184
- Auroral enhancement of IR oxygen band at 1.27 micron compared with molecular nitrogen band intensity
12 p2222 A70-27185
- Monograph on polar aurora with emphasis on solar wind and interplanetary magnetic fields, discussing substorms, particle acceleration in current sheet, etc
13 p2395 A70-28983
- Pulsating auroras X ray association with luminosity via balloon-borne X ray detector and ground based image intensifier TV system
13 p2478 A70-29228
- Auroral oval position with trapping region phi s boundary compared with closed geomagnetic field lines phi c, using Alouette 2 satellite data
13 p2398 A70-29229
- Visual aurora properties attributed to magnetic storm following solar flare, using multiple channel photometer measurements
13 p2478 A70-29231
- Polar ionosphere auroral oval position detection by satellite observations of naturally occurring VLF and man-made HF plasma waves
13 p2371 A70-29924
- Auroral electron precipitation and ground based magnetic field pulsations correlation for magnetic storms inception
13 p2401 A70-30053
- Polar auroral hydrogen emission intensity dependence on K index of geomagnetic activity
14 p2569 A70-30213
- Polar storm simultaneous onset and development, using observational data for geomagnetic field and aurorae
14 p2570 A70-30214
- Pulsating aurorae onset in magnetically conjugate points noting local nature of sources
14 p2572 A70-30241
- Hard electron bremsstrahlung measurement during intense polar aurorae in January and February 1968, determining electron flux penetration region
14 p2575 A70-30816
- Fragmentary arc and band-shaped polar aurora configurations associated with corpuscular rays penetration into upper atmosphere
14 p2576 A70-30833
- Artificial aurora generated by Starfish in northern conjugate region and afterglow spectra
14 p2578 A70-31245
- Magnetospheric dynamic processes leading to energetic and thermal auroras in middle latitudes
14 p2581 A70-31267
- Report to COSPAR on Swedish space research /1969/ including rocket-borne auroral particle experiments, plasma physics, atmospheric, solar, cosmic radiation, etc
15 p2830 A70-31722
- Impulsive proton flux precipitation increase during auroral breakup observed by rocket
18 p3245 A70-36021
- Sporadic E layers structure and dynamic characteristics during polar aurorae, determining critical frequencies
18 p3250 A70-36929
- Sporadic ionization occurrences nighttime observation in auroral E region, describing vertical electron concentration profile
19 p3410 A70-37331
- Auroral phenomena interdisciplinary investigations, discussing electron precipitation and conjugate point drift due to geomagnetic axis position variations
19 p3411 A70-37493
- Auroral substorm temporal relationship to particle kinetic energy increases within trapping region, observing geomagnetic field distortions at higher latitudes during disturbed epochs
19 p3411 A70-37494
- Van Allen electrons acceleration and precipitation during magnetospheric substorms in relation to auroral processes, discussing energy and pitch angle diffusion processes
19 p3411 A70-37495
- Auroral enhancement of IR oxygen band, considering electric field excitation mechanisms
19 p3414 A70-38383
- Auroral photographic and visual observations, discussing satellite results and substorm development
19 p3417 A70-38730
- Postmidnight auroral events precipitating electrons energy spectra components characteristics, using simultaneous X ray, optical and absorption measurements
20 p3699 A70-39334
- Anomalous IR auroral emission observation during rocket flight, indicating unknown energy sources of oxygen excitation
20 p3621 A70-39350
- Auroras and noctilucent clouds simultaneous occurrence in middle latitudes, discussing mesopause temperature variations and mesosphere heating
20 p3621 A70-39402
- Auroral physics, discussing visibility, relations to geomagnetism and sunspots spectrum, morphology, optical emissions and particles in magnetosphere
20 p3623 A70-39929
- Auroral X-ray radiation at magnetoconjugate points Kerguelen/archangel region, using balloon-borne spectrometers
21 p3813 A70-40839
- Transverse magnetic disturbances in auroral oval, examining movement, intensity, particle fluxes and field magnitude
21 p3817 A70-41090
- Auroral proton precipitation oval in antarctic winter based on H Balmer line radiation
21 p3882 A70-41091
- Auroral optical emission measurements, examining oxygen atmospheric and IR bands by rocket sounding
21 p3817 A70-41092
- Auroral pulsations photometric observation data, noting magnetic activity effects
21 p3819 A70-41290
- Magnetosphere storm diagnostics from geomagnetic, auroral and airglow parameters, discussing calibration via satellite observations
22 p4022 A70-43289
- Molecular oxygen ions 1Ng band and molecular nitrogen 1Pg band relative intensities in normal and type B auroras
23 p4191 A70-44408
- Nike-Apache rocket aurora probes using proton detector to measure galactic cosmic ray intensity and relativistic electrons
23 p4192 A70-44879
- Polar auroral hydrogen emission intensity dependence on K index of geomagnetic activity
24 p4331 A70-46288
- Polar storm simultaneous onset and development, using observational data for geomagnetic field and aurorae
24 p4331 A70-46289

- Pulsating aurora onset in magnetically conjugate points noting local nature of sources
24 p4332 A70-46316
- AUSTENITE**
Martensitic steel /AFC 77/ austenite grain size refinement process, noting effects on yield strength, toughness, stress corrosion resistance and fatigue crack growth rate
01 p0120 A70-10739
Optimal thermomechanical treatment for austenitic steel stability to resist propagation and unloading of dislocations in cyclic loading process
05 p0867 A70-17041
Ni effect on nitrogen activity in Fe-Ni-N austenite between 600-1200 C using Strohlein analyzer
06 p1088 A70-17612
Ni influence in high temperature oxidation of austenitic Fe-Cr-Ni alloys investigated thermogravimetrically, metallographically and by electron probe microanalysis
07 p1305 A70-18965
Aluminum nitride morphology in structural Cr-Ni-Mo steel, discussing dependence on austenitization temperature and cooling conditions
08 p1519 A70-21435
Recrystallization in austenite phases of vanadium and columbium HSLA steel alloys determined in high temperature deformation tests
08 p1521 A70-21704
Austenitic Fe-Cr-Ni-Ti alloys at high temperature to determine activation energy for nitrogen diffusion, noting oxygen role
08 p1522 A70-21707
Precipitation in Fe-Ni-Co maraging alloys produced by austenite plates formation from martensite, discussing effects of Ti addition
08 p1524 A70-21955
High-strain fatigue life temperature dependence of austenitic and ferritic power plant materials compared to creep-rupture life
09 p1773 A70-22577
Carbon in austenite derived from composition dependence of diffusivity using first order mixing statistics
12 p2256 A70-27611
First order statistical model for temperature dependence of carbon activity in austenite
13 p2436 A70-29605
Austenization temperature, cooling rate and tempering conditions effect on steel castings structure, strength and impact properties
14 p2596 A70-30875
Alloying elements and austenization conditions effects on hardenability of steels, investigating critical cooling rates based on TTT diagrams
15 p2744 A70-31929
Austenite strength effect on austenite-martensite transformation in alloy steels, measuring resistance to plastic deformation
15 p2760 A70-32376
Martensite-to-austenite reverse transformation in Fe-Ni-Co alloys, using dilatometry and coercive force measurements
15 p2761 A70-32386
Precipitation hardening Co-Cu-Mo stainless steels, determining martensitic structures free from delta ferrite and residual austenite
18 p3262 A70-35965
Fe-Ni-C alloys austenite dispersion matrix effects on martensite structural characteristics
20 p3649 A70-39705
Austenitic formation by rapid heating of Ni maraging steel, noting microstructural characteristics relationship to martensite before phase transformation
24 p4356 A70-45144
Crystallography of martensite transformation on /225/ type planes of austenite in Fe-Mn-Cr-C alloy
24 p4358 A70-45237
- AUSTENITIC STAINLESS STEELS**
Combined aging and plastic deformation treatment effects on breaking point, yield stress, elongation and contraction of austenitic Fe-Ni-Ti alloy
01 p0115 A70-10064
Strain field association with random TaC precipitate particles in austenitic stainless steel shown by electron microscope
01 p0123 A70-11242
Austenitic stainless steels intergranular corrosion model proposed and supported by observations of structural changes and corrosion behavior, suggesting methods to reduce susceptibility
03 p0506 A70-13130
Embrittlement in martensitic and semiaustenitic precipitation hardening stainless steels upon exposure to high temperatures to determine causation and controlling means
03 p0506 A70-13132
Austenitic fcc Cr-Mn-N stainless steels ductile-to-brittle transition behavior noting role of deformation faulting
03 p0506 A70-13133
Serrated plastic flow in stable austenitic stainless steels based on Fe/Ni, showing strength dependence on C and/or Cr presence
03 p0506 A70-13134
- Fe-Cr-Mn-Ni system studied to obtain high Mn austenite and establish boundaries in quaternary system
03 p0509 A70-13278
Monograph on elevated temperature strength data for wrought austenitic stainless steels, considering yield, tensile, creep and rupture strengths for allowable stresses
03 p0510 A70-13300
Stress corrosion of martensitic and austenitic steels, discussing hydrogen embrittlement, mechanical strains, etc
04 p0710 A70-15676
Adverse effects of temperature and strain rate on low cycle fatigue resistance of austenitic stainless steels at elevated temperatures compared with tension tests
06 p1086 A70-17452
Gaseous environments effects on creep of austenitic stainless steel, observing weakening in air and surface cracking in nonoxidizing atmospheres
08 p1519 A70-21453
Temperature, transformation and strain rate effects on tensile ductility properties of stable and metastable compositions of austenitic stainless steels
08 p1524 A70-21956
Metastable austenitic steel mechanical properties after thermomechanical treatment with deformation, discussing stress-strain curves to exhibit yield point
08 p1525 A70-21963
Austenitic stainless steel hydrogen damage noting role of martensite plastic deformation
08 p1525 A70-21965
Thermal treatment function of austenitic grain size and mechanical properties of 18 pct Ni maraging steels
09 p1704 A70-22803
Internal nitridation temperature effect on dispersion hardening of austenitic stainless Fe-Cr-Ni-Ti steels, investigating interparticle spacing and layer thickness effects
09 p1705 A70-22810
Transcrystalline stress corrosion crack initiation in austenitic stainless steel tested in boiling magnesium chloride solution
09 p1706 A70-22940
Austenitic steels and alloys high temperature softening under conditions of stress relaxation and creep, noting hardening action of plastic deformation
09 p1709 A70-23785
Ni-Cr austenitic steel bending, surface temperature variations, crack development and propagation under double fatigue tests
10 p1902 A70-23819
Nitrogen content effect on proportional limit and work hardening rate of austenitic stainless steel at 302 F
10 p1905 A70-25169
Yield point temperature dependence in heat resistant austenitic alloys, showing tendency to brittle failure under short term overloads
10 p1906 A70-25291
Cr-Ni cold worked austenitic steel dislocation structure in tensile tests at different strains
14 p2596 A70-30874
Structure and chemical composition of high Cr diffusion coating on Cr-Ni austenitic steels
15 p2756 A70-31634
Austenitic stainless steel martensitic transformations, using transmission electron microscopy in conjunction with X ray and magnetization methods
15 p2761 A70-32379
Boron effects in austenitic stainless steels, considering chromium carbide formation, high temperature strength, ductility, etc
16 p2916 A70-33079
Void formation and creep during fast neutron irradiation of austenitic stainless steel based on thermodynamic approach, calculating nucleation and growth rates
17 p3123 A70-34626
Physical properties and structure of Cr-Ni austenitic stainless steels with high Mn and N content as function of temperature
17 p3125 A70-35143
Corrosion and mechanical properties of Cr-Ni-Mn-N austenitic stainless steels
17 p3125 A70-35144
High temperature reaging in Ni-Cr-Ti austenitic steel following reversion and interrupted quenching
18 p3274 A70-36054
Vacuum brazed stainless steel hot gas actuators for guided weapons
18 p3265 A70-37202
Austenitic stainless steels high temperature machining with W arc heating, considering constant pressure feeding and chip breaking method
20 p3638 A70-39943
Magnetism in austenitic stainless steels, discussing Mossbauer measurements of temperature dependence of hyperfine field and single line width
22 p4055 A70-43012
Niobium nitride precipitation associated with stacking faults in Cr-Ni-Nb austenitic stainless steels, using electron microscopy
24 p4365 A70-46369
- Cold reduction, refrigeration and annealing effects on stress corrosion cracking of austenitic stainless steels
24 p4365 A70-46389
- AUSTRALIA**
Age data on high sodium tektites from Australia showing distinct fall
03 p0576 A70-14089
Hydromagnetic emissions recordings at two Australian stations indicating simultaneous occurrence
10 p1875 A70-24441
Australite distribution pattern in Southern Central Australia
11 p2119 A70-26846
Report to COSPAR on Australian space research /1969/ including tracking stations, sounding rockets, technology utilization, etc
15 p2829 A70-31706
- AUSTRALITES**
Chemical analysis of Australasian tektites inferring extraterrestrial igneous origin, noting similarity to preimpact parent rock
05 p0916 A70-16832
Magnetic susceptibility of synthetic australite and philippinite-like tektites measured in 77-560 K range, discussing origin
05 p0916 A70-16836
Australasian microtektite compositional trends compared with critical plots enabling distinction between rocks formed by igneous sedimentary and vapor fractionation processes
06 p1150 A70-18477
Australite fall age determination from in situ radioactive carbon and standard geological dating methods
09 p1750 A70-22055
Australite distribution pattern in Southern Central Australia
11 p2119 A70-26846
- AUSTRIA**
Report to COSPAR on Austrian space research covering picture transmissions, solar activity, satellite observation, etc
15 p2829 A70-31707
- AUTOCLAVING**
Synthetic autoclave grown quartz crystals with W and Ga impurities, discussing spectral properties and weak absorption bands after irradiation
14 p2625 A70-30154
- AUTOCOLLIMATORS**
U COLLIMATORS
AUTOCORRELATION
Binocular brightness mixing and autocorrelation function, discussing mathematical model, computer simulation and test results
01 p0025 A70-11053
Autocorrelation function distortion in pseudorandom signal with limited spectrum at RC filter output
03 p0446 A70-13202
Temporal autocorrelation functions of ozone content and concentration from data of Soviet and U.S. stations, obtaining statistical stability
03 p0474 A70-13295
Solar and geomagnetic activity daily parameters persistence, discussing autocorrelation function, variance spectra, sunspot numbers, radiation flux, etc
05 p0906 A70-15877
Maximum gust correlation with gust mean distribution within given hour determined from high speed anemometer
06 p1096 A70-17414
Output autocorrelation properties of ideal limiters driven by binary deterministic signal plus stationary zero-mean Gaussian noise
06 p1013 A70-18625
Laser amplifier effect on autocorrelation function of laser radiation intensity fluctuations, determining emission coherence time
07 p1300 A70-19870
Stereo photographs conjugate image area matching, comparing automatic optical and electronic correlation techniques
09 p1680 A70-23067
Power spectral density and autocorrelation functions of sinusoidal carrier amplitude modulated by split phase PCM and PSK
11 p2008 A70-26203
Autocorrelation and brightness distribution functions for irregular variable star
11 p2115 A70-26579
Optimal phase-manipulated signals synthesis from autocorrelation function using algorithm
11 p2012 A70-26804
Engine firing rate measurement from acoustic waveform autocorrelation analysis
12 p2290 A70-27161
Correlation apparatus for ionospheric drift measurement by spaced receivers using closed loop of magnetic tape
14 p2550 A70-30741
Obliquely incident spherical wave amplitude and phase fluctuations, deriving formulae to compare variances behavior for refractive index fluctuation autocorrelation functions
14 p2574 A70-30750

- Time autocorrelation and power spectrum of radar returns from underdense turbulent ionized gas as function of electron density decay 14 p2551 A70-31035
 - Image coherence of object by laser illumination through moving diffuser related to diffuser autocorrelation 14 p2588 A70-31208
 - Autocorrelation of coherence characteristics of polarized components of light scattered at curved rough surface, showing nonadequate Kirchhoff approximation 15 p2749 A70-31555
 - Clutter signals in radar receiver antenna, determining autocorrelation function and spectral power density 15 p2701 A70-32466
 - Binary coded radar signal autocorrelation function main-to-sidelobe ratio improvement, using echo signal processed in mismatched filter 17 p3043 A70-34590
 - Empirical autocorrelation functions describing statistical properties of vertical temperature gradients in troposphere and lower stratosphere 17 p3132 A70-35337
 - Cyclic block code structures for generating binary sequences with good autocorrelation properties 19 p3375 A70-37284
 - Autocorrelation functions of anomalous gravitational and magnetic fields for ocean lines, relating Mohorovičić boundary and Curie isotherm 19 p3408 A70-37318
 - Ballistocardiogram autocorrelation function and spectrum by scanning graph decoder and computer, determining total power, harmonics periodicity and energy concentration 19 p3370 A70-38211
 - Cardiac contraction rhythm autocorrelation and spectral analysis in healthy subjects and patients with disturbed sinus node functional states 20 p3578 A70-38963
 - Soviet book on complex signals in ranging, navigation and communications, discussing correlation and ambiguity functions and bandwidth effect 20 p3587 A70-39723
 - Optico-acoustic autocorrelator for linear FM signals spatial compression, discussing design and performance 22 p3984 A70-42398
 - Coherent radar backscatter, calculating autocorrelation and power spectrum of spurious noise from periodic random phase injections for filter design to eliminate noise 22 p3992 A70-43591
 - Multibeam communication channel identification from output signal autocorrelation function analysis 23 p4159 A70-43761
 - Threshold output characteristic of FM signals, generalizing Gaussian baseband modulation solution to obtain autocorrelation function of output signal plus FM discriminator noise 24 p4313 A70-46063
- AUTODYNES**
- Frequency locking and control of autodyne oscillating NMR detector for signal averaging 21 p3827 A70-41454
- AUTOGYROS**
- NACA/NASA rotary wing aircraft research covering autogyro and helicopter development, noting flight safety 23 p4142 A70-44851
- AUTOIONIZATION**
- Lifetimes and fine structure of differentially metastable autoionizing states of negative He ion in axial magnetic field, using time of flight techniques 19 p3473 A70-37746
 - P autoionization states of helium and hydrogen negative ions, calculating widths and shifts 19 p3474 A70-38307
 - Autoionization spectral lines growth curves analysis, applying to 3s-4p transition in Ar at 466 Å with specified absorption cross section 21 p3781 A70-41931
 - Autoionization theory application to partial solar photoionization cross sections for production rates of vibrationally excited positive molecular oxygen ions 23 p4222 A70-44785
- AUTOMATA THEORY**
- Linear system theory in abstract algebraic framework applied to nonlinear machines in automata theory, discussing Ho algorithm, convolution and Kalman module theory 03 p0520 A70-14273
 - Human controller in psychology and control engineering, discussing linear and nonlinear modeling of human behavior 05 p0807 A70-16487
 - Stochastic automata for parameter self optimization with multimodal performance criteria 07 p1244 A70-18861
 - Multidimensionality in complex control systems, discussing circuit and oscillation theory, decomposition, variational problems, finite automata and group theory 11 p2023 A70-25602
- Associative analog designed for decision making by man searching for extremum in form of multilayer stochastic automaton 11 p1990 A70-25928
- Optimal strategies for game with nature and two-automata zero sum game under finite memory constraints 11 p2073 A70-26241
- Book on automatic recognition of visual patterns and mechanization of creativity, presenting computer program termed Arithmetic 13 p2373 A70-29451
- Stochastic automata as learning system models in random environments with penalty-nonpenalty expectations, demonstrating convergence 13 p2374 A70-29587
- Discrete time systems, deriving algorithm for testing decomposition property as necessary condition for linearity 13 p2375 A70-29939
- Soviet collection of papers on automation theory and biological systems simulation covering game theory and mathematical models 14 p2542 A70-30630
- Observation space transforming for synthesis of automatic optimization systems with memory tracking randomly walking extremum 18 p3234 A70-36073
- Harmonic linearization method for nonlinear automatic control systems with finite automata, discussing self oscillating modes of operation 22 p4001 A70-42836
- AUTOMATIC CONTROL**
- NT ADAPTIVE CONTROL
- NT AUTOMATIC FLIGHT CONTROL
- NT AUTOMATIC FREQUENCY CONTROL
- NT AUTOMATIC GAIN CONTROL
- NT AUTOMATIC LANDING CONTROL
- NT CASCADE CONTROL
- NT DYNAMIC CONTROL
- NT FEEDBACK CONTROL
- NT FEEDFORWARD CONTROL
- NT LEARNING MACHINES
- NT NUMERICAL CONTROL
- NT OFF-ON CONTROL
- NT OPTIMAL CONTROL
- NT PROPORTIONAL CONTROL
- NT SELF ADAPTIVE CONTROL SYSTEMS
- NT SELF ALIGNMENT
- NT SEQUENTIAL CONTROL
- NT TIME OPTIMAL CONTROL
- Prototype inspection equipment for automatic detection of fatigue damage in helicopter transmission gears teeth by magnetic perturbation method 01 p0097 A70-10011
- Automatic loading control system for tensile test machine permitting creep and creep-rupture testing 01 p0054 A70-10075
- Equivalent linear dynamic systems obtained by analog computers for determining equivalence equations coefficients and by Chebyshev functional to assess discrepancy 01 p0052 A70-10193
- Power supply equipment with automatic control for category 2 airport lighting, discussing reliability and economic efficiency 01 p0055 A70-10300
- Computer program for automatically selecting redundant parts and redundancy types for various aerospace systems characteristics 01 p0103 A70-10488
- Air traffic control system automation, anticipated benefits to users and operators and potential pitfalls associated with implementation [ALAA PAPER 69-1057] 01 p0137 A70-10638
- Tradeoff criteria between man machine and automated space systems applied to lunar and cosmic ray explorations [ALAA PAPER 69-1045] 01 p0034 A70-10644
- Semiautomatic data collection system for IR reflectivity measurements, recording digitized output on punched cards for computer analysis 01 p0088 A70-10747
- Terminal state control systems efficiency from determining permissible range of control parameter variation for steady and unsteady linear dynamic systems 01 p0052 A70-10982
- Information storage in complex automatic control systems with hierarchical structure composed of computers 01 p0047 A70-10983
- Algebraic criteria for absolute stability and equilibrium position in nonlinear continuous automatic control systems, using complex gain amplifier substitution 01 p0053 A70-11041
- Automatic IR control and tracking systems for aviation, space flights and military use, discussing sensor elements 01 p0139 A70-11262
- Automated inspection for defects and dimensions - Conference, Eastbourne, England, May 1969 01 p0105 A70-11394
- Mathematical relations and procedures for automatic satellite tracking by four axis Zeiss camera, discussing motion along small circle approximation and punch tape criteria 02 p0255 A70-11770
- Automatic four axle satellite tracking camera design and operational principle, examining lens aberration 02 p0294 A70-11771
- Automatic camera theodolite at Sophia satellite tracking station, discussing instrument constants 02 p0273 A70-11774
- Built-in, airborne and ground based automatic test equipment /ATE/ for fault finding and serviceability of aircraft electronic systems in civil aviation 02 p0295 A70-11845
- Automatic temperature controller consisting of single element of closed loop feedback system with adjustable transfer characteristics 02 p0296 A70-11874
- Automated structural design program to treat stress, displacement, gauge and cross sectional constraints, discussing applications to aircraft structures 02 p0386 A70-11944
- Secondary surveillance radar to operate autonomously with digital techniques and digital handling systems, discussing design and ATC applications 02 p0266 A70-11957
- Automatic aircraft tracking by returns from secondary surveillance radars, noting correlation of plots with track 02 p0332 A70-11966
- Computer simulation of automated ATC systems, discussing operational gaming and mathematical models 02 p0274 A70-11968
- Computer simulation of automated air traffic control concepts, formulating and implementing generalized model of automated transition/terminal area systems 02 p0335 A70-12133
- Helicopter automatic hybrid navigation system for increased accuracy over unfamiliar terrain and above-human performance, comparing navigating pilot performance with machine 02 p0335 A70-12134
- Algorithms for automatic control of machine elements fabrication 02 p0308 A70-12227
- Optimization potential selection in control system design by analytical method 02 p0272 A70-12412
- Automatic control nonlinear systems with random inputs, determining phase coordinates probability densities 02 p0272 A70-12414
- Automatic inspection data collecting and processing by human operator using display devices and computerized mathematical reduction for real time evaluation 02 p0266 A70-12469
- Instruments and procedures for photogrammetry automation, discussing automatic pattern recognition, data correlation and computer role 02 p0302 A70-12652
- Liapunov function for automatic control systems, deriving theorem to ensure stability 03 p0460 A70-13434
- Dissipativity and asymptotic stability criteria derived for systems of ordinary differential equations, considering application to automatic control problem 03 p0518 A70-13469
- Automatic aiming system for laser range finders using directional information carried by light beam transmission [ONERA-TP-761] 03 p0450 A70-13637
- Unsteady linear automatic control systems transient functions determined by approximation method 03 p0460 A70-13732
- Acceleration and regulating system of free turbine turboprop engines studied by graph-analytical method used for nonlinear circuit analysis 03 p0552 A70-13927
- Controllability conditions for control system described by equation with vectors x and f being non-dimensional and u and r being r dimensional 04 p0660 A70-14491
- Automatic control algorithms for subsystem malfunction identification in multisubsystem plants, analyzing conditions for diagnostic tests existence 04 p0661 A70-14554
- Modified harmonic balance method applied to critical values determination of nonlinear automatic control system parameters 04 p0661 A70-14555
- High gain antenna for 1973 Mars Soft Lander data transmission using sensors and digital computer to achieve autonomous precision pointing to earth [AAS PAPER 69-378] 04 p0716 A70-14653
- Controlled vehicle disturbed trajectory multiple correction, considering constrained control or limited accessible coordinates for observations 04 p0716 A70-15007
- Automatic testing of avionic units, describing electrical stimuli, measuring instruments and signal switching connection to test unit 04 p0663 A70-15042

Inertial navigation system reliability indices and improvement, discussing mission success, mean time between failure and automatic monitoring

04 p0716 A70-15166

Step system of automatic extremal control algorithms for inertial plant in presence of noise

04 p0661 A70-15194

Control system asymptotic stability stabilized by variable structural component applied to critical cases described by multiple zero root equations and imaginary roots

04 p0720 A70-15197

Coefficient matrix-structural method for obtaining transfer function of linear automatic control systems

04 p0662 A70-15277

Parasitic transient process in automatic control system during switching to mode stabilized with respect to certain coordinates

04 p0662 A70-15433

Correction method for single frequency search in extremal control of continuous quick response multivariable plants

04 p0662 A70-15434

Switching-type dekatrons use in automatic control, electronic measuring and computing systems, discussing advantages

04 p0660 A70-15436

Control program debugging for experimental automatic surveillance and tracking radar, noting use for on-line systems

04 p0654 A70-15449

Book on theory of nonlinear control systems covering nonlinear oscillations, Liapunov stability, control systems stability and theory, differential equations, etc

04 p0663 A70-15500

Automatic exposure control system for airborne cameras, providing iris and shutter control through taking lens for sudden light changes

05 p0844 A70-15771

Periodic vibrations of quasi-linear autonomous systems with retardation, deriving sufficient conditions for asymptotic stability

05 p0925 A70-15822

Automatic particle counters and fluid contamination problems, misconceptions relating to sampling, size measurement, calibration, etc

05 p0851 A70-16706

Conjugation principle for control system stabilization based on relation between controlled plant and stabilizing element stability

05 p0824 A70-16851

Automatic measurement of frequency-contrast characteristics of photographic films using linear, photoelectric and high speed comparator devices

05 p0852 A70-16865

Mathematical problem of stability of nonlinear automatic control systems solved using linear criteria

05 p0825 A70-16866

Machines selection for determining low cycle fatigue life, emphasizing automatic control system for regulating load and strain regimes

06 p1164 A70-17407

Automatic temperature stabilizer with high order amplification due to direct heater sensing, noting applicability for synthetic fiber plants and thermophysical laboratories

06 p1064 A70-17783

Nonlinear control systems stability with stochastic coefficients, applying Liapunov function

06 p1026 A70-17971

Approximate linearization of nonlinear automatic control systems with two frequency forced oscillations

07 p1243 A70-18687

Transistorized circuit for automatic control of photographic studies of pupillary reaction transient states in rabbits subjected to light stimulus

07 p1216 A70-18731

N-local controllability conditions for system having persistent controls assumed to be certain piecewise constant vector functions

07 p1244 A70-18766

Autonomy and invariance conditions for control systems composed of multivariable components having same number of inputs and outputs

07 p1244 A70-18768

Self stopping in involute gear mechanisms with external and internal gearing

07 p1290 A70-18818

Band polishing machines slave mechanisms and programmed controllers, describing helicopter longerons finishing process

07 p1291 A70-18829

Information transfer for quantitative relationships to error- and cause-controlled regulations

07 p1216 A70-18859

Soviet book on matrix methods in relay and sampled data control theory described by linear differential and finite difference equations

07 p1244 A70-19069

Collection of papers on control systems theory and applications, Volume 7, covering dynamical systems,

nonlinear filtering, optimal control, feedback control, etc

07 p1244 A70-19090

Automatically controlled rendezvous and docking for orbital assembly of spacecraft, deriving motion equations for mass centers

07 p1393 A70-19481

Control algorithm for vehicle descent after reentry based on descent range prediction by integrating motion equations allowing for motion three dimensionality

07 p1393 A70-19482

Automatic control of continuous medical monitoring in manned space flight

07 p1220 A70-19512

Automatic control theory found effective in studying arterial blood saturation with oxygen during ascent to 4000 m in pressure chamber

07 p1210 A70-19523

Cloudy sky IR background radiation model for designing simulator of IR background for studying noise rejection characteristics of electro-optical automatic control systems

07 p1246 A70-19527

Control system composed of linear and nonlinear components and distributed parameters, deriving stability criterion for simple critical case

07 p1246 A70-19539

Self calibrating radiometer for in-flight measurement of earth surface thermal microwave radiation

07 p1282 A70-19616

Book on control engineering for systems analysis and design, discussing feedback, nonlinear, discrete time and physical systems

07 p1246 A70-19669

Computer-controlled automatic test bench for black box modifications and electronic, hydraulic and pneumatic testing on Concorde aircraft

07 p1249 A70-19742

Reduction method for order of transfer function describing automatic control system, determining coefficients of reduced order transfer functions

07 p1247 A70-19842

Relay control design for model-tracking system with parameter uncertainties and disturbances using semidefinite Liapunov function

07 p1247 A70-20026

Automatic control system identification with respect to optimality criteria, mathematical models, computing techniques and input signals

07 p1247 A70-20029

Linear control circuits transfer function analysis, revising Nyquist criterion

07 p1328 A70-20212

Automatic system for processing data from underground meson telescopes

07 p1238 A70-20347

Magnetic suspension and guidance of high speed vehicles realized via magnetic field interaction of vehicle-mounted superconducting magnets with eddy currents

08 p1543 A70-20576

Automatic support systems for advanced maintainability - IEEE Conference, St. Louis, November 1969

08 p1468 A70-20651

Computer controlled automatic test system (NARF 5500) for naval avionics systems support, discussing system hardware and applications and programming cost reductions

08 p1469 A70-20652

Automatic test equipment from fourth generation computer viewpoint, considering cost and size reduction trends in avionics

08 p1469 A70-20654

Automatic multiple station test system for manufacturing plants, considering centrally controlled vs free standing and intelligent vs nonintelligent remote stations

08 p1470 A70-20655

General purpose automatic test system (GPATS) for electronic equipment fault location, discussing software and hardware for integrating programmable oscilloscope

08 p1470 A70-20656

Automatic test equipment for electronic devices, discussing computerized design of interface adapters for unit under test

08 p1470 A70-20657

Automatic test equipment programming for cost reduction by eliminating duplicated effort between manufacturers of test equipment and unit to be tested

08 p1464 A70-20658

Automatic testing hardware and software compatibility emphasizing versatile avionics shop test (VAST)

08 p1470 A70-20662

Computer program for automated test station simulation, considering station operating characteristics and performance prediction

08 p1465 A70-20666

Onboard automatic test equipment design, evaluating failure detection and reporting ability

08 p1470 A70-20667

Terminal air traffic control automation, discussing Advanced Radar Traffic Control System (ARTS) and control tower data transfer aspects

08 p1540 A70-20678

Soviet book on liquid rocket engines dynamics, emphasizing computational engineering methods and engines automatic control

08 p1558 A70-20757

Soviet book on aircraft engines automated production including plant and machine automatic control, technical and economical factors, etc

08 p1502 A70-20767

Laser systems application to automatic or semiautomatic materials processing in metal working and microelectronics, including hole drilling, silicon wafers scribing, etc

08 p1502 A70-20820

Linear differential controller equations for optimal automatic control system with disturbances

08 p1479 A70-20870

Functions generation to determine probabilistic parameters of automatic air traffic control system

08 p1541 A70-20873

Automatic control system stability with restricted nonlinearity, investigating lumped and distributed parameter systems and unique and nonunique equilibrium positions

08 p1479 A70-20996

Matching operations for difference and differential equations describing discrete control systems dynamics having cyclic interruption of data quantization frequency

08 p1480 A70-20999

Spectral densities of phase coordinates of nonlinear automatic systems in steady states at random disturbances determined by statistic linearization

08 p1480 A70-21016

Diagnostic-control tests for automatic homogeneous microelectronic structures, considering element coupling

09 p1643 A70-22142

Algorithm for controlled plant parameters determination based on sensitivity function calculation

09 p1653 A70-22145

Automatic phase correction for modulated subcarrier microwave systems used for control of industrial processes

09 p1632 A70-22281

Soviet collection of papers on control mechanics and processes, computational mathematics

09 p1772 A70-22532

Automatic spectral data reduction and analysis system consisting of densitometer, analog-digital converter and IBM 1800 process computer with magnetic disk memory

09 p1629 A70-22765

Miniaturized program oriented automatic pipe/tube welding system for in-place joining of fluid systems, controlling timing functions and weld current sequence

09 p1692 A70-22795

Differential equation formulation for pipeline in hydraulic automatic control system considered as lumped or distributed parameter plant

09 p1612 A70-22823

Earth Resources program automatic data correlation system noting lower cost, faster processing, undegraded imagery and compensation for vehicle perturbations and terrain relief

09 p1667 A70-22864

Laser beam with small divergence angle kept in horizontal position by leveling instrument with automatic compensating device, discussing distortion effects on localization

09 p1699 A70-23442

Water cooled space suits automatic control based on physiological changes in astronaut during hard work

09 p1627 A70-23458

Large-base radio interferometer with separate heterodyne receivers and electrical length automatic control, studying causes of phase errors

09 p1650 A70-23631

Radio and automatic control electronic equipment reliability estimation by vibration testing, determining test stand simulation accuracy

09 p1650 A70-23632

Fluidic digital position sensor consisting of fluidic monostable amplifier, analyzing operation by characteristics method

09 p1614 A70-23689

Parabolic antenna for automatic tracking compared for characteristics between multimode and four horn feed systems

10 p1847 A70-23920

Antenna characteristics and parameters as function of position and orientation in radome by automatic system consisting of electromechanical and programming device

10 p1848 A70-23971

Launch vehicle automatic checkout methods emphasizing guidance and control equipment performance in real time operations

10 p1952 A70-24912

- Book on automatic control theory for continuous and sampled data systems based on state variable approach 11 p2022 A70-25369
- Step-Track automatic angle tracking technique for communication satellites, seeking peak of antenna single beam [AIAA PAPER 70-416] 11 p1999 A70-25454
- TATS Master tactical communication satellite network controller with modems and digital computer for semiautomatic control over terminals [AIAA PAPER 70-412] 11 p2002 A70-25491
- Automatic control systems synthesis for plants described by incomplete differential equations, measuring controlled value and input derivatives 11 p2023 A70-25610
- Structural synthesis of automatic control systems for body motion along trajectory, using inverse method and nonlinear coordinate transformations 11 p2077 A70-25611
- Autonomous control system for moving plant based on logic threshold networks and multivariable functional converter 11 p2023 A70-25612
- Fighter aircraft firing accuracy improved by high pass filter to automatically compensate sideslip induced by rudder through follow up slideslipping by aileron 11 p1979 A70-25820
- Automatic maintenance testing of avionics systems, discussing tape controlled equipment and program preparation 11 p2017 A70-25837
- Electronic circuits automated endurance tests by follow-up scanning method, describing error sources in proper operation region cross section determination 11 p2013 A70-25922
- Multidimensional determined automatic control system structure and parameter synthesis by root method 11 p2023 A70-25926
- Self opening em-operated secondary and ternary mylar diaphragms for expansion tubes and tunnels 11 p2031 A70-25982
- Automatic control of continuous medical monitoring in manned space flight 11 p1991 A70-26111
- Automatic base communication system /ABCS/ to handle USAF worldwide base record communications centered on electronic store and forward message switch, utilizing stored programs 11 p2009 A70-26266
- Linear time-varying control process with bounded control amplitudes and rates, deriving conditions for recoverability 11 p2028 A70-26314
- Routing algorithm for computer controlled unmanned autonomous roving vehicle on Martian surface 11 p2081 A70-26317
- Time response deviation correction in hybrid computer control systems with digital feedback elements containing quantized coefficients 11 p2029 A70-26334
- Stochastic control system design methodology noting applications to ASW, law enforcement, document retrieval and autopilots 11 p2029 A70-26336
- Aircraft flight characteristics simulated on trainer with automatic control system and measuring system 11 p2056 A70-26455
- Pneumatically operated lifting mechanism and fluidic control system added to Izod impact testing machine for automatic impact repetition, counting and stopping 11 p2034 A70-26837
- Soviet book on aircraft AC and DC relay pulse generators, emphasizing controllable frequencies and duty factors and neutral and polarized electromagnetic relays 12 p2194 A70-26874
- Automatic in-process inspection testing of electronic products [SME PAPER IQ-70-709] 12 p2241 A70-27083
- Computer programmed automatic circuit analyzers, discussing unit adaptation, wire data processing and analyzer programming [SME PAPER MS-70-727] 12 p2241 A70-27084
- Computerized on-line industrial inspection involving automatic machine sequential control and product geometry error correction, discussing hardware and software requirements [SME PAPER IQ-70-712] 12 p2241 A70-27088
- Control system, operational procedures, aircraft guidance and runway design for increasing runway capacity, noting roles of automation and reduced separation [SAE PAPER 700280] 12 p2206 A70-27440
- Air controllers traffic capacity using automation, discussing airspace loading effect, area navigation and rerouting 12 p2267 A70-27637
- ATC data processing requirements for higher automation level in terms of computer instruction rate and storage 12 p2267 A70-27638
- DC signals measurement in automatic control circuits, ensuring transformer isolation by use of transistorized amplifier 12 p2196 A70-27682
- Flexible vehicle control, using cybernetic model for system design and response [AIAA PAPER 69-115] 12 p2314 A70-27811
- Statistical analysis of control system with nonlinear zero-memory element evaluated for error using Fokker-Planck equation 12 p2204 A70-27985
- Automatic image interpretation and classification using two dimensional digital Fourier transforms 12 p2193 A70-28106
- Computer controlled system for real time measurement and analysis of electromagnetic interference and compatibility with economy of time, manpower and cost 12 p2201 A70-28133
- Spacecraft autonomous control algorithm to ensure geographically specified landing accuracy without considering atmospheric density distribution 12 p2270 A70-28251
- Automatic phase control of demodulating signal in one dimensional extremal system with harmonic tracking oscillations 12 p2205 A70-28338
- Reentry control algorithm for prescribed landing point of space vehicle entering earth atmosphere at parabolic velocity, discussing double-dip reentry and digital simulation 12 p2499 A70-28376
- Automatic rendezvous and mooring-coupling of spin stabilized satellites, discussing configuration, guidance and dynamics model 13 p2499 A70-28397
- Ground stationed automatic orbital operations system /AOOSY/ for satellites and space probes, discussing flow diagram and Siemens computer programming 13 p2372 A70-28398
- Automatic-manual space rendezvous control system for Cosmos and Soyuz satellites, considering terminal phase control at specific closing range and velocity 13 p2499 A70-28402
- Synchronous satellite attitude acquisition and keeping, proposing roll and pitch control law for simulation 13 p2500 A70-28409
- Unmanned vehicles for planet surface exploration, discussing design and control using self adjusting and logic circuits 13 p2384 A70-28418
- Onboard computers automatic reliability control with implementation of self repair, modeling by Markov processes nonhomogeneous in time 13 p2372 A70-28438
- Automatic control systems for scientific experiments, considering algorithms, mathematical models and system designs 13 p2524 A70-28887
- Random reversible failures effect on linear automatic control systems precision treated as randomly varying structure, proposing statistical characteristics calculation 13 p2382 A70-29279
- Automatic test systems - Conference, Birmingham, England, April 1970 13 p2421 A70-29676
- Automatic test equipment performance and effectiveness below customer expectations, discussing design factors 13 p2525 A70-29677
- Automatic test equipment effect on product design, discussing test planning and quality control 13 p2422 A70-29678
- Relative cost benefits estimation of manual and automatic test systems for avionics in maintenance organization, proposing integrated maintenance and ATC data system 13 p2525 A70-29679
- Radio and electronic equipments production testing by automatic equipment combined with semiautomatic manual controller 13 p2379 A70-29680
- Aircraft equipment automatic test methods, comparing in-flight, on ground and second line testings 13 p2348 A70-29681
- Automatic test equipment third generation specifications and design 13 p2525 A70-29682
- MELVIN compact inexpensive multipurpose automatic test system, utilizing MSI single printed circuits to work optimally with computer 13 p2374 A70-29683
- Digital computer controlled test system suitable for verifying response to single input pattern containing time dependent functions 13 p2374 A70-29684
- Test Equipment for Rapid Automatic Checkout and Evaluation /TRACE/ system, describing method for interfacing computer with peripherals 13 p2374 A70-29685
- Automatic test equipment programming procedure including analysis, coding, validation and demonstration 13 p2422 A70-29689
- Digital computers in automatic test equipment, describing required control tasks 13 p2375 A70-29690
- Multistation automatic test equipment assembly management or maintenance organization, using digital computer control 13 p2385 A70-29691
- Quality assurance of automatic testing in military or industrial equipment, including acceptance criteria and statistical proving 13 p2423 A70-29694
- Avionics on military combat-reconnaissance aircraft, discussing automatic systems testing and cost effectiveness model 13 p2380 A70-29698
- Automatic cancelling devices with compensating coils for terrestrial magnetic field vector 13 p2401 A70-30044
- Computer-controlled single-server queueing system with constant access cycle and general service times, calculating mean size and waiting time at statistical equilibrium 14 p2553 A70-30518
- Linear control systems identification and synthesis from data containing modulus and phase information as frequency functions 14 p2559 A70-30520
- Book on automation of mathematical description of controlled plants covering signal generation, information acquisition, statistical disturbance, self adaptive systems, etc 14 p2560 A70-30629
- Soviet book on multivariable automatic control systems analysis and synthesis covering equations of motion, nonlinearities, pulse control, transient responses, etc 14 p2561 A70-30954
- Data flow in computerized automatic data acquisition systems, considering systems traceability of calibration to national standards 14 p2554 A70-31110
- Dual mode algorithm for routing unmanned autonomous roving vehicle around obstacles on planets, using dynamic programming and terrain information [JPL-TR-32-1484] 14 p2655 A70-31183
- Precision reliability indices for automatic dimensional control vibration-inductance sensor 15 p2714 A70-31582
- N-locus controllability of two dimensional holomorphic systems with permissible controls 15 p2715 A70-31641
- Control and guidance theories for biological problems, discussing signal transfer of linear control units and mathematical approaches 15 p2689 A70-31741
- Computer control of nonlinear systems with varying performance specifications, using Popov stability and nonlinear programming 15 p2715 A70-31973
- Soviet book on mathematical theory of linear and nonlinear control systems covering differential and difference equations, calculus variations, etc 15 p2715 A70-32200
- Digital computers in aircraft, discussing automatic control systems, components and advantages over analog systems 15 p2705 A70-32299
- Damping by hemispheric torquing to control spin axis in gyroscope rotor while remaining unchanged with respect to case fixed reference 15 p2741 A70-32505
- Automatically controlled rendezvous and docking for orbital assembly of spacecraft, deriving motion equations for mass centers 15 p2813 A70-32726
- Control algorithm for vehicle descent after reentry based on descent range prediction by integrating motion equations allowing for motion three dimensionality 15 p2813 A70-32727
- Automatic profile measurement and recording, describing equipment and techniques 15 p2742 A70-32777
- Emergency hypotonia regional control with/without blood circulation centralization, describing device consisting of inflatable balloon, extracorporeal shunt, electromagnetic valve, manometer and circuit 15 p2687 A70-32891
- Relay control systems stability bound determination in nonphase variable form, assuming unknown system parameters 16 p2881 A70-33034
- Digital logic control of chromatographic system for measuring instrumental contributions to band broadening 16 p2855 A70-33120

Laser ranging and tracking system consisting of mirror tracking pedestal, instrumentation bay and control van featuring manual/automatic tracking capability
16 p2862 A70-33164

Automatic active optic control of alignment and figure of primary mirror of spacecraft-borne telescope with response time stability
16 p2907 A70-33189

Automatic control - Conference, Atlanta, June 1970
16 p2883 A70-33301

Army missile command /AMICOM/ plasma jet wind tunnel automatic control system design
16 p2888 A70-33303

Upper bound determination for errors due to signal quantization in multirate digital control system through state variable or z transform formulations
16 p2867 A70-33306

Iterative weighted nonlinear least squares parameter estimation for human respiratory control system by transfer function modeling, comparing results with visual curve fitting
16 p2851 A70-33322

Automatic ground based aircraft collision avoidance using combined associative processor- sequential computers
16 p2948 A70-33468

Onboard automatic checkout systems for manned space vehicles, investigating data management development costs for thorough tradeoff studies
16 p2889 A70-33803

Computer controlled frequency surveillance system design and operation
16 p2871 A70-34052

Digital spectrophotometer with automatic continuous wavelength selection, sample feed, measurement and printout
16 p2914 A70-34098

Automatic tracking antenna aiming errors, discussing remedies, design, motion compensation and mechanical resonance damping
16 p2880 A70-34268

Automatic stabilization and control of computerized nonlinear processes, proposing algorithm for stability criteria
17 p3049 A70-34640

Dual flow turbojet engines automatic control and guidance characteristics
17 p3147 A70-34687

Automatic control system stability, allowing for position and velocity loads and compressibility of fluid in force cylinder of hydraulic actuating mechanism
17 p3024 A70-35367

Mechanical and acoustic vibrations signals analyzer, noting automatic or manual operation
17 p3054 A70-35417

Structural vibration test system, using hybrid computer for automatic control and data acquisition and reduction
17 p3061 A70-35488

Test facilities automation, discussing program storage, stimuli, measurement, data accumulation and storage and system control
17 p3062 A70-35503

Structural fatigue testing by computer control of random force cycles
17 p3062 A70-35505

Digital computer controlled positioning of telemetry antennas for tracking spacecraft
17 p3062 A70-35508

Variable loads programming by semicomputers/semihardware method for 747 fatigue testing
17 p3050 A70-35511

Electromagnetic, mechanical and chemical methods for automatic checkout of nonelectronic aerospace propulsion systems
17 p3095 A70-35525

Visual display and automatic taxi guidance system testing for improved aircraft docking accuracy
[AIAA PAPER 70-916] 17 p3064 A70-35828

Automated baggage handling and processing, requiring total aviation community participation
[AIAA PAPER 70-917] 17 p3204 A70-35829

Linear representations of symmetry groups and use in discrete automatic control systems
18 p3290 A70-36070

Multidimensional discrete control for fatigue testing under random loads, discussing model
18 p3234 A70-36074

Left ventricle pumping function self regulation mathematical model, obtaining transfer function
18 p3217 A70-36080

Logarithmic amplitude characteristic of automatic rate stabilization systems for controlled electric actuator systems
18 p3215 A70-36296

Automated radar terminal system, ARTS-III Beacon Tracking Level for continuous aircraft identity on controllers radar display
18 p3288 A70-36393

Data processing system for automatic air traffic control, describing hardware and software
18 p3288 A70-36395

National airspace system /NAS/, describing en route stage A automated air traffic control
18 p3289 A70-36399

Aero gas turbine engines digital computer control, discussing special properties, design and safety problems
[ASME PAPER 70-GT-40] 18 p3304 A70-36870

Algorithm for dynamic processes in unsteady linear automatic control system during finite time interval
19 p3470 A70-37256

Soviet book on statistical calculation methods for linear and nonlinear automatic aircraft control systems design, using correlation theory of stochastic processes
19 p3463 A70-37403

Soviet book on isolated animal heart autoregulation, considering cardio-pulmonary preparations, functional capacity, biometrics and computer technology for heart activity simulation models
19 p3359 A70-37404

Polynomial and logic theories of dynamic systems, explaining linear and nonlinear elements of automatic control systems
19 p3392 A70-37447

Automatic control systems synthesis based on root locus trajectories theory
19 p3392 A70-37808

Automatic control system impulse response points identification by fast Fourier transform
19 p3393 A70-37852

Simultaneous generation of sensitivity functions for linear automatic control system with known characteristic differential equation
19 p3394 A70-37867

Automatic calibration verification of subcarrier telemetry discriminators with selective channel readjustment
19 p3383 A70-37902

Automatic sound monitoring system for measuring aircraft noise in airport vicinity
19 p3397 A70-37908

Computer controlled aircraft noise monitoring system at Stuttgart airport
19 p3397 A70-37909

Computerized automatic ground equipment /CAGE/ as intelligence system for checkout and control of launch vehicles and spacecraft
19 p3397 A70-37915

C-SA engineering flight test /EFT/ computer controlled data processing system operation, illustrating capability, performance and limitations
19 p3355 A70-37917

Digital electrodynamic vibration exciter control for sinusoidal, random and shock spectrum testing of aircraft, missiles and satellites
19 p3383 A70-37920

Automatic ATC with feedback, describing information processing and flight plan algorithm
19 p3464 A70-38161

Iterative adaptation algorithms, using automatic search techniques for single and multiparameter systems
19 p3394 A70-38163

Arterial pressure measurement by automatic control system based on external compression pressure for maximum amplitude intraarterial pressure pulse oscillations
19 p3370 A70-38215

Electroencephalography with automatic frequency analysis to simulate processes involving brain self regulation
19 p3370 A70-38218

Automatic test equipment, considering capability, control and display facilities and system cost
19 p3401 A70-38542

Avionic systems automatic test equipment, discussing maintenance, reliability, cost and time reduction
19 p3402 A70-38544

Electronic components mass production for automatic control equipment, determining parameters probabilistic scatter
19 p3390 A70-38578

ATC automation in France, applying method of filters for controller feed, radar and accident avoidance
19 p3468 A70-38635

Signal automatic air traffic control system /SATCO/ for flight plan processing, using multi-processing real time computer, electronic displays and software facilities
19 p3469 A70-38646

Air traffic controller role in future air traffic system, considering automation in operations
19 p3371 A70-38649

Second order automatic phase control system with proportionately integrating filter, calculating transient response by harmonic linearization method
20 p3584 A70-39253

Semiconductors, ferrites and segnetoelectrics automatic temperature stabilization problem based on heat source energy conversion
20 p3597 A70-39255

Automatic cosmic ray station for recording nucleon and meson components
20 p3629 A70-39314

Guidance and navigation system design for automatic stationkeeping one earth orbiting vehicle with respect to other
[AIAA PAPER 70-1005] 20 p3667 A70-39526

Automatic control system stability error analysis, discussing sensitivity and statistical dispersion analysis
[AIAA PAPER 70-985] 20 p3668 A70-39544

Army Missile Command 8000 kw plasma facility automatic control system design
20 p3606 A70-39689

Invariant automatic control systems - Conference, Kiev, May-June 1966, Volume 2
20 p3601 A70-39826

Automatic control system components parameter variation effects on invariance conditions
20 p3602 A70-39830

Automatic control systems with signal recovery, determining invariance conditions, main operators and reproduction errors
20 p3603 A70-39833

Multidimensional automatic control systems polynomialization, describing compensating cross couplings realization
20 p3603 A70-39834

Complex automatic systems effectiveness synthesis based on invariance principles
20 p3603 A70-39835

VTOL aircraft longitudinal motion automatic stabilization in presence of turbulence and internal disturbances, using rotors and jet engines
20 p3561 A70-39838

Automatic control systems for aircraft approach to landing path and subsequent stabilization on trajectory, compensating for cross wind action and radio noise disturbances
20 p3561 A70-39842

Automatic air conditioning systems for hermetically sealed aircraft cabins, deriving control laws for air pressure, temperature and humidity
20 p3564 A70-39843

Invariant systems structural synthesis for automatic control of plant motion, deriving control laws for thrust and angle of attack
20 p3670 A70-39844

Complex plants process control by experimental statistical methods, considering curves plotting, computer requirements, optimum method selection, etc
20 p3592 A70-39902

Controlled systems characteristics multistep statistical evaluation by extrapolation, analyzing prediction errors
20 p3593 A70-39904

Controlled nonstationary plant dynamic characteristics determination by model, evaluating accuracy
20 p3673 A70-39906

Automatic weight analysis by calculation and orientation of mass properties /COMP/ program, using remote terminal time sharing computer system
[SAWE PAPER 824] 20 p3595 A70-40353

Italian automated ATC system /ATCAS/, discussing subsystem functions, display devices, data acquisition, information distribution, etc
21 p3847 A70-40911

Electromagnetic test equipment transient waveform control using on-line digital computer in near real time configuration
21 p3805 A70-41270

Book on stability of dynamic systems and solid bodies covering variation equations, Liapunov method and functions, approximations, harmonic balance and applications
21 p3850 A70-41370

Optical multilayer metal coatings vacuum deposition by cathode sputtering, using automatic apparatus
22 p4045 A70-42510

Soviet papers on harmonic linearization method in design of nonlinear automatic control systems
22 p3999 A70-42826

Harmonic linearization method for nonlinear automatic control systems, describing theoretical fundamentals
22 p4000 A70-42827

Harmonic linearization of nonlinear hysteretic elements in automatic control systems
22 p4000 A70-42828

Amplitude and phase frequency characteristics of open and closed multiloop nonlinear automatic control systems by graphical methods
22 p4000 A70-42830

Nonlinear automatic control systems transient response by frequency response curves of amplitude and phase characteristics
22 p4001 A70-42831

Harmonic linearization equations for frequency and amplitude of self oscillations in nonlinear automatic control systems
22 p4001 A70-42832

Harmonic linearization method for periodic regimes in discrete nonlinear automatic control systems performing signal quantization with respect to level or time
22 p4001 A70-42833

Asymptotic method for nonlinear automatic control systems involving differential equations in Cauchy form with nonlinearities
22 p4001 A70-42834

Harmonic linearization method for nonlinear automatic control systems with finite automata, discussing self oscillating modes of operation

22 p4001 A70-42836

Self oscillations and dead zones of automatic control systems with variable structures, using harmonic linearization

22 p4001 A70-42837

Periodic solutions to complex nonlinear automatic control systems with initial deviations, considering system stability and self oscillation conditions

22 p4002 A70-42839

Harmonic linearization method application to automatic phase control system with periodic nonlinearities

22 p4002 A70-42840

Harmonic linearization method for automatic control systems having hydraulic or pneumatic actuating device with two nonlinear elements

22 p4002 A70-42841

Soviet papers on statistical methods in nonlinear automatic control systems design

22 p4002 A70-42881

Statistical methods for nonlinear automatic control systems, including Monte Carlo method, equivalent perturbations, linearization and analytical techniques

22 p4002 A70-42882

Signal accuracy prediction in nonlinear steady or unsteady continuous and discrete automatic control systems in random noise, using statistical linearization

22 p4003 A70-42883

Interpolation method for nonlinear automatic control systems accuracy, discussing numerical integration optimal step and node number selection

22 p4003 A70-42886

Quantitative reduction of statistical nodes for nonlinear automatic control system with random noise, using minimal approximating polynomials

22 p4003 A70-42887

Output coordinates probability distribution density of nonlinear automatic control systems at fixed time, using multiple integrals

22 p4003 A70-42888

Digital statistical modeling of nonlinear automatic control systems including accuracy analysis, generation of random perturbations and parameter optimization

22 p4004 A70-42892

Lunik 16 lunar soft landing technique, discussing automatic and ground controlled mission phases

22 p4110 A70-43210

Computerized air cargo clearing, discussing London Airport Cargo Electronic-data-processing Scheme

22 p4007 A70-43272

Soviet cybernetics research, emphasizing discrete and continuous control devices and systems synthesis

22 p4004 A70-43449

Queueing requirements in automatic radar target detection system operating with narrow bandwidth data link

22 p3990 A70-43489

Free motion of second order nonlinear automatic control device with vibration damping

22 p4075 A70-43554

Automatically controlled motion of object with finite degrees of freedom under parametric periodic disturbances

22 p4005 A70-43561

Nonlinear automatic optimal control for discrete system with delay

22 p4005 A70-43563

Automatic control systems small oscillations suppression by nonlinear correcting elements

22 p4005 A70-43564

Universal proportional high accuracy temperature controller using current regulating circuit consisting of light beam galvanometer, photoconductor, photodiodes and thyristors

23 p4194 A70-43999

Automatic conflict detection and resolution in ATC planning, discussing flight paths, zones of protection, etc

23 p4215 A70-44154

Automatic detection of K-complex waveforms in sleep electroencephalograms, using pattern recognition

23 p4151 A70-44379

Automatic shutter for recording holograms with laser light, controlling exposure time by photoconductor cell

23 p4197 A70-44472

Automatic electronics test equipment, discussing choice between tape or computer controlled interpreter systems based on language, time, versatility and cost

23 p4173 A70-44539

Electronic equipment automatic testing systems signal routing and switching trees and matrices design, emphasizing modular approach

23 p4173 A70-44540

Electronic equipment automated testing objectives and requirements, considering man machine interaction, system controls, on-line reporting, and software/hardware availability

23 p4174 A70-44541

Roving vehicle self contained automatic control systems, discussing terrain scanning technique, stereo TV and electronic coordinate measuring and data processing equipment

23 p4260 A70-44628

Automatic Data Processing and Display System for ATC over Belgium, Holland and Germany, relieving traffic controller routine tasks

23 p4216 A70-44860

Iantar 1 automatic ionospheric laboratory flight tests results, investigating Ar ion engine performance

23 p4264 A70-45009

Automatic control of Cosmos spacecraft docking maneuvers in two successive encounter phases

23 p4264 A70-45016

Automated high precision electrical resistance measuring system using digital computer control

24 p4334 A70-45384

Aerial survey cameras exposure time automatic control circuits for high quality photographs with constant integral density

24 p4334 A70-45497

Hydraulic and pneumatic components for logic circuits of automatic controls, considering amplifiers, interlocked systems and use of fluidics

24 p4293 A70-45618

Automatic TV radioscopic X ray control for mass NDT of refractories and grinding wheels

24 p4368 A70-45723

Unmanned Luna 16 landing mission, discussing launching and automatic mission control via onboard computer and earth-radioed data

24 p4412 A70-45982

Automatic control system for Boeing SST engine air intakes, optimizing engine performance and controlling noise propagation

24 p4396 A70-46214

Upper Air Space Control Center Automatic Data Processing and Display System for air traffic control

24 p4323 A70-46238

AUTOMATIC CONTROL VALVES NT PRESSURE REGULATORS NT RELIEF VALVES

Automatic control for filling tanks with stably stratified liquids using analog mixture valve and digital metering pump methods

06 p1062 A70-17617

Fluid system control valve gain dependence on flow characteristics slope due to series resistance or centrifugal pump

09 p1613 A70-23685

AUTOMATIC DATA PROCESSING U DATA PROCESSING AUTOMATIC FLIGHT CONTROL

NT AUTOMATIC LANDING CONTROL

Automatic flight control and instrumentation in civil helicopters, examining military developments and Feranti automatic stabilization system

02 p0329 A70-11834

Inertial navigation systems, discussing role as flight control sensor with advent of all digital interface automatic flight control systems and cost and reliability

02 p0334 A70-11988

Airborne secondary surveillance radar transponders performance and system optimization for automatic altitude reporting, separation standards maintenance and automatic plot extraction

02 p0267 A70-11990

Solid state electronics application in automatic flight control, discussing redundancy, internal failure correction, fault isolation and automatic checkout

02 p0335 A70-12178

UHF ranging system principles, discussing output proportional to approach angle

02 p0257 A70-12179

Automatic flight control systems with aerodynamic characteristic and control parameters deviation from nominal values, discussing mathematical model describing aerodynamic characteristics behavior

02 p0381 A70-12408

Radar visual indicator used with scan converter and as synthetic indicator with computer controlled flight safety system

02 p0263 A70-12700

Ground-airborne steep descent VTOL automatic flight control and vertical path selection using hover augmentation system/HAS/ and remote area terminal system/RATS/

02 p0337 A70-12769

VTOL aircraft fly by wire system eliminating errors automatically, discussing electronic and electrohydraulic control components, flight test model design, prototype, etc

[DGLR-69-41] 04 p0623 A70-15149

Airborne digital letdown computer to guide VTOL aircraft flying complex trajectories to relieve airport congestion

05 p0880 A70-16416

Blind flight and helicopter navigation during prolonged maritime survival operations

07 p1193 A70-19132

Built-in test equipment for automatic flight control systems, discussing testing programs and fail safe hybrid circuitry

08 p1471 A70-20670

Soviet book on control systems for single rotor helicopters covering automatic stabilization system design, autopilots, pilot operation within closed control circuit, etc

08 p1435 A70-20769

Computer managed display system using CRT and appropriate solid state displays providing flight crew with automatically sequenced time varying information

08 p1498 A70-21677

Aircraft instrumentation in automatic flight control, discussing inertial platform, sensors, information transmission and display and digital technology

09 p1676 A70-22607

Flutter suppression in elastic finned beams in supersonic flow controlled automatically by rudder deflection according to flexural strain

09 p1785 A70-23615

Adaptive flight control systems utilization to compensate for variations in aerospace vehicle rigid body dynamics, noting control system performance requirements

[AIAA PAPER 68-970] 12 p2204 A70-28076

Combined radio and physical navigation systems, considering noise rejection and corrections of position and speed

15 p2772 A70-31623

Automatic flight control and instrumentation in civil helicopters, examining military developments and Feranti automatic stabilization system

15 p2772 A70-31771

Optimal adaptive digital autopilot design for reentry vehicle flight path control

16 p2946 A70-33007

V/JSTOL aircraft automatic flight control, guidance and navigation by onboard computer, discussing mathematical model and simulation results

[AIAA PAPER 70-1035] 20 p3665 A70-39502

Automatic aircraft lateral motion stabilization during flight in perturbed atmosphere by HF invariant systems

20 p3670 A70-39839

Metropolitan air transit system design, considering compound helicopters, automatic control by central computer, onboard avionics system and terminal facilities

21 p3956 A70-41250

Maneuver demand control using electric signalling feedback technique in Avro 707C and Hunter Mk 12 aircraft

24 p4374 A70-46203

AUTOMATIC FREQUENCY CONTROL

AFC by digital phase lock loop consisting of zone error detector with phase quantizing circuit and discrete frequency regulator with reversible counter

02 p0258 A70-12542

Frequency monitor design, analyzing relationships between time constants, gain, etc, emphasizing white noise filtration

07 p1227 A70-18991

Optimal control frequency signals for automatic spacecraft docking

08 p1582 A70-21180

Digital sampled-data loop of phase lock control containing digital zone error detector and digital frequency regulator with reversible counter as memory unit

10 p1833 A70-24085

Signal frequency capture probability vs frequency search rates and AFC loop parameters determined in phase locked oscillator

11 p1996 A70-25349

Automatic frequency control of single frequency He-Ne laser, tuning cavity length to extremum output power with Lamb dip

12 p2250 A70-28181

Computer modeling of nonlinear phase automatic frequency control systems under noise and oscillating disturbance

13 p2383 A70-29303

Noise effect on single band modulation receiver using phase automatic frequency control for carrier wave at arbitrary SNR

13 p2370 A70-29739

Phase locked automatic frequency control system, estimating duration of stabilization by theory Markov processes

18 p3228 A70-36625

Signal frequency capture probability vs frequency search rates and AFC loop parameters determined in phase locked oscillator

20 p3589 A70-40461

Automatic frequency control device for power klystron with two cavities, obtaining stabilization at natural frequency of crystal-containing cavity

22 p3998 A70-43236

Phased locked AFC circuit, calculating internal harmonic noise reduction by proportionately integrating filter

23 p4161 A70-43960

Automatic resonance tuning of transmitting and receiving antennas by electronic control for use in mobile communications

23 p4172 A70-44385

AUTOMATIC GAIN CONTROL

Time constant, steady state and tracking error of AGC loops at input/output of FM link in AM-FM telemetry system

12 p2184 A70-27250

Automatic gain ranging amplifier for high speed digital computer controlled data acquisition system used to process input data levels

19 p3383 A70-37919

AUTOMATIC LANDING CONTROL

Automatic landing systems mission and design, discussing pilot-system task coordination, equipment characteristics and reliability, etc

01 p0138 A70-11257

Aircraft pilot-autopilot task division during automatic landing, analyzing man machine interaction in aircraft approach guidance

01 p0139 A70-11258

Integrity monitoring of redundant multiplex control systems for aircraft autoland operations, discussing Triplex autopilot

02 p0329 A70-11833

Automatic landing systems research including VHF ILS accuracy, test equipment for servicing airborne equipment, etc

02 p0333 A70-11981

Hawker Siddeley/Smith Trident Autoland Program, discussing flight test data for Smith autopilot and autothrottle certification

03 p0522 A70-13349

Trident aircraft automatic landing in nearly blind conditions in regular commercial service

11 p2079 A70-25851

Space shuttle automatic landing system based on aircraft low visibility landing, considering economy and safety

14 p2614 A70-30466

All-weather automatic landing in blind conditions, considering Trident system

14 p2615 A70-31392

Automatic landing system assurance of DH 121 aircraft schedule all-weather regularity through high safety level via redundancy

17 p3022 A70-35856

All-weather Autoland control system using inertial smoothing, discussing required redundancy, fault detection, ground beam anomalies compensation, etc

19 p3469 A70-38821

Digital fail-operative flight control computers for automatic landings, describing system requirements and problems and flight test program

20 p3591 A70-39505

AUTOMATIC PATTERN RECOGNITION

U PATTERN RECOGNITION

AUTOMATIC PICTURE TRANSMISSION

Automatic picture transmission /APT/ ground station design for reception of weather satellite cloud cover photographs, discussing SNR

01 p0059 A70-11451

Small read-out stations for automatic picture reception from meteorological satellites, detailing design

02 p0382 A70-12648

Report to COSPAR on Austrian space research covering picture transmissions, solar activity, satellite observation, etc

15 p2829 A70-31707

Report to COSPAR on space research covering satellite tracking telemetry, Apt, meteorology, cosmic rays, solar activity and international cooperative programs, etc

15 p2829 A70-31709

Synoptic surface and upper air analysis and APT mosaics of meridional circulation over Mediterranean by remote satellite images

21 p3846 A70-41399

Picture transmitting systems noise rejection enhancement via redundancy, discussing video coding and decoding and signal filtration

23 p4159 A70-43760

ITOS-1 second generation meteorological satellite launched with Delta N booster, providing direct APT global readout and AVCS TV data recording for playback

23 p4259 A70-44615

AUTOMATIC PILOTS

Aircraft pilot-autopilot task division during automatic landing, analyzing man machine interaction in aircraft approach guidance

01 p0139 A70-11258

Integrity monitoring of redundant multiplex control systems for aircraft autoland operations, discussing Triplex autopilot

02 p0329 A70-11833

Hawker Siddeley/Smith Trident Autoland Program, discussing flight test data for Smith autopilot and autothrottle certification

03 p0522 A70-13349

Harmonic equilibrium method applied in dynamic properties analysis of autopilot electrohydraulic servomechanisms stability

03 p0415 A70-13930

Soviet book on control systems for single rotor helicopters covering automatic stabilization system

design, autopilots, pilot operation within closed control circuit, etc

08 p1435 A70-20769

Digital autopilot design using stochastic noise generator for synchronous random pulse sequence controlled by clock

09 p1720 A70-22418

Computational methods for multiput linear control systems applied to designing lateral and longitudinal autopilots for jet transports subject to gust loads

12 p2203 A70-27417

Minimum-time thrust vector control law in Apollo lunar module computerized autopilot

13 p2499 A70-28399

Aircraft vertical channel landing condition autopilot using state variable feedback control techniques

15 p2773 A70-32553

Optimal adaptive digital autopilot design for reentry vehicle flight path control

16 p2946 A70-33307

Lunar module digital autopilot design, considering attitude state estimator, reaction control system and thrust vector control

[AIAA PAPER 70-991] 20 p3668 A70-39539

Self adjusting autopilot system based on invariance principle for stabilization against wind gusts

20 p3670 A70-39840

Invariant autopilot control system during flight in turbulent atmosphere, allowing for aircraft elastic properties and invariance of coordinates

20 p3561 A70-39845

Flight simulation in SAAB A137 aircraft development, describing analog and digital computers, cockpit simulators, automatic pilots, control and display devices

[ICAS PAPER 70-42] 23 p4178 A70-44140

Elastic fuselage flight vehicle dynamic stability at supersonic speeds, using automatic pilot stabilization

23 p4139 A70-44157

Optimal adaptive digital autopilot design and operation, discussing linear differential equations of motion, algorithms, etc

23 p4215 A70-44504

AUTOMATIC ROCKET IMPACT PREDICTORS

U COMPUTERIZED SIMULATION

U IMPACT PREDICTION

AUTOMATIC TEST EQUIPMENT

Papers on automation in electronic test equipment, Volume 7, covering factory and depot for incoming inspection, production testing, quality control, maintenance and rebuilding

21 p3803 A70-40766

Miniaturized programmer-comparator MINI-BACE /Basic Automatic Checkout Equipment/, discussing design, mechanization, etc

21 p3803 A70-40767

Compact low cost Controller/Programmer/ Evaluator for varied automatic tests, using microminiature components

21 p3803 A70-40768

Electronic equipment test capability, programming methods and operation modes of General Purpose Automatic Test System, describing updating by USN

21 p3803 A70-40769

NASA automatic checkout systems for Saturn 5 stages and instrument units

21 p3803 A70-40770

General Purpose Automatic Test System using building block concept for avionic systems evaluation at military depot level

21 p3803 A70-40771

Computer controlled tester for digital circuits, giving diagrams and operations flow chart

22 p3996 A70-42849

Automated ultrasonic testing and facsimile data recording systems, discussing aerospace, marine and automotive applications

24 p4343 A70-45692

Nondestructive defectoscopic diagnostics, applying cybernetics to materials testing

24 p4344 A70-45694

AUTOMATION

Avionic units automatic testing to increase speed and reliability, discussing system configuration, parts, economics and computer language use

02 p0295 A70-11838

Automated techniques for topographic mapping, considering scales used

07 p1281 A70-19371

Computer and system design automation, considering language problems, microprograms, optimization on subsystem suboptimal basis, etc

10 p1845 A70-24874

Automatic air transportation passenger handling and postflight financial and statistical data processing

12 p2335 A70-27016

Man machine interface between operator and automatic testing equipment based on ergonomic design cost

13 p2360 A70-29687

Automatic laboratory or field testing equipment design requirements

13 p2423 A70-29695

Automatic test equipment for assembly shops, considering skilled personnel shortage, units complexity and repeatable test and repair

13 p2423 A70-29699

Book on automation of mathematical description of controlled plants covering signal generation, information acquisition, statistical disturbance, self adaptive systems, etc

14 p2560 A70-30629

Automated programmed device for fatigue tests based on harmonic oscillator, presenting schematic diagram

16 p2900 A70-33068

Computerized air transportation service including passenger name record, fare quotation, ticketing, etc

17 p3199 A70-34688

National Airspace System air traffic control automation program for en route and terminal facilities

19 p3464 A70-37914

Automatic test technology for avionics systems, discussing equipment and cost reduction

19 p3401 A70-38543

Statistical problems in technical automation - Conference, Moscow, February 1967

20 p3592 A70-39901

Computer calculations automation in mathematical models construction by statistical methods, discussing programs for distributed parameter systems, stochastic approximation, etc

20 p3592 A70-39903

Avionics hardware design guidelines to meet automated testing constraints including malfunction isolation, block requirements, packaging, etc

23 p4173 A70-44538

Air traffic control, future national airspace system improvements in view of air transportation growth, computerized automation technology, etc

24 p4374 A70-45969

AUTOMOBILES

Supersonic transport airworthiness criteria tentatively applied to road characteristics of automobiles

11 p1979 A70-25816

Flying qualities application to automobiles, discussing work load with respect to controllability and pilot behavior

13 p2347 A70-29142

Labyrinthine and sensory information role in driving, discussing car simulator, driver tests with impaired inputs, age factors, etc

22 p3976 A70-43708

AUTONOMIC NERVOUS SYSTEM

NT SYMPATHETIC NERVOUS SYSTEM

Autonomic nervous system role in controlling body functions after rapid decompression, increasing tolerance to pressure gradients by physical training

04 p0630 A70-14575

Cholinergic nervous mechanism of autoregulatory dilatation of pial arteries under decreased blood supply to cerebral cortex in rabbits

09 p1622 A70-23583

Autonomic effects on heart rate, portal, renal, cutaneous and muscle blood flows during arterial hypoxia in unanesthetized sham operated thalamic and pontine rabbits

12 p2170 A70-27899

Neurogenically maintained blood pressure component, discussing autonomic nervous system activity in hypertension and normotension, sympatholytic agents effectiveness in hypertensive treatment, etc

24 p4299 A70-45805

Inherited hypertension genetic and autonomic factors, discussing rats crossbreeding for genetic contribution ratio in males vs females, age effects, etc

24 p4299 A70-45806

AUTONOMY

Party autonomy application to standardized international air transport contracts, discussing international treaties, law court judgments and literature

02 p0402 A70-12267

Autonomy and invariance conditions for control systems composed of multivariable components having same number of inputs and outputs

07 p1244 A70-18768

Local control loop model of multiphase rectifier used as power amplifier, considering extension to nonautonomous and discontinuous conduction systems

21 p3802 A70-42267

AUTOPILOTS

U AUTOMATIC PILOTS

AUTOPSIES

Carboxyhemoglobin saturation in post mortem examination of aircraft accident victims, discussing errors in methodology

17 p3033 A70-35568

In-flight coronary occlusions role in aircraft accidents, discussing need for full autopsies, Double Masters ECG and full medical histories

17 p3033 A70-35570

General aviation aircraft accident post mortem findings, emphasizing standardization of format and terminology

17 p3040 A70-35579

AUTORADIOGRAPHY

Book on photographic action of ionizing radiations in dosimetry and medical, industrial, neutron, auto- and microradiography, emphasizing photographic materials reaction to photons and particles
02 p0337 A70-11696
T4 phage proteins radioisotopic examination, determining quantitative analysis, and molecular weight by autoradiography
20 p3583 A70-40325

AUTOROTATION

Weightless astronaut self rotation by limb maneuvers producing pitch and yaw motion
07 p1219 A70-19245
High powered high speed helicopters autorotation entry characteristics, noting capability of meeting control time delay requirement
17 p3014 A70-34715
Photospheric magnetic field differential rotation using synoptic charts for autocorrelation technique
21 p3885 A70-40951

AUTOTROPHS

NT HYDROGENOMONAS
Assimilation and metabolism of C atoms of pyruvate and acetate by strict autotrophs *Thiobacillus* cell, using radioactive substrates
01 p0021 A70-10788
Quantitative and qualitative differences in enzyme levels of intermediate carbohydrate metabolism in obligate autotrophs *Thiobacillus thioautotrophicus* and *Thiobacillus neapolitanus*
04 p0633 A70-15441
Temperature-synchronized semicontinuous culture and monitoring system for autotrophically growing *Euglenas*
04 p0633 A70-15453

AUXILIARY ELECTRIC POWER UNITS

U AUXILIARY POWER SOURCES
AUXILIARY EQUIPMENT (COMPUTERS)
NT PLOTTERS
NT PRINTERS (DATA PROCESSING)
AUXILIARY POWER SOURCES
NT CHEMICAL AUXILIARY POWER UNITS
NT NUCLEAR AUXILIARY POWER UNITS
NT SNAP
NT SNAP 8
NT SNAP 19
NT SNAP 27
NT SPACE POWER UNIT REACTORS
Emergency auxiliary hydraulic and electric power for commercial and military aircraft control, proposing self contained monofueled turbine system
[SAE PAPER 690658]
05 p0797 A70-15838
Flexible nickel cadmium secondary battery as nocturnal power supply for meteorological balloons transceiver and measuring instruments
08 p1440 A70-20711
Stand-by power supply for emergency lighting of Hamburg airport, discussing circuit connections for generators
08 p1482 A70-21371
Reliable and optimum cost power sources design for long life electronic digital communication equipment
12 p2166 A70-27927
Emergency auxiliary electric and/or hydraulic power for commercial and military aircraft using self contained monofueled gas turbine system
16 p2964 A70-33472
Large capacity sealed nickel cadmium battery for spacecraft, describing mechanical and electrical characteristics
16 p2844 A70-33473
MHD power sources for onboard military aircraft electrical application
16 p2964 A70-33474
High voltage DC electric power systems design for aircraft, considering filtering, transmission and loads interaction
16 p2844 A70-33475
Emergency auxiliary hydraulic and electric power for commercial and military aircraft control, proposing self contained monofueled turbine system
[AIAA PAPER 70-651]
16 p2970 A70-33616
Optimum mounting angles for direct solar radiation flux on solar battery on circular orbit satellite
18 p3215 A70-36176
Micropound extended range thrust stand /MERTS/ for testing electric thrusters for spacecraft auxiliary propulsion, providing three thrust measurement ranges and data telemetry system
[AIAA PAPER 70-1111]
20 p3607 A70-40232
Thermionic reactors for spacecraft auxiliary power and electric propulsion, discussing in-core conversion system and diodes
22 p4071 A70-43191
Hydrazine-fueled battery low power consumption auxiliary system with voltage regulator and gas pumps.
22 p3966 A70-43539
Ni-Zn high energy secondary battery cycle life and discharge capability
22 p3966 A70-43540
Airline selection of Auxiliary Power Unit (APU) for transport aircraft, noting benefits of air conditioning during ground operation
[SAE PAPER 700816]
24 p4394 A70-45901

TSCP700 aircraft auxiliary power unit design, fuel consumption and maintainability
[SAE PAPER 700815]
24 p4395 A70-45902
AUXILIARY POWER SOURCES
NT SNAP 27
AVAILABILITY
Availability model for system with exponential reliability function and constant repair time, determining start-up costs, cost-optimal mean up and down time, etc
01 p0221 A70-11382
Cost model based on initial and support costs for studying availability variations effect on system total cost and maintainability and reliability interrelationship
02 p0401 A70-11674
Computer program /SORCBE/ for systems unavailability tradeoff vs added cost for various versions
15 p2706 A70-32658

AVALANCHES

AVALANCHE DIODES
Read theory application to LF operation of avalanche diodes under large signal conditions
04 p0656 A70-14720
High efficiency oscillator using avalanche square wave diode, considering case of silicon p-i-n diode
05 p0819 A70-15815
Ge IMPATT diodes under pulsed operation to produce LF high efficiency oscillations, recording current and voltage waveforms
05 p0821 A70-16417
Phase, frequency and amplitude fluctuations in avalanche diode oscillators, studying noise origin
05 p0823 A70-16883
Bulk GaAs devices and avalanche /IMPATT and TRAPATT/ diodes compared as microwave sources
06 p1018 A70-17357
Optical and electronic mixing in avalanche photodiode during variable amplitude signal demodulation in optical heterodyne receiver, considering conversion losses
07 p1243 A70-20282
TRAPATT oscillator circuit characteristics determined from measurements and equivalent circuit calculations
08 p1475 A70-21277
Microstrip oscillator circuit design for operating with high power/efficiency avalanche diodes, describing low pass filter tuning section role
08 p1475 A70-21278
Circuit allowing direct combining of power from several avalanche diodes, discussing CW power output, single and multiple diode oscillators, etc
08 p1477 A70-21295
Zener diode used as hydrostatic pressure gauge, describing pressure effects on diode current/voltage characteristics
08 p1477 A70-21644
Short high current pulses generation by avalanche transistors in circuits suitable for investigating low impedance laser diode
09 p1642 A70-22035
P-n junction avalanche and bulk Gunn effect microwave oscillators, analyzing IMPATT and TRAPATT modes
09 p1644 A70-22224
Natural oscillation mode in symmetrically graded p-n junction using Missawa small signal equations for avalanche diode
09 p1653 A70-23804
Avalanche diodes and associated microwave circuits power generation in terms of IMPATT, TRAPATT, parametric, space-charge feedback and thermal modes
10 p1847 A70-23887
Tunable L band high power anomalous mode avalanche diode oscillator with coaxial circuit
10 p1847 A70-23888
Silicon diodes pulse operated in avalanche resonance pumped modes for producing stable microwave amplification
10 p1847 A70-23889
Solid state multistage high power avalanche amplifier at X band
10 p1847 A70-23890
Low power microwave IMPATT oscillator as parametric amplifier pumping sources for use in radar and communication systems
10 p1847 A70-23891
Si avalanche diodes oscillations external current waveform measurement using coaxial current monitoring assembly with negligible phase error
10 p1849 A70-24234
Avalanche diodes in presence of microwave instabilities related to field emission and charge transfer across depleted zone, discussing positive and negative resistance
10 p1850 A70-24621
Silicon avalanche diodes contingencies effect on material choice
10 p1850 A70-24622
Avalanche diodes microwave properties in utilization circuit, discussing negative conductance, nonlinear impedance and intrinsic noise current
10 p1850 A70-24623
Avalanche diodes properties, establishing equivalent circuit accounting for static electricity, carriers transit time and thermal effects
10 p1850 A70-24625
Silicon L-band avalanche diodes as high power pulsed microwave sources, discussing fabrication, circuit requirements, radar applications, etc
10 p1852 A70-24893
High power L-band avalanche diode oscillators fabrication and performance
13 p3736 A70-28977
Microwave avalanche diode emission frequency dependence on charge transfer across drift region, considering varactor diode output, negative resistance and noise factor
14 p2555 A70-30354
Millimeter waves generation by tunnel, Gunn and avalanche diodes, tabulating frequency, efficiency and power data
14 p2548 A70-30435
IMPATT microwave diodes small signal characterization by equivalent circuit using iterative computer procedure
15 p2708 A70-31971
Silicon avalanche transit time diodes as CW microwave generators and amplifiers
16 p2876 A70-33404
Avalanche diode transient temperature response, measuring thermal impedance under pulse bias conditions
16 p2878 A70-33695
Zener diodes as voltage transient suppressors for ground vehicle and aircraft power supplies
16 p2879 A70-34060
K-band high power Si avalanche diode oscillators, discussing decrease in pulse peak power output on basis of quenched plasma effect
16 p2880 A70-34260
Avalanche transit time diode and transferred electron oscillators in microwave systems, discussing design, performance and applications
18 p3232 A70-36675
Avalanche transistor circuits for rectangular pulses generation, considering delay line for optimum results
18 p3233 A70-36774
Small signal oscillation and growth for microwave loaded avalanche diodes with drift and ionization allowance
19 p3389 A70-37968
Etching effects on mesa profiles and edge breakdown of silicon avalanche diodes at high power and temperatures, using scanning electron microscope
19 p3389 A70-37971
Constant false alarm rate bias technique to control avalanche photodiode laser receiver over varying operating conditions of temperature, ambient illumination, etc
20 p3641 A70-39483
Avalanche diode microwave oscillators, considering Impatt and Trapatt oscillation modes
21 p3798 A70-41336
Wave instabilities in avalanche diode bulk semiconductors with negative field dependent drift velocity and carrier temperature, noting validity for gas plasma
21 p3863 A70-41915
Tunable high efficiency high peak power UHF avalanche diode oscillator
21 p3800 A70-42117
CW silicon SHF TRAPATT diode oscillator, discussing double sided design and fabrication
21 p3800 A70-42118
State space method for small signal lumped IMPATT diode model predicting small signal impedance
22 p3998 A70-43251
Miniature avalanche MOS diode, investigating capacitance voltage characteristics of deep depletion regime
23 p4172 A70-44007
Discharge pulse generation and equivalent resistance of relaxation oscillator applied to avalanche transistor
24 p4319 A70-45639

AVALANCHES
NT ELECTRON AVALANCHE
Carrier diffusion effect in large signal analysis of semiconductor avalanches in quasi-static approximation
19 p3387 A70-37768
AVERAGE
NT MEAN
Averaging over finite and infinite intervals derived for nonlinear integrodifferential equations with varying variables
03 p0594 A70-13507
Stepwise averaged parameters of nonuniform three dimensional flow through turbine blade cascade determined from conservation conditions
09 p1606 A70-23611
Averaging over finite and infinite intervals derived for nonlinear integrodifferential equations with varying variables
13 p2440 A70-28656

AVIATION

U AERONAUTICS

AVIATORS

U AIRCRAFT PILOTS

AVIONICS

Civil aviation electronics - Conference, London, September 1969, Part 1, Electronics in flight control

02 p0329 A70-11831

Avionic units automatic testing to increase speed and reliability, discussing system configuration, parts, economics and computer language use

02 p0295 A70-11838

Built-in, airborne and ground based automatic test equipment /ATE/ for fault finding and serviceability of aircraft electronic systems in civil aviation

02 p0295 A70-11845

Helicopter avionic systems man machine capability estimation based on pilot workload, applying results to design evolution

02 p0244 A70-12136

Gas pressure differences and diffusion rates recording using He-Ne laser interferometer, discussing aerodynamic applications and avionic instrumentation problems

02 p0299 A70-12272

Automatic testing of avionic units, describing electrical stimuli, measuring instruments and signal switching connection to test unit

04 p0663 A70-15042

Flammability control requirements and related hazards in avionics systems materials and components, using systems approach

05 p0956 A70-15854

Flight test results of avionics in aircraft

05 p0822 A70-16699

Complex integrated avionics computer system design for navigation, guidance and control of rotary wing aircraft, emphasizing microelectronic modular assembly

06 p1014 A70-17353

Avionic and space electronic equipment converging design, considering chip computer

06 p1017 A70-17354

Airborne computer system program for antisubmarine warfare enhancing human element in man machine system

06 p1185 A70-17974

Civil avionics systems engineering for safety, regularity, weather independence, flight patterns and airport utilization

08 p1468 A70-20649

Computer controlled automatic test system /NARF 5500/ for naval avionics systems support, discussing system hardware and applications and programming cost reductions

08 p1469 A70-20652

Automatic test equipment from fourth generation computer viewpoint, considering cost and size reduction trends in avionics

08 p1469 A70-20654

Carrier-based attack aircraft avionics, describing optimal large scale analysis procedure for flight control, communications and radar subsystems

08 p1470 A70-20660

General purpose support system /GPSS/ simulation for carrier operations and avionic maintenance, considering attack aircraft operations, spare parts, personnel requirements, etc

08 p1470 A70-20661

Automatic testing hardware and software compatibility emphasizing versatile avionic shop test /VAST/

08 p1470 A70-20662

Versatile avionics shop test /VAST/ Implementation Study recommendations on project management for automatic test equipment support system aboard attack aircraft carriers

08 p1601 A70-20663

Avionics maintainability concepts, discussing built-in test equipment, test connectors, automatic test equipment, fault detection and fault isolation

08 p1470 A70-20664

Onboard integrated maintenance system for aircraft avionics in-flight subsystems monitoring

08 p1471 A70-20669

Airplane dependability on basis of improvements in jet engine, avionics, pilot seat cushions and flight control systems

09 p1611 A70-23453

Avionics test station optimum design by computerized simulation involving iteration of computer run, analysis and model change

10 p1861 A70-24907

Automatic maintenance testing of avionic systems, discussing tape controlled equipment and program preparation

11 p2017 A70-25837

Systems engineering study of sensors in fighter aircraft avionics

11 p2081 A70-26501

Soviet book on aircraft AC and DC relay pulse generators, emphasizing controllable frequencies and duty factors and neutral and polarized electromagnetic relays

12 p2194 A70-26874

Avionics technology cost effectiveness effect on airlines and industry, considering systems engineering and specifications

[SAE PAPER 700299] 12 p2335 A70-27447

Multifunctional multimode avionics design integrating communications, navigations and identification subsystems /ICNI/

13 p2368 A70-29619

Relative cost benefits estimation of manual and automatic test systems for avionics in maintenance organization, proposing integrated maintenance and ATC data system

13 p2525 A70-29679

Avionics on military combat-reconnaissance aircraft, discussing automatic systems testing and cost effectiveness model

13 p2380 A70-29698

Flight control and human role in avionics system, discussing stabilization, autopilot and ILS systems

13 p2450 A70-29997

Avionics technology application to air traffic, discussing airborne computers use in navigation and control, secondary radar and correlation protected ILS

14 p2611 A70-30107

Ground and air based avionics for traffic control

14 p2612 A70-30109

Deterministic model for cost effectiveness of avionics support programs based on subsystems support ability, test philosophy and test equipment design and manufacture

14 p2563 A70-30857

Microwaves in integrated military avionics systems, discussing CNI, ECM, component reliability, etc

14 p2551 A70-31177

Avionics and instrumentation, discussing digital techniques application to engine control, electronic head-up and head-down displays, radiation pyrometry, etc

14 p2589 A70-31338

Avionics computers field repair method permitting removal and replacement of flat packs and discrete components on multilayer interconnection boards

15 p2706 A70-32655

Aerospace electronics - IEEE Conference, Dayton, May 1970

16 p2908 A70-33426

Fluidic technology for avionics systems, considering potential cost reduction and reliability improvement

16 p2843 A70-33445

General purpose parallel processor design for avionics, considering radar signal processing

16 p2910 A70-33467

Variable speed constant frequency /VSCF/ generators for avionics systems, discussing power, weight, volume, cost and reliability

16 p2910 A70-33486

Equipment and subsystems application to flight management avionics in military and commercial aircraft, noting role of ground-air information transfer

16 p2878 A70-33724

Space shuttle avionics cost effective design approach, discussing guidance, commonality, reliability, communications and autonomy

16 p2982 A70-33802

Flight deck design since 1920, discussing ergonomics and avionic aspects

16 p2913 A70-34048

Military aircraft avionics central digital computers, discussing memory capacity, computational speed requirements, cost and tradeoffs

17 p3049 A70-34673

Avionics problems in future Army aviation, discussing communications, navigation, instrumentation, automatic flight control, electronic countermeasures, fire control, etc

17 p3051 A70-34725

Aerospace industry instrumentation - Conference, Las Vegas, May 1969, Volume 15

17 p3091 A70-35476

Real time computers design tradeoffs in avionics systems

17 p3050 A70-35510

Flight/accident data recorders and associated equipment for civil and military aircraft requirements

18 p3258 A70-36342

Aircraft electronic equipment cooling techniques, discussing natural and forced convection, phase change and heat pipes

18 p3232 A70-36763

Aircraft digital interior communication systems, combining multiplexing techniques with solid state integrated circuits technology and systems integration

18 p3216 A70-36813

Computerized airborne integrated data acquisition and analysis system, discussing hardware, software and airborne-ground elements interfaces

19 p3382 A70-37393

Avionics role in STOL air transportation operational capabilities in congested air traffic environment

19 p3466 A70-38238

Avionics maintenance effectiveness logistics, discussing symptom pattern observation technique /SPOT/ for in-flight data

19 p3554 A70-38399

Automatic test technology for avionics systems, discussing equipment and cost reduction

19 p3401 A70-38543

Avionic systems automatic test equipment, discussing maintenance, reliability, cost and time reduction

19 p3402 A70-38544

Avionics hardware operational effectiveness assessment method, considering inertial navigation system LN-12D

19 p3442 A70-38837

Aerospace electronics covering fly-by-wire aircraft flight control, ATC, star trackers for spacecraft attitude control, etc

20 p3669 A70-39668

General Purpose Automatic Test System using building block concept for avionic systems evaluation at military depot level

21 p3803 A70-40771

Versatile Avionic Shop Test maintenance system supporting avionic equipment aboard aircraft carriers

21 p3804 A70-40772

Metropolitan air transit system design, considering compound helicopters, automatic control by central computer, onboard avionics system and terminal facilities

21 p3956 A70-41250

Aircraft electronics and instrumentation history, discussing anemometer, barometric altimeter, radar, communications systems, computers, flying control and various flight conditions

21 p3826 A70-41257

Aerospace digital computer and avionics systems man machine relationship optimization, considering human information and control response requirements

21 p3794 A70-41688

Computerized aerospace systems man machine interface mechanization for performance optimization, emphasizing integrated approach to avionic displays

21 p3795 A70-41689

Modular aerospace digital computer system architecture using off-shelf components for rapid avionic computing system realization

21 p3795 A70-41691

Low cost and weight reliable microminiaturized IC automatic cockpit checklist systems for aircraft pilots

22 p3977 A70-42298

Avionics digital computer system using associative memory for executive control functions implementation to mechanize task assignment algorithm

22 p3994 A70-43105

European avionics role in Post Apollo program, noting space shuttles, space tugs, space stations and modules

22 p3999 A70-43501

Aircraft electronics and instrumentation history, discussing anemometer, barometric altimeter, radar, communications systems, computers, flying control and various flight conditions

23 p4193 A70-43888

Avionics system for fighter aircraft, discussing weapons design, navigation-attack systems integration, etc

23 p4173 A70-44413

Avionics hardware design guidelines to meet automated testing constraints including malfunction isolation, block requirements, packaging, etc

23 p4173 A70-44538

High performance military aircraft missile command and control signal data processor microelectronics packaging, using integrated and printed circuit modules

23 p4174 A70-44542

Boeing 747 aircraft passenger entertainment and service system controls electronics design and wire installation improvement by multiplexing techniques

23 p4174 A70-44543

Boeing 747 airliner passenger entertainment and service electronics multiplexing system, discussing cable and connectors selection and design

23 p4174 A70-44544

Avionic components reliability, determining non-steady cooling air environment effects

23 p4175 A70-44744

Fluidics in naval avionics, discussing CH-46A helicopter stability augmentation and approach power compensator for carrier-based aircraft

24 p4293 A70-45428

AVOIDANCE

NT COLLISION AVOIDANCE

AVRO 698 AIRCRAFT

U VULCAN AIRCRAFT

AVRO 707 AIRCRAFT

Maneuver demand control using electric signalling feedback technique in Avro 707C and Hunter Mk 12 aircraft

24 p4374 A70-46203

AXES [COORDINATES]

U COORDINATES

AXES [REFERENCE LINES]

NT AXES OF ROTATION

NT EARTH AXIS

Extensive air shower axis position determined using energy methods and radial distribution geometry of particle density

01 p0171 A70-11252

Individual extensive air showers axes localized by measurement of charged particle densities, assuming age parameter

07 p1365 A70-18777

Earth rotation coordinates, discussing system coupled to earth by fixing of axes to zeniths of selected observatories and equatorial plane orientation

08 p1565 A70-20563

Electrical axis adjustment of east-west antenna array of crossed radio telescope by statistical processing of discrete sources observations

08 p1473 A70-21067

Earth rotation coordinates, discussing system coupled to earth by fixing of axes to zeniths of selected observatories and equatorial plane orientation

15 p2805 A70-32718

Imaginary axes effect of phenomenal space in contrast illusions of distance, discussing division of S field of vision by definite point fixation

20 p3573 A70-39764

Spacecraft principal inertial axis orientation estimation, comparing tangent 2 theta method with eigenvalue solution

[SAWE PAPER 847] 20 p3660 A70-40361

AXES OF ROTATION

NT EARTH AXIS

Shaft misalignment effect on accuracy of precision digital shaft angle encoders, using test fixture and optical methods

05 p0844 A70-15769

Motion equations of rigid vehicle derived in terms of body axes noncoinciding with mass center applied to ships and aircraft

05 p0881 A70-15883

Planets rotation axes inclinations related to Titius-Bode rule of solar distances, noting estimation of unknown inclinations

07 p1386 A70-19557

Asteroids uniaxial rotation as evidence against origin by collisional fragmentation of larger bodies

08 p1581 A70-21951

Spin axis motion of n-body coaxially mounted cluster of differentially spinning bodies, considering combined precession and nutation

11 p2123 A70-26128

Three axis motion simulator for in-orbit spacecraft attitude control evaluation using earth, sun and star sensor references

[AIAA PAPER 69-1029] 11 p2031 A70-26147

Earth rotation perturbations, analyzing secular polar shift dependence on dimensions, depth and location of seismic event

13 p2400 A70-29604

Transparent spherical rotor spin axis orientation by measuring Fresnel drag effect of optical beam inside ring laser cavity

19 p3445 A70-37669

Multiaxis clusters of single axis pendulous accelerometers with coincident centers of angular motion insensitivity

19 p3431 A70-38539

Gyro pendulum mounted on randomly vibrating platform, calculating stability of rotor axis vertical position

22 p4039 A70-43557

AXIAL COMPRESSION LOADS

Thin flat plates effective width under axial edge compression slightly beyond buckling limit, solving von Karman differential equations

01 p0198 A70-10094

Rectangular plates deformation under uniaxial compression, studying postcritical buckling behavior in presence of creep

01 p0201 A70-10937

Sandwich plates plastic buckling stability under uniaxial compressive loads from compressible theory viewpoint

01 p0204 A70-11137

Axially compressed cylindrical shells with edge constraints, determining critical load from inelastic behavior considerations

01 p0205 A70-11141

Reinforced plastics creep rupture strength under compression along elastic symmetry axes

02 p0322 A70-12805

Cylindrical shells buckling under biaxial compression and transverse loads, examining critical loads dependence on shell parameters, end conditions and elastic properties

03 p0590 A70-13380

Cylindrical two layer shells stability under compression and radial pressure, calculating compression and transverse shear strains in carrying layer and filler

03 p0592 A70-13443

Axial compressive forces influence on steel and Al cylindrical shell stability under external pressure

03 p0593 A70-13472

High speed photography for instability onset and subsequent buckling process in photoelastic circular cylindrical shells under axial compression

03 p0594 A70-13659

Far nonlinear postbuckling behavior of noncircular cylindrical shell under axial compression

03 p0598 A70-14241

Supercritical strains and buckling in rib-reinforced cylindrical shells under axial compression using strain-energy method

04 p0766 A70-14478

Elastic orthotropic fiberglass reinforced plastic shells stability under axial compression, analyzing shear modulus influence

04 p0712 A70-14490

Axial compression effect on low cycle fatigue of thin walled metal tubes in torsion

[ASME PAPER 69-MET-H] 04 p0705 A70-14880

Orthotropic axially compressed conical shell stability, evaluating lower critical load and postbuckling state

04 p0772 A70-14921

Orthotropic sandwich cylinders buckling under axial compression, presenting linear theory approximate design equations

04 p0776 A70-15381

Circular cylindrical shells with axisymmetric imperfections tested under axial compressive load, studying imperfection amplitude and wavelength effects on minimum buckling load

04 p0778 A70-15588

Axial compression of elastic circular cylinder in contact with identical elastic half spaces, determining interfacial surface stresses for frictionless and adhesive contacts

05 p0930 A70-16082

Adhesive or frictionless compression /or extension/ under axial load of elastic rectangle between two identical elastic half spaces in condition of plane strain

05 p0931 A70-16132

Incremental stress distribution near circular crack with internal pressure in neo-Hookean solid under deformation due to triaxial compression, illustrating initial stress effect

05 p0956 A70-17108

Thin shell buckling stressing maximum applied loads analysis for circular cylindrical shells with imperfect walls under axial compression

06 p1165 A70-17647

Thin walled cylindrical shell stability under stochastic lateral and axial compression loads using Liapunov method

[AIAA PAPER 70-104] 06 p1169 A70-18037

Local axisymmetric dimple imperfection effects on buckling load of circular cylindrical shell under axial compression

[AIAA PAPER 70-103] 06 p1170 A70-18167

Anisotropic fiberglass reinforced plastics creep properties under biaxial compression, showing compressive to tensile strain elimination or change

07 p1316 A70-19546

Initial perturbation effect of smooth cylindrical shells stability under critical axial compression noting deflection factor

07 p1415 A70-20190

Strain energy method applied to stability analysis of short longitudinally reinforced cylindrical shells under axial compression

08 p1584 A70-20536

Fiberglass reinforced plastics creep behavior under axial compression, studying time dependence of elasticity modulus and Poisson coefficient

08 p1526 A70-21174

Asymptotic analysis for axisymmetric buckling of axially compressed short cylindrical shells with free edges, using Batterman method

08 p1593 A70-21620

Cylindrical shells buckling under axial surface tensions using Donnell stability equations

08 p1593 A70-21624

Buckling and postbuckling equilibrium behavior of fiber reinforced cylindrical shell under uniform axial compression

09 p1780 A70-23207

Random displacement fields in thin circular cylindrical shells with initial imperfections under axial compression using statistical analysis

11 p2129 A70-25562

Stability loss in cylindrical shell under axial compression, noting critical load reduction by local axisymmetric depression

11 p2130 A70-25566

Clamping edges effect on critical parameters of cylindrical orthotropic shell under axial compression using undetermined Lagrange multipliers

11 p2130 A70-25567

Truncated conical shell buckling under axial compression using method for torsion buckling, correlating to equivalent cylindrical shells

11 p2135 A70-25980

Initial geometric imperfections effect on buckling and postbuckling behavior of laminated composite cylindrical shells under axial compression, considering reinforcing fiber orientations

[AIAA PAPER 69-93] 11 p2135 A70-25986

Buckling load calculations for axially compressed circular cylindrical shells under relaxed boundary conditions

11 p2140 A70-26484

Axisymmetric imperfection distributions effect on buckling of circular cylindrical shells under axial compression, constructing test models from photoelastic liquid epoxy

12 p2319 A70-27140

Stiffened cylindrical shells buckling under axial compression, obtaining imperfections and prebuckling growth mappings

12 p2319 A70-27141

Cylindrical shells design under axially compressed loads by elastic stability analysis, predicting critical loads

12 p2320 A70-27142

Thin cylindrical shells elastic buckling under uniform axial compression, considering Kirchhoff-Love hypotheses in critical stress determinations

12 p2324 A70-27396

Transversely isotropic shells stability with respect to subcritical deformation under axial compression using three dimensional linearized equations, determining critical loads

12 p2324 A70-27529

Shear buckling and uniaxial compression dependence on mechanical properties of clamped orthotropic plates, using Ritz method to compute bifurcation type loads

12 p2326 A70-27817

Cylindrical shells stability under axial compression by two dimensional Kirchhoff-Love applied theories, calculating critical stresses

12 p2328 A70-28282

Laminated glass fiber reinforced cylindrical shell stability resting on hinged supports under axial compression

13 p2514 A70-29285

Cylindrical shells under axial compression, using elastic stability analysis for critical loads prediction

15 p2822 A70-32512

In-plane boundary conditions effect on axially compressed conical shell stability under low buckling loads, using linear Donnell-type theory

17 p1886 A70-34971

Buckling loads and postbuckling behavior of curved panels under axial compression, noting dependence on boundary conditions

17 p1888 A70-35225

Stability of circular cylindrical shell reinforced by elastic rings at edges under longitudinal compression

18 p3341 A70-36581

Thin walled cylindrical shell stability under axial compression edge load beyond limit of proportionality

19 p3534 A70-37243

Stiffened thin walled circular cylinders buckling and postbuckling behavior under axial compression or external hydrostatic pressure

[DFVLR-SONDDR-59] 20 p3719 A70-39621

Dynamic stability of cylindrical shell with small curvature under static or periodically variable axial pressure loads

21 p3932 A70-40554

Ti single crystals plastic deformation in axial compression at high temperatures

24 p4358 A70-45239

AXIAL COMPRESSORS

U TURBOCOMPRESSORS

AXIAL FLOW

Design parameter importance in centrifugal axial flow particle separator tubes performance from separator tube development program data

01 p0163 A70-10680

Axial flow reversal in swirling incompressible tube flow, discussing static pressure, velocity profiles and turbulent Navier-Stokes equation

03 p0465 A70-13017

Boundary layer equations for axial laminar and turbulent incompressible flows over slender bodies of revolution solved by finite difference method

[ASME PAPER 69-WA/FE-2] 04 p0667 A70-14786

Motion generated by spherical body moving along axis of uniformly rotating fluid, measuring particle velocities ahead of and behind body

05 p0789 A70-16013

Axial profile characteristics of hypersonic near wake of slender circular cone based on pitot pressure, static pressure and stagnation temperature measurements

06 p0968 A70-17916

Temperature distribution in active elements of explosion proof asynchronous electric motors with multichannel bilateral axial flow ventilation systems

07 p1196 A70-19841

Transverse pressure gradient effect on parameters of turbulent boundary layer on body rotating in axial flow

08 p1483 A70-21193

Second order conical flows around wing-fuselage system, deriving expressions for axial perturbation velocity for various attack geometries

10 p1804 A70-24972

Flow pattern of axial flow of turbine stage calculated from cascade characteristics

11 p1975 A70-25794

Incompressible boundary layers velocity distributions on cylinders rotating in axial flow, considering

- centrifugal force effects, momentum thicknesses, local shearing stress, etc 11 p2038 A70-26477
- Axial compressor stage head determination by measuring axial thrust, noting fluid velocity nonuniform distribution influence 13 p2474 A70-28892
- Axial flow fans performance dependence on aspect ratio from empirical relationships, plotting various component losses and stage efficiency 14 p2529 A70-31418
- Axial wall conduction effects on steady state laminar flow heat transfer 15 p2825 A70-31815
- Turbulent boundary layer instability on rotating cylinder in axial stream, correlating mixing length to Richardson number 15 p2722 A70-32372
- Forced vortex impeller in axial flow fan without inlet vanes, presenting lift and drag coefficients of blade sections, loss of head, etc 19 p3352 A70-38222
- Three dimensional flow through rotor of axial vortex flow fan, using airfoil method for design 19 p3352 A70-38248
- Heat transfer from cylinder in axial air flow with induced turbulence of incident boundary layer, noting temperature effects 20 p3736 A70-39264
- Spatial gain variations transverse to discharge in axially flowing carbon dioxide laser amplifier, noting relationship to flow velocity 20 p3640 A70-39391
- High output CW carbon dioxide laser design, using gas pressure variation and fast axial flow 22 p4048 A70-42322
- Free jet flow axial gradient effects on drag coefficient measurement of slender blunted cones at zero attack angle 23 p4135 A70-44584
- Axisymmetrical nozzle aerodynamic shape design for conical to axially uniform flow conversion, using method of characteristics 23 p4136 A70-44991
- Subsonic flow around bodies of revolution in axial direction, using ALGOL program for numerical calculations 24 p4289 A70-46237
- AXIAL FLOW COMPRESSORS**
- U TURBOCOMPRESSORS**
- AXIAL FLOW PUMPS**
- NT TURBINE PUMPS**
- Axial flow pump impellers suction performance and cavitation conditions 06 p1075 A70-17137
- Liquid hydrogen axial flow pump inducer, describing suction pressure measurements, fluid conditions and flow rate [AIAA PAPER 70-627] 16 p2919 A70-33592
- Axially reciprocating pump, calculating fluid over-flow effect on working cell pressure change 21 p3759 A70-41775
- AXIAL FLOW TURBINES**
- Axial flow turbine stator and impeller blade twist calculated from gas flow stage area diameter using continuity and vorticity equations 01 p0001 A70-10175
- Cascade tests to investigate nature of flow in rotor blade channels of axial flow turbines with partial admission 01 p0162 A70-10329
- Optimal lift-drag ratio of cascades dependence on optimal pitch of cascades calculated for axial flow turbomachinery 02 p0356 A70-12750
- Tip clearance effects in axial flow turbomachinery, predicting blade-to-blade variation in outlet angles and stagnation pressure losses [ASME PAPER 69-WA/FE-26] 04 p0733 A70-14775
- Sound generation in axial-flow subsonic turbomachinery, using two dimensional model [ASME PAPER 69-WA/FE-4] 04 p0733 A70-14785
- Steady and unsteady flow through Napier turboblower axial flow turbine for full and partial admission, estimating mass flow and power output 07 p1189 A70-20294
- Efficiency loss with tip clearance predicted for mixed and axial flow single stage turbomachines, using perfect fluid model 11 p1974 A70-25787
- Optimal efficiency of axial turbomachines limit loading of blade root and hydrodynamical criteria 11 p1975 A70-25791
- Axial flow multistage turbines performance, examining profile manufacturing tolerances effects on cost 16 p2970 A70-33677
- Axial gas turbine performance prediction method improvements based on comparison with tests [ASME PAPER 70-GT-2] 18 p3304 A70-36859
- Three dimensional boundary layer flow on rotating axial flow turbine buckets, determining velocity profiles [ASME PAPER 70-GT-59] 18 p3243 A70-36874
- Annulus wall boundary layers in axial flow turbomachines, taking into account boundary layer growth and associated secondary flows [ASME PAPER 70-GT-92] 18 p3209 A70-36877
- Blade root design for axial flow compressors and turbines, avoiding tensile stress concentration 19 p3490 A70-38616
- AXIAL LOADS**
- NT AXIAL COMPRESSION LOADS**
- Elastoplastic zone and instability of precracked thin sheets under uniaxial loading applied to rectangular center-notched steel foils 03 p0598 A70-14239
- Equipment for cyclic biaxial testing, producing five biaxial stress states by simultaneous direct pressurization and axial loading of thin walled cylindrical specimen 03 p0464 A70-14309
- Transverse vibration of viscoelastic polymethyl methacrylate column with initial curvature under periodic axial load, determining amplitude-frequency curves [ASME PAPER 69-WA/APM-13] 04 p0772 A70-14915
- Dynamic plastic response of finite bar subject to axial impact load noting reflected waves, stress-strain-time histories and residual strain 04 p0779 A70-15599
- Biaxial prebuckling loading effect on compliance tensor in plastic buckling of square plates analyzed by local strain statistical theory 05 p0925 A70-15790
- Isotropic elastic cylindrical shell stability under combined compressive and axisymmetric local loads, using equilibrium equations for shallow shells 05 p0936 A70-16240
- Circular cylindrical shells stiffened by rings and stringers and subjected to periodic axial force, analyzing parametric instability 05 p0940 A70-16513
- Finite element method analysis of axisymmetrically loaded thin shells of revolution, considering non-linearity due to material properties and shell geometry changes 05 p0944 A70-16812
- Shear and linear strain energy criteria for limiting stress state model of solid deformable bodies, considering uniaxial, biaxial and triaxial loading 06 p1166 A70-17657
- Thin walled cylindrical shells design for axisymmetric impulsive loads, calculating strains due to explosive forming in water 06 p1167 A70-17867
- Stress-strain state equations for axisymmetrically loaded shells of revolution made of materials with variable moduli 07 p1399 A70-18660
- Circular plates dynamic response to axisymmetric time dependent loads, analyzing transverse restraint effects on response maxima by plate theory 07 p1404 A70-19251
- Axially uniform stress and strain in cylindrical shells, discussing Saint Venant torsion and displacement relations 07 p1405 A70-19255
- Point matching technique for plane elastic problems extended to axisymmetrically loaded elastic body of revolution, developing general computer program 07 p1416 A70-20303
- Quadrature solution for elastic sphere deformation by axisymmetric normal loads, writing Green function of boundary value problem in finite form 08 p1585 A70-20956
- Free vibrations and dynamic buckling of hinged extensible beam under axial force 09 p1768 A70-22061
- Beam vibration eigenfunctions with allowance for shear compliance used to determine beams dynamic stability under pulsating axial load 09 p1785 A70-23600
- Axisymmetric free vibrations of orthotropic cylindrical shell loaded on ends by constant axial force, investigating nonlinear elasticity 09 p1785 A70-23625
- Shells equilibrium with large plastic deformations, discussing stability under uniaxial/biaxial tension and physical models for material mechanical properties 11 p2130 A70-25569
- Axial strain controlled fatigue tests at elevated temperature, discussing specimen gripping, alignment and break detection for mechanical and closed loop hydraulic test machines 11 p2033 A70-26611
- Viscoelastic polymeric materials tensile failure under multiaxial loading 12 p2321 A70-27205
- Spherically cut space elastic properties, determining normal and tangential stresses for uniform axisymmetric edge loading 12 p2328 A70-28200
- Al-Zn-Mg alloy welds delayed rupture under constant uniaxial load in distilled water or aqueous salt solution 14 p2591 A70-30970
- Shallow shells of revolution under axisymmetrical loads, analyzing plasticity and creep by integral equations algorithm 15 p2817 A70-32164
- Axial stress at notch root of shafts under axially symmetric loading, utilizing integrated birefringent patterns in transmitted light at room temperature [SESA PAPER 1970] 15 p2821 A70-32315
- Axially loaded cylindrical shells prebuckling deformation behavior measurement by holographic interferometry 17 p3086 A70-35012
- High strain fatigue machine with axial loading and servocontrol for short endurance testing 17 p3063 A70-35586
- Pressurized shells of revolution loaded axisymmetrically, formulating equations for calculation of displacements, forces and stresses 18 p3338 A70-36406
- Programmed fatigue testing machine for specimens under cyclic axial loads, transforming angular into linear displacements 18 p3237 A70-36473
- Limit load of cylindrical shell with rigidly clamped edges under varying pressure and axial force, using Tresca yield condition 18 p3343 A70-36722
- Unidirectional composites subjected to free vibration and axial end loading, considering longitudinal stress wave propagation in fiber direction 19 p3540 A70-37954
- Quadrature solution for elastic sphere deformation by axisymmetric normal loads, writing Green function of boundary value problem in finite form 20 p3719 A70-39379
- Perforated steel strip axial tension load limit, considering various hole diameters and numbers 21 p3936 A70-41415
- Parachutes lightweight coated fabrics air permeability under axial tensile loading and load cycling at room temperatures 21 p3843 A70-41835
- Joint strength of three layer fiberglass reinforced plastic panels with bilateral adhesive patches under linear axial force 22 p4115 A70-42812
- Spherically cut space elastic properties, determining normal and tangential stresses for uniform axisymmetric edge loading 22 p4117 A70-43324
- Curved element approximation of orthotropic axisymmetric thin shells under axial loads 24 p4419 A70-45152
- AXIAL STRAIN**
- Out-of-phase or nonsynchronous biaxial straining effects on low cycle fatigue observed on Al specimen by cycling tension-compression and cyclic torsion 03 p0481 A70-12955
- Thin shells of revolution plastic collapse under axisymmetric loads on basis of Tresca-Nakamura yield criterion, using computer algorithm 03 p0598 A70-14238
- Vacancies influence on macrodefect nucleus formation in single metal crystals under uniaxial strain explaining Griffith crack initiation 05 p0861 A70-15784
- Viscoelastic behavior of styrene-butadiene rubber under finite uniaxial and equal biaxial deformations for nonisothermal case 05 p0929 A70-16068
- Plane circular crack in homogeneous and isotropic elastic body under uniform uniaxial tension using linearized couple-stress theory 05 p0931 A70-16089
- Axisymmetrical stress-strain analysis of viscoelastic cylinder enclosed in elastic shell under internal pressure using singular kernels 05 p0933 A70-16207
- Buckling of three layer cylindrical shells under steady creep conditions, deriving axisymmetric deformation 05 p0935 A70-16234
- Steel tube deformation under constant internal pressure and cyclic heating, plotting tangential and axial strain curves as function of cyclic loading 06 p1163 A70-17399
- Solid propellants mechanical properties under uniaxial tension 09 p1741 A70-22423
- Stressed state in region of strain raisers /round holes/ in plate subjected to two axial tension associated with plastic yield 09 p1771 A70-22464
- Uniaxial strain pulse propagation through various materials loaded uniformly with step function pressure by gas dynamic shock wave reflection 09 p1783 A70-23449
- Nonlinear plane deformation of elastic medium with cylindrical cavity under uniform axial tension using successive approximations 09 p1784 A70-23591
- High temperature fatigue tests of materials under uniaxial controlled strain, describing equipment, failure interpretation and data reduction 11 p2033 A70-26613

Finite element method applications to finite axisymmetric deformations of incompressible elastic solids of revolution

13 p2510 A70-28734

Circular cylindrical membrane axially symmetric deformations, determining axial and circumferential stresses

14 p2657 A70-30844

Uniaxial yielding correlation with substructure in Al-stainless steel metal matrix composites, using compressive loading test

15 p2756 A70-31565

Anisotropic glass fiber reinforced plastics strength and deformability under cyclic axial loads

15 p2766 A70-32897

Stress distributions in tapered bolt assemblies due to interference and uniaxial tension

16 p2992 A70-33989

Elastic membrane axisymmetric deformations, reducing nonlinear equations system to quadratures

20 p3718 A70-39230

Elastic and viscoelastic plates, calculating stress concentration and separation of embedded smooth circular inclusion under uniaxial tension

21 p3932 A70-40548

Hollow spheres and hemispheres nonlinear axisymmetric deformation, using shell theory reduced to two point boundary value problem for differential equations

22 p4112 A70-42288

Laminated composites time dependent static strength and reliability under uniaxial tension

22 p4119 A70-43678

Composite laminates under uniform axial strain, determining interlaminar stresses and displacements by finite difference techniques

22 p4060 A70-43684

Plastic postbuckling and imperfection sensitivity of spherical shells under axisymmetric bifurcation

23 p4272 A70-44714

AXIAL STRESS

Plastic flow under biaxial stress, discussing data acquisition system and computer program for comparing test and theory

03 p0480 A70-12954

Equipment for cyclic biaxial stress states testing by simultaneous direct pressurization and axial loading of thin walled cylindrical specimens

03 p0462 A70-12966

Ti-Al-Sn alloy tensile deformation mechanisms at cryogenic temperature under uniaxial and biaxial stress noting twinning, prismatic slip and dislocation characteristics

03 p0507 A70-13141

Limiting equilibrium under axial tension of brittle body with parallel axisymmetric external cracks, studying critical load, crack propagation, etc

03 p0594 A70-13737

Creep rupture and fatigue strength in solid body mechanics, considering triaxial stress state and simplified creep rupture theory variant

03 p0599 A70-14249

Equipment for cyclic biaxial testing, producing five biaxial stress states by simultaneous direct pressurization and axial loading of thin walled cylindrical specimen

03 p0464 A70-14309

Laplace transform of axial stress resultant in impacting semiinfinite elastic cylindrical membrane as exponential function involving wave propagation speed, applying continued fractions

04 p0769 A70-14859

Difference equations and axial stress tensor component for turbomachinery in curvilinear coordinates systems

04 p0776 A70-15268

Axial point force stresses in infinite elastic cylinder determined by superposition of Love solution and normal and shearing tractions

05 p0930 A70-16081

Static and continuity equations of equilibrium of axisymmetric and periodic stressed states of rectilinear helicoidal shell derived for elasticity relations

05 p0934 A70-16228

Membrane stress concentration near circular cutouts in axially stressed sheets reduced by predeforming immediate surroundings of hole

05 p0940 A70-16515

Axial and nonlinear bending performance compared for compression moldings laminated from random glass fiber mat

05 p0870 A70-16577

Vibrational creep curves of Al alloy under uniaxial stress level and amplitude, noting influence of small vibrations

06 p1168 A70-17930

Numerical analysis of axisymmetric elastoplastic deformation of circular plates under combined lateral load and membrane force

07 p1402 A70-18977

Critical stress-strain diagrams for brittle plate possessing notch-type stress raisers under biaxial tension

07 p1408 A70-19547

Atomic bond rupture rate in rubber subjected to uniaxial tensile strain in ozone environment monitored by electron paramagnetic resonance measurements

08 p1527 A70-21454

Unidirectional filamentary composites failure theory for uniaxial and combined stress, considering constituent material properties and fabrication processes

08 p1532 A70-21902

Multiaxial thermal fatigue cracking in carbon steels predicted by elastoplastic stress-strain analysis using finite element method

09 p1773 A70-22578

Axial tensile stress effects on stability of cylindrical shell under nonuniform external pressure

09 p1786 A70-23721

Materials bending fatigue strength calculations for biaxial tension compared with experiments showing agreement

10 p1964 A70-25289

Uniaxial low cycle thermal fatigue test procedure for ductile metals, describing strain measuring system allowing direct recording of load vs mechanical deformation

11 p2034 A70-26615

Aluminum sheets anomalous plastic behavior under balanced biaxial and uniaxial tensions

12 p2324 A70-27398

Al alloy welded sheets strength and plasticity under biaxial tension, examining excess elastic energy effects on strain kinetics and rupture

14 p2597 A70-30967

Stresses in plate containing circular hole with notch under uniaxial tension, determining parametric coefficients by Fourier transforms

14 p2661 A70-31326

Stress distribution in fiberglass unidirectionally reinforced composite material under uniaxial tension

15 p2765 A70-32180

Stress concentration problems for partially strengthened circular hole in plate under uniaxial tension

15 p2819 A70-32185

Biaxial stress effect on fatigue crack propagation in Al alloy plate under reversed bending

15 p2821 A70-32324

Maximum secondary principal stress axis and isotropic points determination in scattered light photoelastic analysis, considering bar in uniaxial tension and rectangular beam

19 p3546 A70-38345

Cross shaped plates with circular hole, determining stress concentrations under uniaxial and biaxial tension

20 p3734 A70-40443

Clad glass fibers axial stress measurement by photoelastic techniques

22 p4060 A70-43415

Full and half journal bearings in axial magnetic field, discussing hydromagnetic noncyclic squeeze fluid films

24 p4349 A70-45995

AXISYMMETRIC BODIES

Symmetrical body rotational motion with asymmetrical mass distribution about center of mass, determining minimum initial value of angular velocity

01 p0192 A70-11482

Steady axially symmetric MHD flow of inviscid incompressible fluid of small conductivity in strong magnetic field past fixed axisymmetric bodies

02 p0347 A70-12234

Maximum power transfer theorem, discussing rotation symmetry with respect to optic axis and confocal optical resonators

02 p0339 A70-12454

Shock wave shapes over axisymmetric power law bodies in hypersonic flow, noting asymptotic flow theory implications

03 p0406 A70-12946

Pseudo two dimensional photoelastic test method applied to axisymmetric solid propellant rocket grains under pressure and thermal loads

[SESA PAPER 1482] 03 p0482 A70-12968

Two dimensional and axisymmetric bodies shapes providing minimum wave drag to supersonic flow of perfect gas, considering bodies around which flow causes bound shock waves

03 p0409 A70-13863

Incompressible boundary layer flow of conducting fluid on solid two dimensional and axisymmetric bodies under transverse magnetic field approximated by momentum method

06 p1031 A70-17199

Hybrid finite element analysis for combination of axisymmetric shell and linear displacement triangular ring elements

[AIAA PAPER 70-137] 06 p1169 A70-18052

Flow field measurements upstream of axisymmetric blunt body in rarefied hypersonic flow used to investigate merging between bow shock and boundary layer

06 p0983 A70-18372

Power series solution of Cauchy problem for axisymmetric state of ideally plastic body

07 p1405 A70-19288

Limiting equilibrium of axisymmetric shells consisting of alternating reinforcement layers separated by layers of homogeneous isotropic material

07 p1415 A70-20184

Aerodynamic drag coefficients and moments for axisymmetric bodies of revolution in rarefied plasma derived for limiting case of delta flux

08 p1432 A70-21088

Aerodynamic coefficients for axisymmetric bodies moving in rarefied plasma, calculating corrections for thermal ion velocities

08 p1432 A70-21089

Axisymmetric or plane bodies temperature distribution from heat conduction analysis using computer program based on finite element method

09 p1788 A70-22581

Hall effect on MGD flow past axisymmetric body by studying incompressible inviscid flow past body of revolution at zero incidence

09 p1661 A70-23074

Boundary layer of MGD flow past axisymmetric insulator body analyzed to determine torque due to Hall effect

09 p1663 A70-23579

Unsteady laminar free convection on heated axially symmetric body under stepwise surface temperature variations and unity Prandtl number

10 p1967 A70-23875

Finite element computer code /AXICRP/ for creep analysis of plane stress, plane strain and axisymmetric bodies of revolution

11 p2015 A70-26682

Gravitational collapse of slightly spherical body with axial symmetry characteristics, taking linear approximation of equation for additions to metric in empty space

12 p2310 A70-28223

Sting diameter and cylindrical protuberance length effects on axisymmetric body base pressure in turbulent supersonic flow

[AIAA PAPER 70-585] 13 p2342 A70-29885

Axisymmetric bodies slow rotation or rotary oscillation in hydrodynamics and MHD using boundary value problems solutions

14 p2527 A70-30276

Maximum impact accelerations of spherical and conical bodies landing on water, using momentum theorem

15 p2722 A70-32524

Laminar compressible boundary layer similar solutions for axisymmetric blunt body, considering viscosity and density variations

16 p2833 A70-33123

Aerodynamic performance of axisymmetric body traveling at transonic Mach numbers for predicting installed nozzle flow fields and efficiency

[AIAA PAPER 70-700] 16 p2835 A70-33562

Laminar and turbulent boundary layer equations solutions for incompressible/compressible flows about two dimensional and axisymmetric bodies, using finite difference method

[ASME PAPER 70-FE-A] 16 p2892 A70-33641

Optimal orientation of axisymmetric spin stabilized rigid bodies as function of moments of inertia ratios, using single jet for alignment

[DFVLR-SONDDR-50] 16 p2976 A70-33773

Heat transfer and pressure drag of axisymmetric body in hypersonic flow, obtaining minimum energy nose and leading edge shapes by Pontryagin principle

[AIAA PAPER 70-825] 16 p3001 A70-33940

Blunt based right circular cylindrical body at subsonic speed, investigating turbulent near wake in wind tunnel

17 p3006 A70-34463

Axisymmetric blunt base cylindrical body with turbulent initial boundary layer, investigating flow structure in annular nozzle wind tunnel

[AIAA PAPER 70-796] 17 p3006 A70-34464

Hypersonic flow of shock heated plasma past axisymmetric blunt body and onboard magnetic source, using numerical method

17 p3008 A70-34491

Nonequilibrium air ionization in hypersonic viscous shock layers in flow about axisymmetric blunt bodies

17 p3008 A70-34501

Axially symmetric parabolic reflector with incident linearly polarized plane wave, determining Poynting vector behavior

17 p3043 A70-34615

Skin friction variation and boundary layer separation for rotating axisymmetric body, using two layer model

17 p3011 A70-35240

Base flow component of total drag for axisymmetric supersonic afterbody with single exhaust jet, considering turbulent mixing

17 p3011 A70-35656

Laminar free convection near two dimensional and axisymmetric nonisothermal bodies, examining surface temperature distribution and heat flux

18 p3345 A70-35999

Optimal orientation control of axisymmetric rotating space vehicle, using cyclic sliding mode theory

18 p3332 A70-36162

Stress concentration on axisymmetric annular wings calculated using method of singularities

18 p3207 A70-36377

Free convection boundary layer on two dimensional or axisymmetric body with sudden temperature increase, determining skin friction and heat transfer coefficients

18 p3346 A70-36487

Axisymmetric structure with elastic contact, analyzing stresses by finite element method with differential displacements

18 p3339 A70-36496

Magnetic three degree of freedom attitude control system for axisymmetric spinning spacecraft, using Kalman filter

[AIAA PAPER 70-974]

20 p3668 A70-39555

Axisymmetric dual spin spacecraft consisting of nonconcentric frictionlessly mounted cylinders equipped with viscous damping mechanisms, evaluating stability criteria by energy method

[AIAA PAPER 70-973]

20 p3715 A70-39556

Axisymmetric contact problem of hollow semi-infinite elastic cylinder subjected to stresses on lower end face, solving by Fourier integral transform

20 p3720 A70-39734

Gravitational collapse of slightly spherical body with axial symmetry characteristics, taking linear approximation of equation for additions to metric in empty space

20 p3710 A70-40098

Slender axisymmetric power-law missile bodies with ballistic factor, using Newton-Busemann centrifugal theory with skin friction

21 p3746 A70-41756

Hypersonic aerodynamic deceleration devices for axisymmetrical bodies with cylindrical main sections and various front sections, using gun tunnel techniques

[AIAA PAPER 70-1174]

21 p3746 A70-41839

Sphere and axisymmetric body with spherical blunting in low density gas flow, measuring local heat transfer flux

21 p3748 A70-42218

Numerical methods for mixed boundary value problem of axisymmetric shells of revolution, using truncated series expansion and finite difference expressions

23 p4272 A70-44712

Axisymmetrical nozzle aerodynamic shape design for conical to axially uniform flow conversion, using method of characteristics

23 p4136 A70-44991

Curved element approximation of orthotropic axisymmetric thin shells under axial loads

24 p4419 A70-45152

German monograph on deformations and tensile stresses calculation in axisymmetric bodies via finite element method involving matrix displacement method

24 p4420 A70-45225

Low gravity fuel sloshing in axisymmetric rigid tank, calculating oscillations by modified Galerkin method

24 p4324 A70-45292

Planetary nebulae NGC 7662 and NGC 7009 axially symmetric models from density distributions, H continuum threshold optical depths and central star temperatures

24 p4409 A70-45757

Time dependent inviscid transonic flow past two dimensional and axisymmetric bodies, presenting numerical procedures including imbedded shock waves as discontinuities

[AIAA PAPER 70-1322]

24 p4288 A70-45943

Viscous heat conducting compressible fluid flow past slender axisymmetric body, presenting Navier-Stokes hypersonic strong interaction theory

24 p4289 A70-46020

AXISYMMETRIC DEFORMATION

U AXIAL STRAIN

AXISYMMETRIC FLOW

NT ANNULAR FLOW

Conservation laws for viscous incompressible two dimensional and axisymmetric flow written in integrodifferential form

01 p0063 A70-10935

Mass transfer analysis for axisymmetric turbulent flow in circular tube, deriving turbulent velocity profile from two part model, based on von Karman similarity hypothesis

01 p0064 A70-11092

Axisymmetric turbulent incompressible and isothermal self preserving jet investigation using linearized constant temperature hot-wire anemometers

01 p0065 A70-11099

Density distributions of electrically charged trace components in axisymmetric jets, considering space charge effect and ambipolar diffusion

01 p0066 A70-11135

Growth rate and shear stress parameter of symmetric, turbulent, two dimensional and axisymmetric self preserving wakes and jets in streaming flow

02 p0223 A70-11861

Steady axially symmetric MHD flow of inviscid incompressible fluid of small conductivity in strong magnetic field past fixed axisymmetric bodies

02 p0347 A70-12234

Low turbulence wind tunnel axisymmetric contraction designed from reformulated Thwaites solution

03 p0462 A70-12935

Turbulent boundary layer of incompressible fluid flow in axisymmetric channels with swirl at inlet, considering components interaction, velocity, circulation profiles and resistance

03 p0466 A70-13389

Axisymmetric incompressible fluid flow aerodynamic properties in flat vortex chamber, studying core and boundary layer interactions and velocity fields

03 p0551 A70-13731

Axisymmetric sonic flow around slender body, determining boundary regions for slender body approximation and Guderley expansion utility

03 p0409 A70-14233

Axisymmetric and three dimensional gas flow around blunt bodies using numerical methods, discussing finite difference algorithms for gas dynamic equations

03 p0410 A70-14251

Asymptotic form of axisymmetric solution with Dirichlet integral for Navier-Stokes equations applied to flow past bodies of revolution with smooth surfaces

03 p0471 A70-14303

Ultrasonic beam scanning measurements in high temperature axisymmetric gas flow, discussing errors and use of numerical transformation methods

04 p0685 A70-14536

Potential axisymmetric vortex flow interaction with stationary flat surface, using existing numerical analysis by transforming boundary value problem to Volterra integral equations

04 p0668 A70-14864

Difference methods application to supersonic gas flow past blunt body and unsteady axisymmetric flow past body of unspecified configuration, analyzing stability

04 p0670 A70-14957

Flow field calculation for axisymmetrical gas flow in axial compressor cascade applicable to optimal blade design

04 p0617 A70-15191

Plane and axisymmetric transonic vortex flow approximate equations of inviscid noneat conducting gas for point on sonic line with entropy having extremal value

04 p0617 A70-15234

Unsteady flow equations for periodic axisymmetric laminar flow of second order fluids in circular cylindrical pipes

05 p0831 A70-15871

Near noise fields of choked axisymmetric air jet, discussing sound pressure levels surrounding jet

05 p0834 A70-16783

Axisymmetric motion of viscous heat conducting gas by constructing indirect analog of Poiseuille gas flow, applying results to slip flow regime

06 p1048 A70-18325

Diffusive separation of Ar 36 and 40 and He in axisymmetric supersonic jet taking into account pressure diffusion

08 p1431 A70-21027

Axisymmetric swirling jet ejection from semiinfinite tube into free space filled by fluid, solving flow equation by Wiener-Hopf method

09 p1658 A70-22153

Second order boundary layer equations for incompressible flow, presenting simplified integral momentum equation for two dimensional and axisymmetric flow

09 p1660 A70-22681

Stability theory application to laminar boundary layer transition prediction on two dimensional and axisymmetric flows having pressure distributions in incompressible flow

09 p1662 A70-23219

Inverse blunt body problem using integral relations method assuming inviscid axisymmetric hypersonic gas flow

10 p1798 A70-24116

Laminar boundary layer characteristics in axisymmetric hypersonic nozzle calculated by finite difference method

10 p1804 A70-25187

Coaxially flowing jets axisymmetric turbulent mixing between inner and outer streams

12 p2211 A70-27837

Incompressible two dimensional and axisymmetric oscillating laminar boundary layer flows approximated by momentum integral equation, discussing flow along flat plate

12 p2158 A70-28205

Blunt base heat transfer in axisymmetric supersonic separated flow in axisymmetric near wake tunnel, comparing to previous data

13 p2523 A70-29989

Electric arc in unbounded axisymmetric steady gas flow, solving energy equation

15 p2780 A70-32129

Nonlinear two dimensional free boundary problem of axisymmetric heat conduction in tubes with internal surface solidification by variational technique

16 p2996 A70-33002

Combustion effects on mixing of axisymmetric supersonic and turbulent free jets to obtain species concentrations, pitot pressures and temperatures

16 p2998 A70-33860

Vortices in axisymmetrically separated flows, comparing results of various experiments

16 p2894 A70-33895

Compressible turbulent boundary layers with heat and mass transfer in two dimensional and axisymmetric flows, using eddy transport coefficients

17 p3066 A70-34506

Turbulent mixing of axisymmetrical supersonic air jet into hot air, investigating Mach number and temperature difference effects on axial decay of velocity

17 p3072 A70-35546

Vortex core diameters calculation methods for axisymmetric angular momentum flows

17 p3074 A70-35750

Supersonic axisymmetric flows past bell-shaped bodies of varying bluntness, using Godunov finite difference method

17 p3012 A70-35887

Axisymmetric ideal incompressible fluid jet outflow from cylindrical vessel with conical bottom, using small parameter technique and conformal mapping

18 p3240 A70-36272

Axisymmetric one dimensional compressible flow theory applications to compressible fluids ducted flow

18 p3243 A70-36882

Incompressible axisymmetric flow through turbomachines, developing flowfield for given velocity distribution along arbitrary streamline

19 p3354 A70-38933

Compressible plasma axisymmetric channel flow under electromagnetic forces and ohmic heating, noting velocity profiles and current density

20 p3683 A70-40239

Axisymmetric jet plasma flow in magnetic nozzle, measuring electric potential, electron temperature and ion density and velocity

21 p3856 A70-41380

Self similar formulations for motion of radiating-absorbing perfect gas symmetric flow

21 p3954 A70-42202

Two layer gas flows in supersonic axisymmetric nozzles, using method of characteristics

21 p3748 A70-42210

Laminar axisymmetric incompressible boundary layer calculation based on Mangler transformation

22 p4008 A70-42414

Iterative method based on slender body approximation applied to axisymmetric sonic flow fields, splitting differential equation into coupled parabolic equations

23 p4132 A70-44124

Axisymmetric laminar compressible jet flow characteristics, allowing for compressibility effects due to temperature dependent density and viscosity variations

24 p4325 A70-45584

AXISYMMETRY

U SYMMETRY

AXLES

U SHAFTS [MACHINE ELEMENTS]

AXONS

Loebster giant axon membrane steady state current fluctuations measured under voltage-clamp conditions, considering current potassium component

11 p1987 A70-26006

AZIDES [INORGANIC]

Lead azide detonation hazards and resulting pressure waves, evaluating protective glove material by dynamic pressure measurements

12 p2289 A70-27665

AZIDES [ORGANIC]

Intramolecular formation of azo-linkage accompanying N elimination from bis-azide

05 p0810 A70-16052

Alpha- and beta-styryl azides catalyzed reactions in ethanolic sulfuric acid

05 p0810 A70-16053

Dicyanostilbene formation from phenylethynyl azide and isocyanate

05 p0811 A70-16054

AZIMUTH

Airborne cartographic azimuthal instrument with reflecting prism type optomechanical assembly and trihedral pyramid gyroscope for stabilization

01 p0093 A70-11269

Coupling coefficients for integral charged component of cosmic rays determined from measuring azimuthal geomagnetic effect on rays observed in crossed telescopes

01 p0172 A70-11545

Azimuth between two stations of triangulation net determined by simultaneous observation of two satellites, discussing mathematical principles and applications in Europe

02 p0289 A70-11797

Gyrotheodolites application to azimuth determination, discussing use for directional control, photogrammetry in geodetic measurements, etc
02 p0295 A70-11800

Azimuth information transmission by PCM signals with equal repetition and scanning frequencies, investigating antenna characteristics
02 p0270 A70-12619

Transit instrument azimuthal stability, investigating horizontal axis support, screw controls and tube position during star observations
04 p0693 A70-15484

Direction fluctuations in radio wave scattering in turbulent gyrotropic medium using Einstein-Fokker-Kolmogoroff equation
04 p0653 A70-15722

Azimuth determination by Vector method based on satellite observations compared to Popovichi method, discussing discrepancy
09 p1670 A70-23329

VLF radio noise statistical parameters observed as functions of azimuth, considering atmospheric distribution and parameters correlations
10 p1884 A70-25259

Azimuth measurement techniques for success-run detectors
11 p2019 A70-26712

Steady state symmetrical model for solar wind near equatorial plane, investigating effects of magnetic forces, viscosity and anisotropic pressure on azimuthal motion
13 p2477 A70-29179

Satellite scintillation index variation with zenith angle and azimuth at ground station
14 p2574 A70-30739

Direction fluctuations in radio wave scattering in turbulent gyrotropic medium using Einstein-Fokker-Kolmogoroff equation
14 p2550 A70-30806

Balloon gondola azimuthal angle control by twisting suspension rope
17 p3090 A70-35315

Reaction jet azimuth control system for balloon-borne gondola
17 p3018 A70-35316

Guidance and navigation systems precision azimuth measurement by star sighting and gyrocompass techniques
22 p4067 A70-42663

Tracking elevation/azimuth errors due to frame misalignment, presenting least squares procedure for determining true bias and misalignment angle and axis
23 p4215 A70-44518

AZINES

Somato-vegetative and behavioral reactions of rabbits to electric stimulation of hypothalamus after injecting aminazine
07 p1209 A70-19521

Vegetative cardiovascular, motor and electrophysiological reactions to electrical stimulation of limbic and reticular formations in cerebrum after adrenalin and aminazine injections
13 p2352 A70-29352

AZO COMPOUNDS

NT RDX

Intramolecular formation of azo-linkage accompanying N elimination from bis-azide
05 p0810 A70-16052

Sterically hindered arylidiazonium salts absorption spectra and quantum yield data interpretation, considering photochemical properties
12 p2182 A70-28300

Photoreaction produced N-cyclohexyldiphenylketenimine from cyclohexyl isocyanide and diphenyldiazomethane
17 p3042 A70-34820

Addition and hydrogenation reactions of azomethines in chemistry of carbon-nitrogen bond, emphasizing Schiff bases
20 p3582 A70-38978

Diazo compounds purity effect on photosensitive photographic film quality, determining color image reproduction density
24 p4334 A70-45498

AZOLES

NT ACETAZOLAMIDE

NT INDOLES

NT OXAZOLE

NT PYRROLES

NT TRYPTOPHAN

Photoclimination of N from fused-ring triazoles in methanol
05 p0810 A70-16046

Aniline and o-anisidine production by photoclimination of nitrogen from fused ring triazoles
17 p3042 A70-34821

AZOTOBACTER

Alternating copolymer of guanylic and cytidylic residues synthesized in RNA polymerase-catalyzed reaction
09 p1630 A70-23274

AZULENE

Isomerization of isocyanide into azulene by irradiation and formation from biphenyl isothiocyanate,

observing ring expansion and electrophilic carbenoid properties
05 p0811 A70-16055

AZUR SATELLITE

Azur satellite launching project by NASA and Germany, describing orbit for investigating earth inner radiation belt, auroral zone and solar flares
03 p0580 A70-13797

Yo-Yo system for satellite Azur to reduce payload angular velocity after separation from booster, analyzing final spin error
04 p0762 A70-15152

Space simulation test results compared with analytical methods for thermal data prediction of Azur satellite
04 p0762 A70-15182

Mission objectives and technical realization of AZUR research satellite and Symphonie communication satellite
04 p0763 A70-15303

Pulse width modulation command coder for German research satellite Azur control
04 p0653 A70-15662

Azur satellite program, describing NASA-German cooperative effort
07 p1391 A70-18815

Yo-Yo system for satellite Azur to reduce payload angular velocity after separation from booster, analyzing final spin error
09 p1767 A70-23430

Azur satellite flight results, noting trajectory accuracy telemetry reception, yo-yo triggering and attitude control
13 p2505 A70-28766

Azur satellite ground control, describing system organization to measure scientific and data information for entire satellite lifetime
13 p2384 A70-28976

Azur satellite p- and n-type Si solar cell system providing both power supply and storage battery charging
13 p2506 A70-29553

PCM telemetry transmitters, command receiver and ground control for German research satellite Azur
16 p2890 A70-34349

Thermal space simulation tests on Azur research satellite relating to temperature control subsystems and qualification and acceptance procedures
19 p3399 A70-38288

Environmental tests and checkout procedures for Azur satellite subsystems and subassemblies integration into flight readiness
19 p3533 A70-38289

Azur satellite magnetic parameters simulation, noting spacecraft structure effect
19 p3400 A70-38295

Space motion simulators for Azur satellite, considering satellite attitude related to sun
19 p3400 A70-38296

Project AZUR organizational structure and post-launch problems, discussing onboard experiments
23 p4262 A70-44685

B

B STARS

Radial velocities determined from prism spectrograms for O and B stars in Milky Way field in Scorpius
02 p0369 A70-12062

Photoelectric line photometry used to study H beta/gamma and He I 4471 absorption line intensities of early B stars, determining projected rotational velocity
02 p0369 A70-12072

Catalog of faint Ob stars between Carina and Centaurus
02 p0370 A70-12075

Anomalous fast OB stars separation method based on spatial kinematic characteristics measurements, noting accuracy
03 p0565 A70-13230

LTE departures in late B stars from measurements of Balmer and Paschen discontinuities
05 p0919 A70-16937

O and B type stars neutral He lines, studying UV line blanketing effects on predicted departures from LTE
08 p1571 A70-20912

Anomalous fast OB stars separation method based on spatial kinematic characteristics measurements, noting accuracy
08 p1580 A70-21663

Radial velocities tabulated for late B-type north and south of equator listed in Catalog of Bright Stars
09 p1763 A70-23452

B3V stars atmospheres by LTE model and spectroscopic techniques
14 p2652 A70-31384

H gamma profiles of B type supergiants, discussing electron density levels, Stark effect, Balmer and Paschen series breaks, etc
14 p2652 A70-31385

Lyman alpha absorption by interstellar neutral hydrogen observed in O and B stars UV spectra
17 p3162 A70-34898

Observational evidence concerning validity of Saha and Boltzmann laws in O, B and A stellar atmospheres
17 p3170 A70-35387

Carina spiral feature progress report covering O and B star distribution, optical and radio H 2 and H 1 sources and cosmic dust
18 p3330 A70-37185

O and B stars velocity dispersion, considering Oort terms and average residual radial velocity
18 p3330 A70-37188

O-B5 stars mean ages estimation by hyperbolic approximation based on distribution in stellar associations
19 p3524 A70-38762

B stars kinematic parameters determination from radial and tangential velocities
19 p3525 A70-38775

Be star HD 37202 zeta Tauri II envelope instability, discussing radial velocities, profiles, line width and electron density in layers
21 p3888 A70-41119

Southern objective prism plates B stars with strong neutral He I absorption lines
21 p3890 A70-41160

Early B stars photometric examination of variable spectral lines, discussing beta Cephei stars possibility
21 p3922 A70-41981

OB star distribution statistical analysis in Southern Milky Way, discussing concentrations, relations and systematic deviations
22 p4100 A70-42854

Be stars hydrogen emission lines widths measurement
22 p4101 A70-42867

Stellar ring 274 reality confirmed by photometric measurements of OB member stars, determining variable shell star P Cygni location
22 p4101 A70-42868

Single normal main sequence stars rotational velocities compared with giant, supergiant, Be, A and metallic line stars and Population II objects
23 p4248 A70-44802

Be stars rotation, considering emission properties and evolutionary state of main sequence
23 p4249 A70-44807

Rapidly rotating B and Be stars interior evolution models, considering mass and radiation pressure
23 p4249 A70-44808

Be star rotation dynamics phenomenon, discussing time variations on main sequence scale
23 p4252 A70-44828

Gamma Cas star time and spectra observations, examining emission line profile variations and envelope and stellar model
24 p4404 A70-45415

B-52 AIRCRAFT

Flight evaluation of direct lift control (DLC) on modified B-52 aircraft, noting controllability improvement during ILS approaches and aerial refueling [SAE PAPER 690406]
03 p0411 A70-12896

Flying qualities criteria and piloted simulator studies during development and flight testing of stability augmentation system for B-52 aircraft [AIAA PAPER 68-1066]
04 p0624 A70-15380

B-70 AIRCRAFT

XB-70 aircraft flight tests in cruise and landing approach to evaluate handling qualities criteria [AIAA PAPER 70-566]
13 p2346 A70-29031

B-103 AIRCRAFT

U BUCCANEER AIRCRAFT

BABBITT METAL

U BEARING ALLOYS

BAC AIRCRAFT

NT BAC 111 AIRCRAFT

Design modifications for BAC Vanguard 953 aircraft conversion to palletized all-cargo service, discussing interior layout, cargo door, air conditioning and weight
16 p2842 A70-34049

BAC 111 AIRCRAFT

BAC 111 short/medium range jet airliner family status report on program activity
10 p1806 A70-24846

BAC 111 commercial aircraft family development, discussing program management
14 p2532 A70-31334

BACILLUS

Assimilation and metabolism of C atoms of pyruvate and acetate by strict autotrophs *Thiobacillus* cell, using radioactive substrates
01 p0021 A70-10788

Growth rate effect on glucose utilization rate using sporogenic strain of *Bacillus subtilis* during N and L-tryptophan limitation
01 p0021 A70-10790

Quantitative and qualitative differences in enzyme levels of intermediate carbohydrate metabolism in obligate autotrophs *Thiobacillus thioautotrophicus* and *Thiobacillus neapolitanus*
04 p0633 A70-15441

- Synthetic carbohydrates effects on A type clostridium perfringens, observing bacterial mass growth and protein elimination 09 p1614 A70-22081
- Chromosome of temperature-sensitive mutant of bacillus subtilis 168, observing multiforked replication at normal temperature and transfer of DNA 09 p1615 A70-22206
- Synthetic carbohydrates effects on A type Clostridium perfringens, observing bacterial mass growth and protein elimination 15 p2685 A70-32677
- Microgram 2-nitro-1-butyl pyridinium sulfate /NBPS/ inhibition of growth of Bacillus subtilis by blocking thymidylate synthetase 23 p4158 A70-44998
- BACK INJURIES**
- Lumbar vertebrae transverse processes fractures in air crashes, considering factors involved, incidence and pathogenesis 17 p3033 A70-35578
- BACKGROUND NOISE**
- Long term storage effects on noise, leakage current and thickness of Li drifted Si surface barrier detectors 03 p0482 A70-13023
- First order pressure gradient microphone design based on electrostatic principle, using foil electrets to discriminate against airborne and solid-borne noises 05 p0821 A70-16402
- Signal parameter quasi-optimal estimation during reception on background of normal noise with unknown correlation function 06 p1009 A70-17671
- Optimal receiver synthesis for signal detection on background noise resulting from nonlinear filtration of Gaussian noise 07 p1226 A70-18760
- HF radio noise environment, discussing local storm effects, noise power estimation, noise measurement methods, etc 07 p1231 A70-19172
- Nonenergetic parameter estimation of signal during optimal reception with random amplitude fluctuation in normal background noise using maximum probability function 08 p1461 A70-20868
- Optimal amplitude modulated radio signal reception on white and narrow band background noise, using nonlinear filtration and phase locked control 09 p1633 A70-22416
- Optimal noncoherent detector for fluctuating radar signals of noise background 13 p2369 A70-29727
- Optimal coherent radar detector for signals with unknown amplitude and background noise intensity 13 p2369 A70-29728
- A priori initial phase distribution influence on optimal nonenergetic parameter estimation of rectangular narrow band radio signals on white noise background 13 p2369 A70-29730
- AM signal reception on strong AM noise background, describing theoretical receiver design 13 p2370 A70-29740
- Optimal temporal and spatial-temporal resolution for unknown parameter of interfering signal on white noise background 17 p3048 A70-35680
- Optimal receiver synthesis for signal detection on background noise resulting from nonlinear filtration of Gaussian noise 18 p3229 A70-37104
- Mechanical parametric amplification, improving SNR of acoustic systems in hostile environments 19 p3422 A70-37695
- Plasma lasers, investigating striation oscillations and excess noise phenomena and generation mechanisms 19 p3446 A70-37858
- Random signal detection on uncorrelated Gaussian noise background with unknown intensity, discussing detector performance 22 p3986 A70-42553
- Optimal reception of phase manipulated signal on noise background with unknown statistics and information parameter a priori probabilities 22 p3987 A70-42561
- Algorithms for analog wideband signals optimal reception in presence of strong Gaussian noise 22 p3988 A70-42568
- Light signals detection on noise background, comparing algorithms based on nonparametric statistics 22 p3989 A70-42569
- Lightning discharge characteristics contributing to electromagnetic background noise at ELF determined from slow tail waveform measurements 22 p4015 A70-42777
- Optimal transducers distribution for estimating random field values in presence of additive noise 22 p4005 A70-43562
- Degraded photographic image enhancement limitations due to film grain noise 23 p4193 A70-43820

BACKGROUND RADIATION

- Millimeter background discrete source model, deriving required source density from small scale anisotropy upper limit 01 p0173 A70-10041
- Model explaining background X radiation spectral properties, assuming production by Compton scattering of radio, IR and optical quanta by relativistic electrons 01 p0171 A70-11124
- Diffused X ray background in isotropic world models in terms of Compton radiation from cosmic ray electrons in intergalactic space 02 p0356 A70-11743
- Extrasolar far IR background radiation observed with liquid He cooled telescope carried by Aerobee rocket 02 p0358 A70-12197
- Gamma ray background near proton synchrocyclotron beam degrader at NASA-LRC Space Radiation Effects Laboratory 02 p0275 A70-12268
- Emission spectrum characteristic distortion in scattering of background X rays at large red shifts by metagalactic electrons, considering photon scattering effect 02 p0358 A70-12491
- Cosmic X ray background interpreted as Compton collisions between cosmic black body photons and relativistic electrons in radio sources 02 p0360 A70-12792
- Diffraction correction of terrestrial, atmospheric and cosmic background radiation at aperture and disk determined by artificial moon method 03 p0442 A70-13084
- Spectral index for diffuse X ray sky background within specific band determined from rocket observations with wide angle telescope 03 p0479 A70-14223
- Sky background brightness temperature measurement at 408 MHz by pyramidal horn antenna 03 p0496 A70-14344
- Neutron monitor calibration method to eliminate natural cosmic ray background, decreasing errors due to ray intensity variation 05 p0846 A70-15938
- Assessing background magnitude caused by earth natural radiation sources during underground detection of solar neutrinos by radiochemical methods 05 p0899 A70-15950
- Galactic synchrotron emission and diffuse X ray background, noting correspondence between spectral indices of radio and X ray emissions in polar directions 05 p0913 A70-16472
- Observational extragalactic dependences obtained within framework of Friedman universe model with matter and neutrino background 07 p1383 A70-19407
- Ion counter circuit using second equivalent condenser for compensating background radiation current, assessing error 07 p1281 A70-19526
- Cloudy sky IR background radiation model for designing simulator of IR background for studying noise rejection characteristics of electro-optical automatic control systems 07 p1246 A70-19527
- Shear and rotation limits on universe from X ray background, using Euclidean shear and vorticity models with open and closed geometries 08 p1561 A70-20901
- Universal X ray background as superposition of nascent pulsars in various galaxies, using Crab Nebula pulsar as guide 09 p1748 A70-23792
- Isotropic background radiation measured in ozone-sphere with balloon-borne far IR radiometer 10 p1917 A70-24630
- Isotropic cosmic background radiation detection in presence of earth and galactic radiation, discussing influence on steady state cosmology 11 p2106 A70-26673
- Cosmic background radiation interactions with matter, discussing molecular excitation and black body radiation interpretation 12 p2291 A70-27054
- Diffuse cosmic X and gamma ray background radiation isotropic component 12 p2295 A70-27887
- Long wave cosmic radio background emission in circumlunar space by Luna 11 and 12 satellites, observing increase in earth magnetosphere tail 12 p2295 A70-28262
- Thermospheric background radiation from Cosmos 225 data 13 p2478 A70-29700
- Low energy neutrino cosmic background, discussing energy density, black body radiation, beta decay, scattering process and origin 13 p2479 A70-30001
- Extrinsic photoconductor with reduced background under uniform illumination, describing frequency response as function of recombination and dielectric relaxation times and load resistances 14 p2586 A70-30989

Cosmic microwaves anomalous absorption by interstellar IR-pumped formaldehyde in dust clouds shock heated layer 17 p3154 A70-34535

- Simultaneous measurement of optical and X ray emission from Scorpius X-1 and X ray diffuse background, using rocket-borne scintillation counter 17 p3157 A70-34831
- UV background radiation observed above atmosphere for intergalactic gas, Galaxy and subcosmic ray components 17 p3163 A70-34903
- Background thermal radiation veiling effect on IR photography extension into long wave spectrum 18 p3257 A70-36282
- Submillimeter wavelength night sky radiation background, observing effects on various cosmic ray phenomena 18 p3308 A70-36330
- Diffuse cosmic X ray background galactic component, using model to predict angular spread 18 p3308 A70-36484
- Centaurus A radio galaxy X ray survey, implying upper limit of background radiation temperature 18 p3308 A70-36516
- Milky Way galaxy continuous background radiation emission observed at various longitude intervals 18 p3322 A70-37130
- Cosmic X ray background measurements, describing ESRO R/73 experiment 19 p3512 A70-38491
- Cosmic electron spectrum formation by acceleration, considering metagalactic background X radiation 20 p3695 A70-39174
- Teleradiometer calibration in background radiation absence, using distant and finite point source method and collimator means 20 p3633 A70-39798
- X ray astronomy proportional counters sensitivity, reducing higher energy radiation background contribution 21 p3821 A70-40653
- Galactic or extragalactic origin of diffuse X ray background, reporting sky survey results 21 p3875 A70-40688
- Diffuse background cosmic X rays in energy range 20-120 keV from balloon observations 21 p3876 A70-40689
- Diffuse background of 2-20 keV X rays over Scorpius to North Galactic Pole sky band by rocket measurements 21 p3876 A70-40693
- Cosmic X ray background measurements at 25-200 keV onboard ESRO Skylark rocket, plotting results against galactic latitude 21 p3876 A70-40695
- Soft X ray background galactic absorption and intensity measurements indicating inverse relation to columnar atomic hydrogen density 21 p3877 A70-40698
- Extragalactic cosmic X ray background source models for intensity and energy spectrum, noting Compton scattering of black body photons by relativistic electrons 21 p3877 A70-40699
- Innerbremsstrahlung of intergalactic protons colliding with electrons as source of cosmic background X rays, interpreting intensity and energy spectrum 21 p3877 A70-40700
- Background gamma ray observations attributed to decay of pi-mesons produced by extragalactic cosmic ray protons collisions, noting radiation sources age 21 p3877 A70-40703
- Gamma ray background anisotropy effects of Sgr A flux arising from Compton scattering and neutral pion decay, discussing complex radio and IR structure 21 p3878 A70-40926
- Cryogenic cooling of IR radiation sensors for increasing sensitivity, considering background radiation interference from sensor optical system and detector/preamplifier noise 21 p3825 A70-41052
- Radio source count formula in zero pressure model universe for background radiation differential density evolution function 21 p3923 A70-42104
- Galactic X ray background due to inner bremsstrahlung associated with suprathermal particles, taking into account interstellar gas self absorption and ionization rate 22 p4093 A70-42465
- Lyman alpha sky background measurements by Mariner 6 UV spectrometer 22 p4094 A70-42932
- Diffuse X ray background attributed to X ray emission during supernova early phases 22 p4095 A70-42998
- BACKLOBES**
- Interference proof characteristics and shielding capability of mirror antennas improved by peripheral sheet metal or wire screens, reducing rear lobe level 09 p1648 A70-23151
- BACKSCATTERING**
- Electromagnetic wave backscattering from composite rough surfaces, using Stratton-Chu integral 02 p0261 A70-12589

Radar pulse scattering from ionized media including nuclear explosion fireballs and high speed reentry vehicle wakes, analyzing to retrieve backscattered pulse signal envelope

02 p0262 A70-12602

Power spectrum of backscattered radiation from turbulent reentry wake illuminated by radar pulse train, discussing electron density decay and pulse shape effects

03 p0408 A70-13585

Radar Thomson backscatter observations of ion temperature and ion-neutral collision frequency used to investigate reversible heating in E region

03 p0477 A70-13988

Backscattering cross sections of metallic bodies of revolution, analyzing statistically echo pattern of complex targets

03 p0452 A70-14225

Tropospheric scattering ability investigation with radar transmitter emitting vertical pulses, considering implications for scatter propagation from backscattering detection

03 p0453 A70-14298

Heat transport conduction mode and earth as heat sink in solar atmosphere, discussing mesopause coldest region, turbulence and solar plasma-earth electromagnetic interactions

[AAS PAPER 69-622]

04 p0677 A70-14644

Raman backscatter of frequency doubled ruby laser beam by water vapor in atmosphere observed by optical radar, calculating water vapor mixing ratio profile

04 p0677 A70-14950

Backscattered signal power density distribution along equivalent propagation path of delayed components, determining reflecting layers characteristics from echo signal phase

04 p0654 A70-15728

Laser atmospheric backscatter measurements using frequency shifted Raman scatter and Rayleigh components for separating returns due to gaseous and aerosol components

05 p0859 A70-16476

Backscatter radar signal phase determination from amplitude data, measuring phase and amplitude in laboratory

05 p0815 A70-16507

Diffuse component of lunar radar echoes, using model with volume backscattering from within lunar regolith, noting rocks permittivity

05 p0816 A70-16826

Backscattered field determination at edge on incidence from thin circular plates illuminated by plane waves

06 p1008 A70-17563

Backscatter observations of F region field-aligned irregularities during IQSY, discussing diurnal variations of echoes

06 p1059 A70-18539

Aspect sensitivity of HF backscatter auroral echoes in F layer, utilizing F supported ground scatter echo to account for ionospheric refraction

06 p1012 A70-18541

CW, pulsed and frequency modulated radar scatterometry, discussing flight, system, terrain and data processing parameters

06 p1012 A70-18594

Field strength predictions for expected returns from backscatter ionospheric soundings, predicting ionospheric propagation modes and losses during sunspot minimum

07 p1229 A70-19161

Ionospheric HF radio wave propagation, describing oblique backscatter sounding during IQSY

07 p1233 A70-19183

Scalar radiative transport equation solved iteratively for microwaves backscattering from turbulent plasma, deriving model for direct and cross polarized cross section

07 p1353 A70-19993

Martian surface radar observation results, discussing data processing method, backscattering behavior evaluation, relief and composition model, etc

08 p1456 A70-20643

Refractive index variations effect on backscattering, scattering and attenuation cross sections of ice sphere at various low temperatures

08 p1536 A70-21098

Atmospheric structure and turbulence relations to radar backscattering from clear air refractive index irregularities

09 p1715 A70-22361

Radar backscattering relationship to refractive index microstructure in turbulent clear atmosphere

09 p1716 A70-22366

Backscattering from rough surface of nuclear fireball measured by two way directive radar antenna on reentry vehicle

09 p1634 A70-22703

Plane electromagnetic wave backscattering from dielectric-coated metallic cylinder calculated as functions of incidence angle and coating external radius

09 p1636 A70-23075

Statistical analysis of aurora backscatter VHF measurements, discussing related stream plasma instability theory and diurnal variation

10 p1885 A70-25263

Sea roughness effect on bandwidth of radar backscatter, analyzing Doppler signals of eight millimeter aircraft navigation system

12 p2228 A70-26906

Axial incidence HF backscattering cross section for absorbing flat based cone assumed to obey impedance boundary condition

12 p2185 A70-27716

Ionospheric probing using pulsed radio waves at oblique incidence, discussing auroral radar, meteor radar, ground backscatter and variable frequency ionosondes techniques

12 p2224 A70-27728

Simultaneous magnetic, photometric and backscatter radio measurement of auroral and ionospheric echoes during geomagnetic storm, confirming electrojet theory

13 p2392 A70-28575

Inclined backscatter sounding of ionosphere in individual channels of multichannel radio link, analyzing data during minimum solar activity

14 p2547 A70-30149

Backscattered signal power density distribution along equivalent propagation path of delayed components, determining reflecting layers characteristics from echo signal phase

14 p2550 A70-30812

Venus radar backscattering properties indicating Muhleman theory applicability, noting radar echoes irregularity

15 p2806 A70-32802

Backscattered radiation depolarization during illumination of aqueous medium by linearly polarized laser beam

15 p2753 A70-32861

Erroneous height correlation coefficients in physical optics formulation of rough surface scatter

16 p2859 A70-32938

Scattered fields evaluation due to creeping waves for smooth convex radar targets, using algebraic expressions

16 p2956 A70-32978

Radar mapping in heavy rain with orthogonal transmit and receive polarization, using backscatter and attenuation to define maximum operating altitude

16 p2863 A70-33434

Millimeter wave radar for high resolution aircraft landing aid, describing experiments to obtain backscatter data from airborne platform

17 p3133 A70-34721

Nonpenetrative reentry vehicle nose thickness ablation sensor using gamma radiation backscatter

17 p3094 A70-35519

Amplitude and phase fluctuations of opposing waves in ring laser with allowance for waves coupling due to backscattering

18 p3267 A70-36618

Backscattering of collimated light beam emitted by pulsed point source into opaque medium

19 p3461 A70-37421

Polar electrojet and VHF auroral radio wave backscattering correlation, discussing geomagnetic disturbances effect

19 p3376 A70-37498

Radar for ionospherically propagated ground backscatter sounding, discussing two-aerial aperture synthesis technique and optical spectrum data recording and processing

20 p3585 A70-39393

Book on molecular and aerosol backscatter measurement from stratosphere by means of ground based laser beams

20 p3623 A70-39925

Multistation observations of long range field aligned backscatter irregularities in F layer, using ray path calculations

21 p3814 A70-40940

Radar backscattering from turbulent rocket exhaust plumes

21 p3791 A70-41730

Holographic interferometry by backscattering, considering displacement and deformation problems

22 p4039 A70-43456

Coherent radar backscatter, calculating autocorrelation and power spectrum of spurious noise from periodic random phase injections for filter design to eliminate noise

22 p3992 A70-43591

EM wave multiple scattering by spheres, attributing cross-polarization absence in backscattered field to spherical symmetry

23 p4160 A70-43767

Laser light polarization and depolarization during backscattering from aqueous suspensions

23 p4215 A70-44271

EM wave backscattering from lossless dielectric sphere, examining diffracted field surface waves role

23 p4165 A70-44960

Radar backscattering cross sections of horizontal and vertical polarizations for thin rectangular plate near grazing incidence

23 p4166 A70-44976

Two identical conducting thin cylinders illuminated by plane wave at arbitrary incidence angle, determining backscattering cross sections and induced current

24 p4314 A70-46133

Positron annihilation in quenched Cd metal from radar backscatter intensities in aircraft model compared with anechoic chamber measurements

24 p4315 A70-46257

BACKWARD WAVE TUBES

Electron trajectories in M-type backward wave tube, TWT and magnetron, giving output power expressions

05 p0823 A70-16885

HF backward wave oscillators with emphasis on limiting factors in millimeter waves generation, discussing ohmic and circuit imperfection losses

14 p2555 A70-30430

Diffraction radiation generator with CW operation in backward wave tube mode, discussing output power dependence on wavelength

18 p3231 A70-36410

BACKWARD WAVES

Backward and complex waves propagation in circular waveguide with coaxial dielectric rod, discussing arbitrary angular dependences

05 p0812 A70-16145

Optical parametric backward-wave instabilities in unbounded medium with stopband dispersion using Fourier-Laplace integral

08 p1552 A70-21595

BACTERIA

NT AZOTOBACTER

NT BACILLUS

NT CLOSTRIDIUM BOTULINUM

NT ESCHERICHIA

NT HYDROGENOMONAS

NT NITROBACTER

NT PSEUDOMONAS

Bacterial and viral detection techniques in liquids based on specific property measurement relevant to biological particle, emphasizing industrial processing applications

01 p0013 A70-10127

Gas chromatography study of fatty acids and polar lipids of thermophilic filamentous bacterial masses from hot Yellowstone Park springs

01 p0021 A70-10791

Chlorobium thiosulfatophilum sulfur bacteria growth on media with/without ammonium chloride exposed to illumination, noting various amino acids effects

02 p0241 A70-12797

Amino acid composition and terminal sequences of ferredoxins from photosynthetic green bacteria

06 p0994 A70-17616

Hydrocarbon distribution of various algae and bacteria, discussing hydrocarbons diagenesis and biological transformations in sediments

06 p0997 A70-18401

Gas mixture composition effect on bacteria growth oxidizing methane and propane, establishing proportional biomass concentration to hydrogen and oxygen in mixture

11 p1991 A70-25938

Hydrocarbon assimilating bacteria cultures selection, considering highest specific growth rate and maximum productivity

11 p1991 A70-25939

Molar growth yields from chemostat cultures of Hydrogenomonas eutropha on succinate and on fumarate, noting equivalence to ATP via oxidation

13 p2350 A70-29113

Nucleated organisms divergence from bacteria compared to nucleated organisms divergence into separate kingdoms by analysis of genetic changes in cytochrome c and transfer RNA

16 p2846 A70-32990

Parental termini-daughter strand linkage in initiation of DNA replication in Bacillus subtilis after thymineless germination

16 p2847 A70-33060

Prototype space foods effects on humans, determining changes in bacterial fecal flora content

17 p3032 A70-35565

Halophilic bacteria electron transport chain, examining hydrophobic forces role in menadione reductase structure

21 p3772 A70-40574

Microbial existence limits in hot springs at varying temperature and pH characteristics

22 p3970 A70-42956

Closed loop life support system employing algae and bacteria cultures to recycle water in addition to atmospheric regeneration

23 p4156 A70-45024

Cosmos 110 satellite experiments concerning radiation effects on lysogenic bacteria and plants

23 p4149 A70-45030

Homogeneous magnetic fields effects on growth rate of Saccharomyces cerevisiae and Micrococcus denitrificans

24 p4306 A70-45102

BACTERICIDES

Natural immunity characteristics in dogs after proton exposure, analyzing integumentary bactericidal activity, oral microflora and neutrophil phagocytic activity

03 p0423 A70-13707

- Activated carbons and ion exchange resins bactericidal action as function of silver coating techniques
04 p0641 A70-14574
- Natural immunity characteristics in dogs after proton exposure, analyzing integumentary bactericidal activity, oral microflora and neutrophil phagocytic activity
11 p1985 A70-25507

BACTERIOLOGY

- Spore and vegetative cell adenylate kinases of *Bacillus subtilis* proved indistinguishable by polyacrylamide gel electrophoresis DEAE cellulose chromatography
01 p0021 A70-10789
- Gnotobiotic mice with orally inoculated microorganisms observed for quantitation and fate of bacteria in intestinal tract
01 p0027 A70-11312
- Synthetic carbohydrates effects on *A. Type clostridium* perfringens, observing bacterial mass growth and protein elimination
09 p1614 A70-22081
- Organic substrates effects on *Hydrogenomonas eutropha* autotrophic and heterotrophic metabolism
10 p1817 A70-24700
- Synthetic carbohydrates effects on *A. Type Clostridium* perfringens, observing bacterial mass growth and protein elimination
15 p2685 A70-32677
- Energy yield measurements of catabolic and anabolic activity in autotrophically growing *Hydrogenomonas eutropha*
23 p4149 A70-44997

BACTERIOPHAGES

- Cytosine-thymine transitions from cytosine-5-H3 decay in bacteriophage S13 DNA, discussing coding change efficiency
05 p0803 A70-16948
- Lambda prophage induction into lysogens, noting nalidixic acid role in DNA synthesis inhibition
20 p3573 A70-39774
- T4 phage proteins radioisotopical examination, determining quantitative analysis and molecular weight by autoradiography
20 p3583 A70-40325

BAFFLES

- Bulk and wall temperature measurements for natural fluid convection in container with and without baffles for various heat flux and aspect ratios
06 p1175 A70-17684

BAGGAGE

- Air terminal design, describing mechanical systems for moving people, baggage and cargo
[SAE PAPER 700259] 12 p2206 A70-27431
- Automated baggage handling and processing, requiring total aviation community participation
[AIAA PAPER 70-917] 17 p3204 A70-35829
- Airport terminal design, describing electromechanical baggage handling and sorting systems
[SAE PAPER 700261] 18 p3237 A70-36822

BAILOUT

- Life support and survival gear design, testing, manufacture, supply and maintenance for combat ejections over rugged enemy terrain, discussing pilot injuries
06 p1002 A70-17706
- RAPIDJET escape, recovery and survival system providing rapid escape for large aircrew complement by manual bailout system utilizing semiautomatic escape slide
06 p0986 A70-17719
- Combat and noncombat ejection/extraction fatalities and major injuries to USAF crewmen
07 p1192 A70-19023
- Combat and noncombat ejection/extraction fatalities and major injuries to USAF crewmen
17 p3039 A70-35576
- Long term effects of ejecting from aircraft, discussing disability incidence after more than ten years
17 p3033 A70-35577
- Pilot airborne recovery device /PAR/ midair rescue system, discussing buoyancy, midair pickup, seat ejection energy absorber, homing avionics and human factors
[AIAA PAPER 70-1206] 21 p3752 A70-41812

BAINITE

- Strain tempering effects on upper and lower bainite, discussing strengthening and fracture toughness as function of temperature
10 p1905 A70-25173

BAINITIC STEEL

- Structure and mechanical properties of martensite and bainite in Fe-Ni-Co-C steels, discussing isothermal aging to obtain tough twinned martensite steels
01 p0119 A70-10733

BAKEOUT

U DEGASSING

BAKER-NUNN CAMERA

- Simple layer model of geopotential from satellite-borne Baker-Nunn camera observations
10 p1876 A70-24645
- Film reduction and time keeping used at Smithsonian Astrophysical Observatory for Baker-Nunn films
11 p2007 A70-26196

BALANCE

- Torsion balance for measuring gravitational constant based on Langevin resonance method
08 p1543 A70-20593
- Wind tunnel balance for measuring small aerodynamic loads on scale models, describing three component construction
17 p3062 A70-35490

BALANCE EQUATIONS

U EQUATIONS

BALANCING

- Balancing method for correcting mathematical model discrepancy with gas turbine based on test data
10 p1930 A70-24289
- Two-disk flexible rotor balancing method based on shaft vibration and bearing forces analysis
10 p1896 A70-25093
- Resistance bridge balancing by time method for dynamic digital measurements
11 p2054 A70-26433
- Color TV tubes white field balancing by spectroradiometer, colorimeter and colorgrad meter
12 p2195 A70-27372
- Tungsten filled urethane in aircraft areas as balancing agent
17 p3126 A70-35418
- Soviet book on vibration and balancing of aircraft engine rotors covering structural deformation and dynamics of turbine engines and compressors
19 p3489 A70-37237
- Asymmetric rotating bodies mass properties measurement on Dynamic Balancing Machine, taking into account aerodynamic forces
[SAE PAPER 69-181] 20 p3634 A70-40351
- Multiplane balancing method for minimizing weight required for spacecraft stability
[SAE PAPER 69-181] 20 p3595 A70-40362

BALL BEARINGS

- Vacuum evaluation of lubricants and techniques applicable to miniature ball bearings and instrument gearing for space systems
[ASME PAPER 69-LUB-30] 01 p0100 A70-10379
- Dry lubricated instrument-size ball bearings operation in vacuum for long life and quality performance
[ASME PAPER 69-LUB-21] 01 p0101 A70-10386
- Gyroscopic bearing cross-torque control techniques, noting ball-group misalignment coupling
[ASME PAPER 69-LUB-17] 01 p0101 A70-10388
- Ball bearing performance prediction using analytical technique based on race profilometry data, considering torque variation
[ASME PAPER 69-WA/LUB-4] 04 p0698 A70-14769
- Equilibrium equations solved for statics of double row radial thrust ball bearing, neglecting load angle changes caused by deformations of races and ball bearings
06 p1077 A70-17929
- Sliding friction and wear of polytetrafluoroethylene ball bearing filled with graphite investigated for irradiation effects
06 p1077 A70-18404
- Spherical radial bearing with gas lubricant, solving Reynolds equation by small parameter method
09 p1690 A70-22450
- Despin ball bearing assemblies performance data for TACSAT and Intelsat 4, discussing technology needed for accelerated testing, higher precision, failure detection and lubricants
[AIAA PAPER 70-459] 11 p2058 A70-25471
- Low temperature tempering effects on steel transformations and axial rigidity of radial thrust ball bearings in aircraft
12 p2243 A70-27568
- Oil-vapor lubricated ball bearing system for deployable spin-free antenna of spin stabilized spacecraft
13 p2349 A70-28843
- Vacuum evaluation of lubricants and techniques applicable to miniature ball bearings and instrument ball bearings and instrument gearing for space systems
13 p2419 A70-29120
- Crack initiation and propagation in rolling contact fatigue, emphasizing electrochemical effects in ball bearing failure
[ASME PAPER 70-DE-46] 16 p2931 A70-33509
- Ball bearings selection criteria, analyzing cost-value tradeoffs
[ASME PAPER 70-DE-48] 16 p2918 A70-33511
- Instrument size ball bearings lubricated with bonded dry or transfer films in simulated interplanetary spacecraft tests
16 p2923 A70-34166
- Disk forced vibration mounted on rotating shaft with ball bearings, assuming nonlinear elastic characteristic of system
16 p2996 A70-34293
- Ball bearing materials for ultrahigh vacuum space environments, determining frictional and wear behavior
17 p3099 A70-34573
- Accelerated vacuum testing of ball bearings and slippers at 30-130 F, considering dry lubricated brush/slipping material combinations
17 p3101 A70-34762
- Instrument ball bearings running torque prediction at high speed under combined radial and axial loads
[ASLE PREPRINT 70AM 3D-3]

- 19 p3438 A70-38803
- Hollow balls for high speed bearings by electron beam welding, describing full scale and rolling element fatigue tests
20 p3637 A70-39236
- Angular contact bearing balls track position on aero gas turbine engines shaft measurement in test rig at high speeds
20 p3638 A70-40141
- Gas turbine ball bearings, measuring effect of rolling elements shape on hydrodynamic power losses
21 p3834 A70-41776
- Electron beam welded hollow balls for high speed ball bearings, comparing fatigue life with solid balls
[ASME PAPER 70-LUBS-17] 22 p4044 A70-42444
- Fluid film lubricated, thrust loaded, angular contact ball bearing high speed performance, predicting skidding by isothermal Newtonian behavior in ball to raceway contact
[ASME PAPER 70-LUBS-7] 22 p4045 A70-42452
- BALLAST [MASS]
Water ballast effect on glider loads, using concept of characteristic velocities
18 p3213 A70-36253
- Water ballast loadings on sailplane Cobra 17, considering wing, aileron, tailplane, fuselage and landing gear
22 p3962 A70-42962
- Nonrigidly supported ballast effects on dynamic characteristics of slender body during atmospheric entry
23 p4258 A70-44594
- BALLISTIC CAMERAS
Photographic techniques for artillery projectile flight evaluation, emphasizing high speed range and drum film image synchronized cameras
13 p2407 A70-29159
- Ballistic photography system for luminous models in gas medium, using collimator for velocity measurement
20 p3632 A70-39746
- High speed photographic systems for ballistic studies, describing high intensity lighting systems
20 p3635 A70-40527
- Impact times measurement by photography, correlating projectile velocity with projectile-target distance
20 p3635 A70-40530
- Stereo synchroballistic shadowgraph system for explosively projected shock wave, using streak camera
[SMPTE PREPRINT 114] 22 p4031 A70-43027
- Ultrahigh speed ballistic-synchrophotography, using Imacon image converter camera for framing and streak modes
[SMPTE PREPRINT 113] 22 p4031 A70-43028
- High speed X ray flash motion picture installation for ballistic photography
[SMPTE PREPRINT 76] 22 p4037 A70-43068
- BALLISTIC MISSILES
NT MINUTEMAN ICBM
Oblate earth gravitational field effect on ballistic missile trajectories, including body range determination and quadratures expressed by elementary functions
01 p0178 A70-10423
- Modern astronautics, discussing postwar rocket motors and ballistic missiles construction, ELDO program, moon and planetary photographs and space walk, etc
05 p0960 A70-16627
- Soviet book on guided ballistic missiles design and construction employing liquid and solid propellant engines with emphasis on aerodynamic heating
06 p1155 A70-17410
- Reentry into earth atmosphere of heavy ballistic missiles with variable and constant geometry compared with light missile
08 p1433 A70-21766
- Radar system for Safeguard ballistic missile system, detailing perimeter acquisition and data processing system
09 p1638 A70-23421
- Rocket sled launching for reusable single stage-to-orbit ballistic transport system, noting increased payload capacity and global application
09 p1767 A70-23434
- Composite and double base solid rocket propellants manufactured by French factory for ballistic missiles, discussing plant installations
11 p2030 A70-25520
- Wide range wind compensated launcher settings for unguided rockets using wind-weighting model and iterative procedure requiring real time computation
13 p2503 A70-28528
- Safeguard defense system against strategic ballistic missiles, discussing Nike X program, PAR and MSR radars and Spartan and Sprint system
15 p2810 A70-32247
- Ballistic missile instrument orientation optimization based on CEP criterion, considering acceleration induced errors
16 p2947 A70-33317
- Scaling relations showing effects of ballistic coefficient, flight path angle and inverse atmospheric scale height on heating of ballistic entry bodies
17 p3012 A70-35667

Atmospheric temperatures from thin walled ballistic rocket surface measurements with high sensitivity photometer 18 p3261 A70-36997

Two-axis electrolytic bubble level as precision vertical reference and tilt indicator for ballistic missiles inertial navigation systems [AIAA PAPER 70-949] 20 p3631 A70-39578

Unguided rockets dispersion firing pattern and accuracy, discussing aerodynamic forces and ballistic coefficients 22 p4110 A70-43156

Warm gas reaction control thrusts via solid propellant exhaust products for ballistic missiles attitude control [SAE PAPER 700780] 24 p4295 A70-45863

BALLISTIC RANGES

Free flight ballistic range method for measuring average drag coefficients for microscopic spherical iron particles in free molecular flow 06 p0983 A70-18378

Anamorphic optics to focus luminous wakes of hypervelocity projectiles onto focal plane of slitless spectrograph in free flight ballistic range launching 07 p1287 A70-20082

Ballistic range tests to study ablation effects on aerodynamic characteristics of ablating and nonablating slender cones [AIAA PAPER 69-179] 11 p2148 A70-25976

Shock wave attenuation and reflection effects on turbulent hypersonic wakes in ballistic ranges 18 p3237 A70-36708

BALLISTIC TRAJECTORIES

Anomalous roll behavior of spinning ballistic reentry vehicles with compound aerodynamic asymmetry consisting of lateral offset combined with trim angle of attack [AIAA PAPER 69-103] 04 p0763 A70-15411

Suboptimal nonlinear state estimation from noise corrupted measurements in ballistic trajectory, using simplified extended Kalman filter 11 p2028 A70-26303

Ordnance flight dynamics, considering trajectory analysis and inaccuracies due to projectile wobble [AIAA PAPER 70-533] 13 p2506 A70-29001

Nonsimilar ablation of graphite sphere cones under ballistic entry conditions, predicting steady state rate and surface temperature 13 p2523 A70-29975

Hodograph theory for family of almost vertical ballistic trajectories 14 p2617 A70-31355

Variational equation of ballistic trajectory applied to two point boundary value guidance problems 15 p2812 A70-32504

Ballistic reentry vehicle roll-pitch coupling, showing influence of nose asymmetries [AIAA PAPER 69-101] 21 p3930 A70-41736

Ballistic trajectory, packageability, deployment and flight stability of attached ram air inflatable decelerator for high speed/low altitude store delivery [AIAA PAPER 70-1199] 21 p3752 A70-41817

BALLISTIC VEHICLES

Range, block speed and fuel-weight ratio formulas for hypervelocity, boost glide and ballistic vehicles 08 p1582 A70-21871

BALLISTICS

NT INTERIOR BALLISTICS

NT TERMINAL BALLISTICS

Ballistic compressor performance as high intensity pulsed light source, discussing Xe gas heating and laser pumping 02 p0311 A70-11921

Hypervelocity projectile size and density effect on ballistic limit of dual sheet spacecraft meteoroid protection structures, considering penetration of low and high density particles 04 p0776 A70-15422

Approximate time solutions to light antiaircraft projectiles velocity, altitude angles, gravity drop and downrange, reducing differential equations of motion to dimensionless forms 04 p0764 A70-15592

Ballistic range measurements of vibrational nonequilibrium effects on leading edge shock wave shape for cone-cylinders fired through chlorine atmosphere at supersonic speeds 04 p0621 A70-15601

German aeroballistic hypersonic test facility with moving model and rest atmosphere, describing acceleration mechanism and several tests 06 p0965 A70-17246

Soviet book on thermodynamic and ballistic fundamentals of designing solid propellant rocket engines 06 p1130 A70-17421

Wind compensation for wind effects with elevation angle in ballistic rocket launching problems 07 p1394 A70-19718

Monopulse ruby lasers for moving object illumination during shadow photography, noting applications to ballistic studies 09 p1698 A70-23173

Temporal echo in plasma for applied rectangular pulses, discussing ballistic approximation 19 p3480 A70-38174

German book on principal characteristics of flight mechanics and ballistics covering mirror symmetric aircraft and axisymmetric bodies such as projectiles and missiles 21 p3749 A70-40738

Slender axisymmetric power-law missile bodies with minimum ballistic factor, using Newton-Busemann centrifugal theory with skin friction 21 p3746 A70-41756

BALLISTOCARDIOGRAPHY

Ballistocardiography and cardiovascular performance - Conference, Atlantic City, May 1968 02 p0240 A70-12675

Display devices for ballistocardiographic test data obtained from professional pilots free of cardiovascular disease subjected to displacement and acceleration 02 p0247 A70-12676

Absolute ULF ballistocardiogram (BCG) values as pulsatile fluid pumping values in cardiodynamic function before and after exercise 02 p0248 A70-12677

Ballistocardiogram force envelopes and pulse pressure relationship, noting perturbation of viscoelastic networks coupling cardiovascular system to ballistic bed 02 p0240 A70-12678

Rigid support properties effect on deformation of ULF ballistocardiogram for quality of recorded curves 02 p0248 A70-12679

Readers interpretation and applications of Starr criteria for ULF ballistocardiograms, showing uniformity for patients with coronary heart disease 02 p0248 A70-12680

Stroke volume formula depending on blood density and viscosity, indicating Hagen-Poiseuille law nonapplicability to ballistocardiography 02 p0248 A70-12681

Chronological age correlations with ballistocardiographic modalities /stroke volume and minute volume indices/ for patients with no cardiovascular disease 02 p0248 A70-12682

Age correlations with ballistocardiogram amplitudes and waveform grades in test pilots 02 p0240 A70-12683

Posture effect on ballistocardiograms, considering ventricular ejection flow changes 02 p0248 A70-12684

Ballistographic psychological evaluation of heart and circulatory system by recording displacement, velocity, acceleration and total forces imparted during each beat 10 p1810 A70-24039

HF ballistocardiograms resonance distortions correction, using electrical selective filters 19 p3369 A70-38210

Ballistocardiogram autocorrelation function and spectrum by scanning graph decoder and computer, determining total power, harmonics periodicity and energy concentration 19 p3370 A70-38211

Ballistocardiography and cardiovascular therapy - Conference, Oporto, Portugal, March-April 1969 21 p3762 A70-41226

Cardiac glycosides and beta receptor blocking agent effect on ULF displacement ballistocardiogram in healthy young men, measuring heart rate and blood pressure 21 p3763 A70-41227

Velocity ballistocardiogram modifications during high altitude stay, observing amplitude and RJ and RI variations 21 p3763 A70-41228

Ballistocardiograms hypertensive observations multivariate analysis, discussing factors for various groups discrimination 21 p3763 A70-41230

Hypoxia and hyperoxia effect on ballistocardiogram of healthy males, determining systolic and minute cardiac forces 21 p3763 A70-41231

Ballistocardiogram relationship to cardiac performance index in hypoxia and hyperoxia conditions, investigating systolic and minute cardiac forces 21 p3770 A70-41232

Work load effect on ballistocardiogram by minute cardiac force (MF) measurement, using bicycle ergometer 21 p3763 A70-41233

ULF ballistocardiogram amplitudes relationship to blood flow velocity for cardiovascular disease diagnosis 21 p3763 A70-41234

Acceleration Bcg dependence on left ventricular ejection flow and properties of vascular system 21 p3763 A70-41237

Algorithm for cardiovascular force computation from phasic regional blood flow and mass motion, interpreting Bcg 21 p3763 A70-41238

Bcg interpretation, discussing degrees of freedom, blood mass displacement, cardiovascular system, etc 21 p3770 A70-41239

BALLOON FLIGHT

Balloon flights for remote sensor systems tests, describing return-beam vidicon and tracking telescope experiments 06 p1061 A70-17153

High energy neutrons searched for during solar flares by balloon flights, giving upper limits for gamma ray and neutron fluxes 06 p1136 A70-18008

Grating spectrometer with Ge-Cu detector used on balloon flights for studying variations of IR solar spectrum with altitude, emphasizing sunset features 06 p1152 A70-18523

Monograph on balloon and satellite borne spark chambers for cosmic gamma radiation energy and direction determination, discussing relativistic electrons multiple scattering 07 p1368 A70-19617

Electronic timing device for light balloon payloads, describing circuit 07 p1286 A70-19975

X ray fluxes upper limits from quasars 3 C 196, 3 186 and 3C 380 measured by balloon flight experiments 09 p1745 A70-23271

Meteorological problems associated with accurate weather prediction affecting launch, trajectory and recovery of ballooning systems 14 p2606 A70-30555

Balloon flight measurements clarifying Arcasonde sensor bias over radiosonde atmospheric temperature data 14 p2585 A70-30570

Free floating balloon position and velocity determination by satellite, using Kalman filter linear estimation theory 14 p2530 A70-30571

Balloon localization with transponder system, measuring payload distance by phase difference in ground transmitted and received CW signal 14 p2588 A70-31308

Stabilized balloon flights during weak winds in stratosphere, discussing pressure vs time curves 14 p2531 A70-31311

Balloon gondola azimuthal angle control by twisting suspension rope 17 p3090 A70-35315

Hunting phenomena of hydrogen gas plastic balloon at ceiling altitude, considering exhaust duct, extra volume and shape 17 p3018 A70-35317

High energy cosmic gamma radiation detection from point source in Sagittarius, using balloon mounted spark chamber with Cerenkov telescope 19 p3500 A70-38078

Thermal design of high altitude balloons and instrument packages, analyzing vertical motion dependence on heat transfer and radiation environment 21 p3755 A70-42077

Position tracking of SOMEX superpressure balloons by solar angle method 24 p4372 A70-45423

BALLOON SOUNDING

Primary cosmic ray nitrogen nuclei intensity and spectrum measured by balloons and Pioneer 8 space probe, obtaining abundance difference from solar atmosphere 01 p0169 A70-10319

Pulsed high energy X rays from Crab Nebula pulsar NP 0532 measured by balloon-borne X ray telescope 01 p0169 A70-10345

Sco X-1 high energy X ray emission intensity changes observed by balloon-borne telescope 01 p0169 A70-10346

Cosmic ray electron intensity diurnal variations measured with combined Cerenkov telescope and Pb-scintillator sandwich detector on balloon flight 01 p0170 A70-10408

Buoyant Venus station using superpressure balloon, discussing requirements for structural design and station position tracking capability [AIAA PAPER 69-1068] 01 p0195 A70-10633

Twilight sky polarization data in visible spectrum obtained by high altitude balloon-borne photoelectric photometers 01 p0079 A70-11219

Gamma ray astronomy using balloon-borne telescope with digitized spark chamber 02 p0364 A70-11785

Celestial X rays from Cygnus XR-1 detected during high altitude balloon flight, noting compatibility with black body radiation or hot thin plasma 02 p0356 A70-11786

Atmospheric IR radiation transmittance in 590 to 750 per cm interval, using balloon-borne spectrometer 02 p0256 A70-11928

Onboard radio altimeter for position finding of research rockets and balloons used for aeronomic investigations 02 p0298 A70-12084

Balloon measurements of cosmic ray alpha particle flux in upper atmosphere over Japan to obtain solar modulation effects data 02 p0357 A70-12122

Superpressure balloon flight trajectories for dynamics of tropical stratosphere, revealing distinctive circulation features

02 p0228 A70-12694

Primary cosmic ray proton energy spectrum determined using balloon-borne ionization spectrometer and spark chamber

02 p0360 A70-12844

GHOST /Global Horizontal Sounding Technique/ balloon for meteorological observation over Southern Hemisphere emphasizing technique to overcome icing in clouds

04 p0622 A70-14550

Stratospheric balloon measurement of near UV from early type stars, discussing gondola, observation method, telescope and photographic recordings analysis

04 p0750 A70-14704

X ray source position determination by balloon observations, estimating intensity in different energy ranges

05 p0904 A70-16978

Atmospheric X ray photons measured regularly by sounding balloons in U.S.S.R., discussing X ray photon flux relation to charged particle fluxes

07 p1367 A70-19445

Pulse radar altimeter design for balloon sounding, discussing flight tests, superregenerative stage, etc

07 p1286 A70-19996

ROBIN superpressure mylar spherical falling balloon deployed from sounding rocket apogee for density and wind measurements via radar tracking

07 p1194 A70-20260

Nitrogen dioxide presence in solar atmosphere from balloon-borne spectrometer observations, presenting graph of sunset solar spectrum

08 p1575 A70-21262

Astronomical sounding balloon to study interplanetary scattered light, discussing actuating and control, structure, onboard and ground electronics

08 p1497 A70-21349

Solar constant measurement by Eppley normal incidence pyrhemometers on high altitude balloons

08 p1501 A70-21920

Tropospheric elevated layers fine structure characteristics by balloon-borne spaced cavity refractometer

09 p1714 A70-22353

Astronomic observation balloon Thisbe, discussing telescope, stabilization, basket control, data processing and objectives including zodiacal light and night sky brightness measurements

10 p1804 A70-23915

Vertical wind components from balloon ascent observations, considering drag, atmospheric density, wind velocity, etc

10 p1911 A70-23927

Ambient temperature measurement by constant level balloon mounted thermistors, discussing errors from differential heating of thermistor support by solar radiation

10 p1886 A70-23935

Balloon observations of Cen XR-2 X ray emission decrease

10 p1948 A70-24999

Motion of incidence regions of X ray radiation in auroral zone using simultaneous balloon measurements

10 p1935 A70-25283

Energy spectra and composition of heavy nuclei in primary cosmic rays during low solar activity by nuclear emulsion stacks exposure in balloon flights

11 p2105 A70-26295

Balloon-borne device for analyzing atmospheric carbon dioxide, moisture and methane, using cyclic analysis by gas chromatography

11 p2052 A70-26371

Solar gamma ray lines search with high resolution balloon-borne directional spectrometer based on lithium-drifted germanium detector

12 p2292 A70-27178

Multiplexer-interface system for digital nuclear and position control data transfer from high altitude balloons to earth monitoring instruments

12 p2233 A70-27407

Primary cosmic ray proton and alpha particle spectral measurements by balloon flights

12 p2293 A70-27586

Balloon-borne measurement of troposphere refractive index vertical distribution using spaced-cavity refractometer

13 p2394 A70-28789

Solar spectra recording by balloon-borne monochromator, measuring stratospheric Ir absorption

13 p2491 A70-29050

Auroral zone rapid motions associated with electron precipitation, discussing balloon flight data

13 p2478 A70-29198

FPS-16/Jimspere wind profiles measurement, discussing effect of data smoothing on accuracy and resolution

14 p2607 A70-30569

Balloon-borne optical dew point hygrometer and radiosonde measurements of atmospheric range refractive index

14 p2585 A70-30573

Balloon-radar soundings of horizontal wind profiles for booster vehicle design

14 p2653 A70-30588

Balloon-borne midinfrared observations of lunar surface composition from interpreting peak emissivity differences

14 p2645 A70-31058

Daytime auroral zone electron precipitation energy spectrum from atmospheric bremsstrahlung X ray balloon data

14 p2580 A70-31257

Auroral zone X rays balloon-borne conjugate recordings from Iceland and Antarctica

14 p2632 A70-31306

Galactic cosmic rays high altitude measurements by balloon-borne Sparmo type multidirectional detectors, revealing azimuthal anisotropy

14 p2632 A70-31309

X ray and proton flux measurement during solar flare of 29 September 1968 by balloon-borne detectors

14 p2633 A70-31310

Balloon systems characterized by day to night altitude variations for permanent atmospheric sounding

14 p2531 A70-31312

Cyg XR-1 X ray spectrum variability by balloon-borne detectors as eclipsing properties of binary system

15 p2799 A70-31750

Atmospheric temperature vertical distribution measurement using sounding balloon and Skylark rocket

15 p2725 A70-31846

Stabilized platform stellar detector for French probe balloons, using semicircular light modulator

15 p2738 A70-32249

Constant altitude helium filled zero pressure polyethylene balloon for stratospheric meteorological data and atmospheric tides studies

17 p3075 A70-34607

Zero pressure balloon as base for stratopause pressure and temperature measurements, analyzing winds and balloon trajectory and dynamics

17 p3075 A70-34608

Carbon isotopes abundance in primary cosmic radiation by nuclear emulsion stack exposure in high altitude balloon flight

17 p3151 A70-34914

Balloon-borne X ray telescope star sensor with one arc minute accuracy, discussing design and Cyg X-1 location measurement

17 p3090 A70-35312

IR balloon observations of absolute solar brightness and stratosphere transparency, discussing BCA and HSRA models

17 p3078 A70-35580

Buoyant Venus station balloon for deployment and inflation during parachute descent into Venus atmosphere tested with scale model balloons in wind tunnels

17 p3063 A70-35658

Gamma ray pulse height spectra during active and quiet solar periods from midlatitude balloon flights

17 p3152 A70-35774

Atmospheric X ray photons measured regularly by sounding balloons in U.S.S.R., discussing X ray photon flux relation to charged particle fluxes

18 p3309 A70-36919

Zodiacal light observations at elongation angles from sun, examining surface brightness, color index and polarization degree by balloon-borne instruments

18 p3318 A70-37012

Atmospheric scattering indicatrices from daytime sky brightness balloon measurements in presence of cloud cover

19 p3460 A70-37420

Primary cosmic ray electron flux, energy spectrum and east-west asymmetry, using balloon-borne spark chamber detector

19 p3503 A70-38104

Sco X-1 X ray source properties in 16-111 keV energy interval, using balloon-borne detectors

19 p3505 A70-38116

Primary cosmic ray proton and alpha particle spectra measurements by balloon-borne equipment

19 p3505 A70-38118

Primary cosmic rays above 4.5 GV, measuring charge composition from balloon flight

19 p3507 A70-38133

Primary cosmic ray particles with Z greater than 40 identified by tracks in balloon-borne nuclear emulsions and plastic detectors

19 p3508 A70-38138

Atmospheric gamma rays vertical intensity dependence on spectrum and altitude from high altitude balloon studies

20 p3697 A70-39286

Earth atmosphere cosmic ray neutron albedo from balloon measurement of flux vertical distribution

20 p3698 A70-39298

Solar constant measurements by high altitude balloon sounding, noting anomalous turbidity in upper atmospheric layers due to nuclear explosions and volcanic eruptions

20 p3703 A70-39375

Buoyant Venus station using superpressure balloon, discussing requirements for structural design and station position tracking capability

20 p3715 A70-39677

PCM command control system for high altitude ballooning operations, discussing component equipment

20 p3587 A70-40085

Balloon-borne measurements of hard X radiation from direction of Virgo

21 p3872 A70-40663

Cyg-X-1 X ray source angular size and position measurements by balloon-borne collimator

21 p3873 A70-40665

Diffuse background cosmic X rays in energy range 20-120 kev from balloon observations

21 p3876 A70-40689

Gamma ray astronomical point sources by balloon flight and satellite observation, discussing detector system and telescope for flux and energy spectrum

21 p3821 A70-40694

High energy gamma rays detection by balloon flights, investigating flux and energy spectrum

21 p3876 A70-40696

Auroral X-ray radiation at magnetoconjugate points Kerguelen/archangel region, using balloon-borne spectrometers

21 p3813 A70-40839

Strong newborn X ray source detection during balloon flight, showing softened low energy spectrum

21 p3892 A70-41190

Orientation system for pointing balloon-borne X ray detector using flux gate magnetometer, DC amplifier and motor control relay circuit

21 p3831 A70-42249

Aeolus A satellite for position fixing and automatic meteorological signal transmission in link with balloons for tropospheric observation

22 p4068 A70-42665

Ionospheric current theoretical model and balloon measurement of ionospheric electric field

22 p4017 A70-42795

Air-earth current density time variation in stratosphere by high altitude balloon, comparing with potential gradient diurnal variation over ocean

22 p4017 A70-42798

Stratospheric electric field and conductivity measurements using balloon-borne electrometer tube circuit

22 p4018 A70-42799

Atmospheric electrical conductivity examination by balloon-borne instruments, discussing temperature and ion mobility height distribution profiles

22 p4018 A70-42800

Pointing systems for balloon-borne telescopes in astronomical investigations

22 p4041 A70-43649

Meteorological NEXAIR /Next Generation Upper Air System/ for atmospheric data from balloon-borne instrument packages

24 p4372 A70-46049

BALLOONS

NT HIGH ALTITUDE BALLOONS

NT METEOROLOGICAL BALLOONS

NT ROBIN BALLOONS

NT TETHERED BALLOONS

Balloon satellite orbital time and eccentricity correlated, investigating earth shadow and solar radiation effects

06 p1142 A70-17892

Fiberglass plastic reinforced high pressure balloons design and fabrication with oblated ellipsoid of revolution, discussing deformability, strength and cyclic loadings resistance

12 p2328 A70-28285

Balloon satellites brightness change from rotation effects, analyzing light curves

16 p2980 A70-34317

Small swing angle detector for balloon payloads, using rate gyro principle

17 p3090 A70-35314

Reaction jet azimuth control system for balloon-borne gondola

17 p3018 A70-35316

Plastic balloon platforms for atmospheric research and engineering applications, discussing design and use of unreinforced polyethylene and reinforced Mylar types

22 p3962 A70-43650

Balloon satellite perturbations in orbital period involving air drag, lunar gravity and solar and terrestrial radiation pressures

24 p4414 A70-45358

Balloon satellites orbital accelerations, considering effects due to air drag, solar radiation pressure and spin

24 p4409 A70-45557

BALLUTES

Pilot Airborne Recovery Device /PARD/ using hot air ballute, noting capability to ascend or descend by flow control valve controlling butane burner

07 p1192 A70-19019

Attached inflated BALLUTE /balloon-parachute/ for stabilization and retardation of aircraft stores, high altitude descent devices and planetary entry vehicles [AIAA PAPER 70-1200]

21 p3752 A70-41816

Drag prediction for Ballute and parachute trailing decelerators at supersonic speed and zero angle of attack, using flow field computations
[AIAA PAPER 70-1177] 21 p3746 A70-41836

BALMER SERIES
Chromospheric slitless spectrograms at 1962 eclipse, discussing Balmer-Paschen line intensities, continuum data, reduction and source error
01 p0175 A70-10244
LTE departures in late B stars from measurements of Balmer and Paschen discontinuities
05 p0919 A70-16937
Solar radiation flux observation-prediction discrepancies due to Fraunhofer line absorption, studying Balmer continuum as atmospheric model criterion
06 p1148 A70-18451
Measured and theoretical stark-broadened line profiles and asymptotic wing approximation of hydrogen Balmer lines at specific electron density and temperature
09 p1732 A70-22782
Chromospheric flares electron concentration and structure from half widths and Balmer lines numbers
13 p2493 A70-29394
Atomic emission in water vapor afterglow, revealing presence of Balmer series of H atom with sodium D line
14 p2579 A70-31255
Luminosity effects in Balmer lines of early type stars, noting H alpha equivalent width decrease
17 p3170 A70-35388
Of stars mean spectrophotometric gradients and Balmer jump data with corrections for interstellar absorption
24 p4409 A70-45632

BANACH SPACE
Generalized transform theory for causal operators developed, using Gelfand theory for commutative Banach algebras
03 p0520 A70-14167
Nonlinear equation solution based on local mapping relations and global implicit function theorems for Banach space problems
06 p1092 A70-17224
Multipoint methods for two point boundary value problems with Banach space self mapped, proving convergence theorems for iterative solutions
09 p1712 A70-23420
Banach space stability in presence of constantly acting perturbations bounded in mean, investigating differential operator equation
13 p2452 A70-29309
Chebyshev method for Banach spaces, discussing location theorem for reducing error bounds
18 p3282 A70-36359
Stability theory for approximate solutions and differential approximations for differential equations in Banach space
23 p4212 A70-44345
Second dual space of E sub 0 /Banach space of analytic functions/ identifiable with subspace of L space infinity
24 p4370 A70-46175

BAND STRUCTURE OF SOLIDS
Indium arsenide crystals conduction band structure with various electron concentrations, determining electron mass dependence on concentration and temperature
01 p0154 A70-10096
Edge luminescence effect in doped p-GaAs single crystals with various hole concentrations, determining band structure at liquid nitrogen and room temperature
01 p0154 A70-10097
Nonstoichiometric GeTe defects nature from band structure analysis based on two carrier model
02 p0350 A70-11698
Energy distributions of emitted electrons from Si, GaP and ZnS semiconductors, determining relative core levels and Si valence band states optical density
03 p0537 A70-12879
Pinch characteristics of simple band structure semiconductors and nondegenerate electron gas during bimolecular current carrier recombination, determining hole pairs spatial and recombination spectral distribution
03 p0538 A70-13062
Electromagnetic wave propagation in semiconductors, considering effects of electric field, energy dissipation law and band structure
03 p0540 A70-13719
Interband transitions and optical absorption edge analysis in indium telluride using dependence on photon energy
03 p0541 A70-13725
Nb metal-like compounds energy band structures using X ray fluorescence technique
04 p0707 A70-15213
Probability of three photon band-band excitation of electron in semiconductors using S-matrix formalism, calculating absorption coefficient for two band approximation
07 p1356 A70-19795

Noble metals band structure effects on shielding cloud around impurity and alloys electronic properties in weak scattering limit
09 p1740 A70-22953
Frequency dependent negative resistance of n-type semiconductor doped at acceptor level near valence band top
10 p1927 A70-24273
Negative resistance and cut-off voltage of doped Si p-n diodes subject to deep acceptor levels
10 p1849 A70-24274
Helicon wave dispersion in cold multicomponent plasma of n-type Si and Ge semiconductors in linear hydrodynamic approximation
10 p1928 A70-24832
Rare earth energy band structure effect on RKKY magnetic interaction between atomic spins
13 p2472 A70-29799
Bi-Sb alloys, discussing structural data, crystal preparation, band structure, pressure, nonohmic conductivity, thermoelectric, thermomagnetic and magnetothermal effects
14 p2625 A70-30332
Ferro-magnetic Ni band structure and Fermi surface including spin-orbit and exchange interactions obtained by Mueller interpolation scheme
14 p2626 A70-30479
Energy bands shape effect on fluctuations in nonequilibrium low resistance semiconductor plasma
15 p2784 A70-32192
Band structure of Brillouin zone and electronic states on pure and contaminated crystal surface
15 p2786 A70-32767
Electron momentum distribution function of p-type semiconductor with arbitrary band structure under electric and magnetic fields
17 p3144 A70-35704
Magneto-optics of semiconductors, taking into account intraband and interband effects with Faraday and Voigt field configurations
18 p3297 A70-35951
Band model of switching states between conducting and high resistance states of amorphous semiconductors
18 p3297 A70-35952
Numerical computation of wave functions and energies in complex band structures for two-band case, using k-p method
19 p3483 A70-37547
Phonons and band structure role in metal-insulator phase transition, developing model of electron interactions with lattice vibrations
20 p3686 A70-39149
Current fluctuations in polar semiconductors in strong electric field, taking into account semiconductor band structure
20 p3686 A70-39589
Electron states localization in disordered binary alloys, describing band structure
20 p3687 A70-40498
Band structure contributions to elastic shear constants of hexagonal close packed metals, using optimized model potential
21 p3839 A70-40600
Apollo 11 lunar rock pyroxenes, examining band structure and magnetic ordering by high voltage electron microscopy and electron diffraction
21 p3898 A70-41523
Amorphous semiconductors optical absorption, thermoelectric effects and switching mechanisms characterized by energy band structure model
22 p4086 A70-42773
X ray K and L emission bands and absorption spectra from TiO, TiN and TiC compared with density of states histograms, considering electronic band structure
22 p4086 A70-43003
Highly alloyed indium arsenide reflection spectra and band structural characteristics
24 p4389 A70-45482

BANDPASS FILTERS
Tunable adjustable solid state bandwidth filter using N path system for low pass to bandpass filter transformation
02 p0270 A70-12666
Frequency responses bounds of nonnormalized low pass and bandpass filters
05 p0820 A70-16360
Frequency monitor design, analyzing relationships between time constants, gain, etc, emphasizing white noise filtration
07 p1227 A70-18991
Narrow band limiter influence on SNR at FM reception output by computer simulation using threshold pulse model
07 p1227 A70-19124
Half wave stepped digital elliptic filter design showing improvements over microwave TEM line narrow band bandpass filter
08 p1476 A70-21284
Electromagnetic wave deceleration in open cylindrical waveguide, noting guide action as bandpass filter
09 p1633 A70-22415

Transistorized pulse repetition frequency bandpass and band elimination filters, using trigger circuit to improve pulse-edge steepness and critical frequency stability
09 p1650 A70-23630
Solid state resonant bandpass electronic filter composed of ferroelectric dielectric capacitors with adaptable voltage gain
09 p1653 A70-23801
Time-bounded pulses with energy maximum in frequency band, solving integral equations for bandpass filters for maximum efficiency and optimum pulse shapes
11 p2004 A70-25799
Threshold extension demodulator /TED/ using bandpass filter without oscillator for FM multiplex
12 p2197 A70-27908
Iris coupled YIG tuned filters for 12-4 GHz region, including high field magnets from vanadium permanent
12 p2202 A70-28165
Active RC bandpass filter with independent linear control of Q peak gain and frequency
13 p2376 A70-28801
Circular shielded three layer dielectric waveguide critical parameters, estimating passbands for phase circulators with ferrite inserts
13 p2364 A70-28873
Evaporated multilayer optical bandpass filters in solar radiation technology, discussing design and construction
13 p2411 A70-29665
Comparative passband of optimal and fixed frequency systems in ionospheric scatter communications during nighttime
14 p2547 A70-30239
Microwave band-stop filters based on ladder network low pass prototypes, comparing performance with bandpass type
14 p2557 A70-31179
FM limiter-discriminator followed with ideal bandpass filter, deriving output signal to noise ratio
14 p2558 A70-31189
Hard limiting bandpass limiter output signal to noise ratio in PM signal detection calculated using probability density function
14 p2552 A70-31194
Quasi-optical filters with bandpass and pseudohigh pass structures for millimeter wave and far IR frequencies
14 p2558 A70-31318
Active RC bandpass filter for space fluxgate magnetometer, using state variable synthesis
17 p3054 A70-35526
Fabry-Perot interferometer series as tunable optical narrow passband filter with high spectral and angular resolution, discussing performance in solar magnetograph
17 p3097 A70-35872
Thin films optical constants and thickness measurements and UV bandpass interference filters design
19 p3488 A70-38204
Active bandpass filter configurations with operational amplifiers, noting resonance frequency and Q factor variation relationship to amplifier gain-bandwidth product
21 p3796 A70-40561
Amplitude instability in vibration testing systems, noting effects of bandpass filters in feedback loop of amplitude servo
22 p4006 A70-43250
Lissajous figures for phase response of N-path signal filter transfer functions, using switched modulators
22 p3998 A70-43256
LF passband ideal filter instantaneous pulse response, using delta function model
22 p4005 A70-43555
Directional periodic linear Yagi-Uda arrays application for open low pass or bandpass filters and open resonators
23 p4166 A70-44971
Comparative passband of optimal and fixed frequency systems in ionospheric scatter communications during nighttime
24 p4316 A70-46314

BANDWIDTH
NT BROADBAND
NT SPECTRAL LINE WIDTH
Phased array antennas bandwidth and range resolution, discussing delay elements and antenna size affecting radiation patterns
01 p0042 A70-10262
IF optimum bandwidth for maximizing output SNR in FM receiver with barrier to noise ratio below discriminator threshold
01 p0051 A70-11119
Rise time relationship with signal bandwidth for class of TEM mode microwave delay line filters
02 p0257 A70-12185
Light pulse demodulator using zero crossing technique to eliminate photomultiplier bandwidth and sensitivity limitations
02 p0271 A70-12744

Bandwidth reduction for interlacing two voice and three additional teletype subchannels in standard phone frequency range for use in VHF/UHF satellite link

03 p0450 A70-13623

Pico-nanosecond light pulses from mode-locked Nd glass laser with spectral mode selector, noting correspondence between pulse duration and inverse bandwidth

03 p0503 A70-14210

Band shaped polar aurora widths from photographs analysis, noting wider bands for midnight hours and winter solstice

04 p0682 A70-15732

Frequency bandwidth reduction for geophysical data transmission from satellites or lunar stations by time correlation of signal and transmission channel band changes

05 p0847 A70-15968

Half octave bandwidth traveling wave X band optical phase modulator, noting multiple interactions of optical and microwave fields in electro-optical crystal

06 p1079 A70-17192

Forbidden bandwidth in Brillouin zone and valence band spin-orbital splitting degree determined for mixed gallium-phosphide-arsenide

06 p1126 A70-17815

Holographic system to obtain time-bandwidth product improvement in spectral analysis without sacrificing multichannel processing capability

07 p1288 A70-20098

Circuit development for realizing narrow bandwidth elliptic function filters at microwave frequencies

08 p1476 A70-21285

Receiver bandwidth effect on audible radio noise bursts parameters of quasi-peak value, burst duration and time interval

08 p1464 A70-21800

Hologram spatial bandwidth reduction by space-time multiplexing

09 p1673 A70-22074

FM noise threshold reduction achieved through narrow bandwidth of self synchronized N-path filter tracking incoming FM carrier

10 p1833 A70-24233

Nomograms simplifying noise and natural loop bandwidths calculation for phase locked loop receiver, determining limiter suppression factor

10 p1844 A70-25244

Fourier and Hadamard transformation codings for multidimensional data channel noise immunity and bandwidth reduction

11 p2011 A70-26329

Narrow band FM noise suggested for masking studies application, discussing noise properties

11 p2011 A70-26496

Sea roughness effect on bandwidth of radar backscatter, analyzing Doppler signals of eight millimeter aircraft navigation system

12 p2228 A70-26906

Radio receiver bandwidth effect on lunar occultation observations

12 p2189 A70-27989

Digital transition tracking symbol synchronizer improving SNR without lowering loop bandwidth

13 p2367 A70-29591

Ionospherically reflected HF radio signal frequency spread measurement involving phase difference crossings counting between antennas

14 p2550 A70-30743

Band shaped polar aurora widths from photographs analysis, noting wider bands for midnight hours and winter solstice

14 p2575 A70-30815

Broadband and narrowband pulse signal noise electromagnetic interference prediction techniques for filter or shielding parameters evaluation

16 p2862 A70-33065

Allowable transmission bandwidth of lens waveguide with curved axis, considering light beam deflection due to chromatic aberration

17 p3050 A70-34583

Bandlimiting in coherent optical matched filtering for pattern recognition, eliminating confusion between cross correlations and autocorrelations

19 p3446 A70-37889

Range channel width effect on radar signal digital detector function and parameters optimal value

19 p3380 A70-38068

Occupied bandwidth definition and measurement based on probability density function computation for radio transmitter spurious, harmonic and fundamental emissions

19 p3380 A70-38176

Holographic bandwidth reduction by periodic dispersion structures, noting large viewfield and compact data recording

20 p3627 A70-39096

He/Ne laser amplifier and oscillator threshold bandwidth measurement by double laser device

20 p3643 A70-40126

PCM/NRZ signal band-limiting effect on bit error probability, using sample detector

22 p3990 A70-43339

Omicron Ceti /Mira/ spectrophotometry before, during and after 1969 maximum, noting TiO bandwidth variations

23 p4242 A70-44294

Natural dispersion effect on bandwidth of glass fiber transmission line using optical glasses

24 p4319 A70-46079

BANG-BANG CONTROL U OFF-ON CONTROL

BANKING FLIGHT

U TURNING FLIGHT

BARDEEN APPROXIMATION

U BARRIER LAYERS

U ELECTRICAL PROPERTIES

U SURFACE PROPERTIES

BARIUM

Test program preceding first German satellite experiment using HEOS satellite for Ba ion cloud injection into deep space

02 p0380 A70-12081

Barium ion artificial clouds motions and striations due to cloud-ionosphere coupling, studying electron density variations below cloud in E layer

07 p1271 A70-20155

Barium ionic cloud formation under action of sunlight and expansion in terrestrial magnetic field using plasma model

12 p2214 A70-26892

Signal decoder for barium USA Germany /BUG/ project command reception system, discussing Ba ion cloud propagation and expansion along geomagnetic field

13 p2367 A70-29557

Ba ion cloud motions agreeing with electric field data from balloon measurement in ionosphere and magnetosphere

13 p2402 A70-30079

Ba II emission lines in solar chromosphere, examining excitation and ionization equilibrium and resonance line intensities by eclipse observations

18 p3317 A70-37010

Submarine basalt sea water alteration effects, examining Sr and rare earth concentrations, Ba enrichments or depletions and trace element data

19 p3413 A70-38015

BARIUM ALLOYS

Electronegative adsorbate effect on work function of Ba-W system

18 p3298 A70-37111

BARIUM COMPOUNDS

NT BARIUM FLUORIDES

NT BARIUM OXIDES

NT BARIUM TITANATES

BARIUM FLUORIDES

Barium fluoride film hygrometer elements for radiosondes, discussing manufacturing and testing methods

13 p2408 A70-29470

Barium fluorides single crystals compression, investigating stress-strain behavior and dislocation mobility

19 p3483 A70-37339

BARIUM OXIDES

Phase transitions in FeW doped strontium and barium oxides, using X ray diffraction and Mossbauer effect for transition temperature

24 p4390 A70-45605

BARIUM TITANATES

Metal/ferroelectric work functions in c-domain barium titanate crystals in short circuited capacitor, noting effect of electrodes presence

01 p0156 A70-10186

Static deformation of radially polarized inhomogeneous rotating cylindrical shaft of barium titanate using elasticity, elec

n, for piezoelectric materials

01 p0118 A70-10549

Pyroelectric coefficient extrema measurement at constant stress in barium titanate ceramic at various temperature ranges for various transition points

03 p0513 A70-14205

Barium titanate ceramics with nonlinear electrical conduction, noting I-V relationship dependence on temperature, impurities and electrodes

05 p0891 A70-15990

Electrical properties of unipolar barium titanate single crystals involving hysteresis loops plotting

05 p0894 A70-17024

Excess titanium dioxide effect on electric resistance of semiconductive barium titanate ceramics suitable for posistors

07 p1355 A70-18654

Thin n-type Ge film electrical conductivity effect on ferromagnetic barium titanate single crystals as function of magnitude and sign of polarizing field

11 p2097 A70-25383

Elastic, piezoelectric and dielectric properties of barium titanate single crystals of laminar domain structure

12 p2288 A70-28329

Temperature dependence of electrical properties and permittivity of barium titanate solid solutions containing Nb, Ta, Sb and La, using bridge-circuit of resonance techniques

13 p2469 A70-28853

Dielectric properties of thin barium titanate films from microwave resonance frequencies and resonance reflection coefficient

19 p3482 A70-37255

Valent state of chromium doped barium titanate from EPR spectra and magnetic susceptibility measurements

22 p4086 A70-43133

BARKHAUSEN EFFECT

Permalloy tapes uncertainty in magnetization process, discussing Barkhausen discontinuities measurement method

20 p3673 A70-40058

BAROCLINIC WAVES

Nongeostrophic baroclinic stability theory predictions test experiment with vertical heating provision, describing fluid motions

02 p0289 A70-11830

Geostrophic baroclinic flow with zonal magnetic field in beta plane channel, analyzing instability, phase velocities, Alfvén-Rossby waves and Eady problem

02 p0291 A70-12284

Stratified air flow above relief in baroclinic atmosphere, considering plane nonlinear and three dimensional linearized flow models

03 p0521 A70-13270

Aerohydrodynamic model of relief waves in baroclinic atmosphere based on convection theory, analyzing strong turbulent vortex regime responsible for CAT

[ONERA-TP-727] 03 p0408 A70-13638

Bottom topography effect on jets stability in baroclinic fluid, discussing two layer model

04 p0715 A70-15518

Quasi-geostrophic baroclinic instability in non-separable parallel flow, using perturbation theory

08 p1539 A70-21604

Motion equation derivation for incompressible fluid flow in baroclinic ocean, allowing for horizontal macro-turbulent exchange

14 p2601 A70-30136

Barotropy, baroclinity and baroclinity induced variations of geostrophic wind vector with altitude within planetary boundary layer

14 p2604 A70-30546

Atmospheric circulation two level quasi-geostrophic model, examining dynamic large scale features of baroclinic wave blocking by high latitude cold anticyclonic cells

20 p3621 A70-39372

BAROMETRIC PRESSURE

U ATMOSPHERIC PRESSURE

BARORECEPTORS

Pulsed noise biological effects on human organism, showing stimulation of auditory duct and baric and mechanical reception system causing neural functional shift

03 p0433 A70-13476

Hypothalamic stimulation effects on cardiac and vascular efferent components of baroreceptor reflexes in spinal cats

07 p1202 A70-18866

BAROTRAUMA

Biophysical symptoms and clinical treatment of ailments resulting from pressure drop, considering exposure to higher and lower pressure changes

01 p0011 A70-10036

Otic Barotrauma with bilateral perforation of ear drums suffered during rapid decompression run in chamber, discussing diagnosis

10 p1811 A70-20440

Hypobaric hypoxia effects on MM virus infection resistance in mice

20 p3572 A70-39428

Rapid decompression due to pressure loss in space vehicle or suit, discussing fulminating hypoxia, mechanical trauma and ebullism

22 p3973 A70-43639

Alpine 11,500 ft air atmosphere for manned orbiting laboratory, noting reduced risk of dysbarism during space suit operations

22 p3980 A70-43645

Decompression disorders after exposures to safe pressure or altitude in cats, noting potential embolia from nongradual high-to-normal pressure passage

23 p4157 A70-45080

BAROTROPIC FLOW

Potential triple traveling space waves in barotropic gas with arbitrary equation of state, analyzing adjacent and three dimensional self similar flows

01 p0068 A70-11582

Jupiter upper atmosphere cloud bands zonal motion velocities, examining barotropic stability criterion and geostrophic balance hypothesis

02 p0368 A70-11828

Numerical procedure for determining horizontal wind from geopotential height in barotropic model, discussing solutions for resultant simultaneous equations

08 p1540 A70-21968

Barotropy, baroclinity and baroclinity induced variations of geostrophic wind vector with altitude within planetary boundary layer

14 p2604 A70-30546

Rosby wave critical level time dependent behavior on latitudinally varying flow 19 p3414 A70-38259

BARRELS
Eigenfrequencies of thin barrel shaped shells on simple supports, noting correspondence of ratio of radius to shell wall thickness 08 p1592 A70-21474

BARRICADES
U BARRIERS
BARRIER LAYERS
Al n-type Si Schottky barrier diode characteristics, discussing I-V, barrier height, temperature dependence, photoemission, LF noise, etc 09 p1644 A70-22210
Volt-ampere characteristics of metal-semiconductor contacts for Schottky barrier diodes, investigating suppression of minority carriers and frequency response 09 p1741 A70-23352
Silicon high resistivity surface barrier detectors fabrication for nondestructive tests, discussing long term sensitivity and calibration 10 p1893 A70-24169
High purity pinhole free films (pyrylene) applicability as barrier coating to keep semiconductor surface free from moisture, ions and contaminants 11 p2099 A70-26395
GaAs-Au surface barrier n-type photodiode structure, electrical parameters and response characteristics 12 p2194 A70-26969
Resonance energies of elastic scattering from one dimensional model potential containing barrier, using stabilization method 13 p2455 A70-29222

BARRIERS
Eigenvalue corresponding to decaying modes for wave equation in exterior of obstacle investigated for dependence on obstacle geometry 06 p1095 A70-18474
Capillary barriers to provide propellant positioning, expulsion capability and slosh dampening for spacecraft propulsion systems during rotational maneuvers [AIAA PAPER 69-529] 11 p2123 A70-26119
Wave properties of nuclear optical model for barrier penetration by charged particles, considering square well reflection, absorption and resonance 14 p2619 A70-30491
Radio wave propagation obstacle gain changes with varying distance between obstacle and path terminal 14 p2549 A70-30514
Optimal longitudinal takeoff trajectories, formulating obstacle clearance criterion function based on aircraft design parameters effects [AIAA PAPER 70-963] 20 p3560 A70-39566

BARS
NT ELASTIC BARS
NT PRISMATIC BARS
Computer calculation in elastoplastic range of statically indeterminate structure of bars, considering collapse load, stress and hinge rotation 01 p0200 A70-10524
Normal and tangential displacements distribution at surface and along cross section of bar with free boundaries computed for symmetric and antisymmetric oscillations 02 p0301 A70-12484
Thin walled uniform open bar stability under arbitrary boundary conditions, using Vlasov assumptions and matrix methods 04 p0774 A70-15099
Dynamic plastic response of finite bar subject to axial impact load noting reflected waves, stress-strain-time histories and residual strain 04 p0779 A70-15599
Neodymium-doped glass bars laser amplification efficiency increased by using conical bar and divergent beam 07 p1302 A70-20096
Unsteady creep of thin walled open section bars under free torsion using successive approximations 09 p1779 A70-23101
Bar produced by sliding thin walled cross section along three dimensional curve, determining twisted shell curvilinear middle plane and deformations by differential geometry 12 p2326 A70-27796
Longitudinal waves propagation in polyethylene bar using Boltzmann-Volterra equation, constructing dynamical stress-strain diagrams by viscous-elastic standard body model 12 p2328 A70-28276
Longitudinal stress waves propagation in polymeric optically active plastic bars using photoelasticity method 12 p2328 A70-28277
Fixed end nonprismatic bar stability in fluid flow, studying form influence on critical flow velocity 13 p2512 A70-28982
Stress and deflection of nonisotropic assembled bar and plate composite structures, using computerized matrix displacement method 14 p2660 A70-31133

Stress-strain vector for straight bar of constant or stepwise cross section, using initial parameter matrix method 15 p2822 A70-32363
Monograph on optimal angles and section partition for buckling strength of twisted and displaced bent bars 16 p2988 A70-33300
Longitudinal wave propagation in variable section bars, solving hyperbolic equation of motion by perturbation method 16 p2993 A70-34088
Titanium alloys quench hardenabilities, determining variations with distance from end of Jominy bars after annealing 17 p3119 A70-34415
Stability conditions in straight bar, taking into account stress direction changes caused by deformation 18 p3337 A70-36372
Maximum secondary principal stress axis and isotropic points determination in scattered light photoelastic analysis, considering bar in uniaxial tension and rectangular beam 19 p3546 A70-38345
Natural flexural vibration frequencies of bars with periodic thickness variations, comparing Hamilton principle, matrix approach and experimental investigations 20 p3735 A70-40536
Elastomechanical system reciprocity relation principles using differential equations for bar with forces in two places 20 p3735 A70-40537
Thermoviscoelasticity stochastic problems for bar with temperature independent viscosity, discussing Fokker-Planck equation for two temperature processes 21 p3937 A70-41435
Acoustic frequency spectra of transverse vibrations in bracketed bar caused by dry friction, using Lagrange method 22 p4073 A70-42612
Elastic-viscoplastic bar quasi-static torsion problem, using approximate method for time dependent torsion function 24 p4425 A70-45993

BARYCENTER
U CENTER OF GRAVITY
BARYON RESONANCES
Proton-deuteron elastic large angle scattering cross sections, noting backward peak consistent with baryon exchange mechanism with resonance transfer 07 p1345 A70-20198

BARYONS
Baryon configurations in relativistic generalized theory of gravitation, discussing field equation transformations, mass distribution, central pressure, etc 09 p1753 A70-22454
Stable hyperon star existence in general relativity, discussing state equations for baryon matter, radial pulsation and superlumina and ultrabarc conditions 21 p3888 A70-41116

BASALT
Lherzolite, anorthosite, Gabbro and basalt dredged from Mid-Indian Ocean Ridge noting geological and geophysical features 04 p0675 A70-14422
Kamchatka regions volcanic deposits structural and mechanical characteristics compared with lunar soil characteristics 04 p0744 A70-14440
Shock and thermal metamorphism of olivine trachybasalt by nuclear explosion at Nevada test site 05 p0843 A70-16946
Earth magnetic field transition recorded in basaltic lavas in southeastern Oregon 07 p1276 A70-20351
Luminescence of powdered silica and basalt bombarded by atomic hydrogen, relating spectral distributions dependence on ion energy to lunar luminescence 10 p1942 A70-24647
Kamchatka regions volcanic deposits structural and mechanical characteristics compared with lunar soil characteristics 13 p2485 A70-28465
Thermal conductivity of particulate basalt as function of density in simulated lunar and Martian environments, noting temperature and pressure effects 18 p3316 A70-36772
Lunar basalt lava bed formations, examining vacuum and gravity effects during cooling 19 p3517 A70-37988
Submarine basalt sea water alteration effects, examining Sr and rare earth concentrations, Ba enrichments or depletions and trace element data 19 p3413 A70-38015
Apollo 11 samples compared to stony meteorites and terrestrial basalt, discussing lunar rock formation processes 21 p3900 A70-41540
Apollo 11 lunar basalt petrogenesis, examining internal constitution and origin by high pressure 21 p3901 A70-41547

Apollo 11 lunar igneous rock mineralogy and petrology, emphasizing ferrobasalt minerals microanalysis electron probe 21 p3903 A70-41557
Apollo 11 lunar rock trace elements, examining basalt, gabbroic igneous rocks, breccias and fines by DC arc emission spectroscopy 21 p3774 A70-41561
Apollo 11 lunar basalt chemical composition and petrogenesis, using stable isotope dilution method 21 p3907 A70-41573
Carbon and nitrogen abundances in Apollo 11 rocks, basaltic achondrites and terrestrial basalts, using meteorite analytical techniques 21 p3776 A70-41592
Apollo 11 lunar rocks oxygen isotope ratios, examining relationship to terrestrial basalts 21 p3776 A70-41596
Apollo 11 lunar, terrestrial and meteoritic basalts relationships, examining Ga, Ge, In, Ir and Au concentrations by neutron activation analyses 21 p3778 A70-41617
Apollo 11 ilmenite basalts petrology from regolith samples 23 p4239 A70-43898
Hawaiian basalt melted in simulated lunar environment, investigating surface characteristics, internal structure and bearing strength 23 p4254 A70-44883
Basalt heating with IR carbon dioxide laser, investigating vapor fractionation for inert atmospheres, very high temperatures and silicon dioxide poor materials 24 p4409 A70-45673

BASE FLOW
Thermal and pressure environments analysis in Saturn S-1C stage base during flight tests, noting base gas flowfield and heating 01 p0195 A70-10833
Roll control method using recirculating base flow reaction against oriented blades or fins attached to reentry vehicle base to produce rolling moments 01 p0003 A70-10847
Base mass injection effects of various gases on slender body supersonic near wake stability, diffusion and cooling [AIAA PAPER 70-110] 06 p0970 A70-18075
Turbulent base flowfields in multinozzle configurations, considering adiabatic flow and determining base pressure distribution from reverse jet impingement [AIAA PAPER 69-570] 13 p2338 A70-28511
Axisymmetric blunt base cylindrical body with turbulent initial boundary layer, investigating flow structure in annular nozzle wind tunnel 17 p3006 A70-34464
Dihedral placed at angle of attack in hypersonic rarefied gas flow, investigating base flow and near wakes 17 p3010 A70-35047
Base flow component of total drag for axisymmetric supersonic afterbody with single exhaust jet, considering turbulent mixing 17 p3011 A70-35656
Transport model for flow field and convective heat transport in planar turbulent supersonic base flow 21 p3744 A70-41030
Subsonic channel incompressible gas flow past semiminfinite flat plate base, using flow pattern for cavitation flow 21 p3748 A70-42213
Reacting gas supersonic flow over two dimensional base, examining reaction rate effects on base pressure 23 p4135 A70-44626

BASE HEATING
Shock tunnel preflight assessment of Apollo Block 2 command module base heating 07 p1394 A70-19722
Convective heat transfer at solid boundaries in separated and reattached subsonic and supersonic flows, considering booster base heating 17 p3007 A70-34484
Short duration tube wind tunnel supersonic testing, noting Saturn S-1C base heating and solid propellant rocket base burning tests 20 p3606 A70-39698

BASE PRESSURE
Shock tunnel type differential sensor for low range base pressure measurements on full scale flight reentry vehicles, discussing ground tests 01 p0089 A70-10843
Combustion effects on base pressure of two dimensional body in supersonic flight, considering air-fuel ratio, combustion length and free stream Mach number 02 p0354 A70-12046
Real gas properties effect on base pressure of blunt nosed vehicle flying through atmosphere at high velocities 04 p0764 A70-15556
Full scale R/V flight test base pressure data for slender cones with ablative heat shields, considering mass flow and addition effects [AIAA PAPER 70-109] 06 p0973 A70-18148
Base pressure effects on cone angle of fixed length conical nozzle yielding maximum thrust 11 p1977 A70-26156

- Turbulent boundary layer and base pressure profiles of supersonic flow past conical models in wind tunnel
12 p2159 A70-28229
- Turbulent base flowfields in multinozzle configurations, considering adiabatic flow and determining base pressure distribution from reverse jet impingement
[AIAA PAPER 69-570] 13 p2338 A70-28511
- Turbulent base pressure on conical afterbodies in supersonic axisymmetric flow, including initial direction effect
[AIAA PAPER 70-555] 13 p2340 A70-29020
- Sting diameter and cylindrical protuberance length effects on axisymmetric body base pressure in turbulent supersonic flow
[AIAA PAPER 70-585] 13 p2342 A70-29885
- Blunt planetary entry body free fall drop tests determining low speed stability and base pressure characteristics
[AIAA PAPER 70-577] 13 p2342 A70-29892
- Full scale R/V flight test base pressure data for slender cones with ablative heat shields, considering mass flow and addition effects
[AIAA PAPER 70-109] 21 p3745 A70-41753
- Base pressure behind supersonic vehicle, examining Crocco-Lees mixing theory critical point in laminar near wake
21 p3747 A70-42109
- Cylindrical afterbodies base pressure drag under powered supersonic flight, modifying Korst flow model recompression criterion
22 p3959 A70-42713
- Reacting gas supersonic flow over two dimensional base, examining reaction rate effects on base pressure
23 p4135 A70-44626
- BASES [CHEMICAL]**
Optically active amino acids synthesis by reduction of Schiff bases with sodium borohydride
17 p3041 A70-34748
- BASES [FOUNDATIONS]**
U FOUNDATIONS
- BATHS**
NT SALT BATHS
- BATHY THERMOGRAPHS**
Sea surface temperature relationship with ocean currents, using bathythermograph data
22 p4014 A70-42768
- BATTERIES**
U ELECTRIC BATTERIES
- BATTERY CHARGERS**
Nickel-cadmium batteries rapid deterioration due to destructive demand pulse charging methods
08 p1439 A70-20706
- Third electrode use in charging secondary zinc air battery, presenting performance data and operation problems
14 p2533 A70-30527
- Automatic and command multiple sequencer for spacecraft solar cell battery charger, providing switching logic by integrated circuits design
21 p3758 A70-41218
- Solar cell array peak power tracker and battery charger for Airlark Vehicle coupling Apollo spacecraft and Saturn IVB stage to form manned orbiting workshop
21 p3759 A70-41221
- BAUSCHINGER EFFECT**
Bauschinger effects in repeated tensile and compressive strains in inelastic media under variable temperatures as function of load vector, using plastic yield
01 p0211 A70-11422
- Microdeformation resistance in Ni alloys with ordered phase diagrams related to strain level, analyzing Bauschinger effect
03 p0505 A70-13106
- Intermediate aging influence on Bauschinger effect in low carbon steel at 270 C and 2 hr holding time
04 p0776 A70-15266
- Metals yield locus in strain hardening range in sigma-tau plane determined using slip theory, considering Bauschinger effects
09 p1771 A70-22395
- Yield condition and Bauschinger effect in transition conditions for isotropic and orthotropic bodies
19 p3542 A70-38061
- BAYES THEOREM**
Human feedback and response mode in performing Bayesian decision task
02 p0237 A70-12382
- Bit transition time /bit synchronization/ estimation, developing bit synchronizer from Bayes estimation and optimization theories
[AAS PAPER 69-608] 04 p0647 A70-14655
- Problems experienced in using computers for medical diagnosis and treatment processes, discussing Bayes formula application
04 p0644 A70-15358
- Telemetry decommutation algorithm for applying Bayesian decisions to demodulated received bits data
11 p2008 A70-26238
- Bayesian probabilistic information processing in psychological decision making in air traffic control, discussing bookbag and poker-chip applications
12 p2178 A70-27047
- Weibull process with unknown scale and shape parameters analyzed by Bayesian decision making model, with application to component reliability problem
12 p2243 A70-28011
- Nondestructive screen test efficiency, determining potential failures of electric components by Bayes theorem
15 p2748 A70-32659
- Computer program for assessment and modification of mechanical component life predictions by discrete formulation of Bayes theorem
19 p3440 A70-38816
- Risk interpretation of prior distributions in acceptance sampling by Bayesian analysis
19 p3440 A70-38817
- Reliability analysis based on Bayesian subjective probability implemented by stored time sharing computer programs for engineering computations and operation analyses
19 p3441 A70-38818
- Kalman filter set for state vector and observation error variance estimation in discrete-time linear system, using empirical Bayes techniques
[AIAA PAPER 70-1058] 19 p3395 A70-38873
- Sequential Bayes procedure for demonstrating mean time to failure beyond minimum acceptable value
20 p3658 A70-39642
- Bayes sequential detection test with constrained error probabilities, investigating properties of thresholds equations
21 p3787 A70-41333
- System parameters identification from short-term signal observations, using Bayesian approach
21 p3802 A70-42253
- Supervisor /monitor/ sampling frequency maximizing payoff function, using Bayesian preprocessor information analysis
22 p4127 A70-43498
- Bayesian identification of system parameters for observable and nonobservable input signals
24 p4316 A70-45474
- BAYESIAN STATISTICS**
U BAYES THEOREM
- BAYS**
Auroral absorption bays meridional motion, observing absorption onset systematic lag at various ground stations
14 p2570 A70-30216
- Auroral absorption bays meridional motion, observing absorption onset systematic lag at various ground stations
24 p4331 A70-46291
- BBGKY HIERARCHY**
Nonlinear Knudsen layer gas flow using BGK model for Boltzmann equation
06 p1048 A70-18322
- BBGKY hierarchy state functional formalism in nonequilibrium statistical mechanics for many particle system using Fourier transformation
11 p2087 A70-26548
- Kinetic equation for electron plasma based on BBGKY hierarchy reducible to set of equations with structure similar to Pines-Schrieffer equations
13 p2458 A70-28561
- BBGKY hierarchy pair correlation function for magnetoplasma under weak external force, using operator method and time periodic ansatz for distribution functions
14 p2623 A70-30697
- Shock and expansion waves formation by moving piston based on kinetic theory of gases, solving Bhatnagar-Gross-Krook equation by numerical method
21 p3808 A70-41377
- BCC LATTICES**
U BODY CENTERED CUBIC LATTICES
- BE B**
U EXPLORER 22 SATELLITE
- BEACON EXPLORER B**
U EXPLORER 22 SATELLITE
- BEACON SATELLITES**
NT EXPLORER 22 SATELLITE
Faraday rotation of radio beacon satellite signals during traveling ionospheric disturbances simulated for spaced ground stations
20 p3590 A70-40481
- Geostationary beacon satellite recording of gravity wave influence on ionospheric electron content
21 p3815 A70-40943
- Radio navigation system using multiple satellite beacons /NAVSTAR/ for large area air and sea coverage
22 p4067 A70-42662
- BEACONS**
NT AIRPORT BEACONS
NT OMNIDIRECTIONAL RADIO RANGES
NT RADAR BEACONS
NT RADIO BEACONS
NT RADIO DIRECTION FINDERS
Personnel danger zones demarcation around radar antennas, using beacons
17 p3040 A70-35913
- BEAM COLUMNS**
U BEAMS (SUPPORTS)
U COLUMNS (SUPPORTS)

BEAM CURRENTS

- Colloid engine propellant mass flow distribution, determining beam current and specific charge effects on thrust, efficiency and specific impulse
[AIAA PAPER 70-1109] 20 p3692 A70-40234
- Glow discharge electron guns for welding and heating, discussing beam current and energy balance
22 p4042 A70-42376

BEAM PLASMA AMPLIFIERS

- Surface wave propagation and amplification by electron beam-plasma interaction, inapplicability of coupled mode theory and use for microwave amplifier
06 p1125 A70-18616
- Spatial electric field variations and electron distribution for beam plasma amplification, using nonlinear approximation
16 p2959 A70-34336
- Spread electron beam excitation of magnetoactive plasma waves in quasi-linear relaxation
21 p3855 A70-40948

BEAM SPLITTERS

- Modified Smith-type reflector for long laser cavities using etalon without coatings instead of usual beam splitter, discussing output characteristics
03 p0501 A70-13648
- Divided photoelectric cell position sensitive detectors in laser alignment systems, obtaining independent signals for displacements in orthogonal directions
06 p1081 A70-17624
- Time variations of reflectance measured for carbon dioxide laser beam splitters
07 p1302 A70-20095

- Laser radiation angular distribution determination by self calibrating method based on dividing light beam into spatially similar beams of various intensities
08 p1510 A70-20515

- Quasi-optical beam splitter, using grid diffraction of plane wave at dielectric cylinder, suitable for millimeter and submillimeter wavelengths and thread measuring
08 p1496 A70-21219

- Power density fluctuations in emission peaks of ruby laser determined by splitting beam into two components and using photosensitive element and photomultiplier recording
15 p2754 A70-32874

- Variable ratio beam splitter design and operation for lasers, using birefringent optics
18 p3270 A70-36755

- Double beam diffraction grating spectrometer for vacuum operation over far IR from 40 microns to 1 mm
24 p4339 A70-46323

BEAM SWITCHING

- CRT color displays advantages and limiting factors, considering beam-penetration tube with high voltage switching
09 p1673 A70-22031

- Beam switching Cassegrain antenna for millimeter wave radio astronomical measurements, describing RF and electronic systems
11 p2019 A70-26374

- Laser field transient properties in switching-on processes, discussing Q switching, detuning switch-off and pump power switch-on
11 p2064 A70-26843

- Q switched laser turn-on nonlinear dynamics, deriving field intensity distribution function
18 p3270 A70-36743

BEAM WAVEGUIDES

- Laser communication system for outer space, beam guiding and fiber optical guiding systems
04 p0649 A70-15038

- Beam fluctuations damping in beam waveguide, determining fluctuations cause as random displacement of lenses
04 p0651 A70-15290

- Injection laser amplifier with emitting and amplifying diodes coupled by planar polyharmonic beam waveguide
04 p0702 A70-15292

- Crosstalk in multiple-beam waveguides due to scattering and distortion caused by surface irregularities of focusers, discussing power profile of Gaussian beam
08 p1462 A70-21507

- Optical and quasi-optical transmission of EM wave beams of type in directional antennas Fresnel region, examining free space and waveguide modes
14 p2549 A70-30445

- Allowable transmission bandwidth of lens waveguide with curved axis, considering light beam deflection due to chromatic aberration
17 p3050 A70-34583

- VLF wave propagation in earth atmosphere waveguide, calculating various atmospheric types from waveguide field dependence on frequencies
19 p3416 A70-38566

- Radio beam trajectory in Fresnel zones of isotropic laminarly inhomogeneous ionosphere, discussing point source field and wave propagation
19 p3381 A70-38569

- Regular beamguides of second kind consisting of nonidentical nonequidistant correctors, calculating energy losses
21 p3785 A70-40629

Beamguides with inhomogeneities regulated for constant radiation losses, systematizing broadening 22 p3984 A70-42389

Prism film device for high efficiency laser beam coupling into light guiding thin film, deriving operation theory by plane wave analysis 22 p4030 A70-42948

Optical waveguides and resonators propagation modes detection and discrimination techniques evaluated for circular cylinder dielectrics /optical fibers/ 22 p4030 A70-42949

BEAMS [RADIATION]

NT ATOMIC BEAMS

NT ELECTRON BEAMS

NT GAMMA RAY BEAMS

NT ION BEAMS

NT LIGHT BEAMS

NT MICROBEAMS

NT MOLECULAR BEAMS

NT NEUTRON BEAMS

NT PARTICLE BEAMS

NT PHOTON BEAMS

NT PION BEAMS

NT PROTON BEAMS

NT RADAR BEAMS

Monk-Gillieson convergent beam dispersion method applied to rocket-borne photoelectric spectrophotometer for far UV stellar spectra observation 01 p0090 A70-10904

Double beam Michelson interferometer for middle IR with moving mirrors operating in constant velocity mode, applying method to atmospheric emission spectra 01 p0091 A70-10909

Gaussian laser beams diffraction by straight edge bounding opaque plane on basis of Kirchhoff scalar wave theory in Fresnel limit 02 p0313 A70-12456

Natural modes and multiple beam interference in open resonators, taking into account centimeter wave experiments and computations 02 p0340 A70-12829

Quasi-optic electromagnetic beams slow spreading in anisotropic media due to propagation in unusual directions 03 p0447 A70-13288

Pencilbeam scanning observations of solar bursts revealing recognizable postincrease phase 03 p0558 A70-13588

Beam transformation laws and matrices for Gaussian beams, discussing propagation, reflection and refraction in geometrical optics 05 p0883 A70-16773

Stationary phase for beam of radio waves propagating in absorber ionosphere as function of mean directions of real and imaginary parts of wave vector 09 p1665 A70-22049

Equivalent angles of slope calculations based on rotary oblique probing data for spherical models of earth and ionosphere, deriving minimum equivalent beam path 11 p2043 A70-25539

Pencil-beam antenna idealized patterns derived from maximum gains and operating wavelengths, discussing sidelobes 12 p2195 A70-27247

Coherence degradation of collimated and focused Gaussian beams in turbulent atmosphere, using small perturbation method 13 p2453 A70-29824

Radio observations of dense briefly visible Leonid meteor shower with fixed pencil beam antenna in coping with wave scattering in trails 15 p2796 A70-31511

Lens antennas for performing radiation collimating function through refraction, discussing solid and artificial dielectrics lens design, beam scanning applications, etc 17 p3052 A70-35069

Multiple narrow beam antenna system with plasma column and electromagnetic wave ring source, discussing radiation pattern and electronic scannability 18 p3294 A70-36346

Pencil beam synthesis for large circular array with arbitrary number of directive elements, determining optimum excitations 18 p3227 A70-36476

Delay time between beams reflected from different parts of meteor trail, using phase invariant and frequency scanning methods 19 p3512 A70-37313

Group delay times criterion of multibeam propagation of ionospheric radio echoes for communications systems 19 p3375 A70-37332

Power flow patterns of near to far field transition of scalar wave pencil beam without reference to specific radiating structure 19 p3536 A70-37703

Object visibility limits when illuminated by laser beam with spatial selection method, discussing atmospheric conditions and light source radiation power 20 p3641 A70-39448

Pulsed ruby free emission mode laser spectrum narrowing, using diffraction lattice adjusted in resonator transversely to beam axis 20 p3643 A70-39757

Equivalent angles of slope calculations based on rotary oblique probing data for spherical models of earth and ionosphere, deriving minimum equivalent beam path 21 p3819 A70-41289

Coherent beam propagation through turbulent atmosphere, discussing limiting resolving power due to random fluctuations of refractive index 22 p4072 A70-42290

Diffusion effect on carbon dioxide Gaussian laser beam amplification, measuring gain saturation via pinhole method 22 p4051 A70-43335

EM radiation beams higher directivity from sources in two layer plasma in planetary atmosphere 23 p4242 A70-44261

BEAMS [SUPPORTS]

NT BOX BEAMS

NT CANTILEVER BEAMS

NT CURVED BEAMS

NT I BEAMS

NT RECTANGULAR BEAMS

Torsional vibration of thin beam of varying cross section, noting moment of inertia and torsional rigidity proportionality 01 p0200 A70-10525

Nonlinear dynamic beam response for classical and shear deformation theories, comparing stresses and deflections using traveling wave approach with finite difference schemes 01 p0206 A70-11147

Semidiscrete approximation of equation for free vibrations of beam with nonuniform cross section, using method of straight lines 01 p0213 A70-11636

Bending strength analysis for high strength beam with thin and long fibers embedded in matrix of viscoelastic material noting maximum stress 03 p0584 A70-12934

Natural frequency calculation accuracy for coupled beam bending vibrations shown dependent on connection stiffness determination 03 p0595 A70-13929

Singular integral equation applied to elasticity theory of composite beam with or without cavity under torsion 04 p0765 A70-14416

Complex uncoupled modes to analyze forced vibrations of three layer damped sandwich beam with arbitrary boundary conditions, discussing orthogonality 04 p0773 A70-15076

Nonlinear connected oscillations of vibrator and rigid bodies, analyzing plane-parallel and spatial motions, including elastic beams self excited oscillations 04 p0720 A70-15446

Boundary value problems of thin beams theory transformed into initial value problems, using dynamic programming and invariant imbedding 05 p0926 A70-15977

Stress distribution in long beams with circular annular inclusion under concentrated load solved in series form 05 p0928 A70-16024

Simply supported beams large deflection analysis in bending under symmetrical pair of forces, based on integration of elastic line differential equation 05 p0941 A70-16521

Transverse vibrations of isotropic truncated-cone beam fixed at ends compared with cylindrical beam 05 p0942 A70-16666

Support moment of beam with ends embedded in elastic medium subject to creep, noting dependence on load 05 p0947 A70-17010

Static buckling load for beam with pinned ends and Wiegardt-type elastic foundation, considering shear stresses effect 05 p0955 A70-17105

Dynamic response of free-free beams on viscoelastic Winkler foundation using complex foundation modulus based on antivibration isolator 06 p1165 A70-17627

Longitudinal vibration equations of beams for nonlinear stress-strain relation reduced to equivalent linear partial differential equations 06 p1106 A70-17863

Thin walled glass fiber reinforced plastics beams strength analysis combined with results from elasticity theory of anisotropic bodies 06 p1167 A70-17913

Minimum weight beams and frames calculation for random loads taking into account material carrying capacity 07 p1400 A70-18821

Minimum weight reliable beams and frames calculation for random loads, using one degree of freedom system to obtain closed form solution 07 p1401 A70-18825

Optimal linear viscoelastic synthetic sandwich structures, investigating test/calculation agreement for simply supported beams and embedded plates [ONERA-TP-702] 07 p1404 A70-19137

Simultaneous partial integrodifferential equations for transverse oscillations of uniform short beams 07 p1406 A70-19306

Minimum weight design of elastic sandwich beams with deflection constraints using n-dimensional space of discretized bending stiffness 07 p1407 A70-19358

Mechanical vibration of beams analyzed by partial differential equations of beam vibration involving mass concentration and flexibility 07 p1411 A70-19786

Vibrating composite beam test method for determining complex dynamic modulus of viscoelastic materials over broad frequency and temperature ranges 07 p1320 A70-19955

Bending tests for characterizing off-axis unidirectional composite beams, discussing errors due to lift off from supports 07 p1412 A70-19963

Bernoulli-Euler beam equation describing natural frequencies and mode shapes for vibrating beam immersed in fluid 07 p1413 A70-20043

Ductile flexure location in bent beams and systems with variable cross sections to determine critical load using plasticity theory 08 p1587 A70-21072

Lateral buckling of simply supported uniform diaphragm using slope-deflection equations for orthogonally intersecting beams, prescribing boundary conditions 08 p1589 A70-21244

Dissipative heating effects on loss factor of viscoelastically damped beam, discussing stiffness effects [ASME PAPER 69-VIBR-37] 08 p1592 A70-21478

Semiinfinite elastic strip supporting thin heavy beam using Airy stress function and Laplace transform, with boundary conditions expressed as Fourier series 08 p1594 A70-21768

Free vibrations and dynamic buckling of hinged extensible beam under axial force 09 p1768 A70-22061

Rotatory inertia and shear deformation effects on structural vibrations of Timoshenko beams and frameworks using matrix formulation 09 p1770 A70-22257

Flexo-torsional elasticity ellipse determining displacements, hyperstatic reactions and influence lines in beams with straight axis and variable cross section 09 p1771 A70-22398

Constant cross section beam bending and torsion with allowance for moment stresses, deriving differential equations for displacement functions 09 p1773 A70-22538

Longitudinal vibrations propagation in nonlinear elastic beam under harmonic kinematic disturbance solved by harmonic linearization method 09 p1773 A70-22541

Weight function minimization of multiweb box beam in pure bending 09 p1777 A70-22769

Elastic beam stability, natural frequencies and critical forces under longitudinal impact with nonuniform compressing force 09 p1780 A70-23116

Free vibrations of plates and beams of pyrolytic graphite type materials, analyzing transverse shear deformation and rotary inertia [AIAA PAPER 69-55] 09 p1780 A70-23210

Beam vibration eigenfunctions with allowance for shear compliance used to determine beams dynamic stability under pulsating axial load 09 p1785 A70-23600

Transition of stress distribution on collision surface of semiinfinite elastic plane with rigid beam, using Fredholm integral equation 10 p1954 A70-23950

Flexural rigidity of thin walled beams, analyzing relationship between loads and displacements taking into account Saint Venant torsional resistance 10 p1955 A70-24052

Stress-strain determination in nonuniformly heated thin walled cylindrical beams with nonlinear stringers and skin 10 p1957 A70-24281

Uniform beams flexural vibration natural frequencies approximate calculation showing effect of shear flexibility and rotatory inertia 10 p1959 A70-24562

Lines of influence of bending moments and cutting force for straight beam using differential equation integration 10 p1959 A70-24777

Beams stability under flexural stress with periodic intensity variations, deriving differential equation of motion 10 p1960 A70-24973

Moving mass effects on Euler beam analysis extended to Timoshenko beam, obtaining numerical solutions by finite difference method
10 p1963 A70-25073

Compressive stress critical moment induced instability and weakening incorporated in thin walled beam design
11 p2131 A70-25590

Free wave propagation constants in periodically supported infinite beams determined for rigid and flexible supports
11 p2132 A70-25727

Finite element matrix structural analysis by direct stiffness method and use of computers, considering thin wall box beams
[SAE PAPER 700218]
11 p2134 A70-25890

Resonant frequencies and Young/shear moduli of unidirectional graphite epoxy composite beams under high modes of vibration
11 p2136 A70-26082

Stress level, block size and constant and variable loading sequence effect on fatigue life of Al alloy box beams
11 p2138 A70-26094

Finite element solution procedures for inextensible beams elastica problem, using galerkin method for element stiffness matrices
11 p2143 A70-26640

Nonuniform beam element stiffness matrices for dynamic and elastic instability analysis, determining frequencies, mode shapes and critical loads
11 p2143 A70-26643

Structural design for allowable plastic deformation under dynamic loads, deriving finite element representation of elastic-plastic plane frame beam
12 p2317 A70-27117

Sandwich beams elastoplastic stability, determining critical load
12 p2323 A70-27342

Vibrating thin beam cross sectional displacement-force equations coefficients included in coefficient matrix, considering shear deformation and rotary inertia effects on vibration modes
12 p2324 A70-27397

Beam-bending and circular plate testing rigs for creep with constant and variable loading, discussing tests repeatability and accuracy
12 p2207 A70-27618

Maximum impact force and central deflection time function of transversely struck beam, assuming no reflected elastic wave effects on stresses
[DFVLR-SONDDR-48]
12 p2325 A70-27619

Elastic beam vibration under constant amplitude and varying frequency periodic forces during passage through resonance
12 p2326 A70-27798

Free elastic rotating beam with tip masses and inertia, developing solutions for flexible modes and natural frequencies of H-type configuration
12 p2273 A70-27820

Clamped beams steady state free and forced response and stability for large amplitude motion, discussing multimode analytical and numerical technique
12 p2327 A70-27821

Euler-Bernoulli and Timoshenko beam impact models compared for case of finite beam resting on spring supports
12 p2327 A70-27843

Stress measurements for eye beams forming of high fatigue strength based on brittle lacquer studies of isotropic material models
13 p2507 A70-28482

Book on torsion emphasizing beam stressed state calculation and civil engineering problems
13 p2512 A70-28850

Plastic symmetrical bending of freely supported beam under transverse local pulsed load, discussing deflection velocity fields during loading and unloading stages
13 p2514 A70-29307

Arbitrary planform plates with edge clamping and elastic beam spanwise support using Green function
14 p2655 A70-30182

Mechanics of solid structures including shells and beams, considering three dimensional behavior laws in plasticity and creep
14 p2656 A70-30294

Differential equations for coupled bending and torsional vibrations of slender beam in centrifugal force field
14 p2661 A70-31226

Numerical method for roots of algebraic equations, computing continuous beam lateral vibrations natural frequencies
14 p2600 A70-31330

Reticulated shell structure buckling using approximate equivalent shell and discrete analysis of individual beams
15 p2816 A70-32007

Constrained and constant coefficient optimal controls compared in optimizing performance criteria of vibrating beams
16 p2886 A70-33332

Composite beam testing concepts and interpretation under three and four point loading, noting shear deformation effect
16 p2989 A70-33385

Macaulay method extended for slope and deflection of statically indeterminate beams, rewriting design equations into index notation for computer programming
[ASME PAPER 70-DE-2]
16 p2989 A70-33419

Infinite elastic plate with beam reinforced circular insert, using classical plate theory and Euler-Bernoulli hypothesis for beams
16 p2990 A70-33679

Twisted uniform beam element flexibility and stiffness matrices, using continuous bending theory
16 p2894 A70-33887

Embedded damped sandwich beams, determining equations for resonant frequency, loss factor and modal roots
16 p2992 A70-34018

Statistically indeterminate Timoshenko beams oscillations natural frequencies and modes by lumping properties of linear and rotary inertia at discrete points
16 p2994 A70-34235

Linear systems with two degrees of freedom modeled as rigid beam on elastic supports, considering vibration damping
16 p2996 A70-34291

Transversely isotropic Timoshenko beam statics and dynamics under initial stress and transverse loading
17 p3182 A70-34561

Nonlinear vibrations of beam harmonically excited by periodic motion of supporting base, using Galerkin method
17 p3185 A70-34962

Infinite elastic beams system supported on two parameter elastic foundation solved by analogy to single beam lying on one-parameter elastic foundation
17 p3189 A70-35229

Optimal design of elastic sandwich, solid beam and plate structures under dynamic harmonically varying loads
18 p3336 A70-36220

Infinite Bernoulli-Euler beam transient and steady state response, considering damping, elastic foundation and constant axial load effects
18 p3339 A70-36490

Torsional vibration of thin beam with varying cross section, formulating fundamental equation and boundary conditions
18 p3339 A70-36519

Vibrations induced by frictional moving force in viscoelastic beam with free ends on elastic base, showing critical load dependence on damping
18 p3343 A70-36720

WKB or eikonal approximation for waves and vibrations in inhomogeneous Euler-Bernoulli beams and plates and Timoshenko beams
19 p3536 A70-37700

Minimum weight thermoelastic design of sandwich beam for given deflection, using potential energy principle
19 p3541 A70-38044

Minimum weight design of sandwich beams with elementwise constant cross section for prescribed compliances under alternative loads
19 p3543 A70-38303

German monograph on creep in statically indeterminate reinforced concrete beams with graduated cross sections
19 p3548 A70-38473

Book on structural analysis by finite difference calculus covering elastic and elastoplastic states, vibration and buckling of beams, gridworks, plates and shells
19 p3548 A70-38599

Elastic-plastic equilibrium bifurcation in geometrically simple frame model with symmetrically loaded beam, comparing characteristics with Shanley uniformly stressed column model
19 p3549 A70-38671

Pretwisted slender beam coupled torsional and longitudinal vibrations under centrifugal force field, obtaining resonant frequency by Rayleigh Quotient method
20 p3719 A70-39601

Thermoelasticity of fiber reinforced materials, considering stress concentration in beams and reinforcing fibers buckling under thermal loading
20 p3730 A70-40037

Elastic beams optimal design for multipurpose loading, considering compliance and minimum cross section constraints
20 p3733 A70-40382

Dynamic response of simply supported non-homogeneous beam and triangular pulse loads
21 p3933 A70-40584

Stress-strain state of finite length elastic beam free of bending moments and coupled to semiinfinite plate
21 p3933 A70-40603

Solid and sandwich beams lateral vibrations under transverse shear, rotary inertia and variable midplane stretching
21 p3938 A70-41761

Analytical iteration method extended to critical load of clamped beam with symmetrically variable cross section
21 p3939 A70-41963

Weight-optimal sandwich beam design for given static deflection, using energy approach
22 p4113 A70-42535

Finite beam element in bending, deriving shear deflection terms in stiffness matrix based on stress assumption
23 p4274 A70-44909

Anisotropic bodies elastic properties, obtaining solutions for nonorthotropic beams under randomly distributed normal loads and for various plates and strips
24 p4424 A70-45589

Periodically supported beams and plates free vibration, calculating natural frequency spectrum distribution and normal modes
24 p4427 A70-46070

BEAMSHAPING U COLLIMATION BEARING [DIRECTION]

Angular resolution dependence on bearing ambiguities in radio direction finders based on interference measurement, using digital logic circuits
04 p0659 A70-15335

Vortices orientation due to unstable Ekman boundary layer, discussing analogy to Taylor-Goertler and thermoconvective vortices
06 p1096 A70-17465

Gradient method applied to onboard analysis of astronavigational bearings of spacecraft
09 p1719 A70-22165

Auroral orientation curves and auroral oval, determining largest difference between locations
11 p2046 A70-26500

Radio direction finding of celestial bodies from moving platform, determining plane rotation effects on angle measurements
18 p3333 A70-36164

Auditory direction finding ability, discussing experimental arrangement, white noise production, test conduction and statistical evaluation
20 p3582 A70-40538

BEARING ALLOYS

Friction, wear and surface evaluation of alloys as bearing materials in prosthetic devices
09 p1690 A70-22044

Bearing materials rolling contact fatigue life, describing three ball-cone test machine
09 p1702 A70-22555

Ball bearing materials for ultrahigh vacuum space environments, determining frictional and wear behavior
17 p3099 A70-34573

BEARINGS

NT ANTIFRICTION BEARINGS

NT BALL BEARINGS

NT FOIL BEARINGS

NT GAS BEARINGS

NT JOURNAL BEARINGS

NT ROLLER BEARINGS

NT THRUST BEARINGS

Inertia effect of electrically conducting lubricant on load capacity of hydromagnetic inclined slider bearing under magnetic field
01 p0104 A70-11389

Newtonian liquid lubricated spiral groove bearing load capacity and power loss dependence on viscosity variations with temperature
[ASLE PREPRINT 69-LC-21]
02 p0309 A70-12533

Bearing strength and rupture of reinforced plastic composites under intense one-sided electric heating and hydrostatic pressure due to pyrolysis of plastic bond
03 p0515 A70-13244

Stability analysis of rotors consisting of disks on massless shaft mounted in unsymmetrical flexible bearings, considering free and forced vibrations with damping neglected
03 p0599 A70-14248

Conducting fluid as MHD lubricant for cylindrical bearings, deriving equations for ideally conducting shaft and bearing and arbitrary Reynolds numbers
04 p0697 A70-14544

Load capacity and power loss of spiral groove bearings lubricated by incompressible liquid with temperature-dependent viscosity, using momentum and energy equations
05 p0853 A70-15778

Spiral gears bearing disks contact fatigue endurance process, deriving critical points cyclic stability from stress distribution considerations
07 p1291 A70-18819

Flexural vibrations of rotor resting on nonlinear elastic bearings under action of exciting forces harmonics using variational method based on Hamilton principle
07 p1403 A70-19112

Aircraft engine vibrational overload reducible by elastic bearings having controllable elastic characteristics
07 p1364 A70-19113

Hydrostatic bearings design for minimum power loss and leakage and maximum stiffness, using geometry-dependent operating parameter
08 p1508 A70-21600

Electromagnetically suspended bearing equivalent to elastic vinculum with limit on linear displacement, relating weight, power consumption, maximum force, etc
09 p1690 A70-22421

Sliding bearings with nonNewtonian lubricants, noting pressure gradient change effect caused by speed fluctuation and material constants
10 p1893 A70-24015
10 p1598 A70-24520

Monograph on critical speeds of nonzero mass shaft supported at both ends by bearings with nonlinear elastic displacements
13 p2416 A70-28373

Hydrodynamically lubricated rectangular taper-land bearing pads, analyzing geometry, viscosity, load capacity, friction and operating temperature conditions
13 p2418 A70-28740

Viscosity variation factor at film inlet in fluid square taper pad bearing investigated by modified Reynolds equation
13 p2418 A70-28746

Flow dynamic lubrication equation for porous bearings under radial load with undefined axial dimension
15 p2745 A70-32442

Thermal constriction resistance between contacting metallic paraboloids applied to instrument bearings [AIAA PAPER 70-857]
16 p2998 A70-33902

Collection of papers on aerospace mechanisms, Part B, Bearings and suspensions
16 p2922 A70-34154

Controlled leakage sealing of hydrodynamic bearing lubrication systems for space vehicles in synchronous orbit
16 p2923 A70-34158

Torque motor driven despin bearing assembly design with integral slip ring for tactical communications satellite /TACOMSAT/
16 p2986 A70-34160

Bearings for nuclear reactor control components in space environment, discussing sliding friction, compatibility and prototype assemblies tests
16 p2923 A70-34162

Conical pivot bearings for impact accelerations tolerance in space environments, discussing optimum dimensions and minimal torque design
16 p2923 A70-34164

Bearing assembly energy dissipation effects on dual spin spacecraft attitude stability, explaining satellite motion anomalies
17 p3100 A70-34756

MHD slider bearing load carrying capacity in tangential magnetic field, observing optimum profile in step form with riser location and step height ratio
18 p3263 A70-36672

Ultrahigh precision microminiature bearing resistance moment measurement with inductive sensors
18 p3264 A70-37069

Pivoted plane pad bearings, calculating design variables from inner products of two vectors and Rayleigh-Ritz matrix function
19 p3435 A70-37612

Bearing strength and rupture of reinforced plastic composites under intense one-sided electric heating and hydrostatic pressure due to pyrolysis of plastic bond
19 p3455 A70-38462

Rotational stability of heavy horizontal shaft supported on plain lubricated bearings with cavitation in lubricant
19 p3438 A70-38669

Three-lobe fluid film bearing configuration for gas turbine concentric rotating shafts/spool shafts/ [ASME PAPER 70-LUBS-10]
22 p4045 A70-42450

Liquid lubricant unsteady motion and pressure distribution during pivot harmonic vibration in hydrodynamic bearing
23 p4200 A70-44163

BEAT
U SYNCHRONISM
BEAT FREQUENCIES

Length shifts measurement with single 2-mode laser by observing beat frequency, obtaining frequency shift proportional to length shifts
05 p0859 A70-16356

Radiation from nonlinear polarization sideband in Ar lasers, discussing anomalous beat notes and mode locking phenomena
06 p1083 A70-17949

Self pulsation in He-Cd laser, noting decreasing number of modes effect on beat frequency stability
07 p1301 A70-20017

Doppler beat spectrum and modulation depth of He-Ne laser emission with backward beam reflected from moving mirror into resonator
10 p1901 A70-25123

He-Ne lasers mode locking by self beat feedback between cavity modes, achieving nonlinearity control by circuit adjustment
12 p2245 A70-27273

Emission spectrum of neon-helium laser receiving Doppler shifted signal from moving mirror, showing memory effect due to beat harmonics
12 p2246 A70-27352

Frequency locked noise effect on beat frequency measurement of angular velocity with ring laser, comparing gyroscope and phase methods
15 p2749 A70-31551

Voltage-frequency conversion technique using FM principle and RF oscillator beating with crystal oscillator output
15 p2705 A70-32705

Beat and synchronization modes of opposed waves in rotating gas ring laser, examining frequency response asymptotic behavior
17 p3108 A70-35683

Aperture size effect on frequency shift and frequency width variation of beat signals observed with laser Doppler velocity meter
19 p3428 A70-38502

M sub L alignment creation due to beam foil excitation process demonstrated with zero field quantum beats in He and H emission spectra
20 p3674 A70-39148

Doppler beat spectrum and modulation depth of He-Ne laser emission with backward beam reflected from moving mirror into resonator
20 p3643 A70-40516

Emission spectrum of neon-helium laser receiving Doppler shifted signal from moving mirror, showing memory effect due to beat harmonics
22 p4052 A70-43596

Magnetic flux dependent interference beats in spontaneous emission of gas discharge of He-Ne laser, estimating Hertzian coherence duration
23 p4202 A70-45052

BED REST

Motion coordination capacity of persons subjected to 40 days bed rest using dynamographic technique, discussing nature of slackening
03 p0425 A70-13896

Prolonged hypokinesia effect on human resistance to physical stress, noting prophylactic influence of physical exercises
03 p0425 A70-13898

Bed rest effects on whole leg venous distensibility, discussing heart rate and leg volume measurements
06 p0999 A70-17288

Recumbency effect on human heel bone density during bed rest using X rays
06 p0996 A70-17850

ECG changes attributed to reduction of blood supply to myocardium during orthostatic tests after prolonged hypokinesia
07 p1209 A70-19513

Human renal function, electrolyte and water metabolism during bed rest with daily leg exercise
07 p1223 A70-19937

Central nervous system activity of white rats during hypokinesia, observing organism shifts and long time effects on functions
09 p1615 A70-22093

Relative value of prolonged bed confinement and hypodynamia in estimating biological effects of weightlessness
10 p1813 A70-24666

Psychic state changes during prolonged bed rest, discussing effects of physical exercise and medicine
10 p1816 A70-24684

Psychic functions stability during prolonged hypodynamia, discussing memory, attention span, sensometer reactions, time estimating, etc
10 p1816 A70-24685

Physical exercise effects on man during prolonged bed rest, investigating muscle performance, static endurance, walking coordination and psychomotor functions
10 p1816 A70-24688

Transverse g-force tolerance and stability after prolonged hypodynamia in bed rest, noting effects of pharmaceuticals, physical exercise and prophylactic measures
10 p1817 A70-24695

Hypodynamia effects on humans during prolonged bed rest, investigating immunological resistance, psychic disorders, myocardium changes, responses to pharmaceuticals, etc
10 p1817 A70-24696

ECG changes attributed to reduction of blood supply to myocardium during orthostatic tests after prolonged hypokinesia
11 p1988 A70-26112

Hypokinesia effects on working capacity of subjects performing manual aircraft control assignments during bed rest
13 p2352 A70-29340

Nine-alpha-fluorohydrocortisone preventing bedrest induced orthostatism, considering plasma volume decrease effects on cardiovascular performance
13 p2358 A70-29433

Central nervous system activity of white rats during hypokinesia, observing organism shifts and long time effects on functions
15 p2685 A70-32689

Human circadian coronary circulatory rhythms during space flight weightlessness or bedrest with and without exercise
16 p2854 A70-33991

Optimum bed rest time schedules for cardiovascular patients from neurological, dynamometric, electromyographic and myogenic-tonus tests
23 p4149 A70-45077

BEDS (PROCESS ENGINEERING)

Cyclic changes in concentration produced in fluid flowing through fixed bed of solid adsorbent, governing separation by beds wave propagation properties
04 p0780 A70-14712

Time dependent transmission of carbon dioxide in air flowing through molecular sieve adsorber beds, developing and programming weighted least squares analysis
04 p0786 A70-15315

Equations and techniques to analyze transient heat and mass transfer characteristics of packed adsorption beds for spacecraft life support systems
04 p0786 A70-15316

Breakthrough curve shape prediction during adsorption from gas stream in fixed bed adsorbers for trace contaminant control applied to activated charcoal
04 p0786 A70-15317

BEER LAW

Absorption cross sections for single and double molecules of oxygen and in UV region noting disagreement with Beer law
06 p1114 A70-18632

BETTER

Space environment and radiation on Biosatellite 2 enhancing radiation effects in developing flour beetle Tribolium confusum
02 p0238 A70-12517

BEHAVIOR
NT HUMAN BEHAVIOR

Collection of articles on chimpanzee central nervous system and behavior
01 p0028 A70-11375

Pigeon response to concurrent variable interval reinforcement schedules, investigating relative and changeover rates regarding key color
05 p0800 A70-16126

Inhibitive stimulus control related to behavioral contrast during discriminative training
08 p1441 A70-20476

Reticular formation of central nervous system in vertebrates described as behavior controlling circuit of interconnected modules, proposing hybrid computer method for operational scheme
08 p1447 A70-21461

Drosophila brain Circadian oscillation as gating device restricting emergence behavior of adult
11 p1989 A70-26661

Feline hypersexuality, aggression and perceptual disorientation resulting from p-chlorophenylalanine administration
12 p2167 A70-27271

Hypothalamic electric stimulation intensity effects on elicited behavior, considering possible neural circuit threshold reduction
13 p2355 A70-29807

Engineering systems construction with behavioral elements of biological objects, describing gyromat
18 p3223 A70-36078

BELGIUM

ATC real time simulation exercises in Brussels Upper Information Region
07 p1250 A70-20227

Real time simulation of air traffic control problems in Brussels upper information region /UIR/
08 p1541 A70-21361

Report to COSPAR on Belgian National Committee for Space Research, discussing efforts of various universities and institutions
15 p2829 A70-31703

BELL AIRCRAFT
NT UH-1 HELICOPTER
NT X-22 AIRCRAFT
BELL MILITARY AIRCRAFT
U MILITARY AIRCRAFT
BELLMAN THEORY

Approximate solutions to Cauchy problem describing controlled pursuit using approximate method of integrating Bellman equation
04 p0713 A70-14602

Optimal terminal control stochastic synthesis for linear systems by Bellman second order nonlinear partial differential equation
21 p3801 A70-40607

BELLOWS

Gas turbine compensating bellows structural strength, discussing low cycle fatigue test under static loads
06 p1167 A70-17664

Expansion bellows fatigue strength based on load and displacement measurements performed during low cycle model tests
10 p1965 A70-25299

BELTRAMI FLOW

Monograph on Beltrami steady state, frictionless flow of incompressible medium past spherical surfaces, assuming vortex and stream lines agreement

11 p2034 A70-25498

MHD nonsteady Beltrami flow between two infinite parallel walls with transverse magnetic field, calculating velocity, skin friction and induced magnetic field

20 p3678 A70-39610

Beltrami flows on spherical surfaces, using scalar equations from kinematic conditions

24 p4326 A70-45990

BENARD CELLS

Atmospheric cellular convection, reducing hydrodynamic equations to amplitude equations for vertical velocity

15 p2770 A70-32064

BENCHES

U SEATS

BENDING

NT ELASTIC BENDING

Photogrammetric deformation measurement of thin steel sheets during static bending tests

02 p0302 A70-12653

Perforated plates bending for multiply connected regions, proving quasi-regularity and uniqueness of boundary value equations

04 p0767 A70-14481

Variable strain bending form design for determining environmental craze resistance of polymers

04 p0713 A70-15375

Electrical network models simulating initial and boundary value problems of applied mechanics, exemplifying with string free vibrations and thin plate bending

06 p1094 A70-17928

Rectangular plates with symmetrical cracks, studying bending under various crack distributions

07 p1399 A70-18662

Stress-strain analysis for rod-shaped structural elements under combined tensile and bending loads

08 p1588 A70-21191

Boundary conditions effect on bending, vibrations and buckling of unsymmetrically laminated rectangular plates

11 p2136 A70-26079

Regular C cubed space curve bending in Euclidean 3-space into piecewise helix, considering torsion and curvature

12 p2260 A70-26973

Tensodiode effect in long plate-shaped semiconductors, noting bend direction effects on I-V characteristics

12 p2195 A70-27312

Reference stress evaluated by numerical analysis techniques, discussing rectangular beam in pure bending

16 p2987 A70-32921

Aircraft wing box beams bending tests to failure loads, considering crushing pressure, bulkhead flexural deformations, structure initial imperfections and instability phenomena

23 p4267 A70-44103

BENDING FATIGUE

Elastoplastic stress concentrations calculations in notched strips and shafts under tension, bending and torsion, using approximate method

01 p0211 A70-11425

Component proportion and porosity effect on fiberglass reinforced plastics properties, establishing relation between bending strength and thermal conductivity coefficient

02 p0323 A70-12814

Reversed bending fatigue tests on stainless steel fibermetal with porous structure to investigate effects of density, thickness, wire diameter, screen stiffening, etc

03 p0481 A70-12957

Low cycle fatigue of alloy and steel materials under bending and cyclic heating, relating strains and number of cycles to failure

05 p0866 A70-17036

Normalized steel low cycle fatigue strength under bending and torsional rotation, testing linear damage accumulation theory

06 p1163 A70-17404

High purity Ni fatigue in reversed bending as function of oxygen pressure and temperature

06 p1086 A70-17454

Ti alloy welded sheets bending fatigue test facility, discussing test stand calibration and optimal welding

07 p1291 A70-18824

Reverse-bend and tension-tension fatigue properties of high strength Cr-Mn-N stainless steel sheet in notched and unnotched conditions

07 p1305 A70-18993

Cyclic bending stresses in web of precessing disk-type gyroscope rotor, considering fatigue failure and forced vibration response

09 p1770 A70-22270

Vertebral injury prediction of seated human subjected to caudocephalad acceleration, suggesting consideration for head and torso forward flexion and external restraints effects

09 p1627 A70-23462

Ni-Cr austenitic steel bending, surface temperature variations, crack development and propagation under double fatigue tests

10 p1902 A70-23819

Materials bending fatigue strength calculations for biaxial tension compared with experiments showing agreement

10 p1964 A70-25289

Stress peak distribution effects on fatigue life of test specimen excited to bending by Gaussian random vibrations

11 p2137 A70-26093

Mechanical notches and saltwater corrosion effects on flexural fatigue behavior of high strength structural alloys, investigating yield strength to density ratio

11 p2066 A70-26097

Low cycle fatigue tests advantages by reversed bending ascribed to simplicity, specimen stability at high strain levels and minimum equipment costs

11 p2034 A70-26614

Biaxial stress effect on fatigue crack propagation in Al alloy plate under reversed bending

15 p2821 A70-32324

Welded Al plates high temperature bend tests, describing materials and procedures

18 p3278 A70-37115

German monograph on refractory materials softening under bending and compression at high temperatures

22 p4061 A70-43742

Double linear damage rule applicability to dual type alloys from two-stress level rotating bending and axial fatigue tests

[ICAS PAPER 70-39]

23 p4267 A70-44137

Plane strain fracture toughness testing of high strength Al alloys and steels, using fatigue cracked bend specimens

23 p4206 A70-44191

Thin Al foil subjected to cyclic bending stresses, investigating substructures and strain regions around fatigue crack

24 p4362 A70-46186

BENDING MOMENTS

Moments and shear forces in plate flexure represented by single valued stress functions of position, stating variational principle for compatibility

01 p0201 A70-10931

Numerical solution of bending stresses in internally pressurized elliptical tubular or ring specimens for testing uniaxial and multiaxial fracture strength

01 p0203 A70-11061

Attachment loads and beam bending moments design curves for linear and right angle fittings on honeycomb inserts to determine internal loading

02 p0386 A70-11949

Stress-strain analysis of rectangular plates under concentrated load, noting sealed liquid compressibility effect on deflections and bending moments

02 p0388 A70-12499

Sinusoidal test for measuring knee moment increase required to flex and extend for various conditions of knee angle, angular velocity and steady knee moment

02 p0238 A70-12546

Finite strain in bending rectangular block into right circular cylindrical shell for transversely isotropic medium along radius vector, using Saint Venant stress-strain relations

03 p0602 A70-14329

Monograph on shear lag measurement in rectangular section beam subjected to bending or torque free from axial restraint, using inductance probe sensors

03 p0603 A70-14351

Stress-strain state under bending of shallow spherical shell having form of circular rectangle with clamped edges

04 p0767 A70-14486

Stress-strain state of circular orthotropic shells under bending, considering distributed loads applied to shell center

05 p0934 A70-16217

Revolving shells local stability developing boundary effect under normal and bending external loads solved by computer program

05 p0935 A70-16237

Compressive forces eccentricity influence on circular cylindrical shell stability noting relation to bending moments

05 p0936 A70-16239

Hammer forces and specimen bending moment-time responses and fracture resistance during notched beam impact test

05 p0938 A70-16479

Simply supported beams large deflection analysis in bending under symmetrical pair of forces, based on integration of elastic line differential equation

05 p0941 A70-16521

Axial and nonlinear bending performance compared for compression moldings laminated from random glass fiber mat

05 p0870 A70-16577

Stress-strain state of plates weakened by reinforced hole and under tensile and bending loads, including boundary conditions

05 p0945 A70-16856

Stress-strain state of drawn and bent circular plate made of rigid viscoplastic work hardened material

05 p0946 A70-16958

Support moment of beam with ends embedded in elastic medium subject to creep, noting dependence on load

05 p0947 A70-17010

Static buckling load for beam with pinned ends and Wighardt-type elastic foundation, considering shear stresses effect

05 p0955 A70-17105

Stress-strain state of curved rod made of anisotropic material under bending loads applied to end face cross sections

07 p1399 A70-18661

Elastic behavior of joint formed by normally intersecting circular cylindrical shells under external bending moment, noting applicability to pipelines and pressure vessels

[ASME PAPER 68-WA/PVP-1]

07 p1400 A70-18710

Bending tests for characterizing off-axis unidirectional composite beams, discussing errors due to lift off from supports

07 p1412 A70-19963

Impact forces and specimen bending moments generated during dynamic tear test interpreted in terms of system dynamics and material fracture characteristics

08 p1518 A70-21319

Stress, strain and strain rate relations determined from dynamic flexural beam tests with bending moment in terms of curvature

08 p1592 A70-21475

End plugs bending moment and shear loads reduction during compression tests of composite orthotropic cylinders

08 p1594 A70-21889

Weight function minimization of multiweb box beam in pure bending

09 p1777 A70-22769

Elastoplastic compressible sheet metals reinforced by isotropic work hardening under action of bending moments, analyzing stresses and strains

10 p1955 A70-24056

Stress distribution in strip with asymmetrically positioned internal row of equal and equally spaced circular holes subjected to longitudinal tension or transverse bending

10 p1955 A70-24082

Lines of influence of bending moments and cutting force for straight beam using differential equation integration

10 p1959 A70-24777

Beams stability under flexural stress with periodic intensity variations, deriving differential equation of motion

10 p1960 A70-24973

Vibrations of combination of cylindrical shells and circular plates, giving bending moment distribution

11 p2139 A70-26415

Thin shell design for minimum bending stresses and transverse shear for composite materials with low interlaminar shear strength

11 p2141 A70-26490

Rectangular beam creep rupture time under bending moment and axial tensile force, using power series to solve integral equations

11 p2142 A70-26635

Orthotropic plates bending with shallow and sharp fillets, determining normal stresses

12 p2325 A70-27533

Postwrinkling nonlinear behavior of conical shell of revolution subjected to bending loads

[AIAA PAPER 69-90]

12 p2326 A70-27816

Rotating shaft model with slight curvature for estimating maximum bending moment through Fourier series analysis

13 p2416 A70-28372

Booster control system reducing maximal wind-induced bending torques, examining booster response to aerodynamic forces

13 p2500 A70-28413

Stability and wind response determining spacecraft structure forces and bending moments

[AGARDGRAPH-115]

13 p2504 A70-28754

Hologram interferometry using moire method to determine bending moments of object surface

13 p2409 A70-29474

Isotropic plates weakened by circular holes, investigating bending by Ambartsumian plate theory

13 p2515 A70-29509

Transverse bending of isotropic rectangular plate with symmetric crack under uniformly distributed load, considering corrections for stress-strain state near cracks

13 p2516 A70-29516

Clamped orthotropic rectangular sandwich plates bending using approximate solution

14 p2661 A70-31429

Pyroceramics transient strength measurements on cylindrical and prismatic samples under static bending

15 p2764 A70-31545

Helicopter rotor blades flapwise bending moments prediction by transfer function/superposition techniques

17 p3013 A70-34704

Normally loaded thin plate displacements, bending moments and stresses determined by hologram interferometry and indirect moiré and superposition of grilles

17 p3085 A70-35011

Plane cross section hypothesis applied to fully developed creep in thin walled tube subjected to internal pressure and bending moments, calculating stress concentration

18 p3340 A70-36571

Static stability requirements relaxation and wing control devices additions for alleviating wing root bending moments in controls configured vehicle /CCV/ design concepts

19 p3355 A70-37395

Concentrated lateral loads effect on elastic stability and moment carrying capacity of circular cylindrical shells in bending

21 p3932 A70-40544

Elastoplastic bending of rotating circular shaft with constant end cross section force couple, assuming small deformations of linearly hardening materials

22 p4118 A70-43570

Cantilever beam optimal stability under concentrated and uniformly distributed bending loads

23 p4268 A70-44171

BENDING THEORY

Elastic support effect on bending of clamped circular, elliptical, rectangular and skewed plates, using variational method and small perturbation technique

01 p0205 A70-11144

Finite element bending stiffness matrices for deflections analysis of pretwisted cantilever plate subjected to static loads

02 p0384 A70-11858

Orthotropic cylindrical shell with initial deflection under long term effect of external hydrostatic pressure, solving bending problem

02 p0390 A70-12809

Triangular conforming plate bending element applied to static and dynamic problems, investigating convergence rates of finite element approximations

03 p0584 A70-12924

Cylindrical bending in laminated plates displaying bending-extensional coupling approximating behavior of rectangular laminated plates with high length-to-width ratio

03 p0587 A70-13125

Simultaneous equations of longitudinal impact bending, introducing temporal and spatial transformations regarding dispersive wave characteristics in elastic rod

03 p0591 A70-13428

R function method for solving plate bending problem by satisfying differential equations coordinates

04 p0767 A70-14489

Bending analysis of cracked plate with arbitrary stress distribution across thickness

[ASME PAPER 69-WA/PPV-2] 04 p0768 A70-14791

Stiffener inclination effect on pressurized cylinder instability under pure bending

[ASME PAPER 69-APM-X] 04 p0769 A70-14868

Fracture criteria in cracked plates under combined extension and cylindrical bending using Sih-Hartman theory

[ASME PAPER 69-MET-L] 04 p0770 A70-14882

Heated isotropic shallow shells results extended to solving nonlinear problem in bending theory of orthotropic shallow shells clamped, heated and under pressure

05 p0927 A70-15993

Bending problem for homogeneous transversely isotropic plate weakened by curvilinear hole

05 p0946 A70-16959

Elastoplastic bending of rectangular plates by finite difference and variational methods assuming homogeneity in elastic region

05 p0946 A70-16962

Rectangular and nonrectangular anisotropic plate bending and stability analysis by difference-differential technique, allowing for combined freely supported and clamped end conditions

06 p1167 A70-17864

Electric network models of nonhomogeneous differential equations applied to elastic beam and thin plate bending and displacement equations

06 p1094 A70-17927

Triangular plate bending elements with enforced compatibility, using cubic interpolation polynomial to describe element displacement

[AIAA PAPER 70-136] 06 p1171 A70-18169

Rectangular three layer plate bending with load carrying central layer obeying Kirchhoff-Love hypotheses and external layers obeying Noether hypothesis

07 p1403 A70-19117

Effect of uniformly distributed circular holes in finite double row on stress distribution in transversely bent strip, based on Kirchhoff bending theory

07 p1407 A70-19385

Anticlastic bending effect on rectangular beam curvature, presenting deflection equations

07 p1414 A70-20175

Ductile flexure location in bent beams and systems with variable cross sections to determine critical load using plasticity theory

08 p1587 A70-21072

Infinitely wide plate bending at small angle of attack in supersonic gas flow, obtaining critical flow rate equal to divergence rate

08 p1588 A70-21175

Linear and nonlinear equilibrium equations for bending deformation of thin elastic cylindrical using Kirchhoff-Love hypotheses

08 p1588 A70-21242

Finite bending elements for static deflections of annular and circular plates loaded by concentrated forces, calculating free vibrations

08 p1588 A70-21243

Yield criterion for plastic bending of transversely anisotropic circular plates under plane stress

08 p1589 A70-21250

Stiffeners inclination effects on instability of pressurized cylinder under bending by Ritz method, considering finite deflection and initial imperfections in strain-displacement relations

08 p1591 A70-21464

Flexural rigidity of thin walled beams, analyzing relationship between loads and displacements taking into account Saint Venant torsional resistance

10 p1955 A70-24052

Bending of homogeneous orthotropic rectangular plate of variable thickness supported on opposite edges, obtaining solution as Fourier series

10 p1955 A70-24083

Plate bending triangular finite element for shell structure analysis, considering displacement functions, stiffness matrix and load vector

10 p1957 A70-24482

Rigid/plastic or rigid/perfectly plastic anisotropic plate under uniform bending, analyzing stress distribution

10 p1964 A70-25092

Elastic bending of clamped and supported elliptic and parabolic plates under external pressure investigated by lines of equal deflection

11 p2133 A70-25839

First order differential equations for unsymmetrical bending of shells of revolution

11 p2135 A70-25978

Transient bending and shear stresses at clamped support of orthotropic circular cylindrical shells

11 p2135 A70-25985

Clamped thin circular plate bending under various loadings due to action of rigid square column on center

11 p2139 A70-26404

Finite element bending stress analysis of thin rectangular and skew plates, discussing computational procedure generating stiffness matrices

11 p2143 A70-26641

Conforming plate bending solution with third degree polynomial deflection functions in triangular finite elements, using Lagrange multipliers as stress parameters

11 p2143 A70-26642

Finite element method solutions for plate bending, improving convergence based on error analysis

11 p2144 A70-26676

Glass fiber reinforced thin rectilinear orthotropic plastic plates bending using finite difference method with allowance for creep

12 p2324 A70-27531

Iteration procedures for boundary value problem of orthotropic rectangular plate under bending loads, discussing convergence of procedures

12 p2325 A70-27552

Derivation procedure for dynamic flexibility matrix including material damping for triangular plate in bending, twisting and shear

13 p2509 A70-28540

Open cross section thin walled prismatic beam twisting and bending based on virtual displacements

13 p2511 A70-28744

Stress distribution in isotropic plates weakened by elliptical holes under bending based on elastic shallow shell theory and small parameter technique

13 p2514 A70-29291

Plastic symmetrical bending of freely supported beam under transverse local pulsed load, discussing deflection velocity fields during loading and unloading stages

13 p2514 A70-29307

Thermoelastic equations for circular sandwich plates bending due to asymmetric temperature distribution

13 p2518 A70-29976

Fourth order differential equations eigenfunctions construction and convergence of expansions in theory of flexure of sector plates

14 p2658 A70-30997

Cosmic rays geomagnetic bending and effective angles of approach for various ground stations

14 p2633 A70-31313

Cylindrical conical shell junction asymmetric bending, using numerical method and exact solution

15 p2822 A70-32360

Elastoplastic bending of thin plate under increasing and uniformly distributed loads, defining statically admissible stresses

16 p2988 A70-33107

Monograph on optimal angles and section partition for buckling strength of twisted and displaced bent bars

16 p2988 A70-33300

Twisted uniform beam element flexibility and stiffness matrices, using continuous bending theory

16 p2894 A70-33887

Shear coupling effect in cylindrical bending of anisotropic composite laminates

17 p3182 A70-34558

Linear bending theory of thin homogeneous isotropic plates

18 p3339 A70-36482

Structure of flexural members, analyzing torsional and lateral stability by finite element method and matrix formulation

18 p3339 A70-36494

Creep bending of rectangular plates with stress-strain and strain displacement nonlinearities

18 p3343 A70-36703

Arbitrary cross sections center of flexure formula, transforming surface integral to line integral dependent on boundary conditions

18 p3343 A70-36716

Bent plates strain analysis using in-plane moiré method for small and large deflections

19 p3535 A70-37383

Straight thin walled elliptical cylindrical shells stability in pure bending, solving boundary value problem

19 p3550 A70-38683

Large deflection of simply supported aluminum alloy annular plate with nonlinear stress-strain curve, considering compressibility effects and membrane force

20 p3718 A70-39138

Anticlastic bending analysis of long narrow plates oscillations and stability based on elastic plates nonlinear theory

20 p3721 A70-39779

Stressed state in thermoelasticity plane steady state problem of thin plate under bending based on dislocations and temperature stresses relationship

20 p3721 A70-39780

Structural mechanics of continuous fiber reinforced composites, discussing bending and stretching of cylinders, pressure vessels, plates and beams

20 p3730 A70-40039

Bending of rigidly fixed or simply supported parallelogram plates, using Ritz and Rubnov-Galerkin variational methods

21 p3933 A70-40742

Cantilever bending under gradual contact with cylindrical supporting surface compared with solution by elasticity theory

21 p3934 A70-41251

Support elasticity role in axisymmetric plates bending, discussing Rayleigh-Ritz solution

21 p3937 A70-41739

Bending stress at clamped support of impulsively loaded semiinfinite conical shell, obtaining formulas from perturbation theory

21 p3938 A70-41759

Third isotropic point in rectangular beam under bending stresses by Hertzian load, using Stokes-Wilson method and photoelastic comparison

21 p3941 A70-42265

Variable thickness flexible plates thermoelastic flexure and buckling, obtaining nonlinear differential matrix equations by difference-differential method

22 p4115 A70-42811

Elastic plate uniform extension with rectangular crack by three dimensional bending theory, using variational principle

22 p4115 A70-42941

Finite element method for bending-extensional coupling in angle-ply laminates deformation behavior

22 p4061 A70-43685

Transverse bending of orthotropic glass fiber reinforced plastic plates under uniformly distributed loads

22 p4120 A70-43720

Two dimensional shell equations derivation from three dimensional elasticity theory, considering rotationally symmetric bending of shells of revolution

23 p4265 A70-43942

Fundamental error in Galerkin method application to bending problem of elastic rods

23 p4268 A70-44172

Finite beam element in bending, deriving shear deflection terms in stiffness matrix based on stress assumption

23 p4274 A70-44909

Prismatic isotropic homogeneous cantilever beams flexure for case of power series conformal mapping function

23 p4275 A70-44944

German monograph on stress-strain state in prestressed, rigidly supported flexible plates subjected to large deflections, using extended Wolmir solution

24 p4418 A70-45083

BENDING VIBRATION

- Spurious flexural vibrations in cylindrical mechanical resonators, transducers and wires used as component parts in electromechanical filters, indicating dependence on material dimensions and properties
02 p0268 A70-12450
- Unidirectional carbon and glass fiber reinforced polyester resins dynamic characteristics under torsional and flexural vibration, showing damping independence of cyclic stress amplitude
03 p0514 A70-13111
- Nonlinear flexural vibration properties of thin circular cylindrical shells with simply supported ends assuming deflection mode
03 p0594 A70-13549
- Complex Young modulus of plastics during flexural vibration, discussing deformation of viscoelastic bodies and test results of various plastics
[ONERA-TP-715] 03 p0487 A70-13645
- Natural frequency calculation accuracy for coupled beam bending vibrations shown dependent on connection stiffness determination
03 p0595 A70-13929
- Frequency equation for flexural vibration of simply supported beam, considering tabular procedure for cantilever beam
03 p0602 A70-14330
- Cyclic bending stress in disk type gyroscope rotor under steady precession, discussing solutions for modal functions and resonant frequencies
[ASME PAPER 69-DE-A] 04 p0689 A70-14873
- Optimal iterative weighted least squares estimation of rotation-coupled flexural oscillations of boom stabilized satellites in earth orbits
04 p0763 A70-15413
- Thin gas turbine disk strength under axisymmetric flexural vibrations, noting agreement of calculated and experimental rotor rpm danger zone
06 p1166 A70-17654
- Energy dissipation during torsional and flexural vibrations of steel and duralumin specimens subjected to plastic deformation, accounting for discrepancies due to methodical errors
06 p1166 A70-17658
- Complex elastic system coupled flexural vibrations resonant frequencies determined with allowance for friction
07 p1363 A70-19111
- Flexural vibrations of rotor resting on nonlinear elastic bearings under action of exciting forces harmonics using variational method based on Hamilton principle
07 p1403 A70-19112
- Inductive sensor design and circuitry for measuring rapidly rotating shaft bending deflections at various vibration frequencies
07 p1279 A70-19115
- Rotating rotor with mass distributed along shaft analyzed for nonlinear flexural and torsional vibrations, determining dynamic instability ranges
08 p1584 A70-20694
- Amplitude-frequency characteristics of arbitrary elastic system performing flexural vibrations determined using computer
08 p1588 A70-21184
- Free in-plane flexural vibrations of circular rings, developing equation of motion to include shear deformation and rotatory inertia effects
08 p1592 A70-21473
- Longitudinal structural vibration and lateral bending response mass and spring coupling in Saturn AS-502 during boost with longitudinal excitation by pogo effect
09 p1766 A70-23239
- Natural bending vibrations of circular plates with allowance for stress tensor asymmetry, deriving transcendental frequency equation
09 p1782 A70-23292
- Static tensile stresses effect on magnetized ferromagnetic materials damping properties explained by anisotropic microplastic strains dissipating energy during bending vibration
10 p1904 A70-24246
- Shrouded aircraft engine turbine blades vibration stresses found minimum by setting up paired blades with fixed tension along shroud
10 p1964 A70-25288
- Flexural vibrations of homogeneous elastic circular cylinder supported at both ends, imposing zero stress conditions on skirt
12 p2321 A70-27154
- Supersonic flutter solutions using finite elements, analyzing rectangular plate bending elements, square simply supported and clamped panels, low aspect ratio configurations, etc
12 p2327 A70-27823
- Energy dissipation during independent flexural-torsional vibrations of rods, noting alternating shear stress superposition effect on damping
15 p2813 A70-31530
- Kinetic instability of elastic cantilever beam under excitation by rotating masses, relating bending and torsional vibrations to masses angular velocity
18 p3334 A70-35960

Flexural vibrations of laminated composite plates, maintaining continuity of displacements and surface tractions at intersurfaces between reinforcing layers and composite matrix
19 p3537 A70-37790

Nodal patterns on thin elastic circular plate vibrating in flexure, considering natural and compounded modes
19 p3543 A70-38245

Low aspect ratio cantilever plate wings supersonic bending torsion flutter speed calculation, using spanwise and chordwise variables and potential energy principle
22 p4112 A70-42276

Nonlinear flexural vibration of thin circular cylindrical shells with clamped ends, using method of averaging for stability
22 p4112 A70-42517

Cross ply laminated plates natural frequencies, approximating flexural vibration by classical theory
22 p4119 A70-43679

Flexural vibrations of clamped circular plate with nonlinear elasticity for small strains and displacements, using variational principle
22 p4120 A70-43719

Bending vibrations of propeller blades calculated by successive approximation
24 p4422 A70-45300

Rope transverse oscillations due to impact taking bending rigidity into account
24 p4424 A70-45627

BENDS [PHYSIOLOGY]

U DECOMPRESSION SICKNESS

BENTONITE

Optimum composition of sand-bentonite materials for aluminum alloy casting in molds compacted by high pressure
08 p1506 A70-21137

Middle Devonian Tioga Bentonite age from Rb, Sr and Sr isotopes in weathered whole rock samples
20 p3615 A70-38989

BENZENE

Thermospectrometric investigation of stimulated Raman lines in benzene to identify generation modes, observing optical sideband effect at 8050 Å
13 p2425 A70-28712

Vapor phase fluorescence spectra from benzene and deuterated benzene at zero point vibrational level
15 p2694 A70-31731

Thermal stability of polymers based on aromatic diamines and isomeric dibenzoylbenzenes
21 p3782 A70-42129

Thermal conductivity of water, toluene and benzene in coaxial cylinders, taking into account edge heat losses
23 p4276 A70-44216

BERENICE ROCKET VEHICLE

Estimated aerodynamic coefficients of reentry body compared with coefficients derived from Antares and Berenice flights
06 p0966 A70-17248

BERNOULLI EQUATION

U BERNOULLI THEOREM

BERNOULLI THEOREM

Martin method for reducing determination of steady plane MHD flow to Bernoulli and direct functions satisfying quasi-linear partial differential equations
03 p0533 A70-14200

Bernoulli-Euler beam equation describing natural frequencies and mode shapes for vibrating beam immersed in fluid
07 p1413 A70-20043

Wind temperature measurement, taking Bernoulli effect and kinetic theory into account
22 p4009 A70-42525

Boundary geometry of region with fluid motions harmonic functions obeying Bernoulli law containing free surface curvature
23 p4218 A70-44337

BERYLLIUM

NT BERYLLIUM 9

NT BERYLLIUM 10

Low speed Ga lubricated sliding electrical contacts of Be in vacuum, discussing Ga film role in friction and contact resistance
01 p0099 A70-10325

Beryllium properties and processing including magnesianothermal reduction, power purity, oxygen content, grain size and temperature effects on mechanical properties
01 p0124 A70-11618

Be oxidation in carbon dioxide at high temperatures, explaining observed kinetic discontinuity in terms of oxide morphology
01 p0124 A70-11638

Ingot and powder metallurgy polycrystalline Be flow and fracture behavior and microstructure pressure dependence at room temperature
02 p0317 A70-12318

Case hardened steels structure and properties, intermetallic phases, hardness variation with depth and hardening techniques by Be and B
03 p0510 A70-13351

Shear testing and data reduction based on torsion analysis to obtain elastic shear constants of thin orthotropic Be sheets
04 p0664 A70-15552

Beryllium single crystals deformation under high pressures at room temperature similar to deformation under atmospheric pressure at elevated temperatures
05 p0863 A70-16203

Atmospheric contamination due to Be solid propellant exhaust products, discussing pollution levels, governmental restrictions on testing, etc
[AIAA PAPER 70-117] 06 p0997 A70-18085

Be atoms effect on lattice structure of three component sodium oxide-beryllia-silicate glasses using IR absorption spectra
07 p1315 A70-18704

Oxide transport and water vapor effects on flash-heated beryllium droplet combustion
10 p1969 A70-25042

High purity beryllium dynamic tests determining Hugoniot equation of state, shock profile and spall threshold/onset of microcracking/for elastic pulses
[AIAA PAPER 69-360] 11 p2066 A70-25964

Isotropic Be billet fabrication by gas pressure consolidation and pressureless sintering techniques
12 p2252 A70-26888

Beryllium proportional counters for satellite X ray astronomy, noting long term stability and environmental resistance
12 p2232 A70-27403

Cleavage cracks initiation and propagation in basal plane of Be single crystals, determining propagation energy as function of temperature, purity and alloying
12 p2256 A70-27614

Surface oxidation effects on thermionic work functions of Be determined by visual observation and X ray diffraction patterns analysis
12 p2288 A70-28004

Plastic deformation of Be single crystals under hydrostatic pressure, considering resolved shear stresses on glide systems
14 p2595 A70-30334

Al and Be single particles combustion in various oxidizers, using pulsed Nd-glass laser and Xe flash heating device and scanning electron microscope
14 p2628 A70-30949

Beryllium fibers and Al matrix interactions at high temperatures and various durations, investigating diffusion by X ray diffraction, electron microscope and microprobe analysis
15 p2757 A70-31812

Polygonized and cellular Be structures formation, examining temperature, strain, annealing and material purity effects
15 p2758 A70-32122

F-4 Be rudders design and tests compared to Al structure
[ASM PAPER W70-12.4] 15 p2676 A70-32336

Bend formability and fracture toughness tests on Be ingot and cross-rolled powdered sheet and brake grade block materials
[ASM PAPER W70-15.3] 15 p2760 A70-32337

Beryllium mirrors optical performance, describing causes and effects of anisotropy and dimensional instability
16 p2904 A70-33146

Lamellar and fibrous Be-reinforced epoxy resin and metal matrix composites, describing preparation and properties
16 p2939 A70-33693

Metallographic observations on slow crack growth in Be monocrystals suggesting explanation for transition regions
16 p2933 A70-32475

Crack initiation in wrought polycrystalline Be sheet, investigating three point loaded bend fractures of powder and ingot samples by optical and electron microscopy
17 p3122 A70-34551

Fine grained Be structure and mechanical properties under tensile deformation at temperatures from 20 to 1000 C
18 p3276 A70-36311

Residual stress of electroless nickel deposits on beryllium from bow deformation measurements, noting role of phosphorus content
19 p3451 A70-37708

Ti-Be composite materials production by coextrusion of powders, investigating microstructure by microprobe analysis and X ray diffraction
20 p3649 A70-39945

Be production, development, potential uses and properties
[ASM PAPER GG8-102] 20 p3650 A70-39970

Beryllium use in inertial navigation as stable platform structure and control gyro, discussing physical properties, design concept, fabrication, service, cost and tradeoffs
20 p3639 A70-40451

Beryllium orbital diamagnetic susceptibility calculated by pseudopotential method compared to experimental data
23 p4208 A70-44886

- High purity Be preparation by Kroll process using Na as reductant, noting mechanical properties and ease of conversion to powder 24 p4341 A70-45242
- BERYLLIUM ALLOYS**
Be-Al-Ti system liquidus surfaces and invariant equilibria by chemical, thermal, X ray and microscopic methods, discussing phase diagrams 14 p2595 A70-30839
Temperature effect on radiation characteristics and cryogenic tensile properties of irradiated Be, Ti and Al alloys 20 p3647 A70-39111
Al-Be eutectic alloys structure, using laue X ray method and electron microscopy in studying fibrous morphology due to unidirectional solidification 24 p4356 A70-45143
- BERYLLIUM COMPOUNDS**
NT BERYLLIUM FLUORIDES
NT BERYLLIUM NITRIDES
NT BERYLLIUM OXIDES
Beryllium sulfate effect on rabbits vascular plasma volumes, using albumin method for blood groups 15 p2681 A70-31884
- BERYLLIUM FLUORIDES**
Solid and liquid lithium tetrafluoroberyllate enthalpy relative to 273 K measured at temperatures between 323-873 K, deriving thermodynamic properties 04 p0646 A70-14583
- BERYLLIUM ISOTOPES**
NT BERYLLIUM 9
NT BERYLLIUM 10
BERYLLIUM NITRIDES
Alpha beryllium nitride enthalpy and thermodynamic properties measured between 273-1173 K using drop calorimetric method 04 p0646 A70-14582
- BERYLLIUM OXIDES**
BeO whiskers formation on burning Be droplets surface using scanning electron microscopy, noting temperature effects 02 p0318 A70-12641
Normal incidence reflectance of BeO single crystals, analyzing data by Kramers-Kronig inversion for dielectric function and energy loss function 05 p0891 A70-16047
Ar ion laser performance improvement by using beryllia for sealed-off discharge tube 09 p1699 A70-23443
- BERYLLIUM POISONING**
Toxicity and downwind diffusion of Be rocket exhaust product measurements, using ADOBE experiment and AFRPL micromet meteorological data system 14 p2628 A70-30611
- BERYLLIUM 9**
Solar neutrons detection from recording high energy electrons in reactions, using Li 7, Be 9 and B 11 as detectors 05 p0899 A70-15964
- BERYLLIUM 10**
Cosmic ray lifetime, investigating radioactive Be 10 nuclei decay effects on intensity ratios Be/B and Be/Li, suggesting nuclei confinement to galactic disk 19 p3509 A70-38148
- BESSEL FUNCTIONS**
NT HANKEL FUNCTIONS
Bessel function applied to unsteady axisymmetric problem of heat conduction in thermally controlled coaxial cylinders with different physical properties 03 p0608 A70-14304
Bessel generalized polynomial series convergence and summability on contour of convergence region 11 p2071 A70-25521
Relationship between fundamental matrices of solutions to boundary value problems of parabolic and elliptical systems with Bessel functions 13 p2441 A70-29314
Computer program for two body problem literal series expansions using Kepler functions with Bessel and Poisson series operation 14 p2638 A70-30702
Zero order Bessel function fringe shape measurement for holographic sinusoidal vibration fringes 17 p3087 A70-35020
Spherical Bessel functions fast generation recurrence technique, presenting real or complex arguments 22 p4062 A70-42920
- BESSEL-BREDICHIN THEORY**
Particle ejection moments from tail of comet Ikeya-Seki determined from photographs having visible terminal synchroes 06 p1140 A70-17732
- BETA PARTICLES**
Two phase density and void fraction measurement using beta, gamma and X ray radiation, considering optimal accuracy and beam collimation 02 p0305 A70-12835
Parachute-borne densitometer using forward scattering of low energy beta particles for direct measurement of atmospheric density at 30-60 km [AAS PAPER 69-570] 04 p0687 A70-14654
- Atmospheric ionization by beta particles due to fission product decay, showing diagram for magnetic shell parameters and postfission periods 04 p0743 A70-15739
Cosine dependence of F 1 critical characteristics on solar zenith angle discriminating alpha neutralization and mixed alpha-beta deionization 06 p1057 A70-17841
Neutron beta decay in strong quantizing magnetic field using Dirac wave function for electron, noting lifetime dependence on field strength 08 p1549 A70-21744
Permeability disturbances in skin capillaries of rabbits and rats following exposure to Sr90-Y90 beta radiation 09 p1619 A70-22789
Electron-neutrino weak interaction and beat decay coupling constants found nearly equal, describing astrophysical tests based on white dwarf stars luminosity intervals 09 p1733 A70-23451
Atmospheric ionization by beta particles due to fission product decay, showing diagram for magnetic shell parameters and postfission periods 14 p2632 A70-30823
Coating thickness measurement and analysis by radioisotope techniques including beta-particle, X or gamma ray backscatter and X ray fluorescence and absorption 15 p2742 A70-32780
Inverse beta decay thermonuclear reactions induced by neutrinos proposed for neutrino detection from solar interior 20 p3704 A70-39471
- BETATONS**
Nondestructive betatron radiographic testing techniques for Ti billets, evaluating various lead screen, film and geometry combinations 08 p1508 A70-21746
Energy spectrum of electrons accelerated in linear plasma betatron close to potential compared to cyclic betatron results 13 p2463 A70-29379
High current betatrons for defectoscopy of manufactured articles and materials compared with other radiation sources 24 p4348 A70-45846
Betatron monoenergetic electron beams in radiometric, spectrometric and radiographic testing of composite materials 24 p4339 A70-45850
- BETHE-SALPETER EQUATION**
Radiation transfer problem in waveguide with statistically uneven walls reduced to Dyson and Bethe-Salpeter equations in quantum field theory 03 p0524 A70-13066
- BIAS**
NT RESPONSE BIAS
Antenna biasing with DC field to improve power handling capacity tested on U-slot and helical antennas 02 p0269 A70-12595
Bias-free estimation of linear process in recursive filtering, avoiding numerical inaccuracies introduced by computations with vectors and matrices 02 p0273 A70-12730
Biased measurement of angular coordinates of phase modulated signals under meter input quantization 11 p2012 A70-26806
Loran C coordinates bias function determination by regression analysis using observed time differences 14 p2615 A70-31195
Extrinsic photoconductive detectors, comparing performance for microwave and DC bias based on gain bandwidth product and SNR analysis 18 p3232 A70-36746
Minimum bias criteria for selecting data fitting curves, allowing for unknown true equation in improving data predictability 20 p3659 A70-40261
Temperature and bias voltage dependence of zero bias tunneling structure in p-type GaAs-Au Schottky junctions 21 p3863 A70-41917
Optimal control of magnetic torque for bias momentum removal from attitude controller, discussing applications to Skylab 23 p4258 A70-44503
- BIBLIOGRAPHIES**
Gunn effect bibliography supplement /1960-1968/ 01 p0159 A70-10799
Water immersion for weightlessness simulation, presenting annotated bibliography covering physiological responses, human performance and simulation techniques and facilities 01 p0038 A70-10965
Soviet bibliography on heat and mass transfer covering thermodynamics, heat conduction, convection and radiation, phase and chemical transitions, aerodynamics, geophysics, etc 03 p0605 A70-13392
Annotated bibliography of laser eye hazards 03 p0434 A70-13680
- Soviet bibliography on heat and mass transfer covering thermodynamics, heat conduction, convective and radiant heat transfer, phase and chemical transformations, combustion, etc 05 p0957 A70-16297
German bibliography on astronomy for 1968 covering astrophysics, astronomical instruments, position determination, solar, terrestrial, planetary and lunar and stellar astronomy, etc 08 p1580 A70-21700
Abstracts with references to literature sources on oceanography from space and aircraft 09 p1665 A70-22014
Soviet bibliography on aviation, high altitude and space biology and medicine 09 p1615 A70-22204
Bibliographies for AIAA technical disciplines 09 p1792 A70-22344
Bibliography of literature on bioengineering, biocontrol, medical physics, biotechnology, safety and human factors in technology 09 p1629 A70-23692
Bibliography for powder metallurgy and related fields covering powder fabrication, compacting and sintering, refractory metals, hard materials, etc 10 p1904 A70-24387
Mechanics of continuous media for noncanonical regions, surveying Soviet literature on stress concentration near shell holes, elasticity theory, fluid aerohydroelasticity, etc 10 p1965 A70-25319
Aeronautics and astronautics bibliographies for college students 12 p2336 A70-27666
Soviet literature on galactic origins and physics including radio emission, star formation, quasars, nuclei activity, etc 12 p2307 A70-27868
Lubrication literature covering rolling bearings, fluid films, seals, automotive, gear and metalworking lubricants, boundary lubrication, friction and wear 13 p2419 A70-29150
Bibliography of far IR spectroscopy with subject index 14 p2586 A70-30987
Graph theory in Soviet literature, applications and bibliographies 14 p2600 A70-31421
Powder metallurgy literature /1968-69/ covering metal powders, sintering, porous materials, etc 15 p2760 A70-32349
Relativistic gravitation theory and experimentation, surveying literature on gravity waves, EM propagation, gyroscopic precession, etc 16 p2973 A70-33230
Thermal radiation configuration factors tables giving reference sources, discussing historical development of factors [AIAA PAPER 70-814] 16 p3002 A70-33947
Boundary layer theory development in U.S.S.R., surveying findings and papers 17 p3067 A70-34662
Solar wind interaction with earth, moon, Venus and Mars, reviewing literature on continuum fluid model, spacecraft observations, plasma characteristics, etc 17 p3150 A70-34669
Cryogenic temperature measurement including metallic and semiconductor resistance thermometers, thermocouples and bibliography 17 p3082 A70-34740
Nonideal plasma thermodynamics data, discussing particle interactions, Coulomb potential, stability, etc 17 p3142 A70-35733
Discrete automatic control theories, including linear, nonlinear, feedback, optimal and adaptive systems and bibliographies 18 p3235 A70-36626
Passive type stable test platforms /slabs/ covering configurations, foundations, vibration isolation, environmental effects, etc 20 p3605 A70-39569
Biographical guide for literature concerning chemical evolution and origin of life 23 p4148 A70-44842
Ferrite junction microwave circulator bibliography /1956-1969/ covering stripline and waveguide versions theory, designs, constructions and applications 24 p4318 A70-45210
Cumulative reference list of published books on microelectronics and reliability 24 p4322 A70-46014
- BICARBONATES**
U CARBONATES
BICRYSTALS
Sintering processes using boundary porosity in welded Nb bicrystal for model of final stages 13 p2434 A70-29081
- BIHARMONIC EQUATIONS**
Fourier transform applied to Riemann boundary value solution to biharmonic equation governing elastic theory for half plane with circular protrusion or indentation 01 p0199 A70-10155

- Alternating direction implicit difference schemes for solving Laplace and biharmonic elliptic equations
03 p0518 A70-13026
- Dirichlet problem of biharmonic operator in boundary region containing infinite number of pieces
05 p0877 A70-16878
- Wedge with symmetric crack at vertex in plane elastostatics, solving biharmonic equation by Wiener-Hopf technique
06 p1164 A70-17441
- Optimal control for distributed parameter systems described by biharmonic linear partial differential equation using dynamic programming
07 p1244 A70-18843
- Biharmonic equation in polar coordinates solved for circular plates and plate sectors with various boundary conditions, using finite difference approximations
08 p1589 A70-21246
- Biharmonic boundary value problems with re-entrant boundaries, comparing Motz and Woods finite difference solution methods
09 p1711 A70-22285
- Biharmonic equation numerical solution by finite differences, discussing outer and inner iteration schemes
14 p2599 A70-30647
- Boundary value problems of biharmonic finite difference equation in rectangular domain, deriving calculation formulas for summary representations solution method
15 p2814 A70-31583
- Reduced dissipation of biharmonic oscillations, examining dynamic model under force and kinematic harmonic perturbation
18 p3344 A70-37070
- BILLETS**
- Nondestructive betatron radiographic testing techniques for Ti billets, evaluating various lead screen, film and geometry combinations
08 p1508 A70-21746
- Isotropic Be billet fabrication by gas pressure consolidation and pressureless sintering techniques
12 p2252 A70-26888
- BIMETALS**
- Rolled bimetallic Ni-Mo mechanical properties produced by powder metallurgy methods
01 p0116 A70-10157
- Solid rocket motor ignition system based on exothermic alloying of bimetallic wire constituents [AIAA PAPER 69-425]
06 p1128 A70-17179
- Welding techniques for Nb-stainless steel bimetal tubing for liquid metal containment, determining structural integrity and bond interface condition after thermal cycling
10 p1897 A70-25309
- Thermal stability of simply supported bimetallic shallow spherical shell, considering rotationally symmetric deflection modes
14 p2657 A70-30845
- Soviet monograph on bimetal and refractory metals production by rolling in vacuum or inert media
19 p3433 A70-37402
- Cu-Ni diffusion couples voids and edges effect on concentration gradients measurement by electron probe microanalysis
22 p4054 A70-42740
- Strained state of Ti and steel sheets during unsymmetric rolling, constructing deformed metal particles displacements rates field based on ideal fluid motion equations
22 p4045 A70-42814
- BINARY ALLOYS**
- Vacuum deposition of Cr-Al film on Ni-Mo alloys, describing operating pressure, temperature and film thickness
01 p0124 A70-11617
- Quenched Ti-Mn alloy omega transition phase microstructure characteristics by transmission electron microscopy using thin foils
01 p0125 A70-11639
- Ti-Mn alloy quenched in brine and aged at high temperature studied for structural transformations using electron microscope
01 p0125 A70-11640
- Co-Cr alloy oxidation behavior at high temperatures and various oxygen pressures
02 p0319 A70-12720
- Mo separation from W during chemical analysis of W in binary Mo-W alloys, using organic reagents for precipitation and extraction
03 p0504 A70-12982
- Nb binary and tertiary alloys density changes found proportional to alloying element content
03 p0511 A70-13489
- Heat treatment effects on mechanical properties of Ti-Fe and Ti-Fe-Al alloys
03 p0512 A70-13855
- Heat treatment produced semicoherent and incoherent precipitations diminished susceptibility to stress corrosion cracking of aluminum binary and ternary alloys
04 p0708 A70-15370

- Binary Al-Y system thermal and microstructural analyses at room temperature and 200 C, obtaining partial diagram and mechanical properties
05 p0864 A70-16546
- Disordered ferromagnetic binary alloys of transition metals magnetic moment distributions based on thermal neutron scattering experiments
05 p0893 A70-16950
- Mn-Bi films Curie point switching with laser, measuring magnetization dependence via magneto-optic effect [IEEE PAPER 9.3]
05 p0893 A70-16997
- Solid solution softening in bcc Ta-Re alloy system attributed to substitutional-interstitial interaction
07 p1310 A70-19736
- Knudsen effusion cells high temperature uses, discussing binary alloys phase boundary determination and volume and surface diffusion studies
07 p1424 A70-19900
- Pyrolytic C-TiC alloys obtained by precipitation from gaseous phase, discussing microstructural properties anisotropy
08 p1517 A70-21146
- Binary and ternary systems phase diagrams construction by diffusion layer method and X ray analysis, studying concentration dependence of diffusion coefficient
09 p1703 A70-22564
- Mechanical and physical properties of Nb-Ti binary annealed alloys as function of compound NbTi using microscopic and X ray phase analysis
09 p1704 A70-22755
- Ordered Ni8Ta phase in nickel-rich binary alloy using electron microscopy and diffraction analysis
09 p1705 A70-22808
- Optical properties of beta prime phase CoAl, CoGa and NiGa as functions of composition and photon energy
10 p1919 A70-23986
- Vapor pressure of binary alloys with volatile components measured by combined Knudsen-torsion method, using thermal balance in vacuum
11 p2065 A70-25773
- Fe-Cr system and Fe-Cr-Ni liquid alloys studied by Knudsen cell-mass spectrometer combination, deriving phase equilibria from ion current ratios
12 p2255 A70-27602
- Dispersion strengthened Ni-Cr alloys elastic and plastic properties at room temperature, studying preferred crystallographic orientation effect
12 p2255 A70-27609
- Binary and ternary Mg alloys ductile fracture mechanism, studying coherent/noncoherent particles effects
12 p2256 A70-27612
- Alloy oxidation at high temperatures emphasizing binary and ternary alloys
12 p2257 A70-28005
- Interstitial atoms arrangement in binary alloys with body centered lattice, describing pressure effects by statistical theory
13 p2435 A70-29321
- Metallic thermoelectric materials, measuring electrical resistivities and Seebeck coefficients of binary Ni alloys
14 p2533 A70-30530
- Binary Co-In system thermal analysis, X ray diffraction and microscopy, discussing phase diagram
14 p2595 A70-30838
- Binary titanium-oxygen and titanium-carbon alloys, investigating interstitial pair mechanism for internal friction peak formation
17 p3115 A70-34383
- Ti interaction with elements of periodic systems, considering binary system phase diagrams
17 p3115 A70-34384
- Ti binary alloys beta phase continuous cooling transformation, investigating additives effects
17 p3118 A70-34408
- Martensitic transformation effects on mechanical properties of beta quenched Ti binary alloys
17 p3119 A70-34414
- Two-component metal coatings on Ni alloys for gaseous corrosion resistance increase, comparing microstructure and properties
17 p3125 A70-35393
- Cobalt binary alloys allotropic transformation and thermal expansion at various temperatures
18 p3271 A70-35967
- Ti-Al binary and Ti-Al-X ternary alloys grain boundary precipitation kinetics and correlation with mechanical properties
18 p3272 A70-36035
- Aligned composite materials preparation by unidirectional lamellar eutectoid decomposition in Co-Si, Cu-Al, Ni-In and in supersaturated solid solution Sn in Pb
18 p3274 A70-36052
- Fe-Ni alloy alpha-gamma phase transformation after heating, noting deformation planes and directions in martensite
18 p3275 A70-36204

- Electron microscopic investigation of alpha-epsilon iron phase transformations in Co-Ni alloys above and under phase equilibrium temperature
18 p3276 A70-36205
- Ti binary alloys with V, Nb and Mo, determining phase boundaries by diffusion layers method and electron microscope analysis
20 p3649 A70-39727
- Electron states localization in disordered binary alloys, describing band structure
20 p3687 A70-40498
- Zr-Nb alloys mechanical strength increase due to beta phase martensitic decomposition
21 p3840 A70-41897
- Allotropic transformation points and linear thermal expansion coefficients of Co-base binary alloy terminal solutions, using dilatometric method
23 p4203 A70-43864
- Self flammability temperature of binary alloy Al-Si powders in aerosol state as function of chemical and phase compositions
23 p4205 A70-44046
- Zr-Cu alloys corrosion resistance in carbon dioxide at high temperatures, noting composition effect on behavior
23 p4208 A70-44875
- Ni-Nb-W and Ni-W alloys phase equilibrium, obtaining diagrams from analysis of liquid and solid phases separated electromagnetically before tempering
24 p4359 A70-45372
- Longitudinal phenomena and two phase structures effect on ductility of low carbon steel-chromium subjected to high temperature torsion
24 p4361 A70-46173
- BINARY CODES**
- Circuit and operation of transistorized RF power attenuator with linear attenuation and binary code control by digital computer
06 p1022 A70-17777
- Capacity and error bounds derived for nonsynchronized channel, discussing binary coding strategy
06 p1012 A70-18623
- Pseudonoise sequence generation with 3-tap linear feedback binary shift registers, citing reduction theorems
11 p2025 A70-26224
- Digital-to-analog converter for voltage representation of signals in 2-4-2-1 binary decimal code
12 p2235 A70-27681
- Binary code distortion in relative phase telegraphy signals under wideband and correlated noise
13 p2364 A70-28870
- Analog computer simulation of command signal detectors for reconstruction of transmitted binary character from noisy binary coded signal
13 p2385 A70-29560
- Noise rejection during synchronous quasi-coherent radio signal reception with binary narrow band linear filter used for voltage shaping
13 p2369 A70-29737
- Noise rejection for optimal reception of incoherent binary signals in one beam Rayleigh dispersion radio channel under ionospheric electron density fluctuations
13 p2369 A70-29738
- Binary division by logic gates cellular arrays, noting accuracy and operating speed
14 p2556 A70-30517
- Rank order statistics for optimum detection of binary pulsed signals in white noise and DC drift
14 p2551 A70-31122
- Image processing and picture enhancement by computer, using fast binary log-antilog conversion
15 p2768 A70-32567
- Binary coded radar signal autocorrelation function main-to-sidelobe ratio improvement, using echo signal processed in mismatched filter
17 p3043 A70-34590
- Lower reliability estimates for block codes of binary channels with feedback noise
18 p2325 A70-36599
- Single-error nongroup binary codes with maximum codewords, including quadratic residue, Reed-Muller and triple-error constructions
24 p4313 A70-46057
- Sequential decoder program for low weight codewords in binary convolutional code over one-half constraint length
24 p4313 A70-46065
- Suboptimum sequential algorithm for recovery decoding errors in convolutional codes, using Hamming distance criterion
24 p4314 A70-46066
- BINARY DATA**
- Binary systems noise resistance with various cross correlation functions and indefinite moment of arrival
03 p0448 A70-13512
- Binary decoding extension to achieve unquantized demodulation performance for nonfading phase shift keyed coherent channel with white Gaussian noise
06 p1008 A70-17525

- Output autocorrelation properties of ideal limiters driven by binary deterministic signal plus stationary zero-mean Gaussian noise
06 p1013 A70-18625
- Communication channel average binary error and stationary Markov chain state probabilities relationship, using mathematical model and HF ionospheric FSK error sequence measurement
08 p1458 A70-20793
- UHF satellite receiver for binary FSK data collection system using matched integrate and dump filter detectors
08 p1459 A70-20804
- Bit error probability after decoding for binary perfect single error correcting codes
11 p2014 A70-26247
- Decision directed receiver with unknown a priori probabilities, obtaining tight bound on runaway for binary and multiple signal detection
14 p2554 A70-31117
- Optimum adaptive reception for binary sequences, using posteriori probability density function computing device synthesized from correlator, instantaneous nonlinearity and multiplier
14 p2552 A70-31188
- Binary data system parameters sudden change detection by noisy observation based on Bayes criterion
17 p3056 A70-34856
- Computer generated holograms, using binary transmittance for wave fronts and three dimensional images construction
17 p3085 A70-35006
- Cyclic block code structures for generating binary sequences with good autocorrelation properties
19 p3375 A70-37284
- Existence theorem concerning arbitrarily long good binary block /nonlinear/ codes preserved under large permutation groups
20 p3594 A70-39974
- Rank permutation codes equivalence to binary code class capable of generation and detection through direct and inverse transformations respectively
20 p3594 A70-39975
- Frequency synchronization channel pulse fluctuations effect on noise stability of binary signal reception
20 p3587 A70-40145
- Statistical pattern recognition and threshold learning in signal detection of noisy binary pulses
21 p3794 A70-41332
- Binary codes linear metric properties description reduced to finite set determination by convex programming procedure
22 p3993 A70-42494
- Binary data transmission via radio channel, discussing phase and frequency modulation and error probability as SNR function
23 p4159 A70-43756
- BINARY DIGITS**
Binary digital radar signal detectors optimization for radiation pattern of sin x/x radar antenna and for non-fluctuating target
02 p0255 A70-11899
- Quasi-logarithmic readout of conventional binary scaler provided by reduced logic system following generalized equations
05 p0851 A70-16844
- Book on numerical control covering principles, electromechanical system using digital logic circuits, binary numbers and arithmetic, etc
10 p1854 A70-24023
- Optimum binary digital detector of radar targets, using confidence ratio as criterion of target presence
12 p2182 A70-26890
- BINARY FLUIDS**
System of equations describing isothermal two phase-two component fluid flows with negligible dissipation effects, emphasizing slug flow
02 p0288 A70-12856
- Shock wave width and temperature expressions for argon-helium mixture
04 p0672 A70-15223
- Electrically heated wire diameter and orientation on heat flux in saturated pool and surface boilings of water and aqueous binary mixtures
07 p1417 A70-18643
- Oscillatory relaxation of binary system of heat conducting viscous gases composed of nonspherical molecules
08 p1547 A70-21085
- Shock wave structure in binary mixture of monoatomic gases based on integral kinetic equations, using iteration process
08 p1483 A70-21086
- Two temperature gasdynamics for binary gas mixtures of differing molecular weight components, analyzing ultrasound and shock wave propagation
08 p1486 A70-21808
- Thermal conductivity of monatomic binary gas mixtures at moderately low temperatures and pressures, considering various Ar-He mixtures
11 p2147 A70-25755
- Heat conductivity of Xe-He binary gas mixtures, allowing for molecular transfer and polarity effects
15 p2827 A70-32107
- Bubble frequencies random distribution during boiling of pure liquids and binary liquid mixtures by optical measurement
21 p3941 A70-40775
- Critical heat flux during forced pipe flow of boiling ethanol-water and acetone-water binary mixtures
23 p4283 A70-44730
- BINARY MIXTURES**
NT BINARY FLUIDS
NT EUTECTIC ALLOYS
NT EUTECTICS
Phase diagrams for binary mixtures at high pressures suggesting layered structures existence in Jupiter and Saturn atmospheres resulting from phase separations in hydrogen-helium mixture
02 p0368 A70-11819
- Gas diffusion coefficients for He-N and nitrogen-carbon dioxide systems in diffusion cell utilizing porous stainless steel barrier
04 p0780 A70-14710
- Free electron formation ahead of strong shock waves traveling into nitrogen-oxygen mixtures in shock tube, observing electron densities
06 p1065 A70-18029
- [AIAA PAPER 70-83] Boltzmann equation for binary mixtures of rarefied gases solution involving specific expansion of distribution functions
06 p1047 A70-18311
- Shock structure in binary gas mixture, discussing governing equations and Chapman-Enskog procedure
06 p1051 A70-18344
- Binary mixture molecular beam apparatus combining aerodynamic acceleration and arc heating techniques, discussing particle energy and density
07 p1341 A70-20106
- Bromine monoxide formation by atomic oxygen-bromine reaction in flash photolysis of bromine-nitrous oxide and bromine-nitrogen dioxide mixtures
08 p1455 A70-21342
- Weak plane waves propagation in binary mixtures of diatomic gases subject to vibrational relaxation, solving piston problem in acoustic approximation
12 p2209 A70-27151
- Translational spectral bands of compressed rare gas binary mixtures, considering mass and temperature effects
12 p2275 A70-27172
- Approximate formula for viscosity of binary polar gas mixtures confirmed for unlike cross sections
16 p2996 A70-33055
- Hypersonic flow of chemically reacting binary mixture of oxygen atoms and molecules past blunt body, presenting viscous shock layer equations and slip boundary conditions
17 p3005 A70-34458
- [AIAA PAPER 70-805] Rarefied binary gas mixture transient Couette flow, considering nonlinear case of plate with equal temperature accelerated impulsively
17 p3067 A70-34546
- Linear corrections formulas for shear stress and heat transfer coefficients associated with boundary layer blowing in binary gas mixture
21 p3748 A70-42207
- Binary gas mixture separation effects by centrifugation in cylindrical tube, calculating maximum radial concentration difference between wall and axis by numerical integration
23 p4181 A70-44206
- Rarefied binary gas mixture, determining temperature gradient effect under various pressures
23 p4284 A70-44984
- Two incompressible isotropic nonlinear elastic solids mixture, investigating entropy production inequality effects
24 p4425 A70-45991
- BINARY STARS**
NT ECLIPSING BINARY STARS
White dwarfs formation in close binary systems ascribed to mass exchange between components, describing evolutionary followup of primary from main sequence by model
01 p0189 A70-11343
- Gravitational finite propagation velocity effects in celestial mechanics, describing binary star motion studies
02 p0380 A70-12783
- Hypotheses for symbiotic stars nature, emphasizing binary with late type giant and hot small star components
03 p0568 A70-13325
- Psi Orionis light variations, using photoelectric photometry, indicating ellipsoidal variability
03 p0570 A70-13552
- Binary star formation using singular solution of Kepler problem in general theory of relativity
04 p0755 A70-15355
- Right ascension and flux density of source in Crab Nebula measured at meter wavelengths, evaluating spectrum and relative position to binary star center
05 p0917 A70-16908
- Binary star frequency and orbital axes distribution, discussing visual orbits, mass ratios, photometrical detection, etc
06 p1138 A70-17308
- Stellar interferometer with superposed beams designed for measurements of close binaries, showing point light modulation convenient for photoelectric recording
08 p1493 A70-20564
- Binary star spectrum analysis establishing seasonal and season-to-season variations in He II emission band intensity and shift toward long wave region
08 p1569 A70-20827
- Cygnus and Perseus symbiotic stars as binaries, studying radial velocities, relative emission line intensities and energy distribution
08 p1569 A70-20830
- Potential flow pertaining to motion of gas surrounding close binary systems generated by orbital motion of stars and matter outflow from stars
10 p1946 A70-24968
- Mass transfer in close binary stars and in highly variable stars
12 p2306 A70-27858
- Stellar intensity interferometer for close binaries and emission line stars, investigating gamma-two Velorum
14 p2640 A70-30733
- Runaway stars and pulsars near Crab Nebula, discussing binary system explosion and remnant motion
14 p2642 A70-30894
- Binary AX Monocerotis brightness variations in UV from photoelectric UVB observations
15 p2796 A70-31610
- Stellar interferometer with superposed beams designed for measurements of close binaries, showing point light modulation convenient for photoelectric recording
15 p2742 A70-32719
- Orbit and component velocities of double line spectroscopic binary HR4072 on high dispersion spectrograms, noting mass ratio close to Guthrie relation
16 p2976 A70-33786
- Frequency spectra of gravitational waves radiated from celestial phenomena, suggesting mass exchange in binary containing neutron star
17 p3067 A70-34619
- Zero moments surface in problem of two immovable centers, taking into account cosmic dust accumulation before binary apex moving forward with periastron of bright component
18 p3324 A70-37147
- Visual binary stars orbits computation catalog from data obtained in 1939-1969 period
19 p3530 A70-38895
- Binary stars dynamical parallaxes, masses, absolute magnitudes and provisional orbits, fitting deduced masses into empirical visual mass-luminosity relations
19 p3531 A70-38896
- Stellar evolution covering formation, structure and time-varying properties of single spherical, nonspherical, magnetic and binary stars
19 p3531 A70-38950
- Cygnus X-2 point X ray source, establishing as spectroscopic binary with peculiarities
21 p3875 A70-40682
- Sco X-1 radio emission models, considering possible binary nature and thermal bremsstrahlung
21 p3875 A70-40685
- Close binary stars evolution, discussing initial parameters effects on mass exchange and orbital period model
21 p3884 A70-40872
- Gravity darkening of tidally and nonuniformly rotating Roche components of close binary systems, calculating surface temperature and spectral distributions
21 p3888 A70-41120
- Circumstellar matter observations between binary star components, considering emission and absorption spectra, velocity and light curve distortion and orbital period changes
21 p3889 A70-41151
- Beta Cephei star discovery criteria, examining mu-mechanism theory by He and N overabundances, far UV flux, spectral line width and binary character
21 p3890 A70-41159
- Sirius components relative photographic positions and magnitude difference, discussing color effect, grating image separations and emulsion contraction
21 p3922 A70-41984
- Intrinsic polarization from Thomson scattering in binary systems with tidal distortions, taking into account gray atmosphere, axial rotation, gravitational interaction and radiative interaction
22 p4103 A70-42988
- Close binary star components axial rotation, considering synchronism, angular velocity and mass exchange
23 p4250 A70-44814
- Upper main sequence and close early type binaries evolution by fission of rapidly rotating protostars
23 p4250 A70-44815
- Synchronous close binary stars primary component structure, using rapidly rotating polytropic method
23 p4250 A70-44816
- Binary star axial rotational correlation, determining coupling between components spin angular momenta
23 p4250 A70-44817

- Stellar rotational velocities in open star clusters, noting evolutionary expansion, tidal coupling in binaries and Ap stars magnetic braking
23 p4251 A70-44820
- A type stars rotation, examining UVB color and rotational velocity relationship, spectral classification and spectroscopic binaries
23 p4251 A70-44822
- BINARY SYSTEMS [DIGITAL]**
U DIGITAL SYSTEMS
- BINARY SYSTEMS [MATERIALS]**
NT BINARY ALLOYS
NT BINARY FLUIDS
NT BINARY MIXTURES
NT EUTECTIC ALLOYS
NT EUTECTICS
- Two phase liquid-vapor system specific heat increase at temperatures approaching critical point, using nonanalytic vapor pressure equation with data for nitrogen and oxygen
04 p0780 A70-14584
- Relative motion of two spheroidal homogeneous rigid bodies of isolated binary system, obtaining potential energy
05 p0880 A70-15760
- Binary system Mo-C determined in temperature range 1250-2270 C, using microscopic and thermal analyses and microhardness testing
05 p0862 A70-16198
- Binary transition metal hydrides consisting of single metal and single hydrogen isotope, discussing preparation and kinetic, thermodynamic and structural properties
05 p0863 A70-16523
- Alpha and beta solid solutions chemical composition in two phase alloys of Ti-Al-Mo and Ti-Al-V determined by electron microprobe analyzer
05 p0864 A70-16549
- Binary CdSb-CdTe systems investigated by X ray and microstructural analyses, showing mechanical mixture constitution and p-type conductivity
07 p1355 A70-18701
- Elastic fields in bimaterial plate under uniform compressive and anti-plane shear loadings, finding stress distribution and induced interfacial shear stresses
07 p1412 A70-19957
- Radar model of shower and hail clouds as two phase system of independently scattering spherical particles, stressing radar properties dependence on particle properties
08 p1536 A70-21097
- Elastic oscillations amplitude-dependent damping during phase transformations in two phase systems
08 p1556 A70-21121
- Enthalpy-entropy, enthalpy-pressure and composition diagrams of fluorine-hydrogen system, noting possible applications to rocket propulsion systems
10 p1929 A70-25100
- Copper alloy composite reinforced by unidirectional solidification of pseudobinary eutectic Cu-ZrCuSi, discussing mechanical properties and electrical conductivity
11 p2066 A70-25775
- Solid-gas phase equilibria of binary systems related to cryogenics
12 p2329 A70-27023
- Titanium base binary systems phase diagrams, describing component activity and compound phases heat of formation
17 p3114 A70-34379
- Nitrogen solubility calculation in transition metals liquid binary systems, using quasi-chemical model
18 p3273 A70-36045
- Binary Nb vapor systems mutual diffusion coefficients concentration and temperature dependences, discussing interatomic bonds and melting point of alloys
19 p3454 A70-38715
- Cd-Se and Cd-Te systems phase diagrams based on regular solutions theory, discussing molecular interaction energy dependence on composition
22 p4085 A70-42678
- Oxides compounds heats of formation isocomponent and primary product composition relationship in binary systems
22 p3982 A70-42679
- Dynamic elastic moduli of model two phase continuous composites, using polymer and metallic foams
22 p4059 A70-43077
- Solid solutions of quasi-binary cross section CdP-CdTe and ZnP-CdTe, using X ray, thermal, microstructural and microhardness analyses
22 p4086 A70-43132
- BINAURAL HEARING**
Loudness lateralization of acoustic signals in right and left ear during binaural interaction
12 p2174 A70-28357
- BINDERS [ADHESIVES]**
U ADHESIVES
- BINDERS [MATERIALS]**
NT PROPELLANT BINDERS
NT SOLID ROCKET BINDERS
- Rational design of structurally anisotropic plane multilayer plates with weak binder, suggesting

- strengthening fibers orientation in internal stresses direction
03 p0516 A70-13379
- Silicon organic binding materials properties, assessing ethyl silicate-50 perspectives in fabrication of precision castings
08 p1506 A70-21144
- Fiberglass reinforcement effects on injection molded thermoplastics physical properties, noting role of binder and glass content
13 p2438 A70-29204
- Polymeric binders adhesion to glass fibers as function of type and chemical structure
16 p2938 A70-33379
- Binder wetting relation to solid film lubricant wear life
[ASLE PREPRINT 70AM 5A-3]
- Unidirectional fiberglass-reinforced plastic, investigating binder content and porosity effects on strength
21 p3841 A70-40647
- Energy absorption and dissipation in friction brakes, investigating brake lining polymer binder contribution through molecular reorientation, crystallinity increase and entropy decrease
24 p4342 A70-45585
- BINOCULAR VISION**
Binocular brightness mixing and autocorrelation function, discussing mathematical model, computer simulation and test results
01 p0025 A70-11053
- Human eye contribution to visual evoked responses under different color stimuli during all possible monocular and binocular combinations
05 p0801 A70-16382
- Macaque monkey stereoscopic vision, obtaining behavioral evidence by random dot stereoscopic patterns and finding cells sensitive to binocular depth in cortex
07 p1205 A70-19276
- Evoked potential /EP/ correlate of binocular depth perception in man, discussing responses to horizontal and vertical changes in retinal disparity
07 p1205 A70-19284
- Binocular fusion and rivalry effects on cortically evoked human potential, obtaining pattern characteristic responses to monocular stimulation
07 p1215 A70-20214
- Optic chiasm damage effects on human depth perception implying interhemispheric link for binocular integration in central vision
09 p1618 A70-22669
- Corpus callosum damage effects on human depth perception implying interhemispheric link for binocular integration in central vision
09 p1618 A70-22670
- Movement information from spatio-temporal integration in binocular-kinetic space perception of time varying optical inputs
09 p1618 A70-22672
- Visually evoked cortical potentials /VECP/ to different probe stimuli to suppressed human eye in binocular rivalry experiments, discussing eye dominance problems
09 p1618 A70-22674
- Choice reaction time task involving right or left hand button pressing in monocular and binocular visual response to directional commands by colored lights
11 p1990 A70-25830
- Neurophysiological framework for binocular single vision and depth discrimination, concerning construction of horopter for cat
14 p2539 A70-31348
- Binocular disparity detectors in human visual response to moving gratings confirmed by electrophysiological evidence
17 p3025 A70-35150
- Panum phenomenon explained by projection, attraction and figure ground psychological theories
19 p3366 A70-38505
- Lighting and background effects on human binocular color vision of signal lights in industry
19 p3366 A70-38923
- Visually evoked responses in man to different light stimuli intensities, noting marked increase in binocular over monocular visual response
22 p3972 A70-43408
- Stroboscopic stereophenomenon, investigating depth shift of oscillating target motion binocularly viewed for interocular luminance differences
23 p4147 A70-44781
- Binocular fundus reflectometry and plethysmography in rabbits and man after dye injection and in patients with carotid occlusion
24 p4310 A70-46345
- BINOMIAL THEOREM**
N binomial events approximations to high probabilities of overall success for reliability situations and mission accomplishment, including operations research implications
01 p0134 A70-11475

BIOACOUSTICS

- Loudness lateralization of acoustic signals in right and left ear during binaural interaction
12 p2174 A70-28357
- BIOASSAY**
Bioscience for recovered lunar samples, discussing Surveyor analyses, Lunar Receiving Laboratory methods and life detection using biological markers
01 p0042 A70-11637
- Microbiological assay procedures for spacecraft sterilization and tabulation of microorganisms found on Surveyor 7
05 p0808 A70-16705
- Human biological organism analysis based on physiological determination of regulating and control functions dependence on oscillatory properties
08 p1452 A70-21460
- Microdissection morphology of vestibular apparatus sensory regions in guinea pig, rabbit, cat, squirrel, monkey and man
10 p1811 A70-24200
- Electron microscope-thin film microprobe techniques in biomaterial studies of chemical segregation, species diffusion and small particle analysis
13 p2411 A70-29808
- Countercurrent sandwich type dialyzer for small animals, noting membrane support function and applicability to human use
13 p2360 A70-29950
- Viable organisms in Apollo 11 lunar fines, discussing tests, laboratory and sterile biological barrier system
21 p3911 A70-41634
- Computer system for ECG interpretation in hospital heart station
22 p3979 A70-43483
- Squid head cartilage properties in terms of light and electron microscopic appearance, amino acid composition and X ray diffraction
24 p4305 A70-46348
- BIOASTRONAUTICS**
Aerospace technology application to biomedical problems in astronautics
01 p0027 A70-11256
- Astronaut vestibular fitness determined from threshold labyrinthine tests on isolated horizontal and vertical semicircular canals
03 p0437 A70-14059
- Collection of papers on spaceflight radiological problems experimentation covering satellite data, dosimetry, solar flares, etc
06 p0989 A70-17259
- Solar proton flare dose rates, discussing tissue-equivalent-ionization-chamber /TEIC/ data usefulness in analyzing possible dose received by man behind shielding
06 p1134 A70-17265
- Spacecraft radiation environment, dosage and shielding problems, discussing high energy protons and electrons exposure hazards for astronauts and mission planning computer codes
06 p0991 A70-17273
- Biomedical concepts for aerospace engineering, discussing human body as self regulating system /homeostasis/ and physiological time regulator /circadian/
- Near zero magnetic fields effect on biological systems studied to determine terrestrial magnetic field absence effect on astronauts
06 p0992 A70-17315
- Bioastronautics and earth ecology, discussing environmental pollution, nutritional, microbiological and psychological problems
08 p1449 A70-20724
- Medicobiological approach to living conditions for sustained residence and human activity during prolonged space flights, describing sealed chamber experiment
18 p3350 A70-36757
- Biological compatibility problem in long duration space operation crew change, discussing human metabolic processes and difference effects
19 p3367 A70-37525
- Orbital biotechnology laboratory requirements concerning man systems integration, life support and protective systems
22 p3980 A70-43641
- Long term space flight crew habitation emphasizing food management, station housekeeping, personal hygiene and waste handling
22 p3980 A70-43644
- Astronaut biological parameters monitored under prolonged space flight conditions for rescue operations
23 p4154 A70-44622
- Calcium metabolic balance reports discrepancies with radiologic indications of astronaut bone loss
23 p4148 A70-44838
- Astronautics - IAF Conference, New York, October 1968, Volume 4, Bioastronautics
23 p4155 A70-45022

- Space biological exploration for determining life origin on earth, emphasizing extraterrestrial life possibilities on other planets 24 p4301 A70-46000
- BIOCHEMISTRY**
- NT BACTERIOLOGY
- NT BIOGEOCHEMISTRY
- NT ENZYMOLOGY
- NT PHYSIOCHEMISTRY
- Book on radiation biochemistry covering effects on biological tissue, nucleic acids, proteins, carbohydrates, lipids, hormones, vitamins, living cells, metabolism and toxic substances formation 01 p0011 A70-10030
- Soviet collection of articles on problems of brain biochemistry, Volume 4 01 p0017 A70-10504
- Book on chemical evolution of life covering molecular paleontology, prebiotic chemistry, membrane structures, molecular evolution and structure, etc 02 p0230 A70-11685
- Biochemical, electron microscopy and experimental medicine data indicating pathogenetic mechanism responsible for arteriosclerosis 03 p0431 A70-14278
- Biochemical disturbances during early myocardial ischemia, examining coronary sinus lactate and K levels using electrocardiographic correlation 06 p0997 A70-18406
- Peptide formation by stepwise tetramer-mediated condensation of alpha-amino acid as possible prebiotic process 07 p1204 A70-19202
- Chlorella species found to contain ergosterol as major sterol 09 p1616 A70-22330
- Mass spectrometric sequence determination of oligopeptides via acetylacetyl derivatives, giving reliable results with small peptides 09 p1630 A70-22976
- Anoxia effects on biochemical processes in human body, comparing chemical energy balances under aerobic and anaerobic conditions 10 p1821 A70-25082
- Structural and functional properties of phosphates in biochemical reactions, discussing linkages 14 p2544 A70-30346
- Molecular respiratory reflex and fluorescent signal in rabbits during hypoxia, determining redox kinetics of intracellular pyridine nucleotides 14 p2539 A70-31346
- Biological conversion of solar energy, discussing photosynthesis and nonphotosynthesis mechanisms 15 p2688 A70-31600
- Parental termini-daughter strand linkage in initiation of DNA replication in *Bacillus subtilis* after thymineless germination 16 p2847 A70-33060
- Systems design and instrumentation for chemical/biochemical space manufacturing at zero g, developing scaling laws for transition to larger production units 16 p2919 A70-33719
- Book on biochemical predestination covering life origin, biomonomer synthesis, polymerization, colloidal systems, etc 17 p3025 A70-34925
- Quantitative and qualitative analysis of biochemically and radiobiologically important thiols and disulfides via gas-liquid chromatography 19 p3373 A70-37836
- Cells chemical origin, discussing terrestrial fractionation, amino acids, macromolecules, metabolism, etc 20 p3569 A70-38992
- Biochemistry of blood group antigens involved in agglutination reactions, discussing effect of proteolytic enzymes on cell membrane structure 21 p3764 A70-41447
- Oxidative enzymes histochemistry in nervous system, liver and kidney of rats in immediate and remote periods after 24-hr artificial hypobiosis 21 p3764 A70-41478
- Cellular irradiation sensitivity in tissue culture modified by propyl gallate as radical reactions inhibitor 21 p3767 A70-42242
- Infused cortisol disappearance rates and distribution volumes in hyper-, hypo- and normocalcemic dogs 24 p4296 A70-45334
- BIOCLIMATOLOGY**
- Human bioclimatology at high altitude, discussing energy balance in terms of net solar and terrestrial radiation balance in mountain area 19 p3367 A70-37369
- BIOCONTROL SYSTEMS**
- Bibliography of literature on bioengineering, biocontrol, medical physics, biotechnology, safety and human factors in technology 09 p1629 A70-23692
- Nine degree of freedom pitch axis model of human postural control system, deriving kinetic and potential energy expressions 11 p1990 A70-25675
- Control and guidance theories for biological problems, discussing signal transfer of linear control units and mathematical approaches 15 p2689 A70-31741
- Serum growth hormone response to hypoglycemia in man following insulin administration, reviewing lumped parameter model 19 p3360 A70-38006
- Muscular activity in regulation of organism functions during aging, considering hypokinesia effects 22 p3968 A70-42894
- Body oxygen control under muscular activity in aging individuals 22 p3969 A70-42899
- Mathematical model of heart beat control during muscular activity in aging individuals, reflecting neutral and hormonal control circuits 22 p3969 A70-42901
- Linear lumped parameter mechanical model of muscle spindle in postural control 22 p3979 A70-43496
- Structure and function of juxtaglomerular apparatus of kidneys controlling synthesis and secretion of renin 24 p4305 A70-46392
- BIODYNAMICS**
- Biomechanics - Conference, Rock Island, Illinois, April 1967 01 p0033 A70-10494
- Biomechanics of microcirculation, discussing rheological characteristics of blood, erythrocyte and vessel wall, hydrodynamics of erythrocyte-shaped bodies mathematical models, etc 01 p0039 A70-11160
- Reactive forces and torques of musculoskeletal system during lifting and carrying materials, using computerized biomechanical models 02 p0247 A70-12549
- Knee joint walking mechanics, calculating forces transmitted by joint tissue 07 p1205 A70-19246
- Aeroelasticity problems, discussing unrestrained flexible structures design, nonconservative systems stability, biomechanics, etc 09 p1777 A70-22972
- Plane flow problem for two hinged plates in motion toward each other with fluid displacement, discussing single vortex application to biomechanics 13 p2338 A70-28481
- Environmental heat stress indices of human subjects in bicycle ergometer experiment 18 p3224 A70-36226
- Muscle function mechanics across knee joint in walking, relating tension to length, velocity and energy absorption 19 p3368 A70-37810
- Biological action of constant magnetic fields, discussing axons electrical properties, biomolecules spatial orientation, electrolytes and liquids 22 p3978 A70-43138
- BIOELECTRIC POTENTIAL**
- EEG investigation of cerebral biocurrents during polar night-day cycle, studying central nervous system nonspecific automatic control mechanism dependence on ecological factors 01 p0030 A70-11466
- Frequency and postextrastolic potentiations in guinea pig isolated auricles and dog heart in vitro and in situ, noting myocardial diagnostic use 02 p0235 A70-12088
- Autocorrelation and cross correlation analysis of slow EEG potentials in rhythm of movement as cortical activity pattern of cerebral hemispheres during work 03 p0421 A70-13687
- Origin and functional designation of associative evoked potentials in orbital cortex of cats, showing phases connected with neuron activity and excitation 03 p0422 A70-13689
- Increased oxygen partial pressure effects on cerebral bioelectric activity from EEG recordings on unanesthetized dogs 03 p0422 A70-13690
- EEG patterns of functional state effect on evoked cortical potentials in response to DC pulses in dogs after nembutal administration 04 p0638 A70-15503
- Norepinephrine-induced depolarization effects on brown fat thermogenesis in cold-acclimated rats determined from in vivo measurement of intracellular potentials 05 p0799 A70-16020
- Rod and cone contributions to S potentials from cat retina using spectral sensitivity observation 05 p0801 A70-16379
- Rod-cone interaction in cat S potentials, analyzing effect of wavelength and intensity upon dark adapted responses 05 p0801 A70-16380
- Rod aftereffect relationship to percent rhodopsin bleached in S potentials from cat retina 05 p0801 A70-16381
- Cats visual analyzer functional rearrangement mechanisms under prolonged light stimulation, considering evoked potential dependence on pulse duration and intensity 07 p1198 A70-18699
- Rabbits visual cortex evoked potential changes due to light flashes under different conditions 07 p1198 A70-18716
- Bioelectrical reactions in anesthetized cats cortical zones in response to stimulation of contralateral sciatic nerve 07 p1199 A70-18722
- Cerebral biopotentials of rabbits exposed to RF weak electromagnetic field indicating cortex inhibition in EEGs 07 p1199 A70-18728
- Hypothalamus influence on potentials and recovery cycles of mesencephalic reticular formation in response to sciatic nerve stimulation in anesthetized rabbits 07 p1204 A70-19138
- Evoked potential /EP/ correlate of binocular depth perception in man, discussing responses to horizontal and vertical changes in retinal disparity 07 p1205 A70-19284
- Electrical recording of retinal and occipital potentials in response to stimulation of human visual system used at levels from receptor to striate cortex 07 p1220 A70-19364
- Auditory averaged evoked potentials to clicks in man subjected to selective listening task, comparing effect on attended and rejected ear 07 p1215 A70-20213
- Binocular fusion and rivalry effects on cortically evoked human potential, obtaining pattern characteristic responses to monocular stimulation 07 p1215 A70-20214
- Direct anatomical couplings between retina and hypothalamus via centripetal and centrifugal fibers by investigating light evoked potentials in rabbits brains 08 p1444 A70-20737
- Hypothalamus stimulation effect on electrical activity of hippocampus at threshold and super-threshold levels in cats 08 p1446 A70-21448
- Heart dipole moment calculation error due to deletion of individual electrode contributions to surface potential map, analyzing multielectrode grids 08 p1453 A70-21753
- Motor performance effects on averaged sensory-evoked potentials in reaction time tasks 10 p1811 A70-24226
- Different retinal regions simultaneous stimulation, describing evoked potentials measurement method 10 p1811 A70-24227
- Psychophysical and evoked potential correlates of changes in stimulus color and intensity compared with minimum subjective flicker conditions 12 p1717 A70-28035
- Human forearm motion control mechanism, examining mechanogram, instantaneous velocity, acceleration and biopotentials of biceps and triceps brachii 12 p1713 A70-28314
- Sensory afterdischarge of human brain under light stimuli during sleep and wakefulness 12 p1713 A70-28354
- Evoked cerebellar potentials time characteristics during spinal cord stimulation in cats, investigating cerebellar intercalated connections effect 13 p3553 A70-29357
- Portable autonomous EEG analyzer for processing brain biopotentials without use of computer hardware and qualified personnel 13 p3660 A70-29522
- HF permittivity variations detector for blood circulation telemetry 14 p2542 A70-30389
- Steady state evoked potentials Fourier analysis from human scalp during psychophysical procedure of heterochromatic flicker photometry, obtaining spectral sensitivity curve 15 p2682 A70-32015
- Electrical potentials in response to auditory stimuli recorded in cat brains by averaging computer 15 p2685 A70-32831
- Cortical evoked potentials in human motor conditioning to photic stimulus 18 p3221 A70-37212
- Evoked potentials in dogs sensorimotor cortex during defensive instrumental conditioning 18 p3221 A70-37213
- Visual attention and temporal cortex stimulation effects on evoked electrical activity in monkey brain 19 p3360 A70-37812
- EEG analysis for poststimulus events, examining contingent negative variation and late positive wave of average evoked potential 19 p3368 A70-37813
- Intracellular myocardium potentials under vagus inhibition by electrometric DC amplifiers with positive and negative feedback 19 p3370 A70-38213
- Multipoint recording of bioelectric potentials based on electroencephalography, discussing multiple leadout, amplification, analysis, etc 19 p3370 A70-38217
- Extracellular spontaneous sequences of action potentials of thalamic neurons during asphyxia in rats under artificial respiration 19 p3361 A70-38306

Enhanced evoked potentials sited by auditory stimuli in complex task, considering EEG and neurophysiological basis of selective attention

19 p3363 A70-38318

Pulse coding system for average evoked EEG potential data acquisition and analysis, describing pulse generation circuitry and computer implemented logic

20 p3578 A70-38985

High fidelity microelectrode recording of phase zero cardiac transmembrane action potentials, utilizing memory oscilloscope

21 p3772 A70-42163

Bioelectric activity changes in rats lumbar neurons, membrane and postsynaptic potential and discharge frequency during and after asphyxiation

22 p3971 A70-43404

Visual system recording neuron pulse potential spatial and temporal responses to sinusoidal stimuli

23 p4144 A70-43922

BIOELECTRICITY

Reversible cold induced deactivation of cat neocortex bioelectric activity in chronic experiment, noting cooling system

01 p0031 A70-10056

Bioelectrically controlled system for indirect heart massage, noting dynamic simulation of system on digital computers using block oriented programming languages

01 p0047 A70-10261

Scaling and refractoriness effect in neutral-pulse train transmission on eye incremental sensitivity, discussing applicability as intraretinal mechanism concept

02 p0247 A70-12466

Synchronizing and desynchronizing systems for cerebral electrical activity, noting roles in sleep and wakefulness mechanisms

03 p0417 A70-13073

Cats cerebral cortex background electrical activity measured during development of conditioned reflexes, noting shift toward higher frequencies

03 p0418 A70-13217

Vascular electrical activity in cats and rats by inserting glass microelectrode into blood vessel, showing blood flow conditioning effect on activity

03 p0422 A70-13691

Aplysia periodic spontaneous gill movements controlled by central neuron activity in abdominal ganglion

04 p0629 A70-14425

Small amplitude discharges and neuron activity in dorsal hippocampus of cats recorded simultaneously with pyramid cell activity

04 p0632 A70-15221

Bioelectrical activity of brain during conditioned motor reflex system operation modes in response to stimulating light pulses

08 p1447 A70-21450

Dogs spinal cord bioelectric activity monitoring by implanted electrodes, noting interelectrode resistances after prolonged operation

09 p1615 A70-22091

Lobster giant axon membrane steady state current fluctuations measured under voltage-clamp conditions, considering current potassium component

11 p1987 A70-26006

Electrical activity of visual cortex, subcortical structures and reticular formations in cats during conditioned reflex stimulation by light

12 p2173 A70-28351

Electronic simulation of neuron membrane demonstrating nervous impulses generation and propagation behavior

14 p2542 A70-30387

Dogs spinal cord bioelectric activity monitoring by implanted electrodes, noting interelectrode resistances after prolonged operation

15 p2685 A70-32687

Gas exchange, body temperature and electrical activity of neck and back muscles of cold-acclimated white rats subjected to various temperatures

18 p3219 A70-36540

Repeated local spine cooling effect on gas exchange and electrical activity of white rats skeletal muscles

18 p3219 A70-36541

Posterior ventral thalamic nucleus neuron reactions converging lemniscus and spinothalamic signals in cats

18 p3221 A70-36639

Cerebrum electrical activity and myogenic tonus relation in subjects performing tasks in response to visual and acoustic stimuli

18 p3221 A70-37216

Human brain LF activity in visual evoked response, determining relationship to stimulation

19 p3360 A70-37846

Time analysis of pulsed activity of neurons, using amplitude analyzer with programmable control unit

22 p3972 A70-43551

Visual system recording neuron pulse potential spatial and temporal responses to sinusoidal stimuli

23 p4144 A70-43922

Intense white pulsed jet engine noise effects on cochlea biocurrents in cats

23 p4157 A70-45076

Sympathetic transmission model, discussing transmitter liberation capacity under various stresses by mobilization of stores, acceleration of synthesis, etc

24 p4299 A70-45804

BIOENGINEERING

NT ANTHROPOMETRY

NT BALLISTOCARDIOGRAPHY

NT BIOINSTRUMENTATION

NT BIOMETRICS

NT BIOTELEMETRY

NT BODY MEASUREMENT [BIOLOGY]

NT CARDIOGRAPHY

NT ELECTROCARDIOGRAPHY

NT ELECTROENCEPHALOGRAPHY

NT ELECTROMYOGRAPHY

NT ELECTRORETINOGRAPHY

NT PLETHYSMOGRAPHY

Humanoid unmanned reconnaissance and assault vehicle maneuvers, describing cover-seeking and obstacle-avoidance functions from physiological and engineering viewpoint

01 p0033 A70-10495

Rocky Mountain Bioengineering - Conference, Laramie, Wyoming, May 1969

02 p0242 A70-12093

Book on engineering in heart and blood vessels stressing technological aspects of artificial internal organs

06 p1001 A70-17649

Minimum ventilation volume requirement for space suit relation to air contaminants and body gas discharge intensities and locations

13 p2358 A70-29333

Medical electronics and biological engineering - Conference, Nancy, France, June-July 1969

14 p2540 A70-30376

Amplifiers with selective feedback and clamping circuits for electrocardiology and electroencephalography

15 p2691 A70-31924

BIOGENESIS

U BIOLOGICAL EVOLUTION

BIOGEOCHEMISTRY

Biogeoecosis applicability to artificial closed ecological systems consisting of plants creating organic matter and heterotrophic organisms

13 p2353 A70-29501

BIOINSTRUMENTATION

NT BIOTELEMETRY

Frequency characteristics of air, water and blood filled pressure transducer systems using various needle and connecting tubing sizes

01 p0031 A70-10275

Skeletal status evaluation in space flight, describing instrumentation for bone mineral measurement and acoustic velocity method for bone elasticity

01 p0032 A70-10369

Constant magnetic fields effects on blood coagulatory processes, describing microcalorimetric determination

01 p0015 A70-10372

Analog time delay device for returning respiratory flow signal to correct time

01 p0035 A70-10654

Piezoelectric ultrasonic crystal on cardiac catheter tip measuring cardiac diameter in vitro and in excised canine hearts

01 p0038 A70-11025

Radiology instrument for examining pulmonary functions during deep inspiration, expiration and rest, describing material, components and assembly, mounting and radiogram development

01 p0040 A70-11401

Respiratory mass spectrometer design specifications, considering sampling and vacuum systems

01 p0041 A70-11649

Stainless steel micropipettes implantation in rat amygdala to study role in gastric secretion

02 p0234 A70-11729

Silicon strain gage transducer for measurement of pressure between tongue and teeth, developing two types of temperature compensated strain gages

02 p0242 A70-12054

Physiological signals of cardiovascular system transducing methods applied to vector ECG, heart sounds, peripheral pulse waves, chest microphone and plethysmography

02 p0243 A70-12095

Monitoring and recording of physiological parameters, discussing heart, muscle, brain potentials, blood pressure, respiration measurements and instrumentation

03 p0439 A70-14267

Blood flow sensors based on electrical conductivity dependence on flow rate, discussing system instrumentation and experimental results

04 p0644 A70-15295

Multiple optical properties measurement instrumentation for cellular specimens to classify biological cells, analyzing and displaying data by on-line computer

04 p0644 A70-15361

Bioelectronic equipment shock hazards reduction by current limiting diodes use in signal and ground leads

06 p0998 A70-17285

Cine recording ophthalmoscope with TV monitoring for retinal photography during centrifugation

06 p1061 A70-17286

Electromagnetic induction blood flowmeter measuring blood velocity as function of voltage in pick-up electrodes

07 p1217 A70-18952

Blood reflection densitometer with linear response to changes in indocyanine green dye concentration, using simple analog computation

07 p1221 A70-19589

Biomedical instrumentation evaluation procedure to minimize redesigns and delays and to bridge communication gap between medical and engineering fields

08 p1450 A70-20791

Simultaneous recording of fast and slow precision manual movements with electroencephalogram and electromyogram

08 p1452 A70-21438

Electromagnetic flowmeter for cardiac output changes in unanesthetized rats, discussing construction, form and associated electronic equipment of implanted probe

09 p1627 A70-23267

Ventricular preexcitation syndrome studied by catheter technique for heart electrical activity recording, noting His bundle bypass effects

10 p1819 A70-24934

ECG telemetry system within small irregular metal chamber

11 p1992 A70-26514

Electromagnetic blood flow determination by catheter in external magnetic field, discussing intravascular EM flow sensor capable of percutaneous introduction into vascular system

11 p1993 A70-26663

Heart dimension measurement by miniature implantable ultrasonic sonomicrometer, describing system design and operation

12 p2174 A70-26897

Transistorized pulsed activity converter for observing analog curve of change in pulse frequency

12 p2179 A70-28316

Transducers for bioimplantable telemetry systems self used by nonhospitalized patients

13 p2357 A70-28816

Neuroregulatory agents instrumentation based on compounds brain level, enzymatic formation and radio labeling

14 p2536 A70-30347

Thoracic impedance changes in premature infants respiration monitoring, noting Respiratory distress syndrome/Rds/physiopathology

14 p2541 A70-30382

Automatic recording respirometer for industrial wastes, discussing design and advantages

14 p2543 A70-31164

Actoballistocardiography based on piezoelectricity for biorthmic activity, respiratory movements and heart rate of small animals

14 p2543 A70-31321

Comparative cardiac output measurements in dogs using left/right heart dye injections and pulmonary/aortic electromagnetic flow probes

15 p2688 A70-31434

Intraarterial hot film constant temperature anemometry for point blood velocity measurements, detecting flow reversal

15 p2688 A70-31435

Miniaturized electromagnetic catheter flowmeter for measuring volume flow rate by potential difference between electrodes

15 p2689 A70-31747

Data system obtaining sampling rate for cardiac volume measurement via fast biplane cineangiography

15 p2691 A70-31922

Aerospace Medical Association Conference, St. Louis, April 1970

17 p3026 A70-35326

Portable hybrid automatic sleep analyzer for on-line EEG and EOG processing

17 p3040 A70-35606

Instrumentation safety for physiological research in hyperbaric chamber environment, taking into account pressure, isolation, atmosphere, electricity and fire

18 p3222 A70-35939

Multichannel time marker network synthesis device for physiological data assembly, transformation and processing, generating pulses

18 p3223 A70-36083

Left ventricular dynamics ultrasonic visualization, involving catheter-borne transducers array and computer for data acquisition and display

18 p3225 A70-36750

Extradural sensor for continuous measurement and recording of human intracranial pressure in neurosurgical practice

19 p3367 A70-37353

- Analog computer for continuous recording of oxygen consumption of muscular area in canine foot via blood flow rate and oxygen saturation
19 p3367 A70-37354
- Exhaled alveolar air data acquisition using mass spectrometer and multichannel analyzer
19 p3367 A70-37356
- Thermal thermesthesiometer for skin heat sensibility studies
19 p3368 A70-37806
- Thermal electronic instrumentation applied to biological flows including blood flow, cardiac outputs and volumes
19 p3368 A70-37843
- Uncoated quartz twin crystal microbalance for monitoring water vapor content of respiratory gases
19 p3368 A70-37844
- Cardiac rhythm, respiration and rhythmical processes of alimentary tract, using digital data device
19 p3370 A70-38214
- Arterial pressure measurement by automatic control system based on external compression pressure for maximum amplitude intraarterial pressure pulse oscillations
19 p3370 A70-38215
- Electronic differentiator for physiological research, discussing electrical voltage derivatives reproduction, sensitivity, etc
19 p3371 A70-38219
- Stabilograph and support dynamograph based on amplitude modulation of carrier frequency for standing stability determination in humans
19 p3371 A70-38220
- Reliability tests of blood carbon dioxide pressure measurement methods, indicating carbon dioxide-electrode method superiority
19 p3365 A70-38371
- Coulometric microrespirometer for long term numerical recording of oxygen consumption in respiratory chamber under sterile conditions
19 p3371 A70-38372
- Electromagnetic blood flowmeters for circulatory research
20 p3579 A70-39371
- Medical monitoring system onboard Soyuz spacecraft, describing equipment design, data acquisition and analysis, telemetric recordings, etc
20 p3581 A70-40193
- High resistance thermistor measurements of rapid blood temperature variation, discussing power dissipation effects
21 p3769 A70-41143
- Blood velocity in ascending aorta in man by transcutaneous ultrasonic Doppler technique, investigating heart hemodynamic performance and systemic perfusion
21 p3770 A70-41235
- Myocardium bioelectric activity electrocardiogram simulator, describing block diagram and operation
22 p3979 A70-43553
- Astronaut physiological monitoring aboard Soyuz spacecraft
22 p3980 A70-43691
- Semiconductor thermometer for skin temperature differences using resistance bridge, transistor amplifier and thermistors
23 p4150 A70-44317
- Miniature respiratory minute volume and rate sensor as pilot personal equipment in flight environment
23 p4155 A70-44840
- Photon-coupled biomedical amplifier for measuring and recording physiological signals
23 p4155 A70-44848
- Indirect blood pressure measurements using motion artifact suppression circuit based on K-sound electrocardiography
24 p4296 A70-45335
- Chronically implantable water perfused thermode system for hypothalamic temperature waveforms generation
24 p4309 A70-46117
- HF sinusoidal fluid pressure generators driven by electromagnetic vibrators for arterial applications
24 p4309 A70-46118
- Subminiature transistor photosensor for direct measurements of capillary blood cell motion
24 p4309 A70-46119
- Recording system errors for measuring pulmonary pressure-volume curves of excised lungs
24 p4309 A70-46122
- Conscious rat systolic blood pressure measurement, using arterial pulse wave detection to occluding cuff by photoconductive cell
24 p4309 A70-46213
- Fluorescent probes inserted into biological membranes for molecular structural and dynamic facets
24 p4304 A70-46231

BIOLOGICAL EFFECTS

- NT RELATIVE BIOLOGICAL EFFECTIVENESS (RBE)
Book on radiation biochemistry covering effects on biological tissue, nucleic acids, proteins, carbohydrates, lipids, hormones, vitamins, living cells, metabolism and toxic substances formation
01 p0011 A70-10030
- Medico-engineering experiment in partially closed ecological system for long term manned space missions
01 p0032 A70-10363
- Constant magnetic fields effects on blood coagulation processes, describing microcalorimetric determination
01 p0015 A70-10372
- Gnotobiotic mice with orally inoculated microorganisms observed for quantitation and fate of bacteria in intestinal tract
01 p0027 A70-11312
- Book on radiation protection, discussing atomic structure, nuclear transformations, effects on biological cells, total body exposures, somatic and genetic effects, etc
01 p0040 A70-11381
- Numerical solutions for laser beams intensity focused by simple lenses with varying primary spherical aberration, demonstrating isophote nonuniformity role in biomedicine
01 p0000 A70-11650
- Guinea pig cochlear hair cell damage after exposure to impulse noise
02 p0236 A70-12322
- Space environment and radiation on Biosatellite 2 enhancing radiation effects in developing flour beetle *Tribolium confusum*
02 p0238 A70-12517
- Biological dosimetry techniques for irradiation damage evaluation
02 p0239 A70-12581
- Pulsed noise biological effects on human organism, showing stimulation of auditory duct and baric and mechanical reception system causing neural functional shift
03 p0433 A70-13476
- Biological hazards of laser radiation, noting eye injuries and cataract from transscleral exposure on rabbits
03 p0434 A70-13679
- Organisms resistance to biological environmental factors, surveying published literature on pressure chamber experiments, tissue resistance, cellular protein stability, etc
03 p0422 A70-13701
- Fraction of Chlorella and Scenedesmus biomass, noting changes in adrenal cortex and renal glomerulus
03 p0425 A70-13889
- Ground-based biological experiments on insects and frog eggs to investigate effects of space flight weightlessness and radiation on mitosis and meiosis
04 p0631 A70-14942
- Nutritive value of mycelium of *Cantharellus cibarius* mushroom on rats compared with eggs and fresh and sour milk
05 p0809 A70-17111
- Nonionizing radiation sources relationship to human targets, discussing damage threshold levels
06 p0998 A70-17201
- Soviet monograph on radiobiological effects of ionizing radiation covering physicochemical and functional cellular changes, recovery mechanisms, etc
06 p0992 A70-17350
- Gravitational effects on organisms - Conference, Warsaw, March 1969
07 p1200 A70-18784
- White rats parenchymatous organs morphological changes following convulsion-producing exposure to pure hyperbaric oxygen
07 p1207 A70-19503
- High energy protons irradiation biological effects, noting qualitative and quantitative variations in radiation disease symptoms
07 p1208 A70-19508
- Microbiological corrosion effects on aluminum alloy fatigue properties inducing further microbiological corrosion compared to chemical corrosion effects
07 p1310 A70-19735
- Near zero magnetic fields effect on biological systems studied to determine terrestrial magnetic field absence effect on astronauts
08 p1449 A70-20724
- Biological effects of laser radiation on human eye, discussing damage caused by long term exposure to visible, IR and UV wavelengths
08 p1451 A70-21043
- Oxygen enhancement ratio and relative biological effectiveness of accelerated helium nuclei on mouse tumor cells, discussing applicability in radiation therapy
09 p1617 A70-22336
- Laser radiation cumulative effects compared to single dose in mice, using hair growth stoppage as test objective
09 p1624 A70-22817

- Laboratory simulations of geomagnetic field suppression, studying biological effects on human, mice, plants and microorganisms
09 p1626 A70-23113
- Microwave radiation thermal and nonthermal biological effects, considering exposure limits
10 p1824 A70-24061
- Orbital space flight effects on dry barley seeds, noting increased intracellular rearrangements
10 p1811 A70-24324
- Mercury arc injection lamp as radiation source for testing sunlight biological effects
10 p1888 A70-24388
- Relative value of prolonged bed confinement and hypodynamia in estimating biological effects of weightlessness
10 p1813 A70-24666
- Organisms resistance to biological environmental factors, surveying published literature on pressure chamber experiments, tissue resistance, cellular protein stability, etc
11 p1985 A70-25501
- Extraterrestrial gravitational effects on microorganisms, describing impulse-applied high g study of freeze dried *Escherichia coli*
11 p1987 A70-26028
- White rats parenchymatous organs morphological changes following convulsion-producing exposure to pure hyperbaric oxygen
11 p1987 A70-26102
- High energy protons irradiation biological effects, noting qualitative and quantitative variations in radiation disease symptoms
11 p1987 A70-26107
- Seed germination in simulated planetary atmospheres, considering biological responses of various organisms
14 p2537 A70-30692
- Wheat seedlings cellular response to weightlessness during NASA Biosatellite II flight compared with simulated weightlessness effects
15 p2688 A70-31662
- Human renal response to various exercise rates, measuring endogenous creatinine clearance, urine volume, solutes, acid, elements and protein excretion
15 p2684 A70-32534
- High strength magnetic fields effect on early embryonic development of frogs, relating growth abnormalities and paramagnetic ferritin motions
16 p2848 A70-33099
- Thermal-chemical damage to carbon particles in egg albumin under ruby laser irradiation, using chemical rate equations for protein denaturation
17 p3035 A70-34577
- Mitotic activity and aberrant mitoses frequency in mice corneal and duodenal epithelium cells under fast fission neutron irradiation
17 p3032 A70-35319
- Transport processes in chemical reactions and biological functions of living systems, using nonequilibrium thermodynamics approach
17 p3032 A70-35539
- Biological tests of fish and invertebrates exposed to Apollo 11 lunar surface material, noting absence of pathological effects
19 p3513 A70-37409
- Lighting effects on phenylethanolamine-N-methyltransferase (PNMT) activity and adrenal epinephrine content in rats
20 p3568 A70-38982
- Toxicity problems from burning or heating of polymeric materials, discussing laboratory experiments and standardized toxicity testing procedures
20 p3579 A70-39406
- Soviet book on dynamics of postradiation damage of biological objects covering dosage and protection effects on various animals
20 p3573 A70-39824
- Mice immunobiological reactivity at simulated high altitude
20 p3575 A70-40189
- Proton irradiation effects on dogs with partial body protection
20 p3575 A70-40192
- Biological action of constant magnetic fields, discussing axons electrical properties, biomolecules spatial orientation, electrolytes and liquids
22 p3978 A70-43138
- Biological compatibility problem in long duration space operation crew change, discussing human metabolic processes and difference effects
22 p3980 A70-43641
- Safety standards and biological effects of microwave radiation, investigating cataractogenesis and heart rate in rabbits
23 p4144 A70-43790
- Mammalian tissues metabolic and genetic alteration during weightlessness, relating rats liver regeneration delay to centrifuging intensity following hepatectomy
23 p4146 A70-44617
- Mice intestinal epithelium, investigating high energy protons irradiation effect on cells
23 p4149 A70-45028

BIOLOGICAL ACTIVITY
U ACTIVITY (BIOLOGY)
BIOLOGICAL ANALYSIS
U BIOASSAY
BIOLOGICAL CELLS
U CELLS (BIOLOGY)

- Cosmos 110 satellite experiments concerning radiation effects on lysogenic bacteria and plants
23 p4149 A70-45030
- Homogeneous magnetic fields effects on growth rate of *Saccharomyces cerevisiae* and *Micrococcus denitrificans*
24 p4306 A70-45102
- Lasers biomedical applications based on thermal and ionization effects on biological targets, considering eye surgery, tumor treatment, etc
24 p4308 A70-45568

BIOLOGICAL EVOLUTION

- NT ABIOTIC GENESIS
Solar system evolution based on Darwin theory, discussing energy inputs effect on primeval atmospheric molecules
02 p0229 A70-11666
- Fatty acids and aliphatic hydrocarbons in 3.4 billion year old metamorphosed sediment, suggesting biological origin
03 p0475 A70-13820
- Replicating molecules on primordial earth, suggesting chemical evolution on Jupiter via demonstrable alpha-aminonitriles synthesis
14 p2536 A70-30364
- Nucleated organisms divergence from bacteria compared to nucleated organisms divergence into separate kingdoms by analysis of genetic changes in cytochrome c and transfer RNA
16 p2846 A70-32990
- Organic compounds detection and identification on Mars surface for living systems existence or evolution
16 p2857 A70-33977
- Precambrian cherts hydrocarbon and fatty acid concentrations and C and S stable isotope ratios, discussing biological evolution rate
18 p3244 A70-35969
- Thermally prepared poly-alpha-amino acids catalytic activity after long term dry state storage, suggesting enzyme activity role in biological evolution
21 p3772 A70-40713
- Apollo 11 lunar dust and microbreccia micropaleontological examination, discussing biological morphology
21 p3778 A70-41620
- Space biological exploration for determining life origin on earth, emphasizing extraterrestrial life possibilities on other planets
24 p4301 A70-46000

BIOLOGICAL MODELS

- U BIONICS
BIOLOGICAL RHYTHM
U RHYTHM [BIOLOGY]
BIOLOGY

- NT MARINE BIOLOGY
Earth orbital experiments synthesis in space programs methodology, discussing examples in astronomy, biology and oceanography research
22 p4097 A70-42500
- Biology of fossil genus *Kakabekia* and living species *Kakabekia borshegniana* Siegel cultured from Alaskan soil samples
24 p4304 A70-46232
- Functional systems in biology, discussing inter-scientific demarcation, research strategy, physiological experiment, operational architectonics, etc
24 p4305 A70-46391

BIO LUMINESCENCE

- Hereditary UV luminescence of transplanted cancerous and lymphosarcomatous cells in mice and rats after ionizing radiation exposure
13 p2358 A70-29341

BIO MECHANICS

- U BIODYNAMICS
BIO MEDICAL DATA
Standard urinary excretion by healthy adult for free adrenaline, noradrenaline, creatine and hydroxymethoxy mandelic acid, making catecholamine determinations
12 p2168 A70-27622
- Cardiac cycle and phases shortening observations from analyzing electro- and phonocardiographic data recorded during Gemini flights
13 p2359 A70-29437
- EKG data automatic classification using discriminant analysis
13 p2360 A70-29627
- Digital filter facilitating biological data analysis through zero or linear phase shift filtering without distorting time relationship in data
14 p2542 A70-30796
- Physiological data analyzer modification for simultaneously estimating scaled interval histograms (SIHs) written in one memory subgroup
14 p2542 A70-30799
- Photon-coupled biomedical amplifier for measuring and recording physiological signals
23 p4155 A70-44848

BIO METEOROLOGY

U BIOCLIMATOLOGY

BIO METRICS

- NT ANTHROPOMETRY
NT BALLISTOCARDIOGRAPHY
NT BODY MEASUREMENT [BIOLOGY]
NT CARDIOGRAPHY
NT ELECTROCARDIOGRAPHY

- NT ELECTROENCEPHALOGRAPHY
NT ELECTROMYOGRAPHY
NT ELECTRORETINOGRAPHY
NT PLETHYSMOGRAPHY
Sinusoidal test for measuring knee moment increase required to flex and extend for various conditions of knee angle, angular velocity and steady knee moment
02 p0238 A70-12546
- Digital computer program for physiological measurements, outlining interpolation of mathematical functions describing signals time variations
03 p0436 A70-13900
- Thorax potential resistivity at sea and high altitude levels measured in children and adults inferring relation to ECG differences
07 p1206 A70-19296
- Pulmonary extravascular (PEV) and intravascular (PBV) fluid volumes measured at rest and exercise
07 p1211 A70-19595
- Deductive model of vision statics formulated for Grassman laws without using operation of color composition
08 p1450 A70-20729
- Postcaloric nystagmus clinical evaluation by analog computer measuring fast-phase eye displacement in Vestibular Function laboratory
08 p1448 A70-21942
- Cardiac output in humans by analog computer program using mass spectrometer analysis of expired air
08 p1454 A70-21948
- Air transport of cardiac patients with auriculoventricular blocks, noting feasibility due to portable surveillance and treatment apparatus
12 p2172 A70-28041
- Pulmonary vital capacity measurements in young recruits for respiratory function, considering relationship to body weight and height
16 p2850 A70-34348
- Soviet book on isolated animal heart autoregulation, considering cardio-pulmonary preparations, functional capacity, biometrics and computer technology for heart activity simulation models
19 p3359 A70-37404
- Frank orthogonal vectorcardiograms on humans during acceleration, using beat-by-beat real time analog-digital computer technique
20 p3572 A70-39435
- BIONICS
Book on dynamics of complex systems represented by control and human operators and animals behavioral activities models
01 p0034 A70-10501
- Analog, analog/digital, digital and hybrid computer simulation current advances, emphasizing physiological problems and optimum solution
02 p0264 A70-11687
- Mechanical properties of human skull specified for construction of physical and mathematical models
02 p0243 A70-12097
- Mathematical model formulated in terms of feedback controller for simulation of horizontal eye movement for positioning upon objects of interest
02 p0243 A70-12098
- Reactive forces and torques of musculoskeletal system during lifting and carrying materials, using computerized biomechanical models
02 p0247 A70-12549
- Arterial model with effects of thick walls, linear viscoelasticity and wall tethering for studying arterial mechanics
02 p0247 A70-12550
- Arrhythmia resembling atrial flutter simulated in dogs by coronary sinus and left atrial pacing and in man by coronary sinus pacing
02 p0240 A70-12696
- Model for simulating normal/abnormal depolarization and repolarization of heart and to reproduce electrocardiograms, describing design and programming
03 p0432 A70-12889
- Electrical analog simulation of cardiovascular system, determining blood flow rate and pressure in aorta and peripheral vessels
03 p0420 A70-13490
- Martian hypothetical organisms biological model, describing nonchlorophyll photosynthesis, epithelial hydrochrome pigments, scale insect morphology, etc
03 p0422 A70-13702
- Real image holography of complex organism or body organs as teaching aid and research tool in medicine and biology
04 p0685 A70-14558
- Biological model describing spacecraft operator sensorimotor activity in response to various spacecraft control stimuli, outlining computer algorithm
05 p0810 A70-17118
- Pavlovian conditioned reflexes theory reappraisal, discussing cortex-subcortical formations interrelations models
07 p1197 A70-18694
- Human head model for craniocerebral trauma analysis, studying fluid filled spherical shell free vibrations axisymmetric response
07 p1219 A70-19243

- Normal and stenosed aortic valve closure wing measurements in model valve in pulsatile water tunnel showing turbulence generation
07 p1220 A70-19249
- Geometrical model of human cardiac excitation stages based on normal heart anatomy, discussing application to study of QRS loop in vectorcardiogram
07 p1211 A70-19592
- Human color vision simulation by mathematical and electronic analogs for photoelectric color measurement and eye resolution
08 p1450 A70-20727
- Psychophysiological regularities of nonlinear human color vision model, analyzing sensitivity curves, achromatic tints and hyperbolic position in perception space
08 p1443 A70-20728
- Cardiovascular control system mathematical model incorporating fundamental properties of heart muscle for digital simulation using FORTRAN program
08 p1453 A70-21513
- Pituitary hormone ACTH stimulatory effect on steroid hormone cortisol secretion by canine adrenal cortex, constructing seventh order state variable model
10 p1819 A70-24868
- Functional model of signal analysis and pulse sequence conversion in nervous system at periphery of hearing
10 p1827 A70-25127
- Information theory, considering biological applications, coding and information content and transmission
10 p1846 A70-25284
- Martian hypothetical organisms biological model, describing nonchlorophyll photosynthesis, epithelial hydrochrome pigments, scale insect morphology, etc
11 p1985 A70-25502
- Nine degree of freedom pitch axis model of human postural control system, deriving kinetic and potential energy expressions
11 p1990 A70-25675
- Cardiovascular model for closed loop analog simulation of congenital heart defects hemodynamics
11 p1990 A70-25705
- Cochlear microphonics in guinea pigs using analog equivalent electrical circuit
11 p1992 A70-26494
- Dimensionless parameters associated with heat transport within living tissues using biothermal model
11 p1992 A70-26513
- Mathematical model for rats nonlinear time-varying glucocorticoid secretion control mechanism, obtaining time dependent characteristics of hypothalamic-hypophyseal complex
12 p2174 A70-26893
- Myocardial individual fibers length calculation based on ellipsoidal model of left ventricle and fibers helicoidal course, noting distension nonuniform effect
12 p2174 A70-27020
- Inert gas absorption from tissue cavities in body, using models with different wall distribution patterns of capillaries and diffusion resistance
12 p2171 A70-28025
- Anatomical and physiological correlations between mathematical model components for vestibular nystagmus mechanisms
13 p2351 A70-29331
- Intracranial pressure pulse waves formation mechanism mathematical model, estimating role of biomechanical factors
13 p2353 A70-29520
- Mathematical models for human adaptive and optimizing characteristics in manual control systems regarding behavior phase
13 p2360 A70-29780
- Soviet collection of papers on automation theory and biological systems simulation covering game theory and mathematical models
14 p2542 A70-30630
- Book on visual perception space covering biological optics, eye model, monocular vision, etc
14 p2539 A70-31349
- Optimal manual control model of human compensatory tracking response
14 p2543 A70-31408
- Model for pilots optimal manual control of hovering VTOL aircraft longitudinal position
14 p2543 A70-31409
- Control and guidance theories for biological problems, discussing signal transfer of linear control units and mathematical approaches
15 p2689 A70-31741
- Mechanical model of arterial viscoelasticity effect on input impedance and wave travel in systematic tree
15 p2691 A70-31941
- Air bubble breaking in blood and water flow passage of simulated cardiopulmonary bypass system with flow constriction
15 p2692 A70-32312
- Human postural motor control systems nonlinearities, describing physiological experiments and mathematical models
15 p2693 A70-32568

Compartmented physiological system dynamics by bilinear control model, relating homeostasis to system 15 p2693 A70-32571

Muscular behavior analog simulation model from generalization of laws governing viscoelastic behavior of polymeric materials 15 p2693 A70-32820

Distributed-lumped parameter model for impled mass transfer and blood-gas maldistribution effects in human respiratory system 15 p2694 A70-32844

Speech signals reflection in nervous system, constructing functional perception model for signals conversion into phonetic patterns 15 p2687 A70-32870

Fluid analog for lung tissue response to gravitational acceleration, examining lung density, transpulmonary pressure, expansion, etc 16 p2850 A70-34257

Arterial wall nonlinear distensibility effects on blood flow velocity profiles, considering various mathematical and physical artery models 17 p3035 A70-34468

Human body radiation shielding, describing development of computerized standing and seated model for space missions [AAS PAPER 70-053] 17 p3036 A70-34794

Mathematical model for short term adaptation effects in human semicircular canal response to rotation, discussing nystagmus 18 p3216 A70-35940

Engineering systems construction with behavioral elements of biological objects, describing gyromat 18 p3223 A70-36078

Continuous functions transformation by artificial neuron networks, investigating electrophysiological data for nerve tissues excitability 18 p3223 A70-36081

Adaptation to extreme stimulation in machine-organism system 18 p3224 A70-36529

Mathematical simulation of human thermoregulatory system, considering automatic control theory 18 p3224 A70-36530

Biophysical model of heat transfer from organism, describing adaptation to ambient temperature 18 p3218 A70-36531

Skin simulation for thermal radiation protection studies, considering fused silica and epoxy resin filled with Al powder 18 p3225 A70-37093

Alpha rhythm phase coherence during photic blocking, examining pacemaker model 19 p3368 A70-37811

Multipurpose microminiature multichannel biomedical telemetry system, discussing design 19 p3368 A70-37856

Electroencephalography with automatic frequency analysis to simulate processes involving brain self regulation 19 p3370 A70-38218

Axiomatic approach to homeostasis, discussing living systems as oscillators with input-output and transit variables in duration and elongation 19 p3365 A70-38411

Computer simulated decision hierarchical model of helicopter and VTOL pilot for multiloop closure and tracking characteristics of man-vehicle system 19 p3372 A70-38921

Mathematical model of human pituitary gland mechanism controlling secretions of serum growth hormone in response to glucose deficiency 20 p3569 A70-38995

Digital computer model of total body ECG surface maps, simulating male torso with lungs 20 p3578 A70-39369

Skeletal muscle force generation stochastic model based on motor unit, discussing Poisson distribution and dynamic force response 21 p3769 A70-41199

Electrokinetic model for semicircular canal transduction, focusing IR beam on exposed ampullae from posterior canals of Rana pipiens 21 p3765 A70-41696

Model for human brain visual information processing networks, considering visual search, selection, storage, correlation, recognition and recall functions 22 p3977 A70-42287

Linear lumped parameter mechanical model of muscle spindle in postural control 22 p3979 A70-43496

Acceleration effects on human organisms, describing centrifuge, rocket sleds and catapult simulators 22 p3979 A70-43528

Semicircular canals dynamic cross coupled responses to rotational movement, discussing mechanical model applicability 22 p3981 A70-43703

Ureter fluid mechanical model from lubrication theory viewpoint, discussing waveforms, pressure distribution, etc 23 p4179 A70-43966

Mathematical model simulating human respiratory physiopathology, based on hypothetical stable autotooscillations dependence on ventilation/pulmonary exchange system 23 p4155 A70-44859

Blood circulatory system and hemodynamic interdependencies simulation by analog computer, using Warner model 23 p4155 A70-44862

Hypogravic skeletal atrophy model, considering bone maintenance as feedback control system 24 p4296 A70-45328

Long wave approximation for peristaltic transport in circular cylindrical tube, noting inertia and wavelength effects on backward flow 24 p4309 A70-46224

Functional systems in biology, discussing inter-scientific demarcation, research strategy, physiological experiment, operational architectonics, etc 24 p4305 A70-46391

BIOPHYSICS

NT HEALTH PHYSICS

Left ventricle confocal prolate spheroid model taking into account physiologic variations of thickness 01 p0040 A70-11373

Biophysics research, discussing supramolecular biological structures, synthesis of proteins, nucleic acids and genetic codes, biological membranes, coding in nervous system, etc 03 p0420 A70-13491

Open circuit gas washout test of lungs under inspiration-expiration transmission symmetry, using Hilbert-Schmidt operators 12 p2175 A70-27021

Physical principles of biological membranes - Conference, University of Miami, December 1968 16 p2847 A70-33026

Molecular structural relationship between cellular membranes and photoreceptors in plants and animals 16 p2847 A70-33028

Cylindrically symmetric transient heat conduction in biological systems for inhomogeneous media and internal sources, using finite difference method 23 p4150 A70-43900

BIOREGENERATION

U REGENERATION [PHYSIOLOGY]

BIOSATELLITE 3

Biosatellite 3 experiment with male marmoset nemes-trima monkey, discussing cardiac rate, vascular data, water balance, weight loss and brain temperature 22 p3973 A70-43646

BIOSATELLITES

Biosatellite Primate Mission Program for component qualification levels validated by flight tests data, performing vibration tests on prime structure spacecraft [AIAA PAPER 70-403] 10 p1951 A70-24902

Biosatellite environmental control coolant loop system design for 30-day mission program, discussing fuel cell power source, cryogenic subsystem, etc 11 p2127 A70-26360

Carbon dioxide output monitoring from biosatellites for circadian system behavior in closed organism-environment systems 16 p2849 A70-33992

Biological satellite experiment, considering long term weightlessness effects on metabolism and biological rhythms of medical leech 16 p2854 A70-33993

Unnatural environment behavior of leeches for long term biosatellite experiment, determining temperature, humidity, oxygen pressure, carbon dioxide concentration, calcium hydroxide limits, etc 16 p2854 A70-33994

GE-RESD primate life support subsystem design for NASA-ARC biosatellite program 17 p3174 A70-34766

Automated orbiting biosatellite program with reentry system, studying long term weightlessness and radiation effects 17 p3178 A70-35258

Xanthine dehydrogenase activity in Drosophila and Habrobracon under hypogravity conditions onboard Biosatellite 23 p4144 A70-43863

Life support systems for biological flight experiments on Biosatellite project and Skylab A mission 23 p4154 A70-44665

BIOSENSORS

U BIOINSTRUMENTATION

BIOSIMULATION

U BIONICS

BIOSPHERE

U EARTH HYDROSPHERE

U LOWER ATMOSPHERE

BIO SYNTHESIS

Catecholamines biosynthesis, distribution, combining, uptake, deposition, release and metabolism in physiological and pathological reactions of organism 01 p0019 A70-10512

Growth rate effect on glucose utilization rate using sporogenic strain of Bacillus subtilis during N and L-tryptophan limitation 01 p0021 A70-10790

Biophysics research, discussing supramolecular biological structures, synthesis of proteins, nucleic acids and genetic codes, biological membranes, coding in nervous system, etc 03 p0420 A70-13491

Melatonin biosynthesis, discussing regulation by light and sympathetic nerves, daily pineal rhythms, estrous rhythms and ovarian hormones 03 p0424 A70-13809

Joint Chlorella-yeast cultivation on metabolites, investigating biomass accumulation and pigment synthesis 07 p1197 A70-18655

Biologically active fragments formation and functions in organism following liberation from inactive proteins via limited proteolysis 10 p1811 A70-24390

Cytoplasm, nucleus and membrane combination techniques for reassembly to form viable amoebae 11 p1986 A70-25849

Space diets with pure nutrition for balanced nutrition obtained through biological and physicochemical synthesis 23 p4157 A70-45027

Nitrogen deficient algae nitrification, showing cellular N compounds oxidized to nitrate and nitrite followed by nitrate reductase 24 p4297 A70-45407

Sympathetic transmission model, discussing transmitter liberation capacity under various stresses by mobilization of stores, acceleration of synthesis, etc 24 p4299 A70-45804

Synthesis regulation of p-hydroxybenzoate hydroxylase and protocatechuate oxygenase in beta-ketoadipate pathway in Pseudomonas putida 24 p4304 A70-46145

Heme biosynthesis defect in vitamin E-deficient rats affecting bone marrow synthesis of delta-aminolevulinic acid and liver formation of porphobilinogen 24 p4304 A70-46146

BIOT METHOD

Weighted residual and Biot variational methods for solving one dimensional heat conduction problems 09 p1789 A70-23260

BIOTECHNOLOGY

Laser radiation effects on eye, quantifying light necessary for coagulation for retinal detachment surgery, discussing risks in laser surgery 01 p0037 A70-10859

Nontoxic method of immobilizing protozoan Tetrahymena pyriformis and bacterium Escherichia coli in acrylamide polymers, discussing microorganism viability 05 p0802 A70-16477

Contamination control of spacecraft for planetary exploration missions emphasizing monitoring equipment and cleaning procedures 05 p0808 A70-16702

Peristaltic motion of viscous incompressible fluid, applying long wave approximation to two dimensional urine flow model 07 p1219 A70-19247

Medical laser systems applications, design criteria, general functions, etc 08 p1450 A70-20819

Soviet papers on biocybernetics covering man and computer, biological and engineering systems, heart self regulation, etc 18 p3223 A70-36076

Mechanical analysis involving clamping apparatus for cardiac muscle contractile response 20 p3570 A70-39362

Ultrasonic detection of tooth surface layer demineralization, noting surface and subsurface enamel structural differences 22 p3978 A70-42955

Orbital biotechnology laboratory requirements concerning man systems integration, life support and protective systems 22 p3980 A70-43644

Biotechnological design of shirt-sleeve side-by-side crew station for shuttle vehicle, including pilot vision and landing experience from X-15 program [AIAA PAPER 70-1327] 24 p4416 A70-45923

BIOTELEMETRY

Radio telemetry of athlete hearts, noting strenuous physical stress induction of transient serum potassium increase, metabolic acidosis, T-wave amplitudes, etc 02 p0230 A70-11694

Vital function telemetry system specifications, design and application to highway accident victims 02 p0243 A70-12096

Civil aviation personnel cardiovascular rehabilitation using single-lead electrocardiographic telemetry for monitoring and assessing cardiovascular status during supervised exercise 03 p0438 A70-14069

Energy converters and radio transmitters for physiological telemetry, using electric power converted from thermal and mechanical energy of human respiratory activity 04 p0644 A70-15276

Miniature piezoresistive pressure transducers for catheter and external physiological measurements in small animals

07 p1220 A70-19297

Dogs spinal cord bioelectric activity monitoring by implanted electrodes, noting interelectrode resistances after prolonged operation

09 p1615 A70-22091

Physiological reactions detection, transmission and data evaluation of aircraft pilots subjected to various stress environments, using radio telemetry

09 p1626 A70-23009

HF permittivity variations detector for blood circulation telemetry

14 p2542 A70-30389

Dogs spinal cord bioelectric activity monitoring by implanted electrodes, noting interelectrode resistances after prolonged operation

15 p2685 A70-32687

Human phasic right ventricular blood velocity, examining respiration, rhythm disturbances and Valsalva maneuver influence by radiotelemetry

16 p2850 A70-33111

Bioradiotelemetry of human cardiac activity during professional activities, using ultrasonic searchless Doppler cardiography

17 p3038 A70-35365

Multipurpose microminiature multichannel biomedical telemetry system, discussing design

19 p3368 A70-37856

Dynamic radio telemetry in physiology and medicine, discussing recordable parameters, multichannel systems, automatic data processing, etc

19 p3370 A70-38216

Cardiovascular stress testing using posterior bipolar lead for radiotelemetry monitoring

20 p3578 A70-39199

Radio telemetry measurements of blood pressure and flow in unrestrained animals

20 p3579 A70-39370

Four channel FM radio telemetry for exercise physiology, measuring EKG, respiration rate and pulmonary ventilation

23 p4151 A70-44380

Digital recording system for body temperature telemetry from small animals, using FM transmitter implanted in peritoneal cavities

23 p4151 A70-44381

Astronaut biological parameters monitored under prolonged space flight conditions for rescue operations

23 p4146 A70-44678

BIOTITE

Static and shock kink bands in biotite deformed by metamorphism, meteorite impact, nuclear explosion and laboratory experiments

09 p1665 A70-22053

Shock deformation of single crystal biotite /lepidomelane/ imbedded in impedance matching NaI, relating kinking intensity to peak pressure and pulse duration

09 p1670 A70-23375

Erasure fission tracks in soda-lime glass, tektite, biotite and apatite by shock loading, determining dynamic pressure and associated temperature effects

19 p3414 A70-38035

BIPROPELLANTS

U LIQUID ROCKET PROPELLANTS

BIRDS

NT CHICKENS

NT PIGEONS

Bird impact damage effect on aircraft structural design, considering forward facing areas and minimum weight

01 p0200 A70-10687

Bird deflection grill device for turboprop engine inlet ducts, noting effects on inlet flow characteristics, engine performance, etc

01 p0165 A70-10688

Bird strikes on aircraft, discussing airport control and environment alteration, radar tracking and link between migratory flights and weather conditions

03 p0411 A70-13075

Icing, bird collisions and static charge problems for jet aircraft, discussing protective devices

03 p0413 A70-13792

Degenerate retinal fibers in duck photoreceptor path connecting to supraoptical hypothalamic region detected following optic nerve dissection

03 p0427 A70-13955

Flight Impact Simulator for simulating bird strikes and bird-proofing of aircraft

16 p2888 A70-33290

Bird hazards to aircraft - Conference, Queens University, Canada, September 1969

18 p3210 A70-35976

Netherlands Air Force bird strike problem and warning system

18 p3211 A70-35977

RAF aircraft damage due to bird strikes in U.K., discussing preventive measures at airfields

18 p3211 A70-35978

German Air Force aircraft bird strikes statistics

18 p3211 A70-35979

West German aircraft bird hazards problems, discussing research activities and recommendations for strike avoidance

18 p3349 A70-35980

Statistical measurement of bird hazards to aircraft in terms of strike rates at airports, considering international strike rate standard

18 p3211 A70-35981

FAA research activities on eliminating birds at airports and improving aircraft components resistance to impact, including interagency committee functions on hazard problems

18 p3349 A70-35982

Bird hazards at Hong Kong airport, considering environmental and ecological problems

18 p3222 A70-35983

U.S. Air Force Bird-aircraft collisions problem and bird control research

18 p3211 A70-35984

Aircraft bird hazards in New Zealand, discussing ecological research techniques and preventive measures

18 p3212 A70-35985

Bird strikes in U.S.S.R., discussing frequency, damage, etc

18 p3212 A70-35986

Aircraft damage from bird impact and alleviating measures, taking into account windshield and intake guard designs, microwave beams for protection and chemical agents as repellent

18 p3212 A70-35987

Military airlift command bird hazard minimization near airfields by environmental control, including uses of scare devices, chemicals, trapping, etc

18 p3212 A70-35988

Canadian civil aircraft bird hazards problem and alleviating measures including airport surrounding lands control

18 p3212 A70-35989

Bird scaring from airfields based on ecological research

18 p3222 A70-35990

Aircraft bird hazards minimization by planning airport location and surroundings

18 p3236 A70-35991

Bird dispersal techniques in use or under study in Britain, including neurophysiological and bioacoustic systems to minimize hazards on airfields

18 p3222 A70-35992

Bird dispersal measure at airports, using behavioral and electrophysiological effects of high power microwave radiation

18 p3222 A70-35993

Aircraft design minimizing damage by bird strikes to gas turbine engine components, discussing service experience, airworthiness demonstration tests and research programs

18 p3300 A70-35994

Gas turbine aero engines damage due to bird strikes, emphasizing rig testing and simulation at first stage rotor blading

18 p3236 A70-35995

Prototype grill device for turboprop aircraft engine inlet protection against bird ingestion, discussing performance tests

18 p3212 A70-35996

International Civil Aviation Organization (ICAO) work on bird hazard reduction, including aircraft airworthiness specifications, bird data dissemination, etc

18 p3349 A70-35997

Airport bird detection equipment /ABDE/ radar to display airfield map for presence and magnitude of bird groups and vegetation on runway

18 p3226 A70-35998

Birdstrikes as aircraft hazard, discussing structural damage, engine ingestion and various countermeasures

18 p3213 A70-36319

Respiratory gas metabolism of liver, heart, brain and muscle tissues in birds exposed to various ambient temperatures for long periods

18 p3220 A70-36547

Soviet monograph on collision hazards between aircraft and birds covering accidents, damage and preventive measures

23 p4137 A70-44099

Soviet civil aircraft-bird collisions, stressing hazard forecast and prevention by bird identification and migration patterns

24 p4289 A70-45644

Birdproofing aircraft research program using pneumatic cannon firing real and simulated bird carcasses

24 p4292 A70-46398

BIREFRINGENCE

Picosecond on-off light gate based on Kerr cell design, using optical pulses to induce birefringence in liquids

01 p0111 A70-10571

Birefringent lens producing spatially separated multiple images, discussing polarization control, thin crystalline lenses and electro-optic control

01 p0091 A70-10915

Birefringences and phase retardations in lithium niobate crystals for light propagation directions near optical axis, considering electro-optic modulation

02 p0313 A70-12451

Optically trapped filaments in liquid carbon disulfide by side illumination and crossed polarizers using glass laser, noting birefringence and duration time

04 p0703 A70-15619

Successive small birefringences undergone by polarized light ray crossing photoelastic model represented by rotations in equatorial plane on Poincare sphere

06 p1168 A70-17918

Birefringence determination from contrast of interfering natural light beams

08 p1543 A70-20521

Electro-optic effects in ferroelectric ceramics with electrically variable coefficients of piezoelectricity and birefringence, discussing applications

09 p1739 A70-22633

Magneto-optical birefringence anisotropy and light propagation in terbium ferrite garnet in presence of Faraday and Cotton-Mouton effects

11 p2097 A70-25377

Solar horizontal telescope monochromator improvement by adding birefringent monochromator and diffraction grating

11 p2057 A70-26590

Photoelastic analysis using fringe multiplication instrument applied to two dimensional models under load and frozen stress slices

11 p2061 A70-26834

Instrument for measuring and recording strains and birefringence in glasses and crystal under compressive, tensile or bending loads at low/high temperatures and in vacuum

12 p2237 A70-28161

Ruby laser radiation frequency control by birefringent calcite plate and KDP electro-optical Q switch

13 p2428 A70-29363

Zero birefringent blend consisting of rigid and flexible polyesters with viscoelastic mechanical and optical response

15 p2765 A70-32318

Hologram interferometry with birefringent objects, showing advantages over polariscope and classical interferometers

17 p3086 A70-35013

Variable ratio beam splitter design and operation for lasers, using birefringent optics

18 p3270 A70-36755

Holographic registration of isochromatic and isopachous diffraction patterns of photoelastic birefringent objects, showing stress concentrations

19 p3422 A70-37649

Thermally induced stress birefringence effect on linearly polarized CW YAG-Nd laser

21 p3834 A70-40566

Thermal and birefringent effects on output of continuous Nd-YAG laser rod, using 6328 A probe

21 p3837 A70-41906

YIG single crystals piezo-optical effect and magnetic double refraction, describing stress measurement technique

23 p4230 A70-43931

Plasticized high polymers mechanical and optical properties, studying birefringence phenomena interrelation with applied external stresses

24 p4424 A70-45590

BIREFRINGENT COATINGS

Stress analysis based on observing birefringence effects in photoelastic surface coating

04 p0689 A70-14922

Fiber-reinforced narrow rectangular beam flexural strain analysis by birefringent coating technique, deriving isochromatic and isoclinic patterns

23 p4275 A70-44915

BIRTH

Gravity effects on perinatal organ growth in chicks

24 p4297 A70-45342

BISMUTH

Electrode surface bismuth coating selected for reducing electrostatic analyzers photocurrents

05 p0851 A70-16734

Bismuth concentrations in various carbonaceous and equilibrated chondrites determination by neutron activation technique

07 p1388 A70-20036

Oscillatory transverse and longitudinal magnetotription in single crystal Bi, obtaining deformation potentials

08 p1557 A70-21838

Far IR radiation transmission through bismuth and gallium normal and superconducting thin films, considering transition temperature role

09 p1739 A70-22323

Bi polycrystalline film grown by vacuum deposition on amorphous substrates investigated for electron microscope beam effects

12 p2285 A70-27261

BISMUTH ALLOYS
Quenched MnBi thin films measured for magnetic, magneto-optical and optical properties, noting Faraday rotation

12 p2284 A70-27246

Bi-Sb alloys, discussing structural data, crystal preparation, band structure, pressure, nonohmic conductivity, thermoelectric, thermomagnetic and magnetothermal effects 14 p2625 A70-30332

BISMUTH COMPOUNDS
NT BISMUTH OXIDES

Laser induced vaporization of Bi compounds with group VIa elements, analyzing vapor species, condensed phase and molecular configurations by mass spectroscopy 08 p1455 A70-21338

Electro-optic device using ferroelectric bismuth titanate, discussing electrical and optical properties and matrix addressed display 21 p3830 A70-42114

Thin film BiSb-oxide-BiSb tunneling junction I-V characteristics anomalies as function of temperature, magnetic field and bias voltage 24 p4390 A70-45662

BISMUTH OXIDES

Bismuth oxide resistivity and structural characteristics at high temperature and during transformation from solid to liquid state 10 p1927 A70-24272

BISTABLE AMPLIFIERS

U FLIP-FLOPS

BISTABLE CIRCUITS

Pneumatic fluidic oscillator consisting of bistable multivibrator, analyzing feedback loop operation based on electropneumatic analog system 02 p0229 A70-12673

Bistable optical resonators with saturable absorbers, discussing hysteresis characteristics and Q switching applications 06 p1105 A70-17449

Transistor bistable multivibrator design by graphic analytic method, considering effects of loading and supply voltages, temperature and component values on circuit performance 10 p1848 A70-23995

BISTATIC REFLECTIVITY

Backscattering, bistatic scattering and current distribution on thin wires during electromagnetic wave incidence 15 p2700 A70-32412

Bistatic lidar/laser radar/ detection of atmospheric aerosol size distribution, using angular scattering measurements of polarization parameters 15 p2704 A70-32609

BIT SYNCHRONIZATION

Bit-slippage errors due to onboard tape recording of PCM/FM telemetry data for Apollo Telescope Mount, noting roles of S/N ratio, data characteristics, etc 01 p0044 A70-10940

Bit transition time /bit synchronization/ estimation, developing bit synchronizer from Bayes estimation and optimization theories [AAS PAPER 69-608] 04 p0647 A70-14655

Random synchronization errors in PN and PSK systems reduce input signal power and introduce additional self noise 07 p1236 A70-20069

PSK demodulation by optimal carrier and bit synchronization methods based on nonlinear filter theory, relating error probability to signal to noise ratios 08 p1458 A70-20795

TDMA system burst synchronizer with periodic channel slots reallocation feature 10 p1835 A70-24331

Bit clock synchronous system for communications satellites TDMA 10 p1839 A70-24368

Review of 1969 London International Conference on Digital Satellite Communication session covering modulation, synchronization and coding [AIAA PAPER 70-464] 11 p1997 A70-25409

Phase noise and cycle slip optimization of steady state digital data transition tracking loop used as bit synchronizer in phase-coherent receiver 11 p2024 A70-26202

Discrete sequential algorithms for bit synchronization implemented with digital computer for optimum data detection 12 p2184 A70-27249

Noise stability of optimal binary detection receiver of rectangular-pulse and discrete pseudorandom signals under nonideal synchronization 13 p2364 A70-28869

Digital transition tracking symbol synchronizer improving SNR without lowering loop bandwidth [JPL-TR-32-1488] 13 p2367 A70-29591

Frame synchronization in biorthogonal coded multiplex communication system, describing PCM, pattern insertion and double encoding methods 17 p3045 A70-35266

PGM noisy high bit rate processing system, describing preprocessor, bit detector and synchronizer 19 p3379 A70-37903

Digital bit synchronization phase locked loop steady state and transient performance in white Gaussian noise 21 p3802 A70-41352

PCM/NRZ signal band-limiting effect on bit error probability, using sample detector 22 p3990 A70-43339

BITERNARY CODE

Bit error probability after decoding for binary perfect single error correcting codes 11 p2014 A70-26247

BITS

Holographic optical memory systems operational principles and potential advantages, discussing feasibility of 100 million bit memory capacity and one microsecond random access time 10 p1892 A70-25245

Fixed information bit rate approach to coding over space channel introducing redundancy and check digits for error probability 11 p2014 A70-26223

Telemetry decommutation algorithm for applying Bayesian decisions to demodulated received bits data 11 p2008 A70-26238

Linear superposition /LSP/ of isolated pulses in tape recording, discussing validity for multibit waveform synthesis 11 p2057 A70-26627

Bits quantity required to represent coefficient within digital controller with high sampling rate 12 p2203 A70-27410

Digital controller bits number determination to meet nominal controller coefficients accuracy requirements 16 p2867 A70-33304

BITUMENS

Powdered metallic additions effect on combustion rates of ammonium perchlorate with bitumen and polymethyl methacrylate and potassium perchlorate with bitumen mixtures 18 p3299 A70-36247

BIVARIATE ANALYSIS

Fifty percent coverage problem /Circular Error Probable/ of general bivariate Gaussian distribution from viewpoint of navigation systems error analysis 16 p2948 A70-33451

BLACK ARROW LAUNCH VEHICLE

U BLACK KNIGHT ROCKET VEHICLE

BLACK BODY RADIATION

Thermodynamic aspects of ray invariance of spectral brightness ratio to square of local index of refraction compared to black body power radiation 01 p0144 A70-11293

Electromagnetic wave diffraction on absorbing black metallic and magnetic cylinders and strip, plotting radar scattering cross sections 05 p0813 A70-16262

Radiation fluxmeters involving black plates and sensor disk respectively for use in space simulation chambers 05 p0849 A70-16636

Antenna calibration by measuring emission of absorbing black disk positioned in Fresnel region 07 p1239 A70-18759

Inverse Compton collisions of relativistic electrons with universal black body photons for diffuse component of cosmic X rays 07 p1369 A70-20166

Black body radiation properties with temperature important only in rest frame, using transformation formulas for coherence and spectral parameters 10 p1968 A70-24631

Cosmic background radiation interactions with matter, discussing molecular excitation and black body radiation interpretation 12 p2291 A70-27054

Observational cosmology, discussing aspects of radio source and quasar counts, intergalactic medium and cosmic black body radiation 12 p2298 A70-27061

Variable reproducible black radiator of resistance heated carbon tube designed for temperatures between carbon glowing and sublimation point 12 p2329 A70-27090

Radiative heat transfer in spherical space bounded by perpendicular annular ring system with gray diffuse and absolutely black body surfaces 12 p2331 A70-27554

Tungsten strip lamps spectral radiance calibration, discussing accuracy requirements for radiation constants, wavelength and black body temperature 13 p2410 A70-29655

Black bodies radiation properties and design for applications as absolute radiation standards 13 p2410 A70-29657

Black body design for radiometry, discussing error sources in calibration 13 p2410 A70-29658

Comet Bennett 1969 photometric observations, showing blackbody-like continuum at short wavelengths with sharp peak due to silicate grains 14 p2642 A70-30895

Reflectivity measurement in near IR using black bodies near room temperature for light sources 14 p2588 A70-31210

Black body cavity type radiometers for high accuracy measurement of irradiance 15 p2737 A70-32036

Uniform model universes containing gaseous matter and background blackbody radiation, solving Einstein equations without zero pressure assumption 18 p3313 A70-36215

Antenna calibration by measuring emission of absorbing black disk positioned in Fresnel region 18 p3233 A70-37103

Reflectance measurements of directional spectral emittance of black body cavities with specific geometries, using laser source and integrating hemi-ellipsoid 20 p3627 A70-39091

Stepwise linear regressions method for estimating black body surface radiances from model atmospheres and corresponding simulated Nimbus 2 window-channel radiances 22 p4013 A70-42617

Ta spectral emissivity, using ratio of specimen surface and black body spectral radiant intensities 23 p4207 A70-44447

Uranus and Neptune millimeter wave observations, showing brightness temperatures in excess of black body equilibrium temperatures derived from solar heating 24 p4403 A70-45398

BLACK KNIGHT ROCKET VEHICLE

Manufacturing and technology of hybrid microelectronics packaging in Black Arrow X-3 satellite equipment 16 p2879 A70-33959

UK space program, describing scientific satellites, Black Arrow launch vehicle and sounding rockets 17 p3167 A70-35206

Black Arrow launch vehicle for inexpensive and reliable payload injection into low polar orbits 17 p3178 A70-35255

Black Arrow X3 spacecraft design and experiments, including silicon cells performance electronic assemblies and micrometeoroid fluxes 17 p3178 A70-35256

BLACKBURN B-103 AIRCRAFT

U BUCCANEER AIRCRAFT

BLACKOUT [PHYSIOLOGY]

NT BLACKOUT PREVENTION

BLACKOUT [PROPAGATION]

NT ATMOSPHERICS

NT COSMIC NOISE

NT DAWN CHORUS

NT ELECTROMAGNETIC NOISE

NT HISS

NT IONOSPHERIC NOISE

NT IONOSPHERICS

NT SHOT NOISE

NT SUDDEN ENHANCEMENT OF ATMOSPHERICS

NT THERMAL NOISE

NT WHISTLERS

Radiation enhancement from spherical antenna by overdense plasma coating, noting use for reentry vehicle blackout prevention 02 p0262 A70-12601

BLACKOUT PREVENTION

Syncope prevention in orthostatic heat test by inflating cuffs around legs and lower abdomen 24 p4306 A70-45331

BLADDER

H ion increased activity effect on sodium transport across short circuited turtle bladder 02 p0234 A70-11730

ADP-ATP catalyzed exchange reaction in turtle bladder microsomes, using chromatographic measurements of conversion rates 17 p3034 A70-35900

Intermediary complexes between Na-K ion stimulated ATPase /adenosine triphosphate/ and microsomal proteins of turtle bladder epithelial cells 18 p3225 A70-36233

Turtle bladder walls osmotic properties, discussing transrenal water flow transient acceleration by sodium transport inhibition 21 p3762 A70-41223

Turtle bladders isolated mucosal and serosal fractions histological and physiological properties, discussing ion transport and oxygen consumption 21 p3762 A70-41224

BLADE TIPS

Tip clearance effects in axial flow turbomachinery, predicting blade-to-blade variation in outlet angles and stagnation pressure losses [ASME PAPER 69-WA/FE-26] 04 p0733 A70-14775

Wire dischargers at helicopter propeller blade tips reducing electrostatic RF interference, substituting stainless steel wire tufts for nichrome wire 05 p0848 A70-16320

Tuft position on rotating helicopter blade in hovering and forward flight, calculating tip path plane and tuftlines 08 p1438 A70-21868

Efficiency loss with tip clearance predicted for mixed and axial flow single stage turbomachines, using perfect fluid model 11 p1974 A70-25787

Tip clearance contactless measurement in jet engine turbine based on radioactive isotopes properties 11 p2055 A70-26446

Inducer tip clearance effect on centrifugal pump section performance with velocity and total head distributions at outlet 14 p2592 A70-31332

Sweep tip rotor blade design, discussing wind tunnel-whirl stand correlations 17 p3015 A70-34736

BLADES

Flexible blades cascade design compared with various correlation criteria, describing cascade and profiles geometry and loss coefficient 05 p0790 A70-16029

Film type solar energy reflector peripheral blades for connection to receiver, discussing precession control and despin for rotating concentrators 07 p1196 A70-19501

Shear flow near walls through cascade of untwisted blades, observing variation in lift coefficient across span 11 p1975 A70-25788

Film type solar energy reflector peripheral blades for connection to receiver, discussing precession control and despin for rotating concentrators 15 p2678 A70-32746

BLADES [CUTTERS]

NT RAZOR BLADES

BLANKS

Impact against elastoplastic blank allowing for base and striker compressibility, giving solution in region of plane wave first reflection from base 05 p0947 A70-17016

Kinematic characteristics of annular-blank elements extruded by pulsed magnetic fields, noting proportionality to energy stored in capacitor bank 05 p0857 A70-17018

Displacement rate measurement in initial portion of blank subjected to explosive forming by capacitance pickup 06 p1076 A70-17868

Explosive forming of large domes from flat blanks with full scale trial-and-error elimination [ASTME PAPER MF-69-186] 12 p2240 A70-27079

BLASIUS EQUATION

Initial value method for solution of nonlinear two point boundary value problems in fluid mechanics, considering Blasius equation and unsteady gas flow [ASME PAPER 69-WA/FE-8] 04 p0667 A70-14782

BLASIUS FLOW

Blasius flow stability on deformable surface of membrane using Orr-Sommerfeld equation to calculate amplitude of function for perturbation flow 09 p1658 A70-22182

Numerical integration of Orr-Sommerfeld equation for flat plate Blasius boundary layer transition 23 p4179 A70-43973

Tollmein-Schlichting waves in flat plate Blasius boundary layer, comparing experimental and theoretical critical Reynolds number 23 p4179 A70-43975

BLAST LOADS

Initial blast wave axisymmetric shock-on-shock interaction for blunt bodies moving supersonically at zero angle of attack solved in Taylor series 10 p1797 A70-23954

Nonsteady flow past duct junctures, investigating ventilation system of underground bomb shelter for blast wave passage prevention 11 p2036 A70-26139

Shock wave diffraction by moving thin wing over flat terrains, discussing aircraft blast encounter 18 p3205 A70-36195

Blast loaded cylindrical shell collapse hinge dynamic instability prediction by mathematical model 19 p3545 A70-38334

BLASTOFF

U ROCKET LAUNCHING

BLEACHING

Wave front reconstruction for perfectly bleached holograms not achievable by simple coherent illumination due to remaining amplitude variation 04 p0691 A70-15033

Bleach process giving high efficiency low noise holograms using potassium ferricyanide, noting drying procedure and developer 06 p1072 A70-18520

Efficiency, low noise and photochromic effects suppression in bleached silver halide holography with various films 20 p3627 A70-39097

BLEED-OFF

U PRESSURE REDUCTION

BLENDS

U MIXTURES

BLIND LANDING

Holographic dynamic head-up display system for aircraft carrier deck landings in low visibility 12 p2232 A70-27371

All-weather automatic landing in blind conditions, considering Trident system 14 p2615 A70-31392

BLINDNESS

NT FLASH BLINDNESS

Bleached eye pressure blinding at bleaching light termination during wavelength settings, discussing effect on interocular hue shifts 03 p0427 A70-13951

Character recognition methods applied to reading machines transforming printed material into forms acceptable to blind 13 p2360 A70-29809

Blind persons susceptibility to acute motion sickness during stressful Coriolis acceleration 15 p2689 A70-31887

BLISTERS [PROTUBERANCES]

U PROTUBERANCES

BLOCKING

Electrocardiographic features and clinical finding in patients with left axis deviation combined with right bundle branch block 01 p0013 A70-10269

Alpha rhythm phase coherence during photic blocking, examining pacemaker model 19 p3368 A70-37811

BLOCKS

Buckling equilibrium equations for thick rectangular block under compression loads, noting bifurcation points 19 p3536 A70-37683

BLOOD

NT EOSINOPHILS

NT ERYTHROCYTES

NT LEUKOCYTES

NT LYMPHOCYTES

NT WHITE BLOOD CELLS

Artificial pulmonary ventilation effects on carbonic anhydrase activity in human blood during hypoventilation and hyperventilation 01 p0025 A70-11029

Blood pH effects on adrenomedullary response to hemorrhage, studying catecholamines release in anesthetized dogs 02 p0235 A70-11733

Oxygen and carbon dioxide partial pressures bloodless determination in mixed venous blood, using platinum electrode and IR carbon dioxide meter 02 p0236 A70-12091

Peripheral blood, neutrophil myeloid hematopoiesis, phagocytic activity and serotonin level in gamma irradiated dogs 03 p0423 A70-13706

Stimulated thyroid gland temperature variations and oxygen metabolism in decorticated dogs and anesthetized rabbits and rats 04 p0639 A70-15511

Ionol concentration variations in oncological patients blood, using liquid gas chromatography to determine removal by urine and feces 07 p1209 A70-19519

Automatic control theory found effective in studying arterial blood saturation with oxygen during ascent to 4000 m in pressure chamber 07 p1210 A70-19523

Blood reflection densitometer with linear response to changes in indocyanine green dye concentration, using simple analog computation 07 p1221 A70-19589

Adaptive reactions in thyroidectomized rats blood and brain during adaptation to hypoxia compared with intact animals 07 p1214 A70-19794

Radial immunodiffusion for serum proteins quantitation adapted to capillary blood and compared with results for venous blood 07 p1214 A70-19932

Biochemical and histochemical parallels of enzymatic activity in blood, cardiac muscle and liver under hypoxia 08 p1446 A70-21445

Acute oxygen deficiency effects on blood electrolyte concentrations in altitude-adapted and nonadapted humans 09 p1616 A70-22217

Blood carbon dioxide and oxygen content determined by respiration mass spectrometer using carrier gas 09 p1629 A70-23584

Physiology and pathophysiology of oxygen transport in human blood, discussing fluctuations in O₂ capacity and affinity 10 p1821 A70-25079

Peripheral blood, neutrophil myeloid hematopoiesis, phagocytic activity and serotonin level in gamma irradiated dogs 11 p1985 A70-25506

High altitude effects on total protein content and composition in rats blood serum 13 p2352 A70-29346

Acceleration effects on Na, K, and pH in rabbits cerebrospinal fluid and cerebral blood 13 p2352 A70-29347

Gas mass diffusivity measurements in plasma and reaction velocity constant in human and dog blood 15 p2692 A70-32311

Pursed lips breathing effects on ventilation and blood gas exchange in patients with chronic airway obstruction 15 p2684 A70-32538

Diffusion coefficient of dissolved oxygen in blood proteins aqueous solutions 15 p2686 A70-32848

Arterial blood carbon dioxide tension effects on rhythmic volley activity of respiratory medulla oblongata neurons in cats 17 p3030 A70-35354

Reliability tests of blood carbon dioxide pressure measurement methods, indicating carbon dioxide-electrode method superiority 19 p3365 A70-38371

Heart stroke volume estimation at submaximal exercise using blood hemoglobin content and heart rate 20 p3576 A70-40328

Lateral and angular acceleration effects on blood and urine contents in specific metabolic indices of healthy young men 22 p3971 A70-43136

Mossbauer spectrum of submolecular changes of oxyhemoglobin in animal blood exposed to microwave irradiation 23 p4144 A70-43788

Blood oxygen, carbon dioxide and pN during hypothermia induced by He-oxygen mixture and cold exposure in hamsters, comparing with hibernation state 23 p4147 A70-44787

Altitude and alcohol intake effects on blood alcohol concentrations 24 p4306 A70-45329

Ganglione and quaterone cholinolytic agents effects on arterial blood acid-base balance indicators in cats 24 p4298 A70-45633

BLOOD CIRCULATION

NT BRAIN CIRCULATION

NT CARBOXYHEMOGLOBIN

NT CORONARY CIRCULATION

NT INTERCRANIAL CIRCULATION

NT INTRAVASCULAR SYSTEM

NT ISCHEMIA

NT OCULAR CIRCULATION

NT PULMONARY CIRCULATION

Pulmonary artery blood sampled before or during rebreathing of carbon dioxide in nitrogen mixtures, at rest and during exercise, discussing oxygen pressure changes 01 p0020 A70-10652

Retinal vessels of humans at 11-2.0 atmosphere oxygen partial pressures, noting arterioles and venules dilation response to hypoxia and vasoconstriction response to hyperoxia 01 p0023 A70-10863

Biomechanics of microcirculation, discussing rheological characteristics of blood, erythrocyte and vessel wall, hydrodynamics of erythrocyte-shaped bodies mathematical models, etc 01 p0039 A70-11160

Humans and dogs breathing CO in closed system, discussing distribution on blood, body stores and oxygen metabolism 02 p0234 A70-11727

Electrical analog simulation of cardiovascular system, determining blood flow rate and pressure in aorta and peripheral vessels 03 p0420 A70-13490

Hemodynamics in cardiosclerosis patients and healthy subjects under hypoxia, investigating heart activity and blood circulation 06 p0994 A70-17667

Biological fluorescent substances passage in rabbit central nervous system as indicators of blood supply to cells 07 p1197 A70-18657

Blood volume and circulation rate in dogs subjected to traumatic shock and hemorrhage under high mountain conditions 07 p1198 A70-18708

Lower limbs circulation of peripheral vascular diseased patients transcutaneously assessed with ultrasonic flow detector, comparing results with arteriograms 07 p1217 A70-18956

ECG changes attributed to reduction of blood supply to myocardium during orthostatic tests after prolonged hypokinesia 07 p1209 A70-19513

German monograph on determination of blood velocity, pressure, pulse rate and vascular structure parameters using Doppler effect 08 p1452 A70-21297

Prolonged hypodynamia effect on human external respiration, arterial blood oxygenation, circulation rate and gas exchange under various physical stress conditions 10 p1814 A70-24674

Human head-up tilt circulatory stress effects on left ventricular systolic time intervals 10 p1820 A70-24937

Brain oxygen supply during cerebral edema, examining venous and arterial blood gases, circulation, oxygen uptake, blood volume and pressure and EEG 10 p1822 A70-25087

ECG changes attributed to reduction of blood supply to myocardium during orthostatic tests after prolonged hypokinesia 11 p1988 A70-26112

Electrical stimulation of dogs hypothalamus effect on blood and lymph circulation and composition
13 p2352 A70-29354

Left ventricle zone as principal reflexogenic zone of heart participating in greater circulation vessel tonus control
13 p2353 A70-29356

HF permittivity variations detector for blood circulation telemetry
14 p2542 A70-30389

Pressure-flow relation for fluid in pipe obeying Casson equation, considering applicability to human blood
15 p2690 A70-31917

Isolated human heart measurements for time course and instantaneous distribution of normal heart excitatory process
15 p2683 A70-32471

Emergency hypotonia regional control with/without blood circulation centralization, describing device consisting of inflatable balloon, extracorporeal shunt, electromagnet valve, manometer and circuit
15 p2687 A70-32891

Arterial pH change effects on circulation and oxygen consumption in dogs, discussing respiratory acidosis heart rate, cardiac output and arterial blood pressure
17 p3024 A70-34593

Atropine effects on circulatory responses to diminished effective blood volume and vasodepressor syncope, noting heart rate increase
17 p3032 A70-35562

Peripheral vasculocapillary blood circulation by television UV capillaroscopy and electronic finger plethysmography
19 p3370 A70-38212

Cardiovascular blood circulation system dynamic characteristics analysis by linear statistical correlation methods, describing test for determining weighting function
20 p3581 A70-39905

Ambient near vacuum pressure effect on blood circulation, examining thoracic aorta blood flow, pressures, gas expansion and water vaporization
20 p3576 A70-40326

Continuous blood oxygen analyzer standardized with atmospheric air, demonstrating on dogs during occlusion of left anterior descending coronary artery
21 p3772 A70-42162

Physical training effects on blood circulation, respiratory and muscular functions in aging persons
22 p3970 A70-42905

Blood-brain and blood-cerebrospinal fluid barriers alterations under various physical environments in manned orbital laboratory
22 p3973 A70-43647

Blood circulatory system and hemodynamic interdependencies simulation by analog computer, using Warner model
23 p4155 A70-44862

Conduit arteries viscoelastic properties in normal and hypertensive dogs from recorded pressure and diameter waves
24 p4299 A70-45808

Arterial hemodynamics in hypertension, discussing pulse changes mechanism as consequence of decreased arterial distensibility via disturbed relationship between ventricular ejection wave and impedance characteristics
24 p4299 A70-45809

BLOOD COAGULATION

Constant magnetic fields effects on blood coagulation processes, describing microcalorimetric determination
01 p0015 A70-10372

Human blood platelets volume measured in Coulter counter, noting relation to temperature
03 p0416 A70-13008

Interactions between nutrition, blood coagulation and atherosclerosis by Duguid theory, emphasizing fibrinolysis, thrombosis and alimentary lipids
03 p0431 A70-14280

Hypokinesia and nutrition deficiency effect on blood coagulation, noting combination with accelerations may lead to hypocoagulation
04 p0630 A70-14578

Blood clotting and fibrinolysis under short term physical work in healthy men measured using thrombelastograms
06 p0992 A70-17423

Hydrodynamic model of blood coagulation in stagnation point flow, analyzing platelet diffusion, white cell bonding stress and thrombus formation
06 p1003 A70-18123

Adhesive and aggregative properties of blood platelets in rats after beta irradiation linked to activity of serum factor
07 p1207 A70-19474

Empirical formulas derived for intuitive estimates of blood coagulability in patients to facilitate medication dosage prescription
07 p1210 A70-19558

Platelet aggregation in whole blood, basing measurement method on filtration pressure with added adenosine diphosphate (ADP)
07 p1210 A70-19591

Flight stress in Starfighter aircraft pilots related to fibrinolysis activity in blood
09 p1625 A70-23003

Flight stress effect on blood clotting stabilization of Starfighter aircraft pilots, observing no change in thrombocytes number
09 p1625 A70-23005

Prolonged hypodynamia effect on human blood coagulation, noting antihemophilic effect of physical exercise
10 p1815 A70-24678

Pro- and anticoagulants dynamics in rats blood during early phases of prolonged sound effect
12 p2168 A70-27347

Blood coagulation process, investigating thermal effects by microcalorimetry and correlating with thromboelastographic indices
13 p2353 A70-29502

Thrombus formation on foreign surface in fresh blood stagnation point flow, applying fluid mechanical and mass transfer models
17 p3035 A70-34470

Blood platelets aggregation and release reaction in thromboembolic disease due to injury
17 p3032 A70-35471

BLOOD FLOW

Physiological interpretation of blood velocity curves recorded in right heart cavities of dogs by ultrasonic directional probe, using Doppler effect
01 p0035 A70-10709

Transcutaneous Doppler-shift flowmeter for arterial blood velocity measurement by ultrasound
01 p0037 A70-10880

On-line electronic integration of aortic flow during systole to provide beat by beat readout of stroke volume
01 p0038 A70-11044

Perfusion pressure and flow effects on coronary resistance, noting venous blood perfusion
01 p0026 A70-11075

Dogs coronary vasodilator responses to hypoxia and induced tachycardia before and after lidoflazine and adenosine
02 p0230 A70-11702

Muscle force and electromyogram behavior with alteration in blood flow and composition in anesthetized cats
02 p0231 A70-11708

Spinal cord blood flow response to carbon dioxide partial pressure in anesthetized goats
02 p0232 A70-11713

Blood flow changes in portal vein and hepatic artery of anesthetized cats following intraportal and intrahepatic arterial administration of isoproterenol, epinephrine and norepinephrine
02 p0232 A70-11718

Canine aortic flow as function of simultaneous mean aortic and mean right atrial pressures
02 p0233 A70-11723

Oxygen consumption, lactic acid production and mechanical performance of anesthetized dog gastrocnemius muscle with increased blood flow
02 p0235 A70-12090

Capillary blood flow, discussing red blood cells deformation, motion, pressure drop and plasma flow/bolus/ between red cells
02 p0238 A70-12545

Stroke volume formula depending on blood density and viscosity, indicating Hagen-Poiseuille law nonapplicability to ballistocardiography
02 p0248 A70-12681

Posture effect on ballistocardiograms, considering ventricular ejection flow changes
02 p0248 A70-12684

Doppler flowmeter-catheter system to record aortic flow velocity in man during cardiac arrhythmias, considering atrial fibrillation, heart block, etc
02 p0241 A70-12697

Time varying blood flow in pulmonary capillaries affecting overall diffusing capacity and alveolar-arterial oxygen tension gradient
03 p0421 A70-13570

Statistical equation of motion of blood by averaging motion of individual blood elements over small volume, finding constitutive equations
03 p0434 A70-13572

Vascular electrical activity in cats and rats by inserting glass microelectrode into blood vessel, showing blood flow conditioning effect on activity
03 p0422 A70-13691

Cardiac output and coronary blood flow changes in patients at rest and during peak exertion, stating correlation coefficients
03 p0428 A70-14065

Pulsatile flows in living animals and model arteries, discussing flow profiles, instability and wall shear
03 p0430 A70-14244

Blood flow through veins and collapsible tubes simulated by physical model, downstream pressure effect and importance of collapse phenomena
04 p0641 A70-14631

Analog computer cardiovascular system model to simulate pressure and flow events in veins including effects of gravity, collapse, breathing and venous valves action
04 p0641 A70-14632

Blood flow sensors based on electrical conductivity dependence on flow rate, discussing system instrumentation and experimental results
04 p0644 A70-15295

Blood flow velocity and pressure measurements on conscious man with catheter-tip velocity probe
04 p0645 A70-15439

Myocardial blood flow in patients with acute myocardial infarction determined from measuring effective capillary flow (ECF) by direct counting of rubidium 86 uptake
04 p0636 A70-15468

Arterial pressure and suprarenal blood flow in dogs under basal conditions and nerve stimulation by stochastic method using analog correlator
05 p0806 A70-16400

Slope and shape of blood-gas dissociation curve as factor influencing pulmonary gas exchange in presence of ventilation-perfusion inequality
06 p0994 A70-17522

Frequency analysis of arterial sounds used in studying atherosclerosis, correlating spectra with jet flow turbulence past occlusion
06 p1003 A70-18220

Haematocrit variations effect on electromagnetic blood flowmeter sensitivity, discussing blood specific impedance changes
07 p1217 A70-18951

Electromagnetic induction blood flowmeter measuring blood velocity as function of voltage in pick-up electrodes
07 p1217 A70-18952

Increased blood flow resistance caused by red cell membrane shrinking due to plasma surface tension alteration
07 p1203 A70-18999

Cylindrical tubes steady axisymmetric inlet flow at lower Reynolds numbers, applying results to blood vessels entry flow
07 p1205 A70-19244

Blood-endothelial surface shear stress in artery inlet, considering asymmetric and radially symmetric plugging effects
07 p1220 A70-19248

Normal and stenosed aortic valve closure wing measurements in model valve in pulsatile water tunnel showing turbulence generation
07 p1220 A70-19249

Phasic aortic blood flow and left ventricular pressure measured at constant heart rates during pulsus alternans, discussing ejection duration and peak flow rate
07 p1210 A70-19588

Posture change effects on vasodilator responses in humans, studying reactive, postexercise and local heat hyperaemia in forearms of subjects lying and standing
07 p1211 A70-19596

Oxygen uptake by brain as function of oxygen tension in rats using venous outflow method and blood gas analysis
08 p1446 A70-21436

Strong magnetic field effects on squirrel monkeys electrical and mechanical cardiac functions determined from vectorcardiogram and aortic blood flow characteristics
09 p1617 A70-22524

Conscious dogs temporary local hypoxia effect on coronary blood flow regulation
09 p1623 A70-23585

Vertical distribution of pulmonary blood flow (DPBF) in dogs without thoracotomy prone, supine, head-up, head-down and right and left decubitus positions
10 p1810 A70-24004

Sodium balance effect on intrarenal distribution of blood flow in normal man determined with Xe washout method
10 p1810 A70-24005

Physiology of oxygen transport in human organism and genesis of tissue hypoxia, discussing pulmonary functions, blood transport properties and tissue blood flow and diffusion
10 p1821 A70-25077

Pulmonary blood flow direction and distribution in dogs during near vacuum exposure and recompression
11 p1984 A70-25351

Shock waves in unsteady aortic blood flow at systole beginning, considering aorta elastic properties and shock formation distances
11 p1992 A70-26479

Electromagnetic blood flow determination by catheter in external magnetic field, discussing intravascular EM flow sensor capable of percutaneous introduction into vascular system
11 p1993 A70-26663

Indicator dispersion model for cardio-pulmonary system based on continuity past sampling site, observing diffusion coefficient nonlinear increase with blood speed
12 p2174 A70-27019

Canoe paddlers physical training effect on cardiac output and local blood flow and metabolism at and during exercise and recovery
12 p2169 A70-27653

Blood flow redistribution during sustained high skin temperatures of men in supine position

12 p2169 A70-27654

Autonomic effects on heart rate, portal, renal, cutaneous and muscle blood flows during arterial hypoxia in unanesthetized sham operated thalamic and pontine rabbits

12 p2170 A70-27899

Systemic hypoxia effect on renal tubule sodium reabsorption in anesthetized mongrel dogs

[AMRL-TR-69-135] 13 p2353 A70-29435

Implantable EM blood flowmeter errors due to nonsymmetrical blood flow velocity distribution and nonuniform magnetic flux density

14 p2542 A70-30797

Comparative cardiac output measurements in dogs using left/right heart dye injections and pulmonary/aortic electromagnetic flow probes

15 p2688 A70-31434

Intraarterial hot film constant temperature anemometry for point blood velocity measurements, detecting flow reversal

15 p2688 A70-31435

Red cell deformability and flow resistance and blood electrical resistance under low g centrifugation

15 p2680 A70-31700

Miniaturized electromagnetic catheter flowmeter for measuring volume flow rate by potential difference between electrodes

15 p2689 A70-31747

Cardiovascular and circulatory phenomena fluid mechanical aspects emphasizing pulsatile blood flow

15 p2720 A70-31789

Doppler effect pulsed ultrasonic blood flowmeter using transducer alternating as transmitter and receiver

15 p2690 A70-31919

Automatic numerical analysis of velocity information from Doppler effect ultrasonic blood flow meter

15 p2691 A70-31920

Phase shift ultrasonic flowmeter measuring transit time between oppositely propagating waves in blood vessels

15 p2691 A70-31921

Data system obtaining sampling rate for cardiac volume measurement via fast biplane cineangiography

15 p2691 A70-31922

Water and blood flow characteristics in converging-diverging plastic tube, considering implications in occlusive vascular disease

15 p2691 A70-31937

Wave propagation through Newtonian fluid in compressible thick walled viscoelastic tube, considering blood flow in arteries

15 p2691 A70-31938

Comparative arterial pressure pulse transmission velocity in dogs, relating wall elasticity with vascular disease

15 p2682 A70-31939

Mechanical model of arterial viscoelasticity effect on input impedance and wave travel in systematic tree

15 p2691 A70-31941

Air bubble breaking in blood and water flow passage of simulated cardiopulmonary bypass system with flow constriction

15 p2692 A70-32312

High altitude liver function and blood flow, determining bromsulphthalein transport maximum and storage capacity and galactose elimination

15 p2683 A70-32531

Human phasic right ventricular blood velocity, examining respiration, rhythm disturbances and Valsalva maneuver influence by radiotelemetry

16 p2850 A70-33111

Arterial wall nonlinear distensibility effects on blood flow velocity profiles, considering various mathematical and physical artery models

17 p3035 A70-34468

Thrombus formation on foreign surface in fresh blood stagnation point flow, applying fluid mechanical and mass transfer models

[ALAA PAPER 70-787] 17 p3035 A70-34470

Weightlessness and gravitational effects on human pulmonary blood flow distribution, considering optimal gas exchange efficiency

[ALAA PAPER 70-785] 17 p3035 A70-34472

Intermittent forced inspirations or expirations effects on venous tone and blood flow in human skin vessels

17 p3024 A70-34595

Eating and digestion effects on arterial pressure and mesenteric and aortic blood flows in intact unanesthetized dogs

17 p3024 A70-34848

Human cardiac flow during acceleration as function of time with and without anti-g suit, using electric plethysmograph

17 p3040 A70-35915

Analog computer for continuous recording of oxygen consumption of muscular area in canine foot via blood flow rate and oxygen saturation

19 p3367 A70-37354

Thermal electronic instrumentation applied to biological flows including blood flow, cardiac outputs and volumes

19 p3368 A70-37843

Circulating blood volume and heart minute and stroke volumes in rabbits, using isotope-labeled albumin

19 p3366 A70-38724

Visceral blood flow during exercise in sled dogs, testing hypothetical compensatory decrease as cardiovascular reserve for skeletal muscle by biotelemetry

20 p3571 A70-39366

Pulmonary hypertension in congenital heart diseases as function of blood flow

20 p3571 A70-39367

Radio telemetry measurements of blood pressure and flow in unrestrained animals

20 p3579 A70-39370

Electromagnetic blood flowmeters for circulatory research

20 p3579 A70-39371

Ambient near vacuum pressure effect on blood circulation, examining thoracic aorta blood flow, pressures, gas expansion and water vaporization

20 p3576 A70-40326

Hypoxia effects on cerebral blood flow in anesthetized dogs, considering acidosis and vasodilation

20 p3577 A70-40330

Liver blood flow in dogs during increased oxygen consumption

20 p3577 A70-40448

Myocardial blood flow response to cardioacceleration by right atrial pacing in normal subjects, using coincidence counting

21 p3760 A70-40576

Viscous fluid motion equations through anisotropic nonrigid porous solid, discussing blood flow in capillary vessels and extracellular fluid through interstitial space

21 p3768 A70-40776

High resistance thermistor measurements of rapid blood temperature variation, discussing power dissipation effects

21 p3769 A70-41143

ULF ballistocardiogram amplitudes relationship to blood flow velocity for cardiovascular disease diagnosis

21 p3763 A70-41234

Blood velocity in ascending aorta in man by transcutaneous ultrasonic Doppler technique, investigating heart hemodynamic performance and systemic perfusion

21 p3770 A70-41235

Acceleration Bcg dependence on left ventricular ejection flow and properties of vascular system

21 p3763 A70-41237

Algorithm for cardiovascular force computation from phasic regional blood flow and mass motion, interpreting Bcg

21 p3763 A70-41238

Bcg interpretation, discussing degrees of freedom, blood mass displacement, cardiovascular system, etc

21 p3770 A70-41239

Reverse curvature silicon transistor linearizer for hot-wire and thin-film constant temperature anemometers for aorta blood flow velocity measurements

21 p3827 A70-41458

Left ventricular surface electrocardiogram T-wave amplitude and circumflex coronary artery blood flow during headward acceleration in unanesthetized dogs, observing velocity decrease

21 p3764 A70-41481

Human leg blood flow distribution between deep and superficial veins during alternate treadmill work-rest periods

21 p3767 A70-42160

Aortic regurgitated flow estimation by dye injection technique, noting correlation with cineangiography method

22 p3977 A70-42301

Blood flow antagonistic changes in various vascular beds following spinal cord central thermal stimulation attributed to sympathetic vasoconstrictor activity

22 p3971 A70-43405

Potential liquid flow in pulsating bulb applied to blood flow

23 p4155 A70-44847

Regional cerebral cortical blood flow measurement, using heat clearance thermistor probe

23 p4157 A70-45082

Intact human forearms venous blood velocity measurements, using nuclear magnetic resonance techniques

24 p4309 A70-45675

Oxygen transport, arterial resistance and consumption in normovolemic and hypovolemic dogs in hemorrhagic shock

24 p4302 A70-46106

Dynamic response of peripheral blood flow to hypothalamic temperature waveforms in baboon, using implanted thermodes

24 p4303 A70-46116

BLOOD GROUPS

Peripheral blood and structural changes in hemopoietic organs of rabbits and mice exposed to microwave radiation

07 p2126 A70-18730

Beryllium sulfate effect on rabbits vascular plasma volumes, using albumin method for blood groups

15 p2681 A70-31884

Biochemistry of blood group antigens involved in agglutination reactions, discussing effect of proteolytic enzymes on cell membrane structure

21 p3764 A70-41447

BLOOD PLASMA

Acid base responses of arterial plasma of anesthetized man during acute carbon dioxide partial pressure changes, discussing anesthesia effects

01 p0020 A70-10651

Capillary blood flow, discussing red blood cells deformation, motion, pressure drop and plasma flow /bolus/ between red cells

02 p0238 A70-12545

Temperature and hemoglobin concentration effect on oxygen solubility in blood, constructing table for Bunsen solubility coefficients

03 p0428 A70-14156

High altitude acclimatization effects on cardiovascular system, external respiration, blood composition, optical and vestibular analyzers in human subjected to various stresses

04 p0630 A70-14576

Plasma free fatty acid level relationship to acute and chronic exposure to cold in rabbits, rats and humans

04 p0631 A70-14983

Nomograms for correlation of dose to methemoglobinemia or plasma monomethylhydrazine /MMH/ concentration observed on dogs, considering human skin contact evaluation

06 p0992 A70-17298

Increased blood flow resistance caused by red cell membrane shrinking due to plasma surface tension alteration

07 p1203 A70-18999

LF ultrasound not producing irreversible denaturation of blood serum proteins but capable of modifying electrophoretic properties

07 p1206 A70-19470

X ray structural and electrophoretic investigation of donor and fibrinolytic blood protein components, observing crystalline to amorphous transition in blood serum and plasma lyophilization

09 p1621 A70-23149

Thyroid gland function following radiation injury by measuring plasma protein bound iodine in irradiated rat blood

09 p1621 A70-23150

Plasma viscosity and aggregation effects on whole-blood viscosity investigated in observation chamber for erythrocyte aggregation

09 p1622 A70-23546

Blood lactate changes during prolonged exhaustive running at varied intensities and durations

10 p1809 A70-24001

Maximum isovolemic hemodilution by volume substitution determined by plasma expanders infusion in dogs

10 p1821 A70-25083

Blood serum enzyme activity in rats during prolonged hypokinesia, noting increase of aminotransferases

13 p2351 A70-29329

Nine-alpha-fluorohydrocortisone preventing bedrest induced orthostatism, considering plasma volume decrease effects on cardiovascular performance

13 p2358 A70-29433

Resting concentrations of fibrinogen, plasminogen and levels of euglobulin fibrinolytic activity, plasmin inhibitors and urokinase in blood in inactive and exercising men

13 p2356 A70-29942

Beryllium sulfate effect on rabbits vascular plasma volumes, using albumin method for blood groups

15 p2681 A70-31884

Blood plasma and red cell volumes simultaneous measurement in native group living at high altitude

15 p2684 A70-32537

Organic solutes diffusion in stagnant blood plasma and red cell suspensions, using models from transport theory

15 p2686 A70-32847

Plasma free fatty acids and glucose relative role in contribution to metabolic state and energy production in partially hepatectomized rats

16 p2850 A70-34319

Blood glucose and plasma immunoreactive insulin concentrations before, during and after intermittent short duration maximal exercise and glucose infusion

17 p0300 A70-35420

Chloride ion shift of respiration occurring between plasma and erythrocytes as function of carbon dioxide, using rapid filtration method

19 p3364 A70-38366

Portable battery operated system for rapid measurements of blood plasma electrolytes during aeromedical evacuation

20 p3579 A70-39433

Water and salt metabolism changes during prolonged hypokinesia of rabbits, noting blood plasma dilution, hematocrit number and hemoglobin concentration reduction, etc 23 p4146 A70-44656

BLOOD PRESSURE

NT HYPERTENSION
NT HYPOTENSION
NT SYSTOLIC PRESSURE

Arterial pressure pulse waves mathematical analysis applied to variations in stroke volume in anesthetized dogs subjected to spine-to-breast accelerations 01 p0012 A70-10125

Male macaque monkey physiological deterioration in Biosatellite 3, noting falling brain temperature, lowered central venous pressure, fluid loss, blood redistribution into visceral pools, etc 01 p0023 A70-10822

Perfusion pressure and flow effects on coronary resistance, noting venous blood perfusion 01 p0026 A70-11075

Canine aortic flow as function of simultaneous mean aortic and mean right atrial pressures 02 p0233 A70-11723

Capillary blood flow, discussing red blood cells deformation, motion, pressure drop and plasma flow /bolus/ between red cells 02 p0238 A70-12545

Ballistocardiogram force envelopes and pulse pressure relationship, noting perturbation of viscoelastic networks coupling cardiovascular system to ballistic bed 02 p0240 A70-12678

Phasic phrenic nerve electrical activity relation to systemic blood pressure oscillations produced in paralyzed dogs by ventilation arrest or hemorrhage 03 p0416 A70-13010

Acceleration component in pelvis to head direction found influencing hyperemia of brain at various g forces 04 p0630 A70-14579

Analog computer cardiovascular system model to simulate pressure and flow events in veins including effects of gravity, collapse, breathing and venous valves action 04 p0641 A70-14632

Polymethylene-bis-lepidine dibromides effect on blood pressure and peripheral vessel tonus in dogs, analyzing depressor reaction as function of binding chain 04 p0632 A70-15204

Arterial pressure and suprarenal blood flow in dogs under basal conditions and nerve stimulation by stochastic method using analog correlator 05 p0806 A70-16400

Blood pressure indirect recording using ceramic crystal pick-up over brachial artery and under pneumatic cuff 06 p0992 A70-17299

Ventilation function, pulse rate and blood pressure measured for adaptation to vertical upright and head-down positions 07 p1201 A70-18794

Phasic aortic blood flow and left ventricular pressure measured at constant heart rate during pulsus alternans, discussing ejection duration and peak flow rate 07 p1210 A70-19588

Screen filtration pressure of human blood, establishing time, anticoagulant, red cells, platelets and leucocytes as physical determinants 07 p1210 A70-19590

German monograph on determination of blood velocity, pressure, pulse rate and vascular structure parameters using Doppler effect 08 p1452 A70-21297

Venous pressure of man in space, investigating return to heart in absence of gravity and distention by hydraulic pressure 08 p1448 A70-21943

Blood pressure variations resulting in permanent irreversible hypertonia in air force pilots subjected to repeated stress situations and emotional irritations 09 p1626 A70-23011

Diastolic and systolic pressure measurement in acute and chronic experiments 09 p1627 A70-23302

Arterial oscillograms, pressure and heart beat rate during prolonged hypodynamia, noting neurocirculatory dystonia 10 p1817 A70-24693

Chronic hypoxia exposure effect on development and maintenance of renal hypertension in rats 14 p2539 A70-30956

Sleep intensity and stages from EEG studies concerning rapid eye movements, vegetative nervous system, heart/respiration rate, blood pressure, body temperature and stomach motility 15 p2680 A70-31743

Phase errors of hydraulic input impedance of arterial bed due to proximal or distal pressure measurements 15 p2682 A70-31940

Heart rate elicitation and blood pressure increase, considering parasympathetic and sympathetic nervous

outflows adjustments of initial cardiovascular response to muscular contraction 15 p2684 A70-32535

Positive pressure breathing effects on cerebral blood pressure and catecholamine content of hypothalamus and adrenal glands in dogs 16 p2849 A70-33997

Eating and digestion effects on arterial pressure and mesenteric and aortic blood flows in intact unanesthetized dogs 17 p3024 A70-34848

Arterial pressure measurement by automatic control system based on external compression pressure for maximum amplitude intraarterial pressure pulse oscillations 19 p3370 A70-38215

Dynamic intravascular pressures measured in small vessels of frog lung using micropressure transducer inserted into vessel lumen 19 p3364 A70-38368

Radio telemetry measurements of blood pressure and flow in unrestrained animals 20 p3579 A70-39370

Human body elastic properties effects on arterial pressure measurement by sphygmomanometer 20 p3581 A70-39879

Ambient near vacuum pressure effect on blood circulation, examining thoracic aorta blood flow, pressures, gas expansion and water vaporization 20 p3576 A70-40326

First derivative of ventricular pressure recorded by conventional cardiac catheters, analyzing in terms of Fourier series 21 p3767 A70-40578

Ethanol ingestion effect on human response to submaximal and maximal exercise, measuring cardiac output and intraarterial pressure 21 p3761 A70-41135

Cardiac glycosides and beta receptor blocking agent effect on ULF displacement ballistocardiogram in healthy young men, measuring heart rate and blood pressure 21 p3763 A70-41227

Systolic and diastolic pressure in central artery of retina in deep-sea divers during oxygen inhalation at atmospheric pressure 23 p4150 A70-45081

Indirect blood pressure measurements using motion artifact suppression circuit based on K-sound electrocardiography 24 p4296 A70-45335

Neurogenically maintained blood pressure component, discussing autonomic nervous system activity in hypertension and normotension, sympatholytic agents effectiveness in hypertensive treatment, etc 24 p4299 A70-45805

HF sinusoidal fluid pressure generators driven by electromagnetic vibrators for arterial applications 24 p4309 A70-46118

BLOOD VESSELS

NT AORTA
NT ARTERIES
NT CAPILLARIES [ANATOMY]
NT VEINS

Vascular electrical activity in cats and rats by inserting glass microelectrode into blood vessel, showing blood flow conditioning effect on activity 03 p0422 A70-13691

Book on engineering in heart and blood vessels stressing technological aspects of artificial internal organs 06 p1001 A70-17649

Cylindrical tubes steady axisymmetric inlet flow at lower Reynolds numbers, applying results to blood vessels entry flow 07 p1205 A70-19244

Aeromedical significance and pathophysiological mechanisms of clinical entities mimicking vasovagal syncope 08 p1454 A70-21946

Perivascular pH influence on arteriolar diameter on brain surface of anesthetized rats and cats by micropipette technique 12 p2168 A70-27623

Dynamic intravascular pressures measured in small vessels of frog lung using micropressure transducer inserted into vessel lumen 19 p3364 A70-38368

Blood vessels constriction in rear limbs, small intestine and spleen of dog with arterial blood heated above rectal temperature 20 p3574 A70-40173

Structure and function of juxtaglomerular apparatus of kidneys controlling synthesis and secretion of renin 24 p4305 A70-46392

BLOWDOWN WIND TUNNELS

60 cm intermittent blowdown type trisonic wind tunnel, discussing main parts basic dimensions and characteristics determination method, detailing design and construction 01 p0055 A70-10148

Local skin friction measurement on model in blowdown hypersonic wind tunnels using floating element transducer, giving results for flat plate and wedge [ONERA-TP-756] 03 p0463 A70-13629

Rotovale induced flow angle variations associated with data repeatability and scatter in blow down wind tunnels at transonic speed 13 p2385 A70-29888

Intermittent blowdown supersonic wind tunnel as economic test facility covering subsonic test velocity range, discussing data quality [AIAA PAPER 70-581] 13 p2342 A70-29889

BLOWERS

Turboblowers and compressors air tests for gas operation performance prediction 06 p1129 A70-17136

Comparative load capacity of disk models of natural gas blowers of different designs under plastic strain 23 p4232 A70-43941

BLOWING

Air cooling with radial and jet blowing on gas turbine stage, discussing influence on aerodynamic characteristics 03 p0551 A70-13486

Blowing intensity influence on turbulent boundary layer of incompressible fluid and friction drag of flat plate 06 p1036 A70-17852

Massive blowing effect on stagnation point radiative energy transfer of ablative heat shield during planetary entry at hypersonic velocities [AIAA PAPER 70-203] 06 p0971 A70-18101

Flow properties and heat transfer of wall jet spreading over permeable surface with suction and blowing 07 p1258 A70-19720

Massive blowing from porous cone with embedded shock wave in supersonic flow, assuming inviscid and conical injected flow field 09 p1662 A70-23216

Flat plate laminar boundary layer blowoff due to wall injection analyzed by parameter matched asymptotic expansion 10 p1862 A70-23844

Two dimensional film cooled turbine blade aerodynamics, investigating massive blowing effect through discrete holes in single blade test facility [AIAA PAPER 70-713] 16 p2834 A70-33537

High lift airfoils boundary layer separation suppression by blowing, describing wall jets streamline development prediction methods [AIAA PAPER 70-872] 17 p3010 A70-34818

Flow field model for large surface blowing problem accounting for upstream and downstream effects with large rate normal injection near trailing edge 20 p3559 A70-40110

Flat plate boundary layer flow with surface blowing and suction /mass transfer/, investigating stability by numerical techniques 20 p3615 A70-40507

Linear corrections formulas for shear stress and heat transfer coefficients associated with boundary layer blowing in binary gas mixture 21 p3748 A70-42207

Wing lift increase by spanwise blowing along upper surface, causing flow reattachment on wing and vortex induced effective aerodynamic camber increase [ICAS PAPER 70-09] 23 p4132 A70-44120

Flat plate film cooling efficiency behind tangential slot at blown-main flow velocity ratio over three 23 p4283 A70-44741

BLUE GREEN ALGAE

NT NOSTOC

Biochemical characteristics, nitrogenase activity and nitrogen fixation in heterocysts of blue green algae 01 p0024 A70-10894

Spacecraft level vibrations and gravity effects on blue-green algae Plectonema Boryanum proposed as gas exchange medium 06 p0999 A70-17292

Amino acid composition of protein in blue green algae Stratonostoc Linckia 14 p2540 A70-30158

Pigments absence in photosystem II of photosynthesis in heterocysts of blue-green algae 23 p4148 A70-44870

BLUE STREAK LAUNCH VEHICLE

Optimum second stage sizes for Blue Streak first stage for maximum payload injection into various orbits, tabulating sizes and payloads 05 p0924 A70-16589

BLUFF BODIES

Wake behind axisymmetric bluff body in steady laminar flow, noting role of Reynolds number 04 p0619 A70-15392

Free recirculation areas in wake of flame holders used for flame stabilization at bluff bodies in supersonic flow 06 p0965 A70-17244

Base bleed fluid injection effect on steady separated flow past two dimensional bluff body, studying streamline pattern near object 06 p0967 A70-17518

Turbulent flames bluff-body stabilization model, measuring recirculation zone concentrations and temperatures for methane and propane-air mixtures 10 p1967 A70-24092

BLUNT BODIES

Boundary layer around blunted cone solved numerically by finite difference method 01 p0001 A70-10297

Flow about blunted wedge with laminar boundary layer at stagnation point and approaching Falkner-Skan flow at infinity, discussing asymptotic behavior
01 p0061 A70-10540

Blunt and conical body optimum heat shield shapes for Jupiter atmospheric entry, noting shallow flight path
[AIAA PAPER 68-1150] 01 p0195 A70-10827

Stagnation point velocity gradients for spherical segment models with bluntness ranging from hemisphere to flatnose cylinder in hypersonic flow
03 p0406 A70-12947

Explosion analogy to study hypersonic flow region behind shock wave including boundary layer at blunt body surface
03 p0406 A70-13332

Approximate solution for hypersonic inviscid flow around spherically blunted bodies at small angle of attack, noting stagnation problems
03 p0407 A70-13547

Supersonic unsteady state three dimensional flow around blunted bodies with detached shock wave
03 p0409 A70-13864

Similarity laws in hypersonic flow of real gas around slender blunted bodies, particularly bodies with rough lateral surface
03 p0409 A70-13866

Axisymmetric and three dimensional gas flow around blunt bodies using numerical methods, discussing finite difference algorithms for gas dynamic equations
03 p0410 A70-14251

Hypersonic flow over blunt bodies, discussing Mach number, specific heat and blast wave limits
04 p0613 A70-14454

Numerical analysis of near equilibrium flow regions in chemically relaxing gas mixtures past blunt bodies at supersonic speeds
04 p0666 A70-14603

Hypersonic blunt body heat transfer prediction, including coupled effects of real gas behavior and slip boundary conditions
[ASME PAPER 69-WA/HT-28] 04 p0614 A70-14809

Axisymmetric radiating flow behind paraboloidal shock in ideal inviscid gas hypersonic stream, using differential approximation method for blunt body solution
04 p0669 A70-14937

Difference methods application to supersonic gas flow past blunt body and unsteady axisymmetric flow past body of unspecified configuration, analyzing stability
04 p0670 A70-14957

Hypersonic flow region about ducted blunt bodies of revolution, assuming correspondent flow conditions to maximum intake through duct
04 p0617 A70-15233

Unsteady pressure at slender blunt body surface in three dimensional hypersonic gas flow
04 p0618 A70-15244

Scaling laws for nose bluntness effects on hypersonic aerodynamics of bodies of revolution
[AIAA PAPER 68-1158] 04 p0620 A70-15530

Viscous shock layer at hypersonic blunt body stagnation point, applying finite difference and nonlinear overrelaxation methods to seven species air model
04 p0620 A70-15539

Real gas properties effect on base pressure of blunt nosed vehicle flying through atmosphere at high velocities
04 p0764 A70-15556

Hypersonic near wake, discussing correlations from optical studies, laminar near wake, blunt body and turbulent wake measurements
05 p0790 A70-16120

Drag reduction on blunt-based body of revolution with boat-tailed afterbodies in low speed flow
05 p0790 A70-16501

Slender wing with blunted leading edge to reduce thermal stresses at supersonic speed studied for aerodynamic characteristics in hypersonic flow
05 p0791 A70-17001

Frictionless hypersonic flow around blunt bodies of revolution, taking into account real gas effects in equilibrium and frozen flow calculations
06 p0965 A70-17242

Laminar hypersonic blunt cone wakes, discussing flow fields and axial static pressure distributions
06 p0968 A70-17553

Inviscid hypersonic blunt body flow of hydrogen-oxygen mixtures in shock layer stagnation region
06 p0968 A70-17555

Melting ablation for two dimensional and axisymmetric blunt bodies with body force, predicting gas-liquid interface temperature for free stream conditions
06 p1176 A70-17690

Nose bluntness, angle of attack and oscillation amplitude effect on hypersonic unsteady aerodynamics of slender cones
[AIAA PAPER 70-216] 06 p0969 A70-18059

Viscous radiating flowfield coupled with ablation for computations on blunt body entering earth atmosphere at interplanetary return velocities
[AIAA PAPER 70-128] 06 p0970 A70-18090

Pressure distributions prediction on blunt bodies at angle of attack, considering bodies of revolution and large angle cones
[AIAA PAPER 70-208] 06 p0971 A70-18104

Knudsen iteration for predicting cooled blunt body near free molecular drag in hypersonic stream, using BGK model for collisions
06 p0979 A70-18313

Density field around leading edge of blunted flat plate, using electron beam measurements in low density hypersonic wind tunnel
06 p0980 A70-18351

Cone bluntness effect on merging onset and downstream flow in merged region at Mach 8 and various Reynolds numbers
06 p0980 A70-18352

Drag coefficients of sharp and blunt cones in rarefied supersonic flow for bluntness ratios and angles of attack
06 p0981 A70-18360

Flow field measurements upstream of axisymmetric blunt body in rarefied hypersonic flow used to investigate merging between bow shock and boundary layer
06 p0983 A70-18372

Stagnation point heating in hypersonic gas flow past blunt bodies, considering radiative transfer effects on shock wave temperature and density distribution, wave separation, etc
06 p0985 A70-18557

Aerodynamic heating of blunt-nosed reentry bodies noting effects of angles of attack
[DGLR-69-0401] 07 p1392 A70-18983

Asymptotic behavior of inviscid radiating gas flow near stagnation point of blunt body
07 p1188 A70-19315

Hypersonic flow past blunted cylinder at Mach number of infinity, investigating real gas effect using Lighthill ideal dissociating gas model
08 p1431 A70-20646

Aerodynamic coefficients for blunt cones in rarefied gas calculated as functions of angle of attack using empirical formulas
08 p1432 A70-21092

Interaction between bodies and spherical detonation wave, measuring force pulse transfer to immobile cylinder and flow patterns past flying blunt body
09 p1659 A70-22186

Aerodynamic heating of blunt bodies, investigating dependence of hypersonic limit distribution on Mach number
09 p1603 A70-22419

Shock layer thickness in supersonic inviscid gas flow past blunt bodies, calculating boundary layer near stagnation point
09 p1603 A70-22442

Aerodynamic characteristics of cooled blunt spherical bodies in low density hypersonic gas flow, discussing heat flux representation for different body surface temperatures
09 p1604 A70-22447

Slender body approximation for shape determination of nonslender hypersonic body of revolution with minimum convective heat transfer rate
09 p1788 A70-22931

Navier-Stokes equations for laminar near wake of blunt based body, obtaining numerical solutions for adiabatic and constant wall temperatures
09 p1605 A70-23176

Wake source model for two dimensional incompressible potential flow past bluff body, considering pressure distribution, flow separation, wake width, etc
09 p1607 A70-23681

Blast wave eigenvalues in asymptotic expansions approximation for hypersonic flows past blunt bodies
10 p1797 A70-23953

Initial blast wave axisymmetric shock-on-shock interaction for blunt bodies moving supersonically at zero angle of attack solved in Taylor series
10 p1797 A70-23954

Inverse blunt body problem using integral relations method assuming inviscid axisymmetric hypersonic gas flow
10 p1798 A70-24116

Shock wave and gas flow structure at constant Mach number past three dimensional blunt bodies, applying method for unsteady flow
10 p1799 A70-24127

Wind tunnel study of entropy extremum upon critical streamline in supersonic three dimensional flow past blunt bodies at zero angle of attack
10 p1800 A70-24131

Plane shock wave interaction with supersonic blunt body, considering pressure-time studies for stagnation point of flow
10 p1801 A70-24145

Vibrational and dissociation relaxation effects on plane shock wave structure and supersonic flow around blunt bodies
10 p1801 A70-24150

Rarefied hypersonic axisymmetric blunt body, examining bow shock and viscous layer upstream merging
10 p1804 A70-24823

Gasdynamic functions of supersonic flow past spherically and ellipsoidally blunted inverted cones
11 p1973 A70-25522

Blunted spherical shells stability under hydrostatic pressure by reducing equilibrium equations to differential
12 p2322 A70-27333

Vibrational relaxation effect on supersonic flow past nose section of blunted body
12 p2159 A70-28231

Radiant shock layer in hypersonic air flow past blunt bodies, showing effects on temperature field and density
12 p2159 A70-28245

Electromagnetic shock tube demonstrations of electrode spark breakdown, strong shock behavior, plasma conductivity and hypersonic shock flow over blunt body
13 p2404 A70-28623

Blunt heat shield effectiveness for trailing payload in reentry capsules, discussing dynamic instability effect
[AIAA PAPER 70-563] 13 p2341 A70-29028

Transonic static and dynamic stability of large angle spherically blunted high-drag cones
[AIAA PAPER 70-564] 13 p2341 A70-29029

Blunt planetary entry body free fall drop tests determining low speed stability and base pressure characteristics
[AIAA PAPER 70-577] 13 p2342 A70-29892

Laminar near wake flow field of two dimensional adiabatic circular cylinder with surface mass transfer
[AIAA PAPER 69-67] 13 p2343 A70-29951

Viscous shock layer equations of laminar hypersonic flow past blunt body at moderate to high Reynolds numbers
13 p2343 A70-29952

Cone boundary layer transition location and Reynolds number as function of nose bluntness combined effect with Ar, air and He mass injection
[AIAA PAPER 69-706] 13 p2343 A70-29954

Surface pressure and heat transfer over blunt conical body in hypersonic flow with uniform mass addition of various gases
[AIAA PAPER 69-716] 13 p2523 A70-29977

Blunt base heat transfer in axisymmetric supersonic separated flow in axisymmetric near wake tunnel, comparing to previous data
13 p2523 A70-29989

Unsteady incompressible laminar boundary layer equations solution after Crocco transformation by implicit finite difference scheme for flow around blunt body
14 p2528 A70-30290

Explosion analogy to study hypersonic flow region behind shock wave including boundary layer at blunt body surface
14 p2528 A70-30711

Viscous gas hypersonic flow past blunt nosed bodies based on Navier-Stokes equation
15 p2671 A70-31481

Finite difference algorithm for supersonic three dimensional steady flow past blunt bodies with generating line bends, allowing for gas equilibrium and frozen states
15 p2671 A70-31495

Internal shock waves in axisymmetric flowfield of perfect gas past blunted cone, noting roles of Mach number and cone half angle
15 p2672 A70-31592

Laminar heat transfer to blunted wedge with constant wall temperature, describing energy field in boundary layer by analytic solution
15 p2825 A70-31818

Laminar compressible boundary layer similar solutions for axisymmetric blunt body, considering viscosity and density variations
16 p2833 A70-33123

Supersonic and hypersonic gas flow past blunt bodies, using finite difference and integral relation methods
16 p2890 A70-33244

Supersonic flows past two dimensional blunted bodies, using method of ascertainment
16 p2833 A70-33248

Book on aerodynamics of bodies of revolution covering hypersonic flow parameters effects, method of characteristics, slender body drag, blunt bodies, rarefied gas aerodynamics, etc
16 p2834 A70-33271

Flow structure in wake of blunt bodies placed perpendicular in parallel airstream determined from hot-wire anemometry
[AIAA PAPER 69-746] 16 p2838 A70-33876

Boundary layer to wake bleed venting for flare-induced separation prevention in hypersonic flow over blunt bodies
16 p2838 A70-33884

Time asymptotic solutions for hypervelocity blunt body flow field with coupled nongray radiation, treating shock as discrete surface
[AIAA PAPER 70-865] 16 p2999 A70-33908

Viscous absorbing emitting shock layer in blunt body stagnation region, calculating skin friction and radiative heat transfer
[AIAA PAPER 70-868] 16 p2999 A70-33911

Transonic flow around perpendicular plate, determining front side velocity and pressure from known stagnation point and transonic region
16 p2839 A70-34236

Axisymmetric detached shock preceding blunt body immersed in hypersonic monatomic gas flow, considering radiative ionization in cold precursor by differential approximation
16 p2839 A70-34252

Hypersonic flow of chemically reacting binary mixture of oxygen atoms and molecules past blunt body, presenting viscous shock layer equations and slip boundary conditions
[AIAA PAPER 70-805] 17 p3005 A70-34458

Blunt based right circular cylindrical body at subsonic speed, investigating turbulent near wake in wind tunnel
17 p3006 A70-34463

Axisymmetric blunt base cylindrical body with turbulent initial boundary layer, investigating flow structure in annular nozzle wind tunnel
[AIAA PAPER 70-796] 17 p3006 A70-34464

Wedge and cylinder high supersonic wakes stability and transition at various Reynolds numbers
17 p3006 A70-34465

Hypersonic flow of shock heated plasma past axisymmetric blunt body and onboard magnetic source, using numerical method
17 p3008 A70-34491

Plasma diagnostic data from onboard Langmuir probes, reflectometers, antenna VSWR and beacon and telemetry attenuation for blunt body reentry flow field
[AIAA PAPER 70-756] 17 p3008 A70-34495

Nonequilibrium air ionization in hypersonic viscous shock layers in flow about axisymmetric blunt bodies
17 p3008 A70-34501

Time dependent solution for inviscid hypersonic flow of chemically reacting gas mixture about blunt bodies
[AIAA PAPER 70-771] 17 p3009 A70-34502

Shock wave and viscous layer structures ahead of blunt body in rarefied hypersonic flow, using continuum theory
17 p3009 A70-34698

Nonadiabatic self absorbing radiative flow of gray gas around sharp cornered blunt body at hyperbolic speed by integral relations method
17 p3010 A70-34974

Adiabatic and chemically inactive hypersonic continuum flow around blunt body, analyzing flow field
17 p3010 A70-35036

Blunt nose effects on drag of flared conical body in supersonic flow, considering pressure loss through shock wave and vorticity
17 p3196 A70-35237

Supersonic axisymmetric flows past bell-shaped bodies of varying bluntness, using Godunov finite difference method
17 p3012 A70-35887

Aerodynamic characteristics of transonic and supersonic blunt vehicles, reviewing numerical methods
17 p3012 A70-35895

Nonequilibrium gas states evolution in detached wave front of hypersonic blunt body, comparing vibrational relaxation in free flight and wind tunnel flow
18 p3335 A70-35962

Unperturbed atmospheric parameters calculation from surface measurements of blunt body at hypersonic speeds under various aerodynamic conditions
18 p3247 A70-36181

Hypersonic gas flow around blown plane of segmentally blunted cones at large angle of attack, using two dimensional model
18 p3206 A70-36258

Viscous hypersonic flow around nonslender bodies with mass supply at small Reynolds numbers, using thin shock layer model
18 p3206 A70-36259

Nonuniform external flow near blunt body stagnation point in diverging hypersonic thin shock layer
18 p3206 A70-36267

Equivalent bodies of revolution method extension for use in semiempirical approximation technique, calculating pressure distribution of nonaxisymmetric blunt bodies
18 p3208 A70-36569

Nonequilibrium ionized hypersonic flow over blunt body at low Reynolds number, using thin shock layer assumption in analysis
18 p3208 A70-36689

Nonequilibrium processes and body geometry as stagnation point conditions in blunt body inviscid flow
20 p3557 A70-39355

Spinning blunt entry vehicles dynamic stability tests in terminal regime, discussing dependence on angle of attack
[AIAA PAPER 70-988] 20 p3714 A70-39541

Stagnation point heat transfer coefficient to elliptical model taking into account pressure, model blunting and diameter, Mach number, etc
20 p3737 A70-39699

Spike effect on nose drag and static stability of blunt bodies, estimating optimum length for drag reduction at zero angle of attack
20 p3558 A70-39702

Laminar viscous effects over blunt cones at hypersonic conditions, taking into account first and second order boundary layer theories
20 p3559 A70-40285

Axisymmetric detached shock before blunt body in hypersonic monatomic gas flow, obtaining radiative ionization patterns in cold precursor
21 p3950 A70-41731

Thin radiating shock layer about axisymmetric blunt bodies, investigating energy-momentum transport coupling
21 p3950 A70-41746

Sphere and axisymmetric body with spherical blunting in low density gas flow, measuring local heat transfer flux
21 p3748 A70-42218

Internal shock waves in axisymmetric flow field of perfect gas past blunted cone, noting poles of Mach number and cone half angle
23 p4133 A70-44276

Heat transfer and shock wave shapes about blunt slender cones in viscous-inviscid coupling hypersonic flow
23 p4134 A70-44569

Radiative energy transfer during interaction between blunt body and hypersonic gas flow, noting effect on flow temperature, shock wave separation, etc
23 p4136 A70-45020

BLUNTNES
U ELLIPTICITY
BLURRING
Ground terrain blurring during aircraft flight at low altitude and high speed, calculating theoretical blur zone
07 p1220 A70-19285

Optimal photometric data processing for planetary characteristics and surface details, considering errors due to image blurring in telescope
07 p1384 A70-19419

Image processing for motion blur removal, discussing methods for measuring degradation and filter design for image restoration
09 p1688 A70-23773

Laser-light spatial-domain scanning function for deconvolution of blurred photographs using point-spread and holographic Fourier transform division filter
11 p2050 A70-25832

Spatial domain deconvolution by laser scanning of blurred photographs, using holographic Fourier transform division filter and photoelectric integration
12 p2230 A70-26979

Blurred photographic image restoration by combining computer generated holographic phase and photographic amplitude filters
12 p2230 A70-26981

Human eye accommodation system, discussing blur detection on retina
13 p2360 A70-29671

Holographic technique to record hypervelocity projectile with front light resolution, discussing image blurring
15 p2736 A70-32031

Photographic image deblurring method, using image forming holograph and amplitude weighting transparency
22 p4042 A70-43670

BO-105 HELICOPTER
Bolkow BO-105 twin turbine rigid rotor helicopter flight tests
08 p1437 A70-21731

BOATTAILS
Cylindrical afterbody drag reduction in transonic flow by combined gas ejection and boat-tailing
11 p1976 A70-25991

Minimum-drag boattail configurations optimization for supersonic flow, determining wave drag coefficients
22 p3961 A70-42714

BODIES OF REVOLUTION
NT CELESTIAL SPHERE
NT CONICAL BODIES
NT CYLINDRICAL BODIES
NT PARABOLIC BODIES
NT POINCARÉ SPHERES
NT ROTATING CYLINDERS
NT ROTATING SPHERES
NT SLENDER CONES
NT SPHERES
NT TORUSES
Thin shells of revolution torsional vibration including bending terms and thickness considerations
01 p0205 A70-11142

Carrying capacity of shells of revolution obtained with threads spun around metallic shell, including stresses during spinning process
01 p0210 A70-11414

Spinning top motion stability in homogeneous incompressible ideal resting fluid, using stability derivative for body of revolution
01 p0145 A70-11438

Symmetrical body rotational motion with asymmetrical mass distribution about center of mass, determining minimum initial value of angular velocity
01 p0192 A70-11482

Axisymmetrical stress-strain state of body of revolution with complex cross sectional geometry under surface loads, deriving computer algorithm for numerical analysis
02 p0384 A70-11665

Kerr physical optics formula usefulness for calculation of radar reflectivity of metallic bodies of revolution in terms of electric and magnetic dipoles
02 p0262 A70-12598

Shells of revolution having arbitrary stiffness distribution and subjected to arbitrary loads and temperatures
03 p0583 A70-12916

Zero-moment theory boundary value problem of shells of revolution with negative curvature under tangential static and geometrical conditions imposed on ends
03 p0589 A70-13337

Approximate method of boundary perturbation to solve elasticity and viscoelasticity problems for non-canonical bodies of revolution applied to stress concentration at ellipsoidal cavity
03 p0591 A70-13439

Stress-strain state of body of revolution having transversely isotropic elastic properties, using perturbation technique
03 p0591 A70-13441

Backscattering cross sections of metallic bodies of revolution, analyzing statistically echo pattern of complex targets
03 p0452 A70-14225

Thin shells of revolution plastic collapse under axisymmetric loads on basis of Tresca-Nakamura yield criterion, using computer algorithm
03 p0598 A70-14238

Asymptotic form of axisymmetric solution with Dirichlet integral for Navier-Stokes equations applied to flow past bodies of revolution with smooth surfaces
03 p0471 A70-14303

Surface singularities method for calculating incompressible potential flow about bodies of revolution with arbitrary thickness ratio and angle of attack
03 p0410 A70-14322

Natural circular frequencies of small axisymmetric vibrations of shells of revolution of arbitrary shape, using Rutishauser algorithm for eigenvalues
04 p0767 A70-14525

Thin elastic revolving shells free axisymmetric oscillations by determining differential equations eigenvalues and eigenfunctions
04 p0768 A70-14604

MHD Stokes flow for magnetized bodies of revolution, rotating with steady motion in viscous conducting fluid at rest at infinity
04 p0726 A70-14615

Boundary layer equations for axial laminar and turbulent incompressible flows over slender bodies of revolution solved by finite difference method
[ASME PAPER 69-WA/FE-2] 04 p0667 A70-14786

Boundary layer transition limits at high Mach numbers, discussing transition on flat plate and bodies of rotation and Reynolds number
04 p0672 A70-15177

Hypersonic flow region about ducted blunt bodies of revolution, assuming correspondent flow conditions to maximum intake through duct
04 p0617 A70-15233

Scaling laws for nose bluntness effects on hypersonic aerodynamics of bodies of revolution
[AIAA PAPER 68-1158] 04 p0620 A70-15530

Geometrically linear anisotropic shell deformation under transverse shear applied to stability analysis of orthotropic shells of revolution sustaining axisymmetric stresses
05 p0933 A70-16212

Stressed state of shallow spherical shells of revolution undergoing large displacements reduced to Kármán equation, solved by small parameter method
05 p0935 A70-16235

Stability and critical load algorithm for flexible shallow spherical and conical shells of revolution derived from variational equation
05 p0935 A70-16236

Revolving shells local stability developing boundary effect under normal and bending external loads solved by computer program
05 p0935 A70-16237

Drag reduction on blunt-based body of revolution with boat-tailed afterbodies in low speed flow
05 p0790 A70-16501

Finite element method analysis of axisymmetrically loaded thin shells of revolution, considering non-

linearity due to material properties and shell geometry changes

05 p0944 A70-16812

Digital computer program for analyzing axisymmetrically loaded ring-stiffened segmented composite elastic shells of revolution, giving vibration frequencies

05 p0944 A70-16814

Lower bound limit analysis of symmetrically loaded thin shells of revolution having arbitrary meridional profiles, demonstrating methods for pressure vessel problems

05 p0944 A70-16815

Axisymmetric deformation of shells of revolution with variable thickness solved by asymptotic method in form of higher Fourier series harmonics

05 p0945 A70-16853

Potential flow over rocket contour containing bends calculated by polygonal distribution of singularities on axis of body of revolution, determining friction effects

06 p0964 A70-17239

Frictionless hypersonic flow around blunt bodies of revolution, taking into account real gas effects in equilibrium and frozen flow calculations

06 p0965 A70-17242

Liquid propellant rocket nozzle configurations maximum stress and stability limits using computer program for composite ring-stiffened shells of revolution [AIAA PAPER 70-138]

06 p0104 A70-18053

Nonlinear aerodynamic moments for arbitrary motions of bodies of revolution in free flight

[AIAA PAPER 70-205] 06 p0971 A70-18102

Flow model for steady axisymmetric vortex system shed from slender body of revolution in coning motion

[AIAA PAPER 70-52] 06 p0971 A70-18118

Stability derivatives for bodies of revolution at subsonic and transonic speeds

[AIAA PAPER 70-190] 06 p0976 A70-18239

Stress-strain state equations for axisymmetrically loaded shells of revolution made of materials with variable moduli

07 p1399 A70-18660

Three dimensional boundary value problems for bodies of revolution rotating in fluid at rest and for bodies at rest in rotating fluids

07 p1252 A70-18709

Cylindrical shell of revolution stress-strain state calculated during shaping in stamp with unclamping dies

07 p1292 A70-18836

Equations for general shells of revolution reduced to simultaneous fourth order ordinary differential equations for stress and displacement functions

07 p1401 A70-18892

Revolving shallow shells steady creep equations solved by approximation adaptable to computer

07 p1402 A70-19051

Integration by orthogonalizations of envelopes of revolution loaded asymmetrically, introducing boundary conditions and structure discontinuities

07 p1404 A70-19128

Segmented elastic shells of revolution supported by rings, studying buckling and vibration by matrix method

07 p1405 A70-19257

Filament wound bodies of revolution manufacture with consideration for linear and nonlinear winding, analyzing mechanically and electronically controlled machines

07 p1295 A70-19765

Natural vibration frequencies and mode shapes for laminated orthotropic shells of revolution using finite element method

07 p1411 A70-19951

Heavy solid body motion about stationary point at small nutation angle, estimating region of series convergence representing periodic solutions to motion equations

07 p1336 A70-20298

Point matching technique for plane elastic problems extended to axisymmetrically loaded elastic body of revolution, developing general computer program

07 p1416 A70-20303

Limiting equilibrium of shells of revolution with different yield points under tension and compression

08 p1583 A70-20527

Boundary value problem solution in study of axisymmetric viscous heat conducting gas flow past body of revolution

08 p1431 A70-20854

Aerodynamic drag coefficients and moments for axisymmetric bodies of revolution in rarefied plasma derived for limiting case of delta flux

08 p1432 A70-21088

Elastic paraboloid of revolution under axisymmetric and nonaxisymmetric loads, using Bessel functions of real and imaginary arguments with trigonometric functions

08 p1587 A70-21165

Thin shells of revolution natural oscillation frequencies approximation based on shell subdivision into series of cylindrical shells

08 p1588 A70-21194

Heat transfer in axially symmetric laminar viscous boundary layer flow due to rotating bodies of revolution, obtaining temperature distribution

08 p1485 A70-21698

Cylindrical shell vibration modal characteristics finite element solutions accuracy compared with exact solutions

08 p1596 A70-21979

Differential equations of motion for body with stationary point, allowing for Kovalevskaya conditions and assuming nonzero gyrostatic moment

09 p1726 A70-22149

Electromagnetic waves diffraction on ideally conducting bodies of revolution, deriving design formulas for electric dipole

09 p1632 A70-22401

Generatrix shape determined for body of revolution moving at supersonic speed with minimum wave drag

09 p1603 A70-22434

Acoustic pressure sensors positioning on bodies of revolution to determine laminar boundary layer stability loss during ideal liquid flow at nonzero angles of attack

09 p1660 A70-22479

Slender body approximation for shape determination of nonslender hypersonic body of revolution with minimum convective heat transfer rate

09 p1788 A70-22931

Hall effect on MGD flow past axisymmetric body by studying incompressible inviscid flow past body of revolution at zero incidence

09 p1661 A70-23074

Transversely isotropic body of revolution under combined surface loads and stationary axisymmetric temperature field, obtaining displacement vector and stress tensor in analytic functions

09 p1778 A70-23086

Axisymmetric thermal stress state in bodies of revolution studied by successive approximation algorithm for digital computer

09 p1778 A70-23088

Elastoplastic stressed state of thin walled shells of revolution under repeated loads, assuming isotropic incompressible material

09 p1779 A70-23092

Endurance limit of momentless shells of revolution under uniform internal pressure, deriving differential equations based on aging and creep theories

09 p1779 A70-23096

Stress distribution in shells of revolution with variable elastic moduli, considering material rigidity and strain state

09 p1781 A70-23286

Carrying capacity of shallow shells of revolution, determining buckling stress and limiting equilibrium of shells with varying thickness under transverse load

09 p1781 A70-23288

Contour immobility effect on load carrying capacity of rigid plastic thin shells of revolution, establishing minimum reinforcement value for edge

09 p1783 A70-23388

Ribs reinforced shells of revolution designs calculations by approximate numerical method, considering surface geometry and cyclic temperature loads effect

09 p1784 A70-23589

Finite deformations of flexible inelastic orthotropic shells of revolution for generalized plastic flow and deformation theories

10 p1955 A70-24079

Shape of minimum drag slender body of revolution in Newtonian flow for given volume, length and maximum cross section determined by stochastic optimality principle

10 p1802 A70-24278

Heat transfer influence on three dimensional boundary layer separation on walled ellipsoid of revolution

10 p1870 A70-24781

Superconducting ellipsoid of revolution in alternating magnetic field, computing disturbed field components using boundary value problem

10 p1917 A70-25201

Stress concentration near ellipsoidal cavity in transversely isotropic body using solutions for transversely isotropic ellipsoid of revolution

11 p2129 A70-25564

Compressible turbulent boundary layer with adverse pressure gradients and crossflow over revolving bodies, integrating numerically three dimensional compressible integral equations

11 p2035 A70-25689

Load carrying capacity of isotropic rigid-plastic shells of revolution with different yield points under tension and compression applied to spherically coupled cylinders

11 p2134 A70-25932

Geometrically exact finite element for thin shells of revolution, using approximation to predict boundary layer stress distribution during vibration

[AIAA PAPER 69-56] 11 p2135 A70-25962

First order differential equations for unsymmetrical bending of shells of revolution

11 p2135 A70-25978

Flat plate flowfield for freestream/jet interaction wrap-around on bodies of revolution, using separation shock model and blast wave analogy

11 p1976 A70-26135

Monograph on shells of revolution and prismatic shells of arbitrary cross sectional shape with arbitrary load covering partial shells, programs, boundary condition methods, etc

11 p2141 A70-26600

Scalar plane wave LF scattering by prolate spheroid of revolution, obtaining iterative solution for Dirichlet problem

11 p2085 A70-26621

Scalar plane wave LF scattering by prolate spheroid of revolution, obtaining iterative solution for Neumann problem

11 p2085 A70-26622

Axisymmetrically loaded shells of revolution with displacement behavior defined by fourth order differential equations, discussing finite difference method suitability for solution

11 p2144 A70-26679

Elastic conical shells of revolution linear theory, calculating stress resultants and couples

11 p2145 A70-26689

Wave propagation in finite length revolving shells, describing advantages of modal superposition method generated by finite element computer program

12 p2317 A70-27124

Stability analysis of ring-stiffened orthotropic, multilayered shells of revolution under axisymmetric torsionless loads by digital computer

12 p2320 A70-27143

Shells of revolution under combined thermal and mechanical loading, presenting analytical basis of BOSOR 3 digital stress analysis program

12 p2320 A70-27144

Large deflection analysis of elastic-plastic shells of revolution by computer program based on nonlinear theory and multisection method of numerical integration

12 p2320 A70-27147

Stress-strain state of thin revolving shells composed of multiple variable thickness layers, assuming layers deformation free of slipping and separation

12 p2322 A70-27332

Postwrinkling nonlinear behavior of conical shell of revolution subjected to bending loads

[AIAA PAPER 69-90] 12 p2326 A70-27816

Thin walled shells of revolution equations boundary conditions formulated by stress state separation, giving small parameter perturbation theorem

12 p2327 A70-28191

Three dimensional laminar boundary layer equations for body of revolution at angle of attack in supersonic gas flow derived for equations

12 p2158 A70-28198

Boundary layer equations with pressure gradient for revolving slender body, examining transverse curvature influence on layer separation and integral characteristics

12 p2214 A70-28249

Finite element method applications to finite axisymmetric deformations of incompressible elastic solids of revolution

13 p2510 A70-28734

Wind tunnel interference for inviscid compressible conducting fluid on slender body of revolution, discussing disturbance potential

13 p2464 A70-29449

Axisymmetric compressible boundary layer on body of revolution transformed into two dimensional turbulent boundary layer

13 p2391 A70-29995

Zero-moment theory boundary value problem of shells of revolution with negative curvature under tangential static and geometrical conditions imposed on ends

14 p2657 A70-30715

Soviet monograph on thermal conductivity of plates and bodies of revolution covering temperature and stress distributions, multilayer shells, etc

14 p2666 A70-30952

Curved finite element for shells of revolution based on minimum potential energy principle, discussing stiffness and equilibrium of domed and branched shells

14 p2659 A70-31130

Wind tunnel tests of flow past oblate ellipsoid of revolution incident on major axis, measuring pressure distribution

15 p2671 A70-31494

Reinforced shells of revolution carrying capacity under limit subjected to internal adiabatic ideal gas flow

15 p2814 A70-31534

Shells of revolution zero moment stressed state calculation by analytical functions, solving boundary value problem for edge loading

15 p2814 A70-31587

Stress-strain state of catenoid, cylindrical and spherical shells of revolution, emphasizing catenoid shell bending problem

15 p2815 A70-31648

Sinusoidal stress and strain in elastic shells of revolution, reducing linear theory to simultaneous second order differential equations

15 p2816 A70-32008

Elastic shells of revolution stability and critical loads, discussing moment stress state and edge effect

15 p2816 A70-32158

Shallow shells of revolution under axisymmetrical loads, analyzing plasticity and creep by integral equations algorithm

15 p2817 A70-32164

Bifurcation stability in geometrically nonlinear shells of revolution under transverse loads, considering tension and compression deformation

15 p2817 A70-32168

Stability characteristics of elastic shallow shells of revolution in temperature field and under compression, reducing variational equation of bending by Ritz method

15 p2817 A70-32169

Elastic two cavity hyperboloid of revolution under stress due to rotating rigid stamp, solving torsional problem numerically

15 p2819 A70-32189

Hyperboloid of revolution acoustic scattering, using Bloom-type method for hard hyperbolic cylinder

15 p2701 A70-32416

Book on aerodynamics of bodies of revolution covering hypersonic flow parameters effects, method of characteristics, slender body drag, blunt bodies, rarefied gas aerodynamics, etc

16 p2834 A70-33271

Shells of revolution nonlinear finite element analysis by matrix displacement method, including higher order strain energy terms

16 p2991 A70-33885

German monograph on supersonic flows calculation past slender bodies of revolution using perturbation approach based on Poincare-Lighthill-Kuo method

16 p2839 A70-34082

Nonlinear dynamic analysis of shells of revolution under symmetric and asymmetric loads, obtaining solutions for shallow cap buckling

16 p2994 A70-34229

Critical load of shallow shell of revolution as function of geometric and material parameters

17 p3192 A70-35717

Flow field on suction side of slender body of revolution with/without wings, investigating by directional probe in wind tunnel

17 p3013 A70-35924

Axisymmetric torsion by terminal loads of elastic shells of revolution, investigating energy inequalities for assessing quality of approximate solution of thin shell problem

18 p3335 A70-36058

Rayleigh-Gans-Born approximation application to thermal radiation of reflecting convex plasma sphere, cylinder and ellipsoid

18 p3294 A70-36146

Pressurized shells of revolution loaded axisymmetrically, formulating equations for calculation of displacements, forces and stresses

18 p3338 A70-36406

Equivalent bodies of revolution method extension for use in semiempirical approximation technique, calculating pressure distribution of nonaxisymmetric blunt bodies

18 p3208 A70-36569

Stress-strain equilibrium of thin isotropic elastic shells of revolution loaded along meridian

18 p3340 A70-36577

Funnel shaped vector radiation pattern realized by synthesizing axisymmetric distribution of elliptically polarized currents on body of revolution

19 p3392 A70-37277

Book on thermoelasticity covering thermal stresses in disks, plates, shells and bodies of revolution under steady and unsteady temperature fields

19 p3541 A70-37974

Axisymmetrical stress-strain state of body of revolution with complex cross sectional geometry under surface loads, deriving computer algorithm for numerical analysis

19 p3547 A70-38439

Modified linearized transonic flow theory application to pressure coefficient distribution on circular arc bodies of revolution

20 p3608 A70-39614

Reentry bodies of revolution subsonic and supersonic aerodynamic characteristics

20 p3558 A70-39704

Complex waveguides with diverging body of revolution shaped horn, solving equation by Frobenius-Latsysheva method

20 p3587 A70-39765

Thin shells of revolution static and dynamic stability under symmetric loads, presenting eigenvalue algorithm for boundary value problems

20 p3725 A70-39863

Stability loss in linear approximation by thin elastic shell of revolution with negative Gaussian curvature

20 p3726 A70-39872

Paraboloid of revolution, examining mixed axisymmetric buckling problem

20 p3727 A70-39892

Transonic flow past bodies of revolution, using finite difference scheme

21 p3743 A70-40611

Elastic-plastic axisymmetric shells of revolution, analyzing large deflection and yielding for internal and external pressures by finite element method

21 p3937 A70-41738

Continuous surface of revolution parachute for supersonic/hypersonic speeds, performing wind tunnel tests

[AIAA PAPER 70-1173]

21 p3754 A70-41840

Conducting fluid supersonic flow past slender body of revolution in circular wind tunnel under inclined magnetic field, investigating MHD interference problem

22 p3958 A70-42669

Thin walled shells of revolution equations boundary conditions formulated by stress state separation, giving small parameter perturbation theorem

22 p4117 A70-43316

Three dimensional laminar boundary layer equations for body of revolution at angle of attack in supersonic gas flow derived from equations

22 p3960 A70-43323

Two dimensional shell equations derivation from three dimensional elasticity theory, considering rotationally symmetric bending of shells of revolution

23 p4265 A70-43942

Three dimensional elasticity for figures close to ellipsoid of revolution with displacements on boundary

23 p4266 A70-43988

Conducting bodies of revolution, calculating surface currents due to axially incident plane electromagnetic wave by computer program

23 p4162 A70-44005

Entrainment theory for incompressible turbulent boundary layer velocity and drag on bodies of revolution employed in fuselage, submersible and cowlings for propulsion design

23 p4182 A70-44400

Numerical methods for mixed boundary value problem of axisymmetric shells of revolution, using truncated series expansion and finite difference expressions

23 p4272 A70-44712

Computer program for geometrical nonlinear static and dynamic structural analysis of arbitrarily loaded shells of revolution

23 p4273 A70-44724

Stress, buckling and vibration analysis of shells of revolution by numerical integration and finite difference methods, summarizing computer programs

23 p4273 A70-44725

Pointed ogival body of revolution in supersonic flow field, investigating local pressure distributed by variational methods

23 p4136 A70-44992

Bodies of revolution optimal configuration, considering minimum head drag coefficient and low heat transfer at hypersonic speeds, using modified Newtonian and hypersonic flow theories

23 p4136 A70-45021

Shell of revolution/pressure vessel/with meridional slope discontinuity, calculating pressurization effect on stresses by computer program

24 p4420 A70-45277

Subsonic flow around bodies of revolution in axial direction, using ALGOL program for numerical calculations

24 p4289 A70-46237

BODY CENTERED CUBIC LATTICES

Strain rate, temperature and alloy content effects on plastic flow in binary substitutional alloys of bcc iron

01 p0119 A70-10735

Interstitial atoms ordering effects on low and high temperature phase transformations in alloys with bcc lattice

03 p0505 A70-13102

Superconducting transition temperature variation in bcc region of Ti-Nb-V ternary alloys measured as function of valence electrons and composition

03 p0538 A70-13154

Surface energy data calculated for bcc and hcp metals and high melting point compounds

06 p1090 A70-17845

Solid solution softening in bcc Ta-Re alloy system attributed to substitutional-interstitial interaction

07 p1310 A70-19736

Cleavage fracture of Ta-Mo bcc alloys, investigating short range ordering and size effects by X ray diffraction

09 p1708 A70-23573

Chemisorption on Mo single crystal surfaces observed by LEED techniques, discussing bcc planes and adsorbed gases

12 p2181 A70-27256

Interstitial atoms arrangement in binary alloys with body centered lattice, describing pressure effects by statistical theory

13 p2435 A70-29321

Superconducting resistive critical field H_c of bcc region of Ti-Nb-V ternary system

15 p2782 A70-31754

Specific heat and enthalpy of body centered cubic refractory metals at high temperatures

15 p2757 A70-31943

Thermodynamic properties of bcc beta phase in Ti-Cu and Ti-Al systems, discussing activities determination technique

17 p3114 A70-34378

Beta Ti-V-Cr-Al phase transformations below 500 C, discussing metastable phase, bcc formation and thermodynamics

20 p3646 A70-39106

Bcc metals and alloys stress relaxation, internal stress and work hardening, discussing temperature dependence and dislocation motion

20 p3647 A70-39108

Orientation and applied stress effects on pure Nb-6W bcc single crystals yield stress, discussing thermal activation strengthening and crystal dislocations

22 p4052 A70-42318

Bcc metals, measuring correlation between residual stress level and fatigue damage by X ray diffraction analysis

23 p4207 A70-44422

Bcc Fe base alloys volume diffusion measurements, determining activation energy and frequency factor dependence on solute content

24 p4357 A70-45232

Fe-Ni-Co martensitic alloys isothermal age hardening, comparing bcc phase energy parameters of binary systems

24 p4362 A70-46182

Fe-Ni-Mn ternary martensitic alloy, discussing metastable miscibility gap island existence in bcc phase

24 p4363 A70-46193

BODY COMPOSITION [BIOLOGY]

Macaca nemestrina total body water measurement by dilution technique

20 p3577 A70-40333

Body composition and weight changes estimation after physical exercise by prediction equations based on skinfold and girth measurements

21 p3766 A70-42155

Ultrasonic velocity in human bones measured for calcium content and density

22 p3979 A70-43522

BODY FLUIDS

NT BLOOD

NT CEREBROSPINAL FLUID

NT ENDOLYMPH

NT EOSINOPHILS

NT ERYTHROCYTES

NT LEUKOCYTES

NT LYMPH

NT LYMPHOCYTES

NT MUCOUS

NT SALIVA

NT SWEAT

NT URINE

NT WHITE BLOOD CELLS

Absolute ULF ballistocardiogram (BCG) values as pulsatile fluid pumping values in cardiodynamic function before and after exercise

02 p0248 A70-12677

Rat body fluids displacement during positive centripetal accelerations by radioisotope tracer compounds, freezing rats in liquid nitrogen to fix hemodynamic changes

07 p1202 A70-18796

Gas bubbles formation in supersaturated solutions and body fluids during decompression

07 p1208 A70-19511

Gas bubbles formation in supersaturated solutions and body fluids during decompression

11 p1988 A70-26110

Systemic hypoxia effect on renal tubule sodium reabsorption in anesthetized mongrel dogs

13 p2353 A70-29435

Macaca nemestrina total body water measurement by dilution technique

20 p3577 A70-40333

Intracellular shifts in body fluids and dehydration tolerance in burro, comparing water content of desert animals

21 p3766 A70-42157

BODY KINEMATICS

Three machine parts problem with relative motion and given active forces distribution and time variation, determining entrainment motion

01 p0142 A70-10554

Stability conditions for helical motions of body bounded by multiply connected surface in fluid

01 p0145 A70-11439

Kirchhoff kinematic analogy applied to solution of gyrostat motion, noting elastic rod deformation under torsion, using Kharlamov equations

01 p0094 A70-11441

Body motions containing cavity filled with viscous fluid under influence of gravity, formulating motion equations for fluid and body

01 p0068 A70-11576

- Motion coordination capacity of persons subjected to 40 days bed rest using dynamographic technique, discussing nature of slackening 03 p0425 A70-13896
- Perturbed motion of solid body with cylindrical cavity partially filled with viscous fluid, using Rabinovich equations 04 p0766 A70-14476
- Hypokinesia effects on transversostriated muscle fibers of mice, noting changes in myofibrillar apparatus, mitochondria and sarcoplasm 04 p0629 A70-14569
- Calcium isotopes tracer migration in caged rats in metabolism study 04 p0630 A70-14571
- Reciprocating force measurement at shake table and subject interface and repetitive circumferential human torso deformation under sinusoidal input at various frequencies and intensities [ASME PAPER 69-WA/BHF-3] 04 p0631 A70-14850
- Time-similar and isotropic geodetic curves simulating paths of test bodies in Riemann space corresponding to gravitational field 06 p1107 A70-18564
- Human body turning/orienting/ in unsupported/weightless/ position by own muscular forces, determining inertia moments of body and parts relative to various axes 07 p1207 A70-19495
- Lagrange rotational motion stability of heavy symmetrical body attached at point to platform moving forward using Liapunov theorem 07 p1334 A70-19641
- Motion of body with cavity completely filled with viscous fluid about center of mass in potential mass-force field, applying small parameter method 08 p1546 A70-21630
- Boundary layer development on body accelerating in viscous incompressible fluid, using straight lines approximation and asymptotic expansions 08 p1485 A70-21631
- Prolonged hypokinesia effect on dynamics of 5-oxindoleacetic acid elimination in rat urine, showing occurrence of shifts in serotonin metabolism 09 p1615 A70-22092
- Human forearm motion control mechanism, examining mechanogram, instantaneous velocity, acceleration and biopotentials of biceps and triceps brachii 12 p2173 A70-28314
- Vibration spectra, kinetic and dispersion equations of solid spherical particles moving in incompressible weakly viscous liquid 13 p2388 A70-29368
- Prolonged hypokinesia effect on dynamics of 5-oxindoleacetic acid elimination in rat urine, showing occurrence of shifts in serotonin metabolism 15 p2685 A70-32688
- Human body turning/orienting/ in unsupported/weightless/ position by own muscular forces, determining inertia moments of body and parts relative to various axes 15 p2685 A70-32740
- Kinematic interpretation of body motion in Hess solution, discussing axoid vector rolling without slip 21 p3849 A70-40617
- Moving stripe stimulus inducing optokinetic turning movements in goldfish, discussing different influence on vestibular organ 21 p3762 A70-41141
- Automatically controlled motion of object with finite degrees of freedom under parametric periodic disturbances 22 p4005 A70-43561
- Gravity gradiometer in moving vehicle for gravity anomaly surveying 22 p4041 A70-43657
- Rigid body rotation about fixed point under oscillatory precession and nutation due to noncentral attractive force, showing errors in Euler equations 23 p4247 A70-44792
- BODY MEASUREMENT [BIOLOGY]**
- NT ANTHROPOMETRY**
- Vital function telemetry system specifications, design and application to highway accident victims 02 p0243 A70-12096
- Dielectrocardiograph for studying cardiovascular and respiratory activities by recording hyperemia-evoked permittivity variations in localized body areas 03 p0435 A70-13714
- High altitude and sea level erythropoietic and somatic development in chick embryos indicating optimal physiological adaptation with prolonged exposure 07 p1202 A70-18864
- Dielectrocardiograph for studying cardiovascular and respiratory activities by recording hyperemia-evoked permittivity variations in localized body areas 11 p1990 A70-25514
- Myocardial individual fibers length calculation based on ellipsoidal model of left ventricle and fibers helicoidal course, noting distension nonuniform effect 12 p2174 A70-27020
- Capillary details in lentiform nucleus region of human brains, measuring blood vessels diameters, lengths and densities 12 p2173 A70-28347
- Mass measuring device used on biological specimens in zero gravity environment, determining normal and disturbed physiological mechanisms 14 p2542 A70-30795
- Ultrasound resonant frequency reproducibility as objective measure of skeletal status, discussing forearm and hand positioning effect 20 p3579 A70-39432
- Intact human forearms venous blood velocity measurements, using nuclear magnetic resonance techniques 24 p4309 A70-45675
- Ox, calf, pig, rabbit, guinea pig and human eye measurements, determining wet and dry weight of iris, ciliary body and choroid 24 p4305 A70-46346
- BODY SIZE [BIOLOGY]**
- Data analysis of compliance, resistance, inertance and natural frequency of chest-lung system, noting trend with body mass 06 p0993 A70-17521
- Mathematical model of human pituitary gland mechanism controlling secretions of serum growth hormone in response to glucose deficiency 20 p3569 A70-38995
- BODY SWAY TEST**
- Human vertical perception with body tilt in median plane tested with luminous rod in upright to supine position with backward and lateral tilt 07 p1224 A70-20045
- BODY TEMPERATURE**
- Photoperiod variation effects on ambulatory primate *Cebus albifrons* deep body temperature/DBT/, locomotor activity/LMA/ phase relationships and DBT waveform 01 p0011 A70-10035
- Cardiac activity temperature coefficients in dogs, specifying physical and chemical cardiac functions 01 p0012 A70-10052
- Human rectal temperature cooling rate during refrigeration in mortuary, applying Newton law 01 p0017 A70-10471
- Male macaque monkey physiological deterioration in Biosatellite 3, noting falling brain temperature, lowered central venous pressure, fluid loss, blood redistribution into visceral pools, etc 01 p0022 A70-10822
- Light synchronization of deep body temperature rhythms in *Macaca nemestrina*, investigating efficiency 03 p0416 A70-13013
- Oxygen consumption and rectal temperature in male mice confined in nitrogen and helium diluted hyperoxic atmosphere at specific temperature and humidity ranges 03 p0425 A70-13891
- Vestibular reactions in rats under hypothermal conditions by measuring postrotatory nystagmus beats number and duration, respiration rates and rectal temperature 03 p0425 A70-13893
- Thin, fat and average men responses to cold during one year period in Antarctica, measuring metabolic rates, skin and rectal temperatures 03 p0429 A70-14163
- Oxygen consumption and body temperatures during acute hypoxia in man, based on low oxygen mixture breathing tests 03 p0439 A70-14291
- Low body temperature effects on convulsive activity elicited by hyperbaric oxygen in unrestrained unanesthetized rats 04 p0629 A70-14448
- Combined hypoxic hypoxia and high ambient temperature found relieving strain on humans by increasing heat release by evaporation 04 p0630 A70-14581
- Temperature variations in organs of man and animals performing physical work as physiological base of metabolic processes and for daily activity timetable development 04 p0638 A70-15502
- Synchronous variations in skin and muscle temperatures of musculus gastrocnemius and flexor carpi in human subjects performing intermittent physical exercises 04 p0639 A70-15507
- Muscle temperature variations and respiratory activity of athletes under various exercise regimens, outlining optimal weight lifting training programs 04 p0639 A70-15507
- Rat survival rate after prolonged gradually decreased body temperature without motion restraint or kept in fixed position 05 p0804 A70-17115
- Heart rate-body temperature relationship during walking in hot environment 06 p0993 A70-17431
- Esthesiometric analysis of cutaneous thermoreceptors reaction dependence on heat production rates of human organisms 07 p1206 A70-19472
- Esophageal, rectal and quadriceps muscle temperatures, oxygen uptake, weight changes, skin conductance and skin evaporation during thermal transients caused by bicycle exercise 10 p1810 A70-24006
- Heat accumulation, oral temperature and heart rate recovery of subjects in various thermal environments 10 p1810 A70-24034
- Extravehicular activity space suits evolution emphasizing appropriate body temperature control under various conditions and work loads 10 p1824 A70-24412
- Body temperature effect on pulmonary ventilation response to exercise 10 p1819 A70-24773
- Thermostability and survival rates of white mice in ambient medium with temperature variations 13 p2351 A70-29330
- Physiological indices criteria for human thermal stress tolerance, discussing rectal temperature, body surface condition, body temperature and local cooling effects 13 p2351 A70-29332
- Intraocular tension due to muscular fatigue in overheated albino rats, determining Na and K content in eye tissue 14 p2535 A70-30159
- Physical methods in applied climatology, analyzing meteorological effects on human body and building thermal conditions and plant biomass growth 15 p2771 A70-32111
- Integrating influence of mediobasilar hypothalamic structures upon temperature regulation of juvenile rat based on Area praeroptica medialis stimulation 16 p2849 A70-33697
- Biological media thermal behavior, discussing maintenance of constant internal temperature under varying conditions in man 16 p2854 A70-33948
- Tympanic membrane and rectal temperatures compared over wide range of ambient environments as indicators of deep body temperature 17 p3029 A70-35332
- Cooling hood effect on physiological responses to work in hot environment, discussing body temperature 17 p3031 A70-35422
- Body temperature-maximum oxygen intake relations in hot humid air 17 p3038 A70-35424
- Aircraft crew oral temperature related to work-rest schedules, discussing hypothermia, flight stress and in-flight depression 17 p3032 A70-35563
- Mathematical simulation of human thermoregulatory system, considering automatic control theory 18 p3224 A70-36530
- Temperature change relation between anterior hypothalamus and concha auricularis in rabbits 18 p3218 A70-36532
- Varying thermoregulatory responses of different rodent species to long term heat and cold 18 p3218 A70-36534
- Gas metabolism, chemical thermoregulation, body temperature and weight of rats during adaptation to repeated high temperature exposure 18 p3219 A70-36538
- Gas exchange, body temperature and electrical activity of neck and back muscles of cold-acclimated white rats subjected to various temperatures 18 p3219 A70-36540
- Prolonged cold adaptation effect on heat transfer during recovery period after hypothermia in white rats 18 p3220 A70-36543
- Repeated snow cooling effect on heat transfer in white rats during temperature homeostasis recovery after hypothermia 18 p3220 A70-36544
- Psychotropic drugs radioprotective effects in mice, noting oxygen consumption and body temperature decrease after X ray exposure 19 p3367 A70-37558
- Human body core temperature control dependence during exercise on heat dissipation, noting sweating control 20 p3570 A70-38997
- Body surface cooling level and rate effects on psychomotor performance tested at various levels of mean weighted skin temperature/MWST/ 20 p3573 A70-39675
- Human peripheral blood flow rewarming in cold ambient temperature, examining skin, rectal and tympanic membrane and oxygen uptake 20 p3576 A70-40327
- Localization and functional topology of thermosensitive central nervous structures in rats cervical spinal cord, discussing role in generating heat to avert coldness 22 p3967 A70-42316

Circadian rhythm in human body temperature by Cosinor method, showing inapplicability for narrow time span

22 p3977 A70-42872

Mean skin temperatures of human body by 10 point method, using cold and hot exposure data

22 p3978 A70-42874

Spinal cord thermal stimulation effects on regional sympathetic activity in rabbits and cats determined from integrated sympathetic efferent discharges

22 p3971 A70-43406

Carbon dioxide exposure limits of rhesus monkeys, examining body temperature, respiratory rate and pressure effects

22 p3973 A70-43642

Digital recording system for body temperature telemetry from small animals, using FM transmitter implanted in peritoneal cavities

23 p4151 A70-44381

Human body heat production and transfer through convection, radiation and evaporation under normal and reduced atmospheric pressure

23 p4154 A70-44654

Hypothermia and body rewarming effects on renal hemodynamics in anesthetized dogs

24 p4301 A70-45998

Chronically implantable water perfused thermode system for hypothalamic temperature waveforms generation

24 p4309 A70-46117

BODY TEMPERATURE REGULATION

U THERMOREGULATION

BODY VOLUME (BIOLOGY)

Bed rest effects on whole leg venous distensibility, discussing heart rate and leg volume measurements

06 p0999 A70-17288

Human lung volume-to-ventilation ratios regional dispersion, using expired nitrogen concentrations analog simulation

24 p4303 A70-46113

BODY WEIGHT

Vasopressin antidiuretic hormone effects on evaporative body weight loss during heat exposure

01 p0020 A70-10516

Chicken body mass and percentage body fat following 24 weeks chronic acceleration determined from fatty acid metabolism, liver citrate cleavage and malic enzyme activities

02 p0233 A70-11720

Thin, fat and average men responses to cold during one year period in Antarctica, measuring metabolic rates, skin and rectal temperatures

03 p0429 A70-14163

Evaporative weight losses by sweating in man exposed to warm environment as function of time, including graphical method for heat storage prediction

03 p0430 A70-14164

Space diets tests for mean DAR of proteins, carbohydrates, fats and water, considering body weight and required energy expenditure

09 p1623 A70-22088

Prolonged hypodynamia effect on human nutritional habits and protein metabolism, noting decrease in energy requirement and body weight

10 p1814 A70-24675

Single and combined hypoxia and hypercapnia effects on growing rats, discussing body weights, blood and histological measurements

13 p2357 A70-29948

Mass measuring device used on biological specimens in zero gravity environment, determining normal and disturbed physiological mechanisms

14 p2542 A70-30795

Space diets tests for mean DAR of proteins, carbohydrates, fats and water, considering body weight and required energy expenditure

15 p2693 A70-32684

Pulmonary vital capacity measurements in young recruits for respiratory function, considering relationship to body weight and height

16 p2850 A70-34348

Astronaut weight loss relation to flight duration during manned space missions

20 p3574 A70-40125

Differential sphygmogram of young men, determining lean body mass on basis of anthropometrical data

21 p3763 A70-41229

Body composition and weight changes estimation after physical exercise by prediction equations based on skinfold and girth measurements

21 p3766 A70-42155

BODY-WING AND TAIL CONFIGURATIONS

Man-computer graphic systems utilization for wing/body aerodynamic design and analysis concept for subsonic vehicles

[AIAA PAPER 69-1130] 01 p0002 A70-10610

Wing-fuselage interference influence in aircraft dihedral effect, discussing role of velocity direction on wing

03 p0406 A70-13020

Aircraft aerodynamics, Volume II, covering profile and wing theory at subsonic and supersonic speeds, fuselage, wing-fuselage and tail assembly, etc

03 p0407 A70-13350

Modified tailed delta configuration selection for U.S. SST, discussing power plant installation choice [RAES PAPER 17]

03 p0411 A70-13544

Blended wing-body design concept for F-15 air superiority fighter, providing fixed wing planform for maneuverability at transonic speed

04 p0622 A70-14395

Variable sweep aircraft aeroelastic stability, considering wing-tail interaction flutter [AIAA PAPER 70-80]

06 p1170 A70-18162

Analog computation in supersonic steady flow and digital technique for wing-fuselage and wing-tail interactions

[ONERA TP-804] 10 p1802 A70-24544

Unsteady supersonic flow past tail-body system with harmonic oscillatory motions

10 p1803 A70-24789

Second order conical flows around wing-fuselage system, deriving expressions for axial perturbation velocity for various attack geometries

10 p1804 A70-24972

Tensile tests on wings and wing components of plastic engine-driven aircraft, discussing design, configurations and mechanical properties

14 p2656 A70-30250

Critical flutter behavior of variable geometry aircraft with wing of 70 degree leading edge sweep, noting wing-tail interference

18 p3338 A70-36445

Aerodynamics of steady, inviscid transonic flows around slender bodies and wing-body combinations at free stream Mach number one

[AIAA PAPER 70-798] 20 p3559 A70-39900

Unsteady supersonic flow around oscillating cross-shaped wing-fuselage system, determining perturbation velocities and pressure distributions

22 p3958 A70-42609

Short wing lift investigated via lateral fluid jets fired in wind tunnel for various lengths

22 p3958 A70-42614

BOEING AIRCRAFT

NT B-52 AIRCRAFT

NT BOEING 707 AIRCRAFT

NT BOEING 727 AIRCRAFT

NT BOEING 737 AIRCRAFT

NT BOEING 747 AIRCRAFT

NT BOEING 2707 AIRCRAFT

NT C-135 AIRCRAFT

NT CH-46 HELICOPTER

NT CH-47 HELICOPTER

Slide and sleeve type servovalves used in Boeing aircraft possessing chip shearing capability of 200 pounds axial force

02 p0229 A70-12863

Boeing 2707 SST horizontal tail multiple channel actuation system features

17 p3020 A70-35827

BOEING MILITARY AIRCRAFT

U BOEING AIRCRAFT

U MILITARY AIRCRAFT

BOEING 707 AIRCRAFT

Boeing 707 B-epoxy composite foreflap design, analysis, fabrication and flight testing

02 p0307 A70-11955

Boeing 707 aircraft operational efficiency optimization by modification program to extend wing life

03 p0497 A70-14052

Thrust control unit in Lufthansa Boeing 707 aircraft designed to maintain landing approach speed by adjusting throttle setting and landing flap position

05 p0845 A70-15903

Boeing 707 and 727 aircraft components on condition maintenance program based on statistical analysis and performance monitoring for replacing scheduled overhauls

15 p2748 A70-32656

BOEING 727 AIRCRAFT

Boeing 707 and 727 aircraft components on condition maintenance program based on statistical analysis and performance monitoring for replacing scheduled overhauls

15 p2748 A70-32656

BOEING 737 AIRCRAFT

Boeing 737 aircraft nose gear gravel deflector and engine vortex dissipator [AIAA PAPER 70-912]

17 p3020 A70-35824

BOEING 747 AIRCRAFT

Area navigation and automatic data communications in air traffic control proposed for New York area STOL aircraft operations and Boeing 747 aircraft [AIAA PAPER 69-1054]

01 p0138 A70-10640

Air traffic problems connected with Boeing 747 introduction, discussing cargo/passenger handling, fueling and maintenance procedures

02 p0227 A70-12620

Positive displacement low pressure air motors for Boeing 747 fan thrust reverser pneumatic actuators and controls

03 p0550 A70-12881

Boeing 747 nacelle development programs involving outdoor and ground test rigs, flying test bed, flight tests, etc

[SAE PAPER 690389] 03 p0550 A70-12894

Ground support and service features present facilities to handle B-747 and DC-10 aircraft [SAE PAPER 690560]

03 p0463 A70-13264

Boeing 747 aircraft family design options related to utilization, performance and economics, discussing development through large turbofan engine availability [AIAA PAPER 68-1020]

04 p0624 A70-15382

Hydrostatic synchronized steering of tow tractor for Boeing 747 and wide body jets compared to mechanical system

05 p0829 A70-16421

Hydraulic jacks for Boeing 747 support during assembly, discussing operation, console, pressure system and safety features

05 p0798 A70-16422

Boeing 747 aircraft container system deployment simulation written in GPSS/360 to minimize stockholding of containers at individual stations

08 p1481 A70-20931

Boeing 747 pretesting work including wind tunnel, components, engines and static structural tests, flight simulation, etc

08 p1437 A70-21730

Boeing 747 aircraft impact on air transportation passenger and freight rates and traffic congestion reduction

10 p1806 A70-24765

Hydraulic systems for Boeing 747 aircraft flight control

12 p2167 A70-28019

Aircraft accidents during descent, approach and landing, discussing B 747, C5A and SST

15 p2675 A70-32216

Variable loads programming by semicomputers/semihardware method for 747 fatigue testing

17 p3050 A70-35511

Boeing 747 aircraft operation in first three months of service, discussing crew training, instrumentation, navigation system improvement, etc

[AIAA PAPER 70-891] 17 p3019 A70-35805

Boeing 747 maintenance and inspection program, discussing condition monitoring, test methods, etc

[AIAA PAPER 70-889] 17 p3019 A70-35806

Boeing 747 aircraft JT9D engine deflections and removals during early service experience and maintenance

[AIAA PAPER 70-890] 17 p3019 A70-35807

Boeing 747 ground operations and airport services, discussing computerized check-in, baggage handling equipment, etc

[AIAA PAPER 70-892] 17 p3019 A70-35808

Boeing 747 aircraft pressure fueling system, describing tanks, feed system, refueling and electrostatic charge minimization

[SAE PAPER 700276] 18 p3214 A70-36816

Engine vibration monitoring system for Boeing 747 aircraft, including piezoelectric transducer, transmission assembly and differential charge converter

19 p3426 A70-37898

Boeing 747 wing panels shot peening process, discussing machine, control technique and operational requirements

19 p3437 A70-38498

Boeing 747 transport airplane flight test data system, discussing recording media, major PCM and FM tape systems, etc

19 p3431 A70-38531

Boeing 747, L-1011 and DC-10 introduction costs, profits and terminal facilities

19 p3357 A70-38951

Boeing 747 pilot transition training, discussing takeoff, landing, eyelevel, flareout taxi speeds, inertial navigation and electrical, fuel and hydraulic systems

20 p3562 A70-40083

Boeing 747 aircraft early operations experience covering airframe, engines and parts, performance, pilot and engineer training, maintenance, etc

[AIAA PAPER 70-886] 21 p3749 A70-40740

Boeing 747 aircraft passenger entertainment and service system controls electronics design and wire installation improvement by multiplexing techniques

23 p4174 A70-44543

Boeing 747 airliner passenger entertainment and service electronics multiplexing system, discussing cable and connectors selection and design

23 p4174 A70-44544

Boeing 747 flight test certification program, describing methods, data systems, inertial navigation, engines, flutter, etc

[SAE PAPER 700828] 24 p4290 A70-45891

BOEING 2707 AIRCRAFT

Boeing 2707 SST design for low community noise, discussing engine-airframe matching effect

[SAE PAPER 700808] 24 p4290 A70-45906

BOGOLIUBOV THEORY

Bogoliubov approach generalized and applied to unstable and inhomogeneous plasmas

07 p1347 A70-19108

BOHR THEORY

Hoyle-Narlikar gravitation theory, considering Bohr quantization of direct interparticle action over all pairs

24 p4403 A70-45405

BOILERS

- Solar radiation heated boilers efficiency and operational temperature range improved by application of coatings, noting surface absorption properties
11 p2148 A70-25930
- Water and alkali metal boilers, predicting helical-flow-promoting inserts effect on pressure drop penalties by constant slip model
21 p3949 A70-41308

BOILING

- NT FILM BOILING
NT LEIDENFROST PHENOMENON
NT NUCLEATE BOILING
- Pseudoboiling heat transfer from platinum wire to carbon dioxide during free convection
03 p6064 A70-13209
- Heat transfer and flux density during bubble boiling of liquid oxygen employing simulated weak gravitational fields
03 p6065 A70-13393
- Electrically heated wire diameter and orientation on heat flux in saturated pool and surface boilings of water and aqueous binary mixtures
07 p1417 A70-18643
- Empirical method for calculating critical thermal flux density during boiling of underheated liquid-vapor systems
07 p1420 A70-19068
- Vapor bubble separation diameter and flow in channel boiling applied to supercooled boiling zone determination
09 p1789 A70-23379
- Fluid boiling heated nonuniformly in pipe, deriving formulas for unsteady temperature field by integrating energy equation
09 p1791 A70-23716
- Empirical method for calculating critical thermal flux density during boiling of underheated liquid-vapor systems
10 p1970 A70-25219
- Surface temperature fluctuations during steady state boiling from tube, using fast response thermocouple
18 p3347 A70-36504
- Heat transfer in boiling liquid from temperature field and temporal changes in liquid above heating surface, determining isotherms by laser interferometry
19 p3447 A70-38455
- Bubble frequencies random distribution during boiling of pure liquids and binary liquid mixtures by optical measurement
21 p3941 A70-40775
- Local or surface boiling phenomenon under triangular channel laminar flow conditions, investigating heat transfer with and without phase change
24 p4429 A70-46089
- Peak pool boiling heat flux on horizontal cylinders, describing interactions of gravity and heater size effects
24 p4429 A70-46176
- BOLKOW AIRCRAFT
NT BO-105 HELICOPTER
BOLKOW BO-105 HELICOPTER
U BO-105 HELICOPTER
- BOLOGRAMS
U BOLOMETERS
BOLOMETERS
- Ge bolometer cooled by liquid helium 3 to near absolute zero to achieve high sensitivity for far IR detection
01 p0091 A70-10910
- Microsecond-response bolometer for measuring thermal fluxes as function of time in high explosion driven shock tubes and plasma jets
06 p1070 A70-18445
- Thin film capacitive bolometer dependent on temperature sensitivity derived from electron trapping effects
09 p1683 A70-23509
- Cryogenic Ge bolometers sensitivity variation and noise, noting radiation absorption by sensor and by coating
12 p2237 A70-28151
- Liquid He temperature fluctuation effects on cryogenic superconducting bolometer noise spectrum, deriving transfer functions
12 p2237 A70-28156
- Superconducting bolometer operating temperature stabilization
13 p2412 A70-29868
- Microsecond response bolometer for measuring thermal radiation fluxes in shock tube, discussing design, calibration and performance
21 p3824 A70-40859
- Superconducting Sn bolometer under isothermal and nonisothermal conditions, measuring noise spectra dependence on displacement current and resistance
22 p4026 A70-42397

BOLTS

- Bolted joints inspection using mechanical impedance algorithm method involving bolt head mechanical shock pulse response in adjacent structure
01 p0098 A70-10017

- Stress analysis of eyebolts in turbine blades hinged locks based on perforated plate theory with concentrated force, discussing stress distributions
01 p0210 A70-11416
- Nut and bolt locking, describing cotter pins, lock washers, elastic washers, prestressing, nut with lock nut and self locking nuts
06 p1075 A70-17436
- Wear resistance of turbine rotor blade stabilizing elements in form of bolts connecting overlapping leading and trailing edges of adjacent tips
09 p1768 A70-22095
- Stress distributions in tapered bolt assemblies due to interference and uniaxial tension
16 p2992 A70-33989
- Ball-lock-bolt separation mechanism for spacecraft applications requiring low shock, controlled release, nonfragmenting fastener
16 p2922 A70-34119
- Stainless maraging steel bolts tensile, shear and fatigue strengths and stress corrosion resistance at room and high temperatures
20 p3650 A70-39964
- Ti alloy bolts mechanical properties improvement by beta heat treatment
20 p3650 A70-39965

BOLTZMANN DISTRIBUTION

- Rotating and oscillating spectra in diatomic molecule excited by slow and fast electrons, discussing Boltzmann distribution of excited molecules
07 p1337 A70-19044
- One dimensional steady neutral shock wave structure, using expanding Boltzmann equation distribution function in terms of Hermite polynomials
07 p1260 A70-19984
- Boltzmann equations for distribution functions of gas, analyzing neutral or ionized components by linearization method
11 p2090 A70-25946
- Boltzmann equation for Knudsen layer and outer region of weakly rarefied gas flow
15 p2777 A70-32131
- Krook gas particle collision model for relaxation from nonequilibrium to equilibrium Boltzmann distribution in spatially uniform gases
17 p3068 A70-34697
- Observational evidence concerning validity of Saha and Boltzmann laws in O, B and A stellar atmospheres
17 p3170 A70-35387
- Gas and semiconductor diode lasers construction and operation principles, discussing terminology, Boltzmann distribution function, excitation methods, population inversion, etc
20 p3643 A70-40535

BOLTZMANN TRANSPORT EQUATION

- Particle diffusion distribution function of two component ionized degenerate gas from Boltzmann transport equation, giving tables for various spin and mass ratios
01 p0151 A70-10318
- Solution existence of linear unsteady Boltzmann equation for single space variable in Hilbert space defined by scalar product
01 p0143 A70-10673
- Chapman-Enskog expansion for Boltzmann equation solution, using PLK method to obtain higher approximations for shock wave structure
01 p0063 A70-10923
- Enskog method for Boltzmann equation, analyzing asymptotic nature of integral kinetic equation for molecular mean free paths and Laplace probabilities
01 p0068 A70-11568
- Hydrostatic equation nonequilibrium terms role in single and multicomponent atmospheres, deriving solutions to Boltzmann equation
02 p0328 A70-12386
- Riccati equation role in solving finite dimensional time invariant transport equations based on equivalent coupled linear equations
02 p0324 A70-12667
- Density effects on transport coefficients of gaseous mixtures, solving modified Boltzmann equation including collisional transfer and three-particle collision effects
03 p0606 A70-13576
- Spatially homogeneous Boltzmann equation containing initial distribution functions expandable into Hermitean polynomials, using ordinary differential equations
03 p0526 A70-14302
- Nonlinear Boltzmann equation for heat transfer in rarefied gases between parallel plates at different temperatures using Monte Carlo method
04 p0782 A70-14811
- Numerical methods for solving Boltzmann gas kinetics equation, assessing various methods effectiveness
06 p1036 A70-17752
- Kinetic Boltzmann equations for spatially uniform two component gas mixture solved with allowance for relaxation processes, assuming differing temperatures
06 p1109 A70-17754

- Boltzmann equation direct numerical integration using successive iterations algorithm
06 p1036 A70-17755

- Kinetic relaxation and Boltzmann equations for studying shock waves propagating in gas composed of rigid ideally elastic spherical molecules without internal degrees of freedom
06 p1036 A70-17756

- Iteration for Boltzmann equation solution for relaxation of gas having solid molecules with time variable and velocity dependent distribution function
06 p1109 A70-17757

- Approximate solution to Boltzmann gas kinetics equation, using moment relations of collision integral and reverse collision operator
06 p1036 A70-17758

- Time dependent transport equations for full Reynolds stress tensor and turbulence decay function using flux approximations and relaxation model [AIAA PAPER 70-3]
06 p1038 A70-18080

- Kinetic flow regime in hypersonic flow past flat plate leading edge, using Boltzmann equation [AIAA PAPER 70-181]
06 p0970 A70-18094

- Boltzmann equation at arbitrary Knudsen numbers and kinetics of polyatomic molecule gases
06 p1047 A70-18310

- Boltzmann equation for binary mixtures of rarefied gases solution involving specific expansion of distribution functions
06 p1047 A70-18311

- Monatomic gas flow past moderate curvature body, obtaining approximate solutions to Boltzmann equation under form of matched asymptotic expansions
06 p0979 A70-18316

- Linear Boltzmann equation in bounded domain, studying solutions existence, uniqueness and structure
06 p1047 A70-18317

- Discrete ordinate technique for nonlinear Boltzmann equation tuned for computing collision integrals to instantaneous nature of distribution function
06 p1047 A70-18319

- Nonlinear Knudsen layer gas flow using BGK model for Boltzmann equation
06 p1048 A70-18322

- Monte Carlo method applied to Boltzmann collision integral in solving heat transfer between plates at different temperatures in elastic spheres gas
06 p1183 A70-18324

- Thermal slip velocity of gas in infinite temperature gradient tangential to solid wall, basing calculation on linearized Boltzmann kinetic equation
06 p1049 A70-18332

- Surface diffusion slip velocity in binary gas mixture above solid surface, basing calculation on distribution functions determined from Boltzmann equation
06 p1049 A70-18333

- Monte Carlo method applied to solving nonlinear Boltzmann equation for plane shock waves in elastic sphere gases
06 p1050 A70-18335

- Least squares method to determine shock thickness at arbitrary Mach number from Boltzmann equation for rigid sphere rarefied gas
06 p1051 A70-18345

- Hyperthermal leading edge analyzed by examining adjacent relevant mean free paths for collisions, establishing basis for formal expansion of Boltzmann equation
06 p0979 A70-18347

- Free molecular heat transfer from sphere at rest in rarefied monatomic gas solved for Krook model of Boltzmann equation
06 p1183 A70-18375

- Time dependent relaxation model for heat flux in metals from quantum mechanical form of Boltzmann transport equation, yielding damped wave equation for temperature
06 p1090 A70-18612

- Weak discontinuities propagation in quasi-linear systems for MGD, obtaining transport equations
07 p1347 A70-18678

- Molecular beam approximation introduced in Boltzmann equation to investigate high speed rarefied flows
07 p1261 A70-20130

- Boltzmann systems dynamics, discussing excitation spectrum, momentum relaxation time, particle diffusion trajectory, macroscopic theory of quasi-collective processes, hydrodynamics, etc
08 p1545 A70-21421

- Kramer problem in kinetic gas theory and gas dynamics applied to Boltzmann equation, discussing uniqueness theorem [ONERA-TP-776]
08 p1486 A70-21845

- Shock wave structure nonequilibrium kinetic model using Boltzmann and Navier-Stokes equations
09 p1662 A70-23306

- Flux equations of single velocity Boltzmann type for unsteady transport problems applied to concentration discontinuity propagation through plane layer
10 p1966 A70-23871

- Coupled Boltzmann and rate equations for free electron distribution function and level populations in monatomic partially ionized gas including nonelastic collisions
10 p1918 A70-23958

Boltzmann collisionless transport equation for relativistic plasma solved by expanding distribution function in terms of unnormalized spherical harmonics 10 p1923 A70-24228

Hydrodynamic equations for ions and electrons of ionized collisional plasma in inhomogeneous magnetic field based on Boltzmann kinetic equations 11 p2088 A70-25710

Boltzmann equation in circular magnetic field solved by Fourier series and Legendre polynomials, correcting distribution function due to Fourier harmonics 13 p2464 A70-29485

Cross coupling relations in Boltzmann equations solution for inhomogeneous plasmas, using spherical harmonics expansion and Laguerre-Sonine polynomials 13 p2464 A70-29539

Ionization coefficient calculation for preionizers through electron distribution function solution to Boltzmann equation 13 p2468 A70-29962

Quantum mechanical Boltzmann equation for atomic gas of composite particles, considering excited level degeneracy 14 p2619 A70-30651

Weak discontinuities propagation in quasi-linear systems for MGD, obtaining transport equations 15 p2777 A70-31470

Soviet book on rarefied gas dynamics involving methods and approaches for kinetic description of gas behavior, emphasizing Boltzmann equation 17 p3067 A70-34604

Exact and normal solutions of Boltzmann equation linearized around total equilibrium, yielding Navier-Stokes and Burnett transport coefficients 17 p3128 A70-34628

Kinetic theory of moderately dense gases, obtaining generalized Boltzmann equation 17 p3072 A70-35534

Chamber solution of Boltzmann time dependent equation in relaxation time approximation 17 p3136 A70-35596

One dimensional steady gas flow, deriving algorithm for iterative solution of Boltzmann kinetic equation by statistical approach 18 p3241 A70-36285

Boltzmann equation for relativistic gas, adapting Grad solution method 19 p3403 A70-37584

Cauchy problem for linearized relativistic Boltzmann equation near equilibrium, using functional analysis 19 p3403 A70-37585

Boltzmann equation for relativistic gas without dissipation, solving for relaxation time and elastic collisions 19 p3403 A70-37586

Magnetoelectric electromotive force in media of ions and neutral molecules, using Boltzmann transport equation 21 p3855 A70-40909

Minimum entropy production in kinetic theory of rarefied gases described by Boltzmann equation 21 p3850 A70-41957

Computerized evaluation of Krook kinetic relaxation equation approximating Boltzmann nonlinear integral equation for rarefied gas motion 21 p3851 A70-42201

Plasma kinetic theory, applying Boltzmann equation, Lorentz gas model and relaxation method 23 p4224 A70-44177

Homogeneous plasma in unidirectional oscillatory electric field, solving Boltzmann equation by electron distribution function expansion 23 p4225 A70-44240

Electron distribution function in homogeneous ionized plasma under oscillating electric fields and steady magnetic fields, solving Boltzmann transport equation 23 p4226 A70-44248

BOLTZMANN-VLASOV EQUATION

Higher order magnetic field-free temporal and spatial plasma wave echoes, solving collisionless Boltzmann equation by method of characteristics 19 p3476 A70-37557

Electron-neutral collisional damping of longitudinal electron oscillations in weakly ionized plasma, solving linearized Boltzmann-Vlasov equation 21 p3860 A70-42014

BOLZA PROBLEMS

Closed loop nonlinear optimal control systems sensitivity to small parameter variations noting influence of feedback 03 p0461 A70-14171

Analytical approach to gradient method within framework of Bolza problem of variational calculus, using linearized differential and isoperimetric constraints 03 p0520 A70-14341

Endpoint sufficiency test based on differential calculus method, considering Bolza problem of continuous state and piecewise control variables 11 p2073 A70-26233

BOMBER AIRCRAFT

NT B-52 AIRCRAFT

NT B-70 AIRCRAFT

NT VULCAN AIRCRAFT

BOMBS [ORDNANCE]

Fin slots and tabs effect on dynamic stability characteristics of low drag bomb, discussing free rolling and pitching tests 21 p3747 A70-41880

BOMBS [PRESSURE GAGES]

U PRESSURE GAGES

BOMBS [SAMPLERS]

U SAMPLERS

BONDING

NT CERAMIC BONDING

NT EXPLOSIVE WELDING

NT METAL BONDING

NT METAL-METAL BONDING

NT RESIN BONDING

Particle, resin and inorganic bonding of solid lubricant to surface and dry lubricant film performance 05 p0855 A70-16043

Resistance strain gauge load cell for measuring compressive loads under high hydrostatic pressure, discussing gauge bonding 05 p0848 A70-16377

Mechanical fastening, adhesive bonding and machining methods for laminated fiberglass reinforced plastic materials 05 p0856 A70-16618

Fiberglass reinforced plastics bonding, discussing structure fabrication and use as material 07 p1295 A70-19759

Longitudinal strength characteristics of filament reinforced composites, discussing bond strength effect on filament fracture 08 p1533 A70-21918

Electrical conductance test for composite materials adhesive bond degradation by liquids 11 p2071 A70-26345

Nondestructive bond inspection by interferometric holography of ultrasonically excited plates 14 p2588 A70-31166

Glass bonding techniques for semiconductor strain gages, discussing outgassing minimization, hysteresis and repeatability and operational temperature range extension 15 p2739 A70-32325

Holographic interferometry for evaluating bond between diaphragm and base in pressure transducer 16 p2904 A70-33138

Adhesive bonds strength parameters, discussing substrate type, surface preparation, etc [ASME PAPER 70-DE-33] 16 p2939 A70-33504

Adhesives selection based on bond performance requirements, considering joint design, stress distribution, temperature effects, etc [ASME PAPER 70-DE-69] 16 p2939 A70-33519

Bond stress distribution in elastic solid with axisymmetrical inclusions under uniform tension, using three function and point matching techniques 17 p3184 A70-34911

IR NDT bond inspection system for helicopter rotor blade honeycomb box assemblies, using closed circuit slow scan video system to detect bondline voids 17 p3101 A70-35184

Joint designs, attachment methods and load introduction in composite structures, suggesting adhesive bonding 20 p3730 A70-40041

Bond stresses between fiber and matrix of fiber reinforced composite materials determined by numerical method based on superposition 21 p3934 A70-41252

Photochromic paint nondestructive testing for survival equipment, detecting bond defects and sandwich water 23 p4197 A70-44490

BONE MARROW

Hypoxic stimulation effect on erythropoiesis in vivo bone marrow 01 p0017 A70-10464

Chronic gamma irradiation effects on bone marrow mitotic activity and chromosome aberrations in dogs 09 p1614 A70-22083

Rhesus monkey active bone marrow distribution and volume studied by radioactive tracing techniques 09 p1616 A70-22301

Therapeutic power of bone marrow transplanted from mice earlier irradiated by high energy protons into newly irradiated mice 09 p1619 A70-22814

Thymidine tracer distribution in bone marrow chromosomes of rats and mice treated with radioprotectors, noting cell metabolic activity reduction by sulfhydryl-type radioprotectors 09 p1619 A70-22818

Therapeutic effects of hemopoietic tissue transplants of bone marrow on irradiated rats, using diffusion chamber for resettlement prevention 13 p2354 A70-29753

Chronic gamma irradiation effects on bone marrow mitotic activity and chromosome aberrations in dogs 15 p2685 A70-32679

Simulated space flight radiation effects on dogs DNA synthesis and bone marrow cell differentiation 20 p3575 A70-40191

Heme biosynthesis defect in vitamin E-deficient rats affecting bone marrow synthesis of delta-aminolevulinic acid and liver formation of porphobilinogen 24 p4304 A70-46146

BONES

NT CARTILAGE

NT CEREBRUM

NT CRANIUM

NT FEMUR

NT MARROW

NT SCIATIC REGION

NT SKULL

NT ULNA

NT VERTEBRAE

Recumbency effect on human heel bone density during bed rest using X rays 06 p0996 A70-17850

Percentage changes in X ray calibration wedge mass equivalency to actual changes in bone Ca content 06 p0997 A70-18015

Long bone necrosis in response to reduced atmospheric pressure exposure, comparing lesions with caisson disease 08 p1449 A70-21944

Mineral saturation in calcaneal bone and hand finger phalanx in humans under prolonged hypodynamia by X ray analysis, observing Ca salts reduction 10 p1815 A70-24676

Bone and muscle tissue morphological changes in caged and immobilized rodents and in myasthenic humans 17 p3030 A70-35357

Ultrasonic velocity in human bones measured for calcium content and density 22 p3979 A70-43522

Weightlessness and immobilization effects on mechanical tolerance of bone compressive and breaking strength in monkeys 22 p3973 A70-43648

BOOLEAN ALGEBRA

NT BOOLEAN FUNCTIONS

BOOLEAN FUNCTIONS

Symmetric Boolean function detection by method using potential concept, determining alpha numbers with potential values for canonical terms 02 p0324 A70-12188

BOOMS [EQUIPMENT]

Deployable STEM/storable tubular extendible member/booms for aerospace gravity gradient stabilization, noting interlocked BI-STEM 04 p0761 A70-14725

TV system for satellite antenna boom position monitoring, describing camera system and programming, imaging techniques, position calibration, etc 10 p1891 A70-24898

Hybrid satellite attitude control system deformation model, utilizing pivoted flexible boom with tip mass as actuator and inertia wheels to dampen gravity induced librations 11 p2123 A70-26127

Orbit eccentricity effect on gravity gradient system with single damping boom, investigating optimum steady state and transient response conditions 11 p2123 A70-26129

Motion stability of rapidly spinning satellite, discussing elastic booms effect 11 p2128 A70-26784

Thermal coated extendable boom for space applications, describing construction and vacuum metallizing technique 12 p2242 A70-27266

Subcaliber cylindrical boom at base of spin stabilized projectile shown to produce aerodynamic changes in static and Magnus moments 13 p2340 A70-29023

Book on tubular spacecraft booms covering design and flight experiences, system performance, evaluation, etc 16 p2983 A70-33961

Spacecraft boom design and performance, including Russian spacecraft photographs 16 p2985 A70-34137

Thermal and mechanical properties of materials for spacecraft booms design 16 p2986 A70-34138

Gearhead DC/AC electric motors with wet/dry lubricants, discussing selection criteria for spacecraft boom deployment 16 p2846 A70-34139

Spacecraft boom selection, discussing parameters, intended use, environment and effect on vehicle 16 p2986 A70-34140

Closed tubular extendible boom [Multiple Applications Storable Tube/ design, fabrication and applications, including stress factors and materials 16 p2846 A70-34142

Space erectable boom with interlocked seam, perforations and coatings to provide torsional rigidity and thermal stability 16 p2986 A70-34143

ATS attitude stabilization boom packages, describing torque transmission, drum synchronization, electrical isolation, lubrication, etc 16 p2846 A70-34145

Radio Astronomy Explorer satellite boom deployment method resulting in gravity gradient capture, emphasizing role of predeployment attitude and antenna Vee angle
[AIAA PAPER 69-920] 21 p3931 A70-41856

Comparative stability of freely spinning satellites for arbitrary number of flexible booms in rotation plane
22 p4111 A70-43440

Spacecraft thin walled tubular booms thermal curvature time constants in relation to solar induced despin of satellites
23 p4258 A70-44521

BOOST

U ACCELERATION (PHYSICS)

BOOSTER RECOVERY

Space shuttle atmospheric maneuvers, examining booster and orbiter entry, flyback and abort
[AAS PAPER 70-047] 17 p3175 A70-34787

BOOSTER ROCKET ENGINES

ELDO booster rocket third stage design and construction, including pictures of parts and devices
03 p0580 A70-13795

Altitude simulation equipment for third stage Europa 1 booster rocket
04 p0664 A70-15302

Fluidics application in sounding rocket guidance control circuits used in space boosters
05 p0797 A70-15809

Air force booster growth inventory, noting combination with space-configured upper stages and strap-on solid motors
[SAE PAPER 690713] 05 p0922 A70-15831

ELGO launcher system with apogee booster for placing payload in geostationary orbit
13 p2505 A70-28768

Digital guidance and control system, discussing communication device providing data transfer between airborne digital computer and control device
[AIAA PAPER 69-988] 14 p2615 A70-30771

Europa 3C light alloy space booster powered by Rolls-Royce engines using kerosene and LOX
15 p2810 A70-32257

Ion electric propulsion system coupled with small booster for geostationary orbit realization
15 p2790 A70-32276

Velocity vector for boost vehicles guidance, comparing implicit and explicit computation
16 p2947 A70-33441

Speed convergence of hybrid vs digital computer synthesis of optimal boost vehicle controller, considering fuel consumption and pitch dynamics
16 p2981 A70-33442

Control systems synthesis with parametric invariance for spacecraft boosters
17 p3177 A70-35219

Launch vehicle injection error sensitivity minimization by trajectory shaping using excess booster capability
[AIAA PAPER 70-1078] 19 p3534 A70-38889

Combustion chamber, turbopump and combustion control system for French turbopump-fed booster rocket motor
20 p3688 A70-39649

Hybrid combustion ram rocket drives, discussing booster initial acceleration, exhaust gas use as fuel and payload gain
[ICAS PAPER 70-50] 23 p4233 A70-44147

Europa 2 booster perigee stage engine design, discussing total and propellant masses, spin stabilization, materials, etc
23 p4234 A70-44672

Saturn 5 Apollo booster stages oscillations induced by coupling between vehicle structure and engine thrust corrected within existing systems
[AIAA PAPER 70-1236] 24 p4417 A70-45954

Italian space satellite booster programs for launching satellite payloads into low orbit
03 p0609 A70-13846

Reusable booster rocket heat protection system design, discussing ablation and insulation methods
05 p0958 A70-16635

Expendable propellant tanks /Tip Tank Concept/ on lifting body reusable booster operations to reduce cost for low earth orbital transport mission
11 p2122 A70-26052

Two stage rocket booster-ram rocket launcher combination compared to single and two stage rockets
11 p2126 A70-26287

Low cost orbital space transportation system with shuttle service, discussing booster and configuration selections, weight, costs, etc
[AIAA PAPER 70-256] 13 p2506 A70-29615

Balloon-radar soundings of horizontal wind profiles for booster vehicle design
14 p2653 A70-30588

Reliable collet release mechanism design for separation and ejection of reentry vehicle payload from booster
16 p2922 A70-34118

Booster parameterized guidance algorithms investigated on basis of steering forms validity, discussing exoatmospheric ascent applications
[AIAA PAPER 70-1006] 20 p3669 A70-39584

BOOSTGLIDE VEHICLES

Space shuttle structural technology for booster and orbiter, discussing hot and cold structure concepts, reentry bodies, military payloads, radiating protective coatings, refractory materials, etc
22 p4111 A70-43516

BORANES

NT CARBORANE

BORES

U CAVITIES

BORESIGHTS

Nonimaging remote sensor data display in spatial registration with ground scene to determine sensor boresight position accuracy
12 p2229 A70-26940

BORIC ACIDS

Third body coefficients of water and heavy water reactions in KCl coated and aged boric acid coated vessels with vibrational-vibrational exchanges
14 p2546 A70-31091

BORIDES

NT TITANIUM BORIDES

Phase content determination in borides and borocarbides mixtures based on compounds different chemical stabilities during hydrolysis and reaction with acids
03 p0514 A70-12984

Metastable tau-phase in Fe-Ni-B melt solidifying into boride, noting lattice constant and solubility
07 p1307 A70-19393

Synthesis procedure for single crystal transition metal diborides, using high pressure capability in controlling stoichiometry
07 p1313 A70-19895

Boride composites with high strength and thermal resistance suitable as nose cap and leading edge materials for reusable lifting reentry systems
[AIAA PAPER 70-278] 07 p1315 A70-20387

Thermal emission cathodes made from lanthanum, yttrium and gadolinium hexaborides, measuring I-V characteristics
22 p3998 A70-43442

Ti, Zr and Hf diborides electrophysical properties, discussing temperature effects and electronic structures
23 p4205 A70-43991

Thermal and electrical conductivities of zirconium and hafnium diborides polycrystalline powders at 300-1300 K
23 p4209 A70-44443

BORN APPROXIMATION

Electron loss in heavy body collisions from free scattering model and Born approximation
02 p0342 A70-11879

Hydrogen-hydrogen double excitation collision cross sections computed by impact parameter method, using Born and two state approximations
02 p0342 A70-11881

Spectrum function in Booker scattering formula /first order Born approximation/ for dielectric constant fluctuations in hypersonic wake plasmas
03 p0529 A70-12908

Born wave for atom-atom inelastic cross sections, calculating He excitation from ground state to higher states by H atom collision
07 p1346 A70-20241

Born approximation used in calculating wave functions of helium atom for determining generalized oscillator strengths in first ionized continuum of helium
10 p1919 A70-24072

Electron-atom collisions, treating elastic and Mott scatterings, Born approximation and ionization
12 p2274 A70-27062

Born approximation limit for plane wave multiple scattering by inhomogeneous electron density distribution in plasma
16 p2957 A70-32981

Rayleigh-Gans-Born approximation application to thermal radiation of reflecting convex plasma sphere, cylinder and ellipsoid
18 p3294 A70-36146

Electron excitation cross sections for light atoms using Slater wave functions and Born-Bethe approximations
21 p3853 A70-41393

BORN-MAYER EQUATION

U BORN APPROXIMATION

BORN-OPPENHEIMER APPROXIMATION

Coupled Schroedinger equations for diatomic molecules internal motion solved using best adiabatic approximation to obtain energy correction to Born-Oppenheimer method
08 p1548 A70-21522

Adiabatic corrections to long range Born-Oppenheimer interatomic potentials from rotationally coupled Schroedinger equations
17 p3138 A70-35199

BORON

NT BORON ISOTOPES

Tensile tests of heat treated silicon carbide coated B filament reinforced metals, discussing fiber strength and interfacial stability
01 p0117 A70-10483

Fiber breakage during powder metallurgy fabrication of compact Al-B composites as function of density
01 p0104 A70-10741

Injected B particles burning in hot gas stream of oxidant mixture with Ar and H, observing trace widening by motion picture technique
01 p0218 A70-11016

Boron fiber reinforced epoxy fatigue life dependence on reinforcing fibers aspect ratio
01 p0129 A70-11082

Al-B composite missile adapter design for aerospace structures
02 p0306 A70-11951

Boeing 707 B-epoxy composite forelap design, analysis, fabrication and flight testing
02 p0307 A70-11955

B and C fiber unidirectionally reinforced plastic composites, discussing mechanical properties, fabrication and testing
02 p0321 A70-12082

Boron combustion in air augmented rockets, examining mixing and burning between subsonic air and supersonic fuel rich exhaust
[AIAA PAPER 68-634] 03 p0603 A70-12910

Quantitative method developed for photometric determination of B in nickel or titanium borides, using magnezon I reagent in alkaline solutions at various pH
03 p0504 A70-2983

Axial and traction loaded boron epoxy laminates tensile and compressive elastic properties and strengths compared from test data including strain gauge measurements
03 p0586 A70-13115

Case hardened steels structure and properties, intermetallic phases, hardness variation with depth and hardening techniques by Be and B
03 p0510 A70-13351

Two step B vacuum diffusion from boron oxide into Si surface using evacuated tube and N atmosphere
05 p0891 A70-15791

Boron and other high performance reinforcements made by vapor plating process, discussing boron filament atomic structure and morphology
05 p0873 A70-16609

Boron-epoxy composite materials for secondary and primary aircraft structural components, discussing multidirectional laminates, joint analysis, etc
05 p0942 A70-16620

Joint design for braze bonding and joining of Al-B composites using Borsic tape backed with alloy brazing foil
07 p1293 A70-18994

Combustion of pure crystalline boron single particles injected into hot oxidizing gases streams at atmospheric pressure
[AIAA PAPER 69-562] 07 p1359 A70-19583

Boron fiber reinforced composites structure and loading capacity, describing network-like fiber winding technique for light reinforced structures
07 p1318 A70-19771

Fatigue tests to relate boron-epoxy laminate fatigue behavior to thermal preconditioning environments
07 p1320 A70-19960

Nickel boronizing in high temperature vacuum, studying mechanical properties and layer thickness time dependence
08 p1517 A70-21148

Graphite crystals surface ribbed growth in Ni-C solutions due to B content observed by scanning electron microscope
08 p1520 A70-21552

Axial constant load creep and strength rupture measurements of B-coated and silicon carbide-coated B filament reinforced Al alloys
08 p1521 A70-21702

Transverse and shear strengths of Al-B composite materials used in F-111 aircraft components, investigating cold work, thermal treatments and steel wire addition effects
08 p1509 A70-21857

Tension, compression and in-plane shear tests to obtain boron epoxy composite materials mechanical properties to design FB-111 wing box extension
08 p1529 A70-21879

Compression test data of Al-B composites used for predicting structural element failure
08 p1523 A70-21886

Test standards for boron epoxy flat laminates, proposing specimen geometries and testing methods
08 p1530 A70-21887

Matrix optimization of boron filament reinforced polymeric for short duration high temperature aerospace applications
08 p1530 A70-21891

Fatigue testing and thermal mechanical treatment effects on uni- and biaxial Al alloy-B composites tensile strength at room and elevated temperatures
08 p1523 A70-21893

Tensile, fatigue, creep and stress-rupture behavior of unidirectional, unidirectional off-axis and cross-piled composites of B filaments in Al alloy matrix
08 p1531 A70-21896

- Laminated anisotropic rectangular plates of boron-epoxy composite material, studying shear stability by potential energy and Ritz method
08 p1595 A70-21903
- Structural analysis of boron filament-epoxy composite laminate tubes for use as spacecraft long column members
08 p1595 A70-21911
- Fractography of Al-B metal matrix composites to study micromechanical behavior, using scanning electron microscopy
08 p1524 A70-21913
- Al-B composites mechanical properties, using heat treatments and transverse steel wires to increase matrix shear and transverse tensile strengths
09 p1701 A70-22551
- Solar boron abundance from BH, BN and BO absorption bands in sunspot spectra, noting no traces in solar atmosphere
11 p2108 A70-25738
- Al and B particles combustion in methane-oxygen system, considering reaction zone models, energy release rate, particle kinetics, instabilities, etc
11 p2149 A70-26284
- Boron epoxy composite structural parts for aerospace vehicles, discussing production times and cost reduction
[ASTME PAPER EM-69-143] 12 p2240 A70-27076
- Boron fibrous composite panels machining methods including drilling, routing, band sawing and reaming
[ASTME PAPER EM-69-141] 12 p2240 A70-27077
- Wide goods fabrication of boron composites, discussing mechanical properties and cost effectiveness
[ASTME PAPER EM-69-142] 12 p2240 A70-27078
- Filament winding process for boron modified phenolic resin tape used in high temperature applications
12 p2242 A70-27204
- Aluminum-boron composite material applications to structural components of F-106 aircraft, noting weight saving and mechanical properties
[AIAA PAPER 68-975] 12 p2257 A70-28082
- Aircraft structure fabrication combining unidirectional strength and stiffness of B composite with metal, including test and weight/cost data
13 p2418 A70-28777
- Aluminum-boron composites for aircraft adapter fabrication
13 p2435 A70-29247
- Boron particles combustion behavior prediction by incorporating condensed phase effect into diffusion controlled model
[WSCI PAPER 70-9] 13 p2472 A70-29612
- Metallic base fiber and particulate composites, emphasizing silicon carbide, sapphire, boron and graphite filaments
14 p2597 A70-31168
- Al-B composites forming and machining, discussing tooling, methods and filament orientation
[ASM PAPER W70-5.2] 15 p2744 A70-32334
- Mechanical properties prediction analysis of boron filament wound reinforced composite structures verified by structural tests
16 p2937 A70-33370
- Boron, silicon carbide and graphite fibers surface properties
16 p2937 A70-33376
- Boron particles ignition and combustion in supersonic air stream, emphasizing axial and lateral two phase flow injection
[AIAA PAPER 70-737] 16 p2856 A70-33496
- Boron epoxy composite wing structures design, fabrication and testing
16 p2990 A70-33703
- Boron-epoxy stiffener reinforced metal wings, examining structural efficiency of multiweb beam aluminum cover skins and Z stiffened panels
16 p2994 A70-34230
- Electrochemical oxidation of p-type boron anode in aqueous solutions, using galvanostatic technique
17 p3041 A70-34514
- Secondary combustion products of air augmented boron loaded solid propellant rocket ram burner, measuring properties by spectroscopy
17 p3196 A70-35196
- Boron thermal diffusion effects on plastic of pure Mo subjected to recrystallization
17 p3102 A70-35408
- Al alloy matrix-boron fiber-stainless steel wire composites fabrication into various shapes with desired mechanical properties for aerospace structural components applications
18 p3263 A70-36837
- Boron composites development for aircraft structures compared with titanium
[ASME PAPER 70-GT-120] 18 p3344 A70-36851
- Refractory metals interaction with boron during vacuum boronizing, investigating kinetics and optimal process conditions
19 p3434 A70-37452
- Boron and boron carbide coatings formation on graphite by vapor deposition, determining optimum parameters for reaction control
19 p3455 A70-38250
- Boron vs carbon fiber reinforced plastics, discussing layer and panel structures, molded and mechanical sections, preimpregnation, cost and structural concepts
21 p3842 A70-41263
- Electronic transitions in B by beam foil technique for spectral lines in 450-5000 Å range, measuring excited levels mean lives
21 p3781 A70-41932
- Particulate boron levitated electrostatically in air and ignited by pulsed laser to avoid contamination, investigating combustion by high speed photography [SMPT PREPRINT 100] 22 p4032 A70-43034
- Boron-Al composite filament fracture behavior and postimpact tensile strength, examining shock loading and impact velocity effects
22 p4060 A70-43682
- Boron-epoxy composites rectangular reinforcing arrays spacing aspect ratios, considering matrix stress concentrations and stiffness estimates
22 p4119 A70-43688
- Boron impurities introduction into InP crystals grown by liquid encapsulation, detecting IR absorption bands due to localized lattice vibration
23 p4231 A70-44891
- Boron and boron-carbide coatings formation by vapor deposition, determining optimum thermodynamic parameters from experiment
24 p4366 A70-45241
- Carbon steel diffusion saturation with Ti and B, investigating layer depth, weight gain and microhardness dependence on powdered mixture composition
24 p4364 A70-46336
- BORON ALLOYS**
B-C alloys chemical composition effect on high temperature stability in pure oxygen
03 p0514 A70-12978
- Isothermal sections in Ti-Ni-B, Mo-Ni-B and W-Ni-B at 800 C determined by X ray analysis
06 p1090 A70-17846
- Isothermal section determination in Mo-Cr-B at 1000 C using X ray, metallographic analyses and microhardness measurements
06 p1090 A70-17847
- Alloying elements effects on vanadium alloys case hardening by boronizing
07 p1303 A70-18742
- Tensile strength of nitrided boron-aluminum alloy composite modules, noting effect of Ti cladding on panel surfaces
11 p2066 A70-26085
- Boron effects in austenitic stainless steels, considering chromium carbide formation, high temperature strength, ductility, etc
16 p2916 A70-33079
- Sintered boron-alloyed Mo electron beam welding behavior examined by texture-revealing color etching method
21 p3833 A70-41411
- BORON CARBIDES**
Phase content determination in borides and borocarbides mixtures based on compounds different chemical stabilities during hydrolysis and reaction with acids
03 p0514 A70-12984
- Boron and boron carbide coatings formation on graphite by vapor deposition, determining optimum parameters for reaction control
19 p3455 A70-38250
- Temperature effect on friction coefficient of boron and silicon carbides, using similar wear pairs in vacuum
23 p4205 A70-44044
- Boron and boron-carbide coatings formation by vapor deposition, determining optimum thermodynamic parameters from experiment
24 p4366 A70-45241
- BORON CHLORIDES**
Luminescence and destruction of gaseous boron trichloride by carbon dioxide laser radiation
11 p2064 A70-26818
- Luminescence and destruction of gaseous boron trichloride by carbon dioxide laser radiation
24 p4351 A70-45190
- BORON COMPOUNDS**
NT BORIC ACIDS
NT BORIDES
NT BORON CARBIDES
NT BORON CHLORIDES
NT BORON FLUORIDES
NT BORON NITRIDES
NT BORON OXIDES
NT CARBORANE
NT DIBORANE
NT TITANIUM BORIDES
- Boron carbonitride soldering with refractory metals by molybdenum disilicide as solder, analyzing electrical resistance and gas tightness
09 p1707 A70-23123
- Amorphous boron arsenide films deposited on Si substrates, measuring current voltage characteristics
15 p2785 A70-32584
- BORON FLUORIDES**
Oxygen difluoride-diborane reaction kinetics and boron fluoride formation rate
[WSCI PAPER 70-11] 13 p2362 A70-29611
- Pressure dependence and high pressure limiting values of rate constants of gas phase reaction of monomethylamine and trimethylamine with boron trifluoride
19 p3373 A70-37775
- BORON HYDRIDES**
NT CARBORANE
BORON ISOTOPES
Solar neutrinos detection from recording high energy electrons in reactions, using Li 7, Be 9 and B 11 as detectors
05 p0899 A70-15964
- BORON NITRIDES**
Thermal stability of turbine sealant mica-ceramic materials containing boron nitride
04 p0712 A70-14467
- Tensile strength of nitrided boron-aluminum alloy composite modules, noting effect of Ti cladding on panel surfaces
11 p2066 A70-26085
- BORON OXIDES**
Density, refractivity, thermal expansion coefficient, softening point and soaking stability for glass containing barium, lead, boron, bismuth and titanium oxides
05 p0871 A70-16594
- Crystallization and dielectric properties of glass containing barium, lead, titanium and boron oxides, noting frequency and temperature dependence
05 p0871 A70-16595
- Ingredient proportions for enamels containing titanium and boron oxides
05 p0871 A70-16597
- BORON TRIFLUORIDE**
U BORON FLUORIDES
BOSE-EINSTEIN STATISTICS
U QUANTUM STATISTICS
BOSON FIELDS
Five dimensional rotations and representation of isomorphic spinor groups by boson operators calculus, expanding Gelfand states in Weyl patterns
01 p0147 A70-10521
- BOSONS**
NT ALPHA PARTICLES
NT MESON RESONANCES
NT MESONS
NT PHOTONS
NT PIONS
- Self gravitating bosons or fermions equilibrium configuration in ground state, confirming Oppenheimer-Volkoff treatment approximation
08 p1581 A70-21741
- Second quantization exciton theory in amorphous disordered materials, discussing hamiltonian, boson annihilation operators and electronic polarization
14 p2627 A70-30693
- BOUGUER LAW**
Bouguer single-scatter theory applicability dependence on angular aperture of receiver and laser beam parameters in water mists
03 p0451 A70-13756
- Configuration factors independence on Lambert law in radiation from spheres and infinitely long cylinders [ASME PAPER 69-HT-J] 04 p0784 A70-14870
- Bouguer single-scatter theory applicability dependence on angular aperture of receiver and laser beam parameters in water mists
10 p1842 A70-25005
- BOUNDARIES**
NT FLUID BOUNDARIES
NT FREE BOUNDARIES
NT GAS-SOLID INTERFACES
NT GRAIN BOUNDARIES
NT JET BOUNDARIES
NT LIQUID-LIQUID INTERFACES
NT LIQUID-SOLID INTERFACES
NT LIQUID-VAPOR INTERFACES
- Magnetosphere boundary configuration calculated with allowance for geomagnetic dipole inclination to geographic axis and nondipole section of geomagnetic field
01 p0082 A70-11522
- Love wave propagation in layers with irregular boundaries, investigating scattered field to determine reflection from triangular notch
13 p2394 A70-28831
- Au-Pd films boundary structure during diffusion annealing, noting polymerized oil vapor effect originating from vacuum pump
15 p2758 A70-32121
- Point source electric field over different sections of impedance piecewise inhomogeneous surface, calculating attenuation function near boundaries
19 p3381 A70-38570
- BOUNDARY LAYER COMBUSTION**
Thermal conditions and graph-analytic solution of laminar boundary layer combustion of disk rotating in free atmosphere and plate in Couette flow
01 p0218 A70-11017
- Inert, oxidizing or reducing fluids wall injection into combustion gas boundary layer of variable composition noting effects on wall temperature
05 p0956 A70-15919

Thermal conditions and graph-analytic solution of laminar boundary layer combustion of disk rotating in free atmosphere and plate in a Couette flow
09 p1787 A70-22266

Laminar boundary layer behind normal shock wave with vaporization and combustion, obtaining profiles on analog computer
11 p2148 A70-25967

Two layer model of burning in turbulent boundary layer on porous surface for carbon monoxide oxidation reaction
18 p3346 A70-36268

BOUNDARY LAYER CONTROL
NT POROUS BOUNDARY LAYER CONTROL
Turbulent boundary layer control by wall jet, analyzing wall jets in adverse pressure gradients for two limiting cases
[AIAA PAPER 70-107] 06 p1041 A70-18160

Aircraft development for subsonic and transonic flight dependent on methods using blowing and boundary layer control and Coanda and Magnus effect
09 p1610 A70-22220

Boundary layer to wake bleed venting for flare-induced separation prevention in hypersonic flow over blunt bodies
16 p2838 A70-33884

Moving skin boundary layer control on airfoil achieved by moving wetted surface in streamwise direction
[AIAA PAPER 70-881] 17 p3010 A70-34808

High lift airfoils boundary layer separation suppression by blowing, describing wall jets streamwise development prediction methods
[AIAA PAPER 70-872] 17 p3010 A70-34818

Suction velocity effects on Rayleigh problem in MHD of flat nonmagnetic nonconducting plate, solving for velocity distribution and skin friction
19 p3481 A70-38448

Turbulent boundary layer control by uniform fluid injection and suction, discussing velocity profiles, wall and wake laws, skin friction and shear stress transport equation
[ICAS PAPER 70-10] 23 p4180 A70-44121

Aircraft longitudinal motion during takeoff and landing due to loss of lift after boundary layer control system failure
24 p4372 A70-45448

BOUNDARY LAYER FLOW
NT BOUNDARY LAYER SEPARATION
NT REATTACHED FLOW
NT SECONDARY FLOW
NT SEPARATED FLOW
Boundary layer equations for plane steady incompressible flow, studying given velocity profiles effects on equations solutions
01 p0060 A70-10144

Boundary layer around blunted cone solved numerically by finite difference method
01 p0001 A70-10297

Turbulent boundary layer computations for flows with various pressure distributions
01 p0063 A70-10928

Laminar airfoils for Reynolds numbers above 4,000,000, utilizing potential and boundary layer flow theories
01 p0063 A70-10930

Boundary layer and singular inviscid stagnation point reacting flow matching, corrections structure and decay and ranking comparison with second order effects in fluid mechanics
01 p0065 A70-11096

Galerkin method applied to boundary layer flows, considering transport problems in unbounded domains
01 p0066 A70-11129

Modified Granville moment of momentum method used with integral equations in integral moment method for turbulent boundary layer flow, considering pressure gradient influence
02 p0282 A70-12334

Heat transfer, three dimensional boundary layers and high speed flow calculations, utilizing original entrainment equation
02 p0284 A70-12341

Differential strip method developed for turbulent boundary layer equations, describing flow by law of wall coupled to wake solution utilizing constant eddy viscosity
02 p0285 A70-12352

Boundary layer prediction methods criteria, discussing advantages and disadvantages of differential and integral methods for various flows
02 p0286 A70-12356

Waves vs eddies in dynamics of turbulent boundary layer fluctuating motions with scale of mean flow
02 p0287 A70-12361

Graphical display of diverse methods of flow predictions by various authors for turbulent boundary layers
02 p0287 A70-12363

Boundary layer calculation for semiinfinite plane turbulent jet on porous wall
02 p0287 A70-12691

Hypersonic flow characteristics on yawed circular cone surface at moderate angle of attack, applying

results to inviscid and boundary layer flow computations
03 p0406 A70-12944

Book on flow and thermal boundary layers covering laminar and turbulent flow velocity profiles, Prandtl equation, heat transfer problems, etc.
03 p0465 A70-13015

Boundary layer processes under unsteady suction allowing for compressibility, relating suction value to external velocity and wall temperature
03 p0465 A70-13275

Boundary layer transition from laminar to turbulent in hypersonic wind tunnel, determining Reynolds and Mach number effects
[ONERA-TP-737D] 03 p0467 A70-13641

Axisymmetric incompressible fluid flow aerodynamic properties in flat vortex chamber, studying core and boundary layer interactions and velocity fields
03 p0551 A70-13731

Hall current effect on steady boundary layer flow of incompressible viscous electrically conducting fluid past semiinfinite flat plate in transverse magnetic field
03 p0469 A70-14183

Magnetic boundary layer equations applied to flow past stationary circular cylinder and sphere, showing graphical variation of slip velocity with angle
03 p0471 A70-14334

Sonic throat formation from two dimensional viscous flow interaction with supersonic inviscid outer stream, using boundary layer equations
04 p0665 A70-14452

Values measured on sharp flat plate in 10.4 Mach boundary layer induced pressure gradient, discussing effects of wall pressure and temperature gradients
04 p0621 A70-15609

Steady state boundary layer of anisotropic Ericksen fluid incident obliquely on infinite cylinder, obtaining differential equations for dynamic behavior
05 p0835 A70-16860

Incompressible boundary layer flow of conducting fluid on solid two dimensional and axisymmetric bodies under transverse magnetic field approximated by momentum method
06 p1031 A70-17199

Flow disturbance calculation for heat transfer between boundary layer flows and adjacent walls modified to allow for wall attachment of thermal boundary layer
06 p1032 A70-17228

Rotta differential equation for turbulent boundary layer flow with fixed profiles of length scale, shear stress and kinetic energy
06 p1035 A70-17694

Porous matrix flow, surface liquid layer and hot gaseous boundary layer interactions at nose tip of reentry vehicle
[AIAA PAPER 70-152] 06 p1037 A70-18028

Boundary layer-induced pressures on flat plate in unsteady hypersonic flight calculated using tangent wedge approximation
[AIAA PAPER 70-184] 06 p1039 A70-18095

Integral moment method for interactions between laminar boundary layer and external supersonic flow applied to hypersonic laminar boundary layer near sharp expansion corner
[AIAA PAPER 70-186] 06 p1039 A70-18111

Higher order boundary layer effects on zero-lift drag of sphere-cones, investigating transverse curvature, shock vorticity, displacement, slip and temperature jump
[AIAA PAPER 70-185] 06 p1041 A70-18173

Flat plate boundary layer flow of partially ionized gas, measuring charged particle density, electron temperature and plasma potential distributions with Langmuir probe
[AIAA PAPER 70-86] 06 p1041 A70-18174

Asymptotic behavior for small mean free path of rarefied gas steady flow over smooth solid boundary
06 p1048 A70-18328

Steady viscoplastic boundary layer near hard wall with power law velocity distribution along outer boundary, deriving self similar solution
07 p1252 A70-18670

Unsteady boundary layer flow with suction, deriving equations for circular cylinder impulsive motion
07 p1253 A70-18862

Nonsimilar laminar boundary layer solutions with negative pressure gradient compared to experimental boundary layer velocity profiles, momentum and displacement thicknesses
[AIAA PAPER 69-35] 07 p1256 A70-19312

Downstream distribution of trace element injected into boundary layer of flat plate or cone with self similar mass transfer
[SAMSO-TR-69-56] 07 p1256 A70-19313

Unsteady boundary layer in compressible fluid laminar flow over accelerating semiinfinite flat plate
07 p1258 A70-19566

Radiation effect on heat transfer during film boiling in forced convection boundary layer of liquid flow past plate, noting vaporization temperature
07 p1423 A70-19812

German book on fluid dynamics for nonideal fluids covering viscosity effects, Prandtl boundary layer, turbulence and aerodynamics
08 p1431 A70-20751

Heat transfer in axially symmetric laminar viscous boundary layer flow due to rotating bodies of revolution, obtaining temperature distribution
08 p1485 A70-21698

Monograph on hypersonic flow boundary layers research conducted by European countries, determining pressures, velocity and temperature profiles, skin friction, heat transfer, displacements, etc.
[ONERA-TP-770] 08 p1601 A70-21844

Turbulent energy spectra in stably stratified atmospheric boundary layer flow
09 p1715 A70-22360

Flow noise measurement for boundary layer pressure fluctuations at rigid wall, analyzing effect of transducer size, shape and orientation on resolution
09 p1675 A70-22387

Shock layer thickness in supersonic inviscid gas flow past blunt bodies, calculating boundary layer near stagnation point
09 p1603 A70-22442

Second order boundary layer equations for incompressible flow, presenting simplified integral momentum equation for two dimensional and axisymmetric flow
09 p1660 A70-22681

Two dimensional equations of boundary layer with arbitrary pressure gradient solved using successive approximations for numerical integration
09 p1605 A70-23168

Boundary layer equations for multicomponent flow with finite chemical reactions solved by finite difference method
09 p1605 A70-23201

Cross hatching on surface of ablating bodies exposed to supersonic turbulent boundary layer flow using mathematical model
09 p1605 A70-23232

Boundary layer equations with heat transfer for laminar and turbulent incompressible flows about two dimensional and axisymmetric flows, using finite difference method
[ASME PAPER 69-HT-7] 09 p1663 A70-23560

Boundary layer of MGD flow past axisymmetric insulator body analyzed to determine torque due to Hall effect
09 p1663 A70-23579

Laminar boundary layer parameters on porous surface in presence of pressure gradient obtained for inner /wall/ and outer regions
09 p1664 A70-23712

Wake-boundary layer interaction in wind tunnel tandem cascades, discussing end wall suction
09 p1609 A70-23750

Upstream influence distance estimation associated with critical pressure rise in two dimensional shock-boundary layer interactions based on Lighthill subsonic inner boundary layer concept
10 p1862 A70-23840

Boundary layer flow near flat plate trailing edge taking into account pressure gradient induced locally in external flow
10 p1862 A70-23846

Orr-Sommerfeld equation of hydrodynamic stability theory solved for incompressible two dimensional boundary layer flow on basis of reduction to integral equation
10 p1867 A70-24161

Laminar boundary layer flow of incompressible fluid in wake of symmetrical disturbance, deriving higher order approximations and introducing Euler transformation
10 p1802 A70-24420

Unsteady compressible laminar boundary layer flow around flat plate influenced by compressibility as function of Mach number
[ONERA-TP-803] 10 p1869 A70-24543

MHD boundary layer flow equations solution by initial value method to eliminate iteration process
10 p1924 A70-24563

Axisymmetric or two dimensional incompressible laminar boundary layer flow field numerical analysis using quasi-linearization and Chebyshev series
11 p2072 A70-25965

Linear viscous theory of steady rotating fluid flows with nonlinear modification of boundary layers, considering inertial modifications
11 p2036 A70-26011

Three dimensional periodic boundary layer flow noting successive approximations method, noting steady streaming in first order cross flow
11 p2037 A70-26296

Laminar boundary layer flow with exponential velocity distribution in outer flow described by differential equations, studying slip velocity at wall
11 p2037 A70-26350

Incompressible boundary layers velocity distributions on cylinders rotating in axial flow, considering centrifugal force effects, momentum thicknesses, local shearing stress, etc.
11 p2038 A70-26477

Motion and shape of interface at separation of turbulent and nonturbulent regions in boundary layer with zero pressure gradient

11 p2040 A70-26539

Harmonic fields with boundary flow losses, discussing similarity on basis of dimensional analysis and pi theorem

12 p2271 A70-26877

Singularities of boundary layer conditions on parabolic cylinder in homogeneous incompressible viscous flow with leading edge, using Weyl integral equation

12 p2210 A70-27559

Compressible turbulent boundary layers velocity profiles, Coles universal wake function, least squares methods, wake-wall representation, etc.

12 p2157 A70-28080

Incompressible two dimensional and axisymmetric oscillating laminar boundary layer flows approximated by momentum integral equation, discussing flow along flat plate

12 p2158 A70-28205

Flow equations for curvilinear boundary layer based on laminar incompressible boundary layer in streamwise corner

13 p2386 A70-28541

MHD boundary layer flow past yawed flat plate in presence of pressure gradient, determining skin friction expansion terms

13 p2461 A70-28804

Wind tunnel boundary interference on V-STOL model calculated in test section with solid vertical and slotted horizontal walls, using image method and Fourier transforms

[AIAA PAPER 70-575]

13 p2343 A70-29894

Gravity effect on conical vortex separator, predicting body force effect on heavy fluid boundary layer flow for limiting condition determination

13 p2391 A70-29978

Transient free convection flow due to arbitrary motion of vertical plate, linearizing equations of boundary layer flow and heat transfer

13 p2523 A70-30009

Incompressible turbulent fluid flow through ducts and pipes by integral boundary layer techniques, considering entrainment principles

14 p2564 A70-30258

Three dimensional boundary layer along semi-infinite swept stagnation line, assessing counteracting effects of cross flow and mass transfer

14 p2565 A70-30278

Boundary layer flow between nodal and saddle points of attachment, comparing matched series and finite difference methods

14 p2565 A70-30281

Unsteady incompressible laminar boundary layer equations solution after Crocco transformation by implicit finite difference scheme for flow around blunt body

14 p2528 A70-30290

Subsonic boundary lift interference in wind tunnels with perforated walls, using point matching method

14 p2563 A70-30869

Steady viscoplastic boundary layer near hard wall with power law velocity distribution along outer boundary, deriving self similar solution

15 p2718 A70-31462

Boundary layer retarded flow past porous surface with suction, using Runge-Kutta computerized integration of Falkner-Scan equation

15 p2720 A70-31586

Viscous incompressible fluid nonstationary flow boundary layer extension around porous plate at Prandtl number equal to unity

15 p2722 A70-32873

Subsonic turbulent boundary layer with mass addition and combustion for combustion effects on velocity profiles in constant pressure and accelerating flows

[AIAA PAPER 70-724]

16 p2997 A70-33498

Outer boundary conditions derivation from asymptotic form of similar boundary layer equations with unit Prandtl number

16 p2894 A70-33874

Equilibrium air boundary layer flows at three dimensional stagnation points, discussing flow characteristics and real gas heat transfer parameters

[AIAA PAPER 70-806]

17 p3005 A70-34455

Steady two dimensional MHD boundary layer flow with uniform suction or injection past semiinfinite flat plate in cross fields

17 p3067 A70-34618

Heat and mass transfer in flowing fluid, deriving conservation and constitutive equations, with application to boundary layer flow of gases

17 p3069 A70-35033

Hypersonic flow past slender bodies, discussing inviscid flows, outer edge singularity of boundary layer and three dimensional interaction on needle-like bodies

17 p3010 A70-35035

Laminar free convection boundary layer on vertical heated plate near discontinuity in plate temperature, discussing velocity field

17 p3198 A70-35593

Incompressible laminar boundary layer equations approximate solution by Galerkin-Kantorovich technique

18 p3238 A70-35972

Laminar flows with surface injection, calculating thermal boundary layer-porous wall coupling effects

[ASME PAPER 70-GT-1]

18 p3243 A70-36860

Boundary layer momentum thickness growth in channels with adverse pressure gradients by stepwise integration of Truckenbrodt equation and extending Gruschwitz-Schmidbauer separation criterion

[ASME PAPER 70-GT-12]

18 p3243 A70-36864

Three dimensional boundary layer flow on rotating axial flow turbine buckets, determining velocity profiles

[ASME PAPER 70-GT-59]

18 p3243 A70-36874

Boundary layer optimization for high turning axial flow compressor blades, using flow theory and conformal mapping

[ASME PAPER 70-GT-88]

18 p3209 A70-36879

Canonical coordinates for numerical computation of free surface flows, considering steady motion and elliptic partial differential equations

19 p3457 A70-37679

Boundary layer equations for two dimensional flow of incompressible constant density micropolar fluid past plane wall, noting skin friction

19 p3404 A70-37962

Velocity distribution and shear stress measurements in three dimensional turbulent boundary layer approaching separation

19 p3405 A70-38021

Multicomponent chemically unstable nonequilibrium gas flow past body, taking into account boundary layer behavior

19 p3373 A70-38182

High temperature gas boundary layer flows with or without magnetic fields, discussing measurement by X ray absorption technique

19 p3405 A70-38192

Two dimensional equations of boundary layer with arbitrary pressure gradient solved using successive approximations for numerical integration

19 p3406 A70-38390

Boundary layer oscillatory flow interaction with nonuniformly rotating lamina, calculating velocity distribution and transitional frequencies

19 p3406 A70-38443

NonNewtonian boundary layer flow having arbitrary potential velocities from methods for Newtonian fluids

19 p3407 A70-38932

Radiation effect on heat transfer during film boiling in forced convection boundary layer of liquid flow past plate, noting vaporization temperature

20 p3736 A70-39259

Spectral lines self rotation effects on plasma temperature and density measurement in MHD duct boundary layer

20 p3678 A70-39632

Combustion driven Hall configuration MHD generator, discussing boundary layer analysis, gas density nonuniformity and electrode drop

20 p3566 A70-40003

Simulated neutral atmospheric boundary layer measurements in wind tunnel, extending power spectral and correlation determinations

20 p3613 A70-40139

Flat plate boundary layer flow with surface blowing and suction / mass transfer, investigating stability by numerical techniques

20 p3615 A70-40507

Nonstationary compressible laminar boundary layer similar solutions by parameter-invariant method, obtaining velocity and temperature profiles by partial differential equations numerical integration

21 p3806 A70-40555

Asymptotic behavior of boundary layer equations solution for viscous incompressible flow past curvilinear obstacle

21 p3806 A70-40613

Flat plate compressible laminar boundary layer flow with variable fluid properties, using series solution by splitting up flow variables into sets of universal functions

21 p3806 A70-40825

Subcritical viscous flow around arbitrary airfoils, calculating boundary layer effect on pressure distribution from inviscid flow approximation

21 p3744 A70-40924

Accelerated self similar compressible laminar boundary layer flows with and without mass transfer, obtaining numerical solutions

21 p3807 A70-41031

Two dimensional body slow motion through stratified fluid bounded by parallel vertical walls, examining flow at different Peclet numbers

21 p3744 A70-41246

Self similar flow instability behind collapsing cavity boundary, examining perfect gas adiabatic equation of state

21 p3808 A70-41500

Rarefied gas flow over plane wall, considering boundary layer thickness of order of mean free path

21 p3809 A70-41715

BOUNDARY LAYER SEPARATION

Upstream mass injection effects on downstream heat transfer of supersonic reacting boundary layer

21 p3952 A70-42079

Incompressible laminar boundary layers thermal response behavior in wedge flow, obtaining surface response, temperature fields, heat flux and steady state data

21 p3811 A70-42164

Three dimensional laminar boundary layer equations for film condensation on curved surface in quiescent vapor, investigating flow at stagnation point

21 p3954 A70-42168

Heat and mass transfer in plane inductionless and dissipationless incompressible MHD boundary layer with longitudinal pressure gradient

21 p3861 A70-42231

Flow past streamlined obstacles under nonNewtonian fluid injection into hydrodynamic laminar and turbulent boundary layer

21 p3812 A70-42266

Elastic plate response to boundary layer pressure fluctuations, estimating vibration modes dependence on fluctuation convection velocity and response magnification as function of flow direction

22 p4007 A70-42283

Viscous flow field in pneumatic vortex rate sensor, discussing boundary layer parameters, velocity profiles and swirling flow theory

[ASME PAPER 70-FLCS-16]

22 p4007 A70-42411

Existence theorem for boundary layer problems, including swirling flow between coaxial rotating disks

22 p4009 A70-42484

Unsteady hydromagnetic boundary layer flow past semiinfinite flat plate under steady magnetic field and small free stream perturbation

22 p4080 A70-42631

Liquid droplet breakup by aerodynamic forces, obtaining solutions for fluid flow inside droplet and in coupled liquid-gaseous boundary layer

22 p4012 A70-43741

Tollmein-Schlichting waves in flat plate Blasius boundary layer, comparing experimental and theoretical critical Reynolds number

23 p4179 A70-43975

Three dimensional hypersonic laminar boundary layer subdivided into inner and outer regions, obtaining flow description by matching inner and outer solutions

23 p4182 A70-44565

Turbulent boundary layer velocity profiles and shear stress distributions computation based on mixing length approach

23 p4182 A70-44574

Highly accelerated boundary layer turbulence structure, measuring intermittency factor distribution with hot-wire probe

23 p4182 A70-44587

Channel vs deflection flow in boundary layer theory, considering Navier-Stokes equations

23 p4183 A70-44736

Friction-originated ageostrophic mass flux in ground friction layer at nonaccelerated geostrophic boundary layer flow

24 p4370 A70-45133

NonNewtonian fluids injection into boundary layer, comparing flow and pressure effects with water injection

24 p4324 A70-45364

Boundary layer instantaneous velocity distributions theoretical and experimental determination

24 p4288 A70-45583

Two dimensional boundary layer growth with suction for oscillating circular cylinder, considering stream functions and phase angles

24 p4326 A70-46002

BOUNDARY LAYER NOISE

U AERODYNAMIC NOISE

U BOUNDARY LAYERS

BOUNDARY LAYER SEPARATION

MHD boundary layers in transverse magnetic field with low Reynolds number, investigating suppression of separation with emphasis on behavior near rear stagnation point

01 p0152 A70-11095

Incompressible turbulent boundary layer and separation flow into forward facing normal step, considering step heights and boundary layer thickness

01 p0066 A70-11133

Prediction criteria regarding turbulent separation in fluid mechanical devices and systems, emphasizing vanishing wall shear stress

02 p0286 A70-12358

Pulsation frequency affecting boundary layer separation from channel wall in incompressible fluid flow calculated by equation

03 p0466 A70-13399

Boundary layer separation in divergent portion of conical ducts in overrelaxed supersonic regime in air and water, showing influence of medium, pressure and thrust

03 p0467 A70-13682

MHD boundary layer separation near rear stagnation point with magnetic field normal to wall solved by

series expansion, calculating skin friction by numerical quadratures

03 p0469 A70-14182

Similarity properties of laminar or turbulent boundary layer separation in uniform supersonic flow, discussing wall cooling, pressure evolution, etc.

03 p0469 A70-14234

Laminar compressible wake behind thin flat plate at zero angle of attack, solving boundary layer equations in von Mises coordinate plane

[ASME PAPER 69-WA/FE-6] 04 p0614 A70-14783

Laminar flow separation, reattachment and transition over downstream step, including visual observations of smoke filaments, velocity fluctuation measurements and velocity profiles

[ASME PAPER 69-WA/FE-5] 04 p0667 A70-14784

Plume-induced flow separation effect on thermal environment using Saturn 5 film and instrument data, attributing heating rate increase to recirculated exhaust gases

[ASME PAPER 69-WA/HT-18] 04 p0761 A70-14815

Stationary and vibrating circular cylinders for boundary layer separation point, determining vortex excited oscillation range

04 p0670 A70-14988

Incompressible laminar Falkner-Skan boundary layer suffering sudden acceleration by moving belt, noting boundary layer separation

[AIAA PAPER 69-40] 04 p0674 A70-15534

Tail screens and spoiler rings aerodynamic braking effect in hypersonic range, discussing separated boundary layer periodic unsteady flow

06 p0965 A70-17247

Rotation and forward flight effects on separation line of laminar incompressible boundary layer along helicopter blade of airfoil shape

[AIAA PAPER 70-49] 06 p0973 A70-18151

Supersonic flow separation over rearward facing step, measuring upstream boundary layer, lip shock and shear layer formation by pitot probe and surface pressure survey

[AIAA PAPER 70-106] 06 p0973 A70-18153

Laminar boundary layer development on cylindrical body set in motion from state of rest, determining time for boundary layer separation occurrence

07 p1253 A70-18771

Supersonic oblique shock wave reflection on turbulent boundary layer, considering layer separation and pressure effects

07 p1255 A70-19210

Air flow disturbances over mountains in terms of turbulent boundary layer separation dissolution

07 p1330 A70-19800

Laminar separation bubble in incompressible flow produced on flat plate by pressure gradients, correlating bursting with Reynolds number and pressure distribution

09 p1660 A70-22770

Laminar boundary layer separation noting effect of mass slot suction

09 p1662 A70-23236

MHD boundary layer on rotating body in viscous incompressible conducting fluid, studying magnetic field effects on time-to-separation

10 p1924 A70-24572

Heat transfer influence on three dimensional boundary layer separation on walled ellipsoid of revolution

10 p1870 A70-24781

Three dimensional incompressible turbulent boundary layer detachment on rotating blading of axial impellers

11 p1975 A70-25793

Turbulent boundary layer in axisymmetric channel having interactions with flow core, calculating flow characteristics and separation point

12 p2209 A70-27289

Electromagnetic effects on separation of turbulent MHD boundary layers allowing for heat transfer

12 p2278 A70-27324

Similar laminar boundary layer solutions exhibiting separation, pressure gradient and mass transfer

12 p2211 A70-27828

Boundary layer equations with pressure gradient for revolving slender body, examining transverse curvature influence on layer separation and integral characteristics

12 p2214 A70-28249

Transonic scaling effects for shock boundary layer interaction on circular and two dimensional airfoil models, discussing separation and reattachment

[AIAA PAPER 70-541] 13 p2339 A70-29008

Backward facing separated step boundary layer flow at Mach 2.25 investigated by diffraction grating interferometer and color schlieren technique

[AIAA PAPER 70-571] 13 p2343 A70-29898

Thermal boundary layer separation in conducting fluids by rotating magnetized blunt body

13 p2469 A70-30008

Magnetoaerodynamic boundary layer of incompressible conducting fluid over right circular cylinder under magnetic field, showing flow separation

14 p2621 A70-30550

Prandtl number effects on adiabatic wall temperature and pressure gradient at separation point for hypersonic compressible laminar boundary layer

14 p2566 A70-31027

Three dimensional boundary layer separation, noting necessity of streamlines perpendicular to pressure gradients near wall

15 p2719 A70-31488

Upper troposphere pressure variations through 20 km separation layer, noting interdiurnal temperature changes

15 p2772 A70-32458

Boundary layer to wake bleed venting for flare-induced separation prevention in hypersonic flow over blunt bodies

16 p2838 A70-33884

Hypersonic cruise vehicles viscous interactions areas, examining compression corners, shock interactions, laminar and turbulent flow, boundary layer separation, etc

[AIAA PAPER 70-781] 17 p3007 A70-34475

Analytical model for jet interaction induced separation of supersonic turbulent boundary layers, conducting flat plate tests at Mach 4

[AIAA PAPER 70-765] 17 p3007 A70-34486

Transitional flow separation upstream of compression corner at trailing edge of sharp leading edge flat plate

[AIAA PAPER 70-764] 17 p3007 A70-34487

High lift airfoils boundary layer separation suppression by blowing, describing wall jets streamwise development prediction methods

[AIAA PAPER 70-872] 17 p3010 A70-34818

Skin friction variation and boundary layer separation for rotating axisymmetric body, using two layer model

17 p3011 A70-35240

Airfoil trailing edge stall in laminar flow, investigating circulation around flat plate

18 p3205 A70-36194

Plane stationary supersonic flows with laminar separation zones at large subcritical Reynolds numbers

18 p3206 A70-36257

Subsonic and supersonic laminar boundary layers separation near sharp corners, considering curvature and Reynolds number effects

18 p3208 A70-36486

Stratford prediction method of separation position for compressible boundary layer flow

19 p3406 A70-38617

Three dimensional boundary layer on lee- and wind-side of protable spheroid, emphasizing separation and embedded streamwise vortices

20 p3608 A70-39359

Boundary layer separation in MHD generators, discussing differences between insulating and electrode wall boundary layers

20 p3680 A70-39985

Turbulent boundary layer in axisymmetric channel having interactions with flow core, calculating flow characteristics and separation point

20 p3613 A70-40339

Loads induced by terminal shock boundary layer interaction on cone-cylinder bodies, discussing angle of attack effect

21 p3746 A70-41863

Electromagnetic effects on separation of turbulent MHD boundary layers allowing for heat transfer

21 p3860 A70-42065

Upstream disturbances propagation during hypersonic flow boundary layer interaction

21 p3748 A70-42205

Three dimensional laminar and turbulent boundary layers separation criteria

21 p3811 A70-42206

Two dimensional incompressible flow, calculating strong surface effects on laminar boundary layer separation by linear model

22 p4010 A70-42630

Perfect gas three dimensional boundary layer separation on circular cone at incidence, comparing numerical calculation and experimental results

23 p4133 A70-44207

Vane type vortex generators to prevent turbulent compressible boundary layer separation, measuring drag in supersonic flow

23 p4133 A70-44527

Three dimensional laminar boundary layer separation at infinite swept stagnation line with high mass injection rates

23 p4182 A70-44568

Unsteady separation criteria for three dimensional laminar boundary layer on finite obstacle

24 p4327 A70-46268

BOUNDARY LAYER STABILITY

Flow visualization of boundary layer transition downstream of Gortler vortices, distinguishing successive instability modes by Te method

01 p0065 A70-11094

Turbulence constant for flows near walls, analyzing viscosity dependence on wall distance by utilizing maximum stability principle

01 p0069 A70-11627

Laminar boundary layer in incompressible liquid, noting effect of variation of kinematic viscosity and density on stability

03 p0468 A70-13870

Vortices orientation due to unstable Ekman boundary layer, discussing analogy to Taylor-Görtler and thermoconvective vortices

06 p1096 A70-17465

Laminar natural convection boundary layer stability over vertical uniform flux surface, measuring disturbance temperature and velocity distributions

06 p1035 A70-17686

Unsteady laminar boundary layers calculation for arbitrary velocity distributions at inner boundary in presence of suction/blowing through porous surface

07 p1254 A70-19080

Solar system origin theory emphasizing brother star approaching nebula for instability of boundary layer

08 p1568 A70-20638

Incompressible laminar boundary layer stability of incompressible fluid for nonparallel oncoming flow, deriving perturbed motion equation

08 p1483 A70-21179

Acoustic pressure sensors positioning on bodies of revolution to determine laminar boundary layer stability loss during ideal liquid flow at nonzero angles of attack

09 p1660 A70-22479

Stability theory application to laminar boundary layer transition prediction on two dimensional and axisymmetric flows having pressure distributions in incompressible flow

[AIAA PAPER 69-10] 09 p1662 A70-23219

Vorticity distribution influence on inviscid laminar jet boundary layer instability investigated for large Reynolds numbers, using shear flow and linearized theory

[DFVLR-SONDDR-14] 10 p1868 A70-24163

Monograph on stability of laminar boundary layer separation at free jets and turbulent free jet flames, considering effects of velocity gradients and temperature

11 p2146 A70-25499

Geometrically exact finite element for thin shells of revolution, using approximation to predict boundary layer stress distribution during vibration

[AIAA PAPER 69-56] 11 p1235 A70-25962

Planview shadowgraph method for observing disturbances generated by spark discharges into laminar boundary layer

13 p2385 A70-29982

Turbulent boundary layer instability on rotating cylinder in axial stream, correlating mixing length to Richardson number

15 p2722 A70-32372

Magnetic field effect on hydromagnetic Görtler instability in boundary layer flow of conducting fluid over concave wall

19 p3481 A70-38352

Multilayered and multiple supersonic jets, deriving dispersion equations for boundaries stability

19 p3354 A70-38663

Turbine blade profiles calculation by hodographs, obtaining compatibility with continuous flow velocity distribution and improved boundary layer stability

19 p3491 A70-38949

Natural convection boundary layer stability on isothermal flat vertical wall or subjected to linear temperature distribution

21 p3950 A70-41443

Combined effects of flow unsteadiness and surface mass transfer on displacement thickness of boundary layer, using flat plate geometry

21 p3811 A70-42092

Neutral stability curve for flat plate boundary layer in zero pressure gradient with increasing thickness, giving critical Reynolds number

23 p4179 A70-43974

BOUNDARY LAYER TRANSITION

Görtler vortices effect on boundary layer transition on concave surface, discussing instability oscillations breakdown leading to turbulent motion

01 p0061 A70-10539

Flow visualization of boundary layer transition downstream of Görtler vortices, distinguishing successive instability modes by Te method

01 p0065 A70-11094

Ablation effects on transition Reynolds number of hypersonic boundary layer on slender cones

03 p0465 A70-12945

Boundary layer transition from laminar to turbulent in hypersonic wind tunnel, determining Reynolds and Mach number effects

[ONERA-TP-737D] 03 p0467 A70-13641

Boundary layer transition limits at high Mach numbers, discussing transition on flat plate and bodies of rotation and Reynolds number

04 p0672 A70-15177

Spin-up of electrically conducting fluid between infinite flat plates under axial magnetic field, considering Ekman-Hartmann boundary layer on single plate

05 p0832 A70-16017

Dynamic stability loss on ablating vehicles ascribed to boundary layer transition effect from turbulent at body heating
[AIAA PAPER 69-106] 06 p0961 A70-17166

Vortices orientation due to unstable Ekman boundary layer, discussing analogy to Taylor-Goertler and thermoconvective vortices
06 p1096 A70-17465

Laminar boundary layer critical height determination using Rouse stability parameter
07 p1257 A70-19336

Laminar to turbulent boundary layer transition and separation on circular cylinder measured by heated end-window film sensor applicable to water flow
07 p1259 A70-19831

Boundary layer research during past decade covering crosshatching during reentry, transition, drag reduction by LFC or compliant surfaces
08 p1483 A70-21040

Laminarization parameter magnitude determination for turbulent boundary layer in convergent channel flow
08 p1484 A70-21518

Plasma sheath in quadrupole and hexapole geometries, investigating magnetic field variation, particle density and electrostatic potential in transition layer
08 p1552 A70-21530

Boundary layer development on body accelerating in viscous incompressible fluid, using straight lines approximation and asymptotic expansions
08 p1485 A70-21631

Stability theory application to laminar boundary layer transition prediction on two dimensional and axisymmetric flows having pressure distributions in incompressible flow
[AIAA PAPER 69-10] 09 p1662 A70-23219

Boundary layer transition measurements on flight tests of experimental 22 degree conical reentry vehicle with Be heat shield and graphite nose
[AIAA PAPER 68-1152] 09 p1606 A70-23243

Laminar-turbulent boundary layer transition in incompressible fluid under surface roughness action, developing theory by generalizing Taylor hypothesis
09 p1664 A70-23713

Two dimensional MHD flow past solid body at large Reynolds numbers, treating boundary layer transition
10 p1922 A70-24011

Transition regime of rarefied gas dynamics using kinetic theory of gases, discussing Couette and Poiseuille flow, heat transfer and time dependent problems
10 p1919 A70-24141

Boundary layer transition detection at supersonic speeds using thin film gages to infer local laminar and turbulent supersonic skin friction
11 p2035 A70-25970

Uncooled leading edge effect on cooled-wall hypersonic flat plate boundary layer transition, discussing leading edge bluntness effects
11 p1976 A70-25984

Boundary layer transition at high Mach numbers on adiabatic wall, showing effects of wind tunnel size, surface roughness and freestream disturbances
[AIAA PAPER 70-586] 13 p2342 A70-29884

Spatial distribution of three dimensional laminar boundary layer transition zone on sharp half angle cone from hypersonic wind tunnel tests
[AIAA PAPER 69-12] 13 p2343 A70-29953

Cone boundary layer transition location and Reynolds number as function of nose bluntness combined effect with Ar, air and He mass injection
[AIAA PAPER 69-706] 13 p2343 A70-29954

Supersonic skin friction measurements in grit type boundary layer transition trips with zero heat transfer
13 p2343 A70-29969

Discrete sonic jets as boundary layer trips producing turbulent hypersonic flows with negligible intrinsic drag and downstream distortions
13 p2523 A70-29973

Axisymmetric compressible boundary layer on body of revolution transformed into two dimensional turbulent boundary layer
13 p2391 A70-29995

Unstable Ekman boundary layer vortex structure analysis by generating similar flow in liquid filled rotating cylinder
14 p2604 A70-30545

Heat transfer from acceleration induced boundary layer reverse transition, considering free stream turbulence effects
14 p2667 A70-31169

Laminar boundary layer transition on sharp cone at zero yaw in supersonic wind tunnels, correlating aerodynamic noise disturbances with transition Reynolds numbers
[AIAA PAPER 70-799] 17 p3006 A70-34462

Acoustic measurement of surface pressure fluctuations in supersonic transitional boundary layers
17 p3092 A70-35482

Asymmetric boundary layer transition effects on slender reentry vehicle motion by changing static stability characteristics
[AIAA PAPER 70-987] 20 p3557 A70-39542

Boundary layer transition application to space shuttle design, relating aerodynamic noise to turbulent boundary layers
21 p3744 A70-41015

Vapor volume entrained in liquid bulk from boundary layer boiling on vertical plate in low gravity field
21 p3947 A70-41055

Boundary layer transition region of flat plate in incompressible flow by subsonic wind tunnel tests, demonstrating harmonic wall perturbation effect
21 p3808 A70-41440

Free stream disturbances influence on hypersonic boundary layer transition Reynolds number in heated and unheated flows
[AIAA PAPER 69-704] 21 p3809 A70-41744

Transitional flow separation upstream of compression corner for two dimensional model relationship to attached flow and boundary layer transition on plate
21 p3746 A70-41864

Numerical integration of Orr-Sommerfeld equation for flat plate Blasius boundary layer transition
23 p4179 A70-43973

Laminar to turbulent boundary layer flow transition over flat plate, using space amplified numerical solutions of Orr-Sommerfeld equation
23 p4181 A70-44234

Wind tunnel testing at transonic speeds, discussing boundary layer transition and dynamic sting interference
23 p4134 A70-44581

Heat exchange on turbine blade profiles, examining boundary layer flow transition region coordinates
23 p4283 A70-44732

Aerodynamic drag and local convective heat transfer on smooth plate for various flow velocities, determining effects of turbulator in boundary layer transition region
23 p4283 A70-44733

Boundary layer transition under small tridimensional perturbations interacting with excitations from wall
24 p4327 A70-46206

BOUNDARY LAYERS

NT COMPRESSIBLE BOUNDARY LAYER

NT HYPERSONIC BOUNDARY LAYER

NT LAMINAR BOUNDARY LAYER

NT SUPersonic BOUNDARY LAYERS

NT THERMAL BOUNDARY LAYER

NT THREE DIMENSIONAL BOUNDARY LAYER

NT TURBULENT BOUNDARY LAYER

Diffusion flame structure in boundary layer with fuel injection from wall, analyzing expansions with single step reversible chemical kinetics, including nonequilibrium case
01 p0214 A70-10334

Turbulent viscosity and thermal conductivity coefficients for entire cross section of fluid flow including wall boundary layers
01 p0069 A70-11624

Aerosol induced light scattering optical properties in atmospheric boundary layer measured with three photometer setup with He-Ne laser
02 p0328 A70-12437

Boundary layer equations describing flow field in turbulent swirling jet diffusion flame solved in von Mises plane
03 p0603 A70-12911

Pitot boundary layer probes with position indicators using extensometric gages for boundary layers on wind tunnel test models
[ONERA-TP-754] 03 p0487 A70-13628

Time of establishment of steady state mixing in plane and axisymmetrical jets determined, using self similar motions in unsteady state boundary layer and free turbulence
03 p0409 A70-13875

Boundary layer equations of motion linearized with self similar profiles
04 p0665 A70-14482

Reflected shock wave velocity, boundary layer disturbance and wall ionization measurements using thin film resistance thermometers
04 p0666 A70-14537

Boundary layer momentum integral equations to predict shear layer behavior, developing method to avoid nonphysical constraint appearance
[ASME PAPER 69-WA/APM-11] 04 p0669 A70-14916

Charge separation effects in boundary layer between cold streaming plasma and perpendicular magnetic field with relativistic electrons
04 p0727 A70-14997

Boundary layer equations closed form similarity solutions for laminar jet of compressible pseudoplastic fluid, discussing velocity transverse behavior
04 p0671 A70-15053

Equilibrium shapes of rotating weightless fluid with surface tension in absence of external force field obtained by boundary layer theory
04 p0673 A70-15241

Mass transfer and viscous interaction combined effects on axisymmetric hypersonic flow of perfect gas over slender bodies
[AIAA PAPER 68-717] 04 p0675 A70-15576

Nozzle boundary layer displacement thickness at Mach 30-70 in helium using Langley hotshot tunnel tests
04 p0675 A70-15603

Optimized compressor blades, examining Le Foll boundary layers theory possibilities as design method
04 p0621 A70-15667

UV radiation propagation in atmospheric boundary layer, analyzing solar UV background and UV signal attenuation along horizontal path
05 p0882 A70-16241

Engineering methods developed for controlling boundary layer, jet and compressor noise, discussing theoretical formulations usefulness
05 p0896 A70-16778

Self similar problems of anisotropic fluid boundary layer involving infinite disk rotation and fluid flow near stagnation point
05 p0835 A70-16857

Boundary layer on sharp flat plate in low density flow computed by continuum approach, obtaining parabolic partial differential equation system
[DVL-914] 06 p1034 A70-17250

Turbulence characteristic scale for atmospheric boundary layer, using wind profile data
06 p1096 A70-17466

Electron distribution functions in weakly ionized plasmas by asymptotic analysis of boundary layer near wall
06 p1121 A70-17903

Ignition and extinction of diffusion flames predicted from studying forced convection in boundary layers
[WSCI PAPER 69-36] 06 p1178 A70-17976

Supersonic exhaust plume/boundary layer interactions, developing integral method and extending to turbulent interactions
[AIAA PAPER 70-230] 06 p1040 A70-18117

Surface shielding from reentry radiation by injecting metal vapors into oxygen bearing boundary layer, calculating particle size distributions, optical depths and attenuation factors
[AIAA PAPER 70-156] 06 p1041 A70-18163

Planetary boundary layer thickness estimation, considering geostrophic wind speed and potential temperature average vertical gradient
07 p1377 A70-18922

Boundary layers calculation for nonporous surface extended to porous with suction by replacing velocity distribution with longitudinal pressure gradient
07 p1254 A70-19083

Electrical effects of boundary layers on insulator wall of MHD generator, considering equilibrium and nonequilibrium ionization generators performance
07 p1196 A70-19321

Ablation products and high temperature boundary layer chemistry of polytetrafluoroethylene (Teflon) in arc jet streams using mass spectrometer
07 p1319 A70-19886

Two dimensional flow field behind shock wave resulting from boundary layer growth in driven gas of shock tube
07 p1260 A70-19983

Reflected molecular beam intensity distribution interpreted in terms of disturbances in boundary layer between gas and solid
07 p1343 A70-20122

Interaction between boundary layer and internal stressed state of thin elastic shell by formulating two dimensional linear theory
08 p1585 A70-20955

Boundary layer research during past decade covering crosshatching during reentry, transition, drag reduction by LFC or compliant surfaces
08 p1483 A70-21040

Perfect fluid sonic flows around weakly lifting three dimensional bodies downstream of shock wave, proving existence of lifting boundary layer
08 p1433 A70-21238

Two dimensional natural convection boundary layer on finite isothermal horizontal plate, examining upward facing cold plate and downward facing hot plate
08 p1598 A70-21580

Atmospheric boundary layer wind and temperature analysis according to similarity scheme for mathematical modeling of atmosphere
08 p1540 A70-21974

Turbulent heat transfer in boundary layer at inlet of porous tube under nonisothermal conditions, studying velocity variations
09 p1787 A70-22169

Solar chromosphere-corona transition region properties, discussing temperature increase within very thin layer and inferring temperature-density structure from emission line intensities
09 p1752 A70-22246

Laminar-turbulent regions boundary, discussing convective layer form and FM-CW microwave and acoustic radar measurement techniques
09 p1717 A70-22378

Potential flow and boundary layer theory application as design tools in aerodynamics, basing calculations on digital computer methods
09 p1605 A70-22947

Doppler-effect-like phenomena of waves or pulses reflected and refracted at moving boundary layers
09 p1728 A70-23072

Cross hatching on various body surfaces due to periodic surface pressure fluctuations, discussing origin from counterrotating longitudinal vortices in boundary layer

[ALAA PAPER 69-11] 09 p1662 A70-23223

Taylor-Goertler vortex formation effect on heat transfer through boundary layer on concave wall

[ASME PAPER 69-HT-3] 09 p1790 A70-23556

Turbulent flow criterion for negligible initial boundary layer case, introducing corrections regarding Korf criterion as function of geometric and aerodynamic flow

10 p1799 A70-24128

Gas viscosity high temperature measurement method in shock tube using boundary layer equations for velocity and static temperature distributions

10 p1867 A70-24151

Carbon oxyfluoride IR radiation from boundary layer formed by arc-heated air passing over Teflon surface

10 p1968 A70-24475

Annulus wall boundary layer effect on spatial flow in subsonic axial compressors by shearing stresses concept between stream surfaces

11 p1974 A70-25777

Seeded dense plasma-electrode system behavior, studying effect of adsorption and emission from boundary surfaces

11 p2090 A70-25952

Conducting fluid incompressible flow in entrance of MHD channel by momentum integral method, permitting edge stress existence at boundary layer free stream interface

[ALAA PAPER 69-724] 11 p2035 A70-25977

Pressure gradient, wind structure and shearing stress in atmospheric boundary layer related by formulation based on quasi-parallelism and boundary condition at Ekman layer top

11 p2076 A70-26071

Uniform asymptotic theory of diffraction by edge of three dimensional body, obtained boundary layer solution applied to scattering by circular cylinder

11 p2084 A70-26422

Variational analysis of fluid flow in hydrodynamic, thermal and diffusional boundary layers including viscous effects, heat and mass transfer and chemical reactions

11 p2041 A70-26652

Pressure fluctuations in acoustic field of boundary layer under slot suction, considering vortex formation and separation on edges

12 p2209 A70-27298

Book on aerodynamics covering flow theory, boundary layers, shock waves, wing design, etc

12 p2157 A70-28148

Chemically reacting stagnation point boundary layers with wall injection of gas, comparing multicomponent solution with binary approximation and chemical simplifications

14 p2565 A70-30265

Radiative heat transfer in optically thick gas between concentric spheres treated by matched asymptotic expansions, comparing results with Rosseland approximation and numerical solution

14 p2663 A70-30266

Variangular wind spirals for vertical wind and shear profile estimation in atmospheric boundary layer

14 p2602 A70-30370

Barotropy, baroclinicity and baroclinity induced variations of geostrophic wind vector with altitude within planetary boundary layer

14 p2604 A70-30546

Velocity and pressure distributions of tornado-like two cell vortices within boundary layer, using different assumptions for eddy diffusion coefficient

14 p2604 A70-30547

Orr-Sommerfeld equation asymptotic solution corresponding to boundary layer velocity distribution

15 p2721 A70-32357

Unequal diffusion film coefficient formulation based on transfer coefficient approach for ablative material coupled multicomponent boundary layer problems

16 p2998 A70-33879

Mechanical erosion concomitant with thermochemical erosion in mass and energy transfer at interface of boundary layer and ablating nylon-silica-phenol material

[ALAA PAPER 70-824] 16 p2941 A70-33942

MHD flow velocity and magnetic flux profiles in rectangular ducts for secondary boundary layer

16 p2959 A70-34239

Boundary layer formation on walls of conical pressure nozzle during vortex flow

16 p2896 A70-34299

Atmospheric contaminants dispersion simulation in meteorological wind tunnel with capability to simulate thermally stratified boundary layers

17 p3065 A70-34496

Boundary layer theory development in U.S.S.R., surveying findings and papers

17 p3067 A70-34662

Atmospheric boundary layer model, considering air-surface interaction, heat and humidity exchange, wind, temperature and humidity profiles, etc

17 p3132 A70-34667

Current sheet structure of hydromagnetic boundary layer formed by mixing two conducting fluid streams containing oppositely directed magnetic fields

17 p3140 A70-34930

Pressure distribution measurements on wedges in compressible flow at Mach 0.5-2.2, discussing wedge angle, Mach number and boundary layer thickness effects

17 p3013 A70-35923

Horizontal boundary layers development on flat plate in nondiffusive stratified flow characterized by Reynolds and Russell numbers

18 p3239 A70-36192

Density diffusion and buoyancy effects on horizontal boundary layers in stratified flow

18 p3239 A70-36193

Soviet book on passenger aircraft aerodynamics covering motions of gases and immersed bodies, similarity laws, boundary layer theory, finite span wing, etc

18 p3208 A70-36507

Unsteady light field spatial moments in turbid medium boundary layer with intense anisotropic scattering during illumination by narrow beam

18 p3285 A70-36631

Subcritical and supercritical boundary layer problems, reviewing various momentum integral solution methods

18 p3242 A70-36705

Annulus wall boundary layers in axial flow turbomachines, taking into account boundary layer growth and associated secondary flows

[ASME PAPER 70-GT-92] 18 p3209 A70-36877

End wall boundary layers effect included in performance prediction method for multistage axial compressors

[ASME PAPER 70-GT-80] 18 p3210 A70-36884

Steady state nonlinear dynamics of low latitude atmospheric global boundary layer, indicating inverse relation between air flow vertical velocity and distance from equator

19 p3460 A70-37417

Supersonic turbine blade rows design, discussing boundary layer interaction around leading edges and flow around trailing edges

19 p3490 A70-38223

Elastic boundary layers analysis based on strain gradient theory of linear elasticity

19 p3544 A70-38331

Meteorological observation on atmospheric boundary layer during winter, determining width and inclination of frontal zones

19 p3463 A70-38758

Flame stabilization in boundary layer during mixing of cold homogeneous fuel mixture and hot gas based on combustion and turbulent jets theories

20 p3736 A70-39267

Interaction between boundary layer and internal stressed state of thin elastic shell by formulating two dimensional linear theory

20 p3719 A70-39378

Parametric boundary layer theory numerical solution in two parameter approximation, solving partial differential equation by finite difference method

20 p3611 A70-39807

Local variables in boundary layer of high temperature ionized gas flowing in magnetic field, using X ray absorption

20 p3613 A70-40344

Electron temperature measurements in flowing high density plasma by cooled Langmuir probe, considering probe temperature variations effects in boundary layer

21 p3854 A70-40557

Secondary flow model for planetary boundary layer, considering flow as finite perturbation

21 p3813 A70-40904

Boundary layer problems with resonance solved by matched asymptotic expansions and WKBJ method

23 p4179 A70-43945

Laser light pulse reflection by atmospheric boundary layer calculated on computer by Monte Carlo method, comparing results with full scale measurement

23 p4166 A70-45072

Porous tube inlet region, calculating fluid injection effect on laminar flow from integral form boundary layer equations

24 p4326 A70-45782

Cold boundary layer effect on chemical kinetic parameters behind reflected shocks in single-pulse shock tube

24 p4323 A70-46044

BOUNDARY LUBRICATION

Finite element solution of incompressible lubrication problem by minimum principle for transient incompressible Reynolds equation with boundary conditions

[ASME PAPER 69-LUB-A] 01 p0100 A70-10378

Film properties of organic liquids squeezed between two solid flats using order liquid model, discussing applications to boundary layer lubrication

08 p1508 A70-21601

Hydrodynamic lubrication film breakdown in cold strip rolling, showing thickness consistency with critical value of modified Sommerfeld number

21 p3833 A70-41256

BOUNDARY VALUE PROBLEMS

NT NEUMANN PROBLEM

General boundary value problem solutions for degenerate second order elliptic equations

01 p0130 A70-10128

Energy inequality solutions properties pertaining to mixed boundary value problem of partial differential equations, using Fourier method

01 p0130 A70-10154

Fourier transform applied to Riemann boundary value solution to biharmonic equation governing elastic theory for half plane with circular protrusion or indentation

01 p0199 A70-10155

Finite difference scheme for linear second order third boundary value problem in ordinary differential equations

01 p0131 A70-10455

Self excited oscillators zero crossing times distribution for Markov process formulated as boundary value problem involving Kolmogoroff backward equation

01 p0143 A70-10891

Functional optimization within partial differential equation solutions class by choosing optimum boundary values

01 p0131 A70-10922

Steady burning process equations numerical solution for boundary conditions prescribed at saddle point singularity

01 p0218 A70-11019

Boundary value problems of elasticity theory in space perforated by cylindrical cavities with parallel axes solved by infinite algebraic equations

01 p0202 A70-11033

Collection of papers on boundary value problems of mathematical physics and related aspects of function theory, Part I

01 p0131 A70-11066

Navier-Stokes equation generalized solutions to initial boundary value problems, considering uniqueness theorem and smoothness

01 p0132 A70-11068

Sound generation by multiblaaded single stage fans operating in free field, deriving model as boundary value problem involving inhomogeneities due to quadrupole distribution

01 p0166 A70-11197

Runge-Kutta method with position dependent optimal parameter alpha for initial value problem solution to minimize total error

01 p0134 A70-11364

Boundary conditions at reinforced edge of shell by separating solution into zero moment stress and edge effect solutions

01 p0209 A70-11407

Nonlinear boundary value problem algorithm in shell theory

01 p0212 A70-11566

Boundary value problem for quasi-linear equation of unsteady transonic gas flow, including linear model and operators for group of transformations

01 p0069 A70-11628

Electrical domain instability in homogeneous hot electron semiconductors, discussing boundary conditions application to fluctuations

02 p0350 A70-11697

Parametric approximation method extended to incompressible laminar boundary layers with surface suction or injection

02 p0277 A70-11857

Integral equation of first kind solution based on two dimensional boundary value problem solution

02 p0323 A70-11994

Three dimensional linear combustion instability in liquid propellant rocket motors using concentrated combustion model, presenting mathematical analysis as boundary value problem

02 p0353 A70-12011

Bounded region satisfying regularity necessary to Korn inequalities and Sobolev immersion theories, discussing plasticity theory operator monotony in Minty-Browder sense

02 p0387 A70-12109

Unstable electron plasma initial value problem solved by numerically integrating Vlasov equation in one dimension

02 p0347 A70-12235

Viscoelastic boundary value problems involving time dependent boundary regions reduced to elastic problems, starting with aging viscoelastic body

02 p0388 A70-12269

Boundary conditions of heat conduction in systems of vessels connected by rods with given heat capacity and unknown temperature

02 p0400 A70-12674

Mixed boundary value problem for viscoelastic body with constant Poisson ratio solved by variables separation method, proving convergence

02 p0390 A70-12802

Summary representation formulas for solving boundary value problems for Helmholtz and Poisson equations in rectangle

03 p0518 A70-13076

Axisymmetric elasticity theory problem of stressed state of space weakened by concentric circular cracks solved using p-analytic functions to generate boundary value problems

03 p0586 A70-13077

Summary representations method to analyze finite difference schemes for integrating parabolic equations with constant coefficients, solving boundary value problems

03 p0518 A70-13078

Summary representations method to determine eigenfrequencies of finite difference Laplace operator for boundary conditions

03 p0518 A70-13079

Zero-moment theory boundary value problem of shells of revolution with negative curvature under tangential static and geometrical conditions imposed on ends

03 p0589 A70-13337

Control problem of linear system with phase coordinate constraints, discussing solution properties, boundary conditions and function minimization procedure

03 p0460 A70-13340

First and second boundary value problems of steady vibrations of viscoelastic bodies reduced to algebraic equations

03 p0589 A70-13345

Elasticity theory contact type problems, proving solutions existence and uniqueness

03 p0589 A70-13346

Static contact mixed boundary value problems in elasticity theory, noting limitations

03 p0590 A70-13383

Discontinuous solutions of nonlinear boundary value problems of heat conduction for second order ordinary differential equations using modified difference method

03 p0604 A70-13390

Eigenfunctions of oscillating infinite perforated membranes for various boundary conditions at holes

03 p0591 A70-13415

Asymptotic behavior at infinity of mixed boundary value problem analyzed for Sobolev equation involving operator

03 p0518 A70-13433

Shallow elliptical planform shell under uniformly distributed normal load calculated with 'ritz and Bubnov-Galerkin variational methods

03 p0593 A70-13496

Boundary value problems for orthotropic half plane and infinite orthotropic plane with cuts, considering loads at various points

03 p0593 A70-13497

Linear functionals over Sobolev spaces and elliptical boundary value problems generated by theorems on homeomorphisms

03 p0519 A70-13505

Three dimensional combustion instability in liquid-propellant rocket engines, investigating dependence on design and operating parameters via boundary value problem analysis

03 p0551 A70-13574

Two point boundary value problem arising from Pontryagin maximum principle application in optimal control, describing solution based on combined existing methods

03 p0460 A70-13699

Variational stress solutions for static case of bounded bodies in Cosserat continuum theory, assuming anisotropic inhomogeneous material and defining boundary value problem solution

03 p0596 A70-13973

Variational principles in linear elasticity theory with couple stresses, solving boundary value problems in Mindlin theory with microstructure and first strain gradient theory

03 p0596 A70-13974

Differential equations system under side condition, examining solutions existence

03 p0519 A70-14073

Fourier expansion method applied to hydrodynamic stability of plane jet, testing boundary conditions

03 p0469 A70-14180

Boundary value problems for partial differential equations representing steady gas flow hydrodynamic problems

03 p0469 A70-14228

Axisymmetric sonic flow around slender body, determining boundary regions for slender body approximation and Guderley expansion utility

03 p0409 A70-14233

Navier-Stokes boundary value problem describing viscous incompressible fluid flow between coaxial fixed and rotating cylinders, emphasizing stability analysis

03 p0470 A70-14242

Elastokinetic three dimensional boundary value vibration problem, involving rectangular area on surface of elastic half space under periodic normal stress

03 p0601 A70-14319

Solutions properties of initial and mixed initial-boundary value problems of wave equations

03 p0537 A70-14384

Perforated plates bending for multiply connected regions, proving quasi-regularity and uniqueness of boundary value equations

04 p0767 A70-14481

Soviet book on boundary value problems involving motion of ideal fluids in unsteady cavities of various geometries, determining attached fluid masses and oscillation frequencies

04 p0666 A70-14678

Initial value method for solution of nonlinear two point boundary value problems in fluid mechanics, considering Blasius equation and unsteady gas flow [ASME PAPER 69-WA/FE-8]

04 p0667 A70-14782

Transient heat conduction solution by finite element methods application to nonlinear boundary condition problems

[ASME PAPER 69-WA/HT-36]

04 p0781 A70-14804

Law for time variations of modulus-restricted control action at trajectory end, two point boundary value problem solution and use of Pontryagin principle

04 p0661 A70-15011

Perturbation technique for numerically sensitive nonlinear two point boundary value problems

04 p0713 A70-15045

Numerical analysis of nonlinear boundary value problems for ordinary differential equations, considering patch bases and monotone methods

04 p0714 A70-15046

Complex uncoupled modes to analyze forced vibrations of three layer damped sandwich beam with arbitrary boundary conditions, discussing orthogonality

04 p0773 A70-15076

Boundary value problems of Cauchy-Riemann differential equations using solution to derive integral equation for stationary infrasonic flow

04 p0671 A70-15094

Thin walled uniform open bar stability under arbitrary boundary conditions, using Vlasov assumptions and matrix methods

04 p0774 A70-15099

Plane static boundary value problems solutions in zero moment elasticity theory, proving solutions existence and uniqueness

04 p0775 A70-15214

Mixed nozzle flows solution complex boundary value problem reducible to Cauchy problem for hyperbolic system with three dependent variables by applying flow stabilization method

04 p0617 A70-15236

Thermoelastic boundary value problems solutions in quadratures applicable to problems with given parameters on boundary sections

04 p0775 A70-15257

Directional pattern of waveguide radiators using Kirchhoff boundary values of electric, magnetic or electric and magnetic fields, discussing aperture reflection coefficient

04 p0653 A70-15397

Soviet book on three dimensional boundary value problems in mathematical theory of elasticity and thermoelasticity

04 p0777 A70-15474

Approximate boundary controllability of heat equation, considering smoothness conditions on piecewise-smooth boundary

05 p0875 A70-15781

Stefan free boundary problems with prescribed flux reduced to form solvable by numerical methods, proving existence and uniqueness theorems

05 p0956 A70-15783

Terminal states and time specifications influence on optimum control systems, using Pontryagin principle for boundary value problems application

05 p0824 A70-15874

Three dimensional elastostatics problems solution method using singular integral equations solvable numerically for surface tractions and displacements of fully mixed boundary value problem

05 p0926 A70-15912

Boundary value problems of thin beams theory transformed into initial value problems, using dynamic programming and invariant imbedding

05 p0926 A70-15977

Dual trigonometric series solution for mixed boundary value problems in two dimensional elasticity

05 p0926 A70-15979

Mixed boundary value problems of plane elasticity, solving stress field of central Griffith crack in wedge using singular integral equations

05 p0932 A70-16173

Mixed boundary value problems of isotropic elastic half space with ring shaped separation region

05 p0935 A70-16232

Unsteady heat conduction numerical approximation for infinite cylinder with variable heating and boundary conditions of third kind

05 p0936 A70-16294

One dimensional unsteady heat conduction with variable boundary conditions solved by difference-differential method using rectangular and cylindrical coordinates

05 p0957 A70-16295

Heat source temperature distribution on surface of infinite cylinder with zero temperature, presenting solution to boundary value problem

05 p0957 A70-16296

Self adjoint boundary value problems with interior point boundary conditions using differential operator in Hilbert space

05 p0876 A70-16423

Displacements and stresses obtained for elastic half plane with variable Poisson ratio under certain traction boundary conditions, using Fourier transform method

05 p0940 A70-16512

Existence and uniqueness of nonlinear boundary value problem solutions formulated by fixed point theorem and Green function

05 p0876 A70-16562

Green operator structure and eigenvalue approximation of boundary value problems regarding vibrations and buckling of clamped plates using orthogonal invariants

05 p0876 A70-16563

Fluid boundary at curved wall under pressure

05 p0834 A70-16680

Dirichlet problem of biharmonic operator in boundary region containing infinite number of pieces

05 p0877 A70-16878

Boundary value problems in closed spaces with fine grained Liapunov boundary described by second order elliptic differential operators

05 p0877 A70-16881

Hydrodynamic coefficients of algebraic equations for boundary value problems in disturbed motion of body with rib-reinforced liquid filled cavity

05 p0836 A70-16956

Thermoelasticity boundary value problems solutions in quadratures based on symmetry property and Fourier integrals

05 p0947 A70-16971

Unsteady temperature field of uniformly thick disk for inhomogeneous boundary conditions and small Fourier numbers solved by Laplace operation

05 p0958 A70-17013

Numerical solution of nonlinear Vlasov equation for collisionless plasma problems, discussing initial value problems, external electric fields, magnetic fields, etc.

06 p1108 A70-17419

Radio wave propagation in stratified media consisting of periodically stacked dielectric slabs solved for boundary condition by reducing Maxwell equations to Hill equation

06 p1007 A70-17463

Electrical network models simulating initial and boundary value problems of applied mechanics, exemplifying with string free vibrations and thin plate bending

06 p1094 A70-17928

Uncoupled quasi-static boundary value problem for linear viscoelastic solids undergoing thermal and mechanical deformation solved by computational algorithm

06 p1168 A70-17937

Boundary conditions and iterative procedures for plasma sheath problems, using matrix equation to represent differenced Poisson equation

06 p1123 A70-18295

Kinetic theory treatment of linearized Rayleigh problem using wall boundary condition models

06 p1049 A70-18329

Transition regime gas flows using Navier-Stokes equations and boundary conditions set, considering heat transfer, torque and drag in spherical geometry

06 p1049 A70-18331

Mixed boundary value potential theory problem numerical solution by integral equation invariant imbedding

06 p1171 A70-18511

Boundary value problems in nonlocal elasticity, considering two one dimensional media coupling with microstructure by Green function analog

07 p1399 A70-18665

Boundary value problems and Cauchy problem considered for mathematical model of turbulent motion in liquid or gas

07 p1252 A70-18671

Equilibrium forms of prolonged rectangular plate in gas flow in terms of nonlinear boundary problem, emphasizing plate with hinged supports

07 p1187 A70-18679

Three dimensional boundary value problems for bodies of revolution rotating in fluid at rest and for bodies at rest in rotating fluids

07 p1252 A70-18709

Soviet collection of papers on boundary problems for differential equations covering variational problems in half space, polynomial behavior at infinity, function spaces, Fourier transformation, etc.

07 p1322 A70-18851

Boundary value problems solutions estimated for heat conduction equation in unbounded domain, considering function satisfying heat induction equation

07 p1419 A70-18852

Existence and uniqueness theorem for boundary value problem solution for parabolic equation in domain with singular points on boundary

07 p1322 A70-18853

First boundary value problem for quasi-elliptic and quasi-parabolic equations, discussing solvability and boundary behavior near characteristic points

07 p1322 A70-18854

Finite element method using cubic polynomials over triangle as trial functions for solving second order boundary value problems in linear theory of elasticity

07 p1324 A70-19075

Inverse boundary value problems for supercavitating bodies, deriving singular integral equations using Prandtl acceleration potential method

07 p1254 A70-19076

Direct boundary value problem for supercavitating profile with finite cavity, deriving singular integral equations by Prandtl acceleration potential method

07 p1254 A70-19077

Circular plates with optimal natural frequency of transverse vibrations, discussing boundary conditions

07 p1405 A70-19256

Stress rate boundary value problem formulation for elastoplastic body by singular integral equations

07 p1405 A70-19258

Flexural elastic behavior of rectangular plates with boundary restraint acting on same side using finite differences method

07 p1406 A70-19348

Plane electromagnetic wave reflection from laminar anisotropic medium, analyzing piecewise-constant permittivity tensor as boundary value problem

07 p1235 A70-19448

Digital computer design of electric and radio equipment using secondary source method for field boundary calculation in inhomogeneous environment

07 p1241 A70-19480

Boundary value problems solution for infinite elastic isotropic plane weakened by arbitrarily distributed circular holes based on using series in Taylor functions

07 p1408 A70-19549

Book on some methods of solving boundary value problems of mathematical physics covering linear operators, boundary conditions, perturbation and Monte Carlo methods

07 p1326 A70-19696

Book on mathematical theory of viscous incompressible flow covering stationary and nonstationary boundary value problems for linearized and nonlinear Navier-Stokes equations

07 p1258 A70-19697

Self adjoint operator generated by differential expression and pseudodifferential boundary conditions, using Berezanskiĭ procedure for operator eigenfunction expansion

07 p1327 A70-19809

Parameters identification in nonlinear boundary value problems by successive approximations technique, using Lagrange multipliers and Newton-Raphson method

07 p1327 A70-20025

Boundary value problem for self conjugate elliptical fourth order differential equation with variable coefficients, proving convergence of iterative process

07 p1328 A70-20143

Two point boundary value problems of quasi-differential equations, discussing conditions for continuous and increasing lower bounds of functions

07 p1328 A70-20349

External and internal three dimensional dynamic problems in elasticity theory for multiply connected region with circular cylinder boundaries

08 p1584 A70-20537

Nonlinear steady state diffusion elliptic boundary value solutions exemplifying enzyme kinetics and radiation cooling

08 p1596 A70-20580

Boundary value problem solution in study of axisymmetric viscous heat conducting gas flow past body of revolution

08 p1431 A70-20854

Optimization of control of oscillatory process with deviating argument in maximum principle form, reducing solution to boundary value problem

08 p1544 A70-20954

Quadrature solution for elastic sphere deformation by axisymmetric normal loads, writing Green function of boundary value problem in finite form

08 p1585 A70-20956

Mixed problems with linear homogeneous boundary conditions with time-independent coefficients for semihyperbolic equations, discussing constraints

08 p1534 A70-21005

Stability of solutions to linear differential equations pair, determining bound conditions having S-property

08 p1534 A70-21100

Boundary value problem for linear elliptic differential operator degenerating on region boundary

08 p1534 A70-21119

Lateral buckling of simply supported uniform diaphragm using slope-deflection equations for orthogonally intersecting beams, prescribing boundary conditions

08 p1589 A70-21244

Biharmonic equation in polar coordinates solved for circular plates and plate sectors with various boundary conditions, using finite difference approximations

08 p1589 A70-21246

Boundary value problems in one speed transport theory, applying Green function technique to neutrons with spherical symmetry

08 p1542 A70-21253

Boundary value contact problems in thermoelastic oscillations theory found to have unique solutions for any frequency

08 p1591 A70-21440

Potential vortex flow interaction with stationary surface calculation extended to Volterra equations by transforming boundary value problem, improving critical Reynolds number bounds

08 p1484 A70-21472

Thermoelastic energy functions bounding by variational principles for anisotropic composite materials properties

08 p1592 A70-21510

Semiinfinite elastic strip supporting thin heavy beam using Airy stress function and Laplace transform, with boundary conditions expressed as Fourier series

08 p1594 A70-21768

Asymptotic distribution of operator eigenvalues for self adjoint elliptic boundary value problem in unbounded region using Green function

09 p1711 A70-22148

Biharmonic boundary value problems with reentrant boundaries, comparing Motz and Woods finite difference solution methods

09 p1711 A70-22285

Mixed system of simultaneous linear differential equations under general boundary conditions, deriving numerical solution in Chebyshev series

09 p1711 A70-22288

Boundary problem for displacement equilibrium equations of elastic body using iterative methods, demonstrating convergence of difference equation solution

09 p1771 A70-22467

Thermo-elastic analysis and optimum start-up in power plant, discussing transfer function for thermally loaded bodies with restricted boundary temperature

09 p1774 A70-22584

Continuous dependence theorem and differentiability properties of free boundary problem solution for heat equation

09 p1788 A70-22609

Hankel integral transforms of half orders for solving boundary value problems in terms of spherical coordinates

09 p1712 A70-22834

Steady harmonic oscillations of half space with circular holes, deriving algebraic equations for boundary value problems

09 p1782 A70-23296

Boundary value problem of torsion for equilibrium of elastic body based on moment theory in absence of bulk forces

09 p1782 A70-23381

Point boundary value problem solution for differential equations with parameters in form of power series, considering Cauchy problem

09 p1712 A70-23383

Boundary value problem for cavitating flow around thin wing reduced to two dimensional singular integral equations from acceleration potential

09 p1663 A70-23393

Multipoint methods for two point boundary value problems with Banach space self mapped, proving convergence theorems for iterative solutions

09 p1712 A70-23420

Soviet monograph on method of functional equations for solving boundary value problems, discussing computer programs and various applications

09 p1712 A70-23548

Stress tensors in initial value problem for incompressible flow with nonlinear viscosity

09 p1663 A70-23570

Reissner-Sagoci transient mixed boundary value problem concerning displacement of infinite half space of isotropic elastic material, deriving surface displacement and reactive torque

09 p1784 A70-23571

Initial value problem of macroscopic disorder-order transformation in random thermal convection phase of fluid heated from below

09 p1791 A70-23679

Progressive shock waves propagation, reflection and transmission through sudden changes in pipe cross sectional area, obtaining boundary conditions for quasi-steady junction flow

09 p1664 A70-23738

Heat conduction analysis for plane body with boundary condition and time variable heat exchange coefficient, applying automatic control technique

10 p1966 A70-23869

Unsteady heat transfer on electronic analog model, using installation prescribing variable boundary conditions of third kind

10 p1966 A70-23872

Integral relations describing laws of conservation and Sobolev theorem used in deriving a priori estimates for nonlinear parabolic equations first boundary value problem

10 p1908 A70-23924

Existence and uniqueness of mixed problem solution for Tricomi equation proved by a priori estimates

10 p1908 A70-23925

Nonstationary thermoelasticity in half space with moving boundary condition described in Cartesian rectilinear coordinates allowing for time term in heat conduction equation

10 p1954 A70-24012

Ill conditioned linear two point boundary value problems solved by Riccati transformation avoiding forward integration

10 p1909 A70-24059

Unsteady MHD flows of viscous, incompressible and electrically conducting fluid, proving boundary value problem solutions existence and uniqueness

10 p1922 A70-24095

Nonautonomous boundary value problems for plates in plane and three dimensional supersonic flows, obtaining eigenfunctions of vibration by Laplace transform

10 p1956 A70-24118

Gas flow from nozzle into duct with enlarged cross section investigated for flow pattern and boundary conditions, noting oscillation behavior

10 p1799 A70-24123

Equilibrium equations integration for body in isotropic linear viscoelastic medium with contact-type boundary conditions

10 p1957 A70-24267

Error analysis and monotone convergence of finite difference approximations to linear one dimensional singular boundary value problems

10 p1909 A70-24406

Quasi-linearization extension to numerical solution of multipoint boundary value problems for ordinary differential equations arising from state constrained optimal control problems

10 p1909 A70-24421

Parameter introduction during boundary value problem solution for second order nonlinear ordinary differential equations

10 p1909 A70-24510

Kinematic analysis of limit loads of equilateral triangular plates under various boundary conditions

10 p1958 A70-24517

MHD boundary layer flow equations solution by initial value method to eliminate iteration process

10 p1924 A70-24563

Adjointness in nonadjoint boundary value problems, extending Neuberger symmetry study to obtain expansion theorem for nonself adjoint p-point problems

10 p1910 A70-24606

Partial differential equation describing one dimensional heat transmission problems solved by eigenvalues for initial and boundary conditions

10 p1969 A70-25098

Superconducting ellipsoid of revolution in alternating magnetic field, computing disturbed field components using boundary value problem

10 p1917 A70-25201

Mixed boundary value problem for linear parabolic equations with discontinuous coefficients, proving solution existence and uniqueness by functional method

10 p1911 A70-25304

Boundary value problem in parallelepiped constructed for linear partial differential equation with constant coefficients using expansions in Riesz bases

10 p1911 A70-25305

Temperature and heat flux in plane, cylindrical and spherical multilayer diaphragms with boundary conditions, assuming harmonic temperature variation

10 p1970 A70-25321

Viscoelastic half plane creep under discontinuous boundary conditions, obtaining exact closed-form solution based on Fourier transforms and distribution theory

10 p1965 A70-25325

Homogeneous boundary value problems in stability theory of circular cylindrical shells axisymmetric equilibrium state

11 p2129 A70-25396

Classical and elastically restrained boundary conditions requirements for anisotropic plates Ritz solution

11 p2135 A70-26076

Boundary conditions effect on bending, vibrations and buckling of unsymmetrically laminated rectangular plates

11 p2136 A70-26079

Guidance boundary value problem estimation by continuous least mean square (CLMS) method, describing application to generation of velocity required coefficients

11 p2081 A70-26322

Spacecraft temperature prediction and heat conduction problems with nonlinear radiation boundary conditions by perturbation theory, applying to heat shield analysis

11 p2150 A70-26355

Monograph on integral calculation method for disk problems with mixed boundary conditions covering two dimensional stress-strain state, extrapolation methods, etc

11 p2140 A70-26474

Elastodynamics mixed initial and boundary value problems numerical solution method applied to deformation of elastic solid

11 p2140 A70-26485

Discrete models for boundary value problems analysis in first strain-gradient elasticity theory, extended finite element method

11 p2142 A70-26637

Asymptotics of linear diffusion processes altered by weak nonlinear effects, discussing deterministic and statistical initial value problems

11 p2074 A70-26686

Book on successive approximation methods in control and oscillation theory covering two point boundary value problems iterative solutions, orbital transfer, etc

12 p2260 A70-26852

Coerciveness /Korn/ inequalities role in boundary value problems for elliptic systems of partial differential equations, noting applications to three dimensional linear elasticity theory

12 p2260 A70-26974

Kantorovich theorem application as weak Newton method used in boundary value problems containing Euler-Lagrange equation for variational problems and ordinary differential equations

12 p2260 A70-27002

Differential equations in two point boundary value problems solved by combining Newton-Raphson iterative method with parameter variation extrapolation

12 p2260 A70-27003

Stable and unstable crack growth in viscoelastic media, solving boundary value problem and continuum mechanics prediction of crack propagation

12 p2315 A70-27092

Heat equation initial value problem with dissipative term nondecreasing and discontinuous function of unknown, discussing existence and uniqueness theorem of periodic solution

12 p2330 A70-27160

Coordinate function selection for boundary value problems solution by Galerkin method demonstrated for heat conduction equation of anisotropic parallelepiped with internal source

12 p2271 A70-27291

Classical eigenvalue problem transformation by invariant imbedding into initial value problem suited for numerical integration, noting applications to columns elastic buckling

12 p2261 A70-27424

Iteration procedures for boundary value problem of orthotropic rectangular plate under bending loads, discussing convergence of procedures

12 p2325 A70-27552

Laminar natural convection plumes behavior above energy sources calculated by simplest variables, indicating optimum formulation of boundary value problem

12 p2332 A70-27700

Spatial relaxation of electron gas colliding with positive ions from plasma velocity distributions, solving time independent Fokker-Planck boundary problem

12 p2280 A70-27791

Linear and nonlinear parabolic boundary value problems with first boundary conditions solved by method of lines, estimating error

12 p2262 A70-28031

Thin walled shells of revolution equations boundary conditions formulated by stress state separation, giving small parameter perturbation theorem

12 p2327 A70-28191

Volterra method applied to solution of mixed boundary value problems for wave equation

12 p2159 A70-28243

Mixed boundary value problems involving time dependent boundary regions for penny-shaped crack in viscoelastic materials with one relaxation function

13 p2508 A70-28489

Inverse boundary value problems involving elliptic equations solved by Newton method and discrete invariant imbedding

13 p2440 A70-28650

Partial differential equations in regions with curvilinear boundaries solved by difference network approximation method

13 p2440 A70-28961

Elliptic equations solved by projection network methods noting estimate derivation for convergence rates

13 p2440 A70-28962

Elastoplastic continuum under specified rates of body forces, surface tractions and displacements, formulating minimum principle for solving boundary value problem

13 p2513 A70-29154

Boundary value problems of ordinary and generalized heat conduction equations using reflection method

13 p2521 A70-29311

Relationship between fundamental matrices of solutions to boundary value problems of parabolic and elliptical systems with Bessel functions

13 p2441 A70-29314

Viscous and inviscid incompressible fluids motion boundary value problems solutions with aid of kinetic stress functions

13 p2388 A70-29319

Nonlinear equations boundary value problem solution by Galerkin method in integrodifferential equations form, determining Lipschitz conditions constant and proving existence and uniqueness

13 p2442 A70-29513

Operator originated by Schroedinger equation having inhomogeneous boundary conditions on portion of boundary of Hilbert spaces orthogonal sum, defining region of self conjugation

13 p2442 A70-29514

Rotating stellar configurations structure consisting of degenerate matter or density dependent temperature describing boundary value problem reduction for Cauchy problem

13 p2494 A70-29518

Variational principles derivation for inelastically deformable body mixed boundary value problem, considering loading conditions with basic functions free of discontinuities

13 p2516 A70-29524

Elastic anisotropic body analysis, formulating boundary value problem solutions

13 p2516 A70-29525

Mixed boundary value problems with radiation-type boundary conditions solved by complex Green function, discussing water waves in irrotational motion

13 p2452 A70-29536

Soviet collection of articles on transactions of seminar on boundary value problems covering plates in weightless fluid, cavitation flow channel, unsteady flows, etc

13 p2390 A70-29643

Generalized Frankl boundary value problem solution uniqueness formulation and proof using auxiliary function

13 p2390 A70-29647

Aerodynamic characteristics of supercavitating airfoil, investigating effect of free surface of unsteady fluid flow with stream separation, solving boundary value problem

13 p2391 A70-29650

Boundedness of solutions and higher derivatives for degenerate matrices, showing dependence on characteristic numbers and linear groups

13 p2443 A70-29744

Boundary conditions and initial value lines for unsteady homentropic flow, performing straight pipe calculations

13 p2392 A70-30023

Multichannel scattering variational bounds reformulation without using projection operators, calculating resonance-energy relations

14 p2619 A70-30490

Closed form solutions of boundary value problems for Burger equation within half plane from zero to infinity

14 p2598 A70-30492

Mixed boundary value problems for pseudoparabolic partial differential equations solved in Hilbert space, demonstrating solution existence and uniqueness

14 p2599 A70-30635

Method of ascent for general representation in boundary value problems associated with differential equation of n variables

14 p2599 A70-30636

Differential equations eigenvalue and boundary value problem finite difference approximation convergence under consistency and stability conditions

14 p2599 A70-30643

Boundary value problems reduction to variational problem by transversality conditions of calculus of variations

14 p2599 A70-30644

Quasi-linear elliptic boundary value problem approximate solution and error bounds, considering linear programming for computation

14 p2599 A70-30646

Zero-moment theory boundary value problem of shells of revolution with negative curvature under tangential static and geometrical conditions imposed on ends

14 p2657 A70-30715

First and second boundary value problems of steady vibrations of viscoelastic bodies reduced to algebraic equations

14 p2657 A70-30720

Recoverability for amplitude and rate bounded optimal control of linear time varying systems

14 p2562 A70-31203

Pontryagin principle for thin vibrating plates under mixed boundary conditions, examining optimal control

14 p2660 A70-31205

Cylindrical shell nonaxisymmetric vibration frequencies and boundary values relation, using Lagrangian

14 p2661 A70-31273

Boundary value problem for Navier-Stokes equations to obtain stationary flows as limits of nonstationary solutions

14 p2600 A70-31347

Cesaro Fourier series summation method for boundary value problems in electrostatics

14 p2600 A70-31419

Boundary value problem of nonlinear one dimensional conduction in radiating heat shields, using perturbation and numerical methods

15 p2824 A70-31450

Boundary value problems and Cauchy problem considered for mathematical model of turbulent motion in liquid or gas

15 p2718 A70-31463

Equilibrium forms of prolonged rectangular plate in gas flow in terms of nonlinear boundary problem, emphasizing plate with hinged supports

15 p2671 A70-31471

Diffraction on strip, investigating for Dirichlet boundary conditions, deriving excited current density and scattered pattern

15 p2696 A70-31515

Boundary value problems of biharmonic finite difference equation in rectangular domain, deriving calculation formulas for summary representations solution method

15 p2814 A70-31583

Cauchy spatial problem of Laplace equation, obtaining approximate solution based on initial conditions

15 p2767 A70-31584

Shells of revolution zero moment stressed state calculation by analytical functions, solving boundary value problem for edge loading

15 p2814 A70-31587

Axissymmetrical boundary value problem solution by net point method via transformation into self adjoint second order elliptic equation, obtaining positively determinate matrix

15 p2767 A70-31588

Natural oscillation frequencies of shallow shells with mixed boundary conditions on clamped edges, using summary representations method

15 p2814 A70-31590

Laminar boundary conditions for heat transfer in gradient flow region for plane turbulent jet impingement on plate normal to flow

15 p2721 A70-32134

Nonlinear higher order canonical time lag equations initial and boundary value problems solutions by approximate iterative two way integration

15 p2767 A70-32171

Heat conductivity equations transformation for Cartesian and cylindrical coordinates and various boundary conditions using static electrointegrator

15 p2827 A70-32172

Nonlinearly elastic bodies under subcritical strain, analyzing boundary value problems for three dimensional stability

15 p2818 A70-32179

Boundary value problem of elastic isotropic material, obtaining pointwise bounds of Cosserat continuum, considering couple stresses and constrained rotation of particles

15 p2821 A70-32340

Boundary value problem in linear elastodynamics, investigating Ignaczak type theorems for microstructure effects in transient heat conduction problems

15 p2822 A70-32343

Riemann-Hilbert problem for discontinuous coefficient solving mixed boundary value problems in infinite elastic strip, discussing shear stress along whole boundary

15 p2822 A70-32355

Orr-Sommerfield equation asymptotic solution corresponding to boundary layer velocity distribution

15 p2721 A70-32357

Wave scattering from elliptic cylinder, solving boundary value problem for two dimensional wave equation

15 p2700 A70-32404

Variational equation of ballistic trajectory applied to two point boundary value guidance problems

15 p2812 A70-32504

Optimal control stochastic problem with initial conditions treated as random variables, using matrix minimum principle

15 p2716 A70-32563

Series expansions convergence of solutions to boundary value problem for Navier-Stokes equations, introducing small parameter in boundary conditions

16 p2890 A70-33243

Difference schemes approximating boundary value problem for heat conductivity and oscillation equations, considering brute force method stability

16 p2951 A70-33245

Elliptic boundary value problems involving pseudodifferential operators on bounded manifold, examining solutions analyticity

16 p2941 A70-33269

State estimation for nonlinear discrete time systems with quantized measurements, obtaining recursive algorithm through boundary value problem linearization

16 p2867 A70-33305

Initial condition sensitivity functions in bang-bang and optimal control, considering discontinuous functions, perturbation equations, iteration algorithms terminal states, cost functions, etc

16 p2885 A70-33325

Particular solutions for nonlinear two point boundary differential equations with initial and final conditions

16 p2942 A70-33692

Continuous space discrete time /CSDT/ method using initial value formulation for partial differential equations, discussing applications to one dimensional problem

16 p2943 A70-33736

Boundary value problem of two dimensional Poisson equation solution procedure with Hockney formulas, applying to unsteady viscous incompressible flow past flat plate

16 p2943 A70-33737

Dwell time boundary and mean values for laminar flows through channel and tube reactors, obtaining field representation from streamline network and isochrones

16 p2893 A70-33745

Optimal design of structures with constraints on strength and natural frequency, developing steepest descent boundary value method

16 p2991 A70-33854

Outer boundary conditions derivation from asymptotic form of similar boundary layer equations with unit Prandtl number

16 p2894 A70-33874

Initial reentry body motion effects on angle of attack envelope value throughout trajectory, including altitude of maximum transient amplification

16 p2982 A70-33892

German monograph on stress-strain state determination for rotors of turbomachines covering strain equations, partial differential equations, boundary conditions, etc

16 p2971 A70-34078

Nonlinear partial differential equations initial value problems asymptotic solution using two time method

16 p2943 A70-34245

Boundedness theorem for solutions to differential equations system in applied mechanics

16 p2944 A70-34287

Canonical variational principle for boundary condition contractions in elastic shell theory

17 p3182 A70-34545

Singular perturbations of boundary value problems, investigating asymptotic solutions to finite difference equations

17 p3128 A70-34613

Boundary conditions for electrodynamics of wave reflection from conducting bodies, using perturbation technique

17 p3128 A70-34633

Boundary value problems for symmetrically excited biconical antennas surrounded by free space, treating spherical and thin wire antennas

17 p3044 A70-35062

Boundary value problem of Hertzian dipole antenna in presence of conducting half space, analyzing lossy earth effects on input impedance and radiation pattern

17 p3044 A70-35074

Antennas in plasma, investigating electromagnetic and electroacoustic waves and boundary value approach

17 p3045 A70-35076

Existence and uniqueness theorem for boundary value problem solutions to nonlinear canonical ordinary differential equations

17 p3131 A70-35339

First boundary value problem solution for parabolic equation by differential invariant method

17 p3131 A70-35340

Shallow shell theory boundary value problems, calculating stress concentration for domes and shells with holes

17 p3192 A70-35694

Axisymmetric mixed boundary problem for elastic infinite cone, obtaining solution by assuming zero shearing stresses

17 p3192 A70-35698

Three dimensional mixed boundary value problems, obtaining solutions for elastic body differential equilibrium equations

17 p3192 A70-35699

Class of third order difference methods for hyperbolic equations in one and two dimensions applicable to nonlinear initial value problems

17 p3131 A70-35893

Two dimensional free boundary problems approximate solution by finite difference method, deriving algorithms for computer program implementation

18 p3230 A70-35941

Elastic layer with circular cylindrical cavity under axial tension /Kirsch problem/, determining stress concentration from boundary value problem

18 p3335 A70-36130

Finite difference theory applied to first boundary value problem of elasticity theory for Lamé equation

18 p3280 A70-36158

Generalized Carleman boundary value problem, discussing analytical function in simply connected region on Liapunov contour

18 p3280 A70-36159

Ritz procedure for problems with eigenvalues in boundary conditions

18 p3336 A70-36222

Boundary value problem for Navier-Stokes equations of viscous incompressible fluid flow, discussing convergence of iterative solution

18 p3241 A70-36290

Boundary value problem approximation method for large numbers, using projective method applicable to linear integral, integrodifferential and differential equations

18 p3282 A70-36360

Monotonic difference schemes for parabolic differential equations with nonlinear boundary conditions, discussing convergence and stability

18 p3282 A70-36361

Linear multistep algorithms in discretization of nonlinear initial value problems of ordinary differential equations

18 p3283 A70-36366

Singular integral equations of elasticity theory, formulating boundary value problem for discontinuous plane stresses

18 p3337 A70-36370

Finite element procedure convergence for fourth order boundary value problems solution

18 p3283 A70-36493

Torsional vibration of thin beam with varying cross section, formulating fundamental equation and boundary conditions

18 p3339 A70-36519

Generalized boundary value problems solution for elliptic differential equations by Schwarz method, proposing algorithm

18 p3283 A70-36573

Thermoelasticity boundary value problems by finite difference method, determining thermal, displacement and stress fields in continuous medium

18 p3342 A70-36671

Closed form solution for minimum fuel constant thrust trajectories for vehicle transfer in vacuum between arbitrary boundary conditions

18 p3316 A70-36683

Arbitrary cross sections center of flexure formula, transforming surface integral to line integral dependent on boundary conditions

18 p3343 A70-36716

Laminar incompressible flow in arbitrary cross sectioned entrance region of ducts by numerical technique after transformation to boundary value problem

[ASME PAPER 70-GT-91] 18 p3243 A70-36878

Plane electromagnetic wave reflection from laminar anisotropic medium, piecewise-constant permittivity tensor as boundary value problem

18 p3229 A70-36922

Boundary value problems in MHD, considering viscous and nonviscous fluids

19 p3479 A70-37592

Initial boundary value problems for hyperbolic partial differential equations, including Cauchy problem

19 p3457 A70-37678

Linear time varying systems optimal control through decoupling of boundary value problems

19 p3393 A70-37866

Mixed boundary value problems approximate solution in linear elasticity by variational method, noting applications to micromechanics

19 p3540 A70-37957

Nonlinear two point boundary value problem, examining quadrature error effects in approximate numerical solutions by variational techniques

19 p3458 A70-37979

Boundary value problem solution in nonlinear viscoelasticity by constitutive equations

19 p3544 A70-38330

Boundary value problems for elastic sphere, extending Kelvin general solution of Cauchy equations

19 p3545 A70-38333

Sandwich panels geometrically and physically nonlinear theory, obtaining equations of motion and boundary conditions consistent with strain displacement relations

19 p3547 A70-38360

Equilibrium equations integration for body in isotropic linear viscoelastic medium with contact-type boundary conditions

19 p3547 A70-38395

Elastoplastic work hardening continua incremental boundary value problem with allowance for distributed dislocations, using quadratic programming concepts

19 p3549 A70-38667

Helmholtz equation initial value problem solution by integral operators

19 p3459 A70-38680

Simultaneous approximation of function and product with given operator, applying to boundary value problems of partial differential equations

19 p3459 A70-38682

Straight thin walled elliptical cylindrical shells stability in pure bending, solving boundary value problem

19 p3550 A70-38683

Initial value or boundary value problems in mathematical physics, solving by process of condition elimination

19 p3472 A70-38727

Coordinate sequences for regions with complex geometries and various boundary conditions, using linear operators

19 p3460 A70-38940

Singular integral equation formulation for torsion from membrane analogy, obtaining boundary value problem solution by computer program

20 p3718 A70-39000

Quadrature solution for elastic shape deformation by axisymmetric normal loads, writing Green function of boundary value problem in finite form

20 p3719 A70-39379

Plane electromagnetic scattering from perfectly conducting bodies, comparing exact numerical solution with experiment

20 p3585 A70-39394

Boundary value problems in potential theory for electrical disk and spherical cap reduced to problems for two dimensional Laplace equation

20 p3657 A70-39446

Spacecraft trajectory initial conditions expressions as parameters dependent functions, applying results to Mars lander mission [AIAA PAPER 70-1016]

20 p3666 A70-39517

Second order approximations to velocity required concept for boundary value problems in guidance, deriving Riccati equation and position required concept

20 p3666 A70-39518

Uniqueness theorem for first boundary value problem of heat conduction equation with discontinuous coefficient

20 p3737 A70-39710

Boundary value problems in dynamic two dimensional elasticity theory for domains bounded by circles and straight lines

20 p3721 A70-39770

Boundary value problems in uniform incompressible inviscid flows past complex profile bodies by R functions method and variational technique

20 p3610 A70-39772

Shock tube with diffuser in low shock wave Mach number range, considering gas flow models to relate wave intensity to initial conditions in chambers

20 p3606 A70-39820

Elasticity theory boundary value problems reduction to one dimensional integral equations

20 p3724 A70-39853

Elastic bodies static stability theory variational principles, introducing equilibrium equations and boundary conditions of initial state by Lagrange multipliers

20 p3724 A70-39857

Elasticity theory equations polynomial solutions for use in boundary value problems

20 p3726 A70-39874

Structurally closed orthotropic circular cylindrical reinforced shell stability, developing approximate method to obtain various boundary conditions

20 p3727 A70-39886

Singular points in elasticity theory solved by correct boundary value problem and homogeneous solutions theorem

20 p3728 A70-39894

Thin elastic shells displacement vector and strain boundary conditions determination from stress-strain relations

20 p3728 A70-39896

Homogeneous boundary value problems in stability theory of circular cylindrical shells axisymmetric equilibrium state

20 p3732 A70-40100

Falkner-Skan type boundary value problem of three dimensional flow near stagnation point

20 p3658 A70-40103

Nonlinear free boundary problem for hyperbolic one dimensional gas dynamics equations

20 p3658 A70-40105

Boundary value problems in dynamic elasticity by perturbation method with displacement components

20 p3732 A70-40111

Boundary conditions on vector and scalar potentials in viscous three dimensional hydrodynamics, investigating compressible flow problems

20 p3612 A70-40115

Boundary value problems for linear ordinary differential equations with singularities, determining eigenvalues by computer oriented method

20 p3659 A70-40134

Hilbert type nonlinear boundary value problem, determining conditions for analytical function solutions based on algebraic isotherms theory

20 p3659 A70-40169

Metallic shell with passive thermal protection coating, solving boundary value problem for high temperature heating with simplified mathematical model

20 p3739 A70-40296

Dynamic external boundary value problems for elastic body bounded by spherical surfaces 20 p3734 A70-40433

Strip array excitation by field with large phase shift per period, deriving approximate solution from averaged boundary conditions 21 p3784 A70-40627

Integral equation of viscoelastic media with unstable properties, solving boundary value problems by approximation method 21 p3933 A70-40643

Boundary value problems for elliptic equations with discontinuous coefficients, using finite element method 21 p3845 A70-40734

Vibration of combined cylindrical shells via Lagrangian minimization regarding unknown boundary values 21 p3934 A70-40897

Assumed vibration modes generation method in beams with arbitrary boundary conditions, applied to cantilevered beams, using modified Rayleigh-Ritz analysis 21 p3934 A70-40923

Supersonic flows with imbedded separated regions, emphasizing cavities with recompression against solid boundary layer 21 p3745 A70-41372

Aerodynamic forces on flexible launch vehicles and missiles in supersonic flight based on first order method, solving boundary value problem for surface velocities 21 p3746 A70-41853

First order linear distributed systems with two point boundary values, obtaining eigenfunction expansion by generalized Fourier method 21 p3846 A70-41949

Viscous laminar parallel flow along cylindrical surfaces, discussing boundaries described by algebraic polynomials 21 p3810 A70-41959

Boundary value problem solution for elliptical crack subjected to impulsive load by method of characteristics and discontinuity relations, calculating stress distribution 21 p3938 A70-41960

Isoperibol calorimetry for laser power and energy measurements, discussing boundary value problem for heat flow 21 p3838 A70-42021

Cracks stress intensity factors in plane problems by combined conformal mapping and boundary collocation technique 21 p3940 A70-42036

Surfaces separated by radiatively nonparticipating medium, determining absorptivities and heat transfer boundary conditions in gray surface problems by irradiation factor method 21 p3953 A70-42085

Dirichlet problem for Tricomi equation emphasizing gap in boundary data 22 p4061 A70-42289

Nonlinear one dimensional conduction in radiating heat shields, solving two point boundary value problem by asymptotic and numerical solutions [ASME PAPER 70-HT-E] 22 p4121 A70-42422

Existence theorem for boundary layer problems, including swirling flow between coaxial rotating disks 22 p4009 A70-42484

Time dependent shock wave structure, considering shock tube flow as initial and boundary value problem 22 p4009 A70-42516

Heat conduction into semiinfinite homogeneous solid with thermal conductivity dependence on temperature, noting temperature profile asymptotic behavior for similarity solution 22 p4123 A70-42641

Harmonic mixed boundary value problem with singularity, deriving approximate solution by dual series technique with conformal transformation and finite difference method 22 p4062 A70-42642

Oscillating wing aerodynamic load boundary value problem reduction to sequence of steady lifting-surface problems 22 p3959 A70-42715

Finite difference method for initial value problems of fokker-Planck equations 22 p4080 A70-42743

Irrational incompressible free falling jet, using asymptotic expansion solution for mixed boundary value potential problems 22 p4012 A70-42938

Viscoelastic continuous shaft whirling motion, discussing boundary conditions and internal linear viscous damping 22 p4012 A70-42939

Stress distribution around moving cracks in finite width strip, obtaining solutions for boundary conditions by Schwarz-Christoffel transformation and complex functions theory 22 p4116 A70-43025

Thin walled shells of revolution equations boundary conditions formulated by stress state separation, giving small parameter perturbation theorem 22 p4117 A70-43316

Newton regularized method for nonlinear boundary value problems in combination with conjugate gradients 22 p4064 A70-43480

Geodetic boundary value problem reformulation based on geometric satellite geodesy involving gravity measurements 22 p4025 A70-43667

Boundary value problems of elasticity for layer and strip with arbitrary inhomogeneity along thickness 22 p4120 A70-43712

Elasticity theory for circular cylinder weakened by cavities, discussing boundary conditions on butt ends and Galerkin solutions 23 p4265 A70-43983

Conducting bodies of revolution, calculating surface currents due to axially incident plane electromagnetic wave by computer program 23 p4162 A70-44005

Notch stress intensity factor representation as boundary traction weighted average, deriving weight functions from stress field boundary displacements 23 p4266 A70-44021

Iterative method for boundary value problems in mathematical physics, showing convergence by heat conduction equation solutions 23 p4276 A70-44218

Ordinary differential equations boundary value problems solution based on continuation and reduction to Cauchy problems 23 p4211 A70-44309

Boundary geometry of region with fluid motions harmonic functions obeying Bernoulli law containing free surface curvature 23 p4218 A70-44337

Approximate method for solving thermal conductivity first boundary value problem via reduction to auxiliary Cauchy problem solved by Laplace transform and power series 23 p4277 A70-44339

Nonlinear free boundary value problems involving region bounded by curvilinear ring consisting of smooth curves, reducing problem to nonlinear equations in Banach space 23 p4212 A70-44342

Boundary value problems of fluid dynamics in dynamic cavities reduced to integral equations system 23 p4182 A70-44347

Homotopic classification of boundary value problems with directional derivatives for harmonic functions 23 p4212 A70-44348

Axially compressed circular cylindrical shells subject to relaxed boundary conditions, calculating buckling loads as function of length to radius ratio [ASME PAPER 70-APM-O] 23 p4269 A70-44397

Temperature dependent materials heat flow analysis using perturbation method for nonlinear boundary value problems 23 p4282 A70-44589

Numerical methods for mixed boundary value problem of axisymmetric shells of revolution, using truncated series expansion and finite difference expressions 23 p4272 A70-44712

Rotating spherical shell equations as initial value problem, noting maximum convective heat transport at equator 23 p4249 A70-44805

Periodic boundary value problems with cyclic totally positive Green functions, considering applications in vibrating physical systems and spline theory 23 p4213 A70-44899

Nonlinear filtering for linear parabolic distributed parameter systems with white noise, considering stochastic boundary value problem 23 p4177 A70-44905

Corrugated plates, closed cylinders and developable shells nonlinear elastic analysis, deriving boundary conditions 23 p4275 A70-44913

Numerical solution of first boundary value problem of elasticity theory involving biharmonic stress function relating to rim loads 23 p4275 A70-44942

Dipole antenna in compressible lossy plasma, calculating sheath and absorptive surface effects on current distribution from boundary value problem formulation 23 p4228 A70-44963

Linear viscoelastic solid quasi-static deformation, deducing associated minimum principles under assumption of unique solutions existence for boundary value problems 24 p4420 A70-45264

Asymptotic properties of integral equations solutions for boundary value problems in theory of elasticity and mathematical physics 24 p4422 A70-45490

Flame propagation limits and damping mechanism in gases under convection, determining boundary and initial conditions 24 p4428 A70-45492

Variational solution of eigenvalues and eigenfunctions of second boundary value problem of elasticity minimizing functional 24 p4424 A70-45629

Asymptotic small-parameter solution of boundary value problem for second-order elliptic equations with variable coefficients in thin regions 24 p4424 A70-45635

Plate constituting doubly connected region bounded by outside curvilinear polygon and inside by eccentrically located circle, using series summation 24 p4424 A70-45636

Nonlinear boundary value problems, deriving existence theorems 24 p4369 A70-46022

Variational principle and reciprocity theorem for initial value problems associated with wave equations, discussing solution uniqueness conditions 24 p4380 A70-46037

Stochastic boundary value problem involving differential equation with random forcing function, proving monotone property of solution covariance variation 24 p4426 A70-46039

Nonlinear parabolic initial value problems, including Navier-Stokes equations 24 p4370 A70-46414

BOUSSINESQ APPROXIMATION

Boussinesq eddy viscosity concept solving equations of two dimensional incompressible turbulent boundary layer, using implicit five point finite difference method 02 p0285 A70-12350

Asymptotic solutions of paraboloidal boundary layer system for thermally driven convective flows governed by nonlinear Boussinesq equations 03 p0519 A70-14077

Solar spin down procedure simulated via Boussinesq fluid spin down in circular cylinder 23 p4252 A70-44832

BOW SHOCK WAVES

U BOW WAVES

U SHOCK WAVES

BOW WAVES

Resonance amplification theory of standing interfacial gravity waves in viscous fluids applied to obtain wavelengths prediction of atmospheric bow waves 01 p0081 A70-11299

Standing bow shock in plasma flow into dipole magnetic field, measuring particle density, electron temperature, magnetic field flux and oscillations 03 p0530 A70-13158

Earth bow shock and magnetopause oscillatory motions with respect to positions assumed under quiet solar wind conditions, discussing satellite observations 05 p0840 A70-16586

Hydromagnetic wave interaction with magnetopause and bow shock, considering solar wind turbulence and magnetopause tail stability 07 p1270 A70-20070

Initial deceleration of solar wind positive ions upstream of earth bow shock determined fromOGO 5 high time resolution plasma measurements 08 p1562 A70-21377

Electron and proton temperature differential near earth bow shock determined from plasma probe measurements by Vela 4B satellite 09 p1670 A70-23486

Supersonic transports bow and rear shock pressure jump lower bounds for various physical constraints 10 p1805 A70-24558

Rarefied hypersonic axisymmetric blunt body, examining bow shock and viscous layer upstream merging 10 p1804 A70-24823

Plasma density and velocity required for simulating solar wind flow over magnetosphere /bow shock/ in plasma wind tunnel 11 p2032 A70-26372

Fast time-resolved spectra of earth bow shock electrostatic turbulence based on broadband analog electric data fromOGO-5 13 p2396 A70-29111

Electron and positive ion velocity distributions measurements near earth bow shock by electrostatic analyzer on Vela 4B satellite 13 p2481 A70-30068

Bow shock associated hydromagnetic waves generation in upstream interplanetary medium, constructing model in terms of ion cyclotron resonance 14 p2631 A70-30359

Solar wind interaction with planetary ionosphere, considering flow behavior across bow MHD shock 14 p2647 A70-31073

Supersonic transport sonic boom theory and effect reduction, discussing Whitham rule, bow shock, overpressure, engine and aircraft design and shock wave control 16 p2843 A70-34263

Electrostatic turbulence in bow shock magnetic structures observed byOGO 5, explaining turbulence as ion acoustic or Buneman mode due to two stream instability

18 p3311 A70-36006

Plasma properties across bow shock and in magnetosheath as function of supersonic solar wind

19 p3494 A70-37481

Solar energetic charged particles interaction with earth bow shock and magnetopause

19 p3494 A70-37482

Magnetic and electric field changes across earth bow shock and magnetosheath, discussing Pioneer 8 andOGO-5 data

19 p3494 A70-37483

Wedge angle large amplitude slow oscillations in hypersonic and supersonic flows, examining attached bow shock

20 p3559 A70-40288

Magnetosheath turbulence generation by hydromagnetic waves amplification carried by solar wind through earth bowshock, computing refracted and incident energy fluxes ratio

21 p3815 A70-41059

Inner magnetosheath large amplitude hydromagnetic waves, discussing power spectrum, earth bow shock and solar wind

21 p3816 A70-41083

Turbulent collisionless plasma shocks formation, wave front steepness and explanation for earth bow shock

23 p4225 A70-44183

BOX BEAMS

Aircraft wing box beams bending tests to failure loads, considering crushing pressure, bulkhead flexural deformation, structure initial imperfections and instability phenomena [ICAS PAPER 70-33]

23 p4267 A70-44103

Rumanian book on torsion in thin walled elastic structures of various cross sections covering calculation methods for box beams, cylindrical and conical shells, aircraft wings, etc

24 p4418 A70-45147

BRADYCARDIA

Artificially induced heart rate changes effect on atrial circumference and pressure in anesthetized cats, showing increase with tachycardia and bradycardia

01 p0017 A70-10473

Ventricular ectopic beats and bradyarrhythmia associated with myocardial infarction, discussing enhanced automaticity, reentry activity, drugs and heart pacing

06 p0998 A70-18407

Bradycardic rhythms in acute myocardial infarction, investigating pathophysiologic, hemodynamic and electrophysiologic aspects and ECG interpretation

06 p0998 A70-18408

Heart rhythm disorders among flying personnel, noting occurrence frequency of sinus bradycardia and arrhythmia

12 p2180 A70-28362

BRAGG ANGLE

Ultrasonic imaging of internal structure by Bragg diffraction, noting reflection and dark field extension and use for flaw detection and medical diagnostics

01 p0111 A70-10570

Aperture dissection scheme to reduce transit time of Bragg angle acousto-optical scanning of laser beam

05 p0860 A70-16657

Bragg reflecting crystals for spectroscopy and polarimetry in X ray astronomy

13 p2489 A70-28904

Laser Doppler heterodyning system for velocity measurements without directional ambiguity, employing incident beams of different frequencies through rotating diffraction grating or Bragg cell application

15 p2751 A70-31986

Integrated Bragg X ray scattering intensities for monatomic crystalline lattices, considering thermal diffuse component contribution

20 p3686 A70-39193

Acoustic Bragg diffraction for laser light deflection, solving high speed photography and holography motion problems [SMPT PREPRINT 5]

22 p4035 A70-43055

BRAIN

NT BRAIN STEM
NT CEREBELLUM
NT CEREBRAL CORTEX
NT CEREBRUM
NT HIPPOCAMPUS

Carbohydrate-phosphorus metabolites content in gophers brains under normal conditions during hypothermia and spontaneous warming at room temperature

01 p0012 A70-10055

Soviet collection of articles on problems of brain biochemistry, Volume 4

01 p0017 A70-10504

Nicotinamide adenine dinucleotide/NAD/ deamination and role of nicotinamide hypoxanthine dinucleotide/deamino-NAD/ in forming ammonia from amino acids in rats/rabbits brain and liver tissue

01 p0018 A70-10505

Indirect ADP deamination and reamination of corresponding deamino form of ionosine diphosphate in rabbit brain tissue

01 p0018 A70-10506

Glutamic and aspartic acid concentrations in brain tissue and incubation medium after adding gamma-aminobutyric acid

01 p0018 A70-10507

Glutamine deamidation enhancement by N-acetyl-L-aspartic acid addition to mitochondrial preparations of rabbit brain incubated in Tris buffer

01 p0018 A70-10508

Gamma-aminobutyric acid effect on oxidative phosphorylation of rabbit and rat brain mitochondria, noting dependence on ionic concentration, temperature and amount of additions

01 p0019 A70-10509

Gamma-aminobutyric acid influence on 5- hydroxytryptamine in rat brain after intraperitoneal administration

01 p0019 A70-10510

Metabolism and biological activity of urea, citrulline, arginosuccinic acid in organism ornithine cycle, discussing role in brain and liver

01 p0019 A70-10513

Polycythemia and hypercapnia effects on apparent oxygenation of rat brain during acute hypoxia by changes in creatine phosphate concentration and lactate/pyruvate ratio

02 p0232 A70-11717

Brain norepinephrine synthesis rate in gonadectomized and control rats treated with alpha-methyl paratyrosine

03 p0416 A70-12987

Noble gases breathing effects on free amino acid pool increase in rat brains, considering O mixtures with He, Ar and Ne

04 p0632 A70-15086

Tetrodotoxin /TTX/ effects on mammalian brain studied by introducing TTX into cat lateral geniculate body /LGB/, causing flash evoked potentials and visual cortex decrease

05 p0799 A70-16049

Hypothalamus influence on potentials and recovery cycles of mesencephalic reticular formation in response to sciatic nerve stimulation in anesthetized rabbits

07 p1204 A70-19138

Mathematical model for oxygen tension changes in dogs brain tissues under hypoxia during altitude simulation

07 p1208 A70-19505

Nucleic acid and protein synthesis dynamics in rat brain and heart during adaptation to high altitude hypoxia

07 p1209 A70-19518

Respiratory neurons pulsating activity in medulla oblongata of anesthetized cats during imposed rhythm

07 p1213 A70-19774

Respiratory neurons activity in respiratory center of medulla oblongata during suspension and forced recovery of respiratory motions

07 p1213 A70-19775

Visual perception of black-and-white photo in aerial photographic interpretation, examining processes in human brain

07 p1221 A70-19777

Adaptive reactions in thyroidectomized rats blood and brain during adaptation to hypoxia compared with intact animals

07 p1214 A70-19794

Oxygen uptake by brain as function of oxygen tension in rats using venous outflow method and blood gas analysis

08 p1446 A70-21436

Bioelectrical activity of brain during conditioned motor reflex system operation modes in response to stimulating light pulses

08 p1447 A70-21450

Time course of changes in rat brain norepinephrine levels after olfactory bulb lesions, discussing automatic and biological mechanisms

08 p1448 A70-21841

Neural information processing taking into account differences between living brain and artificial processor

09 p1617 A70-22496

Machine design similar to human brain for recognition and classification of information

09 p1641 A70-22708

Critical oxygen supply of cerebral mitochondria and intercapillary oxygen transport

10 p1821 A70-25080

Brain oxygen supply during cerebral edema, examining venous and arterial blood gases, circulation, oxygen uptake, blood volume and pressure and EEG

10 p1822 A70-25087

Anterior lobe role of brain limbic region in analysis of afferent pulses arising in receptors of respiratory system

11 p1987 A70-25942

Mathematical model for oxygen tension changes in dogs brain tissues under hypoxia during altitude simulation

11 p1987 A70-26104

Drosophila brain Circadian oscillation as gating device restricting emergence behavior of adult

11 p1989 A70-26661

Memory mechanisms of brain, discussing molecular physiology, information storage in living systems

12 p2168 A70-27278

Sleep biphasic paradoxical stage in cats, correlating brain structures electroencephalographic data with various somatic and vegetative signs

12 p2173 A70-28345

Sensory afterdischarge of human brain under light stimuli during sleep and wakefulness

12 p2173 A70-28354

Acceleration effects on Na, K, and pH in rabbits cerebrospinal fluid and cerebral blood

13 p2352 A70-29347

Portable autonomous EEG analyzer for processing brain biopotentials without use of computer hardware and qualified personnel

13 p2360 A70-29522

Epinephrine uptake and metabolic disposition in rat brain, determining pathways and turnover of endogenous brain hormone and enzymatic synthesis

14 p2536 A70-30348

Rats under constant environmental conditions exhibiting circadian rhythmicity in rate of bar pressing with hypothalamic and septal reinforcing brain electrical stimulation

14 p2539 A70-30986

Electrical potentials in response to auditory stimuli recorded in cat brains by averaging computer

15 p2685 A70-32831

Sodium oxybutyrate effects on brain tissue oxidation during hypoxia in mice

15 p2686 A70-32851

Noise bursts response of positive and inhibitory conditioned eyelid reflexes in cats brain, discussing auditory system function

15 p2687 A70-32871

Daily rhythm in accumulation of rat brain catecholamines synthesized from circulating tritiated tyrosine

16 p2848 A70-33096

Corpus callosum role in auditory information transmission between hemispheres in intact dogs

18 p3221 A70-37215

Human brain LF activity in visual evoked response, determining relationship to stimulation

19 p3360 A70-37846

Electroencephalography with automatic frequency analysis to simulate processes involving brain self regulation

19 p3370 A70-38218

Acetylcholinesterase and simple esterases distribution in squirrel monkey brain, examining activity in neopile and postrema area neurons

20 p3569 A70-38993

Rats brain oxygenation during hyperventilation with air or oxygen-nitrogen mixture, measuring creatine phosphate concentration and lactate/pyruvate ratio

21 p3762 A70-41225

L-dihydroxyphenylalanine intraperitoneal injection effect on S-adenosylmethionine concentration in rat brain

21 p3764 A70-41269

Model for human brain visual information processing networks, considering visual search, selection, storage, correlation, recognition and recall functions

22 p3977 A70-42287

Blood-brain and blood-cerebrospinal fluid barriers alterations under various physical environments in manned orbital laboratory

22 p3973 A70-43647

Biocybernetics of human central nervous system, discussing electronic computers analogy to human brain

23 p4145 A70-44222

Amino acids L-glutamate and gamma-aminobutyric acid as communication agents in brain

23 p4148 A70-44864

Respiration rhythm mechanism from medulla oblongata electric shock stimulation in cats, considering inspiration-expiration phase shift relation to neuron fatigue

24 p4297 A70-45493

BRAIN CIRCULATION

Vestibular analyzer stimulation effects on cerebral blood circulation in humans during angular acceleration using rheoencephalography

03 p0422 A70-13692

Acceleration component in pelvis to head direction found influencing hyperemia of brain at various g forces

04 p0630 A70-14579

Cerebrum hyperemia of dogs subjected to craniocerebral hyperthermia, recording rheoencephalograms by occipitofrontal needle electrodes

07 p1207 A70-19473

Intracerebral, peripheral and central blood circulation relationship in humans during transverse accelerations

07 p1209 A70-19520

Human central nervous system changes during hypodynamia, noting unidirectional shifts in brain

- hemodynamics, rheographic wave propagation time reduction, etc 10 p1815 A70-24680
 - Brain oxygen supply during cerebral edema, examining venous and arterial blood gases, circulation, oxygen uptake, blood volume and pressure and EEG 10 p1822 A70-25087
 - Brain tussular respiration and oxygen consumption in rats during hypothermia 12 p2168 A70-27345
 - Perivascular pH influence on arteriolar diameter on brain surface of anesthetized rats and cats by micropipette technique 12 p2168 A70-27623
 - Cerebral circulatory reactions of smokers and non-smokers exposed to altitude, measuring vasomotor, blood flow and cardiac frequency indexes using scalp electrodes 12 p2172 A70-28042
 - Capillary details in lentiform nucleus region of human brains, measuring blood vessels diameters, lengths and densities 12 p2173 A70-28347
 - Positive pressure breathing effects on cerebral blood pressure and catecholamine content of hypothalamus and adrenal glands in dogs 16 p2849 A70-33997
 - Space flight effects on dogs cardiac activity, brain circulation and systemic-tissue circulation interactions 22 p3972 A70-43635
 - Oxidative phosphorylation and oxygen intake during circulatory hypoxia in mitochondria of liver and brain in rats subjected to acute ischemia 23 p4145 A70-44315
 - Regional cerebral cortical blood flow measurement, using heat clearance thermistor probe 23 p4157 A70-45082
 - Vasodilating carbon dioxide effect on brain circulation in occipital cortical area in cats and rabbits using thermoelectric method 24 p4300 A70-45842
- BRAIN DAMAGE**
- Soviet book on higher cortical functions of man and disorders due to local brain injuries, describing methods for neuropsychological studies of motor functions 01 p0017 A70-10503
 - Oxygen tension and pressure effects on hyperbaric oxygenation induced depletion of brain norepinephrine and 5-hydroxytryptamine in mice 02 p0235 A70-11992
 - Glycogen accumulation in astroglia following brain trauma caused by partial transection of cerebral hemisphere in rats 09 p1620 A70-22898
 - High risk factors for posttraumatic epilepsy /head injury complicated by subdural hematoma and spike EEG abnormality/ precluding return to flying 09 p1622 A70-23470
 - Skin galvanic reaction manifestation degree correlated to EEG changes accompanying injuries of human brain limbic structures 11 p1985 A70-25400
 - Centrifuging as therapeutic device tested on male assault victim with bullet fragment floating freely in brain ventricular system 11 p1993 A70-26523
 - Ionizing X radiation influence in lethal and sublethal doses on cerebral hyaluronic acid in mice and guinea pigs 14 p2536 A70-30186
 - Balloon-borne monkeys possible brain damage due to cosmic rays, discussing thindown tracks and acute vasculitis 21 p3764 A70-41476
 - Forebrain participation in motor response suppression reaction during stimulation of caudate nucleus in rats and cats, noting brain damage effects 24 p4299 A70-45836
 - Pathways of short latency reticulo-cortical responses to thalamic nuclei and hypothalamus destruction in cats 24 p4299 A70-45837
- BRAIN STEM**
- Time sense in human subjects kept in caisson or cave isolation determined as function of upper brain stem paraconsciousness 01 p0041 A70-11474
 - Arterial blood carbon dioxide tension effects on rhythmic volley activity of respiratory medulla oblongata neurons in cats 17 p3030 A70-33534
 - Visual cortical anomalous response to paired photic stimulus in rabbits with ablations in rostral part of brain stem 18 p3221 A70-37214
- BRAKES (FOR ARRESTING MOTION)**
- NT AERODYNAMIC BRAKES
- NT AIRCRAFT BRAKES
- NT BALLUTES
- NT DRAG CHUTES
- NT TRAILING-EDGE FLAPS
- NT WHEEL BRAKES
- NT WING FLAPS
- Air brake with compressed air fed bearings for testing small turbines, determining power and friction moment 08 p1481 A70-21188
 - Parachute decelerator system for 1975 Viking Mars Lander mission, discussing configuration selection, design factors, trajectory simulation, weight and mass analysis, etc 21 p3931 A70-41849
 - [AIAA PAPER 70-1162] Solid cloth personnel parachutes opening forces, discussing loading conditions, flight path shock parameters, mass ratio variations and elasticity of system 23 p4137 A70-43992
 - [AIAA PAPER 70-1167] Self stopping in involute gear mechanisms with external and internal gearing 07 p1290 A70-18818
 - Solar wind interaction with galactic cosmic radiation resulting in wind radial motion braking, discussing possible solar wind focusing 07 p1373 A70-20343
 - Accelerate-stop distance problem in takeoff refusal due to critical engine failure, emphasizing runway limited length hazards 08 p1436 A70-21270
 - Solid body control moments ensuring braking from rotational motion, finite orientation and angular velocity under minimum energy constraint 11 p2023 A70-25609
 - Spacecraft optimal impulsive braking by onboard engine to ensure maximum angle of atmospheric reentry 12 p2310 A70-28253
 - C-5A aircraft six wheel main landing gear bogie pitching control, emphasizing braking torque compensating mechanism design 17 p3020 A70-35826
 - [AIAA PAPER 70-914] Amplitude-phase characteristics of relay slave mechanisms with AC and DC motors under dynamic braking, using harmonic linearization 22 p4002 A70-42842
- BRANCHING (MATHEMATICS)**
- Soviet monograph on branching theory of nonlinear equations, covering solutions with analytical operators dependent on numerical or functional parameters 06 p1093 A70-17412
 - Nonlinear branching point problems in fluid mechanics using perturbation technique 14 p2565 A70-30471
- BRANCHING (PHYSICS)**
- Spheroidal wave function theory, calculating eigenvalues with branch points for propagation constants complex values 24 p4315 A70-46134
- BRASSES**
- Mechanical responses and residual defect structures in brass and stainless steel following explosive shock loading and cold reduction by rolling 03 p0507 A70-13139
 - Metal fiber multiple necking effect on uniaxial metal matrix composites ductility and plastic deformation behavior for brass-W model system 15 p2761 A70-32378
- BRAYTON CYCLE**
- Rankine cycle technology concerning high temperature, refractory alloy and liquid metal experience, showing applicability to nuclear Brayton and thermionic power systems 02 p0229 A70-12513
 - Brayton cycle electric power generator simulation to study turbomachinery startup 03 p0415 A70-14050
 - Brayton, Hg, organic-Rankine and potassium-Rankine dynamic space power systems for use with nuclear energy sources 13 p2450 A70-29492
 - Radiant gas heater for Brayton cycle space power system 18 p3303 A70-36834
 - [ASME PAPER 70-GT-36] Brayton cycles in gas turbines, investigating intercooling or reheat and pressure ratio proportioning influence on efficiency and specific work 18 p3304 A70-36856
 - [ASME PAPER 70-GT-130] Brayton, Hg, organic-Rankine and potassium-Rankine dynamic space power systems for use with nuclear energy sources 22 p4071 A70-43189
 - NERVA Technology Reactor design integrated with Brayton cycle space power conversion systems, considering space bases and shielding analysis 24 p4377 A70-45955
 - [AIAA PAPER 70-1226] NERVA reactor technology applied to closed Brayton cycle MHD power system 24 p4377 A70-45956
 - [AIAA PAPER 70-1225] Software production for Brazilian Advanced Educational Technology System 11 p2152 A70-25403
- BRAZIL**
- NT LOW TEMPERATURE BRAZING
- NT ULTRASONIC SOLDERING
- Ta-V-Cb and Ta-V-Ti alloys used as brazing fillers for refractory metals bonding, noting wetting and flow characteristics, shear strength, remelt temperatures, etc 02 p0319 A70-12753
- BREATHING APPARATUS**
- Brazing time and temperature effect on depth of Ag based brazing alloys penetration into thin Ti-Al-V sheet substantiated by microprobe analysis 06 p1078 A70-18513
 - Joint design for braze bonding and joining of Al-B composites using Borsic tape backed with alloy brazing foil 07 p1293 A70-18994
 - Metal matrix fiber reinforced materials bonding, discussing brazing and fusion and diffusion welding [ASM PAPER W9-23.2] 09 p1690 A70-22557
 - Dip brazing aluminum fan vanes used in high bypass turbofan jet engines 10 p1893 A70-23858
 - Book on metal joining techniques covering various welding and brazing processes 11 p2061 A70-26599
 - Vacuum brazed stainless steel hot gas actuators for guided weapons 18 p3265 A70-37202
- BREAKAWAY**
- U BOUNDARY LAYER SEPARATION
- BREAKDOWN**
- Breakdown of cryptocyanine dye in methanol solution by ruby laser pulses providing passive Q switching mechanism 06 p1083 A70-18524
 - Pulse duration and beam diameter effects on threshold energy density in laser induced transparent dielectric breakdown 13 p2428 A70-29382
 - Threshold light flux densities for thin Al film breakdown by laser radiation 13 p2428 A70-29383
 - Hydrodynamic lubrication film breakdown in cold strip rolling, showing thickness consistency with critical value of modified Sommerfeld number 21 p3833 A70-41256
 - Secondary breakdown meter for semiconductor diodes and transistors with reverse base drive, utilizing I-V characteristics and voltage waveform 21 p3801 A70-42248
 - Breakdown mechanism in Q switched ruby laser triggered spark gap, noting pulse duration and power peak 22 p4049 A70-42352
 - Prebreakdown ionization growth in gases based on initial photocurrents production from high voltage uniform field electrodes 22 p4026 A70-42353
- BREAKERS (ELECTRIC)**
- U CIRCUIT BREAKERS
- BREATHING**
- Endtidal oxygen and carbon dioxide partial pressures, oxygen uptake and carbon dioxide after apnea and during apneic diving 02 p0235 A70-12089
 - Airway resistance effect on ventilation and gas exchange during exercise, discussing minute volume and work of breathing response 03 p0429 A70-14157
 - Inhalation in functional respiratory exploration, describing equipment for aerosol volume measurement in contact with bronchopulmonary effectors 14 p2541 A70-30377
 - Pursed lips breathing effects on ventilation and blood gas exchange in patients with chronic airway obstruction 15 p2684 A70-32538
 - Diaphragmatic muscle reactions and pneumogram changes in rats immediately after air passage obstruction 19 p3360 A70-37804
 - Human sensory perception associated with breathing, comparing physical stimulus intensity with judgement of magnitude 19 p3365 A70-38370
 - Vagus nerve blockage effect on arterial carbon dioxide tension and breathing regulation in dogs 24 p4303 A70-46112
 - Excised perfused dog lungs stratified dead space changes due to transpulmonary pressure and breathing frequency increase, considering pulmonary circulation 24 p4303 A70-46114
- BREATHING APPARATUS**
- NT OXYGEN MASKS
- Dynamic testing instrumentation for oxygen breathing equipment emphasizing demand regulators and masks, connecting hose, helmets and individual components 01 p0041 A70-11458
 - Open loop portable life support system containing light breathing vest within space suit 05 p0806 A70-16123
 - Breathing valve with reduced air resistances based on aerodynamic principles 06 p1000 A70-17433
 - Metabolic Rate Monitor for measuring continuous oxygen consumption during changes in work in real time 15 p2741 A70-32540

BRECCIA

Apollo 11 lunar rocks, breccias, dust and chip mineralogy and petrology, examining composition, texture, grain size and morphologies

21 p3896 A70-41511

Apollo 11 lunar soil and breccia shock metamorphism, examining plastic deformation structures in plagioclase, pyroxene and olivine

21 p3897 A70-41520

Petrography and shock vaporization origin of Apollo 11 lunar breccias and glasses compared to terrestrial impactites and chondrites

21 p3898 A70-41524

Lunar breccia and fine sample metal particles, using optical and scanning electron microscopy and electron probe microanalysis

21 p3899 A70-41529

Apollo 11 lunar rock lavas and breccias, examining opaque minerals and olivine by reflection microscopy, electron probe and optical absorption measurements

21 p3899 A70-41530

Glass spherule lunar particles and breccia from Apollo 11 site, showing passage through impact generated cloud of hot fragmental material

21 p3901 A70-41541

Shock metamorphism in lunar microbreccias and loose regolith materials, assuming crater formation by meteorite impacts

21 p3902 A70-41551

Rare gas analysis of Apollo 11 lunar soil and breccia for surface layer history

21 p3906 A70-41571

Chemical analysis for Li, Na, K, Rb, Cs, Ca, Sr and Ba in achondrites and Apollo 11 lunar rocks, breccia and soil samples

21 p3910 A70-41611

Apollo 11 lunar dust and breccia micromorphology and surface characteristics implying weathering processes

21 p3910 A70-41622

Apollo 11 type C breccia sample remanent magnetism, observing viscous component with several hours time constant

21 p3914 A70-41651

Mossbauer spectra of Apollo 11 lunar fines and microbreccia, showing iron oxidation, site symmetry and magnetic state

21 p3915 A70-41657

Magnetic properties of Apollo 11 lunar breccia samples, determining natural remanent magnetization and susceptibility via paleomagnetism instruments and methods

21 p3916 A70-41668

Apollo 11 lunar crystalline rock and breccias petrography and luminescent properties, spectral analysis, color, emission bands and shock effects

21 p3918 A70-41678

Apollo 11 lunar crystalline rock, microbreccia and fines compressibilities at room temperature, loading-unloading and pressure volume curves

21 p3918 A70-41679

Apollo 11 lunar breccia and fines magnetic properties, examining remanence, composition, oxidation, volcanic activity and stoichiometry

21 p3918 A70-41680

BRECCIES

U CLOSURES

BREMSSTRAHLUNG

Semiconductor laser excitation by bremsstrahlung from electrons and gamma radiation from nuclear reactor

01 p0107 A70-10187

Bremsstrahlung radiation in intense magnetic fields rejected for pulsar radiation mechanism

01 p0169 A70-10344

Electromagnetic showers fluctuations produced by electrons and photons in heavy materials, determining moments of particle numbers and bremsstrahlung differential cross sections

01 p0171 A70-11026

Directional and spectral characteristics of bremsstrahlung X rays from auroral arc in low energy range during cosmic rays sounding rocket measurements

02 p0357 A70-12069

Bremsstrahlung emission from thermal plasma coexisting with relativistic electron tails, noting enhancement at electron plasma frequency harmonics

02 p0348 A70-12240

Electron-electron and electron-atom bremsstrahlung, giving graphical expressions for one and two electron atoms cross sections

04 p0721 A70-14667

Critique of paper on transverse enhanced bremsstrahlung from supraluminous and subluminal longitudinal waves in isotropic homogeneous plasma

04 p0728 A70-15006

Gamma rays due to cosmic ray electrons bremsstrahlung in interstellar medium, predicting diffuse galactic X ray flux

04 p0742 A70-15713

Hard electron bremsstrahlung measurement during intense polar aurorae in January and February 1968, determining electron flux penetration region

04 p0682 A70-15731

Astrophysical plasmas radio emission interpreted as collective bremsstrahlung due to ultrarelativistic electron tails, discussing Crab Nebula, quasars and Jupiter

05 p0904 A70-16932

Electron bremsstrahlung in intense magnetic fields calculated for emission rate and absorption coefficient in large quantum number limits

06 p1104 A70-17182

Cosmic X ray source spectra possibly due to plasma bremsstrahlung

07 p1368 A70-19700

Photon bremsstrahlung from relativistic hydrogen plasma determined by studying electron-positron pairing effect on plasma radiation intensity

09 p1735 A70-22986

Bremsstrahlung radiation in intense magnetic field proposed as emission mechanism from pulsars, discussing absorption coefficient

11 p2104 A70-25697

Bremsstrahlung radiation emitted from homogeneous, field free, nonrelativistic plasma, deriving formulas

13 p2456 A70-28500

Hard electron bremsstrahlung measurement during intense polar aurorae in January and February 1968, determining electron flux penetration region

14 p2575 A70-30816

Daytime auroral zone electron precipitation energy spectrum from atmospheric bremsstrahlung X ray balloon data

14 p2580 A70-31257

High energy electron temperature in beam plasma discharge pulsed laser measured by bremsstrahlung X radiation spectrum

15 p2752 A70-32194

Gravitational bremsstrahlung for small mass with relativistic velocity passing large mass in unbound trajectory, calculating energy flux of emitted waves

17 p3136 A70-34596

Bremsstrahlung from weakly ionized plasma, discussing emission and absorption characteristics, electron-atom collisions and dispersive effects

18 p3294 A70-36347

Neutrino production by synchrotron process /magnetic bremsstrahlung/ in relativistic electron gas under intense magnetic field

20 p3695 A70-39050

Bremsstrahlung and photoneutrons from electron-photon cascades in thick tungsten and tantalum targets bombarded with low energy electrons

20 p3674 A70-39222

Sco X-1 radio emission models, considering possible binary nature and thermal bremsstrahlung

21 p3875 A70-40685

Innerbremsstrahlung of intergalactic protons colliding with electrons as source of cosmic background X rays, interpreting intensity and energy spectrum

21 p3877 A70-40700

Diffuse X rays from nonthermal intergalactic bremsstrahlung, discussing cosmic ray injection models

21 p3878 A70-40705

Nonrelativistic electron bremsstrahlung in dense plasma with strong magnetic field

21 p3855 A70-40721

Electrons optical scale time averaged motion dependence in focused laser beam on light intensity gradient, calculating bremsstrahlung spectrum

21 p3836 A70-40723

Particle acceleration phase in solar flare development, discussing H alpha maximum, hard X ray burst and bremsstrahlung

21 p3880 A70-40971

Angular distribution of thick target bremsstrahlung produced by electron bombardment of Be, Sn and Au surfaces

21 p3854 A70-42020

Galactic X ray background due to inner bremsstrahlung associated with suprathermal particles, taking into account interstellar gas self absorption and ionization rate

22 p4093 A70-42465

Ionospheric bremsstrahlung X ray flux and ionization rate, considering electron-atom and electron-ion collisions as function of altitude

22 p4095 A70-43293

Bremsstrahlung X rays caused by energetic electrons precipitating into upper atmosphere, calculating photoionization rate as function of altitude

22 p4096 A70-43310

Plasmas kinetic theory, considering crossing from instability to stability, waves decay by collisional damping and emission by bremsstrahlung

23 p4224 A70-44178

Fluoroscopes for radiographic examination of materials and products with X ray and hard bremsstrahlung radiation

24 p4348 A70-45847

BREWSTER ANGLE

Longitudinal magnetic field effect on output power and emission polarization of CW Ar laser employing Brewster windows

03 p0500 A70-13529

Ice radiation and reflection characteristics in IR spectral region at certain Brewster angles

14 p2568 A70-30133

Triangular ring laser polarization, using discharge tube with Brewster angle windows in optical circuit

20 p3639 A70-39084

BRIGHTNESS

Current dependence of integral brightness and electroluminescence spectrum of ZnS-GaAs heterojunctions obtained by I vapor reaction in H flow

01 p0155 A70-10142

Near limb solar IR brightness distribution observed during total solar eclipse of 12 November 1966 in Argentina by sounding rocket photometers

01 p0186 A70-11271

Thermodynamic aspects of ray invariance of spectral brightness ratio to square of local index of refraction compared to black body power radiation

01 p0144 A70-11293

Satellite rotation periods determination accuracy from photometric observation data improved by determining initial and terminal moments of maximum brightness

02 p0255 A70-11769

Aerosol size distribution from data on atmospheric spectral transmittance and solar corona brightness spectral and angular variations

02 p0292 A70-12434

Jupiter radio telescope observations at cm wavelengths, describing radiation belt emission characteristics and planetary brightness temperature spectrum

03 p0565 A70-13233

Brightness distribution over source, discussing regularization algorithms for radio astronomical data reduction from crossed telescope

05 p0917 A70-16902

Radio brightness distribution observation over Venus disk, investigating absorption of millimeter radio emission of hot surface by planetary atmosphere

06 p1141 A70-17801

Particles and surface brightness distributions in nonionized cometary tails, considering near nucleus source and particle acceleration

07 p1378 A70-19035

Source power molecule lifetime, acceleration and particle velocity in region near comet nucleus determined from brightness

07 p1378 A70-19036

Surface brightness distribution in comet head investigated photometrically

07 p1379 A70-19038

Kilston comet 1966b brightness correlated with solar flares occurrence

07 p1379 A70-19041

Correlation function prediction of rapid brightness variations in quasar based on variable optical emission model including flares

07 p1383 A70-19403

Mars planet smoothing factor determined from phase curve of integrated brightness distribution on disk

08 p1564 A70-20557

Brightness distribution of spectroheliograms in metal lines reflecting velocity field structure in photosphere

08 p1570 A70-20839

Darkening and brightening of disturbed spot on sun surface determined by abnormal stress in seen layers due to magnetic and velocity fields

08 p1570 A70-20903

Meteors spectral intensity variations along flight path noting color dependence on brightness

08 p1572 A70-20946

Radio sources model brightness distribution and internal magnetic fields deduced from long baseline interferometer observation data

08 p1577 A70-21491

Jupiter radio telescope observations at cm wavelengths, describing radiation belt emission characteristics and planetary brightness temperature spectrum

08 p1580 A70-21666

Hydroxyl emission during auroras, noting absence of correlation with O I brightness fluctuations for IBC II-III aurora of 1 November 1968

09 p1671 A70-23496

Spectral, angular and spatial evolution of earth twilight aureole brightness pattern from visual observation and spectrophotometry on Soyuz 5 spacecraft

10 p1873 A70-24270

Autocorrelation and brightness distribution functions for irregular variable star

11 p2115 A70-26579

Mars and Venus radio temperature measurements by 210 ft telescope, obtaining effective brightness

12 p2309 A70-27896

Brightness temperature of earth atmospheric emission in submillimeter band at 35 km, describing airborne radiometer

12 p2265 A70-28171

Mars border-disk brightness comparison noting atmospheric transparency effects

12 p2311 A70-28303

- Radio brightness distribution observation over Venus disk, investigating absorption of millimeter radio emission of hot surface by planetary atmosphere 13 p2487 A70-28651
- Absolute magnitudes of first brightest galaxies in rich clusters from luminosity model, allowing for mass variation 13 p2495 A70-29795
- Solar magnetic and brightness fields simultaneous measurement by multiimage spectroheliograph 13 p2496 A70-29844
- Solar limb integrated brightness distribution in continuous spectrum during 20 May 1966 solar eclipse 13 p2498 A70-30003
- Mercury mm wave observations, examining longitude dependence of disk average brightness temperature and epilith thermal parameters range 14 p2467 A70-31076
- Lunar occultation observation of Jupiter by radio telescope, determining one dimensional strip brightness distribution 14 p2648 A70-31086
- Clouds and precipitations radio brightness temperature contrasts taking into account underlying surface humidity 15 p2771 A70-32070
- Mars planet smoothing factor determined from phase curve of integrated brightness distribution 15 p2805 A70-32712
- Meteors spectral intensity variations along flight path noting color dependence on brightness 15 p2806 A70-32758
- Balloon satellites brightness change from rotation effects, analyzing light curves 16 p2980 A70-34317
- Cloud brightness as function of illumination and underlying surface conditions, relating macrooptical parameters and microstructure 18 p3284 A70-36628
- Brightness field spatial structure of solar radiation reflected from earth by Cosmos 149 satellite, discussing homogeneity and isotropy 18 p3247 A70-36629
- Ascending long wave radiation brightness from aircraft measurements, observing angular distribution dependence on atmospheric stratification 18 p3287 A70-36970
- Mercury photometric measurement, examining surface brightness for photometric function 18 p3319 A70-37052
- Observed meteor brightness curve shortening with respect to theoretical curves 19 p3514 A70-37645
- Lunar maria distribution, explaining origin and characteristics by surface brightness 19 p3517 A70-37987
- Solid state laser with transverse mode selection to increase brightness, discussing plano-concave resonator 19 p3447 A70-38508
- Soviet book on brightness of irregular and semiregular variable stars by statistical methods 20 p3705 A70-39899
- Holographic exposure and reconstruction processes, considering illumination beam polarization effects on image brightness 22 p4040 A70-43616
- Pluto albedo at various wavelengths from spectrophotometric measurements 24 p4399 A70-45129
- Coherent motion effects on brightness of clouds moving above photosphere, describing H alpha Doppler brightening and Lyman alpha Doppler dimming in solar prominences 24 p4400 A70-45313
- BRIGHTNESS DISCRIMINATION**
- Binocular brightness mixing and autocorrelation function, discussing mathematical model, computer simulation and test results 01 p0025 A70-11053
- Human eye image accumulation effect and meteor brightness estimation dependence on angular velocity based on visual and telescopic observations 03 p0569 A70-13358
- Human eye image accumulation effect and meteor brightness estimation dependence on angular velocity based on visual and telescopic observations 11 p2118 A70-26723
- Optimal spatial discretization and brightness quantization of graphical symbols for pattern recognition, considering illumination and reflection coefficient 14 p2553 A70-30423
- Planetary surface smoothness factor by disk brightness, Mars red light and phase curves methods, indicating superiority of visual observation 18 p3315 A70-36602
- Brightness contrast by human observer binocular matching, discussing neural networks models 19 p3366 A70-38924
- Plate illumination relation to opacity in photometry and spectrophotometry, using digital techniques 20 p3630 A70-39475
- Bilateral cortical cerebellar hemispheric ablations effect on feline light-dark discrimination learning 21 p3762 A70-41142

BRIGHTNESS TEMPERATURE

- X ray differential drift scans of moon, measuring cold limb brightness temperature and temperature distribution 16 p2974 A70-33646
- Radio observations of chromospheric brightness temperature distribution during solar eclipse of March 1970 16 p2977 A70-33846
- IR radiometer for Mariner Mars 1971 project providing surface brightness temperatures 16 p2913 A70-34028
- Hour-angle and declination center-to-limb profiles of quiet sun 3.3mm brightness temperature distribution 17 p3174 A70-35868
- Planetary nebula NGC 7027 radio component, determining brightness temperature from fringe amplitude 18 p3313 A70-36327
- Spectrophotometric solar brightness temperature measurements in far IR, discussing collision type spectral variation of absorption coefficient 18 p3319 A70-37056
- Venus lower atmosphere structure and brightness temperature spectrum analysis for composition, temperature and pressure profiles 18 p3323 A70-37139
- Milky way galactic plane corrugation, discussing maximum hydrogen brightness temperature oscillating in sinusoidal pattern 18 p3328 A70-37167
- Night airglow hydroxyl rotational brightness temperature determined from emission spectra 19 p3412 A70-37777
- Temperature and radio brightness distributions in active regions and upper chromosphere during minimum activity periods 19 p3522 A70-38557
- Passive microwave sensors based on brightness temperature vs frequency model for various atmospheric conditions, presenting vegetation pictures 20 p3626 A70-39054
- Solar equatorial limb brightening at quiet sun from solar disk scanning statistical analysis 20 p3712 A70-40418
- Comet Schwassmann-Wachmann I brightness variations due to interplanetary shock waves in solar wind 22 p4097 A70-42475
- High speed plasma jet propagation, obtaining time of arrival measurements, brightness temperature, pressure and impact data 22 p4012 A70-43014
- Spectral brightness temperature, directional emissivity and surface temperature of earth from remote radiance observations by balloon-borne multidetector grating spectrometer 23 p4194 A70-44035
- Quiet sun and new moon brightness temperature measurements at 3.3 and 5.7 mm wavelengths, giving radiometric maps 23 p4241 A70-44254
- Uranus and Neptune millimeter wave observations, showing brightness temperatures in excess of black body equilibrium temperatures derived from solar heating 24 p4403 A70-45398
- BRILLOUIN EFFECT**
- Brillouin scattering of hypersonic waves produced in liquid medium, using He-Ne laser light source 02 p0313 A70-12471
- Satellite lines from diffraction grating observed by densitometer tracings of plates connected with optical mixing in stimulated Brillouin scattering 04 p0701 A70-15030
- Sound wave velocity and damping in liquid N measured along saturated vapor line using thermal Brillouin scattering techniques 06 p1105 A70-17491
- Acoustic velocity in rarefied argon and nitrogen using Brillouin scatter and Burnett equations 09 p1698 A70-23314
- Waveguide windows for energy outlet in microwave devices analyzed by plane /Brillouin/ modes, discussing dielectric element reflection coefficient 09 p1651 A70-23646
- Stimulated Mandelstam-Brillouin scattering and fracture of molten quartz and silicate glasses produced by laser giant pulse 11 p2061 A70-25380
- Stimulated Mandelstam-Brillouin and entropy backscattering of light pulses, determining intensity and spectral distribution allowing for fluctuations in medium 12 p2248 A70-27550
- Hypersonic sound speeds measured in methane at moderate pressures by spontaneous Brillouin light scattering experiments 21 p3830 A70-41938
- Brillouin effect lines shape dependence on analogous acoustical waves temporal and spatial coherence 21 p3839 A70-42100
- Threshold parameters of liquid and gaseous helium breakdown caused by ruby laser beam, noting Mandelstam-Brillouin scattering in liquid phase 22 p4051 A70-43465

BRILLOUIN ZONES

- Forbidden bandwidth in Brillouin zone and valence band spin-orbital splitting degree determined for mixed gallium-phosphide-arsenide 06 p1126 A70-17815
- Band structure of Brillouin zone and electronic states on pure and contaminated crystal surface 15 p2786 A70-32767
- Thermoelectric power and Hall effect quantum resonances in graphite for locating majority carrier electron and hole Fermi Surfaces in Brillouin zone 24 p4389 A70-45597
- BRITISH AIRCRAFT CORP AIRCRAFT**
- U BAC AIRCRAFT**
- BRITTLENESS**
- Dissolved gases and carbon effect on transition temperature from plastic to brittle state of high melting metals including niobium and vanadium 01 p0124 A70-11615
- Limiting equilibrium under axial tension of brittle body with parallel axisymmetric external cracks, studying critical load, crack propagation, etc 03 p0594 A70-13737
- Brittle fracture in neutron irradiated and nonirradiated Mo specimens tested in tension and compression at low temperature 03 p0513 A70-14013
- InAs-GaAs solid solutions microhardness and brittleness, studying chemical composition effects 04 p0730 A70-14464
- Fracture mechanical theory for crack propagation in brittle ceramics subjected to thermal shock, deriving crack stability criteria 04 p0767 A70-14505
- Erosion characteristics similarities and differences of brittle and ductile materials, noting dependence on particle velocity and diameter (ASME PAPER 69-WA/MET-7) 04 p0704 A70-14761
- Brittleness of joints using Ga solders prevention by high temperature annealing noting application to aluminum alloys 05 p0855 A70-16199
- Three dimensional brittle body limiting axisymmetric stability under tensile stresses and weakened by ring shaped cracks, determining critical tensile loads 05 p0945 A70-16855
- Impurities effect on grain boundaries composition and brittle fracture of metals 06 p1087 A70-17608
- Critical brittleness temperatures of low C steels determined to distinguish main failure types 06 p1166 A70-17655
- Dual model for describing brittleness and plasticity of solid elastic deformable body, formulating criteria for passage into inelastic state 06 p1166 A70-17656
- Critical stress-strain diagrams for brittle plate possessing notch-type stress raisers under biaxial tension 07 p1408 A70-19547
- Brittle failure mechanics application to steels sensitivity to rupture at low temperatures, discussing crack propagation resistance and heat treatment effect on impact toughness 09 p1768 A70-22076
- Quasi-brittle materials limit surface, approximating curve in deviator plane by second order curves leading to strength criteria 10 p1965 A70-25292
- Hollow cylindrical sample scale effect on accuracy of testing heat resistance of brittle materials 10 p1965 A70-25301
- Brittle fracture strength of welded joints in high strength steels 11 p2059 A70-25663
- Phenomenological properties of stress relief embrittlement in nickel steel, noting toughness recovery via retempering 11 p2059 A70-25665
- Interstitial and substitutional impurity effects on fracture strength, plastic properties and ductile-brittle transition temperature of vanadium determined from impact and tensile tests 11 p2066 A70-25913
- Hot shortness of molybdenum alloys under tensile testing due to molybdenum carbide precipitation on grain boundaries 11 p2066 A70-25914
- Critical loads for brittle bodies weakened by sharp holes under combined diffuse thermal fluxes and crack crossing 12 p0000 A70-28321
- Residual gas effects on critical load and brittleness of pure and molybdenum-coated niobium bars after annealing in vacuum 12 p2258 A70-28324
- Thin cut plate quasi-brittle breakdown under tensile stress, considering elastoplastic equilibrium under Tresca-St. Venant yield conditions 12 p2329 A70-28325
- Plastic deformation in brittle and ductile fracture, discussing elastoplastic stress analysis of cracked bodies, plane strain deformation near cracks, etc 13 p2509 A70-28601
- Niobium carbides formation in Nb containing steels during gamma-alpha transformation, establishing rela-

tionship between brittleness and carbide distribution characteristics

15 p2758 A70-32123

Curvilinear cracks development in flat brittle body under asymmetrical loads using small parameter method

15 p2817 A70-32165

Instrumented Charpy impact test evaluating strain rate, alloying and irradiation effects on ductile-brittle transition temperature and fracture of pressure vessel steels

15 p2820 A70-32239

Work to fracture measurements on brittle fiber ductile-matrix metal composites, using Charpy test

15 p2763 A70-32832

Weld brittleness during laser beam welding of Ni-Cu, Ni-Ti and Cu-Ti due to diffusion processes

16 p2916 A70-33052

Microscopic and macroscopic viewpoints of low temperature brittle fracture, noting Inglis, Griffith and Barenblatt theories

16 p2989 A70-33671

Unalloyed Ti hydrogen embrittlement, determining factors affecting brittle-ductile transition temperature

17 p3117 A70-34398

Cone crack closure in brittle solids, discussing optical and X ray studies on glass and silicon during unloading

17 p3183 A70-34621

Elastic crack structure, discussing formalism for force law between faces of brittle and semibrittle fractures

17 p3191 A70-35461

Hydrostatic pressurization effect on ductile-brittle transition temperature of polycrystalline chromium

18 p3274 A70-36053

Chemical composition selection for Ti alloys with low susceptibility to hydrogen induced brittleness

18 p3274 A70-36121

Brittle fibers strand strength as function of statistical distribution of limiting stresses

18 p3342 A70-36648

Nb effects on steel susceptibility to brittle fracture at various temperatures, discussing impact strength and nucleation energy of crack formation

19 p3453 A70-38709

Brittle failure under creep during slow cyclic loading, discussing damage accumulation assumptions

20 p3725 A70-39868

Brittle bodies with sharp pointed defects, constructing limiting equilibrium diagrams by stress concentration factor representations

20 p3733 A70-40393

Cracked brittle body limiting equilibrium, determining critical loads for two half spaces with various circular rib couplings

20 p3733 A70-40393

Intergranular brittleness in powder metallurgy W by Auger Electron Emission Spectroscopy for fracture surfaces chemical analysis

22 p4053 A70-42733

Ceramic composite materials structural application, improving brittleness and thermal shock resistance via reinforcing refractory fibers [ICAS PAPER 70-40]

23 p4267 A70-44138

Brittle fracture of welded notched steels with different stress concentrations, using subzero tensile tests

24 p4347 A70-45732

Precompression and pressurization effects on ductile-brittle transition of polycrystalline cast Cr, W and Mo bcc transition metals

24 p4365 A70-46371

BROADBAND

Small signal opto-electronic wideband transformer with coupling element ensuring fast response and low sensibility to parasitic magnetic fields

03 p0459 A70-14266

Broadband sound attenuation in soft walled /low acoustic impedance/ circular ducts found dependent on frequency

05 p0883 A70-16787

Antenna exciter of crossed radio telescope, discussing design, performance and increased wide band sensitivity

08 p1473 A70-21069

Five resonator broadband frequency doubler design using charge storage diodes

08 p1475 A70-21280

Broadband remote sensing magnetometer for measuring fast-rising pulsed magnetic fields

09 p1676 A70-22716

Probability of given configuration and statistical distribution of peaks between mean crossings of broadband locally stationary and Gaussian processes [ONERA-TP-806]

10 p1805 A70-24546

Wideband stochastic signals for radar range and velocity measurements using polarity coincidence correlation technique

12 p2188 A70-27942

Wideband pulse signal synthesis and optimal filtration by dispersive ultrasonic delay lines, estimating potential noise stability for analog data transmission

15 p2696 A70-31502

Unidirectional tear drop radiation Archimedean spiral broad band frequency independent antenna using printed circuit with cavity

21 p3801 A70-42246

Wideband TEM quarter wave microwave coupler with continuously variable coupling range, employing even and odd mode characteristic impedance levels change

24 p4318 A70-45215

BROADBAND AMPLIFIERS

Wideband HF amplifier development for ionospheric radio sounding, describing various stages

02 p0255 A70-11895

Wideband parametric and tunnel diode amplifiers synthesizing method for obtaining maximum flat amplitude frequency response

03 p0457 A70-13727

Transistorized wideband amplifiers synthesis by combining dynamic parameters method with poles and zeros method

05 p0819 A70-16249

Parasitic effects due to coupling of wideband regenerative amplifier with nonideal ferrite circulators to antenna feeder duct

08 p1468 A70-20575

Multipole coupling circuits for wideband radio amplifiers

08 p1474 A70-21225

Broadbanding method for microwave reflection type amplifiers using additional resonators

09 p1645 A70-22604

S band CW high power broadband power source consisting of transistor amplifier-driven varactor doubler chains in hybrid integrated form

10 p1846 A70-23885

Broad band power amplification with Gunn effect diodes, describing frequency response and saturation characteristics and FM/AM noise spectrum measurements for reflection amplifier in X band

10 p1847 A70-23886

Wideband transistorized DC amplifier circuit and operation for outputs of tensometers, thermoelectric, electrodynamic and resistance sensors

11 p2019 A70-26435

Equivalent circuits for transistors in class A amplification over wide frequency band

11 p2021 A70-26831

Maser amplifier with nonoriented Fe-doped rutile powder as active material, observing broad absorption bands under magnetic field

12 p2249 A70-27649

Broadband traveling wave masers bandwidth increased by staggering direct current magnetic field along active structure length

12 p2249 A70-27690

Single and multistage parametric amplifiers for broadband communications, noting nonideal circulator characteristics by scattering parameter and signal flow graph

12 p2197 A70-27933

Wideband high power output transistor amplifier design features and operational characteristics

12 p2199 A70-27980

Wideband microwave transistor IF amplifier for mm wave communication system

14 p2555 A70-30283

Computerized design of transistorized UHF wideband amplifier, using successive approximations for optimum circuit automatic selection

14 p2556 A70-30668

Low noise wideband amplifier design for Intelsat 3 satellite ground stations

16 p2877 A70-33415

Wideband UHF amplification in bulk n-type GaAs during domain generation, comparing cut-off and Gunn frequency

17 p3143 A70-35684

Computerized design of broadband microwave amplifiers with complex terminations, using transfer scattering parameters for analysis and optimization

24 p4316 A70-45211

BROADCASTING

TV broadcast satellite system operating with home receivers or special receivers, evaluating technological and cost factors [AIAA PAPER 68-1061]

01 p0044 A70-10831

Satellite TV broadcast requirements impact on high power transmitter design, permitting low cost terrestrial receiving systems [AIAA PAPER 70-434]

11 p1999 A70-25450

Wave polarization effects on ionospheric HF radio wave transmission and reception in communication and broadcasting networks

14 p2550 A70-30650

Mechanically despun multifrequency, attitude sensing antenna for spin stabilized spacecraft, deep space probes, tactical communications and community broadcast applications

16 p2986 A70-34159

Satellite broadcasting frequency resources, discussing interference, frequency sharing, antenna transmitting and receiving patterns, etc

17 p3046 A70-35271

Optimal receiving systems for satellite broadcasting, considering costs, power requirements, service area, etc

17 p3046 A70-35272

UN space committee discussion on rules governing direct TV broadcasting by satellite, taking into account frequency allocation, geostationary orbits, etc

17 p3201 A70-35779

International norms establishment for direct TV broadcast by satellites

17 p3201 A70-35780

Satellites for direct radio and TV broadcasting, considering system quality and cost, network planning, frequency economy, etc

20 p3588 A70-40158

BROMIDES

NT DIBROMIDES

NT HYDROBROMIDES

BROMINE

Diatomic Br molecular vibration-rotation coupling effects on energy transfer during Br-Br collisions, determining probability distributions

07 p1339 A70-20054

Scattering cross sections of K atoms on bromine molecules determined as function of particle energy using supersonic atomic beams

07 p1344 A70-20133

Ion production cross sections determined for alkali atoms and bromine molecules collisions, noting charge transfer

07 p1345 A70-20138

Vibrational relaxation time and transition probability in bromine collisions with He, Ne, Ar, Xe atoms determined by shock wave method

12 p2275 A70-27353

BROMINE COMPOUNDS

NT DIBROMIDES

NT HYDROBROMIDES

Tetrafluorodibromoethane combustion inhibitor effects on aircraft hydrocarbon fuels flame propagation rate and explosion pressure

01 p0160 A70-11011

Bromine monoxide formation by atomic oxygen-bromine reaction in flash photolysis of bromine-nitrogen oxide and bromine-nitrogen dioxide mixtures

08 p1455 A70-21342

BRONCHI

Flow profiles in models of human bronchial tree typical junctions, visualizing inspiration and expiration patterns for various Reynolds numbers

01 p0034 A70-10653

Human lung and upper airway pressure drop and fluid flow regime of inspired air

12 p2170 A70-27660

Surface active lipoproteids of lung, discussing quantitative determination and labeling on basis of per-bronchial wash-out procedure over trachea

15 p2680 A70-31725

BRONCHIAL TUBE

NT PHARYNX

NT TRACHEA

Electronic measurement of bronchial flow resistance in pulmonary function to determine impediment in inhaled and exhaled air passage

08 p1449 A70-20676

Resistance to two phase gas-liquid flow in airways simulating human bronchial tree

24 p4303 A70-46111

BRONZES

Thermal porous bronze screened microphones for noise measurements in medium under large heat flow

14 p2555 A70-30298

BROWNIAN MOVEMENTS

Aerosol particles Brownian motion under inertial forces in absence/presence of obstacle

01 p0143 A70-10997

Stochastic processes providing exposition of differential-integral calculus for Brownian motion paths, with applications to diffusion processes and related parabolic partial differential equations

01 p0133 A70-11322

Statistical decision problem of Brownian motion with moving boundaries in automatic daylight star tracker design for aircraft navigation solved by image method

01 p0139 A70-11635

Brownian motion for large viscosity, deriving modified Fokker-Planck equation based on quasi-Huygens relation

11 p2084 A70-26398

BRUSHES

Brush current collectors for strain measurements in rotating machine parts, discussing acceptance testing

11 p1983 A70-26438

Brush collector for strain measurement in jet engine compressor and turbine elements at high RPM

11 p1983 A70-26439

BUBBLE CHAMBERS

Hologram resolution and information storage along depth of reconstructed image related to maximum track density of bubble chamber

10 p1892 A70-25113

- High energy and contemporaneous cosmic ray tracks in bubble chamber picture noting evidence of quarks
12 p2276 A70-27997
- Bubble chamber photography and track image reconstruction by holography, discussing measurement apparatus, accuracy and tolerances
19 p3428 A70-38510
- Criticism of evidence for cosmic ray quark passage through low density bubble chamber
20 p3701 A70-40499
- BUBBLES**
- Organic liquid nucleate pool boiling experiments determining stresses, surface tension, viscosity and gravitation relationships to bubble shape and microlayer formation
01 p0218 A70-11180
- Microlayers evaporation contribution to vapor bubbles growth rate from heated wall in liquid near saturation temperature during nucleate pool boiling
01 p0218 A70-11181
- Heat transfer and flux density during bubble boiling of liquid oxygen employing simulated weak gravitational fields
03 p0605 A70-13393
- Gas bubble formation and equilibrium conditions in air supersaturated fuel stored under atmospheric pressure after injection into evacuated tank
03 p0605 A70-13394
- Sound wave propagation in liquid containing gas bubbles allowing for relative motion of bubbles and liquid, deriving steady shock wave structure
04 p0671 A70-14991
- Bubbles elimination in glass filament wound parts involving total or partial placement of production equipment and process in vacuum
05 p0856 A70-16825
- Time-temperature relation necessary to fine Libyan desert glass and remove gas bubbles calculated by viscosity determination at various temperatures
05 p0843 A70-16833
- Entropy fall in superheated liquid related to vapor bubble growth from finite so-called zero radius to critical radius, noting pressure effects
07 p1418 A70-18645
- Phase growth of free vapor bubbles in water, ethanol and isopropanol at uniform superheats under normal and zero gravity
07 p1418 A70-18646
- Gas bubbles formation in supersaturated solutions and body fluids during decompression
07 p1208 A70-19511
- Initial vapor bubble growth on horizontal heated wall during saturated nucleate boiling using combined streak and high speed frame photography
08 p1542 A70-21584
- Laminar separation bubble in incompressible flow produced on flat plate by pressure gradients, correlating bursting with Reynolds number and pressure distribution
09 p1660 A70-22770
- Vapor bubble separation diameter and flow in channel boiling applied to supercooled boiling zone determination
09 p1789 A70-23379
- Fluid material line growth in grid-generated isotropic turbulent flow measured by tagging lines with hydrogen bubbles
11 p2035 A70-25843
- Gas bubbles formation in supersaturated solutions and body fluids during decompression
11 p1988 A70-26110
- Critical thermal flux and heat transfer coefficients dependence on simulated gravity during bubble and film boiling in inclined flat containers
12 p2331 A70-27325
- Tribonucleation emphasizing viscosity-velocity product in gas nuclei formation and cavitation
12 p2170 A70-27661
- Bubble dynamics in subcooled nucleate boiling, deriving mathematical model based on evaporation-condensation mass transfer mechanism
12 p2333 A70-28113
- Bubbles, steady streaming and surface instability in vibrated liquid columns
14 p2663 A70-30255
- Air bubble breaking in blood and water flow passage of simulated cardiopulmonary bypass system with flow constriction
15 p2692 A70-32312
- Cavitation nuclei in liquids, discussing sources, stability and gas bubble growth
16 p2891 A70-33632
- Gas bubbles thermal rejection and formation in Ni electrodeposit during annealing over 200-1000 C range
18 p3272 A70-36039
- Lagrange equations for translational motion and diameter variation of bubble system moving in hydrostatic field, taking into account dissipative forces
18 p3240 A70-36270
- Oscillations of rigidly clamped elastic liquid filled hemispherical shell with gas bubble
18 p3242 A70-36583
- Erythrocyte suspension subjected to gas bubble ultrasonic oscillation, investigating hemolysis mechanism
20 p3573 A70-39981
- Bubble motion in ideal incompressible fluid, deriving motion equation in low viscosity fluid
20 p3614 A70-40392
- Bubble frequencies random distribution during boiling of pure liquids and binary liquid mixtures by optical measurement
21 p3941 A70-40775
- Vapor bubble response to sinusoidal pressure pulsation in water bulk and on metal wall
21 p3949 A70-41309
- Critical thermal flux and heat transfer coefficients dependence on simulated gravity during bubble and film boiling in inclined flat containers
21 p3952 A70-42066
- Surface tension role in microliquid layer formation on solid surface with growing bubble in nucleate boiling, using optical method
21 p3953 A70-42089
- Gas bubbles effect on recovery and recrystallization in W sheet deposited from tungsten fluoride vapor
24 p4358 A70-45243
- Shock wave structure calculation in liquids containing gas bubbles, taking into account compression wave steepening by convection
24 p4326 A70-45783
- BUCCANEER AIRCRAFT**
- Machine tools used in production of Hawker Siddeley Buccaneer low level strike and reconnaissance aircraft
09 p1691 A70-22608
- BUCKETS**
- Three dimensional boundary layer flow on rotating axial flow turbine buckets, determining velocity profiles
18 p3243 A70-36874
- [ASME PAPER 70-GT-59]
- BUCKLING**
- NT CREEP BUCKLING
- NT ELASTIC BUCKLING
- NT EULER BUCKLING
- NT THERMAL BUCKLING
- Thin flat plates effective width under axial edge compression slightly beyond buckling limit, solving von Karman differential equations
01 p0198 A70-10094
- Sandwich plates plastic buckling stability under uniaxial compressive loads from compressible theory viewpoint
01 p0204 A70-11137
- Static and cyclic stress distributions in buckling shear panel comprising flat plate of clad Cu-Al alloy
02 p0388 A70-12497
- Monograph on buckling and postbuckling behavior of plates tapered in planform, comparing stability of tapered and rectangular plates
03 p0586 A70-13002
- Buckling equations for thin nonlinearly elastic circular plates with affine initial deformation, considering Lure theory and variational principle for uniform compression load
03 p0589 A70-13336
- Far nonlinear postbuckling behavior of noncircular cylindrical shell under axial compression
03 p0598 A70-14241
- Tension field theory describing buckling of membranes or thin plates with boundaries subjected to excessive planar displacements
03 p0599 A70-14246
- Local buckling and failure of thin walled compression column with supported flanges, analyzing strength reduction by eccentricity
03 p0600 A70-14254
- Differential equations solution in terms of elementary functions applied to evaluate critical buckling loads for struts of variable cross sections
03 p0602 A70-14328
- Supercritical strains and buckling in rib-reinforced cylindrical shells under axial compression using strain-energy method
04 p0766 A70-14478
- Thin orthotropic composite circular cylindrical shells buckling under axial and radial loads, satisfying end boundary conditions for clamped and simply supported shells
04 p0771 A70-14910
- [ASME PAPER 69-WA/APM-21]
- Orthotropic axially compressed conical shell stability, evaluating lower critical load and postbuckling state
04 p0772 A70-14921
- Orthotropic sandwich cylinders buckling under axial compression, presenting linear theory approximate design equations
04 p0776 A70-15381
- Clamped and simply supported shallow spherical shells buckling using computer programs
04 p0778 A70-15555
- Circular cylindrical shells with axisymmetric imperfections tested under axial compressive load, studying imperfection amplitude and wavelength effects on minimum buckling load
04 p0778 A70-15588
- Buckling of toroidal shells with reasonably uniform thickness distribution manufactured by casting epoxy resin material
04 p0779 A70-15615
- Biaxial prebuckling loading effect on compliance tensor in plastic buckling of square plates analyzed by local strain statistical theory
05 p0925 A70-15790
- Energy method for analyzing rectangular panels buckling under nonuniform in-plane loading, considering stability under uniform compression
05 p0931 A70-16117
- Galerkin method to formulate buckling problem of homogeneous and fiber reinforced anisotropic plates simply supported under uniform membrane loads
06 p1160 A70-17313
- Stress and buckling measurement of shallow cylindrical steel shells linked to thin plate using resistant strain gauges and high precision indicators
06 p1167 A70-17866
- Nonlinear postbuckling equilibrium of thin cylindrical shell and axisymmetric buckling pressure of imperfect spherical shell calculated by Rayleigh-Ritz method
06 p1169 A70-18036
- [AIAA PAPER 70-102]
- Local axisymmetric dimple imperfection effects on buckling load of circular cylindrical shell under axial compression
06 p1170 A70-18167
- [AIAA PAPER 70-103]
- Buckling-critical composite shell structures, describing pseudo T-rib stiffening and integrated composite design concepts
06 p1171 A70-18235
- [AIAA PAPER 70-101]
- Buckling of clamped skew plates under uniform system of applied stress using Galerkin method
07 p1406 A70-19339
- Inextensional nonlinear theory of arches applied to analysis of hinged-hinged circular arches subjected to downward point load, calculating critical load value
07 p1408 A70-19561
- Buckling stress calculation and measurement in cylindrical fiberglass reinforced composite shells under axial pressure
07 p1409 A70-19756
- Circular cylindrical shells buckling under lateral and hydrostatic pressure using Donnell and Flugge equations, assuming membrane stress state for prebuckling deformation
07 p1414 A70-20168
- Truncated conical shells buckling under hydrostatic pressure using Donnell equations, assuming membrane stress state for prebuckling deformation
07 p1414 A70-20170
- Lateral buckling of simply supported uniform diaphragm using slope-deflection equations for orthogonally intersecting beams, prescribing boundary conditions
08 p1589 A70-21244
- Rectangular plate girder webs buckling under partial edge loadings, using finite element method for flange-web interaction
08 p1589 A70-21247
- Optimal inextensional buckling of uniformly loaded simply supported arches with large opening angle
08 p1589 A70-21310
- Asymptotic analysis for axisymmetric buckling of axially compressed short cylindrical shells with free edges, using Batterman method
08 p1593 A70-21620
- Cylindrical shells buckling under axial surface tensions using Donnell stability equations
08 p1593 A70-21624
- Free vibrations and dynamic buckling of hinged extensible beam under axial force
09 p1768 A70-22061
- Buckling and postbuckling equilibrium behavior of fiber reinforced cylindrical shell under uniform axial compression
09 p1780 A70-23207
- Shallow rectangular shell panels nonsymmetric nonlinear deflection states computed by finite difference equations iteration, discussing snap-through buckling loads
09 p1780 A70-23209
- Plastic buckling of eccentrically stiffened circular cylindrical shells with multiple isotropic layers under combined axial and lateral pressure, deriving stability criterion
09 p1780 A70-23213
- Carrying capacity of shallow shells of revolution, determining buckling stress and limiting equilibrium of shells with varying thickness under transverse load
09 p1781 A70-23288
- Buckling stability of slender knife-edge suspended rods subjected to compression end loads
10 p1955 A70-24053
- Truncated conical shell buckling under axial compression using method for torsion buckling, correlating to equivalent cylindrical shells
11 p2135 A70-25980
- Buckled plates flutter at zero dynamic pressure, considering initial plate imperfections, including aerodynamic damping in quasi-steady supersonic approximation
11 p2135 A70-25988

Boundary conditions effect on bending, vibrations and buckling of unsymmetrically laminated rectangular plates

11 p2136 A70-26079

Dynamic buckling of shell or arch structure determined from response of two degrees of freedom structure to step load application

11 p2138 A70-26158

Buckling load calculations for axially compressed circular cylindrical shells under relaxed boundary conditions

11 p2140 A70-26484

Cylindrical shells plastic flow buckling under radially inward impulsive loading, showing mode number dependence on shell length

11 p2140 A70-26486

Ring buckling under constant and centrally directed pressure, considering small displacement and inextensional deformation

11 p2141 A70-26492

Stiffened cylindrical shells buckling under axial compression, obtaining imperfections and prebuckling growth mappings

12 p2319 A70-27141

Subdivisional method for linear systems vibration and buckling problems, reducing governing equation to ordinary differential equation with variable coefficients

12 p2320 A70-27145

Thin circular cylindrical polyvinyl chloride plastic shells tested under axial compression and end-shortening conditions for buckling

12 p2324 A70-27473

Shear buckling and uniaxial compression dependence on mechanical properties of clamped orthotropic plates, using Ritz method to compute bifurcation type loads

12 p2326 A70-27817

Pressure buckling values of rod and plate profiles with thicknesses graduated across pressure direction in presence of uniform and nonuniform stress distributions

13 p2507 A70-28477

Eccentrically stiffened orthotropic cylinders with intermittently attached stiffeners under bending and axial load, analyzing instability and buckling

13 p2518 A70-29966

Postbuckling of flat variable thickness rectangular plates with unloaded transverse edges, using dynamic relaxation method

13 p2518 A70-30024

Buckling equations for thin nonlinearly elastic circular plates with affine initial deformation, considering hure theory and variational principle for uniform compression load

14 p2657 A70-30714

Thin spherical shell postbuckling behavior with constrained rigid boundary under edge load, using deep and shallow shell theory

14 p2658 A70-30848

Nonlinear dynamic analysis of shells of revolution under symmetric and asymmetric loads, obtaining solutions for shallow cap buckling

16 p2994 A70-34229

In-plane boundary conditions effect on axially compressed conical shell stability under low buckling loads, using linear Donnell-type theory

17 p3186 A70-34971

Axially loaded cylindrical shells prebuckling deformation behavior measurement by holographic interferometry

17 p3086 A70-35012

Mass distribution role in stability theory of rods under nonconservative buckling load

18 p3335 A70-35961

Elastic and plastic cylindrical shells, investigating dynamic buckling under impulsive loads

18 p3338 A70-36436

Flutter design charts for isotropic panels stressed to verge of buckling for tropical values of structural damping

18 p3338 A70-36446

Postbuckled integrally stiffened wide column weight optimization, developing stress equation

18 p3339 A70-36447

Buckling problem numerical analysis by nonlinear programming and minimum energy formulation

18 p3339 A70-36495

Buckling of fiber reinforced composite orthotropic plates

18 p3343 A70-36706

Lateral compression of rocks and global shells multilayers, using equations for buckling of single free stratum

18 p3255 A70-37076

Waveform changes in postbuckling behavior of thin rectangular plates under axial compression

19 p3535 A70-37380

Buckling equilibrium equations for thick rectangular block under compression loads, noting bifurcation points

19 p3536 A70-37683

Edge distribution of transverse reactive forces of rectangular plate with nonuniform flexural rigidity at buckling load

19 p3541 A70-38042

Clamped spherical shells under concentrated, distributed and ring loadings, analyzing large axisymmetric deflections for prebuckled and postbuckled states

19 p3545 A70-38336

Prebuckling deformations effect on buckling of clamped thin walled circular cylindrical shells under axial loading and internal pressure

19 p3546 A70-38346

Asymmetric snap-through buckling in cantilevered column restrained at tip by stiff wire, discussing ratio of flexural rigidity to extensional stiffness

19 p3549 A70-38670

Stiffened thin walled circular cylinders buckling and postbuckling behavior under axial compression or external hydrostatic pressure

20 p3719 A70-39621

Paraboloid of revolution, examining mixed axisymmetric buckling problem

20 p3727 A70-39892

Thermoelasticity of fiber reinforced materials, considering stress concentration in beams and reinforcing fibers buckling under thermal loading

20 p3730 A70-40037

Asymptotic buckling analyses of imperfect columns on nonlinear elastic foundations by perturbation expansions, equivalent linearization and truncated hierarchy approximations

21 p3934 A70-40777

Buckling analysis of stiffened noncircular cross section cylindrical shells constructed by circular arcs and straight line segments

21 p3934 A70-40922

Thin walled column buckling relation to plate element buckling, studying deformation, stress state, failure mechanism and ultimate load

22 p4116 A70-43214

Circular cylindrical orthotropic fiberglass-reinforced shell buckling under longitudinal impact, assuming initial surface imperfections

22 p4117 A70-43347

Fatigue strength of stiffened aircraft panels subjected to repeated buckling by compression loads

23 p4267 A70-44132

Axially compressed circular cylindrical shells subject to relaxed boundary conditions, calculating buckling loads as function of length to radius ratio

23 p4269 A70-44397

Gradient minimization and higher order discrete elements application to shell buckling and vibration eigenproblems, using 48 degree of freedom Bogner cylindrical panel element

23 p4271 A70-44705

Structural eigenvalue problems solved by sparsely populated matrices for structural vibrations and critical buckling, using finite element method

23 p4271 A70-44708

Second approximation for limit loads due to imperfection sensitivity of axisymmetric elastic shell structures with unique harmonic buckling modes

23 p4273 A70-44720

Stress, buckling and vibration analysis of shells of revolution by numerical integration and finite difference methods, summarizing computer programs

23 p4273 A70-44725

Axisymmetrically imperfect spherical thin shell stability analysis, comparing results with theory of initial postbuckling behavior

24 p4421 A70-45282

Truncated spherical shells nonlinear asymmetric buckling calculation from equilibrium equations

24 p4421 A70-45284

Thick isotropic rectangular laminates free vibration and buckling, applying three dimensional linear small deformation theory of elasticity

24 p4422 A70-45296

BUDGETING

Applied space research covering photovoltaic cells, electric propulsion, onboard data storage, vacuum lubrication and NASA-European organizations budgets

06 p1141 A70-17780

Long range army budget forecasting model based on research projects cost distributions and parameters, describing computer program

09 p1794 A70-23415

Product oriented cost data bank for satellite system cost prediction and negotiation designed for USAF communications satellite program

11 p2152 A70-25477

BUFFERS [CHEMISTRY]

Glutamine deamidation enhancement by N-acetyl-L-aspartic acid addition to mitochondrial preparations of rabbit brain incubated in Tris buffer

01 p0018 A70-10508

BUFFETING

F-8D aircraft transonic flight and wind tunnel tests for buffet onset prediction, considering effects of g level and fluctuation amplitude and frequency

09 p1611 A70-23020

Low speed buffet intensity under pressure fluctuations on slender wing aircraft at vortex breakdown, using wind tunnel model

10 p1963 A70-25067

Wind tunnel and flight test methods for determining transonic buffet characteristics on model F-4 aircraft

13 p2348 A70-29886

BUILDING MATERIALS

U CONSTRUCTION MATERIALS

BUILDING STRUCTURES

U BUILDINGS

BUILDINGS

Residential structures vibration response to aircraft flyover noise, discussing noise transmission, rattle phenomenon, spectra, etc

04 p0770 A70-14887

Physical methods in applied climatology, analyzing meteorological effects on human body and building thermal conditions and plant biomass growth

15 p2771 A70-32111

Sonic boom effects on building structures, using Concorde measurements and explosion simulation studies

24 p4289 A70-45151

BULGARIA

Mapping of normal distribution of geomagnetic elements in Bulgaria

08 p1490 A70-21433

Report to COSPAR on space research in Bulgaria, considering ionospheric physics, cosmic rays, satellite observations, meteorology and space communications

15 p2829 A70-31704

BULGING

Lateral pressure bulging of superplastic alloy sheet, considering flat circular sheet and bulging into V grooves

16 p2916 A70-32918

BULK MODULUS

Effective wave propagation velocities, bulk and shear moduli of elastic heterogeneous solids approximated by self consistent method

04 p0777 A70-15496

Adiabatic elastic stiffness of single crystals of Ni-Co alloys, determining bulk modulus dependence on chemical composition

10 p1904 A70-24699

BULKHEADS

Saturn 5 thru-bulkhead initiator for solid propellant rocket motor ignition, discussing transfer design, pressure output and postfire leakage

03 p0546 A70-14105

Design reliability of through-bulkhead initiator explosive train using parametric test program data, discussing shock transmission and acceptor charge sensitivity energy balance

03 p0549 A70-14124

BUMPERS

Bumper materials effect on two component hypervelocity impact shields performance, noting material density influence

07 p1310 A70-19713

BUNCHING

NT ELECTRON BUNCHING

Bunched ion bursts amplitude modulation effects on nonlinear ion acoustic waves in grid plasma system

23 p4229 A70-44989

BUNDLES

Ventricular preexcitation syndrome studied by catheter technique for heart electrical activity recording, noting His bundle bypass effects

10 p1819 A70-24934

BUOYANCY

Rapidly rotating solar interior damping by large scale convection analysis via maximum buoyancy force in water cylinder transition

02 p0373 A70-12391

Buoyancy effects in laminar forced convection on vertical flat plate, obtaining heat transfer coefficient

06 p1172 A70-17141

Plane Poiseuille flow with nonlinear temperature distribution, studying vortex type secondary flow onset due to buoyant forces

09 p1790 A70-23555

Growth rate and spatial distribution of solid deposit freezing onto vertical surface in presence of convective heat transfer at moving phase interface

12 p2331 A70-27696

Buoyancy effects on liquid nitrogen film boiling in vertical flow, using resistance heated test apparatus

17 p3195 A70-34745

Density diffusion and buoyancy effects on horizontal boundary layers in stratified flow

18 p3239 A70-36193

Buoyancy effects on transient free convection heat transfer in revolving tube for zero to 100 g centrifugal acceleration

[ASME PAPER 70-HT-10] 22 p4122 A70-42437

Spherical shape gas or liquid drop steady motion at large Reynolds numbers, examining buoyancy forces and velocity gradients

24 p4326 A70-45996

BURGER EQUATION

Inviscid Burger turbulence spectral equations for cumulant approximation, obtaining energy spectrum and transfer as initial value problems

05 p0832 A70-16147

Burger one dimensional model equation for homogeneous turbulence treated by Fourier transform in space and time, using Bogoliubov expansion method

05 p0833 A70-16331

Error resulting from elasticity modulus and linear thermal field coefficient removal from integral in Burger formula for turbine blade thermal stresses

05 p0954 A70-17061

Navier-Stokes equation approximation for non-homogeneous case obtained by relating Burgers equation to Riccati equation through similarity transformation

09 p1711 A70-22613

Burger turbulence model late decay statistical analysis using kernels of Cameron-Martin-Wiener expansion of random velocity field

13 p2386 A70-28820

Closed form solutions of boundary value problems for Burger equation within half plane from zero to infinity

14 p2598 A70-30492

Turbulent velocity correlation function computation in Burger fluid model, using functional integral expression

19 p3403 A70-37530

Energy spectrum function for Gaussian initial velocity field of inviscid turbulence Burger model, using Cameron-Martin-Wiener exact expansion

20 p3609 A70-39653

BURNERS

Combustion instability of solid propellants using response to pressure perturbations for T and L burners

02 p0352 A70-12013

Slot burner laminar flame front stability loss ascribed to increased slot dimensions and angles between velocity vector and flame front

08 p1598 A70-21208

Methane-air inverted flames blowoff at thin stabilization plates of twin slit inverted flame burner, determining critical values of Karlovitz flame stretch factor

14 p2666 A70-31092

Instantaneous burning rates prediction methods based on flame structure model and steady state burning rate data as pressure and initial temperature functions

[AIAA PAPER 70-667] 16 p2971 A70-33949

Secondary combustion products of air augmented boron loaded solid propellant rocket ramburner, measuring properties by spectroscopy

17 p3196 A70-35196

BURNING

U COMBUSTION

BURNING PROCESS

U COMBUSTION

BURNING RATE

Abnormal burning surface regression in rocket motor solid propellant detected with Flash X ray exposures

01 p0085 A70-10021

Flame propagation rate calculation methods, considering mass burning rate values

01 p0217 A70-11008

Flame propagation in gases with two chemical phases, studying phase interaction effects on burning rate

01 p0217 A70-11010

Gas ignition and burning processes calculation with allowance for hydrodynamics, discussing time saving finite difference solution of differential equations system

01 p0218 A70-11020

Pressure effects on burning rate of magnesium mixtures with solid oxygen containing organic compounds, determining charge density effect on mass velocity

01 p0218 A70-11021

Chemical additives effect on H-Cl-N mixtures burning velocity in air and nitrogen

02 p0398 A70-12031

Chlorine dioxide-methane mixture flame stabilized in low pressure burner, determining emission spectra, burning velocity, activation energy, etc

02 p0251 A70-12033

Ammonia/chlorine dioxide and ammonia/chlorine dioxide/methane flames burner stabilization and burst velocities

02 p0400 A70-12670

Mathematical model for burning rates of solid propellant rocket motors during pressure transients, coupling conservation equations with mass balance equation

03 p0543 A70-12912

Burning constants prediction for suspended hydrocarbon fuel droplets based on modified theoretical equation

03 p0544 A70-13916

Flat flames in stationary gas in tubes useful for flame speed measurements without correction procedure

03 p0607 A70-13917

Burning velocity of methane-air flames inhibited by methyl bromide, using schlieren cone-nozzle burner method involving unburnt gas velocity measurement

03 p0607 A70-13918

Aluminized composite solid propellants burning rates in acceleration fields noting time dependent increase

[AIAA PAPER 68-529] 04 p0709 A70-15581

Polyamide fabric burning rates in oxygen-inert gas mixtures, studying damping effects of density, thermal conductivity, molecular constants and mass flow

06 p1090 A70-17284

Combustion stability in air-liquid fuel zone of jet engine burner with burning rate controlled by droplet vaporization rate controlled mechanism

06 p1178 A70-17980

Gas phase reactions near solid-gas interface of deflagrating double base propellant causing abrupt changes in burning rate-pressure curve

06 p1179 A70-18046

Aluminized solid propellant transient burning rate augmentation during acceleration loads

06 p1129 A70-18047

Burning rates of monopropellant droplet evaluated by variable property models, discussing dimensionless mass flow rate

07 p1358 A70-18914

Polyurethane propellant binders burning rate, studying siloxane moiety effects

07 p1358 A70-19330

Burning rate for composite solid propellant, using model with specific gas phase combustion distribution

07 p1422 A70-19584

Mathematical model for calculating radiative heat transfer from turbulent diffusion buoyant flame and predicting liquid fuel burning rate

07 p1425 A70-20008

Ammonium perchlorate combustion catalysis, studying preflame heating and mixing effects on gas phase flame burning velocity

07 p1425 A70-20010

Condensed fuel mixtures and oxidizers combustion rates as function of pressure and particle size

09 p1786 A70-22104

Combustion rates and temperature distribution in condensed and gaseous phases of ammonium perchlorate sandwich with synthetic resin middle layer

09 p1741 A70-22105

Ammonium perchlorate-polymer mixtures combustion rates with/without cobalt oxide additions, studying ignition temperatures of stable flameless burning

09 p1787 A70-22108

Burning and degradation mechanism of polyester propellants correlated with mass regression rate dependent on surface temperature

11 p2099 A70-25990

Styrene-oxygen copolymer preparation methods, discussing burning rates for rocket solid propellants mixtures with ammonium perchlorate

11 p2100 A70-26146

Flame propagation in slowly combusting fuel-air mixtures using gas chromatography and flame speed

11 p2151 A70-26381

Perfluoropropene, -cyclobutene and -cyclobutane mixing with atmospheric pressure oxygen to determine burning velocities

11 p2100 A70-26383

Nonisothermal burn-up rates of graphite surfaces in turbulent air flow under neutral gas shield estimated by measuring channel diameter

12 p2331 A70-27323

Mode transition characteristics of free burning argon electric arc with transpiration cooled anode, noting current blowing parameter

12 p2281 A70-27806

Low pressure burning rate of double base propellants at various initial temperatures in argon and in air

12 p2332 A70-27844

Pure ammonium perchlorate single crystal self deflagration, determining energy transfer mechanisms from pressure effects, combustion characteristics and subsurface profile

13 p2473 A70-29956

Evaporation and combustion kinetics of droplets and particles in hot air stream, observing luminous trace

14 p2664 A70-30392

Hyperbaric environment combustion, discussing burning rate data and fire resistance scale

14 p2665 A70-30626

Two dimensional transonic flows bounded by free surface and wall with interior heat release and external burning, indicating application to control or propulsion

14 p2665 A70-30947

Burning velocities for methane-air mixtures with water cooled porous metal flat flame burner, discussing surrounding ambient atmospheres effects

14 p2666 A70-31093

Internal ballistics equations solution on basis of pressure index law of burning taking into consideration density approximation

15 p2786 A70-31849

LF unsteady behavior of liquid propellant rockets from droplets evaporation and combustion rates

[AIAA PAPER 70-620] 16 p2968 A70-33589

Composite solid propellants burning rate and initial temperature relationship, investigating granular diffusion flame model

[AIAA PAPER 70-656] 16 p2963 A70-33618

Burning rate increase of nonmetallized composite propellants in acceleration field, assuming surface retention of ammonium perchlorate particles

16 p2963 A70-33861

Acceleration effects on burning rates of double base propellants with and without Al additive

16 p2963 A70-33883

Instantaneous burning rates prediction methods based on flame structure model and steady state burning rate data as pressure and initial temperature functions

[AIAA PAPER 70-667] 16 p2971 A70-33949

Solid propellant combustion, observing burning rate in spin acceleration environments

17 p3145 A70-35209

Combustion efficiency and rate in oxygen enriched spacecraft atmosphere

17 p3177 A70-35210

Chemical kinetics effect on combustion rates of fuel plate in turbulent oxidizer flow, deriving conservation equations in boundary layer and diffusion equation

18 p3346 A70-36245

Powdered metallic additions effect on combustion rates of ammonium perchlorate with bitumen and polymethyl methacrylate and potassium perchlorate with bitumen mixtures

18 p3299 A70-36247

Combustion rates acceleration of ammonium perchlorate mixtures with polystyrene and polymethyl methacrylate by KCl and LiF additions, forming molten layer on charge surface

18 p3299 A70-36248

Combustion rates and self ignition vs pressure and activity in ammonium perchlorate mixtures with Al and Mg powders compressed to maximum densities

18 p3299 A70-36249

Two layer model of burning in turbulent boundary layer on porous surface for carbon monoxide oxidation reaction

18 p3346 A70-36268

Burning rate theory applied to heat and mass transfer rates of monopropellant droplets in heat-up and steady burning at wet bulb temperature

18 p3348 A70-36696

Internal ballistics of composite propellant charge in first stage of burning

19 p3489 A70-38373

Air to air missile launch range maximization for plane trajectories and nonmaneuvering targets, discussing optimal fuel burning rate

[AIAA PAPER 70-980] 20 p3668 A70-39549

Ammonium perchlorate composite solid propellant pressure vs burning rate at various temperatures, discussing granular diffusion flame theory

20 p3694 A70-40266

Deflagration rate measurements by high speed cinematography of ammonium perchlorate single crystals under various ambient temperature and pressure conditions

20 p3688 A70-40468

Methane and hydrogen consumption rates during slow reactions in mixtures of molecular hydrogen, oxygen and nitrogen

21 p3772 A70-40879

Nonisothermal burn-up rates of graphite surfaces in turbulent air flow under neutral gas shield estimated by measuring channel diameter

21 p3952 A70-42064

Combustion rate as function of oxidizer molecular refractivity in perchlorates and nitrates of aliphatic and aromatic mono- and polyamines explosives

21 p3783 A70-42241

Radiant energy flux effect on atmospheric pressure burning rate of composite solid propellant

23 p4232 A70-44552

Combustion velocity in high pressure chamber, determining fire mechanism in overpressure environment

24 p4393 A70-45447

BURNING TIME

Metal particle size relation to combustion time using statistical method applied to polydisperse Mg powder

07 p1419 A70-18756

BURNOUT

Composite programming of vertical ascending rocket with constant thrust phase followed by acceleration and coasting phases, discussing burnout altitude and fuel consumption

08 p1582 A70-21775

Pressure and grain size effect on burnout velocity and combustion capacity of ammonium perchlorate

17 p3145 A70-34639

BURNS [INJURIES]

Ophthalmological treatment of severe thermomechanical eye injuries investigated on radiant-energy burned rabbit eyelids

09 p1617 A70-22473

Nonflammable fibrous textile materials for injury and personnel loss prevention in fires by aircraft accidents

23 p4153 A70-44481

BURSTS

NT RADIO BURSTS
NT SOLAR RADIO BURSTS
NT TYPE 2 BURSTS
NT TYPE 3 BURSTS
NT TYPE 4 BURSTS
NT TYPE 5 BURSTS

X ray bursts rise and fall observed by spectrometer onboard OSO-4

15 p2792 A70-31670

BUSHINGS

Rotating parabolic mirror /antenna/ cantilever suspension rigidity with emphasis on rigidity of central bushing

08 p1586 A70-21056

Test stand based on Froude pendulum for measuring friction coefficients and oscillation parameters of porous bushings

16 p2924 A70-34298

BUTADIENE

Butadiene prepolymers containing carboxyl functional groups used in binder matrix for solid composite propellants

07 p1360 A70-19911

IR absorption spectra of high-cis forms of deuterated polyisoprenes

23 p4157 A70-44274

BUTANES

Photodecomposition of 1,4-dichlorobutane sensitized by n, pi singlet state of acetone as chemical process

04 p0646 A70-15319

Direct sensitized photolysis of various dichlorobutanes yielding HCl

16 p2855 A70-33089

BUTT JOINTS

Welded flat plate specimen to evaluate low cycle crack initiation and propagation of butt welds under compressive loading, discussing design, fabrication and testing

[ASME PAPER 69-SESA-7]

01 p0199 A70-10452

Residual stress distribution in butt joints during welding of sheet Nb measured by extensometer, noting annealing temperature effect on stress relieving

03 p0513 A70-14072

Unsteady heat conduction and thermal stresses in thin isotropic semibonded plates with butt joint possessing internal thermal resistance

04 p0766 A70-14479

Computer analysis of degree of constraint against butt joint transverse shrinkage, using finite element method for stress analysis

12 p2239 A70-26854

Transverse contraction during butt welding of plates of steel and Ti and Al alloys, showing dependence on joint thickness

16 p2916 A70-33053

Magnetic methods of flaw detection, discussing theory and application to welded butt joints

18 p3263 A70-36521

Solid state butt and lap joint welding of TD-nickel bar, evaluating performance by stress rupture and shear tests

21 p3832 A70-40790

Butt joined epoxy Al plates tensile strength, observing fracture strength dependence on stress concentration at bond edges below characteristic crack length

21 p3939 A70-42032

Bar butt current penetration welding, using HF continuous current seam welding process for joining finite length pieces

22 p4046 A70-43148

Thermomechanical contact and heat transfer on reinforced edge in plates butt joined by curvilinear closed rigidity rib

22 p4120 A70-43718

BUTYRIC ACID

Glutamic and aspartic acid concentrations in brain tissue and incubation medium after adding gamma-aminobutyric acid

01 p0018 A70-10507

Gamma-aminobutyric acid effect on oxidative phosphorylation of rabbit and rat brain mitochondria, noting dependence on ionic concentration, temperature and amount of additions

01 p0019 A70-10509

Gamma-aminobutyric acid influence on 5-hydroxytryptamine in rat brain after intraperitoneal administration

01 p0019 A70-10510

Prolonged REM sleep deprivation effect on gamma-aminobutyric acid concentration in mice

23 p4146 A70-44658

Amino acids L-glutamate and gamma-aminobutyric acid as communication agents in brain

23 p4148 A70-44864

BYPASSES

Net thrust determination for high bypass ratio engines in cruise, suggesting performance evaluation in actual flight tests

[SAE PAPER 690652] 05 p0895 A70-15841

Bypass door control system for SST axisymmetric intake operation in external compression mode, obtaining dynamic performance

[AIAA PAPER 70-695] 16 p2966 A70-33558

Kuznetsov NK 8-4 bypass turbojet air entry vanes, pressure compressors, gear case, combustion chamber and turbine drives

17 p3147 A70-34629

C

C BAND

Group delay characteristics of C band nondegenerative parametric amplifier determined by Nyquist method and compared to phase frequency derivative measurement

03 p0458 A70-14037

Spurious output from C band radar magnetrons, discussing measurement procedures and noise reduction by waffle-iron waveguide filters

12 p2201 A70-28141

C band latching ring-and-post ferrite waveguide circulator for radar transmitting-receiving functions, presenting performance and design parameters

12 p2202 A70-28166

C band radar antenna with pencil beam steered in plane by ferrite phase shifters

16 p2875 A70-33394

Steerable C band waveguide arrays design for forming monopulse cluster of sum and difference beams

16 p2875 A70-33395

C-5 AIRCRAFT

MADAR onboard maintenance system designed for C-5 aircraft monitoring line replaceable units in electrical, avionics, environmental, mechanical and propulsion systems

[AIAA PAPER 70-243] 07 p1195 A70-20375

C-5A aircraft testing program covering ground handling, towing, cargo handling, takeoff and landing, cold weather testing, etc

08 p1437 A70-21729

C-5 Galaxy airlifter design, delivery capacity, aerodynamics and flight test program

09 p1609 A70-22020

C-5 design features for entire environment assuring human integration as crew member or troop passenger

09 p1609 A70-22021

C-5 production engineering, discussing welding method for hydraulic stainless steel tubing, bonding of Al floor panels and painting preparation

10 p1893 A70-23853

C-5A airframe composite materials fabrication, tooling, processing, quality assurance and nondestructive test methods

11 p2058 A70-25572

C-5 aircraft electrointerference coupling minimization, applying classification plan for wire categorization and routing

12 p2201 A70-28131

C-5 aircraft failures and system safety program, noting landing gear, pressure equalization, visor nose, crosswind computer, nacelle separation and propulsion design

15 p2675 A70-32215

Aircraft accidents during descent, approach and landing, discussing B 747, C5A and SST

15 p2675 A70-32216

C-5A turbofan engine thrust determination using pressure and temperature values in exhaust nozzles

[AIAA PAPER 70-611] 16 p2969 A70-33606

C-5A propulsion system onboard monitoring for malfunction detection, analysis and subsystem recording

17 p3148 A70-35497

C-5A aircraft six wheel main landing gear bogie pitching control, emphasizing braking torque compensating mechanism design

[AIAA PAPER 70-914] 17 p3020 A70-35826

C-5 aircraft cargo loading system for terminals minimizing ground time

17 p3064 A70-35831

C-5 flight simulation program for design of basic aircraft, flight control and guidance subsystems

[AIAA PAPER 70-922] 17 p3064 A70-35833

C-5A engineering flight test /EFT/ computer controlled data processing system operation, illustrating capability, performance and limitations

19 p3355 A70-37917

Extraction parachute deployment for airdropping multiple loads from C-5A aircraft

[AIAA PAPER 70-1203] 21 p3752 A70-41814

Ultrasonic crack detection in fastener holes in C-5A wings

24 p4341 A70-45571

C5 Malfunction Detection Analysis and Recording /MADAR/ subsystem for onboard fault isolation including engines

[SAE PAPER 700820] 24 p4349 A70-45898

C-9 AIRCRAFT

Ground and ditching emergency evacuation tests of C-9A aeromedical aircraft under worst possible simulated crash conditions

01 p0035 A70-10716

C-47 AIRCRAFT

Airborne multispectral sensing based on modified AN/AAS-5/XE-2/ scanners mounted in C47 aircraft, discussing applications

03 p0491 A70-13669

C-135 AIRCRAFT

Laboratory tests to determine KC-135 air conditioning failure due to turbine wheel icing by flight condition simulation

01 p0005 A70-10694

C-141 AIRCRAFT

Isochronal maintenance inspection management of Military Airlift Command /MAC/, noting C-141 utilization rate

07 p1428 A70-19673

CABIN ATMOSPHERES

NT SPACECRAFT CABIN ATMOSPHERES
Atmosphere classification according to fire hazard based on heat capacity per mole of oxygen, noting exponential growth rate

03 p0607 A70-14054

Portable unit for collection and analysis of toxic gas contaminants in enclosed aircraft and spacecraft cabin atmospheres

07 p1224 A70-20222

Harrier fighter aircraft cabin air conditioning and pressurization system

12 p2166 A70-27890

Heat stress levels in cockpit of AH-1G Hueycobra helicopter parked in sunlight with closed canopy, using sweating copper mannikin

15 p2689 A70-31881

Closed compartment fire mathematical model to analyze combustion parameter effects, atmosphere pressure and temperature during fire

17 p3198 A70-35646

CABLES [ROPES]

Sheath-enclosed steel cable inspection using induction coil transducer in conical sleeve

02 p0301 A70-12490

Cable involving woven multiconductor arrangement and aromatic polyimide insulations to connect thermal moon probe with transmitter for temperature measurements on lunar surface

05 p0798 A70-16034

Dynamic control model of lift helicopters with two cable sling loads using multiple part motion equations

[AIAA PAPER 70-929] 17 p3020 A70-35839

Rotating cable-connected orbital space stations deployment dynamics, considering cable mass and motion equation

23 p4258 A70-44529

Rectangular cable networks covered by or embedded in membrane matrix, calculating vibration response under load by Galerkin method

24 p4421 A70-45279

Rope transverse oscillations due to impact taking bending rigidity into account

24 p4424 A70-45627

CADASTRAL MAPPING

Numerical photogrammetric techniques application to cadastral surveys and mapping, discussing standard errors

10 p1880 A70-24753

CADMIUM

Helium-cadmium laser operation, using DC cathodoresis to maintain spatially uniform optimal Cd vapor concentration

01 p0110 A70-10562

Solar Cd abundance, using spectrograph and synthetic spectral line computer program

06 p1143 A70-17995

Cadmium vapor density distribution by cathodoresis in He-Cd laser discharge tube determined by side light measurements

06 p1084 A70-18613

Radiative lifetime for atomic transitions in UV multiplets of zinc and cadmium atoms and ions measured using phase shift method

11 p2086 A70-25363

He-Cd laser with cathaphoretic transport and diffusion return path, noting condenser critical temperature for radiation noise reduction

15 p2751 A70-31987

CW Cd vapor laser oscillation achieved with slotted hollow cathode discharge containing He carrier gas at pressures of several Torr

15 p2751 A70-31988

He-Cd laser discharge, determining population densities and lifetimes for levels of Cd ion excited by He metastables

17 p3108 A70-35903

He-Cd pulsed laser mode locking at 4416 and 3250 A using intracavity acoustic loss modulator

18 p3266 A70-36314

Helium-like resonance, intercombination and forbidden transitions of Ca, Si and S lines during 3b solar flare decay

20 p3700 A70-40420

Ti embrittlement by liquid Cd, discussing ductile-brittle transition temperature dependence on strain rate

22 p4054 A70-42738

Positron annihilation in quenched Cd metal from radar backscatter intensities in aircraft model compared with anechoic chamber measurements

24 p4315 A70-46257

Radiochemical neutron activation analysis of In, Cd, Y and rare earth elements in rocks

24 p4310 A70-46375

CADMIUM ALLOYS

Binary CdSb-CdTe systems investigated by X ray and microstructural analyses, showing mechanical mixture constitution and p-type conductivity

07 p1355 A70-18701

Cd-Se and Cd-Te systems phase diagrams based on regular solutions theory, discussing molecular interaction energy dependence on composition

22 p4085 A70-42678

CADMIUM ANTIMONIDES

Electrical properties thermally induced irreversible changes in CdSb single crystals measured as function of current intensity and flow

03 p0542 A70-13751

CADMIUM COMPOUNDS

NT CADMIUM ANTIMONIDES

NT CADMIUM FLUORIDES

NT CADMIUM SELENIDES

NT CADMIUM SULFIDES

NT CADMIUM TELLURIDES

Gallium found suitable for doping cadmium/tin arsenide semiconductor, exhibiting hole-type conductivity

01 p0156 A70-10214

Hall effect and electric conductivity of cadmium arsenide at high temperatures as function of carrier concentration dependence on temperature and phase transformation

07 p1357 A70-20314

Optically pumped cadmium phosphide laser, obtaining IR coherent oscillation from Q switched Nd doped YAG laser excitation

15 p2751 A70-31985

CADMIUM FLUORIDES

Lithium-cadmium fluoride battery for aircrew survival beacon radio receivers, considering voltage loss elimination by doping

08 p1439 A70-20708

CADMIUM NICKEL BATTERIES

U NICKEL CADMIUM BATTERIES

CADMIUM SELENIDES

Adsorption influence on electrical and photoelectric properties of CdSse thin films

17 p3143 A70-35674

Heterogeneous solar cells based on polycrystalline cadmium sulfide and selenide, discussing preparation methods and photoelectric and electric properties

18 p3215 A70-36238

Thin optically pumped pulsed CdSe platelet lasers, detecting mode jumping and tuning effects by time-resolved spectroscopy

22 p4049 A70-42946

CADMIUM SULFIDES

Light induced modulation of optical absorption of CdS crystals by chopped laser excitation, noting use for fast recombination center detection

02 p0310 A70-11846

Solder mechanical contact strength to CdS insulating crystal platelets tested in liquid N, noting Ag epoxy

02 p0319 A70-12738

Photoconductivity growth and decay curves green edge emission and integral flux in optical flare of cadmium sulfide crystals due to hole trapping process

03 p0540 A70-13503

Performance degradation in cadmium sulfide solar cells, discussing cause identification technique, I-V curve parameter changes, etc

04 p0628 A70-15329

Vacuum deposited thin cadmium sulfide films semiconducting properties, discussing captured free carriers effects on temperature dependence of dark and photo current

05 p0893 A70-16543

Band extremum loops depth in CdS in electric and magnetic fields determined from calculating linear and nonlinear conductivity

06 p1126 A70-17819

Laser oscillation conditions for CdS crystal pumped by electron beam, using energy loss per unit length for calculations

07 p1298 A70-19681

Minority carriers lifetime following CdS and ZnTe spontaneous luminescence relaxation after electron beam excitation

07 p1302 A70-20318

Two photon photoconductivity of CdS crystals stimulated by ruby laser, showing emission self focusing during pumping

07 p1302 A70-20322

Thermal lens effect produced by photocurrent in CdS, using focused laser beam to generate photocurrent causing local heating changes of refractivity

10 p1898 A70-23980

Self focusing of ruby laser radiation in CdS single crystal, considering effect on crystal photoconductivity

12 p2248 A70-27540

RF-sputtered CdS thin films structural and electrical characteristics from X ray diffractometer tracings, reflection electron diffraction and X ray double crystal spectrometry

13 p2470 A70-29201

Minority carrier diffusion lengths on sides of copper sulfide-cadmium sulfide heterojunctions measured by light microprobes

13 p2471 A70-29709

Vaporization characteristics of solids for relationship between chemical bonding and sublimation mechanism emphasizing NaCl, CdS and GaAs

14 p2545 A70-30906

CdS high field domain modes generation for C parallel to E ascribed to interaction between drift carriers and off-axis shear wave

15 p2784 A70-31984

CdS and cdTe thin film solar cells R and D survey, describing construction and electrical properties

15 p2678 A70-32421

Low threshold electron beam pumped CdS lasers with improved Al coated Fabry-Perot mirrors in end-pumped configuration

16 p2928 A70-33642

Adsorption influence on electrical and photoelectric properties of CdSse thin films

17 p3143 A70-35674

Heterogeneous solar cells based on polycrystalline cadmium sulfide and selenide, discussing preparation methods and photoelectric and electric properties

18 p3215 A70-36238

Electrical conductivity, Hall constant and differential thermal emf n-type GaAs-CdS solid solutions

18 p3298 A70-36596

CdS crystals luminescence spectrum excitation by UV light of ruby laser, noting excitons and phonons recombination

19 p3444 A70-37368

CdS conversion by cation exchange to single crystal CuS, examining phases structural relationship

19 p3486 A70-37766

Cadmium sulfide photocell development, noting plastic support base, film deposition and interconnection

19 p3358 A70-38480

Copper disulfide-cadmium sulfide thin film solar cell degradation under simulated low orbit conditions, investigating thermal stress

21 p3759 A70-41313

Trap filling dependence on intensity, temperature and wavelength of photoexcitation in CdS crystals subjected to electron radiation damage and annealing

21 p3864 A70-42013

Cadmium sulfide pulsed laser spectrum analysis, discussing laser output stabilization by mode selection and electron beam scanning

22 p4049 A70-42405

CdS thin film solar cells, describing manufacture for increased degradation resistance

22 p3966 A70-43537

Electroreflectance at CdS-electrolyte interface, noting field strength effect on relaxation time

23 p4230 A70-43930

CADMIUM TELLURIDES

Current-voltage characteristics of p-n junctions in cadmium telluride, discussing spectral sensitivity bands

01 p0160 A70-11596

Mercury cadmium telluride alloy as photoconductive IR detector material noting properties, composition and temperature dependence of energy gap

03 p0543 A70-14196

Far IR second harmonic generation and frequency mixing in CdTe using pulsed water vapor laser

15 p2751 A70-31983

CdS and cdTe thin film solar cells R and D survey, describing construction and electrical properties

15 p2678 A70-32421

Mercury cadmium telluride photodetectors, analyzing gain, signal current and radiation limits

16 p2905 A70-33153

CdTe nonlinear electro-optical susceptibility predicted by mathematical model using two coupled anharmonic oscillators

19 p3485 A70-37668

Cadmium telluride photocells, discussing performance and mass production

19 p3358 A70-38481

Solid solutions of quasi-binary cross section CdP-CdTe and ZnP-CdTe, using X ray, thermal, microstructural and microhardness analyses

22 p4086 A70-43132

CAFFEINE

Mild temperature and dehydration effects on toxicity of caffeine and dextroamphetamine in mice

09 p1616 A70-22329

Amphetamine, caffeine and secunarine effects on hypodynamic syndrome in subjects during orthostatic tests and transverse G-forces under prolonged hypokinesia

10 p1817 A70-24690

CALCIFICATION

Calcium phosphate crystals precipitation from nutrient gel to determine role of gelatinous ground substance in calcification

10 p1832 A70-25075

Macroscopic architectural changes of cancellous and cortical bone in Rhesus monkey following long term immobilization and chemical removal of calcium

20 p3569 A70-38983

CALCIUM

NT CALCIUM ISOTOPES

Local contractures in K depolarized amphibian skeletal muscle fibers by intracellular injection or by microperfusion, discussing intracellular Ca ion concentration

02 p0234 A70-11728

Release-recovery and dynamic stiffness phenomenon in frog heart muscle at various Ca ion concentrations and temperatures

02 p0241 A70-12771

K line profiles of Ca II for two component chromosome, obtaining line source function and optical depth from steady state and radiative transfer equations

05 p0911 A70-16430

Solar activity centers life history in terms of radio emission and Ca plage intensity, noting radio emission decay faster than plage intensity

05 p0911 A70-16440

Ca II 7323 forbidden line in solar Fraunhofer spectrum, estimating center-limb variation of equivalent width of transition

06 p1143 A70-17994

Percentage changes in X ray calibration wedge mass equivalency to actual changes in bone Ca content

06 p0997 A70-18015

Calcium neutral and ionic lines broadening and shift by microfields measured by plasma flame observations

06 p1148 A70-18453

Solar protuberance radiation polarization in Ca I 4227 A line, discussing depolarization and electron-and photoexcitation

07 p1384 A70-19416

Electron and proton excitation of forbidden transition lines in Ca XV ground configuration determined for coronal densities and temperature

11 p2109 A70-25742

Violet K2 emission in H and K line cores of solar calcium ions using atmospheric model in state of motion

12 p2303 A70-27701

Calcium H and K lines core residual intensities in stars with quiet and active chromosome, suggesting activity due to thermal gradient

12 p2303 A70-27702

Solar IR triplet of singly ionized Ca, suggesting limb darkening caused by chromospheric inhomogeneities for source function inequality

12 p2303 A70-27703

Solar Ca II H and K lines formation, discussing double reversal, limb darkening, plage and spot lines and anomalous line ratios

13 p2494 A70-29481

Ca atom-graphite grain model for interstellar absorption at 4430 A, calculating resonant line shift and width as functions of atom-surface distance

14 p2639 A70-30729

Fine structure in Ca II K line core, determining reduced high dispersion spectra at solar disk center

15 p2804 A70-32618

Serum calcium-digitalis synergism effect on dogs heart excitability, noting hypoxia role in arrhythmia production

17 p3026 A70-35325

Calcium ion role in myocardial cell electrical and mechanical trace processes under normal content and manganese blocking

18 p3221 A70-36640

Ca ion reversible effects of hydrochloric acid and ammonia water on betacyanin leakage from beetroot sections

19 p3365 A70-38375

Spinning cylindrical spicule model with radial and axial gradients in electron number and temperature forming Ca II K line

21 p3879 A70-40955

Ultrasonic velocity in human bones measured for calcium content and density

22 p3979 A70-43522

Ca II chromospheric emission lines for deriving Mn in stellar luminosity, discussing calibration

23 p4242 A70-44293

IR observation of chromospheric Ca II K-line during total eclipse of 7 March 1970

24 p4401 A70-45314

CALCIUM COMPOUNDS

NT CALCIUM FLUORIDES

NT CALCIUM OXIDES

NT CALCIUM PHOSPHATES

NT CALCIUM SILICATES

NT CALCIUM TUNGSTATES

NT PEROVSKITES

Urinary calcium phosphate and carbonate precipitates reduction by protein and carbohydrate

diet change to casein and sucrose in *Macaca nemestrina* 09 p1621 A70-23456

Mineral saturation in calcaneal bone and hand finger phalanx in humans under prolonged hypodynamia by X-ray analysis, observing Ca salts reduction 10 p1815 A70-24676

Compositional variation effect on low silica glass formation based on calcium aluminates 16 p2934 A70-33273

Hydrous Cu-Ca silicate mineral /kinoite/ from Arizona occurring as single crystals and veinlets 24 p4329 A70-45459

Magnetic properties of lanthanum calcium manganate, making stoichiometric specimens by controlling oxygen partial pressure 24 p4390 A70-45602

CALCIUM FLUORIDES

Inorganic photochromic and cathodochromic recording materials, examining transition metal doped strontium titanates, rare earth doped calcium fluorides and Fe or S doped sodalite 22 p4088 A70-43601

CALCIUM ISOTOPES

Calcium isotopes tracer migration in caged rats in metabolism study 04 p0630 A70-14571

CALCIUM METABOLISM

Calcium isotopes tracer migration in caged rats in metabolism study 04 p0630 A70-14571

Autonomic drugs induced contractures of cardiac muscle of frogs, relating inotropic action with Ca influx during low membrane potential 15 p2686 A70-32837

Calcium metabolic balance reports discrepancies with radiologic indications of astronaut bone loss 23 p4148 A70-44838

Infused cortisol disappearance rates and distribution volumes in hyper-, hypo- and normocalcemic dogs 24 p4296 A70-45334

CALCIUM OXIDES

CaO reaction rate with ZrC in effusion cells as function of reactant ion diffusion through product layer 13 p2362 A70-29496

CALCIUM PHOSPHATES

Calcium phosphate crystals precipitation from nutrient gel to determine role of gelatinous ground substance in calcification 10 p1832 A70-25075

Apollo 11 lunar rock fluorapatite and trace minerals, examining pressure and oxidizing conditions of formation, grain and crystallization 21 p3898 A70-41527

CALCIUM SILICATES

Calcium-bearing iron silicate /pyroxferroite/ from Apollo 11 lunar Tranquility Base samples, discussing petrographic environment, physical and optical properties 21 p3895 A70-41504

CALCIUM TUNGSTATES

Absolute quantum efficiency of phosphor calcium tungstate-lead under monochromatic far UV illumination 15 p2729 A70-32017

Calcium tungstate crystals, investigating electron paramagnetic resonance centers produced by neutrons and gamma rays to obtain information on lattice vacancies, defects, etc 16 p2961 A70-33963

CALCIUM 45

U CALCIUM ISOTOPES

CALCULATION

U COMPUTATION

CALCULATORS

Integrated digital circuits for office type desk calculators based on machine concept 01 p0052 A70-11287

Slide rule for calculating electron number density, Debye length and Debye sphere particles in plasma parameters determination 05 p0852 A70-16847

CALCULUS

NT ASYMPTOTIC SERIES

NT CONTINUITY [MATHEMATICS]

NT COPLANARITY

NT DIFFERENTIAL CALCULUS

NT FOURIER SERIES

NT INTEGRAL CALCULUS

NT LIMITS [MATHEMATICS]

NT MACLAURIN SERIES

NT POWER SERIES

NT SERIES [MATHEMATICS]

NT TAYLOR SERIES

NT VECTOR ANALYSIS

NT VORTICITY

Analytic systems theory using Volterra calculus of functionals applied to nonlinear differential equations 10 p1908 A70-23845

CALCULUS OF VARIATIONS

Morse eigenfunctions for variational calculation of diatomic molecules vibrational-rotational energy level

analysis, showing better convergence than harmonic oscillator basis 02 p0344 A70-12519

Variational equation describing thermal diffusion in solid body undergoing deformation 03 p0589 A70-13348

Analytical approach to gradient method within framework of Bolza problem of variational calculus, using linearized differential and isoperimetric constraints 03 p0520 A70-14341

Conjugate points for simple integral problems in calculus of variations extended to multiple integral problems, using Jacobi equation 04 p0713 A70-14674

Calculus of variations used for determining optimum one dimensional MHD slider bearing with bounded control variables 04 p0698 A70-14771

[ASME PAPER 69-WA/LUB-2] Variational analysis of low latitude magnetic sounding data to determine structural differences between various earth mantle regions, noting additional observations required 04 p0682 A70-15735

Euler-Lagrange linear operators in variational embedding with one dependent function 05 p0881 A70-16058

Momentum-energy complex obtained for nonlocalized fields in variational mechanics, deriving integrodifferential identities for Euler equations quadratures 05 p0881 A70-16078

Variational problems of stationarization under constraints, using imbedding integrodifferential equations 05 p0882 A70-16085

Nonlocal variational mechanics with one field variable, developing algorithm for Euler-Lagrange operator calculation 05 p0882 A70-16137

Variational methods in semigeodesic projections of analytic surfaces on plane surface, determining projections impossible by classical cartography 05 p0839 A70-16368

Variational ray path calculation method for HF electromagnetic wave in anisotropic inhomogeneous lossless ionospheric plasma 06 p1055 A70-17592

Book on optimization by variational methods covering use of differential equations, Pontryagin minimum principle, optimal and feedback control, dynamic programming, etc 06 p1093 A70-17650

Growth conditions used in existence theorem for calculus of variations in optimal control problems 06 p1027 A70-18506

Soviet collection of papers on boundary problems for differential equations covering variational problems in half space, polynomial behavior at infinity, function spaces, Fourier transformation, etc 07 p1322 A70-18851

Multiplier and gradient methods in computing variational and optimal control problems 07 p1325 A70-19267

Sufficient condition for calculus of variations problem, applying results to integrands without partial derivatives 07 p1327 A70-20022

Phase space variations method proved not applicable to optimal control problems 08 p1479 A70-20856

TWT model with slow wave structure and realized negative depression coefficient and Q factor described by variational method 09 p1644 A70-22410

Numerical solutions of variational problems concerning symmetrical wings with minimum drag and optimal aerodynamic efficiency in hypersonic flow 09 p1603 A70-22433

Temperature distributions in multidimensional transient conduction heat transfer, using variational method and Laplace transformation 09 p1788 A70-22705

Stability characteristics of near periodic orbits using variational equations, with results applied to phase space and stability problems 09 p1760 A70-22917

Kantorovich variational method extended to thermoelastic plane stress problem of rectangular plates 09 p1781 A70-23278

Soviet book on new methods of variational calculus in aerospace vehicle flight dynamics covering controlled processes optimization theory analysis 09 p1767 A70-23473

Discrete calculus of variations for optimal control involving use of discrete time sequence and functionals 10 p1910 A70-24702

Endpoint sufficiency test based on differential calculus method, considering Bolza problem of continuous state and piecewise control variables 11 p2073 A70-26233

Kantorovich theorem application as weak Newton method used in boundary value problems containing Euler-Lagrange equation for variational problems and ordinary differential equations 12 p2260 A70-27002

Variational equations from Herrick variation of parameters method for Icarus encounter with earth 13 p2488 A70-28823

Satellite time and position observations mean square error analysis using calculus of variations 13 p2367 A70-29528

Extremum criterion for singular solutions to optimal trajectory equations in calculus of variations 13 p2443 A70-29747

Boundary value problems reduction to variational problem by transversality conditions of calculus of variations 14 p2599 A70-30644

Variational equation describing thermal diffusion in solid body undergoing deformation 14 p2657 A70-30722

Variational analysis of low latitude magnetic sounding data to determine structural differences between various earth mantle regions, noting additional observations required 14 p2575 A70-30819

Variational equation of ballistic trajectory applied to two point boundary value guidance problems 15 p2812 A70-32504

Control theory and calculus of variations - Conference, University of California, Los Angeles, July 1968 17 p3129 A70-34866

Unified variational theory of quadratic forms, considering linear functional on real linear space and bilinear and quadratic functionals 17 p3129 A70-34867

Optimal filter problem related to tracking, discussing mathematical formulation and reduction to variational problem 17 p3056 A70-34869

Calculus of variations used for determining optimum one dimensional MHD slider bearing with bounded control variables 19 p3436 A70-37620

[ASME PAPER 69-WA/LUB-2] Variational formalism in mechanics of continuous media in four dimensional event space, considering model with local particle interactions 20 p3724 A70-39855

Soviet book on flight vehicle optimal design algorithms, covering mathematical theory of variational method, multistage spacecraft, etc 20 p3716 A70-39898

Optimal control problem for plant including dynamics and input constraints parameters treated by calculus of variations and Pontryagin maximum principle 21 p3801 A70-40899

Nonlocal variational mechanics, considering case of stationarity with unrestricted nonlocality 21 p3939 A70-42026

Seminormality and upper semicontinuity of variable sets in optimal control 22 p4061 A70-42461

Variational formulation for steady and transient heat conduction with variable thermal conductivity, applying to cylindrical element 22 p4123 A70-42546

Singular and nonsingular optimal control problems, deriving sufficient conditions for nonnegativity of second variation 23 p4213 A70-44908

Linear elasticity with constraint couples, establishing existence theorems by variational methods 24 p4420 A70-45267

Linear elasticity with constraint couples, establishing existence theorems by variational methods 24 p4420 A70-45267

CALIBRATING

NT WIND TUNNEL CALIBRATION

S/N fatigue life gage for nondestructive evaluation of cumulative damage, discussing calibration and two step, block and random tests 01 p0053 A70-10009

Absolute calibration method for daily solar flux density discrepancies measurements at UHF, describing equipment and error analysis 01 p0168 A70-10259

Radiometric method for calibrating loss of multimode antenna-feed components with linear or circular polarization, deriving calibration and error analysis equations 01 p0050 A70-10711

IR spectrum of Jupiter with calibrations from laboratory studies of methane and ammonia bands 02 p0378 A70-12559

Phase measuring scheme for large radio telescope array, describing constant-phase calibration signal production 02 p0269 A70-12583

Turbulence characteristics in liquids measured by hot film anemometry, discussing calibration methods selecting criteria as temperature control, drift influence and relative speed determination 02 p0303 A70-12687

Transient and steady state radiation heat flux sensors calibration by developing and evaluating heat flux source 03 p0606 A70-13558

Cryogenic temperature sensor calibration with automated data readout for spacecraft accuracy requirements, describing potentiometric system 03 p0486 A70-13561

- Surveyor TV camera conversion from qualitative viewing device into quantitative measuring instrument by calibration coupled with data processing program [JPL-TR-32-1374] 03 p0490 A70-13662
- Spectroscopic calibration of laser lines at simultaneous carbon dioxide and nitrous oxide transitions in gas flow, showing abnormal line intensity 03 p0501 A70-13685
- Prelaunch photometric calibration of Surveyor TV system for reconstruction of lunar terrain televised pictures permitting system lunar performance prediction [AIAA PAPER 68-1138] 04 p0692 A70-15405
- Piezoelectric sensing diaphragm for detection of micrometeorites in space, noting vibration mode and effect of small beads contact time on calibration errors 04 p0695 A70-15567
- In-flight radiometric calibration of low brightness OGO 4 airglow photometer 04 p0696 A70-15645
- Airborne system for calibrating remote precision clocks using two way radio transmitter, measuring error by system similar to radar beacon transponder system 05 p0844 A70-15773
- Neutron monitor calibration method to eliminate natural cosmic ray background, decreasing errors due to ray intensity variation 05 p0846 A70-15938
- Solar neutrino detectors calibration with artificial neutrino sources produced by reactors, electron and proton accelerators 05 p0846 A70-15953
- Lasers for optical inspection of components and calibration of machine tools 05 p0860 A70-16823
- Transition probability and Stark profile of H alpha standards for absolute intensity calibration of spectroscopic data from thermal shock tube plasma 05 p0853 A70-17083
- Calibration for five hole spherical pitot probe plotting data for velocity, inclination and static pressure factors 06 p1063 A70-17621
- Turbine flowmeter in-place calibration for measuring cryogenic propellant flow rates in rocket engine testing 06 p1071 A70-18448
- Liquid and slush hydrogen gravimetric flow calibration system for research in slush generation, slush fluid mechanics and flow instrumentation 06 p1031 A70-18449
- HR diagram calibration based on proper motions and radial velocities, deriving absolute magnitudes and statistical parallaxes 06 p1149 A70-18456
- Yawed hot wire measurements of turbulence fluctuations, discussing calibration and mutual interference of adjacent wire and wire supporting prongs in X-ray wire case 06 p1071 A70-18487
- Piezoelectric accelerometer transverse sensitivity calibration using reference accelerometer comparison technique 06 p1073 A70-18599
- Antenna calibration by measuring emission of absorbing black disk positioned in Fresnel region 07 p1239 A70-18759
- Calibrating rods design for vibrating components stress measurement gauges 07 p1400 A70-18822
- Optical density vs illumination amount characteristic curve determined for photometric calibration of astronomical photographs of celestial bodies 07 p1279 A70-19046
- Optical polygon calibration by interferometric method using He-Ne laser light source 07 p1297 A70-19227
- Mechanical shock accelerometer calibration by light frequency Doppler shift measurement using laser interferometer and single sideband carrier insertion circuit 08 p1493 A70-20602
- Sewage water flowmeter calibration, analyzing error propagation and tolerance 09 p1672 A70-22027
- Piezoelectric quartz and tourmaline pressure gages static calibration, evaluating errors 09 p1675 A70-22599
- Flashtube photostimulators for examining human physiological response, discussing design and calibration 09 p1624 A70-22673
- Calibration of shear sensitive cholesteric liquid crystals film, measuring shearing forces and scattering light intensity 09 p1656 A70-22992
- IR thermometers in situ calibration, analyzing maximum error due to reflection effect 09 p1684 A70-23536
- Abbot pyranometer as reference standard for calibration, reporting performance tests of time constant, cosine response and attitude 10 p1886 A70-23933
- Narrow band atmospheric noise peak field strength measurement, describing design and calibration of noise meter output unit 10 p1832 A70-23998
- Thermodynamic properties of periodically variable air volume in pneumatic pressure generator of pressure sensor calibration bench 10 p1863 A70-24027
- Vacuum chamber for adjusting and calibrating spaceborne optical instruments used in studying UV radiations 10 p1860 A70-24479
- Microwave waveguide insertion-loss calibrations, comparing cavity Q and direct measurement methods 10 p1854 A70-25315
- Atomic frequency standards for phase calibration of large aerial arrays applied to radioheliograph 11 p2019 A70-26300
- Precise sweep calibrations and simultaneous spectrum recording for high resolution nuclear magnetic resonance spectroscopy 11 p2052 A70-26375
- Solar magnetograph modified to simplify calibration, using polarimeter with special exit slit geometry 11 p2057 A70-26650
- Electron beam density probe calibration for earth atmospheric reentry vehicles communication 12 p2230 A70-26982
- Digital closed-loop inflight calibration system for spaceborne particle spectrometers, utilizing cesium iodide crystal and programmable photomultiplier dynode supply 12 p2232 A70-27405
- Intra- and extragalactic distance indicators and Hubble constant calibration 12 p2301 A70-27581
- Turbine flow meters dynamic calibration employing sinusoidally perturbed orifice flow 12 p2236 A70-28033
- Ballistic pulsed photometer calibration without etalon light pulse using radiation sensitivity, oscillation period and galvanometer damping 12 p2238 A70-28179
- Black body design for radiometry, discussing error sources in calibration 13 p2410 A70-29658
- Aircraft altimeter measurement for vertical separation based on atmospheric pressure unit changes /Cayleys/ compared with linear measurements in meters and feet 13 p2411 A70-29778
- Narrow band photometry calibration, using model stellar atmospheres and laboratory data for high resolution synthetic spectra of G and K giant stars 14 p2639 A70-30728
- Data flow in computerized automatic data acquisition systems, considering systems traceability of calibration to national standards 14 p2554 A70-31110
- Humidity calibration utilizing precision wide range optically controlled thermoelectrically cooled dew point hygrometer 14 p2587 A70-31165
- Radiometers calibration equipment maintaining radiation standards, investigating long and short waves by digital voltmeter coupled to paper tape punch 15 p2735 A70-31806
- Light sources design with variable uniform luminance for space exploration cameras calibration [JPL-TR-32-1470] 15 p2737 A70-32037
- Photometric calibration changes in EUV solar satellite instruments during orbital operation 15 p2737 A70-32045
- UHF ground communication dish antennas transmit and receive gains calibration by communication satellite repeater 16 p2872 A70-32967
- Simple harmonic scotch yoke mechanical oscillator for strain gauge accelerometer calibration in VLF range 16 p2900 A70-32995
- Admittance calibration of short HF through flow pneumatic lines, using hot-wire anemometer [ASME PAPER 70-FE-10] 16 p2891 A70-33628
- HF shaker for accelerometer calibration and resonance evaluation, discussing construction materials, accuracy and test results 16 p2889 A70-34021
- German monograph on artificially accelerated proton measurements for ionization calorimeter calibration and cosmic radiation energy spectrum analysis during balloon flight 17 p3081 A70-34572
- Laser interferometry for accelerometer and dynamic pressure transducer calibration and vibration measurement 17 p3089 A70-35124
- Humidity measurement and calibration systems, considering automatic optical dew point hygrometry 17 p3089 A70-35172
- Piezoelectric accelerometer reference systems calibration by function separation 17 p3089 A70-35173
- Exciter and instrumentation of vibration transducer calibration system 17 p3089 A70-35179
- Pressure transducers primary calibration to 10 kHz, using shock tube for step function excitation 17 p3093 A70-35486
- Adiabatic calorimeter for heat flux sensor contact calibration, describing operational principles and design 18 p3257 A70-36115
- Error sources in carbon black coating on thin foil heat flux sensors accounting for false altitude effects in vacuum calibration 18 p3262 A70-37100
- Antenna calibration by measuring emission of absorbing black disk positioned in Fresnel region 18 p3233 A70-37103
- Pressure sensors for large frequency and amplitude measurement, discussing calibration with square signal generator 18 p3262 A70-37210
- Ultrahigh vacuum gages absolute calibration by controllable conductance method, discussing accuracy 19 p3421 A70-37463
- Cryogenic temperature sensor with linear characteristics from 150 to minus 452 F, describing calibration and testing 19 p3425 A70-37883
- Dynamic pressure transducer calibration system using fluidic pressure generators 19 p3358 A70-37897
- Automatic calibration verification of subcarrier telemetry discriminators with selective channel readjustment 19 p3383 A70-37902
- ILS glide slope calibration using optically projected digital codes as reference 19 p3464 A70-37912
- Heat flowmeters calibration by conductive method, reducing error due to radiative, conductive and convective losses 19 p3430 A70-38522
- Orbital and physical parameters of calibration satellites launched into right circular cylinder and right circular cone 19 p3382 A70-38894
- Phytoactinometers and phytopyranometer graduating methods, discussing measurement of photosynthetically active radiation 20 p3626 A70-39035
- Short wave calibration system for net pyradiometers, using source with intensity and spectral distribution comparable to solar radiation 20 p3628 A70-39147
- Accelerometer calibration in low g range by mass attraction as equivalent acceleration input [AIAA PAPER 70-1030] 20 p3631 A70-39507
- Self calibrating TRIM gyromonitor inertial platform with gyroflex gyro, describing operation and performance [AIAA PAPER 70-1012] 20 p3667 A70-39521
- Precise sensing systems and instruments calibration with respect to inertial frame of reference for geokinetics [AIAA PAPER 70-958] 20 p3622 A70-39571
- Navigation instrument geometrical calibration by natural satellites and reference stars during interplanetary flight [AIAA PAPER 70-1023] 20 p3669 A70-39586
- Teleradiometer calibration in background radiation absence, using distant and finite point source method and collimator means 20 p3633 A70-39798
- Weighing systems electronic load cells calibration for tension and compression loading, attributing non-repeatability to bending moments [SAWE PAPER 816] 20 p3634 A70-40356
- Optimum calibration intervals determination for obtaining instrument maintenance quality level at low cost 20 p3634 A70-40452
- Installed system calibration thermocouples using temperature plateaus due to pure metals melting and freezing heat of fusion 21 p3823 A70-40857
- Calibration data correlation for constant temperature hot film anemometer for low speed nonisothermal laminar air flow, using modified King law 21 p3828 A70-41475
- Laser heterodyne system for nonisotonic vibration measurements, describing calibration and use 22 p4049 A70-42526
- Ultrahigh vacuum calibration system for vacuum gages and mass spectrometers based on pressure attenuation and molecular beam techniques 22 p4029 A70-42620
- Precision gimbaled sensor pointing system calibration data errors due to misalignments and inaccuracies in transducer readout 22 p4040 A70-43587
- Apparatus characteristics determination for ultrasonic inspection, recommending calibration block 22 p4041 A70-43622

Thermal calibration errors and sensitivity equations for hot-wire anemometers 23 p4195 A70-44288

Pressure sensor testing and calibrating at cryogenic temperatures, describing special test rig structural, insulation, fittings and materials requirements 23 p4178 A70-44846

Cryogenic thermocouples of various metal pairs for low temperature measurements, discussing performance tests and calibrations 24 p4378 A70-45385

CALIFORNIA

California future transport complex, considering STOL and ESTOL /extremely short takeoff landing aircraft/ design requirements 06 p0985 A70-17197

Ozone concentration in San Francisco Bay Area, discussing temperature inversion, air pollution, destruction rate and distribution patterns of oxidants 18 p3284 A70-35945

CALORIC REQUIREMENTS

Space diets tests for mean DAR of proteins, carbohydrates, fats and water, considering body weight and required energy expenditure 09 p1623 A70-22088

Space diets tests for mean DAR of proteins, carbohydrates, fats and water, considering body weight and required energy expenditure 15 p2693 A70-32684

Growth and caloric intake of rats exposed to high altitude dependence on high carbohydrate, protein and fat diets 22 p3967 A70-42458

Extreme environmental temperature effects on hepatic amino acid catabolism in rats attributed to caloric deficiency 23 p4148 A70-44790

CALORIC STIMULI

Norepinephrine-induced depolarization effects on brown fat thermogenesis in cold-acclimated rats determined from in vivo measurement of intracellular potentials 05 p0799 A70-16020

CALORIMETERS

Constant magnetic fields effects on blood coagulatory processes, describing microcalorimetric determination 01 p0015 A70-10372

Adiabatic calorimeter for exothermic chemical reactions determining heats of polymerization, curing rate and thermal decomposition rates as temperature function for high energy propellants 04 p0688 A70-14711

Unsteady calorimetric sensor for measurement of heat transfer between gas jets and solid targets 06 p1064 A70-17857

Wall roughness effects on model heat transfer in high Reynolds number shock tunnel milliseconds flow using thick film fast response calorimeter 06 p1070 A70-18446

Sea level testing of magnetic spectrograph and calorimeter apparatus for studying cosmic ray spectra at different atmospheric depths 08 p1560 A70-20474

Waveguide master short circuit devices reflection coefficient measurements by microcalorimeter 09 p1638 A70-23322

Constant temperature /phase transition/ calorimeter errors in measuring laser energy using ice as working medium 09 p1700 A70-23659

Cascade showers in horizontal flux of cosmic rays measured by ionization calorimeter 09 p1747 A70-23730

Guarded disk type emissometer for hemispherical emittance measurements of sample materials in 88 to 420 K range based on steady state calorimetry [AIAA PAPER 69-600] 13 p2404 A70-28524

Glass disk calorimeter for measuring free running and Q switched laser pulses 15 p2742 A70-32545

Thermal conductivity of gaseous and liquid hydrogen with guarded horizontal flat plate calorimeter, investigating temperature and density effects in critical region 16 p2996 A70-33011

German monograph on artificially accelerated proton measurements for ionization calorimeter calibration and cosmic radiation energy spectrum analysis during balloon flight 17 p3081 A70-34572

Laser energy parameters measurement by calorimetric methods based on radiant heating effect 17 p3106 A70-35099

Adiabatic calorimeter for heat flux sensor control calibration, describing operational principles and design 18 p3257 A70-36115

Liquid nitrogen boil off calorimeter for surface energy measurements, describing construction, calibration and instrument errors 18 p3261 A70-37089

Apollo 11 sample specific heats at 90-350 K, using adiabatic calorimeter 21 p3917 A70-41674

Isoperibol calorimetry for laser power and energy measurements, discussing boundary value problem for heat flow 21 p3838 A70-42021

Guarded electrical cylindrical calorimeter measuring multilayer insulation thermal conductivity, discussing construction, test and error 23 p4195 A70-44366

Differential scanning calorimetry and thermogravimetric analysis combination for thermochemical kinetic measurements, matching analytical and experimental curves for data accuracy 23 p4196 A70-44429

CALORIMETRY

U HEAT MEASUREMENT

CAMBER

NT CONICAL CAMBER

NT WING CAMBER

Casing and suction cone effects on fans with cambered forward curved blading 11 p1975 A70-25796

Numerical solutions of thick cambered jet flap in ground effect for flat plate and diamond shaped airfoil [AIAA PAPER 69-738] 12 p2155 A70-27199

CAMBERED WINGS

Camber and twist distributions for closed ground effect wing optimum design for zero induced drag, employing linearized theory 10 p1801 A70-24158

CAMERA SHUTTERS

Automatic exposure control system for airborne cameras, providing iris and shutter control through taking lens for sudden light changes 05 p0844 A70-15771

Microchannel electron multiplier and optical focusing output shutter tubes for high speed photography 14 p2589 A70-31403

Photographic still and high speed cameras, using Kerr effect electro-optical shutters with transmission line structure 14 p2589 A70-31404

High speed electron cameras with opening time below one nsec, discussing shutter types 14 p2589 A70-31405

Surveyor camera double acting rotary solenoid actuated focal plane shutter utilizing two blades in parallelogram linkage 16 p2914 A70-34148

Combination shutter and filter-changing mechanism for spacecraft vidicon cameras 16 p2914 A70-34150

Spaceborne narrow band TV system with image memory tube and electronic shutter, noting variable exposure time, motion compensation and multimode scanning 17 p3089 A70-35267

Event-triggered high speed spectrograph shutter, studying shock tube plasmas 20 p3630 A70-39484

Partial frame shutter for high speed rotating mirror camera, using explosively driven opaque dust cloud [SMPT PREPRINT 33] 22 p4033 A70-43044

Automatic shutter for recording holograms with laser light, controlling exposure time by photoconductor cell 23 p4197 A70-44472

CAMERA TUBES

NT IMAGE ORTHICON

NT RETURN BEAM VIDICON

NT VIDICON

CAMERAS

NT BAKER-NUNN CAMERA

NT BALLISTIC CAMERAS

NT FRAMING CAMERAS

NT HIGH SPEED CAMERAS

NT LALLEMAND CAMERAS

NT PANORAMIC CAMERAS

NT SCHMIDT CAMERAS

NT TELEVISION CAMERAS

He camera with reduced linear absorption coefficient for contact microradiography, relating exposure, X ray wavelength and atmosphere 01 p0084 A70-10013

Automatic four axle satellite tracking camera design and operational principle, examining lens aberration 02 p0294 A70-11771

Rb-75 adapted reconnaissance cameras error sources on basis of processed Echo 2 satellite photographs 02 p0294 A70-11772

Planetary film system /PFS/ camera-processor-scanner for scientific spaceborne applications, detailing design and performance 03 p0490 A70-13664

Multiband photographic system for automatic earth resources aerial sensing and lunar orbital mapping with manual override provisions [AAS PAPER 69-582] 04 p0687 A70-14657

Cameras photogrammetric parameters determined from stellar photographs, considering distortion components, reference points, etc 05 p0852 A70-16921

Aircraft mounting plate for 70-mm multispectral mapping quadricamera assembly to photograph wildland and agricultural resources 08 p1497 A70-21542

Stars photographic position determination errors with NAFA-3C/25 camera, comparing films and plates 09 p1673 A70-22164

Wide angle electronic camera for astronomical photometry designed to seek photometric standard stars remote from nebular regions 09 p1681 A70-23313

Airborne camera resolution degradations /window losses/ introduced by multilayering wedge, irregularity and structural deformation 09 p1687 A70-23767

Soviet cameras for photographic observation of artificial celestial bodies, noting equatorial platform mount, mirror lenses and installations 10 p1892 A70-25128

Three camera method for studying upper atmosphere winds via smoke trails providing wind velocity, earth coordinate data and error indication 14 p2607 A70-30572

Nimbus weather satellite as laboratory for sensors collecting data for global weather system, describing launching, attitude control systems and cameras 14 p2654 A70-31149

Cloud cover stationary pictures by spin-scan camera in synchronous orbit over Pacific converted into motion pictures showing cloud pattern changes and storm development 14 p2587 A70-31150

Light sources design with variable uniform luminance for space exploration cameras calibration [JPL-TR-32-1470] 15 p2737 A70-32037

Imaging type electro-optical detection systems design for passive night surveillance, building camera system and testing in helicopters and fixed wing aircraft 16 p2903 A70-33127

Aerospectrometric camera facilitating spectral brightness coefficients determination for object identification 16 p2908 A70-33227

Surface temperature changes measurement with thermovision camera, discussing calibration and recording 16 p2911 A70-33775

ATS spin scan cloud cameras mechanical design and operation 16 p2914 A70-34149

Astrophotograph optical center coordinates and camera focal length calculations 18 p3260 A70-36992

Cooled antimony-caesium film photoelectric effect for weak luminous flux, examining electronic camera reciprocity 19 p3427 A70-38175

Artificial satellites photographic observation by camera, describing sighting system, tracking adjustments and shutter controls 19 p3433 A70-38793

Aerial cameras for topographic mapping, emphasizing geometrical image accuracy, optical picture quality and shutter performance 21 p3826 A70-41268

Satellite tracking camera lens-distortion coefficient from comparison of standard stellar and measured X-Y coordinates 22 p4029 A70-42596

Apollo 11 and 12 close-up lunar surface photography, describing specially designed camera 23 p4194 A70-44255

Internal and external orientation elements of aerial cameras from star photographs on clear dark sky 24 p4333 A70-45198

Vibration transfer coefficient of aerial camera-photographic assembly system for shock absorption during surveys 24 p4333 A70-45200

Aerial survey cameras exposure time automatic control circuits for high quality photographs with constant integral density 24 p4334 A70-45497

CANADA

Cosmic ray latitude survey in Canada using airport sites, noting ground snow effect on neutron monitor counting rate 01 p0167 A70-10227

ARCOM earth terminal for Domestic Satellite Communication System bringing telephone, TV and data service to northern Canada 09 p1656 A70-22945

Canadian geostationary satellite communication system design and performance, discussing transponder with six RF channels [AIAA PAPER 70-429] 11 p1996 A70-25402

Canadian domestic satellite communications policy, discussing Telesat Canada for commercial telecommunications services [AIAA PAPER 70-428] 11 p2152 A70-25416

TV network distribution in Canada by communications satellite and terrestrial microwave links, discussing signal to noise ratios and picture quality [AIAA PAPER 70-430] 11 p1998 A70-25417

Report to COSPAR on space research in Canada, covering Alouette satellites, ISIS I, international cooperation, etc 15 p2829 A70-31708

Lake covered ancient meteorite impact crater in Canada, noting eroded rim and microscopic shock criteria
15 p2732 A70-32849

Canadian civil aircraft bird hazards problem and alleviating measures including airport surrounding lands control
18 p3212 A70-35989

CANADAIR AIRCRAFT
NT CL-84 AIRCRAFT
Digital data acquisition system for CF-5A flight test program, discussing recording system design
19 p3384 A70-38532

CANADAIR CF-104 AIRCRAFT
U CANADAIR AIRCRAFT
U F-104 AIRCRAFT
CANADAIR CL-84 AIRCRAFT
U CL-84 AIRCRAFT
CANADIAN SHIELD
Canadian Shield ridges and meteorite impact scars, discussing state of earth crust during meteoritic bombardment of earth and moon
08 p1563 A70-20500

CANARD CONFIGURATIONS
Canard and variable geometry aircraft designs noting SAAB 37 Viggen performance
10 p1805 A70-24764

CANCER
Hereditary UV luminescence of transplanted cancerous and lymphosarcomatous cells in mice and rats after ionizing radiation exposure
13 p2358 A70-29341

Lasers for surgical applications, cancerous tissue treatment, ophthalmology and comparison with RF diathermy
24 p4308 A70-45569

CANISTERS
U CANS
CANONICAL FORMS
Incomplete Airy functions application to wave diffraction problems as canonical functions
01 p0144 A70-11090

Canonic equations of motion of heavy solid body with fixed point
01 p0145 A70-11436

Symmetric Boolean function detection by method using potential concept, determining alpha numbers with potential values for canonical terms
02 p0324 A70-12188

Distribution of zeros of solutions of canonical fourth order linear differential equations
04 p0713 A70-14675

Hori canonical equations solved by eliminating short period terms in general planetary theory, noting reduction to systems of linear differential equations
05 p0907 A70-16160

Perturbation theory based on Lie transforms, reducing Deprit equation to generate general recursion formulas
05 p0908 A70-16336

Birkhoff normalizing canonical transformation built at elliptic type of equilibrium without internal resonance, using Lie transforms
05 p0909 A70-16340

Particles infinite systems equilibrium state by canonical ensemble theory, demonstrating existence and uniqueness of limiting distribution functions dependence on density
07 p1333 A70-18936

Hori canonical equations analytical solution generalization resulting from elimination of short period terms of first order planetary theory
08 p1575 A70-21239

Phase variable canonical form for time varying multivariable systems requiring less computational effort
08 p1463 A70-21645

Random process represented in canonical expansion form simulated by method of prognosis of reliability
11 p2022 A70-25344

Perturbation function of first order general planetary theory using Hori canonical variables, revealing mixed secular term of determining function
13 p2487 A70-28708

Energy and canonical momentum relationship in relativistic mechanics, discussing particle production and annihilation
13 p2453 A70-29721

Critical inclination problem, discussing canonical variables and Bohlin Zeipel technique
14 p2639 A70-30707

Canonical representation for nonlinear differential equations periodic solutions
14 p2658 A70-30846

Localized states reconstructed as superposition of canonical states, using hyperplane generalization
15 p2766 A70-31437

Scalar-tensor theory in canonical form, discussing neutral particle and electron self energy problem
15 p2773 A70-31439

Nonlinear higher order canonical time lag equations initial and boundary value problems solutions by approximate iterative two way integration
15 p2767 A70-32171

Optimal trajectories analysis by canonical transformation for obtaining solution to Hamilton-Jacobi equation without quadratures
16 p2943 A70-33899

First order difference equations for dynamical systems from Hamilton canonical equations
17 p3129 A70-34959

Existence and uniqueness theorem for boundary value problem solutions to nonlinear canonical ordinary differential equations
17 p3131 A70-35339

Canonical coordinates for numerical computation of free surface flows, considering steady motion and elliptic partial differential equations
19 p3457 A70-37679

Sampled data compensators hybrid realization for discrete controllers, selecting canonical representation with minimum number of delay elements
22 p4002 A70-42846

Perturbation theories based on canonical transformations, examining von Zeipel theory and Hamiltonian functions
22 p4109 A70-43749

Static spherically symmetric charged mass distribution exact solutions derived for electrons in scalar tensor theory of gravity by Hamilton-Jacobi method
23 p4222 A70-44403

CANOPES
Parawing canopy behavior during deployment in free flight at specific altitudes and dynamic pressures [AIAA PAPER 70-1189]
21 p3751 A70-41804

Hi-glide personnel canopy /Para-Foil, Parawing, Sailing, Volplane/ technology capability requirements identification from performance parameters tradeoffs [AIAA PAPER 70-1194]
21 p3753 A70-41822

Parachute canopy surfaces transient aerodynamic pressures during unsteady processes, using piston theory [AIAA PAPER 70-1175]
21 p3754 A70-41838

Snatch force during lines-first deployment of aerodynamic decelerator, including effects of canopy skirt acceleration and suspension wave propagation characteristics [AIAA PAPER 70-1171]
21 p3754 A70-41842

CANS
Canister for protecting DC motors in Isis 1 antenna unit, noting pressure monitoring device and shaft seal
17 p3100 A70-34753

CANT
U SLOPES
CANTILEVER BEAMS
Optimal dynamic design of system consisting of elastic cantilever rod with two concentrated masses subjected to harmonic vibrations under force at free end
02 p0384 A70-11739

Finite difference method applied to solving equations of motion for computing natural torsional vibration frequencies of pretwisted cantilever beams
03 p0595 A70-13811

Frequency equation for flexural vibration of simply supported beam, considering tabular procedure for cantilever beam
03 p0602 A70-14330

Dynamic torsion of anisotropic circular cantilever beams and small pitch diameter springs under linear time dependent moment calculated by Saint Venant method
06 p1037 A70-17862

Stress corrosion testing of vanadium alloys using precracked specimens in cantilever beam apparatus, discussing strain hardening exponent role and propagation rates
07 p1306 A70-19299

Saint Venant principle in cantilever sandwich beams under two statically equivalent load systems, considering Young moduli effects
07 p1406 A70-19328

Geometrical-mechanical properties in terms of interlaminar shear stress of composite cantilever beams under end load
07 p1412 A70-19965

Stresses and displacements in largely deflected cantilever beams subjected to gravity using photoelasticity
08 p1593 A70-21619

Rotating cantilever beams mounted on disk periphery, analyzing forced and free vibrations characteristics
09 p1781 A70-23283

Nomogram selecting dimensions of steel or Al alloy cantilever beams for transducer design using strain gages
10 p1890 A70-24593

Finite deflections of nonlinearly elastic cantilevered bar
11 p2140 A70-26481

Cantilevered column stability under constant follower load in presence of external damping
13 p2510 A70-28733

Fracture mechanics and stress analyses comparison for fatigue cracked steel cantilever beam stress corrosion specimens
15 p2755 A70-31473

Free oscillations of Euler-Bernoulli and Timoshenko cantilever beams of variable cross section, obtaining approximate modes and natural frequencies bounds
16 p2994 A70-34234

Time-average holographic interferometry applied to HF transverse vibrations of uniform cantilever beam, noting correlation with Timoshenko beam theory
17 p3083 A70-34961

Kinetic instability of elastic cantilever beam under excitation by rotating masses, relating bending and torsional vibrations to masses angular velocity
18 p3334 A70-35960

Damped linearly tapered cantilever beam elastically restrained against rotation at wall, analyzing displacement under general initial and distributed load conditions
19 p3539 A70-37802

Asymmetric snap-through buckling in cantilevered column restrained at tip by stiff wire, discussing ratio of flexural rigidity to extensional stiffness
19 p3549 A70-38670

Perforated cantilever beams and plates vibration damping capacity improvement by stress concentration introduction
21 p3933 A70-40729

Subminiature three directional cantilever beam accelerometer using semiconductor strain gages
21 p3824 A70-40861

Assumed vibration modes generation method in beams with arbitrary boundary conditions, applied to cantilevered beams, using modified Rayleigh-Ritz analysis
21 p3934 A70-40923

Cantilever bending under gradual contact with cylindrical supporting surface compared with solution by elasticity theory
21 p3934 A70-41251

Postbuckling of wire restrained elastic cantilever column with imperfection sensitivity
22 p4116 A70-43204

Cantilever beam transient response measurement by stored beam /real time/ holographic interferometry combined with high speed motion picture photography
22 p4039 A70-43452

Cantilever beam optimal stability under concentrated and uniformly distributed bending loads
23 p4268 A70-44171

Prismatic isotropic homogeneous cantilever beams flexure for case of power series conformal mapping function
23 p4275 A70-44944

CANTILEVER MEMBERS
NT CANTILEVER BEAMS
NT CANTILEVER PLATES
Cantilevered and doubly supported structures calculated for critical aeroelastic divergence speed resulting from lift and drag
01 p0200 A70-10551

Cantilever cylindrical shell stability under shearing stresses created by transverse force applied to free end
07 p1403 A70-19116

Rotating parabolic mirror /antenna/ cantilever suspension rigidity with emphasis on rigidity of central bushing
08 p1586 A70-21056

Natural vibration analysis of uniform cylindrical and cantilever rectangular tubes with cutouts
10 p1961 A70-25057

Flutter characteristics of uniform cantilever wing with concentrated inertias using Direct Matrix method
10 p1963 A70-25071

Natural frequencies of thin cantilever cylindrical shells, using Flugge equations of motion and Rayleigh-Ritz method
11 p2146 A70-26704

Lateral motions of vertical uniform tubular cantilever conveying fluid, considering oscillatory instability at high flow velocities
13 p2511 A70-28741

Natural vibrations frequency of tubular cantilever pipe with fluid flow, solving differential equation of motion by Ritz method
14 p2567 A70-31426

Cantilevered tube conveying fluid, calculating forced vibration under time dependent loading and arbitrary initial conditions
22 p4010 A70-42650

Undamped elastic cantilever column with concentrated masses, considering transition from stability to divergence under nonconservative forces
24 p4421 A70-45286

CANTILEVER PLATES
Vibration frequencies and modal shapes for square and rhombic cantilever plates with diamond cross section, including commercial resonance test system
01 p0199 A70-10122

Finite element bending stiffness matrices for deflections analysis of pretwisted cantilever plate subjected to static loads
02 p0384 A70-11858

Finite element method for calculating natural frequencies and mode shapes of pretwisted cantilever plates assembly of flat triangular elements
02 p0384 A70-11859

Nonsymmetric planform cantilever plate apparent mass, material properties and geometrical changes effect on vibration frequency

07 p1403 A70-19058
Flutter instability critical velocity and frequency for thin cantilevered plate with follower jet determined by Galerkin and computer simulation

12 p2316 A70-27106
Tapered cantilever Al plate load characteristics, determining elastic and plastic strain due to regular, reverse and second regular deflection sequence

15 p2821 A70-32307
Homogeneous orthotropic cantilevered rectangular plate with reinforcing ribs, calculating flutter in supersonic gas flow

18 p3336 A70-36140
Low aspect ratio cantilever plate wings supersonic bending torsion flutter speed calculation, using spanwise and chordwise variables and potential energy principle

22 p4112 A70-42276
Elastic bar attached to free edge of infinite length cantilever plate, calculating free flexural vibration for comparison with experiment

22 p4114 A70-42648
Cantilever plate random vibration response, calculating eigenvectors and natural frequencies by finite element method

23 p4270 A70-44591

CANTILEVER WINGS

U WINGS

CAPACITANCE

Equivalent circuit for trapped energy resonators and calculations of capacitance ratios for straight crested waves

01 p0088 A70-10777
Tracking method for simultaneously tuned transmitter and receiver with different maximum-to-minimum capacitance ratios in ganged variable capacitors

01 p0051 A70-10888
Shielded multiconductor transmission line capacitance calculated by integral equations with Green function kernel

05 p0820 A70-16383
Oscillatory discharge properties of capacitance power storage circuit used for pumping pulse lasers

06 p1081 A70-17768
DC capacitance measurement based on capacitor discharge using auto-oscillatory macrocharge system variant as transducer of measured capacitance, time constant and insulation resistance

11 p1982 A70-25576
Electron-hole transitions in GaAs obtained by sulfur diffusion, noting capacitance dependence on voltage at 293 and 77 K at various frequencies

12 p2287 A70-27481
Air-damped capacitance accelerometers and velocimeters in data acquisition systems using signal processing

13 p2405 A70-28813
Binary varactor diode microwave device, displaying two capacitance values in reverse bias operation for application in phased array systems and frequency control

14 p2556 A70-30919
Fluidic systems linear lumped components design with allowance for energy factor Q, investigating capacitance and inductance

15 p2678 A70-32675
MOS structures deep depletion capacitance/voltage characteristics by ramp response method

19 p3389 A70-37972
Nonlinear LC circuit with p-n junction capacitance, examining relaxation vibrations during automatic biasing

20 p3596 A70-38970
Degenerate p-n diode junction capacitance calculation, taking into account quantum and temperature effects

20 p3596 A70-39117
Pulsed coaxial plasma accelerator efficiency, examining high capacitance and axial propellant pressure gradients

20 p3693 A70-40250
Integrated directly coupled gyrator operating mode via comparison with switching elements, considering behavior under capacitance load and high pass filter application

21 p3797 A70-40793
Miniature avalanche MOS diode, investigating capacitance voltage characteristics of deep depletion regime

23 p4172 A70-44007

CAPACITIVE FUEL GAGES

Aircraft capacitive fuel gage improvement by integration with flowmeter system, DC torquer display and digital techniques, considering other measurement principles

21 p3821 A70-40619

CAPACITORS

Tracking method for simultaneously tuned transmitter and receiver with different maximum-to-minimum capacitance ratios in ganged variable capacitors

01 p0051 A70-10888

Ceramic capacitors selection considering ionization, third harmonic and HF heating control properties

09 p1642 A70-22003

Charged particle self oscillatory motion in plane condenser field, applying results to electrical measuring instruments theory

09 p1680 A70-23144

Thin film capacitive bolometer dependent on temperature sensitivity derived from electron trapping effects

09 p1683 A70-23509

DC capacitance measurement based on capacitor discharge using auto-oscillatory macrocharge system variant as transducer of measured capacitance, time constant and insulation resistance

11 p1982 A70-25576

RF admittance and electric field of plane grid capacitor in hot collision free magnetoplasma in parallel magnetic field dominated by Bernstein modes

13 p2467 A70-29910

Sawtooth waveform generator using linear discharge of capacitor

15 p2714 A70-32701

Ripple filters for DC power supplies using reliable small capacitance capacitors suitable for spacecraft applications

15 p2714 A70-32806

Matrix condenser for tuning hybrid thin film self excited quartz oscillator with common base transistor configuration, discussing electrical properties and fabrication

20 p3597 A70-39257

Electrolytic capacitor current pulse networks for quasi-steady MPD arc thrusters, determining series resistance effects on energy transfer

[AIAA PAPER 70-1082]

20 p3568 A70-40253

Sheaths effect on capacitance of plane grid capacitor in plasma, discussing satellite aerials admittance

21 p3792 A70-42046

CAPACITY

Capacity bounds in microwave filters computed for periodic cylindrical rods between parallel ground planes using variational principles

10 p1850 A70-24834

CAPE KENNEDY LAUNCH COMPLEX

Cape Kennedy vertical wind speed profiles measured by spectral analysis using fast Fourier transform method

02 p0325 A70-12285

Apollo/Saturn 5 Kennedy Launch Complex 39 /LC-39/ physical characteristics emphasizing high launch rate capability, economy of operation and superior flexibility

[SAE PAPER 690714]

05 p0825 A70-15853

Boundary layer atmospheric turbulence at Kennedy Space Center obtained for engineering spectral model, discussing energy balance

10 p1911 A70-23926

Cape Kennedy peak wind profile probabilities at 10-150 meters for various exposure times

14 p2607 A70-30581

CAPILLARIES

Vapor capillary /melt/ depth in electron beam welding, considering electron energy, radiative dissipation, etc

21 p3833 A70-41124

CAPILLARIES (ANATOMY)

Radial immunodiffusion for serum proteins quantitation adapted to capillary blood and compared with results for venous blood

07 p1214 A70-19932

Permeability disturbances in skin capillaries of rabbits and rats following exposure to Sr90-Y90 beta radiation

09 p1619 A70-22789

Critical oxygen supply of cerebral mitochondria and intercapillary oxygen transport

10 p1821 A70-25080

High altitude acclimatization effect on tissue capillarity, investigating physiological evidence in rats by tissue diffusing capacity measurement

10 p1823 A70-25220

Capillary details in lentiform nucleus region of human brains, measuring blood vessels diameters, lengths and densities

12 p2173 A70-28347

Peripheral vasculocapillary blood circulation by television UV capillaroscopy and electronic finger plethysmography

19 p3370 A70-38212

Lung alveolar and capillary wall structure in mammals under normal conditions, transverse acceleration and mechanically changed pulmonary circulation

20 p3575 A70-40190

CAPILLARY CIRCULATION

U CAPILLARY FLOW

CAPILLARY FLOW

Biomechanics of microcirculation, discussing rheological characteristics of blood, erythrocyte and vessel wall, hydrodynamics of erythrocyte-shaped bodies mathematical models, etc

01 p0039 A70-11160

Capillary blood flow, discussing red blood cells deformation, motion, pressure drop and plasma flow /bolus/ between red cells

02 p0238 A70-12545

Time varying blood flow in pulmonary capillaries affecting overall diffusing capacity and alveolar-arterial oxygen tension gradient

03 p0421 A70-15770

Laminar capillary jet of viscoelastic fluid, discussing breakup, nonNewtonian jet stability and elastic properties

03 p0468 A70-13782

Myocardial blood flow in patients with acute myocardial infarction determined from measuring effective capillary flow /ECF/ by direct counting of rubidium 86 uptake

04 p0636 A70-15468

Ultraminiature pressure sensor for continuous recording of hydrostatic pressure in renal tubules and blood capillaries

05 p0804 A70-15772

Capillary grooves effect on surface wetting and evaporation using heat transfer coefficients for grooves with triangular, semicircular and square cross sections

[ASME PAPER 69-HT-19]

09 p1790 A70-23559

Vertical liquid jets capillary instability under audio frequency disturbances, measuring disturbance growth rates for various wavelengths and fluid viscosities

09 p1664 A70-23678

Partial oxygen pressure in hyperemic earlobe capillary blood under hypoxic conditions, noting correlation with age and body weight

10 p1822 A70-25088

Human peripheral blood circulation during prolonged underwater activity, showing compensation for high humidity, noise levels, low water temperatures, isolation and confinement

10 p1822 A70-25178

Capillary barriers to provide propellant positioning, expulsion capability and slosh dampening for spacecraft propulsion systems during rotational maneuvers

[AIAA PAPER 69-529]

11 p2123 A70-26119

Meniscus curvature correlation to viscosity contrast in capillary during fluid displacement

13 p2390 A70-29633

Hybrid computer simulation of steady state oxygen transport and consumption in capillary-tissue system

15 p2694 A70-32845

Spacecraft propellant expulsion systems, comparing capillary with conventional techniques

[AIAA PAPER 70-685]

16 p2962 A70-33584

Capillary ball game phenomenon under weightlessness, showing photographs of mercury droplet reflection from fluid boundary

18 p3242 A70-36638

Viscous dielectric incompressible fluid cylinder capillary stability under small axisymmetric disturbances and axial electric field, deriving perturbed fluid flow equations

19 p3406 A70-38351

Narrow capillary supermolecular flow density relation to vapor molecule specular reflection, considering Knudsen flow conditions

24 p4381 A70-45491

Subminiature transistor photosensor for direct measurements of capillary blood cell motion

24 p4309 A70-46119

CAPILLARY TUBES

Thermally ionized cesium plasma viscosity at high temperatures in vacuum using capillary tube assembly

11 p2092 A70-26731

Electrocapillary transducers filled with mercury and electrolyte solution for vibration measurement, analyzing seismic operation character

12 p2235 A70-27684

Gas transfer through silicone elastomer capillaries wall in variable pressure chamber

14 p2541 A70-30386

Low noise He-Ne laser with capillary elements, measuring current threshold of noise free operation as function of design parameters

19 p3448 A70-38512

One-step closure sealing of pressurized stainless steel capillary tubes by resistance pinch welding

21 p3832 A70-40789

Capillary boiling and heat transfer for coolant fluids, using motion photography and visual observations

23 p4277 A70-44320

CAPILLARY WAVES

NT BAROCLINIC WAVES

NT GRAVITY WAVES

Stimulated light scattering by capillary waves on incompressible fluid surface or by Rayleigh waves on surface of isotropic solid body with small optoelectronic moduli

16 p2951 A70-33195

Liquid He surface layer thickness as function of temperature, considering capillary waves effect due to gravity

16 p2952 A70-33288

CAPSULES

Pressure and velocity ratios and energy requirements dependence on flow parameters of cylindrical capsule in horizontal pipeline

09 p1665 A70-23747

CAPSULES [SPACECRAFT]

U SPACE CAPSULES

CAPTIVE TESTS

NT STATIC FIRING

NT STATIC TESTS

Ground environmental simulation test for captive carrying cycling of air launched missiles

CAPTURE CROSS SECTIONS

U ABSORPTION CROSS SECTIONS

CAPTURE EFFECT

Sun-planet systems capture and catapult capacity for interstellar bodies under close flyby conditions

Jupiter capture of comets with parabolic orbits taking into account solar gravitational influence

Vacuum deposited thin cadmium sulfide films semiconducting properties, discussing captured free carriers effects on temperature dependence of dark and photo current

Capture and gravity gradient stabilization of LIDOS satellite in eccentric orbit

Neutron formation multiplicity during capture of cosmic ray muons by Zn and Sb nuclei, noting agreement with one-third law

Saturation homogeneity ascribed to resonant photon capture in emission of neon laser

Neutron capture effects in Gd from Norton County meteorite by isotopic composition analysis

Gas laser active medium nonlinear polarizability calculations with allowance for resonance emission capture effect on atomic velocity and population distributions

Solar neutrino fluxes, calculating capture rates and primordial helium abundance

Semiconductor capture level parameter determination, using thermostimulated conductivity

Ion-molecule pair relative motion in capture collisions, using computer-made movies

Capture coefficients and reflected flux measurements for gaseous nitrogen molecular beams impinging on solid nitrogen cryodeposit surface

CAPTURED AIR BUBBLE VEHICLES

Heaving and pitching motion analysis of wave action-induced pressure gradients in captured air bubble /CAB/ ship bubble chamber, discussing fan system design

[ASME PAPER 69-WA/AV-6]

CARBAMATES [TRADENAME]

NT URETHANES

CARBIDES

NT BORON CARBIDES

NT CEMENTITE

NT CHROMIUM CARBIDES

NT MOLYBDENUM CARBIDES

NT NIOBIUM CARBIDES

NT SILICON CARBIDES

NT TANTALUM CARBIDES

NT TITANIUM CARBIDES

NT TUNGSTEN CARBIDES

NT VANADIUM CARBIDES

NT ZIRCONIUM CARBIDES

Tungsten effect on phase transformations and carbide reactions to attain equilibrium at 850 C in Ni-base superalloys

B-C alloys chemical composition effect on high temperature stability in pure oxygen

Carbide rupture energy in wear resistant alloys during abrasion, considering metallographic data and energy parameters

Neutron irradiation and annealing effects on lattice constants of titanium and chromium carbides analyzed for X ray diffractions

Single crystal carbides as high temperature structural materials, noting titanium carbide properties and strength-to-density ratio of B-doped crystals

Carbide layer formation on Ta and Ta-W alloys, discussing Ta-C phase diagram and phases

Microhardness of transition metals carbides measured after hot compression, suggesting dependence on statistical weight of C atoms with stable sp³ configurations

Zr, Ti, Nb and Ta carbides deposition from metal chloride, methane, hydrogen and argon mixture, studying gas concentration and temperature effects on deposition rate

Chemical compositions and structure of carbides in Fe-W-C and Co-W-C systems, clarifying eta phases

Carbide-strengthened Mo alloys dynamic strain aging processes

Methane and ethane released from Apollo 11 lunar samples by crushing or acid treatment, suggesting carbides hydrolysis as main source

Carbide precipitation in metastable beta-Ti alloys, noting precipitations confinement to grain boundaries in alloys containing 15 percent Mo

Portevin-Le Chatelier effect in carburized nickel and Ni-Co alloys, discussing carbide stability and carbon diffusion roles

Ablative composites containing in situ reaction formed refractory metal carbides

Vapor pressures and dissociation energy of yttrium dicarbide and tetracarbide over extended temperature, measured by Knudsen double focusing spectrometer

Metal matrix alloys with base of Co, Fe or Ni reinforced by transition metal carbide fibers, discussing deformation tests at various temperatures

Carbide precipitation and grain boundary migration in solution annealed duplex stainless steel as function of aging time

Mo alloying additions effects on carbide phases in Nb-C alloys

Si-carbide composites electrical conductivity from temperature and thickness dependence, obtaining volt-ampere characteristics via computer method

Pyrolytic carbide protective coating deposition from gaseous phase on spherical particles in boiling layer

CARBOHYDRATE METABOLISM

NT HYPOGLYCEMIA

Carbohydrate-phosphorus metabolites content in gophers brains under normal conditions during hypothermia and spontaneous warming at room temperature

Lipid and carbohydrate behavioral abnormalities in patients with angiographically documented coronary artery disease observed by glucose tolerance tests

Fructose metabolism in liver and extrahepatic tissues of sea level and high altitude natives, noting lactate and pyruvate accumulation in blood

Phagocytic activity and carbohydrate metabolism in peripheral blood neutrophils of men exposed to atmosphere with increased O₂ content, noting neutrophil energy exchange disorder role

Quantitative and qualitative differences in enzyme levels of intermediate carbohydrate metabolism in obligate autotrophs *Thiobacillus thioautotrophicus* and *Thiobacillus neapolitanus*

Z axis acceleration and high temperature effects on guinea pig carbohydrate metabolism, discussing blood and muscle tissues composition

Sialic acids metabolic behavior in cerebrium, liver, myocardium and blood plasma of rats after X ray irradiation

Carbohydrate metabolism disorders in head injury cases, comparing incidence with EEG abnormalities

Anaerobic carbohydrate metabolism in aging individuals under physical loads

Glucose metabolism in chickens under chronic centrifugal acceleration, meeting increased energy requirements

CARBOHYDRATES

NT ADENOSINE DIPHOSPHATE [ADP]

NT ADENOSINE TRIPHOSPHATE [ATP]

NT ADENOSINES

NT CELLULOSE

NT CHOLINE

NT CITRIC ACID

NT FATS

NT GALACTOSE

NT GLUCOSE

NT GLUCOSIDES

NT GLYCOGENS

NT LACTOSE

NT MONOSACCHARIDES

NT NUCLEOSIDES

NT POLYSACCHARIDES

NT SUGARS

Sweet potatoes productivity and nutritive value as carbohydrates source in manned space flights

Physicochemical methods of producing formaldehyde for carbohydrate synthesis in life support systems

Synthetic carbohydrates effects on *A* type clostridium perfringens, observing bacterial mass growth and protein elimination

Penicillium mutant chemical stress tolerance in boric acid and potassium chloride selective media, studying carbohydrate and inosine-5-phosphate effects on growth rate

Radial acceleration effects on tissue carbohydrate in starved female rats, observing blood glucose increase and muscle glycogen levels decrease

Physicochemical methods of producing formaldehyde for carbohydrate synthesis in life support systems

Synthetic carbohydrates effects on *A* type Clostridium perfringens, observing bacterial mass growth and protein elimination

CARBON

NT CARBON ISOTOPES

NT CARBON 12

NT CARBON 13

NT CARBON 14

NT CHARCOAL

Assimilation and metabolism of C atoms of pyruvate and acetate by strict autotrophs *Thiobacillus* cell, using radioactive substrates

Mechanical properties of carbon fiber reinforced Al, Cu and Ni, noting rope and wire applications

High strength high modulus carbon fibers for use in structural reinforced plastics, describing carbonizing and pyrolysis processes

B and C fiber unidirectionally reinforced plastic composites, discussing mechanical properties, fabrication and testing

IR spectra of four carbon stars and Sirius obtained with Michelson interferometer, indicating diatomic carbon and CO bands

Triggered spark source for multiply charged carbon ions applied to collision cross section measurements

Serrated plastic flow in stable austenitic stainless steels based on Fe/Ni, showing strength dependence on C and/or Cr presence

Carbon effect on high temperature elasticity modulus and long term hardness of Nb, indicating diffusion enhancement and counteractive Zr addition

Carbon fiber reinforced plastics /CFRP/ uses in commercial aircraft structural component

Carbon materials manufacture, properties and applications in space technology, discussing carbon fibers, textiles, graphite, pyrolytic carbon, composites and vitreous carbon

Vacuum UV flash photolysis of carbon suboxide, noting pressure dependent reaction rates of carbon atoms with various gases

Porosity in graphitized polyacrylonitrile-based carbon fibers determined from surface area increase during heat treatment in vacuum

Activated carbons and ion exchange resins bactericidal action as function of silver coating techniques

Carbon atom RF recombination lines evaluated for conditions in H II regions and planetary nebulae

Ablation chars, carbon and graphite spectral emittance and reflectance as function of wavelength and temperature, noting applications to atmospheric entry heat shielding

Binary system Mo-C determined in temperature range 1250-2270 C, using microscopic and thermal analyses and microhardness testing

Diatom carbon swan band violet line absence from sunspot suggested in accordance with molecular equilibrium predictions

Stress distribution in restrained hyperelastic sphere based on elastomer reinforcement theory by carbon black

Carbon fiber-reinforced plastics fabrication, discussing leaky mold, prepeg and filament winding methods

C V lines measured near 1s-2p line of C VI, identifying lines belonging to various transitions

05 p0921 A70-16982

Carbon fiber structural model agreeing with experimental results

06 p1092 A70-18025

Quasi-steady radially symmetric theory of liquid drop vaporization and homogeneous combustion extended to burning of solid carbon spheres gasified by chemical attack

07 p1419 A70-18915

Carbon particles formation and growth model for cool variable carbon star atmosphere with sinusoidal carbon star atmosphere with sinusoidal temperature variations

07 p1380 A70-19260

Carbon particles formation and growth in Mira variables atmospheres, considering extinction effects on stellar structure and appearance

07 p1380 A70-19261

Fabrication and properties of carbon fibers and carbon fiber reinforced epoxy resins

07 p1318 A70-19772

Compatibility of single metal coated carbon fibers, discussing structural recrystallization in contact with Ni or Co matrix by dissociation/diffusion/precipitation mechanism

07 p1315 A70-20048

Stress wave propagation in particulate loaded carbonaceous materials induced by homogeneous laser beam

07 p1302 A70-20097

Carbon-bearing materials for modification of Mg-Al-Zn-Mn alloys filtration processes

08 p1505 A70-21132

Carbon fiber composite materials production technology, physical properties and potential applications in aerospace

08 p1527 A70-21520

Test methods for evaluating tensile, compressive, interlaminar shear and bearing strength properties of carbon yarns and flat and tubular composites

08 p1529 A70-21881

Mechanical properties characterization of unidirectional high modulus carbon fiber reinforced epoxy matrix composite

08 p1530 A70-21883

Carbon deposit formation in gas turbine engines with various fuels, studying thermal insulation properties

09 p1742 A70-22472

Combined solubility of group IVA metals and carbon in solid state molybdenum at various temperatures

09 p1704 A70-22754

Carbon fibers and fiber-reinforced composites fabrication, structural properties and uses

09 p1710 A70-22758

Oxygen reduction in sulfuric acid with phthalocyanine-carbon catalysts

10 p1829 A70-24456

Catalytic load carrying capacity of porous carbon electrodes impregnated with nickel salt and nickel boride in anodic fuel cell hydrazine oxidation

10 p1831 A70-24469

Carbon composition resistors investigated for cause of resistance dependence on thermal pulses, suggesting application as stabilization process

10 p1849 A70-24617

Vacuum condensed thin carbon films graphitization stages using electron diffraction

11 p2068 A70-25381

High strength glassy carbon fibers obtained by carbonizing extruded phenol hexamine polymers

11 p2071 A70-26672

Variable reproducible black radiator of resistance heated carbon tube designed for temperatures between carbon glowing and sublimation point

12 p2329 A70-27090

Rotational, vibrational and equilibrium molecular constants for Phillips system of diatomic carbon

12 p2275 A70-27174

Carbon in austenite derived from composition dependence of diffusivity using first order mixing statistics

12 p2256 A70-27611

Recrystallization effect on 3-D graphite orientation in carbon fibers under high temperature heat treatment

12 p2259 A70-27720

High modulus carbon fibers low angle X ray diffraction correlation to physical properties

12 p2259 A70-28050

Gas temperature effects on aerodynamic drag of carbon particles burning during nonisothermal motion

13 p2520 A70-28582

Wool felt based carbon and graphite composite materials for orthogonally isotropic high shear strength compared with rayon felt based composites

13 p2437 A70-28776

Synthetic foam material of hollow carbon microsphere fillers embedded in high compression strength epoxy resin matrix

13 p2437 A70-28780

First order statistical model for temperature dependence of carbon activity in austenite

13 p2436 A70-29605

Carbon and sulfur reactions with solar hydrogen atoms in Apollo 11 lunar samples accounting for isotopic composition of fine-grained basaltic rocks

14 p2545 A70-30791

Lattice resolution of layer planes in polyacrylonitrile based carbon fibers ground and dispersed by ultrasonic irradiation

14 p2598 A70-30793

Colloidal filler /carbon black/ reinforced rubber for various applications, noting fabrication into composite material

15 p2764 A70-31930

Carbon-graphite porous materials thermal conductivity at various temperatures

15 p2765 A70-32141

Carbon reinforcing fibers, discussing mechanical properties, production, cost reduction, etc

15 p2765 A70-32246

Air pollution by turbojets and gas turbines, discussing control of carbon particles and nitrogen oxides

16 p2963 A70-32922

Carbon ground state correlation energy calculation, emphasizing assessment of truncation error sources

16 p2954 A70-33277

Synthetic foams of high filler content, low density, high compression strength and hydrolytic stability using hollow carbon microspheres in epoxy resin matrix

16 p2936 A70-33365

Carbon fiber reinforced plastics potential as fatigue resistant materials

16 p2936 A70-33367

Venus upper atmosphere carbon atoms detection based on low resolution spectra analysis of solar illuminated atmosphere

16 p2979 A70-34036

Ultrahigh strength alpha-beta titanium alloys, examining carbon and oxygen effects on mechanical properties

17 p3121 A70-34429

UV stellar spectra absorption, considering silicon and carbon opacity effect on Balmer discontinuity and Paschen continuum

17 p3159 A70-34880

Solar C II resonance doublet profiles, discussing possible broadening mechanisms

17 p3174 A70-35862

Ultrasonic irradiation effects on steel hardenability and carbon diffusion rate during annealing, noting microstructure

18 p3273 A70-36049

Silicon-containing pyrocarbon, relating microhardness to microstructure

18 p3279 A70-37220

Ti and C effects on Fe-Cr-Ni alloys mechanical properties

19 p3449 A70-37271

Carbon effect on high temperature elasticity modulus and long term hardness of Nb, indicating diffusion enhancement and counteractive Zr addition

19 p3453 A70-38470

Carbon composite technology - Conference, University of New Mexico, January 1970

20 p3652 A70-39201

Composite technology effects on engineering design, emphasizing carbon-carbon materials for aircraft structural weight reduction, performance improvement and high temperature applications

20 p3653 A70-39202

Unidirectional carbon fiber reinforced plastics /CFRP/ interlaminar shear strength measurements using short beam shear, notch overlap and solid rod torsion methods

20 p3653 A70-39203

Carbon/carbon composites constituent characteristics effects on thermal and mechanical properties, using polarized light and scanning electron microscopy

20 p3653 A70-39204

Chemical vapor deposition of carbon matrix material in fiber structure, investigating thermodynamic fundamentals in processes

20 p3654 A70-39207

Carbon fiber/carbon matrix composites fabrication by isotropic casting, flock and spray lay-up and pulp molding, describing physical and mechanical properties

20 p3636 A70-39208

Shaping methods for filament wound carbon structures, emphasizing matrix building by chemical vapor deposition

20 p3636 A70-39209

Unidirectional and multidirectional carbon/carbon composites quality and performance evaluation by NDT methods, including X ray radiography, ultrasonic test, pulse echo mapping, etc

20 p3654 A70-39211

Laser holography for nondestructive testing of C composite structures, reducing fringe patterns to radial deformation and surface strain for cylinders and cones

20 p3718 A70-39212

Carbon/carbon composites thermal and mechanical properties measurements by NDT including image transducer, IR scanning and ultrasonic methods

20 p3636 A70-39213

Carbons and graphites ablation tests for predicting performance under reentry conditions, considering microstructure effects

20 p3735 A70-39214

Carbon resistors negative magnetoresistance measurement near absolute zero temperature by helium cryostat, noting anisotropy

20 p3687 A70-40168

Dynamic response of distended carbon materials to shock loading defined by measuring equation of state, unloading behavior and spallation strength

20 p3657 A70-40263

Boron vs carbon fiber reinforced plastics, discussing layer and panel structures, molded and mechanical sections, preimpregnation, cost and structural concepts

21 p3842 A70-41263

Apollo 11 lunar rocks and soil hydrogen, C and Si concentration and isotopic composition

21 p3774 A70-41568

Carbon and sulfur concentration and isotopic variations in Apollo 11 fines, breccias and fine-grained basalts

21 p3775 A70-41586

Carbon and nitrogen abundances in Apollo 11 rocks, basaltic achondrites and terrestrial basalts, using meteorite analytical techniques

21 p3776 A70-41592

Graphite and carbon fiber surfaces, correlating Raman spectrum and shear strength of composite

22 p4060 A70-43680

Mars atmospheric nitrogen abundance relative to carbon from spacecraft UV spectrometer data

23 p4238 A70-43805

Carbon ionization equilibrium in dense interstellar clouds, discussing grains and neutral atoms attenuation effects

24 p4402 A70-45387

Diffusive carbon redistribution in Mo during interaction with Ni and Cr protective coatings

24 p4364 A70-46334

CARBON COMPOUNDS

NT BORON CARBIDES

NT CARBIDES

NT CARBONATES

NT CEMENTITE

NT CHROMIUM CARBIDES

NT MOLYBDENUM CARBIDES

NT NIOBIUM CARBIDES

NT POLYCARBONATES

NT SILICON CARBIDES

NT TANTALUM CARBIDES

NT TITANIUM CARBIDES

NT TUNGSTEN CARBIDES

NT VANADIUM CARBIDES

NT ZIRCONIUM CARBIDES

CH and CD molecules UV absorption spectra, using flash photolysis of diazomethane

02 p0341 A70-11795

Vacuum UV flash photolysis of carbon suboxide, noting pressure dependent reaction rates of carbon atoms with various gases

04 p0645 A70-14391

Mars surface reddish color due to carbon suboxide suggested based on spectral reflectivity measurements and matching in laboratory

04 p0743 A70-14423

Venus clouds absorption spectra correlation with carbon suboxide frost reflection spectra, suggesting absence of carbon suboxide in atmosphere

08 p1571 A70-20911

Carbon compounds composition and origin in Apollo 11 lunar samples using pyrolytic chromatography and microscopy at elevated temperature

10 p1941 A70-24531

CH molecule line formation mechanism for 4300 Å transition in solar photosphere, noting collisions with hydrogen atoms

12 p2311 A70-28309

Pressure effects on quantum yields of carbon trioxide formation in gas phase ozone photolysis with carbon dioxide

16 p2856 A70-33653

Pressure dependence and efficiency of carbon trioxide formation in Mars and Venus atmospheres

21 p3887 A70-41107

Apollo 11 lunar fines carbon level, finding largest component carbon monoxide in complex form

21 p3778 A70-41621

Apollo 11 lunar samples organic carbon content analysis by pyrolysis hydrogen flame ionization detection

21 p3779 A70-41624

Apollo 11 lunar fines carbon compounds, examining chemical state of porphyrins, fatty and amino acids, purines, pyrimidines and carbohydrates, etc

21 p3779 A70-41625

Chemical etching for revealing structure of carbon-graphite materials subjected to different graphitization stages

23 p4209 A70-44045

CARBON DIOXIDE

- Venus upper atmosphere average rotational temperature determined from high dispersion spectroscopic observations of 7883 A carbon dioxide band
01 p0184 A70-10912
- Carbon dioxide refractivity measured under simulated Martian conditions and standard temperature and pressure, comparing results with radio occultation methods
01 p0186 A70-11085
- Vibrational relaxation times in carbon dioxide and carbon dioxide-argon mixtures at 360-3000 K, using shock tube and laser schlieren method
01 p0148 A70-11355
- Carbon dioxide temperature distribution, absorption and concentration as functions of molecular dissociation behind shock wave determined by measuring IR bands intensity
01 p0069 A70-11623
- Be oxidation in carbon dioxide at high temperatures, explaining observed kinetic discontinuity in terms of oxide morphology
01 p0124 A70-11638
- Spinal cord blood flow response to carbon dioxide partial pressure in anesthetized goats
02 p0232 A70-11713
- Photoelectron energy spectra and partial photoionization cross sections for carbon dioxide determined with spectrometer at monochromatic incident radiation wavelengths
02 p0343 A70-11903
- Martian topographic contours determined from detected carbon dioxide abundances indicating large scale differences from previous data
02 p0373 A70-12390
- Temperature dependence of diffusion coefficient for carbon dioxide filled rigid polyurethane foam, using Fick law
02 p0321 A70-12524
- Atomic oxygen reaction with carbon dioxide and carbon dioxide dissociation in shock waves, using nitrous oxide decomposition for oxygen source
03 p0440 A70-13578
- Carbon dioxide supersonic flows, describing numerical integration procedure for chemical and vibrational relaxation
03 p0440 A70-13743
- Molecular hydrogen destruction by reaction with carbon dioxide ion in Martian ionosphere, discussing conversion into atomic hydrogen
03 p0575 A70-13997
- Xenon sensitized photolysis of carbon dioxide compared with direct photolysis at 1470 A resonance line
03 p0441 A70-14005
- Potential energy surface shapes for lowest states of temporary negative ions of nitrous oxide and carbon dioxide
03 p0441 A70-14008
- LF sound velocity measurement in carbon dioxide near critical point, noting existence of logarithmic divergence
04 p0718 A70-14685
- Ion-neutral reactions in carbon dioxide subjected to electron impact using mass spectrometry
04 p0646 A70-14698
- Integrated intensity measurements of carbon dioxide bands in micron regions, using self-broadening method
04 p0690 A70-15025
- Solid carbon dioxide measured for complex index of refraction at IR wavelengths
04 p0719 A70-15036
- Carbon dioxide electron impact cross sections, analyzing discrete excitation, autoionization, direct and dissociative ionization and use to aeronomy
04 p0722 A70-15121
- Time dependent transmission of carbon dioxide in air flowing through molecular sieve adsorber beds, developing and programming weighted least squares analysis
04 p0786 A70-15315
- Venus-earth carbon dioxide atomic parameters used to determine ionization and optical emission rates in Venus upper atmosphere resulting from solar cosmic rays
05 p0901 A70-16276
- High resolution Venus spectra, obtaining band spectra growth curve of C13O16O18 isotope of carbon dioxide, comparing data reduction methods
05 p0910 A70-16392
- Mariner 6 and 7 missions IR spectrometric records showing evidence of solid carbon dioxide in Martian upper atmosphere
06 p1137 A70-17194
- High fidelity simulations for environmental stress evaluations, describing carbon dioxide effects on pilots simulated ground target tracking and reentry vehicle landing
06 p0999 A70-17291
- Carbon dioxide effect on oxygen uptake during hyperventilation in normal man
07 p1205 A70-19294
- Hydrogen fluoride fundamental vibration rotation band spectral line shift and broadening due to carbon dioxide
07 p1337 A70-19365
- Spectral reflectance of carbon dioxide and water frosts at 0.8-3.2 microns, growing frosts in cold vacuum chamber from high purity gases
07 p1388 A70-19945
- Carbon dioxide adsorption and desorption in Martian bright areas, discussing assumptions relative to temperature, pressure and dust adsorption
08 p1579 A70-21566
- Relative rotational lines intensities of carbon dioxide, considering sigma-sigma transitions for abundant isotopes
08 p1549 A70-21575
- Carbon dioxide molecules dissociation along tube length, measuring temperature drop behind shock front at various pressures and 4300 K
09 p1730 A70-22172
- Temperature effects on IR absorption by water and carbon dioxide vapors measured in narrow spectral intervals
09 p1666 A70-22180
- Carbon dioxide photochemistry of Mars atmosphere, noting complications due to hydrogen compounds
09 p1763 A70-23483
- Blood carbon dioxide and oxygen content determined by respiration mass spectrometer using carrier gas
09 p1629 A70-23584
- Modified apparatus for volumetric determination of alveolar carbon dioxide as indicator of pilot hypernea
10 p1825 A70-24503
- Carbon dioxide dissociation effects on refractive index gradients and decay rates in pulsed carbon dioxide-nitrogen laser mixture
10 p1900 A70-24602
- Hydrogen, oxygen and carbon dioxide in off-gas stream from nuclear reactor experiment using on-line gas chromatography
11 p1994 A70-25615
- Real gas adiabatic lapse rate applied to Venus atmosphere assumed to consist of pure carbon dioxide
11 p2107 A70-25646
- Carbon dioxide fixation in hydrogenomonas eutropha determined from titrating liquid culture with carbon dioxide, showing dependence on oxygen content in gas mixture
11 p1991 A70-25940
- Radiative intensity calculations for carbon dioxide and carbon dioxide-nitrogen plasmas for various temperatures, densities and path lengths, computing UV and continuum spectra
12 p2275 A70-27170
- Spectral absorption characteristics for C atom radiative processes in carbon dioxide-nitrogen mixtures at high temperatures corresponding to Venusian atmosphere
12 p2275 A70-27317
- EHF microwave absorption in compressed carbon dioxide, measuring dielectric loss as function of gas density
12 p2273 A70-27571
- Graphite-carbon dioxide interaction at high temperatures in presence of solid phase diffusion from bulk to reacting surface
13 p2520 A70-28581
- IR spectroscopy, determining relative populations of carbon dioxide vibrational energy levels by comparing emission intensities
13 p2455 A70-29131
- Carbon dioxide molecular vibrational energy levels above carbon monoxide-oxygen premixed flame, discussing vibration modes leading to population inversion and relaxation time variance
13 p2455 A70-29132
- Carbon dioxide jet plumes condensation on model nozzle in vacuum chamber, noting particle size and growth rate
13 p2523 A70-29983
- Venus carbon dioxide absorption bands determining atmospheric scattering model suitability for all data
14 p2642 A70-30889
- Spacecraft measurements revealing hot dense Venusian and cold thin Martian carbon dioxide atmospheres
14 p2646 A70-31066
- Average rotational temperature of Venus atmosphere above cloud tops from carbon dioxide band spectroscopy
14 p2650 A70-31219
- Temperature dependence of laser emission line self broadened half widths in spectral band of carbon dioxide at constant pressure
15 p2752 A70-32056
- Power plant using carbon dioxide planetary atmosphere as working fluid, noting weight reduction
15 p2828 A70-32262
- Martian soil thermal conditions at south pole, considering polar cap annual variations and carbon dioxide sublimation
15 p2802 A70-32492
- Ventilatory response to carbon dioxide in goats during acute and chronic hypoxia
15 p2684 A70-32539
- High temperature reaction kinetics between oxygen difluoride and CO in shock tube, discussing carbon dioxide formation
16 p2855 A70-33010
- Carbon dioxide output monitoring from biosatellites for circadian system behavior in closed organism-environment systems
16 p2849 A70-33992
- Underexpanded carbon dioxide free jet expanding into vacuum from conical nozzles
17 p3070 A70-35246
- Carbon dioxide electric discharge dissociation producing oxygen molecules
17 p3138 A70-35588
- Flux emissivity tables for water vapor, carbon dioxide and ozone based on wavelength dependent absorption coefficients and flux transmissivities
17 p3081 A70-35927
- Positive atomic oxygen ion reactions with carbon dioxide detected using ion cyclotron and double resonance methods
18 p3225 A70-36189
- Carbon dioxide entropy and enthalpy computation covering critical region and wide temperature range [ASME PAPER 70-GT-5]
18 p3348 A70-36861
- Chloride ion shift of respiration occurring between plasma and erythrocytes as function of carbon dioxide, using rapid filtration method
19 p3364 A70-38366
- Reliability tests of blood carbon dioxide pressure measurement methods, indicating carbon dioxide-electrode method superiority
19 p3365 A70-38371
- Water vapor effect on carbon dioxide reaction with lithium hydroxide in dynamic isothermal system
20 p3582 A70-39227
- Carbon dioxide initial dissociation rates in glow discharges and gas mixtures at low pressures, using mass spectrometric sampling and plasma diagnostic methods
20 p3674 A70-39235
- Unicellular hot spring acidophilic alga Cyanidium cadarium cultured in pure carbon dioxide, examining packed cell volume, oxygen production and growth rate
20 p3572 A70-39492
- Satellite-borne conical IR scanner flight data hybrid simulation and error analysis, suggesting carbon dioxide horizon noise model
20 p3631 A70-39513
- Graphites erosion by water and carbon dioxide at high temperatures, using liquid rocket simulator for kinetics study
20 p3736 A70-39587
- Carbon dioxide and CO IR vibration-rotation spectral absorption coefficients, noting harmonic oscillator approximation
21 p3851 A70-40589
- Venusian atmosphere carbon dioxide, water, molecular oxygen and nitrogen contents from Venera 5 and 6 data
21 p3883 A70-40837
- Free and forced convection of supercritical carbon dioxide normal to heated cylinder at constant temperature, measuring heat transfer rates
21 p3945 A70-41034
- Carbon dioxide-atomic oxygen reaction rate constant to investigate Martian ionosphere, discussing reactions involving oxygen, nitrogen molecular ions and NO
21 p3886 A70-41067
- Carbon dioxide-He-nitrogen gas mixture pulsed discharge system afterglow gain measurements up to one atmosphere, using CW laser
21 p3837 A70-41719
- Spectral absorption characteristics for c atom radiative processes in carbon dioxide-nitrogen mixtures at high temperatures corresponding to Venusian atmosphere
21 p3854 A70-42058
- Heat transfer measurement from Pt wire to carbon dioxide near critical pressure, discussing film boiling and free convection flows
21 p3953 A70-42167
- Thermal blooming of 10.6 micron laser beam in carbon dioxide absorption cell
22 p4049 A70-42335
- Carbon dioxide and water cryodeposits refractive indices and densities, using thin film interference technique [ASME PAPER 70-HT-33]
22 p4122 A70-42434
- Interdiffusion coefficients for hydrogen-carbon dioxide and oxygen-carbon dioxide systems at low temperatures
22 p4076 A70-43393
- Martian soil thermal conditions, considering polar cap annual variations and carbon dioxide sublimation
23 p4240 A70-43914
- Vibrational relaxation measurements of specific carbon dioxide vibrational-rotational states from tunable carbon dioxide laser beam absorption
23 p4221 A70-44011
- Venus carbon dioxide band, deriving rotational temperatures at various phase angles
23 p4241 A70-44257

Blood oxygen, carbon dioxide and pN during hypothermia induced by He-oxygen mixture and cold exposure in hamsters, comparing with hibernation state

23 p4147 A70-44787

Zr-Cu alloys corrosion resistance in carbon dioxide at high temperatures, noting composition effect on behavior

23 p4208 A70-44875

Carbon dioxide molecular vibration excitation by Q switched carbon dioxide laser, obtaining accommodation and diffusion coefficients by relaxation measurements

24 p4351 A70-45369

Vasodilating carbon dioxide effect on brain circulation in occipital cortical area in cats and rabbits using thermoelectric method

24 p4300 A70-45842

Transverse flow deuterium fluoride-carbon dioxide chemical laser for CW output without external energy source

24 p4355 A70-46084

CARBON DIOXIDE CONCENTRATION

Martian carbon dioxide band observations using multislit spectrophotometer, indicating surface height variations near Syrtis Major

01 p0182 A70-10723

Carbon dioxide temperature distribution, absorption and concentration as functions of molecular dissociation behind shock wave determined by measuring IR bands intensity

01 p0069 A70-11623

Endtidal oxygen and carbon dioxide partial pressures, oxygen uptake and carbon dioxide after apnea and during apneic diving

02 p0235 A70-12089

Oxygen and carbon dioxide partial pressures bloodless determination in mixed venous blood, using platinum electrode and IR carbon dioxide meter

02 p0236 A70-12091

Vagotomy and carbon dioxide concentration effect on quiet and forced respiration rate, pleural pressure, tidal volume and lung ventilation in cats

03 p0422 A70-13694

Vigilance time degradation, studying effects of breathing gas mixtures with varying oxygen and carbon dioxide content

06 p1000 A70-17293

Respiration behavior of men during inhalation of various gas mixtures, observing spontaneous changes in breathing rates

07 p1206 A70-19471

Atmospheric carbon dioxide and oxygen concentrations effects on white mice low temperature tolerance

09 p1614 A70-22082

Balloon-borne device for analyzing atmospheric carbon dioxide, moisture and methane, using cyclic analysis by gas chromatography

11 p2052 A70-26371

Rhesus monkeys tolerance to graded increase in closed environment carbon dioxide, examining heart rate and cardiac rhythm

11 p1988 A70-26517

Earth atmosphere formation and oxygen-carbon dioxide balance mechanisms, including water vapor photodissociation, photosynthesis, fossil fuel burning, etc

14 p2572 A70-30350

Mars carbon dioxide abundance and surface pressure from growth curve based on high resolution spectra

14 p2650 A70-31218

Atmospheric carbon dioxide and oxygen concentrations effects on white mice low temperature tolerance

15 p2685 A70-32678

Venus atmosphere and surface conditions, describing temperature, accumulation of carbon dioxide and runaway greenhouse effect

15 p2806 A70-32771

Sheep cardiac rate, respiration rate, hematocrit, erythrocytes per cubic mm and hemoglobin concentration responses to elevated ambient carbon dioxide

17 p3030 A70-35421

Carbon dioxide content of dialyzed human hemoglobin measured at specific pressure and varying pH values as function of 2,3 diphosphoglycerate

19 p3364 A70-38367

Spectroscopic detection of sulfur dioxide and carbon dioxide molecules and concentrations in polluted atmosphere by laser-Raman radar technique

20 p3640 A70-39389

NASA aircrew oxygen system, describing carbon dioxide control and oxygen generation subsystems

21 p3768 A70-40990

Low carbon dioxide concentration breathing effects on exercise tolerance, discussing aerobic capacity decrement and hypercapnia occurrence

22 p3973 A70-43637

Carbon dioxide exposure limits of rhesus monkeys, examining body temperature, respiratory rate and pressure effects

22 p3973 A70-43642

Venus vegetative life suggested from algae growth under pure carbon dioxide in hot acid media at high pressures

23 p4253 A70-44836

CARBON DIOXIDE LASERS

Mathematical model for saturable absorbers consisting of molecular gases for use in IR applied to carbon dioxide laser radiation absorption by sulfur hexafluoride

01 p0109 A70-10429

Chirped pulses observation by heterodyning single frequency Q switched carbon dioxide laser with stable CW local oscillator and beat signal display on oscilloscope

01 p0109 A70-10433

Carbon dioxide lasers passive Q switching by gaseous methyl fluoride and phosphorus pentafluoride, presenting absorption coefficients

01 p0110 A70-10561

Nitrogen and helium collisional effect on rotational relaxation rate of carbon dioxide upper laser level, noting thermalization

01 p0110 A70-10567

IR CW sum-frequency up-conversion of carbon dioxide laser radiation using phase matched proustite as nonlinear crystal

01 p0111 A70-10786

Carbon dioxide laser with incorporated grating for measuring line strength to width ratio for various rotational lines

01 p0112 A70-10916

IR radiation absorption from carbon dioxide laser in supersonic gas jet, applying results to nitrogen-carbon dioxide gas dynamic laser action

01 p0148 A70-11123

Thermionic emission characteristics of W and Mo subjected to focused CW carbon dioxide laser radiation, discussing direct energy conversion

02 p0312 A70-12068

Carbon dioxide laser welding equipment and procedures, describing mechanical-electronic control system, target material-laser beam interactions, etc

02 p0310 A70-12752

Vibrational relaxation and optimum population inversion of carbon dioxide molecules under unsteady conditions during pulsed electron excitation, discussing laser output increase

03 p0528 A70-13408

Carbon dioxide laser radar system for studying radar techniques application to IR, discussing automatic tracking capability provision

03 p0450 A70-13676

Chlorotrifluoroethylene and difluorodichloromethane saturable absorbers for wavelength extensions of passively Q switched carbon dioxide lasers

03 p0502 A70-13816

Power stabilization of single mode monochromatic carbon dioxide laser, using grating in cavity

03 p0503 A70-14076

Laser cavity structure for homogeneous transverse discharge in carbon dioxide-nitrogen-helium mixtures, discussing energy and power increase per unit volume

03 p0503 A70-14357

Admixtures effect of chloroform, diethyl ether and acetone vapors on carbon dioxide laser output power

04 p0702 A70-15202

Wavelength selection in Q switched carbon dioxide laser by intracavity gas cell providing selective absorption

04 p0702 A70-15362

Continuous wave chemical laser operation in carbon dioxide pumped by vibrational energy released from DF and HF molecular formation

04 p0704 A70-15686

Power distribution in carbon dioxide laser resonator with external and internal mirror at different power levels

05 p0857 A70-15796

Phase lock technique study of 10.6 micron radiation effect in carbon dioxide laser plasmas on 2.4 micron spontaneous emissions and plasma impedance

05 p0857 A70-16071

Carbon dioxide laser resonator design and operation, discussing performance with dish reflector made of leucosapphire

05 p0859 A70-16272

Center dip formation in curve relating output power and frequency of carbon dioxide laser line operating in single mode on single wavelength

05 p0860 A70-16667

Properties of unstable confocal resonator used with carbon dioxide-nitrogen-helium laser, using geometric models and measurements

06 p1079 A70-17188

Steady state thermal defocusing of carbon dioxide laser radiation in gases as function of beam power, gas absorption coefficient and pathlength

06 p1079 A70-17190

Continuous passive mode locking of carbon dioxide laser cavity using long optical delay line

06 p1080 A70-17446

Electron energy distribution function for carbon dioxide laser plasmas in gas mixtures, discussing dissociation products role in electron energy exchange

06 p1080 A70-17447

Carbon dioxide laser beam modulation by molecular Stark effect

06 p1080 A70-17448

Carbon dioxide and monoxide molecules IR emission in laser noting CO contribution to population of higher laser level

06 p1082 A70-17772

Carbon dioxide-nitrogen laser emission absorption in atmospheric surface layer by wings of distant strong lines investigated statistically

06 p1082 A70-17807

Transverse mode locking for carbon dioxide laser achieved with nonlinear boron chloride absorber, observing emission spatial buildup

06 p1083 A70-18425

Frequency calculation and measurement for acoustic waves produced by carbon dioxide Q switched lasers

06 p1084 A70-18620

Self mode locked pulses with rotating mirror Q switched carbon dioxide laser, attributing pulse shortness to saturation broadening of spectrum

07 p1301 A70-20018

Carbon dioxide gas dynamic laser in shock tube facility, measuring shape, time, output energy, beam diameter, etc

07 p1301 A70-20021

Time variations of reflectance measured for carbon dioxide laser beam splitters

07 p1302 A70-20095

Carbon dioxide laser emission spectrum, considering working mixture emission power and rotational relaxation characteristics

08 p1511 A70-20539

Tunable Q switched pulsed discharge carbon dioxide laser intensity dependence on time delay investigated for various vibrational/rotational lines and gas mixtures

08 p1512 A70-20618

Power output of sealed carbon dioxide-nitrogen-helium laser as function of gas composition and pressure

08 p1514 A70-21751

Refractory oxide submillimeter spherical particle preparation by focused emission from carbon dioxide laser

09 p1697 A70-22984

Nonresonant multipath carbon dioxide laser amplifier small signal gain of 39 dB utilizing White optical reflector design

09 p1699 A70-23365

Scanning spherical mirror interferometer for carbon dioxide lasers radiation spectrum analysis, discussing instrument errors in mode and wavenumber studies

09 p1683 A70-23519

IR holograms real time visual reconstruction by frequency stabilized carbon dioxide lasers

09 p1684 A70-23534

Pulse repetition rate control and stabilization in passively Q switched carbon dioxide laser

09 p1699 A70-23537

Amplifier properties and oscillator mode structure of multipath carbon dioxide laser

09 p1699 A70-23538

Single-pass multimode carbon dioxide laser amplifier power gain optimization

10 p1897 A70-23815

High power CW carbon dioxide laser design and operation for use as heat source in metal fusing, welding and cutting

10 p1897 A70-23816

Ge-Cu IR detector photoconducting characteristics and application to carbon dioxide laser mode pattern measurement

10 p1898 A70-23922

Carbon dioxide-neon-helium flowing lasers gain characteristics determined by transverse-discharge configuration

10 p1901 A70-24944

Carbon dioxide laser frequency stabilization, using plasma tube impedance variations generating error signal

10 p1901 A70-24946

Corneal thermal response model for carbon dioxide laser radiation, computing temperature rise from power distribution and conducting air-cornea interface

11 p2062 A70-25635

Carbon dioxide dissociation in flowing carbon dioxide nitrogen helium laser and effects of carbon monoxide on discharge properties

11 p2063 A70-26068

CW carbon dioxide laser absolute frequency measurements at 28 THz by beating lines with water vapor laser and klystron in tungsten on nickel point contact diode

11 p2063 A70-26070

Saturation of self induced thermal lens resulting from thermal distortion of carbon dioxide laser radiation in wind

11 p2063 A70-26401

Luminescence and destruction of gaseous boron trichloride by carbon dioxide laser radiation

11 p2064 A70-26818

Molecular beam carbon dioxide laser Q switching by ethylene as saturating filter, reducing pulse duration by varying ethylene pressure and active mixture composition

12 p2248 A70-27509

Carbon dioxide CW laser-Doppler velocimeter for detecting aircraft wing tip trailing vortices by measuring atmospheric aerosols backscatter

12 p2249 A70-27630

Carbon dioxide laser gain saturation measurements by intracavity Fresnel loss-plate technique, observing dependence on discharge current

12 p2249 A70-27715

Sum and difference frequency signals generated and propagated by mixing carbon dioxide laser and millimeter wave klystron outputs in GaAs loaded waveguide

12 p2250 A70-28098

Carbon dioxide laser electrical discharge stabilization against transverse gas flow by cross magnetic field

12 p2250 A70-28099

Pulsed CO₂ laser calculating upper level lifetime of carbon dioxide molecule with allowance for gas heating at relaxation

12 p2251 A70-28296

Energy resonances between laser levels of carbon dioxide and diatomic and triatomic molecular impurity species, discussing population inversion due to superelastic collisions

13 p2425 A70-28622

Carbon dioxide laser saturated gain constant calculated for low and high electron densities based on thermodynamic approach

13 p2425 A70-28793

Electron radiation temperature measurements in sealed-off carbon dioxide laser, determining gas mixture effect on discharge properties

13 p2426 A70-28808

Kinetic changes in spectral lines and bands intensity of individual molecular gases and mixtures for carbon dioxide lasers

13 p2428 A70-29361

Giant pulses composed of shorter pulse trains obtained in Q switched carbon dioxide laser with transverse modes

13 p2429 A70-29412

Nitrous oxide and carbon dioxide laser Q switching by ammonia Stark effect

13 p2431 A70-29835

Short term influences on sealed carbon dioxide laser action and lifetime, using mass spectrometry

15 p2750 A70-31752

Linear power scaling-mass flow relationship in multi-Joule pulsed carbon dioxide-nitrogen-helium laser, noting thermal effects role

15 p2751 A70-31977

Laminar to turbulent flow transition observation in laser induced vertical convection, using carbon dioxide-nitrogen laser

15 p2751 A70-31980

Thermal degradation of anhydride-cured epoxy resin by carbon dioxide laser heating through platinum crucible

15 p2695 A70-32828

Pulsed carbon dioxide laser production with electron beam pumping, ascertaining beam effect on discharge parameters and output power

15 p2754 A70-32864

Laser design for production tool applications, noting use of Nd-YAG and carbon dioxide laser [ASME PAPER 70-DE-1]

16 p2917 A70-33418

Carbon dioxide laser action at 10.6 micrometers at pressures up to atmospheric by transverse electrical discharges

16 p2928 A70-33643

Gas breakdown produced by long wave IR pulsed radiation of carbon dioxide laser

16 p2928 A70-33655

Ablative materials performance in high radiative heat flux environments produced by CW carbon dioxide laser

16 p2939 A70-33907

Lasing action and reduced output without beam distortion from misaligned carbon dioxide lasers by DC-Tesla coil pumping

16 p2929 A70-33986

Carbon dioxide laser producing nearly 100 percent amplitude modulation of output by intracavity polarization modulation technique

18 p3270 A70-36747

Modulation of carbon dioxide laser with Stark cell internal to cavity, using methyl chloride electrooptical gas

18 p3270 A70-36748

Carbon dioxide laser passive Q switching, using ethylene and methanol as saturable absorbers

18 p3270 A70-36749

Sealed-off carbon dioxide laser discharge deposits analyzed by mass spectrometry

19 p3445 A70-37670

Folded path transversely excited atmospheric pressure carbon dioxide laser using shower or brush discharges, measuring output pulse characteristics

19 p3445 A70-37674

Carbon dioxide IR laser applications to manufacturing technology, discussing absorption, reflection and heat conduction characteristics of materials

19 p3447 A70-38452

Spatial gain variations transverse to discharge in axially flowing carbon dioxide laser amplifier, noting relationship to flow velocity

20 p3640 A70-39391

Transversely excited atmospheric pressure /TEA/ carbon dioxide laser, noting power output and cost

20 p3641 A70-39424

Carbon dioxide-helium laser hollow cathode negative glow discharge amplifier, discussing construction and advantages compared to other excitation media and discharge structures

21 p3834 A70-40568

Carbon dioxide laser pulse shape, duration and power dependence on repetition rate during continuous pumping

21 p3835 A70-40634

Carbon dioxide laser systems for various space communication links between ground, satellites and Mars probe

21 p3787 A70-41338

Helium and nitrogen role in carbon dioxide laser excitation, discussing optimum gas mixture

21 p3837 A70-41919

Acoustic waves in carbon dioxide at 2-25 torr initial pressures induced by heat from incident carbon dioxide laser pulses

21 p3837 A70-42003

Mass spectroscopy analysis of neutral and ionic population of plasma in carbon dioxide laser gas mixture, discussing collision processes

21 p3838 A70-42006

High output CW carbon dioxide laser design, using gas pressure variation and fast axial flow

22 p4048 A70-42322

Passive Q switching and mode locking of carbon dioxide laser with saturable absorbers and buffer gases, using electric pulse excitation

22 p4050 A70-43023

Wavelength selective carbon dioxide laser using stationary grating to correlate pulses for high J values and line number

22 p4050 A70-43153

Diffusion effect on carbon dioxide Gaussian laser beam amplification, measuring gain saturation via pinhole method

22 p4051 A70-43335

Carbon dioxide laser vibrational temperature measurement, determining ground state vibration level populations in various molecular gases

22 p4051 A70-43391

Carbon dioxide amplification coefficient measurement for lines in laser transition range, determining rotational temperature and upspin levels populations

23 p4201 A70-44204

Carbon dioxide laser adapted for high speed drilling of fine holes in thin rubber sheeting

23 p4201 A70-44474

Narrow resonances in saturated absorption at molecular vibrational-rotational transitions in carbon dioxide laser

23 p4202 A70-45059

Luminescence and destruction of gaseous boron trichloride by carbon dioxide laser radiation

24 p4351 A70-45190

Flow-through carbon dioxide lasers population inversion relation to individual gas components and electron velocity distribution functions

24 p4352 A70-45458

Argon matrix isolated ammonia, examining IR spectra by carbon dioxide laser irradiation

24 p4354 A70-45648

Basalt heating with IR carbon dioxide laser, investigating vapor fractionation for inert atmospheres, very high temperatures and silicon dioxide poor materials

24 p4409 A70-45673

Gas ionization with Q switched carbon dioxide laser radiation, determining breakdown threshold or minimum power density requirement

24 p4355 A70-46261

CARBON DIOXIDE REMOVAL

Granular amine used as regenerable absorbent in cycling two bed system for carbon dioxide removal

01 p0038 A70-10972

Molecular sieve mixed gas adsorption and vacuum desorption of carbon dioxide in Apollo spacecraft cabin

01 p0040 A70-11450

Photolysis of 3-phenyl-oxadiazol-5-one by UV irradiation, eliminating carbon dioxide

17 p3041 A70-34772

Carbon dioxide absorption from gas streams by weak base ion exchange resins

18 p3226 A70-36767

CARBON DIOXIDE TENSION

NT HYPERCAPNIA
NT HYPOCAPNIA

Dogs respiratory response to arterial hydrogen ions at different carbon dioxide pressure levels during hypoxia or hyperoxia, discussing acid-base balance effects

11 p1986 A70-25674

Oxygen and carbon dioxide effects on airway smooth muscle following pulmonary vascular occlusion in dogs

13 p2356 A70-29943

Inspired carbon dioxide pressure effects on human response to physical exercise, noting dyspnea and intercostal muscle pain

13 p2360 A70-29949

Arterial blood carbon dioxide tension effects on rhythmic volley activity of respiratory medulla oblongata neurons in cats

17 p3030 A70-35354

Hyperbaric oxygen exposure produced hypertension and pulmonary edema, discussing carbon dioxide transport mechanism in blood

20 p3572 A70-39430

Rhesus monkeys PCO₂ tolerance in low pressure environments, observing hypothermia and heart and respiratory rates depression

21 p3765 A70-41486

Vagus nerve blockage effect on arterial carbon dioxide tension and breathing regulation in dogs

24 p4303 A70-46112

CARBON DISULFIDE

Optically trapped filaments in liquid carbon disulfide by side illumination and crossed polarizers using glass laser, noting birefringence and duration time

04 p0703 A70-15619

Chemical laser action in spark excited CS₂-O₂ mixtures, attributing emission to combustion product CO

06 p1080 A70-17445

Self phase modulation of stimulated Raman light in carbon disulfide, discussing Stokes and anti-Stokes spectrum regions

18 p3266 A70-36422

Carbon monoxide vibrational population inversion in product molecule produced in free burning carbon disulfide/oxygen flame

21 p3950 A70-41708

CARBON ISOTOPES

NT CARBON 12
NT CARBON 13
NT CARBON 14

Carbon isotopic composition in primary cosmic radiation by nuclear emulsions exposure in balloon flights

19 p3507 A70-38129

Carbon-nitrogen-oxygen isotope bi-cycle function in solar evolution, noting first cycle role in solar energy release and neutrino production

20 p3698 A70-39306

High energy alpha particle beam exposed to plastic scintillators, determining spallation cross section for C12/alpha, alpha n/C11

21 p3852 A70-41138

CARBON MONOXIDE

Sulfur compound effects on carbon monoxide-nitrogen laser emission stability, obtaining continuous operation independently of tube quality

01 p0111 A70-10660

IR spectra of four carbon stars and Sirius obtained with Michelson interferometer, indicating diatomic carbon and CO bands

02 p0372 A70-12252

Low energy electron diffraction structures due to Re crystal surface interaction with CO and molecular oxygen at high temperatures

03 p0440 A70-13098

Opacity-probability distributions for CO, computing theoretical spectra of line absorption coefficient, discussing effects of temperature and/or turbulent velocity

05 p0919 A70-16938

Self broadened semihalf widths measurement in pure rotational spectrum of carbon monoxide compared with vibration-rotation calculation

05 p0886 A70-17086

Pulmonary CO diffusing capacity in young men during muscular exercise

06 p0993 A70-17432

Carbon dioxide and monoxide molecules IR emission in laser noting CO contribution to population of higher laser level

06 p1082 A70-17772

CO vertical distribution near tropopause from photochemical atmospheric model with CO recombination with OH for stratospheric sink

07 p1265 A70-19282

Wave numbers, intensity and half width of lines of vibration-rotation relative to carbon monoxide transition, noting band center displacement dependence on pressure

07 p1338 A70-19380

Kinetics of homogeneous nitrogen dioxide-carbon monoxide atom transfer reaction in single pulse shock tube, carrying out product analysis by vapor phase chromatography

08 p1455 A70-21263

UV absorption cross sections of CO, HCl and ICN, analyzing reactions causing various spectral features

08 p1455 A70-21340

Perturbation rotational levels in triplet states of CO emission spectra attributed to resonance fluorescence process involving optically forbidden transitions

09 p1731 A70-22282

Chemically formed carbon monoxide lasing in fast flow system, discussing reaction and excitation mechanisms

09 p1697 A70-22922

Wave number, intensity and half width of vibrational-rotational lines pertaining to transition of carbon monoxide perturbed by argon

09 p1733 A70-23316

Mars biological activity suggested from metabolic energy cycle based on oxidation of carbon monoxide [NGL-07-004-043]

09 p1765 A70-23798

CO electrochemical oxidation at porous solid electrolyte fuel cell anodes under high temperature, noting current density role

10 p1830 A70-24462

API state lifetime of CO measured using molecular level crossing spectroscopy

10 p1920 A70-24629

Carbon dioxide dissociation in flowing carbon dioxide nitrogen helium laser and effects of carbon monoxide on discharge properties

11 p1063 A70-26068

Effusion steady state pressures time dependence of carbon monoxide and calcium vapors generated during calcium oxide-graphite interaction

11 p1995 A70-26602

CO dissociation kinetics in Ar and mixtures of O in Ar by shock tube study using vacuum UV absorption

12 p180 A70-26857

CO vibration-rotation bands, calculating high resolution and temperature steradiance and spectral absorption coefficient

12 p2275 A70-27171

Carbon monoxide adsorption on rhodium and ruthenium HCP metals emphasizing surface migration, work function increments and desorption

12 p181 A70-27676

CO adsorption on smooth polycrystalline platinum and rhodium electrodes at various potentials

12 p182 A70-27761

High power CO lasers, discussing UV and visible sidelight, gas mixtures, spectral output, gas pressure, etc

13 p2426 A70-28807

Carbon dioxide molecular vibrational energy levels above carbon monoxide-oxygen premixed flame, discussing vibration modes leading to population inversion and relaxation time variance

13 p2455 A70-29132

CW oscillation in carbon monoxide chemical laser

15 p2748 A70-31432

High power CW CO laser operation at room temperature by introducing mercury vapor into discharge

15 p2751 A70-31979

High temperature reaction kinetics between oxygen difluoride and CO in shock tube, discussing carbon dioxide formation

16 p2855 A70-33010

Lung diffusing capacity for CO in Caucasians native to 3100 m noting membrane diffusing capacity, lung capillary volume and age effects

17 p3031 A70-35427

Transverse flow CO chemical laser using atomic oxygen reaction with carbon disulfide, comparing output with longitudinal flow devices

18 p3266 A70-36313

Comet Morehouse CO ions lifetime and density from photometric analysis

18 p3313 A70-36324

Arcturus Co bands, examining equivalent widths, rotational lines and 12C/13C ratio

18 p3318 A70-37015

Solar photosphere temperature constancy in thin CO layer from equivalent spectral line width determination

18 p3322 A70-37134

Carbon monoxide oxidation by molecular oxygen in incident shock waves, accounting for chain branching in shock tubes

19 p3374 A70-38271

Heme catabolism in untreated rats and in animals treated with phenobarbital or porphyrogenic drug, comparing bilirubin and CO production

20 p3583 A70-40450

Carbon monoxide laser efficiency increase through addition of Xe, noting change in laser output spectral intensity distribution

21 p3835 A70-40572

Carbon dioxide and CO IR vibration-rotation spectral absorption coefficients, noting harmonic oscillator approximation

21 p3851 A70-40589

Apollo 11 lunar fines carbon level, finding largest component carbon monoxide in complex form

21 p3778 A70-41621

Carbon monoxide vibrational population inversion in product molecule produced in free burning carbon disulfide/oxygen flame

21 p3950 A70-41708

Carbon monoxide-nitrogen laser mechanism vibrational populations, discussing operational characteristics and walls condition and nature

21 p3837 A70-41716

Carbon monoxide-nitrogen laser luminescent phenomena by electronic spectroscopy

21 p3837 A70-41717

Carbon monoxide-nitrogen system vibrational distribution of populations and kinetics in fundamental and harmonic regions, investigating vibroluminescence

21 p3837 A70-41718

CO vibrational relaxation measurements in shock tube expansion wave generated in argon heat bath

23 p4180 A70-44009

Cryogenic fluids nitrogen, argon and carbon monoxide nucleate boiling from atmospheric to near critical pressure

23 p4279 A70-44359

CARBON MONOXIDE POISONING

Humans and dogs breathing CO in closed system, discussing distribution on blood, body stores and oxygen metabolism

02 p0234 A70-11727

CARBON STEELS

Carbide phase in Cr-Mn heat resistant steels at annealing temperatures, isolating gamma, chromium carbide and niobium carbide phases

03 p0509 A70-13279

Intermediate aging influence on Bauschinger effect in low carbon steel at 270 C and 2 hr holding time

04 p0776 A70-15266

Mechanical properties of nickel steels with carbon after suitable heat treatment found similar to high strength nickel steels properties without carbon

05 p0865 A70-16875

X ray elastic constants measured in cementite phase in high carbon tool steel following plastic deformation at tension, noting residual stresses increase and balance

06 p1084 A70-17126

Loading frequency effect on carbon steel energy dissipation at large stress amplitudes, deriving strain rate relations

08 p1516 A70-20980

Low temperature effects on deformability of middle C steel under complex stress state, showing invalid stress-strain relation and deviator similarity

08 p1516 A70-20983

Multiaxial thermal fatigue cracking in carbon steels predicted by elastoplastic stress-strain analysis using finite element method

09 p1773 A70-22578

Alloying Ni, Cu and Nb effects on grain and strengthening of low carbon precipitation-hardenable ferritic steels

09 p1705 A70-22804

Pure iron and low carbon steel macroscopic stress measurements, determining correlation between residual stress, fatigue damage and fatigue life

15 p2759 A70-32322

Titanizing Armco iron and carbon steels, examining diffusion layer structure and phase composition

19 p3451 A70-37460

Recrystallization kinetics and microstructure of low carbon Ti stabilized steel cold rolled and annealed in 800-1750 F range

22 p4053 A70-42730

Defect effects on welds fatigue properties in low carbon steel plates estimated, using radiographs

24 p4347 A70-45733

Longitudinal phenomena and two phase structures effect on ductility of low carbon steel-chromium subjected to high temperature torsion

24 p4361 A70-46173

Carbon steel diffusion saturation with Ti and B, investigating layer depth, weight gain and microhardness dependence on powdered mixture composition

24 p4364 A70-46336

CARBON TETRACHLORIDE

Upper atmospheric atomic nitrogen reaction with carbon tetrachloride, estimating radiation intensity and brightness of artificial luminescent cloud

18 p3252 A70-36989

Emission spectral distribution of atomic nitrogen reaction with carbon tetrachloride for artificial luminescent clouds

18 p3293 A70-36990

CARBON 12

He to carbon fusion reaction rate enhancement in dense matter by inelastic scattering processes, discussing C 12 deexcitation to ground state

05 p0885 A70-16934

C13/C12 component composition from carbonaceous chondrites and terrestrial samples, showing similar fractional patterns but isotope variations

13 p2497 A70-29860

Carbon isotopes abundance in primary cosmic radiation by nuclear emulsion stack exposure in high altitude balloon flight

17 p3151 A70-34914

Arcturus Co bands, examining equivalent widths, rotational lines and 12C/13C ratio

18 p3318 A70-37015

CARBON 13

Carbonaceous chondrites composition by gas chromatography for light hydrocarbons and carbon, discussing origin of organic matter

10 p1949 A70-25327

C13/C12 component composition from carbonaceous chondrites and terrestrial samples, showing similar fractional patterns but isotope variations

13 p2497 A70-29860

Carbon isotopes abundance in primary cosmic radiation by nuclear emulsion stack exposure in high altitude balloon flight

17 p3151 A70-34914

Arcturus Co bands, examining equivalent widths, rotational lines and 12C/13C ratio

18 p3318 A70-37015

CARBON 14

Cosmic ray flux modulation in earth atmosphere produced by solar wind and geomagnetic variations, considering effects on atmospheric carbon 14 variations

04 p0680 A70-15114

Pinel C14-indoles synthesis in rats noting no direct effect of morphine

11 p1988 A70-26299

Acute hypoxia effects on C14-tagged glycine absorption, distribution and discharge in rats organs and tissues

17 p3030 A70-35360

CARBONACEOUS METEORITES

NT ORGUEIL METEORITE

Allende carbonaceous chondrite radionuclide composition and concentration determined by nondestructive gamma ray spectrometry

04 p0754 A70-15275

Rb 87-Sr 87 age determination of carbonaceous chondrites, showing agreement among petrological classification types

06 p1150 A70-18480

Bismuth concentrations in various carbonaceous and equilibrated chondrites determination by neutron activation technique

07 p1388 A70-20036

Carbonaceous chondrites primordial He and Ne isotopes variations

07 p1388 A70-20037

Micrococcus radiodurans and *Sarcina flava* radiation resistance from proton irradiation tests in carbonaceous chondrite Migei

08 p1441 A70-20550

Carbonaceous material genesis in Tieschitz meteorite from electron microprobe analysis, discussing chondrule formation process residue likelihood

08 p1578 A70-21561

Allende meteorite showing presence of Ca-Al-rich glasses associated with other crystalline phases

08 p1579 A70-21562

Carbonaceous meteorites analyzed for soluble organic compounds, carbonate and residual carbon, showing endogenous nature

10 p1935 A70-23812

Ureilite structures and relationship to carbonaceous chondrites, considering chemical composition, diamond content, age, size, etc

10 p1941 A70-24552

Carbonaceous chondrites composition by gas chromatography for light hydrocarbons and carbon, discussing origin of organic matter

10 p1949 A70-25327

C13/C12 component composition from carbonaceous chondrites and terrestrial samples, showing similar fractional patterns but isotope variations

13 p2497 A70-29860

Ionization potentials of elemental abundances in lunar rocks compared with earth crust and class I carbonaceous chondrites, showing lunar materials differentiation

15 p2801 A70-32463

Chromatographic analysis of organic matter in Pueblito de Allende meteorite

17 p3173 A70-35754

Allende Type III carbonaceous chondrite, examining rare earth and other elemental abundances

19 p3519 A70-38028

Carbonaceous chondrites noble gases measurement by mass spectroscopy, discussing compositional trends and origins

20 p3703 A70-39323

Type 1 carbonaceous chondrites contribution to lunar soil, comparing mineralogical and trace element evidence

21 p3899 A70-41533

Carbonaceous chondrites isomeric alkanes identification by mass spectrometry and gas chromatography

24 p4402 A70-45378

CARBONACEOUS ROCKS

Carbonaceous complex use as indicators of geothermal history and high temperature organic geochemistry

17 p3042 A70-35331

Lunar carbonaceous, organic and organogenic materials analysis by mass spectroscopy, gas chromatography and various other methods

21 p3780 A70-41633

CARBONATES

NT POLYCARBONATES

Thermodynamics of electrochemical cells consisting of Li with lithium chloride or bromide and thallium amalgam with thallium chloride or bromide in propylene carbonate

01 p0042 A70-11107

Fuel cells phase equilibria between carbonate melt and Li, Na and K solid aluminate electrolytes, analyzing thermal and electrical conductances
10 p1830 A70-24458

Propylene carbonate applications in nonaqueous electrolyte batteries, describing impurities identification by gas-liquid chromatographic analysis
12 p2164 A70-27069

Sealed Ni-Cd cells, investigating carbonate effect on performance
22 p3965 A70-43535

CARBONIC ANHYDRASE
Artificial pulmonary ventilation effects on carbonic anhydrase activity in human blood during hypoventilation and hyperventilation
01 p0025 A70-11029

Serologic comparisons of carbonic anhydases in human and other primate erythrocytes
13 p2355 A70-29805

CARBONIZATION
Carbon fabrics and filaments, resin carbonizing and carbon-carbon composites, discussing processing parameters, initial carbonizing resin binder and reinforcement effects on laminate properties
07 p1316 A70-18932

Processing temperature effects on breaking strength-modulus relation for carbonized acrylic fibers
10 p1907 A70-24533

High strength glassy carbon fibers obtained by carbonizing extruded phenol hexamine polymers
11 p2071 A70-26672

CARBONYL COMPOUNDS
Chemical kinetics of carbonyl fluoride thermal decomposition in argon and nitrogen diluent behind shock waves, using IR monitoring method
11 p1995 A70-25824

Polyimideazopyrrolone films relative thermophysical properties, noting polymers thermal stability dependence on carbonyl groups percentage
21 p3783 A70-42132

CARBORANE
Heavy atom skeletal molecular structure of asymmetric close-2,3-dicarbahexaborane from microwave rotational spectra
21 p3773 A70-41392

CARBOXYHEMOGLOBIN
Humans and dogs breathing CO in closed system, discussing distribution on blood, body stores and oxygen metabolism
02 p0234 A70-11727

CARBOXYHEMOGLOBIN TEST
Carboxyhemoglobin saturation in post mortem examination of aircraft accident victims, discussing errors in methodology
17 p3033 A70-35568

CARBOXYLIC ACIDS
NT ACETIC ACID
NT ASPARTIC ACID
NT CITRIC ACID
NT FOLIC ACID
NT HEXOGENES (TRADEMARK)
NT LACTIC ACID
NT LYSINE
NT OLEIC ACID
NT TRYPTOPHAN

CARBURIZING
High chromium stainless steels nitriding and carburizing processes stabilized by nickel galvanic coating, enhancing nitrogen or carbon diffusion into steel
07 p1291 A70-18832

Graphite molds compaction pressure effect on Ti castings nonporosity and surface layers carburization
08 p1506 A70-21143

Carburization resistance of refractory steels, emphasizing chemical composition effect on corrosion rate
08 p1519 A70-21434

Regeneratively cooled stainless steel thrust chamber failure related to internal carburization by fuel decomposition and propellant combustion
12 p2290 A70-27111

Portevin-Le Chatelier effect in carburized nickel and Ni-Co alloys, discussing carbide stability and carbon diffusion roles
15 p2756 A70-31562

Pyrolyzed tetraethoxysilane for carburizing steels and Ti alloys at 850-1050 C
17 p3102 A70-35409

Carburizing spherical powders of Nb, Mo and W to obtain carbides, noting agreement between theoretical and experimental data
17 p3125 A70-35410

Molybdenum carburization in methane-based plasma glow discharge, considering possible pyrocarbon layer formation and temperature effects
19 p3434 A70-37456

Carburization and grain size of tungsten carbide powder from W powder as function of temperature, using optical and electron micrographs
21 p3839 A70-41412

CARCINOMA
U CANCER

CARDIAC AURICLES
Frequency and postextrasystolic potentiations in guinea pig isolated auricles and dog heart in vitro and in situ, noting myocardial diagnostic use
02 p0235 A70-12088

CARDIAC VENTRICLES
Computer analysis and comparison of ST segment on Frank and bipolar lead electrocardiograms of healthy persons and cardiac patients during exercise, noting physiological responses
01 p0013 A70-10270

Reciprocal rhythm occurring with impulses of atrial or atrioventricular [A-V/ nodal or ventricular origin, noting role of A-V nodal pathways
01 p0016 A70-10442

Physiological significance of myocardial fibers curvature in left ventricle wall determined by numerical solutions based on mathematical description
01 p0039 A70-11368

Left ventricular muscle time varying elastic properties, using dynamic model and Fourier series representations
01 p0040 A70-11371

Aortic distensibility and instantaneous left ventricular volume estimation in living man based on elastic reservoir theory and circulatory system model
01 p0040 A70-11372

Left ventricle confocal prolapse spheroid model taking into account physiologic variations of thickness
01 p0040 A70-11373

Hyperbaric oxygenation /OHP/ effect on left ventricular function evaluated by measurement on anesthetized dogs of myocardial contractility
02 p0230 A70-11701

Left ventricular function during paired pulse and single pulse stimulation in dogs, sheep, goats and calves before and after induced heart failure
02 p0233 A70-11719

Left ventricle wall forces and dimensional measurements during cardiac cycle based on stress-strain terms, including results for mitral, aortic and myocardial disease
02 p0238 A70-12512

Posture effect on ballistocardiograms, considering ventricular ejection flow changes
02 p0248 A70-12684

Controlled premature atrial stimulation effects on atrioventricular conduction in man, using electrode catheter technique to record electrical activity of specialized conducting fibers
03 p0415 A70-12886

Atrioventricular conduction in atrial fibrillation and flutter in man, using His bundle recordings
03 p0415 A70-12887

Electrocardiographic criteria for left ventricular hypertrophy diagnosis, using chamber dissection technique
03 p0432 A70-12890

Dogs left ventricle areas supplied by coronary arterial branches visualized utilizing scintillation photography and radioactive Xe
03 p0432 A70-12892

Mathematical model for ejection fraction of human left ventricle incorporated with fiber orientation and ventricular geometry, showing consistent results with biplane angiocardiacographic films
03 p0433 A70-12975

Arterial counterpulsation effect on mechanics of left ventricular contraction and myocardial oxygen consumption in normal and abnormal animals
03 p0416 A70-13009

Stress differential equations of equilibrium for thick prolapse spheroid /left ventricle/, yielding practical values for mean stresses in thick walled ventricles
03 p0434 A70-13571

Computer evaluation of photographic imagery of left ventricle volume obtained by cineangiography, including densitometric measurements
03 p0434 A70-13678

Evidence supporting concept of His bundle and not A-V node as pacemaker site in nodal rhythms using electrode catheter technique
03 p0424 A70-13774

Pathologic findings of left ventricular papillary muscle related to electrocardiogram, discussing papillary muscle dysfunction syndrome
03 p0426 A70-13942

Production mechanism of abnormal Q waves in obstructive cardiomyopathy
03 p0427 A70-13943

Automatic photo-optical technique for processing of cineangiograms to find time-course history of left ventricular volume
04 p0641 A70-14559

QRS and ST-T areas in multiple bipolar chest leads during normal and abnormal activation in patient measured for checking ventricular gradient concept
04 p0632 A70-15307

Ventricular performance as function of infarcting myocardium, discussing dynamic characteristics
04 p0637 A70-15470

Ventricular ectopic beats and bradyarrhythmia associated with myocardial infarction, discussing enhanced automaticity, reentry activity, drugs and heart pacing
06 p0998 A70-18407

Left ventricular wall motion in normal man at rest and after exercise using echocardiogram
07 p1210 A70-19573

Phasic aortic blood flow and left ventricular pressure measured at constant heart rates during pulsus alternans, discussing ejection duration and peak flow rate
07 p1210 A70-19588

Left ventricular function myocardial infarction induced acute depression and subsequent recovery in intact conscious dogs
07 p1211 A70-19615

Cardiovascular control system mathematical model incorporating fundamental properties of heart muscle for digital simulation using FORTRAN program
08 p1453 A70-21513

Various phases of human isometric left ventricle contraction, comparing results with previously published data
09 p1620 A70-23111

Left ventricle pressure rise rate as function of heart contractility and hemodynamics
09 p1623 A70-23587

Vectorcardiographic diagnosis of left ventricular hypertrophy based on changes in MQV magnitude and other QRS vectors
09 p1629 A70-23626

Ventricular preexcitation syndrome studied by catheter technique for heart electrical activity recording, noting His bundle bypass effects
10 p1819 A70-24934

Human head-up tilt circulatory stress effects on left ventricular systolic time intervals
10 p1820 A70-24937

Ultrasonic echography for ventricular size determination, calculating stroke volume and valvular regurgitation severity
10 p1820 A70-24938

Left ventricular volumes, pressure and heart rate in patients and dogs after diagnostic coronary arteriography
10 p1820 A70-24939

Cyclic strain energy method determining oxygen consumption rate of intact working human left ventricle by closed chest measurements
12 p2167 A70-27018

Myocardial individual fibers length calculation based on ellipsoidal model of left ventricle and fibers helicoidal course, noting distension nonuniform effect
12 p2174 A70-27020

Left ventricle zone as principal reflexogenic zone of heart participating in greater circulation vessel tonus control
13 p2353 A70-29356

Cardiac structure-functional relations, discussing muscle strand continuum, basal fibrous skeleton, epicardial, endocardial and myocardial layers
15 p2685 A70-32834

Primary myocardial disease, describing hemodynamic and angiocardiacographic observation of left ventricular volume and wall changes
16 p2848 A70-33110

Human phasic right ventricular blood velocity, examining respiration, rhythm disturbances and Valsalva maneuver influence by radiotelemetry
16 p2850 A70-33111

Involuntary vectorcardiographic signs of right ventricular hypertrophy
17 p3025 A70-34859

Single ventricle and hypoplastic left and right heart syndromes, investigating with reflected ultrasound
17 p3032 A70-35472

Left ventricle pumping function self regulation mathematical model, obtaining transfer function
18 p3217 A70-36080

Left ventricular dynamics ultrasonic visualization, involving catheter-borne transducers array and computer for data acquisition and display
18 p3225 A70-36750

Cardiac ventricular function in compression pump terms, relating mechanical activity to end-diastolic fiber length
20 p3571 A70-39364

Determinants of human ventricular dimensions and myocardial free velocity relations during maximum and submaximum exercise levels
20 p3571 A70-39365

First derivative of ventricular pressure recorded by conventional cardiac catheters, analyzing in terms of Fourier series
21 p3767 A70-40578

Acceleration Bcg dependence on left ventricular ejection flow and properties of vascular system
21 p3763 A70-41237

Left ventricular surface electrocardiogram T-wave amplitude and circumflex coronary artery blood flow during headward acceleration in unanesthetized dogs, observing velocity decrease
21 p3764 A70-41481

Atioventricular conduction in the human heart, analyzing electrocardiogram response patterns recorded by electrode catheter in unanesthetized man
22 p3970 A70-42942

Indirect serial determination of left ventricular systolic ejection time changes in human patients with acute transmural and nontransmural myocardial infarctions
23 p4144 A70-43946

Human left ventricle shape and movements during systolic contraction, using cineangiography and cineradiography of epicardial markers
24 p4302 A70-46076

CARDIOGRAPHY

NT BALLISTOCARDIOGRAPHY

NT ELECTROCARDIOGRAPHY

Cardiac output and coronary blood flow during steady state hypoxia, considering room air and different oxygen concentration breathings
01 p0014 A70-10360

Atrial high gain and HF recordings on three plane vector cardiograms for magnitude and direction for normal and heart diseased patients
01 p0015 A70-10436

Peripheral arterial pizography for cardiological screening tests and checkups of flying personnel
05 p0807 A70-16495

Visual recordings of cardiac rhythm obtained from flashes of miniature indicator tube, describing circuit filter function
08 p1452 A70-21439

Cardiac and respiratory cycles phase coincidence detection device, making photographic plates under physiological conditions
14 p2541 A70-30381

Comparative cardiac output measurements in dogs using left/right heart dye injections and pulmonary/aortic electromagnetic flow probes
15 p2688 A70-31434

Data system obtaining sampling rate for cardiac volume measurement via fast biplane cineangiography
15 p2691 A70-31922

Primary myocardial disease, describing hemodynamic and angiocardigraphic observation of left ventricular volume and wall changes
16 p2848 A70-33110

Bioradiotelemetry of human cardiac activity during professional activities, using ultrasonic searchless Doppler cardiography
17 p3038 A70-35365

Minnesota Impedance Cardiograph method evaluated by applying to cardiac output measurements in postural stress studies
17 p3031 A70-35431

Single ventricle and hypoplastic left and right heart syndromes, investigating with reflected ultrasound
17 p3032 A70-35472

Pressure recording site localization in esophagus, discussing cardiac artifacts morphology and localization over esophagus length
21 p3765 A70-42152

High fidelity microelectrode recording of phase zero cardiac transmembrane action potentials, utilizing memory oscilloscope
21 p3772 A70-42163

Aortic regurgitated flow estimation by dye injection technique, noting correlation with cineangiocardiology method
22 p3977 A70-42301

Human left ventricle shape and movements during systolic contraction, using cineangiography and cineradiography of epicardial markers
24 p4302 A70-46076

CARDIOLOGY

Cardiac activity temperature coefficients in dogs, specifying physical and chemical cardiac functions
01 p0012 A70-10052

Autoimmunity to heart tissues in cardiac diseases, reviewing immune mechanisms in rheumatic fever, postcardiotomy and postinfarction syndromes
01 p0016 A70-10438

Cardiac relaxation mechanics from isolated preparation of cat papillary muscle, noting inotropic influences role
02 p0231 A70-11709

Model for simulating normal/abnormal depolarization and repolarization of heart and to reproduce electrocardiograms, describing design and programming
03 p0432 A70-12889

Electrocardiac events observed in cardiac transplant recipient emphasizing unique finding
03 p0433 A70-12893

Airline stewards cardiovascular and ischaemic heart disease statistics compared with civilian pilots and general population
03 p0438 A70-14070

Cardiac echography applied to diagnosis and therapy evaluation in idiopathic hypertrophic subaortic stenosis
05 p0800 A70-16103

Cardiology role in aviation medicine, evaluating jumbo jet and SST flight stress effects on pilots and passengers in age factor study of arteriosclerosis
05 p0803 A70-16721

Alpha-methyl-DOPA inhibitor effect on catecholamines and cardiac spontaneous activity in pacemaker fibers in rabbits
06 p0992 A70-17422

Acute myocardial ischemic injury and infarction in dogs related to changes in man using oxygraph tracings
06 p0997 A70-18405

Geometrical model of human cardiac excitation stages based on normal heart anatomy, discussing application to study of QRS loop in vectorcardiogram
07 p1211 A70-19592

On-line computer for heart rate, isovolumetric contraction time, ejection time, stroke volume and cardiac output using vibrophonocardiogram signals
07 p1224 A70-20196

Vectorcardiogram variations of clinically normal individuals over forty compared with young adults
08 p1452 A70-21264

Human mitral valve morphology, distinguishing chordae tendineae types by insertion mode
10 p1819 A70-24935

Human mitral valve morphology, studying posterior and anterior leaflets partitioned by chordae tendineae
10 p1819 A70-24936

Stochastic processes for physiological analysis of cardiac rhythm dynamics during work
15 p2680 A70-31609

Electronic simulation of indicator-dilution curves for comparative evaluation of cardiac output computers
24 p4309 A70-46120

CARDIOTACHOMETERS

Cardiac output and coronary blood flow during steady state recumbent exercise, discussing CO and Rb 84 measurements in human subjects
08 p1453 A70-21936

CARDIOVASCULAR SYSTEM

NT AORTA

NT ARTERIES

NT BLOOD VESSELS

NT CAPILLARIES [ANATOMY]

NT CARDIAC AURICLES

NT CARDIAC VENTRICLES

NT DIASTOLE

NT EOSINOPHILS

NT EPICARDIUM

NT ERYTHROCYTES

NT HEART

NT HEMATOPOIESIS

NT HEMATOPOIETIC SYSTEM

NT LEUKOCYTES

NT LYMPHOCYTES

NT MYOCARDIUM

NT SYSTOLE

NT VEINS

Intermittent left anterior hemiblock as natural experiments for changes induced by conduction disturbance on human electrocardiograms
01 p0015 A70-10435

Physiological signals of cardiovascular system transducing methods applied to vector ECG, heart sounds, peripheral pulse waves, chest microphone and plethysmography
02 p0243 A70-12095

Ballistocardiography and cardiovascular performance - Conference, Atlantic City, May 1968
02 p0240 A70-12675

Display devices for ballistocardiographic test data obtained from professional pilots free of cardiovascular disease subjected to displacement and acceleration
02 p0247 A70-12676

Electrical analog simulation of cardiovascular system, determining blood flow rate and pressure in aorta and peripheral vessels
03 p0420 A70-13490

Dielectrocardiograph for studying cardiovascular and respiratory activities by recording hyperemia-evoked permittivity variations in localized body areas
03 p0435 A70-13714

Cardiovascular system, neuromuscular activity and mental fitness of subjects performing physical and mental assignments with prescribed work-rest schedule during confinement
03 p0425 A70-13895

Civil aviation personnel cardiovascular rehabilitation using single-lead electrocardiographic telemetry for monitoring and assessing cardiovascular status during supervised exercise
03 p0438 A70-14069

Airline stewards cardiovascular and ischaemic heart disease statistics compared with civilian pilots and general population
03 p0438 A70-14070

Analog computer model of human cardiovascular control system to reproduce subject response to submaximal workload
03 p0438 A70-14081

Cardiovascular responses to sustained high skin temperature in resting men noting dizziness, impaired vision and extracutaneous vasodilatation
03 p0429 A70-14162

High altitude acclimatization effects on cardiovascular system, external respiration, blood com-

position, optical and vestibular analyzers in human subjected to various stresses
04 p0630 A70-14576

Analog computer cardiovascular system model to simulate pressure and flow events in veins including effects of gravity, collapse, breathing and venous valves action
04 p0641 A70-14632

Catecholine excretion, cardiovascular functions and subjective effort in healthy male subjects under various physical work loads
05 p0801 A70-16141

Hypothalamic stimulation effects on cardiac and vascular efferent components of baroreceptor reflexes in spinal cats
07 p1202 A70-18866

Physical training effects on factors in cardiovascular system influenced by age
07 p1212 A70-19691

Electromechanical graph digital reader for records of cardiovascular studies
07 p1224 A70-20197

German monograph on determination of blood velocity, pressure, pulse rate and vascular structure parameters using Doppler effect
08 p1452 A70-21297

Nervous control of unconditioned cardiovascular reflexes during ontogenesis in children, observing sympathetic and vagal tonicity
08 p1446 A70-21449

Cardiovascular control system mathematical model incorporating fundamental properties of heart muscle for digital simulation using FORTRAN program
08 p1453 A70-21513

Cardiovascular aging and aeromedical maintenance programs for selecting test pilots
08 p1453 A70-21739

Thoracic cage, heart and extirpated lung dimensions measurement for dogs before and after explosive decompression and after ground level recompression
08 p1448 A70-21793

Beta-adrenergic blockade effect on abnormal R-ST segment and T-wave changes, showing propranolol use in stress catecholamine and organic cardiovascular diagnosis
08 p1449 A70-21945

Cardiac output in humans by analog computer program using mass spectrometer analysis of expired air
08 p1454 A70-21948

Hypothalamus stimulus effects on sympathetic nerve activity to heart, spleen, kidney and leg skeletal muscle in anesthetized cats
09 p1614 A70-22001

Soviet book on nervous stress and cardiac activity covering hypothalamus and cardiovascular reactions and cardiac component of complex conditioned reflexes and emotional reactions
10 p1809 A70-23873

Prolonged hypodynamia effects on hemodynamics using dye dilution method, noting adaptability in cardiovascular system
10 p1814 A70-24671

Occlusion training during hypodynamia with inflatable thigh cuffs to prevent unfavorable effects on cardiovascular system
10 p1816 A70-24689

Cardiovascular reactions and orthostatic stability during hypodynamia determined from ECG, seismocardiograms, phonocardiograms, sphygmograms and tachy-oscillograms
10 p1817 A70-24694

Human cardiovascular system function during adaptation at various high altitudes using simultaneous EKG and phono-KG recordings
10 p1823 A70-25179

Dielectrocardiograph for studying cardiovascular and respiratory activities by recording hyperemia-evoked permittivity variations in localized body areas
11 p1990 A70-25514

Cardiovascular model for closed loop analog simulation of congenital heart defects hemodynamics
11 p1990 A70-25705

Pneumatic compression effects on canine cardiovascular dynamics after hemorrhage tested in G-suit inflation
11 p1988 A70-26516

Indicator dispersion model for cardio-pulmonary system based on continuity past sampling site, observing diffusion coefficient nonlinear increase with blood speed
12 p2174 A70-27019

Rats cardiac aerobic and anaerobic pathways response to hyperbaric oxygen exposure
13 p2349 A70-28833

Human proprioceptive reflexes fluctuations correlation with spontaneous respiration and cardiovascular rhythms
13 p2350 A70-29323

Position dependent variations in intrapericardial, pleural and esophageal pressures and cardiac output in thorax of dogs
13 p2356 A70-29946

Cardiovascular and circulatory phenomena fluid mechanical aspects emphasizing pulsatile blood flow
15 p2720 A70-31789

Air bubble breaking in blood and water flow passage of simulated cardiopulmonary bypass system with flow constriction 15 p2692 A70-32312

Heart rate elicitation and blood pressure increase, considering parasympathetic and sympathetic nervous outflows adjustments of initial cardiovascular response to muscular contraction 15 p2684 A70-32535

Long term weightlessness effects on cardiovascular system of rats using miniaturized pump oxygenator 16 p2854 A70-33999

Multistage electrocardiographic exercise tests for cardiovascular performance measurement 17 p3034 A70-35878

Human cardiac flow during acceleration as function of time with and without anti-g suit, using electric plethysmograph 17 p3040 A70-35915

Intact femoral artery pressure-diameter relationship in man, discussing noradrenaline infusions effects 18 p3222 A70-37222

Hemodynamic effect of lidocaine given by infusion and bolus injections in myocardial infarction, examining cardiac output, heart rate, systolic left ventricular and aortic pressures 19 p3366 A70-38575

Cardiovascular stress testing using posterior bipolar lead for radiotelemetry monitoring 20 p3578 A70-39199

Visceral blood flow during exercise in sled dogs, testing hypothetical compensatory decrease as cardiovascular reserve for skeletal muscle by biotelemetry 20 p3571 A70-39366

Hemodynamic changes in Andean native after two years at sea level, measuring intravascular pressures, cardiac output, heart rate and stroke index 20 p3571 A70-39427

Cardiovascular blood circulation system dynamic characteristics analysis by linear statistical correlation methods, describing test for determining weighting function 20 p3581 A70-39905

Ship engineers cardiovascular system functional changes during HF internal combustion engine noise, investigating EKG recordings and arterial pressure 20 p3582 A70-40292

Ballistocardiography and cardiovascular therapy - Conference, Oporto, Portugal, March-April 1969 21 p3762 A70-41226

Algorithm for cardiovascular force computation from phase regional blood flow and mass motion, interpreting Bcg 21 p3763 A70-41238

Bcg interpretation, discussing degrees of freedom, blood mass displacement, cardiovascular system, etc 21 p3770 A70-41239

Adaptation of cardiovascular system in aging and old individuals under muscular activity 22 p3968 A70-42896

Occupational and age composition of working population of U.S.S.R., comparing cardiovascular and respiratory systems 22 p3969 A70-42904

Decompression sickness pathophysiology, discussing cardiovascular system, altitude effects, therapy and prevention 22 p3975 A70-43700

Computer photokymographic recording of gravitational-inertial force environment effects on cardiovascular and respiratory systems on centrifuge 22 p3976 A70-43709

Optimum bed rest time schedules for cardiovascular patients from neurological, dynamometric, electromyographic and myogenic-tonus tests 23 p4149 A70-45077

Hypodynamic effects on human external respiratory function and cardiovascular state under various microclimatic conditions 23 p4149 A70-45078

Human cardiovascular compensatory responses to environmental cold stress, relating heart stroke to increased oxygen consumption 24 p4302 A70-46103

Cardiovascular dimensions changes and heart volume in physically trained young men, comparing with response in old age 24 p4303 A70-46109

CARDS

NT PUNCHED CARDS

CARET WINGS

Energy supply for supersonic flight air suction propellant systems using external supersonic combustion, discussing Caret wing and pressure effect 04 p0785 A70-15160

Shock patterns for simple caret wings generating specific flow patterns 13 p2509 A70-28542

CARGO

NT AIR CARGO

NT BAGGAGE

CARGO AIRCRAFT

NT C-5 AIRCRAFT

NT C-9 AIRCRAFT

NT C-47 AIRCRAFT

NT C-135 AIRCRAFT

NT C-141 AIRCRAFT

Cargo transport aircraft design and operation, discussing costs, cargo density, runway strength, gear design, customer service, etc 02 p0225 A70-12262

Mil-10 Soviet giant helicopter cargo and altitude record, VTOL and STOL capability and weight design 03 p0414 A70-14286

Fiat G-222 aircraft featuring high wing twin engine retractable landing gear for military cargo transport 10 p1805 A70-24381

Onboard cargo loader to make aircraft independent of specialized ground equipment 10 p1862 A70-25330

Book on Polish air cargo transport covering transport volumes, aircraft, preparation and loading operations 13 p2524 A70-29453

Pilots energy expenditure during jet, propeller and helicopter cargo aircraft flight, using expired air samples 15 p2689 A70-31876

Design modifications for BAC Vanguard 953 aircraft conversion to palletized all-cargo service, discussing interior layout, cargo door, air conditioning and weight 16 p2842 A70-34049

Extensible wing flap system for cargo aircraft, discussing structural design details and advantages [AIAA PAPER 70-911] 17 p3020 A70-35823

Swing tail cargo aircraft fuselage section stress analysis by finite element method, discussing displacement models, deformation modes and economics 21 p3935 A70-41260

CARGO SPACECRAFT

Space station-logistics vehicle docking and men-material transfer problem 01 p0193 A70-10612

Orbital space station operations requirements and interactions, considering experimentation, support vehicles, ground support and follow-on growth [AIAA PAPER 69-1062] 01 p0195 A70-10636

Development models for post-Apollo lunar cargo delivery system utilizing Saturn 1B and Centaur stages [DGLR-69-9] 04 p0763 A70-15187

CAROTID SINUS REFLEX

Atrioventricular conduction in atrial fibrillation and flutter in man, using His bundle recordings 03 p0415 A70-12887

Sinocarotid pressor reflexes effects on coronary circulation in anesthetized dogs noting changes in blood pressure, peripheral resistance and cavity pressure 03 p0422 A70-13693

Hypothalamic stimulation effects on cardiac and vascular efferent components of baroreceptor reflexes in spinal cats 07 p1202 A70-18866

Posthypoxic vasodilation in extremities of anesthetized dogs preserved after carotid and aortic reflexogenic zones exclusion 07 p1204 A70-19139

Atmospheric pressure-diameter relationship of common carotid artery in head and neck region of conscious men 08 p1447 A70-21508

Left ventricle zone as principal reflexogenic zone of heart participating in greater circulation vessel tonus control 13 p2353 A70-29356

Sinus and diaphragmatic nerves impulse activity during hypoxia compared with normal respiration in cats 23 p4145 A70-44312

CARRIER FREQUENCIES

Modulation type eddy current flow detector with striding converter, considering envelope shape of carrier frequency oscillations 06 p1079 A70-18631

Digital transmission techniques optimal utilization of assigned frequency spectrum for phase modulation of frequency carriers 10 p1839 A70-24365

Frequency stability characteristics and control in SSB-FDMA/PbM multiple access system tested by ATS [AIAA PAPER 70-411] 11 p2000 A70-25460

Phase lock loop acquisition and tracking of carrier frequency modulated by single sinusoid, obtaining parameter values through mathematical model and digital simulation 15 p2703 A70-32578

Optimum carrier phase delay estimation for one way ranging aircraft navigation, investigating receiver signal processing 16 p2947 A70-33449

Heisenberg uncertainty principle in communications technology, discussing variance products deficiencies and limits in carrier frequency pulses application 20 p3584 A70-39160

Carrier frequency transfer of amplitude modulated signal at two coupled transitions in traveling wave gas laser 23 p4202 A70-45055

CARRIER INJECTION

Double injection in semiconductors at high current densities, discussing procedure yielding space charge and field distribution and voltage drop 01 p0154 A70-10123

Dielectric layers electrical conductivity in ceramics containing Ti during aging, observing different characteristics ascribed to nonequilibrium current carriers injection 01 p0156 A70-10221

Space charge injection-impulse voltage separation technique for nonuniform field breakdown phenomena 01 p0110 A70-10560

Microwave circuit for increasing Gunn oscillators injection locking capabilities and reducing FM resulting from bias-voltage fluctuations 01 p0050 A70-10783

Generation-recombination noise theory extension to nonlinear devices applied to double injection diode in various operation modes 03 p0458 A70-14028

P-n-n structure dynamic I-V characteristics at high injection levels mathematically determined, showing rectifying capability decrease with increasing harmonic signal frequency 05 p0892 A70-16196

Carrier injection luminescence properties useful for display medium applications, discussing group II-VI compounds as injection host crystal materials 08 p1557 A70-21681

Fabrication effects on current instability during injection and breakdown of p-n junctions in GaAs oscillators 09 p1740 A70-23351

Recombination radiation intensity current dependence and I-V characteristics p-n-n diode operating in double injection mode and electrons trapping 14 p2625 A70-30163

CW injection laser frequency stability, noting injection current influence on lasing frequency 15 p2750 A70-31629

Nonequilibrium charge carriers transient accumulation in p-i-n diode at superhigh injection levels 15 p2714 A70-32908

Turbulent charge diffusion during unipolar injection in nitrobenzene between plane-parallel electrodes, discussing liquid motion at high voltages 22 p4080 A70-42719

Carrier injection-limited Gunn diode wideband performance, deriving expression for admittance 24 p4319 A70-46081

CARRIER MOBILITY

NT ELECTRON MOBILITY

NT HOLE MOBILITY

Current carrier mobility in n-InSb calculated by Schwinger variational method over temperature range 01 p0154 A70-10098

Current carrier motion and diffusion capacity in p-i-n junctions with highly doped regions under large variable signal 05 p0892 A70-16197

Activated carrier mobility confirmed in organic solids 06 p1004 A70-17325

Avalanche diodes properties, establishing equivalent circuit accounting for static electricity, carriers transit time and thermal effects 10 p1850 A70-24625

Hall constant and carrier mobility in semiconductor diamond films doped by boron ion injection, observing temperature dependence of mobility 12 p2287 A70-27480

N-type GaAs carrier mobility and concentrations increased slow cooling after heat treatment 12 p2289 A70-28343

Carrier drift due to electromagnetic impulse, deriving expressions for photo emf generated in transverse magnetic field manifesting monopolar photomagnetic effect 13 p2452 A70-29282

Gunn diodes I-V characteristics width as function of carrier concentration/mobility and diode length, noting role of impact ionization in strong electric field 13 p2378 A70-29408

InAs thin films electrical properties and IR reflectance, determining thickness and substrate temperature effects on carrier concentration and mobility 15 p2783 A70-31965

Carrier diffusion effect in large signal analysis of semiconductor avalanches in quasi-static approximation 19 p3387 A70-37768

Current carrier mobility under dynamic regime in p-n junctions by computerized method, emphasizing transitory phase 19 p3487 A70-38169

Photovoltaic effects in semiconductors, considering excess load carrier transport and I-V characteristics 19 p3488 A70-38477

Surface density, charge and field effect mobilities for electrons and holes on MIS insulator-semiconductor structure on narrow bandgap HgCdTe 22 p4086 A70-43018

Intraband absorption in p-type GaAs associated with carrier transitions between heavy and light hole in valence band 23 p4232 A70-45066

Conducting state propagation in p-n-p-n structure involving minority carrier diffusion between regions 23 p4232 A70-45068

CARRIER MODULATION

U MODULATION

CARRIER ROCKETS

U LAUNCH VEHICLES

CARRIER SYSTEMS

U WIRELESS COMMUNICATIONS

CARRIER WAVES

Transient Faraday rotation of S-band telemetry carrier observed during Pioneer 6 occultation by solar corona, correlating with decametric radio radio bursts 02 p0369 A70-12059

Envelope delay and amplitude characteristics measurement of modulated carrier wave channel in radio relay link 02 p0258 A70-12475

Digital controlled phase-locked loop in burst mode operation, comparing recovery characteristics with carrier and bit-timing recovery techniques based on statistical analysis 10 p1835 A70-24333

Power spectral density and autocorrelation functions of sinusoidal carrier amplitude modulated by split phase PCM and PSK 11 p2008 A70-26203

Noise effect on single band modulation receiver using phase automatic frequency control for carrier wave at arbitrary SNR 13 p2370 A70-29739

Demodulators threshold performance for satisfying carrier to noise ratios requirement of Intelsat 4 system 14 p2552 A70-31352

Carrier synchronization system for PSK signals, using direct regenerative repeater and phase locked loop/DR-PLL/ 15 p2697 A70-31826

Automatic calibration verification of subcarrier telemetry discriminators with selective channel readjustment 19 p3383 A70-37902

PCM data transmission, considering baseband code and modulated carrier formats and spectral distributions 19 p3379 A70-37905

Communications satellite carrier instrumentation, using computer controlled frequency shift radiometer for power monitoring 21 p3826 A70-41345

Phase recovery in vestigial sideband (VSB) data transmission, deriving carrier acquisition time required to achieve satisfactory error rate for coherent demodulation of PAM 21 p3793 A70-42178

CARRIERS

Natural vibrations of free autonomous system of carried and carrier solid bodies connected by elastic couplings 18 p3342 A70-36594

CARTESIAN COORDINATES

Initial quaternion for Cartesian time varying transformation matrix based on self alignment method of inertial analytic platform 11 p2072 A70-26150

Military pilots visual estimation of point location coordinates within rectangular area 13 p2357 A70-29121

Heat conductivity equations transformation for Cartesian and cylindrical coordinates and various boundary conditions using static electrointegrator 15 p2827 A70-32172

Curvilinear orthogonal coordinates for gravimetric deduction related to Cartesian coordinates as solvability condition for Molodenskii problem 20 p3617 A70-39071

CARTILAGE

Squid head cartilage properties in terms of light and electron microscopic appearance, amino acid composition and X ray diffraction 24 p4305 A70-46348

CARTOGRAPHY

U MAPPING

CARTRIDGE ACTUATED DEVICES

U ACTUATORS

U EXPLOSIVE DEVICES

CARTRIDGES

Swinging gear drive, breather cartridge and hypocycloid timer mechanisms for reliable aerospace applications 16 p2921 A70-34104

CASCADE CONTROL

Transistorized amplifiers synthesis with multiloop feedback 15 p2707 A70-31518

CASCADE FLOW

Cascade tests to investigate nature of flow in rotor blade channels of axial flow turbines with partial admission 01 p0162 A70-10329

Optimal lift-drag ratio of cascades dependence on optimal pitch of cascades calculated for axial flow turbomachinery 02 p0356 A70-12750

Two dimensional cascade tests of turbine blade airfoil plotted by Legendre hodograph method, discussing pressure distribution measurements 03 p0410 A70-14272

Von Karman transonic similarity law applied to flow through plane turbine blade cascades [DGLR-69-24] 04 p0616 A70-15183

Flow field calculation for axisymmetrical gas flow in axial compressor cascade applicable to optimal blade design 04 p0617 A70-15191

Turbine cascade designs with constant reactivity over blade vertical profiles contributing to effective manufacturing of short and long blades 04 p0617 A70-15192

Flexible blades cascade design compared with various correlation criteria, describing cascade and profiles geometry and loss coefficient 05 p0790 A70-16029

Flow separation angle and loss coefficient in cascades with small aspect ratio blades under secondary vortex pair expansion over channel 06 p1130 A70-17858

Inviscid flow through staggered airfoil cascades in oscillatory and distorted flow simulating axial flow compressor [AIAA PAPER 70-131] 06 p0969 A70-18049

Airfoil cascade flow deflection angle using linearized jet flap theory 08 p1433 A70-21323

Shock wave configurations across compression cascades in transonic approach flow 09 p1604 A70-22657

Secondary losses in axial turbine cascades without end clearance noting correlation with blade loading 09 p1743 A70-22980

Stepwise averaged parameters of nonuniform three dimensional flow through turbine blade cascade determined from conservation conditions 09 p1606 A70-23611

Blade inter-row distances upstream and downstream related to potential flow velocity disturbances created by cascade in turbomachines 09 p1607 A70-23734

Subsonic compressible or incompressible inviscid flow field through turbomachine blade row determined by matrix and streamline curvature methods 09 p1608 A70-23745

Streamwise perturbations in flow downstream of self excited blades cascade calculated by two dimensional theory, discussing periodic circulation shedding 09 p1608 A70-23746

Wake-boundary layer interaction in wind tunnel tandem cascades, discussing end wall suction 09 p1609 A70-23750

Cascade theory of turbulence, applying cascade decomposition resulting from Navier-Stokes application to hydrodynamic turbulence to Riemann equation for atmospheric and plasma turbulence 10 p1868 A70-24167

Singularity carrier auxiliary curves for design calculation of airfoil cascades, discussing existence theorems and case of thin profiles 11 p1974 A70-25783

Singularity carrier auxiliary curves for design calculation of airfoil cascades, discussing profiles with small and large arcs 11 p1974 A70-25784

Velocity distribution of plane airfoil cascade given by geometry, using method of least squares 11 p1974 A70-25785

Circular cascade design from rectangular cascade flow data using conformal transformation, considering aerodynamic properties 11 p1974 A70-25786

Shear flow near walls through cascade of untwisted blades, observing variation in lift coefficient across span 11 p1975 A70-25788

Flow characteristics of airfoil rotating cascades in variable width channel in incompressible liquid 11 p1975 A70-25789

Airfoil cascades flow for given profile shape by singularity method, obtaining velocities 11 p1975 A70-25790

Flow pattern of axial flow of turbine stage calculated from cascade characteristics 11 p1975 A70-25794

Acoustic wave transmission and reflection through blade row in axial flow compressor analysis based on semiautuator disk theory and acceleration potential method 11 p2103 A70-26705

Compressor cascade flutter phenomenon, investigating factors affecting aerodynamic damping force on annular cascade blades 13 p2341 A70-29447

Incompressible two dimensional potential flow analysis with compressibility effects for thick highly cam-

bered multibodies in cascade, noting slotted compressor blade performance 14 p2529 A70-31023

Radial flow impellers design for maximum machine performance, using straight cascade characteristics 15 p2672 A70-31825

Aerodynamic forces exerted by compressible fluid on airfoil cascade in subsonic potential flow 16 p2833 A70-33075

Gas-particle mixture cascade flow over turbine blades, considering momentum/heat transfer and particle trajectories [AIAA PAPER 70-712] 16 p2835 A70-33569

Off-design performance characteristics of supercavitating hydrofoils in cascade for various arrangements, flap angles and flap chord ratios [ASME PAPER 70-FE-24] 16 p2892 A70-33633

Circular blade cascade design for superonic vane diffuser of radial flow centrifugal compressor 16 p2837 A70-33764

German monograph on planar straight cascades in incompressible frictionless potential flow, basing method on singularity method integral equation reversal 16 p2839 A70-34081

Two dimensional compressor cascades of double circular arc and wedge shape blades testing performance in transonic and supersonic wind tunnels [ASME PAPER 70-GT-7] 18 p3302 A70-36829

Plane and annular cascade facilities data application to aerodynamic design of axial flow compressors [ASME PAPER 70-GT-106] 18 p3303 A70-36845

Axial flow compressor cascades, predicting total pressure losses for inlet relative Mach number greater than unity [ASME PAPER 70-GT-57] 18 p3209 A70-36872

Transonic high turning low aspect ratio stator cascades flow field performance prediction, reducing secondary flows by partial slots [ASME PAPER 70-GT-63] 18 p3209 A70-36875

Two dimensional cascades for incompressible plane potential flows with given velocity distribution [ASME PAPER 70-GT-87] 18 p3209 A70-36880

Quasi-two dimensional supersonic cascade flow, taking into account transverse stream contraction effect 18 p3210 A70-37206

Low drag supersonic compressors for aircraft engines, calculating start and cruise conditions of quasi-isentropic flow cascades 21 p3745 A70-41405

Low aspect ratio compressor blade cascade performance at blade span center, discussing pressure loss, angle of attack and staggering 22 p3957 A70-42272

Viscous transonic flow past cascades by semiempirical approach, discussing pressure distribution, boundary layer parameters and compression shock 22 p4088 A70-42343

Two dimensional turbine cascade air flow, examining boundary layer regime, thickness, velocity and pressure coefficient at any point by Mach-Zehnder interferometer 24 p4026 A70-42344

Transonic turbine cascades exit flow parameters taking into account blade profile 22 p4088 A70-42346

Two dimensional transonic cascade flow, using Von Karman similarity law 22 p4089 A70-42347

Cascade flow field analysis from given blade geometry, deriving expressions for numerical solution of inverse turbine design problem 24 p4288 A70-45501

Turbine blades aerodynamic forces theoretical and experimental investigation, noting cascade series interaction induced pressure pulsations 24 p4288 A70-45504

CASCADE WIND TUNNELS

Supersonic cascade wind tunnel performance evaluation, using compressor blades of simple geometric shapes [ASME PAPER 70-GT-110] 18 p3238 A70-36848

Cascade tunnel testing role in designing supersonic compressor rotor blading for lower jet engine weight and fuel consumption [ASME PAPER 70-GT-79] 18 p3305 A70-36885

Airfoil cascade blade design by iteration method equating normal velocity distribution about contour with imposed tangential velocity 01 p0001 A70-10263

Monograph on stochastic theory and cascade processes, discussing branching phenomena, point processes, electromagnetic cascades, extensive air showers, polarization, population growth, etc 01 p0134 A70-11327

Theoretical and experimental cascade curves comparison for heavy materials used for particle absorption in tracking experiments, discussing Coulomb scattering 03 p0527 A70-13051

Longitudinal nuclear-electromagnetic cascade in ionization spectrometer simulated by Monte Carlo

method, noting energy relationship to particle sum recording
08 p1500 A70-21743

Low noise nonreciprocal microwave parametric amplifier with up-and-down converter and idlers in cascade
09 p1647 A70-22850

Circular cascade design from rectangular cascade flow data using conformal transformation, considering aerodynamic properties
11 p1974 A70-25786

Plasma turbulence spectral theory, considering cascade processes in collisional and collisionless dissipation
11 p2095 A70-26756

Atom excited state mean lifetime measurement, using correlated cascade photons method
14 p2620 A70-31378

Three dimensional nucleon-pion cascade equations solution for cosmic ray extensive air showers by pion-links method
17 p3150 A70-34597

Nuclear-electromagnetic cascades longitudinal development in glass, Fe and W absorbers, presenting Monte Carlo simulation
18 p3293 A70-36895

Image intensifier apparatus photographing nuclear electromagnetic cascades in ionization spectrometer
18 p3261 A70-37091

Heavy elements critical energy calculation, taking into account low energy electrons effects on losses in electromagnetic cascade
20 p3674 A70-39303

German monograph on supersonic strongly deflecting retardation cascades covering flow geometry and application to axial flow compressor stage
24 p4287 A70-45095

CASCADES (FLUID DYNAMICS)
U FLUID DYNAMICS

CASE BONDED PROPELLANTS

Sensing device to measure radial stress induced at solid propellant grain-to-case bond interfaces during wide temperature variations, detailing instrumentation and operation
03 p0480 A70-12882

Case bonded solid propellant rocket motors stresses under transverse body force loading as function of load orientation, case stiffness and support method [SESA PAPER 1502]
03 p0579 A70-12961

Two dimensional plane stress photoelastic models of star configurations in elastic case bonded solid propellant rocket motors under transverse body force loading
03 p0582 A70-14312

Cast double base technique for free-standing and case-bonded propellant charges, discussing manufacturing and mathematical model of casting and curing
07 p1360 A70-19906

Adhesive debonding in case-bonded solid propellant rocket motors, describing stress analysis and interfacial surface energy measurement
17 p3146 A70-35222

Sensing device to measure radial stress induced at solid propellant grain-to-case bond interfaces during wide temperature variations, detailing instrumentation and operation
20 p3718 A70-39158

CASE HISTORIES

Long air voyage after exteriorization of Wallenberg syndrome, discussing case history of subject with cerebral vascular accident
12 p2172 A70-28044

Welding failure case histories, discussing design, materials and processes, fabrication and quality control integration
21 p3832 A70-40787

CASES (CONTAINERS)
NT ROCKET ENGINE CASES

Structural design of boron/epoxy front housing for T-56 turboprop reduction gear case achieving reduced weight and increased stiffness
05 p0853 A70-15837

Air cargo transportation systems in 1970s, discussing market expansion, payload capacity and fleet growth, containerization, etc
07 p1250 A70-19875

CASING

Casing and suction cone effects on fans with cambered forward curved blading
11 p1975 A70-25796

CASSEGRAIN ANTENNAS

Shaped-reflector Cassegrainian antenna characteristics calculation, using current distribution method to derive subreflector radiation pattern
02 p0270 A70-12617

Phase center position of field scattered from hyperboloid subreflector in asymmetric Cassegrain antenna feed system
06 p1019 A70-17557

Beam switching Cassegrain antenna for millimeter wave radio astronomical measurements, describing RF and electronic systems
11 p2019 A70-26374

Far field radiation patterns of Cassegrain, offset paraboloid and horn reflector antennas by stationary phase approximation method
11 p2019 A70-26659

Cassegrain antenna feed system for satellite communication earth stations, noting low noise characteristics
11 p2011 A70-26716

Cassegrain antenna with parabolic mirror and switch designed for broadband transhorizon radio relays, using antenna scale model to determine parameters and electrical properties
11 p2020 A70-26823

Field correlation theorem for deducing Cassegrain antennas performance from internal field distributions, considering two reflector diffraction problems
15 p2698 A70-31953

Illumination efficiency in shaped two reflector Cassegrain antenna system related to feed pattern deviation
16 p2861 A70-32968

Cassegrain antennas design parameters using graphs for minimum blockage condition
19 p3376 A70-37690

Millimeter wave high gain Cassegrain antenna for wide bandwidth data link between communications satellites, obtaining accurate parabolic contours
21 p3799 A70-41359

CASSEGRAIN OPTICS

Cassegrain telescopes lens corrector systems, critically examining various published articles
02 p0297 A70-11927

Lund astronomical observatory, describing Cassegrain-Nasmyth reflector and attached electrophotometer for stellar measurements
02 p0275 A70-12061

Optical systems for coude focus spectroscopic telescopes, discussing advantages over Newtonian and Cassegrain foci
04 p0685 A70-14522

Cassegrainian liquid He cooled IR telescope for rocket-borne IR astronomy, discussing optical, cryogenic and electronic designs
04 p0689 A70-15017

CASSIOPEIA A

Cassiopeia A high resolution map at UHF revealing main source physical characteristics and enhanced emission compact components
12 p2309 A70-27976

X ray spectrum analysis for Crab, Cas A and SN 1572 supernova remnants
17 p3156 A70-34830

CASSIOPEIA CONSTELLATION

Supernovae and remnants, data concerning radio brightness distribution of Tycho supernova remnant and Cassiopeia and Crab Nebula origin
09 p1748 A70-21989

VX Cas brightness determination from color plates, giving values in tabular form
11 p2115 A70-26583

Coordinates and brightness characteristics of variable observed during photographic studies of VX Cas
11 p2116 A70-26584

Sounding rocket X ray survey of Cassiopeia region for supernova remnants and galactic source distribution
17 p3153 A70-34528

Gamma Cas star time and spectra observations, examining emission line profile variations and envelope and stellar model
24 p4404 A70-45415

CASTING
NT INVESTMENT CASTING
NT PROPELLANT CASTING

Filamentary casting technique for nonequilibrium alloy structures to produce continuous specimens by rapid solidification
04 p0698 A70-15135

Soviet papers on casting of aluminum, magnesium and titanium alloys
08 p1504 A70-21126

Al-Cr-Zr alloy ingots macrostructural inhomogeneities, studying roles of casting rate and additives in intermetallics primary crystallization
08 p1517 A70-21128

Molten Al alloys flow rate and behavior in various casting systems, considering gate geometry and casting temperature effects
08 p1505 A70-21133

Mold canting effects on nonporosity of Al alloys flat castings noting decreased metal losses
08 p1517 A70-21134

Porosity formation in Al ingots made by semicontinuous casting, considering metal grade and purity, gas content and homogenization conditions
08 p1505 A70-21136

Optimum composition of sand-bentonite materials for aluminum alloy casting in molds compacted by high pressure
08 p1506 A70-21137

Mutual thermal influence zone between parts of die casting during solidification established as function of time
08 p1506 A70-21138

Thermal interaction between casting and mold at beginning of cooling using mathematical model for temperature field
08 p1506 A70-21139

Solidification thermal conditions during Ti casting by melting out patterns in graphite molds, investigating heat accumulation coefficients in molds
08 p1506 A70-21142

Heat resistant cast alloys creep strength reporting criteria, comparing U.S. and European practices [ASM PAPER P9-15.2]
09 p1702 A70-22558

Mono Graf casting process for Ti alloy aerospace applications, utilizing high strength/weight ratio and corrosion resistance
17 p3097 A70-34361

Ti precision casting methods, emphasizing alloys peculiarities
17 p3097 A70-34362

High temperature Ni base superalloy stress-rupture life dependence on casting variables and section size
20 p3648 A70-39413

Creep resistant Ni-base superalloys ductility and thermal shock resistance improvement by precision casting technique, producing columnar grain and single crystal structures
20 p3648 A70-39415

CASTINGS
NT INGOTS
NT PROPELLANT CASTING

Effects of solidification conditions and gas content in melt on continuously cast Al ingots as-cast structure
02 p0316 A70-12297

Al solidification in direct chilling molds effect on as-cast structure, analyzing heat removal, casting rate and application of water to outgoing ingot
02 p0316 A70-12298

Grain refining of continuously cast Al by additions of B and Ti
02 p0309 A70-12299

Electrical resistivity, contact resistance and weldability of cast Cu and Ag contact materials reinforced unidirectionally by W wire compounded to powder composition
04 p0711 A70-14465

Mechanical properties of cast light alloys at low temperatures, showing satisfactory plasticity and insensitivity to stress raisers
05 p0864 A70-16868

Al casting design considering alloy materials selection and casting methods
06 p1076 A70-17602

Heat transfer effects during solidification on mechanical properties of Al alloy castings compared with sand castings [ASM PAPER W9-7.2]
07 p1293 A70-18998

Rare earth elements effects on microstructures and mechanical properties of cast Al, Al-Si and Al-Si-Mg alloys
08 p1516 A70-21127

Graphite shell molds for Al castings mass production
08 p1505 A70-21135

Heat exchange during solidification of castings in molds, studying thermal properties effect for achieving constant mold surface temperature
08 p1506 A70-21141

Graphite molds compaction pressure effect on Ti castings nonporosity and surface layers carburization
08 p1506 A70-21143

Silicon organic binding materials properties, assessing ethyl silicate-50 perspectives in fabrication of precision castings
08 p1506 A70-21144

Foundry facilities for high strength nodular, pearlitic malleable and Cr-Mo gray iron and Al castings
13 p2420 A70-29250

Cellular precipitation in laminar eutectic and cast Ni-Cr alloys
15 p2761 A70-32383

Freckles origin in unidirectionally solidified castings, noting convective jets role
20 p3646 A70-39102

CASUALTIES

Hazards model for probabilistic prediction of casualties by exploding solid propellant rockets, deriving casualty expectation equation [AIAA PAPER 69-461]
06 p1154 A70-17169

CATABOLISM

Heme catabolism in untreated rats and in animals treated with phenobarbital or porphyrogenic drug, comparing bilirubin and Co production
20 p3583 A70-40450

Protein catabolism increase during high altitude exposure to hypoxia in rats, noting amino acid incorporation into tissue proteins
22 p3967 A70-42459

Extreme environmental temperature effects on hepatic amino acid catabolism in rats attributed to caloric deficiency
23 p4148 A70-44790

Energy yield measurements of catabolic and anabolic activity in autotrophically growing *Hydrogenomonas eutropha*
23 p4149 A70-44997

CATALOGS

Catalog systems orientation based on major and minor planets observation, discussing zero points corrections

08 p1574 A70-21152

Catalog in tabular form of discrete celestial X ray sources in energy region above 2 keV

13 p2489 A70-28903

CATALOGS [PUBLICATIONS]

NT ASTRONOMICAL CATALOGS

Fourth Cambridge catalogue radio sources observed for right ascensions using east-west arm of Molonglo radio telescope, presenting data analysis procedures

01 p0191 A70-11362

Catalog of faint Ob stars between Carina and Centaurus

02 p0370 A70-12075

Aerospace ground air conditioning design, discussing ground support equipment, manuals, manufacturer catalogs, etc

07 p1248 A70-18808

Catalog of solar radio bursts recorded at 208 MHz during IGY and IQSY

08 p1570 A70-20843

Position determination for compact radio sources in 3C catalog

08 p1577 A70-21490

Weather situation persistency, using 500 mb contour chart catalog

16 p2945 A70-32950

CATALYSIS

Surface catalysis and variable transport properties effects on chemically frozen dissociated hypersonic air flow boundary layers enveloping flat plates and slender wedges

01 p0067 A70-11179

Ammonium perchlorate combustion catalysis, studying preflame heating and mixing effects on gas phase flame burning velocity

07 p1425 A70-20010

Composite propellant catalysts (copper chromate and chromite) thermal decomposition using simultaneous thermogravimetric and differential thermal analysis

11 p2100 A70-26382

CATALYSTS

NT ELECTROCATALYSTS

IR spectra of N isotopes adsorbed on nickel-on-Aerosil catalysts, investigating effects of intermolecular interaction and isotopic substitution

03 p0440 A70-13099

Silane coupling agents glass-catalyzed hydrolysis without presence of acid, discussing reaction kinetics

06 p1091 A70-17599

Raney alloy catalyst activity and stability in fuel cell anodes, noting properties of ternary phases of nickel, aluminum and iron, molybdenum or titanium

10 p1831 A70-24466

Raney catalyst preparation and continuous operation in molecular hydrogen and oxygen electrodes noting improved voltage, manipulation and energy yield

10 p1831 A70-24467

Electrochemically optimal structure for Raney alloy catalysts based on molecular hydrogen polarization temperature, noting beta and gamma phases and particle size influence

10 p1831 A70-24468

Low temperature fuel cell materials impurity effects on catalyst poisoning, stressing sulfur elimination from rubber molding

10 p1832 A70-25043

Temperature, solvent, catalyst and formaldehyde concentration effects on monosaccharide synthesis from formaldehyde condensation

13 p2362 A70-29327

Ignition delay-reducing catalyst for furfuryl alcohol-red fuming nitric acid hypergolic bipropellant

13 p2473 A70-29992

Liquid hydrazine decomposition by Shell 405 catalyst, determining gaseous products by gas chromatography and titrimetric analysis

16 p2856 A70-33603

Cellulose ion exchanger palladium catalysts preparation and applications in asymmetric hydrogenation reactions

17 p3042 A70-35125

Metal phthalocyanin catalyzed oxidation by oxygen of vanadium and iron couples in externally regenerated redox fuel cell cathode

22 p3966 A70-43536

Catalytic combustion fuel tank inerting techniques for fire protection in military and civilian aircraft

23 p4141 A70-44485

CATALYTIC ACTIVITY

Copper chromite catalyst effects on sublimated ammonium perchlorate dissociation products, noting applications to solid propellants

03 p0544 A70-13923

Ribonucleic acid polymerase bound with initiating purine triphosphate binding to product terminus site and pyrimidine triphosphate engaging in exchange binds to substrate site

03 p0442 A70-14046

Purification and properties of diphosphopyridine nucleotide-linked glycerol 3-phosphate dehydrogenases from chicken breast muscle and liver

03 p0442 A70-14047

Potassium permanganate catalytic effects on ammonium perchlorate deflagration, studying catalyst dispersion degree role

07 p1358 A70-19329

Molten carbonate fuel cells power source for military applications, considering catalytic recycle reformer

08 p1439 A70-20703

Kinetic model for acid catalyzed Delrin decomposition, testing for Delrin-citric acid system and predicting thermograms with nonlinear regression analysis

09 p1630 A70-22896

Oxygen reduction reaction mechanism and catalysis, considering metal electrode surfaces and substrates, hydrogen peroxide role, adsorption, metal-oxygen bonds, etc

10 p1829 A70-24452

Oxygen reduction in sulfuric acid with phthalocyanine-carbon catalysts

10 p1829 A70-24456

Raney alloy catalyst activity and stability in fuel cell anodes, noting properties of ternary phases of nickel, aluminum and iron, molybdenum or titanium

10 p1831 A70-24466

Catalytic load carrying capacity of porous carbon electrodes impregnated with nickel salt and nickel boride in anodic fuel cell hydrazine oxidation

10 p1831 A70-24469

Electrocatalytic activity of oxides in redox reactions without adsorption, noting application to hydrogen oxidation in acid medium

10 p1831 A70-24470

Refutation of Sylven-Snellman report of catalysis of benzoylarginine beta-naphthylamide and leucine beta-naphthylamide hydrolysis by beef spleen cathepsin B

10 p1812 A70-24534

Stannic oxide-chromium oxide catalyst effects on thermal decomposition and ignition of ammonium perchlorate (AP), calculating activation energy

11 p2100 A70-26281

Gold alloys electrocatalytic activity in cathodic reduction of oxygen in potassium hydroxide

12 p2182 A70-27760

Membrane-like properties of synthetic proteinoid microparticle systems, considering catalytic activities, size and ultrastructure

16 p2847 A70-33029

Spacecraft attitude control microthrusters utilizing catalytically reactive gas mixtures during pulse mode and steady state operation

16 p2969 A70-33611

Optically active organic compounds origin on primordial earth, emphasizing role of asymmetric catalyst

17 p3024 A70-34700

ADP-ATP catalyzed exchange reaction in turtle bladder microsomes, using chromatographic measurements of conversion rates

17 p3034 A70-35900

Laminar boundary layer equations on plate with arbitrary catalytic properties in diatomic gas flow undergoing vibrational dissociative relaxation

20 p3611 A70-39802

Thermally prepared poly-alpha-amino acids catalytic activity after long term dry state storage, suggesting enzyme activity role in biological evolution

21 p3772 A70-40713

Oxygen atom catalytic recombination and flame inhibition mechanism literature survey

23 p4157 A70-44002

Catalytic activities of thermal polyanhydro-alpha-amino acids for modeling enzymes and prebiotic protein

24 p4310 A70-45346

CATAPULTS

NT ROCKET CATAPULTS

Sun-planet systems capture and catapult capacity for interstellar bodies under close flyby conditions

04 p0753 A70-15144

Missile and rail launching structure combined dynamic response determined by discrete element dynamic analysis

12 p2312 A70-27116

Portable catapult and arresting gear analog instrumentation data acquisition system testing aboard aircraft carriers and at land-based facilities

19 p3384 A70-38533

CATARACTS

Laser radiation effects on lens lipid content in adult Rana temporaria frogs during cataract development

22 p3978 A70-43139

Safety standards and biological effects of microwave radiation, investigating cataractogenesis and heart rate in rabbits

23 p4144 A70-43790

CATECHOLAMINE

Catecholamines biosynthesis, distribution, combining, uptake, deposition, release and metabolism in physiological and pathological reactions of organism

01 p0019 A70-10512

Rats sympathoadrenomedullary response to increased oxygen tensions, measuring catecholamines, norepinephrine and epinephrine in adrenal gland, hypothalamus, serum and urine

01 p0024 A70-10979

Blood pH effects on adrenomedullary response to hemorrhage, studying catecholamines release in anesthetized dogs

02 p0235 A70-11733

Catechozamine excretion, cardiovascular functions and subjective effort in healthy male subjects under various physical work loads

05 p0801 A70-16141

Alpha-methyl-DOPA inhibitor effect on catecholamines and cardiac spontaneous activity in pacemaker fibers in rabbits

06 p0992 A70-17422

Beta-adrenergic blockade effect on abnormal R-ST segment and T-wave changes, showing propranolol use in stress catecholamine and organic cardiovascular diagnosis

08 p1449 A70-21945

Total body X irradiation effect on tyrosine hydroxylase and catecholamine levels in rats

09 p1616 A70-22318

Hypoxia biphasic effect on adrenal catecholamine content of guinea pigs and rats during short and prolonged periods

11 p1989 A70-26665

Standard urinary excretion by healthy adult for free adrenaline, noradrenaline, creatinine and hydroxymethoxy mandelic acid, making catecholamine determinations

12 p2168 A70-27622

Sympathoadrenals activity in pilots during supersonic flight, investigating urinary catecholamine output

15 p2690 A70-31891

Daily rhythm in accumulation of rat brain catecholamines synthesized from circulating tritiated tyrosine

16 p2848 A70-33096

Positive pressure breathing effects on cerebral blood pressure and catecholamine content of hypothalamus and adrenal glands in dogs

16 p2849 A70-33997

Hemodynamic response to dopamine before and after myocardial infarction in dogs

17 p2026 A70-35200

CATEGORIES

Research problems resulting from observational methods in social-psychological studies, discussing categorization systems and coding reliability

05 p0802 A70-16668

CATENARIES

Stress-strain state of catenoid, cylindrical and spherical shells of revolution, emphasizing catenoid shell bending problem

15 p2815 A70-31648

Single-frequency oscillations mode in nonlinear catenary systems, considering factors promoting stabilization and uniformity

23 p4218 A70-44344

CATENARY CURTAINS

U CURTAINS

CATHETERIZATION

Blood flow velocity and pressure measurements on conscious man with catheter-tip velocity probe

04 p0645 A70-15439

Miniaturized electromagnetic catheter flowmeter for measuring volume flow rate by potential difference between electrodes

15 p2689 A70-31747

First derivative of ventricular pressure recorded by conventional cardiac catheters, analyzing in terms of Fourier series

21 p3767 A70-40578

Atrioventricular conduction in the human heart, analyzing electrocardiogram response patterns recorded by electrode catheter in unanesthetized man

22 p3970 A70-42942

CATHETEROMETERS

Doppler flowmeter-catheter system to record aortic flow velocity in man during cardiac arrhythmias, considering atrial fibrillation, heart block, etc

02 p0241 A70-12697

CATHODE RAY TUBES

Hardware CRT display system based on digital computer for dynamic flight simulation of moving spatial objects

01 p0089 A70-10818

CRT resolution measurements by double slit method, relating light spot response to slit width

01 p0093 A70-11278

Numeric keyboard CRT display for weather data acquisition from ships at sea, utilizing ATS-3 satellite as transmission medium

01 p0048 A70-11279

Display console characteristics for meeting increasing applications, predicting price reduction trends, color emphasis and CRT competition as primary display component

01 p0221 A70-11286

Projected and head-up flight information displays using cathode ray tubes, discussing optical system, lens design and landing aid application
02 p0330 A70-11843

Broad bandwidth electronic analysis of high resolution photographic film using flying spot CRT or rotating mirror devices
02 p0302 A70-12613

Scanned CRT display optimum spot size in relation to raster pitch, assuming Gaussian luminance distribution
04 p0691 A70-15136

Display storage tubes /DST/ for radar systems, describing operating principles and characteristics
04 p0660 A70-15525

CRT display design for command and control with digital symbol and vector generation
05 p0817 A70-16184

Color CRT system to display engineering data based on real time analysis, discussing performance requirements
06 p1061 A70-17349

Alphanumeric and graphic computer driven CRT displays, discussing systems and component selection
08 p1465 A70-20672

Pulse characteristics of scintillator- photomultiplier-cathode ray tube channel for oscillographic recording of nanosecond pulses from neutron, gamma or X ray sources
08 p1496 A70-21218

Computer managed display system using CRT and appropriate solid state displays providing flight crew with automatically sequenced time varying information
08 p1498 A70-21677

CRT display devices and R and D, discussing electron generation, luminescent materials, resolution, brightness, etc
08 p1498 A70-21680

Thermochromic materials feasibility for applications in CRT display devices, observing reversible color changes during electron beam irradiation
08 p1499 A70-21682

Resolution, contrast and gray scale performance of CRT displays compared to dot matrix displays
08 p1500 A70-21763

CRT color displays advantages and limiting factors, considering beam-penetration tube with high voltage switching
09 p1673 A70-22031

Projection CRT with liquid-cooled phosphor faceplate, showing linear relationship between brightness and beam current
09 p1673 A70-22034

Hidden-line determination for computer-drawn polyhedra using edge classification scheme for CRT display applications
09 p1641 A70-22966

CRT laser with gallium arsenide crystal excited by electron gun, describing output characteristics
09 p1698 A70-23161

Temperature limitation on CRT tube performance in high brightness displays imposed by glass breakage danger, discussing liquid cooling of phosphor substrate
09 p1686 A70-23759

CRT displays for business aircraft emphasizing EADI/electronic attitude director indicator/
[SAE PAPER 700210]
11 p2079 A70-25882

Current-sensitive single gun color CRT with phosphor screen for display systems
12 p2195 A70-27373

Virtual infinity CRT display systems testing, discussing effects of large apertures, operational modes and observer physiological requirements on measurements
13 p2411 A70-29790

Dual raster high brightness-high resolution TV display using time sharing with conventional CRT
16 p2903 A70-33131

On-line optical data processing using CRT with electro-optic target crystal
16 p2903 A70-33132

CRT symbol generators design for high speed computer data display as function of electro- optical and human operator constraints
16 p2850 A70-33133

Computer driven on-line CRT graphics displays for data acquisition and reduction
17 p3063 A70-35513

Four dimensional matrix type CRT decoder characterized by large storage capacity and high resolution
18 p3256 A70-36105

Sodalites color centers creation by electron beam, discussing application in dark trace cathode ray storage display tubes
19 p3379 A70-38048

Air traffic control CRT plan position indicators, considering alphanumeric symbols strokes design
19 p3469 A70-38645

Flickerless regeneration rates for CRT displays as function of scan order and phosphor persistence, using computer experiment
24 p4298 A70-45511

CATHODES

NT CELL CATHODES

NT COLD CATHODE TUBES

NT COLD CATHODES

NT HOT CATHODES

NT PHOTOCATHODES

NT PHOTOMULTIPLIER TUBES

NT THERMIONIC CATHODES

NT TUBE CATHODES

NT TUNNEL CATHODES

Spectroscopic determination of radial temperature distribution at various currents in negative glow of hollow cathode discharge, analyzing influence of gas pressure
05 p0888 A70-16358

Optical spectra of discharge chambers of electron bombardment mercury ion thrusters with hollow and oxide cathodes
[AIAA PAPER 70-176]
06 p1132 A70-18157

SERT 2 thruster hollow cathode durability tested in bell jar
[AIAA PAPER 69-304]
07 p1364 A70-19703

Cylindrical magnetrons steady state characteristics with thick and infinitely thin cathodes for full space charge and inclined magnetic field
09 p1651 A70-23641

Hollow cathode mercury electron bombardment thruster design, emphasizing low specific impulse operation and discharge chamber improvements
13 p2473 A70-28505

Microwave harmonic generation by nonlinear plasma- metal junctions noting calcium, gallium, molybdenum, gold, copper and platinum cathodes
14 p2549 A70-30438

Penning pump argon stability, noting influence of pressure and ion incidence angle on cathode surface
15 p2744 A70-31847

Liquid mercury /LM/ cathode thruster characteristics, power conditioning and control requirements
[AIAA PAPER 70-646]
16 p2965 A70-33536

High resistance space charge region formation near crystal cathode in GaAs due to limited contact emissive capacity
18 p3297 A70-36417

Arc luminosity in cathode region of quasi-steady MPD arc jet, using high speed photography and electric and magnetic field probes
[AIAA PAPER 70-1094]
20 p3683 A70-40242

Small-orifice hollow cathode discharge properties in electron bombardment ion thrusters, using vaporized mercury propellant
[AIAA PAPER 70-1087]
20 p3693 A70-40248

Cathode geometry effect on performance of radiation cooled MPD arc thruster in continuous mode
[AIAA PAPER 70-1083]
20 p3693 A70-40252

Cathode spaces electron concentration, time dependence and axial distribution by laser beams interferometric method, noting accuracy and resolution
21 p3836 A70-40796

CATIONS

NT MANGANESE IONS

NT METAL IONS

Flame positive ion concentration measurements with Langmuir probes with mean free path smaller than probe diameter
02 p0397 A70-12019

Direct interaction between hydrogen atom and positive ion with one electron, using Born and two and four state impact parameter treatments
02 p0344 A70-12703

Cross sections determined for formation of secondary positive molecular and atomic hydrogen ions during 1.4-46 kev positive molecular hydrogen passing through hydrogen
02 p0344 A70-12704

Synthesis of 1-oxacyclopent-1-enyl cations from cyclopropyl ketones on heating in strong acids noting rearrangement rates
04 p0646 A70-15088

Bivalent cations effect on crystallization and viscosity of glazed glass
05 p0871 A70-16592

Heavy positive ions pulse counting by spiral-type continuous channel electron multiplier, noting long pulse rise time composed of numerous after pulsing
07 p1286 A70-19970

Secondary electron emission coefficients and energy distributions to investigate interaction between positive ions and Cu/Be dynodes of electron multiplier
07 p1344 A70-20127

Initial deceleration of solar wind positive ions upstream of earth bow shock determined from OGO 5 high time resolution plasma measurements
08 p1562 A70-21377

Cross sections for electron impact excitation of positive helium and hydrogen ions, using non-relativistic Coulomb-Born-Oppenheimer reactance matrices
13 p2455 A70-28988

Plasmapause irregular structure and position indicated by measured distributions of hydrogen and helium thermal positive ions in duskside magnetosphere
13 p2397 A70-29185

Spectrophotometry of comet Honda 1968c, showing free cation and radical emissions and head asymmetry
14 p2635 A70-30304

Semiclassical collision theory for computing fine structure proton impact excitation rates and cross sections for positive ions, presenting excitation rate tables
14 p2652 A70-31383

Positive ion composition in Cs plasma as function of normalized pressure
15 p2779 A70-31978

Triatomic hydrogen positive ion-yielding reactions, using EVA ion-molecule beam apparatus
16 p2855 A70-33012

Gas phase stabilities of bicyclic cations, establishing heats of formation limits by ion- molecule reactions identification
16 p2848 A70-33091

Positive atomic oxygen ion reactions with carbon dioxide detected using ion cyclotron and double resonance methods
18 p3225 A70-36189

D region positive ion density during solar proton event by Arcas rocket-borne cylindrical electrostatic probe
19 p3411 A70-37512

Pi sub u states of positive ionized diatomic oxygen by photoelectron spectrometry
19 p3474 A70-38488

Positive ions energy dispersion effused from RF plasma, presenting ion extraction model for plasma sheath system and equivalent circuit
20 p3678 A70-39608

Positive ionospheric ion species concentration measurements using magnetic deflection mass spectrometer on Explorer 31 satellite
21 p3815 A70-40999

Fe 57 nuclear hyperfine splittings in clinopyroxenes from lunar igneous rocks, determining temperature dependent cation distribution
21 p3915 A70-41659

Atmospheric positive ion composition measurements in D region by rocket-borne mass spectrometers, considering water cluster ions formation
22 p4017 A70-42796

Monovalent cations active transport model in mitochondria, noting membrane potential as driving force and ion pump omission
24 p4304 A70-46230

CATS

Cortex functional interrelationships with hypothalamus and formatio reticularis, studying role of corticofugal effects in anesthetized cats
01 p0012 A70-10051

Corticofugal effects of various cortical regions on neuron activity in hypothalamus posterior lateral sections in cats
01 p0012 A70-10053

Reversible cold induced deactivation of cat neocortex bioelectric activity in chronic experiment, noting cooling system
01 p0031 A70-10056

Microelectrophysiological study of cerebellar neuron responses to stimulation of vestibular apparatus by vertical rocking performed on anesthetized adult cats
01 p0012 A70-10124

Termination mode of primary and secondary vestibular fibers in cerebellar cortex of frog and cat, measuring evoked field and unitary potentials
01 p0014 A70-10353

Integrated static discharge frequencies of cat lingual cold receptors measured as function of constant temperature
01 p0017 A70-10472

Artificially induced heart rate changes effect on atrial circumference and pressure in anesthetized cats, showing increase with tachycardia and bradycardia
01 p0017 A70-10473

Flash blinding of cats using Q switched laser beam, discussing ERG response and retina changes
01 p0113 A70-10920

Morphological analysis of connections between auditory cortex zone and claustrum in anesthetized cats, establishing efferent nerve fibers presence
01 p0025 A70-11039

Human and cat visual neuron properties, discussing encoding orientation and dimensions of retinal images
01 p0028 A70-11360

Vasomotor activity of neurons located in spinal cord lateral crescent in curarized decerebrated and intact cats
01 p0030 A70-11471

Muscle force and electromyogram behavior with alteration in blood flow and composition in anesthetized cats
02 p0231 A70-11708

Cardiac relaxation mechanics from isolated preparation of cat papillary muscle, noting inotropic influences role
02 p0231 A70-11709

Blood flow changes in portal vein and hepatic artery of anesthetized cats following intraportal and in-

trahepatic arterial administration of isoproterenol, epinephrine and norepinephrine

02 p0232 A70-11718

Polarographic method for determining cat papillary muscle oxygen consumption used to investigate Fenn effect involving afterloaded and isometric contractions

02 p0234 A70-11726

Spinal cord and skin temperature effects on tension-extension diagrams in cats red and pale muscles

02 p0236 A70-12092

Skin sensitivity representation in cats cerebellar cortex during electrocutaneous stimulation in chronic experiment, providing information on afferent system

03 p0417 A70-13216

Cats cerebral cortex background electrical activity measured during development of conditioned reflexes, noting shift toward higher frequencies

03 p0418 A70-13217

Somatosensory cortex removal effect on blocking action of skin stimulation on associative response to light flash in cats

03 p0420 A70-13430

Early and late response component of associative cortical area in cerebral hemispheres of cats connected with mono and polysensory neuron activity

03 p0421 A70-13688

Origin and functional designation of associative evoked potentials in orbital cortex of cats, showing phases connected with neuron activity and excitation

03 p0422 A70-13689

Vascular electrical activity in cats and rats by inserting glass microelectrode into blood vessel, showing blood flow conditioning effect on activity

03 p0422 A70-13691

Vagotomy and carbon dioxide concentration effect on quiet and forced respiration rate, pleural pressure, tidal volume and lung ventilation in cats

03 p0422 A70-13694

Immobilization effects on alpha rhythm, locomotor coordination and visual alimentary motor reflexes of cats

04 p0629 A70-14570

Small amplitude discharges and neuron activity in dorsal hippocampus of cats recorded simultaneously with pyramidal cell activity

04 p0632 A70-15221

Cats trained for visual form discrimination tested for retention and reversal performance, studying oxygen deprivation influence

04 p0633 A70-15443

Rod and cone contributions to S potentials from cat retina using spectral sensitivity observation

05 p0801 A70-16379

Rod-cone interaction in cat S potentials, analyzing effect of wavelength and intensity upon dark adapted responses

05 p0801 A70-16380

Rod aftereffect relationship to percent rhodopsin bleached in S potentials from cat retina

05 p0801 A70-16381

Vasomotor center neuron responses to vertical rocking movement stimulus of vestibular apparatus in cats

06 p0995 A70-17805

Cats visual analyzer functional rearrangement mechanisms under prolonged light stimulation, considering evoked potential dependence on pulse duration and intensity

07 p1198 A70-18699

Involvement reactions in dying and reanimated cats with nucleus reticularis hypothalamus stimulated by rectangular electric pulses

07 p1209 A70-19522

Hypothalamus stimulation effect on electrical activity of hippocampus at threshold and super-threshold levels in cats

08 p1446 A70-21448

Body vibration effects in cats on myocardial ECG recordings, discussing electrodes implantation and tracings

10 p1810 A70-24007

Feline hypersexuality, aggression and perceptual disorientation resulting from p-chlorophenylalanine administration

12 p2167 A70-27271

Noise bursts response of positive and inhibitory conditioned eyelid reflexes in cats brain, discussing auditory system function

15 p2687 A70-32871

Spinal reflex activity in normal and altitude exposed cats before, during and after acute hypoxia

17 p3031 A70-35430

Cat lens motion in response to ciliary ganglion step and sinusoidal stimulation, indicating damped accommodative system

19 p3366 A70-38925

Desynchronized sleep phase in cats, discussing activation and hippocampal theta and hippocampal delta rhythm predominance stages

20 p3574 A70-40171

Ganglione and quaterone cholinolytic agents effects on arterial blood acid-base balance indicators in cats

24 p4298 A70-45633

CATTLE

Physicochemical properties of hypothalamic secretions responsible for coronary dilatation in rats, cattle and pigs, using analytical techniques

03 p0417 A70-13215

Enzyme beta-hydroxybutyrate dehydrogenase concentration in mitochondria from bovine and sheep liver

03 p0430 A70-14198

CAUCHY INTEGRAL FORMULA

Cauchy integrals extension to axisymmetric elasticity problems, obtaining numerical results for stressed circularly symmetrical state of hollow cylinder under uniform load

03 p0586 A70-13080

Numerical differentiation of analytic functions involving Cauchy formula and error estimation

18 p3282 A70-36362

CAUCHY PROBLEM

Fourier transform applied to Riemann boundary value solution to biharmonic equation governing elastic theory for half plane with circular protrusion or indentation

01 p0199 A70-10155

Cauchy problem solution asymptotic behavior for linearized system of rotating compressible fluid at time approaching infinity

01 p0064 A70-11031

Cauchy problem of differential equation describing asymptotic nature of conservative system motion resulting from nonperiodic perturbing force

03 p0524 A70-13342

Approximate solutions to Cauchy problem describing controlled pursuit using approximate method of integrating Bellman equation

04 p0713 A70-14602

Mixed nozzle flows solution complex boundary value problem reducible to Cauchy problem for hyperbolic system with three dependent variables by applying flow stabilization method

04 p0617 A70-15236

Right weak solution of Cauchy problem for first order quasi-linear equation

06 p1093 A70-17531

Existence results for Cauchy problem for linear variable coefficient hyperbolic operators with multiple characteristics

06 p1094 A70-17898

Optimal control problem converted Cauchy problem for obtaining numerical solutions through invariant imbedding

06 p1027 A70-18508

Boundary value problems and Cauchy problem considered for mathematical model of turbulent motion in liquid or gas

07 p1252 A70-18671

Nonuniqueness of Cauchy problem for parabolic equation of order 2b with rapidly increasing coefficients at infinity

07 p1322 A70-18855

Power series solution of Cauchy problem for axisymmetric state of ideally plastic body

07 p1405 A70-19288

Infinite order differential operator in S type spaces for Cauchy problem solution uniqueness

08 p1533 A70-20722

Cauchy-Dirichlet problem for linear inhomogeneous polycaloric / polyparabolic / equation with constant coefficients under certain boundary conditions

08 p1597 A70-21006

Nonlinear relativistic wave velocity distribution within spherical nucleus bounded by shock wave in superdense gas determined by Cauchy problem

08 p1484 A70-21403

Cauchy problem solution for linearized Navier-Stokes equations of incompressible rotating viscous fluid, discussing velocity and angular momentum effect on asymptotic behavior

09 p1659 A70-22326

Cauchy problem solution for heat conduction equation stabilization, deriving necessary conditions

09 p1789 A70-23167

Point boundary value problem solution for differential equations with parameters in form of power series, considering Cauchy problem

09 p1712 A70-23383

Algorithm developed for constructing first approximation system from Cauchy matrix for Liapunov stability problem solution

10 p1917 A70-25302

Local uniqueness and instability theorem for Einstein-Liouville equations using energy inequalities, noting relevance to Cauchy problem

11 p2084 A70-26458

Sonic surface and Cauchy problem of Monge-Ampere equations in plane unsteady transonic channel flow solved by hodographic analysis

12 p2156 A70-27299

Asymptotic properties of Cauchy problem solution for heat conduction equation

12 p2331 A70-27300

Cauchy problem for relativistic heat equation for unbounded domain generated by streamlines of future oriented vector field

13 p2451 A70-28709

Rotating stellar configurations structure consisting of degenerate matter or density dependent temperature describing boundary value problem reduction for Cauchy problem

13 p2494 A70-29518

Boundary value problems and Cauchy problem considered for mathematical model of turbulent motion in liquid or gas

15 p2718 A70-31463

Cauchy spatial problem of Laplace equation, obtaining approximate solution based on initial conditions

15 p2767 A70-31584

Nonrigorous hyperbolic systems, discussing existence and uniqueness theorems contradiction in linear equations and proof of Cauchy problem

19 p3478 A70-37582

Cauchy problem for linearized relativistic Boltzmann equation near equilibrium, using functional analysis

19 p3403 A70-37585

Initial boundary value problems for hyperbolic partial differential equations, including Cauchy problem

19 p3457 A70-37678

Polynomial approximation process for scalar nonlinear equation solution, applying to Cauchy problem

22 p4064 A70-43482

Cauchy-Dirichlet type mixed problems for hyperbolic equations in cylindrical domain, using Zygmund-Calderon approximate calculus

23 p4210 A70-43978

Cauchy problem solution for parabolic equation with variable coefficients, using differential invariant method and Volterra integral equation

23 p4210 A70-43979

Ordinary differential equations boundary value problems solution based on continuation and reduction to Cauchy problems

23 p4211 A70-44309

Approximate method for solving thermal conductivity first boundary value problem via reduction to auxiliary Cauchy problem solved by Laplace transform and power series

23 p4277 A70-44339

Cauchy problem for singular parabolic equation, establishing existence, uniqueness and representation theorem by integral operator techniques in conjunction with function-theoretic methods

23 p4212 A70-44895

CAUCHY-RIEMANN EQUATIONS

Error estimation during application of Cauchy approximate integral formulas to numerical differentiation of analytic functions by quadrature

01 p0131 A70-10543

Stress-strain state equations of shallow spherical shells in rectangular and polar coordinates, discussing reduction to plate and Cauchy-Riemann equations

03 p0591 A70-13427

Boundary value problems of Cauchy-Riemann differential equations using solution to derive integral equation for stationary infrasonic flow

04 p0671 A70-15094

CAUSTICS

U ALKALIES

CAVITATION

U CAVITATION FLOW

CAVITATION CORROSION

Liquid oxygen and water cavitation effects on lead, copper, nickel, iron and zinc

01 p0115 A70-10071

Damage data comparison for vibratory cavitation and liquid impact on aluminum alloy, stainless steels and pure nickel

23 p4203 A70-43870

CAVITATION FLOW

Cavitation initial phase flow model, analyzing flow past stepped obstacle in plane channel

01 p0064 A70-11002

Two dimensional plane and axisymmetric free streamline flow problems solved by finite difference methods for supercavitating wedge in potential flows

01 p0065 A70-11127

Cavitating flow in converging channels of hydraulic system, calculating energy distribution at gas-vapor phase using Borda-Carnot theorem

03 p0466 A70-13513

Jet pump cavitation prediction and elimination using limiting-flow equation based on selected index [ASME PAPER 69-WA/FE-29]

04 p0666 A70-14773

Penetration depth calculation of high speed non-deformable sphere into massive body, approximating force on sphere by ideal incompressible fluid cavitating flow

04 p0776 A70-15269

Flow distribution inside triangular shaped cavities of variable depth resembling liquid propellant rocket motor baffle cavities, simulating radial and tangential oscillation modes

04 p0674 A70-15566

Axial flow pump impellers suction performance and cavitation conditions

06 p1075 A70-17137

Sweep angle relationship to cavitation inception on hydrofoils and to hydrofoil performance deterioration due to cavitation

06 p1032 A70-17211

Heat transfer from impinging gas jets on enclosed concave surface, noting self recirculation currents within cavity

07 p1425 A70-20413

Stability and potential cavitation of centrifugal pump operating with four working wheels with different geometric parameters

08 p1558 A70-21196

Flow structure in rectangular cavity in lower wall of two dimensional channel for various aspect ratios and Reynolds numbers

08 p1484 A70-21313

Nonlinear equations for large fluid oscillations in axisymmetric rotating cavities with radial partitions

09 p1660 A70-22438

Boundary value problem for cavitating flow around thin wing reduced to two dimensional singular integral equations from acceleration potential

09 p1663 A70-23393

Cavitational symmetric flow around wedge taking into account gravity and surface tension

10 p1868 A70-24162

Steady two dimensional cavity flow past sharp-edged airfoil and blunt nosed obstacle, using linearization hypothesis

10 p1801 A70-24193

Swirl velocity and cavity stability in rotating container filled radially through porous cylindrical wall at constant and applied pressure

10 p1868 A70-24195

Two dimensional unsteady fluid flow in square cavity numerically analyzed from continuity and Navier-Stokes equations and recorded as computer-generated motion picture

11 p2035 A70-25971

Tribonucleation emphasizing viscosity-velocity product in gas nuclei formation and cavitation

12 p2170 A70-27661

Ideal weightless fluid jet flow past supercavitating plate at incidence using Tulin scheme

12 p2214 A70-28241

Film cavitation between flat annular surfaces in face seal resulting from hydrodynamic pressure generated by misalignment and surface waviness

13 p2417 A70-28613

Longitudinal gravitational field effect on cavitation wedge flow, investigating characteristics by Zhukovskii-Roshko method

13 p2390 A70-29646

Bubbles, steady streaming and surface instability in vibrated liquid columns

14 p2663 A70-30255

Liquid metals pump with cylindrical hydraulic coupling for actuating axial wheel, investigating cavitation and pumping effects on performance

14 p2535 A70-31012

Cavitation in centrifugal pumps, predicting breakdown and inception points variation with temperature and speed

15 p2744 A70-32097

Centrifugal pump performance correlation parameter under cavitation conditions for handling different liquids based on bubble growth theory

15 p2720 A70-32098

Soviet book on hydrodynamics of flows with free boundaries, covering fluids penetration by solid body, hydrofoil motion, cavitation flow, etc

16 p2890 A70-32912

Hydrodynamic internal streamline flow analysis for turboprop inducer blades under cavitating and non-cavitating conditions

16 p2964 A70-33528

[AIAA PAPER 70-629]

Cavitation nuclei in liquids, discussing sources, stability and gas bubble growth

16 p2891 A70-33632

[ASME PAPER 70-FE-23]

External magnetic field effect on cavitation zone behind circular cylinder, proving existence of electric charges

18 p3242 A70-36645

Rotational stability of heavy horizontal shaft supported on plain lubricated bearings with cavitation in lubricant

19 p3438 A70-38669

Nucleation role in boiling and cavitation - ASME Conference, Detroit, May 1970

21 p3948 A70-41201

Self similar flow instability behind collapsing cavity boundary, examining perfect gas adiabatic equation of state

21 p3808 A70-41500

Plunger pump for aircraft hydraulic systems, measuring working fluid temperature effect on cavitation

22 p3965 A70-42817

Cavitation characteristics of jet nozzles, formulating relationship between pressure differential and fluid flow rate

22 p3965 A70-43369

German monograph on flow phenomena in gas containing fluids, covering pressure and ultrasonic induced cavitation in steady and unsteady flow

24 p4324 A70-45098

Partially cavitating flow past plate, calculating characteristics by Riabushinskii scheme

24 p4325 A70-45642

CAVITIES

High temperature solar energy converter cavity absorbers geometry, considering absorption parameters of radiation reflected by concentrator

01 p0010 A70-10761

Boundary value problems of elasticity theory in space perforated by cylindrical cavities with parallel axes solved by infinite algebraic equations

01 p0202 A70-11033

Integral equation for emissivity inside uniform gray isothermal Lambertian cavity solved using successive approximations

02 p0323 A70-11889

Approximate method of boundary perturbation to solve elasticity and viscoelasticity problems for non-canonical bodies of revolution applied to stress concentration at ellipsoidal cavity

03 p0591 A70-13439

Soviet book on boundary value problems involving motion of ideal fluids in unsteady cavities of various geometries, determining attached fluid masses and oscillation frequencies

04 p0666 A70-14678

Stress concentration effects around spherical cavity under uniaxial tension calculated by constitutive equations of micropolar elasticity

05 p0927 A70-15994

Prestrain effect on cavity formation at grain boundaries causing creep strength decrease

07 p1307 A70-19392

Elastic harmonic waves propagation in cylinder with longitudinal cavities and in space with cylindrical cavities solved using series method

09 p1783 A70-23387

Nonlinear plane deformation of elastic medium with cylindrical cavity under uniform axial tension using successive approximations

09 p1784 A70-23591

Stress concentration near ellipsoidal cavity in transversely isotropic body using solutions for transversely isotropic ellipsoid of revolution

11 p2129 A70-25564

Solar energy exchange with radiator surface recessed within specular axisymmetric cylindrical spinning cavity, using deterministic ray tracing scheme

11 p2150 A70-26353

Motion stability of variable mass solid body with ideal liquid filled cavities about stationary point using Liapunov theorem

13 p2452 A70-29310

Plane cavity geometry behind plate in incompressible potential flow, deriving geometrical functions to obtain desirable shapes

13 p2390 A70-29645

Stress and deformations three dimensional solution in semiinfinite elastic body with spherical cavity based on Boussinesq stress function

14 p2661 A70-31328

Perturbed motion of body with partially filled cylindrical cavity with damping ribs, discussing vibrations boundary value problems of liquid filling

15 p2775 A70-32157

Circular cylindrical cavity in elastic space, calculating stresses due to incident plane harmonic compression wave

15 p2819 A70-32204

Nonlinear elasticity equations in displacements by Green and Hencky deformation tensors, discussing stress-strain of body with spherical cavity

16 p2988 A70-33251

Acoustic cavities use in suppressing acoustic modes of combustion instability demonstrated on LM ascent engine

16 p2998 A70-33614

[AIAA PAPER 70-618]

Combustion instability due to narrow cavities in solid propellant engines

17 p3198 A70-35739

Cumulative jets during shock induced collapse of air cavities in thin fluid layers, using high speed motion picture photography

17 p3074 A70-35742

Reflectance measurements of directional spectral emittance of black body cavities with specific geometries, using laser source and integrating hemi-ellipsoid

20 p3627 A70-39091

Radiative transfer among surfaces forming long cavity exposed to collimated incident energy

21 p3944 A70-41022

Cylindrical cavity uniform expansion in compressible elastic plastic solid, calculating pressure by similarity solution

22 p4114 A70-42634

Spherical cavity nonuniform expansion in compressible elastic plastic solid, calculating velocity field and pressure by approximate similarity solution

22 p4114 A70-42635

Cavity radar cross section estimation by simplified models compared to semiempirical prediction with ray tracing procedure

22 p3992 A70-43583

Isotropic nonlinear elasticity problems of stress concentration near spherical cavity in field of triaxial tension, using small parameter method

22 p4120 A70-43714

Elasticity theory for circular cylinder weakened by cavities, discussing boundary conditions on butt ends and Galerkin solutions

23 p4265 A70-43983

Nonlinear elasticity equations in displacements by Green and Hencky deformation tensors, discussing stress-strain of body with spherical cavity

23 p4268 A70-44287

One-dimensional propagation of elastic spherical waves in inhomogeneous unbounded medium under normal stress on cavity surface

24 p4424 A70-45631

CAVITY RESONATORS

Resonant cavity method for measuring varactor diodes cut-off frequency, avoiding errors from circuit losses and parasitic effects

01 p0048 A70-10049

Confocal parameters, spot sizes, waist positions and stability conditions of astigmatic Gaussian beams formed by spherical mirror laser cavity resonators

01 p0108 A70-10426

Laser mode locking due to saturable absorbers taking into account dispersive property of active material, expanding electric field within cavity

01 p0109 A70-10428

Raman effect liquid laser power as function of cavity length, using Q switched ruby laser beam focused by cylindrical lens for optical pump

01 p0111 A70-10674

Unstable laser resonator mode patterns and losses with finite rectangular reflectors of spherical curvature, basing analysis on Cornu spiral

01 p0112 A70-10917

Polarization level dependence of dye lasers emission on angles between direction of forced radiation and pumping laser resonator axis

01 p0113 A70-11037

CW visible ring cavity parametric oscillator, discussing pump depletion, conversion efficiency and improved stability resulting from optical isolation

01 p0052 A70-11173

Thermal resonator effects on YAG-Nd laser rods with dielectric covered ends, using resonant model to study continuous or half wave operation

02 p0311 A70-11850

Mode selection in Ar ion laser by plane resonator mirror with hole, plotting output power vs L/R parameters

03 p0500 A70-13458

Frequency spectrum, Q factor and single mode selectivity of two mirror laser resonator with absorbing thin metallic films, showing agreement for Ag and Ni

03 p0500 A70-13459

Cavity resonator linear excitation by Gunn diode, considering external circuit effects on oscillation conditions and GaAs single crystal parameters

03 p0457 A70-13965

Microwave cavity perturbation measurements of electron densities at electroacoustic resonances excited in afterglow plasma

04 p0728 A70-15004

Rate equation analysis of steady state behavior of double cavity GaAs diode laser, noting solution stability by perturbation method

04 p0703 A70-15618

Microwave spherical resonator and reentrant cavity as diagnostic tools to obtain discrete point data along plasma column compared with cylindrical cavity

04 p0696 A70-15650

Power distribution in carbon dioxide laser resonator with external and internal mirror at different power levels

05 p0857 A70-15796

Power output of gas laser pumped by laser contained in single resonator

05 p0858 A70-16259

Carbon dioxide laser resonator design and operation, discussing performance with dish reflector made of leucosapphire

05 p0859 A70-16272

Wobblator measurement of Q factor of microwave resonator cavities using double modulated klystron signal

05 p0822 A70-16528

Optimal electron bunching in two cavity klystron by varying parameters and nonlinear one dimensional approximation

05 p0823 A70-16888

Convection currents calculation in multicavity klystron allowing for space charge forces influence

05 p0823 A70-16889

Bistable optical resonators with saturable absorbers, discussing hysteresis characteristics and Q switching applications

06 p1105 A70-17449

Weinstein approximation and iteration by digital computer for calculating disturbed Fabry-Perot laser resonator modes

06 p1081 A70-17546

Klystron amplifier output circuit large signal frequency response, showing dependence on distance between cavities

06 p1021 A70-17672

Polarization interference filter as laser resonator frequency selector, showing Q factor measurable within spontaneous emission line

06 p1082 A70-17771

Helmholtz resonator associated flow field analysis in nonlinear regime, considering external pressure, mean flow, velocity fluctuations and orifice flow [AIAA PAPER 70-128]

06 p1038 A70-18065

Apparent resonance frequencies of earth-ionosphere cavity excited by single dipole source, noting dependence on source-observer separation

06 p1058 A70-18414

GaAs lasers fabrication, discussing p-n junctions formation, laser die mounting, low resistance electrical contacts, optical cavities, etc

07 p1298 A70-19398

Resonator aberrations and active element imperfections effect on formation of spatial and angular structures of solid state laser modes

07 p1299 A70-19854

Variable coupler for liquid helium X band EPR cavity during immersion in coolant

07 p1286 A70-19976

Solid state lasers thermal resonator bucking time dependence and compensation, graphing results of resonator field analysis

07 p1303 A70-20359

Laser resonator with concave mirrors and ring aperture as radiation outlet, calculating natural oscillations by wave equation

08 p1510 A70-20508

Stokes components generation in presence of stimulated combination radiation in optical cavity, considering interaction between components and effect of material dispersion on interaction

08 p1510 A70-20511

Polarization anisotropy effect of laser cavity on neodymium glass laser output power

08 p1510 A70-20513

Stokes components simultaneous generation in presence of stimulated combination radiation in optical cavity, noting effects of incident monochromatic beam intensity

08 p1511 A70-20520

Retunable lasers with organic dye dispersive resonators, studying space-angular, spectral and energy emission characteristics

08 p1511 A70-20538

Dispersive resonator for near IR frequency control of neodymium-silicate glass laser

08 p1512 A70-20850

Photodissociation of perfluoroalkyl iodides filler of pulsed laser operating cavity, discussing thermal molecular dissociation and unexcited iodine atoms formation

08 p1513 A70-21418

Double resonator ruby maser dynamic and static characteristics for centimeter band improved by pumping frequency modulation

09 p1695 A70-22188

Natural frequencies and electromagnetic field distributions in rectilinear and cylindrical dielectric resonators used in microwave circuits

09 p1644 A70-22280

Microwave in-cavity modulation of helium-neon laser, obtaining frequency dependence of modulation depth

09 p1696 A70-22628

Amplifier properties and oscillator mode structure of multipath carbon dioxide laser

09 p1699 A70-23538

He-Ne laser emission electro-optical modulation by three mirror optical cavity, considering structural and thermal stability and coupled resonators geometry effects

10 p1899 A70-24260

Microwave pencil triodes and cavities of miniature design for Air Traffic Control Beacon Systems

10 p1852 A70-24886

Microwave IC-compatible resonators for communication systems filters, comparing microstrips, disks, waveguide cavities and dielectric-loaded cavities

10 p1852 A70-24892

Microwave power absorption in plasma investigated by transmission cavity excited in TE mode, determining electron density and collision frequency

11 p2089 A70-25841

Tapered resonance tubes matching supersonic air jet geometries considered for explosion hazards created by pneumatic system seals failure

11 p2035 A70-25981

Optical resonator with active medium and lenses, determining caustic surface, radiation characteristics, transverse modes, focusing conditions, etc

12 p2246 A70-27309

Operator representing anisotropic element in gas laser resonator, considering phase crystalline and rotating plates

13 p2424 A70-28593

Power output dependence on cavity configuration of He-Ne laser in TEM mode operation

13 p2425 A70-28625

Laser cavity modal volume-output power relationship, deriving expression for interaction region

13 p2427 A70-29359

Steady state laser emission of resonator with two crystals with different optical orientation

13 p2428 A70-29371

Self excited cavity oscillators with tunnel and parametric diodes and nonequilibrium medium, noting single and multimodes, energy capabilities and frequency interactions

13 p2366 A70-29405

Laser acoustooptic quartz modulators inserted inside He-Ne and argon cavities for internal power extraction

13 p2430 A70-29705

Transient excitation of Schumann earth-ionosphere cavity resonances by large ELF atmospheric, using propagation model

15 p2726 A70-31865

Equivalent circuits and general formulas for small hole coupling of resonant cavities and waveguides

15 p2714 A70-32817

Instrument for visualization of EM field in open resonators in mm range

16 p2908 A70-33213

Gunn oscillator external negative differential/END/conductance broadband measurement noting effect of cavity control

16 p2875 A70-33398

Laser cavity design with total internal reflection quartz prisms, calculating prism angles tolerances

16 p2915 A70-34219

Solid state laser polarization mechanism, considering isotropic and anisotropic cavities

17 p3106 A70-35103

Microwave self modulating GaAs diode laser, showing coupled external cavity resonator influence on intrinsic resonance frequency

18 p3269 A70-36733

Regular relaxation oscillations of ruby laser by moving resonator mirrors

18 p3271 A70-36954

RF communication signal to noise improvement by time variant tracking filter with high Q superconductive resonant cavity

19 p3391 A70-38892

Microwave apparatus for resonant frequency change and loaded resonator Q measurement during DC discharge afterglow electron removal studies

20 p3679 A70-39715

Cavity mode mixing effects in internally scanned lasers, considering various geometries and coupling parameters for continuous transverse aperture velocity

21 p3835 A70-40720

Optical properties of off-axis multibeam resonators with spherical mirrors, discussing application to He-Ne lasers

21 p3836 A70-40914

Optimum tube diameter for maximum radiation output of single and multimode He-Ne lasers

21 p3836 A70-40916

Circular and nearly rectangular irises for resonant cavities in transmission line for microwave band stop filters, discussing design based on merit factor

21 p3792 A70-41992

Laser oscillator and amplifier characteristics based on ionic Nd dissolved in aprotic solvents, discussing solution loss

21 p3838 A70-42009

Optical waveguides and resonators propagation modes detection and discrimination techniques evaluated for circular cylinder dielectrics/optical fibers

22 p4030 A70-42949

LF cavity loss modulations of homogeneous four-level CW Nd-YAG laser, including relaxation-oscillation regime

22 p4050 A70-43005

High Q frequency stabilized cavity controlled microwave oscillator using Super Invar resonator

23 p4169 A70-43792

Optical transmission and reflection gratings formed by standing light waves evaporation of thin metallic films in ruby laser cavity

23 p4200 A70-43817

Book on guided EM wave theory covering mathematical methods transmission lines cavity resonators, perturbation theory, electrostatics, electric and magnetic fields, propagation, etc

23 p4172 A70-44242

CEILINGS [METEOROLOGY]

Runway low visibility and ceilings frequency and duration at German airports, using 1949-1967 statistical data

19 p3462 A70-37925

CEILOMETERS

U CLOUD HEIGHT INDICATORS

CELESCOPES

Telescope TV photometer system operation on-board OAO by mathematical simulation

16 p2906 A70-33174

CELESTIAL BODIES

NT A STARS

NT ACHONDRITES

NT ANDROMEDA GALAXIES

NT ASTEROIDS

NT AUSTRALITES

NT B STARS

NT BINARY STARS

NT CARBONACEOUS METEORITES

NT CASSIOPEIA A

NT CEPHEID VARIABLES

NT CHONDRITES

NT COMETS

NT CRAB NEBULA

NT DEIMOS

NT DWARF STARS

NT EARLY STARS

NT EARTH [PLANET]

NT ECLIPSING BINARY STARS

NT GALAXIES

NT GEMINID METEORIDS

NT GIANT STARS

NT HERCULES NOVA

NT HOT STARS

NT HUMASON COMET

NT ICARUS ASTEROID

NT IRON METEORITES

NT JUPITER [PLANET]

NT KAPOETA ACHONDRITE

NT LEONID METEORIDS

NT MAGNETIC STARS

NT MAIN SEQUENCE STARS

NT MARS [PLANET]

NT MERCURY [PLANET]

NT METEORITES

NT METEOROID DUST CLOUDS

NT METEOROID SHOWERS

NT METEORIDS

NT MICROMETEORIDS

NT MILKY WAY GALAXY

NT MOON

NT MOREHOUSE COMET

NT NATURAL SATELLITES

NT NEBULAE

NT NEPTUNE [PLANET]

NT NEUTRON STARS

NT NORTON COUNTY ACHONDRITE

NT NOVAE

NT O STARS

NT ODESSA METEORITE

NT OMICRON CETI STAR

NT ORGUEIL METEORITE

NT ORIONID METEORIDS

NT PERSEID METEORIDS

NT PHOBOS

NT PLANETARY NEBULAE

NT PLANETS

NT PLUTO [PLANET]

NT PROTOSTARS

NT PULSARS

NT QUADRANTID METEORIDS

NT QUASARS

NT RADIO GALAXIES

NT RADIO METEORS

NT RADIO SOURCES [ASTRONOMY]

NT RADIO STARS

NT SATURN [PLANET]

NT SCHWASSMANN-WACHMANN COMET

NT SOLAR SYSTEM

NT SPIRAL GALAXIES

NT STAR CLUSTERS

NT STARS

NT STONY METEORITES

NT SUN

NT SUPERGIANT STARS

NT SUPERNOVAE

NT T AURI STARS

NT TEKITES

NT TUNGUSK METEORITE

NT URANUS [PLANET]

NT VARIABLE STARS

NT VENUS [PLANET]

NT VESTA ASTEROID

NT VIRGO STAR CLUSTER

NT WHITE DWARF STARS

NT ZODIACAL DUST

Differential correction procedures, using residuals

to obtain celestial body orbital elements by linear programming

04 p0751 A70-14943

Mass density estimated in solar vicinity for distribution among celestial bodies

05 p0914 A70-16647

Gaseous spheres gravitational stability in proper field, considering convection and radial perturbations effects

07 p1383 A70-19408

Soviet book on celestial bodies radiation transfer and spectra covering light scattering, radiation fields, absorption, etc

08 p1568 A70-20768

Celestial emission bodies forbidden line analysis for physical conditions determination using formulas and graphs

08 p1569 A70-20831

- Celestial X ray sources resolved against diffuse nearly isotropic background radiation by rocket and balloon experiments, noting brightness
09 p1745 A70-22895
- Weak phase objects detection based on interferential and streak photography methods, noting fringe deformation role
10 p1916 A70-24587
- X ray astronomy, discussing emission processes, radiation classification for intensity plot against energy, cosmic sources distribution, etc
11 p2111 A70-26035
- Celestial object position determination, computing local errors for coordinate improvement
11 p2113 A70-26189
- Cosmic IR radiation sources, discussing galactic and stellar masses
14 p2632 A70-30882
- Solar system Eotvos experiments for measuring gravitational to inertial mass ratio of celestial bodies
16 p2978 A70-34033
- Human and divine aspects of space law, discussing ownership and sovereignty problems connected with space and celestial body exploration and utilization
16 p3004 A70-34344
- Multispectral UV sky mapping and heavenly body intensity measurement onboard OAO 2 satellite
17 p3179 A70-35264
- Legal status of natural resources of celestial bodies, discussing limitations of Space Treaty of 27 January 1967
17 p3203 A70-35796
- Regulations existence and application to exploitation of resources in celestial bodies
17 p3203 A70-35798
- Radio direction finding of celestial bodies from moving platform, determining plane rotation effects on angle measurements
18 p3333 A70-36164
- Spherical celestial bodies anomalous rotation problem, noting sunspots zonal character
22 p4106 A70-43261
- OAO 2 for UV telescope sky mapping and spectrophotometric measurements of celestial bodies
23 p4261 A70-44666
- CELESTIAL MECHANICS**
- Stellar systems models numerical construction, using data on star cluster density distribution, centroid velocity, potential distribution, etc
01 p0174 A70-10200
- Final motions of Hamiltonian conservative systems, analyzing Liouville type, homogeneous and similar systems
01 p0146 A70-11561
- Galactic satellite interpretation for high velocity hydrogen clouds at high latitudes
02 p0363 A70-11780
- Soviet collection of articles on structure and dynamics of stellar systems, Part 2
02 p0375 A70-12442
- Statistical analysis of position angles of Berenice cluster galaxies, estimating mass, expansion, rotation period and age
02 p0376 A70-12448
- Gravitational finite propagation velocity effects in celestial mechanics, describing binary star motion studies
02 p0380 A70-12783
- Lagrangian stability of stellar systems of Trapezium in Orion type situated within large stellar cluster or cosmic cloud
03 p0565 A70-13235
- Interplanetary trajectory selection, discussing transfer orbits, energy considerations, launch window computation, hyperbolic encounters and capture maneuvers
03 p0577 A70-14149
- Envelope stars evaporation effects on star cluster contraction, discussing energy inflow from envelope to nucleus
04 p0745 A70-14475
- Stellar systems dynamics, discussing dynamic interactions of point masses, forces in gravitational field, galactic model construction, etc
04 p0754 A70-15353
- Hori canonical equations solved by eliminating short period terms in general planetary theory, noting reduction to systems of linear differential equations
05 p0907 A70-16160
- Disproof of Wintner analytical foundations of celestial mechanics regarding binary collision in three body problem
05 p0909 A70-16338
- Dynamical systems with three degrees of freedom, presenting slice cutting and stereoscopic views graphical techniques for restricted three body problem with perturbations
06 p1149 A70-18462
- Faye comet motion and secular orbital evolution of short period comets
07 p1379 A70-19048
- Approximate method for celestial mechanics problems, considering particle motion under gravitation from central body in cylindrical coordinate system
07 p1387 A70-19266
- Historical survey of celestial mechanics including three body problem and solar system dynamic model construction
08 p1565 A70-20561
- Mass point motion in celestial mechanics, investigating two and three body problems without equal counteraction assumption
08 p1565 A70-20562
- Pulsar formation effect on orbits of preexisting planets and postformation planets effects on pulsar period and phase residuals
08 p1570 A70-20898
- Hori canonical equations analytical solution generalization resulting from elimination of short period terms of first order planetary theory
08 p1575 A70-21239
- Lagrangian stability of stellar systems of Trapezium in Orion type situated within large stellar cluster or cosmic cloud
08 p1580 A70-21668
- Nongravitational effects, systematic residuals and close Jupiter approach problems in motions of comets
09 p1759 A70-22913
- Mechanized Algebraic Operations software package for manipulation on computer Poisson series, noting application to celestial and nonlinear mechanics and astrodynamics
10 p1845 A70-24179
- Hydrodynamic analogy in restricted three body problem of celestial mechanics, discussing mass and momentum conservation and physical properties uniqueness
10 p1938 A70-24180
- Heliometric lunar libration series joined to obtain uniform equation
13 p2490 A70-28949
- Bipolar moment integral in celestial mechanics formed by product of particle kinetic moments for n body problem order reduction
13 p2494 A70-29399
- Book on celestial mechanics covering perturbation methods, two body problems, astronomical coordinates, orbital mechanics, satellite rotation, gravitational effects, etc
15 p2799 A70-31998
- Historical survey of celestial mechanics including three body problem and solar system dynamic model construction
15 p2805 A70-32716
- Mass point motion in celestial mechanics, investigating two and three body problems without equal counteraction assumption
15 p2805 A70-32717
- Celestial mechanics experiment for Mariner Mars 1971 to test general relativity theory and improve Martian ephemeris
16 p2978 A70-34031
- Gravitational variable constant in celestial mechanics, considering theories based on vacuum Jordan Lagrangian
18 p3320 A70-37066
- Spiral structure definition in external galaxies, discussing optical form types, Messier 33 outer and inner parts and differences in arms
18 p3326 A70-37153
- Kinematics of M 33, M 51 and large Magellanic cloud /LMC/
18 p3326 A70-37157
- Milky Way galaxy spiral structure analysis, using neutral H Hat Creek survey with southern observations
18 p3327 A70-37164
- Large scale galactic oscillations, discussing observational evidence and theoretical modal calculations
18 p3330 A70-37191
- Stellar isolated disks spiral structure, examining large numbers of point masses self consistent motion in galactic plane
18 p3331 A70-37195
- Large scale spiral galaxy structure interpretation, examining density wave theory, Milky Way System and spiral form origin
18 p3331 A70-37196
- Planetary theory construction to second order of disturbing masses, applying to motions of any set of two or three planets in solar system
19 p3523 A70-38687
- Stars and stellar gas motions interaction equations, analyzing plasma and gravitation problems
19 p3525 A70-38771
- Rotating stellar systems cooperative phenomena, estimating star-star collisions effect on perturbation rate and damping
19 p3525 A70-38772
- Comet shapes mechanical theory inverse problem approximate solution
19 p3525 A70-38773
- N body numerical integrator using virtual mass technique for computing trajectories with speed and accuracy suitable for spacecraft onboard computer applications
19 p3528 A70-38872
- Spherical celestial bodies anomalous rotation problem, noting sunspots zonal character
22 p4106 A70-43261
- Celestial mechanics covering two body problem, orbital improvement, perturbation theory and dynamics, planetary and satellite theory, lunar motion, etc
23 p4255 A70-45032
- Lunar theory literal solution for average node and perigee movements compared with Delaunay results, using Lie transforms for Hamiltonian function
24 p4399 A70-45141
- Short period hypothetical and real comets in Jupiter sphere of influence distributed according to orbital elements
24 p4409 A70-45637
- CELESTIAL NAVIGATION**
- NT ASTRONAVIGATION**
- Coupled control of space vehicle orientation with reference to three celestial bodies, reducing plane vibrations to dynamic third order system
10 p1914 A70-24307
- Three axis star pointing attitude control system for stabilized Skylark sounding rocket program
13 p2447 A70-28687
- Astronomical navigation on lunar surface with equations for selenographic latitude and longitude
13 p2449 A70-29272
- Celestial methods for lunar navigation, considering terrestrial and selenographic differences
14 p2613 A70-30459
- Spacecraft-based navigation instruments for outer planet missions using celestial directions to outer planet natural satellites
[AIAA PAPER 69-902] 20 p3669 A70-39681
- CELESTIAL OBSERVATION**
- U ASTRONOMY**
- CELESTIAL SPHERE**
- Diurnal and seasonal variations of parameter s of meteor showers on celestial sphere, using radio echo amplitude distribution from radar observations
14 p2635 A70-30307
- Geometrical appearances at relativistic speeds for celestial sphere with multiple constellations, spherical surface features at observer proximity and rectangular box train
19 p3520 A70-38273
- Celestial sphere scanning by spinning symmetric satellite with open loop magnetic control of precession
23 p4216 A70-44524
- CELL ANODES**
- Refuelable Mg-air battery anode, electrolyte and packaging materials selection from standpoint of cell voltage, metal consumption and sludge formation
02 p0253 A70-12721
- Electrochemical cells with lithium anode and nonaqueous electrolyte, discussing research role in designing high specific energy primary batteries
08 p1440 A70-20709
- CO electrochemical oxidation at porous solid electrolyte fuel cell anodes under high temperature, noting current density role
10 p1830 A70-24462
- Electrodes oxidation processes involving fuel cell molecules or derived adsorbed intermediates reacting with anodically generated surface oxide, considering Pt electrochemical reduction
10 p1830 A70-24465
- Raney alloy catalyst activity and stability in fuel cell anodes, noting properties of ternary phases of nickel, aluminum and iron, molybdenum or titanium
10 p1831 A70-24466
- Catalytic load carrying capacity of porous carbon electrodes impregnated with nickel salt and nickel boride in anodic fuel cell hydrazine oxidation
10 p1831 A70-24469
- Anodic breakdown characteristics of Ti alloys as function of metal surface condition
17 p3113 A70-34366
- CELL CATHODES**
- Silver/polytetrafluoroethylene water-repellant air-breathing cathodes for fuel cells with alkaline electrolytes, discussing pressure compatibility
10 p1829 A70-24454
- Silver cathodes and plasma-sprayed anodes for cost effective hydrogen/oxygen fuel cells with solid zirconium dioxide electrolyte, considering carbon precipitation avoidance
10 p1830 A70-24459
- Hydrogen peroxide fuel cell performance in acid and alkaline electrolytes, investigating cathodic reduction of oxygen on platinum
10 p1808 A70-25037
- Hydrogen oxygen fuel cell investigated for oxygen transfer to Pt cathode surface
12 p2166 A70-27848
- CELL DIVISION**
- Growth rate effect on glucose utilization rate using sporogenic strain of *Bacillus subtilis* during N and L-tryptophan limitation
01 p0021 A70-10790
- Temperature-synchronized semicontinuous culture and monitoring system for autotrophically growing *Euglenas*
04 p0633 A70-15453
- Hydrostatic pressure effects on DNA, RNA and protein synthesis and division in *Escherichia coli* cultures
04 p0637 A70-15475

- Local stress effect on immunocompetent cells differentiation in guinea pigs lymphatic ganglia, noting increase in number of antibody producing cells
05 p0803 A70-17114
- Escherichia coli cell division patterns, discussing generation times spread, gamma ray irradiation in nutrient broth, DNA damage and growing points, etc.
08 p1441 A70-20681
- Chromosome of temperature-sensitive mutant of bacillus subtilis 168, observing multiforked replication at normal temperature and transfer of DNA
09 p1615 A70-22206
- Chlorella reproduction rates at steady and variable illumination intensity levels, determining productivity autocorrelation function by statistical analysis
17 p3030 A70-35355
- Circadian rhythms in single cell animals, examining cell division, temperature and light effects
19 p3365 A70-38410
- CELLS**
- Giant cell regular structures in solar atmosphere, using magnetic synoptic charts of solar activity
24 p4400 A70-45305

CELLS [BIOLOGY]

- NT AXONS**
- NT CARBOXYHEMOGLOBIN**
- NT CHROMOSOMES**
- NT EOSINOPHILS**
- NT ERYTHROCYTES**
- NT HEMATOPOIESIS**
- NT HEMOGLOBIN**
- NT LEUKOCYTES**
- NT LYMPHOCYTES**
- NT MITOCHONDRIA**
- NT NEURONS**
- NT OXYHEMOGLOBIN**
- Spore and vegetative cell adenylate kinases of *Bacillus subtilis* proved indistinguishable by polyacrylamide gel electrophoresis DEAE cellulose chromatography
01 p0021 A70-10789
- Biochemical characteristics, nitrogenase activity and nitrogen fixation in heterocysts of blue green algae
01 p0024 A70-10894
- Gnotobiotic techniques for human hematopoietic cell culture establishment and maintenance, considering culture transfer
01 p0027 A70-11311
- Probabilities for cell survival after exposure to ionizing radiation obtained by two compartment model
01 p0028 A70-11370
- High speed fluorescent cell sorting system for sorting mouse spleen cells from Chinese hamster ovarian tumor cells
02 p0240 A70-12695
- DNA penetration into normal and fast neutron irradiated yeast cells, using immunofluorescent microscopy
03 p0417 A70-13072
- Postirradiation free radical processes in cellular organelles of rat liver exposed to gamma irradiation detected by graft copolymerization method
03 p0418 A70-13302
- Radioprotective action of pyridine derivatives in monkey heart and human epithelium cells exposed to gamma radiation evaluated by dioxyphenyl alpha-alanine oxidation
03 p0418 A70-13303
- Ultraweak luminescence intensity, radiation damage kinetics and spectral properties of cellular organelles of rat liver exposed to gamma radiation
03 p0419 A70-13304
- Photodynamic damage in biological cells, discussing free radical originators and protective action of thiourea, mono and polyvinylpyrrolidone, cysteine and antibiotics
03 p0419 A70-13306
- Multiple optical properties measurement instrumentation for cellular specimens to classify biological cells, analyzing and displaying data by on-line computer
04 p0644 A70-15361
- Cortical cells fatigue and performance in subjects doing mental work, using motion picture signal perception method
04 p0639 A70-15509
- Norepinephrine-induced depolarization effects on brown fat thermogenesis in cold-acclimated rats determined in vivo measurement of intracellular potentials
05 p0799 A70-16020
- Hyperbaric oxygenation effects on cellular membrane permeability, analyzing rat plasma behavior of transaminases GOT and GPT and K and Na cations electrolytes
05 p0802 A70-16493
- Biological fluorescent substances passage in rabbit central nervous system as indicators of blood supply to cells
07 p1197 A70-18657
- Vacuum and radiation effects on *Escherichia coli*, noting role of cells water desorption in vacuum damage
07 p1203 A70-18962

- Macaque monkey stereoscopic vision, obtaining behavioral evidence by random dot stereoscopic patterns and finding cells sensitive to binocular depth in cortex
07 p1205 A70-19276
- Density gradient sedimentation of *Escherichia coli* populations irradiated with Co 60 gamma rays, showing correlation between DNA degradation and cell death
08 p1441 A70-20680
- Oxygen enhancement ratio and relative biological effectiveness of accelerated helium nuclei on mouse tumor cells, discussing applicability in radiation therapy
09 p1617 A70-22336
- Cardiac muscle intercellular junctions ultrastructural appearance, considering macula adherens, fascia adherens and nexus junctional specializations
09 p1620 A70-23061
- Orbital space flight effects on dry barley seeds, noting increased intracellular rearrangements
10 p1811 A70-24324
- Aerobic metabolism of heart muscle cells and oxygen utilization of coronary artery blood
10 p1821 A70-25081
- Cytoplasm, nucleus and membrane combination techniques for reassembly to form viable amoebae
11 p1986 A70-25849
- Energy deposition in cells by charged particles during ionizing radiation exposure, discussing RBE/relative biological effectiveness/and dose-effect relation for neutrons
11 p1989 A70-26597
- Field cotton leaves reflectance and transmittance measurement, predicting linear dimension related to cellular structure
12 p2273 A70-28122
- Active and passive ion transport mechanisms in excitable animal cell maintaining constant membrane polarization
13 p2352 A70-29351
- Pure oxygen effect on amino acids uptake and metabolism of *Pseudomonas saccharophila* stationary cells
14 p2536 A70-30343
- Linear density gradients in isopycnic centrifugation technique for selecting synchronous daughter cells from asynchronous *Chlorella* cultures
14 p2546 A70-30985
- Wheat seedlings cellular response to weightlessness during NASA Biosatellite II flight compared with simulated weightlessness effects
15 p2688 A70-31662
- Molecular structural relationship between cellular membranes and photoreceptors in plants and animals
16 p2847 A70-33028
- Lemniscus neurons in switching nucleus of thalamus, showing switching cells with direct cortical projections into somatosensory cortical zones
16 p2848 A70-33262
- Combined ultrasonic and ionizing radiation effects on electrophoretic mobility of tumor cells from albino mice
17 p3034 A70-35762
- Calcium ion role in myocardial cell electrical and mechanical trace processes under normal content and manganese blocking
18 p3221 A70-36640
- Protein solutions and cell cultures changes by ruby and Nd lasers radiation, noting threshold energy
20 p3579 A70-39419
- Simulated space flight radiation effects on dogs DNA synthesis and bone marrow cell differentiation
20 p3575 A70-40191
- Biochemistry of blood group antigens involved in agglutination reactions, discussing effect of proteolytic enzymes on cell membrane structure
21 p3764 A70-41447
- Mammalian cells after X ray irradiation, showing two forms of DNA repair process
21 p3765 A70-42024
- Cellular irradiation sensitivity in tissue culture modified by propyl gallate as radical reactions inhibitor
21 p3767 A70-42242
- Lethal and sublethal radiation dosage effects on cellular Na and K distribution in rat brain, liver, kidneys and muscular tissues
23 p4145 A70-44314
- Mice intestinal epithelium, investigating high energy protons irradiation effect on cells
23 p4149 A70-45028
- Nitrogen deficient algae nitrification, showing cellular N compounds oxidized to nitrate and nitrite followed by nitrate reductase
24 p4297 A70-45407

CELLULOSE

- Cellulose ion exchanger palladium catalysts preparation and applications in asymmetric hydrogenation reactions
17 p3042 A70-35125

CELLULOSE NITRATE

- Slurry-cast filled nitrocellulose plastisols as solid propellants, discussing compositions, performance and applicability to beryllium fuel
07 p1360 A70-19907

**CELSIUS TEMPERATURE SCALE
U TEMPERATURE SCALES
CEMENTITE**

- X ray elastic constants measured in cementite phase in high carbon tool steel following plastic deformation at tension, noting residual stresses increase and balance
06 p1084 A70-17126

CENTAUR LAUNCH VEHICLE

- NT ATLAS CENTAUR LAUNCH VEHICLE**
- Atlas /Centaur and Titan/Centaur launching of Intelsat 4 communication satellites, discussing booster, stage characteristics and payload
[AIAA PAPER 70-483] 11 p2127 A70-26605
- Thermoelectric outer planet spacecraft /TOPS/ flight environment, systems design and Titan 3D/Centaur launch vehicle with Burner II upper stage
21 p3930 A70-41795

CENTAUR PROJECT

- Centaur space guidance equipment design, development, parts control and reliability
14 p2612 A70-30452

CENTAUR VEHICLE**U CENTAUR LAUNCH VEHICLE****CENTAURUS CONSTELLATION**

- Balloon observations of Cen XR-2 X ray emission decrease
10 p1948 A70-24999
- Centaurus A radio galaxy X ray survey, implying upper limit of background radiation temperature
18 p3308 A70-36516
- Extragalactic objects 3C 273 NGC 5128 and M87 X ray emission detection, using proportional counters on Aerobee 150 rocket
18 p3310 A70-37016
- Hydrogen line absorption at 21 cm from Centaurus A /NGC 5128/ radio galaxy
18 p3318 A70-37017

CENTER OF GRAVITY

- Geocentric coordinate system definition by earth mass center and rotation axis and Greenwich meridian plane
01 p0082 A70-11456
- Symmetrical body rotational motion with asymmetrical mass distribution about center of mass, determining minimum initial value of angular velocity
01 p0192 A70-11482
- Integration time reduction for equations of motion of vehicle center of mass during parabolic reentry, using Runge principle
01 p0134 A70-11483
- Gyrostabilized satellite steady state motions in Newtonian force field having displaced satellite center of mass orbital plane relative to center of attraction
01 p0198 A70-11577
- Satellite positions from simultaneous measurement by laser along geocentric arc usable for determining earth mass center position
02 p0253 A70-11752
- Geodetic coordinate system referred to center of mass and earth rotation axis constructible from satellite observations
03 p0472 A70-13186
- Satellite observations used to construct coordinate system referred to earth center of mass and axis of rotation
03 p0474 A70-13733
- Translational-rotational motion of long dumbbell in Newtonian central force field, analyzing plane center of mass trajectory with perpendicular kinetic moment vector
04 p0744 A70-14427
- Randomly oriented vibration effect on noncompensated three degree of freedom gyroscope with displaced center of gravity
04 p0692 A70-15278
- Optical position estimation model based on defining photon density profile center of gravity in noise, using photon Poisson process theory
04 p0652 A70-15337
- Motion equations of rigid vehicle derived in terms of body axes noncoinciding with mass center applied to ships and aircraft
05 p0881 A70-15883
- Automatically controlled rendezvous and docking for orbital assembly of spacecraft, deriving motion equations for mass centers
07 p1393 A70-19481
- Selenocentric coordinate system originating at center of mass, determining lunar figure center from photographs with reference stars
08 p1572 A70-20942
- Center of mass small displacement effects on satellite orbits by solving variational equations for scalar potential function employing matrix formalism
09 p1761 A70-22938
- Ecliptic obliquity secular change rate apparent discrepancy possibly due to earth-moon barycenter motion
10 p1945 A70-24962

Satellite orientation by determining rotation parameters about centers of mass with respect to certain coordinates 11 p2128 A70-26782

Proton 2 satellite orientation and motion about center of mass determined from telemetric data analysis under aerodynamic moment 11 p2128 A70-26783

Aerodynamic moment on satellite with asymmetrically positioned solar cell platforms, analyzing motion around center of mass for diffuse scattering flow 12 p2314 A70-28254

Translational-rotational motion of long dumbbell in Newtonian central force field, analyzing plane center of mass trajectory with perpendicular kinetic moment vector 13 p2485 A70-28452

Earth satellite motion about center of mass, examining effects of random variations in atmospheric density, geomagnetic intensity and solar radiation 15 p2809 A70-31650

Automatically controlled rendezvous and docking for orbital assembly of spacecraft, deriving motion equations for mass centers 15 p2813 A70-32726

Selenocentric coordinate system originating at center of mass, determining lunar figure center from photographs with reference stars 15 p2806 A70-32754

Stable equilibrium positions for satellite consisting of many rigid bodies in circular orbit about center of gravity, using numerical method 18 p3332 A70-35963

Solar radio radiation effective gravity center shift determination, considering directivity diagram scanning phase for radio transit instrument adjustment 19 p3522 A70-35862

L-1011 onboard system for gross weight and center of gravity determination, describing transducers placement, computer design and display panel [SAWE PAPER 837] 20 p3562 A70-40359

Weight, moments and mass centers computer calculation by surface integral method, using FORTRAN language [SAWE PAPER 852] 20 p3660 A70-40373

CENTERBODIES

Turbofanjet powered hypersonic aircraft axisymmetric inlet systems using forward translating cowl and centerbody for various air flow characteristics [AIAA PAPER 70-687] 16 p2835 A70-33586

CENTERS

Geomagnetic center position determined by coordinate system referred to dipole approximating geomagnetic field 06 p1057 A70-17844

CENTIGRADE TEMPERATURE SCALE

U TEMPERATURE SCALES

CENTRAL NERVOUS SYSTEM

NT BRAIN

NT BRAIN STEM

NT CEREBELLUM

NT CEREBRAL CORTEX

NT CEREBRUM

NT HIPPOCAMPUS

NT SPINAL CORD

NT SPINE

NT THALAMUS

Collection of articles on chimpanzee central nervous system and behavior 01 p0028 A70-11375

EEG investigation of cerebral bio currents during polar night-day cycle, studying central nervous system nonspecific automatic control mechanism dependence on ecological factors 01 p0030 A70-11466

Plethysmographic investigation of myogenic load influencing sportsmen central nervous systems state, tabulating short and long distance running results 03 p0420 A70-13403

Quantitative characteristics of central compensatory process, investigating nystagmus responses in guinea pigs subjected to bilateral labyrinthectomy 06 p0995 A70-17806

Biological fluorescent substances passage in rabbit central nervous system as indicators of blood supply to cells 07 p1197 A70-18657

Phase correlation of conditioned and electrophysiological post radiation disturbances in central nervous system of monkeys 08 p1446 A70-21447

Reticular formation of central nervous system in vertebrates described as behavior controlling circuit of interconnected modules, proposing hybrid computer method for operational scheme 08 p1447 A70-21461

Central nervous system activity of white rats during hypokinesia, observing organism shifts and long time effects on functions 09 p1615 A70-22093

X ray effects on central nervous system noting mutations in rats, guinea pigs, chickens, dogs and rabbits 09 p1620 A70-22821

Human central nervous system changes during hypodynamia, noting unidirectional shifts in brain

hemodynamics, rheographic wave propagation time reduction, etc 10 p1815 A70-24680

Mechanisms responsible for sleep-wakefulness rhythm, investigating effect of lesions in CNS, electrical excitation of brain, neurons activity, etc 15 p2680 A70-31744

Sleep-wakefulness cycle regulation role of serotonin, noradrenalin and acetylcholine in CNS of animals 15 p2680 A70-31745

Central nervous system activity of white rats during hypokinesia, observing organism shifts and long time effects on functions 15 p2685 A70-32689

Habituation and dishabituation in semitact Aplysia preparation with central nervous system removed 18 p3217 A70-36517

Plasma tocopherol concentrations and vitamin E deficiency in dogs, noting pathologic changes in smooth muscle, central nervous system, skeletal muscle and retina 20 p3569 A70-38991

Vestibular message flow regulation by central nervous system, describing afference, inhibition and copy formation 22 p3976 A70-43705

Biocybernetics of human central nervous system, discussing electronic computers analogy to human brain 23 p4145 A70-44222

CENTRAL NERVOUS SYSTEM DEPRESSANTS

Reactions to visual emergency signals in humans after administering adrenalin, aminazin, melipramine or andaxine to change control systems functional state of cerebrum 01 p0030 A70-11467

CENTRAL NERVOUS SYSTEM STIMULANTS

Reactions to visual emergency signals in humans after administering adrenalin, aminazin, melipramine or andaxine to change control systems functional state of cerebrum 01 p0030 A70-11467

CENTRAL PROCESSING UNITS

Cosmic ray intensity variations recording device adaptable to computer forming centralized data processing system 05 p0845 A70-15932

CENTRIFUGAL COMPRESSORS

Impeller elastic and elastoplastic strength of centrifugal supercharger with curved disks and radial blades, using variational method 01 p0211 A70-11417

High hub/tip ratio centrifugal compressor with pipe and vane cascade diffusers for turbofan engines, determining impeller performance [ASME PAPER 69-WA/FE-28] 04 p0733 A70-14774

Bladed wheels stability in centrifugal compressors, calculating natural vibration frequencies of rotors 07 p1364 A70-19634

Unsteady relative flow in centrifugal impeller passage running at part capacity and zero flow observed by hydrogen bubble flow visualization method [ASME PAPER 69-GT-35] 14 p2529 A70-31024

Rolls-Royce RB 211 three shaft turbofan engine, discussing centrifugal compressor, tubular combustion chambers and single stage turbine 15 p2787 A70-31949

Circular blade cascade design for supersonic vane diffuser of radial flow centrifugal compressor 16 p2837 A70-33764

Radial compressor diffusers design and technology [ASME PAPER 70-GT-116] 18 p3304 A70-36850

Pressure balanced rotor flow path design for mixed flow centrifugal compressors, calculating losses in rotor and diffuser section [ASME PAPER 70-GT-12] 18 p3209 A70-36863

Centrifugal compressor losses as function of suction chamber exit nonuniform flow field delivered to impeller 21 p3747 A70-41954

Turbofan, turbojet and turboprop engine development in aircraft gas turbine evolution, discussing VTOL propulsion, centrifugal and axial compressor engines 24 p4396 A70-46251

CENTRIFUGAL FORCE

Squeeze film investigation between rotating plane annuli, considering inertia due to centrifugal effect [ASME PAPER 69-LUB-6] 01 p0102 A70-10396

Elastic stability of Coriolis-coupled oscillations of thin rotating disk under influence of centrifugal forces 02 p0389 A70-12650

Ultraharmonic resonance excited by centrifugal force in system with Duffing restoring force characteristic using Ritz method 05 p0925 A70-15886

Load distribution in Christmas tree turbine attachments due to centrifugal force on blades, showing strain diagrams 05 p0939 A70-16488

Centrifugal force induced stressed state in gas turbine blades using photoelastic analysis, emphasizing stress distribution at shroud holes 07 p1403 A70-19118

Elastoplastic stressed state of variable thickness disk under combined effects of nonuniform heating, repeated centrifugal and surface tensile loads 09 p1778 A70-23091

Elastoplastic stress state of variable thickness disk under combined effect of nonuniform heating and centrifugal forces, applying flow theory to stress component determination 09 p1779 A70-23095

Centrifugal forces and nonuniform heating effect on natural vibration frequencies of circular plates using lumped parameter method 09 p1784 A70-23588

Stress-strain state of epoxy resin cylinder situated in centrifugal force field using three dimensional photoelastic method 12 p2323 A70-27340

Differential equations for coupled bending and torsional vibrations of slender beam in centrifugal force field 14 p2661 A70-31226

Disk elements perpendicular mounting by rotation on vibrating shaft, obtaining orientation by centrifugal force 15 p2733 A70-31580

Unanesthetized dogs renal hemodynamic response to negative centrifugal acceleration 15 p2681 A70-31883

Centrifugal atomizer mean drop size dependence on geometry, fluid properties and discharge velocity 18 p3300 A70-36274

Squeeze film investigation between rotating plane annuli, considering inertia due to centrifugal effect [ASME PAPER 69-LUB-6] 19 p3435 A70-37608

Curvilinear motion centrifugal force compared with barometric gradient force in symmetrical cyclone, establishing clockwise direction motion possibility 20 p3663 A70-39275

Gas core nuclear rocket engine light and heavy species centrifugal separation by MHD-driven rotating flow, discussing fluid dynamic simulation results 20 p3671 A70-40256

Dynamics of deployable space structures stiffened by centrifugal forces due to spin, discussing LF radio telescope 21 p3931 A70-41854

Glucose metabolism in chickens under chronic centrifugal acceleration, meeting increased energy requirements 23 p4147 A70-44786

Turbine blades deformation by centrifugal and aerodynamic forces, discussing theory for bending stress free blade design 24 p4288 A70-45505

Altered gravitational field effects on frog eggs centrifuged under various conditions after fertilization, noting time dependence of induced abnormalities 24 p4298 A70-45619

CENTRIFUGAL PUMPS

Stability and potential cavitation of centrifugal pump operating with four working wheels with different geometric parameters 08 p1558 A70-21196

Stability region of hydraulic system containing centrifugal pump calculated from pressure head dependence on pump inlet pressure 09 p1607 A70-23622

Centrifugal pump design optimization, assuming one dimensional throughflow of viscous fluid as driving force 13 p2391 A70-29748

Centrifugal pumps of various metals for liquid oxygen, describing fire and explosion tests 14 p2617 A70-31020

Inducer tip clearance effect on centrifugal pump suction performance with velocity and total head distributions at outlet 14 p2592 A70-31332

Cavitation in centrifugal pumps, predicting breakdown and inception points variation with temperature and speed 15 p2744 A70-32097

Centrifugal pump performance correlation parameter under cavitation conditions for handling different liquids based on bubble growth theory 15 p2720 A70-32098

Centrifugal impellers primary and secondary flows velocity distributions, determining vorticity generation 18 p3243 A70-36871

Power loss reduction from disk friction and gas leakage through rotor seals of low speed centrifugal pumps in aircraft hydraulic systems and liquid propellant rocket engines 22 p4091 A70-42806

CENTRIFUGES

NT HUMAN CENTRIFUGES

Design parameter importance in centrifugal axial flow particle separator tubes performance from separator tube development program data 01 p0163 A70-10680

Optimal data filtering techniques and hardware for centrifuge testing of missile inertial platforms [AIAA PAPER 70-405] 10 p1861 A70-24901

CENTRIFUGING

Powered centrifugal separator for inlet filtering of rotary wing aircraft turbine engines, discussing efficiency and feasibility

01 p0164 A70-10683

Static and centrifugal filters merits for turbine engine lubrication systems, considering mechanical reliability, efficiency, dirt capacity and maintenance

01 p0164 A70-10686

Tolerance level to z axis acceleration from centrifuge techniques, noting irreplacability of intermittent stepwise increasing accelerations tests

07 p1201 A70-18790

Centrifuging as therapeutic device tested on male assault victim with bullet fragment floating freely in brain ventricular system

11 p1993 A70-26523

Linear density gradients in isopycnic centrifugation technique for selecting synchronous daughter cells from asynchronous *Chlorella* cultures

14 p2546 A70-30985

Binary gas mixture separation effects by centrifugation in cylindrical tube, calculating maximum radial concentration difference between wall and axis by numerical integration

23 p4181 A70-44206

CENTRIFUGING STRESS

Rat water intake and urine output during chronic centrifugation at resultant inertial fields of 1.7 and 3.0 g

02 p0231 A70-11705

Circulatory system tests during linear, intermittent and continuous accelerations on centrifuge, noting lack of statistical correlation between centrifuge tests and functional tests

07 p1201 A70-18789

Centrifuging acceleration tolerance of various animals, relating physiological and morphological effects

12 p2174 A70-28361

Red cell deformability and flow resistance and blood electrical resistance under low g centrifugation

15 p2680 A70-31700

Centrifugation effects on human peripheral arterial pulse behavior

17 p3037 A70-35126

Centrophenoxine effects on rabbits centrifugal acceleration resistance

17 p3025 A70-35131

Nystagmic response to directional inert shift of endolymph in semicircular canals in frontal plane head subject rotation

18 p3220 A70-36635

Spatial disorientation of human subjects in centrifuge, examining otolith role in reorientation and eye sensory mechanisms

22 p3976 A70-43707

Computer photokymographic recording of gravitational-inertial force environment effects on cardiovascular and respiratory systems on centrifuge

22 p3976 A70-43709

CENTRIPETAL FORCE

Centripetal acceleration tolerance level correlated with circulatory system functional tests and physical exercises, discussing strength and speed endurance

07 p1201 A70-18787

Rat body fluids displacement during positive centripetal accelerations by radioisotope tracer compounds, freezing rats in liquid nitrogen to fix hemodynamic changes

07 p1202 A70-18796

Pitch illusion in flight personnel under centripetal acceleration

24 p4306 A70-45330

CEPHALAGIA

U HEADACHE

CEPHALOPODS

NT MOLLUSKS

Squid head cartilage properties in terms of light and electron microscopic appearance, amino acid composition and X ray diffraction

24 p4305 A70-46348

CEPHEID VARIABLES

BV photometry of Population I Cepheids in Magellanic Clouds, Galaxy and M31

03 p0578 A70-14287

Cepheid variable 1 Carinae light curve from photoelectric observations, calculating periodicities from best fitting Fourier series

04 p0759 A70-15708

Magellanic Cloud cepheids two color light curves obtained by photoelectric photometry, discussing reddening

07 p1380 A70-19259

Zero-point of period-luminosity-relation of Cepheids based on proper motions, radial velocities and photometric data, applying secular parallax method

10 p1945 A70-24964

Bright southern Cepheids UVB observations, discussing blue companion effect on two color plot

14 p2639 A70-30726

Cepheids distance scale from proper motions data, using maximum likelihood method for period-luminosity relation

14 p2652 A70-31387

Cepheids nonequilibrium continuous emission at maximum brightness, considering phase shift between radiation intensity and stellar contraction

15 p2802 A70-32483

Initial horizontal branch metal poor star models, examining opacities, luminosity and cluster ages of RR Lyrae stars

18 p3317 A70-37006

Young cepheids galactic distribution determined by photometric method, showing correlation with spiral arms

18 p3330 A70-37184

Light curves bumps properties of Population I cepheids in Magellanic Clouds, Milky Way galaxy and M31 as function of period

19 p3523 A70-38691

Cepheids in Galaxy spherical component, determining periodic variations by distribution function technique

19 p3525 A70-38768

Cepheids periodic variations photographic analysis

19 p3525 A70-38769

Intermediate band photometry of companions to RR Lyrae variables, identifying AP Ser K line excess subdwarf

21 p3892 A70-41187

Early B stars photometric examination of variable spectral lines, discussing beta Cephei stars possibility

21 p3922 A70-41981

Cepheids nonequilibrium continuous emission at maximum brightness, considering phase shift between radiation intensity and stellar contraction

23 p4240 A70-43907

CEPHEUS CONSTELLATION

Cepheus light attenuation curve explained by applying polymodal particle size distribution, obtaining interstellar dust density

05 p0918 A70-16915

Beta Cephei star discovery criteria, examining mechanism theory by He and N overabundances, far UV flux, spectral line width and binary character

21 p3890 A70-41159

CERAMAL PROTECTIVE COATINGS

U CERMETS

U PROTECTIVE COATINGS

CERAMALS

U CERMETS

CERAMIC BONDING

Ceramic adhesives with glassy matrix for metal bonding, describing chemical reactions in interface, adhesive processing and application

08 p1526 A70-20883

Bonds strength involving metallic, organic and ceramic adhesives at various temperatures, considering metallic additives effect

08 p1504 A70-20891

CERAMIC COATINGS

Ceramic, cermet and metallic high temperature coatings development and applications, discussing time and cost saving procedures

[SAE PAPER 690478] 03 p0515 A70-13267

Portable megohmmeter for measuring insulation resistance of strain gauge ceramic installations

05 p0848 A70-16378

Optical parameters effect on directional emittance near edge of two dimensional ceramic coating, using Monte Carlo techniques

[AIAA PAPER 70-67] 06 p1106 A70-18138

CERAMICS

NT PYROCERAM [TRADEMARK]

Dielectric layers electrical conductivity in ceramics containing Ti during aging, observing different characteristics ascribed to nonequilibrium current carriers injection

01 p0156 A70-10221

Technical ceramic products physical properties compared with metals, discussing manufacturing methods and industrial and engineering applications

02 p0322 A70-12714

Ceramic plasma containers construction by soldered seal technique for ion lasers, noting moly-manganese process

02 p0314 A70-12746

Raman spectra of lead titanate, sodium tantalate/potassium tantalate and potassium tantalate/potassium niobate solid solutions at various temperatures

03 p0542 A70-13824

Pyroelectric coefficient extrema measurement at constant stress in barium titanate ceramic at various temperature ranges for various transition points

03 p0513 A70-14205

Thermal stability of turbine sealant mica-ceramic materials containing boron nitride

04 p0712 A70-14467

Fracture mechanical theory for crack propagation in brittle ceramics subjected to thermal shock, deriving crack stability criteria

04 p0767 A70-14505

Induction furnace for thermal treatments and melting of solid and liquid metals, alloys and sintering and degassing ceramic and metallic systems in vacuum

04 p0664 A70-15371

Ceramic fibers formation by particles mechanical deformation by extrusion in W matrix, describing grain structure of various extruded metal oxides

04 p0699 A70-15643

Barium titanate ceramics with nonlinear electrical conduction, noting I-V relationship dependence on temperature, impurities and electrodes

05 p0891 A70-15990

Test stand for endurance and creep testing of plastics, glazed ceramics and other brittle materials

06 p1028 A70-17665

Excess titanium dioxide effect on electric resistance of semiconductive barium titanate ceramics suitable for posistors

07 p1355 A70-18654

Turbulence measurement by piezoceramic acoustic sensors, considering capacitance

07 p1284 A70-19829

Ceramic capacitors selection considering ionization, third harmonic and HF heating control properties

09 p1642 A70-22003

Inorganic ceramic materials in design and fabrication of microwave antennas, filters and stable resonators, discussing density and dielectric constant variability by ceramics foaming

09 p1689 A70-22007

Electro-optic effects in ferroelectric ceramics with electrically variable coefficients of piezoelectricity and birefringence, discussing applications

09 p1739 A70-22633

Alkoxy-derived strontium zirconate and titanate preparation and characterization, considering purity control, crystallite size and ceramics synthesis

09 p1740 A70-22981

Acoustic emission monitoring methods to detect crack formation and growth in ceramics

10 p1894 A70-24174

Sputtering method used for applying metallizing layer to ceramics in producing ceramic to metal seals

10 p1895 A70-24555

Piezoelectric effects in ferroelectric ceramics using equivalent circuits and admittance matrices

12 p2283 A70-27005

Supersonic flight simulation in hypersonic wind tunnels for developing hypersonic air breathing propulsion, describing ceramic storage heaters

13 p2384 A70-28666

Book on high temperature, transition and hydrated ceramics covering nomenclature, natural occurrence, mechanical, thermal, sonic, electrical, magnetic and chemical properties

13 p2436 A70-29781

Ceramics microcrack propagation control through small slab with simultaneous microscopic observation of path and force changes, considering grain boundary effects

15 p2741 A70-32434

Ceramic material ranking, using thermal stress crack initiation method

16 p2934 A70-33274

Sapphire and ruby plastic deformation and fracture properties at room temperature, discussing sapphire base ceramics

18 p3278 A70-36046

Spaceborne lightweight mirror blanks made from ceramics fabricated from glass crystallization

18 p3263 A70-36559

Ceramic materials for low cost high inlet temperature gas turbine engine components

[ASME PAPER 70-GT-105] 18 p3279 A70-36889

Strontium titanates ceramics containing various trivalent rare earth ions, observing dielectric relaxation

19 p3486 A70-37755

Transparent ceramic armor fabrication using dense polycrystalline magnesia

19 p3437 A70-38422

Ceramic whisker and continuous filaments reinforced metals, discussing processing, properties, matrices selection of reinforced composites, etc

20 p3650 A70-39948

Hot pressed zirconia-zirconia ceramic fiber reinforced ceramic matrix composites, discussing mechanical properties and failure modes

22 p4057 A70-42285

Ceramic fiber technology, forming processes and matrix composites fabrication, discussing chemical and physical compatibility factors, plastic forming, slip casting, cold pressing, etc

22 p4045 A70-42477

Temperature stable homogeneous single phase zirconate solid solution ceramics for microwave dielectric resonators and microstrip substrates

22 p3996 A70-42922

Reentry protection for radioisotope heat sources, using thermal switch of composite ceramic foam with metal impregnants

22 p4054 A70-42958

Full-swing and incremental Charpy impact and Izod tests for ceramic intrinsic impact strength

23 p4209 A70-43872

- Ceramic composite materials structural application, improving brittleness and thermal shock resistance via reinforcing refractory fibers
[ICAS PAPER 70-40] 23 p4267 A70-44138
- High temperature specific heat terms for refractory metals and ceramics from room temperature to near-melting point 23 p4207 A70-44440
- Refractory materials surface behavior under friction, discussing microscopic nature of wear and surface deterioration due to thermal fatigue, fusion and material transfer, etc 24 p4342 A70-45595
- CEREBELLUM**
- Microelectrophysiological study of cerebellar neuron responses to stimulation of vestibular apparatus by vertical rocking performed on anesthetized adult cats 01 p0012 A70-10124
- Relationships between frog vestibular afferents, cerebellum and efferent vestibular system, using electron microscopy and Nauta degeneration technique 01 p0014 A70-10351
- Cerebello-otolith system represented by axons of Purkinje cells, studying inhibitory vestibular efferent system relation to cerebellum in frog 01 p0014 A70-10352
- Tegmental nucleus neurons of cats cerebellum, considering responses to acceleration changes and natural stimulation of vestibular apparatus 03 p0421 A70-13510
- Evoked cerebellar potentials time characteristics during spinal cord stimulation in cats, investigating cerebellar intercentral connections effect 13 p2353 A70-29357
- CEREBRAL CORTEX**
- Cortex functional interrelationships with hypothalamus and formatio reticularis, studying role of corticofugal effects in anesthetized cats 01 p0012 A70-10051
- Corticofugal effects of various cortical regions on neuron activity in hypothalamus posterior lateral sections in cats 01 p0012 A70-10053
- Reversible cold induced deactivation of cat neocortex bioelectric activity in chronic experiment, noting cooling system 01 p0031 A70-10056
- Termination mode of primary and secondary vestibular fibers in cerebellar cortex of frog and cat, measuring evoked field and unitary potentials 01 p0014 A70-10353
- Soviet book on higher cortical functions of man and disorders due to local brain injuries, describing methods for neuropsychological studies of motor functions 01 p0017 A70-10503
- Neurons and perineuronal glial cells quantitative relations in visual cortex from anesthetized dogs 01 p0025 A70-11030
- Morphological analysis of connections between auditory cortex zone and claustrum in anesthetized cats, establishing efferent nerve fibers presence 01 p0025 A70-11039
- Corticovisceral interrelations concept, summarizing contributions in form of diagram showing interactions between cortical and nervous activity of organs 01 p0029 A70-11463
- Neurons tracing activity and cellular memory mechanisms in cortical projection region of cutaneous analyzer of immobilized rats following electric acoustic stimuli 01 p0030 A70-11468
- Rabbits and cats cortical neurons responses to light and acoustic signals, using microelectrodes inserted at different depths into cortex 01 p0030 A70-11469
- Neuron activity in somatosensory cortex region of guinea pigs and rats with intracortical connections severed by circular incision 01 p0030 A70-11470
- Evoked potentials arising in entorhinal cortex of rabbits in response to stimulation of somatic nerves, light and sound 03 p0417 A70-13070
- Direct links existence between rabbit temporal cortex neurons and neurons in each division of hippocampus, discussing topographic arrangement and axons quantity 03 p0417 A70-13071
- Skin sensitivity representation in cats cerebellar cortex during electrocutaneous stimulation in chronic experiment, providing information on afferent system 03 p0417 A70-13216
- Cats cerebral cortex background electrical activity measured during development of conditioned reflexes, noting shift toward higher frequencies 03 p0418 A70-13217
- Conditioned fear reaction produced by electric stimulation of cat anterior hypothalamus, discussing effect of neocortex removal 03 p0420 A70-13425
- Somatosensory cortex removal effect on blocking action of skin stimulation on associative response to light flash in cats 03 p0420 A70-13430
- Autocorrelation and cross correlation analysis of slow EEG potentials in rhythm of movement as cortical activity pattern of cerebral hemispheres during work 03 p0421 A70-13687
- Early and late response component of associative cortical area in cerebral hemispheres of cats connected with mono and polysensory neuron activity 03 p0421 A70-13688
- Origin and functional designation of associative evoked potentials in orbital cortex of cats, showing phases connected with neuron activity and excitation 03 p0422 A70-13689
- Unrestrained chimpanzees cortical and subcortical electrical activity during sleep recorded by telemetry and compared with human beings and other mammals 03 p0432 A70-14347
- Efferent model to test inhibitory influence of inferotemporal cortex lesions on visual discrimination of monkeys, using paired flashes of light 04 p0629 A70-14449
- Temporary suppression of cortical associative responses in cats with electrocoagulated thalamic relay nuclei lesions 04 p0632 A70-15220
- EEG patterns of functional state effect on evoked cortical potentials in response to DC pulses in dogs after nembutal administration 04 p0638 A70-15503
- Cortical cells fatigue and performance in subjects doing mental work, using motion picture signal perception method 04 p0639 A70-15509
- Tetrodotoxin /TTX/ effects on mammalian brain studied by introducing TTX into cat lateral geniculate body /LGB/, causing flash evoked potentials and visual cortex decrease 05 p0799 A70-16049
- Nonspecific influences on rabbits neurons reaction to nonvisual stimuli in central visual pathway using microelectrodes implantation in visual cortex 05 p0802 A70-16624
- Rhesus monkeys impaired discrimination in recognizing tachistoscopically presented objects following cortical polarization 05 p0802 A70-16625
- Cerebellar cortex reactions to sciatic nerve stimulation in rats under transverse accelerations in centrifuge 05 p0804 A70-17116
- Visually evoked cortical responses to checkerboard patterns, correlating amplitude to visual acuity 06 p0992 A70-17311
- Acetylcholine concentration, esterase activity and synthesis in cerebral tissue of rats under repeated mechanical vibrations combined with noise 06 p0993 A70-17425
- Pavlovian conditioned reflexes theory reappraisal, discussing cortex-subcortical formations interrelations models 07 p1197 A70-18694
- Rabbits sensorimotor and visual cortical responses during defensive conditioning to rhythmic light 07 p1197 A70-18695
- Electrocorticograms frequency spectra from different visual cortex layers of rabbits during exposure to rhythmic light pulses 07 p1198 A70-18698
- Rabbits visual cortex evoked potential changes due to light flashes under different conditions 07 p1198 A70-18716
- Bioelectrical reactions in anesthetized cats cortical zones in response to stimulation of contralateral sciatic nerve 07 p1199 A70-18722
- Thalamic N. VPL role in distributing afferent flux in anesthetized cats cortex, using stimulating contralateral sciatic nerve 07 p1199 A70-18723
- Anticerebral cytotoxic serum effect on white rats conditioned reflex activity 07 p1199 A70-18727
- Cerebral biopotentials of rabbits exposed to RF weak electromagnetic field indicating cortex inhibition in EEGs 07 p1199 A70-18728
- Canines conditioned reflex activity as function of cortex sections following head exposure to X ray irradiation 07 p1199 A70-18729
- Macaque monkey stereoscopic vision, obtaining behavioral evidence by random dot stereoscopic patterns and finding cells sensitive to binocular depth in cortex 07 p1205 A70-19276
- Guinea pigs visual analyzer during stimulations by diffuse light, nonspecific thalamic nuclei and microelectrodes polarization, determining A- neuron activity 07 p1213 A70-19788
- Midbrain reticular neurons activity in cats during response to individual and coincident cortical and hypothalamic stimulations 07 p1213 A70-19789
- Binocular fusion and rivalry effects on cortically evoked human potential, obtaining pattern characteristic responses to monocular stimulation 07 p1215 A70-20214
- Cortical induction phases estimated by retinal mobility index concerning activity of acoustic, olfactory and cutaneous analysors 08 p1443 A70-20735
- Visually evoked cortical potentials /VECP/ to different probe stimuli to suppressed human eye in binocular rivalry experiments, discussing eye dominance problems 09 p1618 A70-22674
- Ionizing radiation effects on tissues of developing cerebellar cortex of rats 09 p1619 A70-22815
- Brain cerebral tissues electrical impedance measurement by electrodes and bridge circuit, discussing chemical and metabolic properties 09 p1620 A70-22897
- Glycogen accumulation in astroglia following brain trauma caused by partial transection of cerebral hemisphere in rats 09 p1620 A70-22898
- Cholinergic nervous mechanism of autoregulatory dilatation of pial arteries under decreased blood supply to cerebral cortex in rabbits 09 p1622 A70-23583
- Cerebral circulatory reactions of smokers and non-smokers exposed to altitude, measuring vasomotor, blood flow and cardiac frequency indexes using scalp electrodes 12 p2172 A70-28042
- Electrical activity of visual cortex, subcortical structures and reticular formations in cats during conditioned reflex stimulation by light 12 p2173 A70-28351
- Neuron activity of cortical motor and visual regions and corpus geniculatum laterale in cats during diffuse thalamic electrostimulation combined with light signals 12 p2173 A70-28355
- Sleep-wakefulness cycle electroencephalogram of auditory and visual portions of neocortex and hippocampus activity in cats, using spectral analysis and integration 14 p2536 A70-30185
- Ionizing X radiation influence in lethal and sublethal doses on cerebral hyaluronic acid in mice and guinea pigs 14 p2536 A70-30186
- Electroencephalographic responses comparison with electroencephalographic record during prolonged torsion swing vestibular tests under cortical and subcortical factors influence 14 p2539 A70-30917
- Human cerebral cortex intercentral relations during repose and afferent stimulation, using electroencephalogram cross correlation 15 p2687 A70-32868
- Thyroxine stimuli transmission from posterior hypothalamus to cerebral cortex ascribed to dorsomedial nucleus of thalamus 16 p2848 A70-33261
- Cortical evoked potentials in human motor conditioning to photic stimulus 18 p3221 A70-37212
- Evoked potentials in dogs sensorimotor cortex during defensive instrumental conditioning 18 p3221 A70-37213
- Visual cortical anomalous response to paired photic stimulus in rabbits with ablations in rostral part of brain stem 18 p3221 A70-37214
- Visual attention and temporal cortex stimulation effects on evoked electrical activity in monkey brain 19 p3360 A70-37812
- Bilateral cortical cerebellar hemispheric ablations effect on feline light-dark discrimination learning 21 p3762 A70-41142
- Orientation detectors in human visual cortex, suggesting mutual lateral inhibition 23 p4144 A70-43813
- Regional cerebral cortical blood flow measurement, using heat clearance thermistor probe 23 p4157 A70-45082
- Auditory cortex projections to caudate nucleus and functions of associative subcortical area in cats 24 p4300 A70-45838
- Mesencephalic reticular formation influence on threshold stimulation of cortex, hippocampus, amygdala, thalamic nuclei and caudatum in rabbits 24 p4300 A70-45839
- Bilateral oligosynaptic interaction between posterior lateral thalamic nucleus and afferent systems in visual and acoustic cortical areas in cats 24 p4300 A70-45840
- Vasodilating carbon dioxide effect on brain circulation in occipital cortical area in cats and rabbits using thermoelectric method 24 p4300 A70-45842
- Brain cortex protein metabolism alterations induced by anticipation stress and ACTH in rats 24 p4301 A70-45999

CEREBRAL VASCULAR ACCIDENTS

Long air voyage after exteriorization of Wallenberg syndrome, discussing case history of subject with cerebral vascular accident 12 p2172 A70-28044

CEREBROSPINAL FLUID

Respiratory waves formation of intracranial pressure in anesthetized cats and dogs, studying various contributing factors 07 p1213 A70-19792

Acceleration effects on Na, K, and pH in rabbits cerebrospinal fluid and cerebral blood 13 p2352 A70-29347

Blood-brain and blood-cerebrospinal fluid barriers alterations under various physical environments in manned orbital laboratory 22 p3973 A70-43647

CEREBRUM

Phospholipid metabolism intensity in brains of adrenalectomized and pseudo operated rats under hypoxia 01 p0012 A70-10054

Glutamic and aspartic acid concentrations in brain tissue and incubation medium after adding gamma-aminobutyric acid 01 p0018 A70-10507

Thyroidin influence on RNA content and nucleotide composition in hypothalamus, cortex and phenolic fractions of cerebral hemispheres resulting in accelerated protein biosynthesis 01 p0019 A70-10511

Reactions to visual emergency signals in humans after administering adrenalin, aminazin, melipramine or andaxine to change control systems functional state of cerebrum 01 p0030 A70-11467

Synchronizing and desynchronizing systems for cerebral electrical activity, noting roles in sleep and wakefulness mechanisms 03 p0417 A70-13073

Increased oxygen partial pressure effects on cerebral bioelectric activity from EEG recordings on unanesthetized dogs 03 p0422 A70-13690

Pilots temporal lobe epilepsy case history and diagnosis 06 p1000 A70-17301

Acute hypoxia effect on mono-, di- and triphosphoinositides metabolism and content in white rats cerebral tissues, using chromatographic analysis 07 p1199 A70-18721

Cranio-cerebral hypothermia effects on phase structure of cardiac thrust in dogs 07 p1204 A70-19140

Cerebrum hyperemia of dogs subjected to cranio-cerebral hypothermia, recording rheoencephalograms by occipitofrontal needle electrodes 07 p1207 A70-19473

Succinic dehydrogenase activity in white rats cerebrum and liver under hypothermia and after warming 07 p1207 A70-19475

Vegetative cardiovascular, motor and electrophysiological reactions to electrical stimulation of limbic and reticular formations in cerebrum after adrenalin and aminazine injections 13 p2352 A70-29352

Cerebrum electrical activity and myogenic tonus relation in subjects performing tasks in response to visual and acoustic stimuli 18 p3221 A70-37216

Hypoxia effects on cerebral blood flow in anesthetized dogs, considering acidosis and vasodilation 20 p3577 A70-40330

CERENKOV COUNTERS

Fast charged particles measurements by Cerenkov counter in Cosmos 137 satellite, noting hard electron flux and cosmic ray radiation spectrum 01 p0172 A70-11509

High energy gamma rays detection from pulsars by fast night sky Cerenkov counter 19 p3500 A70-38083

Periodic high energy gamma rays from pulsars, using night sky Cerenkov light receiver for proton showers 19 p3500 A70-38084

High energy primary electron flux measurements by Cerenkov counter onboard ESO 2 satellite 19 p3504 A70-38107

Rigidity spectra of primary cosmic ray nuclei groups from satellite-borne Cerenkov spectrometer 19 p3508 A70-38135

CERENKOV EFFECT

U CERENKOV RADIATION

CERENKOV RADIATION

Cerenkov radiation from electrons in magnetosphere and ionosphere, analyzing radiated power relationship with frequencies and latitudes 01 p0080 A70-11226

Cerenkov radiation of electron-positron pair as moving radiating dipole in EAS, discussing emission effects of primary energy, production height and inclination angle 03 p0561 A70-14186

Pulsed gamma radiation from pulsars searched for by Cerenkov air shower detection method 04 p0738 A70-14518

Cerenkov light in extensive air shower observed at mountain altitude showing mixed primary cosmic rays in chemical composition 06 p1134 A70-17184

Cerenkov radiation in infinite anisotropic electron plasma linearly polarized in magnetic field having linear electron distribution moving with uniform velocity 06 p1120 A70-17538

VLF and LF auroral or polar hiss as generated by incoherent Cerenkov radiation from high energy electrons 07 p1264 A70-19190

Cerenkov generation of VLF waves in inner magnetosphere at low latitudes 07 p1265 A70-19281

Cosmic rays induced Cerenkov light pulses effect on stellar intensity interferometer from measuring correlated pulses 08 p1497 A70-21492

Non-Cerenkov radiation region produced by passage of oscillating electric dipole at uniform velocity 09 p1728 A70-22958

High energy pulsed gamma rays detection method for pulsars based on search for nanosecond duration Cerenkov light signals 09 p1748 A70-23795

Cerenkov radiation field in infinite parallel dielectric layer by sinusoidally bunched beam of electric charges moving with constant velocity along surface 10 p1916 A70-24408

Electron collision frequency effects on Cerenkov radiation from magnetoplasma, applying results to magnetosphere and ionosphere 13 p2465 A70-29546

Measurable VLF electromagnetic fluxes from Cerenkov effect in ionosphere produced by artificial electron beams 14 p2579 A70-31249

Cerenkov plasma waves generation by fast electron streams in solar corona and conversion into EM waves 17 p1373 A70-35768

Periodic cosmic gamma radiation from pulsars, using reflector detection of shower generated Cerenkov light 19 p3501 A70-38090

Cosmic gamma ray sources detection in 100-1000 GeV range by atmospheric Cerenkov radiation from energetic particle showers 19 p3501 A70-38091

Pc-1 pulsation production by Cerenkov emission of proton beam oscillating along magnetic field line 19 p3417 A70-38590

Spontaneous and induced Cerenkov emission by charged particle in turbulent medium, discussing random fluctuations effect on radiation spectra 21 p3879 A70-40928

Far field power of coherent Cerenkov radio emission from cosmic ray showers in turbulent atmosphere, using radio telescopes 23 p4247 A70-44791

Light flashes observed by Apollo astronauts, proposing Cerenkov radiation or direct excitation of eye retina by cosmic rays 24 p4307 A70-45403

Cerenkov light longitudinal distribution from extensive air showers, using near UV receivers 24 p4398 A70-46225

CERUM

Ce-Ni-Si system X ray and microstructural analysis, constructing phase diagram for Ce contents of 0-33.3 wt percent 08 p1555 A70-21115

CERMETS

Defects development in cermet materials sealing elements in high O content gas flows of turbo-prop and turbojet engines 01 p0161 A70-10160

Chemical composition of cermet material for radial sealing of high temperature gas turbines, ensuring structural stability and oxidation resistance 01 p0124 A70-11621

Ceramic, cermet and metallic high temperature coatings development and applications, discussing time and cost saving procedures [SAE PAPER 690478] 03 p0515 A70-13267

Titanium carbide based cermets with steel matrices, studying heat treatment effects on hardness 04 p0696 A70-14462

Fillers effect on thermal conductivity in porous cermet elements, investigating powdered Ti plates with air replaced by Hg, benzene, ethanol, ether and water vapor 05 p0957 A70-16291

Fission gases trapped in fuel pellets, cladding and matrix of irradiated refractory metal-uranium oxide cermets determined by gamma counting 07 p1332 A70-19851

Solid lubricant crystallographic orientation selection for antifriction cermet material silver-molybdenum disulfide 12 p2254 A70-27286

Ti-Mo cermet alloys properties and production technology, testing corrosion resistance 16 p2931 A70-33220

Wear resistant titanium carbide based cermet material production by impregnation techniques, discussing grain size and heat treatment effects 19 p3450 A70-37453

Copper based cermets production by electrochemical deposition in lieu of powder metallurgy, discussing merits 19 p3450 A70-37455

Aluminum oxide growth rate in molybdenum cermet after high temperature annealing 24 p4359 A70-45478

CERTIFICATION

FAA engineering approach to SST certification involving airworthiness standards development and coordination with industry and foreign governments 03 p4347 A70-14060

Aircraft noise reduction certifications program by tripartite draft plan 07 p1426 A70-18876

Aircraft certification of supersonic and jumbo jet transports assuring acceptable safety level 09 p1610 A70-22948

Certification process for supersonic transports taking into account safety and economic considerations 09 p1610 A70-22949

Apollo Spacecraft Certification Test Program at replaceable hardware assembly level noting future manned spacecraft applications [AIAA PAPER 70-375] 10 p1952 A70-24928

Licensing aspects of Edwards Report, criticizing Air Transport Licensing Board (ATLB) organization 11 p1153 A70-25856

STOL aircraft noise level certification based on aircraft type, landing and takeoff paths and airports [SAE PAPER 700325] 12 p2161 A70-27459

Meteorological problems associated with proposed tests for aircraft noise certification, discussing airport near-surface environments 14 p2610 A70-30612

Charpy impact test accuracy for model machine certification, discussing erroneously high test values 15 p2820 A70-32236

Boeing 747 flight test certification program, describing methods, data systems, inertial navigation, engines, flutter, etc [SAE PAPER 700828] 24 p4290 A70-45891

STOL aircraft FAA airworthiness standards and certification rules, examining noise, control systems, all weather operation, fire protection, handling qualities and performance [AIAA PAPER 70-1331] 24 p4291 A70-45937

CESIUM

NT CESIUM VAPOR

Temperature effect on work function minimum of cesiated W surfaces 01 p0154 A70-10108

Cesium clocks at fixed locations compared for precision and accuracy, noting influence of radio frequency diurnal variations 06 p1139 A70-17474

Phase comparisons between commercial cesium beam frequency standards and NASA experimental hydrogen maser NX-1 08 p1513 A70-21592

Quadratic Stark shifts of absorption lines hyperfine components in cesium atom beam measured using optical spectroscopy 10 p1887 A70-24033

Cs atomic spectral line broadening under simultaneous electric and magnetic fields, observing Zeeman and Stark splitting 13 p2460 A70-28711

Ce atom collision with excited Hg atom, measuring ionization cross section 18 p3292 A70-36154

Critique of paper on electron diffraction study of Ce adsorption on W surface, discussing electron work function changes and data discrepancies 19 p3473 A70-37548

Cesium films structure and work function on W /011/ face, discussing order-disorder transition 19 p3487 A70-37817

Cesium beam velocity attenuation by He, Kr and Xe, determining scattering cross sections from gas pressure and density measurements 20 p3675 A70-39618

Preionization in Cs seeded Ar nonequilibrium plasma for MHD generators, examining discharge characteristics, recombination reactions, etc 20 p3680 A70-39991

Diatom C_s 7667 A band vibrational spectrum analysis 20 p3676 A70-40349

Cesium high temperature saturated liquid and vapor phase density and critical temperature and pressure 23 p4281 A70-44450

Two-bulb switchable pulsed spectral lamp with Cs and Xe for optical pumping studies 23 p4197 A70-44478

CESIUM ALLOYS
Cooled antimony-cesium film photoelectric effect for weak luminous flux, examining electronic camera reciprocity 19 p3427 A70-38175

CESIUM ANTIMONIDES
Photoemitting cesium antimonide thin films for IR detectors 19 p3488 A70-38202

CESIUM COMPOUNDS
NT Cesium Antimonides

CESIUM DIODES
Cs atoms excitation and ionization in Cs diode interelectrode space under Knudsen conditions, considering luminescence and electron energy distribution 10 p1926 A70-25116

CESIUM ENGINES
Thrust vectoring of multiaperture Ce electron bombardment ion engines, determining thrust deflection limit by accelerator current rise 11 p2102 A70-26124
One millipound cesium ion thruster for synchronous ATS-F satellite, describing power conditioning and control logic subsystems [AIAA PAPER 70-1149] 20 p3690 A70-40205
Composite accelerator electrodes on Cs bombardment microthrusters, testing various designs and electrode coatings [AIAA PAPER 70-1089] 20 p3693 A70-40246
Cs and Hg electrostatic thruster effluents effects on spacecraft materials, describing chemical, metallurgical and thermophysical experiments [AIAA PAPER 70-1144] 20 p3652 A70-40519

CESIUM ION
Cs atomic and molecular ions mobilities and drift velocities in Cs vapor at different pressures in low electric fields 04 p0722 A70-14715
Satellite spin stabilization by Cs contact ion microthrusters with beam deflection, investigating performance obtained by optimal and suboptimal laws 13 p2506 A70-29143
Plasma space potential measurement with heavy ion beam probe using cesium gun and electrostatic energy analyzer 16 p2960 A70-34339
Effective collision cross section for reaction resulting in Cs ions neutralization in thermal Cs plasma calculated from measured ion currents 22 p4082 A70-43374

CESIUM PLASMA
Longitudinal and transverse temperature distribution measurement of electrons in electrostatic field and ion current density in ionized Cs plasma beam, determining energy spectra 01 p0149 A70-10170
Negative resistance I-V characteristics of low voltage arc discharge in Cs plasma 01 p0150 A70-10172
Cs seeding effect on bound-free UV photoabsorption of Cs-H plasma at constant electron density and energies below H ionization 02 p0343 A70-11904
Nonequilibrium cesium plasma of low voltage arc discharge, measuring electron temperature and distribution function and diffuse-series excited level populations 03 p0532 A70-13740
Cs plasma research, discussing Q-machines, plasma confinement, magnetic field experiments, LF and HF wave propagation, etc 03 p0533 A70-14015
Plasma instabilities of Ce filled auxiliary discharge thermionic energy converter compared with Langmuir theory 03 p0415 A70-14367
Nonequilibrium Cs plasma electron density, temperature and sustaining field using theoretical analysis and probe measurements 05 p0887 A70-16108
Visible light emission from nonequilibrium Cs plasma measured for spectral intensity distribution, suggesting excitation mechanism in terms of collision-radiation model 05 p0887 A70-16109
Cesium plasma composition as equilibrium mixture of ideal gases assuming chemical equilibrium attainable by specified reactions 07 p1349 A70-19660
Upper cesium levels population inversion during cesium discharge plasma decay 08 p1550 A70-20848
Molecular cesium ion production by arc discharge in inhomogeneous cesium plasma, describing probable reaction mechanism 08 p1551 A70-20849
Longitudinal and transverse temperature distribution measurement of electrons in electrostatic field and ion current density in ionized Cs plasma beam, determining energy spectra 10 p1925 A70-25016
Hg and Cd seeded Ce plasma wide-spaced diode without external light source investigated for Penning effect on diode performance 10 p1808 A70-25038

Thermally ionized cesium plasma viscosity at high temperatures in vacuum using capillary tube assembly 11 p2092 A70-26731
Optimal conditions for obtaining dense low temperature cesium plasma in shock tube with heating calculated by Debye theory 12 p2278 A70-27327
Positive ion composition in Cs plasma as function of normalized pressure 15 p2779 A70-31978
Cesium plasma composition as equilibrium mixture of ideal gases, assuming chemical equilibrium attainable by specified reactions 15 p2781 A70-32697
Probe measurements in Cs plasma formed by contact ionization with hot wire for density, electron temperature and space potential 16 p2958 A70-33624
Photoresonant cesium plasma ionization, discussing pumping spectra, electron gas, molecular-atomic ion ratio and dynamics 19 p3474 A70-37440
Electron and ion transport in cesium plasma for thermionic and MHD energy converters 21 p3859 A70-41912
Optimal conditions for obtaining dense low temperature cesium plasma in shock tube with heating calculated by Debye theory 21 p3860 A70-42068
Cs seeded Ar discharges electron energy distribution, discussing drift velocities, electrons elastic and inelastic collisions with ions and molecules, etc 22 p4081 A70-43198
Effective collision cross section for reaction resulting in Cs ions neutralization in thermal Cs plasma calculated from measured ion currents 22 p4082 A70-43374
Cs ion beam space charge and current neutralization by electron capture for partially ionized plasma formation, investigating longitudinal electrostatic wave excitation 24 p4385 A70-45465

CESIUM VAPOR
Low voltage arc discharge in thermionic converter at low Ce pressures measured for current-voltage characteristics, showing degree of ionization 01 p0150 A70-10173
Threshold laser power density-atom density relation in cesium vapor optical breakdown, suggesting two photon ionization process 01 p0110 A70-10569
Cs atomic and molecular ions mobilities and drift velocities in Cs vapor at different pressures in low electric fields 04 p0722 A70-14715
Cs jet device eliminating wall influence in nonlinear radiation-atom interaction phenomena 07 p1342 A70-20109
Low voltage arc discharge in thermionic converter at low Ce pressures measured for current-voltage characteristics, showing degree of ionization 10 p1925 A70-25018
Nuclear converter with porous metal adsorption reservoir working with or without liquid cesium 10 p1915 A70-25039
Servo type Cs vapor magnetometer performance including sensitivity, orientation effect, dynamic characteristics and operational temperature range 13 p2414 A70-30038
Electron energy loss per collision in Cs vapor discharge, measuring electric field and electron temperature by Langmuir probes 16 p2954 A70-33281
Microwave characteristics in plasma of short discharges in low pressure cesium and mercury vapors, noting spectral and spatial distribution of microwave power and intensities 22 p4083 A70-43392
Cs high temperature vapor and critical pressure and temperature determination for predicting thermodynamic and transport properties, liquid phase nature and state relations 23 p4281 A70-44449

CESSNA AIRCRAFT
Cessna single engine aircraft tubular and flat steel landing gear springs, describing quality control through nondestructive testing 01 p0098 A70-10018
Cessna CITATION aircraft design, considering engineering, marketing and corporate cooperation [SAE PAPER 700241] 11 p1981 A70-25910

CESSNA MILITARY AIRCRAFT
U CESSNA AIRCRAFT
U MILITARY AIRCRAFT

CETYL COMPOUNDS
Cetyl alcohol and water vapor growth by absorption and condensation on hygroscopic nuclei population in atmosphere under cooling 20 p3664 A70-40066

CF-104 AIRCRAFT
U CANADAIIR AIRCRAFT
U F-104 AIRCRAFT

CH-3 HELICOPTER
Flight tests conducted in artificial and natural icing conditions, using CH-3C helicopter with rotor blades equipped with polyethylene anticing tape 01 p0006 A70-10695

CH-46 HELICOPTER
Flight recorder survey to determine combat operating environments of instrumented CH-46D Sea Knight helicopters 01 p0006 A70-10702
Analog/digital system for full scale airframe fatigue amplitude and phase signature measurements on CH-46D tandem rotor helicopter 15 p2739 A70-32323
Fluidics in naval avionics, discussing CH-46A helicopter stability augmentation and approach power compensator for carrier-based aircraft 24 p4293 A70-45428

CH-47 HELICOPTER
Personnel/cargo lowering and retrieval system requirements, design approach and effects on performance for CH-47 helicopter, discussing fabrication and testing on mockup 06 p0985 A70-17711
CH-47C helicopter fiberglass main rotor blade, discussing composite materials impact on design 17 p3013 A70-34702
CH-47 cruise guide indicator for displaying fatigue loading to pilots, discussing design and operation 17 p3082 A70-34705

CH-54 HELICOPTER
CH-54A engine air particle separator /EAPS/ field experience, discussing engine removal times due to erosion, environment evaluation and design improvements 01 p0164 A70-10684
CH-54 engine air inlet antice system design, manufacture and testing, solving heat balance equations describing tapered gap heat exchanger 01 p0165 A70-10693
Crane helicopters characteristics, history and projected applications to petrochemical, shipping, construction and power transmission industries [SAE PAPER 700284] 12 p2160 A70-27427
CH-54A helicopter gas turbine engine air particle separator /EAPS/ field service in Vietnam, noting time before engine removal for erosion [ASME PAPER 70-GT-97] 18 p3303 A70-36844

CH-113 HELICOPTER
U CH-46 HELICOPTER

CHAFF
Rocket-borne radar chaff wind sensor synoptic application above 65 km, describing low fall velocity 07 p1237 A70-20258
Free atmosphere turbulent diffusion coefficient determination, releasing dipole reflectors from helicopter for radio echo observation 19 p3461 A70-37423
Smoke, chaff and flare distress signals design and operation for search and rescue operations 23 p4143 A70-44494

CHAIRS
U SEATS

CHALCOGENIDES
NT ALUMINUM OXIDES
NT BARIUM OXIDES
NT BERYLLIUM OXIDES
NT BISMUTH OXIDES
NT BORON OXIDES
NT CADMIUM SELENIDES
NT CADMIUM SULFIDES
NT CADMIUM TELLURIDES
NT CALCIUM OXIDES
NT CARBON DIOXIDE
NT CARBON DISULFIDE
NT CARBON MONOXIDE
NT CHLORINE OXIDES
NT CHROMITES
NT CHROMIUM OXIDES
NT COBALT OXIDES
NT COPPER OXIDES
NT COPPER SULFIDES
NT DISULFIDES
NT ENSTATITE
NT GALLIUM SELENIDES
NT HAFNIUM OXIDES
NT HEMATITE
NT HYDROGEN PEROXIDE
NT HYDROGEN SULFIDE
NT ILMENITE
NT INDIUM TELLURIDES
NT INORGANIC PEROXIDES
NT IRON OXIDES
NT LANTHANUM OXIDES
NT LEAD SELENIDES
NT LEAD TELLURIDES
NT MAGNESIUM OXIDES
NT MAGNETITE
NT MERCURY TELLURIDES
NT METAL OXIDES
NT MOLYBDENUM DISULFIDES
NT MOLYBDENUM OXIDES
NT MOLYBDENUM SULFIDES
NT MUSCOVITE
NT NICKEL OXIDES

NT NIOBIUM OXIDES
 NT NITRIC OXIDE
 NT NITROGEN DIOXIDE
 NT NITROGEN OXIDES
 NT NITROGEN TETROXIDE
 NT NITROUS OXIDES
 NT OXIDES
 NT PEROXIDES
 NT POLYSULFIDES
 NT POTASSIUM OXIDES
 NT PYROXENES
 NT PYRRHOTITE
 NT QUARTZ
 NT RUTILE
 NT SAPPHIRE
 NT SCANDIUM OXIDES
 NT SELENIDES
 NT SILICON DIOXIDE
 NT SILICON OXIDES
 NT SULFIDES
 NT SULFUR OXIDES
 NT TANTALUM OXIDES
 NT TELLURIDES
 NT THORIUM OXIDES
 NT TIN OXIDES
 NT TIN TELLURIDES
 NT TITANIUM OXIDES
 NT TROLITE
 NT TUNGSTEN OXIDES
 NT URANIUM OXIDES
 NT YTTRIUM OXIDES
 NT ZINC OXIDES
 NT ZINC SELENIDES
 NT ZINC SULFIDES
 NT ZINC TELLURIDES
 NT ZIRCONIUM OXIDES

Glass formation region of chalcogenide semiconductor arsenic triselenide-antimony triselenide system and vitreous-crystalline transformation, investigating electrical and optical properties
 01 p0153 A70-10085

Optical, electrical and structural properties of transition metal dichalcogenides
 05 p0890 A70-15755

Chalcogenide glass based film face threshold switches I-V characteristics, presenting oscillogram and diagrams
 05 p0892 A70-16542

Literature on IV-VI semiconducting Pb compounds PbTe, PbSe, PbS and PbO, discussing PbTe-SnTe and PbSe-SnSe solid solutions
 08 p1555 A70-20584

PbTe-based Sn, Se and Ge alloys lattice constant, thermal EMF and resistance, fusibility and microstructure
 08 p1555 A70-21117

Current-voltage characteristics and lifetime of thin film diodes on chalcogenide glass substrate with symmetrical and asymmetrical electrodes
 09 p1647 A70-22751

Electronic switching effects in amorphous semiconductors emphasizing mass memory for computers based on thin films of chalcogenides
 11 p2017 A70-25524

Superconductive memory type chalcogenide tellurium germanium arsenide, measuring AC magnetic susceptibility and DC electrical resistivity
 23 p4231 A70-44892

CHANCE-VOUGHT MILITARY AIRCRAFT
U MILITARY AIRCRAFT
CHANDRASEKHAR EQUATION
 Solutions of Ambarzumian-chandrasekhar H-equation for radiative transfer
 02 p0340 A70-12661

Nonlinear integral equations for inhomogeneous atmospheres derived from radiative transfer equations global form, noting relations to Ueno and Chandrasekhar equations
 07 p1336 A70-20059

Chandrasekhar polarization upper limit in early type stars noting effects of thermal absorption, wavelengths and effective temperature
 12 p2303 A70-27675

Chandrasekhar H function approximation for isotropic scattering, calculating absorption line contours
 22 p4109 A70-43750

CHANNEL CAPACITY
 Intelsat 4 communication system design and international cooperation, considering satellite design, TV and telephone channels capacity, etc
 01 p0196 A70-10883

Channel constraints on multiple access systems obtained from airborne propagation tests via satellites, studying disparities in received signal strength
 02 p0260 A70-12569

Rate distortion function for class of sources, proving positive and negative sides of Shannon encoding theorem for noisy channels
 02 p0266 A70-12611

Multistop time-to-pulse-height conversion unit to extend capability of pulse height analyzer for multichannel time analysis with narrow channel widths
 02 p0271 A70-12749

Incoherent reception of wideband signals transmitted through multibeam channel with changing random parameters
 05 p0812 A70-16248

Algorithm applied to specific classes of random processes for calculating minimum channel capacity required by transmission system for sources in each class
 06 p1012 A70-18621

Capacity and error bounds derived for nonsynchronized channel, discussing binary coding strategy
 06 p1012 A70-18623

Capacity calculation of N identical discrete memoryless nonsingular channels cascade, discussing dependence on eigenvalues and eigenvectors of subchannel transition matrices
 06 p1013 A70-18628

Digital data transmission over discrete time Gaussian channel with noisy feedback, investigating error-exponent/reliability/and finite SNR
 07 p1235 A70-19362

High attenuation quantum communication channel capacity based on mathematical model
 07 p1335 A70-19864

Millimeter guided wave communication systems information transmission capacity increase, using quaternary and higher order modulation techniques
 08 p1462 A70-21506

Crosstalk in multiple-beam waveguides due to scattering and distortion caused by surface irregularities of focusers, discussing power profile of Gaussian beam
 08 p1462 A70-21507

Digital satellite communication system using multiphase modulation optimized for phase positions number to maximize transmission capacity
 10 p1835 A70-24334

Geostationary orbit capacity based on multichannel telephony, comparing digital and analog modulation techniques
 10 p1836 A70-24343

Communication commercial satellite systems capacity in terms of telephone channels, using frequency modulation and digital methods
 10 p1836 A70-24344

Physical formula for information content in communication signals based on receiver observation concept, noting role of channel properties and encoding
 10 p1844 A70-25223

Satellite communications system optimal parameters and efficiency dependence on working capacity, discussing economic aspects of HF sets increased number
 11 p1995 A70-25345

Satellite capacity utilization for mixed earth stations network using SPADE concept/digital satellite communication system employing demand-assignment and voice-activated carrier techniques
 11 p1996 A70-25404

Geostationary satellite communication bandwidth increase by reusing same frequency band in multiple independent earthward beams, discussing modulation and interference noise allocation effects
 11 p1996 A70-25405

Multiple channel communication satellite interference including preamplifier intermodulation, direct interference, multipath amplification, crosstalk and multiplexer reflections considered for capacity maximization
 11 p2002 A70-25483

Meteorological radar station reception equipment for increased radio telemetry channel reliability in complex radio sounding of atmosphere
 11 p2075 A70-25920

Mariner-type spacecraft telemetry system optimization, considering channel capacity
 11 p2008 A70-26239

Pattern recognition with time interval modulation information coding/TIMIC/, considering channel capacity of switching device, similarity with nervous system, etc
 11 p2010 A70-26267

Memoryless input discrete noisy channels essential equivalence to white Gaussian channel for rates above capacity using extreme value theory
 11 p2010 A70-26326

Quantum mechanical communication system with thermal noise disturbance, analyzing reliability function and channel capacity
 14 p2551 A70-31120

Flexible channel multiplier for particle counting with electron conductive polymer composition, discussing secondary electron emission, gain distribution and degradation
 17 p3054 A70-35279

Asymptotic transmitting capacity of continuous channel with intense independent and additive noise
 18 p3228 A70-36598

Pulse ratio modulation analysis based on information theory, emphasizing magnetic tape channel capacity optimal utilization in signal transmission
 20 p3586 A70-39708

Satellite communications system optimal parameters and efficiency dependence on working capacity,

discussing economic aspects of HF sets increased number
 20 p3589 A70-40457

Earth resources technology satellite data link tradeoff between channel capacity and transmitter power
 22 p4038 A70-43091

High speed PCM Codec with maximum 600 channel capacity applied to Time Division Multiple Access (TDMA)/system for satellite communication
 23 p4166 A70-43774

Communication channel modeling with feedback for small error probability compared to unfolding capacity
 24 p4313 A70-46056

Single-error nongroup binary codes with maximum codewords, including quadratic residue, Reed-Muller and tripple-error constructions
 24 p4313 A70-46057

CHANNEL FLOW

Multiple pulsations mechanism during detonation spherical wavefront propagation in channels with various cross sections, noting volume effect
 01 p0060 A70-10135

Two phase flow in cylindrical channel, formulating maximum momentum flow variational principle for laminated adiabatic vapor- and gas-liquid flows
 01 p0213 A70-10216

Dipolar fluid effect on back flow between parallel plates, considering generalized Couette flow
 01 p0062 A70-10545

Viscous fluid flow due to long flat plate moving rectilinearly inside cylinder, assuming zero pressure gradient
 01 p0062 A70-10801

Power output, Joule dissociation and generator efficiency determined for rectangular MHD channel, considering transverse and longitudinal edge effects
 01 p0152 A70-10992

Cavitation initial phase flow model, analyzing flow past stepped obstacle in plane channel
 01 p0064 A70-11002

Gas jets collision flowing from parallel wall channels, applying solution to calculating geometrical characteristics or fluid jet amplifiers
 01 p0011 A70-11569

Navier-Stokes equations for compressible gas, generalizing viscous channel flow of heat conducting gas to slip flow of rarefied gas
 01 p0068 A70-11579

Mixing length relationship in Prandtl theory for turbulent channel and pipe flow, deriving universal velocity distribution law
 02 p0277 A70-11911

Turbulent boundary layer of incompressible fluid flow in axisymmetric channels with swirl at inlet, considering components interaction, velocity, circulation profiles and resistance
 03 p0466 A70-13389

Boundary layer approximation for natural convection in flat vertical symmetrically heated channel with stabilized laminar flow for local and mean Nusselt numbers
 03 p0605 A70-13395

Pulsation frequency affecting boundary layer separation from channel wall in incompressible fluid flow calculated by equation
 03 p0466 A70-13399

Fluid flow visualization in closed channels, using spherules of pulverized fusible materials prepared in swirl injector
 03 p0485 A70-13473

Cavitating flow in converging channels of hydraulic system, calculating energy distribution at gas-vapor phase using Borda-Carnot theorem
 03 p0466 A70-13513

Viscous compressible heat conducting laminar perfect gas flow in slender axisymmetric channels with adiabatic walls, using equations of motion
 03 p0471 A70-14383

Volumetric flow rate of rare gases, hydrogen and deuterium between parallel plates at various pressures and Knudsen numbers
 04 p0665 A70-14414

Flow viscosity and heat conduction effects on shock wave propagation in bent channel with weak Mach reflection
 04 p0671 A70-15013

Viscous gas self similar channel flow with heat transfer at wall corresponding to fixed Mach number profile in all channel cross sections
 04 p0673 A70-15231

Flow stability of plane channel formed by incompressible viscous fluid injection through porous parallel walls
 04 p0673 A70-15238

Model flow studied for viscous flow near trailing edge of semiinfinite flat plate in middle of moving channel, noting Couette flow tendencies
 05 p0831 A70-15879

Entrance length and pressure drop in MHD parallel plate channel flow using one parameter Pohlhausen method
 05 p0887 A70-15978

- Plane Poiseuille flow stability as function of periodic disturbances of finite amplitude in channel axis direction
05 p0832 A70-16018
- Rarefied H, He, air, carbon dioxide and water vapor flow rates between parallel optically flat glass surfaces measured, giving flow equation describing channel flow
05 p0813 A70-16525
- Steady gravitational waves produced by variable pressure in fluid channel flow assuming small perturbed flow velocity components
05 p0836 A70-16969
- Laminar steady radial flow of simple fluid of short memory between two parallel disks, demonstrating relation to Newtonian fluid
06 p1037 A70-17915
- Velocity profile at entrance of two dimensional channel immersed in rarefied slow moving uniform flow with slip at walls
06 p1052 A70-18384
- Temperature distribution in heated horizontal layer of high Prandtl number silicone fluids at high Rayleigh numbers confined between rigid parallel conducting plates
07 p1418 A70-18647
- Laminar flow of compressible gas in axisymmetrical channel in absence of wall insulation using velocity profiles, heat transfer, etc
07 p1253 A70-19062
- Heat protection effectiveness of rectangular channel plane wall with flow by air injection through aperture on wall
07 p1420 A70-19066
- Electrical conductivity variations effects in subsonic Hartmann plasma flow under transverse magnetic field in channel with cooled walls
07 p1352 A70-19986
- Laminar radial flow between parallel disks, estimating static wall pressure distribution perturbation caused by characteristic time
08 p1484 A70-21237
- Flow structure in rectangular cavity in lower wall of two dimensional channel for various aspect ratios and Reynolds numbers
08 p1484 A70-21313
- Forced convection heat transfer between two parallel plates analyzed numerically for effect of constant heat transfer coefficient boundary condition
08 p1598 A70-21425
- Laminarization parameter magnitude determination for turbulent boundary layer in convergent channel flow
08 p1484 A70-21518
- Viscoelastic fluid steady flow in porous walled channel, examining mass flow solution continuity
08 p1485 A70-21639
- Transient temperature distribution in flow through channel with arbitrary cross section, taking into account internal heat generation and viscous dissipation
08 p1599 A70-21767
- Heat transfer in MHD channel flow of viscous incompressible rarefied gas with slip flow and temperature jump boundary conditions
08 p1554 A70-21769
- Tensor conductivity, magnetic field and electric field effect on heat transfer in MHD channel flow, solving for temperature and Nusselt number
08 p1554 A70-21773
- MHD flow between two parallel plates, noting pressure gradient and skin friction coefficient
08 p1554 A70-21774
- Turbulent MHD channel flow velocity profiles and hydraulic resistance relations for various Reynolds numbers, using two layer model
09 p1658 A70-22175
- Steady turbulent perfect compressible gas flow in axisymmetrical or plane channel, using equations governing channel height and static pressure variations
09 p1659 A70-22429
- Poiseuille and Couette fluid flow with internal rotation in flat channel
09 p1660 A70-22436
- Macroscopic properties of thermal molecular flow between coaxial cylinders and concentric spheres, using transpiration theory in Knudsen gas
09 p1788 A70-22906
- Vapor bubble separation diameter and flow in channel boiling applied to supercooled boiling zone determination
09 p1789 A70-23379
- Local Nusselt numbers beyond abrupt circular channel expansion tested for Reynolds numbers with air as working fluid
09 p1790 A70-23554
- Asymmetry and vorticity effects on linear instability of channel flow with one parameter velocities and inflection points, proving wave speed theorem
10 p1862 A70-23951
- Plane steady flows characteristics of incompressible viscous fluids in rigid walled rectangular channels found asymptotic to Poiseuille and Couette flows
10 p1866 A70-24112
- Optimal MHD generator with constant channel area, assuming small Reynolds numbers and ideal inviscid gas with arbitrary electrical conductivity
10 p1807 A70-24570
- Laminar flow into channel with symmetrical jets along walls, considering velocity profiles and flow establishment lengths
10 p1870 A70-24790
- MHD generator with generator channel consisting of two coaxial cylinders with smooth annular space, discussing internal impedance sensitivity
10 p1807 A70-24855
- Laminar flow of compressible gas in axisymmetrical channel in absence of wall insulation using velocity profiles, heat transfer, etc
10 p1871 A70-25213
- Heat protection effectiveness of rectangular channel plane wall with flow by air injection through aperture on wall
10 p1970 A70-25217
- Flow characteristics of airfoil rotating cascades in variable width channel in incompressible liquid
11 p1975 A70-25789
- Velocity profile and volume flow rate for rarefied gas flowing isothermal parallel plates, solving linearized Boltzmann equation by BGK model
11 p2037 A70-26168
- Plane wave disturbances introduced in turbulent channel flow by vibrating ribbons near each wall, obtaining amplitude and relative phase
11 p2039 A70-26537
- Turbulent three dimensional Poiseuille channel flow at large Reynolds numbers, investigating eddy shapes and energy balance
11 p2041 A70-26546
- Electric arc column properties in channel gas flow, including electric fields distribution of potential and heat conduction function
11 p2092 A70-26729
- Electric arc in cylindrical channel gas flow described by boundary layer equations, assuming equilibrium and quasi-neutral media
11 p2151 A70-26730
- Insulator wall temperature effect on supersonic two temperature MHD generator channel flow at open and short circuit conditions
12 p2163 A70-27067
- Turbulent boundary layer in axisymmetric channel having interactions with flow core, calculating flow characteristics and separation point
12 p2209 A70-27289
- Sonic surface and Cauchy problem of Monge-Ampere equations in plane unsteady transonic channel flow solved by hodographic analysis
12 p2156 A70-27299
- Transverse flow convective instability spectrum in vertical channel with porous walls, noting Peclet number effects
12 p2333 A70-28199
- Hydrodynamic entrance length in channels and tubes of varying cross section with arbitrary initial velocity profile
12 p2212 A70-28210
- Two dimensional irrotational incompressible fluid motion bounded by flexible stretched and unstretched film, noting hydrodynamic shock for closed film
12 p2213 A70-28238
- River bed channel flow instantaneous velocities described by logarithmic law, determining turbulent energy dissipation
12 p2265 A70-28336
- Electric field in rectangular MHD channel with ideally conducting electrodes in uniform magnetic field, considering conditions for maximum channel effectiveness
13 p2461 A70-28966
- Oscillatory flow in porous channel with suction and injection, using Laplace transform technique
13 p2389 A70-29538
- MHD pressure head variations in Hg flow in square channel with conducting and insulating walls under transverse magnetic field
13 p2465 A70-29838
- Laminar or turbulent flow in parallel plate channels with combined forced convective and radiative heat transfer, determining gas temperature field and Nusselt numbers
14 p2663 A70-30253
- Helical vortex generation in rotating flow in straight tube having angular momentum flux sufficiently large relative to linear momentum flux
14 p2565 A70-30277
- Radiation effects on heat transfer in turbulent channel flow for small optical depths and optically thin limit
14 p2665 A70-30548
- Karman vortex shedding phenomenon for flow rate measurement in channel or pipe
14 p2588 A70-31333
- Uniform electric and magnetic fields effects on flow of conducting compressible fluid in channel, using multiple scales method
15 p2779 A70-31914
- Heat transfer between incompressible fluid flow and insulated walls with time varying temperature at channel inlet, applying Laplace transforms
15 p2827 A70-32175
- Stationary hydrodynamic equations of gas channel and nozzle flow with inlet tangential discontinuities
16 p2833 A70-33247
- Turbulent shear flow asymptotic theory, discussing channel, pipe and two dimensional boundary layers
16 p2895 A70-34244
- Hydrodynamic entry length for laminar flow between parallel porous plates, using finite difference theory for flow equations
17 p3069 A70-34983
- Thermal choking of channel flow by radiative transfer from upstream and application to shock waves generation
17 p3195 A70-35039
- Turbulent gas flows shear turbulence structure at various Reynolds numbers in nonconducting channels with and without heat transfer under transverse magnetic field
17 p3141 A70-35245
- Supersonic electrically conducting gas flow in flat channel with dielectric walls in inhomogeneous magnetic field
17 p3141 A70-35334
- Critical heat flux density during annular channel internal heating, examining transfer crisis under forced motion of unheated water
18 p3345 A70-36111
- Critical height phenomenon for vertical jet exhausting into horizontal parallel plates channel simulating aircraft surfaces
18 p3243 A70-36709
- Boundary layer momentum thickness growth in channels with adverse pressure gradients by stepwise integration of Truckenbrodt equation and extending Gruschwitz-Schmidbauer separation criterion [ASME PAPER 70-GT-12]
18 p3243 A70-36864
- Heat transfer characteristics of flows between high speed rotating disk and parallel stationary shroud, discussing experimental facility and procedures [ASME PAPER 70-GT-20]
18 p3349 A70-36865
- Electrically conducting perfect compressible fluid flow in semiinfinite channel under electromagnetic field, using multiple scales method
19 p3479 A70-37595
- Conducting gas channel and jet flow in electric and magnetic fields, using linearizing equations of motion under assumption of small magnetic Reynolds number
19 p3479 A70-37598
- Unsteady laminar incompressible fluid flow in parallel plate channels and circular tubes, solving Navier-Stokes equations for prescribed discharge
19 p3405 A70-38347
- Liquid He 4.2 K in narrow channels with laminar and turbulent flow, measuring boiling heat transfer as function of temperature difference
20 p3735 A70-39155
- MHD flow in channel of arbitrary cross section, deriving velocity and electric potential distribution by variational principle
20 p3677 A70-39360
- One dimensional channel flow theory for ram wings, deriving lift and drag laws for comparison with wind tunnel and free flight tests results [AIAA PAPER 70-971]
20 p3558 A70-39558
- Flow velocity and pressure profiles due to vortex ring confined in cylindrical channel, using electromagnetic analogy
20 p3609 A70-39651
- Unsteady viscous flow of incompressible fluid through porous straight channel under time varying pressure gradient, determining suction and injection effects
20 p3609 A70-39670
- Divergent channel with porous walls, calculating effect of suction on laminar incompressible boundary layer by Runge-Kutta method
20 p3609 A70-39671
- Insulator wall temperature effect on supersonic nonequilibrium MHD generator channel under open and short circuit conditions
20 p3681 A70-39994
- Large MHD generator channel aerodynamics, discussing pressure distributions to stall and stagnation pressure loss
20 p3612 A70-40002
- Conducting wall MHD generator channel current distribution, examining computer program for anode and cathode currents
20 p3566 A70-40013
- Integral transforms applied to convective heat transfer during nonNewtonian fluid flow with power rheology in pipes and channels
20 p3613 A70-40177
- Compressible plasma axisymmetric channel flow under electromagnetic forces and ohmic heating, noting velocity profiles and current density [AIAA PAPER 70-1098]
20 p3683 A70-40239
- Turbulent boundary layer in axisymmetric channel having interactions with flow core, calculating flow characteristics and separation point
20 p3613 A70-40339

Longitudinal averaged and pulsating turbulent flow velocities in rectangular channel with one-sided air injection through porous wall

20 p3614 A70-40346

Steady plane conducting gas flow across magnetic field in channel, calculating flow rate effect on current density distribution

20 p3684 A70-40386

Transient and steady state free convection heat transfer with mercury in vertical rectangular channel, measuring temperature distributions

21 p3941 A70-40773

Wall heat transfer for partially ionized argon laminar flow within square channel conducting walls with and without transverse magnetic field

21 p3856 A70-41032

Incompressible MHD flow in entrance region of channel with electrically conducting walls, calculating interacted laminar heat transfer by integral method

21 p3856 A70-41038

Traveling thermal wave induced channel flow, examining velocity profile thermal boundary conditions and shear stress

21 p3948 A70-41247

Heat transfer in laminar channel flow with random velocity variations, using Monte Carlo technique

21 p3949 A70-41312

Unsteady convective heat transfer and hydrodynamics of laminar and turbulent channel flows

21 p3808 A70-41374

Irrational incompressible flow through two dimensional channel with asymmetric contraction

21 p3809 A70-41757

Single phase flow problem in heated vertical prismatic channel, using dimensional analysis from conservation equations with boundary layer approximation

21 p3954 A70-42170

Decelerated channel flow dynamics of ideal gas with supersonic velocity closed by compression shock, using finite difference method

21 p3747 A70-42203

Subsonic channel incompressible gas flow past semiinfinite flat plate base, using flow pattern for cavitation flow

21 p3748 A70-42213

Nonparallel viscous incompressible fluid flows in channel between parallel porous plates with suction and blowing respectively, calculating stability by numerical solution

21 p3811 A70-42216

One dimensional supersonic flow of ideal conducting gas in linear channel under transverse magnetic field

21 p3861 A70-42228

Jeffery-Hamel flows in symmetric divergent channels with small wall curvature, calculating eigenvalues and nonlinear stability limits

22 p4010 A70-42638

MHD channel flow of suspension for prescribed wall heat flux and temperature, determining flow and heat transfer characteristics

22 p4080 A70-42670

Magnetoacoustic waves in MHD channels, investigating excitation, damping and effects on mean current density and Hall field strength

22 p4081 A70-42822

Ionization waves excitation and damping in MHD channels, investigating effects on electric conductivity, Hall parameter and electron temperature

22 p4081 A70-42823

Shock wave damping by perforated walls in gas channel, visualizing curved fronts with 24-spark HF camera

22 p4032 A70-43031

Isentropic gas two dimensional unsteady flow through channel contraction, using hydraulic analogy

22 p4012 A70-43438

Rotational two dimensional steady shear flows of perfect incompressible fluid, considering channel flow characteristics for various wave modes

23 p4181 A70-44202

Heat transfer by laminar forced convection of viscous fluid in noncircular cylindrical channel with internal heat source and varying wall temperature

23 p4276 A70-44236

Channel vs deflection flow in boundary layer theory, considering Navier-Stokes equations

23 p4183 A70-44736

Turbulent nonadiabatic flow of compressible gas at inlet and main sections of variable cross section plane channel

23 p4183 A70-44739

Optimal load circuits number for maximum power extraction from Hall MHD generator with nonuniform gas flow along channel

23 p4143 A70-44900

Compressible plasma flow in axisymmetric channels under EM body forces and Joule heating

23 p4228 A70-44934

Oscillating viscous conducting fluid laminar flow between parallel nonconducting infinite porous flat plates under suction in transverse magnetic field

24 p4383 A70-45146

Velocity profile in viscous sublayer at wall based on maximum stability principle applied to Karman constant for turbulent channel flow

24 p4325 A70-45495

Local or surface boiling phenomenon under triangular channel laminar flow conditions, investigating heat transfer with and without phase change

24 p4429 A70-46089

CHANNELS

Book on communication and information theories application to fading dispersive communication channels, discussing tropospheric scatter, HF ionospheric links, moon bounds, etc

02 p0253 A70-11700

Conduction liquid metal MHD machine channels design with baffles installed to decrease shunting effect of end zones, calculating segments by circuit theory methods

21 p3760 A70-42233

CHANNELS [DATA TRANSMISSION]

Envelope delay and amplitude characteristics measurement of modulated carrier wave channel in radio relay link

02 p0258 A70-12475

Recognition problem in multipositional symmetrical channel solved by special separation of observational space with preference to signal arriving at reception point

03 p0446 A70-13197

Bandwidth reduction for interlacing two voice and three additional teletype subchannels in standard phone frequency range for use in VHF/UHF satellite link

03 p0450 A70-13623

Coherent and incoherent interference effects on direction finding information derivation, using linear two channel principle

03 p0452 A70-14024

Channels demand assignment between earth terminals of international satellite communication systems, examining multiple access problems

03 p0453 A70-14323

Optimal strategies for observation system subject to recognition using data transmission along symmetrical channel

04 p0647 A70-14401

Soviet book on pulse code telemetry systems covering analog-digital conversion, data transmission in communication channels, noise problem, code selection, etc

04 p0648 A70-14953

Transmission channel nonlinearity effect on signal detector performance for signal received by synthesized antenna indicating SNR change

04 p0659 A70-15287

Multichannel ionization calorimeter data readout into electronic computer using short circuit coil magnetic storage

05 p0816 A70-15947

Adaptive frequency selection of optimum channels for radio communication on noninterference basis, discussing implementation and compatibility problems with nonadaptive systems

05 p0814 A70-16347

Binary decoding extension to achieve unquantized demodulation performance for nonfading phase shift keyed coherent channel with white Gaussian noise

06 p1008 A70-17525

Capacity and error bounds derived for nonsynchronized channel, discussing binary coding strategy

06 p1012 A70-18623

Capacity calculation of N identical discrete memoryless nonsingular channels cascade, discussing dependence on eigenvalues and eigenvectors of subchannel transition matrices

06 p1013 A70-18628

Phase and amplitude modulated signals transmission over band limited channel disturbed by additive white Gaussian noise

07 p1237 A70-20195

Communication channel average binary error and stationary Markov chain state probabilities relationship, using mathematical model and HF ionospheric FSK error sequence measurement

08 p1458 A70-20793

Time-frequency correlation function for fading communication channel between transmitter and receiver sites, using AM transmissions as probing signals

08 p1458 A70-20796

Error statistics recording for digital communications channel performance by extreme value technique

08 p1459 A70-20801

Compatible single sideband transmission realized using iterative signal processing method and ideal band limited channels

08 p1464 A70-21781

Digital computer processing of airborne multispectral data, discussing automatic recognition and mapping of terrain distribution, Earth Resources Technology Satellite data channel efficiency, etc

09 p1668 A70-22878

Coding and decoding efficiency in data transmission over Gaussian channels, comparing error probability, power, bandwidth and equipment complexity

09 p1637 A70-23320

Optimum coding of information for symmetric channel described by code word transformation probability

09 p1639 A70-23694

PCM-TDMA satellite communication system for maximum time slot utility without guard time slots

10 p1834 A70-24330

TDMA system burst synchronizer with periodic channel slots reallocation feature

10 p1835 A70-24331

SNR and system error rate prediction for coherent nonlinear satellite channels based on bounding techniques

10 p1836 A70-24341

Signaling system for communication satellites demand assignment, considering error control, unit negative acknowledgement, system parameters selection, control signals, etc

10 p1837 A70-24347

Traffic simulation in telephone network via communication satellite with presassigned and demand assigned circuits

10 p1838 A70-24356

FM telemetry channel noise effects on digital and analog accelerometer outputs accuracy, suggesting mean square error reduction methods

10 p1893 A70-25318

Channel separation in RF transponder for communication satellite achieved with RF multiplexers consisting of microwave filters and combiners with superior electrical performance

11 p2016 A70-25457

Fixed information bit rate approach to coding over space channel introducing redundancy and check digits for error probability

11 p2014 A70-26223

High speed sequential decoding machine design and performance test for deep space channels

11 p2014 A70-26245

Switched self balancing comparison radiometer with coupling between channels, showing measurement errors due to coupling correctable by phase switching

11 p2018 A70-26269

Channel assignment, considering low cost solution and co-channel interference

11 p2010 A70-26310

Signal selection for phase coherent and incoherent additive noise channels to maximize receiver correct decision probability

11 p2010 A70-26327

Fourier and Hadamard transformation codings for multidimensional data channel noise immunity and bandwidth reduction

11 p2011 A70-26329

Polarization properties of radar channel with random parameters, relating observation range with transmitting-receiving antennas and target fluctuations

11 p2012 A70-26815

Broadband 2 GHz transhorizon radio relay system design and performance for transmission on four channel pairs

11 p2034 A70-26820

Inclined backscatter sounding of ionosphere in individual channels of multichannel radio link, analyzing data during minimum solar activity

14 p2547 A70-30149

Amplitude-frequency characteristics selection for minimum phase channel allowing for intersymbol interference and smooth noise during data transmission, calculating mean error probability

14 p2547 A70-30150

Microwave channelizing filters input ports interconnection techniques for signals sorting into contiguous frequency bands

14 p2558 A70-31319

Noise rejection and spurious reception probability in optimal channel for continuous sequenced signal with undetermined arrival and overlapping spectra

15 p2696 A70-31509

Digital sampled data demodulation, discussing methods of obtaining quadrature channels from single signal

15 p2703 A70-32579

Multimode and dispersive distortion of short quasinonochromatic pulses in earth-ionosphere VLF channel

16 p2858 A70-32930

Data transmission from information sources over communication channels with limit imposed on attainable reliability, discussing coding theorem of information theory

16 p2871 A70-34259

Asymptotic transmitting capacity of continuous channel with intense independent and additive noise

18 p3228 A70-36598

Lower reliability estimates for block codes of binary channels with feedback noise

18 p3235 A70-36599

Range channel width effect on radar signal digital detector function and parameters optimal value

19 p3380 A70-38068

- Apollo digital Range Safety Command System for signal-crowded communications channels
20 p3605 A70-39497
- Signal modulation by pulse ratio variation in magnetic tape channel, discussing SNR characteristics
20 p3586 A70-39707
- Asynchronous delta modulation channels with RLC integrators in feedback circuit, measuring articulation in presence and absence of noise
20 p3587 A70-40144
- Frequency synchronization channel pulse fluctuations effect on noise stability of binary signal reception
20 p3587 A70-40145
- Fluctuating data transmission, using measurement channel with digital logarithmic conversion
20 p3635 A70-40534
- Satellite communications performance improvement by use of multipath signal for channel models including noncoherent FSK
21 p3787 A70-41329
- Single channel per carrier PCM FDMA demand assignment satellite communication system, discussing digital encoding, quadrature PSK modulation, etc
21 p3791 A70-41367
- Digital computer processing of airborne multispectral data, discussing automatic recognition and mapping of terrain distribution, Earth Resources Technology Satellite data, channel efficiency, etc [AIAA PAPER 70-309]
21 p3829 A70-41851
- Optical communication in turbulent media, investigating error rate for binary single path fading channels by photocount detection
21 p3837 A70-41935
- Wideband detection of FSK transmissions in three component two path channel, obtaining channel bit error probability
21 p3792 A70-42176
- Optimal binary and ternary signal system synthesis by information divergence procedure for communication channels with colored Gaussian noise
22 p3985 A70-42491
- Adaptive channel equalization approach leading to adaptive detector for slowly time varying channel
22 p3989 A70-43172
- Binary data transmission via radio channel, discussing phase and frequency modulation and error probability as SNR function
23 p4159 A70-43756
- Multibeam communication channel identification from output signal autocorrelation function analysis
23 p4159 A70-43761
- Polarization properties of radar channel with random parameters, relating observation range with transmitting-receiving antennas and target fluctuations
24 p4311 A70-45187
- Optimal noiseless linear information feedback estimation for additive white Gaussian noise channels, applicable to digital transmission
24 p4313 A70-46064
- Digital PCM telemetry link coding techniques, discussing encoding-decoding complexity, and concatenated block scheme for channel
24 p4315 A70-46258
- CHAPLYGIN EQUATION**
Chaplygin equation algebraic classification with respect to ring admitted by equation, extending results to include lambda function tolerating second order symmetry operators
04 p0613 A70-14412
- Compressible flows with circular sector hodographs, discussing Chaplygin equation for simple wedge flow and theorem on sonic jets
04 p0613 A70-14612
- Chaplygin equation solution for wedge flows applied to Rethy flows, evaluating drag coefficient and approximate hodograph equations for subsonic and transonic regimes
04 p0614 A70-14613
- Chaplygin theorem proof for partial differential equation, using piecewise smooth manifold with unilateral conductivity
08 p1534 A70-21008
- Chaplygin function approximation in subsonic steady gas flow analysis
10 p1909 A70-24293
- Chaplygin approximate hodograph method variants diagrams and tables with numerical values for proper application
13 p2442 A70-29486
- Perfect gas acyclic and cyclic, steady and irrotational motions in subsonic regime around convex profile with constant curvature variation by Chaplygin method
21 p3846 A70-42259
- CHAPMAN SHEAR LAYER**
U SHEAR LAYERS
- CHAPMAN-ENSKOG THEORY**
Chapman-Enskog expansion for Boltzmann equation solution, using PLK method to obtain higher approximations for shock wave structure
01 p0063 A70-10923
- Enskog method for Boltzmann equation, analyzing asymptotic nature of integral kinetic equation for molecular mean free paths and Laplace probabilities
01 p0068 A70-11568
- Shock structure in binary gas mixture, discussing governing equations and Chapman-Enskog procedure
06 p1051 A70-18344
- Kinetic theory of gas composed of identical particles with discrete velocity distribution, using Chapman-Enskog method
12 p2213 A70-28211
- Enskog theory extended to three particle collisions for gas transport properties
23 p4222 A70-44427
- CHAPMAN-FERRARO PROBLEM**
Charge separation effects in boundary layer between cold streaming plasma and perpendicular magnetic field with relativistic electrons
04 p0727 A70-14997
- Chapman-Ferraro two dimensional problem with neutral sheet, investigating magnetospheric flows and time dependence
04 p0679 A70-15109
- CHAPMAN-JOUGET FLAME**
U CHEMICAL EQUILIBRIUM
U DETONATION
U FLAME PROPAGATION
- CHARACTER RECOGNITION**
Recognition problem in multipositional symmetrical channel solved by special separation of observational space with preference to signal arriving at reception point
03 p0446 A70-13197
- Physical identity and name sameness matchings efficiency noting role of interpolated activity
07 p1203 A70-18942
- Algorithms based on continuous-group pattern recognition, distinguishing human faces, speech and handwritten characters
09 p1640 A70-22143
- Machine design similar to human brain for recognition and classification of information
09 p1641 A70-22708
- Character recognition methods applied to reading machines transforming printed material into forms acceptable to blind
13 p2360 A70-29809
- Optical spatial phase modulator array using membrane light modulator for coherent optical processing and character recognition
16 p2904 A70-33147
- Automatic alphabetic characters classification model based on cross correlation and discrete Walsh-Fourier transforms, using computerized simulation
16 p2851 A70-33460
- Holography, discussing light propagation, basic principles, skew reference wave, diffused illumination interferometry, character recognition, microscopy, high density information storage, etc
19 p3427 A70-38449
- CHARACTERISTIC EQUATIONS**
U EIGENVALUES
U EIGENVECTORS
- CHARACTERISTIC FUNCTIONS**
U EIGENVALUES
U EIGENVECTORS
- CHARACTERISTIC METHOD**
U METHOD OF CHARACTERISTICS
- CHARACTERIZATION**
Ti alloys failure-safe design developing procedures for incorporation of stress-corrosion cracking characterizations into ratio analysis diagram system
08 p1519 A70-21456
- Uniaxial and multiaxial stiffness and property characterization of anisotropic composite materials formed as thin walled cylinders
08 p1529 A70-21880
- Mechanical properties characterization of unidirectional high modulus carbon fiber reinforced epoxy matrix composite
08 p1530 A70-21883
- Pattern recognition involving machine extraction of characteristic features and classification based on associated values, discussing design and decision rules for optimal recognition
13 p2373 A70-29577
- Gradient algorithm for sequential identification of features in dynamic linear systems
13 p2383 A70-29582
- CHARACTERS**
U SYMBOLS
- CHARCOAL**
Breakthrough curve shape prediction during adsorption from gas stream in fixed bed adsorbers for trace contaminant control applied to activated charcoal
04 p0786 A70-15317
- CHARGE CARRIERS**
NT FREE ELECTRONS
NT HOLES [ELECTRON DEFICIENCIES]
NT MAJORITY CARRIERS
NT MINORITY CARRIERS
- Hot photoelectrons in semiconductors assuming short lived photoexcited current carriers, deriving expressions for energy distribution function of semiconductor current carriers
01 p0153 A70-10066
- Frequency dependence of intraband absorption of electromagnetic waves by free current carriers in doped semiconductors
01 p0153 A70-10067
- Dielectric layers electrical conductivity in ceramics containing Ti during aging, observing different characteristics ascribed to nonequilibrium current carriers injection
01 p0156 A70-10221
- Metal-nitride-oxide semiconductor [MNOS]/ FET load devices by changing from enhancement to depletion through polarizing voltage
01 p0051 A70-10785
- Voltage-power sensitivity, response time, frequency limit and minimum registered power of hot carrier thermoelectric detectors calculated from characteristic semiconductor parameters
03 p0540 A70-13436
- Magnetic field effect on recombination radiation intensity under pinch effect in semiconductor non-degenerate electron hole plasma with recombination time exceeding carrier lifetime
03 p0540 A70-13508
- Onset conditions for galvanothermal current instability of Ge semiconductors as function of electric field oscillations, carrier concentration and carrier-lattice temperature
03 p0541 A70-13724
- Optical inhomogeneity of GaAs associated with current carrier distribution analyzed quantitatively using magneto-optical Faraday effect and transmittance method
03 p0541 A70-13726
- Competition mechanism for free carriers in junction isolated transistor collector suggested by current dependence of photocurrent
04 p0657 A70-14732
- Heat transmission by current carriers to cryogenic region, ascribing heat flux to Joule effect in conductor
05 p0881 A70-16025
- Energy losses in conductors carrying intense currents to cryogenic regions linked with heat transfer due to high temperature gradients
05 p0881 A70-16026
- Charge carriers recombination and diffusion coefficients for confined gas discharge plasma obtained from data on radial particle distribution profile
05 p0888 A70-16330
- Vacuum deposited thin cadmium sulfide films semiconducting properties, discussing captured free carriers effects on temperature dependence of dark and photo current
05 p0893 A70-16543
- Cascade capture of carriers in semiconductors with negatively charged dislocation explained by diffusion-type equation
06 p1126 A70-17818
- Pulse indicators using thermoelectric effect of hot carriers caused by nonuniform heating of electron gas in HF field
09 p1643 A70-22127
- Semiconductor injection laser, analyzing light absorption by free carriers and gain characteristics
09 p1694 A70-22133
- Carrier recovery circuits synchronization for PSK demodulators used in TDMA satellite communication
10 p1835 A70-24338
- Thermoelectric power and Hall effect quantum resonances in pressure annealed pyrolytic graphite crystals for carrier locations evidence
11 p2097 A70-25616
- Microwave conductance tensor in crystals with non-parabolic carrier energy dissipation under crossed constant electric and magnetic fields
12 p2288 A70-28326
- Electromagnetic waves propagation in semiconductors, allowing for nonlinear effects from field heating of carriers
13 p2469 A70-28877
- Hysteresis in MOS transistors attributed to trapped charge carriers on oxide near silicon oxide interface
14 p2555 A70-30338
- Container wall-collision plasma sheath model for charge carrier investigation using velocity distribution [DFVLR-SONDDR-51]
14 p2622 A70-30662
- CDs high field domain modes generation for C parallel to E ascribed to interaction between drift carriers and off-axis shear wave
15 p2784 A70-31984
- Nonequilibrium charge carriers transient accumulation in p-i-n diode at superhigh injection levels
15 p2714 A70-32908
- Kinetic equation in strong electric fields, describing current carrier behavior in semiconductors
19 p3483 A70-37293
- Stationary DC discharge positive column in helium, determining production balance and loss of charge carriers
19 p3476 A70-37560
- Carrier diffusion effect in large signal analysis of semiconductor avalanches in quasi-static approximation
19 p3387 A70-37768
- Current carrier mobility under dynamic regime in p-n junctions by computerized method, emphasizing transitory phase
19 p3487 A70-38169

High purity surface-free GaAs epitaxial layer carrier lifetime measurement by optical transmission and excitation technique

22 p4086 A70-43017

Coherent reference for demodulating double sideband suppressed carrier (DSB-SC) signals in presence of frequency detuning, using squaring or Costas loop

22 p3990 A70-43326

Frequency multipliers with charge controlled junction diode model, predicting operational behavior

22 p3998 A70-43421

Spectral and threshold emission from optically pumped semiconductor lasers as function of carrier type and concentration in GaAs single crystals

23 p4203 A70-45069

Czochralski thermal probe for current carrier concentration in strip shaped area of n-type GaAs single crystals active growth

24 p4389 A70-45481

CHARGE DISTRIBUTION

Thunderstorm lightning discharge formation mechanism, investigating electric charge concentration and motion of free electrons

01 p0134 A70-10169

Potential distribution outside ideally reflecting charged sphere immersed in resting plasma described by nonlinear integral equation, allowing for polarization

08 p1432 A70-21090

Electrostatic energy converter load current analysis, deriving expression for space charge electric field with axially varying or constant charge distribution

10 p1808 A70-25036

Junction FET potential field and carrier distribution in channel investigated for current saturation mechanism

15 p2708 A70-31841

Alloy junction transistors with emitter larger than collector, analyzing minority carrier distribution in base region and effect on current amplification

15 p2714 A70-32703

Nonequilibrium charge carriers transient accumulation in p-i-n diode at superhigh injection levels

15 p2714 A70-32908

Supersonic plasma flows charge density levels and spatial and temporal variation, discussing theory and use of electrostatic probes

16 p2912 A70-33862

Thin long dipole antenna, determining input admittances, current and charge distributions and field patterns by Wiener Hopf technique

17 p3051 A70-35060

Charge spectrum of heavy relativistic cosmic ray nuclei, using tracks from balloon-borne photographic emulsions

18 p3308 A70-36781

CHARGE EXCHANGE

NT RESONANCE CHARGE EXCHANGE

Ion production cross sections determined for alkali atoms and bromine molecules collisions, noting charge transfer

07 p1345 A70-20138

Charge exchange and electron loss measurements in steam target exposed to high energy hydrogen ions beam, using equilibrium fractions method

07 p1345 A70-20142

Electric field effects on electrification of colliding ice spheres, discussing relaxation time of sphere charges and charge exchange

08 p1538 A70-21114

Elementary processes cross sections in charged states changes during proton-hydrogen molecule interactions

08 p1549 A70-21817

Charge exchange cross section of hydrogen position ion-negative ion collisions

09 p1733 A70-23269

Charge exchange probability in proton-hydrogen atom collisions computed with two state atomic orbital expansion

09 p1733 A70-23270

Ion mobility estimates for air constituents, considering ion-neutral elastic and resonant charge exchange collisions

10 p1919 A70-24427

Optical charge exchange and thermal stimulation effects in Fe doped GaAs crystals, determining iron content role by EPR method

13 p2469 A70-28880

Passive corpuscular diagnostics of high temperature plasma based on charge exchange neutrals, calibrating stripping chamber

20 p3685 A70-40398

Electron exchange coupling of Gd and Gd-Y alloy dihydrides from ESR indicating negative hydrogen ion entry

21 p3862 A70-41703

Charge separated and quasi-neutral solutions of electron heat transfer to spherical body in quiescent nonequilibrium plasma, noting diagnostic applications

21 p3860 A70-42080

CHARGE SEPARATION

U POLARIZATION [CHARGE SEPARATION]

CHARGE TRANSFER

Dissociative charge-transfer reactions of positive He ions with molecular N and O measured in drift tube-mass spectrometer

06 p1109 A70-17490

Plasma charge transfer in unstable beam plasma in magnetic fields system allowing for electron discharge pump operation

09 p1737 A70-23334

Charge transfer reactions of negative ions with oxygen investigated for energy dependence, yielding evidence on oxygen electron affinity

10 p1919 A70-24402

Avalanche diodes in presence of microwave instabilities related to field emission and charge transfer across depleted zone, discussing positive and negative resistance

10 p1850 A70-24621

Charge, hydrogen atom and ion transfer in collisions involving deuterium-labeled methanol- acetaldehyde system and molecular ions

14 p2543 A70-30110

Hydrogen oxygen fuel cells, demonstrating matching of power source and load, charge transfer, porosity, Nernst equation and electrochemical water synthesis

14 p2533 A70-30533

Optical charge transfer transitions in N-alkyl iodide salts, examining transient absorptions due to flash photolysis

18 p3226 A70-36765

He/plus-/H/minus/ collisional charge exchange cross sections, using modulated inclined ion beams technique

21 p3852 A70-40599

Turbulent charge diffusion during unipolar injection in nitrobenzene between plane-parallel electrodes, discussing liquid motion at high voltages

22 p4080 A70-42719

Charge transfer of protons at electron capture in excited states, using proton beam and various target gases

23 p4221 A70-44209

CHARGED PARTICLES

NT ALPHA PARTICLES

NT ANIONS

NT ARTIFICIAL RADIATION BELTS

NT CATIONS

NT CONDUCTION ELECTRONS

NT DEUTERONS

NT ELECTRONS

NT FREE ELECTRONS

NT HIGH ENERGY ELECTRONS

NT HIGH TEMPERATURE PLASMAS

NT HOT ELECTRONS

NT INNER RADIATION BELT

NT MAGNETICALLY TRAPPED PARTICLES

NT MANGANESE IONS

NT METAL IONS

NT N ELECTRONS

NT NEGATONS

NT OUTER RADIATION BELT

NT PHOTOELECTRONS

NT PI-ELECTRONS

NT POSITRONS

NT PROTON BELTS

NT PROTONS

NT RADIATION BELTS

NT SOLAR PROTONS

NT STELLAR WINDS

NT TRITONS

Density distributions of electrically charged trace components in axisymmetric jets, considering space charge effect and ambipolar diffusion

01 p0066 A70-11135

Fast charged particles measurements by Cerenkov counter in Cosmos 137 satellite, noting hard electron flux and cosmic ray radiation spectrum

01 p0172 A70-11509

Coupling coefficients for integral charged component of cosmic rays determined from measuring azimuthal geomagnetic effect on rays observed in crossed telescopes

01 p0172 A70-11545

Polar ionic exosphere electric field polarization, considering positive and negative charges escape fluxes, electric potential, mean ion velocity, etc

02 p0289 A70-12108

Charged particle self resonant motion in field of plane electromagnetic wave, showing trapped particles existence in whistlers

02 p0256 A70-12116

Adiabatic invariance of action integral for motion in nonregular fields, explaining charged particles motion through magnetic shock front in interplanetary space

02 p0359 A70-12788

Charged aerosol charge/mass ratio measurement and colloidal propulsion system thrust, efficiency and exhaust velocity determinations

03 p0551 A70-12936

Charged particles distribution according to multiplicity during pion-nucleon and nucleon-nucleon interactions at high energies

03 p0555 A70-13033

Neutrinos line patterns in Muscovite mica, refuting Russell assumption by analysis of multiple Coulomb scattering of charged particles and track comparison

03 p0556 A70-13047

Charged particles motion in isotropic weakly ionized plasma acoustic wave associated with difference in electrons and ions entrainment by neutral particles

03 p0530 A70-13087

Charged particle distribution in heterogeneous medium using dispersion model to describe quasi-charged particles interaction with internal surfaces

03 p0536 A70-14370

Whistler mode instability due to anisotropic charged particle velocity distribution, establishing general onset conditions for variable density cold plasma containing hot electrons

03 p0537 A70-14378

Circularly polarized synchrotron radiation from distribution of electrically charged particle in magnetic dipole calculated for estimating Jupiter magnetic field

04 p0746 A70-14511

Charged primary cosmic rays sidereal anisotropy generated diurnal/semi-diurnal variations phase characteristics, using energy meson telescopes

04 p0738 A70-14513

High energy dopant ion implants into silicon, discussing implantation profiles and electrical conductivity for use in type conversion and electrical junctions

04 p0730 A70-14727

Optimal outlet velocities of charged particles for spacecraft electrostatic thrusters [DFVLR-SONDDR-28]

04 p0735 A70-15173

Formula for energy radiated from particles system applied to electromagnetic and gravitational radiation and illustrated by charged particle motion in magnetic field

05 p0882 A70-16309

Charged particle concentration emitted by inhomogeneous plasma determinable from emission spectral lines broadening, suggesting error correction procedure

05 p0889 A70-16541

Low energy charged particle motion parallel with magnetic force lines analyzed in magnetosphere model with constant electric field

05 p0903 A70-16726

Electric field determination from charged particle concentration in wake of body moving in rarefied plasma, noting hydrodynamics similarity

05 p0915 A70-16754

Horizontal electric fields relations to charged particle fluxes in polar auroral ionosphere

05 p0842 A70-16756

Charged particles motion in field of whistler mode wave packet, discussing trajectories

06 p1118 A70-17377

Relativity theory and quantum mechanics relation concerning point charge velocity and motion at light speed, deriving elementary particle mass formula

06 p1106 A70-17833

Individual extensive air showers axes localized by measurement of charged particle densities, assuming age parameter

07 p1365 A70-18777

Electromagnetic acceleration and energy losses of charged chromospheric-coronal plasma electrons and protons in unsteady magnetic fields of sunspots

07 p1384 A70-19417

Charged particle replacement by external plasma particles in ionized inhomogeneities moving in ionosphere, considering magnetic field role

07 p1266 A70-19435

Charged particles and He nuclei spatial distribution from recordings in cosmic ray equator region by Cerenkov counter mounted on Proton 2 satellite

07 p1367 A70-19490

Diener kinetic theory for charged particles in EM field with Coulomb interactions taking into account transverse plasma waves

08 p1550 A70-20616

Magnetosphere model for quasi-circular precipitation zones of energetic particles based on geomagnetic activity distribution patterns

08 p1489 A70-21385

Iron peak nuclei synthesis by charged particles under supernova mechanism conditions predicted by hydrodynamic conditions

09 p1749 A70-21994

Excitation cross sections for bound-bound transitions in optical levels in hydrogenlike atoms induced by fast charged particles

09 p1730 A70-22230

Charged particle interaction influence on photoionization cross section of negative hydrogen ion, considering initial state polarization leading to free s wave electron

09 p1732 A70-22826

Charged particle self oscillatory motion in plane condenser field, applying results to electrical measuring instruments theory

09 p1680 A70-23144

- Optimal outlet velocities of charged particles for spacecraft electrostatic thrusters 09 p1744 A70-23428
- Charged particle albedo latitude dependence estimated from balloon-borne Geiger telescopes 09 p1746 A70-23481
- Charged particles velocity profile across shock determined by induction velometry, considering eddy currents effects on induced potential gradient 09 p1738 A70-23677
- Spectrometer design for Helios solar probe using semiconductor detectors to identify particles separated by magnetic field 10 p1888 A70-24487
- Rotating plasma in nonuniform magnetic field analyzed for interchange instability based on MHD fluid and charged particle treatments 10 p1924 A70-24800
- Electrohydrodynamics of charged water drop pairs disintegration in electric field concerning warm cloud electrification 10 p1912 A70-24806
- Ionospheric reaction rate coefficients based on electron concentration curves, discussing maximum number and accuracy obtainable 11 p2043 A70-25538
- Charged particle motion in steady and perturbed dipole fields using laboratory earth magnetosphere plasma model 11 p2104 A70-25546
- Energy deposition in cells by charged particles during ionizing radiation exposure, discussing RBE (relative biological effectiveness/ and dose-effect relation for neutrons 11 p1989 A70-26597
- Adiabatic drawing of quasi-captured charged particles by geomagnetic trap field during phase recovery period of magnetic storm 12 p2295 A70-28258
- Plasma turbulence in Van Allen belts, examining weak turbulent electromagnetic wave properties, with emphasis on trapped energetic particles radiation 13 p2486 A70-28555
- Energy spectrum and equatorial pitch angle distribution of charged particles trapped in magnetosphere resulting from inward diffusion due to third adiabatic invariant violation 13 p2476 A70-28942
- Electric field sense and magnitude determination from lunar particle shadows in solar electron fluxes 13 p2492 A70-29196
- Witness particle electric field as function of non-linear conductivity of weekly turbulent anisotropic plasma by perturbation method 13 p2465 A70-29638
- Serra de Mage meteorite impact history from charge particle track analysis, noting feldspar content 13 p2497 A70-29854
- Magnetospheric convection models and effects on charged particle populations 13 p2402 A70-30064
- Energetic particles measurements in geomagnetic tail by Explorer 33/35 for determining gross magnetic topology of distant tail and electric fields 13 p2481 A70-30070
- Magnetospheric charged particle distributions in plasma sheet, pseudo- and stable-trapping regions by satellite observation 13 p2483 A70-30088
- Low energy charged particle distribution within earth magnetosphere and environs, suggesting solar origin for storm time ring current protons 13 p2483 A70-30089
- Book on space physics covering charged particles in magnetic, electric and dipole fields, cosmic rays, magnetically trapped radiation and interplanetary plasma 14 p2633 A70-30099
- Charged particle acceleration in outer space plasma, deriving ion-acoustic instability equations 14 p2630 A70-30220
- Primary cosmic rays balloon-borne charge composition detector in 3-30 Z range 14 p2587 A70-31002
- Hall, polarization and Pedersen charged particle drift velocities in static magnetic and time dependent electric field 14 p2624 A70-31046
- Charged particles focusing and sorting in bispiral systems, deriving differential equations for relativistic trajectories 15 p2707 A70-31520
- Rocket and satellite data on upper atmospheric neutral/charged particles, short wave solar radiation, temperature and photochemical reactions 15 p2730 A70-32089
- Radial distributions and escape of charged particles across magnetic field in hot cathode Penning discharge plasma with LF oscillations 15 p2780 A70-32191
- Electrostatic analyzer without fringe field effects for measuring low energy particles on spacecraft 15 p2740 A70-32432
- Charged particles and He nuclei spatial distribution from recordings in cosmic ray equator region by Cerenkov counter mounted on Proton 2 satellite 15 p2795 A70-32735
- Book on electrical aspects of combustion processes covering formation, behavior in fields, diagnostics, uses of ions, electrons and charged particles, flame ionization, etc 16 p2996 A70-33030
- Gravitational instability and collapse of thin spherical shell of charged fluid, using energy conservation law 16 p2952 A70-33787
- Miniature multigrad probes for measuring energy spectra of charged particles and absolute plasma densities, comparing results to microwave measurements 18 p3294 A70-36150
- Elongation characteristics of modulation type charged particle traps and analyzers, discussing ions and electrons trapping 18 p3307 A70-36171
- Charge source density during interaction between atmosphere and electron/proton fluxes at prescribed boundary parameters 18 p3307 A70-36178
- Near earth motion equations for electrically charged dust particles in gravitating dipole magnetic fields, using zero-relative-velocity surfaces and energy integral 18 p3315 A70-36606
- Charged particle replacement by external plasma particles in ionized inhomogeneities moving in ionosphere, considering magnetic field role 18 p3249 A70-36909
- Ion composition and charged particle vertical distribution in F region and protonosphere from satellite and ground based observations 18 p3254 A70-37028
- Charged particle balance equations for stratosphere and mesosphere, noting particle composition investigation and formation and annihilation processes 19 p3491 A70-37311
- Solar energetic charged particles interaction with earth bow shock and magnetopause 19 p3494 A70-37482
- Solar particle observations over polar caps, considering spatial and angular distribution measurements 19 p3494 A70-37484
- High energy charged particle observations on OSO 3 at various rigidities 19 p3505 A70-38117
- Primary cosmic radiation singly charged component energy spectra by balloon-borne Cerenkov scintillation counter telescope 19 p3506 A70-38120
- Traversed matter thickness and charge composition for high energy galactic cosmic rays with various propagation modes 19 p3506 A70-38123
- Cosmic ray nuclei charge composition of elements Ne to Ni, using emulsion stacks exposure in balloon flights 19 p3506 A70-38126
- Low energy galactic cosmic radiation energy spectra and charge composition in 2-14 Z range by OGO-5, suggesting two component model for origin 19 p3507 A70-38127
- Charge spectrum of high and low energy heavy cosmic ray nuclei, using balloon-borne nuclear emulsions 19 p3507 A70-38130
- Primary cosmic rays above 4.5 GV, measuring charge composition from balloon flight 19 p3507 A70-38133
- Cosmic ray heavy nuclei charge composition from satellite-borne emulsion stacks exposure 19 p3507 A70-38134
- Highly charged cosmic ray heavy nuclei primaries, examining charge spectra and solar elements abundances 19 p3508 A70-38136
- Super heavy cosmic ray nuclei charge composition and track identification, using LEXAN polycarbonate, cellulose triacetate (CTA) and nuclear emulsion 19 p3508 A70-38137
- Very heavy primary cosmic ray particles propagation calculation, using fragmentation parameters 19 p3508 A70-38139
- High energy charged particles equations of motion in quiet interplanetary magnetic field for primary cosmic ray distribution, calculating diurnal and semidiurnal variations 20 p3698 A70-39297
- High transmission device for quark detection in primary cosmic rays 20 p3629 A70-39315
- Charged particle interaction with fluctuation fields in nonequilibrium magnetoactive plasma 20 p3678 A70-39596
- Charged particle collisions, discussing electron impact ionization of positive ions, detachment from negative ions, ion collisions, etc 20 p3676 A70-40154
- Spontaneous and induced Cerenkov emission by charged particle in turbulent medium, discussing random fluctuations effect on radiation spectra 21 p3879 A70-40928
- Energy losses frequency distributions for fast charged particles in small pathlengths in equimolar He-carbon dioxide mixture 21 p3852 A70-40973
- Ionospheric reaction rate coefficients based on electron concentration curves, discussing maximum number and accuracy obtainable 21 p3819 A70-41288
- Charged particle motion in steady and perturbed dipole fields using laboratory earth magnetosphere plasma model 21 p3882 A70-41296
- Laser light scattering in plasma for charged particle correlation function 23 p4225 A70-44187
- Transition radiation due to charged particle moving in periodically stratified cold isotropic plasma 24 p4384 A70-45254
- Plasma with oriented charged particle fluxes macroscopic parameter measurement by multigrad probes facing and reversed to drift, noting graphical data processing 24 p4385 A70-45454
- Charged particle acceleration in outer space plasma, deriving ion-acoustic instability equations 24 p4399 A70-46295
- CHARPY IMPACT TEST**
- Charpy V notch and dynamic tear tests compared for fracture toughness characterization of Ni-Cr-Mo-V steel 14 p2596 A70-30931
- Impact loaded Griffith-Irwin, Charpy and drop weight tear tests of fracture toughness for design, screening and materials acceptance 15 p2819 A70-32233
- Strength and thickness effects on energy absorption criteria for transition temperatures in Charpy V-notch impact tests 15 p2819 A70-32234
- Charpy impact test evaluation on hot rolled metal plates for low temperature welded structures 15 p2819 A70-32235
- Charpy impact test accuracy for model machine certification, discussing erroneously high test values 15 p2820 A70-32236
- Dynamic fracture toughness measurement of low strength steels via instrumented Charpy impact test with correction factor for inertia loading effects 15 p2820 A70-32237
- Precrack Charpy slow rate straining sensitivity of high strength steel at increased temperatures, comparing fracture energy of impact tests 15 p2758 A70-32328
- Instrumented Charpy impact test evaluating strain rate, alloying and irradiation effects on ductile-brittle transition temperature and fracture of pressure vessel steels 15 p2820 A70-32239
- Plane strain stress intensity factor-Charpy V notch impact test correlations in transition temperature range under slow bend and dynamic loading 15 p2759 A70-32244
- Fracture behavior and tempered martensite embrittlement relationship in steel, using V-notched and fatigue precracked Charpy specimens 22 p4054 A70-42736
- Full-swing and incremental Charpy impact and Izod tests for ceramic intrinsic impact strength 23 p4209 A70-43872
- CHARRING**
- Nonsteady thermal decomposition of plastics subjected to large heat flows, introducing equations governing char layers and pyrolysis zones 02 p0397 A70-12021
- Ablation chars, carbon and graphite spectral emittance and reflectance as function of wavelength and temperature, noting applications to atmospheric entry heat shielding 04 p0787 A70-15590
- Thermal conductivity determination for charring materials by dynamic technique, with application to carbon, graphite and silica cloth phenolics 11 p2068 A70-25766
- Charring ablative plastic thermal properties simultaneous measurement using modified heat transfer model and nonlinear regression analysis 12 p2333 A70-28111
- Gas phase chemical reactions effects on heat transfer to charring ablator, deriving numerical solution for multicomponent stagnation point flow [AIAA PAPER 70-869] 16 p2999 A70-33912
- Charring ablators transient heat transfer model, calculating surface temperature and recession and pyrolysis mass loss [AIAA PAPER 70-1143] 20 p3738 A70-40280
- Charring ablative composites pyrolysis products composition determination, comparing chemical analysis techniques 23 p4158 A70-44519

- NT GRAPHS [CHARTS]
 NT METEOROLOGICAL CHARTS
 NT PATTERSON MAP
 Orbital charts development for space navigation, discussing cartography and orbital navigation
 01 p0138 A70-11251
 Secular variations distribution on earth surface, plotting isopore charts from mean annual values of magnetic elements [1960-1965]
 01 p0083 A70-11540
 Statistical control charts for evaluating instrumentation performance during ordnance devices testing, discussing evolution, interpretation and application
 03 p0494 A70-14126
 Variables control charts based on sample means for determining in-control probability properties
 09 p1691 A70-22575
 Refractive index chart for scattered electromagnetic fields from sphere, evaluating modal coefficient for lossy materials
 09 p1633 A70-22697
 Area navigation system charting, discussing effect on flight information publications
 19 p3465 A70-38231
- CHEBYSHEV APPROXIMATION**
 Transverse nonrecursive digital filters for Hilbert transformation, investigating ideal quadrature filters with Chebyshev approximation errors
 05 p0822 A70-16772
 Chebyshev quadrature formula weighting functions, presenting accuracy estimation method
 07 p1321 A70-18659
 Mathematical programming and conditional extremum problems solution in analytic functions based on Chebyshev function systems and Stieltjes moments
 08 p1534 A70-21451
 Mixed system of simultaneous linear differential equations under general boundary conditions, deriving numerical solution in Chebyshev series
 09 p1711 A70-22288
 Stress concentration analysis using Chebyshev polynomial curve fitting
 09 p1784 A70-23450
 Axisymmetric or two dimensional incompressible laminar boundary layer flow field numerical analysis using quasi-linearization and Chebyshev series
 11 p2072 A70-25965
 Optimum low thrust ion propelled interplanetary trajectory design using two step Chebyshev method
 17 p3167 A70-35232
 Chebyshev method for Banach spaces, discussing location theorem for reducing error bounds
 18 p3282 A70-36359
 Soviet book on numerical methods of Chebyshev approximation covering minimax problems, computer methods, linear programming, etc
 19 p3456 A70-37232
 Consistent dependence of best rational Chebyshev L_p approximator on given function
 23 p4210 A70-44025
 Algorithm for moment problems in Chebyshev system with applications to numerical integration, series summation and function approximation
 23 p4211 A70-44244
 Algorithm for Chebyshev solution of a plus 1 inconsistent linear equations in n unknowns, using minimax technique
 24 p4370 A70-46241
- CHECKOUT**
 Turbine engine checkout techniques, describing oil, sonic-vibration, X ray, gas path and hot section analysis methods
 [AIAA PAPER 69-581] 02 p0356 A70-12526
 Control program debugging for experimental automatic surveillance and tracking radar, noting use for on-line systems
 04 p0654 A70-15449
 Onboard and ground checkout systems for space station and space shuttle operations
 [AIAA PAPER 70-245] 07 p1251 A70-20373
 Aerospace digital computers automatic checkout, considering computers functional and mechanical properties and test equipment configuration and operation
 08 p1469 A70-20653
 Aircraft maintenance, discussing trend toward increased use of quantified methods, failures reclassification, control techniques and check frequencies
 09 p1693 A70-23371
 Tolerance limits for equipment periodic field checkout, considering performance failure effects on system accuracy, costs and availability
 [AIAA PAPER 70-394] 10 p1896 A70-24911
 Automatic Malfunction Analysis /AMA/ digital computer software system supporting checkout and testing, defining normal system status by computer simulation
 [AIAA PAPER 70-383] 10 p1861 A70-24922
 Apollo Applications Program command and service module test requirements to achieve reliable hardware for extended missions
 [AIAA PAPER 70-378] 10 p1952 A70-24925
 Common high order programming language and program debugging in aerospace software
 16 p2868 A70-33430
 Apollo telescope mount postmanufacturing checkout under simulated mission environment, ensuring flight readiness
 16 p2889 A70-33723
 Airline pitot and static altimeter systems and undercarriage maintenance and checkup, discussing water in systems, case leaks, trash, dirt, inoperative heaters, etc
 16 p2842 A70-33823
 Systems operation hybrid simulator for computer checkout of Saturn S-IC stage
 17 p3061 A70-35489
 Electromagnetic, mechanical and chemical methods for automatic checkout of nonelectronic aerospace propulsion systems
 17 p3095 A70-35525
 Test selecting and sequencing for adaptive checkout processes, determining malfunctions
 20 p3659 A70-40106
 Low cost and weight reliable microminiaturized IC automatic cockpit checklist systems for aircraft pilots
 22 p3977 A70-42298
- CHECKOUT EQUIPMENT**
U TEST EQUIPMENT
CHELATE COMPOUNDS
U CHELATES
CHELATES
 Low threshold laser action of Nd-containing chelate in host media consisting of polymethyl methacrylate and organic liquid
 23 p4201 A70-44869
- CHEMICAL ANALYSIS**
NT ELECTROPHOTOMETRY
NT GAS ANALYSIS
NT GAS SPECTROSCOPY
NT MICROANALYSIS
NT NEUTRON ACTIVATION ANALYSIS
NT OZONOMETRY
NT POTENTIOMETRIC ANALYSIS
NT QUANTITATIVE ANALYSIS
NT SPECTROSCOPIC ANALYSIS
NT URINALYSIS
NT VOLUMETRIC ANALYSIS
 Petrological, X ray and chemical analyses of Muz-zaffarpur Ni-rich ataxite, showing kamacite, taenite and minor schreibersite composition
 01 p0177 A70-10328
 Secondary halo in spark source mass spectrography, determining corrections
 02 p0298 A70-12211
 Isolation and structural characterization of adduct formed from propionaldehyde, sym-trinitrobenzene and triethylamine
 02 p0251 A70-12275
 Steranes and triterpanes identification from Green River shale by capillary gas liquid chromatography and mass spectrometry
 02 p0252 A70-12514
 Collection of Soviet papers on chemical properties and analytical methods of refractory compounds
 03 p0504 A70-12977
 Complexonometric analysis of alloys containing Mo without component separation, treating molybdenum aluminides, zirconium boride-molybdenum silicide, molybdenum carbide in Ti, etc
 03 p0504 A70-12980
 Mo separation from W during chemical analysis of W in binary Mo-W alloys, using organic reagents for precipitation and extraction
 03 p0504 A70-12982
 Phase content determination in borides and borocarbides mixtures based on compounds different chemical stabilities during hydrolysis and reaction with acids
 03 p0514 A70-12984
 Chemical analysis of Australasian tektites inferring extraterrestrial igneous origin, noting similarity to preimpact parent rock
 05 p0916 A70-16832
 Microtektites chemical analysis data providing appraisal of strewn field boundaries, implying lunar origin
 05 p0916 A70-16835
 Platelet aggregation in whole blood, basing measurement method on filtration pressure with added adenosine diphosphate /ADP/
 07 p1210 A70-19591
 Gas-liquid chromatographic separation applied in derivatization chemistry of protein amino acids as N-trimethylsilyl /TMS/ esters
 09 p1629 A70-22337
 Solar system objects /earth, moon, planets, meteorites, etc/ chemical composition data and analysis techniques
 10 p1942 A70-24609
 Lunar and planetary surface chemical composition analysis using neutron inelastic scattering as optimum for unmanned missions
 10 p1942 A70-24613
 High energy neutron activation method for remote extraterrestrial in situ rock surface constituents analysis
 10 p1932 A70-24614
- Recovered extraterrestrial material, considering activation analysis, mass spectroscopy, emission spectroscopy, flame photometry, etc
 10 p1942 A70-24615
 Raman and IR spectrum analysis of polywater indicating impurities role in anomalous properties
 11 p1994 A70-25655
 Thermal Analysis - Conference Worcester, Mass., August 1968, Volume 1, Instrumentation, organic materials and polymers
 11 p2069 A70-25801
 Disproportionation to combination ratio of hydrazyl radicals generated in absence of hydrazine direct decomposition
 14 p2544 A70-30120
 Radio astronomical observations of lunar surface material EM properties compared with Surveyor 7 chemical analysis
 14 p2645 A70-31059
 Mobile geochemical laboratory for in situ radiation measurement and elemental analyses in lunar exploration
 15 p2717 A70-31801
 Semiremote laser Raman spectroscopy application in pipes, reactors, hot cells, jet and rocket engines and air pollution studies, discussing LIDAR model for chemical analysis
 16 p2926 A70-33161
 Radioisotopic and complementary surface chemical analysis of coupling agent films on glass surfaces
 16 p2917 A70-33375
 Assay procedures for extraction and determination of N-acetylglucosamine in soil
 18 p3226 A70-36959
 Chemical analysis methods for Apollo 11 lunar rocks, discussing calibration standards, spectral lines and Apollo 12 data
 21 p3777 A70-41610
 Apollo 11 crystalline rocks chemical analysis by argon 40/argon 39 dating techniques
 21 p3778 A70-41613
 Amino acids analysis of Apollo 11 lunar fines by hydrolysis of aqueous extracts
 21 p3778 A70-41623
 Apollo 11 lunar fines chemical analysis for alkanes of 15-30 carbon atom length, obtaining negative results
 21 p3779 A70-41630
 Apollo 11 fines and rocks analysis by chromatography, mass spectrometry and light and scanning electron microscopy
 21 p3779 A70-41631
 Lunar carbonaceous, organic and organogenic materials analysis by mass spectroscopy, gas chromatography and various other methods
 21 p3780 A70-41633
- CHEMICAL ATTACK**
NT INTERGRANULAR CORROSION
 Hot corrosion reactions in Ni, Co and NiAl-base alloys exposed to salt-sulfur containing simulated gas turbine combustion atmospheres
 01 p0118 A70-10728
 Atomic oxygen and chlorine attack on refractory materials studied for kinetics of chemical reactions of free radicals and atoms
 07 p1313 A70-19903
 Corrosion shapes from iodine action on metals in methylic medium, discussing morphology dependence on purity, surface state and reaction products diffusion velocity
 08 p1518 A70-21241
 Zr and stainless steel pitting in acidic and near neutral chloride media, comparing controlled potential and conventional chemical corrosion tests results
 09 p1706 A70-22939
 Chemically active surface decomposition in dissociated gas flow with turbulent boundary layer, determining diffusion fluxes in laminar sublayer
 20 p3612 A70-39812
- CHEMICAL AUXILIARY POWER UNITS**
 Fuel cell development, discussing consumable electrode, hydrogen/oxygen, hydrazine/hydrogen superoxide, hydrazine/air and methanol/air cells
 19 p3359 A70-38497
- CHEMICAL BONDS**
NT HYDROGEN BONDS
 Tungsten metal oxidation retardation by W-F bonds
 02 p0249 A70-11651
 Hydroxy fatty acid methyl esters gas chromatography and mass spectrometry, noting trimethylsilylation usefulness for locating double bond
 02 p0252 A70-12515
 Chemically coupled glass-reinforced polypropylene, studying short term physical properties, creep rupture and deformation, dynamic failure, etc
 02 p0322 A70-12605
 Bimolecular transfer reactions activation energies for multivalent gaseous compounds estimated by bond energy method avoiding use of adjustable parameters
 03 p0441 A70-14045
 Ribonucleic acid polymerase model with initiating purine triphosphate binding to product terminus site and pyrimidine triphosphate engaging in exchange binds to substrate site
 03 p0442 A70-14046

- Chemical bonding of high temperature molecular species, discussing ab initio calculations for diatomic atoms 07 p1225 A70-19882
- Group 4A difluorides vaporization thermodynamics and bond dissociation energies, tabulating mass spectra, vapor composition, reaction enthalpies, heats of polymerization and thermodynamic functions 07 p1319 A70-19889
- Bonding scheme of C-O in ketene described by localized orbital technique 08 p1455 A70-20682
- Adhesives chemistry, discussing ionic, covalent and intermolecular bonds allowing for chemical and physical properties 08 p1455 A70-20880
- Atomic bond rupture rate in rubber subjected to uniaxial tensile strain in ozone environment monitored by electron paramagnetic resonance measurements 08 p1527 A70-21454
- Mechanical properties and fracture behavior of chemically bonded glass matrix-metal composites 08 p1521 A70-21699
- Inductive effect in C-Cl chemical bonds in chloroalkenes, using nuclear quadrupole resonance frequencies shifts 09 p1630 A70-22903
- Isomeric 1-phenylheptenes mass spectra, investigating electron impact induced rearrangements of double bond 09 p1631 A70-23401
- Vaporization characteristics of solids for relationship between chemical bonding and sublimation mechanism emphasizing NaCl, CdS and GaAs 14 p2545 A70-30906
- Gaseous Al oxide bond bending frequency in Ne and Ar matrices at liquid He temperatures, investigating IR spectrum 15 p2695 A70-32830
- Transition probabilities for Markov chain describing bond breaking and molecular energy transfer in vibrational relaxation and dissociation 16 p2953 A70-33009
- Reinforced plastics adhesion to hydrophilic mineral surfaces by using silane coupling agents 16 p2937 A70-33374
- Radioisotopic and complementary surface chemical analysis of coupling agent films on glass surfaces 16 p2917 A70-33375
- Interfacial chemistry of glass fiber reinforced thermoplastics, discussing matrix resin- reinforcement bond 16 p2937 A70-33378
- Reaction kinetics of gas phase pyrolysis of polydifluoroaminomethanes in various reactors, obtaining C-N bond cleavage as rate determining step 16 p2856 A70-33652
- Addition and hydrogenation reactions of azomethines in chemistry of carbon-nitrogen bond, emphasizing Schiff bases 20 p3582 A70-38978
- Barrier heights for hydrogen-iodine reaction from semiempirical four-electron valence bond calculation 21 p3780 A70-41709
- Solid solutions properties in Nb-oxygen system, examining atomic bond nature by elastic modulus measurement 22 p4056 A70-43345
- CHEMICAL CLEANING**
- Chemically treated rolled hair properties following long term use in hair hygrometers 24 p4333 A70-45138
- CHEMICAL COMPOSITION**
- NT CARBON DIOXIDE CONCENTRATION**
- Lubricating oil chemical composition changes influence on combustion engine internal friction, considering surface active Zn, armo-iron and Al 01 p0099 A70-10077
- Chemistry variations effects on mechanical properties, phase stability and microstructure of alloy Unitemp 718 /Ni-Fe-Cr alloy/ via microscopy and X ray analysis 01 p0116 A70-10092
- Nerve cell response to change in chemical constitution of surroundings used to investigate animal periphery sensory mechanisms 01 p0033 A70-10497
- Jupiter chemical composition and atmosphere, considering space probe experiments 01 p0185 A70-11047
- Chemical composition of cermet material for radial sealing of high temperature gas turbines, ensuring structural stability and oxidation resistance 01 p0124 A70-11621
- Laminar counterflow diffusion flame chemical structure and blow-off mechanism established in forward stagnation region of porous cylinder at atmospheric pressure 02 p0398 A70-12032
- B-C alloys chemical composition effect on high temperature stability in pure oxygen 03 p0514 A70-12978
- Phase content determination in borides and borocarbides mixtures based on compounds different chemical stabilities during hydrolysis and reaction with acids 03 p0514 A70-12984
- Major and trace element concentration in contact zones of Precambrian diabase dikes from Wyoming ranges, showing dikes as continental tholeiites 03 p0472 A70-13148
- Abundance levels of K, Rb, Sr and Ba in pyroxenes, olivines and garnets of ultramafic rocks for upper mantle composition 03 p0472 A70-13149
- Heat resistant alloys densities calculated from chemical composition, estimating error 03 p0512 A70-13778
- Aerosols size distribution and chemical composition and carbon monoxide, nitrous oxide and sulfur dioxide concentrations measured in pure atmosphere 03 p0521 A70-14289
- Surveyor 7 alpha scattering experiment and TV image data revealing lunar surface chemical composition, rocks and fragments, etc 04 p0752 A70-15060
- Surveyor 5, 6, 7 missions alpha-scattering experiments, lunar rocks chemical composition compared with earth rocks and chondritic meteorites 04 p0752 A70-15062
- Proton-proton cycle in star interior, calculating isotope concentrations, reaction duration and energy release as function of temperature and chemical composition 05 p0900 A70-15972
- Chemical compositional evidence of Needles /California/ iron meteorite, suggesting distinct fall nature 05 p0912 A70-16465
- Alpha and beta solid solutions chemical composition in two phase alloys of Ti-Al-Mo and Ti-Al-V determined by electron microprobe analyzer 05 p0864 A70-16549
- Correlation between O isotope ratios and composition of tektites investigated for origin of tektites 05 p0917 A70-16840
- Metal content effects on evolution tracks of five solar mass stars with different chemical composition, discussing Magellanic Clouds composition 05 p0919 A70-16936
- Cerenkov light in extensive air shower observed at mountain altitude showing mixed primary cosmic rays in chemical composition 06 p1134 A70-17184
- Chemical abundance data of lunar surface rocks, suggesting basaltic achondrites and eucrites origin from moon 06 p1137 A70-17196
- Amino acid composition and terminal sequences of ferredoxins from photosynthetic green bacteria 06 p0994 A70-17616
- Diffusion layer and protective oxide composition changed to increase chrome plated Mo heat resistance 06 p1089 A70-17742
- Structure, phase composition and heat resistance of diffusion layers obtained by surface alloying of Nb alloy with Cr, Ti and Si 06 p1089 A70-17744
- Sinus Medii lunar surface material chemical composition from alpha scattering experiment on Surveyor 6 06 p1151 A70-18483
- Meteoroids structure, composition and fragmentation, summarizing existing evidence for photographic and radio meteors and meteor luminous and ionizing efficiency 06 p1153 A70-18551
- Chemical composition of scale formation in jet engine injectors for various fuel types tabulated, noting buildup levels in transport aircraft and subsonic jets 07 p1362 A70-18651
- Chemical composition effects on Zr-Ti, Zr-Si, Ni-Al and Ni-Ti alloy aerosols combustion temperature 07 p1419 A70-18755
- Lunar surface samples characteristics correlation with terrestrial igneous rocks /basalts/ and eucrite meteorites based on alpha scattering analysis 07 p1380 A70-19203
- Chemical composition and heat treatment effects on deformation resistance of nonaging aluminum alloys during hot working, noting quenching effect on recrystallization 07 p1294 A70-19388
- Data on Jupiter chemical composition, internal structure and energy sources, discussing Jovian planets origin and role played by gas 07 p1386 A70-19487
- Lunar surface chemical composition determination by radio astronomy, considering SHF electrical properties of silicate earth rocks 08 p1572 A70-20940
- Ti-based alloys with Al and Mo investigated for chemical composition and heat treatment effects on mechanical properties 08 p1518 A70-21200
- Carburization resistance of refractory steels, emphasizing chemical composition effect on corrosion rate 08 p1519 A70-21434
- Apollo 11 lunar material X ray diffraction and microscope studies, noting chemical composition agreement with Surveyor 7 data 09 p1752 A70-22245
- Melting diagram for five element Mo-W-Nb-Ta-V system constructed by optimal projections from known composition-property relations for corresponding ternary systems with common components 09 p1702 A70-22561
- Diffusion layer correspondence to phase diagram in terms of constituent phases and composition 09 p1702 A70-22563
- Twelvelfold solar mass star evolution computed using chemically homogeneous model showing faster evolution rate 09 p1758 A70-22746
- Interstellar dust, discussing effective particle size, composition, formation and effects on astronomical observations 09 p1763 A70-23374
- Solar system objects /earth, moon, planets, meteorites, etc/ chemical composition data and analysis techniques 10 p1942 A70-24609
- Oceanic ridge volcanic rocks alkali metal, alkaline earth, rare earth, nickel and major element content, observing partial melting 10 p1877 A70-24648
- Zero age intermediate and low mass stellar models and evaluation of physical parameters for population I and II chemical compositions 10 p1944 A70-24955
- Radio wave reflection spectra from plane surfaces, determining physical properties and composition 10 p1843 A70-25154
- Gas mixture composition effect on bacteria growth oxidizing methane and propane, establishing proportional biomass concentration to hydrogen and oxygen in mixture 11 p1991 A70-25938
- Temperature distribution in opposed jet diffusion flames, discussing mass fluxes and fuel and oxygen concentrations effect 11 p2151 A70-26385
- Icarus asteroid positions, UVB magnitude, brightness, colors, light curves and polarization, noting stony-iron composition 11 p2113 A70-26470
- Normal and unconstrained vacuum-deposited Permalloy films composition dependence of magnetization-induced uniaxial anisotropy, noting agreement with magnetostrictive constraint theory 12 p2284 A70-27244
- Chemical compositions and structure of carbides in Fe-W-C and Co-W-C systems, clarifying eta phases 12 p2255 A70-27601
- ETA oxides compositions in Hf-Ni-O, Ta-Ni-O and W-Ni-O systems determined by studying 1000 C isothermal sections with X ray diffraction 12 p2255 A70-27607
- Carbon in austenite derived for composition dependence of diffusivity using first order mixing statistics 12 p2256 A70-27611
- Lunar rocks isotopic composition for Gd and variations due to low energy neutron capture produced by cosmic ray interactions 13 p2485 A70-28473
- Mountain climbing and prolonged stays at high altitudes effects on blood composition 13 p2352 A70-29355
- Thick plate titanium alloy welds using filler wire to regulate chemical composition and plate phase constitution 13 p2435 A70-29456
- Weekeroo Station iron meteorite silicate inclusions chemical composition compared to chondrites 13 p2497 A70-29858
- Hydromagnetic fluid model of solar wind for interpreting discontinuities in plasma and magnetic field, interaction with atmosphere, heating mechanism and chemical composition 13 p2481 A70-30067
- Moon rocks nature and mineralogical constitution, describing methods for age determination 14 p2634 A70-30275
- Soviet monograph on V and V alloys covering phase diagrams, mechanical, chemical and physical properties, compounds and chemical composition 14 p2595 A70-30627
- Balloon-borne midinfrared observations of lunar surface composition from interpreting peak emissivity differences 14 p2645 A70-31058
- Radio astronomical observations of lunar surface material EM properties compared with Surveyor 7 chemical analysis 14 p2645 A70-31059
- Lunar surface optical properties differences for lunar and planetary nature and evolution determination 14 p2645 A70-31063

Relativistic cosmic rays primordial chemical composition above atmosphere from abundance data obtained with satellite-borne nuclear emulsion detector 15 p2793 A70-31735

Planetary gamma and X radiation by remote sensing and passive observation for gross chemical composition 15 p2793 A70-31749

Lunar, meteoritic and terrestrial silicate rock chemical individuality based on atomic ratios 15 p2799 A70-31896

Data on Jupiter chemical composition, internal structure and energy sources, discussing Jovian planets origin and role played by gas 15 p2805 A70-32732

Lunar surface chemical composition determination by radio astronomy, considering SHF electrical properties of silicate earth rocks 15 p2805 A70-32752

Composition and heat treatment effects on Fe-Ni alloys structure, using micrographic, autoradiographic and potentiokinetic methods 16 p2916 A70-33080

Chemical structure and room temperature tensile, flexural and compressive properties of metaphenylenediamine cured castings for graphite fiber reinforced epoxy resin matrices 16 p2936 A70-33358

Galactic composition differences, considering stellar and galactic nucleosynthesis 16 p2976 A70-33791

Ti alloy ingot chemical macroinhomogeneity, investigating elimination by vacuum arc melting 17 p3112 A70-34355

Heat treatment and composition effect on mechanical properties of alpha Ti-base alloy, discussing creep resistance, tensile strength, etc 17 p3122 A70-34439

Solar atmosphere structure and chemical composition by UV spectrum analysis 17 p3161 A70-34892

Nonhydrogen spectral lines in interstellar gas, discussing Ca/Na abundance anomaly 17 p3162 A70-34900

Chemical composition selection for Ti alloys with low susceptibility to hydrogen induced brittleness 18 p3274 A70-36121

X ray fluorescence determination of thickness and composition of Permalloy films deposited on wire surface 18 p3258 A70-36466

Heat resistance of cast, forged and annealed Ti-Cu alloys, discussing forged alloys mechanical properties as function of chemical composition and temperature 19 p3449 A70-37273

Simultaneous primary energy spectrum, chemical composition and sidereal daily variation analysis for cosmic ray origin, using Proton measurements 19 p3500 A70-38080

Low energy galactic cosmic radiation energy spectra and charge composition in 2-14 Z range by OGO-5, suggesting two component model for origin 19 p3507 A70-38127

Cosmic ray nuclei chemical composition and energy spectra in 3-30 Z range by balloon flight and Pioneer 8 space probe, noting propagation models 19 p3507 A70-38131

Cosmic ray elements abundance at sources relative to carbon, comparing near-earth composition and solar photosphere 19 p3509 A70-38147

Microstructure and composition of hafnium dioxide stabilized with Ca, Y and Mg oxides using metallographic, X ray and microprobe 20 p3654 A70-39242

Lunar soil from Apollo 12, identifying chemical composition of orthopyroxene-calcic plagioclase rock fragments for origin 20 p3709 A70-39980

Lunar rocks almandine-rich garnet chemical composition and crystallography, noting cell edge and refractive index 21 p3883 A70-40711

Mineralogy and chemistry of Apollo 11 lunar soil samples, using three-channel electron microprobe analyzer 21 p3896 A70-41509

Apollo 11 lunar rock mineralogy, examining petrographic and chemical features by light microscopy, electron microprobe microanalysis and detector system 21 p3898 A70-41525

Bulk chemical compositions, mineral and glass analyses, X ray data and physical properties of Apollo 11 lunar fines and rocks 21 p3898 A70-41526

Apollo 11 lunar rocks, breccias and fines age and chemistry, major element, trace element and rare earth abundances, texture, crystallization and meteoritic effects 21 p3906 A70-41563

Apollo 11 lunar basalt chemical composition and petrogenesis, using stable isotope dilution method 21 p3907 A70-41573

Apollo 11 lunar rocks and soil chemical composition, examining major, minor and trace elements 21 p3776 A70-41591

Apollo 11 lunar rock and soil elemental abundances, discussing composition, volatile element depletion, rare earths, basalt and geochemical processes 21 p3909 A70-41593

Elemental abundances of Apollo 11 lunar rocks and soils, using activation analysis or mass spectrometric isotope dilution 21 p3909 A70-41606

Chemical analysis for Li, Na, K, Rb, Cs, Ca, Sr and Ba in achondrites and Apollo 11 lunar rocks, breccia and soil samples 21 p3910 A70-41611

Oxides compounds heats of formation isocomponent and primary product composition relationship in binary systems 22 p3982 A70-42679

Phase analysis for individual multicomponent alloys, discussing chemical composition in case of invariant equilibria and electron beam microprobe 22 p4053 A70-42734

Computerized calculation of gas turbine cycles thermal efficiency, using hydrocarbon fuel, considering fuel composition and heat of combustion changes 22 p4125 A70-43439

Time constant loci and theoretical luminosity functions for various compositions and ages of metal poor globular clusters 22 p4108 A70-43735

Charring ablative composites pyrolysis products composition determination, comparing chemical analysis techniques 23 p4158 A70-44519

Murchison and Lost City chondrites element abundance analysis by thermal neutron activation and wet chemical techniques, noting low oxygen content 24 p4411 A70-45790

Borgo San Donino chondrite petrology and mineralogical and chemical composition, considering texture and recrystallization features 24 p4411 A70-45791

Chemical composition effects on heat resistance, elastic properties and density of Ti-Ta alloys 24 p4360 A70-45830

Stainless steel oxide films structures and chemical compositions, examining oxidation time, polishing conditions, vapor humidity and temperature effects 24 p4362 A70-46191

X ray powder and chemical data on monoclinic secondary mineral guildite from mine fire at Jerome site 24 p4330 A70-46274

Biochemical heterogeneity of corneal mucopolysaccharides / glycosaminoglycans/, using extraction without proteolytic enzymes 24 p4304 A70-46344

CHEMICAL COMPOUNDS

Morphological box for extracting chemical elements and compounds from lunar materials for manned operations on moon 14 p2634 A70-30200

Magnetically ordered ferroelectric materials properties for various compounds and solid solutions 15 p2785 A70-32749

CHEMICAL EFFECTS

Ni-Cr alloy oxidation resistance dependence on small amount of Al at high temperatures, noting role of protective oxide layer 03 p0514 A70-14315

Aircraft Ti alloys failure due to stress-induced pseudocorrosion caused by trichloroethylene and Freon noting microstructure, heat treatment and welding effects 04 p0710 A70-15679

Mechanical methods locking studs, discussing chemical locking based on hardening of resins by polymerization 06 p1076 A70-17437

Thermal emittance of Cu measured in vacuum in spherical enclosure by calorimetric method to investigate oxidation effect [AIAA PAPER 70-66] 06 p1180 A70-18139

Austenitic stainless steel hydrogen damage noting role of martensite plastic deformation 08 p1525 A70-21965

Molybdenum disulfide dry film lubricant wear life as film sintering process dependent on binder, additive or atmosphere chemical effects 11 p2058 A70-25571

PdH system electrical resistivity, studying hydrogen concentration role 12 p2282 A70-26900

Protein synthesis, dialysis and Mg ion concentration effects on chemical condensation of mixed amino acid adenylates 17 p3042 A70-35146

Ammonium perchlorate filler fraction effect on viscoelastic behavior, relaxation modulus and failure mechanisms of solid composite propellants 17 p3145 A70-35216

Iron cyanide surface additives effect on photodamage to ZnO powder, using ESR method 19 p3372 A70-37543

Sealed Ni-Cd cells, investigating carbonate effect on performance 22 p3965 A70-43535

Chemically treated rolled hair properties following long term use in hair hygrometers 24 p4333 A70-45138

CHEMICAL ELEMENTS

NT ACTINIDE SERIES
NT ALKALI METALS
NT ALUMINUM
NT ALUMINUM ISOTOPES
NT ALUMINUM 26
NT ALUMINUM 27
NT ARGON
NT ARGON ISOTOPES
NT BARIUM
NT BERYLLIUM
NT BERYLLIUM 9
NT BERYLLIUM 10
NT BISMUTH
NT BORON
NT BORON ISOTOPES
NT BROMINE
NT CALCIUM
NT CALCIUM ISOTOPES
NT CARBON
NT CARBON ISOTOPES
NT CARBON 12
NT CARBON 13
NT CARBON 14
NT CERIUM
NT CESIUM
NT CESIUM VAPOR
NT CHARCOAL
NT CHLORINE
NT CHROMIUM ISOTOPES
NT COBALT
NT COBALT ISOTOPES
NT COPPER
NT DEUTERIUM
NT DEUTERIUM PLASMA
NT DYSPROSIUM
NT EUROPIUM
NT FLUORINE
NT GADOLINIUM
NT GALLIUM
NT GERMANIUM
NT GOLD
NT HAFNIUM
NT HALOGENS
NT HELIUM
NT HELIUM ATOMS
NT HELIUM FILM
NT HELIUM ISOTOPES
NT HOLMIUM
NT HYDROGEN
NT HYDROGEN ATOMS
NT HYDROGEN IONS
NT HYDROGEN ISOTOPES
NT HYDROGEN PLASMA
NT INDIUM
NT IODINE
NT IODINE ISOTOPES
NT IODINE 131
NT IRON
NT IRON ISOTOPES
NT IRON 57
NT ISOTOPES
NT KRYPTON ISOTOPES
NT KRYPTON 85
NT LANTHANUM
NT LEAD [METAL]
NT LEAD ISOTOPES
NT LIGHT ELEMENTS
NT LIQUID HELIUM
NT LIQUID HYDROGEN
NT LIQUID NITROGEN
NT LIQUID POTASSIUM
NT LIQUID SODIUM
NT LITHIUM
NT LITHIUM ISOTOPES
NT MAGNESIUM
NT MAGNESIUM ISOTOPES
NT MANGANESE
NT MANGANESE ISOTOPES
NT MERCURY [METAL]
NT MERCURY VAPOR
NT METALLOIDS
NT NEODYMIUM
NT NEON
NT NEON ISOTOPES
NT NICKEL
NT NICKEL ISOTOPES
NT NITROGEN
NT NITROGEN ATOMS
NT NITROGEN IONS
NT NITROGEN ISOTOPES
NT ORTHO HYDROGEN
NT OXYGEN ISOTOPES
NT OXYGEN 18
NT PALLADIUM
NT PARA HYDROGEN
NT PLATINUM
NT PLUTONIUM ISOTOPES
NT POTASSIUM
NT POWDERED ALUMINUM

NT PRASEODYMIUM
NT RADIOACTIVE ISOTOPES
NT RADON
NT RARE EARTH ELEMENTS
NT RARE GASES
NT RHODIUM
NT RUBIDIUM
NT RUBIDIUM ISOTOPES
NT RUBIDIUM 86
NT RUTHENIUM
NT SELENIUM
NT SILICON
NT SILICON ISOTOPES
NT SILVER
NT SINTERED ALUMINUM POWDER
NT SODIUM
NT SODIUM ISOTOPES
NT SODIUM VAPOR
NT SODIUM 22
NT SODIUM 24
NT STRONTIUM
NT STRONTIUM ISOTOPES
NT SULFUR
NT TELLURIUM
NT TELLURIUM ISOTOPES
NT TERBIUM
NT THALLIUM
NT THORIUM
NT THORIUM ISOTOPES
NT TIN
NT TITANIUM
NT TRACE ELEMENTS
NT TRITIUM
NT URANIUM
NT URANIUM ISOTOPES
NT URANIUM 233
NT URANIUM 238
NT VANADIUM
NT XENON
NT XENON ISOTOPES
NT XENON 129
NT XENON 133
NT YTTERBIUM
NT YTTRIUM
NT ZINC
NT ZINC ISOTOPES
NT ZIRCONIUM
Ternary chemical element additions /O, Sn, Zr, Cb, Mo, V/ effects on solubility range of primary alpha region of Ti-Al base alloys 01 p0122 A70-11239
Secondary halo in spark source mass spectrography, determining corrections 02 p0298 A70-12211
Excretion and balance of K, Ca, Mg, P, S and N during prolonged use of dehydrated food diets 03 p0435 A70-13713
Mass and radius relations for zero temperature spheres of chemical elements, using equation of state and numerical integration 04 p0749 A70-14599
Semiconductor compounds application as partial vapor pressure sensors of chemical elements, discussing electrical properties dependence 07 p1356 A70-19554
Excretion and balance of K, Ca, Mg, P, S and N during prolonged use of dehydrated food diets 11 p1989 A70-25513
Thermal diffusivity of elements over wide temperature ranges based on TPRC recommended thermal conductivity and specific heat 11 p2065 A70-25770
Morphological box for extracting chemical elements and compounds from lunar materials for manned operations on moon 14 p2634 A70-30200
Ionization potentials of elemental abundances in lunar rocks compared with earth crust and class I carbonaceous chondrites, showing lunar materials differentiation 15 p2801 A70-32463
Type I carbonaceous chondrites contribution to lunar soil, comparing mineralogical and trace element evidence 21 p3899 A70-41533
Apollo 11 lunar rocks and soil chemical elements analysis by neutron activation scheme 21 p3777 A70-41612
Apollo 11 lunar rocks, soil and core samples major, minor and trace elements abundance by radiochemical and instrumental activation analyses 21 p3910 A70-41614
Alloying elements effects on corrosion resistance of Mg ingot in NaCl aqueous solution 24 p4363 A70-46198
CHEMICAL ENERGY
NT ENERGY OF FORMATION
Anoxia effects on biochemical processes in human body, comparing chemical energy balances under aerobic and anaerobic conditions 10 p1821 A70-25082
Reagent translational energy effect on dynamics of ionic and atomic reactions, using nuclear recoil and chemical accelerator methods 11 p1995 A70-26005

Book on energy conversion statics covering state functions, quasi-static processes, internal energy, chemical energy storage and conversion, dynamics and postulates and laws 12 p2165 A70-27670
Solar, nuclear, chemical and thermal energy sources for short and long duration exploration on moon 14 p2634 A70-30195
Ammonia gas phase IR intensity measurements for hydrogen bonding energy and related parameters 23 p4158 A70-44783
CHEMICAL ENGINEERING
Chemical engineering application to solid propellant rocket motors optimization for specific operations, discussing fuel properties, formulation and additives, mixing and casting [AICHE PAPER 28A] 01 p0166 A70-10971
Chemical engineering problems of resistojets, pulsed plasma, ion bombardment and colloid thrusters 01 p0166 A70-10974
Liquid rocket technology for chemical engineers, discussing insulating tanks, flexible lines, turbopumps and combustion chamber 05 p0896 A70-16168
Liquid rocket technology for chemical engineers, discussing propellant tanks, lines and valves, tank pressurization, turbopumps and combustion chamber problems 12 p2291 A70-27664
Parabolic solar furnace for chemical manufacture of impurity sensitive materials in orbiting spacecraft 21 p3804 A70-41001
CHEMICAL EQUILIBRIUM
NT ACID BASE EQUILIBRIUM
Internal structure of ideal explosive waves at Chapman-Jouguet point, discussing coupling between flow and chemical reactions 02 p0279 A70-12103
Computerized stepwise construction of Hugoniot curve for detonation waves and Chapman-Jouguet detonation and deflagration points 03 p0607 A70-13920
Synthetic and conversion reactions results showing phenylserine and DHEA equilibrium systems in Erlenmeyer reaction 04 p0646 A70-15087
Cesium plasma composition as equilibrium mixture of ideal gases assuming chemical equilibrium attainable by specified reactions 07 p1349 A70-19660
Transport properties of high temperature gases compared with room temperature differences, considering chemical equilibria, heat conduction and atom-free radical forces 07 p1424 A70-19880
Stainless steel corrosion rates in flowing liquid Na from mechanism based on thermodynamic partitioning of oxygen 09 p1706 A70-22942
Fixed low pressures of nitrogen generated by chemical dissociation in system at equilibrium at constant temperature, applying results to vacuum measurement device calibration 09 p1630 A70-22954
Partition functions and equilibrium constants for ScO, YO and LaO computed for 1000-8000 K, assuming doublet ground electronic state 10 p1946 A70-24970
Jet engine pollution reduction for airport areas, discussing chemical equilibrium failure in exhaust gases and combustor design 12 p2291 A70-27993
Cesium plasma composition as equilibrium mixture of ideal gases, assuming chemical equilibrium attainable by specified reactions 15 p2781 A70-32697
Gaseous substances thermodynamic functions and chemical equilibrium constants logarithms dependence on temperature and pressure, deriving internally self consistent formulas 22 p4124 A70-42682
Chemical equilibrium premixed flame composition at given temperature, pressure and mixture strength, using Newton-Raphson iteration technique for simultaneous nonlinear equations 23 p4157 A70-43892
CHEMICAL EXPLOSIONS
NT GAS EXPLOSIONS
Critical detonation diameter as function of concentration and dimensions of inhomogeneities in explosive, assuming chemical reaction generated behind detonation front 01 p0217 A70-11005
Fire and explosion suppression technology for aircraft and hypobaric and hyperbaric oxygen-rich atmospheres, discussing time available for suppression action 03 p0437 A70-14056
Solid rocket motors potential hazards explosive reactions and temperature and blast effects 14 p2629 A70-30782
Centrifugal pumps of various metals for liquid oxygen, describing fire and explosion tests 14 p2617 A70-31020

High energy chemical systems for postcrash emergency evacuation of commercial passenger aircraft, discussing exit opening via explosive methods 15 p2675 A70-32221
CHEMICAL EXTINGUISHERS
U FIRE EXTINGUISHERS
CHEMICAL FUELS
NT AEROCZINE
NT AIRCRAFT FUELS
NT GASOLINE
NT HYDROCARBON FUELS
NT HYDROGEN FUELS
NT JET ENGINE FUELS
NT METAL FUELS
NT SLURRY PROPELLANTS
CHEMICAL KINETICS
U REACTION KINETICS
CHEMICAL LASERS
Continuous wave chemical laser operation in carbon dioxide pumped by vibrational energy released from DF and HF molecular formation 04 p0704 A70-15686
Chemical laser action in spark excited CS₂-O₂ mixtures, attributing emission to combustion product CO 06 p1080 A70-17445
Chemical laser CW operation achieved by mixing gases, obtaining pumping energy from chemical reactions 06 p1080 A70-17492
Supersonic mixing CU chemical lasers, discussing lasing action time duration 06 p1083 A70-17945
Kinetic model developed for Cl-HBr reaction pulsed chemical laser 08 p1513 A70-21337
Chemical high pressure laser action produced by stimulated phototransition of electrons at contact moment between pair of reacting nonexcited gas molecules 08 p1513 A70-21412
CW laser operation at 10.6 microns in DF-carbon dioxide and HF-carbon dioxide molecular systems achieved by purely chemical means 08 p1513 A70-21539
Chemically formed carbon monoxide lasing in fast flow system, discussing reaction and excitation mechanisms 09 p1697 A70-22922
Continuous wave chemical laser operation at 10.6 micron in carbon dioxide pumped by vibrational energy from hydrogen atoms and bromine molecules reaction 10 p1901 A70-25149
CW chemical laser performance using molecular hydrogen diffused into supersonic fluorine atoms streams 11 p2063 A70-26067
Pulsed chemical laser output, considering increase in radiation energy 12 p2251 A70-28292
HF and DF continuous chemical lasers output power, obtaining population inversion by deuterium molecules diffusion into F atoms supersonic free jet 14 p2593 A70-30273
HF and DF continuous chemical lasers vibrational and rotational spectra, comparing lines and relative intensities 14 p2593 A70-30274
CW oscillation in carbon monoxide chemical laser 15 p2748 A70-31432
Chemical energy conversion in lasers, discussing vibrational inversions in diatomic and multiautomic molecules and chain reactions 16 p2927 A70-33233
Transverse flow CO chemical laser using atomic oxygen reaction with carbon disulfide, comparing output with longitudinal flow devices 18 p3266 A70-36313
CW HCl chemical laser action via chlorine atoms reaction with hydrogen iodide in fast flowing mixing device 19 p3444 A70-37542
CW chemical lasers operation from partially inverted transitions of HCl, HF and DF molecules in subsonic flow 22 p4050 A70-43008
Laser kinetics based on exothermal chemical reactions for electron transition stimulation, emphasizing single mode operation 24 p4354 A70-45656
HF chemical laser emission in fluorine-containing organic compounds via arc discharges, noting molecular hydrogen effect on p sub 10 and p sub 21 transitions 24 p4355 A70-46046
Transverse flow deuterium fluoride-carbon dioxide chemical laser for CW output without external energy source 24 p4355 A70-46084
CHEMICAL MACHINING
NT ELECTROCHEMICAL MACHINING
Chemical milling characteristics, development and applications, outlining performance capabilities with Al, Ti, Fe and Mg alloys 12 p2240 A70-26991

Polyurethane swelling in liquid media, measuring surface orientation effects during chemical machining on stress strain state 20 p3654 A70-39249

Asymmetric closed and cylindrical shells variable surface machining for desired wall thickness profile by chemical milling with digital computer numerical control 20 p3637 A70-39942

Chemical etching for revealing structure of carbon-graphite materials subjected to different graphitization stages 23 p4209 A70-44045

CHEMICAL MILLING

U CHEMICAL MACHINING

CHEMICAL PROPERTIES

NT HEAT OF COMBUSTION

NT HEAT OF FORMATION

NT HEAT OF SOLUTION

NT HEAT OF VAPORIZATION

NT THERMOCHEMICAL PROPERTIES

Collection of Soviet papers on chemical properties and analytical methods of refractory compounds 03 p0504 A70-12977

Physicochemical properties of hypothalamic secretions responsible for coronary dilatation in rats, cattle and pigs, using analytical techniques 03 p0417 A70-13215

Peroxides, superoxides and ozonides applications in industrial chemistry, semiconductors and rocket motor fuels, discussing chemical structure and properties and nomenclature 05 p0810 A70-15768

Aluminosilicate glass physical properties and chemical stability in water, alkaline and acidic agents, studying titanium oxides additives effect 05 p0871 A70-16596

Stoichiometric compositions of niobium dioxide to pentoxide range, investigating X ray characteristics and thermal stability 07 p1315 A70-20312

Adhesives chemistry, discussing ionic, covalent and intermolecular bonds allowing for chemical and physical properties 08 p1455 A70-20880

Brain cerebral tissues electrical impedance measurement by electrodes and bridge circuit, discussing chemical and metabolic properties 09 p1620 A70-22897

Chimkurgan reservoir algae life and physicochemical characteristics 09 p1627 A70-23148

Structural materials chemical and metallurgical factors controlling mechanical properties, machinability and finished part productivity [ASTME PAPER MR-69-731] 12 p2240 A70-26992

Visualized multicomponent systems subsolidus structures, studying physicochemical characteristics 13 p2470 A70-28885

Titanium alloys powder metallurgy, considering manufacturing methods and physical, chemical and mechanical properties 13 p2435 A70-29214

Soviet monograph on V and V alloys covering phase diagrams, mechanical, chemical and physical properties, compounds and chemical composition 14 p2595 A70-30627

Boron, silicon carbide and graphite fibers surface properties 16 p2937 A70-33376

Chemical and moisture resistance, electrical and mechanical properties of engineering thermosetting plastics made of HYSTL resins 16 p2938 A70-33380

Soviet reference book on highly refractory elements and compounds covering crystalline, chemical, thermodynamic, thermophysical, electrical, optical and nuclear properties 19 p3451 A70-37470

Organic liquid scintillators with high transparency, describing optical and chemical properties 20 p3629 A70-39319

Fugacities of HCl and HF compared with abundance in volcanic fumarolic emanations, indicating magma undersaturation 20 p3619 A70-39321

Chemical and physical factors effect on smoke evolution from polymers 20 p3736 A70-39405

CHEMICAL PROPULSION

NT HYBRID PROPULSION

Interagency chemical rocket propulsion group method of treating measurement error for liquid rocket engine performance parameters, using uncertainty model [AIAA PAPER 69-734] 07 p1365 A70-19723

Oxygen and fluorine-based liquid fuels and oxidizers development, considering chemical rocket propulsion reaction principles 07 p1361 A70-19917

Book on spaceflight propulsion covering jet thrust, energy release, chemical, nuclear and electric propulsion, transportable and environmental systems 09 p1742 A70-22202

Chemical rocket propulsion systems approximate calculation for characteristic velocity dependence on mixture ratio and pressure in combustion chamber [DFVLR-SONDDR-24] 10 p1929 A70-23842

Chemical high energy rocket propellants, discussing metal combustion, hybrid and tribrid engines, combustion chambers, etc 11 p2100 A70-26282

Book on chemical propellants performance covering properties and parameters effects, rocket performance, chemical thermodynamics, flame temperature, etc 12 p2289 A70-27350

Space vehicles chemical propulsion limitations and potential applications 15 p2786 A70-32268

Chemical rocket propellant research covering composite liquid monopropellants, lateral thrust in solid propellant rockets, ELDO third stage, friction losses, etc 17 p3148 A70-35211

Primer vector theory applied to interplanetary trajectory optimization for high thrust chemically propelled spacecraft, considering 1973 Mars opportunity [AIAA PAPER 70-1039] 19 p3527 A70-38854

Optimal control of composite spacecraft propulsion system incorporating high thrust-weight ratio chemical engine and low thrust ion engine 21 p3865 A70-40831

Electric field control of oscillatory acetylene flame combustion for chemical rocket engines 21 p3942 A70-40885

CHEMICAL REACTIONS

NT ATOMIC RECOMBINATION

NT CARBONIZATION

NT CHLORINATION

NT COPOLYMERIZATION

NT DECARBONATION

NT DEHYDROGENATION

NT DEIONIZATION

NT DENITROGENATION

NT DEOXIDIZING

NT ELECTROCHEMICAL OXIDATION

NT ENDOTHERMIC REACTIONS

NT EXOTHERMIC REACTIONS

NT FERMENTATION

NT FLUORINATION

NT GLYCOLYSIS

NT HYDROGENATION

NT HYDROGENOLYSIS

NT HYDROLYSIS

NT ION RECOMBINATION

NT METAL-WATER REACTIONS

NT METHYLATION

NT NITRATION

NT NITRIDING

NT OXIDATION

NT OXYGEN RECOMBINATION

NT OXYGENATION

NT PHOSPHORYLATION

NT PHOTOCHEMICAL REACTIONS

NT PHOTOCROMISM

NT PHOTODECOMPOSITION

NT PHOTOLYSIS

NT PHOTOOXIDATION

NT PHOTOSYNTHESIS

NT PYROLYSIS

NT RADIOLYSIS

NT REDUCTION [CHEMISTRY]

NT SULFATION

NT THERMAL DISSOCIATION

NT TITRATION

Acetylferrocene preparation by reacting ferrocene with acetic anhydride in phosphoric acid and reducing acetylferrocene to alpha-hydroxyethyl ferrocene by potassium borohydride in methanol 02 p0249 A70-11678

Book on gas kinetics, treating experimental methods, reaction theories, transition state theories, complex processes, etc 02 p0251 A70-12058

Red bicyclic condensation product from reaction of acetone with sym-trinitrobenzene and diethylamine 02 p0251 A70-12278

Statistical model of turbulent chemically reacting shear flows, analyzing wave number fluctuations effect and Couette flow 03 p0464 A70-12928

Aluminum oxide solid state reaction with Ta at high temperatures using chemical analysis 03 p0511 A70-13487

Atomic oxygen reaction with carbon dioxide and carbon dioxide dissociation in shock waves, using nitrous oxide decomposition for oxygen source 03 p0440 A70-13578

Bimolecular transfer reactions activation energies for multivalent gaseous compounds estimated by bond energy method avoiding use of adjustable parameters 03 p0441 A70-14045

Thermodynamics second law application to pyrotechnic systems, discussing solid-solid and reversible reactions 03 p0547 A70-14114

Numerical integration of differential equations governing one dimensional flow of reactive gas, discussing flows of converging-diverging nozzle and normal shock waves 04 p0671 A70-14992

Synthetic and conversion reactions results showing phenylserine and DHEA equilibrium systems in Erlenmeyer reaction 04 p0646 A70-15087

Chemical heat source combined with metals ignition properties considered for spacecraft heating during Mars nighttime landing 04 p0628 A70-15426

Flow fields construction for normal shock waves with nonequilibrium chemical reactions reflected from shock tube end wall [AIAA PAPER 68-732] 04 p0674 A70-15537

Alpha- and beta-styryl azides catalyzed reactions in ethanolic sulfuric acid 05 p0810 A70-16053

Limits of self ignition in reaction of F with H detected photoelectrically 05 p0956 A70-16156

Polyamides chemical welding using HF heating to obtain optimum temperature distribution and to activate polymer reaction with crosslinking agents 06 p1091 A70-17316

Quasi-equilibrium treatment of heterogeneous reactions applied to evaporation rate/desorption/computation for volatile species formed in oxygen reactions with W, Mo and graphite 06 p1004 A70-17330

Quasi-equilibrium treatment of heterogeneous reactions applied to flash desorption data for oxygen reaction with tungsten surface, discussing species desorption dependence on adsorption temperature 06 p1004 A70-17331

Chemical laser CW operation achieved by mixing gases, obtaining pumping energy from chemical reactions 06 p1080 A70-17492

Energy and mass transfer during elastic and inelastic molecular collisions in reacting gas mixtures, using Enskog and variational methods in solving Boltzmann equations 06 p1110 A70-17760

Maxwellian distribution perturbation in chemically reacting gas mixtures with lower inelastic collision frequency than elastic 06 p1110 A70-17761

Gas phase reactions near solid-gas interface of deflagrating double base propellant causing abrupt changes in burning rate-pressure curve [AIAA PAPER 70-124] 06 p1179 A70-18046

Analytical method for design of supersonic flow and maximum thrust nozzles for chemically reacting gases, noting surface geometry [AIAA PAPER 70-129] 06 p0971 A70-18108

Gas dynamic effects of reaction center in explosive gas mixture analyzed by model and numerical computation [AIAA PAPER 70-147] 06 p1181 A70-18144

Thermal conductivity calculation for chemically reacting multicomponent gas mixture, comparing results from Brokaw method and simplified formula 06 p1184 A70-18554

Chemical reaction rates corresponding to initial molecules fixed internal energy levels determinable for multitemperature Maxwell-Boltzmann distribution as function of reagent temperatures 07 p1224 A70-18769

Quasi-steady radially symmetric theory of liquid drop vaporization and homogeneous combustion extended to burning of solid carbon spheres gasified by chemical attack 07 p1419 A70-18915

Inviscid hypersonic flow analysis for chemically relaxing air about wedges and pointed circular cones using Dorodnitsyn integral method [DGLR-69-037] 07 p1188 A70-18986

Chemical synthesis in streaming thermal plasmas including HCN from cold methane and N plasma discharge chemistry 07 p1351 A70-19879

Crossed molecular beam study of reactive asymmetry of oriented methyl iodide molecules reacting with Rb, accounting for observations with hard sphere model 07 p1225 A70-20051

Atomic F reaction with hydrogen studied for vibrational, rotational and translational energy distribution, using IR chemiluminescence method 07 p1225 A70-20055

Ceramic adhesives with glassy matrix for metal bonding, describing chemical reactions in interface, adhesive processing and application 08 p1526 A70-20883

Chemical high pressure laser action produced by stimulated phototransition of electrons at contact moment between pair of reacting nonexcited gas molecules 08 p1513 A70-21412

Physicochemical methods of producing formaldehyde for carbohydrate synthesis in life support systems

09 p1623 A70-22080

Steady flame propagation attainment for chemical reaction initiation in gaseous fuel by heated surface with various wall temperatures

09 p1787 A70-22115

Oxide spinel formation kinetics and reaction mechanisms with emphasis on Ni and Co chromites, discussing cation diffusion

09 p1739 A70-22307

Chemically formed carbon monoxide lasing in fast flow system, discussing reaction and excitation mechanisms

09 p1697 A70-22922

Boundary layer equations for multicomponent flow with finite chemical reactions solved by finite difference method

09 p1605 A70-23201

Peptide formation during glycine reaction with linear polyphosphates and cyclic metaphosphates, considering prebiotic synthesis

09 p1630 A70-23395

Electric discharge reactions in mixtures of phosphine with methane, ammonia and water, obtaining biologically significant inorganic and organic phosphorus compounds

09 p1630 A70-23396

Near equilibrium transonic flows of reacting gas mixtures based on linearization of the thermodynamic and kinetic quantities

10 p1867 A70-24133

Flowing afterglow system below 300 K for rate constants of certain gases association with helium third body, investigating oxygen cluster ions formation and reactions

10 p1920 A70-25144

Deuterium atom reaction with hydrogen molecule yielding HD and H using modulated crossed beams, plotting angular distributions and reaction velocities

10 p1920 A70-25148

Oxygen difluoride-diborane reaction measured for pressure-temperature relationships and gas composition dependence on time, noting possible applications as hypergolic rocket propellants

11 p1995 A70-26138

Recombination in hydrogen-oxygen reaction studied by monitoring IR emission from water vapor formed by shock initiated combustion

11 p1995 A70-26377

Turbulent reacting wakes properties prediction models validity, discussing Lagrangian formulations and eddy diffusivity and mixing models

11 p1978 A70-26772

Compressibility transformation theory extended for turbulent boundary layer, involving mass transfer with/without chemical reactions

12 p2211 A70-27825

Vibrational dissociation relaxation effects on chemical reactions, molecular energy and thermal quanta in air flow behind direct shock wave

12 p2213 A70-28232

Hard sphere model for reactive molecular collisions based on energy and momentum of reactants and products

13 p2361 A70-28497

Graphite-carbon dioxide interaction at high temperatures in presence of solid phase diffusion from bulk to reacting surface

13 p2520 A70-28581

Thermodynamic data for chemical reactions of Ti alloys formation with Al obtained by measuring galvanic cells emf with solid electrolytes at elevated temperatures

13 p2434 A70-28889

Molar growth yields from chemostat cultures of *Hydrogenomonas eutropha* on succinate and on fumarate, noting equivalence to ATP via oxidation

13 p2350 A70-29113

Free jet expansions in molecular beam sampling systems, using Sherman equations and chemical kinetic equations

13 p2389 A70-29608

Oxygen difluoride-diborane reaction kinetics and boron fluoride formation rate

13 p2362 A70-29611

Chemically reacting stagnation point boundary layers with wall injection of gas, comparing multicomponent solution with binary approximation and chemical simplifications

14 p2565 A70-30265

Structural and functional properties of phosphates in biochemical reactions, discussing linkages

14 p2544 A70-30346

Chemically reacting ideal substance model, describing thermodynamic properties and application to energy conversion processes

14 p2533 A70-30529

Statistical transport, energy and chemical reaction rate in turbulent flow field with uniform velocity gradient, using Brownian motion theory

14 p2566 A70-31029

Turbulent chemical reactions invariance preservation for zero diffusivity

14 p2546 A70-31044

Third body coefficients of water and heavy water reactions in KCl coated and aged boric acid coated vessels with vibrational-vibrational exchanges

14 p2546 A70-31091

Gas phase chemical synthesis via AC diffuse discharge superimposed on propane-air flame seeded with potassium carbonate in electrically augmented flame burner

14 p2546 A70-31097

Physicochemical methods of producing formaldehyde for carbohydrate synthesis in life support systems

15 p2693 A70-32676

Triatomic hydrogen positive ion-yielding reactions, using EVA ion-molecule beam apparatus

16 p2855 A70-33012

Formose sugars production from formaldehyde, discussing economic conversion by catalytic reactions

16 p2855 A70-33063

Epoxide ring reactivity and crosslinking related to adjacent electrophilic and electronegative groups, considering epoxy resin technology

16 p2936 A70-33357

Shear flow turbulence effect on chemical reactions, considering two dimensional low speed turbulent mixing layer between high velocity cold gas and air at rest

[AIAA PAPER 70-721] 16 p2855 A70-33493

Turbulent and reacting flows temperature and mixing rates determination, using gaseous HF tracer spectroscopy

[AIAA PAPER 70-726] 16 p2856 A70-33497

Spacecraft attitude control microthrusters utilizing catalytically reactive gas mixtures during pulse mode and steady state operation

[AIAA PAPER 70-614] 16 p2969 A70-33611

Gas phase chemical reactions effect on heat transfer to charring ablator, deriving numerical solution for multicomponent stagnation point flow

[AIAA PAPER 70-869] 16 p2999 A70-33912

Ethylene and ethylene-acetylene mixtures ion-molecule reaction product distributions calculation using quasi-equilibrium theory of unimolecular reactions

16 p2858 A70-34012

Ti interaction with elements of periodic systems, considering binary system phase diagrams

17 p3115 A70-34384

Nonreacting and chemically reacting laminar flows, calculating equilibrium, nonequilibrium and ideal gas laminar boundary and viscous shock layers over hyperboloid

[AIAA PAPER 70-808] 17 p3005 A70-34456

Hypersonic flow of chemically reacting binary mixture of oxygen atoms and molecules past blunt body, presenting viscous shock layer equations and slip boundary conditions

[AIAA PAPER 70-805] 17 p3005 A70-34458

Time dependent solution for inviscid hypersonic flow of chemically reacting gas mixture about blunt bodies

[AIAA PAPER 70-771] 17 p3009 A70-34502

Chemical kinetic and turbulent transport coefficients effects on afterburning rocket exhaust plumes and sea level transverse radar attenuations

[AIAA PAPER 70-733] 17 p3194 A70-34513

Agents for deoxygenation of nitro and nitroso groups

17 p3042 A70-35329

Relaxation gas dynamics with chemical reactions, emphasizing differences and similarities with classical gas dynamics behavior

17 p3071 A70-35467

Nonequilibrium nozzle flows involving molecular vibrational energy relaxation and composition changes from gas phase chemical reactions respectively

17 p3071 A70-35469

Onsager reciprocal relations experimental validity in irreversible processes application to metals, electrokinetics, isothermal diffusion, heat conduction, chemical reactions, etc

17 p3197 A70-35538

Transport processes in chemical reactions and biological functions of living systems, using nonequilibrium thermodynamics approach

17 p3032 A70-35539

Detonation in nonuniformly heated gas capable of chemical reaction, obtaining numerical solution

17 p3198 A70-35737

Gas dynamics of explosions and reacting systems - Conference, Novosibirsk, U.S.S.R., August 1969

17 p3074 A70-35882

ADP-ATP catalyzed exchange reaction in turtle bladder microsomes, using chromatographic measurements of conversion rates

17 p3034 A70-35900

NO in earth atmosphere, describing theory of formation for explaining observed density distribution

18 p3245 A70-36019

Reacting gas relaxation with particle sink removing products from system calculating relaxation processes during equilibrium state approach

18 p3292 A70-36291

Space vehicle reentry hypersonic boundary layer characteristics, considering air components chemical reactions due to excessive heat

18 p3346 A70-36384

Emission spectral distribution of atomic nitrogen reaction with carbon tetrachloride for artificial luminescent clouds

18 p3293 A70-36990

Chemical reactions neutralizing electron-ion gas in F region

18 p3255 A70-37044

Heat transfer coefficient of chemically reacting gas mixture as function of Lewis-Semenov number, discussing nitrogen dioxide decomposition

19 p3550 A70-37251

Multicomponent chemically unstable nonequilibrium gas flow past body, taking into account boundary layer behavior

19 p3373 A70-38182

Chemical reactions of ions and neutral particles in D region, discussing photochemistry of atomic oxygen and ozone and reaction rate constants

19 p3418 A70-38905

Addition and hydrogenation reactions of azomethines in chemistry of carbon-nitrogen bond, emphasizing Schiff bases

20 p3582 A70-38978

Water vapor effect on carbon dioxide reaction with lithium hydroxide in dynamic isothermal system

20 p3582 A70-39227

Hydrogen-oxygen flames recombination rates measurements analysis, taking into account reverse reaction rates

20 p3583 A70-40470

Methane and hydrogen consumption rates during slow reactions in mixtures of molecular hydrogen, oxygen and nitrogen

21 p3772 A70-40879

Carbon dioxide-atomic oxygen reaction rate constant to investigate Martian ionosphere, discussing reactions involving oxygen, nitrogen molecular ions and NO

21 p3886 A70-41067

Shock tube measurements of bimolecular reaction rates in branched chain hydrogen-carbon monoxide-oxygen system, monitoring flame band emission

21 p3773 A70-41314

Adiabatic-transition state theory of chemical reactions in dilute gases with separate binary collisions, considering Morokuma, Eu and Karplus results

21 p3773 A70-41396

Solid phosphorus triamide derivatives as ignition aids in hypergolic propellant systems, testing characteristics in interaction with oxidizers

21 p3865 A70-41404

Barrier heights for hydrogen-iodine reaction from semiempirical four-electron valence bond calculation

21 p3780 A70-41709

Combustion rate as function of oxidizer molecular refractivity in perchlorates and nitrates of aliphatic and aromatic mono- and polyamines explosives

21 p3783 A70-42241

Equilibrium sonic velocity in reacting gas mixture in nozzle flow for unlimited species and independent chemical reactions

22 p4074 A70-42753

Equilibrium performance of closed Stirling cycle with chemically reactive gas as working fluid, discussing power density and thermal efficiency

22 p3982 A70-42756

Nonequilibrium gasdynamic and thermodynamic properties of chemically reacting gas mixtures in high expansion subsonic and supersonic nozzles for selected rocket propellants

22 p3982 A70-42761

Thermosphere, stratosphere and mesosphere reactions involving water, hydrogen, methane, ozone, nitric oxide and nitrogen peroxide

22 p4023 A70-43298

Chemical reaction product fluctuations in reacting and nonreacting turbulent wake of sphere in water tunnel detected by injected salts conductimetric titration

[AIAA PAPER 68-686] 23 p4134 A70-44570

Reacting gas supersonic flow over two dimensional base, examining reaction rate effects on base pressure

23 p4135 A70-44626

Heat transfer in chemically reacting gases boundary layers, obtaining approximate solution by film theory

24 p4428 A70-45101

Air revitalization chemicals reactions with water vapor and gaseous carbon dioxide, describing apparatus for kinetic studies

24 p4307 A70-45348

Al purification by subhalide reaction, discussing contamination sources and thermodynamics

24 p4349 A70-46187

CHEMICAL REACTORS

Mass action law-polynomial optimization analogy, illustrating optimal temperature determination in chemical reactors in series

01 p0143 A70-10925

Reactor surface and propylene role during vapor phase partial oxidation of propane in continuous flow tubular reactors

02 p0250 A70-12017

- Pilot chamber initiated thermal decomposition reactor concept for monopropellant thruster, discussing thrust levels and throttling ratios
[AIAA PAPER 69-420] 13 p2473 A70-28507
- Chemical reactor using successive rapid multiple electrical explosions of metal wires 15 p2717 A70-32436
- Optimal startup control of jacketed tubular reactor with first order reversible exothermic reaction, presenting distributed maximum principle for diffusional parameter system 16 p2885 A70-33330
- CHEMICAL RELAXATION**
U MOLECULAR RELAXATION
CHEMICAL SHIFT
U CHEMICAL EQUILIBRIUM
CHEMICAL STERILIZATION
Reaction kinetics of microbial sterilization in ultrahigh vacuum and in outer space 23 p4148 A70-44841
- CHEMICAL TESTS**
NT CHEMICAL ANALYSIS
NT ELECTROPHOTOMETRY
NT GAS ANALYSIS
NT GAS SPECTROSCOPY
NT MICROANALYSIS
NT NEUTRON ACTIVATION ANALYSIS
NT OZONOMETRY
NT POTENTIOMETRIC ANALYSIS
NT QUANTITATIVE ANALYSIS
NT SALT SPRAY TESTS
NT SPECTROSCOPIC ANALYSIS
NT URINALYSIS
NT VOLUMETRIC ANALYSIS
Synthetic and conversion reactions results showing phenylserine and DHEA equilibrium systems in Erlenmeyer reaction 04 p0646 A70-15087
- CHEMILUMINESCENCE**
Excitation, reemission and absorption spectra of Cr activated powdery Mg titanate prepared, using MgO and Ti dioxide with LiCl as flux 02 p0350 A70-11848
- Chemiluminescence in alkali metals and halogenated methanes diffusion flames, studying diatomic Cs spectral bands 02 p0250 A70-12018
- Graft copolymerization and chemiluminescence analysis of lipids complexes in animal and plant tissue homogenates exposed to gamma radiation 03 p0419 A70-13305
- Chemiluminescent reaction rates measurements for emission of diatomic oxygen molecules Herzberg bands in oxygen and oxygen-inert-gas afterglows 03 p0440 A70-13579
- Flowfield and chemical kinetics model to calculate nitrogen dioxide chemiluminescence wake emission [AIAA PAPER 68-702] 04 p0620 A70-15535
- Nitric oxide free jet expansion, studying molecular cluster formation, inhibition and chemiluminescence 06 p1044 A70-18281
- Atomic F reaction with hydrogen studied for vibrational, rotational and translational energy distribution, using IR chemiluminescence method 07 p1225 A70-20055
- Arcas rocket-borne chemiluminescent ozonesonde for measuring ozone concentration after deployment above stratopause level 07 p1396 A70-20263
- Dual photon emission from chemiluminescent SO-O reaction, proposing two step emission mechanism 09 p1630 A70-23001
- Chemiluminescence from NO adiabatically expanded against supersonic H atoms stream in inert carrier 10 p1831 A70-24566
- Methane oxidation behind reflected shock waves between 1350-1900 K, measuring pressure, chemiluminescence and 3067 A absorption of OH radical 11 p2150 A70-26380
- Atmospheric ozone vertical distribution measurement based on luminescence of solid organic substances, noting chemical and optical methods 14 p2573 A70-30409
- Chemiluminescent processes accounting for radiation from turbulent wake flows behind hypersonic spheres in air 16 p2997 A70-33492
- Rhodamine C chemiluminescent material for atmospheric ozone measurements, describing preparation and luminescence spectrum 19 p3373 A70-37638
- CHEMISORPTION**
IR spectra of N isotopes adsorbed on nickel-on-Aerosil catalysts, investigating effects of intermolecular interaction and isotopic substitution 03 p0440 A70-13099
- Rare gases abundance patterns on earth and in chondrites, proposing chemical adsorption mechanism at planetesimal stage during accretion 09 p1764 A70-23610
- Chemisorption on Mo single crystal surfaces observed by LEED techniques, discussing bcc planes and adsorbed gases 12 p2181 A70-27256

- Carbon monoxide adsorption on rhenium and ruthenium HCP metals emphasizing surface migration, work function increments and desorption 12 p2181 A70-27676
- Nitrous oxide chemisorption by rhenium filament at low pressures at various temperatures, determining sticking probability 12 p2181 A70-27678
- CHEMISTRY**
Cosmochemistry, discussing interdisciplinary nature, goals, nuclear roots, information sources, key concepts involving elements age and origin, nuclear species abundances, chemical fractionation, etc 03 p0578 A70-14346
- Collection of papers on high temperature physics and chemistry covering shock tube chemistry, plasmas, exploding wires, etc 06 p1063 A70-17726
- Shock tube chemistry including ideal and nonideal behavior, instrumentation techniques, etc 06 p1005 A70-17727
- Collection of papers on high temperature chemistry covering gaseous dissociation, molecular beams, thermal plasmas, solids sublimation, solar furnace, etc 14 p2545 A70-30901
- Molecular beams formation from high pressures, discussing detection, diagnosis and applications in high temperature chemistry 14 p2545 A70-30904
- Systems design and instrumentation for chemical/biochemical space manufacturing at zero g, developing scaling laws for transition to larger production units 16 p2919 A70-33719
- CHEMONUCLEAR PROPULSION**
U CHEMICAL PROPULSION
U NUCLEAR PROPULSION
CHEMOTHERAPY
Flight fatigue syndrome origin, therapy and prevention, noting cortical adrenal hormones tests 01 p0031 A70-10234
- Hypercholesterolaemia chemotherapy experimental results with five hypocholesterolemic drugs /nicotinic acid, triparanol, aluminum nicotinate, Atromid and nonfeminizing estrogen/ 03 p0426 A70-13937
- Ionol concentration variations in oncological patients blood, using liquid gas chromatography to determine removal by urine and feces 07 p1209 A70-19519
- Empirical formulas derived for intuitive estimates of blood coagulability in patients to facilitate medication dosage prescription 07 p1210 A70-19558
- Protective ability of various compounds against hyperoxia at 5, 7, 9 and 11 atmosphere of pure oxygen 08 p1441 A70-20629
- Human metabolic study showing effect of yeast RNA and allopurinol on serum and urinary uric acid formation 08 p1454 A70-20679
- Vasoactive agent effects on decompression sickness in rats, noting increased severity of bends by serotonin and platelet role 10 p1811 A70-24176
- L-dihydroxyphenylalanine intraperitoneal injection effect on S-adenosylmethionine concentration in rat brain 21 p3764 A70-41269
- Hypotensive effects of chlorthalidopexide, amobarbital and chlorpromazine on behaviorally induced elevated arterial blood pressure in squirrel monkey 24 p4298 A70-45620
- CHEST**
Chest, abdominal wall and diaphragm displacements of rabbits during partial and whole body exposure to shock waves produced by hexotol charges 02 p0231 A70-11704
- Data analysis of compliance, resistance, inertance and natural frequency of chest-lung system, noting trend with body mass 06 p0993 A70-17521
- Acceleration effects on chest organs by X ray studies noting heart shape changes, pulmonary areas, diaphragm position, etc 07 p1201 A70-18791
- Chest wall vibrations conversion measured by different transducers for simultaneous velocity, displacement, acceleration and phonocardiograms 21 p3770 A70-41236
- CHIASMIS**
Optic chiasm damage effects on human depth perception implying interhemispheric link for binocular integration in central vision 09 p1618 A70-22669
- CHICKENS**
Chicken body mass and percentage body fat following 24 weeks chronic acceleration determined from fatty acid metabolism, liver citrate cleavage and malic enzyme activities 02 p0233 A70-11720
- Erythrocyte sedimentation rate in chicken blood predictable by Stokes equation 02 p0238 A70-12547

- Purification and properties of diphosphopyridine nucleotide-linked glycerol 3-phosphate dehydrogenases from chicken breast muscle and liver 03 p0442 A70-14047
- White single-comb Leghorn chick embryonic development at increased pressures at various hyperbaric gas mixtures for ten day periods 06 p0991 A70-17296
- White Leghorn laying hens parathyroid glands fine structure from electron microscopic studies, noting electron dense membrane bound mature secretory granules in cytoplasm 09 p1619 A70-22800
- Chicken embryogenesis during hypoxia at high altitude, noting metabolic repression effects, hypothermia and brain atrophy 14 p2536 A70-30188
- Chicken lymphopenia and body mass loss resulting in death from chronic restraint, developing physiologically unstressful restraint for space environmental testing 21 p3765 A70-41488
- Space environment husbandry, examining chickens stress response to restraint and parental hydration 24 p4296 A70-45337
- Gravity effects on perinatal organ growth in chicks 24 p4297 A70-45342
- CHILDREN**
Nervous control of unconditioned cardiovascular reflexes during ontogenesis in children, observing sympathetic and vagal tonicity 08 p1446 A70-21449
- Thoracic impedance changes in premature infants respiration monitoring, noting Respiratory distress syndrome /Rds/ physiopathology 14 p2541 A70-30382
- Flotation device for infants and small children incorporating life support and survival capabilities for aviation and marine applications 23 p4153 A70-44480
- CHILLING**
U COOLING
- CHIMES**
U AUDITORY SIGNALS
- CHIMPANZEES**
NT HUMAN BEINGS
NT MONKEYS
Collection of articles on chimpanzee central nervous system and behavior 01 p0028 A70-11375
- Unrestrained chimpanzees cortical and subcortical electrical activity during sleep recorded by telemetry and compared with human beings and other mammals 03 p0432 A70-14347
- Electroencephalograms recorded for chimpanzees performance to play game, selecting parameters by computer analysis to discriminate between game phases and decisions 04 p0640 A70-14387
- CHINA**
Tekite field studies in China concerning strategic occurrence and chemistry 06 p1148 A70-18393
- CHINOOK HELICOPTER**
U CH-47 HELICOPTER
- CHIRP**
Laser mode locking theory, explaining subpicosecond structure and frequency chirp 18 p3266 A70-36315
- CHIRP SIGNALS**
Chirped pulses observation by heterodyning single frequency Q switched carbon dioxide laser with stable CW local oscillator and beat signal display on oscilloscope 01 p0109 A70-10433
- Oblique ionospheric pulse sounding records improvement by use of linear FM /chirp/ transmission, discussing time delay resolution, transmitter power and RF interference rejection 07 p1233 A70-19184
- Maser amplification in Chirp radar signals pulse paramagnetic compressors using electron spin echoes 09 p1637 A70-23321
- Chirp radars energy spectra bounds calculation to insure electromagnetic compatibility 14 p2551 A70-31178
- CHLORATES**
Ammonium chlorate thermal decomposition products as function of temperature using mass spectrometry 05 p0895 A70-17082
- CHLORELLA**
Fraction of Chlorella and Scenedesmus biomass, noting changes in adrenal cortex and renal glomerulus 03 p0425 A70-13889
- Chlorella seaweed hybrid strains containing larger amounts of amino acids than original parent species 04 p0630 A70-14573
- Continuous Chlorella production as function of total illumination in high intensity light system incorporating aerobic fermenter for heterotrophic cells 04 p0645 A70-15454
- Survival rates of continuously cultivated Chlorella plants in air-carbon dioxide atmosphere after single

- exposure to gamma radiation, using microcolony counting technique 05 p0803 A70-17113
- Joint *Chlorella*-yeast cultivation on metabolites, investigating biomass accumulation and pigment synthesis 07 p1197 A70-18655
- Alpha irradiation effect on *Chlorella* survival, cell division and mutation 07 p1208 A70-19507
- Chlorella* species found to contain ergosterol as major sterol 09 p1616 A70-22330
- Alpha irradiation effect on *Chlorella* survival, cell division and mutation 11 p1987 A70-26106
- Linear density gradients in isopycnic centrifugation technique for selecting synchronous daughter cells from asynchronous *Chlorella* cultures 14 p2546 A70-30985
- Hydrogenomonas* vs *Chlorella* spacecraft life support systems, discussing human requirements and equipment for balanced food supply on long duration space missions 16 p2855 A70-34315
- Optimum algae cultivator construction for life support system, using *Chlorella* culture model 17 p3026 A70-35320
- Chlorella* reproduction rates at steady and variable illumination intensity levels, determining productivity autocorrelation function by statistical analysis 17 p3030 A70-35355
- Life support systems based on *Chlorella*-bacterial culture, investigating water exchange and reclamation 20 p3574 A70-40184
- Space cabin atmosphere regeneration by unicellular algae photosynthesis, discussing *Chlorella* cultivation procedures and additional functions in life support systems 23 p4154 A70-44655
- Nitrogen deficient algae nitrification, showing cellular N compounds oxidized to nitrate and nitrite followed by nitrate reductase 24 p4297 A70-45407

CHLORIDES

- NT ALUMINUM CHLORIDES
- NT AMMONIUM CHLORIDES
- NT BORON CHLORIDES
- NT CARBON TETRACHLORIDE
- NT COPPER CHLORIDES
- NT HYDROCHLORIC ACID
- NT HYDROCHLORIDES
- NT IRON CHLORIDES
- NT LITHIUM CHLORIDES
- NT NITROSYL CHLORIDES
- NT PHOSGENE
- NT POTASSIUM CHLORIDES
- NT SODIUM CHLORIDES
- NT SULFUR CHLORIDES
- NT TITANIUM CHLORIDES
- Vibrational spectra and structure of oxalyl chloride in crystalline and fluid states, discussing molecular and space group symmetry 16 p2857 A70-34006
- Niobium oxychloride conversion to niobium pentachloride by vapor phase chlorination with phosgene, examining reaction kinetics 18 p3272 A70-36031
- Chloride ion shift of respiration occurring between plasma and erythrocytes as function of carbon dioxide, using rapid filtration method 19 p3364 A70-38366

CHLORINATION

- Synthesis of alpha-dichloro-seco-A-norcholestanol from diol monoacetate reaction with triphenylphosphine followed by hydrolysis and repeated chlorination 06 p1005 A70-17975
- Niobium oxychloride conversion to niobium pentachloride by vapor phase chlorination with phosgene, examining reaction kinetics 18 p3272 A70-36031

CHLORINE

- Chemical additives effect on H-Cl-N mixtures burning velocity in air and nitrogen 02 p0398 A70-12031
- Ballistic range measurements of vibrational nonequilibrium effects on leading edge shock wave shape for cone-cylinders fired through chlorine atmosphere at supersonic speeds 04 p0621 A70-15601
- Interstitial Cl molecule formation in NaCl lattice, computing strain field and energetics by energy minimization technique based on point ion lattice model 14 p2544 A70-30352
- Gaseous nebulae electron densities based on interpretation of forbidden Cl III lines using collisional strengths and transition probabilities 15 p2798 A70-31746

CHLORINE COMPOUNDS

- NT ALUMINUM CHLORIDES
- NT AMMONIUM CHLORIDES
- NT AMMONIUM PERCHLORATES
- NT BORON CHLORIDES

- NT CARBON TETRACHLORIDE
- NT CHLORATES
- NT CHLORIDES
- NT CHLORINE FLUORIDES
- NT CHLORINE OXIDES
- NT COPPER CHLORIDES
- NT HYDROCHLORIC ACID
- NT HYDROCHLORIDES
- NT IRON CHLORIDES
- NT LITHIUM CHLORIDES
- NT MAGNESIUM PERCHLORATES
- NT NITROSYL CHLORIDES
- NT PERCHLORATES
- NT PHOSGENE
- NT POTASSIUM CHLORIDES
- NT POTASSIUM PERCHLORATES
- NT SODIUM CHLORIDES
- NT SULFUR CHLORIDES
- NT TITANIUM CHLORIDES

Photodecomposition of 1,4-dichlorobutane sensitized by n, pi singlet state of acetone as chemical process 04 p0646 A70-15319

Block diagrams of three stage device for extracting radioactive Ar from perchloroethylene considered for solar nucleus studies 05 p0845 A70-15933

Synthesis of alpha-dichloro-seco-A-norcholestanol from diol monoacetate reaction with triphenylphosphine followed by hydrolysis and repeated chlorination 06 p1005 A70-17975

Inductive effect in C-Cl chemical bonds in chloroalkenes, using nuclear quadrupole resonance frequencies shifts 09 p1630 A70-22903

Flame-resistant trichloromethyl-containing polyester-styrene system, describing curing characteristics at room and higher temperatures 10 p1907 A70-24066

Direct sensitized photolysis of various dichlorobutanes yielding HCl 16 p2855 A70-33089

Dichlorodifluoromethane ionization and attachment coefficients for wide pressure range 22 p4076 A70-42373

CHLORINE FLUORIDES

Materials static tested for compatibility with pure and moisture contaminated chlorine pentafluoride at 160 F and ambient temperatures 09 p1742 A70-23250

Thermal dissociation kinetics in chlorine pentafluoride over high temperature range 11 p1994 A70-25823

CHLORINE OXIDES

Chlorine dioxide-methane mixture flame stabilized in low pressure burner, determining emission spectra, burning velocity, activation energy, etc 02 p0251 A70-12033

Ammonia/chlorine dioxide and ammonia/chlorine dioxide/methane flames burner stabilization and burst velocities 02 p0400 A70-12670

Premixed flames of methane with chlorine dioxide and perchloric acid, comparing properties with methane-oxygen flames, suggesting unified reaction mechanism 07 p1425 A70-20007

Ammonia-chlorine dioxide flame stabilization for simulating ammonium perchlorate combustion at high pressures 11 p2099 A70-25994

CHLOROPHYLLS

Ruby laser Q switching by chlorophyll d and derivatives, discussing peak output power 01 p0114 A70-11391

Backscattered sun and skylight spectra from sea obtained from low flying aircraft as measure of chlorophyll concentration 09 p1666 A70-22250

Remote sensing from aircraft and satellites of chlorophyll concentrations for monitoring of biological productivity of sea 12 p2217 A70-26915

Ruby laser Q switching by chlorophyll thin film, discussing characteristics and mechanics 13 p2429 A70-29670

Cotton plant leaves from high saline soil area, observing chlorophyll content on color photographs 14 p2576 A70-30977

Manganese deficiency effect on chlorophyll fluorescence in algae adapted to hydrogen, determining electron transport mechanism 16 p2848 A70-33291

Visible and near IR radiation reflectance from vegetation, discussing incident solar radiation plant structures, leaf areas shadows and absorption by chlorophylls 22 p4014 A70-42767

CHLOROPLASTS

Electron paramagnetic property in chlorophyll molecules of spinach subchloroplast determined using pulsed ruby laser 03 p0421 A70-13551

UV radiation effects on pea plant chloroplasts photosynthesis at high altitudes, noting disruption of electron-transport chain reactions and cyclic phosphorylation 08 p1445 A70-21216

Streptomycin effects on *euglena gracilis* chloroplasts, comparing effects on chloroplastic ribosomal system to cytoplasmic ribosomal system 09 p1616 A70-22302

Hill reaction color sensitivity in red and blue light during chloroplast disintegration, considering oxygen evolution capacity 15 p2684 A70-32548

CHLOROPRENE RESINS

Radio Influence Voltage (RIV) nondestructive test method for detecting voids in neoprene-steel structures or other elastomers bonded to metal 13 p2420 A70-29245

CHOICE

U SELECTION

CHOLESTEROL

NN dimethylguanidine for prevention of arterial lesions induced by cholesterol in rabbits 01 p0020 A70-10707

Electric field effects on dielectric properties and molecular arrangements of cholesteric liquid crystals with temperature dependent helical pitch 01 p0160 A70-11352

Hypercholesterolemia chemotherapy experimental results with five hypocholesterolemic drugs /nicotinic acid, triparanol, aluminum nicotinate, Atromid and nonfeminizing estrogen/ 03 p0426 A70-13937

Statistical data to demonstrate atherosclerotic diseases affected by cholesterol and saturated fatty acids in foods 03 p0430 A70-14277

Plasma lipids and lipoprotein changes following myocardial infarction, discussing rise and normal return times of free fatty acids, cholesterol and beta lipoproteins 04 p0636 A70-15464

Helical twisting power of steroidal solutes in cholesteric mesophases, discussing nematic temperature shift dependence on ester chain 08 p1455 A70-21524

Room temperature cholesteric liquid crystals retention of information on past electric field excitation by changes in optical transmission properties 09 p1740 A70-22924

Calibration of shear sensitive cholesteric liquid crystals film, measuring shearing forces and scattering light intensity 09 p1656 A70-22992

Liquid crystal of cholesteryl chloride and myristate measured for complex dielectric constant, noting role of molecular rotation modes in dipole relaxation 12 p2180 A70-26859

Coronary heart disease prediction based on clinical suspicion, age, total cholesterol and triglyceride, using relationships established by cinearteriographic studies 23 p4145 A70-43947

Cinecoronary arteriographic investigation of chest pain patients, establishing correlations of clinical symptoms, coronary artery narrowing, arterial lesions, serum cholesterol levels, etc 23 p4145 A70-43948

CHOLINE

Acetylcholine concentration, esterase activity and synthesis in cerebral tissue of rats under repeated mechanical vibrations combined with noise 06 p0993 A70-17425

Sleep-wakefulness cycle regulation role of serotonin, noradrenalin and acetylcholine in CNS of animals 15 p2680 A70-31745

Ganglione and quaterone cholinolytic agents effects on arterial blood acid-base balance indicators in cats 24 p4298 A70-45633

CHOLINERGICS

Cholinergic muscarine-mechanism participation in radioprotective effect after cholinomimetics administration, reducing protective reactions against tissue irradiation and increasing mice survival rate 09 p1624 A70-22820

Cholinergic nervous mechanism of autoregulatory dilatation of pial arteries under decreased blood supply to cerebral cortex in rabbits 09 p1622 A70-23583

CHOLINESTERASE

Acetylcholine concentration, esterase activity and synthesis in cerebral tissue of rats under repeated mechanical vibrations combined with noise 06 p0993 A70-17425

CHONDRITES

NT CARBONACEOUS METEORITES

NT ORGUEIL METEORITE

Chondrite-normalized lanthanide pattern of silicate inclusion of Woodbine iron meteorite, showing differences from mesosiderite phase and chondrite 01 p0177 A70-10340

Nitrogen abundances measured in enstatite chondrites by inert carrier gas fusion extraction technique, noting agglomeration of chondrules

01 p0179 A70-10475

Gray hypersthene Ramsdorf chondrite with thermal and mechanical alterations, discussing shock heating, metal plus troilite melt redistribution, collision and rapid cooling effects

03 p0563 A70-13147

Temperature dependence of sputtering coefficient of quartz and chondrites at 2000 K and mass decrease prior to evaporation

03 p0569 A70-13357

Age and initial strontium for Guarena chondrite, determining differential evolution of Rb/Sr systems involving simple metamorphism of closed systems or multistage processes

03 p0576 A70-14088

Bronzite, hypersthene and amphoteric chondrites examined by X ray diffraction for inert gas retention ages relationship to shock and reheating

05 p0912 A70-16448

X ray diffraction analysis for composition and structure of meteorites found in Kansas, classifying as hypersthene and bronzite chondrites

05 p0912 A70-16466

I-Xe dating of Abee enstatite chondrite by combined neutron activation and mass spectrometric analysis

05 p0915 A70-16829

Pueblo de Allemande chondrite unextractable carbon content using meteorite pyrolysis, obtaining aromatic hydrocarbons

07 p1380 A70-19204

Bismuth concentrations in various carbonaceous and equilibrated chondrites determination by neutron activation technique

07 p1388 A70-20036

Ti demonstrated as predominantly chalcophilic in highly reduced enstatite chondrites and achondrites

07 p1391 A70-20352

Shock wave compression of single olivine crystals and specimens from chondritic meteorites, observing planar deformation microstructures

07 p1391 A70-20353

Uranium abundance in hypersthene chondrites determined by homogenized fission track analysis, comparing age estimation with iron meteorite event occurrence

07 p1391 A70-20354

Micrococcus radiodurans and *Sarcina flava* radiation resistance from proton irradiation tests in carbonaceous chondrite Migé

08 p1441 A70-20550

Rare gases abundance patterns on earth and in chondrites, proposing chemical adsorption mechanism at planetesimal stage during accretion

09 p1764 A70-23610

Enstatite chondrites and achondrites electron microprobe analysis for Si, P and Ni in metal grains and associated schreibersite and perrite

10 p1935 A70-23849

Ureilite structures and relationship to carbonaceous chondrites, considering chemical composition, diamond content, age, size, etc

10 p1941 A70-24552

Chondrites elements fractionation in solar nebula starting from carbonaceous material

10 p1949 A70-25329

Temperature dependence of sputtering coefficient of quartz and chondrites at 2000 K and mass decrease prior to evaporation

11 p2118 A70-26722

Microchondrules from chondritic meteorites, investigating morphology, composition and structure

13 p2487 A70-28696

Holbrook chondrite specimen, discussing effects of weathering, leaching and trace elements enrichment over period of time before recovery

13 p2487 A70-28698

Enstatite chondrites K, Rb and Sr concentrations, measuring ages from Sr87/Sr86 ratios

16 p2974 A70-33649

Chondritic and achondritic meteorites Zr and Hf abundances, distributions and ratios, using thermal and neutron activation analyses

18 p3310 A70-35968

Kingfisher meteorite metal particles microstructures, discussing phase transformation during reheating by shock

18 p3310 A70-35970

Meteorite I-Xe 129, demonstrating cold assembly of unequilibrated chondrite

19 p3519 A70-38036

Chondrites and terrestrial rocks trace elements by neutron activation analysis, discussing radiochemical separation and computer analysis of gamma ray spectra

20 p3582 A70-38980

Allende meteorite age determination, probing K, U and rare gases in whole rock and chondrule samples

21 p3920 A70-41939

Chondrites Ti content by neutron activation analysis

21 p3921 A70-41941

Chondritic meteorites electron and nuclear magnetic resonance spectra at various frequencies

23 p4239 A70-43897

Terrestrial and chondritic vanadium isotopic ratios indicating irradiation histories difference

24 p4402 A70-45381

V and Cu emission spectrographic analyses in chondrite types, noting distribution patterns between groups based on meteorite chemical fractionation mechanisms

24 p4411 A70-45789

Murchison and Lost City chondrites element abundance analysis by thermal neutron activation and wet chemical techniques, noting low oxygen content

24 p4411 A70-45790

Borgo San Donino chondrite petrology and mineralogical and chemical composition, considering texture and recrystallization features

24 p4411 A70-45791

Chemical composition and degree of thermodynamic equilibrium reflected in ferromagnesian silicates of chondrites

24 p4411 A70-45793

CHONDRULE

Carbonaceous material genesis in Tieschitz meteorite from electron microprobe analysis, discussing chondrule formation process residue likelihood

08 p1578 A70-21561

Microchondrules from chondritic meteorites, investigating morphology, composition and structure

13 p2487 A70-28696

Allende meteorite age determination, probing K, U and rare gases in whole rock and chondrule samples

21 p3920 A70-41939

CHOPPERS [ELECTRIC]

U ELECTRIC CHOPPERS

CHOROID MEMBRANES

Ox, calf, pig, rabbit, guinea pig and human eye measurements, determining wet and dry weight of iris, ciliary body and choroid

24 p4305 A70-46346

CHORUS [DAWN PHENOMENON]

U DAWN CHORUS

CHORUS PHENOMENON

U DAWN CHORUS

CHROMATOGRAPHY

Gas-liquid chromatographic separation applied in derivatization chemistry of protein amino acids as N-trimethylsilyl (TMS) esters

09 p1629 A70-22337

Dispersion/peak broadening in gel chromatography measured with nonporous and porous column packings, suggesting diffusion controlled separation with linear permeation isotherm

12 p2181 A70-27474

Time resolving X ray grating polychromator, discussing photoelectric attachment with surface barrier semiconductor detectors

22 p4037 A70-43069

Gel permeation chromatography peak broadening, discussing liquid dispersion factors and column efficiency

24 p4310 A70-46349

CHROME

U CHROMIUM

CHROMITES

Oxide spinel formation kinetics and reaction mechanisms with emphasis on Ni and Co chromites, discussing cation diffusion

09 p1739 A70-22307

Nickel chromite structural changes, thermal conductivity and dilatation during tetragonal-cubic transition, noting phonon-lattice effect

13 p2437 A70-28855

Chromite, zircon and quartz crystals in Muong Nong type tektites by X ray diffraction, discussing possible impact origin

20 p3709 A70-40088

Titanian and aluminian chromites and chromian ulvospinel in Apollo 11 fines, microbreccias and basaltic type igneous rocks

21 p3895 A70-41505

CHROMIUM

NT CHROMIUM ISOTOPES

Thermal diffusivity coefficient and conductivity of Cr at high temperatures determined by plane temperature wave method

01 p0117 A70-10190

Excitation, reemission and absorption spectra of Cr activated powdery Mg titanate prepared, using MgO and Ti dioxide with LiCl as flux

02 p0350 A70-11848

Cr diffusion coating influence on fatigue life of Fe and steel, discussing residual stress measurement technique

02 p0320 A70-12848

Serrated plastic flow in stable austenitic stainless steels based on Fe/Ni, showing strength dependence on C and/or Cr presence

03 p0506 A70-13134

Nonuniformity of dislocation structure and stress distribution in deformation of Cr samples longitudinal sections subjected to upsetting

03 p0511 A70-13488

V and Cr single crystals microhardness anisotropy and causes, noting similarity with W, Nb and silicon ferrite

06 p1088 A70-17613

Chromized molybdenum thermal stability under cyclic induction heating and subsequent air cooling

07 p1304 A70-18743

Chromium films obtained on tungsten by sputtering, studying structure and work function at various temperatures

08 p1516 A70-21123

Transition kinetics during linear to parabolic oxidation of Cr in water-hydrogen gas mixture measured thermogravimetrically

08 p1521 A70-21558

Chromium structural dislocation and cell formation during deformation as function of temperature, impurities and strain rate

10 p1902 A70-23861

Cellular structure and grain size effects on mechanical properties of strained and recrystallized chromium

10 p1902 A70-23862

Diamond burnishing effects on wear and contact endurance of chromium coatings, investigating surface hardening and residual stresses

13 p2419 A70-28868

Diffusion layer microprobe analysis during chromaluminization of Inconel turbine blade

14 p2595 A70-30293

Chromium lattice vibrational properties based on fourth-nearest-neighbor tensor force model, obtaining agreement with inelastic neutron diffraction data and elastic constants

14 p2626 A70-30480

Hydrostatic pressurization effect on ductile-brittle transition temperature of polycrystalline chromium

18 p3274 A70-36053

Fe and Al impurities in bis-ethylene chromium (BEC)/Cr and in chromium films obtained by thermally induced decomposition of metal organic compound

18 p3297 A70-36463

Valent state of chromium doped barium titanate from EPR spectra and magnetic susceptibility measurements

22 p4086 A70-43133

Longitudinal phenomena and two phase structures effect on ductility of low carbon steel-chromium subjected to high temperature torsion

24 p4361 A70-46173

Chromium ions isothermal annealing kinetics in X ray irradiated ruby crystals, using EPR method

24 p4382 A70-46253

CHROMIUM ALLOYS

NT CHROMIUM STEELS

NT RENE 41

Silicide, aluminide and boride coatings transition temperature holdability, considering nitridation/oxidation protection for Cr alloys

01 p0122 A70-11241

Semicoherent interface dislocations in directionally solidified Ni-Al-Cr eutectic, discussing lattice mismatch

01 p0123 A70-11247

Long range order formation in Ni-Cr alloys analyzed by direct neutron diffraction, considering disorder-order transition temperature and chemical composition

01 p0124 A70-11600

Vacuum deposition of Cr-Al film on Ni-Mo alloys, describing operating pressure, temperature and film thickness

01 p0124 A70-11617

Chromium refractory alloys, discussing production difficulties, mechanical properties, engineering applications, etc

02 p0320 A70-12760

Mechanical properties of ordered Ni-Cr alloys, establishing hardening effect of annealing

03 p0505 A70-13105

Solid thoria yttria electrolyte applications in EMF measurements for Cr thermodynamic properties in Fe-Cr and Ni-Cr alloys

03 p0483 A70-13140

Cr alloys applications in high temperature environments, describing alloying elements effects on strength and ductility

03 p0511 A70-13566

Ni-Cr alloy oxidation resistance dependence on small amount of Al at high temperatures, noting role of protective oxide layer

03 p0514 A70-14315

Chromoaluminizing process protecting alloys for gas turbines against oxidation at high temperatures by diffusion mechanism

04 p0711 A70-15683

Ni-Cr alloys oxidation dependence on temperature and Cr concentration

06 p1087 A70-17609

Ni-Cr alloys effects of grain size and surface deformation on oxidation properties at high temperature

06 p1088 A70-17610

Aluminosilicate coatings for increased Ni-Cr alloys heat resistance due to silicon properties

06 p1089 A70-17743

Quadratic precipitate transformation into orthorhombic phase with conservation of maximal atomic density planes in Ni-Cr-Nb and Ni-Cr-Ta alloys during prolonged reheating
08 p1518 A70-21240

Matrix stiffened nickel-chromium welding products featuring high tensile strength at room and elevated temperatures and high impact strength at cryogenic temperatures
08 p1508 A70-21488

Ni-Cr superalloys hot corrosion, studying sulfidation-oxidation in various synthetic controlled gas mixtures
09 p1706 A70-22944

Order-disorder transition temperatures for Ni-Cr alloys determined by neutron diffraction, discussing homogeneous ordering of atoms
09 p1707 A70-23196

Phase diagram of Ti-Ta-Cr system, plotting isothermal and polythermal sections by microstructural and X ray analysis
09 p1709 A70-23787

Ni-Cr alloys hardened by complex alloying with Ti-Al or Ti-Zr-C additions, improving strength at elevated temperatures in oxidizing atmosphere
10 p1904 A70-24836

Binary Ni-Cr alloys tensile mechanical properties at 25 C after water quenching and heat treatments
10 p1905 A70-25172

Resistivity anomalies of nickel-chromium alloy with Al additions subjected to deformation and heating, studying K-state
12 p2254 A70-27496

Dispersion strengthened Ni-Cr alloys elastic and plastic properties at room temperature, studying preferred crystallographic orientation effect
12 p2255 A70-27609

X ray K spectra of Ti-Cr alloy for electron structure in titanium chromide phase region, discussing spectral intensities
13 p2435 A70-29375

Cellular precipitation in lamellar eutectic and cast Ni-Cr alloys
15 p2761 A70-32383

Beta-Ti and Ti-Cr single crystals elastic moduli, determining A ratio temperature dependence
17 p3115 A70-34380

Physical properties and structure of Cr-Ni austenitic stainless steels with high Mn and N content as function of temperature
17 p3125 A70-35143

Binary Co-Cr alloy open circuit potential and microstructure, examining effects of composition, heat treatment, allotropic transformation and precipitation
18 p3271 A70-35966

Microstructural changes of Ni-Cr lamellar eutectic alloy during creep deformation at 625 and 760 C
18 p3272 A70-36034

Cr-Ni system activities and phase boundaries determined by solid electrolyte technique
18 p3273 A70-36040

Sulfidation kinetics and scale morphology of Cr and Cr-Mo alloys at high temperatures in hydrogen/hydrogen sulfide atmosphere
19 p3452 A70-37827

Isothermal section at 1150 C of V-Zr-Cr cast and annealed alloys investigated by X ray and metallographic analyses, establishing various phase regions
19 p3453 A70-38711

Dispersion strengthened Ni-Cr alloys creep properties, investigating temperature, applied stress and thorium dioxide particles effects
20 p3644 A70-38984

Unidirectionally solidified carbide reinforced Co-Cr eutectic alloy, examining tensile strength and creep behavior
24 p4358 A70-45236

Eutectic NiAl-Cr alloys, investigating quaternary additions effect on rod-plate transition to faceted microstructure
24 p4359 A70-45244

Prestraining effect on cellular precipitation in Ni-Cr lamellar eutectic during creep testing
24 p4359 A70-45247

Phase regions and lattice parameters of isothermal section of Mo-Zr-Cr system at 1100 C from microstructural and X ray analyses
24 p4361 A70-45832

High purity Cr-Ni heat resisting steels, investigating phase transformations with microhardness measurements magnetic analysis, X ray diffraction and microstructure examination
24 p4362 A70-46181

Fe-Cr and Fe-Cr-V system miscibility gap, using differential thermal analysis and Mossbauer effect measurements
24 p4362 A70-46190

Fe-Cr alloy powders obtained with thermodynamic saturation from point sources, determining optimal mixture compositions and parameters
24 p4350 A70-46338

CHROMIUM CARBIDES
Quantitative separation of metastable and cubic chromium carbides in alloyed Cr steels utilizing hydrogen peroxide
03 p0504 A70-12981

Boron effects in austenitic stainless steels, considering chromium carbide formation, high temperature strength, ductility, etc
16 p2916 A70-33079

Dissociation energy of vanadium and chromium dicarbide and vanadium tetracarbide, using Knudsen effusion mass spectrometric method
16 p2857 A70-33654

CHROMIUM COMPOUNDS
NT CHROMITES
NT CHROMIUM CARBIDES
NT CHROMIUM OXIDES

CHROMIUM ISOTOPES
Cr 51 osteotropic properties for osseous system studies, discussing binding to bones, experiments on rats and rabbits, applications for human osseous system diagnosis, etc
01 p0029 A70-11403

CHROMIUM OXIDES
NT CHROMITES
Phase diagram of dysprosium oxide-chromium oxide system constructed by microstructural analysis in 1600-2400 C range in argon atmosphere
08 p1556 A70-21118

Stannic oxide-chromium oxide catalyst effects on thermal decomposition and ignition of ammonium perchlorate /AP/, calculating activation energy
11 p2100 A70-26281

CHROMIUM STEELS
Chromium-nickel steel fatigue strength under repeated thermal cycles, showing dependence on long term fatigue buildup and single cycle fatigue damage effects
02 p0383 A70-11653

Quantitative separation of metastable and cubic chromium carbides in alloyed Cr steels utilizing hydrogen peroxide
03 p0504 A70-12981

Intergranular corrosion mechanisms in ferritic stainless steels observed by electronmicroscopic examination on Cr Fe-base alloys vacuum-melt with C and N
03 p0506 A70-13131

Austenitic fcc Cr-Mn-N stainless steels ductile-to-brittle transition behavior noting role of deformation faulting
03 p0506 A70-13133

Microstructure and impact strength of welds of Cr-Mn steel containing nitrogen, observing grain growth dependence on nitrogen content
03 p0509 A70-13277

Fe-Cr-Mn-Ni system studied to obtain high Mn austenite and establish boundaries in quaternary system
03 p0509 A70-13278

Carbaboride phase in Cr-Mn heat resistant steels at annealing temperatures, isolating gamma, chromium carboboride and niobium carbide phases
03 p0509 A70-13279

Initial oxide film on Cr-Ni steel at high temperatures observed by electron microscope, noting Ni role
04 p0708 A70-15311

Crack formation and propagation kinetics in flat and cylindrical Cr-Mo-V steels under tension compression loading cycles
06 p1162 A70-17393

Chromium stainless steels nitrided cases formation and phase composition, studying temperature effects
07 p1304 A70-18744

High chromium stainless steels nitriding and carburizing processes stabilized by nickel galvanic coating, enhancing nitrogen or carbon diffusion into steel
07 p1291 A70-18832

Reverse-bend and tension-tension fatigue properties of high strength Cr-Mn-N stainless steel sheet in notched and unnotched conditions
07 p1305 A70-18993

Cr-Mo steel strength and structural stability during tubular stress-rupture testing with high pressure hydrogen, discussing welding effect on strengths
08 p1519 A70-21455

Structural stability of friction welded joint between high temperature low alloy weld metal from CrMoV electrode and high temperature Cr steel
12 p2244 A70-28349

Structure and chemical composition of high Cr diffusion coating on Cr-Ni austenitic steels
15 p2756 A70-31634

Corrosion and mechanical properties of Cr-Ni-Mn-N austenitic stainless steels
17 p3125 A70-35144

Chromium-nickel steel fatigue strength under repeated thermal cycles, showing dependence on long term fatigue buildup and single cycle fatigue damage effects
19 p3547 A70-38426

Crack propagation resistance-cyclic fracture strength relation for Mn-Cr-V steels, considering thermomechanical working effects
23 p4204 A70-43935

CHROMOSPHERE

CHROMOSOMES
Local gamma irradiation effect on number of chromosome aberrations in lymphocytes of human blood of oncological patients after hysterectomy
01 p0013 A70-10137

Corneal epithelium chromosome rearrangements in gamma irradiated white adult mice, noting radiation dosage and duration
03 p0426 A70-13903

Differential melting for partial purification of chemically distinct region of chromosome mycoplasma sp. /KId/
04 p0647 A70-15448

Whole body microwave irradiation effect on chromosomes and protein synthesis in Chinese hamsters
06 p0998 A70-17203

Hepatic polysome profiles and tyrosine transaminase activity daily rhythms in rats, studying dietary protein role
06 p0997 A70-18402

Soviet book on radiation genetics problems covering radiation damage of chromosomes, sexual and somatic cells, postirradiation cell recovery, etc
08 p1445 A70-20761

Chronic gamma irradiation effects on bone marrow mitotic activity and chromosome aberrations in dogs
09 p1614 A70-22083

Chromosome of temperature-sensitive mutant of bacillus subtilis 168, observing multiforked replication at normal temperature and transfer of DNA
09 p1615 A70-22206

Thymidine tracer distribution in bone marrow chromosomes of rats and mice treated with radioprotectors, noting cell metabolic activity reduction by sulfhydryl-type radioprotectors
09 p1619 A70-22818

Spaceflight effects on dry crepis capillaris seeds in five day orbit, showing chromosome rearrangements and increased mutagenic sensitivity
10 p1811 A70-24323

Computer program for flying spot scanner pattern recognition, analyzing human chromosome contour
12 p2170 A70-27938

Chronic gamma irradiation effects on bone marrow mitotic activity and chromosome aberrations in dogs
15 p2685 A70-32679

Radiation dose estimates by biological and physical methods after radiation accident, discussing chromosome aberration counting
17 p3034 A70-35761

CHROMOSPHERE
Coronal gas pressure boundary conditions on model upper chromosphere, determining temperature and hydrogen density assuming hydrostatic equilibrium
01 p0175 A70-10243

Chromospheric slitless spectrograms at 1962 eclipse, discussing Balmer-Paschen line intensities, continuum data, reduction and source error
01 p0175 A70-10244

Slitless spectrograms of chromosphere obtained during 1962 eclipse to determine H level populations decrements, self absorption in Balmer lines and chromosphere model
01 p0175 A70-10245

Chromospheric structural parameters determined from XUV spectroheliograms, discussing He 2 emission, O 4 and O 5 emission distribution, etc
01 p0175 A70-10246

Chromospheric average velocity field near sunspots determined from M alpha line absorption elements wavelength shifts
01 p0176 A70-10247

Chromospheric flares, loop prominences and filament activation and dissipation attributed to decelerated annihilation of prominence field in upper active region
03 p0557 A70-13218

UV Ceti type flare stars observational and theoretical results related to nebular or chromospheric flare models
03 p0566 A70-13316

One dimensional magnetograph scans studying photospheric velocity oscillations and supergranulation, noting downward flows coincident with chromospheric network
03 p0570 A70-13593

Chromospheric fine structure photographed at H alpha line center, discussing size, lifetimes and relationship between dark and bright mottles
05 p0910 A70-16428

High resolution observations of low chromosphere beyond limb at H-alpha line center revealing fine structures, identifying chromospheric spicules with dark mottles
05 p0910 A70-16429

K line profiles of Ca II for two component chromosphere, obtaining line source function and optical depth from steady state and radiative transfer equations
05 p0911 A70-16430

Monte Carlo radiative transfer techniques applied to develop height dependent spicule model, computing

contrast curves of model against chromospheric background

05 p0911 A70-16431

Flare radiation influence on high photospheric and low chromospheric lines in H alpha, H and K regions

05 p0902 A70-16439

MHD equations including energy dissipation terms applied to irreversible processes occurring in fast hydromagnetic shock waves in solar chromosphere

06 p1143 A70-17999

Strong explosion model for analyzing shock wave propagation after chromospheric flare allowing for quasi-radial motion of unperturbed solar wind

07 p1367 A70-19489

Radiative relaxations of chromospheric oscillations generated by granule, assuming isothermal atmosphere and linearizing equations of motion

08 p1576 A70-21395

Chromospheric flares, loop prominences and filament activation and dissipation attributed to decelerated annihilation of prominence field in upper active region

08 p1562 A70-21651

Solar chromosphere-corona transition region properties, discussing temperature increase within very thin layer and inferring temperature-density structure from emission line intensities

09 p1752 A70-22246

Small scale motions in solar photosphere and chromosphere using solar spectrograms

09 p1757 A70-22729

Solar chromosphere dark and bright mottles mean lifetime from photographs, identifying with spicules

09 p1757 A70-22733

Supergranules /convective cells/ development shown in quiet sun filtergrams of H alpha chromospheric network taken above Arctic Circle

11 p2109 A70-25741

Calcium H and K lines core residual intensities in stars with quiet and active chromosphere, suggesting activity due to thermal gradient

12 p2303 A70-27702

Solar IR triplet of singly ionized Ca, suggesting limb darkening caused by chromospheric inhomogeneities for source function inequality

12 p2303 A70-27703

Solar active regions in chromosphere and corona observed by EUV spectrophotometer aboard OSO-4 spacecraft, discussing ion formation and temperatures

12 p2303 A70-27705

Dark band in H alpha solar chromosphere above photospheric limb, outlining approaches to obtain spectrally pure observational results

13 p2486 A70-28627

Radiative energy transport effect on temperature distribution in conduction heated plane layer applied to solar chromosphere

13 p2488 A70-28716

Solar cosmic rays interaction with interplanetary shock waves, discussing chromospheric eruptions

13 p2476 A70-28959

Chromospheric flares electron concentration and structure from half widths and Balmer lines numbers

13 p2493 A70-29394

Solar chromospheric fine structure from high resolution photographs

13 p2497 A70-29849

Strong explosion model for analyzing shock wave propagation after chromospheric flare allowing for quasi-radial motion of unperturbed solar wind

15 p2795 A70-32734

Coronal structures relationship to chromospheric features in H alpha and Ca II K

16 p2977 A70-33843

Radio observations of chromospheric brightness temperature distribution during solar eclipse of March 1970

16 p2977 A70-33846

Hyades stars between F4 and K5, measuring chromospheric H and K emission lines dependence on bolometric luminosity

17 p3157 A70-34832

Red giant star chromospheric activity, discussing Balmer absorption lines and emission lines

17 p3161 A70-34889

Solar chromosphere resonance lines, observing H and K line profiles of Mg ions

17 p3161 A70-34893

Solar chromosphere model evaluation using sensitivity of flux emission in Lyman continuum

17 p3170 A70-35386

Chromospheric spicules fine structure recorded on H alpha spectrograms and filtergrams from high altitude coronagraph

17 p3174 A70-35863

Chromospheric photoelectric magnetograms with high resolution H alpha pictures for deriving magnetic field directly from filtergrams

17 p3096 A70-35864

Solar atmosphere shock waves frequency and strength, computing radiative energy losses of chromospheric models

17 p3174 A70-35865

Periodic cosmic ray variations near Southern magnetic pole related to chromospheric flares

18 p3307 A70-36102

Ba II emission lines in solar chromosphere, examining excitation and ionization equilibrium and resonance line intensities by eclipse observations

18 p3317 A70-37010

Solar chromospheric Fe abundance, considering f-value effects

19 p3524 A70-38697

Solar eclipse measurements in 1-30 mm range, examining chromosphere, flares and radio emission

19 p3531 A70-38911

Particle ejections in solar atmosphere and chromosphere structure, discussing dark halo exhibited by H alpha line in active region

20 p3699 A70-39464

H alpha chromospheric network lifetime from time lapse photographs

20 p3711 A70-40409

Ratio between mechanical energy flux in nonmagnetic region and magnetic region associated with solar chromospheric mottles

20 p3712 A70-40414

Chromosphere-corona transition region - Conference, Boulder, Colorado, August 1969

21 p3924 A70-42182

Transition region structure between chromosphere and corona, discussing temperature, theoretical models, energy balance and magnetic fields from far UV data

21 p3924 A70-42183

Chromosphere-corona transition region model from limb-disk optically thin line intensities

21 p3924 A70-42184

Oso-4 far UV observations of solar chromosphere and corona active regions

21 p3925 A70-42187

Heating and extension of solar chromosphere and corona via shock waves generated by piston below convection zone surface

21 p3925 A70-42189

Solar chromosphere spicules acceleration via supersonic jet formed by magnetic field under gravity and Melon seed effect

21 p3925 A70-42192

Solar chromosphere elements abundances methods, suggesting Fe differences origin in Fe I and Fe II inconsistencies

21 p3925 A70-42194

Vertical oscillations in solar temperature minimum suggested as acoustic-gravity waves modes dependent on height at chromosphere-corona interface

21 p3926 A70-42196

Transition zone height in corona-chromosphere interface from high resolution disk spectra near limb

21 p3926 A70-42198

Lower chromosphere shock wave heating, analyzing density scale height effects

22 p4105 A70-43001

Spectroscopic differential photosphere and chromosphere rotation with height in solar envelope

23 p4252 A70-44831

Solar chromosphere model convective instability, considering temperature and magnetic field effects

24 p4399 A70-45303

Chromospheric heating in magnetic field above supergranular cell boundaries, using geometric optics method for energy transport by hydromagnetic shock waves

24 p4400 A70-45304

IR observation of chromospheric Ca II K-line during total eclipse of 7 March 1970

24 p4401 A70-45314

CHRONIC CONDITIONS

Glucose metabolism in chickens under chronic centrifugal acceleration, meeting increased energy requirements

23 p4147 A70-44786

CHRONOGRAPHS

U CHRONOMETERS

CHRONOLOGY

Coronary thromboses age estimation based on comparison of blood cells, fibrin, collagenous tissue and neocapillaries quantitative changes

03 p0426 A70-13938

Bronzite, hypersthene and amphibole chondrites examined by X ray diffraction for inert gas retention ages relationship to shock and reheating

05 p0912 A70-16448

Moon rocks nature and mineralogical constitution, describing methods for age determination

14 p2634 A70-30275

Lunar maria absolute age from lunar craters rim height changes via isostatic settling and small craters quantity

14 p2649 A70-31213

CHRONOMETERS

Analog and digital electronically counting chronometers for extremely short times measurements

02 p0295 A70-11868

Multichronometer for multiple time intervals measurement with picosecond resolution, using mixed analog and digital methods

[SMPT PREPRINT 112] 22 p4031 A70-43029

CHRONOPHOTOGRAPHY

Time lapse photographic recording and scoring in-flight performance of helicopter aviator trainees during hypothetical tactical instrument mission

09 p1624 A70-22900

SFR high speed photochronograph for visible and UV raster, stereoscopic and spectral photography

24 p4335 A70-45652

CHRONOTRONS

U PULSE RATE

U TIME LAG

CHUGGING

U COMBUSTION STABILITY

CHUTES

Concorde aircraft design for emergency passenger evacuation, emphasizing overwing inflatable escape slides and kinetic heating effects

15 p2675 A70-32222

CINEFLUOROGRAPHY

U MOTION PICTURES

U RADIOGRAPHY

CINEMATOGRAPHY

Optimum procedure for high speed cinematography of holographic interferograms permitting microsecond exposures while retaining picture quality

02 p0298 A70-12213

Cine recording ophthalmoscope with TV monitoring for retinal photography during centrifugation

06 p1061 A70-17286

Polarization-optical kinematographic method for study of mechanical stresses during dynamic loading

09 p1680 A70-23174

Rapid exposure scanning camera for high speed cinematography, discussing optical system and operation principles

20 p3632 A70-39748

High speed cinematographic recording of wake behind hypervelocity projectiles

[SMPT PREPRINT 102] 22 p4032 A70-43033

Phase locked solid state laser with picosecond pulses applied to high speed cinematography

[SMPT PREPRINT 22] 22 p4034 A70-43051

Cantilever beam transient response measurement by stored beam /real time/ holographic interferometry combined with high speed motion picture photography

22 p4039 A70-43452

CINERADIOGRAPHY

U MOTION PICTURES

U RADIOGRAPHY

CINETHEODOLITES

Real time opto-triangulation by cinetheodolites for data acquisition used in rocket impact prediction

09 p1640 A70-23779

CIRCADIAN RHYTHMS

Photoperiod variation effects on ambulatory primate Cebus albifrons deep body temperature /DBT/, locomotor activity /LMA/ phase relationships and DBT waveform

01 p0011 A70-10035

Male rats locomotor activity responses to altered photoperiods during exposure to varied-light artificial days

01 p0015 A70-10367

Light synchronization of deep body temperature rhythms in Macaca nemestrina, investigating efficiency

03 p0416 A70-13013

Diurnal rhythms of physiological functions and human adaptation to shifted sleep-wakefulness schedule on healthy pilots subjected to solitary confinement

03 p0423 A70-13711

Diurnal periodicity of physiological functions of flight crews flying through several time zones found to correspond to time zone of permanent residence

03 p0425 A70-13894

Circadian rhythms characteristics in humans, animals and plants, noting possible effects of rhythm disturbances on astronauts

04 p0629 A70-14567

Biological rhythm perturbations effect on astronauts, emphasizing waking-sleeping rhythm during space flights

04 p0630 A70-14610

Temperature variations in organs of man and animals performing physical work as physiological base of metabolic processes and for daily activity timetable development

04 p0638 A70-15502

Wake-sleep rhythm of spacecrews for operational capacity to maintain constant watch of spacecraft, suggesting recreation of terrestrial time cycle in space

05 p0799 A70-15766

Hepatic polysome profiles and tyrosine transaminase activity daily rhythms in rats, studying dietary protein role

06 p0997 A70-18402

Circadian rhythm of pilot efficiency and multiple time zone travel effects

[DFVLR-SONDR-29] 08 p1453 A70-21935

Dietary intake and adrenal cortex effects on diurnal rhythm of hepatic tyrosine transaminase activity and adrenal corticosterone content in rats

Diurnal rhythms of physiological functions and human adaptation to shifted sleep-wakefulness schedule on healthy pilots subjected to solitary confinement

Drosophila brain Circadian oscillation as gating device restricting emergence behavior of adult

Daily electrolyte excretion dynamics of subjects with shifted work-rest schedule, noting disagreement with Sharp results

Rats under constant environmental conditions exhibiting circadian rhythmicity in rate of bar pressing with hypothalamic and septal reinforcing brain electrical stimulation

Circadian variation of pituitary-adrenal steroid levels, noting light role

Circadian rhythmic changes in biological organisms by earth rotation, emphasizing diurnal variations role in sleep-wakefulness rhythm

Airline pilots sleep patterns during worldwide east-west routes, considering modification by irregular duty periods and time zone adaptation

Daily rhythm in accumulation of rat brain catecholamines synthesized from circulating tritiated tyrosine

Human circadian coronary circulatory rhythms during space flight weightlessness or bedrest with and without exercise

Carbon dioxide output monitoring from biosatellites for circadian system behavior in closed organism-environment systems

Circadian oscillations and photoperiodic time measurement in *Pectinophora gossypiella*

Circadian and seasonal adaptive function rhythms in animals, discussing terrestrial environment and thermoregulation

Circadian rhythms in single cell animals, examining cell division, temperature and light effects

Tyrosine content and utilization in mouse liver, showing daily rhythm in composite metabolism rate

Human sleep pattern changes due to acute sleep-waking cycle reversal

Circadian rhythms from electrocardiogram and cardiachogram of patient with human heart transplant, noting P waves relationship between donor and recipient tissues

Circadian rhythm in human body temperature by Cosinor method, showing inapplicability for narrow time span

CIRCLES (GEOMETRY)

NT GREAT CIRCLES
Green function of region near circle approximation by matrix method, considering Laplace differential equation solution, conjugate harmonic function and conformal transformation

Autocollimation technique for determining fluxure of tube of Wanschaff vertical circle

Curve arc approximation by circular arc using Chebyshev modulus-minimax principle

Angle of attack for nearly circular reentry motion, deriving expression for lateral rates frequencies

Stellar ring 373, comparing color-magnitude and color-color diagrams to adjacent star fields

CIRCUIT BOARDS

Printed circuit board connector selection techniques based on miniaturization reliability, cost and compatibility with intended application

Monolithic linear IC building blocks for radar systems circuit design

Printed circuit boards vibration control in dynamic environment, noting viscoelastic damping technique

CIRCUIT BREAKERS

Power reduction consumed in vacuum by direct-direct voltage converter by introducing delay into breaker transistor control at output stage

Fluidics for aircraft high pressure hydraulic systems, discussing circuit breaker, feel computer and landing gear sequencing circuit

CIRCUIT DIAGRAMS

Circuit parameter equations for effective circuit synthesis taking into account ratios between coefficients of polynomials in numerator and denominator

Inductive sensor design and circuitry for measuring rapidly rotating shaft bending deflections at various vibration frequencies

Equivalent transformations method for minimizing electronic equipment sensitivity to circuit components value variations during operation

Multipole coupling circuits for wideband radio amplifiers

Circuit allowing direct combining of power from several avalanche diodes, discussing CW power output, single and multiple diode oscillators, etc

Optimal directed circuit and cycle elimination in weighted diagrams by edge reversal orientation

Walsh functions electrical generation with small orthogonality error based on multiplication theory, presenting circuit diagram for 32 channel analyzer

Topology and component values in computerized design of distributed lumped active networks

Fiber optics in functional electronic circuits, considering multichannel optical communication

High speed PCM Codec with maximum 600 channel capacity applied to Time Division Multiple Access (TDMA) system for satellite communication

CIRCUIT PROTECTION

Broadband RF filter/attenuator plug to replace plastic type plugs for protecting wire bridge electroexplosive devices against RF energy

Electroexplosive devices protection from electrostatic discharge by creation of preferential discharge path, considering use of high intensity neon lamp

Philosophical, design, hardware or static sensitivity type myths refutation concerning electroexplosive devices

CIRCUIT RELIABILITY

IR microscope and digitally programmed mirror system for printed circuit inspection, allowing two dimensional scanning and magnetic tape reference

Commercial transport aircraft landing gear electrical circuitry dispatch reliability improvement, considering components causing flight delays due to maintenance problems

Open circuit development in microcircuits metallization and processing to eliminate nonuniformity, voids and microcracks

Digital network reliability with redundancy to mask logic modules failure for asymmetric failure modes

Multichannel spectrometer electronic circuitry for ionization colorimeter providing data on low energy particle interactions, emphasizing reliability and accuracy

Radio and automatic control electronic equipment reliability estimation by vibration testing, determining test stand simulation accuracy

Integrated circuit failure analysis with scanning electron microscopy taking into account ball bond contamination and open metallization at contact windows

Electronic circuits automated endurance tests by follow-up scanning method, describing error sources in proper operation region cross section determination

Solid state proximity switches, sensors, logic and self test circuits for aircraft electrical applications to improve reliability and maintainability over mechanical switches

Onboard computers automatic reliability control with implementation of self repair, modeling by Markov processes nonhomogeneous in time

SCAMP 3 program for calculation of electronic circuit DC performances statistical distribution as function of component parameters variation

Redundant amplifier /RAMP/ for reliability improvement

Circuit design characteristics and reliability relationship in electronic power supplies for performance requirements

Integrated circuits failures due to electromigration in thin films, discussing hole formation and circuit reliability prediction

High usage military system integrated circuit failure modes analysis for reliability improvement

Ripple filters for DC power supplies using reliable small capacitance capacitors suitable for spacecraft applications

Logic circuits reliability with series and parallel connected elements during random malfunctions, obtaining failure formulas for trigger

Microelectronics in space environment, discussing circuit reliability, radiation effects, etc

LSI circuits in space electronics, discussing packaging, reliability, applications, etc

Multichip hybrid microcircuits design and construction, emphasizing reliability and cost reduction

Contact-relay circuits failure free operation probability, taking into account coil winding breakage

Integrated microcircuits reliability prediction models based on failure mode and mechanism knowledge

Digital systems reliability improvement by redundancy at circuit and system levels

DC transistorized Nor logic gates design based on graphic analytic method permitting influence of circuit parameters variations for reliability improvement

Axial propellant density gradients and circuit capacitance correlated with pulsed coaxial plasma gun efficiency

One dimensional cellular logic arrays fault circumvention by bypass switching out defective cells in cascade

Algorithm for communication network synthesis from limited elements selection, considering fixed reliability requirements

RF power transistors failure analysis, describing IR radiometer technique

Integrated circuits failure analysis techniques, including electrical diagnostics, visual inspection, surface examination, shorts location, etc

Commercial satellite system circuit quality and reliability in digital communications, considering Automatic Digital Network Trans-Pac cable cut incident

Cumulative reference list of published books on microelectronics and reliability

Reliability characteristics of standby redundant electronic equipment with imperfect switching and sensing

CIRCUITS

NT ANALOG CIRCUITS

NT AUTODYNES

NT BISTABLE CIRCUITS

NT CIRCULATORS (PHASE SHIFT CIRCUITS)

NT CLIPPER CIRCUITS

NT COINCIDENCE CIRCUITS

NT COUNTING CIRCUITS

NT COUPLING CIRCUITS

NT DELAY CIRCUITS

NT DIGITAL INTEGRATORS

NT DISCRIMINATORS

NT ECHO SUPPRESSORS

NT ELECTRIC BRIDGES

NT EQUIVALENT CIRCUITS

NT FEEDBACK CIRCUITS

NT FIRE CONTROL CIRCUITS

NT FLIP-FLOPS

NT FLUID SWITCHING ELEMENTS

NT GATES (CIRCUITS)

NT INTEGRATED CIRCUITS

NT LC CIRCUITS

NT LIMITER CIRCUITS

NT LINEAR CIRCUITS

NT LOGIC CIRCUITS

NT MAGNETIC CIRCUITS

NT MATRICES (CIRCUITS)

NT MICROWAVE CIRCUITS

NT MIXING CIRCUITS

NT MONOSTABLE MULTIVIBRATORS

NT MULTIVIBRATORS

NT NEGATIVE RESISTANCE CIRCUITS

NT OHMS LAW

NT PHASE DETECTORS

- NT PHASE SHIFT CIRCUITS
 NT PNEUMATIC CIRCUITS
 NT POWER SUPPLY CIRCUITS
 NT PRINTED CIRCUITS
 NT RC CIRCUITS
 NT RLC CIRCUITS
 NT SCALERS
 NT SWEEP CIRCUITS
 NT SWITCHING CIRCUITS
 NT THRESHOLD GATES
 NT TRANSISTOR CIRCUITS
 NT TRANSMISSION CIRCUITS
 NT TRIGGER CIRCUITS
 NT VARACTOR DIODE CIRCUITS
 NT WHEATSTONE BRIDGES
- Resistance, capacitance and inductance in passive hydraulic circuits considered in analogy with electric circuits to determine dynamic characteristics
 03 p0415 A70-13931
- Electric current pulses peak values measurement during aperiodic capacitor discharges, describing circuit with Rogowski coil, diode, capacitor and VTM
 19 p3426 A70-37938
- Conjunctions and traditors circuit realizations, discussing resistive and dynamic nonlinear networks
 22 p3996 A70-42919
- Optimal load circuits number for maximum power extraction from Hall MHD generator with nonuniform gas flow along channel
 23 p4143 A70-44900
- CIRCULAR CONES**
- Elastic bending of thin circular conical shell subject to arbitrary variation of edge loads
 01 p0209 A70-11385
- Hypersonic flow characteristics on yawed circular cone surface at moderate angle of attack, applying results to inviscid and boundary layer flow computations
 03 p0406 A70-12944
- Pressure distribution at circular slender cone with 10 deg semiapex angle in hypersonic vacuum wind tunnel
 06 p0966 A70-17251
- Axial profile characteristics of hypersonic near wake of slender circular cone based on pitot pressure, static pressure and stagnation temperature measurements
 06 p0968 A70-17916
- Hypersonic aerodynamic measurements on cone, investigating effects of oscillatory mass addition on stability
 [AIAA PAPER 70-217] 06 p0974 A70-18171
- Inviscid hypersonic flow analysis for chemically relaxing air about wedges and pointed circular cones using Dorodnitsyn integral method
 [DGLR 69-037] 07 p1188 A70-18986
- Numerical solution for steady supersonic inviscid flow around smooth conical bodies by solving elliptic partial differential equations for conical flow
 12 p2155 A70-27202
- Supersonic and hypersonic motion past circular cone at angle of attack, analyzing for velocity and pressure distributions by linearizing conical motion equations
 12 p2158 A70-28213
- Vortex layer and entropy of supersonic gas flow past circular cones at incidence using surface velocity corrections
 12 p2159 A70-28230
- Equations of supersonic and hypersonic motion past circular cone by linearized method based on small perturbations with respect to nearly incompressible flow
 16 p2835 A70-33746
- Perfect gas three dimensional boundary layer separation on circular cone at incidence, comparing numerical calculation and experimental results
 23 p4133 A70-44207
- CIRCULAR CYLINDERS**
- Transversely isotropic circular cylinder acted upon by transient shearing force at one end, noting forced torsional oscillation using cylindrical coordinates
 01 p0200 A70-10550
- Turbulent heat transfer on heated horizontal circular cylinder rotating freely in space, discussing dimensionless numbers relations and frictional heating
 01 p0215 A70-10926
- MHD wave propagation in electrically conducting fluid contained in finite length circular cylinder subject to axial magnetic field and nonelectromagnetic forces
 01 p0152 A70-10944
- Transient temperature profiles and thermal stress distribution in circular plates and cylinders with eccentric hole determined by conformal mapping
 01 p0207 A70-11153
- Flexural wave propagation in infinitely long circular bimaterial cylinders based on equations of linear elasticity, noting dispersion characteristics different from homogeneous cylinders
 01 p0208 A70-11188
- Horizontal and vertical sound fields local effects on natural convection from heated horizontal circular cylinder, using shadowgraphy
 01 p0219 A70-11198
- Shock wave shapes in hypersonic flow past blunt conical nosed circular cylinders, using analogy with Savic perturbed hypersonic blast wave theory
 02 p0277 A70-11862
- Hypervelocity impact of small different diameter right circular cylinders, describing launching method using light gas gun
 03 p0583 A70-12918
- Gram-Charlier method generalization for curve fitting analytic forms to velocity covariances measured in turbulent wake of circular cylinder
 03 p0480 A70-12950
- Free stream turbulence effect on heat transfer in circular cylinder stagnation region
 03 p0469 A70-14216
- Magnetic boundary layer equations applied to flow past stationary circular cylinder and sphere, showing graphical variation of slip velocity with angle
 03 p0471 A70-14334
- Transverse magnetic fields effects on velocity perturbations and vortices behind circular cylinder in electrolyte flow at various Reynolds and Stewart numbers
 04 p0726 A70-14543
- Long thin cylindrical tube with circumferential restraint analyzed for thermal expansions, obtaining maximum strains, bending moments, shear forces and plastic zone extent
 [ASME PAPER 69-WA/NE-7] 04 p0768 A70-14756
- Stationary and vibrating circular cylinders for boundary layer separation point, determining vortex excited oscillation range
 04 p0670 A70-14988
- Circular cylinder drag in hypersonic transverse flows between continuum and free molecular flow, measuring drag and pressure distribution
 04 p0615 A70-15089
- Hydroelastic sloshing of liquid in partially filled circular cylinder with rigid or elastic walls, including surface tension effect
 04 p0671 A70-15092
- Thermal stresses in transversely isotropic hollow circular cylinder, applying formulas derived to reentry vehicles aerodynamic heating
 04 p0779 A70-15608
- Low Reynolds number flow of variable property gas past infinite heated circular cylinder at large temperature differences, measuring drag on cylinder
 05 p0789 A70-16014
- Perturbation effects on elastic material deformation due to nonorthogonality of curves defining curvilinear aeolotropy, with application to circular cylindrical tube
 05 p0929 A70-16065
- Thermoelastic stresses in rotating circular cylinder, analyzing temperature effect on angular velocity for neo-Hookean material using finite deformation theory
 05 p0930 A70-16080
- Adhesive rocking and parallel translation contact for circular cylindrical punch indenting elastic half space solved using simultaneous equations
 05 p0932 A70-16139
- Secondary vortex generation in near wake of circular cylinders under forced oscillation, analyzing motion dependent transition regimes using hydrogen bubbles flow visualization
 [AIAA PAPER 69-755] 06 p1032 A70-17212
- Mechanical behavior of cylinders with alternating layers of reinforcing and matrix materials derived from governing equations, including equations of motion
 [AIAA PAPER 70-134] 06 p1169 A70-18051
- Rotational and vibrational temperatures measured in hypersonic nonequilibrium rarefied gas flow field of cooled circular cylinder by electron beam technique
 06 p1123 A70-18304
- Circular cylinders drag and pressure distribution in hypersonic range between continuum and free molecular flow
 06 p0983 A70-18376
- Elastic behavior of joint formed by normally intersecting circular cylindrical shells under external bending moment, noting applicability to pipelines and pressure vessels
 [ASME PAPER 68-WA/PVP-1] 07 p1400 A70-18710
- Unsteady boundary layer flow with suction, deriving equations for circular cylinder impulsive motion
 07 p1253 A70-18862
- Plane acoustic wave steady state scattering at circular cylinder in semibounded region
 07 p1334 A70-19089
- Radial heat conduction in infinite hollow cylinder with circular cross section and periodic heat transfer coefficient at inner and outer cylinder surfaces
 07 p1423 A70-19816
- Laminar to turbulent boundary layer transition and separation on circular cylinder measured by heated end-window film sensor applicable to water flow
 07 p1259 A70-19831
- Circular cylindrical shells buckling under lateral and hydrostatic pressure using Donnell and Flugge equations, assuming membrane stress state for prebuckling deformation
 07 p1414 A70-20168
- Unsteady flow behind circular cylinder by flow visualization, determining vortices length variations with time at various Reynolds numbers and dimensionless accelerations
 07 p1261 A70-20236
- Transverse curvature effects on turbulent boundary layer thickness and velocity profiles on circular cylinders in water and air
 07 p1261 A70-20301
- External and internal three dimensional dynamic problems in elasticity theory for multiply connected region with circular cylinder boundaries
 08 p1584 A70-20537
- Multiple scattering of plane time harmonic compressional elastic wave impinged on parallel circular cylindrical inclusions in finite domain, analyzing stress field
 08 p1592 A70-21469
- Free vibration of rib stiffened freely supported circular cylindrical shells, verifying rib eccentricity importance to natural frequencies by numerical solutions
 09 p1780 A70-23211
- Plane electromagnetic wave diffraction on circular cylinder
 09 p1638 A70-23339
- Plane electromagnetic wave scattering by conducting circular cylinder/wire in air/vacuum/, computing scattering cross sections by Wiener-Hopf method
 09 p1638 A70-23347
- Heat transfer from circular cylinder in rarefied gas flow at low Mach number, using B-G-K model of Boltzmann equation
 09 p1791 A70-23582
- Forced inertial oscillations in rotating processing fluid-filled circular cylinder
 09 p1664 A70-23682
- Potential flow resistance theory, deriving monoparameter wake formula for circular cylinder moving through viscous fluid
 10 p1870 A70-24788
- Transient creep analysis of pressurized circular cylindrical shells based on strain and time hardening theories
 10 p1963 A70-25089
- Natural vibrations of truss systems of four circular cylinders hinged along walls, using linear group representation
 11 p1312 A70-25605
- Transient bending and shear stresses at clamped support of orthotropic circular cylindrical shells
 11 p1315 A70-25985
- Spatial correlation effect of unsteady sectional loads in axial direction on average or apparent loads over finite region of circular cylinder immersed in moving fluid
 11 p2036 A70-26148
- Uniform asymptotic theory of diffraction by edge of three dimensional body, obtained boundary layer solution applied to scattering by circular cylinder
 11 p2084 A70-26422
- Coupled effects of transverse curvature and pseudoplasticity on skin friction characteristics of slender circular cylinder in laminar power law fluids
 11 p2038 A70-26493
- Longitudinal vibrations of circular elastic homogeneous cylinders with end restraints
 12 p2321 A70-27152
- Flexural vibrations of homogeneous elastic circular cylinder supported at both ends, imposing zero stress conditions on skirt
 12 p2321 A70-27154
- Thin circular cylindrical polyvinyl chloride plastic shells tested under axial compression and end-shortening conditions for buckling
 12 p2324 A70-27473
- Circular cylinders torsion and plain strain analysis, completing statics by asymmetric shear and moment stresses according to Cosserat theory for plastic flow
 13 p2508 A70-28492
- Hydroelastic oscillations natural frequencies in incompressible and nonviscous liquid in circular cylinder with free surface, demonstrating wall elasticity effects
 13 p2512 A70-28832
- Unsteady fluid flow around circular cylinder with sudden acceleration using flow pattern photographs
 13 p2387 A70-29056
- Two dimensional circular cylinder vortex excitation in uniform flow using linear binary system for flutter analysis
 13 p2341 A70-29057
- Basic flow convergence or divergence effect on steady flow pattern around circular cylinder using fluid motion visualization
 13 p2387 A70-29058
- Laminar near wake flow field of two dimensional adiabatic circular cylinder with surface mass transfer
 [AIAA PAPER 69-67] 13 p2343 A70-29951
- Magnetoaerodynamic boundary layer of incompressible conducting fluid over right circular cylinder under magnetic field, showing flow separation
 14 p2621 A70-30550

Circular cylindrical membrane axially symmetric deformations, determining axial and circumferential stresses

14 p2657 A70-30844

Unsteady aerodynamic forces on oscillating circular cylinder, using wind tunnel two dimensional dynamic model

14 p2529 A70-31050

Shell homogeneity theory, considering uniform states, spheres and circular cylinders

14 p2600 A70-31280

Heat transfer coefficient from circular cylinder subjected to uniform surface heat flux and cooled by ring of holes

14 p2667 A70-31427

Heat transfer through axially symmetric boundary layer on moving circular fiber at uniform temperature

15 p2825 A70-31819

Electromagnetic waves scattering at circular cylinders in semibounded region, showing boundary influence on radiation pattern

15 p2698 A70-32174

Circular cylindrical cavity in elastic space, calculating stresses due to incident plane harmonic compression wave

15 p2819 A70-32204

Wave scattering from circular cylindrical body, considering plane wave primary source, line source, point and dipole source

15 p2700 A70-32403

Initial thermally stressed state of solid bounded by concentric circular cylinders, applying Cauchy thermoelastic stress theory

16 p2987 A70-32993

Far wake linear stability behind circular cylinders at hypersonic speed, comparing experiments and predictions

16 p2838 A70-33898

Asymptotic analysis of wave propagation modes in circular solid elastic cylinder, obtaining displacement components and frequencies as dimensionless wave number power series

16 p2993 A70-34085

Sound wave phase fluctuations from ultrasonic waves traveling through turbulent wakes of circular cylinders and plates, using multichannel pulse height analysis

16 p2839 A70-34086

Free vibration of thin circular cylindrical shells, comparing experimental results to Egle-Sewall analysis

17 p3181 A70-34520

Stress concentration around small elastic spherical inhomogeneous inclusion on circular cylinder in torsion

17 p3183 A70-34631

Analog simulation of elastic wave propagation in thick walled hollow circular cylinders to determine safe impact speed

17 p3185 A70-34964

Supersonic panel flutter of circular cylindrical shells at critical dynamic pressure

17 p3188 A70-35227

Hypersonic rarefied gas flow around flat plate with sharp leading edge and circular cylinder in transition region

17 p3011 A70-35241

German monograph on thermal stresses due to thermal shocks on front surface of infinitely long circular solid cylinder

17 p3189 A70-35371

Natural convection heat transfer from vertical cylinder outer surface to liquids, discussing apparatus design and measurements

17 p3197 A70-35540

Elastic layer with circular cylindrical cavity under axial tension /Kirsch problem/, determining stress concentration from boundary value problem

18 p3335 A70-36130

Circular cylindrical shell with round holes along generatrix subjected to internal pressure, determining stress concentration with aid of computer

18 p3335 A70-36131

Steady incompressible flow past circular cylinder at Reynolds numbers up to 100, using finite difference solutions of motion equations

18 p3238 A70-36191

Two dimensional time dependent solution for impulsive motion of circular cylinder involving viscous cross flow at moderate angles of attack

18 p3207 A70-36454

Stability of circular cylindrical shell reinforced by elastic rings at edges under longitudinal compression

18 p3341 A70-36581

External magnetic field effect on cavitation zone behind circular cylinder, proving existence of electric charges

18 p3242 A70-36645

Shallow circular cylindrical shell with rigid collar on lateral surface, calculating stress under axial tension and internal pressure loading

19 p3534 A70-37245

Torsional and longitudinal vibrations of circular cylinders of micropolar elastic solids in terms of Laplace and Helmholtz equations solutions

19 p3537 A70-37789

Long orthotropic pressurized circular cylindrical shell under radial line loads along equally spaced generators, analyzing stresses and deflections by linearization

19 p3545 A70-38338

Stiffened thin walled circular cylinders buckling and postbuckling behavior under axial compression or external hydrostatic pressure

Three dimensional photoelastic analysis of stresses and strains in hollow circular cylinders with conical ends bonded to shell and shrunk

20 p3719 A70-39621

Liquid fuel behavior in right circular cylindrical tank inclined to earth gravitational field, computing fundamental sloshing frequency

20 p3720 A70-39686

Mechanical behavior of cylinders with alternating layers of reinforcing and matrix materials derived from governing equations, including equations of motion

20 p3610 A70-39694

Perturbation method for stress-strain state of circular cylindrical shell with large curvilinear hole

20 p3732 A70-40267

Local heat transfer between heated circular cylinder and air in transverse slip flow at low Reynolds and Mach numbers

20 p3734 A70-40442

Circular cylindrical hole in uniaxial tension field of elastic media, solving plane strain problem for stress concentration factors

21 p3945 A70-41035

Circular cylindrical shell supersonic panel flutter nonlinear analysis, using averaging and numerical integration methods

21 p3941 A70-42107

Rigid circular cylindrical inclusion elastic bedding dynamic loading, calculating stresses in interface

22 p4112 A70-42275

Nonlinear flexural vibration of thin circular cylindrical shells with clamped ends, using method of averaging for stability

22 p4112 A70-42345

Thin circular cylindrical panels in supersonic gas current parallel to generatrices, calculating heterogeneity effect on flutter

22 p4112 A70-42517

Cylindrical cavity uniform expansion in compressible elastic plastic solid, calculating pressure by similarity solution

22 p4113 A70-42603

Circular cylindrical orthotropic fiberglass-reinforced shell buckling under longitudinal impact, assuming initial surface imperfections

22 p4114 A70-42634

Circular cylindrical shell with varying thickness under circumferential load and radial pressure, calculating critical load

22 p4117 A70-43347

Vortex induced vibration problems, deriving mathematical model for periodic lift on circular cylinder

22 p4117 A70-43347

Circular cylindrical shell under longitudinal line load, deriving closed form solution in Fourier series

22 p4118 A70-43547

Drag estimation for circular cylinders at subcritical Reynolds numbers and subsonic speeds, using Karman vortex street theory for wake

23 p4131 A70-43894

Elasticity theory for circular cylinder weakened by cavities, discussing boundary conditions on butt ends and Galerkin solutions

23 p4265 A70-43983

Thin circular cylindrical shells with clamped-clamped and fixed-fixed edges, calculating natural frequencies of nonsymmetrical free vibrations

23 p4266 A70-43997

Axially compressed circular cylindrical shells subject to relaxed boundary conditions, calculating buckling loads as function of length to radius ratio

23 p4269 A70-44397

Aceroelastic stability for circular cylindrical structures under periodic Karman vortex excitation

23 p4274 A70-44764

Low Reynolds number gas flow past heated circular cylinder, considering Stokes region transport properties

23 p4284 A70-44978

Microwave propagation in circular waveguide with axially magnetized gas or solid state plasma /Faraday configuration/, calculating twist modes

24 p4318 A70-45213

Circular waveguide with axially magnetized plasma, investigating twist mode propagation in InSb at 70 GHz

24 p4311 A70-45214

Two spherical particles rotation and slow motion about axis of circular cylinder in direction perpendicular to line of centers, considering fluid flow characteristics

Two dimensional boundary layer growth with suction for oscillating circular cylinder, considering stream functions and phase angles

24 p4325 A70-45781

Two dimensional incompressible air flow past circular cylindrical body, investigating separation point control by suction and jet injection

24 p4326 A70-46002

Jet momentum for flow separation control of air past circular cylindrical surface

24 p4288 A70-46010

Long wave approximation for peristaltic transport in circular cylindrical tube, noting inertia and wavelength effects on backward flow

24 p4288 A70-46011

Viscous flow stability between two concentric rotating porous cylinders, calculating critical Taylor numbers for wave numbers and velocity ratios

24 p4309 A70-46224

Optimal rendezvous maneuver of two spacecraft in circular orbits with minimum fuel consumption, taking into account propelled vehicle control program and flight path

24 p4328 A70-46366

CIRCULAR ORBITS

NT STATIONARY ORBITS

Optimal rendezvous maneuver of two spacecraft in circular orbits with minimum fuel consumption, taking into account propelled vehicle control program and flight path

01 p0193 A70-10424

Minimum propellant rendezvous maneuver of space vehicles in neighboring circular orbits

01 p0193 A70-10555

Optimal rendezvous between satellite and spacecraft, determining power and time optimal coplanar rendezvous in circular orbit

01 p0139 A70-11479

Periodic motion of satellite with magnetic damper along circular orbit, assuming small value of damping coefficient

01 p0197 A70-11481

Continuous and pulsed parameter stabilization for circular orbits of navigation and communication satellites under perturbing effects of oblateness and atmospheric drag

02 p0374 A70-12402

Gyrost motion stabilization with respect to unperturbed circular orbit vector radius, considering gravitational, aerodynamic, perturbation moments action and zero dry friction moment

03 p0484 A70-13370

Medium duration optimal rendezvous between near circular noncoplanar orbits with close orbital planes, analyzing six impulse solutions

03 p0571 A70-13639

Navy navigation satellite passes predicted by equations for rise and set times, elevation and azimuth in plane circular polar orbit about spherical earth

04 p0764 A70-15431

Hybrid system for allocating domestic synchronous communication satellites in concentric circles within inclined elliptical synchronous orbits

05 p0906 A70-15801

Large spacecraft in circular earth orbit calculated for internal gravitational field

05 p0924 A70-16637

Second order secular perturbations formulas of distant earth satellite motion valid for nearly circular orbits with small inclination to ecliptic plane

06 p1141 A70-17823

Vehicles optimal flights with controlled or boundary level thrust in circular orbit neighborhood, using linearized equations of motion

06 p1142 A70-17876

Optimal landing of spacecraft on moon surface from low circular orbit, analyzing rocket thrust, altitude and landing site distance effect on spacecraft mass

06 p1155 A70-17880

Plane motion of two mass points coupled by flexible inelastic thread assuming system mass center moving along circular orbit

07 p1386 A70-19484

Parameter estimates effectiveness from independent discrete and continuous navigation measurements of circular orbital plane

10 p1914 A70-24303

Optimal pulsed orbital transfer between close nearly circular orbits in central field of gravity realized by geometrical solution

11 p2118 A70-26778

Librational motion of damped gravity oriented satellite in circular orbit

12 p2313 A70-27201

Accelerated gradient projection method applied to rocket trajectory optimization for minimizing fuel required for placing payload in circular orbits

13 p2485 A70-28395

Circular orbit gravitationally stabilized satellite oscillation damping by changes of moments of inertia

13 p2501 A70-28420

Minimum time control for placing circular orbit satellite in gravitationally stable position

13 p2502 A70-28440

Plane motion of two mass points coupled by flexible inelastic thread assuming system mass center moving along circular orbit

15 p2805 A70-32729

Equations of motion for circular periodic orbits extended to elliptic restricted three body problem

15 p2806 A70-32803

Stable equilibrium positions for satellite consisting of many rigid bodies in circular orbit about center of gravity, using numerical method

18 p3332 A70-35963

Minimum-fuel multiple impulse orbital fixed time rendezvous in circular orbit vicinity

18 p3289 A70-36682

Circular orbit stability in stationary axisymmetric space-times dependence on angular momentum per unit mass increases outward from symmetry axis

18 p3317 A70-37004

Nonspinning symmetrical satellite in circular orbit, analyzing laterally oriented rotor effect on attitude stability

19 p3533 A70-38340

Minimum impulse transfer between circular orbit and hyperbolic trajectory velocity vector, assuming fixed transfer times

[AIAA PAPER 70-1038]

19 p3527 A70-38853

Position and velocity of geodetic drag free satellite in near circular orbit, including lunar-solar gravitational effects and zonal and tesseral harmonics

[AIAA PAPER 70-1054]

19 p3528 A70-38869

Aircraft flying at constant speed in circular orbits, calculating flight path under effect of uniform velocity wind

21 p3750 A70-40920

Optimal low thrust transfer between coplanar circular orbits, examining thrust direction and steering as Mayer problem

22 p4097 A70-42489

Nautical loci of constant azimuth of artificial satellite at corridor height in circular orbit at arbitrary inclination, using gyroscope and radio sextant

22 p4068 A70-42664

Orbital eccentricity effects on solutions of eclipsing binary light curves, comparing circular orbits solutions

23 p4242 A70-44290

Moderately elliptic reference orbit perturbed motion, applying linearized perturbation equations for circular orbit

23 p4244 A70-44590

Optimal moments of inertia of rigid satellite in circular orbit by generalization of Beletskij concept, discussing libration boundaries

23 p4261 A70-44677

Relativistic two body system in circular orbits, examining quantum theory with massless and massive scalar fields and energy and angular momentum for bound system

24 p4379 A70-45521

CIRCULAR PLATES

Elastic support effect on bending of clamped circular, elliptical, rectangular and skewed plates, using variational method and small perturbation technique

01 p0205 A70-11144

Circular plate nonlinear analysis under load and uniform midplane temperatures, using stationary potential energy principle

01 p0205 A70-11145

Transient temperature profiles and thermal stress distribution in circular plates and cylinders with eccentric hole determined by conformal mapping

01 p0207 A70-11153

Thin simply supported circular rigid ideally plastic plate subjected to dynamic transverse load uniformly distributed over central circular region

02 p0389 A70-12668

Vibrational response of simply supported and clamped circular plates subjected to gyroscopically induced inertia loads, using equations of motion

03 p0583 A70-12920

Centrally clamped spinning circular disk free transverse vibration analysis within accuracy of numerical computations

03 p0584 A70-12931

Buckling equations for thin nonlinearly elastic circular plates with affine initial deformation, considering Lure theory and variational principle for uniform compression load

03 p0589 A70-13336

Converging series solutions for conducting circular disk in radiation field of vertical and horizontal magnetic dipoles to determine reemitted field

03 p0448 A70-13432

Impulsive and transient load disturbances in thin elastic finite circular plate on Pasternak type viscoelastic foundation

03 p0595 A70-13905

Transient temperature distribution, thermal stresses and deformations in thin finite circular disk due to continuous point heat source, using linear thermoelasticity

[ASME PAPER 69-WA/PVP-6]

04 p0768 A70-14789

Circular sandwich plates fundamental natural frequencies, considering face members membrane characteristics and thickness, face and core isotropy, etc

04 p0778 A70-15559

Reinforced openings effect on burst strength of ductile circular plates subjected to pressure loads

05 p0943 A70-16810

Stress-strain state of drawn and bent circular plate made of rigid viscoplastic work hardened material

05 p0946 A70-16958

Backscattered field determination at edge on incidence from thin circular plates illuminated by plane waves

06 p1008 A70-17563

Numerical analysis of axisymmetric elastoplastic deformation of circular plates under combined lateral load and membrane force

07 p1402 A70-18977

Circular plates dynamic response to axisymmetric time dependent loads, analyzing transverse restraint effects on response maxima by plate theory

07 p1404 A70-19251

Circular plates with optimal natural frequency of transverse vibrations, discussing boundary conditions

07 p1405 A70-19256

Stress-strain state of flexible circular plates as function of thickness distribution using finite difference theory

08 p1583 A70-20529

Aerodynamic forces acting on circular plates in rarefied gases, calculating coefficients as functions of angle of attack

08 p1433 A70-21093

Finite bending elements for static deflections of annular and circular plates loaded by concentrated forces, calculating free vibrations

08 p1588 A70-21243

Biharmonic equation in polar coordinates solved for circular plates and plate sectors with various boundary conditions, using finite difference approximations

08 p1589 A70-21246

Yield criterion for plastic bending of transversely anisotropic circular plates under plane stress

08 p1589 A70-21250

Rotating circular disk under angular acceleration, analyzing stress and deformation distributions

08 p1596 A70-21980

Elasticity theory two dimensional problem solution for circular segment in polar coordinates, applying Lure symbolic notation and Prokopov minimum potential energy principle

09 p1782 A70-23291

Natural bending vibrations of circular plates with allowance for stress tensor asymmetry, deriving transcendental frequency equation

09 p1782 A70-23292

Centrifugal forces and nonuniform heating effect on natural vibration frequencies of circular plates using lumped parameter method

09 p1784 A70-23588

Large amplitude free vibration of heated circular plates, analyzing energy equations by successive approximation method and elliptic integrals

10 p1957 A70-24480

Dynamic postbuckling response of thin elastic circular plates under axisymmetric time dependent radial thrust, discussing response to step loading

10 p1964 A70-25206

Clamped thin circular plate bending under various loadings due to action of rigid square column on center

11 p2139 A70-26404

Vibrations of combination of cylindrical shells and circular plates, giving bending moment distribution

11 p2139 A70-26415

Axisymmetrical stress tensor singularity convergence of rigidly clamped circular plate, showing identity of plane stressed state transcendental equations

12 p2325 A70-27558

Beam-bending and circular plate testing rigs for creep with constant and variable loading, discussing tests repeatability and accuracy

12 p2207 A70-27618

Deflection surface and edge moment prediction for uniformly edge loaded point-supported circular plates, comparing with optical method

13 p2509 A70-28534

Large deflections in impulsively loaded clamped circular Al alloy and steel viscoplastic plates

13 p2511 A70-28736

Elastic isotropic circular perforated plate stress-strain state, proving quasi-regularity of infinite linear algebraic equations

13 p2515 A70-29317

Thermoelastic equations for circular sandwich plates bending due to asymmetric temperature distribution

13 p2518 A70-29976

Buckling equations for thin nonlinearly elastic circular plates with affine initial deformation, considering Lure theory and variational principle for uniform compression load

14 p2657 A70-30714

Liapunov type analysis of linear structural dynamic system excited by stochastic parametric load, discussing radially loaded thin circular plates

14 p2657 A70-30763

Natural frequencies and corresponding mode shapes for free flexural vibrations of circular plates, extending to elastic support cases

17 p3186 A70-34980

Anisotropic disk compressed by isotropic ring of smaller radius, considering elastic equilibrium

18 p3336 A70-36134

Diffraction of EM waves emitted by vertical electric dipole on conducting thin circular disk, using algorithm for integral equation

19 p3375 A70-37432

Rib stiffened elliptical and circular plate vibrations, determining fundamental frequencies by variational techniques

19 p3536 A70-37693

Nodal patterns on thin elastic circular plate vibrating in flexure, considering natural and compounded modes

19 p3543 A70-38245

Disk equations to determine tensions around arbitrary hole or stiffening contours

20 p3720 A70-39623

Elastoplastic deformation of thin circular plates under uniformly distributed transverse loads, using mixed type variational equation

20 p3721 A70-39776

Thin circular plate clamped along edge, calculating large displacements and elastoplastic strains for comparison with measurement

21 p3935 A70-41406

Time average holographic interferometry of circular plate vibrating simultaneously in rationally related modes

21 p3829 A70-41927

Circular plates dynamic stability under variable periodic loads, using differential equations of vibrational motion for median surface

22 p4114 A70-42613

Axisymmetric potential problem of plane circular electrified disk in coplanar gap formulated in triple integral equation, obtaining Wiener-Hopf solution

22 p4080 A70-42632

Forced harmonic vibrations of clamped circular plate in inviscid fluid, calculating radiation pressure and power distributions

22 p4073 A70-42646

Axisymmetric vibrations of cylindrical shell with concentric circular plates at each end, obtaining Lagrangian of combined system

22 p4115 A70-42843

Carrying capacities of simply supported and clamped circular plates under combined lateral pressure and edge compression loads

22 p4118 A70-43548

Flexural vibrations of clamped circular plate with nonlinear elasticity for small strains and displacements, using variational principle

22 p4120 A70-43719

Approximation method for large deflection analysis of impulsively loaded rigid plastic circular plates and symmetric shells

23 p4275 A70-44943

Tempering stress in circular plates and cylinders in casting of solid propellants

24 p4427 A70-46147

CIRCULAR POLARIZATION

MHD model for microwave solar circular polarization bursts interpretation, suggesting Alfvén wave disturbances in solar atmosphere

01 p0168 A70-10254

Circularly polarized synchrotron radiation from distribution of electrically charged particle in magnetic dipole calculated for estimating Jupiter magnetic field

04 p0746 A70-14511

Telescopic circular polarization observations of Jupiter at 9.26 cm related to Jovicentric declination of earth

05 p0906 A70-15896

Circular polarization measurements of Jovian decimeter radiation by 210-ft radio telescope at Goldstone, California

05 p0921 A70-16986

Relativistic electrons synchrotron radiation by calculating magnetoactive plasma permittivity tensor, determining normal waves polarization characteristics

08 p1554 A70-21812

Antenna array circular polarization adjustment using reflections from horn radiator and mirror

09 p1650 A70-23633

Rectangular waveguide with cross shaped slot as polarizer ensuring circular polarization over wide frequency range

09 p1652 A70-23649

Antenna with 3-db slotted waveguide bridge to produce near circular polarization emission field

09 p1652 A70-23651

Waveguide slot antenna with electrical control of field polarization from linear to circular and beam scanning over wide sector

09 p1652 A70-23652

Solar magnetic field measurement emphasizing circular and total polarization characteristics

10 p1939 A70-24275

Circular polarization time dependent reversals during simultaneous microwave solar bursts at different phases, considering relations to coincident flares

10 p1932 A70-24626

Solar radio types I and III sources spatial distribution of circular polarization and coronal magnetic field configurations in active regions

12 p2294 A70-27710

Circularly polarized waves in waveguide loaded with high density magnetoplasma, discussing propagation mode and plasma boundary

13 p2379 A70-29617

Circularly polarized emission from types I and 4 bursts and noise storms, considering mode coupling in warm plasma, gyroradiation and Cerenkov radiation

13 p2479 A70-29851

Antenna gain, efficiency, half power bandwidth, sidelobe level and focal length for circularly polarized metallic lens antenna at X band frequencies

16 p2872 A70-32969

Thin window for circularly polarizing antennas, measuring circularity and VSWR performance on S and X band test sections

16 p2877 A70-33410

Magnetic field effects on Compton scattering and radiative opacity, considering longitudinal and transverse propagation with circular polarization

17 p3154 A70-34538

Sunspot spectrograms analysis, observing wavelength shift in Zeeman triplet circular components and magnetic splitting inequality under different circular polarizations

18 p3322 A70-37136

Impedance measurements on microwave tripole antenna for circular polarization, including expressions for radiation pattern

19 p3388 A70-37868

Quasars and radio galaxies circular polarization at 49 cm wavelength, using radio telescope interferometer

19 p3523 A70-38606

White dwarf star circular polarized light, indicating strong magnetic field

20 p3701 A70-39001

Time and power dependent Lamb shift resonance shapes measurement with circular polarized RF field in beam foil excited H atoms

20 p3675 A70-39498

Parabolic antenna properties generated by dual band circularly polarized focused two channel monopulse feed system, discussing tracking data from helicopter, Apollo 8 and Cassiopeia A

20 p3589 A70-40323

Solar type 4 event flux density and circular polarization radiopolarimetric recording, showing peculiar phases of short duration

22 p4095 A70-43263

Octave bandwidth unidirectional circularly polarized reflector antenna, using crossed conical dipoles near second resonance

23 p4176 A70-44970

Circular polarization time evolution during solar microwave impulsive bursts

24 p4401 A70-45319

White dwarf stars continuum circular polarization as function of time and wavelength, emphasizing magnetic star search

24 p4410 A70-45776

Dual channel circularly polarized feed of monopulse tracking antenna system, noting axial ratio and gain and open loop mode autotracking

24 p4321 A70-46259

CIRCULAR SHELLS

Interior shell equations compared with classical shell theory, considering helicoidal, spherical and circular cylindrical geometry

01 p0200 A70-10542

Natural oscillation frequencies of closed circular orthotropic cylindrical shells having freely supported end faces, particularly with stringers

01 p0210 A70-11413

Circular cylindrical shell stressed state with rectangular opening under compressed torsion, noting opening effect on loads nonuniform distribution

03 p0593 A70-13501

Donnell shallow circular cylindrical shell equation, obtaining approximate solution for stresses in infinitely long circular cylindrical shell with circular hole subjected to edge loading

03 p0601 A70-14320

Finite strain in bending rectangular block into right circular cylindrical shell for transversely isotropic medium along radius vector, using Saint Venant stress-strain relations

03 p0602 A70-14329

Circular cylindrical shells with axisymmetric imperfections tested under axial compressive load, studying imperfection amplitude and wavelength effects on minimum buckling load

04 p0778 A70-15588

Stress-strain state of circular orthotropic shells under bending, considering distributed loads applied to shell center

05 p0934 A70-16217

Stability of clamped, hinged and elastically supported circular cylindrical shells under critical combined torsional and transverse pressure

05 p0934 A70-16227

Stress concentration of circular cylindrical shell weakened by elliptic hole under torsion

05 p0947 A70-16965

Local axisymmetric dimple imperfection effects on buckling load of circular cylindrical shell under axial compression

[AIAA PAPER 70-103] 06 p1170 A70-18167

Stress concentration on isotropic elastic circular cylindrical shallow shell using plane waves and spherical means method, obtaining periodic solutions convergence

08 p1585 A70-20963

Circular cylindrical shell supported along generator under arbitrary forces using finite Fourier transform, simplifying results by Euler sum formula

08 p1589 A70-21312

Three dimensional deformation of finite circular cylindrical shell under plane shock wave solved in linear form

09 p1785 A70-23618

Homogeneous boundary value problems in stability theory of circular cylindrical shells axisymmetric equilibrium state

11 p2129 A70-25396

Characteristic equation roots for circular cylindrical shells deformation under edge load

11 p2135 A70-25960

Inplane and rotary inertia effects on free vibration frequencies of circular cylindrical shells eccentrically stiffened by orthogonal set of stringers and/or rings

11 p2135 A70-25993

Free vibration characteristics of circular cylindrical shells of finite length, utilizing Flugge equations

11 p2135 A70-25997

Axisymmetric imperfection distributions effect on buckling of circular cylindrical shells under axial compression, constructing test models from photoelastic liquid epoxy

12 p2319 A70-27140

Shallow shell solutions complete with respect to finite simply connected surface region applied to circular cylindrical shells

13 p2517 A70-29758

Circular elastic shell response to moving and simultaneous loads, using impulse simulation method

13 p2518 A70-29986

Thin concentric circular cylindrical shells joined at ends by rigid diaphragms, describing free and forced torsional motion

16 p2992 A70-34019

Thin circular cylindrical shell stability subjected to axisymmetric thermal pulse, describing buckling process by mathematical model

18 p3342 A70-36641

Prebuckling deformations effect on buckling of clamped thin walled circular cylindrical shells under axial loading and internal pressure

19 p3546 A70-38346

Shallow shell solutions complete with respect to finite simply connected surface region applied to circular cylindrical shells

19 p3547 A70-38396

Stress concentration on isotropic elastic circular cylindrical shallow shell using plane waves and spherical means method, obtaining periodic solution convergence

20 p3719 A70-39385

Thin walled circular cylindrical steel shells dynamic stability partly filled with liquid and subjected to longitudinal excitation

20 p3723 A70-39852

Long thin circular cylindrical shell resonance velocities in steady response to fluid motion

20 p3727 A70-39884

Structurally closed orthotropic circular cylindrical reinforced shell stability, developing approximate method to obtain various boundary conditions

20 p3727 A70-39886

Circular cylindrical shells theory based on Novozhilov equation, deriving auxiliary formulas for strain and displacement characteristics in terms of stress function

20 p3727 A70-39888

Homogeneous boundary value problems in stability theory of circular cylindrical shells axisymmetric equilibrium state

20 p3732 A70-40100

Closed circular cylindrical shell nonlinear problem solvability extended to anisotropic sandwich shell, using mean deflection theory

21 p3933 A70-40601

CIRCULAR TUBES

Nonaxisymmetric mass transfer in turbulent flow in plain circular tube, considering diametral line and discontinuous ring sources

01 p0065 A70-11093

Flow patterns in circular ducts with circumferential roughness variation, determining axial turbulence, Reynolds number effect and applications as two phase flow analog

01 p0066 A70-11132

Structural similarity hypothesis for fully developed turbulence in smooth circular tubes, using intensity correction procedure

04 p0665 A70-14453

Circular tube entrance upstream and downstream velocity profiles at small axial distances measured by laser Doppler flowmeter

[ASME PAPER 69-WA/FE-13] 04 p0667 A70-14780

Shear modulus of sandwich structure tubular core derived by virtual work principle and matrix approach, comparing results with honeycomb core

[DGLR-69-64] 04 p0774 A70-15156

Three dimensional electromagnetic scattering from thin walled conducting circular tube of finite length normally incident with E or H polarized plane wave

05 p0816 A70-16987

Free molecular flow through long circular tube rotating with constant angular velocity about axis, discussing rotation speed effect on mass flow

05 p0836 A70-16994

Steady laminar flow with frictionless central core surrounded by boundary layer in circular curved pipe, discussing friction factor and flowmeter discharge coefficient

05 p0836 A70-17107

Core length of water jet from circular tube, considering wall roughness, tube diameter and water viscosity and surface tension

06 p1031 A70-17135

Approximate solution for heat transfer in incompressible fluid laminar flow in circular tube

07 p1253 A70-19060

Torsional vibrations of nonhomogeneous anisotropic finite circular tube, computing natural frequencies for various parameters

07 p1414 A70-20173

Single fluid theory for plasma laminar flow in field-free region of circular tube, obtaining friction factor and Nusselt number correlations

08 p1552 A70-21585

Film heat transfer coefficients and thicknesses for condensation and evaporation and two phase flow inside circular tubes

08 p1599 A70-21827

Local heat transfer coefficients determination for unilaterally heated rectangular coolant duct by approximation and experiment applicable to circular tubes

09 p1787 A70-22170

Steady and unsteady viscous incompressible one dimensional flows parameters in deformable cylindrical tube determined, solving continuity and motion equations by Galerkin method

09 p1664 A70-23715

Approximate solution for heat transfer in incompressible fluid laminar flow in circular tube

10 p1871 A70-25211

Rate-sensitive perfectly plastic linear strain hardened rings and tubes, calculating response to impulsive loads

17 p3184 A70-34907

Laminar heat transfer in circular tube under solar radiation in space

18 p3347 A70-36503

Propagation constants in laminar plasma circular waveguides filled with anisotropic linear medium, using Galerkin-Ritz method

19 p3474 A70-37428

Radiation theory circular waveguide in dominant TE mode and flush mounted to infinite conducting flat ground plane covered by plasma or dielectric sheath

20 p3586 A70-39500

High velocity isothermal viscous compressible steam flow in circular tubes, measuring pressure drops

22 p4011 A70-42845

Sound radiation from unflanged circular waveguide duct with flow, calculating reflection coefficients, directivity pattern and power for comparison with approximate methods

23 p4219 A70-44392

Long wave approximation for peristaltic transport in circular cylindrical tube, noting inertia and wavelength effects on backward flow

24 p4309 A70-46224

Microwave transmission in partially dielectric filled circular waveguide, deriving cutoff wavelength and phase velocity vs frequency

24 p4315 A70-46260

CIRCULATION

NT ATMOSPHERIC CIRCULATION

NT BLOOD CIRCULATION

NT BRAIN CIRCULATION

NT CARBOXYHEMOGLOBIN

NT CONGESTION

NT CORONARY CIRCULATION

NT INTERCRANIAL CIRCULATION

NT INTRAVASCULAR SYSTEM

NT ISCHEMIA

NT OCULAR CIRCULATION

NT PERIPHERAL CIRCULATION

NT PULMONARY CIRCULATION

Velocity circulation in laminar motion of fluid in cylindrical tube, assuming equilibrium under dissipative forces

14 p2564 A70-30164

Circulation meter using parallel yawmeters linked to manometer, showing sensitivity in lateral velocity

14 p2589 A70-31397

CIRCULATORS [PHASE SHIFT CIRCUITS]

Magnetron amplifiers with ferrite circulators for synchronizing natural frequency, obtaining I-V characteristics and gain vs bandwidth curves

05 p0823 A70-16886

Lumped element microwave Y circulator, describing device performance and ALGOL program for potentials calculation

07 p1241 A70-19751

Parasitic effects due to coupling of wideband regenerative amplifier with nonideal ferrite circulators to antenna feeder duct

08 p1468 A70-20575

UHF and VHF stacked ferrite loaded junction circulators construction, improving cost to power performance

08 p1476 A70-21292

Photolithographically produced thin film lumped element circulator, assuring physical and electrical symmetry by interweaving junction conductors

08 p1476 A70-21293

Lossless three-port H-plane waveguide junction circulator performance evaluation using computerized design

09 p1646 A70-22710

Ferrite Y-circulator, studying effects of attenuation in ferrite on mean frequency, admittance, forward and reverse losses, etc

09 p1648 A70-23157

C band latching ring-and-post ferrite waveguide circulator for radar transmitting-receiving functions, presenting performance and design parameters

12 p2202 A70-28166

Circular shielded three layer dielectric waveguide critical parameters, estimating passbands for phase circulators with ferrite inserts

13 p2364 A70-28873

Microwave parametric amplifiers with nonideal circulators, deriving gain via scattering matrix theory and signal flow graphs

16 p2874 A70-33389

Signal and noise properties of degenerate and quasi-degenerate nonreciprocal parametric amplifiers without circulators

22 p3990 A70-43423

Stripline and microstrip junction circulators analysis for microwave integrated circuits, based on clockwise and counterclockwise rotation modes

23 p4169 A70-43787

Ferrite junction microwave circulator bibliography /1956-1969/ covering stripline and waveguide versions theory, designs, constructions and applications

24 p4318 A70-45210

CIRCULATORY SYSTEM

NT AORTA

NT ARTERIES

NT BLOOD VESSELS

NT CAPILLARIES [ANATOMY]

NT VASCULAR SYSTEM

NT VEINS

Effect of immersion in thermoindifferent water on circulatory control and work capacity in trained and untrained subjects

02 p0241 A70-12770

Heart rate and circulatory load as ergonomic criteria based on muscular work, environment temperature, mental stress, etc

06 p0997 A70-18017

Centripetal acceleration tolerance level correlated with circulatory system functional tests and physical exercises, discussing strength and speed endurance

07 p1201 A70-18787

Circulatory system tests during linear, intermittent and continuous accelerations on centrifuge, noting lack of statistical correlation between centrifuge tests and functional tests

07 p1201 A70-18789

Orthostatic tilt tolerances in young men and women noting heart rates and blood pressure

09 p1627 A70-23454

Ballistographic psychological evaluation of heart and circulatory system by recording displacement, velocity, acceleration and total forces imparted during each beat

10 p1810 A70-24039

Cyclogometer with powder type electromagnetic brake for respiratory and circulatory measurements and functional rehabilitation

14 p2541 A70-30379

Circulatory phenomenon and deep thoracic impedance changes of ventilatory origin

14 p2537 A70-30385

Cardiovascular and circulatory phenomena fluid mechanical aspects emphasizing pulsatile blood flow

15 p2720 A70-31789

Mountain climbing effects on urinary excretion of vanillylmandelic and homovanillic acids, discussing circulatory system acclimatization

17 p3039 A70-35425

Blood circulatory system and hemodynamic interdependencies simulation by analog computer, using Warner model

23 p4155 A70-44862

CIRCUMLUNAR TRAJECTORIES

Reentry trajectories from lunar surface and orbit obtained by computer with allowance for initial data spread

01 p0191 A70-11476

Earth-moon-earth flight characteristics, discussing spacecraft trajectory, velocity and corrections for close distance placement and return for soft landing

03 p0569 A70-13483

Long wave cosmic radio background emission in circumlunar space by Luna 11 and 12 satellites, observing increase in earth magnetosphere tail

12 p2295 A70-28262

Circumlunar trajectories with return to earth atmosphere, comparing various methods

18 p3312 A70-36165

Multiconic method space flight trajectories analysis, discussing computation time and circumlunar flight altitude and velocity errors

19 p3529 A70-38876

CIRRUS CLOUDS

Cirrus clouds signature analysis, discussing light scattering pertinent to lidar equation

01 p0076 A70-10913

Photographic detection of thin cirrus clouds effect on earth heat budget

04 p0696 A70-15575

IR reflectance of cirrostratus and cirrus clouds and jet contrail measured by spectrometer on high altitude aircraft

11 p2045 A70-25626

Stratospheric water vapor measurement by submillimeter wave sounding, considering signal fluctuations due to scattering by high cirrus clouds

11 p2077 A70-26619

Aircraft ice crystal counter for real-time measurement in cirriform clouds, using contact electrification detection

12 p2264 A70-28091

Clouds upper height boundary relation with radiation temperature field from satellite data, noting cirrus clouds influence

13 p2444 A70-28589

CISLUNAR SPACE

Near parabolic trajectories between moon and cislunar libration point, considering earth perturbative influence

19 p3529 A70-38874

Geolunar space development with transportation based on shuttle stations, describing communication, orbits, logistics, etc

22 p4108 A70-43628

CITIES

Interurban air transportation network structure contribution to airport and airways congestion, considering addition of nonstop links

01 p0005 A70-10647

STOL ports in city environments, discussing elevated building design, assisted takeoff and landing equipment and Navy operational safety potential

01 p0057 A70-10715

CITRATES

Purification and reversible inactivation of isocitrate dehydrogenase /ICDH/ of Halobacterium cutirubrum, overcoming difficulties in purifying halophilic enzymes

01 p0021 A70-10792

CITRIC ACID

Kinetic model for acid catalyzed Delrin decomposition, testing for Delrin-citric acid system and predicting thermograms with nonlinear regression analysis

09 p1630 A70-22896

CIVIL AVIATION

Military inertial navigation technology applied to civil air transport aircraft

01 p0137 A70-10311

Juridical measures against air piracy, discussing civil aviation legislation, unlawful acts aboard aircraft and international agreements

01 p0220 A70-10374

Soviet book on operational maintenance of flight vehicles /civilian/, emphasizing maintenance under various climatic conditions

01 p0004 A70-10502

Military aeronautical R and D contributions to civil aviation since 1905, discussing jet engine and supersonic aircraft introduction, air traffic control, etc

01 p0005 A70-10614

National air traffic control system modernization based on Department of Defense military experience to achieve safe and efficient air space utilization

01 p0137 A70-10616

Air traffic control methods for transport aircraft delay elimination

01 p0139 A70-11367

Civil aviation electronics - Conference, London, September 1969, Part 1, Electronics in flight control

02 p0329 A70-11831

Automatic flight control and instrumentation in civil helicopters, examining military developments and Ferranti automatic stabilization system

02 p0329 A70-11834

Electrical signaling civil aircraft systems, discussing design and integrated maneuver demand controls

02 p0224 A70-11835

Built-in, airborne and ground based automatic test equipment /ATE/ for fault finding and serviceability of aircraft electronic systems in civil aviation

02 p0295 A70-11845

Civil aviation electronics - Conferences, London, September 1969, Part 3, Air traffic control

02 p0330 A70-11956

Civil aviation electronics - Conference, London, September 1969, Part 2

02 p0333 A70-11979

Air traffic congestion alleviation by applying general purpose computers for navigation in civil transport aircraft

02 p0334 A70-11985

Great Britain air transport industry manpower recruitment and training, technology changes effects and costs

02 p0402 A70-12307

Air traffic problems connected with Boeing 747 introduction, discussing cargo/passenger handling, fueling and maintenance procedures

02 p0227 A70-12620

SAS pilot selection system, discussing assessment variables, physiological examinations, psychological tests, recruiting procedure, etc

03 p0433 A70-13262

Aeronautical satellite system for civil flight safety, discussing operational, technical and economic aspects

03 p0522 A70-13610

FAA engineering approach to SST certification involving airworthiness standards development and coordination with industry and foreign governments

03 p0437 A70-14060

Soviet book on air navigation covering civil navigator training, geographic concepts, navigation means, flight and meteorological conditions, instrument errors, etc

06 p1103 A70-17642

Economic flight conditions for civil aviation VTOL aircraft selected by graph-analytical method concerning phases of ascent, cruising and descent

06 p0987 A70-17875

Twinjet helicopter design for business transport, emphasizing redundant systems for safety and bad weather flight capability

07 p1191 A70-18844

Physiological pilot training program of FAA, discussing slides on Aeronautical Center and Civil Aeronautical Institute

07 p1218 A70-19012

Psychiatric disorder in civil aircrew leading to suspension or loss of licence, discussing physicians role and complications of treatments

07 p1223 A70-19940

V/STOL concepts for short haul commercial aircraft compared for gross weight, operating cost, gust sensitivity and noise levels

07 p1195 A70-20409

U.S. Civil Aeronautics Board policy in cooperative agreements involving foreign airlines, highlighting significant cases

08 p1600 A70-20578

V/STOL transport aircraft design in Germany, analyzing demands in military and civil sectors

08 p1435 A70-20639

Civil avionics systems engineering for safety, regularity, weather independence, flight patterns and airport utilization

08 p1468 A70-20649

General aviation urban airport capacity problem, suggesting diversion of training portion of peak-hour traffic

08 p1481 A70-21306

Civil air transportation in India, using mathematical models to estimate optimal development and efficiency of future air traffic potential

08 p1601 A70-21544

Workload relieving displays and controls for general aviation, discussing feasibility of digital computer driven integrated displays

08 p1601 A70-21679

Helicopter utilization in emergency transportation of civilian patients, discussing questionnaire results from medical and police agencies

08 p1454 A70-21937

World air transport system in 1970s, analyzing industry economic performance, discussing fares, rates, technological developments, passenger and air freight increases, etc

09 p1792 A70-22332

Commercial aircraft inertial navigation, examining gyroscope, accelerometer and electronic computer and gyroscopic stabilization

10 p1914 A70-23848

Compound helicopter in civil aviation to alleviate air traffic congestion, discussing design and operative capacities of S-65-200

10 p1804 A70-24046

Commercial aviation safety on basis of aircraft accidents relationship to distance covered, considering clear air turbulence and cosmic radiation dangers

10 p1804 A70-24050

Civil jet VTOL transportation based on Do 31, discussing market, passenger requirements, noise, flight safety and economic factors
[AIAA PAPER 70-001] 10 p1805 A70-24051

Boeing 747 aircraft impact on air transportation passenger and freight rates and traffic congestion reduction
10 p1806 A70-24765

Civil aviation satellites for aircraft communication, navigation and traffic control, discussing technical, political and administrative problems
10 p1842 A70-24974

Edwards Inquiry Report into British Civil Air Transport based on cost effective economic study, involving airlines and regulatory system
11 p2153 A70-25855

Licensing aspects of Edwards Report, criticizing Air Transport Licensing Board /ATLB/ organization
11 p2153 A70-25856

Criticism of public administration aspect of Edwards Report, noting parliamentary and constitutional difficulties in some proposals
11 p2153 A70-25857

Edwards Committee visualization of insurance as air safety aid, discussing insurer specifications and policy conditions
11 p2153 A70-25858

Edwards Report consideration of economic and investment opportunities in civil aviation, discussing denationalizing airways corporations
11 p2153 A70-25859

Commercial aviation gasolines inspection data tabulated and compared for 1969 and 1964
[SAE PAPER 700228] 11 p2099 A70-25897

FAA recommendations on general aviation airports and heliport design standards, explaining standards establishment or modification procedures
[SAE PAPER 700231] 11 p2031 A70-25900

Aircraft interior design styling and material selection, discussing industrial design department function and organization, styling as marketing tool, etc
[SAE PAPER 700233] 11 p1980 A70-25902

Short distance VHF omnirange navigation and distance measuring equipment considered for performance improvements feasibility to meet civil air traffic demands through 1980
12 p2268 A70-27643

VORTAC system providing navigation service to civil and military air traffic on worldwide basis
12 p2269 A70-27919

Civil aircraft weather radar for ground collision hazard warning
13 p2447 A70-28548

Medical wastage of professional aviators in military and civil aviation, discussing reasons for preventing flying license revalidation
13 p2359 A70-29440

Civil aircraft altitude display design, anticipating application to supersonic transport
14 p2582 A70-30287

Economic factors in aviation - RAS Conference, London, May 1970
14 p2668 A70-30935

Commercial aircraft manufacturing industry in UK, discussing SST, wide cabin aircraft, turboprop replacement, engine influence on airframe industry, etc
14 p2668 A70-30936

International airline collaboration in engineering and maintenance for savings in initial and operational costs of aircraft fleets
14 p2669 A70-30940

Commercial aircraft design evolution and trends concerning performance and operating cost reduction
14 p2532 A70-31370

British light aircraft designs, engines and costs, considering business, agricultural, gliding, private, school and club flying
14 p2532 A70-31394

Automatic flight control and instrumentation in civil helicopters, examining military developments and Ferranti automatic stabilization system
15 p2772 A70-31771

High speed civil and commercial transport aircraft, discussing jet-orbital flight
18 p3333 A70-36664

Concorde design limitations for commercial success in civil airlines
18 p3350 A70-36665

International civil aviation, discussing ICAO functions, airports and terminal facilities problems
19 p3553 A70-37748

Aeronautical satellite system for civil flight safety, discussing operational, technical and economic aspects
21 p3848 A70-41131

Light rigid civil aircraft response to continuous atmospheric turbulence estimated using two rigid body degrees of freedom method for vertical and lateral gusts
[AIAA PAPER 69-766] 22 p3961 A70-42703

FAA airport and airway capacity improvement program, considering runway-taxiway configurations,

surface guidance and control, terminal design, takeoff, approach and landing systems, etc
[AIAA PAPER 70-1315] 24 p4431 A70-45946

CL-84 AIRCRAFT
CL-84 tilt wing V/STOL program to develop best configuration for ground support operations
01 p0007 A70-11317

Canadair CL-84 V/STOL aircraft flight characteristics and structural design
23 p4137 A70-44017

CLADDING
Automatic cladding method for submerged arc stainless steel welding, discussing delta ferrite to sigma phase transformation for surfacing with low ferrite stainless steel
08 p1508 A70-21489

Ti explosive bonding and forming, examining peel and shear strengths on Ti clad steel plate
17 p3098 A70-34446

Multicomponent composite materials, discussing fiber reinforced structures, clad metals and bulk materials
20 p3650 A70-39947

Clad glass fibers axial stress measurement by photoelastic techniques
22 p4060 A70-43415

CLARK Y AIRFOIL
U AIRFOIL PROFILES
CLASSICAL MECHANICS
NT ASTRODYNAMICS
NT CELESTIAL MECHANICS
NT KEPLER LAWS
NT ORBITAL MECHANICS
NT SPACE MECHANICS
Mass point motion in inertial reference system of special relativity, finding motion equations analogous to relative motion equations in classical mechanics
01 p0145 A70-11442

Classical mechanics and thermodynamics principles restated using functions of sets, material sets and reciprocal actions between material sets
02 p0339 A70-11896

Lagrangian nonenergetic and unconstrained systems introduced in describing Birkhoff classical dynamics, considering space of motions states as connected analytic manifold
10 p1909 A70-24190

Nonlocal variational mechanics, considering case of stationarity with unrestricted nonlocality
21 p3939 A70-42026

Classical calculations for energy transfer to diatomic molecules with rotational and vibrational degrees of freedom in atom-diatom-molecule collisions
23 p4221 A70-44010

CLASSIFICATIONS
NT DICHOTOMIES
NT HIERARCHIES
NT INDEXES [DOCUMENTATION]
Late stars spectral characteristics, verifying criteria for spectral classification and anomalous spectra determination
03 p0569 A70-13424

Graphic method for classifying EM waves directed by open waveguides, obtaining wave numbers from dispersion equation
05 p0812 A70-16245

Classification and maximal lengths of cometary tails, investigating correlation to type, perihelion distances, absolute magnitudes and spectra
07 p1378 A70-19032

ICAO Juridical Council criteria for nonnational aircraft registration, discussing international airlines recourse to Article 77 of Chicago Convention
07 p1428 A70-19105

Electromagnetic and gravitational fields classification methods using spinor techniques, introducing five dimensional complex linear space with Weyl tensors elements
07 p1337 A70-20302

Small planets observation methods, classification and designation, discussing asteroid belt origin
08 p1572 A70-20939

Spectroscopic instruments for atmospheric temperature measurements classified in terms of filtering, modulating and multiplexing systems
10 p1873 A70-23828

Gadolinium II solar lines classification from photographic IR observations
10 p1947 A70-24990

Systems instabilities classification criterion determination, showing absolute instability conversion into convective by introducing damping
10 p1969 A70-25104

Generalized control theory, discussing optimization and table classifying control theory fields
10 p1856 A70-25238

Statistical classifier for analyzing tape recorded transients
11 p2056 A70-26457

Spectral classification of stars from unbroadened spectra recordings possible when comparing optical depths of lines
11 p2116 A70-26589

Automatic image interpretation and classification using two dimensional digital Fourier transforms
12 p2193 A70-28106

Methodology for machine processing for identification of individual crop types, discussing discriminant photoanalysis
12 p2227 A70-28108

Synoptic processes and meteorological fields computerized automatic classification for weather forecasting applications
12 p2265 A70-28332

Meteorological situations and fields quantitative classification and regional grouping by statistical main components application
12 p2265 A70-28333

Land use classification system of photointerpretation from remote sensor imagery
14 p2576 A70-30976

Remote sensors applied to classification of aerial data concerning housing quality at different scales, using variables observation
14 p2577 A70-31234

Two dimensional quantitative spectral classification of F-G5 stars, using meniscus telescope with preobjective prism at Abastuman observatory
15 p2797 A70-31613

Spectral classification of relatively bright stars in near UV based on moderate and low dispersion spectra including F, G and K stars
15 p2797 A70-31614

Spectral classification and continuous spectrum photometry of weak late stars in visual and near UV regions, noting anomalous C star in CH Cyg
15 p2797 A70-31615

Solar coronal streamers, considering disk locations, evolution, classification and morphological model
15 p2804 A70-32621

Small planets observation methods, classification and designation, discussing asteroid belt origin
15 p2805 A70-32751

G and K stars spectral classification using narrow band photometry
17 p3169 A70-35380

Solar particle events forecasting based on classification scheme, discussing proton active regions
19 p3493 A70-37476

Solar proton events classification system based on solar flux logarithm
19 p3493 A70-37477

Short graphite fiber classification and orientation control in matrix by electrostatic methods
20 p3654 A70-39215

CLASSIFYING
High speed fluorescent cell sorting system for sorting mouse spleen cells from Chinese hamster ovarian tumor cells
02 p0240 A70-12695

Rotary machine for classifying reinforcing fibers and whiskers with respect to length
05 p0855 A70-16583

Classification analysis methods application to plant identification for case with incomplete initial statistical information
06 p1014 A70-17632

International quiet and disturbed magnetic days classification and significance
10 p1873 A70-23833

G and K stars classification /spectral type and luminosity class/ by narrow band photometry
10 p1937 A70-23945

Grain configurations classification for solid propellant rockets by relative web thickness and mean vector direction of burning surface into topological continuum
11 p2100 A70-26288

C-5 aircraft electrointerference coupling minimization, applying classification plan for wire categorization and routing
12 p2201 A70-28131

Pattern recognition involving machine extraction of characteristic features and classification based on associated values, discussing design and decision rules for optimal recognition
13 p2373 A70-29577

Statistical methods for feature selection and ordering, mode estimation and pattern classification in pattern recognition, describing sequential decision model
13 p2374 A70-29578

Error correcting algorithms for pattern classification, finding optimal approximation to unknown optimal decision function
13 p2374 A70-29579

Stochastic approximation methods applied to pattern classification, estimation and control
13 p2442 A70-29586

Pattern recognition procedure for electronic systems data classification
15 p2706 A70-32566

Field classifications for southern extragalactic radio sources with available optical observations, identifying 21 objects
16 p2980 A70-34194

CLATHRATES

Thermodynamic stability of methane clathrate hydrate, building up ice grains halo within comets inner coma 14 p2650 A70-31243

CLAYS

Amino acids asymmetric polymerization on clay minerals, discussing aspartic acid and kaolinite experiments 19 p3455 A70-38030

CLEAN ROOMS

Vacuum probe sampler to monitor particle contamination on surfaces within clean environments 05 p0808 A70-16703

Clean room design problems concerning dampers, high pressure blowers, humidifiers, filters, etc 05 p0808 A70-16709

Clean room complex consisting of quality control analysis laboratory, main and pre-clean rooms and air-lock 05 p0808 A70-16710

Vacuum probe sampler to monitor particle contamination on surfaces within clean environments 09 p1623 A70-22340

Ultraclean technology to eliminate pollution traces present in laboratories, discussing turbulent flow and horizontal and vertical laminar flow rooms 10 p1828 A70-25240

CLEANERS

NT AIR FILTERS

CLEANING

Spacecraft window cleaning with methyl alcohol and low pressure nitrogen providing filming control for Apollo optical experiments 11 p2051 A70-26143

CLEANLINESS

Hydraulic fluid cleanliness requirements for aircraft systems, filtering, servovalve life, solid particles effects on friction, etc 03 p0414 A70-12999

Accommodation coefficients ratio of He 4 to He 3 measured on W and K clean surfaces 06 p1183 A70-18257

Electromagnetic torsion balance measurement of forces exerted on clean Au surfaces by monoenergetic steady state Ar and Kr beams, calculating thermal accommodation coefficients 06 p1066 A70-18258

Particulate contamination in compliance with military standard cleanliness level, using zoom microscope, charts and tables 12 p2174 A70-27010

Ultrasonics for steel cleanliness rating, considering advantages and fatigue life 15 p2743 A70-31768

Cleanliness levels for missile guidance package as function of component design complexity 24 p4349 A70-46250

CLEAR AIR TURBULENCE

High altitude clear air turbulence /HICAT/ occurrence frequency, showing effects of altitude, wind and temperature fields, terrain features, etc 01 p0006 A70-10696

CAT remote sensing for advance aircraft warning, using IR instrument to detect turbulence-associated temperature preceding aircraft 01 p0087 A70-10697

Forward sounding sensors /weather radar/ development for aiding human eye in detecting flight hazards /storms and CAT/ 02 p0297 A70-11989

Aerohydrodynamic model of relief waves in baroclinic atmosphere based on convection theory, analyzing strong turbulent vortex regime responsible for CAT [ONERA-TP-727] 03 p0408 A70-13638

Clear air turbulence and mesoscale structure subsynoptic air motion experiments for numerical weather prediction 04 p0714 A70-14394

Shear generated atmospheric clear air turbulence growth and dependence on atmospheric instabilities calculated numerically by invariant model [AIAA PAPER 70-55] 06 p1098 A70-18031

Depolarization factor measurements of clear atmospheric air by lidar techniques and laser light scattering 06 p1083 A70-18244

Stratospheric clear air turbulence over squall line, discussing turbulence over thunderstorms 06 p1102 A70-18588

Clear air turbulence significance in aviation and atmospheric science, noting Kelvin-Helmholtz model 08 p1539 A70-21559

Free atmosphere clear air turbulence, discussing velocity and temperature spectra, Kelvin-Helmholtz instability, isentropic cross sections, energy budget, etc 09 p1714 A70-22354

Stratospheric CAT layer energy budget analysis, considering energy shear feeding, buoyant extraction and frictional dissipation 09 p1715 A70-22357

Atmospheric structure and turbulence relations to radar backscattering from clear air refractive index irregularities 09 p1715 A70-22361

Potential refractive index mean vertical gradients role in turbulent mixing, noting applications to radar detection of CAT 09 p1716 A70-22365

Radar backscattering relationship to refractive index microstructure in turbulent clear atmosphere 09 p1716 A70-22366

Turbulent energy budgets in atmospheric boundary layer near ground scalar fluctuations and CAT 09 p1717 A70-22380

Clear air turbulence effect on supersonic aircraft safety and comfort, noting shallow zones and effects of topography and thunderstorms 10 p1912 A70-24506

IR sensor for detecting clear air turbulence, discussing design, installation, supporting equipment and inflight test results 12 p2229 A70-26946

IR remote temperature gradient sensor as clear air turbulence detector, presenting inflight test results 12 p2229 A70-26947

Remote measurement of CAT associated temperature gradients, comparing monochromatic and finite bandpass models 12 p2262 A70-26949

Clear air turbulence detection by radar equipped aircraft, considering reflection from refractive inhomogeneities 12 p2262 A70-26952

Statistical analysis of atmospheric wind and temperature variables relationships to high altitude clear air turbulence observed by U-2 flights 12 p2264 A70-28092

Stratospheric clear air turbulence /CAT/ vertical extent above thunderstorm graphically represented 12 p2265 A70-28095

Radar meteorology, discussing convection in lower atmosphere and clear air turbulence observations 13 p2443 A70-28475

CAT parameters sensitivity to horizontal wind and temperature distribution 13 p2444 A70-28587

Wind shear production rate by dynamical processes and relationship to clear air turbulence occurrence 14 p2609 A70-30601

CAT and small scale atmospheric motions in relation to supersonic transport and space shuttle design and operation 14 p2609 A70-30602

Stratospheric CAT-internal wave relationship, using aircraft and radiosonde HICAT measurements 14 p2609 A70-30603

CAT relationship to cyclogenesis and anticyclogenesis, considering synoptic situation and Jacobian values for forecasts 14 p2609 A70-30604

CAT shear spectra above ground frictional layer in jet stream flight conditions, using aircraft measurements 16 p2946 A70-33825

Clear air turbulence /CAT/ remote sensing feasibility by optical signal covariance measurement, taking into account refractive index fluctuations 17 p3132 A70-35723

CAT at subsidence inversion in presence of strong wind shear, noting radar echo pattern as Kelvin-Helmholtz instability indicator 17 p3133 A70-35933

High altitude clear air turbulence structure and evolution examined by high power radar and wind and temperature vertical soundings 18 p3228 A70-36483

Highly localized clear air turbulence at aircraft flight level over Mediterranean, noting simultaneous temperature rise 19 p3463 A70-38948

CAT detection by IR radiation, remotely detecting atmospheric horizontal temperature gradients 20 p3626 A70-39080

CAT as mechanism relieving wind and temperature discontinuities, maintaining Richardson number at limiting value by turbulent energy dissipation 20 p3663 A70-39373

Stratospheric clear air turbulence probability based on vertical temperature gradients and rawinsonde ascensional rates 22 p4064 A70-42619

CAT origin in unstable atmospheric shear and gravity waves, using ultrahigh resolution radar for observation of transition process 23 p4214 A70-44032

Limiting effects of topographic quasi-optical radar propagation above 100 MHz in radar aircraft navigation, clear air disturbances detection and IR warning technique 23 p4163 A70-44230

Clear air turbulence detection by IR radiometry of thermal gradients, using staggered receivers for panoramic visualization 24 p4314 A70-46093

CLEARANCES

Tip clearance effects in axial flow turbomachinery, predicting blade-to-blade variation in outlet angles and stagnation pressure losses 04 p0733 A70-14775

Tip clearance contactless measurement in jet engine turbine based on radioactive isotopes properties 11 p2055 A70-26446

Axial flow compressor clearance control coatings at blade tip paths for efficiency [SAE PAPER 700330] 12 p2291 A70-27462

Aerodynamic characteristics of wing with tip clearance within uniform flow, investigating main stream flow pattern effect 14 p2529 A70-31331

Inducer tip clearance effect on centrifugal pump suction performance with velocity and total head distributions at outlet 14 p2592 A70-31332

Aircraft turbine engines durability estimated from rotor blade minimum tip clearance measurements 22 p4092 A70-43529

CLEARING

Computerized air cargo clearing, discussing London Airport Cargo Electronic-data-processing Scheme 22 p4007 A70-43272

CLEFTAGE

Vacuum cleavage device for producing small area evaporated metal semiconductor contacts free from oxygen or other contamination 02 p0304 A70-12748

Cleavage fracture of Ta-Mo bcc alloys, investigating short range ordering and size effects by X ray diffraction 09 p1708 A70-23573

Cleavage cracks initiation and propagation in basal plane of Be single crystals, determining propagation energy as function of temperature, purity and alloying 12 p2256 A70-27614

CLIMATE

Earth climatic control by reflecting satellites producing artificial solar irradiation 03 p0581 A70-13835

Phenological network observations comparison for phase behavior of trees and plants in open landscapes and in populated areas 15 p2732 A70-32460

CLIMATOLOGY

NT BIOCLIMATOLOGY

NT MICROCLIMATOLOGY

Noctilucent cloud observation stations and international cooperation in exchanging climatological data concerning annual variations, height distribution and latitude dependence 01 p0072 A70-10579

Earth surface hydrology effect incorporated into atmospheric circulation mathematical model for climate, considering ocean as atmospheric moisture reservoir 04 p0680 A70-15296

Two level model for planetary atmospheres adapted to simulate atmospheric circulation and climate of Mars 04 p0756 A70-15515

Aircraft icing effects on conventional and jet aircraft and helicopters, discussing seasonal variations for main climatic regions 07 p1329 A70-18926

Upper atmosphere climatology including latitudinal and longitudinal variations in wind, temperature, density and zonal momentum 07 p1275 A70-20279

Solar radiation variations effect on earth climate, noting atmospheric transparency role in glaciation on thermal regime 08 p1539 A70-21919

Climate variations and earth orbital elements secular perturbations, noting solar radiation and celestial mechanics roles 09 p1666 A70-22177

Lebedev nomogram determination of climatic parameters dependability, considering underlying theory and temperature sums 09 p1718 A70-23171

Management planning for global atmospheric research program /GARP/ applied to climatology and weather forecasting 09 p1795 A70-23545

Climatic phenomena cyclic behavior from forecasting viewpoint, considering geomagnetic, upper atmospheric and solar activity effects 12 p2265 A70-28268

Earth radiation balance climatological characteristics based on satellite and published data, analyzing earth-atmosphere albedo on global scale 14 p2603 A70-30402

Climatology of safe threshold Mach number and airplane ground speed for boomless supersonic cruise, considering San Francisco-New York route 14 p2530 A70-30606

Physical methods in applied climatology, analyzing meteorological effects on human body and building thermal conditions and plant biomass growth 15 p2771 A70-32111

Air mass climatology in terms of pressure temperature and moisture content

15 p2772 A70-32457

Soviet book on statistical analysis of meteorological elements based on expanding natural orthogonal functions covering horizontal, vertical and time distributions including applications

15 p2772 A70-32842

Oceanographic phenomena inference from satellite cloud photographs, developing seasonal cloud climatology for Peru Current area

16 p2897 A70-33713

Shooting star shower and solar eclipse frequencies correlation with long term climatic changes

17 p3168 A70-35310

Climatological maps of earth mean annual radiation balance compared with satellite data

18 p3286 A70-36966

Twenty two year solar activity cycle effect on earth climate, plotting odd and even 11 year cycle curves for pressure and temperature

20 p3662 A70-39189

Soil science and climatology in Central Europe archaeological site location by aerial photography

21 p3826 A70-41402

January climatology simulation experiment based on two layer version of global circulation model, comparing computed and observed results

21 p3847 A70-42120

Global solar radiation climatology of earth including direct and diffusive radiation

22 p4013 A70-42600

Convective heat transport role in determining rotating planets climatic temperature zones

22 p4099 A70-42626

Earth atmospheric boundary layer wind velocity, temperature gradients and specific humidity differences, calculating climatic correlations from mathematical circulation model

23 p4214 A70-44264

CLIMBING FLIGHT

Optimal fuel consumption for climbing, cruising and landing flight conditions for medium range subsonic, high supersonic and hypersonic aircraft

02 p0227 A70-12404

Optimum rocket climbing regime in dense atmospheric layers, including gravitational acceleration investigation in outside layers

06 p1155 A70-17626

Asymptotic expansions and energy methods applied to three dimensional aircraft maneuvers involving energy climbs and turns

07 p1190 A70-20416

CLINICAL MEDICINE

Biophysical symptoms and clinical treatment of ailments resulting from pressure drop, considering exposures to higher and lower pressure changes

01 p0011 A70-10036

Cliniconosographic criteria of flight phobia and differentiation from other psychopathologic syndromes, noting sociofamilial and operative factors

01 p0031 A70-10235

Prospective epidemiological recognition of clinical coronary heart disease, discussing effects of habitual physical inactivity, excessive dietary fat, socioeconomic stresses, etc

01 p0023 A70-10865

Simplified laboratory test program yielding serviceable information for possible direct laboratory diagnosis of risk factors affecting atherosclerosis

03 p0431 A70-14279

Clinicopathological studies of coronary artery occlusion and acute myocardial infarction, discussing coronary thrombosis

04 p0635 A70-15459

Acute myocardial infarction clinical features, discussing gallop rhythm, ventricular arrhythmias, ventricular tachycardia, bradycardia, etc

04 p0637 A70-15471

Asymptomatic pilot with idiopathic paralysis of hemidiaphragm, discussing clinical picture and aeromedical significance

07 p1215 A70-19942

Aeromedical significance and pathophysiological mechanisms of clinical entities mimicking vasovagal syncope

08 p1454 A70-21946

Physiological mechanism and differentiation of alternobaric vertigo in flyers

08 p1449 A70-21947

Hypoxia fundamentals and clinical treatment - Conference, Mainz, Germany, October 1967

10 p1820 A70-25076

Permissible radiation exposure levels during prolonged space flights based on clinical data

13 p2351 A70-29336

Aerospace Medical Association Conference, St. Louis, April 1970

17 p3026 A70-35326

Multiple choice rotation chair for clinical experimental research and pilot vestibular tests

20 p3580 A70-39438

G suit application to clinical therapeutics, noting intraabdominal bleeding control

21 p3767 A70-40737

Automatic diagnosis of clinical electroencephalogram with digital computer, showing maximum and minimum points, basic pattern and paroxysmal wave

22 p3977 A70-42869

Coronary heart disease risk factors and prevention, discussing blood pressure, cholesterol, body weight, smoking, etc

22 p3975 A70-43693

Human retinal detachment treatment by centrifugation

22 p3975 A70-43699

Coronary heart disease prediction based on clinical suspicion, age, total cholesterol and triglyceride, using relationships established by cinearteriographic studies

23 p4145 A70-43947

CLIPPER CIRCUITS

Detection efficiency compared for system containing clipper circuit and quasi-optimal linear system for video pulse signal with additive noise background

03 p0446 A70-13201

Delay locked closed loop system with and without signal clipping in noisy /Gaussian/ environment applied to radar, sonar and seismic propagation

07 p1242 A70-19997

CLOCK PARADOX

Einstein theory of length contraction and time dilation relative to ether regarding slowness of clocks in motion

21 p3849 A70-40550

CLOCKS

NT ATOMIC CLOCKS

NT CHRONOMETERS

Astronomical clock pendulum oscillations isosynchronization noting effects of suspension elastic moment, fabrication, calibration errors and rotation center displacement

03 p0484 A70-13367

Synchronization of ground stations clocks by time scale comparison with overflying aircraft

03 p0487 A70-13642

Semidiurnal lunar tidal wave influence on clock corrections obtained by observations of stellar meridian passages at four localities

04 p0756 A70-15479

Tsl catalog of right ascensions of stars based on photoelectric observations, including clock corrections

04 p0756 A70-15480

Correlation function procedure applied to quartz clock rate analysis, noting operating temperature control

04 p0693 A70-15487

Airborne system for calibrating remote precision clocks using two way radio transmitter, measuring error by system similar to radar beacon transponder system

05 p0844 A70-15773

Clock synchronization system design and test results for PCM time division multiple access satellite communication system

06 p1011 A70-18411

Clock corrections smoothing by linear transformation operator, calculating operator transfer function and averaged errors deviations

08 p1574 A70-21155

Time determination precision dependence on thermal deformations of clock, humidity of atmosphere and most probable value of instrument azimuth

09 p1673 A70-22163

Loran in range-range mode for computing user position based on remote clock synchronization, evaluating accuracy

09 p1719 A70-22192

Clock synchronization system using lunar radar reflections for Deep Space Network needs, discussing remote clock receiver and antenna

09 p1656 A70-23037

Tracking station clock synchronization error measurement using Deep Space Network Mark I ranging system, discussing system theory, design, operation, economy and versatility

09 p1656 A70-23038

Synchronous satellite communication system clock synchronization loop design taking into account delay time

10 p1835 A70-24335

Energy concept in cosmology based on relativistic considerations, indicating universal time by synchronous clocks system

11 p2109 A70-25870

Science of time considered with reference to quantum physics, special theory of relativity, directivity and symmetry and conditional probability, discussing clock designs

12 p2271 A70-27276

Clock synchronization in general relativity theory, investigating temporal and spatial relations in four dimensional continuum using simultaneous hypersurface

12 p2272 A70-27357

Clock corrections determinations by stars pairs situated symmetrically around zenith, obtaining formulas by various methods

18 p3324 A70-37146

CLOSED ECOLOGICAL SYSTEMS

Digital orbital clock and telemetry adapter for TD1A satellite attitude stabilization, describing mechanical structure

21 p3798 A70-41272

Clock synchronization in general relativity theory, investigating temporal and spatial relations in four dimensional continuum using simultaneous hypersurface

22 p4075 A70-43598

CLOSE PACKED LATTICES

Surface energy data calculated for bcc and hcp metals and high melting point compounds

06 p1090 A70-17845

Stacking faults developed in double hexagonal closed-packed phase of Ni-Ti alloy in cold worked and annealed conditions, using X ray line broadening

10 p1906 A70-25228

Superconductivity in noble metal rich hexagonal close packed phases and fcc solid solutions ascribed to Fermi surface-Brillouin zone interaction

15 p2785 A70-32398

CLOSED CIRCUIT TELEVISION

Color closed circuit TV visual cues in flight simulation during flare and touchdown, including ATA requirements and acuity limits

10 p1857 A70-24201

CLOSED CYCLES

Electrothermal instability and critical Hall parameter growth rates in closed cycle linear plasma generators with variable electron mobility, discussing perturbation effects

01 p0151 A70-10655

Closed circuit respiration studies on subjects at rest and work, demonstrating potassium superoxide as oxygen source in breathing apparatus

15 p2688 A70-31500

Space acquired hydrological cycle data relating to water occurrence and movement in atmosphere and earth surface mantle

20 p3616 A70-39063

Equilibrium performance of closed Stirling cycle with chemically reactive gas as working fluid, discussing power density and thermal efficiency

22 p3982 A70-42756

Effective pressure ratio nomographs for mechanical energy conversion and heat transfer of closed regenerative Stirling engines, using isothermal theory

22 p4091 A70-42757

NERVA reactor technology applied to closed Brayton cycle MHD power system

24 p4377 A70-45956

CLOSED ECOLOGICAL SYSTEMS

Medico-engineering experiment in partially closed ecological system for long term manned space missions

01 p0032 A70-10363

Phytotron design and operation, discussing closed air conditioned plant growing system at Stockholm including greenhouse, light controlled rooms, darkrooms, etc

03 p0435 A70-13716

Closed life support systems tests, describing effects of long term /one year/ confinement of three human subjects

04 p0641 A70-14565

Mathematical model of optimal partially closed life support system consisting of man, recycling unit, storage unit and waste disposal outlet

05 p0809 A70-17110

C-5 design features for entire environment assuring human integration as crew member or troop passenger

09 p1605 A70-22021

Phytotron design and operation, discussing closed air conditioned plant growing system at Stockholm including greenhouse, light controlled rooms, darkrooms, etc

11 p1990 A70-25516

Rhesus monkeys tolerance to graded increase in closed environment carbon dioxide, examining heart rate and cardiac rhythm

11 p1988 A70-26517

Plant cultivation in closed biological cycles by hydroponic method using keramsit /alumoferrisilicate/ substrate

13 p2358 A70-29328

Biogeocenosis applicability to artificial closed ecological systems consisting of plants creating organic matter and heterotrophic organisms

13 p2353 A70-29501

Microbial flora in human subjects confined to long term Tektite I underwater habitat

15 p2681 A70-31879

Airborne bacteria and fungi in atmosphere of Tektite I underwater habitat

15 p2681 A70-31880

Carbon dioxide output monitoring from biosatellites for circadian system behavior in closed organism-environment systems

16 p2849 A70-33992

Manned planetary spacecraft and space stations as ecological systems, considering common features

17 p3176 A70-34799

- Systemic bacterial infection resistance in white mice exposed to simulated hypobaric normoxic space cabin environment 20 p3572 A70-39431
- Optimal temperature control for confined spaces and life support systems, using mathematical models of environmental control systems 24 p4295 A70-46373

CLOSED LOOP SYSTEMS U FEEDBACK CONTROL CLOSING

- Cone crack closure in brittle solids, discussing optical and X ray studies on glass and silicon during unloading 17 p3183 A70-34621

CLOSTRIDIUM BOTULINUM

- Thermal stability of glycolytic enzymes from thermophilic clostridia 17 p3042 A70-35327

CLOSURES

- Cascade mechanism of closure associated with non-linear wave interactions between modes in turbulent plasmas, using hydrodynamical model 11 p2087 A70-25358

CLOTH

U FABRICS

CLOTHING

- NT COTTON FIBERS
NT FLIGHT CLOTHING
NT GOGGLES
NT HELMETS
NT PRESSURE SUITS
NT PROTECTIVE CLOTHING
NT SPACE SUITS

- Static electricity generation and discharge in human beings due to clothing layers, analyzing body capacitance, resistance and inductance for ordnance and fuels safety 03 p0439 A70-14133

- Static electricity suppression for textile materials by blending conducting metal fibers into yarn 05 p0870 A70-16299

CLOTTING

- Blood clotting and fibrinolysis under short term physical work in healthy men measured using thrombelastograms 06 p0992 A70-17423

CLOUD CHAMBERS

- Cloud chamber investigation of artificial cloud of water droplets in electrostatic field, discussing cloud precipitation, collection efficiency and fog dissipation 05 p0879 A70-16689
- Critical review of paper on evidence of quarks in air shower cores from cloud chamber tracks, explaining data by statistical fluctuations in particle fluxes 08 p1562 A70-21272
- Fog droplet size growth time dependence and spectral variations during simulated cloud formation by water vapor condensation in chamber 14 p2601 A70-30128

CLOUD COVER

- Automatic picture transmission /APT/ ground station design for reception of weather satellite cloud cover photographs, discussing SNR 01 p0059 A70-11451
- Methane and ammonia absorption bands and possible structure of Jupiter and Saturn cloud layers by spectrophotometric observations 02 p0366 A70-11807
- Two layer model of Jovian clouds including clear space, showing computed and measured equivalent widths of H quadrupole lines 02 p0367 A70-11813
- Decay times for thermal disturbances near cloud tops in Jupiter atmosphere, discussing hydrogen absorption 02 p0368 A70-11827
- Venusian atmosphere low reflectivity reinterpretation based on spectrophotometric data indicating constituents of yellow and upper UV haze layers 02 p0377 A70-12555
- Linear regression equations to relate atmospheric precipitable water to surface dew point, sky cover and weather 03 p0520 A70-13163
- Cloud cover recurrence estimators from set of unconditional probabilities tested against sample of Northern Hemisphere diurnal variation data 03 p0521 A70-13164
- Venusian cloud layer radius, discussing error in determination of occultation level height of regulus by venus 03 p0574 A70-13881
- Cloud layer multiple scattering in Jovian atmosphere, discussing influence on Lorentzian contour of planetary absorption lines 03 p0574 A70-13882
- Global cloud cover and earth atmosphere heat budget measured from weather satellites, discussing Tiros pictures, radiation charts and albedo 03 p0479 A70-14348
- Cloud cover consequence on earth photographing space missions simulated by Monte Carlo method using worldwide statistics [AAS PAPER 69-577] 04 p0676 A70-14636

- Radiometric investigation of energy brightness distribution over clear, cloudy and variable sky at micron wavelengths 06 p1056 A70-17835

- Cloudy sky IR background radiation model for designing simulator of IR background for studying noise rejection characteristics of electro-optical automatic control systems 07 p1246 A70-19527

- Vertical short wave albedo profiles in lower troposphere under cloudiness and clear sky using actinometric sounding 08 p1537 A70-21105

- Cloud layer vertical displacement effects on upper boundary and temperature changes in st-sc using aircraft sounding data 08 p1537 A70-21107

- Side-looking radar used to produce high resolution imagery of Panamanian province under persistent cloud cover 10 p1882 A70-25045

- Communication satellite repeater design requirements to achieve adequate SNR for varying rain and cloud attenuation [AIAA PAPER 70-498] 11 p1998 A70-25425

- Cloud cover effect on earth photographing space missions by Monte Carlo computer simulation, using worldwide cloud statistics 11 p2075 A70-25600

- IR reflectance of cirrostratus and cirrus clouds and jet contrail measured by spectrometer on high altitude aircraft 11 p2045 A70-25626

- Computer plotting of flow patterns and orographic cloud over/in lee wave flow, including rotors, blocking and high level turbulence 12 p2264 A70-27722

- Energy distribution in dark and light details on Venus spectrograms, considering relation to clouds in upper atmosphere 12 p2311 A70-28304

- Spectrographic measurements of Jovian Red Spot and Southern Tropical Zone molecular absorption bands related to cloud cover density and depth 12 p2311 A70-28305

- Cloud cover photographs in deep occluded cyclone by Soyuz 4 spacecraft 14 p2602 A70-30139

- Integral radiation fluxes incident on sloping and horizontal surfaces compared under cloud covers of various intensities 14 p2603 A70-30408

- Cloud size clear area spacing statistics development for satellite mission and simulation analyses 14 p2609 A70-30598

- Venus atmosphere-lithosphere interactions, predicting electrically conducting cloud masses presence 14 p2646 A70-31070

- Cloud cover stationary pictures by spin-scan camera in synchronous orbit over Pacific converted into motion pictures showing cloud pattern changes and storm development 14 p2587 A70-31150

- Retrograde rotation of equatorial spots of Venus cloud exterior layer, using UV photographic and spectroscopic observations 14 p2649 A70-31215

- Geochemistry of venus volatile elements identifying cloud forming species as Hg compounds 14 p2650 A70-31217

- Average rotational temperature of Venus atmosphere above cloud tops from carbon dioxide band spectroscopy 14 p2650 A70-31219

- Cloud cover statistical data applied to planning remote satellite-borne sensing missions, using Monte Carlo method 14 p2611 A70-31232

- Cloud formation and structure determination using aircraft-borne IR stereo imagery 15 p2769 A70-31687

- Temperature profiles and wind velocities during convective cloud banks formation from meteorological satellite data 15 p2770 A70-32065

- Wind field reduction from satellite cloud structure data 15 p2770 A70-32066

- Cloud distribution and optimal satellite picture foreshortening for global meteorological analysis of atmosphere, using Zond 7 photograph 15 p2771 A70-32110

- Martian brightness increase at 1 deg phase angle, explaining by transparent cubic crystals presence in clouds 15 p2803 A70-32499

- Edson layer theory explaining phase anomaly of inner planets in terms of light scattering by thin layer above Venus cloud cover 16 p2973 A70-33113

- Cloud-free earth areas determined via reflected radiance measurements from ATS 3 cloud camera 17 p3133 A70-35930

- Geometric methods for processing TV images of earth cloud cover 18 p3286 A70-36964

- Underlying surface inhomogeneity effect on radiation in presence of solid cloud cover 18 p3287 A70-36975

- Atmospheric scattering indicatrices from daytime sky brightness balloon measurements in presence of cloud cover 19 p3460 A70-37420

- Martian brightness increase at 1 deg phase angle, explaining by transparent cubic crystals presence in clouds 23 p4240 A70-43920

- Venus atmospheric speculations compared to Soviet and American probe findings, discussing composition, evolution cloud layer and ionosphere 23 p4253 A70-44863

CLOUD GLACIATION

- Cloud particles growth and interactions, discussing water vapor condensation, ice phase nucleation, rain droplet growth rate, etc 07 p1262 A70-18897

- Criticism and reply to Venus cloud water drop HCl concentration preventing ice cloud formation 11 p2108 A70-25653

- Aircraft ice crystal counter for real-time measurement in cirriform clouds, using contact electrification detection 12 p2264 A70-28091

CLOUD HEIGHT INDICATORS

- Radiation scattering during upper cloud altitude determination by satellite 06 p1097 A70-17790

- Layered cloud amounts, cloud bases and tops heights analyses based on satellite TV and IR data 10 p1912 A70-23936

- Radiation scattering during upper cloud altitude determination by satellite 10 p1913 A70-25022

- Clouds upper height boundary relation with radiation temperature field from satellite data, noting cirrus clouds influence 13 p2444 A70-28589

- Lidar for cloud height measurements from ground and meteorological satellites 14 p2611 A70-31155

CLOUD PHOTOGRAPHS

- Automatic picture transmission /APT/ ground station design for reception of weather satellite cloud cover photographs, discussing SNR 01 p0059 A70-11451

- Satellite photographs interpretation for cloud types and patterns with allowance for transmission characteristics, image cut-off at corners and sun angle and glint 13 p2394 A70-28786

- Cloud cover photographs in deep occluded cyclone by Soyuz 4 spacecraft 14 p2602 A70-30139

- Cloud cover stationary pictures by spin-scan camera in synchronous orbit over Pacific converted into motion pictures showing cloud pattern changes and storm development 14 p2587 A70-31150

- Oceanographic phenomena inference from satellite cloud photographs, developing seasonal cloud climatology for Peru Current area 16 p2897 A70-33713

- Wind velocity and direction determination from artificial luminescent clouds photographs, calculating topocentric coordinates 18 p3252 A70-36991

- Satellite TV cloud picture digital representation, deriving algorithms for statistical analysis of geometrical features 19 p3463 A70-38755

- Vertical motion determination from satellite cloud pictures based on canonical correlation of initial fields 20 p3664 A70-39401

- Atmospheric global observation for long term weather forecasts, obtaining cloud photographs and radiation data from satellites 21 p3847 A70-42255

CLOUD PHOTOGRAPHY

- Noctilucent clouds morphological and kinematic characteristics based on photographs 03 p0476 A70-13885

- Photographic detection of thin cirrus clouds effect on earth heat budget 04 p0696 A70-15575

- Intertropical convergence zone /ITCZ/ movements, analyzing data obtained by ship and ESSA satellite cloud photography 10 p1912 A70-23939

- Onboard IR receiver and ground photorecorder for Meteor satellite cloud tracking, using computer processed data 15 p2738 A70-32112

- ATS spin scan cloud cameras mechanical design and operation 16 p2914 A70-34149

- Gemini spacecraft photograph patterns revealing relationship between cloud formation and topography 18 p3258 A70-36298

- Geometric methods for processing TV images of earth cloud cover 18 p3286 A70-36964

Electronic data handling and CRT display of ATS satellite cloud pictures
24 p4371 A70-46048

CLOUD PHYSICS

Structure and composition of clouds of ammonia and water bearing condensates, investigating compositional models of Jupiter atmosphere, considering ammonium hydrosulfide cloud layer
01 p0179 A70-10527

Noctilucent cloud observation stations and international cooperation in exchanging climatological data concerning annual variations, height distribution and latitude dependence
01 p0072 A70-10579

Jupiter upper atmosphere cloud bands zonal motion velocities, examining barotropic stability criterion and geostrophic balance hypothesis
02 p0368 A70-11828

Visible radiation reflection, transmission and inside intensities of terrestrial clouds calculated by Monte Carlo program utilizing scattering phase function
02 p0326 A70-12286

Night airglow variations observed during Cosmos satellite orbits, determining atmospheric albedo wavelength dependence for solid and medium cloudiness and clear skies
05 p0841 A70-16728

Stratified cloud transport and evolution, solving kinetic equations by numerical method
06 p1053 A70-17210

Supersaturation during droplet-liquid phase formation in clouds estimated from trough formed on curve of distribution function
06 p1097 A70-17796

One dimensional cumulus convection model modified by incorporating rain evaporation rate and temperature changes from downdrafts
06 p1099 A70-18568

Cloud base updraft field, three dimensional reflectivity pattern and rain and hailfall pattern for thunderstorms in Alberta, discussing shear
06 p1099 A70-18569

Momentum considerations in thunderstorm dissipation by disrupting organized cloud base updraft structure
06 p1100 A70-18570

Air flow in updraft through and around cloud region containing precipitation particles using numerical model, computing horizontal divergence
06 p1100 A70-18572

Dry regions in cumulus cloud near environment interpreted as evidence of compensating motion in environment
06 p1101 A70-18577

Atmospheric electricity phenomena connected with micro, macro and global processes, discussing electrical generation by convective clouds and earth-atmosphere system electrical balance
07 p1262 A70-18896

Cloud particles growth and interactions, discussing water vapor condensation, ice phase nucleation, rain droplet growth rate, etc
07 p1262 A70-18897

Barium ion artificial clouds motions and striations due to cloud-ionosphere coupling, studying electron density variations below cloud in E layer
07 p1271 A70-20155

Nacreous and noctilucent cloud physics, discussing earth-impacting meteor dust accumulation and mesopause water vapor
07 p1273 A70-20265

Rocket-borne sampler for collecting noctilucent cloud particles in mesopause, describing collection and analysis methods and protection against tropospheric contamination
07 p1273 A70-20266

Noctilucent clouds in mesopause over North America, discussing ground stations network, intensity variations, structure and time distribution
07 p1273 A70-20267

Soviet collection of papers on physics of clouds and cloud modifications, covering droplet fusion, radar precipitate measurements, cellular meteorology, ice forming aerosols, stochastic condensation
08 p1535 A70-20770

Soviet collection of papers on cloud physics and modifications covering precipitation agents, droplet growth laws, electrical properties, etc
08 p1535 A70-20876

Vertical plane and axis symmetrical numerical models for cumulus convection of moist atmosphere, discussing initial conditions
08 p1536 A70-21025

Soviet collection of articles on physics of clouds modifications covering precipitations microstructure remote measurements, microwave scattering, etc
08 p1536 A70-21094

Radar model of shower and hail clouds as two phase system of independently scattering spherical particles, stressing radar properties dependence on particle properties
08 p1536 A70-21097

Soviet collection of papers on cloud physics covering stratus variation, radiation, albedo profiles, st-sc

clouds, supercooling, crystallization, condensation nuclei, etc
08 p1536 A70-21101

Time dependent height of lower boundary of subinversion stratus clouds using atmospheric moisture and heat transport equations
08 p1537 A70-21102

Horizontal turbulent diffusion model of cloud, determining particles dispersion as function of time
08 p1538 A70-21111

Optimal atmospheric transmittance windows for underlying surface and cloud temperature determination from satellites
08 p1538 A70-21426

Layered cloud amounts, cloud bases and tops heights analyses based on satellite TV and IR data
10 p1912 A70-23936

Electrohydrodynamics of charged water drop pairs disintegration in electric field concerning warm cloud electrification
10 p1912 A70-24806

Warm clouds electrification calculated for electromagnetic field growth by inductive mechanism, noting role of water drop pair interaction
10 p1913 A70-24807

Pulsed Doppler radar technique for monitoring and diagnosing severe storms, obtaining wind velocity and direction within cloud
10 p1844 A70-25242

Cumulus convection one dimensional time dependent numerical model, considering horizontal mixing, evaporation, precipitation generation and freezing and thermodynamic processes
11 p2075 A70-25648

Initial cloud formation model, computing drop concentration and supersaturation
11 p2075 A70-25917

Scattering particle distribution relation to halo formation in polydisperse clouds, using Kirchhoff approximation for halos theory construction
12 p2264 A70-27522

Model for droplet size spectrum in cloud with spatial inhomogeneity of nuclei concentration, determining characteristic size dependence on altitude
14 p2601 A70-30129

Cloud droplets coagulation growth, calculating aerosols inertial capture coefficient by fine jet method
14 p2602 A70-30390

Time constant equations for hair and film radiosonde hygrometers, allowing for inertial errors in humidity and cloud boundary measurements
14 p2603 A70-30412

Dissection techniques for measuring dynamic parameters of debris clouds expanding from energetic events
14 p2584 A70-30510

Spacecraft design requirements for scientific zero G cloud physics experiments concerning colloidal modification processes
14 p2584 A70-30552

Cloud model development and computer simulation uses, noting applications to aerospace experiment design
14 p2608 A70-30597

Electromagnetic ELF radiation model for multiple return strokes of cloud to ground lightning discharges, considering channel length
15 p2726 A70-31864

Cloud droplet agglomeration by weak shock waves, discussing growth mechanism
17 p3067 A70-34549

Upper atmosphere temperatures from vapor cloud diffusion, eliminating errors from bright sky background at twilight
17 p3076 A70-34940

IR radiation diffuse reflection, transmission and emission in water clouds
18 p3244 A70-35950

Cloud brightness as function of illumination and underlying surface conditions, relating macrooptical parameters and microstructure
18 p3284 A70-36628

Photolytic model of Jupiter belt excess temperatures and coloration compared to solid ammonia clouds, using IR and visual observations
19 p3513 A70-37410

Spectral radiative capacity of lower level clouds in specific transmittance window, using airborne diffraction spectrometer measurements
19 p3461 A70-37424

Isolated cumulus clouds formation numerical simulation, determining movement rates relationship to external wind speed
19 p3463 A70-38756

Prototype cloud physics laser nephelometer design and performance, determining droplet concentration and size from scattered light pulse count and amplitudes
20 p3626 A70-39081

Pulsed laser lidar measurements of atmospheric turbidity, diffusion, pollution, visibility and cloud physics
20 p3584 A70-39127

Noctilucent cloud kinematics, examining wave structure and lengths, velocities and general motion
20 p3622 A70-39403

Cloud motions from IR measurements within overlap region of adjacent Nimbus II orbits compared with wind vectors from constant pressure charts
20 p3665 A70-40068

Cloud structure, atmospheric water vapor and liquid water contents from passive ground based microwave spectrum measurements
21 p3846 A70-40906

Thunderstorm development processes investigated by aircraft measurements of electrical structure in cumulonimbus clouds, noting lightning probability dependence on turbulence within cloud
22 p4064 A70-42775

Cloud droplet growth rapid computation using number density mean value for integrating stochastic coalescence equation into differential equation
22 p4064 A70-42910

Stratus cloud dissipation process in descending vertical currents, using thermohydrodynamic and kinetic equations for cloud droplet distribution function
22 p4066 A70-43377

Noctilucent clouds blue color and rocket sounding results explained by ozone model of mesospheric clouds formation
23 p4188 A70-44048

Computerized simulation of raindrop effects on initiation of cloud-to-ground lightning strokes
24 p4371 A70-45978

CLOUD SEEDING

Visibility improvement in fog at airports, discussing fog-seeding and warm fog modification operations
01 p0135 A70-11320

Satellite surveillance in cloud and weather modification, considering area selection for cloud seeding, atmospheric energy redistribution, etc
04 p0677 A70-14645

[AAS PAPER 69-621]

Seeding effects on isolated cumulus clouds, using numerical model of microphysics and dynamics factors, measuring rainfall amounts and duration
06 p1098 A70-18243

Soviet collection of papers on cloud physics and modifications covering precipitation agents, droplet growth laws, electrical properties, etc
08 p1535 A70-20876

Soviet collection of articles on physics of clouds modifications covering precipitations microstructure remote measurements, microwave scattering, etc
08 p1536 A70-21094

Artificial crystallization theory for supercooled dry-ice seeded stratus clouds, taking into account condensation growth and turbulent diffusion of crystals
08 p1538 A70-21108

Vertical and horizontal expansion rate of crystallization of dry-ice seeded internal stratus clouds
08 p1538 A70-21109

Artificial crystallization zones width measurement error during time intervals after cloud seeding by aircraft and solar reflection methods
08 p1538 A70-21110

Airborne pyrotechnic cloud seeding system development, testing and application, comparing rainfall from test and control clouds
10 p1886 A70-23931

Warm fog clearing effectiveness by seeding with hygroscopic nuclei as function of fog droplet and seeding nuclei distribution
17 p3132 A70-35928

Weather modification by jet aircraft contrails, discussing cloud seeding observations in Alaska
24 p4371 A70-45421

CLOUDS

NT ARTIFICIAL CLOUDS

NT CIRRUS CLOUDS

NT CLOUDS (METEOROLOGY)

NT CUMULONIMBUS CLOUDS

NT CUMULUS CLOUDS

NT ELECTRON CLOUDS

NT NIMBOSTRATUS CLOUDS

NT NOCTILUCENT CLOUDS

NT PLASMA CLOUDS

NT STRATOCUMULUS CLOUDS

NT STRATUS CLOUDS

Galactic satellite interpretation for high velocity hydrogen clouds at high latitudes
02 p0363 A70-11780

Radiative heat transfer through dust clouds in radiative equilibrium and isothermal clouds between parallel plates measured with heat flowmeter
04 p0781 A70-14802

[ASME PAPER 69-WA/HT-41]

Spin angular momentum of planets based on particle accretion, discussing particles cloud condensation
08 p1576 A70-21400

Venus clouds self consistent radiative-convective model with sun as heat source
11 p2107 A70-25647

Radar target optimal detection algorithms in cloud of passive reflectors, noting space surveillance regularities
15 p2696 A70-31516

Aerodynamic drag coefficients of micron size particle clouds in compressible transonic flow, using light extinction method

16 p2894 A70-33882

Interstellar cloud collisions, examining gas and dust particles separation by size

18 p3313 A70-36323

Venus cloud displacement, measuring formations longitudes and latitudes for evidence of cytherean upper atmosphere rapid bulk motion

19 p3518 A70-38027

Venus atmospheric visible clouds circulation, determining zonal flow induced by moving heat sources

19 p3519 A70-38252

Collisions in one, two and three dimensional plasmas of finite sized particles and clouds, obtaining scattering cross sections and Fokker-Planck coefficients

20 p3679 A70-39663

CLOUDS [METEOROLOGY]

NT ARTIFICIAL CLOUDS

NT CIRRUS CLOUDS

NT CUMULONIMBUS CLOUDS

NT CUMULUS CLOUDS

NT NIMBOSTRATUS CLOUDS

NT NOCTILUCENT CLOUDS

NT STRATOCUMULUS CLOUDS

NT STRATUS CLOUDS

Satellite surveillance in cloud and weather modification, considering area selection for cloud seeding, atmospheric energy redistribution, etc

04 p0677 A70-14645

Depth and shape of 0.94 micron water vapor absorption band for clear and cloudy skies, noting radiation distortion for dark dense clouds

04 p0690 A70-15024

Satellite multispectral photometry data in airglow bands correlated with cloud characteristics and surface albedo variations

04 p0715 A70-15522

Spiral cloud vortex model in occluded extratropical cyclone constructed using atmospheric dynamics equations and satellite photographs

05 p0879 A70-16642

Climatological cloud type statistics for simulating earth sensing mission data output as function of sensor field of view and spatial resolution

06 p1065 A70-18098

Ground based radar surveillance for SST to avoid convective clouds and thunderstorm activity during transonic acceleration phase ensuring minimum demands on maneuverability

09 p1610 A70-22242

Reflection patterns of solar radiation from cloud, water and land surfaces measured by airborne radiometer, observing anisotropy

09 p1671 A70-23523

Glider pilots flight above cloudstreets in clear sky, discussing situation for wave soaring over flat ground

10 p1805 A70-24583

Terrestrial clouds near IR light scattering compared to reflectivity of water and ice particles, discussing Mie and multiple scattering

11 p2045 A70-25649

Vertical air velocity in convective clouds by pulsed Doppler radar observations of thunderstorm

11 p2004 A70-25650

Cyclone cloud vortex evolution from satellite photographs, examining reasons for onset and disintegration

13 p2444 A70-28588

Atmospheric moisture balance solution for altitude dependent vertical velocity and turbulence coefficient, considering cloud water content and boundaries height calculation

14 p2601 A70-30137

Clouds and precipitations radio brightness temperature contrasts taking into account underlying surface humidity

15 p2771 A70-32070

Cloud brightness as function of illumination and underlying surface conditions, relating macrooptical parameters and microstructure

18 p3284 A70-36628

Relative effectiveness of radar and visual cloud observations

18 p3287 A70-36999

Steady symmetric flow model for Jupiter cloud banded structure, representing variable concentration of condensing constituents with latitude

19 p3519 A70-38254

Ice crystals growth rate in natural clouds over minus 2-minus 32 C range based on characteristic axial ratio

19 p3462 A70-38261

Soviet book on aircraft electrification in clouds and precipitation during subsonic flight covering atmospheric electrical properties, flight dynamics modification, communications interference, etc

19 p3356 A70-38800

Venus atmosphere and water vapor, finding ice clouds by spectrum analysis

20 p3708 A70-39961

Cloudy planetary atmospheres model, assessing nonlocal thermodynamic equilibrium role

21 p3813 A70-40903

Large scale axisymmetric atmospheric vortex wind velocity determination, using statistical cloud data from meteorological satellites

22 p4065 A70-43376

CLUTCHES

Impact problems of slip clutch and beam scales dynamic characteristics simulation by 1130 CSMP /Continuous System Modeling Program/

10 p1860 A70-24653

Rotary relay for solar array space power transfer using clutch of low moment of inertia capable of recycling once each orbit

17 p3101 A70-34765

CLUTTER

Air traffic control radar velocity resolution for eliminating ground, rain and angel clutter by optimizing wavelengths, pulse length and beam width

02 p0332 A70-11969

Radar system for air traffic control using twin beam antenna to improve performance with respect to ground and angel clutter

02 p0332 A70-11970

Ground clutter characteristics from moving receiver in bistatic radar system, developing method for performance prediction and problem analysis

03 p0449 A70-13586

X band radar with horizontally and vertically polarized antennas to compare sea clutter suppression by decorrelation and constant alarm rate receivers

03 p0451 A70-13935

Nonadaptive processor to detect coherent radar pulse trains with uniform amplitude in clutter-plus-noise environment

04 p0651 A70-15334

Clutter symmetry as indication of matching optimum signal filter pair, comparing mismatched and matched systems

06 p1013 A70-18626

Distributed ground clutter effects computation in airborne pulse Doppler radars, describing high PRF radar

07 p1236 A70-20063

Two frequency moving target indicator system overcoming clutter motion relative to radar

11 p2004 A70-25737

Subclutter visibility /SCV/, resolution and interclutter of MTI or Doppler search radars in land, sea and weather clutter

12 p2188 A70-27940

Radar cross section sea clutter model based on slightly rough surface superposition on swell structure

13 p2366 A70-29215

Clutter signals in radar receiver antenna, determining autocorrelation function and spectral power density

15 p2701 A70-32466

Antenna array system for surface target detection in receiver noise and heavy clutter by space-time decision theory

16 p2860 A70-32954

Recent radar developments covering ground and shipborne systems, clutter suppression and computer techniques

18 p3228 A70-36658

Sea clutter tolerance comparison for frequency agile and fixed frequency radar

20 p3584 A70-39200

Optimum pulse radar signal-receiver design, considering implementation errors for maximum target detectability in clutter

24 p4313 A70-46055

COAGULATION

NT BLOOD COAGULATION

Cloud droplets coagulation growth, calculating aerosols inertial capture coefficient by fine jet method

14 p2602 A70-30390

COALESCENCE

U COALESCING

COALESCING

Physical and chemical phenomena and critical factors underlying, furthering or impeding water droplets coalescence in glass-fiber bed of filter-separator

04 p0625 A70-14709

Electromagnetic theory of forces for coalescence in granular layers during thermal evaporation of thin films, calculating interaction between instantaneous dipoles

13 p2471 A70-29640

COANDA EFFECT

Aircraft development for subsonic and transonic flight dependent on methods using blowing and boundary layer control and Coanda and Magnus effect

09 p1610 A70-22220

Coanda effect in bistable fluid amplifier, using finite difference method for computer programmed solution of flow equations

[ASME PAPER 70-FLCS-12] 22 p4008 A70-42415

COASTAL ECOLOGY

U.S. Coast Guard air delivered antipollution transfer system for oil, discussing deployment method, trajectory analysis, rigging techniques and full scale testing

[AIAA PAPER 70-1205] 21 p3752 A70-41813

COASTING FLIGHT

Constant thrust electric propulsion systems performance with coast trajectories presented for 100 AU extracryptic missions

[AIAA PAPER 68-546] 06 p1137 A70-17160

COASTS

Coastal areas remote sensing instrumentation and techniques, discussing data handling and analysis and ground verification of color and multispectral imagery

[AIAA PAPER 70-299] 09 p1669 A70-22885

Coastal erosion survey by aerial photography, measuring change in beach locations over period of time lapse by corresponding reference points on photograph

10 p1879 A70-24748

Communications satellites for offshore systems, noting development of small earth station

22 p3991 A70-43576

COATING

NT ANODIZING

NT ELECTROPLATING

NT ENCAPSULATING

NT METALLIZING

Glass fiber-reinforcing techniques of polymers, discussing coating and compounding processes

01 p0104 A70-10775

Surface coating optical and thermal properties investigated in preparation for HELIOS solar probe

04 p0762 A70-15163

COATINGS

NT ALUMINUM COATINGS

NT ANODIC COATINGS

NT BIREFRINGENT COATINGS

NT CERAMIC COATINGS

NT ELECTROPLATING

NT ENAMELS

NT ENCAPSULATING

NT GLASS COATINGS

NT GLAZES

NT GOLD COATINGS

NT INORGANIC COATINGS

NT MAGNETIC FILMS

NT METAL COATINGS

NT METALLIZING

NT NICKEL COATINGS

NT PAINTS

NT PLASTIC COATINGS

NT PRIMERS [COATINGS]

NT PROTECTIVE COATINGS

NT RUBBER COATINGS

NT SPRAYED COATINGS

NT ZINC COATINGS

Contact thermographic materials application to non-destructive materials testing based on heat capacity, costs, removal time, equipment, personnel skill and training, etc

01 p0097 A70-10007

Stannic or cobalt oxide film coated glasses optical and energy characteristics determined for potential use in solar energy engineering

01 p0159 A70-10766

Thickness measurement of nonmagnetic coatings on magnetic substrates taking into account surface roughness effect

02 p0302 A70-12672

Solid lubricant films adhesion to metallic surfaces measured using pivot-twist technique

03 p0485 A70-13485

Plane electromagnetic wave backscattering from dielectric-coated metallic cylinder calculated as functions of incidence angle and coating external radius

09 p1636 A70-23075

Solar radiation heated boilers efficiency and operational temperature range improved by application of coatings, noting surface absorption properties

11 p2148 A70-25930

Selective optical coatings of alternate Ni and silicon dioxide layers, describing optical and spectral characteristics of black mirror

12 p2272 A70-27307

Thermal control coatings, windows and mirrors for 1973 Mars Viking Lander vehicles under simulated Martian surface conditions

[AIAA PAPER 69-1023] 13 p3384 A70-28530

Coating thickness measurement and analysis by radioisotope techniques including beta-particle, X and gamma ray backscatter and X ray fluorescence and absorption

15 p2742 A70-32780

Dynamic compensation of thermal pumping-induced deformation of laser active elements via thermal bending of resonator mirrors achieved by coatings

20 p3642 A70-39744

Solar wind effects on thermal control coatings reflectance and absorbance, noting simulation and thermophysical measurement requirements

[AIAA PAPER 70-833] 20 p3653 A70-39825

Polyvinyl chloride sheet steel manufacture, properties and welding methods

22 p4045 A70-42479

Boron and boron-carbide coatings formation by vapor deposition, determining optimum thermodynamic parameters from experiment

24 p3466 A70-45241

Steel surface diffusive saturation with elements of chlorides, noting role of iron chloride phase in promoting coating uniformity

24 p4350 A70-46332

COAXIAL CABLES

Electromagnetic wave diffraction effects on matching plasma waveguide to coaxial power extraction line

03 p0531 A70-13334

Physical model to study coaxial or triaxial cable systems interaction with ionizing radiation fields, emphasizing effects governing induced signals

04 p0658 A70-14746

Backward and complex waves propagation in circular waveguide with coaxial dielectric rod, discussing arbitrary angular dependences

05 p0812 A70-16145

Impedance in coaxial line generated by tee-fed waveguide slot antenna, using equivalent circuit

12 p2198 A70-27966

Frequency sampling adjustable equalizer design and operation, describing coaxial cable system tests

14 p2547 A70-30282

Electromagnetic wave diffraction effects on matching plasma waveguide to coaxial power extraction line

14 p2623 A70-30713

Lossless pulse-shaping active line for unipolar transmission, considering construction by loading two terminal Esaki diode to coaxial cable

15 p2697 A70-13827

Triboelectric noise in mechanically flexed low level signal cables for piezoelectric transducers with high gain amplifiers

21 p3825 A70-40866

Maxwell equations for hybrid modes of shielded ring line with axial and coaxial region at cut-off and near cut-off conductivity

21 p3793 A70-42269

Dielectric filled tubular monopole antenna driven by coaxial line with TEM mode, calculating current distribution from integral equation

23 p4175 A70-44953

Annular aperture /slot/ antenna driven by coaxial line, calculating input admittance and complete near field radiation distribution

23 p4176 A70-44954

COAXIAL FLOW

Dissimilar coaxial axisymmetric jets confined laminar mixing obtained from numerical solution of boundary layer equations, considering binary, isothermal and nonreacting system

04 p0621 A70-15579

Ducted turbulent mixing and burning of coaxial streams, presenting experimental results for rocket-air mixing system

06 p1130 A70-17171

Interacting coaxial supersonic jet flows noise reduction based on noise distribution characteristics measurement in anechoic chamber

06 p1040 A70-18112

Viscous compressible fluid steady laminar flow between coaxial cylinders, studying flow characteristics for uniform inner cylinder velocity

10 p1870 A70-24792

MHD generator with generator channel consisting of two coaxial cylinders with smooth annular space, discussing internal impedance sensitivity

10 p1807 A70-24855

Coaxially flowing jets axisymmetric turbulent mixing between inner and outer streams

12 p2211 A70-27837

Ablation test facilities capability extension by surrounding high enthalpy flow with coaxial cold air jet

13 p2522 A70-29883

Nuclear light bulb reactor and coaxial flow reactor for gas core nuclear rocket engines

16 p2949 A70-33532

Turbulent coaxial flow analysis predicting fuel volume fraction in gas core nuclear rocket reactor cavity, using free-jet computer code and eddy viscosity equation

18 p3290 A70-36560

Extinction condition for diffusion flame formed from opposing coaxial gas jets

20 p3739 A70-40399

Turbulence measurements in ducted coaxial air flow with faster outer stream pertinent to gas core nuclear rocket feasibility

21 p3809 A70-41748

COAXIAL PLASMA ACCELERATORS

Pulsed plasma transfer systems weight analysis, studying propellant density gradients effects on coaxial plasma gun performance

06 p1133 A70-18231

Current sheet velocity in coaxial plasma accelerator, noting drag due to insulator ablation and degassing

09 p1736 A70-23202

Current sheet speed in coaxial plasma accelerator computed as function of time, comparing results with velocity measurements

12 p2281 A70-27833

Coaxial electrode arc discharge plasma accelerators at reduced pressure under crossed fields, employing Hall effect

15 p2779 A70-32104

Pulsed coaxial plasma accelerator efficiency, examining high capacitance and axial propellant pressure gradients

[AIAA PAPER 70-1085] 20 p3693 A70-40250

Deuterium plasma three dimensional flow in coaxial accelerators, examining magnetic structure of filaments /field lines bundles/

21 p3856 A70-41321

Axial propellant density gradients and circuit capacitance correlated with pulsed coaxial plasma gun efficiency

21 p3858 A70-41726

Current distribution of accelerating electrodes of coaxial injector, using differential magnetic probe

22 p3965 A70-42805

Coaxial plasma deflagration gun for accelerating particles to high velocities at low thermal energy for plasma injection experiments

24 p4383 A70-45120

COAXIAL TRANSMISSION

U COAXIAL CABLES

U TRANSMISSION

COBALT

NT COBALT ISOTOPES

Polycrystalline Co strength and plastic properties tested at various temperatures and strain rates

03 p0510 A70-13352

Ionization energies and oscillator strengths for Fe XVI, Co XVII and Ni XVIII by frozen core approximation, noting applications to solar corona

06 p1150 A70-18465

Tensile properties variations of Co whiskers grown by reducing cobaltous bromide in hydrogen-argon mixture

07 p1306 A70-19071

Internal friction and shear modulus of Co under dynamic and steady state conditions, discussing peak at alpha-epsilon transformation

07 p1306 A70-19073

Co role in magnetic materials, discussing high magnetic moments in iron combinations, orbital angular momentum, quantum mechanics explanations, etc

07 p1306 A70-19074

Cobalt modified Ti-6Al-4V plate and billet, testing effects on heat treatment response, microstructure, tensile and fatigue properties, fracture toughness, etc

08 p1523 A70-21852

Cobalt surface X ray analysis after spark erosion treatment, revealing phase with high temperature stability

14 p2596 A70-30840

Cobalt addition to Ti-Al-V alloys, examining yield strength, heat treatment, ductility and microstructure

18 p3271 A70-35964

Dispersion hardened Co strength and plasticity temperature dependence, determining Ti and Nb carbides additives effects

19 p3450 A70-37350

Rotating Ti disk in liquid Co flow, investigating titanium carbide dissolution kinetics

20 p3648 A70-39245

Spark erosion or plasma jet treatment effects on Co surface structure, describing allotropic delta phase

24 p4364 A70-46221

COBALT ALLOYS

NT RENE 41

Hot corrosion reactions in Ni, Co and NiAl- base alloys exposed to salt-sulfur containing simulated gas turbine combustion atmospheres

01 p0118 A70-10728

Vapor pressures of cobalt over pure cobalt and over Ni-Co alloys determined as function of temperature by isotope exchange method

01 p0121 A70-11233

FeCo V plastic deformation and fracture, noting temperature and grain size effects on yield and flow stresses, ductile to brittle transition, etc

01 p0123 A70-11244

Ti-Al-Co alloys melting points and cast structures, discussing reactions with melt

01 p0125 A70-11644

Co-base hardfacing alloys mechanical properties and applications, discussing mechanical and chemical wear processes in cast and wrought types

02 p0319 A70-12712

Co-Cr alloy oxidation behavior at high temperatures and various oxygen pressures

02 p0319 A70-12720

WC-Co alloys noting polishing and grinding effects on residual stress and crack resistance

03 p0508 A70-13145

Co and Fe base alloys corrosion in Hg tested in reflux capsules and forced flow loops

04 p0710 A70-15631

Cobalt alloys physical properties and heat treatment, discussing service conditions and critical problems

04 p0711 A70-15684

Cobalt effects on Ni-W alloys mechanical and metallurgical properties including thermal stability,

fabrication response, weldability and impact resistance

07 p1306 A70-19070

Yield strength of cold worked MP Co-Ni alloys during aging at elevated temperatures, noting behavior in overaged condition

08 p1525 A70-21960

Co-based alloy mechanical properties and physical parameters at high temperatures, discussing oxidation and hot corrosion resistance

09 p1700 A70-22025

Work strengthening and microstructure of Co-Ni base alloys containing Cr and Mo, discussing deformation induced martensitic transformation

09 p1705 A70-22806

Electrical resistivity of TiNi and TiCo compounds and alloys measured at various temperatures after quenching or annealing

09 p1707 A70-23194

Adiabatic elastic stiffness of single crystals of Ni-Co alloys, determining bulk modulus dependence on chemical composition

10 p1904 A70-24699

Residual stresses effect on strength and hardness of tungsten carbide-cobalt alloy by application of small plastic deformations, observing crack formation anisotropy

10 p1904 A70-25168

Co-Fe core ability to adjust roll spacing in model rolling mill determined from magnetostrictive properties

10 p1905 A70-25175

Concentrated Fe-Co alloys, effects of local atomic configurational changes on hyperfine interaction using Mossbauer spectroscopy

12 p2284 A70-27245

Commercial Co base superalloys oxidation and hot corrosion resistance under controlled environments, examining role of various alloying elements

12 p2256 A70-27974

Vacuum annealing treatments effect on oxidation rate of Co-Cr alloy at high temperatures

12 p2257 A70-28007

Binary Co-In system thermal analysis, X ray diffraction and microscopy, discussing phase diagram

14 p2595 A70-30838

Portevin-Le Chatelier effect in carburized nickel and Ni-Co alloys, discussing carbide stability and carbon diffusion roles

15 p2756 A70-31562

Gamma phase particle distribution changes in homogeneous segregation in Co-Ti alloy attributed to elastic interaction during aging temperature changes

16 p2931 A70-33208

Co base superalloys for aircraft structures and parts, discussing temperature stability, corrosion resistance, creep, fatigue and strength

16 p2932 A70-33705

Convective diffusion and liquid velocity in Co and Fe based alloys corrosion in Hg at high temperature, using reflux capsules and forced flow loops

16 p2933 A70-34207

Iron, Ni, Cr and Co corrosion and mass transfer in high temperature Na, examining properties of stainless steels and cobalt base alloys

16 p2933 A70-34209

Binary Co-Cr alloy open circuit potential and microstructure, examining effects of composition, heat treatment, allotropic transformation and precipitation

18 p3271 A70-35966

Cobalt binary alloys allotropic transformation and thermal expansion at various temperatures

18 p3271 A70-35967

Automatic dilatometers for volume variations in steel and Co-W alloy during aging and heat treatment, noting microstructural changes

18 p3257 A70-36202

Electron microscopic investigation of alpha-epsilon phase transformations in Co-Ni alloys above and under phase equilibrium temperature

18 p3276 A70-36205

Fe diffusion in equiatomic Ni-Co alloy, using thin radioactive deposit method with tagged element Fe 59

18 p3277 A70-36440

Ultrahigh vacuum metal bonding by twist compression technique, reporting adhesion and friction coefficients for atomically ordered Pt-Co alloy

21 p3833 A70-41446

Allotropic transformation points and linear thermal expansion coefficients of Co-base binary alloy terminal solutions, using dilatometric method

23 p4203 A70-43864

Ternary Co-Cr-C alloys unidirectional solidification with metal matrix and carbide simultaneous freezing at eutectic liquidus line

24 p4358 A70-45235

Unidirectionally solidified carbide reinforced Co-Cr eutectic alloy, examining tensile strength and creep behavior

24 p4358 A70-45236

Fe-Ni-Co martensitic alloys isothermal age hardening, comparing bcc phase energy parameters of binary systems

24 p4362 A70-46182

COBALT ISOTOPES

- Solar flare proton induced radioactivity in Apollo 11 lunar surface material compared with stony meteorite data, noting cobalt 56 concentration
13 p2489 A70-28910
- Polarized Co59 target using He3-He4 dilution refrigerator, analyzing fast neutron scattering
14 p2584 A70-30508
- Low energy cosmic ray positrons arising from Co decay in Ni 56-Co 56-Fe 56 reaction chain in supernova Si burning shells
21 p3879 A70-40927
- Low temperature anharmonicity in thorium dioxide with Co 57 impurities, using Mossbauer effect of Fe 57
21 p3862 A70-40975

COBALT OXIDES

- Stannic or cobalt oxide film coated glasses optical and energy characteristics determined for potential use in solar energy engineering
01 p0159 A70-10766
- Grain boundary grooves growth kinetics in pure CoO at high temperatures, determining diffusion species and mechanisms
12 p2255 A70-27603

COCHLEA

- Guinea pig cochlear hair cell damage after exposure to impulse noise
02 p0236 A70-12322
- Traveling wave velocity in human cochlea determined by equally loud tonal pairs, comparing results to psychophysical and electrophysiological findings
02 p0237 A70-12323
- Cochlear microphonics in guinea pigs using analog equivalent electrical circuit
11 p1992 A70-26494
- Electrical polarization effects on discharges in individual auditory nerve fibers following current application to cochlear partition
17 p3033 A70-35609
- Intense white pulsed jet engine noise effects on cochlea biocurrents in cats
23 p4157 A70-45076

COCKPIT SIMULATORS

- Flying qualities criteria and piloted simulator studies during development and flight testing of stability augmentation system for B-52 aircraft
[AIAA PAPER 68-1066] 04 p0624 A70-15380
- Dual cockpit wide angle visual cue simulator design, discussing sky-earth-sun projector with four axis gimbal drive
[AIAA PAPER 70-360] 10 p1857 A70-24204
- V/STOL cockpit three degree of freedom multicrew research simulator, utilizing visual display and digital computer
[AIAA PAPER 70-356] 10 p1858 A70-24207
- Landing performance of BLEU static cockpit simulator compared with flight data for night conditions in clear and limited visibility
[AIAA PAPER 70-344] 10 p1859 A70-24215

COCKPITS

- Cockpit information transfer between pilot and flight control information displays improved by on-board data processing system
03 p0436 A70-14021
- Cockpit display system to reduce aircraft pilot workload and aid judgment making during critical operations
[ASME PAPER 69-WA/BHF-12] 04 p0642 A70-14854
- Sound levels and frequency spectra of noises measured in AN-24 and IL-18 turboprop aircraft cockpits
05 p0796 A70-16925
- Flight deck controls and instrument disposition in business aircraft emphasizing size
06 p1061 A70-17318
- Flight deck displays based on digital computer providing signals for CRT and instrumentation
06 p1061 A70-17319
- Collision avoidance system /CAS/ cockpit display equipment design and operation
08 p1492 A70-20480
- Attack aircraft cockpit displays, discussing design requirements and pilot ability as controller
08 p1435 A70-20674
- Thermal tolerance and comfort graph for air conditioned spaces with low air velocity, considering fighter plane cockpits
08 p1454 A70-21949
- V/STOL transport aircraft cockpit design in terms of size, geometry and equipment accommodation
10 p1804 A70-24048
- VFW 614 nose-contoured cockpit panes, discussing structural weight and strength, vision and window frame fabrication
10 p1806 A70-24866
- Inflight aircraft cockpit noise levels effect on pilot hearing sensitivity
11 p1990 A70-25875
- General aviation aircraft fixed-base engineering flight simulator involving use of analog computer, discussing equations of motion and aircraft cockpit
[SAE PAPER 700235] 11 p2031 A70-25904
- Commercial aircraft peak cockpit noise level during cruise and high speed descent, discussing damage risk criteria and interpolator speech interference
11 p1991 A70-26275

Harrier short takeoff fighter aircraft cockpit design, describing layout, lighting, warning and escape systems, etc
12 p2162 A70-27888

- Cockpit data monitor allowing pilot selection of instrumentation parameter readout
13 p2345 A70-28970
- Heat stress levels in cockpit of AH-1G Hueycobra helicopter parked in sunlight with closed canopy, using sweating copper mannikin
15 p2689 A70-31881
- Flight deck design since 1920, discussing ergonomics and avionic aspects
16 p2913 A70-34048
- Heavy lift helicopters cockpit display problems, describing photographic flight research program for data acquisition
17 p3082 A70-34731

- Commercial aircraft flight deck systems controls and time sharing displays, emphasizing crew management
[AIAA PAPER 70-938] 17 p3021 A70-35847
- Low cost and weight reliable microminiaturized IC automatic cockpit checklist systems for aircraft pilots
22 p3977 A70-42298
- U.S. SST flight deck instrumentation and cockpit displays during flight, discussing economic analysis of operations
[ICAS PAPER 70-59] 23 p4139 A70-44155

CODERS

- Pulse width modulation command coder for German research satellite Azur control
04 p0653 A70-15662
- Shaft misalignment effect on accuracy of precision digital shaft angle encoders, using test fixture and optical methods
05 p0844 A70-15769
- Quantizing noise measured for single integration delta modulation coders using unequal positive and negative integrator step sizes
09 p1638 A70-23368
- High speed PCM terminal with 600 channel capacity, evaluating feasibility for high speed PCM codec, examining STN degradation factors
10 p1835 A70-24337
- Coding device for computer storage of graphical information, describing construction and operation
19 p3385 A70-38576
- High speed PCM Codec with maximum 600 channel capacity applied to Time Division Multiple Access /TDMA/ system for satellite communication
23 p4166 A70-43774

CODES

- Binary, ternary and multilevel digital signals transmission codes emphasizing PCM signals
09 p1631 A70-22038
- Beacon identification-friend-foe/selective-identification-feature code-validation schemes for ATC, deriving expression for cumulative probability of validation on or within N interrogations
10 p1914 A70-24446
- Cyclic codes for error correction noting connection with exponential sum theorems
11 p2074 A70-26312
- Graphical data conversion into code for storage in computer memory
15 p2705 A70-31576
- Practical codes in digital space communication systems, reviewing Shannon information theory theorems
15 p2698 A70-31963
- Hypervelocity impact theory, discussing Euler hydrodynamic codes, projectile cratering dimensional analysis, self similar solutions, etc
15 p2823 A70-32785
- Magnetohydrodynamic calculations, discussing various models, difference methods, codes, boundary conditions, etc
18 p3296 A70-36794
- PCM data transmission, considering baseband code and modulated carrier formats and spectral distributions
19 p3379 A70-37905
- Natural language a priori description and linguistic algorithms construction, using statistical phrase contraction with Hoffman codes
22 p3993 A70-42492
- Digital computer codes for production finite element structural analysis, discussing input, output and engineering details
23 p4270 A70-44701
- Cyclic q-ary codes invariant under linear group substitutions using polynomial method
24 p4313 A70-46062

CODING

- NT DECODING
NT REDUNDANCY ENCODING
NT SIGNAL ENCODING
Color coding effects in compatible and noncompatible display control arrangements
02 p0247 A70-12381
- Rate distortion function for class of sources, proving positive and negative sides of Shannon encoding theorem for noisy channels
02 p0266 A70-12611

Technique for coding data on cosmic ray variations based on packing digital information in computer storage, proposing selective statistical control for tape recording phase
05 p0898 A70-15929

- Diagram compression by spatiotemporal coding of antenna array fitted with phase shifters
05 p0811 A70-15989
- Ternary data transmission systems characteristics for modulated codes with known parameters or random initial phases
05 p0816 A70-17006
- Binary cyclic coding schemes for multiplex spectrometry in terms of linear least mean square unbiased estimate
06 p1013 A70-17217
- Radiation Shielding Information Center computer code library for radiation transport or shielding calculations, listing programs available
07 p1239 A70-20364
- Arithmetic codes rate upper bound derived by combinatorial analysis, discussing decoding method for multiple error correction
08 p1465 A70-20792
- Viterbi decoding error probability for convolutional codes using finite Markov chain modeling
08 p1458 A70-20794
- Noise variance extreme value estimator for biorthogonally block coded high rate telemetry system for Mariner missions
08 p1459 A70-20799
- Gigahertz rate circuits requirements for high speed digital data communication from component and system viewpoint, emphasizing coding and multiplexing techniques
09 p1633 A70-22605
- Three dimensional flow field codes for spheres at nonzero angles of attack, comparing numerical and experimental results
09 p1606 A70-23254
- Coding and decoding efficiency in data transmission over Gaussian channels, comparing error probability, power, bandwidth and equipment complexity
09 p1637 A70-23320
- Optimum coding of information for symmetric channel described by code word transformation probability
09 p1639 A70-23694
- Review of 1969 London International Conference on Digital Satellite Communication session covering modulation, synchronization and coding
[AIAA PAPER 70-464] 11 p1997 A70-25409
- Error probability bounds for systematic convolutional codes
12 p2192 A70-27422
- Regular and irregular line-drawing data processing, discussing quantization and encoding methods
12 p2193 A70-28104
- Three phase code transformation task for human subjects, determining memory aid role in problem solving phase from factor analysis
13 p2361 A70-30019
- Digital coding systems operational capabilities, discussing arithmetic procedures and equipment types
14 p2554 A70-30678
- Physical signals continuous to discrete transformation by analog to digital conversion, considering coding process and transfer functions
14 p2554 A70-30679
- Data compression techniques, considering two dimensional image coding problem
15 p2705 A70-32558
- Radiometer employing frequency domain coding of noise-like signal spectrum, comparing with Dicke system
16 p2871 A70-32926
- Coding procedure for Air Force maintenance technicians to record and describe equipment malfunctions compared to experimental codes
16 p2853 A70-33666
- Communication satellite UHF link with FSK or PSK modulation, considering coded digital transmissions
16 p2867 A70-34331
- Majority logic decodability of product of two majority logic decodable cyclic codes
17 p3049 A70-34853
- Inner code concatenation with outer code to yield error probability uniform bound with exponential decrease
17 p3049 A70-34858
- Small digital computer arithmetic unit design, discussing number representation, addition and subtraction methods for performance and cost
21 p3793 A70-40757
- Two dimensional data array contour tracing algorithm for reduction of image coding bits number
21 p3786 A70-41327
- Information transmission and coding theory - Conference, Tashkent, September-October 1969, Section 2, Statistical theory of signals and noise, Optimal reception methods
22 p3986 A70-42551

Selective stimulus encoding and overlearning in paired associate learning

22 p3971 A70-43401

Single-error nongroup binary codes with maximum codewords, including quadratic residue, Reed-Muller and tripple-error constructions

24 p4313 A70-46057

Algebraic structure convolutional codes using minimal encoders with feedback-free delay-free inverses

24 p4313 A70-46058

Codeword weight enumerator for second order Reed-Muller codes, using matrix approach

24 p4313 A70-46060

Weight structure enumerators for codewords of Reed-Muller codes

24 p4313 A70-46061

Digital PCM telemetry link coding techniques, discussing encoding-decoding complexity, and concatenated block scheme for channel

24 p4315 A70-46258

COEFFICIENT OF FRICTION

Surface roughness effects on dry friction between two metals, considering conical asperities and friction coefficients

[ASME PAPER 69-LUB-10] 01 p0102 A70-10394

Friction and wear tests on solid lubricant graphite fluoride compared with molybdenum disulfide at specific temperatures, considering friction coefficient

[ASLE PREPRINT 69-LC-9] 02 p0321 A70-12536

Carrying capacity and moment of friction calculated for cylindrical MHD bearing for small magnitude of radial clearance

03 p0497 A70-13877

Time history of spin and forward motion accuracy of rocket launched from smoothbore, using analytical model and motion coupling through dynamic friction coefficient

03 p0582 A70-14311

Viscous frictional torque on inner cylinder of eccentrically rotating concentric cylinders measured from laminar to turbulent flow

06 p1074 A70-17134

Skin friction law for compressible boundary layer allowing calculation of coefficient of friction for isothermal walls with heat transfer

06 p1033 A70-17232

Metal probes friction coefficient and impact temperature during impingement onto rotating chromium steel disk related to speed under various atmospheres

09 p1708 A70-23425

Synthetic molybdenum disulfide crystal properties compared to natural crystals, discussing friction coefficient, adherence to metal surfaces, etc

10 p1907 A70-24787

Service life and friction coefficient of molybdenum disulfide-silicon lubricating coating as function of load, sliding rate and vacuum level

11 p2060 A70-25943

Die surface composition effects on lubricant efficiency in metal working judged by friction coefficient and surface damage

13 p2418 A70-28830

Transformations on surfaces of molybdenum disulfide-steel system during friction in air, noting Mo oxides formation and friction coefficient increase

13 p2421 A70-29427

Oxide film and liquid effects on friction coefficient, surface relief and dislocation density along depth related to plastic deformation

15 p2743 A70-31638

Lubrication system components behavior in vacuum environment, investigating evaporation, friction, adhesion, wear, etc

16 p2923 A70-34156

Rolamite low friction suspension system, describing components, force generation and applications

16 p2923 A70-34165

Test stand based on Froude pendulum for measuring friction coefficients and oscillation parameters of porous bushings

16 p2924 A70-34298

Friction coefficient theory and measurement, considering definition and measuring equipment

16 p2924 A70-34332

Solid film lubricants deposited by DC and RF sputtering on metal and glass surfaces, determining friction characteristics by electron microscopy

17 p3099 A70-34516

Friction coefficient dependence on hardness of softer element of friction pair determined at constant values of shear strength, using external friction concepts

17 p3102 A70-35672

Turbulent air flow in vertical square duct, investigating local heat transfer and friction coefficients

18 p3347 A70-36506

Turbulent boundary layer on cone in supersonic flow in presence of inflowing foreign substance, considering local surface friction coefficient

20 p3559 A70-39814

Temperature effect on friction coefficient of boron and silicon carbides, using similar wear pairs in vacuum

23 p4205 A70-44044

Pressure gradient effect on skin friction coefficients taking into account Mach, Reynolds and Stanton numbers

23 p4183 A70-44629

Viscous compressible gas flows in pipe initial section, calculating friction and heat transfer coefficients

23 p4135 A70-44734

COEFFICIENTS

NT ACCOMMODATION COEFFICIENT

NT AERODYNAMIC COEFFICIENTS

NT ATTENUATION COEFFICIENTS

NT COEFFICIENT OF FRICTION

NT COHERENCE COEFFICIENT

NT CORRELATION COEFFICIENTS

NT COUPLING COEFFICIENTS

NT DIFFUSION COEFFICIENT

NT DISCHARGE COEFFICIENT

NT FLOW COEFFICIENTS

NT HEAT TRANSFER COEFFICIENTS

NT INFLUENCE COEFFICIENT

NT IONIZATION COEFFICIENTS

NT NOZZLE THRUST COEFFICIENTS

NT RECOMBINATION COEFFICIENT

NT REGRESSION COEFFICIENTS

NT SCATTERING COEFFICIENTS

NT STRUCTURAL INFLUENCE COEFFICIENTS

Mathematical model coefficients determination for planar diffused transistor, obtaining admittance parameters

01 p0048 A70-10050

Coefficients of Legendre polynomial expansion of earth gravitational potential, using Stokes problem solution

03 p0474 A70-13344

Digital computers for calculating coefficients of electronic circuit functions polynomials, developing algorithm

04 p0659 A70-15205

Alternating direction implicit method for solving parabolic equation with variable coefficients in two space dimensions with mixed derivative

09 p1711 A70-22284

Thermomagnetic transport coefficients in anisotropic metals based on theory for galvanometric properties, producing closed form expression for conductivity tensor

11 p2097 A70-25618

Coefficients for linear and nonlinear limb darkening in early type stars

11 p2113 A70-26469

Coefficients for finite difference methods of numerical integration of products of Fourier and ordinary polynomials

11 p2074 A70-26848

Bits quantity required to represent coefficient within digital controller with high sampling rate

12 p2203 A70-27410

Viscosity coefficient for isotropic turbulence using quasi-self-similar solution

13 p2391 A70-29777

Coefficients of Legendre polynomial expansion of earth gravitational potential, using Stokes problem solution

14 p2573 A70-30719

Exact and normal solutions of Boltzmann equation linearized around total equilibrium, yielding Navier-Stokes and Burnett transport coefficients

17 p3128 A70-34628

Liquid Fe-Cr-C, Fe-P-C and Fe-Cr-P systems, evaluating interaction coefficients

18 p3272 A70-36032

COENZYMES

Coenzyme A and acetyl CoA in tissue extracts determined for concentrations by recycling CoA through coupled enzyme system

04 p0640 A70-15754

COERCIVITY

Optimal coercive force selection of residual inductance and energy of magnets for generators with star shaped rotors

01 p0008 A70-10192

Ferroprobe coercimeter with attached electromagnetic for nondestructive hardness testing, describing components and mounting

02 p0301 A70-12489

COGNITION

Heuristic principles for self organization algorithm of cognitive automation system with active learning strategy

08 p1466 A70-20874

Acute mountain sickness symptomatology and cognitive performance, using standardized General High Altitude Questionnaire

20 p3581 A70-40025

COHERENCE

He-Ne laser emission in transverse oscillation mode, analyzing spatial and temporal coherence characteristics

09 p1694 A70-22135

Image coherence of object by laser illumination through moving diffuser related to diffuser autocorrelation

14 p2588 A70-31208

Partial coherence theory in holography with photogrammetry applications, reconstructing images with fringes representing constant range contours

17 p3087 A70-35023

SHF and EHF waves simultaneous propagation over slant line-of-sight overwater path, comparing phase variations and fading for signal coherence

20 p3588 A70-40301

Holographic measurement of general forms of motion based on reconstructed images dependence on coherence

21 p3822 A70-40810

COHERENCE COEFFICIENT

Coherent and incoherent interference effects on direction finding information derivation, using linear two channel principle

03 p0452 A70-14024

Recording of inhomogeneous mutual coherence functions in one hologram by combining image with Fourier /Fresnel/ holography

22 p4038 A70-43151

COHERENT ACOUSTIC RADIATION

Signal processor with ratio-squared predetection combining for adaptive antenna array, discussing radiation patterns for coherent and incoherent signal and noise sources

07 p1242 A70-20066

Brillouin effect lines shape dependence on analogous acoustical waves temporal and spatial coherence

21 p3839 A70-42100

COHERENT ELECTROMAGNETIC RADIATION

NT COHERENT LIGHT

Coherent microwave generation mechanism in indium antimonide at high electric fields, formulating thin plasma layer double stream interaction theory

03 p0534 A70-14214

Maser coherent amplification possibility in comet atmospheres at various frequencies assuming thermodynamic nonequilibrium and nonBoltzmann populations

07 p1378 A70-19034

Laser amplifier effect on autocorrelation function of laser radiation intensity fluctuations, determining emission coherence time

07 p1300 A70-19870

Optical coherence theory functional formalism developed in radiation field probability functional terms, noting role of P representation of density operator

08 p1545 A70-21254

Linear theory of cyclotron resonance maser with TEM standing wave field, considering coherent emission for nonrelativistic electrons oscillating in magnetic field

11 p2061 A70-25392

Mirror adjustment effect on transverse structure, time dependence and spatial coherence of pulsed UV molecular nitrogen laser emission

11 p2062 A70-25394

COHERENT LIGHT

Laser processing applied to optical nondestructive materials tests for surface flaws

01 p0086 A70-10416

Book on coherent optics and holography covering image restoration, holographic interferometry, lensless Fourier transform holography, etc

01 p0144 A70-11074

Coherent light scattering disturbance in level-crossing signals of Rb 85 and Rb 87 second excited state by noble gas atoms

02 p0311 A70-11851

Error probability, signal to noise ratio and average signal level for coherent heterodyne and photon limited laser communication systems, using Poisson distributions

02 p0255 A70-11914

Signal to noise ratio for optical heterodyne with inhomogeneous partially coherent signal and local oscillator fields, using phase-quadrature description

02 p0255 A70-11915

Speckle pattern in image plane of laser illuminated diffuse object, calculating pattern intensity and contrast

02 p0312 A70-12106

Image formation with partially coherent light, summarizing basic properties and diffraction theory of image formation

02 p0315 A70-12831

Surface roughness measurements by coherent optics and interferometry, including theory and experimental verification

04 p0689 A70-15015

Wave front reconstruction for perfectly bleached holograms not achievable by simple coherent illumination due to remaining amplitude variation

04 p0691 A70-15033

Multiple beam interferometer coherence analyzer for temporal and spatial study of laser beams, emphasizing application to pulsed lasers, holography and nonlinear optics

07 p1297 A70-19145

Book on lasers and holography covering coherence, wave diffraction, zone plates, etc

07 p1282 A70-19598

Book on holography principles and applications, discussing imaging properties, coherence, photographic emulsions, optical analog computers, etc
07 p1283 A70-19739

Coherence improvement of ruby laser emission in free mode using corrective holograms in resonator
07 p1303 A70-20323

Coherent light beams scanning and propagation direction control by acoustooptical method for laser applications
09 p1695 A70-22315

Fluorescence produced by resonant coherent light pulse passing through medium assuming infinite relaxation times and negligible pulse attenuation
09 p1726 A70-22321

Coherent optical beam propagation measurement of fine scale turbulent atmosphere structure, inferring microscale size and permittivity spectra
09 p1635 A70-22963

Two beam Fraunhofer holography noting effect of spatially coherent source
09 p1678 A70-22968

Rig using holographic techniques for vibration testing and aircraft engine components inspection
09 p1680 A70-23069

Optical coherence and light fluctuations, determining statistical distributions of light from photoelectric counting experiments
09 p1728 A70-23372

Single and clad glass fibers radii and refractive indices measurements on basis of laser light scattering
09 p1699 A70-23444

Object contrast effects on straight edge images in partially coherent illumination
10 p1898 A70-23910

Instrument localizing-resolving powers relationship as function of luminous source coherence
10 p1898 A70-23911

Granularity spectrum of diffusing screen uniformly illuminated by normally incident coherent light, basing study on long and short distance visual observations
10 p1899 A70-24031

Laser light propagation along strongly inhomogeneous turbulent path, measuring intensity fluctuations dispersion and light amplitude
10 p1844 A70-25161

Semiquantitative study showing variations in degree of laser beam coherence due to turbulence
12 p2245 A70-26980

Holograms formation without reference beam by illuminating transparency with coherent laser light
12 p2233 A70-27505

Strong short coherent light pulses with diffractive divergence generated by ruby lasers in series, showing pulse, emission and far field interferograms
13 p2430 A70-29762

Radiation coherent enhancement of single frequency emission fields in Q modulated coupled ruby lasers
14 p2593 A70-30152

Coherent or spatially incoherent light recordings of Fourier transform holograms, investigating resolution cells film grain and signal to noise ratio
14 p2588 A70-31207

Autocorrelation of coherence characteristics of polarized components of light scattered at curved rough surface, showing nonadequate Kirchhoff approximation
15 p2749 A70-31555

Laser devices design, emission characteristics, coherent light, etc
16 p2926 A70-33071

Optical spatial phase modulator array using membrane light modulator for coherent optical processing and character recognition
16 p2904 A70-33147

Book on holography covering principles, applications, spatial and temporal coherence, interference and diffraction theory and optical filtering
16 p2908 A70-33266

Coherent light pulses propagation through resonant medium, discussing energy loss
16 p2928 A70-33278

Coherent light propagation through turbulent atmosphere observed by applying He-Ne lasers to simultaneous measurements of scintillation effects over homogeneous optical paths
17 p3108 A70-35721

Coherent light communication system quasi-optical lens line output field examination, using laser assembly to study parasitic, radiative and overall power losses
19 p3443 A70-37288

Raman line coherence degree and polarization rate measurement, applying Wolf matrix
19 p3443 A70-37359

Pulsed ruby laser holography with coherent light, discussing applications
19 p3425 A70-37886

Bandlimiting in coherent optical matched filtering for pattern recognition, eliminating confusion between cross correlations and autocorrelations
19 p3446 A70-37889

Strong short coherent light pulses with diffractive divergence generated by ruby lasers in series, showing pulse, emission and far field interferograms
19 p3447 A70-38394

Coherent light beam characteristics with Gaussian radial intensity variation during propagation along optical system axis, determining radius from diffraction theory
20 p3639 A70-39086

Hologram line scattering function dependence on light source spatial coherence, presenting quantitative evaluation, theoretical and experimental data
20 p3633 A70-39760

Short light pulse coherent absorption in homogeneously broadened resonant medium, discussing influence of input pulse area and atomic coherence on propagation properties
21 p3784 A70-40565

Diffraction theory relationship to ray optics for coherent light propagation through lens systems
21 p3829 A70-41929

Radiation coherent enhancement of single frequency emission fields in Q modulated coupled ruby lasers
21 p3839 A70-42076

Photon occurrence moments probability distribution in partially coherent light signals
22 p3988 A70-42563

Laser application to nondestructive testing via holography and hologram interferometry
22 p4028 A70-42587

Ruby laser mode excitation, spatial coherence and free emission kinetics investigated by high speed camera scanning
22 p4051 A70-43461

Solid state high energy light detector for pulsed ruby and glass lasers in long pulse mode
22 p4052 A70-43614

Thermal energy conversion into coherent laser light, examining various thermodynamic limitations
22 p4076 A70-43674

Light source spatial coherence measurement, verifying laser heterodyne interferometer theory
24 p4354 A70-45665

Pb-Sn-Te junction diodes prepared by Sb diffusion, investigating spontaneous and laserlike emission
24 p4355 A70-46086

COHERENT RADAR

Holographic relationship of coherent optical processing applications to coherent or side-looking radar, discussing seismic holography concept
01 p0086 A70-10414

Microwave holography, discussing zone plate lens design, coherent side-looking radar, large antennas, three dimensional radar display applications
01 p0086 A70-10415

Synthetic aperture airborne side-looking radar using coherent optical data processor, discussing system configuration and operation
02 p0263 A70-12632

Nonadaptive processor to detect coherent radar pulse trains with uniform amplitude in clutter-plus-noise environment
04 p0651 A70-15334

Wind velocity measurements by coherent radar pulse method of meteor trail observations
06 p1141 A70-17739

Coherent instrumentation radar for White Sands Missile Range, discussing system design emphasizing pulse Doppler capability
10 p1842 A70-24881

Monostatic and multistatic coherent radar techniques for target mapping, discussing measurements and inverse scattering
14 p2552 A70-31184

Signal processing antennas, discussing synthetic and multiplicative arrays for coherent radar airborne mapping
17 p3052 A70-35078

Passive and cooperative active hologram radar extended from stationary coherent radar, considering use in airport surveillance of aircraft
21 p3792 A70-42119

Coherent radar backscatter, calculating autocorrelation and power spectrum of spuri noise from periodic random phase injections for filter design to eliminate noise
22 p3992 A70-43591

Microwave holography coherent radar with improved focusing, applying to side-looking, bistatic, passive and pulse compression radars
23 p4161 A70-43874

COHERENT RADIATION

NT COHERENT ACOUSTIC RADIATION
NT COHERENT ELECTROMAGNETIC RADIATION

NT COHERENT LIGHT

CW laser perturbation by coupled optical transition at strong pumping with incoherent and coherent perturbing radiation, considering disappearance of laser effect
01 p0108 A70-10231

Coherent short wave and UV radiation generation using continuous ion gas laser, discussing efficiency, stability and feedback effects
01 p0108 A70-10356

Laser radiation coherence origin explainable by mechanism consisting of many photon emission process by many atoms
05 p0883 A70-16500

Spatiotemporal correlation functions of random intensity field during diffuse scattering of coherent radiation by moving reflector
06 p1009 A70-17810

Coherent synchrotron emission in Crab Nebula associated with electron gyromotion, discussing models for high energy particle acceleration
07 p1375 A70-18848

Ionospheric data of local and integral electron concentration obtained by measuring phase shift of satellite emitted coherent radio waves
07 p1276 A70-20422

Coherent and incoherent radio emission from extensive air showers simultaneously detected by radio telescope in VHF-UHF range
08 p1563 A70-20475

Coherent radiation amplification factor for 0.63 micron wavelength in He-Ne mixture, noting dependence on discharge current for various pressures
09 p1698 A70-23304

Coherent wave reflection from random half space, solving scalar Dyson equation in bilocal approximation for oblique incidence
12 p2189 A70-27972

Mutual coherence functions for quasi-monochromatic illumination measured by image holography
12 p2237 A70-28124

Coherence degradation of collimated and focused Gaussian beams in turbulent atmosphere, using small perturbation method
13 p2453 A70-29824

Gas flow velocity measurement by coherent detection of scattered laser radiation from small particles suspended in fluid, using Doppler effect
15 p2751 A70-32030

Coherent pulse propagation in inhomogeneously broadened attenuator, examining degeneracy influence and connection with self induced transparency/SIT in nondegenerate system
15 p2699 A70-32395

Coherent wave propagation in warm turbulent plasma, using perturbation method for wave dispersion
16 p2860 A70-32945

Small angle of rotation measurement of coherent radiation polarization plane, discussing technique for increasing sensitivity and accuracy
20 p3643 A70-39759

Coherent beam propagation through turbulent atmosphere, discussing limiting resolving power due to random fluctuations of refractive index
22 p4072 A70-42290

Optimal detectors for two signals with fluctuating amplitudes and arbitrary mutual coherence, discussing distribution function processing
22 p3987 A70-42556

Coherent reflection waves produced by radio wave propagating through entire earth atmosphere
23 p4159 A70-43757

Multiphoton gas ionization by coherent radiation, showing electron transitions role with gas ionization model
23 p4201 A70-44205

COHERENT SCATTERING

Partial coherence in spontaneous Raman effect, using He-Ne laser source
02 p0313 A70-12465

Spatiotemporal correlation functions of random intensity field during diffuse scattering of coherent radiation by moving reflector
06 p1009 A70-17810

Statistical properties of random intensity field during coherent laser radiation scattering by moving diffuse surface
11 p2064 A70-26812

Three level molecular coherence effects in stimulated Raman scattering, considering molecular relaxation and field inhomogeneity
15 p2752 A70-32350

Mutual coherence function of light scattered by plasma turbulent electron density fluctuations, taking into account refractive index changes
17 p3137 A70-35722

Statistical properties of random intensity field during coherent laser radiation scattering by moving diffuse surface
24 p4351 A70-45184

Partially space coherent diffraction by slit aperture with apodizing filter, calculating tolerance and apodization coefficients for correlation interval numbers
24 p4354 A70-45814

COHERENT SOUND

U COHERENT ACOUSTIC RADIATION

U SOUND WAVES

COHERENT SOURCES

U COHERENT RADIATION

U RADIATION SOURCES

COHERENT TRANSMISSION

U COHERENT RADIATION

COHESION

Nimonic Ni-Cr based alloys fracture characteristics used to determine temperature and time effects on equicohesive points positions
01 p0116 A70-10073

- Elasticity theory two dimensional contact problems, examining cohesion or friction in contact area
17 p3192 A70-35693
- COHOMOLOGY**
U HOMOLOGY
- COILS**
NT MAGNETIC COILS
- COIN AIRCRAFT**
NT F-5 AIRCRAFT
NT OV-10 AIRCRAFT
- COINCIDENCE CIRCUITS**
Statistics and coincidences of Argonne-Maryland gravitational radiation detector array with and without time delays
08 p1545 A70-21271
- COKE**
Structural orientation and defects in graphitized coke crystallites, establishing relation between thermal expansion coefficient and macrostructure
03 p0514 A70-12868
- COLD ACCLIMATIZATION**
Man and animals physiological adaptation and behavior under conditions of polar regions, highland and arid areas
01 p0030 A70-11465
Cross adaptations of physiological functions, discussing results for heat, altitude and cold adapted animals
02 p0242 A70-12824
Plasma free fatty acid level relationship to acute and chronic exposure to cold in rabbits, rats and humans
04 p0631 A70-14983
Ergonomic and medicomilitary aspects of human adaptation to cold environments, discussing metabolic and physical protective reactions, clothing and personnel selection
16 p2850 A70-34346
Soviet papers on physiological adaptation to heat and cold covering thermoregulatory reflexes, bionics, temperature gradients, hypothalamus, gas exchange, heat generation, etc
18 p3217 A70-36526
Physiological mechanisms of cold adaptation in terms of individual, type and population categories, examining thermoregulatory muscular reflex
18 p3218 A70-36527
Human muscular function in conditioned and unconditioned thermoregulatory reflex changes of gaseous metabolism during repeated cooling
18 p3218 A70-36528
Gas exchange, body temperature and electrical activity of neck and back muscles of cold-acclimated white rats subjected to various temperatures
18 p3219 A70-36540
Repeated local spine cooling effect on gas exchange and electrical activity of white rats skeletal muscles
18 p3219 A70-36541
Thermoregulation of hedgehogs during muscular activity in cold environment, recording electrical activity, oxygen consumption and body temperature during work-rest cycles
18 p3219 A70-36542
Prolonged cold adaptation effect on heat transfer during recovery period after hypothermia in white rats
18 p3220 A70-36543
Respiratory activity of internal organs and skeletal muscles in rats exposed to long term heat and cold
18 p3220 A70-36546
Respiratory gas metabolism, tissue respiration and enzyme distribution in white rats skeletal muscles following long term cold acclimatization
18 p3220 A70-36548
Low ambient temperature exposure effect on hamster intestinal absorption capacity, using glucose test compound
19 p3360 A70-37772
Human cardiovascular compensatory responses to environmental cold stress, relating heart stroke to increased oxygen consumption
24 p4302 A70-46103
Hibernation and glycerol production in wasps *Ichneumonidea*, discussing possible physiological cryoprotective function
24 p4304 A70-46140
- COLD CATHODE TUBES**
NT PHOTOMULTIPLIER TUBES
Ionization measurements by OV-3-6 satellite cold cathode ionization gage of Redhead inverted magnetron type in near circular polar orbit
15 p2723 A70-31660
- COLD CATHODES**
Cold cathode soft X ray source with discharge controlled by automatic pressure controller (APC) or metering valve, noting applicability to radiography, luminescence, etc
02 p0271 A70-12743
He-Ne laser using K-activated alumina cold cathode and coaxial construction, discussing output, low noise applications, construction and testing
03 p0501 A70-13583
Steady state plasma generation in metallic waveguide without dielectric container by cold cathode discharge in He
05 p0819 A70-15803
- COLD FLOW TESTS**
Emulsified jet fuels cold flow, combustion and corrosion characteristics in gas turbine combustor compared with JP-4 fuel
[ASME PAPER 69-WA/GT-3] 04 p0732 A70-14892
Ablation test facilities capability extension by surrounding high enthalpy flow with coaxial cold jet
[AIAA PAPER 70-588] 13 p2522 A70-29883
- COLD FORMING**
U COLD WORKING
- COLD GAS**
Protogalaxy formation and molecular processes in primeval hydrogen gas, discussing cold gas cloud cooling mechanism and contraction
03 p0577 A70-14153
Viscosity of nitrogen, hydrogen, Ar and He at high pressures measured by capillary flow viscometer with range extended to minus 100 C
04 p0718 A70-14697
Cool gas inflation systems for evacuation equipment on large aircraft with size and weight fitting into aircraft doors
06 p0986 A70-17721
Acoustic characteristics of high subsonic model cold jet using imaging technique and measurements of energy flux of flow, calculating energy flux from flow-field measurements
[AIAA PAPER 70-234] 06 p1040 A70-18125
Numerical model of thunderstorm cold air outflow, providing horizontal flow as function of height from computer program using vertical velocity and storm motion
06 p1100 A70-18574
Thunderstorm cold air outflow leading edge structure recorded by NASA meteorological tower at Kennedy Space Center
06 p1100 A70-18575
Helium low temperature applications to fuel tank pressurization, superconducting magnet cooling and cryopumping of solar space simulators
11 p2083 A70-25620
MHD generators nonequilibrium ionization improvement by blowing low work function particles into cold working gas to obtain required conductivity
21 p3855 A70-40794
Space vehicle attitude control by cold gas jets, examining principles of operation, optimal conditions for gas consumption and gravitational and gyroscopic effects
[MBB-UR-37-70-0] 23 p4261 A70-44662
Cold boundary layer effect on chemical kinetic parameters behind reflected shocks in single-pulse shock tube
24 p4323 A70-46044
- COLD HARDENING**
Light alloys cold hardening effect and fatigue strength estimation, considering residual stress variability with time
03 p0587 A70-13239
Light alloys cold hardening effect and fatigue strength estimation, considering residual stress variability with time
19 p3548 A70-38457
Structural Ti, investigating effect of surface strain hardening by cold rolling on fatigue strength
20 p3648 A70-39250
- COLD MOLDING**
U COLD PRESSING
- COLD PLASMAS**
Ionization instability in low temperature magnetized plasma, analyzing electron concentration perturbation caused by Joule heating during electron-ion collisions
01 p0153 A70-11598
Probe impedance loss in cold magnetoplasma related to distribution of point charge potentials
02 p0346 A70-12124
LF electromagnetic waves interaction propagating in stream-magnetized cold plasma, discussing waves temporal growth and instability
02 p0262 A70-12603
Acoustic wave excitation and damping in cryogenic He plasma produced by HF pulse discharge, considering nonadiabatic heating and dissipation during reflection
03 p0529 A70-13056
Adsorption properties of pulverized silica gel, quartz, C and graphite under electron bombardment from low temperature plasma, showing surface and physicochemical influence
03 p0516 A70-13468
Whistler mode instability due to anisotropic charged particle velocity distribution, establishing general onset conditions for variable density cold plasma containing hot electrons
03 p0537 A70-14378
Vibrational relaxation and continuous spectrum transition during dissociation of diatomic low temperature plasma
04 p0721 A70-14539
Charge separation effects in boundary layer between cold streaming plasma and perpendicular magnetic field with relativistic electrons
04 p0727 A70-14997
- High density nonlinear and linear growth rates of flute modes instabilities in cold plasma coexisting with low density of energetic electrons
04 p0728 A70-14998
Nonlinear propagation of electron plasma wave in cylindrical waveguide, discussing linear theory of electrostatic waves in cold plasma
04 p0728 A70-15000
Wave dispersion across magnetic field in cold and warm collisionless Maxwellian plasma, discussing electromagnetic and electrostatic Bernstein modes
06 p1116 A70-17364
Transmission and emission of radiation from dense inhomogeneous finite laboratory plasma column in magnetic field with interpretation by cold plasma theory
06 p1116 A70-17367
Electrostatic oscillations in cylindrical column of laboratory plasmas excited by electromagnetic waves, investigating resonances by cold plasma theory
06 p1116 A70-17368
Satellite wake in ionosphere simulated in cold ion plasma without magnetic field, observing complex far wake structure and peculiar electrostatic probes response
06 p1147 A70-18297
Homogenous monoenergetic cylindrical electron beam interaction with homogeneous cold plasma, investigating system stability
06 p1125 A70-18615
Stellar configurations of cold static neutral plasma consisting of nuclei and degenerate electron gas, calculating integral parameters by Newton gravitation theory
07 p1376 A70-18912
Cold plasma approximation of whistler excitation of lower hybrid resonance at wake of body moving through ionosphere, comparing results with Alouette satellite observations
07 p1276 A70-20425
Flute instabilities of cold magnetoactive plasma with radially dependent density and strong azimuthal particle streams, discussing nonzero perpendicular temperature effects on oscillations
08 p1552 A70-21504
Weakly nonlinear dispersive cold plasma waves propagation by two time scale expansion, taking into account amplitude dispersion and coupling
08 p1553 A70-21613
Asymptotic behavior in cold plasma model of magnetopause, describing boundary layer between plasma stream and vacuum magnetic field
10 p1921 A70-23835
Relativistic nonlinear coupled longitudinal-transverse propagation of intense laser beams in cold over-dense plasma
10 p1921 A70-23968
Surface waves stability in cold bounded plasma against background of steady state electron oscillations, using nonlinear approximation
11 p2089 A70-25716
Surface waves excited by oscillating current in cold plasma surrounded by metallic sheath of infinite conductivity, deriving frequencies and growth rates
11 p2089 A70-25717
Population densities of levels of excited atoms and ions in nonthermal plasma including hydrogen-like ion partition function
11 p2086 A70-25835
Ionization equilibrium of atoms and hydrogen-like ions in nonthermal plasma, transforming into Saha formula for high electron densities
11 p2086 A70-25836
Inhomogeneous interatomic magnetic field effects on spectral line widening and shifts of emitting atoms in low temperature plasma
12 p2278 A70-27318
Optimal conditions for obtaining dense low temperature cesium plasma in shock tube with heating calculated by Debye theory
12 p2278 A70-27327
Excitation of surface waves on impedance plane in collisionless cold anisotropic plasma with external magnetic field coinciding with source direction
12 p2278 A70-27538
Linearized dispersion relation for plane wave propagation in uniform unbounded cold plasma permeated by DC magnetic field, considering two stream instability
12 p2281 A70-27881
HF electromagnetic forces on collisionless cold magnetoactive plasma-vacuum boundary using time-averaged stress tensor
13 p2462 A70-29127
Magnetopause model, discussing equilibrium layer between magnetic field and cold plasma field-free stream
13 p2396 A70-29181
Interference holograms of low temperature nitrogen plasma jet using fundamental and second harmonic ruby laser emissions
13 p2464 A70-29384

- Whistler instability examined on gyrating electron beam interaction with cold background plasma propagating parallel to magnetic field
13 p2468 A70-29932
- Gyrosynchrotron from accelerated electron, discussing effects of cold and collisionless magnetoplasma on far field and frequency spectra
15 p2728 A70-31989
- VLF radiation resistance of short filamentary electric dipole at arbitrary angle to magnetic field in cold uniform plasma, using full wave theory
16 p2859 A70-32935
- Refractive index and group velocity in moving dispersive half space /cold plasma or dielectric/ under incident wave from vacuum
16 p2859 A70-32936
- Cylindrical and helical antennas impedance in cold magnetoplasma, using three dimensional integral involving Fourier transform and Green function
16 p2859 A70-32943
- Collisionless damping of electromagnetic waves in regions with strong homogeneity of cold plasma
16 p2957 A70-33199
- Low temperature plasma flow velocity measurements using transit-time technique and high speed filming
17 p3141 A70-35345
- Energy loss of fast protons in cold Li plasma confined by magnetic field, using precession around axis to develop large interaction length
19 p3474 A70-37364
- Soviet papers on transfer phenomena in low temperature plasmas
19 p3480 A70-38180
- Low temperature underexpanded supersonic gas plasma jets behind shock wave, analyzing rarefaction and viscosity effects on parameters distribution
19 p3352 A70-38185
- Permittivity tensor of weakly turbulent magnetoactive cold electron plasma, calculating nonlinear currents
20 p3677 A70-39296
- Cold electron plasma nonlinear oscillations in magnetic field, using mathematical model
20 p3678 A70-39591
- Cold nonuniform plasma slab model for afterglow echoes at upper hybrid resonance in uniform magnetic field
20 p3679 A70-39664
- Ionization stability in low temperature magnetized plasma, using physical plasma model and numerical solution
20 p3679 A70-39983
- Energetic electron precipitation enhancement by cold plasma injection, discussing whistler mode turbulence, particle density and magnetosphere
21 p3818 A70-41105
- Electromagnetic wave propagation through cold slowly varying plasma layers in absence of external magnetic field
21 p3860 A70-42000
- Inhomogeneous interatomic magnetic field effects on spectral line widening and shifts of emitting atoms in low temperature plasma
21 p3860 A70-42059
- Optimal conditions for obtaining dense low temperature cesium plasma in shock tube with heating calculated by Debye theory
21 p3860 A70-42068
- Magnetoplasma interaction with axially slotted delay line, examining coil behavior physical mechanisms by cold plasma model
22 p4079 A70-42365
- Plane plasma waves in homogeneous conducting fluid with magnetic field, considering oscillations of two-fluid, cold and hot plasmas
23 p4224 A70-44179
- Transition radiation due to charged particle moving in periodically stratified cold isotropic plasma
24 p4384 A70-45254
- COLD PLATES**
U **COLD SURFACES**
COLD PRESSING
Relieving microstrains in Ni powders by cold compaction at room temperature using X ray analysis, discussing polygonization process
01 p0117 A70-10161
- COLD ROLLING**
Mechanical responses and residual defect structures in brass and stainless steel following explosive shock loading and cold reduction by rolling
03 p0507 A70-13139
- Al-Ni intermetallic whisker-reinforced Al microstructure and mechanical properties, studying effects of cold rolling
03 p0508 A70-13142
- Cold rolling characteristics of unidirectionally reinforced Al-B fiber composites, measuring hardness and tensile properties
08 p1524 A70-21957
- Cubic texture components preferred orientation shares into rolling texture during cold rolling of aluminum sheets determined quantitatively
09 p1690 A70-22255

- Lubricant ingredients and additives properties effect on surface quality of cold rolled semifinished Al products
14 p2590 A70-30837
- Structural Ti, investigating effect of surface strain hardening by cold rolling on fatigue strength
20 p3648 A70-39250
- Cold form rolling of various metal-shape combinations to close tolerance net shapes without machining
20 p3637 A70-39940
- Hydrodynamic lubrication film breakdown in cold strip rolling, showing thickness consistency with critical value of modified Sommerfeld number
21 p3833 A70-41256
- COLD SURFACES**
Space cold simulation installations, discussing cold wall design
19 p3398 A70-38281
- Pin fin coldplate heat exchanger for cooling Apollo spacecraft electronic equipment, calculating forced convection heat transfer and fluid pressure drop
21 p3797 A70-41025
- Cold plate immersed in warm flowing liquid, calculating two dimensional transient and steady state solidification by conformal mapping
21 p3949 A70-41319
- COLD TOLERANCE**
Thin, fat and average men responses to cold during one year period in Antarctica, measuring metabolic rates, skin and rectal temperatures
03 p0429 A70-14163
- Atmospheric carbon dioxide and oxygen concentrations effects on white mice low temperature tolerance
09 p1614 A70-22082
- Cold air inhalation effect on vital physiological functions of dogs, describing heat exchange simulator of upper respiratory tract
11 p1985 A70-25672
- Atmospheric carbon dioxide and oxygen concentrations effects on white mice low temperature tolerance
15 p2685 A70-32678
- Blood oxygen, carbon dioxide and pN during hypothermia induced by He-oxygen mixture and cold exposure in hamsters, comparing with hibernation state
23 p4147 A70-44787
- COLD WALLS**
U **COLD SURFACES**
U **WALLS**
COLD WATER
Book on survival in cold water covering physiology and treatment of immersion hypothermia and drowning, thermoregulation, etc
19 p3360 A70-37977
- COLD WEATHER**
Upper frontal waves behind quasi-stationary surface cold front using mathematical model
08 p1540 A70-21924
- COLD WEATHER TESTS**
Human peripheral blood flow rewarming in cold ambient temperature, examining skin, rectal and tympanic membrane and oxygen uptake
20 p3576 A70-40327
- COLD WORKING**
NT **COLD ROLLING**
NT **ELECTROHYDRAULIC FORMING**
NT **EXPLOSIVE FORMING**
Beta III Ti alloy cold formability, mechanical properties and heat treatment noting use for fasteners, sheet metal parts, honeycomb sandwich sections and metal matrix composites
03 p0512 A70-13776
- Cold working with subsequent heat treatment increased creep rupture and creep behavior of V alloys
04 p0708 A70-15372
- Cold reduction effects on press formability of pure Al sheet with allowance for tensile properties and crystallographic orientation
06 p1075 A70-17145
- Cold reduction and annealing temperature effects on Al sheet ductility noting roles of hardness, crystallographic orientation and microscopic structure
06 p1075 A70-17146
- Recrystallization behavior of Al alloy containing Mg and Si subjected to maximum aging before cold working
06 p1085 A70-17418
- Strain rate effects in cold metal working processes involving rolling and drawing
08 p1590 A70-21327
- Softening of cold worked alloy by high speed electrical heating, noting supersaturation before natural aging
08 p1520 A70-21496
- Yield strength of cold worked MP Co-Ni alloys during aging at elevated temperatures, noting behavior in overaged condition
08 p1525 A70-21960
- Cold and hot work deformation of aluminum alloys, discussing flow-stress dependence on strain rate, temperature and composition
09 p1692 A70-22642

- Cylindrical coil springs cold winding loading processes, considering initial tension or compression of wire and combined stresses
10 p1894 A70-24297
- Cr-Ni cold worked austenitic steel dislocation structure in tensile tests at different strains
14 p2596 A70-30874
- Pure Mo recrystallization deformed by cold rolling using transmission electron microscopy
14 p2597 A70-31284
- Cold worked metal, estimating lattice imperfections mol fractions based on reversible cell thermodynamics
15 p2676 A70-31564
- Ti alloy suitability for fastener applications noting cold workability, high strength and stress corrosion resistance
15 p2760 A70-32338
- [ASM PAPER W70-17.3]
Glass bead blast induced residual stress and surface cold work effects on Ni base superalloy fatigue crack initiation and propagation
15 p2761 A70-32381
- Cold forming of thermoset-thermoplastic laminate consisting of reinforced epoxy core sandwiched between thermoplastic face sheets
16 p2916 A70-33362
- Ti-Cu alloy sheet material age hardening, considering cold and warm work effects at various stages in aging cycle
17 p3121 A70-34430
- Cold working effects on Zircaloy tubes mechanical properties and hydride orientation, discussing tubes use in nuclear power stations
17 p3123 A70-34645
- Cold metal working techniques, describing electromagnetic, explosive, ultrasonic, high velocity hammering, stretch forming, deep drawing and superalloy shaping
20 p3639 A70-40445
- Dislocation network recovery kinetics of cold worked undoped powder metallurgical W wires by electrical resistivity measurements, determining activation energy
21 p3839 A70-40797
- Space shuttle structural technology for booster and orbiter, discussing hot and cold structure concepts, reentry bodies, military payloads, radiating protective coatings, refractory materials, etc
22 p4111 A70-43516
- Heat treatable beta Ti alloys cold workability, fracture toughness, tensile ductility and applications [SAE PAPER 700856]
24 p4361 A70-45880
- Al and Al alloys cold extrusion, discussing die entry angle, lubrication control, ingot preparation, etc
24 p4349 A70-46217
- Cold reduction, refrigeration and annealing effects on stress corrosion cracking of austenitic stainless steels
24 p4365 A70-46389
- COLLAPSE**
Computer calculation in elastoplastic range of statically indeterminate structure of bars, considering collapse load, stress and hinge rotation
01 p0200 A70-10524
- PreHayashi phase of stellar evolution, discussing protostellar disks /stellisks/ formation from flattened fragments of collapsed interstellar cloud under turbulent viscosity
01 p0190 A70-11346
- Blood flow through veins and collapsible tubes simulated by physical model, downstream pressure effect and importance of collapse phenomena
04 p0641 A70-14631
- Venous pressure of man in space, investigating return to heart in absence of gravity and distention by hydraulic pressure
08 p1448 A70-21943
- COLLECTORS**
U **ACCUMULATORS**
COLLEGES
U **UNIVERSITIES**
COLLIMATION
Time variations and angular collimation of radiation emitted by source with relativistic streaming
06 p1134 A70-17281
- Autocollimation technique for determining fluxure of tube of Wanschaff vertical circle
08 p1496 A70-21158
- Geodesic Luneberg lens Q band antenna design, construction and evaluation, noting point feeding and energy collimation
16 p2876 A70-33408
- Reflecting prism standards rotations effect on autocollimated images positions of optical instruments, investigating focusing method
16 p2915 A70-34214
- Backscattering of collimated light beam emitted by pulsed point source into opaque medium
19 p3461 A70-37421
- Two-component optical system for laser radiation collimation, calculating tolerances for fabrication and assembly
22 p4051 A70-43560

COLLIMATORS

Millimeter and nanosecond resolution of fast neutrons in pulse dense high temperature deuterium plasma discharge with polyethylene collimators and photomultipliers 02 p0303 A70-12739

Autocollimation method for variable profile antenna adjustment and control, describing antenna-mirror array 09 p1648 A70-23155

Electro-optical autocollimating focus sensor for optical systems of high angular resolution, analyzing defocus detection and errors 09 p1687 A70-23764

Bicylindrical microwave lenses, discussing collimating, virtual line source and point fed scanning lenses design 16 p2876 A70-33405

Ballistic photography system for luminous models in gas medium, using collimator for velocity measurement 20 p3632 A70-39746

Teleradiometer calibration in background radiation absence, using distant and finite point source method and collimator means 20 p3633 A70-39798

Large collimator objectives lenses focal lengths measurement in vibrations and temperature gradients 22 p4073 A70-42511

Soft X ray astronomical instrumentation for space experiments, discussing Geiger tubes, gas counters, modulation collimators, telescopes, etc 23 p4196 A70-44416

COLLISION AVOIDANCE

Atomic clock reproducibility short and long term stability, weight and power consumption characteristics, noting Rb gas cell for collision avoidance systems 04 p0688 A70-14724

Air traffic control problems in avoiding midair collisions, satellite utilization in transatlantic flight control and anticollision devices and procedures 04 p0623 A70-15350

Collision safety standards in helicopter services for shore-to-ship transportation of pilots, stores and spares 06 p1103 A70-17639

Pilot limitations role in USAF midair collisions, discussing information systems for collision avoidance 07 p1192 A70-19022

Encounter statistics and operational environment of aircraft collision-hazard warning systems in terminal area 07 p1331 A70-20060

Collision avoidance system /CAS/ cockpit display equipment design and operation 08 p1492 A70-20480

Visual aspects of collision avoidance, describing prudent mid-air maneuvers 08 p1449 A70-20481

Radio air navigation systems by time separation signals with reference to anticollisional methods and ATC 08 p1541 A70-21019

Airborne EROS collision avoidance system, discussing flight performance, range and closing rate measurements 09 p1720 A70-22241

Human psychophysiological inability to avoid mid-air collisions investigated for aviation safety 09 p1611 A70-23465

Optimal two level air traffic control avoiding conflict on runway and in flight and minimizing landing time deviations 11 p2077 A70-25603

Short range aircraft collision pilot warning indicator for low altitude and closure speeds 11 p2078 A70-25706

Light aircraft-airliner collision avoidance, discussing Time-Frequency Collision Avoidance System cost restriction, Pilot Warning Instruments, etc 11 p2079 A70-25872

Collision and missed approach risks in high capacity airport landing operations, discussing parallel runways spacing and aircraft longitudinal separation 12 p2207 A70-27629

Visual aircraft-to-aircraft detection effectiveness in collision avoidance as function of pilot performance and closing speed 12 p2267 A70-27633

Intermittent positive control system for issuing commands to normally uncontrolled aircraft for midair collision avoidance, discussing aircraft and conflict detection 12 p2267 A70-27634

Aircraft separation standards in air traffic control system design regarding collision hazards, noting beacon system role 12 p2267 A70-27635

Pilot midair collision warning instrument based on optical radar MTI, discussing target cross section enhancement by passive retroreflector 12 p2234 A70-27646

Optical IR system as low cost pilot warning indicator providing audible and visual collision warnings to general aviation aircraft 12 p2234 A70-27647

Intermittent positive control /IPC/ role in midair collision avoidance, using mathematical model to determine command frequency and implementation 12 p2269 A70-27913

Civil aircraft weather radar for ground collision hazard warning 13 p2447 A70-28548

General aviation demands on Pilot Warning Indicator systems for collision avoidance 14 p2615 A70-31176

Automatic ground based aircraft collision avoidance using combined associative processor- sequential computers 16 p2948 A70-33468

General aviation growth forecast during next decade, considering economic importance, air traffic control, collision avoidance, etc 16 p3003 A70-33469

Time ordered system for air traffic control providing data link, collision avoidance and navigation data through single channel 16 p2948 A70-33476

Time frequency concept application to air traffic control and collision avoidance systems 16 p2948 A70-33477

Air traffic control, discussing precision instrument landing, approach lighting, collision avoidance, navigation aids, etc 17 p3133 A70-35185

West German aircraft bird hazards problems, discussing research activities and recommendations for strike avoidance 18 p3349 A70-35980

Bird dispersal techniques in use or under study in Britain, including neurophysiological and bioacoustic systems to minimize hazards on airfields 18 p3222 A70-35992

ATA Collision Avoidance System based on time and frequency synchronization via ground stations or other aircraft 19 p3466 A70-38239

Collision avoidance system flight test and evaluation program for airline industry CAS specification 19 p3466 A70-38240

ATC airborne surveillance, communication and control system functioning as CAS after error or failure, discussing minimum parallel runway separation 19 p3466 A70-38241

Ground and cockpit initiated collision avoidance commands system based on satellites surveillance of aircraft position and velocity data 19 p3466 A70-38242

Airborne electronic equipment, collision avoidance systems, displays, instrumentation, human response and ground based control in air traffic control 20 p3665 A70-39198

Airborne three dimensional area navigation equipment for reducing mid-air collision exposure and for raising landing safety in terminal areas 22 p4066 A70-42296

Automatic conflict detection and resolution in ATC planning, discussing flight paths, zones of protection, etc 23 p4215 A70-44154

Collision Avoidance System /CAS/ and Proximity Warning Indicator /PWI/ for preventing midair aircraft collisions 23 p4194 A70-44175

Soviet civil aircraft-bird collisions, stressing hazard forecast and prevention by bird identification and migration patterns 24 p4289 A70-45644

COLLISION PARAMETERS
NT COLLISION RATES

Multistate impact parameter treatment of hydrogen-helium excitation collisions, considering distortion, back- and rotational-coupling and virtual transition sequence 01 p0147 A70-10285

Cross section calculation for spin change in H atoms pair collision, discussing wave number and temperature effects 02 p0341 A70-11796

Energy spectrum of cosmic radiation primary nuclei calculated from collisions against stellar light photons and 3 K black body radiation 03 p0561 A70-14185

Approximate solution to Boltzmann gas kinetics equation, using moment relations of collision integral and reverse collision operator 06 p1036 A70-17758

Discrete ordinate technique for nonlinear Boltzmann equation tuned for computing collision integrals to instantaneous nature of distribution function 06 p1047 A70-18319

Monte Carlo method applied to Boltzmann collision integral in solving heat transfer between plates at different temperatures in elastic spheres gas 06 p1183 A70-18324

Hydrogen atoms collisional excitation cross section expressed in terms of quantum numbers of levels and ratio of colliding electron energy to transition energy 07 p1338 A70-19410

Meteorites explosive fragmentation under aerodynamic loads simulated by steel balls shot into increasing-density target, discussing parameters 08 p1572 A70-20947

Electron impact excitation cross section of /0,0/ first negative band of nitrogen ion from threshold to 3 keV, using photon counting techniques 12 p2276 A70-27880

Heavy particle spectroscopy, deducing collision parameters from empirical observations 13 p2456 A70-29810

Meteorites explosive fragmentation under aerodynamic loads simulated by steel balls shot into increasing-density target, discussing parameters 15 p2806 A70-32759

High velocity center to center collision of two absolutely elastic rods in acoustic medium in terms of Einstein nonclassical mechanics 15 p2775 A70-32890

Meteoroids origin and distribution, examining collisional and radiative processes effects 16 p2974 A70-33650

Multistate impact parameter treatment of heavy particle collisions modified to include higher state couplings for electronic wave functions 16 p2956 A70-34309

Collisions effects on ion collection by Langmuir probes, determining plasma density [AIAA PAPER 70-757] 17 p3139 A70-34494

Coulomb interaction Fermi gas mixture collision integral, obtaining formula from Boltzmann equations and Taylor series expansion 17 p3070 A70-35043

Interstellar cloud collisions, examining gas and dust particles separation by size 18 p3313 A70-36323

Near collisions approximation in Stark broadening of hydrogen Lyman alpha line 18 p3296 A70-37227

Collisional effects on second order spatial ion wave echo, evaluating velocity integral 19 p3475 A70-37539

Periodic collision orbits in plane elliptic three body problem of infinitesimal mass under gravitational field of two finite masses 20 p3705 A70-39603

Elastic bodies collision, determining temperature field variations and contact pressure 20 p3725 A70-39869

Molecular and noble gas rotational collision numbers from thermal transpiration measurements 20 p3738 A70-39995

Electron-neutral interaction parameters for Ohm law coefficients in multicomponent nonisothermal plasmas tabulated as function of electron temperature 22 p4081 A70-43015

Optically thin plasma population and ionization equilibrium, taking into account heavy particle collisions 22 p4082 A70-43219

Collision integral model for multicomponent mixture, investigating partially ionized plasma longitudinal vibrations 22 p4083 A70-43382

Low energy proton-hydrogen collisions, computing differential cross sections for direct elastic scattering, resonant charge exchange and direct and exchange excitation 24 p4382 A70-46226

Plane parallel collision between two solid bodies of similar shape, discussing kinetic energy losses and motion after impact 24 p4427 A70-46376

Plane parallel collision of two solid spherical bodies with mass centers coincident with geometrical centers 24 p4427 A70-46377

COLLISION RATES

Ionospheric reflection coefficients calculations by two full wave theory, using related monoenergetic and collisional frequency profiles and 10-100 kHz frequencies 01 p0076 A70-10870

Molecular reaction rates and ion/electron vertical profile and concentrations in equatorial ionosphere, applying computer simulation to numerical solution of continuity equations 01 p0083 A70-11549

Electron flux parameters determination from ionograms and reflected signal amplitudes between 120-130 km, considering electron collision frequencies 01 p0084 A70-11551

Resonance scattering and drift motion of electrons in gases under pressure, determining ion state lifetime and mean electron-molecule collision frequency for trapping collisions 02 p0342 A70-11883

Collisions effects on cylindrical antenna impedance near plasma frequency of isotropic nonMaxwellian plasma, allowing for collision frequency dependence on electron energy 06 p1020 A70-17567

Ionospheric radio transmission field strength calculation for given electron density and collision frequency profiles, considering electron variations along transmission path

07 p1230 A70-19165

Ionospheric F and E layers collision frequency estimates, comparing pulse absorption and cosmic radio noise measurements

10 p1880 A70-24804

Particle acceleration during solar plasma ejection, disregarding magnetic effects on flux

11 p2107 A70-25526

Electrical conductivity of impact-ionized nitrogen across magnetic field, deriving electron collision frequency

11 p2091 A70-26461

Midair collision frequency under VFR as function of aircraft density derived, noting ATC role in safe separation

12 p2267 A70-27636

Ionospheric D region radio wave probing by cross modulation technique, obtaining electron densities and collision frequencies

12 p2224 A70-27733

Midair collisions incidence correlated with traffic factor proportional to square of number of operations

12 p2269 A70-27912

Collision coefficients of reaction and inverse reaction for nonequilibrium processes with variable distribution functions and cross sections

13 p2461 A70-28920

Electron collision frequency effects on Cerenkov radiation from magnetoplasma, applying results to magnetosphere and ionosphere

13 p2465 A70-29546

D region electron concentration and collision frequency in slowly varying plasma, using rocket-borne probe for ground emitted wave detection

15 p2778 A70-31673

Weakly turbulent plasma dielectric constant nonlinear tensor for frequent Coulomb collisions, using hydrodynamic equations

15 p2781 A70-32824

Electromagnetic field transmission through plasma slab with specified electron density-collision frequency profiles, using integral derived from transmission and reflection coefficients

16 p2957 A70-32979

Microwave diagnostic method for amplitude variations of electron density and collision frequency in weakly ionized plasma

17 p3140 A70-34871

Statistical measurement of bird hazards to aircraft in terms of strike rates at airports, considering international strike rate standard

18 p3211 A70-35981

Vertical profile of electron collisions effective frequencies in auroral ionosphere E region

19 p3409 A70-37330

Absorptivity, transition probability and collision broadening frequency of dimethylether at 3.51 micron He-Xe laser wavelength, noting pressure dependence, transition lifetime and saturation intensity

21 p3835 A70-40573

Electron collision frequency profile for energy loss rate in ionospheric G factor for air, considering rotational excitations of molecular oxygen and nitrogen

21 p3812 A70-40618

Particle acceleration during solar plasma ejection, disregarding magnetic effects on flux

21 p3892 A70-41276

Adiabatic-transition state theory of chemical reactions in dilute gases with separate binary collisions, considering Morokuma, Eu and Karplus results

21 p3773 A70-41396

Plasma concentration and heavy particle-electron collision frequency in open cylindrical cutoff resonator based on frequency shift and passband broadening data

24 p3485 A70-45455

Electron density and collision frequency distributions in lower ionosphere, deriving error limits from VLF and LF sounder data

24 p4314 A70-46127

COLLISION WARNING DEVICES U COLLISION AVOIDANCE U WARNING SYSTEMS COLLISIONLESS PLASMAS

Solar wind-induced drag resulting from collisionless plasma shock on sunward-side of large magnetic comet, using similarity with earth magnetosphere

01 p0168 A70-10258

Mesothermal flow of collisionless plasma around conducting cylinder, calculating densities, velocities, temperatures and electrical potential

02 p0346 A70-12102

Electric potential fluctuations beyond long collisionless plasma cylinder in uniform magnetic field, noting thermal noise intensity

03 p0530 A70-13086

Anomalous H wave absorption in circular waveguide by dense collisionless plasma, connecting to instability excitation with subsequent plasma heating

03 p0537 A70-14379

Neutral particle flux measurements in plasma wind tunnel using BeCu detector, discussing role in collisionless flow dissipation processes

04 p0727 A70-14994

Mixture Mach number defined for collisionless plasma flow about solid body by extending cold-ion theory

[AIAA PAPER 69-78] 04 p0729 A70-15582

Neutral sheet instabilities in magnetotail from collisionless plasma instabilities from shear magnetic field

05 p0887 A70-15911

Whistler mode wave propagation in collisionless Vlasov plasma along nonuniform magnetic field

05 p0889 A70-16533

Wave dispersion across magnetic field in cold and warm collisionless Maxwellian plasma, discussing electromagnetic and electrostatic Bernstein modes

06 p1116 A70-17364

Numerical solution of nonlinear Vlasov equation for collisionless plasma problems, discussing initial value problems, external electric fields, magnetic fields, etc

06 p1108 A70-17419

Collisionless ions trajectories in plasma flowing about cylindrical probe calculated to determine probe ion current, ion density distribution in field and potential distribution

06 p1122 A70-18294

Current collected by cylindrical Langmuir probe immersed in rarefied collisionless plasma streaming with high velocity

06 p1124 A70-18307

Electric and magnetic field perturbation at great distances behind body moving in collisionless magnetized plasma estimated from Fourier transform

07 p1385 A70-19447

Electrical conductivity of collisionless magnetoplasma in weakly turbulent magnetic field, using quasi-linear approach for diffusion equation for distribution function describing test particles

07 p1352 A70-19987

Selective harmonic excitation in one dimensional collisionless plasma conforming to Vlasov equation by counterstreaming electron beams, noting velocity distribution conditions

07 p1353 A70-20202

Asymptotic method for Vlasov equation formulated for weakly Landau damped monochromatic plasma wave in collisionless electron plasma

07 p1353 A70-20231

Electron density calculation for collisionless plasma flow around conducting cylindrical body, accounting for surface absorption and mean electron velocity

08 p1550 A70-20595

Spontaneous echoes amplitude resulting from damped electronic plasma plane wave excitation in collisionless plasma

09 p1735 A70-22843

Oblique E-mode electromagnetic wave in plane stratified collisionless plasma taking into account plasma temperature

09 p1639 A70-23674

Two-stream and cross-stream effects on nonlinear wave stability with shock in collisionless plasma

10 p1921 A70-23967

Stationary collisionless shock waves in hot initial plasma produced by theta pinch discharge, discussing magnetic field, density and electron temperature profiles

10 p1924 A70-24697

Stationary and nonstationary nonlinear waves propagation in multicomponent collisionless plasma, considering dispersion relations for acoustic oscillations

10 p1844 A70-25166

Wakes of cylinder in collision-free plasma wind tunnel simulating ionospheric satellite conditions, noting decaying oscillation

11 p1976 A70-26018

Plasma experiments in space including electric fields measurement, collisionless plasma studies and artificial Ba cloud generation

12 p2214 A70-26868

Excitation of surface waves on impedance plane in collisionless cold anisotropic plasma with external magnetic field coinciding with source direction

12 p2278 A70-27538

Density gradient drift waves stabilization in collisionless plasma by stellarator type windings, observing oscillations amplitude reduction in shear magnetic field

12 p2280 A70-27785

Incoherent scattering of radiation from collisionless plasma in quasi-stationary state, analyzing wave energy from spectral decomposition for given background distribution function

13 p2457 A70-28558

Collisionless plasmas strong turbulence in terms of mixing length and Hamilton-Jacobi theories

13 p2458 A70-28562

Plane electrostatic shock waves propagation in plasma with electrons in potential equilibrium and collision free ions

13 p2461 A70-28730

Collisionless electrostatic shock generation conditions, simulating homogeneous counterstreaming plasmas by computer

13 p2462 A70-29110

HF electromagnetic forces on collisionless cold magnetoactive plasma-vacuum boundary using time-averaged stress tensor

13 p2462 A70-29127

Whistler mode wave packets propagation in hot inhomogeneous collisionless plasma immersed in nonuniform ambient magnetic field

13 p2468 A70-29931

Collisionless alkali plasma diode with two electrodes emitting electrons and ions with half-Maxwellian velocities, analyzing potential distribution

14 p2622 A70-30660

Temporal wave echoes and Landau damping in collisionless plasma using signal averaging and time delay techniques

14 p2622 A70-30687

Ion temperature sensitive end effect in long cylindrical Langmuir probe response in high speed collisionless plasma flow at ionospheric satellite conditions

14 p2577 A70-31038

Sideband instability and trapped particle charge density response of large periodic Bernstein-Green-Kruskal waves in collisionless plasma

14 p2623 A70-31039

Low density collisionless plasma sheath in planar and cylindrical geometry under weak magnetic field, considering ion-electron pair generation

14 p2624 A70-31040

Collisionless plasma confinement using spatially uniform time varying magnetic field

14 p2624 A70-31100

Gyrosynchrotron from accelerated electron, discussing effects of cold and collisionless magnetoplasma on far field and frequency spectra

15 p2728 A70-31989

Low amplitude waves and substantial frequencies interaction by averaging method for hydrodynamics of waves in collisionless plasmas

15 p2720 A70-32114

Solar wind models based on exospheric theory assuming collisionless particles

15 p2794 A70-32613

Collisionless shocks structure in turbulent wave-particle interactions, obtaining ion distribution function

16 p2959 A70-33970

Collisionless plasma theory modification to include effects of finite Larmor radius of ion and electron on perturbation flow mixing

17 p3141 A70-34935

Finite difference methods for collisionless plasma models, taking into account Eulerian form of Vlasov equation in phase space

18 p3296 A70-36792

Electric and magnetic field perturbation at great distances behind body moving in collisionless magnetized plasma estimated from Fourier transform

18 p3316 A70-36921

Hydrodynamic model analogy to water bag/incompressible homogeneous fluid in phase space/, investigating nonlinear collisionless plasma oscillations

19 p3474 A70-37365

Higher order magnetic field-free temporal and spatial plasma wave echoes, solving collisionless Boltzmann equation by method of characteristics

19 p3476 A70-37557

Coulombian drag on body from hybrid calculus of collisionless plasma flow around cylinder

19 p3481 A70-38382

Collisionless plasmas fluid dynamical equations in presence of strong magnetic field, discussing Larmor and electron plasma frequencies

20 p3678 A70-39609

Collisionless cylindrical Langmuir probe response in turbulent plasma for mean and statistical properties

20 p3684 A70-40258

Current driven ion wave plasma turbulence in collisionless shock, measuring frequency and wave number spectra by shock front light scattering

20 p3685 A70-40497

HF electromagnetic field effect on nonhomogeneous collisionless magnetized plasma stability, deriving dispersion equation for drift cyclotron oscillations

21 p3854 A70-40622

Anomalous electromagnetic wave absorption in collisionless plasma attributed to instability excitation causing ion density fluctuations

21 p3855 A70-40754

Collisionless shock wave geometry, determining dispersion relation for ion acoustic waves propagating in plasma

21 p3856 A70-41082

Jump relations for shocks in anisotropic collisionless magnetized plasma

21 p3856 A70-41267

Collisionless nitrogen plasma drift velocity measurement by ion acoustic wave method

21 p3859 A70-41760

Collisionless plasma shock wave instability, discussing resonance and energy dissipation through ion Landau damping 22 p4077 A70-42292

Hot electrons bunch spread deceleration in collisionless plasma, discussing stationary moving jump formation similar to shock wave 22 p4077 A70-42299

Collisionless magnetospheric plasma turbulent conductivities for weak and strong electric fields parallel to magnetic field 22 p4016 A70-42787

Impulse length effect on space echo electric field in collisionless plasma 22 p4082 A70-43237

Collisionless plasma weak turbulence theory derivation from Vlasov equations, considering interactions between oscillation modes 23 p4225 A70-44182

Turbulent collisionless plasma shocks formation, wave front steepness and explanation for earth bow shock 23 p4225 A70-44183

Collisionless plasma shock wave structures from geophysical and astrophysical phenomena standpoint, describing tarantula experiment 23 p4225 A70-44184

One dimensional collisionless electron-proton plasma, obtaining exact electrostatic shock solution to Vlasov and Poisson equations 24 p4382 A70-45107

Ion acoustic wave propagation in collisionless gravity-supported plasma in static magnetic field calculated from linearized Vlasov equation 24 p4382 A70-45109

Collisionless plasma, calculating effects of energy dissipation due to weak firehose instability on steady planar flow, based on quasi-linear fluid equations 24 p4382 A70-45110

Steady state frequency spectra for Alfvén waves and MHD turbulence in collisionless plasma with non-linear interaction by particle scattering 24 p4383 A70-45114

Pressure gradient induced drift waves in collisionless hydrogen plasma in homogeneous magnetic field 24 p4388 A70-46209

COLLISIONS

NT ATOMIC COLLISIONS

NT COULOMB COLLISIONS

NT INELASTIC COLLISIONS

NT IONIC COLLISIONS

NT METEORITE COLLISIONS

NT MOLECULAR COLLISIONS

NT PARTICLE COLLISIONS

Container fluid viscosity effect on container-obstacle interaction solved in Fourier series form 07 p1252 A70-18676

Transition of stress distribution on collision surface of semiinfinite elastic plane with rigid beam, using Fredholm integral equation 10 p1954 A70-23950

Jet collisions solutions for impact of pin at obstacle, solid body impact at surface, cylindrical shells longitudinal impact and jets interactions 13 p2453 A70-29771

Container fluid viscosity effect on container-obstacle interaction solved in Fourier series form 15 p2719 A70-31468

COLLOCATION

Dispersion curves for wave propagation in infinite elastic bars of elliptic cross section obtained by method of collocation 04 p0773 A70-15080

COLLOIDAL GENERATORS

Colloid engine efficiency operating with pulsed positive voltages and square wave and sinusoidal voltages [AIAA PAPER 70-178] 06 p1132 A70-18158

Ground test reactor design based on colloid fueled reactor concept [AIAA PAPER 70-688] 16 p2950 A70-33587

COLLOIDAL PROPELLANTS

Chemical engineering problems of resistojets, pulsed plasma, ion bombardment and colloid thrusters 01 p0166 A70-10974

Charged aerosol charge/mass ratio measurement and colloidal propulsion system thrust, efficiency and exhaust velocity determinations 03 p0551 A70-12936

Dual bellows ball seat valve design for colloid thruster coupled to pressurized feed system, demonstrating thrust decay and flow regulation [AIAA PAPER 70-615] 16 p2919 A70-33610

Electrostatic colloid thrusters operation and technology, including propellants, needle modules and test results 17 p3148 A70-35218

Time-of-flight mass flow rate and thrust stand data comparison for two 100 micropound colloid thrusters [AIAA PAPER 70-1114] 20 p3691 A70-40229

Colloid annular thruster performance, using low mass flow rate data and space charge formulas [AIAA PAPER 70-1113] 20 p3692 A70-40230

Colloid annular thrusters performance tests in vacuum chamber with LN cooled liner, using high speed analog to digital system to acquire time of flight /TOF/ data [AIAA PAPER 70-1112] 20 p3692 A70-40231

Colloid microthruster system life test, discussing design and steady state performance [AIAA PAPER 70-1110] 20 p3692 A70-40233

Colloid engine propellant mass flow distribution, determining beam current and specific charge effects on thrust, efficiency and specific impulse [AIAA PAPER 70-1109] 20 p3692 A70-40234

COLLOIDING

X ray structural and electrophoretic investigation of donor and fibrinolytic blood protein components, observing crystalline to amorphous transition in blood serum and plasma lyophilization 09 p1621 A70-23149

Spacecraft design requirements for scientific zero G cloud physics experiments concerning colloidal modification processes 14 p2584 A70-30552

COLLOIDS

NT AEROSOLS

NT COLLOIDAL PROPELLANTS

NT FOG

Simulator for testing colloid microthruster, discussing spacecraft interfaces and time of flight thrust data [AIAA PAPER 69-314] 01 p0058 A70-10834

Stable colloidal dispersions of subdomain magnetite particles correlated for magnetic properties in terms of size distribution and volumetric concentration by superparamagnetic theory 12 p2284 A70-27241

Colloidal filler /carbon black/ reinforced rubber for various applications, noting fabrication into composite material 15 p2764 A70-31930

Colloidal alumina nonNewtonian suspension in propylene glycol, examining thixotropic behavior at various structural levels 24 p4310 A70-45625

Aeromechanical characteristics of colloidal fuel core nuclear reactor in relation to cavity geometry and propellant gas injection [AIAA PAPER 70-1222] 24 p4377 A70-45958

COLOR

Scattering functions from sky light spectra measurements on high mountain for various sun altitudes, obtaining color value functions 02 p0359 A70-12776

Combining color response in cholesteric liquid crystals generated by trace contaminants applicable to detection of vapors trace amounts 07 p1222 A70-19930

Meteors spectral intensity variations along flight path noting color dependence on brightness 08 p1572 A70-20946

Electroluminescent displays design capable of generating all primary colors in single compact element 08 p1499 A70-21689

CRT color displays advantages and limiting factors, considering beam-penetration tube with high voltage switching 09 p1673 A70-22031

Semiconductor alphanumeric multicolored displays, discussing phosphor coating of GaAs diodes 13 p2408 A70-29217

H II region stellar color anomaly attributed to interstellar extinction 14 p2641 A70-30879

Hill reaction color sensitivity in red and blue light during chloroplast disintegration, considering oxygen evolution capacity 15 p2684 A70-32548

Meteors spectral intensity variations along flight path noting color dependence on brightness 15 p2806 A70-32758

Electric temperature sensors accuracy and stability, considering thermocouples, resistance thermometry, radiation and color pyrometry 15 p2743 A70-32798

Zodiacal light observations at elongation angles from sun, examining surface brightness, color index and polarization degree by balloon-borne instruments 18 p3318 A70-37012

Dispersed stellar clusters color excesses and distance moduli from color-magnitude diagram, considering evolutionary deviation from main sequence 18 p3323 A70-37138

H 2 region galactic clusters and exciting stars, reevaluating distances by color magnitude diagrams 18 p3329 A70-37178

Spectral energy distribution curves and color indices of specific meteor trails observed on 12 August 1959 and 25 July 1963 19 p3526 A70-38780

Magnitude-color relation for Cygnus X-2 and WX Centauri, indicating opposite correlation to Sco X-1 fluctuations 21 p3873 A70-40672

B-V and U-B colors and B and V polarization calculation in single scattering for slab model reflection nebulae with dielectric or graphite grains 22 p4103 A70-42984

Optimal color hierarchy for pyrotechnic markers and signals indicating red, violet and amber hues on top 23 p4146 A70-44459

COLOR BLINDNESS

U COLOR VISION

COLOR CENTERS

KCI F centers isothermal annealing kinetics using EPR, considering electron irradiation levels effects 02 p0350 A70-12719

Emission kinetics variations of ruby laser due to aging attributed to inhomogeneity of active medium developing simultaneously with color centers 07 p1300 A70-19872

Current-sensitive single gun color CRT with phosphor screen for display systems 12 p2195 A70-27373

Defect F centers formation in MgO, discussing optical absorption bands, oscillator strengths, luminescence band, impurity centers, etc [AIAA PAPER 70-828] 16 p2940 A70-33938

Sodalites color centers creation by electron beam, discussing application in dark trace cathode ray storage display tubes 19 p3379 A70-38048

COLOR PERCEPTION

U COLOR VISION

COLOR PHOTOGRAPHY

Holographic color schlieren flow visualization system for three dimensional photography, variable focus shadowgraph, knife edge schlieren, etc 01 p0091 A70-10908

Multicolor Venus photography, discussing anomalous markings association with anomalous UV polarization 02 p0378 A70-12557

Black and white roentgenograms conversion to full color and three dimensional CRT radiograph displays, incorporating electronic data processing circuitry 04 p0641 A70-14560

Semifocusing color schlieren systems for quantitative investigations of flows in fluid mechanics and heat transfer, including photographs of boundary layers 04 p0690 A70-15029

Aerial color IR photography for crop disease identification by tonal and geographic patterns, discussing cameras, films, filters and exposure procedures 05 p0837 A70-16144

Projection display methods using scanned and modulated multicolor laser beams, discussing beam generation, modulation and scanning 05 p0858 A70-16188

Schlieren system modification using diffraction grating to produce color applied to airfoil flowfield analysis [AIAA PAPER 70-223] 06 p1029 A70-18165

Remote sensors for measurement and mapping of ocean color variations, discussing Wierdinger Image Spectrophotometer and Water Color Spectrometer 06 p1073 A70-18592

Barred galaxies colorimetric data to study relative intensities and mean surface brightnesses as function of color 07 p1376 A70-18905

Minimum altitudes for illumination levels of aerial color photographic film calculated for different landscapes 07 p1283 A70-19633

Aerial color photography, considering lens types, exposure, filters, films, etc 08 p1498 A70-21543

Photochromism of dihydroquinoline compounds and absorption spectra of color forms, noting color development upon UV light irradiation and thermal eradication 09 p1629 A70-22334

Color schlieren photography with complete spectrum displayed in single photograph, discussing filter matrix 10 p1857 A70-23913

Color radiography with photographic negative film exposed to X rays, obtaining same thickness latitude with improved detail sensitivity on single emulsion line 10 p1887 A70-24168

Orthophoto Attachment for A8 autograph to produce black and white and color aerial photographs on negative film 10 p1891 A70-24739

Color and color IR aerial photography, discussing effects of solar spectrum, films, filters, etc, in connection with terrain analysis 10 p1880 A70-24751

Faint violet stars in southern galactic latitudes found during scanning of two color plates including halo stars, subdwarfs, white dwarfs and quasi-stellar galaxies 10 p1949 A70-25248

VX Cas brightness determination from color plates, giving values in tabular form 11 p2115 A70-26583

Spaceborne photography for detecting and identifying road networks, using color separation plates and photograph enlargement 12 p2216 A70-26910

Multispectral color aerial photography, describing instrumentation, oceanographic and agricultural applications, atmospheric effects on images, etc 12 p2220 A70-26937

Aerial reconnaissance of soils, rocks, vegetation and streams, comparing color, IR color, and black-and-white photography 12 p2236 A70-27873

Earth colorimetry data improvement by separating signals of each bandwidth on one photographic emulsion or TV tube 13 p2406 A70-28987

Backward facing separated step boundary layer flow at Mach 2.25 investigated by diffraction grating interferometer and color schlieren technique [AIAA PAPER 70-571] 13 p2343 A70-29898

Evaporography at room temperature, showing necessity of recording images on color films 14 p2583 A70-30362

Cotton plant leaves from high saline soil area, observing chlorophyll content on color photographs 14 p2576 A70-30977

Soil characteristics determination from black and white, color and IR aerial photographs 14 p2577 A70-30980

Auxiliary minus-visual filters in high altitude IR aerial color photography, suggesting tests for film sensitometric properties 14 p2588 A70-31235

Lunar color differentiation by computer image processing compared to earth based photoelectric photometry [JPL-TR-32-1472] 16 p2900 A70-33097

Digital color printer with opaque IBM card as filter for sea surface temperature and cloud vortex patterns display 16 p2907 A70-33180

Reactive stream separation high speed color photography for impinging streams of nitrogen tetroxide and hydrazine [AIAA PAPER 70-608] 16 p2998 A70-33605

Large scale aerial color photography over spruce fir stands during 10 year period for assessing damage caused by budworm epidemic 17 p3078 A70-35614

Remote sensing experiment demonstrating utility of multispectral color aerial photography for detection of differences among vegetative species 17 p3095 A70-35615

Color film /XRC/ application in Mexico during solar eclipse of 7 March 1970, showing little color and tone distortion 19 p3423 A70-37751

Aerial terrain analysis by color and color IR photography, analyzing physical factors affecting final image 22 p4018 A70-42963

Color filter schlieren photography for visualization of wind tunnel shock and pressures, liquid mixing and convection currents [SMPTRE PREPRINT 86] 22 p4036 A70-43065

Astronomical color photography, discussing films and filters for exact reproduction 23 p4198 A70-44903

Diazo compounds purity effect on photosensitive photographic film quality, determining color image reproduction density 24 p4334 A70-45498

COLOR TELEVISION

Secondary electron conduction TV camera tube with three color filter wheel for Apollo missions 03 p0493 A70-14025

Color closed circuit TV visual cues in flight simulation during flare and touchdown, including ATA requirements and acuity limits [AIAA PAPER 70-347] 10 p1857 A70-24201

Low cost earth station and antenna for Canadian domestic satellite, bringing color TV to northern territories [AIAA PAPER 70-432] 11 p2000 A70-25458

Ground frequency converters for reception of NTSC color TV transmission from synchronous communication satellites, tabulating cost estimates [AIAA PAPER 70-440] 11 p2002 A70-25490

Color TV tubes white field balancing by spectroradiometer, colorimeter and colorlog meter 12 p2195 A70-27372

Earth colorimetry data improvement by separating signals of each bandwidth on one photographic emulsion or TV tube 13 p2406 A70-28987

Laser color TV display acousto-optic deflectors equalization using prisms 15 p2751 A70-32043

Apollo 10 color TV camera for real time scenes, describing configuration performance and total system operation 16 p2907 A70-33187

SECAM video and audio color TV transmission over Molniia satellite relay path 23 p4162 A70-44091

COLOR VISION

Human foveal color vision in terms of tetrachromatic hypothesis, citing supporting evidence 01 p0026 A70-11054

Color coding effects in compatible and noncompatible display control arrangements 02 p0247 A70-12381

Threshold visibility of uniformly moving colored gratings, noting chromaticity discrimination dependence on spatial and temporal frequencies 02 p0237 A70-12460

Color vision mechanisms spectral sensitivities measured by increment threshold technique for normal and deutan observers 03 p0427 A70-13947

Bleached eye pressure blinding at bleaching light termination during wavelength settings, discussing effect on interocular hue shifts 03 p0427 A70-13951

Color CRT system to display engineering data based on real time analysis, discussing performance requirements 06 p1061 A70-17349

Optimal colors for target and rescue markers, discussing influence on signal detection, response and identification 06 p1002 A70-17713

Human color vision simulation by mathematical and electronic analogs for photoelectric color measurement and eye resolution 08 p1450 A70-20727

Psychophysiological regularities of nonlinear human color vision model, analyzing sensitivity curves, achromatic tints and hyperbolic position in perception space 08 p1443 A70-20728

Deductive model of vision statics formulated for Grassman laws without using operation of color composition 08 p1450 A70-20729

Color vision forms, investigating sensitivity of human retinal receptors and combinations of spectral functions 08 p1443 A70-20731

Binocular achromatic and color thresholds of constant and flickering lights determined from background of different brightness 08 p1443 A70-20732

Microinterval analysis of phased development of human visual color perception in presence of short stimuli 08 p1443 A70-20733

Weightlessness effects on human vision, studying color perception, field of vision and light sensitivity 08 p1444 A70-20743

Dark adaptation correlated with in vivo visual pigments regeneration as function of bleaching during monomolecular time course 08 p1447 A70-21722

Flight personnel color perception requirements and hereditary and acquired anomalies detection 09 p1627 A70-23115

Real time wide angle multicolor scanned laser display for visual flight simulators, utilizing flying-spot camera and rotating optical polygons [AIAA PAPER 70-361] 10 p1857 A70-24203

Visual acuity and light detection after preadaptation to red and orange lights, discussing photopic and scotopic vision 11 p1986 A70-25828

Psychophysical and evoked potential correlates of changes in stimulus color and intensity compared with minimum subjective flicker conditions 12 p2171 A70-28035

Twilight sky color visual estimation from Soyuz 5 spacecraft noting cloudiness effects 15 p2723 A70-31597

Hypoxia and acetazolamide effects on color sensitivity zones in visual field 15 p2684 A70-32533

Exposure duration effect on luminance requirements for hue perception and identification 17 p3040 A70-35724

Lighting and background effects on human binocular color vision of signal lights in industry 19 p3366 A70-38923

Color attributes by subjective estimation of surface colors, discussing correlation with other methods 22 p3972 A70-43409

Central fovea dichromacy tests, using color naming technique 22 p3972 A70-43410

Isochromic change in bleaching of rhodopsin, showing additional intermediate without detectable color change 23 p4147 A70-44776

Monochrome radiography for contrast strengthening to increase color images detectability by human eye 24 p4337 A70-45708

COLORADO

Nitrogenous compounds from Colorado Green River Formation oil shale using high resolution mass spectrometry 11 p2047 A70-26620

COLORATION

U COLOR

COLORIMETRY

Multichannel ionization calorimeter data readout into electronic computer using short circuit coil magnetic storage 05 p0816 A70-15947

Multichannel spectrometer electronic circuitry for ionization colorimeter providing data on low energy particle interactions, emphasizing reliability and accuracy 05 p0846 A70-15948

Barred galaxies colorimetric data to study relative intensities and mean surface brightnesses as function of color 07 p1376 A70-18905

Color TV tubes white field balancing by spectroradiometer, colorimeter and colorlog meter 12 p2195 A70-27372

Integral color indices relation to spectral type on NGC 3077 and M82 galaxies 12 p2308 A70-27871

Earth colorimetry data improvement by separating signals of each bandwidth on one photographic emulsion or TV tube 13 p2406 A70-28987

Twilight colorimetry from horizon spectra obtained by Soyuz 5, computing chromaticity coefficients for purely scattering molecular atmosphere 16 p2896 A70-33260

COLUMBIUM

U NIOBIUM

COLUMNS [PROCESS ENGINEERING]

Thermal conductivity of nitrogen in 350-1500 K range using hot-wire diffusion columns 11 p2147 A70-25756

COLUMNS [SUPPORTS]

NT TAPERED COLUMNS

Dynamic stability of simply supported column of linear viscoelastic materials under sinusoidal loading 01 p0206 A70-11148

Tangential force applied to column end by jet reaction from nozzle clamped to column end, obtaining critical load and oscillation frequency 02 p0389 A70-12644

Visco-elastic column analysis based on mechanical model, investigating relationships between solid viscosities, loading velocities, initial deflections and dynamic buckling loads 03 p0596 A70-14146

Local buckling and failure of thin walled compression column with supported flanges, analyzing strength reduction by eccentricity 03 p0600 A70-14254

Elastic post stability under longitudinal impact on rigid support, considering loading/unloading phases for calculating shock half wave length and critical rate 08 p1591 A70-21443

Clamped thin circular plate bending under various loadings due to action of rigid square column on center 11 p2139 A70-26404

Classical eigenvalue problem transformation by invariant imbedding into initial value problem suited for numerical integration, noting applications to columns elastic buckling 12 p2261 A70-27424

Column end fixity using Euler load and maximum flexibility coefficient for span point lateral load 17 p3188 A70-35226

Postbuckled integrally stiffened wide column weight optimization, developing stress equation 18 p3339 A70-36447

Asymptotic buckling analyses of imperfect columns on nonlinear elastic foundations by perturbation expansions, equivalent linearization and truncated hierarchy approximations 21 p3934 A70-40777

Postbuckling of wire restrained elastic cantilever column with imperfection sensitivity 22 p4116 A70-43204

Thin walled column buckling relation to plate element buckling, studying deformation, stress state, failure mechanism and ultimate load 22 p4116 A70-43214

Undamped elastic cantilever column with concentrated masses, considering transition from stability to divergence under nonconservative forces 24 p4421 A70-45286

COMA

Coma cluster of galaxies morphological and statistical characteristics, determining major and minor axes 10 p1948 A70-25194

Comet tail structures in inner coma region using photographic observations 14 p2650 A70-31220

COMBAT

Air combat model /AIRCOM/ to evaluate close-in air-to-air fighter aircraft combat capability, determining relative changes in kill probability per firing pass 03 p0413 A70-13958

Aircraft life support systems and equipment evaluated in Vietnam combat environment, discussing combat ejection conditions, injuries cause and severity, fatalities, etc 05 p0806 A70-16298

Combat and noncombat ejection/extraction fatalities and major injuries to USAF crewmen
07 p1192 A70-19023

Air combat simulator with attacker and evader pilots control capability, comparing simulated interceptions with flight test maneuvers
[AIAA PAPER 70-340] 09 p1656 A70-23023

Weapon systems combat effectiveness measurements, stressing need for proper data acquisition from early R and D through obsolescence
09 p1794 A70-23414

AH-1G helicopters combat flight loads from on-board oscillograph data recording, defining performance in terms of critical variables
17 p3013 A70-34706

Combat and noncombat ejection/extraction fatalities and major injuries to USAF crewmen
17 p3039 A70-35576

Computerized air combat simulation with comparison of analog and digital approaches, noting Air to Air Combat Fort Worth
18 p3230 A70-36453

COMBINATION
Disproportionation to combination ratio of hydrazyl radicals generated in absence of hydrazine direct decomposition
14 p2544 A70-30120

COMBINATORIAL ANALYSIS
NT PARTITIONS [MATHEMATICS]
NT PERMUTATIONS

COMBINED STRESS
Fracture criteria in cracked plates under combined extension and cylindrical bending using Sih-Hartrant theory
[ASME PAPER 69-MET-L] 04 p0770 A70-14882

Stability of clamped, hinged and elastically supported circular cylindrical shells under critical combined torsional and transverse pressure
05 p0934 A70-16227

Plane deformation of plastic thin walled tubes under complex tensile and torsional load
05 p0935 A70-16233

Shallow spherical shells stability under combined loading, hinging and edge clamping conditions, deriving strain energy expressions
05 p0936 A70-16238

Gas turbine blades thermal fatigue strength under simultaneous temperature cycles and static tensile loads, analyzing temperature and stress fields
05 p0953 A70-17053

Crack formation and propagation kinetics in flat and cylindrical Cr-Mo-V steels under tension compression loading cycles
06 p1162 A70-17393

Numerical analysis of axisymmetric elastoplastic deformation of circular plates under combined lateral load and membrane force
07 p1402 A70-18977

Elastoplastic torsion of combined prismatic bars with transverse distribution of constant properties solved by computer
07 p1415 A70-20189

Unidirectional filamentary composites failure theory for uniaxial and combined stress, considering constituent material properties and fabrication processes
08 p1532 A70-21902

Cylindrical shell stability under combined torsion and internal pressure, noting yield point effect on critical load, obtaining buckling-internal pressure relationship
09 p1786 A70-23722

Cylindrical coil springs cold winding loading processes, considering initial tension or compression of wire and combined stresses
10 p1894 A70-24297

Length effect on modulus determination test for thin laminated tube under combined loading using shell theory
11 p2136 A70-26086

Stress relaxation in combined torsion-tension, developing expressions for torque and axial force
11 p2140 A70-26482

Shells of revolution under combined thermal and mechanical loading, presenting analytical basis of BOSOR 3 digital stress analysis program
12 p2320 A70-27144

Plates elastic-plastic behavior under combined stretching and bending by finite element method
12 p2320 A70-27146

Thin walled tubes plastic instability under combined internal pressure and axial load for open and closed end conditions
12 p2322 A70-27216

Aluminum sheets anomalous plastic behavior under balanced biaxial and uniaxial tensions
12 p2324 A70-27398

Critical loads for brittle bodies weakened by sharp holes under combined diffuse thermal fluxes and crack crossing
12 p0000 A70-28321

Combined internal pressure and axial loading influence on aeroelastic stability of thin walled cylindrical shell in supersonic flow field
16 p2991 A70-33851

Stability analysis of anisotropic cylindrical shells under combined loadings using inverse operators
16 p2994 A70-34246

Optimum filament orientation for maximum strength in composite with combined normal and shear stresses
17 p3183 A70-34563

Zero moment theory for stress-strain state of thin walled anisotropic shells with nonuniform moduli under simultaneous torsion and tension
18 p3340 A70-36578

Strain hardening directionality during creep tests of tubular samples under combined tensile stresses and bending moments
18 p3341 A70-36588

Combined mechanical and cyclic thermal stresses effect on plastic deformation buildup in E1435 alloy preceding breakdown
19 p3449 A70-37349

Circular sandwich arc subject to central concentrated load and symmetrically applied edge couple, obtaining shakedown interaction curve
19 p3546 A70-38354

Cylindrical or tapered composite shell structures optimal design with closed circular or elliptical cross section under combined bending and torsional loads
20 p3730 A70-40043

Solid and sandwich beams lateral vibrations under transverse shear, rotary inertia and variable midplane stretching
21 p3938 A70-41761

Circular cylindrical shell with varying thickness under circumferential load and radial pressure, calculating critical load
22 p4117 A70-43354

Carrying capacities of simply supported and clamped circular plates under combined lateral pressure and edge compression loads
22 p4118 A70-43548

COMBUSTIBILITY
U FLAMMABILITY
COMBUSTIBLE FLOW
Cold ducted supersonic flow of premixed ethylene and air ignition by hot turbulent jet
[AIAA PAPER 70-148] 06 p1131 A70-18057

Combustible gas /hydrogen-air/ subsonic and transonic flow past sphere, approximating combustion zone structure by model
10 p1801 A70-24142

Combustion research prospects, considering turbulence and flame stabilization, pollution control, flame self acceleration, subsonic/ supersonic flow combustion and flame diagnostics
11 p2150 A70-26376

Gas dynamic processes insufficiency for triggering transition to detonation obtained from laser schlieren records of nonsteady flow field ahead of accelerating turbulent flame
11 p2150 A70-26378

Temperature distribution in opposed jet diffusion flames, discussing mass fluxes and fuel and oxygen concentrations effect
11 p2151 A70-26385

Viscid-inviscid equations solution, describing flows with coupled mixing, combustion and lateral pressure gradients
15 p2718 A70-32516

Combustion effects on mixing of axisymmetric supersonic and turbulent free jets to obtain species concentrations, pitot pressures and temperatures
16 p2998 A70-33860

Particle penetration of solid or liquid combustible additives injected into air breathing combustors airstreams
17 p3073 A70-35665

Shock layer and combustion in supersonic flows about conical bodies at various angles of attack
17 p3012 A70-35894

COMBUSTION
NT AFTERBURNING
NT BOUNDARY LAYER COMBUSTION
NT DEFLAGRATION
NT FUEL COMBUSTION
NT HYDROCARBON COMBUSTION
NT HYPERSONIC COMBUSTION
NT METAL COMBUSTION
NT PROPELLANT COMBUSTION
NT SOLID PROPELLANT IGNITION
NT SPONTANEOUS COMBUSTION
NT SUPERSONIC COMBUSTION
Combustion - Conference, Poitiers, France, July 1968
02 p0392 A70-12001

Ignition and combustion in ducted turbulent supersonic flow, discussing premixed and unpremixed ethylene
[AIAA PAPER 70-720] 16 p2997 A70-33488

Boron particles ignition and combustion in supersonic air stream, emphasizing axial and lateral two phase flow injection
[AIAA PAPER 70-737] 16 p2856 A70-33496

COMBUSTION CHAMBERS
Turbojet engines air pollution emissions processes resulting from combustor primary and secondary zone conditions, discussing engine design modifications
[AIAA PAPER 69-1040] 01 p0162 A70-10602

Pressure oscillograms and schlieren photographs of shock wave amplification during interaction of cellular flame of gas mixtures in cylindrical combustion chamber
01 p0217 A70-11014

Combustion chamber traveling oscillating shock wave as driving mechanism of high amplitude axial mode solid rocket combustion instability
02 p0353 A70-12009

Combustion instability in gas turbine main combustors, noting heat release and inlet air flow rates coupling
02 p0353 A70-12012

Premixed methane-oxygen-nitrogen combustion in conical reactor fed by choked sonic flow jet, analyzing reaction products chromatographically
02 p0397 A70-12030

Radiation from flames in gas turbines and rocket engines, discussing effects of soot formation fuel chemical composition, combustor operating conditions, etc.
02 p0354 A70-12050

High pressure tests of primary zone flame radiation, flame and tube metal temperatures in aircraft combustion chambers, including oxygen and vitiated inlet air effects
02 p0355 A70-12051

U-shaped combustion chamber two dimensional model for studying factors influencing flame spread and stabilization and heat transfer in gas turbines
02 p0355 A70-12257

Annular combustion chamber for turboprop engines, analyzing design data and development stages, discussing performance characteristics
03 p0552 A70-13928

Combustion chamber design for engines, considering atomization by rotating disk vs nozzle atomization
03 p0552 A70-14031

Interior ballistics of high-low propulsion system with fixed volume high pressure combustion chamber coupled to variable volume lower pressure action chamber
03 p0548 A70-14116

Liquid fuel film vaporizing combustor for gas turbines, considering combustion efficiency and flame intensity
03 p0552 A70-14324

Cold flow-porous plate simulation of swirling flow-field in spinning end-burning rocket chamber, noting vortex generation and flow characteristics
04 p0764 A70-15541

Thermal and gas dynamic characteristics of aircraft turbine engine annular vaporizing combustion chamber determined from air distribution ratio
05 p0895 A70-15897

Liquid rocket technology for chemical engineers, discussing insulating tanks, flexible lines, turbopumps and combustion chamber
05 p0896 A70-16168

Flight performance prediction for throttling bipropellant rocket engine utilizing ablative combustion chamber throat, discussing lunar module descent engine
[AIAA PAPER 69-452] 06 p1130 A70-17176

Heat transfer to hydrogen calculated with reference to design of cooled rocket nozzles and combustion chambers
06 p1174 A70-17677

Ramjet engines combustion chamber and air intake design for velocities between Mach 2 to 7
06 p1130 A70-17932

Main stream interaction with flame stabilizing jets in combustion chambers and afterburners using gas dynamic models
07 p1419 A70-18754

Propellant sprays behavior in high pressure combustors, calculating jet breakup or atomization length
07 p1257 A70-19331

Transverse and longitudinal combustion chamber oscillations in rocket motors with distributed mass and energy sources
07 p1364 A70-19581

Flame propagation rate and combustion zone extension dependence on chamber dimensions for turbulent flow of homogeneous mixtures
08 p1597 A70-21187

Turbulent combustion stability in chamber, taking into account boundary effects due to acoustic perturbations reflection
09 p1786 A70-22106

Chemical rocket propulsion systems approximate calculation for characteristic velocity dependence on mixture ratio and pressure in combustion chamber
[DFVLR-SONDDR-24] 10 p1929 A70-23842

Gas turbine components, discussing material selection, fabrication and assembly with emphasis on combustion and turbine sections, turbine coatings, shafts, bearings and seals
10 p1929 A70-23851

Entropy or material waves effects on HF pressure oscillations in liquid rocket combustor, assuming concentrated combustion zone and zero length nozzle
10 p1929 A70-24088

Chemical high energy rocket propellants, discussing metal combustion, hybrid and tribrid engines, combustion chambers, etc
11 p2100 A70-26282

Jet engine pollution reduction for airport areas, discussing chemical equilibrium failure in exhaust gases and combustor design 12 p2291 A70-27993

Pilot chamber initiated thermal decomposition reactor concept for monopropellant thruster, discussing thrust levels and throttling ratios [AIAA PAPER 69-420] 13 p2473 A70-28507

Spin detonation of tangential HF vibrations in liquid rocket engine combustion chambers, discussing instability prevention 13 p2474 A70-29422

Tubular gas turbine combustors design by analytical model, summarizing theories of combustor analysis, turbulent flame speed, microvolume burning and stirred reactors [WSCI PAPER 70-2] 13 p2474 A70-29613

Monopropellant rocket combustion one dimensional theory with uniform velocity and size droplets injection, obtaining chamber length 14 p2629 A70-30773

Rolls-Royce RB 211 three shaft turbofan engine, discussing centrifugal compressor, tubular combustion chambers and single stage turbine 15 p2787 A70-31949

Two diaphragm combustion shock tube for plasma radiation energy transfer, describing development, performance, make-up and testing 15 p2779 A70-32019

Rocket motor combustion chamber lining thickness distribution matching to effusor by designing effusor as multiple nozzle made of circular graphite plate 15 p2790 A70-32271

Large scale hydrogen fueled supersonic combustor test at simulated Mach 8 flight, describing fuel injector design [AIAA PAPER 70-715] 16 p2965 A70-33539

Jet engine combustion chamber design, discussing performance range and geometry 16 p2970 A70-33682

Kuznetsov NK 8-4 bypass turbojet air entry vanes, pressure compressors, gear case, combustion chamber and turbine drives 17 p3147 A70-34629

German monograph on gas turbine combustion chambers part-load behavior improvement by load controlled change of flame tube air cross section 17 p3148 A70-35373

Water cooled pressure probes for measuring rocket chamber HF pressure variations 17 p3093 A70-35485

Particle penetration of solid or liquid combustible additives injected into air breathing combustors airstreams 17 p3073 A70-35665

Flameout and ignition correlation for diffusion fuel burnup behind angled stabilizers in annular turbine combustion chamber 18 p3300 A70-36127

Rocket engine with Teflon lined combustion chamber, considering design criteria and tests 18 p3301 A70-36662

High speed combustion chambers for gas turbine applications, using finite rate chemistry and turbulent mixing computer program for burner design [ASME PAPER 70-GT-25] 18 p3304 A70-36866

Aerodynamic stability of branched diffuser systems used in annular combustors of gas turbine engines [ASME PAPER 70-GT-27] 18 p3209 A70-36868

Turbine engine combustion chambers with various frontal devices, investigating burnout mechanism and heat yield in secondary air flow injection zone 19 p3489 A70-37246

Gas turbine engine combustion chamber efficiency dependence on injector characteristics, temperature and fuel physicochemical properties 19 p3489 A70-37247

Air-mechanical fuel injection effect on gas turbine engine combustion chamber working process, investigating heat generation coefficient, temperature field nonuniformity and combustion efficiency 19 p3489 A70-37248

Smoke chamber measurements of opacity developed in polymer pyrolysis or combustion, including Materials Smoke Obscurity Index (MSOI) 20 p3736 A70-39404

Jet engine combustor design and efficiency, discussing heat transfer, cooling and engine materials 20 p3688 A70-39648

Combustion chamber, turbopump and combustion control system for French turbopump-fed booster rocket motor 20 p3688 A70-39649

Reusable rocket engine for space shuttle, discussing propellants, configuration, design, combustion cycle and size 20 p3689 A70-40084

Gas turbine combustion chamber convective and radiant heat transmission, examining steam film cooling of flame tube 22 p4092 A70-43199

Liquid propellant rocket engine nonisobaric cylindrical combustion chamber parameters from thermodynamic data 22 p4092 A70-43355

Gas turbine engine combustion chamber starting, discussing effects of temperature, nozzle characteristics and fuel physicochemical properties 22 p4092 A70-43356

Jet engine air pollution in U.S., discussing fuel types, additives and burner design for smoke emission reduction 23 p4233 A70-44200

Liquid propellant rocket engine combustion instabilities, describing unsteady combustor flow by single nonlinear wave equation with stable and unstable finite amplitude limit cycles 23 p4233 A70-44425

Spinning cold-flow rocket motor, studying rotation effects on chamber flow velocity field 23 p4233 A70-44579

Combustion chamber flow visualization, obtaining information on pressure loss, velocity field, flow pattern and temperature gradients 24 p4393 A70-45444

Jet engine combustion chamber pressure loss, flow velocity through flare tube holes and air supply calculation, noting adaptation for computer use 24 p4393 A70-45446

Reduced smoke combustion chambers for jet aircraft engines tested in full scale JT8D engine 24 p4396 A70-46387

COMBUSTION CONTROL

Burning program for sounding rocket to reach maximum altitude with given initial and propellant masses, discussing numerical parameter optimization technique 01 p0161 A70-10150

Position control of burning solid nonmetalized propellant strand in combustion bomb using closed loop servomechanism 01 p0215 A70-10830

Compression wave mechanism of supersonic combustion controlled by mixing, discussing multiple injector design, thermal compression and geometry effect 02 p0399 A70-12041

Boron particles combustion behavior prediction by incorporating condensed phase effect into diffusion controlled model [WSCI PAPER 70-9] 13 p2472 A70-29612

Ignition delay-reducing catalyst for furfuryl alcohol-red fuming nitric acid hypergolic bipropellant 13 p2473 A70-29992

Solid propellant rocket motor combustion control by fluidic vortex valve, considering thrust variation [AIAA PAPER 70-643] 16 p2965 A70-33535

Optimal water quench of solid rockets using injection normal to propellant surface [AIAA PAPER 70-640] 16 p2968 A70-33598

Combustion extinguishment of composite solid propellant motors by fluid injection, considering binder, curing agent and burning rate catalyst [AIAA PAPER 70-641] 16 p2968 A70-33599

Optimal control for one dimensional compressible gas flow, combustion and heat exchange, described by first order partial differential hyperbolic equations 19 p3402 A70-37240

Combustion chamber, turbopump and combustion control system for French turbopump-fed booster rocket motor 20 p3688 A70-39649

Electric field control of oscillatory acetylene flame combustion for chemical rocket engines 21 p3942 A70-40885

Catalytic combustion fuel tank inerting techniques for fire protection in military and civilian aircraft 23 p4141 A70-44485

COMBUSTION EFFICIENCY

Combustor geometry and heat release effects on supersonic combustor thrust efficiency, considering shock-free, normal and oblique shock situations 02 p0354 A70-12043

Boron combustion in air augmented rockets, examining mixing and burning between subsonic air and supersonic fuel rich exhaust [AIAA PAPER 68-634] 03 p0603 A70-12910

Emulsified jet fuels cold flow, combustion and corrosion characteristics in gas turbine combustor compared with JP-4 fuel [ASME PAPER 69-WA/GT-3] 04 p0732 A70-14892

Optimum injector design for propellant spray mixing using nonreactive simulants and combustion efficiency model 04 p0737 A70-15419

Steady state and dynamic performance of variable geometry free gas turbine using nomogram and analog simulation 06 p1129 A70-17143

Mixture composition and airflow rate of combustion efficiency in turboprop afterburner chamber with air-fuel flame stabilizer 10 p1929 A70-24282

Excess air ratio and heat release efficiency in combustion of kerosene mixture determined by volumetric gas analysis 10 p1968 A70-24283

Residence times distribution in confined round swirling jet, considering mass conservation of 03 p0543 A70-13632

hypothetical tracer substance in combustion efficiency prediction 13 p2522 A70-29609

Liquid rocket engine injector elements design criteria, using noncircular orifice geometry to predict efficiency [AIAA PAPER 70-704] 16 p2967 A70-33565

Motor design parameters effects on solid propellant extinguishment predicted from mathematical combustion model 16 p2962 A70-33571

Pressure and grain size effect on burnout velocity and combustion capacity of ammonium perchlorate 17 p3145 A70-34639

Combustion efficiency and rate in oxygen enriched spacecraft atmosphere 17 p3177 A70-35210

Gas turbine engine combustion chamber efficiency dependence on injector characteristics, temperature and fuel physicochemical properties 19 p3489 A70-37247

Air-mechanical fuel injection effect on gas turbine engine combustion chamber working process, investigating heat generation coefficient, temperature field nonuniformity and combustion efficiency 19 p3489 A70-37248

Jet engine combustor design and efficiency, discussing heat transfer, cooling and engine materials 20 p3688 A70-39648

COMBUSTION HEAT

U HEAT OF COMBUSTION

COMBUSTION INSTABILITY

U COMBUSTION STABILITY

COMBUSTION PHYSICS

Mass loss rate of evaporating liquid droplet with vapor reacting with oxygen of atmosphere in combustion front [DFVLR-SONDDR-16] 01 p0216 A70-10932

Aerodynamic gas flame theory and computations, discussing diffusion burning, turbulent flow burning rate, Reynolds number effects, etc 01 p0217 A70-11006

Unmixed gases diffusion burning calculations, discussing turbulent flame burning aerodynamics in jet flows 01 p0217 A70-11007

Exothermic reaction front propagation in condensed phase, analyzing Novozhilov system of equations 01 p0217 A70-11009

Weightlessness effects on butyl alcohol diffusion flames, studying flame damping mechanism 01 p0217 A70-11012

Combustion time of Al powder, considering concentration, injection into gas flow, oxidizer composition and agglomeration 01 p0161 A70-11015

Injected B particles burning in hot gas stream of oxidant mixture with Ar and H, observing trace widening by motion picture technique 01 p0218 A70-11016

Steady burning process equations numerical solution for boundary conditions prescribed at saddle point singularity 01 p0218 A70-11019

Gas ignition and burning processes calculation with allowance for hydrodynamics, discussing time saving finite difference solution of differential equations system 01 p0218 A70-11020

Solid propellant combustion instability advances, discussing combustion flow interactions, response functions, etc 02 p0351 A70-12008

Three dimensional linear combustion instability in liquid propellant rocket motors using concentrated combustion model, presenting mathematical analysis as boundary value problem 02 p0353 A70-12011

Laminar diffusion flame spread against air stream over solid or liquid fuel bed, noting influence of stoichiometric and thermal properties and data inconsistency 02 p0396 A70-12016

Gas detonation dynamics associated with shock tube self ignition kinetics, noting chemokinetic factors role 02 p0397 A70-12024

Premixed perchloric acid-methane two flame structure, measuring burning velocities, spectra, temperatures and burned gas compositions 02 p0352 A70-12034

Combustion effects on base pressure of two dimensional body in supersonic flight, considering air-fuel ratio, combustion length and free stream Mach number 02 p0354 A70-12046

Ammonia/chlorine dioxide and ammonia/chlorine dioxide/methane flames burner stabilization and burst velocities 02 p0400 A70-12670

Hybrid propellant combustion mechanisms, connecting surface reactions to melting mechanism and subsequent liquid flow [ONERA-TP-736] 03 p0543 A70-13632

Transient response of heterogeneous solid propellant combustion surface determined by step technique regarding pressure buildup and drop conditions [ONERA-TP-748] 03 p0544 A70-13635

Powder and solid propellant combustion, discussing heterogeneous and homogeneous systems, characteristics of foam, fizz and flame zones, etc 03 p0544 A70-13860

Burning constants prediction for suspended hydrocarbon fuel droplets based on modified theoretical equation 03 p0544 A70-13916

Flame structure of liquid methanol burning spheres, discussing temperature and composition profiles 03 p0544 A70-13924

Atmosphere classification according to fire hazard based on heat capacity per mole of oxygen, noting exponential growth rate 03 p0607 A70-14054

Polyamide fabric burning rates in oxygen-inert gas mixtures, studying damping effects of density, thermal conductivity, molecular constants and mass flow 06 p1090 A70-17284

Hydrogen-oxygen difluoride flame burning velocity, diffusion coefficient and light output [WSCI PAPER 69-49] 06 p1178 A70-17982

Ignition of single particles of light metal hydrides, considering combustion stages and heat transfer [WSCI PAPER 69-47] 06 p1179 A70-17984

Heterogeneous ignition mechanism of solid fuels, deriving surface temperature history for time and nature of transition from weak to strong combustion mode [AIAA PAPER 70-119] 06 p1128 A70-18041

Combustion processes and ignition criteria in shock wave ignition of liquid fuel drop in oxidizing atmosphere [AIAA PAPER 70-9] 06 p1180 A70-18142

Shear wave interaction in infinite homogeneous reacting fluid, using Fourier and Taylor series for velocity, temperature, density, pressure and composition [AIAA PAPER 70-146] 06 p1040 A70-18154

Multiphase two dimensional mixing and combustion of flow fields suspended in gaseous medium for propulsion systems problems, obtaining governing equations [AIAA PAPER 70-145] 06 p1181 A70-18175

Main stream interaction with flame stabilizing jets in combustion chambers and afterburners using gas dynamic models 07 p1419 A70-18754

Quasi-steady radially symmetric theory of liquid drop vaporization and homogeneous combustion extended to burning of solid carbon spheres gasified by chemical attack 07 p1419 A70-18915

Integral method for time development of viscous, heat and mass conducting layer over leading edge of volatile drop instantaneously immersed in gas stream 07 p1358 A70-18916

Cold combustible mixture ignition at forward stagnation region of hot projectile, calculating temperatures for propane-air mixture 07 p1422 A70-19577

Metal particles additives behavior in solid rocket propellant combustion, using scanning electron microscope 07 p1359 A70-19585

Minimal initial size of explosion reaction center used to explain ignition process in flammable mixtures, noting dependence on pressure, temperature and composition 07 p1422 A70-19586

Granular diffusion flame theory application to low pressure burning of composite solid AP propellants 07 p1361 A70-19914

Liquid rocket engine combustion processes determined by injector design using similarity principles 07 p1362 A70-19919

Premixed flames of methane with chlorine dioxide and perchloric acid, comparing properties with methane-oxygen flames, suggesting unified reaction mechanism 07 p1425 A70-20007

Ammonium perchlorate combustion catalysis, studying preflame heating and mixing effects on gas phase flame burning velocity 07 p1425 A70-20010

Combustion kinetics in supersonic gas flows past various bodies, assuming exothermal and inverse recombination reactions behind adiabatic shock wave after induction period 08 p1596 A70-20855

Flame propagation rate and combustion zone extension dependence on chamber dimensions for turbulent flow of homogeneous mixtures 08 p1597 A70-21187

Condensed fuel mixtures and oxidizers combustion rates as function of pressure and particle size 09 p1786 A70-22104

Two body collisions reaction mechanisms with small heats of reaction for Be and Al gaseous oxida-

tion, noting low free energy properties of polymerization 10 p1928 A70-24089

Velocity and pressure distribution and flame front shape of confined flame in constant section duct 10 p1969 A70-24786

Combustion research prospects, considering turbulence and flame stabilization, pollution control, flame self acceleration, subsonic/ supersonic flow combustion and flame diagnostics 11 p2150 A70-26376

Artificial carbographites surface combustion processes using mercury porosimetry analysis 13 p2519 A70-28578

Shock wave interaction with burning liquid fuel droplets in gaseous oxygen atmosphere, observing wave amplification due to mass combustion rate increase 13 p2522 A70-29424

Heterogeneous combustion observation by motion picture holography, considering light source requirements and hologram separation at higher sampling rates [WSCI PAPER 70-10] 13 p2409 A70-29610

Boron particles combustion behavior prediction by incorporating condensed phase effect into diffusion controlled model [WSCI PAPER 70-9] 13 p2472 A70-29612

Evaporation and combustion kinetics of droplets and particles in hot air stream, observing luminous trace 14 p2664 A70-30392

Hyperbaric environment combustion, discussing burning rate data and fire resistance scale 14 p2665 A70-30626

Soviet book on rocket engine theory covering liquid and solid propellants, combustion physics, nozzle and thrust chamber geometry, etc 14 p2628 A70-30628

Two dimensional transonic flows bounded by free surface and wall with interior heat release and external burning, indicating application to control or propulsion 14 p2665 A70-30947

Al and Be single particles combustion in various oxidizers, using pulsed Nd-glass laser and Xe flash heating device and scanning electron microscope 14 p2628 A70-30949

Biphase rockets combustion characteristics, comparing results with propellant vaporization and nonlinear instability models 14 p2665 A70-30950

Book on electrical aspects of combustion processes covering formation, behavior in fields, diagnostics, uses of ions, electrons and charged particles, flame ionization, etc 16 p2996 A70-33030

Integral model for combustion of metal particle laden jet mixing with subsonic secondary stream in duct, considering air breathing engine design [AIAA PAPER 70-736] 16 p2964 A70-33490

Subsonic turbulent boundary layer with mass addition and combustion for combustion effects on velocity profiles in constant pressure and accelerating flows [AIAA PAPER 70-724] 16 p2997 A70-33498

Liquid rocket engine combustion analysis, discussing bipropellant spray mass distribution, drop size and velocity, spray evaporation interphase drag and ablative chambers [AIAA PAPER 70-622] 16 p2997 A70-33527

External burning fuels environmental temperature requirements from nonlinear droplet ignition model, emphasizing droplet size importance [AIAA PAPER 70-607] 16 p2997 A70-33604

Composite solid propellants burning rate and initial temperature relationship, investigating granular diffusion flame model [AIAA PAPER 70-656] 16 p2963 A70-33618

Uniform two dimensional turbulent boundary layer with hydrogen-nitrogen mixture injection and combustion at flame front, obtaining velocity distribution by kinetic energy equation 16 p2894 A70-33880

NRL research in flammability and combustion, discussing oxygen concentration effects on ignition and combustion, chemi-ion formation, etc 16 p3002 A70-33967

Pressure histories of burning modes in combustion driven shock tube using ignition of stoichiometric hydrogen-oxygen mixture with He dilution 17 p3195 A70-34922

Closed compartment fire mathematical model to analyze combustion parameter effects, atmosphere pressure and temperature during fire 17 p3198 A70-35646

Powdered metallic additions effect on combustion rates of ammonium perchlorate with bitumen and polymethyl methacrylate and potassium perchlorate with bitumen mixtures 18 p3299 A70-36247

High speed combustion chambers for gas turbine applications, using finite rate chemistry and turbulent mixing computer program for burner design [ASME PAPER 70-GT-25] 18 p3304 A70-36866

Soviet papers on kinetics and aerodynamics of fuel combustion processes covering supersonic flow, flame stabilization, fluid atomization, nonequilibrium recombination, etc 20 p3736 A70-39265

Combustion of decomposition products of Mg based pyrotechnic fuel in supersonic flow, obtaining heating device characteristics 20 p3736 A70-39266

Homogeneous opaque reactive solid heating and ignition by constant energy flux, examining physical and chemical parameters at critical conditions 20 p3738 A70-40078

Multicomponent fuels combustion in air, deriving simplified flame sheet model 21 p3942 A70-40881

Cool flame isothermal theory with oscillatory features accounting for damping time evolution and thermic reaction nature 21 p3942 A70-40886

Gas phase ignition theory with feedback of homogeneous propellant exposed to stagnant gas after shock reflection [AIAA PAPER 69-559] 21 p3950 A70-41728

Book on stationary flame structure, radiation and temperature covering flow visualization, burning velocity, propagation, ionization, etc 22 p4121 A70-42325

Chemical equilibrium premixed flame composition at given temperature, pressure and mixture strength, using Newton-Raphson iteration technique for simultaneous nonlinear equations 23 p4157 A70-43892

Oxygen atom catalytic recombination and flame inhibition mechanism literature survey 23 p4157 A70-44002

Combustion velocity in high pressure chamber, determining fire mechanism in overpressure environment 24 p4393 A70-45447

COMBUSTION PRODUCTS

Expansion isentropes of TNT/hexogen melts explosion products from measured shock wave parameters in Al, organic glass, foam polystyrene, argon and air 01 p0216 A70-11003

Apollo lunar module descent engine exhaust organic combustion products, estimating ion intensities of various species in all mass spectra 02 p0356 A70-12693

Copper chromite catalyst effects on sublimated ammonium perchlorate dissociation products, noting applications to solid propellants 03 p0544 A70-13923

Temperature evolution of detonation products of Na seeded propane-oxygen mixtures, observing periodic variation for helicoidal cases 03 p0608 A70-14356

Flow field between infinitely massive wall and rigid piston accelerated by detonation products, comparing analytical results to finite difference numerical integration 05 p0830 A70-15782

Jet aircraft air pollutant production and dispersion of nitric oxide and soot, discussing mixing process [AIAA PAPER 70-115] 06 p1131 A70-18070

Atmospheric contamination due to Be solid propellant exhaust products, discussing pollution levels, governmental restrictions on testing, etc [AIAA PAPER 70-117] 06 p0997 A70-18085

Preignition products from hydrazine propellants at simulated high altitude conditions using IR spectrophotometry, mass spectrometry and differential thermal analysis 07 p1358 A70-19579

Gas turbine engines contribution to air pollution, using model combustor to study burned gas composition, emphasizing nitric oxide concentration 08 p1559 A70-21481

Earth storable liquid propellants combustion products simulation by combustion of gaseous fuel and oxidizer combination, discussing elemental composition and thermodynamic considerations 08 p1557 A70-21622

Organic compounds chemical reactions during burning in laminar diffusive flames, describing technique for pyrolysis and combustion products sampling 09 p1787 A70-22107

OH, NH and amine radicals concentrations in flame gases from flat ammonia-oxygen-nitrogen flames measured as function of distance from burner surface 09 p1788 A70-22343

Oxygen-kerosene combustion product composition and characteristics in engine thermodynamic design allowing for intermolecular interaction forces 10 p1968 A70-24284

Expansion isentropes of TNT/hexogen melts explosion products from measures shock wave parameters in Al, organic glass, foam polystyrene, argon and air 10 p1960 A70-25008

Temperature and metallic contact effects on composition and structure of solid phase deposits during reactive fuel oxidation 12 p2289 A70-27493

- Detonation model, discussing combustion gases from solid explosives detonation 13 p2520 A70-28803
- Stefan-Boltzmann formula validity for flames and combustion products radiation affected by time dependence of emissivity coefficient, place and wavelength 14 p2662 A70-30179
- Particles shape and phase composition in combustion products of dispersed Al-Mg alloy powders by electron diffraction and X ray analysis 14 p2664 A70-30396
- Toxicity and downwind diffusion of Be rocket exhaust product measurements, using ADOBE experiment and AFRPL micromet meteorological data system 14 p2628 A70-30611
- Air pollution by turbojets and gas turbines, discussing control of carbon particles and nitrogen oxides 16 p2963 A70-32922
- Thermodynamic diagram indicating enthalpy and entropy of oil combustion gases for any state and air excess value 16 p2997 A70-33295
- Nonequilibrium combustion products and condensables containing reactive multiphase rocket nozzle flows and exhaust plumes characterization using generalized kinetics streamtube program [MGKS/ [AIAA PAPER 70-845]] 16 p3001 A70-33928
- Rocket chambers combustion products isotropic expansion effects within nozzle on dissociation degree, assuming shifting and frozen equilibria 16 p2963 A70-34341
- Secondary combustion products of air augmented boron loaded solid propellant rocket ramburner, measuring properties by spectroscopy 17 p3196 A70-35196
- Ni alloys with protective coatings for gas turbine blades, testing corrosion resistance in diesel fuel combustion products with intermittent salt water sprays 17 p3125 A70-35394
- Thermal fatigue cracking of gas turbine blades in fuel combustion product flow, investigating surface composition, microhardness and structure under simulated loads 19 p3490 A70-37338
- Nonequilibrium recombination in supersonic nozzle of dissociated combustion products of hydrogen in air, investigating initial system and rate constants effect 20 p3582 A70-39269
- Chemical and physical factors effect on smoke evolution from polymers 20 p3736 A70-39405
- Toxicity problems from burning or heating of polymeric materials, discussing laboratory experiments and standardized toxicity testing procedures 20 p3579 A70-39406
- Combustion products of 280-400 C oxidation of ethyl acetate, methyl propionate and i-propyl acetate 21 p3864 A70-40882
- Carbon monoxide vibrational population inversion in product molecule produced in free burning carbon disulfide/oxygen flame 21 p3950 A70-41708
- Tank collection and spectrophotometric tests in determining aluminum oxide particle size produced by small rocket engine 21 p3867 A70-41727
- Oxygen-kerosene fuel combustion products thermodynamic properties, tabulating computed values 21 p3865 A70-41771
- Laminar hexane diffusion flame, investigating distribution of final and intermediate combustion products 22 p4123 A70-42522
- German monograph on soot formation and separation in turbulent diffusion flame in power plant combustion chamber, noting pyrolysis role 24 p4428 A70-45087
- COMBUSTION STABILITY**
NT FLAME STABILITY
Hydrogen-oxygen variable length combustor longitudinal instability, studying hydrogen injection temperature effects on pressure interaction index and pressure sensitive time lag 01 p0214 A70-10324
- Composite propellants high pressure burning stability with various binders and oxidizers, showing ammonium perchlorate oxidized formulations susceptibility to instability 01 p0160 A70-10852
- Steady burning process equations numerical solution for boundary conditions prescribed at saddle point singularity 01 p0218 A70-11019
- Nonlinear combustion instabilities in liquid propellant rockets, considering various combustion models and experimental techniques 02 p0351 A70-12007
- Solid propellant combustion instability advances, discussing combustion flow interactions, response functions, etc 02 p0351 A70-12008
- Combustion chamber traveling oscillating shock wave as driving mechanism of high amplitude axial mode solid rocket combustion instability 02 p0353 A70-12009
- Three dimensional linear combustion instability in liquid propellant rocket motors using concentrated combustion model, presenting mathematical analysis as boundary value problem 02 p0353 A70-12011
- Combustion instability in gas turbine main combustors, noting heat release and inlet air flow rates coupling 02 p0353 A70-12012
- Combustion instability of solid propellants using response to pressure perturbations for T and L burners 02 p0352 A70-12013
- Three dimensional combustion instability in liquid-propellant rocket engines, investigating dependence on design and operating parameters via boundary value problem analysis 03 p0551 A70-13574
- Internal stability of turbulent combustion, developing analysis for one dimensional model and deriving sufficient instability criterion 03 p0607 A70-13862
- Cabin interior materials studied and tested for greater fire resistance, lower smoke and toxic gas by-products and flash fire possibility lessening 03 p0437 A70-14057
- Emulsified jet fuels combustion characteristics evaluation by laboratory technique, presenting data on emulsifiers and corrosion inhibitors effect [ASME PAPER 69-WA/GT-2] 04 p0785 A70-14893
- Rocket stability monitoring by temporal radiometry, using exhaust radiance measurement to detect frequencies in thrust chamber combustion pressure [AIAA PAPER 69-580] 04 p0737 A70-15429
- Combustion model for temperature inhomogeneities effect on stability of solid fuels steady combustion 05 p0958 A70-16960
- Combustion stability in air-liquid fuel zone of jet engine burner with burning rate controlled by droplet vaporization rate controlled mechanism [WSCI PAPER 69-44] 06 p1178 A70-17980
- Ammonium perchlorate deflagrations, determining intrinsic stability of one dimensional burning configuration based on flame structure modeling [AIAA PAPER 70-123] 06 p1128 A70-18044
- Liquid rocket motors with concentrated combustion, studying nonlinear longitudinal instabilities with shock waves in combustion chambers 07 p1362 A70-18917
- LF nonacoustic instability of solid propellant rocket motors, using combustion model allowing flame temperature oscillations with chamber pressure [AIAA PAPER 68-179] 07 p1421 A70-19319
- Solid propellant rocket engines design, considering nonlinear longitudinal combustion instability encountered in aluminumized propellants 08 p1558 A70-20623
- Turbine pump systems operation in terms of liquid rocket engine combustion stability, noting altitude effects on pressure pulsations 08 p1559 A70-21849
- Turbulent combustion stability in chamber, taking into account boundary effects due to acoustic perturbations reflection 09 p1786 A70-22106
- Ammonium perchlorate-polymer mixtures combustion rates with/without cobalt oxide additions, studying ignition temperatures of stable flameless burning 09 p1787 A70-22108
- Transient regimes of solid fuel diffusion combustion in channel with oxidizer fed in from outside, proposing finite difference scheme for integrating equations 09 p1741 A70-22114
- Book on fundamental aspects of solid propellant rockets covering nozzle flow, solid propellants performance, ignition, combustion instability, etc [AGARDGRAPH-116] 09 p1743 A70-22635
- Pressure surges originated by tangential instabilities in solid propellant motors, using double base homogeneously compounded cylindrical grains 09 p1743 A70-22661
- Propellant extinction near powder-metal contact to study nonsteady combustion mechanism 09 p1742 A70-23228
- Combustion stability effects of additives on hydrazine/nitrogen tetroxide propellant combination by measuring droplet burning rates 11 p2100 A70-26283
- Oxidizer particle size and binder type effects on nonacoustic combustion instability of solid propellants [AIAA PAPER 69-175] 12 p2332 A70-27804
- Spin detonation of tangential HF vibrations in liquid rocket engine combustion chambers, discussing instability prevention 13 p2474 A70-29422
- Solid fuel steady combustion regime stability dependence on heat generation in reaction zones and temperature and velocity fields inhomogeneity 13 p2522 A70-29423
- Detonation process one dimensional stability in combustible aerosol, considering gas dynamic disturbances effect 14 p2665 A70-30397
- Hybrid rocket engine with solid ammonium perchlorate oxidizer, discussing equilibrium conditions and engine performance 15 p2786 A70-32272
- Hybrid rocket motor with solid oxidizer in ammonium nitrate additive, determining stable combustion conditions 15 p2790 A70-32274
- High temperature combustion wind tunnels for investigating gas and liquid fuel combustion stabilized by shock waves in supersonic flow 16 p2996 A70-32991
- F-1 rocket engine acoustic liner, reevaluating damping data for combustion stability improvement 16 p2968 A70-33588
- LF unsteady behavior of liquid propellant rockets from droplets evaporation and combustion rates [AIAA PAPER 70-620] 16 p2968 A70-33589
- Acoustic cavities use in suppressing acoustic modes of combustion instability demonstrated on LM ascent engine [AIAA PAPER 70-618] 16 p2998 A70-33614
- Combustion instability due to narrow cavities in solid propellant engines 17 p3198 A70-35739
- Nonsteady combustion analysis, using method of flame front penetration through fine metal layer in solid propellant 18 p3300 A70-36704
- Liquid rocket combustion instability due to velocity vector effect, showing importance in longitudinal and transverse modes 20 p3689 A70-40079
- Liquid propellant rocket combustion instability, examining droplet vaporization, wake burning and chemical kinetics 20 p3689 A70-40080
- Solid rocket propellants linear and nonlinear pressure coupled combustion instability behavior relationship to exothermic surface processes 20 p3694 A70-40274
- Liquid propellant rocket engine combustion instabilities, describing unsteady combustor flow by single nonlinear wave equation with stable and unstable finite amplitude limit cycles 23 p4233 A70-44425
- COMBUSTION TEMPERATURE**
Combustion of stationary particle of metal with boiling point lower than ignition temperature in gaseous oxidizing medium 07 p1419 A70-18753
- Chemical composition effects on Zr-Ti, Zr-Si, Ni-Al and Ni-Ti alloy aerosols combustion temperature 07 p1419 A70-18755
- Steady flame propagation attainment for chemical reaction initiation in gaseous fuel by heated surface with various wall temperatures 09 p1787 A70-22115
- Powder combustion on metal plate, investigating unburned layer thickness dependence on initial temperature 17 p3198 A70-35738
- COMBUSTION VIBRATION**
Internal stability of turbulent combustion, developing analysis for one dimensional model and deriving sufficient instability criterion 03 p0607 A70-13862
- COMBUSTION WAVES**
U FLAME PROPAGATION
COMBUSTION WIND TUNNELS
High temperature combustion wind tunnels for investigating gas and liquid fuel combustion stabilized by shock waves in supersonic flow 16 p2996 A70-32991
- Combustion driven shock tunnel applied to tailored interface operating conditions, controlling mass flow into tube by throttling plates 22 p4006 A70-42765
- COMBUSTORS**
U COMBUSTION CHAMBERS
COMETS
NT HUMASON COMET
NT MOREHOUSE COMET
NT SCHWASSMANN-WACHMANN COMET
Stellar emission line spectra from comet-like nebulae, discussing stellar position instability and shell movements 01 p0174 A70-10198
- Solar wind-induced drag resulting from collisionless plasma shock on sunward-side of large magnetic comet, using similarity with earth magnetosphere 01 p0168 A70-10258
- Io and Europa mass and density anomalies, indicating asteroid capture by Jupiter as comet origin theory 01 p0182 A70-10671
- Visual observations of bright comets, deriving photometric parameters from comet head total magnitude 01 p0184 A70-10953

Comet observations analysis, tabulating total head magnitude, photometric parameters, nucleus magnitude, coma diameter, tail type and direction and magnitude correlation with solar activity

01 p0184 A70-10954

Cometary and asteroidal meteors discriminated by orbital elements in region of Jovian comet family adjoining asteroidal belt

02 p0373 A70-12371

Sudden comet brightness changes leading to discovery, tabulating and graphing comet discoveries

02 p0373 A70-12372

Interference filter for photography of comet heads, tabulating filter characteristics

02 p0303 A70-12707

Jupiter capture of comets with parabolic orbits taking into account solar gravitational influence

05 p0905 A70-15757

Photoelectric photometry of comets to obtain principal data and to classify comets by employing same filters and stellar photometric standards

06 p1140 A70-17731

Particle ejection moments from tail of comet Ikeya-Seki determined from photographs having visible terminal synchrones

06 p1140 A70-17732

Stellar light absorption in optically dense cometary atmospheres

06 p1141 A70-17738

Spatial properties of solar wind during maximum and minimum activity inferred from sodium D-line emissions for cometary nuclei

06 p1136 A70-18012

Large scale artificial plasma cloud experiments for magnetosphere, solar wind and cometary physics, discussing Ba ion and ice clouds released by satellites [AIAA PAPER 70-33]

06 p1145 A70-18183

Mass loss rates for short period comets from non-gravitational terms in equations of motion, paying particular attention to secular variations

06 p1151 A70-18490

Space probe investigation of comets, discussing feasibility, instrumentation, mission planning, etc

06 p1153 A70-18550

Single parameter photometric analysis for density distribution of matter in comets atmospheres

07 p1374 A70-18707

Classification and maximal lengths of cometary tails, investigating correlation to type, perihelion distances, absolute magnitudes and spectra

07 p1378 A70-19032

Maser coherent amplification possibility in comet atmospheres at various frequencies assuming thermodynamic nonequilibrium and nonBoltzmann populations

07 p1378 A70-19034

Particles and surface brightness distributions in nonionized cometary tails, considering near nucleus source and particle acceleration

07 p1378 A70-19035

Source power molecule lifetime, acceleration and particle velocity in region near comet nucleus determined from brightness

07 p1378 A70-19036

Recombination processes in comet atmospheres listing ion, atom and electron reactions, cross sections and resonance defects

07 p1379 A70-19037

Surface brightness distribution in comet head investigated photometrically

07 p1379 A70-19038

Dust growth, density distribution and collisions in interior of cometary head atmosphere, considering gravitational attraction to nucleus

07 p1379 A70-19039

Short wave radar tracking of comets, considering tail type criteria for signal reflection

07 p1379 A70-19040

Kilston comet 1966b brightness correlated with solar flares occurrence

07 p1379 A70-19041

Kilston Comet /1966b/ total brightness measurements, discussing integral head magnitudes, observational conditions and stars comparative magnitudes

07 p1379 A70-19042

Photometric observations of Ikeya-Seki comet 1965f by equidensity method, observing CN emission in head

07 p1379 A70-19043

Faye comet motion and secular orbital evolution of short period comets

07 p1379 A70-19048

Alfven wave structure mechanism of geomagnetic micropulsation type in cometary tails, assuming Kelvin-Helmholtz instability at comet plasma-solar wind interface

08 p1565 A70-20567

Tungusk meteorite as comet nucleus, discussing comet structure, composition and behavior analysis

08 p1572 A70-20943

Orbit analysis of hypothetic comets formed by Jupiter surface eruptions using Lagrange origin hypothesis

08 p1573 A70-21012

Comet brightness outbursts monochromatic measurements for lifetime of parent gaseous molecules in solar radiation fields

08 p1575 A70-21373

Nongravitational effects, systematic residuals and close Jupiter approach problems in motions of comets

09 p1759 A70-22913

Photoelectric measurements of dust and CN/C2 molecular emission in atmosphere of Comet Ikeya-Seki

09 p1761 A70-23058

Comets ionized shells, studying plasma expansion in corpuscular solar wind magnetic field

10 p1940 A70-24372

Type I comet tails orientations dispersion attributed to nonradial plasma waves and discontinuities in interplanetary gas, calculating solar angular momentum loss rate

10 p1947 A70-24987

Meteor stream 11 Canis Minoris detected and associated with Comet Melish 1917, discussing true radiant and orbit

11 p2108 A70-25699

Short period hypothetical orbits distribution formed by flaring on Jovian satellites

11 p2109 A70-25925

Comet-asteroid evolutionary relationship based on Hidalgo orbital analysis

11 p2114 A70-26472

Comet model atmospheres for head theoretical spectra computation, considering collisional effects through total gas density distribution

11 p2116 A70-26647

Solar radiation effects on evaporation of dust with high latent heat of vaporization, considering particles in comets and zodiacal cloud

11 p2117 A70-26648

Ring micrometer radius determination and application to right ascension changes in determining positions of comets, planets and planetary moons

11 p2057 A70-26675

Comet tail simulation by using fast acting gas valve to produce gas cloud for interaction with plasma stream

12 p2298 A70-27190

Honda 1968c comet head light polarization measurements, noting correspondence to scattering on dust particles

12 p2300 A70-27499

Attitude control system of three axis stabilized payload for spectral survey of comet head light

13 p2505 A70-28770

Long period comets energy change due to planetary perturbations tabulated, obtaining orbital major axes before and after passage

13 p2489 A70-28906

Orionid and eta Aquarid meteor shower structure and association with comet Halley

13 p2491 A70-29044

Southern and Northern hemispheric comet observations

13 p2494 A70-29483

Spectrophotometry of comet Honda 1968c, showing free cation and radical emissions and head asymmetry

14 p2635 A70-30304

Comet Bennett 1969i photometric observations, showing blackbody-like continuum at short wavelengths with sharp peak due to silicate grains

14 p2642 A70-30895

Comet tail structures in inner coma region using photographic observations

14 p2650 A70-31220

Thermodynamic stability of methane clathrate hydrate, building up ice grains halo within comets inner coma

14 p2650 A70-31243

Gases adsorption on water snows in cometary nucleus, noting sublimation rate role as regulating mechanism in gas production

14 p2650 A70-31244

Churumov-Gerasimenko 1969h comet photographs and preliminary orbital characteristics

15 p2800 A70-32146

Alfven wave structure mechanism of geomagnetic micropulsation type in cometary tails, assuming Kelvin-Helmholtz instability at comet plasma-solar wind interface

15 p2805 A70-32722

Tungusk meteorite as comet nucleus, discussing comet structure, composition and behavior analysis

15 p2806 A70-32755

Comet Alcock flareup on 27-29 May 1969, noting visible rays in coma, dust grains expulsion from nucleus, tail structure, etc

16 p2980 A70-34304

Periodic comet nature, origin and anomalous behavior with space mission planning implications, assuming solar plasma source and solar-interstellar interaction [AAS PAPER 70-029]

17 p3155 A70-34795

Ephemeris of periodic comet Wolf-Harrington for 1970-72 reappearance, assuming non-gravitational motion anomaly and secular acceleration

17 p3158 A70-34862

Periodic comet Slaughter-Burnham improved ephemeris for 1970-71, based on 1958-59 and 1969 orbital elements

17 p3158 A70-34863

Lyman alpha emission from Comet Bennett observed with photometer on board OGO-5 satellite

17 p3163 A70-35049

Comet Bennett 1969 visual observations in Southern Hemisphere, using photometer ocular

18 p3319 A70-37049

Surface temperature distribution over rotating nucleus of comet deficient in volatiles

18 p3319 A70-37058

Comet de Arres 1976 opportunity mission analysis, considering flyby and rendezvous trajectories and guidance problems [AIAA PAPER 70-1073]

19 p3513 A70-37426

Comet nuclei internal structure from photometric measurements, discussing gas emanation and free surface ice evaporation

19 p3514 A70-37640

Physical properties of comet heads, considering apparent diameters and internal magnitudes

19 p3514 A70-37641

Ammonium molecules dissociation and ionization in comet atmospheres due to solar corpuscular and photon radiation

19 p3514 A70-37642

Fine structure of solar radiation-induced electrostatic fields on dielectric surface of comets and meteoroids

19 p3514 A70-37656

Photoelectric and polarimetric observations of comet 1968 c Honda in BV system, noting dust scattering role in emission

19 p3515 A70-37657

Triple polarization astrophotograph observations of comet 1968 c Honda, noting dust component-Wolf number agreement

19 p3515 A70-37658

Lunar and planetary laboratory communications, Volume 8 covering IR astronomy, Mercury, Mars, Uranus, comets, etc

19 p3515 A70-37929

Bester comet 1946k-1947l orbit, showing original and future orbits as long period ellipses

19 p3515 A70-37931

Burnham-Slaughter 1958e-1959l comet orbit, showing nearly parabolic ellipse

19 p3516 A70-37933

Comet shapes mechanical theory inverse problem approximate solution

19 p3525 A70-38773

Comet brightness curves asymmetry with respect to perigee attributed to pre- and post-heating

19 p3526 A70-38781

Atomic hydrogen population distribution in far UV of comets

19 p3526 A70-38782

Photometric cometary parameters from Van Biesbroeck data, using least squares method to compare naked eye, field glasses and small telescope observations

19 p3526 A70-38783

Kylston comet head diameter relation to brightness from photometric observations using north polar sequence stars as reference, noting camera, equipment and exposure times

19 p3526 A70-38784

Comet Ikeya-Seki 1965 f tail formed by dust particles continuous ejection, using preperihelion photographs

19 p3527 A70-38792

Future spacecraft mission for short period comets rendezvous, considering trajectory requirements and launch vehicle payload capabilities [AIAA PAPER 70-1072]

19 p3530 A70-38885

Jupiter swingby trajectory analysis for comet flyby and rendezvous missions, discussing approach velocity and payloads [AIAA PAPER 70-1074]

19 p3530 A70-38886

Ikeya-Seki /1967n/, Thomas /1968b/ and Honda /1968c/ comet photoelectric spectrum examining swan bands, continuum and reflected scattered light

20 p3703 A70-39024

Upper atmosphere ammonia release experiments testing hypothetical mechanisms of radicals and ions formation in comets

20 p3708 A70-39962

Microwave transitions for molecules in comets and interstellar space

21 p3887 A70-41110

Comet Bennett basic characteristics, discussing orbits, periods and observational summaries of other comets

21 p3890 A70-41164

Small craters number density in southern lunar highlands, supporting Tycho Association cometary impact origin

21 p3920 A70-41882

Radio search for formaldehyde rotational transition and H 109 alpha recombination line in comet Bennett during perihelion passage

21 p3921 A70-41976

- Comet Bennett /1969 i/ spectrograms, discussing linear diameter, trajectory, Lyman alpha emission and hydrogen mass 22 p4097 A70-42468
- Jupiter perturbations on short period comets during close approaches, discussing orbital distribution 23 p4241 A70-44252
- Minor planets, comets and natural satellites positions and motions, discussing orbit and ephemerides calculation, Icarus asteroid, etc 23 p4256 A70-45038
- Orbital elements from secular acceleration in motion assumption, proving Comet Harrington identity with Comet Wolf 23 p4257 A70-45045
- Short period hypothetical and real comets in Jupiter sphere of influence distributed according to orbital elements 24 p4409 A70-45637
- COMFORT**
- Comfort plane switch mounting design for helicopter collective controls, noting mock-up evaluation by test pilots 19 p3372 A70-38922
- COMMAND AND CONTROL**
- Analytic guidance and control for minimum fuel expenditure and optimal guidance corrections for low thrust vehicle in Martian orbit [AIAA PAPER 68-862] 04 p0716 A70-15544
- VTOL flight investigation to develop decelerating instrument approach capability with control-command information display for three degrees of freedom [SAE PAPER 690693] 05 p0792 A70-15862
- Displays for command and control centers - NATO/AGARD Conference, Munich, November 1966 05 p0826 A70-16176
- Command control systems characterized as problem solving information processing systems, discussing information requirements specification prior to man-display design 05 p0806 A70-16177
- Command and control display operational requirements within Allied Command Europe (ACE), information flow, decision making and evaluation 05 p0959 A70-16178
- Command and control functions of DOD Manager for Manned Space Flight Support Operations in spacecraft recovery 05 p0827 A70-16180
- BR-90 visual analysis control as flexible and versatile display for command and control, discussing on-line data processing, maintenance, etc 05 p0827 A70-16182
- CRT display design for command and control with digital symbol and vector generation 05 p0817 A70-16184
- Computer generated displays and USAF equipment design for operational command and control systems, discussing Ag halide film technique 05 p0847 A70-16185
- Radar and sonar data processing for display in command and control systems using digital technique, discussing processor configuration 05 p0828 A70-16189
- Large wall display system for USAF command and control with central computer and seven color projector, discussing hardware and operational features 05 p0828 A70-16193
- Display/control system and key technical decisions at Manned Space Mission Control Center, discussing command consoles 05 p0829 A70-16194
- Machinery for management of Sea Dart missile development using managerial concepts of planning, organizing, commanding, coordinating and controlling 08 p1601 A70-21036
- Satellite Integrated Communications, Navigation and Identification System for implementing worldwide command-control system and equipment and signal integration [AIAA PAPER 70-503] 11 p2000 A70-25466
- Pilot leadership qualities as criteria for selection, examining command training 11 p1993 A70-26607
- Intermittent positive control system for issuing commands to normally uncontrolled aircraft for midair collision avoidance, discussing aircraft and conflict detection 12 p2267 A70-27634
- Intermittent positive control (IPC) role in midair collision avoidance, using mathematical model to determine command frequency and implementation 12 p2269 A70-27913
- Remote signal measurement and analysis in hazardous environment by command terminal utilizing manual or computerized control 12 p2201 A70-28134
- Signal decoder for barium USA Germany (BUG)/project command reception system, discussing Ba ion cloud propagation and expansion along geomagnetic field 13 p2367 A70-29557

- Digital signals conversion into command and control TV displays in multiconsole systems 13 p2411 A70-29789
- Intelsat IV command and control system, describing ground stations, control center, telemetry data handling and acquisition, etc 17 p3046 A70-35275
- Ground and cockpit initiated collision avoidance commands system based on satellites surveillance of aircraft position and velocity data 19 p3466 A70-38242
- PCM command control system for high altitude ballooning operations, discussing component equipment 20 p3587 A70-40085
- UpSTAGE interceptor missile flight control system, discussing command logic to capitalize on lifting body advantages to enhance roll maneuver 21 p3927 A70-40782
- COMMAND GUIDANCE**
- Pseudonoise code command system for scientific satellite, describing added bits and decoder 17 p3046 A70-35276
- COMMAND MODULES**
- Nondestructive testing for Apollo Command and Service Module, describing requirements added to quality control scope 01 p0098 A70-10026
- Apollo spacecraft hardware, command, service and lunar modules, discussing design factors and tests contributing to spacecraft reliability [AIAA PAPER 69-1095] 01 p0194 A70-10618
- Materials selection and Apollo command module atmosphere design considerations, discussing fire extinguisher system, equipment design changes, etc 03 p0437 A70-14058
- Spacecraft telecommunication and tracking systems in Gemini, Mercury and Apollo programs, emphasizing Apollo command and lunar modules equipment and mission ground stations 05 p0813 A70-16326
- Shock tunnel preflight assessment of Apollo Block 2 command module base heating 07 p1394 A70-19722
- Fuel cell assemblies as primary electrical source for Apollo command and service modules, discussing heat removal, water vapor control and transient performance 08 p1439 A70-20702
- Apollo mission simulation, discussing Command Module Simulator (CMS), onboard computer system and dynamic visual presentation via infinity-optics display [SMPTE PAPER 105-74] 09 p1655 A70-22226
- Apollo command and service modules from metallurgical viewpoint 09 p1766 A70-22792
- Apollo Command Module inverter experience for post-Apollo spacecraft applications, discussing phase loads and control logic circuits 12 p2165 A70-27693
- Apollo command and service modules environmental control system, discussing redesign of faulty hardware [SAE PAPER 690618] 12 p2167 A70-27948
- NDT techniques in manufacturing of Apollo command and service modules 13 p2420 A70-29243
- Side access hatch system for Apollo command module 16 p2986 A70-34153
- Radiation measurements inside Apollo 4 and 6 command modules during passage through trapped radiation belts 17 p3040 A70-35645
- Command module simulators for Apollo astronaut training in moon landing, using computer, exterior visual scenes and spacecraft interior replica 21 p3804 A70-41195
- Apollo command module land impact capability, discussing impact dynamics, possible landing area, spacecraft structure, crew couch and strut attenuation system, etc [AIAA PAPER 70-1165] 21 p3930 A70-41847
- COMMAND SERVICE MODULES**
- Nondestructive testing of Apollo CSM /Command and Service Module/ spacecraft ordnance explosive devices by indirect and direct neutron radiography 03 p0494 A70-14123
- Apollo Command and Service Modules for lunar orbital science missions, discussing spacecraft-experiment integration 21 p3928 A70-40978
- COMMAND SYSTEMS**
- U COMMAND GUIDANCE**
- COMMAND-CONTROL**
- U COMMAND AND CONTROL**
- COMMERCE**
- Space propulsion systems for public transportation to and from orbit and throughout near solar system, discussing commercial requirements 11 p2102 A70-26060
- COMMERCIAL AIRCRAFT**
- NT BOEING 707 AIRCRAFT
- NT BOEING 727 AIRCRAFT
- NT BOEING 737 AIRCRAFT

- NT BOEING 747 AIRCRAFT
- NT BOEING 2707 AIRCRAFT
- NT DH 121 AIRCRAFT
- NT L-1011 AIRCRAFT
- NT TU-134 AIRCRAFT
- Inertial navigation techniques application to commercial air traffic control, indicating decreased dependence on external navigation aids in oceanic operations 01 p0136 A70-10304
- Data analysis of inertial systems for commercial aircraft overseas operations, classifying systems error propagation as linear time drift or Foucault period oscillation 01 p0137 A70-10314
- Aeronautical satellites for monitoring positions of many commercial aircraft simultaneously crossing North Atlantic, discussing navigational error correction and atmospheres 01 p0178 A70-10454
- Soviet book on operational maintenance of flight vehicles /civilian/, emphasizing maintenance under various climatic conditions 01 p0004 A70-10502
- Economic tradeoffs in airport and commercial aircraft design, considering traffic growth, increased weight impact minimization and costs [AIAA PAPER 69-1087] 01 p0056 A70-10623
- Commercial aircraft design, considering structural allowables effect on economics, using shear web analysis program as example 02 p0225 A70-11947
- Air traffic problems connected with Boeing 747 introduction, discussing cargo/passenger handling, fueling and maintenance procedures 02 p0227 A70-12620
- Computerized airline fleet planning methods for aircraft economics and airline operations [SAE PAPER 690415] 03 p0609 A70-12898
- Flexible pavements for commercial jet planes representative of current and future aircraft 03 p0462 A70-13173
- Turbine noise significance in civil aircraft noise problem [ASME PAPER 69-WA/GT-12] 04 p0734 A70-14884
- Emergency auxiliary hydraulic and electric power for commercial and military aircraft control, proposing self contained monofueled turbine system [SAE PAPER 690658] 05 p0797 A70-15838
- Design safety requirement and philosophy differences distinguishing commercial from military aircraft programs 05 p0792 A70-15855
- British military and civilian aircraft and flying between World War I and II, discussing weapons systems and accidents 05 p0794 A70-16113
- Commercial navigation systems for long range subsonic transports, discussing accuracy, avionics hardware and crew responsibility optimization 06 p1102 A70-17638
- Emergency in-flight evacuation concepts adapted from military experience considered for application to commercial aircraft 06 p0986 A70-17722
- Filamentary composite materials for commercial aircraft and engine construction noting boron, graphite and glass reinforcement 07 p1316 A70-18950
- V/STOL demand for short haul business travel noting time savings, convenient approach, safety records, weather reliability and comfort 07 p1428 A70-19680
- V/STOL concepts for short haul commercial aircraft compared for gross weight, operating cost, gust sensitivity and noise levels [AIAA PAPER 67-938] 07 p1195 A70-20409
- Signal properties of VHF satellite-to-aircraft communications link, discussing results of ATS tests 08 p1463 A70-21779
- Aerodynamics role in large commercial aircraft design, noting mathematics models problem in high speed wing design 09 p1609 A70-22024
- Commercial aircraft inertial navigation, examining gyroscope, accelerometer and electronic computer and gyroscopic stabilization 10 p1914 A70-23848
- Commercial aviation safety on basis of aircraft accidents relationship to distance covered, considering clear air turbulence and cosmic radiation dangers 10 p1804 A70-24050
- VFW 614 nose-contoured cockpit panes, discussing structural weight and strength, vision and window frame fabrication 10 p1806 A70-24866
- Light aircraft-airliner collision avoidance, discussing Time-Frequency Collision Avoidance System cost restriction, Pilot Warning Instruments, etc 11 p2079 A70-25872
- Gas turbine engine technology for military and commercial aircraft, discussing operations economy, design matching to missions and fabrication methods 11 p2101 A70-25873

Commercial aircraft peak cockpit noise level during cruise and high speed descent, discussing damage risk criteria and interplot speech interference
11 p1991 A70-26275

Commercial jet passenger emergency oxygen needs for cabin decompression studied in determining time of safe unconsciousness
11 p1992 A70-26511

Aircraft turbofan and turbojet engines military-commercial interrelationships
[SAE PAPER 700268] 12 p2290 A70-27436

Rigid wing subsonic and supersonic civil and military aircraft utilizing aerodynamic lift at takeoff and landing
13 p2344 A70-28543

Commercial aircraft manufacturing industry in UK, discussing SST, wide cabin aircraft, turboprop replacement, engine influence on airframe industry, etc
14 p2668 A70-30936

Civil aircraft design optimization, considering operating and seat mile costs, speed, wing and fuselage, engine location, etc
14 p2531 A70-30941

BAC 111 commercial aircraft family development, discussing program management
14 p2532 A70-31334

British light aircraft designs, engines and costs, considering business, agricultural, gliding, private, school and club flying
14 p2532 A70-31394

High energy chemical systems for postcrash emergency evacuation of commercial passenger aircraft, discussing exit opening via explosive methods
15 p2675 A70-32221

Emergency auxiliary electric and/or hydraulic power for commercial and military aircraft using self contained monofueled gas turbine system
16 p2964 A70-33472

Emergency auxiliary hydraulic and electric power for commercial and military aircraft control, proposing self contained monofueled turbine system
[AIAA PAPER 70-651] 16 p2970 A70-33616

Equipment and subsystems application to flight management avionics in military and commercial aircraft, noting role of ground-air information transfer
16 p2878 A70-33724

Book on air safety and commercial aviation accidents
16 p2842 A70-33964

Investment risks and technical impact on aircraft development, world aviation growth and airline costs
17 p3200 A70-34915

Airborne data acquisition and flight recorder systems, comparing civil and military aircraft requirements
17 p3094 A70-35515

Wide body commercial jet transport structural design considerations applied to DC 10 aircraft
[AIAA PAPER 70-895] 17 p3193 A70-35812

Commercial air transport mission payload and range capability analysis, noting on-line flight planning computers
[AIAA PAPER 70-899] 17 p3204 A70-35815

Integrated flight management system for commercial aircraft pilot using computer
[AIAA PAPER 70-908] 17 p3134 A70-35820

Commercial aircraft flight deck systems controls and time sharing displays, emphasizing crew management
[AIAA PAPER 70-938] 17 p3021 A70-35847

Heat-up display (HUD) system, discussing development, production, commercial aircraft applications and flight sequences uses
18 p3223 A70-36210

Commercial aircraft strapdown inertial navigation systems, examining initial self alignment techniques
18 p3289 A70-36442

High speed civil and commercial transport aircraft, discussing jet-orbital flight
18 p3333 A70-36664

Military and commercial transports turbofan propulsion systems impact on future aircraft design and development
[SAE PAPER 700267] 18 p3214 A70-36820

Military and commercial aircraft maintenance costs reduction, discussing labor/material ratio, spare parts use, diagnostic systems, etc
21 p3749 A70-40750

Commercial transport aircraft fatigue loading data from NASA VGH /airspeed-acceleration-altitude-program, discussing instrumentation, sample sizes, etc
23 p4270 A70-44548

Hybrid fluidic damper control for yaw axis stability augmentation of commercial jet aircraft
[SAE PAPER 700794] 24 p4294 A70-45853

Commercial STOL aircraft propulsion systems from airline viewpoint, emphasizing subsystem design, engine selection, thrust deterioration and maintainability
[SAE PAPER 700810] 24 p4395 A70-45904

Military helicopter test program application to commercial VTOL operations, discussing military-civil design and development relationships
[AIAA PAPER 70-1242] 24 p4292 A70-46327

COMMERCIAL AVIATION
U CIVIL AVIATION
U COMMERCIAL AIRCRAFT
COMMUNITION
NT GRINDING [COMMINUTION]
COMMITTEE ON SPACE RESEARCH
COSPAS report on UK space research /1969/ covering neutral atmosphere, ionosphere, solar radiation, etc
15 p2831 A70-31723

COMMUNICATING
NT AIRCRAFT COMMUNICATION
NT ELECTROCUTANEOUS COMMUNICATION
NT GROUND-AIR-GROUND COMMUNICATIONS
NT INFORMATION DISSEMINATION
NT INTERSTELLAR COMMUNICATION
NT POINT TO POINT COMMUNICATIONS
NT VERBAL COMMUNICATION
Human communication in pilots and in maintenance and administrative personnel, noting time factor influence
04 p0644 A70-14985

Information transfer for quantitative relationships to error- and cause-controlled regulations
07 p1216 A70-18859

R and D idea flow studies, analyzing liaison, interface, coupling and technology transfer /LINCOTT/
09 p1794 A70-23410

Computer aided on-line test generation for prelaunch checkout, describing interpretive test language for rapid man machine information transfer
[AIAA PAPER 70-384] 10 p1846 A70-24921

Information transfer services potential demand including telephone, telegraph, videophone, electronic mail, etc
[AIAA PAPER 70-443] 11 p2152 A70-25448

Amino acids L-glutamate and gamma-aminobutyric acid as communication agents in brain
23 p4148 A70-44864

COMMUNICATION CABLES
NT BEAM WAVEGUIDES
NT COAXIAL CABLES
NT PLASMA GUIDES
NT WAVEGUIDES
Boeing 747 airliner passenger entertainment and service electronics multiplexing system, discussing cable and connectors selection and design
23 p4174 A70-44544

Commercial satellite system circuit quality and reliability in digital communications, considering Automatic Digital Network Trans-Pac cable cut incident
24 p4311 A70-45223

COMMUNICATION EQUIPMENT
NT CLOSED CIRCUIT TELEVISION
NT RADIO RECEIVERS
NT SATELLITE TELEVISION
NT SPACECRAFT TELEVISION
NT SUPERHETERODYNE RECEIVERS
NT TRANSMITTER RECEIVERS
NT WHISTLER RECORDERS
Airborne DME minimum operational characteristics for air traffic control navigation and communication systems including equipment specifications, environmental conditions, accuracy and range
[DO-141] 01 p0138 A70-11050

Airborne SHF communication system for operation with passive satellites installed in C-121 aircraft
01 p0045 A70-11122

Digital onboard telecommunications and tracking equipment based on Dioscures two satellite system for L band operation
03 p0442 A70-12990

Transmission equipment of Pleumeur-Bodou space communication installation including modulators, converters and amplifiers for telephone and TV carriers
05 p0819 A70-15986

Three frequency heterodyne system for acquisition and tracking of radar and communications signals, noting applicability in optical and microwave ranges
06 p1010 A70-17948

Radio propagation characteristics and communication system performance, discussing concepts of MUF, LUF, error rate, communication system modeling, prediction techniques, etc
07 p1229 A70-19157

Monolithic, thick film, thin film and multichip integrated circuit techniques applied to communication equipment design
08 p1471 A70-20785

Intersite trunk elements design and usage in integrated mission control center /IMCC/ as interface equipment between internal voice communication and worldwide network
08 p1460 A70-20814

Microwave IC-compatible resonators for communication systems filters, comparing microstrips, disks, waveguide cavities and dielectric-loaded cavities
10 p1852 A70-24892

Computerized data communication system /CDCS/ equipment unit capacities and topology specified with aid of vertex weighted linear graph
11 p2009 A70-26253

COMMUNICATION SATELLITES

Nonlinear phase locked loops compared with linear loops in communication and navigation, considering interference vulnerability
12 p2187 A70-27909

Digital guidance and control system, discussing communication device providing data transfer between airborne digital computer and control device. [AIAA PAPER 69-988] 14 p2615 A70-30771

Service multiplex for communications network via satellite, discussing reliability
18 p3229 A70-36667

Magnetic bubbles in miniaturized electronic circuits, discussing fabrication and uses in communication and computers
19 p3484 A70-37574

Coherent receiver as hybrid carrier tracking loop consisting of standard phase locked and modified Costas loop
21 p3802 A70-41351

COMMUNICATION SATELLITES
NT EARLY BIRD SATELLITES
NT INTEL SAT SATELLITES
NT MOLNIYA SATELLITES
NT SYNCOM SATELLITES
Delta boosted electrically raised high power synchronous satellite for communication tasks
[AIAA PAPER 69-1104] 01 p0194 A70-10617

Communication satellite system proposed for small users, assessing viability based on market saturation points estimation
[AIAA PAPER 69-1073] 01 p0043 A70-10629

Dual frequency ranging within narrow bandwidth of VHF communications satellite repeater for transmitted signals correction of ionospheric refraction error
01 p0043 A70-10781

TV broadcast satellite system operating with home receivers or special receivers, evaluating technological and cost factors
[AIAA PAPER 68-1061] 01 p0044 A70-10831

Airborne SHF communication system for operation with passive satellites installed in C-121 aircraft
01 p0045 A70-11122

Satellite mounted mm wave parabolic dish antenna for tracking communication satellite in synchronous orbit
02 p0392 A70-11933

Structural qualification testing of experimental tactical communication satellite /TAC COM SAT/
02 p0274 A70-11936

Continuous and pulsed parameter stabilization for circular orbits of navigation and communication satellites under perturbing effects of oblateness and atmospheric drag
02 p0374 A70-12402

Remote data processing and wideband data transmission between France and U.S. via telecommunication satellites, discussing error detection and correction
02 p0263 A70-12612

Future phase of satellite TV programs distribution in Europe
02 p0403 A70-12645

Operational requirements of shipping for satellite communication systems, discussing distress cases, satellite navigation systems, information distribution traffic control, etc
03 p0522 A70-13605

Low altitude 24-hr orbit twin satellite system joined by long light cord, assessing communications efficiency and physical limitations
03 p0579 A70-13621

German-French communication satellite project Symphonie for radio, TV, telephone, teletype and data transmission, discussing objectives, organization and technical problems
[DVL-910] 03 p0580 A70-13796

Directional transponders for telemetry command, tracking and communications in retrodirective communication satellites
03 p0457 A70-13838

Intelsat communications /1963-1969/, discussing boosters, satellites, system characteristics and ground stations
03 p0451 A70-13840

Experimental Washington Agreement /1964/ governing international juridical rules and regulations regarding telecommunication satellites
03 p0609 A70-13853

Channels demand assignment between earth terminals of international satellite communication systems, examining multiple access problems
03 p0453 A70-14323

Orbit mechanical investigations for increasing Europa 2 booster rocket payload to place German-French communications satellite Symphonie into 24 hr orbit
04 p0754 A70-15153

Mission objectives and technical realization of AZUR research satellite and Symphonie communication satellite
04 p0763 A70-15303

Solar powered communications spacecraft weight, electrical power and communication capacity models for optimizing size and launch vehicle fractionation
04 p0763 A70-15347

Hybrid system for allocating domestic synchronous communication satellites in concentric circles within inclined elliptical synchronous orbits

05 p0906 A70-15801

Satellite communications influence on ground stations design, describing steerable antenna and receive and transmit configurations for domestic station

05 p0811 A70-16095

Satellite relay systems to provide polarization discrimination in antenna main beam to double spectrum for communications

05 p0815 A70-16661

Electric thrusters for putting communications satellite into synchronous orbit analyzed for mission performance, finding hydrogen resistojets as attractive compromise between payload and transfer time

05 p0897 A70-16899

Domestic telecommunication via satellite to reduce terrestrial switching to two levels, discussing system parameters, operation, hardware and cost estimate

06 p1006 A70-17344

Broad beam Tracking Data Relay Satellite (TDRS) for manned and automated spacecraft using VHF bands

06 p1006 A70-17345

Wideband transmission of photographic reconnaissance information over long distances using Initial Defense Communication Satellite Program satellites

06 p1006 A70-17346

Multiple access channel control system operating in variable destination multiple access mode for application in PCM-TDMA satellite communication system

06 p1011 A70-18412

Flywheel stabilization for communication satellites, considering stabilization by reaction wheels, gyros, gas jets, etc

[DGLR-69-058]

07 p1392 A70-18817

Space systems for communications, surveillance and navigation needs of international aviation, discussing service requirements, spectrum utilization, technology limitations and terminal design

07 p1330 A70-19290

Spot III satellite-supported system for transoceanic aircraft navigation, traffic control, voice and data communication, etc

07 p1331 A70-19291

Communication satellite transponders design, cost, reliability, manufacturing, testing and future developments

07 p1241 A70-19620

Optimal distance between satellite communication system ground stations for surface network cost equivalent, analyzing economic efficiency for various cases

08 p1456 A70-20569

Noise mean duration in surface communications links due to communications satellites interference, discussing irradiation emission and termination

08 p1456 A70-20570

Modem selection for satellite communications system, considering bandwidth and power constraints, propagation characteristics, point-to-multipoint operation, etc

08 p1459 A70-20807

Operational figure of merit of high performance antennas in communication satellite earth stations as function of design

08 p1471 A70-20825

Book on navigation and communication satellites for military uses, considering design, operation, computers role, etc

08 p1582 A70-21298

Omega Position Location Experiment with synchronous satellite (ATS-3) as radio relay for merchant shipping, air traffic control and moving vehicle location and communication

09 p1720 A70-22193

Communications satellite technology for earth resources data collection

09 p1634 A70-22857

ARCOM earth terminal for Domestic Satellite Communication System bringing telephone, TV and data service to northern Canada

09 p1656 A70-22945

Digital satellite communication - Conference, London, November 1969

10 p1833 A70-24326

Digital record message communication satellite network system involving synchronous satellites and small earth terminals

10 p1834 A70-24327

Worldwide telephone network optimum interoperation including communication satellites complementation

10 p1834 A70-24328

Satellite communication system using delta modulation for telephone service to large number single channel earth stations

10 p1834 A70-24329

PCM-TDMA satellite communication system for maximum time slot utility without guard time slots

10 p1834 A70-24330

Digital satellite communication system using multiphase modulation optimized for phase positions number to maximize transmission capacity

10 p1835 A70-24334

Communication satellite PSK modulator-demodulator /modem/ implementation requirements and design for optimal performance

10 p1835 A70-24336

Geostationary orbit capacity based on multichannel technology, comparing digital and analog modulation techniques

10 p1836 A70-24343

Communication commercial satellite systems capacity in terms of telephone channels, using frequency modulation and digital methods

10 p1836 A70-24344

Interference problems arising during digital satellite communications, discussing PCM telephone system and PSK modulation

10 p1836 A70-24345

Multiple access PCM satellite communication system with minimum interference to earth radio links, using programmable switch for improved traffic handling and frequency coordination

10 p1837 A70-24346

Signaling system for communication satellites demand assignment, considering error control, unit negative acknowledgement, system parameters selection, control signals, etc

10 p1837 A70-24347

Demand assignment signaling and switching subsystems /DASS/ design for communication satellite, examining voice channels modulation

10 p1837 A70-24348

Transmission performance of telephone calls routed through PCM satellite circuit between London and White Plains

10 p1837 A70-24349

DASS operational parameters and performance in SPADE satellite voice communication system

10 p1837 A70-24350

Demand assignment techniques applicability to TDMA satellite communication systems, discussing operational modes and optimum mode selection

10 p1837 A70-24351

PCM-TDMA satellite communication systems operation modes and applicability, considering efficient circuit utility, equipment cost and control complexity

10 p1837 A70-24352

Time division multiple access /TDMA/ system for Symphonic communication satellite using PCM phase shift keyed RF carrier

10 p1837 A70-24353

FDMA and TDMA systems for demand assignment of satellite circuits noting PCM/TDM operation trends in satellite and ground communications

10 p1838 A70-24355

Traffic simulation in telephone network via communication satellite with presassigned and demand assigned circuits

10 p1838 A70-24356

Demand assignment /DAMA/ and preassignment /PAMA/ Multiple Access Systems mix for cost minimization, developing algorithm for satellite high usage groups and overflow facilities

10 p1838 A70-24357

Adaptive multiple access satellite communication system at millimeter wavelengths in time- and frequency-division modes, compensating rainfall attenuation

10 p1838 A70-24358

Multiple access technique for millimeter wave satellite communications, noting weight and size of on-board equipment

10 p1838 A70-24359

Intermeshed TDMA systems efficiency in interconnecting ground stations in communications satellite systems, discussing rigid and variable burst lengths

10 p1839 A70-24363

Message traffic problems in satellite telephone network, considering traffic distribution characteristics, interarrival mean time, bidirectional traffic, etc

10 p1839 A70-24367

Bit clock synchronous system for communications satellites TDMA

10 p1839 A70-24368

Satellite relayed integrated digital multiple access systems, discussing traffic handling, satellite positioning, demand assignment, etc

10 p1839 A70-24369

Time allocation with sampling interpolation /ATIC/ for TDMA satellite telephone communications, considering auxiliary circuits, transmission quality, bit rates, demand assignment, etc

10 p1840 A70-24370

Soviet book on satellite communication systems for telephone and TV transmission covering orbit selection, signal level calculation, channel characteristics for frequency bands, etc

10 p1840 A70-24378

European space and communication satellite programs priority considerations, noting operational hardware

10 p1970 A70-24568

TDMA communication satellite system compared favorably with FDMA or CDMA systems in efficiency, flexibility and feasibility for commercial and military uses

10 p1842 A70-24884

Satellite communications system optimal parameters and efficiency dependence on working capacity, discussing economic aspects of HF sets increased number

11 p1995 A70-25345

Franco-German telecommunication satellite Symphonic mission objectives and system design [AIAA PAPER 70-406]

11 p1996 A70-25401

Canadian geostationary satellite communication system design and performance, discussing transponder with six RF channels [AIAA PAPER 70-429]

11 p1996 A70-25402

Satellite capacity utilization for mixed earth stations network using SPADE concept/digital satellite communication system employing demand-assignment and voice-activated carrier techniques

[AIAA PAPER 70-420]

11 p1996 A70-25404

Geostationary satellite communication bandwidth increase by reusing same frequency band in multiple independent earthward beams, discussing modulation and interference noise allocation effects

[AIAA PAPER 70-442]

11 p1996 A70-25405

Traveling wave tube amplifier performance in numerous orbiting communication satellites, emphasizing life test data

[AIAA PAPER 70-507]

11 p2015 A70-25406

Signal attenuation and bandwidth limitations imposed by atmospheric hydrometeors on communications satellite systems above 10 GHz, discussing Comsat measurement programs [AIAA PAPER 70-500]

11 p1997 A70-25408

Satellite distribution of TV signal over earth surface as alternative to terrestrial linkups, overcoming rain attenuation by high power spot beam

[AIAA PAPER 70-454]

11 p1997 A70-25410

Radiation environmental model of synchronous communication satellite solar cell degradation by particle fluxes

[AIAA PAPER 70-481]

11 p2103 A70-25411

Report on 1969 London International Conference on digital satellite communication session on operational requirements covering circuit operation modes, demand-assignment control, etc

[AIAA PAPER 70-466]

11 p1997 A70-25412

Canadian domestic satellite communications policy, discussing Telesat Canada for commercial telecommunications services

[AIAA PAPER 70-428]

11 p2152 A70-25416

TV network distribution in Canada by communications satellite and terrestrial microwave links, discussing signal to noise ratios and picture quality

[AIAA PAPER 70-430]

11 p1998 A70-25417

Communication satellites geostationary orbit sharing problem, considering system design and utilization criteria

[AIAA PAPER 70-441]

11 p1998 A70-25419

UK UHF telemetry command station capabilities for Skynet satellites control, discussing equipment

[AIAA PAPER 70-415]

11 p2030 A70-25420

Attitude stabilization of synchronous communications satellites employing multiple narrow beam antennas

[AIAA PAPER 70-457]

11 p2119 A70-25422

Commercial communication satellite earth station technology and operations covering frequency allocations, antennas, orbits, etc

[AIAA PAPER 70-421]

11 p1998 A70-25424

Communication satellite repeater design requirements to achieve adequate SNR for varying rain and cloud attenuation

[AIAA PAPER 70-498]

11 p1998 A70-25425

Communication satellite technology impacts on potential socio-economic developments of emerging nations of Asia, Africa and South America

[AIAA PAPER 70-473]

11 p2152 A70-25426

Communications and attitude control on Phase 2 satellite for Defense Satellite Communication System

[AIAA PAPER 70-493]

11 p1998 A70-25427

Orbit utilization, discussing sharing of satellite communication frequency bands and use of multiple earthward antenna beams

[AIAA PAPER 70-468]

11 p1999 A70-25428

Three axis attitude control of earth oriented non-spinning synchronous communications satellite, using gimbal-mounted momentum wheel and pulsed plasma thrusters

[AIAA PAPER 70-456]

11 p2119 A70-25431

Power sources, transfer and conditioning subsystems design, fabrication and testing for high power communication satellites

[AIAA PAPER 70-433]

11 p2120 A70-25438

Temperature control of USAF tactical communications satellite /TACSAT/ by passive techniques

[AIAA PAPER 70-461]

11 p2120 A70-25441

Italian SIRIO SHF experiment for study of atmospheric effects on satellite link, discussing system design and performance

[AIAA PAPER 70-502]

11 p1999 A70-25442

Air transportation and air traffic control factors relating to satellites applications to surveillance, navigation and communication over contiguous U.S.

[AIAA PAPER 70-488]

11 p2077 A70-25443

Satellite communications subsystem performance testing from initial integration through launch under all environmental exposure
[AIAA PAPER 70-448] 11 p2030 A70-25445

TACSAT 1 communication satellite design, dual-spin stabilization principles and dynamic characteristics, noting nutation behavior
[AIAA PAPER 70-455] 11 p2120 A70-25447

Initial Defense Communication Satellite Program/augmentation satellite design and mission, on-board communications equipment, control subsystems, American-British cooperation, etc
[AIAA PAPER 70-492] 11 p2121 A70-25449

Titan 3 launch vehicles capabilities communication satellites deployment modes, presenting cost and availability data for preliminary mission planning
[AIAA PAPER 70-482] 11 p2121 A70-25451

Step-Track automatic angle tracking technique for communication satellites, seeking peak of antenna single beam
[AIAA PAPER 70-416] 11 p1999 A70-25454

Channel separation in RF transponder for communication satellite achieved with RF multiplexers consisting of microwave filters and combiners with superior electrical performance
[AIAA PAPER 70-509] 11 p2016 A70-25457

Multiple feed waveguide lens in variable coverage communications antenna for geostationary LES-7 satellite
[AIAA PAPER 70-423] 11 p2016 A70-25461

Instructional communication system for U.S. using synchronous satellites over 15 regions
[AIAA PAPER 70-450] 11 p2000 A70-25465

Satellite Integrated Communications, Navigation and Identification System for implementing worldwide command-control system and equipment and signal integration
[AIAA PAPER 70-503] 11 p2000 A70-25466

Electric propulsion system selection for Lockheed Communications Satellite (LCS) based on weight, development status and complexity considerations, discussing optimization procedure
[AIAA PAPER 70-478] 11 p2101 A70-25470

Despin ball bearing assemblies performance data for TACSAT and Intelsat 4, discussing technology needed for accelerated testing, higher precision, failure detection and lubricants
[AIAA PAPER 70-459] 11 p2058 A70-25471

Communications satellite for Alaska and Mountain States TV defined using computerized synthesis program
[AIAA PAPER 70-453] 11 p2001 A70-25473

Wideband transmission media for global communication networks, comparing submarine cables and satellites based on economic tradeoff in terms of circuit density and distance
[AIAA PAPER 70-444] 11 p2001 A70-25475

Product oriented cost data bank for satellite system cost prediction and negotiation designed for USAF communications satellite program
[AIAA PAPER 70-445] 11 p2152 A70-25477

Global commercial communications satellite system arrangements, considering evolutionary political, economic and technological developments within INTELSAT context
[AIAA PAPER 70-446] 11 p2152 A70-25478

Communications satellite systems for developing nations, considering educational TV, economic growth, cost estimates, etc
[AIAA PAPER 70-475] 11 p2152 A70-25479

X band mechanically despun antenna system with RF and motor drive assembly developed for earth coverage communications satellite
[AIAA PAPER 70-422] 11 p2001 A70-25481

Multiple channel communication satellite interchannel interference including preamplifier intermodulation, direct interference, multipath amplification, crosstalk and multiplexer reflections considered for capacity maximization
[AIAA PAPER 70-508] 11 p2002 A70-25483

Horizon sensor design with null operating capabilities for synchronous orbit 3-axis stabilized communication satellites, discussing operation and testing
[AIAA PAPER 70-476] 11 p2121 A70-25484

Low noise wideband uncooled preamplifier for small unattended satellite communication terminals, discussing theory, design and performance
[AIAA PAPER 70-419] 11 p2016 A70-25485

VHF aeronautical communication satellites extended for use in aircraft position determination and surveillance, discussing accuracy and error source reduction
[AIAA PAPER 70-490] 11 p2002 A70-25487

Digital techniques application to military communication satellite systems, discussing 40 Mbps quadriphase modem, convolutional encoders, TDMA, etc
[AIAA PAPER 70-495] 11 p2002 A70-25488

Ground frequency converters for reception of NTSC color TV transmission from synchronous communication satellites, tabulating cost estimates
[AIAA PAPER 70-440] 11 p2002 A70-25490

TATS Master tactical communication satellite network controller with modems and digital computer for semiautomatic control over terminals
[AIAA PAPER 70-412] 11 p2002 A70-25491

Digital satellite communications systems, discussing time division multiplexing, steerable beam antennas and satellite-to-satellite transmission
[AIAA PAPER 70-491] 11 p2003 A70-25492

Ammonia micropropulsion operation modes and performance for stabilizing synchronous communication satellite, noting advantages over chemical and ion propulsions
11 p2122 A70-25817

Symphonic satellite telecommunication network for multiple access telephone, telegraph, data transmission, radio and TV dissemination
11 p2005 A70-26008

Plumeur-Bodou satellite telecommunications center, discussing antennas
11 p2031 A70-26009

Space technology exploitation, describing applications of multimission information transfer satellites
11 p2005 A70-26058

Multiple access to communication satellite by limiting repeater, considering model of a signals plus band limited white Gaussian noise in zero memory device
11 p2008 A70-26229

Trends in military communication satellite repeaters, noting influence by increased payload size, weight and complexity
11 p2009 A70-26258

SHF tactical satellite communications ground terminals, discussing system concepts, relationship to satellites and design problems
11 p2031 A70-26259

Satellite communication systems optimal utilization achievable through supervisory control system
11 p2009 A70-26261

Roll and pitch attitude control for long range station-keeping mission of synchronous flywheel stabilized communication satellite, discussing constraints on on-board equipment and technology
11 p2126 A70-26279

Passive and active satellite systems for point-to-point communication network with multiple access capacity, comparing technical and economic competitiveness
11 p2011 A70-26335

Nonlinear phase shift equation derived from TWT single carrier performance, predicting multicarrier performance of communications satellites
12 p2195 A70-27248

Telecommunication satellite system operation reliability taking into account maintenance and economics, discussing spacecraft acceptance and performance tests
12 p2313 A70-27470

Symphonic communication satellite orbit and attitude stabilization systems components, operation and accuracy requirements
13 p2502 A70-28432

Europa 3D carrier rocket design and operational data, discussing communication satellites
13 p2502 A70-28446

Space traffic control, discussing special problems of synchronous orbiting communications satellites
13 p2449 A70-29268

Earth resources satellite real time wideband relay communication link to ground station
[AIAA PAPER 70-326] 13 p2368 A70-29614

Commercial satellite communications, discussing creation and objectives of Comsat and establishment of Intelsat
13 p2368 A70-29618

Lunar communications systems considering use of satellites, metallic particle belts, rockets, lasers and particle beams
14 p2634 A70-30196

Soviet book on legal aspects of artificial satellites for meteorology and radio communication purposes
14 p2668 A70-30632

Demand assigned domestic satellite communications system with capability of single hierarchy switching and serving terrestrial common carriers and direct users
14 p2552 A70-31351

IR radiating bodies angular displacement determination by vacuum evaporated thermocouple radiation detectors, describing stationary communication satellite altitude control
15 p2740 A70-32422

Integrated tunnel diode amplifiers design using hybrid technique for communications satellites, noting stability and noise performance
15 p2710 A70-32469

UHF ground communication dish antennas transmit and receive gains calibration by communication satellite repeater
16 p2872 A70-32967

Satellite communication/navigation/surveillance systems for domestic and transoceanic ATC
16 p2949 A70-33479

COMMUNICATION SATELLITES

Lens antennas design for communication satellites, discussing power gain, beam width, sidelobe level, temperature distribution, etc
16 p2982 A70-33772

Tactical communications satellite /TACSAT/ design, emphasizing communications repeater characteristics
16 p2983 A70-34051

Artificial pilot phased array /APPA/ for use as multiple narrow beam communication satellite, obtaining beam steering from phase shifter setting
16 p2983 A70-34070

Range and velocity components for ray paths between tracking and data relay satellite and user communication satellite
16 p2866 A70-34073

Torque motor driven despun bearing assembly design with integral slip ring for tactical communications satellite /TACOMSAT/
16 p2986 A70-34160

Brushless despun mechanical drive and control system design and performance for orientation of high gain communications antenna from spin stabilized satellite
16 p2986 A70-34161

Communication satellite UHF link with FSK or PSK modulation, considering coded digital transmissions
16 p2867 A70-34331

Optimal receiving systems for satellite broadcasting, considering costs, power requirements, service area, etc
17 p3046 A70-35272

High power TWT for satellite communications ground stations, including Intelsat experience
17 p3054 A70-35282

Luneberg lens application to construct multiple beam mechanically despun antenna for spin stabilized satellites, discussing temperature problems
17 p3055 A70-35663

Juridical structure, risks and control of satellite telecommunication ensuring equality of nations
17 p3202 A70-35782

Application satellites, discussing uses in communications, meteorology, earth survey and navigation
18 p3333 A70-36348

Service multiplex for communications network via satellite, discussing reliability
18 p3229 A70-36667

Parabolic antennas for satellite communications network and radio telescopes, investigating surface utilization coefficient
19 p3395 A70-37267

Worldwide multichannel air communications system in 10 GHz to IR range by Quasi Laser Link modulation and satellites
19 p3378 A70-37855

U.S. nationwide satellite network for multichannel community antenna TV /CATV/ operated at 12 GHz band
19 p3382 A70-38891

Telecommunication, ATC and navigation satellite systems, examining economic bases for aeronautical and maritime space systems
20 p3740 A70-39407

Space law aspects of direct broadcasting satellites for TV and sound transmission
20 p3740 A70-39408

Communication satellites systems for civil application, considering ground stations design, regional communication, ATC and maritime communications and navigation
20 p3585 A70-39409

Satellites for direct radio and TV broadcasting, considering system quality and cost, network planning, frequency economy, etc
20 p3588 A70-40158

Communication satellites low thrust transfer to synchronous orbit by two-stage operation using hydrogen resistojets and Hg ion motors
[AIAA PAPER 70-1110] 20 p3691 A70-40227

SKYNET PCM telemetry and command station, discussing system design, pseudomonopulse feed, command and computer subsystems, etc
20 p3589 A70-40322

Satellite communications system optimal parameters and efficiency dependence on working capacity, discussing economic aspects of HF sets increased number
20 p3589 A70-40457

Global integrated communications satellite system, discussing International Telecommunication Union regulatory functions, etc
21 p3955 A70-40625

Monograph on communicating by satellite covering INTELSAT system design, pricing, procurement, broadcasting, international community responsibilities, etc
21 p3955 A70-40739

Small ground stations in communication satellite systems involving regional telecommunication, TV distribution, air traffic and maritime applications, data exchange, weather and education service
21 p3785 A70-40764

- Regenerative hydrogen-oxygen secondary fuel cells as rechargeable battery for communication satellites 21 p3756 A70-41007
- Frequency division multiple access satellite communication system, calculating bandwidth variations effects on intermodulation distortion 21 p3787 A70-41328
- FM transmission of multiplex telephone signals by communication satellites, deriving impulse noise due to adjacent channel interference 21 p3787 A70-41330
- Millimeter wave space-to-space and space-to-ground satellite communication links frequency allocation problems 21 p3787 A70-41335
- Communications satellite carrier instrumentation, using computer controlled frequency shift radiometer for power monitoring 21 p3826 A70-41345
- Baseline satellite design for U.S. domestic communications, discussing structural weight, transponders and bandwidth, antennas, etc 21 p3790 A70-41356
- Multiple beam earth station torus microwave antenna for satellite communication with nonplanar field of view over geostationary arc 21 p3798 A70-41357
- Multiple beam antenna system for regional communications satellite directing high radiated power toward specific earth areas 21 p3790 A70-41358
- Millimeter wave high gain Cassegrain antenna for wide bandwidth data link between communications satellites, obtaining accurate parabolic contours 21 p3799 A70-41359
- Single multiple access satellite communication system requirements for worldwide, trunked and local operations, considering transponder allocation and antennas 21 p3790 A70-41365
- Multiple access communication satellite systems providing reliable speech communication for low density use in remote areas [JPL-TR-32-1501] 21 p3791 A70-41368
- Synchronous satellites characteristics and applications to radio connection, light signals, positioning, telecommunications, manned space stations and space shuttles 22 p4109 A70-42467
- Management organization of European operational application satellite systems, concerning interurban telecommunication and air traffic control 22 p4127 A70-43502
- Eurospace Symphonie satellite communication system and ground facilities, discussing international and regional coverage 22 p4111 A70-43504
- Intelsat compatibility with independent regional telecommunication satellite systems 22 p4111 A70-43514
- European space applications program, discussing communication and meteorological satellites 22 p4111 A70-43515
- Communications satellites for offshore systems, noting development of small earth station 22 p3991 A70-43576
- Electromagnetic interference reduction between communication satellite earth stations and microwave radio relay stations by pit shielding 22 p3991 A70-43577
- Ground TV station network operating with communication satellites in remote areas 23 p4159 A70-43758
- Low noise dual receiver system for satellite communication earth station using parametric and transistor amplifiers 23 p4169 A70-43791
- TV broadcast satellites program distribution direct to home by network and by community 23 p4164 A70-44646
- Commercial satellite system circuit quality and reliability in digital communications, considering Automatic Digital Network Trans-Pac cable cut incident 24 p4311 A70-45223
- Military communication satellite requirements considerations including tactical and strategic concepts integration to provide advantages over terrestrial systems [AIAA PAPER 70-1295] 24 p4315 A70-46188
- COMMUNICATION SYSTEMS**
U TELECOMMUNICATION
COMMUNICATION THEORY
 NT WORDS [LANGUAGE]
 Book on communication and information theories application to fading dispersive communication channels, discussing tropospheric scatter, HF ionospheric links, moon bounds, etc 02 p0253 A70-11700
- Electrical analogs for optical systems in communication problem of optimum filtering to improve SNR 04 p0653 A70-15660
- Critique of theory of electromagnetic wave transmission in turbulent atmosphere, considering effects of approximation 05 p0811 A70-16044
- Optimum transmitter strategy and receiver gain for linear feedback communication in nonstationary additive noise 11 p2011 A70-26328
- Stationary phase error variance for second order phase locked loop for low signal to noise ratios 13 p2383 A70-29590
- HF electrical communication based on Kelvin transmission line and Maxwell field theories, noting linear arrays 16 p2860 A70-32951
- Book on random processes, communications and radar covering optimum filtering, detection, information theory, ergodic theory, probability and integration axioms, parameter estimation, coding, etc 17 p3043 A70-34602
- Monograph on state variable approach to continuous estimation of random processes with applications to analog communication theory 17 p3045 A70-35189
- Heisenberg uncertainty principle in communications technology, discussing variance products deficiencies and limits in carrier frequency pulses application 20 p3584 A70-39160
- Uncertainty principle in optimum communication theory, discussing existence and value of minimum product of pulse duration in terms of calculus of variations and differential equations 20 p3584 A70-39161
- Soviet book on complex signals in ranging, navigation and communications, discussing correlation and ambiguity functions and bandwidth effect 20 p3587 A70-39723
- Book on state variable solution techniques for homogeneous and inhomogeneous Fredholm integral equations in communication theory, discussing application to linear estimation theory 21 p3846 A70-41791
- Optimal detectors for two signals with fluctuating amplitudes and arbitrary mutual coherence, discussing distribution function processing 22 p3987 A70-42556
- Communication network approach to submillimeter wave applications in nondestructive testing, deriving transport equations for EM wave propagation 22 p4028 A70-42591
- Microwave communication - Conference, Budapest, April 1970, Volume 1, Communication system theory 23 p4158 A70-43751
- Optimal two-way communication system with feedback and decision constraint, developing algorithm for random code reliability lower bounds 23 p4159 A70-43754
- Radio signal source encoding, investigating error exponent 23 p4159 A70-43755
- Communication channel modeling with feedback for small error probability compared to unfolding capacity 24 p4313 A70-46056
- COMMUNITIES**
 NT CITIES
 NT MOUNTAIN INHABITANTS
 Aviation environment master plan concerning public relations problems confronted by USAF bases with adjoining communities 05 p0960 A70-16634
- COMMUTATION**
 Nonlinear control systems on-off oscillations with instants of commutation determined by simultaneous equations, noting feedback control 11 p2027 A70-26254
- Stress energy tensor equal time commutation, observing metric dependence inability to satisfy relations for linearized gravitational fields 19 p3536 A70-37550
- COMMUTATORS**
 NT DECOMMUTATORS
 Brushless DC motors speed regulation with electronic commutators, discussing photoelectronic, magnetic sensing and magnetic-coil commutation 02 p0229 A70-12616
- Transistorized pistol grip probe design, circuit and operation for testing wobble and asymmetry in rotating ring commutators of electric motors 12 p2165 A70-27495
- Brushless DC motor with rotor position sensor and transistor commutator for armature current switching, describing design and operation 12 p2165 A70-27525
- COMPACTING**
 Book on powder metallurgy treating characterization of powders, compaction, sintering and engineering considerations and applications 02 p0316 A70-11735
- Niobium powder hot pressing compaction in terms of porous body volume viscous flow, determining viscosity shift time dependence 04 p0696 A70-14461
- Titanium carbide sintering under continuous heating in Ar atmosphere, studying ultrasonic waves effects on compaction process 04 p0696 A70-14463
- Optimal temperature for sintering of compact titanium carbide in Ar atmosphere 04 p0697 A70-14468
- Al powder explosive compacting processing, equipment and tests noting heat treatment effect 05 p0894 A70-16324
- Hard alloy mixture shaping by free vibrational compaction of powders 07 p1296 A70-19801
- Optimum composition of sand-bentonite materials for aluminum alloy casting in molds compacted by high pressure 08 p1506 A70-21137
- Contact compaction methods of metal powders involving vibration, shock, detonation and hydrodynamical pressure 09 p1706 A70-23122
- COMPACTNESS**
U VOID RATIO
COMPANION STARS
 Companion galaxies on spiral arms endings, discussing age, expansion and ejection and stopping mechanism 04 p0759 A70-15710
- Bright southern Cepheids UVB observations, discussing blue companion effect on two color plot 14 p2639 A70-30726
- COMPARATORS**
 Comparator design for triplicated attitude indicator instrumentation system in aircraft to achieve reliability, discussing system failure characteristics 02 p0224 A70-11844
- Stereocomparator and electronic computer used to determine aerial photographs relative orientation elements, discussing measurement error elimination 03 p0482 A70-13108
- Comparator for measuring relative phase difference between identical frequency signals within microwave octave band 09 p1647 A70-22715
- Dispersion effect on accuracy of measuring polycrystalline samples electronograms by comparator using statistical method 09 p1682 A70-23392
- Plate coordinate measurements obtained with Zeiss precision monocomparator at satellite observation station 10 p1889 A70-24501
- Heat flow comparator for nondestructive testing of resin-impregnated fiber glass, detecting nonuniformities leading to thermal properties variation 11 p2059 A70-25764
- Thermal comparator for conductivity determination, discussing probe fabrication, surface finish, sensitivity, etc 11 p2050 A70-25765
- Digital frequency and phase flip-flop comparator for slave oscillators fine control by master frequency 22 p3996 A70-42819
- COMPARTMENTATION**
U COMPARTMENTS
COMPARTMENTS
 NT AIR LOCKS
 NT AIRCRAFT COMPARTMENTS
 NT ANECHOIC CHAMBERS
 NT COMMAND MODULES
 NT PRESSURE CHAMBERS
 NT PRESSURIZED CABINS
 NT SPACECRAFT CABINS
 NT TEST CHAMBERS
 NT VACUUM CHAMBERS
 Decompressed crewmember rescue onboard spacecraft and aircraft by compartmentalization combined with air locks 08 p1454 A70-21938
- Petrel payloads taking into consideration rocket stability after launch and compartment design 13 p2503 A70-28683
- COMPASSES**
 NT GYROCOMPASSES
COMPATIBILITY
 Color coding effects in compatible and noncompatible display control arrangements 02 p0247 A70-12381
- Compatibility conditions of theory of micromorphic elastic solids using Riemann theorem 06 p1164 A70-17530
- Compatibility of single metal coated carbon fibers, discussing structural recrystallization in contact with Ni or Co matrix by dissociation/diffusion/precipitation mechanism 07 p1315 A70-20048
- Strain and stress compatibility from extension of Saint Venant and Beltrami-Mitchell equations for physically and geometrically linear to nonlinear media 08 p1585 A70-20962
- Solid state IC-compatible display devices optical, electrical, mechanical and thermal characteristics 09 p1642 A70-22018
- Inlet-engine compatibility testing for aircraft system development program [AIAA PAPER 70-941] 16 p2965 A70-33534
- Strain compatibility equations for continuous shells from physical and mathematical considerations 16 p2991 A70-33893

Strain and stress compatibility from extension of Saint Venant and Beltrami-Mitchell equations for physically and geometrically linear to nonlinear media 20 p3719 A70-39384

Biological compatibility problem in long duration space operation crew change, discussing human metabolic processes and difference effects 22 p3980 A70-43641

COMPENSATION

Quantitative characteristics of central compensatory process, investigating nystagmus responses in guinea pigs subjected to bilateral labyrinthectomy 06 p0995 A70-17806

Lens aberrations compensations in partially coherent image holography 10 p1891 A70-24838

Decoupling by dynamic compensation using algebraic machinery, considering state space extension role in pole assignment 16 p2886 A70-33333

Terminal compensation influence on radiative recombination in n- and p-type GaAs, observing emission band in photoluminescence and electroluminescence spectra 23 p4231 A70-45063

COMPENSATORS

Corrective open-loop circuit, using delay elements for compensation of transient response in linear circuits with lumped parameters for pulse modulation transmissions 06 p1023 A70-17774

Radiometers sensitivity increasable by combining quasi-zero method with compensation circuits 08 p1495 A70-21053

Pulse signal transmission rate increase by transient processes compensator, discussing stability relation to signal to noise ratios 09 p1639 A70-23696

Dynamic force measurement, evaluating hybrid system with reaction force summation and operational compensation subsystems 10 p1889 A70-24580

Random processes correlation coefficients and functions measured by quasi-compensator with potentiometer and digital/analog readout 12 p2235 A70-27770

Automatic cancelling devices with compensating coils for terrestrial magnetic field vector 13 p2401 A70-30044

Computer oriented algebraic method for duplicator control systems applied to loop network, lag, feedback, phase lead and phase lead lag compensator design 14 p2560 A70-30620

Dynamic compensation of thermal pumping-induced deformation of laser active elements via thermal bending of resonator mirrors achieved by coatings 20 p3642 A70-39744

Sampled data compensators hybrid realization for discrete controllers, selecting canonical representation with minimum number of delay elements 22 p4002 A70-42846

Liquid compensators for gamma ray flaw detection of complex metal product configurations, considering radiation source energy spectrum and specimen density 24 p4348 A70-45849

COMPENSATORY TRACKING

Human operator remnant data normalization noting observation noise spectral characteristics for compensatory tracking 10 p1824 A70-23899

Human controllers nonlinear time domain mathematical model for analyzing compensatory tracking task data 11 p1992 A70-26396

Human performance as controller evaluated in man machine control system, considering pursuit or compensatory tracking tasks 12 p2177 A70-27039

Compensatory tracking task with tactile displays determining gains and body locations by describing function and error power analyses 13 p2354 A70-29599

Motion cue requirements in one and two axis closed loop compensatory control tracking tasks, discussing error rates 14 p2540 A70-30247

Optimal manual control model of human compensatory tracking response 14 p2543 A70-31408

Discrete stochastic optimal control model of human operator for single loop compensatory/pursuit tracking situation, considering application to manual control system design 16 p2852 A70-33463

Step and ramp input functions and pursuit and compensatory display modes effects on tracking performance 21 p3767 A70-40753

Vestibular sinusoidal stimulation effects on compensatory tracking under various postures and display conditions 22 p3976 A70-43706

COMPETITION

Optimal control theory applied to oligopoly, considering economic problems and Nash equilibrium solutions 15 p2831 A70-32552

COMPILATION (COMPUTERS)

U COMPILERS

COMPILER PROGRAMS

U COMPILERS

COMPILERS

ALGOL program modification for Fast Fourier Transform to eliminate computation time difference with Fortran 07 p1238 A70-19677

Aerospace compiler design for software cost reduction without affecting reliability, describing input language 16 p2868 A70-33432

COMPLEX NUMBERS

Imaginary numbers of Riabuchinskii, noting irreducibility to ordinary imaginaries 07 p1326 A70-19784

Three stage variable shift iteration algorithm for calculating zeros of polynomial with complex coefficients 09 p1712 A70-23419

Stability of multiconnected nonlinear controlled systems with nonsingle equilibrium position, representing lumped parameter system with characteristic equation having complex roots 11 p2021 A70-25338

COMPLEX SYSTEMS

Complex automatic systems effectiveness synthesis based on invariance principles 20 p3603 A70-39835

Complex plants process control by experimental statistical methods, considering curves plotting, computer requirements, optimum method selection, etc 20 p3592 A70-39902

Statistical analyzer for complex plants dynamic characteristics 20 p3604 A70-39912

COMPLEX VARIABLES

NT AIRY FUNCTION

NT ANALYTIC FUNCTIONS

NT BESSEL FUNCTIONS

NT CAUCHY INTEGRAL FORMULA

NT CONFORMAL MAPPING

NT CONJUGATES

NT ELLIPTIC FUNCTIONS

NT ENTIRE FUNCTIONS

NT EXPONENTIAL FUNCTIONS

NT HANKEL FUNCTIONS

NT HARMONIC FUNCTIONS

NT HYPERBOLIC FUNCTIONS

NT HYPERGEOMETRIC FUNCTIONS

NT LAGUERRE FUNCTIONS

NT LEGENDRE FUNCTIONS

NT LOGARITHMS

NT MATHIEU FUNCTION

NT MEROMORPHIC FUNCTIONS

NT ORTHOGONAL FUNCTIONS

NT RATIONAL FUNCTIONS

NT SCHWARZ-CHRISTOFFEL TRANSFORMATION

NT SINGULARITY [MATHEMATICS]

NT SPHERICAL HARMONICS

Difference set D of k distinct residues, extending Hall search with negative results, discussing multipliers, polynomial congruence, etc 01 p0132 A70-11073

Book on function theoretic methods for partial differential equations covering complex variables, harmonic functions, envelope method for singularities, operators, etc 01 p0133 A70-11325

Operational calculus for semisimple complex Lie group 07 p1321 A70-18658

Algebraic criterion for polynomial with complex coefficients having all zeros in certain regions of complex plane 07 p1324 A70-19201

Prandtl problem solution by reducing integrodifferential equation to linear differential equation in disk of complex variable, noting application to elliptical or rectangular wings 07 p1258 A70-19783

Electromagnetic and gravitational fields classification methods using spinor techniques, introducing five dimensional complex linear space with Weyl tensors elements 07 p1337 A70-20302

Complex Gaussian processes with complex density functions, computing covariances and marginal distributions 10 p1915 A70-24057

Complex variable technique for electrochemical machining of insulated and uninsulated straight sided tool, using minimal computer time 10 p1894 A70-24416

Root-locus approximation technique extended for complex plane analysis of equations with quadratic

term in variable parameter for linear multivariable feedback systems 10 p1855 A70-24449

Complex potentials used in semicomplex variable method for plane-strain problems in two dimensional linearized elasticity with couple stresses 13 p2508 A70-28494

Complex vector parametrization of Lorentz group in relativistic kinematics, discussing Wigner rotation, Lorentz transformation and particles classification during scattering 13 p2453 A70-29722

Asymptotic expansion of contour integrals involving analytic functions of complex variable, using steepest descent method 15 p2767 A70-31696

Point heat source generation of thermal stresses in elliptical plate with circular hole, using functions of complex variable for stress field determination 15 p2818 A70-32182

Stability criteria for differential equations with complex variables, considering boundary value requirements and sufficient conditions theorems 18 p3281 A70-36352

Sufficient conditions for local solvability of linear partial differential equations with operator on complex functions 19 p3457 A70-37682

Two dimensional piezoelectric problems of electroelasticity, formulating general solutions in terms of stress and electric potentials using complex variables 19 p3487 A70-37946

Plane wave reflection from stratified isotropic medium using ray tracing in complex space, noting agreement with phase integral method 19 p3380 A70-38404

Composite materials physical properties based on linearly reinforced media models and complex variable functions theory 20 p3655 A70-39860

Numerical methods, FORTRAN program and table form for complex integrals evaluation along unit circle in positive direction 20 p3605 A70-40120

Perforated infinite plate finite elastic deformation under biaxial tension, using successive approximation in connection with complex variable method of plane elasticity 21 p3932 A70-40551

COMPLEXITY

NT TASK COMPLEXITY

Electronic equipment complexity estimation based on information-recognition characteristics and ease of utilization 08 p1474 A70-21222

COMPLIANCE (ELASTICITY)

U MODULUS OF ELASTICITY

COMPLICATION

U COMPLEXITY

COMPONENT RELIABILITY

Nondestructive evaluation of components and materials in aerospace, weapons systems and nuclear applications - Conference, San Antonio, April 1969 01 p0095 A70-10001

NDT peculiar to airline maintenance, emphasizing inspection of complex parts hidden within assembly 01 p0099 A70-10028

Life-test sampling plan for electron tubes based on exponential failure distribution for reliability demand of military specifications 01 p0099 A70-10112

Cost-effective look at vacuum testing of spacecraft components, noting sensitivity prediction and thermal cycle test 01 p0055 A70-10113

Equipment reliability data application in analytic techniques to predict human requirements for system, using in-space maintenance as reference frame 01 p0055 A70-10117

Cost tradeoff analysis of electronic equipment for systems reliability design, considering component derating, redundancy and selection 01 p0049 A70-10119

Long life subsystems design and testing for orbital space station programs, considering nuclear generation, electromechanical equipment, positive expulsion of fluids, instrumentation, etc 01 p0103 A70-10626

High power TV broadcast satellite subsystems technologies requirements, considering transmitters, power conditioners, solar arrays and component reliability [AIAA PAPER 69-1080] 01 p0194 A70-10632

Commercial transport aircraft landing gear electrical circuitry dispatch reliability improvement, considering components causing flight delays due to maintenance problems 01 p0006 A70-10703

Machine parts fatigue strength under thermal cycles, studying nonlinear dependence of energy dissipation per unit volume on cycles number 02 p0383 A70-11654

Machine parts fatigue behavior and service life, studying endurance margin under load cycles spectra below initial endurance limit

02 p0383 A70-11657

Carrying capacity of heat resistant steel turbomachine elements, discussing plastic deformation and cyclic load effects, breakdown load determination, stress analysis, etc

02 p0352 A70-11659

Magnetic components design, manufacturing and handling for use in space communication satellites, noting design group role in parts construction and quality control

02 p0267 A70-12057

Product reliability using statistical probability technology with product failure studies, discussing performance prediction accuracy

02 p0309 A70-12301

Product reliability engineering analysis, discussing coordination, communication and data accumulation systems

02 p0309 A70-12302

Concorde aircraft main landing gear reliability, discussing design, corrosion, hydraulic contamination, metallurgy, sealing and tests

02 p0226 A70-12366

Electronic integration assembly (EIA)/incorporating modular electronic packaging design techniques to provide reliable mechanical configuration for spacecraft equipment

02 p0268 A70-12579

Optimal use of adaptive renewal capability determined for first order time varying linear systems with quadratic performance index by exponential model of component failure

02 p0273 A70-12729

Failure and defect formation in gas turbine engine disks made of steel alloys, stressing fabrication methods effect on reliability

03 p0588 A70-13251

Neutron radiography for visual nondestructive failure analysis and production inspection of ordnance components compared with X ray radiography

03 p0494 A70-14122

German Space Research Association reliability and testing function, using failure analysis for space projects components and structures

[DGLR-69-30]

04 p0698 A70-15137

Reliability engineering related to general and professional levels, discussing space program methods and Concerto program for electronic components

05 p0853 A70-15810

Design and qualification test criteria for components derived by enveloping peaks of shock response spectra in ground tests of missile stages explosive separation

[SAE PAPER 690616]

05 p0922 A70-15849

Soviet papers on vibrations, strength and structure of aircraft engine elements

07 p1363 A70-19109

Amplifier design effects on device reliability, considering sudden and gradual system failures

07 p1246 A70-19635

Optimal spare parts inventory determined for stochastically failing components using mathematical model

08 p1501 A70-20603

Galvanoplasty process for parts for UHF circuits, discussing cost, safety and quality

08 p1468 A70-20611

Matched filter SNR behavior under time and frequency domains distortion and random distortion, deriving design equations for energy loss coefficients

08 p1474 A70-21223

Nondestructive process control analyzer for spot welds in aircraft structural components, monitoring expansion, current and spotweld properties

08 p1507 A70-21486

Semiconducting components reliability test involving electrical parameters measurement following thermomechanical stresses

09 p1689 A70-22002

Tin oxide film resistors reliability test based on measurement of resistance nonlinearity by third harmonic voltage

09 p1689 A70-22005

Reliability estimations precision evaluated by Monte Carlo simulation, analyzing causes of data inaccuracy

09 p1689 A70-22019

Turbine components design for low cycle fatigue, estimating thermal cycle number for high temperature crack initiation and propagation

09 p1774 A70-22583

Turbine components thermal stress calculations for static and variable loads, considering plastic strain, creep and temperature effects

09 p1775 A70-22592

Turbines rotary shafts and stationary components thermal fatigue analysis, considering cycle numbers and stress concentrations under start-up, continuous operation and shut-down

09 p1775 A70-22593

Fault finding strategy optimization in systems with single defective element

09 p1693 A70-22974

Reliability testing of waveguide ferrite devices based on quantitative technique using circular charts with filled in endurance test results

09 p1652 A70-23661

Qualification and testing procedures for Apollo Spacecraft Program components and systems, discussing vibration tests

09 p1693 A70-23705

Component tolerances effect on transfer function of networks, calculating sum variance for two terminal networks

10 p1833 A70-24223

Optimization of controlled systems with allowance for failures of parallel connected elements dependent on control inputs and phase coordinates

10 p1854 A70-24279

Microwave device test system design, considering measurement ranges and parameters, calibration, repeatability, accuracy, maintainability, etc

10 p1852 A70-24890

Biosatellite Primate Mission Program for component qualification levels validated by flight tests data, performing vibration tests on prime structure spacecraft

[AIAA PAPER 70-403]

10 p1951 A70-24902

Fail-operational fail-safe redundant yaw damper system, comparing reliability requirements with reliability prediction, development and production testing and field usage data

[AIAA PAPER 70-392]

10 p1896 A70-24913

Time-optimal testing sequence for system failure detection, considering maintenance and reliability data

10 p1896 A70-25048

Components life determination from calculating cumulative damage using empirical stress amplitude distributions

11 p2133 A70-25844

Low cycle fatigue problems, environmental influence of operational differences on component life, life limits and controls for safe operation of jet engines

[SAE PAPER 700207]

11 p2102 A70-25879

Algorithm based on component reliability used to determine complex systems reliability

12 p2192 A70-28009

Weibull process with unknown scale and shape parameters analyzed by Bayesian decision making model, with application to component reliability problem

12 p2243 A70-28011

Orifice leak test for electronic components hermeticity

13 p2405 A70-28840

Supply phase voltage loss detection failure by voltage sensors in industry

13 p2378 A70-29349

Severity comparisons of specified and actual impulse tests determining component reliability

14 p2563 A70-30867

Minimum cost systems engineering in aviation equipment maintenance and reliability

14 p2669 A70-30943

Improved standard electrical equipment components development by test by use method, reducing cost and time

15 p2828 A70-31572

Quality assurance R and D for product design and operational integrity in manned space flight, noting space developments application to aircraft safety

15 p2676 A70-32231

Parts standardization in military electronics industry for cost reduction and reliability, discussing design transform from software to hardware

15 p2831 A70-32632

F-111A reliability levels achieved via high reliable hardware and redundancy and alternate mode capability requirements in contract

15 p2676 A70-32638

Electronic equipment reliability performance measurements during tests correlated to performance observed under field use

15 p2712 A70-32645

Electronic components prefailure analysis resulting in reduced failure rates, scrap and rework

15 p2832 A70-32652

Practical electronic components criteria accommodating reliability engineer and circuit designer

15 p2832 A70-32653

Boeing 707 and 727 aircraft components on condition maintenance program based on statistical analysis and performance monitoring for replacing scheduled overhauls

15 p2748 A70-32656

Nondestructive screen test efficiency, determining potential failures of electric components by Bayes theorem

15 p2748 A70-32659

Reliability assurance of LSI components consisting of complex electronic functions fabricated by semiconductor technology on single chip

15 p2713 A70-32662

Wearout life and reliability of rate gyros from field service test data

15 p2748 A70-32668

Mathematical reliability model for quasi-redundant electronic system with two failure modes for each component

15 p2769 A70-32827

Fluidic technology for avionics systems, considering potential cost reduction and reliability improvement

16 p2843 A70-33445

Electrical, electronic, electromechanical, pneumatic and hydraulic subsystems failure pattern determination, discussing sensing techniques in signature analysis

[ASME PAPER 70-DE-34]

16 p2917 A70-33505

Rocket engine thrust chambers and valves, discussing component lifetime extension and operational flexibility of reaction control systems

[AIAA PAPER 70-603]

16 p2964 A70-33526

Monopropellant hydrazine RCS rocket engine module, discussing operating conditions, development, thermal control and valve internal leakage

[AIAA PAPER 70-654]

16 p2965 A70-33544

Design and reliability of digital systems for hard cores of fault tolerant computers /hybrid- redundant systems/, discussing advantages over multiplexed systems

[JPL-TR-32-1490]

16 p2887 A70-33734

Plastic structural components service life estimation based on creep diagrams and short time tests

16 p2941 A70-34323

Aircraft, helicopters and rockets aviation systems design and components service life problems, emphasizing maintenance intervals

17 p3100 A70-34686

High reliability release mechanism with mechanical redundancy on SERT 2 satellite

17 p3174 A70-34759

Linear stress based cumulative damage law for structural component failures

17 p3186 A70-34987

Cost effective reliability apportionment in spacecraft subsystems, allocating failure-risk goals by mathematical model

17 p3101 A70-35160

Space vehicle optimal design based on reliability analysis, taking into account cost of materials strength tests

[JPL-TR-32-1496]

17 p3188 A70-35224

Photoelectric conversion efficiency and radiation resistance of Li-doped Si solar cells, showing improved reliability over Li-free cells

17 p3023 A70-35311

Service multiplex for communications network via satellite, discussing reliability

18 p3229 A70-36667

Critical aviation gas turbine rotating component life limit determination, describing statistical, maintenance, inspection and life evaluation computer program /SMILE/

[ASME PAPER 70-GT-66]

18 p3303 A70-36841

Normalization of mechanical properties of aircraft engine components, increasing weight efficiency and reliability

19 p3490 A70-37254

Electrical tests on satellites and space probes applied to spaceborne subassemblies, subsystems and electronic systems EM compatibility

19 p3532 A70-38287

Environmental tests and checkout procedures for Azur satellite subsystems and subassemblies integration into flight readiness

19 p3533 A70-38289

Space environment simulator for thermal vacuum performance of artificial satellites and components

19 p3401 A70-38308

Machine parts fatigue strength under thermal cycles, studying nonlinear dependence of energy dissipation per unit volume on cycles number

19 p3547 A70-38427

Machine parts fatigue behavior and service life, studying endurance margin under load cycles spectra below initial endurance limit

19 p3547 A70-38430

Carrying capacity of heat resistant steel turbomachine elements, discussing plastic deformation and cyclic load effects, breakdown load determination, stress analysis, etc

19 p3547 A70-38432

Failure and defect formation in gas turbine engine disks made of steel alloys, stressing fabrication methods effect on reliability

19 p3548 A70-38469

Si photocells fabrication, reliability and energy conversion efficiency

19 p3358 A70-38479

Electronic components mass production for automatic control equipment, determining parameters probabilistic scatter

19 p3390 A70-38578

Military electronic equipment reliability limitations in terms of mean time to failure, considering quality control of components

19 p3390 A70-38596

Computer program for assessment and modification of mechanical component life predictions by discrete formulation of Bayes theorem 19 p3440 A70-38816

Technical methods defining, monitoring and controlling life limited aerospace components during storage 19 p3441 A70-38831

Hazard functions, renewal and peril rates for reliability models of nonrepairable parts, sockets and repairable systems 19 p3442 A70-38839

Rotating mechanical components reliability under complex fatigue, presenting design data 19 p3442 A70-38845

Structural design load factors statistical evaluation for element optimal reliability 19 p3550 A70-38850

Fatigue strength distributions at specific cycles of finite life with given cycles-to-failure, calculating reliability 19 p3550 A70-38851

Hollow test platform for gyros and accelerometers used in inertial navigation [AIAA PAPER 70-952] 20 p3606 A70-39577

Automatic control system components parameter variation effects on invariance conditions 20 p3602 A70-39830

Nonrepairable elements reliability under external influences, discussing linear damage accumulation hypothesis 20 p3638 A70-40180

Air navigation Dioscures project satellites, discussing spin or three axis stabilization, system replenishment strategies and subsystem reliability 21 p3929 A70-41259

Electronic parts testing for long duration Mariner spacecraft missions 21 p3799 A70-41798

Ni-Cd cell plates screening and selection by weight for reliability and uniformity improvement 21 p3760 A70-42147

Fluidic oscillators frequency stability evaluation, noting analog circuits superiority over digital [ASME PAPER 70-FLCS-20] 22 p3963 A70-42407

Helicopter parts and assemblies fatigue life estimation and testing, discussing loading spectra, service conditions, etc 22 p4046 A70-43119

Algorithm for communication network synthesis from limited elements selection, considering fixed reliability requirements 23 p4160 A70-43763

Integration operators for transient structural response in qualification tests for internal components of dynamically loaded structures 23 p4273 A70-44719

Avionic components reliability, determining non-steady cooling air environment effects 23 p4175 A70-44744

Electrical and electronic semiconductor device failures from metallurgical viewpoint 23 p4175 A70-44746

Nondestructive testing technology, emphasizing component designer role in facilitating inspection of surface defects 24 p4342 A70-45679

DC potentiometer for nondestructive tests of structural components, obtaining crack detection, depths and angles and wall thicknesses 24 p4338 A70-45740

Si crystal microdefects influence on semiconductor device performance and reliability 24 p4391 A70-46015

COMPONENTS

Pressure sensitive components in cordwood modules noting temperature and pressure damaging stresses during encapsulation 05 p0855 A70-16037

Components and microelectronics - Conference, San Francisco, August 1969, Volume 13, Part 5 06 p1018 A70-17355

Transfer molding process in fabrication of electronic modules components, emphasizing criticality and unfavorable characteristics 13 p2420 A70-29253

Internal stresses in transfer molding of electronic modules by photoelastic technique, discussing component failure 13 p2420 A70-29254

Millimeter waveguide components, discussing impedance measuring equipment, matched loads, variable short circuits and attenuators, power measurement equipment, etc 14 p2556 A70-30446

Design component size index as function of various system demands, using Monte Carlo method 21 p3846 A70-41870

Radio electronic circuits precision, deriving relationship between frequency response and component variations solvable by linear programming 23 p4171 A70-43958

COMPOSITE MATERIALS

NT CERMETS

NT COMPOSITE PROPELLANTS

NT LAMINATES

NT METAL MATRIX COMPOSITES

NT REINFORCED PLASTICS

NT WHISKER COMPOSITES

Ultrasonics inspection applied to reentry vehicle heat shields and composite materials, verifying anomalies by microscopic area examination 01 p0097 A70-10016

Interfaces in composites - ASTM Conference, San Francisco, June 1968 01 p0126 A70-10476

Fiber-matrix interface mechanics in composites, considering shear strength, stress distribution, fiber strength effects, etc 01 p0127 A70-10479

Fiber-composite materials fracture, noting interface mechanical strength effects on composite properties under tension and shear 01 p0127 A70-10481

Microstructural interfacial stability and property retention after elevated temperature exposure of eutectic composites, discussing coarsening rate relationship to interfacial area and energy 01 p0117 A70-10485

Solid glass sphere reinforced nylon resins properties, processing and applications, noting tensile and impact strength and heat distortion 01 p0128 A70-10772

Electrically conductive plastics fabrication and applications limitations, discussing plastic matrix materials loaded with various conductive fillers 01 p0129 A70-10938

Fiber reinforced composites emphasizing refractory fibers, preparation methods, properties and fabrication 01 p0129 A70-10939

Glass reinforced and unreinforced thermoplastics HF fatigue failure modes, discussing isothermal and nonisothermal test procedure 01 p0129 A70-11081

Plane sinusoidal wave propagation through material reinforced with parallel fibers, using integral formulation for multiple scattering in infinite slab 01 p0130 A70-11187

Reinforced metals properties and applications including fibers and lamination, notch sensitivity, brittle fracture, failure and heat resistance characteristics 01 p0124 A70-11619

Expandable space hangar with composite wall for orbiting maintenance shelter, providing radiation and meteoroid protection for occupants 02 p0380 A70-11934

Boron-polyimide composite reinforced Ti fuselage stringers design and test program for SST 02 p0387 A70-11950

Bolted and bonded joints design in composite materials loaded in tension, presenting methods for strength prediction, testing and analysis 02 p0306 A70-11952

Composite fibrous materials applicability to V/STOL rotor blades design and fabrication confirmed by structural analysis 02 p0225 A70-11953

Fiber reinforced composites fabrication, properties and industrial applications, discussing modulus of elasticity and tensile strength equations, bonding and temperature applicability 02 p0322 A70-12713

Stress-optic law for orthotropic composites photoelastic stress analysis, investigating use of transparent filament-resin composites 03 p0481 A70-12956

Fiber composites dimensional changes, stresses and plastic flow during component allotropic transformation, studying temperature variations effects 03 p0585 A70-12973

Momentless design of composite plate and shell structures with variable elastic constants based on loading and shape requirements 03 p0586 A70-13112

Viscosity anisotropy in fluid matrix suspensions of parallel rigid flakes as function of flake content and width-to-thickness ratio 03 p0515 A70-13122

Graphite fiber content determination technique for plastic composites based on epoxy, polyimide and phenolic resins, using concentrated sulfuric acid 03 p0515 A70-13123

Failure mechanisms in notched or damaged fiber reinforced composite materials determined from analysis of axial tensile strength and broken fibers 03 p0515 A70-13124

Constitutive equations for orthotropic bilinear elastic materials in plane stress case, discussing unidirectional composites 03 p0587 A70-13127

Unidirectional composite materials properties, discussing stiffer filaments effect on Young modulus and shear coupling constant relating shear strain to longitudinal strain 03 p0587 A70-13128

Stiffness and expansion properties of oriented short fiber composites, discussing longitudinal modulus and expansion strain dependence on aspect ratio 03 p0587 A70-13129

Deformability calculation of two phase composite solid materials through laminated structural models 03 p0602 A70-14337

Brittle composites /including fiber reinforced material/ deformability and plastic deformation effect on tensile strength, discussing pressure induction of sound flow [ASME PAPER 69-WA/PROD-28] 04 p0705 A70-14834

Thermal damping in gas-filled composite materials during impact loading due to heat transport, discussing role in impact energy dissipation [ASME PAPER 69-APM-V] 04 p0712 A70-14867

Stress intensity and strain energy release rate in elastic fiber-reinforced composites with different thermomechanical properties and imperfect bonding [ASME PAPER 69-WA/APM-15] 04 p0771 A70-14913

Material coupling in two layered orthotropic cylindrical shell subjected to normal external pressure 04 p0778 A70-15547

Structural design of boron/epoxy front housing for T-56 turboprop reduction gear case achieving reduced weight and increased stiffness [SAE PAPER 690666] 05 p0853 A70-15837

Axisymmetric elasticity problem for straight fiber imbedded into infinite matrix, noting homogeneous temperature changes causing residual stresses, tractions at infinity and fiber pulling 05 p0931 A70-16088

Continuum model for plastic-elastic behavior of fiber reinforced composite material, formulating yield condition and constitutive equations 05 p0931 A70-16131

Displacement determination by orthogonality relationship for dynamic vibrations and stresses in composite elastic plates 05 p0937 A70-16406

Composite materials use in nonload bearing and heavily stressed materials, considering applications in aircraft industry and high strength fibers role 05 p0870 A70-16576

High modulus fibers as reinforcing fillers in thermoplastic matrices, discussing cost compensation in low fiber loadings 05 p0870 A70-16578

Composite strength and stiffness prediction from fiber and matrix properties using computer 05 p0870 A70-16579

Handbook on fiberglass and advanced plastics composites covering raw materials, processing methods, design and applications 05 p0872 A70-16601

Glass filled thermoplastics fabrication techniques and composites, discussing molding compounds and processes, reinforced thermoplastics properties and applications 05 p0873 A70-16605

Graphite yarn, cloth and fiber composites physical properties tabulated, discussing multiply laminates for graphite-epoxy composites 05 p0873 A70-16610

Filament winding methods of aerospace industry based on motor case winding, emphasizing reinforcing materials, winding geometry and finished composite evaluation methods 05 p0856 A70-16615

Boron-epoxy composite materials for secondary and primary aircraft structural components, discussing multidirectional laminates, joint analysis, etc 05 p0942 A70-16620

Composite materials properties test methods, discussing nondestructive method for shear or rigidity modulus of square plates 05 p0874 A70-16622

Thermal conductivity and aperiodic temperature distribution in microstructure of composite materials reinforced with solid and hollow fibers 05 p0958 A70-16952

Fibers random curvature effect on thermoelastic properties of unidirectionally reinforced fibrous materials 05 p0946 A70-16953

Mechanical behavior of cylinders with alternating layers of reinforcing and matrix materials derived from governing equations, including equations of motion [AIAA PAPER 70-134] 06 p1169 A70-18051

Dynamic elastic modulus of graphites and composites measured as function of temperature using thin rod resonance method 06 p1070 A70-18447

Reinforced graphite cloth composite for reentry heat shielding of SNAP 27 isotopic heat sources, describing structure, thermal and mechanical properties and ablative characteristics 07 p1332 A70-18933

Filamentary composite materials for commercial aircraft and engine construction noting boron, graphite and glass reinforcement 07 p1316 A70-18950

Arbeitsgemeinschaft Verstärkte Kunststoffe - Conference, Freudenstadt, West Germany, September-October 1969

07 p1316 A70-19753
Stress analysis of multiaxially loaded tubes of fiberglass reinforced composite wound in three directions

07 p1318 A70-19755
Buckling stress calculation and measurement in cylindrical fiberglass reinforced composite shells under axial pressure

07 p1409 A70-19756
Sizing and design of large vessels of fiberglass reinforced composites based on minimum cost

07 p1409 A70-19757
Fiberglass reinforced materials characteristics under stress evaluated by ring test in form of split disk or hydraulic tests

07 p1410 A70-19758
Boron and carbon fiber reinforced composites mechanical properties compared with fiberglass reinforced composites

07 p1318 A70-19770
Boron fiber reinforced composites structure and loading capacity, describing network-like fiber winding technique for light reinforced structures

07 p1318 A70-19771
Heat resistant fibers fabrication and properties for composite materials, noting metal whiskers, C, B, Be and alumina

07 p1318 A70-19802
Compression strength of polyester resin reinforced with hard drawn and softened steel wires, discussing variations from predicted performance

07 p1320 A70-19954
Bending tests for characterizing off-axis unidirectional composite beams, discussing errors due to lift off from supports

07 p1412 A70-19963
Structural composite materials for thermal protection of reusable weight-saving vehicles in space transportation system

07 p1397 A70-20382
[AIAA PAPER 70-272]
Boride composites with high strength and thermal resistance suitable as nose cap and leading edge materials for reusable lifting reentry systems

07 p1315 A70-20387
[AIAA PAPER 70-278]
Residual stresses in continuous fiber reinforced composites with unknown strain history determined by empirical methods

08 p1520 A70-21498
Thermoelectric energy functions bounding by variational principles for anisotropic composite materials properties

08 p1592 A70-21510
Thermal conductivity and diffusivity of two phase composites determined by iterative solution of heat conduction equation with space fluctuating properties

08 p1598 A70-21511
Carbon fiber composite materials production technology, physical properties and potential applications in aerospace

08 p1527 A70-21520
Mechanical properties and fracture behavior of chemically bonded glass matrix-metal composites

08 p1521 A70-21699
Composite materials application to structural members, considering bond or adhesive shear strength

08 p1594 A70-21855
Stress analysis of composite materials reinforced with glass ribbons embedded in epoxy matrix by photoelastic technique, discussing perturbation effect

08 p1594 A70-21862
Composite materials testing and design - ASTM Conference, New Orleans, February 1969

08 p1528 A70-21876
Composite materials shear strength test problems with high modulus fibers

08 p1529 A70-21877
Tension, compression and in-plane shear tests to obtain boron epoxy composite materials mechanical properties to design FB-111 wing box extension

08 p1529 A70-21879
Uniaxial and multiaxial stiffness and property characterization of anisotropic composite materials formed as thin walled cylinders

08 p1529 A70-21880
Test methods for evaluating tensile, compressive, interlaminar shear and bearing strength properties of carbon yarns and flat and tubular composites

08 p1529 A70-21881
Geometry effect on short beam tests for interlaminar shear strength of composite materials

08 p1529 A70-21882
Inplane shear stress-strain response determined for unidirectional composites, using uniaxial test method for laminated plates

08 p1530 A70-21884
Specimen design of laminated angle-ply composite materials for straight-sided axial coupon and long beam flexure tension testing

08 p1530 A70-21885
Split ring load test method for determining shear modulus of isotropic and composite materials

08 p1530 A70-21888

End plugs bending moment and shear loads reduction during compression tests of composite orthotropic cylinders

08 p1594 A70-21889
Failure criteria application to quasi-homogeneous anisotropic materials, discussing material constants

08 p1595 A70-21890
Matrix optimization of boron filament reinforced polymeric for short duration high temperature aerospace applications

08 p1530 A70-21891
Composite materials fatigue determinations providing curves of stress-strain magnitude vs usable life or time to failure, considering environmental effects in service for design criteria

08 p1531 A70-21895
Design allowables and factors of safety for filamentary composite materials, discussing reliability

08 p1595 A70-21900
Unidirectional filamentary composites failure theory for uniaxial and combined stress, considering constituent material properties and fabrication processes

08 p1532 A70-21902
Fiber composites-Ti alloy adhesive, rivet and combined joints for aircraft applications, noting fiber orientation role in joint tensile strength

08 p1509 A70-21905
Filament tensile strengths and pressure strain characteristics of high modulus boron filament wound/resin composite pressure vessels for cryogenic applications

08 p1509 A70-21909
Structural analysis of Titan 3 Stage 2 ablative nozzle extension made of composite material

08 p1595 A70-21910
Fracture processes in homogeneous anisotropic fiber composite materials, describing microcrack initiation, growth and unstable propagation at critical stress level

08 p1532 A70-21912
Composite material tensile strength, discussing statistical scatter in fiber strength and local fiber overstress caused by fiber discontinuities

08 p1532 A70-21914
Failure mode in shear loaded graphite filament reinforced epoxy composites dependent on interfacial bond strength

08 p1533 A70-21915
Longitudinal strength characteristics of filament reinforced composites, discussing bond strength effect on filament fracture

08 p1533 A70-21918
Materials for separator matrix of rechargeable hydrogen oxygen fuel cell, noting use of composite potassium titanate

09 p1612 A70-22045
Strength and plasticity criteria for anisotropic reinforced materials model taking into account material structure, components properties and behavior

09 p1768 A70-22119
Stress-strain characteristics of reinforced elastoplastic layer using mathematical model

09 p1769 A70-22183
Composite materials macroscopic thermoelastic properties relationships to constituents properties, discussing effective thermal expansion coefficients and specific heats

09 p1703 A70-22682
Carbon fibers and fiber-reinforced composites fabrication, structural properties and uses

09 p1710 A70-22758
Composite window permitting visual or photographic observation and IR irradiation of test materials in ultrahigh vacuum system

09 p1698 A70-22994
C-5A airframe composite materials fabrication, tooling, processing, quality assurance and nondestructive test methods

11 p2058 A70-25572
Aircraft turbine engines structural materials and design concepts, describing fiber reinforced materials, oxide dispersion hardened alloys and integral and honeycomb structures

11 p2101 A70-25625
Polyimide resins and composites state of cure determination by thermomechanical analysis (TMA)

11 p2069 A70-25807
Initial geometric imperfections effect on buckling and postbuckling behavior of laminated composite cylindrical shells under axial compression, considering reinforcing fiber orientations

11 p2135 A70-25986
[AIAA PAPER 69-93]
Cost-property index (B/P) to compare economic success of composites, metals, glass and ceramics for load bearing applications

11 p2136 A70-26077
Elastic-plastic shear cracks propagation in two phase composite materials using dislocation model, determining critical fracture strength

11 p2136 A70-26081
Elastic properties determined for reinforced composite material with hollow spherical inclusions embedded in matrix

11 p2136 A70-26083

Tensile strength of nitrided boron-aluminum alloy composite modules, noting effect of Ti cladding on panel surfaces

11 p2066 A70-26085
Elastic moduli of fiber reinforced composites calculated, deriving reinforcement factor in Halpin-Tsai equation from volume fraction

11 p2070 A70-26087
Ultrasonic pulse technique for measuring fiber reinforced composites elastic constants

11 p2052 A70-26341
Flexural stress relaxation properties of thermoplastics and composite materials, assessing strain energy by ballistic pendulum

11 p2070 A70-26342
Open pattern winding technique for composite materials, laying fibers without weaving around pillars at edge of table and to stiff beam

11 p2060 A70-26344
Electrical conductance test for composite materials adhesive bond degradation by liquids

11 p2071 A70-26345
Gas-filled composites under impact loading, studying thermal damping due to heat transfer between compressed gas and solid structure

11 p2140 A70-26480
Anisotropic fiber reinforced composites elastic moduli determined by analytical matrix method

11 p2141 A70-26488
Fiber reinforced composites under longitudinal shear loading, noting orthotropic nature and shear moduli assuming circular fibers

11 p2141 A70-26489
Thin shell design for minimum bending stresses and transverse shear for composite materials with low interlaminar shear strength

11 p2141 A70-26490
Steady state creep of composite material with short fibers, discussing effects of fiber/aspect ratio, fiber volume fraction and distribution

11 p2144 A70-26671
Elastic stiffness of unidirectional glass reinforced epoxy fiber composite determined from ultrasonic velocity measurements

11 p2071 A70-26692
Frequency equation for harmonic waves propagating in composite circular-cylindrical rods consisting of circular core and circular casing of different material

11 p2145 A70-26693
Boron fibrous composite panels machining methods including drilling, routing, band sawing and reaming

12 p2240 A70-27077
[ASTM PAPER EM-69-141]
Wide goods fabrication of boron composites, discussing mechanical properties and cost effectiveness

12 p2240 A70-27078
[ASTM PAPER EM-69-142]
Semiinfinite composite medium displacement caused by nucleus of torsional strain with axis perpendicular to constituent isotropic layers interfaces

12 p2321 A70-27159
Interfacial tractions between matrix and fiber in elastic composite materials reinforced with elastic fibers

12 p2322 A70-27230
Stress and strain in matrix of fiber reinforced material within elastic region, calculating interface shear stress for rectangular fiber

12 p2322 A70-27231
Composite materials fabrication with glass, boron and graphite fibers reinforcement, discussing matrix and binder materials

12 p2253 A70-27267
NDT methods for fiberglass, graphite and boron fiber composites for aircraft structures

12 p2243 A70-27465
Composite reinforced materials similarity criteria to relate static and dynamic fields of various physical parameters, outlining mathematical simulation

12 p2259 A70-27526
Aluminum-boron composite material applications to structural components of F-106 aircraft, noting weight saving and mechanical properties

12 p2257 A70-28082
[AIAA PAPER 68-975]
Glass- and quartz-fabric reinforced polymers for high temperature microwave insulation, evaluating electrical and thermal aging properties

12 p2259 A70-28149
Fiberglass content effects on reinforced polycarbonates long term dimensional stability during compression and tension creep tests

12 p2259 A70-28298
Annealed compressed ground synthetic mica and silver dust composite materials, analyzing physicochemical properties

12 p2260 A70-28319
Al-aluminum oxide composite steady state creep due to grain boundary sliding, accounting for activation energy level

12 p2258 A70-28348
Stress concentration in fiber reinforced materials resulting from thermal self straining, using finite element method and photoelastic analysis

13 p2509 A70-28533

- Complex moduli of isotropic viscoelastic composites from elastic moduli 13 p2511 A70-28735
- Nonlinear theory describing mechanical behavior of prestressed laminated composites subjected to large deformations 13 p2511 A70-28738
- Wool felt based carbon and graphite composite materials for orthogonally isotropic high shear strength compared with rayon felt based composites 13 p2437 A70-28776
- Aircraft structure fabrication combining unidirectional strength and stiffness of B composite with metal, including test and weight/cost data 13 p2418 A70-28777
- Synthetic foam material of hollow carbon microsphere fillers embedded in high compression strength epoxy resin matrix 13 p2437 A70-28780
- Griffith flaws limitation effect on glass matrix-tungsten composites strength, considering dispersed phase with wide particle size distribution 13 p2437 A70-28827
- Unidirectional composite with transversely isotropic fibers, calculating elastic stiffness constants by modified point-matching technique 13 p2515 A70-29466
- Laminated composite materials dynamic elastic properties, outlining resonant frequency effect on apparent Young modulus 13 p2515 A70-29467
- Stainless steel fiber reinforced Sn-Pb eutectic alloy composite mechanical properties, noting tensile strength and rupture behavior 13 p2436 A70-29625
- Filled elastomers elastic and anelastic behavior, investigating strain dependence 13 p2440 A70-29964
- Book on high modulus fibers and composites providing data for preparation, microstructure, structure and properties 14 p2598 A70-31315
- WC as densification aid for NbC-C composites, examining fabrication temperature, mechanical properties, solid solution composition, etc 15 p2757 A70-31797
- Colloidal filler /carbon black/ reinforced rubber for various applications, noting fabrication into composite material 15 p2764 A70-31930
- Fiber reinforced viscoelastic composites complex elastic moduli derivation 15 p2816 A70-32003
- Optimal design for composite material structure, considering internal and external reinforcement 15 p2816 A70-32005
- Stress distribution in fiberglass unidirectionally reinforced composite material under uniaxial tension 15 p2765 A70-32180
- Statistical theory of material strength applied to composite materials reinforced with whiskers and noncontinuous fibers 15 p2763 A70-32833
- Isotropic composite materials with anisotropic components, determining microconstants for heat conduction, elasticity and thermoelasticity problems 15 p2766 A70-32896
- Material data file and retrieval system for designers in automotive, equipment and appliance industries, discussing applications to other FRP markets 16 p2935 A70-33352
- Diluent resins properties for blending with glass fiber reinforced high density polyethylene concentrate 16 p2935 A70-33353
- Mechanical properties of composite materials reinforced with ribbon fibers consisting of stainless steel and polyethylene ionomer resins 16 p2988 A70-33366
- Ablative composites containing in situ reaction formed refractory metal carbides 16 p2937 A70-33371
- Graphite fiber reinforced polyimide composites with low void content, high strength and modulus 16 p2938 A70-33384
- Composite beam testing concepts and interpretation under three and four point loading, noting shear deformation effect 16 p2989 A70-33385
- Laminated multioriented filamentary composites strength and fracture characteristics under longitudinal tension and compression [ASME PAPER 70-DE-31] 16 p2989 A70-33502
- Reinforced polymer composites design for aircraft structures [ASME PAPER 70-DE-67] 16 p2939 A70-33518
- Elastic constants for plates of unidirectional fiber reinforced anisotropic composite material determined by ultrasonic wave propagation 16 p2991 A70-33847
- Constitutive equation for fiber reinforced viscoelastic materials, using continuum theory of mixtures 16 p2994 A70-34231
- Thermal and thermoelastic constants of macroscopically isotropic composite materials based on self consistent calculations 17 p3194 A70-34555
- Inelastic analysis of unidirectional composite subjected to transverse normal loading, discussing linear response up to elastic limit and subsequent crack propagation and failure 17 p3182 A70-34557
- Optimum filament orientation for maximum strength in composite with combined normal and shear stresses 17 p3183 A70-34563
- Longitudinal shear modulus of unidirectional fibrous composite, involving series solution of Laplace equation 17 p3183 A70-34564
- Composite materials in aerospace vehicle design, discussing mechanical behavior, applications and characteristics 17 p3127 A70-34674
- CH-47C helicopter fiberglass main rotor blade, discussing composite materials impact on design 17 p3013 A70-34702
- Composite tail rotor driveshaft for next generation helicopter, discussing materials, fabrication and tests [AHS PREPRINT 451] 17 p3100 A70-34703
- Circular inclusion interface separation in matrix under incident compressive waves interpreted for fiber reinforced composites 17 p3185 A70-34963
- Plastic flow and failure of elastic fiber reinforced composite materials with noninteracting and interacting discontinuities, obtaining stress distribution for various work hardening degrees 17 p3187 A70-34991
- Fiber reinforced composite with ductile matrix, discussing fatigue life prediction from strain hardening characteristics 17 p3128 A70-35465
- Weld transition joints from explosive bonded Al-steel and Al-Cu composite plates, discussing mechanical and electrical properties 17 p3102 A70-35551
- Aligned composite materials preparation by unidirectional lamellar eutectoid decomposition in Co-Si, Cu-Al, Ni-In and in supersaturated solid solution Sn in Pb 18 p3274 A70-36052
- Cracks and tensile failure of interface bonds in elastic composite hollow cylinder, deriving wave front propagation equations 18 p3283 A70-36388
- Boron composites development for aircraft structures compared with titanium [ASME PAPER 70-GT-120] 18 p3344 A70-36851
- Thermal expansion anisotropy in graphite-epoxy composites causing residual stresses [ASME PAPER 70-GT-129] 18 p3279 A70-36855
- Fiber reinforced materials with oriented armoring, calculating stress strain state under transverse shear 19 p3454 A70-37348
- Stress wave propagation based on elasticity theory for reentry heat shield composites reinforced with unidirectional high strength high modulus fibers 19 p3537 A70-37788
- Stress and displacement within internally pressurized composite cylinders having continuous fiber reinforcement in circumferential direction, using finite element method 19 p3538 A70-37797
- Physically nonlinear elastic solid three dimensional and generalized plane strain problem, discussing application to composite materials 19 p3538 A70-37798
- Elastic particulate composite solid with microinclusions, deriving dispersion relations governing plane longitudinal wave propagation modes by analogy with continuum theory 19 p3540 A70-37942
- Fiber reinforced solid material, determining swelling or temperature change induced dilatation by micromechanics and physical chemistry 19 p3540 A70-37943
- Dynamics of composite materials using extensions of continuum theories based on combination of elastic and geometric properties 19 p3455 A70-37950
- Composite bodies under plane deformations, determining stress dependence on elastic constants 19 p3455 A70-37952
- Unidirectional composites subjected to free vibration and axial end loading, considering longitudinal stress wave propagation in fiber direction 19 p3540 A70-37954
- Thermoelastic composite materials, deriving crystal lattice type model of equations for predicting dynamic or thermomechanical behavior 19 p3540 A70-37958
- Micropolar mechanics application to stress and displacement within separate components of fibrous composite material 19 p3541 A70-37961
- Soviet book on fiber reinforced composites covering strength, rheologic and elastic properties, thermal conductivity, diffusion processes, etc 19 p3456 A70-38795
- Hydrofoil and hovering craft design by fiber technology, discussing composite materials, whisker mechanical properties, polycrystalline fibers, matrix materials, etc 19 p3456 A70-38941
- Carbon composite technology - Conference, University of New Mexico, January 1970 20 p3652 A70-39201
- Composite technology effects on engineering design, emphasizing carbon-carbon materials for aircraft structural weight reduction, performance improvement and high temperature applications 20 p3653 A70-39202
- Carbon/carbon composites constituent characteristics effects on thermal and mechanical properties, using polarized light and scanning electron microscopy 20 p3653 A70-39204
- Chemical vapor deposition of carbon matrix material in fiber structure, investigating thermodynamic fundaments in processes 20 p3654 A70-39207
- Carbon fiber/carbon matrix composites fabrication by isotropic casting, flock and spray lay-up and pulp molding, describing physical and mechanical properties 20 p3636 A70-39208
- Composite materials physical properties measurement and defect locations detection by NDT techniques 20 p3636 A70-39210
- Unidirectional and multidirectional carbon/carbon composites quality and performance evaluation by NDT methods, including X ray radiography, ultrasonic test, pulse echo mapping, etc 20 p3654 A70-39211
- Carbon/carbon composites thermal and mechanical properties measurements by NDT including image transducer, IR scanning and ultrasonic methods 20 p3636 A70-39213
- Short graphite fiber classification and orientation control in matrix by electrostatic methods 20 p3654 A70-39215
- Reinforced materials endurance testing, discussing clamping and edge restraints effects 20 p3655 A70-39775
- Composite materials physical properties based on linearly reinforced media models and complex variable functions theory 20 p3655 A70-39860
- Multicomponent composite materials, discussing fiber reinforced structures, clad metals and bulk materials 20 p3650 A70-39947
- Mechanics of composite materials - Conference, Philadelphia, May 1967 20 p3728 A70-40026
- Composite material engineering problems, discussing tensile, compressive and shear strengths, design approaches, unidirectional properties and substance characterizations 20 p3651 A70-40027
- Filamentary composite materials for space vehicles structural design, noting mass reduction, strength, foldability, formability, etc 20 p3656 A70-40030
- Composite materials theory to predict macroscopic physical properties prediction, discussing conductivity, dielectric constant, magnetic permittivity, etc 20 p3729 A70-40032
- Heterogeneous materials statistical theory, evaluating bounds for effective elastic constants by cell model using variational principles and perturbation solution 20 p3729 A70-40033
- Dynamic theories for wave propagation in laminated and fiber reinforced composites, using dispersion curves for transverse and longitudinal motions 20 p3730 A70-40036
- Thermoelasticity of fiber reinforced materials, considering stress concentration in beams and reinforcing fibers buckling under thermal loading 20 p3730 A70-40037
- Continuum mechanics application to elastic composite materials, investigating plane deformation of reinforced medium 20 p3730 A70-40038
- Structural mechanics of continuous fiber reinforced composites, discussing bending and stretching of cylinders, pressure vessels, plates and beams 20 p3730 A70-40039
- Composites potential structural performance, determining mechanical properties for fiber and matrix materials and unidirectional and isotropic composites in cylinders and box beams 20 p3651 A70-40042
- Structural synthesis concept in optimal design of composite material structural systems, considering failure modes of rectangular fiber composite plate 20 p3731 A70-40044

Stress concentrations due to cylindrical inclusions in homogeneous matrix, using stress function methods
20 p3656 A70-40045

Uniaxial fiber composites tensile strength models, including failure analysis
20 p3731 A70-40046

Composite material dynamic properties, discussing modulus and damping during constant strain rate, viscoelasticity, fracture strength and high loading tests
20 p3731 A70-40048

Wire reinforced solid rocket propellant grains mechanical properties and failure modes
20 p3689 A70-40050

Unidirectional fiber reinforced composites strength, obtaining limit load bounds from plasticity analysis
20 p3731 A70-40051

Environmental factors effect on composite materials structural performance, using rate theory
20 p3656 A70-40053

Filament wound composites, investigating interaction of fabrication variables and outward environments by delineating effect of each on structural performance
20 p3731 A70-40055

Composite accelerator electrodes on Cs bombardment microthrusters, testing various designs and electrode coatings
[AIAA PAPER 70-1089] 20 p3693 A70-40246

Mechanical behavior of cylinders with alternating layers of reinforcing and matrix materials derived from governing equations, including equations of motion
20 p3732 A70-40267

Multilayer three dimensionally woven fiberglass-reinforced materials, measuring strength and deformation under tension, compression, bending, torsion and shear tests
21 p3841 A70-40646

Bond stresses between fiber and matrix of fiber reinforced composite materials determined by numerical method based on superposition
21 p3934 A70-41252

Composites reinforced with weakened fibers, investigating weak points effect on fracture toughness by fiber pullout and tensile tests
21 p3843 A70-41889

Fracture toughness and surface energy of fibrous reinforced composites as function of fiber content, strength, diameter, modulus and matrix flow stress
21 p3843 A70-41890

Energy release during flux jump in Nb-Ti single core wires and multifilament composite superconductors
21 p3863 A70-42011

Unidimensional composite materials nonstructural applications, tabulating characteristics
21 p3840 A70-42148

Hot pressed zirconia-zirconia ceramic fiber reinforced ceramic matrix composites, discussing mechanical properties and failure modes
22 p4057 A70-42285

Ceramic fiber technology, forming processes and matrix composites fabrication, discussing chemical and physical compatibility factors, plastic forming, slip casting, cold pressing, etc
22 p4045 A70-42477

High thermal stability glass fibers alternatives improving stiffness-to-weight ratio of resin and Al-based composites used in F-111 boron epoxy wings
22 p4058 A70-42480

Load transfer to elastic fiber in infinite elastic matrix, determining fiber force distribution
22 p4113 A70-42539

Filamentary composites stress wave amplitude distribution calculation and plotting
22 p4114 A70-42645

Ultrasonic wave velocity measurements for flaw detection and modulus of elasticity of carbon-carbon composites
22 p4047 A70-43519

Elastic wave front control volume analysis in laminated and fiber reinforced composite materials
22 p4119 A70-43677

Laminated composites time dependent static strength and reliability under uniaxial tension
22 p4119 A70-43678

Graphite and carbon fiber surfaces, correlating Raman spectrum and shear strength of composite
22 p4060 A70-43680

Unidirectional fiber reinforced composite longitudinal shear deformation, deriving effective shear modulus
22 p4060 A70-43681

Macroscopically homogeneous composites control volume approach, examining Hugoniot equation of state
22 p4060 A70-43683

Mechanical properties and internal stress fields in composite materials reinforced by glass fibrous filler under transverse shear
22 p4061 A70-43724

Ceramic composite materials structural application, improving brittleness and thermal shock resistance via reinforcing refractory fibers
[ICAS PAPER 70-40] 23 p4267 A70-44138

Charring ablative composites pyrolysis products composition determination, comparing chemical analysis techniques
23 p4158 A70-44519

Incremental complementary energy method of stress analysis of orthotropic nonlinear materials having different behavior in tension and compression
[AIAA PAPER 69-119] 23 p4270 A70-44563

German monograph on fiberglass, matrix and filler effect on service life of composites with low fiberglass content
24 p4365 A70-45084

Strong fibrous solids - Conference, London, January 1970
24 p4366 A70-45165

Whiskers and filaments properties compared for fiber reinforcement applications in composite materials production
24 p4356 A70-45167

High melting point fibrous composites, discussing fiber-matrix systems for high temperature applications as in gas turbine blades
24 p4357 A70-45168

Fibrous composites use in compressor blades, discussing materials characteristics requirements relative to environmental and stress conditions in aircraft operational service
24 p4392 A70-45169

Fibrous composites thermomechanical properties derivation by theoretical analysis from basic constituents characteristics, presenting comparisons with experimental results
24 p4366 A70-45170

Fibrous composite interface effects and fracture work, discussing tip stresses of crack normal to fiber, energy dissipation by pullout and debonding in brittle fiber composites, etc
24 p4419 A70-45171

Fibrous composites design for mechanical properties improvement, discussing interfacial properties conflicting requirements as to interlaminar shear, transverse tensile strength, high work of fracture values, etc
24 p4419 A70-45172

Materials design and development for engineering applications, discussing relationships and importance of strength, stiffness, weight, toughness and work of fracture
24 p4419 A70-45174

Unidirectionally solidified carbide reinforced Co-Cr eutectic alloy, examining tensile strength and creep behavior
24 p4358 A70-45236

Unimodal and bimodal distribution of fiber composite properties at different stress levels using quantitative metallography
24 p4359 A70-45250

Thermal IR nondestructive testing of adhesively bonded boron composite/Al honeycomb structures, discussing surface, cross section and instrumentation sensitivity effects
24 p4341 A70-45570

Nonmetallic nonconductive composite materials physical properties by swept microwave frequency nondestructive testing
24 p4345 A70-45705

Stress-strain curves of polycrystalline metals and composites using single crystal elastoplastic model
24 p4425 A70-45779

Betatron monoenergetic electron beams in radiometric, spectrometric and radiographic testing of composite materials
24 p4339 A70-45850

Matched-die compression molding of complex shape structures from composite materials
[SAE PAPER 700751] 24 p4348 A70-45874

Low cost fabrication for solid rocket nozzles using carbon or graphite reinforcements in throat inserts
[SAE PAPER 700796] 24 p4349 A70-45897

Si-carbide composites electrical conductivity from temperature and thickness dependence, obtaining volt-ampere characteristics via computer method
24 p4391 A70-46154

Composite materials tensile strength dependence on reinforced fibers with dispersed tensile strength, using model to predict crack propagation from fiber rupture
24 p4427 A70-46270

COMPOSITE PROPELLANTS

Composite propellants high pressure burning stability with various binders and oxidizers, showing ammonium perchlorate oxidized formulations susceptibility to instability
[AIAA PAPER 69-438] 01 p0160 A70-10852

Aluminized composite solid propellants burning rates in acceleration fields noting time dependent increase
[AIAA PAPER 68-529] 04 p0709 A70-15581

Surface thermal factors influencing ignition delay time of composite solid propellants, using double wavelength optical detector
[AIAA PAPER 70-121] 06 p1128 A70-18043

Burning rate for composite solid propellant, using model with specific gas phase combustion distribution
07 p1422 A70-19584

Heat transfer from composite propellant burning zone to regressing surface measured using microjet burner
07 p1359 A70-19587

Polyvinyl chloride plastisol propellants consisting of fine solid oxidizer and powdered metal, discussing composition, propellant flow, curing time and temperature dependence
07 p1360 A70-19908

Propellants chemistry based on chemically cross-linked binder
07 p1360 A70-19909

Polyurethane-based solid rocket propellants, discussing catalyst modification, mix viscosities, moisture embrittlement, etc
07 p1360 A70-19910

Butadiene prepolymers containing carboxyl functional groups used in binder matrix for solid composite propellants
07 p1360 A70-19911

Processing methods for manufacturing composite solid propellants, describing oxidizer, binder and fuel preparation, propellant mixing and chamber insulation and lining and instrumental analysis
07 p1361 A70-19912

Granular diffusion flame theory application to low pressure burning of composite solid AP propellants
07 p1361 A70-19914

Composite solid propellant ignition characteristics using arc imaging furnace for radiant energy source, discussing minimum initial pressure determined by binder thermal decomposition
09 p1742 A70-23226

Burning solid ammonium perchlorate composite propellants surface structure observation to assess heterogeneous or subsurface reactions, using scanning electron microscope
09 p1742 A70-23234

Composite and double base solid rocket propellants manufactured by French factory for ballistic missiles, discussing plant installations
11 p2030 A70-25520

Composite propellant catalysts /copper chromate and chromite/ thermal decomposition using simultaneous thermogravimetric and differential thermal analysis
11 p2100 A70-26382

Collection of papers on solid propellant technology covering rocket interior ballistics, composite rocket propellants, etc
13 p2472 A70-29602

Low pressure deflagration limit dependence on strand size in terms of cross section dimensions for composite ammonium chlorate propellant
[AIAA PAPER 69-144] 13 p2473 A70-29955

Composite solid propellants surface structure and profile characteristics burning with various oxidizers and polyurethane binder by scanning electron microscopy
14 p2628 A70-30948

Combustion extinguishment of composite solid propellant motors by fluid injection, considering binder, curing agent and burning rate catalyst
[AIAA PAPER 70-641] 16 p2968 A70-33599

Composite solid propellants burning rate and initial temperature relationship, investigating granular diffusion flame model
[AIAA PAPER 70-656] 16 p2963 A70-33618

Burning rate increase of nonmetalized composite propellants in acceleration field, assuming surface retention of ammonium perchlorate particles
16 p2963 A70-33861

Extinction model of composite solid propellant combustion including wall and flame heat release zones
17 p1347 A70-34511

Thermal decomposition of perchlorates evaluated by mass spectrometer, with regard to composite propellants combustion processes
17 p1345 A70-34638

Chemical rocket propellant research covering composite liquid monopropellants, lateral thrust in solid propellant rockets, ELDO third stage, friction losses, etc
17 p1348 A70-35211

Ammonium perchlorate filler fraction effect on viscoelastic behavior, relaxation modulus and failure mechanisms of solid composite propellants
17 p1345 A70-35216

Ignition delay of uncompressed composite solid or hybrid propellant mixtures in rocket engine igniters
18 p3301 A70-36651

Internal ballistics of composite propellant charge in first stage of burning
19 p3489 A70-38373

Ammonium perchlorate composite solid propellant pressure vs burning rate at various temperatures, discussing granular diffusion flame theory
20 p3694 A70-40266

Temperature measurements in gaseous reaction zone near surface of burning composite solid propellant, using modified line reversal pyrometer
20 p3694 A70-40273

- Composite solid propellant thermal ignition from hot wire tests and model 21 p3942 A70-40877
- Multicomponent fuels combustion in air, deriving simplified flame sheet model 21 p3942 A70-40881
- Radiant energy flux effect on atmospheric pressure burning rate of composite solid propellant 23 p4232 A70-44552
- COMPOSITE STRUCTURES**
- NT LAMINATES**
- Structural efficiency of composite tube columns with zero axial coefficient of thermal expansion, discussing three dimensional and planar fiber arrays 01 p0126 A70-10120
- Fiber composite cylinder tensile performance improvement through mechanical residual stress relief by axial straining 01 p0120 A70-10737
- Carrying capacity of shells of revolution obtained with threads spun around metallic shell, including stresses during spinning process 01 p0210 A70-11414
- Bending strength analysis for high strength beam with thin and long fibers embedded in matrix of viscoelastic material noting maximum stress 03 p0584 A70-12934
- Momentless design of composite plate and shell structures with variable elastic constants based on loading and shape requirements 03 p0586 A70-13112
- Singular integral equation applied to elasticity theory of composite beam with or without cavity under torsion 04 p0765 A70-14416
- Thin orthotropic composite circular cylindrical shells buckling under axial and radial loads, satisfying end boundary conditions for clamped and simply supported shells [ASME PAPER 69-WA/APM-21] 04 p0771 A70-14910
- Saint Venant torsion and flexure of composite prismatic and cylindrical bars with circular and concentric interfaces 05 p0936 A70-16318
- Book on analysis of laminated composite structures covering orthotropic materials stress-strain relations, laminated composite shells, plates, beams and columns 05 p0938 A70-16467
- Composite conductors involving conventional conductors and superconductors to obtain satisfactory electrical performance for application to electromagnets 05 p0870 A70-16582
- Digital computer program for analyzing axisymmetrically loaded ring-stiffened segmented composite elastic shells of revolution, giving vibration frequencies 05 p0944 A70-16814
- Dynamics of composite, sandwich and stiffened shell type structures with various geometries 06 p1160 A70-17158
- Thermal and mechanical stresses in rectangular composite beams, considering effects of temperature and reinforcing fiber orientation 06 p1164 A70-17503
- Structural element for discrete element idealization missile and liquid propellant as one composite structure [AIAA PAPER 70-123] 06 p1042 A70-18182
- Buckling-critical composite shell structures, describing pseudo T-rib stiffening and integrated composite design concepts [AIAA PAPER 70-101] 06 p1171 A70-18235
- Rectangular bidirectional composites and sandwich plates three dimensional elasticity solutions 07 p1412 A70-19952
- Vibrating composite beam test method for determining complex dynamic modulus of viscoelastic materials over broad frequency and temperature ranges 07 p1320 A70-19955
- Photoelastic stress analysis of composite structures subjected to gravitational forces using immersion analogy, considering constant acceleration stresses 07 p1413 A70-20038
- Buckling and postbuckling equilibrium behavior of fiber reinforced cylindrical shell under uniform axial compression 09 p1780 A70-23207
- Temperature field distribution in long thin narrow plate composed of materials differing in thermophysical characteristics, creating field by moving heat source on plate 09 p1791 A70-23723
- Vibration behavior theory for elastomechanical systems applied to aircraft and space constructions 10 p1961 A70-25054
- Stiffened fiber composite cylindrical shells minimum weight design, discussing configuration and material parameters 12 p2319 A70-27139
- Composite spherically aeolotropic sphere with isotropic core, analyzing stress concentration during twisting 12 p2327 A70-27836
- Stress concentration in fiberglass reinforced plastic composite cantilever cylindrical shell in round hole region subjected to concentrated load on free supported end 12 p2328 A70-28286
- Axisymmetric postyielded tongue and groove cylindrical joint stress analysis using finite element method 14 p2659 A70-31131
- Stress and deflection of nonisotropic assembled bar and plate composite structures, using computerized matrix displacement method 14 p2660 A70-31133
- Optimal design for composite material structure, considering internal and external reinforcement 15 p2816 A70-32005
- Foamed in place epoxy resins in aircraft composite structures 16 p2937 A70-33369
- Mechanical properties prediction analysis of boron filament wound reinforced composite structures verified by structural tests 16 p2937 A70-33370
- Compact integrated microwave antenna of composite structure involving slotted waveguide planar array capable of operating in three frequency bands 16 p2876 A70-33406
- Boron epoxy composite wing structures design, fabrication and testing 16 p2990 A70-33703
- Optimum fiber orientation for minimum weight boron/epoxy shear panel design 17 p3182 A70-34562
- Composite orthotropic cylindrical shells linear thermoelastic equations solution for fixed end boundary conditions, noting heterogeneity effects on stress distribution 17 p3184 A70-34909
- Composite compression tubes for VTOL aircraft components, describing weight parameters and mechanical properties [AIAA PAPER 70-898] 17 p3193 A70-35809
- Composite wing section design and fabrication utilizing unidirectional glass reinforcement [AIAA PAPER 70-919] 17 p3193 A70-35813
- Honeycomb panels with fiber reinforced facings, obtaining acoustic fatigue design criteria [AIAA PAPER 70-897] 17 p3064 A70-35814
- Buckling of fiber reinforced composite orthotropic plates 18 p3343 A70-36706
- Composite body with free surface under plane deformation, analyzing residual, thermal and dislocation stresses dependence on elastic constants 19 p3544 A70-38332
- Graphite filament composite structure shear strength decrease with modulus increase, examining fiber microstructure effect on interlaminar properties by short beam shear test 20 p3654 A70-39206
- Chemical vapor deposition of carbon matrix material in fiber structure, investigating thermodynamic fundamentals in processes 20 p3654 A70-39207
- Shaping methods for filament wound carbon structures, emphasizing matrix building by chemical vapor deposition 20 p3636 A70-39209
- Laser holography for nondestructive testing of C composite structures, reducing fringe patterns to radial deformation and surface strain for cylinders and cones 20 p3718 A70-39212
- Radial and shearing stresses in hollow composite sphere due to thermoelastic strain nucleus 20 p3719 A70-39602
- Composite structural materials for thermal protection in reentry vehicles applications, evaluating fused quartz yarns, silicone rubber and phenolic resins 20 p3656 A70-40031
- Fiber reinforced composite shell structures stress-strain relations, noting membrane and flexural variables coupling in constitutive relations 20 p3729 A70-40034
- Strains and stresses along interfaces and near fiber ends in composite structures made of reinforced matrix, using photoelastic methods 20 p3730 A70-40035
- Finite element stiffness matrix technique for composite structures, discussing airplane component design program 20 p3730 A70-40040
- Joint designs, attachment methods and load introduction in composite structures, suggesting adhesive bonding 20 p3730 A70-40041
- Cylindrical or tapered composite shell structures optimal design with closed circular or elliptical cross section under combined bending and torsional loads 20 p3730 A70-40043
- Torsion of composite rectangular cross section beam consisting of isotropic media, using Green function and Fourier expansion 20 p3732 A70-40334
- Glass plastic composite electrically heated windshields for aircraft, discussing design, fabrication, qualification testing and service experience 21 p3750 A70-41137
- Linearly elastic skeletal structures, calculating natural frequencies of undamped vibration by computer program 21 p3935 A70-41254
- Darlington composite transistor stability, examining biasing resistance variation effect 22 p3998 A70-43257
- Fiber-reinforced narrow rectangular beam flexural strain analysis by birefringent coating technique, deriving isochromatic and isoclinic patterns 23 p4275 A70-44915
- COMPOSITE WRAPPING**
- Test methods for evaluating tensile, compressive, interlaminar shear and bearing strength properties of carbon yarns and flat and tubular composites 08 p1529 A70-21881
- COMPOSITES**
- U COMPOSITE MATERIALS**
- COMPOSITION [PROPERTY]**
- NT ATMOSPHERIC COMPOSITION**
- NT ATMOSPHERIC MOISTURE**
- NT ATOM CONCENTRATION**
- NT BODY COMPOSITION [BIOLOGY]**
- NT CARBON DIOXIDE CONCENTRATION**
- NT CHEMICAL COMPOSITION**
- NT CONCENTRATION [COMPOSITION]**
- NT GAS COMPOSITION**
- NT IONOSPHERIC COMPOSITION**
- NT LUNAR COMPOSITION**
- NT METEORITIC COMPOSITION**
- NT METEOROID CONCENTRATION**
- NT MOISTURE CONTENT**
- NT PLANETARY COMPOSITION**
- NT PLASMA COMPOSITION**
- Stoichiometric compositions of niobium dioxide to pentoxide range, investigating X ray characteristics and thermal stability 07 p1315 A70-20312
- COMPOUND HELICOPTERS**
- High speed compound helicopters with rigid and hinged rotors noting features, advantages and construction 05 p0794 A70-16351
- Compound helicopter in civil aviation to alleviate air traffic congestion, discussing design and operative capacities of S-65-200 10 p1804 A70-24046
- Second generation helicopter design, considering compound, convertible and electrically powered configurations 17 p3018 A70-35549
- H3-E Sprinter semicompound helicopter with pneumatic rotor drive and side mounted fans for forward flight 17 p3018 A70-35626
- Structural reliability testing methods and loads prediction for rotary wing vehicle components, considering AH-56A compound helicopter 19 p3356 A70-38612
- S-65-200 Commercial Compound Aircraft design for dispatch reliability and maintenance 19 p3356 A70-38823
- Metropolitan air transit system design, considering compound helicopters, automatic control by central computer, onboard avionics system and terminal facilities 21 p3956 A70-41250
- COMPOUNDING**
- Glass fiber-reinforcing techniques of polymers, discussing coating and compounding processes 01 p0104 A70-10775
- COMPRESSED AIR**
- Improvement in power output of ramjet installed under wing using air compression [ONERA-TP-783] 06 p1133 A70-18467
- Rocket roll control by secondary compressed air injection via slender fins inserted into nozzle convergent 21 p3931 A70-41953
- COMPRESSIBILITY**
- P-v-T-x relationships determination method for gaseous mixtures at high pressures and temperatures, studying He-nitrogen mixtures compressibility 07 p1420 A70-19205
- Tantalum single crystals elastic constants temperature dependence, considering compressibility and shear properties 14 p2596 A70-30841
- Finite elements for three dimensional compressible and incompressible solid continua based on minimum potential energy and variational principles 14 p2659 A70-31128
- Human skull porous dipole layer shear and compressive properties, measuring static and dynamic strain rates 15 p2683 A70-32308

- Nonlinear least squares method reducing Burnett data to compressibility factors and virial coefficients
17 p3136 A70-35594
- Compressibility factors and virial coefficients for He-N mixture, He and nitrogen at low temperatures and high pressures
18 p3290 A70-36250
- Gas lubrication with injection at large compressibility numbers, deriving asymptotic solution
20 p3637 A70-39817
- Apollo 11 lunar crystalline rock, microbreccia and fines compressibilities at room temperature, loading-unloading and pressure volume curves
21 p3918 A70-41679
- Transitional flow separation upstream of compression corner for two dimensional model relationship to attached flow and boundary layer transition on plate
21 p3746 A70-41864
- Compressibility, viscosity and thermal conductivity of dense gases, examining high temperature and pressure effects
23 p4222 A70-44431

COMPRESSIBILITY EFFECTS

- Symmetry energy of infinite nuclear matter calculated for cases of constant density and minimum saturation energy by density variation, considering finite compressibility effects
01 p0148 A70-11105
- Stress-strain analysis of rectangular plates under concentrated load, noting sealed liquid compressibility effect on deflections and bending moments
02 p0388 A70-12499
- Impact against elastoplastic blank allowing for base and striker compressibility, giving solution in region of plane wave first reflection from base
05 p0947 A70-17016
- Rarefied gas shear flow over infinite plane wall, using Boltzmann-Krook-Welander equation to determine compressibility effect on Knudsen layer
06 p1048 A70-18327
- Compressibility effect on density explaining Mercury-Venus density near equality to earth-Mars-moon, discussing theory of rotational break-up of parent planets
08 p1563 A70-20496
- Strain energy method applied to stability analysis of short longitudinally reinforced cylindrical shells under axial compression
08 p1584 A70-20536
- Air compressibility effects on aerodynamic characteristics of slender rectangular wings moving at subsonic speed near earth surface approximated by lifting surface theory
10 p1801 A70-24276
- Pneumatic compression effects on canine cardiovascular dynamics after hemorrhage tested in G-suit inflation
11 p1988 A70-26516
- Swirling and meridional flow induced by steady rotation of gravitating sphere in compressible monatomic gas, considering compressibility effects and surface layer
[ASTME PAPER MR-69-714] 11 p1978 A70-26690
- Compression effects in air-oxygen mixture on male mice, observing no adversity on mortality, growth and nitrogen content
13 p2353 A70-29436
- Turbulent boundary layer structure, considering flow properties prediction, wakelike behavior, bursts, compressibility, transport properties, etc
17 p3068 A70-34665
- Helicopter rotors noise intensity prediction for high tip Mach number, including compressibility and thickness effects
17 p3015 A70-34729
- Infinite elastic plates traveling wave flutter in compressible flow, investigating viscous damping effects on critical flow velocity
18 p3343 A70-36701
- Fluid inertia and compressibility effects considered in equations for foil over lubricating film
[ASME PAPER 69-WA/LUB-10] 19 p3435 A70-37615
- Large deflection of simply supported aluminum alloy annular plate with nonlinear stress-strain curve, considering compressibility effects and membrane force
20 p3718 A70-39138
- Umbral flash as magnetoacoustic wave, examining Ca II K line variations formation during adiabatic compression
21 p3885 A70-40958
- Axisymmetric laminar compressible jet flow characteristics, allowing for compressibility effects due to temperature dependent density and viscosity variations
24 p4325 A70-45584
- Precompression and pressurization effects on ductile-brittle transition of polycrystalline cast Cr, W and Mo bcc transition metals
24 p4365 A70-46371

COMPRESSIBLE BOUNDARY LAYER

- Density and heat transfer effects on compressible turbulent boundary layers used to investigate velocity

- and temperature profiles, skin friction, Mach number and Reynolds number
01 p0003 A70-10936
- Unsteady heat transfer from porous flat plate with impulsive motion and rising temperature, analyzing compressible boundary layer equations using Laplace transform
01 p0067 A70-11390
- Finite difference solution of compressible turbulent boundary layer equations of motion, using eddy viscosity concept
02 p0286 A70-12353
- Integral method for studying wall heat transfer influence on compressible boundary layer on cone at angle of attack in supersonic flow
03 p0409 A70-13953
- Numerical integration of equations of motion of three dimensional laminar compressible boundary layers
[DVL-915] 06 p1033 A70-17229
- Skin friction law for compressible boundary layer allowing calculation of coefficient of friction for isothermal walls with heat transfer
06 p1033 A70-17232
- Nonsimilar laminar boundary layer solutions with negative pressure gradient compared to experimental boundary layer velocity profiles, momentum and displacement thicknesses
[AIAA PAPER 69-35] 07 p1256 A70-19312
- Unsteady boundary layer in compressible fluid laminar flow over accelerating semiinfinite flat plate
07 p1258 A70-19566
- Heat insulated plate compressible boundary layer energy equations approximate solutions in hypergeometric functions
10 p1966 A70-23867
- Compressibility transformation theory extended for turbulent boundary layer, involving mass transfer with/without chemical reactions
[AIAA PAPER 69-161] 12 p2211 A70-27825
- Axisymmetric compressible boundary layer on body of revolution transformed into two dimensional turbulent boundary layer
13 p2391 A70-29995
- Laminar compressible boundary layer similar solutions for axisymmetric blunt body, considering viscosity and density variations
16 p2833 A70-33123
- Laminar compressible flat plate boundary layer dependence on Prandtl number and viscosity-temperature relations
16 p2893 A70-33673
- Control efficiency of flaps at hypersonic speeds, considering thick turbulent boundary layer compression process
16 p2836 A70-33751
- Fluctuation measurements at wall and across laminar, transitional and turbulent compressible boundary layers on flat plate, using hot film probes
[AIAA PAPER 70-745] 17 p3066 A70-34498
- Roughness effects on heat transfer to surfaces in supersonic compressible turbulent boundary layer
[AIAA PAPER 70-742] 17 p3066 A70-34505
- Compressible turbulent boundary layers with heat and mass transfer in two dimensional and axisymmetric flows, using eddy transport coefficients
[AIAA PAPER 70-741] 17 p3066 A70-34506
- Favorable pressure gradient effect on compressible two dimensional supersonic turbulent boundary, using temperature and pressure probes and shear balance
18 p3242 A70-36690
- Stratford prediction method of separation position for compressible boundary layer flow
19 p3406 A70-38617
- Compressible hypersonic turbulent boundary layers solution by finite difference method, relating mixing length to velocity profile shape factor
20 p3684 A70-40269
- Nonstationary compressible laminar boundary layer similar solutions by parameter-invariant method, obtaining velocity and temperature profiles by partial differential equations numerical integration
21 p3806 A70-40555
- Flat plate compressible laminar boundary layer flow with variable fluid properties, using series solution by splitting up flow variables into sets of universal functions
21 p3806 A70-40825
- Accelerated self similar compressible laminar boundary layer flows with and without mass transfer, obtaining numerical solutions
21 p3807 A70-41031
- Two dimensional compressible laminar MHD boundary layer flow across flat plate with heat transfer, considering continuity, momentum and energy equations
21 p3856 A70-41039
- Compressible boundary layer equations with second order surface curvature and displacement effects
21 p3809 A70-41751
- Unsteady compressible boundary layer formation on rotating disk, assuming uniform fluid rotation
22 p4009 A70-42616

- Vane type vortex generators to prevent turbulent compressible boundary layer separation, measuring drag in supersonic flow
23 p4133 A70-44527

COMPRESSIBLE FLOW

NT MAGNETOHYDRODYNAMIC FLOW

- Direct and incremental variational formulations for steady compressible lubrication based on finite element method, noting limitations of numerical techniques
[ASME PAPER 69-LUB-12] 01 p0102 A70-10393
- Compressible swirling inviscid nozzle flows approximate solution showing changed choking at throat, axial velocity distributions and reversing in subsonic region
01 p0003 A70-11128
- Compressible gas flow problem in point body gravitational field solved with reference to sun and interstellar gas
01 p0172 A70-11489
- Compressible flows with circular sector hodographs, discussing Chaplygin equation for simple wedge flow and theorem on sonic jets
04 p0613 A70-14612
- Compressible fluid flow satisfying perfect gas equation in presence of thin foil, developing operators characterizing incompressible and compressible flows without Hall effect
05 p0790 A70-16158
- Pressure distribution and drag measurements at flat triangular bodies and rectangular plates with blunt trailing edge in compressible flow
06 p0965 A70-17243
- Viscosity and heat conductivity effects in compressible fluid flow past finite body showing dependence on spatial dimensions
10 p1800 A70-24135
- Unsteady compressible laminar boundary layer flow around flat plate influenced by compressibility as function of Mach number
[ONERA-TP-803] 10 p1869 A70-24543
- Closed streamline low Mach number compressible fluid flow without temperature restrictions, noting incompressible flow behavior
10 p1869 A70-24547
- Compressible flow equations of motion applied to incompressible fluid flow through nozzle with eddies and springs
10 p1871 A70-24796
- One dimensional compressible constant entropy flows stability, noting unstable regions with fluid particles undergoing compression
11 p2034 A70-25679
- Compressible turbulent boundary layer with adverse pressure gradients and crossflow over revolving bodies, integrating numerically three dimensional compressible integral equations
11 p2035 A70-25689
- Numerical techniques and solutions for compressible and incompressible laminar separated flows using time dependent finite difference equations
[AIAA PAPER 68-741] 11 p2035 A70-25972
- One dimensional compound compressible nozzle flow solution dependence on initial conditions and nozzle geometry, discussing applications to bypass turbojets and solid propellant motors
11 p1976 A70-26137
- One dimensional compressible flow with heat addition in nonconstant area duct extended for friction addition, discussing critical thermal shocking
11 p2041 A70-26651
- Compressible turbulent plane Couette flow solution with variable heat transfer based on von Karman model extended to arbitrary wall temperature
12 p2211 A70-27839
- Compressible turbulent boundary layers velocity profiles, Coles universal wake function, least squares methods, wake-wall representation, etc
12 p2157 A70-28080
- Unsteady compressible pipe flows with large cross sectional variations studied by two dimensional difference method
13 p2386 A70-28806
- Viscous and compressible fluid flow in presence of plane plate
13 p2389 A70-29489
- Contraction coefficients for compressible discharge through axisymmetric sharp edged orifice, obtaining approximate analytical expression based on one dimensional theory
13 p2389 A70-29549
- Aerodynamic pressures dependence on angle of incidence for profiles in adiabatic compressible flow
16 p2833 A70-33074
- Laminar and turbulent boundary layer equations solutions for incompressible/compressible flows about two dimensional and axisymmetric bodies, using finite difference method
[ASME PAPER 70-FE-A] 16 p2892 A70-33641
- Aerodynamic drag coefficients of micron size particle clouds in compressible transonic flow, using light extinction method
16 p2894 A70-33882

Forces on two dimensional oscillating airfoil in subsonic compressible wind tunnel flow, solving partial differential equation for pressure potential by integral transform technique

16 p2839 A70-34248

Local skin friction law for turbulent boundary layers in incompressible flow, applying rule for compressible flow conditions

17 p3075 A70-35922

Pressure distribution measurements on wedges in compressible flow at Mach 0.5-2.2, discussing wedge angle, Mach number and boundary layer thickness effects

17 p3013 A70-35923

Compressible flow of two component two phase mixtures through convergent nozzles and orifices, determining initially or annular dispersed flow patterns

18 p3239 A70-36231

Plane compressible sonic flow around symmetrical cylinder subjected to parallel incident flow, using function-theoretic method

18 p3241 A70-36378

Infinite elastic plates traveling wave flutter in compressible flow, investigating viscous damping effects on critical flow velocity

18 p3343 A70-36701

Optimal control for one dimensional compressible gas flow, combustion and heat exchange, described by first order partial differential hyperbolic equations

19 p3402 A70-37240

Compressible fluids flow with conductivity tensor in presence of thin wing under orthogonal fields, reducing integral equation to Fredholm equation

19 p3351 A70-37599

Direct and incremental variational formulations for steady compressible lubrication based on finite element method, noting limitations of numerical techniques

[ASME PAPER 69-LUB-12] 19 p3436 A70-37616

Steady compressible supersonic planar flow of viscous heat conducting fluid under linearization freestream conditions, describing slip flow past finite flat plate

20 p3557 A70-39228

Plasma accelerator compressible turbulent boundary layers numerical calculation taking into account MHD effects, electron thermal nonequilibrium and finite rate ionization

20 p3682 A70-40017

Boundary conditions on vector and scalar potentials in viscous three dimensional hydrodynamics, investigating compressible flow problems

20 p3612 A70-40115

Compressible plasma axisymmetric channel flow under electromagnetic forces and ohmic heating, noting velocity profiles and current density

[AIAA PAPER 70-1098] 20 p3683 A70-40239

Heat transfer from thin plate in compressible gas flow, considering interface temperature as nonanalytic function

21 p3953 A70-42086

Compressible plasma flow in axisymmetric channels under EM body forces and Joule heating

23 p4228 A70-44934

German monograph on casing and hub wall friction effects on three dimensional flow in turbocompressors in subsonic compressible working fluids

24 p4287 A70-45096

Viscous heat conducting compressible fluid flow past slender axisymmetric body, presenting Navier-Stokes hypersonic strong interaction theory

24 p4289 A70-46020

COMPRESSIBLE FLUIDS

Vortex diffusion in viscous compressible fluid, deriving nonlinear differential equations from density velocity and pressure discontinuities considerations

01 p0060 A70-10145

Reflection and transmission characteristics of screens in duct obstructing shock propagating in unsteady compressible fluid, describing theoretical models and experimental detection

01 p0060 A70-10224

Cauchy problem solution asymptotic behavior for linearized system of rotating compressible fluid at time approaching infinity

01 p0064 A70-11031

Navier-Stokes hypersonic weak interaction theory for viscous heat conducting compressible fluid flow past slender axisymmetric body

01 p0003 A70-11097

Pressure waves in accelerated sphere filled with compressible liquid, using convolution integral for pressure distribution on inner surface

01 p0067 A70-11186

Navier-Stokes equations for compressible gas, generalizing viscous channel flow of heat conducting gas to slip flow of rarefied gas

01 p0068 A70-11579

Boundary layer processes under unsteady suction allowing for compressibility, relating suction value to external velocity and wall temperature

03 p0465 A70-13275

Flow characteristics of compressible fluid in compressor or turbine stage, determining radial distribution of downstream Mach number

03 p0410 A70-14271

Boundary layer equations closed form similarity solutions for laminar jet of compressible pseudoplastic fluid, discussing velocity transverse behavior

04 p0671 A70-15053

Laminar and turbulent flows of compressible media in rotating pipes, analyzing velocity distribution, angular velocity and Coriolis effects using Abel equation

04 p0672 A70-15159

Poloidal magnetic field influence on compressible fluid convection in spherical shells, using variational method to obtain stability criteria

04 p0758 A70-15695

Compressible fluid flow velocity profile in turbine stage evaluated by streamline correlation and actuator disk method

06 p0967 A70-17469

Unsteady interaction of compressible fluid and flat circular deforming elastic membrane analyzed by coupled computer program method

[AIAA PAPER 70-75] 06 p1039 A70-18082

Navier-Stokes equations numerical integration in Eulerian coordinates, applying results to compressible and incompressible fluids steady flow

[AIAA PAPER 70-2] 06 p1040 A70-18113

Acoustic impedances of periodically compressed thin fluid layers, discussing effect of mass, viscosity, elasticity and compressibility of medium

06 p1107 A70-18475

Solid surface-compressible liquid drop high speed impact damage, discussing contact pressure

06 p1053 A70-18611

Steady turbulent boundary layer of compressible perfect gas on heat insulated surface with suction and longitudinal pressure gradient

07 p1254 A70-19081

Hydrostatic journal bearing dynamic rigidity for compressible and incompressible fluids, describing fluid film elasticity and damping characteristics

07 p1293 A70-19121

Dense gas effects in free piston hypersonic wind tunnel, discussing Longshot facility, free piston cycle, reservoir conditions decay and hypersonic nozzle flow

[AIAA PAPER 69-169] 07 p1249 A70-19310

Transition from compressible to incompressible fluid assuming isothermal flows and finite stresses for density at or different from initial value

10 p1863 A70-24008

Quasi-one dimensional motion of perfect compressible fluid through pipe, considering one dimensional schemes in aerodynamics

10 p1865 A70-24102

Viscous compressible fluid steady laminar flow between coaxial cylinders, studying flow characteristics for uniform inner cylinder velocity

10 p1870 A70-24792

Heat conduction and viscosity effects on compressible fluids characteristics

11 p2037 A70-26399

Invariant transform of motion and continuity equations for steady three dimensional flows of compressible fluids in absence of massive forces

11 p2041 A70-26598

Regularity domain and singularity location of stream function of transonic two dimensional compressible fluid flow, using integral operators

12 p2260 A70-26972

Thermal boundary layer equations solved for compressible gas at rotating axisymmetric surface with viscosity as linear function of temperature

12 p2331 A70-27698

Reciprocity principle for biased and two component compressible plasmas

12 p2282 A70-27971

Plane electromagnetic wave interaction with compressible plasma fluid moving with uniform velocity in vacuum, calculating reflection and transmission coefficients

13 p2462 A70-29101

Compressible fluids steady state equations invariant transformation, establishing sound speed-Mach number relation

13 p2389 A70-29458

Compressible fluids Alfvén flow with Hall effect presence of thin foils, reducing problem to Fourier integral equation

13 p2442 A70-29484

Compressible fluid two dimensional irrotational flow past Roshko model in channel, deriving exact solution by hodograph method

13 p2341 A70-29487

Linearized two dimensional double vortex sheet model of inviscid compressible jet instabilities over all Mach numbers

15 p2722 A70-32375

Kinetic energy and pressure distribution of three dimensional compressible fluid flow, using invariant transformation of Euler motion equation

16 p2890 A70-33073

Aerodynamic forces exerted by compressible fluid on airfoil cascade in subsonic potential flow

16 p2833 A70-33075

Lagrangian invariants of inviscid compressible fluid dynamics applied to hydrodynamic equations

17 p3070 A70-35333

Free convection in compressible viscous heat conducting fluid, determining parameters leading to onset

17 p3198 A70-35697

Acoustic turbulence spectrum in compressible fluid with potential motion, using complex traveling wave amplitudes in hydrodynamic equations

18 p3242 A70-36637

Axisymmetric one dimensional compressible flow theory applications to compressible fluids ducted flow [ASME PAPER 70-GT-82] 18 p3243 A70-36882

Compressible and incompressible Stokesian fluids motion described by finite element analog of Navier-Stokes equation

20 p3607 A70-38999

Compressible viscous fluid steady plane flow in laminar boundary layer on impermeable isothermic surface, describing parametric method of integrating flow equations

20 p3611 A70-39806

French book on compressible fluid mechanics covering adiabatic, one and two dimensional flows, linear equations, friction factor, heat exchanges, supersonic, subsonic flows, etc

21 p3743 A70-40624

Hodography of compressible fluids three dimensional irrotational isentropic flow

21 p3808 A70-41439

Acoustic wave propagation in continuum of inviscid compressible heat conducting fluid, determining stability criteria

22 p4073 A70-42571

Miles-Howard theorem extension to gravitationally stratified compressible fluid containing parallel shear flow, considering stability against adiabatic perturbations

23 p4179 A70-43976

Turbulent nonadiabatic flow of compressible gas at inlet and main sections of variable cross section plane channel

23 p4183 A70-44739

COMPRESSION

Protein metabolism of mice exposed to compression of air-oxygen mixture containing 27 percent oxygen, showing relationship to food intake

01 p0028 A70-11363

Lateral compression of rocks and global shells multilayers, using equations for buckling of single free stratum

18 p3255 A70-37076

COMPRESSION BUCKLING

U BUCKLING

COMPRESSION LOADS

NT AXIAL COMPRESSION LOADS

NT IMPACT LOADS

Welded flat plate specimen to evaluate low cycle crack initiation and propagation of butt welds under compressive loading, discussing design, fabrication and testing

[ASME PAPER 69-SESA-7] 01 p0199 A70-10452

Curved cylindrical panel flutter in presence of uniform compressive load, taking into account relationship between actual and ideal shape

01 p0202 A70-10946

Molybdenum cylinders strength and plasticity under various compression and cyclic tensile loads

02 p0315 A70-11662

Mathematical model for local postbuckling strength of flat truss core sandwich panels loaded in compression, considering application to Ti structures

02 p0386 A70-11948

Load and strain trajectory vectors components determined for tension followed by transverse compression in five dimensional space

02 p0390 A70-12803

Buckling equations for thin nonlinearly elastic circular plates with affine initial deformation, considering Lure theory and variational principle for uniform compression load

03 p0589 A70-13336

Stability analysis of orthotropically symmetric strip under uniformly distributed compressive forces applied to shorter ends, deriving critical load formula

03 p0590 A70-13402

Elastoplastic bodies stability under compression, using theory of small elastoplastic deformations and linearized equations of nonlinear elasticity theory

03 p0591 A70-13440

Local buckling and failure of thin walled compression column with supported flanges, analyzing strength reduction by eccentricity

03 p0600 A70-14254

Elastoplastic bar stability compressed by tangential force, showing ductility effect on critical parameters, perturbed motion and stability loss process

04 p0767 A70-14484

Spherical shells axisymmetric equilibrium properties under uniformly distributed external compression

04 p0773 A70-15008

Initial deflection effect on elastic cylindrical shell stability under compression, finding critical load by determining limiting point in successive loading

04 p0773 A70-15009

Metals and alloys creep under tension and compression at elevated temperatures, considering plastic deformation equation applicability

04 p0707 A70-15265

Computational procedures for matrix analysis of stability and vibration of thin flat rectangular plates in longitudinal compression

05 p0927 A70-16010

Compressive forces eccentricity influence on circular cylindrical shell stability noting relation to bending moments

05 p0936 A70-16239

Isotropic elastic cylindrical shell stability under combined compressive and axisymmetric local loads, using equilibrium equations for shallow shells

05 p0936 A70-16240

Shape optimization of elastic rod compressed by force directed toward point on undeformed rod axis, deriving optimal bending line

05 p0937 A70-16373

Resistance strain gauge load cell for measuring compressive loads under high hydrostatic pressure, discussing gauge bonding

05 p0848 A70-16377

Buckling behavior of elliptical cylinders under normal pressure using linear thin shell theory and Galerkin method, compared with test results
[AIAA PAPER 70-105]

06 p1169 A70-18038

Elastic membranes deformation compressed by restraints using discrete dynamic programming

07 p1400 A70-18680

Metallic adhesion produced by surfaces compression, discussing asperities plastic deformation and macrodeformation caused by contact area growth

07 p1292 A70-18939

Stress relaxation in polytetrafluoroethylene (PTFE) at various compression deformations and temperatures, considering residual stresses degree

07 p1321 A70-20228

Limiting equilibrium of shells of revolution with different yield points under tension and compression

08 p1583 A70-20527

Rib-reinforced cylindrical shells stability under longitudinal compressive loading, studying stress-strain state using network method

08 p1583 A70-20528

Limiting equilibrium of rigid-plastic cylinder subjected to compression by concave stamps

08 p1583 A70-20533

Hertzian contact stress deformation coefficients defined in transcendental equation with elliptic integrals noting errors

08 p1593 A70-21617

Limiting equilibrium of unbounded cracked elastic plate with circular hole, studying crack propagation under compression

09 p1769 A70-22121

Optimizing shape of elastic bar compressed by polar force obtained by determining functional extremum representing volume of bar at constant critical force

09 p1769 A70-22252

Elastic beam stability, natural frequencies and critical forces under longitudinal impact with nonuniform compressing force

09 p1780 A70-23116

Flat rectangular elastic body stable oscillations with clamped base under compression loads, deriving difference scheme for approximation

09 p1782 A70-23297

Buckling stability of slender knife-edge suspended rods subjected to compression end loads

10 p1955 A70-24053

Cylindrical coil springs cold winding loading processes, considering initial tension or compression of wire and combined stresses

10 p1894 A70-24297

Minimum weight design for symmetrically stiffened cylindrical shells under compression based on linear orthotropic stability theory

10 p1958 A70-24560

Limiting load for annular plates made of material having different yield points in tension and compression

11 p2129 A70-25560

Rectangular conical shells reinforced along ribs by belts under tension/compression calculated by initial functions method

11 p2130 A70-25568

Compressive stress critical moment induced instability and weakening incorporated in thin walled beam design

11 p2131 A70-25590

Compression process in turbulent boundary layer on control surface at hypersonic speeds, noting influence on surface effectiveness and heating
[ONERA-TP-814]

11 p1979 A70-25815

Elastic bending of clamped and supported elliptic and parabolic plates under external pressure investigated by lines of equal deflection

11 p2133 A70-25839

Polycrystalline lanthanides and metals resistance to deformation under compression and tension at different temperatures and strain rates

12 p2257 A70-28273

Cantilevered column stability under constant lower load in presence of external damping

13 p2510 A70-28733

Critical loads and stability of isotropic cylindrical shells under uniformly distributed longitudinal compression loads based on network method

13 p2514 A70-29287

Buckling equations for thin nonlinearly elastic circular plates with affine initial deformation, considering theory and variational principle for uniform compression load

14 p2657 A70-30714

Elastic membranes deformation compressed by restraints using discrete dynamic programming

15 p2813 A70-31472

Bifurcation stability in geometrically nonlinear shells of revolution under transverse loads, considering tension and compression deformation

15 p2817 A70-32168

Stability characteristics of elastic shallow shells of revolution in temperature field and under compression, reducing variational equation of bending by Ritz method

15 p2817 A70-32169

Hysteresis loop behavior under tension-compression cycle fatigue related to Meyer strain hardness values of cyclically strained metals

16 p2934 A70-34334

Temperature and constant compressive loading effects on mechanical characteristics of fiberglass reinforced plastics

17 p3127 A70-35341

Anisotropic disk compressed by isotropic ring of smaller radius, considering elastic equilibrium

18 p3336 A70-36134

Barium fluorides single crystals compression, investigating stress-strain behavior and dislocation mobility

19 p3483 A70-37339

Buckling equilibrium equations for thick rectangular block under compression loads, noting bifurcation points

19 p3536 A70-37683

Molybdenum cylinders strength and plasticity under various compression and cyclic tensile loads

19 p3453 A70-38436

Compressive force on elastic plate of arbitrary shape related to number of equilibrium forms, using Karman equations

20 p3724 A70-39861

Weighing systems electronic load cells calibration for tension and compression loading, attributing non-repeatability to bending moments
[SAWE PAPER 816]

20 p3634 A70-40356

German monograph on refractory materials softening under bending and compression at high temperatures

22 p4061 A70-43742

Fatigue strength of stiffened aircraft panels subjected to repeated buckling by compression loads
[ICAS PAPER 70-35]

23 p4267 A70-44132

Cylindrical shell stability under off-center compression loads applied to end faces, determining collapse conditions

23 p4268 A70-44169

Axially compressed circular cylindrical shells subject to relaxed boundary conditions, calculating buckling loads as function of length to radius ratio
[ASME PAPER 70-APM-O]

23 p4269 A70-44397

German monograph on notched structural steels fatigue properties and crack propagation under tensile-compressive alternating loads

24 p4356 A70-45086

COMPRESSION TESTERS

U COMPRESSION TESTS

COMPRESSION TESTS

Offset yield strengths of TD-Ni and Al-aluminum oxide SAP type two phase alloys in tension and compression

01 p0119 A70-10736

Polyethylene and polypropylene mechanical behavior under tensile and compressive loads and subject to hydrostatic pressure, obtaining tensile nominal stress-strain curves for various pressures

03 p0517 A70-14201

Compression failure of unidirectional fiberglass reinforced plastics

04 p0712 A70-14487

Compression test for ductile materials based on Saint Venant principle of plasticity to reduce friction effects on deformation by lubricant pressurization

04 p0776 A70-15373

P-v-T-x relationships determination method for gaseous mixtures at high pressures and temperatures, studying He-nitrogen mixtures compressibility

07 p1420 A70-19205

Test specimen shapes for determining tensile, compressive and edge-wise shear properties of reinforced plastic laminates

08 p1529 A70-21878

Tension, compression and in-plane shear tests to obtain boron epoxy composite materials mechanical properties to design FB-111 wing box extension

08 p1529 A70-21879

Test methods for evaluating tensile, compressive, interlaminar shear and bearing strength properties of carbon yarns and flat and tubular composites

08 p1529 A70-21881

Compression test data of Al-B composites used for predicting structural element failure

08 p1523 A70-21886

Test standards for boron epoxy flat laminates, proposing specimen geometries and testing methods

08 p1530 A70-21887

End plugs bending moment and shear loads reduction during compression tests of composite orthotropic cylinders

08 p1594 A70-21889

Failure compression tests of flat rectangular Al alloy panels presented in unitary form, adopting structural load index for solution from weight standpoint

09 p1782 A70-23376

High temperature compressive creep tests at constant stress, describing strain measurement techniques and servocontrolled compressive equipment

12 p2206 A70-27214

Stress-strain relationships model for nonlinear restrained cylinders, using compression tests and finite element method

14 p2660 A70-31135

Materials testing machine for tension, compression and flexure at constant strain rate and for fatigue

16 p2900 A70-33067

Plastic materials Poisson ratio and Young modulus measurements by triaxial compression method

17 p3089 A70-35048

Strain measuring apparatus for multiple samples simultaneous compression tests at near absolute zero temperatures

20 p3632 A70-39628

Thin walled column buckling relation to plate element buckling, studying deformation, stress state, failure mechanism and ultimate load

22 p4116 A70-43214

COMPRESSION WAVES

Steady one dimensional flow in gas filled cylindrical tube, studying shock induced compression wave generated by sudden piston acceleration

01 p0062 A70-10804

Compression wave mechanism of supersonic combustion controlled by mixing, discussing multiple injector design, thermal compression and geometry effect

02 p0399 A70-12041

Resonant compression waves in geomagnetic tail estimated for frequency and spatial distribution by single layered two dimensional model

04 p0680 A70-15127

Premixed compression initiated supersonic combustion, noting sensitivity to small perturbations in inlet flow variables
[AIAA PAPER 68-995]

07 p1421 A70-19318

Multiple scattering of plane time harmonic compressional elastic wave impinging on parallel circular cylindrical inclusions in finite domain, analyzing stress field

08 p1592 A70-21469

Shock wave configurations across compression cascades in transonic approach flow

09 p1604 A70-22657

Compression stress wave generated by longitudinal impact of two cylindrical elastic rods, measuring propagation along rod by strain gage stations

12 p2325 A70-27617

Solar radar echo characteristics, discussing coronal compressional waves and refraction by plasma clouds and moving plasma irregularities

13 p2370 A70-29852

Circular cylindrical cavity in elastic space, calculating stresses due to incident plane harmonic compression wave

15 p2819 A70-32204

Gravitational compression of spherical cloud, determining asymptotic features of gas motion near center

15 p2808 A70-32882

Circular inclusion interface separation in matrix under incident compressive waves interpreted for fiber reinforced composites

17 p3185 A70-34963

Omni-directional dynamic stress gage as embedded elastic inclusion, discussing transient response to ground shock compression wave pressure

19 p3422 A70-37699

Compressional sound waves electromagnetic generation in metals in static magnetic fields, examining acoustic amplitude variations

22 p4074 A70-42968

Exponential compression wave propagation in conical rod with smooth tapering cross section

22 p4121 A70-43726

Two dimensional steady flow around slender profiles at free transonic stream with curved compression shocks, approximating by hodographic method

23 p4131 A70-44023

Shock wave structure calculation in liquids containing gas bubbles, taking into account compression wave steepening by convection

24 p4326 A70-45783

COMPRESSIVE STRENGTH

Axial and traction loaded boron epoxy laminates tensile and compressive elastic properties and strengths compared from test data including strain gauge measurements

03 p0586 A70-13115

Creep, ductility and short term tensile and compression strength test facility for graphite in 300-3500 K temperature range

05 p0875 A70-17068

Compression strength of polyester resin reinforced with hard drawn and softened steel wires, discussing variations from predicted performance

07 p1320 A70-19954

Dynamic compressive properties of polypropylene, polystyrene bead and extruded polystyrene foams tested at given strain rate under room temperature

08 p1527 A70-21329

Compressive yield strength of iron meteorites, discussing flow stress, microstructure, grain size, plastic deformation, slip lines, etc

18 p3314 A70-36498

Composite material engineering problems, discussing tensile, compressive and shear strengths, design approaches, unidirectional properties and substance characterizations

20 p3651 A70-40027

Weightlessness and immobilization effects on mechanical tolerance of bone compressive and breaking strength in monkeys

22 p3973 A70-43648

COMPRESSOR BLADES

Ultrasonic detection of service induced cracks near tenon base region of second stage A1 compressor disks

01 p0096 A70-10003

Two stage axial flow compressor with variable pitch guide vanes, discussing HF vibration reduction of rotor blades

01 p0166 A70-11419

Rotating compressor vanes vibration frequencies and modes using shell theory, considering Coriolis forces and rotation rates effects

01 p0211 A70-11427

Single stage experimental front fan designed for aircraft engines, measuring overall and blade element performances

02 p0355 A70-12258

Radiation pyrometers development for in-flight measuring and controlling aircraft engine compressor blades temperature

[SAE PAPER 690432]

03 p0480 A70-12900

Discrete frequency noise generation from axial flow compressor blade row, using experiments in small scale Freon loop

[ASME PAPER 69-WA/FE-22]

04 p0733 A70-14777

Optimized compressor blades, examining Le Foll boundary layers theory possibilities as design method

04 p0621 A70-15667

Bladed wheels stability in centrifugal compressors, calculating natural vibration frequencies of rotors

07 p1364 A70-19634

Stetson-Powell time fringe hologram technique of vibration analysis applied to nodal patterns in compressor blade and turbine disks

09 p1679 A70-22979

Tandem axial compressor performance for various blade stagger and flap angle values of rotor row, investigating gap influence

09 p1608 A70-23736

Transonic two stage compressor design and performance, discussing interblade row traverse data

09 p1608 A70-23742

Compressor blade performance dependence on Reynolds number, turbulence intensity and axial velocity ratio, considering wind tunnel tests with porous side walls

09 p1609 A70-23748

Axial flow compressor blade rings interaction effect on angular speed of rotating stall zones

11 p1974 A70-25780

Compressor cascade flutter phenomenon, investigating factors affecting aerodynamic damping force on annular cascade blades

13 p2341 A70-29447

Incompressible two dimensional potential flow analysis with compressibility effects for thick highly cambered multibodies in cascade, noting slotted compressor blade performance

[ASME PAPER 69-GT-6]

14 p2529 A70-31023

Secondary effect signatures for potential failure detection in jet aircraft engine compressor blades

[ASME PAPER 70-DE-58]

16 p2918 A70-33517

Circular blade cascade design for supersonic vane diffuser of radial flow centrifugal compressor

16 p2837 A70-33764

High strength Ti alloys for aircraft gas turbine engines, determining critical properties for compressor fan blades

17 p3122 A70-34436

Pure impulse principle applied to axial compressor impellers with high solidity high camber blades

18 p3301 A70-36647

Two dimensional compressor cascades of double circular arc and wedge shape blades testing performance in transonic and supersonic wind tunnels

[ASME PAPER 70-GT-7]

18 p3302 A70-36829

Supersonic cascade wind tunnel performance evaluation, using compressor blades of simple geometric shapes

[ASME PAPER 70-GT-110]

18 p3238 A70-36848

Vibration characteristics of low aspect ratio compressor blades, using thin shell theory and Rayleigh-Ritz method

[ASME PAPER 70-GT-94]

18 p3305 A70-36876

Boundary layer optimization for high turning axial flow compressor blades, using flow theory and conformal mapping

[ASME PAPER 70-GT-88]

18 p3209 A70-36879

Cascade tunnel testing role in designing supersonic compressor rotor blading for lower jet engine weight and fuel consumption

[ASME PAPER 70-GT-79]

18 p3305 A70-36885

Blade root design for axial flow compressors and turbines, avoiding tensile stress concentration

19 p3490 A70-38616

Turbocompressor disk materials selection by low cycle fatigue tests, discussing stop and start repetition and cracks in stress concentration zones

21 p3867 A70-41261

Low aspect ratio compressor blade cascade performance at blade span center, discussing pressure loss, angle of attack and staggering

22 p3957 A70-42272

German monograph on three dimensional flow and blade pressure measurements at axial flow compressor casing wall, discussing test control and digital data processing

24 p4332 A70-45093

Fibrous composites use in compressor blades, discussing materials characteristics requirements relative to environmental and stress conditions in aircraft operational service

24 p4392 A70-45169

Turbine compressor blades vibration mode measurements by holographic interferometry

24 p4334 A70-45563

COMPRESSOR EFFICIENCY

Ballistic compressor performance as high intensity pulsed light source, discussing Xe gas heating and laser pumping

02 p0311 A70-11921

Axial compressor aerodynamics and efficiency in aircraft turbine engines

[ONERA-TP-767]

09 p1604 A70-22656

Transonic two stage compressor design and performance, discussing interblade row traverse data

09 p1608 A70-23742

Stagnation pressure losses in radial vaneless diffusers to estimate compressor performance, noting one dimensional analysis

11 p1974 A70-25782

Supersonic axial flow compressors, studying shocks shared by rotor and stator to obtain high efficiency

11 p2101 A70-25819

Axial flow compressor clearance control coatings at blade tip paths for efficiency

[SAE PAPER 700330]

12 p2291 A70-27462

Air intake distortions effect on compressor performance, discussing radial and peripheral gradients

15 p2787 A70-32248

Axial flow compressors off-design performance calculation using radial equilibrium equation

15 p2791 A70-32770

Turbofan engine compressor system performance dependence on circumferential extent, magnitude and rate of change of inlet temperature in altitude test facility

[AIAA PAPER 70-625]

16 p2968 A70-33590

Axial compressor aerodynamics investigation methods concerning compressor flow for efficiency improvement

16 p2836 A70-33757

Axial flow compressor off-design performance optimization by adjustable inlet guide vanes with variable trailing edge flaps

18 p3304 A70-36846

Rotor wakes intrastator transport effects on high Mach number axial flow compressors performance, considering stagnation temperature profile and rotor blade loss factor

[ASME PAPER 70-GT-39]

18 p3209 A70-36869

Axial flow compressor stage efficiency under rotary separation conditions, investigating dependence on flow rate

19 p3490 A70-37252

COMPRESSOR ROTORS

Bladed wheels stability in centrifugal compressors, calculating natural vibration frequencies of rotors

07 p1364 A70-19634

Pressure balanced rotor flow path design for mixed flow centrifugal compressors, calculating losses in rotor and diffuser section

[ASME PAPER 70-GT-12]

18 p3209 A70-36863

Cascade tunnel testing role in designing supersonic compressor rotor blading for lower jet engine weight and fuel consumption

[ASME PAPER 70-GT-79]

18 p3305 A70-36885

Off-design pressure losses in single stage axial flow compressor, using test rotor in annular duct

[ASME PAPER 70-GT-78]

18 p3210 A70-36886

Gas turbine engine compressor rotor roller bearing operation conditions analysis by computer calculation of thermal regime

21 p3834 A70-41777

COMPRESSORS

NT CENTRIFUGAL COMPRESSORS

NT SUPERCHARGERS

NT SUPERSONIC COMPRESSORS

NT TRANSONIC COMPRESSORS

NT TURBOCOMPRESSORS

Corrosion induced fatigue damage suppression in jet engine compressor steel components, describing various surface treatment effects

01 p0165 A70-10699

Free piston compression with sonic flow outlet for determining orifice size by matching with bounce parameters

07 p1249 A70-19334

Martensitic stainless steels corrosion damage in jet engine compressors noting effects of temperature, surface condition, time and chloride presence

12 p2252 A70-26963

Steady and nonsteady engine/inlet flow field simulation for engine/compressor testing, determining feasibility of variable ramp aerodynamic device

[AIAA PAPER 70-591]

15 p2672 A70-31788

F-111A airplane in-flight inlet pressure fluctuations for engine compressor surge, discussing average turbulence factor

[AIAA PAPER 70-624]

16 p2840 A70-33543

Soviet book on vibration and balancing of aircraft engine rotors covering structural deformation and dynamics of turbine engines and compressors

19 p3489 A70-37237

Aircraft noise sources, examining compressors with dynamic pressure devices and jets with turbulence investigations

[ICAS PAPER 70-22]

23 p4232 A70-44111

COMPTON EFFECT

Diffused X ray background in isotropic world models in terms of Compton radiation from cosmic ray electrons in intergalactic space

02 p0356 A70-11743

Cosmic X ray background interpreted as Compton collisions between cosmic black body photons and relativistic electrons in radio sources

02 p0360 A70-12792

Galactic X rays and high energy gamma rays in terms of cosmic ray electrons Compton scattering by submillimeter radiation

05 p0900 A70-16100

Electron momentum distributions from Compton profiles of Li-Mg polycrystalline samples, exhibiting discontinuity at free electron value of Fermi momentum

05 p0892 A70-16471

Induced Compton scattering of plasma and electromagnetic waves under astrophysical conditions, discussing HF radio emission spectra from cosmic objects and quasar

05 p0917 A70-16904

Compton-Getting effect for cosmic ray particles and photons and Lorentz-invariance of distribution functions, discussing thermal background radiation, proton spectra, etc

07 p1369 A70-20071

Inverse Compton collisions of relativistic electrons with universal black body photons for diffuse component of cosmic X rays

07 p1369 A70-20166

Compton scattering of synchrotron radiation from parent electrons in pulsars, calculating Compton-synchrotron radiation from NP 0532 leads to lower limit for magnetic field

07 p1369 A70-20221

Compact nonthermal radio sources in M87 giving rise to X ray source through Compton effect

09 p1744 A70-22520

Magnetic monopole flux limits in primary cosmic radiation derived from moon-poor shower data and inverse Compton scattering

16 p2972 A70-33050

Magnetic field effects on Compton scattering and radiative opacity, considering longitudinal and transverse propagation with circular polarization

17 p3154 A70-34538

Diffuse cosmic X rays produced by Compton scattering of far IR radiation on cosmic ray electrons

19 p3505 A70-38113

Polarization in inverse Compton effect for arbitrary photon and electron distributions, discussing monochromatic photon beam

19 p3524 A70-38696

Diffuse cosmic X and gamma ray spectrum analysis, considering implications for Compton scattering models in intergalactic space

20 p3695 A70-39049

Crab Nebula electromagnetic spectrum deviation from power law in microwave region, investigating origin from Compton scattering of high energy electrons

21 p3875 A70-40683

COMPUTATION

NT ORBIT CALCULATION

- Turbulent boundary layers computations - Conference, Stanford University, August 1968, Volume 2
02 p0280 A70-12271
- Optimization problems computing methods - Conference, San Remo, Italy, September 1968
03 p0461 A70-14338
- Computing methods in optimization problems - Conference, San Remo, September 1968, Volume 2
07 p1324 A70-19266
- Trachtenberg rapid calculation methods for multiplication, describing triangular or double product method and general algebraic theory
07 p1327 A70-19785

Soviet collection of papers on control mechanics and processes, computational mathematics
09 p1772 A70-22532

Artifices to allow computing time reduction in recursive data elaboration for high order differential system
09 p1720 A70-22647

Computational load reduction in aircraft tracking, comparing sensitivity and Hilbert norm methods
11 p2025 A70-26212

Computational methods for multiinput linear control systems applied to designing lateral and longitudinal autopilots for jet transports subject to gust loads
12 p2203 A70-27417

Automatic computation at SNECMA for turbomachines R and D, emphasizing digital computer for scientific calculation and analog simulator for engine regulation
12 p2193 A70-28073

Collection of papers on methods in computational physics, plasma physics covering Vlasov equation, simulation, finite difference, etc
18 p3295 A70-36787

COMPUTER COMPONENTS

NT COMPUTER GRAPHICS

Digital computers in aircraft, discussing automatic control systems, components and advantages over analog systems
15 p2705 A70-32299

Cellular logic arrays design for nonrestoring binary division, with application to Napierian logarithm generation
17 p3050 A70-34571

Dual mode suboptimum minimum time control of high order systems with negative roots and step displacement inputs, using simplified computer switching
21 p3801 A70-40756

Modular aerospace digital computer system architecture using off-shelf components for rapid avionic computing system realization
21 p3795 A70-41691

COMPUTER DESIGN

Aerospace digital computer design development, proposing data processing system with improved flexibility by making subassemblies more independent with multiplexed interface
01 p0047 A70-10305

Digital adaptive-element building blocks in monolithic Si structures for MOS large scale integration, considering serial/parallel multiplier and shift register chips
01 p0047 A70-10458

Aerospace computers stringent design requirements and applications in spacecraft, ballistic missiles and integrated avionic systems
02 p0264 A70-11688

Associative processor with content addressability and simultaneous arithmetic capability to circumvent speed restriction, comparing performance and cost with conventional digital computer
02 p0265 A70-12186

Digital systems design laboratory as instructional tool and experimental model for education
02 p0275 A70-12190

Spaceborne computer system for manned space station to perform functions in addition to guidance and navigation including processing
[AAS PAPER 69-581] 04 p0654 A70-14651

Systems concepts in design of computer operated display systems in air defense and air traffic control systems, discussing alphanumeric display, panoramic display, etc
05 p0827 A70-16183

Federated and integrated computer systems for aerospace applications, discussing system dependent variables
06 p1013 A70-17352

Complex integrated avionics computer system design for navigation, guidance and control of rotary wing aircraft, emphasizing microelectronic modular assembly
06 p1014 A70-17353

Aircraft computer design performing basic arithmetic operations by sampling method noting speed increase
06 p1014 A70-17859

Prototype Onboard Processor (OBP) designed for high reliability, low power dissipation, small size and

low weight, discussing attitude control signal processing
08 p1464 A70-20609

Automatic test equipment from fourth generation computer viewpoint, considering cost and size reduction trends in avionics
08 p1469 A70-20654

Fourth generation systems architecture in microprogramming in terms of control logic, describing inner computer as subroutine processor for controlling interstation communication
08 p1465 A70-20816

Hybrid computers capabilities, programming and operation
09 p1640 A70-22212

Machine design similar to human brain for recognition and classification of information
09 p1641 A70-22708

Computer and system design automation, considering language problems, microprograms, optimization on subsystem suboptimal basis, etc
10 p1845 A70-24874

Airborne computer design for short range attack missile /SRAM/ to perform aircraft navigation and missile fire control
12 p2192 A70-27800

Digital correlator LSI circuits design, layout and mask considerations, diffusion, metallization and dielectric deposition
13 p2378 A70-29551

Biresidue error-correcting codes for digital computers involving use of residue check circuitry working with arithmetic unit
13 p2375 A70-29938

Berkeley array processor /special purpose digital computer/ for correlation, convolution, recursive filtering, matrix multiplication, etc
13 p2376 A70-29941

Parallel associative unstructured element computer design for real time radar track data processing
16 p2869 A70-33466

General purpose parallel processor design for avionics, considering radar signal processing
16 p2910 A70-33467

Design and reliability of digital systems for hard cores of fault tolerant computers /hybrid- redundant systems/, discussing advantages over multiplexed systems
16 p2887 A70-33734

[JPL-TR-32-1490] Coherent optical computer system driven by membrane light modulator /MLM/, describing electro-optical properties and operating characteristics
16 p2871 A70-34055

Real time computers design tradeoffs in avionics systems
17 p3050 A70-35510

Brain-like computer with learning rather than programmable capability, discussing pattern recognition and task performance
18 p3230 A70-36775

Soviet book on computer design and construction covering man machine interfaces, internal languages, interpretation systems, memory distribution, solution processes, etc
19 p3385 A70-38794

Small hybrid computer design, describing algorithms and subsystems for statistical studies
20 p3593 A70-39914

Small digital computer arithmetic unit design, discussing number representation, addition and subtraction methods for performance and cost
21 p3793 A70-40757

Aerospace computers design, considering real time operation and reliability requirements
21 p3794 A70-41686

Aerospace digital computer family structural commonality, considering architecture, hardware and support software
21 p3794 A70-41687

Modular aerospace digital computer system architecture using off-shelf components for rapid avionic computing system realization
21 p3795 A70-41691

Semiconductor circuits large scale integration for aerospace computers, discussing fabrication and design
21 p3799 A70-41692

Aerospace microelectronic digital computer design, discussing optimal packaging by use of integrated circuits
21 p3795 A70-41694

Ultrasurvivable and maintainable computer design involving redundant spare modules and own tester for aerospace applications
21 p3795 A70-41695

Airborne digital computers in aircraft systems, discussing optimization, design and economic effectiveness
21 p3796 A70-41920

Reprogrammable read-mostly memory /RMM/ using integrated circuit array of amorphous and crystalline semiconductor devices, discussing design and applications
22 p3996 A70-42772

Modular plated-wire digital associative processor with content addressable memory, distributed arithmetic and I/O capability at each word
22 p3994 A70-43104

Optical read-write mass memory based on holographic storage and light addressable matrix array, discussing significance to computer design and usage
22 p3994 A70-43606

Digital computer constructed with diodes and transistors logic for evaluating matrix determinants and minors
23 p4166 A70-43955

Computer hardware and software technology for complex problems, discussing switching speeds and parallel and pipeline designs
23 p4167 A70-44716

COMPUTER GRAPHICS

NT DATA PROCESSING TERMINALS

NT PLOTTERS

Man-computer graphic systems utilization for wing/body aerodynamic design and analysis concept for subsonic vehicles
01 p0002 A70-10610

Computer driven display terminal as part-task limited area simulator, examining operational requirements and input characteristics
01 p0059 A70-11277

Dynamic structural analysis using computer graphics display, emphasizing applicability to man machine interaction at key decision making points
02 p0386 A70-11943

ALGOL Dynamic Display System for debugging and optimizing computer source language program, providing real time portrayal of static and dynamic block structure, etc
02 p0264 A70-12128

Display system utilization for diverse graphical operations, discussing interactive tasks and tradeoffs
02 p0265 A70-12153

Two dimensional structural analysis of engineering systems by computer graphics, outlining discrete element representation
02 p0388 A70-12477

Autostereoscopic display using vibrating varifocal mirrors, including laboratory computer generated real time image and movie projection systems
02 p0302 A70-12631

Computer graphics method for determining total magnetic field magnitude for various coil configurations and spacing, indicating optimum field uniformity near Helmholtz spacing
02 p0271 A70-12745

Integrated flight test data acquisition and processing system with real time graphic display, discussing ground station function
05 p0793 A70-15867

Computer-aided design using third generation computers and interactive graphic systems applied to transonic aerodynamics problems
05 p0816 A70-16122

Computer display graphic technique for business decision making, noting electronic aids
05 p0959 A70-16451

Deep reflector antennas mode composition by graphic computer techniques for maximum efficiency feed matches
06 p1021 A70-17575

Spherical frame of reference variations and additions for three dimensional vectorcardiograms composed of solid figures drawn by computer-driven CRT
07 p1221 A70-19594

Digital computer applications to structural analysis, discussing interactive graphics and engineering design
07 p1239 A70-20360

Alphanumeric and graphic computer driven CRT displays, discussing systems and component selection
08 p1465 A70-20672

Computer graphics applications to three dimensional vibration analysis, changing mass, stiffness, exciting load or load frequency at any point with light pen
08 p1467 A70-21050

Display objectives and relationships to recording techniques examined for memory/display system, considering requirement for elastic erasing technique
08 p1467 A70-21761

Airfoil analysis and synthesis, discussing computer graphics application to low speed shape and improved pressure distribution
08 p1594 A70-21867

Computer-generated shaded flicker-free on-line digital video display, allowing superimposed vector graphics with light-pen interaction
09 p1640 A70-22033

Hidden-line determination for computer-drawn polyhedra using edge classification scheme for CRT display applications
09 p1641 A70-22966

Digital computer impact on aerospace sciences and technologies in terms of computerized design, interactive graphics, flight simulation, Apollo systems checkout, etc
09 p1642 A70-23277

Computer-generated holography involving three dimensional object perspective projections computation for incremental rotations

09 p1683 A70-23529

Digital and analog computers applicability to graphic arts noting lack of aesthetic theories

10 p1845 A70-24235

Digital plotters operational characteristics, capabilities and applications

10 p1845 A70-24581

Pattern prerecognition processing for multioject pictures, describing illumination, contour and curvature computation

10 p1845 A70-24659

Real nonnegative function representing transmittance of computer synthesized Fourier transform hologram displayed on flying spot scanner and recorded on film

11 p2049 A70-25631

Aircraft design structural development and substantiation utilizing computer analysis and testing [SAE PAPER 700216]

11 p2134 A70-25888

Computer texture analysis for two dimensional scenery pictures involving periodicity invariance under Fourier transform

11 p2014 A70-26251

Computers graphical display devices for rapid designer-computer communication

12 p2191 A70-27013

Direct view storage tube /DVST/ as graphical display unit for small digital computer installation

12 p2232 A70-27374

Computer plotting of flow patterns and orographic cloud over/in lee wave flow, including rotors, blocking and high level turbulence

12 p2264 A70-27722

Binary-valued digital pictures noise cleaning by propagation processes

12 p2188 A70-27937

Interactive computer graphics using modified Continuous Systems Modeling Program /CSMP/

15 p2705 A70-31773

Plotter induced reconstruction errors minimization in computer generated binary Fourier transform holograms

15 p2737 A70-32044

Filters design by on-line graphic interface computerized synthesis utilizing three screen CRT display

16 p2867 A70-33041

CRT symbol generators design for high speed computer data display as function of electro-optical and human operator constraints

16 p2850 A70-33133

Foreground presence for computer generated and painted three dimensional photographic displays using fly eye lenses

16 p2906 A70-33177

Interactive computer graphics in six degree of freedom control, lunar roving vehicle navigation, orbital elements calculations, drop test simulation, etc

16 p2869 A70-33726

Interactive computer graphics applied to continuous system modeling program /CSMP/, describing hardware system configuration

16 p2870 A70-33727

Computer driven on-line CRT graphics displays for data acquisition and reduction

17 p3063 A70-35513

Ion-polar molecule collision time history plots and computer movies, calculating capture cross sections for mass spectrometry

18 p3292 A70-36561

Apollo spacecraft parts environmental simulation and testing, using real time computer generated graphic display

19 p3532 A70-37918

Coding device for computer storage of graphical information, describing construction and operation

19 p3385 A70-38576

Ion-molecule pair relative motion in capture collisions, using computer-made movies

19 p3474 A70-38796

Computer generated holograms production, reducing memory size and plotter resolution

20 p3627 A70-39098

Aircraft loadability design by computerized loading program using graphic plotter [SAE PAPER 836]

20 p3562 A70-40364

Mathematically defined curve incremental generation by computer, discussing parametric and non-parametric representations and digital differential analyzer technique

22 p3993 A70-43072

Graphical link between operator and digital computer using CRT display and light-pen input system during automatic electronic circuit design

23 p4150 A70-43952

Interactive man computer systems evaluation considering speech communication, SKETCHPAD and graphics capabilities, FORTRAN and programming languages and future manned space missions [AIAA PAPER 70-1292]

24 p4317 A70-45928

COMPUTER METHODS U COMPUTER PROGRAMS

COMPUTER PROGRAMMING NT LANGUAGE PROGRAMMING NT MICROPROGRAMMING NT MULTIPROGRAMMING NT ON-LINE PROGRAMMING

Axisymmetrical stress-strain state of body of revolution with complex cross sectional geometry under surface loads, deriving computer algorithm for numerical analysis

02 p0384 A70-11665

Algebraic properties of indefinite Riemann in integral useful in computer programming, emphasizing invariant algebras

04 p0654 A70-14683

Human controller decision in air traffic control, discussing manpower, on-line computer use and maximized systems

[ASME PAPER 69-WA/AV-1] 04 p0643 A70-14903
Problems experienced in using computers for medical diagnosis and treatment processes, discussing Bayes formula application

04 p0644 A70-15358

Computer aided medical diagnosis

04 p0644 A70-15359

Programming system for Poisson series manipulation on computer, writing subroutines in machine language

05 p0817 A70-16342

Book on digital computer methods in engineering covering numerical and programming methods, algebraic and differential equations solutions, time-frequency domain analysis, etc

05 p0877 A70-16771

Ionospheric data representation in tabular form for computer storage and processing, noting memory cells reduction

07 p1268 A70-19460

Computer scheduling model and timeline plot for Apollo Telescope Module /ATM/ experiments using orbital trajectory simulation

07 p1394 A70-19572

Phased-array radars and parallel processing computers system in high target density environment, input-output, array steering and data storage and handling

07 p1236 A70-20150

Extendable computer simulation model /ECSS/ overcoming programming and debugging problems, discussing language selection, design, specification, work load, etc

08 p1466 A70-20928

Digital differential analyzers improved speed and accuracy by extended resolution on Euler integration for differential equations solution programming

08 p1467 A70-21756

Hybrid computers capabilities, programming and operation

09 p1640 A70-22212

Survey of papers on computer calculation of two and three dimensional gas flows, emphasizing method of characteristics and finite difference techniques

09 p1603 A70-22265

Analog computation in supersonic steady flow and digital technique for wing-fuselage and wing-tail interactions

[ONERA-TP-804] 10 p1802 A70-24544

Eyeball technique smoothing procedure discarding wild data points using minimum computer time for automatic treatment of digitally sampled test data [AIAA PAPER 70-386]

10 p1861 A70-24919

Problem oriented computer programming language and translator for solving partial differential equations

11 p2013 A70-25367

Computer applications in aerospace research involving flutter, supersonic flow, unsteady wing flow, etc

12 p2191 A70-27025

Computer programmed automatic circuit analyzers, discussing unit adaptation, wire data processing and analyzer programming

[SME PAPER MS-70-727] 12 p2241 A70-27084

Automatic test equipment programming procedure including analysis, coding, validation and demonstration

13 p2422 A70-29689

Computer simulation model documentation exemplified by cardiovascular simulation using Continuous Systems Modeling Program /CSMP/ and emphasizing format uniformity

15 p2689 A70-31774

Common high order programming language and program debugging in aerospace software

16 p2868 A70-33430

Aerospace program oriented language /APOL/ requirements for flight programs, discussing cost, design and applicability

16 p2868 A70-33431

Computer generated holograms, using binary transmittance for wave fronts and three dimensional images construction

17 p3085 A70-35006

Two dimensional free boundary problems approximate solution by finite difference method, deriving algorithms for computer program implementation

18 p3230 A70-35941

Human operator and computer interrelations, noting sources of error

18 p3223 A70-36079

Computer language related to ALGOL 60 for handling nonnumerical problems of mechanics

18 p3283 A70-36367

Ionospheric data representation in tabular form for computer storage and processing, noting memory cells reduction

18 p3250 A70-36934

Artificial satellite theory main problem for small and moderate eccentricities, using perturbation techniques based on Lie transforms for computer programming

18 p3334 A70-37062

Computer aided laboratory testing of flight vehicles in real environmental conditions, illustrating vertical stabilizer subject to gust loads

19 p3396 A70-37874

Axisymmetrical stress-strain state of body of revolution with complex cross sectional geometry under surface loads, deriving computer algorithm for numerical analysis

19 p3547 A70-38439

Computerized assembly of production space vehicle with controlled mass properties, discussing automated system of data collection, storage and retrieval [SAWE PAPER 851]

20 p3639 A70-40375

Programming and checkout of computer for ELDO inertial guidance system, including flight simulation and autopilot tests

[AIAA PAPER 69-961] 21 p3795 A70-41862

Binary codes linear metric properties description reduced to finite set determination by convex programming procedure

22 p3993 A70-42494

Computer-aided production engineering involving numerically controlled machines for Rolls-Royce aircraft engines manufacture

24 p4341 A70-45299

Interactive man computer systems evaluation considering speech communication, SKETCHPAD and graphics capabilities, FORTRAN and programming languages and future manned space missions [AIAA PAPER 70-1292]

24 p4317 A70-45928

COMPUTER PROGRAMS

NT COMPILERS

NT COMPUTER SYSTEMS PROGRAMS

NT INPUT/OUTPUT ROUTINES

NT OPERATING SYSTEMS [COMPUTERS]

NT SUBROUTINES

Monograph on future air traffic control concerning radio navigation, color display and computer determined flight paths

01 p0136 A70-10090

Computer program for automatically selecting redundant parts and redundancy types for various aerospace systems characteristics

01 p0103 A70-10488

Computer applications in French missile testing center, describing real and delayed time equipment and computations

01 p0057 A70-10798

Semiautomatic mass condensation transformation for reducing structural vibration calculations, including computer program and mode shape plotting

01 p2000 A70-10868

Textbook on applied numerical methods covering interpolation, approximation, integration, matrices, etc, with emphasis on digital computer algorithms

01 p0132 A70-11306

Book on numerical solution of partial differential equations, discussing methods for physical and chemical problems on digital computer

01 p0134 A70-11326

Stony meteorite trace elements groups neutron activation analysis with computer reduction of Ge/Li spectra

02 p0249 A70-11680

Digital computer program /LANDIT/ for predicting structural impact response of axisymmetric landing vehicles consisting of rigid payload and crushable impact limiter system

02 p0380 A70-11945

Aircraft landing measurement system /ALMS/ designed to provide computer analysis of all traffic landing at airport

02 p0331 A70-11964

Terminal area approach control sequencing, using digital computer to allocate identification mode and landing time slot

02 p0332 A70-11971

Computerized navigation system for controlling aircraft movement on airports under zero visibility conditions

02 p0274 A70-11978

Valvular aortic stenosis severity estimation using digital computer program and tape recorder for determining valve area

02 p0243 A70-12094

Human decision making via man-computer interaction, noting skill role in nonoptimal performance handling of simultaneous factors

02 p0245 A70-12140

Computer application to Navier-Stokes equations numerical integration for incompressible viscous fluid deflected flow with large Reynolds number

02 p0287 A70-12376

Jet aircraft long range flight planning using computer for wind and temperature forecasts, path altitude profile computation and optimization

02 p0403 A70-12841

Computerized airline fleet planning methods for aircraft economics and airline operations [SAE PAPER 690415]

03 p0609 A70-12898

Plastic flow under biaxial stress, discussing data acquisition system and computer program for comparing test and theory

03 p0480 A70-12954

Meteorological data processing computer center of German Weather Service, discussing equipment, data system, forecasting techniques and prediction control

03 p0434 A70-13171

Computer evaluation of photographic imagery of left ventricle volume obtained by cineangiography, including densitometric measurements

03 p0434 A70-13678

Earth satellite orbit parameters determination from angle measurements using computer program and least squares estimation technique

03 p0573 A70-13843

Digital computer program for physiological measurements, outlining interpolation of mathematical functions describing signals time variations

03 p0436 A70-13900

Computerized stepwise construction of Hugoniot curve for detonation waves and Chapman-Jouguet detonation and deflagration points

03 p0607 A70-13920

AMPROD /Automated Mission Profile Design/ generating schedules for long duration missions with real cost and time savings

03 p0581 A70-14023

Computer processing role in film scanning and digitizing for enhancing X ray and radioisotope scanner images in medical radiographs, discussing image noise reduction

04 p0654 A70-14562

Computer method to combine autofluorescence data to produce three dimensional display of absorbed radioactive material from multiview images

04 p0686 A70-14563

Mathematical model based on equivalent electrical circuit for transient radiation analysis by computer /TRAC/ family of circuit analysis programs, simulating semiconductor devices

04 p0657 A70-14737

Reliability analysis formulation for statically indeterminate structures, using modified transition probabilities and computer program for systematic failure paths counting

04 p0768 A70-14747

Computer programs for numerical analysis of shell structures, considering series expansion, numerical integration, finite differences and finite elements

04 p0768 A70-14787

Thermionic converter with oriented W electrodes, describing test method and computerized data acquisition for performance mapping

04 p0627 A70-14945

Diode transistor microelectronic logic circuit reliability, efficiency and optimization using digital computer

04 p0659 A70-15210

Computer program for electrical and transient thermal analysis of satellite electric power subsystem consisting of solar array, battery and power controls

04 p0628 A70-15332

Algorithmic and digital computer method for approximating irrational transfer functions by rational functions in control systems

04 p0662 A70-15336

Equation for disturbance of ILS localizer signals by reflection from flat hangar wall, discussing computer program

04 p0652 A70-15344

Computer program for evaluating measured lung function values by comparison with accepted norms, using matrices containing regression coefficients

04 p0644 A70-15360

Analog computer schemes for solving dynamic plants identification reducible to optimizing parametric problem of many variables function

04 p0654 A70-15435

NASTRAN digital computer program for static and dynamic structural analysis using finite element method [SAE PAPER 690612]

05 p0816 A70-15851

Cosmic ray intensity variations recording device adaptable to computer forming centralized data processing system

05 p0845 A70-15932

Computer program to decide structure for aliphatic ketone from low resolution mass spectrum using DENDRAL algorithm

05 p0810 A70-16048

Display Oriented Computer Usage System /DOCUS/, discussing on-line display console management in multiaccess environment, display oriented language, compiler, etc

05 p0817 A70-16181

Computer generated displays and USAF equipment design for operational command and control systems, discussing Ag halide film technique

05 p0847 A70-16185

Computerized method for processing photographic earth satellite observation results, transforming coordinates by nonconformal approximation of polynomial function

05 p0814 A70-16367

Digital computer program for analyzing axisymmetrically loaded ring-stiffened segmented composite elastic shells of revolution, giving vibration frequencies

05 p0944 A70-16814

MTRAC program for transient analysis of circuits with square loop magnetic cores based on linearization of nonlinear circuit elements and Kirchhoff current law

05 p0825 A70-16999

Computer optimization of spacecraft optical coatings for temperature control, using finite element analysis and matrix inversion [AIAA PAPER 69-979]

06 p1172 A70-17180

Flight deck displays based on digital computer providing signals for CRT and instrumentation

06 p1061 A70-17319

Spatially homogeneous distribution function describing uniform gas motion derived to permit computer calculations in obtaining numerical solutions to kinetic equation

06 p1036 A70-17753

Ionospheric vertical electron concentration computer calculations compared to direct measurements data by satellite and rockets over Sofia

06 p1057 A70-17843

Frontal solution program for symmetric positive definite equations met in finite element applications

06 p1014 A70-17936

Flight software for onboard Apollo Primary Guidance, Navigation and Control System flight qualification by digital simulation, including software diagnostics [AIAA PAPER 70-173]

06 p1029 A70-18060

Apollo-Saturn Launch Vehicle Targeting Program for Lunar Landing Missions, describing functions of integrated digital computer programs [AIAA PAPER 70-172]

06 p1145 A70-18093

Black box modeling of linear integrated circuits for computer analysis in frequency domain

06 p1026 A70-18416

Network analysis for systems application program /NASAP/ computer-aided circuit design program for network analysis, discussing application in education

06 p1015 A70-18418

Computer aided network design course using FORTRAN 4 emphasizing modeling of semiconductor devices

06 p1015 A70-18419

NASAP program FORTRAN subroutine LOOPS for loop detection in circuit analysis, discussing automatic instrumentation process for computation time reduction

06 p1015 A70-18421

Hybrid NASAP program module for direct design of linear dynamic circuits using simple optimization without sophisticated computer programming

06 p1015 A70-18422

Mathematical techniques for selenodesy computer simulation program, solving problems arising from infinite series of spherical harmonics for lunar gravitational potential

06 p1152 A70-18498

Lift fan V/STOL tactical aircraft performance capabilities determination, using digital computer program

07 p1191 A70-18975

LUF for F layer propagation modes, discussing mode cut-off significance using computer ray tracing program

07 p1229 A70-19159

Three dimensional ray tracing computer program in Fortran for determining radio paths in ionosphere

07 p1230 A70-19163

Oblique ionospheric sounder automatic data analysis by computer programs, analog to digital conversion, magnetic tape data recording, signal detection, pattern recognition, etc

07 p1234 A70-19185

Radio signal reception beyond normal horizon by partial reflection from elevated layer in troposphere calculated by computer

07 p1234 A70-19218

Turbulent heat and mass diffusion in catalytic reactors for hydrazine decomposition, developing computer program to calculate temperature and reactant concentration distributions [AIAA PAPER 69-421]

07 p1365 A70-19706

Lumped element microwave Y circulator, describing device performance and ALGOL program for potentials calculation

07 p1241 A70-19751

Computer procedures for solving temperature stresses in thin infinite isotropic viscoelastic plate with heat transfer

07 p1411 A70-19817

Point matching technique for plane elastic problems extended to axisymmetrically loaded elastic body of revolution, developing general computer program

07 p1416 A70-20303

Radiation Shielding Information Center computer code library for radiation transport or shielding calculations, listing programs available

07 p1239 A70-20364

Computer program /SAFETE/ for evaluating missile launch risk on near real time basis [AIAA PAPER 70-248]

07 p1250 A70-20370

Computer program /TACTICS/ for simulating three vehicles simultaneous motion in space, considering interceptor-target guidance and intercept trajectories

07 p1239 A70-20414

Automatic testing hardware and software compatibility emphasizing versatile avionics shop test /VAST/

08 p1470 A70-20662

Computer program for automated test station simulation, considering station operating characteristics and performance prediction

08 p1465 A70-20666

Aircraft roll rate response and aileron step input matching in terms of modal parameters with flight test records by analog computer program

08 p1465 A70-20781

Quasi-linearization technique in computer program for aircraft parameters identification featuring efficient search for optimal parameters in algebraic or differential equations

08 p1465 A70-20784

Computer controlled remote manipulator development, operation, components and applications, describing system programs consisting of executive control programs and subroutines

08 p1465 A70-20817

Extendable computer simulation model /ECSS/ overcoming programming and debugging problems, discussing language selection, design, specification, work load, etc

08 p1466 A70-20928

SOAR /Simulation of Airlift Resources/ model for stochastic productivity variations of strategic airlift systems

08 p1466 A70-20930

Boeing 747 aircraft container system deployment simulation written in GPSS/360 to minimize stockholding of containers at individual stations

08 p1481 A70-20931

Queue control techniques in generating predicted trajectory, discussing queue control logic requiring minimum storage

08 p1467 A70-21049

Analytic solution for computerized vibration analysis of high speed tension test

08 p1590 A70-21332

Computer program predicting thermal response of fusion welding tooling chill bars and holding fixtures, simulating moving heat source and contact

08 p1508 A70-21487

Algorithm for evaluating nth order partial derivatives of network functions and corresponding sensitivity functions

08 p1467 A70-21643

Cardiac output in humans by analog computer program using mass spectrometer analysis of expired air

08 p1454 A70-21948

IR absorption spectral curve interpretation using computer program for iterative solution

09 p1726 A70-22138

Lunar photographs on star-calibrated plates for lunar features coordinates or physical libration determination, outlining photographic technique and computer program

09 p1674 A70-22308

Computer program for generating tables to calculate lunar libration at any epoch

09 p1752 A70-22313

Axisymmetric or plane bodies temperature distribution from heat conduction analysis using computer program based on finite element method

09 p1788 A70-22581

Potential flow and boundary layer theory application as design tools in aerodynamics, basing calculations on digital computer methods

09 p1605 A70-22947

Computer aided design programs as decision-making tool for fighter development projects technical management [AIAA PAPER 70-364]

09 p1611 A70-23024

Aliphatic ethers low resolution mass spectra interpretation using computer program heuristic DENDRAL

09 p1631 A70-23400

Long range army budget forecasting model based on research projects cost distributions and parameters, describing computer program

09 p1794 A70-23415

Soviet monograph on method of functional equations for solving boundary value problems, discussing computer programs and various applications
09 p1712 A70-23548

Geomagnetic field orientation effects on VLF nighttime propagation, checking computer program predictions
09 p1639 A70-23664

Lunar daily variation in geophysical data determined by Chapman-Miller method, improving probable error determination method and giving computer program in FORTRAN
09 p1764 A70-23701

Modified fast Fourier transform for hybrid computer program data processing of human operator describing functions
10 p1824 A70-23900

Continuous media mechanics by applying fractional steps method to numerical solutions, outlining theoretical basis for computer algorithms
10 p1866 A70-24114

Mechanized Algebraic Operations software package for manipulation on computer Poisson series, noting application to celestial and nonlinear mechanics and astrodynamics
10 p1845 A70-24179

Ground based moving-base aircraft flight simulator using computer program to establish motion requirements
[AIAA PAPER 70-348] 10 p1859 A70-24213

Period length calculation method for physiological rhythms by digital computer
10 p1811 A70-24380

ALGOL algorithm for Runge-Kutta type numerical integration of simultaneous differential equations, using Merson method for step length determination
10 p1845 A70-24405

Computer-aided class C amplifier design, discussing algorithm and computer program
10 p1849 A70-24447

Structural behavior during creep by step by step process suitable for computers after linearizing nonlinear equations
[ONERA-TP-805] 10 p1958 A70-24545

Impact problems of slip clutch and beam scales dynamic characteristics simulation by 1130 CSMP /Continuous System Modeling Program/
10 p1860 A70-24653

Remote sensor input radiation at aperture, signals within and sensed data processing by computer techniques, noting automatic image interpretation
10 p1841 A70-24733

Satellite orbit prediction using computer program based on first order secular node-to-node drag perturbations
10 p1943 A70-24822

Flight test programs site selection method using computer program analysis of magnetic tape weather records
[AIAA PAPER 70-397] 10 p1806 A70-24908

Automatic Malfunction Analysis /AMA/ digital computer software system supporting checkout and testing, defining normal system status by computer simulation
[AIAA PAPER 70-383] 10 p1861 A70-24922

Dynamic characteristics of structures measured, using digital computer to analyze transient data from frequency sweep tests
10 p1961 A70-25059

Software production for Brazilian Advanced Educational Technology System
[AIAA PAPER 70-470] 11 p2152 A70-25403

Computerized data communication system /CDCS/ equipment unit capacities and topology specified with aid of vertex weighted linear graph
11 p2009 A70-26253

Linear networks fault detection and isolation using computerized test procedure and symbolic transfer function generation technique
11 p2029 A70-26337

Slender body transonic wave drag double integral, describing computer program for numerical evaluation
11 p1977 A70-26644

Finite element computer code /AXICRP/ for creep analysis of plane stress, plane strain and axisymmetric bodies of revolution
11 p2015 A70-26682

Batch program testing, developing standards for various computer installations by daily work error case examples
12 p2191 A70-27012

Shells of revolution under combined thermal and mechanical loading, presenting analytical basis of BOSOR 3 digital stress analysis program
12 p2320 A70-27144

Computer programs for calculating spectral lines oscillator strength in Coulomb approximation, proposing Fortran program
12 p2192 A70-27595

Multiterminal electronic networks computerized fault detection based on linearized Taylor expansion algorithm
12 p2197 A70-27932

Radio propagation over sea water path, predicting transmission loss by computer programs
12 p2188 A70-27936

Computer program for flying spot scanner pattern recognition, analyzing human chromosome contour
12 p2170 A70-27938

Remote signal measurement and analysis in hazardous environment by command terminal utilizing manual or computerized control
12 p2201 A70-28134

Radar systems EM compatibility simulation, describing FORTRAN IV operational interference prediction program
12 p2193 A70-28139

Phase lattice constants determination by computer method of debyegram line indexing
12 p2258 A70-28350

Navigation satellite systems, analyzing error sources in signal processing and propagation developing computer programs
13 p2447 A70-28429

Dynamic programming applications to optimal stochastic orbital transfer strategy, describing computer program
[AIAA PAPER 68-872] 13 p2447 A70-28502

Configurations stress stability liquid propellant rocket nozzle analysis by BOSOR 3 digital program, describing mathematical model construction
13 p2508 A70-28509

Computer techniques for determining physical libration of moon in longitude
13 p2488 A70-28765

Computerized control of aircraft spare parts inventories, using optimization method maximizing aircraft availability and minimizing handling costs
13 p2524 A70-28836

Dimensional stability derivatives from XV-4B aircraft simulator varied in computer program for extracting roots of lateral-directional characteristic equation
[AIAA PAPER 70-551] 13 p2346 A70-29016

Ordinary differential eigenvalue problems solution by successive transformations, describing computer program and applications to hydrodynamic stability
13 p2440 A70-29085

Computer program for system reliability prediction, using probability tree approach and block probabilities
13 p2373 A70-29565

Computerized Monte Carlo prediction of maintenance time distribution of complex system, concerning man hours, elapsed time and schedule meeting
13 p2524 A70-29566

Configuration management of software concerning automatic test systems in large maintenance depot
13 p2422 A70-29692

Computer techniques for rounding error analysis, stability in linear algebra, matrices factorization, Jacobi rotation method and iteration procedures
13 p2443 A70-29768

Multimode system analysis, using automated technique to calculate effectiveness and cost down to component level
13 p2525 A70-29837

DMC computer code for simulation of two dimensional viscous incompressible flow about arbitrarily shaped bodies
14 p2527 A70-30271

SCAMP I DC statistical circuit analysis program for linear and nonlinear circuits, describing program structure
14 p2560 A70-30664

SCAMP 2 program for statistical analysis of electronic circuit sensitivity to variations in parameters and DC input values
14 p2560 A70-30665

SCAMP 3 program for calculation of electronic circuit DC performances statistical distribution as function of component parameters variation
14 p2560 A70-30666

SCAMP 4 program for electronic circuits statistical analysis in frequency domain, obtaining mathematical models and transfer functions
14 p2561 A70-30667

Computer program for two body problem literal series expansions using Kepler functions with Bessel and Poisson series operation
14 p2638 A70-30702

Real time Apollo lunar module thermal mission data analysis using computer programs
14 p2653 A70-30774

Book on space flight simulation systems examining real time and real performance requirements, mathematical models and various simulation programs
14 p2563 A70-30955

Approximating hazard rate function parameters estimation from failure data, using computer program
14 p2592 A70-31113

Aircraft design optimization by multisearch programs, considering mathematical model role
14 p2532 A70-31400

Interactive computer graphics using modified Continuous Systems Modeling Program /CSMP/
15 p2705 A70-31773

Computer simulation model documentation exemplified by cardiovascular simulation using Continuous Systems Modeling Program /CSMP/ and emphasizing format uniformity
15 p2689 A70-31774

Computer control of nonlinear systems with varying performance specifications, using Popov stability and nonlinear programming
15 p2715 A70-31973

Hybrid rocket engine with solid oxidizer based on ammonium perchlorate and Al, studying performance with FORTRAN 5 program
15 p2787 A70-32273

SIRIO mission algorithm and computer program, determining spacecraft position, ground trace and tracking station visibility
15 p2811 A70-32286

Computerized statistical analysis programs finding plastic stress and acoustic emission as predictors of annealed steel fatigue life
15 p2760 A70-32326

Computer program for limit analysis of rotationally symmetric shells, generating yield point load upper and lower bounds and velocity profile
15 p2822 A70-32351

Heuristic programs and approaches in artificial intelligence
15 p2706 A70-32565

Real time computer algorithm for achieving optimal position of tracking antenna with nonlinear control system
15 p2703 A70-32575

Large signal junction FET model involving piecewise linear approximation for ECAP circuit analysis program
15 p2711 A70-32596

Interrelated computer programs and comprehensive parts data bank /REACT/ for reliability assurance analysis
15 p2706 A70-32654

Computer program /SORCBE/ for systems unavailability tradeoff vs added cost for various versions
15 p2706 A70-32658

Software reliability program development, functional analysis and error sources
15 p2742 A70-32667

Surface temperature color contour maps of objects undergoing aerodynamic testing, utilizing electro-optical and computer techniques
16 p2905 A70-33169

Self alignment for gimballing inertial navigation system fixed base by generating computer programs from error signals derived from inertial sensors
16 p2946 A70-33302

Optimal fixed-form pilot model computer program for VTOL longitudinal control hover task evaluation
16 p2851 A70-33341

Space programming language SPI/J6 replacing machine language programming in flight software capable of expressing complex vector mathematics and decision control
16 p2868 A70-33429

Aerospace program oriented language /APOL/ requirements for flight programs, discussing cost, design and applicability
16 p2868 A70-33431

Interactive computer graphics in six degree of freedom control, lunar roving vehicle navigation, orbital elements calculations, drop test simulation, etc
16 p2869 A70-33726

Interactive computer graphics applied to continuous system modeling program /CSMP/, describing hardware system configuration
16 p2870 A70-33727

Functional equivalence between FS expression and programs
17 p3130 A70-35139

Program for function computation replaced by notion of flow algorithm
17 p3130 A70-35140

Fluid flow longitudinal temperature profiles for inclusion in heat transfer computer program
17 p3198 A70-35659

Dynamic system modeling pulse test data reduction by digital computer and functional approximation for Fourier transform calculations
18 p3230 A70-36458

Left ventricular dynamics ultrasonic visualization, involving catheter-borne transducers array and computer for data acquisition and display
18 p3225 A70-36750

Computer programs for photogrammetric aerial triangulation with independent models
18 p3248 A70-36778

Adjustment program for aerial block triangulation with independent models, using planimetry-height iterations
18 p3248 A70-36779

Electrostatic sheet model for plasma, emphasizing computer solutions of various problems
18 p3295 A70-36788

Potential calculation from given source distribution, including direct and iterative methods, error analysis,
18 p3295 A70-36788

convergence, computer programs and applications in plasma physics 18 p3284 A70-36790

Critical aviation gas turbine rotating component life limit determination, describing statistical, maintenance, inspection and life evaluation computer program (SMILE) 18 p3303 A70-36841 [ASME PAPER 70-GT-66]

High speed combustion chambers for gas turbine engines, using finite rate chemistry and turbulent mixing computer program for burner design 18 p3304 A70-36866 [ASME PAPER 70-GT-25]

Iterative Hansen method of general perturbations programmed for digital computer, evaluating major and minor planetary theory 18 p3320 A70-37060

Soviet book on numerical methods of Chebyshev approximation covering minimax problems, computer methods, linear programming, etc 19 p3456 A70-37232

Ballistocardiogram autocorrelation function and spectrum by scanning graph decoder and computer, determining total power, harmonics periodicity and energy concentration 19 p3370 A70-38211

Kahan Babuska summation method variant in Triplex-ALGOL 60 for reducing roundoff errors in finite series calculation 19 p3385 A70-38678

Many body gravitational problem, computing evolution of two groups by numerical integration with two different computers 19 p3523 A70-38692

Hydrometeorological information processing using ALGOL-60 translator language 19 p3463 A70-38759

Computer program for assessment and modification of mechanical component life predictions by discrete formulation of Bayes theorem 19 p3440 A70-38816

Weapon systems effective reliability analysis, using degraded mode evaluation and deterministic computer program 19 p3442 A70-38833

Singular integral equation formulation for torsion from membrane analogy, obtaining boundary value problem solution by computer program 20 p3718 A70-39000

Computer program transforming spherical harmonic coefficients into arbitrarily tilted coordinate systems, tabulating coefficients of International Geomagnetic Reference Field 1965 in dipole coordinate system 20 p3621 A70-39353

Modified McNish-Lincoln method for Zurich sunspot numbers prediction, adapting for computer operation 20 p3704 A70-39410

Aircraft and rocket guidance systems navigation error analysis, discussing numerical integration techniques and computer program 20 p3667 A70-39527 [AIAA PAPER 70-1004]

Computer calculations automation in mathematical models construction by statistical methods, discussing programs for distributed parameter systems, stochastic approximation, etc 20 p3592 A70-39903

Conducting wall MHD generator channel current distribution, examining computer program for anode and cathode currents 20 p3566 A70-40013

Computer program for systems reliability approximation, giving algorithm for cut and tie sets identification 20 p3594 A70-40060

Numerical methods, FORTRAN program and table form for complex integrals evaluation along unit circle in positive direction 20 p3605 A70-40120

Automatic weight analysis by calculation and orientation of mass properties (COMP) program, using remote terminal time sharing computer system [SAWE PAPER 824] 20 p3595 A70-40353

Aircraft loadability design by computerized loading program using graphic plotter [SAWE PAPER 836] 20 p3562 A70-40364

Weight, moments and mass centers computer calculation by surface integral method, using FORTRAN language [SAWE PAPER 852] 20 p3660 A70-40373

Computer algorithm for optimal linear impulse corrections to satellite orbit under inequality type constraints 21 p3801 A70-40828

Linearly elastic skeletal structures, calculating natural frequencies of undamped vibration by computer program 21 p3935 A70-41254

Aerospace digital computer family structural commonality, considering architecture, hardware and support software 21 p3794 A70-41687

Mission analysis and trajectory simulation (MATTS) program, discussing computer controls, modular design, integration evaluation [AIAA PAPER 69-939] 21 p3920 A70-41872

Electromagnetic wave diffraction at multilayer wire grating, discussing computer program for diffraction field calculation 22 p3985 A70-42399

Horizontal Situation Display (HSD) map computer mechanization transforming earth location to X, Y coordinates for Lambert conformal projection [AIAA PAPER 69-987] 22 p4068 A70-42710

Computerized nonequilibrium thermochemical gas dynamic solutions for nozzle, shock tube and stream tube flow with arbitrary species and kinetic reactions numbers 22 p3982 A70-42762

Automatic diagnosis of clinical electroencephalogram with digital computer, showing maximum and minimum points, basic pattern and paroxysmal wave 22 p3977 A70-42869

Aircraft accident filing system data analysis using Fortran programs 22 p3962 A70-42880

Rational polynomial matrices inversion by automatic computational procedures, considering Gaussian elimination and Faddeev algorithm 22 p4062 A70-42926

Algorithm for fast digital computer recursive estimation of mean of random variable 22 p3993 A70-43074

Computer photokymographic recording of gravitational-inertial force environment effects on cardiovascular and respiratory systems on centrifuge 22 p3976 A70-43709

Hyperthyroidism diagnosis by pattern recognition, using computerized class featuring information compression 22 p3977 A70-43732

Deep penetration radiation shielding calculations using discrete ordinates difference equations and computer program 23 p4216 A70-43808

Radiation shielding calculations using multidimensional Monte Carlo computer programs 23 p4217 A70-43809

Radiation shield design and transport calculations, reviewing kernel methods development and relevant computer programs 23 p4217 A70-43811

Conducting bodies of revolution, calculating surface currents due to axially incident plane electromagnetic wave by computer program 23 p4162 A70-44005

Linear phased arrays computer aided design, discussing search algorithms in multivariable optimization program 23 p4172 A70-44015

Short haul jet transport aircraft design, discussing Computer Aid Design, Airline System Simulator and Traffic Demand Predictor computer programs [ICAS PAPER 70-28] 23 p4284 A70-44105

Computer program for nonlinear differential equations related to nonlinear boundary value problems based on Newtonian iteration process difference analog of linearization method 23 p4212 A70-44338

Automatic electronics test equipment, discussing choice between tape or computer controlled interpreter systems based on language, time, versatility and cost 23 p4173 A70-44539

Electronic equipment automated testing objectives and requirements, considering man machine interaction, system controls, on-line reporting, and software/hardware availability 23 p4174 A70-44541

Computerized algorithm facilitating automatic synthesis of time invariant linear compensation for highly complex multiloop control systems [AIAA PAPER 69-941] 23 p4177 A70-44561

Space shuttle economic risk analysis, using computer program as design and management tool 23 p4261 A70-44674

Digital computer codes for production finite element structural analysis, discussing input, output and engineering details 23 p4270 A70-44701

Asymptotic and computer methods interaction in thin walled shells structural analysis and design, considering pressure vessels, cone vibration and dynamic loads 23 p4271 A70-44703

Thin walled shells structural vibration, buckling and stress analysis by computer methods, discussing shell theory and design 23 p4271 A70-44704

General purpose computer programs for shell structural analysis, using finite element modeling and displacement methods 23 p4271 A70-44707

Arbitrary shells large deflection transient response, using finite difference computer program 23 p4272 A70-44710

Computer hardware and software technology for complex problems, discussing switching speeds and parallel and pipeline designs 23 p4167 A70-44716

Finite element structural analysis (FESTRAN) computer program predicting static structural response of plate and shell structures 23 p4272 A70-44717

Complex structures component modal dynamic analysis technique, describing investigations with combination of finite element and composite modes computer program 23 p4273 A70-44722

Nonlinear shell analysis by finite difference energy method, using BOSOR3 and STAGS computer programs 23 p4273 A70-44723

Computer program for geometrical nonlinear static and dynamic structural analysis of arbitrarily loaded shells of revolution 23 p4273 A70-44724

Stress, buckling and vibration analysis of shells of revolution by numerical integration and finite difference methods, summarizing computer programs 23 p4273 A70-44725

General Optimization Software Package for Electrical network and system design, noting application to engineering problems and education 23 p4177 A70-44750

Gradient iterative solution of large algebraic systems arising from finite element discretization, using computer methods 24 p4419 A70-45153

Matrix-vector computer program for three dimensional perspective projection and shell analysis in FORTRAN IV 24 p4419 A70-45155

Shell of revolution /pressure vessel/ with meridional slope discontinuity, calculating pressurization effect on stresses by computer program 24 p4420 A70-45277

Numerical integration of equations of motion from finite element analysis in structural mechanics, using computer program 24 p4420 A70-45278

Rapid satellite orbit prediction program by numerical integration including oblateness squared and radiation pressure effects over long time spans 24 p4406 A70-45528

Short period lunar perturbation on satellites by computer program with Fortran statements, considering errors, program output and table driven algebraic processors 24 p4406 A70-45532

Air traffic flow digital computer simulation model including departure, enroute and arrival phases for collision avoidance, weather effects and control constraints [AIAA PAPER 70-1316] 24 p4373 A70-45945

COMPUTER SIMULATION
U COMPUTERIZED SIMULATION
COMPUTER STORAGE DEVICES
NT ACCUMULATORS (COMPUTERS)
NT DELAY LINES (COMPUTER STORAGE)
NT MAGNETIC CORES
NT MAGNETIC TAPES
NT SHIFT REGISTERS

Information storage in complex automatic control systems with hierarchical structure composed of computers 01 p0047 A70-10983

Memory volume necessary to store intermediate data estimated for group processing from dependent Poisson information sources 04 p0661 A70-14552

Memory exchange between pairs of electrodes amorphous semiconductors, discussing switch-on and unlocking 04 p0732 A70-15687

Technique for coding data on cosmic ray variations based on packing digital information in computer storage, proposing selective statistical control for tape recording phase 05 p0898 A70-15929

Digital computers structural and operational address format dependence on number of storage readouts expressible with aid of linear function 05 p0818 A70-17004

Memory systems described by integrodifferential equations with distributed time lag, obtaining optimality condition in form of maximum principle 08 p1480 A70-21177

Switching and memory phenomena in semiconducting glasses, thin films and variable threshold metal-oxide-nitride-semiconductor MNOS transistor 08 p1556 A70-21304

Flexible PCM telemetry used in low power plated wire memory system for multiple applications 08 p1462 A70-21359

Display objectives and relationships to recording techniques examined for memory/display system, considering requirement for elastic erasing technique 08 p1467 A70-21761

Holographic optical memory feasibility for digital data storage using Ar ion laser, acousto-optic beam deflector system, hologram storage plane and photodetector array 09 p1642 A70-23780

Holographic optical memory systems operational principles and potential advantages, discussing feasibility of 100 million bit memory capacity and one microsecond random access time 10 p1892 A70-25245

Electronic switching effects in amorphous semiconductors emphasizing mass memory for computers based on thin films of chalcogenides 11 p2017 A70-25524

Holographic memory devices design for information storage 13 p2405 A70-28792

Memory systems in measurement and control equipment, describing applications to linearizing, compression and data refresh operations 14 p2554 A70-30676

Graphical data conversion into code for storage in computer memory 15 p2705 A70-31576

Portable MOS memory module with optical loading and electrical readout, using hybrid array of complementary silicon on sapphire chips 16 p2868 A70-33457

Memory technology based on electrically alterable nonvolatile silicon nitride variable threshold transistor 16 p2868 A70-33458

MOS transistor associative memory cell design utilizing LSI technology 16 p2869 A70-33464

Military aircraft avionics central digital computers, discussing memory capacity, computational speed requirements, cost and tradeoffs 17 p3049 A70-34673

Solar image spectrum magnetic recording for computer, using photomultipliers with coding devices 18 p3256 A70-36107

Three digit hydromechanical step type actuator drives with slide valve assembly for computer data sampling systems 18 p3216 A70-37071

Magnetic bubbles in miniaturized electronic circuits, discussing fabrication and uses in communication and computers 19 p3484 A70-37574

Optically bistable crystal applications, discussing photochromaticity, catochromatic tubes, oscilloscopes, computer storage devices and laser systems 19 p3446 A70-37860

Computer generated holograms production, reducing memory size and plotter resolution 20 p3627 A70-39098

Multichannel cosmic ray recorder providing input to computer memory 20 p3629 A70-39313

Digital optical storage for information system components 21 p3823 A70-40852

Holography application to high capacity permanent memory systems 21 p3825 A70-41125

Computer storage technology, discussing magnetic films, semiconductor cells, content addressable and read-only memories, etc 21 p3795 A70-41693

Airborne test computer for in-flight radar checkout featuring tape storage of computer program and cockpit mounted optical readout 22 p3993 A70-42320

Reprogrammable read-mostly memory /RMM/ using integrated circuit array of amorphous and crystalline semiconductor devices, discussing design and applications 22 p3996 A70-42772

Semiconductor storage unit with decoding circuit, memory matrix and read-out amplifiers 22 p3996 A70-42847

Modular plated-wire digital associative processor with content addressable memory, distributed arithmetic and I/O capability at each word 22 p3994 A70-43104

Avionics digital computer system using associative memory for executive control functions implementation to mechanize task assignment algorithm 22 p3994 A70-43105

Optical read-write mass memory based on holographic storage and light addressable matrix array, discussing significance to computer design and usage 22 p3994 A70-43606

Optical system for read-write holographic memory capable of high storage density 22 p3994 A70-43607

Magnetic holography, considering Faraday and polar Kerr effect reconstructions and potential as computer storage 22 p3994 A70-43608

Integrated ferroelectric photoconductor device for hologram storage, discussing improved phase readout technique for reconstruction 22 p3994 A70-43609

Computer-aided aircraft design, discussing parts geometry data bank, visual display, etc [ICAS PAPER 70-27] 23 p4200 A70-44106

MIS model applied to memory transistor with thin insulator consisting of silicon nitride on silicon dioxide 23 p4172 A70-44197

Optimum finite memory model for sequential minimum-mean-square-error estimation of random variable in added noise 24 p4317 A70-46052

COMPUTER SYSTEMS PROGRAMS

NT INPUT/OUTPUT ROUTINES

NT OPERATING SYSTEMS [COMPUTERS]

Time sharing computer systems for data reduction from semiconductor strain gauges applied to FORTRAN IV programs 03 p0453 A70-12969

Airborne computer system program for antisubmarine warfare enhancing human element in man machine system 06 p1185 A70-17974

Space programming language SPL/J6 replacing machine language programming in flight software capable of expressing complex vector mathematics and decision control 16 p2868 A70-33429

Computer time sharing system for real time mass properties measurements [SAWE PAPER 853] 20 p3595 A70-40374

Computer system for ECG interpretation in hospital heart station 22 p3979 A70-43483

COMPUTERIZED DESIGN

Computer calculation in elastoplastic range of statically indeterminate structure of bars, considering collapse load, stress and hinge rotation 01 p0200 A70-10524

Time sharing computer systems to perform circuit design and analysis, discussing effectiveness in terms of immediate access, accuracy and cost 02 p0265 A70-12187

Linear arrays computerized design with variable element spacing and excitation amplitude 02 p0269 A70-12596

Microwave circuits automatic analysis and design using digital computer in batch mode, describing analysis-optimization program 03 p0457 A70-13562

Optimal synthesis and design of distributed parameter system for waveguides using gradient technique with devised algorithm to overcome convergence problem 03 p0449 A70-13563

Device modeling for computer aided design and analysis of integrated circuits, discussing list of desirable properties and applications to transistor design 03 p0454 A70-14026

Matrix algorithm from parallel element method derived for reducing computer time required in structural modification analysis 04 p0779 A70-15589

Computer-aided design using third generation computers and interactive graphic systems applied to transonic aerodynamics problems 05 p0816 A70-16122

Network analysis for systems application program /NASAP/ computer-aided circuit design program for network analysis, discussing application in education 06 p1015 A70-18418

Computer aided network design course using FORTRAN 4 emphasizing modeling of semiconductor devices 06 p1015 A70-18419

NASAP program FORTRAN subroutine LOOPS for loop detection in circuit analysis, discussing automatic instrumentation process for computation time reduction 06 p1015 A70-18421

Hybrid NASAP program module for direct design of linear dynamic circuits using simple optimization without sophisticated computer programming 06 p1015 A70-18422

Digital computer design of electric and radio equipment using secondary source method for field boundary calculation in inhomogeneous environment 07 p1241 A70-19480

Integrated switching circuits design optimization by ALGOL program, analyzing circuits transient behavior 07 p1242 A70-19752

Large scale integration /LSI/ in electronics, discussing high density microelectronic, memory and logic circuits, fabrication and computer aided design 08 p1468 A70-20468

Automatic test equipment for electronic devices, discussing computerized design of interface adapters for unit under test 08 p1470 A70-20657

Computerized generation of cost optimal decision logic for malfunction analysis 08 p1470 A70-20659

Integrated man machine shipboard maintenance systems design, describing computerized model based on information flow network 08 p1465 A70-20665

Tandem link multichannel LOS FDM-FM communication system cost optimization by computer-aided design 08 p1459 A70-20798

Optimal control synthesis for flight vehicle in vertical plane involving digital and analog computers 08 p1479 A70-20997

Computers impact on engineering science and design, detailing digital computers use in aerodynamics, structures and aeroelasticity 08 p1466 A70-21030

Controllable microwave phase shift varactor diode circuit parameters design optimization using digital computer for transmittance matrix coefficients calculation 08 p1474 A70-21230

Commensurate transmission line circuits design approximating periodic frequency characteristics on digital computer 08 p1476 A70-21286

Airfoil analysis and synthesis, discussing computer graphics application to low speed shape and improved pressure distribution 08 p1594 A70-21867

Lossless three-port H-plane waveguide junction circulator performance evaluation using computerized design 09 p1646 A70-22710

Hidden-line determination for computer-drawn polyhedra using edge classification scheme for CRT display applications 09 p1641 A70-22966

Computer aided design programs as decision-making tool for fighter development projects technical management [AIAA PAPER 70-364] 09 p1611 A70-23024

Digital computer impact on aerospace sciences and technologies in terms of computerized design, interactive graphics, flight simulation, Apollo systems checkout, etc 09 p1642 A70-23277

Concorde SST aerodynamic, structural and thermal analysis and simulation using computers 10 p1849 A70-24382

Computer-aided class C amplifier design, discussing algorithm and computer program 10 p1849 A70-24447

Hybrid computer applications in systems approach to engineering design, discussing design process and computer description 10 p1861 A70-24658

Computer-aided circuit design by imbedding singular elements to transform network synthesis into analysis problem 10 p1855 A70-24762

Computer and system design automation, considering language problems, microprograms, optimization on subsystem suboptimal basis, etc 10 p1845 A70-24874

Avionics test station optimum design by computerized simulation involving iteration of computer run, analysis and model change [AIAA PAPER 70-398] 10 p1861 A70-24907

Poseidon missile optimized and automated computer aided electronic packaging design, considering partitioning, placement, internal and external cable, etc 10 p1853 A70-25210

Communications satellite for Alaska and Mountain States TV defined using computerized synthesis program [AIAA PAPER 70-453] 11 p2001 A70-25473

Computerized design of aircraft contours, determining three dimensional surface by second degree equation [SAE PAPER 700202] 11 p2013 A70-25876

Computerized tradeoff analysis for planetary landing vehicle entry capsule and lander design optimization, emphasizing weight allocation for Mars 1973 missions 11 p2126 A70-26320

Computerized design of microwave circuits with S matrix 11 p2019 A70-26714

Linville bipolar transistor model for computer-aided design programs 11 p2021 A70-26830

Computerized automation of R and D engineering, discussing critical effects of generalization and oversimplification 12 p2334 A70-27006

Computers graphical display devices for rapid designer-computer communication 12 p2191 A70-27013

Aircraft all-movable stabilator computer aided design for optimized structural weight and performance 12 p2319 A70-27137

Automated optimum structural design by variable step direct search algorithm, noting application to stiffened cylindrical shells 12 p2319 A70-27138

Computer aided electronic circuit design, describing calculations, graph and table generation, data storage, etc 12 p2192 A70-27769

Computer-aided MOS/LSI four phase logic circuit design, discussing software, design cycles and testing 13 p2380 A70-28375

Mathematical cartography, discussing uses of electronic computers in network design 13 p2395 A70-28925

Minimum weight structural member size and configuration simultaneous optimization using computer program

13 p2516 A70-29550

Monograph on analysis of reflector antennas covering electromagnetic field equations, computer aided design, etc

13 p2367 A70-29600

Minimum weight design for complex structures subject to frequency constraint using finite element method and computer program

13 p2517 A70-29965

Computer oriented algebraic method for duplicator control systems applied to loop network, lag, feedback, phase lead and phase lead lag compensator design

14 p2560 A70-30620

Electronic systems automatic design problems including man machine communication and data organization

14 p2554 A70-30663

Computerized design of transistorized UHF wide-band amplifier, using successive approximations for optimum circuit automatic selection

14 p2556 A70-30668

Integrated circuits design by combined automatic and manual system

14 p2554 A70-30670

Flat circular parachute stress analysis in steady vertical descent, using computer program for design change effects on shape, drag and stress

14 p2531 A70-30863

Microstrip circuit design, obtaining dimensions by computer programs incorporating subroutine sets

14 p2561 A70-30922

Computerized design of multipad and multirecess incompressible fluid film bearings

15 p2744 A70-31958

Cascade digital filter computerized design with favorable signal to noise ratio, considering round-off errors

15 p2709 A70-32465

Linear time varying low pass filters computer aided design, introducing quadratic performance criterion to calculate steepest descent in function space

15 p2710 A70-32588

Topology and component values in computerized design of distributed lumped active networks

15 p2711 A70-32595

Large signal junction FET model involving piecewise linear approximation for ECAP circuit analysis program

15 p2711 A70-32596

Integrated analog shift register circuits computer aided design, using insulated gate field effect transistor (IGFET)

15 p2711 A70-32597

On-line computer aided design of fixed point digital filters simulating direct, cascade and parallel bit representations

15 p2711 A70-32598

Superdirective small linear antennas computer aided design using Fourier integral and transform techniques

15 p2711 A70-32601

Computer aided design for microwave branch line couplers dimensions practical for integrated circuit microstrip fabrication

15 p2711 A70-32602

Filters design by on-line graphic interface computerized synthesis utilizing three screen CRT display

16 p2867 A70-33041

Nonlinear digital programming techniques for airplane stability augmentation systems design

16 p2840 A70-33343

Fixed and variable sweep wing structure computerized design optimization

[ASME PAPER 70-DE-41] 16 p2869 A70-33506

Fluid power systems computer aided design and optimization, describing modeling and simulation, parameter sensitivity, systems stability, etc

[ASME PAPER 70-DE-44] 16 p2869 A70-33508

Fluid logic systems synthesis by computer aided design programs, proposing referee system

[ASME PAPER 70-DE-47] 16 p2844 A70-33510

Computerized design for radial flow splitters in three dimensional fan exhaust nozzles

18 p3207 A70-36462

Linear feedback control system with dead time compensated by proportional integral derivative action controller, evaluating stability by digital computer

18 p3236 A70-36944

Airport planning and design, discussing role of computers in capacity and site analysis, wind data processing, passenger and baggage flows analysis, etc

19 p3396 A70-37749

DC-to-sinusoidal inverter employing PWM waveform, analyzing circuit parameters effect on harmonic content

19 p3358 A70-37854

Structural weight design optimization by computer aided geometrical programming technique

[SAWE PAPER 822] 20 p3733 A70-40357

Aircraft loadability design by computerized loading program using graphic plotter

[SAWE PAPER 836] 20 p3562 A70-40364

Aircraft manufacturing cost estimation in conceptual design phase, using structural synthesis program for cost buildup simulation

[SAWE PAPER 853] 20 p3741 A70-40371

Structural mass properties solution using programmable printing desk computer for fast data point plotting

[SAWE PAPER 856] 20 p3595 A70-40372

Supersonic aerodynamic design tools, discussing technological application of high speed computer and limitations

[AIAA PAPER 68-1018] 22 p3958 A70-42701

Linear FM radar pulse compression matched filter response calculated by computer evaluation of cross ambiguity function for design tradeoff between resolution and performance

22 p3992 A70-43589

Digital computer algorithm for automatic electronic circuit design using design engineer experience

23 p4171 A70-43953

MOS transistor trigger circuit design parameters statistical calculation and optimization by Monte Carlo method using computer

23 p4171 A70-43957

Linear phased arrays computer aided design, discussing search algorithms in multivariable optimization program

23 p4172 A70-44015

Short haul jet transport aircraft design, discussing Computer Aid Design, Airline System Simulator and Traffic Demand Predictor computer programs

[ICAS PAPER 70-28] 23 p4284 A70-44105

Computer-aided aircraft design, discussing parts geometry data bank, visual display, etc

[ICAS PAPER 70-27] 23 p4200 A70-44106

Aerobee rocket-borne cryogenic air samplers heat exchanger design by mathematical model and computer solution

23 p4280 A70-44365

Optimal design of minimum weight bar and beam structures under static loads, comparing computer time with nonlinear programming methods

23 p4271 A70-44702

Nonlinear shell analysis by finite difference energy method, using BOSOR3 and STAGS computer programs

23 p4273 A70-44723

Electrostatic potential distribution and ion trajectories in extraction gage design by computer

23 p4198 A70-44873

Computerized design of broadband microwave amplifiers with complex terminations, using transfer scattering parameters for analysis and optimization

24 p4316 A70-45211

Optimality criterion selection for asynchronous microelectric motor design by computer

24 p4293 A70-45470

Computer optimization program for solid state components and integrated circuits design with conversational system for man machine dialogues

24 p4317 A70-46321

COMPUTERIZED SIMULATION

NT ANALOG SIMULATION

NT DIGITAL SIMULATION

Equivalent linear dynamic systems obtained by analog computers for determining equivalence equations coefficients and by Chebyshev functional to assess discrepancy

01 p0052 A70-10193

Bioelectrically controlled system for indirect heart massage, noting dynamic simulation of system on digital computers using block oriented programming languages

01 p0047 A70-10261

Hardware CRT display system based on digital computer for dynamic flight simulation of moving spatial objects

01 p0089 A70-10818

Computer model for evolution investigation of disks of stars, discussing methods to obtain gravitational potential

01 p0185 A70-11065

Computer driven display terminal as part-task limited area simulator, examining operational requirements and input characteristics

01 p0059 A70-11277

Analog, analog/digital, digital and hybrid computer simulation current advances, emphasizing physiological problems and optimum solution

02 p0264 A70-11687

Trainers and simulators based on digital computers, eliminating system sensitivity to ambient conditions, power fluctuations, circuit imperfections and digital to analog conversion

02 p0274 A70-11841

Computer simulation of automated ATC systems, discussing operational gaming and mathematical models

02 p0274 A70-11968

Digital real time simulation for training and evaluating ATC controllers, discussing system hardware, software, design and implementation

02 p0274 A70-11977

Computer simulation of automated air traffic control concepts, formulating and implementing general-

ized model of automated transition/terminal area systems

02 p0335 A70-12133

Reactive forces and torques of musculoskeletal system during lifting and carrying materials, using computerized biomechanical models

02 p0247 A70-12549

Photographic negatives analysis, storage and reconstruction using facility permitting photography conditions simulation and computer image treatment

02 p0302 A70-12614

Air combat model /AIRCOM/ to evaluate close-in air-to-air fighter aircraft combat capability, determining relative changes in kill probability per firing pass

03 p0413 A70-13958

Terrain computerized mathematical model for determining unobstructed line of sight between observer and target

03 p0455 A70-14172

Mathematical model for computer simulation of homogeneous neuron nets with recurrent inhibition control, considering activated and inactivated states

04 p0640 A70-14553

Cloud cover consequence on earth photographing space missions simulated by Monte Carlo method using worldwide statistics

04 p0676 A70-14636

Computer modeling of operational amplifier integrated circuit in ionizing radiation environment, using RLC network and voltage transfer curve

04 p0658 A70-14740

Computer program for electrical and transient thermal analysis of satellite electric power subsystem consisting of solar array, battery and power controls

04 p0628 A70-15332

Hybrid computer simulation of small nonlinearities effects in human arterial system, using perturbation techniques

05 p0805 A70-16045

Haze model atmospheres scattering characteristics by computer simulation concerning optical contrast reduction by aerosols for direct and diffuse radiation

[AIAA PAPER 70-194] 06 p1057 A70-18156

Monte Carlo method for modeling gas flow by simulated molecules concurrently followed through collisions and boundary interactions in simulated physical space within computer

06 p1113 A70-18314

Computerized FORTRAN equations simulation of linear and nonlinear circuits for symbolic analysis and transient response

06 p1026 A70-18424

Mathematical techniques for selenodesy computer simulation program, solving problems arising from infinite series of spherical harmonics for lunar gravitational potential

06 p1152 A70-18498

Visual simulation in Lunar Module Mission simulator provided by computer controlled infinity optics system

06 p1031 A70-18603

Narrow band limiter influence on SNR at FM reception output by computer simulation using threshold pulse model

07 p1227 A70-19124

Ionospheric motions and irregularities effects on HF radio propagation using computer simulation involving ray tracing and ionosphere modeling

07 p1264 A70-19192

Computer scheduling model and timeline plot for Apollo Telescope Module (ATM) experiments using orbital trajectory simulation

07 p1394 A70-19572

Computer program /TACTICS/ for simulating three vehicles simultaneous motion in space, considering interceptor-target guidance and intercept trajectories

07 p1239 A70-20414

Man-computer interactions in experiment design analysis, discussing applications to computer simulation

08 p1464 A70-20606

Plasma oscillations analytic second order theory verification by computerized simulation, using Fourier-Hermitian expansion of distribution function in phase space

08 p1550 A70-20636

Extremal statistics for signal and noise error probabilities estimation and computer simulation of digital feedback communication systems

08 p1459 A70-20800

Simulation applications - Conference, Los Angeles, December 1969

08 p1466 A70-20926

Alternative equipment maintenance procedures costs by combined discrete event and continuous system simulation, discussing additional model applications

08 p1466 A70-20927

Extendable computer simulation model /ECSS/ overcoming programming and debugging problems, discussing language selection, design, specification, work load, etc

08 p1466 A70-20928

GPSS simulation for airport capacity, analyzing aircraft ground traffic flow characteristics and developing expansion schemes minimizing investment

08 p1481 A70-20929

SOAR /Simulation of Airlift Resources/ model for stochastic productivity variations of strategic airlift systems

08 p1466 A70-20930

Boeing 747 aircraft container system deployment simulation written in GPSS/360 to minimize stockholding of containers at individual stations

08 p1481 A70-20931

Saturn 5 Prelaunch Systems Simulation Model for launch opportunity containing multiple launch windows, considering last 26 hours of countdown

08 p1582 A70-20933

Real time simulation of air traffic control problems in Brussels upper information region /UIR/

08 p1541 A70-21361

Reticular formation of central nervous system in vertebrates described as behavior controlling circuit of interconnected modules, proposing hybrid computer method for operational scheme

08 p1447 A70-21461

Textured gray-scale imagery by computer simulating lunar display

09 p1642 A70-23771

Ground based moving-base aircraft flight simulator using computer program to establish motion requirements

[AIAA PAPER 70-348]

10 p1859 A70-24213

Computer simulation of six degree of freedom motion system and actual system test, substantiating simulation accuracy

[AIAA PAPER 70-358]

10 p1859 A70-24218

Concorde SST aerodynamic, structural and thermal analysis and simulation using computers

10 p1849 A70-24382

Impact problems of slip clutch and beam scales dynamic characteristics simulation by 1130 CSMP /Continuous System Modeling Program/

10 p1860 A70-24653

SIMCON digital simulation control system optimizing man machine interaction, noting capability to generate solutions with minimum computer memory

10 p1860 A70-24654

Avionics test station optimum design by computerized simulation involving iteration of computer run, analysis and model change

[AIAA PAPER 70-398]

10 p1861 A70-24907

Hybrid simulation, determining vehicle and performance parameters on longitudinal flying qualities of STOL transport in power approach configuration

[AIAA PAPER 70-387]

10 p1806 A70-24918

Cloud cover effect on earth photographing space missions by Monte Carlo computer simulation, using worldwide cloud statistics

11 p2075 A70-25600

Insulators, ablaters, reflectors and computer analyses for aerodynamic and engine heat for aerospace thermal design

11 p1980 A70-25874

Two dimensional unsteady fluid flow in square cavity numerically analyzed from continuity and Navier-Stokes equations and recorded as computer-generated motion picture

11 p2035 A70-25971

Spacecraft launch computerized simulator, discussing operational characteristics applicable to on-line real time process control

11 p2013 A70-26217

Steady state large signal computer model for junction-gate field effect transistors below pitch-off

11 p2019 A70-26711

Electron beam-plasma interaction nonlinear development in time and space using computer simulation

11 p2095 A70-26758

Empennage loads on T tail transport determined for combined vertical and lateral gust loads using real time analog-digital computer simulation

12 p2160 A70-27113

Collisionless electrostatic shock generation conditions, simulating homogeneous counterstreaming plasmas by computer

13 p2462 A70-29110

Delta modulation with slope-overload prediction, showing signal to noise ratio improvement from computer simulation

13 p2365 A70-29146

Computer modeling of nonlinear phase automatic frequency control systems under noise and oscillating disturbance

13 p2383 A70-29303

Cloud model development and computer simulation uses, noting applications to aerospace experiment design

14 p2608 A70-30597

Computer models simulating plasma motion applied to sheet pinch stability, investigating relativistic and nonrelativistic regimes

14 p2623 A70-30696

Gas flow calculations application to gas turbines simulations, considering engine dynamics, one dimensional flow and program structure

14 p2629 A70-30990

Quality control variables optimization for maximum net revenue, using computerized simulation

14 p2592 A70-31105

Electromagnetic interference /EMI/ effects on TALOS missile guidance receiver by expanding computer simulation test results

14 p2655 A70-31345

Computerized thermal modeling of spacecraft environmental control systems /ECS/

15 p2705 A70-32523

On-line computer aided design of fixed point digital filters simulating direct, cascade and parallel bit representations

15 p2711 A70-32598

Complex systems effectiveness analysis by computer simulation technique

15 p2706 A70-32633

Hybrid computer simulation of steady state oxygen transport and consumption in capillary-tissue system

15 p2694 A70-32845

Optimal control solution for dynamic entry vehicle along planar trajectory, using hybrid computer simulation

16 p2981 A70-33443

Automatic alphabetic characters classification model based on cross correlation and discrete Walsh-Fourier transforms, using computerized simulation

16 p2851 A70-33460

Human and machine pattern discrimination correlated by statistical correlation method from pattern recognition task involving computer simulation and humans

16 p2852 A70-33461

Remote real time simulation, using CDC 6600 computers, peripheral equipment and wideband communication link

16 p2870 A70-33732

Real time simulation of space vehicle and ground support equipment by digital computer for launch programs checkout

16 p2870 A70-33733

NERVA XE-Prime test series, discussing computer simulation, full power and high specific impulse operation and startup under varying initial conditions

[AIAA PAPER 70-709]

16 p2951 A70-33950

Human body radiation shielding, describing development of computerized standing and seated model for space missions

[AAS PAPER 70-053]

17 p3036 A70-34794

Real time hybrid computer simulation of guided and controlled rocket flight, noting correlation with digital simulation

17 p3060 A70-35285

Systems operation hybrid simulator for computer checkout of Saturn S-1C stage

17 p3061 A70-35489

Digital computer simulation and analysis of control loops for ion thruster control

[AIAA PAPER 69-239]

17 p3149 A70-35654

Japanese scientific satellite magnetic attitude and spin rate control system design and computer simulation

18 p3332 A70-36065

Computerized simulation role in air traffic control

18 p3236 A70-36398

Optimum approach and departure paths for VTOL aircraft simulated by hybrid computer under constraints

[AIAA PAPER 69-209]

18 p3213 A70-36452

Computerized air combat simulation with comparison of analog and digital approaches, noting Air to Air Combat Fort Worth

18 p3230 A70-36453

Finite size particle physics for plasma computerized simulation, considering longitudinal oscillations, scattering cross sections, diffusion coefficients, etc

18 p3296 A70-36791

Soviet book on isolated animal heart autoregulation, considering cardio-pulmonary preparations, functional capacity, biometrics and computer technology for heart activity simulation models

19 p3359 A70-37404

Airport capacity analysis for terminal areas, using simulation for alternatives to parallel runway operation

19 p3397 A70-38236

Airport capacity and layout, considering air traffic increase, runway occupancy, taxiway and computer simulation

19 p3468 A70-38636

Operational analysis and real time computer simulation models in ATC development

19 p3468 A70-38637

ATC simulation at EUROCONTROL Experimental Center, discussing dynamic simulator, data processor and display

19 p3468 A70-38638

Mariner 7 preencounter anomaly in radio tracking data and trajectory investigated by computerized simulation

[AIAA PAPER 70-1065]

19 p3534 A70-38878

Computer simulated decision hierarchical model of helicopter and VTOL pilot for multiloop closure and tracking characteristics of man-vehicle system

19 p3372 A70-38921

Digital computer model of total body ECG surface maps, simulating male torso with lungs

20 p3578 A70-39369

Satellite-borne conical IR scanner flight data hybrid simulation and error analysis, suggesting carbon dioxide horizon noise model

[AIAA PAPER 70-1021]

20 p3631 A70-39513

Interactive hybrid simulation of TRIAD satellite motions, describing attitude control system with magnetic hysteresis damping

[AIAA PAPER 70-994]

20 p3714 A70-39536

Real time network support simulation allowing network configuration for nominal or perturbed trajectory for Saturn vehicles, applicable to any flight azimuth

[AIAA PAPER 69-936]

20 p3591 A70-39684

Acoustic /microwave/ holography for large masses by crossed linear array of microphones, discussing computer simulation of virtual holograms and image reconstruction

21 p3822 A70-40715

Command module simulators for Apollo astronaut training in moon landing, using computer, exterior visual scenes and spacecraft interior replica

21 p3804 A70-41195

Lunar module simulator for Apollo flight training using computers, digital conversion, cockpit replica, infinity-optics display and instructor control

21 p3805 A70-41196

Computer real time Apollo simulation, checkout and training system duplicating actual mission for flight controllers in Mission Control Center

21 p3805 A70-41198

Gliding parachute air cargo systems using nonproportional and proportional automatic manual control, estimating wind effects on ground track and impact computer simulation

[AIAA PAPER 70-1193]

21 p3753 A70-41823

Mission analysis and trajectory simulation /MATS/ program, discussing computer controls, modular design, integration evaluation

[AIAA PAPER 69-939]

21 p3920 A70-41872

Computer model of self gravitating gas-stars system with spiral structure surviving galactic rotations

22 p4103 A70-42982

Computer synthesis of completely eclipsing binary light curves including limb darkening and simulated observational errors

22 p4103 A70-42990

STOL system traffic analysis simulation model for interurban transportation system as tool for flight hardware evaluation

22 p4007 A70-43731

Computerized mathematical modeling of transistors statistical and dynamic characteristics as functions of structural parameters

23 p4171 A70-43954

Various Frank loops in quenched and annealed Pt, examining dislocations with field ion microscopy and computer simulated approximations

23 p4230 A70-44758

Computerized simulation and hardware for propulsion control of turbine engines

[SAE PAPER 700827]

24 p4394 A70-45892

Computerized simulation of raindrop effects on initiation of cloud-to-ground lightning strokes

24 p4371 A70-45978

Vortices growth in vortex sheets bounding jets flowing from two dimensional slit and circular orifice observed by computer experiments

24 p4327 A70-46244

COMPUTERS

NT AIRBORNE/SPACEBORNE COMPUTERS

NT ANALOG COMPUTERS

NT DIGITAL COMPUTERS

NT HYBRID COMPUTERS

NT IBM 360 COMPUTER

NT SEQUENTIAL COMPUTERS

NT SITE DATA PROCESSORS

Cost effective phased buildup of computerized ATC systems

02 p0401 A70-11961

Instruments and procedures for photogrammetry automation, discussing automatic pattern recognition, data correlation and computer role

02 p0302 A70-12652

Computers - IEEE Conference, Minneapolis, June 1969

05 p0817 A70-16413

Matrix Computer equisolution matrices for nonlinear algebraic and integrodifferential equation systems solution

06 p1014 A70-17427

Management systems growth in relation to computer applications development, noting second industrial revolution

10 p1971 A70-24661

Computerized aircraft navigation utilizing Doppler dead reckoning system and Tacan integration with least square adjustment method

13 p2447 A70-28550

Computer system maintainability demonstration test in accordance with MIL-STD-471, discussing techniques for failure indication and repair crew qualifications and training

15 p2706 A70-32657

Computer applications in radar and air traffic control, large steerable aerials, systems design and graphical displays

15 p2832 A70-32704

Computers - AFIPS Conference, Atlantic City, May 1970

16 p2870 A70-33730

Computer users functions to determine preparation level for effective dialog with computer, discussing teaching stages

18 p3223 A70-36077

Computer merits in test laboratory data acquisition systems

19 p3383 A70-37921

Multichannel computer for statistical investigations of complex nonlinear controlled plants based on recordings of input, output and internal state variables

20 p3594 A70-39921

Biocybernetics of human central nervous system, discussing electronic computers analogy to human brain

23 p4145 A70-44222

Electronic simulation of indicator-dilution curves for comparative evaluation of cardiac output computers

24 p4309 A70-46120

COMSAT PROGRAM

Signal attenuation and bandwidth limitations imposed by atmospheric hydrometeors on communications satellite systems above 10 GHz, discussing Comsat measurement programs

11 p1997 A70-25408

COMSAT measurement of precipitation scatter effects on propagation for frequency sharing with terrestrial radio relay terminals

11 p1997 A70-25413

Commercial communication satellite earth station technology and operations covering frequency allocations, antennas, orbits, etc

11 p1998 A70-25424

Launch vehicle selection, utilization and mission planning and analysis in Comsat programs, discussing INTELSAT I-IV

11 p2002 A70-25489

Commercial satellite communications, discussing creation and objectives of Comsat and establishment of Intelsat

13 p2368 A70-29618

Si and CdS solar cell research at COSMAT laboratories, discussing proton and electron irradiations and thermal cycling

15 p2677 A70-31804

CONCAVITY

Plane stationary shock wave reflection from rigid concave wall at low Mach numbers

21 p3811 A70-42204

CONCENTRATION (COMPOSITION)

NT ATMOSPHERIC MOISTURE

NT ATOM CONCENTRATION

NT CARBON DIOXIDE CONCENTRATION

NT MASCONS

NT METEOROID CONCENTRATION

NT MOISTURE CONTENT

Thermomechanical processing of high strength low alloy steels to evaluate effects of composition, coiling temperature and cooling rate on mechanical properties and microstructures

01 p0118 A70-10726

Vertical concentration and size distribution determinations for aerosols in stratosphere, suggesting volcanic origin

02 p0294 A70-12842

Flame structure of liquid methanol burning spheres, discussing temperature and composition profiles

03 p0544 A70-13924

Laser induced Raman scattering as diagnostic technique for measuring specie concentrations in gas mixtures

[AIAA PAPER 70-224]

06 p1066 A70-18214

Continuous generation of gas trace component quantities into carrier gas flow using dosage device

09 p1672 A70-22028

Initial cloud formation model, computing drop concentration and supersaturation

11 p2075 A70-25917

Analytic expressions for concentration distribution functions in inhomogeneous solids within intermediate stages of homogenization process

12 p2253 A70-27282

Turbulent boundary layer velocity, temperature and concentration instantaneous measurements, describing automatic circuit procedure

17 p3088 A70-35041

Optical observation of laminar convective flow caused by combined action of concentration and temperature fields

18 p3346 A70-36276

Transport ratio for I-131 air to milk concentrations, determining mean value and statistical variation from Project Rover data

19 p3361 A70-38012

Apollo 11 lunar rock and fines primordial radionuclide abundances and concentration gradients by gamma ray spectrometry at Lunar Receiving Laboratory

21 p3776 A70-41595

Apollo 11 lunar surface fine material and rocks cosmogenic radio nuclides Al 26 and Na 22 concentrations determination by gamma ray spectroscopy

21 p3910 A70-41618

Cu-Ni diffusion couples voids and edges effect on concentration gradients measurement by electron probe microanalysis

22 p4054 A70-42740

CONCENTRATORS

Solar energy concentrator with truncated conical mirror and toroidal lens to illuminate cylindrical thermoelectric generators or radiation pumped lasers

01 p0010 A70-10760

Hydrogen-oxygen fuel cell reaction water removal and heat loss using reconcentration device

12 p2163 A70-27066

CONCENTRIC CYLINDERS

Torque upper bounds in Couette flow between concentric rotating cylinders, considering dissipation integral and boundary and continuity conditions validity

03 p0468 A70-13787

Navier-Stokes boundary value problem describing viscous incompressible fluid flow between coaxial fixed and rotating cylinders, emphasizing stability analysis

03 p0470 A70-14242

Bessel function applied to unsteady axisymmetric problem of heat conduction in thermally controlled coaxial cylinders with different physical properties

03 p0608 A70-14304

Rarefied gas heat conduction between concentric cylinders at small Knudsen number and temperature gradient, using integral equations obtained from Krook equation

[ASME PAPER 69-WA/HT-19]

04 p0783 A70-14816

Viscous frictional torque on inner cylinder of eccentrically rotating concentric cylinders measured from laminar to turbulent flow

06 p1074 A70-17134

Rarefied gas flows and heat transfer between parallel plates, concentric cylinders and spheres in presence of fractionally accommodating boundaries

06 p1049 A70-18330

Time dependent stability of viscous rotational Couette flow induced by impulsively started rotating inner cylinder, using dye injection and motion pictures

07 p1255 A70-19209

Viscous compressible fluid steady laminar flow between coaxial cylinders, studying flow characteristics for uniform inner cylinder velocity

10 p1870 A70-24792

Eccentric cylinders with outer cylinder rotating measured for eccentricity and clearance ratios effects on pressure distribution and force on inner cylinder

11 p2060 A70-26409

Homogeneous viscous fluid steady state parallel Stokes flow in annular region between concentric cylinders at low Reynolds numbers

11 p2038 A70-26478

Steady state and transient heat transfer by radiation and conduction in absorbing medium bounded by infinite coaxial cylindrical surfaces

12 p2331 A70-27697

Flow stability of electrically conducting inviscid fluid in coaxial cylindrical annular space under influence of axial magnetic field

12 p2210 A70-27799

Swirling flow between concentric cylinders, studying helical instability modes

13 p2386 A70-28805

Mean field approximations to Couette flow stability between fixed and coaxial rotating inner cylinder, using Roberts preferred mode method

13 p2392 A70-30007

Viscoelastic fluid in Couette flow between coaxial cylinders and flow between fixed plane and rotating cone

14 p2567 A70-31358

Annular turbulent flow between coaxial rotating cylinders, analyzing energy balance of averaged and pulsating motions

15 p2721 A70-32138

Initial thermally stressed state of solid bounded by concentric cylindrical cylinders, applying Cauchy thermoelastic stress theory

16 p2987 A70-32993

Thin concentric circular cylindrical shells joined at ends by rigid diaphragms, describing free and forced torsional motion

16 p2992 A70-34019

Modified discrete ordinate approach in rarefied gas dynamics tested on linearized Couette flow between concentric cylinders, using integral iteration

17 p3067 A70-34548

Couette flow stability between coaxial rotating cylinders, calculating eigenvector in first approximation small perturbation equations

17 p3073 A70-35695

Gunn effect devices with concentric cylindrical electrodes, examining oscillation natural frequency-applied voltage relation

19 p3392 A70-38900

Unsteady temperature field in cylinder surrounded by thin shell under uniformly distributed heat sources

20 p3737 A70-39640

Nonuniform radiation heat transfer between two coaxial cylinders, obtaining temperature distribution by Fourier series expansion

21 p3952 A70-42082

Poiseuille-Couette spiral flow stability between concentric rotating cylinders

22 p4010 A70-42691

Thermal conductivity of water, toluene and benzene in coaxial cylinders, taking into account edge heat losses

23 p4276 A70-44216

Rarefied gas heat conduction between concentric cylinders in slip regime, obtaining perturbed temperature and density variations

23 p4284 A70-44985

Temperature profiles for viscous fluid contained between two concentric rotating porous cylinders

24 p4327 A70-46005

Viscous fluid two dimensional steady natural convection between horizontal concentric cylinders for low Grashof numbers

24 p4429 A70-46007

CONCORDE AIRCRAFT

Concorde aircraft structural acoustics and design problems, discussing noise, fatigue and testing techniques and facilities

01 p0199 A70-10288

Concorde power plant tests using supersonic free jet altitude test facility with Olympus 593 engine

01 p0165 A70-10701

Concorde aircraft flight simulator, describing pilot training system refinement and pilot training

01 p0057 A70-10797

Concorde engine and air intake electronic controls

02 p0353 A70-11837

Concorde aircraft main landing gear reliability, discussing design, corrosion, hydraulic contamination, metallurgy, sealing and tests

02 p0226 A70-12366

Structural aluminum alloy developed for Concorde Mach 2.2 flight, discussing cold mechanical properties, zero creep and fatigue resistance

04 p0706 A70-15041

Concorde microelectronic power plant control system, noting overfueling prevention by throttle actuator during startup and speed governor function

05 p0896 A70-16003

Concorde electronics systems for testing and flight safety, controlling center of gravity, braking, kinetic heating, air conditioning, fuel flow and inertial navigation

07 p1194 A70-19741

Computer-controlled automatic test bench for black box modifications and electronic, hydraulic and pneumatic testing on Concorde aircraft

07 p1249 A70-19742

Concorde simulator for determining aircraft control responses and integrating pilot function into problem

07 p1249 A70-19743

Simulated Concorde kinetic heating system for ground studies of thermal stresses

07 p1250 A70-19744

Laboratory electronics role in Concorde aircraft structural and acoustical fatigue analysis, flight simulation and flight studies

07 p1250 A70-19745

Concorde aerodynamic design compromise between high and low speed requirements, kinetic heat problems and materials selection

[AIAA PAPER 69-759]

07 p1195 A70-20399

Concorde flight testing program, discussing results on prototype, preproduction and production aircraft

08 p1436 A70-21727

Concorde aircraft test flight results, considering ground handling, takeoff, approach and landing, low speed flight, aeroelasticity, stability, power plant, etc

08 p1437 A70-21728

Concorde SST aerodynamic, structural and thermal analysis and simulation using computers

10 p1849 A70-24382

Metal working technology of Ti and alloys for structural parts fabrication for Concorde aircraft, describing laser cutting, electron beam welding, explosive forming, etc

10 p1895 A70-24594

Concorde aircraft radar signal transmission, describing modified Flexwell waveguide

13 p2379 A70-29561

Concorde Olympus 593 power plants air intake and engine control system design for rapid servicing, discussing fault diagnosis and checkout

14 p2535 A70-31337

Aeroelastic test equipment for Concorde, describing operating principles, installation, test results, etc 15 p2717 A70-31810

Hazard analyses of Concorde aircraft design, noting engine control failures and emergency equipment use probabilities 15 p2675 A70-32213

Concorde aircraft design for emergency passenger evacuation, emphasizing overwing inflatable escape slides and kinetic heating effects 15 p2675 A70-32222

Ti alloys use in Olympus 593 engine for Concorde SST, discussing weight saving, mechanical properties and manipulation characteristics 17 p3146 A70-34449

Concorde aircraft man machine simulation and handling using fixed cabin, variable stability and ground based simulators [AIAA PAPER 70-923] 17 p3064 A70-35834

Concorde engine bay thermal insulation combining stainless steel foil and polytetrafluorethylene film, considering noise level, engine fire conditions and molten Ti globules penetration 18 p3346 A70-36345

Suborbital space transports problem solution by recoverable jet orbital or jet assisted aircraft, discussing implications of Concorde supersonic flight 18 p3350 A70-36663

Concorde design limitations for commercial success in civil airlines 18 p3350 A70-36665

Olympus 593 engine for Concorde aircraft, describing design and test procedures [SAE PAPER 700291] 18 p3302 A70-36805

Concorde aircraft powerplant design using fire tunnel test [ASME PAPER 70-GT-128] 18 p3238 A70-36854

Concorde prototype 002 flight test data recording instrumentation, emphasizing digital system for quasi-static parameters 19 p3432 A70-38545

Aeroelastic test equipment for Concorde SST using harmonic method and electromagnetic shakers 19 p3402 A70-38548

Concorde loadability, with comparison of flight balance situation for supersonic and subsonic aircraft, describing fuel system [SAWE PAPER 835] 20 p3563 A70-40365

Concorde aircraft flight test program for verifying design features of wing vortices, fuel transfer, longitudinal stability, etc 21 p3749 A70-40580

Concorde SST horizontal navigation, discussing data sources, equipment specifications, flight rules, man-machine interaction, etc 22 p4067 A70-42660

Concorde downstream thrust reversal nozzle, noting weight saving by use of welded stainless steel honeycomb construction 22 p4092 A70-43213

Sonic boom effects on building structures, using Concorde measurements and explosion simulation studies 24 p4289 A70-45151

Concorde thrust control by employment of variable area nozzle and reheat system, discussing crew work load [SAE PAPER 700817] 24 p4394 A70-45900

Meteorological wind and temperature distributions on selected routes at Concorde cruising level, noting computer use for flight planning 24 p4374 A70-46204

CONCRETES

German monograph on creep in statically indeterminate reinforced concrete beams with graduated cross sections 19 p3548 A70-38473

CONDENSATES

Propellant condensation on surfaces near electric rocket exhaust, calculating particle arrival rates, backflow and desorption energies [AIAA PAPER 69-270] 01 p0166 A70-10836

Smoked-foil technique for transverse wave quantitative study in condensed-phase explosives 03 p0606 A70-13814

CONDENSATION

Nonequilibrium effect of expanding water vapor condensation on supersonic nozzle flows with or without inert carrier gas 01 p0063 A70-10806

Water vapor condensation by homogeneous nucleation measured for cluster number using laser light scattering compared with theory in condensing supersonic flow 02 p0279 A70-12048

Approximate solution for far downstream flow of condensation in hypersonic wind tunnels and nozzles for colloidal thrusters and EHD generators 04 p0621 A70-15600

Irreversible phase transition analysis of atmospheric condensation-crystallization processes 08 p1538 A70-21427

Condensation start dependence on air humidity at inlet and nozzle geometry applied to supersonic wind tunnel using undried atmospheric air 09 p1606 A70-23614

Electrostatic rocket exhaust condensation on spacecraft solar electric panels cover glasses, noting deleterious effects [AIAA PAPER 69-271] 11 p2103 A70-26131

High temperature gaseous molecular beams impingement on Cu surfaces at cryogenic temperatures measured for condensation rates 12 p2271 A70-27265

Carbon dioxide jet plumes condensation on model nozzle in vacuum chamber, noting particle size and growth rate 13 p2523 A70-29983

Protein synthesis, dialysis and Mg ion concentration effects on chemical condensation of mixed amino acid adenylates 17 p3042 A70-35146

Moist air expansion through supersonic nozzle, investigating small ions role in water condensation 22 p4011 A70-42774

Contoured nozzle shock tunnel condensation point, determining flow supercooling over specified pressure range 23 p4182 A70-44588

CONDENSATION TRAILS

U CONTRAILS

CONDENSER RADIATORS

U HEAT RADIATORS

CONDENSING

NT FILM CONDENSATION

Liquid nucleation in vapor condensation on wettable, unwettable, smooth, rough and cavitated surfaces, showing positive effect of roughness elements 06 p1177 A70-17838

Supersonic free jets condensation, examining kinetics of reactions in mono- or diatomic gases 06 p1044 A70-18282

Supersonic molecular free jets using electron diffraction technique, discussing vibrational and condensation states 06 p1044 A70-18301

Cloud particles growth and interactions, discussing water vapor condensation, ice phase nucleation, rain droplet growth rate, etc 07 p1262 A70-18897

Linear kinetic theory for condensation and evaporation at small Knudsen numbers, considering extrapolated temperature jump determination 07 p1422 A70-19656

Atmospheric condensation nuclei activity with rough surface with decreasing spherical hollows 09 p1718 A70-23172

Carrier gas effect on homogeneous condensation in supersonic nozzle using liquid drop theory 12 p2211 A70-27829

Coronal condensations temperature and electron density measurements at meter wavelengths and in white light 13 p2488 A70-28717

Condensed products of vaporized primordial terrestrial material accounting for moon formation, using single stage precipitation earth origin hypothesis 13 p2488 A70-28719

Boron particles combustion behavior prediction by incorporating condensed phase effect into diffusion controlled model 13 p2472 A70-29612

Surface temperature fluctuations during dropwise condensation at various heat fluxes 14 p2663 A70-30256

Linear kinetic theory for condensation and evaporation at small Knudsen numbers, considering extrapolated temperature jump determination 15 p2828 A70-32693

Hygroscopic materials warm fog clearing capabilities comparison, recommending urea and ammonium nitrate 20 p3664 A70-40065

Cetyl alcohol and water vapor growth by absorption and condensation on hygroscopic nuclei population in atmosphere under cooling 20 p3664 A70-40066

Saturated nitrogen vapors condensing coefficients measurement by cryostat, comparing results with theoretical prediction 23 p4218 A70-44364

Aerobee rocket-borne cryogenic air samplers heat exchanger design by mathematical model and computer solution 23 p4280 A70-44365

CONDITIONED RESPONSES

U CONDITIONING [LEARNING]

CONDITIONING [LEARNING]

Conditioned suppression after differential training, discussing shock tests on rats with safe and danger signals 01 p0036 A70-10794

Temporary interneuron connections mechanisms during conditioned reflexes development 01 p0025 A70-11040

Accelerative and decelerative heart rate responses in human subjects given differential conditioning trials by auditory and electric shock stimuli under paced respiration 02 p0239 A70-12628

Cats cerebral cortex background electrical activity measured during development of conditioned reflexes, noting shift toward higher frequencies 03 p0418 A70-13217

Conditioned fear reaction produced by electric stimulation of cat anterior hypothalamus, discussing effect of neocortex removal 03 p0420 A70-13425

Work and exercise conditions effect in early training stages of learning sensorimotor skill, considering different body positions 03 p0432 A70-14295

Complex conditioned reflexes to three component visual-acoustic-tactile stimulus in dogs analyzed by secretory and thermoelectrical techniques 04 p0638 A70-15504

Human macrosaccadic eye movements related to four dial display conditioned by concurrent variable interval schedules of signals 05 p0800 A70-16127

Pavlovian conditioned reflexes theory reappraisal, discussing cortex-subcortical formations interrelations models 07 p1197 A70-18694

Rabbits sensorimotor and visual cortical responses during defensive conditioning to rhythmic light 07 p1197 A70-18695

Human motor reactions rhythmic system, relating reaction-skin-galvanic reflex to formation of successive conditioned connections 07 p1197 A70-18697

Amysyl effects on conditioned passive avoidance reflexes development and reinforcement in white mice under electric shock 07 p1198 A70-18717

Canines conditioned reflex activity as function of cortex sections following head exposure to X ray irradiation 07 p1199 A70-18729

Phase correlation of conditioned and electrophysiological postirradiation disturbances in central nervous system of monkeys 08 p1446 A70-21447

Bioelectrical activity of brain during conditioned motor reflex system operation modes in response to stimulating light pulses 08 p1447 A70-21450

Hippocampus nerve cells protein fractions synthesis in rats, noting relation to learning process during transfer of handedness 12 p2172 A70-28217

Electrical activity of visual cortex, subcortical structures and reticular formations in cats during conditioned reflex stimulation by light 12 p2173 A70-28351

Dynamic interaction between stored and active memory images in apes and monkeys with conditioned alimentary motor reflexes stimulated by visual signals 12 p2173 A70-28352

Threshold excitation of cutaneous analyzer in man under vascular conditioned reflexes in response to acoustic signals with shock 12 p2173 A70-28353

Vestibular nystagmus evocation by conditioned reflexes technique after pure tone stimulation 14 p2538 A70-30910

Thermoregulatory vasodilation conditioned reflexes developed by combination of prolonged physical and acoustic stimuli 15 p2679 A70-31606

Noise bursts response of positive and inhibitory conditioned eyelid reflexes in cats brain, discussing auditory system function 15 p2687 A70-32871

Cortical evoked potentials in human motor conditioning to photic stimulus 18 p3221 A70-37212

Evoked potentials in dogs sensorimotor cortex during defensive instrumental conditioning 18 p3221 A70-37213

Electrophysiological characteristics of man during disorders in rhythmic system of conditioned motor reactions 18 p3221 A70-37217

Soviet monograph on secondary signaling system role in development of speech, thought, conditioned and unconditioned reflexes, human will and hypnosis, noting salivary gland function 19 p3359 A70-37407

Fixed-ratio performance patterns of pigeon key-peck responses to fractional punishments by electric shock 22 p3971 A70-43375

CONDITIONS

NT ADIABATIC CONDITIONS

NT CHRONIC CONDITIONS

NT FLIGHT CONDITIONS

NT LIPSCHITZ CONDITION

NT NONEQUILIBRIUM CONDITIONS

NT RUNWAY CONDITIONS

CONDUCTANCE
U RESISTANCE
CONDUCTING
U CONDUCTION
CONDUCTING FLUIDS

Entrainment of electrically conducting liquid by moving wall in long duct with rectangular cross section and magnetic induction field

01 p0151 A70-10656

Three dimensional instability of perturbed conducting fluid laminar boundary layer flow on concave walls in transverse magnetic field, analyzing various Hartmann numbers

01 p0152 A70-10934

MHD wave propagation in electrically conducting fluid contained in finite length circular cylinder subject to axial magnetic field and nonelectromagnetic forces

01 p0152 A70-10944

Ultrasonic wheel-type portable inspection device with internal coupling immersion fluid contained in silicone tire, allowing angle beam inspection without temperature correction

01 p0105 A70-11396

Unsteady MHD flow of viscous incompressible electrically conducting fluid through rectangular duct under transverse magnetic field

03 p0471 A70-14333

Heat transfer in steady state flow of electrically conducting incompressible viscous fluid in annular channel between coaxial circular cylinders under magnetic field

03 p0608 A70-14335

Conducting fluid laminar flow between parallel planes in traveling magnetic field, integrating Maxwell and Navier-Stokes equations

04 p0726 A70-14542

Conducting fluid as MHD lubricant for cylindrical bearings, deriving equations for ideally conducting shaft and bearing and arbitrary Reynolds numbers

04 p0697 A70-14544

Incompressible electrically conducting fluid flow along rectangular duct under transverse magnetic field, noting equivalency of Hunt solutions and thin wall restriction

04 p0726 A70-14614

MHD Stokes flow for magnetized bodies of revolution, rotating with steady motion in viscous conducting fluid at rest at infinity

04 p0726 A70-14615

Conducting fluid steady convection due to combined effects of thermal gradient and DC electric field predicted by analytical model

04 p0785 A70-14989

Fundamental matrix asymptotic forms obtained for supersonic and subsonic three dimensional steady flows past body in uniform stream of viscous thermally conducting fluid

04 p0673 A70-15320

Electrically driven jets of slightly conducting viscous fluids drawn from conducting tubes, discussing cylindrical soap film instability under radial electric field

05 p0831 A70-15917

Gravitational instability of finitely conducting incompressible fluid layer of finite thickness surrounded by nonconducting medium

05 p0915 A70-16696

Incompressible boundary layer flow of conducting fluid on solid two dimensional and axisymmetric bodies under transverse magnetic field approximated by momentum method

06 p1031 A70-17199

Linearized MHD equations for motion of solids in viscous and electrically conducting fluids

06 p1120 A70-17532

Velocity, magnetic field and drag equations for steady incompressible viscous conducting fluid flow around spherical hollow shell

06 p1122 A70-17917

Hall effect measurements in liquid semiconductors and metals

06 p1127 A70-17919

MHD free convection of electrically conducting fluid in strong cross field using perturbation technique, considering liquid metals and ionized gases

07 p1348 A70-19208

Conducting fluids flow instabilities characterized by incipience at critical electric Hartmann number and convection rate proportional to electric Reynolds number

07 p1348 A70-19265

Incompressible conducting fluid MHD flow at infinite plane wall forward stagnation point, considering suction or injection effects

07 p1354 A70-20237

Finite amplitude effects on MHD thermal convection in rotating layer of conducting fluid, discussing subcritical instability

08 p1563 A70-20472

Steady pressure driven flow of conducting fluid through insulating circular pipe in transverse magnetic field

08 p1549 A70-20502

Model for magnetic field-line reconnection in conducting incompressible fluid, determining maximum reconnection rate entirely by null point conditions

08 p1553 A70-21615

Plane flow of electrically conducting fluids around oscillating plate, using equations linearized by Oseen method

09 p1734 A70-22316

Two dimensional radial flow of inviscid infinitely conducting compressible fluid under influence of magnetic field

09 p1735 A70-22757

Charged particles velocity profile across shock determined by induction velometry, considering eddy currents effects on induced potential gradient

09 p1738 A70-23677

Unsteady MHD flows of viscous, incompressible and electrically conducting fluid, proving boundary value problem solutions existence and uniqueness

10 p1922 A70-24095

Alfven flow of dissipative conducting incompressible fluids in presence of thin airfoil in magnetic field, considering flow turbulence calculation

10 p1922 A70-24143

Conducting gas unsteady efflux from plane tube into vacuum, determining time dependent position of expanding rarefaction wave fronts

10 p1924 A70-24569

MHD boundary layer on rotating body in viscous incompressible conducting fluid, studying magnetic field effects on time-to-separation

10 p1924 A70-24572

MHD exact solutions class, observing conducting flow intensification by magnetic field application

10 p1924 A70-24573

Navier-Stokes-Maxwell equations solutions for conducting fluid flow in azimuthal magnetic field, noting jet acceleration near symmetry axis

10 p1924 A70-24574

Solid body acceleration by ideally conducting gas in constant gravity field under magnetic field, considering rarefaction, reflected waves, motion equation, wall pressure, etc

11 p2082 A70-25389

Conducting fluid incompressible flow in entrance of MHD channel by momentum integral method, permitting edge stress existence at boundary layer free stream interface

[ALAA PAPER 69-724]

11 p2035 A70-25977

Homogeneous turbulent velocity effect on magnetic field distribution in electrically conducting fluid with no external source, observing dynamo action

11 p2091 A70-26545

Velocity fluctuations measurements in conducting fluids flowing through tubes

12 p2230 A70-27091

MHD disturbances in semiinfinite electrically conducting fluid, introducing magnetic dipole to act as source of disturbance

12 p2277 A70-27156

Two dimensional viscous incompressible conducting fluid flow between parallel porous walls in magnetic field, studying skin friction fluctuations

12 p2209 A70-27157

Stability of MHD dissipative circular flow of viscous electrically conducting fluid between concentric stationary cylinders impressed with axial magnetic and radial electric fields

12 p2277 A70-27195

Externally pressurized bearing with electrically conducting gas lubricant under axial magnetic field, considering load capacity

12 p2244 A70-28018

Turbulence energy balance equations for conducting fluid flow in longitudinal magnetic field with Joule dissipation

12 p2282 A70-28227

Plane incompressible conducting fluid laminar jets analysis in magnetic field, using boundary layer equations for zero electric field

13 p2461 A70-28964

Stationary ring vortices in unbounded conducting fluid, investigating self excitation of magnetic field by vortices

13 p2461 A70-28965

Wind tunnel interference for inviscid compressible conducting fluid on slender body of revolution, discussing disturbance potential

13 p2464 A70-29449

Gas parameters determination near singular point of slow magnetosonic wave propagating in conducting medium in uniform magnetic field

13 p2464 A70-29507

Linearized steady plane axisymmetric flows of inviscid finitely conducting incompressible fluid past insulator under magnetic induction with zero components

13 p2464 A70-29541

Incompressible, viscous and electrically conducting fluid flow due to rotating disk in uniform magnetic field, discussing hydromagnetic interaction effect on velocity and friction

13 p2465 A70-29544

Thermal boundary layer separation in conducting fluids by rotating magnetized blunt body

13 p2469 A70-30008

Two dimensional unsteady flow of weakly conducting fluid in perpendicular magnetic field using Green function

14 p2621 A70-30180

Thermal radiative transfer and magnetic field effects on hydromagnetic stability of hot electrically conducting fluid

14 p2623 A70-30996

Conducting incompressible fluid flow past sphere, examining effect on magnetic field for small magnetic Reynolds number

15 p2778 A70-31913

Uniform electric and magnetic fields effects on flow of conducting compressible fluid in channel, using multiple scales method

15 p2779 A70-31914

Conducting incompressible fluid laminar flow between rotating disks in transverse magnetic field with source at center

15 p2779 A70-31915

Hydromagnetic viscous flow of incompressible conducting fluid due to electric current radial divergence from point source

15 p2780 A70-32426

Unsteady hydromagnetic flow of viscous electrically conducting incompressible fluid due to rotating disk under perpendicular magnetic field

16 p2958 A70-33297

Heterogeneous conducting fluid stability between fixed rigid cylinders with radiant gravitational force and magnetic field

16 p2894 A70-33784

Current sheet structure of hydromagnetic boundary layer formed by mixing two conducting fluid streams containing oppositely directed magnetic fields

17 p3140 A70-34930

Supersonic electrically conducting gas flow in flat channel with dielectric walls in inhomogeneous magnetic field

17 p3141 A70-35334

Supersonic conductive gas recombination fronts for arbitrarily oriented magnetic field, allowing for dissipative coefficients

18 p3294 A70-36255

Spatially periodic dynamos, analyzing homogeneous conducting fluid motions and magnetic field forms

18 p3291 A70-36407

Magnetohydrodynamic flow of electrically conducting viscous incompressible fluid past nonconducting semiinfinite flat plate under transverse magnetic field

18 p3295 A70-36431

Thermodynamics and velocity of MHD shock waves in perfect conducting fluid, using compressibility conditions and relativistic Hugoniot equation

19 p3477 A70-37580

Relativistic effects for MHD Riemann waves in electrically conducting fluid

19 p3478 A70-37583

Liquid with small electrical conductivity and kinematic viscosity in intense transverse magnetic field, examining plane and three dimensional duct flow

19 p3478 A70-37589

Electrically conducting perfect compressible fluid flow in semiinfinite channel under electromagnetic field, using multiple scales method

19 p3479 A70-37595

Thin airfoil theory in magnetohydrodynamics, considering steady two dimensional flow of compressible perfectly conducting inviscid fluid in presence of uniform magnetic field

19 p3351 A70-37597

Compressible fluids flow with conductivity tensor in presence of thin wing under orthogonal fields, reducing integral equation to Fredholm equation

19 p3351 A70-37599

Magnetic field effect on hydromagnetic Goertler instability in boundary layer flow of conducting fluid over concave wall

19 p3481 A70-38352

Viscous incompressible electrically conducting fluid steady flow between parallel coaxial rotating disks with transverse magnetic field

19 p3481 A70-38446

Steady compressible supersonic planar flow of viscous heat conducting fluid under linearization freestream conditions, describing slip flow past finite flat plate

20 p3557 A70-39228

Electrically conducting gas flow past slender body of arbitrary cross section in presence of crossed magnetic field by MHD Stokes approximation

20 p3558 A70-39613

Plane parallel viscous conducting fluid flows stability in transverse magnetic field, considering small perturbation spectrum, Hartmann and Reynolds numbers

20 p3684 A70-40397

Elastoviscous incompressible electrically conducting oscillating free stream flow along infinite porous plate with suction in transverse magnetic field

20 p3685 A70-40508

Turbulent incompressible conducting fluid jets velocity and temperature characteristics in presence of longitudinal and transverse magnetic fields

21 p3860 A70-42226

Electrically conducting fluid hydromagnetic spin-up between infinite flat insulating plates in uniform magnetic field normal to boundaries

23 p4223 A70-43972

Gravity waves produced in liquid electric conductor by piston subjected to sinusoidal pulsation, calculating magnetic field effect on amplitude and phase velocity

23 p4425 A70-44208

Conducting viscoelastic fluid flow near harmonically oscillating nonconducting flat plate under uniform transverse magnetic field, considering stress-strain rate relationship

23 p4226 A70-44375

Viscous conducting liquid forced vortex motion, considering radial velocity distribution and rotation effect on free surface shape

24 p4383 A70-45140

Magnetized conducting sphere steady rotation in viscous conducting liquid, solving for fluid velocity and induced magnetic field

24 p4386 A70-45609

Conducting sphere MHD rotation in viscous conducting fluid under uniform magnetic field

24 p4387 A70-46028

CONDUCTING MEDIA

U CONDUCTORS

CONDUCTION

Local control loop model of multiphase rectifier used as power amplifier, considering extension to nonautonomous and discontinuous conduction systems

21 p3802 A70-42267

CONDUCTION BANDS

Indium arsenide crystals conduction band structure with various electron concentrations, determining electron mass dependence on concentration and temperature

01 p0154 A70-10096

Electron surface states bands in insulators induced by image potential, determining lower limits for liquid and solid gases

02 p0345 A70-12823

Negative resistance mechanism model with larger electron accumulation in conduction band than free holes

03 p0539 A70-13212

Piezoelectric scattering effects on electron temperature and mobility in IIB-VIA semiconductor compounds with nonparabolic conduction band

13 p2471 A70-29373

Light absorption coefficient of two band superconductor with nonmagnetic impurity, observing electron pairs removal from condensate and transition into excited states

13 p2472 A70-29723

Ovshinsky switching effect, considering electrothermal initiation and field dependent conductivity at elevated temperatures

14 p2626 A70-30336

Energy zone bending near surface of n-type semiconductor, discussing surface plasma level

18 p3298 A70-36619

Optical density of valence and conduction states by UV photoelectric spectroscopy, outlining experimental techniques and inelastic scattering effects

19 p3471 A70-37711

Fermi energy and bandtail parameters in heavily doped and degenerate n-type GaAs, calculating conduction band density of states by screened Coulomb potential

21 p3864 A70-42018

Direct gap conduction band and alloy composition monitoring InAlP, using electron microprobe cathodoluminescence and X ray emission

22 p4086 A70-43019

Conducting state propagation in p-n-p-n structure involving minority carrier diffusion between regions

23 p4232 A70-45068

CONDUCTION ELECTRONS

Laser emission photons scattering by semiconductor conduction electrons allowing for electron-phonon interaction

07 p1357 A70-19857

MOS field effect transistor, measuring electrons and holes thermal emission rates and activation energies at gold centers in Si

22 p3997 A70-43016

CONDUCTIVE HEAT TRANSFER

Three dimensional thermal conductivity problems solution applied to moving body, body of revolution and hollow cylinder

01 p0213 A70-10218

Flip chip and beam lead methods for microcircuit assembling, discussing heat removal using heat spreader and temperature cycling effects on tensile strength

01 p0050 A70-10330

Steady state heat conduction problems solved by finite element method, with examples involving internal heat generation and various boundary conditions

01 p0215 A70-10558

Length calculation method for nonadiabatic imaginary tip extension of heat exchanger fins, predicting heat conduction rate

01 p0215 A70-10842

Conductive heat transfer coefficients of densely packed electronic subassemblies

01 p0051 A70-10990

Discrete models formulated for thermomechanical behavior of materials with memory, obtaining equations of motion and heat conduction for finite elements of nonlinear continua

01 p0208 A70-11183

Integral theorems for wave-type heat conductivity equation

01 p0219 A70-11398

Radiative, conductive and convective combined heat transfer mechanism in nonisothermal atomic hydrogen plasma laminar flow

02 p0400 A70-12660

Boundary conditions of heat conduction in systems of vessels connected by rods with given heat capacity and unknown temperature

02 p0400 A70-12674

Stefan heat conduction problem with time dependent first kind boundary conditions approximate solution, taking into account unsteady temperature field of solidifying liquid

03 p0604 A70-13210

Discontinuous solutions of nonlinear boundary value problems of heat conduction for second order ordinary differential equations using modified difference method

03 p0604 A70-13390

Periodic process analysis method based on trigonometric Fourier series, noting applications to heat conduction problems

03 p0606 A70-13519

Unsteady heat conduction in hollow cylinder, using transfer functions to solve direct and inverse two dimensional problems

03 p0606 A70-13520

Solid propellants ignition response to radiative and conductive heat transfer

03 p0544 A70-13921

Bessel function applied to unsteady axisymmetric problem of heat conduction in thermally controlled coaxial cylinders with different physical properties

03 p0608 A70-14304

Unsteady heat conduction and thermal stresses in thin isotropic semibounded plates with butt joint possessing internal thermal resistance

04 p0766 A70-14479

Heat transport conduction mode and earth as heat sink in solar atmosphere, discussing mesopause coldest region, turbulence and solar plasma-earth electromagnetic interactions

[AAS PAPER 69-622]

04 p0677 A70-14644

Heat conduction equation solutions, comparing finite element and finite difference methods

[ASME PAPER 69-WA/HT-35]

04 p0781 A70-14805

Finite element method applied to heat conduction in solids with temperature dependent thermal conductivity, using nonlinear constitutive equation for heat flux

[ASME PAPER 69-WA/HT-34]

04 p0782 A70-14806

Rarefied gas heat conduction between concentric cylinders at small Knudsen number and temperature gradient, using integral equations obtained from Krook equation

[ASME PAPER 69-WA/HT-19]

04 p0783 A70-14816

Distribution functions for solving moment equations of Maxwell-Boltzmann equation used in studying heat conduction through rarefied gases within concentric cylinders and spheres

[ASME PAPER 69-WA/HT-17]

04 p0783 A70-14817

Finite element method applied to finite dimensional state variable formulation of transient heat conduction with surface diffusion of thin circular rotating disk

[ASME PAPER 69-DE-B]

04 p0785 A70-14874

Flow viscosity and heat conduction effects on shock wave propagation in bent channel with weak Mach reflection

04 p0671 A70-15013

Steady circulation and temperature perturbations in stratified nonrotating ideal gas atmosphere with viscosity and heat conduction

04 p0681 A70-15517

Numerical solution of transient heat conduction with radiating surface, imposing Runge-Kutta type integration on surface

04 p0787 A70-15613

Thermoelasticity generalization from physically motivated modification of Fourier heat conduction law, postulating constitutive equations valid for finite deformations and temperature variations

05 p0929 A70-16062

Thermal resistance of multicontact heat conducting stainless steel plate stacks with different interface purities in vacuum

05 p0957 A70-16293

Unsteady heat conduction numerical approximation for infinite cylinder with variable heating and boundary conditions of third kind

05 p0936 A70-16294

One dimensional unsteady heat conduction with variable boundary conditions solved by difference-

differential method using rectangular and cylindrical coordinates

05 p0957 A70-16295

Magnetized solar wind steady state inviscid single fluid model developed using MHD, including heat equation with thermal conduction

05 p0902 A70-16445

Heat conduction in anisotropic materials to measure thermophysical parameters, using pulsed point or line heat source

05 p0957 A70-16457

Heat conduction equation containing diffusivity coefficient as Stefan type function

05 p0958 A70-16667

Unsteady inverse heat conduction of semibounded body solved by least squares method

06 p1178 A70-17856

Temperature distribution law for semiinfinite and infinite solid bodies under steady heat conduction in presence of concentrated heat source

06 p1178 A70-17872

Heat conduction transient field problems in two and three dimensional isoparametric finite element solutions using Galerkin method

06 p1178 A70-17938

Transient heat conduction in dual-layer insulated plate exposed to pulse heating, discussing temperature response

[AIAA PAPER 70-14]

06 p1180 A70-18120

Three dimensional ablation calculated for reentry sphere-cone taking into account shape changes and internal heat conduction

[AIAA PAPER 70-199]

06 p1181 A70-18150

Measurement error associated with heat conduction in temperature sensor, using mathematical model

06 p1070 A70-18843

Collisional skewing of electron distribution function associated with heat conduction in solar wind, exciting collisionless ion-acoustic, electrostatic ion cyclotron and magnetoacoustic waves

06 p1136 A70-18527

Rough metal surfaces thermal constriction resistance for total heat flow through microcontacts

07 p1418 A70-18648

Boundary value problems solutions estimated for heat conduction equation in unbounded domain, considering function satisfying heat induction equation

07 p1419 A70-18852

Integral method for time development of viscous, heat and mass conducting layer over leading edge of volatile drop instantaneously immersed in gas stream

07 p1358 A70-18916

Perturbation solution for fins taking into consideration interaction of conduction with radiation and convection

07 p1422 A70-19333

Radial heat conduction in infinite hollow cylinder with circular cross section and periodic heat transfer coefficient at inner and outer cylinder surfaces

07 p1423 A70-19816

Unsteady heat conduction in plate, solid or hollow infinite cylinder and sphere with internal heat source and radiative heat transfer on surface

07 p1423 A70-19818

Penetrative thermal convection stability for statically unstable layer surmounted by statically stable layer from numerical integration of linearized equations of motion and heat conduction

07 p1269 A70-19947

Finite element models for nonlinear problems analysis in coupled thermoelasticity dynamical theory, deriving heat conduction equations from energy balance considerations

07 p1417 A70-20363

Boundary value problem solution in study of axisymmetric viscous heat conducting gas flow past body of revolution

08 p1431 A70-20854

Difference schemes approximating quasi-linear heat conduction equation, demonstrating convergence

08 p1596 A70-20857

One dimensional difference scheme for gas dynamics with heat conduction

08 p1482 A70-20859

Oscillatory relaxation of binary system of heat conducting viscous gases composed of nonspherical molecules

08 p1547 A70-21085

Transient heat conduction and stationary temperature distribution calculation in curvilinear coordinates using finite element method

08 p1590 A70-21362

Thermal conductivity and diffusivity of two phase composites determined by iterative solution of heat conduction equation with space fluctuating properties

08 p1598 A70-21511

Retinal temperature increases produced by intense light absorption described by heat conduction equation

09 p1614 A70-22075

Transient heat conduction of thin circular disk with uninsulated surfaces rotating past stationary point source by finite element method

09 p1787 A70-22269

Lunar internal temperature approximation correcting solution of heat conduction equation for moon thermal histories

09 p1753 A70-22385

Axisymmetric or plane bodies temperature distribution from heat conduction analysis using computer program based on finite element method

09 p1788 A70-22581

Elastic solution and finite element method applied to heat conduction and thermal stress in temperature field determination

09 p1774 A70-22587

Temperature distribution in infinite and finite circular hollow cylinders, considering surface heat flux and linear heat transfer

09 p1788 A70-22595

Temperature distributions in multidimensional transient conduction heat transfer, using variational method and Laplace transformation

09 p1788 A70-22705

Cauchy problem solution for heat conduction equation stabilization, deriving necessary conditions

09 p1789 A70-23167

Weighted residual and Biot variational methods for solving one dimensional heat conduction problems

09 p1789 A70-23260

One dimensional numerical solution for steady state thermal behavior of trapezoidal profile annular fins transferring heat by conduction and radiation

[ASME PAPER 69-HT-6] 09 p1790 A70-23557

Conduction to isothermal insulated cylinder from seminfinit region

09 p1790 A70-23563

Time-temperature charts for one dimensional unsteady conduction with uniform internal heat generation

09 p1791 A70-23567

Temperature field and combined radiative-conductive heat flux in weakly absorbing cylindrical layer bounded by nonblack surfaces

10 p1966 A70-23866

Heat conduction analysis for plane body with boundary condition and time variable heat exchange coefficient, applying automatic control technique

10 p1966 A70-23869

Temperature field and heat conduction equation for two layer polymer cylinder multiply heated from within, considering material decomposition

10 p1966 A70-23870

Nonstationary thermoelasticity in half space with moving boundary condition described in Cartesian rectilinear coordinates allowing for time term in heat conduction equation

10 p1954 A70-24012

One dimensional Navier-Stokes equations solution for viscous heat conducting gas flow involving spherical sink for finite pressure at infinity

10 p1865 A70-24104

Thermal conductivity on coupled heat conducting rods calculated by implicit difference scheme on finite graphs

10 p1969 A70-25189

Radiative heat transfer due to radiation conductivity and transmission in low density glass fiber insulations by heat flowmeter for hot and cold surfaces

11 p2148 A70-25769

Spacecraft temperature prediction and heat conduction problems with nonlinear radiation boundary conditions by perturbation theory, applying to heat shield analysis

11 p2150 A70-26355

Heat conduction and viscosity effects on compressible fluids characteristics

11 p2037 A70-26399

Coordinate function selection for boundary value problems solution by Galerkin method demonstrated for heat conduction equation of anisotropic parallelepiped with internal source

12 p2271 A70-27291

Heat conduction for thermally insulated bilayer metal wall for time-variable heat transfer and ambient temperature, using Green function

12 p2330 A70-27292

Asymptotic properties of Cauchy problem solution for heat conduction equation

12 p2331 A70-27300

Contact and unsteady heat transfer through vacuum cavity applied to hollow cylinders, solving nonlinear integral equations by piecewise linear approximation

12 p2331 A70-27326

Steady state and transient heat transfer by radiation and conduction in absorbing medium bounded by infinite coaxial cylindrical surfaces

12 p2331 A70-27697

Transient heat transfer combining conduction and radiation in absorbing plane layer analyzed by differential approximation

12 p2332 A70-27801

Linearized Fredholm equation solution, describing temperature field for energy transport by radiation and heat conduction

13 p2521 A70-28860

Surface emissivity effects on combined conduction, convection and radiation heat transfer in nonisother-

mal hydrogen plasma, discussing optically thin and thick solutions

13 p2521 A70-29134

Boundary value problems of ordinary and generalized heat conduction equations using reflection method

13 p2521 A70-29311

Time variable dynamic medium nonlinear conductive heat transfer equation obtained by power series procedure

13 p2521 A70-29313

Steady state heat conduction in wedge shaped bodies with boundary conditions of third kind

13 p2522 A70-29515

Time dependent simultaneous solution for continuity, heat conduction and motion equations of system involving neutral, electron and ion gases

14 p2665 A70-30744

Boundary value problem of nonlinear one dimensional conduction in radiating heat shields, using perturbation and numerical methods

15 p2824 A70-31450

Axial wall conduction effects on steady state laminar flow heat transfer

15 p2825 A70-31815

Steady state temperature dependence of heat conduction coefficient using arc approximation

15 p2826 A70-32106

Heat conductivity of Xe-He binary gas mixtures, allowing for molecular transfer and polarity effects

15 p2827 A70-32107

Boundary value problem in linear elastodynamics, investigating Ignaczak type theorems for microstructure effects in transient heat conduction problems

15 p2822 A70-32343

Nonlinear two dimensional free boundary problem of axisymmetric heat conduction in tubes with internal surface solidification by variational technique

16 p2996 A70-33002

Difference schemes approximating boundary value problem for heat conductivity and oscillation equations, considering brute force method stability

16 p2951 A70-33245

Radiation and conduction of open joint multilayer insulation systems, analyzing dependence on contact area by numerical methods

[AIAA PAPER 70-848] 16 p2939 A70-33915

Nonabsorbing gas effect in radiation-conduction heat transfer interaction, predicting magnitude and pressure trends by wideband gas model

[AIAA PAPER 70-836] 16 p3001 A70-33931

Correction techniques for thermal network lumped parameter inaccuracies with conduction and radiation coupling, considering temperature control system

[AIAA PAPER 70-821] 16 p3002 A70-33943

Surface temperature or heat flux density estimation for nonlinear inverse heat conduction problem involving temperature dependent thermal properties

16 p3002 A70-34195

Thermomagnetoelasticity wave equations of heat conduction for thermal and coupled perturbations propagating in isotropic medium at finite velocities

16 p2953 A70-34326

Onsager reciprocal relations experimental validity in irreversible processes application to metals, electrokinetics, isothermal diffusion, heat conduction, chemical reactions, etc

17 p3197 A70-35538

Free convection in compressible viscous heat conducting fluid, determining parameters leading to onset

17 p3198 A70-35697

Viscous heat-conducting one dimensional piston driven gas flow, assuming sharp shock discontinuity

17 p3075 A70-35890

Stationary heat conduction model of two cylinders abutting at ends with internal nonuniform temperature distribution

18 p3345 A70-36128

Elastic continuum conducting heat under general loads, investigating stability thermodynamics- Liapunov criterion relations

18 p3337 A70-36336

Unsteady temperature fields in heat conduction problems associated with high temperature effects on abutted cylinders

18 p3348 A70-36572

Heat conduction three dimensional problem in radiation heated thin crystalline plates with temperature dependent thermophysical characteristics

18 p3348 A70-36644

Book on heat transfer covering conduction, convection, thermal radiation and heat exchange equipment

19 p3550 A70-37231

Book on variational principles in heat transfer covering conduction, convection, dissipation, thermal potential and force boundary layer problem and Lagrangian analysis

20 p3735 A70-39224

Small viscosity and heat conductivity in solutions to critical layer in stratified shear flow

20 p3608 A70-39447

Uniqueness theorem for first boundary value problem of heat conduction equation with discontinuous coefficient

20 p3737 A70-39710

Stellar wind theory and related steady radial flows, discussing gravitating point mass, heat conduction, shocks, viscosity, outflows and inflows

20 p3706 A70-39928

Book on nonuniform gas theory covering viscosity, thermal conduction, diffusion, Maxwell-Boltzmann equations, density, quantum theory, transport phenomena, mixtures, electric fields, etc

20 p3673 A70-40135

Heat conduction problems solved allowing for radiation on electrical models, using nonlinear resistance and composite circuit methods

20 p3738 A70-40178

Eroding surface transient heat conduction problem, considering temperature dependent surface properties, ablation, convective heating, etc

20 p3738 A70-40279

Steady one dimensional temperature field of cylindrical shell spacecraft, allowing for heat conduction and convective and radiative heat transfer within shell

21 p3942 A70-40841

Heat conduction errors in immersion thermocouples and resistance temperature sensors, using mathematical model

21 p3823 A70-40856

Contact and unsteady heat transfer through vacuum cavity applied to hollow cylinders, solving nonlinear integral equations by piecewise linear approximation

21 p3952 A70-42067

Nonlinear one dimensional conduction in radiating heat shields, solving two point boundary value problem by asymptotic and numerical solutions

[ASME PAPER 70-HT-E] 22 p4121 A70-42422

Variational formulation for steady and transient heat conduction with variable thermal conductivity, applying to cylindrical element

22 p4123 A70-42546

Acoustic wave propagation in continuum of inviscid compressible heat conducting fluid, determining stability criteria

22 p4073 A70-42571

Heat conduction into semiinfinite homogeneous solid with thermal conductivity dependence on temperature, noting temperature profile asymptotic behavior for similarity solution

22 p4123 A70-42641

Heat exchange coefficients on side surfaces of constant thickness gas turbine disk, using temperature distribution method and integral transformations

22 p4125 A70-43367

Nonlinear unsteady thermal conductivity problems linearization based on temperature substitution by integral analogs

22 p4125 A70-43370

Cylindrically symmetric transient heat conduction in biological systems for inhomogeneous media and internal sources, using finite difference method

23 p4150 A70-43900

Thermal defocusing and deflection of light beam by lateral wind effect in absorbing media

23 p4200 A70-43950

Thin plates two dimensional dynamic thermoelastic problem, determining hyperbolic type heat conduction for temperature field

23 p4265 A70-43985

Heat conduction of doubly connected square and triangular isotropic plates with hole, applying small parameter method

23 p4276 A70-44217

Iterative method for boundary value problems in mathematical physics, showing convergence by heat conduction equation solutions

23 p4276 A70-44218

Heat conductivity problem of body with variable density and specific thermal conductivity reduced to differential equation via power series

23 p4277 A70-44340

Rarefied gas heat conduction between concentric cylinders in slip regime, obtaining perturbed temperature and density variations

23 p4284 A70-44985

Heat conduction problems numerical solution, using hypermatrices

24 p4428 A70-45127

Contact region structure with viscosity, conduction and radiative transfer effects applied to plane shock wave reflection from heat conducting wall

24 p4326 A70-46001

Viscous heat conducting compressible fluid flow past slender axisymmetric body, presenting Navier-Stokes hypersonic strong interaction theory

24 p4289 A70-46020

One-phase Stefan problem of heat conduction with melting, proving existence and uniqueness theorems for solid and free boundary temperature determination

24 p4429 A70-46036

CONDUCTIVITY

Acoustic conductivity of burning solid propellant surface, discussing critical conditions and variable surface measurement methods

13 p2522 A70-29421

MHD and thermal boundary layer, considering difference scheme for conducting medium flow past body in crossed electric and magnetic fields

18 p3293 A70-36116

CONDUCTORS

NT AIRCRAFT ANTENNAS
 NT ANTENNAS
 NT CASSEGRAIN ANTENNAS
 NT DIPOLE ANTENNAS
 NT DIRECTIONAL ANTENNAS
 NT ELECTRIC CONDUCTORS
 NT ELECTRIC WIRE
 NT ELECTROLYTES
 NT EXPLODING WIRES
 NT FLAT CONDUCTORS
 NT HELICAL ANTENNAS
 NT HORN ANTENNAS
 NT ION EXCHANGE MEMBRANE ELECTROLYTES
 NT LENS ANTENNAS
 NT LOG PERIODIC ANTENNAS
 NT LOOP ANTENNAS
 NT MICROWAVE ANTENNAS
 NT MISSILE ANTENNAS
 NT MOLTEN SALT ELECTROLYTES
 NT MONOPOLE ANTENNAS
 NT MONOPULSE ANTENNAS
 NT MULTIPLE BEAM INTERVAL SCANNERS
 NT OMNIDIRECTIONAL ANTENNAS
 NT PARABOLIC ANTENNAS
 NT PHOTOCONDUCTORS
 NT RADAR ANTENNAS
 NT RADIO ANTENNAS
 NT RHOMBIC ANTENNAS
 NT SLOT ANTENNAS
 NT SPIRAL ANTENNAS
 NT STEERABLE ANTENNAS
 NT SUPERCONDUCTORS
 NT THERMAL CONDUCTORS
 NT TWO REFLECTOR ANTENNAS
 NT WAVEGUIDE ANTENNAS
 NT YAGI ANTENNAS

Eddy currents magnetic field structure over surface defects in conducting objects, noting NDT applications

13 p2404 A70-28661

Plane electromagnetic wave in moving conductive medium, analyzing without approximation of velocity limitation

13 p2462 A70-29104

Concentrated pulsed electromagnetic fields penetration into conductor, assuming magnetic field along metal surface

22 p4041 A70-43621

CONES

NT ABLATIVE NOSE CONES
 NT CIRCULAR CONES
 NT CONICAL BODIES
 NT NOSE CONES
 NT ROCKET NOSE CONES
 NT SLENDER CONES

Boundary layer around blunted cone solved numerically by finite difference method

01 p0001 A70-10297

Monograph on weak interactions on cones in supersonic and hypersonic flows, discussing flow divergence, measurement errors and data reliability

04 p0615 A70-15141

Laminar hypersonic blunt cone wakes, discussing flow fields and axial static pressure distributions

06 p0968 A70-17553

Higher order boundary layer effects on zero-lift drag of sphere-cones, investigating transverse curvature, shock vorticity, displacement, slip and temperature jump

[AIAA PAPER 70-185] 06 p1041 A70-18173

Duality theorem for complex quadratic programming over polyhedral cones

07 p1238 A70-19356

Passive radiant cooler design involving patch cone radiative coupling calculation based on specular image technique

07 p1425 A70-20091

Three dimensional flow field codes for sphere-cones at nonzero angles of attack, comparing numerical and experimental results

09 p1606 A70-23254

Cone roll dynamics-ablation patterns coupling in hypersonic wind tunnels

[AIAA PAPER 70-562] 13 p2340 A70-29025

Internal shock waves in axisymmetric flowfield of perfect gas past blunted cone, noting roles of Mach number and cone half angle

15 p2672 A70-31592

Axisymmetric mixed boundary problem for elastic infinite cone, obtaining solution by assuming zero shearing stresses

17 p3192 A70-35698

Turbulent boundary layer on cone in supersonic flow in presence of inflowing foreign substance, considering local surface friction coefficient

20 p3559 A70-39814

Internal shock waves in axisymmetric flow field of perfect gas past blunted cone, noting poles of Mach number and cone half angle

23 p4133 A70-44276

CONFERENCES

Nondestructive evaluation of components and materials in aerospace, weapons systems and nuclear applications - Conference, San Antonio, April 1969

01 p0095 A70-10001

Interfaces in composites - ASTM Conference, San Francisco, June 1968

01 p0126 A70-10476

Biomechanics - Conference, Rock Island, Illinois, April 1967

01 p0033 A70-10494

GaAs - Conference, Dallas, October 1968

01 p0157 A70-10515

Solar-terrestrial physics, Terrestrial aspects - IQSY and COSPAR Conference, London, July 1967

01 p0071 A70-10577

Environmental effects on aircraft and propulsion systems - Conference, Bordentown, N.J., October 1969

01 p0162 A70-10678

Reinforced thermoplastics - Conference, Hartford, October 1969

01 p0128 A70-10769

Photooptical techniques in simulators - Conference, South Fallsburg, N.Y., April 1969

01 p0057 A70-10807

Occupational and medicative hazards in ophthalmology - Conference, Amsterdam, June 1968

01 p0022 A70-10855

Myocardial infarct and other psychosomatic disturbances - Conference, Wiesbaden, West Germany, August 1967, Part 3

01 p0023 A70-10864

Ultrasonics for industry - Conference, London, October 1969

01 p0089 A70-10877

Developments in mechanics - Conference, Ames, Iowa, August 1969

01 p0203 A70-11126

Information display - Conference, Arlington, Va., May 1969

01 p0048 A70-11276

Germ-free biology experimental and clinical aspects - Conference, Buffalo, June 1968

01 p0027 A70-11309

Low luminosity stars - Conference, Charlottesville, March 1968

01 p0187 A70-11330

Automated inspection for defects and dimensions - Conference, Eastbourne, England, May 1969

01 p0105 A70-11394

Jovian planets atmosphere - Conference, Tucson, April-May 1969

02 p0364 A70-11801

Civil aviation electronics - Conference, London, September 1969, Part 1, Electronics in flight control

02 p0329 A70-11831

Aerospace structures design - Conference, Seattle, Washington, August 1969

02 p0385 A70-11931

Civil aviation electronics - Conferences, London, September 1969, Part 3, Air traffic control

02 p0330 A70-11956

Civil aviation electronics - Conference, London, September 1969, Part 2

02 p0333 A70-11979

Combustion - Conference, Poitiers, France, July 1968

02 p0392 A70-12001

Electronic components - Conference, Washington, D.C., April-May 1969

02 p0267 A70-12052

Rocky Mountain Bioengineering - Conference, Laramie, Wyoming, May 1969

02 p0242 A70-12093

Man machine systems - IEEE/ERS Conference, Cambridge, England, September 1969, Volume 1, Man-computer interaction

02 p0264 A70-12126

Man machine systems - IEEE/ERS Conference, Cambridge, England, September 1969, Volume 2, Transport systems and vehicle control

02 p0334 A70-12130

Man machine systems - IEEE/ERS Conference, Cambridge, England, September 1969, Volume 3, Decision making and mental work load

02 p0244 A70-12137

Adaptive man machine systems, display design - IEEE/ERS Conference, Cambridge, England September 1969, Volume 4

02 p0245 A70-12147

Resources roundup - IEEE Conference, Phoenix, April 1969

02 p0257 A70-12177

Turbulent boundary layers computations - Conference, Stanford University, August 1968, Volume 2

02 p0280 A70-12271

Turbulent boundary layers computation - Conference, Stanford University, California August 1968, Volume 1, Methods, predictions, evaluation and flow structure

02 p0280 A70-12326

CONFERENCES

Application of atmospheric studies to satellite transmissions - Conference, Bedford, Mass., September 1969

02 p0259 A70-12564

Ballistocardiography and cardiovascular performance - Conference, Atlantic City, May 1968

02 p0240 A70-12675

Two phase flow instrumentation - Conference, Minneapolis, August 1969

02 p0304 A70-12833

Service life analysis at randomly varying load - Conference, Muelheim-Ruhr, Germany, April 1969 [DFVLR-SONDDR-4]

02 p0391 A70-12851

Cosmic ray physics - Conference, Tashkent, Uzbek SSR, October 1968

03 p0553 A70-13028

Atom ordering and effects on alloy properties - Conference, Kiev, Ukrainian SSR, 1969

03 p0505 A70-13101

Artificial satellite rotation study on basis of SPIN program photometric data - Conference, Kishinev, Moldavian SSR, September 1968

03 p0443 A70-13176

Geodetic treatment of satellite observation - Conference, Tashkent, Uzbek SSR, November 1968

03 p0444 A70-13182

Nonperiodic phenomena in variable stars - Conference, Budapest, September 1968

03 p0565 A70-13312

Photo-optical instrumentation - Conference, Washington, D.C., August 1968, Volume 1

03 p0487 A70-13651

Earth exploration and service by satellites - Conference, Rome, March 1969

03 p0572 A70-13826

Electroexplosive devices - Conference, San Francisco, July 1969

03 p0544 A70-14101

Applied mechanics - Conference, Stanford, August 1968

03 p0596 A70-14226

Nutrition and atherosclerosis - Conference, Bad Ragaz, Switzerland, October 1968

03 p0430 A70-14276

Theoretical and applied mechanics - Conference, Coimbatore, India, December 1966

03 p0601 A70-14326

Optimization problems computing methods - Conference, San Remo, Italy, September 1968

03 p0461 A70-14338

Phenomena in ionized gases - Conference, Bucharest, September 1969

03 p0534 A70-14359

Astronomy - Conference, Hobart, Australia, May 1969

04 p0746 A70-14506

Applied MHD and high temperature gas dynamics - Conference, Prague, May 1968

04 p0724 A70-14526

Imagery in medicine - Conference, Ann Arbor, May 1969

04 p0640 A70-14556

Nuclear and space radiation effects - IEEE Conference, Pennsylvania State University, July 1969

04 p0656 A70-14726

Numerical methods of solving problems in mechanics of continuous media - Conference, Kiev, Ukrainian SSR, June-July 1966

04 p0669 A70-14956

European space research - Conference, Dusseldorf, West Germany, December 1968

04 p0664 A70-15301

Acute myocardial infarction - Conference, Phoenix, March 1969

04 p0633 A70-15455

Time determination and georotation - Conference, Riga, Latvian SSR, June 1965

04 p0755 A70-15476

Electrical insulation - Conference, Boston, September 1969

05 p0869 A70-16032

Displays for command and control centers - NATO/AGARD Conference, Munich, November 1966

05 p0826 A70-16176

Computers - IEEE Conference, Minneapolis, June 1969

05 p0817 A70-16413

Mechanical engineering and mechanics-Conference, Haifa, June-July 1969

05 p0939 A70-16508

Differential equations and applications - Conference, Bratislava, Czechoslovakia, September 1966

05 p0876 A70-16560

Geoscience electronics - IEEE Conference, Washington, D.C., April 1969

05 p0849 A70-16683

Contamination control - Conference, New York, May 1969

05 p0798 A70-16701

Aerodynamic noise - Conference, University of Toronto, May 1968

05 p0795 A70-16776

Pressure vessel technology - Conference, Delft, Netherlands, September-October 1969
05 p0942 A70-16801

Pressure vessel technology - Conference, Delft, Netherlands, September-October 1969, Part 1, Design and analysis
05 p0943 A70-16808

Magnetics - IEEE Conference, Amsterdam, April 1969
05 p0893 A70-16995

Thermal stability of materials and structural elements - Conference, Kiev, Ukrainian SSR, December 1967
05 p0947 A70-17026

Aerodynamics - Conference, Berlin, October 1968
06 p0961 A70-17226

Electronic circuit packaging - IEEE Conference, San Francisco, August 1960, Part 7
06 p1016 A70-17334

Communications and displays - Conference, North Hollywood, August 1969
06 p1005 A70-17342

Instruments and systems - Conference, San Francisco, August 1969
06 p1017 A70-17351

Components and microelectronics - Conference, San Francisco, August 1969, Volume 13, Part 5
06 p1018 A70-17355

Plasma waves in space and laboratory - NATO Conference, Norway, April 1968
06 p1114 A70-17359

Fatigue at high temperatures - ASTM Conference, San Francisco, June 1968
06 p1086 A70-17451

Flight safety, survival and personal equipment - Conference, Las Vegas, October 1969, Volume 1
06 p1001 A70-17702

Rarefied gas dynamics - Conference, Cambridge, Mass., July 1968, Volume 2
06 p0976 A70-18251

Rarefied gas dynamics - Conference, Cambridge, Mass., July 1968, Volume 1
06 p1044 A70-18309

Instrumentation - ISA Conference, Houston, October 1969, Part 1
06 p1067 A70-18426

Instrumentation - ISA Conference, Houston, October 1969, Part 2
06 p1068 A70-18430

Thunderstorms and thunderstorm phenomena - ASM Conference, Chicago, April 1969
06 p1099 A70-18567

Instrumentation - ISA Conference, Houston, October 1969, Part 3
06 p1072 A70-18590

Instrumentation - ISA Conference, Houston, October 1969, Part 4
06 p1073 A70-18595

Gravitational effects on organisms - Conference, Warsaw, March 1969
07 p1200 A70-18784

Flight safety, survival and personal equipment - Conference, Las Vegas, October 1969, Volume 2
07 p1217 A70-19003

Multivariate analysis - Conference, Dayton, June 1968
07 p1323 A70-19026

Maritime and aeronautics technology - Conference, Paris, May 1969
07 p1192 A70-19126

Oblique ionospheric radio wave propagation at frequencies near lowest usable HF - NATO/AGARD Conference, Leicester, England, July 1966
07 p1227 A70-19151

LF waves and irregularities in ionosphere - Conference, Frascati, Italy, September 1968
07 p1263 A70-19186

Computing methods in optimization problems - Conference, San Remo, September 1968, Volume 2
07 p1324 A70-19266

Arbeitsgemeinschaft Verstärkte Kunststoffe - Conference, Freudenstadt, West Germany, September-October 1969
07 p1316 A70-19753

Photogrammetry - Conference, Karlsruhe, West Germany, September 1969
07 p1284 A70-19776

Numerical calculation and applied mathematics - Conference, Tours, France, July 1965
07 p1326 A70-19781

High temperature technology - Conference, Pacific Grove, California, September 1967
07 p1311 A70-19876

Propellants manufacture, hazards and testing - Conference, Miami Beach, April 1967
07 p1359 A70-19905

High and medium energy molecular beams - Conference, Cannes, July 1969
07 p1339 A70-20101

Cosmic ray physics - Conference, Tashkent, Uzbek SSR, October 1968
07 p1370 A70-20326

Lunar science - NASA Conference, Houston, January 1970, covering moon rock composition, magnetic, electrical and physical properties, etc
08 p1565 A70-20587

Automatic support systems for advanced maintainability - IEEE Conference, St. Louis, November 1969
08 p1468 A70-20651

Power sources - U.S. Army Conference, Atlantic City, May 1969
08 p1438 A70-20701

Electronics - Conference, Chicago, December 1969
08 p1457 A70-20776

Simulation applications - Conference, Los Angeles, December 1969
08 p1466 A70-20926

High speed testing - Conference, Boston, March 1969, Volume 7, Rheology of solids
08 p1526 A70-21326

Display media - Conference, Cambridge, Mass., September 1967
08 p1498 A70-21676

Experimental test pilots - Conference, Beverly Hills, September 1969
08 p1436 A70-21726

Composite materials testing and design - ASTM Conference, New Orleans, February 1969
08 p1528 A70-21876

Supersonic turbojet propulsion systems and components - NATO/AGARD Conference, Varenna, Italy, May 1967
08 p1559 A70-21926

Supernovae and remnants - Conference, New York, November 1967
09 p1748 A70-21987

Photo-optical instrumentation applications and theory - Conference, San Francisco, August 1969
09 p1672 A70-22029

Spectra of meteorological variables - Conference, Stockholm, June 1969
09 p1713 A70-22351

Phase diagrams of metal systems - U.S.S.R. Conference, Moscow, June 1967
09 p1702 A70-22559

Quality control - Conference, Tokyo, October 1969
09 p1690 A70-22568

Instrumentation and measurement - IEEE Conference, Ottawa, May 1969
09 p1647 A70-22713

Navigational techniques - NATO/AGARD Conference, Milan, September 1967
09 p1721 A70-23026

Instrumentation - ISA conference, New York, October 1968
09 p1613 A70-23683

Thermodynamics and fluid mechanics - Conference, Glasgow, March 1970
09 p1607 A70-23733

Photo-optical instrumentation - Conference, San Francisco, August 1969
09 p1684 A70-23751

Advanced fluid dynamics - Conference, Tarda, Poland, September 1967
10 p1863 A70-24101

Digital satellite communication - Conference, London, November 1969
10 p1833 A70-24326

Fuel cells - Conference, Brussels, June 1969
10 p1828 A70-24451

Earth Observation Satellites - BIS-NATO Conference, Cambridge, England, July 1969
10 p1950 A70-24635

Attention and reaction time - Conference, Eindhoven, Netherlands, July-August 1968
10 p1825 A70-24710

Photogrammetry - Conference, Washington, D.C., March 1970
10 p1877 A70-24726

Applied mechanics - Conference, Bucharest, June 1969
10 p1802 A70-24776

Applied mechanics - Conference, Bucharest, June 1969
10 p1870 A70-24794

Structural dynamics - Conference, Loughborough, Leics., England, March 1970, Volume 1
10 p1960 A70-25051

Structural dynamics - Conference, Loughborough, Leics., England, March 1970, Volume 2
10 p1962 A70-25064

Hypoxia fundamentals and clinical treatment - Conference, Mainz, Germany, October 1967
10 p1820 A70-25076

Radio science - Conference, Kleinheubach, West Germany, October 1968
10 p1882 A70-25251

Experimental stress analysis and influence on design - Conference, Cambridge, England, April 1970
11 p2130 A70-25584

Aviation and astronautics - Conference, Tel Aviv and Haifa, March 1970
11 p1978 A70-25676

Radio Technical Commission for Aeronautics - Conference, Washington, D.C., November 1969
11 p2078 A70-25719

Thermal conductivity - Conference, Purdue University, October 1968
11 p2146 A70-25751

Fluid mechanics and fluid machinery - Conference, Budapest, September 1969
11 p1973 A70-25776

Thermal Analysis - Conference Worcester, Mass., August 1968, Volume 1, Instrumentation, organic materials and polymers
11 p2069 A70-25801

Thermal analysis - Conference, Holy Cross College, August 1968, Volume 2, Inorganic materials and physical chemistry
11 p2070 A70-25808

Planetology and space mission planning - Conference, New York, October 1967
11 p2110 A70-26026

Environment and complex load effects on fatigue life - ASTM Conference, Atlanta, September-October 1968
11 p2137 A70-26088

Satellite photographic plate reduction - COSPAR Conference, Prague, April 1968
11 p2006 A70-26179

System sciences - Conference, University of Hawaii, January 1970, Part 1
11 p2024 A70-26201

System sciences - Conference, University of Hawaii, January 1970, Part 2
11 p2026 A70-26226

Space engineering - Conference, Venice, May 1969
11 p2124 A70-26276

Systems sciences - Conference, University of Hawaii, January 1969
11 p2027 A70-26301

Space flight thermodynamics and thermophysics - Conference, Palo Alto, California, March 1970
11 p2149 A70-26351

Measurement of dynamic mechanical quantities - Conference, Warsaw, May-June 1968
11 p2052 A70-26426

Turbulence - Conference, Seattle, June 1969
11 p2038 A70-26526

Turbulent flow - Conference, Seattle, June 1969
11 p2039 A70-26536

Turbulence of fluids and plasmas - Conference, New York, April 1968
11 p2093 A70-26751

Environmental remote sensing - Conference, Ann Arbor, October 1969, Volume 2
12 p2214 A70-26901

Remote environmental sensing - Conference, Ann Arbor, October 1969, Volume 1
12 p2218 A70-26929

Aviation psychological research - Conference, Zurich, September 1969
12 p2175 A70-27026

Growth points of physics - Conference, Florence, April 1969
12 p2297 A70-27053

Materials and structural dynamics - AIAA-ASME Conference, Denver, April 1970
12 p2315 A70-27101

Structures, structural mechanics and materials - AIAA-ASME Conference, Denver, April 1970
12 p2317 A70-27126

Magnetism and magnetic materials - Conference, Philadelphia, November 1969
12 p2283 A70-27238

Vacuum science and technology - Conference, Seattle, October 1969
12 p2284 A70-27251

Nuclear science and nuclear power systems engineering - IEEE Conference, San Francisco, October 1969
12 p2232 A70-27401

Systems theory - Conference, Gainesville, Florida, March 1970
12 p2203 A70-27408

Astronomy - Conference, Mannheim, Germany, September 1969
12 p2300 A70-27576

Manned laboratories in space - Conference, New York, October 1968
12 p2313 A70-27741

Fuel cell systems - ACS Conference, Chicago, September 1967, Part II
12 p2165 A70-27757

Quiescent plasma physics - Conference, Paris, September 1969, Part 1
12 p2279 A70-27776

Physics of quiescent plasmas - Conference, Paris, September 1969, Part 2
12 p2279 A70-27782

Physics of quiescent plasmas - Conference, Paris, September 1969, Part 3
12 p2280 A70-27790

Stars of galactic nebulae - Conference, Biurakan, Armenian SSR, September 1968
12 p2304 A70-27851

Electronics and Aerospace Systems - IEEE Conference, Washington, D.C., October 1969
12 p2185 A70-27901

Automatic image interpretation and classification - Conference, Pisa-Tirrenia, Italy, August-September 1968 12 p2193 A70-28101

Electromagnetic compatibility - IEEE Conference, Atlanta, October 1969 12 p2200 A70-28126

Plasticity and superplasticity exploitation - Conference, Eastbourne, Sussex, England October 1969 12 p2327 A70-28143

Nonlinear effects in plasmas - Conference, Orsay, Essonne, France, September 1966 13 p2456 A70-28551

Solid propellant combustion - Conference, Novosibirsk, November 1965 13 p2519 A70-28576

Fluid sealing - ASLE-ASME Conference, Philadelphia, May 1969 13 p2416 A70-28609

Atmospheric water effects on electromagnetic wave propagation - NATO Conference, University of Western Ontario, August-September 1969 13 p2393 A70-28781

Engineering properties and structure of plastics - Conference, New York, May 1970 13 p2438 A70-29251

System reliability and effectiveness - Conference, Beverly Hills, February 1969 13 p2524 A70-29564

Automatic test systems - Conference, Birmingham, England, April 1970 13 p2421 A70-29676

Plasma waves in space and laboratory - NATO Conference, Roros, Norway, April 1968 13 p2466 A70-29901

Weak magnetic fields in geo- and space physics - Conference, Paris, May 1969 13 p2413 A70-30026

Particles and fields in magnetosphere - Conference, Santa Barbara, August 1969 13 p2479 A70-30058

Air traffic, navigation and community - Conference, London, May 1970 14 p2611 A70-30101

Applied sciences research and utilization of lunar resources - Conference, New York, October 1968 14 p2633 A70-30192

Heat transfer and fluid mechanics - Conference, Stanford, California, June 1970 14 p2662 A70-30251

Medical electronics and biological engineering - Conference, Nancy, France, June-July 1969 14 p2540 A70-30376

Space navigation theory and practice - Conference, Ames Research Center, Moffett Field, California, February 1970 14 p2612 A70-30451

Aerospace meteorology - AMS-AIAA Conference, Las Vegas, May 1970 14 p2604 A70-30551

Otoneurology - Conference, Basel, 1969 14 p2538 A70-30908

Economic factors in aviation - RAS Conference, London, May 1970 14 p2668 A70-30935

Scintillation and semiconductor counters - IEEE Conference, Washington, D.C., March 1970 14 p2586 A70-31001

Planetary atmospheres and surfaces - Conference, Woods Hole, Mass., August 1969 14 p2643 A70-31051

Quality control - ASQC Conference, Pittsburgh, May 1970 14 p2591 A70-31101

Finite element methods application in civil engineering - Conference, Vanderbilt University, November 1969 14 p2658 A70-31126

Flight safety - Conference, Montreux, Switzerland, October 1969 15 p2674 A70-32206

Impact testing of metals - ASTM Conference, Atlantic City, June 1969 15 p2758 A70-32232

Space propulsion evolution in 1970s - Conference, Rome, March 1970 15 p2788 A70-32251

Solar energy - Conference, Athens, September 1969 15 p2677 A70-32418

IEEE Conference, Dallas, April 1970 15 p2701 A70-32551

Reliability - IEEE Conference, Los Angeles, February 1970 15 p2745 A70-32626

Interactions of electrons, phonons and magnons with crystalline surfaces - Conference, University of Lille, France, September 1969 15 p2785 A70-32763

Laser applications in geosciences - Conference, Huntington Beach, California, June-July 1969 16 p2925 A70-33013

Physical principles of biological membranes - Conference, University of Miami, December 1968 16 p2847 A70-33026

Circuits and systems - Conference, Pacific Grove, California, December 1969 16 p2881 A70-33031

Electro-optical systems design - Conference, New York, September 1969 16 p2901 A70-33126

Automatic control - Conference, Atlanta, June 1970 16 p2883 A70-33301

Plastics - Conference, Washington, D.C., February 1970 16 p2934 A70-33351

Microwaves - IEE Conference, London, September 1969 16 p2873 A70-33387

Aerospace electronics - IEEE Conference, Dayton, May 1970 16 p2908 A70-33426

Technology - Conference, Cocoa Beach, Florida, April 1970, Volume 1 16 p2975 A70-33701

Computers - AFIPS Conference, Atlantic City, May 1970 16 p2870 A70-33730

Mechanics - Conference, Bucharest, June 1969 16 p2893 A70-33740

Technology - Conference, Cocoa Beach, Florida, April 1970, Supplement 16 p2982 A70-33801

Sliding electrical contacts in vacuum and space - Conference, Virginia Polytechnic Institute, September-October 1969 16 p2919 A70-33805

Flight safety - Conference, Washington, D.C., May 1969 16 p2841 A70-33813

Electronic packaging and production - Conference, Brighton, England, October 1969 16 p2878 A70-33955

Corrosion by liquid metals - AIME Conference, Philadelphia, October 1969 16 p2932 A70-34201

Linear, nonlinear and random vibrations - Conference, Poznan, Poland, April 1968 16 p2994 A70-34276

Titanium science, technology and applications - Conference, London, May 1968 17 p3109 A70-34351

Optimization - Conference, Toronto, June 1968 17 p3181 A70-34542

Materials research - Conference, Tokyo, September 1969 17 p3123 A70-34651

Control theory and calculus of variations - Conference, University of California, Los Angeles, July 1968 17 p3129 A70-34866

UV stellar spectra and related ground based observations - Conference, Lunteren, Netherlands, June 1969 17 p3158 A70-34876

Engineering uses of holography - Conference, University of Strathclyde, Glasgow, September 1968 17 p3083 A70-35001

Laser measurements - Conference, Warsaw, September 1968 17 p3103 A70-35080

Crab Nebula - Conference, Flagstaff, Arizona, June 1969 17 p3163 A70-35112

Environmental challenge of 1970s - Conference, Boston, April 1970 17 p3058 A70-35151

Space technology and science - Conference, Tokyo, August 1969 17 p3164 A70-35201

Aerospace Medical Association Conference, St. Louis, April 1970 17 p3026 A70-35326

Normal stellar atmospheres - Conference, Cambridge, Mass., April 1968 17 p3168 A70-35379

Aerospace industry instrumentation - Conference, Las Vegas, May 1969, Volume 15 17 p3091 A70-35476

Remote sensing in ecology - Conference, Madison, Wisconsin, June 1968 17 p3078 A70-35611

Outer space law - Conference, Mar del Plata, Argentina, October 1969 17 p3200 A70-35776

Air transportation growth with regularity and safety - Conference, London, November 1969 17 p3021 A70-35851

Gas dynamics of explosions and reacting systems - Conference, Novosibirsk, U.S.S.R., August 1969 17 p3074 A70-35882

Bird hazards to aircraft - Conference, Queens University, Canada, September 1969 18 p3210 A70-35976

Applied mathematics and mechanics - Conference, Aachen, Germany, April 1969 18 p3280 A70-36351

Air traffic - Conference, Versailles, June 1970 18 p3288 A70-36389

Air traffic control - Conference, Versailles, June 1970 18 p3289 A70-36396

Thermodynamics - Conference, University of Pittsburgh, April 1969 18 p3347 A70-36551

Semiconductor lasers - IEEE Conference, Mexico City, December 1969 18 p3267 A70-36726

Electronic packaging - IEEE Conference, Cambridge, Massachusetts, June 1970 18 p3232 A70-36758

Milky Way spiral structure - Conference, Basel, August-September 1969 18 p3324 A70-37151

Classical and relativistic MHD - Conference, Lille, France, June 1969 19 p3476 A70-37576

Ferrite single crystals physical properties - Conference, Krasnoyarsk, U.S.S.R., June-July 1969 19 p3484 A70-37621

Ferrite single crystals physical properties - Conference, Krasnoyarsk, U.S.S.R., June-July 1969 19 p3485 A70-37626

Engineering science - Conference, Princeton University, November 1968 19 p3537 A70-37782

Engineering for 1970s - IEEE Conference, Huntsville, Alabama, November 1969 19 p3392 A70-37842

Instrumentation in aerospace industry - Conference, Seattle, May 1970 19 p3423 A70-37873

Engineering science - Conference, Princeton University, November 1968, Part I 19 p3539 A70-37940

Cosmic rays - Conference, Budapest, August-September 1969, Volume 1, Origin and galactic phenomena, covering supernovae, ray spectra, pulsar gamma rays, etc 19 p3497 A70-38076

Air traffic control - Conference, St. Louis, April 1970 19 p3464 A70-38226

Space simulation for satellites and space probes - Conference, Aachen, Germany, March 1970 19 p3397 A70-38276

Space simulation for satellites and space probes - Conference, Aachen, Germany, March 1970 19 p3398 A70-38285

Attention and performance - Conference, Soesterberg, Netherlands, August 1969 19 p3361 A70-38310

Theoretical and applied mechanics - Conference, Tulane University, February-March 1968 19 p3543 A70-38326

Aerospace instrumentation - Conference, Cranfield Institute of Technology, England, March 1970 19 p3428 A70-38514

Reliability - ASQC Conference, Los Angeles, May 1970 19 p3438 A70-38593

Air traffic control - Conference, Stockholm, March 1969 19 p3466 A70-38629

Reliability and maintainability - Conference, Detroit, July 1970, Volume 9, Assurance technology spinoffs 19 p3440 A70-38815

Solar eclipses and ionosphere - NATO Conference, Lagonissi, Greece, May-June 1969 19 p3417 A70-38901

Aerospace methods for revealing and evaluating earth resources - Conference, Princeton University, September 1969 20 p3615 A70-39051

Physical geodesy - Conference, Prague, September 1969 20 p3617 A70-39068

Carbon composite technology - Conference, University of New Mexico, January 1970 20 p3652 A70-39201

Pathophysiology of congenital heart disease - Conference, University of California, Los Angeles, July 1967 20 p3570 A70-39361

Invariant automatic control systems - Conference, Kiev, May-June 1966, Volume 2 20 p3601 A70-39826

Statistical problems in technical automation - Conference, Moscow, February 1967 20 p3592 A70-39901

Materials technology - Conference, Mexico City, August 1970 20 p3649 A70-39939

Magnetohydrodynamics - MIT Conference, Cambridge, Mass., March 1969 20 p3679 A70-39982

Magnetohydrodynamics - JPL Conference, Padasena, March 1970 20 p3565 A70-40001

Mechanics of composite materials - Conference, Philadelphia, May 1967 20 p3728 A70-40026

Atmospheric studies application to satellite transmissions t USAF Conference, Boston, September 1969 20 p3589 A70-40476

Nonsolar X and gamma ray astronomy - Conference, Rome, May 1969 21 p3870 A70-40651

Test measurement instruments - Conference, Houston, October 1969 21 p3823 A70-40855

Space technology and heat transfer - ASME Conference, Los Angeles, June 1970, Part 1 21 p3927 A70-40976

Space systems and thermal technology - ASME Conference, Los Angeles, June 1970, Part 2 21 p3942 A70-41014

Position finding and navigation in space, air and sea - Conference, Hamburg, October 1969, Volume 1 21 p3847 A70-41126

Astronomy - Conference, Canberra, Australia, December 1969 21 p3890 A70-41176

Nucleation role in boiling and cavitation - ASME Conference, Detroit, May 1970 21 p3948 A70-41201

Power conditioning - IEEE Conference, Greenbelt, Maryland, April 1970 21 p3757 A70-41206

Ballistocardiography and cardiovascular therapy - Conference, Oporto, Portugal, March-April 1969 21 p3762 A70-41226

Communications - IEEE Conference, San Francisco, June 1970, Volume 1 21 p3786 A70-41326

Communications - IEEE Conference, San Francisco, June 1970, Volume 2 21 p3788 A70-41340

Thermoinelasticity - Conference, East Kilbride, Scotland, June 1968 21 p3936 A70-41426

Apollo 11 lunar science - NASA Conference, Houston, January 1970, Volume 1, Mineralogy and petrology 21 p3893 A70-41501

Apollo 11 lunar science - Conference, Houston, January 1970, Volume 2, Chemical and isotope analyses 21 p3903 A70-41560

Apollo 11 lunar science - Conference, Houston, January 1970, Volume 3, Physical properties 21 p3911 A70-41636

Mechanical Engineering - Conference, Haifa, July 1970 21 p3809 A70-41951

Theoretical and applied mechanics - Conference, Haifa, July 1970 21 p3938 A70-41958

Palaeogeophysics - Conference, University of Newcastle-upon-Tyne, England, April 1968 21 p3921 A70-41969

Polymers in space research - ACS Conference, Pasadena, July 1968 21 p3781 A70-42126

Chromosphere-corona transition region - Conference, Boulder, Colorado, August 1969 21 p3924 A70-42182

Gas discharges - IEE Conference, London, September 1970 22 p4077 A70-42351

Information transmission and coding theory - Conference, Tashkent, Uzbek SSR, September-October 1969, Section 1, Data transmission theory, Methods of coding and decoding 22 p3985 A70-42490

Aircraft acoustical duct treatments - ASA Conference, Philadelphia, April 1969 22 p4089 A70-42528

Information transmission and coding theory - Conference, Tashkent, September-October 1969, Section 2, Statistical theory of signals and noise, Optimal reception methods 22 p3986 A70-42551

Astrophysics and general relativity - Waltham, Mass., June-July 1968, Volume 1 22 p4098 A70-42576

Applied mechanics - Conference, Bucharest, June 1969 22 p4113 A70-42601

Applied mechanics - Conference, Bucharest, June 1969 22 p4009 A70-42605

Applied mechanics - Conference, Bucharest, June 1969 22 p4113 A70-42610

High temperature systems - Conference, Pasadena, December 1964, Volume 2 22 p4090 A70-42751

Planetary electrodynamics - Conference, Tokyo, May 1968, Volume 2 22 p4014 A70-42776

Motor activity and aging - Conference, Kiev, April 1968 22 p3967 A70-42893

Aerospace nuclear applications - Conference, Huntsville, Alabama, April 1970 22 p4069 A70-43177

Air cargo - Conference, Frankfurt am Main, September 1970 22 p4006 A70-43267

Nondestructive tests and controls in metallurgy and nuclear technology - Conference, Saclay, France, June 1968 22 p4040 A70-43617

Orbital international laboratory and space sciences - Conference, Cloudcroft, New Mexico, September 1969 22 p4107 A70-43626

Dynamic gravimetry - Conference, Fort Worth, March 1970 22 p4024 A70-43656

Aerospace medicine - Conference, Amsterdam, September 1969 22 p3973 A70-43690

Microwave communication - Conference, Budapest, April 1970, Volume 1, Communication system theory 23 p4158 A70-43751

Microwave communication - Conference, Budapest, April 1970, Volume 3, Electromagnetic theory 23 p4160 A70-43764

Microwave communication - Conference, Budapest, April 1970, Volume 4, Microwave theory and techniques 23 p4168 A70-43776

Microwave communication - Conference, Budapest, April 1970, Volume 5, Microwave electronics, system measurements 23 p4170 A70-43793

Hot plasmas physics - Conference, Newbattle Abbey, Scotland, July-August 1968 23 p4224 A70-44176

Position finding and navigation in space, air and at sea - Conference, Hamburg, October 1969, Volume 2 23 p4162 A70-44227

Environmental engineering - Conference, Delft University, Netherlands, April 1970 23 p4268 A70-44326

Cryogenic engineering - Conference, University of California, Los Angeles, June 1969 23 p4277 A70-44351

X ray analysis - Conference, University of Denver, August 1969 23 p4243 A70-44414

Thermophysical properties - ASME Conference, Newton, Mass., September-October 1970 23 p4219 A70-44426

Survival and flight equipment - Conference, Las Vegas, September-October 1970, Volume 1 23 p4151 A70-44453

Survival and flight equipment - Conference, Las Vegas, September-October 1970, Volume 2 23 p4152 A70-44479

Electronic packaging and production - Conference, Anaheim, California, February 1970 and New York, June 1970 23 p4173 A70-44532

Failure analysis - IEEE Conference, University of Pennsylvania, May 1970 23 p4174 A70-44743

Stellar rotation - Conference, Ohio State University, Columbus, September 1969 23 p4248 A70-44801

Astronautics - IAF Conference, New York, October 1968, Volume 1, Spacecraft systems 23 p4262 A70-45001

Astrodynamics and astronautics - Conference, New York, October 1968, Volume 2 23 p4254 A70-45013

Astronautics - IAF Conference, New York, October 1968, Volume 3, Propulsion reentry physics 23 p4234 A70-45017

Astronautics - IAF Conference, New York, October 1968, Volume 4, Bioastronautics 23 p4155 A70-45022

Strong fibrous solids - Conference, London, January 1970 24 p4366 A70-45165

Fluidics - Conference, Chicago, November 1968 24 p4293 A70-45426

Satellite dynamics - Conference, Prague, May 1969 24 p4405 A70-45526

Applied mechanics - Conference, Bucharest, June 1969 24 p4423 A70-45576

Applied mechanics - Conference, Bucharest, June 1969 24 p4423 A70-45586

Nondestructive testing - Conference, Hanover, June 1970, General problems 24 p4342 A70-45676

Nondestructive testing - Conference, Hanover, June 1970, Ultrasound, Part 1, Instruments, methods and defect evaluation 24 p4342 A70-45680

Nondestructive testing - Conference, Hanover, June 1970, Electric and magnetic methods 24 p4343 A70-45693

Nondestructive testing - Conference, Hanover, June 1970, Radiography 24 p4345 A70-45706

Nondestructive testing - Conference, Hanover, June 1970, Material properties determination 24 p4345 A70-45717

Radiography and stray flux methods in nondestructive testing - Conference, Hanover, June 1970 24 p4346 A70-45722

Nondestructive testing - Conference, Hanover, June 1970, Materials properties determination, Stress measurements 24 p4347 A70-45728

Nondestructive testing - conference, Hanover, June 1970, Material properties determination, covering electric, magnetic, liquid penetrant and thermal methods 24 p4347 A70-45735

Nondestructive testing - Conference, Hanover, June 1970, Neutronradiography and holography 24 p4375 A70-45745

Hypertensive mechanisms - Conference, Canberra, Australia, January 1970 24 p4298 A70-45803

Electronic Packaging and Production - Conference, Chicago, April 1970 24 p4320 A70-46246

CONFIDENCE LIMITS

Confidence limits on percent defective estimates for production processes characterized by two specification limits 16 p2921 A70-34025

Maximum likelihood estimates for setting confidence limits of Weibull percentiles and shape parameters 17 p3128 A70-34579

Aircraft systems safety requirements, consisting of accident probability, confidence level and demonstration test period 19 p3442 A70-38840

Prior distributions computer aided selection for generating Monte Carlo confidence bounds on system reliability 20 p3658 A70-39641

Statistical confidence levels for frequency analysis, detecting peak sinusoid for desired signal to noise ratio 21 p3825 A70-40867

CONFIGURATION MANAGEMENT

Configuration management of software concerning automatic test systems in large maintenance depot 13 p2422 A70-29692

Quality control role in configuration management, considering quality assurance organization of aircraft manufacturer 14 p2669 A70-31104

Space Station long term operations and logistics concerning inventory, configuration and cargo management [SAE PAPER 700757] 24 p4416 A70-45871

CONFINEMENT

Galactic disk model for confinement of cosmic ray electrons, assuming isotropic background radiation 19 p3510 A70-38156

CONFIRMATION

U PROVING

CONFLUENCE

U CONVERGENCE

CONFORMAL MAPPING

Nonlinear modification of Maxwell equations, discussing conformal invariance and nonsingular solutions to neutral and charged states with zero mass 02 p0339 A70-12067

Small parameter method applied to numerical solution of conformal mapping and viscous fluid motion problems 04 p0719 A70-14960

Circular cascade design from rectangular cascade flow data using conformal transformation, considering aerodynamic properties 11 p1974 A70-25786

Jet flow through rectangular orifices in cylindrical wall using conformal mapping for potential, velocity, volume flow rate, viscosity, etc 14 p2567 A70-31359

Equations system for determining constants in Sedov integral for conformal mapping of polygonal airfoil lattice onto Riemann surface 20 p3658 A70-39767

Cold plate immersed in warm flowing liquid, calculating two dimensional transient and steady state solidification by conformal mapping 21 p3949 A70-41319

Cracks stress intensity factors in plane problems by cracked conformal mapping and boundary collocation technique 21 p3940 A70-42036

Horizontal Situation Display (HSD)/ map computer mechanization transforming earth location to X, Y coordinates for Lambert conformal projection [AIAA PAPER 69-987] 22 p4068 A70-42710

CONFORMAL TRANSFORMATIONS

U CONFORMAL MAPPING

CONGENITAL ANOMALIES

Cardiovascular model for closed loop analog simulation of congenital heart defects hemodynamics 11 p1990 A70-25705

CONGENITAL CONDITIONS

U CONGENITAL ANOMALIES

CONGESTION

Human nostril airflow resistance during supported sitting and lateral recumbency and crutch pressure, discussing ipsilateral nasal congestion mechanisms 08 p1448 A70-21874

CONICAL BODIES

NT SLENDER CONES

Surface roughness effects on dry friction between two metals, considering conical asperities and friction coefficients [ASME PAPER 69-LUB-10] 01 p0102 A70-10394

Blunt and conical body optimum heat shield shapes for Jupiter atmospheric entry, noting shallow flight path [AIAA PAPER 68-1150] 01 p0195 A70-10827

Characteristics method for calculating steady supersonic flow of burning gas mixture past wedge and rotating cones 01 p0218 A70-11018

Integral method for studying wall heat transfer influence on compressible boundary layer on cone at angle of attack in supersonic flow 03 p0409 A70-13953

Radiation view factor from differential area to conical surface determined using Stokes theorem and contour integration 04 p0787 A70-15598

Ballistic range measurements of vibrational nonequilibrium effects on leading edge shock wave shape for cone-cylinders fired through chlorine atmosphere at supersonic speeds 04 p0621 A70-15601

Supersonic flow past elliptic cone of small eccentricity treated as axisymmetric conical flow perturbation 05 p0790 A70-16506

Steady and frictionless supersonic flow of ideal gas of constant heat capacity around slightly deformed cone, calculating force exerted by gas 06 p0964 A70-17240

Induced electromotive force method for determining impedance changes of monopole on base of large cone 06 p0109 A70-17558

Radiation patterns from finite conducting cone excited by quarter wave monopole protruding from center of base computed on digital computer 06 p0120 A70-17559

Cone bluntness effect on merging onset and downstream flow in merged region at Mach 8 and various Reynolds numbers 06 p0980 A70-18352

Downstream distribution of trace element injected into boundary layer of flat plate or cone with self similar mass transfer [SAMSO-TR-69-56] 07 p1256 A70-19313

Plane electromagnetic wave scattering at apex of conical body, presenting scattered field calculations for various cone sizes and surface impedances 08 p1461 A70-20974

Aerodynamic coefficients for blunt cones in rarefied gas calculated as functions of angle of attack using empirical formulas 08 p1432 A70-21092

Boundary layer transition measurements on flight tests of experimental 22 degree conical reentry vehicle with Be heat shield and graphite nose [AIAA PAPER 68-1152] 09 p1606 A70-23243

Drag measurement for star-shaped body at hypersonic speeds, comparing results with cone-shaped model 10 p1799 A70-24122

Steel conical disks two dimensional stressed state determined with deformations at elastic and elastoplastic strains using digital computers 10 p1956 A70-24242

Laminar boundary layer in symmetry plane of cone of revolution at angle of attack calculated by finite difference method 10 p1802 A70-24706

Gasdynamic functions of supersonic flow past spherically and ellipsoidally blunted inverted cones 11 p1973 A70-25522

Three dimensional hypersonic steady flow around blunt and pointed cones at nonzero angles of attack calculated by method of characteristics [AIAA PAPER 69-187] 11 p1975 A70-25969

Metal surfaces contact with cones and pyramids asperities, analyzing surface roughness effects on dry friction 11 p2060 A70-26412

Newtonian fluid laminar throughflow between coaxial corotating cones, applying solution for flow between disks 11 p2038 A70-26491

Axial incidence HF backscattering cross section for absorbing flat based cone assumed to obey impedance boundary condition 12 p2185 A70-27716

Wide angle emitter images transformation into circular by reflecting cone and lens system, describing photographic and photoelectric methods 12 p2237 A70-28157

Turbulent boundary layer and base pressure profiles of supersonic flow past conical models in wind tunnel 12 p2159 A70-28229

Pressure distribution over lateral surface of truncated cones in nonequilibrium flow, analyzing physicochemical transformations effect 12 p2159 A70-28246

Turbulent base pressure on conical afterbodies in supersonic axisymmetric flow, including initial direction effect [AIAA PAPER 70-555] 13 p2340 A70-29020

Supersonic rigid cone motion in elastic medium, obtaining partial solutions to motion equation yielding boundary problem solution 13 p2341 A70-29508

Sliding rigid conical indenter friction experiments over work hardenable metal flats in high adhesion conditions, observing forces, stresses and deformation modes 13 p2421 A70-29548

Surface pressure and heat transfer over blunt conical body in hypersonic flow with uniform mass addition of various gases [AIAA PAPER 69-716] 13 p2523 A70-29977

Nonequilibrium dissociation effect on supersonic oxygen flow past inverted blunted cones at angle of attack, considering thermal fluxes and aerodynamic forces 15 p2671 A70-31496

Cone geometry for electromagnetic and acoustic scattering 15 p2701 A70-32417

Incompressible viscous fluid divergent turbulent flow detection in conical tube of revolution based on measuring wall pressure differences along tube generatrix 16 p2894 A70-33849

Turbulent boundary layer growth and thickness on yawed cones, discussing angle of attack effect along windward and leeward rays 16 p2838 A70-33875

Hypersonic flow field around yawed half angle cone from wind tunnel measurements including surface pressure distributions and flow visualization photographs 17 p3007 A70-34485

Blunt nose effects on drag of flared conical body in supersonic flow, considering pressure loss through shock wave and vorticity 17 p3196 A70-35237

Steady supersonic flow past conical bodies at yaw, adapting Telenin numerical method 17 p3012 A70-35889

Shock layer and combustion in supersonic flows about conical bodies at various angles of attack 17 p3012 A70-35894

Hypersonic gas flow around blown plane of segmentally blunted cones at large angle of attack, using two dimensional model 18 p3206 A70-36258

Stress decay rates in Saint Venant boundary region in truncated semiinfinite elastic cone, using Papkovitch-Neuber functions for eigenfunctions formulation 18 p3339 A70-36489

Turbulent mixing in supersonic cone near wake, using laser planogram technique for flow visualization 19 p3351 A70-37529

Heat shield analysis covering high temperature ablation interactions in conical anisotropic structure immersed in hypersonic environment 20 p3738 A70-40054

Hypersonic flat and biconvex conical wings, calculating yaw effects on shock shape and pressure distribution 21 p3761 A70-40918

Loads induced by terminal shock boundary layer interaction on cone-cylinder bodies, discussing angle of attack effect 21 p3746 A70-41863

Surface pressure coefficient dependence on specific heat ratio for yawed conical lifting bodies in supersonic streams 21 p3747 A70-41877

Exponential compression wave propagation in conical rod with smooth tapering cross section 22 p4121 A70-43726

Axisymmetric vibration modal properties /frequencies and mode shapes/ of thin conical shell frustums, considering dimensional and boundary condition influences 23 p4270 A70-44501

Oscillatory motion of triangular wing with conical body of arbitrary cross section in supersonic flow, considering wing-body interference effects 24 p4288 A70-45592

CONICAL CAMBER

Quasi-conical supersonic wings with curved subsonic leading edges, discussing perturbation potential, boundary conditions, homogeneous flow and gothic and ogee planforms 21 p3747 A70-42108

CONICAL FLARE

U CONES

CONICAL FLOW

Supersonic flow past elliptic cone of small eccentricity treated as axisymmetric conical flow perturbation 05 p0790 A70-16506

Small disturbance theory for internal conical inlet hypersonic flows, using method of characteristics for similarity law verification [AIAA PAPER 70-127] 06 p0969 A70-18048

Laminar boundary layer on cone at incidence in supersonic flow evaluated by pressure distribution technique, comparing heat transfer, pitot probe measurements, etc [AIAA PAPER 70-48] 06 p0974 A70-18189

Hypersonic rarefied merged layer flow over sharp slender cones, using strong interaction theory and free molecular flow to analyze surface pressures 06 p0982 A70-18363

Massive blowing from porous cone with embedded shock wave in supersonic flow, assuming inviscid and conical injected flow field 09 p1662 A70-23216

Supersonic flow behind cone, studying bottom pressure and stagnation zone dependence on incident flow parameters and static pressure distribution 09 p1663 A70-23623

Supersonic flow around slender polyhedral wings with nonsymmetrically distributed incidence using method for conical flow around angular wings 10 p1803 A70-24797

Second order conical flows around wing-fuselage system, deriving expressions for axial perturbation velocity for various attack geometries 10 p1804 A70-24972

Nonuniform partitioning of flowfield in three dimensional laminar boundary layer in supersonic conical flow at zero angle of attack, using numerical integration 10 p1804 A70-25192

Numerical solution for steady supersonic inviscid flow around smooth conical bodies by solving elliptic partial differential equations for conical flow 12 p2155 A70-27202

Boundary layer formation on walls of conical pressure nozzle during vortex flow 16 p2896 A70-34299

Shock curvature at wedge or cone tip in radiating gas flow, noting differences between radiative and chemically coupled gas dynamics 23 p4135 A70-44638

Axisymmetrical nozzle aerodynamic shape design for conical to axially uniform flow conversion, using method of characteristics 23 p4136 A70-44991

CONICAL INLETS

Small disturbance and similitude applicability to internal hypersonic conical flows in edge shock and Busemann inlets 09 p1606 A70-23245

CONICAL NOZZLES

Flow development in conical diffusers, delaying stall with high velocity air injection through annular slot at diffuser inlet predicted by finite difference method 02 p0224 A70-12866

One dimensional steady adiabatic source nonisentropic flow of thermally and calorically perfect gas in conical nozzle, considering exit divergence and nonuniform flow effects 04 p0619 A70-15427

Base pressure effects on cone angle of fixed length conical nozzle yielding maximum thrust 11 p1977 A70-26156

Laminar boundary layers in low density supersonic and hypersonic conical and axisymmetric nozzles, treating displacement, transverse curvature, velocity slip and temperature jump [AIAA PAPER 69-653] 13 p2386 A70-28513

Transonic flow in convergent and convergent-divergent conical nozzles with nonuniform inlet predicted by time dependent flow equations, discussing discharge and thrust coefficients [AIAA PAPER 70-635] 16 p2834 A70-33548

Mass flow rate and geometry effects on pressure recovery of conical diffusers with annular secondary injection at inlet [ASME PAPER 70-FE-18] 16 p2835 A70-33631

Shock waves in supersonic conical nozzle flow due to secondary gas injection, using conical lens for flow visualization 17 p3011 A70-35236

Underexpanded carbon dioxide free jet expanding into vacuum from conical nozzles 17 p3070 A70-35246

Conical expansion nozzles manufacturing errors effect on flow expansion considered for large Mach numbers 17 p3011 A70-35662

Conical convergent nozzles discharge coefficient for varying pressure ratios 19 p3352 A70-38243

- Conical diffuser-tailpipe system performance, discussing cone angle, area ratio, Reynolds number and velocity distribution effects on pressure recovery 20 p3559 A70-40082
- LF acoustic disturbances effect on root portion of turbulent jet from conical nozzle 21 p3954 A70-42223
- Twisted incompressible viscous fluid flow in conical diffuser described by differential equation system, considering flow velocity field and separation point 23 p4133 A70-44159
- ### CONICAL SHELLS
- Elastic bending of thin circular conical shell subject to arbitrary variation of edge loads 01 p0209 A70-11385
- Orthotropic axially compressed conical shell stability, evaluating lower critical load and postbuckling state 04 p0772 A70-14921
- Stability analysis of deflected shallow thin walled elastic noncircular conical and cylindrical orthotropic shells using straight lines method 06 p1167 A70-17865
- Retrorocket effects on aerodynamic stability and drag of conical aeroshell planetary entry vehicles, discussing supersonic wind tunnel tests and jet shock interaction [AIAA PAPER 70-219] 06 p0974 A70-18166
- Conical shells stability under uniform pressure, studying varying thickness influence by variational stress and bending equation 07 p1402 A70-19052
- Stress concentrations calculation at holes in plates and shells of positive Gaussian curvature applicable to hyperbolic shells 07 p1408 A70-19548
- Truncated conical shells buckling under hydrostatic pressure using Donnell equations, assuming membrane stress state for prebuckling deformation 07 p1414 A70-20170
- Multilayer orthotropic conical shell cyclic deformation equation obtained in hypergeometric functions 09 p1777 A70-23079
- Layered conical shell creep under axisymmetric load and time dependent temperature field by iterating boundary integral equation 09 p1779 A70-23099
- Liquid motion dynamic effects in open cylindrical and conical tanks with translational motion 09 p1662 A70-23293
- Truncated, structurally orthotropic and round conical shell oscillations taking into account reinforcing ribs eccentricity 10 p1964 A70-25195
- Rectangular conical shells reinforced along ribs by belts under tension/compression calculated by initial functions method 11 p2130 A70-25568
- Truncated conical shell buckling under axial compression using method for torsion buckling, correlating to equivalent cylindrical shells 11 p2135 A70-25980
- Elastic conical shells of revolution linear theory, calculating stress resultants and couples 11 p2145 A70-26689
- Axisymmetric and unsymmetric free vibrational modes of right-circular conical or cylindrical sandwich shells with free edges, discussing Rayleigh-Ritz solution 11 p2145 A70-26700
- Postwrinkling nonlinear behavior of conical shell of revolution subjected to bending loads [AIAA PAPER 69-90] 12 p2326 A70-27816
- Structural strength of fiberglass plastics reinforced conical shells, using impregnation technique of dry package under pressure 12 p2328 A70-28280
- Elastic material filled cylindrical, segmented toroidal and conical shells thermal stability, allowing for stiffer eccentricity 13 p2516 A70-29523
- Cylindrical conical shell junction axisymmetric bending, using numerical method and exact solution 15 p2822 A70-32360
- In-plane boundary conditions effect on axially compressed conical shell stability under low buckling loads, using linear Donnell-type theory 17 p3186 A70-34971
- Shallow conical shell stability under uniformly distributed pressure and concentrated force at apex for rigid and free clamping boundary conditions 18 p3341 A70-36589
- Thin elastic conical shell axisymmetric solution for free vibration in terms of power series 19 p3545 A70-38335
- Stresses around circular hole in shallow conical shell under torsional load, using perturbations in parameters for curvature and cone angle 21 p3934 A70-40779
- Bending stress at clamped support of impulsively loaded semiinfinite conical shell, obtaining formulas from perturbation theory 21 p3938 A70-41759

Radar cross section for thin dielectric plate and spherical and conical shells 23 p4166 A70-44975

Rumanian book on torsion in thin walled elastic structures of various cross sections covering calculation methods for box beams, cylindrical and conical shells, aircraft wings, etc 24 p4418 A70-45147

CONICS

NT HYPERBOLAS
NT PARABOLAS

Lawden primer vector theory applied to matched conic spacecraft trajectories optimization 07 p1381 A70-19325

Space mechanics problem of passing from perigee to radial distance in given time determined by fitting conic to radii, using iteration method 09 p1760 A70-22927

Hybrid patched conic iterative technique for accurate moon-earth/transearth/trajectory generation 09 p1760 A70-22929

CONJUGATE POINTS

Auroral phenomena interdisciplinary investigations, discussing electron precipitation and conjugate point drift due to geomagnetic axis position variations 19 p3411 A70-37493

Cosmic noise absorption diurnal variations at auroral zone conjugate areas during geomagnetically disturbed periods 19 p3414 A70-38379

VLF radiation observation at conjugate points, discussing hisses, choruses and geomagnetic effects 19 p3416 A70-38587

Auroral X-ray radiation at magnetoconjugate points Kerguelen/archangel region, using balloon-borne spectrometers 21 p3813 A70-40839

F 2 region critical frequency cross correlation coefficients for magnetically conjugate stations, considering magnetic disturbances effects 21 p3816 A70-41069

F 2 layer nighttime ionization at mid-latitudes, investigating conjugate point effects on observation point 23 p4188 A70-44055

CONJUGATES

NT CONJUGATE POINTS

Physical processes responsible for conjugate point phenomena involving particles and waves in magnetosphere and IQSY observations 01 p0075 A70-10598

Postbreakup pulsating aurora association with conjugate absorption bays, indicating hard electron precipitation source location 02 p0290 A70-12161

Existence conditions of conjugate points for non-trivial solution of fourth order differential equation 03 p0519 A70-14079

Geomagnetic conjugate point problems involving temporal displacement field line tracing, display, etc 03 p0479 A70-14385

Conjugate points for simple integral problems in calculus of variations extended to multiple integral problems, using Jacobi equation 04 p0713 A70-14674

Explorer 31 Langmuir probe data for electron temperature at conjugate point, tracing magnetic field line passing through spacecraft to earth 04 p0000 A70-14971

Positive correlation between normal ionizations at magnetically conjugate regions in ionospheric F 2 layer from aircraft vertical soundings 04 p0683 A70-15741

F 2 region critical frequency conjugacy latitudinal variations observation at conjugate stations compared with results from nonconjugate stations 05 p0839 A70-16286

High and medium whistler activity in Italy correlated with weather situation in South Africa 05 p0839 A70-16317

Protonospheric heating by photoelectrons from conjugate ionosphere using Explorer 31 data 08 p1489 A70-21387

Conjugate direction procedures for function minimization compared for convergence, recommending modified conjugate gradient procedure 08 p1535 A70-21875

Positive correlation between normal ionizations at magnetically conjugate regions in ionospheric F 2 layer from aircraft vertical soundings 14 p2575 A70-30825

Autofocus for variable magnification systems, discussing conjugate concepts and linkage and cam methods for enlargers and projectors 16 p2907 A70-33182

Auroral cosmic noise absorption, discussing east-west motion, conjugate magnitudes and breakdown 16 p2899 A70-34191

Soviet book on conjugate functions and trigonometric series covering Hilbert transform, Fourier series properties, Cesaro methods, etc 19 p3459 A70-38799

CONJUGATION

Conjugation principle for control system stabilization based on relation between controlled plant and stabilizing element stability 05 p0824 A70-16851

CONNECTIONS

U JOINTS [JUNCTIONS]

CONNECTIVE TISSUE

NT CARTILAGE
NT MARROW

Morphological analysis of connections between auditory cortex zone and claustrum in anesthetized cats, establishing efferent nerve fibers presence 01 p0025 A70-11039

Temporary interneuron connections mechanisms during conditioned reflexes development 01 p0025 A70-11040

Human mitral valve morphology, distinguishing chordae tendinae types by insertion mode 10 p1819 A70-24935

Human mitral valve morphology, studying posterior and anterior leaflets partitioned by chordae tendinae 10 p1819 A70-24936

CONNECTORS

NT ELECTRIC CONNECTORS
NT UNIONS [CONNECTORS]

Film type solar energy reflector peripheral blades for connection to receiver, discussing precession control and despin for rotating concentrators 07 p1196 A70-19501

Film type solar energy reflector peripheral blades for connection to receiver, discussing precession control and despin for rotating concentrators 15 p2678 A70-32746

CONNECTORS [ELECTRIC]

U ELECTRIC CONNECTORS

CONOIDS

U CONICAL BODIES

CONSCIOUSNESS

Rodents hypoxia tolerance following adaptation to hypercapnia by recording time of useful consciousness [TUC] in repeated sloped surface clinging tests 01 p0026 A70-11249

Time sense in human subjects kept in caisson or cave isolation determined as function of upper brain stem paraconsciousness 01 p0041 A70-11474

CONSERVATION EQUATIONS

Angular momentum conservations for solar gas confined by closed field lines or outflowing along open magnetic field lines 01 p0176 A70-10251

Semiempirical potential energy surface generation for triatomic hydrogen from London equation by evaluating Coulomb and exchange integrals taking into account effective orbital overlap 01 p0147 A70-10469

Equations of motion, conservation of mass, momentum and energy for elastic bodies with lattice-type surface defects 01 p0209 A70-11400

Conservation equations for mass, mean momentum and kinetic energy for incompressible turbulent boundary layer, using finite difference procedure 02 p0284 A70-12347

Equations of conservation of mass, energy and momentum applied to rotation effects on convective motion in planetary interiors 05 p0905 A70-15759

Conservation equation for thermal energy in turbulent shear flow, including turbulence kinetic energy equation terms [WSCJ PAPER 69-43] 06 p1179 A70-17983

Similarity model for spherically symmetrical flow following explosion in rarefied atmosphere satisfying hydrodynamic energy conservation equation 07 p1260 A70-19981

Rayleigh number effects on convection in planetary mantles, considering conservation equations of mass, energy and momentum 09 p1752 A70-22312

Hydrodynamic analogy in restricted three body problem of celestial mechanics, discussing mass and momentum conservation and physical properties uniqueness 10 p1938 A70-24180

Solar wind energies spherical surface average and fluctuations from integration of conservation equations 14 p2630 A70-30357

Displacement interacting boundary layer in symmetry plane region of flat hypersonic delta wing by control volume balances for mass, momentum and energy 17 p3010 A70-34975

Heat and mass transfer in flowing fluid, deriving conservation and constitutive equations, with application to boundary layer flow of gases 17 p3069 A70-35033

Non-LTE radiative gas flow conservation equations 24 p4325 A70-45610

CONSERVATION LAWS

Conservation laws for viscous incompressible two dimensional and axisymmetric flow written in integrodifferential form

01 p0063 A70-10935

Integral relations describing laws of conservation and Sobolev theorem used in deriving a priori estimates for nonlinear parabolic equations first boundary value problem

10 p1908 A70-23924

General relativity integral conservation laws of system of bodies in curved space-time obtained from symmetrical energy-momentum tensor

12 p2274 A70-28222

Three dimensional oblique incidence liquid jet impinging on solid surface, evaluating flow force by applying mass and momentum conservation

13 p2389 A70-29540

Liquid metal MHD conservation cycles, discussing evolution and status of power generation at various temperatures

20 p3563 A70-39325

General relativity integral conservation laws of system of bodies in curved space-time obtained from symmetrical energy-momentum tensor

20 p3673 A70-40097

Turbulent flow asymmetrical mechanics equations derivation from conservation laws, discussing Navier-Stokes equation, angular momentum and transport theory

21 p3806 A70-40612

Conservation laws in theory of field with group invariance properties, examining infinitesimal transformations method

22 p4075 A70-43400

MHD equations for one dimensional plane steady flow, considering conservative difference schemes for approximation

23 p4226 A70-44307

CONSOLES

NT REMOTE CONSOLES

Display console characteristics for meeting increasing applications, predicting price reduction trends, color emphasis and CRT competition as primary display component

01 p0221 A70-11286

STRIDA II consoles operation for treating air defense data, discussing data display system, work positions organization and console construction method

05 p0828 A70-16192

Radar consoles with various display components under different illumination levels to determine optimal operator performance, discussing push-button design recommendations

20 p3580 A70-39713

CONSTANTS

NT GRAVITATIONAL CONSTANT

NT GRUNEISEN CONSTANT

NT PERCEPTUAL TIME CONSTANT

NT SOLAR CONSTANT

NT TIME CONSTANT

Reduction constants simultaneous determination in earth figure theory based on astronomical, geodetic and gravimetric data

15 p2731 A70-32147

Universal constant measurement methods in Kolmogoroff third hypothesis for high Reynolds number turbulence in wind over open ocean

23 p4184 A70-44980

CONSTELLATIONS

NT ARIES CONSTELLATION

NT AURIGA CONSTELLATION

NT CASSIOPEIA CONSTELLATION

NT CENTAURUS CONSTELLATION

NT CEPHEUS CONSTELLATION

NT CYGNUS CONSTELLATION

NT LYRAE CONSTELLATION

NT ORION CONSTELLATION

NT SAGITTARIUS CONSTELLATION

NT SCORPIUS CONSTELLATION

NT SCUTUM CONSTELLATION

NT TAURUS CONSTELLATION

Effective temperature of star zeta Puppis from combined angular diameter measurement and model atmospheres, comparing hot stars

24 p4404 A70-45414

CONSTITUTION

Criticism of public administration aspect of Edwards Report, noting parliamentary and constitutional difficulties in some proposals

11 p2153 A70-25857

CONSTITUTIONAL DIAGRAMS

U PHASE DIAGRAMS

CONSTITUTIVE EQUATIONS

Asymmetric thermoelasticity derived for constitutive equations based on the thermodynamics of irreversible processes, formulating variational and reciprocity theorems

01 p0209 A70-11384

Constitutive equations and thermally activated dislocation processes in metals, noting temperature and strain rate relationship

02 p0316 A70-11737

Material functions mathematical forms for Green-Rivlin constitutive equations of nonlinear viscoelasticity

03 p0585 A70-12970

Thermodynamic constitutive equations for large dynamic plastic deformation problems

03 p0585 A70-12971

Constitutive equations for orthotropic bilinear elastic materials in plane stress case, discussing unidirectional composites

03 p0587 A70-13127

Statistical equation of motion of blood by averaging motion of individual blood elements over small volume, finding constitutive equations

03 p0434 A70-13572

Nonlinear solid applied mechanics, emphasizing nonlinear constitutive equations and related subjects, cyclic loading effect on solid materials, etc

03 p0610 A70-14230

Gravity influence on constitutive equations of elasticity for crystals treated as continuous body and particle system, taking into account lattice structure

05 p0925 A70-15869

Integral constitutive relation representing incompressible viscoelastic materials and plane stress and strain conditions

05 p0930 A70-16087

Constitutive equations for isotropic elastic and thermoelastic materials with microstructure derived using free energy function, giving uniqueness theorems

05 p0932 A70-16136

Constitutive equations for Reynolds fluxes in large scale transversely isotropic turbulent mixing using gradients of mean quantities

05 p0836 A70-17103

Electromagnetic fields interaction with nonconducting neutral elastic solid, formulating relativistic variational principle for balance laws and constitutive equations

08 p1545 A70-21252

Stress-strain behavior of Al and Ti alloys, beryllium and nonmetallic structural materials based on constitutive equations describing strain rate and temperature effects

08 p1518 A70-21331

Flow rule for viscoplastic symmetric cylindrical shells, using constitutive equations for strain rate sensitive materials based on Huber-Mises yield condition

10 p1954 A70-24020

Gas passing through shock wave, investigating constitutive relations for stress and heat flux using Maxwell moment method

11 p2036 A70-26015

Isothermal quasi-linear theory of viscoelastic isotropic continuum, considering constitutive equations

13 p2516 A70-29534

Elastoplastic material mechanical theory, considering constitutive equations with plastic deformations and decompositions of total velocity-strain/stretching/

14 p2661 A70-31281

Book on continuum mechanics covering tensor kinematics, energy balance, virtual work, constitutive equations, etc

16 p2987 A70-32914

Constitutive equation for fiber reinforced viscoelastic materials, using continuum theory of mixtures

16 p2994 A70-34231

Heat and mass transfer in flowing fluid, deriving conservation and constitutive equations, with application to boundary layer flow of gases

17 p3069 A70-35033

Viscoplastic solids, computing plane shock wave propagation structure from nonlinear constitutive relations

18 p3338 A70-36435

Nonlinear electromagnetic constitutive equations with coupling to thermal gradients for holohedral and hemihedral materials, extending analysis to orthotropic media

19 p3552 A70-37786

Stress relaxation interpretation at wave fronts in one dimensional media by nonlinear viscoelastic models, giving constitutive equations

19 p3542 A70-38057

Boundary value problem solution in nonlinear viscoelasticity by constitutive equations

19 p3544 A70-38330

Mathematical theory of constitutive relations connecting surface tractions and moments with motion of single body in continuum

20 p3672 A70-39495

Nonhomogeneous shell theory, considering load carrying surfaces with constitutive equations independent of shell curvature

20 p3719 A70-39619

Structures of linear field theories concerning constitutive equations and operators dual relationship

21 p3851 A70-42098

Constitutive equation for homogeneous and isotropic elastic solids

21 p3940 A70-42101

Cosserat elasticity constitutive equations, coupling rotation vectors to eliminate stress indeterminacies

21 p3941 A70-42251

Plane electromagnetic wave propagation at normal incidence in isotropic lossless plane-stratified inhomogeneous gyration medium, calculating varying profiles from constitutive equations

22 p4073 A70-42640

Continuous media theory, deriving first order constitutive differential equations for isotropic tensor functions

24 p4378 A70-45270

Isothermal plasticity thermodynamic foundation, deriving constitutive equations for various deformations

24 p4426 A70-45994

Surface constitutive assumptions restrictions for rigid heat conductor, accounting for radiative heat supply

24 p4429 A70-46032

Constitutive equations in fluid dynamics, discussing Newtonian, Oldroyd and Walter, Reiner-Rivlin, Rivlin-Ericksen, Noll, Bingham and oriented fluids

24 p4327 A70-46149

CONSTRAINTS

NT METEOROLOGICAL PARAMETERS

Out-of-plane displacement restraint at thin photoelastic plates bonded to rigid boundaries of inclusions inducing transverse stress components causing plane stress solution deviation

01 p0202 A70-11059

Automated structural design program to treat stress, displacement, gauge and cross sectional constraints, discussing applications to aircraft structures

02 p0386 A70-11944

Analytical approach to gradient method within framework of Bolza problem of variational calculus, using linearized differential and isoperimetric constraints

03 p0520 A70-14341

Variational problems of stationarization under constraints, using imbedding integrodifferential equations

05 p0882 A70-16085

Algorithm for constrained optimization problems providing rapid convergence

05 p0877 A70-16714

Geometry of limiting surface characterizing strength of isotropic body, discussing material breakdown

05 p0947 A70-16964

Suboptimal closed-loop controller design based on quadratic equivalence for linear time varying process with minimum probability of inequality constraints violation

06 p1024 A70-17951

Slack variable to transform optimal control problem with scalar inequality constraint on state variables into unconstrained problem

06 p1024 A70-17952

Stochastic differential games with constrained state estimators, involving linear system, quadratic cost functional and white Gaussian noises corrupting output measurements

06 p1024 A70-17954

Constraint optimization on phase coordinates and controls noting extension to functional spaces

07 p1330 A70-18683

Optimal control problem solution involving functional minimization along differential vector equation trajectories, considering manifold type constraints on phase coordinates

07 p1244 A70-18747

Dynamical constraints on planetary fission events, calculating maximum possible excursions of planetary orbits

07 p1381 A70-19280

Sequential gradient-restoration algorithm for minimization of function subject to constraint

07 p1325 A70-19355

Constrained complex optimization method for synthesizing distributed-lumped-active networks

11 p2024 A70-26204

Topological symbolic analysis of circuits defined by topological constraints, utilizing digital computers

11 p2029 A70-26330

Circular elastic helix phase velocities determined by internal constraints method, comparing results with other theories

11 p2085 A70-26557

Computer analysis of degree of constraint against butt joint transverse shrinkage, using finite element method for stress analysis

12 p2239 A70-26854

Optimization for control processes with first and higher order constraints on phase coordinates

12 p2205 A70-28195

Optimal control for processes with parameters and state variable inequality constraints using gradient projection method and maximum principle

12 p2205 A70-28337

Terminal constraints affecting matrices comprising linear impulsive guidance law for earth approach, discussing Mars mission

13 p2447 A70-28516

- Geomagnetic noise constraints on weak field measurements in upper magnetosphere 13 p2401 A70-30056
- Optimal control problems constraints and necessary conditions, deriving maximum principle 14 p2600 A70-31202
- Penalty functions for state-space constraints elimination in continuous optimal control problems 14 p2562 A70-31353
- Matrix analysis of discretized dynamical system with constraints, considering case of damped oscillators 15 p2774 A70-31697
- Mechanical system with n material points, deriving control algorithms for realizing constrained programmed motion 16 p2953 A70-34297
- Stability theorem for mechanical systems with constraint damping subjected to energy dissipation 17 p3176 A70-34956
- Constraint optimization in state coordinates by variable structure system flexibility, using mathematical model 18 p3281 A70-36353
- Geometrical interpretation of controlled evolution of optimal systems with mixed state constraints, using Pontryagin and variational methods 19 p3542 A70-38056
- Lifting reentry vehicle two dimensional motion optimization with inequality constraints explicitly containing control by perturbation method 21 p3845 A70-41265
- Inequality constrained optimal control problems by function space method, using integral equation representation of second variation 21 p3802 A70-41266
- Chicken lymphopenia and body mass loss resulting in death from chronic restraint, developing physiologically unstressful restraint for space environmental testing 21 p3765 A70-41488
- Optimization for control processes with first and higher order constraints on phase coordinates 22 p4004 A70-43320

CONSTRUCTIONS

- Air bubble breaking in blood and water flow passage of simulated cardiopulmonary bypass system with flow constriction 15 p2692 A70-32312
- Thermal constriction resistance due to nonuniform metal surface conditions, considering macroscopic contact resistance for nonuniform interface pressure distribution 24 p4429 A70-46177

CONSTRUCTORS

- Transpiration cooling of porous constrictor walls of high intensity electric arc in plasma [ASME PAPER 70-HT-35] 22 p4122 A70-42432

CONSTRUCTION MATERIALS

- Glass-reinforced polypropylene for structural applications, investigating time/temperature dependent creep characteristics 01 p0128 A70-10773
- Ti, Zr and Nb characteristics, properties, processing procedures and applications in corrosive environments, nuclear reactors and aerospace structures 02 p0319 A70-12710
- Carbon fiber reinforced plastics /CFRP/ uses in commercial aircraft structural component 03 p0516 A70-13546
- Structural materials mechanical properties tests during neutron bombardment, discussing atomic reactors optimal parameters calculation 04 p0775 A70-15259
- Creep rupture effect on fatigue damage of structural material, constructing nondimensional stress range diagrams 05 p0943 A70-16806
- Low cycle fatigue life of various structural steels and alloys, studying stress cycle number relations 06 p1085 A70-17402
- Mechanical property factors influencing selection of sintered uncorked refractory metals and alloys for structural applications [AIME PAPER F-69-4] 07 p1290 A70-18810
- Design concept, materials application and performance characteristics of high temperature fasteners [AIME PAPER F-69-6] 07 p1290 A70-18811
- Single crystal carbides as high temperature structural materials, noting titanium carbide properties and strength-to-density ratio of B-doped crystals 07 p1312 A70-19883
- Stress-strain behavior of Al and Ti alloys, beryllium and nonmetallic structural materials based on constitutive equations describing strain rate and temperature effects 08 p1518 A70-21331
- Tubing materials for gas turbine engines covering fabrication, selection, etc 08 p1559 A70-21854
- Microhardness method for property changes in structural materials during sequential cyclic loading, 21 p3944 A70-41023

discussing material identification, statistical fatigue theory, fine structure effects, etc 09 p1701 A70-22299

Aircraft turbine engines structural materials and design concepts, describing fiber reinforced materials, oxide dispersion hardened alloys and integral and honeycomb structures 11 p2101 A70-25625

Aircraft interior design styling and material selection, discussing industrial design department function and organization, styling as marketing tool, etc [SAE PAPER 700233] 11 p1980 A70-25902

Cost-property index /B/P/ to compare economic success of composites, metals, glass and ceramics for load bearing applications 11 p2136 A70-26077

Structural materials chemical and metallurgical factors controlling mechanical properties, machinability and finished part producibility [ASTME PAPER MR-69-731] 12 p2240 A70-26992

Materials and structural dynamics - AIAA-ASME Conference, Denver, April 1970 12 p2315 A70-27101

Materials selection for vibration or shock control based on cost, resonance frequency, strength, weight, etc 13 p2513 A70-29218

Lunar resources classified as rocket fuel, construction and life support materials, discussing implications for manned surface exploration missions 14 p2634 A70-30198

Jet thrust reversers mechanical design limits, objectives and materials 14 p2628 A70-30500

Filament reinforced metal matrix composites fabrication and engineering uses 14 p2590 A70-30542

Radiative properties of construction properties and working media, noting importance to radiative heat transfer calculation 15 p2827 A70-32143

Reinforced polymer composites design for aircraft structures [ASME PAPER 70-DE-67] 16 p2939 A70-33518

Ti hot forming, discussing sheet use as aircraft structural material 17 p3098 A70-34444

Accelerometer installation resonant frequency, discussing mounting methods, structure material, geometry and total mass 17 p3089 A70-35174

Book on materials for structural and mechanical functions covering electrical engineering properties, ferrous and nonferrous metals and alloys, fabrication methods, environmental protection, etc 19 p3453 A70-38622

Polymers industrial applications in textiles, building materials, furniture, aviation, automobile industry and packaging 19 p3455 A70-38700

Scorched aluminum powder /SAF/ materials, discussing fabrication, physical and mechanical properties, applications in aircraft structural components, etc 22 p4055 A70-43084

Caprolon B mechanical properties, comparing properties to other polyamide resins for use in machine parts fabrication 24 p4367 A70-45503

CONSUMPTION

NT FUEL CONSUMPTION

NT OXYGEN CONSUMPTION

NT WATER CONSUMPTION

CONTACT POTENTIALS

Carrier concentration profiles and surface resistance of Ohmic contacts to solution epitaxial n-type GaAs wafers measured by Schottky barrier capacitance 03 p0543 A70-14213

Surface field effect, contact potential and photoconductivity measurements on p- and n-type heteroepitaxial single crystal silicon films on sapphire 13 p2470 A70-29372

Failure mode and mechanism in dielectrically isolated IC attributed to metal bridging under planar oxide 15 p2713 A70-32648

Friction coefficient dependence on hardness of softer element of friction pair determined at constant values of shear strength, using external friction concepts 17 p3102 A70-35672

High resistance space charge region formation near crystal cathode in GaAs due to limited contact emissive capacity 18 p3297 A70-36417

Gadolinium surface work function from contact potential difference against platinum 20 p3687 A70-39996

Surface films effect on thermal contact resistance of microscopically sized contacts 21 p3944 A70-41023

Surface films effect on thermal contact conductance of aluminum surfaces contacting in high vacuum environment 21 p3944 A70-41024

CONTACT RESISTANCE

Space charge barriers AC impedance modification at metal/semiconductor contacts due to trapping 01 p0157 A70-10296

Electrical resistivity, contact resistance and weldability of cast Cu and Ag contact materials reinforced unidirectionally by W wire compared to powder composition 04 p0711 A70-14465

Rough metal surfaces thermal constriction resistance for total heat flow through microcontacts 07 p1418 A70-18648

Contact resistance measurements used in contaminant removal and metallic adhesion on iron surfaces 07 p1293 A70-18940

Thermal resistance for inappropriately spaced contacts using electrolytic analog experiments 08 p1599 A70-21590

Thermal contact resistance of anisotropic materials using mathematical geometric transformation [ASME PAPER 69-HT-47] 09 p1790 A70-23552

Low resistance small area contacts on semiconductor metal oxides 12 p2288 A70-28057

Sinusoidal signal harmonics measurement to determine nonlinear resistance junction I-V equation, discussing applications to circuit analysis 12 p2204 A70-28132

Ohmic contacts for gallium arsenide single crystals, describing fabrication technique and IV characteristics 12 p2202 A70-28187

Thermal contact resistance, discussing behavior at cryogenic temperatures and directional or thermal rectifying effect 17 p3197 A70-35541

Gold foil surface thermal contact resistance, investigating temperature and pressure effects and elastic and plastic deformation of surface structure 21 p3953 A70-42166

Thermal relaxation effect on thermal contact of two semiinfinite walls, showing existence of dynamic contact resistance 22 p4125 A70-43243

Intermaterial adhesion relation to association contact resistance-tension characteristics based on electric potential barrier model for Maxwell-Wagner effect 24 p4379 A70-45617

CONTACTS [ELECTRIC]

U ELECTRIC CONTACTS

CONTAINERS

Air-land demountable cargo containers specifications, establishing dimensional, structural and environmental requirements [SAE-AS-832] 07 p1249 A70-19599

Boeing 747 aircraft container system deployment simulation written in GPSS/360 to minimize stockholding of containers at individual stations 08 p1481 A70-20931

Thermocouple vacuum gauge joined to Apollo lunar sample return containers /ALSRC/, describing two step welding procedure with transition cylinder 08 p1507 A70-21483

Equipment container with sandwich type structure for packing delicate parts 10 p1852 A70-24899

Permittivity cell and encapsulation for liquids subjected to high pressures and temperature extremes 14 p2533 A70-30502

Air cargo container system impact on aircraft requirements, discussing intermodal capability achievement 20 p3607 A70-40128

Free fluid sloshing motion in shallow convex containers, considering isoperimetric problem for planar and axisymmetric vibrations 22 p4009 A70-42534

Air freight containers in continuous air/land transportation chain, discussing weight, performance, cost, technical concepts and inter and nonintermodal prototypes 22 p4007 A70-43273

Controlled filling of container with compressed gas through time-variable cross section inlet, using variable mass thermodynamics 23 p4180 A70-44160

CONTAMINANTS

NT RADIOACTIVE CONTAMINANTS

NT TRACE CONTAMINANTS

Chemical and physical adsorption of gaseous oxygen contaminants to maintain purity for respiratory purposes, noting trichloroethylene and carbon tetrachloride 01 p0031 A70-10236

Volatile contaminants emitted from space cabin construction materials tested under simulated space conditions 01 p0031 A70-10237

Time of useful function /TUF/ determination for human exposure to toxic gas combinations due to fire 06 p1000 A70-17294

Human exhaled air contaminants analysis role in disease diagnosis, metabolism study and spacecraft cabin atmosphere changes 07 p1220 A70-19514

Human exhaled air contaminants analysis role in disease diagnosis, metabolism study and spacecraft cabin atmosphere changes 11 p1991 A70-26113

Carrier distillation DC arc emission spectrography, determining lead, bismuth and tin traces in nickel base alloys after conversion to oxides 14 p2546 A70-30957

Upper atmosphere turbulence spectra of passive contaminants deposited by rockets from radiometrically calibrated photographs of chemical trails 15 p2725 A70-31688

Fe 57 contaminant in Ni, studying Mossbauer effect as function of temperature 15 p2784 A70-32023

Gas turbines, dust and air cleaners interrelationship in preventing failure due to air contaminants [ASME PAPER 70-GT-104] 18 p3305 A70-36890

Method of characteristics for two dimensional steady supersonic gas flows with foreign particles in plane and axisymmetric nozzles 18 p3210 A70-37228

Superpure materials for low background radiation detectors, determining U, Th and Ca radioactive contamination by radiochemical activation analysis 20 p3629 A70-39317

Tungsten-helium arc atmospheric contaminants spectral monitoring parameters under welding conditions, using rotating circular wedge to oscillate emission lines across exit slits 21 p3831 A70-40725

Surface films effect on thermal contact resistance of microscopically sized contacts 21 p3944 A70-41023

CONTAMINATION

NT FUEL CONTAMINATION

NT SPACECRAFT CONTAMINATION

Metal fabrication shop environment contamination effect on bond strength of various adhesive system tested by humidity and salt spraying exposures 02 p0310 A70-12664

Microbiological evaluation of modified vacuum probe surface sampler for handling and fallout contamination compared with swab-rinse technique 05 p0807 A70-16574

Contamination control - Conference, New York, May 1969 05 p0798 A70-16701

Vacuum probe sampler to monitor particle contamination on surfaces within clean environments 05 p0808 A70-16703

Vacuum probe as effective device for sampling surface contamination of airborne microorganisms 05 p0808 A70-16704

Automatic particle counters and fluid contamination problems, misconceptions relating to sampling, size measurement, calibration, etc 05 p0851 A70-16706

Contamination sources covering ball bearing contamination, relay contact failure, instrument window internal fogging, electronic circuit corrosion and air conditioning problems 05 p0809 A70-16712

Liquids particulate contamination sizing and counting by membrane filtration, specifying procedures and apparatus used [SAE-ARP-598A] 07 p1195 A70-18804

Contact resistance measurements used in contaminant removal and metallic adhesion on iron surfaces 07 p1293 A70-18940

Vacuum probe sampler to monitor particle contamination on surfaces within clean environments 09 p1623 A70-22340

Space environment simulation chamber free from oil molecules contamination 09 p1655 A70-22830

Particulate contamination in compliance with military standard cleanliness level, using zoom microscope, charts and tables 12 p2174 A70-27010

Water contaminating effects on thin thermal oxide passivated silicon planar devices 13 p2361 A70-28930

Weld quality relationship to aluminum surface contamination by hydrogen-containing compounds 13 p2407 A70-29108

Ti equipment anodizing methods, observing corrosion resistance reduction and embrittlement hydriding due to Fe contamination 17 p3098 A70-34363

Oxidation and atmospheric contamination protective coatings for high temperature materials, using burner ring tests 17 p3127 A70-34519

Contaminated optical surface investigation technique in near UV, visible and near IR range, in-

vestigating property changes of systems in transmission and reflection 18 p3292 A70-36786

Surface contaminated Langmuir probe measurements in glow discharge plasmas, discussing errors 20 p3633 A70-40161

Surface contamination and degradation effect on reflectance of evaporated vacuum UV mirrors and temperature control coatings under simulated space environments 21 p3842 A70-40815

Optical devices contaminated mirror surfaces restoration with atomic oxygen from RF plasma by noncontaminating nondestructive oxidation of polymer film 22 p4029 A70-42622

Al purification by subhalide reaction, discussing contamination sources and thermodynamics 24 p4349 A70-46187

Cleanliness levels for missile guidance package as function of component design complexity 24 p4349 A70-46250

CONTINENTAL DRIFT

Earth continental drift and polar wandering measurements by laser ranging to two synchronous satellites [AIAA PAPER 70-1069] 19 p3529 A70-38882

Ocean floor-spreading tectonic effects, considering Arabian Shield separation from African continent 24 p4332 A70-46408

CONTINENTAL SHELVES

Continental migration role in lunar maria formation, suggesting similarity with geological formation of earth ocean floor 09 p1765 A70-23797

North Carolina continental shelf discolored water origin, movement and dissipation from Apollo 9 photograph interpretation 24 p4329 A70-45361

CONTINENTS

NT AFRICA

NT ASIA

NT AUSTRALIA

NT EUROPE

NT NORTH AMERICA

Earth rotational velocity irregularities and horizontal motions of continental blocks at expense of oceanic hemisphere, noting seasonal distance changes 04 p0681 A70-15477

CONTINUITY

Space-sampled feedback control of amplifying wave on infinite continuum, discussing system stability 06 p1025 A70-17963

Continuous media geometry with given discrete structure reduced to analyzing relations between functions in denumerable set of points, presenting selected points of subregions 10 p1954 A70-24016

CONTINUITY [MATHEMATICS]

Plate structural analysis by finite element method, obtaining geometric continuity by additional displacements and forces at corner nodes 21 p3932 A70-40553

Seminormality and upper semicontinuity of variable sets in optimal control 22 p4061 A70-42461

Ordinary differential equations boundary value problems solution based on continuation and reduction to Cauchy problems 23 p4211 A70-44309

Approximations by spline functions and polynomials, discussing modulus of continuity 24 p4369 A70-45126

CONTINUITY EQUATION

F 1 layer nonlinear ionospheric continuity equation to investigate role of diurnal variations of loss and production processes in electron density midday bitout effect 01 p0079 A70-11221

Method of weighted residuals /MWR/ for nonlinear partial differential equations applied to incompressible two dimensional turbulent boundary layer momentum and continuity equations 02 p0281 A70-12328

Electromagnetic drifts and neutral air winds effects on F 2 region derived from electron continuity equation, using Jacchia model atmosphere 04 p0677 A70-14966

Na abundance in terrestrial upper atmosphere, solving steady state continuity and momentum equations for Na atoms and ions 05 p0840 A70-16475

Corpuscular radiation as F region ionization source, solving time dependent ionospheric continuity equation 06 p1054 A70-17588

Invariant transform of motion and continuity equations for steady three dimensional flows of compressible fluids in absence of massive forces 11 p2041 A70-26598

Shock wave formation and propagation analyzed by hydrodynamic model of two directional traffic flow based on continuity equations and velocity-density empirical relations 12 p2212 A70-28196

Continuity equation plasma oscillation, discussing ion current waveform flowing from discharge and implications for periodic astrophysical phenomena 14 p2638 A70-30618

Neutral winds effect on F region vertical ion drifts derived from continuity equation, noting diurnal and seasonal variations 14 p2574 A70-30738

Time dependent simultaneous solution for continuity, heat conduction and motion equations of system involving neutral, electron and ion gases 14 p2665 A70-30744

Equations of motion and continuity for early and later stages of expanding universe, explaining matter concentration process of galaxy formation 16 p2976 A70-37813

Neutral atmosphere continuity equation of ionization and equation of motion in F 2 region for different seasons in various solar activity epochs 20 p3623 A70-40478

Shock wave formation and propagation analyzed by hydrodynamic model of two directional traffic flow based on continuity equations and velocity-density empirical relations 22 p4012 A70-43321

CONTINUOUS RADIATION

CW laser perturbation by coupled optical transition at strong pumping with incoherent and coherent perturbing radiation, considering disappearance of laser effect 01 p0108 A70-10231

IR CW sum-frequency up-conversion of carbon dioxide laser radiation using phase matched proustite as nonlinear crystal 01 p0111 A70-10786

CW visible ring cavity parametric oscillator, discussing pump depletion, conversion efficiency and improved stability resulting from optical isolation 01 p0552 A70-11173

Free-bound and free-free continuous emission of hydrogen near Balmer jump in T Tauri star AS209 03 p0566 A70-13315

Energetic and temporal characteristics of CW and pulse laser radiation measured using instrument with absolute sensor 03 p0500 A70-13480

Low threshold injection lasers in IR and visible spectrum at room temperature employing AlAs-GaAs heterojunctions, noting use for CW mode 03 p0501 A70-13723

Frequency pulling and pulse position modulation of CW GaAs injection lasers by locking signal frequency variation 03 p0502 A70-13815

CW and radar type RF signal effects on electroexplosive devices sensitivity in bridgewire heating mode 03 p0550 A70-14142

Geometrical model for characterizing instrument landing system /ILS/ null reference glide path utilizing CW measuring system 04 p0716 A70-15330

Continuous wave chemical laser operation in carbon dioxide pumped by vibrational energy released from DF and HF molecular formation 04 p0704 A70-15686

Radiative excitation in planetary and Orion nebulae by solving transfer equations for Lyman line and continuum radiation, using normalized on-the-spot /NOS/ approximation 04 p0758 A70-15700

Pumping techniques, design and properties of pulsed and CW lasers based on Nd-glass, ruby, barium fluoride and calcium tungstate crystals 05 p0860 A70-16821

Continuous passive mode locking of carbon dioxide laser cavity using long optical delay line 06 p1080 A70-17446

Chemical laser CW operation achieved by mixing gases, obtaining pumping energy from chemical reactions 06 p1080 A70-17492

Phase path variation of stable continuous wave transmission reflected from E region during daytime, discussing night time results 06 p1055 A70-17593

Supersonic mixing CU chemical lasers, discussing lasing action time duration 06 p1083 A70-17945

Continuous signal a posteriori distribution density formed on basis of learning sequence with no a priori information about signal and noise statistics 07 p1226 A70-18761

CW high power operation of transferred-electron oscillators realized by low thermal resistance, describing fabrication 07 p1241 A70-19300

Argon ion CW lasers, discussing design, inverse population, plasma, radiative transition probabilities, pumping, frequency spectra and active medium 07 p1298 A70-19642

Ionosphere absolute phase height measurement methods independent of virtual height, using fixed frequency CW emission and pulsed sounding 07 p1276 A70-20432

Millimeter wave CW Gunn oscillators construction by packaging free from spurious resonance, using sapphire ring and Au cap

08 p1468 A70-20482

Emission saturation in Ar CW laser at high discharge current densities under different pressures and tube channel parameters

08 p1511 A70-20542

Wideband tunable CW Gunn effect oscillator design, discussing microwave circuit effects on performance

08 p1471 A70-20788

CW laser operation at 10.6 microns in DF-carbon dioxide and HF-carbon dioxide molecular systems achieved by purely chemical means

08 p1513 A70-21539

CW GaAs junction laser bistable operation due to saturable absorbing centers in active medium

08 p1513 A70-21598

CW water vapor laser line frequency measurements by beating with radiations from HCN laser in metal-on-metal point contact diode

09 p1697 A70-22925

He-Ne CW and pulsed lasers operation, design and technology, describing measurement methods for output, beam divergence and radiation spectrum distribution

09 p1698 A70-23303

High power CW carbon dioxide laser design and operation for use as heat source in metal fusing, welding and cutting

10 p1897 A70-23816

Continuum radiation of nitrogen plasma at atmospheric pressure at high temperatures

10 p1923 A70-24472

Continuous wave chemical laser operation at 10.6 micron in carbon dioxide pumped by vibrational energy from hydrogen atoms and bromine molecules reaction

10 p1901 A70-25149

Scanned beam holography reducing system stability time for hologram production with CW gas laser

11 p2050 A70-25639

He-Ne optical laser CW operation under DC excitation, considering output power, discharge current, total pressure, mixture ratio, etc

11 p2062 A70-25827

CW carbon dioxide laser absolute frequency measurements at 28 THz by beating lines with water vapor laser and klystrons in tungsten on nickel point contact diode

11 p2063 A70-26070

Pulsed and CW microwave discharge plasmatrons design calculation, providing electrodeless plasma in metallic chamber and nonequilibrium plasma

11 p1984 A70-26741

Emission spectrum of He-Xe CW laser with non-resonant feedback mode achieved with scattering agent and various mirror schemes

12 p2246 A70-27354

Argon CW laser blue beam self focusing in methylene iodide, iodine and liquids under steady state conditions

12 p2248 A70-27545

Ionospheric probing using continuous radio waves at oblique incidence, discussing HF Doppler, VHF forward scatter and radio aurora techniques

12 p2224 A70-27730

Spectra, luminescence and gas dynamic effects in variable stars, discussing nonthermal theory to explain continuous emission

12 p2306 A70-27857

Merop 1/C 349/ nebula, noting luminescence and continuum spectrum fine structure

12 p2307 A70-27867

CW mode locked lasers picosecond pulse widths and shapes measured, determining harmonics and Fourier expansion

13 p2425 A70-28794

CW traveling wave tubes and klystrons LF output signal fluctuations

14 p2555 A70-30303

Continuous operation He-Ne lasers, discussing excitation, structural and optical design, mode selection and performance specifications

14 p2593 A70-30353

GaAs epitaxial layered wafer natural CW R band oscillations in LSA mode

14 p2550 A70-30688

CW oscillation in carbon monoxide chemical laser

15 p2748 A70-31432

CW injection laser frequency stability, noting injection current influence on lasing frequency

15 p2750 A70-31629

Time controllable continuous photon emission from plasma produced by pulsed laser vacuum spark applied to absorption spectroscopy in vacuum UV

15 p2734 A70-31757

High power CW CO laser operation at room temperature by introducing mercury vapor into discharge

15 p2751 A70-31979

CW nonspiking single mode ruby laser operation by end pumping ruby with CW argon ion laser output

15 p2751 A70-31981

CW Cd vapor laser oscillation achieved with slotted hollow cathode discharge containing He carrier gas at pressures of several Torr

15 p2751 A70-31988

Pulsed laser alignment using pentaprism-directed continuous laser light beam

15 p2752 A70-32047

Meteor radiant, drag and altitude via CW radar observation of meteor trails

15 p2800 A70-32150

Cepheids nonequilibrium continuous emission at maximum brightness, considering phase shift between radiation intensity and stellar contraction

15 p2802 A70-32483

Transverse magnetic field effect on CW argon laser operation with linearly polarized radiation

15 p2754 A70-32866

Silicon avalanche transit time diodes as CW microwave generators and amplifiers

16 p2876 A70-33404

Diffraction radiation generator with CW operation in backward wave tube mode, discussing output power dependence on wavelength

18 p3231 A70-36410

Asymptotic transmitting capacity of continuous channel with intense independent and additive noise

18 p3228 A70-36598

CW multifilament GaAs laser diodes measurement, showing cross correlation between light and current noises

18 p3270 A70-36742

Continuous signal a posteriori distribution density formed on basis of learning sequence with no a priori information about signal and noise statistics

18 p3229 A70-37105

Continuum source counts in galactic plane

18 p3327 A70-37165

CW HCl chemical laser action via chlorine atoms reaction with hydrogen iodide in fast flowing mixing device

19 p3444 A70-37542

Rubidium-85 maser, discussing continuous oscillation in low magnetic field

19 p3446 A70-37769

Gallium aluminum arsenide-GaAs laser diodes properties and applications for CW operation, discussing p-GaAs layer thickness effects

19 p3447 A70-38454

Jovian continuum radiation observation by RAE-1 during lunar occultations

19 p3512 A70-38608

CW second harmonic He-Ne laser light second order intensity correlation function measurements

20 p3640 A70-39153

Continuous wave laser action in chlorine, Ar and He gas mixtures, observing energy transfer between Ar and chlorine by pumping action

21 p3834 A70-40570

CW gas laser improvement, discussing optimum efficiency and photon beam spatial distribution

21 p3836 A70-41419

Continuous pseudoacoustic and ion waves excitation and damping in plasma sheath around grid, taking into account transit time effect on ion acceleration

21 p3858 A70-41710

Thermal and birefringent effects on output of continuous Nd-YAG laser rod, using 6328 A probe

21 p3837 A70-41906

CW silicon SHF TRAPATT diode oscillator, discussing double sided design and fabrication

21 p3800 A70-42118

High output CW carbon dioxide laser design, using gas pressure variation and fast axial flow

22 p4048 A70-42322

Water cooled carbon monoxide-He-nitrogen-oxygen laser CW output at room temperature

22 p4048 A70-42327

Host materials for increasing optically pumped solid state CW laser fundamental mode output power

22 p4048 A70-42333

LF cavity loss modulations of homogeneous four-level CW Nd-YAG laser, including relaxation-oscillation regime

22 p4050 A70-43005

CW chemical lasers operation from partially inverted transitions of HCl, HF and DF molecules in subsonic flow

22 p4050 A70-43008

Emission spectrum of He-Xe CW laser with non-resonant feedback mode achieved with scattering agent and various mirror schemes

22 p4052 A70-43597

Cepheids nonequilibrium continuous emission at maximum brightness, considering phase shift between radiation intensity and stellar contraction

23 p4240 A70-43907

CW GaAs semiconductor laser fabrication by liquid epitaxy, noting Ag plating role in output power

24 p4352 A70-45468

Transverse flow deuterium fluoride-carbon dioxide chemical laser for CW output without external energy source

24 p4355 A70-46084

CONTINUOUS WAVE RADAR

CW laser ranging systems power and signal to power ratio characteristics, finding possible advantages over pulsed systems

01 p0114 A70-11321

Active AM scatterer/spiral antenna/used as transponder in elementary CW radar system

04 p0652 A70-15346

CW, pulsed and frequency modulated radar scatterometry, discussing flight, system, terrain and data processing parameters

06 p1012 A70-18594

High resolution FM-CW radar sounder for tropospheric refractive index studies, describing equipment design and performance and clear air scatter observations

09 p1716 A70-22368

Meteor astronomical parameters measurement by pulsed and CW radio methods, considering effects of wind, meteor trails, phase angle, etc

09 p1638 A70-23627

AM and FM CW Doppler radar by combined AM-FM waveform, noting automatic track while scan radar application

10 p1840 A70-24445

Radar transmitter waveforms for multifunction operation, emphasizing phase and frequency modulation for CW radars

12 p2188 A70-27939

CONTINUOUS WAVES

U CONTINUOUS RADIATION

CONTINUUM FLOW

Circular cylinder drag in hypersonic transverse flows between continuum and free molecular flow, measuring drag and pressure distribution

04 p0615 A70-15089

Continuum to free molecule hypersonic flow near flat plate sharp leading edge, studying Knudsen, Reynolds and Mach numbers effects

06 p0982 A70-18365

Circular cylinders drag and pressure distribution in hypersonic range between continuum and free molecular flow

06 p0983 A70-18376

Two phase supersonic continuum flow of dispersed equal gas-liquid volume ratio in shock tunnel using continuum theory, considering sound propagation

07 p1256 A70-19311

Drag on cylinder in transverse rarefied gas flow varying from free molecular to almost continuum

09 p1604 A70-22448

Continuous media mechanics by applying fractional steps method to numerical solutions, outlining theoretical basis for computer algorithms

10 p1866 A70-24114

Supersonic rarefied flow over sharp flat plate with merged shock layer and free molecular-continuum transition, using electron beam fluorescence

14 p2529 A70-31028

Stationary gas flows continuous to rarefied transition analysis based on mean free path anisotropy

15 p2721 A70-32139

Adiabatic and chemically inactive hypersonic continuum flow around blunt body, analyzing flow field

17 p3010 A70-35036

Continuum plasma dynamics with electromagnetic forces of same order of magnitude as gas dynamic forces, discussing various flow problems

17 p3141 A70-35040

Kinetic effects of Barnett equations and slip conditions for continuous dense gas flows at small Knudsen numbers

18 p3239 A70-36256

CONTINUUM MECHANICS

Variational stress solutions for static case of bounded bodies in Cosserat continuum theory, assuming anisotropic inhomogeneous material and defining boundary value problem solution

03 p0596 A70-13973

Three dimensional elasticity theory of generalized continua developed from atomic lattice theory model, discussing frequency spectra, specific heat and applications to crystal defects

03 p0525 A70-14232

Numerical methods of solving problems in mechanics of continuous media - Conference, Kiev, Ukrainian SSR, June-July 1966

04 p0669 A70-14956

Free vibrations of layer of micropolar continuum, analyzing displacements, microrotations and frequencies as wave number power series

04 p0777 A70-15498

Continuum, harmonic and finite element perturbation studies of elastica to yield postbuckling path derivatives from nonlinear energy formulation

05 p0927 A70-16011

Thermodynamics of elastic continuum with microstructure, modifying second law to include microtemperatures

05 p0930 A70-16083

Continuum model for plastic-elastic behavior of fiber reinforced composite material, formulating yield condition and constitutive equations

05 p0931 A70-16131

Convergence of eigenvalues and eigenvectors in torsional vibration problems of continuous systems via improved matrix displacement analysis using points of freedom in segments

05 p0939 A70-16502

Book on mechanics of continuous medium, discussing constitutive equations, fluid mechanics, linearized elasticity, vectors and tensors, stress, strain and deformation, etc

06 p1104 A70-17420

Continuum mechanics equations for calculating strain energy in spherical bottoms production as function of radius and angle

06 p1077 A70-17870

Non-Newtonian fluids in continuum mechanics, classical Navier-Stokes theory limitations and theory of incompressible fluids for viscometric flows

06 p1037 A70-17926

Multiphase fluid continuum model and hydrothermodynamic equations under phase transformations, including dimensionless and similarity parameters

07 p1254 A70-19085

Energy losses due to mixing of primary and secondary flows of jet streams in gas propulsion engine chambers determined by continuum mechanics application

07 p1363 A70-19086

Two phase supersonic continuum flow of dispersed equal gas-liquid volume ratio in shock tunnel using continuum theory, considering sound propagation

07 p1256 A70-19311

Field theory of moving dislocations in Cosserat continuum considered incomplete regarding constitutive equations, basing analysis on Mie-developed mathematical analogy to electrodynamics

07 p1334 A70-19564

Nonlinear thermodynamic theories of plates, elastic shells and rods derived from three dimensional theory of classical continuum mechanics

07 p1414 A70-20172

Structural design analysis techniques for one, two and three dimensional continua, discussing various problem solving methods

07 p1417 A70-20361

Analytical mechanics of discrete and continuous systems covering systems with limited degrees of freedom, statistical and continuum mechanics

08 p1543 A70-20526

Two dimensional continuum of objectivity and isotropy principles applied to study of elastic tridimensional vault

09 p1777 A70-22899

Continuous media mechanics by applying fractional steps method to numerical solutions, outlining theoretical basis for computer algorithms

10 p1866 A70-24114

Mechanics of continuous media for noncanonical regions, surveying Soviet literature on stress concentration near shell holes, elasticity theory, fluid aerohydroelasticity, etc

10 p1965 A70-25319

Stable and unstable crack growth in viscoelastic media, solving boundary value problem and continuum mechanics prediction of crack propagation

12 p2315 A70-27092

Isothermal quasi-linear theory of viscoelastic isotropic continuum, considering constitutive equations

13 p2516 A70-29534

Operator form added to equations of state of continuous media in case of small and large deformations

14 p2656 A70-30473

Spherically symmetric state of slightly ionized gas of unbounded expanse about catalytic conductor by nonequilibrium continuum theory, analyzing Debye number limit for electrostatic probes

14 p2665 A70-30946

Finite elements for three dimensional compressible and incompressible solid continua based on minimum potential energy and variational principles

14 p2659 A70-31128

Book on continuum mechanics covering tensor kinematics, energy balance, virtual work, constitutive equations, etc

16 p2987 A70-32914

Continuum theory of spherical electrostatic probes as measuring devices in high density weakly ionized gases

17 p3140 A70-34931

Finite difference scheme for solving continuum mechanics problems in two space dimensions and time

17 p3131 A70-35885

Thermodynamic application to strained solids, considering paradoxes, irreversible processes and continuum mechanics

18 p3340 A70-36555

Thermodynamics of thermoviscous fluids based on Riemannian space time notions and balance laws of general theory of relativistic continuum mechanics

18 p3347 A70-36557

German book on continuum theory of flowing media covering tensor analysis, equations for kinematics, mechanics, thermodynamics and electrodynamics

18 p3243 A70-37226

Elastic particulate composite solid with microinclusions, deriving dispersion relations governing plane longitudinal wave propagation modes by analogy with continuum theory

19 p3540 A70-37942

Dynamics of composite materials using extensions of continuum theories based on combination of elastic and geometric properties

19 p3455 A70-37950

Continuous one dimensional nonconservative elastic systems under complex forces, examining stability theory

19 p3546 A70-38341

Lumped parameter model for multidimensional solid mechanics problems with inelasticity, discussing stress wave interaction in cylindrical cavity

19 p3458 A70-38357

Discrete finite element models for nonlinear viscoelastic continua

19 p3458 A70-38358

Elastoplastic continua incremental solution for large displacements and small strains, determining sufficient condition of uniqueness

19 p3549 A70-38666

Elastoplastic work hardening continua incremental boundary value problem with allowance for distributed dislocations, using quadratic programming concepts

19 p3549 A70-38667

Continuum bodies strain subjected to shearing stresses in incremental form based on slip theory of metals plasticity

19 p3549 A70-38668

Mathematical theory of constitutive relations connecting surface tractions and moments with motion of single body in continuum

20 p3672 A70-39495

Variational formalism in mechanics of continuous media in four dimensional event space, considering model with local particle interactions

20 p3724 A70-39855

Diffusion processes effect on stress state, allowing for physicochemical coupling between deformed solid bodies based on continuous media theory

20 p3727 A70-39887

Continuum mechanics application to elastic composite materials, investigating plane deformation of reinforced medium

20 p3730 A70-40038

Structural mechanics of continuous fiber reinforced composites, discussing bending and stretching of cylinders, pressure vessels, plates and beams

20 p3730 A70-40039

Sound velocity in isotropic nonlinear elastic Cosserat continuum with constrained particle rotation, analyzing uniaxial and hydrostatic compression

20 p3734 A70-40434

Microelastic solids theory achieved with application of internal constraints from postulate of principal coincidence

21 p3939 A70-42029

Invariance principle in mechanics of deformable continua connecting three dimensional and relativistic space-time formulation

21 p3940 A70-42097

Circular cylindrical hole in uniaxial tension field of elastic media, solving plane strain problem for stress concentration factors

21 p3941 A70-42107

Crack growth study in viscoelastic solids by linear continuum mechanics, discussing cyclic loads, composite solids mechanical behavior and thermodynamics

22 p4115 A70-42937

Sound velocity in isotropic nonlinearly elastic continuum with microstructure, showing dispersion coincident with Cosserat constant

22 p4120 A70-43713

Large element method for stiffness matrix order reduction in two-dimensional continua problems

23 p4275 A70-44940

Continuum media theory, deriving first order constitutive differential equations for isotropic tensor functions

24 p4378 A70-45270

Viscoelastic laminated composite linear anisothermal theory, presenting homogeneous continuum model to describe dynamic characteristics

24 p4368 A70-45992

CONTINUUMS

Equations of state for continuous media, using variational principles within framework of relativity theory

01 p0146 A70-11593

Clock synchronization in general relativity theory, investigating temporal and spatial relations in four dimensional continuum using simultaneous hypersurface

12 p2272 A70-27357

Digital simulation of continuous systems described by differential equations

16 p2870 A70-33728

High current elastic conductors nonlinear mixture theory with inviscid electron gas in elastic continuum under mutual electromagnetic and diffusive forces

19 p3387 A70-37787

Clock synchronization in general relativity theory, investigating temporal and spatial relations in four dimensional continuum using simultaneous hypersurface

22 p4075 A70-43598

CONTOURS

Radiation view factor from differential area to conical surface determined using Stokes theorem and contour integration

04 p0787 A70-15598

Computerized design of aircraft contours, determining three dimensional surface by second degree equation

[SAE PAPER 700202]

11 p2013 A70-25876

Surface contours generation by Moire patterns

12 p2235 A70-27753

Perceptual displacement of hashmark between unequal squares, discussing contour repulsion and perspective interpretation

14 p2537 A70-30899

Stiffness matrix correction for curved element deficient in rigid body motion

18 p3342 A70-36687

He-Ne laser profile-tracing system for contour measurement, suggesting steps for error reduction

20 p3640 A70-39417

Transport aircraft noise at three major airports by noise exposure forecast /NEF/ contours methodology

21 p3750 A70-40896

CONTRACT MANAGEMENT

Spares management of large aircraft contract in relationship to total integrated logistics support systems management

02 p0401 A70-11672

Party autonomy application to standardized international air transport contracts, discussing international treaties, law court judgments and literature

02 p0402 A70-12267

Reliability guarantee vs cost of capital, analyzing contract compliance delay and discounted penalty expenditures

13 p2525 A70-29570

CONTRACT NEGOTIATION

Cost effectiveness tradeoff analysis for reliability incentive contracts, evaluating customer requirements for military procurement

01 p0220 A70-10115

DOD procurement practices for advanced weapon systems, discussing government errors in contracting policies

07 p1428 A70-19678

Midwestern political economy and federal R and D funds distribution, surveying bidding practices and NASA contracts for five year period

07 p1428 A70-19733

Product oriented cost data bank for satellite system cost prediction and negotiation designed for USAF communications satellite program

11 p2152 A70-25477

Contractor all risk incentive contract /CARIC/, discussing innovative features and negotiation elements

14 p2668 A70-30525

CONTRACTION

Low turbulence wind tunnel axisymmetric contraction designed from reformulated Thwaites solution

03 p0462 A70-12935

Transmural stimulation elicited phasic and tonic contractile responses in circular and longitudinal axes of small intestine under nerve-blocking drugs

09 p1622 A70-23547

Hyperbaric oxygen effect on heart muscle contractions in mammals, considering cells enzymatic activity and substrate utilization

09 p1623 A70-23586

Left ventricle pressure rise rate as function of heart contractility and hemodynamics

09 p1623 A70-23587

Contraction coefficients for compressible discharge through axisymmetric sharp edged orifice, obtaining approximate analytical expression based on one dimensional theory

13 p2389 A70-29549

Transverse contraction during butt welding of plates of steel and Ti and Al alloys, showing dependence on joint thickness

16 p2916 A70-33053

Myocardial contractile function in rats under acute overstrain, evaluating role of preliminary training to altitude hypoxia

19 p3360 A70-37805

CONTRACTORS

NASA Source Evaluation Board process for major contractor selection, discussing procurement practices and management techniques

03 p0610 A70-13962

Government environment challenges to government sponsored big technology management illustrated by space nuclear engine research program

09 p1792 A70-22494

- Federal contract research centers objectives, characteristics, crucial issues and future
 - 09 p1793 A70-22971
- Quality evaluation surveys performance by contractors
 - 14 p2669 A70-31106
- Subcontracting for cost optimal parts screening, discussing negotiations and reliability requirements
 - 15 p2747 A70-32651

CONTRACTS

- DOD laser research and development contracts management
 - 14 p2667 A70-30367
- Government defense contract warranties in terms of consumer interests protection and economics
 - 14 p2667 A70-30522
- Incentive earnings and payments in CIPF /cost plus incentive fee/ contracts, considering legal principles
 - 14 p2668 A70-30523
- Book on guide to aerospace defense contracts covering purchase control, marketing solicitation, project management, reports, logistics etc
 - 22 p4126 A70-42723

CONTRAILS

- Lower E region turbulence interpretation based on high resolution photographs of artificial sodium vapor trails
 - 03 p0476 A70-13913
- Winds above 200 km measured from vapor trail observations compared to winds deduced from satellite orbital changes and theoretical models
 - 07 p1269 A70-19950
- IR reflectance of cirrostratus and cirrus clouds and jet contrail measured by spectrometer on high altitude aircraft
 - 11 p2045 A70-25626
- Aircraft condensation trails formation by interactions of exhaust emission, vorticity of wing induced downwash and ambient atmosphere
 - 22 p3958 A70-42684
- Contrail effects on atmospheric thermal radiation budget in heavy jet traffic regions from airborne IR and solar radiometric observations
 - 23 p4214 A70-44033
- Global upper atmosphere circulation pattern by daytime tracking of high altitude rocket vapor trail, using differential radiometer
 - 23 p4214 A70-44039
- Weather modification by jet aircraft contrails, discussing cloud seeding observations in Alaska
 - 24 p4371 A70-45421

CONTRALATERAL FUNCTIONS

- Contralateral remote masking /CRM/ increase of LF tone burst produced by middle ear muscle contractions
 - 04 p0632 A70-15082

CONTRAST

- NT IMAGE CONTRAST
- NT PHASE CONTRAST
 - Visual contrast sensitivity adaptation to temporal frequencies using high modulation sinusoidal grating
 - 17 p3034 A70-35898

CONTROL

- Hamilton modified principal applied to nonlinear control problems including time delay, servosystem with ideal relay and liquid level control
 - 09 p1614 A70-23693
- Generalized control theory, discussing optimization and table classifying control theory fields
 - 10 p1856 A70-25238
- Aircraft design, development and production illustrating systems engineering functions, discussing control process model
 - 16 p3004 A70-33676
- Human postural control system response to mechanical torque disturbance, using second order differential equation with state dependent parameters for approximate analysis
 - 22 p3979 A70-43494

CONTROL BOARDS

- Flight deck controls and instrument disposition in business aircraft emphasizing size
 - 06 p1061 A70-17318
- Comfort plane switch mounting design for helicopter collective controls, noting mock-up evaluation by test pilots
 - 19 p3372 A70-38922
- Pilot influence on dynamic aircraft design, taking into account physiological state during various operational tasks
 - 23 p4138 A70-44134

CONTROL DEVICES

U CONTROL EQUIPMENT

CONTROL EQUIPMENT

- NT CRYOSTATS
- NT PRESSURE REGULATORS
- NT PRESSURE SWITCHES
- NT SERVOAMPLIFIERS
- NT SPEED REGULATORS
- NT TELEOPERATORS
- NT THERMOSTATS
 - Electrical supply and control of monoplex 6.25 Hz ruby laser for use in optical radar, high speed photography, etc
 - 01 p0114 A70-11270

- Phase detector with two value output and pulsed input for measurement and control circuits, noting construction with semiconductor elements
 - 02 p0266 A70-11900

- Aircraft controls response critical speed as function of transmission lag and transfer function of control link elements
 - 02 p0227 A70-12410

- Turbojet engine controls and control devices design, considering fuel properties and fuel consumption
 - 03 p0552 A70-13806

- Structure theorem for time invariant multivariable linear systems proof and formulation for use in controller design and synthesis
 - 03 p0461 A70-14166

- Tactile control in man machine systems using feed-forward loops to provide rate information, noting unmanned aircraft and machine-tool applications [ASME PAPER 69-WA/BHF-14]
 - 04 p0642 A70-14855

- Air traffic control problems in avoiding midair collisions, satellite utilization in transatlantic flight control and anticollision devices and procedures
 - 04 p0623 A70-15350

- Fluidics application in sounding rocket guidance control circuits used in space boosters
 - 05 p0797 A70-15809

- Fluidics background, operational principles, constituent elements, system assemblies and applications, discussing integrated and multiple function circuits, cost and reliability advantages, etc
 - 05 p0798 A70-16146

- Electroluminescent matrix displays, discussing limitations in control element
 - 05 p0827 A70-16186

- Fluidic devices for systems engineering, discussing design and applications of logic simulator, element tester and three mode controller
 - 06 p1015 A70-18428

- Laser beam deflection techniques for directional control of laser beams, noting applications to optical computer memories and active imaging and display devices
 - 09 p1696 A70-22783

- Control system for high speed photographic diagnostics based on rotating mirror action
 - 09 p1679 A70-22993

- Optoelectronic devices for variable resistors controlled by electrical signal, investigating decoupling, capacitance and DC resistance
 - 09 p1649 A70-23353

- Digital sampled-data loop of phase lock control containing digital zone error detector and digital frequency regulator with reversible counter as memory unit
 - 10 p1833 A70-24085

- Equipment design for burst synchronization control in TDMA experiment system
 - 10 p1836 A70-24339

- Multidimensionality in complex control systems, discussing circuit and oscillation theory, decomposition, variational problems, finite automata and group theory
 - 11 p2023 A70-25602

- Decoupling and pole assignments in linear multivariable control systems using geometric method
 - 11 p2072 A70-26160

- Human performance as controller evaluated in man machine control system, considering pursuit or compensatory tracking tasks
 - 12 p2177 A70-27039

- Semifluidic proportional industrial control systems using diaphragm summing junction including applications to temperature control, remote sensing and drill bit adaptive measurement
 - 12 p2164 A70-27073

- Fluidic gas turbine controls, discussing high temperature operation, hybrid sensors and logic in hostile environment applications
 - 12 p2164 A70-27074

- Bits quantity required to represent coefficient within digital controller with high sampling rate
 - 12 p2203 A70-27410

- Solid state power controllers for aircraft electrical power systems [SAE PAPER 700304]
 - 12 p2195 A70-27450

- Semiconductor power controllers for switching aircraft electrical power supplies [SAE PAPER 700308]
 - 12 p2195 A70-27451

- Upper bound on system errors caused by quantization in multirate digital control system
 - 12 p2204 A70-27841

- Lunar vehicle design, discussing dual power steering, switching and joystick control handle
 - 12 p2208 A70-27944

- Control device for micromanipulator with pacing motor during electrophysiological studies involving microelectrodes implantation into tissue
 - 12 p2179 A70-28317

- Cooling system control system for astronaut thermal equilibrium and work output maximization during extravehicular space missions
 - 13 p2357 A70-28526

- Stochastic reinforcement learning model synthesizing control and pattern recognition systems with learning attributes
 - 13 p2374 A70-29584

- Computer oriented algebraic method for duplicator control systems applied to loop network, lag, feedback, phase lead and phase lag compensator design
 - 14 p2560 A70-30620

- Memory systems in measurement and control equipment, describing applications to linearizing, compression and data refresh operations
 - 14 p2554 A70-30676

- Satellite feedback attitude control system resulting in high accuracy earth pointing motions in elliptic orbits
 - 14 p2654 A70-31172

- Control system teaching based on preferred response data, discussing operator determination from purpose control function
 - 15 p2716 A70-32449

- Emergency hypotonia regional control with/without blood circulation centralization, describing device consisting of inflatable balloon, extracorporeal shunt, electromagnetic valve, manometer and circuit
 - 15 p2687 A70-32891

- Bypass door control system for SST axisymmetric intake operation in external compression mode, obtaining dynamic performance [AIAA PAPER 70-695]
 - 16 p2966 A70-33558

- Brushless despin mechanical drive and control system design and performance for orientation of high gain communications antenna from spin stabilized satellite
 - 16 p2986 A70-34161

- Digital logic techniques for pulse modulated radar systems, with application to controlling and timing waveforms for display
 - 17 p3042 A70-34570

- Complex control systems in integrated logic circuits and light laboratory materials production, discussing measurement equipment for quality control
 - 17 p3090 A70-35416

- Characteristic injuries from aircraft controls inflicted in fatal accidents, showing pilot position and hand location upon impact
 - 17 p3039 A70-35573

- Soviet papers on discrete control systems covering linearity, nonlinearity and applications
 - 18 p3233 A70-36068

- Gas turbines dynamics and control system requirements, discussing equipment design and reliability [ASME PAPER 70-GT-76]
 - 18 p3305 A70-36887

- Soviet book on man in aircraft control system covering engineering psychology, complex flight problems, human factors and instrument panels
 - 19 p3367 A70-37236

- Thyristor circuit for storing or generating digital control signals, considering reliability at high noise levels
 - 19 p3385 A70-37377

- Static stability requirements relaxation and wing control devices additions for alleviating wing root bending moments in controls configured vehicle /CCV/ design concepts
 - 19 p3355 A70-37395

- Real time analog display inputs for electronic computers and tracking in physiological control circuits, describing various manual controls
 - 19 p3367 A70-37564

- Analytical adaptation algorithms for PID controllers operation
 - 19 p3394 A70-38162

- Electronic components mass production for automatic control equipment, determining parameters probabilistic scatter
 - 19 p3390 A70-38578

- Bobweights effects on pilot induced oscillations, noting role in flying qualities and control system design [AIAA PAPER 70-1002]
 - 20 p3560 A70-39529

- Invariance conditions for control systems with time varying parameters
 - 20 p3602 A70-39827

- Automatic control system components parameter variation effects on invariance conditions
 - 20 p3602 A70-39830

- Multidimensional control systems synthesized in accord with polyinvariance and coordinating couplings principles
 - 20 p3604 A70-39837

- Multichannel computer for statistical investigations of complex nonlinear controlled plants based on recordings of input, output and internal state variables
 - 20 p3594 A70-39921

- PCM command control system for high altitude ballooning operations, discussing component equipment
 - 20 p3587 A70-40085

- Integrated environmental control/life support resistor systems, surveying NASA programs [AIAA PAPER 70-1130]
 - 20 p3690 A70-40215

- Papers on aerospace vehicle flight control systems covering controller design, flow difference sensors, etc
 - 21 p3926 A70-40780

- Liquid metal hydraulic servoactuation packages for flight control in high temperature environments without coolant systems
 - 21 p3750 A70-40785

- Optimal control problem for plant including dynamics and input constraints parameters treated by calculus of variations and Pontryagin maximum principle
21 p3801 A70-40899
- Integrated circuits for control and telemetry functions in oxide cathode ion thruster power conditioning system operating from solar panel
21 p3798 A70-42126
- Transistorized DC to AC converter providing sinusoidal output to power automatic spacecraft control devices via pulse width modulation
22 p3994 A70-42309
- Fluidic control devices and systems, discussing turbulence amplifiers, impact modulators, logic gates, active and passive elements, etc
[ASME PAPER 70-FLCS-15] 22 p3963 A70-42412
- Fluidic applications in missile components production, discussing various types of fluidic control and logic in relation to functional requirements
[ASME PAPER 70-FLCS-11] 22 p3963 A70-42416
- Fluidic controls for propulsion engines, describing optimum fabrication techniques
[ASME PAPER 70-FLCS-7] 22 p3964 A70-42420
- Harmonic linearization method for periodic regimes in nonlinear control systems based on periodic solution sensitivity to higher harmonics and small parameters
22 p4000 A70-42829
- Thyristor-servomotor temperature control unit, describing circuit and applications
22 p3996 A70-42850
- Fuel delivery and speed control systems for aircraft gas turbine engines, discussing control circuit transfers and block diagrams
22 p4091 A70-43116
- Nonlinear control systems described by linear equations, discussing quasi and local controllability as functions of time and stationary state
22 p4063 A70-43427
- Soviet cybernetics research, emphasizing discrete and continuous control devices and systems synthesis
22 p4004 A70-43449
- Pulse-time multistable state elements for automatic and remote control constructed from pulse sequence interactions with multiple frequency relations
22 p4005 A70-43567
- Manned spacecraft onboard data management systems, discussing information transfer, processing, control, display and man machine interface
23 p4167 A70-44647
- Laser sensors as alignment instrument for control and measurement of five degrees of freedom
24 p4351 A70-45383
- Pilot hand-held and leg-mounted controllers for precision tracking from aircraft under buffeting tested in static and dynamic motion simulator
24 p4308 A70-45513
- Signal flow graphs for selectively invariant autonomous multichannel control systems design
24 p4321 A70-45641
- Engine control concepts for augmented turbofan, discussing integrated electrical/hydraulic/mechanical system
[SAE PAPER 700826] 24 p4394 A70-45893
- Automatic control system for Boeing SST engine air intakes, optimizing engine performance and controlling noise propagation
24 p4396 A70-46214
- Cleanliness levels for missile guidance package as function of component design complexity
24 p4349 A70-46250
- CONTROL MOMENT GYROSCOPES**
- Control moment gyros for spinning satellite stabilization and attitude control
18 p3289 A70-36714
- Control moment gyro (CMG) for spacecraft attitude control, determining optimal gimbal angle rate for desired torque
[AIAA PAPER 70-1042] 19 p3433 A70-38857
- Control moment gyro (CMG) spacecraft attitude control systems, discussing selection and design criteria
[AIAA PAPER 70-976] 20 p3668 A70-39553
- Parametrized design data and selection criteria of biowaste resistor system for orbit keeping and control moment gyro desaturation of manned space station
[AIAA PAPER 70-1132] 20 p3567 A70-40213
- Large earth orbiting spacecraft minimum time attitude maneuvers with control moment gyroscopes, discussing torque calculation and gimbal angle rates
20 p3670 A70-40284
- CONTROL PANELS**
- U CONTROL BOARDS**
- CONTROL ROCKETS**
- Spacecraft trajectory control rockets design and operational characteristics, discussing various propellant types, control valve designs, etc
24 p4393 A70-45640
- CONTROL SIMULATION**
- Book on dynamics of complex systems represented by control and human operators and animals behavioral activities models
01 p0034 A70-10501
- Simulation technique to evaluate TV contrast trackers standard scan performance using video tape recording
01 p0058 A70-10812
- Computer driven display terminal as part-task limited area simulator, examining operational requirements and input characteristics
01 p0059 A70-11277
- Air combat model (AIRCOM) to evaluate close-in air-to-air fighter aircraft combat capability, determining relative changes in kill probability per firing pass
03 p0413 A70-13958
- Two loop control system model of human lens accommodative system derived on basis of muscle mechanics, optics and experiments
03 p0439 A70-14275
- Optimal space vehicle reentry control ensuring minimum scattering of landing points based on accelerometer and free pitch-angle gyroscope data
04 p0760 A70-14431
- Computerized thermal model simulating environment control system, crew and vehicle structure in performance prediction for Apollo lunar module
[SAE PAPER 690621] 05 p0922 A70-15848
- Measurement optimal feedback control algorithm for stochastic discrete time systems, considering nonlinear plant, constrained controls, nonquadratic cost and simulations
06 p1025 A70-17962
- Concorde simulator for determining aircraft control responses and integrating pilot function into problem
07 p1249 A70-19743
- ATC real time simulation exercises in Brussels Upper Information Region
07 p1250 A70-20227
- Air combat simulator with attacker and evader pilots control capability, comparing simulated interceptions with flight test maneuvers
[AIAA PAPER 70-340] 09 p1656 A70-23023
- Digital control systems simulation on analog computer with digital logic, using conventional analog amplifiers and integrators
10 p1860 A70-24655
- Hybrid simulation, determining vehicle and performance parameters on longitudinal flying qualities of STOL transport in power approach configuration
[AIAA PAPER 70-387] 10 p1806 A70-24918
- Spacecraft launch computerized simulator, discussing operational characteristics applicable to on-line real time process control
11 p2013 A70-26217
- Human controllers nonlinear time domain mathematical model for analyzing compensatory tracking task data
11 p1992 A70-26396
- Mathematical model for rats nonlinear time-varying glucocorticoid secretion control mechanism, obtaining time dependent characteristics of hypothalamic-hypophyseal complex
12 p2174 A70-26893
- Synchronous satellite attitude acquisition and keeping, proposing roll and pitch control law for simulation
13 p2500 A70-28409
- Optimal space vehicle reentry control ensuring minimum scattering points based on accelerometer and free pitch-angle gyroscope data
13 p2503 A70-28456
- Stochastic approximation methods applied to pattern classification, estimation and control
13 p2442 A70-29586
- Gunn diode simulation with variable cross section, showing subthreshold and mode oscillograms
15 p2707 A70-31510
- Linear distributed dynamic system simulation using infinite product expansions for transcendental terms in transfer functions
16 p2942 A70-33348
- Tactical missiles electromechanical control actuator with reduced size and weight, describing mathematical model for analog simulation
16 p2845 A70-34111
- Digital computer simulation and analysis of control loops for ion thruster control
[AIAA PAPER 69-239] 17 p3149 A70-35654
- Display/control technology for high performance input/output between man and machine, describing man-in-loop simulation
19 p3369 A70-37875
- Computer real time Apollo simulation, checkout and training system duplicating actual mission for flight controllers in Mission Control Center
21 p3805 A70-41198
- Fighter aircraft higher order control system dynamics effects on longitudinal handling qualities evaluated by in-flight simulator for role of pilot induced oscillations tendencies
[AIAA PAPER 69-768] 22 p3961 A70-42711
- Cryogenic fluid heat exchanger flow oscillation automatic feedback control, discussing design and simulation
23 p4280 A70-44370
- CONTROL STABILITY**
- Popov type nonlinear control systems from synthesis viewpoint, using state variable feedback results to insure absolute stability
02 p0271 A70-12194
- Optimum power and operation mode of space vehicle engine with control error allowance as function of mass and velocity
04 p0760 A70-14433
- Mathematical problem of stability of nonlinear automatic control systems solved using linear criteria
05 p0825 A70-16866
- Satellite launch vehicle attitude control stability study including fuel sloshing and body bending effects
06 p1155 A70-17320
- Absolute stability of automatic control systems with multiple rigid and tachometer feedbacks
06 p1024 A70-17812
- Signal stabilization and performance of nonlinear sampled data systems, suggesting oscillations injection at input
06 p1026 A70-17970
- Nonlinear control systems stability with stochastic coefficients, applying Liapunov function
06 p1026 A70-17971
- Nonlinear feedback control systems frequency domain stability criterion obtained using gain-phase plot
06 p1026 A70-17972
- Linear optimal stochastic control systems described by covariance matrix correlating errors and estimates of state variables, analyzing instability under parameter variations
[AIAA PAPER 70-36] 06 p1095 A70-18054
- Partial stabilization of given quantities on steady motions of nonlinear control systems with initial perturbations based on observation theory
07 p1333 A70-18686
- Absolute stability ranges of forced motions and damping in nonlinear systems determined by Sturm theorem
07 p1243 A70-18688
- Periodic motions and dynamic stability of nonlinear distributed sampled data system of closed loop of pulsed element governed by heat conduction equation
07 p1226 A70-18749
- Control system composed of linear and nonlinear components and distributed parameters, deriving stability criterion for simple critical case
07 p1246 A70-19539
- Book on optimal control and guidance theory covering state and transition equations and canonical forms of linear systems, systems stability, servo loops, etc
07 p1246 A70-19668
- Soviet book on control systems for single rotor helicopters covering automatic stabilization system design, autopilots, pilot operation within closed control circuit, etc
08 p1435 A70-20769
- State observers/filters/ construction in multivariable control systems using phase transformation
08 p1478 A70-20778
- Existence theorem for linear stochastic systems optimal control described by differential equation with random coefficients, providing rms stabilization
08 p1480 A70-21637
- Feedback systems stability treated by functional analysis, describing procedures for generating instability criteria
09 p1654 A70-22348
- Soviet papers on complex control systems covering hierarchical structures, accuracy and stability analysis, optimal and self adjusting control, etc
11 p2022 A70-25601
- Asymptotic stability of multivariable autonomous control systems used Liapunov vector function method
11 p2083 A70-25606
- Asymptotic stabilization of multivariable dynamic systems, using subsystem decomposition and Liapunov second method
11 p2023 A70-25607
- Solid body control moments ensuring braking from rotational motion, finite orientation and angular velocity under minimum energy constraint
11 p2023 A70-25609
- Static longitudinal stick free and stick fixed aircraft stability equations for several configurations and power effects
[SAE PAPER 700238] 11 p1981 A70-25907
- Optimal and suboptimal aircraft lateral directional stability augmentation applying optimal control and model-following techniques
12 p2162 A70-27812
- Admissible controls synthesis for closed loop system/satellite/ stability
13 p2500 A70-28410
- Limit cycle oscillations in satellite attitude control system, producing control moment by pulse modulated controller
13 p2502 A70-28430
- Optimum power and operation mode of space vehicle engine with control error allowance as function of mass and velocity
13 p2503 A70-28458

- Aircraft optimal roll stabilization control system design using performance index with weighting matrix 14 p2532 A70-31395
- Computer control of nonlinear systems with varying performance specifications, using Popov stability and nonlinear programming 15 p2715 A70-31973
- Distributed sampled-data control systems with memoryless nonlinear feedback element, deriving frequency domain stability criterion 16 p2884 A70-33308
- Controllability of nonlinear dynamic feedback systems based on Liapunov-like stability approach and optimal control theory 16 p2885 A70-33321
- Guidance and control and propulsion technology, discussing fluidic systems, digital computers and structural materials, solid and liquid propellant engines 17 p3179 A70-35284
- Automatic control system stability, allowing for position and velocity loads and compressibility of fluid in force cylinder of hydraulic actuating mechanism 17 p3024 A70-35367
- Spacecraft wide angle attitude control system stability analysis, using air bearing table simulation 17 p3134 A70-35651
- Steady forced regime stability in pulse frequency modulated servosystems, using Liapunov method 18 p3234 A70-36071
- Stability conditions for control system third-order differential equations with double nonlinearity, using Liapunov function 18 p3280 A70-36157
- Lumped parameter pipeline and hydraulic systems stability, deriving equations of motion for closed and open cycle control systems 18 p3216 A70-36946
- Stability analysis parameter plane technique for tactical missile control system design, correlating variable parameters with characteristic equation roots location 19 p3532 A70-37853
- Optimal control problems with moving ends in presence of phase constraints, deriving difference approximation stability condition 20 p3601 A70-39730
- Controlled variable perturbation effects on system with internal positive feedback 20 p3602 A70-39829
- Variable wing sweep aircraft angular motion mathematical model, analyzing inertial moments influence on control dynamics 20 p3562 A70-40182
- Linear control plant identification by solving integral equation obtained from input and output signals 22 p4005 A70-43565
- Optimal asymptotic stability laws of control systems with unstable plant, using piecewise coordinate functions 24 p4321 A70-45494
- CONTROL SURFACES**
- NT AERIAL RUDDERS
- NTAILERONS
- NT ELEVATORS [CONTROL SURFACES]
- NT ELEVONS
- NT FLAPS [CONTROL SURFACES]
- NT GUIDE VANES
- NT HORIZONTAL TAIL SURFACES
- NT JET FLAPS
- NT JET VANES
- NT RUDDERS
- NT SPOILERS
- NT TABS [CONTROL SURFACES]
- NT TRAILING-EDGE FLAPS
- NT WING FLAPS
- Two dimensional wing model with harmonically oscillating control surface in transonic range, comparing theoretical with experimental results on unsteady pressure distribution 06 p0966 A70-17252
- Simulated degrading environment effect on spacecraft thermal control surfaces subjected to plume heating during apogee firing and solar irradiation [AIAA PAPER 69-1024] 09 p1657 A70-23259
- Compression process in turbulent boundary layer on control surface at hypersonic speeds, noting influence on surface effectiveness and heating [ONERA-TP-814] 11 p1979 A70-25815
- Rao optimization method for thrust nozzles at given length, analyzing control surface flow field conditions 12 p2158 A70-28202
- Frequency and amplitude during longitudinal control surface pumping by pilots in precise flight path handling for aircraft design [AIAA PAPER 70-567] 13 p2346 A70-29032
- Pressure field due to control surface oscillation in subsonic flow, presenting numerical results for rectangular wing 14 p2528 A70-30295
- Optimal control surface location for flexible aircraft determined by matrix minimum principle and calculus of variations 16 p2840 A70-33316

Lifting reentry vehicles control surface aerodynamics, considering boundary layer separation, shock interference, unsteady flow, etc 18 p3333 A70-36958

Rectangular wing with oscillating control surface, measuring induced unsteady pressure field for comparison with computations based on lifting surface theory 21 p3935 A70-41407

Aircraft control surface aerodynamic characteristics, considering low aspect ratio wing elevons with variable sweep leading edge as longitudinal and lateral controls [ICAS PAPER 70-26] 23 p4131 A70-44107

Unsteady aerodynamic loading of wings with control surfaces, discussing Kuessner integral equation of subsonic lifting theory 23 p4274 A70-44761

ONERA calculations in aeroelasticity including lifting surface optimization, control surface vibration, pressure fields, aircraft transfer functions and panel flutter 23 p4274 A70-44762

High subsonic and transonic effects on pressure distributions for swept wing with oscillating control surface 23 p4274 A70-44763

Pressure measurements on harmonically vibrating sweptback wing with two control surfaces in incompressible flow 23 p4274 A70-44768

Inviscid hypersonic flow fields past lower/compression/surface of delta wing calculated by one strip approximation of integral relations method 24 p4289 A70-46245

CONTROL SYSTEMS

U CONTROL

CONTROL VALVES

Slide and sleeve type servovalves used in Boeing aircraft possessing chip shearing capability of 200 pounds axial force 02 p0229 A70-12863

Static and dynamic characteristics of inertia load driving systems using electrohydraulic pressure and flow control servovalves [ASME PAPER 69-WA/FLCS-15] 04 p0626 A70-14842

Digital control valve for high speed aerospace blending, considering propellant and cryogenics applications 06 p0989 A70-18602

Pilot Airborne Recovery Device [PARD/ using hot air ballute, noting capability to ascend or descend by flow control valve controlling butane burner 07 p1192 A70-19019

Direct digital control valves in fluid flow process evaluated for performance by analog computer simulation 09 p1613 A70-23684

Cage trim control valve designs, outlining properties, advantages and limitations 14 p2534 A70-30682

Solid propellant rocket motor combustion control by fluidic vortex valve, considering thrust variation [AIAA PAPER 70-643] 16 p2965 A70-33535

NERVA engine chamber pressure control, investigating replacement of TPCV with fluidic vortex valve [AIAA PAPER 70-658] 16 p2970 A70-33620

Flow control valve without moving parts used in ATS A and D, describing design, operation and theoretical performance 16 p2846 A70-34132

CONTROLLABILITY

Controllability conditions for control system described by equation with vectors x and f being non-dimensional and u and r being dimensional 04 p0660 A70-14491

Nonlinear control systems with linear controls appearance defined for controllability concepts and sufficient conditions to reduce to lower dimensional problem 04 p0660 A70-14524

Approximate boundary controllability of heat equation, considering smoothness conditions on piecewise-smooth boundary 05 p0875 A70-15781

Reusable lifting entry vehicle flight tests, investigating handling qualities and subsonic-transonic aerodynamics of M2-F2/M2-F3/HL-10 and X-24A [SAE PAPER 690662] 05 p0792 A70-15840

Complex control follow-up systems in transient modes, suggesting synthesis for transfer function of control signal coupling 06 p1023 A70-17775

Unstable spiral precursor to jet upset/Mach tucks/in executive jet transports 06 p0987 A70-18248

N-local controllability conditions for system having permissible controls assumed to be certain piecewise constant vector functions 07 p1244 A70-18766

Structural synthesis of functional control systems represented by first order differential equations, determining hypersurface 08 p1479 A70-20871

Amplitude and Rotational 3-Axis Flight Simulators for handling qualities research, outlining physical constraints and methodology for driving visual display and motion systems 10 p1858 A70-24210

Civil VTOL transport aircraft handling and performance qualities using fixed base simulator with electronically generated display [AIAA PAPER 70-345] 10 p1859 A70-24214

Optimization of controlled systems with allowance for failures of parallel connected elements dependent on control inputs and phase coordinates 10 p1854 A70-24279

Controllability and observability of discrete composite systems in tandem with Jordan canonical form representation noting similarity to continuous systems 10 p1856 A70-24873

XB-70 aircraft flight tests in cruise and landing approach to evaluate handling qualities criteria [AIAA PAPER 70-566] 13 p2346 A70-29031

Pilot-aircraft closed-loop characteristics, using pilot transfer functions for handling qualities prediction [AIAA PAPER 70-568] 13 p2346 A70-29033

Flying qualities application to automobiles, discussing work load with respect to controllability and pilot behavior 13 p2347 A70-29142

Controllability test for second order differential systems, noting applicability to linear first order time dependent systems 13 p2443 A70-29972

Supersonic aircraft lateral stability and controllability design, discussing directional and weathercock stabilities 15 p2673 A70-31625

N-locus controllability of two dimensional holomorphic systems with permissible controls 15 p2715 A70-31641

Multidimensional linear stationary systems controllability and observability with given transfer matrix 15 p2716 A70-32345

Supersonic aircraft stability and controllability during turns about longitudinal and vertical axes 16 p2840 A70-33204

One dimensional controlled plants structure identification with mathematical model composed of aperiodic nonlinear and delay components connected in series 16 p2883 A70-33235

Controllability of nonlinear dynamic feedback systems based on Liapunov-like stability approach and optimal control theory 16 p2885 A70-33321

Control theory and calculus of variations - Conference, University of California, Los Angeles, July 1968 17 p3129 A70-34866

External aerodynamics role in handling qualities of amphibious hovercraft, discussing tests of hull shape, air cushion efflux and hollow models 17 p3017 A70-34919

Pilot induced oscillation rating regression analysis, examining time delay, slope after and time to first peak and stick force per g 18 p3213 A70-36444

Noise effect on signal parameter control in linear measurement devices 22 p3984 A70-42394

Nonlinear control systems described by linear equations, discussing quasi and local controllability as functions of time and stationary state 22 p4063 A70-43427

Stability augmentation in aircraft design for handling and operation benefits, discussing control techniques, autopilot modes and load limitations [ICAS PAPER 70-24] 23 p4138 A70-44109

Wheel force and roll moment nonlinearities effect on light STOL aircraft handling qualities during approach [ICAS PAPER 70-55] 23 p4139 A70-44151

Fluidically augmented artificial feel system for fighter and attack aircraft control, discussing improved handling qualities [SAE PAPER 700785] 24 p4294 A70-45859

STOL aircraft low speed handling characteristics described via approach and landing profiles, power requirements, wind effects, etc [AIAA PAPER 70-1332] 24 p4291 A70-45936

CONTROLLED ATMOSPHERES

NT CABIN ATMOSPHERES

NT INERT ATMOSPHERE

NT SPACECRAFT CABIN ATMOSPHERES

Liquid sodium droplets spontaneous ignition and combustion in controlled oxidizing atmosphere, discussing vapor phase diffusion flame, burning rates and evaporation constants 02 p0396 A70-12005

Oxygen consumption and rectal temperature in male mice confined in nitrogen and helium diluted hyperox- 07 p1244 A70-18766

ic atmosphere at specific temperature and humidity ranges 03 p0425 A70-13891

Photosynthesis and respiration rate in vegetables in controlled temperature, humidity, illumination levels, carbon dioxide and oxygen contents 03 p0425 A70-13892

EKG, EEG, pneumograms and X ray pictures showed no pathological effect after prolonged confinement in sealed chamber having artificial atmosphere with variable gas composition 05 p0810 A70-17121

Gaseous environments effects on creep of austenitic stainless steel, observing weakening in air and surface cracking in nonoxidizing atmospheres [ASME PAPER 68-MET-3] 08 p1519 A70-21453

Human peripheral blood circulation during prolonged underwater activity, showing compensation for high humidity, noise levels, low water temperatures, isolation and confinement 10 p1822 A70-25178

Burning velocities for methane-air mixtures with water cooled porous metal flat flame burner, discussing surrounding ambient atmospheres effects 14 p2666 A70-31093

Ben Franklin submarine life support systems tested during Gulf Stream Drift Mission, discussing atmosphere control, water, waste and food management [ASME PAPER 70-DE-60] 16 p2852 A70-33515

Long term helium-oxygen atmosphere effects on rats and mice, investigating biochemical and metabolic changes 16 p2849 A70-33996

CONTROLLED FUSION

Controlled thermonuclear power generation, considering fusion reactors feasibility and reactor energy balance improvement 04 p0717 A70-14528

Free plasma column discharge in HF field in high pressure deuterium atmosphere, discussing high plasma temperature inside column and reliable thermonuclear reaction achievement 08 p1551 A70-21417

Plasma generation and heating by controlled thermonuclear fusion reactions using pulsed lasers 09 p1734 A70-22249

Worldwide developments in controlled fusion, discussing low beta open ended configurations, open and closed high beta systems, full scale reactors, etc 11 p2089 A70-25718

Plasma production by long wavelength lasers applied to controlled thermonuclear reactions [AIAA PAPER 70-779] 17 p3103 A70-34476

Liquid metal heat pipes in magnetic fields of controlled fusion reactors, considering geometry, compound wick structure and vapor flow 21 p3946 A70-41046

Electrical characteristics of high current two stage DC Hall accelerator for use in controlled thermonuclear fusion 24 p4383 A70-45117

CONTROLLED STABILITY

U CONTROL U STABILITY

CONTROLLERS

NT SERVOAMPLIFIERS
NT SERVOECHANISMS
NT SERVOMOTORS

Automatic temperature controller consisting of single element of closed loop feedback system with adjustable transfer characteristics 02 p0296 A70-11874

Physiological limitations of air traffic controllers, considering stress factors connected with workload 04 p0716 A70-15314

Human controller in psychology and control engineering, discussing linear and nonlinear modeling of human behavior 05 p0807 A70-16487

Observation noise model for human controller remnant 10 p1823 A70-23893

Feedback controller specific suboptimal estimation and control parameters determination using stochastic approximation algorithms 11 p2026 A70-26236

Differential equations of controller providing optimum transient response for plant with indeterminate parameters, allowing for nonadditive random noise 13 p2382 A70-29278

Digital controller bits number determination to meet nominal controller coefficients accuracy requirements 16 p2867 A70-33304

Algorithm for implementing learning controller based on subgoal concept applicable to linear stationary system 16 p2868 A70-33312

Performance cost functions of on-off limit cycle controllers for reaction jet controlled system 17 p3056 A70-35552

Air traffic controller stress reduction, discussing work-rest intervals and various management and human factors 19 p3371 A70-38647

Air traffic controller role in future air traffic system, considering automation in operations 19 p3371 A70-38649

Helicopter stabilization systems design, synthesizing controllers by modal control theory [AIAA PAPER 70-1036] 20 p3560 A70-39501

Conventional closed loop controller design treated as particular formulation of optimal control problem through gain and integration derivations 21 p3927 A70-40783

Sampled data compensators hybrid realization for discrete controllers, selecting canonical representation with minimum number of delay elements 22 p4002 A70-42846

Universal proportional high accuracy temperature controller using current regulating circuit consisting of light beam galvanometer, photoconductor, photodiodes and thyristors 23 p4194 A70-43999

Gas turbine controller design by inverse Nyquist method compared to conventional multivariable design methods 24 p4396 A70-46157

CONVAIR MILITARY AIRCRAFT U MILITARY AIRCRAFT

CONVECTION NT FORCED CONVECTION NT FREE CONVECTION

Core convection consequences with regard to earth figure and continental drift, indicating no changes in magnitude of magnetization 01 p0076 A70-10899

Mesoscale rawinsonde network for convective process resolution, describing reduction and analysis techniques for thunderstorm wind, temperature and moisture data 03 p0521 A70-13165

Poloidal magnetic field influence on compressible fluid convection in spherical shells, using variational method to obtain stability criteria 04 p0758 A70-15695

Equations of conservation of mass, energy and momentum applied to rotation effects on convective motion in planetary interiors 05 p0905 A70-15759

Heat radiation effect on set-up and scale of cellular convection in atmosphere 06 p1097 A70-17789

Solar differential rotation relation to Rossby waves in upper convection zone based on energy conversion rate estimates 06 p1144 A70-18010

Solar and stellar convection regions and coronas using photospheric models, taking into account molecule formation 08 p1581 A70-21953

Rayleigh number effects on convection in planetary mantles, considering conservation equations of mass, energy and momentum 09 p1752 A70-22312

Heat radiation effect on set-up and scale of cellular convection in atmosphere 10 p1882 A70-25021

Cumulus convection one dimensional time dependent numerical model, considering horizontal mixing, evaporation, precipitation generation and freezing and thermodynamic processes 11 p2075 A70-25648

Poloidal magnetic field effects on main sequence stars core convection 11 p2117 A70-26654

Rotation law and circulation velocities in solar hydrogen convection zone under anisotropic turbulent velocity 12 p2302 A70-27588

Radar meteorology, discussing convection in lower atmosphere and clear air turbulence observations 13 p2443 A70-28475

Convection effects in mantle on earth gravitational field using hydrodynamic model 13 p2488 A70-28764

Jupiter Red Spot, explaining motion rate in terms of cellular convection in liquid hydrogen-helium layer 15 p2799 A70-31895

LF oscillatory convection characteristics in polytropic atmosphere in strong magnetic field based on sunspot theory 15 p2802 A70-32487

Waves nonlinear propagation in fluids due to convection, reviewing various solution methods 17 p3068 A70-34666

Energy transfer in convective envelope of rotating star and solar differential rotation, using Lucy gravity-darkening law 18 p3313 A70-36214

Equatorial acceleration of sun, considering rotation and turbulent energy transport in convective zone 23 p4252 A70-44830

Cosmic ray electrons solar modulation, considering diffusion-convection theory 24 p4397 A70-45769

CONVECTION CURRENTS

Periodic cellular convection in troposphere with allowance for anisotropic turbulent mixing, showing cyclone association and intervals 01 p0135 A70-10206

Invariant group study of free atmospheric convection equations at combination of Grashof numbers, Prandtl numbers and boundary conditions, noting infinite flux velocity 02 p0328 A70-12387

Cyclonic convective cell fluctuation and nonuniform core rotation effects on reversal of geomagnetic field, investigating fossil magnetism 04 p0676 A70-14600

Convection currents calculation in multicavity klystron allowing for space charge forces influence 05 p0823 A70-16889

Deflecting forces on nonrotating convecting systems due to environmental shear, comparing magnitude to rotation forces 06 p1100 A70-18571

Convective-current instability in finite length plasma column, analyzing spectrum of unstable harmonics 08 p1554 A70-21802

Integral theorems on vorticity transport derived by Carstou method, suggesting need for redefining Truesdell concepts of convection and diffusion 11 p2037 A70-26175

Magnetospheric convection models and effects on charged particle populations 13 p2402 A70-30064

Atmospheric cellular convection, reducing hydrodynamic equations to amplitude equations for vertical velocity 15 p2770 A70-32064

Temperature profiles and wind velocities during convective cloud banks formation from meteorological satellite data 15 p2770 A70-32065

Solar magnetic field origin and behavior, discussing hydromagnetic dynamos, cyclonic convection and generation times 20 p3706 A70-39927

Differential rotation at solar surface caused by anisotropic turbulent viscosity in hydrogen convection zone, solving via Navier-Stokes equation 20 p3711 A70-40404

CONVECTIVE FLOW

Nonthermal convection permissible modes in planetary mantles, using self gravitating homogeneous nonrotating sphere containing core and overlying viscous mantle 01 p0176 A70-10317

High temperature atmospheric models for red dwarf stars and sun to determine convection effect on atmospheric surface layers and emitted flux 01 p0190 A70-11349

Rapidly rotating solar interior damping by large scale convection analysis via maximum buoyancy force in water cylinder transition 02 p0373 A70-12391

Coupled diffusion of heat and vorticity in gaseous vortex caused by radial mass convection and temperature dependence of gas properties 02 p0400 A70-12858

Solar photosphere temperature fluctuations from model consistent with convection hypothesis agreeing with limb darkening data 03 p0570 A70-13591

Stellar model surface convective zone using diffusion equation taking into account transport due to gravitational separation, noting role of turbulent diffusion 03 p0574 A70-13932

Asymptotic solutions of paraboloidal boundary layer system for thermally driven convective flows governed by nonlinear Boussinesq equations 03 p0519 A70-14077

Free convective flows above flat horizontal plate demonstrating laminar boundary layer existence at intermediate Grashof numbers, using semifocusing color schlieren photography 04 p0780 A70-14456

Conducting fluid steady convection due to combined effects of thermal gradient and DC electric field predicted by analytical model 04 p0785 A70-14989

Steady convective motions in horizontal fluid layer bounded by porous walls of various temperatures at supercritical Rayleigh numbers, noting nonlinear convection equations 04 p0673 A70-15237

Solar atmosphere granular convective velocity field determination methods, using realistic assumptions for typical granulation size and seeing parameter 06 p1142 A70-17990

Free steady convective flow stability relative to three dimensional disturbances between parallel planes reduced to equivalent plane disturbances problem 07 p1252 A70-18669

Conducting fluids flow instabilities characterized by incipience at critical electric Hartmann number and 07 p1252 A70-18669

convection rate proportional to electric Reynolds number

07 p1348 A70-19265

Thermally induced convective mixing motion in rotating cylindrical cryogen space storage tank model under heat flux, calculating critical Rayleigh number

07 p1257 A70-19320

Turbulent velocities of convective motions in active and unperturbed photospheric faculae based on spectral observations

07 p1384 A70-19415

Electronic analog model for simulating convective mass transport in system with stationary and dynamic phases

07 p1423 A70-19740

Fluid motion convective stability between vertical parallel planes with longitudinal temperature gradient, solving boundary value problem for amplitudes of normal perturbations

08 p1482 A70-20952

Vertical plane and axis symmetrical numerical models for cumulus convection of moist atmosphere, discussing initial conditions

08 p1536 A70-21025

Unsteady free convection laminar power-law fluid flow past porous vertical wall, studying similarity solution dependence on wall temperature and suction

08 p1486 A70-21765

Lower atmosphere turbulence under convective conditions, comparing Doppler radar and instrumented aircraft wind speed fluctuation measurements

09 p1716 A70-22367

Radiation effects on polytropic atmosphere convective instability using method of disturbances

09 p1753 A70-22456

Initial value problem of macroscopic disorder-order transformation in random thermal convection phase of fluid heated from below

09 p1791 A70-23679

Supergranules /convective cells/ development shown in quiet sun filtergrams of H alpha chromospheric network taken above Arctic Circle

11 p2109 A70-25741

Temperature profiles in upper symmetric regime of heated rotating water annulus convection obtained by thermocouple probe, noting flow field disturbance and correction

11 p2046 A70-26499

Plasmapause form in equatorial plane in presence of magnetospheric tail subsonic potential convective flow

11 p2047 A70-26796

Laminar natural convection plumes behavior above energy sources calculated by simplest variables, indicating optimum formulation of boundary value problem

12 p2332 A70-27700

Eulerian space-time correlations of velocity and pressure for universal homogeneous turbulence by separating kinematic convection effects of large eddies from velocity assumption

13 p2386 A70-28645

Isolated convective plumes immersed in return flow turbulent downdraft

15 p2769 A70-31440

Free steady convective flow stability relative to three dimensional disturbances between parallel planes reduced to equivalent plane disturbances problem

15 p2718 A70-31461

Laminar to turbulent flow transition observation in laser induced vertical convection, using carbon dioxide-nitrogen laser

15 p2751 A70-31980

Convective flow stability in rotating fluid layer under rigid boundary conditions, calculating critical Taylor number as function of Prandtl number

16 p2893 A70-33686

Angular dependence of instability and Rayleigh number of natural convection flow on inclined flat plates, using electrochemical flow visualization

18 p3345 A70-36190

Optical observation of laminar convective flow caused by combined action of concentration and temperature fields

18 p3346 A70-36276

Freckles origin in unidirectionally solidified castings, noting convective jets role

20 p3646 A70-39102

Fluid motion convective stability between vertical parallel planes with longitudinal temperature gradient, solving boundary value problem for amplitudes of normal perturbations

20 p3608 A70-39377

Laminar convective flow from linear heat source along vertical plate, solving numerically for incompressible fluid by boundary layer approximation

20 p3614 A70-40403

Plane horizontal fluid film convective stability with free boundaries in vertical circular cylinder for periodic modulation of vertical temperature gradient or gravitational field

21 p3941 A70-40608

Ionospheric conductivity effects on plasma convective flow in determining magnetospheric electric fields distribution

21 p3816 A70-41084

Cellular convection in fluid layers with parabolic temperature distribution, calculating stability effects of gravity and surface tension gradients

21 p3952 A70-42078

Supersonic convective electric arcs with magnetic stabilization in sulfur hexafluoride, examining aerodynamic drag and plasma column slanting

23 p4227 A70-44554

Stellar rotation angular momentum loss in premain sequence convective phase, discussing polytropic structure, formation time and velocity changes

23 p4249 A70-44809

Solar chromosphere model convective instability, considering temperature and magnetic field effects

24 p4399 A70-45303

Flame propagation limits and damping mechanism in gases under convection, determining boundary and initial conditions

24 p4428 A70-45492

Shock wave structure calculation in liquids containing gas bubbles, taking into account compression wave steepening by convection

24 p4326 A70-45783

CONVECTIVE HEAT TRANSFER

Heat transfer in tube flow with forced convection, internal radiation exchange, axial wall heat conduction and arbitrary wall heat generation

01 p0214 A70-10294

Horizontal and vertical sound fields local effects on natural convection from heated horizontal circular cylinder, using shadowgraphy

01 p0219 A70-11198

Jovian atmosphere convective energy magnitude determination for various atmospheric thicknesses and temperature gradients

02 p0375 A70-12432

Radiative, conductive and convective combined heat transfer mechanism in nonisothermal atomic hydrogen plasma laminar flow

02 p0400 A70-12660

Transient heat transfer in forced convection flow over curved wall with zero Prandtl number, applying to laminar boundary layer with variable free stream velocity

02 p0400 A70-12857

Pseudoboiling heat transfer from platinum wire to carbon dioxide during free convection

03 p0604 A70-13209

Boundary layer approximation for natural convection in flat vertical symmetrically heated channel with stabilized laminar flow for local and mean Nusselt numbers

03 p0605 A70-13395

Internally air cooled turbine blades and vanes emphasizing coolant aerodynamics, heat transfer and blade life, high temperature in jet engines, etc [RAES PAPER 22]

03 p0551 A70-13545

Convective nongray stellar atmospheres construction for stellar stability studies, accounting for convective flow nonlocality and nongray radiative transfer

04 p0745 A70-14472

Radiation-convection interaction in plasma free jet, using two-thermal-domain model for enthalpy distribution determination

[ASME PAPER 69-WA/HT-50] 04 p0781 A70-14798

Convective heat transfer rates measured on cooled sharp leading edge flat plates at various angles of attack in hypersonic merged flow

[ASME PAPER 69-WA/HT-21] 04 p0614 A70-14813

Instantaneous heat transfer from oscillating wire in free convection in still air as function of time

[ASME PAPER 69-WA/HT-15] 04 p0783 A70-14819

Mechanical vibration effects on natural convective heat transfer in enclosure of rectangular cross section

[ASME PAPER 69-WA/HT-13] 04 p0783 A70-14820

Heat exchangers efficiency taking into account surface, weight and cost

05 p0958 A70-16551

Convective heat and mass transfer augmentation techniques including surface and displaced promoters, vortex flows, etc

06 p1174 A70-17681

Natural convection heat transfer from vertical plate immersed in thermally stratified fluid

06 p1175 A70-17685

Convective and radiative heat fluxes measurement on charring ablative materials surface in rocket nozzle environment

06 p1070 A70-18444

Natural convection flow interactions from individual surfaces in closely spaced array of heated elements, discussing effect on heat transfer, induced flow and temperature field

07 p1418 A70-18644

Ablative materials for thermal protection at low convective heating rates, comparing foam and state-of-art materials performance

07 p1316 A70-18927

Laminar flow forced convection heat transfer in circular pipe entrance region for constant wall temperature and constant wall heat flux

07 p1420 A70-19215

Convective and radiative heat transfer properties of two dimensional circular fin

07 p1421 A70-19316

Perturbation solution for fins taking into consideration interaction of conduction with radiation and convection

07 p1422 A70-19333

Penetrative thermal convection stability for statically unstable layer surmounted by statically stable layer from numerical integration of linearized equations of motion and heat conduction

07 p1269 A70-19947

Natural convection heat transfer from horizontal finned circular cylinder noting effect of distance between fins

07 p1425 A70-20169

Thermal entrance region effect on Nusselt number determination in asymmetrically heated rectangular duct with uniform heat flux

07 p1425 A70-20223

Monograph on convective heat flow in stagnation points of turbulent partly premixed free jet flames at cooled plates

08 p1598 A70-21343

Forced convection heat transfer between two parallel plates analyzed numerically for effect of constant heat transfer coefficient boundary condition

08 p1598 A70-21425

Two dimensional natural convection boundary layer on finite isothermal horizontal plate, examining upward facing cold plate and downward facing hot plate

08 p1598 A70-21580

External convective heat transfer coefficients from quartz-coated cylindrical hot film anemometer probes in mercury

08 p1599 A70-21582

Natural heat convection measurements in vertical annular spaces, noting importance of local density and velocity product

08 p1433 A70-21671

Counterrotating vertical vortices produced by corona discharge on heated flat plate under free convection conditions

08 p1599 A70-21828

Natural heat convection in vertical annular space taking into account variations of volumetric mass, viscosity and thermal conductivity of air with temperature

09 p1786 A70-22047

Vertical heat transfer in silicone oil by single row convection cells, correlating cell number to transport rate and Rayleigh number

09 p1612 A70-22052

Heat transfer coefficient to gas in tube under unsteady heat flow conditions, studying Nusselt number dependence on Reynolds and Prandtl numbers

09 p1787 A70-22173

Slender body approximation for shape determination of nonslender hypersonic body of revolution with minimum convective heat transfer rate

09 p1788 A70-22931

Rectangular fins arrangement on horizontal surfaces for optimum free convection heat transfer coefficient, considering fin weight, height and spacing effects [ASME PAPER 69-HT-44]

09 p1789 A70-23551

Local Nusselt numbers beyond abrupt circular channel expansion tested for Reynolds numbers with air as working fluid

09 p1790 A70-23554

Liquid phase convective heat transfer as rate controlling mechanism for flame propagation, analyzing surface tension driven liquid flow induced by temperature profile

10 p1929 A70-24091

Turbulent gas nonresonant pressure pulsations effects on local convective heat transfer in tube flow

10 p1968 A70-24288

Convective-radiative heating of multilayer plate approximating temperature field by iteration

10 p1969 A70-25143

Heat transport by internal convection through He 2 in two fluid hydrodynamics model noting roles of thermal flux, superfluid component vorticity, normal component turbulence, etc

12 p2329 A70-27022

High temperature, electrically heated convective gas heating system for high velocity atmospheric flight simulation using air-nitrogen working fluids

12 p2205 A70-27100

Growth rate and spatial distribution of solid deposit freezing onto vertical surface in presence of convective heat transfer at moving phase interface

12 p2331 A70-27696

Corona-induced thermal boundary layer breakup effects on convective heat transfer from wire electrode to surrounding gas

12 p2333 A70-28110

Transverse flow convective instability spectrum in vertical channel with porous walls, noting Peclet number effects

12 p2333 A70-28199

Surface emissivity effects on combined conduction, convection and radiation heat transfer in nonisothermal hydrogen plasma, discussing optically thin and thick solutions

13 p2521 A70-29134

Solar thermal convection model, examining effects of rotation about vertical axis

13 p2496 A70-29839

Transient free convection flow due to arbitrary motion of vertical plate, linearizing equations of boundary layer flow and heat transfer

13 p2523 A70-30009

Laminar or turbulent flow in parallel plate channels with combined forced convective and radiative heat transfer, determining gas temperature field and Nusselt numbers

14 p2663 A70-30253

Convective heat transfer from rotating Al spheres in air at rest, investigating structure and boundary layer changes by schlieren method

14 p2665 A70-30398

Overstable convection formation of semiconvective zones in massive stars, noting Schwarzschild and Harm models

14 p2652 A70-31386

Free convection and heat transfer in square region bounded by solid impermeable walls heated from above, using two dimensional model

15 p2824 A70-31492

Convective heat transfer in Cu spherical shell and plate in supersonic rarefied gas flow at zero angle of attack from wind tunnel experiments

15 p2824 A70-31497

Laminar natural convective heat transfer along outer surface of vertical cylinder, giving coefficients nondimensionally by approximate formulas

15 p2826 A70-31821

Thermal boundary layer and heat and mass transfer at porous horizontal heated surface in presence of free convection, considering blowing and suction effects

15 p2827 A70-32133

Mixed forced and natural convection with low speed air flow over horizontal electrically heated cylinders

15 p2740 A70-32373

ATC-S satellite rocket exhaust plume convective heating measurements of VHF whip antennas, discussing nozzle flow and heating rate

[AIAA PAPER 70-843]

16 p3000 A70-33926

Convective heat transfer at solid boundaries in separated and reattached subsonic and supersonic flows, considering booster base heating

17 p3007 A70-34484

Forced convective heat transfer in annular passage with axially varying cross section, noting role of acceleration parameter

17 p3195 A70-34999

Natural convection heat transfer from vertical cylinder outer surface to liquids, discussing apparatus design and measurements

17 p3197 A70-35540

Free convection in compressible viscous heat conducting fluid, determining parameters leading to onset

17 p3198 A70-35697

Unsteady convective heat transfer in pipes in presence of heat flux density and flow rate aperiodic variations

17 p3198 A70-35730

Multiplying factors role in iterative solution of shock wave structures with large radiation-convection ratios

17 p3075 A70-35888

Aircraft electronic equipment cooling techniques, discussing natural and forced convection, phase change and heat pipes

18 p2322 A70-36763

Book on heat transfer covering conduction, convection, thermal radiation and heat exchange equipment

19 p3550 A70-37231

High temperature convective heat transfer in vortex chamber as function of Reynolds number and geometry, measuring pressure variations

19 p3552 A70-38186

Venus atmosphere heat transfer processes from Venera 4, 5 and 6 probes data, evaluating radiative and convective motions model

19 p3520 A70-38256

Book on variational principles in heat transfer covering conduction, convection, dissipation, thermal potential and force boundary layer problem and Lagrangian analysis

20 p3735 A70-39224

Integral transforms applied to convective heat transfer during nonNewtonian fluid flow with power rheology in pipes and channels

20 p3613 A70-40177

Laminar flow of liquid in duct with zero heat resistance of walls, calculating temperature distribution during radiative convective heating

20 p3613 A70-40297

Transient and steady state free convection heat transfer with mercury in vertical rectangular channel, measuring temperature distributions

21 p3941 A70-40773

Convective and radiative heat flux measurement incident on ablative surface in solid rocket nozzles

21 p3824 A70-40858

Forced convection heat transfer from flat plate and cylinder in cross flow to simulated Mars atmosphere

21 p3945 A70-41026

Transport model for flow field and convective heat transport in planar turbulent supersonic base flow

21 p3744 A70-41030

Free and forced convection of supercritical carbon dioxide normal to heated cylinder at constant temperature, measuring heat transfer rates

21 p3945 A70-41034

Freezing and melting of warm water flow at stagnation point over cooled plate for convective condition at solid-liquid interface

21 p3949 A70-41311

Unsteady convective heat transfer and hydrodynamics of laminar and turbulent channel flows

21 p3808 A70-41374

Mass flow rate correlation for nonsteady convective heat transfer in thin walled tubes with turbulent air flow

21 p3953 A70-42087

Heat transfer measurement from Pt wire to carbon dioxide near critical pressure, discussing film boiling and free convection flows

21 p3953 A70-42167

Dynamic nonstationary thermal convection in closed region with heat input from lateral surface for high Rayleigh and Fourier numbers

21 p3954 A70-42214

Nonstationary axisymmetric thermal convection in spherical cavity with boundary heat flux proportional to temperature, using difference scheme and networks method

21 p3954 A70-42215

Natural convection film boiling heat transfer literature, data sources for specific substances, photographic studies, mathematical models, etc

22 p4121 A70-42305

Buoyancy effects on transient free convection heat transfer in revolving tube for zero to 100 g centrifugal acceleration

22 p4122 A70-42437

Convective heat transport role in determining rotating planets climatic temperature zones

22 p4099 A70-42626

Nonaxisymmetric convection of rotating spherical shell in Herring approximation, noting applicability to sun

22 p4104 A70-42994

Gas turbine combustion chamber convective and radiant heat transmission, examining steam film cooling of flame tube

22 p4092 A70-43199

Spherical multilayer shell unsteady temperature fields, assuming mixed convective and radiative transfer at inner surface due to hot gas flow

23 p4276 A70-44165

Heat transfer by laminar forced convection of viscous fluid in noncircular cylindrical channel with internal heat source and varying wall temperature

23 p4276 A70-44236

Jupiter model thermal profiles, examining metallic core and molecular envelope in convective equilibrium

23 p4241 A70-44251

Forced convection heat transfer to liquid nitrogen near critical point, determining coefficients from given wall temperature and heat flux

23 p4279 A70-44358

Aerodynamic drag and local convective heat transfer on smooth plate for various flow velocities, determining effects of turbulator in boundary layer transition region

23 p4283 A70-44733

Rotating spherical shell equations as initial value problem, noting maximum convective heat transport at equator

23 p4249 A70-44805

Heat flux exchange by natural convection along flat vertical isothermal plate in laminar, transition and turbulent flows, using fluxmeters

24 p4429 A70-46207

CONVERGENCE

Rayleigh method convergence for linear development of perturbations in unsteady plane parallel flow of ideal fluid, formulating and proving theorem

01 p0664 A70-11032

Iterative computational procedure for generalized quadratic programming problem, formulating convergence theorem

03 p0460 A70-14165

Convergence of eigenvalues and eigenvectors in torsional vibration problems of continuous systems via improved matrix displacement analysis using points of freedom in segments

05 p0939 A70-16502

Algorithm for constrained optimization problems providing rapid convergence

05 p0877 A70-16714

Integral equations for interpolation process remainder estimation, including convergence of functions interpolation and error analysis

05 p0877 A70-16970

Eigenvalue solutions convergence rates using two finite plate multidegrees of freedom bending elements

06 p1169 A70-17941

Iterative solution of nonlinear optimal control delineated for sufficient conditions for convergence

06 p1027 A70-18507

Indirect methods of trajectory optimization, improving convergence through normalization of state data and Lagrange multipliers

07 p1326 A70-19726

Radiation detector geometrical factor approximation for cylindrical bodies, observing convergence for right square and circular cylinders

07 p1286 A70-19971

Boundary value problem for self conjugate elliptical fourth order differential equation with variable coefficients, proving convergence of iterative process

07 p1328 A70-20143

Turbulent wake behind plate due to confluence of two incompressible fluids with different densities

07 p1261 A70-20463

Convergence role in distance perception during aircraft landing, testing subjects with normal binocular vision, emmetropic refraction and visual acuity

08 p1450 A70-20744

Difference schemes approximating quasi-linear heat conduction equation, demonstrating convergence

08 p1596 A70-20857

Differential descent convergence demonstration based on relation between convex and Liapunov functions

08 p1534 A70-21007

Conjugate direction procedures for function minimization compared for convergence, recommending modified conjugate gradient procedure

08 p1535 A70-21875

Nonorthotropic pinched plates deflections solution, demonstrating asymptotic convergence of small parameter method

09 p1769 A70-22151

Interval of values with stability and convergence for correctors for differential equations

09 p1641 A70-22286

Iterative technique for determining zero of differentiable function

09 p1641 A70-22287

Elastoplastic problems incremental solution by iterative method, demonstrating convergence

09 p1771 A70-22394

Multipoint methods for two point boundary value problems with Banach space self mapped, proving convergence theorems for iterative solutions

09 p1712 A70-23420

Soviet monograph on accelerated convergence method in nonlinear mechanics, discussing quasi-periodic differential equations solutions, smoothing techniques, etc

09 p1729 A70-23726

Power series solution convergence of differential equations system, changing independent variable by conformal mapping

10 p1909 A70-24181

Error analysis and monotone convergence of finite difference approximations to linear one dimensional singular boundary value problems

10 p1909 A70-24406

Analytical aerial triangulation iterative solution mathematical convergence parameters tests, considering photogrammetric relations for standard conditions in variable size block

10 p1878 A70-24729

Dynamic programming successive approximations optimization technique involving system state variables reduction with convergence proofs

10 p1845 A70-24871

Rayleigh method convergence for linear development of perturbations in unsteady plane parallel flow of ideal fluid, formulating and proving theorem

10 p1871 A70-25001

Bessel generalized polynomial series convergence and summability on contour of convergence region

11 p2071 A70-25521

Finite element method solutions for plate bending, improving convergence based on error analysis

11 p2144 A70-26676

Nonlinear equations systems iterative solution convergence by extending classical algorithm with optimization process

11 p2074 A70-26850

Markov renewal processes sums convergence to multidimensional Poisson process, discussing convergence conditions

12 p2260 A70-26884

Differential equations perturbed linear systems convergence, extending Bridgland results

12 p2260 A70-27011

Circular arch finite element solutions compared for convergence rates

12 p2327 A70-27838

Elliptic equations solved by projection network methods noting estimate derivation for convergence rates

13 p2440 A70-28962

Finite difference methods for approximating first order nonlinear hyperbolic differential equations, considering convergence

13 p2441 A70-29098

- Maximum convergence function in image recognition using dynamic programming and sequential optimization 14 p2553 A70-30419
- Differential equations eigenvalue and boundary value problem finite difference approximation convergence under consistency and stability conditions 14 p2599 A70-30643
- Convergence corrections for absorption coefficient measurements by far IR Michelson interferometer 14 p2586 A70-30988
- Fourth order differential equations eigenfunctions construction and convergence of expansions in theory of flexure of sector plates 14 p2658 A70-30997
- Sufficient conditions for convergence of infinite determinant 15 p2766 A70-31448
- Series expansions convergence of solutions to boundary value problem for Navier-Stokes equations, introducing small parameter in boundary conditions 16 p2890 A70-33243
- Limit theorems for sums of multidimensional stochastic step processes, giving necessary and sufficient conditions for convergence to Poisson measures 16 p2942 A70-33700
- Learning scheme with probabilistic teacher for unclassified samples, establishing convergence, comparing with linear estimator 17 p3128 A70-34851
- Convergent spherical rarefaction wave asymptotic behavior 17 p3075 A70-35892
- Boundary value problem for Navier-Stokes equations of viscous incompressible fluid flow, discussing convergence of iterative solution 18 p3241 A70-36290
- Finite element procedure convergence for third order boundary value problems solution 18 p3283 A70-36493
- Quadratures asymptotic properties and convergence for continuous functions and function with singularity 19 p3456 A70-37415
- Turbulent wake behind plate due to confluence of two incompressible fluids with different densities 20 p3557 A70-39263
- Filonenko-Borodich and Papkovitch methods convergence proof based on completeness of cosine binomials system in energy space 20 p3721 A70-39736
- Base function selection for energy calculation optimal convergence conditions of frequencies and stresses in turbomachine blades vibrations 20 p3722 A70-39784
- Linear reinforcement learning technique for accelerating convergence of successive approximation algorithms 22 p3994 A70-43491
- Iterative method for boundary value problems in mathematical physics, showing convergence by heat conduction equation solutions 23 p4276 A70-44218
- ### CONVERGENT NOZZLES
- Swirling flow equations in converging nozzles, comparing analytical and experimental data 03 p0405 A70-12929
- Laminarization parameter magnitude determination for turbulent boundary layer in convergent channel flow 08 p1484 A70-21518
- Aerodynamic and acoustic characteristics of subsonic and supersonic jets from convergent nozzles with room temperature air supply 17 p3005 A70-34460
- Conical convergent nozzles discharge coefficient for varying pressure ratios 19 p3352 A70-38243
- ### CONVERGENT-DIVERGENT NOZZLES
- Air flow density measurements with interferometer in supersonic square Laval nozzle, showing flow core motion and wave structure 01 p0064 A70-11000
- Numerical integration of differential equations governing one dimensional flow of reactive gas, discussing flows of converging-diverging nozzle and normal shock waves 04 p0671 A70-14992
- Supersonic nonequilibrium two phase flow in Laval nozzle from numerical solution of quasi-linear hyperbolic equations 04 p0617 A70-15229
- Solar wind as one dimensional flow analogous to Laval nozzle flow, discussing rotation and magnetic field effect on model with heat conduction 04 p0754 A70-15352
- De Laval nozzle behavior in vacuo, discussing flow rate parameters, viscosity and real gas effects, thermal effects, turbulent jet separation and reattachment, etc [AGARDOGRAPH-120] 08 p1434 A70-21932
- Convergent-divergent nozzle operation at low pressure ratios causing separation of internal flow, discussing stability and flow field 12 p2157 A70-28084
- Specific heat ratio and configuration effects on flow in subsonic, transonic and supersonic sections of Laval nozzle 12 p2159 A70-28233
- Inviscid thermally nonconducting gas unsteady and steady motions in Laval nozzle of known geometry, obtaining solutions for subsonic, transonic and supersonic regions 13 p2391 A70-29756
- Transonic flow in convergent and convergent-divergent conical nozzles with nonuniform inlet predicted by time dependent flow equations, discussing discharge and thrust coefficients [AIAA PAPER 70-635] 16 p2834 A70-33548
- Inviscid air nonequilibrium shock layer properties correlation based on plenum entropy, predicting composition of downstream converging-diverging nozzle expanding air flow 16 p2838 A70-33909
- Convergent-divergent nozzle flow under influence of friction drag, determining heat transfer rate as function of nozzle geometry 17 p3194 A70-34694
- Optimum nozzle geometry for minimum heat transfer to convergent-divergent nozzle wall from high enthalpy flow 17 p3196 A70-35238
- Real gas transonic flow transition through critical velocity in Laval nozzle, examining reasons for increment of viscosity and heat conduction effects 18 p3239 A70-36217
- Convergent-divergent nonequilibrium nozzle flow numerical solution by time dependent technique, investigating rapid vibrational nonequilibrium supersonic expansion of gas mixture with population inversion 20 p3609 A70-39655
- Liquid-gas separator design with reduced friction loss for MHD generators using two phase convergent-divergent nozzles 20 p3612 A70-40014
- Viscous gas flow through Laval nozzle, calculating velocity coefficient and pressure recovery in contracting and expanding parts 21 p3746 A70-41774
- Inviscid thermally nonconducting gas unsteady and steady motions in Laval nozzle of known geometry, obtaining solutions for subsonic, transonic and supersonic regions 21 p3811 A70-42074
- Wave drag due to swirling flow through convergent-divergent nozzle, deriving approximate solution for specified nozzle shape at various swirl ratios 23 p4179 A70-43971
- ### CONVERSION
- Electromagnetic to magnetostatic wave conversion loss reduction at L band by coiled transducer 16 p2913 A70-34038
- ### CONVERTAPLANES
- ### U/VSTOL AIRCRAFT
- ### CONVERTERS
- AC to DC converter design for transforming average AC values into DC voltage 08 p1438 A70-20601
- Linear signal converter analysis using topological method and coordinate transformation 08 p1480 A70-21231
- Exponential pulse time converter investigated for effect of supply voltage variations on duration of generated pulses 08 p1474 A70-21232
- Sensitivity distribution in working field of electro-optical converter tubes, noting use for photometric research 09 p1673 A70-22159
- Negative radix conversion results applied to logical design of serial converter 09 p1642 A70-22967
- Output and frequency limitations of functional converter using photopotentiometer with shaped resistor 09 p1682 A70-23358
- Fluidic curved-wall electropneumatic converter optimization, presenting steady state, step and pulse mode responses for various positions and lengths of resistive heaters 09 p1614 A70-23691
- Superposed converter magnetic field intensity normal component distribution as function of polar coordinate 13 p2348 A70-28659
- Transistorized voltage to pulse width converter based on constant current capacitor discharge 13 p2378 A70-29457
- Statistical output characteristics of harmonic cosine and sinusoidal inertialess phase periodic converters in two channel system with frequency multiplication 13 p2370 A70-29741
- Similarity theory in design of isofunctional electric converters, relating input-output criteria 14 p2533 A70-30374
- Thermal loads on semiconductors in solid state converters during short circuit and overload 15 p2709 A70-32205
- DC-to-DC converter design to supply different isolated voltages from single input 23 p4142 A70-43875
- ### CONVEXITY
- Singularities of solutions of partial differential equations, discussing smallest convex set in manifold with differential operator 19 p3457 A70-37680
- Convex programming solution using quadratic approximation method with objective function 23 p4211 A70-44027
- ### CONVOLUTION INTEGRALS
- Liapunov functionals for time delay systems generated by path integrals in state space in terms of convolution equations 06 p1094 A70-17953
- Convolution formulas for Cauchy and standard normal random variable distributions derived from geometry of circular symmetric distribution on plane 07 p1323 A70-18946
- Convolution equation for kinetic theory of EM field excitation in plasma waveguides 23 p4223 A70-43772
- ### CONVOLUTIONS [MATHEMATICS]
- ### U CONVOLUTION INTEGRALS
- ### COOLANTS
- ### NT ENGINE COOLANTS
- Spacecraft reentry trajectory optimization, considering minimum coolant weight requirement in internal cooling system 02 p0381 A70-12416
- Capillary boiling and heat transfer for coolant fluids, using motion photography and visual observations 23 p4277 A70-44320
- ### COOLERS
- Conical passive radiation coolers for quantum IR detectors on equatorial synchronous earth satellites, determining temperature excursions 16 p2915 A70-34314
- ### COOLING
- ### NT AIR COOLING
- ### NT EVAPORATIVE COOLING
- ### NT FILM COOLING
- ### NT LIQUID COOLING
- ### NT PRECOOLING
- ### NT QUENCHING [COOLING]
- ### NT RADIANT COOLING
- ### NT REGENERATIVE COOLING
- ### NT SODIUM COOLING
- ### NT SUPERCOOLING
- ### NT SURFACE COOLING
- ### NT SWEAT COOLING
- ### NT THERMOELECTRIC COOLING
- Thermomechanical processing of high strength low alloy steels to evaluate effects of composition, cooling temperature and cooling rate on mechanical properties and microstructures 01 p0118 A70-10726
- Artificial hypobiosis state maintenance in animals exposed to cooling after administering lytic mixtures for suppressing oxidation 01 p0029 A70-11464
- Martensite transformation with fcc lattice in Ti alloys containing 5.9 percent Fe as function of cooling rate, using X ray analysis 01 p0124 A70-11590
- Microelectronics equipment high density packaging and heat dissipation, discussing full utilization of high speed 02 p0271 A70-12847
- Widmanstatten structure in iron meteorites relationship to cooling rate and meteoritic origin 04 p0751 A70-15039
- Niobium addition effect on alpha-gamma transformation temperature during continuous cooling of low carbon Ni-Cu steel 04 p0706 A70-15134
- Ablative cooling mechanisms and applications, discussing environmental effects on material performance, pyrolyzed and graphitized plastics, phenolic ablators, etc 05 p0856 A70-16617
- Thermal interaction between casting and mold at beginning of cooling using mathematical model for temperature field 08 p1506 A70-21139
- Olivine and metal compositions of pallastite meteorites by electron microprobe measurements, obtaining cooling rates 12 p2296 A70-26895
- Iron and stony iron meteorite cooling rates and thermal models, showing melting, radioactive heat source redistribution and surface heating effects 13 p2497 A70-29861
- End support cooling in hot-wire anemometry of low density high temperature flows [AIAA PAPER 70-589] 13 p2412 A70-29882
- Alloying elements and austenization conditions effects on hardenability of steels, investigating critical cooling rates based on TTT diagrams 15 p2744 A70-31929
- S-IVB liquid rocket engine and propellant feed systems restart shutdown in orbital operations [AIAA PAPER 70-672] 16 p2967 A70-33574

- Cooling rate effect on beta phase transformation temperature in Ti-Nb and Ti-Al alloys
17 p3118 A70-34406
- Ti binary alloys beta phase continuous cooling transformation, investigating additives effects
17 p3118 A70-34408
- Repeated snow cooling effect on heat transfer in white rats during temperature homeostasis recovery after hypothermia
18 p3220 A70-36544
- Aircraft electronic equipment cooling techniques, discussing natural and forced convection, phase change and heat pipes
18 p3232 A70-36763
- Brayton cycles in gas turbines, investigating inter-cooling or reheat and pressure ratio proportioning influence on efficiency and specific work
[ASME PAPER 70-GT-130] 18 p3304 A70-36856
- Cooling rate effect on Al-Mg equilibrium state during heat treatment after annealing
20 p3644 A70-38959
- Portable contingency transfer life support system for crewman of Apollo missions providing oxygen and cooling
20 p3580 A70-39441
- Fusion welding cooling rates, peak temperatures and heating duration relationships to distance from fusion line predicted by theory for comparison with experiment
21 p3832 A70-40791
- Cryogenic cooling of IR radiation sensors for increasing sensitivity, considering background radiation interference from sensor optical system and detector/preamplifier noise
21 p3825 A70-41052
- Scintillator-film neutron radiography converter combinations efficiency gain for small sources by cooling
24 p4376 A70-45751
- COOLING FINNS**
Length calculation method for nonadiabatic imaginary tip extension of heat exchanger fins, predicting heat conduction rate
01 p0215 A70-10842
- Convective and radiative heat transfer properties of two dimensional circular fin
07 p1421 A70-19316
- Perturbation solution for fins taking into consideration interaction of conduction with radiation and convection
07 p1422 A70-19333
- Natural convection heat transfer from horizontal finned circular cylinder noting effect of distance between fins
07 p1425 A70-20169
- Rectangular fins arrangement on horizontal surfaces for optimum free convection heat transfer coefficient, considering fin weight, height and spacing effects
[ASME PAPER 69-HT-44] 09 p1789 A70-23551
- One dimensional numerical solution for steady state thermal behavior of trapezoidal profile annular fins transferring heat by conduction and radiation
[ASME PAPER 69-HT-6] 09 p1790 A70-23557
- Transient response of fin-tube space radiators sudden steady state operation halting and system cooling
09 p1790 A70-23564
- Increased heat transfer for thermal coupling by interleaving fins in space applications
13 p2519 A70-28522
- Counter current heat exchanger with spiral finned tubing and solid core
14 p2617 A70-31019
- Conical heat radiator system for cooling short cylinders
15 p2827 A70-32142
- Pin fin coldplate heat exchanger for cooling Apollo spacecraft electronic equipment, calculating forced convection heat transfer and fluid pressure drop
21 p3797 A70-41025
- Finned tube-sheet spacecraft radiator transient response for perturbations caused by power supply and heat sink temperature changes
22 p4123 A70-42519
- COOLING SYSTEMS**
Fatigue life of rocket nozzle coolant tubes under thermal cycling environmental conditions, considering design formulas for thermal buckling prediction
03 p0579 A70-12963
- Monograph on application of semicooled thermosiphon system to gas turbine blade cooling, covering heat transfer and temperature distribution analysis, etc
03 p0551 A70-12992
- Helium properties and utilization in NASA projects, discussing pressurization of fuel tanks cooling of superconducting magnets
04 p0720 A70-15633
- Exhaust gas ejectors for engine cooling, discussing ejector design, flow rates, fuel consumption, etc
06 p1129 A70-17144
- Transpiration and film cooling systems comparison for high speed flows with foreign gas injection effects
[AIAA PAPER 70-153] 06 p1179 A70-18073
- Heat pipes to cool electronic circuitry, discussing design and operation
09 p1786 A70-22015
- Lifting entry vehicle thermal protection system (TPS) material performance, analyzing metallic radiator and passive transpiration systems and rigid insulator
11 p2150 A70-26368
- Cooling system control system for astronaut thermal equilibrium and work output maximization during extravehicular space missions
13 p2357 A70-28526
- Energy balance in radiation detector cooling, analyzing refrigerator capacity and thermal load
13 p2412 A70-29870
- Current stability and coil tests of force cooled superconducting systems
14 p2617 A70-31017
- Heat transfer coefficient from circular cylinder subjected to uniform surface heat flux and cooled by ring of holes
14 p2667 A70-31427
- Heat pipes design for rocket engines cooling, discussing connections to space radiator and to heat rejection device and heat transfer capability
[AIAA PAPER 69-582] 15 p2791 A70-32517
- Nuclear rocket nozzle cooling passages, discussing heat transfer and friction correlations for single-phase hydrogen turbulent flow
[AIAA PAPER 70-661] 16 p2950 A70-33622
- Passive radiative coolers role in utilizing IR detector systems for low temperature spacecraft applications, describing staged radiator design, optimization and tests
[AIAA PAPER 70-854] 16 p2983 A70-33921
- Cryogenic attachment for cooling and tilting metal samples in electron microscope
18 p3259 A70-36474
- Diathermic heat exchange cooling systems, analyzing volume boiling in terms of separation into convective and radiative components
19 p3550 A70-37239
- Integrated Cryogenic Isotope Cooling Engine system (ICICLE) for spacecraft sensors refrigeration requirements
21 p3947 A70-41053
- Internally cooled turbine blade with longitudinal cooling channels, calculating temperature field by combined analytical and analog method
21 p3868 A70-41772
- Electrofluid dynamic cooling system for spacecraft environmental control, describing design and operating principles
22 p3965 A70-43142
- Stepwise heat removal for increased continuous combustion gas turbine engine cycle efficiency, deriving equations describing cycles
22 p4092 A70-43372
- Hypersonic airbreathers aerodynamic, structural and propulsive system interactions, discussing hydrogen fuel heat sink, airframe and engine cooling and airframe materials
[ICAS PAPER 70-16] 23 p4138 A70-44127
- High speed internal combustion engine mixed flow type liquid cooling system, deriving dynamic thermal characteristics from differential equations solution
24 p4393 A70-45502
- COOPERATION**
Cooperative differential game with cost functional minimized by each player, discussing problems with linear combinations of state variables final values
11 p2073 A70-26228
- Linear multiplayer differential games absolutely cooperative solution, discussing control variables assumption of interior values
20 p3660 A70-40383
- COORDINATE SYSTEMS**
U COORDINATES
COORDINATE TRANSFORMATIONS
Computerized method for processing photographic earth satellite observation results, transforming coordinates by nonconformal approximation of polynomial function
05 p0814 A70-16367
- Selenodetic investigations based on lunar photographs with background stars, converting equatorial coordinates to orbital using Cracovian formulas
08 p1564 A70-20560
- Linear signal converter analysis using topological method and coordinate transformation
08 p1480 A70-21231
- Satellite photograph equatorial coordinates dependence on magnitude of evaluated region, objective distortion and transformation methods
09 p1679 A70-23056
- Geographic coordinates of intersection points determined directly on sphere, noting reduction on ellipsoid and adjustment for surplus intersections
09 p1670 A70-23441
- Initial quaternion for Cartesian time varying transformation matrix based on self alignment method of inertial analytic platform
11 p2072 A70-26150
- Algorithms for transforming coordinates from photographic plate system to equatorial coordinates, noting applicability with unknown optical center position in plate system
11 p2007 A70-26188
- Heat conductivity equations transformation for Cartesian and cylindrical coordinates and various boundary conditions using static electrointegrator
15 p2827 A70-32172
- Selenodetic investigations based on lunar photographs with background stars, converting equatorial coordinates to orbital using Cracovian formulas
15 p2805 A70-32715
- Horizontal Situation Display /HSD/ map computer mechanization transforming earth location to X, Y coordinates for Lambert conformal projection
[AIAA PAPER 69-987] 22 p4068 A70-42710
- COORDINATES**
NT ASTRONOMICAL COORDINATES
NT CARTESIAN COORDINATES
NT GEOCENTRIC COORDINATES
NT GEODETIC COORDINATES
NT HYLLERAAS COORDINATES
NT INERTIAL COORDINATES
NT LAGRANGE COORDINATES
NT PLANETOCENTRIC COORDINATES
NT POLAR COORDINATES
Geometrical interpretation of motion of body about fixed point in Hess case based on Kharlamov kinematic equations, using special coordinates system
01 p0144 A70-11428
- Periodic motions and integral stability for systems with quasi-cyclic coordinates applied to current carrying conductor oscillations and linear case of Routh equations
01 p0212 A70-11573
- Satellite topocentric equatorial coordinates determination from photographic observations
02 p0363 A70-11773
- Dead zone initial disturbance of sensitive element dynamic coordinate in two rotor gyrocompass determined using method of averages
03 p0484 A70-13419
- R function method for solving plate bending problem by satisfying differential equations coordinates
04 p0767 A70-14489
- Difference equations and axial stress tensor component for turbomachinery in curvilinear coordinates systems
04 p0776 A70-15268
- Coordinates computation method using spherical harmonic expansion of geomagnetic field, discussing direct computations by perturbation method
05 p0837 A70-15820
- Stress functions in three dimensional nonaxisymmetric elastostatics problems in circular cylindrical coordinates, proving representation completeness for cylindrical bodies
05 p0932 A70-16172
- One dimensional unsteady heat conduction with variable boundary conditions solved by difference-differential method using rectangular and cylindrical coordinates
05 p0957 A70-16295
- Geomagnetic center position determined by coordinate system referred to dipole approximating geomagnetic field
06 p1057 A70-17844
- Hybrid coordinate formulation for flexible space vehicle attitude control system design
[AIAA PAPER 70-20] 06 p1158 A70-18180
- Sporadic E layer parameters spatial distribution, describing analytic planetary coordinate system
07 p1267 A70-19453
- Inertial navigation systems errors determined by geometric method, obtaining object coordinates
07 p1332 A70-20145
- Earth rotation coordinates, discussing system coupled to earth by fixing of axes to zeniths of selected observatories and equatorial plane orientation
08 p1565 A70-20563
- Phase coordinates conditional probability density statistical characteristics from continuous reception of random information, deriving differential equations
08 p1479 A70-20998
- Spectral densities of phase coordinates of nonlinear automatic systems in steady states at random disturbances determined by statistic linearization
08 p1480 A70-21016
- Moon rotational constants determination allowing for crater Moesting A coordinate errors
08 p1574 A70-21156
- Transient heat conduction and stationary temperature distribution calculation in curvilinear coordinates using finite element method
08 p1590 A70-21362
- Spherical coordinate intermediaries for calculating satellite orbits
09 p1760 A70-22914
- Televor principle for radial radio coordinates production in all frequency bands, discussing ring antenna feeds
09 p1722 A70-23033
- Satellites equatorial topocentric coordinates determination from photographic observations
09 p1763 A70-23328

Planar restricted three body problem in Thiele coordinates, developing recurrence formulas for coefficients in Taylor series expansions of solution 10 p1938 A70-24178

Three dimensional elasticity by Ritz method, using coordinate system orthonormalized in energy metric of operator to avoid precision loss 10 p1957 A70-24511

Photographic plate reduction method at Polish Academy of Sciences based on sufficient reference stars, correcting x and y coordinates 11 p2007 A70-26194

Automatic input data generation for finite element method using algorithm based on complex geometrical configurations topological classification in terms of natural coordinates [JPL-TR-32-1486] 11 p2144 A70-26678

Explorer 4 magnetic coordinates recalculation using spherical harmonic representation and modified B-L package 12 p2222 A70-27191

Coordinate function selection for boundary value problems solution by Galerkin method demonstrated for heat conduction equation of anisotropic parallelepiped with internal source 12 p2271 A70-27291

Optimization for control processes with first and higher order constraints on phase coordinates 12 p2205 A70-28195

Vinti potential with spheroidal coordinates for equations of motion in earth satellite orbit computation 13 p2486 A70-28503

Soviet book on theory and practice of maps application in aviation, covering coordinates for objects positions determination on ground error estimation, etc 13 p2448 A70-28725

Meteor observation station design and operation, describing calibration difficulties and reflecting points coordinates determination 14 p2583 A70-30331

Loran C coordinates bias function determination by regression analysis using observed time differences 14 p2615 A70-31195

Coordinate systems generation for optimal trajectories, considering Lagrange multiplier as motion constant 14 p2651 A70-31368

Numerical solution to Laplace equation in spherical coordinates with axial symmetry, using Dirichlet method to obtain difference equations 15 p2767 A70-31751

Diurnal vibrations damping in inertial navigation system, demonstrating equations asymptotic stability for coordinates autonomous determination 15 p2775 A70-32156

Earth rotation coordinates, discussing system coupled to earth by fixing of axes to zeniths of selected observatories and equatorial plane orientation 15 p2805 A70-32718

Plasma velocity and moment equations in magnetic dipole field as function of variations along coordinate directions 16 p2956 A70-32934

Modified discrete ordinate approach in rarefied gas dynamics tested on linearized Couette flow between concentric cylinders, using integral iteration 17 p3067 A70-34548

Constraint optimization in state coordinates by variable structure system flexibility, using mathematical model 18 p3281 A70-36353

General relativistic equations for stationary axially symmetric rotating perfect fluid in comoving coordinate system 18 p3292 A70-36900

Sporadic E layer parameters spatial distribution, describing analytic planetary coordinate system 18 p3249 A70-36927

Cylindrical body with gravitational and magnetic anomalies, selecting point coordinates for body parameters 19 p3407 A70-37298

Coordinates for diagonalizing kinetic energy of particle system relative motion, discussing potential energy surface 19 p3373 A70-37841

Coordinate sequences for regions with complex geometries and various boundary conditions, using linear operators 19 p3460 A70-38940

Computer program transforming spherical harmonic coefficients into arbitrarily tilted coordinate systems, tabulating coefficients of International Geomagnetic Reference Field 1965 in dipole coordinate system 20 p3621 A70-39353

Entropy layer in hypersonic flows, determining body configuration from shock wave shape described by coordinates power function 21 p3743 A70-40610

Optimal control of coordinate space cells inspection order during search for unknown number of objects 22 p3999 A70-42552

Output coordinates probability distribution density of nonlinear automatic control systems at fixed time, using multiple integrals 22 p4003 A70-42888

Horizontal passpoint error in block analytic aerotriangulations with dense perimeter ground control 22 p4031 A70-42964

Systematic approach to construction of finite elements, discussing choice of generalized coordinates useful in problems involving singularities 22 p4116 A70-43208

Optimization for control processes with first and higher order constraints on phase coordinates 22 p4004 A70-43320

Field control method for aerial photograph planar tying-in, applying to cartographic reference point coordinate determination in triangulation 24 p4334 A70-45499

COORDINATION

Motion coordination capacity of persons subjected to 40 days bed rest using dynamographic technique, discussing nature of slackening 03 p0425 A70-13896

Human motion coordination under acceleration followed by weightlessness during jet flights along Keplerian orbits, discussing initial disturbance and subsequent subsiding 03 p0425 A70-13897

Machinery for management of Sea Dart missile development using managerial concepts of planning, organizing, commanding, coordinating and controlling 08 p1601 A70-21036

Monograph on systematically disturbed sensorimotor coordination, studying various parameters effects on eye-hand system recoloration 09 p1618 A70-22529

Heterochronism of coordinated cophasal flexor and extensor movements during acrobatic leap in human subjects 12 p2168 A70-27344

Hand-eye coordination in altered gravitational fields, using mirror viewed target in reaching test 15 p2689 A70-31886

COPILOTS

U AIRCRAFT PILOTS

COPLANARITY

Three vector coplanarity equations for space geodetic triangulation grid, discussing role of satellite photographic observation 09 p1667 A70-22488

COPOLYMERIZATION

Graft copolymerization and chemiluminescence analysis of lipids complexes in animal and plant tissue homogenates exposed to gamma radiation 03 p0419 A70-13305

COPOLYMERS

Tuned resonant test for measuring damping characteristics of lead and asbestos filled epoxy-poly sulfide copolymer 08 p1527 A70-21336

Alternating copolymer of guanlylic and cytidylic residues synthesized in RNA polymerase-catalyzed reaction 09 p1630 A70-23274

Styrene-oxygen copolymer preparation methods, discussing burning rates for rocket solid propellants mixtures with ammonium perchlorate 11 p2100 A70-26146

Gas and environmental temperatures, flow rate and sample geometry effects on limiting oxygen index in acrylonitril-butadiene-styrene copolymer, polystyrene and polyester 13 p2439 A70-29261

COPPER

Epitaxial growth of Cu vapor deposited on W single crystal /110/ surface using low energy diffraction, Auger electron and work function techniques 03 p0538 A70-13100

Copper specimens stress-strain diagrams under cyclic loads of various amplitudes, noting three stage process plastic deformation 06 p1162 A70-17386

Thermal emittance of Cu measured in vacuum in spherical enclosure by calorimetric method to investigate oxidation effect [AIAA PAPER 70-66] 06 p1180 A70-18139

Plastic zone around propagating fatigue crack in Cu single crystals, using transmission electron microscopy and X ray topography 06 p1171 A70-18494

Microstrain characteristics of continuously reinforced W-Cu composites as function of volume fraction of fibers and prestrain, discussing dislocation friction stress 08 p1524 A70-21917

Oscillations of longitudinal magnetostriction in silver and copper single crystals at low temperature 11 p2098 A70-25619

Thermal conductivity of neutron irradiated copper at low temperature noting lattice defects 11 p2148 A70-25757

Stress-strain state effects on Cu and Ni tubular samples plasticity and strength using polarization-optical technique 12 p2323 A70-27341

Filamentary crystal growth associated with hyper-velocity microparticles impact upon Cu foil 13 p2513 A70-29264

Tungsten fiber reinforced copper based composite material, investigating moulding and sintering conditions effect on mechanical properties 19 p3450 A70-37454

Copper based cermets production by electrochemical deposition in lieu of powder metallurgy, discussing merits 19 p3450 A70-37455

Cu and Ag low alloying effect on Al single crystals elastic limits and first deformation stages 20 p3644 A70-38960

Silica marker motion in sintering of loose spherical copper powder aggregates 20 p3647 A70-39109

Tungsten wire reinforced copper matrix composite, determining fibers pull-out contribution to fracture work 20 p3651 A70-40047

Copper and Al polycrystalline single crystal substructure changes, examining high temperature, unsteady and diffusion creep 22 p4056 A70-43342

V and Cu emission spectrographic analyses in chondrite types, noting distribution patterns between groups based on meteorite chemical fractionation mechanisms 24 p4411 A70-45789

Cu and Ni doped n-p and p-n silicon solar cells, examining radiation damage and isochronal annealing properties 24 p4294 A70-45810

COPPER ALLOYS

NT BRASSES

NT BRONZES

NT MANGANIN [TRADEMARK]

Stress corrosion cracking in Cu-Al alloys shown dependent on alloy and Cu ion content, solution pH and stress level, discussing tarnish film formation role 01 p0119 A70-10734

Notch-bend strength of titanium, aluminum and copper base alloys, noting geometrical size effect [ASME PAPER 69-MET-D] 04 p0705 A70-14878

Cyclic creep curves plotted from expansion diagrams for steel, copper and brass under small numbers of cyclic compression tension loads 06 p1162 A70-17388

Aged Al-Cu alloys hardness test data normalized and correlated for interpretation in terms of physical metallurgy 08 p1525 A70-21967

Phase diagram of rapidly crystallized Al-Cu-Mn alloys, observing ternary solid solutions formation during high cooling rate of melt 09 p1709 A70-23786

Aluminum and aluminum-copper alloys dislocation damping at high strain rates using impact shear tests 10 p1903 A70-23983

Al-Si and Cu-Ti eutectic alloys showing good ohmic contacts to SiC 10 p1927 A70-23990

Copper alloy composite reinforced by unidirectional solidification of pseudobinary eutectic Cu-ZrCuSi, discussing mechanical properties and electrical conductivity 11 p2066 A70-25775

Cu-Fe-Ti ternary system via microscopic, X ray and thermal analyses, measuring microhardness, electrical resistivity and magnetometry 13 p2433 A70-28863

Specific heat measurements on disordered and ordered phases of Cu-Au alloys at low temperatures 14 p2626 A70-30497

Steel and copper alloys torsion-tension members under nonproportionate loads, predicting creep behavior [SESA PAPER 1615] 15 p2759 A70-32316

Martensite transformations and cellular phase separation in Ti-Cu alloys, using electron microscopy 17 p3119 A70-34412

Heat resistance of cast, forged and annealed Ti-Cu alloys, discussing forged alloys mechanical properties as function of chemical composition and temperature 19 p3449 A70-37273

Oxide dispersed Cu alloys preparation by surface oxidation of powders, considering structural stability and stress rupture properties 20 p3646 A70-39103

Grain boundary damping characteristics of Cu-Ni alloys solid solutions, discussing height, temperature and activation energy of solute peak 22 p4053 A70-42729

Light rare earth metals improving Mg alloys, Al alloys, Cu alloys and superalloys 22 p4057 A70-43575

Short range order and Fermi surface effects in copper-rich Cu-Al alloys single crystals from X ray scattering measurements 23 p4204 A70-43886

Al-Cu alloy unidirectional solidification, investigating interfacial transition from plane to cellular structure and segregation pattern 24 p4362 A70-46179

Cellular breakdown in binary Al-Cu alloys in unidirectional solidification, observing small pit stability on solid-liquid interface 24 p4362 A70-46180

COPPER CHLORIDES

CuCl single crystal refractive index measurement at room temperature using V-block refractometer 02 p0350 A70-12453

High energy density nonaqueous battery with lithium metal anodes, cupric chloride cathodes and organic aprotic solvent electrolyte [AIAA PAPER 70-530] 13 p2349 A70-29038

Cuprous chloride /CuCl/ as low-loss electro-optic material modulating 10.6 micron laser radiation 22 p4051 A70-43334

Formation and radiative recombination of free excitonic molecules in CuCl single crystals via Q switched ruby laser excitation 24 p4353 A70-45604

COPPER COMPOUNDS

NT COPPER CHLORIDES

NT COPPER OXIDES

NT COPPER SULFIDES

Copper chromite catalyst effects on sublimated ammonium perchlorate dissociation products, noting applications to solid propellants 03 p0544 A70-13923

Hydrous Cu-Ca silicate mineral /kinoite/ from Arizona occurring as single crystals and veinlets 24 p4329 A70-45459

COPPER OXIDES

Oxide layers on metal substrate noting emittance dependence on thickness in aluminum-aluminum oxide and Cu-CuO systems [ASME PAPER 69-WA/HT-4] 04 p0705 A70-14825

COPPER SULFIDES

Minority carrier diffusion lengths on sides of copper sulfide-cadmium sulfide heterojunctions measured by light microprobes 13 p2471 A70-29709

CdS conversion by cation exchange to single crystal CuS, examining phases structural relationship 19 p3486 A70-37766

Copper disulfide-cadmium sulfide thin film solar cell degradation under simulated low orbit conditions, investigating thermal stress 21 p3759 A70-41313

CORDITE

U COLLOIDAL PROPELLANTS

U DOUBLE BASE PROPELLANTS

CORE FLOW

Axissymmetric incompressible fluid flow aerodynamic properties in flat vortex chamber, studying core and boundary layer interactions and velocity fields 03 p0551 A70-13731

Core length of water jet from circular tube, considering wall roughness, tube diameter and water viscosity and surface tension 06 p1031 A70-17135

Viscous core of incompressible swirling flow through nozzle using momentum-integral equations [AIAA PAPER 70-51] 06 p1038 A70-18079

Turbulent friction in gas flow core determined on basis of maximum stability principle 07 p1253 A70-18719

Poloidal magnetic field effects on main sequence stars core convection 11 p2117 A70-26654

Turbulent boundary layer in axisymmetric channel having interactions with flow core, calculating flow characteristics and separation point 12 p2209 A70-27289

Vortex core diameters calculation methods for axisymmetric angular momentum flows 17 p3074 A70-35750

Turbulent boundary layer in axisymmetric channel having interactions with flow core, calculating flow characteristics and separation point 20 p3613 A70-40339

CORE SAMPLING

Apollo 11 lunar rocks, soil and core samples major, minor and trace elements abundance by radiochemical and instrumental activation analyses 21 p3910 A70-41614

Amino acid racemization as enantiomers in core sediment samples 21 p3781 A70-41896

CORES

NT EARTH CORE

NT HONEYCOMB CORES

NT MAGNETIC CORES

NT REACTOR CORES

Shear modulus of sandwich structure tubular core derived by virtual work principle and matrix approach, comparing results with honeycomb core [DGLR-69-64] 04 p0774 A70-15156

Jupiter conductive molten metallic hydrogen core of moderate temperature suggested from solids melting point temperature dependence on pressure 07 p1390 A70-20238

Pulsar formation mechanism, showing core collapse to neutron star state 15 p2806 A70-32773

Core flexibility effects on deformation of uniformly loaded clamped parallelogrammic sandwich panels using linear theory 17 p3185 A70-34920

Core-filled thin cylindrical shell under radial ring and band pressure loads, using Boussinesq-Neuber stress function and Flugge shell theory 19 p3543 A70-38247

Circular cylindrical shell with annular orthotropic elastic core, analyzing stress wave propagation under pressure pulse 21 p3938 A70-41740

CORIOLIS EFFECT

Hypothetical magnetic configurations in presence of Coriolis forces from convective cell hydromagnetic activity in solar plasma, considering dynamos with increasing magnetic field 01 p0173 A70-10133

Free convection to rotating central plate in synchronously rotating surroundings with and without consideration of Coriolis forces [AICHE PREPRINT 9] 01 p0216 A70-10968

Coriolis effects in spherical Einstein universe perturbed by rigid body rotation of shell with finite thickness 01 p0186 A70-11272

Rotating compressor vanes vibration frequencies and modes using shell theory, considering Coriolis forces and rotation rates effects 01 p0211 A70-11427

Elastic stability of Coriolis-coupled oscillations of thin rotating disk under influence of centrifugal forces 02 p0389 A70-12650

Adaptation to Coriolis accelerations associated adaptation schedule to with 1-rpm increments developed for preventing motion sickness in slow rotating environment 07 p1223 A70-19938

Hypothetical magnetic configurations in presence of Coriolis forces from convective cell hydromagnetic activity in solar plasma, considering dynamos with increasing magnetic field 08 p1576 A70-21409

Vestibulometric techniques for medical examination and pilot selection using Coriolis accelerations for instability prognosis 09 p1617 A70-22475

Alcoholic beverages effect on positional nystagmus and Coriolis acceleration 11 p1993 A70-26520

Mesoscale waves in jet stream flow within Coriolis force over rotating earth by amplitude functions and phase velocities asymptotic series representation 12 p2265 A70-28334

Coriolis illusions amelioration during space flight, noting cross coupling effects minimization by reflex vestibular stabilization of head 13 p2358 A70-29432

Pitch and Coriolis illusions effects on pilot pitch angle adjustment in simulated takeoff 15 p2689 A70-31885

Blind persons susceptibility to acute motion sickness during stressful Coriolis acceleration 15 p2689 A70-31887

Rotating cold plasma wave propagation modes including Coriolis effect in absence and presence of external magnetic field 21 p3860 A70-41924

Coriolis parameter effects on stream and pressure functions in geostrophic wind equation 22 p4065 A70-43167

Coriolis acceleration effect on inplane vibration resonant frequencies of rotating disks 24 p4425 A70-45780

Cornea UV radiation effects on mucopolysaccharide compounds in tears and on cornea epithelium of albino rabbits 01 p0037 A70-10860

Corneal epithelium chromosome rearrangements in gamma irradiated white adult mice, noting radiation dosage and duration 03 p0426 A70-13903

Corneal stroma transparency analysis based on refractive index and lattice theories 09 p1618 A70-22675

Corneal thermal response model for carbon dioxide laser radiation, computing temperature rise from power distribution and conducting air-cornea interface 11 p2062 A70-25635

Biochemical heterogeneity of corneal mucopolysaccharides [glycosaminoglycans], using extraction without proteolytic enzymes 24 p4304 A70-46344

CORNEA

CORNERS

Three dimensional viscous and inviscid hypersonic flow interaction at rectangular corner, measuring surface and Pitot pressures, heat transfer rates, shear stresses, and Pitot 04 p0620 A70-15533

Hypersonic corner flow in He investigated by heat transfer, surface pressure, pitot surveys, oil and electron beam flow measurements [AIAA PAPER 70-227] 06 p1039 A70-18110

CORONARY CIRCULATION

Flow equations for curvilinear boundary layer based on laminar incompressible boundary layer in stream-wise corner 13 p2386 A70-28541

High Reynolds number flow in moving corner, observing vortex motion at piston and cylinder wall interface by flow visualization techniques 16 p2895 A70-34240

Laminar hypersonic boundary layer interaction with corner expansion wave, presenting numerical solutions to viscous-inviscid equations for small turning angles [AIAA PAPER 70-807] 17 p3065 A70-34457

Incompressible laminar boundary layer along rectangular corner, obtaining similar solutions for velocity distribution 17 p0370 A70-35239

Subsonic and supersonic laminar boundary layers separation near sharp corners, considering curvature and Reynolds number effects 18 p3208 A70-36486

Viscous supersonic flow near sharp convex corner, discussing visual observation and quantitative surveys of velocity and pressure profiles 18 p3208 A70-36659

Radiant heat transfer at vertex of adjoined flat plates separated by vacuum 18 p3243 A70-36711

CORONA DISCHARGES

U ELECTRIC CORONA

CORONAGRAPHS

Ionized iron lines observations under coronal conditions, giving halfwidths and kinetic temperatures for forbidden lines Fe X-Fe XV 14 p2651 A70-31377

Solar catadioptric coronagraph design free from chromatic image defects 15 p2737 A70-32041

Solar limb photographic, isodensity and isothermal data for eclipse of 7 March 1970 from coronagraph observations, noting coronal green line and prominence activity 24 p4402 A70-45389

CORONARY CIRCULATION

Vascular anatomy correlation with human heart conduction tissue structures to study coronary artery disease cases exhibiting major conduction disturbances by ECG 01 p0013 A70-10273

Cardiac output and coronary blood flow during steady state hypoxia, considering room air and different oxygen concentration breathings 01 p0014 A70-10360

Coronary arteries collateral circulation in man using angiographic technique 01 p0016 A70-10439

Prospective epidemiological recognition of clinical coronary heart disease, discussing effects of habitual physical inactivity, excessive dietary fat, socioeconomic stresses, etc 01 p0023 A70-10865

External environmental factors, life habits and personality structure effects on development of coronary artery disease, discussing psychosomatic aspects of myocardial infarction 01 p0023 A70-10866

Perfusion pressure and flow effects on coronary resistance, noting venous blood perfusion 01 p0026 A70-11075

Nervous stress effect on coronary thrombosis, deriving mathematical theory based on biophysical and biochemical approaches 01 p0028 A70-11369

Dogs coronary vasodilator responses to hypoxia and induced tachycardia before and after lidoflazine and adenosine 02 p0230 A70-11702

Heart rate change effect on myocardial oxygen consumption and nutritional circulation with constant coronary blood flow suggesting oxygen extraction independence of capillary surface 02 p0235 A70-11991

Readers interpretation and applications of Starr criteria for ULF ballistocardiograms, showing uniformity for patients with coronary heart disease 02 p0248 A70-12680

Arrhythmia resembling atrial flutter simulated in dogs by coronary sinus and left atrial pacing and in man by coronary sinus pacing 02 p0240 A70-12696

Dogs left ventricle areas supplied by coronary arterial branches visualized utilizing scintillation photography and radioactive Xe 03 p0432 A70-12892

Physicochemical properties of hypothalamic secretions responsible for coronary dilatation in rats, cattle and pigs, using analytical techniques 03 p0417 A70-13215

Sinocarotid pressor reflexes effects on coronary circulation in anesthetized dogs noting changes in blood pressure, peripheral resistance and cavity pressure 03 p0422 A70-13693

Coronary thromboses age estimation based on comparison of blood cells, fibrin, collagenous tissue and neocapillaries quantitative changes

03 p0426 A70-13938

Postmortem coronary angiographies showing role of arterial hypertension in coronary pathology

03 p0426 A70-13939

Cardiac output and coronary blood flow changes in patients at rest and during peak exertion, stating correlation coefficients

03 p0428 A70-14065

Primary and secondary pathological changes in small coronary arteries and role in acute myocardial infarction development, discussing coronary arteries distribution

04 p0635 A70-15457

Platelet function in coronary artery disease and myocardial infarction, considering thrombosis, atherosclerosis, emboli in microcirculation, etc

04 p0635 A70-15458

Clinicopathological studies of coronary artery occlusion and acute myocardial infarction, discussing coronary thrombosis

04 p0635 A70-15459

Coronary atheroma in hyperlipemic dog occurring in arterial tree at most intense physical stress exposure point, discussing interfacial tissue permeation

04 p0635 A70-15460

Acute coronary occlusion effects on adjacent unoccluded artery resistance, discussing responsible mechanisms in ischemic heart

04 p0637 A70-15473

Glucagon infusion effect on human coronary circulation, relating changes in cardiac dynamics to myocardial oxygen consumption and blood flow

05 p0800 A70-16101

Cardiac work limiting factors during exercise under hypoxia, studying cardiac output and coronary blood flow capacities

06 p0991 A70-17282

Biochemical disturbances during early myocardial ischemia, examining coronary sinus lactate and K levels using electrocardiographic correlation

06 p0997 A70-18406

Perfusion pressure effect on myocardial oxygen consumption and coronary flow in stable nonworking rat heart

07 p1202 A70-18865

Physical activity and epidemiology of coronary heart disease

07 p1212 A70-19694

Exercise influence on cardiac output and coronary blood flow during hypoxia, correlating CO and systolic pressure with blood flow changes

07 p1214 A70-19928

Cardiac output and coronary blood flow during steady state recumbent exercise, discussing CO and Rb 84 measurements in human subjects

08 p1453 A70-21936

Conscious dogs temporary local hypoxia effect on coronary blood flow regulation

09 p1623 A70-23585

Left ventricular volumes, pressure and heart rate in patients and dogs after diagnostic coronary arteriography

10 p1820 A70-24939

Aerobic metabolism of heart muscle cells and oxygen utilization of coronary artery blood

10 p1821 A70-25081

Arteriographic determination of severe coronary artery disease in presence of normal resting electrocardiogram

12 p2170 A70-27775

Human circadian coronary circulatory rhythms during space flight weightlessness or bedrest with and without exercise

16 p2854 A70-33991

Left ventricular surface electrocardiogram T-wave amplitude and circumflex coronary artery blood flow during headward acceleration in unanesthetized dogs, observing velocity decrease

21 p3764 A70-41481

Cinecoronary arteriographic investigation of chest pain patients, establishing correlations of clinical symptoms, coronary artery narrowing, arterial lesions, serum cholesterol levels, etc

23 p4145 A70-43948

CORONAS

NT ELECTRIC CORONA

NT SOLAR CORONA

Solar radio types I and III sources spatial distribution of circular polarization and coronal magnetic field configurations in active regions

12 p2294 A70-27710

Corona point discharge current magnitude in transonic wind tunnel, giving current characteristics at different wind speeds

12 p2264 A70-28001

Galactic radio corona existence, measuring northern galactic hemisphere sky brightness and cosmic ray distributions

18 p3322 A70-37129

Stellar coronas X ray fluxes from models of convection zones and corresponding mechanical energy fluxes

21 p3875 A70-40681

Radioheliograph observations of coronal broadening of Crab Nebula at 80 MHz, noting radial scattering and plasma irregularities

21 p3891 A70-41184

CORPUSCULAR RADIATION

NT BETA PARTICLES

NT CYCLOTRON RADIATION

NT ELECTRON BEAMS

NT ELECTRON PRECIPITATION

NT ELECTRON RADIATION

NT ION CYCLOTRON RADIATION

NT PRIMARY COSMIC RAYS

NT SOLAR CORPUSCULAR RADIATION

NT SOLAR COSMIC RAYS

NT SOLAR PROTONS

Corpuscular radiation contributions to D layer ionization determined from intensity measurements

01 p0172 A70-11490

Positive ion concentration profiles in lower nighttime midlatitude ionosphere calculated from corpuscular radiation measurements and ion recombination constants

04 p0738 A70-14436

Solar proton latitude profiles relation to outer radiation zone electron measurements by Alouette 2 satellite charged particle detectors during quiet magnetic conditions

04 p0740 A70-15105

Hysteresis effect on cosmic ray modulation and gradient ionization near solar minimum from measurements made near earth with OGO 1 and 3 ion chambers

04 p0740 A70-15106

Fragmentary arc and band-shaped polar aurora configurations associated with corpuscular rays penetration into upper atmosphere

04 p0684 A70-15749

Magnetic disturbances and corpuscular intrusions in auroral zone, discussing daytime and nighttime magnetic activity of electron fluxes

04 p0684 A70-15752

Neutron flux measurements on Cosmos 53, equipment and calculation of secondary neutrons due to bombardment of satellite components

05 p0905 A70-17112

Corpuscular radiation as F region ionization source, solving time dependent ionospheric continuity equation

06 p1054 A70-17588

Corpuscular radiation distribution function with trapped particles maximum density fixed in equatorial plane and reflection points vicinity of magnetic force line

06 p1135 A70-17894

Atmospheric ground pressure seasonal changes after corpuscular flux arrival shown for Northern Hemisphere

08 p1487 A70-20554

Initial deceleration of solar wind positive ions upstream of earth bow shock determined from OGO 5 high time resolution plasma measurements

08 p1562 A70-21377

Photoelectrons entry into F region detected at conjugate point during winter night by Thomson scatter observations of plasma lines appearing in signal spectrum

08 p1489 A70-21386

Corpuscular radiation intensity measurements in upper atmosphere at midlatitudes by meteorological probe during geomagnetic storm, noting radio wave absorption

11 p2106 A70-26797

Solar flares of 6 and 8 July 1968 correlation regarding electromagnetic radiation emission, radio flux, corpuscular radiation, etc

12 p2294 A70-27708

Solar activity effects on midlatitude upper atmosphere corpuscular radiation intensity via rocket sounding

12 p2296 A70-28266

Positive ion concentration profiles in lower nighttime midlatitude ionosphere calculated from corpuscular radiation measurements and ion recombination constants

13 p2475 A70-28461

Low energy protons penetration into magnetosphere between forbidden regions, using model of constant electric field with charge exchange as loss mechanism

13 p2477 A70-29183

Wave properties of nuclear optical model for barrier penetration by charged particles, considering square well reflection, absorption and resonance

14 p2619 A70-30491

Fragmentary arc and band-shaped polar aurora configurations associated with corpuscular rays penetration into upper atmosphere

14 p2576 A70-30833

Magnetic disturbances and corpuscular intrusions in auroral zone, discussing daytime and nighttime magnetic activity of electron fluxes

14 p2576 A70-30836

Atmospheric ground pressure seasonal changes after corpuscular flux arrival shown for Northern Hemisphere

15 p2732 A70-32709

Solar protons penetration into magnetosphere and magnetotail

18 p3306 A70-36004

Particle flux diagnostics of nonisothermal low pressure plasma, using corpuscular passive method

19 p3476 A70-37556

Space corpuscular radiation simulation to obtain data for increased spacecraft life

19 p3511 A70-38284

Anomalous angular distribution and inelastic cross section of muon-nucleon interaction for penetrating underground cosmic ray particles

22 p4095 A70-43232

CORRECTION

NT OPTICAL CORRECTION PROCEDURE

Secondary halo in spark source mass spectroscopy, determining corrections

02 p0298 A70-12211

Mangler displacement thickness correction for slender cones

08 p1590 A70-21320

Interval of values with stability and convergence for correctors for differential equations

09 p1641 A70-22286

Width corrections in calculation of stress intensity factor for sheet with central crack in uniform uniaxial tension

13 p2510 A70-28608

CORRELATION

NT ANGULAR CORRELATION

NT AUTOCORRELATION

NT CORRELATION COEFFICIENTS

NT CORRELATION DETECTION

NT CROSS CORRELATION

NT DATA CORRELATION

NT SIGNAL ANALYSIS

NT STATISTICAL CORRELATION

Spherical earth wind field correlation matrix, relating scalar fields to isotropic vector field

01 p0135 A70-10204

Four dimensional optimal interpolation for maximum wind velocity components, calculating spatiotemporal correlation functions

01 p0135 A70-10205

Pulse methods for measuring correlation function of incoherent scattered signal, calculating bit estimator errors for large and small SNR

01 p0045 A70-11088

Forward scattering by nonergodic system of identical particles, relating temporal correlation function of scattered radiation and intensity moments

02 p0255 A70-11919

Correlation function estimate of random process represented by sum of steady distributed and independent arbitrary processes

03 p0518 A70-13081

Correlation function for spatial distribution of galaxies determined as function of inverse distance between galaxies

04 p0744 A70-14470

Measurement method for second and third order photon intensity correlation functions, using optical field produced by gas laser operating near oscillation threshold

04 p0700 A70-14686

Correlation function procedure applied to quartz clock rate analysis, noting operating temperature control

04 p0693 A70-15487

Gigacycle correlator involving sampling oscilloscopes for real time display of correlation functions over adjustable time interval, discussing design and performance

05 p0847 A70-16066

Statistical description of geomagnetic field as random vector field, presenting correlation functions from empirical estimates from geomagnetic charts

05 p0842 A70-16748

Dispersion and correlation function for atmospheric transparency due to water vapor, from statistical model of absorption bands and effective mass

06 p1053 A70-17204

Correlation function of velocity fields in two dimensional turbulence determined from hydrodynamic equation assuming normally distributed stream function field

07 p1252 A70-18673

Positive and negative correlations in F 2 layer perturbations by network of paired conjugate ionospheric stations at low latitude

07 p1277 A70-20450

Time-frequency correlation function for fading communication channel between transmitter and receiver sites, using AM transmissions as probing signals

08 p1458 A70-20796

- Correlation functions of spatially inhomogeneous fluctuations in electron gas in strong electric field
08 p1552 A70-21423
- Correlation functions of fluctuations in electrical characteristics of nonequilibrium electron gas during scattering, determining spectral densities and populations by kinetic equation Green function
08 p1554 A70-21806
- Correlation functions for resistance to heat and momentum transfer in viscous sublayer at rough walls defined for varied geometry flows
[ASME PAPER 69-HT-2] 08 p1486 A70-21833
- Correlation function of oscillation modulated in amplitude, phase and frequency by random processes causing spectral density maximum shift away from carrier frequency
09 p1633 A70-22409
- Inertialless nonlinear quadrupole output of oscillations modulated by normal noise, analyzing correlation functions
09 p1637 A70-23159
- Plasma, Coulomb fields and radiation correlations obtained by relativistic kinetic equations, noting bremsstrahlung, synchrotron, cyclotron radiation, radiative and particle diffusion, etc
09 p1736 A70-23182
- Ferromagnetic crystal weakly coupled spin Green and correlation functions calculated for wide temperature range
09 p1740 A70-23193
- Random process noncommutative transformations and correlation functions in linear form of time functions
09 p1655 A70-23695
- Correlation functions of nonlinear auto-oscillatory system under nonstationary conditions determined by statistic linearization
11 p2022 A70-25341
- Time correlation telemetering systems design, describing structural scheme
11 p2004 A70-25929
- Homogeneous turbulence multipoint multimode correlations for fluctuating velocity
11 p2036 A70-26014
- Spatial correlation effect of unsteady sectional loads in axial direction on average or apparent loads over finite region of circular cylinder immersed in moving fluid
11 p2036 A70-26148
- Multipoint time correlations of longitudinal velocity fluctuations in grid-generated turbulence
11 p2039 A70-26532
- Neutral-dominated plasma turbulence, discussing space-time plasma probe correlation functions for electron density fluctuations measurements
11 p2095 A70-26757
- Turbulent flowing plasma, analyzing wavenumber frequency dependent spectral function and space-time correlation function
11 p2096 A70-26768
- Output correlation function of nonlinearity-filter system and phase modulated oscillations influence on system
13 p2366 A70-29411
- Interferometric measurement of spatial correlation function of optical radiation fields propagating through turbulent atmosphere
13 p2454 A70-29825
- Laser beams intensity fluctuations dispersions and correlation functions at various distances
14 p2593 A70-30172
- Correlation characteristics of turbulent motions in atmospheric meteor region, discussing diversity and single point reception methods
14 p2572 A70-30329
- BBGKY hierarchy pair correlation function for magnetoplasma under weak external force, using operator method and time periodic ansatz for distribution functions
14 p2623 A70-30697
- Many body correlation and conditional probability functions of plasma shield clouds surrounding test particles
14 p2623 A70-31034
- Turbulent boundary layer correlations on flat plate, noting inadequate Spalding-Chi predictions
14 p2567 A70-31396
- Correlation function of velocity fields in two dimensional turbulence determined from hydrodynamic equation assuming normally distributed stream function field
15 p2718 A70-31465
- Homogeneous isotropic turbulence velocity field space-time variable correlation functions in fluid flow
15 p2719 A70-31487
- Centrifugal pump performance correlation parameter under cavitation conditions for handling different liquids based on bubble growth theory
15 p2720 A70-32098
- Materials real time strain measurements by optical correlation techniques, noting sensitivity
16 p2913 A70-33980
- Correlation functions of weak quasi-steady plasma turbulence determined by plasmon interactions, using computerized integral equation
17 p3139 A70-34643
- Ionospheric E region winds correlations to lower atmosphere meteorological phenomena
17 p3077 A70-34950
- High intensity noise enveloping space vehicle as distributed excitation, examining correlation effects on structural response
17 p3059 A70-35170
- Wave propagation measurement by correlation techniques, discussing travelling wave representation, delay times, amplitude coefficients, etc
17 p3091 A70-35449
- Time correlation functions approach to calculation of properties of nonequilibrium ensembles in fluid molecular motions
17 p3197 A70-35535
- Solar radio emission slowly varying component, analyzing random aspects, correlation functions and relationship to spot groups
19 p3521 A70-38552
- Correlation spectrometry for earth resources, considering sulfur dioxide, nitrogen oxide and iodine pollution
20 p3626 A70-39055
- CW second harmonic He-Ne laser light second order intensity correlation function measurements
20 p3640 A70-39153
- Kinetic equations derivation for correlation functions and time dependent distribution functions of irreversible processes, using projection operators
20 p3672 A70-39588
- Pair correlations effect in equilibrium and nonequilibrium theory, taking Coulomb collisions into account for ionized plasmas confined to half space by reflecting boundary
20 p3679 A70-39662
- Simulated neutral atmospheric boundary layer measurements in wind tunnel, extending power spectral and correlation determinations
20 p3613 A70-40139
- Multichannel correlation filter devices for processing periodic fluctuating signals in noise background
22 p3987 A70-42557
- Laser light scattering in plasma for charged particle correlation function
23 p4225 A70-44187
- CORRELATION COEFFICIENTS**
Ionization variations and correlation coefficients of F 2 critical frequency variations, using airborne ionospheric sounder over Sogra and Kerguelen Island conjugate areas
01 p0080 A70-11224
- Transverse and longitudinal correlation coefficients of electron density fluctuations in turbulent jet related through equation specifying velocity fluctuations isotropy
04 p0674 A70-15551
- Error correction for correlation coefficient between satellite data of earth radiation intensity and satellite vision field shift
05 p0841 A70-16729
- Random processes correlation coefficients and functions measured by quasi-compensator with potentiometer and digital/analog readout
12 p2235 A70-27770
- Mutual correlation coefficients for signal level changes during short wave space diversity reception and radio wave propagation over two midlatitude paths
14 p2546 A70-30145
- Erroneous height correlation coefficients in physical optics formulation of rough surface scatter
16 p2859 A70-32938
- Correlation distance of VHF fading from irregularities in equatorial ionosphere, using NASA STADAN in Chile
20 p3590 A70-40487
- Flow structure in plane submerged turbulent jet, determining velocity, friction stress and correlation coefficients distributions
21 p3749 A70-42221
- CORRELATION DETECTION**
High and medium whistler activity in Italy correlated with weather situation in South Africa
05 p0839 A70-16317
- Signal detection in correlated noise with two stage prewhitening and matched filter system
10 p1833 A70-24220
- FM demodulation threshold extension by correlation detection implemented in impulse noise cancellation system
19 p3382 A70-38893
- Synthetic aperture radar receivers, discussing cross-product term suppression in correlation detection for image distortion reduction
20 p3585 A70-39392
- Optico-acoustic autocorrelator for linear FM signals spatial compression, discussing design and performance
22 p3984 A70-42398
- Correlation detection methods providing information for ILS in terminal area congestion, discussing role in aircrew-ATC cooperation
22 p4068 A70-42667
- CORRELATION FUNCTIONS**
U CORRELATION
CORRELATORS
Gigacycle correlator involving sampling oscilloscopes for real time display of correlation functions over adjustable time interval, discussing design and performance
05 p0847 A70-16066
- Multichannel correlator for turbulent signal processing in real time scale using natural delay
07 p1284 A70-19832
- FM feedback demodulator performance model using mixer-correlator, showing cross correlation receiver design
08 p1479 A70-20810
- Microwave L-band correlator using YIG delay lines varied by electronically changing magnetic bias
20 p3597 A70-39468
- Electronic correlation signal analysis for localizing noise sources, detecting signals against background noise
20 p3601 A70-39650
- Statistical information processing equipment, describing correlators and digital coding devices design for graphic form information transformation into binary code
20 p3594 A70-39919
- Digital correlator errors due to quantization by levels, designing analyzer of slow processes
20 p3594 A70-39922
- Optico-acoustic autocorrelator for linear FM signals spatial compression, discussing design and performance
22 p3984 A70-42398
- Estimation errors of multilevel modified digital correlator using auxiliary random noise for unbiased output
24 p4312 A70-46054
- CORROSION**
NT CAVITATION CORROSION
NT ELECTROCHEMICAL CORROSION
NT FRETTING CORROSION
NT FUEL CORROSION
NT INTERGRANULAR CORROSION
NT SCALE [CORROSION]
NT STRESS CORROSION
Soviet collection of papers on metal science and corrosion problems covering welding, heat treatment, Cr-Mn steel, Ti alloys, etc
03 p0509 A70-13276
- Corrosion problems in Ti and alloys chemical and aerospace applications, describing thermodynamics and electrochemistry in aqueous media
04 p0710 A70-15677
- Contamination sources covering ball bearing contamination, relay contact failure, instrument window internal fogging, electronic circuit corrosion and air conditioning problems
05 p0809 A70-16712
- Metallic materials homogeneous and nonhomogeneous corrosion kinetics based on superposition principle of independent partial electrode reactions
09 p1707 A70-23422
- Metal corrosion product dissolution in reactor cooling deionized water, investigating Cu, W and Cd using chemical analyses
10 p1904 A70-24398
- Corrosive wear due to oxygen and/or moisture in air indicated as major failure mode in lubricated gears
10 p1895 A70-24852
- Corrosion by liquid metals - AIME Conference, Philadelphia, October 1969
16 p2932 A70-34201
- Metal corrosion effects in Rankine cycle lithium-boiling potassium test loop simulating working fluids of spacecraft nuclear turbopump propulsion system
16 p2933 A70-34204
- Corrosion failures diagnosis, describing visual, electron microscope, metallographic and chemical analysis techniques
20 p3650 A70-39968
- Surface degradation by oxidation, temperature fluctuations and hot corrosion of Ni- and Co-base superalloys in gas turbine engines
22 p4057 A70-43574
- 18-8 stainless steels pitting corrosion, examining grain boundaries influence
24 p4362 A70-46184
- CORROSION PREVENTION**
Corrosion induced fatigue damage suppression in jet engine compressor steel components, describing various surface treatment effects
01 p0165 A70-10699
- Concorde aircraft main landing gear reliability, discussing design, corrosion, hydraulic contamination, metallurgy, sealing and tests
02 p0226 A70-12366
- Emulsified jet fuels combustion characteristics evaluation by laboratory technique, presenting data on emulsifiers and corrosion inhibitors effect
[ASME PAPER 69-WA/GT-2] 04 p0785 A70-14893

Laboratory tests on jet fuels indicating lubricity improvement by corrosion inhibitor addition
[SAE PAPER 690667] 05 p0894 A70-15836

Heat resistant silicate enamel coatings to protect steels and alloys against high temperature gas corrosion, studying properties by various methods
05 p0872 A70-16600

Inhibitive elastomeric sealing compounds and coating systems preventing aluminum alloy corrosion in aircraft
13 p2433 A70-28778

Corrosion resistant paint systems for aircraft structural parts under severe environmental conditions simulated in carrier test stand
14 p2598 A70-31292

Chemical and electrochemical corrosion resisting primers for Mg surface coatings in machine parts
14 p2598 A70-31293

Spilled Hg removal from metal surfaces, describing brush technique based on capillary action
15 p2748 A70-32775

CORROSION RESISTANCE

NT OXIDATION RESISTANCE

Hot corrosion reactions in Ni, Co and NiAl-base alloys exposed to salt-sulfur containing simulated gas turbine combustion atmospheres
01 p0118 A70-10728

Low alloy and stainless steels durability in various natural atmospheres, discussing corrosivity dependence on atmosphere pollutants, temperature and humidity
02 p0318 A70-12476

Ti, Zr and Nb characteristics, properties, processing procedures and applications in corrosive environments, nuclear reactors and aerospace structures
02 p0319 A70-12710

Austenitic stainless steels intergranular corrosion model proposed and supported by observations of structural changes and corrosion behavior, suggesting methods to reduce susceptibility
03 p0506 A70-13130

Surface treatment effects on stainless steels corrosion resistance, relating resistance changes to surface composition, integrity, stability and roughness
03 p0507 A70-13136

Corrosion resistance of Ti-based alloys in humid subtropical climate, discussing sea and rain water effects
03 p0510 A70-13281

Phase structure and corrosion resistance of alloys in Ti-V-Cr system, discussing effects in HCl, sulfuric acid, nitric acid, acetic acid and NaCl solution
03 p0510 A70-13282

Graphite foam reinforced by carburized high polymers used for fabricating highly porous heat and corrosion resistant material
[DGLR-69-57] 04 p0712 A70-15178

Silicon effect on stress corrosion resistance of low alloy high strength steels in NaCl solution for different tensile strength ranges
04 p0707 A70-15272

Welding atmosphere purity effects on Li corrosion resistance of refractory metals in space power systems
04 p0709 A70-15627

Maraging steels microstructure and ductility influence on stress corrosion resistance in magnesium chloride salt chamber
04 p0711 A70-15681

Oxidation, hot corrosion resistance and mechanical properties of aluminide coated superalloys, discussing failure analysis instruments and methods
07 p1305 A70-18969

Stress and intercrystalline corrosion causes and sensitivity in supersaturated Al alloys
07 p1307 A70-19391

Maraging steels stress corrosion sensitivity in marine environment tested in humid atmosphere, salt fog, natural seawater and salt solutions
07 p1310 A70-19749

Performance characteristics of low density epoxy-water emulsion corrosion resistant coating for nonferrous alloys
08 p1526 A70-20648

Al-Mg alloys mechanical properties and corrosion resistance during aging, noting Zr and Mo additives effects
08 p1517 A70-21129

Strength, corrosion resistance and fabricating qualities future improvements in metals and alloys, discussing chemical composition approach, dispersion hardening, superplasticity, etc
08 p1518 A70-21267

Carburization resistance of refractory steels, emphasizing chemical composition effect on corrosion rate
08 p1519 A70-21434

High temperature thermomechanical treatment effects on stainless steels and Ti alloys microheterogeneity, noting corrosion resistance improvement
08 p1519 A70-21444

Co-based alloy mechanical properties and physical parameters at high temperatures, discussing oxidation and hot corrosion resistance
09 p1700 A70-22025

Materials static tested for compatibility with pure and moisture contaminated chlorine pentafluoride at 160 F and ambient temperatures
09 p1742 A70-23250

Corrosion resistance of molybdenum coatings on steel and Pb-Bi eutectic alloy obtained by vacuum contact fusion method
12 p2258 A70-28320

Ti-6Al-4V dissolution in HCl-methanol, investigating corrosion rate
13 p2433 A70-28779

Li and Cr additives effects on Al-Zn-Mg stress corrosion resistance, considering cracking, precipitation hardening and intercrystalline corrosion
13 p2433 A70-28844

Diffuse coatings effect on strength characteristics and corrosion resistance of steels, analyzing structure, thickness and purity of surface layers
13 p2433 A70-28888

Al-Mg, Al-Zn-Mg, Al-Cu and Al-Cu-Mg welded alloy corrosion cracking resistance as function of composition and fabrication techniques
14 p2597 A70-30972

Alloys resistance against erosion-corrosion attack via abrasive slurries in corrosive media in pulp and paper industry
15 p2763 A70-32774

Ti-Mo cermet alloys properties and production technology, testing corrosion resistance
16 p2931 A70-33220

Solvents and chemicals resistant thermosetting resin producing high strength glass reinforced laminates based on polyanhydride crosslinked with monoepoxide
16 p2938 A70-33382

Ta oxygen concentration effects on corrosion resistance to NaK in SNAP 8 boilers
16 p2932 A70-34202

Refractory alloys Li corrosion resistance, examining effects of oxygen contamination during welding
16 p2924 A70-34205

Molten contaminated Li effects on microstructure, tensile strength and stress corrosion of stainless steels and refractory metals
16 p2933 A70-34206

Ti equipment anodizing methods, observing corrosion resistance reduction and embrittlement hydriding due to Fe contamination
17 p3098 A70-34363

Ti corrosion resistance tests in active and passive states
17 p3113 A70-34367

Neutron irradiation effects on stress corrosion susceptibility of Al alloy
17 p3124 A70-34822

Corrosion and mechanical properties of Cr-Ni-Mn-N austenitic stainless steels
17 p3125 A70-35144

Two-component metal coatings on Ni alloys for gaseous corrosion resistance increase, comparing microstructure and properties
17 p3125 A70-35393

Ni alloys with protective coatings for gas turbine blades, testing corrosion resistance in diesel fuel combustion products with intermittent salt water sprays
17 p3125 A70-35394

Aluminum alloy corrosion stimulation and inhibition effects of cathodic polarization
20 p3647 A70-39244

Alloys for aircraft structures design, considering materials strength, corrosion resistance, producibility and cost
20 p3648 A70-39414

Stainless maraging steel bolts tensile, shear and fatigue strengths and stress corrosion resistance at room and high temperatures
20 p3650 A70-39964

Zr-Cu alloys corrosion resistance in carbon dioxide at high temperatures, noting composition effect on behavior
23 p4208 A70-44875

Electrochemical corrosion of metals, discussing passivity and passivating techniques, inhibitors and resistant alloys
24 p4361 A70-46142

Alloying elements effects on corrosion resistance of Mg ingot in NaCl aqueous solution
24 p4363 A70-46198

CORROSION TESTS

NT SALT SPRAY TESTS

Loading frequency effects on Duralumin endurance limit in air and in water, noting stress level role
01 p0115 A70-10070

Austenitic stainless steels intergranular corrosion model proposed and supported by observations of structural changes and corrosion behavior, suggesting methods to reduce susceptibility
03 p0506 A70-13130

Intergranular corrosion mechanisms in ferritic stainless steels observed by electronmicroscopic examination on Cr-Fe-base alloys vacuum-melt with C and N
03 p0506 A70-13131

Al-Zn-Mg-Cu alloy corrosion cracking, studying effects of heat treatment, strain percent, blank parameters and grain size
03 p0512 A70-13734

Stainless steel stress corrosion cracking test in magnesium chloride solution, emphasizing crack crystallographic orientation observation
03 p0513 A70-14299

Emulsified jet fuels cold flow, combustion and corrosion characteristics in gas turbine combustor compared with JP-4 fuel
[ASME PAPER 69-WA/GT-3] 04 p0732 A70-14892

Stress corrosion testing method to separate corrosion and stress effects applied to Al and Ti alloys
04 p0708 A70-15374

Threshold oxygen concentration for corrosion determined for Ta specimens subjected to low pressure contamination in NaK
04 p0709 A70-15628

Co and Fe base alloys corrosion in Hg tested in reflux capsules and forced flow loops
04 p0710 A70-15631

Refluxing capsule tests of refractory metal alloys-boiling alkali metals corrosion compatibility, noting role of capsule geometry
06 p1087 A70-17510

Rankine cycle two loop Li boiling Ka facility for nuclear turbopump simulation, studying alkali metal corrosion for operation with and without hot traps
[AIME PAPER F-69-1] 07 p1304 A70-18809

Heat pipe structural alloys compatibility with different working fluids using capsule tests at high temperatures, noting corrosion behavior
[AIME PAPER F-69-2] 07 p1304 A70-18812

Microbiological corrosion effects on aluminum alloy fatigue properties inducing further microbiological corrosion compared to chemical corrosion effects
07 p1310 A70-19735

Maraging steels stress corrosion sensitivity in marine environment tested in humid atmosphere, salt fog, natural seawater and salt solutions
07 p1310 A70-19749

Duraluminum sheets fatigue life and corrosion fatigue strength decrease with corrosion damage area increase
08 p1515 A70-20921

Corrosion shapes from iodine action on metals in methylic medium, discussing morphology dependence on purity, surface state and reaction products diffusion velocity
08 p1518 A70-21241

Zr and stainless steel pitting in acidic and near neutral chloride media, comparing controlled potential and conventional chemical corrosion tests results
09 p1706 A70-22939

Stainless steel corrosion rates in flowing liquid Na from mechanism based on thermodynamic partitioning of oxygen
09 p1706 A70-22942

Ni-Cr superalloys hot corrosion, studying sulfidation-oxidation in various synthetic controlled gas mixtures
09 p1706 A70-22944

Metals, alloys and galvanic couples corrosion rates in synthetic seawater measured by polarization technique
10 p1887 A70-24044

Filament-reinforced metallic composites corrosion control by specificity of environment and galvanic interactions between components
10 p1904 A70-24651

Mechanical notches and saltwater corrosion effects on flexural fatigue behavior of high strength structural alloys, investigating yield strength to density ratio
11 p2066 A70-26097

Martensitic stainless steels corrosion damage in jet engine compressors noting effects of temperature, surface condition, time and chloride presence
12 p2252 A70-26963

Commercial Co base superalloys oxidation and hot corrosion resistance under controlled environments, examining role of various alloying elements
[ASME PAPER D-8-21-5] 12 p2256 A70-27974

Ti-6Al-4V dissolution in HCl-methanol, investigating corrosion rate
13 p2433 A70-28779

Ni-based heat resisting alloy Inconel 700/ investigated for hot corrosive environment effect on stress rupture and fatigue strengths
13 p2434 A70-29157

NDT for structural corrosion evaluation, including ultrasonics, X rays, penetrating liquids and induced currents
16 p2929 A70-32924

Convective diffusion and liquid velocity in Co and Fe based alloys corrosion in Hg at high temperature, using reflux capsules and forced flow loops
16 p2933 A70-34207

Liquid metal corrosion of heat pipe refractory alloys at high temperatures, noting oxygen role
16 p2933 A70-34208

Iron, Ni, Cr and Co corrosion and mass transfer in high temperature Na, examining properties of stainless steels and cobalt base alloys
16 p2933 A70-34209

Ti corrosion resistance tests in active and passive states
17 p3113 A70-34367

Ti alloys crack initiation and propagation during hot salt stress corrosion 17 p3114 A70-34375

High strength ferrous alloys susceptibility to stress corrosion in seawater environment, tension loading single edge notched and fatigue cracked specimens in NaCl solution 17 p3123 A70-34554

Hot corrosive environment effect on stress rupture and fatigue strength of Ni heat resistant alloy used in gas turbine rotating blade 20 p3647 A70-39241

High temperature Ni, Co and Fe alloys for gas turbines, examining sulfidation-oxidation corrosion test methods 20 p3651 A70-39971

Atmospheric environment effect on residual shear stress corrosion cracking of commercial Al-Zn-Mg alloys subjected to heat treatment regimes 22 p4052 A70-42307

Nb-Zr alloy and yttria corrosion by high velocity Li flow, discussing material removal depth 22 p4055 A70-43100

Metallization systems materials for IC, discussing environmental stability, metals electromigration, electrochemical corrosion tests, etc 23 p4173 A70-44533

Instantaneous corrosion rate measurement, comparing coupon, resistance and polarization methods 24 p4365 A70-46390

CORRUGATED PLATES

Corrugated plates, closed cylinders and developable shells nonlinear elastic analysis, deriving boundary conditions 23 p4275 A70-44913

CORRUGATED SHELLS

Stress distribution in spirally corrugated shell under torsional deformation, calculating twisting moment for stiffness 14 p2661 A70-31327

CORRUGATING

Spherical hybrid modes in corrugated antenna conical horns, obtaining radiation pattern and gain with small flare angle 07 p1243 A70-20284

Corrugated waveguide structures for aperture type feeds for spherical and paraboloidal reflector antennas, discussing experiments on 2-hybrid mode horn 11 p2018 A70-26024

Propagation in corrugated waveguides with surface permitting H-wall boundary condition for choice gap and fin dimensions 14 p2550 A70-30519

Attenuation characteristics for dominant hybrid mode in corrugated circular waveguide for antenna feed 16 p2879 A70-34041

Milky way galactic plane corrugation, discussing maximum hydrogen brightness temperature oscillating in sinusoidal pattern 18 p3328 A70-37167

CORTI ORGAN

Sonic boom effects on guinea pigs Corti organ, comparing auditory damage in cochlea with hair cell damage 24 p4305 A70-46374

CORTICOSTEROIDS

NT ALDOSTERONE

NT CORTISONE

Pituitary hormone ACTH stimulatory effect on steroid hormone cortisol secretion by canine adrenal cortex, constructing seventh order state variable model 10 p1819 A70-24868

Mathematical model for rats nonlinear time-varying glucocorticoid secretion control mechanism, obtaining time dependent characteristics of hypothalamic-hypophyseal complex 12 p2174 A70-26893

Circannual rhythm in levels, amplitudes and acrophases of serum corticosterone in mice compared with phase shift after change of lighting regime 14 p2537 A70-30725

Human mental stress evaluation through chemical analysis of 17-hydrocorticosteroid level in parotid fluid 24 p4308 A70-45509

Desoxycorticosterone action on human kidneys and sweat glands as function of temperature tested with various DOCA and NaCl doses 24 p4301 A70-45988

CORTISONE

Nine-alpha-fluorohydrocortisone preventing bedrest induced orthostatism, considering plasma volume decrease effects on cardiovascular performance 13 p2358 A70-29433

Infused cortisol disappearance rates and distribution volumes in hyper-, hypo- and normocalcemic dogs 24 p4296 A70-45334

CORUNDUM

U ALUMINUM OXIDES

COSINE

U TRIGONOMETRIC FUNCTIONS

COSMIC DUST

NT INTERPLANETARY DUST

NT METEOROID DUST CLOUDS

NT ZODIACAL DUST

IR emission from planetary nebulae, W-R, Of and symbiotic stars, discussing dust hypothesis for IR excess 01 p0173 A70-10039

Cosmic dust particle direction, velocity and mass from ionization and momentum measurements by dust sensor during impact on Pioneer 8 satellite 01 p0088 A70-10748

Diffuse far UV radiation analysis in connection with stars and dust grains distribution and grains optical properties 05 p0903 A70-16571

Cepheus light attenuation curve explained by applying polymodal particle size distribution, obtaining interstellar dust density 05 p0918 A70-16915

Unusual IR object IRC plus 10216 interpreted as galactic source surrounded by optically thick dust shells, noting resemblance to black body energy distribution 05 p0920 A70-16976

Dynamic effect of radiation from massive protostar showing formation of transparent zone free of dust about star and gas density decrease until pressure equalization 06 p1148 A70-18400

Milky way and interstellar clouds brightness fluctuations statistical analysis by surface photometry, studying dust distribution, cloud absorption and dimensions, star distribution, etc 06 p1149 A70-18463

Dust growth, density distribution and collisions in interior of cometary head atmosphere, considering gravitational attraction to nucleus 07 p1379 A70-19039

Optical to IR conversion in circumstellar dust envelope with spherical symmetry based on optical radiation scattering and absorption by dust 08 p1573 A70-21047

Far IR radiation at galactic center suggested as thermal emission by dust particles 09 p1744 A70-22502

Photoelectric measurements of dust and CN/C2 molecular emission in atmosphere of Comet Ikeya-Seki 09 p1761 A70-23058

Interstellar dust, discussing effective particle size, composition, formation and effects on astronomical observations 09 p1763 A70-23374

X ray scattering from pulsar NP 0532 by interstellar grains 09 p1748 A70-23791

Upper atmosphere aerosols and cosmic dust properties investigation by laser beam scattering measurements using photoelectron counters for weak signal detection 10 p1898 A70-23818

Jupiter atmospheric composition, gas and dust cloud formation as clues to origin and evolution of solar system 11 p2108 A70-25654

Singular and nonsingular cosmological models validity for general relativity allowing for cosmic dust 12 p2300 A70-27394

Cold variable stars intrinsic polarization model proposing light scattering in circumstellar dust shells 12 p2307 A70-27865

Book on interstellar medium covering gas dynamics, dust, magnetic fields and nonthermal radio emission, cosmic ray diffusion in galaxy, gravitational instability theory, etc 13 p2490 A70-28996

Stellar light pressure and gravitational force ratios for spherical water, quartz and graphite particles in interstellar space, considering refractive dependence on wavelength 13 p2493 A70-29396

Radar meteor shower rate observation compared with direct cosmic dust measurements on satellites 15 p2798 A70-31682

Cosmic microwaves anomalous absorption by interstellar IR-pumped formaldehyde in dust clouds shock heated layer 17 p3154 A70-34535

Dielectric models of interstellar grains from calculations for smooth particles of homogeneous materials 17 p3159 A70-34879

Hypersonic flow containing dust, investigating for cosmic dust collection and analysis, discussing conditions for collected particle size distribution correspondence to original distribution 17 p3012 A70-35921

Interstellar cloud collisions, examining gas and dust particles separation by size 18 p3313 A70-36323

Zero moments surface in problem of two immovable centers, taking into account cosmic dust accumulation before binary apex moving forward with periastron of bright component 18 p3324 A70-37147

Interstellar dust spatial distribution, indicating galactic spiral structure 18 p3329 A70-37183

Carina spiral feature progress report covering O and B star distribution, optical and radio H 2 and H I sources and cosmic dust 18 p3330 A70-37185

Triple polarization astrophotograph observations of comet 1968 c Honda, noting dust component- Wolf number agreement 19 p3515 A70-37658

Porous matrix explosions during sublimation of dusty ice with nonvolatile particles 19 p3471 A70-37659

Radio wave emission from dust in H II region by dielectric grain photoelectric charging, rotation through stellar photons and rotating dipoles 19 p3518 A70-38024

Cosmic soft X rays scattering by interstellar dust grains, observing source angular size dependence on distance, wavelength and grain properties 20 p3695 A70-39233

Cold neutral atomic hydrogen in Taurus dust clouds from 21 cm line dips in radiotelescope observations 21 p3887 A70-41108

Interstellar spherical dust particles from meteoritic silicates and dirty ice, calculating optical properties and scattering functions 21 p3889 A70-41147

Reflection nebulae dust density, noting lower limit dependence on absolute magnitude of illuminating star 21 p3889 A70-41149

Ic class variables long wavelength anomalous radiation, discussing emission from circumstellar dust shell 22 p4094 A70-42934

Narrow band IR photometry of star alpha Orion, testing hypothetical correlation of emission peak with starlight-reflecting silicate dust 22 p4105 A70-43229

Circumstellar dust cloud model of spectral distribution and anomalous excess emissions in IR T Tauri and red giant stars coincident with photometric measurements 23 p4239 A70-43668

High altitude cosmic dust observations with microphone impact detector onboard L-3H-6 sounding rocket 23 p4257 A70-45049

Crab Nebula X ray pulsation identified with pulsar NP 0532 by rocket measurements, noting implications for interstellar dust density 24 p4401 A70-45371

Interstellar dust clouds, discussing graphite, iron and silicate mixture, solid carbon material, starlight extinction and astrophysical processes 24 p4403 A70-45408

COSMIC GASES

NT INTERPLANETARY GAS

NT INTERSTELLAR GAS

Cosmic ray galactic effects, discussing galactic magnetic field, hydromagnetic wave propagation, etc 02 p0361 A70-11749

Stellar clusters equilibrium state in gravitational field, discussing dispersed clusters formation by gravitational instability in gas containing stars of various ages 02 p0376 A70-12446

Light emission from collapsing nonrotating gas in general relativity, noting restrictions on range and frequency shift 04 p0719 A70-14702

Neutral atomic hydrogen in Virgo A cluster and between Galaxy and Virgo A, using emission and absorption measurements 04 p0758 A70-15707

Noncircular ionized gas motions in NGC 253 central region observed in velocity field analysis, indicating outflow from center 10 p1946 A70-24979

Intergalactic gas condensation rates in galactic nuclei, considering recurrent magnetoplasma cores and quasar-like phenomena 15 p2801 A70-32479

Uniform model universes containing gaseous matter and background blackbody radiation, solving Einstein equations without zero pressure assumption 18 p3313 A70-36215

H 2 regions in Sc galaxies NGC 628, 4254 and 5194 18 p3327 A70-37159

Galactic spiral structure from optical radial velocities of H II regions 18 p3329 A70-37179

Disk shaped galaxy stationary spiral shock pattern, examining gas cloud gravitational collapse for star formation 18 p3331 A70-37198

Sbc galaxy NGC 7320 radio emission and neutral H observations, showing improbability of physical association with Stephan Quintet by distance measurement 19 p3524 A70-38699

Stellar interiors and cosmic He abundance observations, discussing B stars, sun galactic and globular clusters, planetary nebulae, interstellar medium, novae, etc 20 p3706 A70-39931

High velocity intergalactic hydrogen origin, examining galactic evolution by gas infall

21 p3887 A70-41112

Matter and heat balance of cosmic grains surrounded by plasma and neutral gas under radiation

22 p4097 A70-42473

Atomic and molecular spin in cosmic medium

22 p4107 A70-43460

Solar motion apex for neutral hydrogen concentrations at different velocities, suggesting relationship to galaxy

23 p4239 A70-43815

Intergalactic gas condensation rates in galactic nuclei, considering recurrent magnetoplasma cores and quasar-like phenomena

23 p4240 A70-43904

Neutral hydrogen 21 cm line profiles in galactic plane, tabulating terminal positive velocity and brightness temperatures

24 p4414 A70-46381

COSMIC NOISE

Sudden cosmic noise absorption /SCNA/ in polar cap during 7 July 1966 solar proton flare, estimating SCNA latitudinal distribution and protons magnetic cut-off boundary

01 p0172 A70-11527

Spatial and temporal relations between auroral emission at green line 5577 and cosmic noise absorption studied to determine energy spectra and particles distribution

05 p0907 A70-16281

Lunar surface reflectivity determined by measuring reflected cosmic noise, determining dielectric constant and surface material properties

06 p1151 A70-18488

Cosmic radio absorption nightly variations, considering ionospheric structure and composition and various scattering mechanisms

07 p1367 A70-19456

Simultaneous riometer and ionosonde measurements at high latitude suggesting absorption events due to cosmic noise scattering by auroral sporadic E

07 p1271 A70-20165

Ionospheric magnetic activity effects on cosmic radio noise absorption diurnal and seasonal variations in auroral zone, noting K index and lowest reflection frequency roles

11 p2043 A70-25536

Cosmic background radiation interactions with matter, discussing molecular excitation and black body radiation interpretation

12 p2291 A70-27054

Galactic noise and solar type 3 bursts using Alouette 2 satellite HF receiver voltage recordings

12 p2226 A70-28065

Galactic noise spectrum and solar radio bursts in hecto-decametric wave region observed by Alouette 2 satellite

13 p2491 A70-29093

Auroral cosmic noise absorption, discussing east-west motion, conjugate magnitudes and breakdown

16 p2899 A70-34191

Ionospheric cosmic noise absorption diurnal and seasonal variations at Alma-Ata during IQSY, noting chromospheric flares effects

18 p3306 A70-36089

Cosmic radio absorption nightly variations, considering ionospheric structure and composition and various scattering mechanisms

18 p3309 A70-36930

Ionospheric absorption of cosmic noise recorded by riometer and corner reflector antenna directed at pole star, noting seasonal variation

19 p3412 A70-37997

Cosmic noise absorption diurnal variations at auroral zone conjugate areas during geomagnetically disturbed periods

19 p3414 A70-38379

Ionospheric magnetic activity effects on cosmic radio noise absorption diurnal and seasonal variations in auroral zone, noting K index and lowest reflection frequency roles

21 p3819 A70-41286

COSMIC PLASMA

Interplanetary plasma flow simulation around earth magnetosphere and planets not considering initial conditions influence

01 p0172 A70-11488

Hydrogen molecule formation relation to galaxy formation, discussing cosmic plasma neutralization role

03 p0577 A70-14152

Low altitude electric and magnetic measurements of plasma waves in space from OV3-3, Pioneer 8 andOGO 5 satellite observations

06 p1118 A70-17376

Magnetic field and plasma variations in lunar wake using Maxwell equations

06 p1153 A70-18636

VHF propagation variations relationship to changes in interplanetary plasma associated with interplanetary space sectorial structure rotation

07 p1226 A70-18757

Charged particle replacement by external plasma particles in ionized inhomogeneities moving in ionosphere, considering magnetic field role

07 p1266 A70-19435

Spatial and temporal cosmic plasma variations over various energy and wavelength ranges using cosmophysical and aeronomical facility

07 p1372 A70-20339

Proton concentrations, magnetic field strength and temperatures distribution in interplanetary plasma flows as function of latitudinal distance from center of active region

07 p1391 A70-20420

Stellar gas ejection processes in corona-interplanetary plasma system, proposing hydrodynamic model with frequent collision region having finite radius

08 p1573 A70-21060

Solar corona and interplanetary plasma structure and dynamics, calculating solar wind velocity as function of distance from sun

08 p1576 A70-21397

Cosmic rays diffusion through interstellar plasma noting microstabilities role

10 p1931 A70-23972

Plasma experiments in space including electric fields measurement, collisionless plasma studies and artificial Ba cloud generation

12 p2214 A70-26868

Radiation emission and transfer in unsteady outer space plasmas, discussing turbulence mechanisms involving electron and ion motion, relativistic and non-relativistic electron beams, etc

12 p2305 A70-27854

Book on space physics covering charged particles in magnetic, electric and dipole fields, cosmic rays, magnetically trapped radiation and interplanetary plasma

14 p2633 A70-30099

Charged particle acceleration in outer space plasma, deriving ion-acoustic instability equations

14 p2630 A70-30220

Intergalactic gas condensation rates in galactic nuclei, considering recurrent magnetoplasma cores and quasar-like phenomena

15 p2801 A70-32479

Laboratory experiments applicability to interplanetary plasma physics, describing simulations of solar wind interactions, magnetosphere, collisionless shock waves, etc

17 p3164 A70-35123

Charged particle replacement by external plasma particles in ionized inhomogeneities moving in ionosphere, considering magnetic field role

18 p3249 A70-36909

VHF propagation variations relationship to changes in interplanetary plasma associated with interplanetary space sectorial structure rotation

18 p3229 A70-37101

Interplanetary plasma torque due to temperature and pressure anisotropy, considering solar wind angular velocity and sun angular momentum

20 p3712 A70-40423

X ray emission of hot dense intergalactic plasma, discussing evolution equation for temperature and degree of gas ionization vs red shift

21 p3877 A70-40702

Matter and heat balance of cosmic grains surrounded by plasma and neutral gas under radiation

22 p4097 A70-42473

Electric propulsion plasma thrust beam and ambient space plasma electrostatic equilibration, considering various charged particle parameters involved in bi-plasma system interactions

22 p4091 A70-42974

Interplanetary magnetic field and plasma structure observed with Mariners magnetometer, noting 27-day deviations from Parker spiral model

23 p4239 A70-43827

Intergalactic gas condensation rates in galactic nuclei, considering recurrent magnetoplasma cores and quasar-like phenomena

23 p4240 A70-43904

Interplanetary plasma electron density inhomogeneities formation explained by instability due to electron stream curvilinearity obtained from spacecraft data

23 p4240 A70-44070

Charged particle acceleration in outer space plasma, deriving ion-acoustic instability equations

24 p4399 A70-46295

COSMIC RADIATION

U COSMIC RAYS

COSMIC RADIO WAVES

U EXTRATERRESTRIAL RADIO WAVES

COSMIC RAY ALBEDO

Balloon-borne experiments with directional scintillators to measure low energy gamma radiation spectrum in midlatitude atmosphere for photons origin and gamma albedos investigation

03 p0561 A70-13996

Proton injection into radiation belt, comparing solar neutron decay /SND/ and cosmic ray albedo neutron decay /CRAND/ as proton sources

09 p1746 A70-23489

Proton distribution in radiation belt inner zone from radial diffusion addition to cosmic ray produced albedo-neutron decay and atmospheric collision loss

17 p3150 A70-34644

Earth atmosphere cosmic ray neutron albedo from balloon measurement of flux vertical distribution

20 p3698 A70-39298

Cosmic ray albedo neutron flux latitude and altitude dependence, using OGO-6 polar orbiting satellite

20 p3698 A70-39326

COSMIC RAY SHOWERS

Geomagnetic field influence on extensive air shower radio emission, discussing frequency dependency and signal polarization

01 p0069 A70-10281

High energy nuclear interactions defined by computerized determination of sea level lateral distribution of muons from primary cosmic ray air showers

01 p0171 A70-10667

Electromagnetic showers fluctuations produced by electrons and photons in heavy materials, determining moments of particle numbers and bremsstrahlung differential cross sections

01 p0171 A70-11026

Extensive air shower axis position determined using energy methods and radial distribution geometry of particle density

01 p0171 A70-11252

Angular distribution of muon pool extensive air showers flatter than normal showers, discussing initiation by passive particles produced by cosmic ray-atmospheric nuclei

02 p0357 A70-12079

High energy extensive air shower detection by Cerenkov receivers or liquid scintillators, considering 200 and 3000 MHz radio emission mechanisms

02 p0357 A70-12115

Extensive air shower models, noting role of nuclear active component energy decay rate

03 p0556 A70-13038

Spatial distribution function calculation for muons in extensive air shower model and secondary particles mean transverse momentum estimation

03 p0556 A70-13039

Cosmic ray particles high energy interactions during extensive air showers, noting inelastic superhigh energy collisions

03 p0556 A70-13040

Electron numbers in extensive air shower spectra from scintillation counters measurements at high mountain altitude, analyzing electron-photon component spatial distribution

03 p0556 A70-13041

Scintillation counters hodoscopic system for studying spatial distribution of muon and muon-number fluctuations in extensive air showers

03 p0482 A70-13042

Density spectrum exponent of penetrating muon component of extensive air showers determined for hodoscopic assembly of Geiger-Muller counters with lead absorber

03 p0556 A70-13043

Excess electron and combined electron-positron angular distributions compared in electron photon cascade showers, considering Coulomb scattering

03 p0556 A70-13048

Spatial distribution of cascade shower particles in atmosphere described by integrodifferential equations system, considering medium ionization

03 p0557 A70-13049

Electron and photon spatial distributions in cascade air shower, applying moment method to space/angle problem solution

03 p0557 A70-13050

Cerenkov radiation of electron-positron pair as moving radiating dipole in EAS, discussing emission effects of primary energy, production height and inclination angle

03 p0561 A70-14186

Muonic and hadronic component arrival time distribution in EAS measured under rock compared to Monte Carlo computation

03 p0562 A70-14187

Quarks discovery in cores of energetic extensive air showers, discussing results evaluation and interpretation

04 p0722 A70-15299

Isothermal atmospheric temperature effects on extensive air shower characteristics and muon numbers computed at various temperature and observation levels

05 p0898 A70-15945

Extensive air shower characteristics for inelasticity coefficient, nucleon-pion interaction cross sections and secondary particles, noting parameter interchangeability

05 p0898 A70-15946

Angular distribution and production probability of secondary shower particles produced by high energy cosmic ray muons using scintillation counter facility

05 p0899 A70-15957

Extensive air showers with nuclear particle interactions using ionization calorimeters, neutron monitor, scintillation and Cerenkov radiation counters

05 p0846 A70-15958

Muon-electron ratio measurements in extensive air showers, showing anomaly due to chemical composition change of primary cosmic radiation

05 p0901 A70-16274

Density spectra of cosmic ray showers measured by scintillators and GM counters

05 p0902 A70-16458

Cerenkov light in extensive air shower observed at mountain altitude showing mixed primary cosmic rays in chemical composition

06 p1134 A70-17184

Individual extensive air showers axes localized by measurement of charged particle densities, assuming age parameter

07 p1365 A70-18777

Quark search in cores of air showers with four million GeV mean energy, deducing rough production rate

07 p1368 A70-19925

Electromagnetic component of extensive air showers to three dimensional Monte Carlo simulations of hadronic component using electromagnetic cascade theory

07 p1368 A70-19967

Coherent and incoherent radio emission from extensive air showers simultaneously detected by radio telescope in VHF-UHF range

08 p1563 A70-20475

Mathematical model of extensive air showers, calculating lateral distribution of photoelectronic component at all altitudes

08 p1560 A70-20598

Critical review of paper on evidence of quarks in air shower cores from cloud chamber tracks, explaining data by statistical fluctuations in particle fluxes

08 p1562 A70-21272

Extensive air shower simulation for determining inelasticity effect on electrons, hadrons and muons variation at sea level

08 p1563 A70-21674

Cosmic ray air showers simulation, discussing high energy nuclear interaction and linear relation of primary particle energy to number

09 p1744 A70-22048

Cosmic ray air shower detection from radio pulses

09 p1745 A70-23276

Cascade showers in horizontal flux of cosmic rays measured by ionization calorimeter

09 p1747 A70-23730

Highest energy primary cosmic ray particles, considering air shower characteristics and energy spectrum shape

12 p2292 A70-27381

Cosmic ray extensive air showers spectrum at high altitude, describing measuring equipment, techniques and results

12 p2295 A70-28048

Cosmic ray experiment for detecting quarks in low density showers, using hodoscope of wire proportional counters

16 p2972 A70-33048

Magnetic monopole flux limits in primary cosmic radiation derived from muon-poor shower data and inverse Compton scattering

16 p2972 A70-33050

Electron recording by shower counters, noting radiation length importance

16 p2908 A70-33211

Radio receiving system for pulses detection from cosmic ray extensive air showers, discussing sensitivity and noise temperature

16 p2911 A70-33788

Three dimensional nucleon-pion cascade equations solution for cosmic ray extensive air showers by pion-links method

17 p3150 A70-34597

Cosmic ray air showers UHF emission detection at 500 MHz

17 p3151 A70-34850

Electrons lateral distribution in large air showers determining inelasticity of high energy nuclear interactions

18 p3305 A70-35947

Periodic high energy gamma rays from pulsars, using night sky Cerenkov light receiver for proton showers

19 p3500 A70-38084

Periodic cosmic gamma radiation from pulsars, using reflector detection of shower generated Cerenkov light

19 p3501 A70-38090

Cosmic gamma ray sources detection in 100-1000 GeV range by atmospheric Cerenkov radiation from energetic particle showers

19 p3501 A70-38091

Electron energy spectra range from HEOS A1 satellite mounted Cerenkov counter with shower telescope

19 p3503 A70-38103

Primary cosmic rays energy spectrum, investigating extensive air shower /EAS/ size spectrum in 2,000-1,000,000 eV range

19 p3510 A70-38154

Muon deficient showers intensity distribution as function of sidereal time, obtaining anisotropy upper limit by statistical analysis and Monte Carlo method

19 p3511 A70-38483

Air shower radio pulse amplitude dependence on primary energy and core distance

19 p3381 A70-38607

Equilibrium energy spectra of cascade electrons and photons in light and heavy materials as function of total shower energy

20 p3675 A70-39304

Three dimensional Monte Carlo simulation of extensive air shower processes, comparing with hadrons and electrons energy spectra

20 p3699 A70-39442

Cosmic ray jet studies, evaluating nuclear emulsion technique

22 p4096 A70-43399

Far field power of coherent Cerenkov radio emission from cosmic ray showers in turbulent atmosphere, using radio telescopes

23 p4247 A70-44791

Primary mass effects on extensive air shower characteristics, using Monte Carlo simulation

23 p4238 A70-44930

Cerenkov light longitudinal distribution from extensive air showers, using near UV receivers

24 p4398 A70-46225

COSMIC RAYS

NT COSMIC RAY SHOWERS

NT PRIMARY COSMIC RAYS

NT SECONDARY COSMIC RAYS

NT SOLAR COSMIC RAYS

Cosmic ray latitude survey in North America in summer using neutron and muon monitors operating near sea level and on mountains

01 p0167 A70-10226

Cosmic ray latitude survey in Canada using airport sites, noting ground snow effect on neutron monitor counting rate

01 p0167 A70-10227

Cosmic ray latitude survey in western U.S. and Hawaii in summer 1966 using neutron and muon monitors

01 p0167 A70-10228

Cosmic ray survey measurements during IQSY reduced to common atmospheric depth, determining attenuation coefficients of neutron and muon monitors

01 p0167 A70-10230

Cosmic rays nucleon component measurements interpretation in terms of geomagnetic field model

01 p0169 A70-10354

Cosmic ray electron intensity diurnal variations measured with combined Cerenkov telescope and Pb-scintillator sandwich detector on balloon flight

01 p0170 A70-10408

Cosmic ray neutron monitors data comparison for various stations using one factor model, considering atmospheric effects and cut-off rigidities

01 p0087 A70-10460

Seasonal, solar diurnal and semidiurnal variations of cosmic ray soft component observed at sea over seven year period

01 p0170 A70-10467

Tradeoff criteria between man machine and automated space systems applied to lunar and cosmic ray explorations

01 p0034 A70-10644

Interplanetary magnetic field sectoral structure effect on diurnal cosmic ray intensity and geomagnetic field, noting field direction influence

01 p0172 A70-11525

Algorithm for determining readings dispersion during cosmic rays variability, statistical nature and instrument errors

01 p0172 A70-11526

Coupling coefficients for integral charged component of cosmic rays determined from measuring azimuthal geomagnetic effect on rays observed in crossed telescopes

01 p0172 A70-11545

Diffused X ray background in isotropic world models in terms of Compton radiation from cosmic ray electrons in intergalactic space

02 p0356 A70-11743

Meteorites fossil tracks due to cosmic radiation heavy nuclei

02 p0361 A70-11748

Cosmic ray galactic effects, discussing galactic magnetic field, hydromagnetic wave propagation, etc

02 p0361 A70-11749

Cosmic ray primaries and secondaries direct heating of thermal electrons for computation of H I regions electron densities and temperatures

02 p0363 A70-11782

Thermal properties of neutral interstellar gas heated by low energy cosmic rays, noting role of electrons in heating processes

02 p0364 A70-11783

Heavy nuclei survival in cosmic rays Colgate supernova acceleration model, assuming plasma wave instability in shock wave

02 p0357 A70-11788

Balloon measurements of cosmic ray alpha particle flux in upper atmosphere over Japan to obtain solar modulation effects data

02 p0357 A70-12122

Cosmic ray protons, He nuclei and electrons solar modulation by betatron deceleration mechanism during interplanetary space passage

02 p0357 A70-12123

Data collection for ionospheric disturbances, geomagnetic field, radio wave intensity, cosmic rays and solar activity

02 p0290 A70-12125

Cosmic ray origin in high energy H and He isotropic abundances and energy spectra observed by IMP 4 satellite during solar quiet times

02 p0358 A70-12250

HEOS-1 satellite development for ESRO to investigate interplanetary magnetic fields, cosmic radiation, solar wind outside magnetosphere and earth shock wave

02 p0382 A70-12646

Inelastic muon-nucleon scattering implications on cosmic rays, studying equation validity for absorption cross section

02 p0359 A70-12702

Cosmic X ray observations by rockets and balloons noting polarization and line emissions of various sources

02 p0359 A70-12789

Cosmic X ray sources optically observed from ground, discussing identification, distribution, etc

02 p0359 A70-12790

Cosmic X ray background interpreted as Compton collisions between cosmic black body photons and relativistic electrons in radio sources

02 p0360 A70-12792

Cosmic x ray astronomy in near future for source detection concerning spectral bands, polarization, position, instrumentation, etc

02 p0304 A70-12794

Cosmic ray nuclear interactions under paraffin and lead, using counter controlled multiplate cloud chamber

03 p0553 A70-12877

Galaxy model formulated in cylindrical coordinate system using Fokker-Planck equation for cosmic radiation particles propagation, discussing trajectories of high energy particles

03 p0553 A70-12880

Cosmic ray physics - Conference, Tashkent, Uzbek SSR, October 1968

03 p0553 A70-13028

Cosmic ray particles inelastic nuclear interactions mean free path in iron measured in Wilson chamber and ionization calorimeter

03 p0554 A70-13030

Cosmic ray neutrons energy spectrum and angular distribution at sea level based on measurement results

03 p0556 A70-13046

Diffraction correction of terrestrial, atmospheric and cosmic background radiation at aperture and disk determined by artificial moon method

03 p0442 A70-13084

Cosmic ray variations concepts with reference to 11, 22 and 80-90 year solar cycles Wolf number variations

03 p0568 A70-13355

Light-flattering amplitude and intrinsic resolution of large-area flat scintillation detectors used for cosmic rays-nuclear interaction experiments at high energies

03 p0484 A70-13466

Visible solar hemisphere circumstances for 28 January 1967 and ground level cosmic rays enhancement not preceded by intense H alpha flares

03 p0558 A70-13590

Large amplitude wave trains in cosmic ray neutron intensity compared with diurnal variations, determining interplanetary space directional distribution from monitor data

03 p0559 A70-13912

Cosmic ray increases during Forbush decrease onset stage in terms of transient spatial anisotropy

03 p0559 A70-13914

Sidereal cosmic ray diurnal variations from underground muon telescopes in Northern and Southern Hemispheres, proposing model producing variations at earth vicinity

03 p0560 A70-13978

Forbush decrease recorded on 26-27 January 1968 showing large anisotropies in cosmic ray flux after SC magnetic storm

03 p0560 A70-13979

Small amplitude perturbations in interstellar medium, discussing order of magnitude estimates of properties of cosmic rays, thermal gas, dust and magnetic field

03 p0575 A70-14016

Biological experiment on Zond 5 automatic station in earth-moon-earth trajectory determining cosmic radiation absorption and effects on plant seeds, turtles, larvae, etc

03 p0428 A70-14066

Production rates determination for Na 24 and Mg 28 isotopes in Ar exposed to cosmic rays

03 p0561 A70-14092

Electron and positron flux steady state in interstellar space relationship to differential energy spectrum exponent in cosmic rays, discussing galactic halo and age

03 p0561 A70-14151

Lunar neutron flux due to cosmic radiation interaction with lunar surface layer, determining angular distribution and energy spectrum

04 p0738 A70-14442

Low energy cosmic rays effect on electron density in interstellar medium

04 p0738 A70-14509

Cosmic ray origin theories, noting pulsars nature and properties may provide solution

04 p0738 A70-14517

Galactic cosmic rays scattering by solar wind magnetic field fluctuations, considering energy and momentum transfer

04 p0739 A70-14596

Galactic cosmic ray origins, discussing supernovae and galactic nucleus cosmic ray production

04 p0740 A70-15071

Interstellar gas instability, discussing thermal, magnetic and cosmic ray effects

04 p0753 A70-15072

Hysteresis effect on cosmic ray modulation and gradient ionization near solar minimum from measurements made near earth with OGO 1 and 3 ion chambers

04 p0740 A70-15106

Cosmic ray flux modulation in earth atmosphere produced by solar wind and geomagnetic variations, considering effects on atmospheric carbon 14 variations

04 p0680 A70-15114

Fast neutron spectrum produced by galactic cosmic ray protons in atmosphere, presenting Monte Carlo transport calculation results

04 p0742 A70-15130

Ionization losses effect on energy spectra of cosmic ray heavy nuclei with Fermi acceleration, using transfer equation

04 p0742 A70-15201

Gamma rays due to cosmic ray electrons bremsstrahlung in interstellar medium, predicting diffuse galactic X ray flux

04 p0742 A70-15713

Eleven year cosmic ray variation and solar activity cycle analysis, showing variation amplitude dependence on both numbers and heliolatitudinal distribution of sunspots

04 p0742 A70-15718

Cosmic ray energy spectrum variations possible effect on ray intensity amplitude intensity increases preceding Forbush decreases

04 p0743 A70-15719

Lower ionospheric cosmic ray layer state during Forbush decreases from radio absorption observations interpreted on basis of electron production rate analysis

04 p0743 A70-15720

Forbush effect on intensity of neutron component of cosmic rays during quiet sun period

05 p0897 A70-15795

Primordial cosmic ray sources evidence suggesting galaxies and quasars in initial stages of formation

05 p0897 A70-15921

Technique for coding data on cosmic ray variations based on packing digital information in computer storage, proposing selective statistical control for tape recording phase

05 p0898 A70-15929

Block diagram for eliminating counting errors and spurious coincidences in telescope used at cosmic ray stations

05 p0845 A70-15931

Cosmic ray intensity variations recording device adaptable to computer forming centralized data processing system

05 p0845 A70-15932

Transistorized low impedance cascades as amplifiers for proportional counters in studying cosmic ray intensity variations

05 p0845 A70-15934

Diurnal cosmic ray intensity variations first and second harmonics amplitudes during sudden phase variations diagrammed from neutron monitor data during IGY

05 p0898 A70-15936

Azimuthal telescope with proportional counters for underground recording of hard/soft cosmic ray components

05 p0846 A70-15937

Neutron monitor calibration method to eliminate natural cosmic ray background, decreasing errors due to ray intensity variation

05 p0846 A70-15938

Cosmic rays meson component recorded by proportional counters designed for use in large telescopes

05 p0846 A70-15939

Cosmic ray intensity decreases in relation to geomagnetic and F 2 region disturbances characterized by Forbush decreases from vertical sounding data

05 p0898 A70-15940

Cosmic rays neutron component solar-diurnal variations as function of solar activity using magnetically quiet data

05 p0898 A70-15941

Time dependent variation of first and second harmonics amplitudes of diurnal cosmic ray variations during SC magnetic storms

05 p0898 A70-15942

Azimuthal telescope for recording cosmic rays intensity, noting statistical error for vertical and oblique incident component

05 p0846 A70-15967

Solar magnetic discontinuity fluxes analyzed by studying 27-day cosmic ray and geomagnetic activity variations using linear filtration method

05 p0900 A70-15969

Energy spectra of cosmic diffuse X ray component and distribution over northern sky, determining Crab Nebula and Cygnus spectral characteristics

05 p0901 A70-16305

Cosmic ray intensity preceding Forbush effects as function of chromospheric flares solar longitude and solar wind velocity

05 p0903 A70-16730

Relativistic solar proton propagation fluctuation effects in interplanetary magnetic field during cosmic ray intensity increase

05 p0903 A70-16731

Cosmic ray angular distribution spectrum and interplanetary magnetic field properties determined from semi-diurnal cosmic ray variations data

05 p0903 A70-16732

Cosmic protons and high energy heavy nuclei interaction with radiation in expanding universe, including estimates of light radiation influence on cosmic ray spectra

05 p0904 A70-16903

Cosmic gamma radiation sources above 50 Mev investigated by high altitude balloons in Northern Hemisphere with spark chamber system

05 p0904 A70-16930

Relativistic plasma waves in uniform ambient magnetic field analyzed for growth rate to investigate plasma instabilities of streaming cosmic rays

05 p0904 A70-16931

X rays from Sco XR-1 compared with galactic cosmic rays and solar Lyman alpha radiation to determine ionospheric ionization causing radio wave attenuation

06 p1134 A70-17443

Cosmic ray electron spectrum above 200 Gev based on pure nuclear emulsion stack using horizontal sandwich assembly

06 p1135 A70-17473

Cosmic ray triggering of solar system formation by ionizing in solar disk

06 p1135 A70-17539

Cosmic ray time series periodicity using variance analysis allowing for intensity variations and meteorological factors

06 p1135 A70-17543

Proton satellites measurements reconciliation with diurnal stellar variation data and cosmic rays origin models

06 p1135 A70-17885

Solar wind effects on galactic cosmic rays isotropic diffusion and density distribution in interplanetary space in presence of azimuthal asymmetry

07 p1366 A70-19429

Barometric and atmospheric temperature corrections of cosmic ray neutron component intensity fluctuations obtained statistically from monitor recording

07 p1366 A70-19430

Cosmic ray intensity increase preceding Forbush effect using statistical correlation method

07 p1367 A70-19444

Cosmic radio absorption nightly variations, considering ionospheric structure and composition and various scattering mechanisms

07 p1367 A70-19456

Charged particles and He nuclei spatial distribution from recordings in cosmic ray equator region by Cerenkov counter mounted on Proton 2 satellite

07 p1367 A70-19490

Monograph on balloon and satellite borne spark chambers for cosmic gamma radiation energy and direction determination, discussing relativistic electrons multiple scattering

07 p1368 A70-19617

Book on nuclear and astrophysical aspects of cosmic rays covering kinematics in collisions and decays, cascade theory, high energy interactions, origin, etc

07 p1368 A70-19666

Book on cosmic electrodynamics covering cosmic plasmas, sun and solar activity, interplanetary medium and geomagnetic cavity, magnetosphere, geomagnetic disturbance, radiation belt, etc

07 p1387 A70-19667

Cosmic X ray source spectra possibly due to plasma bremsstrahlung

07 p1368 A70-19700

Intensity variations of cosmic ray neutrons and mesons analyzed to isolate lunar day period

07 p1368 A70-20033

Compton-Getting effect for cosmic ray particles and photons and Lorentz-invariance of distribution func-

tions, discussing thermal background radiation, proton spectra, etc

07 p1369 A70-20071

Galactic cosmic rays intensity long term modulation, studying roles of solar corona, solar wind and interplanetary electromagnetic field

07 p1369 A70-20075

Inverse Compton collisions of relativistic electrons with universal black body photons for diffuse component of cosmic X rays

07 p1369 A70-20166

Highly variable component protons and alpha particles identified in low energy cosmic rays by IMP 4

07 p1369 A70-20199

Cosmic ray physics - Conference, Tashkent, Uzbek SSR, October 1968

07 p1370 A70-20326

Cosmic rays origin, discussing galactic theory of supernovae and formation mechanisms for energy spectra and composition of sources

07 p1371 A70-20327

Cosmic rays formation time and evolution in expanding universe, discussing high energy electrons, energy losses and spectra and metagalaxy cascade processes

07 p1371 A70-20328

Hot universe model for determining magnitude constraints on Dirac monopole annihilation cross section and mass in cosmic rays

07 p1371 A70-20330

Plasma physics relating turbulence to cosmic rays covering oscillations, turbulent acceleration, sub-cosmic rays, langmuir turbulence spectra and acceleration, etc

07 p1371 A70-20332

Cosmic ray microvariations relation to solar wind structure, particle scattering models, spatial distribution, time variations, etc

07 p1372 A70-20336

Solar wind structural characteristics determination from cosmic ray variations in interplanetary medium, considering interplanetary magnetic field structure and spatial orientation

07 p1372 A70-20337

Solar system cosmic ray time-space variations analysis based on simulation of meteorite nuclear processes

07 p1372 A70-20338

Forbush decreases of cosmic rays calculated assuming semitransparent magnetic piston action with free particle exchange

07 p1372 A70-20340

Magnetic storms effect on cosmic ray neutron component diurnal variation, determining amplitudes and phases of harmonics by harmonic analysis

07 p1372 A70-20341

Diurnal variations of cosmic ray neutrons following solar proton flares, proposing anisotropic diffusion model for phase and amplitude

07 p1372 A70-20342

Solar wind interaction with galactic cosmic radiation resulting in wind radial motion braking, discussing possible solar wind focusing

07 p1373 A70-20343

27-day variations in ionization layer created by galactic cosmic rays, discussing association with 27-day cosmic ray and geomagnetic field variations

07 p1373 A70-20345

Cosmic rays effect on atmospheric temperature and wind, discussing planetary distribution of neutron component of radiation intensity

07 p1373 A70-20346

Short lived cosmic ray produced nuclides as lower atmospheric motion tracers, studying Na 24 characteristics and activity in rain water

07 p1373 A70-20355

Cosmic rays sudden intensity increases during proton flares of 28 January 1967 and 7 July and 2 September 1966, plotting proton density vs pressure

07 p1374 A70-20445

Sea level testing of magnetic spectrograph and calorimeter apparatus for studying cosmic ray spectra at different atmospheric depths

08 p1560 A70-20474

Cosmic ray intensity increase due to meteor showers magnetic field trapping effect

08 p1560 A70-20568

Neutron formation multiplicity during capture of cosmic ray muons by Zn and Sb nuclei, noting agreement with one-third law

08 p1560 A70-20718

Solar modulation of low energy galactic cosmic ray protons, proposing diffusion-convection model with time dependent diffusion coefficient

08 p1561 A70-20906

Cosmic rays induced Cerenkov light pulses effect on stellar intensity interferometer from measuring correlated pulses

08 p1497 A70-21492

Cosmic ray origin models, considering universal and local metagalactic models and halo and disk galactic models

09 p1744 A70-22057

- Synchrotron emission of relativistic particle in magnetic field with radiative reaction force comparable to Lorentz force, emphasizing pulsar cosmic ray electron acceleration 09 p1731 A70-22273
- Cosmic ray intensity variation correlated with amplitude changes in 27 day variation during solar cycle 18 09 p1745 A70-22740
- Cosmic radio waves discrete sources spectra measured in decametric wavelength range, discussing wave generation and absorption 09 p1762 A70-23189
- Solar wind magnitude and variability effects on geomagnetic activity and cosmic ray intensity modulation from satellite observations 09 p1745 A70-23272
- Low energy positrons and gamma rays from large fluxes of galactic cosmic rays 09 p1746 A70-23477
- Cosmic ray diurnal anisotropy, demonstrating two-solar-cycle variations for nucleonic component 09 p1746 A70-23478
- K-mesons role in high energy cosmic ray muons angular distribution and nuclear interaction 09 p1748 A70-23731
- Heavy particles separation at sea level from overall flux of cosmic radiation, discussing method and device recording subrelativistic particles 09 p1684 A70-23732
- Cosmic rays diffusion through interstellar plasma noting microstabilities role 10 p1931 A70-23972
- Cosmic rays, particles and fields physics in relation to radio and X ray astronomy 10 p1931 A70-24410
- Cosmic ray muons continuous recordings, describing design and performance of plastic scintillators with photomultipliers 10 p1889 A70-24489
- Cosmic radiation low energy positrons flux estimation compared with calculation from solar modulation models 10 p1932 A70-24537
- Cosmic ray electrons during propagation in interstellar space analyzed for energy spectrum modulation 10 p1816 A70-24633
- Sidereal time variations in cosmic ray intensity observed by inclined muon telescopes 10 p1933 A70-24858
- Cosmic layer in lower ionosphere investigated by 164 kHz frequency absorption at night, discussing solar activity effects 10 p1934 A70-25198
- Ionospheric waves positive phases and disturbances related to solar activity variations and cosmic ray modulations 10 p1885 A70-25270
- Multiplicity recorder for cosmic rays neutron component studies, reducing star redistribution errors by coincidence effect compensation 11 p2103 A70-25527
- Isotropic cosmic background radiation detection in presence of earth and galactic radiation, discussing influence on steady state cosmology 11 p2106 A70-26673
- Cosmic ray variations concepts with reference to 11, 22 and 80-90 year solar cycles Wolf number variations 11 p2118 A70-26720
- Cosmic ray intensity fluctuations at geomagnetic equator using power spectrum analysis on mu meson records, discussing solar photosphere and interplanetary magnetic field 12 p2291 A70-27176
- First harmonic of diurnal variation in pressure corrected cosmic ray neutron monitor rate, discussing amplitude variation with height and observed time dependence 12 p2291 A70-27177
- Cosmic X ray sources, considering locations, fluxes and angular sizes from Aerobee rocket observations 12 p2292 A70-27384
- Cosmic X ray sources searched for by Aerobee rockets, noting locations and distribution correlation with galactic novae 12 p2292 A70-27385
- Cosmic gamma rays observation by balloon flight and satellite with scintillation detector, tabulating counting rates in pulse height channels relative to Crab Nebula 12 p2292 A70-27387
- Cosmic neutrinos detection, using inverse beta decay and elastic scattering by electrons to overcome solar neutrino problem 12 p2293 A70-27390
- Cosmic electron detection and measurement techniques, considering presence in solar system, interstellar space and metagalaxy and galactic continuum radio emission 12 p2293 A70-27572
- Cosmic rays origin, discussing choice between galactic halo and radio disk models for trapping region 12 p2295 A70-27883
- Diffuse cosmic X and gamma ray background radiation isotropic component 12 p2295 A70-27887
- Ar 37 and Ar 39 isotopes in recently fallen iron-ataxite and stony meteorites, discussing relevance to cosmic ray variations in space 12 p2309 A70-27950
- Cosmic rays components fluxes, interactions, lifetimes and anisotropy in statistical discrete source model, tabulating and graphing results 12 p2295 A70-27996
- High energy and contemporaneous cosmic ray tracks in bubble chamber picture noting evidence of quarks 12 p2276 A70-27997
- Muon intensity meter for cosmic ray muon flux underground using scintillation telescope consisting of two coincidence counters 12 p2295 A70-28176
- Forbush effects influence on cosmic layer state in lower ionosphere using long radio waves 12 p2295 A70-28220
- Long wave cosmic radio background emission in circumlunar space by Luna 11 and 12 satellites, observing increase in earth magnetosphere tail 12 p2295 A70-28262
- Neutron flux due to cosmic radiation interaction with lunar surface layer, determining angular distribution and energy spectrum 13 p2475 A70-28467
- Gravity radiation detector insensitivity to cosmic rays 13 p2405 A70-28835
- Cosmic rays emission by dipole magnetosphere, applying model to neutron star particle belts 13 p2476 A70-28893
- Cosmic ray muon energy spectra at large zenith angles measured by optical spark chamber magnetic spectrometer 13 p2476 A70-28933
- Cosmic ray muons energy spectra and zenith angle distributions by analyzing tracks recorded in high field heavy liquid bubble chamber 13 p2476 A70-28934
- Cosmic ray vertical muon flux measurements at sea level using spectrometer 13 p2477 A70-29124
- Cosmic rays and cosmic X rays, considering galactic and extragalactic sources, diffuse background, detection devices, etc 13 p2477 A70-29160
- Cosmic radiation yearly semidiurnal anisotropy characteristics based on worldwide neutron monitor stations data analysis 13 p2477 A70-29177
- Cosmic radiation periodic variations measurements noting second harmonic importance of daily variations 13 p2478 A70-29230
- Cosmic rays intensity frequency spectrum near earth, indicating relativistic electron energy spectra similarity in interstellar space and galactic particles existence 13 p2478 A70-29388
- Lower stratosphere ozone formation, suggesting origin in cosmic rays absorption 13 p2400 A70-29472
- High energy cosmic ray muons, investigating arrival from both low and high galactic latitudes 13 p2478 A70-29482
- Cosmic microwave radiation origin based on discrete source models 13 p2479 A70-29787
- Altitude dependence of low latitude cosmic ray diurnal variations from cosmic ray neutron data 13 p2479 A70-29792
- Interstellar electron gas distribution and temperature, suggesting cosmic ray heating as main ionization source 13 p2495 A70-29796
- Low energy neutrino cosmic background, discussing energy density, black body radiation, beta decay, scattering process and origin 13 p2479 A70-30001
- Book on space physics covering charged particles in magnetic, electric and dipole fields, cosmic rays, magnetically trapped radiation and interplanetary plasma 14 p2633 A70-30099
- Cosmic ray energy spectrum in absence of solar activity from eleven year ray variations, noting coincidence with galactic rays 14 p2630 A70-30204
- Diffusion loss model for cosmic ray electron propagation in galaxy, considering direct and radio observations 14 p2631 A70-30538
- Interstellar cosmic ray spectra from nonthermal radio background, obtaining electrons and protons modulation by diffusion-convection energy loss theory 14 p2631 A70-30673
- Galactic cosmic ray actions on interstellar medium for origin of Li, Be and boron in stellar atmospheres and solar system 14 p2640 A70-30786
- Eleven year cosmic ray variation and solar activity cycle analysis, showing variation amplitude dependence on both numbers and heliolatitudinal distribution of sunspots 14 p2632 A70-30802
- Cosmic ray energy spectrum variations possible effect on amplitude of intensity increases preceding Forbush decreases 14 p2632 A70-30803
- Lower ionospheric cosmic layer state during Forbush decreases from radio absorption observations interpreted on basis of electron production rate analysis 14 p2632 A70-30804
- Cosmic ray transport in solar wind generalized with anisotropic diffusion approximation 14 p2632 A70-30887
- Intergalactic medium lukewarm models, considering physical state, cosmic photon spectrum and isothermal and adiabatic expansion 14 p2651 A70-31291
- Galactic cosmic rays high altitude measurements by balloon-borne Sparmu type multidirectional detectors, revealing azimuthal anisotropy 14 p2632 A70-31309
- Cosmic rays geomagnetic bending and effective angles of approach for various ground stations 14 p2633 A70-31313
- Cosmic ray shortest term regular intensity variations, measuring particle dispersion as time function 14 p2633 A70-31314
- Cosmic X ray and gamma ray spectral energy distribution slope change explained by measurement process involving photon spectrum 15 p2792 A70-31431
- Report to COSPAR on space research in Bulgaria, considering ionospheric physics, cosmic rays, satellite observations, meteorology and space communications 15 p2829 A70-31704
- Report to COSPAR on space research covering satellite tracking telemetry, Apt, meteorology, cosmic rays, solar activity and international cooperative programs, etc 15 p2829 A70-31709
- Quark search in cosmic radiation near sea level, using scintillation counter telescope 15 p2793 A70-31737
- Galactic cosmic rays origin in terms of statistical mechanical model of supernova explosions 15 p2799 A70-31793
- Galactic abundances and cosmic ray spectra by IMP-4 satellite, obtaining He ratio 15 p2793 A70-31794
- Quiettime cosmic ray ionization altitude dependence over polar regions from measurements by integrating ionization chamber on OGO-2 15 p2793 A70-31902
- Cosmic ray knee interpretation using polar orbiting ionization chambers data from OGO-2/4 15 p2793 A70-31903
- Polypropylene window proportional counter on board sounding rocket for cosmic soft X ray measurement 15 p2741 A70-32530
- Cosmic ray radial gradients and anisotropies, describing behavior in interplanetary medium 15 p2795 A70-32623
- Cosmic ray intensity increase due to meteor showers magnetic field trapping effect 15 p2795 A70-32723
- Charged particles and He nuclei spatial distribution from recordings in cosmic ray equator region by Cerenkov counter mounted on Proton 2 satellite 15 p2795 A70-32735
- Soviet monograph on modulation of cosmic rays in interplanetary space, covering anisotropic diffusion approximation, diffusion equation, Forbush effects energy spectrum, etc 16 p2971 A70-32911
- German-American HELIOS solar probe for solar wind, interplanetary magnetic field and cosmic rays 16 p2987 A70-34343
- Solar X-ray spectrum and intensity and diffuse cosmic flux measurements, using polar orbiting satellite-borne instruments 17 p3149 A70-34534
- Omnidirectional cosmic gamma ray flux in 1-6 MeV range observed by ERS-18 satellite 17 p3149 A70-34539
- Galactic gamma rays from OSO-3 observations attributed to decay of neutral pions produced by cosmic rays interaction with interstellar gas nucleons 17 p3150 A70-34567
- German monograph on artificially accelerated proton measurements for ionization calorimeter calibration and cosmic radiation energy spectrum analysis during balloon flight 17 p3081 A70-34572
- Energy loss of high energy cosmic rays traversing isotropic radiation field of arbitrary energy spectrum in pair producing collisions with ambient photons 17 p3150 A70-34598
- Galactic cosmic rays eleven year modulation, determining modulating region L depth from dynamical

phase lag between changes in cosmic ray intensity and solar activity

17 p3150 A70-34833

UV background radiation observed above atmosphere for intergalactic gas, Galaxy and subcosmic ray components

17 p3163 A70-34903

Pulsars as cosmic ray sources, emphasizing time properties of acceleration mechanisms

17 p3151 A70-34913

Anthracene, polystyrene and stilbene for scintillation counters measuring cosmic ray protons, analyzing dosimetric properties

17 p3151 A70-35352

Local system interstellar medium thermal electron distribution, synchrotron radiation emissivity, cosmic ray electron flux and spectrum

17 p3152 A70-35583

UV absorption lines in H I regions heated by cosmic rays, discussing possible detection by rocket or satellite spectroscopic observations

17 p3152 A70-35748

Radionuclides production rates in stratosphere from spallation reactions of cosmic rays with Ar

17 p3152 A70-35759

Secular variations calculation in cosmic ray cutoff rigidities by trajectory tracing process with geomagnetic field models

18 p3306 A70-36023

Cosmic ray variations during PCA absorption, relating Forbush decreases to lower ionosphere ionization intensity increase

18 p3306 A70-36096

Statistical analysis of cosmic radiation neutron component monitor error, taking into account generation multiplicity

18 p3307 A70-36097

Recording instrumental noise resolution of standard algorithm for cosmic ray stations

18 p3307 A70-36100

Periodic cosmic ray variations near Southern magnetic pole related to chromospheric flares

18 p3307 A70-36102

High altitude neutron supermonitor investigation of cosmic ray microvariations

18 p3307 A70-36104

Azimuthal muon telescope installation at cosmic ray station, noting photorecorder circuitry

18 p3256 A70-36108

Cosmic ray and radiation belt data from vertical probes, determining instantaneous cross section of atmosphere

18 p3307 A70-36169

Submillimeter wavelength night sky radiation background, observing effects on various cosmic ray phenomena

18 p3308 A70-36330

Superheavy nuclei origin in primary cosmic rays, proposing neutron stars/pulsars as sources

18 p3308 A70-36403

Ionization losses effect on spectrum of cosmic rays accelerated in solar chromosphere, interstellar space, supernovae, radiogalaxies, etc

18 p3308 A70-36425

Diffuse cosmic X ray background galactic component, using model to predict angular spread

18 p3308 A70-36484

Charge spectrum of heavy relativistic cosmic ray nuclei, using tracks from balloon-borne photographic emulsions

18 p3308 A70-36781

Cosmic ray muon intensity deep underground vs depth measured with liquid scintillation detector hodoscope

18 p3308 A70-36897

Cosmic X rays interstellar absorption, giving atomic He total photoionization cross section

18 p3308 A70-36899

Solar wind effects on galactic cosmic rays isotropic diffusion and density distribution in interplanetary space in presence of azimuthal asymmetry

18 p3309 A70-36903

Barometric and atmospheric temperature corrections of cosmic ray neutron component intensity fluctuations obtained statistically from monitor recording

18 p3309 A70-36904

Cosmic ray intensity increase preceding Forbush effect using statistical correlation method

18 p3309 A70-36918

Cosmic radio absorption nightly variations, considering ionospheric structure and composition and various scattering mechanisms

18 p3309 A70-36930

Interstellar gas thermal instability under cosmic ray heating, investigating perturbations causing transition to dense cool phase in pressure equilibrium with intercloud phase

18 p3309 A70-37003

Residual solar modulation of relativistic cosmic ray nuclei in galaxy over eleven years, observing magnitude at solar activity minima

18 p3309 A70-37009

Physical processes in galactic and extragalactic sources of nonthermal radio emission, assuming pulsars as principal magnetic field and cosmic rays sources

18 p3321 A70-37126

Relativistic electron spectra of cosmic rays accelerated by plasma turbulence, examining singularity in solution

18 p3322 A70-37127

Galactic radio corona existence, measuring northern galactic hemisphere sky brightness and cosmic ray distributions

18 p3322 A70-37129

Cosmic ray electron and low energy proton fluxes by satellite-borne detector during solar flare of 25 February 1969

19 p3496 A70-37507

Cosmic rays - Conference, Budapest, August-September 1969, Volume 1, Origin and galactic phenomena, covering supernovae, ray spectra, pulsar gamma rays, etc

19 p3497 A70-38076

Metagalactic and galactic sources of cosmic rays, including composition, electron spectra and radio emission

19 p3500 A70-38077

High energy cosmic gamma radiation detection from point source in Sagittarius, using balloon mounted spark chamber with Cerenkov telescope

19 p3500 A70-38078

High energy electron and photon cascades in Metagalaxy, considering electromagnetic radiation density and cosmic ray origin estimation

19 p3500 A70-38081

Critique of metagalactic origin of high energy cosmic rays, reviewing neutrino hypothesis

19 p3500 A70-38082

Acceleration of high energy cosmic rays by pulsar LF electromagnetic radiation

19 p3501 A70-38085

Cosmic ray high energy electron component intensity and spectra, using nuclear emulsion detector with counter triggered spark array

19 p3502 A70-38095

Cosmic ray electron and positron differential energy spectra during solar quiet times from OGO-5 satellite observations in interplanetary space

19 p3502 A70-38096

Interplanetary cosmic ray positrons energy spectral component with origin different from interstellar mesons decay

19 p3502 A70-38098

Galactic low energy cosmic ray positrons and gamma rays, considering production mechanism in interstellar space

19 p3503 A70-38099

Cosmic ray positrons and negatrons differential energy spectra and solar modulation, using balloon-borne magnetic spectrometer

19 p3503 A70-38100

Cosmic ray positrons and negatrons differential intensities near north geomagnetic pole from balloon flight measurements, noting solar modulation effects

19 p3503 A70-38102

Long term variations of cosmic ray electron spectrum above 500 MeV from balloon and satellite observations, noting reduction during Forbush decreases

19 p3503 A70-38105

Interstellar cosmic ray electron spectrum flattening below 3 GeV from OGO-5 observations

19 p3504 A70-38106

Cosmic ray electron spectrum above 100 GeV by emulsion-lead sandwich assembly, estimating residence time, hydrogen atoms number density in galactic disk, etc

19 p3504 A70-38108

High energy galactic gamma ray and X ray flux explained by cosmic ray electron scattering

19 p3504 A70-38112

Diffuse cosmic X rays produced by Compton scattering of far IR radiation on cosmic ray electrons

19 p3505 A70-38113

High energy galactic gamma rays photons, suggesting two-component cosmic ray source model

19 p3505 A70-38115

Traversed matter thickness and charge composition for high energy galactic cosmic rays with various propagation modes

19 p3506 A70-38123

Galactic cosmic ray energy spectra of light and medium nuclei from IMP-4 satellite measurements, investigating L/M ratio

19 p3506 A70-38124

Cosmic rays deuterons abundance calculation from H and He nuclei collisions with interstellar matter

19 p3506 A70-38125

Cosmic ray nuclei charge composition of elements Ne to Ni, using emulsion stacks exposure in balloon flights

19 p3506 A70-38126

Low energy galactic cosmic radiation energy spectra and charge composition in 2-14 Z range by OGO-5, suggesting two component model for origin

19 p3507 A70-38127

Cosmic rays shock from small mass supernovae explosions

19 p3507 A70-38128

Charge spectrum of high and low energy heavy cosmic ray nuclei, using balloon-borne nuclear emulsions

19 p3507 A70-38130

Cosmic ray nuclei chemical composition and energy spectra in 3-30 Z range by balloon flight and Pioneer 8 space probe, noting propagation models

19 p3507 A70-38131

Heavy cosmic ray abundance attributed to thermal nucleosynthesis during silicon burning at high temperature and density

19 p3507 A70-38132

Cosmic ray heavy nuclei charge composition from satellite-borne emulsion stacks exposure

19 p3507 A70-38134

Super heavy cosmic ray nuclei charge composition and track identification, using Lexan polycarbonate, cellulose triacetate (CTA) and nuclear emulsion

19 p3508 A70-38137

Cosmic ray track sources in meteoritic minerals, considering heavy primaries, secondary spallation and fission products

19 p3508 A70-38142

Galactic cosmic rays temporal and spatial variations in solar system, discussing nuclear active particles and spallation products depth distribution in meteorites

19 p3509 A70-38143

Relativistic cosmic rays nuclei abundances from Gemini 11 flight

19 p3509 A70-38144

Cosmic ray nuclei transformation and propagation in interstellar space, considering diffusion equation, cross sections, solar modulation, etc

19 p3509 A70-38145

Distribution functions of cosmic ray path length, obtaining exponential type for high and low energy data

19 p3509 A70-38146

Cosmic ray elements abundance at sources relative to carbon, comparing near-earth composition and solar photosphere

19 p3509 A70-38147

Cosmic ray lifetime, investigating radioactive Be 10 nuclei decay effects on intensity ratios Be/B and Be/Li, suggesting nuclei confinement to galactic disk

19 p3509 A70-38148

Sideral daily variation in cosmic ray muon intensity at 60 mwe depth, indicating extragalactic origin

19 p3509 A70-38149

Sideral cosmic ray diurnal variations using underground mu-meson telescopes in Northern and Southern Hemispheres

19 p3510 A70-38150

High energy cosmic rays sideral and solar anisotropy, using airborne Cerenkov telescope

19 p3510 A70-38151

Galactic cosmic ray anisotropy, discussing amplitude and phase values of daily sideral variation

19 p3510 A70-38152

Energy spectrum distortion of ultrahigh energy cosmic rays due to interactions with photons and neutrinos in universe

19 p3510 A70-38155

Galactic disk model for confinement of cosmic ray electrons, assuming isotropic background radiation

19 p3510 A70-38156

Cosmic rays propagation and production in Milky Way galaxy, using equilibrium model

19 p3510 A70-38157

Energetic cosmic ray particles transfer through interstellar space based on galactic disk model

19 p3511 A70-38158

Pulsars postulated as supernova remnants sources of local cosmic rays

19 p3511 A70-38159

Cosmic rays relationship to cosmological parameters and galactic radiation source evolution

19 p3511 A70-38160

Cosmic X ray background measurements, describing ESRO R/73 experiment

19 p3512 A70-38491

Galactic cosmic rays lifetime based on nuclei and matter interactions, discussing ionization losses effect

20 p3695 A70-38965

Cosmic ray electron and proton interaction, discussing hydromagnetic waves, synchrotron radiation, magnetic field effects and wave propagation

20 p3695 A70-39012

Diffuse cosmic X and gamma ray spectrum analysis, considering implications for Compton scattering models in intergalactic space

20 p3695 A70-39049

Cosmic electron spectrum formation by acceleration, considering metagalactic background X radiation

20 p3695 A70-39174

Cosmic soft X rays scattering by interstellar dust grains, observing source angular size dependence on distance, wavelength and grain properties

20 p3695 A70-39223

Interplanetary magnetic field large scale structure from cosmic ray intensity secular variations during solar activity cycle

20 p3696 A70-39276

Cosmic ray anisotropy 27 day and seasonal variations, considering neutron component data and sunspot magnetic field strength 20 p3696 A70-39277

Stratospheric cosmic ray intensity increases unassociated with chromospheric flares 20 p3696 A70-39278

Cosmic ray 27 day variations during solar activity minimum, noting unipolar magnetic regions role 20 p3696 A70-39280

Cosmic ray intensity decreases and Forbush effects energy spectra during various solar activity periods 20 p3696 A70-39281

Cosmic ray anisotropy sidereal-diurnal effects isolation by solving simultaneous amplitude and phase modulation problem 20 p3696 A70-39282

High energy cosmic ray-photon interactions, discussing ion production, nuclear fission, proton energy loss, red shift, etc 20 p3696 A70-39283

Cosmic ray neutron semidiurnal variations day and night components with respect to geomagnetic and solar activity 20 p3697 A70-39288

Cosmic ray neutron component differential and integral barometric coefficients, showing dependence on geomagnetic cutoff rigidity and atmospheric depth 20 p3697 A70-39290

Atmospheric dynamic effect on cosmic ray intensity, showing extremum and seasonal variation at midlatitudes 20 p3697 A70-39291

Cosmic ray beta neutron component barometric coefficients planetary distribution during IQSY, establishing latitude dependence for mountain and sea level equations 20 p3697 A70-39292

Electron formation by cosmic rays in atmosphere, taking into account impinging particles energy variations 20 p3697 A70-39293

Cosmic ray intensity variation during maximum meteor showers periods detected on earth, noting relationship to solar activity 20 p3697 A70-39294

Depth distribution of radioactive nuclei generated by cosmic rays in asteroidal sized bodies, calculating primary and secondary surface layer particle fluxes 20 p3698 A70-39295

Cosmic rays cutoff rigidity variations during magnetic storms, investigating flux increase due to current flow along parallel lines on magnetic shell surface 20 p3698 A70-39300

Algorithms for processing of cosmic ray data monitored by space station with multichannels for neutron and meson components recordings 20 p3698 A70-39309

Five-channel azimuthal underground cosmic ray telescope using proportional counters suitable for continuous recording 20 p3629 A70-39312

Multichannel cosmic ray recorder providing input to computer memory 20 p3629 A70-39313

Automatic cosmic ray station for recording nucleon and meson components 20 p3629 A70-39314

Diurnal anisotropy variations of cosmic ray intensity, taking into account neutron monitors data 20 p3699 A70-39346

Barometric coefficient altitude dependence of cosmic ray neutron monitor for vertical flux 20 p3699 A70-39347

Lower atmosphere cosmic ray ionization calculation, using high energy transport code 20 p3699 A70-39348

Fermi momentum upper limit for universe neutrinos in cosmic ray propagation, determining maximum proton energy 20 p3700 A70-39592

Cosmic ray superhigh energy electrons and neutrinos propagation in degenerate neutrino gas universe, considering gas density in cosmological models 20 p3700 A70-39593

Low altitude cosmic rays dosimetric measurement by Cosmos 228 apparatus 20 p3700 A70-39728

Forbush effects influence on cosmic layer state in lower ionosphere using long radio waves 20 p3700 A70-40095

Criticism of evidence for cosmic ray quark passage through low density bubble chamber 20 p3701 A70-40499

COS-B satellite cosmic X ray experiment with high sensitivity and long pointing time for extragalactic sources discovery 21 p3871 A70-40655

Galactic and extragalactic discrete cosmic ray sources by rocket observation with narrow slit collimators 21 p3871 A70-40656

Cosmic hard X ray sources spectra and time variations by balloons and OSO-3 satellite observations of Crab Nebula 21 p3872 A70-40657

Cosmic X ray spectra of Cyg XR-2 in 0.15-20 keV range by spinning rocket-borne detector, noting interstellar absorption 21 p3872 A70-40664

Cosmic gamma radiation from pulsars, examining atmospheric Cerenkov light generated by energetic particle showers 21 p3874 A70-40676

Magnetic field lower limit in Crab Nebula from cosmic gamma ray studies using optical reflector to detect atmospheric Cerenkov radiation 21 p3875 A70-40684

Diffuse cosmic X rays, discussing energy spectrum and contribution of galactic integration 21 p3875 A70-40686

Diffuse background cosmic X rays in energy range 20-120 kev from balloon observations 21 p3876 A70-40689

Low energy diffuse cosmic X radiation flux comparison with power law spectrum, observing asymmetry with respect to galactic latitude 21 p3876 A70-40692

Cosmic X ray background measurements at 25-200 keV onboard ESRO Skylark rocket, plotting results against galactic latitude 21 p3876 A70-40695

Omnidirectional cosmic gamma ray flux near one MeV observed by ERS-18 satellite, plotting spectral energy distribution 21 p3876 A70-40697

Extragalactic cosmic X ray background source models for intensity and energy spectrum, noting Compton scattering of black body photons by relativistic electrons 21 p3877 A70-40699

Innerbremsstrahlung of intergalactic protons colliding with electrons as source of cosmic background X rays, interpreting intensity and energy spectrum 21 p3877 A70-40700

Background gamma ray observations attributed to decay of pi-mesons produced by extragalactic cosmic ray protons collisions, noting radiation sources age 21 p3877 A70-40703

Diffuse X rays from nonthermal intergalactic bremsstrahlung, discussing cosmic ray injection models 21 p3878 A70-40705

Solar wind X ray emission, investigating diffused cosmic ray origin and flow pattern models 21 p3878 A70-40708

Low energy cosmic ray positrons arising from Co decay in Ni 56-Co 56-Fe 56 reaction chain in supernova Si burning shells 21 p3879 A70-40927

Ionospheric D region electron production by cosmic X rays, noting Lyman radiation effects 21 p3882 A70-41099

Multiplicity recorder for cosmic rays neutron component studies, reducing star redistribution errors by coincidence effect compensation 21 p3882 A70-41277

Balloon-borne monkeys possible brain damage due to cosmic rays, discussing thindown tracks and acute vasculitis 21 p3764 A70-41476

Apollo 11 lunar rocks and fines cosmic ray produced radioisotopes, considering surface exposure to high energy component flux 21 p3906 A70-41562

Tritium and Ar radioactivities attributable to galactic and solar cosmic ray interactions in Apollo 11 lunar rocks and soil 21 p3906 A70-41564

Cosmic ray exposure age of lunar surface material by radioactive isotopes Ar 37 and 39 measurement, investigating temperature dependence 21 p3909 A70-41607

Nuclear particle tracks in Apollo 11 samples due to galactic cosmic rays and solar flares relationship to dynamic surface processes 21 p3914 A70-41648

Apollo 11 bulk and core tube fines and rock cosmic ray tracks, discussing material history and corpuscular radiation flux and energy spectra near moon 21 p3916 A70-41667

Fe-group cosmic ray exposure tracks in Apollo 11 lunar rock interior, erosion rate and solar flare paleontology 21 p3917 A70-41673

Galactic evolution and secular variations of cosmic rays, magnetic fields and turbulence, assuming stellar birth rate dependence on gas density and temperature 21 p3919 A70-41700

Cosmic ray signal anisotropy around 0900 h sidereal time and 30-60 degree declination, investigating muon events in liquid scintillator 21 p3882 A70-41994

Cosmic ray energy loss in interplanetary medium, discussing solar wind effects on low energy particles 21 p3883 A70-42111

Cosmic X ray extinction and halo by interstellar grains, applying to light elements identification 21 p3883 A70-42200

High energy neutrinos generated by cosmic ray interactions with earth atmosphere, discussing detection, plotted energy spectrum and underground muons 22 p4093 A70-42310

Galactic soft X ray and subcosmic ray heating and ionizing of interstellar H I regions 22 p4094 A70-42985

Combined space and nuclear radiation effects in manned space flight 22 p3978 A70-43184

Anomalous angular distribution and inelastic cross section of muon-nucleon interaction for penetrating underground cosmic ray particles 22 p4095 A70-43232

Cosmic rays galactic propagation and confinement, discussing matter and star distributions, magnetic fields, positron flux and energy spectrum, etc 22 p4096 A70-43396

Cosmic ray research role in high energy physics, discussing elementary particle interactions 22 p4096 A70-43398

Scale invariance models correlation with cosmic ray data, comparing neutrino- and antineutrino- nucleon scattering 23 p4210 A70-43800

Outer space galactic cosmic rays energy spectrum and modulation region boundary determination, using meteorite observations 23 p4236 A70-44050

Interplanetary magnetic field inhomogeneities structure from galactic cosmic rays intensity fluctuations observation 23 p4237 A70-44053

Cosmic ray 11-year variation pattern change in 19th and 20th solar activity cycles determined by latitude expeditions spectrum analysis 23 p4237 A70-44071

Pioneer 8 and 9 cosmic ray detector system, discussing mechanical, electrical and data conditioning properties 23 p4195 A70-44300

Cosmic X ray sources astronomical observations and implications, considering Crab Nebula, galaxies, constellations, diffuse background radiation, etc 23 p4243 A70-44415

High Energy Astronomy Observatory for space X rays, gamma and cosmic rays research via unmanned spacecraft 23 p4261 A70-44680

Nike-Apache rocket aurora probes using proton detector to measure galactic cosmic ray intensity and relativistic electrons 23 p4192 A70-44879

Cosmic ray events angular distribution from scaling hypothesis 23 p4238 A70-44894

Light flashes observed by Apollo astronauts, proposing Cerenkov radiation or direct excitation of eye retina by cosmic rays 24 p4307 A70-45403

Relativistic cosmic ray LH nuclei abundance via Cerenkov scintillator telescope on polar orbiting OV1-10 satellite 24 p4397 A70-45522

Spallation limits on low energy cosmic and nuclear gamma rays interstellar fluxes, evaluating fast particle effects on interstellar medium 24 p4397 A70-45758

Cosmic ray electrons solar modulation, considering diffusion-convection theory 24 p4397 A70-45769

Excess galactic X rays, discussing synchrotron emission of high energy cosmic ray electrons 24 p4398 A70-46161

High energy electron proton and heavy nuclei absorption in pulsar vicinity, discussing implications for cosmic rays 24 p4398 A70-46170

Cosmic ray energy spectrum in absence of solar activity from eleven year ray variations, noting coincidence with galactic rays 24 p4398 A70-46279

European Space Research and Technology Center space science department, examining cosmic ray, ionospheric and surface physics divisions 24 p4323 A70-46356

COSMOGONY COSMOLOGY

Re 187 to Os 187 nuclear decay rate variability, discussing earth age, temperature and ionization effects 01 p0178 A70-10349

Einstein equations for Bianchi type IX universe model suitable for numerical solution and application to cosmology with pure fluid stress tensor 01 p0142 A70-10522

Coriolis effects in spherical Einstein universe perturbed by rigid body rotation of shell with finite thickness 01 p0186 A70-11272

Einstein-Friedman cosmology of vanishing constants assumed in deducing relations between antipodal radio sources red shifts and universe parameters

01 p0187 A70-12174

Finite rotating universe model construction not possessing Goedel cosmos pathological properties, discussing relation to Mach principle

01 p0191 A70-11358

Lemaître universe and galaxy formation effect on stability of quasi-static epoch, deriving limits for red shift, cosmic ray and electromagnetic fluxes

02 p0363 A70-11779

Universe oscillating closed model dynamics emphasizing conditions of collapse by contraction in terms of relativity theory

02 p0370 A70-12114

Particle-antiparticle creation in galactic nuclei, expelling particles while retaining antiparticles

02 p0371 A70-12195

Symmetric cosmologies within gamma ray measurement context showing antimatter limits in Milky Way and metagalaxy

02 p0371 A70-12196

Radio source ghost images in Lemaître cosmological models, deriving luminosity functions and radio source ages

02 p0371 A70-12198

Soviet papers on universe evolution covering interstellar structure, stellar evolution, multiple galaxies, galactic nuclei, etc

03 p0562 A70-12976

Magnetic cosmological nonuniformity hypothesis leading to galaxies and clusters isolation

03 p0564 A70-13224

Lagrangian gravitational field density related to contraction to expansion transition in terms of cosmological model, discussing quadratic corrections and singularity

03 p0524 A70-13412

Astronomical and space research methods probing fundamental questions concerning universe unsolvable by classical astronomy, discussing solar wind and stellar formation and evolution

03 p0571 A70-13790

Protogalaxy formation and molecular processes in primeval hydrogen gas, discussing cold gas cloud cooling mechanism and contraction

03 p0577 A70-14153

Brans-Dicke cosmological gravitational instability using Lagrangian gage for galaxy formation, discussing density contrast growth in time

03 p0577 A70-14154

Cosmochemistry, discussing interdisciplinary nature, goals, nuclear roots, information sources, key concepts involving elements age and origin, nuclear species abundances, chemical fractionation, etc

03 p0578 A70-14346

Protogalaxy mass limits determined for galactic formation by thermal instability due to radiative cooling and followed by nonlinear gravitational contraction

04 p0744 A70-14469

Double galaxy systems hypothesis with tidal interaction, presenting data from galaxy internal motion studies

04 p0747 A70-14519

Angular diameter data from Cambridge radio telescope for sources with different flux densities for cosmological models red shift tests

04 p0757 A70-15691

Elliptical cosmology, discussing evolutionary geometry, Synge distribution, galactic age and distance from earth, Friedman equations and independence of constants

05 p0905 A70-15794

Primordial cosmic ray sources evidence suggesting galaxies and quasars in initial stages of formation

05 p0897 A70-15921

Local theory alternative to cosmological quasar origin theories, considering red shifts properties

05 p0913 A70-16473

Coordinate system for synthesizing previous work on multifluid cosmologies, investigating noninteracting mixtures of multicomponent fluids

05 p0919 A70-16933

Einstein field equations based on variational principle applied to stability of general self gravitating relativistic gaseous mass obeying specific equation of state

06 p1138 A70-17304

Observation operators and cosmology, constructing equations for cosmological aggregates governed by Einstein field equations

06 p1105 A70-17529

Cosmic ray triggering of solar system formation by ionizing in solar disk

06 p1135 A70-17539

Cosmological theories taking into consideration gravitational collapse, discussing pulsars, quasars and X ray stars evolution

06 p1140 A70-17584

Cosmic evolution of radio sources, discussing observations and data interpretation

07 p1374 A70-18746

Galaxies statistical distribution studied to determine superclusters existence, correlating results with random distribution expectations

07 p1375 A70-18868

Galactic clusters analyzed for identifying possible relationship between cluster configuration, type of component galaxies and radio emission

07 p1376 A70-18907

Distance between objects in Friedman cosmological model determined on basis of red shift, determining relationship between observed and emitted wavelengths

07 p1377 A70-18945

Monograph on relativistic and steady state cosmology covering optical and radio astronomy, matter and galaxies origin, etc

07 p1379 A70-19101

General relativity taking into account astronomical and laboratory tests, cosmology and theoretical studies /1967 to 1969/

07 p1334 A70-19102

Observational extragalactic dependences obtained within framework of Friedman universe model with matter and neutrino background

07 p1383 A70-19407

Circular and radial trajectories in Schwarzschild field applied to isolated metagalaxy with charged central body and nonzero cosmological constant

07 p1385 A70-19426

Radiation catastrophe in universe in terms of cosmological models

07 p1368 A70-19628

Book on cosmic electrodynamics covering cosmic plasmas, sun and solar activity, interplanetary medium and geomagnetic cavity, magnetosphere, geomagnetic disturbance, radiation belt, etc

07 p1387 A70-19667

Signal reception possibly due to gravitational radiation of cosmic origin, estimating energy

07 p1387 A70-19699

Hamiltonian methods applied to homogeneous cosmological models, obtaining Einstein equations, passing to quantum theory by imposing canonical commutation relations

07 p1336 A70-19921

Singularity for absolute zero of time suggested for beginning of universe by Einstein relativity theory

07 p1336 A70-19922

Cosmological gravitation theory for uniformly expanding universe model providing fundamental reference frame and acceleration field

08 p1563 A70-20497

Age dating of earth and universe emphasizing methods based on radioactivity, discussing stellar evolution, galactic age and assessment of cosmic time

08 p1568 A70-20633

Soviet monograph on preplanetary cloud evolution and earth and planet formation covering convection, turbulence, gravitational instability and distribution function of bodies by size

08 p1568 A70-20725

Space-time singularities of gravitational collapse and cosmology indicated by timelike or null geodesic incompleteness

08 p1575 A70-21353

Mathematical model for finite-density nonhomogeneous Newtonian cosmologies, approximating solutions using coupled Vlasov-Poisson equations

08 p1581 A70-21740

Hubble expansion constant and expansion deceleration value roles in cosmological model testing

08 p1581 A70-21752

Cosmic ray origin models, considering universal and local metagalactic models and halo and disk galactic models

09 p1744 A70-22057

Observational verification of cosmological models by examination of red shift discretization in quasars

09 p1750 A70-22098

Neutrinos kinetic theory for anisotropic cosmological models

09 p1753 A70-22453

Gravitating bodies quasi-stationary rotating systems, giving equations of state and evolution

09 p1753 A70-22457

Cosmological solutions of Jordan-Dicke relativistic scalar-tensor theory, giving qualitative analysis of homogeneous isotropic problem at zero pressure

09 p1754 A70-22459

Orthodox cosmology validity, considering density-radius relation for stellar and galactic systems and Charlier hierarchical models

09 p1762 A70-23068

Static gravitation field of spherical mass immersed in cosmological gas, using combined model of Einstein and de Sitter static universes and Schwarzschild solutions

09 p1763 A70-23312

Instability of Godel rotating universe, discussing stability to perturbations in rotation plane and unstable density perturbations along rotation axis

10 p1937 A70-23973

Gravitational instability theory for large density perturbations growth during expansion of matter without pressure

10 p1945 A70-24961

Homogeneous open anisotropic relativistic world model with negative space curvature, observing shear decrease with time and magnitude reciprocal variation with function R/t

11 p2109 A70-25866

Energy concept in cosmology based on relativistic considerations, indicating universal time by synchronous clocks system

11 p2109 A70-25870

Milne special relativistic cosmology consistency with Birkhoff flat space gravitation theory, calculating red shift correction in galactic light

11 p2114 A70-26549

Hyperbolic velocity space physical significance based on cosmological model of light propagation associated with uniformly expanding universe

11 p2114 A70-26551

Evolutionary cosmological models for radio sources at large red shifts, considering source counts, luminosity functions, etc

11 p2117 A70-26655

Isotropic cosmic background radiation detection in presence of earth and galactic radiation, discussing influence on steady state cosmology

11 p2106 A70-26673

High energy break in isotropic gamma ray spectrum predicted from critical test of cosmological pion-decay hypothesis

11 p2106 A70-26844

Iconoclastic cosmology and remote sensing of universe, discussing cosmic scale photometry and extra-galactic red shift spectroscopy

12 p2296 A70-26924

Observational cosmology, discussing aspects of radio source and quasar counts, intergalactic medium and cosmic black body radiation

12 p2298 A70-27061

Singular and nonsingular cosmological models validity for general relativity allowing for cosmic dust

12 p2300 A70-27394

Cosmology theory, models, relativistic and Newtonian cosmology relations, Hubble diagram for cluster galaxies and radio source and quasar distribution

12 p2302 A70-27582

Cosmic rays origin, discussing choice between galactic halo and radio disk models for trapping region

12 p2295 A70-27883

Primordial radiation spectrum, discussing possible distortions due to energy injection before and after recombination

12 p2308 A70-27886

Condensed products of vaporized primordial terrestrial material accounting for moon formation, using single stage precipitation earth origin hypothesis

13 p2488 A70-28719

Soviet monograph on minor planets origin and physical nature, considering orbits, investigative techniques, etc

13 p2488 A70-28800

Cosmological constant role in closed universes with matter and radiation

13 p2490 A70-28936

Closed universe classical and quantum dynamics by ADM Hamiltonian treatment of Einstein equations for homogeneous cosmological models

13 p2495 A70-29812

Microscopic particle mass spectra in six dimensional scalar, spinor and vector fields, noting cosmological implications and eight dimensional theory

14 p2616 A70-30342

Nuclear reactions and elementary particle reactions in Friedman universe with positive lepton abundance and degenerate electrons, discussing prestellar helium synthesis

14 p2620 A70-30877

Adiabatic relation between initial plasma density perturbations and radiation temperature fluctuations during galaxies formation, discussing relic radiation fluctuations

14 p2632 A70-31286

Hot universe model for demonstrating distortions in Rayleigh-Jeans region of microwave relic radiation spectrum by primeval plasma heating before recombination epoch

14 p2632 A70-31287

Intergalactic medium lukewarm models, considering physical state, cosmic photon spectrum and isothermal and adiabatic expansion

14 p2651 A70-31291

Galactic spiral structure effects on residual stellar velocities local distributions

14 p2652 A70-31380

Dynamic spectrum of density fluctuations and galaxy clustering in Einstein universe, considering self gravitation of medium

14 p2652 A70-31389

Cosmogonic phenomena instability, discussing red shift, expanding universe, galactic nuclei and quasars

15 p2800 A70-32144

Stellar associations formation theory including effects of radiation, Rayleigh-Taylor instability and interstellar gas cold regions

15 p2801 A70-32478

Entropy increase, discussing universe heat death, earth energy balance, etc

15 p2809 A70-32907

Equations of motion and continuity for early and later stages of expanding universe, explaining matter concentration process of galaxy formation

16 p2976 A70-33783

Galactic composition differences, considering stellar and galactic nucleosynthesis

16 p2976 A70-33791

Cosmic time varying gravitational constant effects on stellar age determination

16 p2978 A70-33966

Model classification for relativistic universes containing noninteracting matter and radiation by cosmological constant and density parameters

16 p2979 A70-34190

Maxwell equations and equations of massive-vector-meson fields in spatially homogeneous Bianchi cosmologies, obtaining formula for homogeneous EM field

17 p3156 A70-34827

Anisotropic multifluid cosmological models with orthogonal velocity fields

17 p3157 A70-34839

Galactic evolution, reviewing Hubble theory of distances and red shift, Friedman model of expanding universe, big bang model, etc

17 p3168 A70-35328

Globular cluster stars, discussing cosmological importance, stellar development models, main sequence stars, red giant models, He content, age computation, etc

17 p3171 A70-35447

Gaseous disk in equatorial plane of solar nebula, determining dimensions from accretional theory for planets formation

17 p3172 A70-35584

Uniform model universes containing gaseous matter and background blackbody radiation, solving Einstein equations without zero pressure assumption

18 p3313 A70-36215

Cyclic models of evolving universe corresponding to positive, negative or zero cosmological constant

18 p3314 A70-36421

Vacuum-like state of physical medium as initial state of Friedmann cosmology, noting fluctuation instability for conversion into ordinary matter

18 p3315 A70-36643

Log S /flux-log Z /redshift/ diagram for radio galaxies, encouraging steady state cosmology

18 p3320 A70-37074

Cosmological models with matter and radiation for evolution of universe

18 p3322 A70-37132

Galaxies pairs motions, considering disintegrating, rotational and oscillatory types for comparison with observational data

18 p3322 A70-37133

Spiral galaxies structure, considering maintenance problem and effect of possible gas inflow from intergalactic space

18 p3326 A70-37152

Antimatter distribution in universe, investigating mass lower limit

19 p3518 A70-38025

Cosmic rays relationship to cosmological parameters and galactic radiation source evolution

19 p3511 A70-38160

Galactic nuclei activity effect on galactic evolution and cosmology, discussing stellar and gaseous components

20 p3707 A70-39938

Quasar red shift apparent magnitude data analysis, estimating deceleration parameter of universe

20 p3709 A70-40076

Time travel and cosmological model based on Einstein relativity theory, considering hypothetical motor design, energy supply, tachyons and four dimensional orbits implications

20 p3710 A70-40132

Radio source counts from Ohio State University observations, noting faint sources decrease relative to uniform Euclidean universe

20 p3713 A70-40427

Universe homogeneous isotropic model with thermal radiation at outset, considering nucleons and antinucleons interactions

21 p3884 A70-40910

Universe density estimation by galaxy formation theory, discussing spiral galaxies intergalactic gas thermal radiation and soft X rays

21 p3887 A70-41113

Friedmann universe evolution after big bang via Hagedorn hadronic equation of state, noting primordial He abundance criterion

21 p3888 A70-41122

Cosmic evolution of radio sources, discussing observations and data interpretation

21 p3890 A70-41171

Radio source count formula in zero pressure model universe for background radiation differential density evolution function

21 p3923 A70-42104

Extragalactic radio source count interpretation of cosmological model and evolution, discussing luminosity, electron scattering and red shifts effects

21 p3923 A70-42105

Mass spectrometer and high voltage converter powering electrostatic plasma and solar wind analyzer for cosmic space studies on Sputnik 3 and Heos A satellites

22 p4025 A70-42312

Lunar origin by capture, discussing moon orbit evolution, thermal history and surface features, earth evolution and tidal interactions

22 p4098 A70-42550

Einstein gravitational equations solution for expanding universe, discussing possible sudden collapse into zero volume with infinite density

22 p4105 A70-43215

De Sitter nonempty static cosmological model, examining possibility by comparing integral luminosity function for cosmic radio sources to radio galaxies statistics

22 p4106 A70-43258

Universe cold matter structure and distribution from far IR data

22 p4096 A70-43395

Newtonian hydrodynamic analogies for homogeneous anisotropic models in general relativity

22 p4075 A70-43472

Gravitational equations with oscillatory physical singularity, noting Bianchi type IX homogeneous metric

22 p4063 A70-43477

Metric evolution in oscillatory mode of approach to singularity in homogeneous cosmological models in asymptotic region, showing Kasner epoch dependence on perturbation

22 p4075 A70-43478

Friedman-Lemaître model role in big bang cosmology

23 p4238 A70-43812

Optical point characteristics of static spherically symmetric space-times of de Sitter universe, Einstein universe and exterior Schwarzschild field

23 p4239 A70-43821

Stellar associations formation theory including effects of radiation, Rayleigh-Taylor instability and interstellar gas cold regions

23 p4239 A70-43903

Einstein field equations for spatially homogeneous spaces, considering rotating matter model in regularized Euler-Lagrange form

23 p4219 A70-44406

Neutrino processes in lepton era as primeval fireball relic, discussing coupling constant for muon-electron neutrinos interactions

23 p4253 A70-44849

Extragalactic astronomy research covering quasars, Seyfert and related galaxies, cosmology, Magellanic Clouds, supernovae, etc

23 p4256 A70-45040

Primeval cosmic magnetic fields origin, discussing galactic fields and limits on present intergalactic field

24 p4403 A70-45396

Big bang temperature problem, discussing galactic masses determination possibility by gravity-strong interactions interplay in early stages

24 p4403 A70-45402

Nonlinear Lagrangians in relativistic cosmology of open oscillating world model

24 p4404 A70-45409

COSMONAUTS

Soviet book on survival in space covering astronauts training, behavior, impressions, performance, etc, with historical considerations

01 p0033 A70-10493

COSMOS SATELLITES

NT COSMOS 110 SATELLITE

NT COSMOS 149 SATELLITE

COSMOS SATELLITES

NT COSMOS 4 SATELLITE

NT COSMOS 44 SATELLITE

NT COSMOS 110 SATELLITE

NT COSMOS 149 SATELLITE

Solar X ray flare regions size, structure and localization from Cosmos 166 and 230 heliograph observations

01 p0168 A70-10252

Fast charged particles measurements by Cerenkov counter in Cosmos 137 satellite, noting hard electron flux and cosmic ray radiation spectrum

01 p0172 A70-11509

Superconducting magnetic system in magnetic analyzer of positrons and electrons in primary cosmic radiation tested on board Cosmos 213

04 p0685 A70-14443

Scientific equipment on Cosmos 237 satellite for recording extraterrestrial radiation data, discussing specifications, operation and mission purpose

05 p0851 A70-16733

Neutron flux measurements on Cosmos 53, equipment and calculation of secondary neutrons due to bombardment of satellite components

05 p0905 A70-17112

Satellite recording of electron-positron annihilation gamma emission on Cosmos 135 artificial earth satellite relating to meteors antimatter nature

07 p1371 A70-20334

Geoactive low energy particles and fresh photoelectrons interactions with upper atmosphere observed by satellite Cosmos 261

08 p1492 A70-21796

Intercosmos 2 equipment for measurement of positive ion concentration, electron temperature and energy distribution, electron concentration between satellite and ground reception points, etc

12 p2207 A70-27500

Superconducting magnetic system in magnetic analyzer of positrons and electrons in primary cosmic radiation tested on board Cosmos 213

13 p2403 A70-28468

Soviet lunar and interplanetary space missions during 1969 including Venera, Cosmos, Luna and Meteor satellite activities

13 p2505 A70-28901

Nonrecoverable Cosmos satellites lifetimes comparison with last stage rockets

14 p2638 A70-30690

Intercosmos 1 satellite for observing solar UV and X-ray emission in solar flares prediction

15 p2738 A70-32145

Night sky brightness in UV and visible region by photoelectric photometers on Cosmos 51 and 213 satellites

17 p3163 A70-34901

Earth radiation measurement at 10-12 microns by Cosmos 243 satellite-borne radiometer, comparing temperatures for boundary air layers in cloudless conditions

18 p3247 A70-36630

Proton magnetometer measurements from satellite Cosmos 49, observing residual and broad magnetic anomalies

18 p3248 A70-36770

High energy primary gamma quanta intensity limits from Proton-2 and Cosmos-208 measurements

19 p3502 A70-38092

Automatic control of Cosmos spacecraft docking maneuvers in two successive encounter phases

23 p4264 A70-45016

COSMOS 5 SATELLITE

Molecular ion concentrations, using flat probe collector trap on Cosmos 5 satellite at 200-300 km

07 p1276 A70-20421

COSMOS 44 SATELLITE

Cosmos 44 quasi-draconic period analytical and graphical determination, comparing moments of meridian intersection with INTEROBS observations

02 p0363 A70-11767

COSMOS 110 SATELLITE

Cosmos 110 satellite experiments concerning radiation effects on lysogenic bacteria and plants

23 p4149 A70-45030

COSMOS 137 SATELLITE

Cosmos 137 proton spectra data obtained in inner radiation belt agreeing with Relay 1 data

11 p2106 A70-26786

COSMOS 149 SATELLITE

Cosmos 149 meteorological satellite telephotometer, radiometer and other electronic equipment for measuring atmosphere and underlying surfaces physical parameters

01 p0095 A70-11611

Cosmos 149 meteorological satellite telephotometers for measuring reflected solar radiation from earth

01 p0095 A70-11612

COSPAR [COMMITTEE]

U COMMITTEE ON SPACE RESEARCH

COSERAT SURFACES

Cosserat spectrum elastic theory, considering static problems

20 p3726 A70-39876

Sound velocity in isotropic nonlinear elastic Cosserat continuum with constrained particle rotation, analyzing uniaxial and hydrostatic compression

20 p3734 A70-40434

Elastic stability theory Cosserat surface subjected to conservative nongyroscopic surface and edge loading

21 p3939 A70-42027

Cosserat elasticity constitutive equations, coupling rotation vectors to eliminate stress indeterminacies

21 p3941 A70-42251

Stress fields of screw and edge dislocations in linearly elastic isotropic Cosserat continuum using stress functions

23 p4266 A70-44022

COST ANALYSIS

Integrated logistic support for cost effectiveness of ground communication system

01 p0220 A70-10114

Cost effectiveness tradeoff analysis for reliability incentive contracts, evaluating customer requirements for military procurement

01 p0220 A70-10115

Differences in aircraft operating costs, performance characteristics and demand for aircraft by domestic trunk airlines /1932-1965/
[AIAA PAPER 69-1059] 01 p0005 A70-10637

Availability model for system with exponential reliability function and constant repair time, determining start-up costs, cost-optimal mean up and down time, etc
01 p0221 A70-11382

Cost effectiveness analysis applicable to DOD military system selection and acquisition, using model to study airborne electronics subsystem
02 p0401 A70-11673

Cost model based on initial and support costs for studying availability variations effect on system total cost and maintainability and reliability interrelationship
02 p0401 A70-11674

Air cargo transport development and organization trends, considering cost and aircraft types
02 p0401 A70-11736

Cost effective phased buildup of computerized ATC systems
02 p0401 A70-11961

Associative processor with content addressability and simultaneous arithmetic capability to circumvent speed restriction, comparing performance and cost with conventional digital computer
02 p0265 A70-12186

Solar electric propulsion /SEP/ for automated planetary missions, discussing system characteristics, capabilities and costs
[AIAA PAPER 69-1103] 02 p0382 A70-12531

Incremental profit and total airline profit model programs for air cargo systems
[SAE PAPER 690413] 03 p0411 A70-12899

Event probability and cost effects on performance in continuous motor task
03 p0436 A70-13771

R and D effect on aircraft engine business, considering aircraft operating cost, funds allocation, etc
04 p0787 A70-14390

Parametric performance and cost comparison of separate and integral vehicle concepts for manned space activity using payload criterion
04 p0763 A70-15420

Integrated logistic support economics considered in selecting support system for generating quantitative data for cost optimization
[SAE PAPER 690632] 05 p0959 A70-15846

Cost/schedule planning and control system /C/SPCS/ providing early exposure of inadequacies in work execution and initial planning
05 p0959 A70-16461

Aircraft transport tariffs used to determine economic approach to design
07 p1426 A70-18841

Research diets cost analysis including labor, ingredients, preparation and storage
07 p1217 A70-18949

Launch vehicle minimum cost design emphasizing flight vehicle evolution stages via effect on costs
[AIAA PAPER 70-240] 07 p1396 A70-20378

Aerospace vehicles testing cost and technical analysis, discussing component failure, motivation effects, test design optimization, flight simulation, etc
[AIAA PAPER 70-239] 07 p1396 A70-20379

Reusable air breathing launch vehicle for earth orbit shuttle, comparing performance, costs and operation with rocket powered systems
[AIAA PAPER 70-270] 07 p1396 A70-20381

Ground and onboard electronics systems for space shuttle vehicles, discussing role in equipment reliability and maintainability, life cycle costs, management control, etc
[AIAA PAPER 70-261] 07 p1396 A70-20391

Space transportation system objectives including design, operations and economics
[AIAA PAPER 70-263] 07 p1398 A70-20393

Unmanned and manned interorbital shuttle systems for satellite placement and repair and planetary spacecraft insertion, emphasizing cost analysis
[AIAA PAPER 70-267] 07 p1398 A70-20396

Optimal distance between satellite communication system ground stations for surface network cost equivalent, analyzing economic efficiency for various cases
08 p1456 A70-20569

Tandem link multichannel LOS FDM-FM communication system cost optimization by computer-aided design
08 p1459 A70-20798

Alternative equipment maintenance procedures costs by combined discrete event and continuous system simulation, discussing additional model applications
08 p1466 A70-20927

GPSS simulation for airport capacity, analyzing aircraft ground traffic flow characteristics and developing expansion schemes minimizing investment
08 p1481 A70-20929

Economic and social benefits from weather forecasting developments, noting expenditures on satellites and high speed computers
08 p1539 A70-21826

One dimensional Poisson production process under costly surveillance, considering maximum attainable income rate approximation
09 p1653 A70-22347

Earth Resources Satellite Information Systems, discussing NASA Space Application Program relation to national goals, federal spending, cost effectiveness analysis, information sales, etc
[AIAA PAPER 70-333] 09 p1793 A70-22860

Earth resources sensor integration into satellite or aircraft, discussing cost effectiveness
[AIAA PAPER 70-316] 09 p1677 A70-22871

Certification process for supersonic transports taking into account safety and economic considerations
09 p1610 A70-22949

Preamplifier-discriminator-gate generator in printed circuit for use with photomultipliers, noting pulse sensitivity and cost
09 p1679 A70-22997

Fighter flight control design criteria for providing maximum combat effectiveness, safety and survivability without excessive cost or risk
[AIAA PAPER 70-515] 09 p1611 A70-23021

Demand assignment /DAMA/ and preassignment /PAMA/ Multiple Access Systems mix for cost minimization, developing algorithm for satellite high usage groups and overflow facilities
10 p1838 A70-24357

Cost analysis for satellite data system determined for bit rates range and break-even distances
10 p1838 A70-24361

Cost and deadline planning for system development, suggesting theoretical methods tests regarding applicability
10 p1971 A70-24597

Test program effectiveness for Saturn Instrument Unit /IU/, summarizing objectives, costs and results
[AIAA PAPER 70-379] 10 p1891 A70-24924

Cost-property index /B/P/ to compare economic success of composites, metals, glass and ceramics for load bearing applications
11 p2136 A70-26077

Algorithm for infinite dimensional optimal control problems associated with maximum deviation cost functionals distributed systems
11 p2073 A70-26234

Low cost launch and reentry vehicles, surveying technology and economics of spacecraft
11 p2126 A70-26286

Channel assignment, considering low cost solution and co-channel interference
11 p2010 A70-26310

Aircraft turbojet and turbofan engines cost correlation to performance statistically analyzed in terms of various parameters
[SAE PAPER 700270] 12 p2335 A70-27437

Optimal singular controls made nonsingular for decreasing epsilon values by adding integral quadratic functional of control to cost functional
13 p2382 A70-29066

Performance cost functions for reaction-jet controlled spacecraft during on-off-on limit cycle
13 p2382 A70-29072

Reliability guarantee vs cost of capital, analyzing contract compliance delay and discounted penalty expenditures
13 p2525 A70-29570

Air navigation and control systems cost-benefit analysis including ground services, safety and R and D
14 p2667 A70-30103

Guidance system cost and reliability by Monte Carlo analysis of failure statistics
14 p2614 A70-30462

Aircraft manufacturing market research including cost compatibility with resources and capabilities
14 p2668 A70-30937

Civil aircraft design optimization, considering operating and seat mile costs, speed, wing and fuselage, engine location, etc
14 p2531 A70-30941

Designer and operator influence on total aircraft operating costs
14 p2669 A70-30942

Design costs for large subsonic transport engines in terms of size, engine ratings and community noise
14 p2629 A70-30944

Airliner fuselage shape design and effect on manufacturing and flight operation economics
14 p2532 A70-31369

Dynamical systems optimal control approximation without solving differential equations, considering linear systems with quadratic cost functional
14 p2562 A70-31411

Automatic optimal discrete time control for linear distributed parameter systems with quadratic cost function
14 p2562 A70-31412

Filament winding reinforcement and resin noting production equipment and costs
15 p2744 A70-31932

Computer program /SORCBE/ for systems unavailability tradeoff vs added cost for various versions
15 p2706 A70-32658

Maintenance vs redundancy for manned space station economy, considering costing structure and time increase for maintenance
15 p2713 A70-32666

Twin jet light transport Corvette airframe, discussing flight characteristics and economical aspects
15 p2676 A70-32793

Aerospace program oriented language /APOL/ requirements for flight programs, discussing cost, design and applicability
16 p2868 A70-33431

Axial flow multistage turbines performance, examining profile manufacturing tolerances effects on cost
16 p2970 A70-33677

Low cost headup displays /HUD/ for pilot error reduction during takeoff, approach and landing, discussing displayed functions vs cost tradeoffs
16 p2911 A70-33818

Polish Lot airline long haul air transportation cost analysis
17 p3199 A70-34689

Long haul air transportation profitability based on Polish Lot airline ton passenger-km computation comparison
17 p3199 A70-34691

Experiment space module combined with space station and serviced by shuttle for low total cost and maximum flexibility in funding and scheduling
[AAS PAPER 70-034] 17 p3175 A70-34777

Configurational and operational characteristics for space shuttle design, considering economic tradeoffs between expendable and reusable systems
[AIAA PAPER 70-045] 17 p3175 A70-34783

Performance cost functions of on-off limit cycle controllers for reaction jet controlled system
17 p3056 A70-35552

Unmanned and manned interorbital shuttle systems for satellites placement and repair and planetary spacecraft insertion, emphasizing cost analysis
[AIAA PAPER 70-267] 17 p3172 A70-35650

Small earth stations to link isolated areas with Intelsat network, discussing costs
18 p3229 A70-36957

System with N independently failing subsystems minimum cost solution mathematical model based on opportunistic preventive replacement policy
19 p3437 A70-38400

Optimum reliability level in terms of economic benefits and external constraints
19 p3554 A70-38595

Economics of reliability relating risks of failure and cost of failure prevention
19 p3555 A70-38841

Boeing 747, L-1011 and DC-10 introduction costs, profits and terminal facilities
19 p3357 A70-38951

Space shuttle design, considering costs, boosters, payloads and orbits
20 p3716 A70-39795

Technological and economic problems of reusable aeroballistic and ballistic launch vehicles
20 p3562 A70-40150

Weight/cost systems engineering, discussing techniques for using historical data banks and standardized reporting procedures
[SAWE PAPER 866] 20 p3741 A70-40368

Measuring and test equipment economic approach to quality levels and accuracy ratios, deriving cost tradeoffs in optimum inspection fidelity
20 p3634 A70-40453

Optimal and conventional good control systems relationships, considering open and closed loop characteristics, cost functions, etc
21 p3926 A70-40781

Aerospace vehicles testing cost and technical analysis, discussing component failure, motivation effects, test design optimization, flight simulation, etc
[AIAA PAPER 70-239] 21 p3931 A70-41876

Control space properties of pareto-optimal and cooperative solutions for static continuous and differential games involving vector cost criteria
22 p4061 A70-42460

U.S. and European space program costs and resources with particular reference to telecommunication satellites
22 p4126 A70-43247

Long range air transport routes, predicting equipment and expenditures modifications
22 p4128 A70-43533

Space transportation systems cost comparison, taking into account national program goals and near/far orbit traffic fraction
23 p4285 A70-44511

Economic and design aspects of universal Orbit-to-Orbit Shuttle component of Space Transportation System
[SAE PAPER 700763] 24 p4416 A70-45868

Aircraft maintenance cost statistical analysis recursive regression model for aircraft failure and manhour cost data
24 p4292 A70-46125

Technological and economical characteristics of serviced and unserviced automatic hydrometeorological stations and second class nonautomatic station 24 p4340 A70-46406

COST EFFECTIVENESS

Cost effectiveness in Ti forming, discussing materials, tooling and fabrication cost ratios 10 p1970 A70-23852

Ground and flight tests in aeronautical system development process as transfer of basic technology into cost effective operational systems [AIAA PAPER 70-381] 10 p1857 A70-24172

Demand assignment economics relative to ground stations in satellite telecommunication systems 10 p1838 A70-24360

Silver cathodes and plasma-sprayed anodes for cost effective hydrogen/oxygen fuel cells with solid zirconium dioxide electrolyte, considering carbon precipitation avoidance 10 p1830 A70-24459

Integrated microwave systems development taking into account cost effectiveness and anticipating kilowatt and megawatt systems 10 p1851 A70-24880

Nonavionic Aircraft Integrated Data System configurations evaluation by computer model, showing cost effectiveness data in terms of aircraft maintenance and availability [AIAA PAPER 70-396] 10 p1808 A70-24909

Reusable ballistic orbital-global transportation systems using rocket sled-assist-takeoff compared to SST systems in terms of effectiveness and cost 11 p1222 A70-26048

Lunar and planetary exploration costs and technology, discussing role of nuclear propelled passenger vehicles 11 p2082 A70-26061

Electrochemical machining of metals with complex shapes, discussing performance capabilities and cost efficiency [ASTME PAPER MR-69-711] 12 p2239 A70-26989

Wide goods fabrication of boron composites, discussing mechanical properties and cost effectiveness [ASTME PAPER EM-69-142] 12 p2240 A70-27078

Avionics technology cost effectiveness effect on airlines and industry, considering systems engineering and specifications [SAE PAPER 700299] 12 p2335 A70-27447

Manned Mars flyby/orbiter mission, discussing cost, scientific returns, technology advances, popular support, etc 12 p2304 A70-27749

Cost effective data transmission method for high performance under intersymbol interference and noise 12 p2187 A70-27935

Cost optimal carrier rocket system for European satellite TV, communication, navigation and earth survey networks 13 p2502 A70-28448

Cost optimal booster stage for European satellite launchers, comparing liquid and solid propellant rockets 13 p2502 A70-28450

Bora-Sond rocket for cost effective upper atmospheric sounding, discussing Li-Al-O systems performance 13 p2504 A70-28684

System reliability and effectiveness - Conference, Beverly Hills, February 1969 13 p2524 A70-29564

Cost effective spares provisioning models for airline operations, minimizing availability-cost ratio for line replaceable unit and total fleet 13 p2525 A70-29571

Relative cost benefits estimation of manual and automatic test systems for avionics in maintenance organization, proposing integrated maintenance and ATC data system 13 p2525 A70-29679

Avionics on military combat-reconnaissance aircraft, discussing automatic systems testing and cost effectiveness model 13 p2380 A70-29698

Multimode system analysis, using automated technique to calculate effectiveness and cost down to component level 13 p2525 A70-29837

Incentive earnings and payments in CPIF/cost plus incentive fee/ contracts, considering legal principles 14 p2668 A70-30523

International cooperation in military aviation emphasizing cost effectiveness in R and D, production and export prospects 14 p2669 A70-30939

Apollo project overview and quality-cost effectiveness assurance requirements for future space programs 14 p2654 A70-31103

Quality control variables optimization for maximum net revenue, using computerized simulation 14 p2592 A70-31105

System effectiveness apportionment for constraints existing on accountable factors using Lagrange multiple method 14 p2669 A70-31111

Global weather forecasting network costs and benefits evaluated using mathematical criteria 14 p2670 A70-31142

Global weather prediction network economic benefits to key industries, discussing adverse weather effects on production schedules, fuel supplies, construction, harvesting, etc 14 p2610 A70-31143

Cost effective reliability prediction techniques, discussing precision gyros procurement by NASA 15 p2736 A70-31964

Space research cost effectiveness in weather forecasting, TV broadcasting, space biology and medicine, geodesy, aerial and maritime navigation, earth resources, etc 15 p2811 A70-32283

Numerically controlled /N/C/ machines reliability program based on organized failure reporting and analysis system for cost effectiveness and downtime reduction 15 p2747 A70-32635

Subcontracting for cost optimal parts screening, discussing negotiations and reliability requirements 15 p2747 A70-32651

Cost effectiveness of higher order language /HOL/ for airborne computers 16 p3003 A70-33428

Ball bearings selection criteria, analyzing cost-value tradeoffs [ASME PAPER 70-DE-48] 16 p2918 A70-33511

Space shuttle avionics cost effective design approach, discussing guidance, commonality, reliability, communications and autonomy 16 p2982 A70-33802

Aircraft utilization rate vs invested money as factor determining financial justification of corporate aircraft operations, discussing maintenance engineering 16 p2921 A70-33822

Explosively actuated /pyromechanical/, devices for spacecraft, discussing guidelines for design, testing, application and cost efficiency 16 p2963 A70-34125

Candidate products for manufacturing on space station, emphasizing liquid solid transformations, bubbles and droplets, polymerization, and cost effectiveness [AAS PAPER 70-036] 17 p3041 A70-34791

Materials selection for cost effectiveness in 1980s airframe applications [AIAA PAPER 70-870] 17 p3199 A70-34819

Cost effective reliability apportionment in spacecraft subsystems, allocating failure-risk goals by mathematical model 17 p3101 A70-35160

Space vehicle optimal design based on reliability analysis, taking into account cost of materials strength tests [JPL-TR-32-1496] 17 p3188 A70-35224

Start-stop dynamics as cost effective method for computerized testing of digital modules and subassemblies, providing static and dynamic capability 17 p3062 A70-35504

Identification-adaptive control algorithm for quadratic cost control of discrete linear systems 17 p3057 A70-35558

Subsonic aircraft size effect in conventional design, discussing increased weight increments and economic gain rate [AIAA PAPER 70-940] 17 p3021 A70-35849

Air transport operations and economics in 1970 decade, taking into account cost-revenue ratio and cost effectiveness of various aircraft 17 p3204 A70-35852

Air cargo transport growth, considering deterrents of high freight rates, ground movement time and customs clearance 17 p3204 A70-35853

Cost effective spacecraft testing in terms of statistical reliability, program effectiveness and equipment costs 19 p3554 A70-38293

Cost effectiveness methodology for space program, industry, military sector, etc 19 p3554 A70-38402

Automatic test equipment, considering capability, control and display facilities and system cost 19 p3401 A70-38542

Satellite earth resources, discussing cost benefit analysis and economics in agriculture, forestry and mapping 20 p3739 A70-39065

Cost and time optimization for complex aircraft development projects via network planning 20 p3740 A70-39644

Optimum calibration intervals determination for obtaining instrument maintenance quality level at low cost 20 p3634 A70-40452

Cost optimal space shuttle systems, discussing booster configurations, weight and performance factors, technology utilization, etc 21 p3929 A70-40984

Military program cost effectiveness and control, considering resources and products 21 p3955 A70-41173

Airborne digital computers in aircraft systems, discussing optimization, design and economic effectiveness 21 p3796 A70-41920

Nuclear electric space propulsion, emphasizing systems uncertainties and cost aspects 22 p4070 A70-43187

Space shuttle mission and economics, discussing cost effectiveness, capabilities, satellite transportation payloads and traffic forecasts 22 p4127 A70-43505

U.S. SST flight deck instrumentation and cockpit displays during flight, discussing economic analysis of operations [ICAS PAPER 70-59] 23 p4139 A70-44155

Manned space flight regenerative life support systems requirements, considering weight, volume, power, cost effectiveness and integration problems 23 p4156 A70-45023

Cost/design performance management system, noting cost reduction and avoidance needs during design definition [SAE PAPER 700772] 24 p4430 A70-45866

Automatic weather station cost effectiveness criteria based on concepts of loss and error functions 24 p4323 A70-46405

COST ESTIMATES

Cost-effective look at vacuum testing of spacecraft components, noting sensitivity prediction and thermal cycle test 01 p0055 A70-10113

Cost tradeoff analysis of electronic equipment for systems reliability design, considering component derating, redundancy and selection 01 p0049 A70-10119

STOL aircraft configurations optimization including cost effectiveness, considering propulsive lift systems [AIAA PAPER 69-1131] 01 p0162 A70-10609

TV broadcast satellite system operating with home receivers or special receivers, evaluating technological and cost factors [AIAA PAPER 68-1061] 01 p0044 A70-10831

Solid rocket engine components technologies, studying effects of cost consciousness [SAE PAPER 690702] 05 p0922 A70-15828

Manned Mars mission planning, discussing technologies and costs for planetary landing 09 p1757 A70-22676

Long range army budget forecasting model based on research projects cost distributions and parameters, describing computer program 09 p1794 A70-23415

Resource allocation model with cost-effectiveness relationship for Army long range R and D 09 p1795 A70-23417

Satellite communications system optimal parameters and efficiency dependence on working capacity, discussing economic aspects of HF sets increased number 11 p1995 A70-25345

Titan 3 launch vehicles capabilities communication satellites deployment modes, presenting cost and availability data for preliminary mission planning [AIAA PAPER 70-482] 11 p2121 A70-25451

Product oriented cost data bank for satellite system cost prediction and negotiation designed for USAF communications satellite program [AIAA PAPER 70-445] 11 p2152 A70-25477

ATC ground hardware technology implementation, considering national air space system, airports, cost estimates and capacity increase 11 p2078 A70-25722

Edwards Inquiry Report into British Civil Air Transport based on cost effective economic study, involving airlines and regulatory system 11 p2153 A70-25855

Weights, sizes and costs of nuclear and nonnuclear spacecraft power systems with reference to mission duration 11 p2082 A70-26260

Computing optimum flight profiles by Balakrishnan epsilon method, including equations of motion constraint in cost function to be minimized [AIAA PAPER 69-75] 12 p2162 A70-28088

Quality control goals for manufactured products translated into manufacturing process inspection and investment costs terms 13 p2421 A70-29675

Project cost estimate growth pressures on decision making by U.S. Air Force System Program Office director 14 p2667 A70-30521

Price estimate elements interrelationship using three dimensional matrix for computerized cost data extraction 14 p2668 A70-30524

- Deterministic model for cost effectiveness of avionics support programs based on subsystems support ability, test philosophy and test equipment design and manufacture
[AIAA PAPER 69-305] 14 p2563 A70-30857
- Microwave filters developments, performance, production and costs 14 p2559 A70-31374
- Aircraft engine production cost estimating techniques, discussing physical, thermodynamic and metallurgical characteristics
[SAE PAPER 700271] 18 p3350 A70-36818
- Project risk or cost estimation for antipollution, moon mining, tooling, burn-in test and warranties by theory of Takacs processes and correlated queues 19 p3354 A70-38598
- Aircraft manufacturing cost estimation in conceptual design phase, using structural synthesis program for cost buildup simulation
[SAE PAPER 865] 20 p3741 A70-40371
- Satellite communications system optimal parameters and efficiency dependence on working capacity, discussing economic aspects of HF sets increased number 20 p3589 A70-40457
- Worldwide common satellite network for sea and air navigation, discussing cost estimate and economics 23 p4216 A70-44608
- ### COST REDUCTION
- Beacon equipment as means of crashed or force-landed aircraft locator to increase survival possibilities and reduce search cost 01 p0035 A70-10719
- Cost reductions achieved by space payload life extension through manned maintenance and increased transportation economies via refueling and improved space propulsion 01 p0196 A70-10844
- Display console characteristics for meeting increasing applications, predicting price reduction trends, color emphasis and CRT competition as primary display component 01 p0221 A70-11286
- Integrated materiel management for systems or product costs reduction applied to high cost spares management 02 p0401 A70-11671
- AMPROD /Automated Mission Profile Design/ generating schedules for long duration missions with real cost and time savings 03 p0581 A70-14023
- European Ultra-Violet Astronomical Satellite /U-VAS/ to replace Large Astronomical satellite /LAS/ to reduce cost while maintaining scientific objectives 03 p0582 A70-14343
- Design and economic concepts of Lockheed L-1011 wide body trijets, discussing airport and airway congestion alleviation, passenger appeal, etc
[RAES PAPER 15] 04 p0623 A70-15044
- Wind tunnel testing technique innovations, reducing time and cost for low drag aircraft configurations by simultaneous force and pressure model transonic testing
[SAE PAPER 690677] 05 p0825 A70-15868
- Insulating materials and apparatus evaluation in terms of thermal capability to effect competitive cost saving 05 p0869 A70-16033
- Suboptimal control to minimize quadratic cost functional for nonlinear systems, using Taylor series representation for feedback gain matrix 06 p1025 A70-17961
- Quality control manager role in aerospace company overall cost reduction 06 p1185 A70-17987
- Apollo reliability and quality requirements, reviewing changes due to cost reductions in space program 06 p1065 A70-17988
- Integrated space program with merger of manned and automated activities for coming decade permitting costs comparable to aircraft-based scientific programs 07 p1375 A70-18872
- Launch facilities institutionalization for space shuttles launch cost minimization
[AIAA PAPER 70-244] 07 p1251 A70-20374
- Low operating cost space shuttle system for cargo and personnel transportation to earth orbiting stations involving reusable winged vehicles
[AIAA PAPER 70-242] 07 p1396 A70-20376
- Automatic test equipment programming for cost reduction by eliminating duplicated effort between manufacturers of test equipment and unit to be tested 08 p1464 A70-20658
- Computerized generation of cost optimal decision logic for malfunction analysis 08 p1470 A70-20659
- Nickel zinc secondary battery low cost and high performance in military applications, discussing maintenance and rapid recharge requirements 08 p1440 A70-20710
- Low cost programming system for gas tungsten arc welding process for Ti taper and stepped joint designs 08 p1507 A70-21484

- Engineering use of filament reinforced metal matrix composites dependent on fabrication cost reduction, consistent properties and form flexibility 08 p1509 A70-21851
- Equivalent linear programming in integer variables to solve production scheduling for N identical machines, minimizing changeover and inventory costs 10 p1895 A70-24662
- Gas tungsten arc welding application broadened by introducing controlled droplet transfer process 10 p1896 A70-25308
- Low cost lightweight flight control systems for business aircraft providing equivalent performance to larger equipment
[SAE PAPER 700213] 11 p2079 A70-25886
- Light general aviation aircraft production cost reduction, considering adhesive bonding, production certification, etc
[SAE PAPER 700242] 11 p1981 A70-25911
- Expendable propellant tanks /Tip Tank Concept/ on lifting body reusable booster operations to reduce cost for low earth orbital transport mission 11 p2122 A70-26052
- Nonzero sum differential games with cost criteria minimized by inputs control to single dynamic system, emphasizing application to economic competition 11 p2072 A70-26227
- Cooperative differential game with cost functional minimized by each player, discussing problems with linear combinations of state variables final values 11 p2073 A70-26228
- Launch vehicle first stage cost reduction, considering weight factors, mass production, recoverability, etc 11 p2126 A70-26285
- Boron epoxy composite structural parts for aerospace vehicles, discussing production times and cost reduction
[ASTME PAPER EM-69-143] 12 p2240 A70-27076
- Rotating combustion engine design offering low life cycle costs for military applications
[SAE PAPER 700273] 12 p2290 A70-27438
- Reliable and optimum cost power sources design for long life electronic digital communication equipment 12 p2166 A70-27927
- Redundancy optimization based on partial failure modes effect on system reliability to reduce cost 12 p2243 A70-28010
- Beneficial and detrimental effects of value engineering change proposals on system reliability, relating cost improvement and performance factors 13 p2524 A70-29568
- Low cost VHF and UHF navigation aids IFR procedures for low density airports
[SAE PAPER 700230] 13 p2385 A70-29607
- Low cost orbital space transportation system with shuttle service, discussing booster and configuration selections, weight, costs, etc
[AIAA PAPER 70-256] 13 p2506 A70-29615
- Man machine interface between operator and automatic testing equipment based on ergonomic design cost 13 p2360 A70-29687
- Size and cost of Al mirror IR photometric telescopes optimized for scientific information acquisition 14 p2586 A70-30896
- International airline collaboration in engineering and maintenance for savings in initial and operational costs of aircraft fleets 14 p2669 A70-30940
- Minimum cost systems engineering in aviation equipment maintenance and reliability 14 p2669 A70-30943
- Cost reduction and products reliability and quality maintenance by combining accurate cost reporting system with proper quality level control 14 p2669 A70-31108
- Commercial aircraft design evolution and trends concerning performance and operating cost reduction 14 p2532 A70-31370
- Improved standard electrical equipment components development by test by use method, reducing cost and time 15 p2828 A70-31572
- Carbon reinforcing fibers, discussing mechanical properties, production, cost reduction, etc 15 p2765 A70-32246
- Reusable ferry spacecraft program, discussing space shuttles, cost reduction and nuclear propulsion for deep space missions 15 p2791 A70-32300
- Parts standardization in military electronics industry for cost reduction and reliability, discussing design transform from software to hardware 15 p2831 A70-32632
- Aerospace compiler design for software cost reduction without affecting reliability, describing input language 16 p2868 A70-33432
- Fluidic technology for avionics systems, considering potential cost reduction and reliability improvement 16 p2843 A70-33445

- Reliability-cost model to determine optimum failure rate for minimization of systems total life cycle cost
[ASME PAPER 70-DE-43] 16 p3004 A70-33507
- Cost reduction in designing space shuttle system using reusable winged vehicles, suggesting airlines operations method
[AAS PAPER 70-043] 17 p3175 A70-34785
- Space shuttle weight, reliability and reuse cost factors, discussing Phase A ILRV project reducing cost per pound of payload to orbit
[AAS PAPER 70-046] 17 p3175 A70-34786
- Low cost earth-moon transportation system based on shuttle station mode concept
[AAS PAPER 70-058] 17 p3176 A70-34806
- Space station with shuttle and tug service, discussing reduced costs, reusability and commonality 18 p3333 A70-36318
- Worldwide communication satellite network cost optimization and application, discussing Intelsat role 18 p3228 A70-36510
- Multichip hybrid microcircuits design and construction, emphasizing reliability and cost reduction 18 p2322 A70-36759
- Military aircraft engines performance increase and cost reduction
[SAE PAPER 700272] 18 p3302 A70-36817
- Multiaircraft flight test program time compression by management techniques, discussing program length and costs 19 p3355 A70-38530
- Helicopter cost reduction by transmission overhaul frequency reduction, discussing savings with on-condition maintenance 19 p3441 A70-38824
- Microcircuit packaging /primarily hermetic/ and assembly techniques, considering cost reduction 20 p3597 A70-39443
- Nonlinear programming for minimizing inertial guidance systems costs via optimal subsystem selection 20 p3740 A70-39645
- Launch facilities institutionalization for space shuttles launch cost minimization
[AIAA PAPER 70-244] 20 p3606 A70-39697
- Liquid hydrogen balloon inflation system for use at remote locations, discussing characteristics and economy 20 p3607 A70-40086
- Air cargo terminal operations analysis, discussing manpower cost reduction 20 p3607 A70-40127
- Identification adaptive quadratic cost linear system control by mean and covariance correction algorithm 21 p3801 A70-40741
- Military and commercial aircraft maintenance costs reduction, discussing labor/material ratio, spare parts use, diagnostic systems, etc 21 p3749 A70-40750
- Cost optimal space shuttle systems, discussing booster configurations, weight and performance factors, technology utilization, etc 21 p3929 A70-40984
- Silicon solar cell specifications and cost reduction without output or reliability loss 21 p3756 A70-41008
- High strength glass for aircraft structures, discussing applications to passenger cabin windows 21 p3843 A70-41891
- Mathematical model avoiding repetitive tests costs for Nerva nuclear rocket engine 22 p4070 A70-43179
- Space shuttle for low cost transportation, discussing reusable vehicles, payload, design, orbital inclination, mission capabilities and international participation 23 p4261 A70-44676
- Low cost fabrication for solid rocket nozzles using carbon or graphite reinforcements in throat inserts
[SAE PAPER 700796] 24 p4349 A70-45897
- General aviation expansion and competitive position dependence on safety and utility improvements and simultaneous cost reductions
[AIAA PAPER 70-1220] 24 p4291 A70-45953
- ### COSTS
- NT AIRPLANE PRODUCTION COSTS
- NT FREIGHT COSTS
- NT LOW COST
- Seat capacity effect on operational costs of short/medium range high capacity A 300 B aircraft 02 p0402 A70-12368
- Optimality condition for singular control problems derived using differential dynamic programming to obtain expression for change in cost produced by control variation 09 p1653 A70-22345
- Riccati-like linear functional differential equation with quadratic cost, analyzing feedback control solution existence and uniqueness 14 p2600 A70-31204
- ### COTTON FIBERS
- Creep and recovery of polyvinyl chloride reinforced by oriented cotton fibers, considering roles of fiber density and stress magnitude 03 p0516 A70-13499

COUETTE FLOW

Heat and mass transfer in Couette flow of partially ionized symmetric diatomic gas for chemical equilibrium and chemically frozen flow cases 01 p0060 A70-10290

Stiffness values of externally pressurized incompressible fluid-film thrust bearings under turbulent Couette flow, discussing Reynolds number effects [ASME PAPER 69-LUB-25] 01 p0100 A70-10383

Dipolar fluid effect on back flow between parallel plates, considering generalized Couette flow 01 p0062 A70-10545

Thermal conditions and graph-analytic solution of laminar boundary layer combustion of disk rotating in free atmosphere and plate in Couette flow 01 p0218 A70-11017

Petrov proof of plane Couette and Poiseuille flow stability with respect to infinitesimal disturbances, rejecting validity of proof 01 p0064 A70-11071

Unsteady incompressible laminar flow under time dependent body force solved for rectangular and circular conduit and plane and cylindrical Couette flows 01 p0066 A70-11130

Statistical model of turbulent chemically reacting shear flows, analyzing wave number fluctuations effect and Couette flow 03 p0464 A70-12928

Critical thermal regimes in Couette flow, investigating temperature and velocity profiles of nonisothermal steady state Newtonian flow between two parallel plates 03 p0466 A70-13388

Torque upper bounds in Couette flow between concentric rotating cylinders, considering dissipation integral and boundary and continuity conditions validity 03 p0468 A70-13787

Torque and flow patterns in supercritical Taylor instability regime of circular Couette flow 03 p0470 A70-14235

Nonlinear rarefied Couette flow with heat transfer in polyatomic gases, using kinetic theory of gases [ASME PAPER 69-WA/HT-39] 04 p0781 A70-14803

Couette problem for Krook kinetic equation solution, considering shear stress variation at high plate velocities 04 p0672 A70-15228

Classical Couette flow for emitting and conducting gas media, discussing velocity distribution and temperature effects at LTE and non-LTE 04 p0787 A70-15675

Heat transfer in MHD Couette flow influenced by wall electrical conductances with suction 05 p0886 A70-15823

Unsteady nonlinear molecular flow problems concerning plane Couette flow, heat transfer between parallel plates and density discontinuity propagation solved by Monte Carlo method 06 p1113 A70-18321

Plane Couette flow and heat transfer between parallel plates problems treated by generalizing BGK model and applying variational principle to linearized Boltzmann equation 06 p1048 A70-18323

Plane Couette flow and heat transfer problem numerical solution, using Krook kinetic equation and Maxwell boundary condition 06 p1048 A70-18326

Time dependent stability of viscous rotational Couette flow induced by impulsively started rotating inner cylinder, using dye injection and motion pictures 07 p1255 A70-19209

Nonlinear stability of plane Couette flow, computing stream function, vorticity distribution and Reynolds stresses 07 p1255 A70-19211

Instability of plane Couette flow of three superposed layers of fluids of different viscosity between two horizontal planes 07 p1260 A70-19978

Magnetic field and conducting walls effect on laminar steady MHD Couette flow of electrically conducting incompressible viscous rarefied gas in slip regime 08 p1553 A70-21764

MHD flow between two parallel plates, noting pressure gradient and skin friction coefficient 08 p1554 A70-21774

Plane Couette flow stability numerical analysis, predicting eigenvalue behavior for arbitrary Reynolds and wave numbers 09 p1658 A70-22124

Thermal conditions and graph-analytic solution of laminar boundary layer combustion of disk rotating in free atmosphere and plate in a Couette flow 09 p1787 A70-22266

Poiseuille and Couette fluid flow with internal rotation in flat channel 09 p1660 A70-22436

Plane Couette oscillating flow stability to small disturbances under composed unsteady velocity at high Reynolds number 10 p1868 A70-24197

Flow formation in Couette motion of viscous fluids containing suspended rigid spherical particles using theory of fluids with microstructure 11 p2037 A70-26169

Compressible turbulent plane Couette flow solution with variable heat transfer based on von Karman model extended to arbitrary wall temperature 12 p2211 A70-27839

Mean field approximations to Couette flow stability between fixed and coaxial rotating inner cylinder, using Roberts preferred mode method 13 p2392 A70-30007

Nonsteady coupled MHD Couette flow, presenting solution by Fourier series expansion method 14 p2621 A70-30549

Viscometric Poiseuille or Couette flow kinematics, considering nonuniform shear rate 14 p2567 A70-31282

Viscoelastic fluid in Couette flow between coaxial cylinders and flow between fixed plane and rotating cone 14 p2567 A70-31358

Nonstationary MHD Couette flow of viscous incompressible fluid between two parallel walls caused by instantaneous fluctuations of applied transverse magnetic field 15 p2777 A70-31479

Absolute stability and turbulent transport upper bounds in Couette flow, using variational analysis 17 p3066 A70-34543

Rarefied binary gas mixture transient Couette flow, considering nonlinear case of plate with equal temperature accelerated impulsively 17 p3067 A70-34546

Modified discrete ordinate approach in rarefied gas dynamics tested on linearized Couette flow between concentric cylinders, using integral iteration 17 p3067 A70-34548

Couette flow stability between coaxial rotating cylinders, calculating eigenvector in first approximation small perturbation equations 17 p3073 A70-35695

Stiffness values of externally pressurized incompressible fluid-film thrust bearings under turbulent Couette flow, discussing Reynolds number effects [ASME PAPER 69-LUB-25] 19 p3435 A70-37611

Two dimensional MHD couette flow in slip regime, considering constant suction on stationary plate to determine transverse magnetic effects 20 p3677 A70-39047

Slightly rarefied and electrically conducting gas, calculating effects of applied magnetic field on steady laminar low speed plane Couette flow 20 p3685 A70-40504

Poiseuille-Couette spiral flow stability between concentric rotating cylinders 22 p4010 A70-42691

Temperature gradient effect on Couette flow heat transfer and stability 23 p4181 A70-44250

Rarefied gas plane Couette flow, calculating upper and lower bounds on shear stress 24 p4325 A70-45600

COULOMB COLLISIONS

Periodic potential and residual Coulomb interaction effect on inelastic light scattering from electronic excitations in semiconductors, using diagrammatic perturbation theory 01 p0156 A70-10280

Neutrinos line patterns in Muscovite mica, refuting Russel assumption by analysis of multiple Coulomb scattering of charged particles and track comparison 03 p0556 A70-13047

Excess electron and combined electron-positron angular distributions compared in electron photon cascade showers, considering Coulomb scattering 03 p0556 A70-13048

Theoretical and experimental cascade curves comparison for heavy materials used for particle absorption in tracking experiments, discussing Coulomb scattering 03 p0527 A70-13051

Charge-charge scattering model to calculate electron collection by Langmuir probe absorbing surface with and without magnetic field 06 p1124 A70-18308

Thermodynamic properties of nonideal multicomponent gas mixtures including Fermi-Dirac statistics effect, discussing internal partition function for free and confined atoms 06 p1184 A70-18637

Effective potential of electron screening of Coulomb nuclei field leading to thermonuclear reaction rate increase using self consistent field method 07 p1346 A70-20206

Diener kinetic theory for charged particles in EM field with Coulomb interactions taking into account transverse plasma waves 08 p1550 A70-20616

Fokker-Planck Coulomb collisions effect on plasma wave echoes 09 p1736 A70-23181

Coulomb collisions effect on electrostatic lower hybrid resonance waves propagation in ionosphere, noting noise bands cut-off shift 10 p1874 A70-24429

Coulomb interaction effect on diffusion of plasma produced by contact ionization in magnetic field, obtaining density profiles by iterative procedure 12 p2280 A70-27789

Coulomb force effect on electron beam spatial charge for optimal three resonator transit type klystron, regarding buncher length 15 p2707 A70-31507

Weakly turbulent plasma dielectric constant nonlinear tensor for frequent Coulomb collisions, using hydrodynamic equations 15 p2781 A70-32824

Coulomb interaction Fermi gas mixture collision integral, obtaining formula from Boltzmann equations and Taylor series expansion 17 p3070 A70-35043

HF oscillations excitation in decaying plasma-electron beam system, noting Coulomb collisions and nonlinear effects role 18 p3294 A70-36145

Collisional contribution to finite wavelength high frequency dielectric constant of Coulomb plasma 18 p3295 A70-36439

Atmospheric Coulomb interaction influence on longitude dependence of electron intensity in anomaly region 19 p3491 A70-37305

Coulombian drag on body from hybrid calculus of collisionless plasma flow around cylinder [ONERA-TP-819] 19 p3481 A70-38382

Pair correlations effect in equilibrium and nonequilibrium theory, taking Coulomb collisions into account for ionized plasmas confined to half space by reflecting boundary 20 p3679 A70-39662

Minor ion diffusion coefficients in F2 region, noting Coulomb collisions role in ion density sensitivity to ionospheric fluxes 22 p4019 A70-43109

WC radiation damage by resonant absorption following Coulomb excitation observed from gamma ray spectra 23 p4231 A70-44888

LF drift-dissipative instabilities of HF skin layer in nonuniform plasma 24 p4383 A70-45119

COULOMB POTENTIAL

Coulomb, Gaussian and harmonic oscillator potentials for particle pairs in three body system, using S wave expansion 01 p0147 A70-10519

Well depth determination for weak intermolecular potentials based on dimerization enthalpy measurement of rare gas atoms by mass spectrometry 03 p0527 A70-13299

Plasma, Coulomb fields and radiation correlations obtained by relativistic kinetic equations, noting bremsstrahlung, synchrotron, cyclotron radiation, radiative and particle diffusion, etc 09 p1736 A70-23182

Metal-semiconductor transition in magnetite described on band model with electrons breaking symmetry by ordering in self induced Coulomb potential 12 p2283 A70-27239

Radial Schrodinger equation bound state eigenvalues and properties by iterative method, calculating Coulomb potentials 14 p2600 A70-31360

Asymptotic relation between Thomas-Fermi-Dirac and Thomas-Fermi atom models for pressure with and without exchange, considering Coulomb contribution to energy 16 p2953 A70-33004

COUNTERFLOW

Laminar counterflow diffusion flame chemical structure and blow-off mechanism established in forward stagnation region of porous cylinder at atmospheric pressure 02 p0398 A70-12032

State and velocity distribution measurements for air in counterflow vortex tube to determine axial variation of flow quantities 05 p0831 A70-15884

Stable flow distribution of sonic jet exhausting counter to low density supersonic airstream 07 p1189 A70-19982

Incompressible laminar boundary layer stability of incompressible fluid for nonparallel oncoming flow, deriving perturbed motion equation 08 p1483 A70-21179

Asymptotic eigensolutions for equations governing flow between oppositely rotating infinite plane disks in inviscid limit 10 p1870 A70-24607

Thermal design of counter current cryogenic heat exchangers employing spiral finned tubing 14 p2617 A70-31018

Counter current heat exchanger with spiral finned tubing and solid core 14 p2617 A70-31019

Phase shift ultrasonic flowmeter measuring transit time between oppositely propagating waves in blood vessels 15 p2691 A70-31921

COUNTERMEASURES

NT CHAFF
NT ELECTRONIC COUNTERMEASURES
NT JAMMING

COUNTERS

NT CERENKOV COUNTERS
NT ELECTRON COUNTERS
NT GEIGER COUNTERS
NT NEUTRON COUNTERS
NT NEUTRON SPECTROMETERS
NT PARTICLE TELESCOPES
NT PROPORTIONAL COUNTERS
NT QUANTUM COUNTERS
NT RADIATION COUNTERS
NT SCINTILLATION COUNTERS
NT SPARK CHAMBERS

Automatic particle counters and fluid contamination problems, misconceptions relating to sampling, size measurement, calibration, etc 05 p0851 A70-16706

Pulse rate counter for randomly repetitive random processes, noting applications to lightning flash noise bursts in receivers 10 p1848 A70-23996

Aircraft ice crystal counter for real-time measurement in cirriform clouds, using contact electrification detection 12 p2264 A70-28091

Actuating signal at sampling instants determined in phase plane by Mullin-Jury method for sampled data feedback containing quantizer and zero order hold circuit 16 p2886 A70-33336

Pulse counting and encoding system on rocket-borne spectrophotometer for starlight collected by primary telescope mirror 22 p4038 A70-43174

Ionized gas density monitor as meteoroid detector, describing operation in ionization chamber, proportional counter and glow tube modes 23 p4197 A70-44513

COUNTING CIRCUITS

NT SCALERS

Switching-type dekatrons use in automatic control, electronic measuring and computing systems, discussing advantages 04 p0660 A70-15436

Pulse counting frequency divider with discrete phasing device for use with quartz clock and electron beam chronoscope 04 p0694 A70-15492

Vibration decay rate measurement by pulse cycles counting 04 p0695 A70-15571

Ion counter circuit using second equivalent condenser for compensating background radiation current, assessing error 07 p1281 A70-19526

Seven segment in-line digital readout circuit for binary-quinary decade counter, using resistance transistor logic 21 p3793 A70-40763

High resolution electronic time intervalometer using digital counting and analog time expansion circuits 23 p4196 A70-44383

COUPLED MODES

Magnetoelectric mode coupling in satellite transmissions through ionosphere near transverse region, showing diurnal variations and error of electron content 02 p0259 A70-12563

High density nonlinear and linear growth rates of flute modes instabilities in cold plasma coexisting with low density of energetic electrons 04 p0728 A70-14998

Radiation from and panel response to supersonic turbulent boundary layer, emphasizing panel mode coupling to acoustic field 04 p0615 A70-15081

Magnetoelectric mode coupling in satellite transmissions through ionosphere near transverse region, using electron concentration profiles for night and daytime estimates 04 p0650 A70-15131

Quasi-linear mode coupling in confined hot-ion Penning discharge plasma, discussing externally imposed excitation and internally generated oscillations 05 p0888 A70-16166

Noniterative integral solutions of scattering equations extended to coupled channels using matrix notation 06 p1108 A70-17487

Mutual coupling between waveguides radiating through conducting ground planes with orthogonally polarized propagating modes described by first order analysis 06 p1020 A70-17562

Laser mode interaction characteristics determination using resonator field equation taking into account competition and coupled modes 06 p1081 A70-17765

Boundary value problems in nonlocal elasticity, considering two one dimensional media coupling with microstructure by Green function analog 07 p1399 A70-18665

Complex elastic system coupled flexural vibrations resonant frequencies determined with allowance for friction 07 p1363 A70-19111

Coupled mode method, analyzing interaction between slow space charge wave of electron beam and electroacoustic wave of lossless warm plasma 07 p1349 A70-19687

Mode coupling and intensity pulsations observed between two 6328 A He-Ne lasers through nonlinear gain characteristics of inverted population 09 p1699 A70-23363

Wave amplification in semiconductors relationship to coupling between space charge wave and circuit wave based on coupled-mode theory 10 p1927 A70-24619

Undamped natural modes intercoupling resulting from arbitrary linear damping addition to linear dynamic system 10 p1962 A70-25061

Thermal conductivity on coupled heat conducting rods calculated by implicit difference scheme on finite graphs 10 p1969 A70-25189

Coupled panel-cavity vibrations analysis, emphasizing sonic boom excitation of large window-room combinations 11 p2133 A70-25728

Nonlinear parametric excitation of stable resonant drift waves by mode-mode coupling in potassium plasma of Q device 11 p2090 A70-26020

Modulation coupling between electron and ion resonances in magnetoactive plasmas, discussing probeless feedback stabilization scheme 11 p2091 A70-26403

He-Ne lasers mode locking by self beat feedback between cavity modes, achieving nonlinearity control by circuit adjustment 12 p2245 A70-27273

Coupled lasers kinetic operating characteristics, discussing emission power damping 12 p2246 A70-27315

Feedback stabilization and mode coupling of ionization waves in positive column discharges, noting dynamic stabilization of unstable bounded plasma systems 12 p2280 A70-27787

Coupled relaxation dependence on translational and vibrational temperature and number of modes in polyatomic gases, noting molecular dissociation 12 p2276 A70-27797

Coupled microwave oscillators interaction, discussing klystron operation regenerative and non-monotonic frequency pulling modes 12 p2196 A70-27847

Coupling between parallel plate waveguides excited in TE modes using integral and differential equations, noting dielectric plug loading effect 12 p2198 A70-27954

Coupled microstrip transmission lines characteristics from parameters evaluation, considering various geometries, inductive and coupling coefficients, dielectric constant and impedance 12 p2190 A70-28167

Cone roll dynamics-ablation patterns coupling in hypersonic wind tunnels [AIAA PAPER 70-562] 13 p2340 A70-29025

Reentry vehicles dynamic stability analysis involving pitch, yaw and roll motions modes coupled by asymmetries [AIAA PAPER 70-561] 13 p2341 A70-29027

Hydromagnetic coupling between neutral and ionized atmosphere perturbations, noting role of gravity waves 13 p2397 A70-29191

Topside sounder profiles interpretation, discussing ionosphere-protonosphere dynamic coupling 13 p2398 A70-29199

Circularly polarized emission from types 1 and 4 bursts and noise storms, considering mode coupling in warm plasma, gyroradiation and Cerenkov radiation 13 p2479 A70-29851

Differential equations for coupled bending and torsional vibrations of slender beam in centrifugal force field 14 p2661 A70-31226

Incident microwave signal in Tonks-Dattner resonance coupled to discrete LF modes in plasma column 15 p2778 A70-31756

WKB method applied to ionospheric equations with strong wave coupling 15 p2725 A70-31857

Coupled simple harmonic oscillators with almost degenerate energy levels, comparing partitioning perturbation techniques with Rayleigh-Schrodinger approach 16 p2955 A70-34002

Mechanical vibrations models and analysis techniques, emphasizing problem of weak couplings in discrete systems 16 p2996 A70-34290

Coupling processes in daytime D and E regions at LF and VLF, using thin film optics method for reflection and transmission coefficient matrices 19 p3413 A70-38002

Intermode coupling processes in nighttime D and E regions, using thin film optical method for propagation phenomena at LF and VLF 19 p3413 A70-38003

Pretwisted slender beam coupled torsional and longitudinal vibrations under centrifugal force field, obtaining resonant frequency by Rayleigh Quotient method 20 p3719 A70-39601

Ideal fluid-cylindrical tank elastic bottom coupled forced oscillations, determining hydrodynamic pressure for tank reverse translational motion 20 p3615 A70-40444

Thin radiating shock layer about axisymmetric blunt bodies, investigating energy-momentum transport coupling 21 p3950 A70-41746

Coupled rotational vibration system dynamic behavior near critical speed, using graphs of autonomous two degree of freedom system on reduced phase plane 22 p4112 A70-42271

Antifriction number characterizing friction coupling, distinguishing between elastic and plastic modes 22 p4047 A70-43348

Finite element method for bending-extensional coupling in angle-ply laminates deformation behavior 22 p4061 A70-43685

Scattering matrix for external coupling effects in dielectric covered phased array 23 p4160 A70-43766

Neutrino processes in lepton era as primeval fireball relic, discussing coupling constant for muon-electron neutrinos interactions 23 p4253 A70-44849

Elevated horizontal and vertical electric dipole VLF fields, discussing ionospheric TE and TM mode coupling, nighttime variations and amplitude fluctuation 24 p4314 A70-46131

COUPLERS

NT ANTENNA COUPLERS

NT COUPLING CIRCUITS

Asymmetrical and symmetrical directional couplers coupling characteristics during linear and exponential variations of coupling coefficient 04 p0659 A70-15310

Variable coupler for liquid helium X band EPR cavity during immersion in coolant 07 p1286 A70-19976

COUPLING

NT CROSS COUPLING

NT GYROSCOPIC COUPLING

NT MICROWAVE COUPLING

NT OPTICAL COUPLING

NT SPIN-SPIN COUPLING

NT THERMODYNAMIC COUPLING

Coupled nonlinear systems with two degrees of freedom using transformation techniques 04 p0714 A70-15084

Material coupling in two layered orthotropic cylindrical shell subjected to normal external pressure 04 p0778 A70-15547

Coupling between LF oscillations and third harmonic frequency resonances of bounded plasma capacitor system, discussing density profile variation 05 p0890 A70-16654

Integrated electron density determination for plasma sheath on reentry vehicle based on power coupling change measurement 08 p1552 A70-21596

Frequency change for coupled vibrations of slender rotating beam due to hub radius change determined in centrifugal force field by perturbation method 08 p1594 A70-21772

Mutual coupling in arrays of log periodic dipole antennas in terms of impedance and admittance matrices 09 p1645 A70-22690

Soviet book on vibrations of complex oscillatory systems with mechanical, pneumatic and electromagnetic couplings 10 p1959 A70-24650

Shift in nuclear magnetic resonance, investigating transferred hyperfine coupling near Neel temperature for magnetic and nonmagnetic systems 10 p1928 A70-24827

Circular confocal laser with coupling aperture in mirror for maximum power output in specified mode, calculating field distributions and diffraction losses at reflectors 10 p1900 A70-24941

Coupled nonlinear systems analysis based on reducing coupled differential equations to equivalent uncoupled equations amenable to existing techniques 11 p2072 A70-25956

C-5 aircraft electrointerference coupling minimization, applying classification plan for wire categorization and routing 12 p2201 A70-28131

Liquid metals pump with cylindrical hydraulic coupling for actuating axial wheel, investigating cavitation and pumping effects on performance 14 p2535 A70-31012

Electron-acoustic, ion-acoustic and electromagnetic plane waves coupling at shock front in two fluid ionized viscous plasma 16 p2958 A70-33282

Multistate impact parameter treatment of heavy particle collisions modified to include higher state couplings for electronic wave functions 16 p2956 A70-34309

Shear coupling effect in cylindrical bending of anisotropic composite laminates 17 p3182 A70-34558

Magnetic coupling in solid dielectric cylinder under axial magnetic and perpendicular electric fields, noting memory and magnetostrictive effects 19 p3471 A70-37785

Thin shell theory elastic coupling conditions, discussing stress-strain and edge effect states 20 p3726 A70-39875

Ring lasers loss lock-in, attributing frequency synchronization between oppositely directed traveling waves to mutual coupling 21 p3838 A70-42007

Nonlinear coupling in systems with two degrees of freedom, deriving transformation laws for uncoupling 21 p3940 A70-42054

Saturn 5 Apollo booster stages oscillations induced by coupling between vehicle structure and engine thrust corrected within existing systems [AIAA PAPER 70-1236] 24 p4417 A70-45954

COUPLING CIRCUITS

Trigger scaling circuits with pulsed and blanking feedback analysis for minimizing number of couplings 01 p0047 A70-10984

Dispersion equation and coupling impedance of two dimensionally periodic slow wave structure of cellular cylinder type with parallel perpendicular diaphragms 03 p0456 A70-13438

Asymmetrical and symmetrical directional couplers coupling characteristics during linear and exponential variations of coupling coefficient 04 p0659 A70-15310

Three way power divider/summer fabricated symmetrically in stripline by resistive network transformation 05 p0821 A70-16386

Complex control follow-up systems in transient modes, suggesting synthesis for transfer function of control signal coupling 06 p1023 A70-17775

Parasitic effects due to coupling of wideband regenerative amplifier with nonideal ferrite circulators to antenna feeder duct 08 p1468 A70-20575

Multipole coupling circuits for wideband radio amplifiers 08 p1474 A70-21225

Optoelectronic devices for variable resistors controlled by electrical signal, investigating decoupling, capacitance and DC resistance 09 p1649 A70-23353

Directional broadband couplers with lumped elements obtained by insertion of LC networks between sum and difference ports of equal hybrids 10 p1848 A70-24221

Coupled systems stability and oscillatory behavior analysis using Liapunov theory 10 p1855 A70-24763

Switched self balancing comparison radiometer with coupling between channels, showing measurement errors due to coupling correctable by phase switching 11 p2018 A70-26269

Photodetector-electronic circuit matching channels for optical communication system, using minimum risk design criterion 12 p2237 A70-28153

Submillimeter wave devices with prebunched megavolt electron beams in coupling structures, describing electromagnetic beam couplers 14 p2555 A70-30432

Computer aided design for microwave branch line couplers dimensions practical for integrated circuit microstrip fabrication 15 p2711 A70-32602

Transmitter-antenna matching, using Pi-filter for resonance transformation 19 p3389 A70-38071

Wideband TEM quarter wave microwave coupler with continuously variable coupling range, employing even and odd mode characteristic impedance levels change 24 p4318 A70-45215

COUPLING COEFFICIENTS

Coupling coefficients for integral charged component of cosmic rays determined from measuring azimuthal geomagnetic effect on rays observed in crossed telescopes 01 p0172 A70-11545

Unidirectional composite materials properties, discussing stiffer filaments effect on Young modulus and shear coupling constant relating shear strain to longitudinal strain 03 p0587 A70-13128

Ray-optical analysis of electromagnetic scattering in plane and circular waveguides, giving formulas for modal reflection and coupling coefficients 03 p0452 A70-14034

Asymmetrical and symmetrical directional couplers coupling characteristics during linear and exponential variations of coupling coefficient 04 p0659 A70-15310

Electron-neutrino weak interaction and beat decay coupling constants found nearly equal, describing astrophysical tests based on white dwarf stars luminosity intervals 09 p1733 A70-23451

Short cables wire to wire coupling between black boxes, deriving interference transfer function 12 p2204 A70-28130

Interdigital Rayleigh wave transducers piezoelectric coupling coefficient from bulk constants, permitting equivalent circuit parameters prediction 17 p3055 A70-35875

Single crystal yttrium ferrite garnet intrinsic electromagnetic radiation as function of coupling coefficient between specimen and waveguide 19 p3485 A70-37630

Coupling components in homotopic classification of elliptic systems of second-order equations with independent variable 23 p4212 A70-44349

COUPLINGS

Quick-disconnect couplings selection guide for aerospace fluid systems, emphasizing functional and weight considerations [SAE-AIR-1047A] 01 p0197 A70-11461

Elastic couplings applied as sliding contact-free continuous junction between permanently rotating and fixed parts in rotating coil magnetometer 02 p0298 A70-12214

Plane motion of two mass points coupled by flexible inelastic thread assuming system mass center moving along circular orbit 07 p1386 A70-19484

Vibration stability of two identical particles constrained to plane and restrained by three linear springs with initial stress 08 p1591 A70-21466

Passive coupling of spatial six-element mechanical mixer with rotary pairs as function of element axial position and dimensions 11 p1983 A70-25933

Mechanical systems vibrations comprising tension couplings compensating misalignment between non-coaxial shafts 11 p2060 A70-26348

Plane motion of two mass points coupled by flexible inelastic thread assuming system mass center moving along circular orbit 15 p2805 A70-32729

Hard wire hermetically sealed two degrees of freedom rotating coupling design for continuous soldered wire connections between spacecraft and oriented solar array 16 p2924 A70-34172

Natural vibrations of free autonomous system of carried and carrier solid bodies connected by elastic couplings 18 p3342 A70-36594

Structural vibration tests, analyzing errors due to couplings and dampers addition 20 p3734 A70-40439

Equations of motion of mass points connected by inertialess elastic couplings 21 p3933 A70-40615

Antifriction number characterizing friction coupling, distinguishing between elastic and plastic modes 22 p4047 A70-43348

COVARIANCE

Signal waveform algorithmic construction with optimal autocovariance properties, using isosum integer partitions, applied to clustered multipath distribution measurement 02 p0263 A70-12773

Complex Gaussian processes with complex density functions, computing covariances and marginal distributions 10 p1915 A70-24057

First vorticity theorem of Helmholtz derived in general relativistic and covariant differential form, proving invariant kinematical identity 10 p1916 A70-24498

Microwave signals covariance and spectra calculation for amplitude and phase fluctuations propagated over line-of-sight path through turbulent atmosphere 12 p2189 A70-27963

Cratered planetary surface distribution and covariance functions of elevations using statistical model 13 p2488 A70-28763

Covariance propagation via differential equations for time-varying eigenvalues and eigenvectors 13 p2450 A70-29979

Adaptive Kalman filtering with unknown process and measurement noise covariance matrices 16 p2880 A70-32983

X-22 VTOL aircraft initial parameter, state and covariance matrix estimates by Kalman filter and smoothing algorithms 16 p2885 A70-33329

Vector and tensor calculus features, examining contravariance and covariance with bra and ket algebra and absolute differential 18 p3281 A70-36354

Relativistic thermodynamics, developing relativity theories in nonvacuo regimes and discussing covariant scalars and formalisms 18 p3291 A70-36553

Observation classification /image identification/ for two normal sets with common covariance matrix, investigating error probability asymptotic behavior 19 p3375 A70-37283

Covariance matrix of mean square response in structural systems under white noise 19 p3536 A70-37702

Covariance matrices estimates for trajectory parameter tracking of thrust-maneuvering spacecraft [AIAA PAPER 70-1017] 20 p3666 A70-39516

Discrete Kalman-Bucy linear filtering with inaccurate noise covariances, considering optimal and sub-optimal systems, error analysis, probability theory, etc [AIAA PAPER 70-955] 20 p3601 A70-39573

Identification adaptive quadratic cost linear system control by mean and covariance correction algorithm 21 p3801 A70-40741

Suboptimum filter for trajectory estimation from parameters, using modified covariance with least squares formulation in Kalman setting 23 p4177 A70-44601

Stochastic boundary value problem involving differential equation with random forcing function, proving monotone property of solution covariance variation 24 p4426 A70-46039

COVERINGS

Cover plates unsteady motion during explosive welding of metals, discussing edge damage 13 p2416 A70-28484

COWELL METHOD

U NUMERICAL INTEGRATION

COWLINGS

Pressure distribution about finite axisymmetric nacelle determined using Douglas Neumann program for cowl surfaces and inlet external surface 07 p1190 A70-20412

Turboramjet powered hypersonic aircraft axisymmetric inlet systems using forward translating cowl and centerbody for various air flow characteristics [AIAA PAPER 70-687] 16 p2835 A70-33586

CRAB NEBULA

Pulsed high energy X rays from Crab Nebula pulsar NP 0532 measured by balloon-borne X ray telescope 01 p0169 A70-10345

Rotational properties of neutron star models for Crab Nebula energy source, using expressions for angular momentum and rotational kinetic energy 03 p0571 A70-13817

X ray flux pulsations for pulsars near Crab Nebula observed in 2.5-30.0 kev range, determining pulsation profile 03 p0578 A70-14358

Crab Nebula pulsar light intensity fluctuations on very short time scale, noting negative observations 04 p0747 A70-14545

Right ascension and flux density of source in Crab Nebula measured at meter wavelengths, evaluating spectrum and relative position to binary star center 05 p0917 A70-16908

Coherent synchrotron emission in Crab Nebula associated with electron gyromotion, discussing models for high energy particle acceleration 07 p1375 A70-18848

Supernova pulsars parameters prediction based on Crab and Vela observations, discussing dispersion, period, flux density, etc 07 p1389 A70-20218

Relativistic particles formation associated with supernovae outbursts estimated to determine relativistic electrons mechanism in Crab Nebula 08 p1564 A70-20552

Supernovae and remnants, data concerning radio brightness distribution of Tycho supernova remnant and Cassiopeia and Crab Nebula origin 09 p1748 A70-21989

Supernovae remnants X ray emission associated with explosion process generating relativistic particles, indicating Crab Nebula as X ray object 09 p1749 A70-21998

Crab Nebula activity from telescopic plates, illustrating polarization structure on composite plate 09 p1750 A70-21999

Crab Nebula continuing energetic activity study indicating origin in nebula center and association with supernova remnant 09 p1750 A70-22000

Pulsar NP 0532 synchrotron emission reinterpretation related to relativistic particles injection into Crab Nebula

09 p1756 A70-22516

Wispis near Crab Nebula since September 1969 pulsar spin-up, suggesting dynamical changes in neutron star

10 p1947 A70-24994

X ray scattering by interstellar grains in direction of Crab pulsar and Sco XR-1

10 p1933 A70-25044

Dwarf and neutron stars as pulsar energy sources, considering Crab Nebula X ray emission and gravitational collapse

12 p2310 A70-27990

Crab pulsar /neutron star NP 0532/ possible spherical asymmetry indicated by pulse arrival time anomalies

13 p2486 A70-28618

Polarization of strong radio pulses from pulsar NP 0532 in Crab Nebula

13 p2492 A70-29269

Pulsed gamma ray emission from Crab Nebula pulsar NP 0532 investigated by balloon-borne spark chamber detector

13 p2492 A70-29271

Angular size of high energy X ray source in Crab Nebula from balloon-borne X ray modulation collimator

14 p2631 A70-30789

Runaway stars and pulsars near Crab Nebula, discussing binary system explosion and remnant motion

14 p2642 A70-30894

Relativistic particles formation associated with supernovae outbursts estimated to determine relativistic electrons mechanism in Crab Nebula

15 p2805 A70-32707

Angular scattering of interstellar medium resulting in multipath dispersion of pulsar pulses, discussing NP0532 in Crab Nebula

16 p2972 A70-32988

Critique of paper on Crab Nebula pulsar pulsed gamma ray emission, considering photon flux and statistical data analysis

17 p3149 A70-34565

Critique of paper on pulsed gamma rays detection from Crab Nebula pulsar by balloon flights, attributing pulsations to random fluctuations

17 p3149 A70-34566

X ray spectrum analysis for Crab, Cas A and SN 1572 supernova remnants

17 p3156 A70-34830

Crab Nebula pulsar NP 0532, describing quasi-sinusoidal oscillation in arrival times of radio pulses

17 p3157 A70-34842

Crab Nebula - Conference, Flagstaff, Arizona, June 1969

17 p3163 A70-35112

Optical study of Crab Nebula linear expansion and filamentary proper motions, considering line emission

17 p3164 A70-35113

Radio observations of Crab Nebula and radio source, correlating optical and radio features

17 p3164 A70-35114

X ray observations of Crab Nebula

17 p3164 A70-35115

Radio observation of Crab Nebula radio pulsar NP 0532, discussing main and subpulse stability at optical and radio frequencies

17 p3164 A70-35116

Crab Nebula pulsar NP 0532 optical and X ray synchrotron radiation, explaining ratio of pulsar energy flux to nebula

17 p3152 A70-35747

Crab Nebula X ray flux pulsations, analyzing spectra

17 p3152 A70-35756

Small angular diameter radio source in central Crab nebula association with pulsar NP 0532 based on spectra and pulse duration

18 p3322 A70-37128

Crab Nebula electromagnetic spectrum models, considering uniform magnetic field over whole volume and strong fields in small regions

19 p3505 A70-38114

Critique of Ruderman theory of Crab pulsar LF wobble as long wavelength oscillation of superfluid vortex lattice

19 p3522 A70-38604

Crab Nebula filamentary system, examining excitation conditions in terms of ionization and heating by HF radiation

20 p3702 A70-39011

Cosmic hard X ray sources spectra and time variations by balloons and OSO-3 satellite observations of Crab Nebula

21 p3872 A70-40657

X ray emission from Crab Nebula pulsar by rocket-borne proportional counters, comparing with optical observations

21 p3874 A70-40674

Pulsed hard X and gamma rays from NP0532 pulsar in Crab Nebula, comparing with extrapolated optical data

21 p3874 A70-40675

Crab Nebula pulsar NP 0532 electromagnetic spectrum observations, examining radio, optical, IR and X ray emission

21 p3874 A70-40677

Crab Nebula electromagnetic spectrum deviation from power law in microwave region, investigating origin from Compton scattering of high energy electrons

21 p3875 A70-40683

Magnetic field lower limit in Crab Nebula from cosmic gamma ray studies using optical reflector to detect atmospheric Cerenkov radiation

21 p3875 A70-40684

Radioheliograph observations of coronal broadening of Crab Nebula at 80 MHz, noting radial scattering and plasma irregularities

21 p3891 A70-41184

Crab pulsar observations with refractor and on-line data acquisition, indicating optical pulse arrival times at variance with previously assumed 77 day periodic wobble

22 p4097 A70-42464

Crab Nebula pulsar NP 0532 optical timing, measuring frequency, arrival times and pulse interval

22 p4102 A70-42936

Crab Nebula pulsar optical polarization compared with surrounding nebula and radio polarization

22 p4105 A70-43227

Crab Nebula X ray pulsation identified with pulsar NP 0532 by rocket measurements, noting implications for interstellar dust density

24 p4401 A70-45371

CRACK FORMATION

U CRACK INITIATION

CRACK INITIATION

Ultrasonic detection system for crack initiation and propagation in notched low cycle axial fatigue testing using surface and longitudinal waves

01 p0096 A70-10004

Stress corrosion cracking in Cu-Al alloys shown dependent on alloy and Cu ion content, solution pH and stress level, discussing tarnish film formation role

01 p0119 A70-10734

Correlation between sustained-load and fatigue crack growth in high strength steels for aggressive environment effects

02 p0318 A70-12544

Polymethylmethacrylate block breakdown under focused pulsed laser radiation in free emission regime, noting light absorption during crack development

02 p0314 A70-12813

Al alloy rectangular beam stress corrosion crack initiation and propagation measurement using ultrasonic techniques, showing relationship between crack velocity and initial stress

03 p0481 A70-12958

Natural mode shapes of longitudinal oscillations and resonant frequencies of thin rods of constant curvature and rings with slit, noting use for crack determination

03 p0588 A70-13283

Kinetic theory of cracks network formation on LiF crystal surface exposed to plasma jet using high speed camera

04 p0730 A70-14458

Hydrogen embrittlement as delayed rupture origin in high strength steels

04 p0711 A70-15682

Vacancies influence on macrodefect nucleus formation in single metal crystals under uniaxial strain explaining Griffith crack initiation

05 p0861 A70-15784

Plane circular crack in homogeneous and isotropic elastic body under uniform uniaxial tension using linearized couple-stress theory

05 p0931 A70-16089

Planar dislocation array in displacement dependent stress field, investigating tip stress intensification regarding crack nucleation

05 p0932 A70-16170

Steady temperature field and stressed state of elastic plane containing heat resistant arc shaped cracks produced by uniform thermal flux

05 p0935 A70-16231

Scale factor effect on crack development in blanks and structure elements undergoing linear and complex stressed states under cyclic thermal loads

05 p0867 A70-17045

Time to crack formation determined in cylindrical and flat Al and steel specimens having various surface properties under cyclic loads

06 p1084 A70-17392

Crack formation and propagation kinetics in flat and cylindrical Cr-Mo-V steels under tension compression loading cycles

06 p1162 A70-17393

Ultrasonic surface waves detection of transverse fatigue crack initiation in rails under load, applying results to fatigue life determination

06 p1168 A70-17924

Equilibrium cracks in elastic bodies on basis of atomic interaction law, using Griffith problem to estimate bearing capacity

07 p1400 A70-18666

Microfissuring of Ni base alloy weldments as function of grain size produced by solution temperature

07 p1306 A70-18996

Crack formation in resin matrix and effect on fiberglass reinforced composites behavior under loading

07 p1318 A70-19754

Fatigue crack growth in polycrystalline Mo at room temperature under cyclic loads observed along grain boundaries

07 p1314 A70-20013

Quenched and tempered steels ductile fracture with respect to plasticity, structure and crack development conditions using microfractography

08 p1515 A70-20922

Iron base and nickel base alloys susceptibilities to internal hydrogen and hydrogen environment embrittlements, studying crack initiation inside and at metal surface

08 p1520 A70-21515

Nondestructive testing and inspection by acoustic emission from stressed materials, discussing microstructure effect and crack initiation detection

08 p1508 A70-21747

Fracture processes in homogeneous anisotropic fiber composite materials, describing microcrack initiation, growth and unstable propagation at critical stress level

08 p1532 A70-21912

Inertia effect in failure mechanics for steadily developing equilibrium cracks in dynamic system with time dependent periodically variable load

09 p1771 A70-22466

Thermal and high strain fatigue covering cyclic tests, crack initiation and propagation, stress-strain behavior, structural design, frequency and temperature effects, etc

09 p1773 A70-22576

Multiaxial thermal fatigue cracking in carbon steels predicted by elastoplastic stress-strain analysis using finite element method

09 p1773 A70-22578

Turbine components design for low cycle fatigue, estimating thermal cycle number for high temperature crack initiation and propagation

09 p1774 A70-22583

Fatigue life and limit distribution obtained from analysis of crack formation start and final failure in notched and smooth specimens

09 p1776 A70-22619

Transcrystalline stress corrosion crack initiation in austenitic stainless steel tested in boiling magnesium chloride solution

09 p1706 A70-22940

Acoustic emission monitoring methods to detect crack formation and growth in ceramics

10 p1894 A70-24174

Crack development in solid body, considering condition at crack tip not derivable from equation of motion and strain equation

10 p1960 A70-25007

Aluminum alloys hot cracking during welding, ascribing failure to combination of strain and susceptible microstructure

10 p1897 A70-25313

Porosity and intergranular crack formation in tungsten fusion welds using electron fractography

11 p2059 A70-25666

Fatigue crack initiation and propagation in steel using surface plastic replication method, determining propagation rate by stress intensity

12 p2321 A70-27207

Cleavage cracks initiation and propagation in basal plane of Be single crystals, determining propagation energy as function of temperature, purity and alloying

12 p2256 A70-27614

Microdefects as centers of disk shaped destructive cracks in polymer dielectrics under laser irradiation

13 p2437 A70-28621

Kinetic theory of cracks network formation on LiF crystal surface exposed to plasma jet using high speed camera

13 p2510 A70-28655

Brittle rupture cracks theory, discussing unstable /Griffith/ crack, stress intensity coefficient, propagation criterion, etc

13 p2517 A70-29715

Al-Zn-Mg alloy welds delayed rupture under constant uniaxial load in distilled water or aqueous salt solution

14 p2591 A70-30970

Crack initiation and breakdown under thermal stresses of boron nitride containing aluminosilicate

15 p2764 A70-31532

Metallic materials damage accumulation and structural failures due to fatigue, considering surface changes, crack initiation and dislocation pattern

15 p2757 A70-31928

Glass bead blast induced residual stress and surface cold work effects on Ni base superalloy fatigue crack initiation and propagation 15 p2761 A70-32381

Weld cracks in welded joints of Ni-Cr base alloys due to residual stresses during aging, recommending annealing for prevention 16 p2930 A70-33051

Ceramic material ranking, using thermal stress crack initiation method 16 p2934 A70-33274

Crack initiation and propagation in rolling contact fatigue, emphasizing electrochemical effects in ball bearing failure [ASME PAPER 70-DE-46] 16 p2931 A70-33509

Electrochemical mechanism in Ti alloys stress corrosion cracking, formulating mass transport kinetics model 17 p3113 A70-34368

Stress corrosion cracking of alpha-Ti alloys at room temperature, suggesting cathodic polarization promotion of film buildup 17 p3113 A70-34369

Stress corrosion cracking in Ti and alloys, discussing metallurgical and environmental factors emphasizing exposure to hot salt, methanol, seawater, etc 17 p3114 A70-34372

Ti alloys crack formation during oxidation under stress, considering annealing and recrystallizing effects 17 p3114 A70-34374

Ti alloys crack initiation and propagation during hot salt stress corrosion 17 p3114 A70-34375

Single phase alpha Ti alloy welds breaking strength, discussing delayed failure and cold cracking with various oxygen and hydrogen contents 17 p3117 A70-34399

Crack initiation in wrought polycrystalline Be sheet, investigating three point loaded bend fractures of powder and ingot samples by optical and electron microscopy 17 p3122 A70-34551

Void formation and creep during fast neutron irradiation of austenitic stainless steel based on thermodynamic approach, calculating nucleation and growth rates 17 p3123 A70-34626

Membrane and bending stresses at crack tip in cylindrical shell weakened by elliptic hole with major axis perpendicular to shell axis 17 p3186 A70-34981

Elastic field near moving antiplane crack tip to determine energy release rate 17 p3191 A70-35462

Oxygen role in crack initiation and growth in Ni alloys postwelding heat treatment 18 p3277 A70-36525

Thermal fatigue cracking of gas turbine blades in fuel combustion product flow, investigating surface composition, microhardness and structure under simulated loads 19 p3490 A70-37338

Three dimensional stress fracture criterion for initial microcracking derived by generalizing Griffith law theory 19 p3540 A70-37955

Metal cracking and fracture mechanics under creep conditions at elevated temperatures, discussing notch rupture testing 21 p3937 A70-41437

Crack propagation in antiplane shear by opening semipenny shaped cracks straddling front at 45 deg 21 p3940 A70-42035

Polycrystalline aluminas under thermal shock, investigating strength decrease and subcritical crack formation 22 p4059 A70-43413

German monograph on thermally induced elastic stress effects on crack formation and propagation in plates 24 p4422 A70-45524

CRACK PROPAGATION

Holographic interferometry as stress analysis technique for crack propagation studies, discussing advantages over classic interferometric and conventional photoelastic methods 01 p0198 A70-10002

Ultrasonic detection system for crack initiation and propagation in notched low cycle axial fatigue testing using surface and longitudinal waves 01 p0096 A70-10004

Inconel 718 and Al 2219 alloys surface flawed specimens fracture toughness and flaw growth comparison for high pressure hydrogen vessel 01 p0114 A70-10029

Fatigue crack propagation in metals exhibiting initial crystallographic shear mode followed by noncrystallographic tensile mode 01 p0198 A70-10101

Spherical pressure vessel fracture initiation and propagation from long flaws considered from theoretical and experimental approaches 01 p0199 A70-10264

Stress criterion for unstable crack propagation from Al alloy sheet tests, examining fracture data for vessels of various geometries and materials [ASME PAPER 69-SESA-2] 01 p0117 A70-10451

Weak interfaces effects in laminates under triaxial tensions at crack tip, analyzing delamination during crack propagation and fracture resistance 01 p0127 A70-10482

Fatigue crack growth rate for high strength steels from crack length during cyclic loading and striation spacings after fracture 01 p0119 A70-10732

Crack propagation mode in laminated steel-Ni composites, analyzing softer layer effect using impact tests and C replica fractographs 01 p0120 A70-10743

Quasi-brittle fracture of plastic materials based on Griffith theory and crack propagation, analyzing real surface energy and work of plastic strain 01 p0212 A70-11562

Metal fatigue in Al alloys subjected to stress cycles, determining macrocracks propagation stages 01 p0212 A70-11607

Variational principle for admissible functions particular solution in elasticity theory involving solid bodies with cracks 01 p0212 A70-11608

Crack propagation in pure alpha-Ti at room temperature using optical and electron microscopy, considering propagation rate relation to strain amplitude 01 p0125 A70-11643

Fracture surface topography variation with specimen thickness, studying fatigue crack propagation in Al 02 p0317 A70-12317

Al alloy rectangular beam stress corrosion crack initiation and propagation measurement using ultrasonic techniques, showing relationship between crack velocity and initial stress 03 p0481 A70-12958

Discontinuity surfaces /cracks/ propagation in continuous medium having energy and stresses as functions of strain tensor gradient, using variational principle 03 p0589 A70-13330

Limiting equilibrium under axial tension of brittle body with parallel axisymmetric external cracks, studying critical load, crack propagation, etc 03 p0594 A70-13737

Elastoplastic zone and instability of precracked thin sheets under uniaxial loading applied to rectangular center-notched steel foils 03 p0598 A70-14239

Fracture mechanical theory for crack propagation in brittle ceramics subjected to thermal shock, deriving crack stability criteria 04 p0767 A70-14505

Dimensional analysis for describing steel surface microcracks growth under uniaxial fatigue loading, using stress-intensity factor and crack extension concepts of fracture mechanics [ASME PAPER 69-MET-G] 04 p0770 A70-14879

Crack propagation rate in aluminum alloy plates under cyclic tensile and transverse shear loadings, noting sliding mode increasing effect 04 p0705 A70-14881

Swenson shear fatigue crack model expanded to include mean stress effect on cyclic shear crack growth [ASME PAPER 69-WA/APM-8] 04 p0772 A70-14918

Fatigue crack incremental propagation under cyclic shear loading, developing discrete dislocation model for crack and plastic zones [ASME PAPER 69-WA/APM-7] 04 p0772 A70-14919

Stress factor-displacement relation in cruciform line crack deformation in elastic medium under arbitrary internal pressure 05 p0926 A70-15976

Antiplane strain deformation problems concerning crack extension along circular interface separating materials with different shear moduli 05 p0931 A70-16091

Al alloys crack growth effects due to gaseous environment and fatigue frequencies, suggesting role of gas adsorption 05 p0938 A70-16478

Strain energy release rate in terms of propagating crack surface displacements applied to infinite solid loaded in tension 05 p0938 A70-16480

Differential equation for crack propagation applied to threshold conditions for brittle fracture caused by impulsive load 05 p0939 A70-16486

Radially nonsymmetric stress wave propagation from tip of moving crack in infinite plates, deriving minimal group velocity 05 p0941 A70-16516

Dynamical models of relative motions during earthquakes, solving numerically integral equations with nonintegral kernels in crack propagation and elastic wave diffraction 05 p0941 A70-16527

Fatigue crack propagation and fracture toughness in pressurized thin walled cylindrical tubes, basing analysis on shallow shell bending theory 05 p0942 A70-16802

Optimal thermomechanical treatment for austenitic steel stability to resist propagation and unloading of dislocations in cyclic loading process 05 p0867 A70-17041

Incremental stress distribution near circular crack with internal pressure in neo-Hookean solid under deformation due to triaxial compression, illustrating initial stress effect 05 p0956 A70-17108

Crack formation and propagation kinetics in flat and cylindrical Cr-Mo-V steels under tension compression loading cycles 06 p1162 A70-17393

Steels crack propagation direction dependence on load magnitude in low cycle fatigue, noting groove width effects on resistance to static loading 06 p1163 A70-17401

Cracks development in hydrogenated silicon iron, investigating plastic strain relation and brittle rupture propagation 06 p1165 A70-17580

Plastic zone around propagating fatigue crack in Cu single crystals, using transmission electron microscopy and X ray topography 06 p1171 A70-18494

Stress corrosion testing of vanadium alloys using precracked specimens in cantilever beam apparatus, discussing strain hardening exponent role and propagation rates 07 p1306 A70-19299

Three dimensional electrostriction theory for stress and displacement on penny-shaped crack in elastic dielectric with conducting oblate spheroidal inclusion 07 p1409 A70-19569

Corrosion cracking mechanism for notched metal surface in aqueous environment under tensile stress, discussing electron distribution and H ion concentration 07 p1310 A70-19737

Quasi-steady propagation of Prandtl crack in viscoelastic body, noting stress distribution identity for viscoelastic and elastic cases 07 p1414 A70-20181

Rate sensitive materials dynamic fracture test concepts, considering crack speed, division, arrest, toughness, etc 08 p1590 A70-21318

Energy equilibrium for crack growth in elastoplastic media, analyzing crack behavior during plastic deformation concentrated at edge of propagating crack 08 p1590 A70-21414

Stress corrosion-fatigue crack propagation in high strength structural steels, relating growth rates to crack tip stress intensity factor [ASME PAPER 69-MET-5] 08 p1519 A70-21452

Dugdale crack model extended to include effects of linearly varying tensile loading, noting plastic zone length sensitivity 08 p1593 A70-21512

Fracture processes in homogeneous anisotropic fiber composite materials, describing microcrack initiation, growth and unstable propagation at critical stress level 08 p1532 A70-21912

Brittle failure mechanics application to steels sensitivity to rupture at low temperatures, discussing crack propagation resistance and heat treatment effect on impact toughness 09 p1768 A70-22076

Limiting equilibrium of unbounded cracked elastic plate with circular hole, studying crack propagation under compression 09 p1769 A70-22121

Al alloys fatigue cracks propagation rate using electron microfractography 09 p1701 A70-22223

Turbine components design for low cycle fatigue, estimating thermal cycle number for high temperature crack initiation and propagation 09 p1774 A70-22583

Stress and displacement distribution formulas for two and three dimensional crack extension problems in linear viscoelastic body 09 p1775 A70-22611

High temperature fatigue crack growth in metal, suggesting condensation of vacancies at crack front after each loading cycle 09 p1776 A70-22644

Fatigue crack probability distributions under oscillatory stationary random loading, basing analysis on crack propagation model 09 p1776 A70-22683

Dynamic photoelastic analysis of fracturing plastic plates, studying elastic and stress fields around propagating cracks 09 p1783 A70-23448

Crack widening in infinite plane field with wedge in absence of slip, based on elasticity theory, plotting contact forces and stresses on crack boundary 09 p1785 A70-23624

Ni-Cr austenitic steel bending, surface temperature variations, crack development and propagation under double fatigue tests 10 p1902 A70-23819

Acoustic emission monitoring methods to detect crack formation and growth in ceramics

10 p1894 A70-24174

Stress intensity and strain energy of pressurized line crack in cross form in thin elastic plate solved by Wiener-Hopf technique

10 p1956 A70-24192

Subcritical cracking rate behavior estimation in metallic service structures by linear elastic fracture mechanics

10 p1960 A70-24977

Energy methods applied to fatigue crack propagation rate under tensile mean stress

10 p1963 A70-25090

Fatigue crack propagation rate in sheet alloys with holes as stress concentrators related to duration of various development phases

10 p1965 A70-25290

Hypercritical crack growth resistance and notch toughness of aluminum alloys derived from fracture tests

11 p2064 A70-25331

Aircraft structures fatigue durability estimations, studying crack propagation rates under cyclic loadings by fail-safe method

11 p2132 A70-25624

Aircraft structures fatigue, discussing prediction of response to fatigue environment, load distribution, fatigue life, crack propagation rates and residual strength

11 p2132 A70-25677

Crack propagation in tensioned plates subjected to sonically induced vibrations

11 p2133 A70-25731

Two dimensional photoelastic investigation of crack propagation in fiber-reinforced composites consisting of glass and polyester resin layers

11 p2136 A70-26078

Elastic-plastic shear cracks propagation in two phase composite materials using dislocation model, determining critical fracture strength

11 p2136 A70-26081

Stress ratio effects on Al alloy during crack propagation and fatigue, introducing notch stress and strain approximations

11 p2066 A70-26089

Air and salt water tensile and shear mode cracking of titanium alloy sheets examined with electron fractographs

11 p2067 A70-26099

Fatigue crack propagation in high strength steels during fatigue cycling in dry and wet environment containing NaCl

11 p2067 A70-26100

Finite element methods applications to linear fracture mechanics and crack propagation theory, computing stress intensity

11 p2144 A70-26685

Airframe structures fatigue crack propagation with and without strain hardening during variable amplitude loading

12 p2315 A70-27014

Stable and unstable crack growth in viscoelastic media, solving boundary value problem and continuum mechanics prediction of crack propagation

12 p2315 A70-27092

Fatigue crack initiation and propagation in steel using surface plastic replication method, determining propagation rate by stress intensity

12 p2321 A70-27207

Kinetic theory for fatigue crack propagation using cyclic stress-strain relation in connection with strain hardening characteristics

12 p2322 A70-27208

Fracture toughness and cyclic crack propagation of surface cracked high strength aircraft structure steels

12 p2254 A70-27467

Cleavage cracks initiation and propagation in basal plane of Be single crystals, determining propagation energy as function of temperature, purity and alloying

12 p2256 A70-27614

Anisotropy effect on stress distribution at crack apex in elastic plate

12 p2329 A70-28322

Dynamic analysis involving crack extension force for two dimensional multiple radial crack division

13 p2510 A70-28602

Fatigue crack propagation dependence on environment and load frequency in Al alloys, correlating data by stress-intensity factor

13 p2431 A70-28603

Fatigue crack growth dependence on load profile, temperature, test frequency and environment and stress in high strength Al and Ti alloys and steels

13 p2431 A70-28604

Crack extension by alternating shear indicated from slip line flow field comparison at sharp crack tip and blunted crack

13 p2432 A70-28606

Moisture effect on fatigue crack propagation and fracture path through microstructure of 300-grade maraging steel

13 p2432 A70-28607

Viscoelastic plate crack growth analysis within continuum mechanics framework as analog to Griffith problem

13 p2510 A70-28671

Phenomenological theory of crack propagation during fatigue experiments, noting role of work hardening

13 p2510 A70-28672

Secondary crack growth direction from preexisting crack under longitudinal shear loading

13 p2510 A70-28674

Thin walled duralumin cylinders catastrophic fracture analysis by linear elastic fracture mechanics noting fatigue crack propagation

13 p2434 A70-29173

PH variation effect on sea water on stress corrosion cracking behavior of Ti alloys

13 p2435 A70-29174

Brittle rupture cracks theory, discussing unstable /Griffith/ crack, stress intensity coefficient, propagation criterion, etc

13 p2517 A70-29715

Hardened steel embrittlement in low pressure hydrogen caused by crack growth as function of temperature

13 p2436 A70-29804

Fracture mechanics and stress analyses comparison for fatigue cracked steel cantilever beam stress corrosion specimens

15 p2755 A70-31473

Fast brittle crack slowing by mechanical twins in transformer steel and by slip bands in LiF and NaCl crystals

15 p2755 A70-31526

Viscoelastic-plastic solid delayed fracture associated with wedge formation of crazed material at crack tip

15 p2816 A70-32010

Curvilinear cracks development in flat brittle body under asymmetrical loads using small parameter method

15 p2817 A70-32165

High temperature metal fatigue crack growth monitoring by ultrasonic detection

15 p2744 A70-32321

Biaxial stress effect on fatigue crack propagation in Al alloy plate under reversed bending

15 p2821 A70-32324

Metal fatigue cracks, reviewing propagation theories and structure life prediction equations

15 p2822 A70-32358

Heat treatment effect on maraging steel fracture toughness and subcritical crack growth loaded at slow strain rate in laboratory air

15 p2760 A70-32377

Environmental fatigue crack propagation in Al alloys at low cyclic stress intensity levels

15 p2762 A70-32390

Ceramics microcrack propagation control through small slab with simultaneous microscopic observation of path and force changes, considering grain boundaries effects

15 p2741 A70-32434

Fractography of spall cavities and crack growth in ball rolling contact fatigue, using scanning electron microscope

15 p2745 A70-32444

Alternating stress required for edge crack propagation in metal plates under tensile loading cycles

15 p2762 A70-32464

Crack initiation and propagation in rolling contact fatigue, emphasizing electrochemical effects in ball bearing failure

[ASME PAPER 70-DE-46]

16 p2931 A70-33509

Fatigue life estimation from fracture mechanics data, discussing flaw geometry and propagation, mechanical properties, damage accumulation, etc

[AIAA PAPER 70-601]

16 p2989 A70-33601

Kinetic theory of fatigue crack propagation, discussing stochastic nucleation process and power exponent relation

16 p2992 A70-33968

Metallographic observations on slow crack growth in Be monocrystals suggesting explanation for transition regions

16 p2933 A70-34275

Polycarbonate plate fatigue crack propagation, discussing length due to repetitions, striation number relationship to cycles, and stress intensity

16 p2941 A70-34335

Ti alloys crack initiation and propagation during hot salt stress corrosion

17 p3114 A70-34375

Inelastic analysis of unidirectional composite subjected to transverse normal loading, discussing linear response up to elastic limit and subsequent crack propagation and failure

17 p3182 A70-34557

Polymeric materials fatigue tests, investigating correlation between crack propagation and stress intensity factor

17 p3127 A70-34624

Randomized load sequence simulating narrow band Gaussian process for predicting fatigue strength, assuming crack propagation mechanism

17 p3183 A70-34660

Crack propagation, fatigue damage and interaction effects in aircraft structures and materials under flight simulation loading

17 p3185 A70-34924

Elastic field near moving antiplane crack tip to determine energy release rate

17 p3191 A70-35462

Fatigue crack propagation in solids in terms of nucleation theory, explaining temperature dependence of fatigue strength and size effect

17 p3191 A70-35464

Curvilinear crack propagation in elastic plane under balanced loads, using singular integral equations

18 p3341 A70-36584

Finite element method with first order displacement functions to compute crack tip stress intensity factor in various shapes under different loading conditions

19 p3548 A70-38623

Fatigue crack closure in flat sheet specimens under zero-to-peak tension cyclic loading, analyzing stress distribution from fractographic striation patterns

19 p3549 A70-38625

Pop-in fractures analyzed by semiquantitative model, establishing relationship between pop-in length, stress intensity factor and crack-front plastic deformation

19 p3549 A70-38626

Crack tip stress intensity factor in sheet structures, applying complex stress potentials and perturbation techniques in numerical calculations

19 p3549 A70-38627

Fatigue crack propagation under programmed loads, correlating crack growth rates and tip opening displacements

19 p3549 A70-38628

Plastic bodies rupture and crack growth under creep, considering tension of bar with symmetrical angular notches

20 p3727 A70-39882

Longitudinal shear crack propagation in random internal stress field, examining quasi-brittle rupture theory and cyclic loading

20 p3733 A70-40396

Brittle elastic material with wedge shaped void, calculating shear stresses during crack propagation generated by horizontally polarized shear wave

21 p3932 A70-40547

Fatigue crack growth tests on Al alloy sheets under variable amplitude loading

21 p3831 A70-40749

Notched polycrystalline Al-Mg alloy dislocation structure near propagating fatigue crack at various stress levels

21 p3839 A70-40925

Anisotropic material two dimensional crack propagation under deforming stress at infinity, examining fracture criterion, dislocation distributions and crack nucleation

21 p3936 A70-41413

Nondestructive ultrasonic measurements of crack depth in high strength steel plate weldments, studying low cycle fatigue

21 p3834 A70-41943

Crack propagation at supersonic velocities in K Cl crystals, noting plasma induction within specimen by laser pulse

21 p3940 A70-42033

Crack propagation in antiplane shear by opening semipenny shaped cracks straddling front at 45 deg

21 p3940 A70-42035

Acoustic emissions method for monitoring structural stability of solid materials assemblies via crack formation and movement detection

22 p4027 A70-42582

Crack growth study in viscoelastic solids by linear continuum mechanics, discussing cyclic loads, composite solids mechanical behavior and thermodynamics

22 p4115 A70-42937

Stress distribution around moving cracks in finite width strip, obtaining solutions for boundary conditions by Schwarz-Christoffel transformation and complex functions theory

22 p4116 A70-43025

Book on fatigue crack propagation in pure Al covering tension and compression tests, single and polycrystalline materials, elastic stress, notched and smooth specimens, etc

22 p4057 A70-43740

Crack propagation resistance-cyclic fracture strength relation for Mn-Cr-V steels, considering thermomechanical working effects

23 p4204 A70-43935

Fracture toughness testing of metallic materials including fatigue cracking, thickness limitations and crack detection

23 p4206 A70-44190

Crack length and bend specimen thickness effects in plane strain fracture toughness tests of high strength steels

23 p4268 A70-44192

Crack and thickness effects on fracture toughness tests of high strength steel in precracked sheet and bend specimens

23 p4206 A70-44193

Fatigue crack growth detection by acoustic emission techniques

23 p4194 A70-44214

Moire technique application to fracture toughness tests on Zr alloys, measuring crack opening displacements and plastic flow beneath notch

23 p4208 A70-44914

German monograph on notched structural steels fatigue properties and crack propagation under tensile-compressive alternating loads

24 p4356 A70-45086

High strength martensitic stainless steel stress corrosion resistance and fatigue crack growth rate, considering austenite content, strain aging and tempering temperatures

24 p4359 A70-45245

German monograph on thermally induced elastic stress effects on crack formation and propagation in plates

24 p4422 A70-45524

German monograph on fatigue crack propagation in thin notched plate, considering microscopic element fracture probability

24 p4422 A70-45574

Fracture mechanics of craze growth of stressed polymethyl methacrylate in methanol

24 p4368 A70-45778

Composite materials tensile strength dependence on reinforced fibers with dispersed tensile strength, using model to predict crack propagation from fiber rupture

24 p4427 A70-46270

CRACKING [FRACTURING]

Ultrasonic detection of service induced cracks near tenon base region of second stage Al compressor disks

01 p0096 A70-10003

Thermal stresses in infinite layer of transversely isotropic material due to crack with prescribed normal displacement, deriving temperature distribution

01 p0200 A70-10552

Heat transfer effects on corrosion behavior of stainless steel in boiling water, noting stress corrosion cracking increase with chloride ion contamination

03 p0507 A70-13137

Al-Zn-Mg-Cu alloy corrosion cracking, studying effects of heat treatment, strain percent, blank parameters and grain size

03 p0512 A70-13734

Stainless steel stress corrosion cracking test in magnesium chloride solution, emphasizing crack crystallographic orientation observation

03 p0513 A70-14299

Bending analysis of cracked plate with arbitrary stress distribution across thickness

[ASME PAPER 69-WA/PVP-2] Fracture criteria in cracked plates under combined extension and cylindrical bending using Sih-Hartrant theory

04 p0770 A70-14882

Postweld heating cycle for circular patch test to predict strain age cracking susceptibility in welded Rene 41

04 p0700 A70-15654

Stress distributions in infinite elastic solids for shear loadings prescribed over coplanar circular regions, solving integral equations iteratively for coplanar penny-shaped cracks

05 p0928 A70-16057

Failure prediction for arbitrary shape flawed pressurized vessels using structural geometry, crack length, ultimate and yield stresses and fracture toughness

05 p0942 A70-16803

Alloying elements preventing hot cracking in weld metal by converting iron sulfides into higher melting point sulfides

07 p1293 A70-18979

Crack behavior of Al alloy as cryogenic tankage material, establishing relationship of temperature effects and basic crack size to failure stress

07 p1279 A70-18997

Torsion of elastic half space containing circular crack with symmetry axis coinciding with annular stamp rigidly coupled to half space

07 p1414 A70-20183

Ti alloys failure-safe design developing procedures for incorporation of stress-corrosion cracking characterizations into ratio analysis diagram system

08 p1519 A70-21456

Green function for stress intensity factors of rectangular plate edge cracks, noting application to thermal stresses

[ASME PAPER 68-WA/MET-19] Fracture mechanics model for stress corrosion cracking of Al alloys, discussing bond strength lessening by adsorption of damaging species

09 p1706 A70-22941

Polyamides /nylons/ stress cracking by metal halides and halide-like salts, investigating effects of nylon temperature, moisture content, concentration, etc

10 p1907 A70-24224

Polyamide and secondary amide mode compounds stress cracking by metal halides using IR and nuclear magnetic resonance techniques

10 p1907 A70-24299

Nylon 6 polyamide tensile stress cracking by metal thiocyanates in aqueous and nonaqueous solutions, comparing results with cracking by metal halides

10 p1907 A70-24300

Electronic stress wave analysis technique /SWAT/ for delayed weld cracking data acquisition

10 p1897 A70-25312

Low cycle fatigue tests on stainless steel, discussing crack behavior dependence on temperature and plastic strain range

11 p2139 A70-26405

Crack model analysis taking into account nonlinear force-deformation ahead of crack tip

11 p2143 A70-26667

Transient analysis of stress waves around cracks under antiplane strain with time dependent loadings based on integral transforms

11 p2145 A70-26698

Ductile fractures analysis using critical strain near crack tip as criterion

13 p2432 A70-28673

Structural Al-Zn-Mg alloys strain hardening effect on mechanical and corrosion properties, noting relationship between stress corrosion cracking and shear cracks

13 p2434 A70-29155

Al-Mg, Al-Zn-Mg, Al-Cu and Al-Cu-Mg welded alloys corrosion cracking resistance as function of composition and fabrication techniques

14 p2597 A70-30972

Electrochemical processes associated with stress corrosion cracking of Ti-Al-Mo-V alloy in aqueous environments

15 p2755 A70-31474

Stress corrosion cracking of Ti and Ti-Al-V alloy in liquid dinitrogen tetroxide

15 p2755 A70-31475

Stress corrosion cracking of high strength structural, tool and marring steels due to hydride, diffusion controlled and mixed embrittlement

16 p2934 A70-34301

Ti-Al-Mo-V alloy stress corrosion cracking, investigating correlation between dislocation substructure and ambient temperature corrosion susceptibility

17 p3113 A70-34371

Stress corrosion cracking in Ti-Al-V alloy exposed to Freon environments

17 p3114 A70-34373

Stress corrosion cracking of Ti alloys in nitrogen tetroxide and methyl alcohol environments in Apollo spacecraft pressure vessels

17 p3199 A70-34453

Cone crack closure in brittle solids, discussing optical and X ray studies on glass and silicon during unloading

17 p3183 A70-34621

Residual stress concentration at fatigue crack tip, using oscillating crystal X ray microbeam diffraction photographic method

17 p3183 A70-34652

Microscopic residual stress in crystals at fatigue crack tip in notched specimen in terms of flow stress and dislocation density

17 p3183 A70-34653

Papers on cracking during postweld heat treatment of Ni alloys covering Rene 41 mechanical properties and resistance to strain age cracking

18 p3277 A70-36522

Rene 41 resistance to strain-age cracking during postweld heat treatment

18 p3277 A70-36523

Rene 41 ductility reduction by environmental oxygen promoting intergranular cracking at high temperatures

18 p3277 A70-36524

Graphite-epoxy resin cross-ply composites fabrication, analyzing residual thermal stresses role in cracking

[ASME PAPER 70-GT-84] Pop-in fractures analyzed by semiquantitative model, establishing relationship between pop-in length, stress intensity factor and crack-front plastic deformation

19 p3549 A70-38626

Stress intensity factors for complicated crack configurations in finite plates, using finite element method with cracked elements

21 p3940 A70-42034

Two stage aging effects on stress corrosion cracking of Al-Zn-Mg alloys, discussing precipitated particles size, surface roughness change and temperature effects

22 p4052 A70-42306

Atmospheric environment effect on residual shear stress corrosion cracking of commercial Al-Zn-Mg alloys subjected to heat treatment regimes

22 p4052 A70-42307

Centrally cracked sheet, calculating riveted and uniformly spaced stringers effect on stress intensity factor

23 p4270 A70-44549

Fibrous composite interface effects and fracture work, discussing tip stresses of crack normal to fiber, energy dissipation by pullout and debonding in brittle fiber composites, etc

24 p4419 A70-45171

Crack detection in cyclic strained steel and Al alloys, using ultrasonic Rayleigh and longitudinal waves

24 p4424 A70-45718

NDT for aircraft service life extension, discussing fatigue tests and crack detection

24 p4346 A70-45719

Cold reduction, refrigeration and annealing effects on stress corrosion cracking of austenitic stainless steels

24 p4365 A70-46389

CRACKS

NT MICROCRACKS

NT SURFACE CRACKS

Complex stress functions and stress intensity factors at tips of star-shaped contour hole in infinite tensile sheet, including crack forking with arbitrary angle

03 p0585 A70-12974

Axisymmetric elasticity theory problem of stressed state of space weakened by concentric circular cracks solved using p-analytic functions to generate boundary value problems

03 p0586 A70-13077

Integral equations for antisymmetric shallow shell stress-strain state with crack, obtaining asymptotic solution in form of power series

03 p0591 A70-13420

Stress-strain state of arbitrarily cracked cylindrical shell under symmetric and asymmetric loading

03 p0594 A70-13736

Steady thermoelastic state of inhomogeneous plane with circular discontinuity on perimeter, studying stress concentration at thermally insulated crack

03 p0595 A70-13738

Strain distribution measurement in plastically deformed region around crack tip in metals using moire grid and optical interference

03 p0513 A70-14019

Internal pressure deformed cruciform crack energy and stress intensity factor determined by linear equations

04 p0777 A70-15499

Spread criterion and stress distribution near penny shaped crack in elastic solid under axisymmetric body forces distribution

05 p0930 A70-16079

Elastoplastic thick layer with disk-shaped crack analyzed for stress and strain, determining width of plastic zone

05 p0939 A70-16482

Crack stability under tension and thermal stresses caused by uniform disturbed heat flow, using Barenblatt fracture criterion

05 p0939 A70-16483

Stress distribution around crack tip of initially curved sheets

05 p0939 A70-16484

Three dimensional brittle body limiting axisymmetric stability under tensile stresses and weakened by ring shaped cracks, determining critical tensile loads

05 p0945 A70-16855

Wedge with symmetric crack at vertex in plane elastostatics, solving biharmonic equation by Wiener-Hopf technique

06 p1164 A70-17441

Thermal fatigue cracks in gas turbine blade models under simultaneous thermal cycling and static tensile loads simulating pulsed regimes

06 p1166 A70-17652

Rectangular plates with symmetrical cracks, studying bending under various crack distributions

07 p1399 A70-18662

Crack self healing in aluminum foil-polyvinyl acetate sandwich structures

07 p1315 A70-18713

Critical stresses for plate with circular hole and cracks assuming symmetrical load

07 p1402 A70-19054

Infinite strip with longitudinal crack and under loading, analyzing stress-strain state

08 p1585 A70-20938

Steady temperature field and stresses produced by thermal sources in infinite elastic plane containing insulated rectilinear crack, determining thermoelastic state of half plane

08 p1587 A70-21172

Mixed boundary value problems involving time dependent boundary regions for penny-shaped crack in viscoelastic materials with one relaxation function

13 p2508 A70-28489

Stressed state of infinite plate with circular hole induced by displacement discontinuity in form of cracks

13 p2514 A70-29292

Atomic planes around crack, noting configuration dependence on law of interplane interaction

13 p2515 A70-29418

Critical equilibrium of plate under omnidirectional tension with radial rectilinear cracks

13 p2515 A70-29429

Nondestructive noncontacting microwave depth measurement of thin slits and cracks in metal surfaces

14 p2584 A70-30507

- Al-Mg alloy nonpropagating fatigue cracks at roots of sharp notches, discussing cyclic strain hardening
14 p2598 A70-31299
- Double ended dislocation pileups and elastic cracks at bimaterial interface under screw, edge and shear modes
15 p2756 A70-31561
- Stress intensity analysis method for plates with random cracks array under plane stress
17 p3187 A70-34997
- Nonaxisymmetric thermal stress distribution in infinite elastic solid containing external stress-free crack with prescribed heat flux
17 p3196 A70-35437
- Elastic crack structure, discussing formalism for force law between faces of brittle and semibrittle fractures
17 p3191 A70-35461
- Plastic deformation zones at crack tip considered as distributed heat sources, using stress and strain distribution solutions
17 p3191 A70-35463
- Cracks and tensile failure of interface bonds in elastic composite hollow cylinder, deriving wave front propagation equations
18 p3283 A70-36388
- Book on crack problems in classical theory of elasticity, emphasizing mathematical aspects
19 p3534 A70-37234
- Edge dislocation and uniform and radial fissures in elastic isotropic nonhomogeneous bodies under two dimensional deformation
19 p3540 A70-37956
- Cracked brittle body limiting equilibrium, determining critical loads for two half spaces with various circular rib couplings
20 p3733 A70-40432
- Boundary value problem solution for elliptical crack subjected to impulsive load by method of characteristics and discontinuity relations, calculating stress distribution
21 p3938 A70-41960
- Plastic zones between symmetric and collinear edge cracks in thin plexiglass strips, using He-Ne laser interferometry
21 p3939 A70-41967
- Cracks stress intensity factors in plane problems by combined conformal mapping and boundary collocation technique
21 p3940 A70-42036
- Elastic plate uniform extension with rectangular crack by three dimensional bending theory, using variational principle
22 p4115 A70-42941
- Cracked Teflon heat shields ablative behavior for laminar and turbulent boundary layers in supersonic flow, describing heat transfer to substructure
23 p4282 A70-44585
- Commercial fluorescent penetrants for natural and artificial cracks, considering indication characteristics
24 p4348 A70-45742
- Cyclic loaded high purity Al samples, noting substructure around fatigue cracks
24 p4362 A70-46185
- Thin Al foil subjected to cyclic bending stresses, investigating substructures and strain regions around fatigue crack
24 p4362 A70-46186
- CRAFT**
U VEHICLES
CRANES
Crane helicopters characteristics, history and projected applications to petrochemical, shipping, construction and power transmission industries
[SAE PAPER 700284] 12 p2160 A70-27427
- CRANIUM**
Craniocebral hypothermia effects on phase structure of cardiac thrust in dogs
07 p1204 A70-19140
- CRASH INJURIES**
Mathematical elastodynamic model for parametric dynamic study of forced response solution of motion equations during head trauma
02 p0238 A70-12548
- Aircraft passenger tie-down failure, comparing injury patterns in various accidents to aid reconstruction
17 p3039 A70-35572
- Characteristic injuries from aircraft controls inflicted in fatal accidents, showing pilot position and hand location upon impact
17 p3039 A70-35573
- USAF aviation accidents diagnostic patterns of injury and death, noting increase in fire and/or associated complications
17 p3039 A70-35574
- Aircraft accident injuries possible misinterpretation
17 p3039 A70-35575
- CRASH LANDING**
NT DITCHING [LANDING]
Beacon equipment as means of crashed or force-landed aircraft locator to increase survival possibilities and reduce search cost
01 p0035 A70-10719
- Electronic packaging and cabling on Capsule System Advanced Development Lander for Mars rough landing
06 p1016 A70-17335
- Air crash rescue operations by helicopter ambulances of U.S. Army Medical Department, discussing postcrash fire suppression and injured personnel removal, emergency treatment and evacuation
06 p1002 A70-17714
- Emergency evacuation on land of passengers and crew of airliners, discussing training, equipment, standardization, communication and protective fabrics
15 p2675 A70-32220
- Aircraft in-flight and post crash fire protection developments, considering controlled flammability fuel systems and fire fighting methods
[ASME PAPER 70-GT-109] 18 p3215 A70-36847
- Apollo command module land impact capability, discussing impact dynamics, possible landing area, spacecraft structure, crew couch and strut attenuation system, etc
[AIAA PAPER 70-1165] 21 p3930 A70-41847
- Spinal injury prediction during emergency ejection and crash impact protection research
23 p4153 A70-44489
- Near fatal crash in T-33 aircraft, discussing protective clothing, seat harnesses, bodily position and mental attitude
23 p4153 A70-44497
- CRASHES**
NT CRASH LANDING
NT DITCHING [LANDING]
High energy chemical systems for postcrash emergency evacuation of commercial passenger aircraft, discussing exit opening via explosive methods
15 p2675 A70-32221
- CRATERING**
NT PROJECTILE CRATERING
Angle of incidence effect on oblique impact crater formed by high speed solid spherical particles colliding with massive lead targets
03 p0592 A70-13449
- Lunar cratering and erosion from Orbiter 5 photographs, observing crater densities, highland and maria regions, etc
10 p1942 A70-24643
- Nonlunar origin of tektites indicated from molten glass dispersion generated by terrestrial crater-forming meteorite impact
12 p2302 A70-27584
- Lunar cratering rates from Apollo flights data on solidification ages for Mare Tranquillitatis
16 p2979 A70-34037
- Lunar crater size and shape characteristics from Surveyor missions, discussing rimless shallow and cup shaped craters
20 p3707 A70-39954
- Apollo 12 lunar module impact laboratory simulation, investigating possible downrange ballistic effects and cratering process
20 p3709 A70-39976
- CRATERS**
NT LUNAR CRATERS
NT METEORITE CRATERS
NT TYCHO CRATER
Slopes distribution over finite span on planetary surface excavated by primary impact craters, including typical lunar mare crater densities
01 p0178 A70-10443
- Mars craters and crater-like objects catalog from Mariner 4 photographs, statistically analyzing diameter-frequency relations
01 p0179 A70-10523
- Mars primitive atmosphere analyzed from statistics of craters quantity as function of diameter, using Mariner 6 and 7 probe photographs
09 p1763 A70-23318
- Cratered planetary surface distribution and covariance functions of elevations using statistical model
13 p2488 A70-28763
- CRAZING**
U SURFACE CRACKS
CREEP ANALYSIS
Creep propagation determination in pure Al for microscopic and macroscopic continuum points used for determining stiffness and strain time history
01 p0121 A70-11156
- Backreflection X ray microbeam camera with arrangement for positioning preselected area to study grain boundary during creep by Laue method
03 p0492 A70-13759
- Transient creep analysis of simply supported circular cylindrical shells subjected to internal pressure based on strain and time hardening theories
03 p0595 A70-13813
- Plane two body contact creep problem in presence of adhesive forces reduced to solving coupled integral equations with complex valued kernels
04 p0766 A70-14421
- Creep behavior of mascons to infer lunar temperatures at depth compared with electrical conductivity data and heat conduction equation
05 p0906 A70-15892
- Time dependent creep and elastic strain interaction in plates and pressure vessels of cylindrical and spherical geometry
05 p0942 A70-16804
- Creep, ductility and short term tensile and compression strength test facility for graphite in 300-3500 K temperature range
05 p0875 A70-17068
- Vibration frequency influence on vibrational creep of Al-Mg-Si alloy, describing mechanism in terms of strain hardening, additional slip and dislocation movements
06 p1168 A70-17931
- Revolving shallow shells steady creep equations solved by approximation adaptable to computer
07 p1402 A70-19051
- Inelastic behavior of solids strained at high temperature emphasizing hot creep phenomena in aviation materials
07 p1406 A70-19346
- Isothermal steady state creep extension and flexure of laminated beams with alternating layers, indicating nonlinear stress distribution
07 p1412 A70-19964
- Thick walled orthotropic cylinder subjected to internal pressure analyzed for stress distribution and creep rates, using constitutive equations and Norton law
07 p1416 A70-20234
- Dynamic strain aging effect on Mo-Ti-C alloy creep, relating carbides precipitation during plastic deformation to mobile dislocations density
08 p1524 A70-21954
- Limit and shakedown loads in creep range investigated on sheet rolled aluminum at room temperature for structural design applications
09 p1775 A70-22591
- Creep behavior transition analysis, considering activation energies and creep rate dependence on temperature, stress and grain size
09 p1704 A70-22720
- Creep deformation in single crystals of gamma prime precipitation hardened nickel base alloys at intermediate temperatures
09 p1705 A70-22809
- Layered conical shell creep under axisymmetric load and time dependent temperature field by iterating boundary integral equation
09 p1779 A70-23099
- Unsteady creep of thin walled open section bars under free torsion using successive approximations
09 p1779 A70-23101
- High temperature creep of prestrained molybdenum single crystals as function of physical treatment and crystal orientation
10 p1902 A70-23860
- Structural behavior during creep by step by step process suitable for computers after linearizing non-linear equations
[ONERA-TP-805] 10 p1958 A70-24545
- Circular membrane creep under one-sided hydrostatic pressure, using governing equations for finite deformation
10 p1959 A70-24828
- Transient creep analysis of pressurized circular cylindrical shells based on strain and time hardening theories
10 p1963 A70-25089
- Solid and foam polyurethane creep stress, using multiplier for foam stress for comparison
11 p2141 A70-26601
- Finite element computer code /AXICRP/ for creep analysis of plane stress, plane strain and axisymmetric bodies of revolution
11 p2015 A70-26682
- Vibrocreep effect on Al-Mg-Si alloy vibration frequency and mean and maximum stress at constant temperature
13 p2512 A70-28980
- Creep rate intensity approximate solution as invariant function of stress intensity, determining equivalent stresses under creep
15 p2814 A70-31542
- Shallow shells of revolution under axisymmetrical loads, analyzing plasticity and creep by integral equations algorithm
15 p2817 A70-32164
- Phenomenological theory of transient high temperature creep, considering internal back stress
15 p2763 A70-32809
- Steady state high temperature creep theory, including internal back stress and temperature dependencies
15 p2763 A70-32810
- German monograph on two dimensional stress-strain state for material subjected to creep, using differential equations derived from equilibrium conditions
17 p3189 A70-35376
- Plane cross section hypothesis applied to fully developed creep in thin walled tube subjected to internal pressure and bending moments, calculating stress concentration
18 p3340 A70-36571
- Low aspect ratio wings under conditions of creep, calculating stress by method of strains
19 p3534 A70-37244

- German monograph on creep in statically indeterminate reinforced concrete beams with graduated cross sections
19 p3548 A70-38473
- Solid bodies statistical creep analysis, assuming macroscopically homogeneous isotropic polycrystallinity
20 p3725 A70-39866
- Inconel short term creep properties measured for various temperature and stress levels, presenting results in polynomial and graph form
22 p4055 A70-43098
- Equations of state in quadratic viscoelasticity for orthotropic media, deriving tensors of creep and relaxation centers
22 p4119 A70-43711
- Solidified polyglycol maleinate resin optical and mechanical properties under tensile stress creep, using hereditary photoelasticity
22 p4121 A70-43723
- Mg high temperature creep mechanism in high and low stress regions, using isothermal tensile creep tests
23 p4204 A70-43885
- Plastic creep displacement and deformation bounds computation for simple redundant structures, using energy theorems
24 p4422 A70-45288
- CREEP BUCKLING**
Rectangular plates deformation under uniaxial compression, studying postcritical buckling behavior in presence of creep
01 p0201 A70-10937
- Buckling of three layer cylindrical shells under steady creep conditions, deriving axisymmetric deformation
05 p0935 A70-16234
- Circular cylindrical shells creep buckling under nonuniform external loads, considering thermal effects and initial imperfections
07 p1405 A70-19253
- Isothermal steady state creep extension and flexure of laminated beams with alternating layers, indicating nonlinear stress distribution
07 p1412 A70-19964
- Rectangular thin plates in small deformation transient creep bending, using finite element method in iterative procedure
08 p1590 A70-21356
- Microstructure of wrought arc-cast polycrystalline W sheet after high temperature creep deformation at various stress levels
08 p1525 A70-21962
- Stress concentration in elastoplastic and creep deformations determined by approximate solution
11 p2134 A70-25845
- CREEP DIAGRAMS**
Temperature-time-variable stress-strain state of polymer structures, solving creep equation by linear model with rheological properties
01 p0211 A70-11426
- Short term creep and stress-relaxation curves analytic extrapolation for metals and alloys with lifetimes exceeding test duration
03 p0588 A70-13246
- Vibrational creep curves of Al alloy under uniaxial stress level and amplitude, noting influence of small vibrations
06 p1168 A70-17930
- Long time strength and creep rectilinear diagrams constructed for heat resistant alloys to obtain extrapolation values
10 p1903 A70-24239
- Plastic structural components service life estimation based on creep diagrams and short time tests
16 p2941 A70-34323
- Short term creep and stress-relaxation curves analytic extrapolation for metals and alloys with lifetimes exceeding test duration
19 p3548 A70-38464
- CREEP PROPERTIES**
NT SHEAR CREEP
NT STEADY STATE CREEP
NT TENSILE CREEP
Creep deformation modes of Ni-base austenitic superrefractory alloy as function of test temperature
01 p0118 A70-10704
- Intrinsic/extrinsic stacking fault pairs observed during creep of single crystals of gamma prime precipitation hardened Ni-base alloy, developing viscous slip model
01 p0119 A70-10731
- Dislocation climb theories of creep and superplasticity derived, postulating strain hardening and recovery processes with independently determined rates
02 p0317 A70-12315
- Polycrystalline Ni steady state creep characteristics measurement emphasizing temperature dependence of creep rate
03 p0504 A70-13022
- Creep and recovery of polyvinyl chloride reinforced by oriented cotton fibers, considering roles of fiber density and stress magnitude
03 p0516 A70-13499
- Dynamic equilibrium prediction for creep and fatigue of various metals under various loading conditions, using time-temperature and cyclic stress-strain parameters
04 p0704 A70-14759
- Structural metals hysteresis properties under cyclic plastic loading at room temperature, considering cycle dependent creep and stress relaxation
04 p0705 A70-14763
- Creep in single crystal and polycrystalline Nb between 1300-1900 C under stresses, showing stress independent activation energy
05 p0862 A70-16202
- Creep rupture effect on fatigue damage of structural material, constructing nondimensional stress range diagrams
05 p0943 A70-16806
- Unsteady cyclic creep effect on stressed state and margin safety of elements, noting discrepancy of experimental and theoretical characteristics
05 p0866 A70-17030
- Strain hardening equation for anisotropic medium under creep
05 p0952 A70-17035
- Uniform cross section rings creep characteristics testing method, proposing relations for calculating stresses and strains
05 p0952 A70-17037
- Analog to Burger model applied to rotating disk creep problem solution and stress-strain state of plane sample with hyperbolic groove
05 p0952 A70-17038
- Cyclic creep curves plotted from expansion diagrams for steel, copper and brass under small numbers of cyclic compression tension loads
06 p1162 A70-17388
- Creep-low cycle fatigue interactions in Udimet alloy at elevated temperatures, investigating cumulative damage
06 p1086 A70-17455
- Anisotropic fiberglass reinforced plastics creep properties under biaxial compression, showing compressive to tensile strain elimination or change
07 p1316 A70-19546
- Fiberglass reinforced plastics creep behavior under axial compression, studying time dependence of elasticity modulus and Poisson coefficient
08 p1526 A70-21174
- Interstitial sinks effect on structure and creep behavior of dispersion-strengthened Cb base alloy
08 p1521 A70-21703
- Temperature dependence of microplastic yield and flow stress and transient creep responses of gamma prime phase
08 p1522 A70-21709
- Potential function of creep strain rates for incompressible nonstrengthening materials exhibiting different creep characteristics in tension and compression
09 p1769 A70-22122
- Energy storage in creep deformed graphite from stress reduction tests, discussing negative creep, test procedures and results
09 p1709 A70-22386
- Alloy equivalent susceptibility to damage at intermediary service periods and different stress levels under creep conditions at 750 C
09 p1701 A70-22470
- Heat resistant alloys creep ductility, considering grain boundary cavitation, sliding and migration
09 p1701 A70-22554
- Rotating cylinder stress-strain under steady and unsteady creep, using Lagrange variational principle for differential equations
09 p1779 A70-23100
- Soviet book on creep of structural elements at high temperature noting metals, concrete and polymer materials, buckling, variety of structural elements and creep resistance
09 p1781 A70-23266
- Stress concentration at circular hole in plate, considering material creep and aging effects
09 p1782 A70-23290
- Mo single crystals creep behavior temperature and stress dependences using X ray analysis
09 p1708 A70-23543
- Fiberglass reinforced textolite creep strains as function of stress, temperature and time, noting correlation with theory to 200 C
09 p1710 A70-23725
- Austenitic steels and alloys high temperature softening under conditions of stress relaxation and creep, noting hardening action of plastic deformation
09 p1709 A70-23785
- Creep forming application in producing aircraft parts from metal sheets, plates and extrusions, discussing blank forming and drawing
10 p1893 A70-23854
- Viscoelastic half plane creep under discontinuous boundary conditions, obtaining exact closed-form solution based on Fourier transforms and distribution theory
10 p1965 A70-25325
- Creep deflections and collapse times for supported thin shallow spherical shells under uniform pressure predicted using variational theorem
11 p2135 A70-25963
- Glass fiber reinforced thin rectilinear orthotropic plastic plates bending using finite difference method with allowance for creep
12 p2324 A70-27531
- Metallic materials under cyclic stress conditions, investigating creep rate dependence on cycling frequency and impurities during static-to-dynamic transition
13 p2513 A70-28993
- Rotating disk service life and structural failure under creep, using Tresca yield and maximum stress criterion
13 p2514 A70-29290
- Creep properties of torsion-tension metal members subjected to nonproportionate loading at high temperatures
14 p2656 A70-30637
- Two dimensional stress-strain fields under elastic and elastic-plastic strains and steady state creep, calculating stress distribution around hole in cylindrical shell
15 p2813 A70-31533
- Steel and copper alloys torsion-tension members under nonproportionate loads, predicting creep behavior
15 p2759 A70-32316
- Cumulative creep strain and damage based on stress amplitude coefficients, considering continuous single step system of loads
15 p2821 A70-32339
- Thin plates with central circular holes, investigating creep behavior for biaxial edge tractions
15 p2822 A70-32359
- Al-Mg alloys creep characteristics dependence on Ag, Si and Zn additions during aging heat treatments, establishing activation energy and stress exponents
16 p2930 A70-33086
- Polycrystalline NaCl-KCl solid solution alloy, considering high temperature creep under constant compression stress
16 p2961 A70-33275
- Creep and tensile fatigue behavior of notched and unnotched graphite/epoxy composites
16 p2938 A70-33503
- Activation energy for creep at intermediate temperatures, allowing for elastic modulus change
16 p2991 A70-33790
- Ti-Al-Cr-Fe tensile, fatigue and creep properties at various temperatures, considering industrial applications
17 p3121 A70-34428
- Void formation and creep during fast neutron irradiation of austenitic stainless steel based on thermodynamic approach, calculating nucleation and growth rates
17 p3123 A70-34626
- Flexural creep deflections of glass fiber reinforced polycarbonate and Nylon thermoplastics
17 p3127 A70-34657
- Working fluid /Ar/ purity and stability effects on fatigue life and creep of Nb and Mo alloys using gas analysis, microstructure and microhardness data
17 p3126 A70-35715
- Cyclic strain effects on creep for steel at elevated temperatures, discussing overload frequency effects on plastic strain buildup
17 p3127 A70-35719
- Structural members of isotropic and anisotropic polymers, investigating creep behavior under simple stressed state
17 p3192 A70-35740
- Microstructural changes of Ni-Cr lamellar eutectic alloy during creep deformation at 625 and 760 C
18 p3272 A70-36034
- Creep bending of rectangular plates with stress-strain and strain displacement nonlinearities
18 p3343 A70-36703
- High vacuum effects on creep properties of single crystal low carbon nickel base superalloy
19 p3451 A70-37705
- Plane waves superposed on solid during steady state isothermal creep deformation subjected to unidirectional constant initial tensile stress
19 p3537 A70-37791
- Reciprocity theorem for stresses and strains in medium under creep and temperature field
19 p3548 A70-38582
- Alumina effects on Nb creep activation energy at elevated temperatures, noting independence from chemical composition and creep stresses
19 p3453 A70-38710
- Dispersion strengthened Ni-Cr alloys creep properties, investigating temperature, applied stress and thorium dioxide particles effects
20 p3644 A70-38984
- Ni-Cr heat resistant alloys structural transformation kinetics under aging, creep and operational conditions, discussing solid solution decomposition, hardening phases coagulation and dissolution, etc
20 p3645 A70-39037

- Creep and breakdown of thin walled cylindrical shells with circular holes subjected to internal loads at high temperature, discussing time to failure
20 p3721 A70-39777
- Medium thickness shells under thermal creep using Saint Venant semiinverse method
20 p3722 A70-39787
- Plastic bodies rupture and crack growth under creep, considering tension of bar with symmetrical angular notches
20 p3727 A70-39882
- Rotating elastic shafts rectangular shape stability under creep conditions, considering single mass rotor
20 p3727 A70-39883
- Strain component determination for grain boundary sliding influence in creep of alpha iron
20 p3735 A70-40446
- Orthotropic fiberglass-reinforced plastic cylindrical shell with allowance for material creep, calculating stress-strain state during bending under external pressure
21 p3842 A70-40649
- Creep and stability of microstructural Al elements under varying temperatures, noting grain boundary migration
21 p3839 A70-41429
- Duralumin constant speed tensile strength tests at 200 C, discussing creep thresholds statistical distribution in elongations interval
21 p3840 A70-41432
- Copper and Al polycrystalline single crystal substructure changes, examining high temperature, unsteady and diffusion creep
22 p4056 A70-43342
- Fiberglass reinforced plastic strength and deformation properties under creep and stress relaxation, investigating temperature effects and load duration
23 p4209 A70-43980
- Unidirectionally solidified carbide reinforced Co-Cr eutectic alloy, examining tensile strength and creep behavior
24 p4358 A70-45236
- Short-term creep and erosion resistance testing of Ti alloy in high speed air flows under aerodynamic vibrations
24 p4360 A70-45826

CREEP RESISTANCE

U CREEP STRENGTH CREEP RUPTURE STRENGTH

- Mo coated with Ni-base Nimonic and Co-base heat resistant alloys, for working degree effect on creep rupture strength
01 p0126 A70-11646
- Stress rupture strength dependence on specimen geometry /scale effect/ from analyzing metals failure under prolonged loads
02 p0383 A70-11655
- Reinforced plastics creep rupture strength under compression along elastic symmetry axes
02 p0322 A70-12805
- Grain size, forging parameter and microstructure effect on stress-rupture properties of wrought Ni-base alloy
03 p0511 A70-13567
- Creep rupture data processing by computer, performing data collection and processing separately
03 p0487 A70-13569
- Creep rupture and fatigue strength in solid body mechanics, considering triaxial stress state and simplified creep rupture theory variant
03 p0599 A70-14249
- Cold working with subsequent heat treatment increased creep rupture and creep behavior of V alloys
04 p0708 A70-15372
- Stress rupture strength and relaxation and time to failure of AMG-6M sheet under creep using energy dissipation method
05 p0952 A70-17034
- Stress rupture tests with Nb-based alloys in 1273-1673 K temperature range
05 p0952 A70-17039
- Thermocyclic creep and rupture strength of Nb, Ta and Mo refractory alloys under temperature and load variations, showing failure dependence on cycle parameters
05 p0867 A70-17043
- Heat resistant steel and nickel alloys stress rupture strength at operating temperatures, discussing endurance diagrams under cyclic bending loads
05 p0868 A70-17047
- Stress rupture strength of turbine blades fir tree type root joints under prolonged loads at high temperatures, studying disk teeth shearing
05 p0953 A70-17055
- Refractory metal structural elements stress rupture strength in vacuum and inert gas tested up to 2000 K
05 p0829 A70-17071
- Tensile and stress rupture tests facility for microsamples stability at temperatures up to 3300 K, investigating deformation and failure
05 p0830 A70-17073
- Materials stress rupture strength and elastic constants at liquid hydrogen temperature, describing method and facility
05 p0955 A70-17076

- Creep rupture and residual tensile strength tests to evaluate long time properties and structural stability of Inconel 718 alloy, performing phase analysis
07 p1310 A70-19731
- High temperature creep rupture tests of arc cast and powder metallurgy wrought unalloyed W sheets
07 p1313 A70-19884
- Dynamic creep rupture of stainless steel tested at high stress levels and temperatures
08 p1518 A70-21333
- Cr-Mo steel strength and structural stability during tubular stress-rupture testing with high pressure hydrogen, discussing welding effect on strengths
08 p1519 A70-21455
- Gamma-gamma prime mismatch effects on stress rupture of Ni and Fe-Ni based alloys with Al and Ti hardeners
08 p1521 A70-21701
- Axial constant load creep and strength rupture measurements of B-coated and silicon carbide-coated B filament reinforced Al alloys
08 p1521 A70-21702
- Tensile, fatigue, creep and stress-rupture behavior of unidirectional, unidirectional off-axis and cross-ply composites of B filaments in Al alloy matrix
08 p1531 A70-21896
- Creep and rupture of graphite-epoxy composites under unidirectional state of stress and controlled temperature environment, extrapolating long term loading behavior
08 p1531 A70-21897
- Creep failure fatigue life prediction methods involving hold period effects on high temperature fatigue properties
09 p1775 A70-22594
- Diffusion processes rate changes in metals and alloys resulting from radioactive emission, noting role in stress rupture strength mechanisms
11 p2068 A70-26595
- Rectangular beam creep rupture time under bending moment and axial tensile force, using power series to solve integral equations
11 p2142 A70-26635
- Ni-based heat resisting alloy /Inconel 700/ investigated for hot corrosive environment effect on stress rupture and fatigue strengths
13 p2434 A70-29157
- Stress rupture shear strength of fiberglass reinforced plastics under monotonic, prolonged and cyclic loading
15 p2766 A70-32853
- Al, Ga and In effects on creep and rupture stress of Ti at 500 C
17 p3120 A70-34425
- Power and exponential time dependences of long term creep strength for wide stress range, assuming linear heat resistance
19 p3449 A70-37340
- Stress rupture strength dependence on specimen geometry /scale effect/ from analyzing metals failure under prolonged loads
19 p3547 A70-38428
- Oxide dispersed Cu alloys preparation by surface oxidation of powders, considering structural stability and stress rupture properties
20 p3646 A70-39103
- Hot corrosive environment effect on stress rupture and fatigue strength of Ni heat resistant alloy used in gas turbine rotating blade
20 p3647 A70-39241
- High temperature Ni base superalloy stress-rupture life dependence on casting variables and section size
20 p3648 A70-39413
- Metal cracking and fracture mechanics under creep conditions at elevated temperatures, discussing notch rupture testing
21 p3937 A70-41437
- Carbon steel thin walled cylinders creep fracture subjected to combined tension and internal pressure by large strain theory
21 p3840 A70-41438
- Annealing temperature effect on creep rupture strength of Ta-W-Hf alloy
22 p4054 A70-42741
- Refractory metal alloys tensile and creep rupture properties for reactor fuel jackets
24 p4364 A70-46347

CREEP STRENGTH

- Heat and creep resistant Ni- and Fe-base alloys application in gas turbines, superheaters, steam pipes, chemical and petrochemical plants and heat treatment equipment
02 p0319 A70-12711
- Metals and alloys creep under tension and compression at elevated temperatures, considering plastic deformation equation applicability
04 p0707 A70-15265
- Creep and strength criteria reliability for turbomachine disks, determining stresses, destructive rotations and strength margin
05 p0953 A70-17056
- Creep deformation resistance decrease in pure Al tubular specimens at high temperatures under multiple stress reversals
06 p1087 A70-17456

- Book on optimization by variational methods covering use of differential equations, Pontryagin minimum principle, optimal and feedback control, dynamic programming, etc
06 p1093 A70-17650
- Weldability of super alpha high creep strength Ti alloy investigated by synthetic heat affected zone method using thermal cycling tests
06 p1090 A70-18501
- Prestraining effect on cavity formation at grain boundaries causing creep strength decrease
07 p1307 A70-19392
- Creep strain effect on cyclic fatigue life of duralumin at room temperature
08 p1516 A70-20988
- Interstitial sinks effect on structure and creep behavior of dispersion-strengthened Cb base alloy
08 p1521 A70-21703
- Silicon containing alpha matrix Ti alloy with high creep strength and stability at elevated temperatures, studying processing and heat treatment effects on properties
08 p1509 A70-21853
- Heat resistant cast alloys creep strength reporting criteria, comparing U.S. and European practices [ASM PAPER P9-15.2]
09 p1702 A70-22558
- Soviet book on creep of structural elements at high temperature noting metals, concrete and polymer materials, buckling, variety of structural elements and creep resistance
09 p1781 A70-23266
- Nickel base alloy as die material for creep forming titanium
11 p2060 A70-26424
- Fiberglass plastic cylindrical shells stability against creep under prolonged hydrostatic pressure, obtaining critical loading times
12 p2328 A70-28278
- Alloy high temperature creep and long term strength, determining exponential relations between stress, strain rate and durability
15 p2755 A70-31529
- Ti-Al-Sn-Zr system high temperature creep strength and ductility retention
17 p3120 A70-34424
- Ti-Al-Nb system creep strength, oxidation resistance, density, forging and rolling
17 p3120 A70-34426
- Creep resistant Ti alloys with high temperature strength and stability, comparing tensile data for room temperature and 900 F
17 p3122 A70-34440
- Rolled fine grained aluminum-alumina particles composites, determining creep strength dependence on temperature and tensile stress axis orientation
18 p3274 A70-36051
- Heat treatment and alloying element influence on phase and structure transformations in Ti alloys, investigating mechanical properties and creep resistance
20 p3645 A70-39039
- Ti alloy tension creep tests at room temperature, determining strength for correlation with stress relaxation
22 p4055 A70-43097
- Tubular Al creep resistance increase by temperature jumps during steady phase of creep
22 p4056 A70-43344
- Heat treatment effects on dispersion strengthening of Ni alloys, showing enhanced long term creep strength at 1100 C
24 p4360 A70-45828

CREEP TESTS

- Tantalum base alloy T-111 creep tests in vacuum at elevated temperature suggesting diffusion controlled microcreep mechanism
01 p0120 A70-10738
- Apparatus for continuous creep measurement at high temperature for fine wire and thin tubular samples with small cross sectional areas
01 p0088 A70-10746
- Constant stress creep and recovery behavior experiments of polycarbonate under combined tension and torsion stresses in weakly nonlinear range
01 p0130 A70-11083
- Mo coated with Ni-base Nimonic and Co-base heat resistant alloys, for working degree effect on creep rupture strength
01 p0126 A70-11646
- Ti alloys creep and fatigue breakdown under cyclic tensile loads at room temperature
02 p0315 A70-11660
- Integral equation solution in viscoelasticity theory based on creep tests with polymer containing elastic inclusion, improving convergence of approximations method
02 p0390 A70-12801
- Durability of refractory tubes of small thickness under creep with account of scale factor and unsteady conditions, tabulating experimental and theoretical values
03 p0508 A70-13247
- Machine for refractory crystals creep testing in thermal vacuum or inert protective medium
03 p0493 A70-13959

Life fraction hypothesis equation in creep testing derived on basis of chemical reaction rate theory [ASME PAPER 69-MET-A] 04 p0705 A70-14875

Time-to-rupture dependence on temperature and stress related to chemical reaction rate equation in creep testing [ASME PAPER 69-MET-B] 04 p0770 A70-14877

Creep and wear due to microslip under dry rolling contact conditions 05 p0854 A70-15890

LF creep characteristics in Block-wall Permalloy films, using high resolution Bitter pattern technique [IEEE PAPER 5.7] 05 p0893 A70-16996

Effective stress evaluation under cyclic trapezoidal loading and creep noting use in stationary test data conversion 05 p0951 A70-17031

Refractory Ni alloys defects accumulation under creep and cyclic temperature variations assessed by relative lifetime additive method 05 p0866 A70-17032

Stress rupture strength and relaxation and time to failure of AMG-6M sheet under creep using energy dissipation method 05 p0952 A70-17034

Creep effects on structural failure under low cycle fatigue at high temperatures, noting role of plastic deformation 06 p1164 A70-17409

Test stand for endurance and creep testing of plastics, glazed ceramics and other brittle materials 06 p1028 A70-17665

Creep and stress relaxation tests to investigate time dependent fracture strength of unidirectional glass fiber reinforced epoxy composites 07 p1321 A70-19962

Hydrogen penetrability in heat resistant steels subjected to high temperature creep, observing activation energy decrease with increased stress 08 p1515 A70-20923

Cyclic creep and relaxation of heat resistant alloys at high temperatures, showing inapplicability of static load conditions 08 p1516 A70-20982

Gaseous environments effects on creep of austenitic stainless steel, observing weakening in air and surface cracking in nonoxidizing atmospheres [ASME PAPER 68-MET-3] 08 p1519 A70-21453

Internal stresses and substructures dependence on thermomechanical histories of stainless steel during creep, noting subgrain orientation 09 p1705 A70-22805

Creep and stability of perforated and unperforated turbine disks under operating conditions 09 p1779 A70-23097

Mo single crystals dislocation substructure strain dependence after creep using etch pitting techniques 09 p1708 A70-23544

High temperature compressive creep tests at constant stress, describing strain measurement techniques and servocontrolled compressive equipment 12 p2206 A70-27214

Polycrystalline W-Re alloy creep tests in tension, investigating dislocation substructure formation as function of stress, temperature and strain 12 p2255 A70-27606

Beam-bending and circular plate testing rigs for creep with constant and variable loading, discussing tests repeatability and accuracy 12 p2207 A70-27618

Equipment specifications and design for creep testing at variable load and temperature under uniaxial tension, emphasizing test environment control 13 p2509 A70-28537

Short term creep of Ni in vacuum, stationary air and high speed air flow at various temperatures and loads 14 p1594 A70-30167

Polycrystalline Al microstrain distribution nonuniformity under creep and static tension 14 p2595 A70-30173

Optimum diffusion welding temperature for Ti-6Al-4V alloy determined from tensile and creep tests 14 p2591 A70-30934

Ti alloy stability after long term creep exposure at various temperatures 17 p3120 A70-34421

Ultrahigh vacuum creep rate measurements with continuously increasing loads on Ta-base alloy, relating creep life with temperature and stress rate 17 p3122 A70-34552

Creep testing machine with constant load for HF thermal cycling under vacuum 17 p3063 A70-35587

Creep and failure tests for Ti alloys at 500 C, discussing work dissipation during creep process 17 p3126 A70-35714

Polythermal phase equilibrium and heat resistance of Ti-rich Ti-Zr-Al alloys, noting creep and tensile tests 18 p3275 A70-36124

Strain hardening directionality during creep tests of tubular samples under combined tensile stresses and bending moments 18 p3341 A70-36588

Low temperature creep deformation recorder with liquid He coolant, discussing Al and Pb single crystal tests 19 p3395 A70-37352

Ti alloys creep and fatigue breakdown under cyclic tensile loads at room temperature 19 p3452 A70-38434

Durability of refractory tubes of small thickness under creep with account of scale factor and unsteady conditions, tabulating experimental and theoretical values 19 p3453 A70-38465

Brittle failure under creep during slow cyclic loading, discussing damage accumulation assumptions 20 p3725 A70-39868

Contact shaped fiberglass-reinforced plastic tensile creep tests, showing strain property linearity dependence on direction 21 p3841 A70-40642

Ti alloy tension creep tests at room temperature, determining strength for correlation with stress relaxation 22 p4055 A70-43097

Wrought Nimonic alloy, measuring stress redistribution due to creep under variable load and temperature 23 p4274 A70-44911

Servohydraulic testing machine for measuring cyclic stress-strain behavior of materials subjected to fatigue and creep at elevated temperature 23 p4178 A70-44912

Prestraining effect on cellular precipitation in Ni-Cr lamellar eutectic during creep testing 24 p4359 A70-45247

Stress dependent creep rate in nickel based superalloy single crystals 24 p4359 A70-45289

**CRESTATRONS
U TRAVELING WAVE TUBES**

CRESTS
U WAVES
CREVICES
U CRACKS
CRICKETS
NT BEETLES
CRITERIA

Turbine blade materials resonant vibration resistance criterion dependence on temperature and cyclic and static stresses amplitude 04 p0776 A70-15262

Materials in spatial motion criteria of stress power positiveness 05 p0929 A70-16069

Creep and strength criteria reliability for turbomachine disks, determining stresses, destructive rotations and strength margin 05 p0953 A70-17056

Static stability criterion applicable to elastoplastics problems with/without nontrivial equilibrium states, noting effect on buckling loads 06 p1167 A70-17900

Nonlinear feedback control systems frequency domain stability criterion obtained using gain- phase plot 06 p1026 A70-17972

Stability criterion applied to asymmetric rigid cyclic strains and plastic cyclic strains, considering failure of metals 07 p1315 A70-20182

Optimal inertialess nonlinear filters synthesis with various optimality criteria for signal distributions differing from normal 09 p1654 A70-22543

Heat resistant cast alloys creep strength reporting criteria, comparing U.S. and European practices [ASM PAPER P9-15.2] 09 p1702 A70-22558

Spectral criteria for approximating tunnel diode nonlinear characteristics obtained by minimizing deviations of moduli of harmonic amplitudes 09 p1649 A70-23340

Composite reinforced materials similarity criteria to relate static and dynamic fields of various physical parameters, outlining mathematical simulation 12 p2259 A70-27526

Stochastic analog approximation method minimizing criterion functions and for recovering functions from noisy measurements of values in learning systems 13 p2442 A70-29585

Nonlinear feedback control systems forced asymptotic stability, using linear transformation of circle criterion 15 p2716 A70-32554

Popov and circle criteria for stability of nonlinear feedback control systems, using parameter plane representation 16 p2884 A70-33314

CRITICAL FLICKER FUSION

Critical flicker frequency dependence on viewing distance, stimulus angular size and luminance 09 p1618 A70-22671

Visual restriction effects on critical flicker fusion threshold, loudness and pitch discrimination determined using reticular activating system 09 p1622 A70-23576

Reaction time in determining visual transient response at frequencies above flicker fusion 10 p1818 A70-24717

CRITICAL FLOW

Multiple array critical flow venturi air flow metering system constructed for gas turbine engines, developing pressure control valve [ASME PAPER 69-WA/FM-5] 04 p0688 A70-14838

Mass flow rate calculation of methane and natural gas mixtures through critical flow nozzles [ASME PAPER 69-WA/FM-4] 04 p0667 A70-14839

Nonequilibrium models describing two phase critical discharge of initially saturated or subcooled liquid through sharp edged and smooth inlet geometries 05 p0956 A70-16162

Outside-matching functioning of single rotating disk of axial compressor, investigating critical disengagement and rotary detachment [ONERA-TP-701] 07 p1193 A70-19127

One dimensional compressible flow with heat addition in nonconstant area duct extended for friction addition, discussing critical thermal shocking 11 p2041 A70-26651

Small viscosity and heat conductivity in solutions to critical layer in stratified shear flow 20 p3308 A70-39447

Near critical heat transfer in cryogenic fluids, discussing thermodynamic and transport properties 23 p4279 A70-44357

CRITICAL FREQUENCIES

Ionization variations and correlation coefficients of F 2 critical frequency variations, using airborne ionospheric sounder over Sogra and Kerguelen Island conjugate areas 01 p0080 A70-11224

F 2 layer state prediction as function of solar activity by series expansion for describing space-time variations of monthly F 2 medians critical frequencies 01 p0083 A70-11547

Ionospheric critical frequency recorder development for continuous recording of frequency variations with time 02 p0303 A70-12736

Lunar tides in midday critical frequency of F 2 layer, determining phase reversal location 04 p0651 A70-15309

Magnetic declination effect on F 2 layer behavior determined from critical frequencies at two magnetically conjugate points 04 p0683 A70-15742

F 2 region critical frequency conjugacy latitudinal variations observation at conjugate stations compared with results from nonconjugate stations 05 p0839 A70-16286

Midlatitude F 2 perturbations from vertical sounding stations data during solar activity minimum, discussing F 2 region critical frequency variation 07 p1266 A70-19450

Sporadic E layers structure and dynamic characteristics during polar aurorae, determining critical frequencies 07 p1267 A70-19455

Global distribution of F 2 layer critical frequencies by expanding empirical function of diurnal variations into natural orthogonal components 07 p1277 A70-20451

Electrical parameters approximate calculations for waveguides with complex cross sections by Schwarz alternating method, determining critical frequencies of fundamental modes 09 p1632 A70-22406

Midlatitude sporadic E layer critical frequencies dependence on solar activity using vertical ionospheric sounding data, observing ionization correlation 10 p1882 A70-25197

F 2 layer midday ionization equatorial anomaly during summer and winter solstices, using calculated mean critical frequencies 11 p2042 A70-25533

F 2 layer critical frequencies rms deviations approximate dependences on latitude and solar activity for computer calculation of long-range ionospheric forecasts 11 p2043 A70-25549

Flutter instability critical velocity and frequency for thin cantilevered plate with follower jet determined by Galerkin and computer simulation 12 p2316 A70-27106

F 2 region critical frequency from Alouette 2 satellite data compared with ground based measurement 12 p2226 A70-28066

F 2 critical frequencies from Alouette 2 satellite ionogram data compared with ground-based sounding results 13 p2396 A70-29094

F 1 layer occurrence and geometrical parameters relative to critical frequencies of F1/F2 layers 14 p2571 A70-30228

Geomagnetism-sporadic E layer relationship, discussing critical frequencies and H component variations 14 p2571 A70-30236

Magnetic declination effect on F 2 layer behavior determined from critical frequencies at two magnetically conjugate points 14 p2575 A70-30826

Magnetic field effect on critical flutter speed and frequency of elastic plate in ionized gas flow, deriving dispersion equation

15 p2818 A70-32173

Ionospheric small scale ionization discontinuities vertical drift effect on diurnal variations of F 2 layer critical frequency

18 p3246 A70-36086

Midlatitude F 2 perturbations from vertical sounding stations data during solar activity minimum, discussing F 2 region critical frequency variation

18 p3249 A70-36924

Sporadic E layers structure and dynamic characteristics during polar aurorae, determining critical frequencies

18 p3250 A70-36929

F 2 region critical frequency diurnal variation forecasting, using series expansion of natural orthogonal components

19 p3409 A70-37327

Transversely magnetic and electric wave critical frequency spectra in Pi and H section waveguides, using summary representation method

19 p3378 A70-37735

F 2 region critical frequency cross correlation coefficients for magnetically conjugate stations, considering magnetic disturbances effects

21 p3816 A70-41069

F 2 layer midday ionization equatorial anomaly during summer and winter solstices, using calculated mean critical frequencies

21 p3819 A70-41283

F 2 layer critical frequencies rms deviations approximate dependences on latitude and solar activity for computer calculation of long-range ionospheric forecasts

21 p3819 A70-41299

F 2 layer critical frequency and maximum electron concentration statistical characteristics for predicting SW propagation conditions

23 p4188 A70-44056

Ionospheric layers critical frequencies recording, using automatic interplanetary station type probe

23 p4194 A70-44088

F 1 layer occurrence and geometrical parameters relative to critical frequencies of F 1/F 2 layers

24 p4331 A70-46303

Geomagnetism-sporadic E layer relationship, discussing critical frequencies and H component variations

24 p4332 A70-46311

CRITICAL LOADING

Externally pressurized air journal bearings load capacity, film stiffness, attitude-eccentricity locus and mass flow, studying supply pressure and shaft rotation effects

[ASME PAPER 69-LUB-29] 01 p0100 A70-10380

Synchronous dynamic response of gaseous double squeeze film thrust plate with very high frequencies, showing increased load capacity and stiffness

[ASME PAPER 69-LUB-8] 01 p0102 A70-10395

Externally pressurized journal bearing load tests, comparing load capacity data with analytical values

01 p0103 A70-10559

Axially compressed cylindrical shells with edge constraints, determining critical load from inelastic behavior considerations

01 p0205 A70-11141

Carrying capacity of shells of revolution obtained with threads spun around metallic shell, including stresses during spinning process

01 p0210 A70-11414

Carrying capacity of heat resistant steel turbomachine elements, discussing plastic deformation and cyclic load effects, breakdown load determination, stress analysis, etc

02 p0352 A70-11659

Al alloys strips weakened by holes, analyzing limiting tensile load-carrying capacity

02 p0384 A70-11741

Structural support strut design for cryogenic propellant tanks to optimize load carrying capability and heat transfer characteristics

02 p0306 A70-11942

Newtonian liquid lubricated spiral groove bearing load capacity and power loss dependence on viscosity variations with temperature

[ASLE PREPRINT 69-LC-21] 02 p0309 A70-12533

Tangential force applied to column end by jet reaction from nozzle clamped to column end, obtaining critical load and oscillation frequency

02 p0389 A70-12644

Cylindrical shells buckling under biaxial compression and transverse loads, examining critical loads dependence on shell parameters, end conditions and elastic properties

03 p0590 A70-13380

Stability analysis of orthotropically symmetric strip under uniformly distributed compressive forces applied to shorter ends, deriving critical load formula

03 p0590 A70-13402

Limiting equilibrium under axial tension of brittle body with parallel axisymmetric external cracks, studying critical load, crack propagation, etc

03 p0594 A70-13737

Differential equations solution in terms of elementary functions applied to evaluate critical buckling loads for struts of variable cross sections

03 p0602 A70-14328

Supercritical strains and buckling in rib-reinforced cylindrical shells under axial compression using strain-energy method

04 p0766 A70-14478

Turbine blade designs considered for increasing load capacity covering tandem, jet-blade and base plain blade configurations and test results

[ASME PAPER 69-WA/GT-1] 04 p0734 A70-14894

Critical load and instability of smooth and mesh surface mechanical systems subjected to impinging fluid jet, noting static buckling and flutter effects

[ASME PAPER 69-WA/APM-10]

Orthotropic axially compressed conical shell stability, evaluating lower critical load and postbuckling state

04 p0772 A70-14917

Initial deflection effect on elastic cylindrical shell stability under compression, finding critical load by determining limiting point in successive loading

04 p0773 A70-15009

Disk stress concentrations calculation beyond elastic limits taking into account effect on bearing capacity

04 p0775 A70-15261

Carrying capacity and deformation susceptibility of anisotropic fiberglass reinforced conical and cylindrical plastic shells under axial compression

05 p0933 A70-16209

Stability, critical load and strength algorithm for fiberglass reinforced cylindrical plastic shells under external load allowing for shear stresses

05 p0933 A70-16211

Stability and critical loads of transversely isotropic reinforced plastic annular plates with weak shear resistance under axisymmetrical buckling

05 p0933 A70-16213

Stability of clamped, hinged and elastically supported circular cylindrical shells under critical combined torsional and transverse pressure

05 p0934 A70-16227

Stability and critical load algorithm for flexible shallow spherical and conical shells of revolution derived from variational equation

05 p0935 A70-16236

Small amplitude spherical elastic-plastic waves initial behavior studied for critical and supercritical loading

05 p0945 A70-16819

Precooling effect on load carrying capacity of heat resistant plastics subjected to unilateral heating

05 p0874 A70-17065

Fiberglass reinforced plastics load carrying capacity under unsteady unilateral heating described by thermal similarity criteria

05 p0955 A70-17070

Carrying capacity of machine parts under small numbers of cyclic plastic deformation, reviewing breakdown criteria relation to kinetics of stress-strain states

06 p1161 A70-17383

Elastoplastic rod systems under repeated variable loads, calculating carrying capacity from plastic failure considerations

06 p1163 A70-17395

Prismatic pendularly supported beam load-forced vertical vibrations, critical load amplitude and force pulsation in case of stability loss

06 p1165 A70-17586

Thin walled cylindrical shell stability with hollow filler under distributed external loads, determining critical loads

07 p1399 A70-18663

Equilibrium cracks in elastic bodies on basis of atomic interaction law, using Griffith problem to estimate bearing capacity

07 p1400 A70-18666

Critical stresses for plate with circular hole and cracks assuming symmetrical load

07 p1402 A70-19054

Critical slope load calculation for circular elastic embedded and supported arcs under radial and variable force

07 p1404 A70-19136

Inextensional nonlinear theory of arches applied to analysis of hinged-hinged circular arches subjected to downward point load, calculating critical load value

07 p1408 A70-19561

Thin walled strip stability, calculating critical force and rotation angles assuming small subcritical strains

07 p1415 A70-20188

Initial perturbation effect of smooth cylindrical shells stability under critical axial compression noting deflection factor

07 p1415 A70-20190

Ductile flexure location in bent beams and systems with variable cross sections to determine critical load using plasticity theory

08 p1587 A70-21072

Wall material diathermy effects on critical thermal load under radiant transfer, comparing results for quartz glass and stainless steel tubes

08 p1597 A70-21186

Optimizing shape of elastic bar compressed by polar force obtained by determining functional extremum representing volume of bar at constant critical force

09 p1769 A70-22252

Partially loaded clamped plastic shallow spherical caps collapse loads and stress and velocity distributions

09 p1781 A70-23230

Elastic cylindrical shells stability under uniform pressure, calculating critical transverse load by finite-difference computer program

09 p1781 A70-23287

Carrying capacity of shallow shells of revolution, determining buckling stress and limiting equilibrium of shells with varying thickness under transverse load

09 p1781 A70-23288

Contour immobility effect on load carrying capacity of rigid plastic thin shells of revolution, establishing minimum reinforcement value for edge

09 p1783 A70-23388

Cylindrical shell critical load boundaries under uniform external stress and small torsion

09 p1783 A70-23389

Lower critical load for shallow rigidly convex shell expression refined by considering effect of rigid clamping of shell edge on buckling boundary deformation

09 p1784 A70-23594

Solution uniqueness in limit load theory for unbounded regions, obtaining infinity as unique value for critical load from elastoplastic analysis

10 p1954 A70-24013

MHD generators optimum load selection by method of stepwise approach, noting agreement with pressure and density distributions to yield maximum power

10 p1923 A70-24156

Kinematic analysis of limit loads of equilateral triangular plates under various boundary conditions

10 p1958 A70-24517

Limiting load for annular plates made of material having different yield points in tension and compression

11 p2129 A70-25560

Rectangular sandwich plates stability under combined loads, deriving equations for determining critical loads

11 p2129 A70-25563

Stability loss in cylindrical shell under axial compression, noting critical load reduction by local axisymmetric depression

11 p2130 A70-25566

Compressive stress critical moment induced instability and weakening incorporated in thin walled beam design

11 p2131 A70-25590

Optimal efficiency of axial turbomachines limit loading of blade root and hydrodynamical criteria

11 p1975 A70-25791

Critical load, force characteristics and pressure variation on blades of axial compressor under rotating stall

11 p2133 A70-25795

Load carrying capacity of isotropic rigid-plastic shells of revolution with different yield points under tension and compression applied to spherically coupled cylinders

11 p2134 A70-25932

Dynamic buckling of shell or arch structure determined from response of two degrees of freedom structure to step load application

11 p2138 A70-26158

Buckling load calculations for axially compressed circular cylindrical shells under relaxed boundary conditions

11 p2140 A70-26484

Ring buckling under constant and centrally directed pressure, considering small displacement and inextensional deformation

11 p2141 A70-26492

Cylindrical shells design under axially compressed loads by elastic stability analysis, predicting critical loads

12 p2320 A70-27142

Sandwich beams elastoplastic stability, determining critical load

12 p2323 A70-27342

Glass-plastic thin cylindrical shells carrying capacity dependence under axial and external loads on combinations of longitudinal and transverse reinforcing layers

12 p2259 A70-27527

Transversely isotropic shells stability with respect to subcritical deformation under axial compression using three dimensional linearized equations, determining critical loads

12 p2324 A70-27529

Externally pressurized bearing with electrically-conducting gas lubricant under axial magnetic field, considering load capacity

12 p2244 A70-28018

Fiberglass plastic cylindrical shells stability against creep under prolonged hydrostatic pressure, obtaining critical loading times

12 p2328 A70-28278

Critical loads for brittle bodies weakened by sharp holes under combined diffuse thermal fluxes and crack crossing

12 p0000 A70-28321

Residual gas effects on critical load and brittleness of pure and molybdenum-coated niobium bars after annealing in vacuum

12 p2258 A70-28324

Ductile fractures analysis using critical strain near crack tip as criterion

13 p2432 A70-28673

Cantilevered column stability under constant follower load in presence of external damping

13 p2510 A70-28733

Buckling, postbuckling and limit analysis of symmetric elastic structure subjected to increasing loads

13 p2511 A70-28737

Critical loads and stability of isotropic cylindrical shells under uniformly distributed longitudinal compression loads based on network method

13 p2514 A70-29287

Reinforced shells of revolution carrying capacity upper limit subjected to internal adiabatic ideal gas flow

15 p2814 A70-31534

Strength and critical load determination for spherical shells with reinforced hole under internal pressure based on stress-strain state analysis during deformations

15 p2814 A70-31543

Elastic shells of revolution stability and critical loads, discussing moment stress state and edge effect

15 p2816 A70-32158

Cylindrical shells upper critical loads calculation based on linearization of nonlinear shell theory equations

15 p2818 A70-32181

Computer program for limit analysis of rotationally symmetric shells, generating yield point load upper and lower bounds and velocity profile

15 p2822 A70-32351

Cylindrical shells under axial compression, using elastic stability analysis for critical loads prediction

15 p2822 A70-32512

Maximum stress distribution in laminar composites, considering loads on boundary of reinforcing layers

15 p2766 A70-32854

Load carrying capacity of self acting hydrodynamic journal bearings, considering turbulence and whirling motion in closed form solution

17 p3101 A70-35148

Column end fixity using Euler load and maximum flexibility coefficient for span point lateral load

17 p3188 A70-35226

Critical load of shallow shell of revolution as function of geometric and material parameters

17 p3192 A70-35717

Critical stresses and stability of thin Maxwell plates under random temperature fields

18 p3337 A70-36368

Critical loads for notched square Al alloy rods under tension

18 p3343 A70-36718

Optimal distribution of plastic inhomogeneity of torsioned prismatic square bars under maximum loading

18 p3343 A70-36719

Vibrations induced by frictional moving force in viscoelastic beam with free ends on elastic base, showing critical load dependence on damping

18 p3343 A70-36720

Limit load of cylindrical shell with rigidly clamped edges under varying pressure and axial force, using Tresca yield condition

18 p3343 A70-36722

Carrying capacity of nonshallow rectangular shells, showing corner dependent collapse

19 p3535 A70-37345

Nonuniqueness of collapse load for isotropic frictional material with or without cohesion

19 p3433 A70-37385

Optimum one dimensional journal bearing for maximum load with minimum film thickness, using Pontryagin principle [ASME PAPER 69-LUB-9]

19 p3435 A70-37614

Carrying capacity of heat resistant steel turbomachine elements, discussing plastic deformation and cyclic load effects, breakdown load determination, stress analysis, etc

19 p3547 A70-38432

Finite element method with first order displacement functions to compute crack tip stress intensity factor in various shapes under different loading conditions

19 p3548 A70-38623

Load rating methods for cage-type and full complement needle bearings dynamic capacity [ASLE PREPRINT 70AM 3D-2]

19 p3438 A70-38802

Aerostatic journal bearings with double plane admission feeder holes, determining maximum load and stiffness by numerical method

19 p3443 A70-38898

Load bearing capacity of radial gas bearing with annular injection line, discussing gas feeding methods

20 p3637 A70-39816

Unsteadiness effect on load bearing capacity of cylindrical sectoral gas bearing

20 p3637 A70-39819

Unidirectional fiber reinforced composites strength, obtaining limit load bounds from plasticity analysis

20 p3731 A70-40051

Cracked brittle body limiting equilibrium, determining critical loads for two half spaces with various circular rib couplings

20 p3733 A70-40432

Concentrated lateral loads effect on elastic stability and moment carrying capacity of circular cylindrical shells in bending

21 p3932 A70-40544

Thin walled fiberglass-reinforced plastic cylinders in torsion, calculating load carrying capacity as function of temperature

21 p3841 A70-40648

Structural stability analysis by matrix decomposition and iteration, extending to structures with nearly equal critical loads

21 p3934 A70-40888

Perforated steel strip axial tension load limit, considering various hole diameters and numbers

21 p3936 A70-41415

Finite element analysis of critical stress distribution in canopy of deployed twin keel parawing, predicting failure stress levels

[AIAA PAPER 70-1196] 21 p3753 A70-41820

Purity dependent critical resolved shear stress of magnesium oxide single crystals, using compression testing

21 p3862 A70-41910

Analytical iteration method extended to critical load of clamped beam with symmetrically variable cross section

21 p3939 A70-41965

Elastoplastic flexure and critical loading of isotropic rectangular plates of constant and variable thickness, using Lagrange principle with numerical integration

22 p4115 A70-42810

Thin walled column buckling relation to plate element buckling, studying deformation, stress state, failure mechanism and ultimate load

22 p4116 A70-43214

Circular cylindrical shell with varying thickness under circumferential load and radial pressure, calculating critical load

22 p4117 A70-43354

Carrying capacities of simply supported and clamped circular plates under combined lateral pressure and edge compression loads

22 p4118 A70-43548

Stability of elastic stretched ring on thin spherical shell under critical loads

23 p4268 A70-44318

Second approximation for limit loads due to imperfection sensitivity of axisymmetric elastic shell structures with unique harmonic buckling modes

23 p4273 A70-44720

CRITICAL MACH NUMBER

U CRITICAL VELOCITY

U MACH NUMBER

CRITICAL MASS

Nuclear light bulb engine critical fuel mass and design changes effects

[AIAA PAPER 68-571] 01 p0140 A70-10835

Open cycle gas core nuclear rocket reactor, evaluating critical mass for U isotopes

18 p3290 A70-36564

CRITICAL PATH METHOD

Book on project management with critical path method and PERT, covering manual and computerized calculation of scheduling, networks, time-cost tradeoffs, etc

22 p4128 A70-43625

CRITICAL POINT

Mathematical model of spherically symmetric quiescent droplet undergoing quasi-steady vaporization near thermodynamic critical point

01 p0213 A70-10291

Critical detonation diameter as function of concentration and dimensions of inhomogeneities in explosive, assuming chemical reaction generated behind detonation front

01 p0217 A70-11005

Two phase liquid-vapor system specific heat increase at temperatures approaching critical point, using nonanalytic vapor pressure equation with data for nitrogen and oxygen

04 p0780 A70-14584

LF sound velocity measurement in carbon dioxide near critical point, noting existence of logarithmic divergence

04 p0718 A70-14685

Spiral gears bearing disks contact fatigue endurance process, deriving critical points cyclic stability from stress distribution considerations

07 p1291 A70-18819

Critical regions equilibrium thermodynamic properties of fluids and magnets using scaled equation of state

07 p1421 A70-19298

Laminar boundary layer critical height determination using Rouse stability parameter

07 p1257 A70-19336

Elastic stability theory applied to equilibrium and stability of discrete continuous structural systems, detailing discrete critical points

07 p1408 A70-19560

Refractory metals electrical resistivity as function of density near critical point, using exploding wire

07 p1335 A70-19899

Liapunov stability conditions for critical point of ordinary differential equation, determining optimal criterion

09 p1727 A70-22664

Shock and thermodynamic phenomena of real gases near critical points, discussing specific volume and specific enthalpy increases

10 p1867 A70-24136

Plasma cumulation, with and without shell under concentric pressure impulse using perfect gas theory, estimating critical parameters

10 p1926 A70-25322

Coaxial plasmatron pulsation on intensity of heat exchange between high temperature nitrogen jet and axisymmetric body near critical point region of spherical bluntness

11 p1984 A70-26739

Elastic stability of structural systems with generalized coordinates and independent loading parameters associated with critical point

13 p2511 A70-28739

Sound velocity relation with specific heat at constant volume at liquid-gas equilibrium critical point

15 p2826 A70-32022

Steam-water jet discharge heat transfer features, examining critical region parameters from nozzle into submerged space with large counterpressure

18 p3345 A70-36117

Fe-Co alloys critical points during rapid heating, determining alpha-gamma phase transformations onset from dilatometric curves

18 p3275 A70-36203

Critical height phenomenon for vertical jet exhausting into horizontal parallel plates channel simulating aircraft surfaces

18 p3243 A70-36709

Carbon dioxide entropy and enthalpy computation covering critical region and wide temperature range [ASME PAPER 70-GT-5]

18 p3348 A70-36861

Heavy elements critical energy calculation, taking into account low energy electrons effects on losses in electromagnetic cascade

20 p3674 A70-39303

Base pressure behind supersonic vehicle, examining Crocco-Lees mixing theory critical point in laminar near wake

21 p3747 A70-42109

Heat transfer from turbulent axisymmetric jet to normal flat wall at critical point with small Reynolds numbers

23 p4181 A70-44321

Forced convection heat transfer to liquid nitrogen near critical point, determining coefficients from given wall temperature and heat flux

23 p4279 A70-44358

Single component fluid behavior in liquid-vapor critical point vicinity, using LF acoustic resonant cavity technique for isochoric measurements

23 p4222 A70-44432

Critical heat flux during forced pipe flow of boiling ethanol-water and acetone-water binary mixtures

23 p4283 A70-44730

Stability of self-similar flows of second kind near critical point

24 p4327 A70-46004

CRITICAL PRESSURE

Plastic deformation of wedge shaped model asperities influencing gas leakage between contacting surfaces, discussing critical contact pressure

01 p0060 A70-10267

Fuel droplets burning at pressures sufficient to reach critical temperature under zero gravity conditions in free fall apparatus

02 p0351 A70-12002

Dimensionless strength parameter in determining bursting pressure of ductile metal diaphragms in square section shock tubes

08 p1481 A70-21034

Toroidal metallic shells stability under static loads, determining snap-through pressures in pressure chamber with nitrogen working gas

08 p1588 A70-21195

Upstream influence distance estimation associated with critical pressure rise in two dimensional shock-boundary layer interactions based on Lighthill subsonic inner boundary layer concept

10 p1862 A70-23840

Eccentricity and clamping effects on stability and critical pressure of ring-reinforced cylindrical shells under internal pressure

10 p1956 A70-24248

Nonequilibrium plasma MHD generator critical pressures determination, applying electron energy balance equation and relation between plasma conductivity and Hall parameters

10 p1809 A70-25142

- Supersonic panel flutter of circular cylindrical shells at critical dynamic pressure 17 p3188 A70-35227
- Heat transfer measurement from Pt wire to carbon dioxide near critical pressure, discussing film boiling and free convection flows 21 p3953 A70-42167
- Limiting pressure for isotropic plastic plates and spherical shells with stress dependent yield, using flow theory 22 p4120 A70-43717
- Cryogenic fluids nitrogen, argon and carbon monoxide nucleate boiling from atmospheric to near critical pressure 23 p4279 A70-44359
- Cs high temperature vapor and critical pressure and temperature determination for predicting thermodynamic and transport properties, liquid phase nature and state relations 23 p4281 A70-44449
- Cesium high temperature saturated liquid and vapor phase density and critical temperature and pressure 23 p4281 A70-44450
- CRITICAL REYNOLDS NUMBER**
 U CRITICAL VELOCITY
 U REYNOLDS NUMBER
CRITICAL SPEED
 U CRITICAL VELOCITY
CRITICAL STRESS
 U CRITICAL LOADING
CRITICAL TEMPERATURE
 Power and location prediction at critical heat flux onset under nonuniform axial heating conditions, using local approach method 01 p0219 A70-11303
- Fuel droplets burning at pressures sufficient to reach critical temperature under zero gravity conditions in free fall apparatus 02 p0351 A70-12002
- Critical thermal regimes in Couette flow, investigating temperature and velocity profiles of nonisothermal steady state Newtonian flow between two parallel plates 03 p0466 A70-13388
- Superconducting properties of Nb-Ti-N thin films prepared by reactive sputtering process, obtaining transition temperature maximums 04 p0732 A70-15689
- Critical brittleness temperatures of low C steels determined to distinguish main failure types 06 p1166 A70-17655
- Surface tension plotted against density and temperature of hydrocarbon jet fuels, determining critical temperature 07 p1357 A70-18653
- Alloying elements effect on polymorphic alpha-beta transformation temperature of Ti systems, discussing heat resistance 07 p1307 A70-19555
- Hydrogenated Ni activation energy difference for lower and higher critical temperatures due to hydride dislocations binding energy 08 p1522 A70-21705
- He-Cd laser with cathaphoretic transport and diffusion return path, noting condenser critical temperature for radiation noise reduction 15 p2751 A70-31987
- Hydrostatic pressurization effect on ductile-brittle transition temperature of polycrystalline chromium 18 p3274 A70-36053
- Critical heat flux density during annular channel internal heating, examining transfer crisis under forced motion of unheated water 18 p3345 A70-36111
- Thermally induced oscillations and negative resistance in seminsulating oxygen-doped GaAs double injection devices via heating beyond critical temperature 22 p4084 A70-42326
- Self flammability temperature of binary alloy Al-Si powders in aerosol state as function of chemical and phase compositions 23 p4205 A70-44046
- Cs high temperature vapor and critical pressure and temperature determination for predicting thermodynamic and transport properties, liquid phase nature and state relations 23 p4281 A70-44449
- Cesium high temperature saturated liquid and vapor phase density and critical temperature and pressure 23 p4281 A70-44450
- CRITICAL VELOCITY**
 Mathematical model for studying three dimensional whirling shaft stability as function of angular to critical velocity ratio, using Liapunov method for equations of motion 01 p0143 A70-10889
- Aircraft controls response critical speed as function of transmission lag and transfer function of control link elements 02 p0227 A70-12410
- Piston theory application to plates and shells stability in supersonic gas flows, considering critical velocities determination for asymmetric flows and oscillations 04 p0617 A70-15196
- Gas dynamic functions using critical velocity and Laval number 06 p1033 A70-17237
- Flutter instability critical velocity and frequency for thin cantilevered plate with follower jet determined by Galerkin and computer simulation 12 p2316 A70-27106
- Monograph on critical speeds of nonzero mass shaft supported at both ends by bearings with nonlinear elastic displacements 13 p2416 A70-28373
- Fixed end nonprismatic bar stability in fluid flow, studying form influence on critical flow velocity 13 p2512 A70-28982
- Critical Mach numbers for transverse resistive shock waves as function of fluid/magnetic pressure ratio compared with cold plasma theory 14 p2623 A70-31036
- Gas-particle efflux from nozzle at critical velocities, noting particle size and concentration effects on inlet pressure 15 p2721 A70-32136
- Magnetic field effect on critical flutter speed and frequency of elastic plate in ionized gas flow, deriving dispersion equation 15 p2818 A70-32173
- Pilots brake-takeoff decision at critical engine failure speed, discussing operational aspects of accelerate-stop criteria 15 p2675 A70-32219
- Real gas transonic flow transition through critical velocity in Laval nozzle, examining reasons for increment of viscosity and heat conduction effects 18 p3239 A70-36217
- Mechanical systems spontaneous oscillation due to different critical velocities with and without arbitrarily small damping 18 p3338 A70-36430
- Critical rotation rates of gas turbine rotors disk-drum designs, describing initial parameters of model in matrix form 20 p3721 A70-39782
- Alfven critical velocity concept in MPD arcs analysis, obtaining exhaust velocity relationship from one dimensional flow model [AIAA PAPER 70-1096] 20 p3683 A70-40240
- Coupled rotational vibration system dynamic behavior near critical speed, using graphs of autonomous two degree of freedom system on reduced phase plane 22 p4112 A70-42271
- Laminar circular cylindrical shells supersonic flutter characteristics determination by dynamic equilibrium boundary value problem eigenvalues analysis, obtaining critical flutter speeds 24 p4424 A70-45588
- CROCCO-LEE THEORY**
 Base pressure behind supersonic vehicle, examining Crocco-Lees mixing theory critical point in laminar near wake 21 p3747 A70-42109
- CROP GROWTH**
 Aerial IR film optical density related to preharvest crop yield indicators in micro experiments with remote sensors 12 p2217 A70-26918
- Worldwide crop calendar development from repetitive satellite observation to perform agricultural change detection 12 p2218 A70-26922
- Remote photometric and spectrometric measurements for plant structure and productivity of grass and shrub vegetation in desert environments 12 p2218 A70-26923
- Radar imagery for crop discrimination, discussing sensor and data requirements and statistical analysis methods 14 p2578 A70-31237
- CROPS**
 Wheat fields recognition, mapping and acreage measurement by multispectral scanning with real time analog data processing, considering seasonal and observation altitude effects 12 p2219 A70-26930
- Spectral discrimination technique for crops remote sensing, comparing statistical irradiance model with airborne multispectral scanner data 12 p2219 A70-26931
- CROSS CORRELATION**
 Sound radiation from airfoil in turbulent jet flow, discussing direct correlation of fluctuating lift 01 p0004 A70-11192
- Binary systems noise resistance with various cross correlation functions and indefinite moment of arrival 03 p0448 A70-13512
- Visual object images describable in terms of cross correlation functions without loss of information 04 p0662 A70-15437
- Remote sensing of winds and atmospheric turbulence by cross correlation of passive optical signals, discussing results for power spectrum of fluctuations and winds 06 p1072 A70-18553
- Nonstationary correlation function for cross correlation of sample records from random processes, discussing minimum mean square error and weighting method 07 p1238 A70-19250
- Electromyograms cross correlation analysis to study time relationships between motor unit discharges of human musculus biceps and triceps brachii during physical work 07 p1213 A70-19791
- Improper integrals appearing in cross correlation of responses of two single degree of freedom systems to bandwidth limited white noise, deriving Laplace inversion formulas 07 p1236 A70-20067
- Digital cross correlator design for impulse response determination in linear systems, noting real time operation without software and storage problems 07 p1236 A70-20068
- Ionospheric irregularities showing dispersive motions from systematic skewness in cross correlation functions for satellite scintillations at spaced receivers 10 p1881 A70-24810
- Asymmetric cross correlation functions in D and lower E region drift measurements interpreted in terms of moving screens 10 p1881 A70-24811
- Remote monitoring of atmospheric wind and turbulence by cross correlation passive techniques, measuring heat and humidity fluxes 12 p2230 A70-26948
- Optical cross correlator with consecutive recording of mutual correlation function, using transparencies on different side of lens 13 p2412 A70-29865
- Correlation apparatus for ionospheric drift measurement by spaced receivers using closed loop of magnetic tape 14 p2550 A70-30741
- Automatic alphabetic characters classification model based on cross correlation and discrete Walsh-Fourier transforms, using computerized simulation 16 p2851 A70-33460
- CW multifilament GaAs laser diodes measurement, showing cross correlation between light and current noises 18 p3270 A70-36742
- Synthetic aperture radar receivers, discussing cross-product term suppression in correlation detection for image distortion reduction 20 p3585 A70-39392
- F 2 region critical frequency cross correlation coefficients for magnetically conjugate stations, considering magnetic disturbances effects 21 p3816 A70-41069
- Turbulent density fluctuations statistical properties analysis by cross correlation technique with schlieren instruments 21 p3807 A70-41242
- Cross correlation measurement errors for fluid pipe flow with pseudorandom sequence generated temperature fluctuations, considering transport time, impulse response and laminar flow 24 p4333 A70-45111
- CROSS COUPLING**
 Inertia cross coupling during aircraft design stage allowing later flight testing, discussing analysis complexity and sensitivity to aerodynamic data change 01 p0007 A70-11315
- Gyroscopes orientation cross coupling effect on dynamic drift of three axis gyrostabilizer solved by method of successive approximation 07 p1278 A70-18736
- Cross coupled rotational motions of free solid body carrying nutation-damping pendulums 07 p1335 A70-19808
- Longitudinal structural vibration and lateral bending response mass and spring coupling in Saturn AS-502 during boost with longitudinal excitation by pogo effect 09 p1766 A70-23239
- Antenna arrays elements mutual coupling effects on pattern and impedance characteristics 10 p1849 A70-24536
- Roll induced cross coupling evaluation in two dimensional homing systems based on defining roll transfer matrix 11 p2122 A70-25681
- Coriolis illusions amelioration during space flight, noting cross coupling effects minimization by reflex vestibular stabilization of head 13 p2358 A70-29432
- Aircraft lateral and longitudinal motion stability in steady rolling, deriving inertia cross coupled stability criterion 13 p2347 A70-29445
- Cross coupling relations in Boltzmann equations solution for inhomogeneous plasmas, using spherical harmonics expansion and Laguerre-Sonine polynomials 13 p2464 A70-29539
- Multidimensional automatic control systems polyvariance, describing compensating cross couplings realization 20 p3603 A70-39834

Semicircular canals dynamic cross coupled responses to rotational movement, discussing mechanical model applicability

22 p3981 A70-43703

CROSS FLOW

Two dimensional time dependent solution for impulsive motion of circular cylinder involving viscous cross flow at moderate angles of attack

18 p3207 A70-36454

Liquid jets aerodynamic atomization at orifice exit in reentry vehicle under gaseous crossflow, investigating critical Weber number variation with Knudsen number

20 p3610 A70-39701

Forced convection heat transfer from flat plate and cylinder in cross flow to simulated Mars atmosphere

21 p3945 A70-41026

CROSS RELAXATION

Al-27 NMR saturation effects on ruby electron cross relaxation and inversion

23 p4230 A70-43932

CROSS SECTIONS

Multiple pulsations mechanism during detonation spherical wavefront propagation in channels with various cross sections, noting volume effect

01 p0060 A70-10135

Axisymmetrical stress-strain state of body of revolution with complex cross sectional geometry under surface loads, deriving computer algorithm for numerical analysis

02 p0384 A70-11665

Mechanical vibration effects on natural convective heat transfer in enclosure of rectangular cross section [ASME PAPER 69-WA/HT-13]

04 p0783 A70-14820

Torsional vibrations of four cell tube, deriving cross sectional constants and natural frequencies

05 p0936 A70-16321

Uniform cross section rings creep characteristics testing method, proposing relations for calculating stresses and strains

05 p0952 A70-17037

Scattered Lyman alpha radiation intensities measured for mixtures of partially dissociated hydrogen in Ar, measuring quenching cross sections

06 p1053 A70-17327

Equivalent circuit for fluidic transmission line used for studying behavior of lines with circular and rectangular cross sections

06 p0988 A70-17439

Size and shape error distribution law for cross sections of cylindrical components, discussing probability characteristics

07 p1290 A70-18740

Charge exchange cross section of hydrogen position ion-negative ion collisions

09 p1733 A70-23269

Cross sections of fragments emitted in spallation reactions of carbon and nitrogen nuclei emulsion with alpha particles

09 p1733 A70-23549

Shock wave interactions effect on propagation in ducts with gradual or sudden change in cross section, using schlieren spark photography

09 p1664 A70-23735

Finite deflections theory applied to elastic-plastic arches, introducing coefficients depending on shape and degree of yielding of cross section

10 p1955 A70-24080

Solar corpuscular fluxes angular characteristics, derived from observational data analysis, showing circular or elliptical transverse cross sections

11 p2104 A70-25545

Modified method of cross sections applied to solution of scalar Helmholtz equation in infinite symmetrical waveguides

12 p2272 A70-27296

Unsteady compressible pipe flows with large cross sectional variations studied by two dimensional difference method

13 p2386 A70-28806

German monograph on gas turbine combustion chambers part-load behavior improvement by load controlled change of flame tube air cross section

17 p3148 A70-35373

Cross section deformation effect on helicopter rotor blade torsional vibration, using differential equations of vibrating beam

18 p3334 A70-35959

Cosmic ray and radiation belt data from vertical probes, determining instantaneous cross section of atmosphere

18 p3307 A70-36169

Arbitrary cross sections center of flexure formula, transforming surface integral to line integral dependent on boundary conditions

18 p3343 A70-36716

Axisymmetrical stress-strain state of body of revolution with complex cross sectional geometry under surface loads, deriving computer algorithm for numerical analysis

19 p3547 A70-38439

Solar corpuscular fluxes angular characteristics derived from observational data analysis, showing circular or elliptical transverse cross sections

21 p3882 A70-41295

Torsion in rods with rectangular and trapezoidal cross sections, using functional-analytic iterative method

23 p4268 A70-44241

Microwave frequency light modulators waveguides, examining optimal cross sections to increase modulator efficiency

23 p4196 A70-44409

CROSSED FIELD AMPLIFIERS

Duration measurements for sampling function in dynamic crossed field photomultiplier

05 p0849 A70-16655

Crossed field amplifiers properties and applications, comparing performance to TWT

09 p1642 A70-22008

Microwave tubes for high power transmission from space to ground and in deep space communications, discussing klystrons, TWT and crossed field amplifiers [AIAA PAPER 70-435]

11 p2016 A70-25456

CROSSED FIELDS

Electron-hole pair quasi-linear fluctuations at recombination boundary in semiconductor crystal under crossed electric and magnetic fields

01 p0156 A70-10191

Electron transverse and perpendicular drift velocities calculated at moderate and strong magnetic fields for hydrogen, using Maxwellian energy distribution and equivalent pressure concept

02 p0348 A70-12654

Anomalous behavior of arc motion in high pressure cross-field plasma devices in terms of electromagnetic effects

03 p0529 A70-12938

Crossed field plasma accelerator designed as element of hypersonic wind tunnel driver

06 p1119 A70-17471

MHD free convection of electrically conducting fluid in strong cross field using perturbation technique, considering liquid metals and ionized gases

07 p1348 A70-19208

Plasma ion-cyclotron oscillations resonance excitation in crossed electric and magnetic fields, describing instability development

07 p1354 A70-20319

Tensor conductivity, magnetic field and electric field effect on heat transfer in MHD channel flow, solving for temperature and Nusselt number

08 p1554 A70-21773

Landau damping and stability of low density crossed field electron beams using analogy with inviscid shear flows

10 p1918 A70-23964

Multivelocity electron beam critical fluctuation amplitudes in crossed electric and magnetic field

10 p1925 A70-25107

Drift waves relation to anomalous cross field diffusion in fully ionized magnetoplasmas, introducing model predicting amplitude, correlation time, fluctuation spectrum and diffusion process

12 p2280 A70-27788

Carbon dioxide laser electrical discharge stabilization against transverse gas flow by cross magnetic field

12 p2250 A70-28099

Microwave conductance tensor in crystals with non-parabolic carrier energy dissipation under crossed constant electric and magnetic fields

12 p2288 A70-28326

Crossed field nitrogen laser operation in second positive band to obtain high UV pulse output

13 p2429 A70-29669

Parametric oscillation instabilities in plasma under magnetic field perpendicular to circularly polarized or hybrid electric field

14 p2624 A70-31042

Ion-molecule reactions investigation by resonance principle, discussing ion paths in crossed fields

17 p3081 A70-34574

Nonequilibrium plasma from pulsed discharge in crossed electric and magnetic fields

17 p3142 A70-35727

MHD and thermal boundary layer, considering difference scheme for conducting medium flow past body in crossed electric and magnetic fields

18 p3293 A70-36116

Magnetic coupling in solid dielectric cylinder under axial magnetic and perpendicular electric fields, noting memory and magnetostrictive effects

19 p3471 A70-37785

Electron runaway suppression in fully ionized Lorentz plasma by crossed magnetic and electric fields

24 p4382 A70-45105

CROSSLINKING

Diffusion phenomenon in cross linkage theory of biological aging formulated as model in differential equation form, obtaining solution and applications

01 p0028 A70-11374

Polyamides chemical welding using HF heating to obtain optimum temperature distribution and to activate polymer reaction with crosslinking agents

06 p1091 A70-17136

Dicationic crosslinking agents isolation and characterization and formation of polymers with ionic crosslinks

06 p1004 A70-17512

Propellants chemistry based on chemically cross-linked binder

07 p1360 A70-19909

Polymer structure and cross-link density effects on thermal analysis of phenol-formaldehyde polymers pyrolysis products

11 p2069 A70-25804

Epoxide ring reactivity and crosslinking related to adjacent electrophilic and electronegative groups, considering epoxy resin technology

16 p2936 A70-33357

CROSSTALK

NT IONOSPHERIC CROSS MODULATION

Group delay characteristics curvature in radio relay systems, analyzing crosstalk in picture-sound and beamed multiplex signal transmission by nonlinear distortion method

05 p0815 A70-16774

Crosstalk in multiple-beam waveguides due to scattering and distortion caused by surface irregularities of focusers, discussing power profile of Gaussian beam

08 p1462 A70-21507

Crosstalk effects on data transmission in multiplex TV systems for aerospace communications analyzed by signal and noise models

13 p2363 A70-28384

Frequency selection in telemetry taking into account systems for minimum interference and crosstalk

13 p2366 A70-29216

Crosstalk error in binary phase modulated communications systems due to RFI and thermal noise

23 p4158 A70-43752

CROWDING

Short wave ionospheric scatter propagation, observing interference and crowding in 16-23 MHz and relationship to F2 layer maximum usable frequency

18 p3227 A70-36093

CRUCIFORM WINGS

Minimum drag thin symmetrical cruciform wing fitted with central ridge, reducing problem to linear algebraic finite system of equations

10 p1803 A70-24784

Cruciform-finned missiles dynamic stability investigation by nonlinear differential equations of motion, considering roll lock-in, resonance instability and catastrophic yaw [AIAA PAPER 70-969]

20 p3715 A70-39560

CRUDE OIL

Hydrocarbons and fatty acids distribution in living organisms, fossils, sediments and crude oils, discussing slow thermal maturation role and geological applications

02 p0252 A70-12520

CRUISE MISSILES

Otomat surface to surface missile with turbojet engine for extended range subsonic cruise and two solid propellant rocket engines for launch

22 p4110 A70-43211

CRUISING FLIGHT

Minor circle maneuver solution to equations of motion of vehicle in spherical planet atmosphere for gliding and cruising, discussing cylindrical planet case

01 p0184 A70-10949

Optimal fuel consumption for climbing, cruising and landing flight conditions for medium range subsonic, high supersonic and hypersonic aircraft

02 p0227 A70-12404

Deviation angle optimization for cruising hypersonic jet aircraft, noting effect of rotation losses on design

03 p0406 A70-13019

Net thrust determination for high bypass ratio engines in cruise, suggesting performance evaluation in actual flight tests

[SAE PAPER 690652]

05 p0895 A70-15841

Flowfields in lifting-line approximation for finite bladed, lightly loaded propellers in axial cruise and heavily loaded propellers in static operation

07 p1190 A70-20411

XB-70 aircraft flight tests in cruise and landing approach to evaluate handling qualities criteria [AIAA PAPER 70-566]

13 p2346 A70-29031

Northern Hemisphere temperature atlas for SST cruise altitudes, estimating probabilities of enroute temperatures and risk increase

14 p2609 A70-30609

Mariner attitude control system limit cycle operation during cruise, noting variation from ideal case to single side operation [AIAA PAPER 69-844]

15 p2812 A70-32507

Helicopter aerodynamic problems, discussing rotor performance improvement for increased cruising speed

16 p2841 A70-33758

Atmospheric turbulence vertical component spectral density observation by aircraft in steady flight, considering transfer function computation methods

19 p3351 A70-37464

- Thermal protection system based on radiation cooling for high altitude cruising hypersonic flight, achieving zero net mass transfer 21 p3950 A70-41745
- Subsonic high lift cruise wing optimal design using kernel function method of planar lifting surface theory 22 p3959 A70-42709
- Supersonic flight altitude stability, studying effects of velocity, lift-drag ratio, thrust law, wind direction, engine unstarts, etc [AIAA PAPER 69-813] 22 p3961 A70-42712
- Space shuttle transition trajectory optimization for cruising flight entry, considering longitudinal control, pitchup instability and angle of attack 23 p4244 A70-44623
- Meteorological wind and temperature distributions on selected routes at Concorde cruising level, noting computer use for flight planning 24 p4374 A70-46204
- CRUSADER AIRCRAFT**
U F-8 AIRCRAFT
CRUSTS
Pulsars crust plastic deformation leading to rotation damping, higher magnetic moments and rarer starquakes 14 p2638 A70-30672
- CRYODEPOSITS**
Test model thermal balance in space simulator, measuring effects of solar simulator irradiance reflected from carbon dioxide cryopanel deposits [AIAA PAPER 69-1012] 11 p2149 A70-26153
- Capture coefficients and reflected flux measurements for gaseous nitrogen molecular beams impinging on solid nitrogen cryodeposit surface 20 p3675 A70-39390
- Monochromatic radiant flux angular distribution reflected from water and carbon dioxide cryodeposits, discussing incidence, deposit thickness and wavelengths [ASME PAPER 70-HT-34] 22 p4122 A70-42433
- Carbon dioxide and water cryodeposits refractive indices and densities, using thin film interference technique [ASME PAPER 70-HT-33] 22 p4122 A70-42434
- CRYOGENIC EQUIPMENT**
Rocket-borne cryogenic sampler for stratospheric composition measurement by mass spectrometer analysis for computing radiation balance in stratosphere [AAS PAPER 69-569] 04 p0687 A70-14661
- Variable coupler for liquid helium X band EPR cavity during immersion in coolant 07 p1286 A70-19976
- Cryogenic thermometry operating principles, instrument design, measurement techniques, useful temperature ranges and accuracy 09 p1674 A70-22289
- Cryogenic refrigeration below 20 K, analyzing cycles using similarities of work and heat exchange mechanisms 09 p1726 A70-22290
- U.S. cryogenic refrigerators specifications in tabular form 09 p1655 A70-22291
- Rocketborne cryogenic sampler using shock diffuser inlet for air collection at supersonic speeds during rocket ascent 10 p1949 A70-23937
- Cryogenic Ge bolometers sensitivity variation and noise, noting radiation absorption by sensor and by coating 12 p2237 A70-28151
- Thermal anchoring of wire or rod components to heat sinks in cryogenic equipment in vacuum 14 p2584 A70-30501
- Al weldable alloys for cryogenic applications, considering plasticity, brittleness and tensile and yield strengths at low temperatures 14 p2597 A70-30968
- Thermal design of counter current cryogenic heat exchangers employing spiral finned tubing 14 p2617 A70-31018
- Cryogenic single tubes transient cool-down by liquid hydrogen, deriving film boiling heat transfer correlation [AIAA PAPER 70-660] 16 p2998 A70-33621
- Cryogenic attachment for cooling and tilting metal samples in electron microscope 18 p3259 A70-36474
- Liquid nitrogen boil off calorimeter for surface energy measurements, describing construction, calibration and instrument errors 18 p3261 A70-37089
- Cryogenic temperature sensor with linear characteristics from 150 to minus 452 F, describing calibration and testing 19 p3425 A70-37883
- InAs pulsed injection laser at cryogenic temperature for measuring time constant of IR radiation detectors 20 p3630 A70-39449
- Working fluids liquid property variations effects on cryogenic heat pipe performance 21 p3946 A70-41043

- Integrated Cryogenic Isotope Cooling Engine system (ICICLE) for spacecraft sensors refrigeration requirements 21 p3947 A70-41053
- Free vibrating reed apparatus for polymer low temperature internal friction and Young modulus measurements, discussing polystyrene properties 21 p3827 A70-41464
- Low temperature Ge diode thermometer with computer circuit transforming voltage to temperature readout 21 p3828 A70-41473
- Aerobee rocket-borne cryogenic air samplers heat exchanger design by mathematical model and computer solution 23 p4280 A70-44365
- Cryogenic pipelines cooldown to operating temperature, calculating cryogen flow rate limits due to thermal stresses in steel and Al flanges 23 p4280 A70-44368
- Cryogenic fluid heat exchanger flow oscillation automatic feedback control, discussing design and simulation 23 p4280 A70-44370
- Three-stage Gifford-MacMahon cycle regenerative refrigerator in 6.5 K region, using lead shot matrices for coldest regenerators 23 p4280 A70-44371
- CRYOGENIC FLUID STORAGE**
Liquid nitrogen evaporation in PSB foam polystyrene vessels compared with glass vessels for cryogenic application 02 p0305 A70-11875
- Thermally induced convective mixing motion in rotating cylindrical cryogen space tank model under heat flux, calculating critical Rayleigh number 07 p1257 A70-19320
- Liquid helium cryostat for onboard satellite storing designed with allowance for overloads and vibrations during powered flight 08 p1440 A70-21220
- Expandable rigidizable solar shields operational, structural and thermal performance tests conducted with spherical models for cryogenically fueled space vehicles 12 p2312 A70-27131
- Vapor-liquid equilibria predictions for multicomponent cryogenic mixtures, applying to correlation selection in critical and low temperature regions 14 p2616 A70-31015
- Metallic diaphragms design, fabrication and testing for cryogenic fluid and positive expulsion systems [AIAA PAPER 70-683] 16 p2918 A70-33582
- Thermal testing of inflatable solar shields for cryogenic space vehicles, discussing shield misalignment effects on propellant tank temperatures [AIAA PAPER 70-856] 16 p2982 A70-33901
- Al alloys and stainless steels tensile properties and application in lightweight cryogenic propellant tank structures, discussing Ti alloys and reinforced composite materials tests 20 p3651 A70-40123
- Hydrogen slush characteristics, discussing advantages of liquid-solid mixture over liquid hydrogen, production methods, aging effects, transfer and pumping losses, storage, instrumentation, etc 23 p4232 A70-45075
- CRYOGENIC FLUIDS**
NT FLOX
NT LIQUID HYDROGEN
NT LIQUID OXYGEN
NT SOLIDIFIED GASES
- Helium low temperature applications to fuel tank pressurization, superconducting magnet cooling and cryopumping of solar space simulators 11 p2083 A70-25620
- Critical Levitation Loci for floating spheres on cryogenic fluids 17 p3136 A70-34743
- Near critical heat transfer in cryogenic fluids, discussing thermodynamic and transport properties 23 p4279 A70-44357
- Cryogenic fluids nitrogen, argon and carbon monoxide nucleate boiling from atmospheric to near critical pressure 23 p4279 A70-44359
- Cylindrical heaters in corresponding-states fluids, estimating film boiling heat transfer coefficients by correlation procedure using least squares expression 23 p4279 A70-44361
- Cryogenic fluid multipoint level sensing detector circuit using carbon resistors 24 p4339 A70-46200
- CRYOGENIC GYROSCOPES**
Unconventional gyros, discussing nuclear magnetic resonance, induction, cryogenic, electrostatic and laser technology 03 p0481 A70-12960
- Electromagnetic single-coil suspension for cryogenic gyroscope with superconducting sphere rotor, calculating suspension force characteristics 12 p2234 A70-27565

CRYOGENIC MAGNETS

- Cryogenically cooled superconducting electromagnets design, construction and properties for research in plasma and solid state physics, considering coil systems 01 p0143 A70-10970
- Three channel traveling wave maser with cryogenic superconducting magnet for C-band monopulse radar system, describing construction and electrical characteristics 10 p1900 A70-24894
- CRYOGENIC ROCKET PROPELLANTS**
Impingement pressure analysis associated with two phase cryogenic propellant venting to space environment [AIAA PAPER 69-571] 01 p0196 A70-10845
- Wall temperatures and heat transfer coefficients for solid-vapor mixtures of para hydrogen and nitrogen flowing in heated tube 03 p0604 A70-13018
- Turbine flowmeter in-place calibration for measuring cryogenic propellant flow rates in rocket engine testing 06 p1071 A70-18448
- Spacecraft propulsion development guidelines concerning rocket engines with storable propellants, rotating solid propulsion systems, cryogenic propellants, etc 15 p2790 A70-32256
- Liquid or solid Leidenfrost film boiling on saturated cryogenic liquid surface, discussing hydrodynamic model similar to propellant spillage accidents 17 p3194 A70-34744
- Turbofan engine aerodynamic interactions, cryogenic space storable propellants, space station attitude control biowaste resistojet and long burning time solid propellants 20 p3688 A70-39667
- European rocket engine technology, discussing liquid rockets, reliability, restart capability, performance, cryogenic engine, components, facilities and U.S. cooperation 22 p4092 A70-43509
- Pressure sensor testing and calibrating at cryogenic temperatures, describing special test rig structural, insulation, fittings and materials requirements 23 p4178 A70-44846
- CRYOGENIC STORAGE**
Filament tensile strengths and pressure strain characteristics of high modulus boron filament wound/resin composite pressure vessels for cryogenic applications 08 p1509 A70-21909
- Thick superinsulation system design for long term cryogenic storage using superfloc, radiation shield and spacer material 11 p2150 A70-26367
- Supercritical pressure system heat transfer characteristics for cryogenic space oxygen storage and supply 14 p2667 A70-31342
- Cryogenic multilayer insulation (MLI), comparing radiation magnitudes, gas conduction and contact solid conduction to calorimeter and tank data [AIAA PAPER 70-850] 16 p2939 A70-33917
- CRYOGENICS**
Ge bolometer cooled by liquid helium 3 to near absolute zero to achieve high sensitivity for far IR detection 01 p0091 A70-10910
- Ti-Al-Sn alloy tensile deformation mechanisms at cryogenic temperature under uniaxial and biaxial stress noting twinning, prismatic slip and dislocation characteristics 03 p0507 A70-13141
- Cryogenic temperature sensor calibration with automated data readout for spacecraft accuracy requirements, describing potentiometric system 03 p0486 A70-13561
- Thermal conductivity, electrical resistivity, Lorentz ratio and thermopower of aerospace alloys at cryogenic temperatures, considering Inconel, Hastelloy, Ti and Al alloys 03 p0512 A70-13807
- Specific heat, electrical resistivity and thermal conductivity changes in materials properties at cryogenic temperatures, noting parasitic phenomena, mechanical and dielectric properties 03 p0525 A70-14269
- Radiative heat flux between two parallel copper disks at cryogenic temperature, showing dependence on emitter temperature and spacing [ASME PAPER 69-WA/HT-7] 04 p0784 A70-14823
- Cassegrainian liquid He cooled IR telescope for rocket-borne IR astronomy, discussing optical, cryogenic and electronic designs 04 p0689 A70-15017
- Heat transmission by current carriers to cryogenic region, ascribing heat flux to Joule effect in conductor 05 p0881 A70-16025
- Energy losses in conductors carrying intense currents to cryogenic regions linked with heat transfer due to high temperature gradients 05 p0881 A70-16026

Recrystallization annealing third stage of cold worked polycrystalline niobium by measuring electrical resistance at liquid nitrogen temperature
05 p0863 A70-16204

Cryogenics applications to solid state physics and materials research tabulated for experimental methods and objectives
05 p0892 A70-16398

Test apparatus for investigating crystal defects influence on simultaneous measurement of metals thermal and electric conductivity under plastic deformation at cryogenic temperature
05 p0829 A70-16399

Cryogenic temperature effect on short life torsional fatigue properties of Ni-Cr-Mo steel, discussing cyclic strain range effects
05 p0864 A70-16807

Thermal conductivity temperature dependence measured in greases bulk and thin layers at liquid helium temperature
05 p0874 A70-16842

Electronic equipment packaging for operation at cryogenic temperature
06 p1017 A70-17336

Metal lined glass filament-wound pressure vessel performance at cryogenic temperatures, discussing fibers, resins and liners
06 p1091 A70-17615

Digital control valve for high speed aerospace blending, considering propellant and cryogenics applications
06 p0989 A70-18602

Plastic deformation effects on superconductivity of wire specimens of high purity Pb, In and Tl cold worked at liquid He and annealed
06 p1127 A70-18614

Multicomponent Ti alloys mechanical properties for use in cryogenics describing alloying advantages with tantalum
10 p1906 A70-25295

Thermal conductivity of thin metallic films and wires at cryogenic temperatures, discussing electron transport properties
11 p2083 A70-25752

Solid-gas phase equilibria of binary systems related to cryogenics
12 p2329 A70-27023

High temperature gaseous molecular beams impingement on Cu surfaces at cryogenic temperatures measured for condensation rates
12 p2271 A70-27265

Superconducting magnetometers and cryogenic refrigeration techniques, discussing liquid helium refill systems, Joule-Thompson expansion, etc
13 p2414 A70-30027

Cryobiological data for life mechanisms on planets in solar system emphasizing Mars
14 p2536 A70-30344

Cryogenics and nuclear physics, discussing particle beam handling magnets, superconducting accelerators, detectors, moderators, low temperature irradiation facilities, etc
14 p2616 A70-31014

Junction and MOSFET transistors thermal noise characteristics at cryogenic temperatures
15 p2710 A70-32585

High strength Ti alloy for cryogenic applications, comparing plane strain fracture toughness
17 p3122 A70-34438

Cryogenic temperature measurement including metallic and semiconductor resistance thermometers, thermocouples and bibliography
17 p3082 A70-34740

Thermal contact resistance, discussing behavior at cryogenic temperatures and directional or thermal rectifying effect
17 p3197 A70-35541

Nuclear irradiation effect on embrittlement of Ti and Ti alloys at cryogenic temperature, determining radiation damage threshold as function of tensile properties changes
18 p3278 A70-36567

Cryogenically cooled photoconductive IR radiation detectors, determining wideband optical heterodyne performance
20 p3627 A70-39085

Strain measuring apparatus for multiple samples simultaneous compression tests at near absolute zero temperatures
20 p3632 A70-39628

Strain gages for structural stress analysis in cryogenic environments, discussing correction factors for temperature dependent characteristics
21 p3932 A70-40545

Optimum cryogenic heat pipe design, considering gravitational effects for spacecraft applications
21 p3946 A70-41044

Cryogenic cooling of IR radiation sensors for increasing sensitivity, considering background radiation interference from sensor optical system and detector/preamplifier noise
21 p3825 A70-41052

Pressurized liquid nitrogen and hydrogen dielectrics for cryogenic cables, measuring dissipation factor and voltage breakdown by concentric cylindrical test cell
21 p3851 A70-42125

Diluent molecules effect on polymers relaxation behavior at cryogenic temperatures from internal friction measurements, noting loss peaks shift
21 p3844 A70-42138

Polyurethane adhesives differential thermal analysis, rebound resilience and tensile properties at cryogenic temperatures
21 p3844 A70-42141

Polymers as cryogenic adhesives, evaluating role of chain structure below glass transition temperature
21 p3783 A70-42142

Ti and Al alloy weldments plane strain fracture toughness and mechanical properties for cryogenic applications, using gas metal arc and gas tungsten arc welding
22 p4043 A70-42423

[ASME PAPER 70-MET-4] Resilience and tensile properties of polyurethane adhesive at cryogenic temperatures measured by differential thermal analysis
23 p4209 A70-44275

Cryogenic engineering - Conference, University of California, Los Angeles, June 1969
23 p4277 A70-44351

Closed cell polyurethane foam for cryogenic insulation, determining thermal conductivity and net heat flow by analytical model and test
23 p4280 A70-44367

Thermal radiation emissivity predictions for metal surfaces at cryogenic temperatures, comparing anomalous skin effect and Drude single electron theories
23 p4218 A70-44388

Cryogenic thermocouples of various metal pairs for low temperature measurements, discussing performance tests and calibrations
24 p4378 A70-45385

CRYOPUMPING
Helium low temperature applications to fuel tank pressurization, superconducting magnet cooling and cryopumping of solar space simulators
11 p2083 A70-25620

Hydrogen oxygen rocket engine two phase liquid hydrogen pump capability and hydrodynamic design, analyzing constant-quality flow, acoustic effects, compressible flow and cavitation
15 p2791 A70-32511

[AIAA PAPER 69-549] Cryopumping systems of ultrahigh vacuum space environmental chambers
17 p3060 A70-35247

Aerospace coldness and vacuum simulation, discussing uses of cryogenic, titanium sublimation, ion and molecular pumps
19 p3396 A70-37462

CRYOSORPTION
U SORPTION
CRYOSTATS
Liquid helium cryostat for onboard satellite storing designed with allowance for overloads and vibrations during powered flight
08 p1440 A70-21220

Multiple maser-magnet units packaging in single cryostat for maximum tunability
08 p1513 A70-21599

Cryostat design and performance for use with optical telescopes in high altitude balloons
09 p1674 A70-22294

High transmission Mylar window He cryostat for Mossbauer measurements
21 p3828 A70-41470

Saturated nitrogen vapors condensing coefficients measurement by cryostat, comparing results with theoretical prediction
23 p4218 A70-44364

UV excited powdery fluorescent products, describing cryostat for photo and thermoluminescence at various temperatures
24 p4339 A70-46097

CRYSTAL DEFECTS
NT CRYSTAL DISLOCATIONS
NT EDGE DISLOCATIONS
NT FRENKEL DEFECTS
NT POINT DEFECTS
NT SCREW DISLOCATIONS
NT VACANCIES [CRYSTAL DEFECTS]
Epitaxial PbSe films formation mechanism-defect structure relation using moire rotation method, discussing elastic strains, dislocations, boundary formation, etc
01 p0155 A70-10182

Transmission electron microscope study of deformation mode during rapid tensile testing of Ni-base superalloy, discussing twinning and stacking fault modes
01 p0118 A70-10705

Intrinsic/extrinsic stacking fault pairs observed during creep of single crystals of gamma prime precipitation hardened Ni-base alloy, developing viscous slip model
01 p0119 A70-10731

Nonstoichiometric GeTe defects nature from band structure analysis based on two carrier model
02 p0350 A70-11698

Structural orientation and defects in graphitized coke crystallites, establishing relation between thermal expansion coefficient and macrostructure
03 p0514 A70-12868

Austenitic fcc Cr-Mn-N stainless steels ductile-to-brittle transition behavior noting role of deformation faulting
03 p0506 A70-13133

Three dimensional elasticity theory of generalized continua developed from atomic lattice theory model, discussing frequency spectra, specific heat and applications to crystal defects
03 p0525 A70-14232

Radiation effects on swept-synthetic quartz resonators and materials, discussing frequency shift measurements and defect studies
04 p0731 A70-14735

Test apparatus for investigating crystal defects influence on simultaneous measurement of metals thermal and electric conductivity under plastic deformation at cryogenic temperature
05 p0829 A70-16399

X-ray line broadening analysis for lattice damage in kamacite phase of Fe meteorites, evaluating particle size and elastic strain
05 p0915 A70-16828

Meyer-Neldel rule interpretation of distribution width parameter dependence on activation energy annealing of defects in irradiated Si
06 p1106 A70-17925

Stress and intercrystalline corrosion causes and sensitivity in supersaturated Al alloys
07 p1307 A70-19391

Crystal structure imperfections and elastic anisotropy of crystallites in condensed Ni films by X ray analysis
07 p1309 A70-19636

Iron ions EPR lines widening in corundum crystals due to lattice defects, estimating mosaic blocks disorientation parameter and point defects density
08 p1556 A70-21122

Gamma-gamma prime mismatch effects on stress rupture of Ni and Fe-Ni based alloys with Al and Ti hardeners
08 p1521 A70-21701

Lattice defects in Al-Zn alloy due to fatigue investigated for mechanism and effect on aging kinetics by resistivity measurement
09 p1707 A70-23326

Stacking faults developed in double hexagonal closed-packed phase of Ni-Ti alloy in cold worked and annealed conditions, using X ray line broadening
10 p1906 A70-25228

Ion-implanted GaAs junction diodes anneal behavior and defect nature
11 p2098 A70-26391

Radiation defects in Ge single crystals surface layers caused by low energy bombardment with He ions
12 p2287 A70-27486

Radiation defects distribution in GaAs during proton irradiation, noting distribution dependence on proton energy and integral flux
12 p2287 A70-27488

Tungsten crystalline structure defects caused by alpha particles bombardment using helium ion projector at 78 K
12 p2255 A70-27544

Lattice defect influence on EPR spectral and luminescent characteristics of annealed Fe doped gallium arsenide crystals
12 p2288 A70-28330

Cold worked metal, estimating lattice imperfections mol fractions based on reversible cell thermodynamics
15 p2676 A70-31564

Al-Zn eutectoid alloys defect structures and interactions in superplastic deformation process
15 p2756 A70-31567

Twinning lamella formation in Nb single crystals, examining slip and shear roles in surface tilt formation
15 p2761 A70-32382

Defect F centers formation in MgO, discussing optical absorption bands, oscillator strengths, luminescence band, impurity centers, etc
16 p2940 A70-33938

Thermal self focusing filaments observation in form of tracks in KDP and ADP crystals damaged by radiation from free emission mode laser
18 p3266 A70-36612

Radiation flaws in semiconductors, examining effects of gamma quanta, fast electrons and neutrons and heavy charged particles
19 p3483 A70-37295

Fcc metals surface self diffusion temperature dependence, using model based on complex defects contribution to diffusion flux at high temperatures
19 p3483 A70-37545

Superlattice stacking faults in plastically deformed nickel aluminate /gamma prime phase/ due to interaction of antiphase boundary /APB/ type dislocation pairs
19 p3451 A70-37704

Solidification and composition model of macroscopic freckles in nickel base superalloys single crystals
20 p3646 A70-39101

High energy electron irradiation generated defect centers in GaAs p-n electroluminescent diodes, using capacitance and thermally stimulated current measurements

21 p3863 A70-41914

Trap filling dependence on intensity, temperature and wavelength of photoexcitation in CdS crystals subjected to electron radiation damage and annealing

21 p3864 A70-42013

Crack propagation at supersonic velocities in K Cl crystals, noting plasma induction within specimen by laser pulse

21 p3940 A70-42033

Alloys stacking faults thermodynamics based on Gibbs treatment of interfacial free energy

22 p4124 A70-42726

Stacking faults in gamma prime precipitation hardened high temperature Ni base alloys, relating fault energy to strength

22 p4053 A70-42728

Polymer crystal lattice defects and vacancies diffraction patterns observation and interpretation, using optical transformations

24 p4353 A70-45566

Si crystal microdefects influence on semiconductor device performance and reliability

24 p4391 A70-46015

Pure Ni recrystallization, noting stacking faults and parallel sided and thin annealed twins formation during boundary migration

24 p4363 A70-46192

Niobium nitride precipitation associated with stacking faults in Cr-Ni-Nb austenitic stainless steels, using electron microscopy

24 p4365 A70-46369

CRYSTAL DISLOCATIONS

NT EDGE DISLOCATIONS

NT SCREW DISLOCATIONS

Stress-strain effect on dislocation densities of cylindrical Mg single crystals deformed by torsion basal slip compared to tension test

01 p0122 A70-11236

Semicoherent interface dislocations in directionally solidified Ni-Al-Cr eutectic, discussing lattice mismatch

01 p0123 A70-11247

Alloying additions effect on plastic deformation anisotropy in GaAs single crystals, determining dislocation activation energies from creep tests

01 p0160 A70-11606

Constitutive equations and thermally activated dislocation processes in metals, noting temperature and strain rate relationship

02 p0316 A70-11737

Statistical measurements of deformation structures and refractive indices in experimentally shock loaded quartz specimens with different crystallographic orientations

02 p0292 A70-12509

Lattice misfit influence on metastable omega phase morphology and stability in Ti transition metal alloys

03 p0508 A70-13146

Nonuniformity of dislocation structure and stress distribution in deformation of Cr samples longitudinal sections subjected to upsetting

03 p0511 A70-13488

Elastic interaction energy involved in Ti solution hardening by oxygen determined using anisotropic elasticity, presenting atomistic calculations and chemical bonds breaking role

05 p0862 A70-15906

Plasticity theory of single crystals based on dislocations behavior, considering only plane and elastic strains

05 p0928 A70-16061

Beryllium single crystals deformation under high pressures at room temperature similar to deformation under atmospheric pressure at elevated temperatures

05 p0863 A70-16203

Internal friction method for studying dislocation, stacking points and strengthening processes in steels and heat resisting austenitic steel behavior at high temperatures

05 p0864 A70-16870

Optimal thermomechanical treatment for austenitic steel stability to resist propagation and unloading of dislocations in cyclic loading process

05 p0867 A70-17041

Niobium single crystals annealed in ultrahigh vacuum, studying stress-strain behavior, secondary slip geometry and slip line morphology

06 p1090 A70-18493

Dislocations and interstitial atoms interactions in Ta, investigating internal friction and deformation resistance and rate dependence on temperature

07 p1309 A70-19637

Interstitial atoms effect on dislocation relaxation and aging of Mo and Nb single crystals

07 p1309 A70-19638

Tracks shape associated with dislocation motion during etching of Mo single crystals

07 p1309 A70-19639

Dislocation velocity-stress exponent for Nb single crystals calculated from strain rate sensitivity measurements of effective flow stress

07 p1314 A70-20011

Shock wave compression of single olivine crystals and specimens from chondritic meteorites, observing planar deformation microstructures

07 p1391 A70-20353

Deformation amplitude effects on dislocation structure and strengthening mechanism of fcc aluminum under cyclic loading

08 p1516 A70-20985

Critique of paper on diffusion in Si isotopes and excess vacancies generation by motions of diffusion induced dislocations

08 p1553 A70-21696

Metal fatigue by proliferation, diffusion and vanishing of lattice dislocations under varying loadings described by nonlinear inhomogeneous parabolic differential equations

09 p1770 A70-22253

Mo single crystals dislocation substructure strain dependence after creep using etch pitting techniques

09 p1708 A70-23544

Nb-W single crystal low temperature thermally activated deformation, observing slope change in temperature dependence curves of flow stress and strain rate sensitivity

09 p1708 A70-23572

Chromium structural dislocation and cell formation during deformation as function of temperature, impurities and strain rate

10 p1902 A70-23861

Aluminum and aluminum-copper alloys dislocation damping at high strain rates using impact shear tests

10 p1903 A70-23983

Dopant effect on dislocation mobility in elastically loaded silicon crystal using internal friction and modulus defect measurements

11 p2099 A70-26394

Electron bombardment produced clustered displacements, paired vacancies and interstitial atoms in Si, discussing possible mechanism for developing defects

11 p2142 A70-26638

Polycrystalline W-Re alloy creep tests in tension, investigating dislocation substructure formation as function of stress, temperature and strain

12 p2255 A70-27606

Dislocation structure during fretting corrosion in steel plates, analyzing via electron microscopy

12 p2258 A70-28318

High temperature dislocation model based on dislocation dynamics, rate theory and varying back stress ratio

13 p2436 A70-29563

Cr-Ni cold worked austenitic steel dislocation structure in tensile tests at different strains

14 p2596 A70-30874

Single crystal W and W alloys dislocation structures as function of strain, temperature and dilute alloys addition, using electron microscopy

15 p2756 A70-31563

Surface layer dislocations concentration role in metal fatigue, using variable diffusion coefficient

15 p2822 A70-32352

Dislocation distribution in Ta foil following yield point fatigue testing, using thin film electron microscopy

15 p2761 A70-32385

Flow stress and dislocation density dependence on temperature in polycrystalline molybdenum

16 p2930 A70-33085

Dislocation diffusion effects on strength of whiskers and fine grained polycrystals

16 p2934 A70-34327

Ti-Al-Mo-V alloy stress corrosion cracking, investigating correlation between dislocation substructure and ambient temperature corrosion susceptibility

17 p3113 A70-34371

Elastic interactions between anisotropic crystal dislocations and twin and grain boundaries in Ti

17 p3115 A70-34386

Crystallography of deformation twinning in Ti, presenting modes involving shear strains less than unity and simple shuffle mechanisms

17 p3116 A70-34388

Titanium and Ti-Al single crystals microscopic plastic deformation features, slip modes and dislocation substructures

17 p3116 A70-34389

Microscopic residual stress in crystals at fatigue crack tip in notched specimen in terms of flow stress and dislocation density

17 p3183 A70-34653

Parallel edge dislocations in elastically isotropic crystals, discussing climb and glide forces

17 p3126 A70-35454

Barium fluorides single crystals compression, investigating stress-strain behavior and dislocation mobility

19 p3483 A70-37339

Crystal dislocations and microstructure effects on magnetic properties of polycrystalline MnZn ferrites with high permeability, noting eddy currents role

19 p3484 A70-37566

Hexagonal crystal dislocations treatment based on anisotropic elasticity theory, obtaining formulas for displacement and stress fields

19 p3454 A70-38954

Microstresses in plasticity theory, considering continuous elastic body model of crystal with dislocations

20 p3724 A70-39859

Notched polycrystalline Al-Mg alloy dislocation structure near propagating fatigue crack at various stress levels

21 p3839 A70-40925

Orientation and applied stress effects on pure Nb-6W bcc single crystals yield stress, discussing thermal activation strengthening and crystal dislocations

22 p4052 A70-42318

Various Frank loops in quenched and annealed Pt, examining dislocations with field ion microscopy and computer simulated approximations

23 p4230 A70-44758

Steady state creep behavior during multiple deformation process, developing grain boundary sliding relation to grain size

23 p4207 A70-44759

Alpha phase Ti strengthening, investigating interaction between dislocations and interstitial solute atoms

24 p4360 A70-45516

Pure Al thermal cycling tests, investigating effect of minimizing thermal stress during quenching on behavior of dislocations

24 p4360 A70-45518

Crystal elastic dislocations general solution, deriving stress function for stress and displacement fields in bipolar coordinates

24 p4426 A70-46018

Cellular breakdown in binary Al-Cu alloys in unidirectional solidification, observing small pit stability on solid-liquid interface

24 p4362 A70-46180

CRYSTAL FILTERS

UHF satellite receiver for binary FSK data collection system using matched integrate and dump filter detectors

08 p1459 A70-20804

IR light dispersion filters of compressed mixed powdered crystals, discussing optimal preparation procedures, passbands temperature dependence and stability

10 p1915 A70-24256

Holographic interferometry of rapid phase objects by two wavelengths from ruby laser and KDP crystal filter, noting application to dense plasmas

19 p3422 A70-37650

CRYSTAL GROWTH

NT CZOCHRALSKI METHOD

NT EPITAXY

Niobium ditelluride single crystals production with purity dependent on initial materials, discussing X ray structural and chemical analysis and electrical properties

03 p0542 A70-13753

Carrier concentration profiles and surface resistance of Ohmic contacts to solution epitaxial n-type GaAs wafers measured by Schottky barrier capacitance

03 p0543 A70-14213

AsSbSI crystal production technology concerning substitution-type solid solution structure and photoconducting ferroelectric properties

04 p0729 A70-14409

Sliding tube assembly for diverting carrier gas from flow pattern of Verneuil apparatus for flame fusion crystal growth

05 p0829 A70-16849

Tensile properties variations of Co whiskers grown by reducing cobaltous bromide in hydrogen-argon mixture

07 p1306 A70-19071

Electrolyte purity effect on initiation times and growth rate of Zn dendrites in alkaline zincate solution, discussing dendrite initiation retardation

07 p1356 A70-19387

GaAs preparation techniques, crystal structure, electrical and physical properties, single crystal growth, impurities properties and distribution, thermal and optical properties, etc

07 p1356 A70-19397

Ammonium perchlorate decomposition, deflagration, sublimation, crystal growth and surface properties, using scanning electron microscope

07 p1358 A70-19576

Vanadium single crystals substructure on different planes to growth direction using X ray diffraction

07 p1308 A70-19608

Vapor-liquid-solid nucleation mechanism of alpha-aluminum oxide filamentary single crystal growth, suggesting combination with suboxide condensation and disproportionation mechanism

07 p1313 A70-19890

Synthesis procedure for single crystal transition metal diborides, using high pressure capability in controlling stoichiometry
07 p1313 A70-19895

Refractory metal monocarbide single crystal growth by plastic strain induced primary and secondary recrystallization
07 p1313 A70-19902

Graphite crystals surface ribbed growth in Ni-C solutions due to B content observed by scanning electron microscope
08 p1520 A70-21552

Crystal growth of 2H silicon carbide showing temperature profile along susceptor as affecting factor
09 p1739 A70-22498

Growth kinetics of gamma prime precipitate in Ni-Ti alloy noting Ti content variation as function of aging
09 p1706 A70-22812

Yttrium iron garnet sintering and grain growth rates dependence on yttrium/iron ratio
[ACS PAPER 16-BE-68F] 09 p1740 A70-22982

Nucleation and heteroepitaxial GaAs film growth on sapphire using electrical measurements, reflection diffraction and electron microscopy
11 p2098 A70-26393

Filamentary crystal growth associated with hyper-velocity microparticles impact upon Cu foil
13 p2513 A70-29264

Synthetic autoclave grown quartz crystals with W and Ga impurities, discussing spectral properties and weak absorption bands after irradiation
14 p2625 A70-30154

Iodine concentration effects on epitaxial GaAs p-n junctions growth characteristics
14 p2625 A70-30171

Iodine concentrations, temperature gradients and transport ampules etching effects on mass transport rate and crystal growth of MnS-MnSe-iodine system
16 p2960 A70-33088

Surface growth morphology and crystallographic orientation of beta-SiC films formed by chemical conversion and heating
17 p3142 A70-34678

Single and polycrystalline indium arsenide preparation methods and quality control
17 p3143 A70-35119

Grain boundary allotriomorphs growth mechanisms in Al-Cu alloy at high temperatures, indicating interfacial and direct volume diffusion
18 p3271 A70-36027

Growth mechanism and crystal structure of Ge films deposited from molecular beam onto GaAs, Si and Ge substrates
18 p3297 A70-36415

Deformed single crystals of high purity Al of different orientation with respect to growth during recrystallization
19 p3450 A70-37373

Ice crystals growth rate in natural clouds over minus 2-minus 32 C range based on characteristic axial ratio
19 p3462 A70-38261

Boron impurities introduction into InP crystals grown by liquid encapsulation, detecting IR absorption bands due to localized lattice vibration
23 p4231 A70-44891

Single crystal piezoelectric materials growth characteristics and wave propagation properties for surface acoustic wave applications
24 p4367 A70-45399

Aluminum oxide growth rate in molybdenum cermet after high temperature annealing
24 p4359 A70-45478

Czochralski thermal probe for current carrier concentration in strip shaped area of n-type GaAs single crystals active growth
24 p4389 A70-45481

Crystal growth in polycrystalline Au, Ag and Au-Ag thin films annealing, observing by electron microscopy and electron diffraction
24 p4391 A70-45672

CRYSTAL LATTICES
NT BODY CENTERED CUBIC LATTICES
NT CLOSE PACKED LATTICES
NT CUBIC LATTICES
NT FACE CENTERED CUBIC LATTICES

Martensite structure, discussing intensity anomalies in X ray diffraction pattern of intermetallic Ni-Nb
01 p0121 A70-10900

Long range order formation kinetics in lithium ferrite octahedral sublattice after stepwise annealing and quenching in water, using X ray analysis
03 p0537 A70-12867

Atom ordering and effects on alloy properties - Conference, Kiev, Ukrainian SSR, 1969
03 p0505 A70-13101

Steel crystal lattice fine structure and mechanical properties during annealing using X rays as function of temperature
03 p0511 A70-13422

Generalized Watson sums evaluation without series expansions or extensive computer summations, calculating magnetization of anisotropic Heisenberg ferromagnet for cubic, bcc and fcc lattices
04 p0730 A70-14689

Gravity influence on constitutive equations of elasticity for crystals treated as continuous body and particle system, taking into account lattice structure
05 p0925 A70-15869

Divergences in tension textures and values of anisotropy coefficients ascribed to imperfections in cubic texture of aluminum sheet deformed by straining
05 p0927 A70-15995

Stress-strain relations for elastic anisotropic crystal lattice systems derived in terms of orientation vectors and scalar moduli
05 p0932 A70-16135

Orthorhombic form of crystalline formylmethionine transfer RNA, obtaining Patterson function from three dimensional X ray diffraction data
05 p0803 A70-16947

Inert gases scattering from Ni 111/ plane as function of beam temperature and angle of incidence compared to Au and Ag
06 p1110 A70-18263

High energy Ar atomic beams scattering from single crystal face of W measured for distribution pattern
06 p1112 A70-18270

Electron irradiation for reducing thermal coefficient of resistance of Si strain gages, noting crystal orientation dependence of gage factor
06 p1070 A70-18442

Be atoms effect on lattice structure of three component sodium oxide-beryllia-silicate glasses using IR absorption spectra
07 p1315 A70-18704

Metastable tau-phase in Fe-Ni-B melt solidifying into boride, noting lattice constant and solubility
07 p1307 A70-19393

Molybdenum single crystals orientation effect on thermal resistance to argon plasma flow
07 p1309 A70-19614

Metal fatigue by proliferation, diffusion and vanishing of lattice dislocations under varying loadings described by nonlinear inhomogeneous parabolic differential equations
09 p1770 A70-22253

Liquid crystals biaxial smectic C phases tilt and optic axial angles determined from convergent light observations
09 p1738 A70-22271

Metallic solutions formation dependence on alloying elements electron structure assumed by atoms in solvent lattice
09 p1702 A70-22560

Plastic properties of materials to elastic limit of pure metal and ionic solid crystals
12 p2283 A70-27055

Au, Ag and Al films evaporation in ultrahigh vacuum on LiF and MgO surfaces, showing insignificant role of lattice misfit for epitaxy
12 p2285 A70-27260

Chemical compositions and structure of carbides in Fe-W-C and Co-W-C systems, clarifying eta phases
12 p2255 A70-27601

Heat energy transport mechanism in metallic plasma deposited coating, investigating role of elastic crystal lattice vibrations, electrons, molecules, etc
13 p2419 A70-28858

Plastic deformation of Mo-Re single crystals produced by electron beam zone refining, investigating lattice frictional stress, activation volume temperature variation, etc
13 p2436 A70-29562

Ferromagnetic cubic sulfide of Fe easy axis by electron diffraction pattern, aligning sulfide particles along magnetic field
13 p2472 A70-29712

Interstitial Cl molecule formation in NaCl lattice, computing strain field and energetics by energy minimization technique based on point ion lattice model
14 p2544 A70-30352

Localized one electron states in perfect crystals of widely separated atoms, using thermal single determinant/Hartree-Fock/ approximation
14 p2626 A70-30488

Lattice resolution of layer planes in polyacrylonitrile based carbon fibers ground and dispersed by ultrasonic irradiation
14 p2598 A70-30793

Lattice planes and interplanar spacings of small vapor deposited gold crystals, using transmission electron microscopy
16 p2961 A70-33644

Calcium tungstate crystals, investigating electron paramagnetic resonance centers produced by neutrons and gamma rays to obtain information on lattice vacancies, defects, etc
16 p2961 A70-33963

Thermoelectric composite materials, deriving crystal lattice type model of equations for predicting dynamic or themomechanical behavior
19 p3540 A70-37958

Pure metals structure effect on friction and lubrication under steady slip in ultrahigh vacuum at low temperatures
19 p3438 A70-38729

Integrated Bragg X ray scattering intensities for monatomic crystalline lattices, considering thermal diffuse component contribution
20 p3686 A70-39193

Ta single crystal inherent lattice and interstitial solution hardening, discussing impurity doping effect on flow stress thermal component
21 p3839 A70-40902

Monatomic crystal vibrational spectrum, noting quasi-local vibrations near high impurity concentrations
24 p4388 A70-45202

Peroovskite crystals phase transitions based on group theory, considering lattice vibration modes as instability source
24 p4389 A70-45206

Vanadium subnitride crystal structure with ordered array of nitrogen atoms in V sublattice
24 p4360 A70-45519

Polymer crystal lattice defects and vacancies diffraction patterns observation and interpretation, using optical transformations
24 p4353 A70-45566

CRYSTAL OPTICS
Photoconductivity growth and decay curves green edge emission and integral flux in optical flare of cadmium sulfide crystals due to hole trapping process
03 p0540 A70-13503

Optical third harmonic generation in ADP crystals using mode locked and nonmode locked lasers
06 p1082 A70-17943

Group theory investigation of three photon light scattering tensor for all vibration modes of specific crystal classes
07 p1299 A70-19861

Q switched ruby laser light effect on absorption spectra of NaCl crystals
10 p1902 A70-25221

Temperature instability of electro-optical laser modulators using ADP, KDP and DKDP crystals taking into account phase shift between coherent light beams
11 p2063 A70-25848

Twin crystal X ray telescope principle, design and application, discussing radiation sources nature and measurement methods
11 p2057 A70-26824

KDP crystal single cut for laser beam frequency conversion and tuning
12 p2245 A70-27302

IR image conversion into visible using nonlinear KDP crystal
12 p2248 A70-27543

Intensity and photocounts statistical distribution of harmonic generated in nonlinear crystal by laser and thermal radiation
12 p2248 A70-27547

Optical charge exchange and thermal stimulation effects in Fe doped GaAs crystals, determining iron content role by EPR method
13 p2469 A70-28880

Bragg reflecting crystals for spectroscopy and polarimetry in X ray astronomy
13 p2489 A70-28904

Steady state laser emission of resonator with two crystals with different optical orientation
13 p2428 A70-29371

Amplitude and phase modulation of laser beams by tetragonal crystal cuts
13 p2429 A70-29533

CW argon lasers simultaneous mode selection and phase locking by electro-optic KDP crystals
15 p2753 A70-32610

On-line optical data processing using CRT with electro-optic target crystal
16 p2903 A70-33132

Optical rectification/polarization/ and measurement of Q switched laser energy and time parameters, using crystals and parallel plate capacitor
17 p3105 A70-35098

Real time holographic reconstruction by electro-optic light modulation through crystal
18 p3258 A70-36312

Optically bistable crystal applications, discussing photochromaticity, catochromatic tubes, oscilloscopes, computer storage devices and laser systems
19 p3446 A70-37860

Light beam direction variation by crystal deflectors, examining changing internal reflection angle by applied electric field or mechanical stress
23 p4196 A70-44411

Laser light effects on electron beams, considering absence or presence of crystalline optically transparent solid
24 p4353 A70-45564

CRYSTAL OSCILLATORS
NT PIEZOELECTRIC CRYSTALS

Precision frequency analog converter using crystal oscillator and transistor switch reducing errors
09 p1653 A70-23698

Second and third harmonic simultaneous generation in ammonium oxalate crystals achieved by three frequency interactions
10 p1901 A70-25159

High frequency tunnel diode quartz crystal oscillator circuits with inductive element compensating circuit capacitor

13 p2376 A70-28874

Uncoated quartz twin crystal microbalance for monitoring water vapor content of respiratory gases

19 p3368 A70-37844

Electro-optical crystal resonator loss anisotropy, determining natural frequencies and polarizations

20 p3642 A70-39755

Phase and group velocity variations of LF transmission compared against crystal oscillator

23 p4163 A70-44228

CRYSTAL RECTIFIERS

Whisker diode coupling to polarized IR laser beam by orientation based on antenna theory

17 p3048 A70-35902

CRYSTAL STRUCTURE

NT WIDMANSTATTEN STRUCTURE

Structure and mechanical properties of martensite and bainite in Fe-Ni-Co-C steels, discussing isothermal aging to obtain tough twinned martensite steels

01 p0119 A70-10733

Laser transitions to valence band or acceptor in low loss uniformly pumped crystal structure p-type GaAs at 77 K

01 p0113 A70-11168

Diamond-like glassy semiconductor compound of cadmium germanium arsenide, determining optical lattice vibrations from IR reflection spectra

01 p0160 A70-11599

Long range order formation in Ni-Cr alloys analyzed by direct neutron diffraction, considering disorder-order transition temperature and chemical composition

01 p0124 A70-11600

Linear aliphatic polyesters unit cell dimensions and crystalline densities

03 p0517 A70-13808

Optical rotatory power measurement for compensated cholesteric liquid crystal helical structure to observe thermally induced inversion and electric field perturbations

03 p0542 A70-14003

Ge films crystallinity deposited on Ge substrates in vacuum as function of deposition rate, substrate temperature and thermal treatment and background O pressure

03 p0543 A70-14204

Ni addition effects on Mg-Nd and Mg-Nd-Mn alloys structure and heat resistance

04 p0706 A70-15189

Supersaturated Al alloy with Zr addition at high temperatures, showing tetragonal equilibrium phase and intermediate phase with cubic structure

04 p0708 A70-15369

Structures formed during aging of martensite in maraging steels by X ray and chemical analyses using electrolytic isolation of phases

05 p0865 A70-16871

Cliftonite occurrence, internal structure, orientation within kamacite and implications on origin of diamonds in meteorites

05 p0921 A70-17095

Cholesteryl chloride-cholesteryl myristate /CM/ mixture liquid crystal molecular and helical axes orientation from dielectric constant change measurements in magnetic fields

06 p1126 A70-17326

Ni-Fe alloys texture formation, studying strong deoxidizers role in secondary recrystallization

06 p1088 A70-17614

Structure, phase composition and heat resistance of diffusion layers obtained by surface alloying of Nb alloy with Cr, Ti and Si

06 p1089 A70-17744

Carbon fiber structural model agreeing with experimental results

06 p1092 A70-18025

Be atoms effect on lattice structure of three component sodium oxide-beryllia-silicate glasses using IR absorption spectra

07 p1315 A70-18704

GaAs preparation techniques, crystal structure, electrical and physical properties, single crystal growth, impurities properties and distribution, thermal and optical properties, etc

07 p1356 A70-19397

Electron paramagnetic resonance for quality control of crystal structures in quantum electronics applications

07 p1356 A70-19479

Vanadium single crystals substructure on different planes to growth direction using X ray diffraction

07 p1308 A70-19608

Oriented single crystals properties obtained from Mo powder subjected to compacting, annealing in hydrogen and electron beam zone melting

07 p1308 A70-19610

Size effect on structure and mechanical properties of thin wire made of Mo single crystals deformed in recrystallized state

07 p1308 A70-19611

Structure and mechanical properties of Mo single crystals grown from gas phase using metallographic and X ray analysis

07 p1308 A70-19612

Crystal structure imperfections and elastic anisotropy of crystallites in condensed Ni films by X ray analysis

07 p1309 A70-19636

Phonon spectrum of mixed semiconductor crystals based on AlIII-BV and AlI-BVI compounds, studying frequency spectrum as function of crystal composition

07 p1300 A70-19867

Two parameter model for lattice vibrations applicable to diamond structured crystals, calculating phonon dispersion curves from dielectric screening theory

07 p1357 A70-19920

Crystalline structure effect on molecular beam reflection from rough polycrystalline Au surfaces

07 p1343 A70-20123

Quenched and tempered steels ductile fracture with respect to plasticity, structure and crack development conditions using microfractography

08 p1515 A70-20922

Ti additions influence on steel work hardening, specific weight, magnetic properties and structure

08 p1515 A70-20924

Al-Cr-Zr alloy ingots macrostructural inhomogeneities, studying roles of casting rate and additives in intermetallics primary crystallization

08 p1517 A70-21128

Ni-Mo surface alloys investigated by low energy electron diffraction, using tabulated symmetry and extinction properties of space groups and phase diagrams

08 p1557 A70-21603

Hydrides precipitation in Ti-Al-Mo-V alloys using transmission electron microscopy, discussing crystal structure, activation energy, hydride-matrix phase interface, etc

08 p1525 A70-21964

Crystallite orientation distribution function refinement procedure, considering application to isotactic polystyrene

09 p1631 A70-23446

Cellular structure and grain size effects on mechanical properties of strained and recrystallized chromium

10 p1902 A70-23862

Epitaxy of Ag deposited on Ni, observing irreversible crystallographic order transition from metastable nominal orientation by LEED

10 p1927 A70-24076

Synthetic molybdenum disulfide crystal properties compared to natural crystals, discussing friction coefficient, adherence to metal surfaces, etc

10 p1907 A70-24787

Crystal-chemical and geophysical implications concerning earth mantle phase transitions from beta magnesium silicate crystal structure

11 p1994 A70-25333

Extended chain polymer crystals temporary superheating before final melting, discussing hexagonal selenium crystals data

11 p2069 A70-25803

Composition and monoclinic parameters of chromium sulfide mineral breznaitite in metal matrix and silicate inclusions of Tucson meteorite using electron microprobe

11 p2110 A70-26004

Photographs of ferroelectric tungsten oxide crystal domains obtained with photoemission microscope, noting memory effect after electron beam sweeping

11 p2099 A70-26463

Book on tensor calculus in materials science covering thermodynamic equilibrium, gaseous and solid phase heat engines, solids crystalline structure, etc

12 p2282 A70-26866

Soviet monograph on intermetallic compounds with Laves phases, covering crystallographic and thermodynamic characteristics of Mg-Zn, Mg-Cu and Mg-Ni systems

12 p2252 A70-26885

Polyethylene extended chain crystals melting process via electron microscopy and differential thermal analysis

12 p2258 A70-26896

Magnesium arsenide phosphide crystal and magnetic structure using X ray and neutron diffraction

12 p2283 A70-27240

Isostructural crystals of Dy compounds investigated for magnetic behavior using high resolution photoelectric optical spectroscopy

12 p2261 A70-27243

Superconducting thin films of beta-tungsten structure Nb-Al-Ge compound, discussing high purity sputtering preparation techniques and properties in magnetic fields

12 p2285 A70-27259

Tantalum RF sputtered superconducting films structure and properties at various substrate temperatures, observing bcc, fcc and amorphous phases by electron microscopy

12 p2288 A70-27876

Elastic, piezoelectric and dielectric properties of barium titanate single crystals of laminar domain structure

12 p2288 A70-28329

Iron meteorites electrolytic corrosion using potentiostatic technique, noting roles of Ni content and crystal structure

13 p2432 A70-28697

Raman spectrum of lithium formate monohydrate single crystal in polarized He-Ne laser light, discussing crystal structure

13 p2425 A70-28714

Epitaxial Ge deposits on Si control by Kikuchi pseudolines, considering surface polish, crystallinity and substrate orientation

13 p2470 A70-28957

Atomic planes around crack, noting configuration dependence on law of interplane interaction

13 p2515 A70-29418

Fine grained structure effect on steels and Ni alloys short term heat resistance at high temperatures

14 p1594 A70-30168

Bi-Sb alloys, discussing structural data, crystal preparation, band structure, pressure, nonohmic conductivity, thermoelectric, thermomagnetic and magnetothermal effects

14 p2625 A70-30332

Li positive ions in KCl crystals, investigating internal strains effect on paraelectric resonance spectra

14 p2626 A70-30340

Eutectic NiAl-Cr structure and high temperature tensile strength as function of solidification rate

15 p2755 A70-31560

Dielectric constants of zinc tungstate with wolframate structure

15 p2783 A70-31766

Polygonized and cellular Be structures formation, examining temperature, strain, annealing and material purity effects

15 p2758 A70-32122

Thermal-mechanically treated stainless steels structure and properties, discussing stress relief aging effects

15 p2761 A70-32380

Room temperature mechanical properties and structure of age hardened Ti-Cu alloys

15 p2761 A70-32384

Martian brightness increase at 1 deg phase angle, explaining by transparent cubic crystals presence in clouds

15 p2803 A70-32499

Inorganic laser materials containing ionic crystalline structures, including fluorides, oxides, rubies, garnets and oxygen containing complex compounds

16 p2927 A70-33223

Book on refractory metal properties covering nuclear reactor use, atomic, electronic and crystal structures, thermal and electrical characteristics irradiation effects, nuclear properties, etc

16 p2931 A70-33268

Oxidized alpha Ti crystals strain analysis based on X ray divergent beam, discussing hardening effects

17 p3115 A70-34387

Martensitic transformation in Ti and Ti alloys, discussing shear systems influence

17 p3118 A70-34404

Superconducting Nb-Ti-Zr alloy, investigating structure and decomposition at high temperatures by X ray and electron microscopy

18 p3276 A70-36310

Fine grained Be structure and mechanical properties under tensile deformation at temperatures from 20 to 1000 C

18 p3276 A70-36311

Growth mechanism and crystal structure of Ge films deposited from molecular beam onto GaAs, Si and Ge substrates

18 p3297 A70-36415

Heat conduction three dimensional problem in radiation heated thin crystalline plates with temperature dependent thermophysical characteristics

18 p3348 A70-36644

Heavy ions traces in crystals of lunar rocks, discussing applications as detectors

18 p3321 A70-37084

Deformed single crystals of high purity Al of different orientation with respect to growth during recrystallization

19 p3450 A70-37373

Numerical model of piezoelectric surface wave propagation on free and metalized cubic and hexagonal crystals

19 p3486 A70-37754

Fe rich Fe-Al alloys single crystals, determining three dimensional order and atomic displacements coefficients by X ray diffuse scattering

19 p3452 A70-37839

SiC whiskers X ray diffraction studies of crystal structure, suggesting single crystal permanent deformation at ambient temperatures

19 p3455 A70-37941

Solid-solid phase transitions in molecular crystals of organic tetrahedral substances, using differential scanning calorimetry

19 p3373 A70-38193

High modulus graphite fiber tensile strength and structure, using X ray diffraction 20 p3653 A70-39205

Nucleation processes associated with thermal decomposition sites formation in ammonium perchlorate single crystals, using optical and electron microscopy 20 p3582 A70-39494

Crystal orientation dependence of thermal resistance and gage factor in electron irradiated n-type silicon strain gages 21 p3824 A70-40862

Lunar crystalline rock static and dynamic deformation, examining regolith and silicates textures and structures 21 p3897 A70-41515

Apollo 11 lunar crystalline rock samples petrology, discussing shock and other metamorphic effects on mineral structure 21 p3897 A70-41516

Compositions of lunar fines, crystalline rock and glass spherules, showing high normative anorthite 21 p3899 A70-41531

Apollo 11 lunar crystalline rock and breccias petrography and luminescent properties, spectral analysis, color, emission bands and shock effects 21 p3918 A70-41678

Amino acid racemization as enantiomers in core sediment samples 21 p3781 A70-41896

Optical activity of nonenantiomorphous biaxial crystals with mirror planes, investigating polarization plane rotation 21 p3850 A70-41934

Isomorphous mixed ammonium perchlorate and potassium perchlorate crystals structural homogeneity by X ray diffraction and differential thermal and thermogravimetric analyses 21 p3784 A70-42262

Magnetic and structural characteristics of ternary intermetallic systems with lanthanides, considering Ln substitution by other rare earth elements 22 p4085 A70-42481

Orthorhombic martensite tempering behavior in Ti alloys, observing distinct stages for binary and ternary alloys 22 p4054 A70-42742

High strength high Ni maraging steels crystal structure, alloying elements effects on mechanical properties, applications, etc 22 p4055 A70-43121

Copper and Al polycrystalline single crystal substructure changes, examining high temperature, unsteady and diffusion creep 22 p4056 A70-43342

Superconductivity and crystalline structure of laminar solid solutions of niobium-selenide-niobium-telluride single crystals 22 p4088 A70-43464

Martian brightness increase at 1 deg phase angle, explaining by transparent cubic crystals presence in clouds 23 p4240 A70-43920

Chemical etching for revealing structure of carbon-graphite materials subjected to different graphitization stages 23 p4209 A70-44045

Al-Be eutectic alloys structure, using laue X ray method and electron microscopy in studying fibrous morphology due to unidirectional solidification 24 p4356 A70-45143

Cubic titanium oxycarbide structural characteristics, noting lattice constant dependence on component proportions and mutual solubility during formation 24 p4359 A70-45477

Vanadium subnitride crystal structure with ordered array of nitrogen atoms in V sublattice 24 p4360 A70-45519

Al-Cu alloy unidirectional solidification, investigating interfacial transition from plane to cellular structure and segregation pattern 24 p4362 A70-46179

X ray powder and chemical data on monoclinic secondary mineral guildite from mine fire at Jerome site 24 p4330 A70-46274

Vacancies in vanadium carbide /V3C2/ crystals with predicted lattice defects at low temperature, considering entropy 24 p4365 A70-46353

CRYSTAL SURFACES

Si cleaved crystal nature on basis of Auger spectra, discussing impurity stabilization 01 p0159 A70-11175

Solder mechanical contact strength to CdS insulating crystal platelets tested in liquid N, noting Ag epoxy 02 p0319 A70-12738

High temperature heat treatment effects on Mo, W, Ta and Re crystal surface order and faceting observed by electron diffraction, noting contamination role 03 p0538 A70-13097

Low energy electron diffraction structures due to Re crystal surface interaction with CO and molecular oxygen at high temperatures 03 p0440 A70-13098

Pumping energy distribution over cross section of active ruby laser elements in relation to smoothly polished, roughly polished and dull lateral cylindrical surfaces 04 p0700 A70-14607

Molecular He and Ar nozzle-type beams scattering from room temperature LiF crystal surfaces, measuring particles flux and speed distributions 06 p1111 A70-18267

Graphite crystals surface ribbed growth in Ni-C solutions due to B content observed by scanning electron microscope 08 p1520 A70-21552

Low energy electron diffraction pattern from surface steps and facets resulting from recrystallization of Re single crystal 08 p1557 A70-21602

Helium ion bombardment activated tungsten crystal surface migration using field emission microscopy 11 p2097 A70-25378

Chemisorption on Mo single crystal surfaces observed by LEED techniques, discussing bcc planes and adsorbed gases 12 p2181 A70-27256

Ruby crystal surface destruction by laser radiation, studying surface structural and optical properties effect and threshold power dependence on light pulses duration 12 p2248 A70-27541

Contaminated Ni crystal /100/ surface photoelectric yield as function of temperature, considering effects of Ar ion bombardment and annealing 12 p2288 A70-27680

Growing ice crystals surface electric potentials during various stages of water vapor condensation 15 p2769 A70-31444

Interactions of electrons, phonons and magnons with crystalline surfaces - Conference, University of Lille, France, September 1969 15 p2785 A70-32763

Band structure of Brillouin zone and electronic states on pure and contaminated crystal surface 15 p2786 A70-32767

Surface damage of GaAs crystals by mechanical handling and polishing with hard abrasive lapping materials 20 p3686 A70-39119

Clean iron /011/ surfaces, determining sulfur, oxygen and hydrogen sulfide films effects on adhesion behavior 21 p3831 A70-40748

Hydrogen adsorption and coadsorption with oxygen on W single crystal surface measured by mass spectroscopy and low energy electron diffraction method 21 p3862 A70-41887

Holographic recording on n-type Si single crystal surface by photoanodic engraving 22 p4026 A70-42332

GaAs crystal surface Raman scattering from phosphorus impurities localized modes, using Ar ion laser line 24 p4391 A70-46255

CRYSTALLINITY

Linear aliphatic polyesters unit cell dimensions and crystalline densities 03 p0517 A70-13808

Amorphous and partly crystalline polymers low temperature thermal conductivity and heat capacity 21 p3844 A70-42136

CRYSTALLITES

Structural orientation and defects in graphitized coke crystallites, establishing relation between thermal expansion coefficient and macrostructure 03 p0514 A70-12868

X ray diffraction method to determine degree of orientation of crystallites in extruded graphites 03 p0517 A70-13964

Crystal structure imperfections and elastic anisotropy of crystallites in condensed Ni films by X ray analysis 07 p1309 A70-19636

Alkoxy-derived strontium zirconate and titanate preparation and characterization, considering purity control, crystallite size and ceramics synthesis 09 p1740 A70-22981

Crystallite orientation distribution function refinement procedure, considering application to isotactic polystyrene 09 p1631 A70-23446

CRYSTALLIZATION

NT RECRYSTALLIZATION

Iron behavior in GaAs during crystallization, studying Fe distribution ratio, impurity migration and diffusion coefficient 01 p0156 A70-10219

Polysiloxanes morphology crystallized isothermally from melt using electron microscopy, noting fracture ease increment with molecular weight decrease 03 p0517 A70-14203

Bivalent cations effect on crystallization and viscosity of glazed glass 05 p0871 A70-16592

Metal oxides additions effect on Ti glass crystallization, studying small and large ion radii 05 p0871 A70-16593

Crystallization and dielectric properties of glass containing barium, lead, titanium and boron oxides, noting frequency and temperature dependence 05 p0871 A70-16595

Artificial crystallization theory for supercooled dry-ice seeded stratus clouds, taking into account condensation growth and turbulent diffusion of crystals 08 p1538 A70-21108

Vertical and horizontal expansion rate of crystallization of dry-ice seeded internal stratus clouds 08 p1538 A70-21109

Artificial crystallization zones width measurement error during time intervals after cloud seeding by aircraft and solar reflection methods 08 p1538 A70-21110

Al-Cr-Zr alloy ingots macrostructural inhomogeneities, studying roles of casting rate and additives in intermetallics primary crystallization 08 p1517 A70-21128

Irreversible phase transition analysis of atmospheric condensation-crystallization processes 08 p1538 A70-21427

Gaseous species in equilibrium with Apollo 11 holocrystalline rocks during crystallization 09 p1758 A70-22744

High intensity ultrasonics for changing solids properties, discussing effects on metal powder sintering, yield strength, fatigue life, crystallization rate, etc 09 p1728 A70-23348

Phase diagram of rapidly crystallized Al-Cu-Mn alloys, observing ternary solid solutions formation during high cooling rate of melt 09 p1709 A70-23786

Rhyolitic obsidian glass devitrification rate in water and alkali solutions, noting increase in Na or K rich solutions 11 p2070 A70-26003

Amorphous film formation and crystallization, discussing thermal stability 18 p3297 A70-36320

Spaceborne lightweight mirror blanks made from ceramics fabricated from glass crystallization 18 p3263 A70-36559

Lunar crystalline rock melting at atmospheric pressure under partial oxygen pressure, suggesting crystallization temperature 21 p3895 A70-41508

Petrology, crystallization and magma origin of lunar clinopyroxene, ilmenite-rich dolerite and microgabbro from Apollo 11 samples 21 p3900 A70-41536

Lunar sea, mascon and interior composition, discussing crystallization of Apollo 11 Tranquillity samples and synthetic analogs at high pressure 21 p3901 A70-41542

High crystallization temperatures for igneous rocks from Tranquillity Base indicated from late formation of sulfide liquid forming complex troilite intergrowths and iron 21 p3902 A70-41553

Thermochemical method for directional crystallization of wear-resistant alloy coatings on machine parts 23 p4205 A70-44043

CRYSTALLOGRAPHY

Crystals nonlinear permittivity related to temperature-time Green function for electromagnetic radiation, determining crystal polarizability by light-exciton method 07 p1335 A70-19868

Plastic properties of tungsten carbide single crystals at room temperature, determining slip system crystallographic orientations 08 p1520 A70-21557

Intense light effect on refractive index of potassium niobate crystals 09 p1698 A70-23317

Solid lubricant crystallographic orientation selection for friction cermet material silver-molybdenum disulfide 12 p2254 A70-27286

Dispersion strengthened Ni-Cr alloys elastic and plastic properties at room temperature, studying preferred crystallographic orientation effect 12 p2255 A70-27609

Synthetic pyroxenoid stability and crystallography, noting pyroxmangite structure similar to yellow lunar mineral from Mare Tranquillitatis 12 p2226 A70-28022

Fast brittle crack slowing by mechanical twins in transformer steel and by slip bands in LiF and NaCl crystals 15 p2755 A70-31526

Spinel lithium ferrite magnetic and crystallographic properties, considering effects of Li and oxygen losses, sintering temperature and cooling rate 16 p2961 A70-33272

Vibrational spectra and structure of oxaly chloride in crystalline and fluid states, discussing molecular and space group symmetry 16 p2857 A70-34006

Ti-Al alloy crystallographic structure, observing hexagonality for alpha phase 17 p3114 A70-34377

Crystallography of deformation twinning in Ti, presenting modes involving shear strains less than unity and simple shuffle mechanisms

17 p3116 A70-34388

Twinned hexagonal martensites crystallography in Ti alloys, discussing alpha-beta and beta-fcc transformations

17 p3118 A70-34405

Lunar rocks almandine-rich garnet chemical composition and crystallography, noting cell edge and refractive index

21 p3883 A70-40711

Crystallography of euhedral single crystals from lunar troilite indicating hexagonal forms consistent with high temperature NiAs type structure

21 p3898 A70-41522

Apollo 11 lunar rock plagioclases crystallography, obtaining single crystal X ray diffraction patterns by Burger precession method

21 p3903 A70-41555

Potassium acid phthalate crystal X ray spectrometric properties measurements, discussing parallel position rocking curves and reflection coefficients

23 p4230 A70-44420

Crystallography of martensite transformation on /225/ type planes of austenite in Fe-Mn-Cr-C alloy

24 p4358 A70-45237

CRYSTALS

NT BICRYSTALS

NT CRYSTAL OSCILLATORS

NT CRYSTALLITES

NT DENDRITIC CRYSTALS

NT IONIC CRYSTALS

NT LIQUID CRYSTALS

NT METAL CRYSTALS

NT MIXED CRYSTALS

NT PIEZOELECTRIC CRYSTALS

NT POLYCRYSTALS

NT QUARTZ CRYSTALS

NT SINGLE CRYSTALS

NT WHISKERS (SINGLE CRYSTALS)

Microwave conductance tensor in crystals with non-parabolic carrier energy dissipation under crossed constant electric and magnetic fields

12 p2288 A70-28326

Small angle light scattering indicatrices in ruby crystals approximated by Gauss type function

13 p2431 A70-29869

Ronchi test interferometer for optical quality checking of laser crystals

20 p3627 A70-39094

Steady state creep behavior during multiple deformation process, developing grain boundary sliding relation to grain size

23 p4207 A70-44759

CSM

U COMMAND SERVICE MODULES

CUBIC EQUATIONS

Periodic solutions for two dimensional cubic differential equation, covering one dimensional traveling wave and two dimensional types

03 p0519 A70-13581

Regular C cubed space curve bending in Euclidean 3-space into piecewise helix, considering torsion and curvature

12 p2260 A70-26973

CUBIC LATTICES

NT BODY CENTERED CUBIC LATTICES

NT FACE CENTERED CUBIC LATTICES

Quantitative separation of metastable and cubic chromium carbides in alloyed Cr steels utilizing hydrogen peroxide

03 p0504 A70-12981

Cubic texture components preferred orientation shares into rolling texture during cold rolling of aluminum sheets determined quantitatively

09 p1690 A70-22255

Nickel chromite structural changes, thermal conductivity and dilatation during tetragonal-cubic transition, noting phonon-lattice effect

13 p2437 A70-28855

Elastic constants pressure dependence of cubic crystals in NaCl and spinel structures using homogeneous static deformation method

13 p2396 A70-29172

Directional dependence of elastic shear stiffness on cubic axes for Si, Cu and Mo, making polar plots of shear stiffness coefficients

21 p3850 A70-41909

Cubic monocrystalline semiconductor upper critical magnetic field, using correlation function method

23 p4231 A70-44926

Cubic titanium oxycarbide structural characteristics, noting lattice constant dependence on component proportions and mutual solubility during formation

24 p4359 A70-45477

CUES

Distance discrimination experiment in reduced cue setting simulating outer space, confirming Weber power function exponent

04 p0645 A70-15647

Acceleration cues removal effects on vehicular velocity perception, using movie technique to control visual cues

05 p0806 A70-16143

Attention and cue-producing responses in response-mediated stimulus generalization

09 p1617 A70-22342

Color closed circuit TV visual cues in flight simulation during flare and touchdown, including ATA requirements and acuity limits

[AIAA PAPER 70-347] 10 p1857 A70-24201

Airborne simulator program for evaluation of motion and visual cue effects on pilot performance in roll, using compensatory tracking tasks

[AIAA PAPER 70-351] 10 p1857 A70-24202

Dual cockpit wide angle visual cue simulator design, discussing sky-earth-sun projector with four axis gimbal drive

[AIAA PAPER 70-360] 10 p1857 A70-24204

Flight simulation data on motion cues effects in controlling compensatory tracking tasks

[AIAA PAPER 70-352] 10 p1859 A70-24211

Psychophysical metric for space perception visual cues measurement, describing applications to distance discrimination

10 p1827 A70-24768

Motion cue requirements in one and two axis closed loop compensatory control tracking tasks, discussing error rates

14 p2540 A70-30247

Low visibility aircraft landing problem concerning pilot instrument and visual cue and federal regulations governing operational approval

[AIAA PAPER 70-936] 17 p3134 A70-35845

CUFFS

Syncope prevention in orthostatic heat test by inflating cuffs around legs and lower abdomen

24 p4306 A70-45331

CULTIVATION

Growth rate effect on glucose utilization rate using sporogenic strain of *Bacillus subtilis* during N and L-tryptophan limitation

01 p0021 A70-10790

Joint *Chlorella*-yeast cultivation on metabolites, investigating biomass accumulation and pigment synthesis

07 p1197 A70-18655

CULTURE TECHNIQUES

Hypoxic stimulation effect on erythropoiesis in vivo bone marrow

01 p0017 A70-10464

Chemostat culture method for studying control mechanisms during utilization of glucose/lactose and glucose/L-aspartic acid by populations of *Escherichia coli*

01 p0021 A70-10787

Assimilation and metabolism of C atoms of pyruvate and acetate by strict autotrophs *Thiobacillus* cell, using radioactive substrates

01 p0021 A70-10788

Gnotobiotic techniques for human hematopoietic cell culture establishment and maintenance, considering culture transfer

01 p0027 A70-11311

Chlorobium thiosulfatophilum sulfur bacteria growth on media with/without ammonium chloride exposed to illumination, noting various amino acids effects

02 p0241 A70-12797

Mathematical planning of experiments applied to biological mineralization of human wastes, using continuous microorganism cultivation

03 p0435 A70-13715

Temperature-synchronized semicontinuous culture and monitoring system for autotrophically growing *Euglenas*

04 p0633 A70-15453

Microorganisms survivability in agar subjected to simulated Martian freeze-thaw cycles, discussing soil samples collection and composition

09 p1618 A70-22767

Penicillium mutant chemical stress tolerance in boric acid and potassium chloride selective media, studying carbohydrate and inosine-5-phosphate effects on growth rate

10 p1811 A70-24325

Mathematical planning of experiments applied to biological mineralization of human wastes, using continuous microorganism cultivation

11 p1990 A70-25515

Hydrocarbon assimilating bacteria cultures selection, considering highest specific growth rate and maximum productivity

11 p1991 A70-25939

Plant cultivation in closed biological cycles by hydroponic method using *keramsit* /alumoferrisilicate/ substrate

13 p2358 A70-29328

Linear density gradients in isopycnic centrifugation technique for selecting synchronous daughter cells from asynchronous *Chlorella* cultures

14 p2546 A70-30985

Optimum algae cultivator construction for life support system, using *Chlorella* culture model

17 p3026 A70-35320

Wheat culture continuous subirrigation for life support system applications in spacecraft, discussing harvest yields

17 p3026 A70-35321

Unicellular hot spring acidophilic alga *Cyanidium cadarium* cultured in pure carbon dioxide, examining packed cell volume, oxygen production and growth rate

20 p3572 A70-39492

Life support systems based on *Chlorella*-bacterial culture, investigating water exchange and reclamation

20 p3574 A70-40184

CUMULONIMBUS CLOUDS

Thunderstorm development processes investigated by aircraft measurements of electrical structure in cumulonimbus clouds, noting lightning probability dependence on turbulence within cloud

22 p4064 A70-42775

CUMULUS CLOUDS

Near IR reflection spectra of artificial cumulus clouds with progressive droplet sizes

01 p0076 A70-10911

Seeding effects on isolated cumulus clouds, using numerical model of microphysics and dynamics factors, measuring rainfall amounts and duration

06 p1098 A70-18243

One dimensional cumulus convection model modified by incorporating rain evaporation rate and temperature changes from downdrafts

06 p1099 A70-18568

Dry regions in cumulus cloud near environment interpreted as evidence of compensating motion in environment

06 p1101 A70-18577

Vertical plane and axis symmetrical numerical models for cumulus convection of moist atmosphere, discussing initial conditions

08 p1536 A70-21025

Cumulus convection one dimensional time dependent numerical model, considering horizontal mixing, evaporation, precipitation generation and freezing and thermodynamic processes

11 p2075 A70-25648

Radar measured precipitation increase from seeded cloud demonstrated by measurements, numerical cumulus model and physical reasoning

12 p2189 A70-28094

Radar data characteristics for extensive natural cumuli cloud evolution, noting use for precipitation forecasting

18 p3287 A70-37000

Isolated cumulus clouds formation numerical simulation, determining movement rates relationship to external wind speed

19 p3463 A70-38756

CURIE TEMPERATURE

Normal and bottle-green microtektite glass measured for magnetic susceptibility, magnetization and Curie constants

05 p0916 A70-16839

Narrow Curie point switching transfer in Mn-Bi films by controlling magnetization direction within preselected areas

11 p2098 A70-26069

Dilatometric investigation of Fe alloys phase transformations, determining magnetic field effects and Curie temperatures

18 p3276 A70-36206

Autocorrelation functions of anomalous gravitational and magnetic fields for ocean lines, relating Mohorovičić boundary and Curie isotherm

19 p3408 A70-37318

Apollo 11 lunar rock and dust samples thermomagnetic properties, Curie points, magnetization and demagnetization characteristics

21 p3915 A70-41661

CURING

Organic adhesives preparation and application to metal surface for bonding, examining time, pressure and temperature effects on curing

08 p1503 A70-20881

Flame-resistant trichloromethyl-containing polyester-styrene system, describing curing characteristics at room and higher temperatures

10 p1907 A70-24066

Polyimide resins and composites state of cure determination by thermomechanical analysis (TMA/

11 p2069 A70-25807

Thermal stresses and curing in electronic modules transfer molding, discussing various design test models

13 p2420 A70-29252

Low dielectric constant quartz-polyimide for radomes, considering curving methods

16 p2936 A70-33368

Fluid urethane laminating resin for bonding nylon and glass fabrics, giving physical properties as function of room temperature curing time

16 p2938 A70-33381

Poly(perfluoroalkylene oxides) preparation and curing, considering molecular weight and thermal stability

21 p3783 A70-42145

CURL (VECTORS)

NT VORTICITY

CURRENT AMPLIFIERS

NT PHOTOMULTIPLIER TUBES

Magnetron diode current fluctuations in interelectrode space, considering cathode emission current amplification by various modes
10 p1853 A70-25164

Intracellular myocardium potentials under vagus inhibition by electrometric DC amplifiers with positive and negative feedback
19 p3370 A70-38213

M phase thyristor amplifier operation, investigating state and transition equations by state variable methods
22 p3996 A70-42918

Two-cascade amplifying circuits with current and voltage feedback for semiconductor precision devices
24 p4321 A70-46394

CURRENT DENSITY

Photoconductivity and photomagnetic effect measurements in Ge for determining nonequilibrium current carrier concentration produced by Q switched neodymium laser
01 p0107 A70-10099

Double injection in semiconductors at high current densities, discussing procedure yielding space charge and field distribution and voltage drop
01 p0154 A70-10123

Longitudinal and transverse temperature distribution measurement of electrons in electrostatic field and ion current density in ionized Cs plasma beam, determining energy spectra
01 p0149 A70-10170

Critical current density enhancement in Ta-rich Zr alloys in magnetic fields at low temperature after aging
01 p0122 A70-11238

Nonequilibrium potassium seeded Ar plasma electrical conductivity at atmospheric pressure, noting current density role
02 p0347 A70-12232

Current density and electron concentration fluctuations in semiconductors under electric field, obtaining theory of light scattering at hot electrons
03 p0539 A70-13405

Plane electromagnetic wave diffraction at conducting stripline, calculating surface current density and far field scattering using edge wave and factorization methods
03 p0451 A70-13755

Current stream function, Hall current density, force densities and pressure distribution for typical MPD thruster
03 p0552 A70-14372

MHD flow velocity and current density distributions in annular duct with radial magnetic field
04 p0725 A70-14531

Anode work functions from cesiated metal surfaces as parameters for thermionic converter systems analysis
04 p0627 A70-14946

Ionization gage with screened collector, showing limit current in high vacuum equal to X ray radiation component
05 p0847 A70-15997

Energy losses in conductors carrying intense currents to cryogenic regions linked with heat transfer due to high temperature gradients
05 p0881 A70-16026

Electron energy equation for nonequilibrium plasmas, assuming large electron diffusion velocity and current density and enhanceable electron temperature
06 p1123 A70-18299

Induced current density of fully ionized stationary plasma in externally applied HF electric field, discussing frequency range of fluctuations
07 p1352 A70-19988

Thermoelectric stress degradation of injection lasers at high excitation levels, giving critical current densities for short pulse, CW and quasi-CW conditions
08 p1512 A70-20861

Nonlinear wave scattering at plasma particles and weak plasma inhomogeneity effects on plasma current instability
08 p1554 A70-21819

Short high current pulses generation by avalanche transistors in circuits suitable for investigating low impedance laser diode
09 p1642 A70-22035

Fast magnetoacoustic wave propagation in cylindrical plasma column with constant current density, using geometric optics
10 p1923 A70-24229

CO electrochemical oxidation at porous solid electrolyte fuel cell anodes under high temperature, noting current density role
10 p1830 A70-24462

Plane electromagnetic wave diffraction at conducting stripline, calculating surface current density and far field scattering using edge wave and factorization methods
10 p1842 A70-25002

Longitudinal and transverse temperature distribution measurement of electrons in electrostatic field and ion current density in ionized Cs plasma beam, determining energy spectra
10 p1925 A70-25016

Hydromagnetic flute and surface wave instabilities of current-carrying plasma filament in strong longitudinal field, showing radial density stabilization
10 p1926 A70-25117

Current density distribution during electroerosive machining, discussing current diagram construction and tool profile
11 p2060 A70-25935

Nomographic Richardson-Dushman equation solutions for thermionic electron emission devices, giving current density for various work functions and electrode temperatures
12 p2271 A70-26894

Current-sensitive single gun color CRT with phosphor screen for display systems
12 p2195 A70-27373

Argon laser upper levels population measured as function of current strength at constant atom density in capillary
12 p2247 A70-27506

Fuel cells power density improvement under pulsed loading at high current density and constant voltage
12 p2165 A70-27758

Electron density determination, establishing gas pressure relation to discharge current
13 p2460 A70-28710

Current density distributions in Ar-K plasma streams through channel with segmented electrode array, measuring electron temperatures
13 p2461 A70-28732

Sunspot electric current density accounting for magnetic field abrupt reversal
13 p2496 A70-29848

Magnetosphere boundary altitude dependence on longitude, considering role of electric current density along geomagnetic lines of force
14 p2570 A70-30217

Sunspots surface layers azimuthal electric current density, assuming specific magnetic force distribution
18 p3322 A70-37135

High current elastic conductors nonlinear mixture theory with inviscid electron gas in elastic continuum under mutual electromagnetic and diffusive forces
19 p3387 A70-37787

Geomagnetic activity effect on potential gradient and air-earth conduction current density
19 p3413 A70-38000

Argon ion laser inversion saturation at large current densities due to upper working levels depletion
19 p3449 A70-38744

Frequency dependence of impedance of p-n diode with short base in presence of large forward current densities
20 p3598 A70-40021

Steady plane conducting gas flow across magnetic field in channel, calculating flow rate effect on current density distribution
20 p3684 A70-40386

Electromagnetic wave propagation in colloidal plasmas analyzed by kinetic approach, obtaining expressions for current density, DC and microwave conductivities, etc
20 p3685 A70-40502

Hydromagnetic flute and surface waves instabilities of current-carrying plasma filament in strong longitudinal field, showing radial density stabilization
20 p3685 A70-40510

Stainless steel gas tungsten arc welding, considering anode spot size variation and current density
22 p4042 A70-42377

Air-earth current density time variation in stratosphere by high altitude balloon, comparing with potential gradient diurnal variation over ocean
22 p4017 A70-42798

Current densities and fields in quasi-neutral electron beam plasma, solving boundary value problem numerically
22 p4081 A70-42825

Current-phase relationship in short superconducting weak links, using one dimensional model
24 p4389 A70-45224

Strong magnetic fields effect on field emission currents in Bi, Zn, Ta and W
24 p4379 A70-45621

Ferromagnetic cylindrical specimens eddy current density distribution under influence of field strength dependent permeability corresponding to Rayleigh law
24 p4344 A70-45695

Magnetosphere boundary altitude dependence on longitude, considering role of electric current density along geomagnetic lines of force
24 p4331 A70-46292

CURRENT DISTRIBUTION

Current distribution in finite length helical antenna in HF field, using cylindrical model of infinitely good conductivity
01 p0050 A70-10713

Shaped-reflector Cassegrainian antenna characteristics calculation, using current distribution method to derive subreflector radiation pattern
02 p0270 A70-12617

Field patterns of thin resonant and nonresonant antennas in warm plasma, using digital computer to evaluate propagation constant for current distribution
02 p0263 A70-12655

Manganin piezoresistive shock gauge constant current supply using inductor and termination technique eliminating shunting
02 p0303 A70-12737

Onset conditions for galvanothermal current instability of Ge semiconductors as function of electric field oscillations, carrier concentration and carrier-lattice temperature
03 p0541 A70-13724

Optical inhomogeneity of GaAs associated with current carrier distribution analyzed quantitatively using magnetooptical Faraday effect and transmittance method
03 p0541 A70-13726

Direction finding characteristics of nonlinear antenna, including current determination and optimal angle for sidelobe level
06 p1023 A70-18561

Dipole antennas current distribution in dissipative homogeneous medium
07 p1240 A70-19219

Current sheet pattern and gas flow stabilization in pulsed plasma accelerators
07 p1348 A70-19322

Optimal linear antenna synthesis, determining current distribution resulting in specified radiation pattern for superdirective antennas
08 p1472 A70-20972

Current distribution determination necessary for given directional characteristic of antennas in nonlinear synthesis problem
09 p1644 A70-22403

Inert gas glow discharge current change under laser radiation, investigating dependence on discharge region, gas and electrode material and configuration
09 p1696 A70-22484

Quasi-near zone electric field intensity and current distribution of monopole antenna on finite conductive earth
09 p1645 A70-22691

Two dimensional numerical analysis of current saturation mechanism for junction field effect transistors with small and large length-to-width ratio values
09 p1740 A70-23110

Error functional minimization in class of current distribution relay functions noting applications to linear antennas and FM signals synthesis
09 p1637 A70-23154

Current diffusion from magnetic piston into postshock gas upstream observed in electromagnetic shock tube
09 p1736 A70-23185

Anode energy transfer model for measurement of circumferential current and heat flux distributions of MPD arc thruster
09 p1736 A70-23203

Antenna pattern synthesis with circular distributed current source, analyzing directivity characteristics through Fourier series nth order mode concept
10 p1849 A70-24616

Current density distribution during electroerosive machining, discussing current diagram construction and tool profile
11 p2060 A70-25935

Electromagnetic field singularities near sharp edge relating to geometry scatter used for treating singularities in current distribution integral equations
12 p2183 A70-26977

He-Ne laser noise caused by discharge current fluctuation and moving striation in long capillary tubes
12 p2245 A70-27272

Vertical tubular dipole antenna input admittance and current distribution above infinite dissipative half space
12 p2197 A70-27953

Circular loop antenna with traveling wave current distribution, considering phase change effects on radiation pattern and gain
12 p2198 A70-27965

Dipole antenna current distribution in ionized homogeneous anisotropic medium, using dielectric permittivity tensor
13 p2371 A70-29923

Current stability and coil tests of force cooled superconducting systems
14 p2617 A70-31017

Gas kinetic pressure profile and mass density of propagating current sheet in argon pinch discharge, using piezoelectric transducer
14 p2624 A70-31041

Plasma cylinder surface drive current buildup, using theta pinch two dimensional model
14 p2624 A70-31049

Aperture antennas planar finite array, calculating excitation pattern for prescribed surface current distribution
14 p2557 A70-31160

Loop antenna current distribution source from radiation pattern synthesis, using Fourier series
15 p2698 A70-31837

Hydromagnetic viscous flow of incompressible conducting fluid due to electric current radial divergence from point source
15 p2780 A70-32426

Radiation pattern of radial infinitesimal current elements near or on finite length conducting cylinders, using image and geometrical theory of diffraction techniques

16 p2860 A70-32956

Mutual and self admittances for array with two monopoles, solving integral equations for current distributions

16 p2860 A70-32957

Backfire antennas allowing for mutual impedance between dipole elements, determining radiated field from surface current distribution

16 p2861 A70-32958

Current distribution on isolated thin cylindrical center-fed dipole antenna, calculating axial electric fields and radiating properties

16 p2861 A70-32964

Nonuniform parallel element dipole array field patterns and synthesis by three term theory, taking into account current distribution effects

16 p2872 A70-32972

Hall generator measurement of impulse currents, noting error sources and compensation

16 p2900 A70-33072

Simple antenna sources, deriving far zone radiation field from arbitrary current distribution

17 p3043 A70-35052

Linear antennas theory using integral equations for current distributions

17 p3044 A70-35058

Thin long dipole antenna, determining input admittances, current and charge distributions and field patterns by Wiener Hopf technique

17 p3051 A70-35060

Circular loop antenna for transmission and reception, determining current distribution, admittance and radiation field by integral equation

17 p3051 A70-35061

Funnel shaped vector radiation pattern realized by synthesizing axisymmetric distribution of elliptically polarized currents on body of revolution

19 p3392 A70-37277

Scattering structures of two parallel elliptical cylinders, tapes or combinations, deriving surface current density distribution under plane TM wave excitation

19 p3375 A70-37279

Current distribution method for inverse problem of antenna theory, producing radiation pattern

19 p3385 A70-37437

Current and resistance in Hg filled space between two circular electrodes under strong magnetic field, using boundary layer techniques

19 p3477 A70-37578

Cylindrical EM waves diffraction by two parallel ideally conducting elliptical cylinders, discussing field and surface current distributions

19 p3378 A70-37734

Nonuniform emitter current distribution effect on power transistor thermal stability, discussing temperature distribution effects

19 p3387 A70-37821

Center fed cylindrical half wavelength dipole antenna, computing radiation pattern by trigonometric expansion approximation for current distribution

19 p3388 A70-37869

Pulsar radiation mechanisms, discussing magnetic field topology and current distribution estimation

19 p3518 A70-38022

Ionospheric electric current distribution response to horizontal wind induced emf, using lunar tidal wind models

19 p3415 A70-38386

Current fluctuations in polar semiconductors in strong electric field, taking into account semiconductor band structure

20 p3686 A70-39589

Current distribution and interband recombination emission in bipolar semiconductor crystal under pinch effect produced by external magnetic field

20 p3677 A70-39590

Conducting wall MHD generator channel current distribution, examining computer program for anode and cathode currents

20 p3566 A70-40013

Continuous electrode MHD generator ionization instabilities, measuring current distribution and transverse electric field

20 p3567 A70-40018

Antennas with controlled current distribution in medium wavelength range for optimal radiation pattern over desired area, discussing maximum gain tuning for daytime and nighttime operation

22 p3995 A70-42521

Current distribution of accelerating electrodes of coaxial injector, using differential magnetic probe

22 p3965 A70-42805

Eroding-dielectric plasma accelerators energy characteristics, discussing current distribution

22 p4083 A70-43387

Current distribution and near field of cylindrical antennas loaded with built-in lumped elements

22 p3998 A70-43422

Auroral electrojet return current spatial extent from model ionospheric current distribution and geomagnetic variations

23 p4192 A70-44922

Dielectric filled tubular monopole antenna driven by coaxial line with TEM mode, calculating current distribution from integral equation

23 p4175 A70-44953

Electromagnetic scattering by two dimensional periodic arrays of conducting thin plates, calculating induced current and near field radiation distribution

23 p4165 A70-44961

Dipole antenna in compressible lossy plasma, calculating sheath and absorptive surface effects on current distribution from boundary value problem formulation

23 p4228 A70-44963

Radar cross section and current distribution of dipole deformed into low pitch angle helix

23 p4166 A70-44974

Current twisting in double injection ohmic contact long p-n diodes with S-shaped current-voltage curve, showing unstable density at negative resistance segment

23 p4176 A70-45061

Current oscillations in external circuits of semiconductor with low surface recombination in parallel electromagnetic field

23 p4231 A70-45062

Transverse and longitudinal current correlations in fluids from modeled kinetic equations, noting inelastic neutron scattering from liquids

24 p4378 A70-45261

CURRENT REGULATORS

Current oscillations produced in finite-length electron hole semiconductors by strong electric and magnetic fields, discussing HF stabilization

22 p4084 A70-43469

Universal proportional high accuracy temperature controller using current regulating circuit consisting of light beam galvanometer, photoconductor, photodiodes and thyristors

23 p4194 A70-43999

CURRENT SHEETS

Current sheet pattern and gas flow stabilization in pulsed plasma accelerators

07 p1348 A70-19322

Energy transfer from pulse network to mass associated with propagating current sheet in linear pinch discharge, discussing pulsed plasma accelerator efficiency

07 p1348 A70-19323

Pulsars radio, optical and X ray emission spectrum analysis, suggesting oscillating current sheets as radiation source

08 p1561 A70-20914

Current sheet velocity in coaxial plasma accelerator, noting drag due to insulator ablation and degassing

09 p1736 A70-23202

Current sheet speed in coaxial plasma accelerator computed as function of time, comparing results with velocity measurements

12 p2281 A70-27833

Aurora band theory based on three dimensional current system during magnetic substorms, discussing field aligned sheet current instability

14 p2573 A70-30671

Pulse structure, polarization, time varying features and tight beam emission by pulsar model using finite thickness interfaces

17 p3153 A70-34532

Current sheet structure of hydromagnetic boundary layer formed by mixing two conducting fluid streams containing oppositely directed magnetic fields

17 p3140 A70-34930

Electric propulsion research involving MPD thrusters, current sheets and neutral-ion motion coupling

20 p3683 A70-40249

Current sheet motion and pulsar radio, optical and X ray emission, investigating finite thickness oscillating interface radiation with independent particle

24 p4397 A70-45760

CURRENT STABILIZERS

U CURRENT REGULATORS

CURTAINS

Heat and gas curtain efficiency in turbulent boundary layer on flat plate, including heat transfer data

17 p3198 A70-35731

Jet curtain flow recirculation model based on air-bubble flow visualization technique, determining minimum power for air cushion vehicle

22 p3957 A70-42278

CURTISS-WRIGHT MILITARY AIRCRAFT

U MILITARY AIRCRAFT

CURVATURE

Dispersive Doppler shift and Faraday rotation second order theory for curved earth-ionosphere geometry, calculating phase path differences

02 p0260 A70-12574

Zero-moment theory boundary value problem of shells of revolution with negative curvature under tangential static and geometrical conditions imposed on ends

03 p0589 A70-13337

Curvature effects on two dimensional turbulent wall jet flow over plane surface and circular convex and concave surfaces in still air

05 p0832 A70-16118

Stress distribution around crack tip of initially curved sheets

05 p0939 A70-16484

Fibers random curvature effect on thermoelastic properties of unidirectionally reinforced fibrous materials

05 p0946 A70-16953

Steady laminar flow with frictionless central core surrounded by boundary layer in circular curved pipe, discussing friction factor and flowmeter discharge coefficient

05 p0836 A70-17107

Anticlastic bending effect on rectangular beam curvature, presenting deflection equations

07 p1414 A70-20175

Transverse curvature effects on turbulent boundary layer thickness and velocity profiles on circular cylinders in water and air

07 p1261 A70-20301

Electrode curvature effect in radial reflex klystron on processes in electron bunching region

09 p1651 A70-23640

Pressure waves of varying amplitude effect on flow through turbomachine blade passages, discussing interaction with curved diffusers geometry

09 p1608 A70-23743

Streamline curvature technique for two dimensional flow equations, deriving optimal damping factor for quasi-orthogonal method to test stability, convergence and accuracy

09 p1609 A70-23749

Homogeneous open anisotropic relativistic world model with negative space curvature, observing shear decrease with time and magnitude reciprocal variation with function R/t

11 p2109 A70-25866

Zero-moment theory boundary value problem of shells of revolution with negative curvature under tangential static and geometrical conditions imposed on ends

14 p2657 A70-30715

Curved porous wall channels for noise suppression in power plants, ventilation systems, etc

18 p3216 A70-36302

Ricci curvature tensor perturbations of space-time on Alfvén wave fronts

19 p3472 A70-38935

Pool film boiling heat transfer data from small spheres, noting curvature effects and similarities of flat plate, cylinder and sphere theoretical analyses

21 p3949 A70-41310

Steady incompressible turbulent boundary layer form on permeable curvilinear surface with uniform suction, assuming small pressure gradients

22 p4011 A70-42803

Wave front arbitrary curvature, examining integration of weak discontinuities growth equation in quasi-linear hyperbolic system

22 p4062 A70-42953

Earth curvature effects on position of terrain points on planar aerial photographs for various survey altitudes

24 p4333 A70-45197

CURVE FITTING

Gram-Charlier method generalization for curve fitting analytic forms to velocity covariances measured in turbulent wake of circular cylinder

03 p0480 A70-12950

Spline data techniques for error elimination in trajectory optimization to offer improvement over linear interpolation scheme

07 p1325 A70-19340

Space mechanics problem of passing from perigee to radial distance in given time determined by fitting conic to radii, using iteration method

09 p1760 A70-22927

Stress concentration analysis using Chebyshev polynomial curve fitting

09 p1784 A70-23450

Curve arc approximation by circular arc using Chebyshev modulus-minimax principle

13 p2442 A70-29743

Jet flow past arc curve approximation using successive conformal mapping on circle and wedge

13 p2391 A70-29746

Curve approximation quality by method of informative evaluation for determining minimum required number of measured points on ST interval of electrocardiogram

13 p2360 A70-29775

Minimum bias criteria for selecting data fitting curves, allowing for unknown true equation in improving data predictability

20 p3659 A70-40261

Fitting equations to mixture data by linear least squares method with restraints on compositions, using Scheffe polynomials

22 p4064 A70-43728

Model fitting procedure applied to lunar occultation data and models analysis for point sources, close binaries and resolvable stars

24 p4399 A70-45130

Interpolation and smooth curve fitting based on local procedures and piecewise function

24 p4369 A70-45162

CURVED BEAMS

Stiffness matrix derivation for curved beam emphasizing uncoupled normal to plane loads

03 p0584 A70-12949

Natural frequencies upper and lower bounds of elastic clamped vibrating curved beams /arcs/ determined on basis of differential operator theory

05 p0937 A70-16405

Horizontally curved I beams flanges elastic buckling, determining prebuckling flange stresses in longitudinal and radial directions

07 p1413 A70-20001

Multispan horizontally curved beams natural frequencies determination illustrated by developing frequency equation

09 p1770 A70-22388

Elastic circular sandwich beams optimal design for minimum compliance and given weight, considering rings and semicircular arches

24 p4420 A70-45276

CURVED PANELS

Elastic properties of thin curved cylindrical panels with constant mechanical properties subjected to thermal expansion and single face pressure

01 p0201 A70-10943

Equilibrium of thin curved cylindrical panels subjected to thermal expansion and pressure numerically analyzed by Ritz method

01 p0201 A70-10945

Curved cylindrical panel flutter in presence of uniform compressive load, taking into account relationship between actual and ideal shape

01 p0202 A70-10946

Thin elastic cylindrical panel motion induced by plane acoustic shock wave analyzed by integrating nonlinear motion equations using finite difference scheme

03 p0524 A70-13377

Critical radii of curvature in elastoplastic bending of rib-reinforced aircraft components from wafer panels determined using strain energy method

08 p1506 A70-21183

Thin circular cylindrical panels of arbitrary curvature calculated for end support and loading at contour

12 p2323 A70-27335

Hypersonic viscous interaction on curved surfaces, extending Cheng inclined flat plate analysis [AIAA PAPER 70-782]

17 p3007 A70-34474

Frequency analysis of cylindrically curved panel with clamped and elastic boundaries, using mathematical and panel models

17 p3181 A70-34524

Buckling loads and postbuckling behavior of curved panels under axial compression, noting dependence on boundary conditions

17 p3188 A70-35225

Frequency equations derived for cylindrical panels with surface loading, comparing free vibration natural frequencies of panels with attached mass at centers

24 p4422 A70-45297

CURVED SURFACES

U CONTOURS

U SHAPES

U SURFACES

CURVES (GEOMETRY)

NT CATENARIES

Elastic curve deformation of rod in equilibrium under end loads, using equations analogous to Kharlamov kinematic equations and Chaplygin solution

01 p0094 A70-11440

Turbojet performance magnitude data represented by components nondimensional characteristic curves

03 p0551 A70-13021

Theoretical and experimental cascade curves comparison for heavy materials used for particle absorption in tracking experiments, discussing Coulomb scattering

03 p0527 A70-13051

Slope and shape of blood-gas dissociation curve as factor influencing pulmonary gas exchange in presence of ventilation-perfusion inequality

06 p0994 A70-17522

Singularity carrier auxiliary curves for design calculation of airfoil cascades, discussing existence theorems and case of thin profiles

11 p1974 A70-25783

Singularity carrier auxiliary curves for design calculation of airfoil cascades, discussing profiles with small and large arcs

11 p1974 A70-25784

Circular elastic helix phase velocities determined by internal constraints method, comparing results with other theories

11 p2085 A70-26557

Nonlinear dynamic theory describing elastic Cosserat curves plane motion, developing linear displacement equations and dynamic stability concept

11 p2142 A70-26632

Regular C cubed space curve bending in Euclidean 3-space into piecewise helix, considering torsion and curvature

12 p2260 A70-26973

Lambert problem solution for moderate timespan arcs by approximation, offering concise formula without iteration

14 p2639 A70-30705

Parametric representation of brachistochrones of mass point in centrosymmetrical gravitational field

18 p3283 A70-36387

Geometric relations for contact moments of solar eclipse, using crescent cord photographic measurements

18 p3315 A70-36610

Observed meteor brightness curve shortening with respect to theoretical curves

19 p3514 A70-37645

Mathematically defined curve incremental generation by computer, discussing parametric and non-parametric representations and digital differential analyzer technique

22 p3993 A70-43072

CUSHIONS

Airplane dependability on basis of improvements in jet engine, avionics, pilot seat cushions and flight control systems

09 p1611 A70-23453

CUSPS

NT CUSPS [MATHEMATICS]

Trailing edge flow of slender aerodynamic shapes terminating in cusp or wedge, analyzing boundary layer reactions

04 p0613 A70-14457

CUSPS [MATHEMATICS]

NT DOUBLE CUSPS

Optimal three dimensional impulsive orbit transfer at cuspidal point of primer locus in terms of three parameters to facilitate computation and tabulation [AIAA PAPER 70-1037]

19 p3527 A70-38852

CUT-OFF

Geographically smoothed geomagnetic cut-offs for eliminating discontinuity in neutron monitor latitude variation in Mexico City vicinity

01 p0167 A70-10229

Low speed air-propane flame stability, examining holder diameter effects on vibration cutoff wavelength

20 p3738 A70-40281

Synchrotron source spectra natural frequency cut-off in absence of self absorption and electron energy cut-offs, discussing pulsar NP 0532

24 p4410 A70-45774

CUT-OUTS

U OPENINGS

CUTANEOUS PERCEPTION

U TOUCH

CUTTERS

NT RAZOR BLADES

CUTTING

NT METAL CUTTING

NT MILLING [MACHINING]

NT SPARK MACHINING

Ultrasonic machining of glass and cemented carbide, measuring ambient pressure effect on workpiece removal rate

21 p3833 A70-41253

Spatial stability of transferred arc anode spots during cutting with plasma jets, noting currents associated with microspots

22 p4043 A70-42380

CW RADAR

U CONTINUOUS WAVE RADAR

CYANIDES

NT CYANOGEN

NT HYDROGEN CYANIDES

NT IRON CYANIDES

Isomerization of isocyanide into azulene by irradiation and formation from biphenyl isothiocyanate, observing ring expansion and electrophilic carbenoid properties

05 p0811 A70-16055

Radiative lifetimes determination from beta-chi violet transition probabilities of CN

10 p1947 A70-24991

Cyanide gas lasers design for submillimetric region of electromagnetic spectra

11 p2062 A70-25735

Formation mechanism of molecular CN violet bands in solar photosphere

13 p2493 A70-29393

Benzoyl cyanide deoxygenation, describing reaction kinetics and products

17 p3041 A70-34750

Photoreaction produced N- cyclohexyldiphenylketenimine from cyclohexyl isocyanide and diphenyldiazomethane

17 p3042 A70-34820

Numerical molecular rotational transition probabilities and cross sections in HCN-HCN and ICN-ICN collisions, using perturbation theory and multipole potentials

21 p3853 A70-41391

CYANO COMPOUNDS

NT ISOCYANATES

Dicyanostilbene formation from phenylethynyl azide and isocyanate

05 p0811 A70-16054

Cyanoacrylate and anarobic polymer single component adhesives performance

22 p4046 A70-43120

CYANOCOBALAMIN

Hematologic changes in rats under hypergravity, effects of vitamin B12, folic acid and return to 1 g

06 p0991 A70-17283

CYANOGEN

NH bands in stellar spectra by visual inspection of spectrograms, noting abundance of N in normal and strong CN stars

02 p0379 A70-12708

UV absorption cross sections of CO, HCl and ICN, analyzing reactions causing various spectral features

08 p1455 A70-21340

Radiative lifetimes determination from beta-chi violet transition probabilities of CN

10 p1947 A70-24991

Cyanogen-nitrous oxide flame temperature determination for different concentrations of mixture in flat stainless steel diffusion flame burner

11 p2101 A70-26386

CYANOPHYTA

U BLUE GREEN ALGAE

CYBERNETICS

Information transfer for quantitative relationships to error- and cause-controlled regulations

07 p1216 A70-18859

Neural information processing taking into account differences between living brain and artificial processor

09 p1617 A70-22496

Group Method of Data Handling based on heuristic self organization for solving complex system problems, with applications to random processes prediction

10 p1845 A70-24869

Flexible vehicle control, using cybernetic model for system design and response [AIAA PAPER 69-115]

12 p2314 A70-27811

Feedback in electrical networks, discussing transient processes within cybernetics framework

15 p2716 A70-32362

Soviet papers on biocybernetics covering man and computer, biological and engineering systems, heart self regulation, etc

18 p3223 A70-36076

Brain-like computer with learning rather than programmable capability, discussing pattern recognition and task performance

18 p3230 A70-36775

Soviet cybernetics research, emphasizing discrete and continuous control devices and systems synthesis

22 p4004 A70-43449

Biocybernetics of human central nervous system, discussing electronic computers analogy to human brain

23 p4145 A70-44222

Heuristic self organizing systems role in technical cybernetics

24 p4321 A70-45645

CYCLES

NT ACTIVITY CYCLES [BIOLOGY]

NT BRAYTON CYCLE

NT RANKINE CYCLE

NT SOLAR CYCLES

NT STIRLING CYCLE

NT STRESS CYCLES

NT SUNSPOT CYCLE

NT THERMODYNAMIC CYCLES

NT WORK-REST CYCLE

Cyclic changes in concentration produced in fluid flowing through fixed bed of solid adsorbent, governing separation by beds wave propagation properties

04 p0780 A70-14712

Optimal directed circuit and cycle elimination in weighted diagrams by edge reversal orientation

11 p2072 A70-26219

Damped vibrations logarithmic decrement determination during automatic recording of number of cycles, emphasizing error analysis

15 p2733 A70-31531

Computerized calculation of gas turbine cycles thermal efficiency, using hydrocarbon fuel, considering fuel composition and heat of combustion changes

22 p4125 A70-43439

Cyclic q-ary codes invariant under linear group substitutions using polynomial method

24 p4313 A70-46062

CYCLIC ACCELERATORS

NT BETATRONS

NT SYNCHROCYCLOTRONS

NT SYNCHROTRONS

CYCLIC HYDROCARBONS

NT ANTHRACENE

NT CYCLOBUTANE

NT CYCLOPROPANE

Cycloheptane and mixture of exo- and endo-cycloheptene heats of combustion and formation, isomerization and hydrogenation

01 p0213 A70-10134

- Cycloaliphatic epoxy resins for glass and carbon fiber reinforced plastics and laminates
07 p1318 A70-17973
- Cyclization of alkoxy radicals, investigating 4-pentenoxy radical and entropy factors effect
08 p1455 A70-20975
- Cyclohexene oxide mass spectral fragmentation by means of deuterium labeled analogs
09 p1630 A70-23397
- Isomeric 1-phenylheptenes mass spectra, investigating electron impact induced rearrangements of double bond
09 p1631 A70-23401
- Dicyclohexyl (DCH)/endothermic dehydrogenation to diphenyl (DP)/over platinum-alumina catalyst without added hydrogen considered for hypersonic aircraft engine cooling
14 p2546 A70-31175
- Cycloaliphatic epoxy resins tensile and impact strength improvement by modification with elastomeric materials, considering heat distortion temperature
16 p2936 A70-33359
- IR and Raman spectra of gaseous and liquid germylcyclopentane, determining torsional barriers and skeletal ring atom symmetry
16 p2858 A70-34008
- Photoreaction produced N-cyclohexyldiphenylketenimine from cyclohexyl isocyanide and diphenyldiazomethane
17 p3042 A70-34820
- NMR spin-spin coupling constants between vinyl protons in cyclopentadiene, 1,3-cyclohexadiene and 1,3-cyclooctadiene from spectrum analysis
21 p3780 A70-41704
- Heats of combustion and free isomerization energies of exo- and endo-isomers of 2- and 1-methylbicyclo heptane
22 p3982 A70-42680
- Specific heat and thermodynamic functions of endo- and exo-isomers of 2-methylbicyclo heptane in 12-310 K temperature range
22 p3982 A70-42681
- CYCLIC LOADS**
- Nondestructive testing and fatigue life analysis of cyclically loaded mechanism, determining dynamic responses to velocity shocks by computer techniques
01 p0053 A70-10010
- Loading frequency effects on Duralumin endurance limit in air and in water, noting stress level role
01 p0115 A70-10070
- Cyclic loading test apparatus for studying ferromagnetic metals structural changes due to fatigue
01 p0116 A70-10076
- Fatigue crack growth rate for high strength steels from crack length during cyclic loading and striation spacings after fracture
01 p0119 A70-10732
- Fretting corrosion effect on structural steel fatigue strength under asymmetric load cycles
01 p0207 A70-11155
- Bauschinger effects in repeated tensile and compressive strains in inelastic media under variable temperatures as function of load vector, using plastic yield
01 p0211 A70-11422
- Stress concentrations and load cycle asymmetry effect on materials stress and breakdown behavior under various load cycles
02 p0383 A70-11656
- Machine parts fatigue behavior and service life, studying endurance margin under load cycles spectra below initial endurance limit
02 p0383 A70-11657
- Ti alloys creep and fatigue breakdown under cyclic tensile loads at room temperature
02 p0315 A70-11660
- Molybdenum cylinders strength and plasticity under various compression and cyclic tensile loads
02 p0315 A70-11662
- Mechanical losses in fiberglass reinforced textolite converted into thermal energy during cyclic tension and compression
02 p0323 A70-12807
- Fiberglass reinforced textolite fatigue characteristics under impact tensile loads, noting different characteristics under cyclic sinusoidal loads
02 p0323 A70-12815
- Periodic biharmonic stress cycling determination of load influence of fatigue failure used for random load serviceability tests
02 p0391 A70-12855
- Out-of-phase or nonsynchronous biaxial straining effects on low cycle fatigue observed on Al specimen by cycling tension-compression and cyclic torsion
03 p0481 A70-12955
- Equipment for cyclic biaxial stress states testing by simultaneous direct pressurization and axial loading of thin walled cylindrical specimens
03 p0462 A70-12966
- Metals fatigue strength prediction by hysteresis loop method, presenting results for irreversible energy dissipation rules during cyclic loading
03 p0587 A70-13240
- Stress-strain state of infinite isotropic perforated plate under cyclic symmetry, assuming finite strains and nonlinear material
03 p0592 A70-13445
- Equipment for cyclic biaxial testing, producing five biaxial stress states by simultaneous direct pressurization and axial loading of thin walled cylindrical specimen
03 p0464 A70-14309
- Structural metals hysteresis properties under cyclic plastic loading at room temperature, considering cycle dependent creep and stress relaxation
[ASME PAPER 69-WA/MET-4] 04 p0705 A70-14763
- Stress-strain spatial distribution in notched plate fatigue specimen of mild steel determined by finite element method, noting cyclic strain softening effect
[ASME PAPER 69-MET-C] 04 p0770 A70-14876
- Axial compression effect on low cycle fatigue of thin walled metal tubes in torsion
[ASME PAPER 69-MET-H] 04 p0705 A70-14880
- Transverse vibration of viscoelastic polymethyl methacrylate column with initial curvature under periodic axial load, determining amplitude-frequency curves
[ASME PAPER 69-WA/APM-13] 04 p0772 A70-14915
- Swenson shear fatigue crack model expanded to include mean stress effect on cyclic shear crack growth
[ASME PAPER 69-WA/APM-8] 04 p0772 A70-14918
- Fatigue crack incremental propagation under cyclic shear loading, developing discrete dislocation model for crack and plastic zones
[ASME PAPER 69-WA/APM-7] 04 p0772 A70-14919
- Surface work hardening and stress concentrations effects on fatigue strength of alloy under asymmetric tension and compression load cycles at high temperatures
04 p0707 A70-15270
- Summation of cycle ratios for various loading programs to control cumulative damage concept based on French curve, using fatigue tests
05 p0939 A70-16485
- Unsteady cyclic creep effect on stressed state and margin safety of elements, noting discrepancy of experimental and theoretical characteristics
05 p0866 A70-17030
- Effective stress evaluation under cyclic trapezoidal loading and creep noting use in stationary test data conversion
05 p0951 A70-17031
- Optimal thermomechanical treatment for austenitic steel stability to resist propagation and unloading of dislocations in cyclic loading process
05 p0867 A70-17041
- Thermocyclic creep and rupture strength of Nb, Ta and Mo refractory alloys under temperature and load variations, showing failure dependence on cycle parameters
05 p0867 A70-17043
- Gas dynamic stand for testing turbine disks strength under mechanical and cyclic thermal loads, analyzing breakdown data for various disk geometry
05 p0953 A70-17052
- Collection of papers on strength at small number of load cycles, problems of mechanical fatigue
06 p1160 A70-17382
- Carrying capacity of machine parts under small numbers of cyclic plastic deformation, reviewing breakdown criteria relation to kinetics of stress-strain states
06 p1161 A70-17383
- Plastic bodies stress-strain state under variable loads generalized to cases of cyclic loads and plasticity
06 p1162 A70-17384
- Plastic flow theory applied to cyclic deformation of metals under complex cyclic loads
06 p1162 A70-17385
- Copper specimens stress-strain diagrams under cyclic loads of various amplitudes, noting three stage process plastic deformation
06 p1162 A70-17386
- Cylindrical Al, high strength pig iron and heat resistant steels elastoplastic deformation diagrams for cyclic compression tension loads
06 p1084 A70-17387
- Cyclic creep curves plotted from expansion diagrams for steel, copper and brass under small numbers of cyclic compression tension loads
06 p1162 A70-17388
- Complex load strength criterion containing stress and strain invariants applied to simple static loads and cyclic symmetric deformation
06 p1162 A70-17389
- Fatigue breakdown criteria for elastoplastic materials under cyclic loads, deriving equations as functions of stress-strain states kinetic behavior
06 p1162 A70-17390
- Time to crack formation determined in cylindrical and flat Al and steel specimens having various surface properties under cyclic loads
06 p1084 A70-17392
- Crack formation and propagation kinetics in flat and cylindrical Cr-Mo-V steels under tension compression loading cycles
06 p1162 A70-17393
- Structural elements elastoplastic deformation regularities under repeated loadings, using adaptability theory
06 p1163 A70-17394
- Elastoplastic rod systems under repeated variable loads, calculating carrying capacity from plastic failure considerations
06 p1163 A70-17395
- Steel tube deformation under constant internal pressure and cyclic heating, plotting tangential and axial strain curves as function of cyclic loading
06 p1163 A70-17399
- Damage accumulation and failure of low carbon and low alloy steels subjected to repeated static loading, varying cyclic load frequency
06 p1085 A70-17400
- Steels crack propagation direction dependence on load magnitude in low cycle fatigue, noting groove width effects on resistance to static loading
06 p1163 A70-17401
- Low cycle fatigue life of various structural steels and alloys, studying stress cycle number relations
06 p1085 A70-17402
- Structures elastic-plastic behavior under changing cyclic heating, calculating long time strength from linear damage accumulation assumptions
06 p1164 A70-17405
- Ti alloy tensile strength under cyclic loads at room and high temperatures, noting plastic deformation and damage accumulation effects
06 p1085 A70-17406
- Machines selection for determining low cycle fatigue life, emphasizing automatic control system for regulating load and strain regimes
06 p1164 A70-17407
- Fatigue life of unidirectionally glass fiber reinforced composites subjected to low cycle loading, using linear elastic body model for cyclic deformation process
06 p1091 A70-17408
- Creep effects on structural failure under low cycle fatigue at high temperatures, noting role of plastic deformation
06 p1164 A70-17409
- Creep-low cycle fatigue interactions in Udimet alloy at elevated temperatures, investigating cumulative damage
06 p1086 A70-17455
- Glass fiber reinforced thermoplastics fatigue behavior during and after cyclic loading
06 p1091 A70-17600
- Gas turbine compensating bellows structural strength, discussing low cycle fatigue test under static loads
06 p1167 A70-17664
- Cyclic plastic deformation changes with load increase under uniform stress with normal loading and nonuniform stress with impact loading, considering fatigue limit
06 p1168 A70-17923
- Miniature resistance strain gage performance in low cycle fatigue, discussing zero drift and gage sensitivity changes
07 p1281 A70-19241
- Stability criterion applied to asymmetric rigid cyclic strains and plastic cyclic strains, considering failure of metals
07 p1315 A70-20182
- Energy dissipation in heat resistant Ni steels under cyclic tension and compression at room temperature
08 p1516 A70-20981
- Cyclic creep and relaxation of heat resistant alloys at high temperatures, showing inapplicability of static load conditions
08 p1516 A70-20982
- Deformation amplitude effects on dislocation structure and strengthening mechanism of fcc aluminum under cyclic loading
08 p1516 A70-20985
- Electronic recording of cyclic strain diagrams of metals in wide loading frequency range using dynamic hysteresis method
08 p1585 A70-20987
- Creep strain effect on cyclic fatigue life of duralumin at room temperature
08 p1516 A70-20988
- Stress and strain spatial distribution in notched steel plate under cyclic loading determined by finite element method
08 p1590 A70-21315
- Nonmetallic inclusions effect on steels cyclic strength dependence on inclusion composition and metallic matrix properties derived from fatigue tests
08 p1590 A70-21413
- Microhardness method for property changes in structural materials during sequential cyclic loading, discussing material identification, statistical fatigue theory, fine structure effects, etc
09 p1701 A70-22299
- Inertia effect in failure mechanics for steadily developing equilibrium cracks in dynamic system with time dependent periodically variable load
09 p1771 A70-22466

Plastic growth of pressurized shell under cyclic thermal stresses superimposed on steady pressure load, investigating shake down using bending approximation
09 p1774 A70-22586

Damage model for materials failure prediction under cyclic loading developed for strain controlled cycle with hold time
09 p1774 A70-22588

Strain rate and hold time effects on steels low cycle fatigue behavior, graphing various correlations among stress amplitude, time to fracture, etc
09 p1774 A70-22589

Turbines rotary shafts and stationary components thermal fatigue analysis, considering cycle numbers and stress concentrations under start-up, continuous operation and shut-down
09 p1775 A70-22593

Machine parts lifetime dispersion determined by fatigue limits distribution during cyclic loading
09 p1776 A70-22623

High temperature fatigue crack growth in metal, suggesting condensation of vacancies at crack front after each loading cycle
09 p1776 A70-22644

Multilayer orthotropic conical shell cyclic deformation equation obtained in hypergeometric functions
09 p1777 A70-23079

Elastoplastic stressed state of thin walled shells of revolution under repeated loads, assuming isotropic incompressible material
09 p1779 A70-23092

Ti-Al-Zr-W-Si alloy fracture surface concentric markings number related to loading cycles after crack formation
10 p1904 A70-24837

Beams stability under flexural stress with periodic intensity variations, deriving differential equation of motion
10 p1960 A70-24973

Aircraft structures fatigue durability estimations, studying crack propagation rates under cyclic loadings by fail-safe method
11 p2132 A70-25624

Fatigue crack propagation in high strength steels during fatigue cycling in dry and wet environment containing NaCl
11 p2067 A70-26100

Polymer materials fatigue strength and deformability testing in vacuum, air and gas atmospheres at low and high temperatures, subjecting to cyclic loading
13 p2385 A70-29428

Measuring apparatus for cyclic plastic strains at high temperatures, discussing data processing techniques
15 p2733 A70-31538

Plastic deformation and aging effects on fatigue characteristics of steels until rupture under cyclic loads
15 p2755 A70-31540

Temperature measurement of rotating shafts under cyclic loading, using thermistor as thermal radiation sensor
15 p2734 A70-31581

Residual stress measurement in anodic film on duraluminum as function of film thickness and cyclic loadings in air and corrosive media
15 p2757 A70-31635

Environmental fatigue crack propagation in Al alloys at low cyclic stress intensity levels
15 p2762 A70-32390

Anisotropic glass fiber reinforced plastics strength and deformability under cyclic axial loads
15 p2766 A70-32897

Delayed rupture and relaxation in Ti alloys during cyclic deformation, comparing fatigue tests results for continuous and discontinuous cyclic loadings
16 p2931 A70-33209

Fiberglass reinforced anisotropic plastics heating during cyclic axial loading
16 p2934 A70-33215

Hysteresis loop behavior under tension-compression cycle fatigue related to Meyer strain hardness values of cyclically strained metals
16 p2934 A70-34334

Polycarbonate plate fatigue crack propagation, discussing length due to repetitions, striation number relationship to cycles, and stress intensity
16 p2941 A70-34335

Structural fatigue testing by computer control of random force cycles
17 p3062 A70-35505

Cyclic strain effects on creep for steel at elevated temperatures, discussing overload frequency effects on plastic strain buildup
17 p3127 A70-35719

Stainless steel load-strain characteristics and cumulative damage in cyclic fatigue life
18 p3273 A70-36048

Programmed fatigue testing machine for specimens under cyclic axial loads, transforming angular into linear displacements
18 p3237 A70-36473

Cyclic plastic breakdown of thin cylindrical shell under ring shaped load in temperature field, using linear programming method
18 p3341 A70-36585

Failure of materials under multicycle fatigue, deriving general theory of defects
18 p3341 A70-36586

Stress concentrations and load cycle asymmetry effect on materials stress and breakdown behavior under various load cycles
19 p3547 A70-38429

Machine parts fatigue behavior and service life, studying endurance margin under load cycles spectra below initial endurance limit
19 p3547 A70-38430

Ti alloys creep and fatigue breakdown under cyclic tensile loads at room temperature
19 p3452 A70-38434

Molybdenum cylinders strength and plasticity under various compression and cyclic tensile loads
19 p3453 A70-38436

Metal fatigue strength prediction by hysteresis loop method, presenting results for irreversible energy dissipation rules during cyclic loading
19 p3548 A70-38458

Fatigue crack closure in flat sheet specimens under zero-to-peak tension cyclic loading, analyzing stress distribution from fractographic striation patterns
19 p3549 A70-38625

Fatigue crack propagation under programmed loads, correlating crack growth rates and tip opening displacements
19 p3549 A70-38628

Strain multiplier for fatigue sensor in moderate amplitude cyclic strain applications
20 p3628 A70-39159

High temperature endurance strength of temper finished bolt connections under cyclic loads, using programmed fatigue testing machines
20 p3718 A70-39223

Fatigue phenomena based on solid body model, establishing breaking stress dependence on time or load cycles number
20 p3724 A70-39854

Brittle failure under creep during slow cyclic loading, discussing damage accumulation assumptions
20 p3725 A70-39868

Low cycle metal fatigue under stress concentration, examining complex loading, cyclic strain, stress-strain state and plastic deformation
20 p3727 A70-39885

Longitudinal shear crack propagation in random internal stress field, examining quasi-brittle rupture theory and cyclic loading
20 p3733 A70-40396

Dynamic stability of cylindrical shell with small curvature under static or periodically variable axial pressure loads
21 p3932 A70-40554

Fatigue crack growth tests on Al alloy sheets under variable amplitude loading
21 p3831 A70-40749

Turbocompressor disk materials selection by low cycle fatigue tests, discussing stop and start repetition and cracks in stress concentration zones
21 p3867 A70-41261

Slip band formation dislocation-diffusion mechanism for single crystal and polycrystalline metals, considering stress intensity and load cycles effects
21 p3936 A70-41416

Cyclic thermal loading in viscoelastic spherical and cylindrical pressure vessels, investigating thermal frequency effect
21 p3937 A70-41430

Parachutes lightweight coated fabrics air permeability under axial tensile loading and load cycling at room temperatures
21 p3843 A70-41835

[AIAA PAPER 70-1178] Crack growth study in viscoelastic solids by linear continuum mechanics, discussing cyclic loads, composite solids mechanical behavior and thermodynamics
22 p4115 A70-42937

Crack propagation resistance-cyclic fracture strength relation for Mn-Cr-V steels, considering thermomechanical working effects
23 p4204 A70-43935

Load cycle sequences for full scale aircraft structures and components fatigue testing
23 p4266 A70-44101

[ICAS PAPER 70-32] Crack detection in cyclic strained steel and Al alloys, using ultrasonic Rayleigh and longitudinal waves
24 p4424 A70-45718

Miner rule for cumulative fatigue damage, obtaining upper and lower bounds on load cycle number to failure
24 p4426 A70-46024

Cyclic loaded high purity Al samples, noting substructure around fatigue cracks
24 p4362 A70-46185

Thin Al foil subjected to cyclic bending stresses, investigating substructures and strain regions around fatigue crack
24 p4362 A70-46186

CYCLING
U CYCLES
CYCLOBUTANE
Low pressure ionic reactions in gaseous cyclobutane
06 p1004 A70-17328

CYCLOHEXANE
Liquid diethylcyclohexane /DECH/ sprays detonation propagation in gaseous oxygen, studying drop size effect on steady state development
02 p0351 A70-12003

Threshold energy value of organic laser emission from coronene in methyl-cyclohexane-isopentane at 100 K
03 p0498 A70-12878

Mass spectra of 1,2-cyclohexanediol and deuterium labeled analogs data recorded and mechanistic rationalizations of degradation processes given
07 p1225 A70-20200

CYCLONES
NT HURRICANES
Periodic cellular convection in troposphere with allowance for anisotropic turbulent mixing, showing cyclone association and intervals
01 p0135 A70-10206

Cyclone waves development during stationary long wave basic state two dimensional quasi-geostrophic two layer model
03 p0521 A70-14288

Spiral cloud vortex model in occluded extratropical cyclone constructed using atmospheric dynamics equations and satellite photographs
05 p0879 A70-16642

Earth orography shape effect on cyclogenetic properties of atmosphere noting mountain height, slope, air mass thermal properties, etc
10 p1913 A70-25196

Cyclone cloud vortex evolution from satellite photographs, examining reasons for onset and disintegration
13 p2444 A70-28588

Cloud cover photographs in deep occluded cyclone by Soyuz 4 spacecraft
14 p2602 A70-30139

CAT relationship to cyclogenesis and anticyclonogenesis, considering synoptic situation and Jacobian values for forecasts
14 p2609 A70-30604

Radiation fields structural characteristics of fronts, intertropical convergence zones and cyclone formations from radiation charts based on meteorological satellite observations
15 p2770 A70-32068

Right-moving thunderstorm characteristics from mesonet rain rawinsonde updraft observations, considering hydrostatic pressure and cyclonic rotation
19 p3462 A70-38260

Curvilinear motion centrifugal force compared with barometric gradient force in symmetrical cyclone, establishing clockwise direction motion possibility
20 p3663 A70-39275

Mode-generated average variables of atmospheric horizontal heat flux by transient cyclonic eddies used in mean motion circulation model
20 p3664 A70-40063

Tropical cyclone development model for axisymmetric vortex and quasi-balanced conditions, considering vertical heat distribution, rate of intensification and energy budget
23 p4213 A70-43896

CYCLOPROPANE
Cyclopropane-argon mixtures translational and vibrational energies exchange efficiencies analysis based on intermolecular potential
16 p2956 A70-34083

Molecular size dependent steric effects in translation-vibration energy transfer by velocity dispersions in cyclopropane-inert mixtures
21 p3780 A70-41706

CYCLOTRIMETHYLENE TRINITRAMINE
U RDX
CYCLOTRON FREQUENCY
Plasma stability in uniform magnetic and HF electric fields, observing magnetoacoustic wave generation at electron cyclotron frequency greater than HF field frequency
03 p0532 A70-13523

Numerical analysis of cyclotron amplification of geomagnetic micropulsations in magnetosphere based on dispersion relation for three component cold plasma beam system
05 p0838 A70-16284

Cyclotron frequency harmonics emission of PIG discharges linked to nonthermal electron plasma instability
07 p1354 A70-20316

PPi bursts interpreted as proton beams cyclotron instability in geomagnetic field
07 p1277 A70-20439

Excitation of plasma ion-cyclotron oscillations by ion beam passing through neutral gas along magnetic field, noting radial stabilization
10 p1926 A70-25118

Microwave radiation from electron beam generated turbulent magnetoplasma measured, indicating

enhancement near electron cyclotron harmonic frequencies 11 p2095 A70-26760

Beam-plasma system mode coupling near electron cyclotron frequency, obtaining interference patterns 13 p2459 A70-28570

Parametric excitation of potential oscillations in plasma near cyclotron frequency subjected to UHF electric and constant magnetic fields 13 p2463 A70-29281

Alouette 1 plasma resonance observations, analyzing electron density measurements in sheath region and cyclotron harmonic resonant frequencies 13 p2466 A70-29903

Local resonance at upper hybrid frequency from satellite observation, noting effects of electron plasma/cyclotron frequency ratio 13 p2370 A70-29911

Stochastic particle acceleration by VLF in weakly turbulent plasma in magnetic field, considering nonlinear cyclotron damping 13 p2468 A70-29935

Topside plasma frequency resonance below electron cyclotron frequency, discussing ray paths and delay times 20 p3620 A70-39336

Excitation of plasma ion-cyclotron oscillations by ion beam passing through neutral gas along magnetic field, noting radial stabilization 20 p3685 A70-40511

Cyclotron wave rectifier with Cuccia coupler for converting microwave power into DC or LF AC 21 p3756 A70-40730

Plasma and spiraling electron beam interactions, observing oscillations above integral multiples of electron cyclotron frequency 21 p3857 A70-41388

Cyclotron instability of high energy protons in magnetosphere with refraction of growing Alfvén waves 23 p4237 A70-44073

CYCLOTRON RADIATION

Normal and anomalous Doppler shifted cyclotron power radiated by energetic electrons spiralling along geomagnetic line considered as VLF source from magnetosphere 01 p0080 A70-11227

M-type transmission line with cyclotron waves to achieve phase inverter and delay line operation, showing phase sensitivity to magnetic field changes near cyclotron resonance 03 p0447 A70-13292

Cyclotron waves absorption study in bounded rarefied plasma having Larmor electron frequency exceeding plasma frequency 10 p1925 A70-25101

Proton cyclotron echoes in topside ionograms using Alouette 2 satellite data 12 p2226 A70-28064

Proton cyclotron echoes in topside ionograms from Alouette 2 satellite 13 p2396 A70-29092

Landau and Doppler-shifted cyclotron damping effects on helicon-like and plasma excitations of many-valley semiconductors 13 p2472 A70-30016

Warm homogeneous magnetoplasma longitudinal cyclotron harmonic wave propagation perpendicular to static magnetic field, noting instabilities 17 p3140 A70-34927

Nonlinear frequency shift for electronic and ionic cyclotron modes in magnetospheric whistler and hydrodynamic propagation, using Vlasov equation 23 p4187 A70-43880

CYCLOTRON RESONANCE

Cyclotron resonance maser (CRM)/monotron with inclined electron flux and magnetic field, considering design for performance optimization 03 p0499 A70-13455

Output characteristics of cyclotron maser with resonator field due to plane waves interference along static magnetic field, deriving tensor equations 05 p0858 A70-16260

Ionospheric resonances observed by swept frequency Alouette topside sounders, discussing plasma non-linearity 06 p1115 A70-17362

VLF and ULF whistler modes propagating along geomagnetic field-line paths in magnetosphere, studying cyclotron resonance amplification 06 p1118 A70-17379

Harmonic ion cyclotron resonances associated with proton whistlers observed from OGO-4 satellite VLF recordings 07 p1268 A70-19630

Pulsed grid modulation for ion cyclotron resonance spectrometer 07 p1286 A70-19974

Plasma ion cyclotron resonance acceleration in nonuniform magnetic field by RF field 07 p1353 A70-20229

Plasma ion-cyclotron oscillations resonance excitation in crossed electric and magnetic fields, describing instability development 07 p1354 A70-20319

Dialkyl ketone ion in double McLafferty rearrangement, applying ion cyclotron resonance to structural study 08 p1454 A70-20525

Electromagnetic instability measurements in electron cyclotron resonance plasma produced in magnetic mirror field 10 p1921 A70-23963

Nonlinear interaction between plasma and HF field near cyclotron frequency, studying plasma oscillations generation in strong magnetic field 10 p1925 A70-25102

Linear theory of cyclotron resonance maser with TEM standing wave field, considering coherent emission for nonrelativistic electrons oscillating in magnetic field 11 p2061 A70-25392

Ion cyclotron resonance spectroscopy technique for determining electrons photodetachment energy from negative ions in gas phase 11 p1995 A70-26001

Methyl fluoride calculated for ion-molecule reaction rate constants from ion cyclotron resonance spectra 12 p2180 A70-26862

Time decay of higher order cyclotron harmonic resonances with decreasing perpendicular wave number 13 p2467 A70-29908

Emission resonances at harmonics of electron cyclotron frequency in laboratory plasmas, considering stellar optical radiation 13 p2467 A70-29915

Bow shock associated hydromagnetic waves generation in upstream interplanetary medium, constructing model in terms of ion cyclotron resonance 14 p2631 A70-30359

Thermal product distributions and energy dependencies of ion-molecule reactions in allene and propyne, using ion cyclotron resonance 16 p2856 A70-33651

Ion-molecule reactions investigation by resonance principle, discussing ion paths in crossed fields 17 p3081 A70-34574

Fine structure of geomagnetic Pc 1 micropulsations by cyclotron instability due to anisotropic energetic proton velocity 19 p3410 A70-37334

Adiabatic bounce periods of particle gyrophase coherence in earth field for cyclotron echo and triggered emission analyses 20 p3621 A70-39343

Ion cyclotron resonance spectroscopy for detecting trapped gaseous ions in analyzer cell, observing ion-molecule reactions 23 p4196 A70-44390

Plasma heated by cyclotron resonance using waveguide method, considering properties, confinement conditions and instabilities 24 p4385 A70-45453

LF electrostatic ion cyclotron wave energy resonant power absorption in plasma in axially nonuniform magnetic field 24 p4386 A70-45608

LF instability in plasma produced by electron cyclotron resonance in nonuniform magnetic and electromagnetic fields 24 p4386 A70-45613

CYCLOTRONS

NT OMEGATRON
NT SYNCHROCYCLOTRONS

CYGNUS CONSTELLATION

Celestial X rays from Cygnus XR-1 detected during high altitude balloon flight, noting compatibility with black body radiation or hot thin plasma 02 p0356 A70-11786

Photometric measurements in Cygnus, analyzing formulas used for conversion to standard UBV system for Javan reflector/Sweden/ 02 p0297 A70-12065

SS Cygni outburst origin in G type star indicated from radial velocity variations of hydrogen absorption lines during rising light 05 p0915 A70-16695

Cygnus and Perseus symbiotic stars as binaries, studying radial velocities, relative emission line intensities and energy distribution 08 p1569 A70-20830

Brightness curves for eclipsing binary V448 Cygni indicating gas stream flows in system 08 p1577 A70-21441

Cygnus X region surveyed with NRAO radio telescope, estimating visual absorption by comparing radio and H alpha emission 10 p1937 A70-23943

Cygnus loop nebula H alpha line halfwidths and radial velocities 15 p2802 A70-32482

Luminosity criteria in O stars via narrow band photoelectric photometry suggesting VI Cygni proximity 15 p2807 A70-32804

CH Cygni irregular light variations and spectrum peculiarities, considering upper atmosphere perturbation by variable hot satellite 15 p2809 A70-32904

Balloon-borne X ray telescope star sensor with one arc minute accuracy, discussing design and Cyg X-1 location measurement 17 p3090 A70-35312

Soft X ray extended source in Cygnus Loop, indicating supernova remnant 18 p3310 A70-37022

P Cygni line profiles emission and absorption components rectification procedure, considering errors 18 p3321 A70-37123

Local spiral arm H 2 regions distribution in Cygnus direction, discussing symmetry due to magnetic field 18 p3329 A70-37180

Cygnus constellation energetic gamma ray emission by nuclear emulsion and spark chamber telescope on high altitude balloon 19 p3501 A70-38086

Extraterrestrial gamma radiation from Cygnus region of galactic disk, using OGO-5 observations 19 p3501 A70-38087

Spectrum analysis of P Cygni star AG Carinae and derivation of mean radial velocities for different epochs 19 p3523 A70-38694

Cosmic X ray spectra of Cyg XR-2 in 0.15-20 keV range by spinning rocket-borne detector, noting interstellar absorption 21 p3872 A70-40664

Cyg-X-1 X ray source angular size and position measurements by balloon-borne collimator 21 p3873 A70-40665

Cygnus X-2 point X ray source, establishing as spectroscopic binary with peculiarities 21 p3875 A70-40682

Light curve for eclipsing stars with scattering envelopes applied to V444 Cygni binary system 22 p4103 A70-42989

CYLINDERS

Eddy penetration model for heat transfer from trailing face of cylinder in transverse flow 09 p1791 A70-23566

Ideal fluid flow containing small spherical particles past cylinder and flat plate normal to stream using small perturbations method 11 p1976 A70-26012

Wakes of cylinder in collision-free plasma wind tunnel simulating ionospheric satellite conditions, noting decaying oscillation 11 p1976 A70-26018

Thermal stresses in temperature dependent multilayered cylindrically anisotropic hollow cylinders 12 p2321 A70-27203

Singularities of boundary layer conditions on parabolic cylinder in homogeneous incompressible viscous flow with leading edge, using Weyl integral equation 12 p2210 A70-27559

Rigid cylinder acceleration within elastic shell-core structure under pressure pulse distribution over shell semicircumference 13 p2518 A70-29984

Flat plate and cylinder with periodic Joulian heating from time dependent heat source, analyzing transient temperature distribution 14 p2664 A70-30269

Aerodynamic wake structure of cylinders and spheres in hypersonic rarefied gas flow as function of Mach and Knudsen numbers 16 p2836 A70-33756

Laminar near wake of cylinder at free stream Mach 6, using modified Lees-Reeves method 16 p2836 A70-33762

German monograph on shock wave diffraction at spheres and cylinders 17 p3071 A70-35377

Thin cylinder longitudinal two phase dispersed flow, examining heat transfer coefficient 18 p3345 A70-36112

Stationary heat conduction model of two cylinders abutting at ends with internal nonuniform temperature distribution 18 p3345 A70-36128

Electric field equations of plane EM wave diffraction at lattice of conducting cylinders, using Hankel function 19 p3375 A70-37289

Cylindrical EM waves diffraction by two parallel ideally conducting elliptical cylinders, discussing field and surface current distributions 19 p3378 A70-37734

Interference wave functions for diffraction on cylinder and sphere, including noninterfering waves of geometric optics 19 p3380 A70-38398

Heat transfer from cylinder in axial air flow with induced turbulence of incident boundary layer, noting temperature effects 20 p3736 A70-39264

Viscous fluid cylinders electromagnetodynamic stability, discussing viscous forces effects 21 p3858 A70-41699

Comparative analytic and experimental film boiling heat transfer for horizontal cylinders in helium II [ASME PAPER 70-HT-3] 22 p4122 A70-42441

Mach effect on cylinders, tracking triple point of shock interaction using 25-spark camera [SMPT PREPRINT 103] 22 p4032 A70-43032
Forced longitudinal oscillations of cylinder with given surface displacements, using Lamé equations 22 p4118 A70-43571
Tempering stress in circular plates and cylinders in casting of solid propellants 24 p4427 A70-46147

CYLINDRICAL AFTERBODIES

U AFTERBODIES

U CYLINDRICAL BODIES

CYLINDRICAL ANTENNAS

Plasma density and electroacoustic resonance effects on coupled cylindrical antennas self and mutual impedances measured in Hg-arc discharge 01 p0050 A70-10461
Driving point admittance of infinite cylindrical antenna excited by uniform gap and immersed in lossy compressible isotropic plasma, discussing propagation constants 01 p0051 A70-11102

Equatorial patterns measurement of plasma covered axially slotted cylindrical antenna, describing discharge tube, facility and Langmuir probe survey of tube electron density 02 p0269 A70-12590
Electromagnetic radiation patterns from aperture in conducting cylinder coated with moving isotropic plasma sheath, noting sheath velocity and plasma frequency influence 06 p1020 A70-17564

Collisions effects on cylindrical antenna impedance near plasma frequency of isotropic nonMaxwellian plasma, allowing for collision frequency dependence on electron energy 06 p1020 A70-17567
Element pattern derived for circular arrays of axial slits on large perfectly conducting cylinders, comparing properties with planar arrays 06 p1021 A70-17571

Cylindrical antennas immersed in arbitrary homogeneous isotropic media, solving integral equation for current 06 p1074 A70-18607
Thin cylindrical DC pulse driven antenna radiation fields time variation as function of angle 12 p2198 A70-27964

Numerical integration or quadrature technique for evaluating Fourier integrals in theory of infinite cylindrical antenna 13 p2440 A70-29088

Cylindrical electric dipole antenna in magnetoactive ionospheric plasma, noting ion sheath effect on input impedance and active length 13 p2399 A70-29402

Cylindrical antenna admittance during immersion in ionospheric plasma, noting influence of ion sheath and plasma anisotropy 13 p2371 A70-29922

Cylindrical and helical antennas impedance in cold magnetoplasma, using three dimensional integral involving Fourier transform and Green function 16 p2859 A70-32943

Radiation pattern of radial infinitesimal current elements near or on finite length conducting cylinders, using image and geometrical theory of diffraction techniques 16 p2860 A70-32956

Current distribution on isolated thin cylindrical center-fed dipole antenna, calculating axial electric fields and radiating properties 16 p2861 A70-32964

Wedge diffraction analyses of TE sub 10 mode slot radiation characteristics on circular and elliptical cylinder, considering boundary value solutions existence 16 p2861 A70-32965

Excited circular cylindrical dielectric rod antenna radiation patterns derivation by Schelkunoff equivalence principle 16 p2872 A70-33121

Cylindrical antennas and arrays for transmission or reception, determining radiation patterns 17 p3051 A70-35059

Directional solar thermal field /sunlight/ effect on coupled nonplanar transverse and torsional vibrations of satellite cylindrical antennas in orbit 20 p3720 A70-39676

Short cylindrical microwave antenna radiation directivity enhancement by optimum double impedance loading 20 p3599 A70-40318

Ionospheric plasma sheath effect around floating cylindrical high power dipole antenna, obtaining electron, ion and potential profiles 20 p3589 A70-40466

Cylindrical slot antennas radiation patterns in plane perpendicular to axis, discussing field emission and angular position of each slot for phase multiplier 22 p3997 A70-43131

Current distribution and near field of cylindrical antennas loaded with built-in lumped elements 22 p3998 A70-43422

Dielectric filled tubular monopole antenna driven by coaxial line with TEM mode, calculating current distribution from integral equation 23 p4175 A70-44953

CYLINDRICAL BODIES

NT ROTATING CYLINDERS

Lamb wave techniques using guided ultrasonic waves for solid cylindrical objects nondestructive testing 01 p0098 A70-10019

Viscous fluid flow due to long flat plate moving rectilinearly inside cylinder, assuming zero pressure gradient 01 p0062 A70-10801

Taylor model of elastoplastic wave interaction during cylindrical projectile impact 01 p0206 A70-11150

Homogeneous Love-Reissner equations analytical solutions for noncircular pyrolytic graphite cylinders, using asymptotic expansion for transverse materials isotropy 01 p0206 A70-11151

Laminar counterflow diffusion flame chemical structure and blow-off mechanism established in forward stagnation region of porous cylinder at atmospheric pressure 02 p0398 A70-12032

Mesothermal flow of collisionless plasma around conducting cylinder, calculating densities, velocities, temperatures and electrical potential [ONERA-TP-769] 02 p0346 A70-12102

Lamb waves behavior applied to defect evaluation in nondestructive tests of solid elongated cylindrical objects 02 p0276 A70-12552

Motion stability and time dependent deflections of thin flexible cylinder with zero bending rigidity in viscous stream 02 p0595 A70-13783

Wave drag in stratified flow lee waves without upstream influence calculated for cylindrical and three dimensional obstacles 03 p0479 A70-14229

Equipment for cyclic biaxial testing, producing five biaxial stress states by simultaneous direct pressurization and axial loading of thin walled cylindrical specimen 03 p0464 A70-14309

Thermoelastic stresses in solid cylinder under cyclic temperature variation, calculating amplitude for Biot numbers 04 p0766 A70-14477

Mean flow velocity distribution calculated from momentum deficit superposed behind single cylinders in finite array of arbitrarily spaced parallel cylinders [ASME PAPER 69-WA/FE-11] 04 p0614 A70-14781

Stiffener inclination effect on pressurized cylinder instability under pure bending [ASME PAPER 69-APM-X] 04 p0769 A70-14868

Configuration factors independence on Lambert law in radiation from spheres and infinitely long cylinders [ASME PAPER 69-HT-J] 04 p0784 A70-14870

Electromagnetic scattering from perfect conductors by numerical analysis, presenting far field pattern calculation for plane wave scattering from square cylinder 04 p0652 A70-15363

Ballistic range measurements of vibrational nonequilibrium effects on leading edge shock wave shape for cone-cylinders fired through chlorine atmosphere at supersonic speeds 04 p0621 A70-15601

Free stream turbulence effect on drag coefficient of bluff sharp edged cylinders with small square section 05 p0789 A70-15923

Torsion tests on cylindrical plastic metals, considering shear stresses calculation as function of torsion angle and changes determination as function of increasing cold work 05 p0927 A70-15996

Stress functions in three dimensional nonaxisymmetric elastostatics problems in circular cylindrical coordinates, proving representation completeness for cylindrical bodies 05 p0932 A70-16172

Unsteady heat conduction numerical approximation for infinite cylinder with variable heating and boundary conditions of third kind 05 p0936 A70-16294

Heat source temperature distribution on surface of infinite cylinder with zero temperature, presenting solution to boundary value problem 05 p0957 A70-16296

Saint Venant torsion and flexure of composite prismatic and cylindrical bars with circular and concentric interfaces 05 p0936 A70-16318

Cylindrical Al, high strength pig iron and heat resistant steels elastoplastic deformation diagrams for cyclic compression tension loads 06 p1084 A70-17387

Time to crack formation determined in cylindrical and flat Al and steel specimens having various surface properties under cyclic loads 06 p1084 A70-17392

Crack formation and propagation kinetics in flat and cylindrical Cr-Mo-V steels under tension compression loading cycles 06 p1162 A70-17393

Elastic-plastic torsion of convex cylindrical bars 06 p1165 A70-17534

Lift forces and pressure on vibrating cylinders in plane perpendicular to air flow measured in wind tunnel 06 p0968 A70-17545

Heat and mass transfer across laminar boundary layer around stagnation line of cylinder in crossflow affected by free stream turbulence intensity 06 p1176 A70-17693

Drag on infinite cylinder in hypersonic nearly free molecular flow for various angles of attack, using kinetic approach 06 p0983 A70-18380

Cylinder wakes in rarefied gas flow at Mach 20, obtaining density profile data from electron gun, impact pressure and cooled film probe measurements 06 p0984 A70-18387

Size and shape error distribution law for cross sections of cylindrical components, discussing probability characteristics 07 p1290 A70-18740

Laminar boundary layer development on cylindrical body set in motion from state of rest, determining time for boundary layer separation occurrence 07 p1253 A70-18771

Unsteady heat conduction in plate, solid or hollow infinite cylinder and sphere with internal heat source and radiative heat transfer on surface 07 p1423 A70-19818

Temperature stress distribution in cylinder or sphere with variable surface temperature and heated by external sources 07 p1411 A70-19819

Radiation detector geometrical factor approximation for cylindrical bodies, observing convergence for right square and circular cylinders 07 p1286 A70-19971

Gravitating particles systems equilibrium states, solving kinetic equations for sphere and cylinder in isotropic and anisotropic cases 07 p1389 A70-20207

Limiting equilibrium of rigid-plastic cylinder subjected to compression by concave stamps 08 p1583 A70-20533

Heat transfer from inner wall of annular ducted cylindrical body cooled by liquid nitrogen, discussing effects of Teflon, asbestos and vaseline coating and thickness effects 08 p1596 A70-20577

Electron density calculation for collisionless plasma flow around conducting cylindrical body, accounting for surface absorption and mean electron velocity [ONERA-TP-792] 08 p1550 A70-20595

Hypersonic flow past blunt cylinder at Mach number of infinity, investigating real gas effect using Lighthill ideal dissociating gas model 08 p1431 A70-20646

Aerodynamic characteristics of cylinder with wings in free molecular hypersonic flow of monoatomic gas at various angles of attack and slip 08 p1432 A70-21083

Rigid rotating cylindrical shaft vibrations along diameter in viscous fluid using inner and outer expansions method [ASME PAPER 69-APM-S] 08 p1589 A70-21307

External convective heat transfer coefficients from quartz-coated cylindrical hot film anemometer probes in mercury 08 p1599 A70-21582

Interaction between bodies and spherical detonation wave, measuring force pulse transfer to immobile cylinder and flow patterns past flying blunt body 09 p1659 A70-22186

Drag on cylinder in transverse rarefied gas flow varying from free molecular to almost continuum 09 p1604 A70-22448

Stokes flow around sphere moving along axis of cylinder with near-unity diameters relationship 09 p1661 A70-22839

Plane electromagnetic wave backscattering from dielectric-coated metallic cylinder calculated as functions of incidence angle and coating external radius 09 p1636 A70-23075

Elastic harmonic waves propagation in cylinder with longitudinal cavities and in space with cylindrical cavities solved using series method 09 p1783 A70-23387

Conduction to isothermal insulated cylinder from semifinite region 09 p1790 A70-23563

Nonlinear plane deformation of elastic medium with cylindrical cavity under uniform axial tension using successive approximations 09 p1784 A70-23591

Temperature field and combined radiative-convective heat flux in weakly absorbing cylindrical layer bounded by nonblack surfaces 10 p1966 A70-23866

Temperature field and heat conduction equation for two layer polymer cylinder multiply heated from within, considering material decomposition

10 p1966 A70-23870

Air flow turbulence intensity and plug effect influence on local heat exchange on cylinder surface

10 p1797 A70-24028

Stress-strain determination in nonuniformly heated thin walled cylindrical beams with nonlinear stringers and skin

10 p1957 A70-24281

Plane electromagnetic waves scattering from radially inhomogeneous cylindrical structure, deriving expressions for far field and cross section for both polarizations

10 p1841 A70-24856

Two dimensional electromagnetic wave diffraction on arbitrary shaped homogeneous dielectric cylinder, solving integral equations on digital computer

10 p1842 A70-25105

Cylindrical afterbody drag reduction in transonic flow by combined gas ejection and boat-tailing

11 p1976 A70-25991

Radiation heat transfer around interior of long cylinder as function of surface emissivity

11 p2149 A70-26152

Wall pressure fluctuations beneath turbulent boundary layers on flat plate and cylinder

11 p2038 A70-26529

Satellite aerodynamic characteristics, considering orbital position and attitude of cylindrical body and separate plate

11 p2128 A70-26795

Stress-strain state of epoxy resin cylinder situated in centrifugal force field using three dimensional photoelastic method

12 p2323 A70-27340

Plane harmonic wave steady state diffraction at cylinder in elastic half space, applying method of images

13 p2366 A70-29320

Cylinders and airfoils drag tests and simulation in two dimensional sheared flow, considering shapes optimization

[AIAA PAPER 70-576]

13 p2342 A70-29893

Axissymmetric postyielded tongue and groove cylindrical joint stress analysis using finite element method

14 p2659 A70-31131

Stress-strain relationships model for nonlinear restrained cylinders, using compression tests and finite element method

14 p2660 A70-31135

Force acting on cylinder in ideal incompressible fluid plane flow with steady vorticity

15 p2719 A70-31498

Pyroceramics transient strength measurements on cylindrical and prismatic samples under static bending

15 p2764 A70-31545

Monograph on momentum, heat and mass transfer rates to vertical continuous cylinder moving through quiet fluid in forced and free convection

15 p2825 A70-31694

Dimensional measurements of nuclear fuel cylindrical specimens by scanning neutron radiographic negative with microdensitometer, taking into account specimen geometry and neutron cross section

15 p2735 A70-31769

Laminar natural convective heat transfer along outer surface of vertical cylinder, giving coefficients nondimensionally by approximate formulas

15 p2826 A70-31821

Mixed forced and natural convection with low speed air flow over horizontal electrically heated cylinders

15 p2740 A70-32373

Acoustic and EM scattering by hyperbolic cylinder, considering plane wave incidence and line sources

15 p2700 A70-32406

Wave diffraction by parabolic cylinder, solving boundary value problems for two dimensional wave equations via separation of variables

15 p2700 A70-32408

Wave diffraction by half plane limit of parabolic cylinder and wedge, using Fresnel integral and Heaviside step function

15 p2700 A70-32409

Heterogeneous conducting fluid stability between fixed rigid cylinders with radiant gravitational force and magnetic field

16 p2894 A70-33784

Blunt based right circular cylindrical body at subsonic speed, investigating turbulent near wake in wind tunnel

17 p3006 A70-34463

Axissymmetric blunt base cylindrical body with turbulent initial boundary layer, investigating flow structure in annular nozzle wind tunnel

[AIAA PAPER 70-796]

17 p3006 A70-34464

Plane compressible sonic flow around symmetrical cylinder subjected to parallel incident flow, using function-theoretic method

18 p3241 A70-36378

Unsteady temperature fields in heat conduction problems associated with high temperature effects on abutted cylinders

18 p3348 A70-36572

Cylindrical body with gravitational and magnetic anomalies, selecting point coordinates for body parameters

19 p3407 A70-37298

Ring and cylindrical structures comparative stress relaxation at room temperature

19 p3535 A70-37341

Thermal stability test assembly for refractory materials cylindrical specimens, using argon plasma jet

19 p3395 A70-37351

One dimensional integral equations for two dimensional problems of EM wave diffraction by cylindrical bodies

19 p3376 A70-37435

Two axially positioned cylindrical waveguides with slots cut periodically along generatrices /double squirrel cage/, analyzing behavior under excitation by rotating charged filament

19 p3386 A70-37733

Two dimensional electromagnetic fields in presence of cylindrical objects of arbitrary physical properties and cross sections, using scattering matrix approximation

19 p3471 A70-37778

Lumped parameter model for multidimensional solid mechanics problems with inelasticity, discussing stress wave interaction in cylindrical cavity

19 p3458 A70-38357

Coulombian drag on body from hybrid calculus of collisionless plasma flow around cylinder

[ONERA-TP-819]

19 p3481 A70-38382

Cylindrical radiator radiation resistance and mass in waveguide with reflecting boundaries, calculating sound field for effect of medium reaction

19 p3472 A70-38656

Axissymmetric deformation of cylinder based on solution of elasticity theory plane problem for rectangular strip

20 p3724 A70-39858

Motion equation of electron in cylindrical diode subjected to varied voltages

21 p3796 A70-40640

Stagnation point heat transfer of spherical cylinder in argon and air, developing electrically insulated calorimeter gage theory

21 p3941 A70-40774

Forced convection heat transfer from flat plate and cylinder in cross flow to simulated Mars atmosphere

21 p3945 A70-41026

Loads induced by terminal shock boundary layer interaction on cone-cylinder bodies, discussing angle of attack effect

21 p3746 A70-41863

Arbitrarily shaped cylindrical conducting structures with transient incident electromagnetic wave, calculating scattering from integral equation by digital computer

23 p4165 A70-44957

Electromagnetic scattering by homogeneous gyrotropic cylinder, discussing matrix equations formulation and solution by reciprocity theorem

23 p4165 A70-44959

Frequency equations derived for cylindrical panels with surface loading, comparing free vibration natural frequencies of panels with attached mass at centers

24 p4422 A70-45297

Two identical conducting thin cylinders illuminated by plane wave at arbitrary incidence angle, determining backscattering cross sections and induced current

24 p4314 A70-46133

Peak pool boiling heat flux on horizontal cylinders, describing interactions of gravity and heater size effects

24 p4429 A70-46176

CYLINDRICAL CHAMBERS

Sound propagation along cylindrical duct of wind tunnel, discussing fluid flow effect on modal cut-off frequencies

04 p0719 A70-15078

Wall effect on differential spectra distortions in cylindrical ionization chamber and proportional counter type detectors

05 p0900 A70-15971

Time harmonic waves propagation in elastic half-space with submerged cylindrical cavity, assuming linear plane strain conditions

13 p2518 A70-30010

Velocity profiles in steady and unsteady rotating flows for impulsive slow down and acceleration in cylindrical chamber

19 p3403 A70-37527

CYLINDRICAL SHELLS

Steels tested to evaluate proposed incremental strain theories predicting loads on thin walled cylinders subjected to nonproportionate loading, discussing stress-strain diagram

01 p0202 A70-11057

Axially compressed cylindrical shells with edge constraints, determining critical load from inelastic behavior considerations

01 p0205 A70-11141

Nonlinear equations solvability for elastic cylindrical shells found existing for arbitrary load and clamping conditions

01 p0212 A70-11572

Asymptotic dynamic theory for elastic cylindrical shells incorporating thickness effects, considering longitudinal wave propagation in infinite length shell

02 p0385 A70-11877

Circumferential wave propagation around cylinder, demonstrating dependence on incident frequency and surface roughness, noting target surface microscale roughness measurement technique

02 p0339 A70-12184

Orthotropic cylindrical shell with initial deflection under long term effect of external hydrostatic pressure, solving bending problem

02 p0390 A70-12809

Internal hydrostatic or lateral pressure effect on deformations of infinitely long thin cylindrical isotropic shell subjected to equal concentrated radial loads

03 p0584 A70-12922

Incremental strain theories for nonproportionate loading of thin walled cylinders, discussing Tresca flow, von Mises theory and Prandtl-Reuss relations

03 p0480 A70-12953

Cauchy integrals extension to axisymmetric elasticity problems, obtaining numerical results for stressed circularly symmetrical state of hollow cylinder under uniform load

03 p0586 A70-13080

Axial stress pulse induced elastic waves propagation in thin anisotropic circular cylindrical shell of helical wrap construction allowing for shear coupling

03 p0587 A70-13118

Thin elastic cylindrical panel motion induced by plane acoustic shock wave analyzed by integrating nonlinear motion equations using finite difference scheme

03 p0524 A70-13377

Cylindrical shells buckling under biaxial compression and transverse loads, examining critical loads dependence on shell parameters, end conditions and elastic properties

03 p0590 A70-13380

Cylindrical two layer shells stability under compression and radial pressure, calculating compression and transverse shear strains in carrying layer and filler

03 p0592 A70-13443

Natural oscillation frequencies of partially liquid-filled cylindrical shells determined by resonance method

03 p0592 A70-13444

Axial compressive forces influence on steel and Al cylindrical shell stability under external pressure

03 p0593 A70-13472

Flexible cylindrical shell elastoplastic state determined by theory of small elastoplastic deformations, utilizing material incompressibility in plastic state

03 p0593 A70-13500

Circular cylindrical shell stressed state with rectangular opening under compressed torsion, noting opening effect on loads nonuniform distribution

03 p0593 A70-13501

Unsteady heat conduction in hollow cylinder, using transfer functions to solve direct and inverse two dimensional problems

03 p0606 A70-13520

Nonlinear flexural vibration properties of thin circular cylindrical shells with simply supported ends assuming deflection mode

03 p0594 A70-13549

High speed photography for instability onset and subsequent buckling process in photoelastic circular cylindrical shells under axial compression

03 p0594 A70-13659

Stress-strain state of arbitrarily cracked cylindrical shell under symmetric and asymmetric loading

03 p0594 A70-13736

Residual stresses in cylindrical shells eliminated by local heat treatment, determining temperature field in elastic strain regions

03 p0497 A70-13739

Transient creep analysis of simply supported circular cylindrical shells subjected to internal pressure based on strain and time hardening theories

03 p0595 A70-13813

Radial vibration of cylindrical shell of transversely isotropic material determined using finite Hankel transform

03 p0595 A70-13904

Far nonlinear postbuckling behavior of noncircular cylindrical shell under axial compression

03 p0598 A70-14241

Natural oscillations and flutter of three layer cylindrical shell in supersonic gas flow analyzed by semimomentless theory, discussing boundary value problems, damping effects, etc

03 p0600 A70-14301

Donnell shallow circular cylindrical shell equation, obtaining approximate solution for stresses in infinitely long circular cylindrical shell with circular hole subjected to edge loading

03 p0601 A70-14320

Finite strain in bending rectangular block into right circular cylindrical shell for transversely isotropic medium along radius vector, using Saint Venant stress-strain relations

03 p0602 A70-14329

Perturbed motion of solid body with cylindrical cavity partially filled with viscous fluid, using Rabinovich equations

04 p0766 A70-14476

Supercritical strains and buckling in rib-reinforced cylindrical shells under axial compression using strain-energy method

04 p0766 A70-14478

Damping factor of fiberglass-reinforced cylindrical shells, concerning dependence on wave number and energy losses due to medium resistance and acoustic radiation

04 p0712 A70-14488

Gravity and size effects on film boiling from horizontal cylinders, recommending formulas for wavelength and minimum heat flux predictions

[ASME PAPER 69-WA/HT-12] 04 p0784 A70-14821

Elastic postbuckling behavior of axially stiffened and barreled cylindrical shells

[ASME PAPER 69-APM-U] 04 p0769 A70-14866

Thin orthotropic composite cylindrical shells buckling under axial and radial loads, satisfying end boundary conditions for clamped and simply supported shells

[ASME PAPER 69-WA/APM-21] 04 p0771 A70-14910

Initial deflection effect on elastic cylindrical shell stability under compression, finding critical load by determining limiting point in successive loading

04 p0773 A70-15009

Thermal buckling of elliptic cylindrical shells assuming tangential temperature, constant axial pressure and conservation of elastic properties

04 p0775 A70-15203

Principal instability region of hinged cylindrical shell under dynamic loading

04 p0776 A70-15271

Orthotropic sandwich cylinders buckling under axial compression, presenting linear theory approximate design equations

04 p0776 A70-15381

Spectral response of cylindrical shell due to random acoustic pressure input computed using modal approach

04 p0778 A70-15528

Material coupling in two layered orthotropic cylindrical shell subjected to normal external pressure

04 p0778 A70-15547

Circular cylindrical shells with axisymmetric imperfections tested under axial compressive load, studying imperfection amplitude and wavelength effects on minimum buckling load

04 p0778 A70-15588

Thin cylindrical circular shell and three layered plate, analyzing vibration and stability due to loads and temperature

05 p0926 A70-15916

Pseudocylindrical concave polyhedral shells proposed from postbuckling configurations analysis, considering rigidity and structural applications

05 p0928 A70-16039

Buckling equations for neutral equilibrium of arbitrary elastic shells specialized to uniformly loaded circular cylindrical shell with accuracy

05 p0929 A70-16064

Stability, critical load and strength algorithm for fiberglass reinforced cylindrical plastic shells under external load allowing for shear stresses

05 p0933 A70-16211

Statistical stability of cylindrical fiberglass reinforced plastic shells under axial compression, showing breakdown loads vs radius/thickness ratio

05 p0933 A70-16215

Stability of clamped, hinged and elastically supported circular cylindrical shells under critical combined torsional and transverse pressure

05 p0934 A70-16227

Buckling of three layer cylindrical shells under steady creep conditions, deriving axisymmetric deformation

05 p0935 A70-16234

Compressive forces eccentricity influence on circular cylindrical shell stability noting relation to bending moments

05 p0936 A70-16239

Isotropic elastic cylindrical shell stability under combined compressive and axisymmetric local loads, using equilibrium equations for shallow shells

05 p0936 A70-16240

Unsteady vibrations of cylindrical thin walled elastic closed shell under random loads, using correlation method

05 p0937 A70-16371

Rayleigh and Lamb waves propagating on solid and hollow elastic cylinders immersed in water, noting correspondence to symmetric and antisymmetric vibrations in shell

05 p0938 A70-16410

Stress concentration in long thick cylindrical tube under diametrically opposite normal loads using elasticity theory

05 p0939 A70-16505

Circular cylindrical shells stiffened by rings and stringers and subjected to periodic axial force, analyzing parametric instability

05 p0940 A70-16513

Fatigue crack propagation and fracture toughness in pressurized thin walled cylindrical tubes, basing analysis on shallow shell bending theory

05 p0942 A70-16802

Thermal stresses in shell with spherical and circular cylindrical sections, using thin shell approximations and shallow shell theory

05 p0945 A70-16818

Small elastoplastic deformation effects on stress-strain state of rib-reinforced cylindrical shells

05 p0946 A70-16955

Hydrodynamic coefficients of algebraic equations for boundary value problems in disturbed motion of body with rib-reinforced liquid filled cavity

05 p0836 A70-16956

Stress concentration of circular cylindrical shell weakened by elliptic hole under torsion

05 p0947 A70-16965

Cylindrical shell walls vibrations under impact loads, calculating damping factor in differential equation of motion of wall element

05 p0947 A70-17008

Membrane reinforced thin walled cylindrical shells stability as asymmetric contact problem in shell and plate theory

05 p0947 A70-17011

Three dimensional stress-strain analysis of rotating finite hollow cylinder, emphasizing wall thickness effect on stress and strain distribution

06 p1160 A70-17130

Conducting cylindrical shell in constant magnetic field analyzed for magnetoelastic disturbances using Laplace transform

06 p1056 A70-17607

Thin shell buckling stressing maximum applied loads analysis for circular cylindrical shells with imperfect walls under axial compression

06 p1165 A70-17647

Stability analysis of deflected shallow thin walled elastic noncircular conical and cylindrical orthotropic shells using straight lines method

06 p1167 A70-17865

Stress and buckling measurement of shallow cylindrical steel shells linked to thin plate using resistant strain gauges and high precision indicators

06 p1167 A70-17866

Thin walled cylindrical shells design for axisymmetric impulsive loads, calculating strains due to explosive forming in water

06 p1167 A70-17867

Nonlinear postbuckling equilibrium of thin cylindrical shell and axisymmetric buckling pressure of imperfect spherical shell calculated by Rayleigh-Ritz method

[AIAA PAPER 70-102] 06 p1169 A70-18036

Thin walled cylindrical shell stability under stochastic lateral and axial compression loads using Liapunov method

[AIAA PAPER 70-104] 06 p1169 A70-18037

Semiinfinite simply supported cylindrical shell transient response due to axisymmetrically engulfing step pressure wave, investigating moving load critical velocity

[AIAA PAPER 70-18] 06 p1170 A70-18063

Local axisymmetric dimple imperfection effects on buckling load of circular cylindrical shell under axial compression

[AIAA PAPER 70-103] 06 p1170 A70-18167

Thin circular cylindrical shells elastic equilibrium under loads producing deflection, elongation or contraction described by integrating equilibrium equations with constant coefficient

06 p1172 A70-18566

Structural analysis of thin walled cylinder material using normal ultrasonic wave to achieve high resolution determination of components

06 p1172 A70-18630

Elastic behavior of joint formed by normally intersecting circular cylindrical shells under external bending moment, noting applicability to pipelines and pressure vessels

[ASME PAPER 68-WA/PVP-1] 07 p1400 A70-18710

Cylindrical shell of revolution stress-strain state calculated during shaping in stamp with unclamping dies

07 p1292 A70-18836

Cantilever cylindrical shell stability under shearing stresses created by transverse force applied to free end

07 p1403 A70-19116

Notched cylindrical shells of nonuniform thickness using two dimensional photoelastic models mounted on elastic foundations

07 p1249 A70-19239

Circular cylindrical shells creep buckling under nonuniform external loads, considering thermal effects and initial imperfections

07 p1405 A70-19253

Axially uniform stress and strain in cylindrical shells, discussing Saint Venant torsion and displacement relations

07 p1405 A70-19255

Shell elastic constants for multilayered sandwich cylinders using Donnell approximation

07 p1406 A70-19326

Buckling stress calculation and measurement in cylindrical fiberglass reinforced composite shells under axial pressure

07 p1409 A70-19756

Circular cylindrical shells buckling under lateral and hydrostatic pressure using Donnell and Flugge equations, assuming membrane stress state for prebuckling deformation

07 p1414 A70-20168

Axisymmetric elastoplastic deformation theory for elastic cylindrical shell using Saint Venant yield condition, obtaining expressions for strain components, longitudinal deformation, etc

07 p1415 A70-20185

Initial perturbation effect of smooth cylindrical shells stability under critical axial compression noting deflection factor

07 p1415 A70-20190

Natural axisymmetric vibrations of cylindrical shell with hollow filler, analyzing motion by shallow shell and elasticity theory dynamic equations

07 p1415 A70-20191

Equilibrium of torque-free cylindrical shell vertically positioned and partly filled with liquid, obtaining solution for biaxial stress

07 p1415 A70-20192

Rib-reinforced cylindrical shells stability under longitudinal compressive loading, studying stress-strain state using network method

08 p1583 A70-20528

Strain energy method applied to stability analysis of short longitudinally reinforced cylindrical shells under axial compression

08 p1584 A70-20536

Stress concentration on isotropic elastic circular cylindrical shallow shell using plane waves and spherical means method, obtaining periodic solutions convergence

08 p1585 A70-20963

Shear stress in thick cylindrical closed shells subjected to plastic torsion determined from displacement distribution over thickness and generatrix

08 p1588 A70-21182

Thin shells of revolution natural oscillation frequencies approximation based on shell subdivision into series of cylindrical shells

08 p1588 A70-21194

Rectangular planform shallow cylindrical shell parametric vibrations using method applied to large bending vibrations of plates

08 p1588 A70-21212

Linear and nonlinear equilibrium equations for bending deformation of thin elastic cylindrical using Kirchhoff-Love hypotheses

08 p1588 A70-21242

Elastic/perfectly plastic hollow cylinder unloading under monotonic twist during torsion, considering sandhill-membrane analog validity

08 p1589 A70-21249

Circular cylindrical shell supported along generator under arbitrary forces using finite Fourier transform, simplifying results by Euler sum formula

08 p1589 A70-21312

Cylindrical and flat shells equilibrium equations representation using stress, deflection or tangential displacement functions

08 p1591 A70-21442

Stiffeners inclination effects on instability of pressurized cylinder under bending by Ritz method, considering finite deflection and initial imperfections in strain-displacement relations

08 p1591 A70-21464

Transient radial temperature distributions in cylindrical shells via Carslaw and Jaeger procedure involving binomial theorem and asymptotic expansions of Bessel function

08 p1599 A70-21588

Asymptotic analysis for axisymmetric buckling of axially compressed short cylindrical shells with free edges, using Batterman method

08 p1593 A70-21620

Dynamic response of infinite cylindrical shell subjected to arbitrary time and space dependent forcing function in acoustic medium

08 p1593 A70-21621

Cylindrical shells buckling under axial surface tensions using Donnell stability equations

08 p1593 A70-21624

Flugge characteristic equation approximate roots for closed cylindrical shell compared with Donnell equation solution

08 p1593 A70-21625

Cylindrical shell vibration modal characteristics finite element solutions accuracy compared with exact solutions

08 p1596 A70-21979

Elastic body equilibrium forms bifurcation solution for uniform strain applied to cylindrical rod and shell under compressive strain

09 p1773 A70-22539

Temperature distribution in infinite and finite circular hollow cylinders, considering surface heat flux and linear heat transfer

09 p1788 A70-22595

Spherical and cylindrical cavities dynamic plastic expansion analysis by finite element method allowing for inertia forces

09 p1777 A70-22724

Temperature fields in cylindrical shell under axisymmetric heating, ensuring optimal stressed state

09 p1778 A70-23081

Algorithm for stress-strain state calculation of nonuniformly heated cylinder weakened by star-shaped cavity

09 p1779 A70-23094

Buckling and postbuckling equilibrium behavior of fiber reinforced cylindrical shell under uniform axial compression

09 p1780 A70-23207

Buckling of elastic cylinders with rectangular cut-outs and reinforcements under axial or lateral loading, using modified Newton method

[AIAA PAPER 69-92] 09 p1780 A70-23208

Free vibration of rib stiffened freely supported circular cylindrical shells, verifying rib eccentricity importance to natural frequencies by numerical solutions

09 p1780 A70-23211

Plastic buckling of eccentrically stiffened circular cylindrical shells with multiple isotropic layers under combined axial and lateral pressure, deriving stability criterion

09 p1780 A70-23213

Stress analysis for cylindrical shells with reinforced circular holes by collocation method

09 p1781 A70-23280

Elastic cylindrical shells stability under uniform pressure, calculating critical transverse load by finite-difference computer program

09 p1781 A70-23287

Reinforced cylindrical shells stress-strain state under concentrated longitudinal loads, considering ribs of variable rigidity

09 p1782 A70-23289

Cylindrical shell critical load boundaries under uniform external stress and small torsion

09 p1783 A70-23389

Elastic ribs reinforced thin cylindrical shells stress-strain state under arbitrary load distribution allowing for rib spacing discreteness

09 p1784 A70-23590

Three dimensional deformation of finite circular cylindrical shell under plane shock wave solved in linear form

09 p1785 A70-23618

Axisymmetric free vibrations of orthotropic cylindrical shell loaded on ends by constant axial force, investigating nonlinear elasticity

09 p1785 A70-23625

Stress distribution in rib reinforced cylindrical shells under concentrated forces calculated using finite difference scheme

09 p1791 A70-23718

Reinforcing ribs eccentricity effect on closed circular cylindrical shell stability using strain energy method

09 p1786 A70-23720

Axial tensile stress effects on stability of cylindrical shell under nonuniform external pressure

09 p1786 A70-23721

Cylindrical shell stability under combined torsion and internal pressure, noting yield point effect on critical load, obtaining buckling-internal pressure relationship

09 p1786 A70-23722

Flow rule for viscoplastic symmetric cylindrical shells, using constitutive equations for strain rate sensitive materials based on Huber-Mises yield condition

10 p1954 A70-24020

Stress-strain state analysis of prestained thin circular cylindrical shell using Vlasov general shell theory

10 p1955 A70-24021

Eccentricity and clamping effects on stability and critical pressure of ring-reinforced cylindrical shells under internal pressure

10 p1956 A70-24248

Minimum weight design for symmetrically stiffened cylindrical shells under compression based on linear orthotropic stability theory

10 p1958 A70-24560

Forced vibrations of cylindrically curved multispan shell structures, using transfer matrix methods

10 p1962 A70-25062

Transient creep analysis of pressurized circular cylindrical shells based on strain and time hardening theories

10 p1963 A70-25089

Rapid expansion of thin walled aluminum alloy cylinders under pulsed magnetic field pressure using high speed streak camera oscillography

10 p1964 A70-25120

Thin cylindrical shell stresses and displacements enclosed in elastic casing under pressure band using classical theory of Flugge and Love functions

11 p1218 A70-25336

Axisymmetric elasticity theory problem solution for hollow finite cylinder with symmetrical end loading, employing stress function

11 p1218 A70-25388

Homogeneous boundary value problems in stability theory of circular cylindrical shells axisymmetric equilibrium state

11 p1219 A70-25396

Eccentrically stiffened thin circular cylindrical shell stability under torsion emphasizing exact finite formulas derivation

11 p1219 A70-25561

Random displacement fields in thin circular cylindrical shells with initial imperfections under axial compression using statistical analysis

11 p1219 A70-25562

Stability loss in cylindrical shell under axial compression, noting critical load reduction by local axisymmetric depression

11 p1230 A70-25566

Clamping edges effect on critical parameters of cylindrical orthotropic shell under axial compression using undetermined Lagrange multipliers

11 p1230 A70-25567

Load carrying capacity of isotropic rigid-plastic shells of revolution with different yield points under tension and compression applied to spherically coupled cylinders

11 p1234 A70-25932

Panel flutter theory applied to aeroelastic stability of flat unloaded plates and cylindrical shells

11 p1234 A70-25951

Cylindrical shell segments supersonic flutter boundaries engineering estimates related to Saturn 5 booster, obtaining thickness requirement as function of panel geometry

11 p1234 A70-25959

Characteristic equation roots for circular cylindrical shells deformation under edge load

11 p1235 A70-25960

Stiffened cylindrical shells under internal pressure numerically analyzed based on C-5A fuselage material parameters

11 p1235 A70-25961

Truncated conical shell buckling under axial compression using method for torsion buckling, correlating to equivalent cylindrical shells

11 p1235 A70-25980

Transient bending and shear stresses at clamped support of orthotropic circular cylindrical shells

11 p1235 A70-25985

Initial geometric imperfections effect on buckling and postbuckling behavior of laminated composite cylindrical shells under axial compression, considering reinforcing fiber orientations

11 p1235 A70-25986

Inplane and rotary inertia effects on free vibration frequencies of circular cylindrical shells eccentrically stiffened by orthogonal set of stringers and/or rings

11 p1235 A70-25993

Free vibration characteristics of circular cylindrical shells of finite length, utilizing Flugge equations

11 p1235 A70-25997

Membrane theory for thin single layer orthotropic cylindrical shells experiencing harmonic axisymmetric motion

11 p1236 A70-26084

Finite element method using shallow shell stiffness matrix extended to cylindrical shell solution

11 p1238 A70-26159

Thin cylindrical shells of perfectly plastic rigid material, analyzing dynamic plastic deformation under internal impulsive pressure

11 p1239 A70-26413

Vibrations of combination of cylindrical shells and circular plates, giving bending moment distribution

11 p1239 A70-26415

Buckling load calculations for axially compressed circular cylindrical shells under relaxed boundary conditions

11 p1240 A70-26484

Cylindrical shells plastic flow buckling under radially inward impulsive loading, showing mode number dependence on shell length

11 p1240 A70-26486

Vibration equations for closed and open sandwich cylindrical shell with thickness-shear deformation in core and face layers compared with membrane theory

11 p1245 A70-26697

Axisymmetric and unsymmetric free vibrational modes of right-circular conical or cylindrical sandwich shells with free edges, discussing Rayleigh-Ritz solution

11 p1245 A70-26700

Natural frequencies of thin cantilever cylindrical shells, using Flugge equations of motion and Rayleigh-Ritz method

11 p1246 A70-26704

Cylindrical shell response to random acoustic excitation, considering single point transfer functions and equivalent force power spectral densities

12 p2317 A70-27125

Automated optimum structural design by variable step direct search algorithm, noting application to stiffened cylindrical shells

12 p2319 A70-27138

Stiffened fiber composite cylindrical shells minimum weight design, discussing configuration and material parameters

12 p2319 A70-27139

Axisymmetric imperfection distributions effect on buckling of circular cylindrical shells under axial compression, constructing test models from photoelastic liquid epoxy

12 p2319 A70-27140

Stiffened cylindrical shells buckling under axial compression, obtaining imperfections and prebuckling growth mappings

12 p2319 A70-27141

Cylindrical shells design under axially compressed loads by elastic stability analysis, predicting critical loads

12 p2320 A70-27142

Thermal buckling theory for multilayered stiffened cylindrical shells under various combined loads

12 p2321 A70-27149

Axially stiffened and barreled cylindrical shells elastic postbuckling behavior, considering effects of stringer and load eccentricities

12 p2321 A70-27175

Thin cylindrical shells elastic buckling under uniform axial compression, considering Kirchhoff-Love hypotheses in critical stress determinations

12 p2324 A70-27396

Glass-plastic thin cylindrical shells carrying capacity dependence under axial and external loads on combinations of longitudinal and transverse reinforcing layers

12 p2259 A70-27527

Metallic cylindrical shells design reinforced with elastic glass fiber rings, considering elastoplastic deformation

12 p2324 A70-27530

Hollow homogeneous polymer cylinder thermoelastic stressed state, analyzing radial temperature and Poisson Coefficient variations

12 p2325 A70-27532

Pressurized orthotropic cylindrical membrane shells free and forced vibration, considering dynamic response dependence on internal pressure

12 p2326 A70-27815

Fiberglass plastic cylindrical shells stability against creep under prolonged hydrostatic pressure, obtaining critical loading times

12 p2328 A70-28278

Strain induced in laminated orthotropic fiberglass plastic cylindrical shell by normal concentrated load, using equations free from rectilinear normals hypothesis

12 p2328 A70-28279

Cylindrical shells stability under axial compression by two dimensional Kirchhoff-Love applied theories, calculating critical stresses

12 p2328 A70-28282

Stress concentration in fiberglass reinforced plastic composite cantilever cylindrical shell in round hole region subjected to concentrated load on free supported end

12 p2328 A70-28286

Residual stresses in cylindrical shell made of two component solid solution under thermal diffusion

12 p2329 A70-28323

Ablation and temperature effects in hollow viscoelastic cylinder

13 p2508 A70-28487

Slender cylindrical shell loaded by internal pressure analyzed using numerical procedure developed for digital computer

13 p2512 A70-28981

Thin walled duralumin cylinders catastrophic fracture analysis by linear elastic fracture mechanics noting fatigue crack propagation

13 p2434 A70-29173

Laminated glass fiber reinforced cylindrical shell stability resting on hinged supports under axial compression

13 p2514 A70-29285

Initial thermal stresses effect on natural oscillation frequencies of thin cylindrical elastic shells, obtaining linearized equations of motion and boundary conditions

13 p2514 A70-29286

Critical loads and stability of isotropic cylindrical shells under uniformly distributed longitudinal compression loads based on network method

13 p2514 A70-29287

Stability loss of nonreinforced and reinforced cylindrical shells under external pressure

13 p2514 A70-29294

Radial displacements in cylindrical circular shell by impinging spherical waves propagating in acoustic medium, deriving equations by Fourier and Laplace transforms

13 p2515 A70-29318

Thermal stresses dependence on temperature field during axisymmetric heating of rigid cylindrical shells

13 p2421 A70-29426

- Elastic material filled cylindrical, segmented to radial and conical shells thermal stability, allowing for stiffener eccentricity 13 p2516 A70-29523
- Shallow shell solutions complete with respect to finite simply connected surface region applied to circular cylindrical shells 13 p2517 A70-29758
- Linear compressive orthotropic stability theory for shallow-stiffened cylinders 13 p2518 A70-30022
- Cylindrical propellant tanks dynamic stability and parametric resonance, analyzing axial preload, liquid depth top impedance and ullage pressure by Donnell theory 14 p2657 A70-30764
- Stress distribution in aeolotropic cylindrical shell due to shearing force varying linearly and quadratically with depth on inner boundary 14 p2658 A70-30994
- Cylindrical shell nonaxisymmetric vibration frequencies and boundary values relation, using Lagrangian 14 p2661 A70-31273
- Two dimensional stress-strain fields under elastic and elastic-plastic strains and steady state creep, calculating stress distribution around hole in cylindrical shell 15 p2813 A70-31533
- Stress-strain state of catenoid, cylindrical and spherical shells of revolution, emphasizing catenoid shell bending problem 15 p2815 A70-31648
- Thin cylindrical shells flutter analysis in supersonic flow, using linearized potential theory 15 p2815 A70-31916
- Cylindrical shells with longitudinal rib reinforcements, deriving yield surface from strain mapping and collapse under pressure 15 p2816 A70-32006
- Internal pressure deformation of thin cylindrical shells of materials with nonlinear stress-strain relations, considering Al alloy shell and axial strain 15 p2816 A70-32009
- Cylindrical shells upper critical loads calculation based on linearization of nonlinear shell theory equations 15 p2818 A70-32181
- Cylindrical conical shell junction axisymmetric bending, using numerical method and exact solution 15 p2822 A70-32360
- Cylindrical shells under axial compression, using elastic stability analysis for critical loads prediction 15 p2822 A70-32512
- Small displacements in noncircular cylindrical shells under various loads 16 p2987 A70-32992
- Normally intersecting closed cylindrical shells subjected to internal hydrostatic pressure, using Donnell shell theory 16 p2990 A70-33678
- Probabilistic model for radiative transfer of photons in inhomogeneous infinite cylindrical shell medium, noting radiation intensity relation to scattering and transmission functions 16 p2952 A70-33785
- Combined internal pressure and axial loading influence on aeroelastic stability of thin walled cylindrical shell in supersonic flow field 16 p2991 A70-33851
- Thin concentric circular cylindrical shells joined at ends by rigid diaphragms, describing free and forced torsional motion 16 p2992 A70-34019
- Vibrations of shells, plates and membranes carrying dynamic systems at discrete points on surface, obtaining eigenfunction and eigenvalue equations 16 p2993 A70-34090
- Stability analysis of anisotropic cylindrical shells under combined loadings using inverse operators 16 p2994 A70-34246
- Free vibration of thin circular cylindrical shells, comparing experimental results to Egle-Sewall analysis 17 p3181 A70-34520
- Anisotropic and laminated cylindrical shells geometric design for reduction of elastic stress gradients to predetermined limit 17 p3182 A70-34559
- Polycarbonate thin walled cylindrical shells mechanical and material stability under torsion 17 p3127 A70-34656
- Circular cylindrical shells with clamped ends, investigating supersonic panel flutter by two mode approach and Galerkin method 17 p3184 A70-34695
- Displacement bounding principle for finitely deforming rigid plastic structures exhibiting geometric stability, with application to cylindrical shell 17 p3184 A70-34906
- Composite orthotropic cylindrical shells linear thermoelastic equations solution for fixed end boundary conditions, noting heterogeneity effects on stress distribution 17 p3184 A70-34909
- Analog simulation of elastic wave propagation in thick walled hollow circular cylinders to determine safe impact speed 17 p3185 A70-34964
- Solutions for normal and tangential displacements and concentrated forces on shallow cylindrical shells 17 p3186 A70-34969
- Membrane and bending stresses at crack tip in cylindrical shell weakened by elliptic hole with major axis perpendicular to shell axis 17 p3186 A70-34981
- Axially loaded cylindrical shells prebuckling deformation behavior measurement by holographic interferometry 17 p3086 A70-35012
- Supersonic panel flutter of circular cylindrical shells at critical dynamic pressure 17 p3188 A70-35227
- Unsymmetric vibrations of cylindrical shells, analyzing stress states by asymptotic method 18 p3335 A70-36059
- Circular cylindrical shell with round holes along generatrix subjected to internal pressure, determining stress concentration with aid of computer 18 p3335 A70-36131
- Cylindrical shell of variable thickness, deriving axisymmetric thermal stresses in terms of hypergeometric functions 18 p3336 A70-36137
- Cracks and tensile failure of interface bonds in elastic composite hollow cylinder, deriving wave front propagation equations 18 p3283 A70-36388
- Solid or hollow anisotropic elastic cylinders rotating with variable angular velocity, determining dynamic response by Hankel and Laplace transforms 18 p3338 A70-36433
- Elastic and plastic cylindrical shells, investigating dynamic buckling under impulsive loads 18 p3338 A70-36436
- Stability of circular cylindrical shell reinforced by elastic rings at edges under longitudinal compression 18 p3341 A70-36581
- Cyclic plastic breakdown of thin cylindrical shell under ring shaped load in temperature field, using linear programming method 18 p3341 A70-36585
- Thin circular cylindrical shell stability subjected to axisymmetric thermal pulse, describing buckling process by mathematical model 18 p3342 A70-36641
- Limit load of cylindrical shell with rigidly clamped edges under varying pressure and axial force, using Tresca yield condition 18 p3343 A70-36722
- Thin walled cylindrical shell stability under axial compression edge load beyond limit of proportionality 19 p3534 A70-37243
- Shallow circular cylindrical shell with rigid collar on lateral surface, calculating stress under axial tension and internal pressure loading 19 p3534 A70-37245
- Stress and displacement within internally pressurized composite cylinders having continuous fiber reinforcement in circumferential direction, using finite element method 19 p3538 A70-37797
- Core-filled thin cylindrical shell under radial ring and band pressure loads, using Boussinesq-Neuber stress function and Flugge shell theory 19 p3543 A70-38247
- Blast loaded cylindrical shell collapse hinge dynamic instability prediction by mathematical model 19 p3545 A70-38334
- Long orthotropic pressurized circular cylindrical shell under radial line loads along equally spaced generators, analyzing stresses and deflections by linearization 19 p3545 A70-38338
- Thin plates and thin walled cylinders aeroelastic stability in fluid flow, analyzing panel flutter 19 p3546 A70-38342
- Prebuckling deformations effect on buckling of clamped thin walled circular cylindrical shells under axial loading and internal pressure 19 p3546 A70-38346
- Shallow shell solutions complete with respect to finite simply connected surface region applied to circular cylindrical shells 19 p3547 A70-38396
- Sound propagation in cylindrical waveguide with impedance walls in presence of flow 19 p3472 A70-38655
- Straight thin walled elliptical cylindrical shells stability in pure bending, solving boundary value problem 19 p3550 A70-38683
- Stress concentration on isotropic elastic circular cylindrical shallow shell using plane waves and spherical means method, obtaining periodic solution convergence 20 p3719 A70-39385
- Cylindrical shells subjected by sectors to constant radial pressure, investigating stress state and deformation 20 p3719 A70-39620
- Three dimensional photoelastic analysis of stresses and strains in hollow circular cylinders with conical ends bonded to shell and shrunk 20 p3720 A70-39686
- Axisymmetric contact problem of hollow semi-infinite elastic cylinder subjected to stresses on lower end face, solving by Fourier integral transform 20 p3720 A70-39734
- Creep and breakdown of thin walled cylindrical shells with circular holes subjected to internal loads at high temperature, discussing time to failure 20 p3721 A70-39777
- Cylindrical shells dynamic stability under uniform radial pressure 20 p3722 A70-39786
- Thin walled circular cylindrical steel shells dynamic stability partly filled with liquid and subjected to longitudinal excitation 20 p3723 A70-39852
- Long thin circular cylindrical shell resonance velocities in steady response to fluid motion 20 p3727 A70-39884
- Structurally closed orthotropic circular cylindrical reinforced shell stability, developing approximate method to obtain various boundary conditions 20 p3727 A70-39886
- Circular cylindrical shells theory based on Novozhilov equation, deriving auxiliary formulas for strain and displacement characteristics in terms of stress function 20 p3727 A70-39888
- Asymmetric closed and cylindrical shells variable surface machining for desired wall thickness profile by chemical milling with digital computer numerical control 20 p3637 A70-39942
- Cylindrical or tapered composite shell structures optimal design with closed circular or elliptical cross section under combined bending and torsional loads 20 p3730 A70-40043
- Homogeneous boundary value problems in stability theory of circular cylindrical shells axisymmetric equilibrium state 20 p3732 A70-40100
- Finite deflection discrete element analysis of sandwich plates and cylindrical shells with unbalanced laminated faces 20 p3732 A70-40268
- Thin cylindrical shells optimum design with symmetrically paired spiral type stiffeners under uniform axial compressible load and lateral pressure 20 p3732 A70-40287
- Circular rib reinforced cylindrical shells, analyzing error due to Kirchhoff-Love hypothesis 20 p3734 A70-40435
- Stress distribution at hole in orthotropic cylindrical sandwich shell under internal pressure 20 p3734 A70-40440
- Perturbation method for stress-strain state of circular cylindrical shell with large curvilinear hole 20 p3734 A70-40442
- Rapid expansion of thin walled aluminum alloy cylinders under pulsed magnetic field pressure using high speed streak camera oscillography 20 p3735 A70-40513
- Circular cylindrical shell stability under axial compressive load, analyzing buckling process by high speed photographic recording of photoelastic isocline pattern changes 20 p3735 A70-40528
- Concentrated lateral loads effect on elastic stability and moment carrying capacity of circular cylindrical shells in bending 21 p3932 A70-40544
- Dynamic stability of cylindrical shell with small curvature under static or periodically variable axial pressure loads 21 p3932 A70-40554
- Closed circular cylindrical shell nonlinear problem solvability extended to anisotropic sandwich shell, using mean deflection theory 21 p3933 A70-40601
- Thin walled fiberglass-reinforced plastic cylinders in torsion, calculating load carrying capacity as function of temperature 21 p3841 A70-40648
- Orthotropic fiberglass-reinforced plastic cylindrical shell with allowance for material creep, calculating stress-strain state during bending under external pressure 21 p3842 A70-40649
- Steady one dimensional temperature field of cylindrical shell spacecraft, allowing for heat conduction and convective and radiative heat transfer within shell 21 p3942 A70-40841
- Vibration of combined cylindrical shells via Lagrangian minimization regarding unknown boundary values 21 p3934 A70-40897
- Buckling analysis of stiffened noncircular cross section cylindrical shells constructed by circular arcs and straight line segments 21 p3934 A70-40922

Carbon steel thin walled cylinders creep fracture subjected to combined tension and internal pressure by large strain theory

21 p3840 A70-41438

Circular cylindrical shell with annular orthotropic elastic core, analyzing stress wave propagation under pressure pulse

21 p3938 A70-41740

Temperature distribution in rotating thin cylindrical shell with line conduction discontinuity under solar heating, evaluating tubular elements thermal bending on spinning spacecraft

21 p3951 A70-41875

Thin cylindrical shell under nonaxially symmetric concentrated stationary radial loading, calculating random responses and stability

21 p3940 A70-42051

Circular cylindrical shell supersonic panel flutter nonlinear analysis, using averaging and numerical integration methods

22 p4112 A70-42275

Nonlinear flexural vibration of thin circular cylindrical shells with clamped ends, using method of averaging for stability

22 p4112 A70-42517

Thin circular cylindrical panels in supersonic gas current parallel to generatrices, calculating heterogeneity effect on flutter

22 p4113 A70-42603

Elastic cylindrical shell transient response to plane acoustic shock wave traveling through light fluid medium

22 p4114 A70-42647

Axisymmetric vibrations of cylindrical shell with concentric circular plates at each end, obtaining Lagrangian of combined system

22 p4115 A70-42843

Transient elastic vibrations of air and liquid filled cylindrical shells under radial impact, using shadow-optical cinematography [SMPT PREPRINT 107]

22 p4031 A70-43030

Circular cylindrical orthotropic fiberglass-reinforced shell buckling under longitudinal impact, assuming initial surface imperfections

22 p4117 A70-43347

Circular cylindrical shell with varying thickness under circumferential load and radial pressure, calculating critical load

22 p4117 A70-43354

Circular cylindrical shell under longitudinal line load, deriving closed form solution in Fourier series

22 p4118 A70-43547

Natural oscillations of cylindrical shell with elastic filler, using simple load distribution model

22 p4119 A70-43572

Thickness of equally stressed cylindrical shells, using thin elastic shell theory and Kirchhoff-Love hypotheses

22 p4120 A70-43715

Prestressed loadings on two layer fiberglass-reinforced plastic cylindrical shell under internal pressure

23 p4265 A70-43937

Thin circular cylindrical shells with clamped-clamped and fixed-fixed edges, calculating natural frequencies of nonsymmetrical free vibrations

23 p4266 A70-43997

Cylindrical shell stability under off-center compression loads applied to end faces, determining collapse conditions

23 p4268 A70-44169

Axially compressed circular cylindrical shells subject to relaxed boundary conditions, calculating buckling loads as function of length to radius ratio [ASME PAPER 70-APM-O]

23 p4269 A70-44397

Corrugated plates, closed cylinders and developable shells nonlinear elastic analysis, deriving boundary conditions

23 p4275 A70-44913

German monograph on stress concentration around doubly symmetrical cut-out in cylindrical shells subjected to symmetrical load, using elliptical cut-out theory

24 p4418 A70-45092

Rumanian book on torsion in thin walled elastic structures of various cross sections covering calculation methods for box beams, cylindrical and conical shells, aircraft wings, etc

24 p4418 A70-45147

Cylindrical shells with unreinforced openings, determining limit pressures and deformation patterns

24 p4419 A70-45158

Thin cylindrical shell flutter in linearized supersonic potential theory, considering Mach number, aspect ratio and pressure effects on critical wave number

24 p4420 A70-45263

Shell of revolution /pressure vessel/ with meridional slope discontinuity, calculating pressurization effect on stresses by computer program

24 p4420 A70-45277

Cylindrical shells dynamic thermoelastic response to sudden rotating thermal inputs, using Galerkin method

24 p4421 A70-45285

Laminar circular cylindrical shells supersonic flutter characteristics determination by dynamic equilibrium boundary value problem eigenvalues analysis, obtaining critical flutter speeds

24 p4424 A70-45588

Ring-stiffened thin circular cylindrical shells, calculating free vibration natural frequencies and mode shapes by finite element method

24 p4427 A70-46067

CYLINDRICAL TANKS

Simulated low gravity propellant sloshing in spherical, ellipsoidal and cylindrical tanks, discussing Bond number simulation and tank geometry effects [AIAA PAPER 69-1004]

09 p1657 A70-23255

Liquid motion dynamic effects in open cylindrical and conical tanks with translational motion

09 p1662 A70-23293

Liquids relative rotary motion in vertical rotating cylinders under large amplitude axial vibrations and angular velocities

12 p2209 A70-27213

Fluid motion in cylindrical tank with arbitrary sector annular cross section subjected to harmonic longitudinal excitation

12 p2211 A70-27818

Nonlinear effects of oscillatory disturbances produced by viscous excitations in rotating fluid inside of cylindrical tank

13 p2386 A70-28819

Ideal fluid-cylindrical tank elastic bottom coupled forced oscillations, determining hydrodynamic pressure for tank reverse translational motion

20 p3615 A70-40444

CYLINDRICAL WAVES

Radial electron flux interaction with cylindrical electromagnetic wave propagating between conducting planes, noting disturbance development according to power law

01 p0049 A70-10166

HF cylindrical waves propagation by line source in stratified medium, investigating refraction and diffraction at plane boundary using mathematical and ray methods

07 p1335 A70-19683

Electric field diffraction by infinitely long dielectric cylinder due to normally incident cylindrical wave, computing asymptotic value by geometric theory

07 p1235 A70-19684

Anodic precursors of convergent cylindrical shock wave of z-pinch discharges in He and Ar

07 p1261 A70-20357

Kirchhoff theory of elastic wave diffraction in cylindrical case derived on modified Huygens principle, showing edge contribution

08 p1543 A70-20582

Radial electron flux interaction with cylindrical electromagnetic wave propagating between conducting planes, noting disturbance development according to power law

10 p1853 A70-25014

Diffraction of plane cylindrical and spherical waves in wedge-shaped regions with reflecting edge, using asymptotic expansions

10 p1911 A70-25186

Unsteady problems of finite amplitude plane and cylindrical wave propagation in dissipative spatially symmetrical media

11 p2034 A70-25399

Cylindrical shock wave two dimensional propagation in conducting plasma in magnetic field, assuming isentropic flow along streamline

11 p2091 A70-26174

Plane cylindrical and spherical explosion waves propagation in detonating gas mixtures with counter-pressure, calculating perturbed flow parameters by numerical method of integral relations

13 p2388 A70-29308

High Mach number viscous flow past cylinder with cylindrical shock wave

13 p2391 A70-29970

Cylindrical EM waves diffraction by two parallel ideally conducting elliptical cylinders, discussing field and surface current distributions

19 p3378 A70-37734

Unsteady problems of finite amplitude plane and cylindrical wave propagation in dissipative spatially symmetrical media

20 p2673 A70-40093

Cylindrical converging shock waves generation, propagation and structure at high pressures

22 p4012 A70-43431

CYLINDROIDS

U CYLINDRICAL BODIES

CYSTEAMINE

Radiation protective action of cystamin, cysteamine and aminoethyl in mice, noting equal decreases in redox potential

03 p0419 A70-13310

Positive effect of shielding and cystamin administration on tonic and evacuator functions of rats gastrointestinal tract after gamma irradiation

05 p0804 A70-17122

Experimental procedure for investigating radioprotective effectiveness of chemical compounds against

X ray irradiation, discussing Cysteamine protection for golden hamsters and fetuses

06 p0993 A70-17429

CYSTEINE

Chlorella seaweed hybrid strains containing larger amounts of amino acids than original parent species

04 p0630 A70-14573

CYTONEGENESIS

Survival rates of continuously cultivated Chlorella plants in air-carbon dioxide atmosphere after single exposure to gamma radiation, using microcolony counting technique

05 p0803 A70-17113

Cells chemical origin, discussing terrestrial fractionation, amino acids, macromolecules, metabolism, etc

20 p3569 A70-38992

CYTOLOGY

Neurons and perineuronal glial cells quantitative relations in visual cortex from anesthetized dogs

01 p0025 A70-11030

Phagocytic activity and carbohydrate metabolism in peripheral blood neutrophils of men exposed to atmosphere with increased O content, noting neutrophil energy exchange disorder role

03 p0426 A70-13901

Anticerebral cytotoxic serum effect on white rats conditioned reflex activity

07 p1199 A70-18727

CYTOPLASM

Marrow granulocyte reserve restoration in dogs exposed to chronic gamma radiation, discussing leukocyte reaction to pyrogenic agent

13 p2351 A70-29326

CZECHOSLOVAKIA

Czechoslovakian Aeronautical Research and Test Institute history, organization, activities, equipment and achievements

03 p0464 A70-13925

Glassy drops identity and moldavites sculpturing origin in Pannonian sediments in southern Moravia

05 p0916 A70-16838

Report to COSPAR on Czechoslovakian space research /1969/ covering satellite telemetry and tracking, proton flares, aeronomy, etc

15 p2829 A70-31710

CZOCCHRALSKI METHOD

Second phase formation in Czochralski grown Cr-doped GaAs crystals by metallography, radioactive indicators and X ray analysis

01 p0156 A70-10189

Czochralski thermal probe for current carrier concentration in strip shaped area of n-type GaAs single crystals active growth

24 p4389 A70-45481

D

D LAYER

U D REGION

D LINES

Frequency locking of flashlamp pumped Rhodamine 6G dye lasers to D lines of Na vapor by Faraday rotation, noting doublet splitting

01 p0110 A70-10568

Night airglow emission intensities during IQSY concerning Na, OH and H alpha lines compared with intensities during IGY

02 p0292 A70-12433

Spatial properties of solar wind during maximum and minimum activity inferred from sodium D-line emissions for cometary nuclei

06 p1136 A70-18012

Dye laser tuned to sodium D line used for measuring ionospheric atomic sodium

08 p1492 A70-21757

Atomic emission in water vapor afterglow, revealing presence of Balmer series of H atom with sodium D line

14 p2579 A70-31255

Solar prominences monochromatic images in He I D3 and He II 4686 lines allowing for contamination in 4686 images

15 p2803 A70-32614

Na D lines emission cross sections measurement from ionic and neutral gases collisions at simulated meteor conditions

18 p3318 A70-37014

Nightglow Na D line excitation rate in winter and summer

21 p3814 A70-40934

Nightglow Na-D lines excitation, attributing emission to Chapman mechanism

22 p4023 A70-43294

Sodium D lines airglow nocturnal and seasonal variations in upper atmosphere

22 p4023 A70-43295

D REGION

Negative ion reactions relevant to D region measured in ESSA flowing afterglow system as function of temperature

01 p0070 A70-10406

- Stratospheric temperature changes connection with winter D region absorption changes
01 p0073 A70-10583
- Corpuscular radiation contributions to D layer ionization determined from intensity measurements
01 p0172 A70-11490
- Rocket sounding data on ionospheric currents at mid and low latitudes noting absence in D and above E region
01 p0082 A70-11529
- D layer radio absorption during solar eclipse of 22 September 1968 attributed to two solar X-ray sources
03 p0559 A70-13602
- Water vapor ion cluster concentrations in D region, noting discrepancies above mesopause for model atmospheres predictions
03 p0478 A70-13992
- D region electron density distribution during night and presunrise period, using full wave integration method for propagation parameters for waves reflected from electron density model
06 p1054 A70-17587
- Electron density distributions relation to D region diurnal and seasonal variations in radiowave absorption in terms of transport processes near mesopause
06 p1054 A70-17589
- D region positive ion composition measurements by rocket-borne quadrupole mass spectrometer, discussing downleg and upleg data
06 p1137 A70-18537
- Rocket measurement techniques for electron density profiles in D region, giving results from auroral zone disturbed and midlatitude quiet D region
07 p1263 A70-19152
- D and lower E region absorption of short waves, studying absorption distribution with height
07 p1263 A70-19153
- Diurnal vertical shifts of constant electron concentration levels in D region, considering effects of chromosphere, nuclear explosions, solar eclipses, etc
08 p1490 A70-21430
- Hydronium ion formation mechanism for D region, obtaining experimental support from mass spectrometer observation of ion production in oxygen glow discharge
09 p1671 A70-23500
- Nighttime D region ionization irregularities deduced from vertically incident VLF radio wave
09 p1671 A70-23663
- Asymmetric cross correlation functions in D and lower E region drift measurements interpreted in terms of moving screens
10 p1881 A70-24811
- D region electron ion recombination analyzed by two-ion model
10 p1881 A70-24812
- Sunspot cycle and ionospheric D and E layers daily radio wave absorption correlation, observing seasonal variation effect
10 p1885 A70-25267
- Critical review of Meisel paper on solar X ray source identification using D layer ionization behavior during eclipse
11 p2109 A70-25750
- D region synoptic ionization changes investigated by radio waves partial reflection from lower ionosphere, relating wave amplitudes to height
12 p2224 A70-27732
- Ionospheric D region radio wave probing by cross modulation technique, obtaining electron densities and collision frequencies
12 p2224 A70-27733
- Seasonal measurements of ionospheric absorption during sunrise in D region at medium sunspot numbers, noting disagreement with rocket observation
13 p2392 A70-28574
- Mesosphere payload to measure neutral gas density, positive and negative ions concentration and mobility in D region
13 p2393 A70-28682
- Electron density profiles interpretation for quiet daytime D region, noting role of electron-positive ion recombination coefficient
13 p2397 A70-29192
- Lower ionosphere influence on radio reflection from sporadic E layer, determining diurnal variations of D region absorption for various frequencies
14 p2547 A70-30235
- Lunar tide in ionospheric D region absorption near magnetic equator, noting annual variation relationship to sunspots
14 p2574 A70-30747
- D region rocket sounding at geomagnetic equator, measuring electron density, collision frequency, current, temperature, etc
15 p2724 A70-31668
- D region electron concentration and collision frequency in slowly varying plasma, using rocket-borne probe for ground emitted wave detection
15 p2778 A70-31673
- Electron density measurements by partial reflection and rocket techniques during 20 May 1966 solar eclipse, showing agreement below 82 km height
15 p2726 A70-31869
- D region electron density rocket measurements implying recombination coefficient
16 p2896 A70-32939
- D region electron density variations during solar eclipse of 7 March 1970, using wave interaction technique
16 p2898 A70-33832
- Sky wave amplitudes analysis recorded at D region height by loop and short whip antennas during 7 March 1970 solar eclipse
16 p2898 A70-33833
- D region electron energy loss factor during solar eclipse of 7 March 1970, using wave interaction technique
16 p2898 A70-33834
- Transceiving system for recording D region radio signal absorption and reflection, describing component circuitry and operation
16 p2880 A70-34225
- Ionization in ionospheric E and upper D regions, considering solar short wave radiation, small components, atmospheric dynamics and vertical mass transport
19 p3407 A70-37301
- D region positive ion density during solar proton event by Arcas rocket-borne cylindrical electrostatic probe
19 p3411 A70-37512
- Atmospheric turbulence scale and dissipation from 80 to 120 km, using photographic observations of Leonid meteor trails
19 p3515 A70-37663
- Multiple reflection processes in D and E regions at LF and VLF, using Pitteway full wave method
19 p3413 A70-38001
- Coupling processes in daytime D and E regions at LF and VLF, using thin film optics method for reflection and transmission coefficient matrices
19 p3413 A70-38002
- Intermode coupling processes in nighttime D and E regions, using thin film optical method for propagation phenomena at LF and VLF
19 p3413 A70-38003
- Chemical reactions of ions and neutral particles in D region, discussing photochemistry of atomic oxygen and ozone and reaction rate constants
19 p3418 A70-38905
- D region electron density profiles during solar eclipse from X ray rocket and satellite observations
19 p3419 A70-38913
- D region electron densities during 20 May 1966 solar eclipse, using partial reflection and rockets
19 p3419 A70-38914
- D region free electron temperatures at northern auroral zone by dual polarized antenna, observing incident noise radio fluxes
20 p3622 A70-39452
- X ray star effects on ionospheric LF radio wave field strength, examining absorption and ionization in D region
21 p3873 A70-40668
- Ionospheric transition and ozone correction from D region sunrise auroral rocket flight
21 p3814 A70-40935
- D region water vapor chemistry effects on measurements of radio propagation, ionospheric temperature and seasonal changes
21 p3814 A70-40936
- Ionospheric D region irregularities with partially reflected radio wave pulses, using phase path and drift measurements
21 p3814 A70-40941
- D region electron density profiles from high power wave interaction measurements during solar flare, indicating non-X-ray production rate
21 p3879 A70-40942
- Ionospheric D region electron production by cosmic X rays, noting Lyman radiation effects
21 p3882 A70-41099
- D region electron density profiles, using magnetoionic differential-phase partial-reflection technique
21 p3818 A70-41100
- Atmospheric positive ion composition measurements in D region by rocket-borne mass spectrometers, considering water cluster ions formation
22 p4017 A70-42796
- Recombination model of diurnal variation of electron density in midlatitude D region, assuming NO ionization by solar Lyman-alpha radiation
22 p4020 A70-43158
- D region ion chemistry, discussing three body reactions, water cluster ion production, reaction rates and binary collisions
22 p4023 A70-43304
- D region ionization budget, evaluating short wavelength X rays role
23 p4236 A70-43860
- D region LF and VLF sky waves opposite phase perturbation behavior
23 p4162 A70-44006
- Lower ionosphere influence on radio reflection from sporadic E layer, determining diurnal variations of D region absorption for various frequencies
24 p4316 A70-46310
- D-1 SATELLITE
Doppler observations of D1 A satellite, discussing dispersion of data, mean point displacement and resonance harmonics
02 p0362 A70-11756
- Data reduction from D1A satellite VHF and UHF Doppler measurements to attempt geodetic link between Nice and Beirut
07 p1262 A70-18941
- DACRON (TRADEMARK)
Mission sequential environment effects on Dacron parachute material mechanical properties [AIAA PAPER 69-1018]
14 p2563 A70-30770
- DAEMO (DATA ANALYSIS)
U DATA PROCESSING
U DATA REDUCTION
U DATA TRANSMISSION
- DAKOTA AIRCRAFT
U C-47 AIRCRAFT
- DAMAGE
NT IMPACT DAMAGE
NT METEORITIC DAMAGE
NT PROTON DAMAGE
NT RADIATION DAMAGE
NT RAIN IMPACT DAMAGE
Space station damage containment and control, emphasizing safety problems and guidelines
04 p0762 A70-14933
- Structure safety in cumulative damage, considering loading as time dependent stochastic process
05 p0937 A70-16369
- Summation of cycle ratios for various loading programs to control cumulative damage concept based on French curve, using fatigue tests
05 p0939 A70-16485
- Alloy equivalent susceptibility to damage at intermediary service periods and different stress levels under creep conditions at 750 C
09 p1701 A70-22470
- Components life determination from calculating cumulative damage using empirical stress amplitude distributions
11 p2133 A70-25844
- Continually changing residual stress patterns effect defined for predicting cumulative damage in structural fatigue
11 p2137 A70-26090
- Fatigue damage accumulation deterministic models for predicting longevity
14 p2656 A70-30300
- Metallic materials damage accumulation and structural failures due to fatigue, considering surface changes, crack initiation and dislocation pattern
15 p2757 A70-31928
- Aircraft ground damage during maintenance and servicing
15 p2675 A70-32210
- Liability for damages due to supersonic flight sonic booms, discussing pertinent provisions in Dutch and international law
19 p3553 A70-37561
- Double linear damage rule applicability to dual type alloys from two-stress level rotating bending and axial fatigue tests [ICAS PAPER 70-39]
23 p4267 A70-44137
- DAMPERS
Fail-operational fail-safe redundant yaw damper system, comparing reliability requirements with reliability prediction, development and production testing and field usage data [AIAA PAPER 70-392]
10 p1896 A70-24913
- Rectilinear vibration attenuation problem on shop setup, describing adjustable passive and active electromagnetic dampers
14 p2656 A70-30299
- Torsion wire libration damper for satellite gravity-gradient stabilization at near synchronous altitudes
16 p2985 A70-34134
- Two axis eddy current and single axis gravity gradient dampers for satellite stabilization
16 p2985 A70-34135
- Nonlinear structural analysis of Mariner spacecraft solar panel, using damper test characteristics
17 p3022 A70-34769
- Hydraulic and pneumatic dampers operation, analyzing force components
24 p4427 A70-46380

Periodic motion of satellite with magnetic damper along circular orbit, assuming small value of damping coefficient

01 p0197 A70-11481

Rapidly rotating solar interior damping by large scale convection analysis via maximum buoyancy force in water cylinder transition

02 p0373 A70-12391

Elastic stability of Coriolis-coupled oscillations of thin rotating disk under influence of centrifugal forces

02 p0389 A70-12650

Thermal damping in gas-filled composite materials during impact loading due to heat transport, discussing role in impact energy dissipation

[ASME PAPER 69-APM-V]

04 p0712 A70-14867

Gravitational radiation damping effect on motion of two bodies, evaluating field components in approximation by Einstein-Infeld-Hoffman method

05 p0882 A70-16308

Empirical astrophysical damping constants derived for neutral Fe lines using solar spectra, applying constraints to abundances and surface gravity determination

05 p0919 A70-16939

DODGE satellite launched into near-synchronous orbit to demonstrate gravity-gradient stabilization at high altitude and to experiment with damping techniques

[AIAA PAPER 70-69]

06 p1159 A70-18218

Elastic stability theory applied to equilibrium and stability of discrete continuous structural systems, detailing discrete critical points

07 p1408 A70-19560

Kinetic equation for nonlinear interaction of waves, including unstable or damped, using Bogolubov method

09 p1659 A70-22214

Solar IR Fraunhofer line damping constants empirical values and variation with optical depth, noting discrepancy with theoretical constants

09 p1757 A70-22726

Aluminum and aluminum-copper alloys dislocation damping at high strain rates using impact shear tests

10 p1903 A70-23983

Temperature effects on energy dissipation during vibration in ferromagnetic and nonferromagnetic metals, comparing damping capabilities for homologous temperatures

10 p1903 A70-24245

Static tensile stresses effect on magnetized ferromagnetic materials damping properties explained by anisotropic microplastic strains dissipating energy during bending vibration

10 p1904 A70-24246

Systems instabilities classification criterion determination, showing absolute instability conversion into convective by introducing damping

10 p1969 A70-25104

Nutation damping in gyrostabilized for multispin satellites in terms of energy momentum and damping torque arguments

11 p2119 A70-25357

Orbit eccentricity effect on gravity gradient system with single damping boom, investigating optimum steady state and transient response conditions

11 p2123 A70-26129

Gas-filled composites under impact loading, studying thermal damping due to heat transfer between compressed gas and solid structure

11 p2140 A70-26480

Optimum damping and stiffness in nonlinear single degree of freedom systems, discussing protection from ground and velocity shock during landing impact

11 p2145 A70-26695

Elastic moduli and damping coefficients for glass- and boron-epoxy beams determined from resonant frequencies and bandwidths during lateral forced vibrations

12 p2253 A70-27120

Linear periodic coefficient differential equations stability analysis by infinite determinate method, considering applications to damped mechanical systems motion and dual spin satellite

12 p2261 A70-27813

Low aspect ratio wings calculated for roll-damping derivatives, investigating load distribution

12 p2157 A70-27983

Nonlinear rolling motion of four-finned missile, investigating function of angle of attack and cubic damping

13 p2503 A70-28531

Asymmetric missile nonlinear angular motion, describing quasi-linear relations for frequencies, damping rates and swerving motion amplitude

[AIAA PAPER 70-534]

13 p2506 A70-29002

Pitch damping derivatives computation for missile configurations undergoing small amplitude oscillations at subsonic speeds, using static aerodynamic data

[AIAA PAPER 70-537]

13 p2339 A70-29004

Slender wings leading edge vortex flow effect on roll damping at subsonic speeds

[AIAA PAPER 70-540]

13 p2339 A70-29007

Damping by hemispheric torquing to control spin axis in gyroscope rotor while remaining unchanged with respect to case fixed reference

15 p2741 A70-32505

Free rotor air bearing gyros active damping evaluated through experimental studies

[AIAA PAPER 67-590]

15 p2741 A70-32506

Hydrostatic stability and damping characteristics of perforated plates and screens for passive propellant control schemes from drop tower tests

[AIAA PAPER 69-531]

15 p2787 A70-32510

Monograph on elastic stability covering eigenvalues of matrix series, stress-strain state calculation, critical ratio derivation, etc

15 p2823 A70-32550

Phase locked loop damping characteristics optimization based on input rms error rate minimization and transient error integral square value limitation

15 p2704 A70-32604

F-1 rocket engine acoustic line, reevaluating damping data for combustion stability improvement

16 p2968 A70-33588

Stability theorem for mechanical systems with constraint damping subjected to energy dissipation

17 p3176 A70-34956

Mathieu equation with nonlinear terms for damping and restoring forces, investigating first order instability region

18 p3337 A70-36224

Mechanical destabilizing model of nonlinear damping in nonconservative systems with follower forces, using Liapunov method

19 p3542 A70-38065

Transient system decay characteristics, discussing equilibrium point damping time for asymptotically stable systems of ordinary differential equations

19 p3542 A70-38066

Dual spin spacecraft, considering nonlinear damping effect on attitude stability

19 p3533 A70-38859

Interactive hybrid simulation of TRIAD satellite motions, describing attitude control system with magnetic hysteresis damping

[AIAA PAPER 70-994]

20 p3714 A70-39536

Composite material dynamic properties, discussing modulus and damping during constant strain rate, viscoelasticity, fracture strength and high loading tests

20 p3731 A70-40048

Continuous pseudoacoustic and ion waves excitation and damping in plasma sheath around grid, taking into account transit time effect on ion acceleration

21 p3858 A70-41710

Oscillating vane and rotating disk pressure gage theory, considering gas damping and density variations

23 p4198 A70-44948

Flame propagation limits and damping mechanism in gases under convection, determining boundary and initial conditions

24 p4428 A70-45492

Pulsation and turbulence damping in pulsed jet from energy spectra of longitudinal velocity fluctuations

24 p4327 A70-46267

DAMPING FACTOR

U DAMPING

DAMPING IN PITCH

U DAMPING

U PITCH [INCLINATION]

DAMPING IN ROLL

U DAMPING

U ROLL

DAMPING IN YAW

U DAMPING

U YAW

DAMPING TESTS

Machine element materials damping properties, determining energy dissipation during steady resonant vibrations

01 p0211 A70-11423

Tuned resonant test for measuring damping characteristics of lead and asbestos filled epoxy-polysulfide copolymer

08 p1527 A70-21336

DAMPNESS

U MOISTURE CONTENT

DANGER

U HAZARDS

DARK ADAPTATION

Readaptation times of eyes adapted to darkness using night vision training device in relation to helicopter flight safety conditions

03 p0436 A70-13823

Bleached eye pressure blinding at bleaching light termination during wavelength settings, discussing effect on interocular hue shifts

03 p0427 A70-13951

Rod-cone interaction in cat S potentials, analyzing effect of wavelength and intensity upon dark adapted responses

05 p0801 A70-16380

Dark adaptation correlated with in vivo visual pigments regeneration as function of bleaching during monomolecular time course

08 p1447 A70-21722

Human eye sensitization and dark adaptation, noting annular surrounding light addition effect on rod threshold

08 p1447 A70-21723

Visual acuity and light detection after preadaptation to red and orange lights, discussing photopic and scotopic vision

11 p1986 A70-25828

Two dimensional eye position control in dark over prolonged periods, noting role of conjunctiva cues, drifts and saccades

12 p2171 A70-28037

Oxygen effect on night vision tested in men at 5,000 ft above sea level, obtaining threshold curves of dark adaptation

13 p2359 A70-29443

Disadapting photostimulation effect on light sensitivity restoration of human visual analyzer, obtaining dark adaptation curves

15 p2679 A70-31603

Scotopic responses conditions, using stimulus alternation method to elicit electroretinogram

17 p3034 A70-35897

Darkness adaptation of flight personnel in polar regions, discussing effects of physical and nervous strain, sickness and alcoholic intoxication

20 p3576 A70-40290

Bilateral cortical cerebellar hemispheric ablations effect on feline light-dark discrimination learning

21 p3762 A70-41142

Time dependent visual perception probability under prolonged testing at eccentricities, using observer exposed to flashed stimulus with dark-adapted retina

23 p4147 A70-44782

DARKENING

Darkening and brightening of disturbed spot on sun surface determined by abnormal stress in seen layers due to magnetic and velocity fields

08 p1570 A70-20903

Coefficients for linear and nonlinear limb darkening in early type stars

11 p2113 A70-26469

Visual reflectance of wet soils, attributing darkening to internal reflection of radiation in water layer enveloping soil particles

14 p2577 A70-31236

Polar and equatorial limb darkening related to solar rotation and thermal flow, using photospheric models

15 p2807 A70-32812

DARKNESS

Ashen light origin, considering atmospheric refraction of sunlight illuminating dark side of planet

24 p4399 A70-45113

DARKROOMS

Covert solid state imaging system applicability to totally dark laboratory environment

09 p1686 A70-23752

DART TURBOPROP ENGINES

U TURBOPROP ENGINES

DASSAULT AIRCRAFT

Mirage F1 fighter aircraft, describing aerodynamic characteristics, fuselage construction, wing edges, etc

10 p1807 A70-24975

DATA ACQUISITION

Lidar technique using pulsed lasers as energy sources for operational type meteorological data collection including cloud height, visibility, thermal stratification, etc

01 p0042 A70-10081

Data acquisition methods and position in data processing with respect to time and quantity requirements

01 p0047 A70-10260

Noctilucent cloud observation stations and international cooperation in exchanging climatological data concerning annual variations, height distribution and latitude dependence

01 p0072 A70-10579

Sq data acquisition and analysis, noting automatic standard observatories using nuclear magnetometers and ionospheric current information from instrumented rockets

01 p0075 A70-10597

Solar electric spacecraft field interaction with space plasma affecting collection and interpretation of scientific data, emphasizing required system configurations and constraints

[AIAA PAPER 69-1106]

01 p0162 A70-10601

Semiautomatic data collection system for IR reflectivity measurements, recording digitized output on punched cards for computer analysis

01 p0088 A70-10747

On-line electronic integration of aortic flow during systole to provide beat by beat readout of stroke volume

01 p0038 A70-11044

Numeric keyboard CRT display for weather data acquisition from ships at sea, utilizing ATS-3 satellite as transmission medium

01 p0048 A70-11279

Fourth Cambridge catalogue radio sources observed for right ascensions using east-west arm of Molonglo radio telescope, presenting data analysis procedures

01 p0191 A70-11362

- In-flight data acquisition systems to overcome manual methods limitations, discussing applications and system configuration 02 p0224 A70-11839
- Automatic inspection data collection and processing by human operator using display devices and computerized mathematical reduction for real time evaluation 02 p0266 A70-12469
- Two phase flow visualization by various photographic and optical methods, describing equipment and lighting used and types of data obtainable 02 p0305 A70-12834
- Plastic flow under biaxial stress, discussing data acquisition system and computer program for comparing test and theory 03 p0480 A70-12954
- Creep rupture data processing by computer, performing data collection and processing separately 03 p0487 A70-13569
- Ground stations and low orbiting satellite system for automatic collection of meteorological data over Italy 03 p0581 A70-13832
- Thermionic converter with oriented W electrodes, describing test method and computerized data acquisition for performance mapping 04 p0627 A70-14945
- Experiment design and data acquisition for V/STOL aircraft flying qualities simulations, emphasizing pilot rating and comment data and control usage information [SAE PAPER 690695] 05 p0825 A70-15860
- Integrated flight test data acquisition and processing system with real time graphic display, discussing ground station function [SAE PAPER 690678] 05 p0793 A70-15867
- Human performance evaluation and data acquisition as requirements for heuristic analytical models in systems engineering 05 p0805 A70-16008
- Weather data communication, discussing transmission of radar, polar satellite and ATS satellite data to processing center and forecasts dissemination to public media 05 p0814 A70-16327
- High energy solar flare data from neutron monitor stations supplemented by low energy data from interplanetary space probes Pioneer 6 and 7 05 p0902 A70-16443
- Onboard digital data acquisition instrumentation system for scientific satellites, combining existing functional blocks to obtain different configurations and performances 05 p0818 A70-16587
- Remote sensing advantages and limitations of various wavelength bands, resolutions and time spans, discussing instrumentation and environmental limitations 05 p0850 A70-16684
- Meteoroid hazard data comparison from terrestrial and satellite measurements supporting Whipple theory of low density meteoroid 05 p0917 A70-16900
- Earth resources and meteorological data collection from in situ sensors via satellite, discussing system considerations 06 p1006 A70-17343
- Photoelectric photometry of comets to obtain principal data and to classify comets by employing same filters and stellar photometric standards 06 p1140 A70-17731
- Optimal information selection for determining spacecraft trajectory, considering atmosphere, light speed and series expansion coefficients of planetary gravitational potentials 06 p1142 A70-17891
- Climatological cloud type statistics for simulating earth sensing mission data output as function of sensor field of view and spatial resolution [AIAA PAPER 70-196] 06 p1065 A70-18098
- Test facilities and procedures for obtaining aerodynamic data required for studying vehicle-in-tube transportation systems [AIAA PAPER 70-225] 06 p1030 A70-18221
- Acquisition system design and experimental results for time division multiple access satellite communication system 06 p1011 A70-18410
- Computer operated digital system for controlling acoustic test environment and dynamic test data acquisition 06 p1030 A70-18432
- Magnetic, electrostatic and RF fields noise reduced for strain gage data acquisition 06 p1069 A70-18435
- Mariners 6 and 7 range and Doppler tracking data for studying Martian mass and earth-moon mass ratio 06 p1151 A70-18486
- Simultaneous high speed shock tunnel data acquisition system using single tape recorder, analog or digital readout and computerized reduction 06 p1031 A70-18604
- Meteorological data from radiosonde and radar wind observations during Indian Ocean expedition of research vessel Meteor 07 p1329 A70-19350
- Ionospheric data of local and integral electron concentration obtained by measuring phase shift of satellite emitted coherent radio waves 07 p1276 A70-20422
- Geomagnetic storms data compilation /1957-1964/, showing solar activity effect on solar corpuscular stream velocity 07 p1373 A70-20436
- Deep space network /DSN/ functions and characteristics, discussing spacecraft control, data acquisition, orbit determination, data processing, etc 08 p1481 A70-20614
- Celestial emission bodies forbidden line analysis for physical conditions determination using formulas and graphs 08 p1569 A70-20831
- Computer system for real time data acquisition and servicing of asynchronous inertial guidance system test stations 08 p1467 A70-21591
- Global atmospheric research program data requirements analysis based on two level numerical model 08 p1539 A70-21650
- Self similarity concept relevance to atmospheric turbulence demonstrated from ground and airborne observational data 09 p1717 A70-22373
- Communications satellite technology for earth resources data collection 09 p1634 A70-22857
- TIROS Operation Satellite /TOS/ system for daily observation of meteorological phenomena analyzed for problems of general data gathering satellite system [AIAA PAPER 70-283] 09 p1766 A70-22874
- Omega Position Location Equipment /OPL/ system, testing operational feasibility of centralized global meteorological data collection system 09 p1722 A70-23030
- Reference ellipsoids mutual positions determination from observational data by satellites using triangulation points of two triangulations 09 p1763 A70-23327
- Weapon systems combat effectiveness measurements, stressing need for proper data acquisition from early R and D through obsolescence 09 p1794 A70-23414
- Intertropical convergence zone /ITCZ/ movements, analyzing data obtained by ship and ESSA satellite cloud photography 10 p1912 A70-23939
- Satellite system applicability to earth resources data collection from in situ sensors, discussing synoptic, local time, emergency and demand data collection 10 p1840 A70-24371
- Remote sensing and privacy rights, noting political and social trends toward privacy protection 10 p1971 A70-24744
- Aerial photography analysis of drainage basin discharge properties, discussing surface runoff, subsurface flow and underground water movement 10 p1879 A70-24750
- Forest inventory data collection by 70 mm photography, creating correction surface over model area of large scale pair 10 p1880 A70-24754
- Observational data for distributions of physical and optical companions to spiral galactic systems and number of satellites as function of central galaxy size 10 p1948 A70-25247
- Sound speed and horizontal wind velocity components determined in upper atmosphere from measured data of Rocket Grenade Experiment 11 p2121 A70-25678
- Commercial aviation gasoline inspection data tabulated and compared for 1969 and 1964 [SAE PAPER 700228] 11 p2099 A70-25897
- Italian polyvalent data acquisition system for ground space tests, discussing electronic instrumentation system 11 p2032 A70-26293
- Analog-digital real time data automatic acquisition and radar tracking system for air defense and air traffic control 11 p2014 A70-26313
- Residential urban environment data extraction from high and low resolution images 12 p2216 A70-26907
- Gemini 12 photographs examined for urban and transportation data content 12 p2228 A70-26909
- Lumped linear model parameters determined from dynamic test data on mode shapes and frequencies for approximating distributed elastic structure 12 p2317 A70-27122
- Multipath tolerant ranging and data acquisition for air-ground-air links in ATC based on mathematical scattering theory 12 p2268 A70-27642
- Radiological studies of young adult spines for selecting aircrew personnel and collecting data to compile reference dossiers in case of accidents 12 p2171 A70-28039
- Soviet book on discrete system for measuring multivariable probability distributions, covering automatic acquisition and reduction of statistical data 13 p2381 A70-28700
- Deep Space Network /DSN/ data accuracy limitations relation with ability to determine orbit of probe, examining improvements after Mariner 2 and trends 13 p2448 A70-28702
- Meteorological data acquisition by navigational aids, satellites and surface based indirect sensors for computer forecasting 13 p2405 A70-28773
- Signal transduction with differential pulse width modulation applied to data acquisition processes 13 p2405 A70-28812
- Air-damped capacitance accelerometers and velocimeters in data acquisition systems using signal processing 13 p2405 A70-28813
- Azur satellite ground control, describing system organization to measure scientific and data information for entire satellite lifetime 13 p2384 A70-28976
- Integrated computerized data acquisition and reduction system for aircraft flight and wind tunnel tests 13 p2373 A70-29156
- Balloon-borne photometer for collecting twilight and daytime OH intensity and rotational temperature variations data 13 p2399 A70-29240
- Pulsar CP 1919 X ray emission upper limits from balloon flight data, comparing to NP 0532 over entire electromagnetic spectrum 13 p2478 A70-29270
- Aircraft clear line of sight probability data for various altitudes and view angles 14 p2608 A70-30595
- Visual observation, free space traversal, accelerometry and telemetry for measuring and recording human behavior, discussing free space-time traversal data logging system 14 p2542 A70-30794
- Census analysis and population data acquisition using aerial photography 14 p2576 A70-30978
- Data flow in computerized automatic data acquisition systems, considering systems traceability of calibration to national standards 14 p2554 A70-31110
- GHOST free floating balloon system for global atmospheric circulation data acquisition in World Weather Watch 14 p2610 A70-31153
- Alpha-beta and Kalman tracking filters with randomly interrupted data, evaluating transient responses as function of radar measurement accuracy and valid data acquisition probability 14 p2557 A70-31186
- Satellite laser communication system using dual scan acquisition technique 14 p2552 A70-31197
- Remote sensors applied to classification of aerial data concerning housing quality at different scales, using variables observation 14 p2577 A70-31234
- Radar imagery for crop discrimination, discussing sensor and data requirements and statistical analysis methods 14 p2578 A70-31237
- Analog/digital system for full scale airframe fatigue amplitude and phase signature measurements on CH-46D tandem rotor helicopter 15 p2739 A70-32323
- Optimal questionnaires characteristics and design algorithms 15 p2705 A70-32450
- Lidar probing of stratosphere and mesosphere using automatic data acquisition system 16 p2862 A70-33016
- Optimal use of remotely sensed data from NASA Earth Resources Program by matching user models with capabilities of aircraft/satellite remote sensing system 16 p3004 A70-33708
- Airborne flight test data acquisition and ground based automatic bulk data processing system for helicopter test and development programs 17 p3014 A70-34713
- Airborne data acquisition on high density computer tape for aircraft handling and flight dynamics research 17 p3049 A70-35499
- Computer driven on-line CRT graphics displays for data acquisition and reduction 17 p3063 A70-35513
- Airborne data acquisition and flight recorder systems, comparing civil and military aircraft requirements 17 p3094 A70-35515

Ground simulations data of jet lift V/STOL compared with visual flight results, noting hover, lateral quick start and stop maneuver

18 p3236 A70-35954

Data acquisition system applications philosophy, discussing data integrity, expansion facility, flight safety, etc

18 p3258 A70-36339

Flight data recorders and system integration, discussing data replay system backing flight recording

18 p3258 A70-36340

Underwater recovery requirements for flight data recorders, suggesting compressed air instead of explosive charges for ejection force

18 p3258 A70-36343

Left ventricular dynamics ultrasonic visualization, involving catheter-borne transducers array and computer for data acquisition and display

18 p3225 A70-36750

Plane and annular cascade facilities data application to aerodynamic design of axial flow compressors

[ASME PAPER 70-GT-106] 18 p3303 A70-36845

Magnetic tape recorder for panoramic vertical ionospheric sounding data acquisition in digital form

18 p3261 A70-37041

Galaxies and globular clusters, obtaining data by measurements with intermediate bandpass photometry

18 p3321 A70-37121

Radio sources near 2 flux units at 408 MHz, presenting data on positions, optical identifications, angular size and flux densities

18 p3321 A70-37125

Exhaled alveolar air data acquisition using mass spectrometer and multichannel analyzer

19 p3367 A70-37356

Data acquisition and processing system for electronic countermeasure aircraft tests

19 p3383 A70-37900

Rocket engine tests dynamic data oscillographic presentation and digital processing

19 p3490 A70-37916

Automatic gain ranging amplifier for high speed digital computer controlled data acquisition system used to process input data levels

19 p3383 A70-37919

Computer merits in test laboratory data acquisition systems

19 p3383 A70-37921

Soviet papers on physiological data collection and analysis methods

19 p3369 A70-38206

Space corpuscular radiation simulation to obtain data for increased spacecraft life

19 p3511 A70-38284

Signal measurement and processing in thermal vacuum and space simulation tests of Azur and Dial satellites

19 p3400 A70-38298

Flight data acquisition methods standardization, discussing digital recording modes and formats and hardware rationalization

19 p3429 A70-38515

Digital data acquisition system for CF-5A flight test program, discussing recording system design

19 p3384 A70-38532

Portable catapult and arresting gear analog instrumentation data acquisition system testing aboard aircraft carriers and at land-based facilities

19 p3384 A70-38533

Data collection system for prototype flight tests of Fokker F-28 based on DC-8 aircraft digital system

19 p3384 A70-38546

Data acquisition by earth resources technology satellite /ERTS/ for user needs in forestry and agriculture

20 p3616 A70-39062

Space acquired hydrological cycle data relating to water occurrence and movement in atmosphere and earth surface mantle

20 p3616 A70-39063

Morning and evening current reversals in equatorial electrojet, discussing seasonal variation data for refining models

20 p3621 A70-39352

Automatic measurement of drainage networks for lengths and areas by copper plate etching or flying spot scanner on transparencies or radar images

20 p3633 A70-39794

Earth resources observation satellite program and organization for acquiring, processing, utilizing and disseminating remote sensor data

20 p3741 A70-39944

Solar electric propulsion application to out-of-ecliptic mission for interplanetary fields and particles data, comparing performance with chemical systems

[AIAA PAPER 70-1118] 20 p3691 A70-40225

OSO far UV solar spectroheliograms atlas, describing instrumentation, data acquisition, etc

20 p3713 A70-40540

Thermoelectric outer planet spacecraft /TOPS/ data subsystems for 12 year missions compared with Mariner subsystem

21 p3795 A70-41796

TIROS Operation Satellite /TOS/ system for daily observation of meteorological phenomena, analyzing problems of general data gathering satellite system

[AIAA PAPER 70-283] 21 p3931 A70-41868

Airborne data acquisition equipment for accident flight path and engine performance recording

21 p3796 A70-41922

Real time global temperature and geopotential height profiles acquisition from satellite spectrometer measurements by least squares regression method

21 p3820 A70-42121

ERTS line scanning system for cartographic data of water, snow, vegetation and cultural areas

22 p4037 A70-43090

Computer-based seismic data acquisition system using digital vibroseis process for eliminating low signal to noise ratio characteristics

22 p4038 A70-43092

Astronaut physiological monitoring aboard Soyuz spacecraft

22 p3980 A70-43691

Data acquisition and processing in structural modal characteristics analysis during ground resonance tests

[ICAS PAPER 70-36] 23 p4267 A70-44133

EUV reflectance data for optical constants obtained in digital form directly on punched cards by data acquisition system

23 p4197 A70-44470

Information handling for safety design concerning standards, criteria and requirements

23 p4153 A70-44493

Commercial transport aircraft fatigue loading data from NASA VGH /airspeed-acceleration-altitude/ program, discussing instrumentation, sample sizes, etc

23 p4270 A70-44548

Space station program information management system involving data acquisition and extended manned flight operation with minimum ground support

[IBM-70-U60-0015] 23 p4164 A70-44637

Jupiter Orbiting Vehicle for Exploration system for gathering Jupiter atmosphere, magnetic, radiation, gravitation, temperature, topography and interplanetary data

23 p4264 A70-45010

Solar limb photographic, isodensity and isophotal data for eclipse of 7 March 1970 from coronagraph observations, noting coronal green line and prominence activity

24 p4402 A70-45389

Planetary masses determined from radar measurement data and radio tracking of space probes

24 p4407 A70-45535

Geopotential zonal spherical harmonics coefficients revised values determined from reduced Baker-Nunn observations for satellites

24 p4407 A70-45537

Tesseral harmonics of geopotential and station coordinates from combined Baker-Nunn, laser and range data from satellites

24 p4407 A70-45538

Satellite data acquisition and dissemination functions of National Space Science Data Center /NSSDC/

24 p4322 A70-45615

Earth Resources Technology Satellites /ERTS/ providing high resolution image data regarding agriculture, geology, hydrology, geography, etc

[SAE PAPER 700761] 24 p4416 A70-45869

Satellite technology applications to ATC, including communications, navigation, surveillance over water and data acquisition

[AIAA PAPER 70-1301] 24 p4373 A70-45922

DATA ADAPTIVE EVALUATOR/MONITOR

U DATA PROCESSING

U DATA REDUCTION

U DATA TRANSMISSION

DATA ANALYSIS

U DATA PROCESSING

U DATA REDUCTION

DATA COMPRESSORS

U DATA REDUCTION

U DATA TRANSMISSION

DATA CONTROL SYSTEMS

U DATA SYSTEMS

DATA CONVERTERS

NT ANALOG TO DIGITAL CONVERTERS

NT DIGITAL TO ANALOG CONVERTERS

Multistop time-to-pulse-height conversion unit to extend capability of pulse height analyzer for multichannel time analysis with narrow channel widths

02 p0271 A70-12749

Graphical data conversion into code for storage in computer memory

15 p2705 A70-31576

Measurement transducers transforming measured quantity into forms suitable for comparison with standards in metrological sciences

17 p3090 A70-35432

Fluctuating data transmission, using measurement channel with digital logarithmic conversion

20 p3635 A70-40534

Dynamic errors of digital converter for digit-to-digit compensation estimated by probability and information characteristics methods

24 p4340 A70-46404

DATA CORRELATION

NT SIGNAL ANALYSIS

Cosmic ray neutron monitors data comparison for various stations using one factor model, considering atmospheric effects and cut-off rigidities

01 p0087 A70-10460

Spacecraft motion parameters and physical characteristics of space determined from statistical analysis of measurement data

01 p0094 A70-11484

Auroral breakup effects on sporadic E via comparison between sequential ionograms and riometer absorption data indicating transient effect in D/E regions

02 p0288 A70-11744

Instruments and procedures for photogrammetry automation, discussing automatic pattern recognition, data correlation and computer role

02 p0302 A70-12652

Temporal autocorrelation functions of ozone content and concentration from data of Soviet and U.S. stations, obtaining statistical stability

03 p0474 A70-13295

Solar X-ray bursts observations correlation with sudden phase anomalies measured at long VHF propagation paths in lower ionosphere

03 p0558 A70-13601

Solar microwave and soft X ray radiation emission correlation to determine flare peak temperature and solid angle

04 p0741 A70-15126

Ionospheric propagation experiments to measure radio echo height changes, observing correlation between LF signal reflection and MF transmitter power

04 p0650 A70-15132

Space simulation test results compared with analytical methods for thermal data prediction of Azur satellite

04 p0762 A70-15182

Error sources affecting data comparison accuracy between gyro measurements and reference solutions and due to gyro axes misalignment and gimbal angular movement

04 p0692 A70-15327

Positive correlation between normal ionizations at magnetically conjugate regions in ionospheric F 2 layer from aircraft vertical soundings

04 p0683 A70-15741

Hypersonic near wake, discussing correlations from optical studies, laminar near wake, blunt body and turbulent wake measurements

05 p0790 A70-16120

Error correction for correlation coefficient between satellite data of earth radiation intensity and satellite vision field shift

05 p0841 A70-16729

Correlation between O isotope ratios and composition of tektites investigated for origin of tektites

05 p0917 A70-16840

Satellite radiation dose rates in inner Van Allen belt, correlating calculated and measured rates with proton environment model

06 p1134 A70-17264

Radiation data from manned orbital Mercury missions, correlating measurements from various additional sensors with main nuclear emulsion sensors

06 p1134 A70-17267

Balloon satellite orbital time and eccentricity correlated, investigating earth shadow and solar radiation effects

06 p1142 A70-17892

Correlations between 100 percent inspection by automatic equipment and quality control acceptance sampling in vacuum tube industry

06 p1077 A70-17986

Dynamic simulation parameters for sphere drag coefficient data correlation in near free molecular flow

06 p0983 A70-18374

Centripetal acceleration tolerance level correlated with circulatory system functional tests and physical exercises, discussing strength and speed endurance

07 p1201 A70-18787

Lunar surface samples characteristics correlation with terrestrial igneous rocks /basalts/ and eucrite meteorites based on alpha scattering analysis

07 p1380 A70-19203

Time block pooling of atmospheric noise data, basing randomness conclusion on observations correlation

07 p1236 A70-20161

Aircraft roll rate response and aileron step input matching in terms of modal parameters with flight test records by analog computer program

08 p1465 A70-20781

Aged Al-Cu alloys hardness test data normalized and correlated for interpretation in terms of physical metallurgy

08 p1525 A70-21967

Earth resources satellite TV cameras operating on different spectral bands, discussing data preprocessing for correlation with topographic maps

09 p1674 A70-22259

Geogravitational field correlations to geomagnetic fields emphasizing displacements in longitude
09 p1667 A70-22381

Earth Resources program automatic data correlation system noting lower cost, faster processing, un-degraded imagery and compensation for vehicle perturbations and terrain relief
[AIAA PAPER 70-323] 09 p1667 A70-22864

Astronomical high resolution radio interferometers design with autonomous reception, analyzing sensitivity of data processing correlation devices
09 p1647 A70-23132

Balancing method for correcting mathematical model discrepancy with gas turbine based on test data
10 p1930 A70-24289

SID observed as VLF phase anomalies correlated with solar microwave radio bursts
10 p1933 A70-24816

Aerial and ground UHF noise measurement in Phoenix area, correlating air and ground data
[AIAA PAPER 70-437] 11 p2001 A70-25480

Optical and radio homologies of solar flares, studying correlation from astronomical telescope pictures
11 p2105 A70-25747

Small scale and full scale wind tunnel and flight test data correlated for Lear jet aircraft
[SAE PAPER 700237] 11 p1981 A70-25906

Solar wind correlation with geomagnetic activity, comparing Vela 3 and 4 observations with Mariner 2 measurements
11 p2105 A70-26075

Tactical air defense multiple site tracking data correlation equation to select gate sizes
11 p2009 A70-26263

Cosmos 137 proton spectra data obtained in inner radiation belt agreeing with Relay 1 data
11 p2106 A70-26786

Nonimaging remote sensor data display in spatial registration with ground scene to determine sensor bore-sight position accuracy
12 p2229 A70-26940

Maximum oxygen uptake correlation to age of subjects performing physical and sedentary work
13 p2350 A70-29112

Real time signal processor for correlation and spectrum analysis, displaying results on cathode ray oscilloscope
13 p2370 A70-29817

Balloon flight measurements clarifying Arcasonde sensor bias over radiosonde atmospheric temperature data
14 p2585 A70-30570

Positive correlation between normal ionizations at magnetically conjugate regions in ionospheric F 2 layer from aircraft vertical soundings
14 p2575 A70-30825

Magnetic activity intensity comparison in Northern and Southern hemispheres, noting correlation with solstices and equinoxes
14 p2580 A70-31260

Pioneer 8 wave and particle observations correlation showing broadband wave levels reduction during extended geomagnetic tail crossings
15 p2727 A70-31904

F region electron density profiles interpretation by electron balance equation facilitating comparison of aeronomic and ionospheric data
15 p2731 A70-32091

Plane strain stress intensity factor-Charpy V notch impact test correlations in transition temperature range under slow bend and dynamic loading
15 p2759 A70-32244

Intensity correlations in optical parametric noise and second harmonic generation measured by two photon delayed coincidence counting
15 p2753 A70-32603

Electronic equipment reliability performance measurements during tests correlated to performance observed under field use
15 p2712 A70-32645

Cryogenic single tubes transient cool-down by liquid hydrogen, deriving film boiling heat transfer correlation
[AIAA PAPER 70-660] 16 p2998 A70-33621

Polymeric materials fatigue tests, investigating correlation between crack propagation and stress intensity factor
17 p3127 A70-34624

Laminar flow heat transfer in annuli, discussing correlation of local Nusselt numbers
17 p3197 A70-35545

Observation classification /image identification/ for two normal sets with common covariance matrix, investigating error probability asymptotic behavior
19 p3375 A70-37283

Low energy solar protons temporal and spatial variations in magnetosphere by data comparison from polar orbiting satellite and Explorers 33 and 34
19 p3494 A70-37486

Solar flare of 25 February 1969 ground observations comparison to satellite data, measuring magnetic fields, radio emission, sunspots, ionospheric effects, etc
19 p3513 A70-37497

Solar radio emission and optical features correlation, considering integral RF flux, spot groups, main spots and flocculi areas
19 p3521 A70-38553

Digital correlation system for stationary and nonstationary random processes, estimating mathematical expectations and cross- and autocorrelation function
20 p3594 A70-39920

Solar X-ray bursts correlation with H alpha flares and microwave bursts observed by Explorer 34 experiment
21 p3880 A70-40970

Site activation in saturated nucleate boiling tests involving various fluids boiled on transparent oxide coated glass surface, correlating site density data with surface temperature
21 p3948 A70-41202

Scintillation index correlation with mean wind velocity of jet streams
22 p4020 A70-43262

Temporal sequence correlation between surges and associated flares during solar cycle
22 p4095 A70-43265

Damage data comparison for vibratory cavitation and liquid impact on aluminum alloy, stainless steels and pure nickel
23 p4203 A70-43870

Heat transfer measurements compared in free flight and in hypersonic wind tunnel at similar Reynolds number and temperature ratios
[ICAS PAPER 70-06] 23 p4275 A70-44115

Superconducting magnet system design, operation and module tests, noting large and small coil systems performance data relationship
23 p4218 A70-44354

Cylindrical heaters in corresponding-states fluids, estimating film boiling heat transfer coefficients by correlation procedure using least squares expression
23 p4279 A70-44361

Dynamical and geometrical geodesy on European datum, comparing data from Doppler, laser and photographic satellite measurements
24 p4312 A70-45544

DATA HANDLING SYSTEMS
U DATA SYSTEMS
DATA LINKS

Multipath spectral and statistical characteristics in VHF satellite-aircraft link, discussing geometric considerations and reflection from Gaussian surfaces
02 p0259 A70-12565

Design methods for self steerable antenna arrays in unidirectional and two directional radio links
03 p0456 A70-13196

PCM signal transmission testing over radio links with two level phase modulation
03 p0452 A70-14282

Low noise amplification equipment for telecommunications, considering France-Portugal link parametric amplifiers
05 p0819 A70-15983

Optimal design of tropospheric scatter radio link between two localities, investigating power, antenna, diversity, frequency deviation and equipment
05 p0814 A70-16361

High gain paraboloidal reflector antenna with horn feed for satellite and terrestrial microwave links
06 p1022 A70-18022

International data exchange guide for solar-terrestrial physics, including listing of stations active during International Years of Active Sun
07 p1377 A70-18937

Noise mean duration in surface communications links due to communications satellites interference, discussing irradiation emission and termination
08 p1456 A70-20570

Laser and quasi-laser systems modulation for wide spectrum communications, discussing global potentials and application as low cost satellite links
08 p1459 A70-20802

White noise and nonlinear effects in telemetry RF links, analyzing received process to phase coherent receiver
08 p1460 A70-20823

Signal properties of VHF satellite-to-aircraft communications link, discussing results of ATS tests
08 p1463 A70-21779

TV network distribution in Canada by communications satellite and terrestrial microwave links, discussing signal to noise ratios and picture quality
[AIAA PAPER 70-430] 11 p1998 A70-25417

Satellite video-telephone systems promoting economic growth in developing nations through linkage with developed nations advanced centers
[AIAA PAPER 70-474] 11 p2000 A70-25455

Satellite system for air traffic control providing data links for aircraft position determination for U.S. in 1990s using 24-hour inclined elliptical orbits
12 p2270 A70-27926

Earth resources satellite real time wideband relay communication link to ground station
[AIAA PAPER 70-326] 13 p2368 A70-29614

Injection laser communication link for high data rate transmission, discussing design and construction of transmitter and receiver
16 p2862 A70-33139

Deep space optical communications link, fabricating operational prototype of flight hardware for spaceborne terminal
16 p2863 A70-33190

Time ordered system for air traffic control providing data link, collision avoidance and navigation data through single channel
16 p2948 A70-33476

GaAs injection lasers for optical communication, synthesizing high bit rate data link between synchronous relay satellites
16 p2865 A70-33710

Communication satellite UHF link with FSK or PSK modulation, considering coded digital transmissions
16 p2867 A70-34331

Optical communications in space, considering multiple access low earth orbit-to-synchronous and synchronous-to-synchronous links
19 p3379 A70-37878

Millimeter wave propagation measurements by ATS-5 satellite, observing attenuation dependence on meteorological parameters for communication data link performance prediction
20 p3589 A70-40311

Space-to-ground link wideband digital laser communications system design and performance tests
21 p3787 A70-41331

Carbon dioxide laser systems for various space communication links between ground, satellites and Mars probe
21 p3787 A70-41338

ATC data link communications system speeding information flow between controller and pilot
21 p3789 A70-41348

Millimeter wave high gain Cassegrain antenna for wide bandwidth data link between communications satellites, obtaining accurate parabolic contours
21 p3799 A70-41359

High level parametric upconverter for radio link using evanescent mode waveguide
22 p3997 A70-42925

Earth resources technology satellite data link tradeoff between channel capacity and transmitter power
22 p4038 A70-43091

Queueing requirements in automatic radar target detection system operating with narrow bandwidth data link
22 p3990 A70-43489

Optimal two-way communication system with feedback and decision constraint, developing algorithm for random code reliability lower bounds
23 p4159 A70-43754

Global rescue alarm net /GRAN/ using satellites for relaying distress signals, eliminating current line of sight restrictions
23 p4143 A70-44455

Digital PCM telemetry link coding techniques, discussing encoding-decoding complexity, and concatenated block scheme for channel
24 p4315 A70-46258

DATA PROCESSING
NT DATA CORRELATION
NT DATA REDUCTION
NT DATA RETRIEVAL
NT DATA SMOOTHING
NT DATA STORAGE
NT OPTICAL DATA PROCESSING
NT SIGNAL ANALYSIS
NT SIGNAL PROCESSING
NT VOICE DATA PROCESSING

Data acquisition methods and position in data processing with respect to time and quantity requirements
01 p0047 A70-10260

Aerospace digital computer design development, proposing data processing system with improved flexibility by making subassemblies more independent with multiplexed interface
01 p0047 A70-10305

Data analysis of inertial systems for commercial aircraft overseas operations, classifying systems error propagation as linear time drift or Foucault period oscillation
01 p0137 A70-10314

Communications subsystem configuration for orbital manned space station, describing data rates and processing, multiplexing and associated modulation methods
[AIAA PAPER 69-1079] 01 p0043 A70-10627

Fourier transform applied to power spectral distribution determination for two dimensional Fraunhofer holographic data of thin spherical lenses
01 p0090 A70-10907

European Space Operations Center activities in observing HEOS 1 satellite, discussing launch, data processing and S-11 experiment involving ionized Ba cloud creation
01 p0197 A70-11118

Line length effects on sequential blanking in visual perception demonstrated by computer-based CRT display and interpreted with information processing model
01 p0039 A70-11164

Operational planning system for Strategic Air Command for data accessing, generating, displaying and editing using computer complex

01 p0048 A70-11282

Doppler observations of D1 A satellite, discussing dispersion of data, mean point displacement and resonance harmonics

02 p0362 A70-11756

Radar primary plot extraction, suggesting signals summing technique in delay line

02 p0256 A70-11975

Unified Flight Analysis System processing post-flight data from Saturn 5 launches, discussing system components, support programs and performance

02 p0264 A70-12127

Omega position location equipment /OPLE/ experiment data analysis, obtaining quantitative measure of statistical performance of system

02 p0336 A70-12180

Associative processor with content addressability and simultaneous arithmetic capability to circumvent speed restriction, comparing performance and cost with conventional digital computer

02 p0265 A70-12186

Automatic inspection data collecting and processing by human operator using display devices and computerized mathematical reduction for real time evaluation

02 p0266 A70-12469

Remote data processing and wideband data transmission between France and U.S. via telecommunication satellites, discussing error detection and correction

02 p0263 A70-12612

Synthetic aperture airborne side-looking radar using coherent optical data processor, discussing system configuration and operation

02 p0263 A70-12632

Turbojet performance magnitude data represented by components nondimensional characteristic curves

03 p0551 A70-13021

Meteorological data processing computer center of German Weather Service, discussing equipment, data system, forecasting techniques and prediction control

03 p0454 A70-13171

Creep rupture data processing by computer, performing data collection and processing separately

03 p0487 A70-13569

Surveyor TV camera conversion from qualitative viewing device into quantitative measuring instrument by calibration coupled with data processing program

03 p0490 A70-13662

Remote sensing system for earth resources surveys temporal information employing human interpreter and machine for spatial and spectral data processings

03 p0491 A70-13668

Ground stations and low orbiting satellite system for automatic collection of meteorological data over Italy

03 p0581 A70-13832

Cockpit information transfer between pilot and flight control information displays improved by on-board data processing system

03 p0436 A70-14021

Memory volume necessary to store intermediate data estimated for group processing from dependent Poisson information sources

04 p0661 A70-14552

Computer method to combine autofluorescope data to produce three dimensional display of absorbed radioactive material from multiview images

04 p0686 A70-14563

Earth resources satellites capabilities and requirements emphasizing orbit parameters, remote sensing, data handling and telemetry systems

04 p0760 A70-14642

Spaceborne computer system for manned space station to perform functions in addition to guidance and navigation including processing

04 p0654 A70-14651

Integrated flight test data acquisition and processing system with real time graphic display, discussing ground station function

05 p0793 A70-15867

Multichannel ionization calorimeter data readout into electronic computer using short circuit coil magnetic storage

05 p0816 A70-15947

Z term from astronomical latitude data compared with catalog error corrections, showing nearness to absolute star system

05 p0907 A70-16030

Optical, digital and hybrid image processing techniques with objectives of image enhancement and replacement

05 p0847 A70-16121

Radar and sonar data processing for display in command and control systems using digital technique, discussing processor configuration

05 p0828 A70-16189

Ocean surface roughness time variation effect on incident laser beam, analyzing motion picture data by computer program

05 p0860 A70-16687

Riometric data processing method for radio wave absorption measurement, considering nighttime cosmic radio emission intensity

05 p0842 A70-16742

Worldwide Apollo data transmission network emphasizing computer operations for message collection and distribution, command and telemetry processing, etc

06 p1005 A70-17310

Color CRT system to display engineering data based on real time analysis, discussing performance requirements

06 p1061 A70-17349

Atmospheric tides influence on meteors characteristics from processing observation data

06 p1140 A70-17736

Grouping method estimation of statistical data during hydrometeorological information processing to calculate essential data for distribution curve judgement

06 p1096 A70-17786

Optimal timing of measurements to minimize dispersion of navigational observation parameters by least squares method applied to Keplerian orbit elements

06 p1103 A70-17878

Differential game with opponent receiving information on phase coordinates of adversary with delay caused by reception and processing procedures

07 p1244 A70-18718

Methodologies inadequacies for studying information processing rate in visual perception

07 p1203 A70-18943

Oblique ionospheric sounder automatic data analysis by computer programs, analog to digital conversion, magnetic tape data recording, signal detection, pattern recognition, etc

07 p1234 A70-19185

Optimal photometric data processing for planetary characteristics and surface details, considering errors due to image blurring in telescope

07 p1384 A70-19419

Ionospheric data representation in tabular form for computer storage and processing, noting memory cells reduction

07 p1268 A70-19460

Indirect methods of trajectory optimization, improving convergence through normalization of state data and Lagrange multipliers

07 p1326 A70-19726

Divided attention utility for monitoring information processing during encoding, retention and recall of words

07 p1224 A70-20047

Phased-array radars and parallel processing computers system in high target density environment, input-output, array steering and data storage and handling

07 p1236 A70-20150

Martian surface radar observation results, discussing data processing method, backscattering behavior evaluation, relief and composition model, etc

08 p1456 A70-20643

Soviet collection of papers on apparatus for meteorological measurements covering error analysis, reliability engineering, use of computers, etc

08 p1494 A70-20771

Matching operations for difference and differential equations describing discrete control systems dynamics having cyclic interruption of data quantization frequency

08 p1480 A70-20999

Turbulent transfer mechanism in atmospheric surface layer, analyzing micrometeorological data for flux-gradient relationships, relating turbulent scale to eddy diffusivities

09 p1712 A70-22051

Telemetry data processing of Eole scientific weather forecasting program, discussing mathematical model simulating atmospheric circulation in Southern Hemisphere

09 p1674 A70-22200

Earth resources satellite TV cameras operating on different spectral bands, discussing data preprocessing for correlation with topographic maps

09 p1674 A70-22259

Human factors data standardization in NASA Apollo Applications Program for computer data processing

09 p1623 A70-22295

Neural information processing taking into account differences between living brain and artificial processor

09 p1617 A70-22496

Quality information equipment engineering including specifying, development, design, procurement, construction, installation, checkout, etc

09 p1792 A70-22569

Fluidic logic components for automatic data processing, describing circuits designed to solve specific problems

09 p1612 A70-22771

Earth resources satellite imagery processing techniques, discussing sensor and transmission link distortions, image quality and optical or digital approach

[AIAA PAPER 70-297]

09 p1677 A70-22852

Earth Resources Data Processing Center magnitude and facility planning compared with NASA centers

[AIAA PAPER 70-324] 09 p1793 A70-22863

Large scale aerospace data acquisition, processing, handling and dissemination systems analysis and design

[AIAA PAPER 70-322] 09 p1641 A70-22865

Data management functions of National Space Science Data Center /NSSDC/, discussing data processing and information system for secondary usage

[AIAA PAPER 70-320] 09 p1641 A70-22866

Multispectral point scan camera system as remote sensor for Earth Resources Satellite, noting real time automatic data processing and interpretation

[AIAA PAPER 70-319] 09 p1677 A70-22867

Digital computer processing of airborne multispectral data, discussing automatic recognition and mapping of terrain distribution, Earth Resources Technology Satellite data channel efficiency, etc

[AIAA PAPER 70-309] 09 p1668 A70-22878

Coastal areas remote sensing instrumentation and techniques, discussing data handling and analysis and ground verification of color and multispectral imagery

[AIAA PAPER 70-299] 09 p1669 A70-22885

Multidiscipline applications for Earth Resources Satellite data, including data simulation and interpretation techniques

09 p1669 A70-22886

Information extraction efforts using imaging sensors on earth resources satellites compared to data processing for environmental satellite imaging sensors

[AIAA PAPER 70-284] 09 p1669 A70-22894

Hybrid computer for decision-directed estimators of two-class decision boundary, noting applications to medical diagnosis, communications and pattern recognition

09 p1641 A70-22965

Astronomical high resolution radio interferometers design with autonomous reception, analyzing sensitivity of data processing correlation devices

09 p1647 A70-23132

Human operator transinformation sensitivity to display gain and forcing function bandwidth in rate control tracking task

10 p1823 A70-23896

Geophysical measurement curves mechanical transformation by digitizing curve on punched tape followed by processing in computer

10 p1845 A70-24494

Pattern prerecognition processing for multiobject pictures, describing illumination, contour and curvature computation

10 p1845 A70-24659

Information processing stages by reaction time measurements permitting discovery, property assessment and separate testing of stage durations additivity and stochastic independence

10 p1826 A70-24723

Remote sensor input radiation at aperture, signals within and sensed data processing by computer techniques, noting automatic image interpretation

10 p1841 A70-24733

Airborne remote sensing automatic data processing for forest identification through pattern discrimination, utilizing power spectrum analysis

10 p1878 A70-24734

Group Method of Data Handling based on heuristic self organization for solving complex system problems, with applications to random processes prediction

10 p1845 A70-24869

Optimal data filtering techniques and hardware for centrifuge testing of missile inertial platforms

[AIAA PAPER 70-405] 10 p1861 A70-24901

Nonavionics Aircraft Integrated Data System configurations evaluation by computer model, showing cost effectiveness data in terms of aircraft maintenance and availability

[AIAA PAPER 70-396] 10 p1808 A70-24909

Eye-ball technique smoothing procedure discarding wild data points using minimum computer time for automatic treatment of digitally sampled test data

[AIAA PAPER 70-386] 10 p1861 A70-24919

Helicopter flight test and evaluation tools including data processing facilities to improve test validity

[AIAA PAPER 70-373] 10 p1806 A70-24929

Ionospheric fine structure from ionograms, discussing probe and half automatic digital evaluation method

10 p1884 A70-25257

Nimbus high resolution IR radiometer /HRIR/ data processed by color display enhancement system, demonstrating meteorological, oceanographic and geomorphological applications

11 p2049 A70-25636

SAFEGUARD ballistic missile defense radars, discussing terminal defense concept, data processing system and microwave components

11 p2005 A70-26162

Automatic input data generation for finite element method using algorithm based on complex geometrical configurations topological classification in terms of natural coordinates

[JPL-TR-32-1486] 11 p2144 A70-26678

Preprocessing data transformations for multispectral recognition mapping, reducing difficulties due to variations in environmental, observational and sensor conditions

12 p2220 A70-26935
Earth resources satellite ground data handling system providing initial processing, reproduction, indexing, storage, retrieval and dissemination functions

12 p2191 A70-26943
Automatic air transportation passenger handling and postflight financial and statistical data processing

12 p2335 A70-27016
Bayesian probabilistic information processing in psychological decision making in air traffic control, discussing bookbag and poker-chip applications

12 p2178 A70-27047
Discrete sequential algorithms for bit synchronization implemented with digital computer for optimum data detection

12 p2184 A70-27249
ATC data processing requirements for higher automation level in terms of computer instruction rate and storage

12 p2267 A70-27638
Radar beacon target processing system providing ATC information, noting target detecting and locating ability in noisy environment

12 p2268 A70-27640
ATC data processing requirements based on projected traffic growth

12 p2268 A70-27910
Automatic image interpretation and classification - Conference, Pisa-Tirrenia, Italy, August-September 1968

12 p2193 A70-28101
Regular and irregular line-drawing data processing, discussing quantization and encoding methods

12 p2193 A70-28104
Image processing, considering sampled data methods applied to two dimensional data

12 p2193 A70-28107
Methodology for machine processing for identification of individual crop types, discussing discriminant photoanalysis

12 p2227 A70-28108
Spaceborne information processing for manned missions, describing layered system with fault tolerance and onboard checkout

13 p2372 A70-28415
Onboard satellite information processing systems for bandwidth compression using digital filters and error correcting coding

13 p2381 A70-28431
Leonid meteor shower radar observation data, analyzing flux rates and particle size distribution

13 p2487 A70-28694
Soviet book on discrete system for measuring multivariable probability distributions, covering automatic acquisition and reduction of statistical data

13 p2381 A70-28700
Spacecraft based data processing stages to perform navigation during outer planet missions

13 p2448 A70-28704
Hybrid computing techniques for solving parabolic and hyperbolic partial differential equations, discussing serial method accuracy and use of parallel logic for integrator control

13 p2373 A70-29461
Solar probe Helios data processing and transmission system, describing block diagram, PCM/PSK/PM telemetry and transmitter

13 p2367 A70-29558
EEG data automatic classification using discriminant analysis

13 p2360 A70-29627
Time shared computer system providing real time service to multiple laboratory instrumentation, discussing high speed channel, computer control and data abstracting techniques

13 p2375 A70-29830
Analog computer methods applied to aerospace dynamic test data analysis and high speed screening [AIAA PAPER 70-595]

13 p2375 A70-29880
Berkeley array processor /special purpose digital computer/ for correlation, convolution, recursive filtering, matrix multiplication, etc

13 p2376 A70-29941
Price estimate elements interrelationship using three dimensional matrix for computerized cost data extraction

14 p2668 A70-30524
Wind gust data analysis for spacecraft design using power spectrum approach

14 p2607 A70-30580
Electronic systems automatic design problems including man machine communication and data organization

14 p2554 A70-30663
Weibull distribution as statistical method for interpreting fatigue test data

14 p2656 A70-30700
Real time Apollo lunar module thermal mission data analysis using computer programs

14 p2653 A70-30774

People as conservative processors of fallible information, treating stationary data generating process as nonstationary

14 p2537 A70-30898
Approximating hazard rate function parameters estimation from failure data, using computer program

14 p2592 A70-31113
Electronic systems for high speed photography, noting application to data processing and storage

14 p2589 A70-31402
Measuring apparatus for cyclic plastic strains at high temperatures, discussing data processing techniques

15 p2733 A70-31538
Wind field reduction from satellite cloud structure data

15 p2770 A70-32066
Reduction constants simultaneous determination in earth figure theory based on astronomical, geodetic and gravimetric data

15 p2731 A70-32147
Pattern recognition procedure for electronic systems data classification

15 p2706 A70-32566
Interrelated computer programs and comprehensive parts data bank /REACT/ for reliability assurance analysis

15 p2706 A70-32654
System failure rate estimation as function of age using incomplete field reliability data

15 p2748 A70-32660
Regularization techniques for optimal control problems in polynomial algorithms of data handling by groups

16 p2867 A70-33236
Parallel associative unstructured element computer design for real time radar track data processing

16 p2869 A70-33466
Display-control relationships in visual display information processing, considering spatial incompatibility effects on reaction time

16 p2852 A70-33661
Computers - AFIPS Conference, Atlantic City, May 1970

16 p2870 A70-33730
Onboard automatic checkout systems for manned space vehicles, investigating data management development costs for thorough tradeoff studies

16 p2889 A70-33803
Automatic speech recognition and tracking techniques of moving objects, considering applicability to processing data from earth resources satellites

16 p2871 A70-34313
Computerized air transportation service including passenger name record, fare quotation, ticketing, etc

17 p3199 A70-34688
Airborne flight test data acquisition and ground based automatic bulk data processing system for helicopter test and development programs

17 p3014 A70-34713
Real time data processing and display for spacecraft thermal vacuum testing, using hybrid computer

17 p3059 A70-35176
Successful application development and implementation of data processing system, noting sequence, magnitude, manpower and time required

17 p3200 A70-35507
Multichannel time marker network synthesis device for physiological data assembly, transformation and processing, generating pulses

18 p3223 A70-36083
Associative processor concept for air traffic control, discussing tracking and correlation problem

18 p3288 A70-36392
Data processing system for automatic air traffic control, describing hardware and software

18 p3288 A70-36395
Ionospheric data representation in tabular form for computer storage and processing, noting memory cells reduction

18 p3250 A70-36934
Management information systems based on Apollo program experience, considering improvements in data accuracy, display, feedback, etc

19 p3553 A70-37862
Airborne integrated data system /AIDS/ for accepting, processing, recording and displaying aircraft systems data, describing installation and design criteria

19 p3382 A70-37895
Logic, arithmetic, control and instruction capacities of dedicated onboard telemetry preprocessor

19 p3383 A70-37904
Rocket engine tests dynamic data oscillographic presentation and digital processing

19 p3490 A70-37916
Automatic gain ranging amplifier for high speed digital computer controlled data acquisition system used to process input data levels

19 p3383 A70-37919
Automatic ATC with feedback, describing information processing and flight plan algorithm

19 p3464 A70-38161

Soviet papers on physiological data collection and analysis methods

19 p3369 A70-38206
Flight test and airborne data recovery and processing, discussing data format, recorder characteristics, ground equipment and time requirement

19 p3429 A70-38517
Jaguar flight test data processing system, discussing airborne digital computer

19 p3384 A70-38536
Digital computer magnetic tape recording system for flight tests of Jaguar aircraft, discussing data treatment

19 p3384 A70-38537
Ground station to retrieve and process data recorded on airborne digital magnetic tape instrumentation system for Hawker Siddeley Harrier flight development

19 p3384 A70-38550
ATC simulation at EUROCONTROL Experimental Center, discussing dynamic simulator, data processor and display

19 p3468 A70-38638
Digital extraction of primary and secondary radar data for air traffic control

19 p3469 A70-38644
Signal automatic air traffic control system /SATCO/ for flight plan processing, using multi-processing real time computer, electronic displays and software facilities

19 p3469 A70-38646
Hydrometeorological information processing using ALGOL-60 translator language

19 p3463 A70-38759
RAMMIT /reliability and maintainability management improvement techniques/ for processing maintenance data relevant to Army aircraft operations and support

19 p3441 A70-38826
Pulse coding system for average evoked EEG potential data acquisition and analysis, describing pulse generation circuitry and computer implemented logic

20 p3578 A70-38985
Earth resources ground data processing in image formats from sensors in aerospace platforms, discussing collection control, image storage, retrieval, etc

20 p3591 A70-39058
Data processing for Earth Resources Satellite users, investigating partitioning and mosaicking

20 p3591 A70-39059
Algorithms for processing of cosmic ray data monitored by space station with multichannels for neutron and meson components recordings

20 p3698 A70-39309
Real time kalman filtering of Apollo LM/AGS rendezvous radar data [AIAA PAPER 70-957]

20 p3600 A70-39572
Random values analog sensors classification based on physical, algorithmic and data reproduction techniques

20 p3593 A70-39917
Earth resources observation satellite program and organization for acquiring, processing, utilizing and disseminating remote sensor data

20 p3741 A70-39944
Automatic calculations for fuel volume mass properties in tanks at various angles of attack, considering total weight, gravity center moment and inertia product [SAWE PAPER 850]

20 p3563 A70-40376
Papers on information science and technology covering computerized retrieval, automatic indexing, selective dissemination, etc

21 p3955 A70-40894
Digital computer processing of airborne multispectral data, discussing automatic recognition and mapping of terrain distribution, Earth Resources Technology Satellite data, channel efficiency, etc [AIAA PAPER 70-309]

21 p3829 A70-41851
Model for human brain visual information processing networks, considering visual search, selection, storage, correlation, recognition and recall functions

22 p3977 A70-42287
Data handling and processing methods for non-destructive test data translation and interpretation, using scanning test model

22 p3993 A70-42588
Kalman filters for data mixing in optimally aided inertial navigation systems

22 p4067 A70-42661
Spectral signature recognition for automatic interpretation of earth resources multispectral data

22 p4037 A70-43088
Radar information digital processing, deriving criterion for automatic lock-on of target trajectories

22 p3991 A70-43552
Information processing methods in microwave measurement using digital computers, emphasizing active and passive transducers

23 p4193 A70-43795

Data acquisition and processing in structural modal characteristics analysis during ground resonance tests [ICAS PAPER 70-36] 23 p4267 A70-44133

Data management functions of National Space Science Data Center (NSSDC), discussing data processing and information system for secondary usage [AIAA PAPER 70-320] 23 p4285 A70-44514

Scientific/technical information collection, retrieval and dissemination, discussing organization, employment of technical/scientific expert personnel and use of modern data processing equipment 23 p4286 A70-44670

Automatic Data Processing and Display System for ATC over Belgium, Holland and Germany, relieving traffic controller routine tasks 23 p4216 A70-44860

Pattern recognition system design, discussing criteria and algorithm for grouping multivariate data without supervision 24 p4316 A70-45103

Digital frequency filter for data processing 24 p4318 A70-45435

Information theory in physics and engineering, considering data processing, error correction codes, space communication, optical data transmission, noise effects and holography 24 p4379 A70-45616

Onboard digital information processing, discussing applications to tactical missile guidance and manned vehicles [AIAA PAPER 70-1230] 24 p4317 A70-45976

Sapuc-Salut system for evaluating test data measured onboard Viggen aircraft 24 p4339 A70-46229

Upper Air Space Control Center Automatic Data Processing and Display System for air traffic control 24 p4323 A70-46238

DATA PROCESSING EQUIPMENT

NT AIRBORNE/SPACEBORNE COMPUTERS

NT ANALOG COMPUTERS

NT COMPUTERS

NT DATA PROCESSING TERMINALS

NT DIGITAL COMPUTERS

NT HYBRID COMPUTERS

NT IBM 360 COMPUTER

NT PRINTERS (DATA PROCESSING)

NT SEQUENTIAL COMPUTERS

NT SITE DATA PROCESSORS

Apollo program navigation processing using Kalman optimal linear computer, emphasizing position vector and error matrix and command and lunar landing extrapolation module navigation 03 p0522 A70-13604

Planetary film system (PFS)/ camera-processor-scanner for scientific spaceborne applications, detailing design and performance 03 p0490 A70-13664

Installation planning of electronic data processing unit using network and PERT program features 03 p0454 A70-13969

Automatic system for processing data from underground meson telescopes 07 p1238 A70-20347

Neural information processing taking into account differences between living brain and artificial processor 09 p1617 A70-22496

Machine design similar to human brain for recognition and classification of information 09 p1641 A70-22708

Phased array radar system synthesis, discussing small aperture systems, effects of solid state technology and role of data processing 10 p1842 A70-24877

ALSEP component configuration and deployment environment, describing passive thermal control system for data processing equipment 14 p2651 A70-31340

Airborne multiprocessor building blocks, discussing central processor, input/output controller and interface, memory unit and power supply 16 p2869 A70-33465

Electronic data processing by aircraft manufacturer, handling structural and performance problems 16 p2843 A70-34350

Data acquisition and processing system for electronic countermeasure aircraft tests 19 p3383 A70-37900

RMS spectrum analysis system for wideband acoustic data processing, using analog method with digital output 19 p3397 A70-37910

C-5A engineering flight test (EFT)/ computer controlled data processing system operation, illustrating capability, performance and limitations 19 p3355 A70-37917

Data processing systems functions and composition for random data reduction during aircraft flight tests based on analog and digital techniques 19 p3430 A70-38524

Boeing 747 transport airplane flight test data system, discussing recording media, major PCM and FM tape systems, etc 19 p3431 A70-38531

Ground based radar tracking data processing method for real time information concerning lunar module (LM)/ position and velocity during Apollo 12 flight [AIAA PAPER 70-1020] 20 p3591 A70-39514

Statistical information processing equipment, describing correlators and digital coding devices design for graphic form information transformation into binary code 20 p3594 A70-39919

Apollo program navigation processing using Kalman optimal linear computer, emphasizing position vector and error matrix and command and lunar landing extrapolation module navigation 21 p3848 A70-41127

Automated data handling system for satellite environmental testing used by ESRO 21 p3805 A70-42258

Roving vehicle self contained automatic control systems, discussing terrain scanning technique, stereo TV and electronic coordinate measuring and data processing equipment 23 p4260 A70-44628

ATC radar data processing and display systems equipment and operation, emphasizing economy 23 p4216 A70-45044

LSI 4-bit complementary speed (COS/ MOS parallel processor array 24 p4317 A70-46215

DATA PROCESSING TERMINALS

Digital and analog large system data displays, considering CRT, laser, hybrid types, contrast control, etc 06 p1061 A70-17348

DATA PROCESSORS

U DATA PROCESSING EQUIPMENT

DATA READOUT SYSTEMS

U DATA SYSTEMS

U DISPLAY DEVICES

DATA RECORDERS

Automatic universal-code digital data recorder for photogrammetric measurements 03 p0483 A70-13110

On-line system transmitting experimental data from optical spectrometer to central computing facility for magnetic tape recording 05 p0818 A70-16846

Versatile recorder for experimental studies with differing requirements 07 p1283 A70-19670

Flight test and airborne data recovery and processing, discussing data format, recorder characteristics, ground equipment and time requirement 19 p3429 A70-38517

DATA RECORDING

UV sensitive spiropyran films coloration mechanism and color structure stabilization, discussing film and laser applications to optical data recording and storage 01 p0086 A70-10357

Digital computer for data recording in stress-strain curves and data points for mechanical tests 01 p0058 A70-11062

Flight data recorders, examining present systems and planned improvements 02 p0302 A70-12621

Slitless system using interference filter, fixed Fabry-Perot etalon and automatically controlled etalon for recording spectral information for efficient light detection 04 p0685 A70-14523

Scientific equipment on Cosmos 237 satellite for recording extraterrestrial radiation data, discussing specifications, operation and mission purpose 05 p0851 A70-16733

Solar radio bursts time-variable structure at 12 M wavelength recorded on Ediswan pen oscillograph 06 p1144 A70-18005

Holographic recording of information contained in evanescent wave fields in high resolution photographic emulsions 07 p1281 A70-19367

Harmonic ion cyclotron resonances associated with proton whistlers observed from OGO-4 satellite VLF recordings 07 p1268 A70-19630

Holograms in thick absorption recording media in terms of diffraction efficiency, angular orientation and wavelength sensitivities 07 p1287 A70-20093

Display objectives and relationships to recording techniques examined for memory/display system, considering requirement for elastic erasing technique 08 p1467 A70-21761

Duplex schlieren optical system with one channel for data recording and second channel for visual monitoring 09 p1687 A70-23766

Recording nonlinearities effect on image reconstruction from hologram of diffuse object 11 p2050 A70-25641

Atmospheric hydrogen content continuous recording method based on absorption line analysis of mercury vapor from mercuric oxide reduction 11 p2052 A70-26389

Automatic engine maintenance recording system on air transport aircraft noting data reduction [SAE PAPER 700317] 12 p2335 A70-27456

Mesoscale stratospheric turbulence recording using even activated memory recorder 14 p2573 A70-30578

Visual observation, free space traversal, accelerometry and telemetry for measuring and recording human behavior, discussing free space-time traversal data logging system 14 p2542 A70-30794

Automatic recording respirometer for industrial wastes, discussing design and advantages 14 p2543 A70-31164

Damped vibrations logarithmic decrement determination during automatic recording of number of cycles, emphasizing error analysis 15 p2733 A70-31531

Level quantization in time compression systems using storage devices with small dynamic range of recorded signals 15 p2733 A70-31578

Automatic profile measurement and recording, describing equipment and techniques 15 p2742 A70-32777

Semiautomatic ionospheric absorption recorder, describing components circuitry and operation 16 p2915 A70-34223

Holographic velocity data recording (velocimetry), discussing axial resolution enhancement by spherical wave illumination 19 p3423 A70-37859

Digital flight data recording, considering aircraft integrated data systems (AIDS) 19 p3426 A70-37892

Economic payback of AIDS (Aircraft Integrated Data System)/ recording for operational performance monitoring and engine analysis 19 p3382 A70-37894

Flight data acquisition methods standardization, discussing digital recording modes and formats and hardware rationalization 19 p3429 A70-38515

Boeing 747 transport airplane flight test data system, discussing recording media, major PCM and FM tape systems, etc 19 p3431 A70-38531

Concorde prototype 002 flight test data recording instrumentation, emphasizing digital system for quasi-static parameters 19 p3432 A70-38545

Magnetic tape instrumentation system installed aboard Hawker Siddeley Harrier for flight development, discussing digital format recording system 19 p3384 A70-38549

Five-channel azimuthal underground cosmic ray telescope using proportional counters suitable for continuous recording 20 p3629 A70-39312

Tensile test device for continuous recording of sample load and strain 20 p3728 A70-40000

Ionospheric layers critical frequencies recording, using automatic interplanetary station type probe 23 p4194 A70-44088

Image orthicon detection and recording system adapted for spectroscopic measurements in shock tube emission studies 23 p4197 A70-44469

ITOS-1 second generation meteorological satellite launched with Delta N booster, providing direct APT global readout and AVCS TV data recording for playback 23 p4259 A70-44615

Automated ultrasonic testing and facsimile data recording systems, discussing aerospace, marine and automotive applications 24 p4343 A70-45692

DATA REDUCTION

NT DATA SMOOTHING

Data analysis of inertial systems for commercial aircraft overseas operations, classifying systems error propagation as linear time drift or Foucault period oscillation 01 p0137 A70-10314

Stony meteorite trace elements groups neutron activation analysis with computer reduction of Ge/Li spectra 02 p0249 A70-11680

Unified Flight Analysis System processing post-flight data from Saturn 5 launches, discussing system components, support programs and performance 02 p0264 A70-12127

Multidimensional data efficient decomposition for communication interface between man machine system, considering decision making and pattern recognition on digital computers with orthogonal transformations 02 p0265 A70-12149

Omega position location equipment (OPLE)/ experimental data analysis, obtaining quantitative measure of statistical performance of system 02 p0336 A70-12180

Servo systems for analog automatic reduction of time dependent photomechanical model materials fringe data in stress analysis

03 p0482 A70-12967

Time sharing computer systems for data reduction from semiconductor strain gauges applied to FORTRAN IV programs

03 p0453 A70-12969

Mesoscale rawinsonde network for convective process resolution, describing reduction and analysis techniques for thunderstorm wind, temperature and moisture data

03 p0521 A70-13165

Earth satellite tracking data reduction for determining geodetic ground nets, examining errors in triangulation procedures

03 p0445 A70-13184

Gravimetric and satellite tracking data reduction for determining coefficients in mathematical expansion representing earth gravitational field

03 p0473 A70-13189

Photometric reduction of Lunar Orbiter video magnetic tapes for generation of topographic information of proposed Apollo landing sites

03 p0490 A70-13661

Equatorial magnetosphere particle and field data from 18 April 1965 geomagnetic storm reanalyzed in context of drift mirror instability theory

03 p0560 A70-13976

Analog techniques for pulse integration based on sonograph audio spectrum analyzer for pulsar observation by radio telescopes near Hobart, Tasmania

04 p0655 A70-14520

Radar data parameter determination method, discussing false alarm calculation

05 p0811 A70-15988

Diagram compression by spatiotemporal coding of antenna array fitted with phase shifters

05 p0811 A70-15989

Adaptive multiparameter experiment for iterative minimization of investigated data points, based on human response pattern to psychophysical inputs

05 p0805 A70-16006

STRIDA II consoles operation for treating air defense data, discussing data display system, work positions organization and console construction method

05 p0828 A70-16192

High resolution Venus spectra, obtaining band spectra growth curve of C13016018 isotope of carbon dioxide, comparing data reduction methods

05 p0910 A70-16392

Brightness distribution over source, discussing regularization algorithms for radio astronomical data reduction from crossed telescope

05 p0917 A70-16902

Response characteristics of height-based and time-based wind reduction techniques for meteorological rocketsondes

05 p0879 A70-17101

Optimum compression ratio defined for Markov sources for compression algorithm efficiency and data compression schemes

06 p1013 A70-18624

Data reduction from DIA satellite VHF and UHF Doppler measurements to attempt geodetic link between Nice and Beirut

07 p1262 A70-18941

Oblique ionospheric sounder automatic data analysis by computer programs, analog to digital conversion, magnetic tape data recording, signal detection, pattern recognition, etc

07 p1234 A70-19185

Servo systems for analog automatic reduction of time dependent photomechanical model materials fringe data in stress analysis

07 p1286 A70-20040

Turbulent transfer mechanism in atmospheric surface layer, analyzing micrometeorological data for flux-gradient relationships, relating turbulent scale to eddy diffusivities

09 p1712 A70-22051

Automatic spectral data reduction and analysis system consisting of densitometer, analog-digital converter and IBM 1800 process computer with magnetic disk memory

09 p1629 A70-22765

Earth resources remotely sensed data analysis with emphasis on machine analysis over manual photointerpretation, discussing pattern recognition techniques, information systems, etc

09 p1678 A70-22891

Time averaging and length of record effects on horizontal wind speed variance, determining maximum wind gusts as function of height and averaging time

10 p1909 A70-23928

Perceptual selection and integration of sensory data conveyed to brain, explaining various optical illusions

10 p1827 A70-24766

Satellite photographic plate reduction - COSPAR Conference, Prague, April 1968

11 p2006 A70-26179

Stars identification on photographic plates and position computation in FORTRAN, using CONTROL DATA 6600 and IBM 1130 computers

11 p2113 A70-26183

Reduction of satellite photographic data using transformation functions

11 p2007 A70-26186

Satellite observations reduction, determining continuous transformation over whole field of photograph by local transformations

11 p2007 A70-26187

U.S. Coast and Geodetic Survey satellite triangulation data reduction methods, discussing data acquisition system, plate preparation, etc

11 p2046 A70-26190

Passive satellite coordinates correlations to instants of observation in U.S.S.R. ground stations, reducing quasi-synchronous observations by interpolation

11 p2007 A70-26192

Plate reduction method for Schmidt satellite camera, considering satellite position, distortion parameters, etc

11 p2007 A70-26193

Photographic plate reduction method at Polish Academy of Sciences based on sufficient reference stars, correcting x and y coordinates

11 p2007 A70-26194

Film reduction and time keeping used at Smithsonian Astrophysical Observatory for Baker-Nunn films

11 p2007 A70-26196

Photographic reduction techniques at Meudon Observatory, discussing computation of standard and measured coordinates

11 p2007 A70-26197

Photographic satellite plates reduction by astrometric method at geodetic institute at Potsdam, discussing star coordinates, astronomic refraction, etc

11 p2008 A70-26200

Data compression for telemetry transmission with sample choice based on time-varying stream slope thresholds illustrated for Ranger photograph

11 p2010 A70-26305

Delta reprocessing operating system /DEPOS/ for high speed telemetry format-independent decommutation and data compression

11 p2010 A70-26307

High temperature fatigue tests of materials under uniaxial controlled strain, describing equipment, failure interpretation and data reduction

11 p2033 A70-26613

Radiophase and induced pulse transient /input/ remote sensor systems for geological mapping, describing data acquisition and reduction techniques

12 p2221 A70-26961

Nonlinear estimation with quantized measurements, applying algorithms to PCM, predictive quantization and data compression

12 p2192 A70-27420

Relative control data incorporation into sequential or simultaneous analytical triangulation systems, considering extraterrestrial photographs reduction

12 p2308 A70-27875

Skylark sounding rocket telemetry data reduction system providing attitude analysis

13 p2363 A70-28680

Soviet book on discrete system for measuring multivariable probability distributions, covering automatic acquisition and reduction of statistical data

13 p2381 A70-28700

Spaceborne logarithmic variable prescaling counters for automatic compression of particle measurement data, discussing statistical error

13 p2406 A70-28931

Integrated computerized data acquisition and reduction system for aircraft flight and wind tunnel tests

13 p2373 A70-29156

Random data analysis application to aircraft inlet diagnostics

[AIAA PAPER 70-597]

13 p2375 A70-29878

Analog computer methods applied to aerospace dynamic test data analysis and high speed screening

[AIAA PAPER 70-595]

13 p2375 A70-29880

Viper Dart Robin System high altitude data reduction program accuracy, discussing winds and density errors

14 p2606 A70-30566

Wind gust data analysis for spacecraft design using power spectrum approach

14 p2607 A70-30580

Weibull distribution as statistical method for interpreting fatigue test data

14 p2656 A70-30700

Ionospheric electron distribution by true height analysis of oblique incidence HF radio wave sounding data, applying to forward and ground backscatter

14 p2550 A70-30745

Real time Apollo PCM telemetry data compression and transmission using zero order predictor

14 p2550 A70-30768

Saturn rings observations during earth passage through ring plane by Abastuman observatory telescope, describing photometric processing and data reduction

15 p2797 A70-31619

Automatic numerical analysis of velocity information from Doppler effect ultrasonic blood flow meter

15 p2691 A70-31920

Data compression techniques, considering two dimensional image coding problem

15 p2705 A70-32558

On-line reduction of nystagmic data during vestibular bithermal caloric testing by analog technique

15 p2685 A70-32570

Hazard plotting methods for analyzing service life data with different failure modes

16 p2921 A70-34024

Ionospheric irregularities properties from San Marco 2 and BE-B satellites recordings, deriving height variation of irregularity size and occurrence

17 p3076 A70-34942

Static weight tare compensation for V/STOL wind tunnel models, using accelerometer outputs

17 p3062 A70-35500

Nonlinear least squares method reducing Burnett data to compressibility factors and virial coefficients

17 p3136 A70-35594

Dynamic system modeling pulse test data reduction by digital computer and functional approximation for Fourier transform calculations

18 p3230 A70-36458

Airlines data reduction using electronic engine maintenance recorders

18 p3259 A70-36853

Sample images division into teaching and checking sequences in pattern recognition problems, determining coefficients based on statistical properties of set

19 p3382 A70-37449

Signal spectral parameters for reducing VLF atmospheric data from analyzer observations

19 p3412 A70-37998

Data processing systems functions and composition for random data reduction during aircraft flight tests based on analog and digital techniques

19 p3430 A70-38524

Quasar red shift apparent magnitude data analysis, estimating deceleration parameter of universe

20 p3709 A70-40076

Airborne atmospheric turbulent flux measurement system with fast response wind velocity, temperature, humidity and aircraft motion sensors, discussing performance and data reduction

20 p3665 A70-40109

Nonlinear dynamic systems phase coordinate variations statistical characteristics, describing data reduction method

20 p3674 A70-40183

Two dimensional data array contour tracing algorithm for reduction of image coding bits number

21 p3786 A70-41327

Aircraft accident filing system data analysis using Fortran programs

22 p3962 A70-42880

Quantitative reduction of statistical nodes for nonlinear automatic control system with random noise, using minimal approximating polynomials

22 p4003 A70-42887

Spectral signature recognition for automatic interpretation of earth resources multispectral data

22 p4037 A70-43088

Fitting equations to mixture data by linear least squares method with restraints on compositions, using Scheffe polynomials

22 p4064 A70-43728

Multipurpose earth resource satellites design, emphasizing land use factors and data reduction problems

23 p4286 A70-45005

Model fitting procedure applied to lunar occultation data and models analysis for point sources, close binaries and resolvable stars

24 p4399 A70-45130

Plate overlap algorithm for photographic star catalog reduction

24 p4404 A70-45413

DATA RETRIEVAL

Automatic search for data in hydrology and meteorology, describing information search language development

14 p2602 A70-30141

Ground station to retrieve and process data recorded on airborne digital magnetic tape instrumentation system for Hawker Siddeley Harrier flight development

19 p3384 A70-38550

DATA SAMPLING

Supervisor sampling frequency maximizing given value or payoff function, discussing applications to controlling vehicle, information system or institutions

02 p3037 A70-12141

Sampled signal and associated sequence with identical Fourier transforms, noting applications to digital spectral analysis onboard spacecraft

03 p0449 A70-13538

Aircraft computer design performing basic arithmetic operations by sampling method noting speed increase

06 p1014 A70-17859

Signal stabilization and performance of nonlinear sampled data systems, suggesting oscillations injection at input

06 p1026 A70-17970

Model sampling or Monte Carlo applied to normal shock, giving temperature and density profiles for Mach 10 shock

06 p1050 A70-18337

Periodic motions and dynamic stability of nonlinear distributed sampled data system of closed loop of pulsed element governed by heat conduction equation

07 p1226 A70-18749

Soviet book on matrix methods in relay and sampled data control theory described by linear differential and finite difference equations

07 p1244 A70-19069

High speed sampling used with digital computer providing response shock spectrum data

08 p1481 A70-20610

Transfer functions representing continuous dynamic systems, identifying parameters by obtaining coefficients of discrete system transfer function relating input and output sampled sequences

08 p1478 A70-20777

Time allocation with sampling interpolation /ATIC/ for TDMA satellite telephone communications, considering auxiliary circuits, transmission quality, bit rates, demand assignment, etc

10 p1840 A70-24370

Data sampling system compensation based on bending frequency filtering through information obtained by varying sample rate, using saturn 5 launch vehicle simulation

12 p2192 A70-27411

Image processing, considering sampled data methods applied to two dimensional data

12 p2193 A70-28107

Frequency sampling adjustable equalizer design and operation, describing coaxial cable system tests

14 p2547 A70-30282

Nonlinear sampled data system transportation lag effect on limit cycle nature

14 p2560 A70-30623

Mathematical pattern recognition, using potential functions superposition methods for reconstructing probability density from samples

14 p2554 A70-30926

Sampled analog waveforms transmission, deriving optimum pre- and postfilters

15 p2703 A70-32557

Digital sampled data demodulation, discussing methods of obtaining quadrature channels from single signal

15 p2703 A70-32579

Transfer properties of scanning phase discriminator with intermediate storage, explaining sampling method and sample-hold-sample circuit

15 p2714 A70-32672

Finite settling response for single input/output feedback control system obtained by dual rate sampled data control algorithm

16 p2882 A70-33037

Distributed sampled-data control systems with memoryless nonlinear feedback element, deriving frequency domain stability criterion

16 p2884 A70-33308

Physiological tests of sampled data hypothesis in human motor control system

16 p2851 A70-33323

Actuating signal at sampling instants determined in phase plane by Mullin-Jury method for sampled data feedback containing quantizer and zero order hold circuit

16 p2886 A70-33336

Learning scheme with probabilistic teacher for unclassified samples, establishing convergence, comparing with linear estimator

17 p3128 A70-34851

Three digit hydromechanical step type actuator drives with slide valve assembly for computer data sampling systems

18 p3216 A70-37071

Automatic control system impulse response points identification by fast Fourier transform

19 p3393 A70-37852

Electro-optical modulation lock-in techniques for minimizing statistical fluctuations and eliminating internal noise in sampling of light signals

21 p3827 A70-41462

Sampled data compensators hybrid realization for discrete controllers, selecting canonical representation with minimum number of delay elements

22 p4002 A70-42846

Supervisor /monitor/ sampling frequency maximizing payoff function, using Bayesian preposterior information analysis

22 p4127 A70-43498

Time varying signals sampling, noting role of frequency in distortion

24 p4311 A70-45433

Signal distortion dependence on sampling frequency during continuous signals restoration

24 p4312 A70-45440

DATA SMOOTHING

Geographically smoothed geomagnetic cut-offs for eliminating discontinuity in neutron monitor latitude variation in Mexico City vicinity

01 p0167 A70-10229

Sensitivity analysis of discrete filtering and smoothing algorithms, noting in-track motion of circular orbit satellite and marine inertial navigation [AIAA PAPER 68-824]

03 p0459 A70-12913

Statistical testing role in synoptic meteorological analysis, discussing pressure and temperature patterns, front identification, computer applications, etc

07 p1329 A70-19574

High speed sampling used with digital computer providing response shock spectrum data

08 p1481 A70-20610

Clock corrections smoothing by linear transformation operator, calculating operator transfer function and averaged errors deviations

08 p1574 A70-21155

Observational data smoothing method starting from Whittaker method based on probability, recommending use with high speed computer

09 p1669 A70-23057

Eye-ball technique smoothing procedure discarding wild data points using minimum computer time for automatic treatment of digitally sampled test data [AIAA PAPER 70-386]

10 p1861 A70-24919

Kalman-Bucy filtering for estimating initial conditions and smoothing problems in linear dynamic systems, applicable to rectilinear motion of randomly accelerated spacecraft

12 p2186 A70-27905

FPS-16/Jimsphere wind profiles measurement, discussing effect of data smoothing on accuracy and resolution

14 p2607 A70-30569

Dynamic nonlinear estimation, deriving general algorithms for filtering, smoothing and prediction for continuous and discrete systems

14 p2562 A70-31366

Wolf numbers Zurich time series monthly values, evaluating mathematical expectation with probability smoothing by Whittaker operator

15 p2802 A70-32489

Nonlinear differential equations for smoothing density function and smoothed expectation of arbitrary function of state

16 p2941 A70-33057

X-22 VTOL aircraft initial parameter, state and covariance matrix estimates by Kalman filter and smoothing algorithms

16 p2885 A70-33329

Numerical integration of finite difference analogs of nonlinear partial differential equations, investigating data smoothing, filtering and boundary effects on computational instability

19 p3459 A70-38417

Aircraft trajectory postflight reconstruction involving photographic starfield and landmark referenced to inertial navigator output, discussing optimal data smoothing technique [AIAA PAPER 70-1022]

20 p3666 A70-39512

Minimum bias criteria for selecting data fitting curves, allowing for unknown true equation in improving data predictability

20 p3659 A70-40261

Inertial Navigation System /INS/, geodetic reference and optimal data smoothing for estimating vertical deflection and ocean currents

22 p4069 A70-43665

DATA STORAGE

UV sensitive spiropyran films coloration mechanism and color structure stabilization, discussing film and laser applications to optical data recording and storage

01 p0086 A70-10357

Information storage in complex automatic control systems with hierarchical structure composed of computers

01 p0047 A70-10983

SPIRAL system for free-flowing test information storage and retrieval in machine readable library

02 p0264 A70-12129

Information storage and retrieval system development and operation for diversified crew/equipment task data, using general purpose digital computer

02 p0265 A70-12143

Lidar technique capabilities and limitations in meteorological applications, emphasizing data storage and display instrumentation

03 p0450 A70-13673

Memory volume necessary to store intermediate data estimated for group processing from dependent Poisson information sources

04 p0661 A70-14552

ESRO 1 thermal behavior, discussing trajectory effects, onboard temperature measurement, data storage, data transmission, telemetered data and data comparison

04 p0762 A70-15164

Display storage tubes /DST/ for radar systems, describing operating principles and characteristics

04 p0660 A70-15525

Technique for coding data on cosmic ray variations based on packing digital information in computer storage, proposing selective statistical control for tape recording phase

05 p0898 A70-15929

Applied space research covering photovoltaic cells, electric propulsion, onboard data storage, vacuum lubrication and NASA-European organizations budgets

06 p1141 A70-17780

Hologram storage and retrieval in photochromic SrTiO crystals at ruby laser wavelengths

06 p1072 A70-18519

Ionospheric data representation in tabular form for computer storage and processing, noting memory cells reduction

07 p1268 A70-19460

Word organized photodetector array design for holographic read-only optical memories

07 p1288 A70-20148

Hologram data efficiency improvement by spatial offset removal, analyzing plane and spherical reference waves and plane and solid objects

08 p1500 A70-21787

Room temperature cholesteric liquid crystals retention of information on past electric field excitation by changes in optical transmission properties

09 p1740 A70-22924

Holographic optical memory feasibility for digital data storage using Ar ion laser, acousto-optic beam deflector system, hologram storage plane and photodetector array

09 p1642 A70-23780

Hologram resolution and information storage along depth of reconstructed image related to maximum track density of bubble chamber

10 p1892 A70-25113

Holographic optical memory systems operational principles and potential advantages, discussing feasibility of 100 million bit memory capacity and one microsecond random access time

10 p1892 A70-25245

Random phase mask for Fourier Transform hologram recording of data mask, noting minimum space bandwidth required

11 p2049 A70-25637

Automatic base communication system /ABCS/ to handle USAF worldwide base record communications centered on electronic store and forward message switch, utilizing stored programs

11 p2009 A70-26266

Memory mechanisms of brain, discussing molecular physiology, information storage in living systems

12 p2168 A70-27278

Holographic memory devices design for information storage

13 p2405 A70-28792

Level quantization in time compression systems using storage devices with small dynamic range of recorded signals

15 p2733 A70-31578

Reliability criteria documents updating, discussing input vs output, experience retention, tradeoffs, etc

15 p2747 A70-32630

Interrelated computer programs and comprehensive parts data bank /REACT/ for reliability assurance analysis

15 p2706 A70-32654

Transfer properties of scanning phase discriminator with intermediate storage, explaining sampling method and sample-hold-sample circuit

15 p2714 A70-32672

Holographic data storage for random information display and retrieval in wide range consumer credit network

16 p2903 A70-33135

Ionospheric data representation in tabular form for computer storage and processing, noting memory cells reduction

18 p3250 A70-36934

Sodalites color centers creation by electron beam, discussing application in dark trace cathode ray storage display tubes

19 p3379 A70-38048

Coding device for computer storage of graphical information, describing construction and operation

19 p3385 A70-38576

DATA SYSTEMS

Semiautomatic data collection system for IR reflectivity measurements, recording digitized output on punched cards for computer analysis

01 p0088 A70-10747

Unified Flight Analysis System processing post-flight data from Saturn 5 launches, discussing system components, support programs and performance

02 p0264 A70-12127

Information storage and retrieval system development and operation for diversified crew/equipment task data, using general purpose digital computer

02 p0265 A70-12143

Product reliability engineering analysis, discussing coordination, communication and data accumulation systems

02 p0309 A70-12302

ESSA system operation, describing applications of satellite meteorological data

03 p0454 A70-13667

Integrated flight test data acquisition and processing system with real time graphic display, discussing ground station function

[SAE PAPER 690678] 05 p0793 A70-15867

Command control systems characterized as problem solving information processing systems, discussing information requirements specification prior to man-display design

05 p0806 A70-16177

Command and control display operational requirements within Allied Command Europe /ACE/, information flow, decision making and evaluation

05 p0959 A70-16178

Earth resources program data management system, discussing mission control, processing and distribution of data from satellite vidicon cameras and multispectral line sensors

[ALAA PAPER 70-321] 09 p1792 A70-22854

Earth resources data exploitation, describing potential organizational structures for data handling and various political, economic and technological problems

[ALAA PAPER 70-344] 09 p1793 A70-22859

Large scale aerospace data acquisition, processing, handling and dissemination systems analysis and design

[ALAA PAPER 70-322] 09 p1641 A70-22865

Data management functions of National Space Science Data Center /NSSDC/, discussing data processing and information system for secondary usage

[ALAA PAPER 70-320] 09 p1641 A70-22866

Omega Position Location Equipment /OPL/ system, testing operational feasibility of centralized global meteorological data collection system

09 p1722 A70-23030

Cost analysis for satellite data system determined for bit rates range and break-even distances

10 p1838 A70-24361

Thermoelectric outer planet spacecraft /TOPS/ project incorporating adaptable data handling system and self testing and repairing computer with triple redundancy subsystems

11 p1996 A70-25368

Product oriented cost data bank for satellite system cost prediction and negotiation designed for USAF communications satellite program

[ALAA PAPER 70-445] 11 p2152 A70-25477

Air traffic control surveillance and data system using synchronous satellites in inclined elliptical orbits for communications and aircraft position determination

12 p2268 A70-27644

Cockpit data monitor allowing pilot selection of instrumentation parameter readout

13 p2345 A70-28970

Aircraft turbojet engine/inlet compatibility, using data system for acquisition, identification and analysis of critical time variant pressure parameters

[ALAA PAPER 70-594] 13 p2375 A70-29877

Dynamic pressure data acquisition editing and processing system for engine inlet wind tunnel model tests

[ALAA PAPER 70-596] 13 p2375 A70-29879

Data flow in computerized automatic data acquisition systems, considering systems traceability of calibration to national standards

14 p2554 A70-31110

Data system obtaining sampling rate for cardiac volume measurement via fast biplane cineangiography

15 p2691 A70-31922

Experiment information management, discussing data flow patterns, acquisition, processing, storage, etc

[AAS PAPER 70-057] 17 p3199 A70-34807

Pseudonoise code command system for scientific satellite, describing added bits and decoder

17 p3046 A70-35276

Management program for digital data systems maintenance and repair

17 p3200 A70-35487

Low pressure measuring system for aerodynamic models tested in Mach 12-14 wind tunnel, discussing transducers and high speed digital recording and data processing system

17 p3062 A70-35493

On-line final V/STOL Wind Tunnel Data Encoding and Evaluation System /WINDEE/ for complex powered models, using computer monitoring

17 p3049 A70-35494

DC-10 airborne flight test PCM data system, discussing capability, onboard operating characteristics and test results

17 p3093 A70-35498

Digital data acquisition and control system for acoustic testing of large spacecraft

17 p3062 A70-35506

Flight data recording systems for accident investigation and operational purposes, discussing U.S., British and French regulations

18 p3258 A70-36341

Computerized airborne integrated data acquisition and analysis system, discussing hardware, software and airborne-ground elements interfaces

[ALAA PAPER 70-935] 19 p3382 A70-37393

Aircraft nonavionics systems performance condition and minimum maintenance duties diagnosis by integrated data system, discussing engine monitoring instruments

19 p3426 A70-37891

Digital flight data recording, considering aircraft integrated data systems /AIDS/

19 p3426 A70-37892

Flight data recording system /FDRS/ for crashes expanded to aircraft integrated data system /AIDS/ for airlines

19 p3426 A70-37893

Economic payback of AIDS /Aircraft Integrated Data System/ recording for operational performance monitoring and engine analysis

19 p3382 A70-37894

Airborne integrated data system /AIDS/ for accepting, processing, recording and displaying aircraft systems data, describing installation and design criteria

19 p3382 A70-37895

Data acquisition and processing system for electronic countermeasure aircraft tests

19 p3383 A70-37900

RMS spectrum analysis system for wideband acoustic data processing, using analog method with digital output

19 p3397 A70-37910

Data management methodology for test facilities, considering on-line analog/digital computers

19 p3383 A70-37922

Digital computer for high speed wind tunnel data acquisition, processing and operations control

19 p3397 A70-37923

Data collection system for prototype flight tests of Fokker F-28 based on DC-8 aircraft digital system

19 p3384 A70-38546

Integrated data systems for aircraft maintenance, noting information retrieval role in maintenance management for cost reduction and safety

20 p3740 A70-39647

Thermoelectric outer planet spacecraft /TOPS/ data subsystems for 12 year missions compared with Mariner subsystem

21 p3795 A70-41796

Data handling and processing methods for non-destructive test data translation and interpretation, using scanning test model

22 p3993 A70-42588

Automated air cargo and data flow system with on-line computers, discussing handling, document management, load planning, information transmission, storage and mechanized freight systems

22 p3994 A70-43271

NASA safety related research programs based on technology transfer involving information summarizing, indexing and storage from global aerospace research and development

23 p4285 A70-44457

Data management functions of National Space Science Data Center /NSSDC/, discussing data processing and information system for secondary usage

[ALAA PAPER 70-320] 23 p4285 A70-44514

Manned spacecraft onboard data management systems, discussing information transfer, processing, control, display and man machine interface

23 p4167 A70-44647

Space shuttle onboard cost effective data management system, discussing checkout, fault isolation, redundant element switching and crew interaction

[ALAA PAPER 70-1293] 24 p4418 A70-45975

DATA TRANSMISSION

NT AUTOMATIC PICTURE TRANSMISSION

NT CHANNELS [DATA TRANSMISSION]

Area navigation and automatic data communications in air traffic control proposed for New York area STOL aircraft operations and Boeing 747 aircraft

[ALAA PAPER 69-1054] 01 p0138 A70-10640

HEOS 1 satellite telemetry, telecommand and tracking systems, noting data transmission degradation due to high solar activity

01 p0045 A70-11115

FM data and telegraph signal transmission over PCM system analog channel, discussing adaptability to digital modulated signals

01 p0046 A70-11318

Technology transfer techniques within business firm, including specific examples used by successful companies

02 p0403 A70-12635

Optimum balance between program and functional organizations to promote technology transfer

02 p0403 A70-12637

Technology transfer experience in terms of aerospace company policies and technical management mechanics

02 p0389 A70-12638

Interruptions influence in discrete information flow on characteristics of radar tracking system

03 p0446 A70-13198

Bit transition time /bit synchronization/ estimation, developing bit synchronizer from Bayes estimation and optimization theories

[AAS PAPER 69-608] 04 p0647 A70-14655

Data transmission from automatic space stations on Mars and Venus, considering relaying via artificial planet satellite or direct transmission to ground station

04 p0648 A70-14931

Frequency bandwidth reduction for geophysical data transmission from satellites or lunar stations by time correlation of signal and transmission channel band changes

05 p0847 A70-15968

Information transmission capability of hologram without distortion, considering confocal resonator reconstructible transparencies for bounded hologram

05 p0848 A70-16265

Weather data communication, discussing transmission of radar, polar satellite and ATS satellite data to processing center and forecasts dissemination to public media

05 p0814 A70-16327

Ternary data transmission systems characteristics for modulated codes with known parameters or random initial phases

05 p0816 A70-17006

Worldwide Apollo data transmission network emphasizing computer operations for message collection and distribution, command and telemetry processing, etc

06 p1005 A70-17310

Broad beam Tracking Data Relay Satellite /TDRS/ for manned and automated spacecraft using VHF bands

06 p1006 A70-17345

Coding and signal selection for data relay satellite interrogation channel serving many low-powered unattended user terminals

06 p1006 A70-17347

Baseband transmission system information transmission rate improvement, using multivalued PCM signals

06 p1007 A70-17461

Differential game with opponent receiving information on phase coordinates of adversary with delay caused by reception and processing procedures

07 p1244 A70-18718

Digital data transmission over discrete time Gaussian channel with noisy feedback, investigating error-exponent /reliability/ and finite SNR

07 p1235 A70-19362

Terminal air traffic control automation, discussing Advanced Radar Traffic Control System /ARTS/ and control tower data transfer aspects

08 p1540 A70-20678

Digital communications and circuits and components for GHz data rate capability, discussing modulation techniques and bit stream coding

08 p1462 A70-21258

Millimeter guided wave communication systems information transmission capacity increase, using quaternary and higher order modulation techniques

08 p1462 A70-21506

Narrow width pulse-position modulated optical communication system design, determining performance in terms of error probability and information rates

08 p1463 A70-21778

Adaptive equalizer consisting of canonical link structure with minimum number of delay elements applied to fast data transmission

09 p1640 A70-22039

Air safety and navigation systems data transmission, discussing analog to digital conversion and modulation

09 p1720 A70-22550

Gigahertz rate circuits requirements for high speed digital data communication from component and system viewpoint, emphasizing coding and multiplexing techniques

09 p1633 A70-22605

Earth resources data transmission, describing picture reception and reproduction equipment

[ALAA PAPER 70-328] 09 p1634 A70-22856

Rapid and reliable data transfer within limited bandwidth and tracking time in earth resources technology satellites, discussing time division multiplexing, digitizing, etc

[ALAA PAPER 70-325] 09 p1635 A70-22858

Book on information transmission by orthogonal functions covering mathematical foundations, direct signal transmission, carrier transmission, statistical variables, etc

09 p1636 A70-23125

Digital record message communication satellite network system involving synchronous satellites and small earth terminals

10 p1834 A70-24327

Digital satellite communication system using multi-phase modulation optimized for phase positions number to maximize transmission capacity

10 p1835 A70-24334

Equipment design for burst synchronization control in TDMA experiment system

10 p1836 A70-24339

Independent burst and burst coherent TDMA methods compared for ground station-satellite communication

10 p1836 A70-24340

Intermeshed TDMA systems efficiency in interconnecting ground stations in communications satellite systems, discussing rigid and variable burst lengths

10 p1839 A70-24363

Digital transmission techniques optimal utilization of assigned frequency spectrum for phase modulation of frequency carriers

10 p1839 A70-24365

TDMA system control, considering access process control and switching process control, discussing burst transmission phase control and channel selection at receiving end

10 p1839 A70-24366

Physical formula for information content in communication signals based on receiver observation concept, noting role of channel properties and encoding

10 p1844 A70-25223

Information transfer services potential demand including telephone, telegraph, videophone, electronic mail, etc

[AIAA PAPER 70-443]

11 p2152 A70-25448

TATS Master tactical communication satellite network controller with modems and digital computer for semiautomatic control over terminals

[AIAA PAPER 70-412]

11 p2002 A70-25491

Computerized data communication system (CDCS)/equipment unit capacities and topology specified with aid of vertex weighted linear graph

11 p2009 A70-26253

Automatic base communication system (ABCS) to handle USAF worldwide base record communications centered on electronic store and forward message switch, utilizing stored programs

11 p2009 A70-26266

Data compression for telemetry transmission with sample choice based on time-varying stream slope thresholds illustrated for Ranger photograph

11 p2010 A70-26305

Digital river and rainfall data automatic transmission from remote hydrologic platforms via ATS-1, studying system economic and technological feasibility

12 p2205 A70-26939

Materials/design optimization of antenna-aiming mechanism deployed on moon by Apollo 12 astronauts to transmit ALSEP experiments data to earth stations

12 p2231 A70-27130

Multiplexer-interface system for digital nuclear and position control data transfer from high altitude balloons to earth monitoring instruments

12 p2233 A70-27407

Nonlinear estimation with quantized measurements, applying algorithms to PCM, predictive quantization and data compression

12 p2192 A70-27420

ATC radar beacon system, discussing narrow interrogator beams, siting and beam shaping, interrogation environment control, data link transmissions and message content

12 p2268 A70-27641

Optimal linear band limited time invariant data transmission systems, discussing pulse interference tolerance based on eye parameters as quality criteria

12 p2185 A70-27688

Cost effective data transmission method for high performance under intersymbol interference and noise

12 p2187 A70-27935

Statistical characteristics and energy spectra of pulse code signals in data transmission estimated by matrix methods

13 p2364 A70-28871

Solar probe Helios data processing and transmission system, describing block diagram, PCM/PSK/PM telemetry and transmitter

13 p2367 A70-29558

Three dimensional images reconstruction with coherent light, facilitating transmission by holographic information volume reduction

14 p2581 A70-30146

Pulsed noise stability of discrete data transmission system having multipositional frequency manipulation as compared to binary system

14 p2547 A70-30148

Amplitude-frequency characteristics selection for minimum phase channel allowing for intersymbol interference and smooth noise during data transmission, calculating mean error probability

14 p2547 A70-30150

Real time Apollo PCM telemetry data compression and transmission using zero order predictor

14 p2550 A70-30768

Digital guidance and control system, discussing communication device providing data transfer between airborne digital computer and control device

[AIAA PAPER 69-988]

14 p2615 A70-30771

Quantum mechanical communication system with thermal noise disturbance, analyzing reliability function and channel capacity

14 p2551 A70-31120

Optimum interleavers realization procedure for reordering contiguous symbols sequence to satisfy

minimum distance requirement for improving communication system performance

14 p2554 A70-31121

Geostationary tracking and data relay satellites (tdrs), discussing system design and advantages

14 p2615 A70-31182

Analog data transmission over PCM telemetry link, comparing noncoherent FSK vs PSK reception performance for waveform error

14 p2552 A70-31187

Sampled analog waveforms transmission, deriving optimum pre- and postfilters

15 p2703 A70-32557

Injection laser communication link for high data rate transmission, discussing design and construction of transmitter and receiver

16 p2862 A70-33139

Nonlinear least squares method reducing Burnett data to compressibility factors and virial coefficients

17 p3136 A70-35594

Frequency and time information transmission, discussing frequency and time measurement equipment at Czechoslovak facility

18 p3257 A70-36199

Optimal incoherent signal reception in discrete information transmission systems with fluctuation and concentration noise, including Rayleigh fading

18 p3228 A70-36600

Wideband analog signal data transmission, evaluating messages accuracy in terms of error probability

18 p3228 A70-36623

PCM data transmission, considering baseband code and modulated carrier formats and spectral distributions

19 p3379 A70-37905

Information optical transmission parameters with electroluminescent GaAs diode as radiation source, calculating energy received over various distances

19 p3389 A70-38069

Spacecraft data transmission efficiency improvement by budgeting onboard electric energy consumption among data types

21 p3790 A70-41364

Phase recovery in vestigial sideband (VSB) data transmission, deriving carrier acquisition time required to achieve satisfactory error rate for coherent demodulation of PAM

21 p3793 A70-42178

Information transmission and coding theory - Conference, Tashkent, Uzbek SSR, September-October 1969, Section 1, Data transmission theory, Methods of coding and decoding

22 p3985 A70-42490

Optimal binary and ternary signal system synthesis by information divergence procedure for communication channels with colored Gaussian noise

22 p3985 A70-42491

Nonbinary redundant error correcting codes for improving TV transmission speed and fidelity

22 p3985 A70-42493

Information transmission techniques by discrete amplitudes and increments, comparing effectiveness for noise rejection

22 p3986 A70-42495

Information transmission and coding theory - Conference, Tashkent, September-October 1969, Section 2, Statistical theory of signals and noise, Optimal reception methods

22 p3986 A70-42551

Optimal nonlinear filtration for continuous automatic data transmission with radio signal under white, narrow band and Markov noise

22 p4004 A70-42891

Earth resources technology satellite data link tradeoff between channel capacity and transmitter power

22 p4038 A70-43091

Tracking and data relay satellite system in low altitude synchronous orbit

[AIAA PAPER 70-1305]

24 p4311 A70-45085

DATING

U CHRONOLOGY

U TIME MEASUREMENT

DATUM (ELEVATION)

North American datum related to geocentric satellite reference system, using Lambeck method for geodetic parameters

05 p0841 A70-16644

DAWN CHORUS

VLF recordings and X ray flux measurements simultaneous analysis indicating evidence of relation between dawn chorus and electron precipitation, noting ELF whistler development

02 p0293 A70-12689

Dawn chorus frequency relation to solar activity, showing correlation to mean geomagnetic activity

10 p1886 A70-25282

Midlatitude chorus frequency spectrum changes in relation to previous local magnetic conditions

13 p2365 A70-29187

VLF radiation observation at conjugate points, discussing hisses, choruses and geomagnetic effects

19 p3416 A70-38587

DAYGLOW

Mariner 6 spectra establishing Fox-Duffendack-Barker bands and ionized carbon dioxide UV doublet bands as important components of Martian dayglow

10 p1938 A70-24073

Balloon-borne photometer for collecting twilight and daytime OH intensity and rotational temperature variations data

13 p2399 A70-29240

Excitation and radiative transport of 1304 A triplet of atomic oxygen for dayglow and aurora

14 p2578 A70-31241

Sodium dayglow seasonal and diurnal variations observed with Zeeman cell photometer

14 p2579 A70-31253

Sodium and potassium dayglow seasonal and diurnal variations using resonance cell technique and sky polarization effect

14 p2580 A70-31263

Atomic hydrogen emissions in dayglow, considering excitation by resonance absorption of solar radiation

21 p3812 A70-40728

Nitrogen photoelectron excitation in dayglow, examining 3371 A band intensity, energy spectrum and flux in ionosphere

21 p3882 A70-41093

Daytime near horizon atmospheric luminescence measurement by Cosmos 224 satellite, discussing contributions of nitrogen and aerosol and Rayleigh scatterings

23 p4188 A70-44061

DAYTIME

Male rats locomotor activity responses to altered photoperiods during exposure to varied-light artificial days

01 p0015 A70-10367

Quasi-trapped particle currents having discontinuities on daytime and nighttime side of earth

01 p0171 A70-11487

Altitude variation of mesospheric daytime sky brightness from earth based measurements of twilight sky brightness, noting inconsistency in calculations based on standard atmospheres

06 p1053 A70-17207

Atmospheric long wave radiation fluxes and energy balance and daytime radiative temperature variations calculated and compared with thermocell measurements

06 p1098 A70-17831

Day sky Fraunhofer lines filling-in /Ring effect/ considered from analogous effects in surface albedo, suggesting role of Rayleigh wings

10 p1947 A70-24992

Earth-ionosphere cavity resonances diurnal variations by considering different propagation characteristics of day and night hemispheres

15 p2728 A70-31910

Vertical drift contribution to daytime N/h electron profiles in F 2 region, taking into account ionization-recombination processes and ambipolar diffusion

18 p3247 A70-36292

Daylight sky brightness at different wavelengths by airborne photometer, investigating statistical characteristics

19 p3460 A70-37419

Coupling processes in daytime D and E regions at LF and VLF, using thin film optics method for reflection and transmission coefficient matrices

19 p3413 A70-38002

High altitude wind measurement during daytime using photometer for detection of Li trail

20 p3630 A70-39486

Aircraft nighttime and daytime accident rate comparison, considering darkness, flight phase, etc

21 p3751 A70-41489

Daytime ionospheric effect of X ray flare from SCO XR-1, discussing LF radio wave intensity decrease

22 p4095 A70-43165

DC [CURRENT]

U DIRECT CURRENT

DC 8 AIRCRAFT

DC 8 Super 63 aircraft direct lift control flight evaluation

17 p3018 A70-35496

DC 9 AIRCRAFT

DC-9 aircraft instrument subsystems and operating procedures of KLM, discussing series 15 and 30 aircraft

14 p2530 A70-30416

DC-9 aircraft pilot training including jet introduction, DC-9 conversion and route training

14 p2542 A70-30417

Quiet V/STOL transport aircraft from DC-9-10 modification, discussing flying qualities, propulsion and control system interfaces, configurations, etc

[AIAA PAPER 70-1409]

24 p4291 A70-45916

DC 10 AIRCRAFT

Nondestructive inspection program for DC 10 aircraft maintenance

02 p0308 A70-12273

Ground support and service features present facilities to handle B-747 and DC-10 aircraft

03 p0463 A70-13264

- DC-10 aircraft wing engine calibration, isolated- and wing-nacelle testings using air-driven engine simulator [AIAA PAPER 70-590] 13 p2342 A70-29881
- DC-10 airborne flight test PCM data system, discussing capability, onboard operating characteristics and test results 17 p3093 A70-35498
- Wide body commercial jet transport structural design considerations applied to DC 10 aircraft [AIAA PAPER 70-895] 17 p3193 A70-35812
- Boeing 747, L-1011 and DC-10 introduction costs, profits and terminal facilities 19 p3357 A70-38951
- Noise suppression for high-bypass ratio CF6 turbofan engine in DC-10 airplane, considering effect on engine design [SAE PAPER 700804] 24 p4393 A70-45878
- DE HAVILLAND AIRCRAFT**
 NT DH 121 AIRCRAFT
 NT DH 125 AIRCRAFT
DE HAVILLAND DH 121 AIRCRAFT
 U DH 121 AIRCRAFT
DE HAVILLAND DH 125 AIRCRAFT
 U DH 125 AIRCRAFT
DE LAVAL NOZZLES
 U CONVERGENT-DIVERGENT NOZZLES
- DEACCLIMATIZATION**
 U ACCLIMATIZATION
- DEACTIVATION**
 Reversible cold induced deactivation of cat neocortex bioelectric activity in chronic experiment, noting cooling system 01 p0031 A70-10056
- Excited oxygen molecules concentration in upper atmosphere calculated, considering deactivation during interactions in various energy states 04 p0684 A70-15750
- Excited oxygen molecules concentration in upper atmosphere calculated, considering deactivation during interactions in various energy states 14 p2576 A70-30834
- Ketene and diazomethane flash photolytic measurement of reaction rates of singlet-triplet methylene deactivation 15 p2694 A70-31729
- DEAD RECKONING**
 Dead reckoning navigation of manned lunar roving vehicle /MLRV/, describing hardware and coordinate system 12 p2266 A70-27414
- Computerized aircraft navigation utilizing Doppler dead reckoning system and Tacan integration with least square adjustment method 13 p2447 A70-28550
- Manned lunar surface navigation requirements emphasizing dead reckoning system 14 p2613 A70-30458
- Manned lunar roving vehicle /MLRV/ navigation scheme based on dead reckoning concept, discussing instruments effectiveness for vehicle velocity and orientation measurements 19 p3396 A70-37849
- Automatic ship navigation system using Transit satellites and onboard digital computer for routine tasks of dead reckoning 22 p4068 A70-42666
- DEADWEIGHT**
 U STATIC LOADS
- DEAFNESS**
 U AUDITORY DEFECTS
- DEATH**
 Sudden and early death in acute myocardial infarction, discussing prophylactic measures 04 p0637 A70-15472
- USAF aviation accidents diagnostic patterns of injury and death, noting increase in fire and/or associated complications 17 p3039 A70-35574
- Living organisms physiological death as biological problem, discussing hypotheses, theories and facts 23 p4145 A70-44225
- DEBRIS**
 NT RADIOACTIVE DEBRIS
 NT SPACE DEBRIS
- Energy partitioning process under strong shielding with debris acting as energy sink 06 p1130 A70-17181
- Dissection techniques for measuring dynamic parameters of debris clouds expanding from energetic events 14 p2584 A70-30510
- Fireballs atmospheric debris collection by high altitude filtration, describing analysis results 18 p3311 A70-35971
- DEBUGGING**
 U CHECKOUT
- DEBYE LENGTH**
 Spherically symmetric state of slightly ionized gas of unbounded expanse about catalytic conductor by nonequilibrium continuum theory, analyzing Debye number limit for electrostatic probes 14 p2665 A70-30946
- Spherical electrostatic probe in uniform quiescent continuum slightly ionized gas for range of bias potential and radius-Debye length ratio 16 p2912 A70-33863
- DEBYE TEMPERATURE**
 U SPECIFIC HEAT
- DECATETRIC WAVES**
 Rotation period of Jupiter based on decatetric component of radio emission, suggesting anticorrelation with sunspot number for drift observed 01 p0173 A70-10044
- Jovian decatetric radiation polarization during 1966-1967 apparition compared with cyclotron model predictions 02 p0364 A70-11793
- Fine structure morphology in dynamic spectra of Jupiter decatetric radiation determined from spectral recordings 08 p1562 A70-21514
- Jupiter decatetric noise storm commencement time defining constant planetary rotation period 08 p1580 A70-21572
- Baseline measurements of Jupiter decatetric radiation providing upper size limit to coherent and incoherent sources 09 p1755 A70-22512
- Cosmic radio waves discrete sources spectra measured in decatetric wavelength range, discussing wave generation and absorption 09 p1762 A70-23189
- Jupiter decatetric emission modulation by planetary rotation and Io position, suggesting role of magnetic tail diurnal swings 10 p1940 A70-24434
- Decatetric radio sources flux density time variations, discussing possible causes and radio emission spectra 12 p2299 A70-27308
- Twelve year periodicities of Jupiter decatetric radiation, noting correlation with Jupiter magnetic field rotation period 14 p2648 A70-31085
- Jupiter decatetric radio emission modulation by Io simulated by DC circuit model 18 p3321 A70-37120
- DECARBONATION**
 Foil decarbonization process monitored by mass spectrometry of secondary carbon ion emission 12 p2254 A70-27311
- DECAY**
 NT ALPHA DECAY
 NT BIOLUMINESCENCE
 NT CHEMILUMINESCENCE
 NT ELECTROLUMINESCENCE
 NT ELECTRON EMISSION
 NT FIELD EMISSION
 NT FLUORESCENCE
 NT HALF LIFE
 NT INCANDESCENCE
 NT ION EMISSION
 NT LIGHT EMISSION
 NT LUMINESCENCE
 NT LUNAR LUMINESCENCE
 NT NEUTRON DECAY
 NT NEUTRON EMISSION
 NT NUCLEAR FISSION
 NT OPTICAL RESONANCE
 NT PARTICLE EMISSION
 NT PHOSPHORESCENCE
 NT PHOTOELECTRIC EFFECT
 NT PHOTOELECTRIC EMISSION
 NT PHOTOIONIZATION
 NT PHOTOLUMINESCENCE
 NT PLASMA DECAY
 NT RADIO EMISSION
 NT RADIOACTIVE DECAY
 NT SECONDARY EMISSION
 NT SHOCK WAVE LUMINESCENCE
 NT SOLAR RADIO BURSTS
 NT SOLAR RADIO EMISSION
 NT SPECTRAL EMISSION
 NT STIMULATED EMISSION
 NT THERMAL EMISSION
 NT THERMIONIC EMISSION
 NT THERMOLUMINESCENCE
 NT TYPE 2 BURSTS
 NT TYPE 3 BURSTS
 NT TYPE 4 BURSTS
 NT TYPE 5 BURSTS
 NT X RAY FLUORESCENCE
- Transient system decay characteristics, discussing equilibrium point damping time for asymptotically stable systems of ordinary differential equations 19 p3542 A70-38066
- DECAY RATES**
 NT ELECTRON DECAY RATE
- Rapid photoprocesses decay kinetics, using CW Ar ion laser beam interrupted periodically by electro-optical shutter 02 p0314 A70-12742
- Extensive air shower models, noting role of nuclear active component energy decay rate 03 p0556 A70-13038

- Neutron star electrical conductivity, discussing stellar flux and magnetic field decay times 03 p0578 A70-14220
- Maximum plasma decay rate in heterogeneous medium determined from deionization process in rarefied gases 03 p0536 A70-14369
- Vibration decay rate measurement by pulse cycles counting 04 p0695 A70-15571
- Variational and Z-expansion calculations for magnetic quadrupole transitions decay rates of He sequence 05 p0920 A70-16942
- Mean lives measurement for excited levels in singlet system of neutral He using beam foil technique 07 p1338 A70-19821
- Neutron beta decay in strong quantizing magnetic field using Dirac wave function for electron, noting lifetime dependence on field strength 08 p1549 A70-21744
- CH, CD and CH ion excited states decay rates determined from phase shift and frequency data, discussing implications for astrophysics 09 p1731 A70-22513
- Pulsars period distribution not related to decay of magnetic field in rotating neutron star 09 p1756 A70-22518
- Karman trail vortices tangential velocity decay measurement by hot film anemometer experiments 09 p1661 A70-22961
- Carbon dioxide dissociation effects on refractive index gradients and decay rates in pulsed carbon dioxide-nitrogen laser mixture 10 p1900 A70-24602
- Ionospheric loss rates from rocket observation during auroral absorption interpreted by two ion model of recombination 10 p1881 A70-24813
- Time or space decay of turbulent parameters along flow direction in jets, wakes or grid-generated turbulence, illustrating time variation of wave number spectrum 12 p2211 A70-27831
- Burger turbulence model late decay statistical analysis using kernels of Cameron-Martin-Wiener expansion of random velocity field 13 p2386 A70-28820
- Time decay of higher order cyclotron harmonic resonances with decreasing perpendicular wave number 13 p2467 A70-29908
- Polyatomic molecules radiationless transition rate statistical analysis, suggesting role of Franck-Condon principle in determination of nonradiative decay rates 16 p2858 A70-34014
- Plane wave reflection decay rate representation by slowness diagrams 16 p2952 A70-34089
- Stress decay rates in Saint Venant boundary region in truncated semiinfinite elastic cone, using Papkovitch-Neuber functions for eigenfunctions formulation 18 p3339 A70-36489
- Ionospheric inhomogeneities electrodynamic decay rate, using ellipsoidal model with sharp boundary for irregularity 18 p3252 A70-36986
- Isotopic decay rates, solving time dependent atmospheric turbulent dispersion from steady state measurements 22 p4093 A70-42915
- DECCA NAVIGATION**
 Loran and Decca hyperbolic navigation systems 08 p1541 A70-21022
- STOL navigation systems, evaluating Vector Analog Computer, Decca Omnitrac IIB and inertial system 18 p3289 A70-36513
- Decca, Loran C/D and Omega LF and VLF hyperbolic navigation systems 23 p4215 A70-43865
- DECELERATION**
 NT SPIN REDUCTION
- Entry and terminal deceleration systems for unmanned Martian landers, discussing parachute landing and lifting entry vehicles 01 p0195 A70-10828
- Satellite 1965-11-4 /Cosmos 54 rocket/ braking, rotation periods and revolution from INTEROBS and SPIN observations, comparing K-index and solar activity parameters 02 p0363 A70-11768
- Lift-dump system for Hawker Siddeley DH 125, combining aerodynamic drag increase with lift reduction to improve deceleration 02 p0225 A70-12266
- Venus probe high level entry deceleration simulation, discussing test program, equipment and results 03 p0463 A70-13541
- VTOL flight investigation to develop decelerating instrument approach capability with control-command information display for three degrees of freedom [SAE PAPER 690693] 05 p0792 A70-15862

Traumatic rupture of aortic arch and descending thoracic aorta resulting from abrupt linear body deceleration
07 p1206 A70-19295

Two degrees of freedom assemblies transient motions using computer, solving acceleration and deceleration problems in mechanical systems
08 p1502 A70-20699

Initial deceleration of solar wind positive ions upstream of earth bow shock determined fromOGO 5 high time resolution plasma measurements
08 p1562 A70-21377

Hubble expansion constant and expansion deceleration value roles in cosmological model testing
08 p1581 A70-21752

Electromagnetic wave deceleration in open cylindrical waveguide, noting guide action as bandpass filter
09 p1633 A70-22415

Physiopathologic effects on organs of longitudinal and tangential accelerations, decelerations, vibrations and weightlessness
11 p1986 A70-25821

Lambda type pseudoshock /shock during supersonic flow deceleration to subsonic in duct/, investigating mechanism by schlieren photography
11 p2037 A70-26408

Monograph on axially symmetric tandem grids for supersonic flow deceleration to subsonic speeds, using schlieren optical tests and pressure measurements
11 p1977 A70-26525

Intense deceleration effects on mice and rats, including internal organs damage and enzyme activity increase
17 p3025 A70-35132

Repeated decelerations effects on mice and rats, noting fibrotic changes in liver
17 p3025 A70-35133

Meteor deceleration rates in atmosphere, using base line radar measurements
18 p3313 A70-36294

Parachute decelerator towline energy absorber shock attenuation characteristics, discussing drop test results
21 p3752 A70-41815

Earth rotation rate deceleration due to lunar tidal friction taking into account fluctuations from internal processes, discussing moon retreat from earth
21 p3921 A70-41970

Decelerated channel flow dynamics of ideal gas with supersonic velocity closed by compression shock, using finite difference method
21 p3747 A70-42203

Hot electrons bunch spread deceleration in collisionless plasma, discussing stationary moving jump formation similar to shock wave
22 p4077 A70-42299

Aircraft crash protection with preinflated air bag added to conventional seat/lap belt tested with human sled subjects
23 p4140 A70-44456

DECIDERS

U BRAKES [FOR ARRESTING MOTION]

DECIDING WAVES

Decimeter waves propagation along overland path, considering tropospheric radio relay systems development
16 p2863 A70-33238

Jovian decimeter radiation, discussing electron drift velocity in dipole field, characteristic time for energy loss and radiation belt dimensions
16 p2980 A70-34192

Pulsar RF spectral fine structure in decimeter wave range
17 p3163 A70-35050

DECISION ELEMENTS

U LOGICAL ELEMENTS

DECISION MAKING

Book on technological forecasting covering philosophical basis, Federal Government activity, R and D management resource allocation, correlation and regression analysis, etc
01 p0221 A70-11307

Dynamic structural analysis using computer graphics display, emphasizing applicability to man machine interaction at key decision making points
02 p0386 A70-11943

Man machine systems - IEEE/ERS Conference, Cambridge, England, September 1969, Volume 3, Decision making and mental work load
02 p0244 A70-12137

Pattern recognition concepts applied to synthesis of aircraft approach progress monitor as adjunct to pilot decision process, discussing feasibility experiments [SRCC-106]
02 p0335 A70-12138

Human decision making via man-computer interaction, noting skill role in nonoptimal performance handling of simultaneous factors
02 p0245 A70-12140

Multidimensional data efficient decomposition for communication interface between man machine system, considering decision making and pattern recognition on digital computers with orthogonal transformations
02 p0265 A70-12149

Restricted problem solving tasks /perceptual maze test/ formulated as multistage decision making, discussing use of dynamic programming and algorithms
02 p0246 A70-12321

Experienced and naive subject evaluation of probabilistic data, data source determination and prediction of subsequent data in complex decision task
02 p0247 A70-12379

Human feedback and response mode in performing Bayesian decision task
02 p0237 A70-12382

Analytical scoring model design for effective evaluation of competing research and development projects
02 p0402 A70-12634

Flights best day pair and weekly leg schedules concept based on decision making model for traffic volume estimation in airline operations
02 p0403 A70-12787

Decision model for R and D project selection
03 p0609 A70-12991

Signal detection theory analysis indicating within-session changes in human willingness to respond in visual monitoring task, considering optimal decision behavior
03 p0435 A70-13766

Decision analysis in R and D, discussing risk discounting and measure of value selection
03 p0610 A70-13956

NASA Source Evaluation Board process for major contractor selection, discussing procurement practices and management techniques
03 p0610 A70-13962

Managerial practices of problem identification, discussing research study in operating division of large corporation
03 p0610 A70-14051

Weapon systems acquisition projects, studying procurement decisions interactions [ASME PAPER 69-WA/MGT-6]
04 p0788 A70-14833

Human controller decision in air traffic control, discussing manpower, on-line computer use and maximized systems
04 p0643 A70-14903

Command and control display operational requirements within Allied Command Europe /ACE/, information flow, decision making and evaluation
05 p0959 A70-16178

Computer display graphic technique for business decision making, noting electronic aids
05 p0959 A70-16451

DOD systems acquisition management tools and policies, emphasizing role of development concept paper and outside personnel dialogue in DOD decision making
05 p0959 A70-16460

Decision algorithms simulating human controller adaptive behavior in controlling VTOL aircraft in hover following stability augmentation system failure
07 p1216 A70-18860

Risk-reducing information role in decision making using Marschak bidding procedure
07 p1203 A70-18964

Decision trees application to research projects selection, cost stages, probable return on investment and control device
07 p1427 A70-19001

Decision making leading to aircraft selection and buying by airline, evaluating traffic and technological aspects
08 p1601 A70-21866

Decision rules for incomplete a priori data, deriving informational risk estimates for Markov processes and optimal control problems
09 p1653 A70-22144

Computer aided design programs as decision-making tool for fighter development projects technical management [AIAA PAPER 70-364]
09 p1611 A70-23024

Large scale project grading into stepwise decision stages exemplified by aircraft weapon system development program
10 p1971 A70-24596

Response times in deciding same or different between successive visual stimuli
10 p1826 A70-24722

Associative analog designed for decision making by man searching for extremum in form of multilayer stochastic automaton
11 p1990 A70-25928

Aircraft pilot ability tests validity, applying correction methods in decision making regarding applicant acceptance [DFVLR-SONDDR-32]
12 p2176 A70-27031

Bayesian probabilistic information processing in psychological decision making in air traffic control, discussing bookbag and poker-chip applications
12 p2178 A70-27047

Tradeoff decision processes scheduling maintenance frequencies for commercial transport aircraft [SAE PAPER 700328]
12 p2243 A70-27461

Weibull process with unknown scale and shape parameters analyzed by Bayesian decision making
12 p2243 A70-28011

model, with application to component reliability problem
12 p2243 A70-28011

Book on probabilistic systems analysis covering models, decision making, random processes, distribution functions, mass and density functions, etc
13 p2441 A70-29455

Project cost estimate growth pressures on decision making by U.S. Air Force System Program Office director
14 p2667 A70-30521

Weather forecasting for manned space flights, emphasizing Apollo flights and operational decisions due to forecasts
14 p2606 A70-30557

Decision making role in management contribution towards success of research and development based on statistical decision theory
15 p2828 A70-31573

Forecasting necessity and limitations in management decision making process
15 p2829 A70-31574

Pilots brake-takeoff decision at critical engine failure speed, discussing operational aspects of accelerate-stop criteria
15 p2675 A70-32219

Technological forecasting as management concept in decision making process
17 p3199 A70-34679

Component decision logical and temporal arrangement in visual search, defining target by several attribute value combination
19 p3362 A70-38314

Visual sensory storage item selection efficiency
19 p3363 A70-38321

Choice prediction in partially repeatable decision situations, discussing phenomenological analysis
19 p3366 A70-38504

Attitude test validity taking into account selection board subjective decisions on pilot applicant acceptance
19 p3371 A70-38507

Solar system unmanned exploration decision making, discussing resource utilization, sequence optimization, etc
20 p3710 A70-40335

Pursuit evasion game with uncertain state-dependent measurements, modifying Brown-Robinson algorithm for behavior strategies computation
20 p3660 A70-40384

Unitary and compound stimuli and role of response categories in decision time
21 p3767 A70-40751

Subjective probability estimation for R and D decision making, using analytical models incorporating risk and uncertainty
21 p3955 A70-41175

Book on decision making in U.S. manned lunar landing commitment covering space policy, technical planning, national interests, Apollo experience, etc
22 p4126 A70-42314

Training simulation improving ejection decision making in naval aviation
23 p4178 A70-44467

Elastic continua structural optimization analysis decisions for maximizing calculation accuracy, insuring efficient complex numerical analyses
23 p4271 A70-44706

DECISION THEORY

NT STATISTICAL DECISION THEORY

Optimal maneuver decision strategy for space vehicle midcourse trajectory corrections
09 p1760 A70-22928

Hybrid computer for decision-directed estimators of two-class decision boundary, noting applications to medical diagnosis, communications and pattern recognition
09 p1641 A70-22965

Signal selection for phase coherent and incoherent additive noise channels to maximize receiver correct decision probability
11 p2010 A70-26327

Antenna array system for surface target detection in receiver noise and heavy clutter by space-time decision theory
16 p2860 A70-32954

Generalized iterative inverse algorithm for linear inequalities set involved in pattern recognition and threshold logic requiring decision functions determination
16 p2870 A70-33739

Decision theory model evaluation based on experimental findings concerning relationship between stimulus intensity and reaction time
17 p3036 A70-34605

Multidimensional decision models for optimal control, using piecewise constant functions
19 p3394 A70-38679

Water management decision model using earth resources information system with satellite-based remote sensors, evaluating costs and benefits by systems analysis
20 p3616 A70-39066

Discrete decision variable models formulated as linear integer programs, deriving shrinking boundary algorithm for optimization 22 p3994 A70-43497

DECLINATION

Latitude observations at Pulkovo, considering star declinations and proper motions 08 p1574 A70-21162

Positions measurement for 4C radio sources between declinations of 4 and 20 degrees, noting RMS errors 08 p1577 A70-21533

Molonglo pulsars observations, using multiperiod integration technique for declinations, periods and positions 13 p2487 A70-28632

Magnetometer for geomagnetic field declination measurement, eliminating thermal drift by light modulation method 13 p2415 A70-30042

Soviet book on declination observation of bright and faint stars in one system 18 p3314 A70-36402

Magnetic declination data, using spherical harmonics to examine global and secular geomagnetic field variations 23 p4189 A70-44067

DECODERS

High speed PCM terminal with 600 channel capacity, evaluating feasibility for high speed PCM codec, examining STN degradation factors 10 p1835 A70-24337

High speed sequential decoding machine design and performance test for deep space channels 11 p2014 A70-26245

Convolutional code decoder modeled as autonomous stochastic sequential machine, considering finite Markov chain theory for error probability 17 p3049 A70-34854

Pseudonoise code command system for scientific satellite, describing added bits and decoder 17 p3046 A70-35276

Error correcting decoders, investigating lower bounds on three complexity measures to meet error probability requirement 18 p3230 A70-35942

Four dimensional matrix type CRT decoder characterized by large storage capacity and high resolution 18 p3256 A70-36105

Sequential decoder program for low weight code-words in binary convolutional code over one-half constraint length 24 p4313 A70-46065

Suboptimum sequential algorithm for recovery decoding errors in convolutional codes, using Hamming distance criterion 24 p4314 A70-46066

DECODING

Algorithm for optimal decoding of convolutional codes confirmed using error probability upper bound 04 p0654 A70-15067

Binary decoding extension to achieve unquantized demodulation performance for nonfading phase shift keyed coherent channel with white Gaussian noise 06 p1008 A70-17525

Arithmetic codes rate upper bound derived by combinatorial analysis, discussing decoding method for multiple error correction 08 p1465 A70-20792

Viterbi decoding error probability for convolutional codes using finite Markov chain modeling 08 p1458 A70-20794

Bit error probability after decoding for binary perfect single error correcting codes 11 p2014 A70-26247

Digital simulation of linear filter, investigating noise and rounding errors effects on decoding signals from lunar and interplanetary probes 17 p3049 A70-34612

Maximum-likelihood decoding in analog form of linear convolutional codes with respect to constraint length by one-step threshold method 24 p4313 A70-46059

DECOMMUTATORS

Telemetry decommutation algorithm for applying Bayesian decisions to demodulated received bits data 11 p2008 A70-26238

Delta reprocessing operating system (DEPOS) for high speed telemetry format-independent decommutation and data compression 11 p2010 A70-26307

DECOMPOSITION

NT GLYCOLYSIS
NT HYDROGENOLYSIS
NT PHOTODECOMPOSITION
NT PHOTODISSOCIATION
NT PHOTOLYSIS
NT PROPELLANT DECOMPOSITION
NT RADIOLYSIS

Matrix decomposition and full release methods for substructure analysis 09 p1770 A70-22258

Gamma irradiation effects on thermal stability and decomposition of ammonium perchlorate 12 p2289 A70-26870

Self heating accompanying exothermic decomposition of gaseous diethyl peroxide in spherical vessel measured positionally by thermocouple 12 p2330 A70-27223

Thermal testing of decomposition and spontaneous ignition of diethyl peroxide before explosion 12 p3330 A70-27224

Molten lithium sodium carbonate electrolyte decomposition and evaporation at high temperatures in various atmospheres, noting water and carbon dioxide additives effects 12 p2166 A70-27763

Discrete time systems, deriving algorithm for testing decomposition property as necessary condition for linearity 13 p2375 A70-29939

Decomposition of unstable beta solid solution of Ti-V alloy, using X ray and microscopic analyses 17 p3125 A70-35336

Aligned composite materials preparation by unidirectional lamellar eutectoid decomposition in Co-Si, Cu-Al, Ni-In and in supersaturated solid solution Sn in Pb 18 p3274 A70-36052

Superconducting Nb-Ti-Zr alloy, investigating structure and decomposition at high temperatures by X ray and electron microscopy 18 p3276 A70-36310

Beta Ti alloy decomposition study during aging by diffraction electron microscopy, forming finely dispersed coherent precipitates 20 p3645 A70-39041

Chemically active surface decomposition in dissociated gas flow with turbulent boundary layer, determining diffusion fluxes in laminar sublayer 20 p3612 A70-39812

Decomposition kinetics of alumina particles injected into thermal argon induction plasmas 21 p3855 A70-40878

Peroxyacetyl nitrate decomposition products under continued and discontinued irradiations determined by IR spectral analysis 22 p3983 A70-42944

DECOMPRESSION

U PRESSURE REDUCTION

DECOMPRESSION SICKNESS

Biophysical symptoms and clinical treatment of ailments resulting from pressure drop, considering exposure to higher and lower pressure changes [DVL-894] 01 p0011 A70-10036

Lung lipid embolization effect in decompression sickness on obese mice, showing no relationship to dysbaric syndrome 01 p0015 A70-10361

Platelet and lipid changes in thrombocytopenic and control rats subjected to bends producing technique in aeroembolism 01 p0015 A70-10364

Sea-level pressure interval to prevent decompression sickness in humans flying in commercial aircraft after diving 01 p0032 A70-10366

Apollo space cabin atmospheres, evaluating diluent N effect on decompression sickness in intermittently exercising men 01 p0032 A70-10368

Book on subatmospheric decompression sickness in man, covering raised intrapulmonary pressure effects and compensating pressure applications [AGARDGRAPH-125] 01 p0019 A70-10514

Forward and rearward facing passenger seats effects in postdecompression emergency descent of high speed high altitude aircraft 03 p0437 A70-14061

Autonomic nervous system role in controlling body functions after rapid decompression, increasing tolerance to pressure gradients by physical training 04 p0630 A70-14575

Ground level denitrogenation duration effects on decompression sickness occurrence in space cabin atmospheres 06 p0999 A70-17289

Histopathological evidence for pulmonary emboli in experimental decompression sickness in dogs detected by radioisotopic lung scanning 06 p0991 A70-17295

Resistance to decompression sickness increased and mortality rate decreased in mice after adaptation to hypoxia at normal barometric pressure 07 p2106 A70-19469

Gas bubbles formation in supersaturated solutions and body fluids during decompression 07 p2108 A70-19511

Fat embolism and decompression sickness similarities, studying lipid stability changes resulting from liver tissue injury by nitrogen bubbles 07 p2122 A70-19936

Decompressed crewmember rescue onboard spacecraft and aircraft by compartmentalization combined with air locks 08 p1454 A70-21938

Decompression rates effect on altitude tolerance of white rats, discussing hypoxia influence on cardiovascular, respiratory, circulatory, thermal control and central nervous systems 09 p1614 A70-22084

Personnel protection against accidental decompression in transport aircraft at high altitudes, recommending flight stations with capsule to achieve ground level oxygen equivalent 09 p1627 A70-23459

Dogs breathing air or oxygen during slow and rapid decompression, measuring intraocular and cardiovascular pressure changes and retinal responses 09 p1621 A70-23460

Otitic Barotrauma with bilateral perforation of ear drums suffered during rapid decompression run in chamber, discussing diagnosis 10 p1811 A70-24040

Vasoactive agent effects on decompression sickness in rats, noting increased severity of bends by serotonin and platelet role 10 p1811 A70-24176

Gas bubbles formation in supersaturated solutions and body fluids during decompression 11 p1988 A70-26110

Commercial jet passenger emergency oxygen needs for cabin decompression studied in determining time of safe unconsciousness 11 p1992 A70-26511

Swimming activity effect on dysbarism in rats in simulated free ascent from deep water 15 p2681 A70-31877

Decompression rates effect on altitude tolerance of white rats, discussing hypoxia influence on cardiovascular, respiratory, circulatory, thermal control and central nervous systems 15 p2685 A70-32680

Aeroatelectosis and pneumothorax in fighter pilot postflight chest pains, noting decompression role 17 p3041 A70-35920

Decompression hazards in manned orbital systems, considering consciousness time, survival, pathological response, water vapor and denitrogenation effects and recompression rates 22 p3973 A70-43638

Decompression sickness prevention in space flight, discussing suit and capsule pressure, extravehicular activity and alleviation of conditions 22 p3980 A70-43640

Decompression sickness pathophysiology, discussing cardiovascular system, altitude effects, therapy and prevention 22 p3975 A70-43700

Decompression disorders after exposures to safe pressure or altitude in cats, noting potential embolia from nongradual high-to-normal pressure passage 23 p4157 A70-45080

Decompression sickness relationship to physical exercise during simulated Apollo flight 24 p4307 A70-45336

Bends incidence in altitude training, examining denitrogenation role 24 p4307 A70-45339

Critical supersaturation vs phase equilibration of tissue in computing decompression schedules from depth and exposure time 24 p4301 A70-45983

DECONTAMINATION

NT SPACECRAFT STERILIZATION

Vacuum cleavage device for producing small area evaporated metal semiconductor contacts free from oxygen or other contamination 02 p0304 A70-12748

Contamination control of spacecraft for planetary exploration missions emphasizing monitoring equipment and cleaning procedures 05 p0808 A70-16702

Sterile lander recontamination prevention from microorganisms during in-flight transfer from unsterilized carrier vehicle 11 p1991 A70-26049

DECOUPLING

Potential representation of vector fields effecting decoupling of vector wave equation of elasticity for radially heterogeneous isotropic media 01 p0208 A70-11189

Decoupling and pole assignments in linear multivariable control systems using geometric method 11 p2072 A70-26160

Effective moment of inertia in quantum mechanical three body problem, applying specific decoupling to wave functions 13 p2452 A70-29478

Decoupling by dynamic compensation using algebraic machinery, considering state space extension role in pole assignment 16 p2886 A70-33333

Linear second order equation systems decoupling transformation, noting applications to structural feedback, flutter and control systems 16 p2943 A70-33891

Linear time varying systems optimal control through decoupling of boundary value problems 19 p3393 A70-37866

Linear multivariable feedback control system, deriving conditions for existence of triangular decoupling transfer function matrices 20 p3605 A70-40118

Nonlinear coupling in systems with two degrees of freedom, deriving transformation laws for uncoupling 21 p3940 A70-42054

Decoupling and pole assignment in linear multivariable control systems, minimizing dynamic compensation 23 p4213 A70-44904

DEEP DRAWING

Press load prediction for deep drawing Ti-Al-V alloy, stainless steel and Inconel X under various lubrication conditions at room temperature [ASME PAPER 69-WA/PROD-15] 04 p0698 A70-14835

DEEP SCATTERING LAYERS

Illuminating conditions in deep layers of turbid plane-parallel medium for highly elongated scattering characteristic 04 p0745 A70-14497

DEEP SPACE

NT INTERPLANETARY SPACE
NT INTERSTELLAR SPACE

UN General Assembly outer space treaties governing international exploration and use and rescue and return of astronauts and objects 02 p0402 A70-12308

Spherical harmonics expansion for earth surface and outer space geopotential by mapping earth surface onto sphere 05 p0837 A70-15926

Gravitational waves and radiation study based on relativity theory, discussing outer space sources and antenna recording design and properties 10 p1916 A70-24384

Laser systems for deep space communications, considering high data rates, laser types, systems operation, earth atmosphere effects, hardware reliability, etc 11 p2005 A70-26036

Reusable earth-moon and deep space return transportation, assuming extraterrestrial nuclear rocket propellant source 14 p2653 A70-30766

Deep space optical communications link, fabricating operational prototype of flight hardware for spaceborne terminal 16 p2863 A70-33190

Search optimization for object drifting in outer space, considering approximate location and speed 17 p3172 A70-35668

Deep space spacecraft radioisotope thermoelectric generators, discussing testing and evaluating for future missions 18 p3215 A70-36229

Three body numerical solutions to low thrust guidance and navigation for outer planet orbiter with nuclear-electric propulsion [AIAA PAPER 70-1040] 19 p3527 A70-38855

Spacecraft-based navigation instruments for outer planet missions using celestial directions to outer planet natural satellites [AIAA PAPER 69-902] 20 p3669 A70-39681

Deep space microwave and optical communications, describing grand tour requirements 21 p3784 A70-40546

Thermal scale modeling of heat pipe in deep space, using material and heat flux preservation techniques 21 p3946 A70-41048

Reusable space transporter predicted applications evolution from earth circling to space bases and space colonies for deep space missions 21 p3930 A70-41495

Reaction kinetics of microbial sterilization in ultrahigh vacuum and in outer space 23 p4148 A70-44841

DEEP SPACE INSTRUMENTATION FACILITY

RF requirements of deep space-outer planet spacecraft communications for Jupiter, Saturn, Uranus and Neptune flyby missions 21 p3791 A70-41369

DEEP SPACE NETWORK

Deep space network /DSN/ functions and characteristics, discussing spacecraft control, data acquisition, orbit determination, data processing, etc 08 p1481 A70-20614

Clock synchronization system using lunar radar reflections for Deep Space Network needs, discussing remote clock receiver and antenna 09 p1656 A70-23037

Tracking station clock synchronization error measurement using Deep Space Network Mark I ranging system, discussing system theory, design, operation, economy and versatility 09 p1656 A70-23038

High speed sequential decoding machine design and performance test for deep space channels 11 p2014 A70-26245

Deep Space Network /DSN/ data accuracy limitations relation with ability to determine orbit of probe, examining improvements after Mariner 2 and trends 13 p2448 A70-28702

Grand tours navigation system consisting of deep space network radio and onboard TV for future TOPS /Thermoelectric Outer Planet Spacecraft/ applications 21 p3849 A70-41799

DEFECTS

NT AUDITORY DEFECTS
NT CRYSTAL DEFECTS
NT CRYSTAL DISLOCATIONS
NT EDGE DISLOCATIONS

NT FRENKEL DEFECTS

NT INCLUSIONS
NT POINT DEFECTS
NT SCREW DISLOCATIONS
NT SURFACE DEFECTS

NT VACANCIES [CRYSTAL DEFECTS]

Electrodynamic contactless method for ultrasonic nondestructive testing of materials based on natural frequencies shift with and without defects 02 p0301 A70-12483

Lamb waves behavior applied to defect evaluation in nondestructive tests of solid elongated cylindrical objects 02 p0276 A70-12552

Refractory Ni alloys defects accumulation under creep and cyclic temperature variations assessed by relative lifetime additive method 05 p0866 A70-17032

Hyperelastic bodies containing finite number of inclusions and defects analyzed by continuous dynamic model 10 p1954 A70-24014

Axisymmetric imperfection distributions effect on buckling of circular cylindrical shells under axial compression, constructing test models from photoelastic liquid epoxy 12 p2319 A70-27140

Stiffened cylindrical shells buckling under axial compression, obtaining imperfections and prebuckling growth mappings 12 p2319 A70-27141

Spectral analysis of LF pulses from defects obtained by modulation method of monitoring using eddy currents with superposed converter 13 p2404 A70-28660

Electron beam welding, explaining high fusion zone homogeneity and weld defect formation by dynamic model 17 p3100 A70-34637

Viscoelastic materials fracture strength as function of cut length, defect size and temperature 17 p3146 A70-35221

Failure of materials under multicycle fatigue, deriving general theory of defects 18 p3341 A70-36586

Freckles origin in unidirectionally solidified castings, noting convective jets role 20 p3646 A70-39102

Ultrasonic pulse echo flaw detection, relating defect size to echo amplitude 20 p3636 A70-39192

Composite materials physical properties measurement and defect locations detection by NDT techniques 20 p3636 A70-39210

Asymptotic buckling analyses of imperfect columns on nonlinear elastic foundations by perturbation expansions, equivalent linearization and truncated hierarchy approximations 21 p3934 A70-40777

Acoustic fields of circular, rectangular and line focused ultrasonic emitters for small defect detection 22 p4048 A70-43618

Defect grouping role in MIL-STD-105D inspection techniques, discussing costs and acceptance probabilities 22 p4048 A70-43727

Axisymmetrically imperfect spherical thin shell stability analysis, comparing results with theory of initial postbuckling behavior 24 p4421 A70-45282

Angle beam ultrasonic testing of metals, considering beam and depth scanning characteristics and wave reflectability of various flaws 24 p4343 A70-45687

Flaw echo height dependence on ultrasonic testing pulse frequency spectrum 24 p4336 A70-45688

Defect size estimation, using ultrasonic angle beam probes and distance-gain-size /DGS/ diagram 24 p4343 A70-45689

Cylindrical boreholes as reference defects in ultrasonic inspection, discussing geometrical parameters effects on echo height 24 p4343 A70-45691

Defect detection by measurement of magnetic field leakage around flaw 24 p4346 A70-45727

Defect effects on welds fatigue properties in low carbon steel plates estimated, using radiograms 24 p4347 A70-45733

Elastoplastic properties of welded joints containing slag inclusions defects, determining sizes radiographically 24 p4347 A70-45734

Inspection penetrant development for flaw detection, considering entrapment efficiency and dimensional sensitivity 24 p4348 A70-45743

DEFENSE COMMUNICATIONS SATELLITE SYSTEM

Optimum sequence integration and ground testing of Defense Communication System Phase II Satellite, considering vibration, shock, space simulation, spin/despin, RF and acoustic requirements [AIAA PAPER 70-447] 11 p2030 A70-25444

Initial Defense Communication Satellite Program/augmentation satellite design and mission, on-board communications equipment, control subsystems, American-British cooperation, etc [AIAA PAPER 70-492] 11 p2121 A70-25449

Digital techniques application to military communication satellite systems, discussing 40 Mbps quadrature phase modems, convolutional encoders, TDMA, etc [AIAA PAPER 70-495] 11 p2002 A70-25488

X band aircraft antennas selection and design for defense communications satellite systems, emphasizing steerable phased array 16 p2865 A70-33712

DEFENSE COMMUNICATIONS SYSTEM [DCS]

Military communication satellite requirements considerations including tactical and strategic concepts integration to provide advantages over terrestrial systems [AIAA PAPER 70-1295] 24 p4315 A70-46188

DEFENSE INDUSTRY

NT WEAPONS INDUSTRY

Book on guide to aerospace defense contracts covering purchase control, marketing solicitation, project management, reports, logistics etc 22 p4126 A70-42723

DEFENSE PROGRAM

Command and control functions of DOD Manager for Manned Space Flight Support Operations in spacecraft recovery 05 p0827 A70-16180

DOD systems acquisition management tools and policies, emphasizing role of development concept paper and outside personnel dialogue in DOD decision making 05 p0959 A70-16460

DOD laser research and development contracts management 14 p2667 A70-30367

DEFLAGRATION

Aluminum additives effects on stoichiometric ammonium perchlorate/polyformaldehyde mixtures deflagration, determining temperature distribution, burning rate dependence on pressure and heat flow due to radiation 02 p0351 A70-12004

Ammonium perchlorate deflagrations, determining intrinsic stability of one dimensional burning configuration based on flame structure modeling [AIAA PAPER 70-123] 06 p1128 A70-18044

Ammonium perchlorate decomposition, deflagration, sublimation, crystal growth and surface properties, using scanning electron microscope 07 p1358 A70-19576

Low pressure deflagration limit dependence on strand size in terms of cross section dimensions for composite ammonium chlorate propellant [AIAA PAPER 69-144] 13 p2473 A70-29955

Pure ammonium perchlorate single crystal self deflagration, determining energy transfer mechanisms from pressure effects, combustion characteristics and subsurface profile [AIAA PAPER 69-142] 13 p2473 A70-29956

Aluminum particle combustibility in deflagration zone of ammonium perchlorate pellets, measuring combustion rate and pyrolytic behavior 17 p3145 A70-35208

Thermocouple transient response characteristics in deflagrating and ablative low conductivity materials with high temperature gradients [ASME PAPER 70-HT-7] 22 p4122 A70-42440

DEFLATING

U INFLATABLE STRUCTURES

U PRESSURE REDUCTION

DEFLECTION

Infinitesimal deflections of piecewise-regular unfolding scanning surfaces fixed along edge with respect to one point, discussing rigidity 03 p0591 A70-13414

Motion stability and time dependent deflections of thin flexible cylinder with zero bending rigidity in viscous stream 03 p0595 A70-13783

Energy methods used in thermoelastic analysis of thermal stresses and deflections in thin rings 07 p1401 A70-18935

Initial perturbation effect of smooth cylindrical shells stability under critical axial compression noting deflection factor 07 p1415 A70-20190

Static deflection effect on harmonic vibration of system with restoring forces of hardening nonlinear spring, considering gravity effect 08 p1586 A70-21035

Stresses and displacements in largely deflected cantilever beams subjected to gravity using photoelasticity 08 p1593 A70-21619

Laser beam deflection techniques for directional control of laser beams, noting applications to optical computer memories and active imaging and display devices 09 p1696 A70-22783

Elastic bending of clamped and supported elliptic and parabolic plates under external pressure investigated by lines of equal deflection
11 p2133 A70-25839

Finite deflections of nonlinearly elastic cantilevered bar
11 p2140 A70-26481

Deflection surface and edge moment prediction for uniformly edge loaded point-supported circular plates, comparing with optical method
13 p2509 A70-28534

Large deflections in impulsively loaded clamped circular Al alloy and steel viscoplastic plates
13 p2511 A70-28736

Deflection function for annular plate simply supported and loaded with eccentric concentrated force
13 p2518 A70-29981

Stress and deflection of nonisotropic assembled bar and plate composite structures, using computerized matrix displacement method
14 p2660 A70-31133

Radio source 3C279 position during October 1969 occultation by sun, determining SHF deflection in solar gravitational field
16 p2972 A70-33049

Macaulay method extended for slope and deflection of statically indeterminate beams, rewriting design equations into index notation for computer programming
[ASME PAPER 70-DE-2] 16 p2989 A70-33419

Mathematical techniques for optimal design of single purpose structures under dynamic deflection
17 p3182 A70-34544

Deflection behavior of uniformly loaded elliptical elastic plates on elastic foundation, using small parameter perturbation technique
18 p3343 A70-36713

Vertical deflections errors statistical analysis by gravity anomaly measurements, determining autocorrelation functions
18 p3248 A70-36771

Vertical gravimetric deflections calculation based on linear interpolated gravity anomalies
19 p3410 A70-37461

Optimum laser beam deflection for instrument design, considering tandem, rotary mirror and analog methods
19 p3446 A70-37879

Clamped edge thin flat elliptic plate subject to elliptic paraboloidal loading, determining middle surface deformations for nonlinear large deflections
19 p3547 A70-38359

Second approximations of deflection of vertical and quasi-geoid height dependence on difference between unknown earth surface and known hypsometric surface
20 p3617 A70-39072

Integral equations for plumb line deflections on earth surface model, considering Neumann, Molodenskii, Arnold methods, etc
20 p3617 A70-39074

Clamped circular shallow Al arches stability under impulsive loading, obtaining deflection time history by high speed photography and computerized data reduction
20 p3732 A70-40265

Mathematical techniques for optimal design of single purpose structures under dynamic deflection
20 p3733 A70-40381

Elastic-plastic axisymmetric shells of revolution, analyzing large deflection and yielding for internal and external pressures by finite element method
21 p3937 A70-41738

Weight-optimal sandwich beam design for given static deflection, using energy approach
22 p4113 A70-42535

Arbitrary shells large deflection transient response, using finite difference computer program
23 p4272 A70-44710

Approximation method for large deflection analysis of impulsively loaded rigid plastic circular plates and symmetric shells
23 p4275 A70-44943

DEFLECTORS

Light beam deflection for three dimensional fixed and time varying visual displays, discussing mechanical, acousto-optic, electro-optic, digital and holographic techniques
08 p1449 A70-20673

Laser color TV display acousto-optic deflectors equalization using prisms
15 p2751 A70-32043

Boeing 737 aircraft nose gear guard deflector and engine vortex dissipator
[AIAA PAPER 70-912] 17 p3020 A70-35824

Light beam direction variation by crystal deflectors, examining changing internal reflection angle by applied electric field or mechanical stress
23 p4196 A70-44411

DEFOCUSING

Steady state thermal defocusing of carbon dioxide laser radiation in gases as function of beam power, gas absorption coefficient and pathlength
06 p1079 A70-17190

Parabolic antenna radiation pattern synthesis under laboratory conditions with space limitations obtainable by defocused antenna method
10 p1853 A70-25132

Saturation of self induced thermal lens resulting from thermal distortion of carbon dioxide laser radiation in wind
11 p2063 A70-26401

Thermal defocusing and deflection of light beam by lateral wind effect in absorbing media
23 p4200 A70-43950

Monopulse tracking antenna beam broadening by feed displacement defocusing in parabolic reflector
23 p4165 A70-44956

DEFORMATION

NT AXIAL STRAIN

NT ELASTIC BENDING

NT ELASTIC BUCKLING

NT ELASTIC DEFORMATION

NT PLASTIC DEFORMATION

NT STATIC DEFORMATION

NT TENSILE DEFORMATION

NT WAVE FRONT DEFORMATION

Nonlinear dynamic beam response for classical and shear deformation theories, comparing stresses and deflections using traveling wave approach with finite difference schemes
01 p0206 A70-11147

Metallographic examination of impact induced deformation textures of Campo del Cielo iron meteorite, analyzing phase homogeneity, microstructures and shock intensity
02 p0377 A70-12511

Inhomogeneous deformation measurements in stress concentration zones using differential rasters in direction of distance between moire bands
03 p0588 A70-13248

Axial geometry deformations of laser resonator due to fabrication errors and misalignment during operation
03 p0502 A70-13748

Quenching temperature and deformation conditions for Ti alloy bars optimal mechanical properties emphasizing effect of primary structure
03 p0497 A70-13856

Hologram interferometry accuracy, reliability, application to plate deformation and translation measurements, using moire method and correction factors
03 p0493 A70-13945

Antiplane strain deformation problems concerning crack extension along circular interface separating materials with different shear moduli
05 p0931 A70-16091

Refractory materials deformation and failure analysis based on relations between stresses, strains and irreversible energy absorption per cycle in thermal cyclic fatigue testing
05 p0867 A70-17042

Homogeneous gravitating sphere deformation by internal dislocations determined using Green dyad
06 p1055 A70-17605

Motion of gaseous medium with uniform deformation with respect to three dimensional Cartesian coordinates
06 p1036 A70-17854

Body displacement and deformation measurement by fringe separation in holographic interferometry
07 p1280 A70-19143

Chemical composition and heat treatment effects on deformation resistance of nonaging aluminum alloys during hot working, noting quenching effect on recrystallization
07 p1294 A70-19388

Molybdenum rolling-deformed single crystals recovery and recrystallization using diffraction electron spectroscopy
07 p1307 A70-19550

Stability equations of three layer panels with allowance for rigid filler transverse deformations
07 p1415 A70-20186

Deformable bodies subjected to given load using method of equivalences
08 p1584 A70-20589

Low temperature effects on deformability of middle C steel under complex stress state, showing invalid stress-strain relation and deviator similarity
08 p1516 A70-20983

Deformation amplitude effects on dislocation structure and strengthening mechanism of fcc aluminum under cyclic loading
08 p1516 A70-20985

Integration of Saint Venant equations of deformation continuity for region occupied by elastic medium
08 p1587 A70-21166

Green and Cauchy deformation tensors determined from moire fringe pitch and angle measurements, deriving equations by specimen and master grid geometries indicial representation
[ASME PAPER 69-APMW-21] 08 p1591 A70-21462

Hertzian contact stress deformation coefficients defined in transcendental equation with elliptic integrals noting errors
08 p1593 A70-21617

Oscillatory transverse and longitudinal magnetos-triction in single crystal Bi, obtaining deformation potentials
08 p1557 A70-21838

Optimal deformation and minimum wave drag for wings with supersonic leading and straight trailing edge, solving variational problem by Ritz method
09 p1604 A70-22444

Creep deformation in single crystals of gamma prime precipitation hardened nickel base alloys at intermediate temperatures
09 p1705 A70-22809

Shock deformation of single crystal biotite /lepidomelane/ imbedded in impedance matching NaI, relating kinking intensity to peak pressure and pulse duration
09 p1670 A70-23375

Three dimensional deformation of finite circular cylindrical shell under plane shock wave solved in linear form
09 p1785 A70-23618

Membrane deformations in second order rotating surfaces with positive Gaussian curvature investigated for external couple loaded spherical shells
10 p1958 A70-24515

Temperature, stresses and deformations in melting plates of elastic perfectly plastic material, using penetration depth concept with heat balance approach
11 p2138 A70-26134

Ring buckling under constant and centrally directed pressure, considering small displacement and inextensional deformation
11 p2141 A70-26492

Crack model analysis taking into account nonlinear force-deformation ahead of crack tip
11 p2143 A70-26667

Bar produced by sliding thin walled cross section along three dimensional curve, determining twisted shell curvilinear middle plane and deformations by differential geometry
12 p2326 A70-27796

Relaxation function of linear viscoelastic body, defining mechanical deformation process using Stieltjes integral
12 p2327 A70-28046

Atmospheric activity centers movements dependence on latitudinal variation of deformation force horizontal component, noting earth poles motion
12 p2265 A70-28224

Nonlinear theory describing mechanical behavior of prestressed laminated composites subjected to large deformations
13 p2511 A70-28738

Deformation, mechanical properties and processes during recrystallization annealing of nickel and alloys single crystals
13 p2433 A70-28761

Polymer materials fatigue strength and deformability testing in vacuum, air and gas atmospheres at low and high temperatures, subjecting to cyclic loading
13 p2385 A70-29428

Displacement component in chosen direction on deformed object surface, using hologram interferometry with double illumination
13 p2409 A70-29475

Sliding rigid conical indenter friction experiments over work hardenable metal flats in high adhesion conditions, observing forces, stresses and deformation modes
13 p2421 A70-29548

Operator form added to equations of state of continuous media in case of small and large deformations
14 p2656 A70-30473

Core shear deformations effects on stress, deflection and buckling load calculations for sandwich panels
15 p2815 A70-31931

Internal pressure deformation of thin cylindrical shells of materials with nonlinear stress-strain relations, considering Al alloy shell and axial strain
15 p2816 A70-32009

Solid state mechanics of deformable media, surveying development trends with emphasis on rheology and dislocation theory
15 p2818 A70-32176

Small deformation thermoelasticity theory, discussing thermal conductivity, dynamic elasticity, strain field-temperature relationship, etc
15 p2818 A70-32177

Spherical liquid drop deformation time dependence in unbound fluid at low Reynolds number, investigating effects of temperature, pressure, velocity and size
15 p2722 A70-32795

Shock deformation effects on strengthening and microstructure of Ti and Ti-Mo alloys
17 p3120 A70-34420

Core flexibility effects on deformation of uniformly loaded clamped parallelogrammic sandwich panels using linear theory
17 p3185 A70-34920

Metal matrix alloys with base of Co, Fe or Ni reinforced by transition metal carbide fibers, discussing deformation tests at various temperatures
17 p3124 A70-35142

Materials deformational flow theory, relating dislocation motions in solids to fluid viscosity concept
17 p3190 A70-35452

Cross section deformation effect on helicopter rotor blade torsional vibration, using differential equations of vibrating beam
18 p3334 A70-35959

Stability conditions in straight bar, taking into account stress direction changes caused by deformation
18 p3337 A70-36372

Thermodynamics of solids deformation, tracing macroscopic inelastic behavior to deformation induced internal structural changes governed by atomic and molecular processes
18 p3340 A70-36556

Low temperature creep deformation recorder with liquid He coolant, discussing Al and Pb single crystal tests
19 p3395 A70-37352

SiC whiskers X ray diffraction studies of crystal structure, suggesting single crystal permanent deformation at ambient temperatures
19 p3455 A70-37941

Deformation effects on metallic and semiconductor thin films conductivity
19 p3488 A70-38199

Prebuckling deformations effect on buckling of clamped thin walled circular cylindrical shells under axial loading and internal pressure
19 p3546 A70-38346

Clamped edge thin flat elliptic plate subject to elliptic paraboloidal loading, determining middle surface deformations for nonlinear large deflections
19 p3547 A70-38359

Inhomogeneous deformation measurements in stress concentration zones using differential rasters in direction of distance between moiré bands
19 p3548 A70-38466

Duraluminum dislocation structure dependence on deformation temperature by electron microscopy, discussing subgrain boundaries
20 p3646 A70-39045

Cylindrical shells subjected by sectors to constant radial pressure, investigating stress state and deformation
20 p3719 A70-39620

Mirror deformation effect on laser emission angular distribution, estimating output parameters by geometric optics
20 p3642 A70-39741

Diffusion processes effect on stress state, allowing for physicochemical coupling between deformed solid bodies based on continuous media theory
20 p3727 A70-39887

Deformable bodies rupture condition formulation by melting analogy, comparing results to experimental data
20 p3733 A70-40394

Thermally induced mirror deformations and wavefront distortions under radially nonuniform heating
21 p3942 A70-40806

Anisotropic material two dimensional crack propagation under deforming stress at infinity, examining fracture criterion, dislocation distributions and crack nucleation
21 p3936 A70-41413

Mechanical behavior differential equation representation in presence of finite deformations using state variables
21 p3937 A70-41434

Petrology, mineralogy and deformation of Apollo 11 rock samples using microscopic, X ray and electron microprobe methods
21 p3897 A70-41517

Invariance principle in mechanics of deformable continua connecting three dimensional and relativistic space-time formulation
21 p3940 A70-42097

Deformational characteristics of unidirectional glass epoxy composites with ductile and brittle matrices evaluated in flexure
22 p4059 A70-43101

Unidirectional fiber reinforced composite longitudinal shear deformation, deriving effective shear modulus
22 p4060 A70-43681

Fiberglass reinforced plastic strength and deformation properties under creep and stress relaxation, investigating temperature effects and load duration
23 p4209 A70-43980

Spherical shell nonaxisymmetrical deformation under varying loads, relating parameters, Poisson coefficient and complex function
23 p4267 A70-44168

Laser application to deformation and vibration analysis, discussing optical alignment, contactless measurement and holographic interferometry
23 p4201 A70-44335

Steady state creep behavior during multiple deformation process, developing grain boundary sliding relation to grain size
23 p4207 A70-44759

Cylindrical shells with unreinforced openings, determining limit pressures and deformation patterns
24 p4419 A70-45158

German monograph on deformations and tensile stresses calculation in axisymmetric bodies via finite element method involving matrix displacement method
24 p4420 A70-45225

Turbine blades deformation by centrifugal and aerodynamic forces, discussing theory for bending stress free blade design
24 p4288 A70-45505

Spacecraft astronomical instrument structural design, examining aging, vibration and temperature distribution deformations and optical surface contamination
24 p4339 A70-45823

Hydrogen effect on deformation and fracture of polycrystalline nickel
24 p4365 A70-46372

DEFORMETERS

Twin wave interferometer and strain gauge mechanism for press-fit measurements of contact deformation on metallic and polymer samples
03 p0484 A70-13426

DEGASSING

NT DEOXYGENATION

Current sheet velocity in coaxial plasma accelerator, noting drag due to insulator ablation and degassing [AIAA PAPER 69-265]
09 p1736 A70-23202

Degassing kinetics during dry friction in vacuum, suggesting gas separation correspondence to oxide film breakdown
13 p2421 A70-29430

Hydrogen separation from supersaturated solid solution in Zn-Zr alloy, measuring at room temperature with eudiometer
15 p2764 A70-32856

Venus deep mantle water degassing rate from atmospheric hydrogen escape data
17 p3154 A70-34610

DEGENERATION

Linear and nonlinear systems natural frequency and stability determination, using theorems for degenerate systems
16 p2944 A70-34284

DEGENERATIVE FEEDBACK

U NEGATIVE FEEDBACK

DEGRADATION

Tractive behavior in elastohydrodynamic lubrication contact noting role of surface degradation layer
05 p0854 A70-15888

Thermoelastic stress degradation of injection lasers at high excitation levels, giving critical current densities for short pulse, CW and quasi-CW conditions
08 p1512 A70-20861

Burning and degradation mechanism of polyester propellants correlated with mass regression rate dependent on surface temperature
11 p2099 A70-25990

Weather effects on plastic properties, discussing weathering interactions with plastics and polymer degradation
12 p2259 A70-27206

Albumin and IgG degradation, studying high altitude effect on hepatic function in man
15 p2683 A70-32532

Senescent *Drosophila melanogaster* flight muscle electron microscopic examination showing mitochondria in stages of degeneration
20 p3574 A70-40075

High voltage solar arrays for ion engines, discussing spacecraft propulsion, electric generation, insulation integrity, cell degradation and current leakage [AIAA PAPER 70-1138]
20 p3567 A70-40211

CdS thin film solar cells, describing manufacture for increased degradation resistance
22 p3966 A70-43537

DEGREES OF FREEDOM

Optimal damping of flexibly mounted rotor by providing system with additional degrees of freedom and applying damping to additional masses
01 p0199 A70-10121

Autonomous two degrees of freedom Hamiltonian system triangular libration points found stable for all mass ratios in circular restricted three body problem
01 p0192 A70-11575

Flight training simulators recording, playback, demonstration and instructor facilities and six degrees of freedom motion system
02 p0273 A70-11840

Dynamical systems with two degrees of freedom reduced to numerical investigation of quadratic area-preserving mapping
02 p0289 A70-11993

Two degree of freedom gyroscopes stability with hydrodynamic grooved rotor bearings, describing parallel and conical whirling rotor oscillations
02 p0307 A70-12163

N degree of freedom pendulum with suspension point vibrating vertically, determining conditions for parametric resonance occurrence
03 p0524 A70-13368

Distributed parameter systems with arbitrarily many degrees of freedom, studying conditions for destabilization absence
04 p0767 A70-14483

Stability characteristics of two degree of freedom gyroscope having hydrodynamic grooved journal rotor bearings, discussing frequency of self excited oscillation [ASME PAPER 69-LUB-H]
04 p0689 A70-14872

Coupled nonlinear systems with two degrees of freedom using transformation techniques
04 p0714 A70-15084

Single degree of freedom nutation damper motion instability on dual spin stabilized spacecraft ascribed to parametric excitation by transverse angular rates
04 p0764 A70-15585

Two degrees of freedom differentiating gyroscope response time decrease and phase and amplitude error reduction, using differential feedback
05 p0853 A70-17003

Electromagnetic wave scattering from finite plasma, discussing statistical measurement errors in degrees of freedom studies
06 p1007 A70-17464

Eigenvalue solutions convergence rates using two finite plate multidegrees of freedom bending elements
06 p1169 A70-17941

Dynamical systems with three degrees of freedom, presenting slice cutting and stereoscopic views graphical techniques for restricted three body problem with perturbations
06 p1149 A70-18462

Laser alignment sensors for measurement and control of five degrees of freedom with increased sensitivity, faster recording and remote meter readout
06 p1083 A70-18591

Book on gyroscope couple stabilizing role on ships, satellites and stabilized platforms, discussing kinetic motion, gyroscopic precession, degrees of freedom, etc
07 p1283 A70-19665

Improper integrals appearing in cross correlation of responses of two single degree of freedom systems to bandwidth limited white noise, deriving Laplace inversion formulas
07 p1236 A70-20067

Two degrees of freedom assemblies transient motions using computer, solving acceleration and deceleration problems in mechanical systems
08 p1502 A70-20699

Nonlinear quasi-harmonic systems forced vibrations using one degree of freedom system as example
08 p1543 A70-20700

Linear one degree of freedom mechanical system loaded by time dependent force with constraints on loading/unloading rate, studying minimum of dynamic coefficient
09 p1727 A70-22536

Shock absorbing forces for absorber with one degree of freedom optimized for given acceleration during periodic disturbances by variational method
09 p1727 A70-22537

Combination resonance in two degree of freedom dissipative nonlinear system using small parameter and Ritz-Galerkin methods
09 p1727 A70-22667

Three degrees of freedom astatic gyroscopes dynamic characteristics determination by vibration tests
09 p1681 A70-23300

Nonlinear many degrees of freedom systems steady state forced vibrations analysis, expressing response in nonlinear normal coordinates
10 p1954 A70-24010

Periodic orbits for reduced problem of conservative Hamiltonian system with two degrees of freedom, discussing emergence from resonant equilibrium
10 p1939 A70-24187

Flight simulator for advanced aircraft /FSAA/ featuring six degrees of freedom and 100 ft lateral travel [AIAA PAPER 70-359]
10 p1858 A70-24205

Aircraft flight displays, simulating low altitude high speed mission by four degree of freedom Dynamic Flight Simulator [AIAA PAPER 70-343]
10 p1859 A70-24216

Computer simulation of six degree of freedom motion system and actual system test, substantiating simulation accuracy [AIAA PAPER 70-358]
10 p1859 A70-24218

Equations of motion, modal vectors and natural frequencies of n-degree of freedom structurally damped linear system determined directly from test data
10 p1961 A70-25058

Three degrees of freedom astatic gyroscope drift due to base vibrations according to harmonic law
11 p2048 A70-25579

Dynamic buckling of shell or arch structure determined from response of two degrees of freedom structure to step load application
11 p2138 A70-26158

Ground testing apparatus with three degrees of freedom for artificial satellites attitude control

systems, establishing mathematical model by digital and analog techniques

11 p2031 A70-26290

Multidegree of freedom linear vibrating system analysis by dividing differential equation method

11 p2139 A70-26414

Random vibration isolation for two degrees of freedom model system investigated statistically, assuming wide band white noise

11 p2139 A70-26416

Elastic system stability with two degrees of freedom under action of retarded follower forces

11 p2142 A70-26631

Blade torsional degree of freedom effects on stability and flapping response of rotors operating at high advance ratios

13 p2507 A70-28444

Book on vibrations covering natural oscillations, damped and undamped oscillations, energy sources, forced vibrations, resonance and multiple degree of freedom systems

13 p2515 A70-29452

Missile aerodynamic characteristics investigation in subsonic low turbulence wind tunnel with three degrees of freedom angular motions

[AIAA PAPER 70-578]

13 p2342 A70-29891

Nutation damper for dual-spin spacecraft, considering various two degree of freedom systems with two natural frequencies

14 p2655 A70-31367

Equivalent linearization for random vibration, considering stationary statistics of bilinear hysteretic one degree of freedom oscillator response

14 p2661 A70-31428

Navier-Stokes equations derivation for multicomponent gas with internal nonrotary degrees of freedom, using moment equations

15 p2672 A70-31649

Stability loss of dynamic two dimensional mechanical elastic system with single degree of freedom under trajectory bifurcation

15 p2775 A70-32474

Linear systems with two degrees of freedom modeled as rigid beam on elastic supports, considering vibration damping

16 p2996 A70-34291

Tau-decomposition stability analysis method applied to two degrees of freedom system subjected to retarded follower forces

17 p3176 A70-34957

Pisarenko generalized equations for hysteresis loop contour applied to oscillations of one degree of freedom system

17 p3137 A70-35710

Nonlinear differential solutions for free isochronous oscillations of conservative one degree of freedom oscillators

18 p3283 A70-36386

Thermodynamical modeling by regular systems of deformable bodies bound by hyperelastic medium with internal degrees of freedom, formulating equations of motion

18 p3338 A70-36432

Asymptotic, averaging and Ritz methods for steady state periodic vibrations of nonlinear systems with many degrees of freedom

18 p3338 A70-36437

Gyroscope in gimbal suspension on free base of four solid bodies connected by flat hinges

18 p3259 A70-36593

Flutter analysis of n degrees of freedom system, basing stability criteria on energy balance considerations

19 p3542 A70-38244

Linear elastic structure with few degrees of freedom, discussing parameters experimental determination

21 p3935 A70-41409

Single degree of freedom gyroscope design factors applicable to strapdown guidance system, discussing torque-to-balance loop, multiple pulse bursting and error sources

[AIAA PAPER 69-848]

21 p3849 A70-41859

Nonlinear coupling in systems with two degrees of freedom, deriving transformation laws for uncoupling

21 p3940 A70-42054

Parametric phenomena in oscillatory system with unlimited number of degrees of freedom, illustrating segment of long line loaded at one end

22 p3995 A70-42395

Periodic motions of arbitrarily long periods for idealized nonlinear spring-mass systems with two or more degrees of freedom

22 p4073 A70-42699

Light rigid civil aircraft response to continuous atmospheric turbulence estimated using two rigid body degrees of freedom method for vertical and lateral gusts

[AIAA PAPER 69-766]

22 p3961 A70-42703

Classical calculations for energy transfer to diatomic molecules with rotational and vibrational degrees of freedom in atom-diatom-molecule collisions

23 p4221 A70-44010

Laser sensors as alignment instrument for control and measurement of five degrees of freedom

24 p4351 A70-45383

Multidegrees of freedom electronic cabinets dynamic response to AM fast sine sweep

[SAE PAPER 700846]

24 p4380 A70-45884

DEHUMIDIFICATION

Aerodynamics, heat and mass transfer in vapor condensation from humid air on flat plate in longitudinal flow in asymmetrically cooled slot

01 p0004 A70-11178

Vacuum supersonic wind tunnel air continuous dehumidification by using multistage centrifugal blower with/without heat exchanger

12 p2206 A70-27153

DEHYDRATION

Dehydrated food effects on human functional state, noting published literature on food composition, preparation, caloric and nutritional values, digestibility, etc

03 p0435 A70-13703

Excretion and balance of K, Ca, Mg, P, S and N during prolonged use of dehydrated food diets

03 p0435 A70-13713

Prolonged dehydrated food diet effect on metabolism of humans, noting complete adaptation after three or four months

04 p0630 A70-14577

Mild temperature and dehydration effects on toxicity of caffeine and dextroamphetamine in mice

09 p1616 A70-22329

Dehydrated food effects on human functional state, noting food composition, preparation, caloric and nutritional values, digestibility, etc

11 p1989 A70-25503

Excretion and balance of K, Ca, Mg, P, S and N during prolonged use of dehydrated food diets

11 p1989 A70-25513

Dehydration effects on rabbits acceleration resistance

17 p3025 A70-35134

Intracellular shifts in body fluids and dehydration tolerance in burro, comparing water content of desert animals

21 p3766 A70-42157

DEHYDROGENATION

Dicyclohexyl /DCH/ endothermic dehydrogenation to diphenyl /DP/ over platinum-alumina catalyst without added hydrogen considered for hypersonic aircraft engine cooling

14 p2546 A70-31175

Dehydrogenases activities in rabbit retina homogenates exposed to oxygen at high partial pressure for various time periods

21 p3765 A70-41487

DEICERS

Electrothermal helicopter rotor blade deicing system, discussing design, operation and solutions for mechanical and reliability problems

13 p2348 A70-29552

DEICING SYSTEMS

U DEICERS

DEIMOS

Phobos and Deimos photographic reconnaissance feasibility during 1971 orbiter and 1973 Viking missions, studying trajectory

06 p1146 A70-18191

Phobos and Deimos photographic reconnaissance feasibility during 1971 Orbiter and 1973 Viking missions, studying trajectory

23 p4243 A70-44507

DEIONIZATION

Maximum plasma decay rate in heterogeneous medium determined from deionization process in rarefied gases

03 p0536 A70-14369

Cosine dependence of F 1 critical characteristics on solar zenith angle discriminating alpha neutralization and mixed alpha-beta deionization

06 p1057 A70-17841

Metal corrosion product dissolution in reactor cooling deionized water, investigating Cu, W and Cd using chemical analyses

10 p1904 A70-24398

Ni particles induced quenching measured by probes in afterglow plasma of pulsed linear discharge, determining deionization rate

16 p2958 A70-33687

He/plus/-H/minus/ collisional charge exchange cross sections, using modulated inclined ion beams technique

21 p3852 A70-40599

DEKATRONS

U COUNTERS

DELAY

Saddle point existence in determinate integrodifferential games with variable delay, assuming given control function over time interval

10 p1911 A70-25183

Dwell time boundary and mean values for laminar flows through channel and tube reactors, obtaining field representation from streamline network and isochrones

16 p2893 A70-33745

Ignition delay of uncompressed composite solid or hybrid propellant mixtures in rocket engine igniters

18 p3301 A70-36651

DELAY CIRCUITS

Analog time delay device for returning respiratory flow signal to correct time

01 p0035 A70-10654

Axial emission impedance antenna converting strongly delayed surface wave into weakly delayed wave forming cophased front at antenna end

03 p0456 A70-13199

Dispersion equation and coupling impedance of two dimensionally periodic slow wave structure of cellular cylinder type with parallel perpendicular diaphragms

03 p0456 A70-13438

Adjustable pulse delay circuit design utilizing slow switching action of storage diodes emphasizing thermal stability

05 p0820 A70-16343

Microwave variable delay devices, discussing solid state microwave acoustic interactions

06 p1019 A70-17483

Corrective open-loop circuit, using delay elements for compensation of transient response in linear circuits with lumped parameters for pulse modulation transmissions

06 p1023 A70-17774

Delay locked closed loop system with and without signal clipping in noisy /Gaussian/ environment applied to radar, sonar and seismic propagation

07 p1242 A70-19997

Beam delay line for introducing variable gradients in Molonglo radio telescope, discussing circuits and performance

08 p1478 A70-21824

Adaptive equalizer consisting of canonical link structure with minimum number of delay elements applied to fast data transmission

09 p1640 A70-22039

Phase characteristics of nonperiodic slow EM wave delay structures determined by phase shift measurements

12 p2230 A70-26967

Power reduction consumed in vacuum by direct-direct voltage converter by introducing delay into breaker transistor control at output stage

15 p2677 A70-31945

DELAY LINES

NT ACOUSTIC DELAY LINES

NT DELAY LINES [COMPUTER STORAGE]

Radar primary plot extraction, suggesting signals summing technique in delay line

02 p0256 A70-11975

Rise time relationship with signal bandwidth for class of TEM mode microwave delay line filters

02 p0257 A70-12185

M-type transmission line with cyclotron waves to achieve phase inverter and delay line operation, showing phase sensitivity to magnetic field changes near cyclotron resonance

03 p0447 A70-13292

Transversal filters with continuously tapped delay lines, emphasizing synthesis of low pass filter and phase shifter

05 p0822 A70-16652

Wideband transversal coaxial cable delay lines used for improving radar systems target recognition by eliminating misleading signals and distortion

05 p0822 A70-16723

Microwave acoustic transducer and delay line properties determination from mathematical analysis

06 p1062 A70-17481

Multichannel correlator for turbulent signal processing in real time scale using natural delay

07 p1284 A70-19832

Radio telescopes relaying interferometers characteristics noting delay in IF channel and wideband performance

08 p1495 A70-21068

Cross type radio telescope beam forming and steering system, describing switched delay lines and phasing circuits

08 p1477 A70-21823

Beam delay line for introducing variable gradients in Molonglo radio telescope, discussing circuits and performance

08 p1478 A70-21824

Phase modulated optical range finder with RF coaxial delay line

13 p2412 A70-29872

Wideband pulse signal synthesis and optimal filtration by dispersive ultrasonic delay lines, estimating potential noise stability for analog data transmission

15 p2696 A70-31502

Avalanche transistor circuits for rectangular pulses generation, considering delay line for optimum results

18 p3233 A70-36774

Microwave L-band correlator using YIG delay lines varied by electronically changing magnetic bias

20 p3597 A70-39468

Magnetoplasma interaction with axially slotted delay line, examining coil behavior physical mechanisms by cold plasma model

22 p4079 A70-42365

S band tunable free running high Q triode oscillator phase and frequency instability measurement based on delay lines applications

23 p4170 A70-43796

DELAY LINES [COMPUTER STORAGE]

Analogue shift register for use as delay line and digital filter, discussing applications to radio astronomy

18 p3261 A70-37088

DELIVERY

Shot delivery per second per unit area from ejector nozzle during shot peening, determining ideal delivery rates for shot of various sizes

07 p1291 A70-18830

DELIRIN [TRADEMARK]

Kinetic model for acid catalyzed Delrin decomposition, testing for Delrin-citric acid system and predicting thermograms with nonlinear regression analysis

09 p1630 A70-22896

DELTA DART AIRCRAFT

U F-106 AIRCRAFT

DELTA FUNCTION

Green function type solutions of shell equations by small parameter technique for case of free terms consisting of Dirac delta function

01 p0212 A70-11565

Exchange perturbation theories applied to delta function model of molecular hydrogen ion, discussing EL-HAV second order energy at large internuclear separations

05 p0884 A70-15878

Aerodynamic coefficients of nonconvex bodies in free molecular flow of monatomic gases based on delta representation of flow velocity distribution function

08 p1432 A70-21084

Time and spatial evolution of shock and expansion wave evolution from density discontinuity for gas with repulsive delta function interaction between particles

13 p2388 A70-29224

LF passband ideal filter instantaneous pulse response, using delta function model

22 p4005 A70-43555

Delta function approximation in diffuse transmission and reflection of light for phase function with sharp forward peak, using scattering compensation

23 p4214 A70-44034

DELTA LAUNCH VEHICLE

OSO 1-6 spacecraft design, payloads and performance for continuous solar observation, discussing instrumentation and Delta launch vehicle characteristics

14 p2638 A70-30691

Delta launch vehicle for scientific and application satellites, describing three stage liquid and solid propulsion systems

15 p2810 A70-31783

Delta launch vehicle design modifications for increased payload and space research programs

17 p3179 A70-35261

DELTA MODULATION

Satellite communication system using delta modulation for telephone service to large number single channel earth stations

10 p1834 A70-24329

Delta modulation with slope-overload prediction, showing signal to noise ratio improvement from computer simulation

13 p2365 A70-29146

Delta modulation threshold extension technique for phase lock loop FM demodulator

15 p2703 A70-32559

Asynchronous delta modulation channels with RLC integrators in feedback circuit, measuring articulation in presence and absence of noise

20 p3587 A70-40144

Output signal/quantization noise ratio, dynamic range and transmission error effects for syllabically companded delta-sigma modulator systems

24 p4320 A70-46152

DELTA WINGS

Supersonic flow around thin warped delta wing, taking into account current separation at subsonic leading edges for pressure distribution and aerodynamic characteristics

01 p0002 A70-10546

Surface shape determination for thin delta wing with variable geometry to minimize drag for given open and closed configurations and cruising supersonic speeds

01 p0002 A70-10547

Minimum drag hypersonic delta wing, analyzing shape for given planform, lift, pitching moment and volume using correction for pressure coefficient

01 p0002 A70-10557

Leading edge suction analogy for predicting low speed lift and drag-due-to-lift characteristics of sharp edge delta and related wing planforms

[AIAA PAPER 69-1133]

01 p0002 A70-10607

Asymptotic method based on Landahl small perturbation theory applied to perturbation velocity potential for oscillating delta wing in transonic flow

02 p0223 A70-11775

Supersonic flow separation at antisymmetrical delta wing edges, noting eddy layer and vertical velocity fields effects on aerodynamic characteristics

02 p0224 A70-12625

Wave drag dependence of delta wings on thickness distribution

[DVL-888]

03 p0406 A70-13273

Slender delta wing aircraft dynamic behavior under vertical and lateral gusts, particularly during landing approach

[DGLR-69-52]

04 p0623 A70-15145

Delta wing of given volume and planform with maximum lift-drag ratio in hypersonic flow

04 p0618 A70-15243

Aerodynamic characteristics, stability and controllability of swept wing and delta wing supersonic aircraft at subsonic velocities

05 p0796 A70-16966

Three dimensional supersonic flow around delta wings, considering lifting and thickness problems, leading edge characteristics, separated and non-separated shock waves, etc

06 p0964 A70-17241

Nonlinear theory extended to slender triangular and rectangular wings with symmetric profile, taking into account finite wing thickness

06 p0966 A70-17254

Supersonic aircraft aerodynamic properties and control systems performance, considering piloting of delta wing fighters

07 p1194 A70-19640

Swept and delta wing supersonic military aircraft stability and controllability, discussing variation in maximum lift coefficient as function of Mach number

09 p1611 A70-23129

Triangular conical wing with supersonic leading edges analyzed for aerodynamic forces in supersonic flow

10 p1798 A70-24121

Flow past yawed delta wing at supersonic flight velocities, obtaining real velocity near singular surface and replacing Mach number by perturbed parameter

10 p1799 A70-24126

Off-centerline heating on lee surface of supersonic delta wing with separation and vortex initiation at leading edge

11 p1976 A70-25996

Delta wing low aspect ratio aircraft vorticity generating effects, discussing wind tunnel tests for hazardous effects

12 p2156 A70-27692

Tailless delta Avro Vulcan aircraft design, hardware and flight results

14 p2532 A70-31391

Displacement interacting boundary layer in symmetry plane region of flat hypersonic delta wing by control volume balances for mass, momentum and energy

17 p3010 A70-34975

Hypersonic flow around delta wings of finite thickness with supersonic leading edges

18 p3206 A70-36260

Mathematical model of three dimensional separated flows with applications to small aspect ratio delta wing and flat plate

18 p3207 A70-36438

Aerodynamic characteristics of thick sharp edged cropped delta and gothic wings, giving low lift-dependent drag

19 p3353 A70-38615

Hypersonic flow pattern past windward side of triangular wing with supersonic leading edges, joining potential and vortex regions behind shock wave

21 p3743 A70-40609

Wave rider aerodynamic properties at small Reynolds numbers, using non-Weiler wing for flow field, pressure and force measurements at rarefied flow conditions

[AVA-FB-7029]

23 p4135 A70-44668

Oscillatory motion of triangular wing with conical body of arbitrary cross section in supersonic flow, considering wing-body interference effects

24 p4288 A70-45592

Inviscid hypersonic flow fields past lower/compression/ surface of delta wing calculated by one strip approximation of integral relations method

24 p4289 A70-46245

DEMAND [ECONOMICS]

Information transfer services potential demand including telephone, telegraph, videophone, electronic mail, etc

[AIAA PAPER 70-443]

11 p2152 A70-25448

Demand analysis data generation for V/STOL systems suitable for New York-Philadelphia-Washington business travel market, applying model to selected designs

[AIAA PAPER 70-1241]

24 p4374 A70-45961

DEMULATION

Demodulation of signals modulated with respect to wave period, deriving spectral width of pulsed period modulation

03 p0446 A70-13200

Linear phase detection using FM demodulation for Apollo S band communication system eliminating baseband voice interference with telemetry

[AAS PAPER 69-610]

04 p0648 A70-14659

Binary decoding extension to achieve unquantized demodulation performance for nonfading phase shift keyed coherent channel with white Gaussian noise

06 p1008 A70-17525

PSK demodulation by optimal carrier and bit synchronization methods based on nonlinear filter theory, relating error probability to signal to noise ratios

08 p1458 A70-20795

Interferometric combinations of frequency-shifted mode-locked laser pulses achieved by optical modulation-demodulation methods

12 p2249 A70-27755

Automatic phase control of demodulating signal in one dimensional extremal system with harmonic tracking oscillations

12 p2205 A70-28338

Digital sampled data demodulation, discussing methods of obtaining quadrature channels from single signal

15 p2703 A70-32579

FM demodulation threshold extension by correlation detection implemented in impulse noise cancellation system

19 p3382 A70-38893

High speed photodetectors for microwave demodulation of light, discussing electrical properties, equivalent circuits and noise factors

21 p3799 A70-41420

Coherent reference for demodulating double sideband suppressed carrier [DSB-SC] signals in presence of frequency detuning, using squaring or Costas loop

22 p3990 A70-43326

DEMULATORS

NT FREQUENCY COMPRESSION DEMULATORS

NT PHASE DEMULATORS

NT PHASE LOCK DEMULATORS

Light pulse demodulator using zero crossing technique to eliminate photomultiplier bandwidth and sensitivity limitations

02 p0271 A70-12744

Modem selection for satellite communications system, considering bandwidth and power constraints, propagation characteristics, point-to-multipoint operation, etc

08 p1459 A70-20807

Higher order frequency demodulators with feedback in canonical form and with baseband filter

08 p1479 A70-20809

FM feedback demodulator performance model using mixer-correlator, showing cross correlation receiver design

08 p1479 A70-20810

Multichannel performance measurement of threshold extension FM demodulators using click suppression techniques

08 p1460 A70-20812

Communication satellite PSK modulator-demodulator /modem/ implementation requirements and design for optimal performance

10 p1835 A70-24336

Threshold extension demodulator /TED/ using bandpass filter without oscillator for FM multiplex

12 p2197 A70-27908

Modulation-demodulation system for multiple access tactical satellite communication

12 p2187 A70-27915

Demodulators threshold performance for satisfying carrier to noise ratios requirement of Intelsat 4 system

14 p2552 A70-31352

Multilevel FSK system with limiter discriminator followed by low pass filter as demodulator, calculating error rates for comparison with other analyses

23 p4161 A70-44003

DEMONSTRATION

U PROVING

DENDRITIC CRYSTALS

Electrolyte purity effect on initiation times and growth rate of Zn dendrites in alkaline zincate solution, discussing dendrite initiation retardation

07 p1356 A70-19387

DENITROGENATION

Ground level denitrogenation duration effects on decompression sickness occurrence in space cabin atmospheres

06 p0999 A70-17289

Bends incidence in altitude training, examining denitrogenation role

24 p4307 A70-45339

DENSIFICATION

Superplastic nickel superalloys fabrication by controlled densification during direct extrusion

12 p2257 A70-28020

WC as densification aid for NbC-C composites, examining fabrication temperature, mechanical properties, solid solution composition, etc

15 p2757 A70-31797

DENSITOMETERS

Jovian cloud layer light and dark matter albedo determination, applying photographic densitometry

02 p0375 A70-12431

Parachute-borne densitometer using forward scattering of low energy beta particles for direct measurement of atmospheric density at 30-60 km

[AAS PAPER 69-570]

04 p0687 A70-14654

Satellite lines from diffraction grating observed by densitometer tracings of plates connected with optical mixing in stimulated Brillouin scattering
04 p0701 A70-15030

Blood reflection densitometer with linear response to changes in indocyanine green dye concentration, using simple analog computation
07 p1221 A70-19589

Satellite-borne experiments of neutral molecular beam-solid surface interactions, describing Molsink chamber, densitometer, sphere and paddlewheel satellites
07 p1344 A70-20128

Transistor densitometer used for variable star interpretation by amateur photographers
15 p2740 A70-32348

DENSITY [MASS/VOLUME]

NT ATMOSPHERIC DENSITY
NT GAS DENSITY
NT SPACE DENSITY

Icarus asteroidal nature and fragmentation origin suggested from inclusion in angular momentum density-mass diagram
01 p0180 A70-10538

Nb binary and tertiary alloys density changes found proportional to alloying element content
03 p0511 A70-13489

Quarkian substance properties noting possibility of superconducting state at high densities
04 p0753 A70-15074

Turbulent wake behind plate due to confluence of two incompressible fluids with different densities
07 p1261 A70-20463

Inorganic ceramic materials in design and fabrication of microwave antennas, filters and stable resonators, discussing density and dielectric constant variability by ceramics foaming
09 p1689 A70-22007

Ti-Al-Nb system creep strength, oxidation resistance, density, forging and rolling
17 p3120 A70-34426

Thermal conductivity of particulate basalt as function of density in simulated lunar and Martian environments, noting temperature and pressure effects
18 p3316 A70-36772

Equation of state of nuclear neutron matter as function of density
19 p3524 A70-38695

W-Mo-Nb-Ta system with constant 30 percent W, discussing specific weight and hardness
19 p3453 A70-38714

Turbulent wake behind plate due to confluence of two incompressible fluids with different densities
20 p3557 A70-39263

DENSITY [NUMBER/VOLUME]

NT ELECTRON DENSITY [CONCENTRATION]
NT ELECTRON DENSITY PROFILES
NT ELECTRON DISTRIBUTION
NT ION DENSITY [CONCENTRATION]
NT IONOSPHERIC ELECTRON DENSITY
NT IONOSPHERIC ION DENSITY
NT MAGNETOSPHERIC ELECTRON DENSITY
NT MAGNETOSPHERIC ION DENSITY
NT MAGNETOSPHERIC PROTON DENSITY
NT METEOROID CONCENTRATION
NT PACKING DENSITY
NT PARTICLE DENSITY [CONCENTRATION]
NT PLASMA DENSITY
NT PROTON DENSITY [CONCENTRATION]
NT SPACE DENSITY

Neptune data from photoelectric observations of 7 April 1968 occultation of BD-17 deg 4388, determining hydrogen dominance and molecular density
14 p2642 A70-30890

Graphite fibers made from polyacrylonitrile yarn examining density-Young modulus relationship
17 p3127 A70-35149

Trojan asteroids in sun-Jupiter system, determining density near preceding Lagrangian point
17 p3171 A70-35445

Lunar crater number and density vs diameter graph, showing rhythmical deviations from mean asymmetrical cosine curve
19 p3517 A70-37990

K and M star molecular constituent density calculations using model atmospheres and observations
20 p3702 A70-39015

Small craters number density in southern lunar highlands, supporting Tycho Association cometary impact origin
21 p3920 A70-41882

DENSITY [RATE/AREA]

U FLUX DENSITY

DENSITY DISTRIBUTION

Density distribution measurements in flow field using interference methods, including laser light sources
01 p0085 A70-10268

Thermospheric neutral density amplitudes and phases using one dimensional model of geomagnetic activity effect, 27 day variation and semiannual variation
01 p0070 A70-10402

Density distributions of electrically charged trace components in axisymmetric jets, considering space charge effect and ambipolar diffusion
01 p0066 A70-11135

Atmospheric density variations in thermosphere determined from braking satellite data, discussing correlation with solar activity and temperature variations
01 p0077 A70-11202

Atmospheric density on basis of photographic observations of meteors, comparing vertical profile with CIRA profile
01 p0084 A70-11556

Jupiter atmosphere temperature and density profiles determined from thermal models based on thermal structure above dense cloud level
02 p0367 A70-11814

Velocity and density profiles obtained from mass diffusivity time measurements in axisymmetric turbulent air pipe flow over specific Reynolds number range
02 p0295 A70-11853

Chemical kinetics in reaction zone of shock heated hydrogen-carbon monoxide-oxygen mixtures, measuring density field behind normal shock wave by optical interferometry
02 p0250 A70-12022

Measurement techniques for determining density and temperature distributions along radius of plasma cylinder by electron cyclotron resonance, microwave refraction and acoustic resonance
02 p0349 A70-12758

Schlieren photograph intensity variations correlated with statistical parameters for turbulent flow density variations
03 p0464 A70-12941

Density effects on transport coefficients of gaseous mixtures, solving modified Boltzmann equation including collisional transfer and three-particle collision effects
03 p0606 A70-13576

MHD flow velocity and current density distributions in annular duct with radial magnetic field
04 p0725 A70-14531

Statistical electron density distributions and Thomas-Fermi-Dirac screening functions for positive ions with various ionization degrees
04 p0721 A70-14666

Electron beam technique to measure density profiles of strong shock waves in argon
04 p0692 A70-15325

Backscattered signal power density distribution along equivalent propagation path of delayed components, determining reflecting layers characteristics from echo signal phase
04 p0654 A70-15728

Ionospheric air density profiles revision based on satellite orbits analysis
05 p0839 A70-16287

Lunar density gradient, free oscillation and tides study inferring lunar atomic number similarity to Si and earth mantle
05 p0908 A70-16316

Density spectra of cosmic ray showers measured by scintillators and GM counters
05 p0902 A70-16458

Electromagnetic wave phase characteristics after free space passage through statistical medium with wave disturbance producing density and ionization
05 p0815 A70-16735

Ionospheric horizontal discontinuities of electron density distribution parameters effect on penetration frequency, skip distances and arrival angles
05 p0842 A70-16743

Density wave theory and Schmidt model applied to Milky Way spiral structure, considering systematic motion of interstellar neutral hydrogen
05 p0918 A70-16928

Electron density distributions relation to D region diurnal and seasonal variations in radiowave absorption in terms of transport processes near mesopause
06 p1054 A70-17589

Automatic control for filling tanks with stably stratified liquids using analog mixture valve and digital metering pump methods
06 p1062 A70-17617

Pulsed plasma transfer systems weight analysis, studying propellant density gradients effects on coaxial plasma gun performance
06 p1133 A70-18231

[AIAA PAPER 70-168]

Unsteady nonlinear molecular flow problems concerning plane Couette flow, heat transfer between parallel plates and density discontinuity propagation solved by Monte Carlo method
06 p1113 A70-18321

Model sampling or Monte Carlo applied to normal shock, giving temperature and density profiles for Mach 10 shock
06 p1050 A70-18337

Density field around leading edge of blunted flat plate, using electron beam measurements in low density hypersonic wind tunnel
06 p0980 A70-18351

Cylinder wakes in rarefied gas flow at Mach 20, obtaining density profile data from electron gun, impact pressure and cooled film probe measurements
06 p0984 A70-18387

Cadmium vapor density distribution by cataphoresis in He-Cd laser discharge tube determined by side light measurements
06 p1084 A70-18613

Surface tension plotted against density and temperature of hydrocarbon jet fuels, determining critical temperature
07 p1357 A70-18653

Single parameter photometric analysis for density distribution of matter in comets atmospheres
07 p1374 A70-18707

Continuous signal a posteriori distribution density formed on basis of learning sequence with no a priori information about signal and noise statistics
07 p1226 A70-18761

Material inhomogeneity during high temperature fatigue tests taking into account probability density of random failure coordinate distribution
07 p1401 A70-18839

Galaxies statistical distribution studied to determine superclusters existence, correlating results with random distribution expectations
07 p1375 A70-18868

Pressure drop at slender profile performing harmonic vibrations near interface between two media of different density solved by numerical method
07 p1254 A70-19079

Interstellar gas ionization and heating by background X radiation, studying neutral hydrogen density distribution between spiral arms and at galactic peripheries
07 p1383 A70-19401

Bumper materials effect on two component hypervelocity impact shields performance, noting material density influence
07 p1310 A70-19713

Helium and argon atoms number densities radial profiles in supersonic free jets of binary gas mixtures by molecular beam sampling
07 p1341 A70-20105

Integral methods of obtaining electron density profile of planetary ionospheres and interplanetary gases
07 p1388 A70-20160

Compressibility effect on density explaining Mercury-Venus density near equality to earth- Mars-moon, discussing theory of rotational break-up of parent planets
08 p1563 A70-20496

Density profiles of sphere wake in rarefied hypersonic flow compared to free molecular flow calculations
08 p1431 A70-20591

Interplanetary density distribution of cold interstellar origin hydrogen dependent on solar EUV flux, considering interaction with solar wind protons
08 p1562 A70-21401

Laser interferometric technique involving use of unstable external resonator to facilitate electron density measurements in presence of transverse plasma density gradients
08 p1499 A70-21693

Radiation transfer in scattering medium with nonuniform density distribution of absorbing matter expressed in terms of photon distribution
09 p1666 A70-22178

Uniformly rotating gas disk large scale spiral structure analysis, studying density waves due to gravitational disturbance by supersonic particle
09 p1755 A70-22503

Nonlinear stellar density waves in galaxy using gas dynamic equations, assuming one dimensional and steady waves
09 p1762 A70-23073

Blast waves in low Mach number regime with assumption of power law density profile in rear, obtaining particle velocity and pressure distributions
09 p1661 A70-23214

Ion density profile across shock in partially ionized gas measured in plasma jet wind tunnel for comparison with Rankine-Hugoniot relation
09 p1662 A70-23235

Earth shape formulas reduction to Taylor series, considering Molodenski reduction method for simple layer density integral equation
09 p1670 A70-23343

Transition from compressible to incompressible fluid assuming isothermal flows and finite stresses for density at or different from initial value
10 p1863 A70-24008

Latitudinal ionospheric electron density and temperature variations at 1000 km within and near auroral zone
12 p2222 A70-27186

Doped semiconductors electronic state density in forbidden band, assuming fluctuations in impurities in form of homogeneous spheres with varying charges and radii
12 p2286 A70-27363

Shock wave reflection into ideal gas flow with linear density variation analyzed for flow field
12 p2211 A70-27832

Gasdynamic flows strong and weak density discontinuity surfaces determination, using shadowgraphs and interference patterns
12 p2238 A70-28248

Low latitude atmospheric vertical density variations, comparing solar and geomagnetic activities effects

12 p2227 A70-28264

Turbulence spectrum due to density fluctuations in plasma with strong magnetic field, using hydrodynamic theory and Poisson equations

13 p2457 A70-28559

Plasmopause and polar wind, considering density discontinuity due to outer magnetosphere heating during magnetic storms

13 p2491 A70-29059

Time and spatial evolution of shock and expansion wave evolution from density discontinuity for gas with repulsive delta function interaction between particles

13 p2388 A70-29224

Density wave theory and spiral gravitational field effects in migrating stars orbits and origins in Milky Way spiral arm, using Schmidt model

13 p2495 A70-29801

Laminar flow of suspension over flat plate, analyzing particulate velocity and concentration profiles relationships to drag and lift forces

14 p2565 A70-30270

Stratospheric warmings effect on atmospheric density field variations

14 p2608 A70-30592

Backscattered signal power density distribution along equivalent propagation path of delayed components, determining reflecting layers characteristics from echo signal phase

14 p2550 A70-30812

Linear density gradients in isopycnic centrifugation technique for selecting synchronous daughter cells from asynchronous *Chlorella* cultures

14 p2546 A70-30985

Strong shock waves profiles in monatomic perfect gases by Monte Carlo simulation, obtaining maximum density slope thicknesses

14 p2567 A70-31031

Hypersonic low density transitional flow over slender conical vehicle, calculating drag coefficient and density profiles

14 p2529 A70-31365

Temperature and density extreme variations at various levels in stratosphere and mesosphere, analyzing sounding rocket data

15 p2723 A70-31661

Ionospheric density profiles measurement by accelerometers on SPADES and Cannon Ball 1 satellites, comparing results with prediction from atmospheric model

15 p2724 A70-31686

Terrestrial planetary ionospheres, discussing charged particle density distribution of Mars daytime ionosphere and Venus day and dark sides

15 p2799 A70-31748

Internal ballistics equations solution on basis of pressure index law of burning taking into consideration density approximation

15 p2786 A70-31849

Inhomogeneous ion beam plasma LF instability, showing oscillations amplitude maxima in radial density gradient regions

15 p2780 A70-32193

Power density fluctuations in emission peaks of ruby laser determined by splitting beam into two components and using photosensitive element and photomultiplier recording

15 p2754 A70-32874

Shock wave front propagation instability in decreasing density medium, applying to stellar structure

16 p2890 A70-33200

Turbulent kinetic energy equation for determining turbulent flow fields applied to free mixing problem of constant density streams

16 p2894 A70-33856

Turbulent flow in stratified fluids over flat plate, relating density profile curvature and heat transfer

16 p2895 A70-34242

NO in earth atmosphere, describing theory of formation for explaining observed density distribution

18 p3245 A70-36019

Density diffusion and buoyancy effects on horizontal boundary layers in stratified flow

18 p3239 A70-36193

Continuous signal a posteriori distribution density formed on basis of learning sequence with no a priori information about signal and noise statistics

18 p3229 A70-37105

Galactic spiral structure model, examining nonlinear stellar density waves in plasma cylinder

18 p3322 A70-37131

Tightly wound spiral nonlinear density waves in pressureless self gravitating disk with external gravitational field, examining solid body and differential rotation

18 p3331 A70-37192

Electron concentration vertical profile in ionosphere as function of altitude of radio wave reflection and group refraction and velocity characteristics

19 p3409 A70-37329

Light propagation in plane parallel layer of scattering medium containing absorbing substance with random density distribution

19 p3461 A70-37422

Fluctuations in radiation power density of solid state laser near focal plane of convergent lens, using device for selecting and recording individual peaks

20 p3643 A70-40022

Low voltage slotted hollow cathode laser tube design with transverse discharge operation and uniform axial distribution of laser media, including metal vapors

21 p3834 A70-40571

Subsonic air flow around airfoil in wind tunnel, detecting density gradients by pulsed ruby laser holographic visualization

21 p3822 A70-40809

Midlatitude stratosphere and lower ionosphere density model, discussing vertical, diurnal and seasonal variations effects on spacecraft trajectories

21 p3813 A70-40830

Reflection nebulae dust density, noting lower limit dependence on absolute magnitude of illuminating star

21 p3889 A70-41149

Turbulent density fluctuations statistical properties analysis by cross correlation technique with schlieren instruments

21 p3807 A70-41242

Axial propellant density gradients and circuit capacitance correlated with pulsed coaxial plasma gun efficiency

21 p3858 A70-41726

Pressure field behind shock wave after interaction with nonuniform density region, describing shock front shape

21 p3810 A70-41964

Radio source count formula in zero pressure model universe for background radiation differential density evolution function

21 p3923 A70-42104

Star content in Small Magellanic Cloud wing counted to determine detachability from tidal arm and main body

22 p4099 A70-42628

Cloud droplet growth rapid computation using number density mean value for integrating stochastic coalescence equation into differential equation

22 p4064 A70-42910

Stability conditions for relativistic stars, discussing mass-energy density distribution, Taylor instability, Schwarzschild criterion, Newtonian stellar model, gravitational red shift, etc

22 p4104 A70-42999

Lower chromosphere shock wave heating, analyzing density scale height effects

22 p4105 A70-43001

Magnetoplasma density modulation from LF and amplitude magnetic perturbations, using collisionless Boltzmann transport equation

22 p4082 A70-43255

Diurnal atmospheric density variations latitude dependence from satellite data

23 p4185 A70-43842

Oscillating vane and rotating disk pressure gauge theory, considering gas damping and density variations

23 p4198 A70-44948

Rarefied gas heat conduction between concentric cylinders in slip regime, obtaining perturbed temperature and density variations

23 p4284 A70-44985

Quasi-ambipolar diffusion in arc discharges in magnetic field, calculating ions and electrons density distributions between anode and cathode sheaths

24 p4384 A70-45148

Lighthill aerodynamic noise theory fundamental equation for acoustic field density distribution, determining flow fields for surfaces in uniform translational motion

24 p4324 A70-45268

Quasars red shift distribution extrapolated from density evolution and luminosity function

24 p4402 A70-45386

Interplanetary atomic hydrogen density distribution from Lyman alpha scattering calculation, explaining background radiation anisotropy detection by Vela 7 satellite

24 p4403 A70-45392

Sintered material density-sound velocity relation, deriving ultrasonic wave propagation time dependence

24 p4360 A70-45731

Planetary nebulae NGC 7662 and NGC 7009 axially symmetric models from density distributions, H continuum threshold optical depths and central star temperatures

24 p4409 A70-45757

DENSITY MEASUREMENT

NT X RAY DENSITY MEASUREMENT

Absolute calibration method for daily solar flux density discrepancies measurements at UHF, describing equipment and error analysis

01 p0168 A70-10259

Density distribution measurements in flow field using interference methods, including laser light sources

01 p0085 A70-10268

Giant planets structure, calculating Jupiter and Saturn densities using Russell solar mixture and internal heat from central core radioactivity

01 p0181 A70-10663

Air flow density measurements with interferometer in supersonic square Laval nozzle, showing flow core motion and wave structure

01 p0064 A70-11000

Atmospheric density profiles based on laser radar return from ruby laser detected by photomultiplier

01 p0079 A70-11220

Coordination technique for pressure, density and temperature measurements by probes during parachute reentry into planetary atmospheres, taking into account reentry dynamics

01 p0197 A70-11495

Air density variations calculated by visual satellite observations processing, comparing results of IN-TEROBS and average anomalies methods

02 p0288 A70-11766

Time resolved cavity perturbation technique to measure high plasma density in magnetic mirror compression experiment, obtaining total electron number

02 p0347 A70-12236

Optical density measurements in high speed confined air vortex, discussing light deflection mapping of vortex density field at off axis positions

03 p0480 A70-12906

Heat resistant alloys densities calculated from chemical composition, estimating error

03 p0512 A70-13778

Linear aliphatic polyesters unit cell dimensions and crystalline densities

03 p0517 A70-13808

Parachute-borne densitometer using forward scattering of low energy beta particles for direct measurement of atmospheric density at 30-60 km

04 p0687 A70-14654

Atmospheric density measurements from Explorer 17 satellite by density gage and drag techniques resolved for difference by calibration and systematic errors considerations

04 p0691 A70-15120

Vertical air density profile from satellite measurements of atmospheric oxygen radio emission at 40-70 km altitudes

06 p1056 A70-17788

Normal hypersonic shock wave structure in diatomic gas, measuring density by electron beam fluorescence technique

06 p1050 A70-18341

Ar-Kr integral collision cross sections based on density measurements of Ar beam passed through liquid nitrogen cooled Kr filled scattering chamber

07 p1344 A70-20135

Soviet monograph on constant of gravitation, mass and density of earth covering torsion balance, weight experiments and nonlinear vibration techniques

08 p1487 A70-20764

Plasma density measurement by LC tank circuit with plasma contained in induction coil, deriving expressions for circuit resistance and resonant frequency

08 p1550 A70-20846

Kerr cell-shuttered high speed stigmatic spectrograph for shock tube electron density distribution measurement

09 p1682 A70-23503

Plasma electron density errors in measurement by microwave interferometers, noting effects of inaccurate phase shift determination

09 p1738 A70-23634

Electron beam fluorescence probes for rarefied gas flow, describing local density and temperature measurement methods

10 p1888 A70-24399

Vertical air density profile from satellite measurements of atmospheric oxygen radio emission at 40-70 km altitudes

10 p1882 A70-25020

Extraterrestrial electron density precision measurement using HF impedance probe with guard ring to remove ion sheath effects

10 p1892 A70-25255

Pulsed laser holographic interferometry of density field created by high speed projectile motion in air

11 p2051 A70-25987

Rarefied gas stream density measurements with electron beam fluorescence experiment, determining pressures and densities behind plane shock wave and in supersonic nozzles

11 p2087 A70-26743

Air pressure, air density and gravity tables, including corrections for mercury barometer measurements

12 p2222 A70-27008

Stark broadening of neutral helium line in plasmas for electron densities measurements accuracy, comparing to H beta determined densities

13 p2456 A70-29225

Atmospheric density estimation from observation of satellite drag-induced energy dissipation

13 p2400 A70-29530

Hot-wire probe measuring He-ai mixture velocity and concentration following He discharge from circular orifice, noting calibration method

13 p2412 A70-29990

Atmospheric density variations and functional dependence of aerodynamic moment coefficient on incident angle from Saturn Workshop flight experiment

14 p2528 A70-30559

- Pitot probe for high altitude atmospheric density measurements integrated with telemetry system mounted on two stage Super Loki sounding rocket
14 p2585 A70-30576
- Plasma concentration measurement in coaxial accelerator, using gas laser and multiple wave interferometer in vacuum chamber
15 p2781 A70-32858
- Turbulent wakes density fluctuations measurement using pulsed laser holographic interferometry in ballistic range
[AIAA PAPER 70-727] 16 p2834 A70-33494
- Optical system measurement of density and rotational temperature in gaseous plume simulating auxiliary propulsion and oxygen hydrogen burner of S-4B
16 p2913 A70-34023
- Electron density measurements in lower ionosphere by narrow band VLF receiver flown in Tomahawk rocket during quiet daytime
17 p3076 A70-34938
- Air jets from sonic orifice, investigating three zones of isochor families by visualization and density measurement
17 p3070 A70-35046
- Ionospheric plasma disturbances due to moving space vehicle, investigating by electron density measurements in rarefied wake regions using gyro-plasma probe
17 p3142 A70-35763
- HEOS 1 low energy proton measurements in interplanetary space, discussing particle direction during solar event and anisotropy time history
19 p3495 A70-37505
- Whistler density variability correlated with solar activity during IQSY
19 p3462 A70-37924
- Metal vapors electrical conductivity and density measurement at high temperatures and supercritical pressures
20 p3648 A70-39637
- Atomic oxygen density and temperature diurnal variation determination by F region incoherent scatter measurements, using nonlinear regression analysis
21 p3817 A70-41096
- Mean density and temperature measurements in hypersonic Ti spheres wakes in nitrogen atmosphere, using electron beam fluorescence probes
21 p3745 A70-41754
- Carbon dioxide and water cryodeposits refractive indices and densities, using thin film interference technique
[ASME PAPER 70-HT-33] 22 p4122 A70-42344
- Liquids density measurement from digital data obtained from sample subjected to vibrations
22 p4030 A70-42848
- Wollaston prism schlieren interferometer for quantitative density gradient measurements in air
[SMPTE PREPRINT 25] 22 p4034 A70-43050
- Hypersonic projectile turbulent wake measurements, discussing velocity, mass density and temperature determination
[ICAS PAPER 70-07] 23 p4132 A70-44130
- Electron density measurements in ionosphere along rocket trajectory, using sweep frequency RF impedance probe with guard ring
23 p4192 A70-44877
- Air densities from polar satellites orbit analysis
24 p4329 A70-45550
- Density correlation measurements for diffusion coefficient in magnetized He plasma
24 p4386 A70-45614
- DEOXIDIZING**
Ni-Fe alloys texture formation, studying strong deoxidizers role in secondary recrystallization
06 p1088 A70-17614
- Benzoyl cyanide deoxygenation, describing reaction kinetics and products
17 p3041 A70-34750
- DEOXYGENATION**
Agents for deoxygenation of nitro and nitroso groups
17 p3042 A70-35329
- DEOXYRIBONUCLEIC ACID**
DNA penetration into normal and fast neutron irradiated yeast cells, using immunofluorescent microscopy
03 p0417 A70-13072
- Differential melting for partial purification of chemically distinct region of chromosome mycoplasma sp. /KId/
04 p0647 A70-15448
- Hydrostatic pressure effects on DNA, RNA and protein synthesis and division in *Escherichia coli* cultures
04 p0637 A70-15475
- Cytosine-thymine transitions from cytosine-5-H3 decay in bacteriophage S13 DNA, discussing coding change efficiency
05 p0803 A70-16948
- Calf thymus DNA structural and functional changes following exposure to hydrogen atoms and gamma radiation
07 p1215 A70-20050
- Density gradient sedimentation of *Escherichia coli* populations irradiated with Co 60 gamma rays, showing correlation between DNA degradation and cell death
08 p1441 A70-20680
- Escherichia coli* cell division patterns, discussing generation times spread, gamma ray irradiation in nutrient broth, DNA damage and growing points, etc
08 p1441 A70-20681
- DNA enzymatic breakdown in *Escherichia coli* as function of ionizing radiation and temperature
08 p1445 A70-20775
- Chromosome of temperature-sensitive mutant of *Bacillus subtilis* 168, observing multiforked replication at normal temperature and transfer of DNA
09 p1615 A70-22206
- Parental terminid-daughter strand linkage in initiation of DNA replication in *Bacillus subtilis* after thymineless germination
16 p2847 A70-33060
- Monograph on ionizing radiation effects on molecular biology of *Escherichia coli*, discussing cellular damage, DNA degradation and synthesis, incorporating radioactivity, mutations, etc
16 p2848 A70-33098
- Lambda prophage induction into lysogens, noting nalidixic acid role in DNA synthesis inhibition
20 p3573 A70-39774
- Simulated space flight radiation effects on dogs DNA synthesis and bone marrow cell differentiation
20 p3575 A70-40191
- Mammalian cells after X ray irradiation, showing two forms of DNA repair process
21 p3765 A70-42024
- Sunlight induced pyrimidine dimers formation in human cells in vitro, relating DNA lesions by 254 nm irradiation
24 p4304 A70-46139
- DEPENDENCE**
NT SPATIAL DEPENDENCIES
NT TIME DEPENDENCE
Dependence effects on nonparametric mixed statistical tests
06 p1095 A70-18622
- DEPENDENCY**
U DEPENDENCE
DEPENDENT VARIABLES
Short term weather forecast hydrodynamic equations reduced to solving nonlinear differential equations by introducing dependent variables
07 p1329 A70-19647
- Controlled variable perturbation effects on system with internal positive feedback
20 p3602 A70-39829
- DEPERSONALIZATION**
Air traffic controller role in future air traffic system, considering automation in operations
19 p3371 A70-38649
- DEPLOYMENT**
Titan 3 launch vehicles capabilities communication satellites deployment modes, presenting cost and availability data for preliminary mission planning
[AIAA PAPER 70-482] 11 p1212 A70-25451
- Earth-pointing satellites joined by tether, discussing reel back and drag brake orbital deployment techniques and dynamic behavior
15 p2799 A70-31776
- Radio Astronomy Explorer satellite boom deployment method resulting in gravity gradient capture, emphasizing role of predeployment attitude and antenna Vee angle
[AIAA PAPER 69-920] 21 p3931 A70-41856
- Harrier aircraft operation in Marine Corps for fast reaction close support based near maneuver units
[SAE PAPER 700835] 24 p4290 A70-45887
- DEPOLARIZATION**
Right and left atrial polarization time sequence as guide to p wave origin in heart diseased patients following electrical stimulation of atria and ventricles
01 p0015 A70-10437
- Model for simulating normal/abnormal depolarization and repolarization of heart and to reproduce electrocardiograms, describing design and programming
03 p0432 A70-12889
- Norepinephrine-induced depolarization effects on brown fat thermogenesis in cold-acclimated rats determined from in vivo measurement of intracellular potentials
05 p0799 A70-16020
- Scattering and depolarization of plane horizontally polarized electromagnetic wave from slightly rough lossless dielectric layer, using small perturbation theory
06 p1010 A70-18019
- Depolarization factor measurements of clear atmospheric air by lidar techniques and laser light scattering
06 p1083 A70-18244
- Geometrical light depolarization in randomly inhomogeneous medium, discussing light propagation in turbulent atmosphere and ionospheric radio propagation
10 p1844 A70-25162
- Gas laser radiation depolarization coefficient as function of radiation energy, cavity anisotropy and operating transition type
19 p3444 A70-37445
- Laser light polarization and depolarization during backscattering from aqueous suspensions
23 p4215 A70-44271
- Optical solar polarization broadband measurement interpretation with depolarization factor due to elastic collisions or additional source
24 p4414 A70-46172
- DEPOLARIZERS**
U DEPOLARIZATION
DEPOSITION
NT ANODIZING
NT ELECTRODEPOSITION
NT ELECTROPLATING
NT VACUUM DEPOSITION
NT VAPOR DEPOSITION
Reworking of deep-sea sediments as indicated by vertical dispersion of Australasian and Ivory Coast microtektite horizons, implying years of deposition
01 p0178 A70-10474
- Epitaxial Ge deposits on Si control by Kikuchi pseudolines, considering surface polish, crystallinity and substrate orientation
13 p2470 A70-28957
- Adherent Ta films deposition onto Teflon disks by sputtering
18 p3264 A70-37098
- Stellar wind effect on accretion, showing critical intensity of particle ejection replacement
18 p3324 A70-37148
- Lunar formation, investigating accretion rate ratio for earth and moon as function of distance
24 p4409 A70-45674
- DEPOSITS**
NT CRYODEPOSITS
Carbon deposit formation in gas turbine engines with various fuels, studying thermal insulation properties
09 p1742 A70-22472
- Growth rate and spatial distribution of solid deposit freezing onto vertical surface in presence of convective heat transfer at moving phase interface
12 p2331 A70-27696
- Circulated air natural and technical impurities effects on gas turbine time dependent performance emphasizing erosion, deposits and overheating
13 p2475 A70-29713
- Aircraft and engine fuel systems deposit formation and microstructure in various test rigs, using electron microscopy
[SAE PAPER 700258] 18 p3214 A70-36823
- Jet fuel system deposits measurement, noting reliability of oxygen combustion and beta ray backscattering techniques
[SAE PAPER 700257] 18 p3214 A70-36824
- Scaled-off carbon dioxide laser discharge deposits analyzed by mass spectroscopy
19 p3445 A70-37670
- DEPRESSANTS**
NT CENTRAL NERVOUS SYSTEM DEPRESSANTS
Differential effect of hypobaric hypoxia on depressant characteristics of sodium barbital, sodium pentobarbital and chloral hydrate in rats and mice
04 p0631 A70-14680
- DEPRESSURIZATION**
U PRESSURE REDUCTION
DEPRIVATION
NT SENSORY DEPRIVATION
NT SLEEP DEPRIVATION
NT WATER DEPRIVATION
DEPTH MEASUREMENT
Water depth determination by remote measurement of near IR reflectance of underwater plants, discussing effects of water path length changes
10 p1878 A70-24741
- Water depth determination by various remote sensing techniques, discussing bottom reflection, wave analysis, thermal anomalies and laser ranging by time difference
12 p2217 A70-26916
- Depth measurement of gas-saturated surface layer in Ti alloys, using microhardness method
18 p3277 A70-36472
- Lunar regolith depth measurement by Lunar Orbiters 4 and 5 high resolution photographs, discussing thickness relation with sinuous rilles in marial regions
18 p3319 A70-37054
- Vapor capillary /melt/ depth in electron beam welding, considering electron energy, radiative dissipation, etc
21 p3833 A70-41124
- Lava thickness measurement in lunar maria from projecting rim width of partially buried craters
23 p4242 A70-44292
- DEPTH PERCEPTION**
U SPACE PERCEPTION
DERIVATION CALCULUS
U DIFFERENTIAL CALCULUS
DESATURATION
Simultaneous satellite attitude control and flywheel desaturation using external torque
13 p2503 A70-28527

Optimal desaturation of angular momentum exchange controllers in spacecraft attitude control systems, using natural environmental torques
16 p2947 A70-33345

DESCENT

NT PARACHUTE DESCENT

Forward and rearward facing passenger seats effects in postdecompression emergency descent of high speed high altitude aircraft
03 p0437 A70-14061

Differential descent convergence demonstration based on relation between convex and Liapunov functions
08 p1534 A70-21007

Lunar landing training vehicle using Lunar Module free flight simulator for earth practicing of final descent handling
21 p3750 A70-41193

DESCENT PROPULSION SYSTEMS

Apollo lunar module descent engine exhaust organic combustion products, estimating ion intensities of various species in all mass spectra
02 p0356 A70-12693

Flight performance of Apollo LM descent-ascent propulsion systems, considering telemetry data, prediction correlation and modifications
[AIAA PAPER 70-673]
16 p2967 A70-33577

Lunar surface erosion due to Apollo 11 descent engine
18 p3316 A70-36960

DESCENT TRAJECTORIES

NT REENTRY TRAJECTORIES

Optimal control algorithm for spacecraft descent in atmosphere based on nominal trajectory and acceleration measurements
01 p0197 A70-11499

Optimal descent maneuver from planetary orbit for fixed atmospheric reentry angle, considering minimum impulse /fuel consumption/
04 p0745 A70-14496

Airborne digital letdown computer to guide VTOL aircraft flying complex trajectories to relieve airport congestion
05 p0880 A70-16416

Optimal landing of spacecraft on moon surface from low circular orbit, analyzing rocket thrust, altitude and landing site distance effect on spacecraft mass
06 p1155 A70-17880

Distance of spacecraft descending on parachute through planetary atmosphere measured from center of planetary mass using onboard instrument data
06 p1155 A70-17897

Apollo 11 premission planning, real time situation and postflight analysis for lunar descent and ascent phases, providing navigation correction capability for Apollo 12
[AIAA PAPER 70-25]
06 p1159 A70-18227

Control algorithm for vehicle descent after reentry based on descent range prediction by integrating motion equations allowing for motion three dimensionality
07 p1393 A70-19482

Spacecraft trajectory control for hypersonic atmospheric entry
13 p2500 A70-28411

Control algorithm for vehicle descent after reentry based on descent range prediction by integrating motion equations allowing for motion three dimensionality
15 p2813 A70-32727

Lunar Module landing radar system design, discussing antenna and electronics assembly
16 p2865 A70-33681

Optimum guidance and control law for lifting reentry bodies, investigating plane descent trajectories for minimum structural heating
16 p2982 A70-33774

Aircraft climb and descent trajectories approximation compatible with air traffic control operation, noting parameters effects
24 p4375 A70-46239

DESENSITIZING

Initiator desensitization process involving use of volatile inert liquid to increase safety during assembly operations
03 p0549 A70-14137

Multiple wavelength desensitized hologram interferometry to extend displacement measurement range
21 p3822 A70-40814

DESERT ADAPTATION

Man and animals physiological adaptation and behavior under conditions of polar regions, highland and arid areas
01 p0030 A70-11465

Acid mucopolysaccharides in distal segments of medullary substance of kidneys of rodents under high ambient temperature, showing stable morphological characteristics
07 p1204 A70-19141

High temperature adaptation, gas exchange and thermoregulation in dogs during repeated overheatings in open sunshine
18 p3219 A70-36339

Intracellular shifts in body fluids and dehydration tolerance in burro, comparing water content of desert animals
21 p3766 A70-42157

DESERTS

NT LIBYAN DESERT

Remote photometric and spectrometric measurements for plant structure and productivity of grass and shrub vegetation in desert environments
12 p2218 A70-26923

DESIGN OF EXPERIMENTS

U EXPERIMENTAL DESIGN

DESORPTION

Molecular sieve mixed gas adsorption and vacuum desorption of carbon dioxide in Apollo spacecraft cabin
01 p0040 A70-11450

He and Ne adsorption and desorption on field ion microscope tip, determining minimum required field strengths of gas films at different temperatures
05 p0891 A70-15975

Quasi-equilibrium treatment of heterogeneous reactions applied to evaporation rate /desorption/ computation for volatile species formed in oxygen reactions with W, Mo and graphite
06 p1004 A70-17330

Quasi-equilibrium treatment of heterogeneous reactions applied to flash desorption data for oxygen reaction with tungsten surface, discussing species desorption dependence on adsorption temperature
06 p1004 A70-17331

Carbon dioxide adsorption and desorption in Martian bright areas, discussing assumptions relative to temperature, pressure and dust adsorption
08 p1579 A70-21566

Oxygen sticking coefficients and desorption kinetics on tungsten crystal by step desorption/ reflection technique, postulating formation and decomposition of surface oxide phases
10 p1832 A70-25147

Polycrystalline molybdenum desorption of adsorbed hydrogen, oxygen and water by electron impact
12 p2182 A70-27679

Resinous compounds content determination in jet fuels using ice cold acetic acid for desorbent to improve accuracy
16 p2961 A70-33203

Electron impact desorption kinetics of ions and neutrals from polycrystalline W surfaces, using cylindrical magnetic spectrometer
18 p3225 A70-36321

DESPINNING

U SPIN REDUCTION

DESTABILIZATION

Mechanical destabilizing model of nonlinear damping in nonconservative systems with follower forces, using Liapunov method
19 p3542 A70-38065

DESTRUCTION

Scout missile destruct charge system premature operational response to high temperature environment caused by combustion gas leak during stage separation
03 p0550 A70-14140

DESTRUCTIVE TESTS

Soviet book on experimental investigation of thin walled structures elastoplastic work with complex reinforcement, outlining test procedures
03 p0585 A70-12985

Reinforced plastics destructive and nondestructive testing including standard methods, equipment and procedures applicable to materials and parts
05 p0874 A70-16621

Impact forces and specimen bending moments generated during dynamic tear test interpreted in terms of system dynamics and material fracture characteristics
08 p1518 A70-21319

Thermomechanical tests effectiveness and determination of stress level defining boundary between destructive and nondestructive testing
09 p1689 A70-22004

Destructive and nondestructive tests optimum procedure for quality control based on information theory, decision statistics and cost optimization
09 p1691 A70-22573

DESYNCHRONIZED SLEEP

U RAPID EYE MOVEMENT STATE

DETACHMENT

Associative and collisional detachment in H atom and negative ion collisions based on complex adiabatic potential
09 p1733 A70-23431

Turbulent flow detachment in incompressible fluid around thick bodies, considering plane perpendicular to wind
11 p2037 A70-26466

DETECTION

NT AIRCRAFT DETECTION

NT CORRELATION DETECTION

NT FOREST FIRE DETECTION

NT RADAR DETECTION

NT SIGNAL DETECTION

NT TARGET RECOGNITION

Response variation and detection efficiency of funnelled channel electron multipliers for low energy protons and Ar ions
06 p1021 A70-17623

Fire and overheat detection system design for turbine powered vehicles
[ASME PAPER 70-GT-125]
18 p3260 A70-36891

Air hijacking as aviation safety problem, discussing history, prevention and detection methods and equipment, law enforcement, etc
23 p4285 A70-44496

DETECTORS

Voltage-power sensitivity, response time, frequency limit and minimum registered power of hot carrier thermoelectric detectors calculated from characteristic semiconductor parameters
03 p0540 A70-13436

Germanium, silicon and gallium arsenide point contact and Schottky barrier diodes as submillimetric wavelength detectors and mixers
11 p2017 A70-25736

Azimuth measurement techniques for success-run detectors
11 p2019 A70-26712

Stellar sensors and deviation measurement procedures, discussing photosensitive elements, astrophysical data, etc
13 p2407 A70-29140

Thin ferromagnetic film sensitive elements for detection of weak magnetic fields
13 p2415 A70-30041

HF permittivity variations detector for blood circulation telemetry
14 p2542 A70-30389

Photoelectric detector sensitivity variation effect on long term instability of servomagnet variometers
14 p2588 A70-31261

Acoustical holography with single stationary point detector noting reciprocity between detector and point source illuminator
17 p3088 A70-35030

Hydrogen emanation and distribution in metals and alloys by Nd hydrogen metal detection method
20 p3651 A70-40071

DETERMINANTS

Deterministic and stochastic simulation models for obtaining optimal solution in operations research by trial and error
08 p1464 A70-20579

Sufficient conditions for convergence of infinite determinant
15 p2766 A70-31448

Automatic digital device for evaluating matrix determinants
20 p3591 A70-39788

Two dynamic systems synthesis achieving limited influence on each other by coordinates invariance criteria method involving determinant
20 p3604 A70-39841

DETERMINATION

U MEASUREMENT

DETONABLE GAS MIXTURES

Gas detonation dynamics associated with shock tube self ignition kinetics, noting chemokinetic factors role
02 p0397 A70-12024

Spherical detonation waves propagation initiated by laser-induced spark in gaseous explosives, discussing propagation energy regimes
02 p0278 A70-12029

Propane oxidation reaction and ignition delay times
[AIAA PAPER 68-633]
03 p0603 A70-12909

Flat flames in stationary gas in tubes useful for flame speed measurements without correction procedure
03 p0607 A70-13917

Induction distances, transient pressures and wave propagation rates for detonation waves in cylindrical tube low temperature hydrogen-oxygen mixtures
03 p0607 A70-13919

Temperature evolution of detonation products of Na seeded propane-oxygen mixtures, observing periodic variation for helicoidal cases
03 p0608 A70-14356

Ignition of cold premixed fuel by hot projectile, obtaining distance for ignition occurrence
[AIAA PAPER 70-150]
06 p1180 A70-18133

Gas dynamic effects of reaction center in explosive gas mixture analyzed by model and numerical computation
[AIAA PAPER 70-147]
06 p1181 A70-18144

Gas detonation in rough walled pipe, calculating Chapman-Jouguet detonation velocity, deriving existence criterion
07 p1419 A70-18752

Hydrogen concentration effect on self sustained detonation wave propagation in hydrogen-carbon monoxide-oxygen mixtures, using Q switched pulsed laser schlieren photography
07 p1420 A70-18918

Cold combustible mixture ignition at forward stagnation region of hot projectile, calculating temperatures for propane-air mixture
07 p1422 A70-19577

Ignition and extinction in opposed jet diffusion flame for flow of compressible fluid with competitive/chain reactions

07 p1422 A70-19578

Minimal initial size of explosion reaction center used to explain ignition process in flammable mixtures, noting dependence on pressure, temperature and composition

07 p1422 A70-19586

Flame propagation rate and combustion zone extension dependence on chamber dimensions for turbulent flow of homogeneous mixtures

08 p1597 A70-21187

Ternary detonation wave configurations calculated by shock polar method using methane-oxygen and hydrogen-oxygen mixtures in shock tubes

09 p1658 A70-22101

Air shock tube driven by exploding mixture of propane and oxygen investigated for shock overpressure variation with distance

10 p1863 A70-23992

Combustible gas /hydrogen-air/ subsonic and transonic flow past sphere, approximating combustion zone structure by model

10 p1801 A70-24142

Excess air ratio and heat release efficiency in combustion of kerosene mixture determined by volumetric gas analysis

10 p1968 A70-24283

Combustion gases compositions and adiabatic flame temperatures of potassium seeded propane-air mixtures calculated at various equivalence ratios and temperatures assuming thermal equilibrium

12 p2330 A70-27227

Sphere supersonic motion in combustible gas mixture of given temperature and pressure, discussing constant density two front detonation wave model

12 p2334 A70-28242

Unsteady one dimensional motion of reacting gas mixtures in presence of supercompressed detonation waves, discussing transformation into Chapman-Jouguet wave

13 p2522 A70-29772

Detonation process one dimensional stability in combustible aerosol, considering gas dynamic disturbances effect

14 p2665 A70-30397

Burning velocities for methane-air mixtures with water cooled porous metal flat flame burner, discussing surrounding ambient atmospheres effects

14 p2666 A70-31093

Microstructure and reaction kinetics of flat premixed fuel-rich hydrogen-oxygen-nitrogen flame at atmospheric pressure

16 p2998 A70-33900

Tetrafluorodibromo-ethane and bromethyl inhibiting effects on explosion development in constant volume container and flame expansion rates in hydrogen-air mixtures

18 p3345 A70-36241

Flame propagation velocity of gasoline-air mixture during two stage combustion process in laminar and turbulent flows, discussing combustion products effect

19 p3550 A70-37253

Flame stabilization in boundary layer during mixing of cold homogeneous fuel mixture and hot gas based on combustion and turbulent jets theories

20 p3736 A70-39267

MHD measurements of gas flow velocity and boundary layer in oxyhydrogen explosions in detonation tube

21 p3942 A70-40876

Atmospheric pressure hydrocarbon-air mixtures confined by thin plastic membrane, obtaining composition range for detonation initiation limits

21 p3865 A70-40884

DETONATION

Electromagnetic procedures and camera-spectrometer system for studying detonation processes, measuring mass flow rates and explosives spectra

01 p0090 A70-10887

Computerized stepwise construction of Hugoniot curve for detonation waves and Chapman-Jouguet detonation and deflagration points

03 p0607 A70-13920

Shock wave amplitude found strongest influence in explosives initiation to detonation by shock

07 p1359 A70-19675

Detonation mechanism in ammonium perchlorate ascribed to mechanical breakdown of charge occurring at pressure equal or above critical deformation of explosive

09 p1741 A70-22102

Detonation model, discussing combustion gases from solid explosives detonation

13 p2520 A70-28803

Spin detonation of tangential HF vibrations in liquid rocket engine combustion chambers, discussing instability prevention

13 p2474 A70-29422

Detonation process one dimensional stability in combustible aerosol, considering gas dynamic disturbances effect

14 p2665 A70-30397

Detonation in nonuniformly heated gas capable of chemical reaction, obtaining numerical solution

17 p3198 A70-35737

Two dimensional detonations structure by nonlinear theory for systems with hydrodynamically unstable steady state solutions, imposing periodic boundary conditions

20 p3609 A70-39658

DETONATION WAVES

Multiple pulsations mechanism during detonation spherical wavefront propagation in channels with various cross sections, noting volume effect

01 p0060 A70-10135

Critical detonation diameter as function of concentration and dimensions of inhomogeneities in explosive, assuming chemical reaction generated behind detonation front

01 p0217 A70-11005

Strong shocks and high temperature gases production using multistage gaseous detonation driven shock tube

02 p0274 A70-11855

Shock wave shapes in hypersonic flow past blunt conical nosed circular cylinders, using analogy with Savic perturbed hypersonic blast wave theory

02 p0277 A70-11862

Liquid diethylcyclohexane /DECH/ sprays detonation propagation in gaseous oxygen, studying drop size effect on steady state development

02 p0351 A70-12003

Shock and detonation waves stability in arbitrary media, noting overdriven and underdriven waves

02 p0397 A70-12023

Detonation of gaseous systems with marginal compositions, showing sensitivity to physicochemical factors

02 p0251 A70-12025

Detonation front macroscopic properties, Mach configurations, shock spacing, etc, considering effects of tube walls and nonlinear flow

02 p0278 A70-12026

Hydrodynamic structure of multifront detonation waves produced in gases by primary shock interaction with transverse disturbances

02 p0278 A70-12027

Three dimensional picture of wave system of single headed spin detonation constructed by simultaneously considering wave mapping in real and hodograph planes

02 p0278 A70-12028

Spherical detonation waves propagation initiated by laser-induced spark in gaseous explosives, discussing propagation energy regimes

02 p0278 A70-12029

Internal structure of ideal explosive waves at Chapman-Jouguet point, discussing coupling between flow and chemical reactions

02 p0279 A70-12103

Smoked-foil technique for transverse wave quantitative study in condensed-phase explosives

03 p0606 A70-13814

Induction distances, transient pressures and wave propagation rates for detonation waves in cylindrical tube low temperature hydrogen-oxygen mixtures

03 p0607 A70-13919

Computerized stepwise construction of Hugoniot curve for detonation waves and Chapman-Jouguet detonation and deflagration points

03 p0607 A70-13920

Flow field between infinitely massive wall and rigid piston accelerated by detonation products, comparing analytical results to finite difference numerical integration

05 p0830 A70-15782

Sonic bang simulation by linearly distributed explosives, creating blast waves with wide range of shapes and durations

05 p0796 A70-16796

Self similar flow patterns arising during cylindrical shock and detonation waves propagation in gas at rest, considering MGD shock waves

06 p1119 A70-17516

Explosive blast wave effects on flight vehicle in supersonic flow, using conical blast generator and short duration supersonic wind tunnel

06 p0972 A70-18127

Atmospheric thermodynamic properties determined from radar studies of detonation waves from cesium-seeded explosive bursts in lower ionosphere

06 p1012 A70-18542

Detonation front structure stability in gases, discussing spin detonation, transverse waves, perturbation, etc

07 p1418 A70-18751

Gas detonation in rough walled pipe, calculating Chapman-Jouguet detonation velocity, deriving existence criterion

07 p1419 A70-18752

Hydrogen concentration effect on self sustained detonation wave propagation in hydrogen-carbon monoxide-oxygen mixtures, using Q switched pulsed laser schlieren photography

07 p1420 A70-18918

Explosive driver development with hypervelocity gas in thin walled tube surrounded by concentric

cylinder of high explosive, discussing detonation wavefront propagation

07 p1248 A70-19098

Gaseous detonation transverse wave propagation and measurement from smoked foil records

07 p1424 A70-20006

Plane double front detonation wave attenuation by pursuing rarefaction waves, analyzing oscillations, onset mechanism and stability during transition to Chapman-Jouguet mode

08 p1485 A70-21633

Ternary detonation wave configurations calculated by shock polar method using methane-oxygen and hydrogen-oxygen mixtures in shock tubes

09 p1658 A70-22101

One dimensional flow field behind ionizing detonation wave in magnetic field using Chapman-Jouguet hypothesis, accounting for Alfvén speed

09 p1660 A70-22722

Blast waves in low Mach number regime with assumption of power law density profile in rear, obtaining particle velocity and pressure distributions

09 p1661 A70-23214

Plane, cylindrical and spherical blast waves structure with ionization at local thermodynamic equilibrium analyzed using successive approximation to non-similar solution

10 p1967 A70-23991

Wall heat transfer effect on expansion following Chapman-Jouguet detonation wave, calculating pressure and gas velocity profiles from friction coefficient

10 p1869 A70-24423

Oblique blast wave interaction with small bend along plane wall analyzed for diffraction using conformal transformation and complex variable techniques

10 p1869 A70-24524

Explosion aerial blast wave for producing impulsive structural forced response, discussing spatial distribution method for increased wave duration

11 p1213 A70-25729

Lead azide detonation hazards and resulting pressure waves, evaluating protective glove material by dynamic pressure measurements

12 p2289 A70-27665

Computerized numerical integration of nonlinear partial differential equations describing blast wave in ionosphere with finite electric conductivity under uniform magnetic field

12 p2227 A70-28212

Sphere supersonic motion in combustible gas mixture of given temperature and pressure, discussing constant density two front detonation wave model

12 p2334 A70-28242

Plane cylindrical and spherical explosion waves propagation in detonating gas mixtures with counter-pressure, calculating perturbed flow parameters by numerical method of integral relations

13 p2388 A70-29308

Unsteady one dimensional motion of reacting gas mixtures in presence of supercompressed detonation waves, discussing transformation into Chapman-Jouguet wave

13 p2522 A70-29772

Vacuum effect on explosive coupling seismic energy considered in lunar geophysical experiment

16 p2896 A70-33092

Spherical shock from point explosion in medium with varying density, obtaining exact similarity solution for propagation

21 p3808 A70-41448

Detonation front position determination in explosive by photoelectric technique

22 p4121 A70-42341

Orthogonal multistreak recording by framing camera applied to arrival of detonation wave at front surface of explosive charge

22 p4034 A70-43045

Shock wave propagation studies by grating spectrograph with high speed camera, computing equilibrium detonation gases temperature from emitted light

22 p4035 A70-43057

Mammalian eardrum failure due to blast induced pressure variations, examining wave shape, character, magnitude and duration effects

23 p4148 A70-44839

DETONATORS

Linear separation systems for aerospace applications covering mild detonating fuse and cord flexible linear shaped charge, SUPER ZIP concepts, etc

03 p0546 A70-14103

Development and characteristics of inexpensive and reliable detonator for precise synchronization with high speed photographic or electronic experiments

03 p0547 A70-14110

Detonator insensitive to highest level of electrostatic voltage on human body for precise synchronization

03 p0547 A70-14111

Exploding bridgewire detonator electrical input requirements, discussing waveform, peak current and time to peak

03 p0550 A70-14143

DEUTERIUM

Nuclear fusion reactions by focused Q switched Nd doped laser beam on deuterium target, discussing neutrons from flowing plasma, electron temperature and counter experiments

03 p0501 A70-13684

Hydromagnetic normal ionizing shock wave properties in H and D mixtures and pure gases in SUPPER 2 shock wave tube

03 p0536 A70-14365

Lyman alpha transition line in exosphere deuterium line implying enrichment factor ratio to earth surface deuterium

04 p0742 A70-15129

Energy distribution of positive Ar ions scattered from thermal diatomic D noting inelastic collisions

07 p1339 A70-20056

Mass spectra of 1,2-cyclohexanediol and deuterium labeled analogs data recorded and mechanistic rationalizations of degradation processes given

07 p1225 A70-20200

Cross sections measured for symmetric (p, 2p) reactions on deuterium and He, discussing nonsymmetric (p, 2p) events in He

08 p1548 A70-21233

Deuterium Lyman alpha line profiles generated from microwave powered lamp for experimental testing of two layer model characterizing emission line profiles

09 p1730 A70-22066

Deuterium atom reaction with hydrogen molecule yielding HD and H using modulated crossed beams, plotting angular distributions and reaction velocities

10 p1920 A70-25148

Deuterium recovery in Jupiter atmosphere, describing equipment and techniques for hydrogen-helium gathering and processing

11 p2112 A70-26064

High speed shock wave propagation in deuterium gas, observing neutron production

21 p3806 A70-40744

Thermonuclear rate constant for deuterium atom recombination, using orbiting resonance theory

21 p3781 A70-41886

Thermal separation of ortho and para hydrogen and deuterium, discussing kinetic theory of nonspherical molecules in terms of rotational collision numbers

22 p3983 A70-43154

IR absorption spectra of high-cis forms of deuterated polyisoprenes

23 p4157 A70-44274

Extremely high temperature deuterium examination, using coaxial plasma accelerators to determine neutron production and vorticity

23 p4227 A70-44452

DEUTERIUM COMPOUNDS

CH and CD molecules UV absorption spectra, using flash photolysis of diazomethane

02 p0341 A70-11795

CH, CD and CH ion excited states decay rates determined from phase shift and frequency data, discussing implications for astrophysics

09 p1731 A70-22513

Vapor phase fluorescence spectra from benzene and deuterated benzene at zero point vibrational level

15 p2694 A70-31731

Transverse flow deuterium fluoride-carbon dioxide chemical laser for CW output without external energy source

24 p4355 A70-46084

DEUTERIUM PLASMA

Focused deuterium plasma discharge neutrons and X rays energy spectra, flux and time resolved collimation measurement with nuclear emulsions and scintillation detectors

02 p0348 A70-12241

Millimeter and nanosecond resolution of fast neutrons in pulse dense high temperature deuterium plasma discharge with polyethylene collimators and photomultipliers

02 p0303 A70-12739

Fusion reactions generation by high power laser beams focused on solid deuterium target

05 p0857 A70-15992

Temperature measurements in magnetic beach of steady state deuterium plasma, confirming ion-cyclotron waves thermalization

05 p0884 A70-16167

Self sustained fusion reaction in dense deuterium-tritium plasma, considering large atomic number contaminants optimal concentration calculations

07 p1351 A70-19848

Deuterium plasma expansion resulting from thermal shock produced by laser impulse

10 p1923 A70-24526

Controllable thermonuclear reactor with free-floating HF discharge plasma in deuterium

12 p2271 A70-27351

Deuterium plasma three dimensional flow in coaxial accelerators, examining magnetic structure of filaments/field lines bundles/

21 p3856 A70-41321

Controllable thermonuclear reactor with free-floating HF discharge plasma in deuterium

22 p4084 A70-43595

DEUTERONS

Deuteron splitting by solar neutrinos for neutrino detection, describing deuterium scintillation detector characteristics

05 p0899 A70-15954

Proton-deuteron elastic large angle scattering cross sections, noting backward peak consistent with baryon exchange mechanism with resonance transfer

07 p1345 A70-20198

Venusian ionosphere thermal protons and/or deuterons source observed by radio occultation method, suggesting dominance at high altitudes

10 p1938 A70-24068

Cosmic rays deuterons abundance calculation from H and He nuclei collisions with interstellar matter

19 p3506 A70-38125

Collapsing or neutronizing stars detection by recording neutrino and antineutrino flux, calculating antineutrino-deuteron interaction cross section and positron energy and angular distribution

20 p3698 A70-39302

Upper limit to primary deuteron flux and path length in space, using emulsion stack exposed near geomagnetic equator during minimum solar activity

22 p4093 A70-42673

DEVELOPERS [PHOTOGRAPHY]

U PHOTOGRAPHIC DEVELOPERS

DEVIATION

Deviation angle optimization for cruising hypersonic jet aircraft, noting effect of rotation losses on design

03 p0406 A70-13019

DEVITRIFICATION

U CRYSTALLIZATION

DEW

Dew-point temperature of lower troposphere by diffusion equation, noting use for fog and strati forecasting

09 p1717 A70-22655

Thermistor and dew cell as remote air temperature and dewpoint measurement at airports

21 p3822 A70-40760

DEWAR SYSTEMS

U CRYOGENIC EQUIPMENT

DH 121 AIRCRAFT

Trident passenger aircraft development, discussing airframe changes, engine development, weight and drag reduction, etc

05 p0794 A70-16112

Rolls-Royce boost engine fitted to Trident 3B for improving takeoff and climb performance, discussing mounting and effect on aircraft structure and passenger capacity

06 p0985 A70-17156

Trident aircraft automatic landing in nearly blind conditions in regular commercial service

11 p2079 A70-25851

Automatic landing system assurance of DH 121 aircraft schedule all-weather regularity through high safety level via redundancy

17 p3022 A70-35856

DH 125 AIRCRAFT

Lift-dump system for Hawker Siddeley DH 125, combining aerodynamic drag increase with lift reduction to improve deceleration

02 p0225 A70-12266

DIABATIC PROCESSES

U HEAT TRANSFER

DIADEME SATELLITE

French geodetic satellites Diademe I and II experiments in navigation, noting laser and Doppler devices

09 p1725 A70-23049

DIAGNOSIS

Prospective epidemiological recognition of clinical coronary heart disease, discussing effects of habitual physical inactivity, excessive dietary fat, socioeconomic stresses, etc

01 p0023 A70-10865

Simplified laboratory test program yielding serviceable information for possible direct laboratory diagnosis of risk factors affecting atherosclerosis

03 p0431 A70-14279

Automatic control algorithms for subsystem malfunction identification in multisubsystem plants, analyzing conditions for diagnostic tests existence

04 p0661 A70-14554

Computer aided medical diagnosis

04 p0644 A70-15359

Computer program for on-line analysis of exercise ECG considered for improved diagnosis of ischemic heart disease

05 p0805 A70-16105

Human exhaled air contaminants analysis role in disease diagnosis, metabolism study and spacecraft cabin atmosphere changes

07 p1220 A70-19514

Aeromedical significance and pathophysiological mechanisms of clinical entities mimicking vasovagal syncope

08 p1454 A70-21946

Physiological mechanism and differentiation of altitudinal vertigo in flyers

08 p1449 A70-21947

Diagnostic-control tests for automatic homogeneous microelectronic structures, considering element coupling

09 p1643 A70-22142

Vectorcardiographic diagnosis of left ventricular hypertrophy based on changes in MQV magnitude and other QRS vectors

09 p1629 A70-23626

Hypoxia diagnosis based on excess lactate determination as indicator of oxidative metabolism changes

10 p1822 A70-25084

Human exhaled air contaminants analysis role in disease diagnosis, metabolism study and spacecraft cabin atmosphere changes

11 p1991 A70-26113

Focal myocarditis associated with aircraft accidents, discussing difficulties in diagnosis and assessment

17 p3033 A70-35571

Acoustical holography forming optical wavefield analog for nondestructive testing, medical diagnosis, underwater and seismic imaging

19 p3425 A70-37887

Electrocardiogram vs vectorcardiogram for myocardial infarction diagnosis

19 p3371 A70-38362

Astronauts medical examination, using thermal load as functional and diagnostic test

20 p3575 A70-40195

Automatic diagnosis of clinical electroencephalogram with digital computer, showing maximum and minimum points, basic pattern and paroxysmal wave

22 p3977 A70-42869

Atherosclerosis and latent coronary insufficiency diagnosis in flight crews, evaluating various tests

22 p3975 A70-43696

Hyperthyroidism diagnosis by pattern recognition, using computerized class featuring information compression

22 p3977 A70-43732

Obstructive lung diseases clinical, radiological and functional diagnosis in legal medicine

24 p4296 A70-45122

DIAGRAMS

NT CIRCUIT DIAGRAMS

NT CREEP DIAGRAMS

NT FEYNMAN DIAGRAMS

NT HERTZSPRUNG-RUSSELL DIAGRAM

NT PHASE DIAGRAMS

NT S-N DIAGRAMS

NT STRESS-STRAIN DIAGRAMS

Block diagrams of three stage device for extracting radioactive Ar from perchloroethylene considered for solar nucleus studies

05 p0845 A70-15933

Holo-diagrams for simplified evaluation of amplitude and direction displacement in double exposed holograms for interferometric measurements

07 p1287 A70-20086

Diagram extracting Lorentzian line widths from Fabry-Perot interferometer profiles

15 p2737 A70-32050

Holodiagram for making and evaluating holograms for large objects dimension, deformation and vibration measurement

17 p3084 A70-35004

Butterfly diagram for describing latitude distribution of sunspots during solar cycle, considering representation methods

22 p4106 A70-43264

Holo-diagrams for predicting fringe patterns in hologram interferometry caused by translation motion and rotation

22 p4040 A70-43610

DIALS

Human interpolation accuracy for pointer or index position between two scale graduations

24 p4308 A70-45512

DIALYSIS

Countercurrent sandwich type dialyzer for small animals, noting membrane support function and applicability to human use

13 p2360 A70-29950

DIAMAGNETISM

Boundary conditions for equilibrium diamagnetic plasma in magnetic dipole having constant and isotropic pressure in system

01 p0153 A70-11631

Diamagnetic plasma in nonuniform magnetic fields, determining equilibrium plasma configurations in and near neutral point for low and high pressure

09 p1734 A70-22478

Coulomb interaction during optical transitions between Landau subbands of Ge semiconductor valence and conduction bands in magnetic field, observing diamagnetic excitons

10 p1928 A70-25029

Thermal variation of diamagnetism and susceptibility of rhombohedral graphite

21 p3845 A70-42268

Beryllium orbital diamagnetic susceptibility calculated by pseudopotential method compared to experimental data

23 p4208 A70-44886

DIAMANT LAUNCH VEHICLE

Valois motor with nitrogen peroxide oxidizer for Diamant B first stage, describing design and assembly problems

10 p1930 A70-24375

Diamant B satellite launcher testing and construction, discussing DIAL/WIKA scientific satellite launch

12 p2314 A70-28299

DIAMETERS

Critical diameter and detonation parameters of nitromethane and tetranitromethane as function of powder content

01 p0217 A70-11004

Tabular results of Galaxy mean and angular diameters and smallest/largest ratios measured on Palomar Atlas

05 p0906 A70-15797

Atmospheric pressure-diameter relationship of common carotid artery in head and neck region of conscious men

08 p1447 A70-21508

Optical heterodyne interferometer for stellar diameter measurements

16 p2925 A70-33025

Jovian planets polar and equatorial diameters and lateral dimensions of Saturn rings by optical measurements

16 p2979 A70-34034

DIAMINES

NT GUANIDINES

Thermal stability of polymers based on aromatic diamines and isomeric dibenzoylbenzenes

21 p3782 A70-42129

DIAMOND WINGS

U LOW ASPECT RATIO WINGS

W SWEPT WINGS

DIAMONDS

NT METEORITIC DIAMONDS

Evidence disproving interstellar extinction by diamond crystals

03 p0572 A70-13818

Two parameter model for lattice vibrations applicable to diamond structured crystals, calculating phonon dispersion curves from dielectric screening theory

07 p1357 A70-19920

Semiconductor diamond films electrical conductivity obtained by injecting various ions during isochronal stepwise annealing, studying activation energy values

12 p2286 A70-27479

Hall constant and carrier mobility in semiconductor diamond films doped by boron ion injection, observing temperature dependence of mobility

12 p2287 A70-27480

Artificial B-doped semiconductor diamond crystals resistance temperature dependence, determining conductivity and luminescence spectra

15 p2782 A70-31630

Electrical conductivity of semiconductor diamonds made by alloying with Al under high pressure and temperature

19 p3488 A70-38728

DIAPHRAGM [ANATOMY]

Chest, abdominal wall and diaphragm displacements of rabbits during partial and whole body exposure to shock waves produced by hexotol charges

02 p0231 A70-11704

Asymptomatic pilot with idiopathic paralysis of hemidiaphragm, discussing clinical picture and aeromedical significance

07 p1215 A70-19942

Cinereidigraphic analysis of diaphragmatic ventilatory movements, obtaining correlation between lung volume and diaphragm and rib cage movement

14 p2537 A70-30383

Diaphragmatic muscle reactions and pneumogram changes in rats immediately after air passage obstruction

19 p3360 A70-37804

Sinus and diaphragmatic nerves impulse activity during hypoxia compared with normal respiration in cats

23 p4145 A70-44312

DIAPHRAGMS [MECHANICS]

Piezoelectric sensing diaphragm for detection of micrometeorites in space, noting vibration mode and effect of small beads contact time on calibration errors

04 p0695 A70-15567

Impedance and field distribution of bifurcated and stepped waveguide junctions with inserted diaphragm calculated by transformed singular integral equation

05 p0820 A70-16385

Diffused diaphragm pressure sensors in impact probes used in wind tunnel tests of dynamic response of supersonic air induction systems

06 p1074 A70-18605

Dimensionless strength parameter in determining bursting pressure of ductile metal diaphragms in square section shock tubes

08 p1481 A70-21034

Arc driven shock tunnel operation with expansive area change at main diaphragm, evaluating flow characteristics

09 p1657 A70-23279

Temperature and heat flux in plane, cylindrical and spherical multilayer diaphragms with boundary conditions, assuming harmonic temperature variation

10 p1970 A70-25321

Time dependence of shock wave attenuation at multiple reflection in shock tube after diaphragm burst, using damped vibration solution

11 p2034 A70-25495

Self opening em-operated secondary and ternary mylar diaphragms for expansion tubes and tunnels

11 p2031 A70-25982

Remote controlled diaphragm exploding device associated with shock tube for MHD generator

11 p2090 A70-26170

Water cooled metallic diaphragm thermal stability effect on plasmatron electric arc characteristics stabilized by vortex air flow

11 p2093 A70-26736

Semifluidic proportional industrial control systems using diaphragm summing junction including applications to temperature control, remote sensing and drill bit adaptive measurement

12 p2164 A70-27073

Turbulent mixing at contact surface in driven shock wave in shock tube with bursting diaphragm for He-Ar test gas mixtures

14 p2566 A70-31030

Two diaphragm combustion shock tube for plasma radiation energy transfer, describing development, performance, make-up and testing

15 p2779 A70-32019

Electromagnetic diaphragm for use in shock tubes, describing construction and operation

15 p2741 A70-32440

Superplastic deformation of thin circular diaphragms subjected to one-sided hydrostatic pressure, emphasizing thickness variations in bulged shapes

16 p2916 A70-32917

Holographic interferometry for evaluating bond between diaphragm and base in pressure transducer

16 p2904 A70-33138

Metallic diaphragms design, fabrication and testing for cryogenic fluid and positive expulsion systems [AIAA PAPER 70-683]

16 p2918 A70-33582

Diaphragm pressure transducer interaction with solid propellant grain, superposing solutions to clamped circular plate and halfspace

16 p2992 A70-33987

Thin concentric circular cylindrical shells joined at ends by rigid diaphragms, describing free and forced torsional motion

16 p2992 A70-34019

Reliable latch diaphragm release mechanism for separation of payload from spacecraft, discussing design, operation and tests

16 p2921 A70-34117

Pressure transducer diaphragms displacement measurement by holographic interferometry

17 p3085 A70-35010

H and E waves diffraction in circular waveguide by diaphragm thickness, using linear equations and Fourier-Bessel series for representation

19 p3378 A70-37731

DIASTOLE

Diastolic and systolic pressure measurement in acute and chronic experiments

09 p1627 A70-23302

Myocardium potential working capacity in relation to diastole duration of ventricles

13 p2355 A70-29767

Cardiac ventricular function in compression pump terms, relating mechanical activity to end-diastolic fiber length

20 p3571 A70-39364

DIATOMIC GASES

Heat and mass transfer in Couette flow of partially ionized symmetric diatomic gas for chemical equilibrium and chemically frozen flow cases

01 p0060 A70-10290

Collision induced dissociations of 2000 eV diatomic O, N, CO and NO positive molecular ions as function of reactant ion internal energy

01 p0148 A70-11354

Dynamic behavior of dissociating homonuclear diatomic gas, deriving instability equations, proposing stability loss in transonic region

01 p0068 A70-11584

Oscillations and decomposition of diatomic gas molecules at high temperatures during atom-molecule collisions, deriving kinetic equations for energy level changes

01 p0148 A70-11630

Hypersonic flow in thermodynamic equilibrium of diatomic dissociating gas with power law shock, investigating self similar solutions of Van Dyke small disturbance equations

03 p0405 A70-12925

Work function measurement for adsorption of diatomic I, Br and Cl on W crystal using electron beam retarding potential method

05 p0891 A70-15973

Molecular beam continuum model to determine structure of shock waves in diatomic gases, comparing calculated profiles with measurements in nitrogen

06 p1050 A70-18338

Kinetic theory study of shock wave structure in rotationally relaxing diatomic gases

06 p1050 A70-18339

Kinetic model equation for shock structures in rotationally relaxing gas with internal degrees of freedom

06 p1050 A70-18340

Normal hypersonic shock wave structure in diatomic gas, measuring density by electron beam fluorescence technique

06 p1050 A70-18341

Coupled vibrational relaxation in mixtures of diatomic gases, showing energy pumping phenomenon between species

07 p1338 A70-19627

Photodissociation of diatomic O and N molecules in far UV

07 p1338 A70-20052

Diatomic gases, describing rotational distribution function evolution by diffusion equation approximation, discussing apparent relaxation times

08 p1548 A70-21521

Nonequilibrium interaction of radiative and vibrational rate processes in IR-active diatomic gas using macroscopic equations

08 p1549 A70-21574

Rotational-translational energy transfer in collisions between homonuclear diatomic molecules and rotational relaxation time in diatomic gases

10 p1918 A70-23956

Weak plane waves propagation in binary mixtures of diatomic gases subject to vibrational relaxation, solving piston problem in acoustic approximation

12 p2209 A70-27151

Stark cell with high electric fields for studying inactive IR spectrum of homonuclear diatomic gas molecules

13 p2450 A70-28499

Potential energy curves for diatomic He molecules constructed by Rydberg-Klein-Rees procedures

14 p2618 A70-30112

Laminar boundary layer equations on plate with arbitrary catalytic properties in diatomic gas flow undergoing vibrational dissociative relaxation

20 p3611 A70-39802

Absorption diffuse band systems of diatomic argon molecule in vacuum UV region

21 p3853 A70-41395

DIATOMIC MOLECULES

Rotational excitation and scattering of diatomic molecules by structureless atoms, comparing approximation methods

01 p0147 A70-10470

Vibrational energy exchange between colliding diatomic molecules modulated by harmonic oscillators with insignificant frequency difference

01 p0147 A70-11035

CH and CD molecules UV absorption spectra, using flash photolysis of diazomethane

02 p0341 A70-11795

Quadrupole moment matrix elements in adiabatic approximation for transition bands of hydrogen, HD and deuterium molecules in ground electronic state

02 p0342 A70-11822

Rotation-vibration matrix elements of quadrupole moments and absorption coefficients of ground electronic states of hydrogen, HD and deuterium

02 p0342 A70-11823

Morse eigenfunctions for variational calculation of diatomic molecules vibrational-rotational energy level analysis, showing better convergence than harmonic oscillator basis

02 p0344 A70-12519

NH bands in stellar spectra by visual inspection of spectrograms, noting abundance of N in normal and strong CN stars

02 p0379 A70-12708

One and two center Coulomb, hybrid and exchange integrals contributing to orbit-orbit interaction in diatomic molecules evaluated for Slater orbitals combinations

03 p0528 A70-14010

Diatomic oxygen-nitrogen collisions in mixtures with CO, determining vibration-vibration energy exchange probabilities

04 p0723 A70-15562

Diatomic carbon swan band violet line absence from sunspot suggested in accordance with molecular equilibrium predictions

05 p0911 A70-16433

Vibrational energy transfer in oriented nonlinear collisions between diatomic molecule and atom, considering molecular vibration excitation

05 p0885 A70-17080

Electron scattering from diatomic molecular systems including coupling of partial waves in fixed-nuclei approximation

06 p1114 A70-18633

Rotating and oscillating spectra in diatomic molecule excited by slow and fast electrons,

discussing Boltzmann distribution of excited molecules

07 p1337 A70-19044

Chemical bonding of high temperature molecular species, discussing ab initio calculations for diatomic atoms

07 p1225 A70-19882

Coupled Schrodinger equations for diatomic molecules internal motion solved using best adiabatic approximation to obtain energy correction to Born-Oppenheimer method

08 p1548 A70-21522

Compound state resonance energies and widths in elastic scattering of diatomic molecule at energies below rotational excitation threshold

08 p1548 A70-21523

Forward and backward rate constants for diatomic recombination and dissociation in dilute gas

09 p1730 A70-22231

Scattering equations and cross sections for rotational excitation in collisions of rigid diatomic molecules interacting through soft potential

09 p1732 A70-22901

Hoeft-London factors calculated for general doublet transition in diatomic molecules, deriving energy levels

10 p1918 A70-23974

Diatomic molecules vibrational levels distribution near dissociation limit determined using WKB approximation

10 p1919 A70-24041

Free radicals role in astrophysics, considering diatomic or triatomic radicals in atmospheres of earth, sun, planets, comets, stars and interstellar space

10 p1943 A70-24839

Vibrational energy exchange between colliding diatomic molecules modulated by harmonic oscillators with insignificant frequency difference

10 p1920 A70-25004

Threshold photoionization cross sections for homonuclear diatomic N molecules calculated from Slater orbitals and Coulomb waves

11 p2086 A70-25833

Book on rotational structure of diatomic molecules spectra covering multiplets, intensity distributions and perturbations

12 p2274 A70-27094

Rotational, vibrational and equilibrium molecular constants for Phillips system of diatomic carbon

12 p2275 A70-27174

Dissociation energy and long range interatomic potential of diatomic molecules from vibrational spacings of higher levels

13 p2454 A70-28495

Quantum mechanical model of electron scattering by homonuclear diatomic molecule at ground state, calculating differential and integral cross sections for elastic scattering

14 p2618 A70-30113

Gaseous diatomic molecules quantum mechanical treatment, calculating Hamiltonian matrix elements for interpretation of electron resonance spectra

16 p2955 A70-33799

Thermal dissociation mechanism of diatomic molecules in inert diluent behind shock wave, assuming distribution function described by Fokker-Planck equation

18 p3292 A70-36242

HD molecule nuclear relaxation time in liquid state as function of temperature, discussing various mechanisms

19 p3473 A70-37367

Diatomic molecules inelastic collision cross sections for specific rotational transitions, discussing S matrix energy requirements for statistical analysis

19 p3474 A70-38268

Hydrogen molecules rotational excitation cross sections by electron impact in adiabatic excitation, discussing polarization and distortion effects

20 p3675 A70-39606

Diatomic fluorine dissociation energy by mass spectrometry

20 p3582 A70-39615

Resonance excitation of oscillations in diatomic molecules by slow electrons, calculating scattering on spherical potential well

20 p3642 A70-39753

Diatomic Cs 7667 A band vibrational spectrum analysis

20 p3676 A70-40349

Rotational relaxation of diatomic molecular excited electronic state at high temperatures, discussing nonequilibrium region behind shock wave front in nitrogen

21 p3854 A70-42060

Molecular vibrational temperature dependence on electron and neutral gas temperatures and degree of ionization for plasma excitation in nitrogen

22 p4078 A70-42358

Numerical solution of nonlinear master equation for diatomic molecule dissociation and recombination from uncoupled differential equations

22 p4062 A70-42746

Classical calculations for energy transfer to diatomic molecules with rotational and vibrational degrees of freedom in atom-diatom-molecule collisions

23 p4221 A70-44010

Strong coupled rotational excitation problem in atom-diatom molecule scattering system, discussing transition probability matrices statistical analysis

23 p4212 A70-44600

Transition entropy during dissociation, investigating Trouton-Pictet rule applicability to diatomic molecules [DFVLR-SONDDR-58]

24 p4430 A70-46412

DIBORANE

Oxygen difluoride-diborane reaction measured for pressure-temperature relationships and gas composition dependence on time, noting possible applications as hypergolic rocket propellants

11 p1995 A70-26138

Oxygen difluoride-diborane reaction kinetics and boron fluoride formation rate [WSCIPAPER 70-11]

13 p2362 A70-29611

Oxygen difluoride/diborane propellant thrust chamber and injector technology, discussing engine duty cycles and performance [AIAA PAPER 70-717]

16 p2962 A70-33550

Gelled space-storable oxygen difluoride and diborane analysis, including particle preparation, yield stresses, viscosities and storability [AIAA PAPER 70-609]

16 p2962 A70-33607

DIBROMIDES

Polymethylene-bis-lepidine dibromides effect on blood pressure and peripheral vessel tonus in dogs, analyzing depressor reaction as function of binding chain

04 p0632 A70-15204

DICHOTOMIES

Dichotomy of Venus in eastern and western elongations, determining time of occurrence by graphical method

03 p0574 A70-13886

DICHROISM

Ruby green /U/ absorption band magnetic circular dichroism calculations in linear approximation, considering spin-orbital interaction constant and magnetic field strength

01 p0156 A70-10188

Central fovea dichromacy tests, using color naming technique

22 p3972 A70-43410

Flow visualization measuring liquid flow velocity, using flow dichroism

24 p4338 A70-45816

DICKE RADIOMETERS

Absolute sky brightness temperatures measured with horn antennas and Dicke receivers, indicating spectrum change due to galactic nonthermal radiation

12 p2309 A70-27893

DICKE TYPE RADIOMETERS

U DICKE RADIOMETERS

DIELECTRIC CONSTANT

U DIELECTRIC PROPERTIES

DIELECTRIC MATERIALS

U DIELECTRICS

DIELECTRIC PERMEABILITY

Optical permittivity and dielectric permeability of electron gas in magnetic field, considering application to ferromagnetic materials

23 p4221 A70-45051

Doubly excited antiferroelectrics absorption spectrum band and bound states, discussing zero approximation 0-0 transitions of alpha oxygen molecules and permeability tensor

24 p4392 A70-46362

DIELECTRIC PROPERTIES

Thermal emission of inhomogeneous plasma sphere having dielectric constant as function of radius

01 p0149 A70-10164

Dielectric layers electrical conductivity in ceramics containing Ti during aging, observing different characteristics ascribed to nonequilibrium current carriers in junction

01 p0156 A70-10221

Electric field effects on dielectric properties and molecular arrangements of cholesteric liquid crystals with temperature dependent helical pitch

01 p0160 A70-11352

Thick walled incompressible hyperelastic dielectric sphere periodic oscillations, noting dielectric properties influence on amplitude and period

01 p0209 A70-11386

Conductivity and permittivity for ion and electron resonance region of ionospheric plasma model calculated in quasi-hydrodynamic approximation

01 p0082 A70-11528

Two band Drude model validity for analysis of IR optical properties of transition metals obtained from experimental dielectric constant data

02 p0339 A70-12452

Collection of papers on optics covering dielectric multilayer filter synthesis, photographic image, light interaction with free electrons, laser radiation, optical echoes, etc

02 p0340 A70-12828

Spectrum function in Booker scattering formula /first order Born approximation/ for dielectric constant fluctuations in hypersonic wake plasmas

03 p0529 A70-12908

Permittivity tensor calculations of weakly inhomogeneous plasma with monoenergetic component, using distribution function of particles produced by thermonuclear reactions

03 p0529 A70-13055

Three dimensional Gaussian light beam propagation in anisotropic inhomogeneous media with dielectric constant decreasing from energy flow direction

03 p0525 A70-13533

Numerical solutions to determinantal equation for predicting properties of periodically modulated dielectrically filled frequency scanning waveguide as microwave antenna

03 p0457 A70-13696

Dielectric loaded waveguide with symmetric microstrip line, evaluating transverse wave number by finite difference method

03 p0458 A70-14035

Large dielectric constant with small loss determined as function of frequency from resonant frequencies measurement

03 p0493 A70-14039

Normal incidence reflectance of BeO single crystals, analyzing data by Kramers-Kronig inversion for dielectric function and energy loss function

05 p0891 A70-16047

Crystallization and dielectric properties of glass containing barium, lead, titanium and boron oxides, noting frequency and temperature dependence

05 p0871 A70-16595

Cholesteryl chloride-cholesteryl myristate /CM/ mixture liquid crystal molecular and helical axes orientation from dielectric constant change measurements in magnetic fields

06 p1126 A70-17326

Plane light wave diffraction incident upon isotropic dielectric layer traversed by acoustic microwave using guided microwave theory

06 p1105 A70-17484

Transmission losses of plexiglass radome measured as function of frequency and antenna elevation angle, determining material dielectric constant

06 p1019 A70-17505

Plasma dielectric tensor derived quantum mechanically, emphasizing similarity in classical and quantum mechanical methods, discussing linear wave propagation, kinetic equations, etc

06 p1121 A70-17904

Scattering and depolarization of plane horizontally polarized electromagnetic wave from slightly rough lossless dielectric layer, using small perturbation theory

06 p1010 A70-18019

Lunar surface reflectivity determined by measuring reflected cosmic noise, determining dielectric constant and surface material properties

06 p1151 A70-18488

Crystals nonlinear permittivity related to temperature-time Green function for electromagnetic radiation, determining crystal polarizability by light-exiton method

07 p1335 A70-19868

Two parameter model for lattice vibrations applicable to diamond structured crystals, calculating phonon dispersion curves from dielectric screening theory

07 p1357 A70-19920

Spectrum of waves emitted from waveguide of two plane dielectric or isotropic plasma layers, solving dispersion equations numerically by computer

08 p1472 A70-20973

Quasi-optical beam splitter, using grid diffraction of plane wave at dielectric cylinder, suitable for millimeter and submillimeter wavelengths and thread measuring

08 p1496 A70-21219

Slot line wavelength, impedance, transitions and tolerances measured at S band using different dielectric constant materials

08 p1475 A70-21282

Relativistic electrons synchrotron radiation by calculating magnetoactive plasma permittivity tensor, determining normal waves polarization characteristics

08 p1554 A70-21812

Permittivity of thin films in millimeter and submillimeter wavelengths measured by diffraction grating method

08 p1464 A70-21985

Inorganic ceramic materials in design and fabrication of microwave antennas, filters and stable resonators, discussing density and dielectric constant variability by ceramics foaming

09 p1689 A70-22007

Thin resistive layers located in rectangular waveguide assuming constant and surface variable conductivity and permittivity

09 p1644 A70-22279

Natural frequencies and electromagnetic field distributions in rectilinear and cylindrical dielectric resonators used in microwave circuits

09 p1644 A70-22280

Laser measurements of permittivity fluctuations spectrum of turbulent atmosphere, noting proportionality to temperature spectra at optical frequencies 09 p1635 A70-22962

Coherent optical beam propagation measurement of fine scale turbulent atmosphere structure, inferring microscale size and permittivity spectra 09 p1635 A70-22963

Radiation losses of tapered single mode dielectric slab waveguide for TE and TM modes 09 p1650 A70-23369

Microwave signal fading in Venus atmosphere due to turbulence, discussing atmospheric dielectric permittivity variance 09 p1764 A70-23484

Materials permittivity measurement at millimeter and submillimeter wavelengths based on phase shift or sample optical thickness 09 p1684 A70-23648

Solid dielectrics permittivity measurement using beam deflection phenomenon in multislit waveguide antenna 09 p1652 A70-23656

Thermal emission of inhomogeneous plasma sphere having dielectric constant as function of radius 10 p1925 A70-25012

Two dimensional electromagnetic wave diffraction on arbitrary shaped homogeneous dielectric cylinder, solving integral equations on digital computer 10 p1842 A70-25105

Image contrast and diffraction efficiency of dielectric hologram made from diffuse signal beam, bleaching photographic emulsions 11 p2048 A70-25359

Anomalous water /polywater/ dielectric constant and effective parallel conductance, suggesting hydrosol classification 11 p1994 A70-25657

Relative permittivity of small thickness dielectric substrate plates determined from reflection coefficient in rectangular waveguides 11 p2011 A70-26603

Electromagnetic scattering from underdense plasma slabs with randomly varying dielectric constant, calculating reflection coefficient 11 p2095 A70-26763

Liquid crystal of cholesteryl chloride and myristate measured for complex dielectric constant, noting role of molecular rotation modes in dipole relaxation 12 p2180 A70-26859

Monochromatic light propagation in medium with large scale Markov nonuniformities of dielectric constant using parabolic equation approximation 12 p2272 A70-27359

EHF microwave absorption in compressed carbon density, measuring dielectric loss as function of gas density 12 p2273 A70-27571

Quasi-TEM analysis justification for limit cases of guided waves on microstrip transmission lines with dielectric constant approaching free space 12 p2190 A70-28168

Elastic, piezoelectric and dielectric properties of barium titanate single crystals of laminar domain structure 12 p2288 A70-28329

Nonlinear dielectric function and propagators of plasma submitted to electric field by Vlasov equation iterative solution, considering electron plasma in thermodynamic equilibrium 13 p2458 A70-28565

Magnetoplasmas nonlinear dielectric response function and parametric instabilities, discussing homogeneous pumping waves 13 p2459 A70-28568

Quartz-polyimide for missile radome exhibiting low dielectric constant and thin wall for use over broader frequency range 13 p2417 A70-28664

Temperature dependence of electrical properties and permittivity of barium titanate solid solutions containing Nb, Ta, Sb and La, using bridge-circuit of resonance techniques 13 p2469 A70-28853

Radiation characteristics of horn antennas loaded with curved transverse dielectric slabs and radial dielectric strips, discussing axial directivity and half-power beamwidth 13 p2370 A70-29836

Permittivity cell and encapsulation for liquids subjected to high pressures and temperature extremes 14 p2533 A70-30502

Surface wave radiation from plane dielectric waveguide, considering phase constants, directional properties and optimal distance location 15 p2696 A70-31503

Dielectric constants of zinc tungstate with wolframite structure 15 p2783 A70-31766

Earth surface temperature, emissivity and dielectric constant from satellite measurements of SHF radiation 15 p2771 A70-32072

Large amplitude electromagnetic waves propagation along plane parallel nonlinear dielectric layer, considering dispersion and permittivity 15 p2699 A70-32190

Weakly turbulent plasma dielectric constant nonlinear tensor for frequent Coulomb collisions, using hydrodynamic equations 15 p2781 A70-32824

Complex dielectric constant of alpha-AgI measured in microwave region and far IR, noting sample positioning 16 p2960 A70-33225

Low dielectric constant quartz-polyimide for radomes, considering curving methods 16 p2936 A70-33368

H-guide dielectric losses reduction by use of artificial and laminated dielectric slabs 16 p2875 A70-33401

Solid state dipole antenna array miniaturization by etching microstrip components on alumina substrate having high dielectric constant 16 p2876 A70-33409

Electromagnetic wave scattering on resonant dielectric sphere in rectangular waveguide, using reflection coefficient 18 p3227 A70-36419

Collisional contribution to finite wavelength high frequency dielectric constant of Coulomb plasma 18 p3295 A70-36439

Dielectric properties of thin barium titanate films from microwave resonance frequencies and resonance reflection coefficient 19 p3482 A70-37255

Trichroic IR absorption lines of triglycine selenate, computing optical and dielectric constants from transmission and reflection data 19 p3470 A70-37366

Fine structure of solar radiation-induced electrostatic fields on dielectric surface of comets and meteoroids 19 p3514 A70-37656

Strontium titanates ceramics containing various trivalent rare earth ions, observing dielectric relaxation 19 p3486 A70-37755

Breakdown electric field strength in S band microwave cavity for dry air, water vapor and mixture 19 p3423 A70-37757

Permittivity tensor of weakly turbulent magnetoactive cold electron plasma, calculating nonlinear currents 20 p3677 A70-39296

Inclined electromagnetic wave incidence on randomly inhomogeneous medium with changing mean dielectric permittivity, calculating reflected and scattered fields 20 p3587 A70-39726

Thermo-electret surface charge and dielectric constant time variation measurements, considering hole-electron pairs production hypothesis 21 p3797 A70-40890

Wide frequency range dielectric spectrometer for insulating materials permittivity and loss factor measurement and display 21 p3830 A70-41950

Thin two phase film conductivity, noting conditions for equality with geometric mean and for metal-to-dielectric transition 22 p4088 A70-43466

Monochromatic light propagation in medium with large scale Markov nonuniformities of dielectric constant using parabolic equation approximation 22 p4075 A70-43600

EM wave propagation in inhomogeneous media, examining permittivity and permeability 23 p4217 A70-43768

Intermaterial adhesion relation to association contact resistance-tension characteristics based on electric potential barrier model for Maxwell- Wagner effect 24 p4379 A70-45617

Graphite dielectric constant as function of frequency, considering electron energy loss anisotropy in UV 24 p4380 A70-45668

DIELECTRICS

NT RADOME MATERIALS

Dielectric overcoatings effect on Al interconnections electromigration in IC metallization, noting longer intervals between failures 01 p0153 A70-10083

Textolites and ferromagnetodielectric wedges mechanical strengths compared for use in open grooves of compound winding 01 p0008 A70-10195

Quadruple microwave probe applied to phase and attenuation variations measurements of HF wave propagating through dielectric media 02 p0345 A70-11898

Geometrical optics method for obtaining radar cross section of perfectly conducting sphere with inhomogeneous dielectric coating 02 p0262 A70-12599

Wave numbers determined in waveguide formed by laminar inhomogeneous medium enclosed between

homogeneous dielectric media, taking into account radiation losses through wall 03 p0447 A70-13290

Electromagnetic energy transmission factors for metal-dielectric-metal system, calculating net energy flux, noting effects of metal spacing, time, temperature level, etc [ASME PAPER 69-WA/HT-8] 04 p0784 A70-14822

Radiative transfer between two infinite parallel metallic surfaces separated by nonconducting thick film ideal dielectric based on electromagnetic wave theory [ASME PAPER 69-WA/HT-6] 04 p0784 A70-14824

Nonlinear theory of elastic dielectrics with polarization gradients, obtaining jump conditions and field and constitutive equations by variational principle 05 p0882 A70-16092

Backward and complex waves propagation in circular waveguide with coaxial dielectric rod, discussing arbitrary angular dependences 05 p0812 A70-16145

High speed photographic study of breakdown, crack formation, thermal explosions and molecular weight of transparent plastic dielectrics under laser beam 05 p0869 A70-16210

Nonlinear dielectric element /tandem/ for detecting IR radiation in contactless temperature measurement 05 p0848 A70-16363

Parametric coupling between space-time harmonics of electromagnetic wave propagating in dielectrics modulated by pump wave 05 p0815 A70-16660

Radio wave propagation in stratified media consisting of periodically stacked dielectric slabs solved for boundary condition by reducing Maxwell equations to Hill equation 06 p1007 A70-17463

Single mode neodymium laser second harmonic radiation self focusing resulting in filamentary fractures in solid dielectrics 06 p1080 A70-17496

Reflection coefficients, radiation patterns and surface wave excitation calculated from aperture electric field obtained for waveguide radiating through dielectric slab 06 p1020 A70-17561

Traveling wave maser with increased linear gain obtained by slow wave structure through asymmetrical positioning of dielectric 06 p1082 A70-17778

Three dimensional electrostriction theory for stress and displacement on penny-shaped crack in elastic dielectric with conducting oblate spheroidal inclusion 07 p1409 A70-19569

Electric field diffraction by infinitely long dielectric cylinder due to normally incident cylindrical wave, computing asymptotic value by geometric theory 07 p1235 A70-19684

Radiation hardened ICs development, discussing problem of dielectric isolation 08 p1468 A70-20627

Coplanar waveguide consisting of thin metallic film strip on dielectric slab with ground electrodes adjacent and parallel to strip for nonreciprocal gyromagnetic device applications 08 p1475 A70-21281

Circular dielectric waveguide modes self consistent description by asymptotic method, obtaining eigenvalues and eigenfunctions 08 p1476 A70-21288

Rectangular waveguides filled with magnetized ferrite with/without dielectric, calculating phase shift and attenuation by Ritz method 09 p1645 A70-22548

H guide with laminated dielectric strips separated by air layers, analyzing field distribution and characteristics 09 p1634 A70-22709

Polar gas phase dielectric under conditions of power saturation interacting with microwave radiation field in waveguide 09 p1728 A70-22908

Plane electromagnetic wave backscattering from dielectric-coated metallic cylinder calculated as functions of incidence angle and coating external radius 09 p1636 A70-23075

Rectangular coaxial waveguide with internal conductor contained between inhomogeneous magnetodielectric bars, deriving computer algorithm for natural mode fields 09 p1638 A70-23645

Point electric dipole EM radiation in presence of moving dispersive dielectric half space 09 p1639 A70-23669

Radiative capacity measurement for plasmas produced from nonconducting materials by pulsed discharges in magnetic field 10 p1923 A70-24252

Cerenkov radiation field in infinite parallel dielectric layer by sinusoidally bunched beam of electric charges moving with constant velocity along surface 10 p1916 A70-24408

Dielectric coatings resistance to laser radiation, measuring rupture threshold of vacuum coatings consisting of zinc sulfide layers

10 p1901 A70-25111

Radiation patterns widened from plane and circular waveguide ends closed by planoconcave homogeneous dielectric lens

10 p1843 A70-25135

Holographic dielectric gratings analyzed by Raman-Nath formalism modified for losses

11 p2050 A70-25640

Nonisothermal dielectric coating on conductor surface, analyzing temperature distribution effect on thermal emission characteristics

11 p2148 A70-25975

Coupling between parallel plate waveguides excited in TE modes using integral and differential equations, noting dielectric plug loading effect

12 p2198 A70-27954

Variational principle in electromagnetics to produce linear algebraic equations with Rayleigh-Ritz procedure for application to dielectrically coated slot antenna

12 p2198 A70-27957

Transverse electric field distribution in multilayered dielectric loaded rectangular guides determined by ray optics and residue calculus

12 p2199 A70-28051

Plane electromagnetic waves anomalous reflections from diffraction grating with periodic array of rectangular holes in dielectric layer, observing resonant character

12 p2191 A70-28175

Light pulse propagation in dispersive nonlinear dielectric analyzed on nonlinear Lorentz model

12 p2274 A70-28216

Thermoelastic stresses distribution in transmitting dielectric under short nonfocused laser pulses

12 p2251 A70-28327

Microdefects as centers of disk shaped destructive cracks in polymer dielectrics under laser irradiation

13 p2437 A70-28621

Circular shielded three layer dielectric waveguide critical parameters, estimating passbands for phase circulators with ferrite inserts

13 p2364 A70-28873

Plane electromagnetic wave reflection at interface of two semiinfinite dielectric media in relative motion perpendicular to incidence plane, noting polarization change

13 p2365 A70-29102

Pulse duration and beam diameter effects on threshold energy density in laser induced transparent dielectric breakdown

13 p2428 A70-29382

Light transmission losses in optical resonators partially filled with inhomogeneous dielectric, specifying optimal geometrical parameters

13 p2378 A70-29404

Pulsed electron beam irradiated dielectrics secondary electron emission in vacuum, emphasizing inelastic scattering

13 p2471 A70-29409

Electromagnetic energy propagation through absorbing single resonant frequency dielectric, deriving transport velocity and relaxation time

13 p2452 A70-29464

Strip lines transmission characteristics with rectangular outer conductor and multilayered layers within TEM wave approximation, using Green function and variational principle

14 p2558 A70-31316

Electromagnetic wave diffraction by heterogeneous planar dielectric structures, showing field distributions by single variable Fredholm equations

15 p2695 A70-31436

Normally incident plane monochromatic electromagnetic wave reflection and scattering from expanding dielectric slab, using invariant imbedding concept

15 p2695 A70-31438

Large amplitude electromagnetic waves propagation along plane parallel nonlinear dielectric layer, considering dispersion and permittivity

15 p2699 A70-32190

Refractive index and group velocity in moving dispersive half space/cold plasma or dielectric/under incident wave from vacuum

16 p2859 A70-32936

Periodically strip loaded dielectric slab guided electromagnetic waves, discussing attenuation and space harmonics amplitudes relationship

16 p2861 A70-32960

Excited circular cylindrical dielectric rod antenna radiation patterns derivation by Schelkunoff equivalence principle

16 p2872 A70-33121

H-guide dielectric losses reduction by use of artificial and laminated dielectric slabs

16 p2875 A70-33401

Super and subscular maxima in angular distribution of polarized radiation reflected from roughened dielectric surfaces

[ALAA PAPER 70-861]

16 p2999 A70-33906

Lateral heat transfer along parallel conducting and radiating plates spaced by absorbing and isotropically scattering dielectric

[ALAA PAPER 70-849]

16 p2939 A70-33916

Dielectric models of interstellar grains from calculations for smooth particles of homogeneous materials

17 p3159 A70-34879

Radiation from simple slots in moving dispersionless dielectric, using Minkowski electrodynamics

17 p3043 A70-34984

Lens antennas for performing radiation collimating function through refraction, discussing solid and artificial dielectrics lens design, beam scanning applications, etc

17 p3052 A70-35069

Satellite electronics production, discussing dielectric film capacitor, solar probe magnetic oxide memory core and thin film assemblies

17 p3053 A70-35268

Surface destruction of glass dielectric by pulsed laser beam, considering plasma clouds, shock waves, ablation and crack formation

18 p3266 A70-36153

Spatial signal transmission through open resonator determination based on resonator integral equation, extending to dielectric lens with finite Fresnel diffraction number

18 p3259 A70-36480

Maxwell-Wagner migrational polarization resulting from free ions or electrons drift in dielectrics and semiconductors, considering relaxation time

18 p3298 A70-36595

Plane electromagnetic wave diffraction by infinite grid above finite dielectric layer, calculating field distribution

19 p3375 A70-37281

Laser beam alignment system for monitoring dielectric film evaporation

19 p3445 A70-37686

Plane polarized electromagnetic wave diffraction by dielectric grating, obtaining linear algebraic equations for field coefficients

19 p3376 A70-37713

Dielectric layer and screen heat loss effects on diffraction radiation in resonant waveguide

19 p3377 A70-37725

Electromagnetic wave propagation perpendicular to slots of plane dielectric filled waveguide used as slow wave system and antenna

19 p3386 A70-37728

Magnetic coupling in solid dielectric cylinder under axial magnetic and perpendicular electric fields, noting memory and magnetostrictive effects

19 p3471 A70-37785

Viscous dielectric incompressible fluid cylinder capillary stability under small axisymmetric disturbances and axial electric field, deriving perturbed fluid flow equations

19 p3406 A70-38351

Dielectric rod and Yagi antennas radiation mechanism, determining pattern, gain and effective aperture

20 p3585 A70-39398

Radiation theory circular waveguide in dominant TE mode and flush mounted to infinite conducting flat ground plane covered by plasma or dielectric sheath

20 p3586 A70-39500

X band electromagnetic horn antennas, measuring triangular shape dielectrics effects on radiation pattern

20 p3599 A70-40312

Two dimensional and volume diffuse signal beam dielectric holoforms, calculating and measuring diffraction efficiency and signal to noise ratio

21 p3835 A70-40717

Arbitrary mode launching on fiber-optical dielectric waveguides by spatial filtering technique

21 p3829 A70-41930

Pressurized liquid nitrogen and hydrogen dielectrics for cryogenic cables, measuring dissipation factor and voltage breakdown by concentric cylindrical test cell

21 p3851 A70-42125

Ball lightning model assuming radiation field within plasma dielectric region resonant at higher than collision frequency

22 p4016 A70-42780

Self focusing in nonlinear optics, discussing physical processes of wave propagation in dielectrics

22 p4074 A70-43207

Electric strengths of liquid dielectrics during subjection to Q switched laser pulses, determining threshold currents for breakdown

22 p4051 A70-43338

Resonant frequencies of microwave dielectric resonator in magnetic wall waveguide

23 p4169 A70-43784

Electroreflectance at CdS-electrolyte interface, noting field strength effect on relaxation time

23 p4230 A70-43930

Dielectric covered narrow radiating slots in rectangular waveguide broad face, calculating impedance from equivalent circuits

23 p4175 A70-44952

Dielectric filled tubular monopole antenna driven by coaxial line with TEM mode, calculating current distribution from integral equation

23 p4175 A70-44953

EM wave backscattering from lossless dielectric sphere, examining diffracted field surface waves role

23 p4165 A70-44960

Radar cross section for thin dielectric plate and spherical and conical shells

23 p4166 A70-44975

Optical damage center structural defects in transparent dielectrics under high energy ruby laser radiation, noting nontransparent inclusions and dislocation centers

24 p4351 A70-45209

Microwave transmission systems, determining electric potential functions in inhomogeneous dielectrics by Earnshaw theorem and finite difference computation

24 p4318 A70-45217

Microwave transmission in partially dielectric filled circular waveguide, deriving cutoff wavelength and phase velocity vs frequency

24 p4315 A70-46260

DIENCEPHALON

Reduced visual perception time in patients under X ray treatment of diencephalo-hypophyseal region

08 p1443 A70-20736

Vegetative nervous system reactions of patients with diencephalic syndromes, investigating hypothalamo-hypophyseal-adrenal system role

13 p2352 A70-29353

DIENES

NMR spin-spin coupling constants between vinyl protons in cyclopentadiene, 1,3-cyclohexadiene and 1,3-cyclooctadiene from spectrum analysis

21 p3780 A70-41704

DIES

Matched die molding technology working principles, mat materials, mold taper, preforms, etc

05 p0856 A70-16613

Nickel base alloy as die material for creep forming titanium

11 p2060 A70-26424

Die surface composition effects on lubricant efficiency in metal working judged by friction coefficient and surface damage

13 p2418 A70-28830

Matched-die compression molding of complex shape structures from composite materials [SAE PAPER 700751]

24 p4348 A70-45874

DIETS

Human capacity to discriminate between poorly and well balanced diets and liability to select amino acid imbalanced mixtures for deficient nutrient

01 p0028 A70-11314

Diet and feeding method effects on food intake and plasma amino acid concentrations of rats fed low protein diet with amino acid imbalance

02 p0231 A70-11707

Dehydrated food effects on human functional state, noting published literature on food composition, preparation, caloric and nutritional values, digestibility, etc

03 p0435 A70-13703

Excretion and balance of K, Ca, Mg, P, S and N during prolonged use of dehydrated food diets

03 p0435 A70-13713

Fraction of Chlorella and Scenedesmus biomass, noting changes in adrenal cortex and renal glomerulus

03 p0425 A70-13889

Sweet potatoes productivity and nutritive value as carbohydrates source in manned space flights

04 p0641 A70-14572

Prolonged dehydrated food diet effect on metabolism of humans, noting complete adaptation after three or four months

04 p0630 A70-14577

Myocardial infarction therapeutic prevention possibilities on basis of epidemiologic and dietary studies involving hypercholesterolemia and hyperlipemia in coronary disease

04 p0635 A70-15463

Flavor sweetening preference in high protein and high fat diets, basing human subjects experimental range on choice of formulas

07 p1216 A70-18948

Research diets cost analysis including labor, ingredients, preparation and storage

07 p1217 A70-18949

Hyperoxia effects on red blood cell (RBC) survival in rats on normal diets, noting relatively normal erythropoiesis after long term exposure

07 p1214 A70-19935

Unicellular algae protein diet effects on animal and human enteric microflora composition

09 p1615 A70-22087

Dietary intake and adrenal cortex effects on diurnal rhythm of hepatic tyrosine transaminase activity and adrenal corticosterone content in rats

09 p1621 A70-23437

Urinary calcium phosphate and carbonate precipitates reduction by protein and carbohydrate

diet change to casein and sucrose in *Macaca nemestrina*
09 p1621 A70-23456

Dehydrated food effects on human functional state, noting food composition, preparation, caloric and nutritional values, digestibility, etc
11 p1989 A70-25503

Excretion and balance of K, Ca, Mg, P, S and N during prolonged use of dehydrated food diets
11 p1989 A70-25513

Dietary protein and yeast RNA levels effect on uric acid metabolism in normal man
11 p1987 A70-26002

Unicellular algae protein diet effects on animal and human enteric microflora composition
15 p2685 A70-32683

Hypokinesia and reduced diet effects on human tolerance to static loads, discussing acceleration tolerance prediction
20 p3576 A70-40198

Growth and caloric intake of rats exposed to high altitude dependence on high carbohydrate, protein and fat diets
22 p3967 A70-42458

Space diets with pure nutrition for balanced nutrition obtained through biological and physicochemical synthesis
23 p4157 A70-45027

DIFFERENCE EQUATIONS

Difference set D of k distinct residues, extending Hall search with negative results, discussing multipliers, polynomial congruence, etc
01 p0132 A70-11073

Difference method for calculating one dimensional nozzle flow and expansion with allowance for relaxation, friction and heat losses, discussing fluorine-hydrogen mixture application
03 p0408 A70-13804

Difference methods application to supersonic gas flow past blunt body and unsteady axisymmetric flow past body of unspecified configuration, analyzing stability
04 p0670 A70-14957

Unsteady problems of gas dynamics solved by method of characteristics, Godunov method, difference methods, etc
04 p0670 A70-14958

Difference equations and axial stress tensor component for turbomachinery in curvilinear coordinates systems
04 p0776 A70-15268

Finite difference wave equation to obtain asymptotic estimate for magnitude of precursor effects
05 p0875 A70-16310

Homogeneous difference schemes for solving ordinary arbitrary-order differential equation with discontinuous coefficients
05 p0877 A70-16973

Numerical solution of nonlinear hyperbolic systems of differential equations using methods of differences, applying results to invariant cross section gas flow
06 p0964 A70-17236

Turbine machine elements approximation by difference equations of axisymmetrical elasticity theory problem
06 p1167 A70-17663

Ritz method applied to second order nonlinear differential-difference equations subjected to sinusoidal driving functions, studying stability criteria and resonance properties
07 p1327 A70-20023

Error propagation in linear first order difference equations studied to improve accuracy of derivative recursive computation
07 p1328 A70-20249

Steady oscillations under random forces of nonlinear system described by stochastic partial differential difference equations with distributed parameters and delayed argument
08 p1542 A70-20486

Difference schemes approximating quasi-linear heat conduction equation, demonstrating convergence
08 p1596 A70-20857

One dimensional difference scheme for gas dynamics with heat conduction
08 p1482 A70-20859

Matching operations for difference and differential equations describing discrete control systems dynamics having cyclic interruption of data quantization frequency
08 p1480 A70-20999

Nonlinear computational stability of partial difference approximations to meteorological equations
08 p1534 A70-21024

Optimal control with time delays in system model described by constant coefficient linear differential-difference equations
09 p1653 A70-22346

Beginning of table calculations using difference methods for numerical integration of ordinary differential equations
13 p2440 A70-28960

Partial differential equations in regions with curvilinear boundaries solved by difference network approximation method
13 p2440 A70-28961

Numerical solution to Laplace equation in spherical coordinates with axial symmetry, using Dirichlet method to obtain difference equations
15 p2767 A70-31751

Difference schemes approximating boundary value problem for heat conductivity and oscillation equations, considering brute force method stability
16 p2951 A70-33245

Closed form difference equations for finite element models in structural mechanics, noting plate and grid applications
16 p2990 A70-33672

First order difference equations for dynamical systems from Hamilton canonical equations
17 p3129 A70-34959

Class of third order difference methods for hyperbolic equations in one and two dimensions applicable to nonlinear initial value problems
17 p3131 A70-35893

Gasdynamic equations in Euler variables, constructing completely conservative difference schemes with first and second orders of approximation
18 p3241 A70-36288

Monotonic difference schemes for parabolic differential equations with nonlinear boundary conditions, discussing convergence and stability
18 p3282 A70-36361

Two dimensional turbulent film cooling, predicting initial region temperature distribution by solving finite difference form of thermal energy equation
18 p3346 A70-36497

Magnetohydrodynamic calculations, discussing various models, difference methods, codes, boundary conditions, etc
18 p3296 A70-36794

Soviet monograph on gas dynamics one dimensional problems in variable networks, discussing difference schemes, boundary conditions and discontinuities
19 p3407 A70-38930

Deep penetration radiation shielding calculations using discrete ordinates difference equations and computer program
23 p4216 A70-43808

Mathematical models derivation for systems of interconnected elastic segments, using variational method and energy summation via difference equations
23 p4266 A70-44019

MHD equations for one dimensional plane steady flow, considering conservative difference schemes for approximation
23 p4226 A70-44307

MHD nonstationary three dimensional problems, describing difference method
23 p4227 A70-44738

Krylov and Bogoliubov perturbation method extension to difference equations based on analogy between differential and difference equations
24 p4370 A70-46027

DIFFERENTIAL ALGEBRA

U DIFFERENTIAL CALCULUS

U MATRICES [MATHEMATICS]

DIFFERENTIAL AMPLIFIERS

Signal processing by differential data and common mode amplifiers and active filters, emphasizing low level transducers
19 p3431 A70-38529

DIFFERENTIAL ANALYZERS

U ANALOG COMPUTERS

DIFFERENTIAL CALCULUS

Differential properties of class of functions of many real variables
01 p0132 A70-11067

Differential strip method developed for turbulent boundary layer equations, describing flow by law of wall coupled to wake solution utilizing constant eddy viscosity
02 p0285 A70-12352

Boundary layer prediction methods criteria, discussing advantages and disadvantages of differential and integral methods for various flows
02 p0286 A70-12356

Differential correction procedures, using residuals to obtain celestial body orbital elements by linear programming
04 p0751 A70-14943

Second vertical derivative of gravity field, using formulas based on Taylor series expansion method
06 p1055 A70-17604

Infinite order differential operator in S type spaces for Cauchy problem solution uniqueness
08 p1533 A70-20722

Differential calculus for multifunctions using Radstrom embedding theorem for convex sets
09 p1710 A70-22060

Alternating direction implicit method for solving parabolic equation with variable coefficients in two space dimensions with mixed derivative
09 p1711 A70-22284

Iterative technique for determining zero of differentiable function
09 p1641 A70-22287

Endpoint sufficiency test based on differential calculus method, considering Bolza problem of continuous state and piecewise control variables
11 p2073 A70-26233

Differential game theory, discussing two player zero sum situation
20 p3659 A70-40108

DIFFERENTIAL EQUATIONS

NT BIHARMONIC EQUATIONS

NT BLASIVUS EQUATION

NT BURGER EQUATION

NT CAUCHY-RIEMANN EQUATIONS

NT CHANDRASEKHAR EQUATION

NT DUFFING DIFFERENTIAL EQUATION

NT ELLIPTIC DIFFERENTIAL EQUATIONS

NT FALKNER-SKAN EQUATION

NT FOKKER-PLANCK EQUATION

NT GAUSS EQUATION

NT HELMHOLTZ VORTICITY EQUATION

NT LAME WAVE EQUATIONS

NT LIOUVILLE EQUATIONS

NT MONGE-AMPERE EQUATION

NT PARABOLIC DIFFERENTIAL EQUATIONS

NT PARTIAL DIFFERENTIAL EQUATIONS

NT POISSON EQUATION

NT VLASOV EQUATIONS

Differential equation comparison with Liapunov vector function, applying Caratheodory condition
01 p0130 A70-10156

Finite difference scheme for linear second order third boundary value problem in ordinary differential equations
01 p0131 A70-10455

Reentry trajectory dispersions due to atmospheric uncertainties determined using continuous differential equations based on atmospheric random processes method
01 p0183 A70-10846

Autonomous functional differential equations with finite time lag using Liapunov functionals, discussing stability and instability
01 p0132 A70-11070

Two variable expansion method applied to ordinary differential equation and two wave propagation problems, comparing results with matched asymptotic expansions and coordinate stretching methods
01 p0132 A70-11072

Buckling of orthotropic sandwich plates derived for sixth order governing differential equation by variational theorem
01 p0204 A70-11139

Differential and integral inequalities theory and applications, Volume 1, Ordinary differential and Volterra integral equations
01 p0133 A70-11324

Diffusion phenomenon in cross linkage theory of biological aging formulated as model in differential equation form, obtaining solution and applications
01 p0028 A70-11374

Lagrange solution to differential equations of motion of body with fixed point, deriving directrices of mobile and fixed hodograph
01 p0144 A70-11429

Motion of body with fixed point reduced to single second-order differential equation, analyzing special cases of gyrostatic motion
01 p0145 A70-11437

Observation process optimization in system described by linear differential equations of motion reducible to optimal control problem
01 p0047 A70-11574

Second order dynamic systems stability, analyzing nonlinear and self excited oscillations by using two differential equations
01 p0146 A70-11604

Second order ordinary differential equations solution extended to higher order or partial differential equations using numerical integration
02 p0324 A70-12280

Energy dissipation and entrainment methods for calculating turbulent boundary layer development, involving simultaneous numerical solutions of ordinary differential equations for local variables
02 p0283 A70-12337

Integral methods for turbulent boundary layer solutions, emphasizing shape factor improvement in differential equations
02 p0286 A70-12357

Small parameter method for reducing self similar viscous flow problems to ordinary third order differential equations with boundary conditions at wall and infinity
02 p0288 A70-12821

Differential equation with associated boundary conditions constructed for radiative transfer with spherical symmetry, applying to gray gas between concentric black spheres
03 p0603 A70-12904

Generalized multiple scales method for solving linear differential equations with variable coefficients applied to Liouville-Green approximation
03 p0518 A70-12994

Cauchy problem of differential equation describing asymptotic nature of conservative system motion resulting from nonperiodic perturbing force

03 p0524 A70-13342

Gyroplatform angular position with respect to reference stars from solving nonlinear differential equations, applying Liapunov method

03 p0524 A70-13366

Discontinuous solutions of nonlinear boundary value problems of heat conduction for second order ordinary differential equations using modified difference method

03 p0604 A70-13390

Stability criteria for first approximation solutions of nonlinear ordinary differential equations of motion

03 p0524 A70-13431

Liapunov function for automatic control systems, deriving theorem to ensure stability

03 p0460 A70-13434

Dissipativity and asymptotic stability criteria derived for systems of ordinary differential equations, considering application to automatic control problem

03 p0518 A70-13469

Laplace transform applied to ordinary differential equations with variable coefficients, obtaining representations of integral and integrodifferential equations

03 p0519 A70-13506

Stress differential equations of equilibrium for thick prolate spheroid/left ventricle/, yielding practical values for mean stresses in thick walled ventricles

03 p0434 A70-13571

Periodic solutions for two dimensional cubic differential equation, covering one dimensional traveling wave and two dimensional types

03 p0519 A70-13581

Nonlinear differential equations for determining radiation density of three level pulsed gas laser as function of power losses, active medium parameters and time

03 p0502 A70-13745

Differential equations system under side condition, examining solutions existence

03 p0519 A70-14073

Existence conditions of conjugate points for nontrivial solution of fourth order differential equation

03 p0519 A70-14079

Nonlinear stochastic differential equations formulated during random loading processes generation, designing testing devices with stable performance parameters

03 p0598 A70-14236

Spatially homogeneous Boltzmann equation containing initial distribution functions expandable into Hermitian polynomials, using ordinary differential equations

03 p0526 A70-14302

Differential equations solution in terms of elementary functions applied to evaluate critical buckling loads for struts of variable cross sections

03 p0602 A70-14328

Analytical approach to gradient method within framework of Bolza problem of variational calculus, using linearized differential and isoperimetric constraints

03 p0520 A70-14341

R function method for solving plate bending problem by satisfying differential equations coordinates

04 p0767 A70-14489

Distribution of zeros of solutions of canonical fourth order linear differential equations

04 p0713 A70-14675

Transport theory application to differential approximations for radiative transfer problems

[ASME PAPER 69-WA/HT-45] 04 p0781 A70-14801

Numerical analysis of nonlinear boundary value problems for ordinary differential equations, considering patch bases and monotone methods

04 p0714 A70-15046

Differential equations for minimum variance linear filter separating signals from additive correlated noise, using discrete time optimum formulas

[AIAA PAPER 69-73] 04 p0663 A70-15586

Numerical solution for differential equations describing nonlinear beam-plasma interactions based on dispersion relation analysis

05 p0886 A70-15799

Momentum-energy complex obtained for nonlocalized fields in variational mechanics, deriving integrodifferential identities for Euler equations quadratures

05 p0881 A70-16078

Hori canonical equations solved by eliminating short period terms in general planetary theory, noting reduction to systems of linear differential equations

05 p0907 A70-16160

Hydrothermodynamic equations used in forecasting meteorological components solved by assuming equations of motion quasi-linear and reducing to ordinary differential equations

05 p0878 A70-16195

Self adjoint boundary value problems with interior point boundary conditions using differential operator in Hilbert space

05 p0876 A70-16423

Differential equation for crack propagation applied to threshold conditions for brittle fracture caused by impulsive load

05 p0939 A70-16486

Differential equations and applications - Conference, Bratislava, Czechoslovakia, September 1966

05 p0876 A70-16560

Ordinary linear differential equations of high order and normal form with integrable and bounded coefficients in real and complex planes

05 p0876 A70-16561

Liapunov function construction and stability criteria based on linear differential equations containing periodic and aperiodic coefficients and small parameter

05 p0883 A70-16859

Homogeneous difference schemes for solving ordinary arbitrary-order differential equation with discontinuous coefficients

05 p0877 A70-16973

Randomly perturbed linear differential equation involving first derivative of n-vector function of real variable

05 p0878 A70-17096

Existence and uniqueness, stability and asymptotic stability of nonlinear operator differential equation

05 p0878 A70-17098

Existence and stability problems of nonlinear operator differential equations containing linear operator with domain and range contained in real Hilbert space

05 p0878 A70-17099

Numerical solution of nonlinear hyperbolic systems of differential equations using methods of differences, applying results to invariant cross section gas flow

06 p0964 A70-17236

Laplace transform of piecewise continuous function derivative for application to differential equations

06 p1164 A70-17428

Diffusion processes governed by stochastic equations

06 p1093 A70-17581

Nonlinear differential equations variational formulation, giving practical applications

06 p1093 A70-17635

Rotta differential equation for turbulent boundary layer flow with fixed profiles of length scale, shear stress and kinetic energy

06 p1035 A70-17694

Electric network models of nonhomogeneous differential equations applied to elastic beam and thin plate bending and displacement equations

06 p1094 A70-17927

Meksyn asymptotic method of integrating boundary layer equations applied to ordinary differential equations for slip flow past semiinfinite flat plate

06 p0979 A70-18348

Stability and limiting frequency of analog computer solutions of differential equations with root shifts caused by resolver imperfection

07 p1321 A70-18689

Soviet collection of papers on boundary problems for differential equations covering variational problems in half space, polynomial behavior at infinity, function spaces, Fourier transformation, etc

07 p1322 A70-18851

Asymptotic behavior of approximate solutions of nonlinear differential equations

07 p1322 A70-18891

Equations for general shells of revolution reduced to simultaneous fourth order ordinary differential equations for stress and displacement functions

07 p1401 A70-18892

Pursuit games theory with bounded accelerations, using differential equations

07 p1323 A70-18947

Stochastic differential equations for approximate continuous nonlinear minimal variance filtering, discussing existence and uniqueness conditions

07 p1245 A70-19092

Optimal control of dynamical systems with transport lag determined using differential-integral equations

07 p1245 A70-19094

Periodic solution with nondegenerate orbit for functional differential equations taking into account small perturbation

07 p1324 A70-19199

Differential equations of motion for sensitive element of gyrocompass with torsional suspension under small amplitude spatial vibrations, taking into account torsional and flexural rigidities

07 p1282 A70-19534

Convergent power series solution for holonomous mechanical systems stability described by ordinary and partial differential equations

07 p1334 A70-19545

Asymptotically periodic solution of nonlinear differential equations, discussing digital or analog computer utilization

07 p1326 A70-19782

Prandtl problem solution by reducing integrodifferential equation to linear differential equation in disk of complex variable, noting application to elliptical or rectangular wings

07 p1258 A70-19783

Integrodifferential equation derived for energy balance in laminar boundary layer of fluid flow, taking into account viscous energy dissipation, radiative energy transfer, etc

07 p1423 A70-19813

Ritz method applied to second order nonlinear differential-difference equations subjected to sinusoidal driving functions, studying stability criteria and resonance properties

07 p1327 A70-20023

Two point boundary value problems of quasi-differential equations, discussing conditions for continuous and increasing lower bounds of functions

07 p1328 A70-20349

Stability criteria for systems of nonlinear stochastic differential equations on finite time interval, considering stable motion of physical processes

08 p1533 A70-20488

Quasi-stable linear differential equations systems with nearly periodic coefficients, noting application to equations with zero real portions of matrix characteristic roots

08 p1533 A70-20492

Differential correction algorithm for identifying airplane parameters from flight test data, assuming differential equations

08 p1465 A70-20783

Linear differential controller equations for optimal automatic control system with disturbances

08 p1479 A70-20870

Structural synthesis of functional control systems represented by first order differential equations, determining hypersurface

08 p1479 A70-20871

Characteristic equations for differential symmetry operators in homogeneous and nonhomogeneous Maxwell equations

08 p1544 A70-20990

Matching operations for difference and differential equations describing discrete control systems dynamics having cyclic interruption of data quantization frequency

08 p1480 A70-20999

Stability in whole of motion determined by system of nonlinear third order differential equations, using Liapunov functions

08 p1545 A70-21003

Differential descent convergence demonstration based on relation between convex and Liapunov functions

08 p1534 A70-21007

Stability of solutions to linear differential equations pair, determining bound conditions having S-property

08 p1534 A70-21100

Stability of continuously differentiable functions representing approximate solution to system of differential equations of perturbed motion

08 p1545 A70-21167

Nonlinear system oscillations analysis based on small parameter method and difference equations, including resonant case and stability criterion for periodic solutions

08 p1546 A70-21629

Digital differential analyzers improved speed and accuracy by extended resolution on Euler integration for differential equations solution programming

08 p1467 A70-21756

Repetitive electronic differential analyzer with transistorized operational amplifiers for iterated solutions of differential equations

08 p1478 A70-21836

Cup and vane anemometers theory, determining overestimation errors of differential equation for mean values in sinusoidally fluctuating winds

08 p1501 A70-21975

Quadrature formulas with minimum remainder estimate for differentiable functions classes, considering piecewise polynomial/spline/ functions characteristic properties

09 p1711 A70-22147

Interval of values with stability and convergence for correctors for differential equations

09 p1641 A70-22286

Mixed system of simultaneous linear differential equations under general boundary conditions, deriving numerical solution in Chebyshev series

09 p1711 A70-22288

Optimal control with time delays in system model described by constant coefficient linear differential-difference equations

09 p1653 A70-22346

Liapunov stability conditions for critical point of ordinary differential equation, determining optimal criterion

09 p1727 A70-22664

Nonlinear differential equations analysis based on weighted linear approximation applied to singular points and trajectories in phase plane in friction problems

09 p1727 A70-22665

Nonlinear differential equations approximate periodic solutions generation by finding equivalent system in sense of minimum mean square difference

09 p1712 A70-22666

- Differential equation formulation for pipeline in hydraulic automatic control system considered as lumped or distributed parameter plant
09 p1612 A70-22823
- Fourth order differential equation system with complex conjugate eigenvalues, deriving optimal control for fuel minimum
09 p1759 A70-22831
- Ordinary differential and algebraic equations correct analog model, noting residual system stability role
09 p1642 A70-22973
- Asymptotic splitting of system of linear differential equations with slowly varying coefficients in cases with characteristic equation having multiple roots
09 p1712 A70-23119
- Point boundary value problem solution for differential equations with parameters in form of power series, considering Cauchy problem
09 p1712 A70-23383
- Analytic systems theory using Volterra calculus of functionals applied to nonlinear differential equations
10 p1908 A70-23845
- Hodograph or Riemann invariants method generalization for nonelliptic systems, discussing three dimensional potential supersonic flows
10 p1863 A70-24087
- Discontinuous weak solutions of differential equations of gas dynamics as limits in topology of functions
10 p1866 A70-24109
- Power series solution convergence of differential equations system, changing independent variable by conformal mapping
10 p1909 A70-24181
- ALGOL algorithm for Runge-Kutta type numerical integration of simultaneous differential equations, using Merson method for step length determination
10 p1845 A70-24405
- Numerical method for linear differential equations extended to nonlinear ordinary differential equations, liquidating residuals by setting integrals equal to zero
10 p1909 A70-24419
- Quasi-linearization extension to numerical solution of multipoint boundary value problems for ordinary differential equations arising from state constrained optimal control problems
10 p1909 A70-24421
- Parameter introduction during boundary value problem solution for second order nonlinear ordinary differential equations
10 p1909 A70-24510
- Existence theorem for periodic solutions of nonlinear differential equations with deviating arguments
10 p1910 A70-24605
- Numerical integration method for function and solution of differential equation, considering equations governing two dimensional motion of particle in air stream
10 p1910 A70-25099
- Triangular system of linear differential equations reducible to block form by Liapunov transformation, deriving indices stability conditions
10 p1911 A70-25303
- Root loci construction for differential equations with quadratic free parameters applied to aircraft motion with roll control
11 p2071 A70-25393
- Automatic control systems synthesis for plants described by incomplete differential equations, measuring controlled value and input derivatives
11 p2023 A70-25610
- One-step numerical integration of linear differential equations based on Labotto quadrature, including higher order applications and stability analysis
11 p2071 A70-25840
- Coupled nonlinear systems analysis based on reducing coupled differential equations to equivalent uncoupled equations amenable to existing techniques
11 p2072 A70-25956
- First order differential equations for unsymmetrical bending of shells of revolution
11 p2135 A70-25978
- Vector-matrix differential equation for second order sensitivity coefficients applied to trajectory optimization, modeling and compensation and guidance and control
11 p2029 A70-26324
- Stochastic differential equations objectives, limitations and restrictive assumptions in physical problems, discussing electromagnetic wave propagation in random continuum or random d'Alembertian operator
11 p2074 A70-26550
- Random processes correlation functions determined by stochastic differential equations applied to lunar surface statistical characteristics determination
11 p2118 A70-26785
- Markov nonlinear optimal filtration theory exact equations replaced by finite system of approximate differential equations
11 p2012 A70-26805
- Kantorovich theorem application as weak Newton method used in boundary value problems containing Euler-Lagrange equation for variational problems and ordinary differential equations
12 p2260 A70-27002
- Differential equations in two point boundary value problems solved by combining Newton-Raphson iterative method with parameter variation extrapolation
12 p2260 A70-27003
- Differential equations perturbed linear systems convergence, extending Bridgland results
12 p2260 A70-27011
- Subdivisional method for linear systems vibration and buckling problems, reducing governing equation to ordinary differential equation with variable coefficients
12 p2320 A70-27145
- Integral manifolds of third order autonomous differential equations with unstable equilibrium point, investigating forward and negative asymptotic problems
12 p2261 A70-27375
- Differential equations of motion of manometers in log instrument systems with allowance for viscous liquid in sensor and pulse line
12 p2234 A70-27567
- Transient heat transfer combining conduction and radiation in absorbing plane layer analyzed by differential approximation
12 p2332 A70-27801
- Linear periodic coefficient differential equations stability analysis by infinite determinate method, considering applications to damped mechanical systems motion and dual spin satellite
12 p2261 A70-27813
- Algorithm for integrating ordinary differential equations system determined for stability condition by trial-and-error procedure programmed on computer
12 p2262 A70-28030
- Liapunov functions construction through conversion of differential equation with polynomial nonlinearities into auxiliary exact differential equation using algorithm
12 p2262 A70-28070
- Beginning of table calculations using difference methods for numerical integration of ordinary differential equations
13 p2440 A70-28960
- Partial differential equations in regions with curvilinear boundaries solved by difference network approximation method
13 p2440 A70-28961
- Nonlinear differential equations systems, deriving periodic solutions existence conditions
13 p2440 A70-29049
- Ordinary differential eigenvalue problems solution by successive transformations, describing computer program and applications to hydrodynamic stability
13 p2440 A70-29085
- Variable mesh multistep predictor-corrector method for iterative solution of ordinary differential equations, considering numerical stability and algorithm efficiency
13 p2440 A70-29087
- Finite difference methods for approximating first order nonlinear hyperbolic differential equations, considering convergence
13 p2441 A70-29098
- Numerical integration of differential equations with widely separated eigenvalues, outlining solution stability and accuracy problems
13 p2441 A70-29213
- Periodic solutions to linear differential equations with delay, applying numerical-analytical procedure
13 p2441 A70-29315
- Turbulent shear flow direct interaction equations simplification to differential equations amenable to computation
13 p2389 A70-29463
- Finite time stability of differential equations system using Liapunov functions
13 p2442 A70-29488
- Controllability test for second order differential systems, noting applicability to linear first order time dependent systems
13 p2443 A70-29972
- Covariance propagation via differential equations for time-varying eigenvalues and eigenvectors
13 p2450 A70-29979
- Book on differential dynamic programming covering algorithms for continuous time control, bang-bang, discrete time and stochastic systems
14 p2560 A70-30631
- Method of ascent for general representation in boundary value problems associated with differential equation of n variables
14 p2599 A70-30636
- Differential equations eigenvalue and boundary value problem finite difference approximation convergence under consistency and stability conditions
14 p2599 A70-30643
- Differential equations stiff systems numerical solution by linear one step integration methods
14 p2599 A70-30645
- Canonical representation for nonlinear differential equations periodic solutions
14 p2658 A70-30846
- Singular perturbation problems in theory of differential equations with almost periodic coefficients
14 p2599 A70-30847
- Fourth order differential equations eigenfunctions construction and convergence of expansions in theory of flexure of sector plates
14 p2658 A70-30997
- Riccati-like linear functional differential equation with quadratic cost, analyzing feedback control solution existence and uniqueness
14 p2600 A70-31204
- Monograph on nonlinear oscillation equations resonance solutions and solution stability, considering Green matrix, differential equations reduction to integrodifferential equations, etc
14 p2618 A70-31417
- Differential equation for longitudinal vibrations of rod at high temperature, giving asymptotic solution
15 p2814 A70-31589
- Unique solvability of mixed semihyperbolic linear equations of higher order with respect to spatial variables and time
15 p2768 A70-32475
- Nonlinear differential equations for smoothing density function and smoothed expectation of arbitrary function of state
16 p2941 A70-33057
- Particular solutions for nonlinear two point boundary differential equations with initial and final conditions
16 p2942 A70-33692
- Digital simulation of continuous systems described by differential equations
16 p2870 A70-33728
- Hypersonic internal flow investigation by differential equation numerical integration, determining shock shape and surface pressure
16 p2838 A70-33881
- German monograph on calculation and measurement of stress distribution in turbine rotors with radial flow, discussing differential equations for rotating disks
16 p2993 A70-34076
- Neutral type differential equations transformation to time lag system making periodic vibrations existence and stability theorems applicable
16 p2944 A70-34282
- Boundedness theorem for solutions to differential equations system in applied mechanics
16 p2944 A70-34287
- Differential equations numerical integration by one step method of high order accuracy
16 p2945 A70-34333
- Optimal control problems solution using Cartesian product of space of right-hand sides of differential equations with Euclidean n space
17 p3129 A70-34868
- Existence and uniqueness theorem for boundary value problem solutions to nonlinear canonical ordinary differential equations
17 p3131 A70-35339
- Three dimensional mixed boundary value problems, obtaining solutions for elastic body differential equilibrium equations
17 p3192 A70-35699
- Single axis gyroscopic stabilizer with floating-type integrating gyro, describing natural oscillations by differential equations of motion
17 p3096 A70-35701
- Explicit differences scheme for heat and mass transfer differential equations
18 p3345 A70-36114
- Power series solutions to linear and nonlinear differential equations in region of asymptotic stability
18 p3279 A70-36155
- Parametric functions of integral matrices representing linear differential system via continuous coefficients
18 p3279 A70-36156
- Stability conditions for control system third-order differential equations with double nonlinearity, using Liapunov function
18 p3280 A70-36157
- Stability criteria for differential equations with complex variables, considering boundary value requirements and sufficient conditions theorems
18 p3281 A70-36352
- Nonlinear second order differential equations with periodic coefficients and solutions, examining stability by phase and amplitude plots by marginal range diagrams
18 p3282 A70-36356
- Linear differential equation integration method, using Eulerian technique for error reduction
18 p3282 A70-36358
- Boundary value problem approximation method for large numbers, using projective method applicable to linear integral, integrodifferential and differential equations
18 p3282 A70-36360
- Eigenvalues and errors in asymptotic approximation of ordinary differential equations of second and fourth order
18 p3283 A70-36365
- Linear multistep algorithms in discretization of nonlinear initial value problems of ordinary differential equations
18 p3283 A70-36366

Inverse Laplace transform of network function with allowance for initial differential equation solution, determining circuit temporal characteristics

19 p3456 A70-37269

Soviet book on dynamic systems with cylindrical phase space covering differential equations with angular coordinates, parameter estimation, multidimensional and discontinuous systems, pendulums, etc

19 p3470 A70-37468

Differential equations for odd and even parity Regge-Wheeler perturbations on Schwarzschild metric

19 p3457 A70-37573

Uniform asymptotic solutions of second order linear differential equations with arbitrarily many turning points or Stokes lines

19 p3457 A70-37681

Modified differential equation for stability of oscillating nonlinear system

19 p3458 A70-37823

Periodic solutions of nonlinear second order differential systems containing symmetries, noting Marlin criteria

19 p3458 A70-38064

Round laminar jet with swirl, reducing Navier-Stokes equations to ordinary differential equations by similarity transformations

19 p3405 A70-38349

Ordinary differential equations piecewise polynomial approximation using subpartitioning to liquidate residuals

19 p3458 A70-38356

Stress differential equations of micropolar elasticity, considering mass forces and moments of inertia

19 p3459 A70-38672

Liapunov stability analysis of dynamic systems described by simultaneous ordinary and partial differential equations of motion, applying to satellite spin stabilization

[AIAA PAPER 70-1045]

19 p3472 A70-38860

Differential equations approximate solution by interval differential equations, obtaining graphs with analog computer

19 p3459 A70-38931

Linear homogeneous differential equations nonautonomous systems integration techniques, deriving finite forms of solutions

19 p3460 A70-38938

Integrodifferential equation derived for energy balance in laminar boundary layer of fluid flow, taking into account viscous energy dissipation, radiative energy transfer, etc

20 p3736 A70-39261

Upper atmospheric wind currents differential equations, obtaining physical data in terms of asymptotic expansion of Gaussian error functions

20 p3622 A70-39763

Nonlinear differential equations solutions in power series with indefinite coefficients, determining type of singular points

20 p3658 A70-39766

Perturbation theory for nonlinear systems of differential equations

20 p3658 A70-40104

Boundary value problems for linear ordinary differential equations with singularities, determining eigenvalues by computer oriented method

20 p3659 A70-40134

Multidimensional linear differential equations with periodic coefficients, proving analog of Floquet-Liapunov theorem

20 p3659 A70-40170

Elastomechanical system reciprocity relation principles using differential equations for bar with forces in two places

20 p3735 A70-40537

Symmetric two-step algorithms for differential equations

21 p3845 A70-40735

Circumstellar system crushing processes described by integrodifferential equations, deriving particle size distribution of fragments in interplanetary space

21 p3889 A70-41148

Control processes and optimization problems solutions by stochastic differential equations, discussing dynamic models and programming, linear filtering and optimal feedback

21 p3802 A70-41275

Recursive differential equation for moments of time-to-cycle slip in first and second order phase lock loops

21 p3802 A70-41350

Mechanical behavior differential equation representation in presence of finite deformations using state variables

21 p3937 A70-41434

Numerical procedure for second order nonlinear differential equations, discussing temperature distribution in seminfinitesimal solid homogeneous medium

21 p3950 A70-41449

Circular plates dynamic stability under variable periodic loads, using differential equations of vibrational motion for median surface

22 p4114 A70-42613

Quasi-linear higher order differential equations, examining periodic solutions existence and stability

22 p4062 A70-42698

Numerical solution of nonlinear master equation for diatomic molecule dissociation and recombination from uncoupled differential equations

22 p4062 A70-42746

Asymptotic method for nonlinear automatic control systems involving differential equations in Cauchy form with nonlinearities

22 p4001 A70-42834

Harmonic linearization for nonsearching self adaptive automatic control systems described by nonlinear differential equations

22 p4001 A70-42835

Cloud droplet growth rapid computation using number density mean value for integrating stochastic coalescence equation into differential equation

22 p4064 A70-42910

Nonlinear differential equations system under small perturbation, considering uniqueness for autonomous unperturbed system

22 p4062 A70-42969

Linear differential equation solution associated with FM signal generation, presenting analytical methods for FM and AM components

22 p4063 A70-43209

Differential rendezvous game theory with non-separated control inputs on right side of equations of motion applied to guidance problem

22 p4063 A70-43346

Two phase liquid one dimensional motion in variable cross section tube, deriving mass transfer, motion and phase interaction differential equations

22 p4012 A70-43721

Free jet stream effect on thin jet-flapped airfoil with fully developed wake, using linear theory

22 p3960 A70-43737

Whole operator with infinite defective numbers for Sturm-Liouville differential equation, describing spectral functions

23 p4210 A70-43977

Minimal deviation estimates for linear approximations by seminorms for space defined by differential equations

23 p4210 A70-44018

Shooting method for computing eigenvalues of Hermitian differential operators

23 p4210 A70-44020

Nonlinear differential equation systems overall stability, using qualitative methods

23 p4211 A70-44092

Differential equation systems with Jordan form block-triangular matrix, discussing homeomorphic mapping

23 p4211 A70-44093

Linear methods for approximate solutions of ordinary differential equations and Fredholm integral equations by polynomials

23 p4211 A70-44249

Ordinary differential equations boundary value problems solution based on continuation and reduction to Cauchy problems

23 p4211 A70-44309

Differential equations of motion for machine assembly, using Appel equations

23 p4200 A70-44319

Computer program for nonlinear differential equations related to nonlinear boundary value problems based on Newtonian iteration process difference analog of linearization method

23 p4212 A70-44338

Heat conductivity problem of body with variable density and specific thermal conductivity reduced to differential equation via power series

23 p4277 A70-44340

Weak compactness of set of measures in functional space corresponding to stochastic differential equations solutions for n-dimensional Euclidean space

23 p4212 A70-44341

Nonlinear properties of first order differential equations for axisymmetric velocity vector fields of ideal incompressible fluid, using nonlinear singular integral equation

23 p4181 A70-44343

Stability theory for approximate solutions and differential approximations for differential equations in Banach space

23 p4212 A70-44345

Restricted osculating two body orbit with time derivative of eccentric anomalies difference position as independent variable in perturbation differential equations

23 p4244 A70-44635

Sufficient condition for bounded solution of matrix Riccati differential equation

23 p4212 A70-44896

German monograph on Hamilton principle and Hermitian polynomials for solving linear and nonlinear differential equations via computer method

24 p4369 A70-45091

Runge-Kutta formulas with multiple nodes for differential equations solution

24 p4369 A70-45099

Fifth-order pseudo-Runge-Kutta methods for numerical solution of ordinary differential equations, determining optimal parameters

24 p4369 A70-45163

Continuous media theory, deriving first order constitutive differential equations for isotropic tensor functions

24 p4378 A70-45270

Virtual work equations steady state subharmonic solutions by Newton-Raphson method, developing generalized iterative procedure for nonlinear differential equations

24 p4423 A70-45577

Nonlinear second order differential equation periodic solutions, describing water column oscillation in U-tube

24 p4369 A70-46021

Krylov and Bogoliubov perturbation method extension to difference equations based on analogy between differential and difference equations

24 p4370 A70-46027

Differential equations with integrable coefficients, proposing asymptotic integration for second order system

24 p4370 A70-46031

Stochastic boundary value problem involving differential equation with random forcing function, proving monotone property of solution covariance variation

24 p4426 A70-46039

DIFFERENTIAL GEOMETRY

NT LIE GROUPS

NT RIEMANN MANIFOLD

NT SPINOR GROUPS

NT TENSOR ANALYSIS

Steady three dimensional motions using classical differential geometry, considering Navier-Stokes and helical flows

05 p0884 A70-17100

Bar produced by sliding thin walled cross section along three dimensional curve, determining twisted shell curvilinear middle plane and deformations by differential geometry

12 p2326 A70-27796

DIFFERENTIAL INTERFEROMETRY

Differentiating Fabry-Perot interferometer, obtaining emission spectrum derivatives respecting frequency in millimeter range

12 p2238 A70-28177

Time average hologram interferometry, calculating light beam modulation effects on fringe loci and localization

22 p4030 A70-42950

Low pressure supersonic wake measurement by differential interferometer in double pass polarized light [SMPT PREPRINT 95]

22 p4036 A70-43060

DIFFERENTIAL OPERATORS

U DIFFERENTIAL EQUATIONS

U OPERATORS [MATHEMATICS]

DIFFERENTIAL THERMAL ANALYSIS

Kinetic energy of atomic motions for vitreous and crystalline high polymers measured by differential scanning calorimetry and thermal analysis

02 p0253 A70-12522

Curve characteristics of differential thermalgram of high alumina allophane, observing endothermal peak for water loss

06 p1004 A70-17225

Composite propellant catalysts /copper chromate and chromite/ thermal decomposition using simultaneous thermogravimetric and differential thermal analysis

11 p2100 A70-26382

Differential thermal analyzer coupled to mass spectrometer for kinetics of reactions giving volatile products at high temperature, considering ablative materials

14 p2664 A70-30292

Premature exothermic decomposition suppression in propellant grade ammonium perchlorate, using differential thermal analysis

18 p3300 A70-36699

Simultaneous mass spectrometric differential thermal analysis of low pressure decompositions of nitrate salts of monomethylhydrazine and methylamine

20 p3688 A70-40475

High temperature combined differential thermal analysis and spectrophotometric cell for phase transformation monitoring of evaporated thin film and bulk phthalocyanine

21 p3827 A70-41459

Polyurethane adhesives differential thermal analysis, rebound resilience and tensile properties at cryogenic temperatures

21 p3844 A70-42141

Solid propellant ingredients and explosives differential thermal analyses, discussing thermogravimetry, isothermal or adiabatic constant volume decomposition, crystallographic phase changes, etc

21 p3865 A70-42263

Differential scanning calorimetry and thermogravimetric analysis combination for thermochemical kinetic measurements, matching analytical and experimental curves for data accuracy

23 p4196 A70-44429

Fe-Cr and Fe-Cr-V system miscibility gap, using differential thermal analysis and Mossbauer effect measurements 24 p4362 A70-46190

DIFFERENTIATION
Numerical differentiation of analytic functions involving Cauchy formula and error estimation 18 p3282 A70-36362

DIFFERENTIATORS
Electronic differentiator for physiological research, discussing electrical voltage derivatives reproduction, sensitivity, etc 19 p3371 A70-38219

DIFFRACTION
NT ELECTRON DIFFRACTION
NT FRESNEL DIFFRACTION
NT NEUTRON DIFFRACTION
NT PULSE DIFFRACTION
NT WAVE DIFFRACTION
NT X RAY DIFFRACTION
Diffraction limited resolution criteria for geoscene imagery 02 p0297 A70-11924
Multiparticle processes in acceleration energy region, comparing various models, noting role of diffraction 03 p0526 A70-13044
Electric field diffraction by infinitely long dielectric cylinder due to normally incident cylindrical wave, computing asymptotic value by geometric theory 07 p1235 A70-19684
Diffraction effects for bilinear screen with irregular apertures determined using correction weighting function for solution 09 p1639 A70-23668
Book on holography covering principles, applications, spatial and temporal coherence, interference and diffraction theory and optical filtering 16 p2908 A70-33266
Ray theory of diffraction from open-ended parallel plate waveguides, using Wiener-Hopf technique 23 p4219 A70-44404

DIFFRACTION GRATINGS
U GRATINGS [SPECTRA]
DIFFRACTION PATHS
Topside ray trajectories near upper hybrid resonance 04 p0650 A70-15119
Pulsars dispersions, setting upper limit to emission measure of dense plasma 05 p0921 A70-16984
Oblique measurements in HF on Kiruna-Stockholm path with two fixed frequency pulsed transmitters, comparing results to ionosonde measurements 07 p1232 A70-19175
Coherence degradation of collimated and focused Gaussian beams in turbulent atmosphere, using small perturbation method 13 p2453 A70-29824
Earth-space path attenuation measurements by 8-14 micrometer telescope appended to sun tracker 16 p2861 A70-32989

DIFFRACTION PATTERNS
NT RAINBOWS
Michelson interferometer with movable mirror using laser beam to measure linear by counting fringes number, discussing design features 01 p0085 A70-10032
Ultrasonic imaging of internal structure by Bragg diffraction, noting reflection and dark field extension and use for flaw detection and medical diagnostics 01 p0111 A70-10570
Martensite structure, discussing intensity anomalies in X ray diffraction pattern of intermetallic Ni-Nb 01 p0121 A70-10900
Optical spatial amplitude filtering techniques application to moire fringe patterns processing 01 p0058 A70-11060
Diffraction plates for classroom demonstrations of Fraunhofer patterns, Babinet principle and Rayleigh resolution by computer generation 01 p0093 A70-11292
Field pattern near paraboloid reflectors focus for low f/D ratios, considering vectorial character of electromagnetic field 02 p0268 A70-12474
Image formation with partially coherent light, summarizing basic properties and diffraction theory of image formation 02 p0315 A70-12831
Schwerd color drawings of amplitude and intensity distributions of Fraunhofer diffraction patterns, verifying accuracy with computer generated diffraction plate photographs 04 p0719 A70-15014
Simultaneous recording of near and far field diffraction patterns at several exposures for single laser pulse 04 p0701 A70-15022
Gabor holography producing interference phenomena, discussing far field fringes, circular fringes, diffuser, etc 05 p0849 A70-16529

Laser interferometer for earth strain study, measuring Michelson arm length changes by counting fringes in interference pattern 05 p0861 A70-16843
Electron transmission diffraction patterns of thin monocrystal films using Ar laser 06 p1080 A70-17444
Holographic method for reconstructing polarization of light emitted by photoelastic model, obtaining isochromatic and isoclinic fringe patterns 06 p1063 A70-17643
Telescope resolution limit dependence on refractive index mean square fluctuation and effective aperture in turbulent medium 06 p1067 A70-18396
Body displacement and deformation measurement by fringe separation in holographic interferometry 07 p1280 A70-19143
Hologram interference fringes formation and location using grating model of diffusely reflecting surface 07 p1280 A70-19144
Diffraction pattern drift velocity increase with temporal frequency of Fourier components by dispersion analysis of interplanetary scintillation, noting solar wind structure 07 p1388 A70-20076
Vacuum UV spectrum interferometer with grazing incidence reflections between plane parallel mirrors to obtain coherent beams, discussing fringe patterns 07 p1286 A70-20081
Ionospheric irregularities-diffraction patterns relative drifts, verifying point source effect for radio waves reflected from E and sporadic E layers 07 p1236 A70-20162
Multibeam interferometer sensitivity restrictions due to diffraction effects on interference patterns near transparent inhomogeneities 08 p1493 A70-20540
Green and Cauchy deformation tensors determined from moire fringe pitch and angle measurements, deriving equations by specimen and master grid geometries indicial representation [ASME PAPER 69-APMW-21] 08 p1591 A70-21462
Low energy electron diffraction pattern from surface steps and facets resulting from recrystallization of Re single crystal 08 p1557 A70-21602
Electro-optical analogies application to sidelobe reduction of radar antenna illumination patterns and optics far field diffraction patterns in terrain image formation 09 p1631 A70-22009
LEED pattern and germanium surface conductivity during oxidation indicating electron states annihilation 09 p1738 A70-22215
Turbulent medium refractive index fluctuations effect on parameters of focused plane light wave, calculating diffraction patterns center of gravity 09 p1636 A70-23138
Compound semioaque thin films quality control for thickness uniformity by observing fringe patterns generated by optical data processing techniques 09 p1687 A70-23765
Diffraction pattern sampling for automatic pattern recognition in photographic imagery 09 p1689 A70-23802
Bragg diffraction imaging for sound fields visualization 10 p1893 A70-24170
TV camera with diffraction limited pinhole lens for visual simulation, solving depth of field and extending field of view without distortion 10 p1887 A70-24217
Image contrast and diffraction efficiency of dielectric hologram made from diffuse signal beam, bleaching photographic emulsions 11 p2048 A70-25359
Moire-holographic technique for deformed plane spatial displacements determination, describing diffraction patterns generation and stress analysis 11 p2140 A70-26487
Two dimensional remote sensing displays based on diffraction patterns generated by coherent light, discussing optical processing of photographs, drawings, maps, etc 12 p2229 A70-26944
Holographic method for reconstructing polarization of light emitted by photoelastic model, obtaining isochromatic and isoclinic fringe patterns 13 p2405 A70-28726
Fringe interpretation in stress-holo- interferometry, emphasizing isopachic-isochromatic interaction effects in photoelastic analysis [SESA PAPER 1642] 15 p2739 A70-32309
Fringe visibility and localization in double exposure holographic interferometry of diffusely reflecting flat objects 15 p2740 A70-32430
Rayleigh type holographic interferometer featuring production method for base pattern of variable fringe density 15 p2741 A70-32438
Wedge diffraction analyses of TE sub 10 mode slot radiation characteristics on circular and elliptical

cylinder, considering boundary value solutions existence 16 p2861 A70-32965
Holography techniques, discussing fringe pattern formation, various systems advantages and optical elements 17 p3084 A70-35002
Vibration measurement by hologram interferometry, discussing wave front reconstruction and fringe theory based on Rayleigh integral formulation of light propagation 17 p3086 A70-35017
Zero order Bessel function fringe shape measurement for holographic sinusoidal vibration fringes 17 p3087 A70-35020
Lunar occultation photoelectric measurement covering star angular diameters and diffraction patterns, ephemeris theory, astrometry close double star detection, etc 17 p3170 A70-35440
Shadow current method for asymptotic solution to two dimensional problem of electromagnetic wave far diffraction field on ideally conducting plane with infinite rectilinear slot 18 p3227 A70-36142
Plane electromagnetic waves diffraction by periodic structure of infinite system of parallel strips, reducing problem to solution of linear algebraic equations 18 p3227 A70-36287
Holographic registration of isochromatic and isopachous diffraction patterns of photoelastic birefringent objects, showing stress concentrations 19 p3422 A70-37649
Gas laser iterative alignment of Mach-Zehnder interferometer for monochromatic and white light fringes 19 p3424 A70-37880
Far field diffraction, radiation and gain of wide flare angle corrugated conical horns 19 p3389 A70-37970
High accuracy length measurement by fringe counting using laser interferometer 19 p3447 A70-38050
Photographic patterns from brittle coatings, grids, photoelasticity and moire, considering variability, association with other images and esthetic value 19 p3546 A70-38343
Interference wave functions for diffraction on cylinder and sphere, including noninterfering waves of geometric optics 19 p3380 A70-38398
Characteristic functions for frequency analysis of fringes obtained by time-average holographic interferometry of generalized time dependent optical phase function 20 p3628 A70-39133
Fresnel diffraction using He-Ne gas laser and opaque wire 21 p3834 A70-40549
Two dimensional and volume diffuse signal beam dielectric holograms, calculating and measuring diffraction efficiency and signal to noise ratio 21 p3835 A70-40717
Mach-Zehnder interferometer for plasma diagnostics measurements, discussing optical interference method, fringe shift determination and dispersion equations 21 p3856 A70-41150
Apollo 11 lunar rock plagioclases crystallography, obtaining single crystal X ray diffraction patterns by Buerger precession method 21 p3903 A70-41555
Equal thickness interference fringe networks behavior in singularities region of photoelasticity 21 p3941 A70-42260
Electromagnetic wave diffraction at multilayer wire grating, discussing computer program for diffraction field calculation 22 p3985 A70-42399
Tracking of point object in Fresnel zone from observation of amplitude-phase pattern in aperture plane 22 p4026 A70-42555
Elastic wave diffraction by rigid inclusion, calculating far field displacement and cross section by integral equation method 22 p4073 A70-42636
Ultrasonic transducer diffraction fields in highly anisotropic crystals obtained by plane waves angular spectrum 22 p4029 A70-42643
Time average hologram interferometry, calculating light beam modulation effects on fringe loci and localization 22 p4035 A70-43058
Holo-diagrams for predicting fringe patterns in hologram interferometry caused by translation motion and rotation 22 p4040 A70-43610

Cross slip between screw dislocations coplanar arrays in Ti-Al alloy, noting fringe pattern and bowing absence 24 p4359 A70-45248

Polymer crystal lattice defects and vacancies diffraction patterns observation and interpretation, using optical transformations 24 p4353 A70-45566

Holographic interference pattern interpretation, measuring object rotation 24 p4336 A70-45666

Al alloys structural analysis using electron diffraction pattern techniques 24 p4360 A70-45737

Partially space coherent diffraction by slit aperture with apodizing filter, calculating tolerance and apodization coefficients for correlation interval numbers 24 p4354 A70-45814

Multiple light beam interferences, using complex diagrams for reflection fringe visualization 24 p4381 A70-46096

Interference fringes on gas laser beam reflected by total reflection prism 24 p4356 A70-46272

DIFFRACTION PROPAGATION

Diffraction by single wire waveguide with obstacle, considering propagation phenomena of symmetrical modes 08 p1472 A70-21042

Diffraction radiation generator with CW operation in backward wave tube mode, discussing output power dependence on wavelength 18 p2321 A70-36410

Diffraction by star bounded by closed contour scalar field created by surrounding medium, reducing solution to boundary value problem via algorithm 19 p3470 A70-37431

Microwave aperture antenna in finite size ground plane, calculating radiation pattern distortion by superposition of boundary value and wedge diffraction solutions 20 p3599 A70-40314

DIFFRACTION TELESCOPES

U SPECTROSCOPIC TELESCOPES

DIFFRACTOMETERS

Nondestructive X ray stress measurement equipment for large specimen, using diffractometer focusing 01 p0085 A70-10022

DIFFUSE RADIATION

Diffuse illumination in holography indicating spread increase dependence on product of phase mean-square value and spatial frequency bandwidth 02 p0296 A70-11891

Speckle pattern in image plane of laser illuminated diffuse object, calculating pattern intensity and contrast 02 p0312 A70-12106

Double exposure holograms in diffuse radiation used to reconstruct in white light interferogram images localized in hologram plane 03 p0483 A70-13259

Spectral index for diffuse X ray sky background within specific band determined from rocket observations with wide angle telescope 03 p0479 A70-14223

Energy spectra of cosmic diffuse X ray component and distribution over northern sky, determining Crab Nebula and Cygnus spectral characteristics 05 p0901 A70-16305

Diffuse far UV radiation analysis in connection with stars and dust grains distribution and grains optical properties 05 p0903 A70-16571

Diffuse component of lunar radar echoes, using model with volume backscattering from within lunar regolith, noting rocks permittivity 05 p0816 A70-16826

Spatiotemporal correlation functions of random intensity field during diffuse scattering of coherent radiation by moving reflector 06 p1009 A70-17810

Haze model atmospheres scattering characteristics by computer simulation concerning optical contrast reduction by aerosols for direct and diffuse radiation [AIAA PAPER 70-194] 06 p1057 A70-18156

Inverse Compton collisions of relativistic electrons with universal black body photons for diffuse component of cosmic X rays 07 p1369 A70-20166

Diffuse radiation intensity determination in finite optical thickness atmosphere illuminated by parallel light beams 07 p1389 A70-20204

Monochromatic plane electromagnetic wave incident from vacuum on plane boundary of plasma half space, discussing specular reflection and diffuse scattering boundary conditions 08 p1553 A70-21611

Granularity spectrum of diffusing screen uniformly illuminated by normally incident coherent light, basing study on long and short distance visual observations 10 p1899 A70-24031

Diffuse light transmission from point sources over horizontal paths in lower atmosphere, discussing effect of range 10 p1912 A70-24424

Lunar radar echoes wavelength dependence in terms of backscattering behavior 10 p1841 A70-24644

Radiant heat transfer predictions between isothermal plates based on diffuse plus specular directional property model [AIAA PAPER 69-624] 11 p2149 A70-26157

Surface parameters influence on energy transfer to arc jet anode, discussing work function, accommodation coefficient and diffuse reflection coefficient of electrons [AIAA PAPER 69-107] 12 p2281 A70-27809

Diffuse galactic radiation and absorbing clouds luminescence illuminated by integral stellar radiation in Milky Way 12 p2307 A70-27866

Diffuse cosmic X and gamma ray background radiation isotropic component 12 p2295 A70-27887

Compton electron scattering generated galactic gamma ray flux effects on diffuse IR 13 p2476 A70-28630

Cosmic rays and cosmic X rays, considering galactic and extragalactic sources, diffuse background, detection devices, etc 13 p2477 A70-29160

Solar and terrestrial radiation measurements and computations in meteorology, considering diffuse radiation and radiative transfer in atmosphere 13 p2410 A70-29661

Angular distribution of diffusely reflected solar rays over spherical shell planetary atmosphere, determining halo brightness 14 p2632 A70-31222

Diffusely transmitted and reflected radiation fields for planetary isotropically scattering atmosphere bounded by Lambert law reflector 14 p2617 A70-31305

Planetary atmospheric light diffuse reflection and transmission, applying anisotropic scattering theory 15 p2802 A70-32493

Solar stray light, determining spread function, limb profile and aureole at various wavelengths 15 p2795 A70-32625

Diffuse specular rough surface measure for imperfect reflections in thermal radiation transfer through slot passages [AIAA PAPER 70-860] 16 p2999 A70-33905

Diffuse-specular models for radiant heat interchange prediction for isothermal-adiabatic surface enclosure tested for steel and gold 16 p3003 A70-34197

Shadow moire method for comparing diffusely reflecting component against holographically recorded master shape, noting turbine blade measurement 17 p3088 A70-35025

IR radiation diffuse reflection, transmission and emission in water clouds 18 p3244 A70-35950

Interstellar hot low density intercloud medium in H I region, estimating diffuse emission in forbidden lines O I at 6300 Å and N I at 5200 Å 18 p3310 A70-37020

Diffuse cosmic X rays produced by Compton scattering of far IR radiation on cosmic ray electrons 19 p3505 A70-38113

Diffuse cosmic X and gamma ray spectrum analysis, considering implications for Compton scattering models in intergalactic space 20 p3695 A70-39049

Integrated Bragg X ray scattering intensities for monatomic crystalline lattices, considering thermal diffuse component contribution 20 p3686 A70-39193

Diffuse cosmic X rays, discussing energy spectrum and contribution of galactic integration 21 p3875 A70-40686

Diffuse background cosmic X rays in energy range 20-120 keV from balloon observations 21 p3876 A70-40689

Low energy diffuse cosmic X radiation flux comparison with power law spectrum, observing asymmetry with respect to galactic latitude 21 p3876 A70-40692

Diffuse background of 2-20 keV X rays over Scorpius to North Galactic Pole sky band by rocket measurements 21 p3876 A70-40693

Diffuse X rays from nonthermal intergalactic bremsstrahlung, discussing cosmic ray injection models 21 p3878 A70-40705

Lunar surface specific effective radio signal scattering area measured by Luna 9 and 13, describing signal fluctuations 21 p3884 A70-40838

Diffuse X ray background attributed to X ray emission during supernova early phases 22 p4095 A70-42998

Planetary atmospheric light diffuse reflection and transmission, applying anisotropic scattering theory 23 p4240 A70-43915

Delta function approximation in diffuse transmission and reflection of light for phase function with sharp forward peak, using scattering compensation 23 p4214 A70-44034

Scattered photon effects on cosmic diffuse X ray spectrum at balloon altitude, noting overcorrection for absorption of primary X rays 23 p4237 A70-44794

Planetary atmosphere diffuse radiative transfer reflection and transmission, deriving reciprocity relations from integrodifferential equations 24 p4409 A70-45756

Discrete source interpretation of isotropic component of diffuse gamma radiation in Milky Way galaxy 24 p4398 A70-46166

DIFFUSERS

Wind tunnel tests of isentropic inlet diffusers, describing two dimensional model, test apparatus and modification and results 06 p0963 A70-17235

Vortex refrigerators characteristics, examining configurations with cylindrical and conical hot ends with and without diffuser 06 p0988 A70-17855

Straight-walled two dimensional diffusers with incompressible steady flow, noting effects of inlet blockage and aspect ratio on performance 08 p1433 A70-21322

Pressure waves of varying amplitude effect on flow through turbomachine blade passages, discussing interaction with curved diffusers geometry 09 p1608 A70-23743

Pressure recovery and energy loss efficiencies of two dimensional diffusers with suction at entrance 11 p1977 A70-26418

Rotor wakes and diffuser blades interactions visualization using hydraulic setup 14 p2528 A70-30297

Image coherence of object by laser illumination through moving diffuser related to diffuser autocorrelation 14 p2588 A70-31208

Mass flow rate and geometry effects on pressure recovery of conical diffusers with annular secondary injection at inlet [ASME PAPER 70-FE-18] 16 p2835 A70-33631

Shrouded propeller diffusers, considering diffusion effects on propulsion performance 16 p2970 A70-33754

Collisionless monatomic gas flow density and velocity distribution on axis of diffusely reflecting circular cone at zero attack angle with free stream 16 p2839 A70-34273

Plane diffuser grid profiles for subcritical velocities of oncoming flow, using wind tunnel test data 18 p3205 A70-36129

Shock tube with diffuser in low shock wave Mach number range, considering gas flow models to relate wave intensity to initial conditions in chambers 20 p3606 A70-39820

Conical diffuser-tailpipe system performance, discussing cone angle, area ratio, Reynolds number and velocity distribution effects on pressure recovery 20 p3559 A70-40082

Total reflectance of composite light diffuser with nonuniform absorption by two beam model, noting application to photochemistry 21 p3829 A70-41936

SNR of moving diffuser illuminated by laser light, considering image plane and Fresnel field observations 24 p4354 A70-45670

DIFFUSION

- NT AMBIPOLAR DIFFUSION
- NT ATMOSPHERIC DIFFUSION
- NT ELECTRON DIFFUSION
- NT GASEOUS DIFFUSION
- NT IONIC DIFFUSION
- NT MAGNETIC DIFFUSION
- NT MOLECULAR DIFFUSION
- NT PARTICLE DIFFUSION
- NT PLASMA DIFFUSION
- NT SPECIES DIFFUSION
- NT SURFACE DIFFUSION
- NT THERMAL DIFFUSION
- NT TURBULENT DIFFUSION

Tantalum base alloy T-111 creep tests in vacuum at elevated temperature suggesting diffusion controlled microcreep mechanism 01 p0120 A70-10738

Constant-inflow and constant-pressure perfusion effect on vascular responses of dog 02 p0232 A70-11716

Perfusion pressure effect on myocardial oxygen consumption and coronary flow in stable nonworking rat heart 07 p1202 A70-18865

Nonlinear steady state diffusion elliptic boundary value solutions exemplifying enzyme kinetics and radiation cooling 08 p1596 A70-20580

Collection of papers on diffusion processes in metals covering welded joints layers, radiation effects, radioactivity, nickel grain growth

11 p2067 A70-26593
Diffusion processes rate changes in metals and alloys resulting from radioactive emission, noting role in stress rupture strength mechanisms

11 p2068 A70-26595
Shock slip analysis of merged layer stagnation point air ionization, clarifying effects of reaction rates, species diffusion, etc

13 p2343 A70-29987
Molecular Markov processes application to vibrational relaxation and dissociation, small system kinetics, nucleation and droplet growth, thermalization kinetics and diffusion processes

14 p2619 A70-30615
Fluid quantum corrections to viscosity, thermal conductivity and diffusion, expanding Wigner operator in Planck constant

14 p2665 A70-30655
Organic solutes diffusion in stagnant blood plasma and red cell suspensions, using models from transport theory

15 p2686 A70-32847
Weld brittleness during laser beam welding of Ni-Cu, Ni-Ti and Cu-Ti due to diffusion processes

16 p2916 A70-33052
Chemical and structural microinhomogeneity, diffusion and mechanical properties of Ti alloys in connection with phase transformation characteristics

17 p3112 A70-34354
Density diffusion and buoyancy effects on horizontal boundary layers in stratified flow

18 p3239 A70-36193
Perfusion peristaltic pump for determining smooth muscle reaction in vascular bed, discussing applications to physiological and pharmacological investigations

19 p3372 A70-38958
Diffusion processes effect on stress state, allowing for physicochemical coupling between deformed solid bodies based on continuous media theory

20 p3727 A70-39887
Diffusion effect on carbon dioxide Gaussian laser beam amplification, measuring gain saturation via pin-hole method

22 p4051 A70-43335
Bcc Fe base alloys volume diffusion measurements, determining activation energy and frequency factor dependence on solute content

24 p4357 A70-45232
Round pulsed jet diffusion rate from velocity measurements, considering Strouhal number and pulse amplitude

24 p4327 A70-46205

DIFFUSION BONDING
U DIFFUSION WELDING
DIFFUSION COEFFICIENT

Diffusion coefficients for laminar multicomponent dissociating boundary layer at surfaces of thermally decomposing protective coatings

01 p0042 A70-11583
Mutual diffusion coefficient of hydrogen atoms and molecules in upper atmospheres of major planets calculated as function of temperature, using Chapman-Enskog theory

02 p0342 A70-11817
Static atmosphere model above 120 km, assuming oxygen atoms and molecules and nitrogen molecules presence to determine diffusion velocity and recombination coefficient

02 p0327 A70-12385
Temperature dependence of diffusion coefficient for carbon dioxide filled rigid polyurethane foam, using Fick law

02 p0321 A70-12524
Gas diffusion coefficients for He-N and nitrogen-carbon dioxide systems in diffusion cell utilizing porous stainless steel barrier

04 p0780 A70-14710
Hydrogen diffusion in pure Ti and beta Ti alloy VT15, determining diffusion coefficient for various temperatures

04 p0707 A70-15190
Diffusion rates in refractory metal alloys for thermionic emitters as function of time and temperature [GA-9495]

05 p0892 A70-16075
Charge carriers recombination and diffusion coefficients for confined gas discharge plasma obtained from data on radial particle distribution profile

05 p0888 A70-16330
Meteor trail drift characteristics from telescopic observations, determining velocity and diffusion coefficient

05 p0920 A70-16975
Thermal conductivity and diffusion-thermal coefficients analysis for nonequilibrium and highly ionized plasmas based on particle velocities

06 p1120 A70-17698
Radioactive sodium and potassium diffusion in single crystal and polycrystalline Mo and Nb at various temperatures, calculating activation energies and coefficients

06 p1089 A70-17745

Atmospheric density determined by using diffusion coefficients obtained from artificial luminous clouds observations

06 p1096 A70-17785
Hydrogen-oxygen difluoride flame burning velocity, diffusion coefficient and light output [WSC1 PAPER 69-49]

06 p1178 A70-17982
Solid electrolyte cells discharge characteristics and open-circuit voltage, evaluating diffusion coefficient of Ag from time dependent behavior of I-V relationship

07 p1196 A70-19386
Kirkendall effect in Fe-Ni and Fe-Co systems using measurement of radiotracer and intrinsic diffusion coefficients

07 p1314 A70-20015
Diffusion coefficient of charged particles in HF stabilization of current-convective instability measured in Ge semiconductor electron hole plasma

07 p1355 A70-20365
Atmospheric turbulence parameters in meteor zone determined from simultaneous photographic and radar observations, determining turbulent diffusion coefficient dependence on height

08 p1563 A70-20546
Binary and ternary systems phase diagrams construction by diffusion layer method and X ray analysis, studying concentration dependence of diffusion coefficient

09 p1703 A70-22564
Oxygen diffusion time into nitrogen in dichotomously branched human lung model calculated by finite difference technique, discussing alveolar plateau

10 p1809 A70-24003
Electron diffusion in trap with magnetic mirrors under pulsed field perturbations, determining coefficients by numerical integration of drift equation

10 p1931 A70-24311
Helium ions diffusion perpendicular to magnetic field in He gas, measuring coefficients as function of field strength and for various gas pressures

10 p1925 A70-25108
Electrons thermodiffusion and energy transport coefficients in noble gases at mean reduced electric field intensities, obtaining distribution functions

11 p2089 A70-25868
Wind velocity and direction and diffusion coefficients measurements by artificial luminous clouds, injecting appropriate reagents from rockets

11 p2075 A70-25918
Indicator dispersion model for cardio-pulmonary system based on continuity past sampling site, observing diffusion coefficient nonlinear increase with blood speed

12 p2174 A70-27019
Turbulent heat diffusion coefficients in air and water tube flow calculated from statistical characteristics, extending method to boundary layers

12 p2210 A70-27322
Oxygen and hydrogen diffusion coefficients in aqueous potassium hydroxide electrolyte solutions at various temperatures and concentrations

12 p2181 A70-27575
Diffusion coefficients measurements in velocity space from ion-ion collisions and ion wave microturbulence, supporting theoretical calculations and diffusion equations in plasma

12 p2279 A70-27777
Turbulent diffusion coefficients and time dependent velocity pulsations in air flow, considering relation between Eulerian and Lagrangian turbulence characteristics

12 p2213 A70-28235
Thermal diffusion effects on F 2 region ion densities, deriving diffusion coefficients for partially ionized atomic oxygen plasma

13 p2398 A70-29232
Self diffusion coefficient for gaseous ammonia at specific temperature range, applying polar gases theory

13 p2453 A70-29800
Atmospheric turbulence parameters in meteor zone determined from simultaneous photographic and radar observations, determining turbulent diffusion coefficient dependence on height

15 p2796 A70-31455
Propylene carbonate, dimethyl formamide, acetonitrile and methyl formate diffusion coefficients measurement for estimating nonaqueous Li batteries transport limitations

15 p2766 A70-32528
Diffusion coefficient of dissolved oxygen in blood proteins aqueous solutions

15 p2686 A70-32848
Heterodiffusion coefficients and activation energy for Cu, Ag and Au impurities in Al, using gamma spectrometry and X ray emission microanalysis

16 p2930 A70-33081
Unequal diffusion film coefficient formulation based on transfer coefficient approach for ablative material coupled multicomponent boundary layer problems

16 p2998 A70-33879

Diffusion during high temperature exposure of protective coatings on Mo, noting compact layers and carbide forming elements effect on thermal stability

17 p3125 A70-35404
Fe diffusion in equiatomic Ni-Co alloy, using thin radioactive deposit method with tagged element Fe 59

18 p3277 A70-36440
Finite size particle physics for plasma computerized simulation, considering longitudinal oscillations, scattering cross sections, diffusion coefficients, etc

18 p3296 A70-36791
Alloying elements effect on diffusion coefficient of hydrogen in low-alloyed alpha titanium

19 p3449 A70-37274
Free atmosphere turbulent diffusion coefficient determination, releasing dipole reflectors from helicopter for radio echo observation

19 p3461 A70-37423
Nitrogen diffusion coefficient in Mo and W using degassing method

19 p3452 A70-37828
Alkali metal vapors diffusion coefficients in inert gases, determining atomic interaction parameters

19 p3473 A70-38190
Binary Nb vapor systems mutual diffusion coefficients concentration and temperature dependences, discussing interatomic bonds and melting point of alloys

19 p3454 A70-38715
Argon hydrostatic pressure effect on self diffusion coefficients and activation energy of Al and Be single crystals

20 p3644 A70-38961
Primary cosmic ray intensity variation during solar activity half cycle, expressing diffusion coefficient as function of sunspot group number

20 p3696 A70-39279
Solar cosmic rays emission spectrum for 23 February 1956 flare, taking into account nucleon diffusion coefficient dependence on particle rigidity and distance to sun

20 p3697 A70-39287
Turbulent heat diffusion coefficients in air and water tube flow calculated from statistical characteristics, extending method to boundary layers

21 p3811 A70-42063
Oxygen diffusion coefficient of alpha-Ti from oxidation of saturated and unsaturated beta phase in 932-1142 C range

22 p4053 A70-42731
Minor ion diffusion coefficients in F 2 region, noting Coulomb collisions role in ion density sensitivity to ionospheric fluxes

22 p4019 A70-43109
Interdiffusion coefficients for hydrogen-carbon dioxide and oxygen-carbon dioxide systems at low temperatures

22 p4076 A70-43393
Carbon dioxide molecular vibration excitation by Q switched carbon dioxide laser, obtaining accommodation and diffusion coefficients by relaxation measurements

24 p4351 A70-45369
Density correlation measurements for diffusion coefficient in magnetized He plasma

24 p4386 A70-45614

DIFFUSION EFFECT
U DIFFUSION
DIFFUSION FLAMES

Diffusion flame structure in boundary layer with fuel injection from wall, analyzing expansions with single step reversible chemical kinetics, including nonequilibrium case

01 p0214 A70-10334
Aerodynamic gas flame theory and computations, discussing diffusion burning, turbulent flow burning rate, Reynolds number effects, etc

01 p0217 A70-11006
Unmixed gases diffusion burning calculations, discussing turbulent flame burning aerodynamics in jet flows

01 p0217 A70-11007
Weightlessness effects on butyl alcohol diffusion flames, studying flame damping mechanism

01 p0217 A70-11012
Liquid sodium droplets spontaneous ignition and combustion in controlled oxidizing atmosphere, discussing vapor phase diffusion flame, burning rates and evaporation constants

02 p0396 A70-12005
Laminar diffusion flame spread against air stream over solid or liquid fuel bed, noting influence of stoichiometric and thermal properties and data inconsistency

02 p0396 A70-12016
Chemiluminescence in alkali metals and halogenated methanes diffusion flames, studying diatomic Cs spectral bands

02 p0250 A70-12018
Laminar counterflow diffusion flame chemical structure and blow-off mechanism established in forward stagnation region of porous cylinder at atmospheric pressure

02 p0398 A70-12032

Volumetric reaction rates and mass transport coefficients as function of position for ducted two dimensional turbulent hydrogen-air diffusion flame
02 p0398 A70-12036

Turbulence intensity, light intensity fluctuations and frequency optical measurement in diffusion flames of city gas with air, deriving turbulence spectral functions
02 p0398 A70-12038

Noise generation in turbulent premixed flames, turbulent diffusion flames and liquid-spray combustion of hydrocarbon fuels, using optical method
02 p0399 A70-12040

Supersonic diffusion flames produced by subsonic and supersonic free jet injection of hydrogen into high enthalpy airstream
02 p0399 A70-12042

Structure of hydrogen-oxygen diffusion flame in equilibrium using iterative solution
02 p0352 A70-12796

Boundary layer equations describing flow field in turbulent swirling jet diffusion flame solved in von Mises plane
03 p0603 A70-12911

Ignition and extinction of diffusion flames predicted from studying forced convection in boundary layers [WSCI PAPER 69-36]
06 p1178 A70-17976

Laminar flow mixing stability and diffusion flame flow field measurements revealing role of Tollmien-Schlichting waves in enclosed flames vibrations [WSCI PAPER 69-46]
06 p1179 A70-17985

HF periodic velocity oscillations effect on axisymmetric wake diffusion flames
06 p1182 A70-18179

Ignition and extinction in opposed jet diffusion flame for flow of compressible fluid with competitive/chain reactions
07 p1422 A70-19578

Granular diffusion flame theory application to low pressure burning of composite solid AP propellants
07 p1361 A70-19914

Mathematical model for calculating radiative heat transfer from turbulent diffusion buoyant flame and predicting liquid fuel burning rate
07 p1425 A70-20008

Organic compounds chemical reactions during burning in laminar diffusive flames, describing technique for pyrolysis and combustion products sampling
09 p1787 A70-22107

Turbulent flames bluff-body stabilization model, measuring recirculation zone concentrations and temperatures for methane and propane-air mixtures
10 p1967 A70-24092

Temperature distribution in opposed jet diffusion flames, discussing mass fluxes and fuel and oxygen concentrations effect
11 p2151 A70-26385

Hydrogen-air turbulent diffusion flame structure at differing air and hydrogen velocities
11 p2151 A70-26387

Temperature estimation of micro hydrogen-air diffusion flame from hydrogen content of unburned gas mixture
14 p2666 A70-31095

Diffusion flame development in homologous turbulent shear flow, investigating flame structure and chemical reaction by statistical theory
16 p2997 A70-33499

Velocity fluctuations in temperature gradient turbulent jets in diffusion flames, using hot wire in cooled pitot tube
17 p3096 A70-35749

Ethyl alcohol fuel diffusion flame, examining thermal decomposition pyrolysis and free electron concentration distribution
18 p3345 A70-36113

Ammonium perchlorate composite solid propellant pressure vs burning rate at various temperatures, discussing granular diffusion flame theory
20 p3694 A70-40266

Extinction condition for diffusion flame formed from opposing coaxial gas jets
20 p3739 A70-40399

Ducted laminar and turbulent diffusion flames, examining electric fields effect on heat transfer, geometry and velocity field
20 p3739 A70-40471

Gravitational effects on laminar gas jet diffusion flame stability, including zero gravity environment
21 p3949 A70-41316

Book on stationary flame structure, radiation and temperature covering flow visualization, burning velocity, propagation, ionization, etc
22 p4121 A70-42325

Laminar hexane diffusion flame, investigating distribution of final and intermediate combustion products
22 p4123 A70-42522

German monograph on soot formation and separation in turbulent diffusion flame in power plant combustion chamber, noting pyrolysis role
24 p4428 A70-45087

DIFFUSION THEORY

Complex formation mechanisms and effects on impurity diffusion profiles in semiconductors
01 p0155 A70-10180

Diffusion phenomenon in cross linkage theory of biological aging formulated as model in differential equation form, obtaining solution and applications
01 p0208 A70-11374

One dimensional diffusion equation serial solution implementation by hybrid computation, using equivalence between differential and integral equations
02 p0324 A70-12259

Impurity diffusion in Ni using diffusion theory, considering activation energies for Mo and W
02 p0317 A70-12396

Diffusion processes governed by stochastic equations
06 p1093 A70-17581

Temperature fields creation in infinite or finite regions by moving surfaces with given time dependence of temperature studied by subjecting diffusion equation to transformations
08 p1597 A70-20959

Atoms diffusion mobility enhancement in metal systems during irradiation suggested due to change in electrons energy states
09 p1707 A70-23192

Integral theorems on vorticity transport derived by Carstou method, suggesting need for redefining Truesdell concepts of convection and diffusion
11 p2037 A70-26175

Asymptotics of linear diffusion processes altered by weak nonlinear effects, discussing deterministic and statistical initial value problems
11 p2074 A70-26686

Analytic expressions for concentration distribution functions in inhomogeneous solids within intermediate stages of homogenization process
12 p2253 A70-27282

Grain boundary grooves growth kinetics in pure CoO at high temperatures, determining diffusion species and mechanisms
12 p2255 A70-27603

Diffusion processes on multidimensional cylindrical phase space for studying stochastic processes for physical systems with angular measurements, developing model for satellite under torque
12 p2273 A70-28067

Diffusion loss model for cosmic ray electron propagation in galaxy, considering direct and radio observations
14 p2631 A70-30538

Thermodynamic effects and transport phenomena in discontinuous system of gas filled containers connected by membrane, deriving entropy production and diffusion flux in membrane
17 p3197 A70-35531

Unsteady state Newtonian liquid diffusion in laminar flow in circular tube, using mathematical model
17 p3072 A70-35544

Fcc metals surface self diffusion temperature dependence, using model based on complex defects contribution to diffusion flux at high temperatures
19 p3483 A70-37545

Soviet book on diffusion kinetics in stationary media covering membranes, combustion, flame propagation, hydrodynamics, exothermal reactions, thermodynamics, heat transfer, thermal explosion, insulation, etc
20 p3673 A70-39800

Heavy elements diffusive separation as explanation of metallic and magnetic A stars abundance anomalies at outer convective envelope bases
24 p4410 A70-45775

DIFFUSION WELDING

Diffusion welding of dissimilar metals with or without intermediate layers, assessing joint strength factors
03 p0498 A70-14071

Roll diffusion bonding applicability to Ti, Ni and Fe alloys, discussing fabrication temperatures and tooling [AIME PAPER F-69-3]
07 p1290 A70-18813

Stainless steel wire-reinforced Al alloy diffusion bonded scarf joints, considering aluminum oxide coating and bonding times effects
08 p1509 A70-21906

Metal matrix fiber reinforced materials bonding, discussing brazing and fusion and diffusion welding [ASM PAPER W9-23.2]
09 p1690 A70-22557

Diffusion and electron beam welding combined with forging for cost reduction and production enhancement of titanium structural components
12 p2241 A70-27087

Diffusion bonding processes for Ti aerospace structural elements, describing electric blanket, roll and press bondings
12 p2242 A70-27089

Solid state diffusion bonding techniques for aerospace Ti structural components
12 p2242 A70-27093

HF resistance welding and roll diffusion bonding fabrication of thin complex structures from Ti alloys in aerospace industry
13 p2418 A70-28828

Solid state welding processes for space, nuclear and deep submergence technologies, discussing diffusion bonding of Al and stainless steels
13 p2419 A70-29117

Low pressure diffusion welding for joining Ti-6Al-4V alloy in Ar atmosphere under compressive loading, evaluating performance
14 p2591 A70-30933

Optimum diffusion welding temperature for Ti-6Al-4V alloy determined from tensile and creep tests
14 p2591 A70-30934

Solid state diffusion bonding applied to rocket engine injectors manufacture [AIAA PAPER 70-639]
16 p2968 A70-33597

Nondestructive testing of diffusion bonded metals for quality assurance
19 p3437 A70-38423

Optimum conditions and methods for vacuum diffusion welding of heat resistant alloys, removing thermodynamically stable surface oxide films by gaseous reaction products
20 p3636 A70-39197

DIFFUSIVITY

Velocity and density profiles obtained from mass diffusivity time measurements in axisymmetric turbulent air pipe flow over specific Reynolds number range
02 p0295 A70-11853

Voltage-step method to measure diffusivity of structured region in polar liquid electrolyte solutions, considering iodine near Pt microelectrodes in aliphatic alcohols
03 p0441 A70-14044

Diffusivities of argon, krypton and xenon determined in olive oil by curve-fitting analysis of sorption curves
03 p0429 A70-14159

Carbon in austenite derived for composition dependence of diffusivity using first order mixing statistics
12 p2256 A70-27611

Turbulent chemical reactions invariance preservation for zero diffusivity
14 p2546 A70-31044

Gas mass diffusivity measurements in plasma and reaction velocity constant in human and dog blood
15 p2692 A70-32311

DIFFUSION

NT CALCIUM FLUORIDES
Hydrogen-oxygen difluoride flame burning velocity, diffusion coefficient and light output [WSCI PAPER 69-49]
06 p1178 A70-17982

NT POLYTETRAFLUOROETHYLENE
Dichlorodifluoromethane ionization and attachment coefficients for wide pressure range
22 p4076 A70-42373

DIGESTING

Appetitive behavior of rats following cessation of hypothalamic stimulation, observing eating and drinking inhibition
01 p0027 A70-11275

Eating and digestion effects on arterial pressure and mesenteric and aortic blood flows in intact unanesthetized dogs
17 p3024 A70-34848

DIGESTIVE SYSTEM

NT ESOPHAGUS
NT GASTROINTESTINAL SYSTEM
NT INTESTINES
NT MOUTH
NT RECTUM
NT STOMACH
NT TONGUE

DIGITAL COMMAND SYSTEMS

MOSFET uses in spacecraft electronic subsystems, describing digital control unit and typical logic circuitry
03 p0456 A70-13534

Digital signals conversion into command and control TV displays in multiconsole systems
13 p2411 A70-29789

DIGITAL COMMUNICATION

U PULSE COMMUNICATION
DIGITAL COMPUTERS
NT IBM 360 COMPUTER
NT SEQUENTIAL COMPUTERS

Aerospace digital computer design development, proposing data processing system with improved flexibility by making subassemblies more independent with multiplexed interface
01 p0047 A70-10305

Table lookup/interpolation function generation for fixed point digital computations, illustrating sine-cosine generator
01 p0047 A70-10459

Digital computer for data recording in stress-strain curves and data points for mechanical tests
01 p0058 A70-11062

Digital computer display techniques relationship with man in modern environment, considering human

- engineering and educational problems and future impact on intellectual qualities
01 p0221 A70-11281
Integrated digital circuits for office type desk calculators based on machine concept
01 p0052 A70-11287
Analog, analog/digital, digital and hybrid computer simulation current advances, emphasizing physiological problems and optimum solution
02 p0264 A70-11687
Trainers and simulators based on digital computers, eliminating system sensitivity to ambient conditions, power fluctuations, circuit imperfections and digital to analog conversion
02 p0274 A70-11841
Digital computers in air traffic control, discussing reliability, automated area choice, controller tasks, planning, etc
02 p0331 A70-11960
Associative processor with content addressability and simultaneous arithmetic capability to circumvent speed restriction, comparing performance and cost with conventional digital computer
02 p0265 A70-12186
Hardware-software integrated time sharing computer system for testing transmission control units and associated terminals on line
02 p0275 A70-12189
Digital computer program for physiological measurements, outlining interpolation of mathematical functions describing signals time variations
03 p0436 A70-13900
Digital computers for calculating coefficients of electronic circuit functions polynomials, developing algorithm
04 p0659 A70-15205
Large wall display system for USAF command and control with central computer and seven color projector, discussing hardware and operational features
05 p0828 A70-16193
Real time computer control system queueing model to optimize preemptible and nonpreemptible job priority assignment
05 p0817 A70-16414
Special purpose computer organized as time-shared digital filter for real time applications with adaptable coefficients, programming and multiplexing scheme
05 p0818 A70-16415
Digital computer interface for ELDO launcher inertial guidance system linking with platform, autopilots, telemetry equipment and rocket subsequencers
05 p0818 A70-16572
Book on digital computer methods in engineering covering numerical and programming methods, algebraic and differential equations solutions, time-frequency domain analysis, etc
05 p0877 A70-16771
Digital computers structural and operational address format dependence on number of storage readouts expressible with aid of linear function
05 p0818 A70-17004
Worldwide Apollo data transmission network emphasizing computer operations for message collection and distribution, command and telemetry processing, etc
06 p1005 A70-17310
Computer operated digital system for controlling acoustic test environment and dynamic test data acquisition
06 p1030 A70-18432
Space rendezvous navigation and guidance based on optical sightings with hand-held sextant entered into and processed by small digital computer
07 p1331 A70-20061
Digital computer applications to structural analysis, discussing interactive graphics and engineering design
07 p1239 A70-20360
Aerospace digital computers automatic checkout, considering computers functional and mechanical properties and test equipment configuration and operation
08 p1469 A70-20653
Computers impact on engineering science and design, detailing digital computers use in aerodynamics, structures and aeroelasticity
08 p1466 A70-21030
Digital differential analyzers improved speed and accuracy by extended resolution on Euler integration for differential equations solution programming
08 p1467 A70-21756
Digital computer impact on aerospace sciences and technologies in terms of computerized design, interactive graphics, flight simulation, Apollo systems checkout, etc
09 p1642 A70-23277
Computer-generated holography involving three dimensional object perspective projections computation for incremental rotations
09 p1683 A70-23529
Signal converter for centimeter band-DC voltage transformation, noting applications to microwave power measurement by digital computers
09 p1650 A70-23629
Digital and analog computers applicability to graphic arts noting lack of aesthetic theories
10 p1845 A70-24235
TATS Master tactical communication satellite network controller with modems and digital computer for semiautomatic control over terminals
[AIAA PAPER 70-412] 11 p2002 A70-25491
Direct view storage tube /DVST/ as graphical display unit for small digital computer installation
12 p2232 A70-27374
Terminal automation system /ARTS/ digital computerized beacon tracking for future ATC facilities, noting add-on packages to increase system reliability
[SAE PAPER 700282] 12 p2206 A70-27441
Automatic computation at SNECMA for turbomachines R and D, emphasizing digital computer for scientific calculation and analog simulator for engine regulation
12 p2193 A70-28073
Digital correlator LSI circuits design, layout and mask considerations, diffusion, metallization and dielectric deposition
13 p2378 A70-29551
Digital computer controlled test system suitable for verifying response to single input pattern containing time dependent functions
13 p2374 A70-29684
Digital computers in automatic test equipment, describing required control tasks
13 p2375 A70-29690
Time shared computer system providing real time service to multiple laboratory instrumentation, discussing high speed channel, computer control and data abstracting techniques
13 p2375 A70-29830
Biresidue error-correcting codes for digital computers involving use of residue check circuitry working with arithmetic unit
13 p2375 A70-29938
Berkeley array processor /special purpose digital computer/ for correlation, convolution, recursive filtering, matrix multiplication, etc
13 p2376 A70-29941
Computer-controlled single-server queueing system with constant access cycle and general service times, calculating mean size and waiting time at statistical equilibrium
14 p2553 A70-30518
Digital computers for interplanetary spacecraft, comparing centralized and decentralized approaches for implementing onboard functions
[AIAA PAPER 68-840] 14 p2554 A70-30757
Spacecraft onboard computer for prelaunch targeting constants verification through checksum equation and error detection scheme, using generated number sequence
[AIAA PAPER 69-946] 14 p2599 A70-30769
Digital computers in aircraft, discussing automatic control systems, components and advantages over analog systems
15 p2705 A70-32299
Speed convergence of hybrid vs digital computer synthesis of optimal boost vehicle controller, considering fuel consumption and pitch dynamics
16 p2981 A70-33442
Fast Fourier digital processor for real time filtering of radar signals, discussing applications as Fourier transform system
16 p2870 A70-33738
Military aircraft avionics central digital computers, discussing memory capacity, computational speed requirements, cost and tradeoffs
17 p3049 A70-34673
Digital computer technology impact on advanced aircraft design, discussing airborne computers, distributed and lumped computer systems, outer loop control, engine control and system integrity
17 p3049 A70-34993
Nuclear rocket engine testing, monitoring reactor and facility performance with real time digital computer
17 p3135 A70-35212
Digital computer controlled positioning of telemetry antennas for tracking spacecraft
17 p3062 A70-35508
Digital computer six degree of freedom wind tunnel separation simulator for air launched missile trajectory analysis
17 p3063 A70-35509
High speed digital computer input device for reading data from magnetic tape, discussing design and operation principles
18 p3230 A70-36095
Hypotheses concerning optimal methods of solving mathematical physics problems, choosing algorithms employable in digital computers
18 p3291 A70-36284
Computerized air combat simulation with comparison of analog and digital approaches, noting Air to Air Combat Fort Worth
18 p3230 A70-36453
Brain-like computer with learning rather than programmable capability, discussing pattern recognition and task performance
18 p3230 A70-36775
Aero gas turbine engines digital computer control, discussing special properties, design and safety problems
[ASME PAPER 70-GT-40] 18 p3304 A70-36870
Iterative Hansen method of general perturbations programmed for digital computer, evaluating major and minor planetary theory
18 p3320 A70-37060
Automatic gain ranging amplifier for high speed digital computer controlled data acquisition system used to process input data levels
19 p3383 A70-37919
Digital electrodynamic vibration exciter control for sinusoidal, random and shock spectrum testing of aircraft, missiles and satellites
19 p3383 A70-37920
Data management methodology for test facilities, considering on-line analog/digital computers
19 p3383 A70-37922
Digital computer for high speed wind tunnel data acquisition, processing and operations control
19 p3397 A70-37923
Digital computer magnetic tape recording system for flight tests of Jaguar aircraft, discussing data treatment
19 p3384 A70-38537
Emmanuel magnetic recording system used with airborne digital computers for aircraft in-flight tests
19 p3432 A70-38547
Digital computer input language with multiple access for engineering calculations
19 p3385 A70-38577
Neutron monitor NM-64 design and operation, using Setun digital computer for around clock processing
20 p3629 A70-39310
Digital fail-operative flight control computers for automatic landings, describing system requirements and problems and flight test program
[AIAA PAPER 70-1032] 20 p3591 A70-39505
Small digital computer arithmetic unit design, discussing number representation, addition and subtraction methods for performance and cost
21 p3793 A70-40757
Fast pseudorandom number generators for digital computers
21 p3793 A70-40851
Electromagnetic test equipment transient waveform control using on-line digital computer in near real time configuration
21 p3805 A70-41270
Aerospace digital computers impact on aerospace systems design
21 p3794 A70-41685
Aerospace digital computer family structural commonality, considering architecture, hardware and support software
21 p3794 A70-41687
Aerospace digital computer and avionics systems man machine relationship optimization, considering human information and control response requirements
21 p3794 A70-41688
Aerospace system design, considering use of microprogram-controlled digital computers
21 p3795 A70-41690
Modular aerospace digital computer system architecture using off-shelf components for rapid avionic computing system realization
21 p3795 A70-41691
Aerospace microelectronic digital computer design, discussing optimal packaging by use of integrated circuits
21 p3795 A70-41694
Airborne digital computers in aircraft systems, discussing optimization, design and economic effectiveness
21 p3796 A70-41920
Automatic ship navigation system using Transit satellites and onboard digital computer for routine tasks of dead reckoning
22 p4068 A70-42666
Modular plated-wire digital associative processor with content addressable memory, distributed arithmetic and I/O capability at each word
22 p3994 A70-43104
Avionics digital computer system using associative memory for executive control functions implementation to mechanize task assignment algorithm
22 p3994 A70-43105
Automated air cargo and data flow system with on-line computers, discussing handling, document management, load planning, information transmission, storage and mechanized freight systems
22 p3994 A70-43271
Information processing methods in microwave measurement using digital computers, emphasizing active and passive transducers
23 p4193 A70-43795
Graphical link between operator and digital computer using CRT display and light-pen input system during automatic electronic circuit design
23 p4150 A70-43952
Digital computer constructed with diodes and transistors logic for evaluating matrix determinants and minors
23 p4166 A70-43955
Flight simulation in SAAB AJ37 aircraft development, describing analog and digital computers, cockpit simulators, automatic pilots, control and display devices
[ICAS PAPER 70-42] 23 p4178 A70-44140

- Automated high precision electrical resistance measuring system using digital computer control
24 p4334 A70-45384
- DIGITAL DATA**
- Semiautomatic data collection system for IR reflectivity measurements, recording digitized output on punched cards for computer analysis
01 p0088 A70-10747
- Man machine digital display low cost system for displaying black and white image data with gray levels, color image data and dot patterns
02 p0265 A70-12152
- Automatic universal-code digital data recorder for photogrammetric measurements
03 p0483 A70-13110
- Technique for coding data on cosmic ray variations based on packing digital information in computer storage, proposing selective statistical control for tape recording phase
05 p0898 A70-15929
- Onboard digital data acquisition instrumentation system for scientific satellites, combining existing functional blocks to obtain different configurations and performances
05 p0818 A70-16587
- Digital and analog large system data displays, considering CRT, laser, hybrid types, contrast control, etc
06 p1061 A70-17348
- Arithmetical divisible codes with error correction in single digit for nonbinary positional number systems, using comparison and group theories
07 p1246 A70-19645
- Error statistics recording for digital communications channel performance by extreme value technique
08 p1459 A70-20801
- Digital data display system designed for central station of German ground station system
08 p1462 A70-21369
- Automatic photographic data processing system with transient reproducer to obtain digital format for computer analysis
09 p1673 A70-22030
- Binary, ternary and multilevel digital signals transmission codes emphasizing PCM signals
09 p1631 A70-22038
- Gigahertz rate circuits requirements for high speed digital data communication from component and system viewpoint, emphasizing coding and multiplexing techniques
09 p1633 A70-22605
- Digital transmission techniques optimal utilization of assigned frequency spectrum for phase modulation of frequency carriers
10 p1839 A70-24365
- Phase noise and cycle slip optimization of steady state digital data transition tracking loop used as bit synchronizer in phase-coherent receiver
11 p2024 A70-26202
- Controlled digital data relay satellite system to provide multiple access between central station and user terminals, noting computer time sharing operation
11 p2008 A70-26230
- Digital air data system vibrating diaphragm pressure sensor
11 p1983 A70-26508
- Digital river and rainfall data automatic transmission from remote hydrologic platforms via ATS-1, studying system economic and technological feasibility
12 p2205 A70-26939
- Binary-valued digital pictures noise cleaning by propagation processes
12 p2188 A70-27937
- Digital signals transmission codes comparison for transient response by reducing channel bandwidth to obtain error probability
13 p2372 A70-28899
- Digital recording of geomagnetic field variations, using IBM or international telex code for radio transmission
13 p2415 A70-30043
- Harmonic analysis of digital data from satellite measurements of periodic phenomena with unknown periodicity
14 p2554 A70-31415
- Digital data detection in presence of noise and double sided intersymbol interference, deriving error rates for known and stochastic signals
15 p2703 A70-32561
- Digital sampled data demodulation, discussing methods of obtaining quadrature channels from single signal
15 p2703 A70-32579
- Digital color printer with opaque IBM card as filter for sea surface temperature and cloud vortex patterns display
16 p2907 A70-33180
- Digital data acquisition and control system for acoustic testing of large spacecraft
17 p3062 A70-35506
- Magnetic tape recorder for panoramic vertical ionospheric sounding data acquisition in digital form
18 p3261 A70-37041
- Digital flight data recording, considering aircraft integrated data systems /AIDS/
19 p3426 A70-37892
- Range channel width effect on radar signal digital detector function and parameters optimal value
19 p3380 A70-38068
- Cardiac rhythm, respiration and rhythmical processes of alimentary tract, using digital data device
19 p3370 A70-38214
- Piezoresistive Si pressure transducer design for Digital Air Data Computers, achieving optimum resistor matching and long term stability
19 p3430 A70-38521
- Digital data acquisition system for CF-5A flight test program, discussing recording system design
19 p3384 A70-38532
- Data collection system for prototype flight tests of Fokker F-28 based on DC-8 aircraft digital system
19 p3384 A70-38546
- Digital extraction of primary and secondary radar data for air traffic control
19 p3469 A70-38644
- Digital readout test equipment characteristics and parameters for electrical properties measurement, proposing pulse counting analog-digital conversion technique
19 p3432 A70-38701
- Satellite TV cloud picture digital representation, deriving algorithms for statistical analysis of geometrical features
19 p3463 A70-38755
- Digital correlation system for stationary and nonstationary random processes, estimating mathematical expectations and cross- and autocorrelation function
20 p3594 A70-39920
- Digital correlator errors due to quantization by levels, designing analyzer of slow processes
20 p3594 A70-39922
- Liquids density measurement from digital data obtained from sample subjected to vibrations
22 p4030 A70-42848
- EUV reflectance data for optical constants obtained in digital form directly on punched cards by data acquisition system
23 p4197 A70-44470
- DIGITAL FILTERS**
- Digital filters output error due to roundoff accumulation and input quantization calculated by floating point arithmetic
01 p0050 A70-10778
- Special purpose computer organized as time-shared digital filter for real time applications with adaptable coefficients, programming and multiplexing scheme
05 p0818 A70-16415
- Transverse nonrecursive digital filters for Hilbert transformation, investigating ideal quadrature filters with Chebyshev approximation errors
05 p0822 A70-16772
- Half wave stepped digital elliptic filter design showing improvements over microwave TEM line narrow band bandpass filter
08 p1476 A70-21284
- Roundoff noise output-dynamic range interaction in digital filters, discussing filter synthesis with transpose configurations concept
09 p1649 A70-23366
- Collection of papers on digital signal processing covering digital filter synthesis, Fourier transforms, algorithms, etc
11 p2003 A70-25575
- Digital filters response errors due to signal amplitude quantization, resulting from analog-to-digital conversion and arithmetic operations
11 p2029 A70-26333
- Satellite signal scintillation spectrum analysis by digital filtering of magnetic tape recording
11 p2012 A70-26718
- Bits quantity required to represent coefficient within digital controller with high sampling rate
12 p2203 A70-27410
- Digital range tracking, Doppler filtration and moving target selection in multichannel automatic surveillance radars
13 p2380 A70-29735
- Digital filter facilitating biological data analysis through zero or linear phase shift filtering without distorting time relationship in data
14 p2542 A70-30796
- Cascade digital filter computerized design with favorable signal to noise ratio, considering round-off errors
15 p2709 A70-32465
- On-line computer aided design of fixed point digital filters simulating direct, cascade and parallel bit representations
15 p2711 A70-32598
- Real time variable range digital filter design in suitable form for LSI realization, satisfying reduced dead-band requirement for input interface element
16 p2882 A70-33040
- Digital self optimizing distortionless filter for hybrid navigation system
17 p3054 A70-35281
- Analog shift register for use as delay line and digital filter, discussing applications to radio astronomy
18 p3261 A70-37088
- Digital filter synthesis, discussing transfer function determination based on prescriptions for frequency or time response properties
19 p3391 A70-38746
- Recursive digital filters for flight control system airborne computer, considering quantization effects and eigenvalue sensitivity
20 p3601 A70-39575
- Digital filtering of sampled narrowband sinusoidal signal embedded in wideband white noise, assessing hard clipping effect on performance by simulation on digital computer
21 p3791 A70-41948
- Adaptive channel equalization approach leading to adaptive detector for slowly time varying channel
22 p3989 A70-43172
- Digital frequency filter for data processing
24 p4318 A70-45435
- Analog and digital low pass filters for radiometric postdetector filtering
24 p4321 A70-45622
- Multifunction programmable digital filter design performing bandpass, bandstop, comb, nonlinear phase and matched filtering of signals
24 p4319 A70-46082
- DIGITAL INTEGRATORS**
- Digital differential analyzers one step integration method with iteration procedure truncation to single step
22 p3996 A70-42921
- DIGITAL NAVIGATION**
- Inertial navigation systems, discussing role as flight control sensor with advent of all digital interface automatic flight control systems and cost and reliability
02 p0334 A70-11988
- Digital guidance computer compatibility with analog attitude control loop in Digital Inertial Guidance System used in ELDO launch vehicle
11 p2080 A70-26280
- Global digital navigation and traffic control system via satellites, discussing position determination, surveillance and communication requirements
21 p3848 A70-41133
- Aircraft navigation control system by digital computer combined with inertial platform, considering emergency backup, slow drift and system malfunctions
24 p4374 A70-46092
- DIGITAL SIMULATION**
- IBM System/360 Operating System submodel simulator for multiprogramming, discussing language and structure
02 p0266 A70-12281
- Optimum numerical integration with application to real time digital simulation of continuous systems, deriving three step methods
03 p0455 A70-14173
- Nuclear rocket engine core thermal and neutronic transient and steady state dynamics digital simulation, showing advantages over lump model analysis [ASME PAPER 69-WA/NE-3]
04 p0717 A70-14757
- Dodge satellite postlaunch attitude stabilization and flight data comparison with digital simulation, underlining simulation use in design analyses
04 p0765 A70-15674
- Book on digital simulation of continuous systems covering programming, engineering and mathematical applications, equipment logic and construction, etc
06 p1014 A70-17475
- Flight software for onboard Apollo Primary Guidance, Navigation and Control System flight qualification by digital simulation, including software diagnostics [AIAA PAPER 70-173]
06 p1029 A70-18060
- Computer program for automated test station simulation, considering station operating characteristics and performance prediction
08 p1465 A70-20666
- Mars lander atmospheric entry digital simulation for deceleration system design, discussing ballistic coefficient, aeroshell diameter, parachute size and deployment altitude, etc
08 p1582 A70-20932
- Cardiovascular control system mathematical model incorporating fundamental properties of heart muscle for digital simulation using FORTRAN program
08 p1453 A70-21513
- DICAP system to analyze digital sequential switching circuits, studying simulation technique range and limitations of applicability
10 p1845 A70-24236
- Combined discrete event and continuous systems simulation language, discussing mathematical modeling and various applications
10 p1860 A70-24652
- Digital simulation of complex dynamic systems using homing missile as example, basing algorithm on 1 transforms for linear systems
11 p2013 A70-25692
- Digital computer simulation of Bake concept as related to tropospheric CW signal scatter measurement
11 p2009 A70-26240

Mars landing analysis and simulation for unmanned lander prototype, discussing digital simulation by Monte Carlo techniques and physical tests
11 p2032 A70-26291

Radar systems EM compatibility simulation, describing FORTRAN IV operational interference prediction program
12 p2193 A70-28139

Attitude control system for pointing rocket nose cone at sun examined by digital computer simulation
13 p2501 A70-28419

Fixed wing aircraft and associated subsystems simulation by digital computer, having full FORTRAN capability
[AIAA PAPER 70-572] 13 p2385 A70-29897

DMC computer code for simulation of two dimensional viscous incompressible flow about arbitrarily shaped bodies
14 p2527 A70-30271

Gas turbine performance dynamic modeling by analog and digital computer simulation providing clear picture of transient behavior
14 p2629 A70-30991

Interactive computer graphics using modified Continuous Systems Modeling Program /CSMP/
15 p2705 A70-31773

Computer simulation model documentation exemplified by cardiovascular simulation using Continuous Systems Modeling Program /CSMP/ and emphasizing format uniformity
15 p2689 A70-31774

Magnetic hysteresis dynamic model for digital simulation of stabilized satellite attitude motions
15 p2812 A70-32509

Digital simulation for turbine engine propulsion system testing
[AIAA PAPER 70-633] 16 p2869 A70-33593

Multibody lifting entry vehicle clusters separation dynamics, describing digital simulation, wind tunnel tests, separation mechanisms, etc
16 p2981 A70-33704

Interactive computer graphics applied to continuous system modeling program /CSMP/, describing hardware system configuration
16 p2870 A70-33727

Digital simulation of continuous systems described by differential equations
16 p2870 A70-33728

Digital simulation of linear filter, investigating noise and rounding errors effects on decoding signals from lunar and interplanetary probes
17 p3049 A70-34612

Satellite interference distribution prediction from digital simulation
17 p3177 A70-35250

Aircraft traffic on ground at airports by digital simulation, investigating influence of constraint represented by infrastructure of taxi tracks
18 p3236 A70-36390

Gas turbine engine dynamic performance simulation, using analog and digital techniques
[ASME PAPER 70-GT-23] 18 p3237 A70-36830

Global scale atmospheric circulation processes numerical simulation leading to long range weather forecasts for Northern Hemisphere
19 p3462 A70-38753

Isolated cumulus clouds formation numerical simulation, determining movement rates relationship to external wind speed
19 p3463 A70-38756

Apollo service module retrograde motion due to propellants reorientation after reentry jettison predicted by digital simulation
[AIAA PAPER 70-1047] 19 p3534 A70-38862

Variable parameter nutation damper SAS-A dual spin satellite, discussing design and expected in-flight performance by digital simulation
[AIAA PAPER 70-972] 20 p3669 A70-39557

Image detection in pattern recognition through bipolar correlation, discussing reference generating algorithms and digital simulation results
20 p3633 A70-39972

Digital filtering of sampled narrowband sinusoidal signal embedded in wideband white noise, assessing hard clipping effect on performance by simulation on digital computer
21 p3791 A70-41948

January climatology simulation experiment based on two layer version of global circulation model, comparing computed and observed results
21 p3847 A70-42120

Digital statistical modeling of nonlinear automatic control systems including accuracy analysis, generation of random perturbations and parameter optimization
22 p4004 A70-42892

Air traffic flow digital computer simulation model including departure, enroute and arrival phases for collision avoidance, weather effects and control constraints
[AIAA PAPER 70-1316] 24 p4373 A70-45945

DIGITAL SYSTEMS

Secondary surveillance radar to operate autonomously with digital techniques and digital handling systems, discussing design and ATC applications
02 p0266 A70-11957

Multiplying digital device for measuring motor speed, torque and power, discussing optional applications and design
02 p0297 A70-12076

Digital systems design laboratory as instructional tool and experimental model for education
02 p0275 A70-12190

Spatial registration of digitized multispectral video imagery obtained from multilens cameras, multichannel optical-mechanical line scanners and multiple TV camera systems
03 p0453 A70-13000

Binary systems noise resistance with various cross correlation functions and indefinite moment of arrival
03 p0448 A70-13512

Digital network reliability with redundancy to mask logic modules failure for asymmetric failure modes
03 p0454 A70-14022

Solid state digital pressure transducer incorporating Si diaphragm with piezoresistive sensing elements for computerized supersonic and subsonic data applications
03 p0496 A70-14194

Frequency selection systems synthesis with digital AND type logical elements, noting basic design relations
04 p0647 A70-14404

CRT display design for command and control with digital symbol and vector generation
05 p0817 A70-16184

Radar digital indicators generating deflection signals for digital PPI display, discussing scale ranges, symbols and digital circuits application
05 p0828 A70-16191

Computational algorithms transformation to forms convenient for aircraft computer adaptation for reducing digital network length with small accuracy penalty
05 p0818 A70-17005

Binary cyclic coding schemes for multiplex spectrometry in terms of linear least mean square unbiased estimate
06 p1013 A70-17217

Adjustment process dynamics in digital adaptive system with task of ensuring minimum quadratic criterion for parameters using gradient search technique
08 p1480 A70-21017

Digital communications and circuits and components for GHz data rate capability, discussing modulation techniques and bit stream coding
08 p1462 A70-21258

Error probability upper and lower bounds determined for self synchronized binary PSK communication systems, presenting maximum-likelihood and Monte Carlo computer simulation
08 p1463 A70-21777

Computer-generated shaded flicker-free on-line digital video display, allowing superimposed vector graphics with light-pen interaction
09 p1640 A70-22033

Digital autopilot design using stochastic noise generator for synchronous random pulse sequence controlled by clock
09 p1720 A70-22418

Book on numerical control covering principles, electromechanical system using digital logic circuits, binary numbers and arithmetic, etc
10 p1854 A70-24023

Digital sampled-data loop of phase lock control containing digital zone error detector and digital frequency regulator with reversible counter as memory unit
10 p1833 A70-24085

Error probability degradation for digital satellite communication systems, employing multiphase signal sets distorted by bandlimited filtering
10 p1836 A70-24342

Satellite relayed integrated digital multiple access systems, discussing traffic handling, satellite positioning, demand assignment, etc
10 p1839 A70-24369

SIMCON digital simulation control system optimizing man machine interaction, noting capability to generate solutions with minimum computer memory
10 p1860 A70-24654

Digital control systems simulation on analog computer with digital logic, using conventional analog amplifiers and integrators
10 p1860 A70-24655

Ionospheric fine structure from ionograms, discussing probe and half automatic digital evaluation method
10 p1884 A70-25257

Optimal fixed digital control for handling wide range plant parameters uncertainty involving random disturbances and measurement errors
11 p2026 A70-26248

Binary-coded sequential acquisition spacecraft ranging system operating at weak signals using HF digital logic
11 p2009 A70-26252

Upper bound on system errors caused by quantization in multirate digital control system
12 p2204 A70-27841

Digital transition tracking symbol synchronizer improving SNR without lowering loop bandwidth
[JPL-TR-32-1488] 13 p2367 A70-29591

Digital coding systems operational capabilities, discussing arithmetic procedures and equipment types
14 p2554 A70-30678

Iterative cellular logical array for nonrestoring binary division
14 p2556 A70-30685

Digital guidance and control system, discussing communication device providing data transfer between airborne digital computer and control device
[AIAA PAPER 69-988] 14 p2615 A70-30771

Stripline skin effect in digital equipment transmitting fast rising pulses
15 p2708 A70-31828

High pulse repetition rate digital systems signal processing using Gunn effect diodes
15 p2710 A70-32583

Digital logic control of chromatographic system for measuring instrumental contributions to band broadening
16 p2855 A70-33120

Digital controller bits number determination to meet nominal controller coefficients accuracy requirements
16 p2867 A70-33304

Upper bound determination for errors due to signal quantization in multirate digital control system through state variable or z transform formulations
16 p2867 A70-33306

Algebraic computation of diagnostic tests for combinational digital circuits single gate failure detection and location
16 p2868 A70-33455

High speed MOS circuitry design with application to digital equipment, noting low power and high packaging density
16 p2887 A70-33456

Design and reliability of digital systems for hard cores of fault tolerant computers /hybrid-redundant systems/, discussing advantages over multiplexed systems
[JPL-TR-32-1490] 16 p2887 A70-33734

Computer controlled frequency surveillance system design and operation
16 p2871 A70-34052

Digital spectrophotometer with automatic continuous wavelength selection, sample feed, measurement and printout
16 p2914 A70-34098

Coherent digital communication systems optimal design based on unified theory, discussing tradeoffs between error rates, Doppler tracking capability and time and frequency division multiplexing
16 p2866 A70-34258

Interference free high speed monolithic digital integrated gate, determining current swing, lead inductances and switching times
17 p3048 A70-34587

Binary data system parameters sudden change detection by noisy observation based on Bayes criterion
17 p3056 A70-34856

Management program for digital data systems maintenance and repair
17 p3200 A70-35487

Start-stop dynamics as cost effective method for computerized testing of digital modules and subassemblies, providing static and dynamic capability
17 p3062 A70-35504

Aircraft digital interior communication systems, combining multiplexing techniques with solid state integrated circuits technology and systems integration
[SAE PAPER 700302] 18 p3216 A70-36813

LSI technology effect on digital circuits and systems designs
19 p3387 A70-37847

Concorde prototype 002 flight test data recording instrumentation, emphasizing digital system for quasi-static parameters
19 p3432 A70-38545

Magnetic tape instrumentation system installed aboard Hawker Siddeley Harrier for flight development, discussing digital format recording system
19 p3384 A70-38549

Digital frequency synthesizer design, operation and stability
19 p3390 A70-38581

Apollo digital Range Safety Command System for signal-crowded communications channels
20 p3605 A70-39497

Statistical information processing equipment, describing correlators and digital coding devices design for graphic form information transformation into binary code
20 p3594 A70-39919

Digital systems reliability improvement by redundancy at circuit and system levels
21 p3797 A70-40762

Digital bit synchronization phase locked loop steady state and transient performance in white Gaussian noise
21 p3802 A70-41352

- Book on digital electronics with engineering applications covering switching circuits and logic designs, integrated circuits, error correcting codes, information storage and control, etc
22 p3999 A70-42324
- Optimal binary and ternary signal system synthesis by information divergence procedure for communication channels with colored Gaussian noise
22 p3985 A70-42491
- Nonbinary redundant error correcting codes for improving TV transmission speed and fidelity
22 p3985 A70-42493
- Computer controlled tester for digital circuits, giving diagrams and operations flow chart
22 p3996 A70-42849
- Computer-based seismic data acquisition system using digital vibroseis process for eliminating low signal to noise ratio characteristics
22 p4038 A70-43092
- Digital recording system for body temperature telemetry from small animals, using FM transmitter implanted in peritoneal cavities
23 p4151 A70-44381
- Optimal adaptive digital autopilot design and operation, discussing linear differential equations of motion, algorithms, etc
23 p4215 A70-44504
- Onboard digital information processing, discussing applications to tactical missile guidance and manned vehicles
[AIAA PAPER 70-1230] 24 p4317 A70-45976
- Dynamic errors of digital converter for digit-to-digit compensation estimated by probability and information characteristics methods
24 p4340 A70-46404
- ### DIGITAL TECHNIQUES
- Moving targets automatic identification by radar signals digital processing, describing radar echoes properties, moving window detector system and circuits design
01 p0137 A70-10358
- Digital log-linear companding technique for nonuniform quantization of speech and image signals
01 p0044 A70-10784
- Integrated digital circuits for office type desk calculators based on machine concept
01 p0052 A70-11287
- Textbook on applied numerical methods covering interpolation, approximation, integration, matrices, etc, with emphasis on digital computer algorithms
01 p0132 A70-11306
- Secondary surveillance radar to operate autonomously with digital techniques and digital handling systems, discussing design and ATC applications
02 p0266 A70-11957
- AFC by digital phase lock loop consisting of zone error detector with phase quantizing circuit and discrete frequency regulator with reversible counter
02 p0258 A70-12542
- Sampled signal and associated sequence with identical Fourier transforms, noting applications to digital spectral analysis onboard spacecraft
03 p0449 A70-13538
- Digital microcircuits for one kva three phase DC-AC inverter control to generate sinusoidal 400 Hz output using HF bridge chopper techniques
04 p0628 A70-15340
- Radar and sonar data processing for display in command and control systems using digital technique, discussing processor configuration
05 p0828 A70-16189
- Computer controlled radar guided tactical missile system using digital techniques in performing target detection, acquisition, tracking and illumination
05 p0814 A70-16328
- Theoretical performance computation of on-line analyzer for radar echo detection by digital techniques
05 p0814 A70-16359
- Computerized statistical analysis of digital filters used to eliminate digital radar interference
05 p0822 A70-16530
- Radiation patterns of scanning antenna using digital phase shifters to obtain suitable phase distribution to move sidelobes into invisible region
05 p0822 A70-16676
- Displacement measurement using single reflecting phase grating
06 p1060 A70-17148
- Digital control valve for high speed aerospace blending, considering propellant and cryogenics applications
06 p0989 A70-18602
- Oblique radio ray tracing at 2-10 MHz and application to signal strength calculation, concentrating on digital techniques
07 p1230 A70-19162
- Digital cross correlator design for impulse response determination in linear systems, noting real time operation without software and storage problems
07 p1236 A70-20068
- Electromechanical graph digital reader for records of cardiovascular studies
07 p1224 A70-20197

- Digital differential analyzers improved speed and accuracy by extended resolution on Euler integration for differential equations solution programming
08 p1467 A70-21756
- Digital image processing applied to picture generation, intensity and geometric manipulation, spatial frequency operations and image analysis
[JPL-TR-32-1482] 09 p1682 A70-23507
- Digital wavemeter description using interferometer with parallel plates and automatic frequency readout for submillimeter band
09 p1652 A70-23658
- Direct digital control valves in fluid flow process evaluated for performance by analog computer simulation
09 p1613 A70-23684
- Optimizing control system design using fluidic digital circuitry and FM type transducers
09 p1614 A70-23690
- Digital controlled phase-locked loop in burst mode operation, comparing recovery characteristics with carrier and bit-timing recovery techniques based on statistical analysis
10 p1835 A70-24333
- Communication commercial satellite systems capacity in terms of telephone channels, using frequency modulation and digital methods
10 p1836 A70-24344
- Digital plotters operational characteristics, capabilities and applications
10 p1845 A70-24581
- Book on principles of pulse code modulation covering analog to digital conversion, sampling, quantizing, coding, etc
10 p1841 A70-24775
- Digital techniques application to military communication satellite systems, discussing 40 Mbps quadriphase modem, convolutional encoders, TDMA, etc
[AIAA PAPER 70-495] 11 p2002 A70-25488
- Collection of papers on digital signal processing covering digital filter synthesis, Fourier transforms, algorithms, etc
11 p2003 A70-25575
- Digital control program parameters synthesis to realize time optimality with pure delay for ensuring absence of auto-oscillations under steady conditions
11 p2022 A70-25577
- Controlled missile reentry trajectory through dense atmosphere, describing digital computer solution of differential equations of motion
12 p2314 A70-27768
- Pipeline fast Fourier transform signal processor for digital spectrum analysis of wideband radars
12 p2186 A70-27904
- Automatic image interpretation and classification using two dimensional digital Fourier transforms
12 p2193 A70-28106
- Radiation patterns of phased array scanning antenna using digital phase shifter, reducing peak sidelobe level
13 p2380 A70-29785
- Airphoto interpretation, discussing descriptive, digital and photographic methods of representing recognition process results
14 p2585 A70-30642
- Avionics and instrumentation, discussing digital techniques application to engine control, electronic head-up and head-down displays, radiation pyrometry, etc
14 p2589 A70-31338
- Radiograph images digital processing by linear and nonlinear position invariant techniques, obtaining contrast enhancement
15 p2706 A70-32569
- Digital logic techniques for pulse modulated radar systems, with application to controlling and timing waveforms for display
17 p3042 A70-34570
- Associative processor concept for air traffic control, discussing tracking and correlation problem
18 p3288 A70-36392
- Recent radar developments covering ground and shipborne systems, clutter suppression and computer techniques
18 p3228 A70-36658
- Three digit hydromechanical step type actuator drives with slide valve assembly for computer data sampling systems
18 p3216 A70-37071
- Long period duration digital sinusoidal voltage generator, presenting schematic diagram and theoretical and operational characteristics
19 p3385 A70-37376
- ILS glide slope calibration using optically projected digital codes as reference
19 p3464 A70-37912
- Neutron flux measurement in nuclear reactors based on logarithmic techniques and digital approach, discussing temperature effects compensation
19 p3427 A70-37939
- High resolution successive approximation voltmeters using digital carry to improve speed and accuracy
19 p3427 A70-38049

- Solid state, digital, Resonant Capsule Pressure Transducer based on natural frequency variation of aneroïd capsules by pressure induced curvature changes
19 p3430 A70-38520
- Data processing systems functions and composition for random data reduction during aircraft flight tests based on analog and digital techniques
19 p3430 A70-38524
- Random values statistical characteristics by digital methods, deriving errors as function of quantization parameters
19 p3432 A70-38705
- Crystal controlled digital frequency setting for microwave oscillators in mobile FM radio links with remote handling
20 p3596 A70-39162
- Lunar module digital autopilot design, considering attitude state estimator, reaction control system and thrust vector control
[AIAA PAPER 70-991] 20 p3668 A70-39539
- Automatic digital device for evaluating matrix determinants
20 p3591 A70-39788
- Aircraft capacitive fuel gage improvement by integration with flowmeter system, DC torquer display and digital techniques, considering other measurement principles
21 p3821 A70-40619
- Seven segment in-line digital readout circuit for binary-quinary decade counter, using resistance transistor logic
21 p3793 A70-40763
- Digital optical storage for information system components
21 p3823 A70-40852
- Space-to-ground link wideband digital laser communications system design and performance tests
21 p3787 A70-41331
- Digital radar receiver based on pseudo Bayes likelihood ratio algorithms
21 p3789 A70-41353
- Remote digital mean wind speed indicator with numerical display, using photoanemometer for airport application
21 p3831 A70-42247
- Digital frequency and phase flip-flop comparator for slave oscillators fine control by master frequency
22 p3996 A70-42819
- Mathematically defined curve incremental generation by computer, discussing parametric and non-parametric representations and digital differential analyzer technique
22 p3993 A70-43072
- Digitally controlled milling machine for complex aerodynamic profiles and prismatic blades
22 p4046 A70-43117
- Digital Doppler ambiguity resolution method for pulsed S-band radar, using integrating interval approach
22 p3992 A70-43592
- Phased array radar for missile defense, discussing development trends toward adaptive system logic control and microwave digital circuitry for signal processing
23 p4172 A70-44012
- Functions of two variables, using digital method for curve family modeling
23 p4166 A70-44350
- Estimation errors of multilevel modified digital correlator using auxiliary random noise for unbiased output
24 p4312 A70-46054
- Digital to analog converters for signal processing in CRT character and sweep generation, programmable power supplies, resolver positioning, shaft angle conversion, etc
24 p4320 A70-46083
- Digital PCM telemetry link coding techniques, discussing encoding-decoding complexity, and concatenated block scheme for channel
24 p4315 A70-46258
- ### DIGITAL TO ANALOG CONVERTERS
- Direct, indirect, quasi A to D digital transducers principles and features
06 p1073 A70-18596
- Digital-to-analog converter for voltage representation of signals in 2-4-2-1 binary decimal code
12 p2235 A70-27681
- Digital to analog converters for signal processing in CRT character and sweep generation, programmable power supplies, resolver positioning, shaft angle conversion, etc
24 p4320 A70-46083
- ### DIGITAL TRANSDUCERS
- Direct, indirect, quasi A to D digital transducers principles and features
06 p1073 A70-18596
- Surface acoustic wave delay lines using interdigital transducers based on piezoelectrics with applications in VHF and UHF signal processing
11 p2005 A70-26165
- Interdigital Rayleigh wave transducers piezoelectric coupling coefficient from bulk constants, permitting equivalent circuit parameters prediction
17 p3055 A70-35875

DIGITALIS

Serum calcium-digitalis synergism effect on dogs heart excitability, noting hypoxia role in arrhythmia production

17 p3026 A70-35325

DIGITIZERS

U ANALOG TO DIGITAL CONVERTERS

DIGITS

NT BINARY DIGITS

DIHEDRAL ANGLE

Supersonic flow in dihedral angle between intersecting wings and in space between parallel wings, using integrating wave equation by Volterra method

03 p0407 A70-13492

Secondary velocities analysis in turbulent boundary layer in dihedral interior based on turbulence anisotropy and effects on wall pressure gradient

03 p0471 A70-14354

Linear model of edge effect in supersonic gas flow past dihedral angle of intersecting wings, using Abel equations

15 p2672 A70-32127

DIHEDRAL EFFECT

U LATERAL STABILITY

DIHYDRIDES

Titanium and zirconium dihydrides room and higher temperature electrical resistivity, Hall effect and thermal expansion coefficients

08 p1517 A70-21149

Electron exchange coupling of Gd and Gd-Y alloy dihydrides from ESR indicating negative hydrogen ion entry

21 p3862 A70-41703

DILATION

U STRETCHING

DILATOMETERS

U EXTENSOMETERS

DILATOMETRY

Dilatometric diagrams of phase transformations at low temperatures in Re steels, studying dilatation coefficient behavior

05 p0862 A70-16201

Volt-watt sensitivity of dilatocapacitor types of thermal radiation receivers, noting low natural noise levels

07 p1284 A70-19815

Phase transformations in TiNi with equiatomic composition, using internal friction, electrical resistivity and dilatometry

13 p2435 A70-29499

Fe-Co alloys critical points during rapid heating, determining alpha-gamma phase transformations onset from dilatometric curves

18 p3275 A70-36203

Dilatometric investigation of Fe alloys phase transformations, determining magnetic field effects and Curie temperatures

18 p3276 A70-36206

DILUENTS

Combustion characteristics of blended droplets composed of monopropellant and diluent, using theoretical model to predict life histories

06 p1180 A70-18141

Diluent resins properties for blending with glass fiber reinforced high density polyethylene concentrate

16 p2935 A70-33353

Diluent molecules effect on polymers relaxation behavior at cryogenic temperatures from internal friction measurements, noting loss peaks shift

21 p3844 A70-42138

DILUTION

Maximum isovolemic hemodilution by volume substitution determined by plasma expanders infusion in dogs

10 p1821 A70-25083

DIMENSIONAL ANALYSIS

Correlation characteristics and dimensionality of speech spectra from statistical properties derived from continuous speech and summarized by covariance-matrix eigenvectors

02 p0237 A70-12324

Dimensional analysis for describing steel surface microcracks growth under uniaxial fatigue loading, using stress-intensity factor and crack extension concepts of fracture mechanics

04 p0770 A70-14879

Scale dependence and optimal sample dimensions for strength tests of brittle refractory materials

05 p0955 A70-17064

Heat conduction transient field problems in two and three dimensional isoparametric finite element solutions using Galerkin method

06 p1178 A70-17938

Coaxial fluid streams mixing within finite length tube based on dimensional analysis of aerodynamic noise generation, discussing subsonic and supersonic flows within ejector

13 p2474 A70-29080

Microstrip circuit design, obtaining dimensions by computer programs incorporating subroutine sets

14 p2561 A70-30922

Hypervelocity impact theory, discussing Euler hydrodynamic codes, projectile cratering dimensional analysis, self similar solutions, etc

15 p2823 A70-32785

One dimensional analysis of stress and strain concentration resulting from longitudinal impact of viscoelastic rods

17 p3185 A70-34965

Viscoelastic materials fracture strength as function of cut length, defect size and temperature

17 p3146 A70-35221

Orifice length-to-diameter ratio effect on spray mixture uniformity from unlike impinging jets

17 p3073 A70-35671

Kylston comet head diameter relation to brightness from photometric observations using north polar sequence stars as reference, noting camera, equipment and exposure times

19 p3526 A70-38784

Single phase flow problem in heated vertical prismatic channel, using dimensional analysis from conservation equations with boundary layer approximation

21 p3954 A70-42170

DIMENSIONAL MEASUREMENT

Michelson interferometer with movable mirror using laser beam to measure linear by counting fringes number, discussing design features

01 p0085 A70-10032

Length measuring systems based on Michelson type interferometers, laser sources, fringe counting electronics, ambient air compensation, fringe-inch conversion and digital display

01 p0108 A70-10418

Light curve and relative dimensions of eclipsing system V338 Herculis, from photoelectric measurements, discussing component stars

01 p0184 A70-10951

Light curves of Algol eclipsing variable AD Herculis and semidetached system relative dimensions from BV photoelectric observations

01 p0184 A70-10952

Automated inspection for defects and dimensions - Conference, Eastbourne, England, May 1969

01 p0105 A70-11394

Left ventricle wall forces and dimensional measurements during cardiac cycle based on stress-strain terms, including results for mitral, aortic and myocardial disease

02 p0238 A70-12512

Thickness measurement of nonmagnetic coatings on magnetic substrates taking into account surface roughness effect

02 p0302 A70-12672

Pressure-volume-temperature measurements on H, calculating fugacity coefficients

04 p0719 A70-15057

Artificial crystallization zones width measurement error during time intervals after cloud seeding by aircraft and solar reflection methods

08 p1538 A70-21110

Meteor trail angular dimensions determined by frequency scanning method involving minimum points on reflected signal characteristics

11 p2107 A70-25556

Heart dimension measurement by miniature implantable ultrasonic sonomicrometer, describing system design and operation

12 p2174 A70-26897

Economical inspection of numerical-control produced parts through critical dimensions determination and dimension measurement reduction

12 p2241 A70-27086

Radio meteor train initial radius determination, discussing radio echo observation method

12 p2309 A70-27977

Decreasing gravitational constant effects on secular earth figure and dimension changes using Clairaut equation

14 p2568 A70-30143

Dimensional measurements of nuclear fuel cylindrical specimens by scanning neutron radiographic negative with microdensitometer, taking into account specimen geometry and neutron cross section

15 p2735 A70-31769

Thickness measurement for thin films in inaccessible locations using scanning electron microscope, comparing accuracy with interferometric techniques

15 p2741 A70-32435

Holodiagram for making and evaluating holograms for large objects dimension, deformation and vibration measurement

17 p3084 A70-35004

High accuracy length measurement by fringe counting using laser interferometer

19 p3447 A70-38050

Solar disk dimensions and RF emission characteristics from eclipse observation and flux recordings, considering brightness temperature distribution and lunar edge diffraction effects

19 p3521 A70-38551

Characteristic dimensions of large and small scale atmospheric turbulence by meteor trails photographic observations, determining energy dissipation

19 p3526 A70-38790

Meteor trail angular dimensions determined by frequency scanning method involving minimum points on reflected signal characteristics

21 p3892 A70-41306

DIMENSIONAL STABILITY

NT SHELL STABILITY

NT STRUCTURAL STABILITY

Dimensional stability of nickel maraging steel at ambient temperature measured for applications as gage block materials

01 p0120 A70-10742

Low melt viscosity prepolymers of diallyl phthalate and isophthalate in mold encapsulation showing dimensional, electrical and mechanical stabilities under adverse environments

05 p0869 A70-16035

Fiberglass content effects on reinforced polycarbonates long term dimensional stability during compression and tension creep tests

12 p2259 A70-28298

Precision reliability indices for automatic dimensional control vibration-contact sensor

15 p2714 A70-31582

Beryllium mirrors optical performance, describing causes and effects of anisotropy and dimensional instability

16 p2904 A70-33146

DIMENSIONLESS NUMBERS

NT FROUDE NUMBER

NT GRASHOF NUMBER

NT HARTMANN NUMBER

NT LAVAL NUMBER

NT LEWIS NUMBERS

NT MACH NUMBER

NT NUSSELT NUMBER

NT PECLET NUMBER

NT PRANDTL NUMBER

NT RAYLEIGH NUMBER

NT REYNOLDS NUMBER

NT RICHARDSON NUMBER

NT SCHMIDT NUMBER

NT STROUHAL NUMBER

Parachute inflation dispersion studied by plotting dimensionless products characterizing incompressible flow process

01 p0006 A70-10849

Contacting metal surfaces thermal conductance prediction in vacuum, formulating dimensionless parameters in terms of properties, surface measurements and load/temperature conditions of contact

[AIAA PAPER 70-852] 16 p2932 A70-33919

Dimensionless heat transfer and resistance coefficients during stabilized nonNewtonian fluid flow in circular pipe

20 p3613 A70-40176

DIMENSIONS

NT DIAMETERS

NT FILM THICKNESS

NT HEIGHT

NT LENGTH

NT RADII

NT SCALE HEIGHT

NT TARGET THICKNESS

NT THICKNESS

NT WIDTH

Resilience coefficient of intermediate elements of threaded connection related to transverse and axial nut dimensions by least squares method

05 p0856 A70-17012

Weight-dimensions correlation for gas turbine engine/airplane optimization analyses, determining tradeoffs among performance, noise, drag characteristics, etc

[AIAA PAPER 70-669] 16 p2967 A70-33575

Hot gas pipe thermoelastic reduction factors, determining elastic support, material and dimensions

20 p3720 A70-39624

Space three dimensionality compared with Huygens principle via quantum mechanics, discussing past and current theories and empirical arguments

24 p4380 A70-45643

DIMERIZATION

Well depth determination for weak intermolecular potentials based on dimerization enthalpy measurement of rare gas atoms by mass spectrometry

03 p0527 A70-13299

DIMERS

Ar and nitric oxide free jets dimmer and cluster abundance dependence on nozzle diameter and reservoir temperature and pressure

09 p1733 A70-22907

Sunlight induced pyrimidine dimers formation in human cells in vitro, relating DNA lesions by 254 nm irradiation

24 p4304 A70-46139

DIMETHYLHYDRAZINES

Raman and IR spectra of unsymmetrical dimethylhydrazine and unsymmetrical dimethylhydrazine-d2 recorded in liquid and gaseous states

06 p1128 A70-17329

Odor threshold levels for unsymmetrical dimethylhydrazine/UDMH/ and nitrogen tetroxides

18 p3224 A70-36227

DIMPLING

Local axisymmetric dimple imperfection effects on buckling load of circular cylindrical shell under axial compression

[AIAA PAPER 70-103] 06 p1170 A70-18167

Lunar dimple /drainage/ craters formation mechanisms, considering analogous earth drainage craters associated with lava tubes
09 p1666 A70-22311

DIODES

NT AVALANCHE DIODES
NT CESIUM DIODES
NT CRYSTAL RECTIFIERS
NT GERMANIUM DIODES
NT JUNCTION DIODES
NT PARAMETRIC DIODES
NT PHOTODIODES
NT PLASMA DIODES
NT THERMIONIC DIODES
NT TUNNEL DIODES
NT VARACTOR DIODES

Schottky barrier diodes design for wideband radiometer mixers to obtain optimum noise performance and broadband operation by DC bias application
03 p0457 A70-13968

Generation-recombination noise theory extension to nonlinear devices applied to double injection diode in various operation modes
03 p0458 A70-14028

Diodes on cordwood module measured for stress during soldering, foaming and operation, describing methods for mounting semiconductor strain gages
05 p0854 A70-16036

Adjustable pulse delay circuit design utilizing slow switching action of storage diodes emphasizing thermal stability
05 p0820 A70-16343

Laser harmonic-frequency mixing techniques extended into IR with IR metal-metal point contact diode
06 p1083 A70-17944

Step-recovery diodes to shape pulses with steep leading and trailing edges noting transient processes
07 p1241 A70-19734

Schottky barrier diodes microwave power rectification efficiency, developing diode losses theory based on back capacitance, series and front resistance and knee voltage
08 p1474 A70-21274

Five resonator broadband frequency doubler design using charge storage diodes
08 p1475 A70-21280

Current-voltage characteristics and lifetime of thin film diodes on chalcogenide glass substrate with symmetrical and asymmetrical electrodes
09 p1647 A70-22751

Iterative solution for balanced diode modulator performance, obtaining output spectrum using Fourier transformation
10 p1849 A70-24232

Negative resistance and cut-off voltage of doped Si p-i-n diodes subject to deep acceptor levels
10 p1849 A70-24274

Magnetron diode current fluctuations in interelectrode space, considering cathode emission current amplification by various modes
10 p1853 A70-25164

Impact ionization effects in electric field domain on stability of current-voltage characteristics of Gunn diodes
11 p2020 A70-26813

GaAs vapor phase epitaxial growth characteristics noting applications to Gunn diodes
11 p2020 A70-26826

Epitaxial or bulk GaAs for Gunn diodes in high power microwave oscillators
11 p2021 A70-26828

Tensodiode effect in long plate-shaped semiconductors, noting bend direction effects on I-V characteristics
12 p2195 A70-27312

He-Ne laser focused beam effect on negative Si diodes base I-V characteristics
13 p2378 A70-29517

Gunn diode simulation with variable cross section, showing subthreshold and mode oscillograms
15 p2707 A70-31510

Analog simulation of frequency multipliers and dividers with step recovery diodes
15 p2709 A70-32467

Nonequilibrium charge carriers transient accumulation in p-i-n diode at superhigh injection levels
15 p2714 A70-32908

High power microwave pulse generation in SHF region, discussing use of boat-grown and epitaxial GaAs diodes
16 p2875 A70-33396

Thermal noise in space charge limited solid state diodes by Langevin equation, relating spectral intensity for open and short circuit voltage and current
16 p2878 A70-33694

Doped Gunn diode domain field width, nucleation and annihilation dependence on electron drift velocity
16 p2879 A70-34044

Frequency multipliers with charge storage diodes, examining recombination and hysteresis effects on performance
17 p3050 A70-34588

Switching circuit with Se diode, comparing I-V characteristics with Se rectifiers
17 p3054 A70-35411

Current oscillations of GaAs Gunn diodes over wide voltage range, discussing diode behavior dependence on polarity and applied voltage
18 p3230 A70-36197

Gunn phenomenon, discussing GaAs Gunn diodes preparation and applications
18 p3231 A70-36198

GaAs laser diodes thermal degradation, observing nature, extent and occurrence of permanent damage
19 p3446 A70-37818

IMPATT diode microwave oscillator with modulated bias current, discussing amplitude and frequency modulation sensitivity, thermal effects and load parameters
19 p3390 A70-38363

Gallium aluminum arsenide-GaAs laser diodes properties and applications for CW operation, discussing p-GaAs layer thickness effects
19 p3447 A70-38454

Semiconductor silicon power diodes nondestructive quality control, discussing optimal sampling procedures
20 p3595 A70-38969

Projected nuclear MHD system conditions, examining electrical measurements in K vapor with diode at atmosphere pressure and high temperatures
20 p3681 A70-40006

GaAs Gunn diodes design and fabrication, discussing material selection and operating heat removal
21 p3799 A70-41424

Secondary breakdown meter for semiconductor diodes and transistors with reverse base drive, utilizing I-V characteristics and voltage waveform
21 p3801 A70-42248

Electron beam interaction with external harmonic microwave field in planar diode gap, calculating electric field current and voltage distribution functions
22 p3995 A70-42396

GaAs point contact diodes quick response performance with glass-metal or metal-ceramic bases, obtaining Schottky-type rectifying barriers by half period currents
22 p3995 A70-42406

Gunn diode oscillators in domain suppression mode, showing dynamic I-V curve shape relationship to donor concentration and crystal thickness
22 p3997 A70-43128

Spectrum generator with step recovery diode multiplier, discussing line spacing, energy and phase coherence
22 p3990 A70-43485

Frequency measurement extension to 5 micron region by IR laser harmonic frequency mixing in point contact diode as multiplier chain
23 p4201 A70-44917

Impact ionization effects in electric field domain on stability of current-voltage characteristics of Gunn diodes
24 p4317 A70-45185

DIOXIDES

NT CARBON DIOXIDE
NT ENSTATITE
NT HYDROGEN PEROXIDE
NT PYROXENES
NT QUARTZ
NT SILICON DIOXIDE

DIPHENYL COMPOUNDS

Dicyclohexyl /DCH/ endothermic dehydrogenation to diphenyl /DP/ over platinum-alumina catalyst without added hydrogen considered for hypersonic aircraft engine cooling
14 p2546 A70-31175

DIPHOSPHATES

NT ADENOSINE DIPHOSPHATE [ADP]
Indirect ADP deamination and reamination of corresponding deamino form of inosine diphosphate in rabbit brain tissue
01 p0018 A70-10506

DIPOLE ANTENNAS

Impedance and radiation pattern of quarter wave monopole and half wave dipole antennas in isotropic plasma, considering plasma density role
06 p1117 A70-17372

Two port isotropic antenna excited by independent noise sources for uniform power radiation in all directions and polarizations
06 p1021 A70-17574

Dipole antennas current distribution in dissipative homogeneous medium
07 p1240 A70-19219

Impedance radiation pattern and actual height of receiving dipole antenna in magnetoactive plasma calculated by electrodynamic reciprocity theorem
08 p1472 A70-20970

Standing wave measurements on radiating traveling wave dipole arrays with glide symmetric excitation, showing multimode propagation and effect on log periodic balancing
09 p1633 A70-22688

Mutual coupling in arrays of log periodic dipole antennas in terms of impedance and admittance matrices
09 p1645 A70-22690

Square Van Atta reflector with/without conducting plate used for mounting antenna half wave dipoles, considering scattering cross sections
09 p1646 A70-22695

Vertical Hertzian doublet with large circular screen placed above earth, calculating radiation pattern, directive gain, efficiency and radiation resistance
09 p1637 A70-23152

Reactive portion of mutual impedance of arbitrary antennas calculated from radiation patterns by interpolation method
09 p1648 A70-23162

Radiation field of electric and magnetic dipole in double layer medium, solving Sommerfeld integrals
09 p1650 A70-23550

Superwideband dipole antenna array reproducing radiation patterns in horizontal plane for signal polarization
12 p2196 A70-27539

Input impedances of small vertical and horizontal dipole and loop antennas above conducting ground plane, noting effect of refractive index
12 p2196 A70-27714

Vertical tubular dipole antenna input admittance and current distribution above infinite dissipative half space
12 p2197 A70-27953

Log-periodic dipole /LPD/ antennas compressed along transmission-line axis, considering frequency dependent behavior in narrow bands and radiation pattern
12 p2198 A70-27955

Optimum scattering from linear array of half-wave dipoles at bistatic angle, employing coupled impedance loading network
12 p2198 A70-27958

Dipole and monopole antenna radiation patterns, considering effects of soil conductivity and elevation above ground
12 p2199 A70-27979

Cylindrical electric dipole antenna in magnetoactive ionospheric plasma, noting ion sheath effect on input impedance and active length
13 p2399 A70-29402

Infinitesimal dipole moving through hot uniform electron plasma in magnetic field, investigating asymptotic time behavior of plasma resonance
13 p2467 A70-29912

Radiation from electric dipole oriented normal to magnetostatic field in plasma column improving antenna transmission characteristic during reentry
13 p2467 A70-29913

Dipole antenna current distribution in ionized homogeneous anisotropic medium, using dielectric permittivity tensor
13 p2371 A70-29923

Javelin rocket measurements of ionospheric AC electromagnetic fields, determining amplitude/frequency spectra and dipole antenna performance
13 p2401 A70-29926

Double sphere dipole antenna detecting VLF electrostatic plasma waves, discussing induced and contact potentials
13 p2372 A70-29927

Synthesis of vertically polarized omnidirectional pattern with cascade dipole antennas on conducting cylinder
15 p2697 A70-31832

Medium wave thin cylindrical dipole antenna arrays design, discussing operating impedance determination
15 p2714 A70-32816

Dipole antenna arrays feeds design and performance for spherical aberration correction, discussing polarization mismatch
16 p2871 A70-32955

Backfire antennas allowing for mutual impedance between dipole elements, determining radiated field from surface current distribution
16 p2861 A70-32958

Current distribution on isolated thin cylindrical center-fed dipole antenna, calculating axial electric fields and radiating properties
16 p2861 A70-32964

Mutual impedance between coplanar skew dipoles with arbitrary lengths and terminal positions, noting convenience for computer programming
16 p2861 A70-32970

Nonuniform parallel element dipole array field patterns and synthesis by three term theory, taking into account current distribution effects
16 p2872 A70-32972

Dipole and loop antennas in isotropic compressible plasma under wave incidence, using reciprocity theorem for receiving voltages and maximum powers
16 p2957 A70-32982

Solid state dipole antenna array miniaturization by etching microstrip components on alumina substrate having high dielectric constant
16 p2876 A70-33409

Dipole antenna finite three dimensional array, calculating excitation patterns
17 p3042 A70-34589

Thin long dipole antenna, determining input admittances, current and charge distributions and field patterns by Wiener Hopf technique
17 p3051 A70-35060

Log periodic antennas, discussing dipole array and planar sheath spiral structures, base current and far field pattern calculations, etc
17 p3052 A70-35073

Boundary value problem of Hertizian dipole antenna in presence of conducting half space, analyzing lossy earth effects on input impedance and radiation pattern
17 p3044 A70-35074

Infinitesimal electric and magnetic dipoles embedded in lossy media, investigating earth effect on electromagnetic field
17 p3045 A70-35075

Center fed cylindrical half wavelength dipole antenna, computing radiation pattern by trigonometric expansion approximation for current distribution
19 p3388 A70-37869

Dipole antenna radiation in compressible anisotropic electron plasma overlying imperfectly conducting half space, solving for lunar environment
19 p3381 A70-38407

Dipole antenna radiation in compressible anisotropic electron plasma overlying imperfectly conducting half space, evaluating Fourier-Bessel integrals for lunar environment
19 p3381 A70-38408

Ionospheric plasma sheath effect around floating cylindrical high power dipole antenna, obtaining electron, ion and potential profiles
20 p3589 A70-40466

Two identical parallel arbitrarily located thin asymmetrical dipole antennas, calculating self and mutual admittances
21 p3800 A70-41945

Log periodic dipole antenna arrays, calculating HF performance and patterns in presence of ground
22 p3997 A70-43176

Infinite periodic phased array over ground plane with dipole elements in parallelogram lattice, calculating driving impedance and gain loss due to mismatch
23 p4172 A70-44004

Broadside-endfire array of cylindrical dipoles and monopoles driven by interconnecting transmission lines, calculating admittance and field patterns
23 p4176 A70-44955

Dipole antenna in compressible lossy plasma, calculating sheath and absorptive surface effects on current distribution from boundary value problem formulation
23 p4228 A70-44963

Skew arrays of coupled linear antennas, calculating planar and nonplanar configurations mutual admittance vs rotation angle between dipoles
23 p4166 A70-44969

Octave bandwidth unidirectional circularly polarized reflector antenna, using crossed conical dipoles near second resonance
23 p4176 A70-44970

Elevated horizontal and vertical electric dipole VLF fields, discussing ionospheric TE and TM mode coupling, nighttime variations and amplitude fluctuations
24 p4314 A70-46131

DIPOLE MOMENTS

NT ELECTRIC MOMENTS

NT MAGNETIC MOMENTS

Molecular hydrogen Lyman bands radiative transition probabilities, using electronic dipole moment functions
02 p0344 A70-12659

Molecular dipole moments-electric field interaction induction of cholesteric liquid crystal transition to nematic phase
07 p1225 A70-20053

Heart dipole moment calculation error due to deletion of individual electrode contributions to surface potential map, analyzing multielectrode grids
08 p1453 A70-21753

Power spectrum of light scattered by two level atom driven by monochromatic electric field obtained from atomic dipole moment correlation function
10 p1920 A70-24632

Geomagnetic dipole field disturbances by trapped particles, calculating self consistent equilibrium configuration for ring current dipole moments
15 p2727 A70-31905

Plasma velocity and moment equations in magnetic dipole field as function of variations along coordinate directions
16 p2956 A70-32934

Elastic materials consisting of particles with rotary inertia, long range force and dipole interactions, deriving constitutive relations
19 p3538 A70-37794

DIPOLARS

Dipole shielding tensor of atom in arbitrary time dependent field, giving conditions for general variational calculations yielding results
04 p0721 A70-14389

Geomagnetic field variations represented by optimal electric current loops or dipoles, noting advantages over spherical polynomials
07 p1266 A70-19442

Spherical harmonic coefficients of eccentric dipole potential and coinciding magnetic and mass center, noting geophysical prospecting applicability
11 p2047 A70-26571

Plasma resonance excitation by small pulsed dipole in weakly inhomogeneous plasma determined using WKB solutions and stationary phase approximations
12 p2277 A70-27188

Alouette plasma resonance stimulated perpendicularly to magnetic field by planar dipole charge sheet and permeable grids
13 p2467 A70-29907

Geomagnetic field variations represented by optimal electric current loops or dipoles, noting advantages over spherical polynomials
18 p3249 A70-36916

Computer program transforming spherical harmonic coefficients into arbitrarily tilted coordinate systems, tabulating coefficients of International Geomagnetic Reference Field 1965 in dipole coordinate system
20 p3621 A70-39353

Plane electromagnetic waves diffraction on thin filaments cloud/passive dipoles/, discussing field fluctuations and mean power
20 p3588 A70-40298

Mutual impedance of interacting dipoles at wedge tip, determining errors for short spacing distances
21 p3796 A70-40638

DIRECT CURRENT

Potential created by DC point source in ionosphere at high and medium geomagnetic latitudes, taking into account electrical conductivity anisotropy and altitude variation
01 p0080 A70-11225

Hall generator DC brushless motor operation and applications, obtaining motor action by rotor and stator magnetic fields interaction
02 p0228 A70-12053

Brushless DC motors speed regulation with electronic commutators, discussing photoelectronic, magnetic sensing and magnetic-coil commutation
02 p0229 A70-12616

Longitudinal pressure gradient measurement for DC discharges in He, Ne and Ar, investigating effects of gas purity, tube geometry, etc
04 p0671 A70-14995

Digital microcircuits for one kva three phase DC-AC inverter control to generate sinusoidal 400 Hz output using HF bridge chopper techniques
04 p0628 A70-15340

DC electric arc with superimposed axial subsonic gas flow breakdown voltage and anode heat transfer using high speed photography
06 p1177 A70-17697

Colloid engine efficiency operating with pulsed positive voltages and square wave and sinusoidal voltages
06 p1132 A70-18158

[AIAA PAPER 70-178] AC to DC converter design for transforming average AC values into DC voltage
08 p1438 A70-20601

Static power processing efficiency illustrated by application to DC to DC converters
08 p1439 A70-20704

Plasma finite DC resistivity quantum theory, considering electron-molecule collisions energy absorption, noise generation, etc
08 p1551 A70-21099

Signal converter for centimeter band-DC voltage transformation, noting applications to microwave power measurement by digital computers
09 p1650 A70-23629

DC capacitance measurement based on capacitor discharge using auto-oscillatory macrocharge system variant as transducer of measured capacitance, time constant and insulation resistance
11 p1982 A70-25576

He-Ne optical laser CW operation under DC excitation, considering output power, discharge current, total pressure, mixture ratio, etc
11 p2062 A70-25827

Brushless DC motor with rotor position sensor and transistor commutator for armature current switching, describing design and operation
12 p2165 A70-27525

DC signals measurement in automatic control circuits, ensuring transformer isolation by use of transistorized amplifier
12 p2196 A70-27682

Electromagnetic wave penetration in plasma under uniform DC magnetic field, considering wave propagational direction and electric field
12 p2279 A70-27781

Magnetically constrained steady state plasma production by hot cathode DC arc discharge in He
13 p2465 A70-29819

Ionospheric DC electric fields long period oscillations at high latitudes observed by polar orbiting Injun 5 satellite
13 p2403 A70-30081

SCAMP 3 program for calculation of electronic circuit DC performances statistical distribution as function of component parameters variations
14 p2560 A70-30666

Ripple filters for DC power supplies using reliable small capacitance capacitors suitable for spacecraft applications
15 p2714 A70-32806

High voltage DC electric power systems design for aircraft, considering filtering, transmission and loads interaction
16 p2844 A70-33475

Helium plasma ionization rate in positive column with DC discharge, considering gas pressure, electron density, electric field strength and plasma radius
19 p3476 A70-37559

Stationary DC discharge positive column in helium, determining production balance and loss of charge carriers
19 p3476 A70-37560

Satellite electrometer for weak DC currents due to charged particle flux
19 p3428 A70-38485

Brushless DC motor types and sources, describing electronic commutation, AC inverter and limited rotation torque
20 p3564 A70-39725

Modular DC to DC switching mode converter for space power system
21 p3758 A70-41217

Thin titania films electrical breakdown under high DC fields in high vacuum, suggesting reduction to lower order semiconducting oxide
22 p4085 A70-42621

Space DC electric field measurement by quadrupole probe, discussing geomagnetic field and contact potential effects
22 p4029 A70-42792

DC-to-DC converter design to supply different isolated voltages from single input
23 p4142 A70-43875

Fluidic networks nonlinear component AC and DC behavior, discussing Bernoulli equation, nonlinear resistances, transmission lines and various flows
23 p4142 A70-44296

External DC electric field effect on microwave absorption in plasma
23 p4226 A70-44372

DIRECT POWER GENERATORS

NT ALKALINE BATTERIES

NT DRY CELLS

NT ELECTROSTATIC GENERATORS

NT FUEL CELLS

NT HYDROGEN OXYGEN FUEL CELLS

NT MAGNESIUM CELLS

NT MAGNETOHYDRODYNAMIC GENERATORS

NT METAL AIR BATTERIES

NT NICKEL ZINC BATTERIES

NT PHOTOELECTRIC GENERATORS

NT RADIOISOTOPE BATTERIES

NT REGENERATIVE FUEL CELLS

NT SNAP 19

NT SNAP 27

NT SOLAR CELLS

NT THERMIONIC CONVERTERS

NT THERMOELECTRIC GENERATORS

Conducted interference on input power lines of AC to DC power supplies with diode rectification and smoothing capacitors predicted by Fourier analysis
01 p0049 A70-10089

High temperature solar energy converter cavity absorbers geometry, considering absorption parameters of radiation reflected by concentrator
01 p0010 A70-10761

Energy converters and radio transmitters for physiological telemetry, using electric power converted from thermal and mechanical energy of human respiratory activity
04 p0644 A70-15276

Static power processing efficiency illustrated by application to DC to DC converters
08 p1439 A70-20704

DC to DC switching power processor design considerations for avoiding system failures
08 p1439 A70-20705

Operation mode for full-bridge programmed waveform static inverter permitting saturation of power transistors in DC power conversion
08 p1439 A70-20707

Electrostatic energy converter load current analysis, deriving expression for space charge electric field with axially varying or constant charge distribution
10 p1808 A70-25036

Electrostatic generator with spatial charge neutralization for direct thermal-to-electrical energy conversion at high gas pressures
12 p2165 A70-27330

Electrostatic generator with spatial charge neutralization for direct thermal-to-electrical energy conversion at high gas pressures
21 p3760 A70-42071

Book on batteries and energy systems covering theoretical concepts, construction, operation principles, characteristics and applications of various types of primary and secondary cells
22 p3964 A70-42454

DIRECTION FINDERS [RADIO]

U RADIO DIRECTION FINDERS

DIRECTIONAL ANTENNAS

- NT DIPOLE ANTENNAS
- NT HELICAL ANTENNAS
- NT HORN ANTENNAS
- NT LENS ANTENNAS
- NT LOG PERIODIC ANTENNAS
- NT LOOP ANTENNAS
- NT PARABOLIC ANTENNAS
- NT RADAR ANTENNAS
- NT RHOMBIC ANTENNAS
- NT SLOT ANTENNAS
- NT STEERABLE ANTENNAS
- NT TWO REFLECTOR ANTENNAS
- NT YAGI ANTENNAS

Satellite tracking antennas servo design including adaptive and compensation methods and digital computer applications

Design methods for self steerable antenna arrays in unidirectional and two directional radio links

Rapid fading intensity distribution formula for analysis of aperture phase and amplitude errors influence on antenna arrays directional characteristics

High gain antenna for 1973 Mars Soft Lander data transmission using sensors and digital computer to achieve autonomous precision pointing to earth [AAS PAPER 69-578]

Asymmetrical and symmetrical directional couplers coupling characteristics during linear and exponential variations of coupling coefficient

Shell directional antennas operational behavior at 2 and 4 GHz and mechanical properties

Radiation patterns of scanning antenna using digital phase shifters to obtain suitable phase distribution to move sidelobes into invisible region

Deep reflector antennas mode composition by graphic computer techniques for maximum efficiency feed matches

High gain paraboloidal reflector antenna with horn feed for satellite and terrestrial microwave links

Paraboloidal- and spherical-reflector antennas efficiency optimization obtained from optimum combination of amplitude and phase of hybrid modes propagating in guide

Optimal linear antenna synthesis, determining current distribution resulting in specified radiation pattern for superdirective antennas

Current distribution determination necessary for given directional characteristic of antennas in non-linear synthesis problem

Antenna pattern synthesis with circular distributed current source, analyzing directivity characteristics through Fourier series nth order mode concept

Nonlinear synthesis for direction-finding plane antenna aperture

Materials/design optimization of antenna-aiming mechanism deployed on moon by Apollo 12 astronauts to transmit ALSEP experiments data to earth stations

Linearly tapered zigzag antenna of constant pitch angle observed for radiation and impedance characteristics

Radiation characteristics of horn antennas loaded with curved transverse dielectric slabs and radial dielectric strips, discussing axial directivity and half-power beamwidth

Microwave axicon with dielectric cone at aperture of focused antenna to reduce far-field radiation pattern beamwidth

Electronically tracking antenna system for satellite reception in VHF range suitable for unmanned receiving stations

Real time computer algorithm for achieving optimal position of tracking antenna with nonlinear control system

Superdirective small linear antennas computer aided design using Fourier integral and transform techniques

Automatic tracking antenna aiming errors, discussing remedies, design, motion compensation and mechanical resonance damping

Receiver for artificial satellite transmission and optical tracking time signals, using crossed dipole directional antenna

Reflector antennas analysis, design principles and uses, with emphasis on paraboloidal and spherical reflecting surface types

Traveling wave antennas, analyzing modal characteristics of various waveguiding structures

Leaky wave antennas, deriving radiation field distribution in terms of power leakage from interior by Sommerfeld integral and Kirchhoff-Huygens integration

Surface wave antennas, operated on guided wave mode parallel to interface and with radiation at discontinuities, calculating excitation and radiation characteristics

Digital computer controlled positioning of telemetry antennas for tracking spacecraft

Highly directive radio telescope antenna parameters in near zone, using focusing at minimum distance

Statistical directivity, radiation pattern, drift and dispersion of segmented traveling wave antennas

Linear and circular apertures sum and difference radiation patterns for minimum sidelobe power

S band telemetry antenna with electronic tracking and polarity diversity for remote location missile testing

Millimeter wave reflector antennas, considering various system designs, performance, pointing capabilities, limitations and applications

Uniformly and nonuniformly spaced microwave antenna arrays, investigating directivity function and gain characteristics dependence on spacing

Unidirectional tear drop radiation Archimedean spiral broad band frequency independent antenna using printed circuit with cavity

Directional microwave transmitter for 300 frequency division multiplexed telephone channels, discussing transmission quality, reliability, design and operation

Monopulse tracking antenna beam broadening by feed displacement defocusing in parabolic reflector

Octave bandwidth unidirectional circularly polarized reflector antenna, using crossed conical dipoles near second resonance

Feed voltages and directional gain maximization for loaded long thin-wire antennas with multiple excitations, using matrix methods

Nonlinear synthesis for direction-finding plane antenna aperture

Dual channel circularly polarized feed of monopulse tracking antenna system, noting axial ratio and gain and open loop mode autotragging

DIRECTIONAL CONTROL

NT THRUST VECTOR CONTROL

Gyrotheodolites application to azimuth determination, discussing use for directional control, photogrammetry in geodetic measurements, etc

Automatic aiming system for laser range finders using directional information carried by light beam transmission

Coherent light beams scanning and propagation direction control by acoustooptical method for laser applications

Laser beam deflection techniques for directional control of laser beams, noting applications to optical computer memories and active imaging and display devices

North-finding gyroscope applicability for directional gyros and stabilized platforms

Solid body control moments ensuring braking from rotational motion, finite orientation and angular velocity under minimum energy constraint

Antenna system with linear polarization direction electronically changeable in microsecond

Main rotor wake adverse effects on tail rotor directional control in low velocity wind

Light beam direction variation by crystal deflectors, examining changing internal reflection angle by applied electric field or mechanical stress

DIRECTIONAL STABILITY

NT GYROSCOPIC STABILITY

Probability theory for gimbal errors in directional gyroscopes under irregular rocking, using linearization of functions of random arguments

Pitch angle anisotropy instabilities of electromagnetic waves in space, discussing warm plasma, solar wind and Van Allen belts

Optimal and suboptimal aircraft lateral directional stability augmentation applying optimal control and model-following techniques

Opposing mode interaction effect on ring laser unidirectional emission instability, discussing homogeneous and inhomogeneous line broadening

Hovercraft wind directional stability and control by cam operated fin-tab assembly

Turbulence effects on lateral directional flying qualities, examining pilot task performance, control workload and compensatory behavior [AIAA PAPER 70-998]

Directional solar thermal field/sunlight effect on coupled nonplanar transverse and torsional vibrations of satellite cylindrical antennas in orbit

Manual attitude control for Lunar Module employing directional stability, coordinated turn and attitude command

DIRECTIVITY

Directional transponders for telemetry command, tracking and communications in retrodirective communication satellites

Directivity characteristics of planar antenna arrays with discrete identical elements and uniform phase progression

Uniformly and nonuniformly spaced microwave antenna arrays, investigating directivity function and gain characteristics dependence on spacing

Short cylindrical microwave antenna radiation directivity enhancement by optimum double impedance loading

EM radiation beams higher directivity from sources in two layer plasma in planetary atmosphere

DIRECTORIES

U INDEXES [DOCUMENTATION]

DIRECTORS [ANTENNA ELEMENTS]

Electronic narrow sweep antenna array active element number reduction, discussing optical considerations

Pencil beam synthesis for large circular array with arbitrary number of directive elements, determining optimum excitations

DIRICHLET PROBLEM

Algorithm for solving Dirichlet problem of nonlinear elliptical differential equations representing atmospheric dynamics balance equation

Dirichlet problem of biharmonic operator in boundary region containing infinite number of pieces

Cauchy-Dirichlet problem for linear inhomogeneous polycaloric/polyparabolic equation with constant coefficients under certain boundary conditions

Second order elliptic differential equations solution involving Dirichlet problem reduced to equivalent singular integral equations

Thin airfoil theory, discussing harmonic Dirichlet problem for complex plane

Geomagnetic field upward calculation in lower ionosphere, discussing accurate data acquisition difficulties in Dirichlet problem solution

Scalar plane wave LF scattering by prolate spheroid of revolution, obtaining iterative solution for Dirichlet problem

Diffraction on strip, investigating for Dirichlet boundary conditions, deriving excited current density and scattered pattern

Dirichlet problem for elliptic linear system of partial differential equations with constant first order coefficients

Geomagnetic field upward calculation in lower ionosphere, discussing accurate data acquisition difficulties in Dirichlet problem solution

Dirichlet problem for Tricomi equation emphasizing gap in boundary data

Cauchy-Dirichlet type mixed problems for hyperbolic equations in cylindrical domain, using Zygmund-Calderson approximate calculus

23 p4210 A70-43978
23 p4211 A70-44239

DIRIGIBLES

U AIRSHIPS

DISARMAMENT

Soviet SS-9 ICBM role in international debates over antiballistic missile, multiple independently targeted reentry vehicles, superhard silos and offensive forces

04 p0760 A70-14501

DISCHARGE COEFFICIENT

Statistical model equations to predict discharge coefficients for concentric orifice plates as function of line size, diameter ratio and Reynolds number [ASME PAPER 69-WA/FM-6] 04 p0667 A70-14837
Contraction coefficients for compressible discharge through axisymmetric sharp edged orifice, obtaining approximate analytical expression based on one dimensional theory

13 p2389 A70-29549
15 p2721 A70-32137

Rarefied gas mixtures efflux from opening at various pressures, calculating component discharge coefficients for molecular flow conditions

Transonic flow in convergent and convergent-divergent conical nozzles with nonuniform inlet predicted by time dependent flow equations, discussing discharge and thrust coefficients [AIAA PAPER 70-635] 16 p2834 A70-33548
Conical convergent nozzles discharge coefficient for varying pressure ratios 19 p3352 A70-38243

DISCHARGE TUBES

U GAS DISCHARGE TUBES

DISCHARGERS

NT STATIC DISCHARGERS

DISCOLORATION

Cotton leaves ammonia induced discoloration spectrophotometric examination, discussing light reflectance, transmittance and absorbance 22 p4014 A70-42771

DISCONTINUITY

NT SHOCK DISCONTINUITY

Geographically smoothed geomagnetic cut-offs for eliminating discontinuity in neutron monitor latitude variation in Mexico City vicinity 01 p0167 A70-10229

Particle trajectory and associated wave determined for nonclassical trajectory problem from nonprobabilistic point of view, discussing discontinuity arising from unbounded velocities 01 p0142 A70-10657

Dynamic stress concentration factor in strut containing symmetrically located elliptical discontinuity, using photoelastic technique with modulated ruby laser light source 02 p0388 A70-12495

Solar wind discontinuity surfaces observed by spacecraft magnetometers determined from measured time delays and solar wind speed 03 p0558 A70-13600

Two dimensional wave diffraction problems involving discontinuity line, analyzing instability behavior of geometrically induced singularities by applying integral transform on Helmholtz equations 03 p0525 A70-14199

Tangential solar wind discontinuity observed by Vela 2A satellite, producing ground magnetic disturbances conjunctively with magnetospheric, ground and ionospheric currents 05 p0903 A70-16727

Irreversible radiative energy transfer effect on stability of flow with two dimensional stationary infinite contact discontinuity 09 p1731 A70-22431

Discontinuous weak solutions of differential equations of gas dynamics as limits in topology of functions 10 p1866 A70-24109

Gasdynamic flows strong and weak density discontinuity surfaces determination, using shadowgraphs and interference patterns 12 p2238 A70-28248

Stationary hydrodynamic equations of gas channel and nozzle flow with inlet tangential discontinuities 16 p2833 A70-33247

Initial condition sensitivity functions in bang-bang and optimal control, considering discontinuous functions, perturbation equations, iteration algorithms terminal states, cost functions, etc 16 p2885 A70-33325

Elastic wave with discontinuities propagation, calculating decay velocities and stresses at leading wave front by theory of characteristics 17 p3189 A70-35436

F region small scale ionization discontinuities parameters observational data concerning anisotropy, dimensions, velocity and lifetime 18 p3246 A70-36088

Cu-Ni diffusion couples voids and edges effect on concentration gradients measurement by electron probe microanalysis 22 p4054 A70-42740

Wave front arbitrary curvature, examining integration of weak discontinuities growth equation in quasi-linear hyperbolic system 22 p4062 A70-42953

DISCOVERING

U EXPLORATION

DISCRETE FUNCTIONS

Radiative transfer in plane parallel atmospheres computed by discrete space techniques based on invariance concept for application to planetary atmospheres 02 p0338 A70-11825

Discrete statistical stellar system relation existence with continuous model proved by introducing unique volume concept for discrete systems 02 p0376 A70-12443

Discrete space theory for radiative transfer in one dimensional scattering media of arbitrary constitution 02 p0340 A70-12642

Discrete spectrum of fourth order differential operator estimating number of eigenvalues in bounded interval of real line 06 p1094 A70-17740

Primal and dual algorithms for discrete optimal control incorporating antijamming procedures 07 p1245 A70-19271

Dynamic discrete systems unsteady motions stability, formulating theorem for finite characteristic numbers existence 08 p1543 A70-20493

Discrete process max-min problem, using dynamic programming to obtain upper and lower bounds 08 p1533 A70-20604

One dimensional discrete time nonlinear filters synthesis using Bayes theorem and digital techniques 09 p1654 A70-22934

Continuous media geometry with given discrete structure reduced to analyzing relations between functions in denumerable set of points, presenting selected points of subregions 10 p1954 A70-24016

Discrete calculus of variations for optimal control involving use of discrete time sequence and functionals 10 p1910 A70-24702

Random fields entropy estimation technique taking into account higher than immediately adjacent spatial dependencies 12 p2192 A70-27771

Discretized linear theory of arbitrary shell forms 13 p2513 A70-29151

Discrete time systems, deriving algorithm for testing decomposition property as necessary condition for linearity 13 p2375 A70-29939

Soviet papers on discrete control systems covering linearity, nonlinearity and applications 18 p3233 A70-36068

Spectral densities of input and output signals of discretely continuous systems as function of comparison moment 18 p3233 A70-36069

Nonlinear stochastic discrete time processes prediction and filtering by Monte Carlo techniques 18 p3234 A70-36338

Linear multistep algorithms in discretization of nonlinear initial value problems of ordinary differential equations 18 p3283 A70-36366

Discrete signals synthesis optimal with respect to given criterion, determining ambiguity function extremum 19 p3374 A70-37270

Nonlinear discrete uniform approximation of real valued functions by gradient method 19 p3459 A70-38677

Information transmission techniques by discrete amplitudes and increments, comparing effectiveness for noise rejection 22 p3986 A70-42495

Maximum principle for discrete systems of recurrence equations, applying Pontryagin principle 22 p4073 A70-42696

Nonlinear automatic optimal control for discrete system with delay 22 p4005 A70-43563

DISCRIMINATION

NT BRIGHTNESS DISCRIMINATION

NT SENSORY DISCRIMINATION

NT TACTILE DISCRIMINATION

NT VISUAL DISCRIMINATION

Retroactive and proactive inhibition in verbal discrimination learning, using paradigms characteristic of paired-associate retention studies 03 p0435 A70-13768

Age discrimination in employment policies of air carriers, discussing legislative measures, hiring practices and retirement rules concerning stewardesses and FAA pilots 12 p2336 A70-27772

DISCRIMINATORS

NT FRAUNHOFER LINE DISCRIMINATORS

Wide range pulse height discriminator with milliwatt power drain for use in nuclear experiments on scientific satellites 01 p0088 A70-10749

Unsaturable frequency discriminator influence in semiconductor laser feedback loop on laser emission spectrum 08 p1514 A70-21821

Static error of varactor-controlled tuning-locked discriminator using computer 09 p1638 A70-23323

Probability density function of click duration in FM discriminator 11 p2018 A70-26270

FM limiter-discriminator followed with ideal band-pass filter, deriving output signal to noise ratio 14 p2558 A70-31189

Wideband PCM/FM discriminator detection, predicting effects of predetection and postdetection filtering on system performance 14 p2558 A70-31192

Asymmetrical transient attenuation effects of bridge circuit phase discriminator on accuracy of phase difference measurements 15 p2707 A70-31508

Transfer properties of scanning phase discriminator with intermediate storage, explaining sampling method and sample-hold-sample circuit 15 p2714 A70-32672

Frequency discrimination circuits for multiple remote control receiver systems with high harmonic noise levels 18 p3235 A70-36428

Automatic calibration verification of subcarrier telemetry discriminators with selective channel readjustment 19 p3383 A70-37902

Frequency discriminators output voltages under action of fluctuating signal and noise with arbitrary energy spectrum 20 p3584 A70-39254

Threshold output characteristic of FM signals, generalizing Gaussian baseband modulation solution to obtain autocorrelation function of output signal plus FM discriminator noise 24 p4313 A70-46063

DISEASES

NT AIRBORNE INFECTION

NT ARTERIOSCLEROSIS

NT ATELECTASIS

NT CANCER

NT CARBON MONOXIDE POISONING

NT EDEMA

NT EMPHYSEMA

NT EPILEPSY

NT FAT EMBOLISMS

NT FIBROSIS

NT HEADACHE

NT HEART DISEASES

NT INFARCTION

NT INFECTIOUS DISEASES

NT LITHIASIS

NT PARALYSIS

NT PULMONARY LESIONS

NT RADIATION SICKNESS

NT RESPIRATORY DISEASES

NT RHEUMATIC DISEASES

NT TACHYCARDIA

NT THROMBOSIS

NT TOOTH DISEASES

NT TOXIC DISEASES

NT TUMORS

Aerial color IR photography for crop disease identification by tonal and geographic patterns, discussing cameras, films, filters and exposure procedures 05 p0837 A70-16144

Flying disability period due to coccidioidomycosis in southwestern U.S., giving recommendations for earlier return to flying duty 06 p1000 A70-17300

Stomatologic diseases during prolonged space flights simulation, discussing gingivitis, stomatitis, dental caries, parodontitis and odontogenous inflammations 13 p2352 A70-29338

Long rhythms of periodic disparate heritable diseases in man 19 p3365 A70-38414

DISHES

U PARABOLIC REFLECTORS

DISINTEGRATION

Disintegration of charged distilled water jets, discussing drops size, velocity distribution and instabilities 03 p0467 A70-13781

DISKS

Monograph on integral calculation method for disk problems with mixed boundary conditions covering two dimensional stress-strain state, extrapolation methods, etc 11 p2140 A70-26474

Book on thermoelasticity covering thermal stresses in disks, plates, shells and bodies of revolution under steady and unsteady temperature fields 19 p3541 A70-37974

DISKS [SHAPES]

NT ACTUATOR DISKS

NT ROTATING DISKS

Laser beam technique applied to thermal shock testing of metal disks, using solid state laser, compared to predicted results

01 p0113 A70-11058

Turbine disk strength calculations, obtaining matrix expressions and optimum algorithm for arbitrary disk shapes

03 p0588 A70-13242

Disk stress concentrations calculation beyond elastic limits taking into account effect on bearing capacity

04 p0775 A70-15261

Forced torsional vibration of elastic stratum produced by rigid circular disk approximated by Fredholm equations

04 p0777 A70-15497

Unsteady temperature field of uniformly thick disk for inhomogeneous boundary conditions and small Fourier numbers solved by Laplace operation

05 p0958 A70-17013

Turbine disk strength calculations, obtaining matrix expressions and optimum algorithm for arbitrary disk shapes

08 p1580 A70-21657

Stress distribution in anisotropic disk shaped into wedge loaded at vertex by concentrated moment determined by complex potentials method

10 p1956 A70-24084

Steel conical disks two dimensional stressed state determined with deformations at elastic and elastoplastic strains using digital computers

10 p1956 A70-24242

Dynamic stresses, temperature and displacements fields in thin circular disk under transient heat sources, considering mechanical resonance vibration

10 p1958 A70-24518

Nonaxisymmetric free oscillations of self gravitating disk reduced to eigenvalue problem to investigate galactic spiral structures

10 p1917 A70-25207

Gasdynamic test stand analyzing elastoplastic strains in aircraft gas turbine disks and liquid-propellant rocket engines turbopumps under alternating nonisothermal loads

10 p1862 A70-25298

Pinhole expansion in anisotropic plastic disks determined by obtaining solutions for Tresca and Mises yield functions, assuming plane stressed state

11 p2138 A70-26171

Electromagnetic waves diffraction and scattering from acoustically soft and hard and perfectly conducting disks in plane or arbitrary incidence directions

15 p2701 A70-32414

Plane wave incident on oblate spheroid or disk, deriving LF field scattering

18 p3335 A70-35974

Anisotropic disk compressed by isotropic ring of smaller radius, considering elastic equilibrium

18 p3336 A70-36134

Turbine disk strength calculations, obtaining matrix expressions and optimum algorithm for arbitrary disk shapes

19 p3548 A70-38460

Boundary value problems in potential theory for electrical disk and spherical cap reduced to problems for two dimensional Laplace equation

20 p3657 A70-39446

Disk equations to determine tensions around arbitrary hole or stiffening contours

20 p3720 A70-39623

Incompressible Newtonian fluid laminar radial flow between parallel stationary disks, obtaining integral solution for Navier-Stokes equation

22 p4007 A70-42302

Radiation patterns and scattering cross sections of plane black disks excited by electromagnetic and acoustic waves

22 p3984 A70-42391

Comparative load capacity of disk models of natural gas blowers of different designs under plastic strain

23 p4232 A70-43941

DISLOCATIONS [MATERIALS]

NT CRYSTAL DISLOCATIONS

NT EDGE DISLOCATIONS

NT SCREW DISLOCATIONS

Dislocation climb theories of creep and superplasticity derived, postulating strain hardening and recovery processes with independently determined rates

02 p0317 A70-12315

Inhomogeneous deformation measurements in stress concentration zones using differential rasters in direction of distance between moire bands

03 p0588 A70-13248

Fatigue crack incremental propagation under cyclic shear loading, developing discrete dislocation model for crack and plastic zones

[ASME PAPER 69-WA/APM-7] 04 p0772 A70-14919

Planar dislocation array in displacement dependent stress field, investigating tip stress intensification regarding crack nucleation

05 p0932 A70-16170

Field theory of moving dislocations in Cosserat continuum considered incomplete regarding constitutive equations, basing analysis on Mie-developed mathematical analogy to electrodynamics

07 p1334 A70-19564

Static and shock kink bands in biotite deformed by metamorphism, meteorite impact, nuclear explosion and laboratory experiments

09 p1665 A70-22053

Dislocations maximal concentration during metal fatigue

10 p1955 A70-24081

Metallic materials damage accumulation and structural failures due to fatigue, considering surface changes, crack initiation and dislocation pattern

15 p2757 A70-31928

Solid state mechanics of deformable media, surveying development trends with emphasis on rheology and dislocation theory

15 p2818 A70-32176

Book on elasticity theory covering end effects, Saint Venant principle, edge and screw dislocations, moire method, thermoelasticity, cavity and inclusion effects, Muskhelishvili methods, etc

17 p1383 A70-34603

Imperfect solid deformation, presenting formalism for elastic theory nonlinear aspects of continuous distributions of dislocations and point defects

17 p3190 A70-35456

Orowan stress calculation, discussing line tension, screw or edge character, spatial distribution and yield strength

17 p3191 A70-35457

Soft metal and dilute alloy dynamic yielding, describing high dislocation mobility effects on mechanical properties

17 p3191 A70-35459

Inhomogeneous deformation measurements in stress concentration zones using differential rasters in direction of distance between moire bands

19 p3548 A70-38466

Elastoplastic work hardening continua incremental boundary value problem with allowance for distributed dislocations, using quadratic programming concepts

19 p3549 A70-38667

Al-Zn-Mg alloys structural transformations by diffraction electron microscopy, investigating grain boundary and dislocation structure as function of heat treatment and chemical composition

20 p3646 A70-39044

Duraluminum dislocation structure dependence on deformation temperature by electron microscopy, discussing subgrain boundaries

20 p3646 A70-39045

Dislocation network recovery kinetics of cold worked undoped powder metallurgical W wires by electrical resistivity measurements, determining activation energy

21 p3839 A70-40797

Maraging steels hardening mechanisms, discussing dislocations density and distribution and Ni, Mo and Co additives effects

23 p4208 A70-44919

Plastic deformation dislocation motion and incompatibility relationship, describing strain rate, velocity and stresses

24 p4420 A70-45229

DISORDERS

Carbohydrate metabolism disorders in head injury cases, comparing incidence with EEG abnormalities

10 p1810 A70-24037

DISORIENTATION

Spatial disorientation of human subjects in centrifuge, examining otolith role in reorientation and eye sensory mechanisms

22 p3976 A70-43707

DISPERSING

Temperature limit of efficiency threshold for ground based liquid propane sprayer for supercooled fog dispersal at Orly airport

02 p0324 A70-11872

Wastes dispersion discharged into sea analyzed by aerial photography, measuring diffusion

10 p1879 A70-24749

Polarized light scattering angle relationship with Mueller matrix elements for polydisperse systems of irregular randomly oriented particles

15 p2775 A70-32040

DISPERSION

Single dispersion statistical analysis by simultaneous parameters tolerances application

03 p0518 A70-12937

Dispersion and correlation function for atmospheric transparency due to water vapor, from statistical model of absorption bands and effective mass

06 p1053 A70-17204

Dispersion function and measured line profile distortion by rectangular detector slit of order scanning Fabry-Perot spectrometer

06 p1063 A70-17622

Dispersion equation harmonic analysis for three dimensional periodic structure

09 p1637 A70-23156

Dispersion function model based on mixed second order kinetics with distributed relaxation times

11 p2086 A70-25831

Dispersion/peak broadening in gel chromatography measured with nonporous and porous column packings, suggesting diffusion controlled separation with linear permeation isotherm

12 p2181 A70-27474

Dispersion relations for linearized Grad equations of three dimensional rarefied gas dynamics, including nonequilibrium pressure term for bulk viscosity

12 p2210 A70-27520

Radiant dispersion, position, areas and orbital axis in meteor showers by double-station photographic observations, noting Apollo group detection

21 p3884 A70-40875

Dispersion relations for linearized Grad equations of three dimensional rarefied gas dynamics, including nonequilibrium pressure term for bulk viscosity

21 p3807 A70-41168

Convergent numerical method for principal value integrals in dispersion relations of coupled channel scattering problem involving wave phase shifts

22 p4062 A70-42748

Isotopic decay rates, solving time dependent atmospheric turbulent dispersion from steady state measurements

22 p4093 A70-42915

Unguided rockets dispersion firing pattern and accuracy, discussing aerodynamic forces and ballistic coefficients

22 p4110 A70-43156

Sounding rockets dispersion, considering deviations from predicted point of impact due to wind effects, thrust vector errors and manufacturing inaccuracies

23 p4262 A70-44845

Natural dispersion effect on bandwidth of glass fiber transmission line using optical glasses

24 p4319 A70-46079

Gel permeation chromatography peak broadening, discussing liquid dispersion factors and column efficiency

24 p4310 A70-46349

DISPERSION PRECIPITATION HARDENING

U PRECIPITATION HARDENING

DISPERSIONS

NT AEROSOLS

NT COLLOIDAL PROPELLANTS

NT COLLOIDS

NT EMULSIONS

NT FOG

NT LIQUID-GAS MIXTURES

NT NUCLEAR EMULSIONS

NT PHOTOGRAPHIC EMULSIONS

NT PLASTISOLS

NT SMOKE

Reworking of deep-sea sediments as indicated by vertical dispersion of Australasian and Ivory Coast microtektite horizons, implying years of deposition

01 p0178 A70-10474

Surface interactions in incompressible dynamics and stability of ferrofluid with nonlinear magnetization properties

04 p0665 A70-14451

Vibration spectra, kinetic and dispersion equations of solid spherical particles moving in incompressible weakly viscous liquid

13 p2388 A70-29368

DISPLACEMENT

Normal and tangential displacements distribution at surface and along cross section of bar with free boundaries computed for symmetric and antisymmetric oscillations

02 p0301 A70-12484

Integral formulas of thermoelasticity theory for calculating displacements and rotations caused by temperature field action in micropolar Cosserat and Hooke media

02 p0391 A70-12817

Nozzle boundary layer displacement thickness at Mach 30-70 in helium using Langley hotshot tunnel tests

04 p0675 A70-15603

Dynamics theory of displacement on basis of equations of motion solution by stress functions

05 p0931 A70-16133

Shear stress in thick cylindrical closed shells subjected to plastic torsion determined from displacement distribution over thickness and generatrix

08 p1588 A70-21182

Stress and displacement distribution formulas for two and three dimensional crack extension problems in linear viscoelastic body

09 p1775 A70-22611

Linearly exact displacement and strain variations in transverse coordinate within shell structure

09 p1781 A70-23233

Stresses and displacements determinations in spherical shells under concentrated loads, considering transverse shear deformation effect

11 p2139 A70-26347

Semiinfinite composite medium displacement caused by nucleus of torsional strain with axis perpendicular to constituent isotropic layers interfaces

12 p2321 A70-27159

Indentation pressures in rigid perfectly plastic solids correlated with ratio between indenter strain and material yield strain for various indenter geometries

12 p2322 A70-27232

Iteration solution for three dimensional equations of equilibrium of elastic body in boundary displacements, discussing convergence rate and computer applications

12 p2272 A70-27553

Stressed state of infinite plate with circular hole induced by displacement discontinuity in form of cracks

13 p2514 A70-29292

Vector displacement numerical calculations for rectangular parallelepipeds of infinite and finite lengths

15 p2767 A70-32018

Shallow shells displacement theory, representing solution in terms of analytical functions

15 p2817 A70-32160

Small displacements in noncircular cylindrical shells under various loads

16 p2987 A70-32992

Displacements and stresses in freely vibrating aeolotropic deep spherical shells, including effects of shear deformation, rotary inertia and transverse normal strain

16 p2993 A70-34091

Solutions for normal and tangential displacements and concentrated forces on shallow cylindrical shells

17 p3186 A70-34969

German monograph on stress and displacement in plane elastic circular rings, disk strips and wedges, considering single load distributions

17 p3189 A70-35370

Shell theory for shear deformations in covariant notation involving displacement power series expansion

18 p3337 A70-36371

Pressurized shells of revolution loaded axisymmetrically, formulating equations for calculation of displacements, forces and stresses

18 p3338 A70-36406

Discrete element stress and displacement analysis of elastoplastic plates

18 p3342 A70-36686

Flexural vibrations of laminated composite plates, maintaining continuity of displacements and surface tractions at interfaces between reinforcing layers and composite matrix

19 p3537 A70-37790

Infinite linearly elastic solid response with random variations in material elastic properties, obtaining average energy in displacement field by method of moments

19 p3538 A70-37796

Stress and displacement within internally pressurized composite cylinders having continuous fiber reinforcement in circumferential direction, using finite element method

19 p3538 A70-37797

Electric dipole displacement of heart estimation by supplementing orthogonal with precordial lead, discussing stationary and moving point dipole hypotheses

19 p3369 A70-38209

Sandwich panels geometrically and physically nonlinear theory, obtaining equations of motion and boundary conditions consistent with strain displacement relations

19 p3547 A70-38360

Elastoplastic continua incremental solution for large displacements and small strains, determining sufficient condition of uniqueness

19 p3549 A70-38666

Compressible boundary layer equations with second order surface curvature and displacement effects

21 p3809 A70-41751

Displacement effect of hot-wire anemometric probes near wall as function of support orientation

22 p4038 A70-43241

Composite laminates under uniform axial strain, determining interlaminar stresses and displacements by finite difference techniques

22 p4060 A70-43684

Three dimensional elasticity for figures close to ellipsoid of revolution with displacements on boundary

23 p4266 A70-43988

DISPLACEMENT MEASUREMENT

Elastic sensor for measuring linear displacements using fine crossed filaments and torsion principle

03 p0485 A70-13482

Simple harmonic oscillator vibrations due to local random processes in spacecraft launching, calculating oscillator displacement variance

04 p0774 A70-15102

Beam fluctuations damping in beam waveguide, determining fluctuations cause as random displacement of lenses

04 p0651 A70-15290

Saint Venant torsion problem using finite element method, establishing direct matrix relation between forces and displacements

04 p0778 A70-15527

Stereophotogrammetric measurement for dynamic deformation of circular membrane subjected to underwater detonation

05 p0927 A70-16009

Displacement measurement using single reflecting phase grating

06 p1060 A70-17148

Displacement measurement to fractions of micron using laser interferometer

06 p1060 A70-17149

Displacement rate measurement in initial portion of blank subjected to explosive forming by capacitance pickup

06 p1076 A70-17868

Body displacement and deformation measurement by fringe separation in holographic interferometry

07 p1280 A70-19143

Holo-diagrams for simplified evaluation of amplitude and direction displacement in double exposed holograms for interferometric measurements

07 p1287 A70-20086

Mangler displacement thickness correction for slender cones

08 p1590 A70-21320

Grid shadow moire method to measure displacement contours of large plates, discussing sensitivity changes

11 p1311 A70-25589

Moire-holographic technique for deformed plane spatial displacements determination, describing diffraction patterns generation and stress analysis

11 p1240 A70-26487

Central shock and target displacement of underexpanded supersonic jets with obstacle at nozzle exit, using Toepler schlieren photographs

12 p1256 A70-27293

Displacement component in chosen direction on deformed object surface, using hologram interferometry with double illumination

13 p2409 A70-29475

Displacement sensor based on interference fringes counting by laser interferometry

14 p2594 A70-30683

Stress analysis for plate with large displacements by multicamera photogrammetry, comparing results with numerical solution by finite differences

15 p2821 A70-32313

IR radiating bodies angular displacement determination by vacuum evaporated thermocouple radiation detectors, describing stationary communication satellite altitude control

15 p2740 A70-32422

Displacement and velocity measurements using strain gauges, linear potentiometers and seismic transducers

15 p2743 A70-32799

Pressure transducer diaphragms displacement measurement by holographic interferometry

17 p3085 A70-35010

Optical correlator for displacement measurements using laser produced speckle patterns of scattered coherent light

17 p3088 A70-35026

Small swing angle detector for balloon payloads, using rate gyro principle

17 p3090 A70-35314

Deflection behavior of uniformly loaded elliptical elastic plates on elastic foundation, using small parameter perturbation technique

18 p3343 A70-36713

Damped linearly tapered cantilever beam elastically restrained against rotation at wall, analyzing displacement under general initial and distributed load conditions

19 p3539 A70-37802

Micropolar mechanics application to stress and displacement within separate components of fibrous composite material

19 p3541 A70-37961

Thin elastic shells displacement vector and strain boundary conditions determination from stress-strain relations

20 p3728 A70-39896

Holographic measurement of general forms of motion based on reconstructed images dependence on coherence

21 p3822 A70-40810

Fraunhofer holography for small spherical particles three dimensional position and velocity measurements

21 p3822 A70-40811

Multiple wavelength desensitized hologram interferometry to extend displacement measurement range

21 p3822 A70-40814

Thin circular plate clamped along edge, calculating large displacements and elastoplastic strains for comparison with measurement

21 p3935 A70-41406

Nondestructive measurement of elastic and plastic deformation in soldered joints and printed circuit boards by holographic interferometry

22 p4047 A70-43521

Various Frank loops in quenched and annealed Pt, examining dislocations with field ion microscopy and computer simulated approximations

23 p4230 A70-44758

DISPLAY DEVICES

NT ANEMOMETERS

NT APPROACH INDICATORS

NT FLOW DIRECTION INDICATORS

NT GYRO HORIZONS

NT HOT-WIRE ANEMOMETERS

NT MICROVISION LANDING AID

NT PLAN POSITION INDICATORS

NT POSITION INDICATORS

NT RADARSCOPES

NT RADIO DIRECTION FINDERS

NT SONIC ANEMOMETERS

NT SPACECRAFT POSITION INDICATORS

NT SPEED INDICATORS

NT TACHOMETERS

NT WIND VANES

Monograph on future air traffic control concerning radio navigation, color display and computer determined flight paths

01 p0136 A70-10090

Optical data display involving laser light deflection by vibrating mirrors actuated by mechanical resonators

01 p0108 A70-10355

Length measuring systems based on Michelson type interferometers, laser sources, fringe counting electronics, ambient air compensation, fringe-inch conversion and digital display

01 p0108 A70-10418

Duty factor and contrast in scanned displays, discussing light modulator and emitting displays

01 p0043 A70-10780

Real time recording and permanent display, using high power energy density focused Ar laser beam for ink transfer

01 p0111 A70-10782

Visual simulation limitations, discussing parallax error correction in display system, wraparound system, image generation, TV and motion picture film systems

01 p0036 A70-10813

Display systems used in space capsule window simulation for flight training, discussing erecting eyepieces, field of view and exit pupils

01 p0058 A70-10814

Hardware CRT display system based on digital computer for dynamic flight simulation of moving spatial objects

01 p0089 A70-10818

Line length effects on sequential blanking in visual perception demonstrated by computer-based CRT display and interpreted with information processing model

01 p0039 A70-11164

Visual flight displays technological and human engineering development

01 p0039 A70-11259

Electronic displays role in pilot-aircraft interaction, considering flight safety, cost effectiveness, onboard data input, etc

01 p0039 A70-11260

Information display - Conference, Arlington, Va., May 1969

01 p0048 A70-11276

Computer driven display terminal as part-task limited area simulator, examining operational requirements and input characteristics

01 p0059 A70-11277

Numeric keyboard CRT display for weather data acquisition from ships at sea, utilizing ATS-3 satellite as transmission medium

01 p0048 A70-11279

Digital computer display techniques relationship with man in modern environment, considering human engineering and educational problems and future impact on intellectual qualities

01 p0221 A70-11281

Operational planning system for Strategic Air Command for data accessing, generating, displaying and editing using computer complex

01 p0048 A70-11282

Moving map displays applications in marine and air navigation, discussing human factors and impact on ATC

01 p0139 A70-11284

ATC terminal displays procurement and use, discussing effects of traffic growth and FAA automation program

01 p0139 A70-11285

Display console characteristics for meeting increasing applications, predicting price reduction trends, color emphasis and CRT competition as primary display component

01 p0221 A70-11286

Electronic head-up display experience in transport aircraft flight tests including human factor, installation, operational applications, etc

02 p0224 A70-11836

Head-up display for horizon, desired and actual approach paths information to assist pilot during approach, landing and overshoot

02 p0330 A70-11842

Projected and head-up flight information displays using cathode ray tubes, discussing optical system, lens design and landing aid application

02 p0330 A70-11843

Dynamic structural analysis using computer graphics display, emphasizing applicability to man machine interaction at key decision making points

02 p0386 A70-11943

ATC display devices, discussing digital systems requirements, data storage, etc

02 p0331 A70-11962

Secondary surveillance radar (SSR) automatic plot extractors and display processors for providing information on aircraft height and identity for air traffic control

02 p0256 A70-11963

Alphanumeric label and vector scan converted bright display operation, characteristics and equipment, discussing line scanning method, visual storage, display phosphor problems, etc

02 p0256 A70-11974

TV raster scan display using CRT and beam steering scan systems, comparing alphanumeric capability for airport information and control problems

02 p0274 A70-11976

Aircraft navigation systems performance, discussing navigation aid integration by digital management computer coupling navigation sensors to display and control devices

02 p0334 A70-11984

Airborne computer civil navigation system designed for output coordination from navigation sensors

02 p0334 A70-11986

ALGOL Dynamic Display System for debugging and optimizing computer source language program, providing real time portrayal of static and dynamic block structure, etc

02 p0264 A70-12128

Adaptive man machine systems, display design - IEEE/ERS Conference, Cambridge, England September 1969, Volume 4

02 p0245 A70-12147

Display system for Apollo Telescope Mount designed for unclouded sun view by orbiting astronaut-scientists, discussing human factors, film budgeting, etc

02 p0298 A70-12151

Man machine digital display low cost system for displaying black and white image data with gray levels, color image data and dot patterns

02 p0265 A70-12152

Display system utilization for diverse graphical operations, discussing interactive tasks and tradeoffs

02 p0265 A70-12153

Vigilance of human monitors detecting additions and deletions of relevant and irrelevant signals presented on computer matrix display

02 p0246 A70-12377

Color coding effects in compatible and noncompatible display control arrangements

02 p0247 A70-12381

Autostereoscopic display using vibrating varifocal mirrors, including laboratory computer generated real time image and movie projection systems

02 p0302 A70-12631

Small read-out stations for automatic picture reception from meteorological satellites, detailing design

02 p0382 A70-12648

Display devices for ballistocardiographic test data obtained from professional pilots free of cardiovascular disease subjected to displacement and acceleration

02 p0247 A70-12676

Lidar technique capabilities and limitations in meteorological applications, emphasizing data storage and display instrumentation

03 p0450 A70-13673

Cockpit information transfer between pilot and flight control information displays improved by on-board data processing system

03 p0436 A70-14021

Three dimensional display of human body surface potential distributions as diagnostic tool of cardiac abnormalities

04 p0641 A70-14557

Black and white roentgenograms conversion to full color and three dimensional CRT radiograph displays, incorporating electronic data processing circuitry

04 p0641 A70-14560

Computer method to combine autofluorescence data to produce three dimensional display of absorbed radioactive material from multiview images

04 p0686 A70-14563

Variable anamorphic motion picture system to produce visual display for use with flight simulator [ASME PAPER 69-WA/BHF-8]

04 p0642 A70-14852

Cockpit display system to reduce aircraft pilot workload and aid judgment making during critical operations [ASME PAPER 69-WA/BHF-12]

04 p0642 A70-14854

Scanned CRT display optimum spot size in relation to raster pitch, assuming Gaussian luminance distribution

04 p0691 A70-15136

Pilot visual information display systems influence on flight safety, discussing aircraft accidents and human error factors

04 p0691 A70-15143

Display storage tubes /DST/ for radar systems, describing operating principles and characteristics

04 p0660 A70-15525

VTOL flight investigation to develop decelerating instrument approach capability with control-command information display for three degrees of freedom

[SAE PAPER 690693]

05 p0792 A70-15862

Gigacycle correlator involving sampling oscilloscopes for real time display of correlation functions over adjustable time interval, discussing design and performance

05 p0847 A70-16066

Human macrosaccadic eye movements related to four dial display conditioned by concurrent variable interval schedules of signals

05 p0800 A70-16127

Displays for command and control centers - NATO/AGARD Conference, Munich, November 1966

05 p0826 A70-16176

Command control systems characterized as problem solving information processing systems, discussing information requirements specification prior to man-display design

05 p0806 A70-16177

Command and control display operational requirements within Allied Command Europe /ACE/, information flow, decision making and evaluation

05 p0959 A70-16178

Operational/technical system improving air traffic control services efficiency by increased utilization of automation, displaying radar information and synthetic air situation presentations

05 p0827 A70-16179

Display Oriented Computer Usage System /DOCUS/, discussing on-line display console management in multiaccess environment, display oriented language, compiler, etc

05 p0817 A70-16181

BR-90 visual analysis control as flexible and versatile display for command and control, discussing on-line data processing, maintenance, etc

05 p0827 A70-16182

Systems concepts in design of computer operated display systems in air defense and air traffic control systems, discussing alphanumeric display, panoramic display, etc

05 p0827 A70-16183

CRT display design for command and control with digital symbol and vector generation

05 p0817 A70-16184

Computer generated displays and USAF equipment design for operational command and control systems, discussing Ag halide film technique

05 p0847 A70-16185

Electroluminescent matrix displays, discussing limitations in control element

05 p0827 A70-16186

Ferroelectric control circuits controlling electroluminescent cells in matrix, pointer, bargraph, alphanumeric and other displays

05 p0827 A70-16187

Projection display methods using scanned and modulated multicolor laser beams, discussing beam generation, modulation and scanning

05 p0858 A70-16188

Real time large screen display systems operation, brightness, accuracy, resolution, contrast ratio, data rates, reliability, fail-safe and management functions

05 p0828 A70-16190

STRIDA II consoles operation for treating air defense data, discussing data display system, work positions organization and console construction method

05 p0828 A70-16192

Large wall display system for USAF command and control with central computer and seven color projector, discussing hardware and operational features

05 p0828 A70-16193

Display/control system and key technical decisions at Manned Space Mission Control Center, discussing command consoles

05 p0829 A70-16194

Computer display graphic technique for business decision making, noting electronic aids

05 p0959 A70-16451

Information display devices, discussing interactive graphic consoles, reusable film, magneto-optics, broadband laser, etc

05 p0851 A70-16725

Aircraft visual flight control displays development, considering liquid crystals in alpha numeric data output devices and holograms for three dimensional structures reproduction

05 p0853 A70-17090

Flight deck controls and instrument disposition in business aircraft emphasizing size

06 p1061 A70-17318

Flight deck displays based on digital computer providing signals for CRT and instrumentation

06 p1061 A70-17319

Communications and displays - Conference, North Hollywood, August 1969

06 p1005 A70-17342

Digital and analog large system data displays, considering CRT, laser, hybrid types, contrast control, etc

06 p1061 A70-17348

Color CRT system to display engineering data based on real time analysis, discussing performance requirements

06 p1061 A70-17349

Electronic sine-cosine converters construction in devices for visual display of hydroacoustic transducers radiation patterns

06 p1064 A70-17773

Multichannel magnetograph display for pattern recognition of solar feature morphology compared with spectroheliograms

06 p1142 A70-17993

Holographic recording and reconstruction for wide angle three dimensional displays noting limitations

07 p1287 A70-20085

Enhanced real time operational impact and casualty analysis /ERIOCA/ for range safety, discussing computer-driven CRT display and missile flight parameters selection

[AIAA PAPER 70-247]

07 p1251 A70-20371

Flight test evaluation program for airborne multisensor electro-optical display systems performance in TV mode under variety of optical conditions

07 p1289 A70-20403

Collision avoidance system /CAS/ cockpit display equipment design and operation

08 p1492 A70-20480

Electronic displays and flight control system of Multi-Role Combat Aircraft developed by Germany, Italy and UK

08 p1493 A70-20631

Aircraft gas discharge displays, discussing segmented alphanumeric annunciator devices with field effect electroluminescent elements and incandescent lamps

08 p1493 A70-20671

Alphanumeric and graphic computer driven CRT displays, discussing systems and component selection

08 p1465 A70-20672

Light beam deflection for three dimensional fixed and time varying visual displays, discussing mechanical, acousto-optic, electro-optic, digital and holographic techniques

08 p1449 A70-20673

Attack aircraft cockpit displays, discussing design requirements and pilot ability as controller

08 p1435 A70-20674

Optical suitability to pilot visual requirements in head-up displays, discussing telecentric viewed system permitting binocular disparity tests

08 p1449 A70-20675

Machine-plotted pseudo three dimensional turbocharger rotor whirl display, discussing amplitude and frequency

08 p1496 A70-21300

Display design for improved target detection performance taking into account human attention to display field areas

08 p1452 A70-21301

Digital data display system designed for central station of German ground station system

08 p1462 A70-21369

Display media - Conference, Cambridge, Mass., September 1967

08 p1498 A70-21676

Computer managed display system using CRT and appropriate solid state displays providing flight crew with automatically sequenced time varying information

08 p1498 A70-21677

Control display requirements for manned spacecraft, integrating human operator with vehicle control system and determining man machine relations in stabilization, control and guidance

08 p1498 A70-21678

Workload relieving displays and controls for general aviation, discussing feasibility of digital computer driven integrated displays

08 p1601 A70-21679

CRT display devices and R and D, discussing electron generation, luminescent materials, resolution, brightness, etc

08 p1498 A70-21680

Carrier injection luminescence properties useful for display medium applications, discussing group II-VI compounds as injection host crystal materials

08 p1557 A70-21681

Thermochromic materials feasibility for applications in CRT display devices, observing reversible color changes during electron beam irradiation

08 p1499 A70-21682

Fluidic display, discussing applications for fluidic computers and control systems

08 p1441 A70-21684

Magnetic display devices covering magneto-optical displays, magnetic-electrostatic technique combinations and ferromagnetography

08 p1499 A70-21685

Display devices using electrostatic forces, discussing electrostatic printing, magnetic display system, etc

08 p1499 A70-21686

Laser display systems, discussing mechanical, diffractive and refractive beam deflection techniques, electro-optical polarization devices, holographic displays, etc
08 p1499 A70-21687

Plasma display system characteristics and history, discussing gas discharge cell construction and behavioral mechanisms
08 p1499 A70-21688

Electroluminescent displays design capable of generating all primary colors in single compact element
08 p1499 A70-21689

Display media development and implementation from engineering psychology viewpoint for information transfer in form compatible to sensory-perceptual capabilities
08 p1447 A70-21690

Visual display media requirements of future high performance vehicles, considering spacecraft and aircraft
08 p1499 A70-21691

Aircraft electronic attitude display indicators using symbology generation to combine several flight monitors indications
08 p1500 A70-21737

Integrated display for crowded tactical aircraft cockpits, presenting multisensor information for weapons and fire control systems
08 p1500 A70-21760

Display objectives and relationships to recording techniques examined for memory/display system, considering requirement for elastic erasing technique
08 p1467 A70-21761

Display devices luminance and luminous efficiency measurement as function of angle
08 p1500 A70-21762

Resolution, contrast and gray scale performance of CRT displays compared to dot matrix displays
08 p1500 A70-21763

Solid state IC-compatible display devices optical, electrical, mechanical and thermal characteristics
09 p1642 A70-22018

CRT color displays advantages and limiting factors, considering beam-penetration tube with high voltage switching
09 p1673 A70-22031

Fluidic logic elements to control firing and extinction of plasma matrix display system cells with constant electrical power supply
09 p1673 A70-22032

Computer-generated shaded flicker-free on-line digital video display, allowing superimposed vector graphics with light-pen interaction
09 p1640 A70-22033

Projection CRT with liquid-cooled phosphor faceplate, showing linear relationship between brightness and beam current
09 p1673 A70-22034

Apollo mission simulation, discussing Command Module Simulator /CMS/, onboard computer system and dynamic visual presentation via infinity- optics display
09 p1655 A70-22226

Computer-generated holography involving three dimensional object perspective projections computation for incremental rotations
09 p1683 A70-23529

Fluidic logic elements for controlling selected cells extinction in hybrid plasma-fluidic display
09 p1738 A70-23758

Temperature limitation on CRT tube performance in high brightness displays imposed by glass breakage danger, discussing liquid cooling of phosphor substrate
09 p1686 A70-23759

Textured gray-scale imagery by computer simulating lunar display
09 p1642 A70-23771

Alphanumeric solid state displays with vertically stacked character rows for text format reading, using injection electroluminescence technology
10 p1846 A70-23882

Light-emitting integrated circuit semiconductor display devices with inherent memory permitting logic and optical output functions performed on surface
10 p1846 A70-23883

Human operator transinformation sensitivity to display gain and forcing function bandwidth in rate control tracking task
10 p1823 A70-23896

Real time wide angle multicolor scanned laser display for visual flight simulators, utilizing flying-spot camera and rotating optical polygons
[AIAA PAPER 70-361] 10 p1857 A70-24203

V/STOL cockpit three degree of freedom multicrew research simulator, utilizing visual display and digital computer
[AIAA PAPER 70-356] 10 p1858 A70-24207

Amplitude and Rotational 3-Axis Flight Simulators for handling qualities research, outlining physical constraints and methodology for driving visual display and motion systems
[AIAA PAPER 70-353] 10 p1858 A70-24210

Aircraft flight displays, simulating low altitude high speed mission by four degree of freedom Dynamic Flight Simulator
[AIAA PAPER 70-343] 10 p1859 A70-24216

Data display systems parameters and functional elements, considering resolution, brightness, contrast, command and control, storage, etc
10 p1889 A70-24576

Digital plotters operational characteristics, capabilities and applications
10 p1845 A70-24581

Functional visual field selective process, studying performance as function of display angle
10 p1827 A70-24769

Symbols design for machine displays based on Gestalt pattern perception theory, considering symbol learning, perceptibility, detail, boundaries, etc
10 p1827 A70-24771

Spatial and amplitude modulators for laser-photochromatic display system producing real time TV pictures or images
11 p2062 A70-25734

CRT displays for business aircraft emphasizing EADI/electronic attitude director indicator/
[SAE PAPER 700210] 11 p2079 A70-25882

Business aircraft fuel management system using capacitance and mass flow rate measurements, displaying fuel quantity and flow rate and flight time remaining
[SAE PAPER 700225] 11 p1983 A70-25896

Nonimaging remote sensor data display in spatial registration with ground scene to determine sensor boresight position accuracy
12 p2229 A70-26940

Two dimensional remote sensing displays based on diffraction patterns generated by coherent light, discussing optical processing of photographs, drawings, maps, etc
12 p2229 A70-26944

Computers graphical display devices for rapid designer-computer communication
12 p2191 A70-27013

Holographic dynamic head-up display system for aircraft carrier deck landings in low visibility
12 p2232 A70-27371

Current-sensitive single gun color CRT with phosphor screen for display systems
12 p2195 A70-27373

Direct view storage tube /DVST/ as graphical display unit for small digital computer installation
12 p2232 A70-27374

Acoustographic imaging system /AGIS/ using liquid crystal detection screen to provide color display of ultrasonic wave information
12 p2235 A70-27724

Human detection capability for objects on electro-optical imaging displays calculated as function of SNR, viewing distances and brightness levels
12 p2236 A70-27903

Course deviation indicator /CDI/ display applicability to tracking Omega lines of position, providing reduction in weight, volume, cost and complexity
12 p2269 A70-27920

Chrysler lunar vehicle design featuring flexible metal wheels and Ackerman front wheel steering, noting back-to-back seating and centrally mounted control display panel
12 p2208 A70-27947

Cockpit data monitor allowing pilot selection of instrumentation parameter readout
13 p2345 A70-28970

Tactical aid displays /TAD/ for lightweight multisensor airborne ASW localization missions, discussing mission planning, avionic design, operator direction airborne tactical decision structures, etc
[AIAA PAPER 70-517] 13 p2407 A70-29036

Pictorial display area navigation system for air traffic control in terms of cockpit utilization, interface with ground navigation aids, parallel multiple routes, etc
[AIAA PAPER 69-798] 13 p2449 A70-29171

Semiconductor alphanumeric multicolored displays, discussing phosphor coating of GaAs diodes
13 p2408 A70-29217

Visual acuity determination by tape with staggered squares rotating behind screen with window
13 p2350 A70-29298

Vibrotactile display operational skill acquisition, discussing stimuli quality and spacing effects on lumen of temporal ordering of sensory events in haptic space
13 p2354 A70-29596

Compensatory tracking task with tactile displays determining gains and body locations by describing function and error power analyses
13 p2354 A70-29599

Digital signals conversion into command and control TV displays in multiconsole systems
13 p2411 A70-29789

Virtual infinity CRT display systems testing, discussing effects of large apertures, operational modes and observer physiological requirements on measurements
13 p2411 A70-29790

Holographic display requirements anticipating applications to motion pictures and TV
13 p2411 A70-29791

Real time signal processor for correlation and spectrum analysis, displaying results on cathode ray oscilloscope
13 p2370 A70-29817

AC and DC driven gas discharge aircraft displays, discussing capabilities and applications
13 p2412 A70-29875

Visual display reference system rotation effect on control quality and tracking error compensation using stick signal control
14 p2540 A70-30249

Civil aircraft altitude display design, anticipating application to supersonic transport
14 p2582 A70-30287

Avionics and instrumentation, discussing digital techniques application to engine control, electronic head-up and head-down displays, radiation pyrometry, etc
14 p2589 A70-31338

Passive optical crossed beam detection systems monitoring meteorological parameters in rocket or aircraft environments, noting real time display
15 p2736 A70-32032

Laser color TV display acousto-optic deflectors equalization using prisms
15 p2751 A70-32043

Visual IR laser beam displacer, using cathode ray tube phosphor with variable sensitivity and range control
15 p2752 A70-32441

X ray inspection with direct TV viewing, discussing specimen geometry effects, equipment, applications, etc
15 p2742 A70-32778

Dual raster high brightness-high resolution TV display using time sharing with conventional CRT
16 p2903 A70-33131

Holographic data storage for random information display and retrieval in wide range consumer credit network
16 p2903 A70-33135

Real time angular readout system for declination axis of U.S. Naval Observatory six inch transit circle, using Inductosyn as basic transducer
16 p2906 A70-33176

Foreground presence for computer generated and painted three dimensional photographic displays using fly eye lenses
16 p2906 A70-33177

Solid state electroluminescent phosphor displays for aircraft/spacecraft instrument panels
16 p2906 A70-33178

Drosograph high brilliance display device for rapid line-pattern projections and optical signal processing
16 p2906 A70-33179

Real time video data display at visual and thermal IR wavelengths, demonstrating performance improvement for target recognition
16 p2910 A70-33436

Human factors requirements for effective utilization of electronic reconnaissance displays, noting SNR and TV lines over target effects on performance
16 p2851 A70-33459

Display-control relationships in visual display information processing, considering spatial incompatibility effects on reaction time
16 p2852 A70-33661

Electronic pulsarium displaying flashing or beeping properties of pulsars
16 p2911 A70-33795

Electronic attitude director indicator /EADI/ integrated vertical situation display, noting information volume and TV format flexibility
16 p2911 A70-33817

Low cost headup displays /HUD/ for pilot error reduction during takeoff, approach and landing, discussing displayed functions vs cost tradeoffs
16 p2911 A70-33818

Head up display /HUD/ flight tests, examining effects decreasing quality of manually handled instrument approach, discussing space myopia and disorientation
16 p2912 A70-33819

INTIC tube memory image intensifier with contrast enhancement, describing design and performance
16 p2880 A70-34269

Metal grid capacitive memory for INTIC and direct view storage tubes, describing image contrast control
16 p2880 A70-34270

Digital logic techniques for pulse modulated radar systems, with application to controlling and timing waveforms for display
17 p3042 A70-34570

CH-47 cruise guide indicator for displaying fatigue loading to pilots, discussing design and operation
17 p3082 A70-34705

Heavy lift helicopters cockpit display problems, describing photographic flight research program for data acquisition
17 p3082 A70-34731

Real time data processing and display for spacecraft thermal vacuum testing, using hybrid computer 17 p3059 A70-35176

On-line display of pulsed rocket engine performance data using hybrid computer 17 p3063 A70-35512

Computer driven on-line CRT graphics displays for data acquisition and reduction 17 p3063 A70-35513

Solid state display for on-line information retrieval using light emitting crystals, integrated circuits and hybrid packaging 17 p3063 A70-35514

Visual display and automatic taxi guidance system testing for improved aircraft docking accuracy [AIAA PAPER 70-916] 17 p3064 A70-35828

Aircraft perspective display as independent landing monitor based on electronic runway lights, discussing simulator development and flight validation [AIAA PAPER 70-924] 17 p3064 A70-35835

Commercial aircraft flight deck systems controls and time sharing displays, emphasizing crew management [AIAA PAPER 70-938] 17 p3021 A70-35847

Heat-up display [HUD] system, discussing development, production, commercial aircraft applications and flight sequences uses 18 p3223 A70-36210

Automated radar terminal system, ARTS-III Beacon Tracking Level for continuous aircraft identity on controllers radar display 18 p3288 A70-36393

Left ventricular dynamics ultrasonic visualization, involving catheter-borne transducers array and computer for data acquisition and display 18 p3225 A70-36750

Real time analog display inputs for electronic computers and tracking in physiological control circuits, describing various manual controls 19 p3367 A70-37564

Display/control technology for high performance input/output between man and machine, describing man-in-loop simulation 19 p3369 A70-37875

Electronic attitude director indicator [EADI] for supersonic transport, employing CRT display, head down TV and microvision sensors 19 p3463 A70-37911

Apollo spacecraft parts environmental simulation and testing, using real time computer generated graphic display 19 p3532 A70-37918

Sodalites color centers creation by electron beam, discussing application in dark trace cathode ray storage display tubes 19 p3379 A70-38048

Airline area navigation in national airspace system, emphasizing moving map display for navigation charting 19 p3465 A70-38233

Pictorial display methods for pilot error reduction in area navigation via guidance control and capability beyond visual field 19 p3465 A70-38234

Human monitoring behavior, discussing display, task and organismic variables effects 19 p3363 A70-38323

Automatic test equipment, considering capability, control and display facilities and system cost 19 p3401 A70-38542

ATC simulation at EUROCONTROL Experimental Center, discussing dynamic simulator, data processor and display 19 p3468 A70-38638

TV display simulation of instrument and visual aircraft landing approaches, investigating color, collimation and resolution effects on pilot evaluations 20 p3578 A70-39172

Aircraft landing maneuver optimization by in-flight monitoring of approach and landing phases, furnishing decision making display [AIAA PAPER 70-1000] 20 p3560 A70-39531

Radar consoles with various display components under different illumination levels to determine optimal operator performance, discussing push-button design recommendations 20 p3580 A70-39713

Airborne integrated computerized ASW system, describing navigation, flight control, display and sensor subsystems 21 p3821 A70-40575

Aircraft capacitive fuel gage improvement by integration with flowmeter system, DC torque display and digital techniques, considering other measurement principles 21 p3821 A70-40619

Oscilloscope polar coordinate displays for multidimensional analog signals, noting human detection capability 21 p3823 A70-40853

Computerized aerospace systems man machine interface mechanization for performance optimization, emphasizing integrated approach to avionic displays 21 p3795 A70-41689

Electro-optic device using ferroelectric bismuth titanate, discussing electrical and optical properties and matrix addressed display 21 p3830 A70-42114

Airborne test computer for in-flight radar checkout featuring tape storage of computer program and cockpit mounted optical readout 22 p3993 A70-42320

Area navigation for aircraft guidance with radio aids, discussing advantages, airborne equipment, Dynamic Map Displays, etc 22 p4067 A70-42658

Horizontal Situation Display [HSD] map computer mechanization transforming earth location to X, Y coordinates for Lambert conformal projection [AIAA PAPER 69-987] 22 p4068 A70-42710

Visual system recording neuron pulse potential spatial and temporal responses to sinusoidal stimuli 23 p4144 A70-43922

Computer-aided aircraft design, discussing parts geometry data bank, visual display, etc [ICAS PAPER 70-27] 23 p4200 A70-44106

Flight simulation in SAAB A137 aircraft development, describing analog and digital computers, cockpit simulators, automatic pilots, control and display devices [ICAS PAPER 70-42] 23 p4178 A70-44140

U.S. SST flight deck instrumentation and cockpit displays during flight, discussing economic analysis of operations [ICAS PAPER 70-59] 23 p4139 A70-44155

Real time contourgraphic electrocardiographic display determining heart rate from CRT face on beat-by-beat basis 23 p4150 A70-44377

Optimal color hierarchy for pyrotechnic markers and signals indicating red, violet and amber hues on top 23 p4146 A70-44459

Enhanced real time operational impact and casualty analysis for range safety, discussing computer-driven CRT display and missile flight parameters selection [AIAA PAPER 70-247] 23 p4178 A70-44517

Manned spacecraft onboard data management systems, discussing information transfer, processing, control, display and man machine interface 23 p4167 A70-44647

Automatic Data Processing and Display System for ATC over Belgium, Holland and Germany, relieving traffic controller routine tasks 23 p4216 A70-44860

ATC radar data processing and display systems equipment and operation, emphasizing economy 23 p4216 A70-45044

Aircraft binocular head-up display, discussing system operation, history and potential applications 24 p4372 A70-45349

Human tracking performance as function of information precision in electrocutaneous display 24 p4308 A70-45508

Flickerless regeneration rates for CRT displays as function of scan order and phosphor persistence, using computer experiment 24 p4298 A70-45511

Readability of segmented numerals under critical accuracy and limited exposure time, comparing with conventional displays 24 p4308 A70-45514

Aircraft onboard radar system with landing monitor perspective display of runway operating independently of ground based electronic equipment [AIAA PAPER 70-1336] 24 p4373 A70-45932

Electronic data handling and CRT display of ATS satellite cloud pictures 24 p4371 A70-46048

Human compensatory two dimensional visual display tracking performance with superimposed apparent vertical vibration, studying frequency dependent eye pursuit movements 24 p4309 A70-46078

Upper Air Space Control Center Automatic Data Processing and Display System for air traffic control 24 p4323 A70-46238

DISPLAY SYSTEMS

U DISPLAY DEVICES

DISPOSAL

NT WASTE DISPOSAL

DISSECTION

Electrocardiographic for left ventricular hypertrophy diagnosis, using chamber dissection technique 03 p0432 A70-12890

DISSIPATION

NT ENERGY DISSIPATION

NT OHMIC DISSIPATION

Turbulent boundary layer calculations by integral dissipation method, using various dissipation coefficient laws 02 p0283 A70-12340

Dissipativity and asymptotic stability criteria derived for systems of ordinary differential equations, considering application to automatic control problem 03 p0518 A70-13469

Magnetic moment fluctuations of arbitrary solid body by fluctuation-dissipation theorem for thermal equilibrium 13 p2454 A70-30033

DISSIPATORS

U DISSIPATION

DISSOCIATION

NT AUTOIONIZATION

NT GAS DISSOCIATION

NT PHOTODISSOCIATION

NT THERMAL DISSOCIATION

Vibrational relaxation and continuous spectrum transition during dissociation of diatomic low temperature plasma 04 p0721 A70-14539

Dissociative recombination coefficient ratio between O ion and nitrogen oxide ion in ionosphere using rocket data 04 p0683 A70-15743

Equilibrium existing at gaseous-condensed phases interface inferred as mechanism for dissociative sublimation of ammonium perchlorate 05 p0894 A70-17079

Electron energy distribution function for carbon dioxide laser plasmas in gas mixtures, discussing dissociation products role in electron energy exchange 06 p1080 A70-17447

Dissociative charge-transfer reactions of positive He ions with molecular N and O measured in drift tube-mass spectrometer 06 p1109 A70-17490

Projection operators in dissociative attachment theory, considering use of truncated diagonalization method 07 p1347 A70-20248

Fixed low pressures of nitrogen generated by chemical dissociation in system at equilibrium at constant temperature, applying results to vacuum measurement device calibration 09 p1630 A70-22954

Dissociative-recombination rate coefficient measured for dissociative recombination reaction in inviscid nozzle flow of reflected shock tunnel, using high temperature and pressure nitrogen 09 p1737 A70-23225

Diatomic molecules vibrational levels distribution near dissociation limit determined using WKB approximation 10 p1919 A70-24041

Molecular I ground state dissociation energy value, proposing spectroscopic reassignment 12 p2180 A70-26861

Integral Hellmann-Feynman formula for dissociation energies in H, Li and LiH molecules, discussing transition densities and dissociation energy 12 p2275 A70-27569

Dissociation energy and long range interatomic potentials of diatomic molecules from vibrational spacings of higher levels 13 p2454 A70-28495

Predissociation of excited molecules in molecular hydrogen and deuterium by electric field as linear function of field strength 13 p2362 A70-29479

Dissociative recombination coefficient ratio between O ion and nitrogen oxide ion in ionosphere using rocket data 14 p2576 A70-30827

Transition probabilities for Markov chain describing bond breaking and molecular energy transfer in vibrational relaxation and dissociation 16 p2953 A70-33009

Dissociation energy of vanadium and chromium dicarbide and vanadium tetracarbide, using Knudsen effusion mass spectrometric method 16 p2857 A70-33654

Weak predissociation effects of hydroxyl compounds electron state on radiative lifetime via phase shift method 19 p3374 A70-38270

Electron-ion recombination in Ar plasma, discussing transition from collisional-radiative to dissociative process as function of electron density and temperature 21 p3858 A70-41711

Transition entropy during dissociation, investigating Trouton-Pictet rule applicability to diatomic molecules [DFVLR-SONDDR-58] 24 p4430 A70-46412

DISSOLUTION

U DISSOLVING

DISSOLVING

Metal corrosion product dissolution in reactor cooling deionized water, investigating Cu, W and Cd using chemical analyses 10 p1904 A70-24398

Lead ion effects on single crystal zinc dissolution and electrodeposition in alkaline solutions investigated microscopically 13 p2361 A70-28928

Rotating Ti disk in liquid Co flow, investigating titanium carbide dissolution kinetics 20 p3648 A70-39245

Isothermal kinetic rates of polymer swelling and dissolution, using thermomechanical analyzer 22 p4059 A70-43078

DISSYMMETRY U ASYMMETRY

DISTANCE NT DEBYE LENGTH NT MISS DISTANCE NT MISSILE RANGES NT RADAR RANGE NT RADIO RANGE NT REENTRY RANGE

Pulsar distance and distribution estimation, considering galactic spiral structure and nature of interstellar medium

02 p0371 A70-12201

Flight crews spatial vision, estimating absolute distance perception of pilots and navigators with emmetropic refraction

08 p1450 A70-20742

Convergence role in distance perception during aircraft landing, testing subjects with normal binocular vision, emmetropic refraction and visual acuity

08 p1450 A70-20744

Head wave distance from body determined for slender pointed profile in subsonic region of transonic flow

10 p1803 A70-24780

DISTANCE MEASURING EQUIPMENT

NT ALTIMETERS NT GEODIMETERS NT LASER RANGE FINDERS NT OPTICAL RANGE FINDERS NT RADIO ALTIMETERS NT RANGE FINDERS NT TELLURIMETERS

Minimum operational characteristics /MOC/ for vertical guidance in airborne area navigation systems, including VOR-DME accuracy criteria

01 p0138 A70-11049

Airborne DME minimum operational characteristics for air traffic control navigation and communication systems including equipment specifications, environmental conditions, accuracy and range

01 p0138 A70-11050

Space triangulation net using direction and distance measurements from satellite photographic and Doppler observations, including tracking data leveling

03 p0446 A70-13194

Electronic distance measurements involving transit time determination for signal from instrument to far point and back

03 p0495 A70-14176

Microwave and IR distance measuring devices design and operational principles, discussing main circuits and reading displays

05 p0851 A70-16799

Distance of spacecraft descending on parachute through planetary atmosphere measured from center of planetary mass using onboard instrument data

06 p1155 A70-17897

Lasers industrial application to distance and flow rate measurement, automated machining and tunneling, inspection, die hole punching, welding, etc

06 p1078 A70-18431

European air transport navigation, discussing air traffic control and planned VHF omnirange/distance measuring equipment network /VOR/DME/

07 p1332 A70-20226

Doppler VOR offering increased course accuracy and allowing precise area coverage in conjunction with DME ground station

09 p1723 A70-23036

Sequential collation of range /SECOR/ satellite tracking system using electronic phase comparison for measuring ground station-satellite distance

09 p1724 A70-23047

Apollo 11 lunar laser reflector for earth-moon distance measurement

10 p1898 A70-23847

Galactic radio source W 31 distance from sun determined from measurements of OH, H I and formaldehyde absorption lines

10 p1937 A70-23949

Laser methods for industrial length measurements

11 p2061 A70-25355

Intra- and extragalactic distance indicators and Hubble constant calibration

12 p2301 A70-27581

Short distance VHF omnirange navigation and distance measuring equipment considered for performance improvements feasibility to meet civil air traffic demands through 1980

12 p2268 A70-27643

Radiotelescope measurements for geodetic purposes, applying interferometric principles to quasar radiation

13 p2396 A70-29163

Short range VOR/DME area navigation techniques in U.S. National Airspace System

16 p2948 A70-33470

Pulsar distance calculation, assuming immersion in uniform average electron density medium

18 p3328 A70-37174

H 2 region galactic clusters and exciting stars, reevaluating distances by color magnitude diagrams

18 p3329 A70-37178

Association Carina OB 2 photometric investigation of mean distances

18 p3330 A70-37186

Eurocontrol evaluation of navigational aid systems air traffic control, examining HARCO and VORDAC systems

19 p3468 A70-38641

Ultrasonic sensor for detecting altitude and vertical velocity of aircraft near ground, applying to helicopter hovering flight or conventional airplane takeoff and landing

[AIAA PAPER 70-1031]

20 p3631 A70-39506

Onboard velocity sensors for VOR/DME navigation systems positional accuracy improvement, describing optimal and suboptimal data filtering

[AIAA PAPER 70-1024]

20 p3666 A70-39511

Pulsar observational data and theories, discussing main pulse shape, wavelength, polarization, fine structure distance estimates, intensity and scintillations

20 p3706 A70-39935

Extragalactic radio sources observable and intrinsic properties relationship for distance estimates, considering surface brightness, diameter, luminosity, etc

21 p3889 A70-41145

Position experiments for navigation satellite system parameters determination, using satellite ATS-3 distance measurements

22 p4066 A70-42653

Position fixing by distance measuring to geostationary satellites, discussing ATS-3 and ship experiment accuracy and orbit interference

23 p4215 A70-44232

Flueric position and distance sensor characteristics

24 p4293 A70-45427

DISTANCE PERCEPTION

U SPACE PERCEPTION

DISTILLATION

Propylene carbonate applications in nonaqueous electrolyte batteries, describing impurities identification by gas-liquid chromatographic analysis

12 p2164 A70-27069

Carrier distillation DC arc emission spectrography, determining lead, bismuth and tin traces in nickel base alloys after conversion to oxides

14 p2546 A70-30957

DISTILLATION EQUIPMENT

Vacuum distillation vapor filtered catalytic oxidation for water reclamation from human waste, using radioisotopes for thermal energy

20 p3579 A70-39437

Vacuum distillation vapor filtered catalytic oxidation water recovery system, using radioisotopes for thermal energy supply

21 p3769 A70-40994

Potable water recovery from urine by vacuum distillation and vapor pyrolyzation

21 p3769 A70-40995

DISTORTION

NT FLOW DISTORTION NT SIGNAL DISTORTION NT SURFACE DISTORTION

Heat treatment induced shape distortions measurements in maraging steel bars, plates and sheets, noting dependence on number of anneals and product form

14 p2595 A70-30544

Distorting and distorted components during geometrical illusions stereoscopic registration

19 p3366 A70-38926

Al alloy products heat treatment, using synthetic quenchants for distortion control

20 p3650 A70-39967

Satellite tracking camera lens-distortion coefficient from comparison of standard stellar and measured X-Y coordinates

22 p4029 A70-42596

Spheroidal three mirror telescopes distortion involving dioptrics combination

23 p4194 A70-44213

DISTRIBUTED AMPLIFIERS

Input conductance variation for common-emitter triode distributed-gain wideband amplifier, deriving energy equations improving tube characteristics

08 p1472 A70-20862

Noise and gain formulas for wideband distributed-gain amplifiers using quadrupole elements and transmission line configurations

08 p1472 A70-20863

Multivibrators with improved stability and frequency-division capacity, using distributed R-C-NR structures

24 p4321 A70-46396

LF narrow band-pass amplifiers with distributed RC structures

24 p4321 A70-46397

DISTRIBUTION [PROPERTY]

NT ANGULAR DISTRIBUTION NT ANTENNA RADIATION PATTERNS NT BOLTZMANN DISTRIBUTION NT CHARGE DISTRIBUTION NT CURRENT DISTRIBUTION NT DIFFRACTION PATTERNS NT ELECTRON DENSITY PROFILES NT ELECTRON DISTRIBUTION NT ENERGY DISTRIBUTION NT FLOW DISTRIBUTION

NT FORCE DISTRIBUTION NT FREQUENCY DISTRIBUTION NT HOLE DISTRIBUTION [ELECTRONICS] NT HOLE DISTRIBUTION [MECHANICS] NT INTERFERENCE LIFT NT ION DISTRIBUTION NT LOAD DISTRIBUTION [FORCES] NT MASS DISTRIBUTION NT MOMENT DISTRIBUTION NT NEUTRON DISTRIBUTION NT PRESSURE DISTRIBUTION NT RADIAL DISTRIBUTION NT RADIATION DISTRIBUTION NT RAINBOWS NT SIDELOBES NT SPATIAL DISTRIBUTION NT SPECTRAL ENERGY DISTRIBUTION NT STAR DISTRIBUTION NT STRESS CONCENTRATION NT TEMPERATURE DISTRIBUTION NT VELOCITY DISTRIBUTION NT VERTICAL DISTRIBUTION

Iron behavior in GaAs during crystallization, studying Fe distribution ratio, impurity migration and diffusion coefficient

01 p0156 A70-10219

Far and near side lunar crater chains regularities in distribution and size

03 p0574 A70-13879

Australite distribution pattern in Southern Central Australia

11 p2119 A70-26846

V and Cu emission spectrographic analyses in chondrite types, noting distribution patterns between groups based on meteoric chemical fractionation mechanisms

24 p4411 A70-45789

DISTRIBUTION FUNCTIONS

Particle diffusion distribution function of two component ionized degenerate gas from Boltzmann transport equation, giving tables for various spin and mass ratios

01 p0151 A70-10318

Satellite orbital elements optical determination accuracy by differential corrections, presenting computations for data distributed along small arc

02 p0254 A70-11754

Collective interactions effect on electron scattering opacity in stellar interiors, using Debye-Huckel radial distribution function and neglecting collisions

02 p0364 A70-11789

Molecular velocity distribution function measured in normal He shock wave in low density wind tunnel by electron beam fluorescence technique

02 p0299 A70-12229

Electron distribution function for steady homogeneous plasma of arbitrary ionization degree under strong electric fields, discussing kinetic equations for elastic and nonelastic encounters

02 p0346 A70-12231

Spatial distribution function calculation for muons in extensive air shower model and secondary particles mean transverse momentum estimation

03 p0556 A70-13039

Kinetic equation describing variation of distribution function of stellar residual velocities under action of gravitational field, discussing stellar diffusion in velocity field

03 p0564 A70-13227

Energy distribution function of electrons in weakly ionized plasma layer at electrode calculated, allowing for possible plasma concentration inhomogeneities

03 p0540 A70-13525

Electrostatic instability criterion for plasma with distribution function having discontinuities and sharp bend at minima

03 p0532 A70-13526

Formation of Maxwell and nonMaxwellian energy distribution in gases, noting reduction of time reversible to time irreversible equations

03 p0606 A70-13861

Laser amplifier electromagnetic field in arbitrary quantum mechanical state, deriving complex amplitude distribution function to calculate phase uncertainty

03 p0503 A70-14174

Spatially homogeneous Boltzmann equation containing initial distribution functions expandable into Hermitean polynomials, using ordinary differential equations

03 p0526 A70-14302

Maximum entropy principle used in rarefied gas dynamics for optimal representation of distribution function, examining difficulties associated with constraints on boundary conditions

04 p0718 A70-14492

Distribution of zeros of solutions of canonical fourth order linear differential equations

04 p0713 A70-14675

Distribution functions for solving moment equations of Maxwell-Boltzmann equation used in studying heat conduction through rarefied gases within concentric cylinders and spheres

[ASME PAPER 69-WA/HT-17]

04 p0783 A70-14817

Stars distribution in depleted globular clusters determined by integral equations describing distribution as function of cluster parameters

04 p0754 A70-15256

Eleven year cosmic ray variation and solar activity cycle analysis, showing variation amplitude dependence on both numbers and heliolatitudinal distribution of sunspots

04 p0742 A70-15718

Kinetic theory for calculating electron distribution function of weakly ionized plasmas in arbitrarily time dependent electromagnetic fields

05 p0886 A70-15800

Electron distribution function in quasi-static free moderately ionized plasma with partial radiation trapping determined from electron-electron collisions

05 p0889 A70-16452

Plane magnetopause models assuming ionospheric electrons ability to short circuit electric fields, constructing distribution functions by Vlasov theory

05 p0840 A70-16568

Characteristic equation for phase velocity of surface wave propagating on helix for forbidden zone, suggesting current distribution function

05 p0815 A70-16775

Maximum gust correlation with gust mean distribution within given hour determined from high speed anemometer

06 p1096 A70-17414

Spatially homogeneous distribution function describing uniform gas motion derived to permit computer calculations in obtaining numerical solutions to kinetic equation

06 p1036 A70-17753

Iteration for Boltzmann equation solution for relaxation of gas having solid molecules with time variable and velocity dependent distribution function

06 p1109 A70-17757

Supersaturation during droplet-liquid phase formation in clouds estimated from trough formed on curve of distribution function

06 p1097 A70-17796

Distribution function distortions produced in counting devices due to simultaneous arrival of particles, correcting errors

06 p1064 A70-17830

Corpuscular radiation distribution function with trapped particles maximum density fixed in equatorial plane and reflection points vicinity of magnetic force line

06 p1135 A70-17894

Solar wind temperature, using distribution function for solar wind ions in anisotropic Maxwell distribution form

06 p1135 A70-17895

Electron distribution functions in weakly ionized plasmas by asymptotic analysis of boundary layer near wall

06 p1121 A70-17903

Boltzmann equation for binary mixtures of rarefied gases solution involving specific expansion of distribution functions

06 p1047 A70-18311

Discrete ordinate technique for nonlinear Boltzmann equation tuned for computing collision integrals to instantaneous nature of distribution function

06 p1047 A70-18319

Boltzmann equation fourth moment numerically solved to study distribution function characteristics during monatomic gases spherical expansions into vacuum

06 p1048 A70-18320

Surface diffusion slip velocity in binary gas mixture above solid surface, basing calculation on distribution functions determined from Boltzmann equation

06 p1049 A70-18333

Particles infinite systems equilibrium state by canonical ensemble theory, demonstrating existence and uniqueness of limiting distribution functions dependence on density

07 p1333 A70-18936

Convolution formulas for Cauchy and standard normal random variable distributions derived from geometry of circular symmetric distribution on plane

07 p1323 A70-18946

Particles and surface brightness distributions in nonionized cometary tails, considering near nucleus source and particle acceleration

07 p1378 A70-19035

Kinetic processes in plasma subjected to randomly fluctuating electric field, obtaining chain of single particle distribution functions

07 p1349 A70-19553

Statistical methods for characterizing interval sequences of ECG, treating interval distribution and joint probability density function of adjacent interval pairs

07 p1211 A70-19593

Compton-Getting effect for cosmic ray particles and photons and Lorentz-invariance of distribution functions, discussing thermal background radiation, proton spectra, etc

07 p1369 A70-20071

Stellar velocity distribution function for small mass stars in nonrotating systems

07 p1389 A70-20208

Plasma oscillations analytic second order theory verification by computerized simulation, using Fourier-Hermitian expansion of distribution function in phase space

08 p1550 A70-20636

Diatom gases, describing rotational distribution function evolution by diffusion equation approximation, discussing apparent relaxation times

08 p1548 A70-21521

Kinetic equation describing variation of distribution function of stellar residual velocities under action of gravitational field, discussing stellar diffusion in velocity field

08 p1580 A70-21660

Fatigue limits distribution functions of full-scale machine parts estimated by rupture similarity criterion, discussing stress concentration and scale factor effects

09 p1776 A70-22616

Crystallite orientation distribution function refinement procedure, considering application to isotactic polystyrene

09 p1631 A70-23446

Boltzmann collisionless transport equation for relativistic plasma solved by expanding distribution function in terms of unnormalized spherical harmonics

10 p1923 A70-24228

Independent identically distributed random variables sequence, obtaining asymptotic expansion for large deviations of distribution function

10 p1910 A70-24799

Observational data for distributions of physical and optical companions to spiral galactic systems and number of satellites as function of central galaxy size

10 p1948 A70-25247

Dispersion function model based on mixed second order kinetics with distributed relaxation times

11 p2086 A70-25831

Components life determination from calculating cumulative damage using empirical stress amplitude distributions

11 p2133 A70-25844

Electrons velocity distribution function in homogeneous stationary weakly ionized Lorentz plasma in neon, investigating effect on mobility, collision frequency, diffusion and kinetic energy

11 p2089 A70-25871

Boltzmann equations for distribution functions of gas, analyzing neutral or ionized components by linearization method

11 p2090 A70-25946

Transformed distribution function of particle velocity of plasma in Debye thermodynamic equilibrium approximation based on statistical mechanics

11 p2091 A70-26459

Autocorrelation and brightness distribution functions for irregular variable star

11 p2115 A70-26579

Analytic expressions for concentration distribution functions in inhomogeneous solids within intermediate stages of homogenization process

12 p2253 A70-27282

Limiting distributions of sums of random variables coupled in homogeneous Markov chain with finite number of states

12 p2261 A70-27551

Free electrons non-Maxwellian equilibrium kinetic energy distribution function, considering partially ionized hydrogen-like plasma in thermal equilibrium

13 p2459 A70-28634

Cratered planetary surface distribution and covariance functions of elevations using statistical model

13 p2488 A70-28763

Jeans escape rate error for atmospheric H and He attributed to perturbed velocity distribution function, using realistic atom-atom elastic scattering cross sections

13 p2398 A70-29226

Self gravitating collisionless particles instability related to anisotropic random velocity distribution function in presence of disk-galaxy type spiral wave perturbations

13 p2492 A70-29299

Type 3 solar bursts theory covering beam-type instabilities and quasi-linear relaxation of fast electron distribution functions

13 p2478 A70-29389

Book on probabilistic systems analysis covering models, decision making, random processes, distribution functions, mass and density functions, etc

13 p2441 A70-29455

Boltzmann equation in circular magnetic field solved by Fourier series and Legendre polynomials, correcting distribution function due to Fourier harmonics

13 p2464 A70-29485

Light scattering from plasmas with nonMaxwellian electron velocity distribution function

14 p2622 A70-30694

BBGKY hierarchy pair correlation function for magnetoplasma under weak external force, using

operator method and time periodic ansatz for distribution functions

14 p2623 A70-30697

Eleven year cosmic ray variation and solar activity cycle analysis, showing variation amplitude dependence on both numbers and heliolatitudinal distribution of sunspots

14 p2632 A70-30802

Kinetic processes in plasma subjected to randomly fluctuating electric field, obtaining chain of single particle distribution functions

15 p2777 A70-31460

Linear distributed dynamic system simulation using infinite product expansions for transcendental terms in transfer functions

16 p2942 A70-33348

Electron momentum distribution function of p-type semiconductor with arbitrary band structure under electric and magnetic fields

17 p3144 A70-35704

Pontryagin stability for distributed delay or parameter systems, using Brin criterion

18 p2335 A70-36478

Q switched laser turn-on nonlinear dynamics, deriving field intensity distribution function

18 p2370 A70-36743

Book on abstract methods in partial differential equations, covering functional analysis and distributions, elliptic theory, linear and nonlinear problems, evolution equations, etc

18 p3284 A70-36782

Two dimensional phase distribution function of mixture of Gaussian noise with amplitude modulated signal

18 p3229 A70-37110

Density and distribution functions for quotient of ellipsoids of variance volumes, yielding probabilities and fractiles in three dimensional sets of points

19 p3382 A70-37835

Distribution functions of cosmic ray path length, obtaining exponential type for high and low energy data

19 p3509 A70-38146

Risk interpretation of prior distributions in acceptance sampling by Bayesian analysis

19 p3440 A70-38817

Kinetic equations derivation for correlation functions and time dependent distribution functions of irreversible processes, using projection operators

20 p3672 A70-39588

Random radio signals distributions properties with parameters subject to random variation

21 p3785 A70-40639

Homogeneous plasma in unidirectional oscillatory electric field, solving Boltzmann equation by electron distribution function expansion

23 p4225 A70-44240

Electron distribution function in homogeneous ionized plasma under oscillating electric fields and steady magnetic fields, solving Boltzmann transport equation

23 p4226 A70-44248

Limiting distribution of additive nonnegative continuous functional of homogeneous Markovian process with conditional transfer function

23 p4212 A70-44346

Quasi-homogeneous approximation validity for electron velocity distribution function disturbance in gas plasma column ionization waves discharge involving high currents

24 p4386 A70-45794

High resolution cylindrical capacitor observation of fine structure of distribution function of electron beam interacting with plasma

24 p4387 A70-45820

DISTRIBUTION MOMENTS

NT MEAN

NT STANDARD DEVIATION

NT VARIANCE [STATISTICS]

Electron and photon spatial distributions in cascade air shower, applying moment method to space/angle problem solution

03 p0557 A70-13050

Recursive differential equation for moments of time-to-cycle slip in first and second order phase lock loops

21 p3802 A70-41350

Five-moments approximation calculation of magnetoplasma dynamic hydrogen arc radial pressure profile as function of ambient pressure and superimposed magnetic field

23 p4228 A70-44935

Magnetoplasma dynamic hydrogen arc radial pressure profile as function of ambient pressure and superimposed magnetic field, using thirteen-moments approximation

23 p4228 A70-44936

DISTURBANCE THEORY

U PERTURBATION THEORY

DISTURBANCES

Incompressible inviscid free shear layer stability with respect to spatially growing three and two dimensional disturbances, considering hyperbolic tangent velocity profile

[DFVLR-SONDDR-10]

03 p0468 A70-13786

Initial disturbances propagation in gas mixtures by asymptotic analysis, observing diffusely and viscously damped modes
05 p0833 A70-16404

Linear differential controller equations for optimal automatic control system with disturbances
08 p1479 A70-20870

Three axis large angle attitude control system global analysis, determining system stability, responsiveness and sensitivity to disturbances
[ALAA PAPER 70-996]
20 p3668 A70-39534

DISTURBING FUNCTIONS

Tidal disturbing functions developed with amplitude factor and lag angle expressed as sums of zonal spherical harmonics, discussing lunar formation and orbit evolution
03 p0576 A70-14083

Stationary and periodic solutions for commensurable cases of mean motions in restricted three body problems by expanding disturbing functions
04 p0745 A70-14474

Periodic solutions with moderate eccentricities and high inclinations for three dimensional restricted three body problem by expanding disturbing functions by high speed computer
09 p1759 A70-22773

DISULFIDES

NT CARBON DISULFIDE

Quantitative and qualitative analysis of biochemically and radiobiologically important thiols and disulfides via gas-liquid chromatography
19 p3373 A70-37836

Transition metal disulfides and diselenides as solid lubricants, investigating sliding friction characteristics
[ASLE PREPRINT 70AM 6E-1]
19 p3438 A70-38801

DITCHING [LANDING]

Ground and ditching emergency evacuation tests of C-9A aeromedical aircraft under worst possible simulated crash conditions
01 p0035 A70-10716

DC-8 aircraft ditching in San Francisco Bay on 22 November 1968, discussing accident sequence, evacuation operations, life raft stowage and deployment, etc
06 p0985 A70-17705

Passenger survival and evacuation of civil jet transport aircraft after ditching at sea
15 p2676 A70-32223

Modeling techniques based on Froude scaling laws for helicopter ditching and flotation stability characteristics
17 p3016 A70-34738

Model testing for helicopters, considering scaling, ditching and rotor performance
19 p3402 A70-38610

DITHIOLS

U THIOLS

DIURNAL RHYTHMS

U CIRCADIAN RHYTHMS

DIURNAL VARIATIONS

Harmonic analysis of upper atmospheric wind periodic data from radar sounding of meteor trails, defining principal diurnal wind variations
01 p0134 A70-10201

Underground and surface telescope measurements of second harmonic of primary cosmic ray daily variation and upper solar modulation limit
01 p0170 A70-10405

Cosmic ray electron intensity diurnal variations measured with combined Cerenkov telescope and Pb-scintillator sandwich detector on balloon flight
01 p0170 A70-10408

Nonlinear flow conductance and convective terms effects on planetary thermospheres heating diurnal variations, emphasizing solar EUV heating
01 p0178 A70-10413

Seasonal, solar diurnal and semidiurnal variations of cosmic ray soft component observed at sea over seven year period
01 p0170 A70-10467

Wind oscillations in stratosphere, lower mesosphere and meteor heights noting periodicities
01 p0074 A70-10591

Diurnal variation for structure and energy balance of thermosphere, noting effect of global wind pattern
01 p0074 A70-10592

Rocket and satellite studies of geomagnetic field during IQSY, confirming ionospheric currents responsible for magnetic diurnal variations
01 p0075 A70-10596

Magnetic bay microstructures occurrences at low latitude not restricted to day or night hemisphere
01 p0076 A70-10668

HF radio waves propagation between antipodal transmitter and receiver, discussing diurnal variations and reception over polar caps and water
01 p0045 A70-11103

Thermospheric horizontal winds diurnal bulge, discussing maximum density-maximum temperature phase relationship
01 p0078 A70-11210

F 1 layer nonlinear ionospheric continuity equation to investigate role of diurnal variations of loss and

production processes in electron density midday biteout effect
01 p0079 A70-11221

Ionosphere total electron content diurnal and seasonal variations at midlatitudes, based on data analysis from Explorer 22 in polar orbit
01 p0080 A70-11223

Stable geomagnetic pulsations related to plasma density shock position in magnetosphere and to magnitude of diurnal variations
01 p0082 A70-11508

Secondary corpuscular stream effect on diurnal variations in cosmic ray intensity obtained from statistical analysis
01 p0172 A70-11524

Interplanetary magnetic field sectoral structure effect on diurnal cosmic ray intensity and geomagnetic field, noting field direction influence
01 p0172 A70-11525

Auroral electron energy diurnal variation, noting ground observations of polar auroras, riometric absorption, vertical changes in ionization layer maximum position, etc
01 p0083 A70-11535

Lunar diurnal variation parameters at Irkutsk determined from IGY data concerning geometric field components
01 p0083 A70-11538

Diurnal variations in sporadic E layer and wind in ionosphere during equinox and solstice periods, noting wind shear mechanisms and ambient electron density
01 p0084 A70-11552

Air density variations calculated by visual satellite observations processing, comparing results of INTEROBS and average anomalies methods
02 p0288 A70-11766

Diurnal variations of intensity and height profile of diametric O concentration from photometric rocket measurements compared with balloon data
02 p0297 A70-12066

Predawn O I 6300 A airglow enhancement, observing time variations and suggesting mechanism
02 p0289 A70-12120

Seasonal effect on F region midlatitude slab thickness diurnal variations during magnetic disturbances using monitoring VHF signals from geostationary satellites
02 p0290 A70-12160

Lunar atmospheric tidal wind semidiurnal variations from Hong Kong and Uppsala data, discussing agreement with theory
02 p0325 A70-12217

Canary Bird synchronous satellite radio signal transmissions scintillations from recordings, noting diurnal scintillation pattern
02 p0260 A70-12573

Earth daily rotation effects on magnetosphere electric currents, discussing Pederson currents in dynamo region and E region ionization
02 p0293 A70-12775

Cloud cover recurrence estimators from set of unconditional probabilities tested against sample of Northern Hemisphere diurnal variation data
03 p0521 A70-13164

Large amplitude wave trains in cosmic ray neutron intensity compared with diurnal variations, determining interplanetary space directional distribution from monitor data
03 p0559 A70-13912

Sidereal cosmic ray diurnal variations from underground muon telescopes in Northern and Southern Hemispheres, proposing model producing variations at earth vicinity
03 p0560 A70-13978

Winter diurnal behavior of northern high latitude ionospheric electron density using temperature data from Langmuir probes
03 p0478 A70-13993

Diurnal variations of phase coupling between heart beat and respiration under resting conditions and modification by quantitatively regulated physical effort
03 p0431 A70-14294

Charged primary cosmic rays sidereal anisotropy generated diurnal/semidiurnal variations phase characteristics, using energy meson telescopes
04 p0738 A70-14513

Lunar tide in E region phase height from measurements of diurnal phase path change for continuous wave
04 p0678 A70-14973

Lunar tides in midday critical frequency of F 2 layer, determining phase reversal location
04 p0651 A70-15309

Diurnal fluctuations of quiet F 2 region intensity at midlatitude based on vertical probe observations during solar activity minimum
04 p0684 A70-15745

Upper atmosphere wind and semidiurnal and diurnal tide interactions observed by meteoric radar, noting relation to gravity waves
05 p0878 A70-15818

Diurnal cosmic ray intensity variations first and second harmonics amplitudes during sudden phase

variations diagrammed from neutron monitor data during IGY
05 p0898 A70-15936

Cosmic rays neutron component solar-diurnal variations as function of solar activity using magnetically quiet data
05 p0898 A70-15941

Time dependent variation of first and second harmonics amplitudes of diurnal cosmic ray variations during SC magnetic storms
05 p0898 A70-15942

Meteor rate data tabulated from controlled parameter radar survey of Southern Hemisphere activity, noting diurnal and annual variations
05 p0907 A70-16001

Daily variations of winter stratospheric zonal wind and planetary waves based on synoptic charts from balloon observation
05 p0878 A70-16148

Meteorological parameters influence on diurnal variations of radionuclide activity and resulting global air pollution
05 p0903 A70-16662

Diurnal and seasonal variations of mortality due to cardiac and circulatory failure using model representing daylight regulation of human organism
05 p0802 A70-16663

Cosmic ray angular distribution spectrum and interplanetary magnetic field properties determined from semidiurnal cosmic ray variations data
05 p0903 A70-16732

Time and altitude induced variations in daytime NO and molecular and atomic oxygen ions
05 p0841 A70-16736

Polar aurora rays mean length diurnal variations determined from photographic and visual observations in Tiksi bay
05 p0843 A70-16763

Solar daily atmospheric oscillations from pressure, wind and temperature recordings at ground level, discussing seasonal and worldwide variations of daily component
06 p1053 A70-17307

Cesium clocks at fixed locations compared for precision and accuracy, noting influence of radio frequency diurnal variations
06 p1139 A70-17474

Electron density distributions relation to D region diurnal and seasonal variations in radiowave absorption in terms of transport processes near mesopause
06 p1054 A70-17589

Phase path variation of stable continuous wave transmission reflected from E region during daytime, discussing night time results
06 p1055 A70-17593

Proton satellites measurements reconciliation with diurnal stellar variation data and cosmic rays origin models
06 p1135 A70-17885

Ionospheric absorption diurnal and seasonal variations determined from field strength recordings
07 p1263 A70-19154

Effective LUF fade-out and fade-in times seasonal and diurnal variations for oblique ionospheric propagation paths, noting sunspot number effects
07 p1233 A70-19180

Diurnal variations of lower F region ion composition and recombination coefficient based on numerical modeling of continuity equations for electrons and molecular species
07 p1265 A70-19431

Cosmic radio absorption nightly variations, considering ionospheric structure and composition and various scattering mechanisms
07 p1367 A70-19456

Pc micropulsations with periods of 4-12 sec, discussing occurrence probability and diurnal characteristics
07 p1268 A70-19465

Intensity variations of cosmic ray neutrons and mesons analyzed to isolate lunar day period
07 p1368 A70-20033

Topside ionosphere morphology during IQSY, emphasizing plasma scale height diurnal and latitudinal variations role in satellite data interpretation
07 p1270 A70-20073

Magnetic storms effect on cosmic ray neutron component diurnal variation, determining amplitudes and phases of harmonics by harmonic analysis
07 p1372 A70-20341

Diurnal variations of cosmic ray neutrons following solar proton flares, proposing anisotropic diffusion model for phase and amplitude
07 p1372 A70-20342

Global distribution of F 2 layer critical frequencies by expanding empirical function of diurnal variations into natural orthogonal components
07 p1277 A70-20451

Electron, oxygen and NO molecular ions concentrations for E region from computer calculations of diurnal model compared to observations
08 p1490 A70-21391

Diurnal vertical shifts of constant electron concentration levels in D region, considering effects of chromosphere, nuclear explosions, solar eclipses, etc
08 p1490 A70-21430

Atmospheric density in thermosphere observed by satellites, noting daily and semiannual variations related to solar and geomagnetic activities
09 p1667 A70-22626

Cosmic ray diurnal anisotropy, demonstrating two-solar-cycle variations for nucleonic component
09 p1746 A70-23478

Equatorial electrojet diurnal variability in intensity, position and width obtained from H records of magnetometers
09 p1747 A70-23495

Lunar daily variation in geophysical data determined by Chapman-Miller method, improving probable error determination method and giving computer program in FORTRAN
09 p1764 A70-23701

Asian zone solar daily and storm time ionospheric disturbance variations synoptic study during IGY-IGC period
10 p1872 A70-23822

Loran C radio wave field intensity diurnal variations measurements, investigating ionospheric waves characteristics
10 p1832 A70-23921

Ionospheric electron content diurnal, latitudinal variations and equivalent slab thickness determined from observing satellite signals Faraday fading
10 p1874 A70-24426

Daily horizontal intensity spectrum for equatorial observatories, computing power densities near 27 day variation during high, moderate and low solar activity
10 p1875 A70-24440

Diurnal variations of concentrations of ions and neutral components of NO, O and N in E region from analysis of chemical and photochemical processes
10 p1881 A70-24809

Scintillation sudden inception in Faraday rotation in Sodankyl and Oulu, noting diurnal north-south frontier movements in polar ionosphere
10 p1884 A70-25262

Statistical analysis of aurora backscatter VHF measurements, discussing related stream plasma instability theory and diurnal variation
10 p1885 A70-25263

Near IR radiation diurnal variations in corn canopy accounted for by Duntley equations for unidirectionally incident light propagation through diffusing medium
11 p2082 A70-25364

Diurnal variation of equatorial ionospheric electron concentration from Schooner observations
11 p2043 A70-25548

Electron temperature diurnal variations data from rocket soundings used for determining recombination coefficient in E region
11 p2044 A70-25550

Annular current effect on auroral oval location during morning and evening hours, noting airglow region shift toward equator and expansion
11 p2044 A70-25555

Lunar semidiurnal tidal oscillations of surface pressure in atmosphere, observing constant amplitude with maximum and minimum phase lag variations
11 p2045 A70-25645

Lunar tides relationship with equatorial electrojet currents using daily variations at fixed lunar ages and monthly variations at solar hours of horizontal magnetic field
11 p2114 A70-26564

First harmonic of diurnal variation in pressure corrected cosmic ray neutron monitor rate, discussing amplitude variation with height and observed time dependence
12 p2291 A70-27177

Solar and lunar daily geomagnetic variations, correcting harmonic components calculated values
12 p2303 A70-27673

Long term ionospheric absorption measurements in Japan from IGY through IQSY using A1 method, discussing annual and diurnal variations correlation with solar activity
12 p2226 A70-28059

Long term ionospheric absorption measurements in Northern Hemisphere from IGY through IQSY, discussing annual and diurnal variations correlation with solar activity
12 p2226 A70-28060

Cosmic radiation yearly semidiurnal anisotropy characteristics based on worldwide neutron monitor stations data analysis
13 p2477 A70-29177

Cosmic radiation periodic variations measurements noting second harmonic importance of daily variations
13 p2478 A70-29230

Balloon-borne photometer for collecting twilight and daytime OH intensity and rotational temperature variations data
13 p2399 A70-29240

Altitude dependence of low latitude cosmic ray diurnal variations from cosmic ray neutron data
13 p2479 A70-29792

Mesospheric daytime/nighttime ozone abundance vertical profile diurnal variations
14 p2568 A70-30130

Diurnal and seasonal variations of sporadic E layer observed at ionospheric station
14 p2568 A70-30134

F 1 region ion structure diurnal variations, calculating photoionization rates
14 p2571 A70-30227

Lower ionosphere influence on radio reflection from sporadic E layer, determining diurnal variations of D region absorption for various frequencies
14 p2547 A70-30235

UHF propagation measurement over sea for varying surface refractivity and meteorological conditions, noting diurnal variations
14 p2549 A70-30513

Neutral winds effect on F region vertical ion drifts derived from continuity equation, noting diurnal and seasonal variations
14 p2574 A70-30738

F region horizontal drift velocity height and diurnal variations, using ionograms
14 p2574 A70-30751

Daily variations of geomagnetic field horizontal component at dip equator associated with ionospheric current
14 p2575 A70-30792

Diurnal fluctuations of quiet F 2 region intensity at midlatitude based on vertical probe observations during solar activity minimum
14 p2576 A70-30829

Mars surface material properties from radio emission observations, considering daily temperature variations distribution
14 p2648 A70-31083

Stratospheric and mesospheric ozone diurnal variation by rocket-borne ozonesonde in January 1968
14 p2577 A70-31170

5577 A /OI/ airglow emission diurnal variations during IGY by normalization method, observing seasonal effects
14 p2578 A70-31239

Nonlinear diurnal tide and gravity wave interactions at meteor heights below mesopause
14 p2579 A70-31251

Sodium dayglow seasonal and diurnal variations observed with Zeeman cell photometer
14 p2579 A70-31253

Sodium and potassium dayglow seasonal and diurnal variations using resonance cell technique and sky polarization effect
14 p2580 A70-31263

Balloon systems characterized by day to night altitude variations for permanent atmospheric sounding
14 p2531 A70-31312

Circadian rhythmical changes in biological organisms by earth rotation, emphasizing diurnal variations role in sleep-wakefulness rhythm
15 p2680 A70-31742

Atomic hydrogen escape effects on altitude distribution, discussing lateral flow limitations on thermospheric diurnal variation
15 p2725 A70-31796

Correlated daily variations of ionospheric drift and anisotropy parameters in E and F regions at Thumba, India
15 p2725 A70-31858

Daily amplitude variability of equatorial electrojet current related to solar extreme ultraviolet radiation /XUV/ influx
15 p2727 A70-31873

Numerical model of diurnal variations of minor neutral constituents in mesosphere and lower atmosphere including molecular and eddy diffusion
15 p2727 A70-31909

Earth-ionosphere cavity resonances diurnal variations by considering different propagation characteristics of day and night hemispheres
15 p2728 A70-31910

Superposed effects in solar quiet daily variations of geomagnetic horizontal component, using Lerwick and Eskdalemuir data
15 p2728 A70-31991

Diurnal, seasonal and latitudinal variations of maximum electron concentration in F 2 region, using global network observations
15 p2729 A70-32077

F 2 layer afternoon and evening ionization maxima dependence on season, zenith angle and solar activity
15 p2730 A70-32084

Diurnal vibrations damping in inertial navigation system, demonstrating equations asymptotic stability for coordinates autonomous determination
15 p2775 A70-32156

Upper troposphere pressure variations through 20 km separation layer, noting interdiurnal temperature changes
15 p2772 A70-32458

Ionospheric small scale ionization discontinuities vertical drift effect on diurnal variations of F 2 layer critical frequency
18 p3246 A70-36086

Ionospheric cosmic noise absorption diurnal and seasonal variations at Alma-Ata during IQSY, noting chromospheric flares effects
18 p3306 A70-36089

Short wave propagation above F2 maximum usable frequency, observing field intensity and SNR seasonal and diurnal variations
18 p3226 A70-36092

Diurnal variations of lower F region ion composition and recombination coefficient based on numerical modeling of continuity equations for electrons and molecular species
18 p3249 A70-36905

Cosmic radio absorption nightly variations, considering ionospheric structure and composition and various scattering mechanisms
18 p3309 A70-36930

Pc micropulsations with periods of 4-12 sec, discussing occurrence probability and diurnal characteristics
18 p3250 A70-36939

Ionization-recombination parameters based on diurnal variations of electron concentration in F 2 layer maximum, discussing latitudinal variations
18 p3254 A70-37033

F 2 layer maximum electron concentration diurnal variations dependence on ionization intensity and dissociative recombination and ion-molecular reactions rate coefficients
18 p3255 A70-37039

Global diurnal variations in F 2 layer seasonal anomaly during high and low solar activity, noting corpuscular radiation role
19 p3491 A70-37326

F 2 region critical frequency diurnal variation forecasting, using series expansion of natural orthogonal components
19 p3409 A70-37327

Diurnal variations in polarization axis direction of Pc 1 pulsations
19 p3410 A70-37333

Polar cap absorption correlation with solar protons flux into magnetosphere, discussing diurnal and spatial variations and magnetic storm effects
19 p3411 A70-37492

LF geomagnetic micropulsations recordings by two component induction magnetometer, relating diurnal frequency and occurrence variations to local K-index changes
19 p3412 A70-37995

HF geomagnetic micropulsations recordings by two component induction magnetometer, relating diurnal frequency and occurrence variations to local K-index
19 p3412 A70-37996

Simultaneous primary energy spectrum, chemical composition and sidereal daily variation analysis for cosmic ray origin, using Proton measurements
19 p3500 A70-38080

Sidereal daily variation in cosmic ray muon intensity at 60 mwe depth, indicating extragalactic origin
19 p3509 A70-38149

Sidereal cosmic ray diurnal variations using underground mu-meson telescopes in Northern and Southern Hemispheres
19 p3510 A70-38150

Galactic cosmic ray anisotropy, discussing amplitude and phase values of daily sidereal variation
19 p3510 A70-38152

Cosmic noise absorption diurnal variations at auroral zone conjugate areas during geomagnetically disturbed periods
19 p3414 A70-38379

Upper atmospheric density and temperature diurnal phase and amplitude discrepancy reconciled by dynamic diffusion model
19 p3414 A70-38381

Diurnal variations of thermospheric atomic hydrogen, investigating lateral flow effects on global distribution
19 p3415 A70-38419

Sporadic E layer occurrence probability over Dushanbe from ionospheric station data, discussing curves for diurnal and annual PE variations
19 p3417 A70-38785

Cosmic ray anisotropy sidereal-diurnal effects isolation by solving simultaneous amplitude and phase modulation problem
20 p3696 A70-39282

Cosmic ray neutron semidiurnal variations day and night components with respect to geomagnetic and solar activity
20 p3697 A70-39288

Solar cosmic rays diurnal and semidiurnal variations modulation by noncoincidence between earth rotation axis and normal to ecliptic plane
20 p3697 A70-39289

High energy charged particles equations of motion in quiet interplanetary magnetic field for primary cosmic ray distribution, calculating diurnal and semidiurnal variations
20 p3698 A70-39297

Maximum to minimum exospheric temperature ratio determination, concluding solar wind dependence of diurnal variation in thermosphere
20 p3621 A70-39345

- Diurnal anisotropy variations of cosmic ray intensity, taking into account neutron monitors data
20 p3699 A70-39346
- Morning and evening current reversals in equatorial electrojet, discussing seasonal variation data for refining models
20 p3621 A70-39352
- Ionospheric VLF diurnal transmission loss differences on two long paths, analyzing values for first and second modes
20 p3585 A70-39455
- Diurnal variations and spatial distribution of total electron content in equatorial ionosphere
20 p3623 A70-40477
- Ionospheric electron density response to geomagnetic storms at midlatitudes, noting diurnal variations detected by ATS 3 VHF signals
20 p3623 A70-40479
- Scintillation LF observations with synchronous satellite radio signals at low latitude station, noting magnetic activity effects on night and day scintillations
20 p3590 A70-40488
- Diurnal variations of sudden enhancements and decreases of ELF atmospherics, using mode theory
21 p3814 A70-40939
- Atomic oxygen density and temperature diurnal variation determination by F region incoherent scatter measurements, using nonlinear regression analysis
21 p3817 A70-41096
- Diurnal variation of equatorial ionospheric electron concentration from schooner observations
21 p3819 A70-41298
- Electron temperature diurnal variations data from rocket soundings used for determining recombination coefficient in E region
21 p3819 A70-41300
- Annular current effect on auroral oval location during morning and evening hours, noting airglow region shift toward equator and expansion
21 p3819 A70-41305
- Transmeridian flights effect on diurnal urinary excretion of unconjugated 17-hydroxycorticosteroids in males, evaluating time shift effects
21 p3770 A70-41477
- Recombination model of diurnal variation of electron density in midlatitude D region, assuming NO ionization by solar Lyman-alpha radiation
22 p4020 A70-43158
- F region electron content day-to-day changes observed by Early Bird satellite, determining cross correlation with magnetic indices
22 p4020 A70-43161
- Day and nighttime E and sporadic E layer drifts over low latitude station recorded by spaced receiver technique
22 p4020 A70-43166
- Geomagnetic daily variations analysis in terms of universal time components, considering solar wind-magnetosphere interactions, auroral zone effects, etc
22 p4021 A70-43278
- High altitude outer radiation zone boundary region electron energy measurement by satellite Injun 3, noting angular distribution dependence on local time, latitude, etc
23 p4236 A70-43833
- Diurnal atmospheric density variations latitude dependence from satellite data
23 p4185 A70-43842
- Exospheric neutral hydrogen temperature diurnal variation from satellite resonance filter data, suggesting Lyman alpha source external to geocorona
23 p4186 A70-43852
- Air current in upper atmosphere meteor zone above equator, noting diurnal and semidiurnal harmonics in wind velocity components
23 p4188 A70-44049
- Diurnal variation symmetry of upper atmosphere molecular oxygen concentration in terms of ozone photodissociation
23 p4190 A70-44083
- Thermosphere diurnal thermal influx theory, allowing for heat conductivity
23 p4214 A70-44265
- Hough eigenfunctions of lunar diurnal and semidiurnal atmospheric oscillations using matrix and group methods
24 p4328 A70-45351
- F I region ion structure diurnal variations, calculating photoionization rates
24 p4331 A70-46302
- Lower ionosphere influence on radio reflection from sporadic E layer, determining diurnal variations of D region absorption for various frequencies
24 p4316 A70-46310
- DIVERGENCE**
Gas laser beams divergence at various laser power levels vs resonator nonconfocality
01 p0106 A70-10062
- Thin airfoil magnetoaerodynamics problem revised solution to avoid divergent integrals expressing kernels of integral equations
03 p0405 A70-12933
- Laser beam trajectory equation in scanning ultrasonic cell for nonzero incidence angle, relating input and output beam divergence
07 p1300 A70-19865
- Axial-vector current divergence in external gravitational field, using perturbation approach in Minkowski space
07 p1336 A70-20167
- Divergence measurement of beam emitted by ruby laser in relaxation mode as function of cavity length and excitation voltage
11 p2063 A70-26462
- Nondiverging filter with single additional multiplication by fixed scalar s at each observation time, proposing algorithm
16 p2887 A70-33872
- Radiation divergence from gas laser resonator with coupling aperture
20 p3642 A70-39752
- DIVERGENT NOZZLES**
Boundary layer separation in divergent portion of conical ducts in overrelaxed supersonic regime in air and water, showing influence of medium, pressure and thrust
03 p0467 A70-13682
- Supersonic jet flow from diverging nozzle into space with given pressure or into supersonic slipstream, noting barrel shock formation inside jet
04 p0617 A70-15235
- DIVERTERS**
Plasma jet motion stability in axial magnetic field of stellarator diverter and solenoid
24 p4386 A70-45660
- DIVIDING [MATHEMATICS]**
Binary division by logic gates cellular arrays, noting accuracy and operating speed
14 p2556 A70-30517
- Iterative cellular logical array for nonrestoring binary division
14 p2556 A70-30685
- Semigroup B, uniquely divisible range space for compact divisible commutative semigroups
16 p2941 A70-33095
- Cellular logic arrays design for nonrestoring binary division, with application to Napierian logarithm generation
17 p3050 A70-34571
- DIVING (UNDERWATER)**
Endtidal oxygen and carbon dioxide partial pressures, oxygen uptake and carbon dioxide after apnea and during apneic diving
02 p0235 A70-12089
- Systolic and diastolic pressure in central artery of retina in deep-sea divers during oxygen inhalation at atmospheric pressure
23 p4150 A70-45081
- Critical supersaturation vs phase equilibration of tissue in computing decompression schedules from depth and exposure time
24 p4301 A70-45983
- DME-A SATELLITE**
U EXPLORER 31 SATELLITE
DNA
U DEOXYRIBONUCLEIC ACID
DO-31 AIRCRAFT
V/STOL supersonic fighter VJ 101, transport Do 31 and VTOL fighter/reconnaissance VAK 191 development in West Germany, discussing control and stabilization during hovering
03 p0413 A70-13794
- Civil jet VTOL transportation based on Do 31, discussing market, passenger requirements, noise, flight safety and economic factors
10 p1805 A70-24051
- [AIAA PAPER 70-001]
- DOCKING**
U SPACECRAFT DOCKING
DOCUMENT STORAGE
Aircraft accident filing system data analysis using Fortran programs
22 p3962 A70-42880
- DOCUMENTATION**
Signature theory application to space mission planning and archeological project
11 p2051 A70-26034
- Computer simulation model documentation exemplified by cardiovascular simulation using Continuous Systems Modeling Program /CSMP/ and emphasizing format uniformity
15 p2689 A70-31774
- DOCUMENTS**
NT ABSTRACTS
NT BIBLIOGRAPHIES
NT CATALOGS [PUBLICATIONS]
NT DRAWINGS
NT HANDBOOKS
NT PAPERS
NT RECORDS
Reliability criteria documents updating, discussing input vs output, experience retention, tradeoffs, etc
15 p2747 A70-32630
- DODGE SATELLITE**
Dodge satellite postlaunch attitude stabilization and flight data comparison with digital simulation, underlining simulation use in design analyses
04 p0765 A70-15674
- DODGE satellite launched into near-synchronous orbit to demonstrate gravity-gradient stabilization at high altitude and to experiment with damping techniques
06 p1159 A70-18218
- [AIAA PAPER 70-69]
- DODGE satellite gravity gradient stabilization at synchronous altitude by flywheel and magnetic sample-and-hold damping, noting boom bending
13 p2501 A70-28425
- Torsion wire libration damper for satellite gravity-gradient stabilization at near synchronous altitudes
16 p2985 A70-34134
- DOGHOUSES**
U PROTUBERANCES
DOGS
Cardiac activity temperature coefficients in dogs, specifying physical and chemical cardiac functions
01 p0012 A70-10052
- Arterial pressure pulse waves mathematical analysis applied to variations in stroke volume in anesthetized dogs subjected to spine-to-breast accelerations
01 p0012 A70-10125
- Thermoregulatory salivary responses of dog to various ambient temperatures, emphasizing hypothalamic temperature, threshold and proportionality constant
01 p0017 A70-10465
- Physiological interpretation of blood velocity curves recorded in right heart cavities of dogs by ultrasonic directional probe, using Doppler effect
01 p0035 A70-10709
- Piezoelectric ultrasonic crystal on cardiac catheter tip measuring cardiac diameter in vitro and in excised canine hearts
01 p0038 A70-11025
- Neurons and perineuronal glial cells quantitative relations in visual cortex from anesthetized dogs
01 p0025 A70-11030
- Erythropoietic response in anesthetized dogs subjected to sublethal whole-body proton irradiation followed by hypoxic hypoxia, discussing test procedure and results
01 p0027 A70-11300
- Hyperbaric oxygenation /OHP/ effect on left ventricular function evaluated by measurement on anesthetized dogs of myocardial contractility
02 p0230 A70-11701
- Constant-inflow and constant-pressure perfusion effect on vascular responses of dog
02 p0232 A70-11716
- Oxygen uptake increase following sodium L-lactate isomer infusion into anesthetized dogs
02 p0233 A70-11721
- Canine aortic flow as function of simultaneous mean aortic and mean right atrial pressures
02 p0233 A70-11723
- Lactate rise diminution in anesthetized paralyzed dogs subjected to hypoxia by gas mixtures before and after beta-adrenergic blockade
02 p0233 A70-11724
- Phasic phrenic nerve electrical activity relation to systemic blood pressure oscillations produced in paralyzed dogs by ventilation arrest or hemorrhage
03 p0416 A70-13010
- Increased oxygen partial pressure effects on cerebral bioelectric activity from EEG recordings on unanesthetized dogs
03 p0422 A70-13690
- Sinocarotid pressor reflexes effects on coronary circulation in anesthetized dogs noting changes in blood pressure, peripheral resistance and cavity pressure
03 p0422 A70-13693
- Peripheral blood, neutrophil myeloid hematopoiesis, phagocytic activity and serotonin level in gamma irradiated dogs
03 p0423 A70-13706
- Experiments on frozen dogs to determine localized shielding effectiveness in astronauts protection from radiation
03 p0423 A70-13710
- Pleural space of dogs investigated by spheres injection of varying density and diameter, discussing sedimentation velocities
03 p0429 A70-14160
- Solar and geomagnetic effects on variations in physiological tests using alimentary reflex of dogs
04 p0639 A70-15512
- Blood volume and circulation rate in dogs subjected to traumatic shock and hemorrhage under high mountain conditions
07 p1198 A70-18708
- Posthypoxic vasodilation in extremities of anesthetized dogs preserved after carotid and aortic reflexogenic zones exclusion
07 p1204 A70-19139
- Oxygen uptake increase phenomena in passively hyperventilated anesthetized and paralyzed dogs
07 p1205 A70-19293
- Cerebrum hyperemia of dogs subjected to craniocerebral hypothermia, recording rheoencephalograms by occipitofrontal needle electrodes
07 p1207 A70-19473
- Left ventricular function myocardial infarction induced acute depression and subsequent recovery in intact conscious dogs
07 p1211 A70-19615

- Thoracic cage, heart and extirpated lung dimensions measurement for dogs before and after explosive decompression and after ground level recompression 08 p1448 A70-21793
- Chronic gamma irradiation effects on bone marrow mitotic activity and chromosome aberrations in dogs 09 p1614 A70-22083
- Conscious dogs temporary local hypoxia effect on coronary blood flow regulation 09 p1623 A70-23585
- Vertical distribution of pulmonary blood flow /DPBF/ in dogs without thoracotomy prone, supine, head-up, head-down and right and left decubitus positions 10 p1810 A70-24004
- Pulmonary blood flow direction and distribution in dogs during near vacuum exposure and recompression 11 p1984 A70-25351
- Peripheral blood, neutrophil myeloid hematopoiesis, phagocytic activity and serotonin level in gamma irradiated dogs 11 p1985 A70-25506
- Experiments on frozen dogs to determine localized shielding effectiveness in astronauts protection from radiation 11 p1985 A70-25510
- Cold air inhalation effect on vital physiological functions of dogs, describing heat exchange simulator of upper respiratory tract 11 p1985 A70-25672
- X ray irradiation effects on phonocardiograms, EKGs, cardiac activity phases and Kunos-Garan mechano-electrical coefficient in dogs 13 p2350 A70-28890
- Comparative cardiac output measurements in dogs using left/right heart dye injections and pulmonary/aortic electromagnetic flow probes 15 p2688 A70-31434
- Unanesthetized dogs renal hemodynamic response to negative centrifugal acceleration 15 p2681 A70-31883
- Chronic gamma irradiation effects on bone marrow mitotic activity and chromosome aberrations in dogs 15 p2685 A70-32679
- Evoked potentials in dogs sensorimotor cortex during defensive instrumental conditioning 18 p3221 A70-37213
- Mongrel dogs pulmonary and systemic circulatory responses to dopamine infusion 20 p3569 A70-38986
- Blood vessels constriction in rear limbs, small intestine and spleen of dog with arterial blood heated above rectal temperature 20 p3574 A70-40173
- Skeletal muscles static tension influence on dog respiratory center functional properties, showing increased frequency volume and sensitivity under stimulation 20 p3574 A70-40174
- Excised perfused dog lungs stratified dead space changes due to transpulmonary pressure and breathing frequency increase, considering pulmonary circulation 24 p4303 A70-46114
- DOMAIN WALL**
- Magnetic trap chamber walls adverse effect on plasma heating produced by electron beam injected at low hydrogen pressures 07 p1350 A70-19845
- Ferromagnetic domain wall-dislocations magnetoelastic interaction in Fe and Ni computed as function of relative separation, discussing effects on magnetic properties 09 p1705 A70-22811
- DOMAINS**
- NT MAGNETIC DOMAINS**
- Algebraic criterion for polynomial with complex coefficients having all zeros in certain regions of complex plane 07 p1324 A70-19201
- Gunn oscillator voltage supply influence on domain capacity, considering frequency stability 13 p2377 A70-29302
- Saint Venant principle treating Neumann problem with nonthin two dimensional domain 15 p2767 A70-31855
- Semiconducting gallium arsenide LF oscillations, considering domain behavior and illumination effects 15 p2783 A70-31972
- CDs high field domain modes generation for C parallel to E ascribed to interaction between drift carriers and off-axis shear wave 15 p2784 A70-31984
- Magnetic dislocations effect on domain structure of postcritical Permalloy films subjected to alternating magnetic field 16 p2930 A70-33206
- Doped Gunn diode domain field width, nucleation and annihilation dependence on electron drift velocity 16 p2879 A70-34044
- Hysteresis effects during retuning of n-type GaAs Gunn oscillator with bias source and LCR circuit, showing range of domain damping by low field 17 p3055 A70-35689

- Gunn effect pulse regenerators, describing random domain triggering rate voltage dependence comparison with Johnson noise predictions 19 p3387 A70-37820
- GaAs stripline domains and guided EM waves, discussing velocity, conductivity, drift and transmission amplification gain 22 p3996 A70-42917
- Linear operator convex closed set, considering range-domain or output-input implications 24 p4369 A70-46023
- DOMES (STRUCTURAL FORMS)**
- NT RADOMES**
- Explosive forming of large domes from flat blanks with full scale trial-and-error elimination [ASTME PAPER MF-69-186] 12 p2240 A70-27079
- Membrane stresses on nonspherical domes with axisymmetric loads 16 p2990 A70-33743
- Shallow shell theory boundary value problems, calculating stress concentration for domes and shells with holes 17 p3192 A70-35694
- Dynamic axisymmetrical loading of thin elastic shallow spherical rigidly clamped dome, using variational method 18 p3341 A70-36582
- DOMINANCE**
- NT EYE DOMINANCE**
- DONNELL EQUATIONS**
- Donnell shallow circular cylindrical shell equation, obtaining approximate solution for stresses in infinitely long circular cylindrical shell with circular hole subjected to edge loading 03 p0601 A70-14320
- Shell elastic constants for multilayered sandwich cylinders using Donnell approximation 07 p1406 A70-19326
- Truncated conical shells buckling under hydrostatic pressure using Donnell equations, assuming membrane stress state for prebuckling deformation 07 p1414 A70-20170
- Cylindrical shells buckling under axial surface tensions using Donnell stability equations 08 p1593 A70-21624
- Donnell-Vlasov shallow shell equations error analysis 20 p3734 A70-40441
- DONOR MATERIALS**
- Excited terminal states emission in bound exciton-donor materials to determine donor ionization energies, electron effective masses and electron G values 02 p0350 A70-11847
- Solubility isotherms of alloying elements in Ge-Al-P semiconductor-acceptor-donor system at high temperatures 24 p4391 A70-46143
- DOORS**
- Emergency life saving instant exits for transport aircraft, using electromechanical confined transfer shaped explosive device 23 p4141 A70-44487
- DOPING (ADDITIVES)**
- U ADDITIVES**
- DOPPLER EFFECT**
- Solar radiation pressure effects on zodiacal dust particle orbital velocity, computing Doppler shift of H-beta absorption line as function of elongation 01 p0070 A70-10348
- Transcutaneous Doppler-shift flowmeter for arterial blood velocity measurement by ultrasound 01 p0037 A70-10880
- Normal and anomalous Doppler shifted cyclotron power radiated by energetic electrons spiraling along geomagnetic line considered as VLF source from magnetosphere 01 p0080 A70-11227
- Horizontal gradients below satellite orbit effect on reduced and minimum difference in Doppler frequency shifts of coherent radio waves from satellite in inhomogeneous ionosphere 01 p0046 A70-11517
- Doppler observations of D1 A satellite, discussing dispersion of data, mean point displacement and resonance harmonics 02 p0362 A70-11756
- Receiving station geodetic coordinates computed from Doppler curves of artificial satellite, using method of differential corrections 02 p0254 A70-11757
- Navigation system with twin gyro platform and Doppler sensor, discussing performance and cost advantage over inertial systems 02 p0334 A70-11987
- Doppler spectrum and radio troposcatter beam swinging in thin homogeneous turbulent scatter layer as function of height, crosswind speed and refractivity 02 p0326 A70-12288
- Dispersive Doppler shift and Faraday rotation second order theory for curved earth-ionosphere geometry, calculating phase path differences 02 p0260 A70-12574

- Cylindrical axial plasma flow fields velocity radial dependence measurement by double-wedge spectroscopy using Abel unfolding of Doppler shifts 02 p0349 A70-12657
- Ultrasonic Doppler method for timing mitral and aortic valves rapid movements, using filter to eliminate LF signals due to heart walls 03 p0432 A70-12891
- Nonducted VLF walking trace whistlers and Doppler shifts in fixed frequency transmissions identified on OGO midlatitude spectrographic records 04 p0649 A70-15116
- Signal amplitude and Doppler shift statistical characteristics calculated from sounding data on scattering at lower ionospheric discontinuities 04 p0650 A70-15284
- Axial and rotational velocity profiles of plasma jet from Doppler shift of spectral lines [DFVLR-SONDDR-27] 04 p0729 A70-15612
- Anomalous Doppler shift interaction between positive ions and right-hand polarized EM waves propagating at small angle to interplanetary magnetic field 05 p0905 A70-15761
- Transverse Doppler effect of laser beam retroreflected from artificial satellite predicted by special relativity theory, noting transformations 05 p0860 A70-16653
- Laser Doppler velocimeter directly measuring detected frequency with passive confocal Fabry-Perot interferometer 05 p0860 A70-16658
- H alpha line for emission nebulae analyzed by Fabry-Perot etalon, noting Doppler profile 05 p0917 A70-16907
- Doppler shift of laser beam reflected from shock wave measuring velocity through optical mixing 05 p0852 A70-16993
- Microwave frequency radar terrain echoes simulation concerning variation of echo delay, Doppler shift, random fine structure and time variation 06 p1008 A70-17482
- Rate of change of radio ray path length for transionospheric satellite VHF signals determined from Doppler and Faraday effect analyses 06 p1008 A70-17578
- Doppler technique for HF ionospheric radio signal fading, observing frequency spreading during flutter fading conditions in low geomagnetic latitudes 07 p1231 A70-19169
- Doppler shift measurements of axial and rotational velocities in MPD arc, using references from iron arc [AIAA PAPER 69-110] 07 p1364 A70-19324
- Short coherent laser radar detection of backscattered signal in measuring Doppler shift due to atmospheric temperature 07 p1297 A70-19368
- Ionospheric electron content and concentration variations analysis based on data of radio waves propagating from satellite, considering Doppler shift and Faraday effect 07 p1237 A70-20427
- Mechanical shock accelerometer calibration by light frequency Doppler shift measurement using laser interferometer and single sideband carrier insertion circuit 08 p1493 A70-20602
- German monograph on determination of blood velocity, pressure, pulse rate and vascular structure parameters using Doppler effect 08 p1452 A70-21297
- Monograph on normal frequency generator serving devices measuring differential Doppler effect, discussing generator design for ionospheric research satellites frequencies 09 p1645 A70-22531
- Plasma electron density determination by number of extreme resolved line, considering broadening action by Doppler effect for Balmer, Lyman and Paschen series 09 p1734 A70-22731
- Signal properties and measurement accuracy of noncontacting optical heterodyne velocity sensing method used in differential Doppler velocity measurements 09 p1678 A70-22926
- Doppler VOR offering increased course accuracy and allowing precise area coverage in conjunction with DME ground station 09 p1723 A70-23036
- Doppler-effect-like phenomena of waves or pulses reflected and refracted at moving boundary layers 09 p1728 A70-23072
- Doppler effect induced small spectral line shifts measured by modified duochromator in MPD arc jet 09 p1684 A70-23531
- Laser Doppler velocimeter optics, noting minimal heterodyne alignment needs and stress and vibration stability 10 p1889 A70-24556
- Doppler beat spectrum and modulation depth of He-Ne laser emission with backward beam reflected from moving mirror into resonator 10 p1901 A70-25123

Optical heterodyning of Doppler shifted signal with minimal instrumental spectral broadening and high SNR, applying to turbulence structure measurement by CW laser

11 p2062 A70-25630

Circumterrestrial dust component in Doppler shifted zodiacal light, considering Mie theory

11 p2045 A70-25698

Ionospheric electron and ion temperatures information extraction from Doppler broadening of radar returns based on correlation measurement

12 p2183 A70-27163

Emission spectrum of neon-helium laser receiving Doppler shifted signal from moving mirror, showing memory effect due to beat harmonics

12 p2246 A70-27352

Carbon dioxide CW laser-Doppler velocimeter for detecting aircraft wing tip trailing vortices by measuring atmospheric aerosols backscatter

12 p2249 A70-27630

Satellite based random Doppler environmental measurement technique for Global Atmospheric Research Program /GARP/, receiving signals from balloons, buoys and land stations

13 p2407 A70-29176

Ionic temperature difference from Arecibo data indicated in Injun 3 and Alouette 1 sonograms of proton whistlers propagation time, noting Doppler shift role

13 p2372 A70-29928

Vertical ionospheric electron concentration profiles, horizontal gradients and integral component from Doppler and Faraday signal recording on geophysical rockets, using diversity reception

14 p2569 A70-30205

Phased array monopulse autotracking, radiointerferometer and Doppler frequency methods for radar tracking systems for artificial satellite orbits

15 p2697 A70-31836

Doppler effect pulsed ultrasonic blood flowmeter using transducer alternating as transmitter and receiver

15 p2690 A70-31919

Laser Doppler heterodyning system for velocity measurements without directional ambiguity, employing incident beams of different frequencies through rotating diffraction grating or Bragg cell application

15 p2751 A70-31986

Gas flow velocity measurement by coherent detection of scattered laser radiation from small particles suspended in fluid, using Doppler effect

15 p2751 A70-32030

Laser Doppler velocimeter for measuring turbulence in gas and fluid flows

16 p2926 A70-33140

Laser Doppler-shift velocimeter with self aligning optics, discussing performance parameters

16 p2926 A70-33143

Pressure broadened line widths in electric field induced fundamental hydrogen spectral band, noting linear variation with density

16 p2954 A70-33276

Recursive estimation and Kalman filtering for space vehicle trajectory tracking, using Doppler shift measurements

16 p2866 A70-34071

Doppler shifted radiation production, using time and space dependent radiant energy sources

16 p2952 A70-34255

Ionospheric refraction during radio wave propagation using space diversity recordings of Faraday and Doppler effects for coherent signals from geophysical rockets

19 p3407 A70-37306

Dual scatter laser Doppler velocimeter /LDV/ technique, considering system design, performance and experimental verifications

19 p3424 A70-37876

Aperture size effect on frequency shift and frequency width variation of beat signals observed with laser Doppler velocity meter

19 p3428 A70-38502

Velocity measurement by Doppler effect in two-point direction finding, calculating error dependence on angular coordinates and distance

20 p3587 A70-39792

Amplitude-phase data from gathering receiving antenna array, obtaining Doppler frequency spectrum as arrival angle function

20 p3599 A70-40319

Ionosphere and magnetosphere total electron content from beacon method of measuring difference-differential-doppler /DDD/ and Faraday effects via synchronous satellite signal frequencies

20 p3590 A70-40484

Doppler beat spectrum and modulation depth of He-Ne laser emission with backward beam reflected from moving mirror into resonator

20 p3643 A70-40516

Doppler frequency shift of reflected radio waves for ionospheric disturbances, discussing solar flares, geomagnetic variations, etc

21 p3820 A70-42256

Doppler effect in interference fringe formation in holographic vibration analysis, discussing path length variation

22 p4038 A70-43152

Emission spectrum of neon-helium laser receiving Doppler shifted signal from moving mirror, showing memory effect due to beat harmonics

22 p4052 A70-43596

Flowing medium turbulent velocity measurement using laser Doppler device

22 p4040 A70-43615

ELF acoustic gravity wave arrival from Apollo launches recorded by Doppler shift ionospheric sounder channeled near mesopause and lower thermosphere

23 p4187 A70-43859

Optical FM system with laser interferometer and sideband carrier circuit for measuring mechanical shock by Doppler shift

23 p4193 A70-43964

Doppler effect simplification to classical Laplacian orbit determination, deriving equations in perturbed gravity field for initial point determination

23 p4246 A70-44697

Coherent motion effects on brightness of clouds moving above photosphere, describing H alpha Doppler brightening and Lyman alpha Doppler dimming in solar prominences

24 p4400 A70-45313

Doppler satellite measurements in semidynamic geodesy using data from Mediterranean ground stations

24 p4312 A70-45543

Ionospheric HF Doppler frequency dispersion at low latitudes under various geomagnetic disturbance conditions

24 p4314 A70-46129

Aircraft Doppler VHF omnidirectional radio range /DVOR/ performance test, noting improvement over VOR system

24 p4375 A70-46240

Vertical ionospheric electron concentration profiles, horizontal gradients and integral component from Doppler and Faraday signal recording on geophysical rockets, using diversity reception

24 p4330 A70-46280

Laser Doppler shift theory and applications to vibration and flow velocity field measurements

24 p4340 A70-46351

DOPPLER NAVIGATION

Doppler memory mode of ground speed and drift angle calculations analyzed by operators for possible errors

04 p0716 A70-14629

Computerized aircraft navigation utilizing Doppler dead reckoning system and Tacan integration with least square adjustment method

13 p2447 A70-28550

Preflight error statistics of earth based Doppler tracking for Mariner navigation concerning Mars 1971 and Venus-Mercury 1973 missions

[AIAA PAPER 70-1077]

20 p3670 A70-40023

Integrated air navigation by least square adjustment, analyzing Doppler navigation errors

22 p4067 A70-42655

DOPPLER RADAR

Ferrite-type phase shifter production by microstrip technique and integrated microwave system use in Gunn element Doppler radar

01 p0052 A70-11290

Doppler radar spectrum mean and variance derived for reflectivity gradients combined with linear wind shear velocity gradient

02 p0328 A70-12508

Reliability of Doppler radar hail detection, discussing corrupting effects of turbulence and shear, size-sorting and vertical air motions

03 p0443 A70-13167

Self excited microwave mixer and transmitting oscillator using Gunn diode applied to short distance Doppler radar

05 p0822 A70-16678

Gravity anomalies of moon mapped by time differentiation of Doppler-tracked satellite velocities, noting isostatic equilibrium

05 p0915 A70-16827

X band Doppler radar observation of horizontal motion of precipitation particles in low levels of slow moving thunderstorm

06 p1101 A70-18580

Navigational accuracy of two way Doppler tracking of interplanetary spacecraft during heliocentric and planetary encounter trajectory phases

[AIAA PAPER 69-899]

07 p1331 A70-19727

Precipitations microstructure remote measurements using Doppler method and attenuation coefficients measurements, estimating errors

08 p1536 A70-21095

Atmospheric small scale turbulence observation by Doppler radar, noting role of tracers radial velocity spectrum

09 p1716 A70-22364

Lower atmosphere turbulence under convective conditions, comparing Doppler radar and instrumented aircraft wind speed fluctuation measurements

09 p1716 A70-22367

AM and FM CW Doppler radar by combined AM-FM waveform, noting automatic track while scan radar application

10 p1840 A70-24445

Pulsed Doppler radar technique for monitoring and diagnosing severe storms, obtaining wind velocity and direction within cloud

10 p1844 A70-25242

Vertical air velocity in convective clouds by pulsed Doppler radar observations of thunderstorm

11 p2004 A70-25650

Turbulent ionized wakes Doppler radar scattering spectrum parameters in terms of wake characteristics using double convolution integral

11 p2010 A70-26271

Sea roughness effect on bandwidth of radar backscatter, analyzing Doppler signals of eight millimeter aircraft navigation system

12 p2228 A70-26906

Subclutter visibility /SCV/, resolution and interclutter of MTI or Doppler search radars in land, sea and weather clutter

12 p2188 A70-27940

Doppler radar aircraft navigation system with gyroscopic reference platform and computer, showing error propagation dependence on velocity and latitude

13 p2449 A70-29621

Radar reflectivity correlations with lunar surface structure in Mare Imbrium, using delay-Doppler radar maps

17 p3154 A70-34568

Doppler radar frequency tracker with servomechanism applicable to velocity computation of aircraft for self contained navigation

18 p3226 A70-36063

Vortex signature recognition from radial velocity field by Doppler radar

20 p3664 A70-40067

Digital Doppler ambiguity resolution method for pulsed S-band radar, using integrating interval approach

22 p3992 A70-43592

DORNIER AIRCRAFT

NT DO-31 AIRCRAFT

DO-231 fixed wing V/STOL airliner project based on DO-31 development, construction and flight tests, considering design problems, controls, safety, performance targets, etc

05 p0793 A70-15901

V/STOL Do 231 design, discussing propulsion, control, safety, traffic control and economic factors

08 p1435 A70-20640

DORNIER DO-31 AIRCRAFT

U DO-31 AIRCRAFT

DOSAGE

NT RADIATION DOSAGE

Empirical formulas derived for intuitive estimates of blood coagulability in patients to facilitate medication dosage prescription

07 p1210 A70-19558

Venturi tube optimal design and operation parameters for small liquid quantities dosage

11 p2035 A70-25778

Antimotion sickness drugs evaluated for effectiveness under standardized stress conditions in slow rotation room

20 p3572 A70-39439

DOSE

U DOSAGE

DOSIMETERS

NT THRESHOLD DETECTORS [DOSIMETERS]

Radiation dosimetry and shielding onboard Cosmos 110 artificial satellite, noting earth belt proton radiation

01 p0198 A70-11518

Book on photographic action of ionizing radiations in dosimetry and medical, industrial, neutron, auto- and microradiography, emphasizing photographic materials reaction to photons and particles

02 p0337 A70-11696

Biological dosimetry techniques for irradiation damage evaluation

02 p0239 A70-12581

Space environment radiation dose monitoring systems requirements and implementation, discussing material distribution, dose equivalence, parameters accuracy, etc

06 p0990 A70-17262

Radiation dose measurements from satellite and space probe experiments, considering radiation and shielding characteristics, sensor orientation effects, etc

06 p0990 A70-17266

Dosimetry data and personal radiation sensors from Apollo and Gemini flights, noting spacecraft geometry shielding effects

06 p1134 A70-17268

Soviet manned space flight radiation dosimetry evaluation, comparing U.S. and Soviet techniques for astronaut protection

06 p0990 A70-17271

- Thermoluminescent glass X ray dosimeter sensitivity tested as function of rigidity of gamma and X radiation, noting compensating filters for incident radiation
08 p1496 A70-21217
- Continuous generation of gas trace component quantities into carrier gas flow using dosage device
09 p1672 A70-22028
- Anthracene, polystyrene and stilbene for scintillation counters measuring cosmic ray protons, analyzing dosimetric properties
17 p3151 A70-35352
- CW laser beam power density distribution monitoring by self calibrating photographic dosimetry technique
24 p4307 A70-45343
- DOSIMETRY**
U **DOSIMETERS**
DOUBLE BASE PROPELLANTS
NT **DOUBLE BASE ROCKET PROPELLANTS**
Reaction heat for flameless combustion of double-base propellant using differential scanning calorimetry and thermogravimetric analysis, noting pressure effects
[AIAA PAPER 70-125] 06 p1179 A70-18045
Low pressure burning rate of double base propellants at various initial temperatures in argon and in air
12 p2332 A70-27844
Acceleration effects on burning rates of double base propellants with and without Al additive
16 p2963 A70-33883
Autoignition, ignition and surface temperatures of M-2 double base propellant at low pressure, correcting thermocouple measurements by theoretical model
18 p3299 A70-36697
Thermocouple and IR temperature measurement techniques comparison for double base solid propellants at low pressures
20 p3694 A70-40275
- DOUBLE BASE ROCKET PROPELLANTS**
Cast double base technique for free-standing and case-bonded propellant charges, discussing manufacturing and mathematical model of casting and curing
07 p1360 A70-19906
Pressure surges originated by tangential instabilities in solid propellant motors, using double base homogeneously compounded cylindrical grains
09 p1743 A70-22661
Composite and double base solid rocket propellants manufactured by French factory for ballistic missiles, discussing plant installations
11 p2030 A70-25520
- DOUBLE CUSPS**
Minor planets orbits coordinates and velocities data at osculation time
09 p1756 A70-22654
- DOUBLE SIDEBAND TRANSMISSION**
Coherent reference for demodulating double sideband suppressed carrier (DSB-SC) signals in presence of frequency detuning, using squaring or Costas loop
22 p3990 A70-43326
- DOUGLAS AIRCRAFT**
NT C-9 AIRCRAFT
NT C-47 AIRCRAFT
NT DC 8 AIRCRAFT
NT DC 9 AIRCRAFT
DOUGLAS DC-8 AIRCRAFT
U DC 8 AIRCRAFT
DOUGLAS DC-9 AIRCRAFT
U DC 9 AIRCRAFT
DOUGLAS MILITARY AIRCRAFT
U MILITARY AIRCRAFT
DOVAP
U **DOPPLER EFFECT**
DOWNTIME
Reliability figure of merit variations for predicted microwave radio system outages, using computer method
20 p3583 A70-38987
- DOWNWASH**
Test chamber to simulate helicopter rotor downwash for engine inlet air particle separator optimization
01 p0056 A70-10676
Optimal control conditions for elastic aircraft motion with delayed wing downwash determined by hyperbolic partial differential equations with delay
08 p1480 A70-21178
Isolated convective plumes immersed in return flow turbulent downdraft
15 p2769 A70-31440
Aircraft condensation trails formation by interactions of exhaust emission, vorticity of wing induced downwash and ambient atmosphere
22 p3958 A70-42684
Downwash angle behind straight wing for unsteady aperiodic flight at subsonic speeds, using vorticity model
22 p3959 A70-42802
Small airplane unsteady motion downwash angle at low speeds, comparing results from rectilinear steady flights
[ICAS PAPER 70-25] 23 p4138 A70-44108
- DRAFTING (DRAWING)**
Engineering design and drafting techniques in aerospace industry, emphasizing cost reduction
13 p2423 A70-29820

DRAG

- NT **AERODYNAMIC DRAG**
NT **ELECTROSTATIC DRAG**
NT **FRICTION DRAG**
NT **INTERFERENCE DRAG**
NT **MINIMUM DRAG**
NT **PRESSURE DRAG**
NT **SATELLITE DRAG**
NT **SUPERSONIC DRAG**
NT **VISCOUS DRAG**
NT **WAVE DRAG**
Solar wind-induced drag resulting from collisionless plasma shock on sunward-side of large magnetic comet, using similarity with earth magnetosphere
01 p0168 A70-10258
Chaplygin equation solution for wedge flows applied to Rethy flows, evaluating drag coefficient and approximate hodograph equations for subsonic and transonic regimes
04 p0614 A70-14613
Aligned electric current effect on drag of sphere with arbitrary conductivity moving in current carrying fluid
04 p0671 A70-14993
Free stream turbulence effect on drag coefficient of bluff sharp edged cylinders with small square section
05 p0789 A70-15923
Transonic flow theory, investigating thin three dimensional lifting wings, similarity for lift and drag, plane flow past airfoil, far field and hodograph solutions
[D1-82-0878] 05 p0834 A70-16693
One dimensional compressible flow analysis for near field aerodynamics of tube-vehicles, showing drag coefficient dependence
[AIAA PAPER 70-140] 06 p1038 A70-18077
Drag of diffusely reflecting and cool slender cone in hypersonic flow, using nonlinear Boltzmann equation for hard spheres
06 p0981 A70-18359
Dynamic simulation parameters for sphere drag coefficient data correlation in near free molecular flow
06 p0983 A70-18374
Free flight ballistic range method for measuring average drag coefficients for microscopic spherical iron particles in free molecular flow
06 p0983 A70-18378
Sphere and sharp slender cone drag coefficients in hypersonic transitional flow measured by flow modulation technique
06 p0984 A70-18389
Nonlinear pursuit problem solution taking into account drag and lift in pursuing object equations of motion
07 p1330 A70-18682
Aerodynamic drag coefficients and moments for axisymmetric bodies of revolution in rarefied plasma derived for limiting case of delta flux
08 p1432 A70-21088
Current sheet velocity in coaxial plasma accelerator, noting drag due to insulator ablation and degassing
[AIAA PAPER 69-265] 09 p1736 A70-23202
Variations after one revolution in semimajor axis, period and eccentricity computed for orbit using variable drag coefficient involving satellite and air thermal speeds
10 p1951 A70-24824
Hypersonic low density transitional flow over slender conical vehicle, calculating drag coefficient and density profiles
14 p2529 A70-31365
Interstellar drag resulting from relativistic rocket elastic collisions with interstellar matter, discussing effects on minimum time acceleration limited relativistic trajectories
17 p3155 A70-34752
Steady state tangential drag by solar wind on geomagnetic cavity, describing unipolar induction
22 p4013 A70-42469
Relaxation gas dynamics, discussing vorticity and drag generation by relaxation, linearized theory and shock waves structure
23 p4178 A70-43889
Parachute trajectory and opening load prediction based on inflation process and added mass, determining drag area as function of distance
[AIAA PAPER 70-1168] 23 p4137 A70-43993
Bodies of revolution optimal configuration, considering minimum head drag coefficient and low heat transfer at hypersonic speeds, using modified Newtonian and hypersonic flow theories
23 p4136 A70-45021
- DRAG BALANCE**
U **AERODYNAMIC BALANCE**
U **LIFT DRAG RATIO**
DRAG CHUTES
Tractor rocket powered escape system of 600 knot extraction capability using drogue parachute and barometric time delay device
[AIAA PAPER 70-1209] 21 p3751 A70-41809
Reentry vehicle recovery deployment initiation, comparing performances of conical wake drogue and body attached spoilers hypersonic deceleration devices
[AIAA PAPER 70-1207] 21 p3752 A70-41811

DRAG COEFFICIENT

- U **AERODYNAMIC COEFFICIENTS**
U **DRAG**
DRAG DEVICES
NT **AERODYNAMIC BRAKES**
NT **BALLUTES**
NT **DRAG CHUTES**
NT **SPOILERS**
NT **TRAILING-EDGE FLAPS**
NT **WING FLAPS**
Streamers (drag devices) tests at subsonic speeds, measuring drag dependence on size, weight, shape and velocity
20 p3559 A70-40282
Euler buckling of inflated toroidal drag bodies, including packaging and load deflection tests for Mylar, dacron-neoprene and stainless steel-silicone fabrics
[AIAA PAPER 70-1198] 21 p3932 A70-41818
Attached Inflatable Decelerator for planetary atmospheric entry, discussing mission applications and wind tunnel models performance
[AIAA PAPER 70-1163] 21 p3931 A70-41848
- DRAG EFFECT**
U **DRAG**
DRAG MEASUREMENT
Air-glass particle suspensions flows in shock tubes, deriving effective drag coefficients from simultaneous particle concentration and pressure measurements
[ASME PAPER 69-WA/FE-21] 04 p0667 A70-14778
Periodic drag of vibrating cylinders as function of excitation amplitude and frequency, noting similarity to nonlinear oscillator subjected to forced vibration
04 p0691 A70-15148
Pressure distribution and drag measurements at flat triangular bodies and rectangular plates with blunt trailing edge in compressible flow
06 p0965 A70-17243
Sphere drag measurements in low density hypersonic transition and near free molecular flow
06 p1124 A70-18373
Plastic lubricants motion in circular pipes, determining drag and cross sectional velocity profile of laminar flows
07 p1290 A70-18652
Drag on sharp cones in hypersonic flow, studying effects of intense transverse mass injection through porous walls
09 p1603 A70-22441
Drag coefficients for spheres and sharp cones in rarefied hypersonic air flow obtained in shock tunnel using free flight technique
09 p1605 A70-23221
Drag measurement for star-shaped body at hypersonic speeds, comparing results with cone-shaped model
10 p1799 A70-24122
Boundary layer equations for laminar flow, drag and heat transfer of gas in circular tube, considering parabolic and uniform entrance velocity profiles
15 p2722 A70-32692
Exhaust nozzle model tests at high subsonic Mach numbers, investigating differences in nozzle drag in contrast to engine conditions
[AIAA PAPER 70-668] 16 p2967 A70-33573
Wing camber and twist effects on transonic drag, using wind tunnel measurements
16 p2840 A70-34321
Magnetic field and permeability effects on drag in steady axisymmetric MHD flow of incompressible fluid around full and hollow spheres
19 p3477 A70-37577
Cylindrical afterbodies base pressure drag under powered supersonic flight, modifying Korst flow model recompression criterion
22 p3959 A70-42713
Strike fighter aircraft fuselage side air intakes, measuring external drag as function of design at subsonic and supersonic speeds
[ICAS PAPER 70-49] 23 p4133 A70-44146
Entrainment theory for incompressible turbulent boundary layer velocity and drag on bodies of revolution employed in fuselage, submersible and cowlings for propulsion design
23 p4182 A70-44400
Free jet flow axial gradient effects on drag coefficient measurement of slender blunted cones at zero attack angle
23 p4135 A70-44584
- DRAG REDUCTION**
Monograph on aircraft aerodynamic nozzle asymmetry effects for pressure drag reduction in critical conditions
03 p0465 A70-13003
Laser velocimeter measurements on drag reducing polyacrylamide solution compared to water
03 p0502 A70-13821
Supersonic missile drag reduction through wake heating assuming conical shaped missile tail and flow nonseparation
[DFVLR-SONDDR-36] 04 p0616 A70-15165
Drag reduction on blunt-based body of revolution with boat-tailed afterbodies in low speed flow
05 p0790 A70-16501

- Frictional drag reducing polymer solution injection into boundary for turbulent pipe flow, discussing Reynolds number, injection rate, injection points and concentration
06 p1032 A70-17215
- Long chain molecule additive effect on drag reduction in turbulent flow of aqueous polymeric solutions [AIAA PAPER 70-56]
06 p1037 A70-18030
- Boundary layer research during past decade covering crosshatching during reentry, transition, drag reduction by LFC or compliant surfaces
08 p1483 A70-21040
- Camber and twist distributions for closed ground effect wing optimum design for zero induced drag, employing linearized theory
10 p1801 A70-24158
- Viscous fluid dynamics for reducing hydrodynamic resistance, discussing aquatic animals speeds, vortex flows, etc
10 p1871 A70-25193
- Cylindrical afterbody drag reduction in transonic flow by combined gas ejection and boat-tailing
11 p1976 A70-25991
- Maximum thrust and drag reduction for supersonic missiles by base burning, showing dependence on chemical reaction and Mach number
12 p2158 A70-28208
- Model for hydraulic resistance reduction for turbulent fluid flows by injecting suspended impurities
15 p2719 A70-31489
- Long chain molecule additive effect on drag reduction in turbulent flow of aqueous polymeric solutions
17 p3066 A70-34525
- Drag optimal stern section of plane body at supersonic flow, allowing for friction forces
18 p3206 A70-36261
- Spike effect on nose drag and static stability of blunt bodies, estimating optimum length for drag reduction at zero angle of attack
20 p3558 A70-39702
- Minimum-drag boattail configurations optimization for supersonic flow, determining wave drag coefficients
22 p3961 A70-42714
- DRAGULATORS**
U BRAKES [FOR ARRESTING MOTION]
U DRAG DEVICES
- DRAINAGE**
Aerial photography analysis of drainage basin discharge properties, discussing surface runoff, subsurface flow and underground water movement
10 p1879 A70-24750
- Automatic measurement of drainage networks for lengths and areas by copper plate etching or flying spot scanner on transparencies or radar images
20 p3633 A70-39794
- DRAINING**
U DRAINAGE
- DRAWINGS**
Regular and irregular line-drawing data processing, discussing quantization and encoding methods
12 p2193 A70-28104
- Mars 1969 planetary surface drawing and photograph evaluation, noting dark spot east of Nodus Lacoontis
17 p3154 A70-34677
- DREAMS**
Collection of articles on fatigue, sleep and dreams covering mechanisms, biochemistry, pathological physiology, etc
15 p2680 A70-31739
- DRIFT**
HF instabilities effect on magnetospheric drift waves, considering Alfvén mode in auroral plasma
13 p2482 A70-30084
- DRIFT [INSTRUMENTATION]**
Doppler memory mode of ground speed and drift angle calculations analyzed by operators for possible errors
04 p0716 A70-14629
- Telescope servocontrol system with low pointing error and drift rate, permitting extended time exposure photography of star or deep space probe
12 p2202 A70-26869
- Drift of two platform gyroazimuth with stabilized base under harmonic or random vibrations
15 p2734 A70-31622
- Viscous friction force moments effect on gyroscope drift in gimbal suspension during base angular vibrations, obtaining drift velocity
15 p2738 A70-32153
- Open faced polyimide-backed strain gage for transducer and/or long term applications, considering drift and zero shifts
15 p2739 A70-32329
- Drift reducing NMR stabilization of Hall regulated electromagnet, applying error signal to bias coil
21 p3827 A70-41456
- DRIFT RATE**
Ionospheric discontinuities drift velocities from diversity reception data indicating no dependence on solar activity
01 p0083 A70-11531
- Electron transverse and perpendicular drift velocities calculated at moderate and strong magnetic fields for hydrogen, using Maxwellian energy distribution and equivalent pressure concept
02 p0348 A70-12654
- Interplanetary plasma inhomogeneity size, shape and spatial orientation and drift velocity and direction determined from radio telescope data
03 p0565 A70-13231
- Kinetic equation of helicons interactions in electron-hole plasma, discussing turbulence spectrum and effect on current carrier drift velocity
03 p0531 A70-13407
- Magnetic activity effect on ionospheric drift speeds variation with latitude, observing correlation with electron density
05 p0837 A70-15922
- Large scale ionospheric inhomogeneities anisotropy, dimensions and drift velocities from simultaneously measured irregular refraction
05 p0841 A70-16739
- Radio astronomical observations of shape and drift velocity of focusing ionospheric discontinuities
05 p0841 A70-16740
- Meteor trail drift characteristics from telescopic observations, determining velocity and diffusion coefficient
05 p0920 A70-16975
- HF drift instabilities of plasma with nonuniform magnetic field, studying anomalous ion heating and resistance in Zeta instabilities
06 p1119 A70-17502
- Propagation in perturbed magnetically focused electron beams, noting influence of spatially varying drift velocity and damping effect
07 p1239 A70-18867
- Diffraction pattern drift velocity increase with temporal frequency of Fourier components by dispersion analysis of interplanetary scintillation, noting solar wind structure
07 p1388 A70-20076
- Interplanetary plasma inhomogeneity size, shape and spatial orientation and drift velocity and direction determined from radio telescope data
08 p1580 A70-21664
- Horizontal ionospheric drift rates and traveling wave disturbances, showing differences between winter and summer
09 p1667 A70-22493
- Drift dissipative instability of weakly ionized plasma, considering ion motion along magnetic lines in dispersion equation
10 p1923 A70-24407
- Solid state plasma drift velocity effect on helicon propagation constant assuming isotropic momentum relaxation time and effective mass
10 p1928 A70-24831
- Archeomagnetic measurements showing westward drift of geomagnetic intensity and correlation of magnetic earth moment with radiocarbon production
11 p2044 A70-25599
- Spherical electroacoustic waves in drifting thermal plasma, describing ion acoustic perturbations
12 p2279 A70-27779
- Drift wave instabilities nonlinearities, discussing plasma growth rate and saturation coefficients, damping rate as function of amplitude and lower mode modification
12 p2280 A70-27786
- Drift waves relation to anomalous cross field diffusion in fully ionized magnetoplasmas, introducing model predicting amplitude, correlation time, fluctuation spectrum and diffusion process
12 p2280 A70-27788
- Lower ionosphere nonuniformities drift velocity and direction using space diversity reception
14 p2571 A70-30233
- Hall, polarization and Pedersen charged particle drift velocities in static magnetic and time dependent electric field
14 p2624 A70-31046
- Barium ion clouds striation formation above E layer ascribed to LF gradient drift instability
15 p2727 A70-31908
- Electron mobility, diffusion, drift velocity and attachment in oxygen, determining Townsend primary ionization coefficient
15 p2776 A70-31969
- Viscous friction force moments effect on gyroscope drift in gimbal suspension during base angular vibrations, obtaining drift velocity
15 p2738 A70-32153
- Doped Gunn diode domain field width, nucleation and annihilation dependence on electron drift velocity
16 p2879 A70-34044
- Drift velocity for bound electron orbital motion in static axisymmetric magnetic field
16 p2959 A70-34187
- Refractive index equation for Whistler propagation in weakly drifting magnetoplasma
16 p2959 A70-34224
- VHF auroral scatter signal correlation analysis, determining scale size and drift velocity of scattered field
17 p3047 A70-35548
- Ionospheric drift velocity fluctuations by similar fading method, discussing applicability and errors
19 p3408 A70-37312
- Auroral phenomena interdisciplinary investigations, discussing electron precipitation and conjugate point drift due to geomagnetic axis position variations
19 p3411 A70-37493
- Electron drift velocity longitudinal variation in equatorial electrojet, noting land-sea boundary and magnetic anomalies effects
20 p3620 A70-39337
- Slow ions mobility, diffusion and reactions in gases by drift tubes, developing mathematical analysis of drifting ion swarm space-time behavior
20 p3676 A70-40152
- Gaseous neon plasma positive column electrons density and drift velocities measurements by Langmuir probe technique
20 p3683 A70-40163
- Pulsars subpulse intensities and shapes in magnetic field, noting drift speed sawtooth patterns
20 p3713 A70-40428
- Satellite-borne sensor for ionospheric ions velocity measurement, describing design and principles of operation
21 p3813 A70-40834
- Ionospheric ions drift velocity horizontal and vertical components distribution, using satellite-borne sensor
21 p3813 A70-40835
- Collisionless nitrogen plasma drift velocity measurement by ion acoustic wave method
21 p3859 A70-41760
- Dynamo region electrostatic fields effects on magnetospheric drift, taking electrical conductivities and solar and lunar tidal modes into account
23 p4185 A70-43836
- Electron precipitation latitude extent and drift rate magnetospheric substorms from ESSA riometer data
23 p4186 A70-43850
- Plasma with oriented charged particle fluxes macroscopic parameter measurement by multigrad probes facing and reversed to drift, noting graphical data processing
24 p4385 A70-45454
- Pressure gradient induced drift waves in collisionless hydrogen plasma in homogeneous magnetic field
24 p4388 A70-46209
- Lower ionosphere nonuniformities drift velocity and direction using space diversity reception
24 p4331 A70-46308
- DRILLING**
Equations for deep hole drilling errors calculations ensuring accuracy
07 p1291 A70-18826
- Electrochemical machining for drilling deep holes in alloys and refractory metals used in jet engine hardware
10 p1893 A70-23857
- Drilling rates improvement for Ti by adding ultrasonic vibration to conventional process
19 p3437 A70-38421
- Carbon dioxide laser adapted for high speed drilling of fine holes in thin rubber sheeting
23 p4201 A70-44474
- Drilling machinability of wrought Al alloys, relating tool force to hardness, feeding and cutting speed
24 p4349 A70-46195
- Si content and chip treatment effects on drilling machinability of Al-Si alloys
24 p4349 A70-46199
- DRINKING**
Hunger, thirst and environmental stimuli roles in development and elicitation of stimulus bound eating and drinking in animals
13 p2355 A70-29806
- Photoperiod effects on rats food and water intake, noting endogenous feeding rhythm correlation with activity patterns
24 p4296 A70-45332
- DRIVES**
Simulator servo drive system dynamic requirements for single-axis manual control task using pilot models and computer
10 p1858 A70-24208
- [AIAA PAPER 70-355]
Hypothalamic motivation, presenting data supporting less anatomical specificity
13 p2355 A70-29794
- DROGE PARACHUTES**
U DRAG CHUTES
- DROGUES**
U TOWED BODIES
- DRONE AIRCRAFT**
NT TARGET DRONE AIRCRAFT
TV system for controlling QF-9 drone aircraft landing, takeoff and BQM-34A target drone in-flight test operations
01 p0058 A70-10815
- Remote control turboprop drone aircraft for long unmanned electronic intelligence or tactical communications relay missions
08 p1435 A70-20625
- Negative g Drone aircraft surface tension fuel system preventing air inclusion in turbojet engine fuel by tank filters/screens/ [AIAA PAPER 70-910]
17 p3019 A70-35822

DRONE HELICOPTERS

U DRONE AIRCRAFT
U HELICOPTERS

DRONE VEHICLES

NT DRONE AIRCRAFT
NT TARGET DRONE AIRCRAFT

Parachute recovery system for surveillance drone and landing bag subsystem
[AIAA PAPER 68-935] 14 p2531 A70-30858

DROP SIZE

Holograms of light scattered by clouds of water droplets to determine drop size, noting agreement with Mie theory 02 p0296 A70-11890

Liquid diethylcyclohexane /DECH/ sprays detonation propagation in gaseous oxygen, studying drop size effect on steady state development 02 p0351 A70-12003

Supersaturated vapor condensation in supersonic nozzles, obtaining flow and droplet growth equations for local equilibrium condition 02 p0279 A70-12049

Disintegration of charged distilled water jets, discussing drops size, velocity distribution and instabilities 03 p0467 A70-13781

Frozen wax measurement of droplet sizes and sprays from impinging injector elements, concerning like and unlike doublets and quintuplets 04 p0786 A70-15416

Cloud chamber investigation of artificial cloud of water droplets in electrostatic field, discussing cloud precipitation, collection efficiency and fog dissipation 05 p0879 A70-16689

N-heptane and Freon-13 droplets vaporizing size and temperature at supercritical pressures in heated air stream [AIAA PAPER 70-6] 06 p1182 A70-18204

Airborne precipitation drop sampler imprint size relationship to water drop diameter 10 p1857 A70-23932

Nozzle fuel and air system geometrical parameters to determine mean diameter of fuel droplets, dispersion angle and spectrum and flame jet shape 10 p1930 A70-24295

Fog droplet size growth time dependence and spectral variations during simulated cloud formation by water vapor condensation in chamber 14 p2601 A70-30128

Model for droplet size spectrum in cloud with spatial inhomogeneity of nuclei concentration, determining characteristic size dependence on altitude 14 p2601 A70-30129

Monopropellant rocket combustion one dimensional theory with uniform velocity and size droplets injection, obtaining chamber length 14 p2629 A70-30773

External burning fuels environmental temperature requirements from nonlinear droplet ignition model, emphasizing droplet size importance [AIAA PAPER 70-607] 16 p2997 A70-33604

Cloud droplet agglomeration by weak shock waves, discussing growth mechanism 17 p3067 A70-34549

Centrifugal atomizer mean drop size dependence on geometry, fluid properties and discharge velocity 18 p3300 A70-36274

Prototype cloud physics laser nephelometer design and performance, determining droplet concentration and size from scattered light pulse count and amplitudes 20 p3626 A70-39081

Water droplet size measurement by forward light scatter holography, evaluating reconstructed wave front by Fresnel transform 20 p3628 A70-39132

Aerosol IR emission, discussing relative humidity, water droplet size and temperature effects on atmospheric radiance levels 21 p3846 A70-40804

Fuel nozzle sprays mean droplet diameter based on computerized analysis of small angle forward scattered light profile 21 p3806 A70-40805

Fuel atomization drop size calculation for mechanical swirl injectors with and without air input 21 p3867 A70-41770

Fuel atomization drop size calculation for mechanical swirl injectors with and without air input 21 p3867 A70-41770

Fuel atomization drop size calculation for mechanical swirl injectors with and without air input 21 p3867 A70-41770

Fuel atomization drop size calculation for mechanical swirl injectors with and without air input 21 p3867 A70-41770

Fuel atomization drop size calculation for mechanical swirl injectors with and without air input 21 p3867 A70-41770

Fuel atomization drop size calculation for mechanical swirl injectors with and without air input 21 p3867 A70-41770

Fuel atomization drop size calculation for mechanical swirl injectors with and without air input 21 p3867 A70-41770

Fuel atomization drop size calculation for mechanical swirl injectors with and without air input 21 p3867 A70-41770

Fuel atomization drop size calculation for mechanical swirl injectors with and without air input 21 p3867 A70-41770

Fuel atomization drop size calculation for mechanical swirl injectors with and without air input 21 p3867 A70-41770

Drop-weight tear test evaluation taking into account operator, test machine, specimen thickness, notch type and strength level effects 15 p2759 A70-32241

Hydrostatic stability and damping characteristics of perforated plates and screens for passive propellant control schemes from drop tower tests [AIAA PAPER 69-531] 15 p2787 A70-32510

Drop weight tests U DROP TESTS

DROPS (LIQUIDS)
NT RAINDROPS

Mathematical model of spherically symmetric quiescent droplet undergoing quasi-steady vaporization near thermodynamic critical point 01 p0213 A70-10291

Mass loss rate of evaporating liquid droplet with vapor reacting with oxygen of atmosphere in combustion front [DFVLR-SONDDR-16] 01 p0216 A70-10932

Fuel droplets burning at pressures sufficient to reach critical temperature under zero gravity conditions in free fall apparatus 02 p0351 A70-12002

Liquid sodium droplets spontaneous ignition and combustion in controlled oxidizing atmosphere, discussing vapor phase diffusion flame, burning rates and evaporation constants 02 p0396 A70-12005

Burning constants prediction for suspended hydrocarbon fuel droplets based on modified theoretical equation 03 p0544 A70-13916

Flame structure of liquid methanol burning spheres, discussing temperature and composition profiles 03 p0544 A70-13924

Physical and chemical phenomena and critical factors underlying, furthering or impeding water droplets coalescence in glass-fiber bed of filter-separator 04 p0625 A70-14709

Frozen wax measurement of droplet sizes and sprays from impinging injector elements, concerning like and unlike doublets and quintuplets 04 p0786 A70-15416

Ignition of freely falling single fuel droplets, considering initial size, oxidizer temperature, fuel composition, droplet spacing, etc 04 p0733 A70-15540

Supersaturation during droplet-liquid phase formation in clouds estimated from trough formed on curve of distribution function 06 p1097 A70-17796

Combustion processes and ignition criteria in shock wave ignition of liquid fuel drop in oxidizing atmosphere [AIAA PAPER 70-9] 06 p1180 A70-18142

Evaporation rate from spherical drop into vacuum influenced by molecular collisions occurring in gas cloud formed by emitted particles 06 p1113 A70-18283

Solid surface-compressible liquid drop high speed impact damage, discussing contact pressure 06 p1053 A70-18611

Burning rates of monopropellant droplet evaluated by variable property models, discussing dimensionless mass flow rate 07 p1358 A70-18914

Integral method for time development of viscous, heat and mass conducting layer over leading edge of volatile drop instantaneously immersed in gas stream 07 p1358 A70-18916

Quasi-steady adiabatic vaporization and exothermic decomposition of monopropellant spherical droplet in inert and reactive environments 07 p1359 A70-19580

Metal erosion under liquid drop impingement attack, investigating damage from microplastic deformation to surface material removal using wheel and jet apparatus 08 p1519 A70-21354

Electrohydrodynamics of charged water drop pairs disintegration in electric field concerning warm cloud electrification 10 p1912 A70-24806

Warm clouds electrification calculated for electromagnetic field growth by inductive mechanism, noting role of water drop pair interaction 10 p1913 A70-24807

Oxide transport and water vapor effects on flash-heated beryllium droplet combustion 10 p1969 A70-25042

Initial cloud formation model, computing drop concentration and supersaturation 11 p2075 A70-25917

Deposition zone on sphere and aerosol particles flux onto sphere as functions of flow Reynolds and Stokes numbers, discussing drop deformation effects 12 p2263 A70-27513

Carrier gas effect on homogeneous condensation in supersonic nozzle using liquid drop theory 12 p2211 A70-27829

Solid particles or liquid drops admixture effect on propagation of inhomogeneous turbulent gas jet, using

Prandtl mixing length theory to estimate pulsation velocities 12 p2213 A70-28218

Radiating drop unsteady vaporization or growth for uniformly distributed internal heat sources, discussing gas temperature distribution and diffusion thermal effect 13 p2521 A70-29417

Shock wave interaction with burning liquid fuel droplets in gaseous oxygen atmosphere, observing wave amplification due to mass combustion rate increase 13 p2522 A70-29424

Surface temperature fluctuations during dropwise condensation at various heat fluxes 14 p2663 A70-30256

Cloud droplets coagulation growth, calculating aerosols inertial capture coefficient by fine jet method 14 p2602 A70-30390

Droplets collision and coagulation for processes in aqueous aerosols, discussing interaction with collectors 14 p2603 A70-30391

Evaporation and combustion kinetics of droplets and particles in hot air stream, observing luminous trace 14 p2664 A70-30392

Liquid fuel droplet ignition quasi-stationary theory occurring at maximum chemical reaction rate 14 p2664 A70-30393

Flameout from burning liquid fuel droplet within reduced film theory 14 p2664 A70-30394

Spherical liquid drop deformation time dependence in unbound fluid at low Reynolds number, investigating effects of temperature, pressure, velocity and size 15 p2722 A70-32795

Gaseous flows and local droplet velocity measurement in dense gas/liquid sprayfields, using noninterference technique [AIAA PAPER 70-728] 16 p2910 A70-33491

LF unsteady behavior of liquid propellant rockets from droplets evaporation and combustion rates [AIAA PAPER 70-620] 16 p2968 A70-33589

Liquid nitrogen drops anomalous behavior in film boiling, resolving vaporization time discrepancies 17 p3194 A70-34741

Capillary ball game phenomenon under weightlessness, showing photographs of mercury droplet reflection from fluid boundary 18 p3242 A70-36638

Nonisothermal condensation in ionized vapor as function of energy additions to droplets 20 p3680 A70-39989

Solid particles or liquid drops admixture effect on propagation of inhomogeneous turbulent gas jet, using Prandtl mixing length theory to estimate pulsation velocities 20 p3612 A70-40091

Interfacial instability effect on heat transfer to liquid nitrogen drops undergoing film boiling on flat Al surface, obtaining vaporization rates and times 21 p3948 A70-41203

Liquid droplet shape effect flow field velocity and pressure distribution over windward surface in high speed gas streams 21 p3809 A70-41762

Gas velocity and static pressure effects on evaporation rate of moving liquid fuel droplets 21 p3953 A70-42094

Cloud droplet growth rapid computation using number density mean value for integrating stochastic coalescence equation into differential equation 22 p4064 A70-42910

Water drop-solid surface collision experiments to study rain impact erosion process, using gas gun projectiles, high speed photography, photomicrography and profilometry techniques 22 p4116 A70-43096

Liquid droplet breakup by aerodynamic forces, obtaining solutions for fluid flow inside droplet and in coupled liquid-gaseous boundary layer 22 p4012 A70-43741

Liquid nitrogen drops undergoing film boiling on Al surface, measuring heat transfer coefficient 23 p4279 A70-44360

Spherical shape gas or liquid drop steady motion at large Reynolds numbers, examining buoyancy forces and velocity gradients 24 p4326 A70-45996

Photographic measurement of droplets size, velocity and number during sprayed liquid fuel combustion, using Xe flash bulbs 24 p4429 A70-46008

Photographic measurement of droplets size, velocity and number during sprayed liquid fuel combustion, using Xe flash bulbs 24 p4429 A70-46008

Photographic measurement of droplets size, velocity and number during sprayed liquid fuel combustion, using Xe flash bulbs 24 p4429 A70-46008

Photographic measurement of droplets size, velocity and number during sprayed liquid fuel combustion, using Xe flash bulbs 24 p4429 A70-46008

Photographic measurement of droplets size, velocity and number during sprayed liquid fuel combustion, using Xe flash bulbs 24 p4429 A70-46008

Photographic measurement of droplets size, velocity and number during sprayed liquid fuel combustion, using Xe flash bulbs 24 p4429 A70-46008

Photographic measurement of droplets size, velocity and number during sprayed liquid fuel combustion, using Xe flash bulbs 24 p4429 A70-46008

Photographic measurement of droplets size, velocity and number during sprayed liquid fuel combustion, using Xe flash bulbs 24 p4429 A70-46008

Photographic measurement of droplets size, velocity and number during sprayed liquid fuel combustion, using Xe flash bulbs 24 p4429 A70-46008

Photographic measurement of droplets size, velocity and number during sprayed liquid fuel combustion, using Xe flash bulbs 24 p4429 A70-46008

Photographic measurement of droplets size, velocity and number during sprayed liquid fuel combustion, using Xe flash bulbs 24 p4429 A70-46008

Xanthine dehydrogenase activity in *Drosophila* and *Habrobracon* under hypogravity conditions onboard Biosatellite

23 p4144 A70-43863

DROWSINESS

U SLEEP

DRUG THERAPY

U CHEMOTHERAPY

DRUGS

NT ADRENERGICS
NT ANTIHYPERTENSIVE AGENTS
NT ANTIDIURETICS
NT ANTIDOTES
NT ANTIHYPERTENSIVE AGENTS
NT ANTIRADIATION DRUGS
NT ATROPINE
NT CAFFEINE
NT CENTRAL NERVOUS SYSTEM DEPRESSANTS
NT CENTRAL NERVOUS SYSTEM STIMULANTS
NT CHOLINERGICS
NT CORTISONE
NT CYCLOPROPANE
NT CYSTEINE
NT DIGITALIS
NT EPINEPHRINE
NT HISTAMINES
NT INSULIN
NT MORPHINE
NT MOTION SICKNESS DRUGS
NT NORADRENALINE
NT NOREPINEPHRINE
NT PENTOBARBITAL SODIUM
NT SEDATIVES
NT STIMULANT
NT STREPTOMYCIN
NT TRANQUILIZERS
NT VASOCONSTRICTOR DRUGS

Drug-alcohol and hypoxia effects on multiple task operator performance tested at altitude and pressure chamber treatments

08 p1448 A70-21939

Vasodilator agent effects on decompression sickness in rats, noting increased severity of bends by serotonin and platelet role

10 p1811 A70-24176

Acceleration and hypoxia resistance of mice and rats after injections of phenamine, sidoncarb, strychnine, secunarine, araeside, trioxazine, banactisine and chlordiazepoxide

13 p2358 A70-29344

Sodium oxybutyrate effects on brain tissue oxidation during hypoxia in mice

15 p2686 A70-32851

Hemodynamic response to dopamine before and after myocardial infarction in dogs

17 p3026 A70-35200

General aviation aircraft accident investigation toxicological findings, describing methods of examination for drugs and toxic agents

17 p3033 A70-35569

Psychotropic drugs radioprotective effects in mice, noting oxygen consumption and body temperature decrease after X ray exposure

19 p3367 A70-37558

Hemodynamic effect of lidocaine given by infusion and bolus injections in myocardial infarction, examining cardiac output, heart rate, systolic left ventricular and aortic pressures

19 p3366 A70-38575

DRY CELLS

NT MAGNESIUM CELLS

NT NICKEL ZINC BATTERIES

Nickel cadmium battery construction capabilities and limitations from design engineer and aircraft operator viewpoint

11 p1983 A70-25898

DRY FRICTION

Surface roughness effects on dry friction between two metals, considering conical asperities and friction coefficients

[ASME PAPER 69-LUB-10] 01 p0102 A70-10394

Unlubricated wear characteristics of polyimide resin sliding against carbon steel in air, noting effects of surface temperature, bearing pressure and velocity

01 p0103 A70-10448

Harmonic vibration testing of aircraft structural nonlinearities caused by dry friction, describing pitch control system

02 p0387 A70-12215

Power gyro stabilizer stability with dry friction at bearings, using point mapping to obtain system phase image

03 p0484 A70-13365

Particle, resin and inorganic bonding of solid lubricant to surface and dry lubricant film performance

05 p0855 A70-16043

Metal surfaces contact with cones and pyramids asperities, analyzing surface roughness effects on dry friction

11 p2060 A70-26412

Degassing kinetics during dry friction in vacuum, suggesting gas separation correspondence to oxide film breakdown

13 p2421 A70-29430

Dry friction and wear tests of various materials in vacuum at low temperatures

18 p3263 A70-36471

Polymethyl methacrylate glasses microcracks removal by dry friction

21 p3841 A70-40645

Moving object coordinates autonomous determination errors in accelerometers with dry friction, investigating inertial navigation system with integral horizon correction

23 p4193 A70-43981

DRY HEAT

Dry heat resistance of bacillus subtilis var. niger spores on selected planetary lander capsule surface materials

04 p0645 A70-15442

DRYING

NT DEHUMIDIFICATION

NT DEHYDRATION

DSIF [INSTRUMENTATION FACILITY]

U DEEP SPACE INSTRUMENTATION FACILITY

DTA [ANALYSIS]

U DIFFERENTIAL THERMAL ANALYSIS

DTMB-111 GROUND EFFECT MACHINE

U GROUND EFFECT MACHINES

DTMB-430 GROUND EFFECT MACHINE

U GROUND EFFECT MACHINES

DUAL THRUST NOZZLES

Dual flow turbojet engine rotor slip constraints during turning, investigating turbine blade strength, thrust deviation, fuel consumption and compressor stability

10 p1930 A70-24285

DUCTED BODIES

Hypersonic flow region about ducted blunt bodies of revolution, assuming correspondent flow conditions to maximum intake through duct

04 p0617 A70-15233

Heat transfer from inner wall of annular ducted cylindrical body cooled by liquid nitrogen, discussing effects of Teflon, asbestos and vaseline coating and thickness effects

08 p1596 A70-20577

DUCTED FAN ENGINES

NASA acoustically treated nacelle program reducing noise under commercial transport flight path near airports

22 p4089 A70-42529

Acoustic lining technology and materials for turbofan engine ducts, considering environmental factors and noise spectra

22 p4089 A70-42530

Structural and environmental design criteria for acoustical duct-lining materials in turbofan noise suppression

22 p4089 A70-42531

Duct lining parameters effects on engine inlet and fan discharge noise reduction during fan jet landing

22 p4090 A70-42532

Acoustically treated inlet and fan exhaust duct configurations for JT3D turbofan engine on DC 8 aircraft

22 p4090 A70-42533

DUCTED FANS

Optimum low speed ducted fan design for minimum noise generation

[ASME PAPER 69-WA/GT-4] 04 p0734 A70-14891

Rotating acoustic modes generated at blade passing frequencies in inlet duct of axial flow fan or compressor measured

04 p0691 A70-15079

Design parameters for optimum heavily loaded single rotation ducted fan characterized by ultimate wake vortex system

[AIAA PAPER 69-222] 12 p2157 A70-28083

Shock wave radiation from supersonic ducted rotor, determining sound power at blade passing harmonic frequency

19 p3353 A70-38614

DUCTED FLOW

NT KNUDSEN FLOW

Reflection and transmission characteristics of screens in duct obstructing shock propagating in unsteady compressible fluid, describing theoretical models and experimental detection

01 p0060 A70-10224

Entrainment of electrically conducting liquid by moving wall in long duct with rectangular cross section and magnetic induction field

01 p0151 A70-10656

Unsteady incompressible laminar flow under time dependent body force solved for rectangular and circular conduit and plane and cylindrical Couette flows

01 p0066 A70-11130

Flow patterns in circular ducts with circumferential roughness variation, determining axial turbulence, Reynolds number effect and applications as two phase flow analog

01 p0066 A70-11132

Modified shock layer theory for predicting hypersonic internal flow in axisymmetric converging duct with attached shock at leading edge

02 p0276 A70-11854

Laminar isothermal entrance flows in circular cross section ducts with uniform mass injection at wall from

boundary layer equations, discussing molecular weight effects

02 p0288 A70-12859

Monograph on laminar flow heat transfer in thermal entrance region of flat and profiled ducts, treating construction and efficiency of plate heat exchangers

03 p0603 A70-12988

Temperature sensor location for accurate averaging in fluid flowing through heated or cooled circular duct

03 p0486 A70-13557

Incompressible viscous fluid rectilinear flow along arbitrary cross section duct under pressure gradients oscillating at large frequencies

03 p0468 A70-14147

Unsteady MHD flow of viscous incompressible electrically conducting fluid through rectangular duct under transverse magnetic field

03 p0471 A70-14333

Heat transfer coefficient in turbulent duct flow of fine particles suspension, using coupled similar equations

03 p0608 A70-14382

Striated plasma flow in MHD duct of conducting rings using Ar with K vapor detected by high speed camera

04 p0725 A70-14533

Ideal fluid flow past sphere in rectangular duct and slot solved in series form in spherical functions

04 p0666 A70-14605

Incompressible electrically conducting fluid flow along rectangular duct under transverse magnetic field, noting equivalency of Hunt solutions and thin wall restriction

04 p0726 A70-14614

Hypersonic flow region about ducted blunt bodies of revolution, assuming correspondent flow conditions to maximum intake through duct

04 p0617 A70-15233

Ducted turbulent mixing and burning of coaxial streams, presenting experimental results for rocket-air mixing system

[AIAA PAPER 69-85] 06 p1130 A70-17171

Dynamic characteristics of systems consisting of train and air in tunnel using one dimensional incompressible fluid description

[AIAA PAPER 70-141] 06 p1042 A70-18216

Thermal entrance region effect on Nusselt number determination in asymmetrically heated rectangular duct with uniform heat flux

07 p1425 A70-20223

MHD flow in rectangular duct with arbitrary conductivity via modified Fourier method, obtaining magnetic induction and current for various Hartmann numbers

[ASME PAPER 69-WA/APM-17] 08 p1551 A70-21308

Instantaneous velocities measured for wall region of smooth duct during turbulent fluid flow by chronophotography of particles

09 p1658 A70-22046

Steady laminar gas flow on duct wall boundary layer considering external swirling flow and wall heat transfer

09 p1659 A70-22428

Average velocities profile measurement in wall region of turbulent fluid flow in smooth duct

09 p1661 A70-22838

Shock wave initiated two dimensional time dependent ducted flows in nonuniform regions using fluid-in-cell method, discussing density, pressure and energy distributions

09 p1665 A70-23740

Spectrum analysis of unsteady duct flow caused by pressure loss induced instability

10 p1863 A70-24026

Gas flow from nozzle into duct with enlarged cross section investigated for flow pattern and boundary conditions, noting oscillation behavior

10 p1799 A70-24123

Wall shear stress distribution in rectangular ducts, discussing secondary currents and main flow prediction

11 p2035 A70-25779

Nonsteady flow past duct junctures, investigating ventilation system of underground bomb shelter for blast wave passage prevention

11 p2036 A70-26139

Lambda type pseudoshock /shock during supersonic flow deceleration to subsonic in duct, investigating mechanism by schlieren photography

11 p2037 A70-26408

One dimensional compressible flow with heat addition in nonconstant area duct extended for friction addition, discussing critical thermal shocking

11 p2041 A70-26651

Wall shear stress distribution in noncircular ducts with steady incompressible fluid flow

12 p2209 A70-27217

Turbulent and laminar heat transfer to gases in circular ducts entry region, considering various gas properties

12 p2212 A70-28114

Inflow and pressure difference for mean flow in straight suction duct with porous walls, using elementary momentum analysis 13 p2392 A70-30020

Incompressible turbulent fluid flow through ducts and pipes by integral boundary layer techniques, considering entrainment principles 14 p2564 A70-30258

MHD power generation, investigating replenishment of zirconia electrodes from plasma in open flame and duct configurations 14 p2534 A70-30535

MHD experiments showing effects of local water supply electrical conductivity from measurements of voltage distribution, pressure gradients and extracted power 16 p2957 A70-32998

Ignition and combustion in ducted turbulent supersonic flow, discussing premixed and unpremixed ethylene [AIAA PAPER 70-720] 16 p2997 A70-33488

Integral model for combustion of metal particle laden jet mixing with subsonic secondary stream in duct, considering air breathing engine design [AIAA PAPER 70-736] 16 p2964 A70-33490

MHD flow velocity and magnetic flux profiles in rectangular ducts for secondary boundary layer 16 p2959 A70-34239

Turbulent air flow in vertical square duct, investigating local heat transfer and friction coefficients 18 p3347 A70-36506

Sound transmission and suppression in turbomachinery fans and compressor ducts, using three dimensional wave equation [ASME PAPER 70-GT-58] 18 p3304 A70-36873

Laminar incompressible flow in arbitrary cross sectioned entrance region of ducts by numerical technique after transformation to boundary value problem [ASME PAPER 70-GT-91] 18 p3243 A70-36878

Axissymmetric one dimensional compressible flow theory applications to compressible fluids ducted flow [ASME PAPER 70-GT-82] 18 p3243 A70-36882

Liquid with small electrical conductivity and kinematic viscosity in intense transverse magnetic field, examining plane and three dimensional duct flow 19 p3478 A70-37589

Velocity profiles of laminar flow through rectangular duct with moving wall and arbitrary cross section under nonslip boundary condition 19 p3405 A70-38043

Perturbation method for nonlinear acoustic wave propagation in steady one dimensional flow through variable cross section duct 20 p3673 A70-39612

Plasma inhomogeneities effects on MHD generators I-V characteristics, energy conversion efficiency and optimum duct geometry 20 p3564 A70-39636

Mach number effect on sound propagation in tuning acoustically lined rectangular duct with uniform flow 20 p3673 A70-39709

Laminar flow of liquid in duct with zero heat resistance of walls, calculating temperature distribution during radiative convective heating 20 p3613 A70-40297

Turbulence measurements in ducted coaxial air flow with faster outer stream pertinent to gas core nuclear rocket feasibility 21 p3809 A70-41748

Multiple tube manometer with selector switch for measuring flow channel wall pressures 23 p4194 A70-44000

Sound radiation from unflanged circular waveguide duct with flow, calculating reflection coefficients, directivity pattern and power for comparison with approximate methods 23 p4219 A70-44392

Incompressible laminar flow in entrance region of rectangular duct allowing direct computation of eigenvalues 24 p4287 A70-45294

DUCTED PROPELLERS

U SHROUDED PROPELLERS

DUCTILITY

Transformation induced plasticity steels tensile properties measurement indicating loss of ductility due to H embrittlement 01 p0118 A70-10729

Polycrystalline Mo ductility at low pressures in tension at ambient temperature, discussing H type embrittlement mechanism 01 p0121 A70-11234

Tensile tests of polycrystalline Nb-H alloys at low temperatures, noting cooling rate effect on ductility in terms of microstructure 01 p0122 A70-11240

High temperature ductility improvement in stainless steels containing He, analyzing lattice damage and interphase cavities after fast neutron irradiation 01 p0123 A70-11246

Cr alloys applications in high temperature environments, describing alloying elements effects on strength and ductility 03 p0511 A70-13566

Elastoplastic bar stability compressed by tangential force, showing ductility effect on critical parameters, perturbed motion and stability loss process 04 p0767 A70-14484

Erosion characteristics similarities and differences of brittle and ductile materials, noting dependence on particle velocity and diameter [ASME PAPER 69-WA/MET-7] 04 p0704 A70-14761

Prealloyed powders of Ni base alloys, made by inert gas atomization for improved strength and ductility 04 p0706 A70-14951

Maraging steels microstructure and ductility influence on stress corrosion resistance in magnesium chloride salt chamber 04 p0711 A70-15681

Alloy E1 602 ingots low ductility during forging ascribed to nonferrous metal atoms, decreasing iron diffusion and forming brittle nitride and carbide compounds 05 p0863 A70-16545

Continuous metal fiber composites tensile strength and ductility in terms of plastic instability 05 p0946 A70-16924

Creep, ductility and short term tensile and compression strength test facility for graphite in 300-3500 K temperature range 05 p0875 A70-17068

Cold reduction and annealing temperature effects on Al sheet ductility noting roles of hardness, crystallographic orientation and microscopic structure 06 p1075 A70-17146

Polycarbonate ductile fracture measured for strain energy release rates and plastic zone size and shapes to correlate with existing theories and experimental data 07 p1321 A70-20041

Temperature, transformation and strain rate effects on tensile ductility properties of stable and metastable compositions of austenitic stainless steels 08 p1524 A70-21956

Heat resistant alloys creep ductility, considering grain boundary cavitation, sliding and migration 09 p1701 A70-22554

Microstructure and ductility of air- and vacuum-melted heats of corrosion resistant steels, investigating tensile and yield strengths for all grain directions 10 p1905 A70-25170

Interstitial and substitutional impurity effects on fracture strength, plastic properties and ductile-brittle transition temperature of vanadium determined from impact and tensile tests 11 p2066 A70-25913

Ti alloys tensile properties correlated with microstructure for multiple heat treatment cycle variations for high strength and adequate ductility 12 p2252 A70-27107

Rhenium alloying effect on room temperature ductility of Cr, Mo and W, measuring lattice parameters by Debye-Scherrer method 12 p2256 A70-27616

Metals and metal alloys ductility development, discussing plastic flow problem in metal working 12 p2327 A70-28144

Engineering development role in metal forming industry expansion, discussing metals ductility or plasticity increase for extending processes 12 p2244 A70-28146

Plastic deformation in brittle and ductile fracture, discussing elastoplastic stress analysis of cracked bodies, plane strain deformation near cracks, etc 13 p2509 A70-28601

Ductile fractures analysis using critical strain near crack tip as criterion 13 p2432 A70-28673

Plastic strain state effect on ductility and toughness of structural steels 13 p2432 A70-28675

Ductile fracture in Al matrix composite reinforced with unidirectional stainless steel fibers described by critical crack tip displacement and fracture strain criteria 13 p2512 A70-28917

Instrumented Charpy impact test evaluating strain rate, alloying and irradiation effects on ductile-brittle transition temperature and fracture of pressure vessel steels 15 p2820 A70-32239

Metal fiber multiple necking effect on uniaxial metal matrix composites ductility and plastic deformation behavior for brass-W model system 15 p2761 A70-32378

Work to fracture measurements on brittle fiber ductile-matrix metal composites, using Charpy test 15 p2763 A70-32832

Ti alloys beta forging effect on physical properties and tensile ductility 17 p3097 A70-34358

Unalloyed Ti hydrogen embrittlement, determining factors affecting brittle-ductile transition temperature 17 p3117 A70-34398

High yield strength alpha-beta Ti alloys ductility control, observing fracture strength dependence on morphology, grain location and size for constant heat treatment 17 p3119 A70-34417

Ti-Al-Sn-Zr system high temperature creep strength and ductility retention 17 p3120 A70-34424

Plastic deformation of two phase alloy with small nondeformable particles in ductile matrix, discussing cross slip, yield and flow stress, work hardening etc 17 p3126 A70-35460

Fiber reinforced composite with ductile matrix, discussing fatigue life prediction from strain hardening characteristics 17 p3128 A70-35465

Cobalt addition to Ti-Al-V alloys, examining yield strength, heat treatment, ductility and microstructure 18 p3271 A70-35964

Hydrostatic pressurization effect on ductile-brittle transition temperature of polycrystalline chromium 18 p3274 A70-36053

Rene 41 ductility reduction by environmental oxygen promoting intergranular cracking at high temperatures 18 p3277 A70-36524

Creep resistant Ni-base superalloys ductility and thermal shock resistance improvement by precision casting technique, producing columnar grain and single crystal structures 20 p3648 A70-39415

Hot work effect on properties and microstructure of wrought Waspaloy, observing temperature decrease effect on fracture ductility 22 p4054 A70-42739

Heat treatable beta Ti alloys cold workability, fracture toughness, tensile ductility and applications [SAE PAPER 700856] 24 p4361 A70-45880

Longitudinal phenomena and two phase structures effect on ductility of low carbon steel-chromium subjected to high temperature torsion 24 p4361 A70-46173

Zn-Al alloy high velocity deformation characteristics, examining ductility and aging at various temperatures and heat treatments 24 p4363 A70-46194

Precompression and pressurization effects on ductile-brittle transition of polycrystalline cast Cr, W and Mo bcc transition metals 24 p4365 A70-46371

DUCTS

NT ACOUSTIC DUCTS

NT AIR DUCTS

Fast neutron transport characteristics of helical ducts using Monte Carlo code FASTER, computing neutron fluxes and attenuation 05 p0884 A70-16163

Shock wave interactions effect on propagation in ducts with gradual or sudden change in cross section, using schlieren spark photography 09 p1664 A70-23735

Curved porous wall channels for noise suppression in power plants, ventilation systems, etc 18 p3216 A70-36302

DUFFING DIFFERENTIAL EQUATION

Large amplitude free vibration of rectangular plates subjected to aerodynamic heating with different boundaries and temperature distribution, deriving Duffing nonlinear differential equation 10 p1957 A70-24417

DUMMIES

Flotation dummy to simulate unconscious survivors characteristics analyzed for life jacket design 07 p1218 A70-19004

DUMMY LOADS

U IMPEDANCE

U LOADING

U OUTPUT

DUNGEYS WIND SHEAR MECHANISM

U WIND SHEAR

DUOCHROMATORS

Doppler effect induced small spectral line shifts measured by modified duochromator in MPD arc jet 09 p1684 A70-23531

Concentric polarization Fabry-Perot duochromator for spectral line displacement measurements applied to ion drifts in hollow cathode plasma 15 p2737 A70-32042

DUPLEX OPERATION

Duplex aging treatment effect on Ni-Co-Mo-Ti maraging steels mechanical properties 10 p1905 A70-25171

DUPLEXERS

Antenna-duplexer assembly comprising log periodic antennas, power divider and hybrid loop 09 p1649 A70-23324

DUPLICATING

U REPRODUCTION [COPYING]

DURABILITY

HF endurance tests of Al sheet alloy used in welded aircraft structural components, plotting curves for heat treated and untreated specimens 02 p0315 A70-11658

Low alloy and stainless steels durability in various natural atmospheres, discussing corrosivity dependence on atmosphere pollutants, temperature and humidity 02 p0318 A70-12476

Molybdenum disulfide surface and bulk properties, comparing endurance of fractions and grades with synthetic chalcogenides at same layer thickness in dry atmospheres
[ASLE PREPRINT 69-LC-7] 02 p0322 A70-12538
Cyclic heating and thermal stresses effect on fatigue strength and durability of turbine blade alloys and structural elements 09 p1771 A70-22463

Materials durability in presence of stress concentration under biharmonic loading 15 p2813 A70-31527

HF endurance tests of Al sheet alloy used in welded aircraft structural components, plotting curves for heat treated and untreated specimens 19 p3452 A70-38431

Step-amplitude stress cycle program effects on durability of heat resistant alloy for turbine blades under cyclic loading 23 p4204 A70-43934

Statistical analysis of durability data of heat resistant alloys for gas turbine engines, using long term strength tests of melts in mass production 23 p4204 A70-43940

DURATION

U TIME

DUST

NT COSMIC DUST
NT INTERPLANETARY DUST
NT LUNAR DUST
NT METEOROID DUST CLOUDS
NT TERRESTRIAL DUST BELT
NT ZODIACAL DUST

Sand and dust environmental test of T-63 regenerative engine, discussing performance depreciation, recuperator inspection and comparison with non-regenerative t63-a-5a engine 01 p0164 A70-10685

Ice nucleating properties of dust particles above 80 km compared with soil and AgI particles 01 p0081 A70-11296

Turbulence in hypersonic nozzle due to two phase flow of ideal gas and solid spherical particles, discussing thermal and dynamic differences 03 p0407 A70-13494

Materials science experimental and diagnostic phases in mechanisms of metal erosion by impacting dust particles [ASME PAPER 69-WA/MET-8] 04 p0704 A70-14760

Radiative heat transfer through dust clouds in radiative equilibrium and isothermal clouds between parallel plates measured with heat flowmeter [ASME PAPER 69-WA/HT-41] 04 p0781 A70-14802

Dust devil wind velocity relationship to environmental parameters including atmospheric temperature, wind direction and vorticity, etc 07 p1269 A70-19948

Ar-arc-produced dust of iron, carbon, silicon carbide and silica, investigating shapes, sizes, grouping and optical absorption to simulate interstellar grains 10 p1944 A70-24957

Solid particle motions in dusty gas in inviscid hypersonic shock layers of slender wedges and cones and stagnation regions of cylinders and spheres 12 p2156 A70-27827

Dusty gas dynamics, examining shock wave structure, boundary layers stability, flow equations, acoustic damping, velocity and density perturbations, etc 17 p3068 A70-34671

Gas turbines, dust and air cleaners interrelationship in preventing failure due to air contaminants [ASME PAPER 70-GT-104] 18 p3305 A70-36890

Upper atmospheric dust composition and optical properties by crepuscular technique, using photometric measurements in 5200 A region 18 p3251 A70-36978

Dust content effect on hypersonic wind tunnel flow test results, noting drag force on slender and blunt nosed models 21 p3749 A70-42224

Atmospheric vorticity and dust devil rotation direction relationship, suggesting shear in horizontal flows associated with convective activity in unstable atmosphere 22 p4065 A70-42912

H II region dust grains thermal emission, examining effect on diffuse nebulae 24 p4413 A70-46158

DUST COLLECTORS

Boeing inertial separator system for eliminating air dust taken by CH-46 helicopter engines during takeoff and landing on unprepared areas 01 p0162 A70-10677

Particle removal efficiency of engine inlet separator-filter devices evaluated at Naval inlet test facility for simulated engine airflows, scavenging conditions, etc 01 p0163 A70-10679

DWARF STARS

NT WHITE DWARF STARS

M dwarf stars spectroscopic, spectral and photometric parallaxes calibration based on trigonometric measurements 01 p0188 A70-11333

Duplicity characteristics of low luminosity stars, considering nearby M dwarfs, white dwarfs and high velocity subdwarfs 01 p0188 A70-11334

Convective red dwarfs Kr 60 A and 60 B structure and stability taking into account electrostatic interactions between gas particles 01 p0188 A70-11337

Faint, metal poor, subluminoous and red degenerate stars occurrence and properties, considering spectra of candidate degenerates 01 p0188 A70-11338

Cool dwarf stars atmospheric models including IR opacity due to water vapor and pressure induced dipole of molecular hydrogen 01 p0190 A70-11347

M dwarf stars model atmosphere construction taking into account molecular opacities in cool stellar atmospheres 01 p0190 A70-11348

High temperature atmospheric models for red dwarf stars and sun to determine convection effect on atmospheric surface layers and emitted flux 01 p0190 A70-11349

Nongray and constant radiative flux model atmosphere for K dwarf stars with 4000 K effective temperature and 4.5 log surface gravity 01 p0191 A70-11350

Electron pressure and negative H ion population in late type dwarfs atmospheres by Ca I resonance line observation, noting non-LTE mechanism 01 p0191 A70-11351

Isophote flattening functions of elliptical galaxies including identification of giant and dwarf galaxies 02 p0377 A70-12449

Barnard two planet solar system, dwarf star perturbations, orbital parameters and comparison with Solar system 10 p1943 A70-24758

Hydrogen recombination and hydrogen molecules formation may explain sharp brightness variations in later dwarf stars 11 p2115 A70-26581

Red dwarfs and supernovae determination in stellar clusters, outlining statistical probability technique for total number of flare stars 12 p2308 A70-27872

Dwarf and neutron stars as pulsar energy sources, considering Crab Nebula X ray emission and gravitational collapse 12 p2310 A70-27990

Dwarf Me stars flare spectra, examining hydrogen recombination layer and impulse heating of photosphere 20 p3702 A70-39013

Soviet book on red dwarf star flares covering data acquisition, flare frequency, mechanisms and nebular model 20 p3705 A70-39722

Intermediate band photometry of companions to RR Lyrae variables, identifying AP Ser K line excess subdwarf 21 p3892 A70-41187

High velocity stars in Large Magellanic Cloud from spectroscopic observations, including A dwarfs and G-K giants 23 p4240 A70-44212

G8, IV subdwarf 31 Aql spectrum at 4000-6600 A, discussing Ba II 4554 A, G and CN bands and spectral lines 24 p4414 A70-46329

DWELL

Dwell time boundary and mean values for laminar flows through channel and tube reactors, obtaining field representation from streamline network and isochrones 16 p2893 A70-33745

DYADICS

Homogeneous gravitating sphere deformation by internal dislocations determined using Green dyad 06 p1055 A70-17605

Planetary motion zero-rank effects numerical integration, using Hill secular perturbation method and trace of dyadics 14 p2639 A70-30704

DYES

Photochromic aminotriarylmethane filter solutions for flash blindness protection, noting stability against xenon flash UV exposure 04 p0690 A70-15028

Saturable Q switch of cryptocyanine used in ruby laser for pulse sharpening, describing dye sensitivity to solar radiation 04 p0701 A70-15035

Flash lamp pumped tunable organic dye laser, using capacitor bank for reliable operation 05 p0861 A70-16845

Breakdown of cryptocyanine dye in methanol solution by ruby laser pulses providing passive Q switching mechanism 06 p1083 A70-18524

Blood reflection densitometer with linear response to changes in indocyanine green dye concentration, using simple analog computation 07 p1221 A70-19589

Dye laser stimulation by pumping with pulsed nitrogen laser line to obtain entire visible spectrum 07 p1301 A70-26016

Optical pumping energy effects on lasing pulse duration during pulse excitation of alcohol solutions of rhodamine 6G 08 p1511 A70-20522

Retunable lasers with organic dye dispersive resonators, studying space-angular, spectral and energy emission characteristics 08 p1511 A70-20538

Dye laser tuned to sodium D line used for measuring ionospheric atomic sodium 08 p1492 A70-21757

Organic dyes investigated for amplification characteristics of Raman emission stimulated by Q switched ruby laser 09 p1694 A70-22134

Dye laser small signal gain via pumping by UV nitrogen laser 13 p2426 A70-28811

Bleachable dye filters selection for periodic undamped output power oscillations in laser 15 p2753 A70-32859

Rhodamine C chemiluminescent material for atmospheric ozone measurements, describing preparation and luminescence spectrum 19 p3373 A70-37638

Organic dye lasers output bandwidth and tunability extension by acidification of solution 19 p3445 A70-37675

Power, energy and efficiency of emission from dye solutions pumped by incoherent light pulses, allowing for particle accumulation at metastable level 19 p3448 A70-38738

Flash lamp pumped organic dye laser intensity for dye solutions in contact with different argon-oxygen compositions, noting effect of oxygen partial pressure 21 p3834 A70-40569

Aortic regurgitated flow estimation by dye injection technique, noting correlation with cineangiography method 22 p3977 A70-42301

Excited state complexes laser action in coumarin dyes indicated from stimulated fluorescence time dependence 22 p4048 A70-42328

Rhodamine 6G triplet lifetime under continuous pumping by Ar laser 22 p4050 A70-43225

Amplification factor time dependence of dye lasing under rectangular pumping pulse, noting threshold conditions and burnout time relation to material parameters and resonator 24 p4352 A70-45473

Laser gain coefficient increased via organic compounds addition to rhodamine 6G aqueous solution 24 p4356 A70-46273

DYNAMIC CHARACTERISTICS

NT AERODYNAMIC DRAG
NT AERODYNAMIC STABILITY
NT AIRCRAFT STABILITY
NT ATTITUDE STABILITY
NT BOUNDARY LAYER STABILITY
NT COMBUSTION STABILITY
NT CONTROL STABILITY
NT DIRECTIONAL STABILITY
NT DRAG
NT DYNAMIC PRESSURE
NT DYNAMIC STABILITY
NT ELECTROSTATIC DRAG
NT FLAME STABILITY
NT FLOW CHARACTERISTICS
NT FLOW DISTRIBUTION
NT FLOW STABILITY
NT FLOW VELOCITY
NT FREQUENCY STABILITY
NT FRICTION DRAG
NT GYROSCOPIC STABILITY
NT HOVERING STABILITY
NT INTERFERENCE DRAG
NT INTERFERENCE LIFT
NT JET LIFT
NT LATERAL STABILITY
NT LIFT
NT LONGITUDINAL STABILITY
NT LOW SPEED STABILITY
NT MAGNETOHYDRODYNAMIC STABILITY
NT MINIMUM DRAG
NT MOTION STABILITY
NT PRESSURE DRAG
NT ROTARY STABILITY
NT ROTOR LIFT
NT SATELLITE DRAG
NT SPACECRAFT STABILITY
NT SUPERSONIC DRAG
NT TRANSIENT RESPONSE
NT VISCOUS DRAG
NT WAVE DRAG

Nonlinear closed-loop automatic control systems steady state characteristics calculation by graphic method 01 p0052 A70-10194

Book on dynamics of complex systems represented by control and human operators and animals behavioral activities models 01 p0034 A70-10501

Two velocity hydrodynamic scheme for describing dynamic behavior of two phase supersonic flow past slender body 01 p0003 A70-10995

Dynamic characteristics of model of spacecraft-astonaut-tether system during approach, deriving kinetic potential 01 p0192 A70-11587

Characteristics of dynamic mechanical systems including solid state and hydrodynamic analogs of ideal incompressible fluids, based on statistical theory of turbulence 01 p0068 A70-11594

Planetary atmospheres dynamics, discussing rotational and MHD effects, energy sources, etc 02 p0366 A70-11806

Dynamical systems with two degrees of freedom reduced to numerical investigation of quadratic area-preserving mapping 02 p0289 A70-11993

Waves vs eddies in dynamics of turbulent boundary layer fluctuating motions with scale of mean flow 02 p0287 A70-12361

Self gravitating galaxies theoretical properties, including structural and dynamic characteristics of interacting and colliding galaxies 02 p0376 A70-12444

Self consistent field method to calculate effective dynamic characteristics of elastic media with filler for plane longitudinal wave propagation 02 p0388 A70-12485

Steady, homogeneous, electromagnetic plasma acceleration fields, demonstrating electric and magnetic fields effects on dynamic behavior 03 p0529 A70-12989

Unidirectional carbon and glass fiber reinforced polyester resins dynamic characteristics under torsional and flexural vibration, showing damping independence of cyclic stress amplitude 03 p0514 A70-13111

Phonon-photon scattering intensity and line shape used to study laser-excited impurity centers dynamic characteristics in stimulated induction regime 03 p0499 A70-13256

Dead zone initial disturbance of sensitive element dynamic coordinate in two rotor gyrocompass determined using method of averages 03 p0484 A70-13419

Stability and dynamics of dielectrophoretic equilibria, considering circular cylindrical column of inviscid liquid with rigid body rotation 03 p0525 A70-13784

Harmonic equilibrium method applied in dynamic properties analysis of autopilot electrohydraulic servomechanisms stability 03 p0415 A70-13930

Resistance, capacitance and inductance in passive hydraulic circuits considered in analogy with electric circuits to determine dynamic characteristics 03 p0415 A70-13931

Perturbed motion of solid body with cylindrical cavity partially filled with viscous fluid, using Rabinovich equations 04 p0766 A70-14476

Time transient and step-jump dynamic analyses of gas lubricated bearing, illustrating hybrid journal and Rayleigh-Step thrust bearings [ASME PAPER 69-WA/LUB-5] 04 p0697 A70-14768

Static and dynamic characteristics of inertia load driving systems using electrohydraulic pressure and flow control servovalves [ASME PAPER 69-WA/FLCS-15] 04 p0626 A70-14842

Fluidic component linearized characteristics in coupled or uncoupled environment determined for wide frequency range, discussing application to proportional fluidic amplifier [ASME PAPER 69-WA/FLCS-2] 04 p0626 A70-14847

Boundary layer momentum integral equations to predict shear layer behavior, developing method to avoid nonphysical constraint appearance [ASME PAPER 69-WA/APM-11] 04 p0669 A70-14916

Soviet monograph on numerical determination of dynamic characteristics of plates and shells by method of summary representations, covering oscillation and stability problems 04 p0773 A70-14954

Integral-criterion optimization of transient processes in mechanical systems synthesis with favorable dynamic and damping characteristics 04 p0720 A70-15218

Sound vibrations effect on pulsation characteristics of turbulent gas jet 04 p0618 A70-15248

Dynamic vibration absorbers /DVA/ efficiency in limiting excessive vibrations in mechanical systems by transferring motion to auxiliary system 04 p0699 A70-15306

Multiple skirt air cushion vehicle /ACV/ pitch and heave dynamic characteristics, describing mathematical modeling and analog computer simulation 04 p0624 A70-15389

Parasitic transient process in automatic control system during switching to mode stabilized with respect to certain coordinates 04 p0662 A70-15433

Thermal and gas dynamic characteristics of aircraft turbine engine annular vaporizing combustion chamber determined from air distribution ratio 05 p0895 A70-15897

Rotor-driven vibrational gyroscopic device dynamic characteristics, stability, transient delta function, signal response and sensitivity assessment 05 p0848 A70-16222

Dynamic strain measurement by solid state direct coupled amplifier with flat frequency response 05 p0936 A70-16322

Radio waves propagation along polar auroras region, obtaining ionospheric parameters for magnetic disturbances based on penetration probability 05 p0842 A70-16744

Plane and cylindrical elastic waves dynamic characteristics propagating in half space with holes, reducing boundary value problem and deriving formulas for interacting waves 05 p0946 A70-16858

Dynamic characteristics from equations of motion of gyroscope with allowance for structural damping forces between inner gimbal and rotor 05 p0852 A70-16961

Kinematic characteristics of annular-blank elements extruded by pulsed magnetic fields, noting proportionality to energy stored in capacitor bank 05 p0857 A70-17018

Dynamics of composite, sandwich and stiffened shell type structures with various geometries 06 p1160 A70-17158

Dynamic behavior of earth magnetosphere, discussing geophysical micropulsations, geomagnetic field diagnostics, cold plasma density, etc 06 p1139 A70-17535

Laser mode interaction characteristics determination using resonator field equation taking into account competition and coupled modes 06 p1081 A70-17765

Adaptive control algorithm for parameter adjustment of unknown dynamic characteristics of linear systems 06 p1025 A70-17956

Transducer for pressure fluctuations measurement in wide frequency range based on piezoelectric microphones, discussing dynamic characteristics 06 p1071 A70-18472

Two mode gas laser behavior under external signal action showing mode locking possibility by combination frequencies due to medium nonlinearity 07 p1296 A70-18764

Thermoelasticity equations derived for regular systems of M bodies in dynamic and thermal interaction using nonlocal continuous model 07 p1407 A70-19381

Sporadic E layers structure and dynamic characteristics during polar aurorae, determining critical frequencies 07 p1267 A70-19455

Dynamic characteristics approximation in transfer functions class with singularity at infinity 07 p1327 A70-19806

Microwave mixer design to increase dynamic range applied to communications and video systems 07 p1243 A70-20216

Uniqueness theorem for coupled dynamic problem of linear thermoviscoelastic theory assuming contact-type boundary conditions 07 p1416 A70-20296

Soviet collection of articles on machine dynamics covering various rotor vibrations, machine/operator system, etc 08 p1501 A70-20693

Human operator dynamic properties working to maintain given process parameters, obtaining differential equations for closed machine operator system 08 p1449 A70-20696

Soviet book on liquid rocket engines dynamics, emphasizing computational engineering methods and engines automatic control 08 p1558 A70-20757

Transfer functions representing continuous dynamic systems, identifying parameters by obtaining coefficients of discrete system transfer function relating input and output sampled sequences 08 p1478 A70-20777

Model characteristics selection for dynamic system behavior simulation, studying characteristics variability extent without changing trajectory behavior dependence on parameter space 08 p1544 A70-20953

Matching operations for difference and differential equations describing discrete control systems dynamics having cyclic interruption of data quantization frequency 08 p1480 A70-20999

Adjustment process dynamics in digital adaptive system with task of ensuring minimum quadratic criterion for parameters using gradient search technique 08 p1480 A70-21017

Spatially inhomogeneous semiconductor structures dynamic characteristics, obtaining equations 08 p1474 A70-21207

Dynamic compressive properties of polypropylene, polystyrene bead and extruded polystyrene foams tested at given strain rate under room temperature 08 p1527 A70-21329

Dynamic tensile properties of monolithic and pyrolytic graphite compared with static tensile strength 08 p1527 A70-21334

Dynamic mechanical properties of filled polymers as function of filler concentration, particle agglomeration and ratio of particle to polymer modulus 08 p1527 A70-21335

Human biological organism analysis based on physiological determination of regulating and control functions dependence on oscillatory properties 08 p1452 A70-21460

Auroral zone electrojets spatial structure and dynamic behavior based on IGY and IQSY geomagnetic data 08 p1491 A70-21717

Strength and plasticity criteria for anisotropic reinforced materials model taking into account material structure, components properties and behavior 09 p1768 A70-22119

Double resonator ruby maser dynamic and static characteristics for centimeter band improved by pumping frequency modulation 09 p1695 A70-22188

Geometric, cinematic and dynamic conditions of ideal fluid adiabatic nonstationary movement expressed by differential external system /s/ 09 p1659 A70-22254

Linear one degree of freedom mechanical system loaded by time dependent force with constraints on loading/unloading rate, studying minimum of dynamic coefficient 09 p1727 A70-22536

Soviet book on servo systems for radar automatic tracking and control stations covering static, dynamic and frequency characteristics, amplifiers and correction devices 09 p1654 A70-22597

Dynamical characteristics of variable-mass flexible spinning rocket with internal flow, investigating rigid body motion, elastic displacements and vibrations 09 p1767 A70-23252

Three degrees of freedom astatic gyroscopes dynamic characteristics determination by vibration tests 09 p1681 A70-23300

Simulator servo drive system dynamic requirements for single-axis manual control task using pilot models and computer [AIAA PAPER 70-355] 10 p1858 A70-24208

Amplitude and Rotational 3-Axis Flight Simulators for handling qualities research, outlining physical constraints and methodology for driving visual display and motion systems [AIAA PAPER 70-353] 10 p1858 A70-24210

Geomagnetic pulsations /pc 4/ characteristics from analyzing magnetosphere model yielding plasma densities consistent with experimental data 10 p1875 A70-24483

Impact problems of slip clutch and beam scales dynamic characteristics simulation by 1130 CSMP /Continuous System Modeling Program/ 10 p1860 A70-24653

Dynamic characteristics of structures measured, using digital computer to analyze transient data from frequency sweep tests 10 p1961 A70-25059

Linear steady and unsteady systems time optimal control switching points determination by introducing parameterization to reduce number of transcendental equations 11 p2021 A70-25339

TACSAT 1 communication satellite design, dual-spin stabilization principles and dynamic characteristics, noting nutation behavior [AIAA PAPER 70-455] 11 p2120 A70-25447

Thermal conductivity determination for charring materials by dynamic technique, with application to carbon, graphite and silica cloth phenolics 11 p2068 A70-25766

Analog integrating moving window detector performance analysis for use with scanning pulse radar allowing for antenna radiation pattern and detection process dynamic characteristics 11 p2009 A70-26262

Microscopic behavior and excitational processes found similar in argon ion lasers with hollow cathode or conventional heated oxide cathode discharge 11 p2063 A70-26370

Connecting wires length effect on sensitivity and current-voltage characteristics of sensors for dynamic values measurement, deriving integral electrical parameters 11 p2055 A70-26445

Turbine flowmeter dynamic characteristics dependence on individual parameters, deriving equations of motion and time constant

11 p2055 A70-26450

Dynamic measurements of aerospace mechanical quantities covering tensometry, vibration, torque, angular velocity, pressure, telemetry and data processing

11 p2057 A70-26750

Gyroscopic platform stabilizers (GPS) dynamic properties improved by compensation of perturbing torques

12 p2237 A70-28155

Coupled microstrip transmission lines characteristics from parameters evaluation, considering various geometries, inductive and coupling coefficients, dielectric constant and impedance

12 p2190 A70-28167

Laminar MHD boundary layer equations at nonconducting surface, determining flow core parameters influence on boundary characteristics

13 p2462 A70-28967

High speed dynamic systems synthesis with optimal damping of elastic vibrations, using gradient method

14 p2617 A70-31354

Stochastic terminal optimal control for nonlinear dynamical systems with state independent noise

14 p2600 A70-31420

Stochastic medium mathematical model for loose medium motion in potential field of forces

15 p2821 A70-32342

No-inertia line, lumped parameter and distributed parameter models for dynamic characteristics of fluid transmission lines

15 p2678 A70-32526

Servocontrolled laser strainmeter based on Michelson-Morley interferometer, determining dynamic characteristics dependence on feedback loop filter type

16 p2925 A70-33022

Bypass door control system for SST axisymmetric intake operation in external compression mode, obtaining dynamic performance

16 p2966 A70-33558

Vibrations of shells, plates and membranes carrying dynamic systems at discrete points on surface, obtaining eigenfunction and eigenvalue equations

16 p2993 A70-34090

Linear system under ergodic random processes, determining optimal dynamic characteristics by approximation of spectral density by Laguerre series

16 p2944 A70-34280

Dynamics of continuously operating linear servosystems stimulated by stochastic signals, using vectorial equation and impulse response matrix

16 p2944 A70-34295

Transversely isotropic Timoshenko beam states and dynamics under initial stress and transverse loading

17 p3182 A70-34561

Dynamic behavior of eccentric annular mercury nutation damper, using variational principle of least viscous frictional power loss

17 p3023 A70-34770

Parameter variation effects on iterative identification of linear system by learning method

17 p3130 A70-35299

Dynamic characteristics of hydraulic fatigue testing machines, using hydraulic activation efficiency factor

17 p3064 A70-35718

Magnetospheric plasmopause duskside bulge dynamic behavior during substorms, using whistler data

18 p3312 A70-36013

Supply valve influence on dynamic characteristics of volumetric hydraulic actuator

18 p3215 A70-36126

Structurally similar models, investigating space vehicles dynamic characteristics

18 p3332 A70-36161

Quasi-equilibration of static or dynamic universal solutions of compressible or incompressible simple bodies, investigating homogeneity of symmetry and objectivity conditions

18 p3336 A70-36221

Polymers dynamic properties in hyperelastic and vitreous states as function of temperature, using torsion pendulum method

18 p3263 A70-36469

Damped vibrations of single-mass elastic systems, determining E function singularity effect on dynamic characteristics

18 p3341 A70-36587

Sporadic E layers structure and dynamic characteristics during polar aurorae, determining critical frequencies

18 p3250 A70-36929

Meteorological prediction methods based on dynamic or thermodynamic considerations

18 p3285 A70-36949

Two mode gas laser behavior under external signal action showing mode locking possibility by combination frequencies due to medium nonlinearity

18 p3271 A70-37108

Late-type barred spiral galaxies structure and dynamics with asymmetric mass distribution, using

model consisting of small prolate spheroid displaced from disk center

18 p3331 A70-37194

Algorithm for dynamic processes in unsteady linear automatic control system during finite time interval

19 p3470 A70-37256

Polynomial and logic theories of dynamic systems, explaining linear and nonlinear elements of automatic control systems

19 p3392 A70-37447

Time transient and step-jump dynamic analyses of gas lubricated bearing, illustrating hybrid journal and Rayleigh-Step thrust bearings

[ASME PAPER 69-WA/LUB-5] 19 p3436 A70-37619

Dynamics of composite materials using extensions of continuum theories based on combination of elastic and geometric properties

19 p3455 A70-37950

Thermoelastic composite materials, deriving crystal lattice type model of equations for predicting dynamic or thermomechanical behavior

19 p3540 A70-37958

Equilibrium homogeneous steady state highly ionized non-Debye plasma for investigation of electrical conductivity, viscosity, dynamic properties, etc

19 p3480 A70-38183

Upper atmosphere semiannual variations dependence on lower thermosphere dynamic properties seasonal variations, using steady state models

19 p3415 A70-38384

Elastoplastic oscillator dynamic behavior with one degree of freedom compared with bilinear hysteretic model results, investigating mechanical scheme with continuous skeleton intrinsic curve

19 p3432 A70-38665

Feedback regulator synthesis for linear time invariant dynamic system with quadratic performance index, using computer algorithm for algebraic Riccati matrix equation

19 p3395 A70-38937

Low power thyristors in relaxation oscillation circuits, considering static and dynamic characteristics in large signal mode

20 p3596 A70-38971

Free wing aircraft dynamic characteristics, discussing gust alleviation and handling qualities

[AIAA PAPER 70-947] 20 p3561 A70-39580

Boundary value problems in dynamic two dimensional elasticity theory for domains bounded by circles and straight lines

20 p3721 A70-39770

Thermal stress and changes in modulus of elasticity and expansion coefficient effects on dynamical properties of turbine disks at high temperatures

20 p3721 A70-39783

Cardiovascular blood circulation system dynamic characteristics analysis by linear statistical correlation methods, describing test for determining weighting function

20 p3581 A70-39905

Controlled nonstationary plant dynamic characteristics determination by model, evaluating accuracy

20 p3673 A70-39906

Uncontrolled plant dynamic characteristics analysis based on signal recordings, using black box without input method

20 p3705 A70-39909

Statistical analyzer for complex plants dynamic characteristics

20 p3604 A70-39912

Dynamic theories for wave propagation in laminated and fiber reinforced composites, using dispersion curves for transverse and longitudinal motions

20 p3730 A70-40036

Composite material dynamic properties, discussing modulus and damping during constant strain rate, viscoelasticity, fracture strength and high loading tests

20 p3731 A70-40048

Nonlinear dynamic systems phase coordinate variations statistical characteristics, describing data reduction method

20 p3674 A70-40183

Elastic body steady forced oscillations under monoharmonic excitation, investigating hereditary nonlinearity effects on systems dynamic characteristics

20 p3733 A70-40395

Solar corona streamer and interstreamer regions, examining geometrical and dynamic structure by energy transport process

20 p3712 A70-40417

Dynamical theorems to control number of collisions for sequences in generalized Boltzmann equation, discussing binary collisions involving three molecules

21 p3852 A70-40946

Coupled rotational vibration system dynamic behavior near critical speed, using graphs of autonomous two degree of freedom system on reduced phase plane

22 p4112 A70-42271

Gas lubricated three-foil bearing for high speed rotor support, considering dynamic and static behavior in zero gravity environment

[ASME PAPER 70-LUBS-18] 22 p4044 A70-42443

Dynamic characteristics of turborotor simulator supported on gas lubricated foil bearings, considering rotor response to imbalance

[ASME PAPER 70-LUBS-11] 22 p4044 A70-42449

Dynamical linear thermoelasticity theorem generalization with time dependent conductivities, elasticities and density

22 p4112 A70-42483

Dynamic characteristics of autooscillatory nonlinear self adaptive systems under random noise, using statistical and harmonic linearization

22 p4003 A70-42884

Computerized mathematical modeling of transistors statistical and dynamic characteristics as functions of structural parameters

23 p4171 A70-43954

Dynamic elasticity theory for multiply connected region

23 p4266 A70-43990

Structural optimization of designs with requirements including restrictions on structure dynamic response and characteristics

23 p4270 A70-44562

Nonrigidly supported ballast effects on dynamic characteristics of slender body during atmospheric entry

23 p4258 A70-44594

NACA/NASA rotating wing aircraft research history 1915-1970, Part 2, autogyro flight test experiences, rotor blade dynamics research, interest in helicopters, etc

23 p4142 A70-44852

Viscoelastic laminated composite linear anisothermal theory, presenting homogeneous continuum model to describe dynamic characteristics

24 p4368 A70-45992

Dynamic errors of digital converter for digit-to-digit compensation estimated by probability and information characteristics methods

24 p4340 A70-46404

DYNAMIC CONTROL

Gyroscope bearing cross-torque control techniques, noting ball-group misalignment coupling

[ASME PAPER 69-LUB-17] 01 p0101 A70-10388

Posture and motion control for functional organizations of nervous systems, emphasizing reflexes and relation between suprasegmental structures and controlling organs

01 p0017 A70-10499

Adaptive man machine system for automated training of pilot dynamic control skills/decision and motion/, describing synthesis procedure

02 p0246 A70-12148

Analog computer model of human cardiovascular control system to reproduce subject response to submaximal workload

03 p0438 A70-14081

Nonlinear control systems with linear controls appearance defined for controllability concepts and sufficient conditions to reduce to lower dimensional problem

04 p0660 A70-14524

Algorithmic and digital computer method for approximating irrational transfer functions by rational functions in control systems

04 p0662 A70-15336

Differential game analysis of dynamic systems feedback control, presenting extremal aiming for successful pursuit completion

07 p1332 A70-18681

Statistical analysis of dynamic plant based on steady signal, showing numerical determination of operator by least squares method

07 p1226 A70-18726

Optimal control mathematical modeling for dynamic systems under statistically indeterminate disturbances based on game theory and pattern recognition

09 p1653 A70-22141

TDMA system control, considering access process control and switching process control, discussing burst transmission phase control and channel selection at receiving end

10 p1839 A70-24366

Low altitude operational meteorological and navigation spacecraft, discussing need for orbit adjustment by dynamic control

13 p2500 A70-28404

Training algorithms in designing multilevel quasi-optimal controllers for dynamic processes, using pattern recognition methods

13 p2383 A70-29581

Third order dynamic relay control system, determining periodic motion and motion stability

13 p2507 A70-29719

Electrohydraulic control system dynamics, examining executive component loading at low speeds and nonlinear resistances

13 p2345 A70-29720

Controllability test for second order differential systems, noting applicability to linear first order time dependent systems

13 p2443 A70-29972

Dynamical optimal control for infinite dimensional linear systems, examining Balakrishnan solution technique

14 p2562 A70-31201

Dynamical systems optimal control approximation without solving differential equations, considering linear systems with quadratic cost functional

14 p2562 A70-31411

Decoupling by dynamic compensation using algebraic machinery, considering state space extension role in pole assignment

16 p2886 A70-33333

Linear distributed dynamic system simulation using infinite product expansions for transcendental terms in transfer functions

16 p2942 A70-33348

Recurrence scheme for parameter estimation by quasi-linear equations of motion method and Kalman filtering for nonlinear dynamical systems

16 p2887 A70-33349

Mechanical system with n material points, deriving control algorithms for realizing constrained programmed motion

16 p2953 A70-34297

Dynamic control model of lift helicopters with two cable sling loads using multiple part motion equations. [AIAA PAPER 70-29]

17 p3020 A70-35839

Spectral densities of input and output signals of discretely continuous systems as function of comparison moment

18 p3233 A70-36069

Soviet book on dynamic systems with cylindrical phase space covering differential equations with angular coordinates, parameter estimation, multidimensional and discontinuous systems, pendulums, etc

19 p3470 A70-37468

Book on optimal control covering optimization, estimation, dynamic and linear control systems, programming, probability and random processes, environmental influence, etc

20 p3600 A70-39124

Two dynamic systems synthesis achieving limited influence on each other by coordinates invariance criteria method involving determinant

20 p3604 A70-39841

Dynamic plants optimal control, deriving algorithm for determining a posteriori probability density of generalized state vector

20 p3604 A70-39907

Extremal dynamic controlled plant with random input signals, identifying components weighting functions by statistical approximation

20 p3604 A70-39908

Amplitude-phase characteristics of relay slave mechanisms with AC and DC motors under dynamic braking, using harmonic linearization

22 p4002 A70-42842

German monograph on dynamic control behavior of jet engines covering computation for normal external actions and perturbation effects

23 p4233 A70-44396

Decoupling and pole assignment in linear multivariable control systems, minimizing dynamic compensation

23 p4213 A70-44904

DYNAMIC LOADS

NT AERODYNAMIC LOADS

NT BLAST LOADS

NT CYCLIC LOADS

NT GUST LOADS

NT IMPACT LOADS

NT LANDING LOADS

NT ROLLING CONTACT LOADS

NT SHOCK LOADS

NT THRUST LOADS

NT TRANSIENT LOADS

NT VIBRATORY LOADS

NT WING LOADING

Stiffeners reinforced rectangular plates parametric stability under dynamic load, deriving equilibrium equations and boundary conditions by averaging stiffener effects

01 p0205 A70-11146

Dynamic loads calculation on teeth of cylindrical straight tooth gears under engaged and disengaged conditions, performing strength analysis

01 p0105 A70-11421

Two asymptotic dimensional moment theory of elasticity, analyzing stress concentration at curvilinear holes and fluctuating boundary loads

01 p0212 A70-11563

Thin simply supported circular rigid ideally plastic plate subjected to dynamic transverse load uniformly distributed over central circular region

02 p0389 A70-12668

Linear isothermal response of viscously damped thin homogeneous polygonal plates subjected to uniform dynamic loading, calculating forced solutions by numerical integration

03 p0601 A70-14318

Thin elastic plate oscillations plane two dimensional steady state problem assuming constant thickness, finite dimension and moving load

04 p0766 A70-14420

Principal instability region of hinged cylindrical shell under dynamic loading

04 p0776 A70-15271

Parametric oscillations of unclamped rod under variable longitudinal force applied to end, approximating resonance boundaries and instability regions

05 p0934 A70-16226

Dynamic torsion of anisotropic circular cantilever beams and small pitch diameter springs under linear time dependent moment calculated by Saint Venant method

06 p1037 A70-17862

Semiinfinite simply supported cylindrical shell transient response due to axisymmetrically engulfing step pressure wave, investigating moving load critical velocity

[AIAA PAPER 70-18]

06 p1170 A70-18063

Three dimensional latching dynamics and loads induced during Apollo spacecraft docking, using linear stiffness or flexibility matrices for structural elasticity

[AIAA PAPER 70-21]

06 p1158 A70-18181

Shallow orthotropic shell of rectangular platform with edges under dynamic load, studying forced vibrations by anisotropic shell theory

07 p1403 A70-19057

Inhomogeneous elastic half space surface response to moving line loads

08 p1584 A70-20645

Strain rate effects on mechanical properties of solids under dynamic loading

08 p1590 A70-21328

Transient waves propagation in homogeneous isotropic linearly elastic half space excited by traveling normal point load on surface, deriving displacements

[ASME PAPER 69-APMW-12]

08 p1592 A70-21468

Popping pressure of relief valve with helical spring under dynamic load noting frequency dependence

[ASME PAPER 69-VIBR-48]

08 p1441 A70-21479

Machine parts fatigue strength calculated from failure probability parameter during unsteady loading

09 p1776 A70-22622

Dynamic stresses during abrupt temperature changes of medium, showing internal stress waves amplitude increasability by suitable internal stress source selection

09 p1778 A70-23089

Polarization-optical kinematographic method for study of mechanical stresses during dynamic loading

09 p1680 A70-23174

Dynamic force measurement, evaluating hybrid system with reaction force summation and operational compensation subsystems

10 p1889 A70-24580

Space vehicle residual thrust oscillation and dynamic response using power spectral density functions from flight data

10 p1953 A70-25068

High purity beryllium dynamic tests determining Hugoniot equation of state, shock profile and spall threshold/onset of microcracking for elastic pulses

[AIAA PAPER 69-360]

11 p2066 A70-25964

Cylindrical shells plastic flow buckling under radially inward impulsive loading, showing mode number dependence on shell length

11 p2140 A70-26486

Stresses in dynamically loaded struts with one or three holes by photoelasticity, using Fastax camera

12 p2315 A70-26878

Airframe structures fatigue crack propagation with and without strain hardening during variable amplitude loading

12 p2315 A70-27014

Structural design for allowable plastic deformation under dynamic loads, deriving finite element representation of elastic-plastic plane frame beam

12 p2317 A70-27117

Filament reinforced composites tested under dynamic compression loads for determining relations among strain rate, constituent properties, stress-strain behavior, fracture energy and mode

12 p2253 A70-27119

Dynamic behavior and moments of oscillatory systems under steady perturbations using linear differential equations

12 p2261 A70-27555

Plastic symmetrical bending of freely supported beam under transverse local pulsed load, discussing deflection velocity fields during loading and unloading stages

13 p2514 A70-29307

Slope deflection method for computing spatial trusses and plane frameworks under dynamic aperiodic forces

13 p2516 A70-29532

S glass fibers strength characteristics at quasi-static strain rates, considering temperature effects on elastic modulus

13 p2439 A70-29707

Inertial load-time effects in instrumented impact tests, showing corrections for bending stress and dynamic fracture toughness measurements

15 p2820 A70-32240

Dynamic fracture toughness test on heat treated precracked steel specimens under dynamic loading

15 p2759 A70-32243

Plane strain stress intensity factor-Charpy V notch impact test correlations in transition temperature range under slow bend and dynamic loading

15 p2759 A70-32244

Stress rupture shear strength of fiberglass reinforced plastics under monotonic, prolonged and cyclic loading

15 p2766 A70-32853

Sandwich rings inplane transient response to concentrated radial impulsive loads based on Timoshenko type theory, noting dependence on extensional to shear stiffness ratio

16 p2993 A70-34093

Wave propagation from two dimensional expanding load on liquid half space with load fronts decelerating monotonically from initial supersonic speed

17 p3069 A70-34976

Dynamical stresses in members and structures under impulsive loads, taking into account solid viscosities and frequencies effects

17 p3187 A70-34998

Holographic measurement of transient behavior of structures under unsteady or impulsive loading, using pulsed lasers

17 p3085 A70-35008

Shakedown theory of elastic-plastic structures under time dependent loadings

17 p3188 A70-35191

Variable loads programming by semicomputers/semihardware method for 747 fatigue testing

17 p3050 A70-35511

Optimal design of elastic sandwich, solid beam and plate structures under dynamic harmonically varying loads

18 p3336 A70-36220

Elastic Cosserat half plane, analyzing wave propagation of small amplitude thermoelastic disturbances and uniform motion of concentrated line load along surface

18 p3338 A70-36434

Dynamic axisymmetrical loading of thin elastic shallow spherical rigidly clamped dome, using variational method

18 p3341 A70-36582

Dynamic and static stress effects on martensite formation temperature in Fe-Ni-C alloys

19 p3451 A70-37569

Magnetomotive loading of cantilevers, beams and frames, studying dynamic loading of structures

19 p3541 A70-38045

Load rating methods for cage-type and full complement needle bearings dynamic capacity

[ASLE PREPRINT 70AM 3D-2]

19 p3438 A70-38802

Elastic shell stability criterion during short duration dynamic loading

20 p3725 A70-39864

Clamped circular shallow Al arches stability under impulsive loading, obtaining deflection time history by high speed photography and computerized data reduction

20 p3732 A70-40265

Lunar crystalline rock static and dynamic deformation, examining regolith and silicates textures and structures

21 p3897 A70-41515

Boundary value problem solution for elliptical crack subjected to impulsive load by method of characteristics and discontinuity relations, calculating stress distribution

21 p3938 A70-41960

Rigid circular cylindrical inclusion elastic bedding dynamic loading, calculating stresses in interface

22 p4112 A70-42345

Cantilevered tube conveying fluid, calculating forced vibration under time dependent loading and arbitrary initial conditions

22 p4010 A70-42650

Transient stresses and strains in plane wedge under dynamic load, using photoelastic, high speed photographic and strain gage studies

[SMPE PREPRINT 93]

22 p4036 A70-43062

Rigid and elastic rectangular plates vibration under uniformly distributed dynamic load, investigating bending behavior by Galerkin method

23 p4268 A70-44170

Dynamic deformation in thin walled axisymmetric plastic shells and filaments under time variable loads applied to high energy rate forming techniques

23 p4200 A70-44235

Integration operators for transient structural response in qualification tests for internal components of dynamically loaded structures

23 p4273 A70-44719

Wrought Nimonic alloy, measuring stress redistribution due to creep under variable load and temperature

23 p4274 A70-44911

DYNAMIC MODELS

Two band Drude model validity for analysis of IR optical properties of transition metals obtained from experimental dielectric constant data
02 p0339 A70-12452

Mathematical elastodynamic model for parametric dynamic study of forced response solution of motion equations during head trauma
02 p0238 A70-12548

Multiparticle processes in acceleration energy region, comparing various models, noting role of diffraction
03 p0526 A70-13044

Model gas turbine engine blades fatigue strength under stress conditions, considering tensile stresses reproducibility from centrifugal loads
03 p0587 A70-13241

Magnetosphere dynamic morphology model, including qualitative phenomena
03 p0475 A70-13850

Device modeling for computer aided design and analysis of integrated circuits, discussing list of desirable properties and applications to transistor design
03 p0454 A70-14026

Analog computer model of human cardiovascular control system to reproduce subject response to submaximal workload
03 p0438 A70-14081

Visco-elastic column analysis based on mechanical model, investigating relationships between solid viscosities, loading velocities, initial deflections and dynamic buckling loads
03 p0596 A70-14146

Pulsatile flows in living animals and model arteries, discussing flow profiles, instability and wall shear
03 p0430 A70-14244

Electron scattering by molecules, demonstrating formal equivalence of fixed nucleus and free rotator scattering models
04 p0722 A70-14949

Dynamic model for Martian ionosphere modification by solar wind, assuming negligible Mars magnetic moment and neutral atmosphere
04 p0753 A70-15103

Flutter investigation on model designed and constructed for tail unit of HFB 320 Hansa jet aircraft, discussing classical and statistical methods
04 p0775 A70-15180

Decaying isotropic turbulence spectrum evolution model, verifying numerical integration of differential equations
04 p0673 A70-15249

Circulation model of joint ocean-atmosphere system constructed with ocean and atmospheric models, discussing heat transfer by ocean currents
04 p0680 A70-15297

Energy state approximation for supersonic aircraft performance optimization with extension to maximum range problems, noting comparison with complex dynamic models
04 p0623 A70-15376

Nonsimple dynamic model of regular system of interacting deformable bodies, deriving motion equations for nonlocal and local model
05 p0928 A70-16023

Magnetized solar wind steady state inviscid single fluid model developed using MHD, including heat equation with thermal conduction
05 p0902 A70-16445

Dynamical models of relative motions during earthquakes, solving numerically integral equations with nonintegral kernels in crack propagation and elastic wave diffraction
05 p0941 A70-16527

He excitation by low energy He ions giving support for Rosenthal-Foley postcollisional interaction model, testing model predictions
05 p0885 A70-16556

Control system employing adaptive modeler to estimate state, dynamics and future trajectory of unknown plant through performance index minimization
06 p1025 A70-17965

Unified model for transverse gaseous jet penetration into supersonic stream agreeing with measured flow field properties
06 p0976 A70-18201

One dimensional cumulus convection model modified by incorporating rain evaporation rate and temperature changes from downdrafts
06 p1099 A70-18568

Ciliary nerve stimulation and lens motion data to identify open-loop plant dynamics of lens accommodation
07 p1216 A70-18858

Burning rates of monopropellant droplet evaluated by arbitrary property models, discussing dimensionless mass flow rate
07 p1358 A70-18914

Three dimensional unsteady and steady sediment distribution obtained by Monte Carlo simulation method, using stochastic hydrodynamics model for transport
07 p1255 A70-19103

Two parameter model for lattice vibrations applicable to diamond structured crystals, calculating phonon dispersion curves from dielectric screening theory
07 p1357 A70-19920

Similarity model for spherically symmetrical flow following explosion in rarefied atmosphere satisfying hydrodynamic energy conservation equation
07 p1260 A70-19981

Hydromagnetic ionizing shock wave structure in electromagnet fields, using model composed of strong adiabatic shock to translational equilibrium followed by ionization initiation
07 p1351 A70-19985

Model of ideal accelerometer in form of mass point suspended within body of accelerometer mounted in spatial elastic weightless suspension on moving object
07 p1288 A70-20178

Historical survey of celestial mechanics including three body problem and solar system dynamic model construction
08 p1565 A70-20561

Stellar gas ejection processes in corona-interplanetary plasma system, proposing hydrodynamic model with frequent collision region having finite radius
08 p1573 A70-21060

Kinetic model developed for Cl-HBr reaction pulsed chemical laser
08 p1513 A70-21337

Turbulence model, noting possibility of turbulence energy to vanish with distance from tunnel central point of entrance
08 p1486 A70-21770

Fracture mechanics model for stress corrosion cracking of Al alloys, discussing bond strength lessening by adsorption of damaging species
09 p1706 A70-22941

Constant flux gas core nuclear rocket acoustic instabilities, presenting idealized physical model with gas dynamic field perturbed by wave phenomena
09 p1725 A70-23227

Electrical narrowband noise model for laser speckle pattern, obtaining image intensity statistical properties
09 p1638 A70-23370

Discrete dynamic models construction using Gaussian quadrature formula with Jacobian weight, noting Raleigh function role
09 p1785 A70-23597

Hyperelastic bodies containing finite number of inclusions and defects analyzed by continuous dynamic model
10 p1954 A70-24014

Model testing gas flow calculation in system emitting electron beam into atmosphere through supersonic gas seal
10 p1895 A70-24590

Digital simulation of complex dynamic systems using homing missile as example, basing algorithm on 1 transforms for linear systems
11 p2013 A70-25692

Hybrid satellite attitude control system deformation model, utilizing pivoted flexible boom with tip mass as actuator and inertia wheels to dampen gravity induced librations
11 p2123 A70-26127

Nonlinear viscoelastic turbulence model with monotone increasing time scale to predict behavior in homogeneous shear and in pure strain
11 p2040 A70-26544

Crack model analysis taking into account nonlinear force-deformation ahead of crack tip
11 p2143 A70-26667

Spacecraft orientation control system optimization by plotting controlled motion kinematic models
13 p2501 A70-28417

Homogeneous and stationary turbulence in incompressible fluid, proposing dynamic model for strong wave interactions during cascade process
13 p2457 A70-28557

Fracture kinetics model for polymers emphasizing quantum effects even at room temperature
13 p2510 A70-28670

Dynamic linear system simplification and order reduction, showing utilization precautions and validity
13 p2381 A70-28938

Earth core flow velocity field to construct kinematic model of hydromagnetic dynamo, discussing magnetic field development
13 p2398 A70-29209

Turbulent diffusion random model of foreign substance, investigating latent parameters existence
13 p2387 A70-29211

Time variable dynamic medium nonlinear conductive heat transfer equation obtained by power series procedure
13 p2521 A70-29313

Earth dipole field disk dynamo model, studying connection between polarity intervals and precession effects
14 p2638 A70-30619

Biphase rockets combustion characteristics, comparing results with propellant vaporization and nonlinear instability models
14 p2665 A70-30950

Magnetic hysteresis dynamic model for digital simulation of stabilized satellite attitude motions
15 p2812 A70-32509

No-inertia line, lumped parameter and distributed parameter models for dynamic characteristics of fluid transmission lines
15 p2678 A70-32526

Compartmental physiological system dynamics by bilinear control model, relating homeostasis to system
15 p2693 A70-32571

Nonlinear time-invariant lumped parameter dynamic systems, determining mathematical model by piecewise continuous power series expansions
15 p2768 A70-32576

Historical survey of celestial mechanics including three body problem and solar system dynamic model construction
15 p2805 A70-32716

Gas-core nuclear rocket engine simulation by induction coupled plasma torch, determining gas flow patterns
[AIAA PAPER 70-691] 16 p2950 A70-33555

Exhaust nozzle model tests at high subsonic Mach numbers, investigating differences in nozzle drag in contrast to engine conditions
[AIAA PAPER 70-668] 16 p2967 A70-33573

Grain boundary sliding model subjected to shear strain, discussing effect on mechanical properties
16 p2932 A70-33789

Frequency analysis of cylindrically curved panel with clamped and elastic boundaries, using mathematical and panel models
17 p3181 A70-34524

Thermodynamical modeling by regular systems of deformable bodies bound by hyperelastic medium with internal degrees of freedom, formulating equations of motion
18 p3338 A70-36432

Necessary and sufficient conditions for optimal control law existence for model following system, discussing applications to aircraft control
18 p3235 A70-36443

Reduced dissipation of biharmonic oscillations, examining dynamic model under force and kinematic harmonic perturbation
18 p3344 A70-37070

Hydrodynamic model analogy to water bag/incompressible homogeneous fluid in phase space, investigating nonlinear collisionless plasma oscillations
19 p3474 A70-37365

Linear damping theory, discussing simple harmonic motion model extension to transient motion
19 p3472 A70-38041

Model gas turbine engine blades fatigue strength under stress conditions, considering tensile stresses reproducibility from centrifugal loads
19 p3548 A70-38459

Dynamic airfoil stall simulation in wind tunnels, considering pitch rate, Reynolds number, oscillation and test equipment effects
[AIAA PAPER 70-945] 20 p3558 A70-39582

Controlled nonstationary plant dynamic characteristics determination by model, evaluating accuracy
20 p3673 A70-39906

Magnetoplasma interaction with axially slotted delay line, examining coil behavior physical mechanisms by cold plasma model
22 p4079 A70-42365

Free and forced oscillations of dynamic system with linear hysteretic damping, using nonlinear model
22 p4114 A70-42700

Rotating magnetic star dynamic evolution, discussing magnetic and rotation axes inclinations for oblique rotator model
23 p4252 A70-44827

Be star rotation dynamics phenomenon, discussing time variations on main sequence scale
23 p4252 A70-44828

Atmospheric response to heating in stable auroral red arc by two dimensional steady state dynamic model of neutral thermosphere
24 p4329 A70-45357

DYNAMIC PRESSURE

Flight maneuver for roll modulated lifting reentry vehicle to reduce deployment dynamic pressure
07 p1394 A70-19724

Buckled plates flutter at zero dynamic pressure, considering initial plate imperfections, including aerodynamic damping in quasi-steady supersonic approximation
11 p2135 A70-25988

Dynamic pressure data acquisition editing and processing system for engine inlet wind tunnel model tests
[AIAA PAPER 70-596] 13 p2375 A70-29879

Magnetotail plasma sheet temporal variations during substorms and plasma pressure as related to dynamic pressure of solar wind from Vela satellites observation
13 p2480 A70-30061

Dynamic pressure transducer calibration system using fluidic pressure generators
19 p3358 A70-37897

- Dynamic intravascular pressures measured in small vessels of frog lung using micropressure transducer inserted into vessel lumen
19 p3364 A70-38368
- Solar wind static and dynamic pressures on earth magnetosphere, using geomagnetic parameters
21 p3878 A70-40845
- Parawing canopy behavior during deployment in free flight at specific altitudes and dynamic pressures [AIAA PAPER 70-1189]
21 p3751 A70-41804
- Surface pressure coefficient dependence on specific heat ratio for yawed conical lifting bodies in supersonic streams
21 p3747 A70-41877
- ### DYNAMIC PROGRAMMING
- Optimization of distributed parameter control systems described by linear integro-partial differential parabolic equation with delayed argument, using dynamic programming
01 p0131 A70-10548
- Dynamic programming for optimizing distributed parameter control systems described by parabolic linear integrodifferential equation with delayed argument
01 p0131 A70-10556
- Boundary value problems of thin beams theory transformed into initial value problems, using dynamic programming and invariant imbedding
05 p0926 A70-15977
- Circular antenna arrays synthesis, minimizing peak sidelobe level by dynamic programming
06 p1022 A70-18021
- Optimal control for distributed parameter systems described by biharmonic linear partial differential equation using dynamic programming
07 p1244 A70-18843
- Primal-dual algorithm for optimal control with fixed or free terminal time
07 p1238 A70-19269
- Optimum systems synthesis in computation of programmed movements including dynamical programming methods, control under uncertainty and division problem
07 p1325 A70-19270
- Discrete process max-min problem, using dynamic programming to obtain upper and lower bounds
08 p1533 A70-20604
- Apportionment optimization of reliability and maintainability by Lagrange multipliers and dynamic programming, discussing maintainability cost model and computerized simulation
09 p1792 A70-22211
- Optimality condition for singular control problems derived using differential dynamic programming to obtain expression for change in cost produced by control variation
09 p1653 A70-22345
- Narrow throat problems of linear dynamic programming concerning maximum linear functional determination in set of vector functions, giving algorithm for solution
10 p1855 A70-24393
- Dynamic programming successive approximations optimization technique involving system state variables reduction with convergence proofs
10 p1845 A70-24871
- Dynamic programming successive approximation method application to airline scheduling, reviewing real time dispatching, operations, schedule and fleet planning
11 p2013 A70-26209
- Nonlinear discrete time sampled systems optimal control by dynamic programming, with application to stochastic systems
12 p2204 A70-28068
- Dynamic programming applications to optimal stochastic orbital transfer strategy, describing computer program [AIAA PAPER 68-872]
13 p2447 A70-28502
- Terminal guidance by dynamic programming to obtain optimal feedback control law in nominal trajectory neighborhood for minimum energy consumption
13 p2449 A70-29963
- Maximum convergence function in image recognition using dynamic programming and sequential optimization
14 p2553 A70-30419
- Book on differential dynamic programming covering algorithms for continuous time control, bang-bang, discrete time and stochastic systems
14 p2560 A70-30631
- Interplanetary low thrust orbit transfer optimization by dynamic programming, including gravitational perturbation effects from earth, Mars and Jupiter
14 p2640 A70-30759
- Minimum energy feedback control for electrically driven vehicles by dynamic programming
16 p2884 A70-33310
- Optimal control problem solution methods, comparing Euler-Lagrange equations, Pontryagin principle, dynamic programming and invariant imbedding
17 p3057 A70-35589
- Differential dynamic programming algorithm for discrete time orbit transfer optimization
21 p3919 A70-41737
- ### DYNAMIC PROPERTIES
- #### U DYNAMIC CHARACTERISTICS
- #### DYNAMIC RESPONSE
- ##### NT TRANSIENT RESPONSE
- Nondestructive testing and fatigue life analysis of cyclically loaded mechanism, determining dynamic responses to velocity shocks by computer techniques
01 p0053 A70-10010
- Dynamic response to step transverse loads of viscoelastic annulus of constant Poisson ratio in plane strain, analyzing work and spring-dashpot model [ASME PAPER 69-LUB-23]
01 p0101 A70-10384
- Synchronous dynamic response of gaseous double squeeze film thrust plate with very high frequencies, showing increased load capacity and stiffness [ASME PAPER 69-LUB-8]
01 p0102 A70-10395
- Nonlinear dynamic beam response for classical and shear deformation theories, comparing stresses and deflections using traveling wave approach with finite difference schemes
01 p0206 A70-11147
- Linear structures response to pressure fields of deterministic excitation with input function spectra as meromorphic functions of wave number and frequency
01 p0208 A70-11191
- Time independent kernel integral equations in dynamic contact problems of elasticity and mathematical physics
01 p0146 A70-11571
- Turbulent boundary layer response to sudden changes in surface conditions or pressure gradients, considering equilibrium attainment
02 p0287 A70-12360
- Aircraft controls response critical speed as function of transmission lag and transfer function of control link elements
02 p0227 A70-12410
- Vibrational response of simply supported and clamped circular plates subjected to gyroscopically induced inertia loads, using equations of motion
03 p0583 A70-12920
- Solid propellants ignition response to radiative and conductive heat transfer
03 p0544 A70-13921
- Spectrum deductions from profile excited random vibration response, considering single profile imposed displacements
03 p0600 A70-14250
- Linear isothermal response of viscously damped thin homogeneous polygonal plates subjected to uniform dynamic loading, calculating forced solutions by numerical integration
03 p0601 A70-14318
- Pulse width modulated /PWM/ electrohydraulic servo response characteristics from modulator transfer characteristic determination by Fourier series analysis of PWM signal [ASME PAPER 69-WA/AUT-2]
04 p0625 A70-14831
- Slender delta wing aircraft dynamic behavior under vertical and lateral gusts, particularly during landing approach [DGLR-69-52]
04 p0623 A70-15145
- Spectral response of cylindrical shell due to random acoustic pressure input computed using modal approach
04 p0778 A70-15528
- Response characteristics of asymptotic or Gordan type thin foil heat flux transducer, discussing heat transfer coefficient effect on response time and curve
04 p0694 A70-15548
- Dynamic plastic response of finite bar subject to axial impact load noting reflected waves, stress-strain-time histories and residual strain
04 p0779 A70-15599
- Aircraft engine support system dynamic loads induced by fan unbalance analyzed by coupling pylon and engine vibration modes [SAE PAPER 690613]
05 p0895 A70-15850
- Dynamic response of simply supported rectangular plate under suddenly applied transverse load, comparing solutions of classical and improved plate theories
05 p0933 A70-16174
- Thermometer dynamic response under various working conditions predicted from time constant curves
05 p0849 A70-16518
- Pseudosound field wall pressure correlation obtained to predict response characteristics of aircraft panel mounted along jet wake
05 p0835 A70-16785
- Dynamic response of constant resistance anemometers, investigating unsteady probe thermal equilibrium, inductance and feedback equations
06 p1063 A70-17620
- Dynamic response of free-free beams on viscoelastic Winkler foundation using complex foundation modulus based on antivibration isolator
06 p1165 A70-17627
- Single and double cylindrical Langmuir probe responses in highly expanded low density flowing Ar plasma [AIAA PAPER 70-85]
06 p1066 A70-18207
- Airframes dynamic response during simulated launchings of externally carried missile measured in laboratory, describing dynamic load simulation and structural analysis
06 p1159 A70-18439
- Diffused diaphragm pressure sensors in impact probes used in wind tunnel tests of dynamic response of supersonic air induction systems
06 p1074 A70-18605
- Dynamic response of gas lubricated radial sliding bearing from transfer function derived from pH linearized mathematical model of gas lubrication
07 p1290 A70-18739
- Circular plates dynamic response to axisymmetric time dependent loads, analyzing transverse restraint effects on response maxima by plate theory
07 p1404 A70-19251
- Improper integrals appearing in cross correlation of responses of two single degree of freedom systems to bandwidth limited white noise, deriving Laplace inversion formulas
07 p1236 A70-20067
- Digital cross correlator design for impulse response determination in linear systems, noting real time operation without software and storage problems
07 p1236 A70-20068
- Dynamic response of joined elastic quarter spaces of solids to time varying free surface shear tractions parallel to plane of juncture [ASME PAPER 69-APMW-16]
08 p1591 A70-21467
- Dynamic response of infinite cylindrical shell subjected to arbitrary time and space dependent forcing function in acoustic medium
08 p1593 A70-21621
- Inplane shear stress-strain response determined for unidirectional composites, using uniaxial test method for laminated plates
08 p1530 A70-21884
- Vibration theory damping using mathematical model emphasizing controlling response under steady state resonance and random excitation
09 p1769 A70-22238
- Longitudinal structural vibration and lateral bending response mass and spring coupling in Saturn AS-502 during boost with longitudinal excitation by pogo effect
09 p1766 A70-23239
- Roundoff noise output-dynamic range interaction in digital filters, discussing filter synthesis with transposition configurations concept
09 p1649 A70-23366
- Nonlinear many degrees of freedom systems steady state forced vibrations analysis, expressing response in nonlinear normal coordinates
10 p1954 A70-24010
- Channel electron multipliers design and operation, investigating parameters influencing amplification, resolving power and response probability
10 p1888 A70-24484
- Shell dynamics equations role in natural frequencies, determining dynamic response with damping allowance
10 p1960 A70-25052
- Forced vibration of rib-skin structures under random pressure and heavy damping using wave group theory
10 p1963 A70-25066
- Space vehicle residual thrust oscillation and dynamic response using power spectral density functions from flight data
10 p1953 A70-25068
- Aircraft arresting hook response to impact regarding beam flexibility and internal damping using numerical wave propagation methods
10 p1963 A70-25069
- Explosion aerial blast wave for producing impulsive structural forced response, discussing spatial distribution method for increased wave duration
11 p2133 A70-25729
- Sinusoidal and random loading response of age hardening aluminum alloy determined by fatigue testing
11 p2133 A70-25732
- Light aircraft lateral and longitudinal response to atmospheric turbulence, presenting equations and charts for design load calculations [SAE PAPER 700239]
11 p1981 A70-25908
- Transfer functions estimation by taking Fourier transform ratio of finite length samples of input and response measurements, considering error term probability density
11 p2071 A70-25954
- Dynamic buckling of shell or arch structure determined from response of two degrees of freedom structure to step load application
11 p2138 A70-26158
- Reaction impulse during steel spheres impacts at lead surface in vacuum dependent on kinetic energy, velocity and spheres material
11 p2146 A70-26794
- Missile and rail launching structure combined dynamic response determined by discrete element dynamic analysis
12 p2312 A70-27116

Complex structures vibration using component vibration modes, considering dynamic behavior from interface reactions effects

12 p2317 A70-27123

Cylindrical shell response to random acoustic excitation, considering single point transfer functions and equivalent force power spectral densities

12 p2317 A70-27125

Pressurized orthotropic cylindrical membrane shells free and forced vibration, considering dynamic response dependence on internal pressure

12 p2326 A70-27815

Gust response calculations compared with flight measurements for two fighter aircraft and jet transport to determine accuracy
[AIAA PAPER 68-892]

12 p2162 A70-28077

Spin stabilized nonrigid satellite dynamics, considering liquid propellant behavior effect

13 p2499 A70-28401

Prelaunch dynamic response test parameter selection for control systems for space complexes with form of Nyquist locus

13 p2381 A70-28423

Stability and wind response determining spacecraft structure forces and bending moments
[AGARDOGRAPH-115]

13 p2504 A70-28754

Spacecraft parameters role in response to atmospheric disturbances, considering model design and control systems effects
[AGARDOGRAPH-115]

13 p2504 A70-28757

Aircraft dynamic response to homogeneous isotropic atmospheric turbulence analyzed for power spectral density, taking into account spacewise variations in airframe loading

[AIAA PAPER 70-544]

13 p2345 A70-29010

Rudder control of aircraft nullifying yawing and sideslip angles, analyzing rolling response to proportional control by ailerons

13 p2348 A70-29450

Automatic dynamic response system for testing logic and semiconductor devices

13 p2379 A70-29693

Temporal structure and spectral evolution of Nd laser emission with self locking axial modes, noting gain saturation effects

13 p2430 A70-29776

Circular elastic shell response to moving and simultaneous loads, using impulse simulation method

13 p2518 A70-29986

Human temporal motor response models relating reaction, movement and manipulation time to stimulus, movement and manipulation information

14 p2540 A70-30248

Helicopter gust response at high forward speed for various rotor loads noting effects of gust shape, gradual penetration, nonsteady aerodynamics and blade aeroelasticity

[AIAA PAPER 68-981]

14 p2531 A70-30855

Plane frames with and without shear walls, determining dynamic response under vibration by finite element method

14 p2660 A70-31137

Piezoelectric annular disk transducer mechanical response to step voltage input with prescribed temperature field

14 p2588 A70-31228

Equivalent linearization for random vibration, considering stationary statistics of bilinear hysteretic one degree of freedom oscillator response

14 p2661 A70-31428

Upper atmospheric short lived disturbances connected with geomagnetic storms characterized by determining equivalent duration D/I value

15 p2723 A70-31651

Finite settling response for single input/output feedback control system obtained by dual rate sampled data control algorithm

16 p2882 A70-33037

Flight vehicle dynamic response prediction from elastic filler stiffness contained between rigid sphere and ellipsoidal shell

16 p2991 A70-33878

Dynamic response of simply supported elastic bodies due to oscillating point mass executing longitudinal harmonic motion based on linear theory

16 p2993 A70-34092

Rate-sensitive perfectly plastic linear strain hardened rings and tubes, calculating response to impulsive loads

17 p3184 A70-34907

Tracked air cushion vehicle dynamic heave response, examining flow characteristics, active lip control, guideway contact, acceleration response, etc

17 p3017 A70-35178

Shock wave response of metals and nonmetals under high strain rates

17 p3188 A70-35223

Elastic plate vibration with damping under random load, calculating linear response by harmonic analysis

18 p3334 A70-35958

Solid or hollow anisotropic elastic cylinders rotating with variable angular velocity, determining dynamic response by Hankel and Laplace transforms

18 p3338 A70-36433

Elastic and plastic cylindrical shells, investigating dynamic buckling under impulsive loads

18 p3338 A70-36436

Infinite Bernoulli-Euler beam transient and steady state response, considering damping, elastic foundation and constant axial load effects

18 p3339 A70-36490

Shock function response and Fourier spectra relationship, using Fourier transform for equation of motion solution

19 p3456 A70-37381

Dynamic response to step transverse loads of viscoelastic annulus of constant Poisson ratio in plane strain, analyzing work and spring-dash model
[ASME PAPER 69-LUB-23]

19 p3435 A70-37607

Infinite linearly elastic solid response with random variations in material elastic properties, obtaining average energy in displacement field by method of moments

19 p3538 A70-37796

Automatic control system impulse response points identification by fast Fourier transform

19 p3393 A70-37852

Group variational procedure for first integrals of nonconservative dynamical systems

19 p3458 A70-38060

High order servosystems approximation characterized by gain, time constant and dead time, discussing application to response prediction

19 p3394 A70-38503

Three axis large angle attitude control system global analysis, determining system stability, responsiveness and sensitivity to disturbances

[AIAA PAPER 70-996]

20 p3668 A70-39534

Pneumatic actuator control system improvement, using invariance theory to compensate load variability and dynamic response of medium

20 p3564 A70-39848

Long thin circular cylindrical shell resonance velocities in steady response to fluid motion

20 p3727 A70-39884

Dynamic response of distended carbon materials to shock loading defined by measuring equation of state, unloading behavior and spallation strength

20 p3657 A70-40263

Dynamic response of simply supported nonhomogeneous beam and triangular pulse loads

21 p3933 A70-40584

Thin cylindrical shell under nonaxially symmetric concentrated stationary radial loading, calculating random responses and stability

21 p3940 A70-42051

Light rigid civil aircraft response to continuous atmospheric turbulence estimated using two rigid body degrees of freedom method for vertical and lateral gusts

[AIAA PAPER 69-766]

22 p3961 A70-42703

Wind tunnel response tests of cup, vane and propeller wind sensors, determining wind direction and speed parameters, damped and natural frequencies, etc

22 p4030 A70-42914

Conjunctors and traditors circuit realizations, discussing resistive and dynamic nonlinear networks

22 p3996 A70-42919

Strain rate sensitivity and stress waves effects on dynamic response and adhesion failures of rain erosion resistant coatings

22 p4059 A70-43102

Resistance strain foil gage response to dynamic plastic strain

22 p4039 A70-43451

Linear FM radar pulse compression matched filter response calculated by computer evaluation of cross ambiguity function for design tradeoff between resolution and performance

22 p3992 A70-43589

Differential equations of motion for machine assembly, using Appel equations

23 p4200 A70-44319

Rubber mount vibration and shock isolation problems, discussing dynamic response to reaction forces and force concentration

23 p4269 A70-44330

Mechanical structure dynamic response to vibration environment, using mobility method analysis

23 p4269 A70-44334

Structural optimization of designs with requirements including restrictions on structure dynamic response and characteristics

23 p4270 A70-44562

Cantilever plate random vibration response, calculating eigenvectors and natural frequencies by finite element method

23 p4270 A70-44591

Lightly damped second order linear system mean square response to nonstationary random load excitation

24 p4421 A70-45280

Cylindrical shells dynamic thermoelastic response to sudden rotating thermal inputs, using Galerkin method

24 p4421 A70-45285

Gyroscope system steady states, showing dynamic couplings centering in finite angular precession rate case

24 p4335 A70-45630

Multidegrees of freedom electronic cabinets dynamic response to AM fast sine sweep
[SAE PAPER 700846]

24 p4380 A70-45884

DYNAMIC STABILITY

NT AERODYNAMIC STABILITY

NT AIRCRAFT STABILITY

NT ATTITUDE STABILITY

NT BOUNDARY LAYER STABILITY

NT COMBUSTION STABILITY

NT CONTROL STABILITY

NT DIRECTIONAL STABILITY

NT FLAME STABILITY

NT FLOW STABILITY

NT FREQUENCY STABILITY

NT GYROSCOPIC STABILITY

NT HOVERING STABILITY

NT LATERAL STABILITY

NT LONGITUDINAL STABILITY

NT LOW SPEED STABILITY

NT MAGNETOHYDRODYNAMIC STABILITY

NT MOTION STABILITY

NT ROTARY STABILITY

NT SPACECRAFT STABILITY

High speed rotor supported by air lubricated foil bearings subjected to periodic unidirectional excitation by vibrator, noting stability at high speeds
[ASME PAPER 69-LUB-E]

01 p0099 A70-10376

Dynamic unbalance effects in rigid body rotors, discussing lubricant temperature changes and instability hysteresis

[ASME PAPER 69-LUB-14]

01 p0101 A70-10391

Dynamic stability of simply supported column of linear viscoelastic materials under sinusoidal loading

01 p0206 A70-11148

Second order dynamic systems stability, analyzing nonlinear and self excited oscillations by using two differential equations

01 p0146 A70-11604

Nongeostrophic baroclinic stability theory predictions test experiment with vertical heating provision, describing fluid motions

02 p0289 A70-11830

Shock and detonation waves stability in arbitrary media, noting overdriven and underdriven waves

02 p0397 A70-12023

Snap-through dynamic instability of clamped shallow arches subjected to timewise step loads, establishing stability and instability conditions

03 p0583 A70-12919

Lagrangian stability of stellar systems of Trapezium in Orion type situated within large stellar cluster or cosmic cloud

03 p0565 A70-13235

Dynamic stability of flexible aircraft fuselage in controlled supersonic flight at zero angle of attack, basing analysis on elastic oscillation equations

03 p0579 A70-13418

Elastoplastic bodies stability under compression, using theory of small elastoplastic deformations and linearized equations of nonlinear elasticity theory

03 p0591 A70-13440

Energy requirement for nonconservative elastic system unperturbed state stability, using direct Liapunov method

03 p0594 A70-13502

Energetic stability theorems of dynamical feedback system, removing assumption concerning local square integrability

03 p0460 A70-13971

Two dimensional wave diffraction problems involving discontinuity line, analyzing instability behavior of geometrically induced singularities by applying integral transform on Helmholtz equations

03 p0525 A70-14199

Lumped model formulated for dynamics of proportional fluidic amplifiers, describing flow visualization experiments for resonances and instabilities mechanisms
[ASME PAPER 69-WA/FLCS-3]

04 p0627 A70-14848

Interstellar gas instability, discussing thermal, magnetic and cosmic ray effects

04 p0753 A70-15072

Spherical caps axisymmetric static and dynamic buckling under load, using axisymmetric nonlinear elastic shell theory approximation and finite difference equations
[AIAA PAPER 69-89]

04 p0778 A70-15587

Rate equation analysis of steady state behavior of double cavity GaAs diode laser, noting solution stability by perturbation method

04 p0703 A70-15618

Helicoid precession in reentry problem found unstable in sense of Liapunov and Lagrange and asymptotically stable in sense of Poincare

04 p0765 A70-15666

Stability conditions for relief valves assumed to be part of closed hydraulic line simulating receiving part

05 p0797 A70-15899

Stereophotogrammetric measurement for dynamic deformation of circular membrane subjected to underwater detonation

05 p0927 A70-16009

Soviet book on anisotropic plates theory, strength, stability and oscillations including corrections to classical theory

05 p0928 A70-16016

Stability of nonlinear plasma waves set up by counterstreaming cold electron beams immersed in background of stationary ions

05 p0889 A70-16531

Liapunov second method extension to dynamical systems stability, illustrating wing torsional divergence and panel supersonic flutter

05 p0941 A70-16564

Conjugation principle for control system stabilization based on relation between controlled plant and stabilizing element stability

05 p0824 A70-16851

Transonic dynamic stability of free flight half angle cones in wind tunnel for high drag planetary entry vehicles, discussing Mars entry trajectories

[AIAA PAPER 69-105] 06 p1154 A70-17164

Dynamic stability loss on ablating vehicles ascribed to boundary layer transition effect from turbulent aft body heating

[AIAA PAPER 69-106] 06 p0961 A70-17166

Einstein field equations based on variational principle applied to stability of general self gravitating relativistic gaseous mass obeying specific equation of state

06 p1138 A70-17304

Parasitic elements influence on stability of linear equivalent circuits with tunnel diodes

06 p1022 A70-17674

Three dimensional motion of nonrigid parachute and payload system analyzed for dynamic stability

[AIAA PAPER 70-209] 06 p0987 A70-18062

Dynamic stability of complex aeroelastic structures including V/STOL aircraft using simplified technique, noting application to tilt rotor aircraft design

[AIAA PAPER 70-22] 06 p1170 A70-18119

Dynamic instability of finned missiles occurring as angle of attack undamping and caused by differential lift from windward and leeward fins

[AIAA PAPER 70-206] 06 p1158 A70-18178

Whistler amplification in magnetosphere for electron interaction with background plasma to produce wave growth, discussing stability of various anisotropic velocity distributions

06 p1059 A70-18533

Gyroscopes orientation cross coupling effect on dynamic drift of three axis gyrostabilizer solved by method of successive approximation

07 p1278 A70-18736

Periodic motions and dynamic stability of nonlinear distributed sampled data system of closed loop of pulsed element governed by heat conduction equation

07 p1226 A70-18749

Detonation front structure stability in gases, discussing spin detonation, transverse waves, perturbation, etc

07 p1418 A70-18751

Gaseous spheres gravitational stability in proper field, considering convection and radial perturbations effects

07 p1383 A70-19408

Gravitating particles systems equilibrium states, solving kinetic equations for sphere and cylinder in isotropic and anisotropic cases

07 p1389 A70-20207

Dynamic stability of pendulum-weight system during vertical HF small amplitude vibration of suspension point by averaging method

08 p1543 A70-20494

Central equilibrium position stability of gas bearing supported rotor allowing for inertia and lubricant compressibility

08 p1502 A70-20695

Dynamic stability of shallow shells, taking into account longitudinal inertial forces and nonlinear geometry

08 p1587 A70-21170

Stability and potential cavitation of centrifugal pump operating with four working wheels with different geometric parameters

08 p1558 A70-21196

Vibration stability of two identical particles constrained to plane and restrained by three linear springs with initial stress

08 p1591 A70-21466

Lagrangian stability of stellar systems of Trapezium in Orion type situated within large stellar cluster or cosmic cloud

08 p1580 A70-21668

Free vibrations and dynamic buckling of hinged extensible beam under axial force

09 p1768 A70-22061

Fluids equilibrium stability within medium at constant temperature and pressure, discussing time behavior of thermodynamic processes

09 p1786 A70-22062

Variational principle application to stability in failure mechanics of arbitrary linearly elastic bodies, discussing inertia effect on steady state vibrations of cracked bodies

09 p1771 A70-22465

Dynamic stability of Jeans spheroid and Roches ellipsoid using small perturbations method

09 p1759 A70-22749

Free flight static, dynamic stability and drag data for 10 degree semiangle cone obtained at 8-16 Mach numbers

[AIAA PAPER 69-133] 09 p1605 A70-23218

Lifting reentry dynamic stability of flare stabilizers and flap controls

09 p1766 A70-23242

Elastic chain systems stability and natural vibrations using parameter coupling method permitting integral equation construction

09 p1784 A70-23596

Beam vibration eigenfunctions with allowance for shear compliance used to determine beams dynamic stability under pulsating axial load

09 p1785 A70-23600

Computer simulation of six degree of freedom motion system and actual system test, substantiating simulation accuracy

[AIAA PAPER 70-358] 10 p1859 A70-24218

Pulsed solid state laser power output stability in terms of kinetic theory noting laser action threshold role

10 p1899 A70-24254

Coupled control of space vehicle orientation with reference to three celestial bodies, reducing plane vibrations to dynamic third order system

10 p1914 A70-24307

Horizontal fluid layer heated from above or below analyzed for gravitational field sinusoidal modulation effects on stability

10 p1968 A70-24523

Thin elastic plates and shells parametric resonance amplitudes by solving nonlinear differential equations, considering dynamic stability

11 p2129 A70-25523

Balanced rotor with radial sliding bearing bushings, studying lubricant gas restoring force effect on stability with allowance for bushings translational movements

11 p2058 A70-25581

Asymptotic stabilization of multivariable dynamic systems, using subsystem decomposition and Liapunov second method

11 p2023 A70-25607

Nonlinear dynamic theory describing elastic Cosserat curves plane motion, developing linear displacement equations and dynamic stability concept

11 p2142 A70-26632

Electric arc stability with descending static I-V characteristics in plasmatrons using direct Liapunov method

11 p2093 A70-26734

Equations of motion for dynamic stability of flexible freely spinning Alouette-type satellite with crossed dipole configuration

12 p2312 A70-27194

Three dimensional variational dynamic and static large deformation equations solutions for stability and natural frequencies and wave propagation in bodies under initial strains

12 p2322 A70-27331

Dynamic systems absolute stability, optimality and passivity algebraic criterion in terms of real even polynomial coefficients

12 p2261 A70-27412

Dynamic stability of multipoint servocontrol system actuating thin deformable primary mirror of orbiting telescope

12 p2203 A70-27413

Amplitude and phase fluctuations in laser with nonlinear absorption due to spontaneous emission, studying lasing instability near hysteresis threshold

12 p2248 A70-27548

Dynamics of gravity stabilized satellite having maximum damping rate

13 p2499 A70-28391

Minimum time control for placing circular orbit satellite in gravitationally stable position

13 p2502 A70-28440

Blade torsional degree of freedom effects on stability and flapping response of rotors operating at high advance ratios

13 p2507 A70-28444

Two mirror astigmatic resonator mode fields and stability determined by writing Fredholm equation suitable to geometrical optics approximation

13 p2424 A70-28596

Soviet book on dynamics of rockets covering solid and liquid fuel rocket stability, controllability and transfer functions

13 p2505 A70-28799

Reentry vehicles dynamic stability analysis involving pitch, yaw and roll motions modes coupled by asymmetries

[AIAA PAPER 70-561] 13 p2341 A70-29027

Blunt heat shield effectiveness for trailing payload in reentry capsules, discussing dynamic instability effect

[AIAA PAPER 70-563] 13 p2341 A70-29028

Transonic static and dynamic stability of large angle spherically blunted high-drag cones

[AIAA PAPER 70-564] 13 p2341 A70-29029

Pulsed noise stability of discrete data transmission system having multipositional frequency manipulation as compared to binary system

14 p2547 A70-30148

Liapunov type analysis of linear structural dynamic system excited by stochastic parametric load, discussing radially loaded thin circular plates

14 p2657 A70-30763

Cylindrical propellant tanks dynamic stability and parametric resonance, analyzing axial preload, liquid depth top impedance and ullage pressure by Donnell theory

14 p2657 A70-30764

Dynamic stability derivatives calculation using steady and oscillatory lifting surface theory with allowance for Bryan limitations

14 p2529 A70-30864

Static and dynamic stability of wind tunnel models with flexible support, considering binary rigid body freedoms

14 p2564 A70-31398

Stability loss of dynamic two dimensional mechanical elastic system with single degree of freedom under trajectory bifurcation

15 p2775 A70-32474

Massive hydrogen burning stars evolution with pulsational mass loss based on minimizing pulsational instability degree to specify mass loss rate

15 p2803 A70-32612

Shock wave front propagation instability in decreasing density medium, applying to stellar structure

16 p2890 A70-33200

Linear dynamic systems under nonconservative and harmonic forces, examining stability conditions

16 p2952 A70-33896

Nonlinear dynamic stability of fluid layer heated from below in time dependent bounded domain

16 p2943 A70-34249

Nonlinear dynamic systems described by matrix equation, formulating asymptotically stable conditions, discussing motion equations of two degree of freedom system

16 p2995 A70-34281

Neutral type differential equations transformation to time lag system making periodic vibrations existence and stability theorems applicable

16 p2944 A70-34282

Tau-decomposition stability analysis method applied to two degrees of freedom system subjected to retarded follower forces

17 p3176 A70-34957

Equilibria stability of linear discrete dynamic systems involving elastic, nonconservative, dissipative and gyroscopic forces, using Liapunov-type energy method

17 p3129 A70-34958

First order difference equations for dynamical systems from Hamilton canonical equations

17 p3129 A70-34959

Minimal interference thin metal strap support system for dynamic stability tests of high fineness ratio wind tunnel models

17 p3063 A70-35657

Solar prominences thermal and dynamical stability in terms of optically thin plasma supported by magnetic field against gravity

17 p3174 A70-35867

Constraint torque elimination from vector equations canonical system for attitude dynamics of satellite consisting of arbitrarily interconnected rigid bodies

[AIAA PAPER 69-923] 18 p3316 A70-36679

Flat model galaxy stability, examining unstable two armed density wave by numerical methods

18 p3330 A70-37190

Dynamic unbalance effects in rigid body rotors, discussing lubricant temperature changes and instability hysteresis

[ASME PAPER 69-LUB-14] 19 p3435 A70-37606

Transient system decay characteristics, discussing equilibrium point damping time for asymptotically stable systems of ordinary differential equations

19 p3542 A70-38066

Blast loaded cylindrical shell collapse hinge dynamic instability prediction by mathematical model

19 p3545 A70-38334

Gravity effects on impact damper performance, investigating dynamic stability and kinematic viability of various steady state motion solutions

20 p3717 A70-38974

Gravitational effects on impact damper performance, discussing dynamic stability and kinematically viable periodic motion and resonant conditions

20 p3717 A70-38975

Relativistic gas spheres and collisionless star cluster models with large red shifts, showing radial perturbation stability

20 p3703 A70-39175

Spinning blunt entry vehicles dynamic stability tests in terminal regime, discussing dependence on angle of attack [AIAA PAPER 70-988] 20 p3714 A70-39541

Nonrolling lifting gliding vehicle hypersonic longitudinal dynamic stability, applying analysis to space shuttles [AIAA PAPER 70-977] 20 p3715 A70-39552

Cruciform-finned missiles dynamic stability investigation by nonlinear differential equations of motion, considering roll lock-in, resonance instability and catastrophic yaw [AIAA PAPER 70-969] 20 p3715 A70-39560

Two dimensional detonations structure by nonlinear theory for systems with hydrodynamically unstable steady state solutions, imposing periodic boundary conditions 20 p3609 A70-39658

Thin walled circular cylindrical steel shells dynamic stability partly filled with liquid and subjected to longitudinal excitation 20 p3723 A70-39852

Elastic shell stability criterion during short duration dynamic loading 20 p3725 A70-39864

Rotating elastic shafts rectangular shape stability under creep conditions, considering single mass rotor 20 p3727 A70-39883

Dynamic stability of cylindrical shell with small curvature under static or periodically variable axial pressure loads 21 p3932 A70-40554

Be star HD 37202 zeta Tauri II envelope instability, discussing radial velocities, profiles, line width and electron density in layers 21 p3888 A70-41119

Inlet data for engine stability analyses, developing technical management procedure patterns for pretest test and posttest results [AIAA PAPER 70-1214] 21 p3745 A70-41320

Book on stability of dynamic systems and solid bodies covering variation equations, Liapunov method and functions, approximations, harmonic balance and applications 21 p3850 A70-41370

Static and dynamic longitudinal stability of semirigid parafoil gliding descent system in pitching motion [AIAA PAPER 70-1191] 21 p3753 A70-41825

Fin slots and tabs effect on dynamic stability characteristics of low drag bomb, discussing free rolling and pitching tests 21 p3747 A70-41880

Spatial stability of transferred arc anode spots during cutting with plasma jets, noting currents associated with microspots 22 p4043 A70-42380

Linear dynamic systems stability under various types of forces 22 p4061 A70-42536

Elastic bodies under motion-dependent loads, examining thermodynamic conditions of equilibrium states stability 22 p4123 A70-42538

Circular plates dynamic stability under variable periodic loads, using differential equations of vibrational motion for median surface 22 p4114 A70-42613

Earth gravity deforming effect on flexible crossed-dipole satellite configuration, considering dynamic stability and spin stabilization 22 p4110 A70-43434

Heavy homogeneous material free elastic rod dynamic stability under distributed scanning load, investigating plane transverse vibrations by differential equations 22 p4121 A70-43722

Dynamic systems stability with periodically varying parameters analyzed by Hill type infinite determinant, exemplifying helicopter rotor aeroelastic stability in forward flight 23 p4220 A70-44556

Pendulum dynamic stability under parametric excitation, presenting transient and steady state solutions by linear and nonlinear theory applications 24 p4379 A70-45587

Formation flight stability in dynamic environment, using stationkeeping geometry simulation [AIAA PAPER 70-1337] 24 p4373 A70-45931

DYNAMIC STRUCTURAL ANALYSIS

Random vibration of interconnected systems, analyzing power flow and energy levels in linear oscillator interacting with environments, using Thevenin-Norton representations 01 p0207 A70-11161

Transfer matrix method analysis of dynamic behavior of beam structures applied to single rows of aircraft panels 01 p0209 A70-11200

Book on vibrational motions of straight and curved shafts, covering dynamic analysis for noncircular cross sections, applications to machine tools and vehicles design, etc 01 p0209 A70-11378

Asymptotic dynamic theory for elastic cylindrical shells incorporating thickness effects, considering longitudinal wave propagation in infinite length shell 02 p0385 A70-11877

Dynamic structural analysis using computer graphics display, emphasizing applicability to man machine interaction at key decision making points 02 p0386 A70-11943

Rigid body dynamics of turborotors in fluid film journal bearings, investigating initial transients effect on motion stability by Runge-Kutta technique [ASME PAPER 68-LUB-7] 02 p0307 A70-12165

Triangular conforming plate bending element applied to static and dynamic problems, investigating convergence rates of finite element approximations 03 p0584 A70-12924

Visco-elastic column analysis based on mechanical model, investigating relationships between solid viscosities, loading velocities, initial deflections and dynamic buckling loads 03 p0596 A70-14146

Axisymmetric structures under load and temperature distribution analyzed by matrix displacement method [DGLR-69-62] 04 p0774 A70-15167

Postdamage structural analysis based on Hardy-Cross method, describing mathematical techniques 04 p0776 A70-15391

Transient excitation methods for structures dynamic analysis, discussing suitable forcing transients choice 06 p1165 A70-17646

Three dimensional latching dynamics and loads induced during Apollo spacecraft docking, using linear stiffness or flexibility matrices for structural elasticity [AIAA PAPER 70-21] 06 p1158 A70-18181

Elastic membranes deformation compressed by restraints using discrete dynamic programming 07 p1400 A70-18680

Natural oscillations of three dimensional bundle of parallel strapped rods with variable elastic mass parameters determined by Hamilton-Ostrogradskii variational principle 08 p1583 A70-20485

Inhomogeneous elastic half space surface response to moving line loads 08 p1584 A70-20645

Stress-strain analysis for rod-shaped structural elements under combined tensile and bending loads 08 p1588 A70-21191

Lateral buckling of simply supported uniform diaphragm using slope-deflection equations for orthogonally intersecting beams, prescribing boundary conditions 08 p1589 A70-21244

Prismatic thin walled shells with box type cross section under torsion using Vlasov variational method in conjunction with transfer matrices 08 p1589 A70-21248

Dynamic buckling of thin circular ring subjected to radially directed impulsive load, investigating in-plane and out-of-plane modes 08 p1596 A70-21978

Rotating circular disk under angular acceleration, analyzing stress and deformation distributions 08 p1596 A70-21980

Potential function of creep strain rates for incompressible nonstrengthening materials exhibiting different creep characteristics in tension and compression 09 p1769 A70-22122

Rotatory inertia and shear deformation effects on structural vibrations of Timoshenko beams and frameworks using matrix formulation 09 p1770 A70-22257

Four point supported square plate fundamental frequency by finite difference and energy methods 09 p1770 A70-22389

Matrix theory of elastic locking structures, programming for analysis under given loads and displacements 09 p1771 A70-22396

Flexo-torsional elasticity ellipse determining displacements, hyperstatic reactions and influence lines in beams with straight axis and variable cross section 09 p1771 A70-22398

Self excited vibrations in balanced vertical shaft running on plain lubricated bearings, making numerical analysis of small perturbation transition to fully developed swirl 09 p1690 A70-22399

Inertia effect in failure mechanics for steadily developing equilibrium cracks in dynamic system with time dependent periodically variable load 09 p1771 A70-22466

Soviet book on rocket structure mechanics covering acting loads and selection of tanks, stage segments, nose section and propulsion units 09 p1772 A70-22527

Constant cross section beam bending and torsion with allowance for moment stresses, deriving differential equations for displacement functions 09 p1773 A70-22538

Forced vibrations of trusses calculated by dynamic rigidities method allowing for friction forces 09 p1773 A70-22540

Truss vibrations calculations by method of dynamic rigidities, describing numerical methods for solving frequency equation to save computer storage capacity 09 p1773 A70-22546

Spherical and cylindrical cavities dynamic plastic expansion analysis by finite element method allowing for inertia forces 09 p1777 A70-22724

Sensors design for studying temperature fields and stressed state of structures 09 p1680 A70-23106

External plane dynamic problems reduction to infinite algebraic equations in elasticity theory for simply connected domains based on Helmholtz equation solution in curvilinear coordinates 09 p1783 A70-23391

Dynamic photoelastic analysis of fracturing plastic plates, studying elastic and stress fields around propagating cracks 09 p1783 A70-23448

Finite deformations of flexible inelastic orthotropic shells of revolution for generalized plastic flow and deformation theories 10 p1955 A70-24079

Finite deflections theory applied to elastic-plastic arches, introducing coefficients depending on shape and degree of yielding of cross section 10 p1955 A70-24080

Bending of homogeneous orthotropic rectangular plate of variable thickness supported on opposite edges, obtaining solution as Fourier series 10 p1955 A70-24083

Dynamic shear modulus and depth of dominant layer of vibrating elastic medium, assuming foundation as isotropic stratum on rigid bed 10 p1957 A70-24481

Kinematic analysis of limit loads of equilateral triangular plates under various boundary conditions 10 p1958 A70-24517

Dynamic stresses, temperature and displacements fields in thin circular disk under transient heat sources, considering mechanical resonance vibration 10 p1958 A70-24518

Structural behavior during creep by step by step process suitable for computers after linearizing non-linear equations [ONERA-TP-805] 10 p1958 A70-24545

Structural dynamics - Conference, Loughborough, Leics., England, March 1970, Volume 1 10 p1960 A70-25051

Shell dynamics equations role in natural frequencies, determining dynamic response with damping allowance 10 p1960 A70-25052

Structural dynamics - Conference, Loughborough, Leics., England, March 1970, Volume 2 10 p1962 A70-25064

Moving mass effects on Euler beam analysis extended to Timoshenko beam, obtaining numerical solutions by finite difference method 10 p1963 A70-25073

Torsional vibration of rotating tapered and twisted turbomachine blade, constructing digital computer program for convergence and boundary conditions [SAE PAPER 700180] 11 p2128 A70-25373

Momentum theory of small elastic-plastic deformations, proving minimum potential energy, simple loading and elastic unloading theorems 11 p2128 A70-25387

Explosion arial blast wave for producing impulsive structural forced response, discussing spatial distribution method for increased wave duration 11 p2133 A70-25729

Dynamic synthesis of hinged four-element mechanism with respect to driven link position, transmission relations and allowance for transmission angle 11 p1983 A70-25934

Dynamic buckling of shell or arch structure determined from response of two degrees of freedom structure to step load application 11 p2138 A70-26158

Thin cylindrical shells of perfectly plastic rigid material, analyzing dynamic plastic deformation under internal impulsive pressure 11 p2139 A70-26413

Nonuniform beam element stiffness matrices for dynamic and elastic instability analysis, determining frequencies, mode shapes and critical loads 11 p2143 A70-26643

Elastic postbuckling and imperfection sensitivity of discrete structural systems using perturbation approach 11 p2143 A70-26668

Lunar Orbiter spacecraft vibration responses based on mathematical models, comparing results with experiment 12 p2315 A70-27098

Materials and structural dynamics - AIAA-ASME Conference, Denver, April 1970 12 p2315 A70-27101

Apollo lunar module structural integrity for lunar landing verified by Monte Carlo dynamic analysis
12 p2312 A70-27114

Airframe structural tests in elevated temperature environment by applied load ratios and room temperature static results
12 p2205 A70-27134

Space shuttle structural dynamic problems, discussing stall flutter due to transition from high angle of attack to normal aircraft flying attitude [AIAA PAPER 70-740]
12 p2312 A70-27150

Semiinfinite composite medium displacement caused by nucleus of torsional strain with axis perpendicular to constituent isotropic layers interfaces
12 p2321 A70-27159

Elastic-plastic plane stress analysis of two dimensional structures based on Tresca yield criterion, using finite element technique
12 p2326 A70-27795

Dynamic analysis involving crack extension force for two dimensional multiple radial crack division
13 p2510 A70-28602

Dynamic instability of multirecess hydrostatic journal bearings at critical shaft rotation velocity
13 p2418 A70-28745

Self similar dynamic problems in two dimensional elasticity theory for slot with point source in boundless body
13 p2517 A70-29763

Eigenvalue and eigenvector derivatives in dynamic system designs involving vibrations and oscillations, discussing applications in modeling
13 p2518 A70-29971

Dynamic stiffness, natural frequencies and mode shapes of prismatic and thin walled open grids, including warping and shear flange deformation
14 p2659 A70-31132

Plane frames with and without shear walls, determining dynamic response under vibration by finite element method
14 p2660 A70-31137

Elastic membranes deformation compressed by restraints using discrete dynamic programming
15 p2813 A70-31472

Matrix analysis of discretized dynamical system with constraints, considering case of damped oscillators
15 p2774 A70-31697

Dynamic structures design optimization subject to shock spectrum, describing conversational type computer program [ASME PAPER 70-DE-28]
16 p2989 A70-33501

Dynamic seal effectiveness prediction, considering bearing and sealing pressure distributions, friction coefficient, flow characteristics, etc [ASME PAPER 70-DE-53]
16 p2918 A70-33514

Nonlinear dynamic analysis of shells of revolution under symmetric and asymmetric loads, obtaining solutions for shallow cap buckling
16 p2994 A70-34229

Mechanical vibrations models and analysis techniques, emphasizing problem of weak couplings in discrete systems
16 p2996 A70-34290

Mathematical techniques for optimal design of single purpose structures under dynamic deflection
17 p3182 A70-34544

Dynamical stresses in members and structures under impulsive loads, taking into account solid viscosities and frequencies effects
17 p3187 A70-34998

Impulsive loading of structures via light-initiated sprayed explosives
17 p3059 A70-35162

Impulse loading of rings using magnetically accelerated flyer plates
17 p3187 A70-35163

Torsional vibration of thin beam with varying cross section, formulating fundamental equation and boundary conditions
18 p3339 A70-36519

Three dimensional dynamic analysis of small harmonic stress wave propagation in elastic-plastic and viscoplastic materials, using finite differences
18 p3344 A70-36724

Magnetomotive loading of cantilevers, beams and frames, studying dynamic loading of structures
19 p3541 A70-38045

Rectangular plates free and forced vibrations, including rotatory inertia and shear deformation effects in dynamic response analysis
19 p3544 A70-38327

Rectangular plate with three clamped edges, analyzing free vibration by Ritz method with deflection functions
19 p3544 A70-38328

Circular sandwich arc subject to central concentrated load and symmetrically applied edge couple, obtaining shakedown interaction curve
19 p3546 A70-38354

Dynamic testing of turbine machine parts using strength and vibration equations and similarity method
19 p3437 A70-38472

Self similar dynamic problems in two dimensional elasticity theory for slot with point source in boundless body
20 p3732 A70-40101

Mathematical techniques for optimal design of single purpose structures under dynamic deflection
20 p3733 A70-40381

Stress-strain characteristics at high strain rates, obtaining materials dynamic plastic properties by thin wafer technique
21 p3932 A70-40543

Dynamic response of simply supported non-homogeneous beam and triangular pulse loads
21 p3933 A70-40584

Skew panels supersonic flutter and vibration calculated by matrix displacement method
21 p3933 A70-40586

Free vibration optimization analysis by reducing stiffness and mass matrices
21 p3933 A70-40587

Dynamics of deployable space structures stiffened by centrifugal forces due to spin, discussing L F radio telescope
21 p3931 A70-41854

Analytical iteration method extended to critical load of clamped beam with symmetrically variable cross section
21 p3939 A70-41965

Cylindrical cavity uniform expansion in compressible elastic plastic solid, calculating pressure by similarity solution
22 p4114 A70-42634

Cantilevered tube conveying fluid, calculating forced vibration under time dependent loading and arbitrary initial conditions
22 p4010 A70-42650

Strapdown inertial attitude indication, describing static and dynamic tests, error propagation profiles, performance prediction, etc
22 p4068 A70-42668

Rectangular plates natural vibration problem, using straight line method with approximate separation of variables
23 p4265 A70-43982

Data acquisition and processing in structural modal characteristics analysis during ground resonance tests [ICAS PAPER 70-36]
23 p4267 A70-44133

Mechanical structure dynamic response to vibration environment, using mobility method analysis
23 p4269 A70-44334

Thin shells static and dynamic finite element analysis
23 p4273 A70-44721

Complex structures component modal dynamic analysis technique, describing investigations with combination of finite element and composite modes computer program
23 p4273 A70-44722

Dynamic structural stability analysis, describing integral equation matrix technique
24 p4419 A70-45156

Rectangular cable networks covered by or embedded in membrane matrix, calculating vibration response under load by Galerkin method
24 p4421 A70-45279

Lightly damped second order linear system mean square response to nonstationary random load excitation
24 p4421 A70-45280

Natural frequencies of elastic bodies with variable properties, using external forcing function and continued fractions approximation
24 p4422 A70-45295

DYNAMIC TESTS

Dynamic testing instrumentation for oxygen breathing equipment emphasizing demand regulators and masks, connecting hose, helmets and individual components
01 p0041 A70-11458

Metal adhesive joints peeling and stripping strength determinations, describing static and dynamic tests
08 p1503 A70-20884

Stress, strain and strain rate relations determined from dynamic flexural beam tests with bending moment in terms of curvature
08 p1592 A70-21475

Dynamic force measurement methods, considering reaction force and operational compensation
09 p1672 A70-22013

Analog computer methods applied to aerospace dynamic test data analysis and high speed screening [AIAA PAPER 70-595]
13 p2375 A70-29880

Charpy V notch and dynamic tear tests compared for fracture toughness characterization of Ni-Cr-Mo-V steel
14 p2596 A70-30931

Impact test machines, specimen design and energy measurement in dynamic tear test method for steel fracture strength
15 p2759 A70-32242

Start-stop dynamics as cost effective method for computerized testing of digital modules and subassemblies, providing static and dynamic capability
17 p3062 A70-35504

Gyro test package, dynamic test facility and real time attitude algorithm to investigate operational capabilities of strapdown inertial attitude package
17 p3134 A70-35652

Dynamic system modeling pulse test data reduction by digital computer and functional approximation for Fourier transform calculations
18 p2320 A70-36458

Rocket engine tests dynamic data oscillographic presentation and digital processing
19 p3490 A70-37916

Magnetic perturbations effect neutralization for satellite attitude stabilization by real time simulation of satellite angular motion in magnetic field
19 p3399 A70-38286

Inertial platform with integral dynamic self test and fault monitoring scheme, describing design and operation [AIAA PAPER 70-1013]
20 p3667 A70-39520

Helicopter dynamic tests for aeroelastic and mechanical instabilities and forced vibration problems
21 p3749 A70-40583

Shock and bump testing for dynamic mechanical environments effects encountered by vehicle equipment and components
23 p4195 A70-44331

DYNAMICS

Dynamic discrete systems unsteady motions stability, formulating theorem for finite characteristic numbers existence
08 p1543 A70-20493

Book on dynamics of mechanisms with elastic connections and impact systems covering differential and finite difference equations, equations of motion, friction effects, etc
08 p1502 A70-20753

Dynamics dominant on different scales in atmosphere by spectral analysis, showing marked gap under most synoptic conditions
09 p1717 A70-22376

Insular system energy and momentum definition in external gravitational field, using dynamic equations and Einstein theory
19 p3513 A70-37412

Dynamic systems stability in sense of Poisson, relating motions commutative and stable families
19 p3472 A70-38936

Hamilton-Jacobi theorem for nonlinear dynamic system moving with holonomic Cetaev constraints, investigating necessary and sufficient conditions
23 p4210 A70-44024

DYNAMO THEORY

Hypothetical magnetic configurations in presence of Coriolis forces from convective cell hydromagnetic activity in solar plasma, considering dynamos with increasing magnetic field
01 p0173 A70-10133

Two layer truncated harmonic model of Rossby wave dynamo for solar cycle, accounting for maintenance and reversal of magnetic fields
01 p0174 A70-10238

Polar magnetic disturbances during IQSY characterized by SP field superposed on Sq field generated by ionospheric dynamo
01 p0075 A70-10599

DC dynamo models for planetary electromagnetic conditions, considering nonrotationally symmetric turbulence induction actions and critical values for field maintenance
01 p0185 A70-10956

Dynamo theory of stellar and planetary magnetic fields, discussing mathematical analysis and electronic computation of eigenvalue problems and field parameters
01 p0185 A70-10957

Earth daily rotation effects on magnetosphere electric currents, discussing Pederson currents in dynamo region and E region ionization
02 p0293 A70-12775

F 2 small scale inhomogeneities drift relation to current systems of dynamo region, discussing solar activity effects on ionospheric conductivity
07 p1267 A70-19452

Stratosphere-ionosphere coupling, dynamo theory on geomagnetic Sq variation and ionosphere radio wave absorption and reflection
07 p1274 A70-20271

Hypothetical magnetic configurations in presence of Coriolis forces from convective cell hydromagnetic activity in solar plasma, considering dynamos with increasing magnetic field
08 p1576 A70-21409

Ionospheric wind velocity fields calculated from atmospheric dynamo effects taking into account electric field, current density and conductivity tensor
10 p1881 A70-24819

Homogeneous turbulent velocity effect on magnetic field distribution in electrically conducting fluid with no external source, observing dynamo action
11 p2091 A70-26545

Ionosphere dynamo region thermal input by Joule heating and solar radiation and coupling to various thermotidal modes, observing semidiurnal and semianual effects
11 p2047 A70-26569

Earth core flow velocity field to construct kinematic model of hydromagnetic dynamo, discussing magnetic field development 13 p2398 A70-29209

Earth hydromagnetic dynamo spectrum fluctuation related to secular geomagnetic field variations, using unsteady kinematic models 14 p2568 A70-30202

Earth dipole field disk dynamo model, studying connection between polarity intervals and precession effects 14 p2638 A70-30619

Spatially periodic dynamos, analyzing homogeneous conducting fluid motions and magnetic field forms 18 p3291 A70-36407

F 2 small scale inhomogeneities drift relation to current systems of dynamo region, discussing solar activity effects on ionospheric conductivity 18 p3249 A70-36926

Solar magnetic field origin and behavior, discussing hydromagnetic dynamos, cyclonic convection and generation times 20 p3706 A70-39927

Earth magnetic dipole represented by Rikitake two-disk MHD dynamo system 22 p4013 A70-42633

Dynamo region electrostatic fields effects on magnetospheric drift, taking electrical conductivities and solar and lunar tidal modes into account 23 p4185 A70-43836

Dynamo role in magnetospheric disturbances and ionospheric inhomogeneities, allowing for charged particle concentration height dependence 23 p4237 A70-44059

Earth hydromagnetic dynamo spectrum fluctuation related to secular geomagnetic field variations, using unsteady kinematic models 24 p4330 A70-46277

DYNAMOMETERS

Multiplying digital device for measuring motor speed, torque and power, discussing optional applications and design 02 p0297 A70-12076

Dynamic hysteresis loop measurement of energy dissipation in materials, showing deformation effects on accuracy 19 p3535 A70-37346

Stabilograph and support dynamograph based on amplitude modulation of carrier frequency for standing stability determination in humans 19 p3371 A70-38220

DYNODES

Fatigue effects of incident illumination on area sensitivity, dynode gain stability and anode output for end-on photomultipliers 09 p1683 A70-23511

Hybrid Cockroft Walton multidynode photomultiplier supply for space applications, using miniature components and thick film technology 12 p2233 A70-27406

DYSON THEORY

Radiation transfer problem in waveguide with statistically uneven walls reduced to Dyson and Bethe-Salpeter equations in quantum field theory 03 p0524 A70-13066

Coherent wave reflection from random half space, solving scalar Dyson equation in bilocal approximation for oblique incidence 12 p2189 A70-27972

DYSPROSIUM

Absorption spectra of single crystals TbAlG and DyAlG garnets, investigating Verdet constant dependence on ion concentration 07 p1355 A70-18705

Phase diagram of dysprosium oxide-chromium oxide system constructed by microstructural analysis in 1600-2400 C range in argon atmosphere 08 p1556 A70-21118

Isotropical crystals of Dy compounds investigated for magnetic behavior using high resolution photoelectric optical spectroscopy 12 p2261 A70-27243

E

E LAYERS

U E REGION

E REGION

NT E-2 LAYER

NT SPORADIC E LAYER

Heat sources in E region from electron temperature data analysis recorded by rockets during eclipses in July 1963 01 p0082 A70-11491

Electron gas heating at E region altitudes as function of ionization of atmospheric gases, noting rocket experiments during solar eclipse 01 p0082 A70-11492

Rocket sounding data on ionospheric currents at mid and low latitudes noting absence in D and above E region 01 p0082 A70-11529

Auroral breakup effects on sporadic E via comparison between sequential ionograms and riometer absorption data indicating transient effect in D/E regions 02 p0288 A70-11744

E layer kinetic energy viscous dissipation and transfer to potential energy by turbulence and irregular winds shear 02 p0327 A70-12292

Lower E region turbulence interpretation based on high resolution photographs of artificial sodium vapor trails 03 p0476 A70-13913

Radar Thomson backscatter observations of ion temperature and ion-neutral collision frequency used to investigate reversible heating in E region 03 p0477 A70-13988

Uniform stratified layers in equatorial E region determined from Centaur rocket capacitance probe electron density observations, suggesting internal atmospheric gravity waves mechanism 03 p0478 A70-14222

Lunar tide in E region phase height from measurements of diurnal phase path change for continuous wave 04 p0678 A70-14973

F region ionograms processing with correction for ionization effects between E and F layers 04 p0684 A70-15748

Magnetic disturbance associated with E layer east-west electric current calculated in terms of ionization production and loss 05 p0838 A70-16282

Phase path variation of stable continuous wave transmission reflected from E region during daytime, discussing night time results 06 p1055 A70-17593

Seasonal variations of maximum electron concentration in stratified E-F region, including E 2 layer recombination coefficient and F layer characteristics probability 06 p1057 A70-17842

D and lower E region absorption of short waves, studying absorption distribution with height 07 p1263 A70-19153

Lowest useful frequency /LUF/ prediction on long distance quasi-antipodal circuit, considering E layer blanketing 07 p1232 A70-19178

Barium ion artificial clouds motions and striations due to cloud-ionosphere coupling, studying electron density variations below cloud in E layer 07 p1271 A70-20155

Ionospheric irregularities-diffraction patterns relative drifts, verifying point source effect for radio waves reflected from E and sporadic E layers 07 p1236 A70-20162

Radar measurements of magnetic dip in E region compared with surface values and spherical harmonic models for dip angles 07 p1271 A70-20163

Reactions determining ion composition in E region, discussing neutral composition variations from day to night and during solar activity cycles 07 p1276 A70-20431

E layer atmospheric circulation model for meteor zone, noting solar thermal radiation role 08 p1575 A70-21215

Electron, oxygen and NO molecular ions concentrations for E region from computer calculations of diurnal model compared to observations 08 p1490 A70-21391

Deviating and nondeviating absorption of radiowaves in ionosphere, deriving vertical distribution of particle collisions in E layer 08 p1490 A70-21431

Excessive absorption in night E layer with and without geomagnetic disturbances for almost complete solar cycle, discussing winter increases /anomalies/ 09 p1669 A70-23170

Ionospheric F and E layers collision frequency estimates, comparing pulse absorption and cosmic radio noise measurements 10 p1880 A70-24804

Diurnal variations of concentrations of ions and neutral components of NO, O and N in E region from analysis of chemical and photochemical processes 10 p1881 A70-24809

Asymmetric cross correlation functions in D and lower E region drift measurements interpreted in terms of moving screens 10 p1881 A70-24811

Nocturnal E layer electron density profile dependence on solar activity 10 p1885 A70-25265

Sunspot cycle and ionospheric D and E layers daily radio wave absorption correlation, observing seasonal variation effect 10 p1885 A70-25267

Ion component drift displacing components from E and F layers ascribed to vertical electric field presence in hydrogen arc 11 p2104 A70-25541

Electron temperature diurnal variations data from rocket soundings used for determining recombination coefficient in E region 11 p2044 A70-25550

Wind shear caused ionospheric E region irregularities investigated by horizontal plasma density gradients determination 11 p2045 A70-25652

E and F layer ion chemistry dependence on ion-neutral reactions and dissociative recombination 12 p2223 A70-27720

E region plasma parameters measurement by in situ probes, considering electron density and temperature 12 p2225 A70-27737

Three-point simultaneous observations for ionospheric drift characteristics in E and F regions 13 p2396 A70-29097

Vlasov interaction of magnetically coupled E layer with dissipative structures including injection, trapping and drag effects 14 p2623 A70-30698

F region ionograms processing with correction for ionization effects between E and F layers 14 p2576 A70-30832

Hydrogen UV geocorona photoionizing effect on nighttime E region electron density in low and midlatitudes, comparing with ionosonde data 14 p2581 A70-31270

E region ion composition from rocket-borne mass spectrometer data 15 p2725 A70-31689

Correlated daily variations of ionospheric drift and anisotropy parameters in E and F regions at Thumba, India 15 p2725 A70-31858

Barium ion clouds striation formation above E layer ascribed to LF gradient drift instability 15 p2727 A70-31908

Ionization-neutralization processes and recombination coefficient in F and E regions, using radiophysical measurements 15 p2730 A70-32083

Single pulse ionospheric sounding system for detecting and identifying E region echoes 16 p2859 A70-32940

Nighttime E region structure variations observed by Wallops Island rocket flights, obtaining electron density profiles by Langmuir probe during ascent 17 p3076 A70-34941

Ionospheric E layer formation, investigating role of solar X ray control by electron production rate and density calculations 17 p3151 A70-34943

Ionospheric E region winds correlations to lower atmosphere meteorological phenomena 17 p3077 A70-34950

Nighttime E region molecular ion production rate estimation, taking into account windshear effect 18 p3245 A70-36022

Lower E region electron concentration variations relationship with geomagnetic field disturbances 18 p3255 A70-37037

Ionization in ionospheric E and upper D regions, considering solar short wave radiation, small components, atmospheric dynamics and vertical mass transport 19 p3407 A70-37301

E layer electron concentrations, effective recombination coefficient and ionization sources during solar eclipse, noting soft X radiation intensity 19 p3408 A70-37310

Ionization rate experimental profiles during maximum solar activity compared with calculations, showing additional source of ionization in E region 19 p3409 A70-37322

Vertical profile of electron collisions effective frequencies in auroral ionosphere E region 19 p3409 A70-37330

Multiple reflection processes in D and E regions at LF and VLF, using Pitteway full wave method 19 p3413 A70-38001

Coupling processes in daytime D and E regions at LF and VLF, using thin film optics method for reflection and transmission coefficient matrices 19 p3413 A70-38002

Intermode coupling processes in nighttime D and E regions, using thin film optical method for propagation phenomena at LF and VLF 19 p3413 A70-38003

Solar eclipse effects on E and F layers, discussing photoionization rate, electron density and temperature, plasma diffusion, electric fields, etc 19 p3418 A70-38903

E and F region electron density response to incident radiation intensity on upper atmosphere during solar eclipses 19 p3419 A70-38916

Ion component drift displacing components from E and F layers ascribed to vertical electric field presence in hydrogen arc 21 p3882 A70-41291

Electron temperature diurnal variations data from rocket soundings used for determining recombination coefficient in E region 21 p3819 A70-41300

Nighttime equatorial E region small scale irregularities detected by rocket-borne Langmuir and plasma noise probes, discussing generation mechanism

22 p4018 A70-43108

Lower E region recombination coefficients from electron density and flux measurements in glow aurora by Nike-Apache rocket

22 p4020 A70-43163

Day and nighttime E and sporadic E layer drifts over low latitude station recorded by spaced receiver technique

22 p4020 A70-43166

Upper atmosphere ionization balance, examining metastable species in E and F regions

22 p4106 A70-43306

E region winds response to solar radiation variations, including geomagnetism role

23 p4186 A70-43848

Wind induced modification of E region ionization density profiles, using coupled continuity equations for ion species

23 p4214 A70-44040

E region ion composition nighttime variations, examining nitrogen monoxide and O ion nonequilibrium concentrations by ionic-molecular reactions

23 p4189 A70-44074

E region additional ionization source during solar activity maximum, analyzing ion production function and electron concentration

23 p4190 A70-44077

E region electron concentration profiles, using ground sounding equipment allowing accurate signal reflection altitude measurements

23 p4190 A70-44078

Equatorial E region electrojet plasma irregularities, discussing electron density, drift velocity, profile structure, etc

24 p4384 A70-45150

E-2 LAYER

Soviet book on ionospheric interlayer formations covering electron concentration distribution, E-2 layer occurrence frequency, recombination coefficient, etc

20 p3622 A70-39823

EAR

NT COCHLEA
NT CORTI ORGAN
NT EARDRUMS
NT LABYRINTH
NT MIDDLE EAR
NT SEMICIRCULAR CANALS
NT VESTIBULES

Frequency function of sound localization in median plane measured psychoacoustically at both ears with narrow band signals

09 p1624 A70-22762

Microdissection morphology of vestibular apparatus sensory regions in guinea pig, rabbit, cat, squirrel, monkey and man

10 p1811 A70-24200

Partial oxygen pressure in hyperaemic earlobe capillary blood under hypoxic conditions, noting correlation with age and body weight

10 p1822 A70-25088

Loudness lateralization of acoustic signals in right and left ear during binocular interaction

12 p2174 A70-28357

Temperature change relation between anterior hypothalamus and concha auricularae in rabbits

18 p3218 A70-36532

Auditory perception by neuroelectrical tests based on logic coincidence among several detectors, discussing bullfrog inner ear

21 p3765 A70-41991

EAR PRESSURE TEST

Hearing threshold and ear canal pressure levels, using circumaural enclosure with varying acoustic field

06 p0994 A70-17598

EAR PROTECTORS

Army aviation personnel ear protection, evaluating APH-5 and SPH-4 helmets

06 p1002 A70-17703

Ear protection for persons exposed to various jet aircraft noise environments

24 p4306 A70-45121

EARDRUMS

Otic Barotrauma with bilateral perforation of ear drums suffered during rapid decompression run in chamber, discussing diagnosis

10 p1811 A70-24040

Mammalian eardrum failure due to blast induced pressure variations, examining wave shape, character, magnitude and duration effects

23 p4148 A70-44839

EARLY BIRD SATELLITES

Syncom and Early Bird systems development, launch procedure and operation, discussing common components

14 p2654 A70-31144

EARLY STARS

NT PROTOSTARS
NT T TAURI STARS

Stratospheric balloon measurement of near UV from early type stars, discussing gondola, observation

method, telescope and photographic recordings analysis

04 p0750 A70-14704

Statistical analysis of rotation and macroturbulence in early type Ia and IaB supergiants, discussing evolutionary effects

08 p1571 A70-20908

Coefficients for linear and nonlinear limb darkening in early type stars

11 p2113 A70-26469

Chandrasekhar polarization upper limit in early type stars noting effects of thermal absorption, wavelengths and effective temperature

12 p2303 A70-27675

Young stars evolution rates in expanding and disintegrating stellar associations, giving age estimates

12 p2306 A70-27862

UV interstellar extinction, examining reddened and unreddened early stars with OAO satellite spectrophotometric scans

17 p3159 A70-34878

Early-type star spectral scan analysis from OAO observation, comparing model atmosphere calculations

17 p3161 A70-34887

Luminosity effects in Balmer lines of early type stars, noting H alpha equivalent width decrease

17 p3170 A70-35388

Young cepheids galactic distribution determined by photometric method, showing correlation with spiral arms

18 p3330 A70-37184

Early B stars photometric examination of variable spectral lines, discussing beta Cephei stars possibility

21 p3922 A70-41981

Stellar rotation effects on atmospheres of early type main sequence stars, using models for surface gravity and temperature variations

23 p4249 A70-44810

Early type Ia and IaB supergiant stars macroturbulence and rotation, investigating spectral line broadening, mass loss and angular momentum

23 p4250 A70-44813

Upper main sequence and close early type binaries evolution by fission of rapidly rotating protostars

23 p4250 A70-44815

Southern early stars away from galactic plane, reporting magnitudes and colors on UBV system and MK spectral classifications

24 p4404 A70-45412

EARLY WARNING SYSTEMS

Tiros solar proton monitor program, describing detector design, operational data processing and early warning network

17 p3180 A70-35304

EARTH (PLANET)

Spherical earth wind field correlation matrix, relating scalar fields to isotropic vector field

01 p0135 A70-10204

Human activities inadvertent effects on planet earth, discussing catastrophic physical environment changes and compensation methods

01 p0077 A70-11045

Satellite positions from simultaneous measurement by laser along geocentric arc usable for determining earth mass center position

02 p0253 A70-11752

Geogravitational constants and mass determination, discussing Cavendish constant and measurement theory and technique

03 p0473 A70-13236

Penumbra visibility of earth on lunar disk related to moon distance during lunar eclipse, discussing moon vanishing

03 p0569 A70-13361

Earth exploration and service by satellites - Conference, Rome, March 1969

03 p0572 A70-13826

Cloud cover consequence on earth photographing space missions simulated by Monte Carlo method using worldwide statistics

04 p0676 A70-14636

Heat transport conduction mode and earth as heat sink in solar atmosphere, discussing mesopause coldest region, turbulence and solar plasma-earth electromagnetic interactions

04 p0677 A70-14644

Earth model based on free air gravity anomaly with condensed topography for eliminating gravity reduction difficulties, noting use in Vening-Meinsz formula

05 p0840 A70-16640

Magnetovariational sounding procedure for determining vertical distribution of earth mean electrical conductivity using geomagnetic field spatial derivatives for spherical earth

05 p0843 A70-16767

Solar wind flow different interactions with earth, Venus and moon

06 p1136 A70-18284

Soviet monograph on constant of gravitation, mass and density of earth covering torsion balance, weight experiments and nonlinear vibration techniques

08 p1487 A70-20764

Geogravitational constants and mass determination, discussing Cavendish constant and measurement theory and technique

08 p1491 A70-21669

Earth shadow effect on solar radiation pressure induced short periodic perturbations of satellite orbits

09 p1761 A70-23054

Rare gases abundance patterns on earth and in chondrites, proposing chemical adsorption mechanism at planetesimal stage during accretion

09 p1764 A70-23610

Earth mechanical properties and composition compared with moon and other terrestrial planets

11 p2047 A70-26616

Penumbra visibility of earth on lunar disk related to moon distance during lunar eclipse, discussing moon vanishing

11 p2118 A70-26726

Terrestrial external gravitational field approximation using sphere and ellipsoid attraction, showing mass, angular velocity and size dependence

12 p2300 A70-27477

Variational equations from Herrick variation of parameters method for Icarus encounter with earth

13 p2488 A70-28823

Replicating molecules on primordial earth, suggesting chemical evolution on Jupiter via demonstrable alpha-aminonitriles synthesis

14 p2536 A70-30364

Brightness field spatial structure of solar radiation reflected from earth by Cosmos 149 satellite, discussing homogeneity and isotropy

18 p3247 A70-36629

Lunar surface mapping and comparison of geological features with earth, considering mass, volume, density, gravity, rotation and energy and matter balance

19 p3518 A70-37994

Space environment physical properties near earth, discussing neutral atmosphere, solar radiation, ionosphere, electric and magnetic fields and radiation belts

19 p3520 A70-38277

Earthshine bright parts relationship to average brilliance of sun during total eclipse

21 p3893 A70-41445

Earth ellipticity in past, using hydrostatic equations based on density distribution and angular velocity to obtain oblateness

21 p3820 A70-41973

EARTH ALBEDO

Satellite multispectral photometry data in airglow bands correlated with cloud characteristics and surface albedo variations

04 p0715 A70-15522

Night airglow variations observed during Cosmos satellite orbits, determining atmospheric albedo wavelength dependence for solid and medium cloudiness and clear skies

05 p0841 A70-16728

Earth and atmosphere effect on solar radiation balance in Southern Hemisphere

06 p1054 A70-17413

Vertical short wave albedo profiles in lower troposphere under cloudiness and clear sky using actinometric sounding

08 p1537 A70-21105

Day sky Fraunhofer lines filling-in /Ring effect/ considered from analogous effects in surface albedo, suggesting role of Rayleigh wings

10 p1947 A70-24992

Polarization of radiation reflected and transmitted by earth atmosphere, calculating scattering matrix for aerosol size distribution model

21 p3820 A70-41725

Planetary albedo changes due to pollution aerosols, showing absorption-to-backscattering ratio function in atmospheric heating or cooling

22 p4096 A70-43419

Echo 1 and PAGEOS 1 orbital elements variations, determining perturbing effects of earth albedo radiation pressure

24 p4409 A70-45558

EARTH ATMOSPHERE

NT ARTIFICIAL RADIATION BELTS

NT D REGION

NT E REGION

NT E-2 LAYER

NT EXOSPHERE

NT F REGION

NT F 1 REGION

NT F 2 REGION

NT FREE ATMOSPHERE

NT INNER RADIATION BELT

NT IONOSPHERE

NT LOWER ATMOSPHERE

NT LOWER IONOSPHERE

NT MAGNETOPAUSE

NT MAGNETOSPHERE

NT MESOPAUSE

NT MESOSPHERE

NT MIDLATERAL ATMOSPHERE

NT OUTER RADIATION BELT

NT OZONOSPHERE

NT PROTON BELTS

NT RADIATION BELTS

NT SPORADIC E LAYER

Atmospheric density variations during solar maximum and minimum, discussing solar corpuscular stream and EUV radiation

01 p0075 A70-10594

Atmospheric water vapor photodissociation and resulting O evolution recalculated for determining O abundance in absence of biological activity

01 p0081 A70-11294

Wave structure function dependence on altitude, comparing function ratio for up/down propagation through atmosphere

02 p0258 A70-12461

Space research photography role in studying earth and moon atmospheres and surfaces, determining spectral bands for contrast

03 p0483 A70-13168

D-2 experiments measuring atomic oxygen emission from terrestrial atmosphere and polarization rate and emission intensity from geocoronal hydrogen

03 p0559 A70-13828

Venus-earth carbon dioxide atomic parameters used to determine ionization and optical emission rates in Venus upper atmosphere resulting from solar cosmic rays

05 p0901 A70-16276

Earth, Venus and Mars atmospheric structure, discussing gases escape, temperature, density, IR radiation and solar radiation absorption

05 p0914 A70-16628

Surface impedance of spherical earth isolated by nonconducting atmosphere from ionospheric currents producing alternating electromagnetic field

05 p0843 A70-16768

Earth and atmosphere effect on solar radiation balance in Southern Hemisphere

06 p1054 A70-17413

Meteor motions at cosmic velocities in real atmosphere studies to determine cause of sudden flares

06 p1140 A70-17735

Earth oxygen atmosphere age estimated from sulfur isotope composition of geological phlogopite and lazurite deposits from South Baikal region

06 p1056 A70-17798

Optimal control program using multiple maxima method for maneuvering spacecraft in earth atmosphere with aim of changing orbital plane

07 p1331 A70-19483

Mariner 4 and 5 and Venera 4 data used for comparing terrestrial planets ionospheres

07 p1386 A70-19488

Extra-atmospheric submillimeter astronomy, discussing emission observations between IR and RF region and astrophysical-cosmological applications

07 p1387 A70-19643

Atmospheric regions interactions concerning stratosphere, mesosphere, troposphere, etc, noting solar activity effects

08 p1490 A70-21428

IR energy interaction with earth atmosphere, determining multispectral scanner optimum wavelength intervals for earth resources applications [AIAA PAPER 70-289]

09 p1669 A70-22892

Spectral, angular and spatial evolution of earth twilight aureole brightness pattern from visual observation and spectrophotometry on Soyuz 5 spacecraft

10 p1873 A70-24270

Satellite studies geoeactive particles and photoelectrons, including interactions with earth atmosphere

10 p1874 A70-24312

Atomic oxygen IR emission in earth atmospheric models, using reduction factor for comparison with optically thin atmosphere

10 p1875 A70-24439

Earth orography shape effect on cyclogenetic properties of atmosphere noting mountain height, slope, air mass thermal properties, etc

10 p1913 A70-25196

Earth atmosphere circulation mechanisms, discussing zonal and meridional components and eddy motions

11 p2075 A70-26030

Antimatter motion in solar system and earth atmosphere, discussing vaporization and annihilation energy in collisions with interplanetary gas atoms

11 p2119 A70-26793

Satellite based random Doppler environmental measurement technique for Global Atmospheric Research Program /GARP/, receiving signals from balloons, buoys and land stations

13 p2407 A70-29176

Jeans escape rate error for atmospheric H and He attributed to perturbed velocity distribution function, using realistic atom-atom elastic scattering cross sections

13 p2398 A70-29226

Earth atmosphere formation and oxygen-carbon dioxide balance mechanisms, including water vapor photodissociation, photosynthesis, fossil fuel burning, etc

14 p2572 A70-30350

Solar activity predictions for earth upper atmosphere models emphasizing linear repression method

14 p2638 A70-30565

Quartz crystal particulate sensor instrument for terrestrial and Mars atmospheres

14 p2585 A70-30575

Earth atmosphere model for weather forecasting using space technology, noting Global Atmospheric Research Project /GARP/

14 p2576 A70-30973

Numerical modeling for earth atmosphere in terms of six pressure levels using digital computers

14 p2577 A70-31151

Absorption spectrum of terrestrial atmosphere with sun as source, obtaining formaldehyde line with rotating grid spectrometer

14 p2579 A70-31256

Terrestrial planetary ionospheres, discussing charged particle density distribution of Mars daytime ionosphere and Venus day and dark sides

15 p2799 A70-31748

Earth-ionosphere cavity resonances diurnal variations by considering different propagation characteristics of day and night hemispheres

15 p2728 A70-31910

Atmospheric optical properties at various altitudes, using lunar disk photometric observations at different wavelengths during eclipse

15 p2801 A70-32476

Optimal control program using multiple maxima method for maneuvering spacecraft in earth atmosphere with aim of changing orbital plane

15 p2813 A70-32728

Mariner 4 and 5 and Venera 4 data used for comparing terrestrial planets ionospheres

15 p2805 A70-32733

Earth/atmosphere system outgoing microwave radiation calculations, surveying aircraft/ satellite measurements at various wavelengths

16 p2896 A70-33217

Atmospheric oxygen history, using primeval anoxic terrestrial atmosphere simulation to show organic molecule formation by abiogenic process

16 p2898 A70-33990

Earth atmosphere transmission coefficients determination by relation between transparency and daytime sky brightness, noting limits of applicability

16 p2899 A70-34180

Earth atmosphere transmission coefficient and optical stability based on solar aureole observation

16 p2899 A70-34186

Cloud-free earth areas determined via reflected radiance measurements from ATS 3 cloud camera

17 p3133 A70-35930

NO in earth atmosphere, describing theory of formation for explaining observed density distribution

18 p3245 A70-36019

Meteor deceleration rates in atmosphere, using base line radar measurements

18 p3313 A70-36294

Simultaneous measurements of earth atmosphere radiation, comparing short and long wave data consistencies at various altitudes

18 p3286 A70-36963

Soviet papers on physical processes in earth upper atmosphere covering emissions, dust, particle distribution, Rayleigh scattering, temperature, inhomogeneities, etc

18 p3250 A70-36976

Terrestrial atmospheric tidal theory applicability to Venus and Mars, considering dependence on parameters variation among planets

19 p3519 A70-38253

Moon as standard radio source for eliminating earth atmosphere influence during solar radio radiation measurements

19 p3522 A70-38564

VLF wave propagation in earth atmosphere waveguide, calculating various atmospheric types from waveguide field dependence on frequencies

19 p3416 A70-38566

Earth atmosphere cosmic ray neutron albedo from balloon measurement of flux vertical distribution

20 p3698 A70-39298

Soviet book on physical atmospheric parameters covering model, solar and earth radiation fluxes and spectral energy distribution

20 p3664 A70-39799

Earth-moon system formation theory, discussing condensation from terrestrial hot extended silicate atmosphere

22 p4098 A70-42548

Aircraft condensation trails formation by interactions of exhaust emission, vorticity of wing induced downwash and ambient atmosphere

22 p3958 A70-42684

Coherent reflection waves produced by radio wave propagating through entire earth atmosphere

23 p4159 A70-43757

Atmospheric optical properties at various altitudes, using lunar disk photometric observation at different wavelengths during eclipse

23 p4239 A70-43901

Statistical-dynamical atmosphere model for global circulation simulation, taking into account meteorological variables of velocity, temperature, pressure and eddy statistics

23 p4213 A70-44029

Earth atmospheric boundary layer wind velocity, temperature gradients and specific humidity differences, calculating climatic correlations from mathematical circulation model

23 p4214 A70-44264

Earth/atmosphere system outgoing microwave radiation calculations, surveying aircraft/ satellite measurements at various wavelengths

24 p4328 A70-45192

EARTH AXIS

Geodetic coordinate system referred to center of mass and earth rotation axis constructible from satellite observations

03 p0472 A70-13186

Earth poles motion influence on latitude, longitude, azimuth and geocentric rectangular coordinates of points determinations on earth surface

03 p0473 A70-13187

Satellite observations used to construct coordinate system referred to earth center of mass and axis of rotation

03 p0474 A70-13733

Earth axis position and displacements measured by earth-moon laser telemetry

06 p1058 A70-18452

Triaxial earth attraction potential from expanding certain elliptical functions into series, noting consistency with concepts of astronomy and geodesy

15 p2731 A70-32148

Statistical test of Melchior laws governing Chandlerian motion of earth pole based on polar coordinates

15 p2732 A70-32497

Statistical test of Melchior laws governing Chandlerian motion of earth pole based on polar coordinates

23 p4187 A70-43918

EARTH CORE

Core convection consequences with regard to earth figure and continental drift, indicating no changes in magnitude of magnetization

01 p0076 A70-10899

Cyclonic convective cell fluctuation and nonuniform core rotation effects on reversal of geomagnetic field, investigating fossil magnetism

04 p0676 A70-14600

Geomagnetic field secular variations relation to variations of magnetic field of optimum dipoles, noting earth core role

05 p0842 A70-16747

Earth central region chemical exploration using antineutrino flux produced by natural radioactive isotopes

09 p1761 A70-22985

Seismology as tool for investigation of planets, discussing earth rigidity, tides and long period oscillations

11 p2111 A70-26040

Earth core flow velocity field to construct kinematic model of hydromagnetic dynamo, discussing magnetic field development

13 p2398 A70-29209

Earth hydromagnetic dynamo spectrum fluctuation related to secular geomagnetic field variations, using unsteady kinematic models

14 p2568 A70-30202

Sulphur in earth core composition, considering volatile element abundances and iron melt in thermal models

18 p3256 A70-37078

Geomagnetic axial dipole deviation from true north associated with earth core asymmetric motion, discussing geomagnetic reversal

22 p4020 A70-43231

Earth hydromagnetic dynamo spectrum fluctuation related to secular geomagnetic field variations, using unsteady kinematic models

24 p4330 A70-46277

EARTH CRUST

Canadian Shield ridges and meteorite impact scars, discussing state of earth crust during meteoritic bombardment of earth and moon

08 p1563 A70-20500

Gravity long wave variations correlation with crust and upper mantle geological activity, describing anomaly distribution

08 p1488 A70-21014

Geometrical analysis of partial fusion in earth crust and mantle formation, discussing solid solution and boundaries in MgO-iron oxide-silicon dioxide system

09 p1670 A70-23398

Continental migration role in lunar maria formation, suggesting similarity with geological formation of earth ocean floor

09 p1765 A70-23797

Lunar-earth early crust anorthosites comparison, including occurrence sites, physical and chemical properties, etc

13 p2486 A70-28616

Ionization potentials of elemental abundances in lunar rocks compared with earth crust and class I carbonaceous chondrites, showing lunar materials differentiation

15 p2801 A70-32463

Carbonaceous complex use as indicators of geothermal history and high temperature organic geochemistry 17 p3042 A70-35331

Phase delay of solid earth tide, minimizing ocean and atmosphere loading by strain seismograph measurement 18 p3255 A70-37077

Astronomically determined latitude longitude and azimuth reduction to common epoch, discussing secular nonperiodic pole motion due to crust drift 18 p3323 A70-37144

EARTH CURRENTS

U TELLURIC CURRENTS

EARTH ENVIRONMENT

Earth climatic control by reflecting satellites producing artificial solar irradiation 03 p0581 A70-13835

Satellite observation of energetic particles and magnetic fields, discussing radiation belts, magnetosphere, galactic cosmic rays, etc 04 p0740 A70-14620

Earth environmental satellite data for oceanography and hydrology, discussing sea surface temperature mapping, low level wind conditions, snow and ice mapping, etc [AAS PAPER 69-596] 04 p0676 A70-14635

Satellite monitoring of air pollution, discussing sulfur dioxide measurement in UV, optical correlation techniques, IR and visible spectra, stratospheric balloon tests, etc [AIAA PAPER 70-305] 09 p1668 A70-22875

Satellites application to studying and monitoring earth ecology, discussing environmental space research and space program priorities 09 p1794 A70-23333

Soviet book on solar activity influence on earth natural processes covering atmospheric circulation and pressure, air temperature, precipitations and hydrological changes 09 p1719 A70-23471

Cryobiotic potentialities on earth, investigating life forms physiological response to temperature, cryotolerance mechanisms, etc 16 p2848 A70-33093

Bioastronautics and earth ecology, discussing environmental pollution, nutritional, microbiological and psychological problems 18 p3350 A70-36757

Circadian and seasonal adaptive function rhythms in animals, discussing terrestrial environment and thermoregulation 19 p3365 A70-38409

Optical solar observatory for investigation of solar activity and impact on earth environment, discussing site selection and equipment 22 p4005 A70-42349

EARTH FIGURE

U GEODESY

EARTH HYDROSPHERE

Earth surface hydrology effect incorporated into atmospheric circulation mathematical model for climate, considering ocean as atmospheric moisture reservoir 04 p0680 A70-15296

Circulation model of joint ocean-atmosphere system constructed with ocean and atmospheric models, discussing heat transfer by ocean currents 04 p0680 A70-15297

EARTH MANTLE

Shear velocity variation with depth in upper mantle for Basin and Range province of western North America, using S waves measurements 02 p0292 A70-12505

Abundance levels of K, Rb, Sr and Ba in pyroxenes, olivines and garnets of ultramafic rocks for upper mantle composition 03 p0472 A70-13149

Pb isotope data from young mantle derived volcanics suggesting mantle evolution and lunar capture 04 p0743 A70-14396

Variational analysis of low latitude magnetic sounding data to determine structural differences between various earth mantle regions, noting additional observations required 04 p0682 A70-15735

Melting zone evolution in thermal history of earth, investigating upper mantle heat transfer effect on layer motion due to radioactive decay 06 p1056 A70-17804

Gravity long wave variations correlation with crust and upper mantle geological activity, describing anomaly distribution 08 p1488 A70-21014

Rayleigh number effects on convection in planetary mantles, considering conservation equations of mass, energy and momentum 09 p1752 A70-22312

Geometrical analysis of partial fusion in earth crust and mantle formation, discussing solid solution and boundaries in MgO-iron oxide-silicon dioxide system 09 p1670 A70-23398

Crystal-chemical and geophysical implications concerning earth mantle phase transitions from beta magnesium silicate crystal structure 11 p1994 A70-25333

Geogravity-geomagnetic fields correlation due to lateral temperature variations in upper mantle 13 p2393 A70-28620

Convection effects in mantle on earth gravitational field using hydrodynamic model 13 p2488 A70-28764

Variational analysis of low latitude magnetic sounding data to determine structural differences between various earth mantle regions, noting additional observations required 14 p2575 A70-30819

Earth mantle electrical conductivity profiles, using Lahiri-Price model and spherical harmonic analysis of quiet day daily variations 16 p2896 A70-33077

Earth upper mantle phase change instability, discussing temperature gradient, transformation influence on fluid, olivine-spinel phase flow patterns and tectonics 21 p3820 A70-41895

Electromagnetic variational soundings of ocean floor earth crust upper mantle near magnetic equator 23 p4189 A70-44066

EARTH MOTION

Earth rotational velocity irregularities and horizontal motions of continental blocks at expense of oceanic hemisphere, noting seasonal distance changes 04 p0681 A70-15477

Earth axis position and displacements measured by earth-moon laser telemetry 06 p1058 A70-18452

EARTH MOVEMENTS

NT EARTHQUAKES

Collapse prone land detected by multispectral scanning and photography with analog data processing 12 p2220 A70-26933

Seismic measurements of sonic boom induced ground vibrations for hazard to structures 12 p2227 A70-28078

Gutenberg-Bullen interior model applied to fading of earth spheroidal oscillations 14 p2568 A70-30153

Surface waves free period partial derivative correlation and relation to resolution of gross earth data 19 p3414 A70-38374

EARTH ORBITAL RENDEZVOUS

Optimal rendezvous maneuver of two spacecraft in circular orbits with minimum fuel consumption, taking into account propelled vehicle control program and flight path 01 p0193 A70-10424

EARTH ORBITING SPACE STATIONS

U EOSS

EARTH ORBITS

NT APOGEES

NT PERIGEEES

Space rescue techniques and equipment in NASA recovery programs, considering low earth orbit and water landing 01 p0035 A70-10717

Space programs to monitor earth resources from synchronous orbit of 19,400 nautical miles, discussing geostationary systems characteristics related to optics and telemetry 01 p0093 A70-11280

Geocentric orbital elements of lunar particles expelled into space by meteorite impact, using spheres of influence method 03 p0574 A70-13880

Satellite motion in earth gravitational field under additional forces using Stockel theorem 04 p0760 A70-14432

Drift, anti-Fermi retardation, convective transfer and diffusion effects on solar cosmic ray energy spectrum in earth orbit proximity 05 p0898 A70-15943

Second order secular perturbations formulas of distant earth satellite motion valid for nearly circular orbits with small inclination to ecliptic plane 06 p1141 A70-17823

Satellite temperature determination in earth orbit, testing mathematical thermal model in simulation chamber 06 p1155 A70-17935

Reusable space shuttle employing two stages resembling subsonic aircraft for carrying passengers and cargo between earth surface and orbit 07 p1392 A70-18873

Climate variations and earth orbital elements secular perturbations, noting solar radiation and celestial mechanics roles 09 p1666 A70-22177

Optimal acceleration from earth orbit to hyperbolic velocities of low thrust space vehicle, constructing asymptotic expansions near and far from central field 10 p1940 A70-24305

Space propulsion systems for public transportation to and from orbit and throughout near solar system, discussing commercial requirements 11 p2102 A70-26060

Earth orbital parameters estimation in manned flight by manual space navigation sensors and computer 13 p2446 A70-28406

Satellite motion in earth gravitational field under additional forces using Stockel theorem 13 p2503 A70-28457

Magnetic moment measurement of satellite in near earth orbit, using data transmitted by rectangular magnetic sensors 13 p2454 A70-30032

Synchronous navigation satellite system for ships and aircraft applicable to earth orbital and lunar operations 14 p2614 A70-30463

Primary mirror development problems for large orbiting telescopes 17 p3083 A70-34873

Solar eclipse calculation and prediction, discussing relationship between possible forms and earth-moon orbital configurations 21 p3924 A70-42173

Radiation pressure effects on artificial satellite motion, including earth shadow perturbation 24 p4408 A70-45554

EARTH PLANETARY STRUCTURE

Moon-earth historical relationship, comparing differences in figure and interior with terrestrial planets 03 p0562 A70-12875

Earth oblateness effects on lunar and interplanetary trajectories, using algorithm based on orbital elements variations [AIAA PAPER 70-97] 06 p1146 A70-18203

Earth surface mapping and shape and internal constitution determination by satellite geodesy 10 p1876 A70-24642

Earth interior structure models using geophysical data in Monte Carlo inversion procedure 11 p2042 A70-25332

Earth continents and ocean basins as clues to planetary evolution, considering crust composition, moon origin, continental drift, etc 11 p2111 A70-26032

Seismology as tool for investigation of planets, discussing earth rigidity, tides and long period oscillations 11 p2111 A70-26040

Precession-nutation dependence on earth structure based on oscillations theory of ellipsoid with rotating fluid contained in rigid envelope 16 p2980 A70-34316

EARTH RADIATION

U TERRESTRIAL RADIATION

EARTH RESOURCES

NT CRUDE OIL

NT DESERTS

NT FARM CROPS

NT FORESTS

NT GRAINS (FOOD)

NT LAKES

NT LAVA

NT LIMESTONE

NT RIVERS

NT ROCKS

NT SANDS

NT SHALES

NT VEGETATION

Terrain imaging radar applied to sensing earth resources 02 p0298 A70-12181

Remote sensing system for earth resources surveys temporal information employing human interpreter and machine for spatial and spectral data processings 03 p0491 A70-13668

Aircraft multispectral IR scanning systems for earth resources remote sensing, discussing capabilities 03 p0491 A70-13670

Multispectral scanner technology for earth resources exploration from space 03 p0492 A70-13671

Earth resources applications of Apollo 6 photography, describing camera system and photographic coverage 03 p0474 A70-13672

Remote sensing aerial and space surveys application to agriculture, forestry and water resources, discussing imaging systems and information acquisition and analysis techniques 05 p0838 A70-16164

Geostationary mode application to earth sensing, examining resolution requirements for earth scanning tracking telescope 06 p1154 A70-17152

Satellites for meteorological and geographical studies using information from TV and IR pictures 08 p1487 A70-20716

Aircraft mounting plate for 70-mm multispectral mapping quadricamera assembly to photograph wildland and agricultural resources 08 p1497 A70-21542

Electromagnetic radiation sources for remote sensing application to identification of water, moist soil and vegetation, discussing optical properties of diverse materials 09 p1667 A70-22851

Earth resources data exploitation, describing potential organizational structures for data handling and various political, economic and technological problems [AIAA PAPER 70-344] 09 p1793 A70-22859

International legal and political aspects of earth resource surveying by satellite remote sensors, considering U.S. policy
[AIAA PAPER 70-331] 09 p1793 A70-22862

Specifications nomographs for earth resources IR radiometers, considering ground resolution, aperture diameters, detector arrays, etc
[AIAA PAPER 70-317] 09 p1677 A70-22870
Earth resources sensor integration into satellite or aircraft, discussing cost effectiveness
[AIAA PAPER 70-316] 09 p1677 A70-22871
Synthetic aperture radar in earth resource monitoring by satellite, determining topography and surface nature from spatial patterns
09 p1635 A70-22872

Multiband high resolution spaceborne imagery telemetry with optical mechanical scanners from earth orbiting satellites in earth resource applications
[AIAA PAPER 70-314] 09 p1677 A70-22873

Automatic change discrimination applications to weather prediction, land resource management and city planning, using photographic, IR and radar sensor imagery
[AIAA PAPER 70-311] 09 p1677 A70-22876

Remote sensing systems for vegetation analysis, discussing machine-aided photointerpretation methods for data analysis
[AIAA PAPER 70-308] 09 p1678 A70-22879

Remote sensors for earth resources observation by satellites, discussing electromagnetic spectrum, device operation, atmospheric transmission, measuring instruments, etc
09 p1678 A70-22888

Earth resources remotely sensed data analysis with emphasis on machine analysis over manual photointerpretation, discussing pattern recognition techniques, information systems, etc
[AIAA PAPER 70-292] 09 p1678 A70-22891

Multipurpose multiband photographic system used for aerial remote sensing of earth resources
09 p1686 A70-23755

Photointerpretation applications to kaolin deposit detection, railway tunnel collapse analysis and highway drainage
10 p1873 A70-24075

Satellite system applicability to earth resources data collection from in situ sensors, discussing synoptic, local time, emergency and demand data collection
10 p1840 A70-24371

Earth Observation Satellites - BIS-NATO Conference, Cambridge, England, July 1969
10 p1950 A70-24635

Spacecraft and boosters for earth resources surveys, discussing design, payloads, orbits, etc
10 p1950 A70-24641

Aerial photographic surveys of urban land use and natural resources, considering data analysis, display, computer compilation, updating and remote sensing
10 p1891 A70-24738

Remote sensing techniques for water resources evaluation and hydrobiological features mapping with multiband scanner imagery
10 p1879 A70-24742

Remote sensing techniques for earth resources inventory, describing image enhancement role in multiband space photography
12 p2220 A70-26936

Microwave radiometry assumptions relating to absorptivity, emissivity and reflectivity data for earth resources remote sensing applications
12 p2230 A70-26959

Terrain spectral imagery from satellites for natural resources investigations
12 p2235 A70-27745

Earth resource observation from orbiting spacecraft, discussing photo-image map construction for continents and continental shelves, terrain analysis, delta formation, etc
12 p2225 A70-27747

Orbital earth resources sensors, outlining user oriented method of determining measurement requirements
15 p2735 A70-31777

Correlation spectrometry for earth resources, considering sulfur dioxide, nitrogen oxide and iodine pollution
20 p3626 A70-39055

Data acquisition by earth resources technology satellite /ERTS/ for user needs in forestry and agriculture
20 p3616 A70-39062

Spectral signature recognition for automatic interpretation of earth resources multispectral data
22 p4037 A70-43088

Earth orbital space stations as long term investment for future benefit of mankind, considering earth resources management, environmental and pollution control, etc
22 p4128 A70-43652

EARTH RESOURCES PROGRAM

Space programs to monitor earth resources from synchronous orbit of 19,400 nautical miles, discussing geostationary systems characteristics related to optics and telemetry
01 p0093 A70-11280

University/industry team project Bonanza conducting aircraft flight over Colorado to investigate earth resources remote sensing techniques
[AAS PAPER 69-574] 04 p0788 A70-14637

Remote sensor capability in land use, urban and soil moisture analysis data acquired by NASA Earth Resources Program
[AAS PAPER 69-575] 04 p0676 A70-14641

Orbital spacecraft/sensor systems for earth resource surveys and measurement, considering agriculture, forestry, geology, mineralogy, hydrology, etc
[AAS PAPER 69-584] 04 p0761 A70-14643

Apollo 9 space photography of earth surface and use for quantitative analysis of earth resources, including supporting aircraft photography
[AAS PAPER 69-572] 04 p0687 A70-14650

Multiband photographic system for automatic earth resources aerial sensing and lunar orbital mapping with manual override provisions
[AAS PAPER 69-582] 04 p0687 A70-14657

Earth resources remote sensing investigations from spacecraft and aircraft, noting Gemini and Apollo photography, hydrological surveys and radar techniques
05 p0849 A70-16450

Earth resources observation satellite /EROS/ program, discussing geologic terrain and land-use planning maps
[SPE PAPER 2703] 06 p1053 A70-17155

Earth resources program data management system, discussing mission control, processing and distribution of data from satellite vidicon cameras and multispectral line sensors
[AIAA PAPER 70-321] 09 p1792 A70-22854

Multidiscipline systems analysis of satellite assisted information system improving earth resource management, developing User Decision Models
[AIAA PAPER 70-335] 09 p1792 A70-22855

Earth resources data transmission, describing picture reception and reproduction equipment
[AIAA PAPER 70-328] 09 p1634 A70-22856

Communications satellite technology for earth resources data collection
09 p1634 A70-22857

Earth Resources Satellite Information Systems, discussing NASA Space Application Program relation to national goals, federal spending, cost effectiveness analysis, information sales, etc
[AIAA PAPER 70-333] 09 p1793 A70-22860

Earth resources observation satellite /EROS/ program, describing remote sensor data acquisition, processing, dissemination and utilization
[AIAA PAPER 70-332] 09 p1667 A70-22861

Earth Resources Data Processing Center magnitude and facility planning compared with NASA centers
[AIAA PAPER 70-324] 09 p1793 A70-22863

Earth Resources program automatic data correlation system noting lower cost, faster processing, degraded imagery and compensation for vehicle perturbations and terrain relief
[AIAA PAPER 70-323] 09 p1667 A70-22864

Ground truth calibration for aircraft and spacecraft earth resource sensors, discussing ground truth instrumentation, procurement procedures, reduction techniques, etc
[AIAA PAPER 70-296] 09 p1678 A70-22887

EROS program earth imaging models characteristics, describing airborne and spaceborne film return and global and geosynchronous space data transmission
[AIAA PAPER 70-294] 09 p1678 A70-22889

User information traffic forecasting method for operational Earth Resource Satellite System, discussing user expectations
[AIAA PAPER 70-293] 09 p1793 A70-22890

IR energy interaction with earth atmosphere, determining multispectral scanner optimum wavelength intervals for earth resources applications
[AIAA PAPER 70-289] 09 p1669 A70-22892

Earth resources program function of early orbital manned space station in remote sensing
09 p1687 A70-23760

Aerial remote sensing package for Earth Resources Program
09 p1687 A70-23761

Operational planning for earth resources surveys using spacecraft
09 p1672 A70-23762

Manned and unmanned earth resources observation satellite program, noting international cooperation
10 p1971 A70-24636

Worldwide crop calendar development from repetitive satellite observation to perform agricultural change detection
12 p2218 A70-26922

Earth resources satellite systems synthesis, describing analytical techniques in R and D preceding operational status
12 p2334 A70-26942

Earth resources satellite ground data handling system providing initial processing, reproduction, indexing, storage, retrieval and dissemination functions
12 p2191 A70-26943

Optimal use of remotely sensed data from NASA Earth Resources Program by matching user models with capabilities of aircraft/satellite remote sensing system
16 p3004 A70-33708

Aerospace methods for revealing and evaluating earth resources - Conference, Princeton University, September 1969
20 p3615 A70-39051

Earth resources data from man operated airborne/spaceborne sensors and data handling systems, examining Apollo Applications Program
20 p3616 A70-39056

Earth resources ground data processing in image formats from sensors in aerospace platforms, discussing collection control, image storage, retrieval, etc
20 p3591 A70-39058

Aircraft/spacecraft assisted agricultural resource information system design concerning nongovernmental user and remote sensing needs
20 p3740 A70-39067

Multispectral photography in earth resources research, noting three return beam vidicons for technology satellites
20 p3628 A70-39128

EROS program earth imaging models characteristics, describing airborne and spaceborne film return and global and geosynchronous space data transmission
[AIAA PAPER 70-294] 21 p3829 A70-41871

Multispectral IR scanner system for earth resources survey programs
22 p4037 A70-43087

Multispectral hydrometeorological environment monitoring in Earth Resources Survey Program
23 p4191 A70-44664

Earth resources information systems using space, aerial and ground measurements, discussing Apollo 9 IR color photograph of Mississippi Valley and timber inventory applications
23 p4192 A70-44679

EARTH RESOURCES SURVEY AIRCRAFT

Remote sensing application to agriculture, forestry and range resources in terms of human priority over monetary benefits, noting high altitude aircraft use
[AAS PAPER 69-583] 04 p0788 A70-14638

Earth resources survey aircraft system producing optical spectrum imagery of continental U.S. with photometric and photogrammetric fidelity
05 p0850 A70-16686

Optimal use of remotely sensed data from NASA Earth Resources Program by matching user models with capabilities of aircraft/satellite remote sensing system
16 p3004 A70-33708

Aircraft/spacecraft assisted agricultural resource information system design concerning nongovernmental user and remote sensing needs
20 p3740 A70-39067

EARTH RESOURCES TECHNOLOGY SATELLITES

Earth resources satellites use in agriculture, considering materials reflectance and emittance, electromagnetic spectrum wavelengths identification and data accuracy standards
[AIAA PAPER 69-1083] 01 p0220 A70-10624

Multispectral scanner for Earth Resources Technology Satellite, discussing agriculture applications and advantages over return beam vidicon
03 p0493 A70-13957

Earth resources satellites capabilities and requirements emphasizing orbit parameters, remote sensing, data handling and telemetry systems
[AAS PAPER 69-587] 04 p0760 A70-14642

Earth resources observation satellite /EROS/ program, discussing geologic terrain and land-use planning maps
[SPE PAPER 2703] 06 p1053 A70-17155

Earth resources and meteorological data collection from in situ sensors via satellite, discussing system considerations
06 p1006 A70-17343

Return Beam Vidicon /RBV/ system compatibility with requirements for Earth Resources Observation Satellite /EROS/, featuring high resolution image sensor for decreasing signal noise
07 p1280 A70-19231

Earth resources satellite TV cameras operating on different spectral bands, discussing data preprocessing for correlation with topographic maps
09 p1674 A70-22259

Earth resources satellite imagery processing techniques, discussing sensor and transmission link distortions, image quality and optical or digital approach
[AIAA PAPER 70-297] 09 p1677 A70-22852

Rapid and reliable data transfer within limited bandwidth and tracking time in earth resources technology satellites, discussing time division multiplexing, digitizing, etc
[AIAA PAPER 70-325] 09 p1635 A70-22858

Earth resources observation satellite /EROS/ program, describing remote sensor data acquisition, processing, dissemination and utilization
[AIAA PAPER 70-332] 09 p1667 A70-22861

Multispectral point scan camera system as remote sensor for Earth Resources Satellite, noting real time automatic data processing and interpretation [AIAA PAPER 70-319] 09 p1677 A70-22867

Digital computer processing of airborne multispectral data, discussing automatic recognition and mapping of terrain distribution, Earth Resources Technology Satellite data channel efficiency, etc [AIAA PAPER 70-309] 09 p1668 A70-22878

ERTS satellite role in resource policy, management and remote sensing [AIAA PAPER 70-304] 09 p1668 A70-22881

Photographic and IR multiband spectral discrimination for rock and soil mapping from orbiting ERTS satellites [AIAA PAPER 70-303] 09 p1668 A70-22882

Philosophy and technology of spacecraft-borne sensors for earth resource surveys, noting ERTS-A satellite [AIAA PAPER 70-302] 09 p1668 A70-22883

Multidiscipline applications for Earth Resources Satellite data, including data simulation and interpretation techniques 09 p1669 A70-22886

User information traffic forecasting method for operational Earth Resource Satellite System, discussing user expectations [AIAA PAPER 70-293] 09 p1793 A70-22890

Atmospheric limitations on remote sensors using visible sunlight, noting applications to Earth Resources Technology Satellite and human vision [AIAA PAPER 70-288] 09 p1718 A70-22893

Information extraction efforts using imaging sensors on earth resources satellites compared to data processing for environmental satellite imaging sensors [AIAA PAPER 70-284] 09 p1669 A70-22894

Tiros M requirements for earth resources sensor systems, discussing spacecraft structure, dynamics, power, command and communications subsystems 10 p1950 A70-24638

ERTS multispectral scanner with optimal sensitivity and resolution for agricultural scenes signature analysis 12 p2229 A70-26941

Earth resources satellite real time wideband relay communication link to ground station [AIAA PAPER 70-326] 13 p2368 A70-29614

Optimal use of remotely sensed data from NASA Earth Resources Program by matching user models with capabilities of aircraft/satellite remote sensing system 16 p3004 A70-33708

Earth resources technology satellite /ERTS-A/ for Eros program, producing telemetric imagery spatially correlated to earth surface 16 p2898 A70-34046

Earth resources satellite /ERS/ TV camera configurations, return beam vidicon camera characteristics and devices for TV picture reproduction on film 16 p2915 A70-34312

Automatic speech recognition and tracking techniques of moving objects, considering applicability to processing data from earth resources satellites 16 p2871 A70-34313

Space legal problems involving earth resource survey /ERS/ satellites and weather modification 17 p3203 A70-35799

Earth resources survey satellite programs, examining aspects of international participation 18 p3349 A70-36297

Satellite observations of earth by human or automatic methods, discussing principle applications of Earth Resources Technological Satellite 19 p3410 A70-37387

Earth resources satellite missions TV systems design, using vidicon as sensing element 20 p3626 A70-39052

Earth resources satellite orbits and imaging sensors, discussing multispectral spin scanner design 20 p3626 A70-39053

Unmanned spacecraft for earth resources survey, investigating ERTS payload, performance characteristics and ground station 20 p3713 A70-39057

Data processing for Earth Resources Satellite users, investigating partitioning and mosaicking 20 p3591 A70-39059

Earth Resources Satellites political background, investigating international implications 20 p3739 A70-39060

Data acquisition by earth resources technology satellite /ERTS/ for user needs in forestry and agriculture 20 p3616 A70-39062

ERTS programs status and prospects from international utility viewpoint 20 p3739 A70-39064

Satellite earth resources, discussing cost benefit analysis and economics in agriculture, forestry and mapping 20 p3739 A70-39065

Water management decision model using earth resources information system with satellite-based remote sensors, evaluating costs and benefits by systems analysis 20 p3616 A70-39066

Aircraft/spacecraft assisted agricultural resource information system design concerning nongovernmental user and remote sensing needs 20 p3740 A70-39067

Earth Resources Technology Satellite program and international participation, taking into account UN involvement in outer space 20 p3741 A70-39796

Earth resources observation satellite program and organization for acquiring, processing, utilizing and disseminating remote sensor data 20 p3741 A70-39944

Digital computer processing of airborne multispectral data, discussing automatic recognition and mapping of terrain distribution, Earth Resources Technology Satellite data, channel efficiency, etc [AIAA PAPER 70-309] 21 p3829 A70-41851

ERTS line scanning system for cartographic data of water, snow, vegetation and cultural areas 22 p4037 A70-43090

Earth resources technology satellite data link tradeoff between channel capacity and transmitter power 22 p4038 A70-43091

Multipurpose earth resource satellites design, emphasizing land use factors and data reduction problems 23 p4286 A70-45005

Earth Resources Technology Satellites /ERTS/ providing high resolution image data regarding agriculture, geology, hydrology, geography, etc [SAE PAPER 700761] 24 p4416 A70-45869

EARTH ROTATION

Geocentric coordinate system definition by earth mass center and rotation axis and Greenwich meridian plane 01 p0082 A70-11456

Random variations of terrestrial rotation rate effects on pulsar observations, discussing methods to minimize effects 02 p0371 A70-12203

Earth daily rotation effects on magnetosphere electric currents, discussing Pederson currents in dynamo region and E region ionization 02 p0293 A70-12775

Geodetic coordinate system referred to center of mass and earth rotation axis constructible from satellite observations 03 p0472 A70-13186

Cyclonic convective cell fluctuation and nonuniform core rotation effects on reversal of geomagnetic field, investigating fossil magnetism 04 p0676 A70-14600

Time determination and georotation - Conference, Riga, Latvian SSR, June 1965 04 p0755 A70-15476

Earth rotational velocity irregularities and horizontal motions of continental blocks at expense of oceanic hemisphere, noting seasonal distance changes 04 p0681 A70-15477

Earth rotation seasonal fluctuations analyzed from astronomical observations using frequency markers and quartz clocks 04 p0681 A70-15478

Geophysical-solar phenomenological interrelationships, considering earth rotation and nutation, sunspot area, earthquake energy, etc 06 p1056 A70-17636

Earth rotation coordinates, discussing system coupled to earth by fixing of axes to zeniths of selected observatories and equatorial plane orientation 08 p1565 A70-20563

Earth free diurnal nutation parameters determination from latitude observations, establishing amplitude and phase time-independent variations 08 p1488 A70-21154

Terrestrial rotation changes effects on pulsar period observations 08 p1575 A70-21260

Gerstenkorn moon capture theory taking into account tidal evolution of earth-moon system, discussing marine organisms time rate synopsis for earth rotation retardation 10 p1943 A70-24840

Magnetosphere large-scale motions dependence on earth magnetic axis inclination against rotational axis 10 p1885 A70-25279

Mesoscale waves in jet stream flow within Coriolis force over rotating earth by amplitude functions and phase velocities asymptotic series representation 12 p2265 A70-28334

Upper atmosphere superrotation velocity based on satellite polar orbit calculation of 1968-59A, correcting for lunisolar perturbations 13 p2394 A70-28895

Earth rotation perturbations, analyzing secular polar shift dependence on dimensions, depth and location of seismic event 13 p2400 A70-29604

Circadian rhythmical changes in biological organisms by earth rotation, emphasizing diurnal variations role in sleep-wakefulness rhythm 15 p2680 A70-31742

Earth rotation coordinates, discussing system coupled to earth by fixing of axes to zeniths of selected observatories and equatorial plane orientation 15 p2805 A70-32718

Earth continental drift and polar wandering measurements by laser ranging to two synchronous satellites 19 p3529 A70-38882

Earth rotation rate deceleration due to lunar tidal friction taking into account fluctuations from internal processes, discussing moon retreat from earth 21 p3921 A70-41970

Tidal friction theories relating to earth rotation and lunar evolution 21 p3921 A70-41972

Upper atmosphere average rotation speed and height variation, presenting atmospheric and earth angular velocity ratio from satellite orbit inclinations 24 p4328 A70-45353

EARTH SATELLITES

NT ACTIVE SATELLITES

NT AEROS SATELLITE

NT ALOUETTE SATELLITES

NT ALOUETTE 1 SATELLITE

NT ALOUETTE 2 SATELLITE

NT APPLICATIONS TECHNOLOGY SATELLITES

NT ARIEL SATELLITES

NT ARIEL 3 SATELLITE

NT ATS 1

NT ATS 3

NT ATS 5

NT BEACON SATELLITES

NT BIOSATELLITES

NT COMMUNICATION SATELLITES

NT COSMOS SATELLITES

NT COSMOS 5 SATELLITE

NT COSMOS 44 SATELLITE

NT COSMOS 110 SATELLITE

NT COSMOS 149 SATELLITE

NT D-1 SATELLITE

NT DIADEME SATELLITE

NT DODGE SATELLITE

NT EARLY BIRD SATELLITES

NT EARTH RESOURCES TECHNOLOGY SATELLITES

NT ECHO SATELLITES

NT ECHO 1 SATELLITE

NT ECHO 2 SATELLITE

NT ELEKTRON 2 SATELLITE

NT ELEKTRON 4 SATELLITE

NT ENVIRONMENTAL RESEARCH SATELLITES

NT EOSS

NT ESRO SATELLITES

NT ESRO 1 SATELLITE

NT ESRO 2 SATELLITE

NT ESSA SATELLITES

NT ESSA 9 SATELLITE

NT EXPLORER 1 SATELLITE

NT EXPLORER 4 SATELLITE

NT EXPLORER 17 SATELLITE

NT EXPLORER 19 SATELLITE

NT EXPLORER 20 SATELLITE

NT EXPLORER 22 SATELLITE

NT EXPLORER 31 SATELLITE

NT EXPLORER 32 SATELLITE

NT EXPLORER 33 SATELLITE

NT EXPLORER 38 SATELLITE

NT EXPLORER 40 SATELLITE

NT GEODETIC SATELLITES

NT GEOPHYSICAL SATELLITES

NT GEOS 1 SATELLITE

NT GEOS 2 SATELLITE

NT HEOS 4 SATELLITE

NT HEOS SATELLITES

NT INTLSAT SATELLITES

NT ISIS-A

NT LINCOLN EXPERIMENTAL SATELLITES

NT METEOROLOGICAL SATELLITES

NT MIDAS 4 SATELLITE

NT MOLNIYA SATELLITES

NT MOON

NT NAVIGATION SATELLITES

NT NIMBUS SATELLITES

NT NIMBUS 2 SATELLITE

NT NIMBUS 3 SATELLITE

NT NIMBUS 4 SATELLITE

NT OAO

NT OGO

NT OGO-A

NT OGO-B

NT OGO-D

NT OGO-E

NT OGO-F

NT ORBIS CAL SATELLITE

NT OSO

NT OSO-B

NT OSO-1

NT OUTER PLANETS EXPLORERS

NT PAGEOS SATELLITE

NT PROTON SATELLITES

NT PROTON 4 SATELLITE

NT RADIO ASTRONOMY EXPLORER SATELLITE

- NT RELAY SATELLITES
NT SAN MARCO SATELLITE
NT SAN MARCO 2 SATELLITE
NT SYCOM SATELLITES
NT TIROS SATELLITES
NT TRANSIT SATELLITES
NT VELA SATELLITES
NT VENERA SATELLITES
- Earth satellites magnetic survey contributions to World Magnetic Survey project /WMS/, discussing international reference standards and magnetic mapping
01 p0075 A70-10595
- Unmanned teleoperator spacecraft /UTS/ for future orbital demonstration, discussing manipulators, multifunction viewing, stabilization, human factors, etc [AIAA PAPER 69-1067]
01 p0195 A70-10649
- Earth satellite orbit parameters determination from angle measurements using computer program and least squares estimation technique
03 p0573 A70-13843
- Earth environmental satellite data for oceanography and hydrology, discussing sea surface temperature mapping, low level wind conditions, snow and ice mapping, etc [AAS PAPER 69-596]
04 p0676 A70-14635
- Temperature distribution causes in earth orbiting satellite, outlining thermal control and temperature calculation methods and prelaunch ground tests
05 p0956 A70-15813
- Large spacecraft in circular earth orbit calculated for internal gravitational field
05 p0924 A70-16637
- Relative motion of two bodies linked by flexible weightless tether in artificial earth satellite orbit, simulating extravehicular walk
06 p1142 A70-17882
- Instantaneous and integral solar irradiance of earth oriented satellite surface, noting solar illumination nomogram representation
06 p1155 A70-17893
- Artificial earth satellites photographic observation without chronometric recording aids, determining location and time by single indicator
09 p1635 A70-23055
- Angular motion of deformable earth satellite as solid-elastic system with distributed masses, applying automatic control transfer function
10 p1914 A70-24308
- Extraneous earth satellites interferences in ground communication line, determining combined duration and numbers average values
11 p1996 A70-25346
- Cloud cover effect on earth photographing space missions by Monte Carlo computer simulation, using worldwide cloud statistics
11 p2075 A70-25600
- Method of dependence involving triangulation applied to reducing photographs of earth satellites
11 p2006 A70-26185
- Artificial earth satellites orientation determined by onboard telemetric measurements, constructing model for rotational motion around center of mass
12 p2314 A70-28255
- Vinti potential with spheroidal coordinates for equations of motion in earth satellite orbit computation
13 p2486 A70-28503
- Scanning celestial attitude determination system /SCADS/, providing triaxial information for earth stabilized satellites
16 p2946 A70-33159
- Satellite path geometry along Keplerian elliptical orbit, taking earth flattening into consideration
18 p3312 A70-36167
- Extraneous earth satellites interferences in ground communication line, determining combined duration and numbers average values
20 p3589 A70-40458
- Secondary propulsion subsystem earth synchronous orbital mission requirements, discussing thrust vector alignment and control, colloidal propellants and pulsing [ASME PAPER 70-AV/SPT-31]
21 p3866 A70-40870
- Terrestrial satellites ground tracks by FORTRAN IV computer program, investigating orbital parameters effects
21 p3892 A70-41325
- Earth orbital experiments synthesis in space programs methodology, discussing examples in astronomy, biology and oceanography research
22 p4097 A70-42500
- EARTH SHAPE**
U GEODESY
EARTH SURFACE
- Remote sensors to determine atmospheric characteristics and underlying earth surface structure, using electromagnetic and acoustic waves as signal carriers
01 p0093 A70-11266
- Secular variations distribution on earth surface, plotting isopore charts from mean annual values of magnetic elements /1960-1965/
01 p0083 A70-11540
- Space research photography role in studying earth and moon atmospheres and surfaces, determining spectral bands for contrast
03 p0483 A70-13168
- Lyman alpha transition line in exosphere deuterium line implying enrichment factor ratio to earth surface deuterium
04 p0742 A70-15129
- Spherical harmonics expansion for earth surface and outer space geopotential by mapping earth surface onto sphere
05 p0837 A70-15926
- IR imagery by InSb detectors applied to mapping earth surface thermal distribution
05 p0840 A70-16498
- Surface impedance of spherical earth isolated by nonconducting atmosphere from ionospheric currents producing alternating electromagnetic field
05 p0843 A70-16768
- Atmospheric difficulties in earth surface remote sensing by satellites, describing absorption, emission and scattering as wavelength functions [AIAA PAPER 70-193]
06 p1057 A70-18083
- Geophysical parameters of atmosphere and underlying surfaces from outgoing thermal radio emission measurements on Cosmos 243 satellite
07 p1261 A70-18724
- Reusable space shuttle employing two stages resembling subsonic aircraft for carrying passengers and cargo between earth surface and orbit
07 p1392 A70-18873
- Self calibrating radiometer for in-flight measurement of earth surface thermal microwave radiation
07 p1282 A70-19616
- Altitude asymmetry of instantaneous auroral oval plotted for geomagnetic pole and earth surface
07 p1277 A70-20456
- Earth deviations from isostatic equilibrium, showing irregularities dependence on distance from surface for various tectonic zones
08 p1487 A70-20715
- Reflection patterns of solar radiation from cloud, water and land surfaces measured by airborne radiometer, observing anisotropy
09 p1671 A70-23523
- Reflected solar radiation polarization over land, sea and cloud surfaces to determine atmospheric pollution
09 p1747 A70-23603
- Terrestrial surface radiometric imaging by sensing thermal radiation at centimeter wavelengths to reduce atmospheric scattering attenuation
09 p1687 A70-23763
- Ionospheric current flow past circular inhomogeneous spot with Pedersen and Hall conductivities, calculating earth surface magnetic field by Lipshits-Hankel integral
10 p1873 A70-24309
- Downward ozone transport from troposphere to atmospheric boundary layer by turbulent diffusion calculated by model, estimating annihilation rate
10 p1875 A70-24486
- Earth surface mapping and shape and internal constitution determination by satellite geodesy
10 p1876 A70-24642
- Earth profile influence on two dimensional nonlinear lee waves in troposphere, discussing Helmholtz perturbation equation and stream function field
11 p2075 A70-25391
- Atmospheric hemispheric general circulation model numerical time integration with moist processes and uniform earth surface
12 p2262 A70-26882
- Spatial-temporal distribution of meteorological elements allowing for effects of underlying surface
12 p2263 A70-27511
- Nonlunar origin of tektites indicated from molten glass dispersion generated by terrestrial crater-forming meteorite impact
12 p2302 A70-27584
- Meteorite craters on U.S.S.R. territory, discussing impact, explosive and complex craters
12 p2311 A70-28308
- Earth colorimetry data improvement by separating signals of each bandwidth on one photographic emulsion or TV tube
13 p2406 A70-28987
- Plane stationary nonlinear problem of air flow over earth surface roughnesses, using three layer atmospheric model
14 p2602 A70-30160
- High winds simultaneous occurrence and duration to 150 meter height, showing coherence tendencies
14 p2607 A70-30583
- Transient excitation of Schumann earth-ionosphere cavity resonances by large ELF atmospherics, using propagation model
15 p2726 A70-31865
- Earth surface temperature, emissivity and dielectric constant from satellite measurements of SHF radiation
15 p2771 A70-32072
- Lake covered ancient meteorite impact crater in Canada, noting eroded rim and microscopic shock criteria
15 p2732 A70-32849
- Earth resources technology satellite /ERTS-A/ for Eros program, producing telemetric imagery spatially correlated to earth surface
16 p2898 A70-34046
- Boundary value problem of Hertzian dipole antenna in presence of conducting half space, analyzing lossy earth effects on input impedance and radiation pattern
17 p3044 A70-35074
- Tiros satellites window radiation applied to day and night surface temperature measurements on land and sea
17 p3081 A70-35932
- Air surface layer stationary electric field, considering ionization balance equation, turbulent diffusion coefficient, ion concentration vertical distribution, etc
18 p3247 A70-36520
- Airborne IR scanner as geophysical research tool depicting surface emission and heat mass transfer
18 p3259 A70-36558
- Gravitational field on Liapunov surface approximating earth relief, using double sphere solution
19 p3407 A70-37299
- Geological and cartographical data acquisition and processing, considering aircraft and satellite-borne photography of earth surface
20 p3616 A70-39061
- Second approximations of deflection of vertical and quasi-geoid height dependence on difference between unknown earth surface and known hypsometric surface
20 p3617 A70-39072
- Integral equations for gravity field and plumb line deflections solved by Neumann and Molodenskii methods
20 p3617 A70-39073
- Integral equations for plumb line deflections on earth surface model, considering Neumann, Molodenskii, Arnold methods, etc
20 p3617 A70-39074
- Earth surface pressure changes related to PCA of high energy protons
20 p3695 A70-39187
- Lunar and earth surfaces imaging for astronaut training in LEM simulator
20 p3607 A70-40320
- Distribution functions of errors in earth and moon horizon sighting due to planetary surface unevenness
21 p3884 A70-40840
- Mapping from satellite-collected earth surface images, emphasizing optical/mechanical scanner images
22 p4037 A70-43089
- Solar wind intensity and direction correlated with intensity of earth surface magnetic disturbances and geomagnetic pi-2 type pulsations
22 p4022 A70-43284
- Spectral brightness temperature, directional emissivity and surface temperature of earth from remote radiance observations by balloon-borne multidetector grating spectrometer
23 p4194 A70-44035
- Anomalous multiple reflections from ionosphere showing concave surface focusing
23 p4164 A70-44374
- Electromagnetic ground wave propagation, deriving exact solution from two dimensional cylindrical earth model with any number of homogeneous sections
23 p4164 A70-44405
- Space technology applications to earth survey, discussing use of automatic satellites and manned space laboratories for meteorological, geophysical and related purposes
23 p4191 A70-44634
- Spectrophotometry of earth surface from manned Soyuz spacecraft, obtaining transfer function of atmosphere by aircraft flights
23 p4191 A70-44636
- Gravitational field fine structure representation near earth surface as sum of global model in spherical harmonics and local model in harmonic B functions
24 p4328 A70-45287
- EARTH-MARS TRAJECTORIES**
- Solar electric propulsion Mars high data rate orbiter trajectory design and analysis, including landing site selection and spacecraft parameters optimization [AIAA PAPER 70-1119]
20 p3710 A70-40224
- EARTH-MOON SYSTEM**
- Moon-earth historical relationship, comparing differences in figure and interior with terrestrial planets
03 p0562 A70-12875
- Moon origin theories emphasizing fission from earth, noting objections to capture theory
04 p0751 A70-15058
- Interplanetary magnetic field fluctuations stimulated by lunar wake, using Explorer 35 satellite measurements
04 p0753 A70-15122
- Mariners 6 and 7 range and Doppler tracking data for studying Martian mass and earth-moon mass ratio
06 p1151 A70-18486
- Lunar periodicity detected from radio aurora data as possible cause of lunar interaction with magnetosphere
07 p1389 A70-20164
- Tidal friction induced secular changes in earth-moon system near minimum of angular momentum of moon orbit, including temporal changes in moments of inertia
08 p1579 A70-21570

- Solar attraction effects on zero-mass body planar motion near triangular earth-moon libration points, obtaining variational equations of motion
09 p1754 A70-22477
- Lunar surface luminescence considered for correlation with tidal forces of earth
09 p1758 A70-22748
- Apollo 11 lunar laser reflector for earth-moon distance measurement
10 p1898 A70-23847
- Gerstenkorn moon capture theory taking into account tidal evolution of earth-moon system, discussing marine organisms time rate synopsis for earth rotation retardation
10 p1943 A70-24840
- Ecliptic obliquity secular change rate apparent discrepancy possibly due to earth-moon barycenter motion
10 p1945 A70-24962
- Book on moon covering motion, earth-moon system, internal structure, hydrostatic equilibrium, thermal history, global form, gravitation, topography, etc
12 p2298 A70-27096
- Lunar spring board effect to minimize impulses for given velocity at great distance of earth-moon system, discussing nonimpulsive grazing passage
14 p2635 A70-30289
- Celestial methods for lunar navigation, considering terrestrial and selenographic differences
14 p2613 A70-30459
- Earth/moon mass ratio and Mars mass and ephemeris from Mariners range and Doppler tracking data, noting relativistic time delay measurement possibility
15 p2798 A70-31652
- Earth and moon meteor fall probabilities calculation using hyperbolic encounters method and lunar near and far sides crater densities difference interpretation
15 p2798 A70-31658
- Translational-rotational motion of axisymmetrical moon in earth gravitational field
15 p2803 A70-32496
- Lunar gravitational field effect on sun-earth exterior libration point location, examining placement on line passing through sun and earth-moon barycenter
18 p3320 A70-37059
- Near parabolic trajectories between moon and cislunar libration point, considering earth perturbative influence
19 p3529 A70-38874
- Distribution functions of errors in earth and moon horizon sighting due to planetary surface unevenness
21 p3884 A70-40840
- Earth rotation rate deceleration due to lunar tidal friction taking into account fluctuations from internal processes, discussing moon retreat from earth
21 p3921 A70-41970
- Earth-moon system age and origin from tidal evolution equations, considering growth line counts on living and fossil marine invertebrates
21 p3921 A70-41971
- Ephemerides for lunar-orbiting observation of dust clouds in earth-moon system libration points L4 and L5 by observer orbiting over lunar equator
22 p4097 A70-42308
- Earth-moon system formation theory, discussing condensation from terrestrial hot extended silicate atmosphere
22 p4098 A70-42348
- Translational-rotational motion of axisymmetrical moon in earth gravitational field
23 p4240 A70-43917
- Interplanetary mission propellant reduction by using earth-moon-sun gravity field properties, discussing swingby techniques, low energy trajectories, etc
23 p4244 A70-44607
- Lunar formation from ejected terrestrial magma, considering distribution of seas, gravitational anomalies and craters with rays
23 p4247 A70-44772
- Lunar formation, investigating accretion rate ratio for earth and moon as function of distance
24 p4409 A70-45674
- Earth-moon laser distance measurements, examining relationship between Newtonian and relativistic field coordinates
24 p4413 A70-46160
- EARTH-MOON TRAJECTORIES**
- Earth-moon-earth flight characteristics, discussing spacecraft trajectory, velocity and corrections for close distance placement and return for soft landing
03 p0569 A70-13483
- Translunar Apollo orbit analysis from elementary equations relating to elliptical and hyperbolic orbits in inverse square force field
06 p1148 A70-18397
- Hybrid patched conic technique as iterative procedure for generating translunar and transearth trajectories emphasizing computing time saving
06 p1152 A70-18495
- Apollo 8 mission, spacecraft and booster details, calculating earth-moon flight parameters based on laws of mechanics
07 p1375 A70-18776
- RF EMI propagation between manned spaceflight network and Apollo 10 launch vehicle in translunar mission, considering cochannel interference possibilities
12 p2189 A70-28137
- Lunar spring board effect to minimize impulses for given velocity at great distance of earth-moon system, discussing nonimpulsive grazing passage
14 p2635 A70-30289
- Reusable earth-moon and deep space return transportation, assuming extraterrestrial nuclear rocket propellant source
14 p2653 A70-30766
- French photographic observations of Apollo 12 translunar trajectory
15 p2697 A70-31676
- Low cost earth-moon transportation system based on shuttle station mode concept
17 p3176 A70-34806
- Saturn 5 launch vehicle targeting methods for lunar missions, solving earth departure variables via iterative process
19 p3528 A70-38867
- Interplanetary trajectories calculation using constant and/or slowly varying functions for accuracy, noting application to earth-moon spacecraft
19 p3530 A70-38888
- EARTH-VENUS TRAJECTORIES**
- Solar probe trajectory optimization, using Venus gravitational field for braking
23 p4243 A70-44506
- EARTHQUAKES**
- Dynamical models of relative motions during earthquakes, solving numerically integral equations with nonintegral kernels in crack propagation and elastic wave diffraction
05 p0941 A70-16527
- Earth rotation perturbations, analyzing secular polar shift dependence on dimensions, depth and location of seismic event
13 p2400 A70-29604
- Ionospheric acoustic wave propagation from seismic waves of Kurile Islands earthquake on 11 August 1969
17 p3075 A70-34569
- Thermoelastic seismic-energy release as source mechanism for volcanic earthquakes, describing thermal microfracture tests
20 p3619 A70-39217
- EATING**
- Hunger, thirst and environmental stimuli roles in development and elicitation of stimulus bound eating and drinking in animals
13 p2355 A70-29806
- Eating and digestion effects on arterial pressure and mesenteric and aortic blood flows in intact unanesthetized dogs
17 p3024 A70-34848
- Photoperiod effects on rats food and water intake, noting endogenous feeding rhythm correlation with activity patterns
24 p4296 A70-45332
- Alpha and beta reciprocal hunger regulating systems localized in rats hypothalamus areas by varying injection sites of alpha and beta adrenergic drugs
24 p4304 A70-46233
- EBULLITION**
- U BOILING**
- ECCENTRIC ORBITS**
- HEOS 1 satellite for interplanetary space exploration, describing eccentric orbit, structure, power supply, attitude measurement and control, spin rate control, telemetry and telecommand systems
01 p0196 A70-11114
- Jupiter capture of comets with parabolic orbits taking into account solar gravitational influence
05 p0905 A70-15757
- HEOS-A2 project development plan for investigating unexplored interplanetary space in eccentric orbit
05 p0923 A70-16588
- Capture and gravity gradient stabilization of LIDOS satellite in eccentric orbit
06 p1154 A70-17175
- Eccentric and inclined motions of satellite of spherical planet in planet centered coordinate system, applying formulas to Jupiter motion
07 p1374 A70-18693
- Nonspinning satellite orbit eccentricity effect on attitude stability
09 p1766 A70-23229
- Orbit eccentricity effect on gravity gradient system with single damping boom, investigating optimum steady state and transient response conditions
11 p2123 A70-26129
- Errors in determining controlled satellite rotation periods, proposing scheme for corrected trajectory calculation of small eccentricity orbits
11 p2118 A70-26779
- Resonant and nonresonant satellite eccentric orbits for determination of high order terms in geopotential
20 p3709 A70-40073
- Orbital eccentricity effects on solutions of eclipsing binary light curves, comparing circular orbits solutions
23 p4242 A70-44290
- Practical stability of highly eccentric orbits quasi-normal to ecliptic, discussing lunar effects on orbital lifetime
23 p4243 A70-44510
- ECCENTRICITY**
- Misalignment and eccentricity effect on face seal, discussing leakage dependence on phase angle
[ASLE FICFS PREPRINT 15A] 02 p0308 A70-12171
- Eccentric face seal with tangentially varying film thickness, analyzing leakage flow proportional to eccentricity and surface waviness
[ASLE FICFS PREPRINT 15B] 02 p0308 A70-12176
- Periodic solutions with moderate eccentricities and high inclinations for three dimensional restricted three body problem by expanding disturbing functions by high speed computer
09 p1759 A70-22773
- Reinforcing ribs eccentricity effect on closed circular cylindrical shell stability using strain energy method
09 p1786 A70-23720
- Eccentricity and clamping effects on stability and critical pressure of ring-reinforced cylindrical shells under internal pressure
10 p1956 A70-24248
- Eccentric cylinders with outer cylinder rotating measured for eccentricity and clearance ratios effects on pressure distribution and force on inner cylinder
11 p2060 A70-26409
- ECHELETTE GRATINGS**
- High dispersion stellar spectroscopy with echelle grating, discussing instrument design, operation and performance
22 p4040 A70-43613
- ECHO SATELLITES**
- NT ECHO 1 SATELLITE
NT ECHO 2 SATELLITE
Solar UV radiation reflected from Echo satellites measured and compared with UV fluxes from Lyrae
01 p0095 A70-11614
- ECHO SUPPRESSORS**
- Radio wave reflection from ionosphere, discussing suppression of magnetoionic component with fluctuating elliptical polarization
11 p2003 A70-25534
- Transmission delay and echo effects in long distance satellite relay telephony links, describing echo suppression and speech quality
12 p2183 A70-27004
- Radio wave reflection from ionosphere, discussing suppression of magnetoionic component with fluctuating elliptical polarization
21 p3786 A70-41284
- ECHO 1 CARRIER ROCKET**
- U THOR DELTA LAUNCH VEHICLE**
- ECHO 1 SATELLITE**
- Echo 1 satellite orbital acceleration correlated with solar activity, determining atmospheric density from drag observations using PERLO computer program
24 p4408 A70-45552
- ECHO 2 SATELLITE**
- Echo 2 satellite orbital elements from optical observations covering last passages over Milan before orbital decay
17 p3172 A70-35628
- ECHOES**
- NT ANGELS
NT AURORAL ECHOES
NT CLUTTER
NT LUNAR ECHOES
NT LUNAR RADAR ECHOES
NT RADAR ECHOES
NT RADIO ECHOES
NT SIGNAL REFLECTION
NT SOLAR RADAR ECHOES
NT VENUS RADAR ECHOES
Optical echoes using model of spins precessing in magnetic field, presenting time dependent theory of perturbation
02 p0341 A70-12830
- Ionogram conjugate echoes observed at Singapore longitudes by Alouette 2 topside sounder, attributing sequential occurrence to field-aligned irregularities in magnetosphere
03 p0477 A70-13986
- Cardiac echography applied to diagnosis and therapy evaluation in idiopathic hypertrophic subaortic stenosis
05 p0800 A70-16103
- Light inductions and echo intensities in liquids and gases, investigating thermal vibrations, translational Brownian motion, particle collisions and laser diffusion effects
06 p1082 A70-17809
- Spontaneous echoes amplitude resulting from damped electronic plasma plane wave excitation in collisionless plasma
09 p1735 A70-22843
- Fokker-Planck Coulomb collisions effect on plasma wave echoes
09 p1736 A70-23181

Ultrasonic echography for ventricular size determination, calculating stroke volume and valvular regurgitation severity 10 p1820 A70-24938

Seismic echo produced by jettisoned Apollo 12 S-4B stage impact at lunar surface analyzed by multiscascade scattering theory 12 p2298 A70-27280

Proton cyclotron echoes in topside ionograms using Alouette 2 satellite data 12 p2226 A70-28064

Delayed ionospheric resonance echoes radiated from topside plasma after pulse sequence stimulation by Alouette 2 satellite 13 p2370 A70-29904

Dispersion and group velocity characteristics of topside resonance oblique echoes near plasma frequencies observed by satellite 13 p2467 A70-29909

Temporal wave echoes and Landau damping in collisionless plasma using signal averaging and time delay techniques 14 p2622 A70-30687

Plasma echo oscillations due to superposition of consecutive perturbations separated by intervals greater than characteristic decay time 16 p2957 A70-33198

Electron spin-echo device as programmable linear matched filter for PN modulated carrier waveforms detection 16 p2864 A70-33480

Collisional effects on second order spatial ion wave echo, evaluating velocity integral 19 p3475 A70-37539

Higher order magnetic field-free temporal and spatial plasma wave echoes, solving collisionless Boltzmann equation by method of characteristics 19 p3476 A70-37557

Temporal echo in plasma for applied rectangular pulses, discussing ballistic approximation 19 p3480 A70-38174

Ultrasonic pulse echo flaw detection, relating defect size to echo amplitude 20 p3636 A70-39192

Adiabatic bounce periods of particle gyrophase coherence in earth field for cyclotron echo and triggered emission analyses 20 p3621 A70-39343

Cold nonuniform plasma slab model for afterglow echoes at upper hybrid resonance in uniform magnetic field 20 p3679 A70-39664

Low latitude observations of spread F echoes and stationary satellite scintillations, correlating with ionospheric disturbances and geomagnetic activity 21 p3818 A70-41097

Plasma wave echo, observing oscillatory behavior of perturbed distribution with different phases and amplitudes 21 p3858 A70-41389

Impulse length effect on space echo electric field in collisionless plasma 22 p4082 A70-43237

Neutron-electron collision damping and displacing of space echo in plasmas, indicating use for density measurement 22 p4082 A70-43244

Anomalous multiple reflections from ionosphere showing concave surface focusing 23 p4164 A70-44374

Flaw echo height dependence on ultrasonic testing pulse frequency spectrum 24 p4336 A70-45688

Echoes with ion sonar waves in ionized gases, considering ion density disturbances under local excitation 24 p4387 A70-45795

ECLIPSES

NT LUNAR ECLIPSES

NT SOLAR ECLIPSES

ECLIPSING BINARY STARS

Light curve and relative dimensions of eclipsing system V338 Herculis, from photoelectric measurements, discussing component stars 01 p0184 A70-10951

Light curves of Algol eclipsing variable AD Herculis and semidetached system relative dimensions from BV photoelectric observations 01 p0184 A70-10952

Photometric results on beta Lyrae from various observatories during 1959 international campaign with data reduced to BV system, showing reddening at primary eclipse 02 p0369 A70-12064

Orbits computation from double lined spectra of eclipsing binaries 31 Men and 9 Cha, emphasizing systemic velocity and mass ratio derivation method 03 p0565 A70-13268

U Geminorum type variables properties, orbital period changes in close binaries and origin of outbursts 03 p0567 A70-13322

Light variation curves for distorted white dwarf hypothetical secondaries in close binary systems calculated by integrating monochromatic fluxes 03 p0567 A70-13323

Binary system Nova WZ Sge model with nonnegligible secondary component contribution to total light explaining W UMa type light curve 03 p0568 A70-13324

Nonperiodic changes in radiation connected with orbital period in eclipsing conventional binaries observed in R Canis Majoris 03 p0568 A70-13326

Beta lyrae light curve changes by comparing international program observations with 1958 Lick Observatory results, discussing period, brightness, spectra, etc 03 p0568 A70-13326

AD Herculis components as Algol system with gas flow based on observed absorption effects 03 p0577 A70-14100

Color photoelectric study of eclipsing binary RY Gemini for determining orbital elements and structure 04 p0754 A70-15217

Bolometric albedo of main sequence stars with deep convective envelopes in close binary systems derived as function of photometric proximity using entropy invariance 05 p0914 A70-16694

Brightness curves for eclipsing binary V448 Cygni indicating gas stream flows in system 08 p1577 A70-21441

Secondary minimums role in studying eclipsing variable stars, correlating observability with detection of line of apsides motion 08 p1581 A70-21759

Phase variations in polarization parameters of eclipsing binary Z Vul during polarimetric studies for interstellar polarization component 09 p1751 A70-22156

Eclipsing binary beta Aurigae effective temperature and surface gravity determination from photoelectric spectrum and abundance analyses 10 p1938 A70-24100

Algol variable RV Ophiuchi photoelectric observation in B and V, representing light curve characteristics by gas stream model 10 p1945 A70-24967

WZ Sagittae ultrashort period binary evolution, considering mass-radius relation, initial separation and present position 11 p2108 A70-25696

Cyg XR-1 X ray spectrum variability by balloon-borne detectors as eclipsing properties of binary system 15 p2799 A70-31750

Helium abundance in unevolved main sequence eclipsing binaries by comparing to homogeneous models in mass luminosity plane 18 p3318 A70-37023

Eclipsing binary with very hot white dwarf, discussing effective temperature and photometric observations 21 p3889 A70-41158

BM Orionis eclipsing binary spectra, determining radial velocity curve 21 p3890 A70-41161

Light curve for eclipsing stars with scattering envelopes applied to V444 Cygni binary system 22 p4103 A70-42989

Computer synthesis of completely eclipsing binary light curves including limb darkening and simulated observational errors 22 p4103 A70-42990

Orbital eccentricity effects on solutions of eclipsing binary light curves, comparing circular orbits solutions 23 p4242 A70-44290

Algol type semidetached eclipsing binaries main sequence components rotational velocities, determining deviations from synchronism 23 p4251 A70-44818

Eclipsing binary stars minima variations related to orbit perturbations and rotational angular momentum of component interiors 23 p4251 A70-44819

ECLIPTIC

Minor meteor showers radiants determined close to ecliptic plane from systematic visual observations during November, December and January 1961-67 08 p1577 A70-21532

Ecliptic obliquity secular change rate apparent discrepancy possibly due to earth-moon barycenter motion 10 p1945 A70-24962

ECOLOGICAL SYSTEMS

U ECOLOGY

ECOLOGY

NT COASTAL ECOLOGY

EEG investigation of cerebral biocurrents during polar night-day cycle, studying central nervous system nonspecific automatic control mechanism dependence on ecological factors 01 p0030 A70-11466

Organisms resistance to biological environmental factors, surveying published literature on pressure

chamber experiments, tissue resistance, cellular protein stability, etc 03 p0422 A70-13701

Radiobiological and radioecological aspects of radioactive pollution of earth atmosphere, considering international cooperation for preventive measures 07 p1199 A70-18781

Satellites application to studying and monitoring earth ecology, discussing environmental space research and space program priorities 09 p1794 A70-23333

Organisms resistance to biological environmental factors, surveying published literature on pressure chamber experiments, tissue resistance, cellular protein stability, etc 11 p1985 A70-25501

Remote sensing in ecology - Conference, Madison, Wisconsin, June 1968 17 p3078 A70-35611

Ecological potentials in spectral signature analysis, using laboratory leaf and soil spectral reflectance data 17 p3078 A70-35612

Remote multispectral sensing of environmental and vegetative gradients in Yellowstone National Park by intercomparison of thermal IR and visible band imagery 17 p3079 A70-35617

Shallow water bottom biota, sediments and morphology determination by aerial and satellite photography 17 p3079 A70-35620

Multispectral remote sensing for detection and mapping of ecological objects and energy budget parameters measurement 17 p3079 A70-35622

Aircraft bird hazards in New Zealand, discussing ecological research techniques and preventive measures 18 p3212 A70-35985

Bird scaring from airfields based on ecological research 18 p3222 A70-35990

Bioastronautics and earth ecology, discussing environmental pollution, nutritional, microbiological and psychological problems 18 p3350 A70-36757

Holography application to marine ecological studies, using laser beam reduction techniques for image recording and reconstruction of large areas and volumes 21 p3823 A70-40821

Biological life support systems mass exchange processes analysis based on mathematical models, predicting artificial ecological systems stability 23 p4149 A70-45029

ECONOMICS

NT DEMAND [ECONOMICS]

Economic tradeoffs in airport and commercial aircraft design, considering traffic growth, increased weight impact minimization and costs 01 p0056 A70-10623

Communication satellite system proposed for small users, assessing viability based on market saturation points estimation 01 p0043 A70-10629

Commercial aircraft design, considering structural allowables effect on economics, using shear web analysis program as example 02 p0225 A70-11947

Aeronautical satellite system for civil flight safety, discussing operational, technical and economic aspects 03 p0522 A70-13610

Boeing 747 aircraft family design options related to utilization, performance and economics, discussing development through large turbofan engine availability 04 p0624 A70-15382

Integrated logistic support economics considered in selecting support system for generating quantitative data for cost optimization 05 p0959 A70-15846

Integrated space program with merger of manned and automated activities for coming decade permitting costs comparable to aircraft-based scientific programs 07 p1375 A70-18872

Demand assignment economics relative to ground stations in satellite telecommunication systems 10 p1838 A70-24360

Direct domestic reception of TV signals from satellites, discussing microwave components, economics and reliability 10 p1840 A70-24448

Communication satellite technology impacts on potential socio-economic developments of emerging nations of Asia, Africa and South America [AIAA PAPER 70-473] 11 p2152 A70-25426

Educational satellite TV for developing countries, giving model relating economic development to education and applied technology 11 p2152 A70-25429

Satellite video-telephone systems promoting economic growth in developing nations through linkage with developed nations advanced centers [AIAA PAPER 70-474] 11 p2000 A70-25455

Wideband transmission media for global communication networks, comparing submarine cables and satellites based on economic tradeoff in terms of circuit density and distance
[AIAA PAPER 70-444] 11 p2001 A70-25475

Communications satellite systems for developing nations, considering educational TV, economic growth, cost estimates, etc
[AIAA PAPER 70-475] 11 p2152 A70-25479

Edwards Report consideration of economic and investment opportunities in civil aviation, discussing denationalizing airways corporations
11 p2153 A70-25859

Edwards Report on UK domestic air services, considering unprofitability, trunk route competition and V/STOL development exploitation
11 p2153 A70-25860

Nonzero sum differential games with cost criteria minimized by inputs control to single dynamic system, emphasizing application to economic competition
11 p2072 A70-26227

Passive and active satellite systems for point-to-point communication network with multiple access capacity, comparing technical and economic competitiveness
11 p2011 A70-26335

Economical inspection of numerical-control produced parts through critical dimensions determination and dimension measurement reduction
[SME PAPER IQ-70-710] 12 p2241 A70-27086

VTOL profitability in Northeast Corridor, discussing city center ports accessibility for S-65-200 short hauls and economic and ground acreage advantages
[SAE PAPER 700310] 12 p2335 A70-27452

Economic factors in developing STOL and VTOL metroflight service, proposing evolutionary process beginning with short term demonstration
[SAE PAPER 700313] 12 p2335 A70-27454

Telecommunication satellite system operation reliability taking into account maintenance and economics, discussing spacecraft acceptance and performance tests
12 p2313 A70-27470

STT feasibility for U.S., considering program costs, financing, investment return and airport and community noise aspects
12 p2162 A70-27991

High speed commercial transport hovercraft economic factors, considering traffic needs, fares, service frequency, reliability, etc
13 p2347 A70-29158

Gear pumps for hydraulic systems, discussing costs, types and applications
14 p2590 A70-30302

Government defense contract warranties in terms of consumer interests protection and economics
14 p2667 A70-30522

Economic factors in aviation - RAS Conference, London, May 1970
14 p2668 A70-30935

Military aviation economics in UK emphasizing aircraft industry and government cooperation in meeting RAF requirements
14 p2668 A70-30938

R and D impact on transport aircraft design economics
14 p2669 A70-30945

Airliner fuselage shape design and effect on manufacturing and flight operation economics
14 p2532 A70-31369

Optimal control theory applied to oligopoly, considering economic problems and Nash equilibrium solutions
15 p2831 A70-32552

General aviation growth forecast during next decade, considering economic importance, air traffic control, collision avoidance, etc
16 p3003 A70-33469

Power plants development for air transport propulsion system economics, noting engine reliability, traffic delays, etc
16 p2841 A70-33770

Long haul air transportation profitability based on Polish Lot airline ton passenger-km computation comparison
17 p3199 A70-34691

Power plant efficiency, size, maintenance and operating economics of propulsion systems for air transport
17 p3200 A70-34917

Air transport operations and economics in 1970 decade, taking into account cost-revenue ratio and cost effectiveness of various aircraft
17 p3204 A70-35852

Aircraft accident prevention and investigation, noting economic factors as deterrent to safety measures implementation
17 p3022 A70-35860

Ignition surges role in combustion economics
18 p3348 A70-36652

STOL systems 1975 technical and economic characteristics in terms of passenger market, aircraft design, terminal facilities and ATC capability
[SAE PAPER 700311] 18 p3350 A70-36812

Optimum reliability level in terms of economic benefits and external constraints
19 p3554 A70-38595

Value engineering for British aerospace industry management planning
19 p3555 A70-38619

Economics of reliability relating risks of failure and cost of failure prevention
19 p3555 A70-38841

Satellite earth resources, discussing cost benefit analysis and economics in agriculture, forestry and mapping
20 p3739 A70-39065

Telecommunication, ATC and navigation satellite systems, examining economic bases for aeronautical and maritime space systems
20 p3740 A70-39407

Air transport regulatory system, considering operational, technological and economic factors
21 p3954 A70-40579

Aeronautical satellite system for civil flight safety, discussing operational, technical and economic aspects
21 p3848 A70-41131

Worldwide common satellite network for sea and air navigation, discussing cost estimate and economics
23 p4216 A70-44608

Nondestructive testing for aircraft maintenance, considering economics
24 p4342 A70-45677

Wide-bodied and SST aircraft impact on airport design based on economic, social and environmental considerations
[AIAA PAPER 70-1269] 24 p4323 A70-45970

Technological and economical characteristics of serviced and unserved automatic hydrometeorological stations and second class nonautomatic station
24 p4340 A70-46406

ECONOMY

Fighter aircraft design combining optimal qualities with economy
05 p0793 A70-15902

Economic flight conditions for civil aviation VTOL aircraft selected by graph-analytical method concerning phases of ascent, cruising and descent
06 p0987 A70-17875

Midwestern political economy and federal R and D funds distribution, surveying bidding practices and NASA contracts for five year period
07 p1428 A70-19733

Satellite TV transmission economic, technical and practical feasibility, describing direct transmission system
09 p1634 A70-22766

Project economic evaluation, discussing value analysis from market research recommendations
19 p3555 A70-38620

EDDIES

U VORTICES

EDDINGTON APPROXIMATION

Eddington equation for white dwarf pulsation solved by treating eigenfunctions as differential moment of inertia functions
04 p0751 A70-15050

EDDY CURRENTS

Eddy current inspection method for detecting fatigue cracks location and depth in fastener holes
01 p0097 A70-10008

Spherical conducting body effect on induction coil impedance and EMF in nondestructive testing using eddy current probes
02 p0300 A70-12478

Inductive eddy current strain gage for repeated strains measurement in magnetic and nonmagnetic sheets offering direct readout and remote recording
03 p0485 A70-13475

Modulation type eddy current flaw detector with striding converter, considering envelope shape of carrier frequency oscillations
06 p1079 A70-18631

Magnetic suspension and guidance of high speed vehicles realized via magnetic field interaction of vehicle-mounted superconducting magnets with eddy currents
08 p1543 A70-20576

Nondestructive testing of small metal tubing, discussing eddy current, ultrasonic and electromagnetic inspection and dye penetrants
08 p1509 A70-21748

Spectral analysis of LF pulses from defects obtained by modulation method of monitoring using eddy currents with superposed converter
13 p2404 A70-28660

Eddy currents magnetic field structure over surface defects in conducting objects, noting NDT applications
13 p2404 A70-28661

Two axis eddy current and single axis gravity gradient dampers for satellite stabilization
16 p2985 A70-34135

Eddy currents in Hall generator with conducting side wall, studying velocity and temperature effects for turbulent boundary layer and laminar flows
21 p3859 A70-41733

Multiparameter eddy current test methods, describing test coil output signal amplification, demodulation and recombination
22 p4028 A70-42592

Pulsed eddy currents in metals nondestructive testing, discussing masked probes, reflection systems, correlation and filtering methods, etc
22 p4028 A70-42593

Ferromagnetic cylindrical specimens eddy current density distribution under influence of field strength dependent permeability corresponding to Rayleigh law
24 p4344 A70-45695

Finite thickness metal plate eddy current response to pulsed field from aperture probe
24 p4344 A70-45696

Eddy current nondestructive tests for surface defects detection, determining optimum test parameters based on calculation
24 p4344 A70-45697

Eddy current magnetic probe with frequency scanning for signal-noise discrimination in nondestructive testing of tubes
24 p4336 A70-45698

Metal sheets thickness measurement and monitoring by through-transmission eddy current nondestructive testing, using phase locked amplifier
24 p4344 A70-45699

Magnetic and nonmagnetic metals flaw detection, using orthogonal eddy current probe to reduce permeability and conductivity variations effects
24 p4344 A70-45700

Metals flaw detection, using electronic balancing type eddy current detecting coil
24 p4336 A70-45701

Encasing and welded pipes flaws detection with high resolution by nondestructive testing, using eddy current method
24 p4345 A70-45702

Nondestructive tests of work-hardening Al alloy structural deterioration due to overheating, using eddy current conductivity techniques
24 p4345 A70-45703

EDDY DIFFUSION

U TURBULENT DIFFUSION

EDDY VISCOSITY

Boussinesq eddy viscosity concept solving equations of two dimensional incompressible turbulent boundary layer, using implicit five point finite difference method
02 p0285 A70-12350

Differential strip method developed for turbulent boundary layer equations, describing flow by law of wall coupled to wake solution utilizing constant eddy viscosity
02 p0285 A70-12352

Finite difference solution of compressible turbulent boundary layer equations of motion, using eddy viscosity concept
02 p0286 A70-12353

Eddy viscosity equation derived from flat plate turbulent boundary layer velocity data, considering shear stresses and mixing length profiles
03 p0464 A70-12943

Turbulent boundary layer model using two region characterization for eddy viscosity and similarity solution taking into account interfacial conditions
[ASME PAPER 69-WA/APM-27] 04 p0668 A70-14905

Viscosity superposition principle applied to isotropic turbulence analysis, approximating self similar solution by time factor averaging
07 p1258 A70-19698

Turbulent Prandtl number and eddy viscosity distribution in thermally stratified turbulent boundary layer of air shear flow dependent on wall distance and thermal stability
08 p1599 A70-21581

Turbulent trailing vortex decay calculated from circumferential velocity and eddy viscosity dependent on Reynolds number
10 p1802 A70-24561

Reynolds momentum and mass transport at velocity half radius of coaxial jet compared to eddy viscosity models
14 p2564 A70-30260

Plane turbulent impinging jet by iterative finite difference technique, assuming eddy viscosity dependence on energy fluctuations and turbulence length scale
[ASME PAPER 70-FE-27] 16 p2835 A70-33634

Oscillatory flow in turbulent boundary layer modeled by eddy viscosity distribution, deriving mass transport velocity induced by progressive and standing waves
20 p3608 A70-39358

Turbulent boundary layers calculation with and without mass addition based on eddy viscosity concept, including accelerating flows
21 p3807 A70-41029

EDEMA

Brain oxygen supply during cerebral edema, examining venous and arterial blood gases, circulation, oxygen uptake, blood volume and pressure and EEG
10 p1822 A70-25087

Hyperbaric oxygen exposure produced hypertension and pulmonary edema, discussing carbon dioxide transport mechanism in blood 20 p3572 A70-39430

EDGE DISLOCATIONS

Temperature effects on tensile deformation mechanism of Mo single crystals, investigating stress-strain characteristics and slip geometry 02 p0316 A70-11699

Steady creep process microscopic mechanisms, discussing creep due to glide of jogged screw dislocations, climbing of edge dislocations and stress directed vacancy diffusion 08 p1593 A70-21519

Plastic properties of tungsten carbide single crystals at room temperature, determining slip system crystallographic orientations 08 p1520 A70-21557

Temperature effect on plastic flow in Ti-scavenged Fe, attributing microyielding to edge dislocations motion 08 p1525 A70-21959

Ferromagnetic domain wall-dislocations magnetoelastic interaction in Fe and Ni computed as function of relative separation, discussing effects on magnetic properties 09 p1705 A70-22811

Fast brittle crack slowing by mechanical twins in transformer steel and by slip bands in LiF and NaCl crystals 15 p2755 A70-31526

Double ended dislocation pileups and elastic cracks at bimaterial interface under screw, edge and shear modes 15 p2756 A70-31561

Elastic properties of dislocations in Ti basal, prismatic and pyramidal slip systems, discussing dilatational fields of edge and screw dislocations 17 p3115 A70-34385

Parallel edge dislocations in elastically isotropic crystals, discussing climb and glide forces 17 p3126 A70-35454

Edge dislocation and uniform and radial fissures in elastic isotropic nonhomogeneous bodies under two dimensional deformation 19 p3540 A70-37956

Slip band formation dislocation-diffusion mechanism for single crystal and polycrystalline metals, considering stress intensity and load cycles effects 21 p3936 A70-41416

Plastic zones between symmetric and collinear edge cracks in thin plexiglass strips, using He-Ne laser interferometry 21 p3939 A70-41967

Half plane with stress-free surface deformed by protrusions or notches, deriving edge force or screw dislocation by linear elastic analysis 21 p3939 A70-42028

Optimal weight design of axisymmetric rotating elastic disks for specific edge radial displacement 22 p4112 A70-42463

Stress fields of screw and edge dislocations in linearly elastic isotropic Cosserat continuum using stress functions 23 p4266 A70-44022

EDGE LOADING

Thin flat plates effective width under axial edge compression slightly beyond buckling limit, solving von Karman differential equations 01 p0198 A70-10094

Axially compressed cylindrical shells with edge constraints, determining critical load from inelastic behavior considerations 01 p0205 A70-11141

Elastic bending of thin circular conical shell subject to arbitrary variation of edge loads 01 p0209 A70-11385

Donnell shallow circular cylindrical shell equation, obtaining approximate solution for stresses in infinitely long circular cylindrical shell with circular hole subjected to edge loading 03 p0601 A70-14320

Structural analysis of rectangular plates simply supported on two edges subjected to free edge uniform moments 03 p0602 A70-14332

Stress analysis of shell loaded at free edge by concentrated forces and moments 04 p0772 A70-14920

Fiberglass reinforced rectilinear plastic plates bending under various edge loads, noting shear pliability 05 p0934 A70-16220

Shallow orthotropic shell of rectangular planform with edges under dynamic load, studying forced vibrations by anisotropic shell theory 07 p1403 A70-19057

Rectangular plate girder webs buckling under partial edge loadings, using finite element method for flange-web interaction 08 p1589 A70-21247

Elastically symmetric thin plate stress-strain state under uniformly distributed load applied to edges 08 p1591 A70-21415

Green function for stress intensity factors of rectangular plate edge cracks, noting application to thermal stresses [ASME PAPER 68-WA/MET-19] 08 p1591 A70-21457

Stress concentration in elastic plate reinforced at edge by straight rib analyzed in finite form by Cauchy integrals and Fourier transforms 08 p1594 A70-21635

Axisymmetric free vibrations of orthotropic cylindrical shell loaded on ends by constant axial force, investigating nonlinear elasticity 09 p1785 A70-23625

Stress distribution in infinite strip of finite thickness under symmetric edge loading analyzed by linear couple stress theory using Fourier transforms 10 p1954 A70-24017

Influence coefficients for toroidal shells under axisymmetric edge loads, taking one term in asymptotic expansion of Hankel function 11 p2132 A70-25693

Characteristic equation roots for circular cylindrical shells deformation under edge load 11 p2135 A70-25960

Thin circular cylindrical panels of arbitrary curvature calculated for end support and loading at contour 12 p3232 A70-27335

Deflection surface and edge moment prediction for uniformly edge loaded point-supported circular plates, comparing with optical method 13 p2509 A70-28534

Stress concentration factors determined for u-shaped and semielliptical edge notches in semiinfinite sheet under uniaxial tension parallel to edge 13 p2509 A70-28535

Postbuckling of flat variable thickness rectangular plates with unloaded transverse edges, using dynamic relaxation method 13 p2518 A70-30024

Thin spherical shell postbuckling behavior with constrained rigid boundary under edge load, using deep and shallow shell theory 14 p2658 A70-30848

Shells of revolution zero moment stressed state calculation by analytical functions, solving boundary value problem for edge loading 15 p2814 A70-31587

Linear model of edge effect in supersonic gas flow past dihedral angle of intersecting wings, using Abel equations 15 p2672 A70-32127

Nonlinear bearing surface of symmetrical rectangular edge wings without slipping in incompressible flow, using oblique horseshoe vortex model 15 p2673 A70-32128

Thin plates with central circular holes, investigating creep behavior for biaxial edge tractions 15 p2822 A70-32359

Alternating stress required for edge crack propagation in metal plates under tensile loading cycles 15 p2762 A70-32464

Thin walled cylindrical shell stability under axial compression edge load beyond limit of proportionality 19 p3534 A70-37243

Edge distribution of transverse reactive forces of rectangular plate with nonuniform flexural rigidity at buckling load 19 p3541 A70-38042

Elastic stability theory Cosserat surface subjected to conservative nongyroscopic surface and edge loading 21 p3939 A70-42027

EDGES

NT LEADING EDGES

NT SHARP LEADING EDGES

NT TRAILING EDGES

Boundary conditions at reinforced edge of shell by separating solution into zero moment stress and edge effect solutions 01 p0209 A70-11407

Edge smear in far field holography as function of interference orders, using short-cut trace technique 09 p1684 A70-23532

Object contrast effects on straight edge images in partially coherent illumination 10 p1898 A70-23910

Shear deformation of sandwich plate cross sections with hinged opposite edges, constructing transfer matrix for state variables 13 p2508 A70-28483

Steady expansion flows at three dimensional supersonic edges with small corner angles using analytical method of characteristics 13 p2338 A70-28491

Focusing lens edge diffraction effect on angular distribution of laser radiation, considering zero mode field distribution 13 p2428 A70-29367

EDUCATION

NT ASTRONAUT TRAINING

NT EJECTION TRAINING

NT FLIGHT TRAINING

NT PILOT TRAINING

NT SPACE FLIGHT TRAINING

Human subjects performances on fixed interval reinforcement schedules, emphasizing effects of instruction 01 p0035 A70-10793

Digital computer display techniques relationship with man in modern environment, considering human engineering and educational problems and future impact on intellectual qualities 01 p0221 A70-11281

System analysis and synthesis processes applied to educational requirements identification and programs implementation, emphasizing use of functional model with man machine interface 01 p0221 A70-11283

Student development and exercising of electron physics principles by designing, assembling, operating and studying electron and ion devices 01 p0093 A70-11291

Diffraction plates for classroom demonstrations of Fraunhofer patterns, Babinet principle and Rayleigh resolution by computer generation 01 p0093 A70-11292

Digital systems design laboratory as instructional tool and experimental model for education 02 p0275 A70-12190

Great Britain air transport industry manpower recruitment and training, technology changes effects and costs 02 p0402 A70-12307

Network analysis for systems application program /NASAP/ computer-aided circuit design program for network analysis, discussing application in education 06 p1015 A70-18418

Computer aided network design course using FORTRAN 4 emphasizing modeling of semiconductor devices 06 p1015 A70-18419

Critical comments on teaching switching theory concerning mathematics role, logic functions, Boolean equations, etc 06 p1026 A70-18423

Survival training for safety promotion in emergency, discussing psychological factors, communication, living off land and shelter 07 p1218 A70-19007

Inhibitive stimulus control related to behavioral contrast during discriminative training 08 p1441 A70-20476

Direct broadcast voice satellite for educational system improvement, discussing lesson formatting, ground receiver/programmer, multichannel capacity, etc [AIAA PAPER 70-449] 11 p1998 A70-25423

Systems analysis approach to problem solving, discussing application to sociological and educational considerations 17 p3130 A70-35297

ATC personnel training at International ATC Academy, discussing objectives and syllabus 19 p3372 A70-38650

Oxygen pressure effects on tracking control training for stable reactions, investigating muscles bioelectrical activity changes during elevated pressure breathing 20 p3581 A70-40291

Age, grade, educational institution and attitude effects on pilot personality test performance 22 p3977 A70-42870

Aerospace medicine approach to medical investigator training for aircraft accidents, noting flight surgeon role as life support specialists chief 23 p4152 A70-44454

Survival training program preparing physicians as advisors regarding survival equipment and medicine 23 p4152 A70-44463

Heat transfer and viscous flow pedagogy, discussing classroom use of remote time sharing computer terminals 23 p4166 A70-44642

Industry-university interaction in competitive teaching of spacecraft design 23 p4285 A70-44643

EDUCATIONAL TELEVISION

Software production for Brazilian Advanced Educational Technology System [AIAA PAPER 70-470] 11 p2152 A70-25403

Educational satellite TV for developing countries, giving model relating economic development to education and applied technology [AIAA PAPER 70-514] 11 p2152 A70-25429

Satellite ETV/ITV broadcast system, discussing frequency, receiver population, channel number, beam number, minimum cost solutions, etc [AIAA PAPER 70-452] 11 p1999 A70-25437

Satellite video-telephone systems promoting economic growth in developing nations through linkage with developed nations advanced centers [AIAA PAPER 70-474] 11 p2000 A70-25455

Instructional communication system for U.S. using synchronous satellites over 15 regions [AIAA PAPER 70-450] 11 p2000 A70-25465

Communications satellite systems for developing nations, considering educational TV, economic growth, cost estimates, etc [AIAA PAPER 70-475] 11 p2152 A70-25479

- Microwave converter system for ETV satellite reception, discussing characteristics and costs for mass production
[AIAA PAPER 70-439] 11 p2017 A70-25493
- Low cost microwave receiver and antenna for instructional satellite TV broadcasting in developing nations
21 p3789 A70-41355
- Educational TV system via satellite, discussing social benefits for Spanish speaking countries in South America
23 p4285 A70-44602
- Juridical problems in satellite direct TV broadcasting, discussing regulation proposals submitted to UN and educational applications
24 p4430 A70-45596

EEG [ELECTROENCEPHALOGRAMS]

U ELECTROENCEPHALOGRAPHY

- EFFECTIVENESS**
NT COST EFFECTIVENESS
NT SYSTEM EFFECTIVENESS
Complex systems effectiveness analysis by computer simulation technique
15 p2706 A70-32633
- Systems consisting of redundant and different modules, deriving vector and matrix expressions for effectiveness
17 p3099 A70-34581

EFFECTORS

U CONTROL EQUIPMENT

- EFFERENT NERVOUS SYSTEMS**
Relationships between frog vestibular afferents, cerebellum and efferent vestibular system, using electron microscopy and Nauta degeneration technique
01 p0014 A70-10351
- Cerebello-otolith system represented by axons of Purkinje cells, studying inhibitory vestibular efferent system relation to cerebellum in frog
01 p0014 A70-10352
- Morphological analysis of connections between auditory cortex zone and claustrum in anesthetized cats, establishing efferent nerve fibers presence
01 p0025 A70-11039
- Efference role in eye tracking of moving targets, discussing oculomotor system role
03 p0439 A70-14345

- Astronauts physical training for space flight requirements
04 p0629 A70-14564
- Immobilization effects on alpha rhythm, locomotor coordination and visual alimentary motor reflexes of cats
04 p0629 A70-14570
- Postrest upswing or muscles warm-up in motor skill learning
05 p0803 A70-16671
- Human motor reactions rhythmic system, relating reaction-skin-galvanic reflex to formation of successive conditioned connections
07 p1197 A70-18697
- Efferent and afferent fibers presence in optic nerves determined by unilateral and bilateral enucleation of dogs and cats
07 p1207 A70-19476

- Bioelectrical activity of brain during conditioned motor reflex system operation modes in response to stimulating light pulses
08 p1447 A70-21450
- Discrete motor act short term retention measurement to investigate decay and interference effects
09 p1621 A70-23378
- Startle auditory stimuli effects on motor performance and recovery characteristics from heart rate and skin conductance recordings
09 p1628 A70-23577
- Neuron activity of cortical motor and visual regions and corpus geniculatum laterale in cats during diffuse thalamic electrostimulation combined with light signals
12 p2173 A70-28355

- Excitation conduction velocity maximum along motor fibers of peripheral nerves as function of age in healthy subjects
15 p2679 A70-31602
- Human postural motor control systems nonlinearities, describing physiological experiments and mathematical models
15 p2693 A70-32568
- Physiological tests of sampled data hypothesis in human motor control system
16 p2851 A70-33323

- Moving stripe stimulus inducing optokinetic turning movements in goldfish, discussing efferent influence on vestibular organ
21 p3762 A70-41141
- Active recreation in motor function regulation in aging individuals
22 p3968 A70-42897
- Kinesophilia mechanisms of motor-visceral integration in aging organism
22 p3969 A70-42902
- Spinal cord thermal stimulation effects on regional sympathetic activity in rabbits and cats determined from integrated sympathetic efferents discharges
22 p3971 A70-43406

- Auditory cortex projections to caudate nucleus and functions of associative subcortical area in cats
24 p4300 A70-45838

EFFICIENCY

- NT COMBUSTION EFFICIENCY
NT COMPRESSOR EFFICIENCY
NT ENERGY CONVERSION EFFICIENCY
NT NOZZLE EFFICIENCY
NT POWER EFFICIENCY
NT PROPELLER EFFICIENCY
NT PROPULSIVE EFFICIENCY
NT THERMODYNAMIC EFFICIENCY
NT TRANSMISSION EFFICIENCY
Efficiency of terminal state control systems defined, relating efficiency, random parameters and reliability
07 p1246 A70-19528

- Efficiency loss with tip clearance predicted for mixed and axial flow single stage turbomachines, using perfect fluid model
11 p1974 A70-25787
- Aircraft stretch efficiency factor as function of productivity and payload growth
[SAWE PAPER 838] 20 p3563 A70-40369

EFFLUENTS

- Environmental surveillance associated with ground tests of nuclear rocket engine prototypes, determining statistical nature of radioactive effluent
19 p3470 A70-38013

EFFLUX

- Conducting gas unsteady efflux from plane tube into vacuum, determining time dependent position of expanding rarefaction wave fronts
10 p1924 A70-24569
- Gas-particle efflux from nozzle at critical velocities, noting particle size and concentration effects on inlet pressure
15 p2721 A70-32136
- Rarefied gas mixtures efflux from opening at various pressures, calculating component discharge coefficients for molecular flow conditions
15 p2721 A70-32137

EFFUSIVES

- CaO reaction rate with ZrC in effusion cells as function of reactant ion diffusion through product layer
13 p2362 A70-29496

EGGS

- Organism reactions to gravity forces, discussing experimental zero and hyper g simulation studies with frog and nematode eggs
23 p4146 A70-44630
- Altered gravitational field effects on frog eggs centrifuged under various conditions after fertilization, noting time dependence of induced abnormalities
24 p4298 A70-45619

EGRESS

- High energy emergency exit systems for passenger survival in aircraft accidents
23 p4140 A70-44466

EIGENFUNCTIONS

U EIGENVECTORS

EIGENSTATES

U EIGENVECTORS

EIGENVALUES

- Dynamo theory of stellar and planetary magnetic fields, discussing mathematical analysis and electronic computation of eigenvalue problems and field parameters
01 p0185 A70-10957

- Characteristic equations developed for two-spatial dimensional elastic wave propagating in linear elastic, isotropic and homogeneous medium
01 p0208 A70-11185

- Lower bounds of Stekloff and free membrane eigenvalues for sloshing of incompressible inviscid fluid, subject to gravity in rigid tank with free surface
02 p0278 A70-11999

- Summary representations method to determine eigenfrequencies of finite difference Laplace operator for boundary conditions
03 p0518 A70-13079

- Eigenfunctions of oscillating infinite perforated membranes for various boundary conditions at holes
03 p0591 A70-13415

- Homogeneous waveguide solutions by finite element method using matrix operator and function minimization to assure rapid convergence to eigenvalue
03 p0457 A70-13936

- Upper and lower bounds for eigenvalues of lumped parameter straight line torsional system determined by receptance synthesis based on Holzer method
04 p0773 A70-15083

- Eigenvalue and eigenfunction of H01 wave in bend of cross shaped waveguide, determining field components and propagation constant change
04 p0651 A70-15291

- Surface wave spectrum and propagation in non-homogeneous bounded elastic solid, considering existence and eigenvalues approximation
05 p0925 A70-15789

- Eigenvalues upper and lower bounds of vibrating anisotropic material with multiple elastic constants, predicting free vibration frequencies by bounding isotropic moduli
05 p0937 A70-16408

- Convergence of eigenvalues and eigenvectors in torsional vibration problems of continuous systems via improved matrix displacement analysis using points of freedom in segments
05 p0939 A70-16502

- Green operator structure and eigenvalue approximation of boundary value problems regarding vibrations and buckling of clamped plates using orthogonal invariants
05 p0876 A70-16563

- Discrete spectrum of fourth order differential operator estimating number of eigenvalues in bounded interval of real line
06 p1094 A70-17740

- Eigenvalues of spheroidal wave functions calculations dependent on complex propagation constants, discussing branch point values in tabular form
06 p1009 A70-17907

- Eigenvalue solutions convergence rates using two finite plate multidegrees of freedom bending elements
06 p1169 A70-17941

- Eigenvalue corresponding to decaying modes for wave equation in exterior of obstacle investigated for dependence on obstacle geometry
06 p1095 A70-18474

- Capacity calculation of N identical discrete memoryless nonsingular channels cascade, discussing dependence on eigenvalues and eigenvectors of subchannel transition matrices
06 p1013 A70-18628

- Characteristic equations for differential symmetry operators in homogeneous and nonhomogeneous Maxwell equations
08 p1544 A70-20990

- Circular dielectric waveguide modes self consistent description by asymptotic method, obtaining eigenvalues and eigenfunctions
08 p1476 A70-21288

- Fluge characteristic equation approximate roots for closed cylindrical shell compared with Donnell equation solution
08 p1593 A70-21625

- Natural oscillation frequencies of subsonic gas flow past plate array, solving eigenvalue problem by splitting method
09 p1603 A70-22117

- Plane Couette flow stability numerical analysis, predicting eigenvalue behavior for arbitrary Reynolds and wave numbers
09 p1658 A70-22124

- Asymptotic distribution of operator eigenvalues for self adjoint elliptic boundary value problem in unbounded region using Green function
09 p1711 A70-22148

- Eigenvalues and eigenvectors evaluation for real symmetric matrices by iterating simultaneously with trial vectors
09 p1641 A70-22283

- Fourth order differential equation system with complex conjugate eigenvalues, deriving optimal control for fuel minimum
09 p1759 A70-22831

- Asymptotic splitting of system of linear differential equations with slowly varying coefficients in cases with characteristic equation having multiple roots
09 p1712 A70-23119

- Blast wave eigenvalues in asymptotic expansions approximation for hypersonic flows past blunt bodies
10 p1797 A70-23953

- Closed loop control system design with preassigned eigenvalues based on multipoint linear stationary system synthesis with dynamic feedback
10 p1855 A70-24394

- Asymptotic eigensolutions for equations governing flow between oppositely rotating infinite plane disks in inviscid limit
10 p1870 A70-24607

- Stability of multiconnected nonlinear controlled systems with nonsingle equilibrium position, representing lumped parameter system with characteristic equation having complex roots
11 p2021 A70-25338

- Elastic wave propagation, deriving characteristic equations in generalized curvilinear coordinates using linear elastic, isotropic and homogeneous constitutive equations
11 p2132 A70-25680

- Nonlinear partial differential operators eigenvalue solution using modified Newton iteration method, noting advantages over perturbation method
11 p2074 A70-26423

- Classical eigenvalue problem transformation by invariant imbedding into initial value problem suited for numerical integration, noting applications to columns elastic buckling
12 p2261 A70-27424

- Dimensional stability derivatives from XV-4B aircraft simulator varied in computer program for extracting roots of lateral-directional characteristic equation
[AIAA PAPER 70-551] 13 p2346 A70-29016

- Ordinary differential eigenvalue problems solution by successive transformations, describing computer program and applications to hydrodynamic stability
13 p2440 A70-29085

- Quasi-pyramidal horn waveguide TE and TM modes eigenvalues computed by asymptotic formula
13 p2377 A70-29147
- Numerical integration of differential equations with widely separated eigenvalues, outlining solution stability and accuracy problems
13 p2441 A70-29213
- Eigenvalue and eigenvector derivatives in dynamic system designs involving vibrations and oscillations, discussing applications in modeling
13 p2518 A70-29971
- Covariance propagation via differential equations for time-varying eigenvalues and eigenvectors
13 p2450 A70-29979
- Differential equations eigenvalue and boundary value problem finite difference approximation convergence under consistency and stability conditions
14 p2599 A70-30643
- Eigenvalues of membranes and plates, comparing asymptotic and numerical values
14 p2600 A70-31223
- Radial Schrodinger equation bound state eigenvalues and properties by iterative method, calculating Coulomb potentials
14 p2600 A70-31360
- Natural oscillation frequencies in rectangular shallow shells weakened by cuts, using summary representations method for eigenvalues determination
15 p2814 A70-31585
- Feedback gains for repeated eigenvalues in Simon-Mitter pole allocation algorithm
16 p2941 A70-32986
- Radial energy eigenvalue problem conversion into one dimensional by infinite set of transformations, considering WKB quantization condition
16 p2942 A70-33691
- Complex matrix eigenvalues bound derivation by constructing integral equation with degenerate kernel
17 p3131 A70-35934
- Hurwitz matrix of real Hurwitzian polynomial, discussing relation between eigenvalues and zeros locations
18 p3279 A70-36062
- Ritz procedure for problems with eigenvalues in boundary conditions
18 p3336 A70-36222
- Eigenvalues of transfer matrix and vibrations generation for passive mechanical systems with n degrees of freedom based on Laplace transformation
18 p3337 A70-36225
- Eigenvalues and errors in asymptotic approximation of ordinary differential equations of second and fourth order
18 p3283 A70-36365
- Nontrivial eigenvalues of stochastic matrices
19 p3456 A70-37414
- Noniterative homogeneous solutions of integral equations for coupled open channel and coupled eigenvalue scattering
19 p3473 A70-38264
- Electromagnetic wave propagation in spherical impedance waveguide, determining eigenvalues with negligible refraction
19 p3381 A70-38565
- Perturbation calculation for linear ordinary differential operators, considering equivalence to eigenvalue problems
19 p3459 A70-38681
- Neighboring normal matrix pairs eigenvalues determination
19 p3459 A70-38685
- Mode clamping theorems for eigenvalues upper and lower bounds
20 p3657 A70-39232
- Recursive digital filters for flight control system airborne computer, considering quantization effects and eigenvalue sensitivity
20 p3601 A70-39575 [AIAA PAPER 70-953]
- Thin shells of revolution static and dynamic stability under symmetric loads, presenting eigenvalue algorithm for boundary value problems
20 p3725 A70-39863
- Vibrating plate thickness function, applying eigenvalue problem
20 p3726 A70-39877
- Feedback control system characteristic equation generalized root locus following technique using straight line approximation
20 p3659 A70-40121
- Boundary value problems for linear ordinary differential equations with singularities, determining eigenvalues by computer oriented method
20 p3659 A70-40134
- Jeffery-Hamel flows in symmetric divergent channels with small wall curvature, calculating eigenvalues and nonlinear stability limits
22 p4010 A70-42638
- Nesbet algorithm modified for iterative evaluation of eigenvalues and corresponding eigenvectors for large matrices
22 p4062 A70-42749
- Shooting method for computing eigenvalues of Hermitian differential operators
23 p4210 A70-44020
- Multidimensional correspondences between Helmholtz equation eigenfunctions and eigenvalues, including involutorial transformations
23 p4218 A70-44211
- Approximate bounds for differential eigenvalues of self adjoint linear operators in Hilbert space
23 p4211 A70-44245
- Iterative Rayleigh-Ritz method for eigenvalue determination in natural vibration problems
23 p4270 A70-44580
- Gradient minimization and higher order discrete elements application to shell buckling and vibration eigenproblems, using 48 degree of freedom Bogner cylindrical panel element
23 p4271 A70-44705
- Structural eigenvalue problems solved by sparsely populated matrices for structural vibrations and critical buckling, using finite element method
23 p4271 A70-44708
- Eigenvalue problem in elasticity theory, treating nonlinear equations solutions multiplicity by topological methods
24 p4420 A70-45273
- Variational solution of eigenvalues and eigenfunctions of second boundary value problem of elasticity minimizing functional
24 p4424 A70-45629
- Ionospheric wave propagation, using medium model, perturbation theory for vertical variation and computer eigenvalues of matrix system
24 p4314 A70-46132
- Spheroidal wave function theory, calculating eigenvalues with branch points for propagation constants complex values
24 p4315 A70-46134
- EIGENVECTORS**
- Characteristic equations developed for two-spatial dimensional elastic wave propagating in linear elastic, isotropic and homogeneous medium
01 p0208 A70-11185
- Morse eigenfunctions for variational calculation of diatomic molecules vibrational-rotational energy level analysis, showing better convergence than harmonic oscillator basis
02 p0344 A70-12519
- Eddington equation for white dwarf pulsation solved by treating eigenfunctions as differential moment of inertia functions
04 p0751 A70-15050
- Eigenvalue and eigenfunction of H₀₁ wave in bend of cross shaped waveguide, determining field components and propagation constant change
04 p0651 A70-15291
- Convergence of eigenvalues and eigenvectors in torsional vibration problems of continuous systems via improved matrix displacement analysis using points of freedom in segments
05 p0939 A70-16502
- Capacity calculation of N identical discrete memoryless nonsingular channels cascade, discussing dependence on eigenvalues and eigenvectors of subchannel transition matrices
06 p1013 A70-18628
- Self adjoint operator generated by differential expression and pseudodifferential boundary conditions, using Berezanskii procedure for operator eigenfunction expansion
07 p1327 A70-19809
- Characteristic equations for differential symmetry operators in homogeneous and nonhomogeneous Maxwell equations
08 p1544 A70-20990
- Circular dielectric waveguide modes self consistent description by asymptotic method, obtaining eigenvalues and eigenfunctions
08 p1476 A70-21288
- Fluge characteristic equation approximate roots for closed cylindrical shell compared with Donnell equation solution
08 p1593 A70-21625
- Eigenvalues and eigenvectors evaluation for real symmetric matrices by iterating simultaneously with trial vectors
09 p1641 A70-22283
- Asymptotic splitting of system of linear differential equations with slowly varying coefficients in cases with characteristic equation having multiple roots
09 p1712 A70-23119
- Beam vibration eigenfunctions with allowance for shear compliance used to determine beams dynamic stability under pulsating axial load
09 p1785 A70-23600
- Nonautonomous boundary value problems for plates in plane and three dimensional supersonic flows, obtaining eigenfunctions of vibration by Laplace transform
10 p1956 A70-24118
- Stability of multiconnected nonlinear controlled systems with nonsingular equilibrium position, representing lumped parameter system with characteristic equation having complex roots
11 p2021 A70-25338
- Elastic wave propagation, deriving characteristic equations in generalized curvilinear coordinates using linear elastic, isotropic and homogeneous constitutive equations
11 p2132 A70-25680
- Dimensional stability derivatives from XV-4B aircraft simulator varied in computer program for extracting roots of lateral-directional characteristic equation [AIAA PAPER 70-551]
13 p2346 A70-29016
- Geopotential fields seasonal statistical analysis over first natural synoptic region, using expansion into orthogonal eigenfunctions
13 p2446 A70-29674
- Eigenvalue and eigenvector derivatives in dynamic system designs involving vibrations and oscillations, discussing applications in modeling
13 p2518 A70-29971
- Covariance propagation via differential equations for time-varying eigenvalues and eigenvectors
13 p2450 A70-29979
- Fourth order differential equations eigenfunctions construction and convergence of expansions in theory of flexure of sector plates
14 p2658 A70-30997
- Couette flow stability between coaxial rotating cylinders, calculating eigenvector in first approximation small perturbation equations
17 p3073 A70-35695
- Feedback control system characteristic equation generalized root locus following technique using straight line approximation
20 p3659 A70-40121
- First order linear distributed systems with two point boundary values, obtaining eigenfunction expansion by generalized Fourier method
21 p3846 A70-41949
- Steepest descent method for determining lowest ground state eigenvectors for molecular wave configurations
22 p4062 A70-42747
- Nesbet algorithm modified for iterative evaluation of eigenvalues and corresponding eigenvectors for large matrices
22 p4062 A70-42749
- Multidimensional correspondences between Helmholtz equation eigenfunctions and eigenvalues, including involutorial transformations
23 p4218 A70-44211
- Cantilever plate random vibration response, calculating eigenvectors and natural frequencies by finite element method
23 p4270 A70-44591
- Variational solution of eigenvalues and eigenfunctions of second boundary value problem of elasticity minimizing functional
24 p4424 A70-45629
- EINSTEIN EQUATIONS**
- Einstein equations for Bianchi type IX universe model suitable for numerical solution and application to cosmology with pure fluid stress tensor
01 p0142 A70-10522
- Conformally plane solutions to Einstein equations derived with energy momentum tensor characteristics of pulverized material representing gravitational fields
01 p0193 A70-11629
- Einstein equations for five dimensional spherically symmetric space solved using gravitational constant without singularities on Schwarzschild sphere
05 p0880 A70-15793
- Shear-free gravitational radiation described by Einstein equations, analyzing physical properties including energy, angular momentum, radiation flux and trapped surfaces
06 p1104 A70-17185
- Einstein field equations based on variational principle applied to stability of general self gravitating relativistic gaseous mass obeying specific equation of state
06 p1138 A70-17304
- Observation operators and cosmology, constructing equations for cosmological aggregates governed by Einstein field equations
06 p1105 A70-17529
- Lagrangian invariance transformation application to steady state solution for Einstein-Maxwell equations interpreted as external field of charged isolated rotating source
06 p1106 A70-17747
- Stationary solutions of Einstein-Maxwell equations constructed from Einstein-Maxwell or vacuum fields
06 p1106 A70-17748
- Einstein-Maxwell equations solutions relation to Robinson and Robinson metrics compared with Reissner-Nordstrom solution relation to Schwarzschild
07 p1333 A70-18961
- Cosmological solution of Einstein gravitational equations with singularity in time
07 p1381 A70-19361
- Hamiltonian methods applied to homogeneous cosmological models, obtaining Einstein equations, passing to quantum theory by imposing canonical commutation relations
07 p1336 A70-19921

- Singularity for absolute zero of time suggested for beginning of universe by Einstein relativity theory
07 p1336 A70-19922
- News function relation with far fields of sources obtained in linear approximation for axisymmetric case in integrating Einstein field equation
08 p1543 A70-20721
- Matter distribution and motion in conformally flat gravitational fields, analyzing Friedmann solution to Einstein equations
08 p1544 A70-20991
- Gravitational waves in general relativity theory, discussing Kaigorodov exact solution to Einstein equations
08 p1545 A70-20993
- Einstein gravitational equations general solution having physical singularity with respect to time
08 p1546 A70-21424
- Local uniqueness and instability theorem for Einstein-Liouville equations using energy inequalities, noting relevance to Cauchy problem
11 p2084 A70-26458
- Metric analyticity around each point of C cubed static vacuum space-time for Einstein equations
11 p2084 A70-26553
- Gravitational collapse of star and general relativity role, considering Schwarzschild solution to Einstein vacuum equations
12 p2298 A70-27058
- Einstein equations derivation in comoving reference frame for spatially homogeneous gravitational fields
12 p2310 A70-28221
- Kerr-Schild space-time manifolds with electromagnetic field, solving Einstein equations
13 p2451 A70-29166
- Four dimensional Einstein space metric of signature 2 with N type Weyl tensor and nonintegrable rays
13 p2453 A70-29636
- Closed universe classical and quantum dynamics by ADM Hamiltonian treatment of Einstein equations for homogeneous cosmological models
13 p2495 A70-29812
- Dynamic spectrum of density fluctuations and galaxy clustering in Einstein universe, considering self gravitation of medium
14 p2652 A70-31389
- High velocity center to center collision of two absolutely elastic rods in acoustic medium in terms of Einstein nonclassical mechanics
15 p2775 A70-32890
- Uniform model universes containing gaseous matter and background blackbody radiation, solving Einstein equations without zero pressure assumption
18 p3313 A70-36215
- Schwarzschild exterior metric stability against perturbations from asymptotic behavior of Einstein field equations solution in Kruskal coordinates
18 p3291 A70-36650
- Insular system energy and momentum definition in external gravitational field, using dynamic equations and Einstein theory
19 p3513 A70-37412
- Variational principle application to relativistic MHD, deriving Einstein field equations, Maxwell equations and equations of motion for self gravitating charged fluid
19 p3478 A70-37591
- Einstein equations derivation in comoving reference frame for spatially homogeneous gravitational fields
20 p3710 A70-40096
- Time travel and cosmological model based on Einstein relativity theory, considering hypothetical motor design, energy supply, tachyons and four dimensional orbits implications
20 p3710 A70-40132
- Einstein equations solved for steady axisymmetric physical schemes by varying Kerr metric constants, considering electromagnetic field case
22 p4073 A70-42717
- Einstein gravitational equations solution for expanding universe, discussing possible sudden collapse into zero volume with infinite density
22 p4105 A70-43215
- Optical point characteristics of static spherically symmetric space-times of de Sitter universe, Einstein universe and exterior Schwarzschild field
23 p4239 A70-43821
- Einstein field equations for spatially homogeneous spaces, considering rotating matter model in regularized Euler-Lagrange form
23 p4219 A70-44406
- Newton and Einstein gravitation theories applied to light velocity in gravitational field
24 p4379 A70-45487
- Einstein equations internal solution other than Schwarzschild for case of central symmetry and static source
24 p4379 A70-45628
- Hermitian symmetry in Einstein unified field theory in terms of pseudotensor
24 p4380 A70-45819
- Mathematical model for ejection fraction of human left ventricle incorporated with fiber orientation and ventricular geometry, showing consistent results with biplane angiocardiographic films
03 p0433 A70-12975
- Aircraft life support systems and equipment evaluated in Vietnam combat environment, discussing combat ejection conditions, injuries cause and severity, fatalities, etc
05 p0806 A70-16298
- Materials jet-like ejection from metal surfaces under high density laser radiation action, investigating erosion and plasma spectrum
19 p3448 A70-38734
- In-flight escape systems and survival equipment reliability in U.S. Navy ejections
23 p4143 A70-44460
- EJECTION INJURIES**
Helmet loss and failure role in major and fatal head injuries of USAF ejections
01 p0032 A70-10370
- Fatal ejections in USN, suggesting initiation delay as prime causal factor
07 p1191 A70-19006
- Combat and noncombat ejection/extraion fatalities and major injuries to USAF crewmen
07 p1192 A70-19023
- Pathogenic mechanisms of fatal injuries during supersonic ejection determinable by radiography
09 p1627 A70-23114
- Vertebral injury prediction of seated human subjected to caudocephalad acceleration, suggesting consideration for head and torso forward flexion and external restraints effects
09 p1627 A70-23462
- Multiple emergency noncombat ejections by USAF aircraft pilots, investigating success rates on second ejection relation to injuries on first
13 p2359 A70-29444
- Combat and noncombat ejection/extraion fatalities and major injuries to USAF crewmen
17 p3039 A70-35576
- Long term effects of ejecting from aircraft, discussing disability incidence after more than ten years
17 p3033 A70-35577
- Spinal injury prediction during emergency ejection and crash impact protection research
23 p4153 A70-44489
- EJECTION SEATS**
Aircraft escape/rescue capability /AERCAB/ flying ejection seat design and test programs, noting rotary wing, fixed wing and parawing feasibility
01 p0035 A70-10714
- Aircraft seat ejection systems using SCID /small column insulated delay/ distribution system taking advantage of standard end devices
01 p0035 A70-10718
- Rocket catapult design, development and qualification for Advanced Concept Ejection Seat System /ACES/
06 p0987 A70-17724
- Advanced concept ejection seat /ACES/ system design and performance, considering gyro-controlled vernier rocket motor and electronic time delays
07 p1192 A70-19016
- Flying ejection seat providing capability for leaving hostile area before vertical descent by parachute, using Princeton Sailing and bypass fanjet
07 p1192 A70-19020
- Search and rescue /SAR/ concepts behind advanced Navy systems, emphasizing flying ejection seat /AERCAB/ for air to air self rescue
07 p1192 A70-19024
- AERCAB /Aircraft Escape/Rescue Capability/ flying ejection seat, considering rotary wings, fixed wings and parawings
21 p3751 A70-41806
- SIIS-3 ejection seat escape system design, considering minimum weight, cost and maximum performance
21 p3751 A70-41808
- Tractor rocket powered escape system of 600 knot extraction capability using drogue parachute and barometric time delay device
21 p3751 A70-41809
- Optimum drogue gun firing angle of stabilization times for MEW /Minimal Envelope and Weight/ ejection seat system, considering zero and high velocities
21 p3751 A70-41810
- Pilot airborne recovery device /PAR/ midair rescue system, discussing buoyancy, midair pickup, seat ejection energy absorber, homing avionics and human factors
21 p3752 A70-41812
- Modularized multiple use SIIS-3 ejection seat escape system, discussing weight, envelope and low cost
23 p4143 A70-44499
- EJECTION TRAINING**
Emergency ejection from lunar landing training vehicles, describing working sequence and experimental results on astronaut and test pilot
06 p1003 A70-17717
- Training simulation improving ejection decision making in naval aviation
23 p4178 A70-44467
- EJECTORS**
Exhaust gas ejectors for engine cooling, discussing ejector design, flow rates, fuel consumption, etc
06 p1129 A70-17144
- Coaxial fluid streams mixing within finite length tube based on dimensional analysis of aerodynamic noise generation, discussing subsonic and supersonic flows within ejector
13 p2474 A70-29080
- High secondary/primary mass ratio multinozzle jet pump /ejector/ operation feasibility
13 p2342 A70-29890
- Supersonic cylindrical ejectors without induced flow for rocket engine studies
16 p2837 A70-33763
- Underwater recovery requirements for flight data recorders, suggesting compressed air instead of explosive charges for ejection force
18 p3258 A70-36343
- Ejector maximum compression ratio calculation based on inlet nozzle gas flow model
21 p3746 A70-41767
- Two stream ejector type propelling nozzles for supersonic aircraft, investigating various configuration effects over range of secondary/primary air flow ratios
23 p4133 A70-44145
- VTOL aircraft ejector thrust augmentors, discussing configurations in wing root section
23 p4139 A70-44152
- EKKMAN LAYER**
U BOUNDARY LAYER TRANSITION
ELASTIC ANISOTROPY
Elastic interaction energy involved in Ti solution hardening by oxygen determined using anisotropic elasticity, presenting atomistic calculations and chemical bonds breaking role
05 p0862 A70-15906
- Stress-strain relations for elastic anisotropic crystal lattice systems derived in terms of orientation vectors and scalar moduli
05 p0932 A70-16135
- Crystal structure imperfections and elastic anisotropy of crystallites in condensed Ni films by X ray analysis
07 p1309 A70-19636
- Strength conditions for orthotropic Hooke law materials with complex elasticity, giving elastic potential boundary values in tensor form
12 p2325 A70-27560
- Nonlinearly elastic bodies under subcritical strain, analyzing boundary value problems for three dimensional stability
15 p2818 A70-32179
- Anisotropic elastic solids linear dynamic theory, discussing uniqueness theorem, reciprocal identity and far elastodynamic field quiescence
20 p3718 A70-39231
- ELASTIC BARS**
Elastic bending of pretwisted elliptical bars, showing stiffness response
02 p0387 A70-12216
- Elastoplastic bar stability compressed by tangential force, showing ductility effect on critical parameters, perturbed motion and stability loss process
04 p0767 A70-14484
- Dispersion curves for wave propagation in infinite elastic bars of elliptic cross section obtained by method of collocation
04 p0773 A70-15080
- Kacner method applied to longitudinal vibrations study of nonhomogeneous nonuniform bars, noting applicability to geometrical and elastic properties variations
04 p0779 A70-15702
- Shape optimization of elastic rod compressed by force directed toward point on undeformed rod axis, deriving optimal bending line
05 p0937 A70-16373
- Elastic bars self excited oscillations at audible frequencies, determining natural frequencies from analyzing sound
07 p1401 A70-18847
- Optimizing shape of elastic bar compressed by polar force obtained by determining functional extremum representing volume of bar at constant critical force
09 p1769 A70-22252
- Finite deflections of nonlinearly elastic cantilevered bar
11 p2140 A70-26481
- High velocity center to center collision of two absolutely elastic rods in acoustic medium in terms of Einstein nonclassical mechanics
15 p2775 A70-32890
- Infinite elastic beams system supported on two parameter elastic foundation solved by analogy to single beam lying on one-parameter elastic foundation
17 p3189 A70-35229
- Kinetic instability of elastic cantilever beam under excitation by rotating masses, relating bending and torsional vibrations to masses angular velocity
18 p3334 A70-35960

EJECTION

NT STELLAR MASS EJECTION

One dimensional magnetostrictive bar electromagnetically forced vibration, using Lagrange equations and normal mode analysis

19 p3472 A70-37959

Nonlinear stress-strain model of unloading in symmetric longitudinal impact of two elastic-plastic bars, using numerical method

19 p3541 A70-38046

Elastic beams optimal design for multipurpose loading, considering compliance and minimum cross section constraints

20 p3733 A70-40382

Stress-strain state of finite length elastic beam free of bending moments and coupled to semiinfinite plate

21 p3933 A70-40603

Elastic bar attached to free edge of infinite length cantilever plate, calculating free flexural vibration for comparison with experiment

22 p4114 A70-42648

Heavy homogeneous material free elastic rod dynamic stability under distributed scanning load, investigating plane transverse vibrations by differential equations

22 p4121 A70-43722

ELASTIC BENDING

Elastic bending of thin circular conical shell subject to arbitrary variation of edge loads

01 p0209 A70-11385

Attachment loads and beam bending moments design curves for linear and right angle fittings on honeycomb inserts to determine internal loading

02 p0386 A70-11949

Elastic bending of pretwisted elliptical bars, showing stiffness response

02 p0387 A70-12216

Bending strength analysis for high strength beam with thin and long fibers embedded in matrix of viscoelastic material noting maximum stress

03 p0584 A70-12934

Linear nonaxisymmetric bending of infinite plate coupled to elastic half space under concentrated loads using double Fourier transforms

04 p0766 A70-14480

Fiberglass reinforced rectilinear plastic plates bending under various edge loads, noting shear flexibility

05 p0934 A70-16220

Shape optimization of elastic rod compressed by force directed toward point on undeformed rod axis, deriving optimal bending line

05 p0937 A70-16373

Electric network models of nonhomogeneous differential equations applied to elastic beam and thin plate bending and displacement equations

06 p1094 A70-17927

Bending stress concentrations in elastic square plate with central hole under uniform load, using finite element solutions of modified Rayleigh-Ritz method

06 p1168 A70-17940

Effect of uniformly distributed circular holes in infinite double row on stress distribution in transversely bent strip, based on Kirchhoff bending theory

07 p1407 A70-19385

Stressed state of plate with reinforced circular hole under tension and bending using Airy stress functions

07 p1407 A70-19540

Nonuniqueness theorems for von Karman equations governing thin flat elastic plate deflections clamped at edges and subjected to normal and edge loading

09 p1768 A70-22063

Constant cross section beam bending and torsion with allowance for moment stresses, deriving differential equations for displacement functions

09 p1773 A70-22538

Transverse Dember effect in elastically bent Ge single crystal illuminated by light beam, considering EMF distribution and photocell application

09 p1740 A70-23191

Finite deflections of nonlinearly elastic cantilevered bar

11 p2140 A70-26481

Finite element solution procedures for inextensible beams elastica problem, using galerkin method for element stiffness matrices

11 p2143 A70-26640

Residual stress determination in flat strip elastoplastically deformed by finite bending

13 p2508 A70-28485

Elastic bending of perforated inhomogeneous plane with circular holes or inclusions

18 p3340 A70-36579

Elastoplastic flexure and critical loading of isotropic rectangular plates of constant and variable thickness, using Lagrange principle with numerical integration

22 p4115 A70-42810

Symmetrical bending of isotropic elastic half-strip with free longitudinal edges and end displacements, indicating use for plate and shell theory

22 p4118 A70-43568

Soviet bibliography on flexible plates covering elastic bending, elastoplastic state under transverse load and bending beyond elastic limit

22 p4119 A70-43710

ELASTIC BODIES

Book on nonlinear stress waves propagation in elastic solids covering adiabatic shocks, isentropic

plane waves, Lagrange equation, spherical waves, heat conduction effect, etc

01 p0202 A70-10966

Nonlinear vibrations in mechanical systems of elastic components having equivalent circuits represented by finite number of discrete masses interconnected by weightless infinite rod

01 p0143 A70-11027

Stresses in plane elastic bodies analyzed by generalizing biharmonic stress function equation in polar coordinates, assuming constant Poisson ratio and nonhomogeneity

01 p0206 A70-11152

Equations of motion, conservation of mass, momentum and energy for elastic bodies with lattice-type surface defects

01 p0209 A70-11400

Optimal dynamic design of system consisting of elastic cantilever rod with two concentrated masses subjected to harmonic vibrations under force at free end

02 p0384 A70-11739

Aerodynamic load distribution due to wind action on elastic structures, calculating various ratios between wind and critical divergence velocity

02 p0385 A70-11913

Viscoelastic boundary value problems involving time dependent boundary regions reduced to elastic problems, starting with aging viscoelastic body

02 p0388 A70-12269

Singular perturbation problem solution asymptotic expansions applied to linearized theory of elasticity equilibrium problem with stress couples

02 p0389 A70-12685

Integral equation solution in viscoelasticity theory based on creep tests with polymer containing elastic inclusion, improving convergence of approximations method

02 p0390 A70-12801

Mixed boundary value problem for viscoelastic body with constant Poisson ratio solved by variables separation method, proving convergence

02 p0390 A70-12802

Elastoplastic bodies stability under compression, using theory of small elastoplastic deformations and linearized equations of nonlinear elasticity theory

03 p0591 A70-13440

Natural oscillation frequencies lower bounds of orthotropic plates determined as coupled elastic systems

03 p0592 A70-13451

Energy requirement for nonconservative elastic system unperturbed state stability, using direct Liapunov method

03 p0594 A70-13502

Axisymmetric problem analysis for cylindrically anisotropic elastic bodies with restricted orthotropy based on Love-Lekhnitsky stress function generalization

03 p0601 A70-14327

Nonlinearity sources in elastic structures under large displacements, developing general matrix formulation

04 p0768 A70-14748

Nonlinear connected oscillations of vibrator and rigid bodies, analyzing plane-parallel and spatial motions, including elastic beams self excited oscillations

04 p0720 A70-15446

Forced torsional vibration of elastic stratum produced by rigid circular disk approximated by Fredholm equations

04 p0777 A70-15497

Plane Lamb problem in semiinfinite micropolar elastic body solved by transformation to one dimensional wave propagation problem in elastic half space

05 p0925 A70-15785

Surface wave spectrum and propagation in non-homogeneous bounded elastic solid, considering existence and eigenvalues approximation

05 p0925 A70-15789

Three dimensional analysis of nonhomogeneous elastic solids based on finite element method and equilibrium equations, discussing iterative solution

05 p0926 A70-15915

Nonsimple dynamic model of regular system of interacting deformable bodies, deriving motion equations for nonlocal and local model

05 p0928 A70-16023

Stress distributions in infinite elastic solids for shear loadings prescribed over coplanar circular regions, solving integral equations iteratively for coplanar penny-shaped cracks

05 p0928 A70-16057

Spread criterion and stress distribution near penny shaped crack in elastic solid under axisymmetric body forces distribution

05 p0930 A70-16079

Thermodynamics of elastic continuum with microstructure, modifying second law to include microtemperatures

05 p0930 A70-16083

Stress distribution in vicinity of stress-free Griffith crack in elastic solid acted upon by symmetric distribution of body forces

05 p0930 A70-16084

Plane circular crack in homogeneous and isotropic elastic body under uniform uniaxial tension using linearized couple-stress theory

05 p0931 A70-16089

Adhesive or frictionless compression /or extension/ under axial load of elastic rectangle between two identical elastic half spaces in condition of plane strain

05 p0931 A70-16132

Static deformation fields producible in isotropic homogeneous incompressible elastic body with uniform transverse stretch

05 p0931 A70-16134

Linear and nonlinear inelastic spherical inclusion in elastic and viscoelastic isotropic matrix with constant strain or stress fields at infinity

05 p0932 A70-16171

Mixed boundary value problems of isotropic elastic half space with ring shaped separation region

05 p0935 A70-16232

Natural frequencies upper and lower bounds of elastic clamped vibrating curved beams /arcs/ determined on basis of differential operator theory

05 p0937 A70-16405

Stress distribution in restrained hyperelastic sphere based on elastomer reinforcement theory by carbon black

05 p0940 A70-16510

Dynamic strength calculation for linear viscoelastic body and elastic-viscous liquid with retardation and relaxation times spectra respectively

05 p0940 A70-16511

Inherent stresses in elastic solid assuming inherent strain as stress source, integrating stress functions

06 p1160 A70-17131

Compatibility conditions of theory of micromorphic elastic solids using Riemann theorem

06 p1164 A70-17530

Dual model for describing brittleness and plasticity of solid elastic deformable body, formulating criteria for passage into inelastic state

06 p1166 A70-17656

Model for impact behavior of elastic body at elastic half space, measuring gas molecule impulse exchange at metal surfaces

06 p1171 A70-18260

Micropolar homogeneous and anisotropic elastic solids linear dynamic theory, deriving reciprocity and variational theorems

06 p1172 A70-18512

Equilibrium cracks in elastic bodies on basis of atomic interaction law, using Griffith problem to estimate bearing capacity

07 p1400 A70-18666

Prestrain effect on waves propagation along slender low density unoriented polyethylene rod, indicating uniform phase velocity change over audio frequency range

07 p1248 A70-19237

Isotropic elastic body occupying half plane assuming elasticity coefficients of certain class

07 p1407 A70-19376

Piecewise linear elastic material with jump-like nonhomogeneity, analyzing stress-strain relation

07 p1407 A70-19384

Three dimensional nonlinear viscoelastic body stability under triaxial compression, extending results obtained for elastic body

07 p1408 A70-19542

Quasi-steady propagation of Prandtl crack in viscoelastic body, noting stress distribution identity for viscoelastic and elastic cases

07 p1414 A70-20181

Point matching technique for plane elastic problems extended to axisymmetrically loaded elastic body of revolution, developing general computer program

07 p1416 A70-20303

Two dimensional wave front shapes induced in finitely strained elastic body by impulsive point body force, discussing normal and double inflection points

08 p1584 A70-20581

Elastic body with incompressible fluid filled cavities, studying motion and stability by deriving motion equations starting from principle of least action

08 p1544 A70-20951

Quadrature solution for elastic sphere deformation by axisymmetric normal loads, writing Green function of boundary value problem in finite form

08 p1585 A70-20956

Elastic systems vibrations calculated with allowance for amplitude and frequency dependent energy dissipation using hysteresis loop contour expression

08 p1585 A70-20978

Optimal control conditions for elastic aircraft motion with delayed wing downwash determined by hyperbolic partial differential equations with delay

08 p1480 A70-21178

Amplitude-frequency characteristics of arbitrary elastic system performing flexural vibrations determined using computer

08 p1588 A70-21184

Thermomechanical coupling effect on stability of elastic continuous systems subjected to nonconservative forces, reducing flutter load by thermal damping

08 p1589 A70-21245

Electromagnetic fields interaction with nonconducting neutral elastic solid, formulating relativistic variational principle for balance laws and constitutive equations

08 p1545 A70-21252

Constitutive inequalities for isotropic elastic solids under finite strain generated by introducing concept of conjugate pairs of stress

08 p1590 A70-21351

Elastic post stability under longitudinal impact on rigid support, considering loading/unloading phases for calculating shock half wave length and critical rate

08 p1591 A70-21443

Astatic equilibrium in Saint Venant principle applied to surface of linear elastic body, discussing stress field produced by boundary loading

08 p1591 A70-21463

Transient waves propagation in homogeneous isotropic linearly elastic half space excited by traveling normal point load on surface, deriving displacements

[ASME PAPER 69-APMW-12] 08 p1592 A70-21468

Semiinfinite elastic strip supporting thin heavy beam using Airy stress function and Laplace transform, with boundary conditions expressed as Fourier series

08 p1594 A70-21768

Matrix theory of elastic locking structures, programming for analysis under given loads and dislocations

09 p1771 A70-22396

Variational principle application to stability in failure mechanics of arbitrary linearly elastic bodies, discussing inertia effect on steady state vibrations of cracked bodies

09 p1771 A70-22465

Boundary problem for displacement equilibrium equations of elastic body using iterative methods, demonstrating convergence of difference equation solution

09 p1771 A70-22467

Optimum control for shock absorber of elastic body solved by graph analytic method

09 p1727 A70-22535

Elastic body equilibrium forms bifurcation solution for uniform strain applied to cylindrical rod and shell under compressive strain

09 p1773 A70-22539

Two dimensional continuum of objectivity and isotropy principles applied to study of elastic tridimensional vault

09 p1777 A70-22899

Temperature fields and stress-strain state in elastic bodies with thin walled cylindrical shell inclusions during uniform heat flow at infinity

09 p1778 A70-23083

Thermal stress state of nonuniformly heated elastic body with bounding surfaces formed by parts of coordinate surfaces

09 p1778 A70-23087

Elastic beam stability, natural frequencies and critical forces under longitudinal impact with nonuniform compressing force

09 p1780 A70-23116

Flat rectangular elastic body stable oscillations with clamped base under compression loads, deriving difference scheme for approximation

09 p1782 A70-23297

Boundary value problem of torsion for equilibrium of elastic body based on moment theory in absence of bulk forces

09 p1782 A70-23381

Numerical solution of three dimensional equation of elastic body equilibrium in displacements, giving convergence rate of iteration processes

09 p1783 A70-23384

Hyperelastic bodies containing finite number of inclusions and defects analyzed by continuous dynamic model

10 p1954 A70-24014

Finite deflections theory applied to elastic-plastic arches, introducing coefficients depending on shape and degree of yielding of cross section

10 p1955 A70-24080

Material elasticity effects on librational motion of arbitrary shaped satellite

10 p1950 A70-24177

Angular motion of deformable earth satellite as solid-elastic system with distributed masses, applying automatic control transfer function

10 p1914 A70-24308

Elastic stress-strain states in spherical reservoir and thick walled tube during nuclear radiation induced phase transformations

10 p1894 A70-24513

Elastic shaft with central unbalanced disk, deriving equation of motion for rotation in flexible bearings

10 p1958 A70-24520

Free vibration analysis of elastic structures using Rayleigh-Ritz method and finite element methods

10 p1961 A70-25055

Contact stresses in elastic half plane with boundary connected to rod and moment applied at arbitrary point

10 p1965 A70-25324

Semiinfinite elastic body with instantaneous heat source on surface, analyzing temperature and thermal stress distributions

11 p2139 A70-26406

Stress concentration around elastic spheroidal inclusions in isotropic elastic body under shear

11 p2140 A70-26483

Circular elastic helix phase velocities determined by internal constraints method, comparing results with other theories

11 p2085 A70-26557

Elastic wedge under spatially uniform but time dependent shear tractions, studying shear stress and transient wave propagation

11 p2142 A70-26629

Elastic system stability with two degrees of freedom under action of retarded follower forces

11 p2142 A70-26631

Lumped linear model parameters determined from dynamic test data on mode shapes and frequencies for approximating distributed elastic structure

12 p2317 A70-27122

Reissner variational theorem applied to stress analysis of vertically accelerated end burning solid propellant grain in studying elastic rocket launch failure

12 p2313 A70-27196

Iteration solution for three dimensional equations of equilibrium of elastic body in boundary displacements, discussing convergence rate and computer applications

12 p2272 A70-27553

Elastic beam vibration under constant amplitude and varying frequency periodic forces during passage through resonance

12 p2326 A70-27798

Free elastic rotating beam with tip masses and inertia, developing solutions for flexible modes and natural frequencies of H-type configuration

12 p2273 A70-27820

Finite element method applications to finite axisymmetric deformations of incompressible elastic solids of revolution

13 p2510 A70-28734

Elastic stability of structural systems with generalized coordinates and independent loading parameters associated with critical point

13 p2511 A70-28739

Oscillatory perturbed motion of elastic body in general relativity space time, discussing energy tensor, unitary speed vector and density

13 p2451 A70-28954

Rigid solid replacement by elastic body in relativistic mechanics

13 p2451 A70-28955

Isotropic elastic three dimensional body steady stressed state under large subcritical triaxial strains described by solving linearized equations

13 p2515 A70-29316

Elastic anisotropic body analysis, formulating boundary value problem solutions

13 p2516 A70-29525

Stress, strain, temperature, electric and magnetic field distributions resulting from magneto-thermoelastic interactions in infinite elastic solid subjected to transient heat source

14 p2661 A70-31229

Stress and deformations three dimensional solution in semiinfinite elastic body with spherical cavity based on Boussinesq stress function

14 p2661 A70-31328

Elastic two cavity hyperboloid of revolution under stress due to rotating rigid stamp, solving torsional problem numerically

15 p2819 A70-32189

Boundary value problem of elastic isotropic material, obtaining pointwise bounds of Cosserat continuum, considering couple stresses and constrained rotation of particles

15 p2821 A70-32340

Elastic micropolar body thermal stresses induced by discontinuous temperature field, using differential equations of thermoelasticity

15 p2822 A70-32353

Deformation formulas for simply connected micropolar isotropic homogeneous centrosymmetric elastic body under external forces and heating

16 p2990 A70-33742

Flight vehicle dynamic response prediction from elastic filler stiffness contained between rigid sphere and ellipsoidal shell

16 p2991 A70-33878

Dynamic response of simply supported elastic bodies due to oscillating point mass executing longitudinal harmonic motion based on linear theory

16 p2993 A70-34092

Safety, microdamages and lifetime of elastic structures under random Poisson pulsed loads

16 p2996 A70-34328

Bond stress distribution in elastic solid with axisymmetrical inclusions under uniform tension, using three function and point matching techniques

17 p3184 A70-34911

Axisymmetric mixed boundary problem for elastic infinite cone, obtaining solution by assuming zero shearing stresses

17 p3192 A70-35698

Three dimensional mixed boundary value problems, obtaining solutions for elastic body differential equilibrium equations

17 p3192 A70-35699

Stress decay rates in Saint Venant boundary region in truncated semiinfinite elastic cone, using Papkovitch-Neuber functions for eigenfunctions formulation

18 p3339 A70-36489

Spinning body with rigid and elastic parts, using Liapunov direct method for attitude stability analysis

18 p3292 A70-36677

Acceleration wave propagation in materially uniform inhomogeneous isotropic elastic bodies, using tensor analysis

19 p3536 A70-37563

Torsional and longitudinal vibrations of cylindrical cylinders of micropolar elastic solids in terms of Laplace and Helmholtz equations solutions

19 p3537 A70-37789

Physically nonlinear elastic solid three dimensional and generalized plane strain problem, discussing application to composite materials

19 p3538 A70-37798

Edge dislocation and uniform and radial fissures in elastic isotropic nonhomogeneous bodies under two dimensional deformation

19 p3540 A70-37956

Continuous one dimensional nonconservative elastic systems under complex forces, examining stability theory

19 p3546 A70-38341

Elastic body with incompressible fluid filled cavities, studying motion and stability by deriving motion equations starting from principle of least action

20 p3672 A70-39376

Quadrature solution for elastic sphere deformation by axisymmetric normal loads, writing Green function of boundary value problem in finite form

20 p3719 A70-39379

Elastic bodies stability criteria, investigating loss under nonconservative forces influence

20 p3722 A70-39785

Elastic bodies static stability theory variational principles, introducing equilibrium equations and boundary conditions of initial state by Lagrange multipliers

20 p3724 A70-39857

Microstresses in plasticity theory, considering continuous elastic body model of crystal with dislocations

20 p3724 A70-39859

Elastic bodies collision, determining temperature field variations and contact pressure

20 p3725 A70-39869

Rotating elastic shafts rectangular shape stability under creep conditions, considering single mass rotor

20 p3727 A70-39883

Linear relations between stress state and Euler strain rate in isotropic elastic bodies during superposition of small deformation on finite strain

20 p3728 A70-39893

Elastic body steady forced oscillations under monoharmonic excitation, investigating hereditary nonlinearity effects on systems dynamic characteristics

20 p3733 A70-40395

Dynamic external boundary value problems for elastic body bounded by spherical surfaces

20 p3734 A70-40433

Elastic deformable satellite motion stability in central Newtonian force field

21 p3927 A70-40827

Linear elastic structure with few degrees of freedom, discussing parameters experimental determination

21 p3935 A70-41409

Anisotropic elastic solid body thermal stresses, investigating static plain strain problem in thermoelastic linear theory

21 p3936 A70-41414

Thermoelasticity theory for elastic material with different moduli in tension and compression, noting heteroresistance

21 p3937 A70-41428

Microlelastic solids theory achieved with application of internal constraints from postulate of principal coincidence

21 p3939 A70-42029

Constitutive equation for homogeneous and isotropic elastic solids

21 p3940 A70-42101

Elastic bodies under motion-dependent loads, examining thermodynamic conditions of equilibrium states stability

22 p4123 A70-42538

Load transfer to elastic fiber in infinite elastic matrix, determining fiber force distribution

22 p4113 A70-42539

Deformations with constant strain invariants for elastic bodies under surface traction

22 p4113 A70-42543

Hyperelastic bodies stability subject to conservative configuration dependent forces, formulating surface potential for hydrostatic loading

22 p4114 A70-42695

- Stability of elastic stretched ring on thin spherical shell under critical loads 23 p4268 A70-44318
- Elastic structure equilibrium state stability, discussing damping and stiffening effects 23 p4275 A70-44941
- Rumanian book on torsion in thin walled elastic structures of various cross sections covering calculation methods for box beams, cylindrical and conical shells, aircraft wings, etc 24 p4418 A70-45147
- Undamped elastic cantilever column with concentrated masses, considering transition from stability to divergence under nonconservative forces 24 p4421 A70-45286
- Natural frequencies of elastic bodies with variable properties, using external forcing function and continued fractions approximation 24 p4422 A70-45295
- Controllable states with prescribed heat flux for incompressible isotropic thermoelastic bodies with temperature dependent response functions 24 p4426 A70-46041
- ELASTIC BUCKLING**
- Buckling of orthotropic sandwich plates derived for sixth order governing differential equation by variational theorem 01 p0204 A70-11139
- Finite element method for postbuckling analysis of thin elastic plates, using iterative method to obtain equilibrium configurations 03 p0583 A70-12917
- Cylindrical shells buckling under biaxial compression and transverse loads, examining critical loads dependence on shell parameters, end conditions and elastic properties 03 p0590 A70-13380
- Visco-elastic column analysis based on mechanical model, investigating relationships between solid viscosities, loading velocities, initial deflections and dynamic buckling loads 03 p0596 A70-14146
- Buckling in one dimensional elastic media, discussing pendulum equations for Jacobi elliptic functions, critical loads determination, Timoshenko energy method, etc 03 p0597 A70-14227
- Elastic postbuckling behavior of axially stiffened and barreled cylindrical shells [ASME PAPER 69-APM-U] 04 p0769 A70-14866
- Continuum, harmonic and finite element perturbation studies of elastica to yield postbuckling path derivatives from nonlinear energy formulation 05 p0927 A70-16011
- Buckling equations for neutral equilibrium of arbitrary elastic shells specialized to uniformly loaded circular cylindrical shell with accuracy 05 p0929 A70-16064
- Closed form solutions describing nonlinear motions of incompressible fluid flowing in thin walled tube buckled by uniform external pressure 05 p0832 A70-16090
- Simply supported skew plates calculated for buckling loads by Rayleigh-Ritz method using double Fourier series 05 p0940 A70-16514
- Static buckling load for beam with pinned ends and Wiegardt-type elastic foundation, considering shear stresses effect 05 p0955 A70-17105
- Static stability criterion applicable to elastoplastic problems with/without nontrivial equilibrium states, noting effect on buckling loads 06 p1167 A70-17900
- Buckling behavior of elliptical cylinders under normal pressure using linear thin shell theory and Galerkin method, compared with test results [AIAA PAPER 70-105] 06 p1169 A70-18038
- Shallow spherical caps elastic buckling under uniform pressure, considering symmetric and asymmetric deformation modes 07 p1405 A70-19252
- Segmented elastic shells of revolution supported by rings, studying buckling and vibration by matrix method 07 p1405 A70-19257
- Elliptical cylinders buckling under normal pressure analyzed on polyvinyl chloride sheet models 07 p1406 A70-19304
- Horizontally curved I beams flanges elastic buckling, determining prebuckling flange stresses in longitudinal and radial directions 07 p1413 A70-20001
- Dynamic buckling of thin circular ring subjected to radially directed impulsive load, investigating in-plane and out-of-plane modes 08 p1596 A70-21978
- Buckling of elastic cylinders with rectangular cut-outs and reinforcements under axial or lateral loading, using modified Newton method [AIAA PAPER 69-92] 09 p1780 A70-23208
- Dynamic postbuckling response of thin elastic circular plates under axisymmetric time dependent radial thrust, discussing response to step loading 10 p1964 A70-25206
- Initial geometric imperfections effect on buckling and postbuckling behavior of laminated composite cylindrical shells under axial compression, considering reinforcing fiber orientations [AIAA PAPER 69-93] 11 p2135 A70-25986
- Elastic stability of discrete conservative structures under combined loads 11 p2142 A70-26636
- Elastic postbuckling and imperfection sensitivity of discrete structural systems using perturbation approach 11 p2143 A70-26668
- Axisymmetric imperfection distributions effect on buckling of circular cylindrical shells under axial compression, constructing test models from photoelastic liquid epoxy 12 p2319 A70-27140
- Axially stiffened and barreled cylindrical shells elastic postbuckling behavior, considering effects of stringer and load eccentricities 12 p2321 A70-27175
- Thin cylindrical shells elastic buckling under uniform axial compression, considering Kirchhoff-Love hypotheses in critical stress determinations 12 p2324 A70-27396
- Classical eigenvalue problem transformation by invariant imbedding into initial value problem suited for numerical integration, noting applications to columns elastic buckling 12 p2261 A70-27424
- Clamped shallow spherical cap elastic buckling and initial postbuckling behavior under uniformly distributed load over circular region centered at apex 12 p2326 A70-27814
- Buckling, postbuckling and limit analysis of symmetric elastic structure subjected to increasing loads 13 p2511 A70-28737
- Reticulated shell structure buckling using approximate equivalent shell and discrete analysis of individual beams 15 p2816 A70-32007
- Cylindrical shells under axial compression, using elastic stability analysis for critical loads prediction 15 p2822 A70-32512
- Monograph on optimal angles and section partition for buckling strength of twisted and displaced bent bars 16 p2988 A70-33300
- Buckling loads and postbuckling behavior of curved panels under axial compression, noting dependence on boundary conditions 17 p3188 A70-35225
- Elastic systems impact buckling approximate solution by finite difference method 18 p3342 A70-36591
- Complete elastic spherical shell axisymmetric buckling mode under pressure 19 p3539 A70-37801
- Frames nonlinear elastic postbuckling behavior, using static perturbation technique 19 p3542 A70-38058
- Overbraced frame loaded at joints, limiting elastic buckling examinations to geometrically perfect structures 20 p3717 A70-38973
- Circular cylindrical shell stability under axial compressive load, analyzing buckling process by high speed photographic recording of photoelastic isoclinic pattern changes 20 p3735 A70-40528
- Variable thickness flexible plates thermoelastic flexure and buckling, obtaining nonlinear differential matrix equations by difference-differential method 22 p4115 A70-42811
- Postbuckling of wire restrained elastic cantilever column with imperfection sensitivity 22 p4116 A70-43204
- ELASTIC COLLISIONS**
- U ELASTIC SCATTERING**
- ELASTIC CONSTANTS**
- U ELASTIC PROPERTIES**
- ELASTIC CYLINDERS**
- Hydrodynamic and elasticity equations for squeeze films between elastic cylinders in normal approach reduced to integral equation [ASME PAPER 69-LUB-13] 01 p0102 A70-10392
- Flexural wave propagation in infinitely long circular bimaterial cylinders based on equations of linear elasticity, noting dispersion characteristics different from homogeneous cylinders 01 p0208 A70-11188
- Laplace transform of axial stress resultant in impacting semiinfinite elastic cylindrical membrane as exponential function involving wave propagation speed, applying continued fractions [ASME PAPER 69-APM-K] 04 p0769 A70-14859
- Axial point force stresses in infinite elastic cylinder determined by superposition of Love solution and normal and shearing tractions 05 p0930 A70-16081
- Axial compression of elastic circular cylinder in contact with identical elastic half spaces, determining interfacial surface stresses for frictionless and adhesive contacts 05 p0930 A70-16082
- Rayleigh and Lamb waves propagating on solid and hollow elastic cylinders immersed in water, noting correspondence to symmetric and antisymmetric vibrations in shell 05 p0938 A70-16410
- Stress concentration in long thick cylindrical tube under diametrically opposite normal loads using elasticity theory 05 p0939 A70-16505
- Disturbances in infinite aeolotropic inhomogeneous medium due to transient forces and twists on elastic cylindrical source surface 07 p1407 A70-19382
- Stress concentration in plate with hole reinforced by elastic cylinder described by equations of three dimensional elasticity theory 09 p1784 A70-23592
- Axisymmetric elasticity theory problem solution for hollow finite cylinder with symmetrical end loading, employing stress function 11 p2128 A70-25388
- Longitudinal vibrations of circular elastic homogeneous cylinders with end restraints 12 p2321 A70-27152
- Flexural vibrations of homogeneous elastic circular cylinder supported at both ends, imposing zero stress conditions on skirt 12 p2321 A70-27154
- Isotropic slab with implanted elastic circular disk, analyzing stress-strain state due to torsional and bending moments 15 p2824 A70-32895
- Internal pressure maximization for compound cylinders in elastic condition using accelerated direct search technique 16 p2987 A70-32919
- Asymptotic analysis of wave propagation modes in circular solid elastic cylinder, obtaining displacement components and frequencies as dimensionless wave number power series 16 p2993 A70-34085
- Plane strain vibrations of two layered elastic cylinders, analyzing results for lobar mode numbers 2, 3 and 4 16 p2994 A70-34096
- Cracks and tensile failure of interface bonds in elastic composite hollow cylinder, deriving wave front propagation equations 18 p3283 A70-36388
- Solid or hollow anisotropic elastic cylinders rotating with variable angular velocity, determining dynamic response by Hankel and Laplace transforms 18 p3338 A70-36433
- Nonhomogeneous elastic cylinder under internal pressure with modulus in terms of Fermi-Dirac distribution function series, discussing fibers rigidity and modulus change 20 p3731 A70-40052
- Maxwellian fluid oscillating flow in thin walled elastic circular tube as function of tube dimensions, elastic properties, oscillation frequency, etc 21 p3810 A70-41963
- Isotropic homogeneous elastic cylindrical rods, investigating nonlinear longitudinal dispersive waves corresponding to water wave theory analogs 22 p4115 A70-42952
- ELASTIC DAMPING**
- Vibration damping by sandwich structure consisting of viscoelastic layer between two high Youngs modulus metal sheets 07 p1401 A70-18845
- Elastic oscillations amplitude-dependent damping during phase transformations in two phase systems 08 p1556 A70-21211
- Forced vibrations amplitude of rotor mounted on elastically damping supports 08 p1588 A70-21181
- Dissipative heating effects on loss factor of viscoelastically damped beam, discussing stiffness effects [ASME PAPER 69-VIBR-37] 08 p1592 A70-21478
- Temperature effect on plate damping by constrained viscoelastic layers, emphasizing transition and operating temperature compatibility 10 p1962 A70-25063
- Metal plates vibration under viscoelastic damping layers using electromagnetic transducer and impact excitation 11 p2145 A70-26702
- Vibration control by alternate layers of high damping viscoelastic material, discussing damping and loss factors, beams design and attachment 13 p2513 A70-29079
- Damped vibrations of single-mass elastic systems, determining E function singularity effect on dynamic characteristics 18 p3341 A70-36587
- Constrained viscoelastic layer optimal length for vibration damping of metallic structures 19 p3536 A70-37696
- External and material damped three dimensional rotating elastic shaft-disk system, using energy technique and nonlinear model 19 p3542 A70-38062

Hot gas pipe thermoelastic reduction factors, determining elastic support, material and dimensions 20 p3720 A70-39624

ELASTIC DEFORMATION

NT ELASTIC BENDING
NT ELASTIC BUCKLING

Nonlinear stress relation in elastic media incompatible deformations, eliminating elastic distortions for known temperature distribution and thermal distortion 01 p2021 A70-10890

Elastic curve deformation of rod in equilibrium under end loads, using equations analogous to Kharlamov kinematic equations and Chaplygin solution 01 p0094 A70-11440

Kirchhoff kinematic analogy applied to solution of gyrostat motion, noting elastic rod deformation under torsion, using Kharlamov equations 01 p0094 A70-11441

Linear theory of second grade elastic materials for small deformations, discussing special case of couple stress 02 p0387 A70-11995

Lubrication problem for centrally pivoted tilting-pad sector thrust bearings with temperature and elasticity effects, noting iterative solution for coupled equations [ASME PAPER 68-LUB-4] 02 p0307 A70-12166

Elastic deformation of plates with circular holes, determining stress concentration factors for compressible and incompressible materials on digital computer 02 p0390 A70-12810

Buckling equations for thin nonlinearly elastic circular plates with affine initial deformation, considering Lure theory and variational principle for uniform compression load 03 p0589 A70-13336

Flexible cylindrical shell elastoplastic state determined by theory of small elastoplastic deformations, utilizing material incompressibility in plastic state 03 p0593 A70-13500

Deformability calculation of two phase composite solid materials through laminated structural models 03 p0602 A70-14337

Nonlinearity sources in elastic structures under large displacements, developing general matrix formulation 04 p0768 A70-14748

Energy balance relations for elastic material with different elastic moduli in two regions of deformation space 05 p0925 A70-15824

Nonlinear stress-strain laws and yield conditions derived for anisotropic materials on basis of one, two and three invariants 05 p0926 A70-15914

Stress factor-displacement relation in cruciform line crack deformation in elastic medium under arbitrary internal pressure 05 p0926 A70-15976

Dual trigonometric series solution for mixed boundary value problems in two dimensional elasticity 05 p0926 A70-15979

Perturbation effects on elastic material deformation due to nonorthogonality of curves defining curvilinear aeolotropic, with application to circular cylindrical tube 05 p0929 A70-16065

Viscoelastic behavior of styrene-butadiene rubber under finite uniaxial and equal biaxial deformations for nonisothermal case 05 p0929 A70-16068

Static deformation fields producible in isotropic homogeneous incompressible elastic body with uniform transverse stretch 05 p0931 A70-16134

Adhesive rocking and parallel translation contact for circular cylindrical punch indenting elastic half space solved using simultaneous equations 05 p0932 A70-16139

Static and dynamic solutions for isothermal deformation of elastic cylindrical and spherical Cosserat surfaces with holohedral isotropy 05 p0932 A70-16140

Static-geometric analogy of Kirchhoff-Love shell theory applied to Timoshenko complex equations allowing for transverse shear deformation 05 p0934 A70-16219

Displacement determination by orthogonality relationship for dynamic vibrations and stresses in composite elastic plates 05 p0937 A70-16406

Displacements and stresses obtained for elastic half plane with variable Poisson ratio under certain traction boundary conditions, using Fourier transform method 05 p0940 A70-16512

Simply supported beams large deflection analysis in bending under symmetrical pair of forces, based on integration of elastic line differential equation 05 p0941 A70-16521

Asymmetric deformation of shells of revolution with variable thickness solved by asymptotic method in form of higher Fourier series harmonics 05 p0945 A70-16853

Incremental stress distribution near circular crack with internal pressure in neo-Hookean solid under deformation due to triaxial compression, illustrating initial stress effect 05 p0956 A70-17108

Structural elements elastoplastic deformation regularities under repeated loadings, using adaptability theory 06 p1163 A70-17394

Unsteady interaction of compressible fluid and flat circular deforming elastic membrane analyzed by coupled computer program method [AIAA PAPER 70-75] 06 p1039 A70-18082

Elastic membranes deformation compressed by restraints using discrete dynamic programming 07 p1400 A70-18680

Elastic and plastic deformation zones stress-strain state under complex stresses, obtaining relation for stress and strain components 07 p1401 A70-18834

Numerical analysis of axisymmetric elastoplastic deformation of circular plates under combined lateral load and membrane force 07 p1402 A70-18977

Isotropic shells with shear deformations, investigating stress-strain relations in Cosserat continuum applied to plates [DFVLR-SONDDR-23] 07 p1404 A70-19233

Disturbances in infinite aeolotropic inhomogeneous medium due to transient forces and twists on elastic cylindrical source surface 07 p1407 A70-19382

Fundamental integral for small deformations superposed on finite triaxial extension of neo-Hookean elastic material 07 p1409 A70-19563

Abrasive wear of polymers subject to plastic and elastic deformation, considering papers, metal gauze and rough metal surfaces 07 p1296 A70-20003

Axisymmetric elastoplastic deformation theory for elastic cylindrical shell using Saint Venant yield condition, obtaining expressions for strain components, longitudinal deformation, etc 07 p1415 A70-20185

Stress relaxation in polytetrafluoroethylene (PTFE) at various compression deformations and temperatures, considering residual stresses degree 07 p1321 A70-20228

Quadrature solution for elastic sphere deformation by axisymmetric normal loads, writing Green function of boundary value problem in finite form 08 p1585 A70-20956

Rotating parabolic mirror /antenna/ on multisupported suspension analyzed for static rigidity, determining elastic deformation under mirror weight 08 p1586 A70-21055

Rectangular thin plates in small deformation transient creep bending, using finite element method in iterative procedure 08 p1590 A70-21356

Nonorthotropic pinched plates deflections solution, demonstrating asymptotic convergence of small parameter method 09 p1769 A70-22151

Variable modular elasticity theory demonstrated for anisotropic body subjected to plane stressed state, deriving expression for potential energy of deformation 09 p1769 A70-22152

Boundary problem for displacement equilibrium equations of elastic body using iterative methods, demonstrating convergence of difference equation solution 09 p1771 A70-22467

Two dimensional Poiseuille flow stability at deformable walls, assuming pressure proportionality to displacement and rate 09 p1660 A70-22533

Irreversible processes thermodynamics during thermoelastic deformation of solid bodies, deriving thermodynamic potentials, state and coupled heat equations 09 p1777 A70-23077

Multilayer orthotropic conical shell cyclic deformation equation obtained in hypergeometric functions 09 p1777 A70-23079

Thermal stress concentrations at arbitrary holes for nonlinearly elastic materials, developing small deformation theory for two dimensional problem 09 p1779 A70-23093

Numerical solution of three dimensional equation of elastic body equilibrium in displacements, giving convergence rate of iteration processes 09 p1783 A70-23384

Nonlinear plane deformation of elastic medium with cylindrical cavity under uniform axial tension using successive approximations 09 p1784 A70-23591

Asymmetric deformation of spherical shell by solving homogeneous differential equation in spherical functions, assessing approximation error 09 p1786 A70-23719

Shear and cross sectional deformation of prismatic rectilinear rods with unicellular or multicellular thin walls, determining elastic behavior under arbitrary loads 10 p1955 A70-24055

Thin cylindrical shell stresses and displacements enclosed in elastic casing under pressure band using classical theory of Flugge and Love functions 11 p2128 A70-25336

Momentum theory of small elastic-plastic deformations, proving minimum potential energy, simple loading and elastic unloading theorems 11 p2128 A70-25387

Stress concentration in elastoplastic and creep deformations determined by approximate solution 11 p2134 A70-25845

Plane electromagnetic waves propagation in nonabsorbing photoelastic material with finite deformations, formulating theory from Eulerian and Lagrangian point of view 11 p2139 A70-26173

Elastodynamics mixed initial and boundary value problems numerical solution method applied to deformation of elastic solid 11 p2140 A70-26485

Nonlinear dynamic theory describing elastic Cosserat curves plane motion, developing linear displacement equations and dynamic stability concept 11 p2142 A70-26632

Deformation theory for small elastic-plastic strains in orthotropic material and discretization and iterative solution techniques 11 p2144 A70-26684

Large deflection analysis of elastic-plastic shells of revolution by computer program based on nonlinear theory and multisegment method of numerical integration 12 p2320 A70-27147

Transversely isotropic shells stability with respect to subcritical deformation under axial compression using three dimensional linearized equations, determining critical loads 12 p2324 A70-27529

Metallic cylindrical shells design reinforced with elastic glass fiber rings, considering elastoplastic deformation 12 p2324 A70-27530

Maximum impact force and central deflection time function of transversely struck beam, assuming no reflected elastic wave effects on stresses [DFVLR-SONDDR-48] 12 p2325 A70-27619

Residual stress determination in flat strip elastoplastically deformed by finite bending 13 p2508 A70-28485

Radial displacements in cylindrical circular shell by impinging spherical waves propagating in acoustic medium, deriving equations by Fourier and Laplace transforms 13 p2515 A70-29318

Filled elastomers elastic and anelastic behavior, investigating strain dependence 13 p2440 A70-29964

Buckling equations for thin nonlinearly elastic circular plates with affine initial deformation, considering Lure theory and variational principle for uniform compression load 14 p2657 A70-30714

Al alloy welded sheets strength and plasticity under biaxial tension, examining excess elastic energy effects on strain kinetics and rupture 14 p2597 A70-30967

Stress and deformations three dimensional solution in semiinfinite elastic body with spherical cavity based on Boussinesq stress function 14 p2661 A70-31328

Elastic membranes deformation compressed by restraints using discrete dynamic programming 15 p2813 A70-31472

Elastic body bounded by parallel planes, solving three dimensional equilibrium problem by eigenfunction expansion of nonself adjoint differential operator 15 p2814 A70-31593

Elastic half plane with crack perpendicular to free surface and under arbitrary pressure distribution, obtaining exact solution for stress and displacement fields 15 p2767 A70-31854

Mechanical and morphological characteristics of overload and fatigue in dog ulnas, showing elastic and plastic deformation zones 15 p2682 A70-31935

Thin two dimensional shells static linear elastic deformations analysis using difference based variational method 15 p2815 A70-32001

Thin elastic shell deformation, considering random imperfections in regions adjacent to contour 15 p2817 A70-32162

Axisymmetric elastoplastic deformation of compressible plate with arbitrary hardening under uniform load, solving in quadratures 15 p2817 A70-32167

Nonlinearly elastic bodies under subcritical strain, analyzing boundary value problems for three dimensional stability

15 p2818 A70-32179

Elastic equilibrium of unbounded body with central hole and concentric cracks under symmetric load

15 p2819 A70-32188

Elastic and optical properties of polyurethane rubber under large deformation using natural stress concept derived from stress-strain linear relationship [SESA PAPER 1608]

15 p2821 A70-32319

Semiclamped strut supported rectangular plate deflection determined holographically, mechanically and analytically

15 p2740 A70-32331

Transverse vibration of thin circular elastic turbine disk of variable thickness rotating axially at constant angular velocity

16 p2916 A70-32994

Nonlinear elasticity equations in displacements by Green and Hencky deformation tensors, discussing stress-strain of body with spherical cavity

16 p2988 A70-33251

Deformation formulas for simply connected micropolar isotropic homogeneous centrosymmetric elastic body under external forces and heating

16 p2990 A70-33742

Arterial wall nonlinear distensibility effects on blood flow velocity profiles, considering various mathematical and physical artery models

17 p3035 A70-34468

Elastic thin walled toroidal shell under internal pressure, investigating large deformation and stress behavior

17 p3184 A70-34910

Anisotropy and variable thickness effects on elastic stress distribution in rotating disks, discussing limiting cases

17 p3185 A70-34912

Imperfect solid deformation, presenting formalism for elastic theory nonlinear aspects of continuous distributions of dislocations and point defects

17 p3190 A70-35456

Perturbation method for finite elastodynamic deformation of nonlinear systems

17 p3191 A70-35590

Equilibrium theory of finite deformation of elastic solids, discussing applications and approximate solution methods

18 p3335 A70-35975

Elastoplastic deformations during explosive extrusion of pipes of different materials with linear strain hardening law

18 p3335 A70-36132

Spherical shell of variable thickness, calculating stress-strain state around reinforced circular hole during elastoplastic deformation

18 p3336 A70-36138

Forced vibration in Cartesian half space filled with elastic medium, investigating uniqueness conditions

18 p3337 A70-36289

Shell theory for shear deformations in covariant notation involving displacement power series expansion

18 p3337 A70-36371

Thermodynamical modeling by regular systems of deformable bodies bound by hyperelastic medium with internal degrees of freedom, formulating equations of motion

18 p3338 A70-36432

Elastic and plastic cylindrical shells, investigating dynamic buckling under impulsive loads

18 p3338 A70-36436

Axisymmetric structure with elastic contact, analyzing stresses by finite element method with differential displacements

18 p3339 A70-36496

Damped linearly tapered cantilever beam elastically restrained against rotation at wall, analyzing displacement under general initial and distributed load conditions

19 p3539 A70-37802

Composite bodies under plane deformations, determining stress dependence on elastic constants

19 p3455 A70-37952

Edge dislocation and uniform and radial fissures in elastic isotropic nonhomogeneous bodies under two dimensional deformation

19 p3540 A70-37956

Minimum weight thermoelastic design of sandwich beam for given deflection, using potential energy principle

19 p3541 A70-38044

Composite body with free surface under plane deformation, analyzing residual, thermal and dislocation stresses dependence on elastic constants

19 p3544 A70-38332

Quadrature solution for elastic sphere deformation by axisymmetric normal loads, writing Green function of boundary value problem in finite form

20 p3719 A70-39379

Elastoplastic deformation of thin circular plates under uniformly distributed transverse loads, using mixed type variational equation

20 p3721 A70-39776

Soviet papers on mechanics of solid deformed body covering elasticity and plasticity theories, shell stability, eigenvalue problems, etc

20 p3722 A70-39851

Axisymmetric deformation of cylinder based on solution of elasticity theory plane problem for rectangular strip

20 p3724 A70-39858

Anisotropic plasticity yield conditions, analyzing elastic to plastic deformation transition geometry

20 p3727 A70-39889

Linear relations between stress state and Euler strain rate in isotropic elastic bodies during superposition of small deformation on finite strain

20 p3728 A70-39893

Continuum mechanics application to elastic composite materials, investigating plane deformation of reinforced medium

20 p3730 A70-40038

Perforated infinite plate finite elastic deformation under biaxial tension, using successive approximation in connection with complex variable method of plane elasticity

21 p3932 A70-40551

Multilayer three dimensionally woven fiberglass-reinforced materials, measuring strength and deformation under tension, compression, bending, torsion and shear tests

21 p3841 A70-40646

Cantilever bending under gradual contact with cylindrical supporting surface compared with solution by elasticity theory

21 p3934 A70-41251

Elastic-plastic deformation analysis at finite strain by two component thermodynamic model

21 p3937 A70-41431

Elastic stability theory Cosserat surface subjected to conservative nongyroscopic surface and edge loading

21 p3939 A70-42027

Half plane with stress-free surface deformed by protrusions or notches, deriving edge force or screw dislocation by linear elastic analysis

21 p3939 A70-42028

Microelastic solids theory achieved with application of internal constraints from postulate of principal coincidence

21 p3939 A70-42029

Deformations with constant strain invariants for elastic bodies under surface traction

22 p4113 A70-42543

High speed camera rotating mirror dynamic surface deformations, discussing reflected waves, astigmatism, gas turbulence and pressure effects

22 p4033 A70-43043

[SMPTE PREPRINT 34] Elastic bending, vibration and buckling of simply supported thick orthotropic rectangular plates and laminates

22 p4116 A70-43205

Stress fields of screw and edge dislocations in linearly elastic isotropic Cosserat continuum using stress functions

23 p4266 A70-44022

Nonlinear elasticity theory, deriving geometrical relations applicable to small deformation tensor components

23 p4267 A70-44167

Elastic body bounded by parallel planes, solving three dimensional equilibrium problem by eigenfunction expansion of nonself adjoint differential operator

23 p4268 A70-44286

Nonlinear elasticity equations in displacements by Green and Hencky deformation tensors, discussing stress-strain of body with spherical cavity

23 p4268 A70-44287

Linear viscoelastic solid quasi-static deformation, deducing associated minimum principles under assumption of unique solutions existence for boundary value problems

24 p4420 A70-45264

Thick isotropic rectangular laminates free vibration and buckling, applying three dimensional linear small deformation theory of elasticity

24 p4422 A70-45296

Inhomogeneous anisotropic elastic plates large deflection, using asymptotic integration of nonlinear elasticity equations to obtain successive field equations systems

24 p4423 A70-45580

Crystal elastic dislocations general solution, deriving stress function for stress and displacement fields in bipolar coordinates

24 p4426 A70-46018

ELASTIC MEDIA

Nonlinear stress relation in elastic media incompatible deformations, eliminating elastic distortions for known temperature distribution and thermal distortion

01 p0201 A70-10890

Nonlinear stress-strain equations for incompressible hyperelastic media developed for undeformed and deformed continuum states

01 p0201 A70-10892

Elastic support effect on bending of clamped circular, elliptical, rectangular and skewed plates, using variational method and small perturbation technique

01 p0205 A70-11144

Characteristic equations developed for two-spatial dimensional elastic wave propagating in linear elastic, isotropic and homogeneous medium

01 p0208 A70-11185

Linear theory of second grade elastic materials for small deformations, discussing special case of couple stress

02 p0387 A70-11995

Self consistent field method to calculate effective dynamic characteristics of elastic media with filler for plane longitudinal wave propagation

02 p0388 A70-12485

Mixed anisotropic linear elastic solids stability with internal friction due to mechanical interaction, considering asymptotic motion stability

03 p0586 A70-13116

Buckling in one dimensional elastic media, discussing pendulum equations for Jacobi elliptic functions, critical loads determination, Timoshenko energy method, etc

03 p0597 A70-14227

Elastoplastic media revised mathematical model with allowance for cumulative damages effect on elastoplastic property under variable loads

04 p0775 A70-15199

Energy balance relations for elastic material with different elastic moduli in two regions of deformation space

05 p0925 A70-15824

Nonlinear theory of elastic dielectrics with polarization gradients, obtaining jump conditions and field and constitutive equations by variational principle

05 p0882 A70-16092

Constitutive equations for isotropic elastic and thermoelastic materials with microstructure derived using free energy function, giving uniqueness theorems

05 p0932 A70-16136

Time-varying loads effect on linear elastically hereditary media described by generalized fractional-order exponential functions and Rzhantitsyn type viscoelastic kernels

05 p0946 A70-16954

Support moment of beam with ends embedded in elastic medium subject to creep, noting dependence on load

05 p0947 A70-17010

Uniqueness and reciprocity theorems in elastic medium occupying infinite domain extended to electromagnetic wave propagation in plasma

05 p0890 A70-17097

Boundary value problems in nonlocal elasticity, considering two one dimensional media coupling with microstructure by Green function analog

07 p1399 A70-18665

Flexural vibrations of rotor resting on nonlinear elastic bearings under action of exciting forces harmonics using variational method based on Hamilton principle

07 p1403 A70-19112

Fundamental integral for small deformations superposed on finite triaxial extension of neo-Hookean elastic material

07 p1409 A70-19563

Torsion of elastic half space containing circular crack with symmetry axis coinciding with annular stamp rigidly coupled to half space

07 p1414 A70-20183

Integration of Saint Venant equations of deformation continuity for region occupied by elastic medium

08 p1587 A70-21166

Elastic equilibrium of semiinfinite two dimensional medium with Griffith crack under axisymmetric load and free and rigidly clamped edges

08 p1594 A70-21771

Reissner-Sagoci transient mixed boundary value problem concerning displacement of infinite half space of isotropic elastic material, deriving surface displacement and reactive torque

09 p1784 A70-23571

Cylindrically isotropic elastic medium statics, deriving general solutions to Lamé equations

09 p1784 A70-23593

Mixed thermoelastic problem in elastic layer with arbitrarily prescribed temperature in upper free surface

10 p1954 A70-23878

Wave propagation in bounded homogeneous elastic anisotropic media solved as sum of eigenvalue and static problems without transform calculus

10 p1915 A70-24058

Longitudinal shock wave oblique reflection in nonlinear harmonic elastic material in terms of wave propagation

10 p1956 A70-24097

Interfacial tractions between matrix and fiber in elastic composite materials reinforced with elastic fibers

12 p2322 A70-27230

Stress concentration coefficients in multiply connected plates and bulky elements made of nonlinearly elastic materials

12 p2323 A70-27336

Spherically cut space elastic properties, determining normal and tangential stresses for uniform axisymmetric edge loading

12 p2328 A70-28200

Uniqueness theorem in Mindlin theory of elastic materials with microstructure

13 p2508 A70-28488

Supersonic rigid cone motion in elastic medium, obtaining partial solutions to motion equation yielding boundary problem solution

13 p2341 A70-29508

Time harmonic waves propagation in elastic half-space with submerged cylindrical cavity, assuming linear plane strain conditions

13 p2518 A70-30010

Unloading shock waves propagation in elastoplastic medium, investigating strain hardening effect on shock strength decay, residual strains and radial stresses

15 p2815 A70-32002

Circular cylindrical cavity in elastic space, calculating stresses due to incident plane harmonic compression wave

15 p2819 A70-32204

Induced strain plane state in elastic micropolar medium by temperature effect, discussing thermoelastic problem stress functions

15 p2821 A70-32341

Riemann-Hilbert problem for discontinuous coefficient solving mixed boundary value problems in infinite elastic strip, discussing shear stress along whole boundary

15 p2822 A70-32355

Stress wave propagation in solid infinite elastic medium and laminated materials

15 p2823 A70-32784

Stress wave generation in elastic temperature-dependent absorbing solids by impulsive EM radiation

17 p3185 A70-34967

Parallel edge dislocations in elastically isotropic crystals, discussing climb and glide forces

17 p3126 A70-35454

Stationarity of complementary energy in nonlinear elasticity theory, using Piola stress tensor representation for isotropic elastic media

17 p3192 A70-35692

Plane strain and stress produced in elastic micropolar medium by action of temperature

18 p3338 A70-36429

Symmetric functions of second rank tensors with syngonies in elastic anisotropic media

18 p3340 A70-36576

Elastic materials consisting of particles with rotary inertia, long range force and dipole interactions, deriving constitutive relations

19 p3538 A70-37794

Wave propagation in linear elastic surfaces, calculating wave speeds, shapes and strength decay

19 p3473 A70-38943

Sound velocity in isotropic nonlinear elastic Cosserat continuum with constrained particle rotation, analyzing uniaxial and hydrostatic compression

20 p3734 A70-40434

Brittle elastic material with wedge shaped void, calculating shear stresses during crack propagation generated by horizontally polarized shear wave

21 p3932 A70-40547

External field perturbations by local inhomogeneities in elastic medium, deriving expressions for interaction energy and forces between defects

21 p3933 A70-40604

Sommerfeld type radiation conditions for linear homogeneous isotropic elastic materials with microstructure, discussing field equations, displacement and rotation vector and scalar conditions

21 p3936 A70-41417

Circular cylindrical hole in uniaxial tension field of elastic media, solving plane strain problem for stress concentration factors

21 p3941 A70-42107

Rigid circular cylindrical inclusion elastic bedding dynamic loading, calculating stresses in interface

22 p4112 A70-42345

Finite difference method for stress wave propagation and multiple reflection in elastic bar with discontinuities

22 p4115 A70-42744

Arbitrary form acceleration waves growth equation in deformed hyperelastic material, discussing growth and decay criteria

22 p4115 A70-42940

Spherically cut space elastic properties, determining normal and tangential stresses for uniform axisymmetric edge loading

22 p4117 A70-43324

Spatial problem of elastic spherical transversal isotropic medium solved by reducing Lamé equations

22 p4118 A70-43481

Three dimensional elasticity for figures close to ellipsoid of revolution with displacements on boundary

23 p4266 A70-43988

Finite amplitude longitudinal shock waves in nonlinear hyperelastic materials, deriving solutions for various shock types in accordance with second law of thermodynamics and Lax stability criterion

24 p4420 A70-45265

Polar elastic materials constitutive relations for thermoelastic couple stresses by general theory of in-

compatible strains, obtaining linearization for isotropic materials

24 p4428 A70-45578

Two incompressible isotropic nonlinear elastic solids mixture, investigating entropy production inequality effects

24 p4425 A70-45991

Elastic-viscoplastic bar quasi-static torsion problem, using approximate method for time dependent torsion function

24 p4425 A70-45993

Semiinfinite elastic medium under variable dynamic pressure on boundary, investigating couple stresses effect on stress distribution

24 p4426 A70-46006

ELASTIC MODULUS U MODULUS OF ELASTICITY

ELASTIC PLATES

Out-of-plane displacement restraint at thin photoelastic plates bonded to rigid boundaries of inclusions inducing transverse stress components causing plane stress solution deviation

01 p0202 A70-11059

Flexural and longitudinal waves propagation in infinite elastic plate, using solutions to approximate nonlinear equations of plate motion

01 p0213 A70-11634

Finite element method for postbuckling analysis of thin elastic plates, using iterative method to obtain equilibrium configurations

03 p0583 A70-12917

Momentless design of composite plate and shell structures with variable elastic constants based on loading and shape requirements

03 p0586 A70-13112

Plane elasticity solution for differential expansion stresses on interface of laminated elastic rectangular strip

03 p0586 A70-13114

Thin elastic cylindrical panel motion induced by plane acoustic shock wave analyzed by integrating nonlinear motion equations using finite difference scheme

03 p0524 A70-13377

Elliptic system of twelfth order equations describing elastic equilibrium of plate with kinematic functions analyzed by integration procedure

03 p0600 A70-14306

Thin elastic plate oscillations plane two dimensional steady state problem assuming constant thickness, finite dimension and moving load

04 p0766 A70-14420

R function method for solving plate bending problem by satisfying differential equations coordinates

04 p0767 A70-14489

Transient processes of strain wave propagation in elastic shells and plates under time varying loads

04 p0773 A70-15010

Steady temperature field and stressed state of elastic plane containing heat resistant arc shaped cracks produced by uniform thermal flux

05 p0935 A70-16231

Displacement determination by orthogonality relationship for dynamic vibrations and stresses in composite elastic plates

05 p0937 A70-16406

Unsteady interaction of compressible fluid and flat circular deforming elastic membrane analyzed by coupled computer program method

[AIAA PAPER 70-75]

06 p1039 A70-18082

Contact stresses between elastic half planes and elastic cover plates determined by integrodifferential equation with Hilbert kernel

07 p1400 A70-18667

Boundary value problems solution for infinite elastic isotropic plane weakened by arbitrarily distributed circular holes based on using series in Taylor functions

07 p1408 A70-19549

Plane anisotropic elastic bodies stress determination using Somigliana type integral formula to relate elastic displacement field to boundary traction and displacement vectors

07 p1412 A70-19953

Shear wave and plate velocity expressions derived for orthotropic elastic plate with shear coupling, considering propagation direction

07 p1412 A70-19961

Stress-strain state of flexible circular plates as function of thickness distribution using finite difference theory

08 p1583 A70-20529

Stress concentration in elastic plate reinforced at edge by straight rib analyzed in finite form by Cauchy integrals and Fourier transforms

08 p1594 A70-21635

Limiting equilibrium of unbounded cracked elastic plate with circular hole, studying crack propagation under compression

09 p1769 A70-22121

Transition of stress distribution on collision surface of semiinfinite elastic plane with rigid beam, using Fredholm integral equation

10 p1954 A70-23950

Stress intensity and strain energy of pressurized line crack in cross form in thin elastic plate solved by Wiener-Hopf technique

10 p1956 A70-24192

Energy dissipation in free oscillations of multilayer shells consisting of alternating rigid elastic layers and soft fillers, deriving equations of motion

10 p1956 A70-24249

Thin elastic plates and shells parametric resonance amplitudes by solving nonlinear differential equations, considering dynamic stability

11 p2129 A70-25523

Plane tension in elastic infinite strip covered by elastic plate, considering applicability to strain measurement errors calculation

11 p2129 A70-25565

Elastic bending of clamped and supported elliptic and parabolic plates under external pressure investigated by lines of equal deflection

11 p2133 A70-25839

Vibration of thin elastic plates under random driving forces simulated digitally, using power residue method for pseudorandom number generation

11 p2139 A70-26277

Stress tensor and displacement vector in thin elastic shells/plates derived from three dimensional nonlinear equations using asymptotic integration

11 p2142 A70-26634

Extensional waves asymptotic nature and stress distributions in infinite elastic plate of finite thickness under axisymmetric and in-plate disturbances using perturbation

11 p2145 A70-26696

Kane-Mindlin equations and frequency spectra determined for free extensional vibrations in isotropic elastic plate strips

11 p2146 A70-26703

Anisotropy effect on stress distribution at crack apex in elastic plate

12 p2329 A70-28322

Stress analysis of infinite elastic plate containing elastic rectangular inclusion subjected to uniform stress field

13 p2508 A70-28486

Elastic isotropic circular perforated plate stress-strain state, proving quasi-regularity of infinite linear algebraic equations

13 p2515 A70-29317

Plane stress state equations for micropolar elastic plates using complex potentials

13 p2517 A70-29629

Elastic waves propagation in finite thickness elastic plate under transient load, assuming material behavior in conformity with nonlinear Hooke's law

15 p2814 A70-31544

Elastic body bounded by parallel planes, solving three dimensional equilibrium problem by eigenfunction expansion of nonself adjoint differential operator

15 p2814 A70-31593

Magnetic field effect on critical flutter speed and frequency of elastic plate in ionized gas flow, deriving dispersion equation

15 p2818 A70-32173

Infinite elastic plate with beam reinforced circular insert, using classical plate theory and Euler-Bernoulli hypothesis for beams

16 p2990 A70-33679

Wave propagation in infinite elastic plate in contact with inviscid incompressible liquid layer, deriving dispersion relation

16 p2993 A70-34094

Transversely isotropic elastic plates vibrations without initial specification of field variables spatial dependence on thickness coordinate by two dimensional asymptotic theory

16 p2994 A70-34232

Elastic plate vibration with damping under random load, calculating linear response by harmonic analysis

18 p3334 A70-35958

Elastic layer with circular cylindrical cavity under axial tension /Kirsch problem/, determining stress concentration from boundary value problem

18 p3335 A70-36130

Plane nonconducting elastic plate with one side impinged upon by supersonic conducting gas flow, determining magnetic field effect on flutter vibrations

18 p3336 A70-36135

Nonlinearly elastic plate with hole of general shape, determining stress concentration

18 p3336 A70-36139

Optimal design of elastic sandwich, solid beam and plate structures under dynamic harmonically varying loads

18 p3336 A70-36220

Curvilinear crack propagation in elastic plane under balanced loads, using singular integral equations

18 p3341 A70-36584

Infinite elastic plates traveling wave flutter in compressible flow, investigating viscous damping effects on critical flow velocity

18 p3343 A70-36701

Deflection behavior of uniformly loaded elliptical elastic plates on elastic foundation, using small parameter perturbation technique

18 p3343 A70-36713

Thickness determination of external elastic plates in freely supported three layer structures of uniform strength under perpendicular loads

18 p3343 A70-36717

Stress concentrations in edge-bonded elastic quarter planes with normal and shear loading at boundary

19 p3535 A70-37384

Nodal patterns on thin elastic circular plate vibrating in flexure, considering natural and compounded modes

19 p3543 A70-38245

Elastic panel nonlinear free vibrations, analyzing small amplitude phenomena

20 p3672 A70-39493

Infinite elastic plate with pair of insulated unequal circular holes, calculating thermal stresses

20 p3720 A70-39672

Anticlastic bending analysis of long narrow plates oscillations and stability based on elastic plates nonlinear theory

20 p3721 A70-39779

Compressive force on elastic plate of arbitrary shape related to number of equilibrium forms, using Karman equations

20 p3724 A70-39861

Thin plane bars elasticity theory, constructing integrals of equations by asymptotic series expansion

20 p3726 A70-39881

Elastic and viscoelastic plates, calculating stress concentration and separation of embedded smooth circular inclusion under uniaxial tension

21 p3932 A70-40548

Elastic plate response to boundary layer pressure fluctuations, estimating vibration modes dependence on fluctuation convection velocity and response magnification as function of flow direction

22 p4007 A70-42283

Elastic plate uniform extension with rectangular crack by three dimensional bending theory, using variational principle

22 p4115 A70-42941

Elastic plane equilibrium with thin walled flexible rectangular finite inclusion under symmetrical concentrated load, including computer calculated tangential stresses

22 p4118 A70-43569

Soviet bibliography on flexible plates covering elastic bending, elastoplastic state under transverse load and bending beyond elastic limit

22 p4119 A70-43710

Flexural vibrations of clamped circular plate with nonlinear elasticity for small strains and displacements, using variational principle

22 p4120 A70-43719

Rigid and elastic rectangular plates vibration under uniformly distributed dynamic load, investigating bending behavior by Galerkin method

23 p4268 A70-44170

Elastic body bounded by parallel planes, solving three dimensional equilibrium problem by eigenfunction expansion of nonself adjoint differential operator

23 p4268 A70-44286

Elastic orthotropic plates vibration analysis by finite strip method via eigenvalue matrix, obtaining natural frequencies and modal vectors by small computer

24 p4423 A70-45579

ELASTIC PROPERTIES

NT AEROELASTICITY
NT AEROTHERMOELASTICITY
NT ANELASTICITY
NT ELASTOPLASTICITY
NT HYDROELASTICITY
NT MAGNETOSTRICTION
NT MODULUS OF ELASTICITY
NT PHOTOELASTICITY
NT PHOTOVISCOELASTICITY
NT PROPORTIONAL LIMIT
NT THERMOELASTICITY
NT THERMOVISCOELASTICITY
NT VISCOELASTICITY

Fourier transform applied to Riemann boundary value solution to biharmonic equation governing elastic theory for half plane with circular protrusion or indentation

01 p0199 A70-10155

Polycrystalline rocks elastic constant and nonelastic behavior, discussing Voigt, Reuss and Hill averaging methods

01 p0071 A70-10446

Elastic properties of thin curved cylindrical panels with constant mechanical properties subjected to thermal expansion and single face pressure

01 p0201 A70-10943

Boundary value problems of elasticity theory in space perforated by cylindrical cavities with parallel axes solved by infinite algebraic equations

01 p0202 A70-11033

Axially compressed cylindrical shells with edge constraints, determining critical load from inelastic behavior considerations

01 p0205 A70-11141

Potential representation of vector fields effecting decoupling of vector wave equation of elasticity for radially heterogeneous isotropic media

01 p0208 A70-11189

Left ventricular muscle time varying elastic properties, using dynamic model and Fourier series representations

01 p0040 A70-11371

Aortic distensibility and instantaneous left ventricular volume estimation in living man based on elastic reservoir theory and circulatory system model

01 p0040 A70-11372

Bauschinger effects in repeated tensile and compressive strains in inelastic media under variable temperatures as function of load vector, using plastic yield

01 p0211 A70-11422

Thin anisotropic elliptical plate elastic equilibrium weakened by hole and under concentrated loads

01 p0211 A70-11445

Stressed state of isotropic nonlinear multiply connected media with large deformations, using nonlinear elasticity theory

01 p0212 A70-11446

Two asymptotic dimensional moment theory of elasticity, analyzing stress concentration at curvilinear holes and fluctuating boundary loads

01 p0212 A70-11563

Error estimates of stress concentration at free hole determined by two dimensional elasticity theory of thick plates

01 p0212 A70-11564

Time independent kernel integral equations in dynamic contact problems of elasticity and mathematical physics

01 p0146 A70-11571

Variational principle for admissible functions particular solution in elasticity theory involving solid bodies with cracks

01 p0212 A70-11608

Elastic couplings applied as sliding contact-free continuous junction between permanently rotating and fixed parts in rotating coil magnetometer

02 p0298 A70-12214

Elasticity theory equilibrium equations derivation using distribution theory

02 p0388 A70-12270

Oxides and silicates universal equations of state based on experimental data including elastic properties, density, mean atomic weight relations and geophysics interpretations

02 p0294 A70-12778

Axisymmetric elasticity theory problem of stressed state of space weakened by concentric circular cracks solved using p-analytic functions to generate boundary value problems

03 p0586 A70-13077

Cauchy integrals extension to axisymmetric elasticity problems, obtaining numerical results for stressed circularly symmetrical state of hollow cylinder under uniform load

03 p0586 A70-13080

Axial and traction loaded boron epoxy laminates tensile and compressive elastic properties and strengths compared from test data including strain gauge measurements

03 p0586 A70-13115

Constitutive equations for orthotropic bilinear elastic materials in plane stress case, discussing unidirectional composites

03 p0587 A70-13127

Rigid and flexible pavements response to jumbo jets load using elastic theory

03 p0462 A70-13175

Elasticity theory contact type problems, proving solutions existence and uniqueness

03 p0589 A70-13346

Spherical shell elasticity having circular hole at apex using asymptotic method, calculating stress concentration at hole

03 p0590 A70-13381

Static contact mixed boundary value problems in elasticity theory, noting limitations

03 p0590 A70-13383

Approximate method of boundary perturbation to solve elasticity and viscoelasticity problems for non-canonical bodies of revolution applied to stress concentration at ellipsoidal cavity

03 p0591 A70-13439

Stress-strain state of body of revolution having transversely isotropic elastic properties, using perturbation technique

03 p0591 A70-13441

Elastic sensor for measuring linear displacements using fine crossed filaments and torsion principle

03 p0485 A70-13482

Variational principles in linear elasticity theory with couple stresses, solving boundary value problems in Mindlin theory with microstructure and first strain gradient theory

03 p0596 A70-13974

Three dimensional elasticity theory of generalized continua developed from atomic lattice theory model, discussing frequency spectra, specific heat and applications to crystal defects

03 p0525 A70-14232

Singular integral equation applied to elasticity theory of composite beam with or without cavity under torsion

04 p0765 A70-14416

Elastic equilibrium of quasi-completely regular rectangular parallelepiped with rigidly clamped lateral faces, obtaining Lamé equations in double Fourier series

04 p0765 A70-14418

HF expansions of harmonic solutions concentrated at waves propagating in inhomogeneous medium to dynamic equations in elasticity theory

04 p0767 A70-14499

Astatic equilibrium loadings in Saint Venant principle for linear elasticity, analyzing physical distinction from self equilibrated loadings to explain smaller long range stresses

[ASME PAPER 69-APM-L]

04 p0769 A70-14860

Spherical shells axisymmetric equilibrium properties under uniformly distributed external compression

04 p0773 A70-15008

Plane static boundary value problems solutions in zero moment elasticity theory, proving solutions existence and uniqueness

04 p0775 A70-15214

Soviet book on three dimensional boundary value problems in mathematical theory of elasticity and thermoelasticity

04 p0777 A70-15474

Shear testing and data reduction based on torsion analysis to obtain elastic shear constants of thin orthotropic Be sheets

04 p0664 A70-15552

Gravity influence on constitutive equations of elasticity for crystals treated as continuous body and particle system, taking into account lattice structure

05 p0925 A70-15869

Stress concentration effects around spherical cavity under uniaxial tension calculated by constitutive equations of micropolar elasticity

05 p0927 A70-15994

Axisymmetric elasticity problem for straight fiber imbedded into infinite matrix, noting homogeneous temperature changes causing residual stresses, tractions at infinity and fiber pulling

05 p0931 A70-16088

Mixed boundary value problems of plane elasticity, solving stress field of central Griffith crack in wedge using singular integral equations

05 p0932 A70-16173

Eigenvalues upper and lower bounds of vibrating anisotropic material with multiple elastic constants, predicting free vibration frequencies by bounding isotropic moduli

05 p0937 A70-16408

Finite element method for large displacement elastic-plastic analysis of plates and shells, using geometric stiffness matrices and stress-strain relationships

05 p0943 A70-16809

X ray elastic constants measured in cementite phase in high carbon tool steel following plastic deformation at tension, noting residual stresses increase and balance

06 p1084 A70-17126

Compatibility conditions of theory of micromorphic elastic solids using Riemann theorem

06 p1164 A70-17530

Turbine machine elements approximation by difference equations of axisymmetrical elasticity theory problem

06 p1167 A70-17663

Thin circular cylindrical shells elastic equilibrium under loads producing deflection, elongation or contraction described by integrating equilibrium equations with constant coefficient

06 p1172 A70-18566

Plane elasticity problem for Cosserat medium rectangular region with parallel boundaries free of force and moment stresses solved by Airy and Mindlin stress functions

07 p1400 A70-18668

Elastic behavior of joint formed by normally intersecting circular cylindrical shells under external bending moment, noting applicability to pipelines and pressure vessels

[ASME PAPER 68-WA/PVP-1]

07 p1400 A70-18710

Soviet monograph on theory and calculations of impact systems covering solid body collisions, elasticity, wave mechanics and nonflat rod applications

07 p1400 A70-18732

Aircraft engine vibrational overload reducible by elastic bearings having controllable elastic characteristics

07 p1364 A70-19113

Critical slope load calculation for circular elastic embedded and supported arcs under radial and variable force

07 p1404 A70-19136

Shell elastic constants for multilayered sandwich cylinders using Donnell approximation

07 p1406 A70-19326

Inelastic behavior of solids strained at high temperature emphasizing hot creep phenomena in aviation materials

07 p1406 A70-19346

Flexural elastic behavior of rectangular plates with boundary restraint acting on same side using finite differences method

07 p1406 A70-19348

Finite element method applied to two dimensional variational first order problems in plane elasticity of triangular or rectangular elements

07 p1409 A70-19562

Toupin and Knowles elasticity theory applied to spatial decay estimate for parabolic heat equation used in diffusive temperature field

07 p1409 A70-19565

Singular part of half plane stress field solution using Cosserat elasticity theory

07 p1409 A70-19570

Rectangular bidirectional composites and sandwich plates three dimensional elasticity solutions

07 p1412 A70-19952

Elastic and optical properties anisotropy in fiberglass reinforced epoxy plates using photoelastic method

07 p1416 A70-20295

Natural oscillations of three dimensional bundle of parallel strapped rods with variable elastic mass parameters determined by Hamilton-Ostrogradskii variational principle

08 p1583 A70-20485

Book on dynamics of mechanisms with elastic connections and impact systems covering differential and finite difference equations, equations of motion, friction effects, etc

08 p1502 A70-20753

Integral equations arising in contact problems of elasticity reduced to infinite linear algebraic equations

08 p1585 A70-20957

Elastic contact between bodies in presence of friction or adhesion by reducing singular integral equations to Fredholm equation

08 p1585 A70-20958

Paired integral equations of elasticity with kernels containing Legendre spherical harmonics, admitting exact solution in quadratures

08 p1544 A70-20960

Half space elasticity problems solved by operator method

08 p1586 A70-21013

Elastic paraboloid of revolution under axisymmetrical and nonaxisymmetrical loads, using Bessel functions of real and imaginary arguments with trigonometric functions

08 p1587 A70-21165

Elastic coatings effect on turbulent friction using turbulence flow theory based on mixing length concept

08 p1483 A70-21227

Polarization-optical studies of large deformations in nonlinear theory of elasticity and plasticity, considering procedures based on photoelastic coatings and transparent models

09 p1768 A70-22120

Flexo-torsional elasticity ellipse determining displacements, hyperstatic reactions and influence lines in beams with straight axis and variable cross section

09 p1771 A70-22398

Elastic solution and finite element method applied to heat conduction and thermal stress in temperature field determination

09 p1774 A70-22587

Elasticity theory two dimensional problem solution for circular segment in polar coordinates, applying Lure symbolic notation and Prokopyov minimum potential energy principle

09 p1782 A70-23291

Vibration decrement of nonlinear elastic system from resonance peak width of displacement amplitude curve of perturbing force

09 p1782 A70-23295

External plane dynamic problems reduction to infinite algebraic equations in elasticity theory for simply connected domains based on Helmholtz equation solution in curvilinear coordinates

09 p1783 A70-23391

Crack widening in infinite plane field with wedge in absence of slip, based on elasticity theory, plotting contact forces and stresses on crack boundary

09 p1785 A70-23624

Elasticity stratification stabilization effect on two layer flows down inclined plane found dependent on time response difference between layers

10 p1863 A70-24009

Shear and cross sectional deformation of prismatic rectilinear rods with unicellular or multicellular thin walls, determining elastic behavior under arbitrary loads

10 p1955 A70-24055

Material elasticity effects on librational motion of arbitrary shaped satellite

10 p1950 A70-24177

Three dimensional elasticity by Ritz method, using coordinate system orthonormalized in energy metric of operator to avoid precision loss

10 p1957 A70-24511

Linearization of elastic forces in vibration system with percussion

10 p1958 A70-24516

Adiabatic elastic stiffness of single crystals of Ni-Co alloys, determining bulk modulus dependence on chemical composition

10 p1904 A70-24699

Complex redundant structures matrix analysis by substructure approach, obtaining elastic properties of system by subdivision and synthesis [SAE PAPER 700217]

11 p2134 A70-25889

Heat resistance and elastic properties of binary Ti-Mo alloys as function of phase structure and chemical composition

11 p2066 A70-25915

Classical and elastically restrained boundary conditions requirements for anisotropic plates Ritz solution

11 p2135 A70-26076

Elastic properties determined for reinforced composite material with hollow spherical inclusions embedded in matrix

11 p2136 A70-26083

Ultrasonic pulse technique for measuring fiber reinforced composites elastic constants

11 p2052 A70-26341

Work and energy theorems in linear elasticity, discussing potential energy, real work, complementary energy and energy coefficients

11 p2142 A70-26625

Equilibrium displacement equations for linear infinitesimal isotropic Cosserat elasticity solved in terms of stress functions

11 p2142 A70-26630

Discrete models for boundary value problems analysis in first strain-gradient elasticity theory, using extended finite element method

11 p2142 A70-26637

Elastic stiffness of unidirectional glass reinforced epoxy fiber composite determined from ultrasonic velocity measurements

11 p2071 A70-26692

Coerciveness / Korn/ inequalities role in boundary value problems for elliptic systems of partial differential equations, noting applications to three dimensional linear elasticity theory

12 p2260 A70-26974

Dispersion strengthened Ni-Cr alloys elastic and plastic properties at room temperature, studying preferred crystallographic orientation effect

12 p2255 A70-27609

Book on three dimensional problems of linear elasticity of homogeneous and isotropic solids, discussing prismatic bodies, bodies of revolution, notch effect, etc

12 p2326 A70-27669

Elastic, piezoelectric and dielectric properties of barium titanate single crystals of laminar domain structure

12 p2288 A70-28329

Monograph on critical speeds of nonzero mass shaft supported at both ends by bearings with nonlinear elastic displacements

13 p2416 A70-28373

Complex potentials used in semicomplex variable method for plane-strain problems in two dimensional linearized elasticity with couple stresses

13 p2508 A70-28494

Ni and Ni alloys elastic properties relationship with ferromagnetic and magnetostriction effects, determining modulus of elasticity for wide temperatures and heat treatment

13 p2432 A70-28760

Hydroelastic oscillations natural frequencies in incompressible and nonviscous liquid in circular cylinder with free surface, demonstrating wall elasticity effects

13 p2512 A70-28832

Linear theory of homogeneous and anisotropic elastic media with microstructure, establishing reciprocity and variational theorems

13 p2512 A70-28951

Dual controlled elastically twisting rotor blade performance during flight with azimuthal and collective variations compared to direct control rotor [AIAA PAPER 70-547]

13 p2345 A70-29012

Elastoplastic continuum under specified rates of body forces, surface tractions and displacements, formulating minimum principle for solving boundary value problem

13 p2513 A70-29154

Elastic constants pressure dependence of cubic crystals in NaCl and spinel structures using homogeneous static deformation method

13 p2396 A70-29172

Unidirectional composite with transversely isotropic fibers, calculating elastic stiffness constants by modified point-matching technique

13 p2515 A70-29466

Laminated composite materials dynamic elastic properties, outlining resonant frequency effect on apparent Young modulus

13 p2515 A70-29467

Variational principles of linear asymmetric elasticity for dynamic problems with initial and boundary conditions, using Laplace transforms

13 p2517 A70-29724

Self similar dynamic problems in two dimensional elasticity theory for slot with point source in boundless body

13 p2517 A70-29763

Torsion of variable diameter rods based on moment theory of elasticity, solving integral equations system

13 p2517 A70-29774

Stress distribution and pressure distending air spaces in lungs, using mechanical pulmonary elasticity model

13 p2356 A70-29945

Filled elastomers elastic and anelastic behavior, investigating strain dependence

13 p2440 A70-29964

Chromium lattice vibrational properties based on fourth-nearest-neighbor tensor force model, obtaining agreement with inelastic neutron diffraction data and elastic constants

14 p2626 A70-30480

Tantalum single crystals elastic constants temperature dependence, considering compressibility and shear properties

14 p2596 A70-30841

Double ended dislocation pileups and elastic cracks at bimaterial interface under screw, edge and shear modes

15 p2756 A70-31561

Elasticity theory in general relativity formulated from classical nonlinear three dimensional theory, discussing thermodynamics and weak field limit

15 p2774 A70-31734

Reinforced shallow shells and plates stability beyond elastic limit, obtaining optimal parameters under compressive loads

15 p2816 A70-32159

Addition theorems for cylindrical functions, discussing applications to shell stress analysis and three dimensional elasticity theory

15 p2819 A70-32187

Tapered cantilever Al plate load characteristics, determining elastic and plastic strain due to regular, reverse and second regular deflection sequence

15 p2821 A70-32307

Elastic and optical properties of polyurethane rubber under large deformation using natural stress concept derived from stress-strain linear relationship [SESA PAPER 1608]

15 p2821 A70-32319

Stability loss of dynamic two dimensional mechanical elastic system with single degree of freedom under trajectory bifurcation

15 p2775 A70-32474

Monograph on temperature dependent material properties effect on elastic stress distribution in thin rotating disks of arbitrary profile

15 p2823 A70-32700

Book on structural mechanics with introduction to elasticity and plasticity

16 p2987 A70-32915

Heating rate effect on Ti-V martensite decomposition, discussing elastic properties effects of partial tempering

16 p2931 A70-33256

Elastic constants for plates of unidirectional fiber reinforced anisotropic composite material determined by ultrasonic wave propagation

16 p2991 A70-33847

Disk forced vibration mounted on rotating shaft with ball bearings, assuming nonlinear elastic characteristic of system

16 p2996 A70-34293

Thermomagnetoelasticity wave equations of heat conduction for thermal and coupled perturbations propagating in isotropic medium at finite velocities

16 p2953 A70-34326

Elastic properties of dislocations in Ti basal, prismatic and pyramidal slip systems, discussing dilatational fields of edge and screw dislocations

17 p3115 A70-34385

Elastic interactions between anisotropic crystal dislocations and twin and grain boundaries in Ti

17 p3115 A70-34386

Strain gage measurements of elastic properties of Ti sheet alloys, computing polycrystalline properties from single crystal values

17 p3121 A70-34433

Three dimensional linear small deformation theory of elasticity solution for free vibration of simply supported homogeneous isotropic thick laminated rectangular plates

17 p3181 A70-34522

Inelastic analysis of unidirectional composite subjected to transverse normal loading, discussing linear response up to elastic limit and subsequent crack propagation and failure

17 p3182 A70-34557

Anisotropic and laminated cylindrical shells geometric design for reduction of elastic stress gradients to predetermined limit

17 p3182 A70-34559

Book on elasticity theory covering end effects, Saint Venant principle, edge and screw dislocations, moire method, thermoelasticity, cavity and inclusion effects, Muskhelishvili methods, etc

17 p3183 A70-34603

Stress concentration around small elastic spherical inhomogeneous inclusion on circular cylinder in torsion

17 p3183 A70-34631

Elastic and equilibrium matrices for semimonocoque membrane /plane stress/ elements using skin and reinforcing member transformations

17 p3185 A70-34921

Second order incompressible elastic torsion problems reduction to two dimensional classical linear elasticity problem without body force

17 p3189 A70-35434

Nonaxisymmetric thermal stress distribution in infinite elastic solid containing external stress-free crack with prescribed heat flux

17 p3196 A70-35437

Isotropic body screw dislocations, using finite elasticity approach

17 p3190 A70-35453

Elastic properties of complex screw dislocation arrays from equations for stress fields of dislocation segments

17 p3190 A70-35455

Elastic crack structure, discussing formalism for force law between faces of brittle and semibrittle fractures

17 p3191 A70-35461

Low temperature effects on Ti alloys welded joints elasticity

17 p3126 A70-35637

Elasticity theory two dimensional contact problems, examining cohesion or friction in contact area

17 p3192 A70-35693

Equilibrium theory of finite deformation of elastic solids, discussing applications and approximate solution methods

18 p3335 A70-35975

Micropolar elasticity theory, discussing difficulties from erroneous thermodynamic inequality

18 p3335 A70-36061

Anisotropic disk compressed by isotropic ring of smaller radius, considering elastic equilibrium

18 p3336 A70-36134

Finite difference theory applied to first boundary value problem of elasticity theory for Lamé equation

18 p3280 A70-36158

Singular integral equations of elasticity theory, formulating boundary value problem for discontinuous plane stresses

18 p3337 A70-36370

Thermodynamics of solids deformation, tracing macroscopic inelastic behavior to deformation induced internal structural changes governed by atomic and molecular processes

18 p3340 A70-36556

Silicon elastic constant measurement by Debye-Sears effect, using He-Ne laser source

18 p3298 A70-36952

Book on crack problems in classical theory of elasticity, emphasizing mathematical aspects

19 p3534 A70-37234

Viscoelastic fluids stratified flow down inclined plane, examining liquids elasticity role in stability

19 p3403 A70-37531

Plane electromagnetic wave diffraction by thin metal gratings, using mathematical method of elasticity theory

19 p3376 A70-37712

Elastic constants of ZnTe and ZnSe single crystals over 77-300 K range, using ultrasonic pulse echo method

19 p3486 A70-37761

Hydrostatic pressure dependences of second order elastic constants of ZnTe and ZnSe at 295 K, using ultrasonic pulse echo method

19 p3486 A70-37762

Single crystalline mercury elastic constants calculated from propagation velocity measurements of polarized sound waves

19 p3486 A70-37770

High current elastic conductors nonlinear mixture theory with inviscid electron gas in elastic continuum under mutual electromagnetic and diffusive forces

19 p3387 A70-37787

Stress wave propagation based on elasticity theory for reentry heat shield composites reinforced with unidirectional high strength high modulus fibers

19 p3537 A70-37788

Linear micropolar elasticity theory of shells and plates, considering transverse shear and normal strains and rotary inertia

19 p3538 A70-37793

Linear micromorphic material constants determination from constituent properties based on microelasticity theory

19 p3538 A70-37795

Infinite linearly elastic solid response with random variations in material elastic properties, obtaining average energy in displacement field by method of moments

19 p3538 A70-37796

Elastic particulate composite solid with microinclusions, deriving dispersion relations governing plane

longitudinal wave propagation modes by analogy with continuum theory

19 p3540 A70-37942

Two dimensional piezoelectric problems of electroelasticity, formulating general solutions in terms of stress and electric potentials using complex variables

19 p3487 A70-37946

Dynamics of composite materials using extensions of continuum theories based on combination of elastic and geometric properties

19 p3455 A70-37950

Composite bodies under plane deformations, determining stress dependence on elastic constants

19 p3455 A70-37952

Mixed boundary value problems approximate solution in linear elasticity by variational method, noting applications to micromechanics

19 p3540 A70-37957

Elastic boundary layers analysis based on strain gradient theory of linear elasticity

19 p3544 A70-38331

Composite body with free surface under plane deformation, analyzing residual, thermal and dislocation stresses dependence on elastic constants

19 p3544 A70-38332

Lumped parameter model for multidimensional solid mechanics problems with inelasticity, discussing stress wave interaction in cylindrical cavity

19 p3458 A70-38357

Stress differential equations of micropolar elasticity, considering mass forces and moments of inertia

19 p3459 A70-38672

Hexagonal crystal dislocations treatment based on anisotropic elasticity theory, obtaining formulas for displacement and stress fields

19 p3454 A70-38954

Cu and Ag low alloying effect on Al single crystals elastic limits and first deformation stages

20 p3644 A70-38960

Integral equations arising in contact problems of elasticity reduced to infinite linear algebraic equations

20 p3719 A70-39380

Elastic contact between bodies in presence of friction or adhesion by reducing singular integral equations to Fredholm equation

20 p3719 A70-39381

Paired integral equations of elasticity with kernels containing Legendre spherical harmonics, admitting exact solution in quadratures

20 p3672 A70-39382

Boundary value problems in dynamic two dimensional elasticity theory for domains bounded by circles and straight lines

20 p3721 A70-39770

Invariant autopilot control system during flight in turbulent atmosphere, allowing for aircraft elastic properties and invariance of coordinates

20 p3561 A70-39845

Elasticity theory boundary value problems reduction to one dimensional integral equations

20 p3724 A70-39853

Elasticity theory equations polynomial solutions for use in boundary value problems

20 p3726 A70-39874

Thin shell theory elastic coupling conditions, discussing stress-strain and edge effect states

20 p3726 A70-39875

Cosserat spectrum elastic theory, considering static problems

20 p3726 A70-39876

Human body elastic properties effects on arterial pressure measurement by sphygmomanometer

20 p3581 A70-39879

Singular points in elasticity theory solved by correct boundary value problem and homogeneous solutions theorem

20 p3728 A70-39894

Composite materials theory to predict macroscopic physical properties prediction, discussing conductivity, dielectric constant, magnetic permittivity, etc

20 p3729 A70-40032

Heterogeneous materials statistical theory, evaluating bounds for effective elastic constants by cell model using variational principles and perturbation solution

20 p3729 A70-40033

Self similar dynamic problems in two dimensional elasticity theory for slot with point source in boundless body

20 p3732 A70-40101

Boundary value problems in dynamic elasticity by perturbation method with displacement components

20 p3732 A70-40111

Elastomechanical system reciprocity relation principles using differential equations for bar with forces in two places

20 p3735 A70-40537

Band structure contributions to elastic shear constants of hexagonal close packed metals, using optimized model potential

21 p3839 A70-40600

Equations of motion of mass points connected by inertialless elastic couplings

21 p3933 A70-40615

Micro-breccia, igneous rocks and lunar fines elastic properties at ambient conditions and as function of pressure, discussing near surface mare region models

21 p3913 A70-41640

Support elasticity role in axisymmetric plates bending, discussing Rayleigh-Ritz solution

21 p3937 A70-41739

Spacecraft parachute stress analysis, using finite elements with nonlinear elastic properties to obtain shape and load distribution

21 p3753 A70-41821

Decelerator fabric elastic constants for structural analyses using generalized Hooke's law

21 p3843 A70-41834

Directional dependence of elastic shear stiffness on cubic axes for Si, Cu and Mo, making polar plots of shear stiffness coefficients

21 p3850 A70-41909

Elastic bounce of body resulting from falling to ground with calf muscles in sustained contraction and without knee bending

21 p3765 A70-42151

Cosserat elasticity constitutive equations, coupling rotation vectors to eliminate stress indeterminacies

21 p3941 A70-42251

Linear elasticity problem approximation by elastic energy expression modification, deriving upper bounds for errors

22 p4113 A70-42537

Natural oscillations of cylindrical shell with elastic filler, using simple load distribution model

22 p4119 A70-43572

Thin metal matrix composite rods elastic properties, examining Al-W system by Young and shear modulus measurements

22 p4061 A70-43687

Boundary value problems of elasticity for layer and strip with arbitrary inhomogeneity along thickness

22 p4120 A70-43712

Isotropic nonlinear elasticity problems of stress concentration near spherical cavity in field of triaxial tension, using small parameter method

22 p4120 A70-43714

Two dimensional shell equations derivation from three dimensional elasticity theory, considering rotationally symmetric bending of shells of revolution

23 p4265 A70-43942

Elasticity theory for circular cylinder weakened by cavities, discussing boundary conditions on butt ends and Galerkin solutions

23 p4265 A70-43983

Dynamic elasticity theory for multiply connected region

23 p4266 A70-43990

Fundamental error in Galerkin method application to bending problem of elastic rods

23 p4268 A70-44172

Heating rate effect on Ti-V martensite decomposition, discussing elastic properties effects of partial tempering

23 p4206 A70-44285

Parachute opening load amplification due to suspension line elasticity, using two-body spring-mass model

23 p4142 A70-44531

Elastic continua structural optimization analysis decisions for maximizing calculation accuracy, insuring efficient complex numerical analyses

23 p4271 A70-44706

Corrugated plates, closed cylinders and developable shells nonlinear elastic analysis, deriving boundary conditions

23 p4275 A70-44913

Hydrogenated Ni elastic limit discontinuity, discussing Portevin-Le Chatelier effect

23 p4208 A70-44921

Rumanian book on spatial problems in elasticity theory covering deformation geometry, temperature effects, elastic parallelepipeds, etc

23 p4275 A70-44999

Numerical solutions of three dimensional static elasticity, using physical analogies

24 p4419 A70-45195

Linear elasticity with constraint couples, establishing existence theorems by variational methods

24 p4420 A70-45267

Eigenvalue problem in elasticity theory, treating nonlinear equations solutions multiplicity by topological methods

24 p4420 A70-45273

Asymptotic properties of integral equations solutions for boundary value problems in theory of elasticity and mathematical physics

24 p4422 A70-45490

Anisotropic bodies elastic properties, obtaining solutions for nonorthotropic beams under randomly distributed normal loads and for various plates and strips

24 p4424 A70-45589

Variational solution of eigenvalues and eigenfunctions of second boundary value problem of elasticity minimizing functional

24 p4424 A70-45629

Chemical composition effects on heat resistance, elastic properties and density of Ti-Ta alloys

24 p4360 A70-45830

Infinite plate perforated with rounded corner square hole under uniform partial loading, examining elasticity with conformal mapping

24 p4427 A70-46367

ELASTIC SCATTERING

Differential elastic and rotational excitation cross sections for electron-hydrogen scattering in close coupling approximation with electron exchange neglected

02 p0342 A70-11880

Differential elastic scattering cross section of Ar nozzle beam in nitrogen considered with rainbow effect in determining intermolecular potential well depth

02 p0344 A70-12722

Rotational compound state resonances in subthreshold atom-diatom scattering determined for lowest state molecular hydrogen and deuterium model systems scattered by Xe

03 p0526 A70-13006

Slow electrons elastic scattering by diatomic hydrogen molecule, analyzing cross sections in two center prolate spheroidal coordinates emphasizing polarization effect

03 p0528 A70-14179

Elastic and inelastic scattering of proton beams from magnesium and silicon isotopes, using optical model

04 p0723 A70-15637

Maxwellian distribution perturbation in chemically reacting gas mixtures with lower inelastic collision frequency than elastic

06 p1110 A70-17761

Gas stream-elastic solid surface scattering characteristics, calculating trajectories, particle flux angular distributions, velocities, transfer coefficients, etc

06 p1111 A70-18265

Electron elastic scattering from surface plane of Au and W fcc lattices using quantum mechanics

07 p1343 A70-20120

Energy dependence of elastic total collision cross section of identical He molecules, using velocity selected primary beams at low target temperature

07 p1345 A70-20137

Atmospheric gases atomic and molecular binary short range repulsive forces, determining interaction potentials from elastic scattering cross sections

07 p1345 A70-20141

Proton-deuteron elastic large angle scattering cross sections, noting backward peak consistent with baryon exchange mechanism with resonance transfer

07 p1345 A70-20198

Multiple scattering of plane time harmonic compressional elastic wave impinged on parallel circular cylindrical inclusions in finite domain, analyzing stress field

08 p1592 A70-21469

Compound state resonance energies and widths in elastic scattering of diatomic molecule at energies below rotational excitation threshold

08 p1548 A70-21523

High energy electrons elastic scattering from 2s-1d shell nuclei based on Dirac equation solution in Glauber approximation

09 p1730 A70-22043

Quantum mechanical inverse problem of elastic scattering theory, discussing Hylleraas solution for determining potential energy function from phase shift

12 p2274 A70-26899

Elastic scattering effect on photoelectron transport and escape in upper sunlit atmosphere

12 p2222 A70-27187

Slow electrons interaction with periodic and non-periodic solid surfaces, investigating elastic scattering

12 p2275 A70-27252

Resonance energies of elastic scattering from one dimensional model potential containing barrier, using stabilization method

13 p2455 A70-29222

Elastic scattering formation and decay of unstable particle gases, discussing density and corrections to chemical and nuclear statistical equilibrium equations

13 p2455 A70-29223

High energy proton-He 3 elastic scattering cross section measurement, comparing result with Glauber model calculation

13 p2456 A70-29459

Quantum mechanical model of electron scattering by homonuclear diatomic molecule at ground state, calculating differential and integral cross sections for elastic scattering

14 p2618 A70-30113

Elastic scattering of electrons by hydrogen as function of vibrational excitation, discussing intensities and cross sections

14 p2618 A70-30114

Measuring instrument for total cross section of proton elastic scattering during sigma R reactions

16 p2908 A70-33210

Li ion elastic scattering by He, calculating ground state interaction potential

16 p2956 A70-34310

Elastic energy transfer cross sections calculation of H-H scattering to estimate neutralized solar wind particles thermalization

18 p3309 A70-36951

Energy and momentum exchange between gases in elastic collisions at different temperatures and velocities

19 p3551 A70-37538

Asymptotic high energy behavior of Feynman integrals in scalar field theory models for elastic scattering

19 p3457 A70-37549

Boltzmann equation for relativistic gas without dissipation, solving for relaxation time and elastic collisions

19 p3403 A70-37586

Elastic bodies collision, determining temperature field variations and contact pressure

20 p3725 A70-39869

Configuration space three body elastic scattering theory for initially free independently moving particles collisions under short range forces

21 p3852 A70-40595

Differential elastic cross sections of 42 MeV alpha particles scattering from He 3, using optical model with spin-orbit potential

22 p4076 A70-42722

Optical solar polarization broadband measurement interpretation with depolarization factor due to elastic collisions or additional source

24 p4414 A70-46172

ELASTIC SHEETS

Plane tension in elastic infinite strip covered by elastic plate, considering applicability to strain measurement errors calculation

11 p2129 A70-25565

Plane waves propagation in elastic layer using Cauchy theory of initial stress

14 p2658 A70-30998

Energy balance criterion for continuum mechanics analysis of fracture threshold for blistered adhesive elastic layer between elastic material and rigid substrate

19 p3536 A70-37774

Elastic membrane axisymmetric deformations, reducing nonlinear equations system to quadratures

20 p3718 A70-39230

Carbon dioxide laser adapted for high speed drilling of fine holes in thin rubber sheeting

23 p4201 A70-44474

ELASTIC SHELLS

Thin elastic shells parallel surface nonlinear tangential strains derived in terms of midsurface tangential and bending strain components

01 p0205 A70-11143

Thick walled incompressible hyperelastic dielectric sphere periodic oscillations, noting dielectric properties influence on amplitude and period

01 p0209 A70-11386

Nonlinear equations solvability for elastic cylindrical shells found existing for arbitrary load and clamping conditions

01 p0212 A70-11572

Asymptotic dynamic theory for elastic cylindrical shells incorporating thickness effects, considering longitudinal wave propagation in infinite length shell

02 p0385 A70-11877

Momentless design of composite plate and shell structures with variable elastic constants based on loading and shape requirements

03 p0586 A70-13112

Wave front discontinuities during pressure wave propagation in membranes and elastic shells by asymptotic procedure using Laplace transform

03 p0589 A70-13331

Shallow flexible shells similarity conditions derived in dimensionless form, assessing error

03 p0592 A70-13450

Nonlinear theory for thin elastic shells with small strains and rotations, analyzing nonzero Gaussian curvature

03 p0594 A70-13622

Thin elastic laminar shells nonlinear physical theory assuming Love-Kirchhoff hypothesis validity, rigidly connected layers and nonlinear mechanical behavior

04 p0765 A70-14419

Elastic orthotropic fiberglass reinforced plastic shells stability under axial compression, analyzing shear modulus influence

04 p0712 A70-14490

Thin elastic revolving shells free axisymmetric oscillations by determining differential equations eigenvalues and eigenfunctions

04 p0768 A70-14604

Torospherical heads attached to cylinders and under internal pressure as elastic and/or elastic-plastic shells, using finite element

[ASME PAPER 69-WA/PVP-7]

04 p0769 A70-14792

Free vibrations of reinforced elastic shell structures subject to constraints imposed by reinforcing elements, utilizing equivalent models without reinforcing elements

[ASME PAPER 69-WA/APM-25]

04 p0770 A70-14907

Elastic spherical shell excited by point force, analyzing HF response in terms of near field and flexural wave field

[ASME PAPER 69-WA/APM-18]

04 p0771 A70-14912

Initial deflection effect on elastic cylindrical shell stability under compression, finding critical load by determining limiting point in successive loading

04 p0773 A70-15009

Transient processes of strain wave propagation in elastic shells and plates under time varying loads

04 p0773 A70-15010

Thin elastic shallow shell static problem solved using numerical integration of differential equation

04 p0778 A70-15558

Buckling equations for neutral equilibrium of arbitrary elastic shells specialized to uniformly loaded circular cylindrical shell with accuracy

05 p0929 A70-16064

Axisymmetrical stress-strain analysis of viscoelastic cylinder enclosed in elastic shell under internal pressure using singular kernels

05 p0933 A70-16207

Static and continuity equations of equilibrium of axisymmetric and periodic stressed states of rectilinear helicoidal shell derived for elasticity relations

05 p0934 A70-16228

Stability and critical load algorithm for flexible shallow spherical and conical shells of revolution derived from variational equation

05 p0935 A70-16236

Isotropic elastic cylindrical shell stability under combined compressive and axisymmetric local loads, using equilibrium equations for shallow shells

05 p0936 A70-16240

Unsteady vibrations of cylindrical thin walled elastic closed shell under random loads, using correlation method

05 p0937 A70-16371

Finite element analysis of elastic thin shells, approximating shell surface by network of triangular plate elements

05 p0944 A70-16813

Digital computer program for analyzing axisymmetrically loaded ring-stiffened segmented composite elastic shells of revolution, giving vibration frequencies

05 p0944 A70-16814

Stability analysis of deflected shallow thin walled elastic noncircular conical and cylindrical orthotropic shells using straight lines method

06 p1167 A70-17865

Segmented elastic shells of revolution supported by rings, studying buckling and vibration by matrix method

07 p1405 A70-19257

Axisymmetric elastoplastic deformation theory for elastic cylindrical shell using Saint Venant yield condition, obtaining expressions for strain components, longitudinal deformation, etc

07 p1415 A70-20185

Dynamic calculation of oscillating liquid filled elastic cavity on elastic kinematic system under random load, using random signals transmission theory

07 p1416 A70-20194

Soviet book on free, forced and parametric vibrations of thin walled shells containing liquid, gas and continuous elastic medium

08 p1584 A70-20762

Interaction between boundary layer and internal stressed state of thin elastic shell by formulating two dimensional linear theory

08 p1585 A70-20955

Stress concentration on isotropic elastic circular cylindrical shallow shell using plane waves and spherical means method, obtaining periodic solutions convergence

08 p1585 A70-20963

Radial vibrations of hollow elastic sphere in acoustic medium, considering Laplace transform of field equations with respect to time

08 p1587 A70-21076

Linear and nonlinear equilibrium equations for bending deformation of thin elastic cylindrical using Kirchhoff-Love hypotheses

08 p1588 A70-21242

Elastic cylindrical shells stability under uniform pressure, calculating critical transverse load by finite-difference computer program

09 p1781 A70-23287

Elastic shell theory, deriving dynamic bidimensional equations from tridimensional elasticity equations asymptotic integration

10 p1959 A70-24793

Thin elastic plates and shells parametric resonance amplitudes by solving nonlinear differential equations, considering dynamic stability

11 p2129 A70-25523

Cylindrical shell segments supersonic flutter boundaries engineering estimates related to Saturn 5 booster, obtaining thickness requirement as function of panel geometry

[AIAA PAPER 68-284]

11 p2134 A70-25959

Stress tensor and displacement vector in thin elastic shells/plates derived from three dimensional nonlinear equations using asymptotic integration

11 p2142 A70-26634

Elastic conical shells of revolution linear theory, calculating stress resultants and couples

11 p2145 A70-26689

Initial thermal stresses effect on natural oscillation frequencies of thin cylindrical elastic shells, obtaining linearized equations of motion and boundary conditions 13 p2514 A70-29286

Geometrical theory of nonlinearly elastic inhomogeneous flexible shells, deriving variational equation in terms of displacement component and stress function 13 p2514 A70-29288

Rigid cylinder acceleration within elastic shell-core structure under pressure pulse distribution over shell semicircumference 13 p2518 A70-29984

Circular elastic shell response to moving and simultaneous loads, using impulse simulation method 13 p2518 A70-29986

Wave front discontinuities during pressure wave propagation in membranes and elastic shells by asymptotic procedure using Laplace transform 14 p2657 A70-30710

Sinusoidal stress and strain in elastic shells of revolution, reducing linear theory to simultaneous second order differential equations 15 p2816 A70-32158

Elastic shells of revolution stability and critical loads, discussing moment stress state and edge effect 15 p2816 A70-32158

Thin elastic shell deformation, considering random imperfections in regions adjacent to contour 15 p2817 A70-32162

Stability characteristics of elastic shallow shells of revolution in temperature field and under compression, reducing variational equation of bending by Ritz method 15 p2817 A70-32169

Plane acoustic wave interaction with elastic spherical shell, discussing effects of membrane, bending, rotatory inertia and shear deformation 16 p2993 A70-34087

Canonical variational principle for boundary condition contractions in elastic shell theory 17 p3182 A70-34545

Thin elastic shells linear theory, examining three dimensional stress distribution and displacement field 17 p3191 A70-35608

Axisymmetric torsion by terminal loads of elastic shells of revolution, investigating energy inequalities for assessing quality of approximate solution of thin shell problem 18 p3335 A70-36058

Stress-strain equilibrium of thin isotropic elastic shells of revolution loaded along meridian 18 p3340 A70-36577

Dynamic axisymmetrical loading of thin elastic shallow spherical rigidly clamped dome, using variational method 18 p3341 A70-36582

Oscillations of rigidly clamped elastic liquid filled hemispherical shell with gas bubble 18 p3242 A70-36583

Complete elastic spherical shell asymmetric buckling mode under pressure 19 p3539 A70-37801

Forced torsional vibrations of thin elastic spherical and hemispherical shells with free or restrained edge, using Gegenbauer transform 19 p3541 A70-38037

Boundary value problems for elastic sphere, extending Kelvin general solution of Cauchy equations 19 p3545 A70-38333

Thin elastic conical shell axisymmetric solution for free vibration in terms of power series 19 p3545 A70-38335

Anisotropic axisymmetric elastic shell theory including transverse stress effects, with application to orthotropic cylinder 19 p3545 A70-38337

Interaction between boundary layer and internal stressed state of thin elastic shell by formulating two dimensional linear theory 20 p3719 A70-39378

Stress concentration on isotropic elastic circular cylindrical shallow shell using plane waves and spherical means method, obtaining periodic solution convergence 20 p3719 A70-39385

Long hollow nonlinearly viscoelastic cylinder in elastic shell, calculating stress and strain under internal pressure 20 p3720 A70-39731

Axisymmetric contact problem of hollow semi-infinite elastic cylinder subjected to stresses on lower end face, solving by Fourier integral transform 20 p3720 A70-39734

Thin elastic shell natural vibrations, examining orthogonality of form shapes 20 p3724 A70-39862

Elastic shell stability criterion during short duration dynamic loading 20 p3725 A70-39864

Stability loss in linear approximation by thin elastic shell of revolution with negative Gaussian curvature 20 p3726 A70-39872

Thin elastic shells displacement vector and strain boundary conditions determination from stress-strain relations 20 p3728 A70-39896

Perturbed motion linear equations of body rigidly coupled to thin walled elastic shell partially filled with heavy compressible fluid 21 p3806 A70-40602

Circular cylindrical shell with annular orthotropic elastic core, analyzing stress wave propagation under pressure pulse 21 p3938 A70-41740

Fluid filled elastic spherical shell, calculating free vibration axisymmetric response and fundamental mode 21 p3940 A70-42053

Novozhilov complex transformation method extended to Timoshenko theory of elastic shells constructed with allowance for transverse shear deformation 21 p3941 A70-42237

Elastic cylindrical shell transient response to plane acoustic shock wave traveling through light fluid medium 22 p4114 A70-42647

Curved finite element for thin elastic shells satisfying rigid body motions and energy convergence 22 p4116 A70-43202

Thickness of equally stressed cylindrical shells, using thin elastic shell theory and Kirchhoff-Love hypotheses 22 p4120 A70-43715

Second approximation for limit loads due to imperfection sensitivity of axisymmetric elastic shell structures with unique harmonic buckling modes 23 p4273 A70-44720

ELASTIC STABILITY

U DAMPING

ELASTIC STRENGTH

U PROPORTIONAL LIMIT

ELASTIC SYSTEMS

Photoelasticity extension to plane elastic problems with stress state depending on Poisson ratio, discussing multiple connected body with nonzero surface tractions on internal boundaries [SESA PAPER 1570] 03 p0583 A70-12884

Finite element method using cubic polynomials over triangle as trial functions for solving second order boundary value problems in linear theory of elasticity 07 p1324 A70-19075

Complex elastic system coupled flexural vibrations resonant frequencies determined with allowance for friction 07 p1363 A70-19111

Transient process statistical calculation in discrete elastic mechanical system possessing energy dissipation under time dependent cross correlated random forces 09 p1729 A70-23595

Elastic chain systems stability and natural vibrations using parameter coupling method permitting integral equation construction 09 p1784 A70-23596

Thermal effects on aircraft elastic vibration mode shapes, recommending investigation to develop analysis and design tools 18 p3213 A70-36459

Natural vibrations of free autonomous system of carried and carrier solid bodies connected by elastic couplings 18 p3342 A70-36594

Linear elastomechanical systems natural vibration parameters by harmonic excitation method 22 p4116 A70-43200

Shock response of passive nonlinear elastic isolators under pulse excitation with viscous damping 22 p4117 A70-43249

Solid cloth personnel parachutes opening forces, discussing loading conditions, flight path shock parameters, mass ratio variations and elasticity of system [AIAA PAPER 70-1167] 23 p4137 A70-43992

Mathematical models derivation for systems of interconnected elastic segments, using variational method and energy summation via difference equations 23 p4266 A70-44019

ELASTIC WAVES

NT AERODYNAMIC NOISE

NT AIRCRAFT NOISE

NT BAROCLINIC WAVES

NT CAPILLARY WAVES

NT COHERENT ACOUSTIC RADIATION

NT COMPRESSION WAVES

NT DETONATION WAVES

NT ELECTROSTATIC WAVES

NT ENGINE NOISE

NT GRAVITY WAVES

NT IONIC WAVES

NT JET AIRCRAFT NOISE

NT LAMB WAVES

NT LOVE WAVES

NT MACH CONES

NT MAGNETOACOUSTIC WAVES

NT MAGNETOELASTIC WAVES

NT MAGNETOHYDRODYNAMIC STABILITY

NT MAGNETOHYDRODYNAMIC WAVES

NT MICROSEISMS

NT NOISE [SOUND]

NT NORMAL SHOCK WAVES

NT OBLIQUE SHOCK WAVES

NT P WAVES

NT PHONONS

NT PLASMA WAVES

NT POLARIZED ELASTIC WAVES

NT RAYLEIGH WAVES

NT RIEMANN WAVES

NT ROCKET ENGINE NOISE

NT S WAVES

NT SEISMIC WAVES

NT SHOCK WAVES

NT SONIC BOOMS

NT SOUND WAVES

NT STRESS WAVES

NT THERMAL NOISE

NT TOLLMEIN-SCHLICHTING WAVES

NT ULTRASONIC RADIATION

NT UNLOADING WAVES

Characteristic equations developed for two-spatial dimensional elastic wave propagating in linear elastic, isotropic and homogeneous medium 01 p0208 A70-11185

Pressure waves in accelerated sphere filled with compressible liquid, using convolution integral for pressure distribution on inner surface 01 p0067 A70-11186

Microbarographic oscillations associated with geomagnetic activity during observation of infrasonic waves on geomagnetically disturbed days 01 p0081 A70-11298

Pressure waves propagation velocity dependence on flow regime in gas-liquid mixtures 01 p0067 A70-11302

Flexural and longitudinal waves propagation in infinite elastic plate, using solutions to approximate nonlinear equations of plate motion 01 p0213 A70-11634

Arc phenomena for producing interaction effects, discussing reflected shocks rarefaction waves and gas dynamics 02 p0345 A70-11863

Forward air cushion performance of tracked hovercraft entering tunnel, determining arrival of reflected expansion wave at vehicle front 02 p0226 A70-12313

Periodic shock fronted longitudinal pressure wave effect on instantaneous heat flux rates at tube end wall 02 p0400 A70-12860

Axial stress pulse induced elastic waves propagation in thin anisotropic circular cylindrical shell of helical wrap construction allowing for shear coupling 03 p0587 A70-13118

Wave front discontinuities during pressure wave propagation in membranes and elastic shells by asymptotic procedure using Laplace transform 03 p0589 A70-13331

Plane longitudinal elastic monochromatic wave diffraction on stress free circular holes in infinite plate, calculating stresses between holes 03 p0589 A70-13375

Mechanical behavior of anesthetized dog abdominal vena cava from pressure wave transmission characteristics, discussing chemical and electrical stimuli 04 p0630 A70-14630

Dispersion curves for wave propagation in infinite elastic bars of elliptic cross section obtained by method of collocation 04 p0773 A70-15080

Gas dynamics of intense explosion with expanding inner contact surface in Newtonian limit, discussing shock layer reattachment 04 p0619 A70-15322

Effective wave propagation velocities, bulk and shear moduli of elastic heterogeneous solids approximated by self consistent method 04 p0777 A70-15496

Sonic waves induced by shock of laser produced brass and graphite vapor in air at atmospheric pressure using high speed shadowgraphs 05 p0857 A70-15802

Pressure wave formation induced by absorption of radiation in oxygen, noting wave driving after radiation pulse decay by frozen dissociation energy 05 p0833 A70-16306

Dynamical models of relative motions during earthquakes, solving numerically integral equations with nonintegral kernels in crack propagation and elastic wave diffraction 05 p0941 A70-16527

Plane and cylindrical elastic waves dynamic characteristics propagating in half space with holes, reducing boundary value problem and deriving formulas for interacting waves 05 p0946 A70-16858

Guided elastic waves propagation on layered media, considering elastic wave circuitry design for true microminiaturization 06 p1018 A70-17476

Wave equation for elastic waves in isotropic solid solved in Cartesian and circular cylindrical coordinates 06 p1018 A70-17476

dinates for studying microsonic wave guiding structures

06 p1105 A70-17479

Semiinfinite simply supported cylindrical shell transient response due to axisymmetrically engulfing step pressure wave, investigating moving load critical velocity

[AIAA PAPER 70-18] 06 p1170 A70-18063

Plane elastic-relaxing plastic shock wave yielding of Fe numerically integrated by two step stable difference scheme without pseudoviscosity

06 p1172 A70-18618

Kirchhoff theory of elastic wave diffraction in cylindrical case derived on modified Huygens principle, showing edge contribution

08 p1543 A70-20582

Vibration insulation of rib estimated with respect to diffuse flexural wave field in reinforced plate

08 p1586 A70-21010

Plane double front detonation wave attenuation by pursuing rarefaction waves, analyzing oscillations, onset mechanism and stability during transition to Chapman-Jouguet mode

08 p1485 A70-21633

Atmospheric pressure waves generated by high energy disturbance in South Pacific, using ionospheric Doppler signals correlated with ground-level pressure signals

08 p1490 A70-21646

Relaxational oscillations produced by interaction between rarefaction wave in external two dimensional supersonic flow and turbulent near wake

09 p1603 A70-22426

Monatomic gas rarefaction wave structure in unsteady one dimensional flow from high to low pressure zones, describing numerical solution technique

09 p1604 A70-22449

Elastic harmonic waves propagation in cylinder with longitudinal cavities and in space with cylindrical cavities solved using series method

09 p1783 A70-23387

Pressure waves of varying amplitude effect on flow through turbomachine blade passages, discussing interaction with curved diffusers geometry

09 p1608 A70-23743

Quasi-transverse constant profile wave in finite elasticity with isothermal shock at discontinuity compared to Whitham breakdown

10 p1956 A70-24191

Elastic wave propagation, deriving characteristic equations in generalized curvilinear coordinates using linear elastic, isotropic and homogeneous constitutive equations

11 p2132 A70-25680

High purity beryllium dynamic tests determining Hugoniot equation of state, shock profile and spall threshold/onset of microcracking/for elastic pulses

[AIAA PAPER 69-360] 11 p2066 A70-25964

Extensional waves asymptotic nature and stress distributions in infinite elastic plate of finite thickness under axisymmetric and in-plate disturbances using perturbation

11 p2145 A70-26696

Plane periodic diffraction of elastic waves propagating in medium with infinite sequence of circular holes

12 p2325 A70-27557

Interaction of laminar hypersonic boundary layer and supersonic corner expansion wave, discussing upstream influence, transverse pressure gradients and external flow

[AIAA PAPER 69-137] 12 p2211 A70-27826

Lunar elastic waves anomalous propagation, considering Apollo seismographic records and earth rocks specific dissipation function measurements

13 p2486 A70-28617

Time and spatial evolution of shock and expansion wave evolution from density discontinuity for gas with repulsive delta function interaction between particles

13 p2388 A70-29224

Elastic plane wave diffraction and scattering at convex obstacle in semibounded regions, using method of images

13 p2452 A70-29289

Variable temperature plasma with two ion species, noting rarefaction wave propagation during one dimensional expansion into vacuum

13 p2464 A70-29415

High temperature elastic moduli of slender polycrystalline aluminum rods with elastic waves generated by Q switched laser energy

14 p2595 A70-30638

Wave front discontinuities during pressure wave propagation in membranes and elastic shells by asymptotic procedure using Laplace transform

14 p2657 A70-30710

Elastic waves propagation in finite thickness elastic plate under transient load, assuming material behavior in conformity with nonlinear Hooke's law

15 p2814 A70-31544

Rarefaction wave analytical construction by successive approximation, solving hyperbolic equations for longitudinal vibrations of rods

15 p2815 A70-31644

High temperature elastic moduli in polycrystalline Al rods from propagation velocity of elastic waves generated by Q switched laser

[SESA PAPER 1641] 15 p2759 A70-32304

Propellant flame temperature and emission spectra during depressurization by rarefaction waves, using rapid scanning spectrometer

[AIAA PAPER 70-663] 16 p2962 A70-33570

Quasi-linear hyperbolic systems interactions for rarefaction waves, applying Glimm difference method

16 p2943 A70-33782

Laminar hypersonic boundary layer interaction with corner expansion wave, presenting numerical solutions to viscous-inviscid equations for small turning angles

[AIAA PAPER 70-807] 17 p3065 A70-34457

Elastic waves on isotropic and anisotropic surfaces, discussing excitation methods, surface probing, propagation characteristics, etc

17 p3136 A70-34650

Analog simulation of elastic wave propagation in thick walled hollow circular cylinders to determine safe impact speed

17 p3185 A70-34964

Elastic wave with discontinuities propagation, calculating decay velocities and stresses at leading wave front by theory of characteristics

17 p3189 A70-35436

Elastic field near moving antipane crack tip to determine energy release rate

17 p3191 A70-35462

Convergent spherical rarefaction wave asymptotic behavior

17 p3075 A70-35892

Heat transfer across boundary between two stationary fluids, applying elastic wave theory in isotropic media

18 p3345 A70-36118

Elastic Cosserat half plane, analyzing wave propagation of small amplitude thermoelastic disturbances and uniform motion of concentrated line load along surface

18 p3338 A70-36434

Acceleration wave propagation in materially uniform inhomogeneous isotropic elastic bodies, using tensor analysis

19 p3536 A70-37563

Transient polymers stress-strain state induced by elastic waves, using model with space and time dependence of laser beam

20 p3654 A70-39248

Elastic quasi-stationary waves, discussing waveforms and resonance phenomena

20 p3727 A70-39890

Elastic wave propagation mathematics in visual form for ultrasonic testing

21 p3831 A70-40746

Elastic wave propagation in isotropic homogeneous bodies, considering free vibrations and propagation velocity

21 p3940 A70-42099

Surface elastic waves, considering propagation, electromagnetic transduction, amplification, guiding, focusing, reflection and applications

21 p3830 A70-42115

Elastic wave diffraction by rigid inclusion, calculating far field displacement and cross section by integral equation method

22 p4073 A70-42636

Analytic shock front velocity as function of initial parameters in continuous inhomogeneous medium, verifying propagation through rarefaction wave

22 p4010 A70-42687

Striations due to mechanical oscillations in fast wire explosions, using dispersion for elastic waves in solid cylinders

22 p4074 A70-43002

Transient elastic vibrations of air and liquid filled cylindrical shells under radial impact, using shadow-optical cinematography

[SMPTE PREPRINT 107] 22 p4031 A70-43030

Elastic wave front control volume analysis in laminated and fiber reinforced composite materials

22 p4119 A70-43677

CO vibrational relaxation measurements in shock tube expansion wave generated in argon heat bath

23 p4180 A70-44009

Heat transfer from turbulent boundary layer interacting with shock and expansion waves in supersonic flow

23 p4134 A70-44573

Electromagnetic-surface elastic waves conversion in superconductors, considering thin plate forced vibrations and standing waves excitation

24 p4389 A70-45205

One-dimensional propagation of elastic spherical waves in inhomogeneous unbounded medium under normal stress on cavity surface

24 p4424 A70-45631

ELASTICITY

U ELASTIC PROPERTIES

ELASTODYNAMICS

NT ELASTIC DAMPING

NT ELASTOHYDRODYNAMICS

Anisotropic shells and plates dynamic field equations derived, taking into account mechanical forces and nonuniform temperature field

01 p0200 A70-10553

Mathematical elastodynamic model for parametric dynamic study of forced response solution of motion equations during head trauma

02 p0238 A70-12548

Variational principles in dynamic viscoplasticity theory, based on operator approach combined with time independent variations in elasticity theory

02 p0391 A70-12818

Elastokinetic three dimensional boundary value vibration problem, involving rectangular area on surface of elastic half space under periodic normal stress

03 p0601 A70-14319

Governing equations of plane elasticity to define suitable approximate theories for structural analysis

[ASME PAPER 69-WA/APM-22] 04 p0771 A70-14909

Static and dynamic solutions for isothermal deformation of elastic cylindrical and spherical Cosserat surfaces with holohedral isotropy

05 p0932 A70-16140

Integral equation for time development of harmonic oscillations in finite one dimensional chain of elastically coupled discrete elements, using Bessel functions for solution

08 p1547 A70-20535

External and internal three dimensional dynamic problems in elasticity theory for multiply connected region with circular cylinder boundaries

08 p1584 A70-20537

Inhomogeneous elastic half space surface response to moving line loads

08 p1584 A70-20645

Gas dynamics regarding velocity field excited by vibrations propagating over elastic wing surface at finite velocity

10 p1803 A70-24779

Vibration behavior theory for elastomechanical systems applied to aircraft and space constructions

10 p1961 A70-25054

Elastodynamics mixed initial and boundary value problems numerical solution method applied to deformation of elastic solid

11 p2140 A70-26485

Dynamic asymmetric elasticity problems, considering longitudinal and torsional wave propagation in bounded and unbounded micropolar media

15 p2818 A70-32178

Boundary value problem in linear elastodynamics, investigating Ignaczak type theorems for microstructure effects in transient heat conduction problems

15 p2822 A70-32343

Perturbation method for finite elastodynamic deformation of nonlinear systems

17 p3191 A70-35590

Dynamic elasticity theory for multiply connected region

23 p4266 A70-43990

Elastic coupling and dynamic equations for flight elastomechanical vibration systems, including tiptanks on aircraft wings

23 p4274 A70-44767

Elastic orthotropic plates vibration analysis by finite strip method via eigenvalue matrix, obtaining natural frequencies and modal vectors by small computer

24 p4423 A70-45579

ELASTOHYDRODYNAMICS

Roller bearing endurance dependence on shaft speed, surface finish and elastohydrodynamic lubricants temperature, viscosity and film thickness

[ASME PAPER 69-LUB-18] 01 p0101 A70-10387

Hydrodynamic and elasticity equations for squeeze films between elastic cylinders in normal approach reduced to integral equation

[ASME PAPER 69-LUB-13] 01 p0102 A70-10392

Tractive behavior in elastohydrodynamic lubrication contact noting role of surface degradation layer

05 p0854 A70-15888

Rheology applied to motor oil viscosity, elastohydrodynamic (EHD) and extremely thin film lubrication, examining viscosity relationship to film thickness

07 p1293 A70-18954

Frictional traction-sliding speed relation in elastohydrodynamic lubrication in Barlow-Lamb model of viscoelastic liquid, discussing oscillatory and continuous shear

09 p1691 A70-22600

Elastohydrodynamic lubrication of rollers relationship to pressure

09 p1693 A70-22978

Elastohydrodynamic monochromatic wave coupling in liquid filled container as model for Alfvén and magnetoacoustic waves transmission in plasma

14 p2625 A70-31356

Rolling element bearings fatigue life prediction and extension, using elastohydrodynamic lubrication theory

[ASME PAPER 70-DE-19] 16 p2917 A70-33423

ELASTOMERS

NT CHLOROPRENE RESINS

Incompressible elastomer viscoelastic response to exponential extension ratio history in simple tension based on constitutive equations 01 p0201 A70-10893

Synthetic polymers properties and processing, discussing thermoplastics, elastomers, thermosets, etc 02 p0322 A70-12715

Poisson ratio of elastomers determination for defining compliant surface fluid film thrust bearings behavior, considering method and error analysis [ASME PAPER 69-WA/LUB-7] 04 p0712 A70-14751

Strain energy function for swollen crosslinked elastomers, extending application range by including third invariant 05 p0927 A70-15980

Elastomeric silicone ablator reinforced by carbon cloth or fibers for Venus entry heat protection [AIAA PAPER 70-201] 06 p1157 A70-18086

Elastomeric seals and sealants selection for SST, describing tests in air, fuel vapors and hydraulic fluids at elevated temperatures 13 p2418 A70-28668

Ethylene-propylene elastomers compatibility with hydrazine determined under ambient conditions from gas evolution rate by catalytic decomposition 13 p2472 A70-28669

Inhibitive elastomeric sealing compounds and coating systems preventing aluminum alloy corrosion in aircraft 13 p2433 A70-28778

Radio Influence Voltage /RIV/ nondestructive test method for detecting voids in neoprene-steel structures or other elastomers bonded to metal 13 p2420 A70-29245

Elastomeric liner material for missile launch system design, developing bowed-knotted strut for compression-deflection characteristics 13 p2513 A70-29256

Missile tube liner design with cast polyurethane elastomers, discussing effect of polymer composition and processing on physical properties 13 p2439 A70-29257

Filled elastomers elastic and anelastic behavior, investigating strain dependence 13 p2440 A70-29964

Stress distributions in elastomers under different loads, proposing appropriate measuring technique 14 p2655 A70-30178

Gas transfer through silicone elastomer capillaries wall in variable pressure chamber 14 p2541 A70-30386

Cycloaliphatic epoxy resins tensile and impact strength improvement by modification with elastomeric materials, considering heat distortion temperature 16 p2936 A70-33359

Poisson ratio of elastomers determination for defining compliant surface fluid film thrust bearings behavior, considering method and error analysis [ASME PAPER 69-WA/LUB-7] 19 p3434 A70-37602

Cycloaliphatic epoxy resins toughness improvement by modification with elastomers, maintaining high heat distortion temperature 21 p3842 A70-40733

Saturated hydrocarbon prepolymers for solid propellant elastomeric binders 21 p3865 A70-42144

ELASTOPLASTICITY

Computer calculation in elastoplastic range of statically indeterminate structure of bars, considering collapse load, stress and hinge rotation 01 p0200 A70-10524

Taylor model of elastoplastic wave interaction during cylindrical projectile impact 01 p0206 A70-11150

Residual stress determination in elastoplastic body with known plastic strains, using Hilbert space for symmetric tensor fields 01 p0209 A70-11399

Propagation equations for spherical waves in elastoplastic work hardening materials 03 p0585 A70-12972

Soviet book on experimental investigation of thin walled structures elastoplastic work with complex reinforcement, outlining test procedures 03 p0585 A70-12985

Elastoplastic bodies stability under compression, using theory of small elastoplastic deformations and linearized equations of nonlinear elasticity theory 03 p0591 A70-13440

Flexible cylindrical shell elastoplastic state determined by theory of small elastoplastic deformations, utilizing material incompressibility in plastic state 03 p0593 A70-13500

Elastoplastic analysis of strain hardening materials under multiaxial states of stress based on von Mises yield condition and stress-strain relationship 03 p0596 A70-14012

Elastoplastic zone and instability of precracked thin sheets under uniaxial loading applied to rectangular center-notched steel foils 03 p0598 A70-14239

Elastoplastic strains in machine element surface layers under static friction force using polarization-optical techniques 04 p0696 A70-14410

Elastoplastic bar stability compressed by tangential force, showing ductility effect on critical parameters, perturbed motion and stability loss process 04 p0767 A70-14484

Long thin cylindrical tube with circumferential restraint analyzed for thermal expansions, obtaining maximum strains, bending moments, shear forces and plastic zone extent [ASME PAPER 69-WA/NE-7] 04 p0768 A70-14756

Torispherical heads attached to cylinders and under internal pressure as elastic and/or elastic-plastic shells, using finite element [ASME PAPER 69-WA/PVP-7] 04 p0769 A70-14792

Elastoplastic media revised mathematical model with allowance for cumulative damages effect on elastoplastic property under variable loads 04 p0775 A70-15199

One dimensional stress waves propagation in elastoplastic medium, determining stress and velocity fields due to heat sources motion by characteristics method 04 p0776 A70-15447

Unloading wave in elastic-plastic half space with rigid unloading for two parameter loads, discussing deformation body model 05 p0925 A70-15825

Finite element discretization and linear programming methods for shakedown theory in perfect elastoplasticity with associated and nonassociated flow laws 05 p0925 A70-15873

Continuum model for plastic-elastic behavior of fiber reinforced composite material, formulating yield condition and constitutive equations 05 p0931 A70-16131

Elastoplastic thick layer with disk-shaped crack analyzed for stress and strain, determining width of plastic zone 05 p0939 A70-16482

Torispherical heads design pressures compared from results of elastic-plastic and elastic-stress analyses to examine use of limiting stress criteria 05 p0944 A70-16816

Small amplitude spherical elastic-plastic waves initial behavior studied for critical and supercritical loading 05 p0945 A70-16819

Small elastoplastic deformation effects on stress-strain state of rib-reinforced cylindrical shells 05 p0946 A70-16955

Elastoplastic bending of rectangular plates by finite difference and variational methods assuming homogeneity in elastic region 05 p0946 A70-16962

Impact against elastoplastic blank allowing for base and striker compressibility, giving solution in region of plane wave first reflection from base 05 p0947 A70-17016

Fatigue breakdown criteria for elastoplastic materials under cyclic loads, deriving equations as functions of stress-strain states kinetic behavior 06 p1162 A70-17390

Elastoplastic rod systems under repeated variable loads, calculating carrying capacity from plastic failure considerations 06 p1163 A70-17395

Structures elastic-plastic behavior under changing cyclic heating, calculating long time strength from linear damage accumulation assumptions 06 p1164 A70-17405

Elastic-plastic torsion of convex cylindrical bars 06 p1165 A70-17534

Stability criterion applicable to elastoplastics problems with/without nontrivial equilibrium states, noting effect on buckling loads 06 p1167 A70-17900

Stress rate boundary value problem formulation for elastoplastic body by singular integral equations 07 p1405 A70-19258

Elastoplastic torsion of combined prismatic bars with transverse distribution of constant properties solved by computer 07 p1415 A70-20189

Elastoplastic bending of inhomogeneous rectangular plates with modulus of elasticity and yield stress varying over plate thickness 08 p1583 A70-20530

Elastic/perfectly plastic hollow cylinder unloading under monotonic twist during torsion, considering sandhill-membrane analog validity 08 p1589 A70-21249

Energy equilibrium for crack growth in elastoplastic media, analyzing crack behavior during plastic deformation concentrated at edge of propagating crack 08 p1590 A70-21414

Elastic-plastic plane strain solutions in infinitesimal plastic flow theory with separable stress fields [ASME PAPER 69-APMW-13] 08 p1592 A70-21470

Elastic-plastic work hardening sandwich arch under given loading rate analyzed for stress rates using integral equation [ASME PAPER 69-APM-21] 08 p1593 A70-21616

Stress-strain characteristics of reinforced elastoplastic layer using mathematical model 09 p1769 A70-22183

Elastoplastic problems incremental solution by iterative method, demonstrating convergence 09 p1771 A70-22394

Plane and cylindrical stress wave propagation in elastoplastic medium, studying stress interrelations 09 p1775 A70-22610

Solution uniqueness in limit load theory for unbounded regions, obtaining infinity as unique value for critical load from elastoplastic analysis 10 p1954 A70-24013

Elastoplastic compressible sheet metals reinforced by isotropic work hardening under action of bending moments, analyzing stresses and strains 10 p1955 A70-24056

Optimal trusses design, considering minimal volume /weight/ and elastoplastic stability in compressed and stretched bars 10 p1958 A70-24514

Photoplastic method for modeling of plane elastoplastic problems, comparing results with photoelastic coating method to estimate transition errors from model to prototype 10 p1965 A70-25320

Macrodon elastic-plastic strain model, studying stress-strain relationship and optico-mechanical properties 11 p2128 A70-25385

Elastic-plastic shear cracks propagation in two phase composite materials using dislocation model, determining critical fracture strength 11 p2136 A70-26081

Energy principle providing upper bounds on plastic deformation in elastoplastic structures subjected to blast loading 11 p2144 A70-26670

Deformation theory for small elastic-plastic strains in orthotropic material and discretization and iterative solution techniques 11 p2144 A70-26684

Plates elastic-plastic behavior under combined stretching and bending by finite element method 12 p2320 A70-27146

Large deflection analysis of elastic-plastic shells of revolution by computer program based on nonlinear theory and multisegment method of numerical integration 12 p2320 A70-27148

Two dimensional structures large strain elastoplastic analysis by finite element method, using variational principles to derive equilibrium equations 12 p2320 A70-27148

Sandwich beams elastoplastic stability, determining critical load 12 p2323 A70-27342

Elastic-plastic plane stress analysis of two dimensional structures based on Tresca yield criterion, using finite element technique 12 p2326 A70-27795

Thin cut plate quasi-brittle breakdown under tensile stress, considering elastoplastic equilibrium under Tresca-St. Venant yield conditions 12 p2329 A70-28325

Elastoplastic thermal stress analysis using finite element matrix method exemplified by cylindrical bar induction quenching 13 p2513 A70-28992

Minimum principles for rate solution in elastoplastic work hardening materials with regular yield surface 13 p2513 A70-29152

Piecewise linear elastoplastic matrix structural theory with interacting yield planes, discussing kinematic and isotropic hardening 14 p2656 A70-30475

Finite element displacement method for elastoplastic bilinear strain hardening orthotropic plates and shells, comparing initial and tangent stiffness 14 p2660 A70-31136

Elastoplastic material mechanical theory, considering constitutive equations with plastic deformations and decompositions of total velocity-strain /stretching/ 14 p2661 A70-31281

Elastoplastic torsion problems solution by strain theory of plasticity, describing torsion function in hypergeometric series form 14 p2661 A70-31329

Two dimensional stress-strain fields under elastic and elastic-plastic strains and steady state creep, calculating stress distribution around hole in cylindrical shell 15 p2813 A70-31533

Equation of state of solids measured by shock wave techniques, considering elastic-plastic flow in plane wave geometry 15 p2824 A70-32789

Elastoplastic bending of thin plate under increasing and uniformly distributed loads, defining statically admissible stresses 16 p2988 A70-33107

Elastoviscoplastic medium filled half space motion under pressure front moving along surface with time varying velocity, analyzing penetrating wave fronts form 16 p2990 A70-33780

Heat transfer in tungsten-tungsten and Armco Iron-Armco Iron specimens, confirming Bowden-Tabor model of elastoplastic events during cyclic engagement of surfaces 16 p3000 A70-33920
[AIAA PAPER 70-853]

Finite element formulation for large strain and displacement problems with emphasis on elastic-plastic behavior in metals 17 p3184 A70-34905

One dimensional elastoplastic wave propagation in rate-sensitive viscoplastic rod with thermal gradient 17 p3185 A70-34966

Shakedown theory of elastic-plastic structures under time dependent loadings 17 p3188 A70-35191

Discrete element stress and displacement analysis of elastoplastic plates 18 p3342 A70-36686

Three dimensional dynamic analysis of small harmonic stress wave propagation in elastic-plastic and viscoplastic materials, using finite differences 18 p3344 A70-36724

Elastic-plastic behavior of fine grained fcc polycrystals based on single crystal slip data, satisfying displacement compatibility, equilibrium condition, etc 19 p3538 A70-37792

Nonlinear stress-strain model of unloading in symmetric longitudinal impact of two elastic-plastic bars, using numerical method 19 p3541 A70-38046

Elastoplastic oscillator dynamic behavior with one degree of freedom compared with bilinear hysteretic model results, investigating mechanical scheme with continuous skeleton intrinsic curve 19 p3432 A70-38665

Elastoplastic continua incremental solution for large displacements and small strains, determining sufficient condition of uniqueness 19 p3549 A70-38666

Elastoplastic work hardening continua incremental boundary value problem with allowance for distributed dislocations, using quadratic programming concepts 19 p3549 A70-38667

Elastic-plastic equilibrium bifurcation in geometrically simple frame model with symmetrically loaded beam, comparing characteristics with Shanley uniformly stressed column model 19 p3549 A70-38671

Plasticity and strain hardening in sintered metals, considering pressure at pores and elastoplastic limit under small plastic deformation 20 p3644 A70-38962

Q switched lasers time dependent loss elimination from elastoplastic relaxation effect in lithium niobate and KDP Pockel cells 20 p3640 A70-39093

Elastoplastic deformation in strip with symmetrical semicircular notches simulating stress-strain-state on celluloid models by polarization-optical method 20 p3720 A70-39735

Elastoplastic equilibrium of thin infinite plate with periodic slit system along straight line under tension, investigating localized plastic deformation domains 20 p3721 A70-39769

Uniformly loaded thin elastoplastic spherical shells, calculating strain hardening and strain rate effects on transient response 21 p3935 A70-41255

Thin circular plate clamped along edge, calculating large displacements and elastoplastic strains for comparison with measurement 21 p3935 A70-41406

Elastic-plastic deformation analysis at finite strain by two component thermodynamic model 21 p3937 A70-41431

Elastic-plastic axisymmetric shells of revolution, analyzing large deflection and yielding for internal and external pressures by finite element method 21 p3937 A70-41738

Cylindrical cavity uniform expansion in compressible elastic plastic solid, calculating pressure by similarity solution 22 p4114 A70-42634

Spherical cavity nonuniform expansion in compressible elastic plastic solid, calculating velocity field and pressure by approximate similarity solution 22 p4114 A70-42635

Elastoplastic flexure and critical loading of isotropic rectangular plates of constant and variable thickness, using Lagrange principle with numerical integration 22 p4115 A70-42810

Antifriction number characterizing friction coupling, distinguishing between elastic and plastic modes 22 p4047 A70-43348

Strain gage stress measurement under elastoplastic strain conditions at high temperature 22 p4117 A70-43454

Elastoplastic bending of rotating circular shaft with constant end cross section force couple, assuming small deformations of linearly hardening materials 22 p4118 A70-43570

Soviet bibliography on flexible plates covering elastic bending, elastoplastic state under transverse load and bending beyond elastic limit 22 p4119 A70-43710

Elastoplastic properties of welded joints containing slag inclusions defects, determining sizes radiographically 24 p4347 A70-45734

ELASTOSTATICS

Three dimensional elastostatics problems solution method using singular integral equations solvable numerically for surface tractions and displacements of fully mixed boundary value problem 05 p0926 A70-15912

Static and dynamic solutions for isothermal deformation of elastic cylindrical and spherical Cosserat surfaces with holohedral isotropy 05 p0932 A70-16140

Stress functions in three dimensional nonaxisymmetric elastostatics problems in circular cylindrical coordinates, proving representation completeness for cylindrical bodies 05 p0932 A70-16172

Wedge with symmetric crack at vertex in plane elastostatics, solving biharmonic equation by Wiener-Hopf technique 06 p1164 A70-17441

Cylindrically isotropic elastic medium statics, deriving general solutions to Lamé equations 09 p1784 A70-23593

Inhomogeneous anisotropic elastic plates large deflection, using asymptotic integration of nonlinear elasticity equations to obtain successive field equations systems 24 p4423 A70-45580

Anisotropic bodies elastic properties, obtaining solutions for nonorthotropic beams under randomly distributed normal loads and for various plates and strips 24 p4424 A70-45589

ELDO LAUNCH VEHICLE

ELDO booster rocket third stage design and construction, including pictures of parts and devices 03 p0580 A70-13795

ELDO-PAS apogee motor prequalification test to determine specifications for constructing units for qualification testing 03 p0581 A70-13854

Digital computer interface for ELDO launcher inertial guidance system linking with platform, autopilots, telemetry equipment and rocket subsequenceurs 05 p0818 A70-16572

ELDO launch vehicle achievements, potential and use, showing relationship to possible satellite payloads 05 p0924 A70-16896

Radio and inertial guidance of Europa 1 and 2 ELDO launch vehicles 08 p1542 A70-21870

ELDO rocket tracking error, considering guidance antenna angular precision and UHF circuit performance in signal comparison 09 p1720 A70-22649

Digital guidance computer compatibility with analog attitude control loop in Digital Inertial Guidance System used in ELDO launch vehicle 11 p2080 A70-26280

Modular launch vehicle system for European commercial satellites using Eldo-A/I Astris and French rocket stages 16 p2987 A70-34342

ELDO launch vehicle FE /flat earth/ guidance, discussing perturbations, trajectory optimization, inertial navigation system, onboard computer, etc 18 p3288 A70-36299

ELDO launch vehicle design, describing high energy upper stages 18 p3333 A70-36300

ELDO project planning and progress monitoring system for management provided by Central Planning and Progress Monitoring Service 21 p3956 A70-41497

Programming and checkout of computer for ELDO inertial guidance system, including flight simulation and autopilot tests 21 p3795 A70-41862

[AIAA PAPER 69-961]

ELDO Europa 1 and 2 launchers configurations tendencies, discussing use of liquid propellant boosters, chemical, electrostatic or thermonuclear propulsion system, etc 23 p4263 A70-45002

Gyroscopically stabilized solid propellant apogee motor for experimental satellite of CECLES/ELDO Europa 2 program 23 p4235 A70-45018

Satellite launch vehicle guidance equations for programmed optimization applied to Eldo inertial guidance system 24 p4375 A70-46359

ELECTRETS

First order pressure gradient microphone design based on electrostatic principle, using foil electrets to discriminate against airborne and solid-borne noises 05 p0821 A70-16402

Electret microphones application for pressure fluctuations measurements on thin aerodynamic profiles noting operation, vibration insensitivity, robustness and cost 06 p1071 A70-18473

Thermo-electret surface charge and dielectric constant time variation measurements, considering hole-electron pairs production hypothesis 21 p3797 A70-40890

ELECTRIC ANALOGIES

U ANALOGIES

ELECTRIC APPLIANCES

U ELECTRIC EQUIPMENT

ELECTRIC ARCS

NT MERCURY ARCS

Pulsed arcs in argon and helium at superhigh pressures, noting plasma ionization and temperature and charged particle density 01 p0149 A70-10168

Ground based space simulation of arc-type electrothermal propulsion systems, discussing test facilities 01 p0161 A70-10225

Gas-stabilized electric arc heater electrical and gas dynamic parameters, studying velocity and enthalpy radial distributions and IV characteristics 03 p0531 A70-13386

Pulsed high current arc burning in hydrogen at pressures to 400 atm, discussing stability and discharge plasma parameters 04 p0729 A70-15224

Transpiration-cooled electric arcs for high temperature high density plasma generation, considering uncertainties in plasma transport properties and temperature distributions 04 p0729 A70-15591

DC electric arc with superimposed axial subsonic gas flow breakdown voltage and anode heat transfer using high speed photography 06 p1177 A70-17697

Thermal conductivity of argon, nitrogen and air plasmas at atmospheric pressure and 6500-16500 K range, discussing electric arc source 11 p2148 A70-25760

Electric arc shape moving at hypersonic speed investigated by Newtonian pressure distribution for thin shock layer 11 p2090 A70-25992

Electric arc column properties in channel gas flow, including electric fields distribution of potential and heat conduction function 11 p2092 A70-26729

Electric arc in cylindrical channel gas flow described by boundary layer equations, assuming equilibrium and quasi-neutral media 11 p2151 A70-26730

Electric arc stability with descending static I-V characteristics in plasmatrons using direct Liapunov method 11 p2093 A70-26734

Plasmatron geometrical parameters effect on electric arc I-V characteristics, using various gas vortex flows for arc stabilization 11 p2093 A70-26735

Water cooled metallic diaphragm thermal stability effect on plasmatron electric arc characteristics stabilized by vortex air flow 11 p2093 A70-26736

Ignitron converters for feeding power plasmatrons and arc reactors, describing circuit and operation 11 p1984 A70-26742

Mode transition characteristics of free burning argon electric arc with transpiration cooled anode, noting current blowing parameter [AIAA PAPER 69-696] 12 p2281 A70-27806

High argon plasma temperatures via pulsing constricted electric arc 14 p2621 A70-30504

Heat exchange measurements between solid body and high enthalpy gas flow at stagnation point using electric arc heater 15 p2826 A70-32102

Teflon and polymethyl methacrylate sublimation breakdown in plasma jets, using electric arc heated argon, nitrogen, air and oxygen 15 p2765 A70-32103

Electric arc in unbounded axisymmetric steady gas flow, solving energy equation 15 p2780 A70-32129

Laminar Cu-W electrode erosion resistivity in single chamber electric arc hydrogen plasmatrons with gas vortex stabilization 15 p2780 A70-32130

Microwave probe for measuring electron density profile in supersonic arc jet plasma 15 p2741 A70-32433

Experimental and theoretical investigation of mass injection effect on high current MPD arc [AIAA PAPER 69-266] 16 p2959 A70-33869

German monograph on temperature distribution and motion of free burning arcs in transversal magnetic fields and gas flows, covering aerodynamic model concept 16 p2959 A70-34077

Fluid transpiration arc radiation source based on forced convection effect on electric arc
17 p3023 A70-35153

Spectral radiation and polar distribution from high power Ar, Kr and Xe arcs
17 p3023 A70-35156

Homopolar device electric arc dynamics dependence on gas type, noting flow geometry-Hall effect competition
20 p3681 A70-40009

Low voltage arc nonequilibrium ionization rate, taking into account atom-electron collisions
20 p3684 A70-40389

Transpiration cooling of porous constrictor walls of high intensity electric arc in plasma
[ASME PAPER 70-HT-35]
22 p4122 A70-42432

Dissociated and ionized hypersonic flows of hydrogen heated by electric arc techniques, investigating flows in wind tunnel nozzles
22 p4011 A70-42759

Supersonic convective electric arcs with magnetic stabilization in sulfur hexafluoride, examining aerodynamic drag and plasma column slanting
23 p4227 A70-44554

High speed radiographic observation of electric arc movement and metal transfer during submerged arc welding
24 p4322 A70-45724

ELECTRIC BATTERIES

NT ALKALINE BATTERIES

NT DRY CELLS

NT MAGNESIUM CELLS

NT METAL AIR BATTERIES

NT NICKEL CADMIUM BATTERIES

NT NICKEL ZINC BATTERIES

NT SILVER ZINC BATTERIES

NT STORAGE BATTERIES

Lithium-cadmium fluoride battery for aircrew survival beacon radio receivers, considering voltage loss elimination by doping
08 p1439 A70-20708

Sealed cells failure analysis procedures analogous to medical examination in external and internal inspection and diagnosis
08 p1440 A70-20713

Organic semiconductor electrodes for electrochemical generators, discussing redox association with ion and electron conductivity in polyanilines
10 p1830 A70-24463

Low temperature fuel cell materials impurity effects on catalyst poisoning, stressing sulfur elimination from rubber molding
10 p1832 A70-25043

Weights, sizes and costs of nuclear and nonnuclear spacecraft power systems with reference to mission duration
11 p2082 A70-26260

Liquid hydrocarbon-air battery with fuel transport operation, considering electrode structure, boiling range, carbon dioxide rejection, etc
12 p2166 A70-27764

Natural gas-air fuel cell battery with sulfuric acid electrolyte for low temperature operation
12 p2166 A70-27766

High energy density nonaqueous battery with lithium metal anodes, cupric chloride cathodes and organic aprotic solvent electrolyte
[AIAA PAPER 70-530]
13 p2349 A70-29038

Azur satellite p- and n-type Si solar cell system providing both power supply and storage battery charging
13 p2506 A70-29553

Solar cell/battery systems for spacecraft, discussing power system evaluator, NiCd thermal control, lightweight rigid panels design, etc
21 p3757 A70-41011

Book on batteries and energy systems covering theoretical concepts, construction, operation principles, characteristics and applications of various types of primary and secondary cells
22 p3964 A70-42454

Solid state batteries based on highly conducting solid electrolyte rubidium silver iodide, testing discharge performance
22 p3966 A70-43543

Batteries and fuel cells as portable and transportable electrochemical power sources
24 p4295 A70-46399

ELECTRIC BRIDGES

NT WHEATSTONE BRIDGES

Bridging joints resistance effect on thermoelement efficiency, describing W and Co coatings deposition on GeTe based thermoelectric alloys
01 p0159 A70-10757

Molten bridging alloy deposition on p and n type thermoelectric materials, utilizing diffusion process brief duration during contact
01 p0009 A70-10758

Electronic transistorized harmonic signal integrator operating in connection with static-dynamic bridge
03 p0493 A70-13975

Vacuum deposited thin film bridges in electroexplosive devices, discussing composition, surface condi-

tions, substrate temperature, bell jar atmosphere and deposition rate
03 p0546 A70-14107

Design, performance and manufacturing information on various microcircuit bridges in conjunction with production of squibs, detonators and pressure cartridges
03 p0547 A70-14112

Frequency characteristics optimization of symmetrical octupole bridge networks based on relationships between electrical parameters functions and impedance matrices eigenvalues
08 p1468 A70-20572

Operation mode for full-bridge programmed waveform static inverter permitting saturation of power transistors in DC power conversion
08 p1439 A70-20707

Electric bridge for measuring complex impedances and admittances in 60 kHz-30 MHz frequency range
09 p1650 A70-23402

Planar Ge and Si diodes application in pulsed bridge elements, investigating current-voltage and resistance-voltage characteristics
11 p2015 A70-25350

Multichannel tensometric AC bridge network for static and dynamic measurements of mechanical quantities in structural elements
11 p2054 A70-26436

Asymmetrical transient attenuation effects of bridge circuit phase discriminator on accuracy of phase difference measurements
15 p2707 A70-31508

Failure mode and mechanism in dielectrically isolated IC attributed to metal bridging under planar oxide
15 p2713 A70-32648

Planar Ge and Si diodes application in pulsed bridge elements, investigating current-voltage and resistance-voltage characteristics
20 p3600 A70-40462

Polar microwave interferometer using single null path bridge and klystron repeller voltage modulation
22 p4048 A70-42323

Varied-frequency signals separation using bridge circuits for splitting process resulting in unchanged phase ratio and changed amplitude ratio
23 p4159 A70-43759

Superheterodyne EPR spectrometer microwave bridge using single X band klystron
23 p4170 A70-43798

ELECTRIC CELLS

Q switched lasers time dependent loss elimination from elastoplastic relaxation effect in lithium niobate and KDP Pockel cells
20 p3640 A70-39093

ELECTRIC CHARGE

NT ELECTRIC DIPOLES

NT ELECTROSTATIC CHARGE

NT ION CHARGE

NT SPACE CHARGE

NT TRAVELING CHARGE

Thunderstorm lightning discharge formation mechanism, investigating electric charge concentration and motion of free electrons
01 p0134 A70-10169

Disintegration of charged distilled water jets, discussing drops size, velocity distribution and instabilities
03 p0467 A70-13781

Flux, energy spectrum and charge composition of primary cosmic ray electrons measured, determining energy spectrum of primary positrons above 220 Mev
04 p0739 A70-14595

Electrically charged earth satellite motion under action of Lorentz force produced by geomagnetic field interaction, relating field trajectories to acceleration
06 p1142 A70-17879

Dynamics of multicomponent plasma involving charged or neutral gases with transport phenomena for case of no magnetic field
09 p1738 A70-23580

Cerenkov radiation field in infinite parallel dielectric layer by sinusoidally bunched beam of electric charges moving with constant velocity along surface
10 p1916 A70-24408

DC capacitance measurement based on capacitor discharge using auto-oscillatory macrocharge system variant as transducer of measured capacitance, time constant and insulation resistance
11 p1982 A70-25576

Einstein-Maxwell equations for monopolar point electrical charge, calculating proper energy for electromagnetic and gravitational fields
13 p2451 A70-28956

Shot noise effect in antennas to measure electric charge density fluctuations in plasma, noting thermal equilibrium with Maxwellian distribution function
13 p2371 A70-29920

Quantum-electrodynamic renormalization for electron charge in metal environment, using solid state many-body techniques
14 p2619 A70-30476

External magnetic field effect on cavitation zone behind circular cylinder, proving existence of electric charges
18 p3242 A70-36645

Two axially positioned cylindrical waveguides with slots cut periodically along generatrices /double squirrel cage/, analyzing behavior under excitation by rotating charged filament
19 p3386 A70-37733

Ni-Zn high energy secondary battery cycle life and discharge capability
22 p3966 A70-43540

ELECTRIC CHOPPERS

Electrodynamic and electrohydraulic vibrators for frequency sweep, wideband random and sweep random vibration test methods
23 p4195 A70-44333

ELECTRIC CIRCUITS

U CIRCUITS

ELECTRIC COILS

NT MAGNETIC COILS

ELECTRIC CONDUCTORS

Inertia effect of electrically conducting lubricant on load capacity of hydromagnetic inclined slider bearing under magnetic field
01 p0104 A70-11389

Mesothermal flow of collisionless plasma around conducting cylinder, calculating densities, velocities, temperatures and electrical potential
02 p0346 A70-12102

Spherical conducting body effect on induction coil impedance and EMF in nondestructive testing using eddy current probes
02 p0300 A70-12478

Geometrical optics method for obtaining radar cross section of perfectly conducting sphere with inhomogeneous dielectric coating
02 p0262 A70-12599

Electromagnetic scattering from perfect conductors by numerical analysis, presenting far field pattern calculation for plane wave scattering from square cylinder
04 p0652 A70-15363

Static electricity suppression for textile materials by blending conducting metal fibers into yarn
05 p0870 A70-16299

Shielded multiconductor transmission line capacitance calculated by integral equations with Green function kernel
05 p0820 A70-16383

Reflection coefficients of circular posts in rectangular waveguides computed by Green function and method of moments
05 p0820 A70-16384

Composite conductors involving conventional conductors and superconductors to obtain satisfactory electrical performance for application to electromagnets
05 p0870 A70-16582

Three dimensional electromagnetic scattering from thin walled conducting circular tube of finite length normally incident with E or H polarized plane wave
05 p0816 A70-16987

Conducting cylindrical shell in constant magnetic field analyzed for magnetoelastic disturbances using Laplace transform
06 p1056 A70-17607

Numerical analysis of rarefied plasma flow interaction with charged conducting bodies of various forms and dimensions
06 p1123 A70-18298

Rectangular coaxial waveguide with internal conductor contained between inhomogeneous magneto-electric bars, deriving computer algorithm for natural mode fields
09 p1638 A70-23645

Electrodeless electrolysis of solid ionic conductors and fused salts without contact leads, using electron beams and glow discharge
13 p2361 A70-28929

Book on materials for conductive and resistive functions covering superconductive and contacting functions and applications
14 p2557 A70-30951

Electrical conductors specific heat measurement at high temperatures, using optical techniques and digital systems
15 p2826 A70-31942

Boundary conditions for electrodynamics of wave reflection from conducting bodies, using perturbation technique
17 p3128 A70-34633

Diffraction of EM waves emitted by vertical electric dipole on conducting thin circular disk, using algorithm for integral equation
19 p3375 A70-37432

High current elastic conductors nonlinear mixture theory with inviscid electron gas in elastic continuum under mutual electromagnetic and diffusive forces
19 p3387 A70-37787

Plane electromagnetic scattering from perfectly conducting bodies, comparing exact numerical solution with experiment
20 p3585 A70-39394

Conduction liquid metal MHD machine channels design with baffles installed to decrease shunting effect of end zones, calculating segments by circuit theory methods

21 p3760 A70-42233

Flutter of elastic current-carrying shell containing incompressible inviscid nonconducting fluid flow

22 p4117 A70-43383

Arbitrarily shaped cylindrical conducting structures with transient incident electromagnetic wave, calculating scattering from integral equation by digital computer

23 p4165 A70-44957

Electromagnetic scattering by two dimensional periodic arrays of conducting thin plates, calculating induced current and near field radiation distribution

23 p4165 A70-44961

Two monopole antennas on perfectly conducting sphere, calculating radiation pattern by numerical technique

23 p4165 A70-44968

ELECTRIC CONNECTORS

Electrical lead sealing in hydrostatic high pressure systems with gaseous pressure transmitting medium, considering pipestone cone seals, frozen oil seals, epoxy seals, etc

01 p0104 A70-10744

Printed circuit board connector selection techniques based on miniaturization reliability, cost and compatibility with intended application

02 p0268 A70-12473

Lead resistance effects on resistance strain gauge measurements as function of utilized measurement system and procedure

11 p2054 A70-26432

Multiple wiring algorithm for automatic pattern design for AI interconnections and printed wiring in integrated circuits

15 p2715 A70-31842

Connectors for supersonic jetliners, discussing butyl rubber grommet, power distribution collector, modular terminal blocks and passenger service connector

16 p2878 A70-33956

Wire wrapped, soldered, welded and crimped joints and plug/socket connections in electronic packaging for spacecraft

16 p2879 A70-33958

Silicon solar cell array interconnector design based on analysis of stresses caused by thermal expansion and vibrational motion

21 p3756 A70-41009

Boeing 747 airliner passenger entertainment and service electronics multiplexing system, discussing cable and connectors selection and design

23 p4174 A70-44544

Superjet airliners wiring connectors for power distribution, signal circuitry and self ejecting push buttons for passenger seats

23 p4174 A70-44545

Failure analysis methods for connectors and interconnections, discussing visual inspection, X ray vidicon analysis, electrical evaluation, etc

24 p4320 A70-46249

ELECTRIC CONTACTS

Low speed Ga lubricated sliding electrical contacts of Be in vacuum, discussing film role in friction and contact resistance

01 p0099 A70-10325

Vacuum cleavage device for producing small area evaporated metal semiconductor contacts free from oxygen or other contamination

02 p0304 A70-12748

Moving contact pressure transducer for remote signaling

03 p0494 A70-14048

GaAs lasers fabrication, discussing p-n junctions formation, laser die mounting, low resistance electrical contacts, optical cavities, etc

07 p1298 A70-19398

Ohmic contacts to n- and p-type semiconductors obtained by ruby laser, noting linear current-voltage characteristics

07 p1299 A70-19797

Al-Si and Cu-Ti eutectic alloys showing good ohmic contacts to SiC

10 p1927 A70-23990

Electrical, physical and technological requirements and methods of preparation of ohmic contacts on GaAs, noting use of Au-Ge-Ni alloy

10 p1927 A70-24225

Nonsliding rotary electrical connector for conducting current and signals from satellite solar panel [AIAA PAPER 70-458]

11 p2016 A70-25453

Germanium, silicon and gallium arsenide point contact and Schottky barrier diodes as submillimetric wavelength detectors and mixers

11 p2017 A70-25736

Brush current collectors for strain measurements in rotating machine parts, discussing acceptance testing

11 p1983 A70-26438

Brush collector for strain measurement in jet engine compressor and turbine elements at high RPM

11 p1983 A70-26439

Low resistance small area contacts on semiconductor metal oxides

12 p2288 A70-28057

Ohmic contacts for gallium arsenide single crystals, describing fabrication technique and IV characteristics

12 p2202 A70-28187

Metallic contacts deposition on p- or n-GaAs using vacuum evaporation by electron bombardment

12 p2202 A70-28188

Age hardenable monolithic spring material composed of Ag-Pd-Cu alloys for make-break electrical contact

13 p2376 A70-28839

Junction and contact regions in electronic devices using X ray microanalysis and electron probe

14 p2590 A70-30355

Book on materials for conductive and resistive functions covering superconductive and contacting functions and applications

14 p2557 A70-30951

Sliding electrical contacts in vacuum and space - Conference, Virginia Polytechnic Institute, September-October 1969

16 p2919 A70-33805

Reliability life tests preventing sliding electrical contacts failure in space vehicles, discussing data dissemination

16 p2920 A70-33806

Literature review of sliding electrical contacts in space vehicles, covering heavy aromatic hydrocarbons, molybdenum disulfide and other lubrication materials

16 p2920 A70-33807

Fluid lubricants applications to electrical contacts, discussing hydrodynamic and boundary lubrication, film formation on solid surfaces, etc

16 p2920 A70-33808

Sliding electrical contacts for unmanned scientific satellites, discussing Nimbus AVCS camera iris motors

16 p2920 A70-33809

Solid lubricated contacts performance in Nimbus and OAO spacecraft, discussing slip ring assembly and noise problems in Ag-graphite brushes

16 p2920 A70-33810

Slip ring assemblies for spacecraft devices, evaluating sliding electrical contact industry technological capabilities

16 p2920 A70-33811

Materials test fixture design and fabrication for vacuum testing and evaluation of slip rings and brushes, discussing dry film lubrication

16 p2920 A70-33812

Contact-relay circuits failure free operation probability, taking into account coil winding breakage

19 p3390 A70-38579

Epitaxially grown Si contact for area reduction of MOS transistor circuits

20 p3596 A70-39099

In-Au contacts for GaAs, discussing fabrication and performance tests on transverse Gunn mode oscillator

20 p3686 A70-39118

Conjunctors and traditors circuit realizations, discussing resistive and dynamic nonlinear networks

22 p3996 A70-42919

ELECTRIC CONTROL

Triple mode control strategy to provide near optimal stable transient response in variably loaded electrohydraulic servomechanisms

02 p0272 A70-12728

Electrical and hydraulic units controlling second antenna at Pleumeur-Bodou space communication center

05 p0819 A70-15984

Book on hydraulic and electrohydraulic mechanisms covering power transmission by fluids under pressure, data for designing and utilizing equipment, etc

09 p1612 A70-22636

Electrohydraulic fast response servosystem design and operation, describing nonlinear model based on component limitations

10 p1807 A70-24578

Electrohydraulic control system dynamics, examining executive component loading at low speeds and nonlinear resistances

13 p2349 A70-29720

Bang-bang control of electrohydraulic servomechanisms, approximating optimal control by quasi-optimal controls

16 p2887 A70-33685

SST electrohydraulic primary and standby brake control systems, discussing design and advantages [AIAA PAPER 70-913]

17 p3024 A70-35825

Electric field control of oscillatory acetylene flame combustion for chemical rocket engines

21 p3942 A70-40885

ELECTRIC CORONA

Space charge injection-impulse voltage separation technique for nonuniform field breakdown phenomena

01 p0110 A70-10560

Atmospheric humidity effects on ionization and positive corona-current pulses development, discussing radio interference

02 p0258 A70-12425

Counterrotating vertical vortices produced by corona discharge on heated flat plate under free convection conditions

08 p1599 A70-21828

Thin wire glow during corona discharge in metal cylinders analyzed by photomultiplier

11 p2083 A70-25924

Corona-induced thermal boundary layer breakup effects on convective heat transfer from wire electrode to surrounding gas

12 p2333 A70-28110

Corona and voltage breakdown for spacecraft electrical components in low pressure helium-oxygen atmospheres, measuring between parallel plates

21 p3851 A70-42124

Corona discharges from fine W points in liquid He initiated by field ionization or emission, noting anomalous characteristics

23 p4221 A70-44889

ELECTRIC CURRENT

NT ALTERNATING CURRENT

NT ARC DISCHARGES

NT AURORAL ELECTROJETS

NT BEAM CURRENTS

NT DIRECT CURRENT

NT EDDY CURRENTS

NT ELECTRIC ARCS

NT ELECTRIC CORONA

NT ELECTRIC DISCHARGES

NT ELECTRIC SPARKS

NT ELECTRODELESS DISCHARGES

NT ELECTROJETS

NT EQUATORIAL ELECTROJET

NT GAS DISCHARGES

NT IONOSPHERIC CURRENTS

NT LIGHTNING

NT MERCURY ARCS

NT PENNING DISCHARGE

NT RADIO FREQUENCY DISCHARGE

NT RING CURRENTS

NT RING DISCHARGE

NT TELLURIC CURRENTS

NT THRESHOLD CURRENTS

NT TOROIDAL DISCHARGE

Electron-hole pair quasi-linear fluctuations at recombination boundary in semiconductor crystal under crossed electric and magnetic fields

01 p0156 A70-10191

H ion increased activity effect on sodium transport across short circuited turtle bladder

02 p0234 A70-11730

Electrical exploding wire experiments at constant current with inductive energy storage system, discussing experiments with various cross sectioned copper wires

02 p0338 A70-11870

Polarohydrodynamics method applied to electrochemical kinetics of electrode cathodic or anodic current by coupling surface reaction with mass transfer

03 p0534 A70-14268

GaAs tunnel diodes excess current nature and voltage dependence, considering thermal current measurements, depletion layer processes, electron barrier height, etc

04 p0656 A70-14713

Competition mechanism for free carriers in junction isolated transistor collector suggested by current dependence of photocurrent

04 p0657 A70-14732

Silicon bipolar transistors primary photocurrent calculation using manufacturers data

04 p0657 A70-14736

Aligned electric current effect on drag of sphere with arbitrary conductivity moving in current carrying fluid

04 p0671 A70-14993

Plasma acceleration by induced Hall currents, discussing Hall-to-current ratio maximum at critical magnetic field [AIAA PAPER 69-280]

04 p0729 A70-15596

Cylindrical antennas immersed in arbitrary homogeneous isotropic media, solving integral equation for current

06 p1074 A70-18607

Hall current effects on anisotropic plasma magnetogravitational instability under uniform magnetic field, considering electron inertia role and plasma perturbations

07 p1348 A70-19228

Magnetic field variation rates characteristics during magnetic storms investigated for longitudinal dependence and influence of equatorial electric current

07 p1276 A70-20437

Magnetic spikes in polar cap region due to poleward shift of narrow westward electric current filament

08 p1491 A70-21716

Chapman-Vestine and Birkeland-Alfven electric current systems equivalence in ground geomagnetic effect explained for polar magnetic storms

08 p1491 A70-21719

Transistor current gain measurement at HF by two channel method 09 p1632 A70-22234

Pinched plasma reversed current induction due to relativistic electron beam injection 09 p1736 A70-23183

Segmented anode current and heat distribution in MPD engine measured with current shunts and calorimetric methods 09 p1613 A70-23238

Thermal lens effect produced by photocurrent in CdS, using focused laser beam to generate photocurrent causing local heating changes of refractivity 10 p1898 A70-23980

Si avalanche diodes oscillations external current waveform measurement using coaxial current monitoring assembly with negligible phase error 10 p1849 A70-24234

Electric current flow effect on thermoelectric figure of merit from thermal conductivity measurements on thermoelement 10 p1808 A70-25034

Surface waves excited by oscillating current in cold plasma surrounded by metallic sheath of infinite conductivity, deriving frequencies and growth rates 11 p2089 A70-25717

Temperature effects on base and surface currents of plane bipolar transistors, testing validity of surface recombination process model 11 p2021 A70-26832

Current flow across metal-semiconductor contacts via electron tunneling 12 p2285 A70-27254

Corona point discharge current magnitude in transonic wind tunnel, giving current characteristics at different wind speeds 12 p2264 A70-28001

Electron density determination, establishing gas pressure relation to discharge current 13 p2460 A70-28710

Operational amplifier with Darlington circuit for high output current 13 p2377 A70-29114

Electric current direction effect on wake of copper sphere moving in electrolyte 13 p2391 A70-29968

Flueric sensor for RF induced currents providing alternative to bridge wires as initiators of explosive charges 14 p2534 A70-30681

Sunspot electric current evaluation from analyzing transverse component of magnetic field, discussing difficulties and errors in data reduction 15 p2804 A70-32615

Near cathode magnetic field effect on instability in linear Hall current accelerators, using geometry of field extending from anode to cathode region [AIAA PAPER 69-381] 16 p2959 A70-33870

Current oscillations of GaAs Gunn diodes over wide voltage range, discussing diode behavior dependence on polarity and applied voltage 18 p3230 A70-36197

CW multifilament GaAs laser diodes measurement, showing cross correlation between light and current noises 18 p3270 A70-36742

Thin metal film electrical conduction current noise characteristics 19 p3487 A70-38196

Helicon electromagnetic wave attenuation control by steady current of uniform density in propagation direction, considering Hall effect role 20 p3585 A70-39396

Nonequilibrium plasma stability, conductivity and Hall parameter influenced by current flow parallel to magnetic field, discussing Ar-Cs and He-Cs plasma data 20 p3682 A70-40019

High voltage solar arrays for ion engines, discussing spacecraft propulsion, electric generation, insulation integrity, cell degradation and current leakage [AIAA PAPER 70-1138] 20 p3567 A70-40211

Low density plasma in region of orbital-motion-limited /OML/ currents in presence of cylindrical Langmuir probes 22 p4078 A70-42360

Photocurrent multiplication in single crystal n-type epitaxial GaAs due to impact ionization of shallow donors 22 p4087 A70-43218

Ti and Zr based superconducting alloys with Nb content, measuring longitudinal critical currents in wire and ribbon samples 22 p4087 A70-43462

Conducting bodies of revolution, calculating surface currents due to axially incident plane electromagnetic wave by computer program 23 p4162 A70-44005

Laminar geoelectromagnetic field excited by coaxial circular current, determining impedance and magnetic field ratios of spherical harmonics 23 p4189 A70-44064

Force-reduced superconducting toroidal magnet coils built with Cu plated Nb-Zr wire, investigating current enhancement characteristics 23 p4230 A70-44356

Electron recombination effect on current transmission through insulator-semiconductor junction with large diffusion length of minority carriers 24 p4390 A70-45634

ELECTRIC DIPOLES

Radiation from dipole in dispersive anisotropic magnetized plasmas using Fourier analysis 06 p1116 A70-17363

Vertical electric dipole transient response over circular ground screen, studying low angle radiation patterns 06 p1021 A70-17573

Electromagnetic field of horizontal LF electric dipole formed by thin ionosphere layer between anisotropic planes 07 p1277 A70-20447

Polarization of interacting atoms resonance fluorescence and coherence transfer due to excitation exchange, considering electrostatic dipole-dipole and electromagnetic radiative interactions 08 p1548 A70-21341

Electromagnetic waves diffraction on ideally conducting bodies of revolution, deriving design formulas for electric dipole 09 p1632 A70-22401

Non-Cerenkov radiation region produced by passage of oscillating electric dipole at uniform velocity 09 p1728 A70-22958

Electric dipole emission near ideally conducting screen with variable surface impedance parallel strips, analyzing radiation pattern 09 p1636 A70-23140

Radiation field of electric and magnetic dipole in double layer medium, solving Sommerfeld integrals 09 p1650 A70-23550

Point electric dipole EM radiation in presence of moving dispersive dielectric half space 09 p1639 A70-23669

Integral equation for radiation patterns from vertical antenna over variable impedance surface [AFCL-69-0315] 09 p1639 A70-23670

Radiation from electric dipole in moving isotropic plasma analyzed for plasma velocity effect on pattern and far fields 11 p2091 A70-26178

Rectangular tolerancing of dipole impedance values scatter for random passive network samples 12 p194 A70-26968

Electric dipole radiation field in homogeneous anisotropic compressible plasma, obtaining asymptotic expressions by saddle point integration method 12 p2282 A70-27970

Diffraction and scattering of electromagnetic waves emitted by electric dipole arbitrarily oriented in space on inhomogeneous sphere 12 p2190 A70-28172

Cylindrical electric dipole antenna in magnetoactive ionospheric plasma, noting ion sheath effect on input impedance and active length 13 p2399 A70-29402

Elevation and ground conductivity effects on horizontal dipole excitation of earth-ionosphere waveguide, considering east-west propagation 16 p2858 A70-32932

VLF radiation resistance of short filamentary electric dipole at arbitrary angle to magnetic field in cold uniform plasma, using full wave theory 16 p2859 A70-32935

Electric and magnetic dipole VLF radiation patterns in lossy two component magnetoplasma 16 p2860 A70-32944

Electromagnetic field determination from oscillating vertical and horizontal electric dipoles above flat earth, demonstrating Sommerfeld formulation and dyadic Green function technique equivalence 16 p2861 A70-32974

Infinitesimal electric and magnetic dipoles embedded in lossy media, investigating earth effect on electromagnetic field 17 p3045 A70-35075

Diffraction of EM waves emitted by vertical electric dipole on conducting thin circular disk, using algorithm for integral equation 19 p3375 A70-37432

Electrocardiography electrical bridge type leads system based on potential quenching phenomenon, determining electric dipole displacement of heart in transverse plane of body 19 p3369 A70-38208

Electric dipole displacement of heart estimation by supplementing orthogonal with precordial lead, discussing stationary and moving point dipole hypotheses 19 p3369 A70-38209

Electric and magnetic field components of step function excited electric dipole immersed in dissipative homogeneous medium with specified conductivity and dielectric constant 20 p3589 A70-40464

Elevated horizontal and vertical electric dipole VLF fields, discussing ionospheric TE and TM mode coupling, nighttime variations and amplitude fluctuation 24 p4314 A70-46131

ELECTRIC DISCHARGES

NT ARC DISCHARGES

NT ELECTRIC ARCS

NT ELECTRIC CORONA

NT ELECTRIC SPARKS

NT ELECTRODELESS DISCHARGES

NT GAS DISCHARGES

NT LIGHTNING

NT MERCURY ARCS

NT PENNING DISCHARGE

NT RADIO FREQUENCY DISCHARGE

NT RING DISCHARGE

NT TOROIDAL DISCHARGE

Soviet book on plasma physics covering noninteracting and colliding particle motion, elementary processes, electric discharges, kinetic equations, macrocharacteristics, plasmoids, etc 01 p0151 A70-10500

Organic synthesis by electrical discharge in simulated Jovian atmosphere, noting appearance of orange-red cyanogen-ammonia polymer nonvolatile fraction 01 p0179 A70-10529

Equilibrium state of high current discharge in low conductivity plasmas, obtaining light sources at low temperatures 01 p0152 A70-10993

Electrical discharge machining showing close tolerance sizing capability on honeycomb panels 02 p0310 A70-12665

Respiratory muscles neuromotor units activity as function of volley from electric discharge features study on dogs and cats 03 p0417 A70-13068

Transverse magnetic field effects on electrode heat fluxes in heavy-current discharge, discussing anodic space thermal ionization 03 p0531 A70-13205

Electrical discharge machining using electrical spark eroding action for machining tough metals in burr-free intricate configurations, including narrow slots and blind holes 03 p0497 A70-13564

Electroexplosive devices protection from electrostatic discharge by creation of preferential discharge path, considering use of high intensity neon lamp 03 p0549 A70-14134

Axial neutral gas pressure gradient calculated in cylindrical positive column of DC discharge due to driving volume force 04 p0671 A70-15003

Exploding wire discharges in high vacuum, discussing particle emission MHD instabilities, plasma temperature and electron density 05 p0890 A70-16820

Ball lightning mechanism proposal based on mathematical model for electric discharge current in parabolic plasma shell forming vortex-type storm front 05 p0879 A70-17021

Oscillatory discharge properties of capacitance power storage circuit used for pumping pulse lasers 06 p1081 A70-17768

Organic compounds synthesis by electric discharges in simulated primitive atmosphere, considering mechanism for biologically significant molecules formation 07 p1225 A70-19104

Solid electrolyte cells discharge characteristics and open-circuit voltage, evaluating diffusion coefficient of Ag from time dependent behavior of I-V relationship 07 p1196 A70-19386

He-Ne laser plasma vibrations and radiation power during active medium discharge excitation by DC current, noting characteristic energy hysteresis 08 p1511 A70-20519

Discharge current effect on shape and position of resonance curves for electron concentrations during microwave oscillation conversion in magnetoactive plasma 08 p1551 A70-20866

He-Ne laser investigated for He and Ne population inversion as function of discharge parameters 09 p1694 A70-22006

Fast neutral particles produced in electron-ion oscillation discharge as function of gas pressure and magnetic field 09 p1736 A70-23190

Electric discharge reactions in mixtures of phosphine with methane, ammonia and water, obtaining biologically significant inorganic and organic phosphorus compounds 09 p1630 A70-23396

Radiative capacity measurement for plasmas produced from nonconducting materials by pulsed discharges in magnetic field 10 p1923 A70-24252

Plasma instability in RF discharge in Ar in magnetic field 10 p1840 A70-24540

DC capacitance measurement based on capacitor discharge using auto-oscillatory macrocharge system variant as transducer of measured capacitance, time constant and insulation resistance 11 p1982 A70-25576

- Electric discharge machining technology, discussing quality control factors 12 p2239 A70-26990
- Carbon dioxide laser electrical discharge stabilization against transverse gas flow by cross magnetic field 12 p2250 A70-28099
- Gas phase chemicals synthesis via AC diffuse discharge superimposed on propane-air flame seeded with potassium carbonate in electrically augmented flame burner 14 p2546 A70-31097
- Discharged cleaned surface effect on accuracy and reliability of electron density and temperature measurements by Langmuir probes 15 p2778 A70-31765
- CW Cd vapor laser oscillation achieved with slotted hollow cathode discharge containing He carrier gas at pressures of several Torr 15 p2751 A70-31988
- Beam current instability and plasma heating by electron beam generated in linear discharge, discussing electron beam-cold plasma interactions 16 p2957 A70-33191
- Carbon dioxide laser action at 10.6 micrometers at pressures up to atmospheric by transverse electrical discharges 16 p2928 A70-33643
- Carbon dioxide electric discharge dissociation producing oxygen molecules 17 p3138 A70-35588
- Laser oscillation in atomic fluorine from electrically pulsed discharge of fluoride compounds-helium mixtures, identifying as 3p-2P and 3s-2P transitions in fluorine I 17 p3108 A70-35910
- Electric current pulses peak values measurement during aperiodic capacitor discharges, describing circuit with Rogowski coil, diode, capacitor and VTVM 19 p3426 A70-37938
- Energy distribution of ions transversal to magnetic field in argon plasma source with oscillating electrons, showing dependence on induction and discharge current 19 p3482 A70-38956
- Microwave apparatus for resonant frequency change and loaded resonator Q measurement during DC discharge afterglow electron removal studies 20 p3679 A70-39715
- Gas dynamics turbulence of controlled properties effect on electrical discharge across plasma stream, preventing filamentary nature 20 p3681 A70-40008
- Intense high ionization degree discharge plasma initiation at low gas pressures, using auxiliary discharge 22 p4078 A70-42356
- ### ELECTRIC ENERGY STORAGE
- Oscillatory discharge properties of capacitance power storage circuit used for pumping pulse lasers 06 p1081 A70-17768
- ### ELECTRIC EQUIPMENT
- Acoustic noise control on Boeing aircraft electromagnetic components, noting iron-core magnetostriiction demanding transformer redesign 09 p1647 A70-22764
- Design criteria for minimizing EMC problems confronting engineers of aircraft electrical and electronic equipment [SAE PAPER 700215] 11 p1980 A70-25887
- Similarity theory in design of isofunctional electric converters, relating input-output criteria 14 p2533 A70-30374
- Feedback in electrical networks, discussing transient processes within cybernetics framework 15 p2716 A70-32362
- Logarithmic amplitude characteristic of automatic rate stabilization systems for controlled electric actuator systems 18 p3215 A70-36296
- ### ELECTRIC EQUIPMENT TESTS
- Test setup to determine safe limits of atmospheric potential gradients in electroexplosive device initiation 03 p0549 A70-14136
- Fluidic curved-wall electro pneumatic converter optimization, presenting steady state, step and pulse mode responses for various positions and lengths of resistive heaters 09 p1614 A70-23691
- Improved standard electrical equipment components development by test by use method, reducing cost and time 15 p2828 A70-31572
- Soviet book on aircraft electrical and radio systems manufacturing, assembling and testing methods, considering effectiveness and standardization 19 p3357 A70-37405
- ### ELECTRIC FIELD STRENGTH
- Electron distribution function for steady homogeneous plasma of arbitrary ionization degree under strong electric fields, discussing kinetic equations for elastic and nonelastic encounters 02 p0346 A70-12231
- Cs atomic and molecular ions mobilities and drift velocities in Cs vapor at different pressures in low electric fields 04 p0722 A70-14715
- Ground wave electric field intensity prediction model in EMC applications, discussing soil conditions and polarization effects 07 p1336 A70-20217
- Quasi-near zone electric field intensity and current distribution of monopole antenna on finite conductive earth 09 p1645 A70-22691
- Polar gas phase dielectric under conditions of power saturation interacting with microwave radiation field in waveguide 09 p1728 A70-22908
- Millimeter band direct-transit klystrons oscillation and amplification at improved output power obtained by electron bunching in nonuniform drift fields 09 p1651 A70-23637
- Electrostatic energy converter load current analysis, deriving expression for space charge electric field with axially varying or constant charge distribution 10 p1808 A70-25036
- Plasma turbulence theory, discussing particles stochastic acceleration in strong electric field 11 p2094 A70-26753
- Electric field heating effect on edge photoluminescence of n-type GaAs, noting increase in electron energy 12 p2286 A70-27368
- Stark cell with high electric fields for studying inactive IR spectrum of homonuclear diatomic gas molecules 13 p2450 A70-28499
- Electric field sense and magnitude determination from lunar particle shadows in solar electron fluxes 13 p2492 A70-29196
- Predissociation of excited molecules in molecular hydrogen and deuterium by electric field as linear function of field strength 13 p2362 A70-29479
- Ionized impurity scattering in polar semiconductors by strong electric fields, using energy and momentum conservation equations in electron temperature approximation 13 p2472 A70-30017
- Electric field intensity and extension of space charge sheath for ion extraction from nitrogen plasma 14 p2622 A70-30661
- Earth-ionosphere waveguide electric field strength calculation based on nighttime ionospheric models, comparing results to measurements 14 p2574 A70-30748
- Nickel-doped p- and n-type Ge hot electrons recombination characteristics in strong electric fields, examining electron capture cross section 15 p2782 A70-31628
- Kinetic equation in strong electric fields, describing current carrier behavior in semiconductors 19 p3483 A70-37293
- Multivalley semiconductors electrical conductivity anisotropy, discussing redistribution and electron transfer under strong electric field 19 p3483 A70-37294
- Electric field strength in earth ionosphere and magnetosphere during irregular motion of fast ions and electrons 19 p3407 A70-37303
- Ion density and electron temperature variations as function of maximum electric field density in independently excited plasma column striations 19 p3475 A70-37552
- Breakdown electric field strength in S band microwave cavity for dry air, water vapor and mixture 19 p3423 A70-37757
- High field noise emission from indium antimonide, suggesting electron-hole plasma as source 19 p3486 A70-37767
- Current fluctuations in polar semiconductors in strong electric field, taking into account semiconductor band structure 20 p3686 A70-39589
- Electric strengths of liquid dielectrics during subjection to Q switched laser pulses, determining threshold currents for breakdown 22 p4051 A70-43338
- Homogeneous plasma in unidirectional oscillatory electric field, solving Boltzmann equation by electron distribution function expansion 23 p4225 A70-44240
- Ultrasonic absorption in SbSI semiconductors as function of temperature, illumination and constant electric field strength, noting absorption coefficient rise near Curie point 24 p4389 A70-45207
- Temperature, densities and electric field strength of cascaded arcs burning in He under normal pressure 24 p4384 A70-45425
- ### ELECTRIC FIELDS
- Laser mode locking due to saturable absorbers taking into account dispersive property of active material, expanding electric field within cavity 01 p0109 A70-10428
- Electric field effects on flame structure and propagation rate in methane-air mixture 01 p0217 A70-11013
- Electric field effects on dielectric properties and molecular arrangements of cholesteric liquid crystals with temperature dependent helical pitch 01 p0160 A70-11352
- Local thermodynamic equilibrium conditions in superhigh pressure He plasma produced by laser action, obtaining threshold electric field relationship with gas pressure and temperature 02 p0312 A70-12078
- Polar ionic exosphere electric field polarization, considering positive and negative charges escape fluxes, electric potential, mean ion velocity, etc 02 p0289 A70-12108
- Propulsion efficiency in air and in space measured according to relativity concepts, including electric field inertia explanation 02 p0355 A70-12364
- Antenna biasing with DC field to improve power handling capacity tested on U-slot and helical antennas 02 p0269 A70-12595
- Dynamic electric field in solar coronal exosphere on basis of kinetic and hydrodynamic theories, giving estimate of solar wind 02 p0359 A70-12609
- Electric fields in rotating magnetic relativistic neutron stars, analyzing static fields in corotating frame and pulsar emission 02 p0379 A70-12726
- Current density and electron concentration fluctuations in semiconductors under electric field, obtaining theory of light scattering at hot electrons 03 p0539 A70-13405
- Plasma stability in uniform magnetic and HF electric fields, observing magnetoacoustic wave generation at electron cyclotron frequency greater than HF field frequency 03 p0532 A70-13523
- Analytic solutions for focal plane electric field components in parabolic reflector antennas 03 p0457 A70-13697
- Electromagnetic wave propagation in semiconductors, considering effects of electric field, energy dissipation law and band structure 03 p0540 A70-13719
- GaAs nonlinear I-V characteristics and negative differential conductivity associated with electron heating by electric field 03 p0540 A70-13720
- Onset conditions for galvanothermal current instability of Ge semiconductors as function of electric field oscillations, carrier concentration and carrier-lattice temperature 03 p0541 A70-13724
- Optical rotatory power measurement for compensated cholesteric liquid crystal helical structure to observe thermally induced inversion and electric field perturbations 03 p0542 A70-14003
- Earth magnetosphere electric fields associated with magnetic disturbances, using satellite observations 04 p0676 A70-14459
- Resonance frequency shift in motional field-averaging system due to nonuniformities in static magnetic or electric field may cause unexpected systematic errors 04 p0721 A70-14665
- Inhomogeneous plasma oscillations in counterstreaming plasmas analyzed for electric fields and resonant frequencies from Vlasov equation 04 p0726 A70-14671
- Aperture electric field bounds presented for TE, TM and TE/TM excitation over azimuthally symmetric slotted cylinder subject to constraint of specified radiated power 04 p0649 A70-14969
- Conducting fluid steady convection due to combined effects of thermal gradient and DC electric field predicted by analytical model 04 p0785 A70-14989
- Electrostatic field effects of electromagnetic wave propagation in anisotropic plasma 04 p0728 A70-15002
- Rarefied ionospheric plasma flow around rockets and satellites, studying electric field effect on ion motion by kinetic equation and similarity law 04 p0680 A70-15188
- Directional pattern of waveguide radiators using Kirchhoff boundary values of electric, magnetic or electric and magnetic fields, discussing aperture reflection coefficient 04 p0653 A70-15397
- Coaxial electrodes with electric and magnetic fields to study instability in MPD arcs [AIAA PAPER 69-230] 04 p0737 A70-15542
- Electrically driven jets of slightly conducting viscous fluids drawn from conducting tubes, discussing cylindrical soap film instability under radial electric field 05 p0831 A70-15917
- Equivalent pressure concept for breakdown processes and sparking voltage of gas moving at angle to electric field across uniformly stressed gap 05 p0881 A70-16000

Nonequilibrium Cs plasma electron density, temperature and sustaining field using theoretical analysis and probe measurements

05 p0887 A70-16108

Plane magnetopause models assuming ionospheric electrons ability to short circuit electric fields, constructing distribution functions by Vlasov theory

05 p0840 A70-16568

Cloud chamber investigation of artificial cloud of water droplets in electrostatic field, discussing cloud precipitation, collection efficiency and fog dissipation

05 p0879 A70-16689

Low energy charged particle motion parallel with magnetic force lines analyzed in magnetosphere model with constant electric field

05 p0903 A70-16726

Electric field determination from charged particle concentration in wake of body moving in rarefied plasma, noting hydrodynamics similarity

05 p0915 A70-16754

Horizontal electric fields relations to charged particle fluxes in polar auroral ionosphere

05 p0842 A70-16756

Electromagnetic energy spectra of lightning expressed as function of electric field spectral density of atmospheric

05 p0843 A70-16762

Synchronous and asynchronous electrostatic motors based on action of electric fields charges, discussing design and construction

06 p0988 A70-17150

Numerical solution of nonlinear Vlasov equation for collisionless plasma problems, discussing initial value problems, external electric fields, magnetic fields, etc

06 p1108 A70-17419

Lagrangian invariance transformation application to steady state solution for Einstein-Maxwell equations interpreted as external field of charged isolated rotating source

06 p1106 A70-17747

Band extremum loops depth in CDS in electric and magnetic fields determined from calculating linear and nonlinear conductivity

06 p1126 A70-17819

Electric field in earth magnetotail via Explorer 33 and 35 satellite observation of solar electrons above 50 keV energy

06 p1058 A70-18528

Electric and magnetic fields of waterspouts measured by instrumented U.S. Navy aircraft

06 p1101 A70-18582

Unipolar induction to calculate moon interior electric field profiles, noting magnetic back pressure as limb shock wave and interaction with solar wind

07 p1377 A70-18970

Electric and magnetic field perturbation at great distances behind body moving in collisionless magnetized plasma estimated from Fourier transform

07 p1385 A70-19447

Digital computer design of electric and radio equipment using secondary source method for field boundary calculation in inhomogeneous environment

07 p1241 A70-19480

Kinetic processes in plasma subjected to randomly fluctuating electric field, obtaining chain of single particle distribution functions

07 p1349 A70-19553

Electric field diffraction by infinitely long dielectric cylinder due to normally incident cylindrical wave, computing asymptotic value by geometric theory

07 p1235 A70-19684

Induced current density of fully ionized stationary plasma in externally applied HF electric field, discussing frequency range of fluctuations

07 p1352 A70-19988

Molecular dipole moments-electric field interaction induction of cholesteric liquid crystal transition to nematic phase

07 p1225 A70-20053

Particle flux densities in electric field near spherical body moving in rarefied plasma

07 p1355 A70-20368

Lower ionosphere electric fields and currents vertical profiles above geomagnetic equator under quiet geomagnetic conditions from rocket data

07 p1277 A70-20453

Rarefied plasma flow past bodies, considering determination of aerodynamic coefficients, charged states, electric and magnetic fields and plasma parameters

08 p1432 A70-21087

Electric field effects on electrification of colliding ice spheres, discussing relaxation time of sphere charges and charge exchange

08 p1538 A70-21114

Polarized light electroreflection from GaAs single crystal, noting useful signal linear dependence on electric field

08 p1556 A70-21124

TEM waves penetration into magnetoactive semibounded plasma using Vlasov and Maxwell equations, obtaining electric field for specular reflection of electrons

08 p1551 A70-21255

Correlation functions of spatially inhomogeneous fluctuations in electron gas in strong electric field

08 p1552 A70-21423

Acoustic wave propagation in partially ionized gas in external electric field, solving differential equations by Laplace transformation

08 p1552 A70-21503

Trapped particle vibrations stability during quasi-neutral plasma disturbance due to centrifugal drift in stellarator electric field

08 p1555 A70-21982

Bounds on near electric field outside rectangular slot in conducting ground plane applied to microwave breakdown limitation

09 p1646 A70-22696

Room temperature cholesteric liquid crystals retention of information on past electric field excitation by changes in optical transmission properties

09 p1740 A70-22924

Charged particle self oscillatory motion in plane condenser field, applying results to electrical measuring instruments theory

09 p1680 A70-23144

Electrical narrowband noise model for laser speckle pattern, obtaining image intensity statistical properties

09 p1638 A70-23370

MGD model of plasma with dissipation due to finite electrical conductivity described by differential equations

10 p1922 A70-24144

Solar wind model with electrons, protons and alpha particles coupled by electric field and expanding due to pressure gradient and solar gravitation

10 p1931 A70-24433

Mapping electric field components perpendicular to magnetic field line in ionosphere at equatorial plane, discussing discrepancy with convection patterns

10 p1875 A70-24437

Electrodynamic generator channel electric field model, evaluating electric body forces on ionized working fluid flow

10 p1807 A70-24571

Power spectrum of light scattered by two level atom driven by monochromatic electric field obtained from atomic dipole moment correlation function

10 p1920 A70-24632

Microfluctuations frequency and wavelength of electromagnetic, electric and magnetic field distributions in plasma shock wave front found consistent with ion-acoustic origin hypothesis

10 p1925 A70-25031

Electrons radial motion and beam focusing in linear accelerator allowing for perturbing forces, calculating particle trajectory

10 p1926 A70-25110

Electric field structure at shock wave front propagating in weakly ionized gas under Ramsauer effect

10 p1871 A70-25121

Radiation fields of sources in plane stratified plasma medium calculated for amplitude transformation coefficient

10 p1843 A70-25155

Extraterrestrial electrical and magnetic fields effect on meteorological observations, noting relationship between atmospheric pressure distribution and ionospheric developments

10 p1913 A70-25269

EPR line width angle and temperature dependences assuming line widening due to electric field of lattice defects, dipole-dipole interactions and spin-lattice relaxation

11 p2097 A70-25382

Ion component drift displacing components from E and F layers ascribed to vertical electric field presence in hydrogen arc

11 p2104 A70-25541

Nonlinear effects in beam-plasma type interactions, studying particle redistribution under inhomogeneous oscillating electric field

11 p2095 A70-26759

Impact ionization effects in electric field domain on stability of current-voltage characteristics of Gunn diodes

11 p2020 A70-26813

Trumpet-type plane waves instability thresholds in plasma driven by electric field, including calculation of thermodynamic equilibrium

12 p2184 A70-27236

Impurity centers thermal and autoionization and effective capture cross section dependent on free carrier concentration in GaAs under electric field, allowing for plasma shielding

12 p2285 A70-27361

Electromagnetic wave penetration in plasma under uniform DC magnetic field, considering wave propagational direction and electric field

12 p2279 A70-27781

Transverse electric field distribution in multilayered dielectric loaded rectangular guides determined by ray optics and residue calculus

12 p2199 A70-28051

Electric field propagation model in proximal region above plane earth permitting solutions of EMI propagation problems

12 p2190 A70-28138

Electric field distribution in rectangular waveguide loaded with magnetized n-InSb at room temperature obtained by solving boundary value problem by variational method

12 p2202 A70-28163

Alternating electric field effect on weakly ionized gases, analyzing electronic temperature and harmonics generation

13 p2458 A70-28560

Cs atomic spectral line broadening under simultaneous electric and magnetic fields, observing Zeeman and Stark splitting

13 p2460 A70-28711

Electric field in rectangular MHD channel with ideally conducting electrodes in uniform magnetic field, considering conditions for maximum channel effectiveness

13 p2461 A70-28966

Polarized Lyman alpha radiation emitted in electron collisions with atomic and molecular hydrogen and by electric field quenching of metastable atom

13 p2455 A70-29221

Parametric excitation of potential oscillations in plasma near cyclotron frequency subjected to UHF electric and constant magnetic fields

13 p2463 A70-29281

Witness particle electric field as function of non-linear conductivity of weakly turbulent anisotropic plasma by perturbation method

13 p2465 A70-29638

Satellite plasma diagnostics for electric and magnetic fields and fine structure of collisionless shocks in solar wind plasma flows and interplanetary shocks

13 p2481 A70-30069

Energetic particles measurements in geomagnetic tail by Explorer 33/35 for determining gross magnetic topology of distant tail and electric fields

13 p2481 A70-30070

Ba ion cloud motions agreeing with electric field data from balloon measurement in ionosphere and magnetosphere

13 p2402 A70-30079

Auroral and polar cap ionospheric electric fields and tensor conductivity elements using ion clouds data of Ba release experiment

13 p2402 A70-30080

Ionospheric DC electric fields long period oscillations at high latitudes observed by polar orbiting Injun 5 satellite

13 p2403 A70-30081

Ionospheric electric fields variations in ELF-VLF, confirming OV-1 satellite measurements with OGO 6 data

13 p2403 A70-30082

Plasma wave particle interactions in outer magnetosphere, magnetosheath and solar wind, noting role of AC electric fields

13 p2483 A70-30085

Parametric oscillation instabilities in plasma under magnetic field perpendicular to circularly polarized or hybrid electric field

14 p2624 A70-31042

Hall, polarization and Pedersen charged particle drift velocities in static magnetic and time dependent electric field

14 p2624 A70-31046

Stress, strain, temperature, electric and magnetic field distributions resulting from magneto-thermoelastic interactions in infinite elastic solid subjected to transient heat source

14 p2661 A70-31229

Kinetic processes in plasma subjected to randomly fluctuating electric field, obtaining chain of single particle distribution functions

15 p2777 A70-31460

Spherical ionized cloud movement in ionosphere uniform anisotropic plasma as function of electric field applied to rocket released ion clouds

15 p2726 A70-31867

Uniform electric and magnetic fields effects on flow of conducting compressible fluid in channel, using multiple scales method

15 p2779 A70-31914

Longitudinal electric field effect on trapped particle motion in asymmetrical magnetosphere, considering electron precipitation

15 p2728 A70-31990

Diurnal variations in attenuation of ELF atmospherics over different propagation paths from recordings at distant ground stations

15 p2728 A70-31994

Electric field measurements in ionosphere using satellite and rocket experiments

15 p2729 A70-32082

Film condensation in tubes, considering liquid-vapor interface, zero gravity and electrostatic field conditions

15 p2828 A70-32541

Pressure broadened line widths in electric field induced fundamental hydrogen spectral band, noting linear variation with density

16 p2954 A70-33276

Electrostatic near wake model for ionospheric satellites, using low speed fluid dynamic blunt body similarities

[AIAA PAPER 69-674] Longitudinal and transverse electric field effects in magnetospheric electron precipitation, discussing trapped particle drift

16 p2837 A70-33867

Spatial electric field variations and electron distribution for beam plasma amplification, using nonlinear approximation

16 p2959 A70-34336

Rod antenna radiation representation by instantaneous pictures of electric field lines, considering wave detachment mechanism

17 p3050 A70-34575

Plasma waves parametric excitation by external electric field, using perturbation method of multiple scales

17 p3140 A70-34933

Two component fully ionized plasma in HF electric field, demonstrating suppression of runaway electrons in Lorentz plasma

17 p3140 A70-34934

Electric field component of waves in auroral ionosphere measured by double Langmuir probe field detectors, discussing wave-particle interactions and turbulence

17 p3096 A70-35767

Magnetospheric electric field configuration from trapped particle flux asymmetries, using Explorer 14 electron data

18 p3306 A70-36024

Electric fields in lower ionosphere during solar activity minimum above magnetic equator, using vertical profiles of ionospheric current magnetic fields and electron concentration

18 p3246 A70-36098

Air surface layer stationary electric field, considering ionization balance equation, turbulent diffusion coefficient, ion concentration vertical distribution, etc

18 p3247 A70-36520

Electric and magnetic field perturbation at great distances behind body moving in collisionless magnetized plasma estimated from Fourier transform

18 p3316 A70-36921

Polarization electric field in drifting ionospheric inhomogeneities, examining role of longitudinal currents

18 p3252 A70-36987

Ionospheric electric field formation from polarization of electron density inhomogeneities under anisotropic conditions

18 p3252 A70-36988

Electric field equations of plane EM wave diffraction at lattice of conducting cylinders, using Hankel function

19 p3375 A70-37289

High latitudes magnetospheric electric field structure, using electrostatic probes and artificial clouds

19 p3410 A70-37489

Fine structure of solar radiation-induced electrostatic fields on dielectric surface of comets and meteoroids

19 p3514 A70-37656

Electric field component equations of electromagnetic wave traveling through stratified plasma, considering incident and reflected ordinary and extraordinary waves

19 p3379 A70-37863

Auroral enhancement of IR oxygen band, considering electric field excitation mechanisms

19 p3414 A70-38383

Striation formation in artificial ion clouds aligned with local geomagnetic fields, considering visual indication of ionospheric electric field transfer along magnetic field

19 p3415 A70-38387

Point source electric field over different sections of impedance piecewise inhomogeneous surface, calculating attenuation function near boundaries

19 p3381 A70-38570

Skin effect for unsteady radio waves emitted into homogeneous nonmagnetic isotropic half space, calculating electric field

19 p3381 A70-38571

Thunderclouds electric fields and conductivities measurement by differential rotating mill, noting insensitivity to space charge and frictional charging

20 p3661 A70-39146

Whistler mode wave propagation amplitude, polarization and dispersion in lower ionosphere, discussing electric field experiment with Nike-Tomahawk sounding rocket

20 p3622 A70-39456

Electric fields influence on emission lines shape of multiply charged ions in coronal plasma, discussing kinetic temperature

20 p3704 A70-39462

Steady electric field effect on dense plasma cyclotron instability

20 p3678 A70-39595

Wave particle resonances broadening by particles random motion in turbulent electric field, determining cyclotron instabilities saturation level from vanishing nonlinear growth rate

20 p3679 A70-39661

Continuous electrode MHD generator ionization instabilities, measuring current distribution and transverse electric field

20 p3567 A70-40018

Electric and magnetic field components of step function excited electric dipole immersed in dissipative homogeneous medium with specified conductivity and dielectric constant

20 p3589 A70-40464

Ducted laminar and turbulent diffusion flames, examining electric fields effect on heat transfer, geometry and velocity field

20 p3739 A70-40471

Electric field structure at shock wave front propagating in weakly ionized gas under Ramsauer effect

20 p3685 A70-40514

Constant emf in bulk Ge and Si N-type semiconductors under multifrequency microwave electric field

21 p3861 A70-40636

Steady state magnetic and electric fields in magnetosheath by linear superposition of field vectors, using axisymmetric velocity function from gas dynamics

21 p3815 A70-41063

Rarefied ionospheric plasma flow around rockets and satellites, studying electric field effect on ion motion by kinetic equation and similarity law

21 p3819 A70-41169

Ion component drift displacing components from E and F layers ascribed to vertical electric field presence in hydrogen arc

21 p3882 A70-41291

Electron beam interaction with external harmonic microwave field in planar diode gap, calculating electric field current and voltage distribution functions

22 p3995 A70-42396

Large scale electric fields in ionosphere, magnetosphere and interplanetary space, considering further needs for theoretical and observational investigations

22 p4099 A70-42782

Ionospheric electric field origin theory in terms of charge separation due to neutral wind drag

22 p4016 A70-42785

LF electrostatic instability of Van Allen belt in outer trapping zone causing electric field in plasmopause

22 p4099 A70-42786

Collisionless magnetospheric plasma turbulent conductivities for weak and strong electric fields parallel to magnetic field

22 p4016 A70-42787

Upper atmosphere electric field nature, considering solar radiation as major source of ionization

22 p4017 A70-42788

Space electric field considered for solar wind plasma drift origin and possible energy source for spacecraft propulsion, estimating intensity on lunar surface

22 p4100 A70-42789

Upper atmosphere and magnetosphere DC electric field measurement using artificial clouds

22 p4017 A70-42791

Space DC electric field measurement by quadrupole probe, discussing geomagnetic field and contact potential effects

22 p4029 A70-42792

Rocket-borne double probe electric field detector design and operation, discussing error sources

22 p4030 A70-42793

Auroral zone electric field measurements from rocket-borne instruments

22 p4017 A70-42794

Ionospheric current theoretical model and balloon measurement of ionospheric electric field

22 p4017 A70-42795

Lower atmosphere electric field vertical distribution measurement by combined balloon and rocket soundings

22 p4017 A70-42797

Stratospheric electric field and conductivity measurements using balloon-borne electrometer tube circuit

22 p4018 A70-42799

Current densities and fields in quasi-neutral electron beam plasma, solving boundary value problem numerically

22 p4081 A70-42825

Impulse length effect on space echo electric field in collisionless plasma

22 p4082 A70-43237

Electronic damped plasma oscillations eigenfrequency in presence of external electric field

22 p4082 A70-43253

Oxidized Si surface recombination rate measurement by electric field effect, noting electron bombardment effects on electrical properties

22 p3998 A70-43443

Electric field finite amplitude oscillations of electron hole plasma during pinch effect, considering impurities stabilizing effect

22 p4084 A70-43468

Auroral electrojet, arcs, electric and magnetic fields relationship investigated by rocket-borne magnetometers and photometers

23 p4184 A70-43835

Dynamo region electrostatic fields effects on magnetospheric drift, taking electrical conductivities and solar and lunar tidal modes into account

23 p4185 A70-43836

Solar wind electric field relation to ground magnetic disturbances during magnetic storm from Explorer 28 and ground data

23 p4188 A70-44062

Electron distribution function in homogeneous ionized plasma under oscillating electric fields and steady magnetic fields, solving Boltzmann transport equation

23 p4226 A70-44248

External DC electric field effect on microwave absorption in plasma

23 p4226 A70-44372

Stark effect in hydrogen atoms for nonuniform electric fields, considering correction of energy eigenvalues of Schrodinger equation by WKB method

23 p4221 A70-44401

FSRO satellites missions and payloads, emphasizing studies of earth magnetic and electric field environment and of polar region particle measurements

23 p4191 A70-44663

Electric field radial distribution measured for stationary hydrogen arc with axial magnetic field

23 p4227 A70-44933

Electron runaway suppression in fully ionized Lorentz plasma by crossed magnetic and electric fields

24 p4382 A70-45105

Uniform HF electric field effect on ion-acoustic oscillation instability in nonisothermal magnetized current-carrying plasma

24 p4383 A70-45118

Impact ionization effects in electric field domain on stability of current-voltage characteristics of Gunn diodes

24 p4317 A70-45185

Franz-Keldysh and hot electron effects in interband absorption of semiconductors in external electric field

24 p4392 A70-46361

ELECTRIC FILTERS

NT BANDPASS FILTERS

NT DIGITAL FILTERS

NT ELECTROMAGNETIC WAVE FILTERS

NT INFRARED FILTERS

NT LINEAR FILTERS

NT LOW PASS FILTERS

NT MICROWAVE FILTERS

NT OPTICAL FILTERS

NT RADAR FILTERS

NT RADIO FILTERS

NT TRACKING FILTERS

NT ULTRAVIOLET FILTERS

NT WAVEGUIDE FILTERS

Spurious flexural vibrations in cylindrical mechanical resonators, transducers and wires used as component parts in electromechanical filters, indicating dependence on material dimensions and properties

02 p0268 A70-12450

Autocorrelation function distortion in pseudorandom signal with limited spectrum at RC filter output

03 p0446 A70-13202

Distributed RC notch filter normalized constants for dominant and nondominant transmission zero

09 p1654 A70-23025

Reactance filters for matching circuits design with optimum transforming performance

09 p1650 A70-23404

Vibrational motion sensors amplitude-frequency characteristics correction by passive electrical filters, deriving spectral transmittances

11 p2055 A70-26444

Ripple filters for DC power supplies using reliable small capacitance capacitors suitable for spacecraft applications

15 p2714 A70-32806

HF ballistocardiograms resonance distortions correction, using electrical selective filters

19 p3369 A70-38210

Stripline bandstop filter design method, discussing response shape and resonator number determination, reactance calculation, etc

22 p3999 A70-43488

ELECTRIC GENERATORS

NT AC GENERATORS

NT ALKALINE BATTERIES

NT DIRECT POWER GENERATORS

NT DRY CELLS

NT DYNAMOMETERS

NT ELECTROSTATIC GENERATORS

NT FUEL CELLS

NT HYDROGEN OXYGEN FUEL CELLS

NT MAGNESIUM CELLS

NT MAGNETOHYDRODYNAMIC GENERATORS

NT METAL AIR BATTERIES

NT NICKEL ZINC BATTERIES

NT PHOTOELECTRIC GENERATORS

NT RADIOISOTOPE BATTERIES

NT REGENERATIVE FUEL CELLS

NT SNAP 19
NT SNAP 27
NT SOLAR CELLS
NT SOLAR GENERATORS
NT THERMIONIC CONVERTERS
NT THERMOELECTRIC GENERATORS
NT TURBOGENERATORS
Output voltage stabilizers for thermal compensation in semiconductor power generating circuits, using stabiltron reference source
01 p0049 A70-10139
Optimal coercive force selection of residual inductance and energy of magnets for generators with star shaped rotors
01 p0008 A70-10192
Brayton cycle electric power generator simulation to study turbomachinery startup
03 p0415 A70-14050
High power giant pulse YAG laser using nonlinear material to achieve complete second harmonic conversion in intracavity experiment
05 p0859 A70-16470
Stand-by power supply for emergency lighting of Hamburg airport, discussing circuit connections for generators
08 p1482 A70-21371
Generator regulator for Ni-Cd batteries capable of sensing temperature, reducing charge rate and limiting output to increase batteries life
[SAE PAPER 700212]
11 p1983 A70-25884
Harrier fighter aircraft electrical supply system, considering generator design and installation
12 p2166 A70-27891
EGD energy converter system geometries for maximum power efficiencies, comparing slender conversion channels, abrupt expansion, free jet and divergent for operating characteristics
14 p2534 A70-30536
Variable speed constant frequency (VSCF) generators for avionics systems, discussing power, weight, volume, cost and reliability
16 p2910 A70-33486
Aircraft electric power generators performance, discussing transients, modulation and regulation of voltage and frequency
16 p2844 A70-33487
Invariance conditions in two parameter frequency control unit for electric power generator driven by variable speed motor
20 p3565 A70-39850
Axial pressure, electric current and potential distribution in two-phase particulate electrodynamic flow, discussing space charge electric field effect
20 p3683 A70-40257
Modular Dc to Dc switching mode converter for space power system
21 p3758 A70-41217
Mass spectrometer and high voltage converter powering electrostatic plasma and solar wind analyzer for cosmic space studies on Sputnik 3 and Heos A satellites
22 p4025 A70-42312
Planetary unipolar electric generator system theoretical model based on polarization charges deposition by solar wind
22 p4100 A70-42790
ELECTRIC IGNITION
Exploding bridgewire detonator electrical input requirements, discussing waveform, peak current and time to peak
03 p0550 A70-14143
ELECTRIC IMPULSES
U ELECTRIC PULSES
ELECTRIC LEADS
U ELECTRIC WIRE
ELECTRIC MOMENTS
Normal shock waves produced in argon and helium flow by holder with variable downstream porosity, measuring DC moments, component velocities and density
06 p1051 A70-18342
ELECTRIC MOTORS
NT MICROMOTORS
NT SYNCHRONOUS MOTORS
NT TORQUE MOTORS
Hall generator DC brushless motor operation and applications, obtaining motor action by rotor and stator magnetic fields interaction
02 p0228 A70-12053
Brushless DC motors speed regulation with electronic commutators, discussing photoelectric, magnetic sensing and magnetic-coil commutation
02 p0229 A70-12616
Temperature field in thermally stressed electric machine rotor obtained by solving Poisson and Laplace equations with digital computer, using network method
03 p0414 A70-13517
Synchronous and asynchronous electrostatic motors based on action of electric fields charges, discussing design and construction
06 p0988 A70-17150
Temperature distribution in active elements of explosion proof asynchronous electric motors with multichannel bilateral axial flow ventilation systems
07 p1196 A70-19841

Optimal traction drive system design for lunar roving vehicle, considering weight, energy consumption, operational flexibility, power supply, motor and power train
[SAE PAPER 700023]
11 p2030 A70-25375
Transistorized pistol grip probe design, circuit and operation for testing wobble and asymmetry in rotating ring commutators of electric motors
12 p2165 A70-27495
Brushless DC motor with rotor position sensor and transistor commutator for armature current switching, describing design and operation
12 p2165 A70-27525
Brushless DC motor consisting of permanent magnet rotor, wound stator and optical rotor position sensing
16 p2843 A70-33000
Gearhead DC/AC electric motors with wet/dry lubricants, discussing selection criteria for spacecraft boom deployment
16 p2846 A70-34139
Canister for protecting DC motors in Isis 1 antenna unit, noting pressure monitoring device and shaft seal
17 p3100 A70-34753
Electric machines magnetic circuit and motor shape, evaluating current, flux, resistance and reluctance
19 p3357 A70-37362
Brushless DC motor types and sources, describing electronic commutation, AC inverter and limited rotation torque
20 p3564 A70-39725
Closed loop automatic speed control system for working shaft of two stage alternating current electric servomotor, using invariance principle
20 p3564 A70-39849
ELECTRIC NETWORKS
Unconditional stability criterion of active two port in scattering and admittance matrix notation equivalent to conjugate matching for maximum power gain with part impedances
02 p0271 A70-12820
Electric network models of nonhomogeneous differential equations applied to elastic beam and thin plate bending and displacement equations
06 p1094 A70-17927
Electrical network models simulating initial and boundary value problems of applied mechanics, exemplifying with string free vibrations and thin plate bending
06 p1094 A70-17928
Linear networks fault detection and isolation using computerized test procedure and symbolic transfer function generation technique
11 p2029 A70-26337
Rectangular tolerancing of dipole impedance values scatter for random passive network samples
12 p2194 A70-26968
Distributed-lumped-active network to produce transfer function with pair of high Q zero real part sensitivity poles
12 p2196 A70-27652
Communication network approach to submillimeter wave applications in nondestructive testing, deriving transport equations for EM wave propagation
22 p4028 A70-42591
General Optimization Software Package for Electrical network and system design, noting application to engineering problems and education
23 p4177 A70-44750
ELECTRIC POTENTIAL
NT BIOELECTRIC POTENTIAL
NT CONTACT POTENTIALS
NT COULOMB POTENTIAL
NT PHOTOVOLTAGES
NT SPIKE POTENTIALS
EMI/electromagnetic interference/ antennas relative received voltage vs height above ground as functions of effective length, impedance, etc
01 p0042 A70-10087
Double injection in semiconductors at high current densities, discussing procedure yielding space charge and field distribution and voltage drop
01 p0154 A70-10123
Potential created by DC point source in ionosphere at high and medium geomagnetic latitudes, taking into account electrical conductivity anisotropy and altitude variation
01 p0080 A70-11225
Evoked potentials arising in entorhinal cortex of rabbits in response to stimulation of somatic nerves, light and sound
03 p0417 A70-13070
Electric potential fluctuations beyond long collisionless plasma cylinder in uniform magnetic field, noting thermal noise intensity
03 p0530 A70-13086
Voltage-step method to measure diffusivity of structured region in polar liquid electrolyte solutions, considering iodine near Pt microelectrodes in aliphatic alcohols
03 p0441 A70-14044
MOS devices radiation testing for estimating anticipated threshold voltage shift at various dose levels, including gate bias intermittent application during irradiation
04 p0658 A70-14745

Hall voltage measurements on Ta thin films using square wave generator current, discussing parasitic effects and suppression possibilities
05 p0863 A70-16366
Modulated high voltage pulse generator, using rectification of voltage obtained from HF oscillator
06 p1022 A70-17776
Circuit and operation of transistorized linear voltage-to-frequency converter performing current integration proportional to input signal
06 p1022 A70-17779
Multiple electrode probe characteristics in rarefied plasma flow created by ion source, noting electrode potential role
06 p1064 A70-17886
Instability of semiconductor circuit with nonlinear current-voltage characteristics, showing potential negative differential conductivity effect
07 p1240 A70-19274
Lumped element microwave Y circulator, describing device performance and ALGOL program for potentials calculation
07 p1241 A70-19751
Potential distribution outside ideally reflecting charged sphere immersed in resting plasma described by nonlinear integral equation, allowing for polarization
08 p1432 A70-21090
Potential gradient radiosonde field distortion formula, deriving form factors
09 p1671 A70-23602
Vacuum arc discharge phases before total breakdown, studying high combustion voltage relation to interplasma double layer potential difference
10 p1969 A70-25115
Digital-to-analog converter for voltage representation of signals in 2-4-2-1 binary decimal code
12 p2235 A70-27681
Gunn oscillator voltage supply influence on domain capacity, considering frequency stability
13 p2377 A70-29302
Shock waves in partially ionized gas discharge argon plasma, recording potential jump at wavefront
13 p2388 A70-29419
Transistorized voltage to pulse width converter based on constant current capacitor discharge
13 p2378 A70-29457
Frequency conversion during multiple phase modulation of supply voltage by pulse width technique
14 p2548 A70-30372
Reactive filter synthesis for step-voltage output inverter smoothing, using network theory
14 p2559 A70-30373
Cell electrode potential interphasial components, defining problems due to relevant interfacial electrochemistry concepts
14 p2533 A70-30526
Coupled temperature and electric potential distribution in finite rotational symmetric hydrogen arc column in axial magnetic field
14 p2621 A70-30656
Piezoelectric annular disk transducer mechanical response to step voltage input with prescribed temperature field
14 p2588 A70-31228
Growing ice crystals surface electric potentials during various stages of water vapor condensation
15 p2769 A70-31444
Regenerative semiconductor parametric amplifier saturation in forward current mode, assuming harmonic voltages /signal, pumping and difference frequencies/ action at p-n junction
15 p2708 A70-31522
B, In or Ga doped Si photosensitivity dependence on sample temperature, supply voltage and illumination intensity, determining optimal operating conditions
15 p2782 A70-31631
Power reduction consumed in vacuum by direct-current voltage converter by introducing delay into breaker transistor control at output stage
15 p2677 A70-31945
Ladder networks total transmittance and voltage transfer ratio and impedance or admittance, investigating signal flow graph open paths and Fibonacci sequence
15 p2715 A70-32344
Zener diodes as voltage transient suppressors for ground vehicle and aircraft power supplies
16 p2879 A70-34060
Space charge sign distribution sounding in atmosphere by electrode potential difference measurement
18 p3246 A70-36180
Current oscillations of GaAs Gunn diodes over wide voltage range, discussing device behavior dependence on polarity and applied voltage
18 p3230 A70-36197
Gunn effect pulse regenerators, describing random domain triggering rate voltage dependence comparison with Johnson noise predictions
19 p3387 A70-37820
Induction flometers operation, emphasizing various factors effects on induced voltage
19 p3426 A70-37936

- Two dimensional piezoelectric problems of electroelasticity, formulating general solutions in terms of stress and electric potentials using complex variables 19 p3487 A70-37946
- MOS structures deep depletion capacitance/voltage characteristics by ramp response method 19 p3389 A70-37972
- Gunn effect devices with concentric cylindrical electrodes, examining oscillation natural frequency-applied voltage relation 19 p3392 A70-38900
- Frequency discriminators output voltages under action of fluctuating signal and noise with arbitrary energy spectrum 20 p3584 A70-39254
- MHD flow in channel of arbitrary cross section, deriving velocity and electric potential distribution by variational principle 20 p3677 A70-39360
- Voltage programmed RF oscillator /VPO/ for spaceborne quadrupole mass spectrometer, describing transistorized circuitry 20 p3630 A70-39487
- Emitting plasma probes floating potential, discussing emission rate dependence on probe temperature and surface coverage by seed 20 p3632 A70-39607
- Voltage-to-frequency transducers with negative feedback, analyzing errors and conversion transconductance 20 p3601 A70-39789
- SERT 2 measurements for spacecraft and ion beam potential as function of thruster and orbital parameters, using hot wire emissive probes [AIAA PAPER 70-1127] 20 p3691 A70-40218
- Maintenance voltage of RF argon thermal induction plasma at atmospheric pressure as function of ring probe 21 p3859 A70-41904
- Corona and voltage breakdown for spacecraft electrical components in low pressure helium-oxygen atmospheres, measuring between parallel plates 21 p3851 A70-42124
- Rayleigh wave scalar electric potential analysis on piezoelectric medium, using iterative techniques for Poisson equation 22 p4074 A70-42967
- Stochastic heating of plasma in toroidal trap/stellarator, showing discharge ignition potential dependence on microwave oscillator frequency 22 p4084 A70-43394
- DC-to-DC converter design to supply different isolated voltages from single input 23 p4142 A70-43875
- Electrostatic potential distribution and ion trajectories in extraction gage design by computer 23 p4198 A70-44873
- Microwave transmission systems, determining electric potential functions in inhomogeneous dielectrics by Earnshaw theorem and finite difference computation 24 p4318 A70-45217
- Intermaterial adhesion relation to association contact resistance-tension characteristics based on electric potential barrier model for Maxwell-Wagner effect 24 p4379 A70-45617
- ELECTRIC POWER**
- Antenna biasing with DC field to improve power handling capacity tested on U-slot and helical antennas 02 p0269 A70-12595
- Electrodynamic compressor with direct conversion of electric energy into mechanical energy, improving conversion efficiency by using plasma as working medium 07 p1196 A70-19658
- Integrated electron density determination for plasma sheath on reentry vehicle based on power coupling change measurement 08 p1552 A70-21596
- Integrated microwave systems development taking into account cost effectiveness and anticipating kilowatt and megawatt systems 10 p1851 A70-24880
- Hybrid ring microwave power divider /rat race/ for equal or unequal power splitting 13 p2377 A70-29061
- Electrodynamic compressor with direct conversion of electric energy into mechanical energy, improving conversion efficiency with plasma as working medium 15 p2678 A70-32695
- High voltage DC electric power systems design for aircraft, considering filtering, transmission and loads interaction 16 p2844 A70-33475
- Solid state switching effect on aerospace electric power conditioning equipment [SAE PAPER 700306] 18 p3302 A70-36802
- One wavelength MHD induction generator, discussing field pressure gradients, fluid velocities, excitation and electrical output power 20 p3566 A70-40015

ELECTRIC POWER CONVERSION

U ELECTRIC GENERATORS

ELECTRIC POWER PLANTS

NT NUCLEAR POWER PLANTS

Mission model construction for power limited systems, discussing flight concepts, propulsion mixes and electric propulsion 01 p0183 A70-10848

High-strain fatigue life temperature dependence of austenitic and ferritic power plant materials compared to creep-rupture life 09 p1773 A70-22577

Solid state power controllers for aircraft electrical power systems [SAE PAPER 700304] 12 p2195 A70-27450

Power plant using carbon dioxide planetary atmosphere as working fluid, noting weight reduction 15 p2828 A70-32262

ELECTRIC POWER TRANSMISSION

Solid state multiplexed electrical power distribution system for future generation military and commercial airplanes [SAE PAPER 700301] 18 p3216 A70-36803

Aircraft electrical system multiplexing, discussing design features and advantages over conventional hard wired systems [SAE PAPER 700303] 18 p3216 A70-36811

ELECTRIC PROPULSION

NT ELECTROMAGNETIC PROPULSION

NT ELECTROSTATIC PROPULSION

NT ION PROPULSION

NT PLASMA PROPULSION

Solar electric spacecraft field interaction with space plasma affecting collection and interpretation of scientific data, emphasizing required system configurations and constraints [AIAA PAPER 69-1106] 01 p0162 A70-10601

Solar and nuclear electric propelled spacecraft applications to planetary and interplanetary missions, considering asteroid survey, out-of-ecliptic, Mercury orbiter, comet rendezvous, etc [AIAA PAPER 69-1108] 01 p0181 A70-10619

Propellant condensation on surfaces near electric rocket exhaust, calculating particle arrival rates, backflow and desorption energies [AIAA PAPER 69-270] 01 p0166 A70-10836

Advanced reconnaissance electric planetary spacecraft /AREPS/ concept for repeated coverage of Mars or Venus surface, using solar-photovoltaic system [AIAA PAPER 69-253] 01 p0196 A70-10837

Electric propulsion technology status for auxiliary and solar electric prime propulsion applications [AIAA PAPER 69-1107] 02 p0356 A70-12530

Solar electric propulsion /SEP/ for automated planetary missions, discussing system characteristics, capabilities and costs [AIAA PAPER 69-1103] 02 p0382 A70-12531

German developments in electric propulsion and energy supply systems for commercial satellites in geostationary orbits [DGLR-69-20] 04 p0735 A70-15169

Solar or nuclear energy powered electric propulsion systems for transferring satellite from low to geostationary orbit, discussing feasibility and costs of various designs 04 p0735 A70-15174

Solar powered electric propulsion systems for automated missions throughout solar system by extending range of Atlas Centaur-Titan 3-C launch vehicles [AIAA PAPER 68-1120] 04 p0736 A70-15401

Spacecraft design, trajectory and mission analyses for multipurpose solar electric propulsion missions, emphasizing modular ion engine and fixed attitude spacecraft designs [AIAA PAPER 69-252] 04 p0763 A70-15412

Pulsed MPD arc jet electric propulsion system requirements, examining physical constraints, pulse duration, duty cycle, power network structural details, etc [AIAA PAPER 69-269] 04 p0737 A70-15424

Nuclear and electric propulsion systems performance, considering applications in future European space activities 05 p0897 A70-16898

Electric propulsion system and initial gross weights estimation for manned Mars missions 05 p0924 A70-17093

Constant thrust electric propulsion systems performance with coast trajectories presented for 100 AU extraecliptic missions [AIAA PAPER 68-546] 06 p1137 A70-17160

Satellite electric propulsion system and configuration for orbital transfer maneuvers, describing ELDO launcher, Black Arrow, orbital dynamics, sensor system, etc 06 p1130 A70-17648

Applied space research covering photovoltaic cells, electric propulsion, onboard data storage, vacuum lubrication and NASA-European organizations budgets 06 p1141 A70-17780

Low thrust trajectory and performance analysis of solar electric propulsion system for unmanned interplanetary exploration [AIAA PAPER 70-212] 06 p1145 A70-18081

Space electric rocket test /SERT/ II thruster system, discussing flight worthiness and mercury bombardment discharges [AIAA PAPER 67-700] 07 p1364 A70-19701

Book on spaceflight propulsion covering jet thrust, energy release, chemical, nuclear and electric propulsion, transportable and environmental systems 09 p1742 A70-22202

Electric propulsion design, considering effects of weight, impedance matching, beam voltage regulation and operating point variations in formulating system mass and reliability 09 p1743 A70-23248

Electric propulsion system selection for Lockheed Communications Satellite /LCS/ based on weight, development status and complexity considerations, discussing optimization procedure [AIAA PAPER 70-478] 11 p2101 A70-25470

Space charge sheath electric thruster principles, construction and performance using laboratory test model [AIAA PAPER 69-282] 11 p2102 A70-26121

Minimum energy feedback control for electrically driven vehicles by dynamic programming 16 p2884 A70-33310

Solar electric spacecraft for interplanetary missions including asteroid belt survey, Jupiter flyby and out-of-elliptic survey [AIAA PAPER 70-645] 16 p2981 A70-33531

Hollow cathode ion thruster and lightweight power conditioner of solar-electric propulsion system for unmanned deep space probes [AIAA PAPER 70-648] 16 p2966 A70-33546

Unmanned electric propulsion spacecraft with external fuel and flashlight thermionic reactors, discussing thruster arrays, weight and performance for reference Jupiter orbiter mission [AIAA PAPER 70-644] 16 p2966 A70-33547

Low thrust high impulse nuclear and electric space propulsion systems, discussing performance capability for space missions 18 p3290 A70-36566

ESRO applied research program, discussing IR technology, onboard computers, electric propulsion, etc 19 p3553 A70-37870

Electric propulsion systems design and performance, surveying various types 20 p3688 A70-39238

Solar electric propulsion system performance consisting of thrusters with thrust vector aligning actuators, switching network and flight type power conditioner 20 p3688 A70-39687

Algorithm for trajectory analysis in closed loop terminal guidance of solar electrically thrusted interplanetary spacecraft [AIAA PAPER 70-1152] 20 p3670 A70-40203

Solar panel flexibility effect on attitude control of solar electric spacecraft for deep space mission [AIAA PAPER 70-1140] 20 p3716 A70-40209

Electric propulsion systems integration into SERT 2 spacecraft, discussing launch imposed environment, thrust vector control, thruster breakdown, power conditioning, etc [AIAA PAPER 70-1123] 20 p3691 A70-40222

Optimized trajectories and spacecraft for solar-electric missions to asteroids, using chemical booster for injection [AIAA PAPER 70-1120] 20 p3710 A70-40223

Solar electric propulsion Mars high data rate orbiter trajectory design and analysis, including landing site selection and spacecraft parameters optimization [AIAA PAPER 70-1119] 20 p3710 A70-40224

Solar electric propulsion application to out-of-ecliptic mission for interplanetary fields and particles data, comparing performance with chemical systems [AIAA PAPER 70-1118] 20 p3691 A70-40225

Interplanetary solar electric spacecraft performance improvement by mission mode including earth swingby maneuver in solar orbit inclined to ecliptic [AIAA PAPER 70-1117] 20 p3710 A70-40226

Primary solar electric propulsion for automated space transportation propulsion program, considering performance and technology readiness [AIAA PAPER 70-1115] 20 p3691 A70-40228

Thermionic reactor program for electric propulsion, considering internally fueled flashlight concept [AIAA PAPER 70-1108] 20 p3568 A70-40235

Kaufman ion thruster providing electric propulsion for satellite spiraling from parking to synchronous orbit [AIAA PAPER 70-1101] 20 p3692 A70-40237

Electric propulsion research involving MPD thrusters, current sheets and neutral-ion motion coupling [AIAA PAPER 70-1086] 20 p3683 A70-40249

Solar electric propulsion systems technology development at JPL, discussing performance data and relationship to spacecraft requirements [AIAA PAPER 70-1153] 20 p3695 A70-40520

Thermionic reactor electric propulsion for unmanned outer planets exploration, discussing spacecraft design, launch vehicle, weight factors, etc [AIAA PAPER 70-1122] 20 p3717 A70-40524

Solar electric propulsion unmanned asteroid belt probe, discussing propulsion system, flux data acquisition, etc [AIAA PAPER 70-1121] 20 p3717 A70-40525

Vapor biowaste electric spacecraft propulsion system, discussing recovery cycles and subsystem tradeoffs, specific impulse, chamber heating, power input and reaction products 21 p3866 A70-40869

Low specific impulse hollow cathode mercury thruster for deep space electric propulsion, using SERT 2 configuration [AIAA PAPER 70-1099] 21 p3866 A70-40893

Power conditioning requirements and specifications for spacecraft electric propulsion ion thruster 21 p3758 A70-41209

Scientific payloads integration with multimission electric propulsion interplanetary spacecraft, discussing possible contamination effects due to solar electric propulsion system [AIAA PAPER 70-1141] 21 p3930 A70-41781

Three axis attitude ion thrust vector control mechanism for solar electric propulsion spacecraft, discussing gimbal and translation actuators, array and cabling [AIAA PAPER 70-1156] 21 p3759 A70-41784

Multimission solar electric spacecraft propulsion module design for Asteroid Belt, Jupiter and out-of-ecliptic missions, including thruster failure and power conditioning requirements [AIAA PAPER 70-1155] 21 p3868 A70-41785

Mars and Venus orbiter spacecraft electric propulsion system, discussing Hg electron bombardment ion engine [AIAA PAPER 70-1154] 21 p3868 A70-41786

Liquid metal/mercury/cathode thruster system for operation at reduced beam voltages, discussing design and performance [AIAA PAPER 70-1103] 21 p3868 A70-41788

Spacecraft electric propulsion system performance, discussing exhaust velocity optimization 21 p3869 A70-42043

Electric propulsion plasma thrust beam and ambient space plasma electrostatic equilibration, considering various charged particle parameters involved in bi-plasma system interactions [AIAA PAPER 70-1142] 22 p4091 A70-42974

Nuclear electric space propulsion, emphasizing systems uncertainties and cost aspects 22 p4070 A70-43187

Thermionic reactors for spacecraft auxiliary power and electric propulsion, discussing in-core conversion system and diodes 22 p4071 A70-43191

Attitude and orbit control electric propulsion systems for long term space stations, discussing resistojets and electron bombardment and contact ionization ion thrusters 22 p4092 A70-43654

Space vehicle for testing electric propulsion systems in space, powering by cluster of six electrostatic ion motors regulated by automatic thrust control 23 p4259 A70-44616

ELECTRIC PULSES

Wide range pulse height discriminator with milliwatt power drain for use in nuclear experiments on scientific satellites 01 p0088 A70-10749

Atmospheric humidity effects on ionization and positive corona-current pulses development, discussing radio interference 02 p0258 A70-12425

Modulated high voltage pulse generator, using rectification of voltage obtained from HF oscillator 06 p1022 A70-17776

Repetitively pulsed quasi-steady vacuum arc magnetoplasmadynamic accelerator for propulsion, using electrolytic capacitors as power source [AIAA PAPER 70-167] 06 p1133 A70-18228

Pulsed current gas tungsten arc welding in inert gas atmosphere and applications 12 p2238 A70-26853

Fuel cells power density improvement under pulsed loading at high current density and constant voltage 12 p2165 A70-27758

Thin cylindrical DC pulse driven antenna radiation fields time variation as function of angle 12 p2198 A70-27964

Magnesium pulse arc welding, describing procedure, techniques testing and advantages 17 p3100 A70-34635

Pulsed signal amplitude and delay time measurement in presence of interfering /reverberated/ signals and steady noise 19 p3375 A70-37285

Electric current pulses peak values measurement during aperiodic capacitor discharges, describing circuit with Rogowski coil, diode, capacitor and VTVM 19 p3426 A70-37938

Electrolytic capacitor current pulse networks for quasi-steady MPD arc thrusters, determining series resistance effects on energy transfer [AIAA PAPER 70-1082] 20 p3568 A70-40253

Finite thickness metal plate eddy current response to pulsed field from aperture probe 24 p4344 A70-45696

ELECTRIC REACTORS

Optoelectronic devices for variable resistors controlled by electrical signal, investigating decoupling, capacitance and DC resistance 09 p1649 A70-23353

ELECTRIC RELAYS

Soviet book on matrix methods in relay and sampled data control theory described by linear differential and finite difference equations 07 p1244 A70-19069

Soviet book on aircraft AC and DC relay pulse generators, emphasizing controllable frequencies and duty factors and neutral and polarized electromagnetic relays 12 p2194 A70-26874

Diode coil suppression effect on two coil magnetic latching relays, showing operating time increment due to transformer action 13 p2378 A70-29348

Relay stabilization system for flight vehicle motion about center of mass, using point transformations method and bifurcations theory 15 p2674 A70-32151

Relay control systems stability bound determination in nonphase variable form, assuming unknown system parameters 16 p2881 A70-33034

Contact-relay circuits failure free operation probability, taking into account coil winding breakage 19 p3390 A70-38579

Space vehicle self oscillatory pulsed relay attitude control system with jet nozzles, determining angular motion 22 p4001 A70-42838

Amplitude-phase characteristics of relay slave mechanisms with AC and DC motors under dynamic braking, using harmonic linearization 22 p4002 A70-42842

Fluidic logic devices compared with electric relay and hydraulic/pneumatic valve equivalents 24 p4293 A70-45429

ELECTRIC ROCKET ENGINES

NT ELECTROSTATIC ENGINES

Tangential thrust, constant acceleration trajectories for close solar probe missions using low thrust electric engines 06 p1137 A70-17177

SERT 2 thruster hollow cathode durability tested in bell jar [AIAA PAPER 69-304] 07 p1364 A70-19703

Quantum electronic space vehicle, discussing time reversing motor or inverse /anti-/ atomic engine 17 p3148 A70-35213

Micropound extended range thrust stand /MERTS/ for testing electric thrusters for spacecraft auxiliary propulsion, providing three thrust measurement ranges and data telemetry system [AIAA PAPER 70-1111] 20 p3607 A70-40232

ELECTRIC SPARKS

Triggered spark source for multiply charged carbon ions applied to collision cross section measurements 02 p0303 A70-12747

Detonator insensitive to highest level of electrostatic voltage on human body for precise synchronization 03 p0547 A70-14111

Fixed gap electrostatic spark discharge apparatus for booster type explosive sensitivity tests, discussing construction of two models, safety features and results 03 p0548 A70-14120

Equivalent pressure concept for breakdown processes and sparking voltage of gas moving at angle to electric field across uniformly stressed gap 05 p0881 A70-16000

Discharge circuit parameters and heat physical constants of electrode material effects on electrical erosion of metals 07 p1294 A70-19351

Spark track plasma of electrical discharge in fluid, describing energy dissipation, particle formation and density, plasma temperature, etc 08 p1551 A70-21202

High resolution multiple spark photography, discussing facility 09 p1680 A70-23070

Gas flow rate measurement by repeated spark method suitable for stationary and nonstationary flows past surfaces of complex shape 10 p1892 A70-25119

Ruby laser beam used to trigger high voltage spark discharge in vacuum, studying auxiliary photoionization during firing delay or failure 12 p2249 A70-27999

Electromagnetic shock tube demonstrations of electrode spark breakdown, strong shock behavior,

plasma conductivity and hypersonic shock flow over blunt body 13 p2404 A70-28623

Planview shadowgraph method for observing disturbances generated by spark discharges into laminar boundary layer 13 p2385 A70-29982

Metallic fuels preparation by electric spark discharge process 17 p3145 A70-35214

Aircraft streamer /spark/ discharges formation, waveforms and RF noise levels, using mathematical model for electric field strength 19 p3380 A70-38179

Metallic surfaces vacuum electric spark alloying, investigating pressure effects on coating layer thickness and area 20 p3636 A70-39195

Gas flow rate measurement by repeated spark method suitable for stationary and nonstationary flows past surfaces of complex shape 20 p3635 A70-40512

Sparks channel resistance temporal variation, using resistivity of fully and singly ionized plasma 22 p4072 A70-42354

Spark erosion or plasma jet treatment effects on Co surface structure, describing allotropic delta phase 24 p4364 A70-46221

ELECTRIC STIMULI

Right and left atrial polarization time sequence as guide to p wave origin in heart diseased patients following electrical stimulation of atria and ventricles 01 p0015 A70-10437

Object carrying behavior of rats, using electrical stimulation of hypothalamic structures 02 p0237 A70-12395

EEG patterns of functional state effect on evoked cortical potentials in response to DC pulses in dogs after nembutal administration 04 p0638 A70-15503

Amysyl effects on conditioned passive avoidance reflexes development and reinforcement in white mice under electric shock 07 p1198 A70-18717

Hypothalamic stimulation effects on cardiac and vascular efferent components of baroreceptor reflexes in spinal cats 07 p1202 A70-18866

Somato-vegetative and behavioral reactions of rabbits to electric stimulation of hypothalamus after injecting aminazine 07 p1209 A70-19521

Involvement reactions in dying and reanimated cats with nucleus reticular hypothalamicus stimulated by rectangular electric pulses 07 p1209 A70-19522

Hypothalamus stimulation effect on electrical activity of hippocampus at threshold and super-threshold levels in cats 08 p1446 A70-21448

Hypothalamus stimulus effects on sympathetic nerve activity to heart, spleen, kidney and leg skeletal muscle in anesthetized cats 09 p1614 A70-22001

Orthostatic tolerance in humans increased by lower limb muscles electrostimulation, correlating subjective feelings with heart and pulse rate measurements 09 p1615 A70-22089

Transmural stimulation elicited phasic and tonic contractile responses in circular and longitudinal axes of small intestine under nerve-blocking drugs 09 p1622 A70-23547

Vegetative cardiovascular, motor and electrophysiological reactions to electrical stimulation of limbic and reticular formations in cerebrum after adrenalin and aminazine injections 13 p2352 A70-29352

Electrical stimulation of dogs hypothalamus effect on blood and lymph circulation and composition 13 p2352 A70-29354

Evoked cerebellar potentials time characteristics during spinal cord stimulation in cats, investigating cerebellar intercentral connections effect 13 p2353 A70-29357

Hypothalamic motivation, presenting data supporting less anatomical specificity 13 p2355 A70-29794

Hypothalamic electric stimulation intensity effects on elicited behavior, considering possible neural circuit threshold reduction 13 p2355 A70-29807

Eating, drinking and gnawing motivation interchangeability under hypothalamic stimulation, noting role of neural substrate activation 13 p2356 A70-29814

Conditioned reflex type fear reaction by electric stimulation of hippocampus in cats 14 p2535 A70-30184

Rats under constant environmental conditions exhibiting circadian rhythmicity in rate of bar pressing with hypothalamic and septal reinforcing brain electrical stimulation 14 p2539 A70-30986

- Orthostatic tolerance in humans increased by lower limb muscles electrostimulation, correlating subjective feelings with heart and pulse rate measurements
15 p2685 A70-32685
- Human tracking performance in position, rate and acceleration control systems under short term psychological stress induced by electric shocks
16 p2853 A70-33689
- Electrical stimulation in rostromedial hypothalamus effects on thermogenesis of juvenile rats, calculating heat transfer at trunk
16 p2849 A70-33696
- Electrical polarization effects on discharges in individual auditory nerve fibers following current application to cochlear partition
17 p3033 A70-35609
- Nonreciprocal double-pumped parametric converter eliminating separate pump signals
22 p3998 A70-43252
- Fixed-ratio performance patterns of pigeon key-peck responses to fractional punishments by electric shock
22 p3971 A70-43375
- Respiration rhythm mechanism from medulla oblongata electric shock stimulation in cats, considering inspiration-expiration phase shift relation to neuron fatigue
24 p4297 A70-45493
- Forebrain participation in motor response suppression reaction during stimulation of caudate nucleus in rats and cats, noting brain damage effects
24 p4299 A70-45836
- ELECTRIC STRAIN GAGES**
U STRAIN GAGES
- ELECTRIC SWITCHES**
NT THERMOSTATS
- Chalcogenide glass based film face threshold switches I-V characteristics, presenting oscillogram and diagrams
05 p0892 A70-16542
- Electronic switching effects in amorphous semiconductors emphasizing mass memory for computers based on thin films of chalcogenides
11 p2017 A70-25524
- Multibandswitch AC Wheatstone bridge design with large circuit factor
17 p3051 A70-34616
- Air spark gap to switch stored charge in LC circuit, using auxiliary triggering circuit to clamp magnetic flux
23 p4177 A70-44471
- ELECTRIC WELDING**
NT ARC WELDING
NT ELECTRON BEAM WELDING
NT GAS TUNGSTEN ARC WELDING
NT PLASMA ARC WELDING
- HF resistance welding and roll diffusion bonding fabrication of thin complex structures from Ti alloys in aerospace industry
13 p2418 A70-28828
- Quality control organization for miniature resistance welding of electronic equipment, examining planning phase and personnel training program
14 p2592 A70-31107
- One-step closure sealing of pressurized stainless steel capillary tubes by resistance pinch welding
21 p3832 A70-40789
- Stainless steel sheet-to-plate tee joint resistance welded by Magnetic Force Upset Welding process, testing performance
21 p3832 A70-40792
- Bar butt current penetration welding, using HF continuous current seam welding process for joining finite length pieces
22 p4046 A70-43148
- ELECTRIC WIRE**
NT EXPLODING WIRES
- Electrical exploding wire experiments at constant current with inductive energy storage system, discussing experiments with various cross sectioned copper wires
02 p0338 A70-11870
- Radar cross section computation for thin wires bent into circular arcs and V shapes using numerical method
02 p0262 A70-12597
- Solid rocket motor ignition system based on exothermic alloying of bimetallic wire constituents [AIAA PAPER 69-425]
06 p1128 A70-17179
- Electrically heated wire diameter and orientation on heat flux in saturated pool and surface boilings of water and aqueous binary mixtures
07 p1417 A70-18643
- Rapid guiding system for high resolution astronomical observations using thermal expansion of electrically conducting wires
09 p1721 A70-22741
- Transverse and longitudinal resistive critical fields of Nb wires, discussing superconductivity in dislocation cell walls created by drawing or swaging
09 p1704 A70-22802
- Evanothm alloy resistance wire for applications in magnetic field, illustrating percentage change at 4.2 K
09 p1679 A70-22998

- Thermal conductivity of thin metallic films and wires at cryogenic temperatures, discussing electron transport properties
11 p2083 A70-25752
- Connecting wires length effect on sensitivity and current-voltage characteristics of sensors for dynamic values measurement, deriving integral electrical parameters
11 p2055 A70-26445
- Short cables wire to wire coupling between black boxes, deriving interference transfer function
12 p2204 A70-28130
- Electrocardiography leads system optimal selection based on electrophysical modeling
19 p3369 A70-38207
- Electrocardiography electrical bridge type leads system based on potential quenching phenomenon, determining electric dipole displacement of heart in transverse plane of body
19 p3369 A70-38208
- Electric dipole displacement of heart estimation by supplementing orthogonal with precordial lead, discussing stationary and moving point dipole hypotheses
19 p3369 A70-38209
- Strain measurement on filament-wound structural members, incorporating electric resistance wire as strain gage within windings
19 p3550 A70-38719
- Cardiovascular stress testing using posterior bipolar lead for radiotelemetry monitoring
20 p3578 A70-39199
- Energy release during flux jump in Nb-Ti single core wires and multifilament composite superconductors
21 p3863 A70-42011
- Feed voltages and directional gain maximization for loaded long thin-wire antennas with multiple excitations, using matrix methods
23 p4176 A70-44972
- ELECTRIC WIRING**
U ELECTRIC WIRE
U WIRING
- ELECTRICAL BREAKDOWN**
U ELECTRICAL FAULTS
ELECTRICAL CONDUCTIVITY
U ELECTRICAL RESISTIVITY
ELECTRICAL ENERGY
U ELECTRIC POWER
ELECTRICAL ENGINEERING
- Resources roundup - IEEE Conference, Phoenix, April 1969
02 p0257 A70-12177
- Electronics and Aerospace Systems - IEEE Conference, Washington, D.C., October 1969
12 p2185 A70-27901
- Electromagnetic compatibility /EMC/ design criteria including gain, selectivity, nonlinearity and filter types
12 p2202 A70-28142
- Altimeter-telemetry system for small sounding rockets, discussing ground and flight test results
13 p2363 A70-28688
- IEEE Conference, Dallas, April 1970
15 p2701 A70-32551
- Thermal design factors in electronic components packaging, considering equipment failure types and rates, fabrication processes, etc [ASME PAPER 70-DE-17]
16 p2877 A70-33422
- Electronic packaging and production - Conference, Brighton, England, October 1969
16 p2878 A70-33955
- Operational amplifier with high output current for use as thermostatic regulator, power supply unit, AC/DC converter, etc
16 p2880 A70-34100
- Fiber optics in functional electronic circuits, considering multichannel optical communication
18 p3290 A70-36235
- Optoelectronics conversion for functional electronic circuits, discussing optical coupling, digital and analog computers and information display systems, injection diode light sources, etc
19 p3385 A70-37266
- Book on materials for structural and mechanical functions covering electrical engineering properties, ferrous and nonferrous metals and alloys, fabrication methods, environmental protection, etc
19 p3453 A70-38622
- ELECTRICAL FAULTS**
Space charge injection-impulse voltage separation technique for nonuniform field breakdown phenomena
01 p0110 A70-10560
- P-n junction and microplasmas voltage temperature coefficients during avalanche breakdown
03 p0541 A70-13729
- Static breakdown voltage of air and nitrogen measured under uniform field conditions for specific gas number densities, comparing results with Paschen law
03 p0528 A70-14086
- Electron radiation-induced second breakdown in transistors indicated by time delay and failure by collector-to-emitter short
04 p0657 A70-14734

- Gas discharge avalanche breakdown in Si semiconductors, analyzing microplasmas, ionization coefficients, p-n junction voltage, electron and light emissions
04 p0731 A70-15494
- Variational principle used in microwave breakdown predictions for rectangular aperture antenna
05 p0824 A70-16988
- DC electric arc with superimposed axial subsonic gas flow breakdown voltage and anode heat transfer using high speed photography
06 p1177 A70-17697
- General purpose automatic test system /GPATS/ for electronic equipment fault location, discussing software and hardware for integrating programmable oscilloscope
08 p1470 A70-20656
- Avionics maintainability concepts, discussing built-in test equipment, test connectors, automatic test equipment, fault detection and fault isolation
08 p1470 A70-20664
- Electrode erosion during high voltage vacuum breakdown measured by neutron activation analysis and gamma ray spectrometry, noting plasma formation from electrode material
10 p1854 A70-25317
- Integrated circuit failure analysis with scanning electron microscopy taking into account ball bond contamination and open metallization at contact windows
11 p2015 A70-25366
- Permanent memory faults effects on sequential machines finite-state behavior, considering masking role in synthesis of fault-tolerant sequential networks
11 p2072 A70-26220
- Linear networks fault detection and isolation using computerized test procedure and symbolic transfer function generation technique
11 p2029 A70-26337
- Multiterminal electronic networks computerized fault detection based on linearized Taylor expansion algorithm
12 p2197 A70-27932
- Autodiagnosis of logic module failure in complex electronic systems, examining fault simulation methods and Safe system program and apparatus
14 p2561 A70-30669
- Failure mode and mechanism in dielectrically isolated IC attributed to metal bridging under planar oxide
15 p2713 A70-32648
- Microscopic data importance in recognizing IC semiconductor failure characteristic traits, revealing current direction, voltage magnitude, microsurface temperature excursion and approximate transient duration
15 p2693 A70-32664
- Anodic breakdown characteristics of Ti alloys as function of metal surface condition
17 p3113 A70-34366
- Spacecraft flight systems voltage breakdown due to DC gas discharge, discussing occurrence and preventive techniques
17 p3053 A70-35164
- Channeling and guidance of electrical breakdown streamer via laser induced gas ionization trail
17 p3108 A70-35905
- Corona and voltage breakdown for spacecraft electrical components in low pressure helium-oxygen atmospheres, measuring between parallel plates
21 p3851 A70-42124
- Pressurized liquid nitrogen and hydrogen dielectrics for cryogenic cables, measuring dissipation factor and voltage breakdown by concentric cylindrical test cell
21 p3851 A70-42125
- Thin titania films electrical breakdown under high DC fields in high vacuum, suggesting reduction to lower order semiconducting oxide
22 p4085 A70-42621
- Electrical and electronic semiconductor device failures from metallurgical viewpoint
23 p4175 A70-44746
- ELECTRICAL IMPEDANCE**
NT CONTACT RESISTANCE
NT ELECTRICAL RESISTANCE
NT LC CIRCUITS
NT REACTANCE
NT SKIN RESISTANCE
- Mathematical model coefficients determination for planar diffused transistor, obtaining admittance parameters
01 p0048 A70-10050
- Space charge barriers AC impedance modification at metal/semiconductor contacts due to trapping
01 p0157 A70-10296
- Driving point admittance of infinite cylindrical antenna excited by uniform gap and immersed in lossy compressible isotropic plasma, discussing propagation constants
01 p0051 A70-11102
- Input impedance of monopole antenna in rectangular waveguide assuming sinusoidal current distribution, noting accuracy limitation to specific monopole lengths
03 p0457 A70-13698

- Transistor admittance and diffusion parameters in direct measurement with varying frequency, evaluating reliability
03 p0459 A70-14285
- Surface function and impedance distribution for unilateral surface wave antenna excitation by slot emitter above surface impedance segment
04 p0655 A70-14403
- Phase lock technique study of 10.6 micron radiation effect in carbon dioxide laser plasmas on 2.4 micron spontaneous emissions and plasma impedance
05 p0857 A70-16071
- Impedance and field distribution of bifurcated and stepped waveguide junctions with inserted diaphragm calculated by transformed singular integral equation
05 p0820 A70-16385
- Surface impedance of spherical earth isolated by nonconducting atmosphere from ionospheric currents producing alternating electromagnetic field
05 p0843 A70-16768
- Spherical probe impedance in infinite collisional isotropic plasma investigated for ionospheric applications, selecting electron density
06 p1117 A70-17369
- RF probe admittance in ionosphere investigated for cold anisotropic and warm isotropic plasma diagnostics
06 p1117 A70-17370
- Impedance and radiation pattern of quarter wave monopole and half wave dipole antennas in isotropic plasma, considering plasma density role
06 p1117 A70-17372
- Immittance, transfer and scattering characteristics for interdigital acoustic surface wave transducers, using linear equivalent circuit model
06 p1062 A70-17478
- Electrical impedance, conversion loss and bandwidth for piezoelectric film or plate transducers used for generating planar volume-acoustic waves at microwave frequencies
06 p1062 A70-17480
- Rectangular-slot antenna pair self and mutual admittances in inhomogeneous plasma layer on slender conical body, calculating VSWR and isolation
06 p1020 A70-17565
- Collisions effects on cylindrical antenna impedance near plasma frequency of isotropic nonMaxwellian plasma, allowing for collision frequency dependence on electron energy
06 p1020 A70-17567
- Inhomogeneous plasma cylinder skin effect, surface impedance, radiation transport and mean noise temperature
07 p1347 A70-19107
- Impedance behavior of inductive posts with small capacitive gap in waveguide
08 p1468 A70-20644
- Impedance radiation pattern and actual height of receiving dipole antenna in magnetoactive plasma calculated by electrodynamic reciprocity theorem
08 p1472 A70-20970
- Plane electromagnetic wave scattering at apex of conical body, presenting scattered field calculations for various cone sizes and surface impedances
08 p1461 A70-20974
- Thin metal plate surface impedance during excitation by HF electromagnetic field as function of magnetic field, calculating line shapes
08 p1557 A70-21754
- Equivalent circuit for radiation admittance of infinite planar array of phased rectangular waveguide apertures
09 p1646 A70-22692
- Brain cerebral tissues electrical impedance measurement by electrodes and bridge circuit, discussing chemical and metabolic properties
09 p1620 A70-22897
- Electric dipole emission near ideally conducting screen with variable surface impedance parallel strips, analyzing radiation pattern
09 p1636 A70-23140
- Electric bridge for measuring complex impedances and admittances in 60 kHz-30 MHz frequency range
09 p1650 A70-23402
- Small loop impedance in magnetoplasma determined for magnetic field normal and parallel to loop plane
09 p1738 A70-23671
- Antenna arrays elements mutual coupling effects on pattern and impedance characteristics
10 p1849 A70-24536
- Avalanche diodes microwave properties in utilization circuit, discussing negative conductance, nonlinear impedance and intrinsic noise current
10 p1850 A70-24623
- Two dimensional impedance horn antennas synthesis by aperture field distribution and radiation pattern configuration relationship, deriving energy balance equation
11 p2015 A70-25348
- Piezoelectric effects in ferroelectric ceramics using equivalent circuits and admittance matrices
12 p2283 A70-27005
- Excitation of surface waves on impedance plane in collisionless cold anisotropic plasma with external magnetic field coinciding with source direction
12 p2278 A70-27538
- Input impedances of small vertical and horizontal dipole and loop antennas above conducting ground plane, noting effect of refractive index
12 p2196 A70-27714
- Vertical tubular dipole antenna input admittance and current distribution above infinite dissipative half space
12 p2197 A70-27953
- Impedance in coaxial line generated by tee-fed waveguide slot antenna, using equivalent circuit
12 p2198 A70-27966
- Magnetospheric plasma density effects on impedance of VLF electric field spacecraft antenna
13 p2397 A70-29186
- Cylindrical electric dipole antenna in magnetoactive ionospheric plasma, noting ion sheath effect on input impedance and active length
13 p2399 A70-29402
- Grid assemblies as electrostatic plasma wave antennas, computing driving point and transimpedances for approximating single pole impedance in heavy Landau damping regime
13 p2371 A70-29918
- Cylindrical antenna admittance during immersion in ionospheric plasma, noting influence of ion sheath and plasma anisotropy
13 p2371 A70-29922
- Dipole antenna current distribution in ionized homogeneous anisotropic medium, using dielectric permittivity tensor
13 p2371 A70-29923
- Medium wave thin cylindrical dipole antenna arrays design, discussing operating impedance determination
15 p2714 A70-32816
- Cylindrical and helical antennas impedance in cold magnetoplasma, using three dimensional integral involving Fourier transform and Green function
16 p2859 A70-32943
- Mutual and self admittances for array with two monopoles, solving integral equations for current distributions
16 p2860 A70-32957
- Backfire antennas allowing for mutual impedance between dipole elements, determining radiated field from surface current distribution
16 p2861 A70-32958
- Thin long dipole antenna, determining input admittances, current and charge distributions and field patterns by Wiener Hopf technique
17 p3051 A70-35060
- Circular loop antenna for transmission and reception, determining current distribution, admittance and radiation field by integral equation
17 p3051 A70-35061
- Radiation patterns and impedance properties of slot antenna in ground plane, slot on cylinder and sphere and waveguide slot arrays
17 p3051 A70-35064
- Boundary value problem of Hertzian dipole antenna in presence of conducting half space, analyzing lossy earth effects on input impedance and radiation pattern
17 p3044 A70-35074
- Flush mounted lightweight antennas for rockets, discussing construction radiation patterns, input impedance, etc
17 p3053 A70-35273
- Transverse impedance in semiconductor surface layer, taking into account charge in diffusion region
20 p3686 A70-39594
- Frequency dependence of impedance of p-n-n diode with short base in presence of large forward current densities
20 p3598 A70-40021
- Ga-as Gunn diodes small signal admittance in dipole oscillation mode, analyzing RC model
20 p3598 A70-40062
- Aperture antennas admittance calculation, considering upper bound on error involved in approximating finite ground plane conductivity by perfect conductivity
20 p3599 A70-40316
- Two dimensional impedance horn antennas synthesis by aperture field distribution and radiation pattern configuration relationship, deriving energy balance equation
20 p3600 A70-40460
- Two identical parallel arbitrarily located thin asymmetrical dipole antennas, calculating self and mutual admittances
21 p3800 A70-41945
- Sheaths effect on capacitance of plane grid capacitor in plasma, discussing satellite aerials admittance
21 p3792 A70-42046
- Microwave output power and impedance for InP and GaAs bulk negative resistance oscillators, using velocity/field characteristics
21 p3800 A70-42049
- Admittance matrix of microwave networks, referring to coaxial line-waveguide coupling through 3 kMc adapter
21 p3802 A70-42250
- Intermodulation distortion reduction in four frequency parametric converter by low impedance path
23 p4169 A70-43785
- Asymptotic solution for thick linear antenna admittance
23 p4171 A70-43882
- Infinite periodic phased array over ground plane with dipole elements in parallelogram lattice, calculating driving impedance and gain loss due to mismatch
23 p4172 A70-44004
- Laminar geoelectromagnetic field excited by coaxial circular current, determining impedance and magnetic field ratios of spherical harmonics
23 p4189 A70-44064
- Dielectric covered narrow radiating slots in rectangular waveguide broad face, calculating impedance from equivalent circuits
23 p4175 A70-44952
- Annular aperture /slot/ antenna driven by coaxial line, calculating input admittance and complete near field radiation distribution
23 p4176 A70-44954
- Broadside-endfire array of cylindrical dipoles and monopoles driven by interconnecting transmission lines, calculating admittance and field patterns
23 p4176 A70-44955
- Skew arrays of coupled linear antennas, calculating planar and nonplanar configurations mutual admittance vs rotation angle between dipoles
23 p4166 A70-44969
- Plasma positive column impedance in low current noble gas discharges, using Boltzmann equation for electrons
24 p4387 A70-45796
- Carrier injection-limited Gunn diode wideband performance, deriving expression for admittance
24 p4319 A70-46081

ELECTRICAL INSULATION

- Electrical lead sealing in hydrostatic high pressure systems with gaseous pressure transmitting medium, considering piston cone seals, frozen oil seals, epoxy seals, etc
01 p0104 A70-10744
- Electrical insulation - Conference, Boston, September 1969
05 p0869 A70-16032
- Electrical effects of boundary layers on insulator wall of MHD generator, considering equilibrium and nonequilibrium ionization generators performance
07 p1196 A70-19321
- Glass- and quartz-fabric reinforced polymers for high temperature microwave insulation, evaluating electrical and thermal aging properties
12 p2259 A70-28149
- Laser beam method sensitivity for spectral emission analysis of nonconducting materials
20 p3642 A70-39743
- Thermally stable polyimide resins for carbon fiber composites, noting high temperature strength, oxidizing resistance and electrical insulation properties
22 p4058 A70-42478
- Semiconductor junctions passivation by silicon nitride insulation layers, discussing pyrolysis and cathode sputtering fabrication methods
22 p4087 A70-43444

ELECTRICAL LEADS

U ELECTRIC CONDUCTORS

ELECTRICAL MEASUREMENT

NT POLAROGRAPHY

- Feedback time sharing analog electronic multiplier for two quantities, noting linearity, accuracy and stability of measurements
02 p0268 A70-12422
- Terrestrial solid powdered rocks HF electrical properties measurements for lunar radar observation
04 p0678 A70-15054
- Hall voltage measurements on Ta thin films using square wave generator current, discussing parasitic effects and suppression possibilities
05 p0863 A70-16366
- Portable megaohmmeter for measuring insulation resistance of strain gauge ceramic installations
05 p0848 A70-16378
- Errors arising in torsion-type ponderomotive wattmeter connected in homogeneous microwave transmission line with mismatched oscillator at input and mismatched load at output
06 p1024 A70-17861
- Hall effect measurements in liquid semiconductors and metals
06 p1127 A70-17919
- Thermal diffusivity measurements for Ta-W, Ta-W-Hf, Hf-Ta-Mo alloys using pulse technique
07 p1305 A70-18960
- Semiconducting components reliability test involving electrical parameters measurement following thermomechanical stresses
09 p1689 A70-22002
- Specimen holder for 300 K/4.2 K resistance ratio measurement
09 p1655 A70-22645
- Segmented anode current and heat distribution in MPD engine measured with current shunts and calorimetric methods
[AIAA PAPER 69-244]
09 p1613 A70-23238

- Tropospheric electrical path length estimated by microwave radiometry using atmospheric models
09 p1640 A70-23806
- Different retinal regions simultaneous stimulation, describing evoked potentials measurement method
10 p1811 A70-24227
- Si avalanche diodes oscillations external current waveform measurement using coaxial current monitoring assembly with negligible phase error
10 p1849 A70-24234
- Figure of merit for thermoelectric generator determined experimentally, assuming temperature difference between heated and cooled junctions
10 p1808 A70-25035
- Hydrogen, nitrogen and argon electrical and thermal conductivity measured at high temperature using electric arc as plasma source
11 p2148 A70-26016
- Dynamic errors of electric measurement devices during three dimensional polyharmonic vibrations of foundation
12 p2233 A70-27561
- Radio Influence Voltage (RIV) nondestructive test method for detecting voids in neoprene-steel structures or other elastomers bonded to metal
13 p2420 A70-29245
- Hall generator measurement of impulse currents, noting error sources and compensation
16 p2900 A70-33072
- Teflon bucket and Be-Cu cap seal against hydrostatic pressure, discussing applications for high pressure superconductivity measurements
18 p3262 A70-37097
- Electric current pulses peak values measurement during aperiodic capacitor discharges, describing circuit with Rogowski coil, diode, capacitor and VTVM
19 p3426 A70-37938
- InSb semiconductor, measuring small signal microwave conductivity for hot electron region at 9.4 GHz in high electric DC fields
19 p3488 A70-38747
- Automatic measurement of drainage networks for lengths and areas by copper plate etching or flying spot scanner on transparencies or radar images
20 p3633 A70-39794
- MHD induction generator design, considering electrical and friction loss measurement and control
20 p3565 A70-39988
- Projected nuclear MHD system conditions, examining electrical measurements in K vapor with diode at atmosphere pressure and high temperatures
20 p3681 A70-40006
- Effective dissociation potential measurement for alkali compound seed in MHD generator working fluid
20 p3682 A70-40159
- Manganin in wire and thin foil geometries, measuring shock piezoresistance coefficient as function of deformation
20 p3687 A70-40166
- Carbon resistors negative magnetoresistance measurement near absolute zero temperature by helium cryostat, noting anisotropy
20 p3687 A70-40168
- Subnanosecond risetime milliohm Faraday cup for measuring electron beams from pulsed accelerators
21 p3799 A70-41466
- Secondary breakdown meter for semiconductor diodes and transistors with reverse base drive, utilizing I-V characteristics and voltage waveform
21 p3801 A70-42248
- Ti and Zr based superconducting alloys with Nb content, measuring longitudinal critical currents in wire and ribbon samples
22 p4087 A70-43462
- Information processing methods in microwave measurement using digital computers, emphasizing active and passive transducers
23 p4193 A70-43795
- Microwave p-n diode RLC equivalent circuit parameters experimental determination
23 p4171 A70-43956
- Packaged microwave junction diodes in reduced-height waveguide, discussing parasitics and equivalent circuit parameters measurement technique
24 p4318 A70-45220
- NT PIEZOELECTRICITY
NT PLASMA CONDUCTIVITY
NT POLARIZATION CHARACTERISTICS
NT PYROELECTRICITY
NT REACTANCE
NT SKIN RESISTANCE
NT SUPERCONDUCTIVITY
Electrical properties of Si-doped GaAs p-n structures obtained by liquid phase epitaxy, considering charge buildup
01 p0155 A70-10132
- Variational methods for investigation of thermal and electrical properties of semiconducting materials, noting accuracy
01 p0159 A70-10759
- Electrical domain instability in homogeneous hot electron semiconductors, discussing boundary conditions application to fluctuations
02 p0350 A70-11697
- Gradual linear p-n junctions characteristics, including diffusion voltage value and temperature coefficient, space charge zone thickness and junction capacitance
02 p0268 A70-12493
- MOS structure electrical characteristics dependence on silicon/silicon dioxide interfacial energy and electric charges, considering fabrication difficulties
02 p0350 A70-12541
- Gas-stabilized electric arc heater electrical and gas dynamic parameters, studying velocity and enthalpy radial distributions and IV characteristics
03 p0531 A70-13386
- Thin superconducting films nonlinear microwave properties including impedance-amplitude relation, superconducting current threshold decrease, mode production, frequency mixing, etc
03 p0539 A70-13409
- Electrical properties of Cu-diffused GaAs, studying temperature effects on acceptor concentration and electron population growth
03 p0541 A70-13730
- Electrical properties thermally induced irreversible changes in CdSb single crystals measured as function of current intensity and flow
03 p0542 A70-13751
- Niobium ditelluride single crystals production with purity dependent on initial materials, discussing X ray structural and chemical analysis and electrical properties
03 p0542 A70-13753
- Thermal conductivity, electrical resistivity, Lorentz ratio and thermopower of aerospace alloys at cryogenic temperatures, considering Inconel, Hastelloy, Ti and Al alloys
03 p0512 A70-13807
- Resistance, capacitance and inductance in passive hydraulic circuits considered in analogy with electric circuits to determine dynamic characteristics
03 p0415 A70-13931
- Electrical and thermal factors in mathematical characterization of electroexplosive devices, including heuristic predictions
03 p0548 A70-14119
- Josephson effect in superconductors emphasizing Josephson junction electrical properties and applications to devices and measuring techniques
03 p0542 A70-14190
- Electrical and mechanical instability of jets, threads and sheets of viscous fluid, noting role of deceleration
03 p0471 A70-14253
- Field effect transistors with controlled p-n junction and metal-dielectric-semiconductor transistors investigated for radiation effects on physical and electrical properties
04 p0730 A70-14500
- Terrestrial solid powdered rocks HF electrical properties measurements for lunar radar observation
04 p0678 A70-15054
- Epitaxial GaAs FET using evaporated Au-Ge-Ni contacts and Ni Schottky barrier, describing fabrication and electrical properties measurement
04 p0660 A70-15367
- Biplanar photocell in various holders noting intrinsic properties, emphasizing rise time characteristics
04 p0695 A70-15572
- N-type layer formation with ion implanted nitrogen or Sb in p-type alpha-SiC, evaluating electrical characteristics, discussing junction devices formed
04 p0732 A70-15685
- Vapor deposited GaN single crystals tested for electrical and optical properties, determining band gap energy, electron concentration, etc
04 p0732 A70-15688
- Optical, electrical and structural properties of transition metal dichalcogenides
05 p0890 A70-15755
- Low melt viscosity prepolymers of diallyl phthalate and isophthalate in mold encapsulation showing dimensional, electrical and mechanical stabilities under adverse environments
05 p0869 A70-16035
- Doped beta-iron disilicide thermocouples measured for electrical characteristics and energy conversion efficiency at various temperatures
05 p0798 A70-16357
- Doped n-type Ga-As electrophysical parameters determinable from IR reflection spectra
05 p0892 A70-16540
- Composite conductors involving conventional conductors and superconductors to obtain satisfactory electrical performance for application to electromagnets
05 p0870 A70-16582
- Electrical properties of unipolar barium titanate single crystals involving hysteresis loops plotting
05 p0894 A70-17024
- Fabrication and electrical properties of p-ZnTe/n-InAs heterojunctions obtained by interface alloying, suggesting p-n structure from characteristics and capacitance behavior
06 p1125 A70-17123
- Steady state electrical characteristics of double diffused planar transistor calculated by iterative algorithm under arbitrary bias conditions
06 p1016 A70-17125
- Oxygen tension change effects on rats smooth vascular muscles electrical and contractile properties
07 p1198 A70-18715
- Electrical effects of boundary layers on insulator wall of MHD generator, considering equilibrium and nonequilibrium ionization generators performance
07 p1196 A70-19321
- GaAs preparation techniques, crystal structure, electrical and physical properties, single crystal growth, impurities properties and distribution, thermal and optical properties, etc
07 p1356 A70-19397
- Electrical and thermal characteristics of stabilized gas heating by electric arc at high pressures calculated by successive approximation
07 p1350 A70-19840
- Lunar surface chemical composition determination by radio astronomy, considering SHF electrical properties of silicate earth rocks
08 p1572 A70-20940
- Titanium and zirconium dihydrides room and higher temperature electrical resistivity, Hall effect and thermal expansion coefficients
08 p1517 A70-21149
- Electrical properties of Si-doped GaAs p-n structures obtained by liquid phase epitaxy, considering charge buildup
08 p1556 A70-21408
- Correlation functions of fluctuations in electrical characteristics of nonequilibrium electron gas during scattering, determining spectral densities and populations by kinetic equation Green function
08 p1554 A70-21806
- Electrical and photographic methods for measuring microcracking in fiber reinforced plastics
08 p1501 A70-21916
- Semiconducting components reliability test involving electrical parameters measurement following thermomechanical stresses
09 p1689 A70-22002
- Hybrid microwave integrated circuits technology and design, discussing distributed and lumped-element structures and component properties
09 p1644 A70-22225
- Electrical parameters approximate calculations for waveguides with complex cross sections by Schwarz alternating method, determining critical frequencies of fundamental modes
09 p1632 A70-22406
- Spectral criteria for approximating tunnel diode nonlinear characteristics obtained by minimizing deviations of moduli of harmonic amplitudes
09 p1649 A70-23340
- Capacity bounds in microwave filters computed for periodic cylindrical rods between parallel ground planes using variational principles
10 p1850 A70-24834
- Air and solar activity electrical parameters relationship, observing ionizing radiation increase in upper atmosphere during solar activity
10 p1885 A70-25268
- Epitaxial surface morphology layer electrical properties and autoping at GaAs-Ge heterojunctions as function of substrate temperature, orientation and HCl concentration
11 p2098 A70-26392
- Mechanically rechargeable zinc-air battery, discussing electrical performance, advantages and military applications
12 p2167 A70-27928
- Glass- and quartz-fabric reinforced polymers for high temperature microwave insulation, evaluating electrical and thermal aging properties
12 p2259 A70-28149
- Temperature dependence of electrical properties and permittivity of barium titanate solid solutions containing Nb, Ta, Sb and La, using bridge-circuit of resonance techniques
13 p2469 A70-28853
- Silicon and alpha-alumina support interface reactions during nucleation-coalescence and after epitaxial growth, investigating electrical properties
13 p2470 A70-28958

Electrodynamic transducer electrical and mechanical parameters measurement, comparing various techniques

13 p2406 A70-28991

Undoped GaAs lattice constants and electrical properties before and after heat treatment

13 p2471 A70-29504

Stagnation point electrostatic probe for measuring local electrical properties of solid propellant rocket exhausts

[AIAA PAPER 69-573]

13 p2475 A70-29960

Evaporated Au-Ni-Cr alloy resistor films physical and electrical characteristics, noting dependence on composition

14 p2625 A70-30285

Semiconductors as igniter material for ignitrons, tabulating electrical characteristics

14 p2590 A70-30640

Broadband frequency multipliers optimum efficiency solutions, realizing linear charge-voltage characteristics with MIS varactors

14 p2557 A70-31159

Portal vein smooth muscles electrical properties, using double saccharose bridge method

15 p2679 A70-31605

InAs thin films electrical properties and IR reflectance, determining thickness and substrate temperature effects on carrier concentration and mobility

15 p2783 A70-31965

Diffused p-n junction devices impurity profile from capacitance-voltage measurements

15 p2710 A70-32562

Lunar surface chemical composition determination by radio astronomy, considering SHF electrical properties of silicate earth rocks

15 p2805 A70-32752

Semiconductor surfaces electrical equilibrium, considering statistical occupation of surface energy and Fermi levels for given doping of bulk material

15 p2786 A70-32766

Book on electrical aspects of combustion processes covering formation, behavior in fields, diagnostics, uses of ions, electrons and charged particles, flame ionization, etc

16 p2996 A70-33030

Ion implantation doping for MOS devices, discussing improved HF performance, integrated circuitry and threshold voltage selection

16 p2872 A70-33054

Book on refractory metal properties covering nuclear reactor use, atomic, electronic and crystal structures, thermal and electrical characteristics irradiation effects, nuclear properties, etc

16 p2931 A70-33268

Chemical and moisture resistance, electrical and mechanical properties of engineering thermosetting plastics made of HYSTL resins

16 p2938 A70-33380

Sandwich wire planar antenna array design, noting electrical performance, ruggedness, volume and weight

16 p2877 A70-33416

Large capacity sealed nickel cadmium battery for spacecraft, describing mechanical and electrical characteristics

16 p2844 A70-33473

ZnO coating pigment for spacecraft thermal control, examining UV irradiation effects on electrical properties

16 p2961 A70-34056

Physical and electrical sizes in large antennas, discussing paraboloid reflectors, arrays, slot antennas, etc

17 p3053 A70-35079

Indium arsenide p-n junctions fabrication and electrical and photoelectric properties

17 p3143 A70-35120

Adsorption influence on electrical and photoelectric properties of CdSe thin films

17 p3143 A70-35674

Electrical properties of n-type GaAs epitaxial films grown by gas transport method

17 p3144 A70-35706

Position sensitive planar photocells based on silicon-silicon dioxide systems, discussing photoelectromotive force generation mechanism, light intensity and load characteristics

18 p3297 A70-36236

MOS devices, investigating laser radiation effects on electrical behavior

18 p3266 A70-36237

Heterogeneous solar cells based on polycrystalline cadmium sulfide and selenide, discussing preparation methods and photoelectric and electric properties

18 p3215 A70-36238

InAs p-n junction laser electrical and optical characteristics during spontaneous and stimulated radiative recombination

18 p3269 A70-36739

Ge and Si surface electrical properties, discussing conductivity, field effect, work function, current carriers, photoconductivity, photocurrent carrier capture, etc

19 p3483 A70-37297

Electric machines magnetic circuit and motor shape, evaluating current, flux, resistance and reluctance

19 p3357 A70-37362

Soviet reference book on highly refractory elements and compounds covering crystalline, chemical, thermodynamic, thermophysical, electrical, optical and nuclear properties

19 p3451 A70-37470

Electroacoustic transducer driven by acoustic pressure and electronic generator, describing electrical properties for functioning as characteristic impedance of acoustic transmission line

19 p3422 A70-37701

Iron phosphate semiconducting glasses, determining electrical and magnetic properties dependence on thermal treatment

19 p3487 A70-37861

Superconductor thin films, discussing transition temperature, critical field and current, solid state applications, etc

19 p3488 A70-38198

Digital readout test equipment characteristics and parameters for electrical properties measurement, proposing pulse counting analog-digital conversion technique

19 p3432 A70-38701

Electrophysical properties of refractory and rare earth metallic single crystals, discussing work function, transition temperature, resistivity and superconductivity

19 p3454 A70-38731

Thermoresistor parameters of organic semiconductor polymers with conjugated bond system, plotting temperature and EV characteristics

20 p3595 A70-38966

One-component rigid epoxy foam system suitable for lightweight electronic potting determining mechanical, electrical and thermal properties

20 p3652 A70-39167

Matrix condenser for tuning hybrid thin film self excited quartz oscillator with common base transistor configuration, discussing electrical properties and fabrication

20 p3597 A70-39257

Langley 20 megawatt plasma accelerator design and operation, describing arc heater modifications, exit parameters, electrical properties, etc

20 p3606 A70-40010

Noble gas mixture large shock tunnel driven linear MHD generator, examining electron density, operating characteristics and electrical properties

20 p3682 A70-40012

Apollo 11 lunar powder optical and HF electrical properties, discussing reflectivity, polarization, absorption, differential mass spectrum and albedo

21 p3915 A70-41655

Electrical and thermal characteristics of DC magnetic annular arc operating continuously at atmospheric pressure

21 p3805 A70-41758

Electro-optic device using ferroelectric bismuth titanate, discussing electrical and optical properties and matrix addressed display

21 p3830 A70-42114

Plasma arc welding torches nozzle dimensions and shape dependence on thermal and electrical characteristics, optimizing energy output

22 p4042 A70-42378

Silicon solar cell design optimization for near solar missions, discussing electrical characteristics and performance obtainable under various solar radiation conditions

22 p3964 A70-42496

Addition effects on lattice and electrophysical properties of trititanate prepared by Ba, Pb, Ca and Ti precipitation

22 p4087 A70-43134

Oxidized Si surface recombination rate measurement by electric field effect, noting electron bombardment effects on electrical properties

22 p3998 A70-43443

In thin film resistance thermometers fabrication by vapor deposition in vacuum, considering electrical properties dependence on temperature

22 p4039 A70-43446

Electroreflectance at CdS-electrolyte interface, noting field strength effect on relaxation time

23 p4230 A70-43930

Live skin tissue electrical parameters changes due to laser radiation, showing coagulative necrosis by histomorphological studies

23 p4150 A70-44313

Electrical characteristics of high current two stage DC Hall accelerator for use in controlled thermonuclear fusion

24 p4383 A70-45117

ELECTRICAL RESISTANCE

NT CONTACT RESISTANCE

NT LC CIRCUITS

NT SKIN RESISTANCE

Bridging joints resistance effect on thermoelement efficiency, describing W and Co coatings deposition on GeTe based thermoelectric alloys

01 p0159 A70-10757

Continuous measurement and automatic recording of metals electrical resistance during fatigue testing in vacuum at elevated temperatures

01 p0092 A70-11108

Recrystallization annealing third stage of cold worked polycrystalline niobium by measuring electrical resistance at liquid nitrogen temperature

05 p0863 A70-16204

Portable megaohmmeter for measuring insulation resistance of strain gauge ceramic installations

05 p0848 A70-16378

Excess titanium dioxide effect on electrical resistance of semiconductive barium titanate ceramics suitable for posistors

07 p1355 A70-18654

Graphite-polyester plastic material with electrical resistance for eliminating static charges leading to explosions

07 p1295 A70-19764

Tin oxide film resistors reliability test based on measurement of resistance nonlinearity by third harmonic voltage

09 p1689 A70-22005

Specimen holder for 300 K/4.2 K resistance ratio measurement

09 p1655 A70-22645

Electron tunneling into amorphous Ge films using Al-aluminum sesquioxide-germanium tunnel junctions, observing conductance dependence on bias voltage

09 p1739 A70-22918

SnTe of various nominal hole concentrations measured for longitudinal piezoresistance effect along different crystallographic directions

10 p1927 A70-23993

Carbon composition resistors investigated for cause of resistance dependence on thermal pulses, suggesting application as stabilization process

10 p1849 A70-24617

Electrode shape and background resistance effects on power rationing between gas tungsten arc and electrode

10 p1897 A70-25314

Planar Ge and Si diodes application in pulsed bridge elements, investigating current-voltage and resistance-voltage characteristics

11 p2015 A70-25350

Lead resistance effects on resistance strain gage measurements as function of utilized measurement system and procedure

11 p2054 A70-26432

Extrinsic photoconductor with reduced background under uniform illumination, describing frequency response as function of recombination and dielectric relaxation times and load resistances

14 p2586 A70-30989

Thermal and electrical resistances of Na at low temperatures measured by germanium thermometers and galvanometer amplifier

14 p2617 A70-31021

Artificial B-doped semiconductor diamond crystals resistance temperature dependence, determining conductivity and luminescence spectra

15 p2782 A70-31630

Red cell deformability and flow resistance and blood electrical resistance under low g centrifugation

15 p2680 A70-31700

Ultrahigh vacuum gages absolute calibration by controllable conductance method, discussing accuracy

19 p3421 A70-37463

Current and resistance in Hg filled space between two circular electrodes under strong magnetic field, using boundary layer techniques

19 p3477 A70-37578

Electric resistance adjustment of thick and thin film resistors on ceramic substrate, using laser for material evaporation

20 p3640 A70-39416

Manganin in wire and thin foil geometries, measuring shock piezoresistance coefficient as function of deformation

20 p3687 A70-40166

Planar Ge and Si diodes application in pulsed bridge elements, investigating current-voltage and resistance-voltage characteristics

20 p3600 A70-40462

Solar cell array maximum power point in scientific satellites via closed loop conductance matching regulator

21 p3758 A70-41220

High resistivity single crystal silicon wafers induced IR absorption measurement, using Nd doped glass laser

21 p3837 A70-41916

Sparks channel resistance temporal variation, using resistivity of fully and singly ionized plasma

22 p4072 A70-42354

Darlington composite transistor stability, examining biasing resistance variation effect

22 p3998 A70-43257

Automated high precision electrical resistance measuring system using digital computer control

24 p4334 A70-45384

Discharge pulse generation and equivalent resistance of relaxation oscillator applied to avalanche transistor

24 p4319 A70-45639

ELECTRICAL RESISTIVITY

NT IONOSPHERIC CONDUCTIVITY

NT MAGNETORESISTIVITY

NT PHOTOCONDUCTIVITY

NT PLASMA CONDUCTIVITY

NT SUPERCONDUCTIVITY

Dielectric layers electrical conductivity in ceramics containing Ti during aging, observing different characteristics ascribed to nonequilibrium current carriers injection

01 p0156 A70-10221

Current distribution in finite length helical antenna in HF field, using cylindrical model of infinitely good conductivity

01 p0050 A70-10713

GeTe thermoelectric power, electrical/thermal conductivity and expansion coefficient measured at 20-600 C, determining suitability as thermoelectric material

01 p0158 A70-10755

Electrically conductive plastics fabrication and applications limitations, discussing plastic matrix materials loaded with various conductive fillers

01 p0129 A70-10938

Relativistic formulation of radiation for sources in uniformly moving isotropic dispersionless conducting medium in terms of Green functions

01 p0144 A70-11091

Periodic motions and integral stability for systems with quasi-cyclic coordinates applied to current carrying conductor oscillations and linear case of Routh equations

01 p0212 A70-11573

Electrical conductivity of air behind incident and reflected shock wave fronts as function of temperature and Mach numbers measured by electrode method

01 p0095 A70-11622

Nonequilibrium potassium seeded Ar plasma electrical conductivity at atmospheric pressure, noting current density role

02 p0347 A70-12232

Electromagnetic scattering from randomly rough surface with finite conductivity, using Kirchhoff approximation

02 p0261 A70-12587

Titanium aluminide-Mo system hardness, electrical conductivity and density as function of chemical composition, presenting creep test results

03 p0510 A70-13353

DC electrical conduction in In and In-Pb alloy foils sandwich structures, discussing size effect and Pb diffusion rate

03 p0540 A70-13624

Electrical conductivity of GaSe thin films developed in vacuum by electron bombardment as function of temperature

03 p0540 A70-13686

Titanium carbide hemispherical and spectral emissivity and electrical resistivity measured at high temperature

03 p0512 A70-13752

Neutron star electrical conductivity, discussing stellar flux and magnetic field decay times

03 p0578 A70-14220

Specific heat, electrical resistivity and thermal conductivity changes in materials properties at cryogenic temperatures, noting parasitic phenomena, mechanical and dielectric properties

03 p0525 A70-14269

Electrical resistivity, contact resistance and weldability of cast Cu and Ag contact materials reinforced unidirectionally by W wire compared to powder composition

04 p0711 A70-14465

High energy dopant ion implants into silicon, discussing implantation profiles and electrical conductivity for use in type conversion and electrical junctions

04 p0730 A70-14727

Equivalent conductances and resistances vs pumping oscillation modes of p-n junction in parallel and series-connected three-frequency parametric circuits

04 p0659 A70-15209

Elliptically polarized microwave scattering at electrically conducting rough surface, considering probability distribution of profile angles and random reflection coefficients

04 p0650 A70-15286

Heat transfer in MHD Couette flow influenced by wall electrical conductances with suction

05 p0886 A70-15823

Barium titanate ceramics with nonlinear electrical conduction, noting I-V relationship dependence on temperature, impurities and electrodes

05 p0891 A70-15990

Phenomenology theory on conduction and switching behavior of amorphous semiconductor diodes

05 p0891 A70-16021

Magnetovariational sounding procedure for determining vertical distribution of earth mean electrical conductivity using geomagnetic field spatial derivatives for spherical earth

05 p0843 A70-16767

Maraging steels mechanical properties, studying changes in lattice constant and electric resistance to determine Al strengthening effect nature

05 p0865 A70-16872

Band extremum loops depth in CdS in electric and magnetic fields determined from calculating linear and nonlinear conductivity

06 p1126 A70-17819

Heat flux, electrical and thermal conductivity of H measured on plasma in cascade arc chamber of high power load at 1 atm pressure

06 p1107 A70-18525

Lunar interior electrical conductivity estimated using lunar interaction with solar wind and interplanetary electric and magnetic fields

06 p1153 A70-18544

Hall voltage and electric conductivity measurements in alternating magnetic field and current by narrow band amplifier with synchronous detector

07 p1279 A70-18944

Lunar surface magnetometer data interpretation by analysis of moon motion relative to interplanetary magnetic field spatial irregularities, using lunar electrical conductivity models

07 p1378 A70-18974

Thorax potential resistivity at sea and high altitude levels measured in children and adults inferring relation to ECG differences

07 p1206 A70-19296

Interrelation of precipitation state, mechanical properties and electrical conductivity of wrought aluminum age hardened alloy under varied heat treatment conditions

07 p1294 A70-19389

High electrical conductivity effects on alignment between magnetic field and flow velocity vector in two dimensional plasma flow

07 p1349 A70-19568

Active and compensating sensors resistances, strain sensitivities, temperature gradients and lead resistances differences effect on accuracy of resistance strain gage measurements

07 p1283 A70-19747

Refractory metals electrical resistivity as function of density near critical point, using exploding wire

07 p1335 A70-19899

Electrical conductivity variations effects in subsonic Hartmann plasma flow under transverse magnetic field in channel with cooled walls

07 p1352 A70-19986

Electrically conductive ablative materials rapidly heated to 7000 F in test facility, discussing heating method and high strain rate testing

07 p1250 A70-20042

Electrical conductivity of fully ionized plasma in strong magnetic field computed as application of method for plasma transport coefficients

07 p1354 A70-20246

Hall effect and electric conductivity of cadmium arsenide at high temperatures as function of carrier concentration dependence on temperature and phase transformation

07 p1357 A70-20314

Terrestrial electrical conductivity measurement from electromagnetic field variations determination by geomagnetic sounding

07 p1277 A70-20458

Polarization structure of electromagnetic wave scattered by slanted two dimensional statistically rough surface of finite conductivity

08 p1456 A70-20573

Electron density calculation for collisionless plasma flow around conducting cylindrical body, accounting for surface absorption and mean electron velocity [ONERA-TP-792]

08 p1550 A70-20595

MHD flow in rectangular duct with arbitrary conductivity via modified Fourier method, obtaining magnetic induction and current for various Hartmann numbers

[ASME PAPER 69-WA/AFM-17]

08 p1551 A70-21308

Plane shock wave stability propagating in external magnetic field determined by temperature dependence of medium electrical conductivity

09 p1658 A70-22168

Thin resistive layers located in rectangular waveguide assuming constant and surface variable conductivity and permittivity

09 p1644 A70-22279

Electrical conductivity and conductive opacity for relativistic electron gas in presence of ions taking into account ion-ion interaction

09 p1727 A70-22509

Quasi-near zone electric field intensity and current distribution of monopole antenna on finite conductive earth

09 p1645 A70-22691

Transverse and longitudinal resistive critical fields of Nb wires, discussing superconductivity in dislocation cell walls created by drawing or swaging

09 p1704 A70-22802

Microwave conductivity and limiting frequency in Gunn effect GaAs using drifted Maxwellian

09 p1739 A70-22849

Molybdenum heat capacity, electrical resistivity and thermal radiation measurements at high temperatures with millisecond resolution

09 p1706 A70-22955

Gages for static strain measurements at high temperatures, discussing resistivity temperature coefficient compensation

09 p1680 A70-23109

Electrical resistivity of TiNi and TiCo compounds and alloys measured at various temperatures after quenching or annealing

09 p1707 A70-23194

Algorithm for inversion of geomagnetic induction problem, determining earth radial conductivity distribution

09 p1669 A70-23305

Bismuth oxide resistivity and structural characteristics at high temperature and during transformation from solid to liquid state

10 p1927 A70-24272

Longitudinal electrical conductivity of relativistic gas in intense magnetic field

10 p1924 A70-24634

Thin n-type Ge film electrical conductivity effect on ferromagnetic barium titanate single crystals as function of magnitude and sign of polarizing field

11 p2097 A70-25383

Anomalous water /polywater/ dielectric constant and effective parallel conductance, suggesting hydrosol classification

11 p1994 A70-25657

Thermal conductivity, electrical resistivity, Lorentz ratio and thermopower of aerospace alloys in 4-300 K range, separating electronic and lattice contributions

11 p2065 A70-25758

Copper alloy composite reinforced by unidirectional solidification of pseudobinary eutectic Cu-ZrCuSi, discussing mechanical properties and electrical conductivity

11 p2066 A70-25775

Electrical conductance test for composite materials adhesive bond degradation by liquids

11 p2071 A70-26345

Electrical conductivity of impact-ionized nitrogen across magnetic field, deriving electron collision frequency

11 p2091 A70-26461

Electrical conductivity hypothesis based on concept of transition temperature being inversely proportional to ionic mass square root

12 p2282 A70-26880

pH system electrical resistivity, studying hydrogen concentration role

12 p2282 A70-26900

MHD disturbances in semiinfinite electrically conducting fluid, introducing magnetic dipole to act as source of disturbance

12 p2277 A70-27156

Read-diode microwave oscillators performance degradation due to space charge and series resistance, discussing RF power optimization

12 p2194 A70-27167

Low resistivity films synthesized on seminsulating GaAs by xenon, krypton, selenium and zinc ions bombardment

12 p2286 A70-27364

Semiconductor diamond films electrical conductivity obtained by injecting various ions during isochronal stepwise annealing, studying activation energy values

12 p2286 A70-27479

Electroacoustic conversion in low resistivity GaAs crystal surface layer, applying external magnetic field to tune converter in wide frequency range

12 p2287 A70-27483

Resistivity anomalies of nickel-chromium alloy with Al additions subjected to deformation and heating, studying K-state

12 p2254 A70-27496

Shock ionized xenon electrical conductivity measurement at high temperatures as function of Mach number, noting equilibrium effects

12 p2281 A70-27807

Dipole and monopole antenna radiation patterns, considering effects of soil conductivity and elevation above ground

12 p2199 A70-27979

Decomposition of supersaturated solid solutions in granulated Al alloys with Mn, Cr, Zr, Ti, V and Mo, studying microhardness and electrical resistivity

12 p2258 A70-28274

Temperature dependence of electrical conductivity and optical properties of strontium titanate semiconductor single crystals doped with Ce and Nb

12 p2288 A70-28328

RF method for recording temperature dependence of electrical conductivity of solids, liquids and multicomponent plasma mixtures

13 p2459 A70-28583

Electrical conductivity without particle-particle or wave-particle collisional noise or radiation
13 p2463 A70-29238

Witness particle electric field as function of non-linear conductivity of weekly turbulent anisotropic plasma by perturbation method
13 p2465 A70-29638

Attenuation, resistivity and surface roughness measurements in rectangular waveguides
14 p2555 A70-30440

Band and localized models for electrical conduction of metal oxides, discussing Mott and semiconductor to metal transitions
14 p2627 A70-30498

Conductive rubber pressure transducers for fluid flow measurement
14 p2584 A70-30503

Metallic thermoelectric materials, measuring electrical resistivities and Seebeck coefficients of binary Ni alloys
14 p2533 A70-30530

Book on materials for conductive and resistive functions covering superconductive and contacting functions and applications
14 p2557 A70-30951

Critical Mach numbers for transverse resistive shock waves as function of fluid/magnetic pressure ratio compared with cold plasma theory
14 p2623 A70-31036

Venus atmosphere-lithosphere interactions, predicting electrically conducting cloud masses presence
14 p2646 A70-31070

Thermal and electric conductivities for interface separating two parts of system with different temperature and chemical and electrical potential
14 p2617 A70-31296

Semiconductors surface energy levels based on conductivity, metal-dielectric-semiconductor capacity and optics
15 p2785 A70-32765

Elevation and ground conductivity effects on horizontal dipole excitation of earth-ionosphere waveguide, considering east-west propagation
16 p2858 A70-32932

MHD experiments showing effects of local water supply electrical conductivity from measurements of voltage distribution, pressure gradients and extracted power
16 p2957 A70-32998

Earth mantle electrical conductivity profiles, using Lahiri-Price model and spherical harmonic analysis of quiet day daily variations
16 p2896 A70-33077

Electrical conductivity of partially ionized gas in magnetic field by Frost mixture rules extension
17 p3141 A70-34985

Ni-Fe ferrites resistivity and thermoelectric power as function of temperature, proposing two energy level model for Fe ions
17 p3143 A70-35604

IV characteristics of high resistivity Ti-doped GaAs single crystals and S-diodes, using Hall constant and conductivity measurements
17 p3144 A70-35709

Negative resistance and conductivity segments in I-V curves of diode structures, taking into account injection junction imperfections
18 p3231 A70-36413

Electrical conductivity, Hall constant and differential thermal emf n-type GaAs-CdS solid solutions
18 p3298 A70-36596

Degenerate relativistic electrons in intense magnetic field, computing transverse electrical conductivity
18 p3296 A70-36896

Multivalley semiconductors electrical conductivity anisotropy, discussing redistribution and electron transfer under strong electric field
19 p3483 A70-37294

Semiconductor capture level parameter determination, using thermostimulated conductivity
19 p3483 A70-37296

Electromagnetic induction in plate with two dimensional conductivity distribution for case of E polarization, representing field by Green functions
19 p3408 A70-37314

Magnetite and ferrite spinels Hall effect, magnetoresistance and electrical conductivity over wide temperature range
19 p3485 A70-37627

Electrical conduction and surface properties of beta-SiC films obtained by heating Si wafer in presence of hydrocarbon
19 p3485 A70-37685

Low temperature electrical resistivities of Al, Ni, Cu, Ti and Fe alloys for different heat treated conditions
19 p3452 A70-37825

Electrical conductivity of thin semiconductor films for FETs, investigating excessive conductivity scattering
19 p3389 A70-38067

Deformation effects on metallic and semiconductor thin films conductivity
19 p3488 A70-38199

Electrical conductivity of semiconductor diamonds made by alloying with Al under high pressure and temperature
19 p3488 A70-38728

InSb semiconductor, measuring small signal microwave conductivity for hot electron region at 9.4 GHz in high electric DC fields
19 p3488 A70-38747

Electrical and thermal conductivities in white dwarf stars cores and neutron stars outer layers, calculating electron-photon collisions transition probability
20 p3702 A70-39016

Thunderclouds electric fields and conductivities measurement by differential rotating mill, noting insensitivity to space charge and frictional charging
20 p3661 A70-39146

Metal vapors electrical conductivity and density measurement at high temperatures and supercritical pressures
20 p3648 A70-39637

Lithium-diffused silicon, investigating heat treatment and electron irradiation effects on electrical resistivity at high temperatures
20 p3687 A70-40164

Coaxial three coil probe measuring local electrical conductivity and velocity in plasma streams, discussing operations in electrolytes and axisymmetric plasma stream
20 p3684 A70-40259

Liquid and solid semiconductors thermal emf and electrical and heat conductivities measurement over wide temperature range
20 p3634 A70-40300

Aperture antennas admittance calculation, considering upper bound on error involved in approximating finite ground plane conductivity by perfect conductivity
20 p3599 A70-40316

Dislocation network recovery kinetics of cold worked undoped powder metallurgical W wires by electrical resistivity measurements, determining activation energy
21 p3839 A70-40797

Impurities concentration estimate in metals by low temperature residual resistivity, investigating contact and contactless measurements
22 p4052 A70-42573

Atmospheric electrical conductivity examination by balloon-borne instruments, discussing temperature and ion mobility height distribution profiles
22 p4018 A70-42800

Conjunctors and traditors circuit realizations, discussing resistive and dynamic nonlinear networks
22 p3996 A70-42919

Rb and Cs ions implanted Si analyzed by Hall effect and sheet resistivity measurements and channeling techniques
22 p4087 A70-43143

Ti phase transformation effects on thermal conductivity, electrical resistivity and spectral and total emittances at 1100-1500 K
22 p4056 A70-43222

Thin two phase film conductivity, noting conditions for equality with geometric mean and for metal-to-dielectric transition
22 p4088 A70-43466

Conducting epoxy shielding and bonding efficiency and bulk resistivity at high frequencies for bonding cover onto compartmentalized module
23 p4170 A70-43866

Thermal and electrical conductivities of zirconium and hafnium diborides polycrystalline powders at 300-1300 K
23 p4209 A70-44443

N type GaAs doped with Si, conductivity anisotropy observed from measurement and explanation in terms of electron distribution
23 p4231 A70-44890

Superconductive memory type chalcogenide tellurium germanium arsenide, measuring AC magnetic susceptibility and DC electrical resistivity
23 p4231 A70-44892

P-n junction conductance at superhigh frequencies in breakdown region with simultaneous tunneling and impact ionization
23 p4232 A70-45064

Electrical conductivity in inhomogeneous photosphere and sunspots, suggesting sunspot plasma instabilities
24 p4400 A70-45311

Neutron star crust conductivity, obtaining electrical conductivity formula for outer kilometer
24 p4403 A70-45394

Amorphous semiconductor alloys in As-Se system, measuring DC and AC electrical conductivity dependence on temperature
24 p4390 A70-45657

Metallic rods and tubes permeability and resistivity nondestructive measurement by AC apparatus with self balancing sensing coil, using computer program for data reduction
24 p4345 A70-45704

Si-carbide composites electrical conductivity from temperature and thickness dependence, obtaining volt-ampere characteristics via computer method
24 p4391 A70-46154

Thin epitaxial Ag films on mica, measuring electrical resistivity strain dependence
24 p4391 A70-46266

ELECTRICALLY SUSPENDED GYROSCOPES

U ELECTROSTATIC GYROSCOPES

ELECTRICITY

NT ALTERNATING CURRENT
NT ATMOSPHERIC ELECTRICITY
NT AURORAL ELECTROJETS
NT ELECTROJETS
NT EQUATORIAL ELECTROJET
NT GEOELECTRICITY
NT IONOSPHERIC CURRENTS
NT STATIC ELECTRICITY
NT TELLURIC CURRENTS

ELECTRIFICATION

Electric field effects on electrification of colliding ice spheres, discussing relaxation time of sphere charges and charge exchange
08 p1538 A70-21114

Soviet book on aircraft electrification in clouds and precipitation during subsonic flight covering atmospheric electrical properties, flight dynamics modification, communications interference, etc
19 p3356 A70-38800

ELECTRO-OPTICAL EFFECT

Birefringences and phase retardations in lithium niobate crystals for light propagation directions near optical axis, considering electro-optic modulation
02 p0313 A70-12451

Half octave bandwidth traveling wave X band optical phase modulator, noting multiple interactions of optical and microwave fields in electro-optical crystal
06 p1079 A70-17192

Electro-optic effects in ferroelectric ceramics with electrically variable coefficients of piezoelectricity and birefringence, discussing applications
09 p1739 A70-22633

He-Ne laser emission electro-optical modulation by three mirror optical cavity, considering structural and thermal stability and coupled resonators geometry effects
10 p1899 A70-24260

Mariner spacecraft electro-optically controlled star sensors design and performance, discussing star simulation and stray light test techniques
15 p2736 A70-32033

CW argon lasers simultaneous mode selection and phase locking by electro-optic KDDP crystals
15 p2753 A70-32610

Solid state subnanosecond electro-optic light switch for mode locked laser controller or light shutter
15 p2753 A70-32815

CdTe nonlinear electro-optical susceptibility predicted by mathematical model using two coupled anharmonic oscillators
19 p3485 A70-37668

Tantalum oxide thin films electro-optical effects due to refractivity changes
19 p3488 A70-38203

Grid system with alternating filament potentials, deriving potential distribution for fields and electro-optical effect
21 p3835 A70-40632

Electro-optic device using ferroelectric bismuth titanate, discussing electrical and optical properties and matrix addressed display
21 p3830 A70-42114

Light modulator design based on Fabry-Perot interferometer controlled by electro-optical effect
22 p4026 A70-42507

Liquid crystals as solid state organic material with physical properties of liquid, discussing electro-optical properties and applications
22 p4085 A70-42724

Electro-optical light speed measurements with interference comparator using He-Ne lasers with light modulators
24 p4353 A70-45562

ELECTRO-OPTICAL PHOTOGRAPHY

Spatial registration of digitized multispectral video imagery obtained from multilens cameras, multichannel optical-mechanical line scanners and multiple TV camera systems
03 p0453 A70-13000

Wide angle electronic camera for astronomical photometry designed to seek photometric standard stars remote from nebular regions
09 p1681 A70-23313

Photo-optical instrumentation - Conference, San Francisco, August 1969
09 p1684 A70-23751

Electronic camera instrumental profile, information capacity and object recognition
14 p2583 A70-30363

Surface temperature color contour maps of objects undergoing aerodynamic testing, utilizing electro-optical and computer techniques
16 p2905 A70-33169

Short pulse length X ray flash electro-optical recording equipment for explosive processes, describing technique, experimental setup, optical characteristics and information retrieval [SMFTE PREPRINT 69] 22 p4037 A70-43071

ELECTRO-OPTICS

Ferroelectric sodium nitrite single crystals L.F. linear electro-optical coefficients as function of temperature 01 p0154 A70-10104

Electrical supply and control of monopulse 6.25 Hz ruby laser for use in optical radar, high speed photography, etc 01 p0114 A70-11270

Small signal opto-electronic wideband transformer with coupling element ensuring fast response and low sensitivity to parasitic magnetic fields 03 p0459 A70-14266

Electrical analogs for optical systems in communication problem of optimum filtering to improve SNR 04 p0653 A70-15660

Laser beam modulation by electro-optic devices, investigating modulator characteristics in longitudinal and transverse configurations 05 p0860 A70-16489

Two cavity mode locking of He-Ne laser using electro-optic phase modulator 06 p1083 A70-17947

Cloudy sky IR background radiation model for designing simulator of IR background for studying noise rejection characteristics of electro-optical automatic control systems 07 p1246 A70-19527

Electro-optical shutter for optical pumping experiments using Kerr cell controlled by high voltage modulator 07 p1286 A70-19972

Mode locked laser pulse chopping by interferometrically combined electro-optical frequency shifters 08 p1513 A70-21541

Laser display systems, discussing mechanical, diffractive and refractive beam deflection techniques, electro-optical polarization devices, holographic displays, etc 08 p1499 A70-21687

Electro-optical analogies application to sidelobe reduction of radar antenna illumination patterns and optics far field diffraction patterns in terrain image formation 09 p1631 A70-22009

Sensitivity distribution in working field of electro-optical converter tubes, noting use for photometric research 09 p1673 A70-22159

Nonlinear parameter of two intersecting laser beams in interaction with free electrons plane wave external field coupling 09 p1695 A70-22213

Optoelectronic devices for variable resistors controlled by electrical signal, investigating decoupling, capacitance and DC resistance 09 p1649 A70-23353

Electro-optical technique for size distributions of cloud and precipitations particles using linear array of photodetectors 10 p1912 A70-23929

Electrical analogs for optical systems based on linear system concepts and communication theory analysis 10 p1854 A70-25246

IR electro-optical tracker Oculometer using human eye motions for pointing and tracking 11 p1989 A70-25352

Temperature instability of electro-optical laser modulators using ADP, KDP and DKDP crystals taking into account phase shift between coherent light beams 11 p2063 A70-25848

Electro-optical Q switches for generating laser radiation pulses 11 p2064 A70-26809

Monopulse laser operating on ruby and neodymium glass using quarter-wave electro-optical Q switch 11 p2064 A70-26810

Human detection capability for objects on electro-optical imaging displays calculated as function of SNR, viewing distances and brightness levels 12 p2236 A70-27903

Electro-optical light modulators representation by two port matrices, deriving amplitude modulation methods 13 p2427 A70-28924

Ruby laser radiation frequency control by birefringent calcite plate and KDP electro-optical Q switch 13 p2428 A70-29363

Photodetector properties influence on opton transfer functions achieving light conversion by separating photocarriers with p-n junction 14 p2555 A70-30161

CW HCN laser driven phase matched traveling wave lithium niobate electro-optic light modulator performance 15 p2750 A70-31976

Electro-optical systems design - Conference, New York, September 1969 16 p2901 A70-33126

Imaging type electro-optical detection systems design for passive night surveillance, building camera system and testing in helicopters and fixed wing aircraft 16 p2903 A70-33127

Electronic zoom for low light level TV sensor employing electrostatic image intensifier coupled optically to SEC camera tube 16 p2903 A70-33128

On-line optical data processing using CRT with electro-optic target crystal 16 p2903 A70-33132

CRT symbol generators design for high speed computer data display as function of electro-optical and human operator constraints 16 p2850 A70-33133

Electro-optical transducers based on photoconductive cells, phototransistors and microminiature incandescent and solid state light emitters 16 p2904 A70-33144

Airborne electro-optical imaging sensor subsystems performance optimization, comparing mathematical and graphical methods for providing maximum SNR 16 p2906 A70-33172

Airborne electro-optical array system design and performance for particle size measurement 16 p2906 A70-33175

Light modulation electro-optical device with liquid crystals, determining liquid nematic stability 16 p2907 A70-33181

Electro-optical sensor night time capabilities with laser illuminator, determining current per unit area from photocathode 16 p2907 A70-33183

Free generation regime of ruby laser studied by electro-optical method of smoothing spatial inversion inhomogeneities 16 p2907 A70-33192

Methods and equipments for light dispersion measurements for determining atmospheric refraction in terrestrial angle and electrooptical distance measurements 16 p2911 A70-33523

Modulation method for phase detection in electro-optical light modulator of optical range finder 16 p2914 A70-34213

Tactical aircraft performance, discussing electro-optical devices, weaponry, communication and navigational networks, information displays and real time remotely manned control systems 17 p3013 A70-34672

Ar plasma generation by focused Q switched ruby laser beam, measuring density and temperature by electro-optical spectroscopy 17 p3107 A70-35111

Real time holographic reconstruction by electro-optic light modulation through crystal 18 p3258 A70-36312

Optoelectronics conversion for functional electronic circuits, discussing optical coupling, digital and analog computers and information display systems, injection diode light sources, etc 19 p3385 A70-37266

Electro-optical SHF modulator characteristics calculation from light wave interaction with traveling wave 19 p3443 A70-37291

Single frequency ruby laser with electro-optical Q switching, selecting transverse and longitudinal modes by stepwise voltage application to shutter 19 p3448 A70-38737

High speed electro-optic spectral scanning in UV, visible and IR regions, using monochromator deflection of dispersed light 20 p3671 A70-39090

Electro-optical crystal resonator loss anisotropy, determining natural frequencies and polarizations 20 p3642 A70-39755

Electro-optical modulation lock-in techniques for minimizing statistical fluctuations and eliminating internal noise in sampling of light signals 21 p3827 A70-41462

Oscilloscope design involving optimum bandwidth and input sensitivity, reference measurement and second time base 22 p3996 A70-42820

Cuprous chloride (CuCl) as low loss electro-optic material modulating 10.6 micron laser radiation 22 p4051 A70-43334

Ultrasound time perceiving electron-optical conversion methods, discussing image quality and brightness, quantum yield and time resolution 22 p4038 A70-43424

Electro-optical Q switches for generating laser radiation pulses 24 p4351 A70-45181

Monopulse laser operating on ruby and neodymium glass using quarter-wave electro-optical Q switch 24 p4351 A70-45182

ELECTROACOUSTIC TRANSDUCERS

NT LOUDSPEAKERS

NT MICROPHONES

Selectivity and pulsation sensitivity of electroacoustic transducers in turbulent flow under non-coherent reception of random pressure field 03 p0467 A70-13514

Equivalent circuit for acoustoelectric oscillator providing practical device analog, discussing oscillation suppression and resonant frequency changes under reactive load 04 p0656 A70-14719

Microwave acoustic transducer and delay line properties determination from mathematical analysis 06 p1062 A70-17481

Electroacoustic conversion in low resistivity GaAs crystal surface layer, applying external magnetic field to tune converter in wide frequency range 12 p2287 A70-27483

Electroacoustic transducer driven by acoustic pressure and electronic generator, describing electrical properties for functioning as characteristic impedance of acoustic transmission line 19 p3422 A70-37701

Thin film microwave acoustic transducers, calculating top electrode thickness effect on frequencies of infinite conversion loss 24 p4333 A70-45218

Noncontact electromagnetic acoustic transducer (EMAT) for metallic products ultrasonic thickness testing 24 p4336 A70-45682

ELECTROACOUSTIC WAVES

Plasma density and electroacoustic resonance effects on coupled cylindrical antennas self and mutual impedances measured in Hg-arc discharge 01 p0050 A70-10461

Microwave cavity perturbation measurements of electron densities at electroacoustic resonances excited in afterglow plasma 04 p0728 A70-15004

Coupled mode method, analyzing interaction between slow space charge wave of electron beam and electroacoustic wave of lossless warm plasma 07 p1349 A70-19687

Spherical electroacoustic waves in drifting thermal plasma, describing ion acoustic perturbations 12 p2279 A70-27779

Electron-acoustic, ion-acoustic and electromagnetic plane waves coupling at shock front in two fluid ionized viscous plasma 16 p2958 A70-33282

Antennas in plasma, investigating electromagnetic and electroacoustic waves and boundary value approach 17 p3045 A70-35076

ELECTROCARDIOGRAMS

U ELECTROCARDIOGRAPHY

ELECTROCARDIOGRAPHY

Electrocardiographic features and clinical finding in patients with left axis deviation combined with right bundle branch block 01 p0013 A70-10269

P wave changes in serial ECG in patients with acute myocardial infarction 01 p0013 A70-10272

Vascular anatomy correlation with human heart conduction tissue structures to study coronary artery disease cases exhibiting major conduction disturbances by ECG 01 p0013 A70-10273

Oral potassium chloride usefulness and toxicity in EKG nonspecific T wave abnormality evaluation 01 p0014 A70-10274

Intermittent left anterior hemiblock as natural experiments for changes induced by conduction disturbance on human electrocardiograms 01 p0015 A70-10435

Right and left atrial polarization time sequence as guide to p wave origin in heart diseased patients following electrical stimulation of atria and ventricles 01 p0015 A70-10437

Radio telemetry of athlete hearts, noting strenuous physical stress induction of transient serum potassium increase, metabolic acidosis, T-wave amplitudes, etc 02 p0230 A70-11694

Intermittent EKG recordings during hypoxia test for detection and diagnosis of heart disorders in airmen 02 p0242 A70-12850

Model for simulating normal/abnormal depolarization and repolarization of heart and to reproduce electrocardiograms, describing design and programming 03 p0432 A70-12889

Electrocardiographic criteria for left ventricular hypertrophy diagnosis, using chamber dissection technique 03 p0432 A70-12890

Electrocardiac events observed in cardiac transplant recipient emphasizing unique finding 03 p0433 A70-12893

Dielectrocardiograph for studying cardiovascular and respiratory activities by recording hyperemia-evoked permittivity variations in localized body areas 03 p0435 A70-13714

Human atrial flutter studies using electrocardiographic electrodes placed within esophagus and right atrium 03 p0424 A70-13773

Pathologic findings of left ventricular papillary muscle related to electrocardiogram, discussing papillary muscle dysfunction syndrome 03 p0426 A70-13942

Civil aviation personnel cardiovascular rehabilitation using single-lead electrocardiographic telemetry for monitoring and assessing cardiovascular status during supervised exercise

03 p0438 A70-14069

Three dimensional display of human body surface potential distributions as diagnostic tool of cardiac abnormalities

04 p0641 A70-14557

Propranolol effects on human cardiac conduction and intraventricular conduction in dogs studied by recording His bundle electrograms, noting P-H interval prolongation

05 p0800 A70-16102

Myocardial scarring sites localized in human subjects by HF ECG components

05 p0800 A70-16104

Computer program for on-line analysis of exercise ECG considered for improved diagnosis of ischemic heart disease

05 p0805 A70-16105

Electrocardiographic changes during positive headward acceleration of normal human subjects after oxygen breathing and propranolol administration

05 p0808 A70-16675

Periodic components distribution of human cardiac activity rhythm noting slow waves

07 p1210 A70-19556

Statistical methods for characterizing interval sequences of ECG, treating interval distribution and joint probability density function of adjacent interval pairs

07 p1211 A70-19593

Arrhythmia monitor for cardiac distress prediction, using small hybrid computer for detection of abnormal rhythm and ECG complex comparison

07 p1221 A70-19604

Multistage treadmill exercise tests on healthy business executives noting S-T-segment responses

08 p1445 A70-21265

P wave and P loop changes during transvenous pacing of specific locations in coronary sinus and left atrium in dogs and man

08 p1445 A70-21266

Heart dipole moment calculation error due to deletion of individual electrode contributions to surface potential map, analyzing multielectrode grids

08 p1453 A70-21753

Beta-adrenergic blockade effect on abnormal R-ST segment and T-wave changes, showing propranolol use in stress catecholamine and organic cardiovascular diagnosis

08 p1449 A70-21945

Orthogonal electrocardiograms of patients with pulmonary emphysema analyzed by computer, discussing diagnostic classification and correlation with physiologic parameters

09 p1616 A70-22276

Postinfectious noncoronarygenic afflictions of myocardium in flight personnel, discussing clinical record, arteriosclerotic differentiation and ECG variation

09 p1617 A70-22474

Various phases of human isometric left ventricle contraction, comparing results with previously published data

09 p1620 A70-23111

Wolff-Parkinson-White syndrome simulation of myocardial infarction, indicating false positive tests for exercise electrocardiograms

09 p1622 A70-23468

Body vibration effects in cats on myocardial ECG recordings, discussing electrodes implantation and tracings

10 p1810 A70-24007

EKG and cardiac rhythm changes during prolonged hypodynamia /bed rest/ with restricted physical activity

10 p1814 A70-24669

Electrocardiac activity, myocardium and hemodynamic disorders in subjects after prolonged hypodynamia with or without physical exercises and during orthostatic test

10 p1817 A70-24692

Ventricular preexcitation syndrome studied by catheter technique for heart electrical activity recording, noting His bundle bypass effects

10 p1819 A70-24934

Ischemic heart disease /IHD/ prognosis using abnormal electrocardiographic stress test

10 p1820 A70-24940

Dielectrocardiograph for studying cardiovascular and respiratory activities by recording hyperemia-evoked permittivity variations in localized body areas

11 p1990 A70-25514

ECG telemetry system within small irregular metal chamber

11 p1992 A70-26514

Dry electrodes application to ECG monitoring under primitive field conditions, noting materials storage and transportation advantages

11 p1993 A70-26524

Arteriographic determination of severe coronary artery disease in presence of normal resting electrocardiogram

12 p2170 A70-27775

X ray irradiation effects on phonocardiograms, EKGs, cardiac activity phases and Kunos-Garan mechanoelectrical coefficient in dogs

13 p2350 A70-28890

Curve approximation quality by method of informative evaluation for determining minimum required number of measured points on ST interval of electrocardiogram

13 p2360 A70-29775

Asymptotic myocardial infarction in USAF flyers detected by annual electrocardiograms

15 p2690 A70-31889

Amplifiers with selective feedback and clamping circuits for electrocardiology and electroencephalography

15 p2691 A70-31924

In-flight coronary occlusions role in aircraft accidents, discussing need for full autopsies, Double Masters ECG and full medical histories

17 p3033 A70-35570

Electrocardiograms amplitude probability densities, noting variations for different heart diseases

17 p3034 A70-35877

Multistage electrocardiographic exercise tests for cardiovascular performance measurement

17 p3034 A70-35878

Electrocardiography leads system optimal selection based on electrophysical modeling

19 p3369 A70-38207

Electrocardiography electrical bridge type leads system based on potential quenching phenomenon, determining electric dipole displacement of heart in transverse plane of body

19 p3369 A70-38208

Electrocardiogram vs vectorcardiogram for myocardial infarction diagnosis

19 p3371 A70-38362

Circadian rhythms from electrocardiogram and cardiostachogram of patient with human heart transplant, noting P waves relationship between donor and recipient tissues

20 p3570 A70-39166

Isopotential surface maps for body surface potential relation to ECG and Frank vectorcardiogram during QRS stages in children

20 p3571 A70-39368

Digital computer model of total body ECG surface maps, simulating male torso with lungs

20 p3578 A70-39369

Human arterial hypertension, correlating ECG changes with systemic hemodynamics

20 p3573 A70-40069

Left ventricular surface electrocardiogram T-wave amplitude and circumflex coronary artery blood flow during headward acceleration in unanesthetized dogs, observing velocity decrease

21 p3764 A70-41481

Postexercise electrocardiogram detection of latent coronary heart disease in flyers prior to myocardial infarction

21 p3771 A70-41494

Atrioventricular conduction in the human heart, analyzing electrocardiogram response patterns recorded by electrode catheter in unanesthetized man

22 p3970 A70-42942

Computer system for ECG interpretation in hospital heart station

22 p3979 A70-43483

Myocardium bioelectric activity electrocardiogram simulator, describing block diagram and operation

22 p3979 A70-43553

Cardiological examination of flying personnel, taking ECG anomalies and artery wall elasticity into account

22 p3981 A70-43694

Real time contourographic electrocardiographic display determining heart rate from CRT face on beat-by-beat basis

23 p4150 A70-44377

ELECTROCATALYSTS

Liquid metal alloys surface composition and electronic structure roles in electrocatalysis evaluated by studying hydrogen-ion discharge reaction and electrical double layer

06 p1005 A70-18392

Oxygen reduction reaction mechanism and catalysis, considering metal electrode surfaces and substrates, hydrogen peroxide role, adsorption, metal-oxygen bonds, etc

10 p1829 A70-24452

Oxygen reduction in sulfuric acid with phthalocyanine-carbon catalysts

10 p1829 A70-24456

Electrocatalytical activity of oxides in redox reactions without adsorption, noting application to hydrogen oxidation in acid medium

10 p1831 A70-24470

Fuel cell electrolytes, describing porous tungsten carbide as catalyst

12 p2164 A70-27068

ELECTROCHEMICAL CORROSION

Porous hydrogen electrode performance with Ni skeleton catalyst, studying effects of temperature, active layer thickness, etc

12 p2182 A70-27759

Gold alloys electrocatalytic activity in cathodic reduction of oxygen in potassium hydroxide

12 p2182 A70-27760

Electrocatalysts, electrode structure and design of fuel cells using air at cathode, describing applications to hybrid systems

12 p2166 A70-27765

ELECTROCHEMICAL CELLS

NT ALKALINE BATTERIES

NT DRY CELLS

NT ELECTRIC BATTERIES

NT FUEL CELLS

NT HYDROGEN OXYGEN FUEL CELLS

NT MAGNESIUM CELLS

NT METAL AIR BATTERIES

NT NICKEL CADMIUM BATTERIES

NT NICKEL ZINC BATTERIES

NT REGENERATIVE FUEL CELLS

NT SILVER ZINC BATTERIES

NT STORAGE BATTERIES

Thermodynamics of electrochemical cells consisting of Li with lithium chloride or bromide and thallium amalgam with thallium chloride or bromide in propylene carbonate

01 p0042 A70-11107

Electrochemical generators based on thermodynamic equilibrium processes, deriving expressions for EMF, efficiency, and I-V characteristics

07 p1196 A70-20462

Electrochemical cells with lithium anode and nonaqueous electrolyte, discussing research role in designing high specific energy primary batteries

08 p1440 A70-20709

Organic semiconductor electrodes for electrochemical generators, discussing redox association with ion and electron conductivity in polyanilines

10 p1830 A70-24463

Electrochemically optimal structure for Raney alloy catalysts based on molecular hydrogen polarization temperature, noting beta and gamma phases and particle size influence

10 p1831 A70-24468

Cell electrode potential interphasal components, defining problems due to relevant interfacial electrochemistry concepts

14 p2533 A70-30526

Book on batteries and energy systems covering theoretical concepts, construction, operation principles, characteristics and applications of various types of primary and secondary cells

22 p3964 A70-42454

ELECTROCHEMICAL CORROSION

Corrosion problems in Ti and alloys chemical and aerospace applications, describing thermodynamics and electrochemistry in aqueous media

04 p0710 A70-15677

Al-Zn-Mg alloys anodic corrosion behavior under various heat treatment regimes using potentiostatic method

06 p1090 A70-17922

Zr and stainless steel pitting in acidic and near neutral chloride media, comparing controlled potential and conventional chemical corrosion tests results

09 p1706 A70-22939

Iron meteorites electrolytic corrosion using potentiostatic technique, noting roles of Ni content and crystal structure

13 p2432 A70-28697

Chemical and electrochemical corrosion resisting primers for Mg surface coatings in machine parts

14 p2598 A70-31293

Crack initiation and propagation in rolling contact fatigue, emphasizing electrochemical effects in ball bearing failure

[ASME PAPER 70-DE-46]

16 p2931 A70-33509

Upstream wear of small metal orifices under large pressure drops in phosphate ester hydraulic fluids due to current driven electrochemical corrosion

[ASME PAPER 70-FE-15]

16 p2919 A70-33629

Electrochemical mechanism in Ti alloys stress corrosion cracking, formulating mass transport kinetics model

17 p3113 A70-34368

Pre-corrosion effects on strained Al alloy electrochemical response, examining strain test results graphically

19 p3451 A70-37780

Aluminum alloy corrosion stimulation and inhibition effects of cathodic polarization

20 p3647 A70-39244

Electrode and electrolyte additives effect on corrosion and polarization of alkaline zinc electrode

22 p3965 A70-43417

Metallization systems materials for IC, discussing environmental stability, metals electromigration, electrochemical corrosion tests, etc

23 p4173 A70-44533

Electrochemical corrosion of metals, discussing passivity and passivating techniques, inhibitors and resistant alloys

24 p4361 A70-46142

ELECTROCHEMICAL MACHINING

Electrochemical machining based on reverse plating useful in gas turbine industry

04 p0699 A70-15398

Anodic dissolution initial stages of Ti alloys in neutral salt solutions from viewpoint of electrochemical dimensional processing, noting temperature effect on anodic activation potential

07 p1294 A70-19352

Electrochemical machining for drilling deep holes in alloys and refractory metals used in jet engine hardware

10 p1893 A70-23857

Sludge removal from electrolyte in electrochemical machining by settling system, discussing temperature control, flow requirements, concentration control and balance system

10 p1893 A70-23859

Complex variable technique for electrochemical machining of insulated and uninsulated straight sided tool, using minimal computer time

10 p1894 A70-24416

Electrochemical machining of metals with complex shapes, discussing performance capabilities and cost efficiency

[ASTME PAPER MR-69-711] 12 p2239 A70-26989

Electrochemical machining effects on surface integrity and fatigue properties of steel, Ti and Al alloys

[ASTME PAPER MR-69-110] 12 p2241 A70-27081

Electrochemical machining /ECM/ effects on components surface integrity, discussing jet engine materials

[ASME PAPER 70-GT-111] 18 p3264 A70-36849

Electrochemical dimensional machining of complex profile components, using servosystem with feedback for interelectrode gap control

20 p3636 A70-39196

Electrochemical shaping by stationary plane electrodes and by constant velocity electrodes, comparing shaped surface accuracy

22 p4047 A70-43534

ELECTROCHEMICAL OXIDATION

Oxygen-hydrazine interactions on partially immersed metal electrodes, studying conjugated electrochemical reactions

10 p1830 A70-24457

CO electrochemical oxidation at porous solid electrolyte fuel cell anodes under high temperature, noting current density role

10 p1830 A70-24462

Hydrocarbon fuel components relative reactivities in direct electrochemical oxidation on platinum black/Teflon electrodes in phosphoric acid

12 p2182 A70-27762

Electrochemical oxidation of p-type boron anode in aqueous solutions, using galvanostatic technique

17 p3041 A70-34514

ELECTROCHEMISTRY

NT ELECTROLYSIS

Free energies of formation determined for tantalum silicides from EMF measurements on cells with solid thoria-yttria electrolytes

01 p0041 A70-10084

Electrochemical mechanisms of nervous tension generation and expansion based on neural impulse expansion theory, noting ion transport

01 p0020 A70-10518

Polarohydrodynamics method applied to electrochemical kinetics of electrode cathodic or anodic current by coupling surface reaction with mass transfer

03 p0534 A70-14268

Thermodynamics of LiBr in anhydrous dimethyl sulfoxide determined at several temperatures using EMF method

06 p1003 A70-17219

Book on electrochemical processes in fuel cells covering mass transport processes, electrode reactions, anodic oxidation, etc

06 p0989 A70-18250

Electrochemically optimal structure for Raney alloy catalysts based on molecular hydrogen polarization temperature, noting beta and gamma phases and particle size influence

10 p1831 A70-24468

Book on fuel cells electrochemistry covering direct energy conversion methods, electrode kinetics, electrocatalysis, organic substances, electrochemical combustion, research techniques, etc

14 p2532 A70-30100

Hydrogen oxygen fuel cells, demonstrating matching of power source and load, charge transfer, porosity, Nernst equation and electrochemical water synthesis

14 p2533 A70-30533

Electrochemical processes associated with stress corrosion cracking of Ti-Al-Mo-V alloy in aqueous environments

15 p2755 A70-31474

Binary Co-Cr alloy open circuit potential and microstructure, examining effects of composition, heat treatment, allotropic transformation and precipitation

18 p3271 A70-35966

Electrochemical properties of sintered and film nickel hydroxide electrodes

22 p3966 A70-43542

ELECTROCONDUCTIVITY

High temperature fuel cell electrolytes, analyzing electrical conductivity of ternary systems of zirconium, cesium or tantalum and yttrium oxides in fluorite phase

10 p1830 A70-24460

Electric conductivity, thermal emf and EPR spectra of oxide semiconductor glasses based on vanadium and phosphorus oxides, correlating unpaired electron and charge carrier concentrations

15 p2784 A70-32201

Microwave conductivity of thick film screen-printed microstrip circuits, measuring closed resonators SHF Q factors

19 p3388 A70-37964

EM induction in flat plates with two dimensional conductivity distribution, describing approximation method

23 p4217 A70-44054

ELECTROCUTANEOUS COMMUNICATION

Skin sensitivity representation in cats cerebellar cortex during electrocutaneous stimulation in chronic experiment, providing information on afferent system

03 p0417 A70-13216

ELECTRODELESS DISCHARGES

Microwave transmission through afterglow of RF excited electrodeless He discharge approximating low collision frequency plasma slab of uniform electron density in magnetic field

03 p0530 A70-13152

Electrodeless electrolysis of solid ionic conductors and fused salts without contact leads, using electron beams and glow discharge

13 p2361 A70-28929

Numerical analysis of inductive electrodeless discharge of thermal Ar plasma column heated by RF axial magnetic field

21 p3859 A70-41902

Superimposed external DC magnetic field effect on electrodeless HF plasma density, discussing electron cyclotron waves resonance excitation and plasma electron energy gain

22 p4079 A70-42364

ELECTRODEPOSITION

NT ELECTROPLATING

Galvanoplasty process for parts for UHF circuits, discussing cost, safety and quality

08 p1468 A70-20611

Lead ion effects on single crystal zinc dissolution and electrodeposition in alkaline solutions investigated microscopically

13 p2361 A70-28928

Gas bubbles thermal rejection and formation in Ni electrodeposition during annealing over 200-1000 C range

18 p3272 A70-36039

Copper based cermets production by electrochemical deposition in lieu of powder metallurgy, discussing merits

19 p3450 A70-37455

Residual stress of electrodeless nickel deposits on beryllium from bow deformation measurements, noting role of phosphorus content

19 p3451 A70-37708

Uniaxial magnetic anisotropy in electrodeposited Permalloy films in terms of magnetostriuctive mechanism

20 p3687 A70-40160

Sn and tetraethylammonium ions effects on Zn electrodeposition on Zn single crystals in aqueous KOH, using scanning electron microscopy

21 p3772 A70-40726

ELECTRODERMAL RESPONSE

U GALVANIC SKIN RESPONSE

ELECTRODES

NT ANODES

NT CATHODES

NT CELL ANODES

NT CELL CATHODES

NT COLD CATHODE TUBES

NT DYNODES

NT HOT CATHODES

NT PHOTOCATHODES

NT PHOTOMULTIPLIER TUBES

NT PLASMA ELECTRODES

NT THERMIONIC CATHODES

NT TUBE CATHODES

NT TUBE GRIDS

NT TUNNEL CATHODES

Metal/ferroelectric work functions in c-domain barium titanate crystals in short circuited capacitor, noting effect of electrodes presence

01 p0156 A70-10186

Planar Gunn effect devices using various surface electrode configurations, discussing limitations by breakdown on Ga arsenide exposed surface

01 p0049 A70-10287

Transverse magnetic field effects on electrode heat fluxes in heavy-current discharge, discussing anodic space thermal ionization

03 p0531 A70-13205

Human atrial flutter studies using electrocardiographic electrodes placed within esophagus and right atrium

03 p0424 A70-13773

Voltage-step method to measure diffusivity of structured region in polar liquid electrolyte solutions, considering iodine near Pt microelectrodes in aliphatic alcohols

03 p0441 A70-14044

Detached electrode electroexplosive devices consisting of cylindrical column of explosive loaded into tube with thin closure disk at input end

03 p0547 A70-14109

Polarohydrodynamics method applied to electrochemical kinetics of electrode cathodic or anodic current by coupling surface reaction with mass transfer

03 p0534 A70-14268

Anode work functions from cesiated metal surfaces as parameters for thermionic converter systems analysis

04 p0627 A70-14946

Coaxial electrodes with electric and magnetic fields to study instability in MPD arcs

[AIAA PAPER 69-230] 04 p0737 A70-15542

Memory exchange between pairs of electrodes amorphous semiconductors, discussing switch-on and unlocking

04 p0732 A70-15687

Electrode surface bismuth coating selected for reducing electrostatic analyzers photocurrents

05 p0851 A70-16734

Coplanar waveguide consisting of thin metallic film strip on dielectric slab with ground electrodes adjacent and parallel to strip for nonreciprocal gyromagnetic device applications

08 p1475 A70-21281

Electrode curvature effect in radial reflex klystron on processes in electron bunching region

09 p1651 A70-23640

Oxygen electrode ring and disk currents analysis, studying oxygen reduction on platinum via peroxy intermediates

10 p1829 A70-24453

Teflon-bonded gas diffusion electrode flooded agglomerate model, determining porosity, surface area, IR drop, etc

10 p1829 A70-24455

Oxygen-hydrazine interactions on partially immersed metal electrodes, studying conjugated electrochemical reactions

10 p1830 A70-24457

Solid electrolyte high temperature fuel cells electrode materials, investigating various metal oxides

10 p1830 A70-24461

Organic semiconductor electrodes for electrochemical generators, discussing redox association with ion and electron conductivity in polyanilines

10 p1830 A70-24463

Hydrogen oxygen fuel cells with porous electrodes based on Eloflux principle, discussing diaphragms, electrolyte flow and heat removal

10 p1830 A70-24464

Raney catalyst preparation and continuous operation in molecular hydrogen and oxygen electrodes noting improved voltage, manipulation and energy yield

10 p1831 A70-24467

Electrode structural parameters effect on polarization characteristics of air-hydrogen cells to obtain optimum performance, reliability and service life

10 p1831 A70-24471

Electrode erosion or entrainment in MPD arcs due to excess current density, considering inner cathode and outer ring anode with axial magnetic field

10 p1925 A70-25040

Electrode shape and background resistance effects on power rationing between gas tungsten arc and electrode

10 p1897 A70-25314

Electrode erosion during high voltage vacuum breakdown measured by neutron activation analysis and gamma ray spectrometry, noting plasma formation from electrode material

10 p1854 A70-25317

Dry electrodes application to ECG monitoring under primitive field conditions, noting materials storage and transportation advantages

11 p1993 A70-26524

Porous hydrogen electrode performance with Ni skeleton catalyst, studying effects of temperature, active layer thickness, etc

12 p2182 A70-27759

CO adsorption on smooth polycrystalline platinum and rhodium electrodes at various potentials

12 p2182 A70-27761

Electrocatalysts, electrode structure and design of fuel cells using air at cathode, describing applications to hybrid systems

12 p2166 A70-27765

Corona-induced thermal boundary layer breakup effects on convective heat transfer from wire electrode to surrounding gas

12 p2333 A70-28110

Control device for micromanipulator with pacing motor during electrophysiological studies involving microelectrodes implantation into tissue

12 p2179 A70-28317

Electrode placement ancillary technique for obtaining stereotaxic atlas of infant rat hypothalamus

13 p2350 A70-30322

Cell electrode potential interphasial components, defining problems due to relevant interfacial electrochemistry concepts

14 p2533 A70-30526

Third electrode use in charging secondary zinc air battery, presenting performance data and operation problems

14 p2533 A70-30527

Twisted bipolar electrode in needle with controlled separation between bare areas for electrocytography

14 p2542 A70-30398

Tissue respiration measurement with membrane-covered oxygen electrode, discussing effects of electrode deterioration and diffusion artifacts on accuracy

17 p3026 A70-35186

Current and resistance in Hg filled space between two circular electrodes under strong magnetic field, using boundary layer techniques

19 p3477 A70-37578

Electrocardiography leads system optimal selection based on electrophysical modeling

19 p3369 A70-38207

Posterior electrode structural modification for reducing silicon photovoltaic cells absorptivity and operating temperature

19 p3358 A70-38492

Gunn effect devices with concentric cylindrical electrodes, examining oscillation natural frequency-applied voltage relation

19 p3392 A70-38900

Electrochemical dimensional machining of complex profile components, using servosystem with feedback for interelectrode gap control

20 p2636 A70-39196

Interactions between moving alkali-metal seeded dense plasma and metallic thermionically emitting electrode with surface properties influenced by seed particle absorption

20 p3681 A70-40007

Homopolar device electric arc dynamics dependence on gas type, noting flow geometry-Hall effect competition

20 p3681 A70-40009

Composite accelerator electrodes on Cs bombardment microthrusters, testing various designs and electrode coatings

20 p3693 A70-40246

High fidelity microelectrode recording of phase zero cardiac transmembrane action potentials, utilizing memory oscilloscope

21 p3772 A70-42163

Axisymmetric potential problem of plane circular electrified disk in coplanar gap formulated in triple integral equation, obtaining Wiener-Hopf solution

22 p4080 A70-42632

Turbulent charge diffusion during unipolar injection in nitrobenzene between plane-parallel electrodes, discussing liquid motion at high voltages

22 p4080 A70-42719

Pulsed spray welding electrode melting rates for Al alloy, mild steel and stainless steel electrodes over range of pulse current levels

22 p4046 A70-43147

Electrode and electrolyte additives effect on corrosion and polarization of alkaline zinc electrode

22 p3965 A70-43417

Electrochemical shaping by stationary plane electrodes and by constant velocity electrodes, comparing shaped surface accuracy

22 p4047 A70-43534

Electrochemical properties of sintered and film nickel hydroxide electrodes

22 p3966 A70-43542

Thin film microwave acoustic transducers, calculating top electrode thickness effect on frequencies of infinite conversion loss

24 p4333 A70-45218

ELECTRODISSOLUTION

Quantitative analysis of nonmetallic inclusions in steels containing Ti after electrochemical anodic dissolution

18 p3277 A70-36464

ELECTRODYNAMICS

NT ELECTROHYDRODYNAMICS

NT QUANTUM ELECTRODYNAMICS

Nonlinear electrodynamic equations solutions for electromagnetic media with one dimensional unsteady electromagnetic field based on wave functions determined from boundary conditions

01 p0149 A70-10165

Periodic motions and integral stability for systems with quasi-cyclic coordinates applied to current carrying conductor oscillations and linear case of Routh equations

01 p0212 A70-11573

Electrodynamic contactless method for ultrasonic nondestructive testing of materials based on natural frequencies shift with and without defects

02 p0301 A70-12483

Neutral gas ionization and ion recombination effect on electrodynamic plasma acceleration in coaxial and flat electrode accelerators

04 p0728 A70-15222

Relativistic length contraction, time dilation and classical electrodynamics formulated in terms of special relativity using Galilean transformations

05 p0881 A70-15875

Book on cosmic electrodynamics covering cosmic plasmas, sun and solar activity, interplanetary medium and geomagnetic cavity, magnetosphere, geomagnetic disturbance, radiation belt, etc

07 p1387 A70-19667

Earth ionosphere and magnetosphere electrodynamic state as function of neutral gas small scale motions, considering magnetic disturbances and ionospheric discontinuities

07 p1276 A70-20426

Book on electrodynamics of particles and plasmas covering Cerenkov and gyro radiation, point charge motion, magneto-ionic theory, Boltzmann-Vlasov equations, etc

09 p1734 A70-22637

Nonlinear electrodynamic equations solutions for electromagnetic media with one dimensional unsteady electromagnetic field based on wave functions determined from boundary conditions

10 p1925 A70-25013

Vibration generators based on magnetic field electrodynamic effect, giving design, schematic diagram and exploitation properties

11 p2032 A70-26441

Mass transfer in electrodynamically accelerated plasma, discussing recombination, ambipolar diffusion, electrode sputtering, charge exchange, electron capture and resistance forces effect on acceleration

13 p2461 A70-28862

Electrodynamic transducer electrical and mechanical parameters measurement, comparing various techniques

13 p2406 A70-28991

Laser beam scattering by free electrons in terms of classical electrodynamics, discussing radiation damping effects

15 p2752 A70-32451

H alpha and H beta lines electrodynamic broadening with linear Stark effect, calculating relative intensity

15 p2777 A70-32490

Asymptotic motion stability bound for non-holonomic nonlinear electrodynamic systems, using energy metric algorithm for Liapunov functions generation

15 p2768 A70-32556

Electrodynamic-gravitational model of radio galaxies and quasars accounting for complex field, particle acceleration, angular momentum, luminosity and line emission

15 p2807 A70-32811

Boundary conditions for electrodynamics of wave reflection from conducting bodies, using perturbation technique

17 p3128 A70-34633

Radiation from simple slots in moving dispersionless dielectric, using Minkowski electrodynamics

17 p3043 A70-34984

Pulsars electrodynamics concerning EM emissions, discussing roles of rotation and magnetic field

17 p3172 A70-35591

Ionospheric inhomogeneities electrodynamic decay rate, using ellipsoidal model with sharp boundary for irregularity

18 p3252 A70-36986

Fabry-Perot microwave interferometer, examining resonant system electrodynamic properties by matrix method

19 p3422 A70-37722

Slot type oscillations electrodynamic suppression in coaxial magnetrons resonator systems, calculating long wave oscillation frequencies

19 p3387 A70-37738

Planetary electrodynamics - Conference, Tokyo, May 1968, Volume 2

22 p4014 A70-42776

Mass transfer effects on plasma electrodynamic acceleration, discussing plasma recombination and diffusion

22 p4083 A70-43386

H alpha and H beta lines electrodynamic broadening with linear Stark effect, calculating relative intensity

23 p4221 A70-43912

Contactless electrodynamic ultrasonic transducers design and operation, discussing applications and developmental state

24 p4343 A70-45684

ELECTRODYNAMOMETERS

U DYNAMOMETERS

ELECTROENCEPHALOGRAPHY

U ELECTROENCEPHALOGRAPHY

ELECTROENCEPHALOGRAPHY

Human EEG relationship to verbal behavior, discussing separation of stressful from nonstressful verbal stimuli, semantics and question-answer sequences

02 p0236 A70-12119

Autocorrelation and cross correlation analysis of slow EEG potentials in rhythm of movement as cortical activity pattern of cerebral hemispheres during work

03 p0421 A70-13687

Frequency amplitude-threshold EEG analyzer with automatic distribution of filter signals over recording levels

03 p0434 A70-13695

Electroencephalograms recorded for chimpanzees performance to play game, selecting parameters by computer analysis to discriminate between game phases and decisions

04 p0640 A70-14387

Noise effects on tracking performance, electroencephalography /EEG/ and galvanic skin resistance /GSR/

04 p0643 A70-14977

EEG patterns of functional state effect on evoked cortical potentials in response to DC pulses in dogs after nembutal administration

04 p0638 A70-15503

Electroencephalographic study of flying personnel utilizing nasopharyngeal electrodes to determine neurological disorders

06 p1000 A70-17302

Visually evoked cortical responses to checkerboard patterns, correlating amplitude to visual acuity

06 p0992 A70-17311

Electrocorticograms frequency spectra from different visual cortex layers of rabbits during exposure to rhythmic light pulses

07 p1198 A70-18698

Simultaneous recording of fast and slow precision manual movements with electroencephalogram and electromyogram

08 p1452 A70-21438

Brain cerebral tissues electrical impedance measurement by electrodes and bridge circuit, discussing chemical and metabolic properties

09 p1620 A70-22897

Skin galvanic reaction manifestation degree correlated to EEG changes accompanying injuries of human brain limbic structures

11 p1985 A70-25400

Pilot electroencephalograms during F-104 flights recorded by telemetering noting alpha, beta and theta activities

11 p1990 A70-25668

Sensory afterdischarge of human brain under light stimuli during sleep and wakefulness

12 p2173 A70-28354

Sensory deprivation induced EEG changes, discussing duration effect on postisolation occipital alpha frequency

13 p2350 A70-29242

Pilots EEG characteristics, noting alpha and beta rhythms prevalence

13 p2358 A70-29342

Portable autonomous EEG analyzer for processing brain biopotentials without use of computer hardware and qualified personnel

13 p2360 A70-29522

EEG data automatic classification using discriminant analysis

13 p2360 A70-29627

Sleep-wakefulness cycle electroencephalogram of auditory and visual portions of neocortex and hippocampus activity in cats, using spectral analysis and integration

14 p2536 A70-30185

Electronystagmographical responses comparison with electroencephalographic record during prolonged torsion swing vestibular tests under cortical and sub-cortical factors influence

14 p2539 A70-30917

Forced hyperventilation effect in human subject based on indices regarding changes in respiration rhythm, EEG and finger plethysmogram

15 p2679 A70-31607

Amplifiers with selective feedback and clamping circuits for electrocardiology and electroencephalography

15 p2691 A70-31924

Electrical potentials in response to auditory stimuli recorded in cat brains by averaging computer

15 p2685 A70-32831

Human cerebral cortex intercentral relations during repose and afferent stimulation, using electroencephalogram cross correlation

15 p2687 A70-32868

Portable hybrid automatic sleep analyzer for on-line EEG and EOG processing

17 p3040 A70-35606

EEG analysis for poststimulus events, examining contingent negative variation and late positive wave of average evoked potential

19 p3368 A70-37813

Multipoint recording of bioelectric potentials based on electroencephalography, discussing multiple leadout, amplification, analysis, etc
19 p3370 A70-38217

Electroencephalography with automatic frequency analysis to simulate processes involving brain self regulation
19 p3370 A70-38218

Enhanced evoked potentials sited by auditory stimuli in complex task, considering EEG and neurophysiological basis of selective attention
19 p3363 A70-38318

Noise effects on arousal level in auditory vigilance from EEG parameters
19 p3364 A70-38325

Pulse coding system for average evoked EEG potential data acquisition and analysis, describing pulse generation circuitry and computer implemented logic
20 p3578 A70-38985

Automatic diagnosis of clinical electroencephalogram with digital computer, showing maximum and minimum points, basic pattern and paroxysmal wave
22 p3977 A70-42869

Jet pilot EEG radio telemetry showing psychomotor stresses during takeoff and acceleration
22 p3978 A70-42877

EEG dynamics during normal and altered human sleep-wakefulness regimens
22 p3971 A70-43137

Automatic detection of K-complex waveforms in sleep electroencephalograms, using pattern recognition
23 p4151 A70-44379

Human EEG alpha rhythm during surface-tapping test with rod at time-limited maximum frequency, noting slowdown to preferred frequency
24 p4301 A70-45987

ELECTROEROSION

U SPARK MACHINING

ELECTROEXPLOSIVE DEVICES

U INITIATORS [EXPLOSIVES]

ELECTROGENERATORS

U ELECTRIC GENERATORS

ELECTROHYDRAULIC CONTROL

U ELECTRIC CONTROL

U HYDRAULIC CONTROL

ELECTROHYDRAULIC FORMING

Facility for studying energy characteristics of electrohydraulic stamping, discussing copper wire exploding in water
06 p1077 A70-17869

ELECTROHYDRODYNAMICS

Hydrodynamic stability of high purity insulating incompressible fluid subjected to unipolar ion injection
01 p0151 A70-10669

Critical conditions for hydrodynamic stability of incompressible nonconducting fluids subjected to unipolar injection, establishing variational principle leading to characteristic relation
01 p0152 A70-10672

Density distributions of electrically charged trace components in axisymmetric jets, considering space charge effect and ambipolar diffusion
01 p0066 A70-11135

Equations governing electrofluid dynamic energy conversion processes and indicating differences between EFD and magnetofluid dynamic processes presented for mechanical engineering problems [ASME PAPER 69-WA/ENER-9]
04 p0627 A70-14899

Ohms law of electromagnetohydrodynamics derived on basis of Lorentz hydrodynamic plasma model, considering plasma conductivity
05 p0890 A70-16852

Electrohydrodynamic (EHD) technique for generating ions from liquid metals by using electrostatic forces to overcome surface tension forces for field emission of ions
06 p1125 A70-18610

Conducting fluids flow instabilities characterized by incipience at critical electric Hartmann number and convection rate proportional to electric Reynolds number
07 p1348 A70-19265

Hydraulic regenerative servoamplifier system for electrohydraulic actuator design, discussing specifications and test results
09 p1614 A70-23686

Electrostatic generator channel electric field model, evaluating electric body forces on ionized working fluid flow
10 p1807 A70-24571

Electrohydrodynamics of charged water drop pairs disintegration in electric field concerning warm cloud electrification
10 p1912 A70-24806

Viscous dielectric incompressible fluid cylinder capillary stability under small axisymmetric disturbances and axial electric field, deriving perturbed fluid flow equations
19 p3406 A70-38351

Earth atmospheric electricity problems formulated as continuous macroscopic electrohydrodynamic model
22 p4016 A70-42784

Electrofluid dynamic cooling system for spacecraft environmental control, describing design and operating principles
22 p3965 A70-43142

ELECTROJET

NT AUROREAL ELECTROJET

NT EQUATORIAL ELECTROJET

Simultaneous magnetic, photometric and backscatter radio measurement of auroral and ionospheric echoes during geomagnetic storm, confirming electrojet theory
13 p2392 A70-28575

ELECTROKINETICS

Polarohydrodynamics method applied to electrochemical kinetics of electrode cathodic or anodic current by coupling surface reaction with mass transfer
03 p0534 A70-14268

Electrokinetic model for semicircular canal transduction, focusing IR beam on exposed ampullae from posterior canals of Rana pipiens
21 p3765 A70-41696

ELECTROLUMINESCENCE

Current dependence of integral brightness and electroluminescence spectrum of ZnS-GaAs heterojunctions obtained by I vapor reaction in H flow
01 p0155 A70-10142

Electroluminescent matrix displays, discussing limitations in control element
05 p0827 A70-16186

Ferroelectric control circuits controlling electroluminescent cells in matrix, pointer, bargraph, alphanumeric and other displays
05 p0827 A70-16187

Carrier injection luminescence properties useful for display medium applications, discussing group II-VI compounds as injection host crystal materials
08 p1557 A70-21681

Thermochromic materials feasibility for applications in CRT display devices, observing reversible color changes during electron beam irradiation
08 p1499 A70-21682

Electroluminescent displays design capable of generating all primary colors in single compact element
08 p1499 A70-21689

Electroluminescence recombination emission spectra during avalanche breakdown in AlGaAs n-p and p-n heterojunctions
12 p2286 A70-27367

Solid state electroluminescent phosphor displays for aircraft/spacecraft instrument panels
16 p2906 A70-33178

Photosensitivity and electroluminescence spectra of GaAs-indium gallium arsenide p-n heterojunctions at room temperature
17 p3144 A70-35708

GaAs diodes electroluminescence dependence on temperature and injection current
18 p3297 A70-36234

Information optical transmission parameters with electroluminescent GaAs diode as radiation source, calculating energy received over various distances
19 p3389 A70-38069

High energy electron irradiation generated defect centers in GaAs p-n electroluminescent diodes, using capacitance and thermally stimulated current measurements
21 p3863 A70-41914

Direct gap conduction band and alloy composition monitoring InAlP, using electron microprobe cathodoluminescence and X ray emission
22 p4086 A70-43019

ELECTROLUMINESCENT LAMPS

U ELECTROLUMINESCENCE

U LUMINAIRES

ELECTROLYSIS

Water electrolysis module long term operation in providing oxygen for life support systems
05 p0804 A70-15843

Electrodeless electrolysis of solid ionic conductors and fused salts without contact leads, using electron beams and glow discharge
13 p2361 A70-28929

Life support water electrolysis system design, discussing alkaline or acid electrolysis selection
21 p3768 A70-40993

ELECTROLYTE METABOLISM

Human renal function, electrolyte and water metabolism during bed rest with daily leg exercise
07 p1223 A70-19937

Daily electrolyte excretion dynamics of subjects with shifted work-rest schedule, noting disagreement with Scharp results
13 p2358 A70-29343

Electrolyte changes after marathon running noting increase in serum sodium and serum potassium
24 p4302 A70-46108

ELECTROLYTES

NT ION EXCHANGE MEMBRANE ELECTROLYTES

NT MOLTEN SALT ELECTROLYTES

Refuelable Mg-air battery anode, electrolyte and packaging materials selection from standpoint of cell voltage, metal consumption and sludge formation
02 p0253 A70-12721

Voltage-step method to measure diffusivity of structured region in polar liquid electrolyte solutions, considering iodine near Pt microelectrodes in aliphatic alcohols
03 p0441 A70-14044

Transverse magnetic fields effects on velocity perturbations and vortices behind circular cylinder in electrolyte flow at various Reynolds and Stewart numbers
04 p0726 A70-14543

Electrolyte purity effect on initiation times and growth rate of Zn dendrites in alkaline zincate solution, discussing dendrite initiation retardation
07 p1356 A70-19387

Electrochemical cells with lithium anode and nonaqueous electrolyte, discussing research role in designing high specific energy primary batteries
08 p1440 A70-20709

Acute oxygen deficiency effects on blood electrolyte concentrations in altitude-adapted and nonadapted humans
09 p1616 A70-22217

Sludge removal from electrolyte in electrochemical machining by settling system, discussing temperature control, flow requirements, concentration control and balance system
10 p1893 A70-23859

High temperature fuel cell electrolytes, analyzing electrical conductivity of ternary systems of zirconium, cesium or tantalum and yttrium oxides in fluorite phase
10 p1830 A70-24460

Fuel cells with alkaline electrolyte consuming H and O and operating near ambient temperature, discussing electrodes composition and performance
12 p1263 A70-26993

Fuel cells with solid oxide electrolyte, principles, advantages and drawbacks
12 p1263 A70-26994

Fuel cell electrolytes, describing porous tungsten carbide as catalyst
12 p1264 A70-27068

Acceleration effects on Na, K, and pH in rabbits cerebrospinal fluid and cerebral blood
13 p3352 A70-29347

Electric current direction effect on wake of copper sphere moving in electrolyte
13 p2391 A70-29968

Wustite partial oxygen pressure measurements using emf in zirconia solid electrolyte
16 p2961 A70-33965

Cr-Ni system activities and phase boundaries determined by solid electrolyte technique
18 p3273 A70-36040

Portable battery operated system for rapid measurements of blood plasma electrolytes during aeromedical evacuation
20 p3579 A70-39433

Myocardial Na and K content of rats exposed to high altitude, preparing isolated right ventricular strip
20 p3577 A70-40541

High temperature fuel cell with thin disk solid electrolyte, evaluating performance as function of electrolyte, electrode and current collector resistance ratio
22 p3964 A70-42499

Solid state batteries based on highly conducting solid electrolyte rubidium silver iodide, testing discharge performance
22 p3966 A70-43543

ELECTROLYTIC CELLS

Galvanic cell using liquid Mg chloride or Mg chloride-Ca chloride mixtures as electrolyte used to determine activities in Mg-Al liquid alloys
03 p0507 A70-13138

Solid thorium yttria electrolyte applications in EMF measurements for Cr thermodynamic properties in Fe-Cr and Ni-Cr alloys
03 p0483 A70-13140

Titanium alloy wastes electrorefining by electrolytic cell with solid bipolar electrodes to eliminate non-metallic inclusions
05 p0863 A70-16544

Solid electrolyte cells discharge characteristics and open-circuit voltage, evaluating diffusion coefficient of Ag from time dependent behavior of I-V relationship
07 p1196 A70-19386

Solid electrolyte high temperature fuel cells electrode materials, investigating various metal oxides
10 p1830 A70-24461

Hydrogen oxygen fuel cells with porous electrodes based on Eloflux principle, discussing diaphragms, electrolyte flow and heat removal
10 p1830 A70-24464

Hydrogen peroxide fuel cell performance in acid and alkaline electrolytes, investigating cathodic reduction of oxygen on platinum
10 p1808 A70-25037

Fuel cells with solid oxide electrolyte, principles, advantages and drawbacks
12 p1263 A70-26994

SUBJECT INDEX

Prototype electrolyzer for generating oxygen from water vapor under various atmospheric conditions, noting spacecraft cabin application
20 p3564 A70-39696

ELECTROLYTIC GRINDING

U ELECTROCHEMICAL MACHINING

ELECTROLYTIC POLARIZATION

Aluminum alloy corrosion stimulation and inhibition effects of cathodic polarization
20 p3647 A70-39244

ELECTROLYTIC POLISHING

U ELECTROPOLISHING

ELECTROMAGNETIC ABSORPTION

NT AURORAL ABSORPTION

NT MOLECULAR ABSORPTION

NT PHOTOABSORPTION

NT POLAR CAP ABSORPTION

NT X RAY ABSORPTION

Frequency dependence of intraband absorption of electromagnetic waves by free current carriers in doped semiconductors
01 p0153 A70-10067

Semiconductor laser active element radiation absorbing inhomogeneities effect on I-V characteristics, considering oscillation modes excitation
01 p0106 A70-10095

Disk-shaped Mo and Nb specimens solar radiation reflection and absorption characteristics observed for temperature effect
01 p0117 A70-10176

Stratospheric temperature changes connection with winter D region absorption changes
01 p0073 A70-10583

Synoptic ionospheric observations during IQSY, discussing electron density profiles, absorption, drifts, etc
01 p0084 A70-11555

Solution crystallization method to obtain gallium indium phosphide semiconductor alloys, discussing optical absorption thresholds and transitions
01 p0158 A70-10661

Midlatitude ionospheric disturbances accompanied by auroral type radio absorption observed by radio astronomy and probes during 26 May 1967 storm
01 p0084 A70-11555

Light induced modulation of optical absorption of CdS crystals by chopped laser excitation, noting use for fast recombination center detection
02 p0310 A70-11846

Ionospheric absorption associated with sudden stratospheric warmings following geomagnetic disturbances in 1958 and 1963
02 p0290 A70-12159

Free carrier light absorption in n-type GaAs, InAs and Ge semiconductors with mechanically polished surfaces as function of thickness and crystal structure
03 p0538 A70-13057

Interband transitions and optical absorption edge analysis in indium telluride using dependence on photon energy
03 p0541 A70-13725

Anomalous H wave absorption in circular waveguide by dense collisionless plasma, connecting to instability excitation with subsequent plasma heating
03 p0537 A70-14379

Photon absorption and emissivity of nonequilibrium cylindrical plasma in Doppler broadened lines and hemisphere approximation
04 p0724 A70-14411

Interstellar formaldehyde absorption from radio observations with parametric amplifier
04 p0747 A70-14515

Collimated light beam enhanced scattering and anomalous absorption due to decay into plasma waves
04 p0727 A70-14996

Ionospheric inhomogeneities motion and vertical profile of atomic oxygen concentration associated with solar particle absorption in upper layer
04 p0681 A70-15724

Electromagnetic wave diffraction on absorbing black metallic and magnetic cylinders and strip, plotting radar scattering cross sections
05 p0813 A70-16262

Seasonal variation in ionospheric radiation absorption related to time variation between sunrise and constant angle attainment of sun
05 p0842 A70-16758

Radio wave absorption coefficient in lower ionosphere related to total radiation absorption and electron concentration profile
05 p0843 A70-16761

Cepheus light attenuation curve explained by applying polymodal particle size distribution, obtaining interstellar dust density
05 p0918 A70-16915

Absorption transition fine structure measurements for bulk rare earth garnets single crystals using reflectivity techniques
05 p0894 A70-16998

Steady state thermal defocusing of carbon dioxide laser radiation in gases as function of beam power, gas absorption coefficient and pathlength
06 p1079 A70-17190

Electron density distributions relation to D region diurnal and seasonal variations in radiowave absorption in terms of transport processes near mesopause
06 p1054 A70-17589

Large scale horizontal gradients in auroral radio absorption and effects on absorption height measurement by multifrequency riometry
06 p1055 A70-17595

Color difference method for interstellar extinction laws applied to O stars study
06 p1140 A70-17641

Stellar light absorption in optically dense cometary atmospheres
06 p1141 A70-17738

Transmission and reflection coefficients calculated for electromagnetic waves incident on inhomogeneous absorbing layer applicable to ionosphere, plasma and p-n junction
06 p1009 A70-17834

Nighttime radio wave absorption in ionosphere during moderate solar activity based on echo observations
06 p1056 A70-17840

Ionospheric absorption at oblique incidence during IQSY, studying seasonal and diurnal variations as solar zenith angle function
06 p1009 A70-17905

D and lower E region absorption of short waves, studying absorption distribution with height
07 p1263 A70-19153

Ionospheric absorption diurnal and seasonal variations determined from field strength recordings
07 p1263 A70-19154

Ray tracing calculation and experimental observation for mode structure and absorption loss of oblique incidence HF radio wave propagation
07 p1234 A70-19217

Synchrotron radiation negative reabsorption possibility for relativistic electrons dipped into and in absence of unrelativistic plasma
07 p1348 A70-19413

Sunrise effects in lower ionosphere at midlatitude, discussing long wave absorption measurements, summer electron concentration profile and consistency of aeronomic model
07 p1235 A70-19436

Graphic method of calculating radio wave absorption in ionosphere and field strength at reception point with aid of vertical sounding data
07 p1235 A70-19437

Probability of three photon band-band excitation of electron in semiconductors using S-matrix formalism, calculating absorption coefficient for two band approximation
07 p1356 A70-19795

Holograms in thick absorption recording media in terms of diffraction efficiency, angular orientation and wavelength sensitivities
07 p1287 A70-20093

Extrema behavior in nonlinear absorption of organic compounds under high power laser radiation interpreted by triple absorption molecular energy level models
07 p1302 A70-20100

S- and p-polarized electromagnetic wave incident on semiinfinite laminar plasma layers, analyzing reflection and absorption characteristics
08 p1456 A70-20504

Absorption and luminescence in complex molecules and semiconductors, describing particle distribution and Fermi quasi-levels dependence on temperature and excitation intensity
08 p1555 A70-20510

UHF telescopic survey of southern sky for studying galactic plane in absorption
08 p1578 A70-21536

CW GaAs junction laser bistable operation due to saturable absorbing centers in active medium
08 p1513 A70-21598

Retinal temperature increases produced by intense light absorption described by heat conduction equation
09 p1614 A70-22075

Semiconductor injection laser, analyzing light absorption by free carriers and gain characteristics
09 p1694 A70-22133

Photographic emulsions design for increased water depth penetration during aerial multispectral recording of light absorption and scattering in water masses
09 p1674 A70-22261

Nonresonant electromagnetic absorption in high density plasma used for RF heating in magnetostatic field
09 p1735 A70-22923

Intense laser radiation effect on light absorption, gas breakdown and formation of spark at focus
10 p1899 A70-24154

He-Ne laser Q factor modulator based on Fabry-Perot interferometer with alternating absorption
10 p1899 A70-24255

Shock pressure and impulse caused by Q switched laser light absorption, considering temperature dependence of EM radiation penetration depth
10 p1900 A70-24422

ELECTROMAGNETIC ABSORPTION

Light scattering, turbulent disturbances and absorption by binary oxygen complexes in atmospheric layers
10 p1843 A70-25126

Cosmic layer in lower ionosphere investigated by 164 kHz frequency absorption at night, discussing solar activity effects
10 p1934 A70-25198

Q switched ruby laser light effect on absorption spectra of NaCl crystals
10 p1902 A70-25221

Tunable nitrous oxide laser cavity losses and absorption by carbon dioxide determined spectroscopically
11 p2061 A70-25361

Sporadic E formation correlation to geomagnetic activity from ionospheric radio absorption observed at midlatitude and polar zone stations
11 p2044 A70-25554

Radio wave absorption at 2.2 MHz measured by vertical incidence pulse method, observing maxima in February and in September-October due to auroral activity
11 p2006 A70-26176

Layered electromagnetic absorbers performance analysis by variable metric optimization method, handling functions defined over polyhedral region of real space
11 p2019 A70-26713

Corpuscular radiation intensity measurements in upper atmosphere at midlatitudes by meteorological probe during geomagnetic storm, noting radio wave absorption
11 p2106 A70-26797

Microwaves reflection, absorption and thermal emission at smooth air-water interface, tabulating calculated coefficients
12 p2183 A70-27169

Nonlinear optical effects in solids, gases and liquids with light from laser sources, discussing self focusing and absorption of light, transclucidity, harmonics, etc
12 p2245 A70-27277

Light absorption coefficient frequency dependence related to interband transitions in highly doped semiconductors
12 p2287 A70-27487

Ionospheric absorption measurements by HF and VHF techniques, discussing electron density profiles, collision frequencies, anomalies and aeronomic and ionospheric implications
12 p2224 A70-27735

Optical resonator longitudinal modes selection, comparing Michelson interferometer, internal slanted Fabry-Perot interferometer and absorbing film methods
12 p2251 A70-28290

Seasonal measurements of ionospheric absorption during sunrise in D region at medium sunspot numbers, noting disagreement with rocket observation
13 p2392 A70-28574

Macroscopic plasma response to absorption of high intensity laser radiation in one dimensional geometry
13 p2459 A70-28636

Electromagnetic radiation attenuation in rain at cm and mm wavelengths, determining rainfall rates and drop size distribution
13 p2364 A70-28783

Solar spectra recording by balloon-borne monochromator, measuring stratospheric IR absorption
13 p2491 A70-29050

Q switched ruby laser pulses nonlinear absorption by partially ionized plasma behind reflected shock wavefront, observing absorptivity dependence on light intensity
13 p2429 A70-29420

Optical absorption due to imperfections in CdS by sensitive differential technique using laser excitation
13 p2430 A70-29708

Light absorption coefficient of two band superconductor with nonmagnetic impurity, observing electron pairs removal from condensate and transition into excited states
13 p2472 A70-29723

Rossland stellar opacity calculation allowing for photon absorption in spectral lines using non-relativistic dipole approximation
13 p2495 A70-29752

Ionospheric inhomogeneities motion and vertical profile of atomic oxygen concentration associated with solar particle absorption in upper layer
14 p2575 A70-30808

H II region stellar color anomaly attributed to interstellar extinction
14 p2641 A70-30879

Nonhomogeneous atmosphere with absorbing gas of constant mixing ratio, deriving transmission along isothermal and nonisothermal paths
14 p2617 A70-31304

Electromagnetic absorption of Martian matter based on vertical temperature variations in planet surface layer
15 p2802 A70-32491

Laser beam anticorrelation after attenuation by two photon amplifier, deriving density matrix in time dependent perturbation theory

16 p2928 A70-33283

Semiautomatic ionospheric absorption recorder, describing components circuitry and operation

16 p2915 A70-34223

Winter anomaly of radio wave absorption in midlatitude lower ionosphere in terms of meteorological influences and particle influx enhancements

17 p3076 A70-34936

Photon capture cross sections for surface silicon electronic states using IR photoconductivity measurements

17 p3144 A70-35707

Proton flares showing enhancement of ionospheric absorption and complex magnetic disturbances

18 p3306 A70-36087

Ionospheric radio wave absorption measurements, noting winter anomaly during maximum solar activity year

18 p3227 A70-36101

Quantum mechanical model of stimulated thermal, Brillouin and molecular excitation scattering of light due to absorption

18 p3266 A70-36409

Sunrise effects in lower ionosphere at midlatitude, discussing long wave absorption measurements, summer electron concentration profile and consistency of aeronomic model

18 p3249 A70-36910

Graphic method of calculating radio wave absorption in ionosphere and field strength at reception point with aid of vertical sounding data

18 p3229 A70-36911

Light propagation in plane parallel layer of scattering medium containing absorbing substance with random density distribution

19 p3461 A70-37422

Two photon absorption-fluorescence measurement of laser pulse width, using three level model of absorber

19 p3422 A70-37671

Ionospheric absorption of cosmic noise recorded by riometer and corner reflector antenna directed at pole star, noting seasonal variation

19 p3412 A70-37997

Solar X ray emission during flares from ionospheric absorption measurements, discussing continuous ionograms method

19 p3512 A70-38912

Light characteristics and geometry of photoelectric photometer system measuring light attenuated by atmosphere, discussing error sources

20 p3625 A70-39030

Multiphoton absorption coefficient for semiconductors, using interband absorption method

20 p3687 A70-40020

Millimeter waves atmospheric attenuation vs frequency and altitude due to oxygen absorption, tabulating for graphical and seasonal model atmospheres

20 p3588 A70-40302

Millimeter and decimeter waves atmospheric absorption as function of pressure, temperature and water vapor density

20 p3588 A70-40303

Short light pulse coherent absorption in homogeneously broadened resonant medium, discussing influence of input pulse area and atomic coherence on propagation properties

21 p3784 A70-40565

Earth magnetic field effects on midlatitude F2 layer deviative absorption

21 p3812 A70-40727

Anomalous electromagnetic wave absorption in collisionless plasma attributed to instability excitation causing ion density fluctuations

21 p3855 A70-40754

Low latitude boundary of ionospheric absorption during winter anomaly showing enhancement dependence on solar zenith angle

21 p3815 A70-40944

Sporadic E formation correlation to geomagnetic activity from ionospheric radio absorption observed at midlatitude and polar zone stations

21 p3819 A70-41304

Total reflectance of composite light diffuser with nonuniform absorption by two beam model, noting application to photochemistry

21 p3829 A70-41936

Rossland stellar opacity calculation allowing for photon absorption in spectral lines using non-relativistic dipole approximation

21 p3923 A70-42072

Atmospheric scattering governed by Rayleigh phase function with absorption, calculating radiative transfer by numerical solution of Chandrasekhar integral equations

22 p4072 A70-42340

Cotton leaves ammonia induced discoloration spectrophotometric examination, discussing light reflectance, transmittance and absorbance

22 p4014 A70-42771

Electromagnetic absorption of Martian matter based on vertical temperature variations in planet surface layer

23 p4240 A70-43913

Radiative transfer equation solution for polarized light in Rayleigh scattering atmosphere with absorption, using singular eigenfunction expansion technique

23 p4219 A70-44402

Dipole antenna in compressible lossy plasma, calculating sheath and absorptive surface effects on current distribution from boundary value problem formulation

23 p4228 A70-44963

Short and long term stabilized optical frequency standard of gas laser, using two absorption cells

23 p4202 A70-45057

Monthly and annual root-mean-square deviations of ionosphere radio wave absorption

24 p4312 A70-45485

Solid solution of GaAs with CdSe and CdS compounds, investigating intrinsic absorption edge dependence on temperature

24 p4390 A70-45663

Doubly excited antiferroelectrics absorption spectrum band and bound states, discussing zero approximation 0-0 transitions of alpha oxygen molecules and permeability tensor

24 p4392 A70-46362

ELECTROMAGNETIC COMPATIBILITY

Electroexplosive devices (EED) in electromagnetic environments, discussing principles of warship safety

03 p0549 A70-14129

RF hazard measuring system for complete guided weapons electromagnetic compatibility tests with instrumented inert device replacing live igniter

03 p0495 A70-14132

Instrumentation concepts for electromagnetic compatibility measurements on electroexplosive devices, considering thin film thermocouple, electrical diode detector and microstrip transmission line techniques

03 p0495 A70-14138

Ground wave electric field intensity prediction model in EMC applications, discussing soil conditions and polarization effects

07 p1336 A70-20217

Design criteria for minimizing EMC problems confronting engineers of aircraft electrical and electronic equipment

11 p1980 A70-25887

Electromagnetic compatibility - IEEE Conference, Atlanta, October 1969

12 p2200 A70-28126

Electromagnetic interference filters design for equipment power lines from electromagnetic compatibility and reliability viewpoints

12 p2201 A70-28129

Computer controlled system for real time measurement and analysis of electromagnetic interference and compatibility with economy of time, manpower and cost

12 p2201 A70-28133

Radar systems EM compatibility simulation, describing FORTRAN IV operational interference prediction program

12 p2193 A70-28139

Measured electronic equipment characteristics trends improving electromagnetic compatibility design

12 p2190 A70-28140

Electromagnetic compatibility (EMC) design criteria including gain, selectivity, nonlinearity and filter types

12 p2202 A70-28142

Chirp radars energy spectra bounds calculation to insure electromagnetic compatibility

14 p2551 A70-31178

Frequency allocation in EM environment of 1970s based on interference compatibility analysis

17 p3045 A70-35158

Wire antennas array analysis and beam pattern synthesis by method of moments, considering application to electromagnetic compatibility

19 p3380 A70-38178

Electrical tests on satellites and space probes applied to spaceborne subsystems, subsystems and electronic systems EM compatibility

19 p3532 A70-38287

ELECTROMAGNETIC CONTROL

U ELECTROMAGNETS

U REMOTE CONTROL

ELECTROMAGNETIC DEDUCTION

U MAGNETIC INDUCTION

ELECTROMAGNETIC FIELDS

NT FAR FIELDS

Nonlinear electrodynamic equations solutions for electromagnetic media with one dimensional unsteady electromagnetic field based on wave functions determined from boundary conditions

01 p0149 A70-10165

Current distribution in finite length helical antenna in HF field, using cylindrical model of infinitely good conductivity

01 p0050 A70-10713

Field pattern near paraboloid reflectors focus for low f/D ratios, considering vectorial character of electromagnetic field

02 p0268 A70-12474

Reinforced plastics models for determining internal stress, temperature and electromagnetic fields of multicomponent reinforced plastics

02 p0323 A70-12806

Steady, homogeneous, electromagnetic plasma acceleration fields, demonstrating electric and magnetic fields effects on dynamic behavior

03 p0529 A70-12989

Electron flux interaction with electromagnetic field in comb type waves via linear approximation assuming small space charge

03 p0447 A70-13291

Electromagnetic field spectrum and spatial distribution in ring laser, considering transverse modes influence

03 p0500 A70-13462

Laser amplifier electromagnetic field in arbitrary quantum mechanical state, deriving complex amplitude distribution function to calculate phase uncertainty

03 p0503 A70-14174

Electromagnetic field sources in two dimensional problem of diffraction by slit

03 p0526 A70-14355

Transient electromagnetic fields coupling transfer functions for two wire uniform transmission line cable models, using long wire antenna as radiation source

04 p0658 A70-14739

Electromagnetic structure of interplanetary space on basis of secondary cosmic ray intensity gradient annual variations as function of earth heliographic latitude

05 p0900 A70-15970

Output characteristics of cyclotron maser with resonator field due to plane waves interference along static magnetic field, deriving tensor equations

05 p0858 A70-16260

HF electromagnetic field penetration of plasma with finite conductivity and Hall constant for containment of hot plasmas, formulating nonlinear electrodynamic problem

05 p0889 A70-16490

Surface impedance of spherical earth isolated by nonconducting atmosphere from ionospheric currents producing alternating electromagnetic field

05 p0843 A70-16768

Waves and differential equations for electromagnetic field in nonuniform magnetized plasma described for all orders in electron and ion temperature

07 p1350 A70-19823

Hydromagnetic ionizing shock wave structure in electromagnetic fields, using model composed of strong adiabatic shock to translational equilibrium followed by ionization initiation

07 p1351 A70-19985

Electromagnetic and gravitational fields classification methods using spinor techniques, introducing five dimensional complex linear space with Weyl tensors elements

07 p1337 A70-20302

Electromagnetic field of horizontal LF electric dipole formed by thin ionosphere layer between anisotropic planes

07 p1277 A70-20447

Terrestrial electrical conductivity measurement from electromagnetic field variations determination by geomagnetic sounding

07 p1277 A70-20458

Scattered field from rough ionospheric irregularities or earth surface for arbitrary polarization of incident wave

08 p1456 A70-20574

Diener kinetic theory for charged particles in EM field with Coulomb interactions taking into account transverse plasma waves

08 p1550 A70-20616

Momentum vector and spin tensor definitions for extended body moving in arbitrary gravitational and electromagnetic fields, considering test body in de Sitter universe

08 p1545 A70-21352

Electron-positron pair formation in electromagnetic field created by coherent laser light focused into vacuum with ideal lens

08 p1513 A70-21411

Unified geometric description of gravitational and electromagnetic fields, determining electromagnetic field influence on geometry from dimensional constant

08 p1546 A70-21811

Natural frequencies and electromagnetic field distributions in rectilinear and cylindrical dielectric resonators used in microwave circuits

09 p1644 A70-22280

Plasma conductivity measuring device using phenomenon of change of coil induction in electromagnetic field

09 p1737 A70-23380

Argon plasma interaction with RF electromagnetic field using MGD model, noting plasma-field coupling and plasma temperature exhibition of skin effect

09 p1737 A70-23433

Electromagnetic fields in electron plasma with electron density variations due to transient ionization processes

10 p1921 A70-23978

Momentum-energy tensor and angular momentum for hydrodynamic and electrodynamic fields determined in transformations of m-parametric Lie group
10 p1922 A70-24098

Wave propagation in homogeneous cone region of broadband radiator, calculating field distribution by retarded potentials method
10 p1848 A70-24222

Warm clouds electrification calculated for electromagnetic field growth by inductive mechanism, noting role of water drop pair interaction
10 p1913 A70-24807

Nonlinear electrodynamic equations solutions for electromagnetic media with one dimensional unsteady electromagnetic field based on wave functions determined from boundary conditions
10 p1925 A70-25013

Microfluctuations frequency and wavelength of electromagnetic, electric and magnetic field distributions in plasma shock wave front found consistent with ion-acoustic origin hypothesis
10 p1925 A70-25031

Homogeneous plasma turbulence growth limits, determining bounds on density and electromagnetic field nonlinear fluctuations in thermodynamic terms
11 p2096 A70-26767

Electromagnetic effects on separation of turbulent MHD boundary layers allowing for heat transfer
12 p2278 A70-27324

Book on electromagnetic fields and waves covering electrostatic and magnetic fields, relativity, vectors, Maxwell equations and propagation
12 p2273 A70-28150

Electromagnetic fields features in VLF spectral range for propagation in earth-ionosphere waveguide, discussing effects of ionospheric irregularities
12 p2190 A70-28169

Parametric and Raman instabilities predicted by linear theory for plasma in electromagnetic field
13 p2458 A70-28563

Wire loop inductive probe with compensation spur as precision sensor for magnetic field intensity in EM fields
13 p2376 A70-28817

Quasi-monochromatic radiation field polarization representation and transformation of state, including instrumental effects
13 p2451 A70-28829

Einstein-Maxwell equations for monopolar point electrical charge, calculating proper energy for electromagnetic and gravitational fields
13 p2451 A70-28956

Kerr-Schild space-time manifolds with electromagnetic field, solving Einstein equations
13 p2451 A70-29166

Monograph on analysis of reflector antennas covering electromagnetic field equations, computer aided design, etc
13 p2367 A70-29600

Electromagnetic theory of forces for coalescence in granular layers during thermal evaporation of thin films, calculating interaction between instantaneous dipoles
13 p2471 A70-29640

Javelin rocket measurements of ionospheric AC electromagnetic fields, determining amplitude/frequency spectra and dipole antenna performance
13 p2401 A70-29926

Frequency dependence of gravitational-electromagnetic fields interaction assumption inconsistent with general relativity and consistent with data on deflection of radiation by massive bodies
14 p2573 A70-30616

Thermal EM field as function of coherent states, outlining quantum theory for thermal radiation and solar energy
15 p2678 A70-32423

Electromagnetic field determination from oscillating vertical and horizontal electric dipoles above flat earth, demonstrating Sommerfeld formulation and dyadic Green function technique equivalence
16 p2861 A70-32974

Electromagnetic field intensity measurements in focal region of wide angle spherical reflector antenna illuminated by polarized plane wave
16 p2872 A70-32976

Instrument for visualization of EM field in open resonators in mm range
16 p2908 A70-33213

Maxwell equations and equations of massive-vector-meson fields in spatially homogeneous Bianchi cosmologies, obtaining formula for homogeneous EM field
17 p3156 A70-34827

Plane electromagnetic wave diffraction by infinite grid above finite dielectric layer, calculating field distribution
19 p3375 A70-37281

Electromagnetic induction in plate with two dimensional conductivity distribution for case of E polarization, representing field by Green functions
19 p3408 A70-37314

Electrically conducting perfect compressible fluid flow in semiinfinite channel under electromagnetic field, using multiple scales method
19 p3479 A70-37595

Wave diffraction by finite dimension grating, determining EM field strength distribution by approximate method
19 p3377 A70-37716

Diffacted-field structure on two-element gratings in near zone, calculating amplitude, phase and energy flux for normal and slant incidence of EM fields
19 p3377 A70-37720

Metallic core shielded squirrel cage waveguide excitation by charged filament, giving equations for Fourier coefficients of electromagnetic fields
19 p3386 A70-37732

Cylindrical EM waves diffraction by two parallel ideally conducting elliptical cylinders, discussing field and surface current distributions
19 p3378 A70-37734

Two dimensional electromagnetic fields in presence of cylindrical objects of arbitrary physical properties and cross sections, using scattering matrix approximation
19 p3471 A70-37778

Magnetic coupling in solid dielectric cylinder under axial magnetic and perpendicular electric fields, noting memory and magnetostrictive effects
19 p3471 A70-37785

Nonlinear electromagnetic constitutive equations with coupling to thermal gradients for holohedral and hemihedral materials, extending analysis to orthotropic media
19 p3552 A70-37786

Terrestrial ELF electromagnetic wave fields strength variation with distance over earth surface, using residue series zero-order term
19 p3380 A70-38405

Earth EM field short period pulsations distribution within magnetic storms
19 p3416 A70-38585

Correction to Wu theory of microstrip leading to exponentially increasing fields
21 p3784 A70-40558

Optical communication waveguides with diffused boundaries, calculating modal propagation fields by perturbation theory
21 p3792 A70-42045

Electromagnetic effects on separation of turbulent MHD boundary layers allowing for heat transfer
21 p3860 A70-42065

Einstein equations solved for steady axisymmetric physical schemes by varying Kerr metric constants, considering electromagnetic field case
22 p4073 A70-42717

Compressional sound waves electromagnetic generation in metals in static magnetic fields, examining acoustic amplitude variations
22 p4074 A70-42968

Einstein-Maxwell fields in presence of matter and pressure, expressing existence conditions in terms of eigenvalues and eigenvectors of Ricci tensor
22 p4074 A70-43206

Concentrated pulsed electromagnetic fields penetration into conductor, assuming magnetic field along metal surface
22 p4041 A70-43621

Convolution equation for kinetic theory of EM field excitation in plasma waveguides
23 p4223 A70-43772

Secondary source distribution of EM field induced on ground-air interface by antenna
23 p4161 A70-43773

F region equatorial anomaly formation, investigating vertical EM drift effect
23 p4187 A70-43857

Laminar geoelectromagnetic field excited by coaxial circular current, determining impedance and magnetic field ratios of spherical harmonics
23 p4189 A70-44064

Lower ionosphere electromagnetic induction effect on geomagnetic field guided MHD wave propagation, considering Hall effect
23 p4189 A70-44072

Compressible plasma flow in axisymmetric channels under EM body forces and Joule heating
23 p4228 A70-44934

Current oscillations in external circuits of semiconductor with low surface recombination in parallel electromagnetic field
23 p4231 A70-45062

Relativistic and nonrelativistic generalizations of classical approach in quantum mechanics applied to equations of motion in electromagnetic field
24 p4378 A70-45275

Pre-Maxwellian electromagnetic equations application to MHD, investigating existence theorems generalization from system at rest to system with motion
24 p4386 A70-45593

Helicons and transverse optical phonons coupling in degenerate polar semiconductors investigated from electromagnetic linear response theory and field method
24 p4390 A70-45603

Quantum detector with impinging EM field, discussing photoelectron counting distribution and signal with white noise
24 p4312 A70-46051

VHF and UHF radio field strength changes due to tropospheric reflecting layers disintegration during anticyclonic weather, using ray tracing technique
24 p4315 A70-46153

ELECTROMAGNETIC INTERACTIONS

NT PLASMA-ELECTROMAGNETIC INTERACTION

Radial electron flux interaction with cylindrical electromagnetic wave propagating between conducting planes, noting disturbance development according to power law
01 p0049 A70-10166

Soviet book on quantum electrodynamics covering photon mechanics, electron relativistic mechanics, electromagnetic interactions, corrections to Green functions, particle interactions, etc
02 p0345 A70-12827

Electromagnetic field structure and interaction inside and outside of spherical shell of arbitrary linear media excited by monochromatic plane wave
03 p0443 A70-13151

Half octave bandwidth traveling wave X band optical phase modulator, noting multiple interactions of optical and microwave fields in electro-optical crystal
06 p1079 A70-17192

Laser mode interaction characteristics determination using resonator field equation taking into account competition and coupled modes
06 p1081 A70-17765

Light pulse propagation in nonlinearly amplifying or absorbing medium, discussing coherent and non-coherent interaction between pulse and medium
07 p1296 A70-18745

Electron density dependence on electron temperature during self and mutual interaction of electromagnetic waves in magnetoplasma, tabulating numerical results
07 p1351 A70-19968

Cs jet device eliminating wall influence in nonlinear radiation-atom interaction phenomena
07 p1342 A70-20109

Stokes components generation in presence of stimulated combination radiation in optical cavity, considering interaction between components and effect of material dispersion on interaction
08 p1510 A70-20511

Electromagnetic fields interaction with nonconducting neutral elastic solid, formulating relativistic variational principle for balance laws and constitutive equations
08 p1545 A70-21252

Polarization of interacting atoms resonance fluorescence and coherence transfer due to excitation exchange, considering electrostatic dipole-dipole and electromagnetic radiative interactions
08 p1548 A70-21341

Galaxies and stars interactions, explaining observed peculiarities by electrostatic and electromagnetic forces
09 p1750 A70-22097

Multilevel quantum systems interaction with electromagnetic fields at frequencies near quantum transitions using small signal analysis
09 p1695 A70-22256

IR energy interaction with earth atmosphere, determining multispectral scanner optimum wavelength intervals for earth resources applications
09 p1669 A70-22892

Excited gas kinetic state determination from observed spectral profiles during interaction with radiation
10 p1919 A70-24147

Radial electron flux interaction with cylindrical electromagnetic wave propagating between conducting planes, noting disturbance development according to power law
10 p1853 A70-25014

Injection semiconductor lasers emission characteristics, discussing gallium arsenide diodes, nonlinear losses in pulsed mode, laser interactions, etc
15 p2749 A70-31453

Light propagation-shift relationships in optically pumped atomic vapors, discussing susceptibilities, birefringence, conversion efficiencies, coupling, etc
17 p1303 A70-35000

Linear phased antenna arrays, calculating influence of interaction between radiating elements on radiation pattern
17 p3048 A70-35686

Nuclear-electromagnetic cascades longitudinal development in glass, Fe and W absorbers, presenting Monte Carlo simulation
18 p3293 A70-36895

Three level gas laser amplifier theory, considering quantum mechanical atomic system in interaction with two monochromatic EM waves
19 p3446 A70-37829

Laser radiation and solid target interaction, calculating temperature and plasma density as function of intensity
19 p3447 A70-38166

Laser beam and matter interaction models for positive energy balance in nuclear fusion, obtaining Lawson criterion

19 p3447 A70-38168

Light pulse propagation in nonlinearly amplifying or absorbing medium, discussing coherent and non-coherent interaction between pulse and medium

21 p3836 A70-41170

Quantum theory of inhomogeneously broadened laser, considering atomic motion-electromagnetic field interactions and detuning effects

22 p4048 A70-42293

Electron beam interaction with external harmonic microwave field in planar diode gap, calculating electric field current and voltage distribution functions

22 p3995 A70-42396

Current oscillations produced in finite-length electron hole semiconductors by strong electric and magnetic fields, discussing HF stabilization

22 p4084 A70-43469

Electron loss by resonant interaction with whistlers in nonuniform magnetic field, taking Fokker-Planck equation as distribution function

23 p4237 A70-44052

Pulsed radio wave interactions with various lower ionosphere models, estimating cross modulation by computer calculation for comparison with measurements

23 p4162 A70-44080

ELECTROMAGNETIC INTERFERENCE

NT ATMOSPHERICS

NT BLACKOUT [PROPAGATION]

NT COSMIC NOISE

NT CROSSTALK

NT DAWN CHORUS

NT ELECTROMAGNETIC NOISE

NT HISS

NT IONOSPHERIC CROSS MODULATION

NT IONOSPHERIC NOISE

NT IONOSPHERICS

NT JAMMING

NT RADIO FREQUENCY INTERFERENCE

NT SHOT NOISE

NT SUDDEN ENHANCEMENT OF AT-

MOSPHERICS

NT THERMAL NOISE

NT WHISTLERS

NT WHITE NOISE

EMI [electromagnetic interference/ antennas relative received voltage vs height above ground as functions of effective length, impedance, etc

01 p0042 A70-10087

Conducted interference on input power lines of AC to DC power supplies with diode rectification and smoothing capacitors predicted by Fourier analysis

01 p0049 A70-10089

Signal discrimination from sequence of interference and noise by determining parameter value probability density using random process

01 p0044 A70-11024

Natural modes and multiple beam interference in open resonators, taking into account centimeter wave experiments and computations

02 p0340 A70-12829

Interference wave formula for multiple reflections from smooth inhomogeneous region with arbitrary boundary

03 p0442 A70-13093

Opposing cavity modes interference effect on passive Q switched ruby laser energy yield

03 p0499 A70-13213

Coherent and incoherent interference effects on direction finding information derivation, using linear two channel principle

03 p0452 A70-14024

Microwave radio refraction analysis for controlling interference between radio relay antenna and geostationary satellites

07 p1235 A70-19363

FM spectral density model with applications to radio transmitter bandwidth estimation and interference analysis

08 p1456 A70-20473

Optimal satellite communication system design concerning spectrum and interference limits

08 p1459 A70-20805

Interference proof characteristics and shielding capability of mirror antennas improved by peripheral sheet metal or wire screens, reducing rear lobe level

09 p1648 A70-23151

Interference problems arising during digital satellite communications, discussing PCM telephone system and PSK modulation

10 p1836 A70-24345

Earth station antenna radiation diagrams with respect to interference isolation capability

[AIAA PAPER 70-418]

Multiple channel communication satellite interchannel interference including preamplifier intermodulation, direct interference, multipath amplification, crosstalk and multiplexer reflections considered for capacity maximization

[AIAA PAPER 70-508]

11 p2002 A70-25483

Channel assignment, considering low cost solution and co-channel interference

11 p2010 A70-26310

Optimal linear band limited time invariant data transmission systems, discussing pulse interference tolerance based on eye parameters as quality criteria

12 p2185 A70-27688

Nonlinear phase locked loops compared with linear loops in communication and navigation, considering interference vulnerability

12 p2187 A70-27909

Cost effective data transmission method for high performance under intersymbol interference and noise

12 p2187 A70-27935

Electromagnetic interference filters design for equipment power lines from electromagnetic compatibility and reliability viewpoints

12 p2201 A70-28129

Short cables wire to wire coupling between black boxes, deriving interference transfer function

12 p2204 A70-28130

C-5 aircraft electrointerference coupling minimization, applying classification plan for wire categorization and routing

12 p2201 A70-28131

Computer controlled system for real time measurement and analysis of electromagnetic interference and compatibility with economy of time, manpower and cost

12 p2201 A70-28133

Electric field propagation model in proximal region above plane earth permitting solutions of EMI propagation problems

12 p2190 A70-28138

Radar systems EM compatibility simulation, describing FORTRAN IV operational interference prediction program

12 p2193 A70-28139

Beam-plasma system mode coupling near electron cyclotron frequency, obtaining interference patterns

13 p2459 A70-28570

EM interference origins, transmission and prevention, noting equipment sources and measurement methods

13 p2367 A70-29460

VHF wave interference from heavy ion layers in lower ionosphere

14 p2574 A70-30737

Interference free and frequency stable transistorized multivibrator circuits using High Level Logic/HLL/units

14 p2561 A70-31163

Electromagnetic interference [EMI/ effects on TALOS missile guidance receiver by expanding computer simulation test results

14 p2655 A70-31345

Digital data detection in presence of noise and double sided intersymbol interference, deriving error rates for known and stochastic signals

15 p2703 A70-32561

Amplitude and intensity interference relations from pseudothermal light sources, noting applicability to stellar interferometry

16 p2900 A70-32999

Broadband and narrowband pulse signal noise electromagnetic interference prediction techniques for filter or shielding parameters evaluation

16 p2862 A70-33065

Solid state spectrum centered receiver for eliminating externally generated pulse type interference between radar sets

16 p2862 A70-33066

Interference free high speed monolithic digital integrated gate, determining current swing, lead inductances and switching times

17 p3048 A70-34587

Frequency allocation in EM environment of 1970s based on interference compatibility analysis

17 p3045 A70-35158

Pulsed signal amplitude and delay time measurement in presence of interfering [reverberated/ signals and steady noise

19 p3375 A70-37285

Electromagnetic interference in aircraft communication due to jet engine charging, considering various prevention measures

20 p3561 A70-39724

Cryogenic cooling of IR radiation sensors for increasing sensitivity, considering background radiation interference from sensor optical system and detector/preamplifier noise

21 p3825 A70-41052

Fences and pits effectiveness for shielding satellite earth stations from local terrestrial facilities interference

21 p3789 A70-41342

Multicarrier FM communication system, calculating adjacent channel interference due to impulse noise

21 p3789 A70-41343

Electromagnetic interference reduction between communication satellite earth stations and microwave radio relay stations by pit shielding

22 p3991 A70-43577

Spacecraft radioisotope thermoelectric generator interference in onboard instrument operation, using analytical models to determine necessary shielding

24 p4375 A70-45175

ELECTROMAGNETIC MEASUREMENT

Electromagnetic procedures and camera-spectrometer system for studying detonation processes, measuring mass flow rates and explosives spectra

01 p0090 A70-10887

Diffraction loss measurement in solid state laser to determine laser material contribution to total cavity loss

01 p0113 A70-10919

Measurement techniques for determining density and temperature distributions along radius of plasma cylinder by electron cyclotron resonance, microwave refraction and acoustic resonance

02 p0349 A70-12758

Electronic distance measurements involving transit time determination for signal from instrument to far point and back

03 p0495 A70-14176

Horizontal ionospheric small scale inhomogeneity drift measurements at two closely spaced points, noting agreement with global network stations

04 p0684 A70-15747

Gain measurement in He-Ne laser based on small modulation of discharge current

05 p0859 A70-16267

Low altitude electric and magnetic measurements of plasma waves in space from OV3-3, Pioneer 8 and OGO 5 satellite observations

06 p1118 A70-17376

Electromagnetic induction blood flowmeter measuring blood velocity as function of voltage in pick-up electrodes

07 p1217 A70-18952

Submillimeter wave applications in measurement and communication, developing submillimeter gas maser sources

09 p1676 A70-22784

Electromagnetic instability measurements in electron cyclotron resonance plasma produced in magnetic mirror field

10 p1921 A70-23963

Italian SIRIO SHF experiment for study of atmospheric effects on satellite link, discussing system design and performance

11 p1999 A70-25442

Aerial and ground UHF noise measurement in Phoenix area, correlating air and ground data

11 p2001 A70-25480

Sequential filter equations for nonlinear system dynamics and observational model with linear estimator, comparing difference between white and colored noise filter results

11 p2024 A70-26126

Electromagnetic blood flow determination by catheter in external magnetic field, discussing intravascular EM flow sensor capable of percutaneous introduction into vascular system

11 p1993 A70-26663

Plasma experiments in space including electric fields measurement, collisionless plasma studies and artificial Ba cloud generation

12 p2214 A70-26868

Electromagnetic differential flowmeter design and performance, considering SNR

12 p2231 A70-27162

Upper atmosphere electromagnetic probing theory and techniques, noting applications to aeronomic problems

12 p2223 A70-27726

Computer controlled system for real time measurement and analysis of electromagnetic interference and compatibility with economy of time, manpower and cost

12 p2201 A70-28133

Microwave field component distribution in plasma waveguide covered by metallic sheath in magnetic field, using counterbalanced antenna probes for field measurements

13 p2463 A70-29378

Collection of papers on precision radiometry in geophysics covering radiation detectors and electromagnetic radiation measurements in atmosphere

13 p2409 A70-29651

Precision radiometry of electromagnetic energy transfer in atmospheric and space physics emphasizing solar and terrestrial radiative fluxes measurements

13 p2409 A70-29652

Satellite position fixing based on electromagnetic angle measurements from observation station, using least squares method

14 p2612 A70-30187

Statistical variation of number of VLF atmospherics per unit time above given vertical electric field strength threshold

14 p2550 A70-30515

Horizontal ionospheric small scale inhomogeneity drift measurements at two closely spaced points, noting agreement with global network stations

14 p2576 A70-30831

Radio astronomical observations of lunar surface material EM properties compared with Surveyor 7 chemical analysis

14 p2645 A70-31059

Measurable VLF electromagnetic fluxes from Cerenkov effect in ionosphere produced by artificial electron beams

14 p2579 A70-31249

Correction method for near field antenna measurements made with measuring antenna of arbitrary but known characteristics

15 p2698 A70-31954

High gain helix radiators for spacecraft phased arrays, measuring performance vs design parameters

15 p2678 A70-32600

Absolute cosmic ray ionization in lower atmosphere, using air-filled ionization chamber

18 p3305 A70-36001

Equatorial electrojet measurements by Nike-Apache rockets

18 p3244 A70-36018

Millimeter wave and optical astronomical refraction differential measurements, showing dependence on atmospheric water vapor

20 p3588 A70-40305

Electromagnetic test equipment transient waveform control using on-line digital computer in near real time configuration

21 p3805 A70-41270

Induced voltage electromagnetic flowmeter, assessing performance in terms of weight vector to obtain conditions for ideal flow patterns

22 p4029 A70-42692

Global thunderstorm activity location found by measuring differences between time of arrival of electromagnetic energy at three satellites

22 p4016 A70-42779

Upper atmosphere and magnetosphere DC electric field measurement using artificial clouds

22 p4017 A70-42791

Lower atmosphere electric field vertical distribution measurement by combined balloon and rocket soundings

22 p4017 A70-42797

Electromagnetic variational soundings of ocean floor earth crust upper mantle near magnetic equator

23 p4189 A70-44066

ELECTROMAGNETIC NOISE

NT ATMOSPHERICS

NT COSMIC NOISE

NT DAWN CHORUS

NT HISS

NT IONOSPHERIC NOISE

NT IONOSPHERICS

NT SHOT NOISE

NT SUDDEN ENHANCEMENT OF ATMOSPHERICS

NT WHISTLERS

NT WHITE NOISE

Absorbed RF plasma wave noise spectrum in region of anomalous dispersion, noting peak in far IR region

01 p0150 A70-10286

Gain, noise temperature and gain to noise temperature ratio measurement techniques for electrically large earth station antenna, recommending radio star technique

01 p0051 A70-11121

Square root filters algorithms based on covariance and invariance matrices extended to include process noise effects

01 p0144 A70-11193

Molecular beam laser short term frequency instability found dependent on laser and measuring device noise

03 p0455 A70-13091

HF admittance and noise in forward-biased majority carrier Ge-Si n-n heterojunctions and Schottky barrier

03 p0539 A70-13159

He-Ne laser using K-activated alumina cold cathode and coaxial construction, discussing output, low noise applications, construction and testing

03 p0501 A70-13583

Generation-recombination noise theory extension to nonlinear devices applied to double injection diode in various operation modes

03 p0458 A70-14028

Burst noise in forward biased silicon diodes and transistors, discussing measurements on gate controlled devices

03 p0458 A70-14029

Frequency shift and FM noise of uncontrolled Gunn effect diode and reflex klystron oscillators

05 p0818 A70-15774

Antenna far field noise effect on monopulse type and conical scanning radar angle meters performance

05 p0813 A70-16256

Monograph on He-Ne laser beam noise properties and intensity fluctuations during single mode operation

05 p0860 A70-16559

Phase, frequency and amplitude fluctuations in avalanche diode oscillators, studying noise origin

05 p0823 A70-16883

Optical parameters of Martian surface and temperature, discussing brightness distribution along diameter in red spectral region, based on photoelectric cross sections

05 p0918 A70-16917

Reentry plasma RF noise temperature in-flight measurements by Trailblazer 2 compared with computed data

06 p1008 A70-17568

Slowly varying component filtration from multiplicative mixture of two random processes by statistical analysis

06 p1009 A70-17670

Magnetic, electrostatic and RF fields noise reduced for strain gage data acquisition

06 p1069 A70-18435

VLF noise phenomena observed with satellite electric dipole antennas compared with lower hybrid resonance frequency of ionospheric medium in vicinity

06 p1011 A70-18534

HF radio noise environment, discussing local storm effects, noise power estimation, noise measurement methods, etc

07 p1231 A70-19172

Random synchronization errors in PN and PSK systems reduce input signal power and introduce additional self noise

07 p1236 A70-20069

Spectroradiometer with paramagnetic traveling wave quantum amplifier applied to radio telescope, studying noise, temperature and fluctuation sensitivity at given time constant

08 p1495 A70-21054

Large carrier to noise ratios in FM receivers as function of correlation between Gaussian and impulse shot noise /clicks/

08 p1463 A70-21776

Receiver bandwidth effect on audible radio noise bursts parameters of quasi-peak value, burst duration and time interval

08 p1464 A70-21800

Low noise TWT, discussing dynamic range, gain and phase tracking, environmental performance, life behavior and noise factor interrelations

09 p1644 A70-22233

Intermodulation noise performance of FM FDM trunk radio systems in two path fading situations, calculating noise/power ratio and baseband enhancements

09 p1632 A70-22237

Quantizing noise measured for single integration delta modulation coders using unequal positive and negative integrator step sizes

09 p1638 A70-23368

Pulse rate counter for randomly repetitive random processes, noting applications to lightning flash noise bursts in receivers

10 p1848 A70-23996

Gunn oscillator current noise correlation with frequency modulation noise

10 p1848 A70-24230

Microwave devices excess AM and FM noise levels measurement by carrier suppression methods

10 p1841 A70-24579

Avalanche diodes microwave properties in utilization circuit, discussing negative conductance, nonlinear impedance and intrinsic noise current

10 p1850 A70-24623

FM telemetry channel noise effects on digital and analog accelerometer outputs accuracy, suggesting mean square error reduction methods

10 p1893 A70-25318

Ambiguities during brightness temperature distributions reconstruction from intensity interferograms

11 p2048 A70-25335

Sequential filter equations for nonlinear system dynamics and observational model with linear estimator, comparing difference between white and colored noise filter results

11 p2024 A70-26126

Signal selection for phase coherent and incoherent additive noise channels to maximize receiver correct decision probability

11 p2010 A70-26327

Noise effects during mechanical parameters measurement by electronic devices, noting noise from resistors, potentiometers, power lines and wiper-type distributors

11 p2056 A70-26454

T2L logic circuits design and coherent noise immunity

11 p2021 A70-26833

He-Ne laser noise caused by discharge current fluctuation and moving striation in long capillary tubes

12 p2245 A70-27272

Very low frequency radio noise in ionosphere, magnetosphere and solar wind, using multiple receivers to measure mathematical relations between direction magnitude and polarization characteristics

12 p2184 A70-27574

Cost effective data transmission method for high performance under intersymbol interference and noise

12 p2187 A70-27935

Quantum noises in laser systems, deriving kinetic equation for traveling wave generation field density matrix

13 p2428 A70-29360

Pulsed noise stability of discrete data transmission system having multipositional frequency manipulation as compared to binary system

14 p2547 A70-30148

Amplitude-frequency characteristics selection for minimum phase channel allowing for intersymbol interference and smooth noise during data transmission, calculating mean error probability

14 p2547 A70-30150

Noise sources and identification in low noise RF amplifiers via noise temperature or factors

15 p2708 A70-31952

Piezoelectric field effect strain gage with semiconducting film for extremely small strains in electrically noisy background

[SESA PAPER 1676]

15 p2739 A70-32317

Intensity correlations in optical parametric noise and second harmonic generation measured by two photon delayed coincidence counting

15 p2753 A70-32603

Antenna array system for surface target detection in receiver noise and heavy clutter by space-time decision theory

16 p2860 A70-32954

Adaptive Kalman filtering with unknown process and measurement noise covariance matrices

16 p2880 A70-32983

Low light level TV systems performance relationship to visual acuity requirements, considering interfering noise characteristics effect on target recognition

16 p2903 A70-33130

Electron spin-echo device as programmable linear matched filter for PN modulated carrier waveforms detection

16 p2864 A70-33480

Packaging and grounding for electrical noise control in nanosecond switching circuits using transmission line design

16 p2879 A70-33960

Weak narrow band noise measurements using FM radiometer insensitive to gain fluctuations

17 p3053 A70-35278

Frequency discrimination circuits for multiple remote control receiver systems with high harmonic noise levels

18 p3235 A70-36428

Radio frequency indigenous noise measurement in urban areas

18 p3228 A70-36568

CW multifilament GaAs laser diodes measurement, showing cross correlation between light and current noises

18 p3270 A70-36742

Gunn effect pulse regenerators, describing random domain triggering rate voltage dependence comparison with Johnson noise predictions

19 p3387 A70-37820

Aircraft streamer /spark/ discharges formation, waveforms and RF noise levels, using mathematical model for electric field strength

19 p3380 A70-38179

Thin metal film electrical conduction current noise characteristics

19 p3487 A70-38196

FM demodulation threshold extension by correlation detection implemented in impulse noise cancellation system

19 p3382 A70-38893

Automatic control systems for aircraft approach to landing path and subsequent stabilization on trajectory, compensating for cross wind action and radio noise disturbances

20 p3561 A70-39842

Triboelectric noise in mechanically flexed low level signal cables for piezoelectric transducers with high gain amplifiers

21 p3825 A70-40866

FM transmission of multiplex telephone signals by communication satellites, deriving impulse noise due to adjacent channel interference

21 p3787 A70-41330

Multicarrier FM communication system, calculating adjacent channel interference due to impulse noise

21 p3789 A70-41343

Mode intensity fluctuations in unlocked multiple mode He-Ne laser related to LF noise

21 p3837 A70-41918

Noise effect on signal parameter control in linear measurement devices

22 p3984 A70-42394

Transfer function optimization for linear follow-up frequency filter with controlled resonance, analyzing noise band performance

22 p3985 A70-42402

Pulse angle modulation and PTM-AM equivalence, examining noise effect on conversion

22 p3989 A70-42570

Lightning discharge characteristics contributing to electromagnetic background noise at ELF determined from slow tail waveform measurements

22 p4015 A70-42777

Silicon MOSTs LF noise model, discussing noise and gate voltages and trapping efficiency of surface states

22 p3996 A70-42916

Optical parametric noise from barium sodium niobate crystal pumped at 4358 Å by compact source mercury lamp

22 p4074 A70-43022

Minimum noise microwave parametric amplifiers incorporating varactor diodes with frequency dependent apparent loss resistance

23 p4169 A70-43786

Signal arrival time variance in optical communication system with high lag photodetectors, examining input, detection and amplification noise

23 p4196 A70-44410

Equation for antenna noise temperature calculation

23 p4165 A70-44967

ELECTROMAGNETIC PROPAGATION

U ELECTROMAGNETIC WAVE TRANSMISSION

ELECTROMAGNETIC PROPERTIES

DC dynamo models for planetary electromagnetic conditions, considering nonrotationally symmetric turbulence induction actions and critical values for field maintenance

01 p0185 A70-10956

Nonlinear characteristics of electromagnetic actuating mechanism induced by magnetic field of coil

07 p1281 A70-19529

Dense plasma thermodynamic and electromagnetic properties, discussing correlation energy

19 p3480 A70-38181

Lower ionospheric structure and electromagnetic resonance phenomena, describing radio equipment for solar activity effects studies

21 p3812 A70-40620

ELECTROMAGNETIC PROPULSION

Plasma devices for spacecraft propulsion taking into account electrothermal, electromagnetic and electrostatic systems

05 p0895 A70-15817

Plasma accelerators for nuclear EM propulsion, considering power supply requirements and differences between plasma and ion engines

22 p4070 A70-43186

ELECTROMAGNETIC PULSES

Electromagnetic pulse duration formed by spectral content in HF bandwidth received after ionospheric reflection

02 p0258 A70-12419

Electromagnetic pulse scattering in time varying inhomogeneous medium, applying finite difference method to Maxwell equations

02 p0261 A70-12588

Light pulses propagation in nonlinear laser medium, obtaining equations of motion for density matrix

04 p0700 A70-14687

Self induced light pulses from GaAs injection lasers in pulse driven diodes at liquid nitrogen temperatures, noting pulse width and frequency

04 p0703 A70-15623

Pulsed radio signals time delay due to molecular microwave resonance in earth atmosphere and interstellar medium

08 p1461 A70-20915

Acousto-optic receiver and spectrum analyzer for electromagnetic signals in VHF-UHF range

08 p1463 A70-21780

Thermoacoustic waves formation and propagation in metallic rods by light pulses, studying pulse rise time influence on waves shape and amplitude

09 p1778 A70-23090

Laser pulse energy ponderomotive meter using mechanical action exerted by light on movable sapphire plate in air at atmospheric pressure

09 p1700 A70-23657

Distortion of electromagnetic pulse undergoing total internal reflection in inhomogeneous isotropic plasmas in lower ionosphere

09 p1639 A70-23672

Self opening em-operated secondary and ternary mylar diaphragms for expansion tubes and tunnels

11 p2031 A70-25982

Optimal linear band limited time invariant data transmission systems, discussing pulse interference tolerance based on eye parameters as quality criteria

12 p2185 A70-27688

Electromagnetic pulse distortion with Gaussian envelope in longitudinally inhomogeneous anisotropic ionized media to investigate radio wave communication with ionospheric propagation

12 p2189 A70-27962

Ni-Mo-Fe magnetic alloy for EM pulse shielding, verifying saturated regions diffusion theory

12 p2201 A70-28128

Electromagnetic pulse generator for simulation of EMP associated with nuclear explosions, describing electronic equipment vulnerability testing

12 p2208 A70-28135

Electromagnetic pulse /EMP/ testing, discussing sensor types and sensitivity, data acquisition and recording, instrumentation, etc

13 p2377 A70-29073

Carrier drift due to electromagnetic impulse, deriving expressions for photo emf generated in transverse magnetic field manifesting monopolar photomagnetic effect

13 p2452 A70-29282

Q switched ruby laser pulses nonlinear absorption by partially ionized plasma behind reflected shock wavefront, observing absorptivity dependence on light intensity

13 p2429 A70-29420

Pulse characteristics received by loop antenna in field of second antenna excited with step functions, calculating radiation characteristics

16 p2871 A70-32961

Radar and DC pulse signatures of multiple reflection from dry, damp and wet earth for vertical and horizontal polarization

16 p2861 A70-32977

Coherent light pulses propagation through resonant medium, discussing energy loss

16 p2928 A70-33278

Radio receiving system for pulses detection from cosmic ray extensive air showers, discussing sensitivity and noise temperature

16 p2911 A70-33788

Crab Nebula pulsar NP 0532, describing quasiperiodic oscillation in arrival times of radio pulses

17 p3157 A70-34842

Argon and helium breakdown induced by ruby laser 50-picosec pulse at various pressures

18 p3267 A70-36616

Self induced intensity pulsations frequency stabilization and narrowing in continuously operating GaAs injection lasers

18 p3269 A70-36734

Self induced sustained light pulsations from GaAs injection lasers with tandem double section stripe geometry based on repetitively Q switched model

18 p3269 A70-36735

Power, energy and efficiency of emission from dye solutions pumped by incoherent light pulses, allowing for particle accumulation at metastable level

19 p3448 A70-38738

Self focusing schlieren observation in gas breakdown, discussing cubic polarizability of excited atoms in electron cascade due to laser pulses

21 p3835 A70-40594

Crab pulsar observations with refractor and on-line data acquisition, indicating optical pulse arrival times at variance with previously assumed 77 day periodic wobble

22 p4097 A70-42464

Fluctuating light pulse packet detection by inertialless photodetector, deriving optimal algorithm

22 p3987 A70-42554

Fluctuating light pulses detection and arrival time estimation for heterodyne reception

22 p3987 A70-42560

Impulse length effect on space echo electric field in collisionless plasma

22 p4082 A70-43237

Nd laser single picosecond pulse energy, duration and frequency width

24 p4354 A70-45664

Earth-ionosphere cavity ELF electromagnetic pulse propagation from atmospheric source, considering transient field as frequency and time functions

24 p4314 A70-46130

ELECTROMAGNETIC PULSES

Liquid metal pump design and performance in SNAP 8 Mercury Rankine and Advanced Rankine fluid power systems, including containment materials and corrosion effects

04 p0718 A70-15641

ELECTROMAGNETIC RADIATION

NT AIRGLOW

NT BLACK BODY RADIATION

NT BREMSSTRAHLUNG

NT CERENKOV RADIATION

NT COHERENT ELECTROMAGNETIC RADIATION

NT COHERENT LIGHT

NT CYCLOTRON RADIATION

NT DAYGLOW

NT DECA-METRIC WAVES

NT DECIMETER WAVES

NT ELECTROMAGNETIC PULSES

NT EXTRATERRESTRIAL RADIO WAVES

NT FAR INFRARED RADIATION

NT FAR ULTRAVIOLET RADIATION

NT GALACTIC RADIO WAVES

NT GAMMA RAY BEAMS

NT GAMMA RAYS

NT GEOCORONAL EMISSIONS

NT H WAVES

NT INFRARED RADIATION

NT LIGHT [VISIBLE RADIATION]

NT LIGHT BEAMS

NT LONG WAVE RADIATION

NT LYMAN ALPHA RADIATION

NT MICROWAVES

NT MILLIMETER WAVES

NT MONOCHROMATIC RADIATION

NT NEAR INFRARED RADIATION

NT NEAR ULTRAVIOLET RADIATION

NT NIGHTGLOW

NT NONEQUILIBRIUM RADIATION

NT PHOTON BEAMS

NT PLANETARY RADIATION

NT POLARIZED ELECTROMAGNETIC RADIATION

NT POLARIZED LIGHT

NT RADIO EMISSION

NT RADIO WAVES

NT SHORT WAVE RADIATION

NT SKY RADIATION

NT SKY WAVES

NT SOLAR RADIO BURSTS

NT SOLAR RADIO EMISSION

NT SOLAR X-RAYS

NT SOMMERFELD WAVES

NT SUBMILLIMETER WAVES

NT SUNLIGHT

NT SYNCHROTRON RADIATION

NT TERRESTRIAL RADIATION

NT THERMAL RADIATION

NT TROPOSPHERIC RADIATION

NT TWILIGHT GLOW

NT TYPE 2 BURSTS

NT TYPE 3 BURSTS

NT TYPE 4 BURSTS

NT TYPE 5 BURSTS

NT ULTRAVIOLET RADIATION

NT X RAYS

NT ZODIACAL LIGHT

LF electromagnetic waves theory for turbulent plasma based on expansion of particle collision and turbulent pulsation integrals

01 p0150 A70-10211

Equivalent circuit for trapped energy resonators and calculations of capacitance ratios for straight crested waves

01 p0088 A70-10777

Reflection coefficient of electromagnetic wave reflected from thin ionization layer, using frequency dependence of amplitude to estimate ionospheric layer thickness

01 p0083 A70-11532

Book on scattering of light and other electromagnetic radiation, treating scattering by spheres, cylinders, liquids, Rayleigh-Debye scattering, particle size analysis, etc

02 p0337 A70-11689

Charged particle self resonant motion in field of plane electromagnetic wave, showing trapped particles existence in whistlers

02 p0256 A70-12116

Electromagnetic plane wave diffraction by slit and circular apertures in nonplanar conducting screens, presenting equireadance contour maps

02 p0340 A70-12455

Numerical integration methods in electromagnetic theory, discussing scattering and radiation from thin wire structures

02 p0262 A70-12600

Hyperon and resonance particle effects on neutron star vibration, discussing vibrational energy storage and atmospheric electromagnetic generation

02 p0379 A70-12699

Plane electromagnetic wave diffraction at periodic arrays obtained by direct summation of multiple reflection between arrays

03 p0442 A70-13095

Fourier and perturbation methods applied to radiation from uniformly moving charge in inhomogeneous magnetoactive medium, deriving expressions for radiation spectrum and energy losses

03 p0531 A70-13285

Quasi-optic electromagnetic beams slow spreading in anisotropic media due to propagation in unusual directions

03 p0447 A70-13288

Electromagnetic energy transmission factors for metal-dielectric-metal system, calculating net energy flux, noting effects of metal spacing, time, temperature level, etc

[ASME PAPER 69-WA/HT-8] 04 p0784 A70-14822

Fields and power transfer for electromagnetic waves in hot plasma calculated using Fourier integral and Fourier series methods

05 p0888 A70-16165

TEM wave reflection incident on conducting thin strips semiinfinite array in free space not accompanied by emission

05 p0812 A70-16243

Graphic method for classifying EM waves directed by open waveguides, obtaining wave numbers from dispersion equation

05 p0812 A70-16245

Formula for energy radiated from particles system applied to electromagnetic and gravitational radiation and illustrated by charged particle motion in magnetic field

05 p0882 A70-16309

Radiation environment in space and effect on man, discussing particulate and high energy electromagnetic radiation components

05 p0903 A70-16630

- Electromagnetic energy spectra of lightning expressed as function of electric field spectral density of atmospheric
05 p0843 A70-16762
- Induced Compton scattering of plasma and electromagnetic waves under astrophysical conditions, discussing HF radio emission spectra from cosmic objects and quasar
05 p0917 A70-16904
- Radiation from dipole in dispersive anisotropic magnetized plasmas using Fourier analysis
06 p1116 A70-17363
- Transmission and emission of radiation from dense inhomogeneous finite laboratory plasma column in magnetic field with interpretation by cold plasma theory
06 p1116 A70-17367
- Electromagnetic radiation patterns from aperture in conducting cylinder coated with moving isotropic plasma sheath, noting sheath velocity and plasma frequency influence
06 p1020 A70-17564
- Turbulence spectra and generated power determined for plasma turbulence in objects with high electromagnetic radiation density /quasars and supernova shells/
07 p1384 A70-19412
- Plane electromagnetic wave reflection from laminar anisotropic medium, analyzing piecewise-constant permittivity tensor as boundary value problem
07 p1235 A70-19448
- Electromagnetic component of extensive air showers to three dimensional Monte Carlo simulations of hadronic component using electromagnetic cascade theory
07 p1368 A70-19967
- Plane electromagnetic wave diffraction on conducting plate with circular hole
08 p1456 A70-20503
- Book on mathematical theory of electromagnetic waves covering vector analysis, reduced wave equation, linear transformations, boundary value problems and radiation patterns
08 p1533 A70-20759
- Whistler type electromagnetic waves excitation by electron beam in plasma, noting intensity dependence on electron frequency
08 p1554 A70-21804
- Matrix multidimensional singular linear integral equation applied to electromagnetic radiation transfer through stratified atmosphere
09 p1711 A70-22349
- Electromagnetic waves diffraction on ideally conducting bodies of revolution, deriving design formulas for electric dipole
09 p1632 A70-22401
- Electromagnetic wave diffraction by sphere and spheroid at resonance frequencies with incident wavelength comparable to bodies dimensions
09 p1632 A70-22402
- Electromagnetic wave deceleration in open cylindrical waveguide, noting guide action as bandpass filter
09 p1633 A70-22415
- Book on radiation and propagation of electromagnetic waves covering plane waves in anisotropic and inhomogeneous media, spectral representation of sources, radiation in plasma, diffraction, etc
09 p1633 A70-22639
- Electromagnetic radiation sources for remote sensing application to identification of water, moist soil and vegetation, discussing optical properties of diverse materials
09 p1667 A70-22851
- Electromagnetic wave theory and applications covering propagation modes, properties of media, communications, equipment, etc
09 p1635 A70-22950
- Plane electromagnetic wave diffraction on circular cylinder
09 p1638 A70-23339
- Point electric dipole EM radiation in presence of moving dispersive dielectric half space
09 p1639 A70-23669
- Oblique E-mode electromagnetic wave in plane stratified collisionless plasma taking into account plasma temperature
09 p1639 A70-23674
- Maxwell electromagneticism analogy to Einstein gravitation inferred from asymptotic studies of electromagnetic and gravitational radiation
10 p1915 A70-24029
- HF electromagnetic wave detector based on study of volt-ampere characteristics of luminescent plasma discharge
10 p1922 A70-24030
- Electromagnetic radiation frequency shift during passage by sun or earth not caused by electrostatic or magnetic fields
10 p1917 A70-24860
- Two dimensional electromagnetic wave diffraction on arbitrary shaped homogeneous dielectric cylinder, solving integral equations on digital computer
10 p1842 A70-25105
- Phase characteristics of nonperiodic slow EM wave delay structures determined by phase shift measurements
12 p2230 A70-26967
- Book on antennas and waves covering EM radiation, configurations, insulation, dissipative media, coupling, transmission lines, etc
12 p2194 A70-27095
- Solar flares of 6 and 8 July 1968 correlation regarding electromagnetic radiation emission, radio flux, corpuscular radiation, etc
12 p2294 A70-27708
- Book on electromagnetic fields and waves covering electrostatic and magnetic fields, relativity, vectors, Maxwell equations and propagation
12 p2273 A70-28150
- Annular gas laser, considering external periodic perturbation effect on difference frequency of oppositely moving waves
12 p2251 A70-28291
- Textbook reissue on diffraction of electromagnetic and acoustic waves at open end of waveguide, using Wiener-Hopf-Fock factorization method
13 p2363 A70-28724
- Plasma instability in TEM wave field, considering nonpotential HF oscillations buildup with frequency near external wave frequency
13 p2463 A70-29283
- Fabry-Perot resonator higher modes excitation by external TEM wave, discussing optimal mismatch for maximum intensity
13 p2408 A70-29358
- Magnetospheric particles, fields, electromagnetic waves and data on collisionless bow shock structure
13 p2484 A70-30098
- Superhigh energy particles detection by transition radiation, measuring Lorentz factor of emitted spectra
14 p2616 A70-31003
- Strip lines transmission characteristics with rectangular outer conductor and multilayered layers within TEM wave approximation, using Green function and variational principle
14 p2558 A70-31316
- Electromagnetic wave diffraction by heterogeneous planar dielectric structures, showing field distributions by single variable Fredholm equations
15 p2695 A70-31436
- Electromagnetic ELF radiation model for multiple return strokes of cloud to ground lightning discharges, considering channel length
15 p2726 A70-31864
- Third harmonic generation using hot electron nonlinearity characteristics of semiconductors, considering plane-polarized electromagnetic wave nonlinear interaction with sample
15 p2783 A70-31970
- Electromagnetic waves scattering at circular cylinders in semibounded region, showing boundary influence on radiation pattern
15 p2698 A70-32174
- Electromagnetic waves diffraction and scattering from acoustically soft and hard and perfectly conducting disks in plane or arbitrary incidence directions
15 p2701 A70-32414
- Periodically strip loaded dielectric slab guided electromagnetic waves, discussing attenuation and space harmonics amplitudes relationship
16 p2861 A70-32960
- Collisionless damping of electromagnetic waves in regions with strong homogeneity of cold plasma
16 p2957 A70-33199
- Monochromatic electromagnetic wave diffraction on moving ideally conducting half plane, deriving parameters and spectral composition after diffraction
16 p2863 A70-33216
- Electron-acoustic, ion-acoustic and electromagnetic plane waves coupling at shock front in two fluid ionized viscous plasma
16 p2958 A70-33282
- Electromagnetic to magnetostatic wave conversion loss reduction at L band by coiled transducer
16 p2913 A70-34038
- Stress wave generation in elastic temperature-dependent absorbing solids by impulsive EM radiation
17 p3185 A70-34967
- Radiation from simple slots in moving dispersionless dielectric, using Minkowski electrodynamics
17 p3043 A70-34984
- Prolate and oblate wave functions for EM radiation from spheroidal antenna in surrounding inhomogeneous medium
17 p3044 A70-35063
- OGO 5 observations of quasi-trapped electromagnetic waves in solar wind at 70 kHz
18 p3306 A70-36005
- Shadow current method for asymptotic solution to two dimensional problem of electromagnetic wave far diffraction field on ideally conducting plane with infinite rectilinear slot
18 p3227 A70-36142
- Plane electromagnetic waves diffraction by periodic structure of infinite system of parallel strips, reducing problem to solution of linear algebraic equations
18 p3227 A70-36287
- Electromagnetic wave scattering on resonant dielectric sphere in rectangular waveguide, using reflection coefficient
18 p3227 A70-36419
- Phase plane method for Hill equation in problems involving EM wave expansion in elliptical waveguides or single circuit parametric systems analysis
18 p3227 A70-36424
- Plane electromagnetic wave reflection from laminar anisotropic medium, piecewise-constant permittivity tensor as boundary value problem
18 p3229 A70-36922
- Electric field equations of plane EM wave diffraction at lattice of conducting cylinders, using Hankel function
19 p3375 A70-37289
- Electromagnetic propagation in flat waveguide with local gyrotropic filling and transverse magnetization, using Galerkin method
19 p3470 A70-37430
- Diffraction of EM waves emitted by vertical electric dipole on conducting thin circular disk, using algorithm for integral equation
19 p3375 A70-37432
- Plane EM wave diffraction by conducting strip, using algorithm for reducing integral to linear algebraic equations
19 p3376 A70-37433
- One dimensional integral equations for two dimensional problems of EM wave diffraction by cylindrical bodies
19 p3376 A70-37435
- Electromagnetic wave diffraction by inhomogeneous anisotropic body, applying Fredholm integral equations
19 p3376 A70-37436
- Single crystal yttrium ferrite garnet intrinsic electromagnetic radiation as function of coupling coefficient between specimen and waveguide
19 p3485 A70-37630
- Plane electromagnetic wave diffraction by thin metal gratings, using mathematical method of elasticity theory
19 p3376 A70-37712
- Plane polarized electromagnetic wave diffraction by dielectric grating, obtaining linear algebraic equations for field coefficients
19 p3376 A70-37713
- Polarized plane EM wave diffraction by inclined half plane grating, obtaining transformation matrices coefficients
19 p3376 A70-37714
- Diffraction grating systems resonance properties, obtaining transcendental equations for natural slow wave and radiation modes
19 p3377 A70-37717
- Plane EM wave diffraction by ribbon periodic grating, determining diffraction spectrum wave amplitudes
19 p3377 A70-37718
- Plane EM wave diffraction by bounded and unbounded periodic gratings
19 p3377 A70-37719
- Rectangular waveguide EM radiation into plane parallel region through asymmetrical longitudinal slot
19 p3386 A70-37727
- H and E waves diffraction in circular waveguide by diaphragm thickness, using linear equations and Fourier-Bessel series for representation
19 p3378 A70-37731
- Transversely magnetic and electric wave critical frequency spectra in Pi and H section waveguides, using summary representation method
19 p3378 A70-37735
- Quasi-static thickness-shear approximation of radiation of electromagnetic energy accompanying oscillation of piezoelectric crystal plates
19 p3487 A70-37945
- High energy electron and photon cascades in Metagalaxy, considering electromagnetic radiation density and cosmic ray origin estimation
19 p3500 A70-38081
- Acceleration of high energy cosmic rays by pulsar LF electromagnetic radiation
19 p3501 A70-38085
- Various light velocities, including controvercity for describing EM radiation transport
19 p3472 A70-38274
- Holography, discussing light propagation, basic principles, skew reference wave, diffused illumination interferometry, character recognition, microscopy, high density information storage, etc
19 p3427 A70-38449
- Geomagnetic pulsations propagation through horizontally inhomogeneous ionosphere, solving EM wave diffraction problem
19 p3416 A70-38589
- Book on electromagnetic waves in stratified media covering reflection, propagation, waveguide mode theory, superrefraction and tropospheric ducting
20 p3586 A70-39604
- Electromagnetic waves and oscillations excited by magnetic current ring source around infinitely long

- compressible plasma column, deriving radiation field distribution 20 p3685 A70-40506
- Radiation patterns and scattering cross sections of plane black disks excited by electromagnetic and acoustic waves 22 p3984 A70-42391
- Electromagnetic wave diffraction at multilayer wire grating, discussing computer program for diffraction field calculation 22 p3985 A70-42399
- Book on guided EM wave theory covering mathematical methods transmission lines cavity resonators, perturbation theory, electrostatics, electric and magnetic fields, propagation, etc 23 p4172 A70-44242
- EM radiation beams higher directivity from sources in two layer plasma in planetary atmosphere 23 p4221 A70-44261
- EM wave effects on radio receiver, using Maxwell equations without taking photons into account 23 p4221 A70-44798
- Expansion of laser produced plasma into uniform magnetic field, calculating electromagnetic radiation 24 p4382 A70-45108
- Electromagnetic-surface elastic waves conversion in superconductors, considering thin plate forced vibrations and standing waves excitation 24 p4389 A70-45205
- ### ELECTROMAGNETIC SCATTERING
- #### NT IONOSPHERIC F-SCATTER PROPAGATION
- #### NT LIGHT SCATTERING
- #### NT MICROWAVE SCATTERING
- #### NT MIE SCATTERING
- #### NT RAMAN SPECTRA
- #### NT RAYLEIGH SCATTERING
- #### NT X RAY SCATTERING
- Harmonic generation in scattering of electromagnetic waves by anharmonically bound electrons, noting light source intensity 01 p0141 A70-10278
- Book on scattering of light and other electromagnetic radiation, treating scattering by spheres, cylinders, liquids, Rayleigh-Debye scattering, particle size analysis, etc 02 p0337 A70-11689
- Element relations of phase transformation matrix for scattering, relating radiation field vector to scattered field vector 02 p0339 A70-12283
- Electromagnetic scattering from randomly rough surface with finite conductivity, using Kirchhoff approximation 02 p0261 A70-12587
- Electromagnetic pulse scattering in time varying inhomogeneous medium, applying finite difference method to Maxwell equations 02 p0261 A70-12588
- Electromagnetic wave backscattering from composite rough surfaces, using Stratton-Chu integral 02 p0261 A70-12589
- Plane electromagnetic wave diffraction at conducting stripline, calculating surface current density and far field scattering using edge wave and factorization methods 03 p0451 A70-13755
- Ray-optical analysis of electromagnetic scattering in plane and circular waveguides, giving formulas for modal reflection and coupling coefficients 03 p0452 A70-14034
- Electromagnetic scattering from perfect conductors by numerical analysis, presenting far field pattern calculation for plane wave scattering from square cylinder 04 p0652 A70-15363
- Electromagnetic inverse diffraction solved by Bojarski identity determining target geometry 04 p0720 A70-15703
- Direction fluctuations in radio wave scattering in turbulent gyrotropic medium using Einstein-Fokker-Kolmogoroff equation 04 p0653 A70-15722
- Small scale disturbances and radio wave scattering effects on signal transmission and radiophysical observations in ionosphere 04 p0653 A70-15723
- Radio wave scattering increase in moving body wake near caustic in vertically inhomogeneous ionosphere 04 p0653 A70-15725
- Three dimensional electromagnetic scattering from thin walled conducting circular tube of finite length normally incident with E or H polarized plane wave 05 p0816 A70-16987
- Electromagnetic wave scattering from finite plasma, discussing statistical measurement errors in degrees of freedom studies 06 p1007 A70-17464
- Scattering and depolarization of plane horizontally polarized electromagnetic wave from slightly rough lossless dielectric layer, using small perturbation theory 06 p1010 A70-18019
- Electromagnetic wave scattering from charged particle in hot electron plasma in magnetic field, considering relativistic corrections for scattered radiation spectra 07 p1352 A70-19992
- Polarization structure of electromagnetic wave scattered by slanted two dimensional statistically rough surface of finite conductivity 08 p1456 A70-20573
- Scattered field from rough ionospheric irregularities or earth surface for arbitrary polarization of incident wave 08 p1456 A70-20574
- Plane electromagnetic wave scattering at apex of conical body, presenting scattered field calculations for various cone sizes and surface impedances 08 p1461 A70-20974
- Plane electromagnetic wave scattering by perfectly conducting cylinder coated with moving dielectric or plasma sheath, using relativity theory, Lorentz transformations, etc 08 p1551 A70-21251
- Monochromatic plane electromagnetic wave incident from vacuum on plane boundary of plasma half space, discussing specular reflection and diffuse scattering boundary conditions 08 p1553 A70-21611
- Scattering cross sections of electromagnetic waves in rectangular plasma-filled waveguide based on reciprocity theorem 08 p1464 A70-21983
- Electromagnetic wave diffraction on array of plane waveguides, determining scattered field by solving infinite system of algebraic equations 09 p1632 A70-22407
- Output energies of Stokes components of stimulated combination scattering excited by pulsed laser 09 p1696 A70-22482
- Refractive index chart for scattered electromagnetic fields from sphere, evaluating modal coefficient for lossy materials 09 p1633 A70-22697
- Plane electromagnetic wave backscattering from dielectric-coated metallic cylinder calculated as functions of incidence angle and coating external radius 09 p1636 A70-23075
- Plane electromagnetic wave scattering by conducting circular cylinder/wire in air/vacuum, computing scattering cross sections by Wiener-Hopf method 09 p1638 A70-23347
- Plane electromagnetic wave diffraction at conducting stripline, calculating surface current density and far field scattering using edge wave and factorization methods 10 p1842 A70-25002
- COMSAT measurement of precipitation scatter effects on propagation for frequency sharing with terrestrial radio relay terminals 11 p1997 A70-25413
- [AIAA PAPER 70-499] Polarization effects during HF EM wave interaction in plasma, discussing plasma scattering effects in polarization transport equations 11 p2004 A70-25937
- Electromagnetic scattering from underdense plasma slabs with randomly varying dielectric constant, calculating reflection coefficient 11 p2095 A70-26763
- Intermittency role in free turbulent flow and EM wave scattering by hypersonic wakes 11 p1978 A70-26776
- Electromagnetic field singularities near sharp edge relating to geometry scatter used for treating singularities in current distribution integral equations 12 p2183 A70-26977
- Electromagnetic wave scattering on passively reflecting statistical clusters of inhomogeneities 12 p2184 A70-27498
- Mutual impedance coupling among minimum scattering antennas with electromagnetic properties expressed in terms of radiation patterns 12 p2198 A70-27956
- Optimum scattering from linear array of half-wave dipoles at bistatic angle, employing coupled impedance loading network 12 p2198 A70-27958
- Diffraction and scattering of electromagnetic waves emitted by electric dipole arbitrarily oriented in space on inhomogeneous sphere 12 p2190 A70-28172
- Electromagnetic waves extraordinary mode scattering by small diameter nonuniform plasma column in magnetic field 13 p2460 A70-28644
- Radio sources scintillation due to scattering medium with refractive index irregularities under detection of finite bandwidth receiver 13 p2365 A70-29148
- Electromagnetic wave scattering from atmospheric ellipsoidal plasma formations, using arbitrary permittivity and magnetic permeability tensors 13 p2366 A70-29376
- Interstellar grains potential model, discussing plane electromagnetic waves scattering by infinite concentric homogeneous circular cylinders at oblique incidence 14 p2639 A70-30732
- Direction fluctuations in radio wave scattering in turbulent gyrotropic medium using Einstein-Fokker-Kolmogoroff equation 14 p2550 A70-30806
- Small scale disturbances and radio wave scattering effects on signal transmission and radiophysical observations in ionosphere 14 p2550 A70-30807
- Radio wave scattering increase in moving body wake near caustic in vertically inhomogeneous ionosphere 14 p2550 A70-30809
- Normally incident plane monochromatic electromagnetic wave reflection and scattering from expanding dielectric slab, using invariant imbedding concept 15 p2695 A70-31438
- Solar radiation and aureole measuring instrument composed of telescope, double monochromator, amplifier and recorder 15 p2735 A70-31807
- Collection of papers on electromagnetic and acoustic scattering by simple shapes 15 p2699 A70-32401
- EM and acoustic scattering by simple shapes covering Maxwell equations, boundary and radiation conditions, radar cross sections, EM potentials, etc 15 p2700 A70-32402
- Acoustic and EM scattering by hyperbolic cylinder, considering plane wave incidence and line sources 15 p2700 A70-32406
- Backscattering, bistatic scattering and current distribution on thin wires during electromagnetic wave incidence 15 p2700 A70-32412
- EM wave scattering and diffraction by acoustically soft and hard oblate spheroids 15 p2701 A70-32413
- Electromagnetic waves diffraction and scattering from acoustically soft and hard and perfectly conducting disks in plane or arbitrary incidence directions 15 p2701 A70-32414
- Convex infinite paraboloid of revolution, describing geometry and applications to electromagnetic wave scattering and antennas 15 p2701 A70-32415
- Cone geometry for electromagnetic and acoustic scattering 15 p2701 A70-32417
- Radiative transfer in scattering medium with nonuniform absorption 15 p2775 A70-32906
- Angular scattering of interstellar medium resulting in multipath dispersion of pulsar pulses, describing NP0532 in Crab Nebula 16 p2972 A70-32988
- Electromagnetic waves scattering in uniformly moving media, using transformation formulas for plane waves 16 p2865 A70-33690
- Rough surface radiative properties, determining electromagnetic wave scattering by Maxwell equation solution [AIAA PAPER 70-862] 17 p3135 A70-34508
- Microwave antenna with aperture in infinite conducting plane, analyzing radiation patterns, scattering and diffraction 17 p3043 A70-35053
- Electromagnetic wave scattering at ellipsoidal bodies in microwave rectangular and circular waveguides 17 p3046 A70-35346
- Plane wave incident on oblate spheroid or disk, deriving LF field scattering 18 p3335 A70-35974
- Thomson theory of arbitrarily intense elliptically polarized plane electromagnetic wave scattering by free electrons, solving electron equations of motion 18 p3267 A70-36649
- Lunar rocks permittivity and density and surface roughness from radio wave scattering data 19 p3512 A70-37276
- Plane TM wave scattering by systems of two parallel conducting elliptical cylinders, metal tapes and combinations 19 p3374 A70-37278
- Scattering structures of two parallel elliptical cylinders, tapes or combinations, deriving surface current density distribution under plane TM wave excitation 19 p3375 A70-37279
- Plane electromagnetic scattering from perfectly conducting bodies, comparing exact numerical solution with experiment 20 p3585 A70-39394
- Electromagnetic waves scattering from dense turbulent plasma, calculating radar cross sections of inhomogeneous plasma for peak electron densities 20 p3586 A70-39459
- Time harmonic waveguide scattering involving metallic obstacles, obtaining numerical solution by finite difference Green function method 20 p3586 A70-39469

- Inclined electromagnetic wave incidence on randomly inhomogeneous medium with changing mean dielectric permittivity, calculating reflected and scattered fields
20 p3587 A70-39726
- Langmuir wave beam nonlinear transformation in isothermal plasma due to induced scattering by ions
20 p3684 A70-40385
- Electromagnetic wave diffraction by ideally conducting wedge of finite radius, deriving asymptotic formula for plane wave scattering
21 p3784 A70-40626
- Electromagnetic field amplitude and phase scattering diagrams analysis for shape information capacity
21 p3785 A70-40637
- Electromagnetic scattering power spectrum from underdense turbulent plasmas, deriving first and second moments
21 p3858 A70-41732
- Electromagnetic radiation power spectrum scattered by relativistic particles, considering reflected waves resemblance to HF radio spectra of quasars
22 p4100 A70-42856
- Scattering indicatrix of electromagnetic radiation in plasma caused by electron-ion interactions
22 p3989 A70-43141
- Laser radiation hyper Raman scattering intensity enhancement via resonance processes, using density matrix method
22 p4075 A70-43233
- EM wave multiple scattering by spheres, attributing cross-polarization absence in backscattered field to spherical symmetry
23 p4160 A70-43767
- Millimeter band electromagnetic scattering from weakly doped GaAs, calculating reflection coefficient and phase angle
23 p4229 A70-43926
- Conducting bodies of revolution, calculating surface currents due to axially incident plane electromagnetic wave by computer program
23 p4162 A70-44005
- Lyman alpha radiation scattering intensity during solar radiation period, discussing dependence of interstellar hydrogen density in interplanetary space on solar EUV
23 p4237 A70-44753
- Arbitrarily shaped cylindrical conducting structures with transient incident electromagnetic wave, calculating scattering from integral equation by digital computer
23 p4165 A70-44957
- Two dimensional electromagnetic scattering body geometry reconstruction from given incident and scattered far field distributions
23 p4165 A70-44958
- Electromagnetic scattering by homogeneous gyrotropic cylinder, discussing matrix equations formulation and solution by reciprocity theorem
23 p4165 A70-44959
- EM wave backscattering from lossless dielectric sphere, examining diffracted field surface waves role
23 p4165 A70-44960
- Electromagnetic scattering by two dimensional periodic arrays of conducting thin plates, calculating induced current and near field radiation distribution
23 p4165 A70-44961
- Interplanetary atomic hydrogen density distribution from Lyman alpha scattering calculation, explaining background radiation anisotropy detection by Vela 7 satellite
24 p4403 A70-45392
- Radiative flaw detection problems, calculating gamma radiation scattering
24 p4348 A70-45848
- Phase and tracking errors due to mutual scattering in phase monopulse phase-scanned antenna
24 p4315 A70-46135
- ELECTROMAGNETIC SHIELDING**
NT RADIO FREQUENCY SHIELDING
Ruby laser energy threshold dependence on partial shielding of rod by stainless steel tubing
09 p1694 A70-22136
- Interference proof characteristics and shielding capability of mirror antennas improved by peripheral sheet metal or wire screens, reducing rear lobe level
09 p1648 A70-23151
- Ni-Mo-Fe magnetic alloy for EM pulse shielding, verifying saturated regions diffusion theory
12 p2201 A70-28128
- Anechoic chambers and test equipment for microwave antenna pattern measurements, discussing electromagnetic shielding and construction
14 p2557 A70-31180
- Fences and pits effectiveness for shielding satellite earth stations from local terrestrial facilities interference
21 p3789 A70-41342
- Maxwell equations for hybrid modes of shielded ring line with axial and coaxial region at cut-off and near cut-off conductivity
21 p3793 A70-42269
- Conducting epoxy shielding and bonding efficiency and bulk resistivity at high frequencies for bonding cover onto compartmentalized module
23 p4170 A70-43866
- ELECTROMAGNETIC SHOCK TUBES**
U SHOCK TUBES
ELECTROMAGNETIC SPECTRA
NT BALMER SERIES
NT D LINES
NT ELECTRONIC SPECTRA
NT FRAUNHOFER LINES
NT H ALPHA LINE
NT H BETA LINE
NT H GAMMA LINE
NT H LINES
NT INFRARED SPECTRA
NT K LINES
NT LINE SPECTRA
NT LYMAN SPECTRA
NT MICROWAVE SPECTRA
NT PASCHEN SERIES
NT RADIO SPECTRA
NT RAMAN SPECTRA
NT RYDBERG SERIES
NT SOLAR SPECTRA
NT STELLAR SPECTRA
NT TELLURIC LINES
NT ULTRAVIOLET SPECTRA
NT VIBRATIONAL SPECTRA
Intensity and spectral distribution measurement techniques for nonvisible extraterrestrial radiation, discussing rocket spectroscopy results
04 p0757 A70-15648
- Cyanide gas lasers design for submillimetric region of electromagnetic spectra
11 p2062 A70-25735
- Chorioretinal damage thresholds spectral dependence of intense light sources, describing temporal, axial and radial temperature distributions
15 p2682 A70-32014
- Crab Nebula electromagnetic spectrum models, considering uniform magnetic field over whole volume and strong fields in small regions
19 p3505 A70-38114
- Crab Nebula pulsar NP 0532 electromagnetic spectrum observations, examining radio, optical, IR and X ray emission
21 p3874 A70-40677
- Crab Nebula electromagnetic spectrum deviation from power law in microwave region, investigating origin from Compton scattering of high energy electrons
21 p3875 A70-40683
- ELECTROMAGNETIC WAVE FILTERS**
NT INFRARED FILTERS
NT MICROWAVE FILTERS
NT OPTICAL FILTERS
NT RADAR FILTERS
NT ULTRAVIOLET FILTERS
NT WAVEGUIDE FILTERS
Signal orientation insensitive filter for pattern recognition
02 p0266 A70-12701
- Photoelectric photometry of comets to obtain principal data and to classify comets by employing same filters and stellar photometric standards
06 p1140 A70-17731
- Polarization interference filter as laser resonator frequency selector, showing Q factor measurable within spontaneous emission line
06 p1082 A70-17771
- Discrete analog filters circuits for optimal non-coherent processing of phase manipulated signals
08 p1456 A70-20571
- Interference emission filtering in high power microwave transmitters, discussing spurious emissions removal or rejection by transmission line filters
08 p1474 A70-21257
- Optimal decomposition of nth order filter into cascaded second order sections
09 p1650 A70-23367
- Signal detection in correlated noise with two stage prewhitening and matched filter system
10 p1833 A70-24220
- Electromagnetic interference filters design for equipment power lines from electromagnetic compatibility and reliability viewpoints
12 p2201 A70-28129
- Signal-arrival-time invariance and SNR resolution of discretely analog filters matched to complex radio signals
13 p2380 A70-29736
- Wideband pulse signal synthesis and optimal filtration by dispersive ultrasonic delay lines, estimating potential noise stability for analog data transmission
15 p2696 A70-31502
- Combination shutter and filter-changing mechanism for spacecraft vidicon cameras
16 p2914 A70-34150
- Spectral filtration methods in diffraction instruments at vacuum UV region, discussing ambient storage conditions and fabrication effects
23 p4219 A70-44412
- ELECTROMAGNETIC WAVE TRANSMISSION**
NT DOUBLE SIDEBAND TRANSMISSION
NT IONOSPHERIC F-SCATTER PROPAGATION
NT IONOSPHERIC PROPAGATION
NT LIGHT SCATTERING
NT LIGHT TRANSMISSION
NT MICROWAVE TRANSMISSION
NT MULTIPATH TRANSMISSION
NT RADAR TRANSMISSION
NT RADIO TRANSMISSION
NT SCATTER PROPAGATION
NT SHORT WAVE RADIO TRANSMISSION
NT SINGLE SIDEBAND TRANSMISSION
NT TELEVISION TRANSMISSION
NT TRANSEQUATORIAL PROPAGATION
Radial electron flux interaction with cylindrical electromagnetic wave propagating between conducting planes, noting disturbance development according to power law
01 p0049 A70-10166
- Transmission and reflection of electromagnetic waves by bounded moving plasma layer in slow wave space
01 p0042 A70-10167
- Electromagnetic propagation in linear dispersive media, discussing energy transport velocities of total stored energy density and electromagnetic energy
01 p0043 A70-10779
- LF electromagnetic waves interaction propagating in stream-magnetized cold plasma, discussing waves temporal growth and instability
02 p0262 A70-12603
- Electromagnetic wave propagation in homogeneous plasma waveguide satisfying Appleton-Hartree approximation without collisions in presence of longitudinal magnetic induction
02 p0349 A70-12724
- Energy transfer formula and scattering of electromagnetic waves at ideally reflecting bodies in inhomogeneous medium using geometrical optics approximation
03 p0442 A70-13094
- Electromagnetic wave propagation through stratified positive plasma column in waveguide, noting stratification travel effects on wave amplitude and phase shift
03 p0443 A70-13096
- Quasi-optic electromagnetic beams slow spreading in anisotropic media due to propagation in unusual directions
03 p0447 A70-13288
- Electromagnetic wave diffraction effects on matching plasma waveguide to coaxial power extraction line
03 p0531 A70-13334
- Electromagnetic finite amplitude wave beams self action in magnetoactive plasma, noting nonlinear characteristics
03 p0448 A70-13411
- Method of characteristic calculation of field amplitude of electromagnetic waves propagating in inhomogeneous nonlinear medium applicable for computer
03 p0448 A70-13461
- Electromagnetic wave propagation in semiconductors, considering effects of electric field, energy dissipation law and band structure
03 p0540 A70-13719
- Fabry-Perot resonator misalignment effect on TEM wave transmission coefficient in gas laser
03 p0492 A70-13749
- Refractive index profile analysis for hypergeometric functions solutions for vertically polarized electromagnetic waves propagating in horizontally stratified isotropic media
04 p0647 A70-14616
- Electrostatic field effects of electromagnetic wave propagation in anisotropic plasma
04 p0728 A70-15002
- Electromagnetic waves amplification in semiconductor plasma with high electron concentration, analyzing equations describing waves drift instability
04 p0731 A70-15216
- Electromagnetic wave growth effect on wave field propagating along beam-plasma slab, showing Poynting vector component
04 p0651 A70-15293
- Anomalous Doppler shift interaction between positive ions and right-hand polarized EM waves propagating at small angle to interplanetary magnetic field
05 p0905 A70-15761
- Critique of theory of electromagnetic wave transmission in turbulent atmosphere, considering effects of approximation
05 p0811 A70-16044
- UV radiation propagation in atmospheric boundary layer, analyzing solar UV background and UV signal attenuation along horizontal path
05 p0882 A70-16241
- Whistler mode wave propagation in collisionless Vlasov plasma along nonuniform magnetic field
05 p0889 A70-16533
- Polarization transfer equations for electromagnetic waves propagating in inhomogeneous magnetized plasma solved analytically for homogeneous magnetized plasma
05 p0890 A70-16570
- Parametric coupling between space-time harmonics of electromagnetic wave propagating in dielectrics modulated by pump wave
05 p0815 A70-16660

Electromagnetic wave phase characteristics after free space passage through statistical medium with wave disturbance producing density and ionization
05 p0815 A70-16735

Symmetrical and asymmetrical electromagnetic wave modes in conical waveguide calculated, relating critical cross section plane position to aperture angle
05 p0816 A70-16892

Uniqueness and reciprocity theorems in elastic medium occupying infinite domain extended to electromagnetic wave propagation in plasma
05 p0890 A70-17097

Propagation, reflection and dispersion equation for electromagnetic waves in longitudinally magnetized plasma filled coaxial waveguide using rotating coordinates
06 p1016 A70-17124

Wave dispersion across magnetic field in cold and warm collisionless Maxwellian plasma, discussing electromagnetic and electrostatic Bernstein modes
06 p1116 A70-17364

VLF and ULF whistler modes propagating along geomagnetic field-line paths in magnetosphere, studying cyclotron resonance amplification
06 p1118 A70-17379

Pitch angle anisotropy instabilities of electromagnetic waves in space, discussing warm plasma, solar wind and Van Allen belts
06 p1118 A70-17380

Power reflection and transmission coefficients for polarized electromagnetic waves incident on plasma slab moving along magnetostatic field
06 p1008 A70-17566

Eigenvalues of spheroidal wave functions calculations dependent on complex propagation constants, discussing branch point values in tabular form
06 p1009 A70-17907

Electromagnetic-acoustic probe for remote wind velocity sensing and radar range performance
06 p1071 A70-18509

Satellite observations of equatorial erosion and defocusing of VLF waves propagating at low magnetic latitudes
06 p1058 A70-18532

Electromagnetic waves phase modulation index during propagation in nonlinear media found dependent on mismatch between interacting waves group velocities, relaxation time and losses
07 p1227 A70-18763

Plane electromagnetic wave penetration into ferromagnetic half space solved for nonlinear parabolic equations using difference method
07 p1227 A70-18992

S- and p-polarized electromagnetic wave incident on semiinfinite laminar plasma layers, analyzing reflection and absorption characteristics
08 p1456 A70-20504

TEM waves penetration into magnetoactive semibounded plasma using Vlasov and Maxwell equations, obtaining electric field for specular reflection of electrons
08 p1551 A70-21255

Electromagnetic wave instability propagating across static magnetic field in presence of thermal anisotropy, considering interplanetary plasma and plasma devices stability
08 p1553 A70-21610

Book on radiation and propagation of electromagnetic waves covering plane waves in anisotropic and inhomogeneous media, spectral representation of sources, radiation in plasma, diffraction, etc
09 p1633 A70-22639

H guide with laminated dielectric strips separated by air layers, analyzing field distribution and characteristics
09 p1634 A70-22709

Nonlinear effects related to plane electromagnetic wave propagation in weakly ionized plasma
09 p1735 A70-22842

Electromagnetic wave propagation in gyromagnetic medium, solving for field vectors in degenerate hypergeometric form
09 p1637 A70-23158

Diagnostics of inhomogeneous plane stratified plasma with arbitrary electron concentration distribution, solving differential equation for electromagnetic wave propagation normal to plasma layers
09 p1735 A70-23160

Meteor ionized trails initial expansion and diffusion resulting in dissociation and ionization of air molecules through collision, using electromagnetic wave scattering
09 p1762 A70-23177

Plane electromagnetic waves scattering from radially inhomogeneous cylindrical structure, deriving expressions for far field and cross section for both polarizations
10 p1841 A70-24856

Radial electron flux interaction with cylindrical electromagnetic wave propagating between conducting planes, noting disturbance development according to power law
10 p1853 A70-25014

Transmission and reflection of electromagnetic waves by bounded moving plasma layer in slow wave space
10 p1842 A70-25015

Electromagnetic waves propagation in nonlinear medium, investigating polarized plane wave incident on vacuum-plasma interface in magnetic field
10 p1844 A70-25156

Plane electromagnetic waves propagation in nonabsorbing photoelastic material with finite deformations, formulating theory from Eulerian and Lagrangian point of view
11 p2139 A70-26173

Stochastic differential equations objectives, limitations and restrictive assumptions in physical problems, discussing electromagnetic wave propagation in random continuum or random d'Alembertian operator
11 p2074 A70-26550

Atmospheric turbulence effects on line-of-sight electromagnetic wave propagation, deriving signal statistics for nonvalid weak scattering solutions case
11 p2012 A70-26764

Electromagnetic wave propagation problem in periodic slow wave structures reduced to Hamiltonian using parametric resonance theory
11 p2012 A70-26802

Plane electromagnetic wave diffraction by perfectly reflecting half plane calculated by elementary method
12 p2184 A70-27234

Electromagnetic wave penetration in plasma under uniform DC magnetic field, considering wave propagational direction and electric field
12 p2279 A70-27781

Radiation transfer models for diffuse reflection of quanta from turbulent medium applied to electromagnetic wave propagation in turbulent atmosphere
12 p2306 A70-27855

Electromagnetic waves emission and propagation in chaotically inhomogeneous media, analyzing mean field and permittivity tensor for isotropic and anisotropic media
12 p2190 A70-28170

Diffraction and scattering of electromagnetic waves emitted by electric dipole arbitrarily oriented in space on inhomogeneous sphere
12 p2190 A70-28172

Frequency spectra of log amplitude fluctuations of electromagnetic wave propagating in turbulent atmosphere, using geometrical optics approximation
12 p2190 A70-28173

Plane electromagnetic waves anomalous reflections from diffraction grating with periodic array of rectangular holes in dielectric layer, observing resonant character
12 p2191 A70-28175

Atmospheric water effects on electromagnetic wave propagation - NATO Conference, University of Western Ontario, August-September 1969
13 p2393 A70-28781

Radar meteorology in electromagnetic communications to provide storm systems data, noting clear air radar echoes
13 p2445 A70-28791

Electromagnetic waves propagation in semiconductors, allowing for nonlinear effects from field heating of carriers
13 p2469 A70-28877

Plane electromagnetic wave interaction with compressible plasma fluid moving with uniform velocity in vacuum, calculating reflection and transmission coefficients
13 p2462 A70-29101

Plane electromagnetic wave reflection at interface of two semiinfinite dielectric media in relative motion perpendicular to incidence plane, noting polarization change
13 p2365 A70-29102

Plane electromagnetic wave in moving conductive medium, analyzing without approximation of velocity limitation
13 p2462 A70-29104

Electromagnetic energy propagation through absorbing single resonant frequency dielectric, deriving transport velocity and relaxation time
13 p2452 A70-29464

Circularly polarized waves in waveguide loaded with high density magnetoplasma, discussing propagation mode and plasma boundary
13 p2379 A70-29617

Book on millimeter and submillimeter waves covering generation, transmission, components and detection
14 p2548 A70-30426

Optical and quasi-optical transmission of EM wave beams of type in directional antennas Fresnel region, examining free space and waveguide modes
14 p2549 A70-30445

Electromagnetic wave diffraction effects on matching plasma waveguide to coaxial power extraction line
14 p2623 A70-30713

Lossless waveguide propagation analysis as transient problem by means of Laplace transform
14 p2556 A70-30923

Ordinary mode electromagnetic wave propagation instability in high beta plasma, determining lower bound on growth rate
14 p2624 A70-31048

Em wave reflection and transmission at boundary between free space and semiinfinite anisotropic plasma
15 p2778 A70-31830

Plane EM wave reflection and transmission at moving boundary, discussing frequency disparity with incident wave
15 p2697 A70-31834

Electromagnetic wave propagation in cylindrical guide containing anisotropic sheets, observing TE and TM modes existence
15 p2774 A70-31946

Large amplitude electromagnetic waves propagation along plane parallel nonlinear dielectric layer, considering dispersion and permittivity
15 p2699 A70-32190

Plane electromagnetic waves propagation in isotropic medium in electromagnetic nonequilibrium conditions
15 p2790 A70-32275

Coherent pulse propagation in inhomogeneously broadened attenuator, examining degeneracy influence and connection with self induced transparency /SIT/ in nondegenerate system
15 p2699 A70-32395

Elevation and ground conductivity effects on horizontal dipole excitation of earth-ionosphere waveguide, considering east-west propagation
16 p2858 A70-32932

Electromagnetic field transmission through plasma slab with specified electron density-collision frequency profiles, using integral derived from transmission and reflection coefficients
16 p2957 A70-32979

Pulsar models distinguishing by Huygens principle in flat space-time, describing electromagnetic propagation in Riemann space
17 p3173 A70-35757

Electromagnetic wave Poynting vector trajectories in absorbing inhomogeneous media, discussing reversibility and energy propagation of spherical and plane structures
18 p3293 A70-36144

Electromagnetic waves phase modulation index during propagation in nonlinear media found dependent on mismatch between interacting waves group velocities, relaxation time and losses
18 p3229 A70-37107

Bounded electromagnetic wave propagation in randomly inhomogeneous medium, calculating correlation in amplitude and phase fluctuations
19 p3375 A70-37282

Ponderomotive forces of plane electromagnetic wave incident at arbitrary angle on metal grating, based on diffraction results
19 p3377 A70-37723

Electromagnetic wave propagation perpendicular to slots of plane dielectric filled waveguide used as slow wave system and antenna
19 p3386 A70-37728

Diffraction amplitudes in plane H-polarized electromagnetic wave incident obliquely on grating with closely spaced conducting rectangular bars, obtaining transmission coefficient
19 p3378 A70-37745

Electric field component equations of electromagnetic wave traveling through stratified plasma, considering incident and reflected ordinary and extraordinary waves
19 p3379 A70-37863

Electromagnetic wave propagation in spherical impedance waveguide, determining eigenvalues with negligible refraction
19 p3381 A70-38565

Helicon electromagnetic wave attenuation control by steady current of uniform density in propagation direction, considering Hall effect role
20 p3585 A70-39396

Book on electromagnetic waves in stratified media covering reflection, propagation, waveguide mode theory, superrefraction and tropospheric ducting
20 p3586 A70-39604

Plane electromagnetic waves diffraction on thin filaments cloud/passive dipoles/, discussing field fluctuations and mean power
20 p3588 A70-40298

Electromagnetic wave propagation in colloidal plasmas analyzed by kinetic approach, obtaining expressions for current density, DC and microwave conductivities, etc
20 p3685 A70-40502

Correction to Wu theory of microstrip leading to exponentially increasing fields
21 p3784 A70-40558

Electromagnetic wave propagation in one dimensional periodic waveguide slow wave systems, deriving dispersion curves by perturbation theory
21 p3784 A70-40628

Electromagnetic wave propagation in inhomogeneous anisotropic linear media, discussing ray tracing, permittivity and relativistic electrodynamics
21 p3785 A70-40798

- Electromagnetic wave propagation through cold slowly varying plasma layers in absence of external magnetic field 21 p3860 A70-42000
- Dynamic potentials equations of guided electromagnetic wave propagating in laterally bounded plasma along magnetic field axis 21 p3860 A70-42005
- Plane electromagnetic waves diffraction by moving periodic metal strip grating, writing E polarized wave of unit amplitude by Lorentz transforms 22 p3984 A70-42388
- Plane electromagnetic wave propagation at normal incidence in isotropic lossless plane-stratified inhomogeneous gyration medium, calculating varying profiles from constitutive equations 22 p4073 A70-42640
- Russian monograph on propagation of LF electromagnetic waves in waveguide formed between earth and ionosphere 22 p3989 A70-42674
- GaAs stripline domains and guided EM waves, discussing velocity, conductivity, drift and transmission amplification gain 22 p3996 A70-42917
- Lower ionosphere ionization anomalies, discussing sunrise seasonal change effects in VLF-LF propagation, winter radio wave absorption and geomagnetic storm after-effects 22 p4024 A70-43311
- Weak EM transmission through resonant medium of two-level atoms in presence of intense monochromatic wave, obtaining absorption coefficient and refractive index 22 p4075 A70-43473
- EM wave propagation in inhomogeneous media, examining permittivity and permeability 23 p4217 A70-43768
- Electromagnetic ground wave propagation, deriving exact solution from two dimensional cylindrical earth model with any number of homogeneous sections 23 p4164 A70-44405
- Electromagnetic wave propagation problem periodic slow wave structures reduced to Hamiltonian, using parametric resonance theory 24 p4311 A70-45177
- Electromagnetic waves nonlinear interaction at various threshold powers, inducing propagation in solid body plasma 24 p4388 A70-45201
- Electromagnetic radiation propagation through resonant medium 24 p4378 A70-45260
- ELECTROMAGNETIC WAVES**
U ELECTROMAGNETIC RADIATION
ELECTROMAGNETICS
U ELECTROMAGNETISM
ELECTROMAGNETISM
NT MAGNETOSTATICS
Variational principle in electromagnetics to produce linear algebraic equations with Rayleigh-Ritz procedure for application to dielectrically coated slot antenna 12 p2198 A70-27957
- One dimensional magnetostrictive bar electromagnetically forced vibration, using Lagrange equations and normal mode analysis 19 p3472 A70-37959
- Maxwell electromagnetism and Einstein gravitation analogy in vacuum field equations, showing metric analytical for inverse distance parameter 24 p4377 A70-45142
- ELECTROMAGNETS**
NT HIGH FIELD MAGNETS
NT SUPERCONDUCTING MAGNETS
Ferromagnetic coercimeter with attached electromagnets for nondestructive hardness testing, describing components and mounting 02 p0301 A70-12489
- Composite conductors involving conventional conductors and superconductors to obtain satisfactory electrical performance for application to electromagnets 05 p0870 A70-16582
- Mechanical electromagnet model of MHD dynamo achieving direct conversion of mechanical to magnetic field energy 06 p1121 A70-17803
- Dynamic mathematical model of proportional electromagnetic transducer in pneumatic servomechanisms derived by Lagrange-Maxwell method assuming circuit linearity 07 p1195 A70-18750
- Electromagnetically suspended bearing equivalent to elastic vinculum with limit on linear displacement, relating weight, power consumption, maximum force, etc 09 p1690 A70-22421
- Electromagnetic control system for spin rate and axis orientation of ISIS ionospheric research satellites, describing design parameters 13 p2501 A70-28414
- Mechanical electromagnet model of MHD dynamo achieving direct conversion of mechanical to magnetic field energy 13 p2460 A70-28654
- Drift reducing NMR stabilization of Hall regulated electromagnet, applying error signal to bias coil 21 p3827 A70-41456
- ELECTROMECHANICAL DEVICES**
Spurious flexural vibrations in cylindrical mechanical resonators, transducers and wires used as component parts in electromechanical filters, indicating dependence on material dimensions and properties 02 p0268 A70-12450
- Solid lubricant films adhesion to metallic surfaces measured using pivot-twist technique 03 p0485 A70-13485
- Nonlinear characteristics of electromagnetic actuating mechanism induced by magnetic field of coil 07 p1281 A70-19529
- Electromechanical graph digital reader for records of cardiovascular studies 07 p1224 A70-20197
- Time optimal control synthesis for electromechanical devices, considering acoustical vibrations elimination in magnetically controlled contacts 08 p1472 A70-21001
- Electromechanical start-up time, inertia and synchronous electromagnetic moment of wave-type electric servomotor calculated by energy method 10 p1809 A70-25202
- Miniature electromechanical gallium antimonide tunnel diode transducer theory fabrication and performance 12 p2236 A70-28055
- Electromechanical position sensor for locating and holding operations 15 p2741 A70-32437
- Electromagnetic diaphragm for use in shock tubes, describing construction and operation 15 p2741 A70-32440
- Electromechanical velocity feeder redesign for functional performance in random vibration environments [ASME PAPER 70-DE-25] 16 p2917 A70-33425
- Electromechanical servomotor for positioning and handling of objects in weightless environment, discussing design and operations 16 p2919 A70-33720
- Tactical missiles electromechanical control actuator with reduced size and weight, describing mathematical model for analog simulation 16 p2845 A70-34111
- Materials and noncontacting design for 50,000 hour lifetime electromechanical components, noting magnetically suspended motor 17 p3100 A70-34754
- Airport terminal design, describing electromechanical baggage handling and sorting systems [SAE PAPER 700261] 18 p3237 A70-36822
- Digital electrodynamic vibration exciter control for sinusoidal, random and shock spectrum testing of aircraft, missiles and satellites 19 p3383 A70-37920
- Optimality criterion selection for asynchronous microelectric motor design by computer 24 p4293 A70-45470
- ELECTROMETERS**
Satellite electrometer for weak DC currents due to charged particle flux 19 p3428 A70-38485
- ELECTROMIGRATION**
Dielectric overcoatings effect on Al interconnections electromigration in IC metallization, noting longer intervals between failures 01 p0153 A70-10083
- Integrated circuits failures due to electromigration in thin films, discussing hole formation and circuit reliability prediction 15 p2713 A70-32649
- Metallization systems materials for IC, discussing environmental stability, metals electromigration, electrochemical corrosion tests, etc 23 p4173 A70-44533
- IC metallization systems in semiconductor devices fabrication and packaging, assessing metals alternate to Al for electromigration difficulties avoidance 24 p4319 A70-46075
- ELECTROMOTIVE FORCES**
Electrochemical generators based on thermodynamic equilibrium processes, deriving expressions for EMF, efficiency, and I-V characteristics 07 p1196 A70-20462
- Transverse Dember effect in elastically bent Ge single crystal illuminated by light beam, considering EMF distribution and photocell application 09 p1740 A70-23191
- Transient processes in n-stage aperiodic amplifier during instantaneous change in phase and amplitude of emf at input 12 p2195 A70-27536
- Electromotive force appearance in fissionable material semiconductor during thermal neutrons irradiation 13 p2469 A70-28879
- Carrier drift due to electromagnetic impulse, deriving expressions for photo emf generated in transverse magnetic field manifesting monopolar photomagnetic effect 13 p2452 A70-29282
- Electric conductivity, thermal emf and EPR spectra of oxide semiconductor glasses based on vanadium and phosphorus oxides, correlating unpaired electron and charge carrier concentrations 15 p2784 A70-32201
- W-3 percent Re-W-25 percent Re thermocouple reliability and stability, describing emf vs temperature table in 0-2400 C range 18 p3257 A70-36200
- Liquid and solid semiconductors thermal emf and electrical and heat conductivities measurement over wide temperature range 20 p3634 A70-40300
- Constant emf in bulk Ge and Si N-type semiconductors under multifrequency microwave electric field 21 p3861 A70-40636
- Magnetoelectric electromotive force in media of ions and neutral molecules, using Boltzmann transport equation 21 p3855 A70-40909
- Global atmospheric electrical structure, considering emf from thermally driven tidal motions in lower atmosphere 22 p4016 A70-42783
- ELECTROMYOGRAMS**
U ELECTROMYOGRAPHY
ELECTROMYOGRAPHS
U ELECTROMYOGRAPHY
ELECTROMYOGRAPHY
Muscle force and electromyogram behavior with alteration in blood flow and composition in anesthetized cats 02 p0231 A70-11708
- Pathological Q waves in various diseases in absence of myocardial infarction, discussing electrophysiological mechanism 03 p0426 A70-13941
- Production mechanism of abnormal Q waves in obstructive cardiomyopathy 03 p0427 A70-13943
- Electromyograms cross correlation analysis to study time relationships between motor unit discharges of human musculus biceps and triceps brachii during physical work 07 p1213 A70-19791
- Simultaneous recording of fast and slow precision manual movements with electroencephalogram and electromyogram 08 p1452 A70-21438
- Mg ion metabolism in neuromuscular excitability maintenance, discussing quantity requirements, detection and electromyographic recording 12 p2172 A70-28045
- Twisted bipolar electrode in needle with controlled separation between bare areas for electromyography 14 p2542 A70-30798
- Fatigue effects on relationship between oxygen consumption, electromyographic activity and isometric contraction in human leg muscles 21 p3766 A70-42159
- Signal processing methods application to myoelectric studies of muscular fatigue, employing surface electrodes 23 p4151 A70-44378
- ELECTRON ACCELERATORS**
NT BETATRONS
Reactor gamma in-pile effects on thermionic diodes simulated in electron accelerator, noting ion production insufficient to support saturation currents 04 p0717 A70-14948
- Subnanosecond risetime milliohm Faraday cup for measuring electron beams from pulsed accelerators 21 p3799 A70-41466
- ELECTRON ATTACHMENT**
Dissociative attachment of low energy electrons in nitrous oxide as function of gas temperature 03 p0441 A70-14006
- Slow electron attachment to O molecules forming stable O-ions, discussing formation rate constant 06 p1109 A70-17488
- Electron affinity and compound formation in hydrogen/nitrogen/oxygen flames containing potassium and boron using mass spectrometry 10 p1832 A70-25150
- Coupled differential rate equations governing growth and decay of positive and negative ion and electron concentrations in afterglow with ambipolar diffusion and electron attachment 11 p2088 A70-25703
- Electron mobility, diffusion, drift velocity and attachment in oxygen, determining Townsend primary ionization coefficient 15 p2776 A70-31969
- Electron attachment rate to sulfur hexafluoride in He buffered flowing afterglow 21 p3853 A70-41394
- ELECTRON AVALANCHE**
P-n junction and microplasmas voltage temperature coefficients during avalanche breakdown 03 p0541 A70-13729
- Gas discharge avalanche breakdown in Si semiconductors, analyzing microplasmas, ionization coefficients, p-n junction voltage, electron and light emissions 04 p0731 A70-15494

- Electron losses from avalanches in hydrogen in cylindrical tube with plane parallel end electrodes, assuming elastic electron collision 22 p4076 A70-42355
- ELECTRON BEAM WELDING**
- Electron beam welding at Oak Ridge Y-12 plant, discussing applications, disadvantages, welding parameters, unweldable materials, welder maintenance, personnel training and safety 02 p0310 A70-12751
- Electron beam welding of AH-56A helicopter rotor hubs outside of vacuum chamber, discussing modifications of machine 04 p0699 A70-15651
- Inertia bonded and electron beam welded joints of Waspaloy compared for suitability in aircraft gas turbine engines 04 p0700 A70-15655
- Convergent ribbon electron beam shaping for vacuum welding with double anode gun, considering space charge effect 06 p1076 A70-17784
- Electron beam gun for drilling and perforation modified to include micromachining and welding 08 p1502 A70-20821
- Fatigue properties of electron beam welded precipitation hardening stainless steels 11 p2059 A70-25664
- Flash, gas-pressure and electron-beam welding of airframe steels 12 p2239 A70-26987
- [ASTME PAPER MR-69-712] Diffusion and electron beam welding combined with forging for cost reduction and production enhancement of titanium structural components 12 p2241 A70-27087
- [SME PAPER AD-70-735] Titanium electron beam welding in aerospace industry, discussing alloy properties and strength behavior 16 p2919 A70-33683
- Electron beam welding of Ti alloys in partial vacuum, describing mechanical tests and metallographic examinations 17 p3098 A70-34442
- Electron beam welding, explaining high fusion zone homogeneity and weld defect formation by dynamic model 17 p3100 A70-34637
- Spiking in deep partial penetration electron beam weld in U dependence on machine parameters 18 p3264 A70-37116
- Precision electron beam welding for metal joints, discussing equipment and quality control factors 19 p3436 A70-38072
- Electron beam welding for thin steel, nonferrous metals and reactive metals sheets 19 p3436 A70-38073
- Electron beam welding for instrument components including torsion shafts, heat sensing membranes, etc 19 p3436 A70-38074
- Electron beam welding for thin copper, carbon and Cr-Ni steel sheets in precision mechanical and optical devices 19 p3436 A70-38075
- Hollow balls for high speed bearings by electron beam welding, describing full scale and rolling element fatigue tests 20 p3637 A70-39236
- Vapor capillary /melt/ depth in electron beam welding, considering electron energy, radiative dissipation, etc 21 p3833 A70-41124
- Sintered boron-alloyed Mo electron beam welding behavior examined by texture-revealing color etching method 21 p3833 A70-41411
- Magnesium Al and Ti alloys electron beam welding for aerospace industry, discussing material requirements, weld quality and optimum conditions 22 p4042 A70-42338
- Glow discharge electron guns for welding and heating, discussing beam current and energy balance 22 p4042 A70-42376
- Welding electron beams metal penetration dependence on ionization phenomena, discussing model based on self focusing 22 p4043 A70-42379
- Electron beam welded hollow balls for high speed ball bearings, comparing fatigue life with solid balls [ASME PAPER 70-LUBS-17] 22 p4044 A70-42444
- ELECTRON BEAMS**
- Langmuir oscillations excited by electron beam in plasma during instability development investigated for temporal and spatial structure, using visualization 01 p0150 A70-10174
- Quasi-linear relaxation of electron beam in plasma with concentration nonuniformities, noting electron velocity role 01 p0150 A70-10213
- UHF signal amplification by electron beam-plasma interaction, defining amplification frequency ranges 01 p0043 A70-10658
- Plasma arc wind tunnel gas velocity measurement with electron beam probe using closed-loop electronic controller to stabilize beam position 01 p0092 A70-11195

- Inhomogeneous plasma containing weak electron beam using Vlasov equation, noting wave-wave coupling effect 02 p0345 A70-11882
- Molecular velocity distribution function measured in normal He shock wave in low density wind tunnel by electron beam fluorescence technique 02 p0299 A70-12229
- Electron multiple scattering theory graphic approximation showing angular distribution in electron beam 03 p0527 A70-13053
- Laser emission action at 4880 Å in plasma discharge from injecting electron beam into Ar at different pressures 03 p0530 A70-13063
- Temporal and statistical characteristics of HF oscillations from electron beam interaction with plasma in magnetic field 03 p0532 A70-13524
- Electron beam technique to measure density profiles of strong shock waves in argon 04 p0692 A70-15325
- Stability of nonlinear plasma waves set up by counterstreaming cold electron beams immersed in background of stationary ions 05 p0889 A70-16531
- Magnetron electron beam amplifier large signal operation analysis using model with thin beam to calculate space charge 05 p0823 A70-16884
- Nonlinear equations for TWT derived allowing for electron beam defocusing and slow wave structure deposition current 05 p0823 A70-16887
- Phase velocities of intrinsic normal waves of electron beam in three frequency parametric amplifier of space charge waves, determining optimal wave interaction conditions 05 p0823 A70-16890
- Two frequency electron beam modes produced by O-type TWT at simultaneous input of HF signals of different amplitudes and frequencies 05 p0824 A70-16894
- Thermophysical characteristics of annealed Ta and Mo alloy welded joints under electron beam and ray heating, noting use for short term tests 05 p0865 A70-17028
- Minority current carriers diffusion in heterojunctions and p-n junctions in AlAs-GaAs, using X ray microanalyzer performing electron beam scanning 06 p1126 A70-17816
- P-n junction depth in semiconductors, using electron beam of scanning electron microscope 06 p1127 A70-17820
- Species concentration, jet structure and diatomic nitrogen rotational temperature measured for diffusive separation of nitrogen-helium mixture free jets, using electron beam 06 p1043 A70-18253
- Electron beam generated plasma behavior, showing electron pressure local nonisotropy capability for generating supersonic-subsonic transitions 06 p1123 A70-18296
- Electron beam fluorescence in rarefied air flow at low static temperature used to study influence of secondary electron emission on rotational temperature measurements 06 p1123 A70-18300
- Excitation emission of diatomic nitrogen molecule for first negative band broadening, considering high energy primary beam with secondary electrons 06 p1124 A70-18305
- Density effects on rotational temperature measurements in nitrogen by electron beam excitation, discussing emission intensity distribution 06 p1067 A70-18306
- Homogenous monoenergetic cylindrical electron beam interaction with homogeneous cold plasma, investigating system stability 06 p1125 A70-18615
- Surface wave propagation and amplification by electron beam-plasma interaction, inapplicability of coupled mode theory and use for microwave amplifier 06 p1125 A70-18616
- Propagation in perturbed magnetically focused electron beams, noting influence of spatially varying drift velocity and damping effect 07 p1239 A70-18867
- Laser oscillation conditions for CdS crystal pumped by electron beam, using energy loss per unit length for calculations 07 p1298 A70-19681
- Coupled mode method, analyzing interaction between slow space charge wave of electron beam and electroacoustic wave of lossless warm plasma 07 p1349 A70-19687
- Magnetic trap chamber walls adverse effect on plasma heating produced by electron beam injected at low hydrogen pressures 07 p1350 A70-19845
- Gruneisen parameter for metal and semiconductor single crystals obtained from measuring one dimensional thermoelastic response during exposure to pulsed electron beam 07 p1357 A70-20020

- Selective harmonic excitation in one dimensional collisionless plasma conforming to Vlasov equation by counterstreaming electron beams, noting velocity distribution conditions 07 p1353 A70-20202
- Plasma-electron beam system LF dispersion characteristics noting ion instability 08 p1549 A70-20505
- Neodymium-glass laser under action of electron beam investigated for population inversion 08 p1512 A70-21204
- Population inversion in neodymium glass impurities in four level laser dependent on electron beam intensity and energy 08 p1512 A70-21205
- Light ions acceleration to high energy by pulsed high intensity electron beams 08 p1553 A70-21694
- Whistler type electromagnetic waves excitation by electron beam in plasma, noting intensity dependence on electron frequency 08 p1554 A70-21804
- Radial self focusing of low density electron beam by interaction with plasma in presence of beam plasma instability 08 p1554 A70-21818
- Pinched plasma reversed current induction due to relativistic electron beam injection 09 p1736 A70-23183
- Plasma charge transfer in unstable beam plasma in magnetic fields system allowing for electron discharge pump operation 09 p1737 A70-23334
- Multibeam O-type TWT characteristic equation analyzed for arbitrary space diversity, calculating gain for various velocity parameter values and electrical lengths 09 p1651 A70-23638
- TWT characteristic equation with arbitrary coupling between two electron beams over wide range of velocity difference, analyzing wave amplitude constant 09 p1651 A70-23639
- Wave propagation constants in electron wave TWT, studying nonuniformity parameter influence to determine relationships between beam and system parameters 09 p1652 A70-23655
- Landau damping and stability of low density crossed field electron beams using analogy with inviscid shear flows 10 p1918 A70-23964
- Electron beam fluorescence probes for rarefied gas flow, describing local density and temperature measurement methods 10 p1888 A70-24399
- Electron-ion beam plasma system, using one dimensional quasi-linear equations for describing electron heating and stabilization 10 p1923 A70-24403
- Electron beam probe applied to flow visualization in rarefied gas wind tunnels 10 p1860 A70-24549
- Model testing gas flow calculation in system emitting electron beam into atmosphere through supersonic gas seal 10 p1895 A70-24590
- Langmuir oscillations excited by electron beam in plasma during instability development, investigating temporal and spatial structure using visualization 10 p1925 A70-25019
- Multivelocity electron beam critical fluctuation amplitudes in crossed electric and magnetic field 10 p1925 A70-25107
- Electrons radial motion and beam focusing in linear accelerator allowing for perturbing forces, calculating particle trajectory 10 p1926 A70-25110
- Stability of realistic inhomogeneous plasmas with sheaths, examining electron beam-stable Maxwellian plasma interaction 11 p2090 A70-26021
- Electrostatic wave propagation and growth rate in electron beam-inhomogeneous plasma confined by magnetic field 11 p2091 A70-26460
- Rarefied gas stream density measurements with electron beam fluorescence experiment, determining pressures and densities behind plane shock wave and in supersonic nozzles 11 p2087 A70-26743
- Electron beam-plasma interaction nonlinear development in time and space using computer simulation 11 p2095 A70-26758
- Microwave radiation from electron beam generated turbulent magnetoplasma measured, indicating enhancement near electron cyclotron harmonic frequencies 11 p2095 A70-26760
- Bi polycrystalline film grown by vacuum deposition on amorphous substrates investigated for electron microscope beam effects 12 p2285 A70-27261

- Spiraling electron beam energy conversion and distribution using retarding-field velocity analyzer
12 p2196 A70-27651
- Radiation emission and transfer in unsteady outer space plasmas, discussing turbulence mechanisms involving electron and ion motion, relativistic and non-relativistic electron beams, etc
12 p2305 A70-27854
- Electron beam interaction with plasma in absence of magnetic field, discussing microwave radiation emission and incoherent scattering and instability spatial growth
13 p2459 A70-28569
- Beam-plasma system mode coupling near electron cyclotron frequency, obtaining interference patterns
13 p2459 A70-28570
- Electron beam interaction with Maxwellian plasma, investigating temperature effects on instabilities
13 p2460 A70-28639
- Electrodeless electrolysis of solid ionic conductors and fused salts without contact leads, using electron beams and glow discharge
13 p2361 A70-28929
- Type 3 solar bursts theory covering beam-type instabilities and quasi-linear relaxation of fast electron distribution functions
13 p2478 A70-29389
- Landau damping in plasma cyclotron wave interaction by symmetrical counterstreaming double electron beam with uniform magnetic field
13 p2468 A70-29917
- Whistler instability examined on gyrating electron beam interaction with cold background plasma propagating parallel to magnetic field
13 p2468 A70-29932
- Electron beam measurement of rotational and high vibrational temperature in molecular nitrogen
13 p2412 A70-29980
- Megavolt prebunched electron beam systems for electronic sources in millimeter and submillimeter region, describing microwave accelerators and bunchers
14 p2555 A70-30431
- Submillimeter wave devices with prebunched megavolt electron beams in coupling structures, describing electromagnetic beam couplers
14 p2555 A70-30432
- Low energy electron beam diffraction, calculating intensity as wavelength function
14 p2619 A70-30489
- Measurable VLF electromagnetic fluxes from Cerenkov effect in ionosphere produced by artificial electron beams
14 p2579 A70-31249
- Transverse kinetic energy of electrons at outlet of magnetron-injection gun as function of cathode inclination and magnetic induction
15 p2707 A70-31504
- Coulomb force effect on electron beam spatial charge for optimal three resonator transit type klystron, regarding buncher length
15 p2707 A70-31507
- Space charge waves in electron beams with velocity distribution, considering dispersion equation and Landau damping
15 p2708 A70-31831
- Plasma beam systems dispersion equation with allowance for electron collisions with heavy particles
15 p2779 A70-32117
- VHF radiation from plasma during electron beam interaction with fast magnetoacoustic wave stimulated by external spatially periodic currents
15 p2780 A70-32118
- High purity V and V-Cr-Ti process, describing aluminothermic reduction and electron beam purification
15 p2761 A70-32387
- Pulsed carbon dioxide laser production with electron beam pumping, ascertaining beam effect on discharge parameters and output power
15 p2754 A70-32864
- Beam current instability and plasma heating by electron beam generated in linear discharge, discussing electron beam-cold plasma interactions
16 p2957 A70-33191
- Low threshold electron beam pumped CdS lasers with improved Al coated Fabry-Perot mirrors in end-pumped configuration
16 p2928 A70-33642
- Spatial electric field variations and electron distribution for beam plasma amplification, using nonlinear approximation
16 p2959 A70-34336
- Low Reynolds number flow inside Delaval nozzle, examining gas density and rotational temperatures by electron beam techniques
[AIAA PAPER 70-810] 17 p3065 A70-34454
- Single gap klystron output resonator optimization, showing maximum electronic efficiency during bunched beam excitation
17 p3055 A70-35681
- HF oscillations excitation in decaying plasma-electron beam system, noting Coulomb collisions and nonlinear effects role
18 p3294 A70-36145
- Microwave devices with harmonized electron beam constructed from klystrons, TWT, backward wave tubes, magnetrons
18 p3231 A70-36414
- Electron beam interaction with ionized K plasma, considering Langmuir waves instability, turbulence and electron heating
18 p3295 A70-36614
- ONERA low pressure wind tunnel equipped with electron beam probing device to visualize flows too rarefied for optical methods
18 p3210 A70-37208
- Finite electron beam plasma system, investigating relationship between linear fluctuations temporal growth and resulting stationary oscillations spatial growth
19 p3475 A70-37540
- Monochromatic radiation from laser modulated electron beams
19 p3444 A70-37572
- Plane EM wave diffraction in cylindrical plasma-electron beam system
19 p3378 A70-37740
- Traveling wave tube with two mixed different velocity electron beams, analyzing nonlinear operation by integro-differential equations
19 p3387 A70-37742
- Laser and electron beam removal of material in manufacturing technology
19 p3447 A70-38451
- Pulsed laser emission at IR transitions of xenon and neon under electron beam pumping
19 p3449 A70-38743
- Rarefied plasma flute oscillation stabilization in magnetic field, using controlled electron beams
20 p3677 A70-39173
- Magnetron type backward wave tube with negatively charged slow wave structure, analyzing electron beam wave interaction for starting conditions
20 p3596 A70-39251
- Square cross section waveguide with cutoff frequency, calculating density wave propagation in helical electron beam trajectories directed by magnetic field
20 p3584 A70-39256
- High resolution electron beams application to electron spectroscopy, discussing elastic and inelastic scattering, resonances and atomic and diatomic molecular ionization
20 p3676 A70-40156
- Time varying flow properties effects on hypersonic wind tunnel spectroscopic measurements, considering direct emission and electron beam techniques
20 p3607 A70-40271
- Superradiant light /SRL/ converted from electron beam energy by semiconductor targets applied to nanosecond photography
20 p3635 A70-40529
- Statistical analysis of random oscillations excited in electron beam-plasma system based on signal recording data
21 p3855 A70-40631
- Spread electron beam excitation of magnetoactive plasma waves in quasi-linear relaxation
21 p3855 A70-40948
- Thermal processes during electron beam metal working, deriving relations for temperature field
21 p3833 A70-41123
- Plasma and spiraling electron beam interactions, observing oscillations above integral multiples of electron cyclotron frequency
21 p3857 A70-41388
- High power pulsed relativistic annular electron beam production and focusing by injection gun using magnetic field control
21 p3827 A70-41461
- Subnanosecond risetime milliohm Faraday cup for measuring electron beams from pulsed accelerators
21 p3799 A70-41466
- Plasma source design using stellarator type magnetic field, eliminating electron beam and electrode produced impurities
21 p3858 A70-41713
- Spatial energy loss and ionization deposition distributions of fluorescent radiation emission induced by electron beam in nitrogen gas
21 p3853 A70-41913
- Electron beam interaction with external harmonic microwave field in planar diode gap, calculating electric field current and voltage distribution functions
22 p3995 A70-42396
- Electron beam instability in cylindrical magnetically confined plasma column, calculating quasi-static spatial growth increments
22 p4080 A70-42403
- Potassium plasma-electron beam interaction, studying LF instability due to electron and ion heating
22 p4083 A70-43385
- Nonlinear collective ionic acceleration by relativistic electron beam, assuming blob dimensions of plasma wavelength
22 p4077 A70-43471
- Ion source emitter plasma column generated by electron beam injection through gas filled chamber, compensating ion space charge with fast discharge electrons
24 p4385 A70-45451
- Plasma-electron beam interaction instability transition from absolute to convective in hydrogen tube system at various pressures, considering electron collision effects
24 p4385 A70-45452
- Laser light effects on electron beams, considering absence or presence of crystalline optically transparent solid
24 p4353 A70-45564
- High resolution cylindrical capacitor observation of fine structure of distribution function of electron beam interacting with plasma
24 p4387 A70-45820
- Betatron monoenergetic electron beams in radiometric, spectrometric and radiographic testing of composite materials
24 p4339 A70-45850

ELECTRON BOMBARDMENT

- Adsorption properties of pulverized silica gel, quartz, C and graphite under electron bombardment from low temperature plasma, showing surface and physicochemical influence
03 p0516 A70-13468
- Electron bombardment effects on epoxy based textolites mechanical properties, studying structural changes spectroscopically
03 p0516 A70-13735
- Optical spectra of discharge chambers of electron bombardment mercury ion thrusters with hollow and oxide cathodes
06 p1132 A70-18157
- Ni L alpha X ray emission line shape and position as function of bombarding electron energy, observing differential self absorption in anode
09 p1731 A70-22777
- Ion accelerator for doping semiconductors, discussing electronic bombardment of low pressure vapors, electrostatic extraction, focusing and mass spectrometer
09 p1649 A70-23325
- Energy spectra of electrons transmitted through Be, Al and Au targets measured for incident electron energy
10 p1918 A70-23984
- Metallic contacts deposition on p- or n-GaAs using vacuum evaporation by electron bombardment
12 p2202 A70-28188
- Molecular nitrogen excitation under electron bombardment at auroral and airglow impact levels, using computerized Monte Carlo method
14 p2620 A70-31269
- Spatial distribution of energy deposited by auroral electrons in upper atmosphere, using Monte Carlo method
15 p2725 A70-31860
- Nitrogen and air bombardment by relativistic electrons, determining absolute fluorescence intensity of nitrogen molecular ion first negative band
16 p2954 A70-33279
- Submillipound mercury electron bombardment ion thruster efficiency, noting cathode pole piece, baffle position and geometry influence on ion chamber performance
16 p2969 A70-33612
- Electron bombardment effect on volt-ampere, voltage-capacitance and pulse characteristics of GaAs point contact pulse diodes
17 p3055 A70-35675
- Bremsstrahlung and photoneutrons from electron-photon cascades in thick tungsten and tantalum targets bombarded with low energy electrons
20 p3674 A70-39222
- Electron gun for high current density electron bombardment of semiconductor lasers
20 p3641 A70-39482
- Critical components effect on small Hg electron bombardment thruster performance, considering glass coated accelerator grids, hollow cathodes and plasma bridge neutralizers
20 p3692 A70-40238
- Mercury electron bombardment thruster, measuring effect of geometry and magnetic field inside pole piece region on discharge losses and propulsion efficiency
20 p3693 A70-40247
- Small-orifice hollow cathode discharge properties in electron bombardment ion thrusters, using vaporized mercury propellant
20 p3693 A70-40248
- Angular distribution of thick target bremsstrahlung produced by electron bombardment of Be, Sn and Au surfaces
21 p3854 A70-42020
- Light generation by free electrons interaction with metallic diffraction grating, devising experiments for explaining incompatibility with simple electrostatic image theory
22 p4074 A70-42943
- Oxidized Si surface recombination rate measurement by electric field effect, noting electron bombardment effects on electrical properties
22 p3998 A70-43443

ELECTRON BUNCHING

Optimal electron bunching in two cavity klystron by varying parameters and nonlinear one dimensional approximation

05 p0823 A70-16888

Millimeter band direct-transit klystrons oscillation and amplification at improved output power obtained by electron bunching in nonuniform drift fields

09 p1651 A70-23637

Electrode curvature effect in radial reflex klystron on processes in electron bunching region

09 p1651 A70-23640

Megavolt prebunched electron beam systems for electronic sources in millimeter and submillimeter region, describing microwave accelerators and bunchers

14 p2555 A70-30431

Submillimeter wave devices with prebunched megavolt electron beams in coupling structures, describing electromagnetic beam couplers

14 p2555 A70-30432

Single gap klystron output resonator optimization, showing maximum electronic efficiency during bunched beam excitation

17 p3055 A70-35681

Hot electrons bunch spread deceleration in collisionless plasma, discussing stationary moving jump formation similar to shock wave

22 p4077 A70-42299

ELECTRON CAPTURE

High latitude capture region boundary for electrons in upper radiation belt determined relative to current electrojets in ionosphere from satellite observations

01 p0172 A70-11516

Inhomogeneous fast electron clouds stability and perturbation dynamics captured in magnetosphere geomagnetic field described by hydrodynamic equations

04 p0743 A70-15721

Cascade capture of carriers in semiconductors with negatively charged dislocation explained by diffusion-type equation

06 p1126 A70-17818

Heavy negative charges formation in ionized Hg vapor by electron capture, basing demonstration on magnetic field effects on free electrons or charged droplets

08 p1550 A70-20594

Heavy particle collisions impact parameter and wave equations for direct excitation and electron capture processes

08 p1548 A70-21502

Recombination radiation intensity current dependence and I-V characteristics p-n-n diode operating in double injection mode and electrons trapping

14 p2625 A70-30163

Inhomogeneous fast electron clouds stability and perturbation dynamics captured in magnetosphere geomagnetic field described by hydrodynamic equations

14 p2632 A70-30805

Nickel-doped p- and n-type Ge hot electrons recombination characteristics in strong electric fields, examining electron capture cross section

15 p2782 A70-31628

Electron capture involving iron nuclei in contracting iron stars treated as endothermic nuclear reaction

22 p4104 A70-42992

Charge transfer of protons at electron capture in excited states, using proton beam and various target gases

23 p4221 A70-44209

Cs ion beam space charge and current neutralization by electron capture for partially ionized plasma formation, investigating longitudinal electrostatic wave excitation

24 p4385 A70-45465

ELECTRON CLOUDS

Inhomogeneous fast electron clouds stability and perturbation dynamics captured in magnetosphere geomagnetic field described by hydrodynamic equations

04 p0743 A70-15721

Ion resonance instability in nonneutral plasmas, considering ions addition to low density electron cloud with low kinetic energy

07 p1352 A70-19991

Electron clouds injection and containment by magnetic field in toroidal vacuum chamber, studying causes of cloud instability

07 p1353 A70-19994

Inhomogeneous fast electron clouds stability and perturbation dynamics captured in magnetosphere geomagnetic field described by hydrodynamic equations

14 p2632 A70-30805

Upper atmospheric wind velocity and diffusion coefficient measurement by radar observation of artificial electron cloud from atomic K ejection

18 p3253 A70-36993

ELECTRON COLLISIONS

U ELECTRON SCATTERING

ELECTRON COUNTERS

Satellite-borne scintillation spectrometers for medium and high energy electron and proton measurements

10 p1931 A70-24315

Electron recording by shower counters, noting radiation length importance

16 p2908 A70-33211

Electron intensity long term variations above 500 MeV byOGO-5 satellite-borne cosmic ray electron detector, supporting diffusion-convection theory of solar modulation

19 p3497 A70-37522

ELECTRON DECAY RATE

Time autocorrelation and power spectrum of radar returns from underdense turbulent ionized gas as function of electron density decay

14 p2551 A70-31035

ELECTRON DENSITY (CONCENTRATION)

NT ELECTRON DENSITY PROFILES

NT IONOSPHERIC ELECTRON DENSITY

NT MAGNETOSPHERIC ELECTRON DENSITY
Indium arsenide crystals conduction band structure with various electron concentrations, determining electron mass dependence on concentration and temperature

01 p0154 A70-10096

Auroral light emission and electron density simultaneous measurements by rocket flights into auroral glow, deriving recombination rates

01 p0171 A70-10872

Upper atmospheric contribution to Faraday rotation angle above 5000 km determined from beacon frequencies of geostationary satellite, noting geomagnetism weighting and electron content decrement role

01 p0076 A70-10874

Mach numbers, electron density and temperature in partially ionized frozen equilibrium flows of Ar in hypersonic nozzle

01 p0063 A70-10994

White dwarf spectra interpretation based on model atmosphere method, discussing chemical composition, low luminosity high pressure atmospheres, electron density, etc

01 p0189 A70-11340

Ionization instability in low temperature magnetized plasma, analyzing electron concentration perturbation caused by Joule heating during electron-ion collisions

01 p0153 A70-11598

Cosmic ray primaries and secondaries direct heating of thermal electrons for computation of H I regions electron densities and temperatures

02 p0363 A70-11782

Time resolved cavity perturbation technique to measure high plasma density in magnetic mirror compression experiment, obtaining total electron number

02 p0347 A70-12236

Equatorial patterns measurement of plasma covered axially slotted cylindrical antenna, describing discharge tube, facility and Langmuir probe survey of tube electron density

02 p0269 A70-12590

Electron surface states bands in insulators induced by image potential, determining lower limits for liquid and solid gases

02 p0345 A70-12823

Atomic and electron densities measurements in shock wave interactions with magnetic fields, using interferometric and spectroscopic method

03 p0529 A70-12876

Electron numbers in extensive air shower spectra from scintillation counters measurements at high mountain altitude, analyzing electron-photon component spatial distribution

03 p0556 A70-13041

Negative resistance mechanism model with larger electron accumulation in conduction band than free holes

03 p0539 A70-13212

Current density and electron concentration fluctuations in semiconductors under electric field, obtaining theory of light scattering at hot electrons

03 p0539 A70-13405

Laser irradiation of RF plasmoid producing electron density increase, discussing resonance sustained RF discharges, mode locking, laser photodetachment, etc [ONERA-TP-751]

03 p0501 A70-13630

Electron density and temperature in ionized gas created by thermal collisions between neutral particles, analyzing chemical ionization and inelastic collisions influence

03 p0532 A70-13631

Electrical properties of Cu-diffused GaAs, studying temperature effects on acceptor concentration and electron population growth

03 p0541 A70-13730

Tonks-Dattner resonances peaks in rare gas plasmas, considering electron densities variations role

03 p0534 A70-14211

Spectral line widths in MPD arc jet measured to determine plasma electron density and heavy particle temperature

03 p0536 A70-14371

Low energy cosmic rays effect on electron density in interstellar medium

04 p0738 A70-14509

Statistical electron density distributions and Thomas-Fermi-Dirac screening functions for positive ions with various ionization degrees

04 p0721 A70-14666

High density nonlinear and linear growth rates of flute modes instabilities in cold plasma coexisting with low density of energetic electrons

04 p0728 A70-14998

Microwave cavity perturbation measurements of electron densities at electroacoustic resonances excited in afterglow plasma

04 p0728 A70-15004

Electromagnetic waves amplification in semiconductor plasma with high electron concentration, analyzing equations describing waves drift instability

04 p0731 A70-15216

Transverse and longitudinal correlation coefficients of electron density fluctuations in turbulent jet related through equation specifying velocity fluctuations isotropy

04 p0674 A70-15551

Electron quench additives electrophilic effects in high temperature air plasma flow, simulating reentry flight conditions

04 p0664 A70-15561

Precursor electron densities measured in nitrogen and air ahead of shock waves, noting shock tube wall reflectivity

04 p0694 A70-15565

NO ion dissociative recombination rate coefficient determined in high temperature air plasma from electron temperature and number density measurements

04 p0675 A70-15583

Mercury plasma flow rate change effect on electron temperature and density in thermoelectric converter determined by spectroscopy

05 p0887 A70-16028

Nonequilibrium Cs plasma electron density, temperature and sustaining field using theoretical analysis and probe measurements

05 p0887 A70-16108

Electron recombination in inert gases at various pressures, studying electron density decrease in time by UHF and optical methods

06 p1109 A70-17495

Free electron formation ahead of strong shock waves traveling into nitrogen-oxygen mixtures in shock tube, observing electron densities

06 p1065 A70-18029

Charge-charge scattering model to calculate electron collection by Langmuir probe absorbing surface with and without magnetic field

06 p1124 A70-18308

Light scattering from free electrons in laboratory plasma, showing frequency spectrum equal to electron density fluctuations

07 p1347 A70-18899

Electron density dependence on electron temperature during self and mutual interaction of electromagnetic waves in magnetoplasma, tabulating numerical results

07 p1351 A70-19968

Electron density calculation for collisionless plasma flow around conducting cylindrical body, accounting for surface absorption and mean electron velocity [ONERA-TP-792]

08 p1550 A70-20595

Electron density, excited state density and neutral particle temperature in Ar and Ne nonequilibrium laminar plasma jets

08 p1550 A70-20596

Discharge current effect on shape and position of resonance curves for electron concentrations during microwave oscillation conversion in magnetoactive plasma

08 p1551 A70-20866

Electron wake measurements on Explorer 8 and 31 and Ariel 1, discussing order of magnitude discrepancy

08 p1497 A70-21392

Alkali seeded plasma electron density and temperature enhancement by laser resonance pumping

08 p1552 A70-21576

Integrated electron density determination for plasma sheath on reentry vehicle based on power coupling change measurement

08 p1552 A70-21596

Extensive air shower simulation for determining inelasticity effect on electrons, hadrons and muons variation at sea level

08 p1563 A70-21674

Laser interferometric technique involving use of unstable external resonator to facilitate electron density measurements in presence of transverse plasma density gradients

08 p1499 A70-21693

Radial self focusing of low density electron beam by interaction with plasma in presence of beam plasma instability

08 p1554 A70-21818

Refractive index variation regions and mapping along propagation path in random medium, noting application to solar wind electron density structures measurements

09 p1634 A70-22699

Plasma electron density determination by number of extreme resolved line, considering broadening action by Doppler effect for Balmer, Lyman and Paschen series

09 p1734 A70-22731

Transient partially ionized plasmas observation by two wavelength holographic interferometry, describing electron density measurements

09 p1736 A70-23186

Electron density reduction in plasma surrounding reentry vehicle due to N atom removal by water droplets injection

09 p1737 A70-23237

Kerr cell-shuttered high speed stigmatic spectrograph for shock tube electron density distribution measurement

09 p1682 A70-23503

Plasma electron density errors in measurement by microwave interferometers, noting effects of inaccurate phase shift determination

09 p1738 A70-23634

Simultaneous Thomson scatter measurements for middle and low latitudes, comparing electron density and temperature and exospheric and global temperature distributions

10 p1872 A70-23821

Temperature, pressure and electron density measurements behind reflected shocks in gas driven diaphragm shock tube compared with Rankine-Hugoniot predictions

10 p1967 A70-23960

High electron density plasma generation by ionized gaseous filament explosion, noting plasma frequency effect on spectral brightness

10 p1915 A70-23961

Electromagnetic fields in electron plasma with electron density variations due to transient ionization processes

10 p1921 A70-23978

Type 3 burst sources velocity calculated by frequency drift and Newkirk model of electron density, discussing frequency range extension of Weissenau radiospectrograph

10 p1934 A70-25274

Coupled differential rate equations governing growth and decay of positive and negative ion and electron concentrations in afterglow with ambipolar diffusion and electron attachment

11 p2088 A70-25703

Electron temperature and concentration in decaying He and Ar plasmas with cesium vapor additions

11 p2092 A70-26733

Electron density decrease in F 2 layer ascribed to 9 July 1962 thermonuclear explosion, noting dissociative recombination role

11 p2047 A70-26791

Electron concentration measurement range expansion in plasma by laser interferometer with optical signal phase modulation

12 p2278 A70-27328

N-type GaAs carrier mobility and concentrations increased slow cooling after heat treatment

12 p2289 A70-28343

Electron density determination, establishing gas pressure relation to discharge current

13 p2460 A70-28710

Coronal condensations temperature and electron density measurements at meter wavelengths and in white light

13 p2488 A70-28717

Carbon dioxide laser saturated gain constant calculated for low and high electron densities based on thermodynamic approach

13 p2425 A70-28793

Free carriers mobility and concentration in microwave semiconductors measurable by two mode resonator over temperature ranges and magnetic fluxes

13 p2470 A70-28881

Photon lifetime dependence on hole and electron concentration in GaAs from IR reflection spectra analysis

13 p2470 A70-28882

Metallic state basic parameters determined by electron transfer technique, discussing ion charges, electron and hole concentrations current scattering cross sections, etc

13 p2433 A70-28886

Electron density and transverse electron temperature of magnetoactive plasma generated in circular waveguide by microwave signal with variable polarization

13 p2462 A70-29128

Stark broadening of neutral helium line in plasmas for electron densities measurements accuracy, comparing to H beta determined densities

13 p2456 A70-29225

Radio wave transmission through magnetized plasma layer as function of electron concentration and collision frequency, using coaxial accelerator

13 p2366 A70-29377

Chromospheric flares electron concentration and structure from half widths and Balmer lines numbers

13 p2493 A70-29394

Gunn diodes I-V characteristics width as function of carrier concentration/mobility and diode length, noting role of impact ionization in strong electric field

13 p2378 A70-29408

Electron temperature and concentration determined from longitudinal electron cyclotron harmonic waves in finite plasma column

13 p2467 A70-29916

Electron density, characteristic dimensions and vertical density gradient of coronal enhancements in white light, observing elliptical cross section

13 p2479 A70-30004

Mossbauer temperature dependent isomer shift, proposing electron density change at resonant nucleus site by lattice phonons

14 p2626 A70-30483

Plasma refractive index determination by propagation method allowing simultaneous electron concentration and density measurements by reflected damped wave

14 p2622 A70-30658

Electron temperatures and electron and negative ion concentrations in low pressure hydrocarbon flames

14 p2666 A70-31098

Gaseous nebulae electron densities based on interpretation of forbidden Cl III lines using collisional strengths and transition probabilities

15 p2798 A70-31746

Electron density measurements by partial reflection and rocket techniques during 20 May 1966 solar eclipse, showing agreement below 82 km height

15 p2726 A70-31869

Glass tube surrounded nonuniform plasma column interaction with TM microwave field of cylindrical cavity for electron density measurements

15 p2780 A70-32347

Plasma electron density measurement for microwave-excited pulsed discharges based on skin effect

15 p2780 A70-32367

Electromagnetic field transmission through plasma slab with specified electron density-collision frequency profiles, using integral derived from transmission and reflection coefficient

16 p2957 A70-32979

Electron density fluctuation measurements in wakes behind hypersonic sphere projectiles, using Langmuir probes

[AIAA PAPER 70-730]

16 p2834 A70-33489

Electron density fluctuations in transitional zone of turbulent plasma jet, using digital analysis of Langmuir probe signals

[AIAA PAPER 70-731]

16 p2958 A70-33495

Thin wire Langmuir probe measurements of electron temperature and density in transition and free molecular nozzle flow of short duration reflected shock tunnel

16 p2912 A70-33864

Turbulence spectrum functions time variations, examining electron density fluctuations in ionized gas

16 p2894 A70-33886

Compact ionized hydrogen components inside galactic H II regions of lower electron density, explaining existence and evolution by various models

16 p2980 A70-34308

Reflected shock waves generation by shock produced plasma flow interaction with strong magnetic fields, determining electron density and ionization relaxation times

[AIAA PAPER 70-761]

17 p3139 A70-34490

Microwave diagnostic method for amplitude variations of electron density and collision frequency in weakly ionized plasma

17 p3140 A70-34871

Magnetized plasma electron density measurement by laser self heterodyne

17 p3141 A70-34996

Absorption coefficient of n-type indium arsenide single crystals with varying electron and doping concentrations, investigating spectral dependence

17 p3144 A70-35705

Ethyl alcohol fuel diffusion flame, examining thermal decomposition pyrolysis and free electron concentration distribution

18 p3345 A70-36113

Meteor radar echoes of parallel and perpendicular polarization from ionized transient trails with linear electron densities

18 p3317 A70-36995

Pulsar galactic longitudinal distribution, discussing observability impaired by high electron density in spiral

18 p3328 A70-37173

Pulsar distance calculation, assuming immersion in uniform average electron density medium

18 p3328 A70-37174

Electron photodetachment rate from meteor radar echo duration during night and daytime observations

19 p3515 A70-37664

Ionized argon supersonic flow velocity and local electron density by optical methods

19 p3480 A70-38173

Solar wind velocity variations showing relationship with electron density excess and localized region temperature of corona

19 p3512 A70-38693

Electron density irregularities convected past space probe relationship to radio intensity power spectrum scintillations

20 p3703 A70-39023

Particulate matter interaction with ionized gas in external magnetic field and nonequilibrium state, examining free electron density

20 p3677 A70-39324

Laminar thermal boundary layer at atmospheric pressure adjacent to cooled wall, measuring electron temperature and number density

20 p3737 A70-39990

Noble gas mixture large shock tunnel driven linear MHD generator, examining electron density, operating characteristics and electrical properties

20 p3682 A70-40012

Exhaust velocity, electron density and temperature of pulsed megawatt nitrogen MPD-ARC thruster, using Thomson scattering of pulsed laser light

[AIAA PAPER 70-1081]

20 p3694 A70-40254

Cathode spaces electron concentration, time dependence and axial distribution by laser beams interferometric method, noting accuracy and resolution

21 p3836 A70-40796

Solar radio U burst second branch low relative intensity, contradicting previous theory for trajectories

21 p3880 A70-40966

Electron-ion recombination in Ar plasma, discussing transition from collisional-radiative to dissociative process as function of electron density and temperature

21 p3858 A70-41711

Electron concentration measurement range expansion in plasma by laser interferometer with optical signal phase modulation

21 p3860 A70-42069

Electron densities between inner edge plasma sheet and plasmasphere as function of geocentric radial distance fromOGO-3 electrostatic measurements

23 p4236 A70-43834

Interplanetary plasma electron density inhomogeneities formation explained by instability due to electron stream curvilinearity obtained from spacecraft data

23 p4240 A70-44070

Limit analysis for ionization potential reduction effect on ionized gas atomic composition, considering temperature and electron density

23 p4220 A70-44435

Local thermal equilibrium validity for electron temperature and density determination in reflected shock waves in He plasma, comparing laser scattering and spectroscopic methods

23 p4229 A70-44986

Microwave recombination H lines, deriving electron temperature, electron density and emission measure sequentially

24 p4402 A70-45388

ELECTRON DENSITY PROFILES

Coronal electron densities and magnetic fields determined from K-coronameter and type 4 radio burst data

01 p0168 A70-10255

Magnetoionic mode coupling in satellite transmissions through ionosphere near transverse region, showing diurnal variations and error of electron content

02 p0259 A70-12563

Electromagnetic wave reflection on thin plasma layer with Epstein electron density profile, noting use in microwave diagnostics

03 p0529 A70-13016

Primary protons energy estimated from energy ratio with maximum extremal distribution of electron numbers in lower half of atmosphere

03 p0527 A70-13054

Carrier concentration profiles and surface resistance of Ohmic contacts to solution epitaxial n-type GaAs wafers measured by Schottky barrier capacitance

03 p0543 A70-14213

Electron density profiles alongOGO 1 orbit portions calculated by measuring harmonic radio beacon transmissions differential Doppler frequencies and Faraday polarization rotation angle

04 p0741 A70-15118

Solar helium-like ion line intensities, determining electron densities and excitation rate ratios

04 p0758 A70-15696

Ionospheric reaction coefficients estimate to correlate equatorial electron density profile and Jacchia model of neutral atmosphere

04 p0683 A70-15744

D region electron density distribution during night and presunrise period, using full wave integration method for propagation parameters for waves reflected from electron density model

06 p1054 A70-17587

Rocket measurement techniques for electron density profiles in D region, giving results from auroral zone disturbed and midlatitude quiet D region

07 p1263 A70-19152

Ionospheric radio transmission field strength calculation for given electron density and collision frequency

cy profiles, considering electron variations along transmission path

07 p1230 A70-19165

Electron concentration profiles calculated during vertically moving perturbations to evaluate ionospheric state

07 p1267 A70-19458

Descending and albedo electron fluxes at specific geomagnetic latitude and various atmospheric depths, obtaining electron energy spectrum vertical profiles

07 p1372 A70-20335

Venus ionosphere, discussing day and night electron density profiles, carbon dioxide presence, plasma interaction model, etc

09 p1750 A70-22058

Interstellar gas electron number density fluctuations effect on pulsar signals in terms of frequency dependent dispersion, noting long wavelength disturbances

09 p1764 A70-23609

Plasmaspheric columnar electron content determination up to plasmopause by ATS-3 beacon transmitter and combining differential Doppler frequency and Faraday rotation angle methods

10 p1874 A70-24430

Nocturnal E layer electron density profile dependence on solar activity

10 p1885 A70-25265

Nocturnal F layer electron density profile and temperature dependence on solar activity

10 p1885 A70-25266

Polar ionosphere inhomogeneous electron concentration by analyzing satellite signal amplitude fluctuations received by spaced interferometers

11 p2042 A70-25528

Neutral-dominated plasma turbulence, discussing space-time plasma probe correlation functions for electron density fluctuations measurements

11 p2095 A70-26757

Microwave scattering by turbulent plasma electron density fluctuations

11 p2096 A70-26765

Gas and electron density fluctuations in weakly ionized turbulent wake behind hypersonic spheres and cones

11 p1978 A70-26773

Electron beam density probe calibration for earth atmospheric reentry vehicles communication

12 p2230 A70-26982

Topside ionosphere structural analysis, considering electron density profiles deduced from Alouette 2 satellite data

12 p2226 A70-28062

Ionospheric electron density profiles at various altitudes, using HF impedance probe method

12 p2227 A70-28261

Topside ionosphere structure deduced from electron density profiles observed by Alouette 2 satellite

13 p2395 A70-29090

Electron density profiles interpretation for quiet daytime D region, noting role of electron-positive ion recombination coefficient

13 p2397 A70-29192

Alouette 1 plasma resonance observations, analyzing electron density measurements in sheath region and cyclotron harmonic resonant frequencies

13 p2466 A70-29903

Electron density profile calculation method using ionograms on analog-digital computer

14 p2569 A70-30209

Ionospheric reaction coefficients estimate to correlate equatorial electron density profile and Jacchia model of neutral atmosphere

14 p2576 A70-30828

Mars upper atmosphere refractivity, free electron number density and plasma temperature altitude profiles from Mariner 1969 radio occultation measurements

14 p2646 A70-31072

Ionospheric electron density profiles between two locations calculated from oblique incidence ionograms, plotting radio path for ground range

15 p2726 A70-31861

Microwave probe for measuring electron density profile in supersonic arc jet plasma

15 p2741 A70-32433

Radiative transfer in spherical stellar atmosphere, considering free electrons density gradient and thermal motions, atmospheric layer curvature, optical thickness, etc

15 p2732 A70-32905

Iterative solution for electron density profiles from topside ionograms

16 p2900 A70-29391

Electron concentration profiles in blunt nose vehicle shock layer during atmospheric near orbital entry at high altitudes, using finite rate chemistry

16 p2837 A70-33865

Mean electron density profiles and fluctuations in equilibrium high speed turbulent boundary layers, calculating temperature effects

[AIAA PAPER 70-743]

17 p3066 A70-34500

Time span in total electron content (TEC)/measurements on BE-B and BE-C ionospheric satellites by differential Doppler method, applying chi sub O super 2 test

17 p3077 A70-34986

Mutual coherence function of light scattered by plasma turbulent electron density fluctuations, taking into account refractive index changes

17 p3137 A70-35722

Electron concentration distribution over plasma discharge cross section, using interferometry

17 p3142 A70-35732

Electron density large scale structure in plasmasphere identified from whistlers recorded at Antarctica near sunspot minimum

18 p3311 A70-36012

Latitude profiles made of low energy solar electrons over polar cap, finding latitude knee position

18 p3306 A70-36020

Spatial-temporal distribution of laser spark plasma electron density and temperature based on holographic interferometry

18 p3265 A70-36152

Electron concentration profiles calculated during vertically moving perturbations for evaluation of ionospheric state

18 p3250 A70-36932

F 1 region unsteady model, examining vertical distribution profile of electron concentration on summer day

19 p3409 A70-37323

Vertical electron density profile variations during ionospheric perturbations in years of solar activity maximum and minimum

19 p3409 A70-37328

Sporadic ionization occurrences nighttime observation in auroral E region, describing vertical electron concentration profile

19 p3410 A70-37331

Electron temperature and concentration profiles behind shock front from IR emission and absorption simultaneous measurement, applying method to xenon ionization and recombination processes

19 p3402 A70-37443

Electron density measurements by rocket observation during PCA after solar flare of 25 February 1969, deriving effective loss rates in terms of recombination model

19 p3496 A70-37511

D region electron density profiles during solar eclipse from X ray rocket and satellite observations

19 p3419 A70-38913

Vertical electron concentrations in upper F region during solar eclipses in South Atlantic from satellite observation

19 p3419 A70-38920

Laser interferometry with unstable external resonator, determining radial electron density distributions during implosion phase of linear z-pinch discharge in argon

20 p3630 A70-39420

D region electron density profiles from high power wave interaction measurements during solar flare, indicating non-X-ray production rate

21 p3879 A70-40942

Solar wind free electron number density measurement by Pioneer 6 spacecraft after solar proton flare, constructing plasma cloud models

21 p3881 A70-41079

D region electron density profiles, using magnetoionic differential-phase partial-reflection technique

21 p3818 A70-41100

Polar ionosphere inhomogeneous electron concentration by analyzing satellite signal amplitude fluctuations received by spaced interferometers

21 p3819 A70-41278

Electron density profiles calculation from model atmosphere, deriving F 2 layer ionization vertical distribution

22 p4023 A70-43303

Ionization rate and electron density height profiles for typical auroral proton energy spectrum, noting radio noise absorption, sporadic E and radio aurora

22 p4024 A70-43307

E region electron concentration profiles, using ground sounding equipment allowing accurate signal reflection altitude measurements

23 p4190 A70-44078

Electron density and collision frequency distributions in lower ionosphere, deriving error limits from VLF and LF sounder data

24 p4314 A70-46127

Electron density profile calculation method using ionograms on analog-digital computer

24 p4330 A70-46284

ELECTRON DETECTORS

U ELECTRON COUNTERS

ELECTRON DIFFRACTION

Precipitation in Ni-base superalloy analysis with dark field electron microscopy and electron and X ray diffraction

01 p0119 A70-10730

Cu, W and oxidized W adhesion to Ni surface, examining before and after adhesion contact with low energy electron diffraction

[ASLE PREPRINT 69-LC-13]

02 p0318 A70-12535

Low energy electron diffraction structures due to Re crystal surface interaction with CO and molecular oxygen at high temperatures

03 p0440 A70-13098

Electron transmission diffraction patterns of thin monocrystal films using Ar laser

06 p1080 A70-17444

Supersonic molecular free jets using electron diffraction technique, discussing vibrational and condensation states

06 p1044 A70-18301

Inelastic scattering of electrons by surface plasma oscillation for low energy electron diffraction and photoemission, interpreting surface plasmon excitation

07 p1337 A70-19359

Low energy electron diffraction pattern from surface steps and facets resulting from recrystallization of Re single crystal

08 p1557 A70-21602

Ni-Mo surface alloys investigated by low energy electron diffraction, using tabulated symmetry and extinction properties of space groups and phase diagrams

08 p1557 A70-21603

Intensity vs voltage curves for LEED beams from clean Ni surface, calculating Bragg spectrum with energy diagram method

10 p1927 A70-24077

Ferromagnetic cubic sulfide of Fe easy axis by electron diffraction pattern, aligning sulfide particles along magnetic field

13 p2472 A70-29712

Low energy electron beam diffraction, calculating intensity as wavelength function

14 p2619 A70-30489

Thin film sandwich Ag/Ni/Cu, demonstrating multiple electron diffraction

14 p2627 A70-30724

Critique of paper on electron diffraction study of Ce adsorption on W surface, discussing electron work function changes and data discrepancies

19 p3473 A70-37548

Dielectric layer and screen heat loss effects on diffraction radiation in resonant waveguide

19 p3377 A70-37725

Multichannel monitor for repetitive short scan Auger electron spectroscopy for surface composition changes, using low energy electron diffraction

21 p3827 A70-41467

Al alloys structural analysis using electron diffraction pattern techniques

24 p4360 A70-45737

ELECTRON DIFFUSION

Resonance scattering and drift motion of electrons in gases under pressure, determining ion state lifetime and mean electron-molecule collision frequency for trapping collisions

02 p0342 A70-11883

Transistor admittance and diffusion parameters in direct measurement with varying frequency, evaluating reliability

03 p0459 A70-14285

Current carrier motion and diffusion capacity in p-n junctions with highly doped regions under large variable signal

05 p0892 A70-16197

Electron energy equation for nonequilibrium plasmas, assuming large electron diffusion velocity and current density and enhanceable electron temperature

06 p1123 A70-18299

Electron diffusion in magnetosphere, describing experimental model

07 p1367 A70-19494

Electron diffusion in trap with magnetic mirrors under pulsed field perturbations, determining coefficients by numerical integration of drift equation

10 p1931 A70-24311

Cosmic ray electrons during propagation in interstellar space analyzed for energy spectrum modulation

10 p1816 A70-24633

Electrons thermodiffusion and energy transport coefficients in noble gases at mean reduced electric field intensities, obtaining distribution functions

11 p2089 A70-25868

Minority carrier diffusion lengths on sides of copper sulfide-cadmium sulfide heterojunctions measured by light microprobes

13 p2471 A70-29709

Electron mobility, diffusion, drift velocity and attachment in oxygen, determining Townsend primary ionization coefficient

15 p2776 A70-31969

Electron diffusion in magnetosphere, describing experimental model

15 p2795 A70-32739

Outer zone electrons radial diffusion coefficients and lifetimes determined as functions of magnetic shell parameter, based on satellite measurement following geomagnetic storm

23 p4236 A70-43831

Conducting state propagation in p-n-p structure involving minority carrier diffusion between regions

23 p4232 A70-45068

- Cosmic ray electrons solar modulation, considering diffusion-convection theory 24 p4397 A70-45769
- ELECTRON DISTRIBUTION**
- NT ELECTRON DENSITY PROFILES**
- Quasi-linear ion oscillation theory for Maxwellian plasma, considering electron and ion distribution perturbations and energy transfer 02 p0346 A70-12105
- Characteristic X radiation intensity in atmosphere calculated using irradiating electrons spatial and energy distribution data 02 p0358 A70-12156
- Electron distribution function for steady homogeneous plasma of arbitrary ionization degree under strong electric fields, discussing kinetic equations for elastic and nonelastic encounters 02 p0346 A70-12231
- Excess electron and combined electron-positron angular distributions compared in electron photon cascade showers, considering Coulomb scattering 03 p0556 A70-13048
- Electron multiple scattering theory graphic approximation showing angular distribution in electron beam 03 p0527 A70-13053
- Kinetic theory for calculating electron distribution function of weakly ionized plasmas in arbitrarily time dependent electromagnetic fields 05 p0886 A70-15800
- Angular distribution of particles in electron photon showers without recourse to Landau approximation 05 p0899 A70-15960
- Electron distribution function in quasi-static free moderately ionized plasma with partial radiation trapping determined from electron-electron collisions 05 p0889 A70-16452
- Cerenkov radiation in infinite anisotropic electron plasma linearly polarized in magnetic field having linear electron distribution moving with uniform velocity 06 p1120 A70-17538
- Electron distribution functions in weakly ionized plasmas by asymptotic analysis of boundary layer near wall 06 p1121 A70-17903
- Collisional skewing of electron distribution function associated with heat conduction in solar wind, exciting collisionless ion-acoustic, electrostatic ion cyclotron and magnetoacoustic waves 06 p1136 A70-18527
- Quasi-linear feedback effect of enhanced ion-wave fluctuations on average electron distribution in current-carrying plasma 07 p1338 A70-19822
- Mathematical model of extensive air showers, calculating lateral distribution of photoelectronic component at all altitudes 08 p1560 A70-20598
- Anisotropic angular distribution of electrons and ions emitted from W targets irradiated by ruby laser pulses 08 p1512 A70-21211
- Plasma instabilities in solar wind for frequencies near proton gyrofrequency, driving instabilities by electron and proton thermal anisotropies 08 p1561 A70-21261
- Relativistic electrons synchrotron radiation by calculating magnetoactive plasma permittivity tensor, determining normal waves polarization characteristics 08 p1554 A70-21812
- Ionospheric electron content and distribution determination from Explorer 22 satellite signal amplitude recordings, considering wave propagation and polarization and Faraday effect 09 p1633 A70-22530
- Solar cosmic ray ionization of upper atmosphere, calculating electron production rate distribution 10 p1934 A70-25199
- Ultrarelativistic electrons cone instability in Van Allen radiation belts, discussing distribution function, relativistic effects and electron lifetimes 11 p2104 A70-25529
- Photomultipliers single electron response by measuring electron pulse height distribution 12 p2236 A70-27850
- Electric field sense and magnitude determination from lunar particle shadows in solar electron fluxes 13 p2492 A70-29196
- X ray K spectra of Ti-Cr alloy for electron structure in titanium chromide phase region, discussing spectral intensities 13 p2435 A70-29375
- Type 3 solar bursts theory covering beam-type instabilities and quasi-linear relaxation of fast electron distribution functions 13 p2478 A70-29389
- Interstellar electron gas distribution and temperature, suggesting cosmic ray heating as main ionization source 13 p2495 A70-29796
- Ionization coefficient calculation for preionizers through electron distribution function solution to Boltzmann equation 13 p2468 A70-29962
- Van Allen radiation belts energetic electrons injection and distribution due to magnetic storms, using satellite-borne spectrometers 13 p2483 A70-30090
- Ionospheric electron distribution by true height analysis of oblique incidence HF radio wave sounding data, applying to forward and ground backscatter 14 p2550 A70-30745
- Electron distribution for transport coefficients in Lorentzian plasma under magnetic field, determining electrical conductivity, thermal diffusion and viscosity 14 p2623 A70-31033
- Transport properties of partially ionized argon based on electron velocity distribution function, comparing to Chapman-Enskog calculations 15 p2774 A70-31799
- Spatial electric field variations and electron distribution for beam plasma amplification, using nonlinear approximation 16 p2959 A70-34336
- Local system interstellar medium thermal electron distribution, synchrotron radiation emissivity, cosmic ray electron flux and spectrum 17 p3152 A70-35583
- Electron momentum distribution function of p-type semiconductor with arbitrary band structure under electric and magnetic fields 17 p3144 A70-35704
- Electrons lateral distribution in large air showers determining inelasticity of high energy nuclear interactions 18 p3305 A70-35947
- Multivalley semiconductors electrical conductivity anisotropy, discussing redistribution and electron transfer under strong electric field 19 p3483 A70-37294
- ESRO 1 satellite and ground observations of energetic auroral electrons angular distribution during solar event, using Geiger counters 19 p3412 A70-37519
- Stepwise ionization effect on electron distribution, transport and balance coefficients in low voltage low pressure neon plasma 19 p3476 A70-37555
- Primary cosmic ray electron flux, energy spectrum and east-west asymmetry, using balloon-borne spark chamber detector 19 p3503 A70-38104
- Polarization in inverse Compton effect for arbitrary photon and electron distributions, discussing monochromatic photon beam 19 p3524 A70-38696
- Phase rate of plasma potential variations in fast ionization waves without electron distribution assumptions 21 p3856 A70-40949
- Ultrarelativistic electrons cone instability in Van Allen radiation belts, discussing distribution function, relativistic effects and electron lifetimes 21 p3882 A70-41279
- Homogeneous plasma in unidirectional oscillatory electric field, solving Boltzmann equation by electron distribution function expansion 23 p4225 A70-44240
- Electron distribution function in homogeneous ionized plasma under oscillating electric fields and steady magnetic fields, solving Boltzmann transport equation 23 p4226 A70-44248
- Static spherically symmetric charged mass distribution exact solutions derived for electrons in scalar tensor theory of gravity by Hamilton-Jacobi method 23 p4222 A70-44403
- N type GaAs doped with Si, conductivity anisotropy observed from measurement and explanation in terms of electron distribution 23 p4231 A70-44890
- ELECTRON EMISSION**
- NT FIELD EMISSION**
- NT PHOTOELECTRIC EMISSION**
- NT SECONDARY EMISSION**
- Energy distributions of emitted electrons from Si, GaP and ZnS semiconductors, determining relative core levels and Si valence band states optical density 03 p0537 A70-12879
- Autoelectron and autophotoelectron emission from Fe-doped p-type GaAs cathodes in vacuum, noting I-V and emission characteristics dependence on light flux 03 p0538 A70-13067
- Electron efflux effectiveness from discharge plasma into vacuum, investigating various electrodes influence 04 p0724 A70-14415
- MHD generator cathode current-sheath voltage characteristics for thermionic arc spot emission mode, noting role of cathode temperature [ASME PAPER 69-WA/HT-51] 04 p0625 A70-14797
- Anode work functions from cesiated metal surfaces as parameters for thermionic converter systems analysis 04 p0627 A70-14946
- Physical conditions required to explain observations of radio galaxies through electrons of secondary origin, considering spectral characteristics and evolution 04 p0742 A70-15716
- Electron work function variation of W in Ba-Cs-Sr vapor combinations determined using thermionic diode 05 p0891 A70-15974
- Electron ejections from nuclei of radio galaxies and quasars on basis of plasma stability, discussing role of relativistic electrons and resulting unstable pinch 05 p0917 A70-16901
- Electron beam fluorescence in rarefied air flow at low static temperature used to study influence of secondary electron emission on rotational temperature measurements 06 p1123 A70-18300
- Secondary electron emission coefficients and energy distributions to investigate interaction between positive ions and Cu/Be dynodes of electron multiplier 07 p1344 A70-20127
- Laser-induced electron emission from metals and insulators in form of evaporated films and single crystals, discussing many-photon photoelectric effects and thermionic emission 08 p1556 A70-21509
- Seeded dense plasma-electrode system behavior, studying effect of adsorption and emission from boundary surfaces 11 p2090 A70-25952
- Electrostatic probes response due to thermionic electron emission, considering I-V characteristics and space-charge-limited current 13 p2459 A70-28635
- Emission resonances at harmonics of electron cyclotron frequency in laboratory plasmas, considering stellar optical radiation 13 p2467 A70-29915
- Photoemission of electrons and holes from Al into aluminum oxide, giving approximate energy band diagram of Al-aluminum oxide interface 15 p2783 A70-31759
- Low energy electron emission during solar flares relation to radio and X ray emission 15 p2795 A70-32622
- Electron emission effects on ion sheath and probe characteristics in continuum argon plasma 17 p3083 A70-34994
- Tungsten exploding wires electron emission during vacuum melting 17 p3137 A70-35726
- Low energy ion beam system for studying electron ejection from controlled metal surfaces, describing vacuum, ion source, lens and mass spectrometer components 18 p3261 A70-37086
- Photoelectron production and escape flux at midlatitudes, using spectrometric measurements from ISIS-1 satellite 21 p3818 A70-41102
- Precious metals, measuring tension, grinding and polishing induced surface plastic deformation effects on electron work function and exoemission 23 p4204 A70-43927
- Surface potential and electron work function of single crystal plane W/110 under zero-field and strong-field conditions 23 p4230 A70-44797
- Pi geomagnetic micropulsations relation to magnetotelluric energetic electron bursts, from ground based midlatitude magnetic observatories and IMP-1 data 23 p4193 A70-44924
- Microwave recombination H lines, deriving electron temperature, electron density and emission measure sequentially 24 p4402 A70-45388
- Laser operation instability with nonlinear filter, deriving electrons differential velocity distribution functions on inhomogeneous emitter 24 p4352 A70-45469
- Field emission from narrow 3d bands of ferromagnetic nickel, calculating 3d and free electron transmission coefficients ratio, using triangular surface barrier model 24 p4391 A70-45671
- ELECTRON ENERGY**
- NT ELECTRON STATES**
- Longitudinal and transverse temperature distribution measurement of electrons in electrostatic field and ion current density in ionized Cs plasma beam, determining energy spectra 01 p0149 A70-10170
- Energy spectrum of electrons and holes in semiconductors under strong electromagnetic wave field, calculating electron-phonon interaction Green function 01 p0155 A70-10184
- Daytime ionospheric electron temperature as function of electron-neutral particle collision reaction and nonlocal heating effect 01 p0170 A70-10407
- Internal gravity waves theory to interpret large amplitude oscillations in electron density and temperature and ion temperature and velocity observed in thermosphere 01 p0079 A70-11215

Heat sources in E region from electron temperature data analysis recorded by rockets during eclipses in July 1963

01 p0082 A70-11491

Electron gas heating at E region altitudes as function of ionization of atmospheric gases, noting rocket experiments during solar eclipse

01 p0082 A70-11492

Ionospheric measurements of electron density, electron and ion temperature profiles from strength of incoherent radio wave scattering

01 p0082 A70-11530

Auroral electron energy diurnal variation, noting ground observations of polar auroras, riometric absorption, vertical changes in ionization layer maximum position, etc

01 p0083 A70-11535

Calorimetric measurement of electron temperature in collisionless shock wave propagating in plasma column, discussing role of H beta line Stark broadening

01 p0153 A70-11589

Cosmic ray primaries and secondaries direct heating of thermal electrons for computation of H I regions electron densities and temperatures

02 p0363 A70-11782

Characteristic X radiation intensity in atmosphere calculated using irradiating electrons spatial and energy distribution data

02 p0358 A70-12156

Plasma electron temperature and density in Tokamak T3 toroidal discharge measured by Thomson scattering of laser light

02 p0346 A70-12199

Electron transverse and perpendicular drift velocities calculated at moderate and strong magnetic fields for hydrogen, using Maxwellian energy distribution and equivalent pressure concept

02 p0348 A70-12654

Quiet time primary cosmic ray electron flux and energy spectrum from 10 to 200 Mev in interplanetary space observed byOGO 5 satellite

03 p0553 A70-12902

Ionization and electron temperature dependence on shock wave structure in partially ionized hydrogen plasma allowing for luminescent energy losses

03 p0465 A70-13060

Neutron star X synchrotron radiation from gas accretion producing strong magnetic field with high electron temperature

03 p0557 A70-13220

Semiconductors low temperature electron energy losses due to inelastic electron scattering at neutral impurity donors shown to exceed scattering losses at phonons

03 p0539 A70-13423

Energy distribution function of electrons in weakly ionized plasma layer at electrode calculated, allowing for possible plasma concentration inhomogeneities

03 p0540 A70-13525

Electron density and temperature in ionized gas created by thermal collisions between neutral particles, analyzing chemical ionization and inelastic collisions influence

[ONERA-TP-752] 03 p0532 A70-13631

Electron temperature and density data obtained during Alouette satellite passage over middle latitude red arc, noting influence of intersecting magnetic field lines

03 p0476 A70-13911

Dissociative attachment of low energy electrons in nitrous oxide as function of gas temperature

03 p0441 A70-14006

Electron temperature anisotropy in ionospheric plasma for case of ionizing sunlight propagating along geomagnetic field

03 p0479 A70-14376

Electron temperature of hydrogen-oxygen flame plasma obtained by floating probe method compared to spectroscopic method results

03 p0608 A70-14380

Electron thermal capacity of d-transition metals for stable configurations determined by X ray spectral analysis

04 p0721 A70-14408

Electron temperature and particle density measurements in annular MHD duct, demonstrating Hall effect existence

04 p0725 A70-14532

Flux, energy spectrum and charge composition of primary cosmic ray electrons measured, determining energy spectrum of primary positrons above 220 Mev

04 p0739 A70-14595

Electron heat transfer to spherical body in nonequilibrium quiescent plasma by asymptotic solution

[ASME PAPER 69-WA/HT-56] 04 p0727 A70-14793

Explorer 31 Langmuir probe data for electron temperature at conjugate point, tracing magnetic field line passing through spacecraft to earth

04 p0000 A70-14971

NO ion dissociative recombination rate coefficient determined in high temperature air plasma from electron temperature and number density measurements

04 p0675 A70-15583

Hard electron bremsstrahlung measurement during intense polar aurorae in January and February 1968, determining electron flux penetration region

04 p0682 A70-15731

Mercury plasma flow rate change effect on electron temperature and density in thermoelectric converter determined by spectroscopy

05 p0887 A70-16028

Nonequilibrium Cs plasma electron density, temperature and sustaining field using theoretical analysis and probe measurements

05 p0887 A70-16108

Electron temperature dependence of molecular neon ions recombination with electrons using microwave afterglow/mass spectrometer, obtaining recombination coefficient

05 p0885 A70-16468

Electron momentum distributions from Compton profiles of Li-Mg polycrystalline samples, exhibiting discontinuity at free electron value of Fermi momentum

05 p0892 A70-16471

Electron energy distribution function for carbon dioxide laser plasmas in gas mixtures, discussing dissociation products role in electron energy exchange

06 p1080 A70-17447

Ion and electron density, electron temperature and space potential measured in ion wake formed by Gemini spacecraft using sensors on Agena Target Vehicle

06 p1066 A70-18285

Electron energy equation for nonequilibrium plasmas, assuming large electron diffusion velocity and current density and enhanceable electron temperature

06 p1123 A70-18299

Electric field in earth magnetotail via Explorer 33 and 35 satellite observation of solar electrons above 50 kev energy

06 p1058 A70-18528

Temporal behavior of energetic particle precipitation during auroral substorm, discussing electron energy spectra and pitch angle distributions

06 p1059 A70-18536

Equivalent excited-state temperature of high pressure plasma calculated for unequal electron and gas temperature, considering ion and electron recombination

06 p1114 A70-18634

Midlatitude upper atmosphere soft electron energy flux nighttime measurements by sounding rocket

07 p1368 A70-19500

Waves and differential equations for electromagnetic field in nonuniform magnetized plasma described for all orders in electron and ion temperature

07 p1350 A70-19823

Electron density dependence on electron temperature during self and mutual interaction of electromagnetic waves in magnetoplasma, tabulating numerical results

07 p1351 A70-19968

Descending and albedo electron fluxes at specific geomagnetic latitude and various atmospheric depths, obtaining electron energy spectrum vertical profiles

07 p1372 A70-20335

Auroral electron energy distribution and ionization rates characteristics based on satellite and rocket measurements

08 p1487 A70-20642

Plasma temperatures in magnetosphere, investigating ion energy balance, electron heating and agreement with rocket measurements

08 p1489 A70-21381

Electron-to-ion temperature ratio determined from ion and plasma line components of radar Thomson scatter signal from ionosphere

08 p1489 A70-21389

Neutron star X synchrotron radiation from gas accretion producing strong magnetic field with high electron temperature

08 p1563 A70-21653

Statistical correlation between polar magnetic disturbances and magnetospheric energetic electron flux increase from IMP-1 satellite observations

08 p1491 A70-21714

Thermal and nonthermal plasmas for ion production, discussing gas pressure, voltage and discharge current effects on electron temperature

09 p1734 A70-22037

High energy electrons elastic scattering from 2s-1d shell nuclei based on Dirac equation solution in Glauber approximation

09 p1730 A70-22043

Electron temperature distribution in thermal boundary layer about probe electrodes calculated by successive approximations allowing for electron heating by arc

09 p1734 A70-22167

Electron temperature resonance probe to eliminate effects of geomagnetic field, rocket velocity and random noise

09 p1675 A70-22422

Photoemission analyzer with finite emitter in spherically symmetric retarding field with magnetic field present, analyzing energy resolution

09 p1679 A70-22988

Fast electrons spatial distribution for multiple scattering in nitrogen and argon, noting target thickness and incident energy

09 p1735 A70-23179

Electron and proton temperature differential near earth bow shock determined from plasma probe measurements by Vela 4B satellite

09 p1670 A70-23486

Satellite observational data on time history of inner radiation belt /October 1963-December 1968/

09 p1746 A70-23488

Multibeam O-type TWT characteristic equation analyzed for arbitrary space diversity, calculating gain for various velocity parameter values and electrical lengths

09 p1651 A70-23638

TWT characteristic equation with arbitrary coupling between two electron beams over wide range of velocity difference, analyzing wave amplitude constant

09 p1651 A70-23639

Ionospheric photoelectrons resulting from solar UV radiation interaction with atmospheric gases, obtaining escape fluxes using Monte Carlo method

09 p1747 A70-23667

Energy spectra of electrons transmitted through Be, Al and Au targets measured for incident electron energy

10 p1918 A70-23984

Laser radiation conversion into kilovolt X rays using planar heated plasma, discussing electron temperature role

10 p1921 A70-23987

Electron-ion beam plasma system, using one dimensional quasi-linear equations for describing electron heating and stabilization

10 p1923 A70-24403

Rocket-borne spectrometer for measuring 1-13 kev electron fluxes in auroral zone, describing design, operation and calibration

10 p1889 A70-24493

Bright rims in North America Nebula, measuring electron temperature to derive profile characteristics

10 p1944 A70-24956

Longitudinal and transverse temperature distribution measurement of electrons in electrostatic field and ion current density in ionized Cs plasma beam, determining energy spectra

10 p1925 A70-25016

Electron temperature distribution behind strong shock wavefront in air measured by electrostatic probe and compared to results of spectral line inversion method

10 p1871 A70-25114

Small parameter structure and propagation velocity of ionization front in gas, applying nonequilibrium plasma model and electron equation

10 p1926 A70-25191

Electron energy loss spectrum in Ti measured by bombarding thin films vacuum deposited on NaCl crystal with electrons of intermediate energy

11 p2065 A70-25376

Electron temperature diurnal variations data from rocket soundings used for determining recombination coefficient in E region

11 p2044 A70-25550

Foreign gases effects on He-Ne lasers IR emission, describing quenching due to positive column electron temperature decrease

11 p2062 A70-25826

Electron temperature and concentration in decaying He and Ar plasmas with cesium vapor additions

11 p2092 A70-26733

Ionospheric electron and ion temperatures information extraction from Doppler broadening of radar returns based on correlation measurement

12 p2183 A70-27163

Energetic electron layer near magnetopause attributed to geomagnetic activity from satellite observations of fluxes

12 p2292 A70-27180

Latitudinal ionospheric electron density and temperature variations at 1000 km within and near auroral zone

12 p2222 A70-27186

Electric field heating effect on edge photoluminescence of n-type GaAs, noting increase in electron energy

12 p2286 A70-27368

Low energy electron flux as interplanetary radiation primary component, considering data from IMP-1 observations

12 p2292 A70-27383

Electromagnetic inductive shock tube design and wave velocity, electron temperature and plasma conductivity measurements

12 p2206 A70-27400

Ionospheric electron density, electron and ion temperature profiles measurements, comparing relative merits of radio-rocket ground-based radar and satellite methods

12 p2223 A70-27727

E region plasma parameters measurement by in situ probes, considering electron density and temperature

12 p2225 A70-27737

Electron impact excitation cross section of $/0,0/$ first negative band of nitrogen ion from threshold to 3 keV, using photon counting techniques

12 p2276 A70-27880

Alternating electric field effect on weakly ionized gases, analyzing electronic temperature and harmonics generation

13 p2458 A70-28560

Free electrons non-Maxwellian equilibrium kinetic energy distribution function, considering partially ionized hydrogen-like plasma in thermal equilibrium

13 p2459 A70-28634

Probe diagnostic techniques for ionospheric electron density and temperature measurement, describing results from P53H firing

13 p2404 A70-28691

Precipitated energetic electrons attenuation and impact ionization in ionosphere, determining vertical energy distribution profile

13 p2476 A70-28722

Current density distributions in Ar-K plasma streams through channel with segmented electrode array, measuring electron temperatures

13 p2461 A70-28732

Ionospheric electrons velocity distribution function in steady state with oscillating electric field imposed in arbitrary direction with respect to magnetic field

13 p2395 A70-28941

Electron density and transverse electron temperature of magnetoactive plasma generated in circular waveguide by microwave signal with variable polarization

13 p2462 A70-29128

Rotational and vibrational temperature effects on neutral gas and electron temperature and density in high pressure discharge plasma diagnostics

13 p2462 A70-29129

Northern auroral regions low energy electron fluxes survey by Injun 4 satellite during minimum solar activity

13 p2477 A70-29184

Piezoelectric scattering effects on electron temperature and mobility in IIB-VIA semiconductor compounds with nonparabolic conduction band

13 p2471 A70-29373

Energy spectrum of electrons accelerated in linear plasma betatron close to potential compared to cyclic betatron results

13 p2463 A70-29379

Cosmic rays intensity frequency spectrum near earth, indicating relativistic electron energy spectra similarity in interstellar space and galactic particles existence

13 p2478 A70-29388

Attenuation length of vacuum UV photoexcited electrons in evaporated metal films, observing lack of dependence on photon energy

13 p2472 A70-29711

Interstellar electron gas distribution and temperature, suggesting cosmic ray heating as main ionization source

13 p2495 A70-29796

Electron temperature and concentration determined from longitudinal electron cyclotron harmonic waves in finite plasma column

13 p2467 A70-29916

Ionized impurity scattering in polar semiconductors by strong electric fields, using energy and momentum conservation equations in electron temperature approximation

13 p2472 A70-30017

Electron and positive ion velocity distributions measurements near earth bow shock by electrostatic analyzer on Vela 4B satellite

13 p2481 A70-30068

Spatial distribution and directional anisotropies of tail plasma sheet energetic electrons from measurements by electrostatic analyzer and energetic particle experiments on Vela 4

13 p2482 A70-30071

Diffusion loss model for cosmic ray electron propagation in galaxy, considering direct and radio observations

14 p2631 A70-30538

Light scattering from plasmas with nonMaxwellian electron velocity distribution function

14 p2622 A70-30694

Hard electron bremsstrahlung measurement during intense polar aurorae in January and February 1968, determining electron flux penetration region

14 p2575 A70-30816

Small amplitude HF electromagnetic wave penetration in hot plasma slab, showing wave period/transit time ratio dependence of electromagnetic field distribution

14 p2551 A70-31037

Flame ionization, extra-equilibrium excitation and electronic temperature resulting from electron collisions with gas molecules

14 p2666 A70-31096

Electron temperatures and electron and negative ion concentrations in low pressure hydrocarbon flames

14 p2666 A70-31098

Electron and ion temperature and electron density relationship in F region during sunspot maximum, using incoherent scatter experiment

14 p2581 A70-31271

Scalar-tensor theory in canonical form, discussing neutral particle and electron self energy problem

15 p2773 A70-31439

Transverse kinetic energy of electrons at outlet of magnetron-injection gun as function of cathode inclination and magnetic induction

15 p2707 A70-31504

Ionospheric electron concentration and temperature measurements by cylindrical Langmuir probe on rockets and satellites, emphasizing error sources

15 p2723 A70-31657

Langmuir probe comparison to electron temperature probe measurements of ionospheric electron temperature during rocket flights

15 p2734 A70-31674

Collisionless shock waves in magnetized plasma as function of Alfvén-Mach number, measuring electron temperature jump on wave front spectroscopically

15 p2779 A70-32116

High energy electron temperature in beam plasma discharge pulsed laser measured by bremsstrahlung X radiation spectrum

15 p2752 A70-32194

Midlatitude upper atmosphere soft electron energy flux nighttime measurements by sounding rocket

15 p2795 A70-32745

Electron energy losses at interface of helium inclusions in aluminum irradiated by radioactive lithium

15 p2785 A70-32764

Gas dynamic molecular laser with electrons in ground state, using incoherent optical pumping from stationary shock wave

16 p2927 A70-33255

Electron energy loss per collision in Cs vapor discharge, measuring electric field and electron temperature by Langmuir probes

16 p2954 A70-33281

Probe measurements in Cs plasma formed by contact ionization with hot wire for density, electron temperature and space potential

16 p2958 A70-33624

Low energy electron impact spectrometry, discussing apparatus, procedures, electronic excitation of gas molecules, etc

16 p2857 A70-33797

Equatorial F 2 region response during solar eclipse of 7 March 1970, emphasizing ionization production and loss, transport processes and electron temperature

16 p2897 A70-33826

D region electron energy loss factor during solar eclipse of 7 March 1970, using wave interaction technique

16 p2898 A70-33834

Thin wire Langmuir probe measurements of electron temperature and density in transition and free molecular nozzle flow of short duration reflected shock tunnel

16 p2912 A70-33864

Jovian decimeter radiation, discussing electron drift velocity in dipole field, characteristic time for energy loss and radiation belt dimensions

16 p2980 A70-34192

Lorentz plasma electron velocity distribution with allowance for elastic and inelastic collisions, using Legendre polynomial and spherical harmonic expansions in Boltzmann equation

16 p2945 A70-34337

Time resolved measurements of ion and electron temperature in pulsed Ar ion laser discharge, observing heating

17 p3108 A70-35907

Hydrogen, He and oxygen ion density, and ion and electron temperatures in upper ionosphere from OGO 4 observations

18 p3244 A70-36016

Magnetic probes effectiveness study of electron heating behind shock wave front in plasma, measuring electron temperature

18 p3294 A70-36149

Orion nebula core radio recombination line intensities, showing variations in mean electron temperatures and physical conditions

18 p3313 A70-36329

Sample dimensions effect on shape of I-V curve caused by overheating in media with ambiguous dependence of electron temperature on field

18 p3298 A70-36621

Electron energy effect on output power and beam divergence of electron beam pumped GaAs lasers

18 p3269 A70-36740

Electronic excitation contribution to frozen properties and cut-off criteria of high temperature gas plasma

18 p3296 A70-36955

Stellar atmosphere radiation field quantity vs quality, deriving electron temperature as function of tau

18 p3309 A70-37007

Electron temperature in 500-1000 km range during minimum solar activity based on Alouette satellite data and atmospheric model, observing latitudinal variation

18 p3254 A70-37029

Electron temperature and concentration profiles behind shock front from IR emission and absorption simultaneous measurement, applying method to xenon ionization and recombination processes

19 p3402 A70-37443

Solar cosmic ray protons and electrons increase during 25 February-5 March 1969 observed by Venus 5 and 6 space probes, discussing interplanetary medium disturbance

19 p3495 A70-37504

Cosmic ray electron and low energy proton fluxes by satellite-borne detector during solar flare of 25 February 1969

19 p3496 A70-37507

Ionospheric electron density and temperature variation measurements after solar proton event of 25 February 1969, using ESO 1 satellite

19 p3411 A70-37514

Trapped and precipitated electron observations at northern high latitudes in 45-450 keV range, using ESO-1 satellite

19 p3496 A70-37515

Low energy electron and proton measurements by ESO 1 satellite, discussing electron spectra, auroral zones and proton precipitation

19 p3412 A70-37516

ESRO 1 satellite and ground observations of energetic auroral electrons angular distribution during solar event, using Geiger counters

19 p3412 A70-37519

High energy solar electrons observed by HEOS-A1 satellite, discussing semitransparent barrier existence at distance from sun

19 p3497 A70-37521

Electron intensity long term variations above 500 MeV by OGO-5 satellite-borne cosmic ray electron detector, supporting diffusion-convection theory of solar modulation

19 p3497 A70-37522

Ion density and electron temperature variations as function of maximum electric field density in independently excited plasma column striations

19 p3475 A70-37552

Microwave diagnostics of electron density, temperature and light emission in self excited moving striations in hydrogen plasma

19 p3475 A70-37553

Sodium line in meteor spectrum, determining electron temperature and number of atoms as velocity and height function

19 p3514 A70-37600

Helium to electron excitation ratios for population inversion in helium-neon laser

19 p3445 A70-37758

Primary interplanetary electron energy spectrum, using Pioneer 8 measurements

19 p3502 A70-38094

Quiet time intensity increases and long term solar modulation of interplanetary low energy electrons, using IMP observations

19 p3502 A70-38097

Electron energy spectra range from HEOS A1 satellite mounted Cerenkov counter with shower telescope

19 p3503 A70-38103

Cosmic ray electron spectrum above 100 GeV by emulsion-lead sandwich assembly, estimating residence time, hydrogen atoms number density in galactic disk, etc

19 p3504 A70-38108

Positron fraction among primary cosmic ray low energy electrons, using pure emulsion stack exposed under residual atmosphere

19 p3504 A70-38109

Heavy elements critical energy calculation, taking into account low energy electrons effects on losses in electromagnetic cascade

20 p3674 A70-39303

Stable midlatitude red arc observation by Alouette 2 satellite for electron temperature and density structure measurement, calculating intensity and extent

20 p3620 A70-39333

Three dimensional Monte Carlo simulation of extensive air shower processes, comparing with hadrons and electrons energy spectra

20 p3699 A70-39442

D region free electron temperatures at northern auroral zone by dual polarized antenna, observing incident noise radio fluxes

20 p3622 A70-39452

Cosmic ray superhigh energy electrons and neutrinos propagation in degenerate neutrino gas universe, considering gas density in cosmological models

20 p3700 A70-39593

Laminar thermal boundary layer at atmospheric pressure adjacent to cooled wall, measuring electron temperature and number density

20 p3737 A70-39990

Exhaust velocity, electron density and temperature of pulsed megawatt nitrogen MPD-ARC thruster, using Thomson scattering of pulsed laser light

20 p3694 A70-40254

Solar soft X ray flare spectra of 16 November 1967, examining electron temperatures and emission lines by OSO-4

20 p3700 A70-40419

Electron temperature measurements in flowing high density plasma by cooled Langmuir probe, considering probe temperature variations effects in boundary layer

21 p3854 A70-40557

Interplanetary medium energetic electrons and isotopes measurement, discussing spectrometer electronics of IMP H and J

21 p3825 A70-41000

F region synoptic electron densities and electron and ion temperatures from Thomson scatter radar data

21 p3816 A70-41065

Artificial injection of trapped electrons into geomagnetic field by low altitude nuclear explosions, examining electron flux and energy

21 p3816 A70-41086

Midlatitude F region electron and ion temperatures during magnetic storms, examining Thomson scattering, density and time dependence

21 p3817 A70-41094

F region heating by magnetic storms, discussing electron temperature, ring current conduction and red arcs

21 p3817 A70-41095

Electron temperature incoherent scatter radar and satellite-borne Langmuir probe measurements discrepancy

21 p3825 A70-41104

Energetic electron precipitation enhancement by cold plasma injection, discussing whistler mode turbulence, particle density and magnetosphere

21 p3818 A70-41105

Electron temperature diurnal variations data from rocket soundings used for determining recombination coefficient in E region

21 p3819 A70-41300

Two probe electron energy distribution measurements in gaseous discharges with random and coherent oscillations, giving xenon results at low pressures

21 p3828 A70-41471

Electron-ion recombination in Ar plasma, discussing transition from collisional-radiative to dissociative process as function of electron density and temperature

21 p3858 A70-41711

Ruby giant pulse laser produced plasmas from aluminum and copper surfaces, measuring electron and ion energies by time of flight and retarding potential techniques

21 p3860 A70-41925

Molecular vibrational temperature dependence on electron and neutral gas temperatures and degree of ionization for plasma excitation in nitrogen

22 p4078 A70-42358

Probe technique for plasma electron temperature measurements at medium and high pressures, examining thermal boundary effects

22 p4078 A70-42362

Constricted arc characteristics in air and nitrogen at various pressures, considering spectral lines radiation transfer and electron, atom and ion temperature difference effects

22 p4079 A70-42369

One fluid solutions for solar wind with reduced electron heat conduction in agreement with observed characteristics at corona base

22 p4093 A70-42472

Ion and electron ambipolar velocity distribution near plasma sheath boundary in collisional positive column

22 p4080 A70-42542

Nonzero electron temperature effect on mutual impedance of quadrupole probe in hot isotropic plasma

22 p4080 A70-42720

Electron-neutral interaction parameters for Ohm law coefficients in multicomponent nonisothermal plasmas tabulated as function of electron temperature

22 p4081 A70-43015

Cs seeded Ar discharges electron energy distribution, discussing drift velocities, electrons elastic and inelastic collisions with ions and molecules, etc

22 p4081 A70-43198

Electron energy distribution in time-varying plasmas, using difference quotient circuits for Langmuir probe characteristics measurement

22 p4082 A70-43220

Nonequilibrium ionization during plasma flow into magnetic field, examining electrons selective heating

22 p4083 A70-43384

Electron energies correlation in relativistic theory of atoms applied to multielectron atoms energy levels

22 p4076 A70-43470

High altitude outer radiation zone boundary region electron energy measurement by satellite Injun 3, noting angular distribution dependence on local time, latitude, etc

23 p4236 A70-43833

Gas dynamic molecular laser with electrons in ground state, using incoherent optical pumping from stationary shock wave

23 p4201 A70-44284

Soft particle spectrometer in Isis-1 satellite using electrostatic deflection for differential energy spectra measurements for electrons and protons

23 p4197 A70-44468

Atomic levels occupation numbers and ionization degree for optically thin hydrogen plasma with self consistent electron velocity distribution

23 p4227 A70-44932

Local thermal equilibrium validity for electron temperature and density determination in reflected shock waves in He plasma, comparing laser scattering and spectroscopic methods

23 p4229 A70-44986

X ray spectra from paraboloidal plasma focus devices, measuring electron energy produced by photoelectric effect and by Compton scattering

23 p4229 A70-44990

Spectroscopic features of mercury laser associated with electron energy levels and spontaneous emission line structure, giving excitation and disruption mechanisms

23 p4202 A70-45054

Microwave recombination H lines, deriving electron temperature, electron density and emission measure sequentially

24 p4402 A70-45388

Flow-through carbon dioxide lasers population inversion relation to individual gas components and electron velocity distribution functions

24 p4352 A70-45458

Graphite dielectric constant as function of frequency, considering electron energy loss anisotropy in UV

24 p4380 A70-45668

LF plasma waves amplification by beam-plasma interaction, considering electron and ion temperatures effects

24 p4387 A70-45797

ELECTRON FLUX

U ELECTRONS

U FLUX (RATE)

ELECTRON FLUX DENSITY

Radial electron flux interaction with cylindrical electromagnetic wave propagating between conducting planes, noting disturbance development according to power law

01 p0049 A70-10166

Cosmic ray electron intensity diurnal variations measured with combined Cerenkov telescope and Pb-scintillator sandwich detector on balloon flight

01 p0170 A70-10408

Quiet time primary cosmic ray electron flux and energy spectrum from 10 to 200 Mev in interplanetary space observed byOGO 5 satellite

03 p0553 A70-12902

Cyclotron resonance maser /CRM/ monotron with inclined electron flux and magnetic field, considering design for performance optimization

03 p0499 A70-13455

Explorer observations of large temporal variations of midlatitude outer zone energetic electron intensities interpreted as redistribution during geomagnetic disturbances

03 p0560 A70-13989

Flux, energy spectrum and charge composition of primary cosmic ray electrons measured, determining energy spectrum of primary positrons above 220 Mev

04 p0739 A70-14595

Solar proton latitude profiles relation to outer radiation zone electron measurements by Alouette 2 satellite charged particle detectors during quiet magnetic conditions

04 p0740 A70-15105

Magnetic disturbances and corpuscular intrusions in auroral zone, discussing daytime and nighttime magnetic activity of electron fluxes

04 p0684 A70-15752

Electron flux-atmosphere interaction solved by numerical integration on computer, discussing auroral ionosphere

05 p0842 A70-16755

Sporadic electron flux contribution to high latitude geomagnetic disturbances at outer radiation belt boundary estimated from Elektron 1 and 2 observations

05 p0843 A70-16765

Collisions effects on ion saturation and electron currents in electron retarding region of cylindrical and spherical electrostatic probes, noting applicability over wide range

06 p1123 A70-18303

Outer radiation belt high energy electron fluxes correlated with VLF hiss ground observations

07 p1367 A70-19498

Electron and gamma quanta concentrations measurements by high altitude balloon, noting fluctuations at various altitudes

07 p1374 A70-20446

Electron flux independence of pitch angle distribution /0-90 degrees/ observed from sounding rocket measurements in auroral arc

10 p1932 A70-24492

Rocket-borne spectrometer for measuring 1-13 kev electron fluxes in auroral zone, describing design, operation and calibration

10 p1889 A70-24493

Radial electron flux interaction with cylindrical electromagnetic wave propagating between conducting planes, noting disturbance development according to power law

10 p1853 A70-25014

Energetic electron layer near magnetopause attributed to geomagnetic activity from satellite observations of fluxes

12 p2292 A70-27180

Low energy electron flux as interplanetary radiation primary component, considering data from IMP-1 observations

12 p2292 A70-27383

Soft electron fluxes spatial distribution and temporal variations in magnetosphere based on Elektron 2 charged particle trap data

12 p2295 A70-28259

Northern auroral regions low energy electron fluxes survey by Injun 4 satellite during minimum solar activity

13 p2477 A70-29184

Trapped and polar proton and electron flux observations during 9 June 1968 magnetic storm

13 p2482 A70-30072

Outer belt electron intensity variations related to geomagnetic activity indices, using Elektron measurements

14 p2630 A70-30201

Magnetic disturbances and corpuscular intrusions in auroral zone, discussing daytime and nighttime magnetic activity of electron fluxes

14 p2576 A70-30836

Discharged cleaned surface effect on accuracy and reliability of electron density and temperature measurements by Langmuir probes

15 p2778 A70-31765

Outer radiation belt high energy electron fluxes correlated with VLF hiss ground observations

15 p2795 A70-32743

Born approximation limit for plane wave multiple scattering by inhomogeneous electron density distribution in plasma

16 p2957 A70-32981

Magnetospheric electric field configuration from trapped particle flux asymmetries, using Explorer 14 electron data

18 p3306 A70-36024

Charge source density during interaction between atmosphere and electron/proton fluxes at prescribed boundary parameters

18 p3307 A70-36178

Atmospheric Coulomb interaction influence on longitude dependence of electron intensity in anomaly region

19 p3491 A70-37305

Cosmic ray electron and low energy proton fluxes by satellite-borne detector during solar flare of 25 February 1969

19 p3496 A70-37507

Electron intensity long term variations above 500 MeV byOGO-5 satellite-borne cosmic ray electron detector, supporting diffusion-convection theory of solar modulation

19 p3497 A70-37522

Cosmic ray high energy electron component intensity and spectra, using nuclear emulsion detector with counter triggered spark array

19 p3502 A70-38095

Quiet time intensity increases and long term solar modulation of interplanetary low energy electrons, using IMP observations

19 p3502 A70-38097

Primary cosmic ray electron flux, energy spectrum and east-west asymmetry, using balloon-borne spark chamber detector

19 p3503 A70-38104

High energy primary electron flux measurements by Cerenkov counter onboard ESR0 2 satellite

19 p3504 A70-38107

Primary cosmic ray electron flux above 30 GeV, using nuclear emulsion plate chamber

19 p3504 A70-38110

Interstellar electron and positron intensity, observing pion production spectrum from nuclear collisions at machine energies

19 p3504 A70-38111

Square cross section waveguide with cutoff frequency, calculating density wave propagation in helical electron beam trajectories directed by magnetic field

20 p3584 A70-39256

Pitch-angle distribution of electron fluxes in auroral zone as function of geomagnetic latitude

23 p4192 A70-44878

Outer belt electron intensity variations related to geomagnetic activity indices, using Elektron measurements

24 p4398 A70-46276

ELECTRON GAS

Electron gas heating at E region altitudes as function of ionization of atmospheric gases, noting rocket experiments during solar eclipse

01 p0082 A70-11492

Thermal properties of neutral interstellar gas heated by low energy cosmic rays, noting role of electrons in heating processes

02 p0364 A70-11783

Pinch characteristics of simple band structure semiconductors and nondegenerate electron gas dur-

ing bimolecular current carrier recombination, determining hole pairs spatial and recombination spectral distribution

03 p0538 A70-13062

Recombination emission of InSb semiconductor at low temperature during pinch effect with electron gas degeneration, calculating spectral distribution and effective temperature vs current

03 p0539 A70-13406

Landau Orbital Ferromagnetism in electron gas as magnetic field source for neutron stars

07 p1380 A70-19279

Correlation functions of spatially inhomogeneous fluctuations in electron gas in strong electric field

08 p1552 A70-21423

Collective approach to thermodynamics of N- particle electron gas including transverse radiation, calculating internal energy and pressure of modes

08 p1553 A70-21612

Correlation functions of fluctuations in electrical characteristics of nonequilibrium electron gas during scattering, determining spectral densities and populations by kinetic equation Green function

08 p1554 A70-21806

Pulse indicators using thermoelectric effect of hot carriers caused by nonuniform heating of electron gas in HF field

09 p1643 A70-22127

Electrical conductivity and conductive opacity for relativistic electron gas in presence of ions taking into account ion-ion interaction

09 p1727 A70-22509

Longitudinal electrical conductivity of relativistic gas in intense magnetic field

10 p1924 A70-24634

Spatial relaxation of electron gas colliding with positive ions from plasma velocity distributions, solving time independent Fokker-Planck boundary problem

12 p2280 A70-27791

Interstellar electron gas distribution and temperature, suggesting cosmic ray heating as main ionization source

13 p2495 A70-29796

Energy transfer processes of electron gas for pipe flow of weakly ionized nonequilibrium plasmas, noting electron temperature decrease exponentially along tube axis

17 p3142 A70-35438

Chemical reactions neutralizing electron-ion gas in F region

18 p3255 A70-37044

Photoresonant cesium plasma ionization, discussing pumping spectra, electron gas, molecular-atomic ion ratio and dynamics

19 p3474 A70-37440

High current elastic conductors nonlinear mixture theory with inviscid electron gas in elastic continuum under mutual electromagnetic and diffusive forces

19 p3387 A70-37787

Neutrino production by synchrotron process [magnetic bremsstrahlung/ in relativistic electron gas under intense magnetic field

20 p3695 A70-39050

Optical permittivity and dielectric permeability of electron gas in magnetic field, considering application to ferromagnetic materials

23 p4221 A70-45051

ELECTRON GUNS

Convergent ribbon electron beam shaping for vacuum welding with double anode gun, considering space charge effect

06 p1076 A70-17784

Electron gun onboard reentering spacecraft to measure densities and temperatures in flowing gases

06 p1066 A70-18286

Electron beam gun for drilling and perforation modified to include micromachining and welding

08 p1502 A70-20821

CRT laser with gallium arsenide crystal excited by electron gun, describing output characteristics

09 p1698 A70-23161

Magnetron-type electron gun structure with high design pervance for TWT applications

09 p1651 A70-23642

Current-sensitive single gun color CRT with phosphor screen for display systems

12 p2195 A70-27373

Electron gun for high current density electron bombardment of semiconductor lasers

20 p3641 A70-39482

High power pulsed relativistic annular electron beam production and focusing by injection gun using magnetic field control

21 p3827 A70-41461

Glow discharge electron guns for welding and heating, discussing beam current and energy balance

22 p4042 A70-42376

ELECTRON IMPACT

Total cross section for electron impact excitation and ionization in He, CO, nitrogen, oxygen, carbon dioxide, ethylene and benzene, emphasizing threshold values

01 p0147 A70-10489

Negative O, NO and nitrous oxide ions formation by electron impact on nitrous oxide as function of pressure

03 p0441 A70-14007

Ion-neutral reactions in carbon dioxide subjected to electron impact using mass spectrometry

04 p0646 A70-14698

Carbon dioxide electron impact cross sections, analyzing discrete excitation, autoionization, direct and dissociative ionization and use to aeronomy

04 p0722 A70-15121

Rotating and oscillating spectra in diatomic molecule excited by slow and fast electrons, discussing Boltzmann distribution of excited molecules

07 p1337 A70-19044

Electron impact induced fragmentation of androstane using deuterium labeling

08 p1454 A70-20524

Singly ionized Mg resonance lines electron impact broadening quantum mechanical calculation

09 p1732 A70-22827

Isomeric 1-phenylheptenes mass spectra, investigating electron impact induced rearrangements of double bond

09 p1631 A70-23401

Electron and proton impact excitations of He using Born two and four state versions of impact parameter treatment

11 p2086 A70-25834

N and O ions electron impact ionization rates calculated from approximate cross sections

12 p2275 A70-27173

Polycrystalline molybdenum desorption of adsorbed hydrogen, oxygen and water by electron impact

12 p2182 A70-27679

Helium excitation from ground to excited state by electron impact, determining differential and integral scattering cross sections

12 p2276 A70-27879

Electron impact excitation cross section of /O,0/ first negative band of nitrogen ion from threshold to 3 keV, using photon counting techniques

12 p2276 A70-27880

Cross sections for electron impact excitation of positive helium and hydrogen ions, using non-relativistic Coulomb-Born-Oppenheimer reactance matrices

13 p2455 A70-28988

Evidence against electron impact induced alkyl shifts in mass spectra of alpha-hydroxy-ketones, showing thermal rearrangements

13 p2363 A70-29803

Electron impact promoted phenyl migration of trans phenyltolalene, considering mass spectrometry and stereochemistry

14 p2544 A70-30189

Electron impact excitation cross sections of oxygen ion first negative bands, considering relationship to oxygen ionization cross section

14 p2620 A70-31363

Hydrogen atom excitation at various energy levels by electron impact, applying Glauber theory

16 p2954 A70-33287

Low energy electron impact spectrometry, discussing apparatus, procedures, electronic excitation of gas molecules, etc

16 p2857 A70-33797

Electron impact desorption kinetics of ions and neutrals from polycrystalline W surfaces, using cylindrical magnetic spectrometer

18 p3225 A70-36321

Hydrogen molecules rotational excitation cross sections by electron impact in adiabatic excitation, discussing polarization and distortion effects

20 p3675 A70-39606

Emission cross sections of nitrogen in vacuum UV by electron impact

20 p3675 A70-39617

Electron impact excitation and ionization cross sections, describing various approximation methods

20 p3675 A70-39937

Charged particle collisions, discussing electron impact ionization of positive ions, detachment from negative ions, ion collisions, etc

20 p3676 A70-40154

Nitrogen, hydrogen, oxygen and He total ionization cross sections due to electron impact

21 p3852 A70-40597

Decay lifetimes and electron impact cross sections of vacuum UV O I and O II emission multiplets, using pulsed electron beam in low pressure gases

21 p3852 A70-40718

Electron impact induced transitions in ions with configurations 3p/q/ responsible for forbidden lines in gaseous nebulae

22 p4105 A70-43234

ELECTRON INTENSITY

U ELECTRON FLUX DENSITY

ELECTRON INTERACTIONS

U ELECTRON SCATTERING

ELECTRON IONIZATION

U IONIZATION

ELECTRON IRRADIATION

Complementary symmetry MOS/CMOS/integrated circuit transient response to electron irradiation

04 p0657 A70-14733

Silicon semiconductor irradiated strain gages for precision measurement of low level strain

06 p1069 A70-18441

Electron irradiation for reducing thermal coefficient of resistance of Si strain gages, noting crystal orientation dependence of gage factor

06 p1070 A70-18442

Si-NP solar cell damage coefficient dependence on energy of irradiating electrons and protons, determining diffusion length from short circuit current

06 p1127 A70-18504

Thermochromic materials feasibility for applications in CRT display devices, observing reversible color changes during electron beam irradiation

08 p1499 A70-21682

Thrust vectoring of multipartite Ce electron bombardment ion engines, determining thrust deflection limit by accelerator current rise

11 p2102 A70-26124

Electron bombardment produced clustered displacements, paired vacancies and interstitial atoms in Si, discussing possible mechanism for developing defects

11 p2142 A70-26638

Electron bombardment ion engine thrust variations, considering effects of electrode misalignment and ion current changes

12 p2291 A70-27808

Causes and magnitudes of thrust misalignment of Kaufman type electron bombardment ion thruster [AIAA PAPER 69-303]

13 p2473 A70-28506

Proton and electron irradiation producing oxygen vacancies in silicates, minerals and rocks, indicating similar processes in lunar surface materials erosion and transport

13 p2395 A70-28908

N-type Te-doped gallium antimonide conversion to p-type by electron irradiation, noting thermal conductivity variations

13 p2470 A70-29167

Pulsed electron beam irradiated dielectrics secondary electron emission in vacuum, emphasizing inelastic scattering

13 p2471 A70-29409

Kinetics for two free radical conversion processes in electron irradiated D, L-valine, measuring activation energies by electron spin spectroscopy

14 p2544 A70-30111

MOSFET integrated circuits radiation resistance measurements under electron irradiation, determining changes in threshold voltage, transconductance and on-resistance for applications in spacecraft

14 p2559 A70-31372

Discharge chamber plasma processes in electron bombardment ion thrusters, considering factors affecting thruster performance

15 p2791 A70-32501

Electron radiation damage and stage 3 annealing effects on polycrystalline Mo properties

19 p3451 A70-37570

Crystal orientation dependence of thermal resistance and gage factor in electron irradiated n-type silicon strain gages

21 p3824 A70-40862

High energy electron irradiation generated defect centers in GaAs p-n electroluminescent diodes, using capacitance and thermally stimulated current measurements

21 p3863 A70-41914

Trap filling dependence on intensity, temperature and wavelength of photoexcitation in CdS crystals subjected to electron radiation damage and annealing

21 p3864 A70-42013

Irradiation influence on emission power of GaAs laser excited by high energy electron beam

23 p4203 A70-45060

ELECTRON MASS

Indium arsenide crystals conduction band structure with various electron concentrations, determining electron mass dependence on concentration and temperature

01 p0154 A70-10096

Excited terminal states emission in bound exciton-donor materials to determine donor ionization energies, electron effective masses and electron Q values

02 p0350 A70-11847

Electron mass evaluation, using fluid dynamic flow process

22 p4076 A70-43672

ELECTRON MICROSCOPES

Machined surface evaluation of fabricated components by electron microscopy to identify defects

01 p0097 A70-10012

Precipitation in Ni-base superalloy analysis with dark field electron microscopy and electron and X ray diffraction

01 p0119 A70-10730

Biochemical, electron microscopy and experimental medicine data indicating pathogenetic mechanism responsible for arteriosclerosis

03 p0431 A70-14278

Thin film transmission electron microscopy study of precipitation in Fe-Ni-Cr-Mo alloy with added Be and specific thermoelastic properties

05 p0862 A70-16022

Duplex Fe-Cr-Ni-Ti alloy sigma phase formation mechanism using electron microscope

08 p1525 A70-21958

Integrated circuit failure analysis with scanning electron microscopy taking into account ball bond contamination and open metallization at contact windows

11 p2015 A70-25366

Microtopography of fracture surfaces by stereo electron fractography, using large angle tilting of specimens

13 p2431 A70-28605

Electron microscope-thin film microprobe techniques in biomaterial studies of chemical segregation, species diffusion and small particle analysis

13 p2411 A70-29808

Composite solid propellants surface structure and profile characteristics burning with various oxidizers and polyurethane binder by scanning electron microscopy

14 p2628 A70-30948

Thickness measurement for thin films in inaccessible locations using scanning electron microscope, comparing accuracy with interferometric techniques

15 p2741 A70-32435

Lattice planes and interplanar spacings of small vapor deposited gold crystals, using transmission electron microscopy

16 p2961 A70-33644

Electron microscopic investigation of alpha-epsilon phase transformations in Co-Ni alloys above and under phase equilibrium temperature

18 p3276 A70-36205

Nb-based Ti-Zr alloy surface phase recrystallization characteristics, using field emission microscope

18 p3276 A70-36309

Cryogenic attachment for cooling and tilting metal samples in electron microscope

18 p3259 A70-36474

Fossil nuclear particle tracks in extraterrestrial matter using high voltage electron microscope and chemical etching

19 p3519 A70-38031

Soviet papers on heat resistant alloys and steels structure by electron microscopes

20 p3644 A70-39036

Senescent *Drosophila melanogaster* flight muscle electron microscopic examination showing mitochondria in stages of degeneration

20 p3574 A70-40075

ELECTRON MICROSCOPY

U ELECTRON MICROSCOPES

ELECTRON MOBILITY

Electron mobility in single component aromatic hydrocarbons, considering crystals structures and electrical properties, energy dissipation and fluctuation, etc

01 p0158 A70-10517

Electrothermal instability and critical Hall parameter growth rates in closed cycle linear plasma generators with variable electron mobility, discussing perturbation effects

01 p0151 A70-10655

Electron transverse and perpendicular drift velocities calculated at moderate and strong magnetic fields for hydrogen, using Maxwellian energy distribution and equivalent pressure concept

02 p0348 A70-12654

Electron relaxation in shock heated Ar plasma estimated by measuring radiation intensity at various frequencies

03 p0535 A70-14363

Neutron irradiation effect on space charge limited current of electrons in high purity silicon, noting SCLC sensitivity in detecting traps and changes

04 p0731 A70-14730

Electron mobility transition in infinite system of random hard core scatterers relation to switching effect in semiconductors

08 p1549 A70-21840

F region vertical electron drift velocity determined from Thomson scatter observations

09 p1671 A70-23665

Resistive parametric mixing in GaAs oscillators at microwave frequencies resulting in negative mobility at signal frequency

10 p1849 A70-24231

Acoustic wave amplification and generation in piezoelectric semiconductors and semimetals by supersonic carrier drift currents

10 p1925 A70-25030

Electrons velocity distribution function in homogeneous stationary weakly ionized Lorentz plasma in neon, investigating effect on mobility, collision frequency, diffusion and kinetic energy

11 p2089 A70-25871

Kaufman thruster with predominant radial field, noting electron mobility across ion extraction screen and advantages of uniform plasma distribution [AIAA PAPER-69-259]

11 p2102 A70-26120

Electron amplification and phase velocity of plane harmonic Rayleigh wave in gallium arsenide crystals under constant electric field

12 p2285 A70-27294

Free carriers mobility and concentration in microwave semiconductors measurable by two mode resonator over temperature ranges and magnetic fluxes

13 p2470 A70-28881

High resistivity Si electron drift velocity measurement by exciting surface barrier diode with subnanosecond superradiant laser pulses

14 p2594 A70-30924

Electron mobility, diffusion, drift velocity and attachment in oxygen, determining Townsend primary ionization coefficient

15 p2776 A70-31969

Manganese deficiency effect on chlorophyll fluorescence in algae adapted to hydrogen, determining electron transport mechanism

16 p2848 A70-33291

Doped Gunn diode domain field width, nucleation and annihilation dependence on electron drift velocity

16 p2879 A70-34044

Maxwell-Wagner migrational polarization resulting from free ions or electrons drift in dielectrics and semiconductors, considering relaxation time

18 p3298 A70-36595

Electron drift velocity longitudinal variation in equatorial electrojet, noting land-sea boundary and magnetic anomalies effects

20 p3620 A70-39337

Motion equation of electron in cylindrical diode subjected to varied voltages

21 p3796 A70-40640

Electrons optical scale time averaged motion dependence in focused laser beam on light intensity gradient, calculating bremsstrahlung spectrum

21 p3836 A70-40723

Electron and ion transport in cesium plasma for thermionic and MHD energy converters

21 p3859 A70-41912

Quasi-homogeneous approximation validity for electron velocity distribution function disturbance in gas plasma column ionization waves discharge involving high currents

24 p4386 A70-45794

Plasma positive column impedance in low current noble gas discharges, using Boltzmann equation for electrons

24 p4387 A70-45796

ELECTRON MULTIPLIERS

U PHOTOMULTIPLIER TUBES

ELECTRON OPTICS

Laser optoelectronic and spectroscopic methods using fixed gap spherical mirror confocal Fabry-Perot interferometer and multiple beam image tube framing camera

01 p0112 A70-10901

Microprobe analyzer for light elements using electronic optics probe, sample visualization devices and equipment for X photon detection and measurement [ONERA-TP-774]

02 p0275 A70-12210

Vidicon electron optics, describing triode emission system, focusing section, deflection component, collimating lens, beam landing error, etc

09 p1674 A70-22216

High resolution electron return beam vidicon cameras, comparing transfer functions and SNR with photographic films

20 p3630 A70-39496

ELECTRON ORBITALS

Semiempirical potential energy surface generation for triatomic hydrogen from London equation by evaluating Coulomb and exchange integrals taking into account effective orbital overlap

01 p0147 A70-10469

One and two center Coulomb, hybrid and exchange integrals contributing to orbit-orbit interaction in diatomic molecules evaluated for Slater orbitals combinations

03 p0528 A70-14010

Hartree-Fock method to study doubly even nuclei in 2s-1d shell, generating basis functions by Wood-Saxon well

04 p0722 A70-15318

First order wave functions orbital correlation energies and electron affinities of first row atoms for low lying electronic states of B, C, N, O, F and Ne

06 p1108 A70-17333

Bonding scheme of C-O in ketene described by localized orbital technique

08 p1455 A70-20682

Energy levels predicted for various electron orbital configurations in Fe V by Slater parameters

10 p1944 A70-24953

Drift velocity for bound electron orbital motion in static axisymmetric magnetic field

16 p2959 A70-34187

Metastable excitation levels in np/4 configuration for population inversion, discussing free electron collisions, forbidden line intensity and flow density pressure

20 p3642 A70-39751

ELECTRON OSCILLATIONS

Electron-hole pair quasi-linear fluctuations at recombination boundary in semiconductor crystal under crossed electric and magnetic fields

01 p0156 A70-10191

Harmonic generation in scattering of electromagnetic waves by anharmonically bound electrons, noting light source intensity

01 p0141 A70-10278

He-Ne gas laser simultaneous oscillation detection based on output power modulation due to variable path length element placed in cavity

01 p0109 A70-10434

Linear theory of cyclotron resonance maser with TEM standing wave field, considering coherent emission for nonrelativistic electrons oscillating in magnetic field

11 p2061 A70-25392

Surface waves stability in cold bounded plasma against background of steady state electron oscillations, using nonlinear approximation

11 p2089 A70-25716

Modulation coupling between electron and ion resonances in magnetoactive plasmas, discussing probeless feedback stabilization scheme

11 p2091 A70-26403

Self excited electron-phonon-spin spontaneous oscillations generation, deriving dispersion equation

16 p2878 A70-33779

Energy distribution of ions transversal to magnetic field in argon plasma source with oscillating electrons, showing dependence on induction and discharge current

19 p3482 A70-38956

Electron-neutral collisional damping of longitudinal electron oscillations in weakly ionized plasma, solving linearized Boltzmann-Vlasov equation

21 p3860 A70-42014

Electric field finite amplitude oscillations of electron hole plasma during pinch effect, considering impurities stabilizing effect

22 p4084 A70-43468

LF instability in plasma produced by electron cyclotron resonance in nonuniform magnetic and electromagnetic fields

24 p4386 A70-45613

ELECTRON PARAMAGNETIC RESONANCE

X band electron paramagnetic resonance spectrometer with ruby maser preamplifier, correcting misinterpretation and noise figure analysis

01 p0114 A70-11196

Zeeman interaction for super SS term in ESR Hamiltonian determined, using trivalent GD magnetic spectrum at eightfold coordinated cubic sites of thorium

02 p0340 A70-12718

KCl F centers isothermal annealing kinetics using EPR, considering electron irradiation levels effects

02 p0350 A70-12719

Electron paramagnetic property in chlorophyll molecules of spinach subchloroplast determined using pulsed ruby laser

03 p0421 A70-13551

Electron paramagnetic resonance for quality control of crystal structures in quantum electronics applications

07 p1356 A70-19479

Variable coupler for liquid helium X band EPR cavity during immersion in coolant

07 p1286 A70-19976

Gadolinium ions in zinc tungstate single crystals, studying low symmetry effects on EPR spectrum

08 p1556 A70-21120

Iron ions EPR lines widening in corundum crystals due to lattice defects, estimating mosaic blocks disorientation parameter and point defects density

08 p1556 A70-21122

Atomic bond rupture rate in rubber subjected to uniaxial tensile strain in ozone environment monitored by electron paramagnetic resonance measurements

08 p1527 A70-21454

Electron paramagnetic resonance absorption curve influence on power transfer characteristics and maximum passband of multicavity maser

09 p1695 A70-22278

LEPR spectrometer with sample cavity as part of HCN laser for experiments with gases, noting improved sensitivity

09 p1698 A70-22991

Spin-lattice NMR and EPR relaxation time measurements, using train signals and free induction decays

09 p1679 A70-22995

EPR line width angle and temperature dependences assuming line widening due to electric field of lattice defects, dipole-dipole interactions and spin-lattice relaxation

11 p2097 A70-25382

Light-induced electron paramagnetic resonance signal detected in *Anacystis nidulans*

11 p1989 A70-26847

Steady state EPR signal I kinetic behavior in wild type *Chlamydomonas reinhardtii* and in mutant strain AC-206 lacking cytochrome 53

12 p2168 A70-27468

Lattice defect influence on EPR spectral and luminescent characteristics of annealed Fe doped gallium arsenide crystals
12 p2288 A70-28330

Optical charge exchange and thermal stimulation effects in Fe doped GaAs crystals, determining iron content role by EPR method
13 p2469 A70-28880

Strontium chloride lanthanum ion system with dynamic Jahn-Teller effect, indicating isotropic EPM spectrum resulting from averaging by relaxation
13 p2470 A70-29109

High sensitivity conditions for rapid electronic spin resonance magnetometer
13 p2415 A70-30049

Electric conductivity, thermal emf and EPR spectra of oxide semiconductor glasses based on vanadium and phosphorus oxides, correlating unpaired electron and charge carrier concentrations
15 p2784 A70-32201

Electron paramagnetic resonance of Mn ions in single crystal and powder forsterite, testing heat treatment and proton irradiation effect on ordering
16 p2960 A70-33008

Electron paramagnetic resonance of viscous nematic liquid crystal, investigating order as function of temperature
16 p2960 A70-33058

Gaseous diatomic molecules quantum mechanical treatment, calculating Hamiltonian matrix elements for interpretation of electron resonance spectra
16 p2955 A70-33799

Calcium tungstate crystals, investigating electron paramagnetic resonance centers produced by neutrons and gamma rays to obtain information on lattice vacancies, defects, etc
16 p2961 A70-33963

Iron cyanide surface additives effect on photodamage to ZnO powder, using ESR method
19 p3372 A70-37543

ESR spectrum of gamma irradiated cyclohexatriene silver perchlorate, indicating free radicals and trapped electrons
19 p3374 A70-38272

Microwave frequency marginal oscillator for electron spin resonance spectrometer, using Gunn diode in sample cavity
21 p3827 A70-41460

Apollo 11 lunar fines, rocks and breccias luminescence, electron paramagnetic resonance and optical properties, discussing reflection spectra, heating effects and dipole resonance
21 p3914 A70-41654

Radiation induced free radicals in thymidine single crystals, attributing electron spin resonance spectral observations to nature of various radicals
22 p3981 A70-42348

Valent state of chromium doped barium titanate from EPR spectra and magnetic susceptibility measurements
22 p4086 A70-43133

EPR method for elementary reaction kinetics of vapor phase oxygen atoms interacting with molecular hydrogen
22 p3983 A70-43349

Superheterodyne EPR spectrometer microwave bridge using single X band klystron
23 p4170 A70-43798

Chondritic meteorites electron and nuclear magnetic resonance spectra at various frequencies
23 p4239 A70-43897

ESR intensities and line widths at X and Q bands of Cr and Fe molecular ions in water/glycerol mixtures
24 p4310 A70-46045

ELECTRON PATHS

U ELECTRON TRAJECTORIES

ELECTRON PHONON INTERACTIONS

Light Raman scattering in semiconductors under constant magnetic field, studying electron-phonon spectrum characteristics
01 p0155 A70-10183

Energy spectrum of electrons and holes in semiconductors under strong electromagnetic wave field, calculating electron-phonon interaction Green function
01 p0155 A70-10184

Electron-phonon interaction model of temperature dependence of luminescence produced by multiphonon nonradiative transitions in Cr ions of ruby crystal, deriving transition probability
03 p0538 A70-13058

Laser emission photons scattering by semiconductor conduction electrons allowing for electron-phonon interaction
07 p1357 A70-19857

Intense laser radiation effect on electrons interactions with acoustic and optical phonons and ionized impurities in semiconductors
12 p2246 A70-27360

Photocurrent multiplication in single crystal n-type epitaxial GaAs due to impact ionization of shallow donors
22 p4087 A70-43218

Tunneling electron and local mode phonon interaction in MIS n-type semiconductors
23 p4231 A70-44916

Vanadium carbide single crystals superconductivity from upper limit on electron phonon interactions at 30 mK
24 p4391 A70-46252

ELECTRON PHOTON CASCADES

Monograph on stochastic theory and cascade processes, discussing branching phenomena, point processes, electromagnetic cascades, extensive air showers, polarization, population growth, etc
01 p0134 A70-11327

Excess electron and combined electron-positron angular distributions compared in electron photon cascade showers, considering Coulomb scattering
03 p0536 A70-13048

Spatial distribution of cascade shower particles in atmosphere described by integrodifferential equations system, considering medium ionization
03 p0557 A70-13049

Electron and photon spatial distributions in cascade air shower, applying moment method to space/angle problem solution
03 p0557 A70-13050

Light collecting properties of polystyrene scintillator designed for counting particles of electron-photon showers generated by high energy cosmic ray particles
05 p0846 A70-15944

Angular distribution of particles in electron photon showers without recourse to Landau approximation
05 p0899 A70-15960

High energy electron and photon cascades in Metagalaxy, considering electromagnetic radiation density and cosmic ray origin estimation
19 p3500 A70-38081

Bremsstrahlung and photoneutrons from electron-photon cascades in thick tungsten and tantalum targets bombarded with low energy electrons
20 p3674 A70-39222

Equilibrium energy spectra of cascade electrons and photons in light and heavy materials as function of total shower energy
20 p3675 A70-39304

Laplace and Mellin transforms inversion in one dimensional cascade theory problems, using numerical methods for primary electron and photon spectra
20 p3675 A70-39305

ELECTRON PLASMA

Magnetic field effects on point Coulomb impurity charge static shielding by quantum electron plasma
01 p0151 A70-10449

Cerenkov radiation from electrons in magnetosphere and ionosphere, analyzing radiated power relationship with frequencies and latitudes
01 p0080 A70-11226

Electron trapping effect on ion-wave instability in plasma, deriving expression for saturation energy spectrum
01 p0152 A70-11361

Unstable electron plasma initial value problem solved by numerically integrating Vlasov equation in one dimension
02 p0347 A70-12235

Kinetic equation of helicons interactions in electron-hole plasma, discussing turbulence spectrum and effect on current carrier drift velocity
03 p0531 A70-13407

Magnetic field effect on recombination radiation intensity under pinch effect in semiconductor nondegenerate electron hole plasma with recombination time exceeding carrier lifetime
03 p0540 A70-13508

Shock wave structure in quasi-neutral weakly ionized plasma using Mott-Smith functions
03 p0535 A70-14362

Intensity, spectrum and polarization of gyrosynchrotron radiation from magnetoactive plasma electrons distribution
04 p0749 A70-14594

Electron plasma frequency exchange corrections temperature dependence at high densities, using equation of motion for coupled particle-hole pair operators
04 p0727 A70-14714

Nonlinear propagation of electron plasma wave in cylindrical waveguide, discussing linear theory of electrostatic waves in cold plasma
04 p0728 A70-15000

Electromagnetic waves amplification in semiconductor plasma with high electron concentration, analyzing equations describing waves drift instability
04 p0731 A70-15216

Boltzmann-type kinetic equation for homogeneous electron plasma in uniform magnetic field, describing relaxation to thermal equilibrium by convergent collision integral
05 p0888 A70-16329

Cerenkov radiation in infinite anisotropic electron plasma linearly polarized in magnetic field having linear electron distribution moving with uniform velocity
06 p1120 A70-17538

Relativistic electron low beta plasma oscillations in external magnetic field using covariant dispersion relations
06 p1120 A70-17542

Electron plasma wave damping by ion sound wave scattering using Vlasov equation
06 p1125 A70-18638

Plasma properties produced in mirror magnetic trap by electron beam determined during transition from hot electron dense plasma into cold electron low density plasma
07 p1350 A70-19846

Asymptotic method for Vlasov equation formulated for weakly Landau damped monochromatic plasma wave in collisionless electron plasma
07 p1353 A70-20231

Cyclotron frequency harmonics emission of PIG discharges linked to nonthermal electron plasma instability
07 p1354 A70-20316

Inhomogeneities in interplanetary plasma formation due to instability of electron flows moving along interplanetary magnetic field lines of force
08 p1570 A70-20845

Alkali seeded plasma electron density and temperature enhancement by laser resonance pumping
08 p1552 A70-21576

Electromagnetic instability measurements in electron cyclotron resonance plasma produced in magnetic mirror field
10 p1921 A70-23963

Electromagnetic fields in electron plasma with electron density variations due to transient ionization processes
10 p1921 A70-23978

Fokker-Planck equation solution for electron scattering and energy loss in mirror confined hot electron plasma
11 p2090 A70-26022

Drift instability of Alfvén waves at electron plasma sheet edge as source of auroral micropulsation instability
12 p2222 A70-27184

Active region characteristics of double injection laser employing electron-hole plasma in p-type indium antimonide
12 p2247 A70-27491

Resonant and nonresonant coupling between two coherent electron plasma waves propagating in opposite directions, considering parametric decay
12 p2279 A70-27780

Nonequilibrium solid state electronic plasma instabilities due to interactions with strong electric and magnetic fields
12 p2289 A70-28363

Kinetic equation for electron plasma based on BBGKY hierarchy reducible to set of equations with structure similar to Pines-Schrieffer equations
13 p2458 A70-28561

Nonlinear dielectric function and propagators of plasma submitted to electric field by Vlasov equation iterative solution, considering electron plasma in thermodynamic equilibrium
13 p2458 A70-28565

Transition radiation in plasma sheet in vacuum assuming specular reflection of electrons at vacuum boundary
13 p2464 A70-29512

Degenerate pinch in bipolar electron-hole plasma in semiconductors
13 p2472 A70-29760

Local resonance at upper hybrid frequency from satellite observation, noting effects of electron plasma/cyclotron frequency ratio
13 p2370 A70-29911

Infinitesimal dipole moving through hot uniform electron plasma in magnetic field, investigating asymptotic time behavior of plasma resonance
13 p2467 A70-29912

Thermal relaxation rate in one and two dimensional electron plasma models with positive background, using particle in cell simulation
14 p2624 A70-31047

Surface oscillations energy and attenuation in damped spectral region of semibounded degenerate electron plasma
18 p3293 A70-36143

Relaxation properties of nonequilibrium electronic solid state plasma during nonlinear interaction with external fields, using kinetic equation
18 p3297 A70-36423

Energy zone bending near surface of n-type semiconductor, discussing surface plasma level
18 p3298 A70-36619

Finite electron beam plasma system, investigating relationship between linear fluctuations temporal growth and resulting stationary oscillations spatial growth
19 p3475 A70-37540

High field noise emission from indium antimonide, suggesting electron-hole plasma as source
19 p3486 A70-37767

Dipole antenna radiation in incompressible anisotropic electron plasma overlying imperfectly conducting half space, solving for lunar environment
19 p3381 A70-38407

Dipole antenna radiation in incompressible anisotropic electron plasma overlying imperfectly conducting half space, evaluating Fourier-Bessel integrals for lunar environment
19 p3381 A70-38408

Nonuniform electron plasma trapped in one dimensional potential well, determining linear oscillations by normal mode approach

19 p3482 A70-39844

Permittivity tensor of weakly turbulent magnetoactive cold electron plasma, calculating nonlinear currents

20 p3677 A70-39296

Cold electron plasma nonlinear oscillations in magnetic field, using mathematical model

20 p3678 A70-39591

Collisionless plasmas fluid dynamical equations in presence of strong magnetic field, discussing Larmor and electron plasma frequencies

20 p3678 A70-39609

Low electron temperature plasma measurements by electrostatic planar guard ring probe with floating potential electrode, discussing electronic circuit

21 p3830 A70-42015

Superimposed external DC magnetic field effect on electrodeless HF plasma density, discussing electron cyclotron waves resonance excitation and plasma electron energy gain

22 p4079 A70-42364

Current densities and fields in quasi-neutral electron beam plasma, solving boundary value problem numerically

22 p4081 A70-42825

Electron plasma oscillations excitation by ion-acoustic waves

24 p4386 A70-45607

Large amplitude high phase velocity oscillations anomalous damping in electron-ion plasma resulting from MHD instability

24 p4387 A70-46091

ELECTRON PRECIPITATION

Postbreakup pulsating aurora association with conjugate absorption bays, indicating hard electron precipitation source location

02 p0290 A70-12161

VLF recordings and X ray flux measurements simultaneous analysis indicating evidence of relation between dawn chorus and electron precipitation, noting ELF whistler development

02 p0293 A70-12689

Temporal behavior of energetic particle precipitation during auroral substorm, discussing electron energy spectra and pitch angle distributions

06 p1059 A70-18536

Ionospheric radio wave/auroral/absorption during substorm investigated for longitudinal and latitudinal variations by multistation riometer measurements, inferring electron precipitation characteristics

07 p1269 A70-20030

Daylight ionospheric scatter propagation and absorption during energetic electron precipitation event in auroral zone using bremsstrahlung observations at balloon altitude

07 p1271 A70-20154

Electron and proton precipitation measurements in auroral zone by soft particle spectrometer in ISIS-1 satellite

08 p1560 A70-20501

Quasi-trapped electrons precipitating at high latitudes measured from low altitude polar orbiting satellite

08 p1562 A70-21382

Magnetosphere model for quasi-circular precipitation zones of energetic particles based on geomagnetic activity distribution patterns

08 p1489 A70-21385

Electron precipitation modulation exponential dependence on micropulsation amplitude derived from idealized model

09 p1747 A70-23492

Two phase process for electron precipitation during polar substorm observed from balloon measurements of X rays produced by precipitated electrons in atmosphere

10 p1932 A70-24490

Precipitated energetic electrons attenuation and impact ionization in ionosphere, determining vertical energy distribution profile

13 p2476 A70-28722

Postdusk and predawn seasonal variations of forbidden OI 6300 A airglow, discussing photoelectron precipitation

13 p2395 A70-28945

Auroral zone rapid motions associated with electron precipitation, discussing balloon flight data

13 p2478 A70-29198

Auroral electron precipitation and ground based magnetic field pulsations correlation for magnetic storms inception

13 p2401 A70-30053

Daytime auroral zone electron precipitation energy spectrum from atmospheric bremsstrahlung X ray balloon data

14 p2580 A70-31257

Longitudinal electric field effect on trapped particle motion in asymmetrical magnetosphere, considering electron precipitation

15 p2728 A70-31990

Longitudinal and transverse electric field effects in magnetospheric electron precipitation, discussing trapped particle drift

16 p2972 A70-34188

Pi 2 pulsation power spectra change with magnetospheric substorm development, relating pulsations and electron precipitation

17 p3080 A70-35641

Acceleration and precipitation of Van Allen outer zone energetic electrons, using correlation experiment between magnetosphere and auroral zone

18 p3306 A70-36010

Auroral phenomena interdisciplinary investigations, discussing electron precipitation and conjugate point drift due to geomagnetic axis position variations

19 p3411 A70-37493

Van Allen electrons acceleration and precipitation during magnetospheric substorms in relation to auroral processes, discussing energy and pitch angle diffusion processes

19 p3411 A70-37495

Trapped and precipitated electron observations at northern high latitudes in 45-450 keV range, using ESRO-1 satellite

19 p3496 A70-37515

Postmidnight auroral events precipitating electrons energy spectra components characteristics, using simultaneous X ray, optical and absorption measurements

20 p3699 A70-39334

Electron precipitation at geomagnetic storm sudden commencement in auroral zone from X ray balloon observations

21 p3814 A70-40937

Universal time control of south polar F layer during IGY attributed to low energy electron precipitation, comparing IGY and recent satellite data

21 p3818 A70-41101

Energetic electron precipitation enhancement by cold plasma injection, discussing whistler mode turbulence, particle density and magnetosphere

21 p3818 A70-41105

Bremsstrahlung X rays caused by energetic electrons precipitating into upper atmosphere, calculating photoionization rate as function of altitude

22 p4096 A70-43310

Electron precipitation latitude extent and drift rate magnetospheric substorms from ESSA riometer data

23 p4186 A70-43850

ELECTRON PRESSURE

Electron pressure and negative H ion population in late type dwarfs atmospheres by Ca I resonance line observation, noting non-LTE mechanism

01 p0191 A70-11351

ELECTRON PROBES

Plasma arc wind tunnel gas velocity measurement with electron beam probe using closed-loop electronic controller to stabilize beam position

01 p0092 A70-11195

Electron microprobe determinations of Si concentrations in metal of iron meteorites, showing weak evidence for Si presence in earth core

05 p0921 A70-17094

Electron temperature resonance probe to eliminate effects of geomagnetic field, rocket velocity and random noise

09 p1675 A70-22422

Electron beam probe applied to flow visualization in rarefied gas wind tunnels

10 p1860 A70-24549

Electron beam density probe calibration for earth atmospheric reentry vehicles communication

12 p2230 A70-26982

Probe diagnostic techniques for ionospheric electron density and temperature measurement, describing results from P53H firing

13 p2404 A70-28691

Electron microscope-thin film microprobe techniques in biomaterial studies of chemical segregation, species diffusion and small particle analysis

13 p2411 A70-29808

Electron emission effects on ion sheath and probe characteristics in continuum argon plasma

17 p3083 A70-34994

Elongation characteristics of modulation type charged particle traps and analyzers, discussing ions and electrons trapping

18 p3307 A70-36171

ONERA low pressure wind tunnel equipped with electron beam probing device to visualize flows too rarefied for optical methods

18 p3210 A70-37208

Two probe electron energy distribution measurements in gaseous discharges with random and coherent oscillations, giving xenon results at low pressures

21 p3828 A70-41471

Electron microprobe and petrographic analyses of crystalline rock and separates from Apollo 11 lunar soil samples

21 p3895 A70-41506

Quantitative optical and electron probe studies of opaque phases in Apollo 11 lunar rocks

21 p3902 A70-41552

ELECTRON RADIATION

NT BETA PARTICLES

NT ELECTRON BEAMS

Electron and hard photon /X and gamma ray/ production and propagation in expanding metagalaxy, deducing universe matter density, cosmic ray sources, etc

03 p0557 A70-13225

Electron radiation-induced second breakdown in transistors indicated by time delay and failure by collector-to-emitter short

04 p0657 A70-14734

Electron bremsstrahlung in intense magnetic fields calculated for emission rate and absorption coefficient in large quantum number limits

06 p1104 A70-17182

Synchrotron radiation rate from deexcitation of electrons in magnetic orbits of low quantum numbers, stressing electrons radiation in intense magnetic fields

06 p1108 A70-17183

Electron and hard photon /X and gamma ray/ production and propagation in expanding metagalaxy, deducing universe matter density, cosmic ray sources, etc

08 p1563 A70-21658

Solar microwave bursts polarization reversal mechanism, considering radiating electrons gyrosynchrotron absorption

11 p2106 A70-26617

Electron radiation temperature measurements in sealed-off carbon dioxide laser, determining gas mixture effect on discharge properties

13 p2426 A70-28808

Solar protons and electrons spatial and angular distributions over polar caps by USAF-OAR satellites 1966-70A, 1967-72D and 1968-59A

13 p2482 A70-30073

Electrons, positrons and photon energy distribution inside hydrogen plasma injected with high energy electrons

15 p2781 A70-32429

Plasma wave radiation by electron stream in active solar corona, obtaining spectrum and growth rate

16 p2979 A70-34189

Latitude profiles made of low energy solar electrons over polar cap, finding latitude knee position

18 p3306 A70-36020

Satellite radiation dosage in space proton and electron environment

19 p3511 A70-38490

Nonrelativistic electron bremsstrahlung in dense plasma with strong magnetic field

21 p3855 A70-40721

Electron radiation damaged Si, investigating p type defect concentration effect on isochronal temperature in annealing by fractionation experiment

23 p4231 A70-44887

ELECTRON RECOMBINATION

NT RADIATIVE RECOMBINATION

Electron-hole pair quasi-linear fluctuations at recombination boundary in semiconductor crystal under crossed electric and magnetic fields

01 p0156 A70-10191

Light induced modulation of optical absorption of CdS crystals by chopped laser excitation, noting use for fast recombination center detection

02 p0310 A70-11846

Dielectronic recombination rate coefficient determined by quantum theory of resonance-collision processes, considering coupling, degeneracy and overlapping resonances

05 p0920 A70-16943

Electron recombination in inert gases at various pressures, studying electron density decrease in time by UHF and optical methods

06 p1109 A70-17495

Ionization equilibria and ionization and recombination rates for Fe and Ni ions, discussing dielectronic recombination

14 p2631 A70-30727

Nickel-doped p- and n-type Ge hot electrons recombination characteristics in strong electric fields, examining electron capture cross section

15 p2782 A70-31628

F region electron content and recombination times during solar eclipse of 7 March 1970, using Faraday rotation technique

16 p2897 A70-33829

Electron recombination effect on current transmission through insulator-semiconductor junction with large diffusion length of minority carriers

24 p4390 A70-45634

ELECTRON SCATTERING

Collective interactions effect on electron scattering opacity in stellar interiors, using Debye-Huckel radial distribution function and neglecting collisions

02 p0364 A70-11789

Electron loss in heavy body collisions from free scattering model and Born approximation

02 p0342 A70-11879

Differential elastic and rotational excitation cross sections for electron-hydrogen scattering in close coupling approximation with electron exchange neglected

02 p0342 A70-11880

Emission spectrum characteristic distortion in scattering of background X rays at large red shifts by metagalactic electrons, considering photon scattering effect

02 p0358 A70-12491

Electron multiple scattering theory graphic approximation showing angular distribution in electron beam

03 p0527 A70-13053

Semiconductors low temperature electron energy losses due to inelastic electron scattering at neutral impurity donors shown to exceed scattering losses at phonons

03 p0539 A70-13423

Slow electrons elastic scattering by diatomic hydrogen molecule, analyzing cross sections in two center prolate spheroidal coordinates emphasizing polarization effect

03 p0528 A70-14179

Electron-electron and electron-atom bremsstrahlung, giving graphical expressions for one and two electron atoms cross sections

04 p0721 A70-14667

Electron scattering by molecules, demonstrating formal equivalence of fixed nucleus and free rotator scattering models

04 p0722 A70-14949

Galactic X rays and high energy gamma rays in terms of cosmic ray electrons Compton scattering by submillimeter radiation

05 p0900 A70-16100

Scattering matrix noniterative integral solutions applied to singlet and triplet s-wave Hartree-Fock phase shifts for electron-H-atom scattering

06 p1108 A70-17486

Charge-charge scattering model to calculate electron collection by Langmuir probe absorbing surface with and without magnetic field

06 p1124 A70-18308

Electron scattering from diatomic molecular systems including coupling of partial waves in fixed-nuclei approximation

06 p1114 A70-18633

Ionospheric radio transmission field strength calculation for given electron density and collision frequency profiles, considering electron variations along transmission path

07 p1230 A70-19165

Monograph on balloon and satellite borne spark chambers for cosmic gamma radiation energy and direction determination, discussing relativistic electrons multiple scattering

07 p1368 A70-19617

Electron elastic scattering from surface plane of Au and W fcc lattices using quantum mechanics

07 p1343 A70-20120

Fast electron ionization losses due to multiple scattering with atoms during passage through thin layer, calculating spatial energy distribution function

08 p1547 A70-20989

Transition metal alloys electronic effect on solubility of interstitials

08 p1521 A70-21695

Correlation functions of fluctuations in electrical characteristics of nonequilibrium electron gas during scattering, determining spectral densities and populations by kinetic equation Green function

08 p1554 A70-21806

Electron mobility transition in infinite system of random hard core scatterers relation to switching effect in semiconductors

08 p1549 A70-21840

High energy electrons elastic scattering from 2s-1d shell nuclei based on Dirac equation solution in Glauber approximation

09 p1730 A70-22043

Molecular vibration spectra from inelastic interaction between electrons and absorbed molecules at metal-vacuum interface

09 p1732 A70-22904

Noble metals band structure effects on shielding cloud around impurity and alloys electronic properties in weak scattering limit

09 p1740 A70-22953

Fast electrons spatial distribution for multiple scattering in nitrogen and argon, noting target thickness and incident energy

09 p1735 A70-23179

Electron-neutrino weak interaction and beat decay coupling constants found nearly equal, describing astrophysical tests based on white dwarf stars luminosity intervals

09 p1733 A70-23451

F region electrons collision frequency from short radio waves amplitude and group path relationship

10 p1876 A70-24535

Electron-hole pair creation in semiconductors /Zener effect and impact ionization/ defined from qualitative study of electron-phonon collisions

10 p1928 A70-24624

Fokker-Planck equation solution for electron scattering and energy loss in mirror confined hot electron plasma

11 p2090 A70-26022

Electrical conductivity of impact-ionized nitrogen across magnetic field, deriving electron collision frequency

11 p2091 A70-26461

Electron-atom collisions, treating elastic and Mott scatterings, Born approximation and ionization

12 p2274 A70-27062

Slow electrons interaction with periodic and non-periodic solid surfaces, investigating elastic scattering

12 p2275 A70-27252

Ar ions excitations by low energy electron collisions, noting excitation functions and cross sections of lines and levels by optical methods

12 p2278 A70-27501

Compton electron scattering generated galactic gamma ray flux effects on diffuse IR

13 p2476 A70-28630

Low energy solar flare electrons scatter-free propagation through interplanetary medium, considering rise, decay and travel times

13 p2477 A70-29194

Polarized Lyman alpha radiation emitted in electron collisions with atomic and molecular hydrogen and by electric field quenching of metastable atom

13 p2455 A70-29221

Pulsed electron beam irradiated dielectrics secondary electron emission in vacuum, emphasizing inelastic scattering

13 p2471 A70-29409

Electron collision frequency effects on Cerenkov radiation from magnetoplasma, applying results to magnetosphere and ionosphere

13 p2465 A70-29546

Quantum mechanical model of electron scattering by homonuclear diatomic molecule at ground state, calculating differential and integral cross sections for elastic scattering

14 p2618 A70-30113

Elastic scattering of electrons by hydrogen as function of vibrational excitation, discussing intensities and cross sections

14 p2618 A70-30114

Differential cross sections for electron scattering by hydrogen with and without vibrational excitation, discussing inelastic processes

14 p2618 A70-30115

Ion line Stark broadening, considering electron-ion quadrupole excitation and electron resonant scattering

14 p2620 A70-31376

D region electron concentration and collision frequency in slowly varying plasma, using rocket-borne probe for ground emitted wave detection

15 p2778 A70-31673

F 2 layer heating by photoelectrons reconsidered in terms of electron inelastic collisions effect on temperature

15 p2727 A70-31870

Plasma beam systems dispersion equation with allowance for electron collisions with heavy particles

15 p2779 A70-32117

Laser beam scattering by free electrons in semiclassical radiation theory, discussing intensity dependent frequency shift

15 p2753 A70-32452

Electron energy loss per collision in Cs vapor discharge, measuring electric field and electron temperature by Langmuir probes

16 p2954 A70-33281

Resonant electron scattering processes in atoms and molecules, discussing mechanistic models and use in interpretation of experiments

16 p2955 A70-33798

Two component fully ionized plasma in HF electric field, demonstrating suppression of runaway electrons in Lorentz plasma

17 p3140 A70-34934

Electron correlations and solar neutrino counts, correcting frequency independent Thomson cross section

18 p3308 A70-36485

Relaxation time for nitrogen molecule vibration temperature in ionosphere due to thermal electron collisions

19 p3409 A70-37324

Vertical profile of electron collisions effective frequencies in auroral ionosphere E region

19 p3409 A70-37330

Maxwell field quantization theory for case of interaction with Dirac field, calculating S matrix for interacting electrons

19 p3473 A70-37413

Electrons nonlinear interaction with field in traveling wave tube, using approximate quasi-classical quantum mechanics method

19 p3387 A70-37741

High energy galactic gamma ray and X ray flux explained by cosmic ray electron scattering

19 p3504 A70-38112

Weakly ionized gas subjected to pulsed DC electric field, analyzing transient relaxation of electrons velocity distribution

19 p3482 A70-38899

Resonance excitation of oscillations in diatomic molecules by slow electrons, calculating scattering on spherical potential well

20 p3642 A70-39753

Electron collision frequency profile for energy loss rate in ionospheric G factor for air, considering rotational excitations of molecular oxygen and nitrogen

21 p3812 A70-40618

Crab Nebula electromagnetic spectrum deviation from power law in microwave region, investigating origin from Compton scattering of high energy electrons

21 p3875 A70-40683

Electron excitation cross sections for light atoms using Slater wave functions and Born-Bethe approximations

21 p3853 A70-41393

Electron collisional detachment from negative fluorine ions in shock tube following nonequilibrium ion overshoot in CsF dissociation in argon, noting correlation with temperature

21 p3853 A70-41705

Electron-ion wave interaction due to scattering by electrons, using kinetic wave equation to describe wave-particle interaction

21 p3858 A70-41712

Electron losses from avalanches in hydrogen in cylindrical tube with plane parallel end electrodes, assuming elastic electron collision

22 p4076 A70-42355

Silicon line collisional broadening by electrons and hydrogen atoms, discussing Stark effect and van der Waal interactions

22 p4076 A70-42861

Neutron-electron collision damping and displacing of space echo in plasmas, indicating use for density measurement

22 p4082 A70-43244

Gunn effect, comparing intervalley scattering model to diffusion model for dynamic domain equilibrium

23 p4229 A70-43794

Solar wind instability from TEM waves propagating parallel to magnetic field in electron-proton plasma

23 p4235 A70-43826

Electron loss by resonant interaction with whistlers in nonuniform magnetic field, taking Fokker-Planck equation as distribution function

23 p4237 A70-44052

Auger spectra characteristics obtained with X rays and electrons from radioactive alpha sources

23 p4222 A70-44421

Electron runaway suppression in fully ionized Lorentz plasma by crossed magnetic and electric fields

24 p4382 A70-45105

Plasma-electron beam interaction instability transition from absolute to convective in hydrogen tube system at various pressures, considering electron collision effects

24 p4385 A70-45452

Plasma concentration and heavy particle-electron collision frequency in open cylindrical cutoff resonator based on frequency shift and passband broadening data

24 p4385 A70-45455

Semiconductors with bipolar conductivity under electron-hole scattering, calculating plasma pinch effect on I-V characteristics

24 p4390 A70-45659

ELECTRON SOURCES
Ionization gate with reverse biased silicon carbide p-n junction hot electron emitter as source

12 p2231 A70-27263

Electron formation by cosmic rays in atmosphere, taking into account impinging particles energy variations

20 p3697 A70-39293

Ionospheric D region electron production by cosmic X rays, noting Lyman radiation effects

21 p3882 A70-41099

Photoelectron production and escape flux at midlatitudes, using spectrometric measurements from ISIS-1 satellite

21 p3818 A70-41102

Electron pulse generator for imaging of glass microspheres simulating meteorite flight and impact in evacuated vessel [SMPE PREPRINT 96]

22 p4036 A70-43059

ELECTRON SPIN
Spin exchange theory for collisions between atoms extended to include target polarization

04 p0722 A70-14672

Maser amplification in Chirp radar signals pulse paramagnetic compressors using electron spin echoes

09 p1637 A70-23321

Electron spin-echo device as programmable linear matched filter for PN modulated carrier waveforms detection

16 p2864 A70-33480

Temperature gradient spectra on complexes of metmyoglobin and methemoglobin with ligands, discussing boundary forms equilibria for various electron spin configurations

24 p4301 A70-45985

ELECTRON SPIN RESONANCE
U ELECTRON PARAMAGNETIC RESONANCE
ELECTRON STATES
Resonance scattering and drift motion of electrons in gases under pressure, determining ion state lifetime

and mean electron-molecule collision frequency for trapping collisions

02 p0342 A70-11883

NH emission systems radiative lifetimes and SiD and SiH transition probabilities measured, noting effects of radiative cascading

05 p0885 A70-16424

First order wave functions orbital correlation energies and electron affinities of first row atoms for low lying electronic states of B, C, N, O, F and Ne

06 p1108 A70-17333

Nitrogen IR emission spectra from atomic and molecular excited electronic states transitions, studying DC discharges at various pressures

07 p1339 A70-20092

Electron density, excited state density and neutral particle temperature in Ar and Ne nonequilibrium laminar plasma jets

08 p1550 A70-20596

Te nuclear magnetic resonance in amorphous semiconducting sample cycled between conducting and nonconducting states

08 p1557 A70-21697

LEED pattern and germanium surface conductivity during oxidation indicating electron states annihilation

09 p1738 A70-22215

Atoms diffusion mobility enhancement in metal systems during irradiation suggested due to change in electrons energy states

09 p1707 A70-23192

Electron and proton impact excitations of He using Born two and four state versions of impact parameter treatment

11 p2086 A70-25834

Atomic Russell-Saunders coupling states classification from equivalent electrons configurations, using Young diagrams method

14 p2618 A70-30450

Localized one electron states in perfect crystals of widely separated atoms, using thermal single determinant/Hartree-Fock/approximation

14 p2626 A70-30488

NaLi molecular and ionic electronic states, discussing valence formulation, Hartree-Fock calculations, wave functions, excited state potential, etc

15 p2776 A70-31728

Band structure of Brillouin zone and electronic states on pure and contaminated crystal surface

15 p2786 A70-32767

Electronic wave functions for atoms from atomic configuration-interaction/CI expansion for open shell states

18 p3292 A70-36185

Weak predissociation effects of hydroxyl compounds electron state on radiative lifetime via phase shift method

19 p3374 A70-38270

Pi sub u states of positive ionized diatomic oxygen by photoelectron spectrometry

19 p3474 A70-38488

Photon states localization in disordered binary alloys, describing band structure

20 p3687 A70-40498

Rotational relaxation of diatomic molecular excited electronic state at high temperatures, discussing nonequilibrium region behind shock wave front in nitrogen

21 p3854 A70-42060

Thermodynamic parameters of stellar matter in electronic degeneration conditions, discussing energy balances discrepancies

22 p4106 A70-43260

ELECTRON SWEEPING

U SWEEP FREQUENCY

ELECTRON TELESCOPES

U PARTICLE TELESCOPES

ELECTRON TEMPERATURE

U ELECTRON ENERGY

ELECTRON TRAJECTORIES

Tunable adjustable solid state bandwidth filter using N path system for low pass to bandpass filter transformation

02 p0270 A70-12666

Velocity field characteristic for electrons in GaAs in negative differential mobility region by method involving probe measurements

04 p0732 A70-15690

Electron trajectories in M-type backward wave tube, TWT and magnetron, giving output power expressions

05 p0823 A70-16885

Interplanetary plasma electron density inhomogeneities formation explained by instability due to electron stream curvilinearity obtained from spacecraft data

23 p4240 A70-44070

ELECTRON TRANSFER

CW high power operation of transferred-electron oscillators realized by low thermal resistance, describing fabrication

07 p1241 A70-19300

Metallic state basic parameters determined by electron transfer technique, discussing ion charges, elec-

tron and hole concentrations current scattering cross sections, etc

13 p2433 A70-28886

Electron transfer mechanism between photoact I and II from redox reactions observation with modulated polarograph

13 p2363 A70-29815

Bulk n-type InP single crystal transferred-electron oscillators, investigating current instabilities

14 p2556 A70-30686

GaAs slices efficiency as transferred electron devices, correlating impurity profiles with microwave performance

15 p2708 A70-31957

Bilinear scalar spin Hamiltonian inadequacy to describe electron exchange in systems containing orbitally degenerate ions, considering cobalt magnon spectra

15 p2777 A70-32399

Partitioning formalism for degenerate, almost degenerate and electron exchange perturbation problems

16 p2955 A70-34001

Partitioning perturbation theory for electron exchange problems, generalizing Hirschfelder-Silbey formalism

16 p2955 A70-34003

Microwave oscillator performance of InP three level transferred electron devices

17 p3048 A70-35874

Multivalley semiconductors electrical conductivity anisotropy, discussing redistribution and electron transfer under strong electric field

19 p3483 A70-37294

Halophilic bacteria electron transport chain, examining hydrophobic forces role in menadiene reductase structure

21 p3772 A70-40574

Charge separated and quasi-neutral solutions of electron heat transfer to spherical body in quiescent nonequilibrium plasma, noting diagnostic applications

21 p3860 A70-42080

Heitler-London curves calculation for electron exchange in H-H collisions as function of internuclear distance and velocity

24 p4381 A70-45252

ELECTRON TRANSITIONS

Laser transitions to valence band or acceptor in low loss uniformly pumped crystal structure p-type GaAs at 77 K

01 p0113 A70-11168

Molecular hydrogen Lyman bands radiative transition probabilities, using electronic dipole moment functions

02 p0344 A70-12659

Dynamic time constants for specific transition and relaxation times of hydrogen maser, noting coupling between hyperfine differences and atomic polarization

03 p0498 A70-13007

Temperature dependence of luminescence quantum yields and lifetimes in transitions during excitation of ruby crystal atoms

03 p0538 A70-13059

Electron spectrometer for nitrogen energy loss spectrum in 12-14 eV region, detailing relative intensities of transition bands

03 p0528 A70-13577

He isoelectronic sequence 3d-nf transitions, determining UV wavelengths and oscillator strengths

04 p0739 A70-14601

Two phase transitions existence in Hubbard model of interacting electrons using one particle Green function solution

05 p0884 A70-16099

Radiative lifetimes of transitions to ground state for CS, SO and diatomic sulfur, showing relationship to absolute transition probabilities in terms of physicochemical applications

05 p0885 A70-16456

C V lines measured near 1s-2p line of C VI, identifying lines belonging to various transitions

05 p0921 A70-16982

Absorption transition fine structure measurements for bulk rare earth garnets single crystals using reflectivity techniques [IEEE PAPER 19.6]

05 p0894 A70-16998

Unified model for pulsars involving electron population inversion and laser type transition

07 p1375 A70-18893

Probability of three photon band-band excitation of electron in semiconductors using S-matrix formalism, calculating absorption coefficient for two band approximation

07 p1356 A70-19795

Kinetic theory of laser emission on direct band-band semiconductor transitions

07 p1299 A70-19853

Nitrogen IR emission spectra from atomic and molecular excited electronic states transitions, studying DC discharges at various pressures

07 p1339 A70-20092

Microwave absorption by rotational transition of interstellar formaldehyde in direction of Sgr B2, Sgr A and W51

08 p1570 A70-20896

Chemical high pressure laser action produced by stimulated phototransition of electrons at contact moment between pair of reacting nonexcited gas molecules

08 p1513 A70-21412

Relative rotational lines intensities of carbon dioxide, considering sigma-sigma transitions for abundant isotopes

08 p1549 A70-21575

Allowed and forbidden transitions probability in isoelectron sequences of solar corona, using scale factor method and variational wave functions

09 p1751 A70-22155

Collision effects on saturation of He line transition in He-Ne laser, determining power output dependence on cavity tuning and gas pressure

09 p1695 A70-22322

Laser action in 5d-6p electron transitions of neutral atomic iodine, measuring electron temperature and density

09 p1699 A70-23517

Hoeon-London factors calculated for general doublet transition in diatomic molecules, deriving energy levels

10 p1918 A70-23974

Transitions in interstellar OH observed at National Radio Astronomy Observatory

10 p1948 A70-25000

Sulfur beam foil spectrum in 600-4000 Å range, identifying transitions in S I-S VI

11 p1994 A70-25362

Radiative lifetime for atomic transitions in UV multiples of zinc and cadmium atoms and ions measured using phase shift method

11 p2086 A70-25363

Electron-hole transitions in GaAs obtained by sulfur diffusion, noting capacitance dependence on voltage at 293 and 77 K at various frequencies

12 p2287 A70-27481

Light absorption coefficient frequency dependence related to interband transitions in highly doped semiconductors

12 p2287 A70-27487

Plasma ionization enhancement by laser line radiation matched to specific atomic transitions [AIAA PAPER 69-47]

13 p2468 A70-29958

Semiconductor laser emission at band-band transitions with free carriers participation under quantizing magnetic field, using kinetic equations

15 p2749 A70-31627

Polyatomic molecules radiationless transition rate statistical analysis, suggesting role of Franck-Condon principle in determination of nonradiative decay rates

16 p2858 A70-34014

Laser oscillation in atomic fluorine from electrically pulsed discharge of fluoride compounds-helium mixtures, identifying as 3p-2P and 3s-2P transitions in fluorine I

17 p3108 A70-35910

Atomic H electron transition induced by H atom collisional-excitation rates at various thermal energies, explaining anomalous recombination lines in H I regions

18 p3253 A70-37021

Closed coupled partial wave calculation of cross section for fine structure transitions in Na in collisions with He

19 p3372 A70-37541

Pulsed emission in midinfrared region at neutral atomic transitions of inert gases and mixtures, tabulating wavelengths, intensity, component ratios and optimal pressure

19 p3448 A70-38736

Time and power dependent Lamb shift resonance shapes measurement with circular polarized RF field in beam foil excited H atoms

20 p3675 A70-39498

Autoionization spectral lines growth curves analysis, applying to 3s-4p transition in Ar at 466 Å with specified absorption cross section

21 p3781 A70-41931

Electronic transitions in B by beam foil technique for spectral lines in 450-5000 Å range, measuring excited levels mean lives

21 p3781 A70-41932

Quark in stars, discussing electronic transitions and UV spectral lines

21 p3921 A70-41975

Multiphoton gas ionization by coherent radiation, showing electron transitions role with gas ionization model

23 p4201 A70-44205

Laser kinetics based on exothermal chemical reactions for electron transition stimulation, emphasizing single mode operation

24 p4354 A70-45656

HF chemical laser emission in fluorine-containing organic compounds via arc discharges, noting molecular hydrogen effect on p sub 10 and p sub 21 transitions

24 p4355 A70-46046

Doubly excited antiferroelectrics absorption spectrum band and bound states, discussing zero approximation 0-0 transitions of alpha oxygen molecules and permeability tensor

24 p4392 A70-46362

ELECTRON TUBES

- NT IMAGE ORTHICONS
- NT RETURN BEAM VIDICONS
- NT VACUUM TUBE OSCILLATORS
- NT VACUUM TUBES
- NT VIDICONS
- Life-test sampling plan for electron tubes based on exponential failure distribution for reliability demand of military specifications

- 01 p0099 A70-10112
- Microwave low power electron tube oscillators and solid state technology
- 05 p0823 A70-16882
- Gyrotron efficiency increment at fundamental gyroresonance by applying magnetostatic field variable along length of interaction space
- 12 p2233 A70-27535

ELECTRON TUNNELING

- Electron tunneling into amorphous Ge films using Al-aluminum sesquioxide-germanium tunnel junctions, observing conductance dependence on bias voltage
- 09 p1739 A70-22918
- Current flow across metal-semiconductor contacts via electron tunneling
- 12 p2285 A70-27254
- Metal-Ge n-type semiconductor tunnel junctions, discussing Sb and As doped units and conductance and barrier heights air cleavage effects
- 14 p2626 A70-30482
- Field-ion microscope image formation, determining periodic surface potential variation effects on high field tunneling
- 21 p3862 A70-40974
- Electron tunneling through p-type GaAs point contacts on Pb single crystals at liquid He temperatures
- 21 p3864 A70-42017
- Double tunneling electrothermal initiation of threshold electronic switching in semiconducting glasses, discussing temperature profile and current density saturation effects
- 21 p3864 A70-42019
- P-n junction conductance at superhigh frequencies in breakdown region with simultaneous tunneling and impact ionization
- 23 p4232 A70-45064
- Thin film BiSb-oxide-BiSb tunneling junction I-V characteristics anomalies as function of temperature, magnetic field and bias voltage
- 24 p4390 A70-45662

ELECTRON-ION RECOMBINATION

- NT RADIATIVE RECOMBINATION
- Electron temperature dependence of molecular neon ions recombination with electrons using microwave afterglow/mass spectrometer, obtaining recombination coefficient
- 05 p0885 A70-16468
- Equivalent excited-state temperature of high pressure plasma calculated for unequal electron and gas temperature, considering ion and electron recombination
- 06 p1114 A70-18634
- Spectral line shapes determination for radiating atoms immersed in plasma developed without neglecting ion-electron interaction and static ion assumption
- 07 p1346 A70-20247
- Projection operators in dissociative attachment theory, considering use of truncated diagonalization method
- 07 p1347 A70-20248
- Electron ion recombination rate in atomic collision process in rare gases ionization path, considering scintillation mechanism
- 08 p1549 A70-21815
- D region electron ion recombination analyzed by two-ion model
- 10 p1881 A70-24812
- Electron density profiles interpretation for quiet daytime D region, noting role of electron-positive ion recombination coefficient
- 13 p2397 A70-29192
- Electron-ion gas ionization, neutralization and ambipolar diffusion effects on F region vertical profile
- 15 p2730 A70-32090
- Rare gas ions recombination with electrons, describing microwave cavity method and light and mass spectrometer techniques
- 20 p3676 A70-40155
- Electron-ion recombination in Ar plasma, discussing transition from collisional-radiative to dissociative process as function of electron density and temperature
- 21 p3858 A70-41711
- Partially ionized gas electron-ion recombination rate coefficients calculation methods compared with Ar plasma data
- 23 p4226 A70-44436

ELECTRONIC AMPLIFIERS

U AMPLIFIERS

ELECTRONIC CONTROL

- Concorde engine and air intake electronic controls
- 02 p0353 A70-11837

Solid state electronics application in automatic flight control, discussing redundancy, internal failure correction, fault isolation and automatic checkout

- 02 p0335 A70-12178
- RB.211 aircraft engine control, describing fuel and electronic control systems design and operation
- 03 p0551 A70-12895
- Concorde microelectronic power plant control system, noting overfueling prevention by throttle actuator during startup and speed governor function
- 05 p0896 A70-16003

Laboratory Electronic Servo Controller for structural fatigue tests, aircraft material tests, model position and velocity control in wind tunnels

- 06 p0989 A70-18606
- Concorde electronics systems for testing and flight safety, controlling center of gravity, braking, kinetic heating, air conditioning, fuel flow and inertial navigation
- 07 p1194 A70-19741

Parabolic reflectors profile error compensation by means of multiclement feed array with controllable phasing

- 09 p1644 A70-22236
- Airport capacity increase via electronic aids enhancing guidance, flight control, reduced aircraft separation, ATC automation and runway configurations
- 12 p2208 A70-27914

Electronically tracking antenna system for satellite reception in VHF range suitable for unmanned receiving stations

- 14 p2558 A70-31196
- Antenna system with linear polarization direction electronically changeable in microseconds
- 16 p2873 A70-33265
- Steerable microwave circular array to provide 360 deg electronic beam steering with computerized adaptive amplitude and phase control
- 16 p2874 A70-33392

Aircraft electronic propulsion control system using flight type computers and analog to digital conversion equipment

- [AIAA PAPER 70-693]
- 16 p2966 A70-33556
- Electronic pulsarium displaying flashing or beeping properties of pulsars
- 16 p2911 A70-33795

Electronically despun antenna for spin stabilized medium altitude satellites

- 17 p3179 A70-35270
- Stress tolerant thyristor and transistor switching electronic converter for ion propulsion engine
- [AIAA PAPER 70-1157]
- 21 p3866 A70-40901

Signal controlled microwave modulator as filter or attenuator, using rectangular waveguide and varactor diode switching

- 22 p3995 A70-42718

High speed three-frame electronic camera with storage tube, slow scanning and magnetic recording

- [SMPTE PREPRINT 55]
- 22 p4033 A70-43038
- Boeing 747 aircraft passenger entertainment and service system controls electronics design and wire installation improvement by multiplexing techniques
- 23 p4174 A70-44543

ELECTRONIC COUNTERMEASURES

- NT CHAFF
- Pulse position modulation focused TWT for airborne electronic countermeasure broadband jamming, considering output power and thermal design
- 04 p0653 A70-15656
- Traveling wave tubes used in electronic countermeasure chain or repeater for deception jammer, discussing design and performance
- 04 p0653 A70-15658
- Input and memory-storage traveling wave tubes for electronic countermeasures
- 10 p1852 A70-24888
- Automatic meteor station jamming protection using ferrite diode logical elements
- 19 p3422 A70-37652
- Data acquisition and processing system for electronic countermeasure aircraft tests
- 19 p3383 A70-37900

ELECTRONIC EQUIPMENT

- NT AVALANCHE DIODES
- NT CRYSTAL RECTIFIERS
- NT ELECTRONIC FILTERS
- NT ELECTRONIC MODULES
- NT ELECTRONIC PACKAGING
- NT ELECTRONIC RECORDING SYSTEMS
- NT ELECTRONIC TRANSDUCERS
- NT GALLIUM ARSENIDE LASERS
- NT GERMANIUM DIODES
- NT JUNCTION DIODES
- NT JUNCTION TRANSISTORS
- NT METAL OXIDE SEMICONDUCTORS
- NT MIS [SEMICONDUCTORS]
- NT PARAMETRIC DIODES
- NT PHOTODIODES
- NT PHOTOTRANSISTORS
- NT PHOTOVOLTIC CELLS
- NT RUBY LASERS
- NT SEMICONDUCTOR DEVICES
- NT SEMICONDUCTOR LASERS
- NT SILICON TRANSISTORS
- NT SOLID STATE DEVICES

- NT SOLID STATE LASERS
- NT THERMISTORS
- NT THYRISTORS
- NT TRANSISTOR AMPLIFIERS
- NT TRANSISTORS
- NT VARACTOR DIODES

Cost tradeoff analysis of electronic equipment for systems reliability design, considering component derating, redundancy and selection

- 01 p0049 A70-10119
- Semiconductor solar thermoelectric generator allowing thermoelement replacement during service including construction, bridging methods and characteristics
- 01 p0009 A70-10751

Student development and exercising of electron physics principles by designing, assembling, operating and studying electron and ion devices

- 01 p0093 A70-11291
- Handbook of transducers for electronic measuring systems covering operating principles, design features, etc
- 01 p0094 A70-11301

Rumanian book on shock tubes covering facility construction, gas flow, electronic measuring equipment, etc

- 01 p0059 A70-11379
- Electronic gauging machine for multipoint measurement at preselected points around turbine blade airfoil produced by electrochemical machining
- 01 p1015 A70-11397

Electronics in all-weather operations systems concerned with approach, landing and takeoff, considering components of airborne, ground and supporting systems

- 02 p0401 A70-11832
- Analog and digital electronically counting chronometers for extremely short times measurements
- 02 p0295 A70-11868

Civil aviation electronics - Conferences, London, September 1969, Part 3, Air traffic control

- 02 p0330 A70-11956
- Electronic scanning role in ATC radar, discussing combined search and track radar with elevation and azimuth scanning
- 02 p0331 A70-11959

Alphanumeric label and vector scan converted bright display operation, characteristics and equipment, discussing line scanning method, visual storage, display phosphor problems, etc

- 02 p0256 A70-11974
- Electronic components - Conference, Washington, D.C., April-May 1969
- 02 p0267 A70-12052

Photoelectronic measurement of distance from laser beam axis to reference plane, discussing applications to surveying, vibration measurements and atmospheric investigations

- 02 p0314 A70-12785
- Installation planning of electronic data processing unit using network and PERT program features
- 03 p0454 A70-13969

Electronic transistorized harmonic signal integrator operating in connection with static-dynamic bridge

- 03 p0493 A70-13975
- Small signal opto-electronic wideband transformer with coupling element ensuring fast response and low sensibility to parasitic magnetic fields
- 03 p0459 A70-14266

Radiation hardening of electronic systems for nuclear weapons using shielding, circuit design techniques and hardened components

- 04 p0657 A70-14738
- Digital computers for calculating coefficients of electronic circuit functions polynomials, developing algorithm
- 04 p0659 A70-15205

Switching-type dekatrons use in automatic control, electronic measuring and computing systems, discussing advantages

- 04 p0660 A70-15436
- Electronic search and rescue system developed for West German Air Force, consisting of personal transceiver and automatic distress signal transmitter unit, etc
- 05 p0793 A70-15904

Rotator and symmetrizer negative resistance circuits application in electronic function generator

- 05 p0824 A70-15991
- Semiconductor electronic devices applications in microelectronics, optical/dielectric electronics and photography and electron-acoustical phenomena and negative differential conductivity
- 05 p0822 A70-16863

Bioelectronic equipment shock hazards reduction by current limiting diodes use in signal and ground leads

- 06 p0998 A70-17285
- Electronic equipment packaging for operation at cryogenic temperature
- 06 p1017 A70-17336

Mechanical latching crossbar switches for space division electronic switching, discussing structure, performance, reliability, etc

- 06 p1023 A70-18413

Static electricity hazards and problems in electronic and aerospace industries

07 p1333 A70-18930

Electronic analog model for simulating convective mass transport in system with stationary and dynamic phases

07 p1423 A70-19740

Laboratory electronics role in Concorde aircraft structural and acoustical fatigue analysis, flight simulation and flight studies

07 p1250 A70-19745

Electronic timing device for light balloon payloads, describing circuit

07 p1286 A70-19975

Electronic displays and flight control system of Multi-Role Combat Aircraft developed by Germany, Italy and UK

08 p1493 A70-20631

Equivalent transformations method for minimizing electronic equipment sensitivity to circuit components value variations during operation

08 p1474 A70-21221

Electronic equipment complexity estimation based on information-recognition characteristics and ease of utilization

08 p1474 A70-21222

Astronomical sounding balloon to study interplanetary scattered light, discussing actuating and control, structure, onboard and ground electronics

08 p1497 A70-21349

Aircraft electronic attitude display indicators using symbology generation to combine several flight monitors indications

08 p1500 A70-21737

Display devices luminance and luminous efficiency measurement as function of angle

08 p1500 A70-21762

Heat pipes to cool electronic circuitry, discussing design and operation

09 p1786 A70-22015

Electronic equipment optimal design variant selection method, based on relative characteristics of feasible versions, widening weighting coefficients determination basis

09 p1643 A70-22129

Stereo photographs conjugate image area matching, comparing automatic optical and electronic correlation techniques

09 p1680 A70-23067

Electronic radio equipment with encapsulated structure and natural ventilation, calculating heated zone and casing mean surface temperatures

09 p1648 A70-23147

Structural and material design of contactless photopotentiometers operating in forward and reverse modes with given output characteristics

09 p1681 A70-23357

Book on integrated electronic systems covering integrated circuit design, device and material properties, quality control, applications, etc

10 p1853 A70-25049

Heating rate of radio electronic equipment with variable power shown dependent on initial dissipated power

10 p1853 A70-25134

Air ventilated cassette-type electronic equipment steady thermal regime, measuring local excess temperatures relative to ambient temperature

11 p2017 A70-25583

Design criteria for minimizing EMC problems confronting engineers of aircraft electrical and electronic equipment [SAE PAPER 700215]

11 p1980 A70-25887

Noise effects during mechanical parameters measurement by electronic devices, noting noise from resistors, potentiometers, power lines and wiper-type distributors

11 p2056 A70-26454

Reliable and optimum cost power sources design for long life electronic digital communication equipment

12 p2166 A70-27927

Photodetector-electronic circuit matching channels for optical communication system, using minimum risk design criterion

12 p2237 A70-28153

Hazardous X ray bremsstrahlung from military radio electronic equipment, discussing radiation protection and operating safety standards

12 p2180 A70-28360

Active antennas definition with integrated, amplifying electronic components based on designations in two port theory

13 p2376 A70-28897

Electronic systems automatic design problems including man machine communication and data organization

14 p2554 A70-30663

Quality control organization for miniature resistance welding of electronic equipment, examining planning phase and personnel training program

14 p2592 A70-31107

Quality control of electronic equipment using technical and management approach for attaining specified reliability

14 p2592 A70-31109

Ultrahigh speed photographic equipment with electronic systems, investigating integral images and slit cameras

14 p2589 A70-31401

Electronic systems for high speed photography, noting application to data processing and storage

14 p2589 A70-31402

Microchannel electron multiplier and optical focusing output shutter tubes for high speed photography

14 p2589 A70-31403

High speed electron cameras with opening time below one nsec, discussing shutter types

14 p2589 A70-31405

Electron camera with two stage image intensifier control electrode tube for rapidly evolving and slightly luminous phenomena, discussing exposure times

14 p2590 A70-31406

Pattern recognition procedure for electronic systems data classification

15 p2706 A70-32566

Parts standardization in military electronics industry for cost reduction and reliability, discussing design transform from software to hardware

15 p2831 A70-32632

Decreasing failure rate (DFR) with time in electronic systems operating in avionics applications

15 p2712 A70-32646

Electronic components prefailure analysis resulting in reduced failure rates, scrap and rework

15 p2832 A70-32652

Practical electronic components criteria accommodating reliability engineer and circuit designer

15 p2832 A70-32653

Electronic equipment maintainability in military environment, discussing myths for hardware and human performance conditions

16 p2852 A70-33664

High speed digital computer input device for reading data from magnetic tape, discussing design and operation principles

18 p3230 A70-36095

Standard units and assembling of electrical driving mechanism for telescope, using audio reference oscillator, electronic power amplifier and synchronous motor

18 p3259 A70-36609

Optoelectronics conversion for functional electronic circuits, discussing optical coupling, digital and analog computers and information display systems, injection diode light sources, etc

19 p3385 A70-37266

Electronic differentiator for physiological research, discussing electrical voltage derivatives reproduction, sensitivity, etc

19 p3371 A70-38219

Electronic components mass production for automatic control equipment, determining parameters probabilistic scatter

19 p3390 A70-38578

Military electronic equipment reliability limitations in terms of mean time to failure, considering quality control of components

19 p3390 A70-38596

Soviet book on operational tolerances in radio electronic equipment from reliability criteria

20 p3597 A70-39400

Weighing systems electronic load cells calibration for tension and compression loading, attributing non-repeatability to bending moments

[SAWE PAPER 816]

20 p3634 A70-40356

Papers on automation in electronic test equipment, Volume 7, covering factory and depot for incoming inspection, production testing, quality control, maintenance and rebuilding

21 p3803 A70-40766

Interplanetary medium energetic electrons and isotopes measurement, discussing spectrometer electronics of IMP H and J

21 p3825 A70-41000

Book on digital electronics with engineering applications covering switching circuits and logic designs, integrated circuits, error correcting codes, information storage and control, etc

22 p3999 A70-42324

Book on plastic coatings for electronics covering chemical structure, properties, applications, manufacturing technology, etc

22 p4058 A70-42455

Optimal design of electronic circuits, using mathematical methods for solving nonlinear multivariable function extremum

23 p4171 A70-43951

Graphical link between operator and digital computer using CRT display and light-pen input system during automatic electronic circuit design

23 p4150 A70-43952

Digital computer algorithm for automatic electronic circuit design using design engineer experience

23 p4171 A70-43953

High resolution electronic time intervalometer using digital counting and analog time expansion circuits

23 p4196 A70-44383

Multidegrees of freedom electronic cabinets dynamic response to AM fast sine sweep [SAE PAPER 700846]

24 p4380 A70-45884

Stochastic behavior of failed standby redundant electronic equipment with imperfect switching and opportunistic repairs

24 p4319 A70-46016

Reliability characteristics of standby redundant electronic equipment with imperfect switching and sensing

24 p4319 A70-46017

Electronic data handling and CRT display of ATS satellite cloud pictures

24 p4371 A70-46048

ELECTRONIC EQUIPMENT TESTS

IR microscope and digitally programmed mirror system for printed circuit inspection, allowing two dimensional scanning and magnetic tape reference

01 p0054 A70-10024

Avionic units automatic testing to increase speed and reliability, discussing system configuration, parts, economics and computer language use

02 p0295 A70-11838

Built-in, airborne and ground based automatic test equipment (ATE) for fault finding and serviceability of aircraft electronic systems in civil aviation

02 p0295 A70-11845

Automatic testing of avionic units, describing electrical stimuli, measuring instruments and signal switching connection to test unit

04 p0663 A70-15042

VTOL aircraft fly by wire system eliminating errors automatically, discussing electronic and electrohydraulic control components, flight test model design, prototype, etc

04 p0623 A70-15149

Flight test results of avionics in aircraft

05 p0822 A70-16699

Weld quality monitor for production testing of welding strength in electronic circuitry

05 p0856 A70-16722

Integrated circuit technology impact on electronic equipment designers and organization relationships within industry

07 p1239 A70-18800

General purpose automatic test system (GPATS) for electronic equipment fault location, discussing software and hardware for integrating programmable oscilloscope

08 p1470 A70-20656

Automatic test equipment for electronic devices, discussing computerized design of interface adapters for unit under test

08 p1470 A70-20657

Automatic testing hardware and software compatibility emphasizing versatile avionic shop test (VAST)

08 p1470 A70-20662

Versatile avionics shop test (VAST) Implementation Study recommendations on project management for automatic test equipment support system aboard attack aircraft carriers

08 p1601 A70-20663

Avionics maintainability concepts, discussing built-in test equipment, test connectors, automatic test equipment, fault detection and fault isolation

08 p1470 A70-20664

Altitude influence on forced ventilation of cooled electronic apparatus, analyzing flow change and temperature roles

09 p1643 A70-22040

Diagnostic-control tests for automatic homogeneous microelectronic structures, considering element coupling

09 p1643 A70-22142

Transistor current gain measurement at HF by two channel method

09 p1632 A70-22234

Low power semiconductor diode rectifying test apparatus for analysis of fusing and shaping effects on dynamic current-volt and frequency characteristics

09 p1649 A70-23355

Radio and automatic control electronic equipment reliability estimation by vibration testing, determining test stand simulation accuracy

09 p1650 A70-23632

Microwave equipment reliability achievement emphasizing tests and analyses on RF amplifiers, duplexers, antennas, etc

10 p1851 A70-24882

Microwave device test system design, considering measurement ranges and parameters, calibration, repeatability, accuracy, maintainability, etc

10 p1852 A70-24890

Test program effectiveness for Saturn Instrument Unit (IU), summarizing objectives, costs and results [AIAA PAPER 70-379]

10 p1891 A70-24924

Integrated Test Program for S-3A Weapon System, detailing test sequence flow and interfaces to assure vehicle and avionics systems reliability and maintainability

[AIAA PAPER 70-370]

10 p1959 A70-24931

Optimum sequence integration and ground testing of Defense Communication System Phase II Satellite, considering vibration, shock, space simulation, spin/despin, RF and acoustic requirements [AIAA PAPER 70-447]

11 p2030 A70-25444

Spacecraft S band power amplifier TWT electrical, environmental and life tests under saturated conditions [AIAA PAPER 70-506] 11 p2016 A70-25468

Electronic circuits automated endurance tests by follow-up scanning method, describing error sources in proper operation region cross section determination 11 p2013 A70-25922

Test pattern generation algorithm and program for failure detection in asynchronous sequential logic circuits, using combinational method 11 p2024 A70-26205

Automatic in-process inspection testing of electronic products [SME PAPER IQ-70-709] 12 p2241 A70-27083

Computer programmed automatic circuit analyzers, discussing unit adaptation, wire data processing and analyzer programming [SME PAPER MS-70-727] 12 p2241 A70-27084

Multiterminal electronic networks computerized fault detection based on linearized Taylor expansion algorithm 12 p2197 A70-27932

Electromagnetic pulse generator for simulation of EMP associated with nuclear explosions, describing electronic equipment vulnerability testing 12 p2208 A70-28135

Measured electronic equipment characteristics trends improving electromagnetic compatibility design 12 p2190 A70-28140

Orifice leak test for electronic components hermeticity 13 p2405 A70-28840

Electromagnetic pulse (EMP) testing, discussing sensor types and sensitivity, data acquisition and recording, instrumentation, etc 13 p2377 A70-29073

Radio and electronic equipments production testing by automatic equipment combined with semiautomatic manual controller 13 p2379 A70-29680

Digital computer controlled test system suitable for verifying response to single input pattern containing time dependent functions 13 p2374 A70-29684

Automatic Failure Rate Assessment Machine /FRAM/ for subjecting guided weapons electronic modules to cyclic stresses inducing failure of inherent weakness 13 p2379 A70-29686

Quality assurance of automatic testing in military or industrial equipment, including acceptance criteria and statistical proving 13 p2423 A70-29694

Feedback control systems automatic testing by examining frequency response 13 p2423 A70-29696

Virtual infinity CRT display systems testing, discussing effects of large apertures, operational modes and observer physiological requirements on measurements 13 p2411 A70-29790

Reliability and environmental testing of residual magnetic field measurements of satellite HEOS-A1 electronic equipment, using Rb vapor magnetometers 13 p2380 A70-30031

Frequency sampling adjustable equalizer design and operation, describing coaxial cable system tests 14 p2547 A70-30282

Junction and contact regions in electronic devices using X ray microanalysis and electron probe 14 p2590 A70-30355

Autodiagnosis of logic module failure in complex electronic systems, examining fault simulation methods and Safe system program and apparatus 14 p2561 A70-30669

Electronic components environmental testing, examining temperature, humidity and vibration effects 14 p2558 A70-31295

Micro-Hall device as tool for evaluating epitaxial silicon in integrated circuit processing 15 p2710 A70-32573

Solid state UHF and microwave device testing by computer automated network analyzers, measuring scatter parameters 15 p2742 A70-32590

Electronic equipment reliability performance measurements during tests correlated to performance observed under field use 15 p2712 A70-32645

Nondestructive screen test efficiency, determining potential failures of electric components by Bayes theorem 15 p2748 A70-32659

Reliability test facilities for military shipboard electronic equipment, subjecting equipment to combined thermal shock and vibration cycles 16 p2888 A70-33125

Algebraic computation of diagnostic tests for combinational digital circuits single gate failure detection and location 16 p2868 A70-33455

Electrical tests on satellites and space probes applied to spaceborne subassemblies, subsystems and electronic systems EM compatibility 19 p3532 A70-38287

Electronic equipment reliability improvement, based on reliability control group qualification, burn-in and diagnostic tests 19 p3554 A70-38401

Avionic systems automatic test equipment, discussing maintenance, reliability, cost and time reduction 19 p3402 A70-38544

Airborne electronic equipment guarantees, discussing USAF experience with full life, maximum failure rate and failure free plans 19 p3391 A70-38843

Electronic equipment test capability, programming methods and operation modes of General Purpose Automatic Test System, describing updating by USN 21 p3803 A70-40769

General Purpose Automatic Test System using building block concept for avionic systems evaluation at military depot level 21 p3803 A70-40771

Versatile Avionic Shop Test maintenance system supporting avionic equipment aboard aircraft carriers 21 p3804 A70-40772

Electronic parts testing for long duration Mariner spacecraft missions 21 p3799 A70-41798

Visual binary state transistor tester for positive and negative logic circuits, illuminating lamp for specific logic states 21 p3801 A70-42244

Computer controlled tester for digital circuits, giving diagrams and operations flow chart 22 p3996 A70-42849

Avionics hardware design guidelines to meet automated testing constraints including malfunction isolation, block requirements, packaging, etc 23 p4173 A70-44538

Automatic electronics test equipment, discussing choice between tape or computer controlled interpreter systems based on language, time, versatility and cost 23 p4173 A70-44539

Electronic equipment automatic testing systems signal routing and switching trees and matrices design, emphasizing modular approach 23 p4173 A70-44540

Electronic equipment automated testing objectives and requirements, considering man machine interaction, system controls, on-line reporting, and software/hardware availability 23 p4174 A70-44541

Avionic components reliability, determining non-steady cooling air environment effects 23 p4175 A70-44744

Integrated circuits failure analysis techniques, including electrical diagnostics, visual inspection, surface examination, shorts location, etc 23 p4175 A70-44749

ELECTRONIC FILTERS

Rise time relationship with signal bandwidth for class of TEM mode microwave delay line filters 02 p0257 A70-12185

Informative filter automatic selection for describing visual object with aid of frequency spectrum, taking filter output voltage mean square value as criterion 04 p0662 A70-15438

Transversal filters with continuously tapped delay lines, emphasizing synthesis of low pass filter and phase shifter 05 p0822 A70-16652

Self adaptive servosystems operating with incomplete input signal information, proposing schemes for parameter adjustment by employing differential circuit containing frequency filters 07 p1239 A70-18734

Higher order frequency demodulators with feedback in canonical form and with baseband filter 08 p1479 A70-20809

Matched filter SNR behavior under time and frequency domains distortion and random distortion, deriving design equations for energy loss coefficients 08 p1474 A70-21223

Transistorized pulse repetition frequency bandpass and band elimination filters, using trigger circuit to improve pulse-edge steepness and critical frequency stability 09 p1650 A70-23630

Solid state resonant bandpass electronic filter composed of ferroelectric dielectric capacitors with adaptable voltage gain 09 p1653 A70-23801

Distributed gain amplifier circuits with K-type filters, deriving analytical relations for pulsed and transient characteristics 10 p1853 A70-25131

Output correlation function of nonlinearity- filter system and phase modulated oscillations influence on system 13 p2366 A70-29411

Statistical linearization synthesis of nonlinear self adjusting systems with frequency filters and input signal under white noise 14 p2559 A70-30156

Reactive filter synthesis for step-voltage output inverter smoothing, using network theory 14 p2559 A70-30373

Root locus of active distributed RC circuit for synthesis of magnitude response of parabolic filters 14 p2562 A70-31323

Filter circuits composed of stripline resonators, determining input impedance and attenuation by digital computer 15 p2701 A70-32468

Filters design by on-line graphic interface computerized synthesis utilizing three screen CRT display 16 p2867 A70-33041

Optimal filters design predicting electronic systems parameters, preventing equipment failure due to wear and aging 17 p3055 A70-35744

Frequency filters in nonlinear self adaptive system design for noncorrelated input and noise signals 18 p2324 A70-36119

Optimal synthesis of linear active RC filters with controlled source, using feedforward and feedback weighted signals 20 p3596 A70-39163

Multichannel correlation filter devices for processing periodic fluctuating signals in noise background 22 p3987 A70-42557

Active filter operation, examining angle modulated signal at input by various approximation methods 22 p3997 A70-43130

Phased locked AFC circuit, calculating internal harmonic noise reduction by proportionately integrating filter 23 p4161 A70-43960

Multifunction programmable digital filter design performing bandpass, bandstop, comb, nonlinear phase and matched filtering of signals 24 p4319 A70-46082

ELECTRONIC LEVELS

U ELECTRON ENERGY

U ENERGY LEVELS

ELECTRONIC MODULES

Electronic integration assembly/EIA/ incorporating modular electronic packaging design techniques to provide reliable mechanical configuration for spacecraft equipment 02 p0268 A70-12579

Packaging and placement algorithms for modules in automated design of microelectron equipment 04 p0659 A70-15193

Diodes on cordwood module measured for stress during soldering, foaming and operation, describing methods for mounting semiconductor strain gages 05 p0854 A70-16036

Pressure sensitive components in cordwood modules noting temperature and pressure damaging stresses during encapsulation 05 p0855 A70-16037

Electronic modulo-M counter driven by HF pulse generator used for generating random numbers sequence 10 p1848 A70-23976

Thermal stresses and curing in electronic modules transfer molding, discussing various design test models 13 p2420 A70-29252

Transfer molding process in fabrication of electronic modules components, emphasizing criticality and unfavorable characteristics 13 p2420 A70-29253

Internal stresses in transfer molding of electronic modules by photoelastic technique, discussing component failure 13 p2420 A70-29254

Transfer molding of electronic modules, discussing materials for evaluating selection and processing guidelines 13 p2421 A70-29255

Monolithic linear IC building blocks for radar systems circuit design 15 p2704 A70-32581

Portable MOS memory module with optical loading and electrical readout, using hybrid array of complementary silicon on sapphire chips 16 p2868 A70-33457

Thermal design of hybrid microelectronics modules, considering resistance, assembly, joining, encapsulation and final packaging 16 p2879 A70-33957

Transmit only solid state radar module built with microstrip techniques for phased array systems operating at L and S dual bands 17 p3056 A70-35899

S band CW power amplifier and varactor doubler module for airborne phased arrays 18 p3231 A70-36674

Modular aerospace digital computer system architecture using off-shelf components for rapid avionic computing system realization 21 p3795 A70-41691

Ultrasurvivable and maintainable computer design involving redundant spare modules and own tester for aerospace applications

21 p3795 A70-41695

Strapdown inertial system mechanization and modularized instrument packaging with self contained failure isolation, temperature control and redundant components

[AIAA PAPER 70-1027] 22 p4066 A70-42315

Modular plated-wire digital associative processor with content addressable memory, distributed arithmetic and I/O capability at each word

22 p3994 A70-43104

Phased array radar systems microwave circuit modules packaging techniques, discussing interconnections, assembly, hermetic sealing and leak testing

23 p4173 A70-44535

Electronic equipment automatic testing systems signal routing and switching trees and matrices design, emphasizing modular approach

23 p4173 A70-44540

ELECTRONIC PACKAGING

Conductive heat transfer coefficients of densely packed electronic subassemblies

01 p0051 A70-10990

Electronic wafer packages heat transfer coefficients determined analytically, considering roles of geometrical and physical parameters

01 p0051 A70-10991

Electronic integration assembly (EIA) incorporating modular electronic packaging design techniques to provide reliable mechanical configuration for spacecraft equipment

02 p0268 A70-12579

Beam-lead substrate package for six stage TTL shift register, discussing metallization systems for interconnections and beams

02 p0271 A70-12846

Microelectronics equipment high density packaging and heat dissipation, discussing full utilization of high speed

02 p0271 A70-12847

Packaging and placement algorithms for modules in automated design of microelectron equipment

04 p0659 A70-15193

Diodes on cordwood module measured for stress during soldering, foaming and operation, describing methods for mounting semiconductor strain gages

05 p0854 A70-16036

Thick film hybrid circuit technology providing higher packaging density and better cooling

06 p1016 A70-17276

Electronic circuit packaging - IEEE Conference, San Francisco, August 1960, Part 7

06 p1016 A70-17334

Electronic packaging and cabling on Capsule System Advanced Development Lander for Mars rough landing

06 p1016 A70-17335

Electronic equipment packaging for operation at cryogenic temperature

06 p1017 A70-17336

Spacecraft electronics packaging methods, discussing mechanical engineering aspect of high density component packing in single housing

06 p1017 A70-17337

Millimeter wave CW Gunn oscillators construction by packaging free from spurious resonance, using sapphire ring and Au cap

08 p1468 A70-20482

Multiple maser-magnet units packaging in single cryostat for maximum tunability

08 p1513 A70-21599

Equipment container with sandwich type structure for packing delicate parts

10 p1852 A70-24899

Poseidon missile optimized and automated computer aided electronic packaging design, considering partitioning, placement, internal and external cable, etc

10 p1853 A70-25210

Short cables wire to wire coupling between black boxes, deriving interference transfer function

12 p2204 A70-28130

Resin systems for encapsulation of microelectronic packages, using thermal expansion dilatometer and gravimetric and differential analyses

13 p2439 A70-29258

Epoxy resin with low shrinking effect for encapsulation of electronic components by flexibilizing procedure

13 p2439 A70-29262

Rigid one component epoxy foam system mechanical, electrical and thermal properties for foamed-in-place electronic potting and encapsulation

13 p2439 A70-29263

Electronic packages design for vibration resistance, discussing isolators and damped laminate structures

13 p2516 A70-29616

Microwave power transistors design and packaging

15 p2711 A70-32589

Microwave transmission techniques with packaging designs for radiation energy losses control, discussing functions of components

15 p2714 A70-32750

Thermal design factors in electronic components packaging, considering equipment failure types and rates, fabrication processes, etc

[ASME PAPER 70-DE-17] 16 p2877 A70-33422

Electronic packaging and production - Conference, Brighton, England, October 1969

16 p2878 A70-33955

Thermal design of hybrid microelectronics modules, considering resistance, assembly, joining, encapsulation and final packaging

16 p2879 A70-33957

Wire wrapped, soldered, welded and crimped joints and plug/socket connections in electronic packaging for spacecraft

16 p2879 A70-33958

Manufacturing and technology of hybrid microelectronics packaging in Black Arrow X-3 satellite equipment

16 p2879 A70-33959

Packaging and grounding for electrical noise control in nanosecond switching circuits using transmission line design

16 p2879 A70-33960

Satellite electronics production, discussing dielectric film capacitor, solar probe magnetic oxide memory core and thin film assemblies

17 p3053 A70-35268

LSI circuits in space electronics, discussing packaging, reliability, applications, etc

17 p3053 A70-35274

Thermal control through fusible materials for missile S band transmitter package, using computer analysis

18 p3231 A70-36349

Electronic packaging - IEEE Conference, Cambridge, Massachusetts, June 1970

18 p3232 A70-36758

LSI packaging effects on systems design, discussing physical integration

18 p3232 A70-36761

LM-Apollo rendezvous radar and transponder electronic assemblies packaging and mechanical design

18 p3232 A70-36762

Microwave power transistors, considering figure of merit, performance and packaging

19 p3386 A70-37691

Microcircuit packaging /primarily hermetic/ and assembly techniques, considering cost reduction

20 p3597 A70-39443

Microelectronic packages encapsulation by resin systems with emphasis on thermal expansion, discussing effects of curing temperature, reactive diluents, etc

20 p3655 A70-39444

High power IC technical limits involving packaging, bonding wires, interconnect metal, power transistors

21 p3797 A70-41213

Aerospace microelectronic digital computer design, discussing optimal packaging by use of integrated circuits

21 p3795 A70-41694

Electronic packaging and production - Conference, Anaheim, California, February 1970 and New York, June 1970

23 p4173 A70-44532

Phased array radar systems microwave circuit modules packaging techniques, discussing interconnections, assembly, hermetic sealing and leak testing

23 p4173 A70-44535

Microelectronic phase lock microwave receiver packaging, discussing subassemblies interconnection minimization, shielding, RF interference, low loss and testing problems

23 p4164 A70-44536

Miniaturized VHF transmitter with bonded circular printed circuits for withstanding high shock loads, discussing design, production, packaging and testing

23 p4164 A70-44537

Avionics hardware design guidelines to meet automated testing constraints including malfunction isolation, block requirements, packaging, etc

23 p4173 A70-44538

High performance military aircraft missile command and control signal data processor microelectronics packaging, using integrated and printed circuit modules

23 p4174 A70-44542

Boeing 747 aircraft passenger entertainment and service system controls electronics design and wire installation improvement by multiplexing techniques

23 p4174 A70-44543

IC metallization systems in semiconductor devices fabrication and packaging, assessing metals alternate to Al for electromigration difficulties avoidance

24 p4319 A70-46075

Electronic Packaging and Production - Conference, Chicago, April 1970

24 p4320 A70-46246

Miniwire method of packaging high density electronic equipment shown in photographs, including OAO applications

24 p4320 A70-46247

High density packaging of micrologic flatpacks using high interconnection method for two-side use of double-sided card in space flight applications

24 p4320 A70-46248

Cleanliness levels for missile guidance package as function of component design complexity

24 p4349 A70-46250

ELECTRONIC PHOTOGRAPHY

U ELECTRO-OPTICAL PHOTOGRAPHY

ELECTRONIC RECORDING SYSTEMS

On-line electronic integration of aortic flow during systole to provide beat by beat readout of stroke volume

01 p0038 A70-11044

Electronic recorder design and operation for mean moments of star transit times

04 p0694 A70-15491

Whistler activity continuous recording by autocorrelation method using electronic analog computation with fixed delay time

10 p1886 A70-25281

Airlines data reduction using electronic engine maintenance recorders

18 p3259 A70-36853

ELECTRONIC SIGNAL MEASUREMENT

U SIGNAL MEASUREMENT

ELECTRONIC SPECTRA

Electron spectrometer for nitrogen energy loss spectrum in 12-14 eV region, detailing relative intensities of transition bands

03 p0528 A70-13577

Resonance, intercombination and forbidden lines observed in solar He isoelectronic sequence of oxygen, Ne, Al, Si and sulfur with Bragg crystal spectrometer

10 p1944 A70-24954

Local system interstellar medium thermal electron distribution, synchrotron radiation emissivity, cosmic ray electron flux and spectrum

17 p3152 A70-35583

Vertical secondary cosmic gamma spectra from primary nucleon and electron spectra, discussing effects of solar cycle and geomagnetic cut-off

18 p3308 A70-36500

Long term variations of cosmic ray electron spectrum above 500 MeV from balloon and satellite observations, noting reduction during Forbush decreases

19 p3503 A70-38105

Interstellar cosmic ray electron spectrum flattening below 3 GeV fromOGO-5 observations

19 p3504 A70-38106

ELECTRONIC STRUCTURE

U ATOMIC STRUCTURE

ELECTRONIC SWITCHES

U SWITCHING CIRCUITS

ELECTRONIC TRANSDUCERS

Miniature electromechanical gallium antimonide tunnel diode transducer theory fabrication and performance

12 p2236 A70-28055

Electromechanical transducer to sense and record strain cycles, describing motion magnification principle, system and prototype evaluation

15 p2739 A70-32310

Voltage-to-frequency transducers with negative feedback, analyzing errors and conversion transconductance

20 p3601 A70-39789

Surface elastic waves, considering propagation, electromagnetics transduction, amplification, guiding, focusing, reflection and applications

21 p3830 A70-42115

Information processing methods in microwave measurement using digital computers, emphasizing active and passive transducers

23 p4193 A70-43795

ELECTRONICS

Book on quantum electronics covering energy levels of materials, matter-radiation interactions and laser theory and applications

01 p0112 A70-10876

Civil aviation electronics - Conference, London, September 1969, Part 2

02 p0333 A70-11979

Geoscience electronics - IEEE Conference, Washington, D.C., April 1969

05 p0849 A70-16683

Book on quantum electronics, discussing dipole transitions, resonant processes, lasers, nonlinear effects in quantized media, field quantization, radiation-photon interactions, etc

05 p0893 A70-16800

Electronics - Conference, Chicago, December 1969

08 p1457 A70-20776

Electronics and Aerospace Systems - IEEE Conference, Washington, D.C., October 1969

12 p2185 A70-27901

Explosive metal bonding in electronics, noting explosive strength and initial surface angle effects on bond physical and chemical properties

19 p3438 A70-38752

ELECTRONEUROGRAPHY

Dispersion effect on accuracy of measuring polycrystalline samples electronograms by comparison using statistical method

09 p1682 A70-23392

Shifts method applicability to electronic camera for stellar magnitude photometry, studying instrument limitations and errors

14 p2589 A70-31379

Electroneurographic camera for ultrahigh speed photography, using nuclear emulsion as recording medium [SMPT PREPRINT 54]

22 p4033 A70-43039

ELECTRONS

NT CONDUCTION ELECTRONS

NT FREE ELECTRONS

NT HIGH ENERGY ELECTRONS

NT HOT ELECTRONS

NT N ELECTRONS

NT NEGATONS

NT PHOTOELECTRONS

NT PI-ELECTRONS

Electron flux parameters determination from ionograms and reflected signal amplitudes between 120-130 km, considering electron collision frequencies

01 p0084 A70-11551

Cosmic ray protons, He nuclei and electrons solar modulation by betatron deceleration mechanism during interplanetary space passage

02 p0357 A70-12123

Soviet book on quantum electrodynamics covering photon mechanics, electron relativistic mechanics, electromagnetic interactions, corrections to Green functions, particle interactions, etc

02 p0345 A70-12827

Electron and proton accelerators design characteristics, performance capabilities and specifications, emphasizing opposite-beam techniques for elementary particles interactions studies

03 p0527 A70-13045

Electron flux interaction with electromagnetic field in comb type waves via linear approximation assuming small space charge

03 p0447 A70-13291

Muon-electron ratio measurements in extensive air showers, showing anomaly due to chemical composition change of primary cosmic radiation

05 p0901 A70-16274

Electron-positron pair formation in electromagnetic field created by coherent laser light focused into vacuum with ideal lens

08 p1513 A70-21411

Ion cyclotron resonance spectroscopy technique for determining electrons photodetachment energy from negative ions in gas phase

11 p1995 A70-26001

Cosmic electron detection and measurement techniques, considering presence in solar system, interstellar space and metagalaxy and galactic continuum radio emission

12 p2293 A70-27572

Flat emission spectra of quasars in 3CP catalog attributed to anisotropic relativistic electron fluxes

13 p2493 A70-29387

HF electrostatic waves generation by electrons in magnetosphere

13 p2482 A70-30083

Quantum-electrodynamic renormalization for electron charge in metal environment, using solid state many-body techniques

14 p2619 A70-30476

Cosmic ray electron and positron differential energy spectra during solar quiet times from OGO-5 satellite observations in interplanetary space

19 p3806 A70-38096

Cosmic ray electron and proton interaction, discussing hydromagnetic waves, synchrotron radiation, magnetic field effects and wave propagation

20 p3695 A70-39012

Cosmic electron spectrum formation by acceleration, considering metagalactic background X radiation

20 p3954 A70-39174

Magnetic field and electron flux observations near magnetopause via magnetometer and triaxial electron spectrometer on OGO-E

24 p4328 A70-45350

Resonant electrons interaction with turbulent ion-acoustic plasma oscillations consisting of superimposed three dimensional random phase wave packets

24 p4386 A70-45658

ELECTROPHORESIS

Helium-cadmium laser operation, using DC cataphoresis to maintain spatially uniform optimal Cd vapor concentration

01 p0110 A70-10562

Stability and dynamics of dielectrophoretic equilibria, considering circular cylindrical column of inviscid liquid with rigid body rotation

03 p0525 A70-13784

Cadmium vapor density distribution by cataphoresis in He-Cd laser discharge tube determined by side light measurements

06 p1084 A70-18613

LF ultrasound not producing irreversible denaturation of blood serum proteins but capable of modifying electrophoretic properties

07 p1206 A70-19470

X ray structural and electrophoretic investigation of donor and fibrinolytic blood protein components, observing crystalline to amorphous transition in blood serum and plasma lyophilization

09 p1621 A70-23149

He-Cd laser with cathaphoretic transport and diffusion return path, noting condenser critical temperature for radiation noise reduction

15 p2751 A70-31987

Hematology of sea level and high altitude native Sonoran deer mice, correlating hemoglobin electrophoretic patterns with oxygen affinity

15 p2686 A70-32835

Combined ultrasonic and ionizing radiation effects on electrophoretic mobility of tumor cells from albino mice

17 p3034 A70-35762

ELECTROPHOTOMETERS

Twilight sky polarization data in visible spectrum obtained by high altitude balloon-borne photoelectric photometers

01 p0079 A70-11219

Lund astronomical observatory, describing Cassegrain-Nasmyth reflector and attached electrophotometer for stellar measurements

02 p0275 A70-12061

Three dimensional photoelastic case bonded solid propellant motor model, analyzing stress distribution using scattered light photoelasticity [SESA PAPER 1587]

03 p0583 A70-12885

Atmospheric extinction observed photometrically in South Africa and southern France in narrow bands and astronomical UVB bands

08 p1490 A70-21647

Photoelectric photometer for astronomical observations, discussing design and performance

10 p1886 A70-23917

Optical instruments for space measurements, discussing photoelectric spectroscopic devices, Michelson interferometer, etc

12 p2234 A70-27597

Light characteristics and geometry of photoelectric photometer system measuring light attenuated by atmosphere, discussing error sources

20 p3625 A70-39030

Pulse counting photoelectric photometer for lunar occultation recording of stars, discussing design, associated equipment and operation principles

22 p4030 A70-42860

ELECTROPHOTOMETRY

Stellar interferometer with superposed beams designed for measurements of close binaries, showing point light modulation convenient for photoelectric recording

08 p1493 A70-20564

Stellar interferometer with superposed beams designed for measurements of close binaries, showing point light modulation convenient for photoelectric recording

15 p2742 A70-32719

Lunar color differentiation by computer image processing compared to earth based photoelectric photometry

[JPL-TR-32-1472]

16 p2900 A70-33097

ELECTROPHYSICS

NT ELECTRO-OPTICS

NT MOLECULAR ELECTRONICS

Elementary chemical reaction kinetics effect on electrophysical parameters of low temperature plasma jets, calculating relaxation time for C fuels

19 p3481 A70-38184

Electrocardiography leads system optimal selection based on electrophysical modeling

19 p3369 A70-38207

Ti, Zr and Hf diborides electrophysical properties, discussing temperature effects and electronic structures

23 p4205 A70-43991

ELECTROPHYSIOLOGY

Controlled premature atrial stimulation effects on atrioventricular conduction in man, using electrode catheter technique to record electrical activity of specialized conducting fibers

03 p0415 A70-12886

Phasic phrenic nerve electrical activity relation to systemic blood pressure oscillations produced in paralyzed dogs by ventilation arrest or hemorrhage

03 p0416 A70-13010

Pathological Q waves in various diseases in absence of myocardial infarction, discussing electrophysiological mechanism

03 p0426 A70-13941

Unrestrained chimpanzees cortical and subcortical electrical activity during sleep recorded by telemetry and compared with human beings and other mammals

03 p0432 A70-14347

Book on sense of time covering psychological and physiological aspects and electrophysiological experimental results in man

05 p0800 A70-16129

Rhesus monkeys impaired discrimination in recognizing tachistoscopically presented objects following cortical polarization

05 p0802 A70-16625

Phase correlation of conditioned and electrophysiological postirradiation disturbances in central nervous system of monkeys

08 p1446 A70-21447

Control device for micromanipulator with pacing motor during electrophysiological studies involving microelectrodes implantation into tissue

12 p2179 A70-28317

Electrophysiological characteristics of rabbit eye muscles tonic fibers, measuring postsynaptic and membrane rest potentials

15 p2679 A70-31604

Binocular disparity detectors in human visual response to moving gratings confirmed by electrophysiological evidence

17 p3025 A70-35150

Continuous functions transformation by artificial neuron networks, investigating electrophysiological data for nerve tissues excitability

18 p3223 A70-36081

Electrophysiological characteristics of man during disorders in rhythmic system of conditioned motor reactions

18 p3221 A70-37217

ELECTROPLATING

Bridging joints resistance effect on thermoelement efficiency, describing W and Co coatings deposition on GeTe based thermoelectric alloys

01 p0159 A70-10757

Electrochemical machining based on reverse plating useful in gas turbine industry

04 p0699 A70-15398

ELECTROPOLISHING

Two stage electropolishing technique for preparation of multiphase alloys for transmission electron microscopy

08 p1510 A70-21966

ELECTROREFINING

Titanium alloy wastes electrorefining by electrolytic cell with solid bipolar electrodes to eliminate non-metallic inclusions

05 p0863 A70-16544

ELECTRORETINOGRAPHY

Flash blinding of cats using Q switched laser beam, discussing ERG response and retina changes

01 p0113 A70-10920

Electrical recording of retinal and occipital potentials in response to stimulation of human visual system used at levels from receptor to striate cortex

07 p1220 A70-19364

Operator analysis of electroretinograms, investigating eye reaction dependence on stimulation using amplitude-phase-frequency characteristics

08 p1450 A70-20730

Ionizing radiation effect on isolated frog retina using ERG recordings noting reduction of b wave

08 p1444 A70-20739

Human eye early receptor potential, investigating contributions of rods and cones

17 p3034 A70-35896

Scotopic responses conditions, using stimulus alternation method to elicit electroretinogram

17 p3034 A70-35897

Nervous inhibition effect on electroretinogram b wave during flash sequences

24 p4301 A70-45986

ELECTROSEISMIC EFFECT

U ELECTRIC CURRENT

U SEISMIC WAVES

ELECTROSLAG REFINING

Electroslag melted titanium wrought shapes mechanical properties, comparing with double vacuum arc melted material properties

17 p3112 A70-34356

ELECTROSTATIC CHARGE

Icing, bird collisions and static charge problems for jet aircraft, discussing protective devices

03 p0413 A70-13792

Detonator insensitive to highest level of electrostatic voltage on human body for precise synchronization

03 p0547 A70-14111

Fixed gap electrostatic spark discharge apparatus for booster type explosive sensitivity tests, discussing construction of two models, safety features and results

03 p0548 A70-14120

Synchronous and asynchronous electrostatic motors based on action of electric fields charges, discussing design and construction

06 p0988 A70-17150

Electrostatic methods considered for using earth electric field in smog dispersion in polluted areas and for airport fog clearing [AIAA PAPER 70-118]

06 p1058 A70-18217

Electrostatic ignition discharge prevention on fiberglass reinforced depot tanks, noting ground connection safeguard

07 p1295 A70-19763

- Graphite-polyester plastic material with electrical resistance for eliminating static charges leading to explosions 07 p1295 A70-19764
- Heavy negative charges formation in ionized Hg vapor by electron capture, basing demonstration on magnetic field effects on free electrons or charged droplets 08 p1550 A70-20594
- Solar charge effects on Mercury perihelion motion, relativistic light deflection and gravitational red shift, using Reissner-Nordstrom solution 11 p2107 A70-25395
- Electrostatic charging hazard and flight evaluation of aviation fuels with static dissipator additive [SAE PAPER 700278] 12 p2289 A70-27439
- Supersonic air flow control by electrostatic discharges tested by Mach 3 wind tunnels, using schlieren system for bow shock wave [AIAA PAPER 70-759] 17 p3008 A70-34492
- Boeing 747 aircraft pressure fueling system, describing tanks, feed system, refueling and electrostatic charge minimization [SAE PAPER 700276] 18 p3214 A70-36816
- Gravitationally induced /Machian/ magnetic field by rotating mass-shell with centrally located stationary charged sphere, using linearized relativity theory 19 p3471 A70-37815
- Electromagnetic interference in aircraft communication due to jet engine charging, considering various prevention measures 20 p3561 A70-39724
- Electrostatic potential distribution and ion trajectories in extraction gage design by computer 23 p4198 A70-44873
- ELECTROSTATIC DRAG**
- Coulombian drag on body from hybrid calculus of collisionless plasma flow around cylinder [ONERA-TP-819] 19 p3481 A70-38382
- ELECTROSTATIC ENGINES**
- Electrostatic charged particle acceleration and ion thruster function in geostationary satellite station-keeping and attitude control, orbital transfer and drag compensation [ONERA-TP-764] 04 p0735 A70-14934
- Electrostatic rocket exhaust condensation on spacecraft solar electric panels cover glasses, noting deleterious effects [AIAA PAPER 69-271] 11 p2103 A70-26131
- Electrostatic colloid thrusters operation and technology, including propellants, needle modules and test results 17 p3148 A70-35218
- RF ion source for electrostatic spacecraft propulsion, discussing RIT-10 performance optimization and development [AIAA PAPER 70-1102] 20 p3692 A70-40236
- Cs and Hg electrostatic thruster effluents effects on spacecraft materials, describing chemical, metallurgical and thermophysical experiments [AIAA PAPER 70-1144] 20 p3652 A70-40519
- ELECTROSTATIC EROSION**
- U SPARK MACHINING**
- ELECTROSTATIC FIELDS**
- U ELECTRIC FIELDS**
- ELECTROSTATIC GENERATORS**
- Electrostatic compressor with direct conversion of electric energy into mechanical energy, improving conversion efficiency by using plasma as working medium 07 p1196 A70-19658
- HF electrostatic waves generation by electrons in magnetosphere 13 p2482 A70-30083
- Electrostatic compressor with direct conversion of electric energy into mechanical energy, improving conversion efficiency with plasma as working medium 15 p2678 A70-32695
- ELECTROSTATIC GYROSCOPES**
- Unconventional gyros, discussing nuclear magnetic resonance, induction, cryogenic, electrostatic and laser technology 03 p0481 A70-12960
- Moments equations for electrostatic gyroscope drift caused by rotor asphericity 11 p2048 A70-25559
- Spherical shaped rotor unbalance effect on electrostatic gyroscope runout time, discussing energy dissipation 15 p2738 A70-32152
- ELECTROSTATIC PLASMA**
- U PLASMAS [PHYSICS]**
- ELECTROSTATIC PROBES**
- Spherical and cylindrical electrostatic probe operation analyzed under conditions producing collision-dominated sheaths 01 p0149 A70-10105
- Disturbances effect in Langmuir layer at cathode on ionization rate in arc discharge, estimating ion density and width of nonequilibrium ionization region 01 p0150 A70-10171

- Flame positive ion concentration measurements with Langmuir probes with mean free path smaller than probe diameter 02 p0397 A70-12019
- Plasma velocity, electron temperature and density and ion density determined by two mutually perpendicular probes 03 p0529 A70-12940
- Ionization studies in collision dominated high pressure flame plasma using electrostatic probes 03 p0534 A70-14212
- Explorer 31 Langmuir probe data for electron temperature at conjugate point, tracing magnetic field line passing through spacecraft to earth 04 p0000 A70-14971
- Electrode surface bismuth coating selected for reducing electrostatic analyzers photocurrents 05 p0851 A70-16734
- Microwave nonlinear effects including mixing, harmonic generation and current rectification observed in plasma sheath surrounding Langmuir probe using PIG discharge 05 p0852 A70-16992
- Spherical cylindrical and toroidal electrostatic analyzers with symmetrical angular characteristics for solar wind investigations 06 p1135 A70-17896
- Electrostatic probe measurements of radial distributions of mean ion density in N and air wakes behind hypervelocity spheres compared with electron microwave measurements 06 p0975 A70-18197
- Single and double cylindrical Langmuir probe responses in highly expanded low density flowing Ar plasma [AIAA PAPER 70-85] 06 p1066 A70-18207
- Satellite wake in ionosphere simulated in cold ion plasma without magnetic field, observing complex far wake structure and peculiar electrostatic probes response 06 p1147 A70-18297
- Collisions effects on ion saturation and electron currents in electron retarding region of cylindrical and spherical electrostatic probes, noting applicability over wide range 06 p1123 A70-18303
- Current collected by cylindrical Langmuir probe immersed in rarefied collisionless plasma streaming with high velocity 06 p1124 A70-18307
- Charge-charge scattering model to calculate electron collection by Langmuir probe absorbing surface with and without magnetic field 06 p1124 A70-18308
- Plasma space potential measurement by RF characteristics of Langmuir probe 07 p1288 A70-20233
- Time dependent electrostatic probe theory relating measurements to internal properties of plasma, calculating free stream ion density from collected electric charge 07 p1289 A70-20466
- Solar wind properties and helium abundance determined from satellite-borne electrostatic analyzers 09 p1746 A70-23482
- Disturbances effect in Langmuir layer at cathode on ionization rate in arc discharge, estimating ion density and width of nonequilibrium ionization region 10 p1925 A70-25017
- Electron temperature distribution behind strong shock wavefront in air measured by electrostatic probe and compared to results of spectral line inversion method 10 p1871 A70-25114
- Electrostatic cylindrical probes applicability to hypersonic flow field diagnostics 11 p2086 A70-25684
- Flush-mounted electrostatic probes behavior in shock tube over wide range of freestream conditions and bias voltage 12 p2236 A70-27810
- Electrostatic probes response due to thermionic electron emission, considering I-V characteristics and space-charge-limited current 13 p2459 A70-28635
- Electrostatic probe behavior in RF excited plasma, illustrating perturbation effect of potential drop on I-V characteristics 13 p2406 A70-28935
- Stagnation point electrostatic probe for measuring local electrical properties of solid propellant rocket exhausts [AIAA PAPER 69-573] 13 p2475 A70-29960
- Surface type airborne electrostatic probes in ambipolar diffusion flux measuring ion saturation current, discussing electrode contamination and temperature and ablation tests [AIAA PAPER 69-700] 13 p2412 A70-29967
- Langmuir probe characteristics and field response in low pressure nonstationary plasma diagnostics in weak magnetic field 14 p2623 A70-30785
- Spherically symmetric state of slightly ionized gas of unbounded expanse about catalytic conductor by

- nonequilibrium continuum theory, analyzing Debye number limit for electrostatic probes 14 p2665 A70-30946
- Ion temperature sensitive end effect in long cylindrical Langmuir probe response in high speed collisionless plasma flow at ionospheric satellite conditions 14 p2577 A70-31038
- Ionospheric electron concentration and temperature measurements by cylindrical Langmuir probe on rockets and satellites, emphasizing error sources 15 p2723 A70-31657
- Langmuir probe comparison to electron temperature probe measurements of ionospheric electron temperature during rocket flights 15 p2734 A70-31674
- Discharged cleaned surface effect on accuracy and reliability of electron density and temperature measurements by Langmuir probes 15 p2778 A70-31765
- Electrostatic analyzer without fringe field effects for measuring low energy particles on spacecraft 15 p2740 A70-32432
- Electron density fluctuation measurements in wakes behind hypersonic sphere projectiles, using Langmuir probes [AIAA PAPER 70-730] 16 p2834 A70-33489
- Electron density fluctuations in transitional zone of turbulent plasma jet, using digital analysis of Langmuir probe signals [AIAA PAPER 70-731] 16 p2958 A70-33495
- Supersonic plasma flows charge density levels and spatial and temporal variation, discussing theory and use of electrostatic probes 16 p2912 A70-33862
- Spherical electrostatic probe in uniform quiescent continuum slightly ionized gas for range of bias potential and radius-Debye length ratio 16 p2912 A70-33863
- Thin wire Langmuir probe measurements of electron temperature and density in transition and free molecular nozzle flow of short duration reflected shock tunnel 16 p2912 A70-33864
- Electrostatic probe measurements of vortex streets growth in plasmas bounded shear flow [AIAA PAPER 70-758] 17 p3139 A70-34493
- Collisions effects on ion collection by Langmuir probes, determining plasma density [AIAA PAPER 70-757] 17 p3139 A70-34494
- Continuum theory of spherical electrostatic probes as measuring devices in high density weakly ionized gases 17 p3140 A70-34931
- Langmuir probe position-dependent ion flow effects on plasma density measurement in low pressure mercury discharge 17 p3083 A70-34995
- Surface contaminated Langmuir probe measurements in glow discharge plasmas, discussing errors 20 p3633 A70-40161
- Electrostatic plasma probe inverse process I-V properties from current voltage characteristics, improving accuracy and reliability by theory in terms of new variables 20 p3683 A70-40162
- Gaseous neon plasma positive column electrons density and drift velocities measurements by Langmuir probe technique 20 p3683 A70-40163
- Collisionless cylindrical Langmuir probe response in turbulent plasma for mean and statistical properties 20 p3684 A70-40258
- Electron temperature measurements in flowing high density plasma by cooled Langmuir probe, considering probe temperature variations effects in boundary layer 21 p3854 A70-40557
- Electron temperature incoherent scatter radar and satellite-borne Langmuir probe measurements discrepancy 21 p3825 A70-41104
- Book on electrical probes for plasma diagnostics covering kinetic theory, carrier distribution, current characteristics, plasma resonance, etc 21 p3829 A70-41790
- Low electron temperature plasma measurements by electrostatic planar guard ring probe with floating potential electrode, discussing electronic circuit 21 p3830 A70-42015
- Low density plasma in region of orbital-motion-limited /OML/ currents in presence of cylindrical Langmuir probes 22 p4078 A70-42360
- Electron energy distribution in time-varying plasmas, using difference quotient circuits for Langmuir probe characteristics measurement 22 p4082 A70-43220
- Shock wave electrical precursor measurements in weakly ionized gas, describing approximate electrostatic probe theory and high sensitivity gages 23 p4184 A70-44995
- ELECTROSTATIC PROPULSION**
- NT ION PROPULSION**

Optimal outlet velocities of charged particles for spacecraft electrostatic thrusters
[DFVLR-SONDDR-28] 04 p0735 A70-15173

Plasma devices for spacecraft propulsion taking into account electrothermal, electromagnetic and electrostatic systems 05 p0895 A70-15817

Optimal outlet velocities of charged particles for spacecraft electrostatic thrusters 09 p1744 A70-23428

Electrostatic colloid thrusters operation and technology, including propellants, needle modules and test results 17 p3148 A70-35218

Space vehicle for testing electric propulsion systems in space, powering by cluster of six electrostatic ion motors regulated by automatic thrust control 23 p4259 A70-44616

ELECTROSTATIC SHIELDING

Magnetic field effects on point Coulomb impurity charge static shielding by quantum electron plasma 01 p0151 A70-10449

Electrostatic shielding of nuclei Coulomb field during thermonuclear reactions in degenerate gases of arbitrary densities 11 p2087 A70-26578

ELECTROSTATIC WAVES

Saturation of linear or nonlinearly /explosively/ unstable HF electrostatic flute modes in mirror confined plasma 03 p0529 A70-13005

Electrostatic instability criterion for plasma with distribution function having discontinuities and sharp bend at minima 03 p0532 A70-13526

Plasma quasi-stationary turbulence spectrum determination from nonlinear equations for Langmuir waves interaction, considering fast particles effects 06 p1119 A70-17499

Coulomb collisions effect on electrostatic lower hybrid resonance waves propagation in ionosphere, noting noise bands cut-off shift 10 p1874 A70-24429

LF ion-acoustic wave nonlinear interaction with HF Langmuir waves in nonisothermal plasma, establishing criteria for ion plasma turbulence 10 p1925 A70-25103

Long-time cross modulation field resulting from triggering electrostatic waves in one dimensional plasma, discussing supraluminous waves interactions 11 p2088 A70-25704

Electrostatic wave propagation and growth rate in electron beam-inhomogeneous plasma confined by magnetic field 11 p2091 A70-26460

Electrostatic wave modes in inhomogeneous adiabatic plasma, discussing waves with gamma-fold ion and electron drift velocity 12 p2280 A70-27783

LF electrostatic waves oblique to magnetic field in plasma, evaluating dispersion relation near ion cyclotron frequency 13 p2363 A70-28641

Plane electrostatic shock waves propagation in plasma with electrons in potential equilibrium and collision free ions 13 p2461 A70-28730

Collisionless electrostatic shock generation conditions, simulating homogeneous counterstreaming plasmas by computer 13 p2462 A70-29110

Fast time-resolved spectra of earth bow shock electrostatic turbulence based on broadband analog electric data from OGO-5 13 p2396 A70-29111

Electrostatic waves for upper ionospheric plasma model, obtaining solutions to dispersion relation at multiples of electron cyclotron frequency 13 p2400 A70-29914

Double sphere dipole antenna detecting VLF electrostatic plasma waves, discussing induced and contact potentials 13 p2372 A70-29927

HF electrostatic waves generation by electrons in magnetosphere 13 p2482 A70-30083

Particle acceleration by electrostatic waves propagation in inhomogeneous plasma in terms of phase velocity, magnetic field and wave amplitude 15 p2778 A70-31912

Electrostatic near wake model for ionospheric satellites, using low speed fluid dynamic blunt body similarities [AIAA PAPER 69-674] 16 p2837 A70-33867

Nonlinear electrostatic vibrations in colliding antiparallel flows of rarefied plasma 17 p3141 A70-35335

Type I burst effects on type III and V bursts occurrence, suggesting Langmuir waves excited by suprathermal electrons 17 p3173 A70-35746

Electrostatic turbulence in bow shock magnetic structures observed by OGO 5, explaining turbulence

as ion acoustic or Buneman mode due to two stream instability 18 p3311 A70-36006

Homogeneous plasma electrostatic oscillations excitation by electromagnetic waves nonlinear interaction in magnetic field, deriving expression for density perturbation 19 p3475 A70-37536

Electrostatic ion waves in uniform magnetic field, calculating phase and group velocities as function of propagation angle for comparison with dispersion measurements 20 p3678 A70-39659

LF electrostatic instability of Van Allen belt in outer trapping zone causing electric field in plasmapause 22 p4099 A70-42786

Ionospheric parametric amplification and frequency mixing due to polarized TEM waves nonlinear interaction with longitudinal electrostatic waves 23 p4185 A70-43838

One dimensional collisionless electron-proton plasma, obtaining exact electrostatic shock solution to Vlasov and Poisson equations 24 p3482 A70-45107

Cs ion beam space charge and current neutralization by electron capture for partially ionized plasma formation, investigating longitudinal electrostatic wave excitation 24 p4385 A70-45465

LF electrostatic ion cyclotron wave energy resonant power absorption in plasma in axially nonuniform magnetic field 24 p4386 A70-45608

ELECTROSTATICS

Hazards due to nonohmic materials responsible for electrostatic failures in missile and space programs and ground equipment 01 p0141 A70-10088

Convective red dwarfs Kr 60 A and 60 B structure and stability taking into account electrostatic interactions between gas particles 01 p0188 A70-11337

Electrostatic drift-dissipative plasma instability and nocturnal equatorial spread F irregularities, discussing amplification in collision dominated medium 03 p0477 A70-13990

Electroexplosive devices protection from electrostatic discharge by creation of preferential discharge path, considering use of high intensity neon lamp 03 p0549 A70-14134

Philosophical, design, hardware or static sensitivity type myths refutation concerning electroexplosive devices 03 p0549 A70-14135

First order pressure gradient microphone design based on electrostatic principle, using foil electrets to discriminate against airborne and solid-borne noises 05 p0821 A70-16402

Semi-Lagrangian formulation of Vlasov equation in two and three dimensional electrostatic problems, investigating tensor determinants and perturbation 08 p1553 A70-21614

Display devices using electrostatic forces, discussing electrostatic printing, magnetic display system, etc 08 p1499 A70-21686

Galaxies and stars interactions, explaining observed peculiarities by electrostatic and electromagnetic forces 09 p1750 A70-22097

Perfect gas mixtures thermodynamic functions at high temperatures with correction for Debye-type electrostatic interaction effects 10 p1968 A70-24707

Gravitational field and ellipsoidal gravitational waves anisotropy, deriving gravitistics results from electrostatics 11 p2083 A70-25944

Electrostatically focused klystron design, discussing gain, bandwidth, efficiency, noise and reliability 13 p2379 A70-29666

Grid assemblies as electrostatic plasma wave antennas, computing driving point and transimpedances for approximating single pole impedance in heavy Landau damping regime 13 p2371 A70-29918

Convective or absolute electrostatic instability in weakly inhomogeneous hot magnetoplasma, determining density and frequency for onset 14 p2622 A70-30695

Normal wave propagation modes existence in magnetized plasma, deriving criteria for electrostatic approximation validity 14 p2624 A70-31045

Cesaro Fourier series summation method for boundary value problems in electrostatics 14 p2600 A70-31419

Electrostatic sheet model for plasma, emphasizing computer solutions of various problems 18 p3295 A70-36788

Short graphite fiber classification and orientation control in matrix by electrostatic methods 20 p3654 A70-39215

Scaling laws for turbulent plasma anomalous conductivity dependent on electrostatic fluctuation spectrum 23 p4227 A70-44796

ELECTROSTRICTION

Three dimensional electrostriction theory for stress and displacement on penny-shaped crack in elastic dielectric with conducting oblate spheroidal inclusion 07 p1409 A70-19569

ELECTROTHERMAL ENGINES

Ground based space simulation of arc-type electrothermal propulsion systems, discussing test facilities 01 p0161 A70-10225

Refractory metals in rocket propulsion devices, applying tungsten in uncooled rocket nozzles and tungsten and rhenium to electrothermal propulsion 03 p0512 A70-13617

Performance analysis for electrothermal thruster using lithium propellant with supersonic heat addition [AIAA PAPER 69-286] 06 p1129 A70-17159

Electrothermal thruster with liquid propellant, describing energy dissipation and high specific impulse 15 p2791 A70-32280

Electrothermal thruster with biowaste propellants, discussing design and performance with various propellant compositions [AIAA PAPER 70-1161] 20 p3567 A70-40201

ELEKTRON SATELLITES

NT ELEKTRON 2 SATELLITE

NT ELEKTRON 4 SATELLITE

ELEKTRON 2 SATELLITE

Elektron 2 and 4 satellites orientation based on on-board solar and magnetic sensors 12 p2314 A70-28256

Soft electron fluxes spatial distribution and temporal variations in magnetosphere based on Elektron 2 charged particle trap data 12 p2295 A70-28259

ELEKTRON 4 SATELLITE

Elektron 4 satellite radio emission data transmitted from July to December 1964, noting month-to-month variations in mean radiation level 01 p0172 A70-11496

Elektron 2 and 4 satellites orientation based on on-board solar and magnetic sensors 12 p2314 A70-28256

ELEMENT ABUNDANCE

U ABUNDANCE

ELEMENTARY EXCITATIONS

NT EXCITONS

NT MAGNONS

NT PHONONS

NT PLASMONS

ELEMENTARY PARTICLE INTERACTIONS

NT ELECTRON CAPTURE

Cosmic ray electron and proton interaction, discussing hydromagnetic waves, synchrotron radiation, magnetic field effects and wave propagation 20 p3695 A70-39012

Potential fluctuations in intersecting plasma jet streams attributed to ion-electron instability, using external probe 20 p3682 A70-40136

Cosmic ray research role in high energy physics, discussing elementary particle interactions 22 p4096 A70-43398

ELEMENTARY PARTICLES

NT ALPHA PARTICLES

NT ANTINEUTRINOS

NT ANTIPARTICLES

NT BARYON RESONANCES

NT BETA PARTICLES

NT BOSONS

NT CONDUCTION ELECTRONS

NT DEUTERONS

NT ELECTRONS

NT FAST NEUTRONS

NT FERMIONS

NT FREE ELECTRONS

NT HADRONS

NT HIGH ENERGY ELECTRONS

NT HOT ELECTRONS

NT HYPERONS

NT LEPTONS

NT MESON RESONANCES

NT MESONS

NT N ELECTRONS

NT NEGATONS

NT NEUTRINOS

NT NEUTRON BEAMS

NT NEUTRONS

NT NUCLEONS

NT PHOTOELECTRONS

NT PHOTONEUTRONS

NT PHOTONS

NT PI-ELECTRONS

NT PIONS

NT POSITRONS

NT PROTONS

NT QUARKS

NT SOLAR PROTONS

NT THERMAL NEUTRONS

- Gravity effect on atoms, neutrons, electrons and photons, measurement techniques and comparison with macroscopic bodies 03 p0524 A70-13172
- Bethe function for ionization losses in energy of elementary particles heavier than electron 05 p0899 A70-15961
- Scintillation spectrometer design for mass and energy spectra of elementary particles, discussing block diagram 05 p0846 A70-15962
- Elementary particles gravitational interactions, identifying tensor field with local gravitation 15 p2776 A70-31732
- ### ELEVATION ANGLE
- HF oblique ionospheric soundings over long temperate latitude path, discussing measured angles of elevation and multipath time dispersion 05 p0847 A70-15998
- Wind compensation for wind effects with elevation angle in ballistic rocket launching problems 07 p1394 A70-19718
- Low elevation angle focusing of oblique radio waves after reflection from E and F layers 19 p3379 A70-37965
- Tracking elevation/azimuth errors due to frame misalignment, presenting least squares procedure for determining true bias and misalignment angle and axis 23 p4215 A70-44518
- ### ELEVATIONS [DRAWINGS]
- ### U DRAWINGS
- ### ELEVATORS [CONTROL SURFACES]
- Mounted-above-wing jet engine effect on wing pressure distribution and elevator unit, using fluid mechanical model 04 p0735 A70-15146
- Wind tunnel investigated flow stabilization at horizontal control surfaces by vortex BCL technique, considering angles of attack, elevator deflection and shape 06 p0968 A70-17853
- High performance aircraft self adaptive feedback control system, using airborne digital computer with inputs of elevator deflection and pitch rate for effectiveness identification 20 p3605 A70-40119
- ### ELEVONS
- Structural design and fabrication of load bearing Ta alloy radiation cooled elevon control surface for high L/D hypersonic flight vehicle 02 p0306 A70-11941
- ### ELIMINATION
- Barometric pressure reduction effect on gaseous and volatile metabolic products elimination in men wearing oxygen-supplied rubberized suits 17 p0308 A70-35363
- ### ELLIPSOIDS
- Material particles unrealizability of periodic motion near libration points of triaxial ellipsoid rotating steadily about polar axis 08 p1543 A70-20491
- Dynamic stability of Jeans spheroid and Roches ellipsoid using small perturbations method 09 p1759 A70-22749
- Reference ellipsoids mutual positions determination from observational data by satellites using triangulation points of two triangulations 09 p1763 A70-23327
- Aluminized epoxy integrating hemiellipsoid reflector, discussing fabrication, focusing properties and selection of detector size 09 p1683 A70-23530
- Book on liquid masses ellipsoidal figures of equilibrium extended into coherent mathematical theory, discussing virial equations, potentials of homogeneous and heterogeneous ellipsoids, etc 10 p1917 A70-24701
- Heat transfer influence on three dimensional boundary layer separation on walled ellipsoid of revolution 10 p1870 A70-24781
- Superconducting ellipsoid of revolution in alternating magnetic field, computing disturbed field components using boundary value problem 10 p1917 A70-25201
- Stress concentration near ellipsoidal cavity in transversely isotropic body using solutions for transversely isotropic ellipsoid of revolution 11 p2129 A70-25564
- Triaxial earth ellipsoid best fitting parameters for geoidal surface radius vector by spherical harmonics with coefficients computed from satellite observations 13 p2398 A70-29207
- Wind tunnel tests of flow past oblate ellipsoid of revolution incident on major axis, measuring pressure distribution 15 p2671 A70-31494
- Hypersonic gas flow characteristics incident on elliptic paraboloid and triaxial ellipsoid at arbitrary angles of attack 15 p2672 A70-31647
- Electromagnetic wave scattering at ellipsoidal bodies in microwave rectangular and circular waveguides 17 p3046 A70-35346

- Inhomogeneous plasma ellipsoid equilibrium in external HF field, assuming parabolic density distribution 19 p3479 A70-37739
- Density and distribution functions for quotient of ellipsoids of variance volumes, yielding probabilities and fractiles in three dimensional sets of points 19 p3382 A70-37835
- Jacobi ellipsoid quasi-static evolution by gravitational radiation, discussing direction of increasing angular velocity toward nonradiating state at bifurcation point with Maclaurin sequence 20 p3702 A70-39018
- Three dimensional elasticity for figures close to ellipsoid of revolution with displacements on boundary 23 p4266 A70-43988
- Stable ellipsoidal plasma configurations in alternating electrode annular system, considering longitudinal magnetic field strength, electrode voltage and gas discharge chamber pressure 24 p4385 A70-45456
- Galactic evolutionary models using disklike Riemann ellipsoids with internal motions and gravitational gas equilibria 24 p4410 A70-45759

ELLIPSOIDS

- Anions adsorption at platinum determined by ellipsometry, finding perchlorate and fluoride ions adsorption below detection limit 03 p0441 A70-14043
- Parameters defining elliptic vibration of light reflected from surface using photoelectric ellipsometer 08 p1546 A70-21673
- Hertzian differential polarimeter-ellipsometer with single detector designed for multiwave oscillations analysis 10 p1888 A70-24477
- Ellipsometry with Poincare sphere representation, describing application to automatic two and three dimensional photoelasticity by scattered light 17 p3086 A70-35014

ELLIPTIC DIFFERENTIAL EQUATIONS

- ### NT MONGE-AMPERE EQUATION
- General boundary value problem solutions for degenerate second order elliptic equations 01 p0130 A70-10128
- Interior estimates for second order elliptic differential or finite difference equations, applying maximum principle 01 p0131 A70-10375
- Algorithm for solving Dirichlet problem of nonlinear elliptic differential equations representing atmospheric dynamics balance equation 01 p0134 A70-11609
- Alternating direction implicit difference schemes for solving Laplace and biharmonic elliptic equations 03 p0518 A70-13026
- Elliptic system of twelfth order equations describing elastic equilibrium of plate with kinematic functions analyzed by integration procedure 03 p0600 A70-14306
- Boundary value problems in closed spaces with fine grained Liapunov boundary described by second order elliptic differential operators 05 p0877 A70-16881
- First boundary value problem for quasi-elliptic and quasi-parabolic equations, discussing solvability and boundary behavior near characteristic points 07 p1322 A70-18854
- Boundary value problem for self conjugate elliptical fourth order differential equation with variable coefficients, proving convergence of iterative process 07 p1528 A70-20143
- Nonlinear steady state diffusion elliptic boundary value solutions exemplifying enzyme kinetics and radiation cooling 08 p1596 A70-20580
- Boundary value problem for linear elliptic differential operator degenerating on region boundary 08 p1534 A70-21119
- Second order elliptic differential equations solution involving Dirichlet problem reduced to equivalent singular integral equations 10 p1908 A70-23923
- Coerciveness /Korn/ inequalities role in boundary value problems for elliptic systems of partial differential equations, noting applications to three dimensional linear elasticity theory 12 p2260 A70-26974
- Second order self conjugate elliptical differential equation for modulus of gravitational field strength, giving geometrical interpretation of coefficient 12 p2223 A70-27349
- Inverse boundary value problems involving elliptic equations solved by Newton method and discrete invariant imbedding 13 p2440 A70-28650
- Elliptic equations solved by projection network methods noting estimate derivation for convergence rates 13 p2440 A70-28962
- Axisymmetrical boundary value problem solution by net point method via transformation into self ad-

joint second order elliptic equation, obtaining positive-definite matrix 15 p2767 A70-31588

- Finite difference schemes for systems of elliptic and parabolic equations, using brute force algorithm 16 p2941 A70-33246
- Generalized boundary value problems solution for elliptic differential equations by Schwarz method, proposing algorithm 18 p3283 A70-36573
- Boundary value problems for elliptic equations with discontinuous coefficients, using finite element method 21 p3845 A70-40734
- Iterative solutions for systems of nonlinear equations and discretization of elliptic differential equations 21 p3845 A70-40736
- Coupling components in homotopic classification of elliptic systems of second-order equations with independent variable 23 p4212 A70-44349
- Asymptotic small-parameter solution of boundary value problem for second-order elliptic equations with variable coefficients in thin regions 24 p4424 A70-45635
- ### ELLIPTIC FUNCTIONS
- Elliptic integrals for plane motion of stars, assuming stationary gravitational potential of stellar system 01 p0174 A70-10138
- Book on integrals and elliptic functions in real domain, solving fourth degree Hermitian equation and integral reduction 02 p0323 A70-11897
- Birkhoff normalizing canonical transformation built at elliptic type of equilibrium without internal resonance, using Lie transforms 05 p0909 A70-16340
- Half wave stepped digital elliptic filter design showing improvements over microwave TEM line narrow band bandpass filter 08 p1476 A70-21284
- Circuit development for realizing narrow bandwidth elliptic function filters at microwave frequencies 08 p1476 A70-21285
- Hertzian contact stress deformation coefficients defined in transcendental equation with elliptic integrals noting errors 08 p1593 A70-21617
- Flexo-torsional elasticity ellipse determining displacements, hyperstatic reactions and influence lines in beams with straight axis and variable cross section 09 p1771 A70-22398
- Triaxial earth attraction potential from expanding certain elliptical functions into series, noting consistency with concepts of astronomy and geodesy 15 p2731 A70-32148
- Elliptic boundary value problems involving pseudodifferential operators on bounded manifold, examining solutions analyticity 16 p2941 A70-33269
- Book on abstract methods in partial differential equations, covering functional analysis and distributions, elliptic theory, linear and nonlinear problems, evolution equations, etc 18 p3284 A70-36782
- German book on functional theory, Volume 6, tabulating theta and elliptic functions for application to applied physics, potential theory, fluid dynamics and oscillation theory 19 p3459 A70-38600
- ### ELLIPTIC INTEGRALS
- ### U ELLIPTIC FUNCTIONS
- ### ELLIPTICAL CYLINDERS
- Thermal buckling of elliptic cylindrical shells assuming tangential temperature, constant axial pressure and conservation of elastic properties 04 p0775 A70-15203
- Buckling behavior of elliptical cylinders under normal pressure using linear thin shell theory and Galerkin method, compared with test results [ALAA PAPER 70-105] 06 p1169 A70-18038
- Large Froude number solution for nonseparative impact of elliptical cylinder floating on incompressible fluid surface in half space extended to small Froude numbers 07 p1253 A70-18770
- Elliptic cylinders buckling under normal pressure analyzed on polyvinyl chloride sheet models 07 p1406 A70-19304
- Circulating flow around elliptical cylinder in inviscid liquid vortex 09 p1659 A70-22435
- Wave scattering from elliptic cylinder, solving boundary value problem for two dimensional wave equation 15 p2700 A70-32404
- Plane wave scattering by strip of elliptical cylinder, considering geometrical diffraction theory 15 p2700 A70-32405
- Plane TM wave scattering by systems of two parallel conducting elliptical cylinders, metal tapes and combinations 19 p3374 A70-37278

Scattering structures of two parallel elliptical cylinders, tapes or combinations, deriving surface current density distribution under plane TM wave excitation
19 p3375 A70-37279

Straight thin walled elliptical cylindrical shells stability in pure bending, solving boundary value problem
19 p3350 A70-38683

Stationary elliptic cylinders in subcritical flow, determining Strouhal number, pressure fluctuations and wake geometry as functions of angle of attack
[AIAA PAPER 69-745] 23 p4134 A70-44564

Microwave propagation in hollow conducting elliptical pipe waveguide, calculating successive modes cut-off wavelengths by numerical analysis
24 p4318 A70-45212

ELLIPTICAL ORBITS
NT APOGEES
NT INTERPLANETARY TRANSFER ORBITS
NT PERIGEEES
NT PERIHELIONS
NT TRANSFER ORBITS

Minimum propellant maneuver during docking of elliptical orbit rendezvous between propelled and passive target vehicles, analyzing as variational problems
02 p0380 A70-12784

Elliptic restricted three body problem singularities dynamical meaning and character, presenting regularization transformations for equations of motion
03 p0576 A70-14074

Satellites gravity-gradient stabilization by flywheels in elliptical orbits, deriving control system for orientation and optimal motion damping
03 p0582 A70-14321

Hybrid system for allocating domestic synchronous communication satellites in concentric circles within inclined elliptical synchronous orbits
05 p0906 A70-15801

Lunar module rendezvous with command and service module by coelliptic sequence establishing standard lighting and relative position and velocity for final approach
[AIAA PAPER 70-26] 06 p1157 A70-18129

Optimum impulsive velocity calculation for the three dimensional deorbit from elliptical orbits to achieve specified reentry angle
06 p1152 A70-18496

Time optimal rendezvous maneuver between neighboring elliptic orbits, discussing propulsive jet system with variable thrust
07 p1381 A70-19357

Optimal transfer ellipse obtained by complete rotation in gravitational field of axisymmetric planet
09 p1751 A70-22161

Planetary satellites perturbation by sun for elliptical solar orbit, applying Zeipel method to equations of motion
09 p1754 A70-22480

Minimal characteristic velocity of single impulse transfer between coplanar elliptical orbits with allowance for thrust action finite time
10 p1940 A70-24304

Minimum fuel continuous thrust elliptical orbit transfer problem, obtaining optimal steering function for departure and arrival points
11 p2124 A70-26214

Kalman filter modifications for spinning satellite attitude determination in elliptical orbit prior to apogee maneuver, using sun and IR earth sensors
11 p2028 A70-26304

Characteristic exponents for periodic orbits of infinitesimal body attracted according to Newtonian law by two finite bodies revolving in ellipses about mass center
13 p2498 A70-30005

Satellite feedback attitude control system resulting in high accuracy earth pointing motions in elliptic orbits
14 p2654 A70-31172

Equations of motion for circular periodic orbits extended to elliptic restricted three body problem
15 p2806 A70-32803

Satellite path geometry along Keplerian elliptical orbit, taking earth flattening into consideration
18 p3312 A70-36167

Intermediate elliptical orbits for planetary satellites with small inclination to equatorial plane
18 p3312 A70-36174

Bester comet 1946k-1947I orbit, showing original and future orbits as long period ellipses
19 p3515 A70-37931

Burnham-Slaughter 1958e-1959I comet orbit, showing nearly parabolic ellipse
19 p3516 A70-37933

Lunar module rendezvous with command and service module by coelliptic sequence, establishing standard lighting and relative position and velocity for final approach
[AIAA PAPER 70-26] 21 p3931 A70-41860

Two particles relative motion in elliptical orbits in inverse square central force field
23 p4244 A70-44576

Moderately elliptic reference orbit perturbed motion, applying linearized perturbation equations for circular orbit
23 p4244 A70-44590

German monograph on Milky Way spiral structure, describing elliptic orbit model
24 p4399 A70-45100

ELLIPTICAL POLARIZATION
Pulsar synchrotron emission model, discussing elliptic polarization, pulse shape, duration and negative absorption /wave amplification/
01 p0183 A70-10897

Elliptically polarized microwave oscillations conversion to linearly polarized oscillations with polarization plane in original orientation
04 p0655 A70-14608

Elliptically polarized microwave scattering at electrically conducting rough surface, considering probability distribution of profile angles and random reflection coefficients
04 p0650 A70-15286

Polarization loss for elliptically polarized antennas, using curves based on Hatkin equation
06 p1019 A70-17504

Slot transmission line applicability to miniature ferrite phase shifter design exploiting elliptically polarized H field existence
08 p1475 A70-21283

Radio wave reflection from ionosphere, discussing suppression of magnetoionic component with fluctuating elliptical polarization
11 p2003 A70-25534

Radio wave reflection from ionosphere, discussing suppression of magnetoionic component with fluctuating elliptical polarization
21 p3786 A70-41284

ELLIPTICITY
Supersonic flow past elliptic cone of small eccentricity treated as axisymmetric conical flow perturbation
05 p0790 A70-16506

Aerodynamic effects of bluntness on slender cones in free flight tests at Mach 17
[AIAA PAPER 70-554] 13 p2340 A70-29019

Clamped edge thin flat elliptic plate subject to elliptic paraboloidal loading, determining middle surface deformations for nonlinear large deflections
19 p3547 A70-38359

ELONGATION
Ni maraging steel sheets tensile strength and elongation anisotropy, studying effects of directional cold work, aging and annealing
07 p1306 A70-19072

Elongation measurement in tensile testing of thin films and sheeting, coupling with gripping test program
10 p1887 A70-24042

Thickness effects on elongation of sheet type Al alloys, tabulating tensile test results
10 p1887 A70-24043

EMBEDDING
Euler-Lagrange linear operators in variational embedding with one dependent function
05 p0881 A70-16058

Embedded damped sandwich beams, determining equations for resonant frequency, loss factor and modal roots
16 p2992 A70-34018

EMBOLISMS
NT AEROEMBOLISM
NT FAT EMBOLISMS

EMBRIEMENT
Transformation induced plasticity steels tensile properties measurement indicating loss of ductility due to H embrittlement
01 p0118 A70-10729

Polycrystalline Mo ductility at low pressures in tension at ambient temperature, discussing H type embrittlement mechanism
01 p0121 A70-11234

Ferritic stainless steel embrittlement caused by He injected into tensile samples by alpha particle cyclotron irradiation tested at elevated temperatures
01 p0122 A70-11235

Nb-Mo alloys in various proportions prepared by vacuum casting, showing embrittlement under hydrogen atmosphere
02 p0318 A70-12671

Embrittlement in martensitic and semiaustenitic precipitation hardening stainless steels upon exposure to high temperatures to determine causation and controlling means
03 p0506 A70-13132

Austenitic fcc Cr-Mn-N stainless steels ductile-to-brittle transition behavior noting role of deformation faulting
03 p0506 A70-13133

Polycrystalline metals strength factors in aircraft and aerospace applications as relation between rupture time and embrittled grain boundary at high temperatures
04 p0779 A70-15671

Delayed failure due to hydrogen embrittlement of structural high strength steels, discussing stress corrosion
04 p0710 A70-15678

Hydrogen embrittlement as delayed rupture origin in high strength steels
04 p0711 A70-15682

Cracks development in hydrogenated silicon iron, investigating plastic strain relation and brittle rupture propagation
06 p1165 A70-17580

Hydrogen embrittlement of landing gear steels, discussing plating bath program additions for optimum safety conditions
07 p1294 A70-19349

Iron base and nickel base alloys susceptibilities to internal hydrogen and hydrogen environment embrittlements, studying crack initiation inside and at metal surface
08 p1520 A70-21515

Ti-8Al alloy embrittlement from ordered phase precipitation during aging using tensile, impact and hardness tests, optical and electron transmission microscopies
13 p2436 A70-29624

Hardened steel embrittlement in low pressure hydrogen caused by crack growth as function of temperature
13 p2436 A70-29804

Hydrogen embrittlement of martensitic Fe-Ni alloys as function of temperature via slow strain rate tensile tests
15 p2755 A70-31559

Omega phase embrittlement in aged Ti-V alloys, discussing precipitation effect on tensile properties
15 p2756 A70-31570

Stress corrosion cracking of high strength structural, tool and maraging steels due to hydride, diffusion controlled and mixed embrittlement
16 p2934 A70-34301

Ti equipment anodizing methods, observing corrosion resistance reduction and embrittlement hydriding due to Fe contamination
17 p3098 A70-34363

Ti alloys embrittlement, investigating time temperature dependence of brittle subsurface layer formation during elevated temperature air exposure
17 p3112 A70-34365

Titanium hydride deformation assisted nucleation in alpha-beta titanium alloy, showing low strain rate embrittlement and stress corrosion crack propagation in aqueous environments
17 p3116 A70-34395

Hydrogen embrittlement of Ti and Ti alloys under plastic deformation and critical hydrogen concentration
17 p3117 A70-34397

Unalloyed Ti hydrogen embrittlement, determining factors affecting brittle-ductile transition temperature
17 p3117 A70-34398

Transformation induced plasticity (TRIP)/high strength steels resistance to hydrogen embrittlement
18 p3273 A70-36047

Nuclear irradiation effect on embrittlement of Ti and Ti alloys at cryogenic temperature, determining radiation damage threshold as function of tensile properties changes
18 p3278 A70-36567

Fracture behavior and tempered martensite embrittlement relationship in steel, using V- notched and fatigue precracked Charpy specimens
22 p4054 A70-42736

Ti embrittlement by liquid Cd, discussing ductile-brittle transition temperature dependence on strain rate
22 p4054 A70-42738

EMBRYOS
White single-comb Leghorn chick embryonic development at increased pressures at various hyperbaric gas mixtures for ten day periods
06 p0991 A70-17296

High altitude and sea level erythropoietic and somatic development in chick embryos indicating optimal physiological adaption with prolonged exposure
07 p1202 A70-18864

Chick embryogenesis during hypoxia at high altitude, noting metabolic repression effects, hypothermia and brain atrophy
14 p2536 A70-30188

High strength magnetic fields effect on early embryonic development of frogs, relating growth abnormalities and paramagnetic ferritin motions
16 p2848 A70-33099

Human hemoglobin chain, noting zeta chain synthesis during embryonic development
24 p4297 A70-45406

EMERGENCIES
Ground and ditching emergency evacuation tests of C-9A aeromedical aircraft under worst possible simulated crash conditions
01 p0035 A70-10716

Space flight emergencies causes and consequences, underlying life threats and crew survival times, considering equipment failures, personnel errors, etc
04 p0761 A70-14926

Medical kit utility for colds, sore throats, scrapes, cuts and bruises
07 p1219 A70-19021

Human acceleration resistance and psychomotor behavior under emergency flight conditions, including

high temperature exposure and remaining in clino-static position 17 p3037 A70-35135

Manned spacecraft abort guidance and control problems, discussing various modes and emergency conditions 24 p4374 A70-46210

EMERGENCY BREATHING TECHNIQUES

Aircraft passengers and crew fire protection in crashes via insulating air-carrying foam ejected into compartment from fuselage 23 p4140 A70-44465

EMERGENCY LIFE SUSTAINING SYSTEMS

Three man space escape system, describing emergency situations, parachute descent, life raft design, rescue operations and engineering tests [AIAA PAPER 68-936] 04 p0763 A70-15403

DC-8 aircraft ditching in San Francisco Bay on 22 November 1968, discussing accident sequence, evacuation operations, life raft stowage and deployment, etc 06 p0985 A70-17705

Solid propellant cool gas generating systems applications to inflating emergency escape slides, rafts, pontoons and flotation bags 06 p0986 A70-17720

Survival training for safety promotion in emergency, discussing psychological factors, communication, living off land and shelter 07 p1218 A70-19007

Spacecraft incorporated emergency rescue systems, discussing design of nonseparable crew escape compartment and separable capsule 07 p1218 A70-19010

Emergency equipment for aircraft accidents with dual channel radio beacons installed on life rafts, noting electronically conducted search 07 p1191 A70-19011

Helicopter utilization in emergency transportation of civilian patients, discussing questionnaire results from medical and police agencies 08 p1454 A70-21937

Decompressed crewmember rescue onboard spacecraft and aircraft by compartmentalization combined with air locks 08 p1454 A70-21938

Survival on sea following air accident, based on medical and technical considerations, emphasizing life jackets 09 p1625 A70-23008

Commercial jet passenger emergency oxygen needs for cabin decompression studied in determining time of safe unconsciousness 11 p1992 A70-26511

Patients emergency transportation by helicopter, discussing vehicle types and onboard medical treatment 14 p2540 A70-30191

Hazard analyses of Concorde aircraft design, noting engine control failures and emergency equipment use probabilities 15 p2675 A70-32213

Aircraft passengers and crew fire protection in crashes via insulating air-carrying foam ejected into compartment from fuselage 23 p4140 A70-44465

High energy emergency exit systems for passenger survival in aircraft accidents 23 p4140 A70-44466

Flotation device for infants and small children incorporating life support and survival capabilities for aviation and marine applications 23 p4153 A70-44480

Nonflammable fibrous textile materials for injury and personnel loss prevention in fires by aircraft accidents 23 p4153 A70-44481

Presentation styles of passenger emergency evacuation briefing cards, noting preference for sequential action graphic displays with minimum key wording 23 p4141 A70-44486

Emergency life saving instant exits for transport aircraft, using electromechanical confined transfer shaped explosive device 23 p4141 A70-44487

Spinal injury prediction during emergency ejection and crash impact protection research 23 p4153 A70-44489

Civilian survival in emergency situations, discussing basic requirements, environments, vehicles and equipment for survival kits 23 p4153 A70-44495

Modularized multiple use SIIS-3 ejection seat escape system, discussing weight, envelope and low cost 23 p4143 A70-44499

EMISSION

NT BIOLUMINESCENCE
NT CHEMILUMINESCENCE
NT ELECTROLUMINESCENCE
NT ELECTRON EMISSION
NT FIELD EMISSION
NT FLUORESCENCE
NT INCANDESCENCE
NT ION EMISSION

NT LIGHT EMISSION
NT LUMINESCENCE
NT LUNAR LUMINESCENCE
NT NEUTRON EMISSION
NT OPTICAL RESONANCE
NT PARTICLE EMISSION
NT PHOSPHORESCENCE
NT PHOTOELECTRIC EFFECT
NT PHOTOELECTRIC EMISSION
NT PHOTOIONIZATION
NT PHOTOLUMINESCENCE
NT RADIO EMISSION
NT SECONDARY EMISSION
NT SHOCK WAVE LUMINESCENCE
NT SOLAR RADIO BURSTS
NT SOLAR RADIO EMISSION
NT SPECTRAL EMISSION
NT SPONTANEOUS EMISSION
NT STIMULATED EMISSION
NT THERMAL EMISSION
NT THERMIONIC EMISSION
NT THERMOLUMINESCENCE
NT TYPE 2 BURSTS
NT TYPE 3 BURSTS
NT TYPE 4 BURSTS
NT TYPE 5 BURSTS
NT X RAY FLUORESCENCE

EMISSION SPECTRA

Chromospheric structural parameters determined from XUV spectroheliograms, discussing He 2 emission, O 4 and O 5 emission distribution, etc 01 p0175 A70-10246

X ray line emission from Sco X-1 using Monte Carlo estimates of spectral distribution of scattered photons in terms of Fe line and cosmic abundance 01 p0169 A70-10338

Upper atmospheric atomic H and He concentration height distribution, considering L alpha and H alpha emissions, He emission, light components and direct measurements 01 p0074 A70-10589

Nova Delphini 1967 emission line spectrum at 8400-9600 A, using diffraction spectrograph attached to astronomical telescope 01 p0182 A70-10675

Quasars emission and absorption red shifts distribution analysis suggesting cluster interpretation 01 p0183 A70-10895

Spectrometer scanning .20-15 microns in 3 sec, measuring absorption and emission spectra of hot samples alternately, discussing resolutions at various bands 01 p0091 A70-10914

Antarctic twilight observation by photoelectric scanning spectrometer in search for metallic emission lines in upper atmosphere 01 p0081 A70-11231

Excitation, reemission and absorption spectra of Cr activated powdery Mg titanate prepared, using MgO and Ti dioxide with LiCl as flux 02 p0350 A70-11848

Giant pulse Q switched lasers generated plasmas, noting VUV spectral line shifts, asymmetries and existence of satellite lines 02 p0345 A70-11894

Chlorine dioxide-methane mixture flame stabilized in low pressure burner, determining emission spectra, burning velocity, activation energy, etc 02 p0251 A70-12033

Jupiter Red Spot continuous spectrum intensity distribution and methane/ammonia absorption between 3300-6500 A 02 p0374 A70-12427

Emission spectrum characteristic distortion in scattering of background X rays at large red shifts by metagalactic electrons, considering photon scattering effect 02 p0358 A70-12491

Emission lines origin in radio galaxies optical spectra explained by using energy gained from radioactive elements decay 03 p0563 A70-13214

Eta Carinae IR region emission and absorption spectra characteristics in tabular form 03 p0565 A70-13269

Free-bound and free-free continuous emission of hydrogen near Balmer jump in T Tauri star AS209 03 p0440 A70-13315

Chemiluminescent reaction rates measurements for emission of diatomic oxygen molecules Herzberg bands in oxygen and oxygen-inert-gas afterglows 03 p0440 A70-13379

Low molecular weight organic semiconductors photoelectron UV emission spectra, studying electron energy distribution and optical ionization, dark bulk conductivity, etc 03 p0541 A70-13728

Dynamic spectra of quasi-periodic VLF emissions noting association with geomagnetic micropulsations 03 p0477 A70-13985

Radiative lifetimes and total transition probabilities measured in polyatomic gases using phase shift method and electron beam excitation 03 p0441 A70-14009

Photoelectric intensity measurements on emission bands of oxygen Herzberg I system excited in argon-oxygen afterglow 03 p0528 A70-14350

Photon absorption and emissivity of nonequilibrium cylindrical plasma in Doppler broadened lines and hemisphere approximation 04 p0724 A70-14411

Transient emissions on He I wavelength during breakup phase of auroral events, discussing observational interference by OH bands 05 p0907 A70-16277

Absolute values of emission cross sections for vibrational Meinel bands of molecular nitrogen ions excited by electron impact 05 p0901 A70-16279

Solar cosmic ray flare /28 January 1967/ observed by neutron monitors, determining emission and particle spectrum at atmosphere boundary 05 p0903 A70-16752

H alpha line for emission nebulae analyzed by Fabry-Perot etalon, noting Doppler profile 05 p0917 A70-16907

Nd glass laser emission spectral width reproducibility as function of flash intervals and pump energy 07 p1297 A70-18869

Photometric observations of Ikeya-Seki comet 1965f by equidensity method, observing CN emission in head 07 p1379 A70-19043

Hydrogen and helium emissions in upper atmosphere, observing amplifications towards geomagnetic poles and in winter hemisphere 07 p1266 A70-19439

Exciton spectrum in semiconductor laser emission, investigating location in Brillouin zone and temperature dependence 07 p1298 A70-19478

Extra-atmospheric submillimeter astronomy, discussing emission observations between IR and RF region and astrophysical-cosmological applications 07 p1387 A70-19643

Laser emission from organic molecules under neodymium laser harmonics excitation, describing absorption and photochemical inversions effects and emission spectra characteristics 07 p1300 A70-19866

Emission kinetics variations of ruby laser due to aging attributed to inhomogeneity of active medium developing simultaneously with color centers 07 p1300 A70-19872

Nitrogen IR emission spectra from atomic and molecular excited electronic states transitions, studying DC discharges at various pressures 07 p1339 A70-20092

Predawn enhancement of emission rate of 6300 A forbidden O I line in nightglow spectrum, discussing onset time 07 p1275 A70-20286

Carbon dioxide laser emission spectrum, considering working mixture emission power and rotational relaxation characteristics 08 p1511 A70-20539

Emission flame spectrometer based on double diffraction monochromator, describing design features and operating characteristics 08 p1493 A70-20545

Cygnus and Perseus symbiotic stars as binaries, studying radial velocities, relative emission line intensities and energy distribution 08 p1569 A70-20830

Celestial emission bodies forbidden line analysis for physical conditions determination using formulas and graphs 08 p1569 A70-20831

Pulsars radio, optical and X ray emission spectrum analysis, suggesting oscillating current sheets as radiation source 08 p1561 A70-20914

Sunspots narrow and double K lines probable emission by quiescent type prominences 08 p1575 A70-21372

Excitation and layers heights for 5577 A and O2 bands of atmospheric and Herzberg systems in night airglow estimated, suggesting Chapman reaction for emission 08 p1492 A70-21755

Unsaturable frequency discriminator influence in semiconductor laser feedback loop on laser emission spectrum 08 p1514 A70-21821

Deuterium Lyman alpha line profiles generated from microwave powered lamp for experimental testing of two layer model characterizing emission line profiles 09 p1730 A70-22066

Lyman-Birge-Hopfield nitrogen bands high resolution emission spectrum, giving energy values of particular states together with corresponding rotational constants and band origins 09 p1730 A70-22067

Active element inhomogeneity effects on semiconductor injection lasers emission spectra and radiation intensity distribution 09 p1695 A70-22481

- Water vapor emission detection from IR stars, discussing radial velocities of microwave lines 09 p1756 A70-22523
- Ni L alpha X ray emission line shape and position as function of bombarding electron energy, observing differential self absorption in anode 09 p1731 A70-22777
- Relative transition probabilities of Si I and II determined from emission spectra obtained by injecting SiC14 vapor into argon plasma jet 09 p1737 A70-23315
- Optically variable compact galaxy with broad emission lines similar to Seyfert and N-type galaxies, noting no stellar contribution in continuous spectrum 09 p1765 A70-23808
- Ruby monopulse laser emission spectrum wavelength stabilization by frequency tuning of generated radiation using Fabry-Perot interferometer 10 p1898 A70-23970
- Pulsars dynamic spectra in 110-420 MHz range, observing emission bandwidths to formulate power law 10 p1938 A70-24099
- Emission and absorption by nonhomogeneous gases with vibration-rotation bands determined by scaling approximation 10 p1968 A70-24474
- IR oxygen emission transmission characteristics in atmosphere compared with ground-based observation 10 p1876 A70-24538
- Elongated neutral-hydrogen emission feature in Sco-Oph region, comparing with interstellar sodium lines for distance from sun 10 p1945 A70-24966
- Bremsstrahlung radiation in intense magnetic field proposed as emission mechanism from pulsars, discussing absorption coefficient 11 p2104 A70-25697
- Airborne geological mapping by IR emission spectroscopy, describing instrumentation, materials discrimination capability, data processing, etc 12 p2230 A70-26957
- Ruby laser with electro-optical Q switching, using polarization element for emission spectrum narrowing to single longitudinal mode 12 p2245 A70-27303
- Inhomogeneous interatomic magnetic field effects on spectral line widening and shifts of emitting atoms in low temperature plasma 12 p2278 A70-27318
- Emission spectrum of neon-helium laser receiving Doppler shifted signal from moving mirror, showing memory effect due to beat harmonics 12 p2246 A70-27352
- Emission spectrum of He-Ne CW laser with non-resonant feedback mode achieved with scattering agent and various mirror schemes 12 p2246 A70-27354
- Electroluminescence recombination emission spectra during avalanche breakdown in AlGaAs n-p and p-n heterojunctions 12 p2286 A70-27367
- Nonthermal radiation effects on emission line spectra of Seyfert galaxies and quasars determined from ionization equilibrium of gas envelope 12 p2293 A70-27585
- Emission asymmetry of solar limb flares, inferring luminescent layer contraction-expansion from spectral qualitative analysis 12 p2294 A70-27859
- Mathematical models for radar transmitters emission spectra envelopes calculation, considering effects of pulse width, rise and fall times, corner smoothing and frequency modulation 12 p2189 A70-28136
- Differentiating Fabry-Perot interferometer, obtaining emission spectrum derivatives respecting frequency in millimeter range 12 p2238 A70-28177
- Far UV emission spectrum of plasma produced by laser beam impact on Al target observed as function of time, determining electron temperature 13 p2460 A70-28729
- Laser field structure effect on spectrum of Q switched laser nonmonochromatic emission after amplitude modulation 13 p2426 A70-28872
- DC plasma arc jet excitation and emission characteristics for solution analysis with economical inert gas flow rates 13 p2362 A70-29107
- Steady state laser emission of resonator with two crystals with different optical orientation 13 p2428 A70-29371
- Flat emission spectra of quasars in 3CP catalog attributed to anisotropic relativistic electron fluxes 13 p2493 A70-29387
- Stellar upper atmospheric shock wave motion, discussing emission spectra interpretation and temperature gradients 13 p2493 A70-29395
- Lunar crater Aristarchus red spot spectrum analysis, determining emission bands 13 p2494 A70-29398
- Star HBV 475 emission spectra in near IR due to H, He I, OI and Ca II, confirming symbiotic character 13 p2495 A70-29641
- Electron beam-pumped ZnO laser emission wavelength at various temperatures 13 p2430 A70-29833
- VLF auroral and low latitude emissions along N-S chain of stations, discussing daytime and nighttime observations 13 p2371 A70-29925
- Spectrophotometry of comet Honda 1968c, showing free cation and radical emissions and head asymmetry 14 p2635 A70-30304
- Lunar surface thermal emission spectra, calculating IR emissivities 14 p2637 A70-30495
- Lunar surface thermal emission spectra based on laboratory analysis of rocks and minerals emissivity 14 p2637 A70-30496
- Carrier distillation DC arc emission spectrography, determining lead, bismuth and tin traces in nickel base alloys after conversion to oxides 14 p2546 A70-30957
- Superhigh energy particles detection by transition radiation, measuring Lorentz factor of emitted spectra 14 p2616 A70-31003
- Satellite probing method for transmission absorption spectroscopy of planetary atmospheres 14 p2650 A70-31230
- 5577 A /OI/ airglow emission diurnal variations during IGY by normalization method, observing seasonal effects 14 p2578 A70-31239
- Atomic emission in water vapor afterglow, revealing presence of Balmer series of H atom with sodium D line 14 p2579 A70-31255
- Laser devices design, emission characteristics, coherent light, etc 16 p2926 A70-33071
- Uranium plasma emission coefficients as function of DC arc operation, measuring intensity spectrum with scanning spectrometer [AIAA PAPER 70-692] 16 p2950 A70-33554
- Propellant flame temperature and emission spectra during depressurization by rarefaction waves, using rapid scanning spectrometer [AIAA PAPER 70-663] 16 p2962 A70-33570
- Near IR electronic emission spectrum of positive column in flowing oxygen electric discharge, noting vibrational temperature 16 p2955 A70-33981
- Hyades stars between F4 and K5, measuring chromospheric H and K emission lines dependence on bolometric luminosity 17 p3157 A70-34832
- Solar X-ray flux measurements in selected emission lines, using curved crystal Bragg spectrometers in low altitude sounding rockets 17 p3150 A70-34834
- Quasar and radio galaxies, observing absorptions at red shifts close to emission line 17 p3157 A70-34846
- Red giant star chromospheric activity, discussing Balmer absorption lines and emission lines 17 p3161 A70-34889
- He-Ne CW laser emission line width measurement, describing apparatus and technique 17 p3106 A70-35108
- Optical study of Crab Nebula linear expansion and filamentary proper motions, considering line emission 17 p3164 A70-35113
- German monograph on spectral emission behavior of pulsed ruby laser with regard to output intensity 17 p3107 A70-35369
- Solar chromosphere model evaluation using sensitivity of flux emission in Lyman continuum 17 p3170 A70-35386
- Solar corona radiation at 1-100 A for 1-10 million K, using Jordan ionization equilibrium calculations 17 p3151 A70-35582
- Spectral and temporal characteristics of ruby laser operating with dielectric coated mirror scatterer 17 p3108 A70-35673
- Direction and time variations of O I 4368 A emission following evening twilight 18 p3245 A70-36026
- Nonequidistant structure of axial mode spectrum of ruby laser with plane dielectric mirrors 18 p3266 A70-36418
- Spectral emission kinetics from neodymium glass laser with rod in translational motion during laser action 18 p3267 A70-36613
- Hydrogen and helium emissions in upper atmosphere, observing amplifications towards geomagnetic poles and in winter hemisphere 18 p3249 A70-36913
- Emission spectral distribution of atomic nitrogen reaction with carbon tetrachloride for artificial luminescent clouds 18 p3293 A70-36990
- Na D lines emission cross sections measurement from ionic and neutral gases collisions at simulated meteor conditions 18 p3318 A70-37014
- CdS crystals luminescence spectrum excitation by UV light of ruby laser, noting excitons and phonons recombination 19 p3444 A70-37368
- Radial profiles of emission and absorption coefficients and temperatures in cylindrically symmetric plasmas 19 p3475 A70-37551
- Photoelectric and polarimetric observations of comet 1968 c Honda in BV system, noting dust scattering role in emission 19 p3515 A70-37657
- Night airglow hydroxyl rotational brightness temperature determined from emission spectra 19 p3412 A70-37777
- Galactic plane hard X ray emission measurements, considering gamma and X ray origin from Compton scattering of photons by galactic electrons 19 p3497 A70-38023
- Cygnus constellation energetic gamma ray emission by nuclear emulsion and spark chamber telescope on high altitude balloon 19 p3501 A70-38086
- Astronomical gamma ray emission measurement by balloon-borne spark chamber, presenting results for discrete and diffuse sources and albedo intensities 19 p3501 A70-38088
- Nitrogen dioxide continuous visible emission under thermal and recombination excitation, examining spectral characteristics 19 p3374 A70-38267
- Transverse magnetic field effect on emission spectrum of He-Ne laser, using scanning interferometer 19 p3448 A70-38735
- Pulsed emission in midinfrared region at neutral atomic transitions of inert gases and mixtures, tabulating wavelengths, intensity, component ratios and optimal pressure 19 p3448 A70-38736
- Power, energy and efficiency of emission from dye solutions pumped by incoherent light pulses, allowing for particle accumulation at metastable level 19 p3448 A70-38738
- M sub L alignment creation due to beam foil excitation process demonstrated with zero field quantum beats in He and H emission spectra 20 p3674 A70-39148
- Solar cosmic rays emission spectrum for 23 February 1956 flare, taking into account nucleon diffusion coefficient dependence on particle rigidity and distance to sun 20 p3697 A70-39287
- Microwave emission from GaAs due to EM wave amplification within biased sample 20 p3686 A70-39397
- Giant pulse neodymium glass laser emission spectrum structure, showing cavity geometry effect on fine structure 20 p3641 A70-39450
- Electric fields influence on emission lines shape of multiply charged ions in coronal plasma, discussing kinetic temperature 20 p3704 A70-39462
- Current distribution and interband recombination emission in bipolar semiconductor crystal under pinch effect produced by external magnetic field 20 p3677 A70-39590
- Emission cross sections of nitrogen in vacuum UV by electron impact 20 p3675 A70-39617
- Laser beam method sensitivity for spectral emission analysis of nonconducting materials 20 p3642 A70-39743
- Lunar environment diagnostic features enhancement on IR emission spectra, making moon excellent target for remote sensing 20 p3709 A70-39979
- X ray sources location, distribution and spectral characteristics, investigating emission from supernova remnants 21 p3872 A70-40662
- Galactic K series emission at 1-10 kev by low energy cosmic rays and diffuse X rays interaction with H I region heavy ions 21 p3877 A70-40704
- Tungsten-helium arc atmospheric contaminants spectral monitoring parameters under welding conditions, using rotating circular wedge to oscillate emission lines across exit slits 21 p3831 A70-40725
- Atomic hydrogen emissions in daylight, considering excitation by resonance absorption of solar radiation 21 p3812 A70-40728
- Aerosol IR emission, discussing relative humidity, water droplet size and temperature effects on atmospheric radiance levels 21 p3846 A70-40804
- Solar X-ray spectra of active regions, examining emission lines, fluxes electron temperature and density and transitions 21 p3879 A70-40963
- Laser characteristics of Nd doped lithium germanate and silicate glasses, discussing spectroscopic properties 21 p3838 A70-42010

Inhomogeneous interatomic magnetic field effects on spectral line widening and shifts of emitting atoms in low temperature plasma

21 p3860 A70-42059

Spontaneous emission intensification at 6911 Å in potassium to evaluate plasma local conditions, using low pressure arc and Q switched ruby laser

22 p4049 A70-42359

T tauri star mass loss, observing variations in spectral emission line widths

22 p4101 A70-42858

Be stars hydrogen emission lines widths measurement

22 p4101 A70-42867

Scorpius X-1 X ray line emission, discussing continuum and background counts and cosmic abundance of iron

22 p4094 A70-42931

Planetary nebula NGC 7027 IR line spectra emission, examining S IV and AR III line intensities

22 p4094 A70-42933

X ray K and L emission bands and absorption spectra from TiO, TiN and TiC compared with density of states histograms, considering electronic band structure

22 p4086 A70-43003

Planetary atmospheres X ray fluorescence, calculating Mercury, Venus, earth, Mars and Jupiter emissions

22 p4105 A70-43230

Saturated absorption spectroscopy of various molecules using emission spectra of carbon dioxide and nitrous oxide lasers

22 p4050 A70-43239

Nightglow Na-D lines excitation, attributing emission to Chapman mechanism

22 p4023 A70-43294

Emission spectrum of neon-helium laser receiving Doppler shifted signal from moving mirror, showing memory effect due to beat harmonics

22 p4052 A70-43596

Emission spectrum of He-Xe CW laser with non-resonant feedback mode achieved with scattering agent and various mirror schemes

22 p4052 A70-43597

H II regions density-size relationship, using emission measurements and radio data

22 p4109 A70-43746

CA II chromospheric emission lines for deriving M_{av} in stellar luminosity, discussing calibration

23 p4242 A70-44293

Omicron Ceti (Mira) spectrophotometry before, during and after 1969 maximum, noting TiO bandwidth variations

23 p4242 A70-44294

Be stars rotation, considering emission properties and evolutionary state of main sequence

23 p4249 A70-44807

Earth and atmosphere thermal emission spectra via Nimbus 4 Michelson interferometer, obtaining atmospheric temperature, humidity and ozone profiles

23 p4192 A70-44866

Terminal compensation influence on radiative recombination in n- and p-type GaAs, observing emission band in photoluminescence and electroluminescence spectra

23 p4231 A70-45063

Solar limb emission spectrum between 300-2803 Å, using Skylark rocket instrumentation

24 p4399 A70-45301

Microwave emission from Maxwellian magnetoplasma in uniform magnetic field

24 p4386 A70-45606

HF chemical laser emission in fluorine-containing organic compounds via arc discharges, noting molecular hydrogen effect on p sub 10 and p sub 21 transitions

24 p4355 A70-46046

Spectral anomalies due to inhomogeneous optical pumping in masked ruby laser, using mathematical model

24 p4355 A70-46264

EMISSION

Integral equation for emissivity inside uniform gray isothermal Lambertian cavity solved using successive approximations

02 p0323 A70-11889

Titanium carbide hemispherical and spectral emissivity and electrical resistivity measured at high temperature

03 p0512 A70-13752

Monochromatic radiation emissivity temperature dependence of monocarbides of Ti, Nb and alloys in homogeneity region

08 p1516 A70-20994

Tungsten emissivity and radiance properties obtained at high surface temperatures

09 p1725 A70-22068

Radiation heat transfer around interior of long cylinder as function of surface emissivity

11 p2149 A70-26152

Hemispherical emissivity measurement in vacuum chamber for thermal testing of space satellite structural materials

12 p2332 A70-27984

Earth surface temperature, emissivity and dielectric constant from satellite measurements of SHF radiation

15 p2771 A70-32072

Flux emissivity tables for water vapor, carbon dioxide and ozone based on wavelength dependent absorption coefficients and flux transmissivities

17 p3081 A70-35927

Synchrotron radiation emissivity function containment in dispersion equation for plane wave propagation in magnetoactive plasma

19 p3480 A70-38017

Thermal radiation emissivity predictions for metal surfaces at cryogenic temperatures, comparing anomalous skin effect and Drude single electron theories

23 p4218 A70-44388

Ta spectral emissivity, using ratio of specimen surface and black body spectral radiant intensities

23 p4207 A70-44447

Directional emissivity and thermal diffusivity of solids at 1000-3000 K by radiation comparison method, applying to sintered and plasma sprayed Mu, Ta and W

23 p4207 A70-44661

EMISSOGRAPHS

U ACTINOMETERS

U RECORDING INSTRUMENTS

EMITTANCE

Oxide layers on metal substrate noting emittance dependence on thickness in aluminum-aluminum oxide and Cu-CuO systems

[ASME PAPER 69-WA/HT-4] 04 p0705 A70-14825
Series emittance thermal control coatings of polymeric dielectric films overlaying reflectors vacuum exposed to UV, X ray and proton radiation

[ALAA PAPER 70-64] 06 p1106 A70-18069
Temperature and pressure effects as function of time in spectral and total normal emittance of metal coated refractory metals

[ALAA PAPER 70-68] 06 p1092 A70-18136
Optical parameters effect on directional emittance near edge of two dimensional ceramic coating, using Monte Carlo techniques

[ALAA PAPER 70-67] 06 p1106 A70-18138
Thermal emittance of Cu measured in vacuum in spherical enclosure by calorimetric method to investigate oxidation effect

[ALAA PAPER 70-66] 06 p1180 A70-18139
Calorimetric measurements determining total hemispherical emittance of thin gold films as function of temperature, demonstrating film thickness effect

[ALAA PAPER 70-63] 06 p1180 A70-18140
Emittance measurement by thermal decay integration method

06 p1184 A70-18597
Thermal conductivities and total emittance of Ta, W, Re and alloys at high temperatures compared with NBS values

07 p1313 A70-19894
Guarded disk type emissometer for hemispherical emittance measurements of sample materials in 88 to 420 K range based on steady state calorimetry

[ALAA PAPER 69-600] 13 p2404 A70-28524
Ge and Si hemispherical emittance, showing doping and temperature effects

15 p2784 A70-32055
Kirchhoff law validity for freely radiating metallic surfaces, using emissometer to measure hemispherical emittance

[ALAA PAPER 70-858] 16 p2999 A70-33903
Reflectance measurements of directional spectral emittance of black body cavities with specific geometries, using laser source and integrating hemi-ellipsoid

20 p3627 A70-39091

EMITTERS

NT THERMIONIC EMITTERS

Successive approximations method for incorrectly posed problems in synthesis of radiating systems, discussing radiation patterns of linear emitter

01 p0044 A70-11036
Input conductance variation for common-emitter triode distributed-gain wideband amplifier, deriving energy equations improving tube characteristics

08 p1472 A70-20862
Germanium p-n-p-m transistor frequency oscillation dependence on emitter current, noting forced air cooling effect

09 p1741 A70-23354
Successive approximations method for incorrectly posed problems in synthesis of radiating systems, discussing radiation patterns of linear emitter

10 p1842 A70-25006
Nonuniform emitter current distribution effect on power transistor thermal stability, discussing temperature distribution effects

19 p3387 A70-37821

EMOTIONAL FACTORS

Pilot emotional state during stressful situations from tape recorded vocal utterances of air to ground radio communications using spectrographic analysis

06 p1000 A70-17297

Emotional stability relationship to pilot acceleration tolerance tested on centrifuge, confirming instability correlation to poor resistance

07 p1201 A70-18793

Blood pressure variations resulting in permanent irreversible hypertonia in air force pilots subjected to repeated stress situations and emotional irritations

09 p1626 A70-23011

Minnesota Multiphasic Personality Inventory scores compared with various pilot training proficiency levels, noting low correlation

12 p2176 A70-27032

EMOTIONS

Exercise habits and environmental emotional stresses role in origin and prevention of degenerative heart disease

07 p1212 A70-19692

EMPHYSEMA

Commercial pilots susceptibility to emphysema and respiratory impairment in hypobaric environment, discussing flying disability implications

03 p0438 A70-14068

Orthogonal electrocardiograms of patients with pulmonary emphysema analyzed by computer, discussing diagnostic classification and correlation with physiologic parameters

09 p1616 A70-22276

Human lung internal surface area automated measurement by computerized image processing techniques, grading emphysema

17 p3035 A70-34578

EMPLOYMENT

Flying safety and human factors from job dissatisfaction in Japan Air Self Defense Force

08 p1453 A70-21794

Age discrimination in employment policies of air carriers, discussing legislative measures, hiring practices and retirement rules concerning stewardesses and FAA pilots

12 p2336 A70-27772

EMULSIONS

NT NUCLEAR EMULSIONS

NT PHOTOGRAPHIC EMULSIONS

Emulsified jet fuels cold flow, combustion and corrosion characteristics in gas turbine combustor compared with JP-4 fuel

[ASME PAPER 69-WA/GT-3] 04 p0732 A70-14892

Emulsified jet fuels combustion characteristics evaluation by laboratory technique, presenting data on emulsifiers and corrosion inhibitors effect

[ASME PAPER 69-WA/GT-2] 04 p0785 A70-14893

Performance characteristics of low density epoxy-water emulsion corrosion resistant coating for nonferrous alloys

08 p1526 A70-20648

ENAMELS

Ingredient proportions for enamels containing titanium and boron oxides

05 p0871 A70-16597

Silicate enamel coating formulas for application on titanium exhibiting adequate adhesion

05 p0872 A70-16599

ENCAPSULATING

Low melt viscosity prepolymers of diallyl phthalate and isophthalate in mold encapsulation showing dimensional, electrical and mechanical stabilities under adverse environments

05 p0869 A70-16035

Pressure sensitive components in cordwood modules noting temperature and pressure damaging stresses during encapsulation

05 p0855 A70-16037

Resin systems for encapsulation of microelectronic packages, using thermal expansion dilatometer and gravimetric and differential analyses

13 p2439 A70-29258

Plastic encapsulated semiconductor reliability test programs with emphasis on accelerated humidity-temperature method

13 p2377 A70-29259

Epoxy resin with low shrinking effect for encapsulation of electronic components by flexibilizing procedure

13 p2439 A70-29262

Rigid one component epoxy foam system mechanical, electrical and thermal properties for foamed-in-place electronic potting and encapsulation

13 p2439 A70-29263

Permittivity cell and encapsulation for liquids subjected to high pressures and temperature extremes

14 p2533 A70-30502

Microelectronic packages encapsulation by resin systems with emphasis on thermal expansion, discussing effects of curing temperature, reactive diluents, etc

20 p3655 A70-39444

Plastic encapsulated IC for military environments, discussing cooker, corrosion and thermal shock tests

23 p4173 A70-44534

ENCKE METHOD

Three body problem involving sun and perturbing and perturbed planets, examining perturbed motion equations of Brouwer and Encke methods

07 p1374 A70-18773

- ENCLOSURES**
Diffuse-specular models for radiant heat interchange prediction for isothermal-adiabatic surface enclosure tested for steel and gold
16 p3003 A70-34197
- Script-F radiative interchange matrix for enclosures with arbitrary surface emission and reflection characteristics
21 p3944 A70-41020
- ENCODERS**
U CODERS
- ENCODING**
U CODING
- END PLATES**
End plugs bending moment and shear loads reduction during compression tests of composite orthotropic cylinders
08 p1594 A70-21889
- Planar wing with end plates in ground effect, calculating minimum induced drag by approximation theory
21 p3743 A70-40919
- ENDFIRE ARRAYS**
NT YAGI ANTENNAS
Backfire antennas allowing for mutual impedance between dipole elements, determining radiated field from surface current distribution
16 p2861 A70-32958
- Dolph-Pritchard technique limitations for transformation of array factor into Chebyshev polynomial as related to element spacing for single lobe endfire arrays
20 p3599 A70-40315
- Broadside-endfire array of cylindrical dipoles and monopoles driven by interconnecting transmission lines, calculating admittance and field patterns
23 p4176 A70-44955
- ENDOCRINE GLANDS**
NT ADRENAL GLAND
NT GONADS
NT OVARIES
NT PARATHYROID GLAND
NT PINEAL GLAND
NT PITUITARY GLAND
NT THYMUS GLAND
NT THYROID GLAND
Ionizing radiation effects on endocrine system, studying ACTH metabolism in rats under X ray irradiation
19 p3372 A70-38723
- ENDOCRINE SECRETIONS**
NT HORMONES
NT INSULIN
Chloride and sulphydryl activators in glucagon degradation and secretion by purified rat liver dipeptidyl aminopeptidase I/Cathepsin C/
04 p0631 A70-14682
- Circannual rhythm in levels, amplitudes and acrophases of serum corticosterone in mice compared with phase shift after change of lighting regime
14 p2537 A70-30725
- Human cortisol intermittent secretion during early morning sleep and sleep-wake cycle, examining adrenal activity
24 p4305 A70-46410
- ENDOCRINE SYSTEMS**
Broad spectrum light sources effects on mammalian endocrine apparatus development and function determined in rats
09 p1617 A70-22335
- ENDOGENOUS CONDITIONS**
U PHYSIOLOGY
- ENDOLYMPH**
Nystagmic response to directional inert shift of endolymph in semicircular canals in frontal plane head subject rotation
18 p3220 A70-36635
- ENDOTHELIUM**
Blood-endothelial surface shear stress in artery inlet, considering asymmetric and radially symmetric plugging effects
07 p1220 A70-19248
- ENDOTHERMIC REACTIONS**
Dicyclohexyl /DCH/ endothermic dehydrogenation to diphenyl /DP/ over platinum-alumina catalyst without added hydrogen considered for hypersonic aircraft engine cooling
14 p2546 A70-31175
- Electron capture involving iron nuclei in contracting iron stars treated as endothermic nuclear reaction
22 p4104 A70-42992
- ENDURANCE**
Heart rate augmentation during constant performance in excess of endurance limit, considering muscle fatigue
03 p0431 A70-14292
- 2000 meter race for endurance testing, using heart rate radiotelemetry before, during and after
14 p2543 A70-31173
- ENERGY**
Electroexplosive devices output energy measurement through metal deformation by lead block and projectile penetration methods
03 p0548 A70-14121
- Energy concept in cosmology based on relativistic considerations, indicating universal time by synchronous clocks system
11 p2109 A70-25870
- Energy derivation for mechanics and thermodynamics with generalization to systems of more than two dynamic variables, considering transformations and Newton and Kepler laws
12 p2164 A70-27070
- Stationarity of complementary energy in nonlinear elasticity theory, using Piola stress tensor representation for isotropic elastic media
17 p3192 A70-35692
- Insular system energy and momentum definition in external gravitational field, using dynamic equations and Einstein theory
19 p3513 A70-37412
- Energy and impulse tensor of nonviscous relativistic fluid, excluding sound velocity greater than light velocity
19 p3404 A70-37593
- ENERGY ABSORPTION**
NT AURORAL ABSORPTION
NT ELECTROMAGNETIC ABSORPTION
NT MOLECULAR ABSORPTION
NT NEUTRON THERMALIZATION
NT PHOTOABSORPTION
NT POLAR CAP ABSORPTION
NT SELF ABSORPTION
NT THERMAL ABSORPTION
NT THERMALIZATION [ENERGY ABSORPTION]
NT X RAY ABSORPTION
Refractive index perturbation from energy absorbed from long pulsed and Q switched Nd doped glass lasers, observing sonic waves generated by Q switched laser
03 p0498 A70-13156
- Refractory materials deformation and failure analysis based on relations between stresses, strains and irreversible energy absorption per cycle in thermal cyclic fatigue testing
05 p0867 A70-17042
- Fast electron ionization losses due to multiple scattering with atoms during passage through thin layer, calculating spatial energy distribution function
08 p1547 A70-20989
- Strength and thickness effects on energy absorption criteria for transition temperatures in Charpy V-notch impact tests
15 p2819 A70-32234
- Size effects on impact energy disposition in plastically deformed thick steel specimens at shelf temperature, using similitude laws
15 p2760 A70-32332
- Nonlinear resonant heating in magneto-plasma, calculating energy absorption by ions and plasma wave amplitude
20 p3685 A70-40467
- Energy deposition in solar corona associated with momentum transfer from heating wave in transition region, discussing wave pressures
21 p3925 A70-42190
- Ground Effect Takeoff and Landing /GETOL/ aircraft, evaluating energy absorption capability of air cushion landing gear in touch-down condition
22 p3961 A70-42282
- Energy absorption and dissipation in friction brakes, investigating brake lining polymer binder contribution through molecular reorientation, crystallinity increase and entropy decrease
24 p4342 A70-45585
- LF electrostatic ion cyclotron wave energy resonant power absorption in plasma in axially nonuniform magnetic field
24 p4386 A70-45608
- Franz-Keldysh and hot electron effects in interband absorption of semiconductors in external electric field
24 p4392 A70-46361
- ENERGY BANDS**
NT CONDUCTION BANDS
NT FORBIDDEN BANDS
Compact 4 micron radiation band from high temperature air and gases measured on arc jet and shock tube, noting molecular O and N source
02 p0392 A70-11901
- Nb metal-like compounds energy band structures using X ray fluorescence technique
04 p0707 A70-15213
- Rare earth energy band structure effect on RKKY magnetic interaction between atomic spins
13 p2472 A70-29799
- Numerical computation of wave functions and energies in complex band structures for two-band case, using k-p method
19 p3483 A70-37547
- Amorphous semiconductors optical absorption, thermoelectric effects and switching mechanisms characterized by energy band structure model
22 p4086 A70-42773
- ENERGY BUDGETS**
NT ATMOSPHERIC HEAT BUDGET
Upper atmosphere structure and energy budget based on IGY/IQSY spectroscopic observations of temperature distribution and stratosphere-mesosphere composition
01 p0072 A70-10578
- Algorithm for fixed time minimum energy discrete optimal control problems of linear plants with convex constraints imposed on terminal state
02 p0273 A70-12731
- Controlled thermonuclear power generation, considering fusion reactors feasibility and reactor energy balance improvement
04 p0717 A70-14528
- Energy balance relations for elastic material with different elastic moduli in two regions of deformation space
05 p0925 A70-15824
- Integrodifferential equation derived for energy balance in laminar boundary layer of fluid flow, taking into account viscous energy dissipation, radiative energy transfer, etc
07 p1423 A70-19813
- Stratospheric CAT layer energy budget analysis, considering energy shear feeding, buoyant extraction and frictional dissipation
09 p1715 A70-22357
- Turbulent energy budgets in atmospheric boundary layer near ground scalar fluctuations and CAT
09 p1717 A70-22380
- Nonturbulent fluid entrainment into turbulent flow dependent on flow properties controlling energy balance
11 p2038 A70-26528
- Dissipating instability in plasma by variational method, using relation between energy balance of wave and medium
15 p2779 A70-32115
- Atmospheric temperature fluctuation spectrum determination by energy budget solution, considering spectral density dependence on Richardson number
15 p2732 A70-32542
- Entropy increase, discussing universe heat death, earth energy balance, etc
15 p2809 A70-32907
- Multispectral remote sensing for detection and mapping of ecological objects and energy budget parameters measurement
17 p3079 A70-35622
- Human bioclimatology at high altitude, discussing energy balance in terms of net solar and terrestrial radiation balance in mountain area
19 p3367 A70-37369
- Planetary atmospheres energy balance, considering models in terms of radiative control or large scale fluid motions
19 p3521 A70-38499
- Atmospheric zonal kinetic energy balance for Northern Hemisphere, assuming frictional destruction due to stresses across horizontal surfaces
20 p3661 A70-39145
- Integrodifferential equation derived for energy balance in laminar boundary layer of fluid flow, taking into account viscous energy dissipation, radiative energy transfer, etc
20 p3736 A70-39261
- Spacecraft data transmission efficiency improvement by budgeting onboard electric energy consumption among data types
21 p3790 A70-41364
- Temperature, metal vapor density and energy balance in Ar shielded welding arc with Fe electrodes
22 p0403 A70-42381
- Tropical cyclone development model for axisymmetric vortex and quasi-balanced conditions, considering vertical heat distribution, rate of intensification and energy budget
23 p4213 A70-43896
- ENERGY CONVERSION**
Thermionic emission characteristics of W and Mo subjected to focused CW carbon dioxide laser radiation, discussing direct energy conversion
02 p0312 A70-12068
- Equations governing electrofluid dynamic energy conversion processes and indicating differences between EFD and magnetofluid dynamic processes presented for mechanical engineering problems [ASME PAPER 69-WA/ENER-9]
04 p0627 A70-14899
- Temperature measurements in magnetic beach of steady state deuterium plasma, confirming ion-cyclotron waves thermalization
05 p0884 A70-16167
- Doped beta-iron disilicide thermocouples measured for electrical characteristics and energy conversion efficiency at various temperatures
05 p0798 A70-16357
- Mechanical electromagnet model of MHD dynamo achieving direct conversion of mechanical to magnetic field energy
06 p1121 A70-17803
- Spiraling electron beam energy conversion and distribution using retarding-field velocity analyzer
12 p2196 A70-27651
- Book on energy conversion states covering state functions, quasi-static processes, internal energy,

chemical energy storage and conversion, dynamics and postulates and laws

12 p2165 A70-27670

Mechanical electromagnet model of MHD dynamo achieving direct conversion of mechanical to magnetic field energy

13 p2460 A70-28654

Book on fuel cells electrochemistry covering direct energy conversion methods, electrode kinetics, electrocatalysis, organic substances, electrochemical combustion, research techniques, etc

14 p2532 A70-30100

Chemically reacting ideal substance model, describing thermodynamic properties and application to energy conversion processes

14 p2533 A70-30529

Switch controlled resonant current pulse modulation for power converters, noting integration with spacecraft ion propulsion engine

14 p2535 A70-31324

Biological conversion of solar energy, discussing photosynthesis and nonphotosynthesis mechanisms

15 p2688 A70-31600

Solar type 3 burst theory, considering plasma wave energy conversion into radio emission

15 p2802 A70-32484

Chemical energy conversion in diatomic and multiatomic molecules and chain reactions

16 p2927 A70-33233

Axial pressure, electric current and potential distribution in two-phase particulate electrodynamic flow, discussing space charge electric field effect

20 p3683 A70-40257

Superradiant light (SRL) converted from electron beam energy by semiconductor targets applied to nanosecond photography

20 p3635 A70-40529

Cyclotron wave rectifier with Cuccia coupler for converting microwave power into DC or LF AC

21 p3756 A70-40730

Effective pressure ratio nomographs for mechanical energy conversion and heat transfer of closed regenerative Stirling engines, using isothermal theory

22 p4091 A70-42757

Thermal energy conversion into coherent laser light, examining various thermodynamic limitations

22 p4076 A70-43674

Solar type 3 burst theory, considering plasma wave energy conversion into radio emission

23 p4240 A70-43908

ENERGY CONVERSION EFFICIENCY

Hot junctions nonuniform heating influence on thermoelectric generator efficiency, taking into account temperature dependence of thermoelement materials properties

01 p0009 A70-10753

Cascaded thermoelements with high figure of merit for increasing solar thermoelectric generator efficiency, noting high temperature materials effect

01 p0158 A70-10754

Power output, Joule dissipation and generator efficiency determined for rectangular MHD channel, considering transverse and longitudinal edge effects

01 p0152 A70-10992

Mo/Mo cylindrical thermionic converter steady state performance, measuring efficiency and power density at various low emitter and collector temperatures

04 p0627 A70-14947

Performance degradation in cadmium sulfide solar cells, discussing cause identification technique, I-V curve parameter changes, etc

04 p0628 A70-15329

Heat exchangers efficiency taking into account surface, weight and cost

05 p0958 A70-16551

Solar cell for improved performance during extreme temperature fluctuations, discussing wraparound contact

05 p0799 A70-16724

Electrical impedance, conversion loss and bandwidth for piezoelectric film or plate transducers used for generating planar volume-acoustic waves at microwave frequencies

06 p1062 A70-17480

Experimental data to define idealized thruster discharge model power efficiency limits, computing probabilities for excitation, ionization, propellant escape and wall interception of ions

06 p1131 A70-18034

Electrical effects of boundary layers on insulator wall of MHD generator, considering equilibrium and nonequilibrium ionization generators performance

07 p1196 A70-19321

Electrodynamic compressor with direct conversion of electric energy into mechanical energy, improving conversion efficiency by using plasma as working medium

07 p1196 A70-19658

Optical and electronic mixing in avalanche photodiode during variable amplitude signal demodulation in optical heterodyne receiver, considering conversion losses

07 p1243 A70-20282

Electrochemical generators based on thermodynamic equilibrium processes, deriving expressions for EMF, efficiency, and I-V characteristics

07 p1196 A70-20462

Schottky barrier diodes microwave power rectification efficiency, developing diode losses theory based on back capacitance, series and front resistance and knee voltage

08 p1474 A70-21274

GaAs solar cells performance as function of doping levels, ascribing poor efficiencies to surface recombinations

08 p1557 A70-21721

Electrodynamic generator with spatial charge neutralization for direct thermal-to-electrical energy conversion at high gas pressures

12 p2165 A70-27330

Thermospheric heating and conversion efficiency of short wave radiation as functions of solar radiation spectral flux, atmospheric components concentration and elementary processes cross sections

14 p2569 A70-30212

MHD induction generator efficiency, investigating winding slot finite spacing and width effects

14 p2533 A70-30531

EGD energy converter system geometries for maximum power efficiencies, comparing slender conversion channels, abrupt expansion, free jet and divergent for operating characteristics

14 p2534 A70-30536

Photomultiplier tubes high quantum efficiency attainment by optical enhancement techniques

15 p2735 A70-31767

Absolute quantum efficiency of phosphor calcium tungstate-lead under monochromatic far UV illumination

15 p2729 A70-32017

Flow nonuniformity effects on heat exchangers efficiency

15 p2827 A70-32140

Solar thermoelectric generator (STEG) with two stage converter, discussing weight factors and efficiency

15 p2678 A70-32425

Homopolar Inductor Alternators of minimum weight and maximum efficiency for aerospace power supplies

15 p2710 A70-32587

Electrodynamic compressor with direct conversion of electric energy into mechanical energy, improving conversion efficiency with plasma as working medium

15 p2678 A70-32695

Ruby laser second harmonic radiation generation efficiency, using cylindrical lens beam forming optical system

16 p2929 A70-34212

Photoelectric conversion efficiency and radiation resistance of Li-doped Si solar cells, showing improved reliability over Li-free cells

17 p3023 A70-35311

Brayton cycles in gas turbines, investigating intercooling or reheat and pressure ratio proportioning influence on efficiency and specific work

18 p3304 A70-36856

[ASME PAPER 70-GT-130]

Si photocells fabrication, reliability and energy conversion efficiency

19 p3358 A70-38479

Cadmium telluride photocells, discussing performance and mass production

19 p3358 A70-38481

Plasma inhomogeneities effects on MHD generators I-V characteristics, energy conversion efficiency and optimum duct geometry

20 p3564 A70-39636

MHD induction generator efficiency reduction due to finite winding slots spacing and width

20 p3565 A70-39987

Carbon monoxide laser efficiency increase through addition of Xe, noting change in laser output spectral intensity distribution

21 p3835 A70-40572

Collection efficiency and spectral response calculations for semiconductor heterojunction solar cells

21 p3861 A70-40623

Electrodynamic generator with spatial charge neutralization for direct thermal-to-electrical energy conversion at high gas pressures

21 p3760 A70-42071

Ruby laser second harmonics generation in low loss lithium iodate crystal with high conversion efficiency

24 p4355 A70-46085

Thermospheric heating and conversion efficiency of short wave radiation as functions of solar radiation spectral flux, atmospheric components concentration and elementary processes cross sections

24 p4331 A70-46287

ENERGY CONVERTERS

U DIRECT POWER GENERATORS

ENERGY DENSITY

U FLUX DENSITY

ENERGY DISSIPATION

Minimum weight sandwich plates complying with von Mises criterion, providing constant dissipated energy density

01 p0202 A70-10947

Machine element materials damping properties, determining energy dissipation during steady resonant vibrations

01 p0211 A70-11423

Machine parts fatigue strength under thermal cycles, studying nonlinear dependence of energy dissipation per unit volume on cycles number

02 p0383 A70-11654

Decay times for thermal disturbances near cloud tops in Jupiter atmosphere, discussing hydrogen absorption

02 p0368 A70-11827

Geodesic motion of massless particles inside static sphere of small volume, analyzing relativistic effect of energy accumulation and release

02 p0339 A70-12117

E layer kinetic energy viscous dissipation and transfer to potential energy by turbulence and irregular winds shear

02 p0327 A70-12292

Dissipation spectrum /viscous dissipation of turbulent kinetic energy as function of wave number magnitude/ data compared and plotted

02 p0327 A70-12294

Energy dissipation and entrainment methods for calculating turbulent boundary layer development, involving simultaneous numerical solutions of ordinary differential equations for local variables

02 p0283 A70-12337

Dissipation integral method for turbulent boundary layer problem based on nonequilibrium flow, analyzing inner and outer regions

02 p0283 A70-12338

Mechanical losses in fiberglass reinforced textile converted into thermal energy during cyclic tension and compression

02 p0323 A70-12807

Ionization and electron temperature dependence on shock wave structure in partially ionized hydrogen plasma allowing for luminescent energy losses

03 p0465 A70-13060

Metals fatigue strength prediction by hysteresis loop method, presenting results for irreversible energy dissipation rules during cyclic loading

03 p0587 A70-13240

Stress cycle asymmetry effects on energy dissipation in rods under torsional vibration

03 p0588 A70-13249

Linearly polarized radiation in Nd-glass laser obtained without energy loss by placing glass plates in resonator at Brewster angle to axis

03 p0499 A70-13257

Fourier and perturbation methods applied to radiation from uniformly moving charge in inhomogeneous magnetoactive medium, deriving expressions for radiation spectrum and energy losses

03 p0531 A70-13285

Semiconductors low temperature electron energy losses due to inelastic electron scattering at neutral impurity donors shown to exceed scattering losses at phonons

03 p0539 A70-13423

Electron spectrometer for nitrogen energy loss spectrum in 12-14 eV region, detailing relative intensities of transition bands

03 p0528 A70-13577

Electromagnetic wave propagation in semiconductors, considering effects of electric field, energy dissipation law and band structure

03 p0540 A70-13719

Power losses in ruby laser with polarized spontaneous luminescence determined as function of laser parameters and light polarization

03 p0502 A70-13747

Difference method for calculating one dimensional nozzle flow and expansion with allowance for relaxation, friction and heat losses, discussing fluorine-hydrogen mixture application

03 p0408 A70-13804

Large dielectric constant with small loss determined as function of frequency from resonant frequencies measurement

03 p0493 A70-14039

Book on rational thermodynamics covering homogeneous processes, internal dissipation, Coleman theorem, wave propagation in dissipative materials, diffusion, chemical reactions, Onsager relationship, etc

03 p0525 A70-14042

Fiberglass reinforced plastics energy dissipation during fatigue failure phases, studying mechanical-thermal energy transformation under cyclic strain

04 p0713 A70-15263

Very high energy cosmic rays disintegration and energy degradation by intense blue shifted photon fields of supernovae quasars and pulsar models

04 p0742 A70-15300

Pneumatic line losses due to friction in pneumatic control systems

04 p0628 A70-15399

Interstellar propagation effect on spectra and charge ratios due to ionization energy loss and nuclear spallation during traversal of matter

05 p0897 A70-15762

- Bethe function for ionization losses in energy of elementary particles heavier than electron
05 p0899 A70-15961
- Energy losses in conductors carrying intense currents to cryogenic regions linked with heat transfer due to high temperature gradients
05 p0881 A70-16026
- Normal incidence reflectance of BeO single crystals, analyzing data by Kramers-Kronig inversion for dielectric function and energy loss function
05 p0891 A70-16047
- Kinetic, potential and dissipative energies computed in systems of randomly excited coupled oscillators, using Liapunov stability method
05 p0821 A70-16407
- Bipolar n-p-n transistors fabrication to increase driving capabilities of complementary MOS transistors while retaining low power dissipation
05 p0821 A70-16419
- Galactic expansion due to mass energy loss by gravitational radiation
05 p0913 A70-16557
- Inertial parameters and functions of dissipative and restoring forces in quasi-linear oscillatory system determined from free motion characteristics
05 p0884 A70-16951
- Work of plastic deformation in two dimensional rolling determined by energy dissipation function
05 p0857 A70-17017
- Energy dissipation patterns of metal fatigue failure during static and cyclic loading applied to untreated and heat treated steel samples
06 p1166 A70-17651
- Energy dissipation during torsional and flexural vibrations of steel and duralumin specimens subjected to plastic deformation, accounting for discrepancies due to methodical errors
06 p1166 A70-17658
- MHD equations including energy dissipation terms applied to irreversible processes occurring in fast hydromagnetic shock waves in solar chromosphere
06 p1143 A70-17999
- Energy losses due to mixing of primary and secondary flows of jet streams in gas propulsion engine chambers determined by continuum mechanics application
07 p1363 A70-19086
- Mass variation laws in light of Tsiolkovskii hypothesis, considering particle separation rates and thermal energy losses for actual jet engines
07 p1363 A70-19088
- Laser oscillation conditions for CdS crystal pumped by electron beam, using energy loss per unit length for calculations
07 p1298 A70-19681
- Elastic systems vibrations calculated with allowance for amplitude and frequency dependent energy dissipation using hysteresis loop contour expression
08 p1585 A70-20978
- Martensitic stainless steels structure related to energy dissipation capability, obtaining damping mechanism as magnetomechanical hysteresis
08 p1515 A70-20979
- Loading frequency effect on carbon steel energy dissipation at large stress amplitudes, deriving strain rate relations
08 p1516 A70-20980
- Energy dissipation in heat resistant Ni steels under cyclic tension and compression at room temperature
08 p1516 A70-20981
- Flow turbulence effect on heat turbines efficiency using energy losses in blade cascades
08 p1432 A70-21073
- Mechanical system undergoing internal mass redistribution, showing energy dissipation during motion
08 p1545 A70-21203
- Matched filter SNR behavior under time and frequency domains distortion and random distortion, deriving design equations for energy loss coefficients
08 p1474 A70-21223
- Dissipative heating effects on loss factor of viscoelastically damped beam, discussing stiffness effects
[ASME PAPER 69-VIBR-37] 08 p1592 A70-21478
- Transient temperature distribution in flow through channel with arbitrary cross section, taking into account internal heat generation and viscous dissipation
08 p1599 A70-21767
- Turbulence model, noting possibility of turbulence energy to vanish with distance from tunnel central point of entrance
08 p1486 A70-21770
- Transparent gas radiation behind strong shock wave front with small pressure gradient due to energy losses
08 p1486 A70-21986
- Three dimensional RC network simulating temperature fields in IC at different heat source power dissipation laws, discussing harmonic heat source field
09 p1643 A70-22128
- Free and forced vibrations of three layer freely suspended plate with allowance for energy dissipation
09 p1772 A70-22468
- Energy losses in gas turbine flows ascribed to combined exhaust and internal losses, noting usefulness of entropy loss concept
09 p1743 A70-22659
- Secondary losses in axial turbine cascades without end clearance noting correlation with blade loading
09 p1743 A70-22980
- Radiation losses of tapered single mode dielectric slab waveguide for TE and TM modes
09 p1650 A70-23369
- Transient process statistical calculation in discrete elastic mechanical system possessing energy dissipation under time dependent cross correlated random forces
09 p1729 A70-23595
- Neutrino emission effect on collapse of supermassive stars, estimating energy radiated, discussing envelope explosion
10 p1938 A70-24022
- Viscosity and heat conductivity effects in compressible fluid flow past finite body showing dependence on spatial dimensions
10 p1800 A70-24135
- Energy dissipation-fatigue strength relationships during vibrations for prestrained metals and alloys
10 p1956 A70-24244
- Temperature effects on energy dissipation during vibration in ferromagnetic and nonferromagnetic metals, comparing damping capabilities for homologous temperatures
10 p1903 A70-24245
- Static tensile stresses effect on magnetized ferromagnetic materials damping properties explained by anisotropic microplastic strains dissipating energy during bending vibration
10 p1904 A70-24246
- Energy dissipation in free oscillations of multilayer shells consisting of alternating rigid elastic layers and soft fillers, deriving equations of motion
10 p1956 A70-24249
- Multilayer plate vibrations calculated with allowance for energy dissipation in material, deriving equations of motion
10 p1965 A70-25297
- Electron energy loss spectrum in Ti measured by bombarding thin films vacuum deposited on NaCl crystal with electrons of intermediate energy
11 p2065 A70-25376
- HF energy nonresonance dissipation in polycrystalline yttrium-garnet ferrites subjected to constant magnetizing field
11 p2097 A70-25384
- Unsteady problems of finite amplitude plane and cylindrical wave propagation in dissipative spatially symmetrical media
11 p2034 A70-25399
- Vibration damping theory validity, discussing response curve for frequency dependence of energy dissipation
11 p2133 A70-25733
- Fokker-Planck equation solution for electron scattering and energy loss in mirror confined hot electron plasma
11 p2090 A70-26022
- Pressure recovery and energy loss efficiencies of two dimensional diffusers with suction at entrance
11 p1977 A70-26418
- Turbulence theory based on Wiener-Hermite expansion of velocity distribution to predict energy decay rate for Reynolds numbers greater than two
11 p2040 A70-26542
- Heat equation initial value problem with dissipative term nondecreasing and discontinuous function of unknown, discussing existence and uniqueness theorem of periodic solution
12 p2330 A70-27160
- Solar plasma and energy and radiation fading during microwave bursts due to synchrotron radiation losses, determining magnetic field strength
12 p2294 A70-27593
- Laser output energy decreased by microscopic fractures masking effect in neodymium glass laser rod during monopulse operation
12 p2250 A70-28152
- Suspended Stokes particle-single wave interaction effect on energy dissipation and vorticity of random turbulent incompressible fluid approximated by Fourier-Stieltjes integral
12 p2213 A70-28236
- Microwave conductance tensor in crystals with non-parabolic carrier energy dissipation under crossed constant electric and magnetic fields
12 p2288 A70-28326
- River bed channel flow instantaneous velocities described by logarithmic law, determining turbulent energy dissipation
12 p2265 A70-28336
- Dissipation mechanism and period rate increase in neutron star pulsar model with neutrino emission for damping
12 p2312 A70-28368
- Energy loss radial dependence due to K resonance radiation for infinitely long plasma cylinder, using approximation method for integrals
13 p2461 A70-28731
- Low energy protons penetration into magnetosphere between forbidden regions, using model of constant electric field with charge exchange as loss mechanism
13 p2477 A70-29183
- Energy dissipation effect on complex parametric resonance and stability of two rotor gyrocompass on ship in motion
13 p2408 A70-29295
- Two body system with Newtonian force interaction, calculating gravitational wave energy losses and spectral decomposition
13 p2453 A70-29668
- Induction plasmas in thermal equilibrium dominated by radial conduction losses, discussing energy balance equation and Ar plasmas at atmospheric pressure
13 p2465 A70-29701
- Thermal induction plasma discharge characteristics, considering radiation and conduction losses
13 p2465 A70-29702
- F-type close stars residual spatial motions and rotational velocity relationship, discussing angular momentum loss
13 p2498 A70-30015
- HF backward wave oscillators with emphasis on limiting factors in millimeter waves generation, discussing ohmic and circuit imperfection losses
14 p2555 A70-30430
- Vlasov interaction of magnetically coupled E layer with dissipative structures including injection, trapping and drag effects
14 p2623 A70-30698
- Starting criterion for hypersonic inlets with large turbulent boundary layers, considering total pressure recovery from all shock and viscous losses
14 p2529 A70-30865
- Energy dissipation during independent flexural-torsional vibrations of rods, noting alternating shear stress superposition effect on damping
15 p2813 A70-31530
- Pilots energy expenditure during jet, propeller and helicopter cargo aircraft flight, using expired air samples
15 p2689 A70-31876
- Power reduction consumed in vacuum by direct-voltage converter by introducing delay into breaker transistor control at output stage
15 p2677 A70-31945
- Dissipating instability in plasma by variational method, using relation between energy balance of wave and medium
15 p2779 A70-32115
- Spherical shaped rotor unbalance effect on electrostatic gyroscope runout time, discussing energy dissipation
15 p2738 A70-32152
- Electrothermal thruster with liquid propellant, describing energy dissipation and high specific impulse
15 p2791 A70-32280
- Microwave transmission techniques with packaging designs for radiation energy losses control, discussing functions of components
15 p2714 A70-32750
- Electron energy losses at interface of helium inclusions in aluminum irradiated by radioactive lithium
15 p2785 A70-32764
- Collisionless shock waves model in solar wind plasma, discussing instability and energy dissipation
15 p2795 A70-32825
- Annular lasers energy, polarization, radiation loss and frequency characteristics dependence on phase shift due to anisotropic plate introduction
15 p2753 A70-32860
- Coherent light pulses propagation through resonant medium, discussing energy loss
16 p2928 A70-33278
- Electron energy loss per collision in Cs vapor discharge, measuring electric field and electron temperature by Langmuir probes
16 p2954 A70-33281
- Laminar boundary layer model for viscous losses during transient turbulent liquid flow in tube, assuming slug flow for core
[ASME PAPER 70-FE-8] 16 p2891 A70-33627
- D region electron energy loss factor during solar eclipse of 7 March 1970, using wave interaction technique
16 p2898 A70-33834
- Inelastic energy losses in oxygen ion beams collisions with neutral molecules, determining vibrational transition probabilities
16 p2955 A70-34011
- Spacecraft gravity gradient stabilization by damping out oscillatory motions by energy dissipation, using combined eddy current and hysteresis dampers/Combination Passive Damper/
16 p2985 A70-34133
- Energy loss of high energy cosmic rays traversing isotropic radiation field of arbitrary energy spectrum in pair producing collisions with ambient photons
17 p3150 A70-34598
- Bearing assembly energy dissipation effects on dual spin spacecraft attitude stability, explaining satellite motion anomalies
17 p3100 A70-34756

Hydromagnetic shock waves structure, investigating resistive, viscous and thermal conduction dissipation effects on discontinuities

17 p3140 A70-34928

Stability theorem for mechanical systems with constraint damping subjected to energy dissipation

17 p3176 A70-34956

Infinitesimal electric and magnetic dipoles embedded in lossy media, investigating earth effect on electromagnetic field

17 p3045 A70-35075

Elastic field near moving antipane crack tip to determine energy release rate

17 p3191 A70-35462

Damping characteristics/absorption coefficient/ of dissipative systems, defining authentic value of energy dissipation characteristic determination from natural vibrations damping

17 p3192 A70-35711

Energy dissipation measurement in materials during fatigue testing by dynamic hysteresis loop method

17 p3096 A70-35712

Creep and failure tests for Ti alloys at 500 C, discussing work dissipation during creep process

17 p3126 A70-35714

Solar atmosphere shock waves frequency and strength, computing radiative energy losses of chromospheric models

17 p3174 A70-35865

Stellar thermal and vibrational energy losses due to URCA shells in interiors

18 p3310 A70-35935

Energy dissipation and viscosity effects on isotropic turbulence in extreme short wave region at large Reynolds numbers

18 p3239 A70-36263

Turbulent energy dissipation in lower atmospheric layer on meteorological mast during various temperature stratifications

18 p3247 A70-36627

Fluid dynamics of pulsed plasma accelerators, discussing energy transfer and losses limitations

18 p3301 A70-36660

Radiative energy loss and wall sublimation effects on gas flow parameters behind reflected strong plane shock wave, taking into account small disturbances

18 p3348 A70-36673

Al spheres hypervelocity impact against dry quartz sand targets in light gas gun facility, discussing energy partitioning

18 p3344 A70-36769

Reduced dissipation of biharmonic oscillations, examining dynamic model under force and kinematic harmonic perturbation

18 p3344 A70-37070

Gyroscope dissipative function, using quasi-elastic gyroscope model and forced oscillation method

19 p3420 A70-37260

Coherent light communication system quasi-optical lens line output field examination, using laser assembly to study parasitic, radiative and overall power losses

19 p3443 A70-37288

Dynamic hysteresis loop measurement of energy dissipation in materials, showing deformation effects on accuracy

19 p3535 A70-37346

Energy dissipation in material under complex vibrations, noting role of summary shear stress

19 p3535 A70-37347

Energy loss of fast protons in cold Li plasma confined by magnetic field, using precession around axis to develop large interaction length

19 p3474 A70-37364

Initial condition effects on weak homogeneous turbulence with uniform shear, studying energy transfer and dissipation

19 p3403 A70-37537

Diffraction radiation excitation by electron beam moving within resonant system formed by ribbon grating and metal plane, taking into account screen conduction losses

19 p3377 A70-37724

Monograph on gas laser dynamics, emphasizing single mode intensity measurement as function of cavity loss in He-Ne laser

19 p3446 A70-37978

Polar gas rotational relaxation time calculation, comparing volume viscosity and energy equation definitions

19 p3473 A70-38266

Machine parts fatigue strength under thermal cycles, studying nonlinear dependence of energy dissipation per unit volume on cycles number

19 p3547 A70-38427

Metal fatigue strength prediction by hysteresis loop method, presenting results for irreversible energy dissipation rules during cyclic loading

19 p3548 A70-38458

Stress cycle asymmetry effects on energy dissipation in rods under torsional vibration

19 p3548 A70-38467

Heat flowmeters calibration by conductive method, reducing error due to radiative, conductive and convective losses

19 p3430 A70-38522

Characteristic dimensions of large and small scale atmospheric turbulence by meteor trails photographic observations, determining energy dissipation

19 p3526 A70-38790

Human body core temperature control dependence during exercise on heat dissipation, noting sweating control

20 p3570 A70-38997

Maclaurin spheroid secular stability, examining energy dissipation of gravitational radiation

20 p3702 A70-39017

Q switched lasers time dependent loss elimination from elastoplastic relaxation effect in lithium niobate and KDP Pockel cells

20 p3640 A70-39093

Power diffraction losses at mirrors of asymmetric confocal laser interferometers with output coupling apertures

20 p3628 A70-39130

Thermoelastic seismic-energy release as source mechanism for volcanic earthquakes, describing thermal microfracture tests

20 p3619 A70-39217

Book on variational principles in heat transfer covering conduction, convection, dissipation, thermal potential and force boundary layer problem and Lagrangian analysis

20 p3735 A70-39224

Heavy elements critical energy calculation, taking into account low energy electrons effects on losses in electromagnetic cascade

20 p3674 A70-39303

CAT as mechanism relieving wind and temperature discontinuities, maintaining Richardson number at limiting value by turbulent energy dissipation

20 p3663 A70-39373

Positive ions energy dispersion effused from RF plasma, presenting ion extraction model for plasma sheath system and equivalent circuit

20 p3678 A70-39608

Electro-optical crystal resonator loss anisotropy, determining natural frequencies and polarizations

20 p3642 A70-39755

Gas dynamic functions of point explosions, determining flow parameters for instantaneous energy release in quiescent, inviscid, nonheat conducting perfect gas

20 p3612 A70-39821

Unsteady problems of finite amplitude plane and cylindrical wave propagation in dissipative spatially symmetrical media

20 p3673 A70-40093

Power loss due to cumulative meteoroid impacts on solar cells during extended planetary missions, investigating hypervelocity particle impacts into glass [AIAA PAPER 70-1139]

20 p3567 A70-40210

Energy dissipation in laminar unsteady incompressible viscous fluid flows, discussing velocity fields, boundaries, tangential motion and entrainment

20 p3614 A70-40402

Electric and magnetic field components of step function excited electric dipole immersed in dissipative homogeneous medium with specified conductivity and dielectric constant

20 p3589 A70-40464

Electron collision frequency profile for energy loss rate in ionospheric G factor for air, considering rotational excitations of molecular oxygen and nitrogen

21 p3812 A70-40618

Regular beamguides of second kind consisting of nonidentical nonequidistant correctors, calculating energy losses

21 p3785 A70-40629

Energy losses frequency distributions for fast charged particles in small pathlengths in equimolar He-carbon dioxide mixture

21 p3852 A70-40973

Gas turbine ball bearings, measuring effect of rolling elements shape on hydrodynamic power losses

21 p3834 A70-41776

Spatial energy loss and ionization deposition distributions of fluorescent radiation emission induced by electron beam in nitrogen gas

21 p3853 A70-41913

Wide frequency range dielectric spectrometer for insulating materials permittivity and loss factor measurement and display

21 p3830 A70-41950

Ring lasers loss lock-in, attributing frequency synchronization between oppositely directed traveling waves to mutual coupling

21 p3838 A70-42007

Energy release during flux jump in Nb-Ti single core wires and multifilament composite superconductors

21 p3863 A70-42011

Cosmic ray energy loss in interplanetary medium, discussing solar wind effects on low energy particles

21 p3883 A70-42111

Pressurized liquid nitrogen and hydrogen dielectrics for cryogenic cables, measuring dissipation factor and voltage breakdown by concentric cylindrical test cell

21 p3851 A70-42125

Collisionless plasma shock wave instability, discussing resonance and energy dissipation through ion Landau damping

22 p4077 A70-42292

Beamguides with inhomogeneities regulated for constant radiation losses, systematizing broadening

22 p3984 A70-42389

Power loss reduction from disk friction and gas leakage through rotor seals of low speed centrifugal pumps in aircraft hydraulic systems and liquid propellant rocket engines

22 p4091 A70-42806

Energy attenuation parameters measurements for monoenergetic source neutrons in shielding materials, using Van de Graaff accelerator

23 p4216 A70-43807

Wideband wattmeter for measurement and analysis of power dissipation in semiconductor switching devices, considering occurrence of peaks, frequency dependency of average dissipation, etc

23 p4174 A70-44597

Freely spinning gyrostal satellites with dissipation, deriving rotational motion equations by osculating elements method

23 p4261 A70-44681

Solid surface interaction between surface with normal molecular beam, generalizing model by energy parameter simulating dissipative forces

23 p4223 A70-44994

Collisionless plasma, calculating effects of energy dissipation due to weak firehose instability on steady planar flow, based on quasi-linear fluid equations

24 p4382 A70-45110

Acoustic plasma wave excitation by transverse electromagnetic wave beam, calculating LF instabilities and energy losses

24 p4384 A70-45149

Fibrous composite interface effects and fracture work, discussing tip stresses of crack normal to fiber, energy dissipation by pullout and debonding in brittle fiber composites, etc

24 p4419 A70-45171

Energy absorption and dissipation in friction brakes, investigating brake lining polymer binder contribution through molecular reorientation, crystallinity increase and entropy decrease

24 p4342 A70-45585

Graphite dielectric constant as function of frequency, considering electron energy loss anisotropy in UV

24 p4380 A70-45668

ENERGY DISTRIBUTION

NT SPECTRAL ENERGY DISTRIBUTION

Hot photoelectrons in semiconductors assuming short lived photoexcited current carriers, deriving expressions for energy distribution function of semiconductor current carriers

01 p0153 A70-10066

Direct solar radiation concentration by paraboloid mirrors, analyzing energy transport and distribution functions, based on statistically distributed imperfections of reflecting surfaces

01 p0010 A70-10762

Absorber positioning inaccuracy influence in concentrating solar unit mirror on unit energy parameters, discussing defocusing

01 p0010 A70-10763

Energy reversal zones in turbulent shear flows with asymmetric mean velocity distribution, implying zones of opposing shear

02 p0279 A70-12228

Energy distributions of emitted electrons from Si, GaP and ZnS semiconductors, determining relative core levels and Si valence band states optical density

03 p0537 A70-12879

Pulsation energy distribution in free turbulent incompressible jets, noting role of mean velocity distribution

03 p0466 A70-13384

Energy distribution function of electrons in weakly ionized plasma layer at electrode calculated, allowing for possible plasma concentration inhomogeneities

03 p0540 A70-13525

Formation of Maxwell and nonMaxwellian energy distribution in gases, noting reduction of time reversible to time irreversible equations

03 p0606 A70-13861

Design reliability of through-bulkhead initiator explosive train using parametric test program data, discussing shock transmission and acceptor charge sensitivity energy balance

03 p0549 A70-14124

Pumping energy distribution over cross section of active ruby laser elements in relation to smoothly polished, roughly polished and dull lateral cylindrical surfaces

04 p0700 A70-14607

Satellite HEOS-1 S 73 experiment launched during solar maximum to determine flux and energy distribution of solar wind positive component

05 p0900 A70-16077

Energy partitioning process under strong shielding with debris acting as energy sink

06 p1130 A70-17181

Pumping light distribution in rectangular laser rods showing corner maxima and overall nonhomogeneity

07 p1300 A70-19871

Atomic F reaction with hydrogen studied for vibrational, rotational and translational energy distribution, using IR chemiluminescence method

07 p1225 A70-20055

Energy distribution of positive Ar ions scattered from thermal diatomic D noting inelastic collisions 07 p1339 A70-20056

Angular and energy distributions of hyperthermal K atoms scattered and ionized by W surface measured as function of beam particle energy 07 p1342 A70-20115

Secondary electron emission coefficients and energy distributions to investigate interaction between positive ions and Cu/Be dynodes of electron multiplier 07 p1344 A70-20127

Molecular vibration energy distributions of polyatomic molecules, formulating energy criterion valid for nth order general case 08 p1511 A70-20597

Auroral electron energy distribution and ionization rates characteristics based on satellite and rocket measurements 08 p1487 A70-20642

Spatial and energy characteristics of laser with nonuniform transmittance across resonator mirrors, analyzing transverse modes interaction 08 p1514 A70-21816

Energy distribution of solar wind alpha particles in magnetosheath observed by Heos A satellite 09 p1744 A70-23205

Photoemission analyzer with finite emitter in spherically symmetric retarding field with magnetic field present, analyzing energy resolution 09 p1679 A70-22988

Photoemission energy distribution curves measuring circuit using AC retarding potential method, offering improved noise performance 09 p1679 A70-22996

Finite difference methods stability for time dependent Navier-Stokes equations coupled to energy equation with quadratic terms in velocity gradients 10 p1866 A70-24106

Solar radiation energy distribution simulated using vacuum monochromator, discussing Ar-Kr-Xe-methane mixture 10 p1931 A70-24317

Electron temperature distribution behind strong shock wavefront in air measured by electrostatic probe and compared to results of spectral line inversion method 10 p1871 A70-25114

Statistical energy concepts application to Mariner Mars 1969 spacecraft, estimating coupling of damping factors to analyze structural vibration [SAE PAPER 700171] 11 p2128 A70-25374

Pulsation energy distribution in turbulent flow of incompressible fluid near tube wall, defining energy diffusion, production and dissipation terms in energy balance equation 12 p2210 A70-27321

Spiraling electron beam energy conversion and distribution using retarding-field velocity analyzer 12 p2196 A70-27651

Turbulence energy balance equations for conducting fluid flow in longitudinal magnetic field with Joule dissipation 12 p2282 A70-28227

Free electrons non-Maxwellian equilibrium kinetic energy distribution function, considering partially ionized hydrogen-like plasma in thermal equilibrium 13 p2459 A70-28634

Long period comets energy change due to planetary perturbations tabulated, obtaining orbital major axes before and after passage 13 p2489 A70-28906

Solid state laser optical pumping energy density calculations for case of circular cylindrical image of pumping lamp formed in rod 13 p2429 A70-29476

Energy balance in radiation detector cooling, analyzing refrigerator capacity and thermal load 13 p2412 A70-29870

Solar wind energies spherical surface average and fluctuations from integration of conservation equations 14 p2630 A70-30357

Photoemission from evaporated gold films, measuring quantum yield, photoelectric energy distribution curves and optical density states 14 p2626 A70-30481

Laminar heat transfer to blunted wedge with constant wall temperature, describing energy field in boundary layer by analytic solution 15 p2825 A70-31818

Spatial distribution of energy deposited by auroral electrons in upper atmosphere, using Monte Carlo method 15 p2725 A70-31860

Annular turbulent flow between coaxial rotating cylinders, analyzing energy balance of averaged and pulsating motions 15 p2721 A70-32138

Electrons, positrons and photon energy distribution inside hydrogen plasma injected with high energy electrons 15 p2781 A70-32429

Composition dependence of optical energy gap and diffuse reflectance in MnSe-CdSe solid solutions 16 p2960 A70-33094

Plane turbulent impinging jet by iterative finite difference technique, assuming eddy viscosity dependence on energy fluctuations and turbulence length scale [ASME PAPER 70-FE-27] 16 p2835 A70-33634

Anisotropic energy gap model in superconducting Zn to describe microwave absorption measurements 16 p2961 A70-33777

Monte Carlo model of V groove surface roughness effects on directional reflections in plane of incidence, employing energy localization circle [AIAA PAPER 70-820] 16 p3002 A70-33944

Stellar UV and visual continuum observations, discussing recalibration of absolute energy distribution of alpha Lyr to improve model atmospheres 17 p3160 A70-34881

Reaction rate kinetics characteristics from isothermal data, investigating relationship to activation energy distribution 17 p3042 A70-35330

Turbulent energy distribution in plane wake in incompressible fluid, using pulsational energy balance equation 17 p3011 A70-35348

Energy distribution of laser spark spectrum in air, He and Ar, determining transmission coefficients of spark plasmas by self absorption method 18 p3265 A70-36151

Central pulsars effects on supernova envelopes, examining luminosity, energy input, shape and light curve 18 p3314 A70-36333

Infinite linearly elastic solid response with random variations in material elastic properties, obtaining average energy in displacement field by method of moments 19 p3538 A70-37796

Radiation transfer in plane parallel layers consisting of two atomic energy levels, assuming free electrons Maxwellian energy distribution 19 p3525 A70-38764

Pulsation energy distribution in turbulent flow of incompressible fluid near tube wall, defining energy diffusion, production and dissipation terms in energy balance equation 21 p3810 A70-42062

Approximate lasing condition from coupled rate and radiative transfer equations, determining population, energy density and power output 22 p4050 A70-43006

Cs seeded Ar discharges electron energy distribution, discussing drift velocities, electrons elastic and inelastic collisions with ions and molecules, etc 22 p4081 A70-43198

Electron energy distribution in time-varying plasmas, using difference quotient circuits for Langmuir probe characteristics measurement 22 p4082 A70-43220

Energy rotation in electromagnetic wavefields, noting TE-MODE excitation in rectangular guides 23 p4164 A70-44384

Spectral bidirectional reflectance measurements of rough metallic surfaces for reflected energy spatial distribution determination in radiative heat transfer problems 23 p4281 A70-44446

Rotating stellar atmospheric models for middle and late A star masses, emphasizing Altair observed and predicted energy distribution 23 p4250 A70-44812

Discontinuity in solar wind energy and angular distribution from 2 January 1970 ESRO satellite HEOS-1 observation 24 p4396 A70-45326

ENERGY EXCHANGE

U ENERGY TRANSFER

ENERGY LEVELS

NT ATOMIC ENERGY LEVELS

NT ELECTRON STATES

NT GROUND STATE

NT INTERMOLECULAR FORCES

NT MOLECULAR ENERGY LEVELS

Hydrogen type excitation model applied to analysis of intermediate exciton state role in two quantum absorption in semiconductors 01 p0153 A70-10068

Nitrogen and helium collisional effect on rotational relaxation rate of carbon dioxide upper laser level, noting thermalization 01 p0110 A70-10567

Ionized Ne, Ar and Kr first excited p states lifetime and transition probabilities, tabulating energy levels and mixing coefficients 02 p0343 A70-11887

Amplification cross section of 1.06 micron transition of trivalent Nd ion in alkaline silicate glass host material, based on three level energy level diagram 02 p0312 A70-12111

Energy distributions of emitted electrons from Si, GaP and ZnS semiconductors, determining relative core levels and Si valence band states optical density 03 p0537 A70-12879

Multiple particle production at high energy levels and associated peripheral interaction and statistical theories 03 p0555 A70-13035

Matrix elements systematic calculation method in terms of inelastic transition densities to evaluate nuclear properties 04 p0723 A70-15634

Degenerate and nondegenerate energy states and wave functions formulated by Rayleigh-Schrodinger perturbation theory 06 p1110 A70-17764

Possible pairing without superconductivity at low carrier concentrations in bulk and thin film superconducting semiconductors 06 p1127 A70-18641

Upper cesium levels population inversion during cesium discharge plasma decay 08 p1550 A70-20848

Ruby laser energy threshold dependence on partial shielding of rod by stainless steel tubing 09 p1694 A70-22136

Multilevel quantum systems interaction with electromagnetic fields at frequencies near quantum transitions using small signal analysis 09 p1695 A70-22256

Probability coefficients computation for transitions between energy levels of ion A XIV in solar corona 09 p1761 A70-23060

Bowen levels of O III radiative lifetimes and transition probabilities measurements by beam-foil spectroscopy 10 p1936 A70-23909

Hoeft-London factors calculated for general doublet transition in diatomic molecules, deriving energy levels 10 p1918 A70-23974

Energy levels predicted for various electron orbital configurations in Fe V by Slater parameters 10 p1944 A70-24953

Population densities of levels of excited atoms and ions in nonthermal plasma including hydrogen-like ion partition function 11 p2086 A70-25835

Methanol proton transfer reaction rate energy dependence 12 p2180 A70-26863

Iron impurity energy level behavior in seminsulating GaAs from determining temperature dependences of Hall coefficient, resistivity, optical absorption and steady spectral photoconductivity 12 p2286 A70-27370

Argon laser upper levels population measured as function of current strength at constant atom density in capillary 12 p2247 A70-27506

Energy levels of Th lines computed from weighted averages of interferometrically measured wavelengths data 12 p2277 A70-28119

Ruby laser output calculated as function of pumping power, taking into account pumping energy density spatial distribution and laser level depopulation 13 p2427 A70-28985

Hadron energy levels description by Lorentz invariant wave equation in form of supermultiplets 15 p2776 A70-31736

Semiconductors surface energy levels based on conductivity, metal-dielectric-semiconductor capacity and optics 15 p2785 A70-32765

Semiconductor surfaces electrical equilibrium, considering statistical occupation of surface energy and Fermi levels for given doping of bulk material 15 p2786 A70-32766

He II 3s and 3d states mean lives and initial population as function of energy, analyzing emitted radiation intensity 16 p2954 A70-33059

Gas dynamic molecular laser with electrons in ground state, using incoherent optical pumping from stationary shock wave 16 p2927 A70-33255

Radial energy eigenvalue problem conversion into one dimensional by infinite set of transformations, considering WKB quantization condition 16 p2942 A70-33691

Surface recombination centers protecting against discoloration of thermal control coatings due to chemical changes induced by photoproduced holes and electrons in oxide pigments 16 p2940 A70-33935

Coupled simple harmonic oscillators with almost degenerate energy levels, comparing perturbation techniques with Rayleigh-Schrodinger approach 16 p2955 A70-34002

Multistate impact parameter treatment of heavy particle collisions modified to include higher state couplings for electronic wave functions 16 p2956 A70-34309

Inverted coexistence possibility of spherical and deformed states in Si 28 and S 32 nuclei 17 p3137 A70-34518

Ni-Fe ferrites resistivity and thermoelectric power as function of temperature, proposing two energy level model for Fe ions 17 p3143 A70-35604

He-Cd laser discharge, determining population densities and lifetimes for levels of Cd ion excited by He metastables 17 p3108 A70-35903

Energy levels and spectral broadening of neodymium ions in laser glass from fluorescence and absorption spectra 19 p3445 A70-37760

Argon ion laser inversion saturation at large current densities due to upper working levels depletion 19 p3449 A70-38744

Electronic transitions in B by beam foil technique for spectral lines in 450-5000 Å range, measuring excited levels mean lives 21 p3781 A70-41932

Electron energies correlation in relativistic theory of atoms applied to multielectron atoms energy levels 22 p4076 A70-43470

Carbon dioxide amplification coefficient measurement for lines in laser transition range, determining rotational temperature and upslon levels populations 23 p4201 A70-44204

Gas dynamic molecular laser with electrons in ground state, using incoherent optical pumping from stationary shock wave 23 p4201 A70-44284

Level relaxation constants measurements by three-level laser spectroscopy, using line shape of stimulated shifted resonance scattering in gas 24 p4354 A70-45821

ENERGY LOSSES

U ENERGY DISSIPATION

ENERGY METHODS

NT STRAIN ENERGY METHODS

Extensive air shower axis position determined using energy methods and radial distribution geometry of particle density 01 p0171 A70-11252

Energy equation for thermal turbulent boundary layer on adiabatic flat plate 03 p0466 A70-13421

Energy method for analyzing rectangular panels buckling under nonuniform in-plane loading, considering stability under uniform compression 05 p0931 A70-16117

Acoustic characteristics of high subsonic model cold jet using imaging technique and measurements of energy flux of flow, calculating energy flux from flow-field measurements [AIAA PAPER 70-234] 06 p1040 A70-18125

Energy methods used in thermoelastic analysis of thermal stresses and deflections in thin rings 07 p1401 A70-18935

Nonsimilar energy and species equations for flow velocities described by Falkner-Skan equation 07 p1256 A70-19307

Toupin and Knowles elasticity theory applied to spatial decay estimate for parabolic heat equation used in diffusive temperature field 07 p1409 A70-19565

Asymptotic expansions and energy methods applied to three dimensional aircraft maneuvers involving energy climbs and turns 07 p1190 A70-20416

Thermoelastic energy functions bounding by variational principles for anisotropic composite materials properties 08 p1592 A70-21510

Stress, strain and acceleration spatial variation in plate structures under broad frequency band excitation using statistical energy method 10 p1962 A70-25065

Energy methods applied to fatigue crack propagation rate under tensile mean stress 10 p1963 A70-25090

Energy equations solved for step change of wall temperature and heat flux, determining turbulent heat transfer in tube, discussing asymptotic solutions validity 11 p2146 A70-25334

Plasma energy confinement time as function of discharge parameters for plasma thermal insulation in Tokamak-3 11 p2088 A70-25713

Energy dependence and threshold behavior of ion Ar lines excited in low-energy He ion-Ar collisions 11 p2087 A70-26402

Work and energy theorems in linear elasticity, discussing potential energy, real work, complementary energy and energy coefficients 11 p2142 A70-26625

Energy principle providing upper bounds on plastic deformation in elastoplastic structures subjected to blast loading 11 p2144 A70-26670

Stability analysis using energy method applied to Navier-Stokes equations for unsteady viscous flow 11 p2042 A70-26849

Sonic boom minimization methods involving mass or energy addition 14 p2531 A70-30868

Thermal response of passive heliotrope solar array orientation device using rotating bimetallic helix, performing energy balance analysis for helix temperature distribution 17 p3082 A70-34761

Buckling problem numerical analysis by nonlinear programming and minimum energy formulation 18 p3339 A70-36495

Gyroscope dissipative function, using quasi-elastic gyroscope model and forced oscillation method 19 p3420 A70-37260

Book on extremum principles covering energy methods of static and dynamic structural analysis 19 p3541 A70-37976

Complementary energy bounding theorem for statically loaded bodies composed of time independent plastic material 19 p3546 A70-38353

Encircled energy calculation in optical systems with central obstruction, observing focus error, spherical aberration and central stop effects on image contrast 20 p3627 A70-39088

Axissymmetric dual spin spacecraft consisting of nonconcentric frictionlessly mounted cylinders equipped with viscous damping mechanisms, evaluating stability criteria by energy method 20 p3715 A70-39556

Filonenko-Borodich and Papkovitch methods convergence proof based on completeness of cosine binomials system in energy space 20 p3721 A70-39736

Base function selection for energy calculation optimal convergence conditions of frequencies and stresses in turbomachine blades vibrations 20 p3722 A70-39784

Energy methods for stability of linear inflatable pouch actuator based on energy change in pouch deflection 21 p3760 A70-41966

Lagrange formulation for deriving energy-conserving numerical approximations for Vlasov plasmas 22 p4080 A70-42750

Correctable gyroscope stability estimation by energy method taking into account nutation and precession motions 22 p4039 A70-43556

MHD flow universal stability, investigating nonlinear system by energy methods 23 p4223 A70-43967

Mathematical models derivation for systems of interconnected elastic segments, using variational method and energy summation via difference equations 23 p4266 A70-44019

Incremental complementary energy method of stress analysis of orthotropic nonlinear materials having different behavior in tension and compression [AIAA PAPER 69-119] 23 p4270 A70-44563

Nonlinear shell analysis by finite difference energy method, using BOSOR3 and STAGS computer programs 23 p4273 A70-44723

Plastic creep displacement and deformation bounds computation for simple redundant structures, using energy theorems 24 p4422 A70-45288

Energy-mass analysis for steady state plasma by electrostatic analyzer and time of flight mass spectrometer, determining ion species temperature and density ratios 24 p4387 A70-45813

ENERGY OF FORMATION

Free energies of formation determined for tantalum silicides from EMF measurements on cells with solid thorium-yttria electrolytes 01 p0041 A70-10084

ENERGY REQUIREMENTS

Energy requirement for nonconservative elastic system unperturbed state stability, using direct Liapunov method 03 p0594 A70-13502

External work and energy expenditure relations of heart, including myocardial oxygen consumption 03 p0426 A70-13940

Mass-energy content of universe, discussing galactic formation in positive energy systems and missing mass problems 04 p0753 A70-15073

Energy optimal osculating elliptical transfer orbit from low eccentricity orbit constructed for prolonged circling in equatorial plane of axisymmetric planet 07 p1374 A70-18774

Energy cost and heart rate responses to single stage nonsteady state submaximal exercise procedures used in diagnostic and functional testing 07 p1211 A70-19690

Extragalactic radio sources evolution, discussing energy requirements of hollow-shell models 12 p2299 A70-27377

Initial period of muscular energy expenditure in athletes performing exercises on veloergometer, considering oxygen consumption 12 p2172 A70-28313

Linear systems approximate minimum energy controller, suggesting algorithm for mathematical model evaluation 16 p2886 A70-33344

Space vehicles dimensions effects on working fluid mass and power required for orientation 21 p3927 A70-40826

Deorbiting target intercept energy optimization by game theory approach [AIAA PAPER 70-1019] 21 p3848 A70-41778

Eroding-dielectric plasma accelerators energy characteristics, discussing current distribution 22 p4083 A70-43387

ENERGY SOURCES

Rotational properties of neutron star models for Crab Nebula energy source, using expressions for angular momentum and rotational kinetic energy 03 p0571 A70-13817

Meteoroid impacts as sources of seismic energy on moon, using projectile impact coupling to seismic waves in vacuum chamber experiment 04 p0751 A70-15056

Energy supply for supersonic flight air suction propellant systems using external supersonic combustion, discussing Caret wing and pressure effect 04 p0785 A70-15160

Proton-proton cycle in star interior, calculating isotope concentrations, reaction duration and energy release as function of temperature and chemical composition 05 p0900 A70-15972

Data on Jupiter chemical composition, internal structure and energy sources, discussing Jovian planets origin and role played by gas 07 p1386 A70-19487

Nucleons split-up into quarks disregarded as energy source for quasars 08 p1547 A70-20583

Thermospheric molecular nitrogen vibrational temperature, studying various chemical reactions and collisions as energy sources 10 p1872 A70-23827

Shock propagation from point explosion energy source into cold exponential atmosphere with radiative heat transfer in rear of shock front 10 p1869 A70-24525

IR radiation sources /irtrons/ accounting for energy releases by continuous matter and antimatter creation 10 p1947 A70-24997

Thermal explosion in degenerate nucleus of white dwarf due to formation of laminar energy source in presence of hydrogen 11 p2115 A70-26577

Primitive earth prebiological organic synthesis via amino acids shock heating in atmosphere-simulating gas mixture, suggesting energy sources from atmospheric entry 12 p2167 A70-27269

Laminar natural convection plumes behavior above energy sources calculated by simplest variables, indicating optimum formulation of boundary value problem 12 p2332 A70-27700

Dwarf and neutron stars as pulsar energy sources, considering Crab Nebula X ray emission and gravitational collapse 12 p2310 A70-27990

Solar, nuclear, chemical and thermal energy sources for short and long duration exploration on moon 14 p2634 A70-30195

Jupiter luminosity as indication of internal energy magnitude, comparing limb darkening with predicted brightness distribution 14 p2643 A70-30984

Data on Jupiter chemical composition, internal structure and energy sources, discussing Jovian planets origin and role played by gas 15 p2805 A70-32732

Book on batteries and energy systems covering theoretical concepts, construction, operation principles, characteristics and applications of various types of primary and secondary cells 22 p3964 A70-42454

Energy yield measurements of catabolic and anabolic activity in autotrophically growing Hydrogenomonas eutropha 23 p4149 A70-44997

Energy production of extragalactic radio sources, discussing objects associated with quasars 24 p4403 A70-45395

Gas tight lead storage battery with negative plates for oxygen absorption 24 p4295 A70-46352

ENERGY SPECTRA

NT ELECTRONIC SPECTRA

NT NEUTRON SPECTRA

Longitudinal and transverse temperature distribution measurement of electrons in electrostatic field and ion current density in ionized Cs plasma beam, determining energy spectra 01 p0149 A70-10170

Relaxation time approximation formulas for galvanomagnetic effects in graphite based on energy spectrum model 01 p0126 A70-10181

Energy spectrum of electrons and holes in semiconductors under strong electromagnetic wave field, calculating electron-phonon interaction Green function 01 p0155 A70-10184

Energy dependence of intensity ratio of Li, Be and B on C, N, O and F nuclei L/M ratio in primary cosmic rays, analyzing data discrepancy 01 p0169 A70-10316

Photoelectron energy spectra and partial photoionization cross sections for carbon dioxide determined with spectrometer at monochromatic incident radiation wavelengths 02 p0343 A70-11903

Cosmic ray origin in high energy H and He isotopic abundances and energy spectra observed by IMP 4 satellite during solar quiet times 02 p0358 A70-12250

Primary cosmic ray proton energy spectrum determined using balloon-borne ionization spectrometer and spark chamber 02 p0360 A70-12844

Threshold energy value of organic laser emission from coronene in methyl-cyclohexane-isopentane at 100 K 03 p0498 A70-12878

Quiet time primary cosmic ray electron flux and energy spectrum from 10 to 200 Mev in interplanetary space observed by OGO 5 satellite 03 p0553 A70-12902

Cosmic ray neutrons energy spectrum and angular distribution at sea level based on measurement results 03 p0556 A70-13046

Spectral energy transfer measurements in isotropic grid turbulence to determine validity of dynamical equation 03 p0468 A70-13785

Electron and positron flux steady state in interstellar space relationship to differential energy spectrum exponent in cosmic rays, discussing galactic halo and age 03 p0561 A70-14151

Energy spectrum of cosmic radiation primary nuclei calculated from collisions against stellar light photons and 3 K black body radiation 03 p0561 A70-14185

Flux, energy spectrum and charge composition of primary cosmic ray electrons measured, determining energy spectrum of primary positrons above 220 Mev 04 p0739 A70-14595

Ionization losses effect on energy spectra of cosmic ray heavy nuclei with Fermi acceleration, using transfer equation 04 p0742 A70-15201

Shear-dependent nearly isotropic turbulence energy spectrum theory, considering effects of viscous loss, shear production and inertial and velocity gradient transfer 04 p0674 A70-15520

Cosmic ray energy spectrum variations possible effect on ray intensity amplitude intensity increases preceding Forbush decreases 04 p0743 A70-15719

Interstellar propagation effect on spectra and charge ratios due to ionization energy loss and nuclear spallation during traversal of matter 05 p0897 A70-15762

Drift, anti-Fermi retardation, convective transfer and diffusion effects on solar cosmic ray energy spectrum in earth orbit proximity 05 p0898 A70-15943

Spectral intensity recording facility design for high energy electrons and hard gamma quanta in upper layer and beyond atmosphere 05 p0846 A70-15959

Scintillation spectrometer design for mass and energy spectra of elementary particles, discussing block diagram 05 p0846 A70-15962

Inviscid Burger turbulence spectral equations for cumulant approximation, obtaining energy spectrum and transfer as initial value problems 05 p0832 A70-16147

Energy spectra of cosmic diffuse X ray component and distribution over northern sky, determining Crab Nebula and Cygnus spectral characteristics 05 p0901 A70-16305

Energy spectrum time dependence of solar cosmic ray event of 28 January 1967 measured in Northern Hemisphere, discussing particle diffusion and magnetic trap 05 p0902 A70-16459

Electromagnetic energy spectra of lightning expressed as function of electric field spectral density of atmospheric 05 p0843 A70-16762

Energetic particle intensity fluctuations during bright aurora, using rocket-borne measurements 06 p1060 A70-18548

Turbulence spectra and generated power determined for plasma turbulence in objects with high electromagnetic radiation density /quasars and supernova shells/ 07 p1384 A70-19412

Midlatitude upper atmosphere soft electron energy flux nighttime measurements by sounding rocket 07 p1368 A70-19500

Turbulent energy and velocity spectra of air flow at atmospheric boundary layer over water analyzed statistically, assuming rippling surface activity 07 p1259 A70-19838

Pulsar short term pulse energy fluctuations presented in pulse amplitude histograms and power spectra 07 p1389 A70-20219

Descending and albedo electron fluxes at specific geomagnetic latitude and various atmospheric depths, obtaining electron energy spectrum vertical profiles 07 p1372 A70-20335

Sea level testing of magnetic spectrograph and calorimeter apparatus for studying cosmic ray spectra at different atmospheric depths 08 p1560 A70-20474

Ultrahigh energy primary cosmic rays model, considering galactic origin and energy spectrum 08 p1560 A70-20479

Damped isotropic turbulence kinetic and temperature fluctuation energy spectra, neglecting viscosity and molecular heat conduction 08 p1483 A70-20961

Intensity and altitude profile of H beta light emission and energetic hydrogen fluxes during auroral breakup using rocket soundings 08 p1489 A70-21383

Modified diffusion approximation for spectral transfer of isotropic turbulent pulsation energy for temperatures with low Prandtl number 08 p1538 A70-21429

Auroral electrons and photoelectrons spatial, energy and angular distributions measurements using low energy electron spectrometer onboard satellite Cosmos-261 08 p1500 A70-21797

Atmospheric variables /velocity, temperature, energy, etc/ spectra in lowest few hundred meters 09 p1714 A70-22352

Turbulent energy spectra in stably stratified atmospheric boundary layer flow 09 p1715 A70-22360

Flare star burst energy from radio telescope observations compared with solar flares 10 p1936 A70-23916

Energy spectra of electrons transmitted through Be, Al and Au targets measured for incident electron energy 10 p1918 A70-23984

Satellite-borne spectrometer for low energy electrons measurement, describing virgin photoelectrons equilibrium energy spectrum for different latitudes and pitch angles 10 p1874 A70-24313

Cosmic ray electrons during propagation in interstellar space analyzed for energy spectrum modulation 10 p1816 A70-24633

Canopus energy curve derived from UV spectrophotometry on Gemini 11 flight, noting agreement with model atmosphere 10 p1946 A70-24983

Longitudinal and transverse temperature distribution measurement of electrons in electrostatic field and ion current density in ionized Cs plasma beam, determining energy spectra 10 p1925 A70-25016

Time-bounded pulses with energy maximum in frequency band, solving integral equations for band-pass filters for maximum efficiency and optimum pulse shapes 11 p2004 A70-25799

Three dimensional turbulent flow, using direct interaction approximation for growth and propagation of point-to-point velocity field deviations energy spectrum 11 p2036 A70-26013

Energy spectra and composition of heavy nuclei in primary cosmic rays during low solar activity by nuclear emulsion stacks exposure in balloon flights 11 p2105 A70-26295

Energy spectrum of homogeneous isotropic incompressible turbulence, discussing eddy relaxation and direct interaction approximation 11 p2040 A70-26541

High energy break in isotropic gamma ray spectrum predicted from critical test of cosmological pion-decay hypothesis 11 p2106 A70-26844

Highest energy primary cosmic ray particles, considering air shower characteristics and energy spectrum shape 12 p2292 A70-27381

Turbulent shear flow energy spectrum theory for unstratified fluid with arbitrary eddies-mean velocity gradient interaction 12 p2214 A70-28364

Energy resonances between laser levels of carbon dioxide and diatomic and triatomic molecular impurity species, discussing population inversion due to superelastic collisions 13 p2425 A70-28622

Statistical characteristics and energy spectra of pulse code signals in data transmission estimated by matrix methods 13 p2364 A70-28871

Cosmic ray muon energy spectra at large zenith angles measured by optical spark chamber magnetic spectrometer 13 p2476 A70-28933

Cosmic ray muons energy spectra and zenith angle distributions by analyzing tracks recorded in high field heavy liquid bubble chamber 13 p2476 A70-28934

Energy spectrum and equatorial pitch angle distribution of charged particles trapped in magnetosphere resulting from inward diffusion due to third adiabatic invariant violation 13 p2476 A70-28942

Resonance energies of elastic scattering from one dimensional model potential containing barrier, using stabilization method 13 p2455 A70-29222

Energy spectrum of electrons accelerated in linear plasma betatron close to potential compared to cyclic betatron results 13 p2463 A70-29379

Cosmic ray energy spectrum in absence of solar activity from eleven year ray variations, noting coincidence with galactic rays 14 p2630 A70-30204

Temperature dependence of short wavelength magnon energies correlated with heat capacity 14 p2619 A70-30487

Cosmic ray energy spectrum variations possible effect on amplitude of intensity increases preceding Forbush decreases 14 p2632 A70-30803

Chirp radars energy spectra bounds calculation to insure electromagnetic compatibility 14 p2551 A70-31178

Daytime auroral zone electron precipitation energy spectrum from atmospheric bremsstrahlung X ray balloon data 14 p2580 A70-31257

Magnetospheric protons and electron energy spectrum time and magnetic activity dependence during solar maximum 15 p2792 A70-31671

Quiet time proton and alpha particle flux and differential energy spectra measured by cosmic ray detectors on OGO 3 satellite 15 p2793 A70-31795

Kinetic energy turbulence spectrum in free atmosphere from rawinsonde and aircraft data 15 p0000 A70-32369

Midlatitude upper atmosphere soft electron energy flux nighttime measurements by sounding rocket 15 p2795 A70-32745

Ions energy spectra in plasma heated by shock wave, using passive corpuscular diagnostic technique 15 p2781 A70-32821

Anisotropic superconducting energy gap of pure Zn from microwave absorption measurements 16 p2961 A70-33776

German monograph on artificially accelerated proton measurements for ionization calorimeter calibration and cosmic radiation energy spectrum analysis during balloon flight 17 p3081 A70-34572

Miniature multigrad probes for measuring energy spectra of charged particles and absolute plasma densities, comparing results to microwave measurements 18 p3294 A70-36150

Protons and alpha particles energy spectra during 25 February 1969 solar event from Centaur rocket measurements 19 p3496 A70-37509

Protons and alpha particles energy spectra following solar flares of 24-25 February 1969 from rocket measurements, estimating proton mean free path 19 p3496 A70-37510

Simultaneous primary energy spectrum, chemical composition and sidereal daily variation analysis for cosmic ray origin, using Proton measurements 19 p3500 A70-38080

Primary interplanetary electron energy spectrum, using Pioneer 8 measurements 19 p3502 A70-38094

Cosmic ray high energy electron component intensity and spectra, using nuclear emulsion detector with counter triggered spark array 19 p3502 A70-38095

Cosmic ray electron and positron differential energy spectra during solar quiet times from OGO-5 satellite observations in interplanetary space 19 p3502 A70-38096

Interplanetary cosmic ray positrons energy spectral component with origin different from interstellar mesons decay 19 p3502 A70-38098

Cosmic ray positrons and negatrons differential energy spectra and solar modulation, using balloon-borne magnetic spectrometer 19 p3503 A70-38100

Energy spectrum of primary cosmic ray electrons /negatron and positron/ in interstellar region observed near 1965 solar minimum 19 p3503 A70-38101

Electron energy spectra range from HEOS A1 satellite mounted Cerenkov counter with shower telescope 19 p3503 A70-38103

Primary cosmic ray electron flux, energy spectrum and east-west asymmetry, using balloon-borne spark chamber detector

19 p3503 A70-38104

Long term variations of cosmic ray electron spectrum above 500 MeV from balloon and satellite observations, noting reduction during Forbush decreases

19 p3503 A70-38105

Cosmic ray electron spectrum above 100 GeV by emulsion-lead sandwich assembly, estimating residence time, hydrogen atoms number density in galactic disk, etc

19 p3504 A70-38108

Sco X-1 X ray source properties in 16-111 keV energy interval, using balloon-borne detectors

19 p3505 A70-38116

Primary cosmic radiation singly charged component energy spectra by balloon-borne Cerenkov scintillation counter telescope

19 p3506 A70-38120

Primary cosmic rays energy spectra in interstellar space in relation to sunspot group number

19 p3506 A70-38121

Galactic cosmic ray energy spectra of light and medium nuclei from IMP-4 satellite measurements, investigating L/M ratio

19 p3506 A70-38124

Low energy galactic cosmic radiation energy spectra and charge composition in 2-14 Z range by OGO-5, suggesting two component model for origin

19 p3507 A70-38127

Cosmic ray nuclei chemical composition and energy spectra in 3-30 Z range by balloon flight and Pioneer 8 space probe, noting propagation models

19 p3507 A70-38131

Highly charged cosmic ray heavy nuclei primaries, examining charge spectra and solar elements abundances

19 p3508 A70-38136

Heavy and super heavy nuclei steady state spectra, comparing propagation parameters of light and medium nuclei

19 p3508 A70-38140

Primary cosmic ray proton energy spectra from satellite observation, presenting spectrum approximating function

19 p3510 A70-38153

Primary cosmic rays energy spectrum, investigating extensive air shower /EAS/ size spectrum in 2,000-1,000,000 eV range

19 p3510 A70-38154

Energy spectrum distortion of ultrahigh energy cosmic rays due to interactions with photons and neutrinos in universe

19 p3510 A70-38155

Cosmic electron spectrum formation by acceleration, considering metagalactic background X radiation

20 p3695 A70-39174

Frequency discriminators output voltages under action of fluctuating signal and noise with arbitrary energy spectrum

20 p3584 A70-39254

Cosmic ray intensity decreases and Forbush effects energy spectra during various solar activity periods

20 p3696 A70-39281

Equilibrium energy spectra of cascade electrons and photons in light and heavy materials as function of total shower energy

20 p3675 A70-39304

Solar B8-Be8 decay neutrinos energy spectrum and absorption cross sections calculation

20 p3698 A70-39307

Postmidnight auroral events precipitating electrons energy spectra components characteristics, using simultaneous X ray, optical and absorption measurements

20 p3699 A70-39334

Damped isotropic turbulence kinetic and temperature fluctuation energy spectra, neglecting viscosity and molecular heat conduction

20 p3608 A70-39383

Three dimensional Monte Carlo simulation of extensive air shower processes, comparing with hadrons and electrons energy spectra

20 p3699 A70-39442

Energy spectrum function for Gaussian initial velocity field of inviscid turbulence Burger model, using Cameron-Martin-Wiener exact expansion

20 p3609 A70-39653

High resolution electron beams application to electron spectroscopy, discussing elastic and inelastic scattering, resonances and atomic and diatomic molecular ionization

20 p3676 A70-40156

Ratio between mechanical energy flux in nonmagnetic region and magnetic region associated with solar chromospheric mottles

20 p3712 A70-40414

X ray flux and energy spectrum of Cen-X2, Sco-X1 and Tau-X1 sources by rocket flight observation

21 p3872 A70-40659

Hard X ray sources energy spectra in 20-120 keV range by balloon flights, presenting Sco X-1 intensities

21 p3872 A70-40660

Cosmic X ray spectra of Cyg XR-2 in 0.15-20 keV range by spinning rocket-borne detector, noting interstellar absorption

21 p3872 A70-40664

Diffuse cosmic X rays, discussing energy spectrum and contribution of galactic integration

21 p3875 A70-40686

High energy gamma rays detection by balloon flights, investigating flux and energy spectrum

21 p3876 A70-40696

Atmospheric neutron flux increase during solar proton event, measuring flux and energy spectrum of particles by balloon sounding

21 p3881 A70-41076

Total energies of stars with velocities perpendicular to galactic plane, examining absolute luminosities, galaxy size and local gravitational potential

21 p3890 A70-41162

Secondary periodicities in energy spectrum of strong pulsars from 80 MHz radioheliograph observations

21 p3892 A70-41186

Turbulent energy balance and spectra of axisymmetric wake behind sphere in incompressible fluid, measuring flow velocity

21 p3745 A70-41376

High energy neutrinos generated by cosmic ray interactions with earth atmosphere, discussing detection, plotted energy spectrum and underground muons

22 p4093 A70-42310

Extragalactic variable radio sources as clue for quasars and galactic nuclei energy, using long baseline interferometry

22 p4105 A70-43226

Ionization rate and electron density height profiles for typical auroral proton energy spectrum, noting radio noise absorption, sporadic E and radio aurora

22 p4024 A70-43307

Outer space galactic cosmic rays energy spectrum and modulation region boundary determination, using meteorite observations

23 p4236 A70-44050

Soft particle spectrometer in Isis-I satellite using electrostatic deflection for differential energy spectra measurements for electrons and protons

23 p4197 A70-44468

Energy loss spectra and collision cross sections for positive ion impact on molecular nitrogen, noting Lyman-Birge-Hopfield system excitation

24 p4381 A70-45599

Field emission from narrow 3d bands of ferromagnetic nickel, calculating 3d and free electron transmission coefficients ratio, using triangular surface barrier model

24 p4391 A70-45671

Cosmic ray energy spectrum in absence of solar activity from eleven year ray variations, noting coincidence with galactic rays

24 p4398 A70-46279

ENERGY STORAGE

NT ELECTRIC ENERGY STORAGE

NT HEAT STORAGE

Solar energy absorbers and thermal storage devices for high temperature energy conversion to electric power by thermionic or thermoelectric method

01 p0010 A70-10764

Equivalent circuit for trapped energy resonators and calculations of capacitances ratios for straight crested waves

01 p0088 A70-10777

Electrical exploding wire experiments at constant current with inductive energy storage system, discussing experiments with various cross sectioned copper wires

02 p0338 A70-11870

Electrical power system adaptable to intermediate solar probes, discussing thermoelectric, thermionic, photovoltaic systems and battery for energy storage [ASME PAPER 69-WA/SOL-5]

04 p0625 A70-14753

Energy storage in creep deformed graphite from stress reduction tests, discussing negative creep, test procedures and results

09 p1709 A70-22386

Input and memory-storage traveling wave tubes for electronic countermeasures

10 p1852 A70-24888

Book on energy conversion statics covering state functions, quasi-static processes, internal energy, chemical energy storage and conversion, dynamics and postulates and laws

12 p2165 A70-27670

Frequency multipliers with charge storage diodes, examining recombination and hysteresis effects on performance

17 p3050 A70-34588

Thermoluminescence, X ray and stored energy measurements of Apollo 11 samples, comparing surface outputs to interior

21 p3916 A70-41665

ENERGY STORAGE DEVICES

U ENERGY STORAGE

ENERGY TRANSFER

NT COUPLING CIRCUITS

Hydrodynamics, mass and energy transfer equations for moderately dense gases multicomponent mixtures, using Bogoliubov theory

01 p1146 A70-10129

Soviet monograph on transfer processes theory in statistical mechanical systems based on probabilistic approach to random particle walk

01 p0215 A70-10650

Electromagnetic propagation in linear dispersive media, discussing energy transport velocities of total stored energy density and electromagnetic energy

01 p0043 A70-10779

Vibrational energy exchange between colliding diatomic molecules modulated by harmonic oscillators with insignificant frequency difference

01 p0147 A70-11035

Perturbation method developed for linearizing non-linear singular equation for inhomogeneous stratified atmosphere H-function in theory of radiative transfer

02 p0338 A70-11791

Radiative transfer in plane parallel atmospheres computed by discrete space techniques based on invariance concept for application to planetary atmospheres

02 p0338 A70-11825

Absorption spectra computation for model planetary atmosphere using Neumann series for solving semimfinite radiative transfer equation

02 p0342 A70-11826

Radiative transfer in nongray gas between parallel walls, solving heat flux and temperature distribution

02 p0392 A70-11907

Transient energy transfer during expansion of plane layer of radiating gas bounded by strong shock, assuming LTE and perfect inviscid nonconducting gas

02 p0279 A70-12230

Radiative energy transport in sunspot region via model computations, obtaining reduced subphotospheric flux estimates for given magnetic field

02 p0372 A70-12254

Intramolecular triplet-triplet energy transfer between nonconjugated molecular chromophores held together by rigid molecular frame at known separation distance and mutual orientation

02 p0251 A70-12277

Discrete space theory for radiative transfer in one dimensional scattering media of arbitrary constitution

02 p0340 A70-12642

Numerically stable solutions existence for one dimensional monochromatic radiative transfer, using linear algebra including vector and matrix norms, convergence, etc

02 p0340 A70-12643

Solutions of Ambarzumian-chandrasekhar H-equation for radiative transfer

02 p0340 A70-12661

Stratospheric air intrusion into troposphere calculated for speed and frequency of occurrence, considering mass and energy transfer

02 p0329 A70-12690

Resonant energy transfer of trivalent Yb into trivalent Eb for optical pumping improvement for fluorophosphate glass lasing

02 p0314 A70-12725

Radiative energy transfer from single small sphere to quiescent nonconducting gas with constant volumetric absorption coefficient, using method of matched asymptotic expansions

02 p0400 A70-12861

Differential equation with associated boundary conditions constructed for radiative transfer with spherical symmetry, applying to gray gas between concentric black spheres

03 p0603 A70-12904

Radiation transfer problem in waveguide with statistically uneven walls reduced to Dyson and Bethe-Salpeter equations in quantum field theory

03 p0524 A70-13066

Spectral energy transfer measurements in isotropic grid turbulence to determine validity of dynamical equation

03 p0468 A70-13785

Vibrational energy exchange between molecules during collision behind normal shock front as function of wave velocity

03 p0468 A70-13873

Electromagnetic energy transmission factors for metal-dielectric-metal system, calculating net energy flux, noting effects of metal spacing, time, temperature level, etc

[ASME PAPER 69-WA/HT-8]

04 p0784 A70-14822

Radiative transfer between two infinite parallel metallic surfaces separated by nonconducting thick film ideal dielectric based on electromagnetic wave theory

[ASME PAPER 69-WA/HT-6]

04 p0784 A70-14824

Temperature distribution around radiating sphere in homogeneous gas medium with molecular heat transfer, solving energy transport equation

04 p0785 A70-15012

Temporal behavior of energy injection into geomagnetic ring current found burst-like and similar to Dp at all magnetic levels

04 p0679 A70-15108

Diatomic oxygen-nitrogen collisions in mixtures with CO, determining vibration-vibration energy exchange probabilities

Rectennas design, construction and power output

Inviscid Burger turbulence spectral equations for cumulant approximation, obtaining energy spectrum and transfer as initial value problems

Formula for energy radiated from particles system applied to electromagnetic and gravitational radiation and illustrated by charged particle motion in magnetic field

Monte Carlo radiative transfer techniques applied to develop height dependent spicule model, computing contrast curves of model against chromospheric background

Vibrational energy transfer in oriented nonlinear collisions between diatomic molecule and atom, considering molecular vibration excitation

Monte Carlo calculations of nonequilibrium radiative transport, including weighting and biasing techniques

Electron energy distribution function for carbon dioxide laser plasmas in gas mixtures, discussing dissociation products role in electron energy exchange

Kolmogoroff constant determined by Heisenberg turbulence formula and model for transfer of turbulent energy between different wave numbers

Energy and mass transfer during elastic and inelastic molecular collisions in reacting gas mixtures, using Enskog and variational methods in solving Boltzmann equations

Radiative transfer equations for Zeeman multiplets of electric and magnetic dipoles and quadrupole radiation in solar Fraunhofer spectrum

Monte Carlo analysis of free and near free molecular flow through circular tubes for mass, momentum and energy transfer

Energy transfer from pulse network to mass associated with propagating current sheet in linear pinch discharge, discussing pulsed plasma accelerator efficiency

Coupled vibrational relaxation in mixtures of diatomic gases, showing energy pumping phenomenon between species

Radiative heat transfer in radiant energy flux incident on plane surface of nonisothermal absorbing and dissipating layer

Diatomic Br molecular vibration-rotation coupling effects on energy transfer during Br-Br collisions, determining probability distributions

Radiant energy transport in plane semiinfinite atmosphere with scattering indicatrix and quantum survival probability as arbitrary functions of optical depth

Multiple pass tube heat exchangers efficiency, solving energy and heat transfer equations from fluids homogeneity and constant thermal capacity considerations

Soviet book on celestial bodies radiation transfer and spectra covering light scattering, radiation fields, absorption, etc

Hydrodynamics, mass and energy transfer equations for moderately dense gases multicomponent mixtures using Bogoliubov theory

Modified diffusion approximation for spectral transfer of isotropic turbulent pulsation energy for temperatures with low Prandtl number

Einstein power transfer theory used for demonstrating energy transfer rate by gravitational radiation from emitter to absorber

Troposphere-stratosphere kinetic energy transfer during 1967-1968 midwinter warming, comparing calculation by pressure interaction term with direct calculation of vertical velocity fields

Excitation energy transfer processes in oxide glasses containing trivalent Tb ions in combination with other rare earth activators

Radiation transfer in semiinfinite medium illuminated by parallel light beams assuming triominal scattering indicatrix, deriving radiative effects and radiation field

Radiation transfer in scattering medium with nonuniform density distribution of absorbing matter expressed in terms of photon distribution

Vacuum UV atomic nitrogen and oxygen lines contribution to energy transfer in high density plasma, noting f values and Stark half widths

Irreversible radiative energy transfer effect on stability of flow with two dimensional stationary infinite contact discontinuity

Resonance radiation transport in optically thick layer, obtaining conservative light scattering solution

Anode energy transfer model for measurement of circumferential current and heat flux distributions of MPD arc thruster

Radiative heat transfer along adjacent layers of multilayer insulation blanket determined as energy transport mode

Nongray surfaces radiative interchange calculation, considering surface radiation properties

Waveguide windows for energy outlet in microwave devices analyzed by plane /Brillouin/ modes, discussing dielectric element reflection coefficient

Coaxial energy outlets satisfying vacuum maintenance requirements of dielectric waveguide windows in dismountable prototype microwave devices

Rotational-translational energy transfer in collisions between homonuclear diatomic molecules and rotational relaxation time in diatomic gases

Radiation transport calculations based on approximate method restricted to X ray and low energy gamma ray region of electromagnetic spectrum

Hydrodynamic energy flow down horizontal tunnel from nuclear explosive detonated underground, recording shock front luminosity and time of arrival

Radiative transfer in inhomogeneous atmospheres using simplified matrix equations in perturbation method

Polarized radiation transfer through inhomogeneous semiinfinite atmosphere by matrix perturbation method, giving nonlinear singular integral equation

Time dependent radiative transfer equation for plane-parallel isotropic scattering medium in first Gaussian approximation

Vibrational energy exchange between colliding diatomic molecules modulated by harmonic oscillators with insignificant frequency difference

Adenosine phosphates hydrolysis in solutions containing Ca ions and in synthetic seawater, investigating living systems energy transfer and prebiological evolution

Energy balance of self sustaining thermonuclear reaction with nonuniform magnetic field in wall-contained dense plasma, allowing for radiation losses

Electrons thermodiffusion and energy transport coefficients in noble gases at mean reduced electric field intensities, obtaining distribution functions

Solar energy exchange with radiator surface recessed within specular axisymmetric cylindrical spinning cavity, using deterministic ray tracing scheme

Laminar boundary layer equations solved for mass and energy transfer in binary gas mixture, investigating forced and free convection

Turbulence in incompressible electrically conducting fluid with uniform applied magnetic field, discussing nonlinear energy transfer mechanisms and magnetic effects

Radiative energy transfer in hydrogen plasma having uniform heat source and bounded by parallel black plates

Surface parameters influence on energy transfer to arc jet anode, discussing work function, accommodation coefficient and diffuse reflection coefficient of electrons

Nonlinear integral equations of radiation transfer of stellar and planetary atmospheres

Radiation transfer models for diffuse reflection of quanta from turbulent medium applied to electromagnetic wave propagation in turbulent atmosphere

Primal radiation spectrum, discussing possible distortions due to energy injection before and after recombination

Q switched CO-HE laser IR fluorescence, considering population inversion recovery by vibrational energy transfer

Radiative energy transport effect on temperature distribution in conduction heated plane layer applied to solar chromosphere

Linearized Fredholm equation solution, describing temperature field for energy transport by radiation and heat conduction

Nonlinear integrodifferential equations of radiative transfer solved by invariant imbedding approach, discussing Rayleigh phase matrix

Planar absorbing and emitting layer exposed to monochromatic collimated radiation, analyzing line or band shape effect on radiative transfer

Band or line shape effect on radiative transfer in nongray medium between parallel walls, discussing temperature distribution and radiative flux

Electromagnetic energy propagation through absorbing single resonant frequency dielectric, deriving transport velocity and relaxation time

Precision radiometry of electromagnetic energy transfer in atmospheric and space physics emphasizing solar and terrestrial radiative fluxes measurements

Solar and terrestrial radiation measurements and computations in meteorology, considering diffuse radiation and radiative transfer in atmosphere

Pure ammonium perchlorate single crystal self deflagration, determining energy transfer mechanisms from pressure effects, combustion characteristics and subsurface profile

Excitation and radiative transport of ^{130}A triplet of atomic oxygen for dayglow and aurora

Troposphere-stratosphere kinetic energy transfer /1964-1968/, annual variations and vertical flux correlation to circulation pattern

Sound propagation in atmospheric fog, considering mass, momentum and energy transfer mechanisms between particles and gas

Radiant energy transport in plane semiinfinite atmosphere with scattering indicatrix and quantum survival probability as arbitrary functions of optical depth

Linear integral equations for radiative transfer between parallel plates, using least squares method

Spatial distribution of energy deposited by auroral electrons in upper atmosphere, using Monte Carlo method

Two diaphragm combustion shock tube for plasma radiation energy transfer, describing development, performance, make-up and testing

Molecular velocity influence of optically active medium in gas dynamic quantum amplifier on monochromatic radiation transport, using corpuscular light model

Radiative transfer in spherical stellar atmosphere, considering free electrons density gradient and thermal motions, atmospheric layer curvature, optical thickness, etc

Radiative transfer in scattering medium with nonuniform absorption

Transition probabilities for Markov chain describing bond breaking and molecular energy transfer in vibrational relaxation and dissociation

Book on stellar spectra theory covering line absorption coefficient expressions, radiative transfer, line source function, line broadening, etc

Probabilistic model for radiative transfer of photons in inhomogeneous infinite cylindrical shell medium, noting radiation intensity relation to scattering and transmission functions

Thermal conductivity along parallel radiation shields, proposing calculation method for energy transport

Mechanical erosion concomitant with thermochemical erosion in mass and energy transfer at interface of

boundary layer and ablating nylon-silica-phenol material
[AIAA PAPER 70-824] 16 p2941 A70-33942

Cyclopropane-argon mixtures translational and vibrational energies exchange efficiencies analysis based on intermolecular potential 16 p2956 A70-34083

Nucleosynthesis in supernova models based on neutrino energy transport 17 p3153 A70-34529

Vibrational relaxation and energy transfer processes in gas dynamic flows, discussing cross sections, atom-molecule interactions, molecular rotation, kinetic equations, etc 17 p3068 A70-34670

Nonadiabatic self absorbing radiative flow of gray gas around sharp cornered blunt body at hyperbolic speed by integral relations method 17 p3010 A70-34974

Energy transfer processes of electron gas for pipe flow of weakly ionized nonequilibrium plasmas, noting electron temperature decrease exponentially along tube axis 17 p3142 A70-35438

Energy transfer in convective envelope of rotating star and solar differential rotation, using Lucy gravity-darkening law 18 p3313 A70-36214

Free turbulent incompressible jet, analyzing pulsating characteristics and energy balance with Reynolds stress equations 18 p3240 A70-36264

Fluid dynamics of pulsed plasma accelerators, discussing energy transfer and losses limitations 18 p3301 A70-36660

Elastic energy transfer cross sections calculation of H-H scattering to estimate neutralized solar wind particles thermalization 18 p3309 A70-36951

Radiative transfer equation for spectral line formed in multidimensional atmosphere, solving for two dimensional atmospheric model 18 p3317 A70-37008

Coupled fiber lasers maximum energy transfer between passive conductors, determining minimum pulse duration 19 p3443 A70-37286

Initial condition effects on weak homogeneous turbulence with uniform shear, studying energy transfer and dissipation 19 p3403 A70-37537

Energy and momentum exchange between gases in elastic collisions at different temperatures and velocities 19 p3551 A70-37538

Energy flow between two superfluid helium baths at different temperatures and separated by thin plate 19 p3471 A70-37648

Monoatomic inert gas molecules interaction with continuous elastic solid of alkaline and nonalkaline metals, calculating energy exchange 19 p3373 A70-37816

Various light velocities, including controvelocity for describing EM radiation transport 19 p3472 A70-38274

Atmospheric energy flow cycle involving large scale circulation components measured by wave number around latitude circles, using equations for closed global system 19 p3415 A70-38416

Radiation transfer in plane parallel layers consisting of two atomic energy levels, assuming free electrons Maxwellian energy distribution 19 p3525 A70-38764

Intercomponent momentum and energy exchange in weakly ionized gases, examining kinetic theory of subsonic and supersonic transport processes 19 p3482 A70-38945

Radiation field multidimensionality effect on radiating gas jet flow, taking into account radiative energy transfer by differential approximation 20 p3611 A70-39808

Nonisothermal condensation in ionized vapor as function of energy additions to droplets 20 p3680 A70-39989

Homogeneous opaque reactive solid heating and ignition by constant energy flux, examining physical and chemical parameters at critical conditions 20 p3738 A70-40078

Electrolytic capacitor current pulse networks for quasi-steady MPD arc thrusters, determining series resistance effects on energy transfer [AIAA PAPER 70-1082] 20 p3568 A70-40253

Exponential kernel approximation effect on radiative energy transfer in high temperature hydrogen plasma 20 p3684 A70-40278

Solar corona streamer and interstreamer regions, examining geometrical and dynamic structure by energy transport process 20 p3712 A70-40417

Continuous wave laser action in chlorine, Ar and He gas mixtures, observing energy transfer between Ar and chlorine by pumping action 21 p3834 A70-40570

Lorentz lines radiative transfer in nonisothermal gases, developing Landenburg-Reiche analysis for isolated unshifted lines growth curves 21 p3852 A70-40590

Atmospheric temperature and water vapor profiles from iterative solution of radiative transfer equation for comparison with spectral radiance observation from Nimbus satellites 21 p3846 A70-40803

Surface roughness effects on thermal radiant energy interchange between opaque interacting surfaces formulated for unequal temperature adjoining plates 21 p3944 A70-41018

Script-F radiative interchange matrix for enclosures with arbitrary surface emission and reflection characteristics 21 p3944 A70-41020

Radiative transfer among surfaces forming long cavity exposed to collimated incident energy 21 p3944 A70-41022

Radiation line transfer in Wolf-Rayet envelopes with rapid radial expansion by escape probability method, including radiation effect from stellar core 21 p3892 A70-41248

Molecular size dependent steric effects in translation-vibration energy transfer by velocity dispersions in cyclopropane-inert mixtures 21 p3780 A70-41706

Thin radiating shock layer about axisymmetric blunt bodies, investigating energy-momentum transport coupling 21 p3950 A70-41746

Magnesium-sodium nitrate porotectonic flare spectral radiant energy comparison with radiative transfer theory data, considering Na resonance continuum formation 21 p3850 A70-41937

Radiative transfer equations quantum theoretical deduction in spectral line regime, considering Planck law, Einstein coefficients and kinetic equations 22 p4072 A70-42339

Stepwise linear regressions method for estimating black body surface radiances from model atmospheres and corresponding simulated Nimbus 2 window-channel radiances 22 p4013 A70-42617

Classical calculations for energy transfer to diatomic molecules with rotational and vibrational degrees of freedom in atom-diatom-molecule collisions 23 p4221 A70-44010

Relaxation method for inverse radiative transfer equation solution, determining temperature profiles and atmospheric parameters 23 p4214 A70-44036

Energy transfer methods for hybrid air breathing ramjet propulsion systems with rocket motor S gas source [ICAS PAPER 70-61] 23 p4233 A70-44156

Radiative transfer equation solution for polarized light in Rayleigh scattering atmosphere with absorption, using singular eigenfunction expansion technique 23 p4219 A70-44402

Radiative transfer upstream absorption effect on inviscid stagnation region shock layer radiation 23 p4133 A70-44551

Equatorial acceleration of sun, considering rotation and turbulent energy transport in convective zone 23 p4252 A70-44830

Radiative energy transfer during interaction between blunt body and hypersonic gas flow, noting effect on flow temperature, shock wave separation, etc 23 p4136 A70-45020

Electronic energy collisional transfer between atomic and molecular hydrogen, measuring excited molecule vibrational distribution 24 p4381 A70-45650

Radiative transfer and magnetic dispersion for three dimensional wave propagation in radiation magnetogasdynamics 24 p4387 A70-46148

ENGINE ANALYZERS

Engine performance monitoring system/EPMS/ for aircraft jet onboard operation analysis and failure detection 08 p1558 A70-20668

Aircraft turbojet engine/inlet compatibility, using data system for acquisition, identification and analysis of critical time variant pressure parameters [AIAA PAPER 70-594] 13 p2375 A70-29877

ENGINE CONTROL

NT ROCKET ENGINE CONTROL

NT TURBOJET ENGINE CONTROL

Concorde engine and air intake electronic controls 02 p0353 A70-11837

RB.211 aircraft engine control, describing fuel and electronic control systems design and operation [SAE PAPER 690404] 03 p0551 A70-12895

Optimum power and operation mode of space vehicle engine with control error allowance as function of mass and velocity 04 p0760 A70-14433

30 cm diameter mercury bombardment low impulse thruster development for potential space applications, discussing performance and control [AIAA PAPER 69-238] 07 p1365 A70-19704

Fluidic devices and applications to gas turbine control, discussing beam deflection amplifiers design parameters [AGARDOGRAPH-120] 08 p1559 A70-21933

Algorithm for propellant flow rate increase of nuclear rocket in minimum time without exceeding maximum allowable stress in reactor core 10 p1914 A70-24870

Fluidic gas turbine controls, discussing high temperature operation, hybrid sensors and logic in hostile environment applications 12 p2164 A70-27074

Optimum power and operation mode of space vehicle engine with control error allowance as function of mass and velocity 13 p2503 A70-28458

Concorde Olympus 593 power plants air intake and engine control system design for rapid servicing, discussing fault diagnosis and checkout 14 p2535 A70-31337

Avionics and instrumentation, discussing digital techniques application to engine control, electronic head-up and head-down displays, radiation pyrometry, etc 14 p2589 A70-31338

Aircraft electronic propulsion control system using flight type computers and analog to digital conversion equipment [AIAA PAPER 70-693] 16 p2966 A70-33556

Aircraft propulsion control system accommodating transients and yielding higher steady state performance 16 p2966 A70-33557

Inlet and engine control vector size and weight reduction, reliability, accuracy, etc [AIAA PAPER 70-696] 16 p2967 A70-33559

F-14A engine air inlet control, describing variable geometry system open loop design [AIAA PAPER 70-697] 16 p2841 A70-33560

Digital computer simulation and analysis of control loops for ion thruster control [AIAA PAPER 69-239] 17 p3149 A70-35654

Helicopter gas turbine governor systems for engine and rotor speed control, minimizing pilot activity [ASME PAPER 70-GT-37] 18 p3214 A70-36835

Flight test program for helicopter gas turbine engines, considering engine-airframe-control systems integration and environmental tests [ASME PAPER 70-GT-38] 18 p3303 A70-36836

Control system considerations for small shaft-type aircraft gas turbines providing torque, temperature, load sharing and overspeed limiting functions [ASME PAPER 70-GT-132] 18 p3304 A70-36858

Aero gas turbine engines digital computer control, discussing special properties, design and safety problems [ASME PAPER 70-GT-40] 18 p3304 A70-36870

Gas turbines dynamics and control system requirements, discussing equipment design and reliability [ASME PAPER 70-GT-76] 18 p3305 A70-36887

Two stage turbine engine parts adjustment optimization in terms of fuel consumption or thrust control by linear programming techniques 19 p3489 A70-37241

Gas turbine propulsion systems design, performance and applications for industrial and military uses, discussing sensors for measurement and control of critical engine parameters 19 p3424 A70-37881

Nuclear rocket engine fluidic chamber pressure control, discussing design concepts for static and dynamic subsystems [AIAA PAPER 70-1010] 20 p3688 A70-39585

Fluidic controls for propulsion engines, describing optimum fabrication techniques [ASME PAPER 70-FLCS-7] 22 p3964 A70-42420

Low and medium power turboprop engines for V/STOL aircraft, discussing development trends concerning operational control 22 p4091 A70-43081

Fuel delivery and speed control systems for aircraft gas turbine engines, discussing control circuit transfers and block diagrams 22 p4091 A70-43116

German monograph on dynamic control behavior of jet engines covering computation for normal external actions and perturbation effects 23 p4233 A70-44396

Computerized simulation and hardware for propulsion control of turbine engines [SAE PAPER 700827] 24 p4394 A70-45892

Engine control concepts for augmented turbofan, discussing integrated electrical/hydraulic/mechanical system [SAE PAPER 700826] 24 p4394 A70-45893

High temperature gas turbine aircraft engine control system requirements, noting stoichiometric fuel-air ratio [SAE PAPER 700823] 24 p4394 A70-45895

Direct drive turbine engine control components and airframe accessories, noting weight and frontal area reduction
[SAE PAPER 700821] 24 p4394 A70-45896

Propulsion control integration for aircraft power management
[SAE PAPER 700818] 24 p4394 A70-45899

Gas turbine controller design by inverse Nyquist method compared to conventional multivariable design methods
24 p4396 A70-46157

ENGINE COOLANTS

Exhaust gas ejectors for engine cooling, discussing ejector design, flow rates, fuel consumption, etc
06 p1129 A70-17144

Dicyclohexyl (DCH)/ endothermic dehydrogenation to diphenyl (DP)/ over platinum-alumina catalyst without added hydrogen considered for hypersonic aircraft engine cooling
14 p2546 A70-31175

Heat pipes design for rocket engines cooling, discussing connections to space radiator and to heat rejection device and heat transfer capability
[AIAA PAPER 69-582] 15 p2791 A70-32517

Hypersonic airbreathers aerodynamic, structural and propulsive system interactions, discussing hydrogen fuel heat sink, airframe and engine cooling and airframe materials
[ICAS PAPER 70-16] 23 p4138 A70-44127

ENGINE DESIGN

Rolls-Royce RB 211 three shaft turbofan engines development and tests, noting preparation, building, cradle installment, open air facilities and noise measurements
01 p0161 A70-10079

Optimum R and D organization in aircraft engine production illustrated on turbofan engine
01 p0161 A70-10080

Turbojet engines air pollution emissions processes resulting from combustor primary and secondary zone conditions, discussing engine design modifications
[AIAA PAPER 69-1040] 01 p0162 A70-10602

A-7 aircraft TF-41 engine tolerance to steam ingestion, discussing test program and results and engine modifications
01 p0165 A70-10700

Nuclear light bulb engine critical fuel mass and design changes effects
[AIAA PAPER 68-571] 01 p0140 A70-10835

Turbine engine starting system design requirements, outlining lifetime improvement of hot section parts
01 p0167 A70-11460

Helicopter turbine engine bleed air requirements obtained by compressor extraction for engine designers
01 p0167 A70-11462

Fuel injection and mixing and piloted ignition in supersonic flow design principles for scramjet engine, evaluating eddy viscosity model for parallel injection
02 p0354 A70-12047

Optimum performance for Mach 3 to 7 fixed geometry ramjet with successive subsonic and supersonic combustion, noting lifting wing conjunction
02 p0355 A70-12365

Annular combustion chamber for turboprop engines, analyzing design data and development stages, discussing performance characteristics
03 p0552 A70-13928

Combustion chamber design for engines, considering atomization by rotating disk vs nozzle atomization
03 p0552 A70-14031

Design specifications for low noise turbofan engine used on long range subsonic transport aircraft
[ASME PAPER 69-WA/GT-7] 04 p0734 A70-14888

Optimum low speed ducted fan design for minimum noise generation
[ASME PAPER 69-WA/GT-4] 04 p0734 A70-14891

Stirling free piston engine operating principles, performance limitations, heat transfer problems, fluid flow, mechanical design, test results and applications
[ASME PAPER 69-WA/ENER-15] 04 p0627 A70-14895

Aircraft power plant technology trends, discussing noise and installation, rear fan engine layout, anticipated bypass and compressor pressure ratios and fuel consumption
04 p0735 A70-15043

Solar or nuclear energy powered electric propulsion systems for transferring satellite from low to geostationary orbit, discussing feasibility and costs of various designs
04 p0735 A70-15174

Small three stage hydraulic turbine for aerospace and commercial applications, discussing design and performance
04 p0628 A70-15640

Optimized compressor blades, examining Le Flo boundary layers theory possibilities as design method
04 p0621 A70-15667

Noise suppressor research for jet engine components, describing test equipment and facilities for models work
05 p0825 A70-15808

Engine cycle and low pressure-intermediate pressure compressor aerodynamic design of TF41 turbofan engine
[SAE PAPER 690687] 05 p0895 A70-15864

Engine development for 3 and 4 engine large capacity jet aircraft, discussing fan cowl size and weight, installation drag effects, etc
05 p0895 A70-15928

Aircraft engine prospects in terms of power and thermal efficiency, pressure ratio and turbine entry temperature, materials and fuel cooling improvement, etc
05 p0896 A70-16111

Aircraft power plant development, discussing thrust, specific weight, speed, jet engine and noise suppression efforts
05 p0896 A70-16346

Development trends, design and gas dynamic characteristics of turbine engines for helicopter propulsion systems including pressure, turbofan and integral engines
05 p0896 A70-16350

Steady state and dynamic performance of variable geometry free gas turbine using nomogram and analog simulation
06 p1129 A70-17143

Resistojet design criteria for performance modeling of ammonia propellant thrusters and manned space stations using biowaste propellants
[AIAA PAPER 70-211] 06 p1131 A70-18026

Solid propellant rocket engines design, considering nonlinear longitudinal combustion instability encountered in aluminized propellants
08 p1558 A70-20623

Aerodynamic and mechanic design of gas turbine for light helicopters, including flight tests and program objectives
08 p1558 A70-20686

Aircraft power plant development, discussing thrust, specific weight speed, jet engine and noise suppression efforts
08 p1558 A70-21029

Aircraft engines development and reliability, discussing rejection causes, data retrieval, repair and salvage techniques
08 p1558 A70-21031

Soviet helicopter and aircraft engines characteristics covering designer, power, rpm limits, fuel consumption, weight, geometry and applications
08 p1559 A70-21366

Helicopter turboshaft engines design and performance
08 p1559 A70-21517

Tubing materials for gas turbine engines covering fabrication, selection, etc
08 p1559 A70-21854

Supersonic burning ramjet /scramjet/ performances, discussing vehicle engine integration, superiority to ordinary ramjets at hypersonic speeds, combustion process-flow field interaction, etc
[AGARDOGRAPH-120] 08 p1600 A70-21930

Turbine blade and vane air cooling need established by advantages of operating aircraft turbines at high turbine entry temperatures
[AGARDOGRAPH-120] 08 p1559 A70-21931

V/STOL aircraft turbojet engine design and quality control for in-service reliability
09 p1743 A70-22572

Harrier engine nozzle actuation system role in short ground takeoff run facility, discussing pneumatic system, air motor servo unit and pilot control
09 p1610 A70-22606

Oxygen-kerosene combustion product composition and characteristics in engine thermodynamic design allowing for intermolecular interaction forces
10 p1968 A70-24284

Aircraft turbine engines structural materials and design concepts, describing fiber reinforced materials, oxide dispersion hardened alloys and integral and honeycomb structures
11 p2101 A70-25625

Three spool turbofan engine design regarding maintainability, noting on-condition module removal and overhaul
[SAE PAPER 700204] 11 p2101 A70-25877

Small turboprop engine development, flight tests, performance and weight reduction
[SAE PAPER 700206] 11 p2102 A70-25878

Engine design for future small passenger and sports aircraft, discussing piston, shaft turbine, Wankel and bypass engines and synthetic materials application
11 p1981 A70-25949

Rotating combustion engine design offering low life cycle costs for military applications
[SAE PAPER 700273] 12 p2290 A70-27438

CF6 engine experience effects on current engine manufacturing, servicing and support in airline service, discussing maintainability, component repair and reliability, etc
[SAE PAPER 700289] 12 p2290 A70-27444

Aerojet engine minimum weight design, suggesting use of welding and brazing instead of nut-and-bolt joints in component fabrication
[SAE PAPER 700319] 12 p2243 A70-27457

Hollow cathode mercury electron bombardment thruster design, emphasizing low specific impulse operation and discharge chamber improvements
13 p2473 A70-28505

Altitude Test Facility in air breathing aircraft engine design, discussing plant, test cells design and flight representation and systems accuracy
13 p2473 A70-28538

Jet engines for civil and military aircraft, discussing turbine designs and noise reduction
13 p2474 A70-28546

French jet engines, outlining various models built by SNECMA and Turbomeca
13 p2474 A70-29144

Tubular gas turbine combustors design by analytical model, summarizing theories of combustor analysis, turbulent flame speed, microvolume burning and stirred reactors
[WSCI PAPER 70-2] 13 p2474 A70-29613

Aircraft smoke emission reduction and elimination by engine modifications
14 p2628 A70-30190

Design costs for large subsonic transport engines in terms of size, engine ratings and community noise
14 p2629 A70-30944

V/STOL propulsion for commercial needs, considering best tradeoff between propulsion size, weight, noise generation and fuel consumption
14 p2629 A70-31277

Jet engine technology, discussing thrust/weight ratio, compressors, fans, combustors, turbines, materials, manufacturing, maintainability and noise
15 p2787 A70-31698

Soviet book on liquid propellant rocket motors construction, discussing combustion chambers, frame, ducts, turbopump feed system, etc
15 p2744 A70-31850

NERVA rocket engine program reliability, design, performance and managerial approaches
[AIAA PAPER 70-711] 16 p2950 A70-33568

Heat pipes in nuclear aircraft propulsion system, describing core, heat exchangers, and reactor to jet engine heat transport system
[AIAA PAPER 70-662] 16 p2950 A70-33623

Jet engine combustion chamber design, discussing performance range and geometry
16 p2970 A70-33682

Ti alloys use in jet engines design, considering weight, structural stability, useful temperature range, cost, etc
17 p3146 A70-34448

Kuznetsov NK 8-4 bypass turbojet air entry vanes, pressure compressors, gear case, combustion chamber and turbine drives
17 p3147 A70-34629

V/STOL 5000 hp engine design optimization, considering component arrangements, rotor design, blade cooling method and fuel control
17 p3147 A70-34709

Convertible fan-shaft engine for V/STOL tactical and transport aircraft, discussing design and performance
17 p3147 A70-34710

Solid propellant rocket motor, discussing manufacture, materials and configuration of 156 inch engine
17 p3148 A70-35217

Aircraft design minimizing damage by bird strikes to gas turbine engine components, discussing service experience, airworthiness demonstration tests and research programs
18 p3300 A70-35994

Prototype grill device for turboprop aircraft engine inlet protection against bird ingestion, discussing performance tests
18 p3212 A70-35996

High temperature radial turbine design for small gas turbine engines, discussing aerodynamic, structure and thermal analyses
18 p3301 A70-36450

High speed and long life bearings and dampers for future jet engines, considering design factors
[SAE PAPER 700318] 18 p3263 A70-36800

High bypass turbofan engine design concepts and development program for airline operation
[SAE PAPER 700292] 18 p3302 A70-36804

Olympus 593 engine for Concorde aircraft, describing design and test procedures
[SAE PAPER 700291] 18 p3302 A70-36805

JT9D engine design and performance, describing operational problems
[SAE PAPER 700288] 18 p3302 A70-36807

Aircraft engine production cost estimating techniques, discussing physical, thermodynamic and metallurgical characteristics
[SAE PAPER 700271] 18 p3350 A70-36818

Lightweight lift jet engine design, testing and performance for V/STOL aircraft
[ASME PAPER 70-GT-32] 18 p3302 A70-36833

Helicopter gas turbine engines protection against salt spray, dust, sand, ice, cut grass, etc
[ASME PAPER 70-GT-96] 18 p3263 A70-36843

Concorde aircraft powerplant design using fire tunnel test
[ASME PAPER 70-GT-128] 18 p3238 A70-36854

Cascade tunnel testing role in designing supersonic compressor rotor blading for lower jet engine weight and fuel consumption
[ASME PAPER 70-GT-79] 18 p3305 A70-36885

Aircraft gas turbine engine development, considering gas dynamic and structural parameters
19 p3489 A70-37238

Jumbo jets turbofan engines design, considering fuel consumption, maintenance, reliability, noise reduction, etc
19 p3491 A70-38953

Jet engine combustor design and efficiency, discussing heat transfer, cooling and engine materials
20 p3688 A70-39648

Aircraft engine design combining turbojet and ramjet features to ensure optimum performance
20 p3690 A70-40148

Parametrized design data and selection criteria of biowaste resistor system for orbit keeping and control moment gyro desaturation of manned space station
20 p3567 A70-40213

Colloid microthruster system life test, discussing design and steady state performance
[AIAA PAPER 70-1110] 20 p3692 A70-40233

RF ion source for electrostatic spacecraft propulsion, discussing RIT-10 performance optimization and development
[AIAA PAPER 70-1102] 20 p3692 A70-40236

Single stage gas turbines rational design based on minimum diametric dimensions
21 p3867 A70-41768

Rocket engines propulsion systems design and performance based on thermodynamical theory, involving expanding gas
21 p3869 A70-42038

Solid propellant rocket motors performance, manufacture and hardware, discussing mechanical properties, storage, combustion, nozzle expansion, etc
21 p3869 A70-42040

M 3.5 two dimensional mixed compression inlet system with self restart using flexible variable ramp system
[AIAA PAPER 69-447] 22 p3959 A70-42707

Gas turbine design by nomograms with minimal preliminary calculations
22 p3960 A70-43368

Allison/Rolls-Royce TF41 turbofan engine improved power and reduced weight versions, comparing afterburning Model 912-B23 to nonafterburning TF41-A-2
23 p4234 A70-44596

Europa 2 booster perigee stage engine design, discussing total and propellant masses, spin stabilization, materials, etc
23 p4234 A70-44672

Optimal propeller selection for given aircraft and engine designs, considering aerodynamic and acoustic characteristics
24 p4393 A70-45441

Cascade flow field analysis from given blade geometry, deriving expressions for numerical solution of inverse turbine design problem
24 p4288 A70-45501

Turbine blades deformation by centrifugal and aerodynamic forces, discussing theory for bending stress free blade design
24 p4288 A70-45505

L-1011 aircraft optimum minimum noise pod design, describing technology, restraints and system requirements
[SAE PAPER 700805] 24 p4393 A70-45877

Noise suppression for high-bypass ratio CF6 turbofan engine in DC-10 airplane, considering effect on engine design
[SAE PAPER 700804] 24 p4393 A70-45878

TSCP700 aircraft auxiliary power unit design, fuel consumption and maintainability
[SAE PAPER 700815] 24 p4395 A70-45902

V/STOL powerplant development, discussion airframe and engine design, application to large aircraft and planned evolutionary process
[SAE PAPER 700809] 24 p4395 A70-45905

Noise reduction design for subsonic transport turbofan engines
[SAE PAPER 700807] 24 p4395 A70-45907

Hydrogen oxygen engine designs for space vehicle auxiliary propulsion systems, considering long life thrust chamber performance with compatible heat transfer characteristics
[SAE PAPER 700803] 24 p4395 A70-45908

NERVA nuclear rocket engine design technology program, discussing probabilistic techniques for reliability engineering
[SAE PAPER 700801] 24 p4377 A70-45910

Radial inflow turbine optimum design geometry, calculating nozzle and rotor geometrical parameters efficiency
24 p4395 A70-46012

German book on aircraft thermal propulsion systems calculation, design and evaluation, covering thermodynamic principles and atmospheric composition and properties
24 p4396 A70-46150

ENGINE FAILURE

Defects development in cermet materials sealing elements in high O content gas flows of turboprop and turbojet engines
01 p0161 A70-10160

Engine performance monitoring system /EPMS/ for aircraft jet onboard operation analysis and failure detection
08 p1558 A70-20668

Aircraft engines development and reliability, discussing rejection causes, data retrieval, repair and salvage techniques
08 p1558 A70-21031

Accelerate-stop distance problem in takeoff refusal due to critical engine failure, emphasizing runway limited length hazards
08 p1436 A70-21270

Equivalent test results, studying damaging factors in aircraft engine compared with regular tests
10 p1929 A70-24241

Regeneratively cooled stainless steel thrust chamber failure related to internal carburization by fuel decomposition and propellant combustion
12 p2290 A70-27111

Hazard analyses of Concorde aircraft design, noting engine control failures and emergency equipment use probabilities
15 p2675 A70-32213

Vibration monitoring for turbine engine malfunction detection
17 p3061 A70-35480

Aircraft engine failures advanced detection by spectrometric lubricating oil analysis
17 p3061 A70-35481

Boeing 747 aircraft JT9D engine deflections and removals during early service experience and maintenance
[AIAA PAPER 70-890] 17 p3019 A70-35807

Gas turbines, dust and air cleaners interrelationship in preventing failure due to air contaminants
[ASME PAPER 70-GT-104] 18 p3305 A70-36890

Integrated structural analysis for reliability prediction of solid propellant rocket motors
19 p3489 A70-38844

Automated aircraft flight safety, concerning probabilities and onboard elimination of servomotor failures in hydraulic system due to fuel contamination
22 p3961 A70-42804

ENGINE INLETS

Test chamber to simulate helicopter rotor downwash for engine inlet air particle separator optimization
01 p0056 A70-10676

Particle removal efficiency of engine inlet separator-filter devices evaluated at Naval inlet test facility for simulated engine airflows, scavenging conditions, etc
01 p0163 A70-10679

Powered centrifugal separator for inlet filtering of rotary wing aircraft turbine engines, discussing efficiency and feasibility
01 p0164 A70-10683

Bird deflection grill device for turboprop engine inlet ducts, noting effects on inlet flow characteristics, engine performance, etc
01 p0165 A70-10688

CH-54 engine air inlet anti-ice system design, manufacture and testing, solving heat balance equations describing tapered gap heat exchanger
01 p0165 A70-10693

Air inlet and exhaust nozzle form and location effect in afterburning turbofan engines, discussing stalling, afterburner blowouts and thrust losses prevention
05 p0895 A70-15807

Aircraft turbojet engine/inlet compatibility, using data system for acquisition, identification and analysis of critical time variant pressure parameters
[AIAA PAPER 70-594] 13 p2375 A70-29877

Dynamic pressure data acquisition editing and processing system for engine inlet wind tunnel model tests
[AIAA PAPER 70-596] 13 p2375 A70-29879

Steady and unsteady engine/inlet flow field simulation for engine/compressor testing, determining feasibility of variable ramp aerodynamic device
[AIAA PAPER 70-591] 15 p2672 A70-31788

SST inlet steady state pressure defects and random pressure fluctuations determining TF30 engine/inlet compatibility
[AIAA PAPER 70-632] 16 p2834 A70-33530

Inlet and engine control vector size and weight reduction, reliability, accuracy, etc
[AIAA PAPER 70-696] 16 p2967 A70-33559

High temperature and pressure hot gas source for testing fluidic temperature sensor used in gas turbine engine inlet simulation
17 p3058 A70-35157

Airframe-inlet integration for supersonic tactical fighters, testing wind tunnel models
[AIAA PAPER 70-933] 17 p3149 A70-35843

Aerodynamic stability of branched diffuser systems used in annular combustors of gas turbine engines
[ASME PAPER 70-GT-27] 18 p3209 A70-36868

Ceramic materials for low cost high inlet temperature gas turbine engine components
[ASME PAPER 70-GT-105] 18 p3279 A70-36889

Inlet data for engine stability analyses, developing technical management procedure patterns for pretest and posttest results
[AIAA PAPER 70-1214] 21 p3745 A70-41320

Acoustically treated inlet and fan exhaust duct configurations for JT3D turbofan engine on DC 8 aircraft
22 p4090 A70-42533

Subsonic jet engine intake duct radar cross section calculation using waveguide model
22 p3992 A70-43584

Automatic control system for Boeing SST engine air intakes, optimizing engine performance and controlling noise propagation
24 p4396 A70-46214

ENGINE MONITORING INSTRUMENTS

Engine performance monitoring system /EPMS/ for aircraft jet onboard operation analysis and failure detection
08 p1558 A70-20668

Book on aircraft flight and engine instruments covering fuel gages, altitude and speed indicators, altimeters, magnetic compasses, gyroscopes, tachometers, pressure, gages, flowmeters etc
11 p2048 A70-25574

Spectrometric oil analysis program /SOAP/ for engine and transmission components damage detection and preventive maintenance in military aircraft
12 p2240 A70-27017

Aircraft turbine engines gaseous emission measurements, discussing instrumentation for continuous pollutant concentration monitoring
[SAE PAPER 700249] 12 p2290 A70-27428

Automatic engine maintenance recording system on air transport aircraft noting data reduction
[SAE PAPER 700317] 12 p2335 A70-27456

Vibration monitoring for turbine engine malfunction detection
17 p3061 A70-35480

C-5A propulsion system onboard monitoring for malfunction detection, analysis and subsystem recording
17 p3148 A70-35497

Jet transport aircraft turbine engine performance monitoring by flight data, discussing historical highlights and future prospects
[SAE PAPER 700314] 18 p3301 A70-36801

Airlines data reduction using electronic engine maintenance recorders
[ASME PAPER 70-GT-127] 18 p3259 A70-36853

Electronic gas turbine diagnostic systems, discussing engine parameters and analysis system
[ASME PAPER 70-GT-131] 18 p3259 A70-36857

Gas turbine propulsion systems design, performance and applications for industrial and military uses, discussing sensors for measurement and control of critical engine parameters
19 p3424 A70-37881

Aircraft nonavionics systems performance condition and minimum maintenance duties diagnosis by integrated data system, discussing engine monitoring instruments
19 p3426 A70-37891

Economic payback of AIDS /Aircraft Integrated Data System/ recording for operational performance monitoring and engine analysis
19 p3382 A70-37894

Engine vibration monitoring system for Boeing 747 aircraft, including piezoelectric transducer, transmission assembly and differential charge converter
19 p3426 A70-37898

Aircraft compressor and turbine vibration monitor, using velocity coil or piezoelectric transducers
19 p3430 A70-38525

Airborne data acquisition equipment for accident flight path and engine performance recording
21 p3796 A70-41922

C5 Malfunction Detection Analysis and Recording /MADAR/ subsystem for onboard fault isolation including engines
[SAE PAPER 700820] 24 p4349 A70-45898

ENGINE NOISE

NT ROCKET ENGINE NOISE

Jet engine noise sources and design of noise suppressors used during airport runway engine tests
02 p0275 A70-12222

Aerodynamic sound generation by subsonic jet engines noting jet thrust relation to emitted acoustic power
03 p0552 A70-13926

Turbine noise significance in civil aircraft noise problem
[ASME PAPER 69-WA/GT-12] 04 p0734 A70-14884

Design specifications for low noise turbofan engine used on long range subsonic transport aircraft
[ASME PAPER 69-WA/GT-7] 04 p0734 A70-14888

Noise suppressor research for jet engine components, describing test equipment and facilities for models work
05 p0825 A70-15808

Airport noise silencers for aircraft engines, discussing design, operation and damping efficiency
05 p0829 A70-16353

Aircraft noise suppression, discussing community aspects of jet and fan noise and physical mechanisms of jet noise

05 p0795 A70-16777

Discrete noise generation and propagation due to fan engine rotor forcing excitation and interaction with downstream stator

05 p0896 A70-16791

Temporary and permanent threshold shifts in hearing of guinea pigs exposed to intense rocket booster engine noise

07 p1214 A70-19931

Jet aircraft engine noise control, discussing noise sources and built-in acoustic absorbers

09 p1743 A70-22759

In-flight shock cell noise generation by static jets, discussing frequency prediction formula

13 p2347 A70-29078

Commercial jet aircraft engine noise evaluation, discussing noise reduction and effects on airport neighbors

14 p2630 A70-31335

Rolls-Royce RB 211 turbofan engine, discussing fuel consumption, specific weight, noise and smoke level, reliability and maintainability

15 p2787 A70-31948

Jet engine noise technology evaluation, noting effects on airport neighbor

16 p2971 A70-34262

Aircraft gas turbine propulsion, discussing engine performance characteristics, thermodynamics, noise and installation

[AIAA PAPER 70-873]

17 p3147 A70-34810

Ground test noise measurements accuracy and repeatability on J78D turbojet engine

17 p3060 A70-35183

Buzz-saw noise of transonic compressor due to rotating pressure field at supersonic blade tip speeds

[ASME PAPER 70-GT-54]

18 p3303 A70-36838

Flow noise mechanisms, considering discharge, propeller, ventilator, jet engine, boundary layer, water pipe and supersonic aircraft sources

19 p3406 A70-38474

Ship engineers cardiovascular system functional changes during HF internal combustion engine noise, investigating EKG recordings and arterial pressure

20 p3582 A70-40292

Acoustic lining technology and materials for turbofan engine ducts, considering environmental factors and noise spectra

22 p4089 A70-42530

Duct lining parameters effects on engine inlet and fan discharge noise reduction during fan jet landing

22 p4090 A70-42532

Test rig vehicle design for noise research on single stage high bypass ratio fans for quieter turbofan power plants

[AIAA PAPER 69-492]

22 p4090 A70-42708

Jet engine compressor noise analysis, noting inlet swirl role

22 p4090 A70-42725

Aircraft noise reduction, discussing generation sources in propulsion system, noise levels and subjective responses

23 p4140 A70-44395

Jet engine noise propagation near porous surface, predicting anomalous LF dip from direct and reflected waves interference with phase delay

24 p4395 A70-46068

ENGINE PARTS

Solid rocket engine components technologies, studying effects of cost consciousness

[SAE PAPER 690702]

05 p0922 A70-15828

Soviet papers on vibrations, strength and structure of aircraft engine elements

07 p1363 A70-19109

Supersonic fluid turbomachine components and systems innovations and performance trends

[AGARDOGRAPH-120]

08 p1434 A70-21927

Abradable and abrasive types thermal spray coatings application to jet engine parts

10 p1893 A70-23856

Electrochemical machining for drilling deep holes in alloys and refractory metals used in jet engine hardware

10 p1893 A70-23857

Dip brazing aluminum fan vanes used in high bypass turbofan jet engines

10 p1893 A70-23858

Aircraft turbine engine components vibrational testing by holographic interferometry methods

16 p2903 A70-33134

Ti fabrications in aircraft engines, discussing alloys properties, sheet deformation, fusion welding, porosity, etc

17 p3099 A70-34450

Cooperative airline program for aircraft turbofan engine parts aging and performance deterioration evaluations

[SAE PAPER 700329]

18 p3301 A70-36798

Critical aviation gas turbine rotating component life limit determination, describing statistical, maintenance, inspection and life evaluation computer program [SMILE/

[ASME PAPER 70-GT-66]

18 p3303 A70-36841

Electrochemical machining [ECM] effects on components surface integrity, discussing jet engine materials

[ASME PAPER 70-GT-111]

18 p3264 A70-36849

Two stage turbine engine parts adjustment optimization in terms of fuel consumption or thrust control by linear programming techniques

19 p3489 A70-37241

Dynamic testing of turbine machine parts using strength and vibration equations and similarity method

19 p3437 A70-38472

Jet engine roller bearings retainer candidate cage materials and coatings evaluation on test rig simulating engine conditions

[ASLE PREPRINT 70AM 2D-1]

19 p3439 A70-38805

Critical components effect on small Hg electron bombardment thruster performance, considering glass coated accelerator grids, hollow cathodes and plasma bridge neutralizers

[AIAA PAPER 70-1100]

20 p3692 A70-40238

Aircraft engine diagnostics and defectoscopy, considering radioactive isotopes testing for component wear and performance

22 p4046 A70-43083

Aircraft flight propulsion systems performance improvement via materials technology for gas turbine engine components

22 p4057 A70-43573

NASA research in turbojet aircraft propulsion noting inlet, compressor, combustor, turbine and nozzle component technology

[ICAS PAPER 70-46]

23 p4233 A70-44144

ENGINE STARTERS

Turbine engine starting system design requirements, outlining lifetime improvement of hot section parts

01 p0167 A70-11460

Acceleration and regulating system of free turbine turboprop engines studied by graph-analytical method used for nonlinear circuit analysis

03 p0552 A70-13927

M 3.5 two dimensional mixed compression inlet system with self restart using flexible variable ramp system

[AIAA PAPER 69-447]

22 p3959 A70-42707

Gas turbine engine combustion chamber starting, discussing effects of temperature, nozzle characteristics and fuel physicochemical properties

22 p4092 A70-43356

Start-up characteristics for three-phase synchronous reactive motors with various starting unit designs

24 p4293 A70-45471

ENGINE TESTING LABORATORIES

Ice tunnel testing facility at Naval Air Propulsion Test Center [NAPTC], describing methods, systems, instrumentation and various turbofan and turbojet engine tests

01 p0056 A70-10691

Air breathing engine testing at propulsion Wind Tunnel Facility at Arnold Engineering Development Center

11 p2031 A70-25852

Aircraft propulsion system test facilities, discussing altitude simulation, large subsonic and supersonic engines and component development

[ICAS PAPER 70-45]

23 p4178 A70-44143

ENGINE TESTS

NT COLD FLOW TESTS

NT SPACE ELECTRIC ROCKET TESTS

NT STATIC FIRING

Rolls-Royce RB 211 three shaft turbofan engines development and tests, noting preparation, building, cradle installation, open air facilities and noise measurements

01 p0161 A70-10079

Sand and dust environmental test of T-63 regenerative engine, discussing performance depreciation, recuperator inspection and comparison with non-regenerative t63-a-5a engine

01 p0164 A70-10685

Multifan cross wind jet engine test facility to produce variable wind velocity in various directions

01 p0056 A70-10698

Corrosion induced fatigue damage suppression in jet engine compressor steel components, describing various surface treatment effects

01 p0165 A70-10699

A-7 aircraft TF-41 engine tolerance to steam ingestion, discussing test program and results and engine modifications

01 p0165 A70-10700

Concorde power plant tests using supersonic free jet altitude test facility with Olympus 593 engine

01 p0165 A70-10701

Jet engine noise sources and design of noise suppressors used during airport runway engine tests

02 p0275 A70-12222

Turbine engine checkout techniques, describing oil, sonic-vibration, X ray, gas path and hot section analysis methods

[AIAA PAPER 69-581]

02 p0356 A70-12526

ELDO-PAS apogee motor prequalification test to determine specifications for constructing units for qualification testing

03 p0581 A70-13854

Stirling free piston engine operating principles, performance limitations, heat transfer problems, fluid flow, mechanical design, test results and applications

[ASME PAPER 69-WA/ENER-15]

04 p0627 A70-14895

Predicted and measured low density plume impingement effects on loads and heat transfer compared on orbiting Saturn 5 with oxygen-hydrogen burner engine

04 p0737 A70-15430

Noise suppressor research for jet engine components, describing test equipment and facilities for models work

05 p0825 A70-15808

Net thrust determination for high bypass ratio engines in cruise, suggesting performance evaluation in actual flight tests

[SAE PAPER 690652]

05 p0895 A70-15841

Hot air breather test facility design to increase flowrate range at maximum pressure level

[WSCI PAPER 69-45]

06 p1028 A70-17981

Turbine flowmeter in-place calibration for measuring cryogenic propellant flow rates in rocket engine testing

06 p1071 A70-18448

Analog-numerical measurements on French liquid oxygen and hydrogen motor

07 p1364 A70-19129

Twin spool hydrogen turbopump performance at zero net positive suction pressure [NPSP] saturated fluid in propellant tank, including steady state and simulated transient engine tests

[AIAA PAPER 69-550]

07 p1295 A70-19709

Interagency chemical rocket propulsion group method of treating measurement error for liquid rocket engine performance parameters, using uncertainty model

[AIAA PAPER 69-734]

07 p1365 A70-19723

Saturn ULLAGE solid propellant rocket motor vibration test evaluation

07 p1365 A70-20039

Boeing 747 pretesting work including wind tunnel, components, engines and static structural tests, flight simulation, etc

08 p1437 A70-21730

Rig using holographic techniques for vibration testing and aircraft engine components inspection

09 p1680 A70-23069

Equivalent test results, studying damaging factors in aircraft engine compared with regular tests

10 p1929 A70-24241

Air breathing engine testing at propulsion Wind Tunnel Facility at Arnold Engineering Development Center

11 p2031 A70-25852

Free jet test facility for supersonic engine/ intake combination testing, discussing benefits to aircraft flying hours, development costs and safety

11 p2101 A70-25854

Engine firing rate measurement from acoustic waveform autocorrelation analysis

12 p2290 A70-27161

Turboprop engine testing in ground level facilities with automatic instrument reading and parameters calculation

13 p2474 A70-29688

Dynamic pressure data acquisition editing and processing system for engine inlet wind tunnel model tests

[AIAA PAPER 70-596]

13 p2375 A70-29879

DC-10 aircraft wing engine calibration, isolated- and wing-nacelle testings using air-driven engine simulator

[AIAA PAPER 70-590]

13 p2342 A70-29881

Turboprop aircraft engine service life extension, correcting deficiencies via accelerated tests based on relation between failure rate and usage

15 p2787 A70-31535

Steady and nonsteady engine/inlet flow field simulation for engine/compressor testing, determining feasibility of variable ramp aerodynamic device

[AIAA PAPER 70-591]

15 p2672 A70-31788

Inlet-engine compatibility testing for aircraft system development program

[AIAA PAPER 70-941]

16 p2965 A70-33534

Monopropellant hydrazine RCS rocket engine module, discussing operating conditions, development, thermal control and valve internal leakage

[AIAA PAPER 70-654]

16 p2965 A70-33544

Fluid mechanics and engine dynamics and start-up experiments simulating thermal environment in nuclear light bulb engine

16 p2949 A70-33552

NERVA rocket engine program reliability, design, performance and managerial approaches

[AIAA PAPER 70-711]

16 p2950 A70-33568

Digital simulation for turbine engine propulsion system testing

[AIAA PAPER 70-633]

16 p2869 A70-33593

Supersonic cylindrical ejectors without induced flow for rocket engine studies

16 p2837 A70-33763

- NERVA XE-Prime test series, discussing computer simulation, full power and high specific impulse operation and startup under varying initial conditions [AIAA PAPER 70-709] 16 p2951 A70-33950
- Nuclear rocket engine testing, monitoring reactor and facility performance with real time digital computer 17 p3135 A70-35212
- Cooperative airline program for aircraft turbofan engine parts aging and performance deterioration evaluations [SAE PAPER 700329] 18 p3301 A70-36798
- Jet transport aircraft turbine engine performance monitoring by flight data, discussing historical highlights and future prospects [SAE PAPER 700314] 18 p3301 A70-36801
- Olympus 593 engine for Concorde aircraft, describing design and test procedures [SAE PAPER 700291] 18 p3302 A70-36805
- High bypass ratio aircraft turbofan engines, discussing program of factory, flight and operational suitability testing [SAE PAPER 700290] 18 p3302 A70-36806
- Flight test program for helicopter gas turbine engines, considering engine-airframe-control systems integration and environmental tests [ASME PAPER 70-GT-38] 18 p3303 A70-36836
- Concorde aircraft powerplant design using fire tunnel test [ASME PAPER 70-GT-128] 18 p3328 A70-36854
- Time of acceleration to rated speed for three-phase asynchronous gyroengine rotor 19 p3420 A70-37259
- Rocket engine tests dynamic data oscillographic presentation and digital processing 19 p3490 A70-37916
- Environmental surveillance associated with ground tests of nuclear rocket engine prototypes, determining statistical nature of radioactive effluent 19 p3470 A70-38013
- Dynamic testing of turbine machine parts using strength and vibration equations and similarity method 19 p3437 A70-38472
- Long term life test and vacuum tests of high temperature resistojets using ammonia and hydrogen propellants [AIAA PAPER 70-1136] 20 p3567 A70-40212
- Colloid annular thrusters performance tests in vacuum chamber with LN cooled liner, using high speed analog to digital system to acquire time of flight /TOF/data [AIAA PAPER 70-1112] 20 p3692 A70-40231
- Inlet data for engine stability analyses, developing technical management procedure patterns for pretest test and posttest results [AIAA PAPER 70-1214] 21 p3745 A70-41320
- Aircraft engine diagnostics and defectoscopy, considering radioactive isotopes testing for component wear and performance 22 p4046 A70-43083
- Mathematical model avoiding repetitive tests costs for Nerva nuclear rocket engine 22 p4070 A70-43179
- Two stage gas turbine engine optimal tuning for RPM, thrust, fuel rate and gas temperature, describing automated bench tests 22 p4092 A70-43361
- ENGINEERING**
- Papers on engineering materials covering refractory creep resistant materials, fiber reinforcement, ceramics, polymers, alloys, etc 02 p0318 A70-12709
- Polymers application as engineering materials, discussing properties, physical states, etc 02 p0322 A70-12716
- Book on digital computer methods in engineering covering numerical and programming methods, algebraic and differential equations solutions, time-frequency domain analysis, etc 05 p0877 A70-16771
- Holography application in engineering, discussing strains and distortions detection, vibration testing, design optimization, etc 10 p1887 A70-24198
- Engineering science - Conference, Princeton University, November 1968 19 p3537 A70-37782
- Engineering science - Conference, Princeton University, November 1968, Part I 19 p3539 A70-37940
- ENGINEERING DEVELOPMENT**
- U PRODUCT DEVELOPMENT**
- ENGINES**
- NT AIR BREATHING ENGINES
- NT BOOSTER ROCKET ENGINES
- NT CESIUM ENGINES
- NT CONTROL ROCKETS
- NT DUCTED FAN ENGINES
- NT ELECTRIC ROCKET ENGINES
- NT ELECTROSTATIC ENGINES
- NT F-1 ROCKET ENGINE
- NT GAS TURBINE ENGINES
- NT HOT WATER ROCKET ENGINES
- NT HYBRID PROPELLANT ROCKET ENGINES
- NT HYDRAZINE ENGINES
- NT HYDROGEN OXYGEN ENGINES
- NT INTERNAL COMBUSTION ENGINES
- NT ION ENGINES
- NT J-2 ENGINE
- NT JET ENGINES
- NT LIQUID PROPELLANT ROCKET ENGINES
- NT MICROROCKET ENGINES
- NT NUCLEAR ENGINE FOR ROCKET VEHICLES
- NT NUCLEAR ROCKET ENGINES
- NT PISTON ENGINES
- NT PLASMA ENGINES
- NT PULSED JET ENGINES
- NT RAMJET ENGINES
- NT RESTARTABLE ROCKET ENGINES
- NT RETROCKET ENGINES
- NT ROCKET ENGINES
- NT SOLID PROPELLANT ROCKET ENGINES
- NT SUPERSONIC COMBUSTION RAMJET ENGINES
- NT T-56 ENGINE
- NT TURBINE ENGINES
- NT TURBOFAN ENGINES
- NT TURBOJET ENGINES
- NT TURBOPROP ENGINES
- NT TURBORAMJET ENGINES
- NT ULLAGE ROCKET ENGINES
- NT VERNIER ENGINES
- NT WANKEL ENGINES
- Kaufman thruster performance dependence on transmission of ion extraction optics and magnetic field shape [AIAA PAPER 69-257] 07 p1365 A70-19705
- Book on tensor calculus in materials science covering thermodynamic equilibrium, gaseous and solid phase heat engines, solids crystalline structure, etc 12 p2282 A70-26866
- ENGLISH LANGUAGE**
- Analysis method permitting English speech sound recognition by computer for different speakers 08 p1460 A70-20815
- ENGRAVING**
- Helical engraving influence on aerodynamic stability of bullets at long range, discussing wind tunnel tests [AIAA PAPER 70-557] 13 p2340 A70-29022
- ENLARGING**
- U EXPANSION**
- ENSKOG-CHAPMAN THEORY**
- U CHAPMAN-ENSKOG THEORY**
- ENSTATITE**
- Nitrogen abundances measured in enstatite chondrites by inert carrier gas fusion extraction technique, noting agglomeration of chondrules 01 p0179 A70-10475
- Enstatite luminescence response for bulk specimens, powders and individual grains, considering selenological implications 05 p0909 A70-16391
- I-Xe dating of Abee enstatite chondrite by combined neutron activation and mass spectrometric analysis 05 p0915 A70-16829
- Ti demonstrated as predominantly chalcophilic in highly reduced enstatite chondrites and achondrites 07 p1391 A70-20352
- Enstatite chondrites and achondrites electron microprobe analysis for Si, P and Ni in metal grains and associated schreibersite and perryite 10 p1935 A70-23849
- Enstatite chondrites K, Rb and Sr concentrations, measuring ages from Sr87/Sr86 ratios 16 p2974 A70-33649
- ENSTROM AIRCRAFT**
- NT F-28 HELICOPTER**
- ENTHALPY**
- Radiation effect on enthalpy and velocity distributions of laminar compressible planar free jet 01 p0061 A70-10295
- Well depth determination for weak intermolecular potentials based on dimerization enthalpy measurement of rare gas atoms by mass spectrometry 03 p0527 A70-13299
- Radiation-convection interaction in plasma free jet, using two-thermal-domain model for enthalpy distribution determination [ASME PAPER 69-WA/HT-50] 04 p0781 A70-14798
- Ion exchange entropy and enthalpy functions calculated from experimental constants and temperature dependence data 06 p1177 A70-17837
- Liquid nitrogen tetroxide enthalpy measured by indirect heating techniques, obtaining data at supercritical temperatures 06 p1005 A70-18560
- Enthalpy of nitrogen tetroxide in liquid phase using direct heating of test substance in calorimeter 07 p1358 A70-19207
- State equation for entropy of dissociated air with enthalpy and pressure as independent variables for calculating gas dynamic processes on computers 10 p1966 A70-23839
- High intensity shock wave propagation and generation of high enthalpy hypersonic flow studied to determine IMF-2 hypersonic shock tube performance limit 10 p1871 A70-24795

- Multiband radiative cooling effect on enthalpy distribution behind incident wave in cylindrical shock tube for air, using differential approximation 14 p2663 A70-30268
- Specific heat and enthalpy of body centered cubic refractory metals at high temperatures 15 p2757 A70-31943
- Heat exchange measurements between solid body and high enthalpy gas flow at stagnation point using electric arc heater 15 p2826 A70-32102
- Free energy and enthalpy of single ion solvation in water and propylene carbonate, using electrostatic model 15 p2695 A70-32829
- Thermodynamic diagram indicating enthalpy and entropy of oil combustion gases for any state and air excess value 16 p2997 A70-33295
- Optimum nozzle geometry for minimum heat transfer to convergent-divergent nozzle wall from high enthalpy flow 17 p3196 A70-35238
- Laminar gas flow enthalpy determination in stagnation regions based on energy balance equation across separation streamline 18 p3240 A70-36266
- Carbon dioxide entropy and enthalpy computation covering critical region and wide temperature range [ASME PAPER 70-GT-5] 18 p3348 A70-36861
- Meridional mean eddy transport of enthalpy in Southern Hemisphere during IGY, comparing results with Northern Hemisphere 20 p3661 A70-39143
- Radiative cooling of shock heated air in cylindrical shock tubes, calculating enthalpy profiles for nonadiabatic air flow 23 p4282 A70-44586
- ENTIRE FUNCTIONS**
- News function relation with far fields of sources obtained in linear approximation for axisymmetric case in integrating Einstein field equation 08 p1543 A70-20721
- Entire functions for analysis and representation of distant atmospheres, using concentrated spectrum and zero coordinate readings 14 p2569 A70-30210
- Entire functions for analysis and representation of distant atmospheres, using concentrated spectrum and zero coordinate readings 24 p4330 A70-46285
- ENTRAINMENT**
- Three machine parts problem with relative motion and given active forces distribution and time variation, determining entrainment motion 01 p0142 A70-10554
- Entrainment of electrically conducting liquid by moving wall in long duct with rectangular cross section and magnetic induction field 01 p0151 A70-10656
- Energy dissipation and entrainment methods for calculating turbulent boundary layer development, involving simultaneous numerical solutions of ordinary differential equations for local variables 02 p0283 A70-12337
- Heat transfer, three dimensional boundary layers and high speed flow calculations, utilizing original entrainment equation 02 p0284 A70-12341
- Integral method for computing two dimensional incompressible turbulent boundary layer development, including entrainment process of irrotational fluid 02 p0284 A70-12343
- Porous wall material entrainment in turbulent boundary layer during supplementary inert gas injection, including nonisothermicity effects in heat and mass transfer equations 03 p0440 A70-13385
- Entrainment rate of ambient medium by MPD arc jet, discussing flow field in and around jet and pressure distribution along vacuum tank wall 03 p0553 A70-14373
- Vorticity entrainment effects in zonal jet flows, considering Long asymptotic series, shear enhancement, etc 04 p0715 A70-15519
- Electrode erosion or entrainment in MPD arcs due to excess current density, considering inner cathode and outer ring anode with axial magnetic field 10 p1925 A70-25040
- Nonturbulent fluid entrainment into turbulent flow dependent on flow properties controlling energy balance 11 p2038 A70-26528
- Solid particles interactions during entrainment by viscous incompressible fluid in pipe, calculating interaction force as function of radius, distance and Reynolds number 23 p4181 A70-44310
- Entrainment theory for incompressible turbulent boundary layer velocity and drag on bodies of revolution employed in fuselage, submersible and cowlings for propulsion design 23 p4182 A70-44400

ENTRANCES

Entrance length and pressure drop in MHD parallel plate channel flow using one parameter Pohlhausen method 05 p0887 A70-15978

ENTRAPMENT

Inspection penetrant development for flaw detection, considering entrapment efficiency and dimensional sensitivity 24 p4348 A70-45743

ENTROPY

Evolution and entropy of partially ionized collision dominated plasmas interacting with radiation based on statistical analogs of irreversible thermodynamics 02 p0346 A70-11902

Thermodynamics second law application to pyrotechnic systems, discussing solid-solid and reversible reactions 03 p0547 A70-14114

Maximum entropy principle used in rarefied gas dynamics for optimal representation of distribution function, examining difficulties associated with constraints on boundary conditions 04 p0718 A70-14492

Dynamic response of solid propellant flame to oscillating pressure field using T-tube rocket motor, discussing entropy waves produced in oscillatory combustion [AIAA PAPER 68-499] 04 p0737 A70-15580

Numerical results for perturbed downstream flow field resulting from entropy wave interaction with normal shock and oblique shock generated by wedge flow 05 p0835 A70-16788

Combustion and pyrolysis of carbonaceous solids considered for hybrid rocket fuels, using integrating factors in Caratheodory multiple entropies 06 p1172 A70-17468

Ion exchange entropy and enthalpy functions calculated from experimental constants and temperature dependence data 06 p1177 A70-17837

Laminar boundary layer in hypersonic flow calculated by integral method, including effects of entropy gradient and induced pressure gradient [ONERA-TP-784] 06 p0984 A70-18468

Entropy fall in superheated liquid related to vapor bubble growth from finite so-called zero radius to critical radius, noting pressure effects 07 p1418 A70-18645

Entropy analysis of feedback control systems leading to separation theorem and feedback process information interpretation 07 p1245 A70-19095

State equation for entropy of dissociated air with enthalpy and pressure as independent variables for calculating gas dynamic processes on computers 10 p1966 A70-23839

Entropy or material waves effects on HF pressure oscillations in liquid rocket combustor, assuming concentrated combustion zone and zero length nozzle 10 p1929 A70-24088

One dimensional compressible constant entropy flows stability, noting unstable regions with fluid particles undergoing compression 11 p2034 A70-25679

Information theory as basis for statistical thermodynamics, discussing maximum entropy principle and probability as frequency in Gibbs ensemble 11 p2083 A70-25694

Geometric and predictive methods for developing bounds on epsilon-entropy for infinity error norm constraint 11 p2014 A70-26306

Random fields entropy estimation technique taking into account higher than immediately adjacent spatial dependencies 12 p2192 A70-27771

Self organization and adaptive routing communication system for military network, describing routing algorithm and entropy organization measure based on stochastic switching matrices 12 p2187 A70-27934

Vortex layer and entropy of supersonic gas flow past circular cones at incidence using surface velocity corrections 12 p2159 A70-28230

Stagnation point position and entropy at surfaces of supersonic paraboloids in perfect gas 12 p2160 A70-28250

Minimum entropy production at microscopic level, obtaining stationary state by Pauli master equation 14 p2616 A70-30654

Entropy increase, discussing universe heat death, earth energy balance, etc 15 p2809 A70-32907

Shock wave stability in plane steady flow at uniform entropy and limiting velocity 16 p2890 A70-33101

Thermodynamic diagram indicating enthalpy and entropy of oil combustion gases for any state and air excess value 16 p2997 A70-33295

Thermodynamic effects and transport phenomena in discontinuous system of gas filled containers connected by membrane, deriving entropy production and diffusion flux in membrane 17 p3197 A70-35531

Carbon dioxide entropy and enthalpy computation covering critical region and wide temperature range [ASME PAPER 70-GT-5] 18 p3348 A70-36861

Entropy layer in hypersonic flows, determining body configuration from shock wave shape described by coordinates power function 21 p3743 A70-40610

Shock wave extinction point within plane steady upstream flow with uniform entropy and limit velocity 21 p3808 A70-41441

Minimum entropy production in kinetic theory of rarefied gases described by Boltzmann equation 21 p3850 A70-41957

Octahedral solid-solid phase transitions by differential thermal analyzer and scanning calorimeter module, discussing entropy change causes 21 p3784 A70-42264

Linear aliphatic polyesters, calculating conformational contribution to heats and entropies of fusion 22 p3981 A70-42501

Linear aliphatic polyesters melting point, fusion heat and entropy correlations to molecular parameters 22 p3982 A70-42502

Al-Mg alloys solid phases free energy, entropies and formation heats determination by electromotive force measurement 24 p4357 A70-45230

Two incompressible isotropic nonlinear elastic solids mixture, investigating entropy production inequality effects 24 p4425 A70-45991

Transition entropy during dissociation, investigating Trouton-Picet rule applicability to diatomic molecules [DFVLR-SONDDR-58] 24 p4430 A70-46412

ENTRY

Multivariable nonlinear systems absolute stability criteria, emphasizing nonzero entry functions 19 p3394 A70-38171

ENVELOPES

Integration by orthogonalizations of envelopes of revolution loaded asymmetrically, introducing boundary conditions and structure discontinuities 07 p1404 A70-19128

Partially polarized wave with log-normal distribution law of component envelopes, investigating statistical characteristics of polarization parameters 18 p3228 A70-36624

ENVIRONMENT MODELS

Satellite radiation dose rates in inner Van Allen belt, correlating calculated and measured rates with proton environment model 06 p1134 A70-17264

Geophysical environment, discussing vibrations, foundation conditions, local gravity vector and atmospheric conditions in relation to precision instruments tests and operation [AIAA PAPER 70-959] 20 p3622 A70-39570

Structural fatigue design loads computation for fighter aircraft using multivariable load environment model from oscillograph recorded multichannel aircraft response data [AIAA PAPER 70-948] 20 p3719 A70-39579

ENVIRONMENT SIMULATION

NT ACOUSTIC SIMULATION

NT ALTITUDE SIMULATION

NT SPACE ENVIRONMENT SIMULATION

NT THERMAL SIMULATION

NT WEIGHTLESSNESS SIMULATION

Laboratory tests to determine KC-135 air conditioning failure due to turbine wheel icing by flight condition simulation 01 p0005 A70-10694

Hot corrosion reactions in Ni, Co and NiAl-base alloys exposed to salt-sulfur containing simulated gas turbine combustion atmospheres 01 p0118 A70-10728

Simulated lunar environmental facility to investigate effects of high risk vacuum, lunar gravity and terrain characteristics and spacesuit encumbrances on astronaut performance 01 p0037 A70-10961

Venus atmosphere simulation at condensation level in uniform temperature mixing cloud chamber, studying artificial and natural ice nuclei nucleation 02 p0373 A70-12293

Optical properties changes of various transmitting materials under simulated micrometeoroid environment, using silicon carbide particles accelerated in shock tube 03 p0523 A70-13027

High fidelity simulations for environmental stress evaluations, describing carbon dioxide effects on pilots simulated ground target tracking and reentry vehicle landing 06 p0999 A70-17291

Emergency ejection from lunar landing training vehicles, describing working sequence and experimental results on astronaut and test pilot 06 p1003 A70-17717

Organic compounds synthesis by electric discharges in simulated primitive atmosphere, considering

mechanism for biologically significant molecules formation 07 p1225 A70-19104

Preignition products from hydrazine propellants at simulated high altitude conditions using IR spectrophotometry, mass spectrometry and differential thermal analysis 07 p1358 A70-19579

Acceleration environment duplication difficulties, considering human physiological responses dependence on centrifuges performance characteristics and geometries 07 p1222 A70-19927

Flight simulators for pilot training, discussing need for aircraft motion cues 09 p1655 A70-22296

Microorganisms survivability in agar subjected to simulated Martian freeze-thaw cycles, discussing soil samples collection and composition 09 p1618 A70-22767

Laboratory simulations of geomagnetic field suppression, studying biological effects on human, mice, plants and microorganisms 09 p1626 A70-23113

TV camera with diffraction limited pinhole lens for visual simulation, solving depth of field and extending field of view without distortion 10 p1887 A70-24217

Cold air inhalation effect on vital physiological functions of dogs, describing heat exchange simulator of upper respiratory tract 11 p1985 A70-25672

Thermal control coatings, windows and mirrors for 1973 Mars Viking Lander vehicles under simulated Martian surface conditions [AIAA PAPER 69-1023] 13 p2384 A70-28530

Energy consumption in male subjects during walking and running in erect and supine position under simulated gravity 13 p2351 A70-29335

Similarity and scaling between atmospheric and wind tunnel simulated shear flows near earth surface 14 p2602 A70-30369

Supersonic nonequilibrium gas mixture flow past segmental bodies nose areas to simulate Venusian atmosphere, determining temperature, pressure and concentration distributions 15 p2796 A70-31483

Ionospheric spacecraft flight conditions simulation in vacuum chamber, discussing low energy ion sources 15 p2717 A70-31814

Fluid mechanics and engine dynamics and start-up experiments simulating thermal environment in nuclear light bulb engine 16 p2949 A70-33552

Atmospheric contaminants dispersion simulation in meteorological wind tunnel with capability to simulate thermally stratified boundary layers 17 p3065 A70-34496

Ground environmental simulation test for captive carrying cycling of air launched missiles 17 p3060 A70-35182

Gas turbine aero engines damage due to bird strikes, emphasizing rig testing and simulation at first stage rotor blading 18 p3236 A70-35995

Apollo spacecraft parts environmental simulation and testing, using real time computer generated graphic display 19 p3532 A70-37918

Jet engine roller bearings retainer candidate cage materials and coatings evaluation on test rig simulating engine conditions [ASLE PREPRINT 70AM 2D-1] 19 p3439 A70-38805

Simulated neutral atmospheric boundary layer measurements in wind tunnel, extending power spectral and correlation determinations 20 p3613 A70-40139

Accelerated vibration equipment testing for reducing test time, discussing vibration environment simulation 23 p4269 A70-44336

Hawaiian basalt melted in simulated lunar environment, investigating surface characteristics, internal structure and bearing strength 23 p4254 A70-44883

ENVIRONMENT SIMULATORS

NT HIGH VACUUM ORBITAL SIMULATOR

NT LUNAR GRAVITY SIMULATOR

NT SOLAR SIMULATORS

NT SPACE SIMULATORS

Test chamber to simulate helicopter rotor downwash for engine inlet air particle separator optimization 01 p0056 A70-10676

Real-world physical simulators application to tactical and strategical optical hardware 01 p0089 A70-10819

Reduced gravity simulators for studies of human mobility in space and lunar missions 01 p0037 A70-10958

Prototype lunar gravity simulator for studies of reduced gravity effects on human self locomotive

capability, using magnetic air bearings and body support system

01 p0037 A70-10960

Cloudy sky IR background radiation model for designing simulator of IR background for studying noise rejection characteristics of electro-optical automatic control systems

07 p1246 A70-19527

Space environment simulators and test facilities for solar cells and arrays, describing solar and magnetic field simulators and universal battery charger

13 p2385 A70-29555

Magnetic field simulator for investigating magnetic properties of satellites designed for magnetometric experiments

13 p2385 A70-29556

Aerospace coldness and vacuum simulation, discussing uses of cryogenic, titanium sublimation, ion and molecular pumps

19 p3396 A70-37462

Optical system mtf measurement by photographic technique for comparing telescopic sight with simulator, discussing performance

19 p3428 A70-38511

ENVIRONMENTAL CHAMBERS

U TEST CHAMBERS

ENVIRONMENTAL CONTROL

Granular amine used as regenerable absorbent in cycling two bed system for carbon dioxide removal

01 p0038 A70-10972

Human activities inadvertent effects on planet earth, discussing catastrophic physical environment changes and compensation methods

01 p0077 A70-11045

Phytotron design and operation, discussing closed air conditioned plant growing system at Stockholm including greenhouse, light controlled rooms, darkrooms, etc

03 p0435 A70-13716

Fire prevention problems in closed oxygen-rich environments, discussing ignition temperature and flame propagation rate

03 p0607 A70-13961

Fire safety in hyperbaric systems isolated from environment by gas tight barrier

[ASME PAPER 69-WA/SAF-2] 04 p0784 A70-14836

Environmental control of Apollo applications program orbital assembly, analyzing thermal and life support systems

[SAE PAPER 690622] 05 p0922 A70-15847

Computerized thermal model simulating environment control system, crew and vehicle structure in performance prediction for Apollo lunar module

[SAE PAPER 690621] 05 p0922 A70-15848

Si fluid thermal actuator as temperature sensor and prime mover for active thermal controller in spacecraft

05 p0806 A70-16124

Manned space flight requirements connected with cabin atmosphere, food/water supplies and waste disposal and environmental conditioning

05 p0807 A70-16632

Aviation environment master plan concerning public relations problems confronted by USAF bases with adjoining communities

05 p0960 A70-16634

Contamination control - Conference, New York, May 1969

05 p0798 A70-16701

Contamination control of spacecraft for planetary exploration missions emphasizing monitoring equipment and cleaning procedures

05 p0808 A70-16702

Environmental control underground low level radiation counting facility of Lunar Receiving Laboratory for gamma ray spectrometry, including radon adsorption system

05 p0829 A70-16707

Sterile access system using pilot assembly sterilizer system /PASS/ for NASA Planetary Quarantine Program

05 p0808 A70-16708

Clean room design problems concerning dampers, high pressure blowers, humidifiers, filters, etc

05 p0808 A70-16709

Clean room complex consisting of quality control analysis laboratory, main and pre-clean rooms and air-lock

05 p0808 A70-16710

Spacecraft contamination control teamwork operation, examining procedures and processes to ensure components cleanliness

05 p0809 A70-16713

Computer operated digital system for controlling acoustic test environment and dynamic test data acquisition

06 p1030 A70-18432

Book on aircraft environmental control covering design, construction and operation of various systems

10 p1809 A70-25203

Fluorocarbon fluid Rankine cycle system utilizing gas turbine exhaust heat for environmental control

[SAE PAPER 700160] 11 p1982 A70-25371

Phytotron design and operation, discussing closed air conditioned plant growing system at Stockholm including greenhouse, light controlled rooms, darkrooms, etc

11 p1990 A70-25516

Biosatellite environmental control coolant loop system design for 30-day mission program, discussing fuel cell power source, cryogenic subsystem, etc

11 p2127 A70-26360

Environmental control of confined spaces and life support systems by Pontryagin maximum principle of optimal control theory, discussing cabins, heat exchanger, etc

11 p1991 A70-26363

Harrier fighter aircraft cabin air conditioning and pressurization system

12 p2166 A70-27890

Apollo command and service modules environmental control system, discussing redesign of faulty hardware

[SAE PAPER 690618] 12 p2167 A70-27948

Equipment specifications and design for creep testing at variable load and temperature under uniaxial tension, emphasizing test environment control

13 p2509 A70-28537

Computerized thermal modeling of spacecraft environmental control systems /ECS/

15 p2705 A70-32523

Microbial contamination levels on Apollo 6 spacecraft, discussing intramural environments for assembly and testing

16 p2849 A70-33995

Habitability factors in space station crew quarter design, discussing hygiene and dining facilities

17 p3036 A70-34803

Statistical measurement of bird hazards to aircraft in terms of strike rates at airports, considering international strike rate standard

18 p3211 A70-35981

U.S. Air Force bird-aircraft collisions problem and bird control research

18 p3211 A70-35984

Military airlift command bird hazard minimization near airfields by environmental control, including uses of scare devices, chemicals, trapping, etc

18 p3212 A70-35988

Canadian civil aircraft bird hazards problem and alleviating measures including airport surrounding lands control

18 p3212 A70-35989

Aircraft bird hazards minimization by planning airport location and surroundings

18 p3236 A70-35991

Adaptation to extreme stimulation in machine-organism system

18 p3224 A70-36529

Integrated environmental control/life support resistojet systems, surveying NASA programs

[AIAA PAPER 70-1130] 20 p3690 A70-40215

Book on environment and human efficiency covering stress mechanisms, experimentation, exposure to chemicals, radiation, noise, heat, cold, machines, etc

22 p3967 A70-42457

Particulate boron levitated electrostatically in air and ignited by pulsed laser to avoid contamination, investigating combustion by high speed photography

[SMPT PREPRINT 100] 22 p4032 A70-43034

Electrofluid dynamic cooling system for spacecraft environmental control, describing design and operating principles

22 p3965 A70-43142

Manned orbiting laboratory microclimate including atmosphere composition, temperature, humidity and weightlessness effects, radiation and noise protection, etc

22 p3980 A70-43636

Earth orbital space stations as long term investment for future benefit of mankind, considering earth resources management, environmental and pollution control, etc

22 p4128 A70-43652

Metallization systems materials for IC, discussing environmental stability, metals electromigration, electrochemical corrosion tests, etc

23 p4173 A70-44533

Earth orbital space station electrical power systems, discussing power sources, effect on structural configuration, environmental control and launch and resupply operations

[MDAC-WD-1461] 23 p4143 A70-44605

Long term space flight crew habitation emphasizing food management, station housekeeping, personal hygiene and waste handling

23 p4154 A70-44622

Multispectral hydrometeorological environment monitoring in Earth Resources Survey Program

23 p4191 A70-44664

Earth-to-orbit space shuttle environmental control and life support system

[AIAA PAPER 70-1253] 24 p4418 A70-45967

Wide-bodied and SST aircraft impact on airport design based on economic, social and environmental considerations

[AIAA PAPER 70-1269] 24 p4323 A70-45970

ENVIRONMENTAL ENGINEERING

Conventional inertial gyro modified to provide specification performance for aircraft environments

01 p0086 A70-10312

Mercury atmospheric models for preliminary environmental criteria to be used in spacecraft design and engineering tradeoff studies

[AIAA PAPER 69-54] 01 p0183 A70-10838

Gear materials evaluation program for space environment application with unlubricated or solid film lubricated operation mode

[ASLE PREPRINT 69-LC-6] 02 p0309 A70-12539

Gear materials evaluation program for space environment application with unlubricated or solid film lubricated operation mode

10 p1893 A70-23837

Environmental engineering at NASA MSC, surveying Lunar Receiving Laboratory, micro incinerator, radon adsorption, Apollo Post-Landing Environmental Test Tank and vacuum chamber

10 p1860 A70-24411

Book on thermal environmental engineering covering refrigeration, psychometrics, solar radiation and heat transmission in buildings

12 p2163 A70-26865

Space environment effects on spacecraft payload materials and performance, discussing atmospheric pressure, outgassing, radiation and meteoroid collision

13 p2485 A70-28434

Robot motion optimal control in partially unknown environment, using dynamic programming and heuristic methods

14 p2543 A70-31413

Environmental challenge of 1970s - Conference, Boston, April 1970

17 p3058 A70-35151

Aircraft bird hazards minimization by planning airport location and surroundings

18 p3236 A70-35991

Metropolitan airports environmental considerations, noting aircraft noise role in planning

[SAE PAPER 700253] 18 p3237 A70-36826

Environmental factors effect on composite materials structural performance, using rate theory

20 p3656 A70-40053

Orbital photography interpretation from test rockets and Apollo-Gemini spacecraft, considering environmental applications

20 p3634 A70-40321

Structural and environmental design criteria for acoustical duct-lining materials in turbofan noise suppression

22 p4089 A70-42531

Environmental engineering - Conference, Delft University, Netherlands, April 1970

23 p4268 A70-44326

Spacecraft design to overcome space and launch environment, including environmental protection

23 p4257 A70-44327

Materials problems in space and spacecraft environments, discussing particle density, composition and UV radiation, spacecraft structure, payloads, vibration, etc

23 p4209 A70-44328

Civilian survival in emergency situations, discussing basic requirements, environments, vehicles and equipment for survival kits

23 p4153 A70-44495

Fireproof nonmetallic materials for spacecraft and aircraft, discussing functional utility, durability and aesthetic requirements relative to environmental conditions

23 p4210 A70-44610

Optimal temperature control for confined spaces and life support systems, using mathematical models of environmental control systems

24 p4295 A70-46373

ENVIRONMENTAL INDEX

Residential urban environment data extraction from high and low resolution images

12 p2216 A70-26907

Environmental heat stress indices of human subjects in bicycle ergometer experiment

18 p3224 A70-36226

Environmental factors effect on composite materials structural performance, using rate theory

20 p3656 A70-40053

Acoustic lining technology and materials for turbofan engine ducts, considering environmental factors and noise spectra

22 p4089 A70-42530

ENVIRONMENTAL LABORATORIES

Laboratory simulation for shock waves around earth, moon and Venus based on artificial solar wind and magnetic dipole interaction study

10 p1948 A70-25182

Surveyor spacecraft testing at Environmental Test Laboratory, describing facilities and innovations designed for temperature extremes

19 p3532 A70-37960

ENVIRONMENTAL RESEARCH SATELLITES

Incipient tropical storm location and synoptic weather pattern analysis from environmental satellite system data utilization

07 p1329 A70-19196

- Satellite based random Doppler environmental measurement technique for Global Atmospheric Research Program /GARP/, receiving signals from balloons, buoys and land stations 13 p2407 A70-29176
- Earth orbital space stations as long term investment for future benefit of mankind, considering earth resources management, environmental and pollution control, etc 22 p4128 A70-43652
- ENVIRONMENTAL TEMPERATURE**
- U AMBIENT TEMPERATURE**
- ENVIRONMENTAL TESTS**
- NT COLD WEATHER TESTS
- NT CORROSION TESTS
- NT HIGH TEMPERATURE TESTS
- NT LOW TEMPERATURE TESTS
- NT SALT SPRAY TESTS
- NT UNDERWATER TESTS
- Volatile contaminants emitted from space cabin construction materials tested under simulated space conditions 01 p0031 A70-10237
- Environmental effects on aircraft and propulsion systems - Conference, Bordentown, N.J., October 1969 01 p0162 A70-10678
- CH-54A engine air particle separator /EAPS/ field experience, discussing engine removal times due to erosion, environment evaluation and design improvements 01 p0164 A70-10684
- Sand and dust environmental test of T-63 regenerative engine, discussing performance depreciation, recuperator inspection and comparison with non-regenerative T63-a-5a engine 01 p0164 A70-10685
- High speed hail impact damage on flat Al alloy plates observed for effects of impact angle and velocity, plate material properties and thickness 01 p0056 A70-10690
- Hemoglobin concentration in red blood cells in men of various ages as function of altitude, discussing correlations with body weight and plasma protein 01 p0024 A70-10978
- Continuous measurement and automatic recording of metals electrical resistance during fatigue testing in vacuum at elevated temperatures 01 p0092 A70-11108
- Low alloy and stainless steels durability in various natural atmospheres, discussing corrosivity dependence on atmosphere pollutants, temperature and humidity 02 p0318 A70-12476
- Correlation between sustained-load and fatigue crack growth in high strength steels for aggressive environment effects 02 p0318 A70-12544
- Metal fabrication shop environment contamination effect on bond strength of various adhesive system tested by humidity and salt spraying exposures 02 p0310 A70-12664
- Transillumination holography in environmental tests, discussing camera design, particle field and applications, including flow visualization in wind tunnel tests 03 p0486 A70-13539
- Nuclear environmental testing techniques, discussing radiation effects, measurements, instrumentation hardening, simulation source selection, dosimetry, noise sources and noise reduction, etc 03 p0523 A70-13540
- Artillery type projectiles field photography in flight in connection with service integrity evaluation of weapon components under real environment conditions 03 p0490 A70-13658
- Organisms resistance to biological environmental factors, surveying published literature on pressure chamber experiments, tissue resistance, cellular protein stability, etc 03 p0422 A70-13701
- Electro-pyrotechnic initiators for space applications subjected to dry heat sterilization cycles and to post-sterilization mechanical and electrical environments 03 p0495 A70-14131
- Thermal comfort in disparate environments, discussing human subjects skin mean temperature and body water loss 03 p0429 A70-14158
- Material evaluation and selection for compact nuclear reactor control bearings operating at high temperature in vacuum [ASME PAPER 69-WA/LUB-1] 04 p0697 A70-14765
- High altitude simulation installations design for rocket motors starting tests under long term high vacuum exposure 04 p0736 A70-15179
- Variable strain bending form design for determining environmental craze resistance of polymers 04 p0713 A70-15375
- Solar and geomagnetic effects on variations in physiological tests using alimentary reflex of dogs 04 p0639 A70-15512
- Heat exchanges between man and environment due to incidents or accidents during aircraft operation evaluated by combined heat transfer coefficient 05 p0799 A70-15764
- Microbial contamination levels and types detected on Apollo 9 spacecraft and related effects of various test and assembly environments 05 p0809 A70-16711
- White single-comb Leghorn chick embryonic development at increased pressures at various hyperbaric gas mixtures for ten day periods 06 p0991 A70-17296
- External environment changes effect on animal activity, considering reactions on molecular, physiological and behavioral levels 07 p1199 A70-18782
- Physical discomfort and miseries contribution to psychological deterioration during water survival tests on life raft 07 p1218 A70-19009
- U.S., U.S.S.R. and European space environment simulation chambers accommodating assembled spacecraft for thermal tests, describing design and characteristics 07 p1249 A70-19659
- Radiative heating rates and gas environments effects on ablative material performance from tests at arc image facility 07 p1319 A70-19888
- Environmental test facilities for space transportation systems, discussing aerodynamic, propulsion and structural problems, operational requirements and existing capabilities [AIAA PAPER 70-275] 07 p1251 A70-20384
- Metal adhesive joints permanence under various environmental conditions, considering surface properties effect 08 p1504 A70-20890
- Gaseous environments effects on creep of austenitic stainless steel, observing weakening in air and surface cracking in nonoxidizing atmospheres [ASME PAPER 68-MET-3] 08 p1519 A70-21453
- Ni-Cr superalloys hot corrosion, studying sulfidation-oxidation in various synthetic controlled gas mixtures 09 p1706 A70-22944
- Biological performance studies under extreme environmental stresses for gaining insight into potential of earth-type life here and in universe 09 p1623 A70-23699
- Satellite communications subsystem performance testing from initial integration through launch under all environmental exposure 11 p2030 A70-25445
- Spacecraft S band power amplifier TWT electrical, environmental and life tests under saturated conditions [AIAA PAPER 70-506] 11 p2016 A70-25468
- Organisms resistance to biological environmental factors, surveying published literature on pressure chamber experiments, tissue resistance, cellular protein stability, etc 11 p1985 A70-25501
- Environment and complex load effects on fatigue life - ASTM Conference, Atlanta, September-October 1968 11 p2137 A70-26088
- Air and salt water tensile and shear mode cracking of titanium alloy sheets examined with electron fractographs 11 p2067 A70-26099
- Fatigue crack propagation in high strength steels during fatigue cycling in dry and wet environment containing NaCl 11 p2067 A70-26100
- Environmental remote sensing - Conference, Ann Arbor, October 1969, Volume 2 12 p2214 A70-26901
- Hyperbaric environment combustion, discussing burning rate data and fire resistance scale 14 p2665 A70-30626
- Mission sequential environment effects on Dacron parachute material mechanical properties [AIAA PAPER 69-1018] 14 p2563 A70-30770
- Simulated Venusian atmosphere effects on polymeric plastic and rubber materials, comparing with high temperature air and nitrogen exposures 14 p2640 A70-30781
- Corrosion resistant paint systems for aircraft structural parts under severe environmental conditions simulated in carrier test stand 14 p2598 A70-31292
- Electronic components environmental testing, examining temperature, humidity and vibration effects 14 p2558 A70-31295
- Environmental fatigue crack propagation in Al alloys at low cyclic stress intensity levels 15 p2762 A70-32390
- U.S., U.S.S.R. and European space environment simulation chambers accommodating assembled spacecraft for thermal test, describing design and characteristics 15 p2718 A70-32696
- Cryobiotic potentialities on earth, investigating life forms physiological response to temperature, cryotolerance mechanisms, etc 16 p2848 A70-33093
- Materials test fixture design and fabrication for vacuum testing and evaluation of slip rings and brushes, discussing dry film lubrication 16 p2920 A70-33812
- Carbon dioxide output monitoring from biosatellites for circadian system behavior in closed organism-environment systems 16 p2849 A70-33992
- Unnatural environment behavior of leeches for long term biosatellite experiment, determining temperature, humidity, oxygen pressure, carbon dioxide concentration, calcium hydroxide limits, etc 16 p2854 A70-33994
- Stress corrosion cracking in Ti and alloys, discussing metallurgical and environmental factors emphasizing exposure to hot salt, methanol, seawater, etc 17 p3114 A70-34372
- Tektite II program safety planning for ambient pressure habitat under saturation diving conditions [AAS PAPER 70-053] 17 p3036 A70-34796
- Humidity resistance test method involving flight simulation for airborne equipment in tropical environment 17 p3058 A70-35159
- Combined environments testing to reveal potential flight failure modes 17 p3059 A70-35165
- Automatic shock spectrum synthesizer/analyzer for shock testing of field environments 17 p3059 A70-35175
- Forcing time functions prediction for structures under shock tube test, relating aerodynamic parameters to mechanics terminology 17 p3060 A70-35180
- Test machine for partial gravity environment simulation for aerospace subsystem testing in vacuum chamber 17 p3060 A70-35181
- Flight test program for helicopter gas turbine engines, considering engine-airframe-control systems integration and environmental tests [ASME PAPER 70-GT-38] 18 p3303 A70-36836
- Helicopter gas turbine engines protection against salt spray, dust, sand, ice, cut grass, etc [ASME PAPER 70-GT-96] 18 p3263 A70-36843
- CH-54A helicopter gas turbine engine air particle separator /EAPS/ field service in Vietnam, noting time before engine removal for erosion [ASME PAPER 70-GT-97] 18 p3303 A70-36844
- Computer aided laboratory testing of flight vehicles in real environmental conditions, illustrating vertical stabilizer subject to gust loads 19 p3396 A70-37874
- Apollo spacecraft parts environmental simulation and testing, using real time computer generated graphic display 19 p3532 A70-37918
- Surveyor spacecraft testing at Environmental Test Laboratory, describing facilities and innovations designed for temperature extremes 19 p3532 A70-37960
- Environmental surveillance associated with ground tests of nuclear rocket engine prototypes, determining statistical nature of radioactive effluent 19 p3470 A70-38013
- Environmental tests and checkout procedures for Azur satellite subsystems and subassemblies integration into flight readiness 19 p3533 A70-38289
- Heos 1 research satellite space simulation tests at ESTEC test facility 19 p3399 A70-38292
- Seismic measurements at inertial test facilities, considering vibration environment relevant to single degree of freedom gyroscope performance tests [AIAA PAPER 70-951] 20 p3606 A70-39576
- Filament wound composites, investigating interaction of fabrication variables and untoward environments by delineating effect of each on structural performance 20 p3731 A70-40055
- Apollo spacecraft tests in Space Environment Simulation Laboratory, discussing thermal data, astronaut training, extravehicular activity, reaction control system, etc 21 p3805 A70-41271
- Automated data handling system for satellite environmental testing used by ESRO 21 p3805 A70-42258
- Shock and bump testing for dynamic mechanical environments effects encountered by vehicle equipment and components 23 p4195 A70-44331
- Deterministic vs stochastic signals for equipment and installations short cycle reliability tests over service life during changing environments 23 p4166 A70-44332

ENVIRONMENTS

- Viruses response to environmental exposure emphasizing temperature, humidity, light and extraterrestrial conditions
23 p4146 A70-44398
- Man-rated chamber facilities at Manned Spacecraft Center /MSC/, discussing safety requirements and criteria, environmental test chamber design and test results
23 p4152 A70-44458
- Extreme environmental temperature effects on hepatic amino acid catabolism in rats attributed to caloric deficiency
23 p4148 A70-44790
- Cosmos 110 satellite experiments concerning radiation effects on lysogenic bacteria and plants
23 p4149 A70-45030
- Ear protection for persons exposed to various jet aircraft noise environments
24 p4306 A70-45121

ENVIRONMENTS

- NT AEROSPACE ENVIRONMENTS
NT CHROMOSPHERE
NT CISLUNAR SPACE
NT DEEP SPACE
NT EXTRATERRESTRIAL ENVIRONMENTS
NT FRICTIONLESS ENVIRONMENTS
NT HIGH ALTITUDE ENVIRONMENTS
NT HIGH GRAVITY ENVIRONMENTS
NT HIGH TEMPERATURE ENVIRONMENTS
NT INTERPLANETARY SPACE
NT INTERSTELLAR SPACE
NT JUPITER ATMOSPHERE
NT LOW TEMPERATURE ENVIRONMENTS
NT LUNAR ATMOSPHERES
NT LUNAR ENVIRONMENT
NT MARS ATMOSPHERE
NT MARS ENVIRONMENT
NT PLANETARY ATMOSPHERES
NT PLANETARY ENVIRONMENTS
NT ROTATING ENVIRONMENTS
NT SOLAR ATMOSPHERE
NT SPACECRAFT ENVIRONMENTS
NT STELLAR ATMOSPHERES
NT THERMAL ENVIRONMENTS
- Soviet collection of papers on physiology of vision under normal and extremal conditions
08 p1442 A70-20726
- Airport operations effects on total environment, considering jet aircraft noise pollution [AIAA PAPER 70-887]
19 p3395 A70-37391

ENZYME ACTIVITY

- NT FERMENTATION
- Phosphopentomutase activity in rabbit tissue, reporting probable PG-mutase subsidiary function and activity of previously unrecognized enzyme
01 p0012 A70-10091
- Spore and vegetative cell adenylate kinases of *Bacillus subtilis* proved indistinguishable by polyacrylamide gel electrophoresis DEAE cellulose chromatography
01 p0021 A70-10789
- Biochemical characteristics, nitrogenase activity and nitrogen fixation in heterocysts of blue green algae
01 p0024 A70-10894
- Artificial pulmonary ventilation effects on carbonic anhydrase activity in human blood during hypoventilation and hyperventilation
01 p0025 A70-11029
- Renal and hepatic glutamine synthetase distribution in mammals, studying relation between glutaminase and urinary activities /ammonia metabolism/
02 p0232 A70-11710
- Enzymatic hydroxylation mechanism of p-hydroxybenzoate hydroxylase from *Pseudomonas putida*, describing product separation and purification
02 p0236 A70-12100
- Separate gamma irradiation effect of enzyme and hemoglobin-albumin-globulin substrates on proteolysis dynamics
03 p0419 A70-13308
- Ribonucleic acid polymerase model with initiating purine triphosphate binding to product terminus site and pyrimidine triphosphate engaging in exchange binds to substrate site
03 p0442 A70-14046
- Purification and properties of diphosphopyridine nucleotide-linked glycerol 3-phosphate dehydrogenases from chicken breast muscle and liver
03 p0442 A70-14047
- Spacecraft cabin atmosphere effects on mice primary and secondary immunological responses relative to spleen histochemical and biochemical changes in enzyme activity
03 p0437 A70-14063
- Enzyme beta-hydroxybutyrate dehydrogenase concentration in mitochondria from bovine and sheep liver
03 p0430 A70-14198
- Chloride and sulphydryl activators in glucagon degradation and secretion by purified rat liver dipeptidyl aminopeptidase I /Cathepsin C/
04 p0631 A70-14682
- Quantitative and qualitative differences in enzyme levels of intermediate carbohydrate metabolism in

obligate autotrophs *Thiobacillus thioparus* and *Thiobacillus neapolitanus*
04 p0633 A70-15441

- Histochemical detection of L-gulonolactone-phenazine methosulfate oxidoreductase activity in mammals with emphasis on vitamin C synthesis in primates
04 p0647 A70-15753
- Hyperbaric oxygenation effects on cellular membrane permeability, analyzing rat plasma behavior of transaminases GOT and GPT and K and Na cations electrolytes
05 p0802 A70-16493
- Acetylcholine concentration, esterase activity and synthesis in cerebral tissue of rats under repeated mechanical vibrations combined with noise
06 p0993 A70-17425
- Hepatic polysome profiles and tyrosine transaminase activity daily rhythms in rats, studying dietary protein role
06 p0997 A70-18402
- Succinic dehydrogenase activity in white rats cerebrum and liver under hypothermia and after warming
07 p1207 A70-19475
- Nonlinear steady state diffusion elliptic boundary value solutions exemplifying enzyme kinetics and radiation cooling
08 p1596 A70-20580
- DNA enzymatic breakdown in *Escherichia coli* as function of ionizing radiation and temperature
08 p1445 A70-20775
- Biochemical and histochemical parallels of enzymatic activity in blood, cardiac muscle and liver under hypoxia
08 p1446 A70-21445
- Total body X irradiation effect on tyrosine hydroxylase and catecholamine levels in rats
09 p1616 A70-22318
- Amino acid metabolism time dependent variations, studying tyrosine transaminase rhythm in rat liver
09 p1618 A70-22525
- Flight stress in Starfighter aircraft pilots related to fibrinolysis activity in blood
09 p1625 A70-23003
- Alternating copolymer of guanylic and cytidylic residues synthesized in RNA polymerase-catalyzed reaction
09 p1630 A70-23274
- Dietary intake and adrenal cortex effects on diurnal rhythm of hepatic tyrosine transaminase activity and adrenal corticosterone content in rats
09 p1621 A70-23437
- Serum lactate dehydrogenase /LDH/ isoenzyme in males before and after muscular exertion, observing change in skeletal muscle and liver fraction
10 p1809 A70-24002
- Refutation of Sylven-Snellman report of catalysis of benzoylarginine beta-naphthylamide and leucine beta-naphthylamide hydrolysis by beef spleen cathepsin B
10 p1812 A70-24534
- Prolonged hypodynamia effect on human blood serum mineral content and enzyme activity
10 p1815 A70-24677
- Pesinogens A, C and D from stomach mucosae of smooth dogfish separated by chromatography on DEAE cellulose
11 p1987 A70-26007
- Glycolysis and glycolytic enzymes activity increase in tissues observed during training of rats to hypoxia, discussing adaptive reactions at cellular level
12 p2167 A70-26975
- Stereospecificity and reaction rate of enzymatic hydrolysis of racemic substrate by pepsin determined by nuclear magnetic resonance spectroscopy
12 p2181 A70-27472
- Blood serum enzyme activity in rats during prolonged hypokinesia, noting increase of aminotransferases
13 p2351 A70-29329
- Partial nucleotide sequences for fragments isolated from ribonuclease digests of tobacco mosaic virus RNA, suggesting genetic duplication possibility
13 p2363 A70-29798
- Serologic comparisons of carbonic anhydrases in human and other primate erythrocytes
13 p2355 A70-29805
- Epinephrine uptake and metabolic disposition in rat brain, determining pathways and turnover of endogenous brain hormone and enzymatic synthesis
14 p2536 A70-30348
- Ammonia incorporation in chemolithotrophic *Hydrogenomonas eutropha*, investigating responsible enzyme
15 p2682 A70-32000
- Nicotinamide adenine dinucleotide phosphate /NADP/ specific isocitrate dehydrogenase /ICDH/ inactivation from obligate halophile at low NaCl levels
15 p2685 A70-32671
- Intense deceleration effects on mice and rats, including internal organs damage and enzyme activity increase
17 p3025 A70-35132

Thermal stability of glycolytic enzymes from thermophilic clostridia
17 p3042 A70-35327

- Intermediary complexes between Na-K ion stimulated ATPase /adenosine triphosphate/ and microsomal proteins of turtle bladder epithelial cells
18 p3225 A70-36233
- Field test for microbiological contamination of jet fuel, discussing phosphates detection
18 p3299 A70-36344
- Respiratory gas metabolism, tissue respiration and enzyme distribution in white rats skeletal muscles following long term cold acclimatization
18 p3220 A70-36548
- Anomalous substrate oxidizing specificities among red brown and green algal peroxidases and land plants
19 p3360 A70-37773
- Lighting effects on phenylethanolamine-N-methyltransferase /PNMT/ activity and adrenal epinephrine content in rats
20 p3568 A70-38982
- Acetylcholinesterase and simple esterases distribution in squirrel monkey brain, examining activity in neuropil and postrema area neurons
20 p3569 A70-38993
- Thermally prepared poly-alpha-amino acids catalytic activity after long term dry state storage, suggesting enzyme activity role in biological evolution
21 p3772 A70-40713
- Serotonin, 5-hydroxyindoleacetic acid /5-HIAA/ and monoamine oxidase in bovine pituitary organ and median eminence
21 p3761 A70-40850
- Biochemistry of blood group antigens involved in agglutination reactions, discussing effect of proteolytic enzymes on cell membrane structure
21 p3764 A70-41447
- Oxidative enzymes histochemistry in nervous system, liver and kidney of rats in immediate and remote periods after 24-hr artificial hypobiosis
21 p3764 A70-41478
- Serum enzymes lactate dehydrogenase, creatine phosphokinase and isoenzymes in conditioned male after marathon run, noting little myocardium damage
21 p3766 A70-42158
- Xanthine dehydrogenase activity in *Drosophila* and *Habrobracon* under hypogravity conditions onboard Biosatellite
23 p4144 A70-43863
- Microgram 2-nitro-1-butyl pyridinium sulfate /NBPS/ inhibition of growth of *Bacillus subtilis* by blocking thymidylate synthetase
23 p4158 A70-44998
- Nitrogen deficient algae nitrification, showing cellular N compounds oxidized to nitrate and nitrite followed by nitrate reductase
24 p4297 A70-45407
- Light effect on cis-trans-isomerization of cinnamoyl-alpha-chymotrypsin, considering molecular modeling of visual reception
24 p4298 A70-45496
- Lipoprotein lipase activation on emulsified triglycerides by specific glycopeptides of human serum lipoproteins
24 p4298 A70-45802
- Synthesis regulation of p-hydroxybenzoate hydroxylase and protocatechuate oxygenase in beta-ketoadipate pathway in *Pseudomonas putida*
24 p4304 A70-46145
- Structure and function of juxtaglomerular apparatus of kidneys controlling synthesis and secretion of renin
24 p4305 A70-46392
- ENZYMES
- NT CARBONIC ANHYDRASE
NT CHOLINESTERASE
NT COENZYMES
NT OXIDASE
NT PEPSIN
- Ammonia incorporation in chemolithotrophic *Hydrogenomonas eutropha*, investigating responsible enzyme
15 p2682 A70-32000
- Halophilic bacteria electron transport chain, examining hydrophobic forces role in menadione reductase structure
21 p3772 A70-40574
- Catalytic activities of thermal polyanhydro-alpha-amino acids for modeling enzymes and prebiotic protein
24 p4310 A70-45346
- Synthesis regulation of p-hydroxybenzoate hydroxylase and protocatechuate oxygenase in beta-ketoadipate pathway in *Pseudomonas putida*
24 p4304 A70-46145
- ENZYMOMOLOGY
- Purification and reversible inactivation of isocitrate dehydrogenase /ICDH/ of *Halobacterium cutirubrum*, overcoming difficulties in purifying halophilic enzymes
01 p0021 A70-10792
- FOR [RENDEZVOUS]
U EARTH ORBITAL RENDEZVOUS

EOSINOPHILS

Eosinophilic leukocytes behavior in blood of Starfighter aircraft pilots due to flight stress
09 p1625 A70-23004

EOSS

Attitude sensing and target pointing instrumentation in earth orbiting stellar telescopes in inertial space
16 p2905 A70-33155

Juridical condition of earth orbiting space stations, discussing term definitions in treaty on outer space
17 p3202 A70-35785

Space station with shuttle and tug service, discussing reduced costs, reusability and commonality
18 p3333 A70-36318

Reusable space transporter predicted applications evolution from earth circling to space bases and space colonies for deep space missions
21 p3930 A70-41495

Earth orbital space stations as long term investment for future benefit of mankind, considering earth resources management, environmental and pollution control, etc
22 p4128 A70-43652

EPHEMERIDES

NT PLANET EPHEMERIDES

Solar and lunar disks instant of contact during solar eclipse determined by chord measurements, comparing three methods for successive time intervals
01 p0191 A70-11473

Ts1 catalog of right ascensions of stars based on photoelectric observations, including clock corrections
04 p0756 A70-15480

Catalog of right ascensions of stars obtained from photoelectric observations, comparing equatorial and zenith region with F6 catalog
04 p0756 A70-15481

Tabular results of Galaxy mean and angular diameters and smallest/largest ratios measured on Palomar Atlas
05 p0906 A70-15797

Lunar ephemeris, lunar theory constants and coordinate system corrections based on conditional equations formulated by analytical partial derivatives
05 p0908 A70-16334

Meridian circle observations before and after occultation of ZC 2232 by Neptune on 7 April 1968, correcting ephemeris for star and Neptune
06 p1151 A70-18489

Moon observation in megalithic times by means of menhirs
09 p1751 A70-22194

Latitude determination from observations of pairs of bright stars at equal altitudes, using computer ephemeris calculations
14 p2633 A70-30142

Delaunay reduced Hamiltonian verification in lunar ephemeris theory based on Lie transforms
16 p2978 A70-33972

Ephemeris of periodic comet Wolf-Harrington for 1970-72 reappearance, assuming nongravitational motion anomaly and secular acceleration
17 p3158 A70-34862

Periodic comet Slaughter-Burnham improved ephemeris for 1970-71, based on 1958-59 and 1969 orbital elements
17 p3158 A70-34863

Lunar ephemeris computerized analytical solution, considering literal expansions generation
20 p3705 A70-39479

Ephemerides for lunar-orbiting observation of dust clouds in earth-moon system libration points L4 and L5 by observer orbiting over lunar equator
22 p4097 A70-42308

EPHEMERIS TIME

Selenodetic control systems orientation based on lunar features correlation with reference stars, considering ephemeris times corrections
08 p1572 A70-20941

Planetary ephemerides accuracy and navigation during interplanetary missions, discussing machine readable ephemerides for outer planets
13 p2448 A70-28703

Selenodetic control systems orientation based on lunar features correlation with reference stars, considering ephemeris times corrections
15 p2806 A70-32753

EPICARDIUM

Myocardium, endocardium and/or epicardium disease characteristics, discussing primary and secondary cardiomyopathy groups
09 p1616 A70-22277

Cardiac structure-functional relations, discussing muscle strand continuum, basal fibrous skeleton, epicardial, endocardial and myocardial layers
15 p2685 A70-32834

EPIDEMOLOGY

Prospective epidemiological recognition of clinical coronary heart disease, discussing effects of habitual physical inactivity, excessive dietary fat, socioeconomic stresses, etc
01 p0023 A70-10865

Physical activity and epidemiology of coronary heart disease
07 p1212 A70-19694

Epidemiologic investigation of physical activity and fitness effect on prevention of premature clinical coronary heart disease
07 p1212 A70-19695

Large scale aerial color photography over spruce fir stands during 10 year period for assessing damage caused by budworm epidemic
17 p3078 A70-35614

EPIDERMIS

Keratinocyte development on epidermal surface of female patient exposed to cosmetic UV irradiation with quartz lamp
01 p0029 A70-11406

EPILEPSY

Pilots temporal lobe epilepsy case history and diagnosis
06 p1000 A70-17301

High risk factors for posttraumatic epilepsy /head injury complicated by subdural hematoma and spike EEG abnormality/ precluding return to flying
09 p1622 A70-23470

Student pilot case diagnosis of hysterical neurosis with syncopal and epileptiform symptoms
21 p3771 A70-41493

EPINEPHRINE

Rats sympathoadrenomedullary response to increased oxygen tensions, measuring catecholamines, norepinephrine and epinephrine in adrenal gland, hypothalamus, serum and urine
01 p0024 A70-10979

Ambient temperature effects on rats excretion of epinephrine, norepinephrine and major metabolites
02 p0232 A70-11714

Blood flow changes in portal vein and hepatic artery of anesthetized cats following intraportal and intrahepatic arterial administration of isoproterenol, epinephrine and norepinephrine
02 p0232 A70-11718

Adrenaline effects on rats peripheral blood leukocyte content used for X-irradiation sensitivity estimation
10 p1822 A70-25177

Vegetative cardiovascular, motor and electrophysiological reactions to electrical stimulation of limbic and reticular formations in cerebrum after adrenalin and aminazine injections
13 p2352 A70-29352

Vegetative nervous system reactions of patients with diencephalic syndromes, investigating hypothalamo-hypophyseal-adrenal system role
13 p2352 A70-29353

Epinephrine uptake and metabolic disposition in rat brain, determining pathways and turnover of endogenous brain hormone and enzymatic synthesis
14 p2536 A70-30348

Pressor response to epinephrine in hyperbaric atmospheres measured in cats under change of sympathetic tone
17 p3032 A70-35566

Lighting effects on phenylethanolamine-N-methyltransferase (PNMT) activity and adrenal epinephrine content in rats
20 p3568 A70-38982

EPITAXY

Electrical properties of Si-doped GaAs p-n structures obtained by liquid phase epitaxy, considering charge buildup
01 p0155 A70-10132

GaAs - Conference, Dallas, October 1968
01 p0157 A70-10515

Epitaxial growth of Cu vapor deposited on W single crystal /110/ surface using low energy diffraction, Auger electron and work function techniques
03 p0538 A70-13100

Carrier concentration profiles and surface resistance of Ohmic contacts to solution epitaxial n-type GaAs wafers measured by Schottky barrier capacitance
03 p0543 A70-14213

Epitaxial GaAs FET using evaporated Au-Ge-Ni contacts and Ni Schottky barrier, describing fabrication and electrical properties measurement
04 p0660 A70-15367

Epitaxial beta-SiC films formation on sapphire by chemical conversion
06 p1127 A70-17946

Electrical properties of Si-doped GaAs p-n structures obtained by liquid phase epitaxy, considering charge buildup
08 p1556 A70-21408

Epitaxy of Ag deposited on Ni, observing irreversible crystallographic order transition from metastable nominal orientation by LEED
10 p1927 A70-24076

Gallium arsenide phosphide epitaxial films electroluminescence spectra noting composition effect
10 p1928 A70-24833

Epitaxial surface morphology layer electrical properties and autoping at GaAs-Ge heterojunctions as function of substrate temperature, orientation and HCl concentration
11 p2098 A70-26392

Nucleation and heteroepitaxial GaAs film growth on sapphire using electrical measurements, reflection diffraction and electron microscopy
11 p2098 A70-26393

Epitaxial magnetic oxide films grown by chemical vapor deposition
11 p2099 A70-26626

GaAs vapor phase epitaxial growth characteristics noting applications to Gunn diodes
11 p2020 A70-26826

Au, Ag and Al films evaporation in ultrahigh vacuum on LiF and MgO surfaces, showing insignificant role of lattice misfit for epitaxy
12 p2285 A70-27260

Epitaxial Ge deposits on Si control by Kikuchi pseudolines, considering surface polish, crystallinity and substrate orientation
13 p2470 A70-28957

Silicon and alpha-alumina support interface reactions during nucleation-coalescence and after epitaxial growth, investigating electrical properties
13 p2470 A70-28958

Ternary phase diagram of liquid epitaxially grown gallium arsenide antimonide, considering use as high quantum efficiency long wavelength photoemitter
15 p2782 A70-31758

ZnO epitaxial layers deposition by chemical vapor transport on sapphire single crystal substrates
15 p2784 A70-31982

Hydrogen effect on impurity redistribution in heteroepitaxial Si layers on sapphire substrate
15 p2785 A70-32529

Micro-Hall device as tool for evaluating epitaxial silicon in integrated circuit processing
15 p2710 A70-32573

Solar cells based on homogeneous diffusion p-n junctions in epitaxial GaAs films grown on Ge single crystal substrate
16 p2843 A70-33202

GaAs microwave devices including diffused varactor, Schottky barrier and Gunn diode, discussing single crystals preparation and epitaxial growth layers
16 p2873 A70-33293

Electrical properties of n-type GaAs epitaxial films grown by gas transport method
17 p3144 A70-35706

MIS structures with silicon nitride film deposited by RF glow discharge, observing doping increase in epitaxial substrate
17 p3055 A70-35873

Epitaxial beta SiC film formation on SiC by reactive evaporation or sputtering at low temperature
17 p3144 A70-35906

Heteroepitaxial ZnO film on anisotropic sapphire substrate, calculating dispersion for fundamental Rayleigh wave mode
17 p3144 A70-35908

Epitaxial growth of GaAs thin films in vapor phase using hydrogen, gallium and arsenic trichloride as sources
19 p3488 A70-38200

Impurity distribution in diffused p-n junction in thin epitaxial film, calculating space charge region width and junction capacitance
20 p3685 A70-38967

Epitaxially grown Si contact for area reduction of MOS transistor circuits
20 p3596 A70-39099

Epitaxial GaAs films growth from solid solutions of InAs-GaAs system deposited on GaAs substrates, noting electron mobility and temperature effect
20 p3686 A70-39629

Niobium suboxide formation in Nb-O system from supersaturated solution of oxygen in niobium after annealing
20 p3648 A70-39630

Temperature dependence of titanium-zirconium oxide semiconductor compounds growth, using samples arc melted in purified He
20 p3687 A70-39631

Transmission electron microscopy observation of thermal annihilation of stacking faults in epitaxial layers of GaAs grown from liquid phase
21 p3863 A70-42004

High purity surface-free GaAs epitaxial layer carrier lifetime measurement by optical transmission and excitation technique
22 p4086 A70-43017

CW GaAs semiconductor laser fabrication by liquid epitaxy, noting Ag plating role in output power
24 p4352 A70-45468

EPITHELIUM

Temporary mitotic activity depression with decrease in aberrant mitoses observed in mice intestinal epithelium cells after exposure to 50 Mev proton doses
03 p0423 A70-13708

Corneal epithelium chromosome rearrangements in gamma irradiated white adult mice, noting radiation dosage and duration
03 p0426 A70-13903

Photoconductivity detected in pigmented epithelium of eye during illumination by visible light
08 p1444 A70-20738

Laser irradiation effects on mice skin and internal organs, observing inflammatory symptoms, hair follicles destruction and epithelial atrophy
09 p1624 A70-22816

- Temporary mitotic activity depression with decrease in aberrant mitoses in mice intestinal epithelium cells after exposure to 50 Mev proton doses
11 p1985 A70-25508
- Mitotic activity and aberrant mitoses frequency in mice corneal and duodenal epithelium cells under fast fission neutron irradiation
17 p3026 A70-35319
- Intermediary complexes between Na-K ion stimulated ATPase /adenosine triphosphate/ and microsomal proteins of turtle bladder epithelial cells
18 p3225 A70-36233
- Mice intestinal epithelium, investigating high energy protons irradiation effect on cells
23 p4149 A70-45028

EPOCHS

U TIME MEASUREMENT

EPOCHS

U EPOXY COMPOUNDS

EPOXY COMPOUNDS

Axial and traction loaded boron epoxy laminates tensile and compressive elastic properties and strengths compared from test data including strain gage measurements
03 p0586 A70-13115

Epoxy-phenolic coatings effect on fatigue durability of bent steel samples
08 p1587 A70-21075

Glass-epoxy composites failure mode dependence on matrix characteristics and fiber orientation, observing flexural strength increase with strain rate
10 p1908 A70-25174

Boron epoxy composite structural parts for aerospace vehicles, discussing production times and cost reduction
12 p2240 A70-27076

Reinforced epoxy models as precursor to prototype design and analysis of aircraft structures, discussing stress analysis methods
12 p2318 A70-27129

Rigid one component epoxy foam system mechanical, electrical and thermal properties for foamed-in-place electronic potting and encapsulation
13 p2439 A70-29263

Epoxy ring reactivity and crosslinking related to adjacent electrophilic and electronegative groups, considering epoxy resin technology
16 p2936 A70-33357

EPOXY RESINS

Graphite fiber-epoxy resin composites interfacial bonding, describing various surface treatments for increased interlaminar shear strength
01 p0127 A70-10477

Stress-strain state of epoxy resin plates with single or paired wire reinforcement, using polarization-optical method
02 p0384 A70-11664

Reinforced epoxy resin performance prediction from correlation between unfilled resin and laminates mechanical properties
02 p0322 A70-12606

Interlaminar shear stress and fabrication of high modulus graphite-reinforced epoxy matrix composites
03 p0515 A70-13119

Electron bombardment effects on epoxy based textolites mechanical properties, studying structural changes spectroscopically
03 p0516 A70-13735

Buckling of toroidal shells with reasonably uniform thickness distribution manufactured by casting epoxy resin material
04 p0779 A70-15615

Tetrabromophthalic anhydride (TBPA) in polyester and epoxy resins, studying fire retardant capabilities by comparative combustion tests
05 p0811 A70-16584

Boron-epoxy composite materials for secondary and primary aircraft structural components, discussing multidirectional laminates, joint analysis, etc
05 p0942 A70-16620

Fabrication and properties of carbon fibers and carbon fiber reinforced epoxy resins
07 p1318 A70-19772

Cycloaliphatic epoxy resins for glass and carbon fiber reinforced plastics and laminates
07 p1318 A70-19773

Tensile strength test and clamping of epoxy impregnated fiber strands
07 p1250 A70-19959

Fatigue tests to relate boron-epoxy laminate fatigue behavior to thermal preconditioning environments
07 p1320 A70-19960

Performance characteristics of low density epoxy-water emulsion corrosion resistant coating for nonferrous alloys
08 p1526 A70-20648

Mechanical properties characterization of unidirectional high modulus carbon fiber reinforced epoxy matrix composite
08 p1530 A70-21883

Test standards for boron epoxy flat laminates, proposing specimen geometries and testing methods
08 p1530 A70-21887

Adhesion characteristics in composites, investigating correlation between short beam and torsion shear tests in glass and graphite reinforced epoxy materials
08 p1531 A70-21892

Fiberglass-epoxy laminates mechanical behavior under biaxial loading, describing test equipment and procedures
08 p1532 A70-21904

Failure mode in shear loaded graphite filament reinforced epoxy composites dependent on interfacial bond strength
08 p1533 A70-21915

Antifriction reinforced plastics based on polyamide fibers in epoxy phenolic resins, determining optimum ratios to obtain desired mechanical properties
09 p1710 A70-23675

Epoxy glass fiber composites pyrolyzates IR spectra as function of time, observing changes in fingerprint region
10 p1828 A70-24065

Transient and steady state thermal stress distribution measured by strain gages embedded in epoxy models
11 p2130 A70-25585

Glass epoxy cross ply laminates with brittle or ductile epoxy matrices tensile tested, comparing mechanical performance
11 p2068 A70-25686

Elastic moduli and damping coefficients for glass- and boron-epoxy beams determined from resonant frequencies and bandwidths during lateral forced vibrations
12 p2253 A70-27120

Stress-strain state of epoxy resin cylinder situated in centrifugal force field using three dimensional photoelastic method
12 p2323 A70-27340

Syntactic foam material of hollow carbon microsphere fillers embedded in high compression strength epoxy resin matrix
13 p2437 A70-28780

Versamid cured epoxies time-dependent mechanical properties, determining loading mode, strain level and reinforcing agent effects on time-temperature shift factors
13 p2438 A70-29205

Epoxy resin with low shrinking effect for encapsulation of electronic components by flexibilizing procedure
13 p2439 A70-29262

Thermal degradation of anhydride-cured epoxy resin by carbon dioxide laser heating through platinum crucible
15 p2695 A70-32828

Epoxy ring reactivity and crosslinking related to adjacent electrophilic and electronegative groups, considering epoxy resin technology
16 p2936 A70-33357

Chemical structure and room temperature tensile, flexural and compressive properties of metaphenylendiamine cured castings for graphite fiber reinforced epoxy resin matrices
16 p2936 A70-33358

Cycloaliphatic epoxy resins tensile and impact strength improvement by modification with elastomeric materials, considering heat distortion temperature
16 p2936 A70-33359

Epoxy laminating resin evaluation for tooling industry, considering diluent, fillers, thixotropy, hardeners and physical property testing
16 p2936 A70-33360

Cold forming of thermoset-thermoplastic laminate consisting of reinforced epoxy core sandwiched between thermoplastic face sheets
16 p2916 A70-33362

Syntactic foams of high filler content, low density, high compression strength and hydrolytic stability using hollow carbon microspheres in epoxy resin matrix
16 p2936 A70-33365

Foamed in place epoxy resins in aircraft composite structures
16 p2937 A70-33369

Fiber reinforced prepreg properties measurements in high modulus graphite/epoxy and fiberglass/epoxy prepreg sheets and tapes
16 p2938 A70-33386

Beta transition mechanism dynamic mechanical properties in bisphenol-A based epoxy resins prepared with different curatives
16 p2856 A70-33500

Creep and tensile fatigue behavior of notched and unnotched graphite/epoxy composites
16 p2938 A70-33503

Lamellar and fibrous Be-reinforced epoxy resin and metal matrix composites, describing preparation and properties
16 p2939 A70-33693

Boron epoxy composite wing structures design, fabrication and testing
16 p2990 A70-33703

Boron-epoxy stiffener reinforced metal wings, examining structural efficiency of multiweb beam aluminum cover skins and Z stiffened panels
16 p2994 A70-34230

Graphite-epoxy resin cross-ply composites fabrication, analyzing residual thermal stresses role in cracking
18 p3279 A70-36828

Stress-strain state of epoxy resin plates with single or paired wire reinforcement, using polarization-optical method
19 p3547 A70-38438

One-component rigid epoxy foam system suitable for lightweight electronic potting, determining mechanical, electrical and thermal properties
20 p3652 A70-39167

Cycloaliphatic epoxy resins toughness improvement by modification with elastomers, maintaining high heat distortion temperature
21 p3842 A70-40733

Epoxy and polyurethane adhesives stress-strain behavior in lap joints, examining bond thickness and cryogenic temperature effects
21 p3844 A70-42139

Deformational characteristics of unidirectional glass epoxy composites with ductile and brittle matrices evaluated in flexure
22 p4059 A70-43101

Glass-epoxy composites, measuring embedding filaments effect on time-temperature relationship under ultimate stress conditions
22 p4118 A70-43549

Boron-epoxy composites rectangular reinforcing arrays spacing aspect ratios, considering matrix stress concentrations and stiffness estimates
22 p4119 A70-43688

Conducting epoxy shielding and bonding efficiency and bulk resistivity at high frequencies for bonding cover onto compartmentalized module
23 p4170 A70-43866

EQUATIONS

Equations for converting satellite geodetic latitude and altitude into geocentric Cartesian system
20 p3669 A70-39691

EQUATIONS OF MOTION

NT EULER EQUATIONS OF MOTION
NT HELMHOLTZ VORTICITY EQUATION
NT HYDRODYNAMIC EQUATIONS
NT KINEMATIC EQUATIONS
NT KINETIC EQUATIONS
NT NAVIER-STOKES EQUATION
NT REYNOLDS EQUATION

Motion equations for vibratory two degrees of freedom spring mass system subjected to rotation, discussing use for small rates of turn measurement
01 p0199 A70-10266

Minor circle maneuver solution to equations of motion of vehicle in spherical planet atmosphere for gliding and cruising, discussing cylindrical planet case
01 p0184 A70-10949

Discrete models formulated for thermomechanical behavior of materials with memory, obtaining equations of motion and heat conduction for finite elements of nonlinear continua
01 p0208 A70-11183

Equations of motion, conservation of mass, momentum and energy for elastic bodies with lattice-type surface defects
01 p0209 A70-11400

Lagrange solution to differential equations of motion of body with fixed point, deriving directrices of mobile and fixed hodograph
01 p0144 A70-11429

Mobile hodograph in problem of gyrostat motion about fixed point
01 p0094 A70-11430

Kharlamova solution for solid body motion in Newtonian force field represented as rolling, without slipping, of mobile hodograph of angular velocity vector
01 p0145 A70-11431

Kharlamova motion equations solution for solid body with fixed point in potential force field, assuming fixed center of gravity
01 p0145 A70-11432

Kharlamov motion equations solution for solid body with fixed point subjected to zero-potential forces
01 p0145 A70-11433

Kharlamov conditions for existence of linear and quadratic invariant relationships between equations of motion of body about fixed point
01 p0145 A70-11435

Canonical equations of motion of heavy solid body with fixed point
01 p0145 A70-11436

Motion of body with fixed point reduced to single second-order differential equation, analyzing special cases of gyrostatic motion
01 p0145 A70-11437

Mass point motion in inertial reference system of special relativity, finding motion equations analogous to relative motion equations in classical mechanics
01 p0145 A70-11442

Motion equations of material point in general relativity theory found analogous to equations in classical mechanics for metric in introduced physical space
01 p0146 A70-11443

Lagrange and Hamilton equations of motion of mass point in physical space of general theory of relativity based on least action principle

01 p0146 A70-11444

Integration time reduction for equations of motion of vehicle center of mass during parabolic reentry, using Runge principle

01 p0134 A70-11483

Motion stability over finite interval of time for perturbed mechanical systems

01 p0146 A70-11560

Final motions of Hamiltonian conservative systems, analyzing Liouville type, homogeneous and similar systems

01 p0146 A70-11561

Observation process optimization in system described by linear differential equations of motion reducible to optimal control problem

01 p0047 A70-11574

Flexural and longitudinal waves propagation in infinite elastic plate, using solutions to approximate nonlinear equations of plate motion

01 p0213 A70-11634

Aerodynamic derivatives in equations of motion governing aircraft longitudinal short period motion estimated using least squares methods

02 p0224 A70-11866

Temperature fields and universal motions in homogeneous isotropic thermoelastic body in absence of body forces and external heat supply

02 p0387 A70-12000

Mean velocity and mean turbulent energy field methods of calculating boundary layer behavior based on numerical solutions of equations of motions

02 p0285 A70-12349

Finite difference solution of compressible turbulent boundary layer equations of motion, using eddy viscosity concept

02 p0286 A70-12353

Soviet book on rocket motion and flight theory covering equations of motion, launching and flight optimization, data acquisition and correction, etc

03 p0579 A70-12872

Vibrational response of simply supported and clamped circular plates subjected to gyroscopically induced inertia loads, using equations of motion

03 p0583 A70-12920

Optimal strategies for controlled plant guidance into convex space assuming linear differential equations of motion

03 p0459 A70-13339

Stability criteria for first approximation solutions of nonlinear ordinary differential equations of motion

03 p0524 A70-13431

Statistical equation of motion of blood by averaging motion of individual blood elements over small volume, finding constitutive equations

03 p0434 A70-13572

Spectral energy transfer measurements in isotropic grid turbulence to determine validity of dynamical equation

03 p0468 A70-13785

Finite difference method applied to solving equations of motion for computing natural torsional vibration frequencies of pretwisted cantilever beams

03 p0595 A70-13811

Time of establishment of steady state mixing in plane and axisymmetrical jets determined, using self similar motions in unsteady state boundary layer and free turbulence

03 p0409 A70-13875

Elliptic restricted three body problem singularities dynamical meaning and character, presenting regularization transformations for equations of motion

03 p0576 A70-14074

MHD laminar flow between parallel porous disks for large suction Reynolds number, solving equations of motion with singular perturbation technique

03 p0469 A70-14181

Relative satellite motion equations derived in generalized parameters, obtaining expressions for coefficients of correcting impulses sensitivity to measurement errors

04 p0760 A70-14430

Boundary layer equations of motion linearized with self similar profiles

04 p0665 A70-14482

Light pulses propagation in nonlinear laser medium, obtaining equations of motion for density matrix

04 p0700 A70-14687

Linear stress distribution insertion into equations of motion for turbulent boundary layer, considering velocity profile in wall region

04 p0670 A70-14987

Nonlinear wave propagation in relaxing gas with internal energy characterized by translational and internal temperature, using model equation for piston induced motion

04 p0786 A70-15324

Approximate time solutions to light aircraft projectiles velocity, altitude angles, gravity drop and downrange, reducing differential equations of motion to dimensionless forms

04 p0764 A70-15592

Motion equations of rigid vehicle derived in terms of body axes noncoinciding with mass center applied to ships and aircraft

05 p0881 A70-15883

Nonlinear dynamic model of regular system of interacting deformable bodies, deriving motion equations for nonlocal and local model

05 p0928 A70-16023

Materials in spatial motion criteria of stress power positiveness

05 p0929 A70-16069

Dynamics theory of displacement on basis of equations of motion solution by stress functions

05 p0931 A70-16133

Von Zeipel method applied to stellar three body problem, eliminating short period terms and establishing two integrals of motion

05 p0909 A70-16337

Nonlinear equations for TWT derived allowing for electron beam defocusing and slow wave structure deposition current

05 p0823 A70-16887

Inertial parameters and functions of dissipative and restoring forces in quasi-linear oscillatory system determined from free motion characteristics

05 p0884 A70-16951

Dynamic characteristics from equations of motion of gyroscope with allowance for structural damping forces between inner gimbal and rotor

05 p0852 A70-16961

Numerical integration of equations of motion of three dimensional laminar compressible boundary layers

[DVL-915] 06 p1033 A70-17229

Equations of motion for hypersonic friction layers integrated using quadrature procedures

[DVL-913] 06 p1033 A70-17230

Variable stars, discussing equation of motion for envelope structure properties and determining oscillation energy change rate from linear theory

06 p1138 A70-17309

Wave functions of asymmetric gyroscope in rotating coordinate system, presenting quantum equation of motion solution

06 p1105 A70-17500

Linearized MHD equations for motion of solids in viscous and electrically conducting fluids

06 p1120 A70-17532

Longitudinal vibration equations of beams for nonlinear stress-strain relation reduced to equivalent linear partial differential equations

06 p1106 A70-17863

Gyrostatt satellite equilibrium positions in circular equatorial orbit under action of gravitational magnetic and aerodynamic moments based on gyrostatized satellite equations of motion

06 p1155 A70-17884

Mechanical behavior of cylinders with alternating layers of reinforcing and matrix materials derived from governing equations, including equations of motion

[AIAA PAPER 70-134] 06 p1169 A70-18051

Flexible spacecraft equations of motion derived by modeling as rigid central body with arbitrary subsidiary flexible bodies

[AIAA PAPER 70-19] 06 p1157 A70-18116

Mass loss rates for short period comets from non-gravitational terms in equations of motion, paying particular attention to secular variations

06 p1151 A70-18490

Routh theorem and Chetaev method for construction of Liapunov function to investigate steady state motions, obtaining stability conditions

07 p1332 A70-18677

Nonlinear pursuit problem solution taking into account drag and lift in pursuing object equations of motion

07 p1330 A70-18682

Error analysis for pendulum type gyrocompass with indirect correction during irregular rolling, taking into account second infinitesimal order terms of equations of motion

07 p1278 A70-18735

Three body problem involving sun and perturbing and perturbed planets, examining perturbed motion equations of Brouwer and Encke methods

07 p1374 A70-18773

Inertial acceleration in relative motion of two bodies subjected to external forces, basing equations of motion on rotating coordinates

07 p1375 A70-18890

Rocket rectilinear motion, comparing Meshcherskii and Gantmacher-Levin equations in light of contact interaction hypothesis

07 p1392 A70-19087

Gyrocompass with sensitive element mounted on horizontally stabilized platform and aligned with meridian by applied correcting moments, deriving equations of motion

07 p1282 A70-19532

Differential equations of motion for sensitive element of gyrocompass with torsional suspension under small amplitude spatial vibrations, taking into account torsional and flexural rigidities

07 p1282 A70-19534

Penetrative thermal convection stability for statically unstable layer surmounted by statically stable layer from numerical integration of linearized equations of motion and heat conduction

07 p1269 A70-19947

Exact solutions class of nonlinearized equations of motion of adjustable two rotor gyrohorizon compass

07 p1288 A70-20176

Natural axisymmetric vibrations of cylindrical shell with hollow filler, analyzing motion by shallow shell and elasticity theory dynamic equations

07 p1415 A70-20191

Heavy solid body motion about stationary point at small nutation angle, estimating region of series convergence representing periodic solutions to motion equations

07 p1336 A70-20298

Mass point motion in celestial mechanics, investigating two and three body problems without equal counteraction assumption

08 p1565 A70-20562

Soviet monograph on inertial methods of flight vehicle motions parameters measurement

08 p1540 A70-20692

Matter distribution and motion in conformally flat gravitational fields, analyzing Friedmann solution to Einstein equations

08 p1544 A70-20991

Stability of continuously differentiable functions representing approximate solution to system of differential equations of perturbed motion

08 p1545 A70-21167

Spherical pendulum equations of motion solved using Hamilton-Jacobi theory

08 p1546 A70-21465

Minimization of motion deviation from prescribed motion as differential game of converging motions using equations of motion

08 p1546 A70-21626

Equations of motion of holonomic and non-holonomic mechanical systems obtained by displacement operators

08 p1546 A70-21627

Motion of body with cavity completely filled with viscous fluid about center of mass in potential mass-force field, applying small parameter method

08 p1546 A70-21630

Differential equations of motion for body with stationary point, allowing for Kovalevskia conditions and assuming nonzero gyrostatic moment

09 p1726 A70-22149

Motion equations and decay of rotating equal mass triple systems for random configuration integrated numerically on computer

09 p1751 A70-22160

Plastic bodies plane flow Lagrangian description applied for prescribed deformation path of material fibers

09 p1769 A70-22251

Planetary satellites perturbation by sun for elliptical solar orbit, applying Zeipel method to equations of motion

09 p1754 A70-22480

Solar system planetary mean motions calculation from characteristic equations roots at equilibrium points of restricted three body problem, using Taylor series solution

09 p1760 A70-22915

Motion equations and dynamic lateral stability of towed glider in steady horizontal flight treated by small perturbations method, including design and handling influence

09 p1611 A70-23063

Equations of motion integration for solid body in potential forces field induced by elastic springs

09 p1728 A70-23386

Laminar boundary layer with blowing through wedge surface, solving linearized motion equation analytically

10 p1862 A70-23868

Spherical isotropic shells motion equations solved in terms of associated Legendre functions, considering surface loads and body forces

10 p1953 A70-23876

Transfer coefficients calculation for equations of motion of medium, presenting mathematical experiment requiring molecular interactions only

10 p1919 A70-24157

Elastic shaft with central unbalanced disk, deriving equation of motion for rotation in flexible bearings

10 p1958 A70-24520

Compressible flow equations of motion applied to incompressible fluid flow through nozzle with eddies and springs

10 p1871 A70-24796

Crack development in solid body, considering condition at crack tip not derivable from equation of motion and strain equation

10 p1960 A70-25007

Equations of motion, modal vectors and natural frequencies of n-degree of freedom structurally damped linear system determined directly from test data

10 p1961 A70-25058

Linearized equations of motion solved for stability of dual spin satellite with two dampers, comparing to Floquet analysis

[AIAA PAPER 70-431] 11 p2120 A70-25440

General aviation aircraft fixed-base engineering flight simulator involving use of analog computer, discussing equations of motion and aircraft cockpit [SAE PAPER 700235] 11 p2031 A70-25904

Static longitudinal stick free and stick fixed aircraft stability equations for several configurations and power effects

[SAE PAPER 700238] 11 p1981 A70-25907

Invariant transform of motion and continuity equations for steady three dimensional flows of compressible fluids in absence of massive forces

11 p2041 A70-26598

Nonlinear dynamic theory describing elastic Cosserat curves plane motion, developing linear displacement equations and dynamic stability concept

11 p2142 A70-26632

Natural frequencies of thin cantilever cylindrical shells, using Flugge equations of motion and Rayleigh-Ritz method

11 p2146 A70-26704

Equations of motion for dynamic stability of flexible freely spinning Alouette-type satellite with crossed dipole configuration

12 p2312 A70-27194

Rigid and stretch yo-yo device equations of motion for despinning rotating rigid body derived for two and three dimensional model

12 p2271 A70-27228

Differential equations of motion of manometers in log instrument systems with allowance for viscous liquid in sensor and pulse line

12 p2234 A70-27567

Controlled missile reentry trajectory through dense atmosphere, describing digital computer solution of differential equations of motion

12 p2314 A70-27768

Aerodynamic coefficients from observed motion of body in flight, eliminating need for closed form solutions by employing numerical solutions to equations of motion

[AIAA PAPER 69-134] 12 p2156 A70-27824

Computing optimum flight profiles by Balakrishnan epsilon method, including equations of motion constraint in cost function to be minimized

[AIAA PAPER 69-75] 12 p2162 A70-28088

Turbulent flow of incompressible fluid, obtaining closed system of approximate equations for probability distribution of velocities

12 p2213 A70-28237

Sphere supersonic motion in combustible gas mixture of given temperature and pressure, discussing constant density two front detonation wave model

12 p2334 A70-28242

Rendezvous trajectory control problems solution by regularization techniques, emphasizing equations of motion in gravitational field

13 p2446 A70-28380

Relative satellite motion equations derived in generalized parameters, obtaining expressions for coefficients of correcting impulses sensitivity to measurements errors

13 p2503 A70-28455

Vinti potential with spheroidal coordinates for equations of motion in earth satellite orbit computation

13 p2486 A70-28503

Wind-launch vehicle interaction in flight, using equations of motion for aerodynamic loads

[AGARDGRAPH-115] 13 p2504 A70-28756

Stability of single periodic symmetrical solutions of plane circular restricted three body problem, using digital computer for numerical integration of equations of motion

13 p2490 A70-28950

Rotating spherical galaxy evolution, using equations of motion for mass points representing mass distribution

13 p2492 A70-29385

Supersonic rigid cone motion in elastic medium, obtaining partial solutions to motion equation yielding boundary problem solution

13 p2341 A70-29508

Material system equations of motion, determining programmed motion variable mass systems stability

13 p2453 A70-29717

Time dependent simultaneous solution for continuity, heat conduction and motion equations of system involving neutral, electron and ion gases

14 p2665 A70-30744

Soviet book on multivariable automatic control systems analysis and synthesis covering equations of motion, nonlinearities, pulse control, transient responses, etc

14 p2561 A70-30954

Single mode gas laser theory for arbitrary field intensities in terms of ensemble averaged form of density-matrix equations of motion

14 p1594 A70-31361

Natural vibrations frequency of tubular cantilever pipe with fluid flow, solving differential equation of motion by Ritz method

14 p2567 A70-31426

Routh theorem and Chetaev method for construction of Liapunov function to investigate steady state motions, obtaining stability conditions

15 p2774 A70-31469

Relay stabilization system for flight vehicle motion about center of mass, using point transformations method and bifurcations theory

15 p2674 A70-32151

Mass point motion in celestial mechanics, investigating two and three body problems without equal counteraction assumption

15 p2805 A70-32717

Equations of motion for circular periodic orbits extended to elliptic restricted three body problem

15 p2806 A70-32803

Linearization error bound analysis in solution of equations of motion of reentry vehicle

16 p2974 A70-33319

Quasi-linearization for VTOL aircraft equations of motion, using spline functions for unknown parameters initial estimation

16 p2942 A70-33328

Recurrence scheme for parameter estimation by quasi-linear equations of motion method and Kalman filtering for nonlinear dynamical systems

16 p2887 A70-33349

Rigid body motion about fixed point with angular velocity vector parallel to fixed straight line plane in space and comoving plane

16 p2952 A70-33741

Equations of supersonic and hypersonic motion past circular cone by linearized method based on small perturbations with respect to nearly incompressible flow

16 p2835 A70-33746

Equations of motion and continuity for early and later stages of expanding universe, explaining matter concentration process of galaxy formation

16 p2976 A70-33783

Two body torque free gyrostat equations of rotational motion, relating rotational, spin and precession angular velocities

16 p2912 A70-33877

Vibrational motion equations of interconnected bodies based on Newtonian approach, investigating gyroscopic vibration absorber

16 p2992 A70-34020

Longitudinal wave propagation in variable section bars, solving hyperbolic equation of motion by perturbation method

16 p2993 A70-34088

Nonlinear dynamic systems described by matrix equation, formulating asymptotically stable conditions, discussing motion equations of two degree of freedom system

16 p2995 A70-34281

Nonlinear systems excitation by two harmonic forces, analyzing vibration by linearization of differential equation of motion

16 p2995 A70-34286

Satellite equations of motion in noninertial instantaneous astronomical system, taking into account perturbation equations terms

17 p3155 A70-34684

Independent integrals of perturbed motion equations of spatial gyrohorizon compass

17 p3090 A70-35344

Harmonic oscillator with exponentially decreasing spring constant, obtaining closed form solution for equation of motion

17 p3137 A70-35602

Single axis gyroscopic stabilizer with floating-type integrating gyro, describing natural oscillations by differential equations of motion

17 p3096 A70-35701

Spinning symmetric satellite attitude stability in hyperbolic orbit on flyby mission, examining by numerical integrations of equations of motion

17 p3181 A70-35753

Motion perturbation equations for guided space vehicles, allowing for sloshing liquid propellant viscosity effects

18 p3332 A70-36160

Quasi-equilibration of static or dynamic universal solutions of compressible or incompressible simple bodies, investigating homogeneity of symmetry and objectivity conditions

18 p3336 A70-36221

Two dimensional reverse trajectory reaction and mass behavior for motion of material point with changing mass, using Mesherskij equation

18 p3283 A70-36401

Thermodynamical modeling by regular systems of deformable bodies bound by hyperelastic medium with internal degrees of freedom, formulating equations of motion

18 p3338 A70-36432

Significant terms in equations of motion for parachutes inflating in free air and in wind tunnel experiments

[AIAA PAPER 68-924] 18 p3213 A70-36449

Nonperturbability conditions and equations of motion of bigyroscopic vertical below escape velocity

18 p3259 A70-36592

Integrals of motion for minimum fuel rocket trajectories in inverse square field calculated for constant power and constant exhaust rockets

18 p3316 A70-36678

Nonrigid satellites dynamical equations derivation in modeling by generalized coordinates

18 p3333 A70-36702

Shock function response and Fourier spectra relationship, using Fourier transform for equation of motion solution

19 p3456 A70-37381

Variational principle application to relativistic MHD, deriving Einstein field equations, Maxwell equations and equations of motion for self gravitating charged fluid

19 p3478 A70-37591

Conducting gas channel and jet flow in electric and magnetic fields, using linearizing equations of motion under assumption of small magnetic Reynolds number

19 p3479 A70-37598

Sandwich panels geometrically and physically nonlinear theory, obtaining equations of motion and boundary conditions consistent with strain displacement relations

19 p3547 A70-38360

Stars and stellar gas motions interaction equations, analyzing plasma and gravitation problems

19 p3525 A70-38771

Liapunov stability analysis of dynamic systems described by simultaneous ordinary and partial differential equations of motion, applying to satellite spin stabilization

[AIAA PAPER 70-1045] 19 p3472 A70-38860

Closed form approximate solution for restricted three body motion of lunar or interplanetary spacecraft, demonstrating accuracy and flexibility in lunar mission trajectory calculations

[AIAA PAPER 70-1061] 19 p3529 A70-38875

High energy charged particles equations of motion in quiet interplanetary magnetic field for primary cosmic ray distribution, calculating diurnal and semidiurnal variations

20 p3698 A70-39297

High velocity gas motion in laminar boundary layer, describing universal motion equations two parameter solution

20 p3611 A70-39805

Invariant systems structural synthesis for automatic control of plant motion, deriving control laws for thrust and angle of attack

20 p3670 A70-39844

Mechanical behavior of cylinders with alternating layers of reinforcing and matrix materials derived from governing equations, including equations of motion

20 p3732 A70-40267

Bubble motion in ideal incompressible fluid, deriving motion equation in low viscosity fluid

20 p3614 A70-40392

Neutral atmosphere continuity equation of ionization and equation of motion in F 2 region for different seasons in various solar activity epochs

20 p3623 A70-40478

Perturbed motion linear equations of body rigidly coupled to thin walled elastic shell partially filled with heavy compressible fluid

21 p3806 A70-40602

Equations of motion of mass points connected by inertialess elastic couplings

21 p3933 A70-40615

Kinematic interpretation of body motion in Hess solution, discussing axoid vector rolling without slip

21 p3849 A70-40617

Motion equation of electron in cylindrical diode subjected to varied voltages

21 p3796 A70-40640

Viscous fluid motion equations through anisotropic nonrigid porous solid, discussing blood flow in capillary vessels and extracellular fluid through interstitial space

21 p3768 A70-40776

Relativistic observer in rotational motion relative to inertial observer, imposing velocity onto perfect relativistic fluid

21 p3851 A70-42096

Computerized evaluation of Krook kinetic relaxation equation approximating Boltzmann nonlinear integral equation for rarefied gas motion

21 p3851 A70-42201

Circular plates dynamic stability under variable periodic loads, using differential equations of vibrational motion for median surface

22 p4114 A70-42613

Macroscopic equations of motion established by Maxwell transport equations for relativistic perfect gas

22 p4011 A70-42716

Differential rendezvous game theory with non-separated control inputs on right side of equations of motion applied to guidance problem

22 p4063 A70-43346

Hamilton-Jacobi theorem for nonlinear dynamic system moving with holonomic Cetaev constraints, investigating necessary and sufficient conditions

23 p4210 A70-44024

- Differential equations of motion for machine assembly, using Appel equations 23 p4200 A70-44319
- Nonlinear equations of motion approximate solution, determining ordnance weapons aerodynamic stability coefficients from angle of attack [AIAA PAPER 69-135] 23 p4133 A70-44515
- Tornado vortex motion equation derivation based on kinematical modification of Kelvin theorem 23 p4215 A70-44547
- Two particles relative motion in elliptical orbits in inverse square central force field 23 p4244 A70-44576
- Freely spinning gyrostal satellites with dissipation, deriving rotational motion equations by osculating elements method 23 p4261 A70-44681
- Partially ionized viscous plasma longitudinal wave propagation, formulating motion equations for electrons, ions and neutrals from Maxwell and Boltzmann equations 23 p4229 A70-44987
- Relativistic and nonrelativistic generalizations of classical approach in quantum mechanics applied to equations of motion in electromagnetic field 24 p4378 A70-45275
- Numerical integration of equations of motion from finite element analysis in structural mechanics, using computer program 24 p4420 A70-45278
- Continuous structural systems stability under random load excitation from linear partial differential equations of motion 24 p4421 A70-45281
- Boundedness theorem for nonlinear Mathieu equation describing motion of parametrically excited system 24 p4380 A70-46042
- EQUATIONS OF STATE**
- NT HUGONOT EQUATION OF STATE
- Statistical mechanical method deriving ionization equilibrium and equations of state for low mass stars, considering Coulombic interactions, nonideal effects, etc 01 p0188 A70-11336
- Equations of state for continuous media, using variational principles within framework of relativity theory 01 p0146 A70-11593
- Oxides and silicates universal equations of state based on experimental data including elastic properties, density, mean atomic weight relations and geophysics interpretations 02 p0294 A70-12778
- Thermodynamic potential of meson-nucleon plasma, showing variation of Landau equation of state in hydrodynamic theory of multiple particle production 03 p0527 A70-13052
- Equation of state for neutron, proton and electron gas mixture associated with cold matter above white dwarf densities and below nuclear density 05 p0905 A70-15756
- P-v-T-x relationships determination method for gaseous mixtures at high pressures and temperatures, studying He-nitrogen mixtures compressibility 07 p1420 A70-19205
- Critical regions equilibrium thermodynamic properties of fluids and magnets using scaled equation of state 07 p1421 A70-19298
- Neutron stars equation of state derived, suggesting three body forces inclusion at high densities 07 p1388 A70-19924
- Transformed thermodynamics equations derived automatically by substitution codes, noting exceptions for real gas and discharge flow 08 p1597 A70-20918
- Thermodynamic properties of real gases estimated using Hirschfelder equation of state 08 p1598 A70-21363
- Self gravitating bosons or fermions equilibrium configuration in ground state, confirming Oppenheimer-Volkoff treatment approximation 08 p1581 A70-21741
- Gravitating bodies quasi-stationary rotating systems, giving equations of state and evolution 09 p1753 A70-22457
- Equation of state for cold matter at neutron star densities, deriving equilibrium equations for nuclear interactions among hadrons 09 p1764 A70-23606
- Neutron star models based on equation of state for cold degenerate matter, taking into account nuclear forces and clustering 09 p1764 A70-23607
- BBGKY hierarchy state functional formalism in nonequilibrium statistical mechanics for many particle system using Fourier transformation 11 p2087 A70-26548
- Book on energy conversion states covering state functions, quasi-static processes, internal energy, chemical energy storage and conversion, dynamics and postulates and laws 12 p2165 A70-27670
- Nitrogen tetroxide thermodynamic properties calculation from pressure-volume-temperature equation of state in gas and liquid phases 12 p2332 A70-27975
- State estimation in linear discrete time systems operating in Markov dependent switching environments, using Bayes theorem for filtering 13 p2381 A70-29062
- Plane stress state equations for micropolar elastic plates using complex potentials 13 p2517 A70-29629
- Operator form added to equations of state of continuous media in case of small and large deformations 14 p2656 A70-30473
- Plane deformation of anisotropic plastic nonstrain-hardenable material, analyzing state equations for stresses and strain rates 15 p2818 A70-32184
- Aircraft vertical channel landing condition autopilot using state variable feedback control techniques 15 p2773 A70-32553
- Equation of state of solids measured by shock wave techniques, considering elastic-plastic flow in plane wave geometry 15 p2824 A70-32789
- Thermodynamic equations of state for dissociating and ionizing air in equilibrium, noting applications to vertical and oblique compression shocks [DGLR-70-026] 15 p2828 A70-32840
- Neutron core star models based on realistic nuclear matter calculations and hyperons equation of state 17 p3157 A70-34844
- Equation of state of nuclear neutron matter as function of density 19 p3524 A70-38695
- Neutron stars, discussing equations of state and stellar interiors, models, atmosphere, cooling, vibration, rotation and magnetic fields 20 p3706 A70-39932
- Stable hyperon star existence in general relativity, discussing state equations for baryon matter, radial pulsation and superlumina and ultrablastic conditions 21 p3888 A70-41116
- Friedmann universe evolution after big bang via Hagedorn hadronic equation of state, noting primordial He abundance criterion 21 p3888 A70-41122
- Mechanical behavior differential equation representation in presence of finite deformations using state variables 21 p3937 A70-41434
- Self similar flow instability behind collapsing cavity boundary, examining perfect gas adiabatic equation of state 21 p3808 A70-41500
- Book on state variable solution techniques for homogeneous and inhomogeneous Fredholm integral equations in communication theory, discussing application to linear estimation theory 21 p3846 A70-41791
- Viscoelastic liquids state equations, surveying various fluid models 22 p4009 A70-42541
- M phase thyristor amplifier operation, investigating state and transition equations by state variable methods 22 p3996 A70-42918
- Linear distributed parameter systems state estimation from noisy measurements, developing sequential algorithms for prediction, filtering and smoothing 22 p4063 A70-43026
- Thermodynamic properties, tables and equations of state of liquid para hydrogen from liquid-gas and liquid-solid phase equilibria 23 p4220 A70-44434
- Perfect gas statistical relations by perturbation form of state equation for atmosphere 24 p4372 A70-46071
- EQUATORIAL ELECTROJET**
- Electrostatic drift-dissipative plasma instability and nocturnal equatorial spread F irregularities, discussing amplification in collision dominated medium 03 p0477 A70-13990
- Equatorial electrojet diurnal variability in intensity, position and width obtained from H records of magnetometers 09 p1747 A70-23495
- Equatorial geomagnetic micropulsations using earth current technique, discussing night and diurnal variations 10 p1875 A70-24435
- Blanketing type sporadic E layer associated with equatorial electrojet as thin layer of enhanced ionization 10 p1880 A70-24801
- Lunar tides relationship with equatorial electrojet currents using daily variations at fixed lunar ages and monthly variations at solar hours of horizontal magnetic field 11 p2114 A70-26564
- Equatorial electrojet Lorentz coupling to neutral atmosphere as source of long period traveling ionospheric disturbances 13 p2399 A70-29235
- Daily amplitude variability of equatorial electrojet current related to solar extreme ultraviolet radiation /XUV/ influx 15 p2727 A70-31873
- Type 2 irregularities in equatorial electrojet associated with plasma density vertical gradients 18 p3244 A70-36017
- Equatorial electrojet measurements by Nike-Apache rockets 18 p3244 A70-36018
- Geomagnetic latitudinal variations in Sq/H/ and Sq/Z/ in equatorial region, using electric simulation 18 p3246 A70-36099
- Electron drift velocity longitudinal variation in equatorial electrojet, noting land-sea boundary and magnetic anomalies effects 20 p3620 A70-39337
- Morning and evening current reversals in equatorial electrojet, discussing seasonal variation data for refining models 20 p3621 A70-39352
- Equatorial E region electrojet plasma irregularities, discussing electron density, drift velocity, profile structure, etc 24 p4384 A70-45150
- EQUATORIAL ORBITS**
- NT STATIONARY ORBITS
- Global and European geodetic satellite network, discussing San Marco equatorial satellite and observation stations 03 p0581 A70-13829
- Energy optimal osculating elliptical transfer orbit from low eccentricity orbit constructed for prolonged circling in equatorial plane of axisymmetric planet 07 p1374 A70-18774
- Quasi-sinusoidal fluctuations of magnetic field during geomagnetic storms measured by ATS 1 in synchronous equatorial orbit 12 p2223 A70-27192
- Intermediate elliptical orbits for planetary satellites with small inclination to equatorial plane 18 p3312 A70-36174
- Europa III SLV payload for geostationary equatorial orbit, describing engine thrust and propellant capacity for high energy second stage 24 p4414 A70-46357
- EQUATORS**
- NT MAGNETIC EQUATOR
- Solar eclipse effects on equatorial F 2 layer by transient solutions of time dependent continuity equation, calculating electron concentrations 20 p3622 A70-39453
- F region equatorial anomaly formation, investigating vertical EM drift effect 23 p4187 A70-43857
- EQUILIBRIUM**
- Stellar clusters equilibrium state in gravitational field, discussing dispersed clusters formation by gravitational instability in gas containing stars of various ages 02 p0376 A70-12446
- Singular perturbation problem solution asymptotic expansions applied to linearized theory of elasticity equilibrium problem with stress couples 02 p3899 A70-12685
- Limiting equilibrium under axial tension of brittle body with parallel axisymmetric external cracks, studying critical load, crack propagation, etc 03 p0594 A70-13737
- Stability and dynamics of dielectrophoretic equilibria, considering circular cylindrical column of inviscid liquid with rigid body rotation 03 p0525 A70-13784
- Dynamic equilibrium prediction for creep and fatigue of various metals under various loading conditions, using time-temperature and cyclic stress-strain parameters [ASME PAPER 69-WA/MET-9] 04 p0704 A70-14759
- Astatic equilibrium loadings in Saint Venant principle for linear elasticity, analyzing physical distinction from self equilibrated loadings to explain smaller long range stresses [ASME PAPER 69-APM-L] 04 p0769 A70-14860
- De Sitter hydrostatic equations solution possible with help of boundary condition from external potential theory with/without assumed equilibrium in earth interior 04 p0678 A70-15051
- Elastic stability theory applied to equilibrium and stability of discrete continuous structural systems, detailing discrete critical points 07 p1408 A70-19560
- Central equilibrium position stability of gas bearing supported rotor allowing for inertia and lubricant compressibility 08 p1502 A70-20695
- Earth deviations from isostatic equilibrium, showing irregularities dependence on distance from surface for various tectonic zones 08 p1487 A70-20715
- Steady state finite difference solution of equations governing arbitrarily biased bipolar transistor action in two dimensions 08 p1477 A70-21641

- Stable equilibrium of rotor in pressurized gas bearing, considering perturbed rotor motion equation together with Reynolds equations for pressures in lubricant layer 09 p1690 A70-22544
- Book on liquid masses ellipsoidal figures of equilibrium extended into coherent mathematical theory, discussing virial equations, potentials of homogeneous and heterogeneous ellipsoids, etc 10 p1917 A70-24701
- Solid-gas phase equilibria of binary systems related to cryogenics 12 p2329 A70-27023
- Phase equilibria in quasi-ternary alloys by microstructural, thermographic and X ray analyses, showing continuous solid solutions formation in titanium-niobium-titanium aluminide 12 p2258 A70-28275
- Metal surfaces friction and wear processes dynamic equilibrium noting loading conditions effects 13 p2423 A70-29766
- Equilibrium and steady state Hall and thermoelectric effects in inhomogeneous semiconductor materials 15 p2783 A70-31760
- Metal surfaces friction and wear processes dynamic equilibrium noting loading conditions effects 20 p3638 A70-40099
- Krylov-Bogoliubov virtual work principal, investigating nonlinear vibrations, extending to heteronomous vibrations 23 p4266 A70-44028
- EQUILIBRIUM DIAGRAMS**
- U PHASE DIAGRAMS**
- EQUILIBRIUM EQUATIONS**
- Elasticity theory equilibrium equations derivation using distribution theory 02 p0388 A70-12270
- Stress differential equations of equilibrium for thick prolate spheroid (left ventricle), yielding practical values for mean stresses in thick walled ventricles 03 p0434 A70-13571
- Elliptic system of twelfth order equations describing elastic equilibrium of plate with kinematic functions analyzed by integration procedure 03 p0600 A70-14306
- Equilibrium shapes of rotating weightless fluid with surface tension in absence of external force field obtained by boundary layer theory 04 p0673 A70-15241
- Buckling equations for neutral equilibrium of arbitrary elastic shells specialized to uniformly loaded circular cylindrical shell with accuracy 05 p0929 A70-16064
- Static and continuity equations of equilibrium of axisymmetric and periodic stressed states of rectilinear helicoidal shell derived for elasticity relations 05 p0934 A70-16228
- Steady state electrical characteristics of double diffused planar transistor calculated by iterative algorithm under arbitrary bias conditions 06 p1016 A70-17125
- Equilibrium equations solved for statics of double row radial thrust ball bearing, neglecting load angle changes caused by deformations of races and ball bearings 06 p1077 A70-17929
- Thin circular cylindrical shells elastic equilibrium under loads producing deflection, elongation or contraction described by integrating equilibrium equations with constant coefficient 06 p1172 A70-18566
- Soviet book on mathematical physics covering equilibrium equations of vibration, thermal conductance and diffusion with emphasis on Laplace equations 08 p1544 A70-20763
- Linear and nonlinear equilibrium equations for bending deformation of thin elastic cylindrical using Kirchhoff-Love hypotheses 08 p1588 A70-21242
- Cylindrical and flat shells equilibrium equations representation using stress, deflection or tangential displacement functions 08 p1591 A70-21442
- Elastic equilibrium of semiinfinite two dimensional medium with Griffith crack under axisymmetric load and free and rigidly clamped edges 08 p1594 A70-21771
- Boundary problem for displacement equilibrium equations of elastic body using iterative methods, demonstrating convergence of difference equation solution 09 p1771 A70-22467
- Boundary value problem of torsion for equilibrium of elastic body based on moment theory in absence of bulk forces 09 p1782 A70-23381
- Numerical solution of three dimensional equation of elastic body equilibrium in displacements, giving convergence rate of iteration processes 09 p1783 A70-23384

- Equilibrium equations integration for body in isotropic linear viscoelastic medium with contact-type boundary conditions 10 p1957 A70-24267
- Rotating degenerate gravitating fluid cylinders equilibrium configuration 10 p1917 A70-25208
- Equilibrium displacement equations for linear infinitesimal isotropic Cosserat elasticity solved in terms of stress functions 11 p2142 A70-26630
- General relativistic hydrodynamics near equilibrium, discussing velocity and kinetic energy increase spherically symmetric large masses as function of radius change 12 p2300 A70-27392
- Collapsed spherical bodies equilibrium structure, considering density-pressure state equations for cold neutron gas and gas-radiation mixture 12 p2300 A70-27395
- Iteration solution for three dimensional equations of equilibrium of elastic body in boundary displacements, discussing convergence rate and computer applications 12 p2272 A70-27553
- Equilibrium equations for thin multilayer shells with variable thickness, assuming simultaneous work without friction under loads 12 p2325 A70-27556
- Elastic scattering formation and decay of unstable particle gases, discussing density and corrections to chemical and nuclear statistical equilibrium equations 13 p2455 A70-29223
- Thermoelastic equations for circular sandwich plates bending due to asymmetric temperature distribution 13 p2518 A70-29976
- Minimum entropy production at microscopic level, obtaining stationary state by Pauli master equation 14 p2616 A70-30654
- Oscillations and stability of rotating masses for axisymmetric equilibrium configurations with toroidal magnetic field based on virial equations 14 p2642 A70-30886
- Orbiting gyrostats equilibrium orientations under gravitational torques, considering internal angular momentum effects 14 p2655 A70-31364
- Elastic body bounded by parallel planes, solving three dimensional equilibrium problem by eigenfunction expansion of nonself adjoint differential operator 15 p2814 A70-31593
- Elastic equilibrium of unbounded body with central hole and concentric cracks under symmetric load 15 p2819 A70-32188
- Axial flow compressors off-design performance calculation using radial equilibrium equation 15 p2791 A70-32770
- Three dimensional mixed boundary value problems, obtaining solutions for elastic body differential equilibrium equations 17 p3192 A70-35699
- Quasi-equilibration of static or dynamic universal solutions of compressible or incompressible simple bodies, investigating homogeneity of symmetry and objectivity conditions 18 p3336 A70-36221
- Cauchy problem for linearized relativistic Boltzmann equation near equilibrium, using functional analysis 19 p3403 A70-37585
- Buckling equilibrium equations for thick rectangular block under compression loads, noting bifurcation points 19 p3536 A70-37683
- Equilibrium equations integration for body in isotropic linear viscoelastic medium with contact-type boundary conditions 19 p3547 A70-38395
- Gravity effects on impact damper performance, investigating dynamic stability and kinematic viability of various steady state motion solutions 20 p3717 A70-38974
- Equilibrium theory of white dwarfs, neutron and hyperon stars, deriving equations for nonrotating objects composed of degenerate cold electron or neutron gas 20 p3704 A70-39472
- Elastic bodies static stability theory variational principles, introducing equilibrium equations and boundary conditions of initial state by Lagrange multipliers 20 p3724 A70-39857
- Cracked brittle body limiting equilibrium, determining critical loads for two half spaces with various circular rib couplings 20 p3733 A70-40432
- Membrane theory of shells, reducing equilibrium equations to single second order partial differential equation through transformation in terms of stress function derivatives 21 p3939 A70-42031
- Matter and heat balance of cosmic grains surrounded by plasma and neutral gas under radiation 22 p4097 A70-42473

- Stellar envelope physical structure studied to solve equilibrium equation, applying results to stellar model 22 p4097 A70-42545
- Nonlinear shell theory formulated in Lagrangian stress and moment resultants, deriving equilibrium equations 22 p4118 A70-43545
- Plasma physics computational problems concerning controlled thermonuclear reactions, considering instability and equilibrium numerical calculations 23 p4224 A70-44181
- Elastic body bounded by parallel planes, solving three dimensional equilibrium problem by eigenfunction expansion of nonself adjoint differential operator 23 p4268 A70-44286
- Elastic structure equilibrium state stability, discussing damping and stiffening effects 23 p4275 A70-44941
- Truncated spherical shells nonlinear asymmetric buckling calculation from equilibrium equations 24 p4421 A70-45284
- EQUILIBRIUM FLOW**
- NT FROZEN EQUILIBRIUM FLOW**
- Momentum integral method for turbulent boundary layers based on equilibrium profiles family, considering weighting function specification techniques 02 p0284 A70-12345
- Experimentation in fluid mechanics research, discussing equilibrium flows, relaxation processes, turbulence structure and digital techniques 02 p0286 A70-12355
- Time of establishment of steady state mixing in plane and axisymmetrical jets determined, using self similar motions in unsteady state boundary layer and free turbulence 03 p0409 A70-13875
- Numerical analysis of near equilibrium flow regions in chemically relaxing gas mixtures past blunt bodies at supersonic speeds 04 p0666 A70-14603
- Finite difference theory applied to numerical analysis of laminar equilibrium MHD flow in circular tube [ASME PAPER 69-WA/HT-55] 04 p0727 A70-14794
- Equilibrium forms of prolonged rectangular plate in gas flow in terms of nonlinear boundary problem, emphasizing plate with hinged supports 07 p1187 A70-18679
- Near equilibrium transonic flows of reacting gas mixtures based on linearization of thermodynamic and kinetic quantities 10 p1867 A70-24133
- Equilibrium properties of nearly normal turbulence assuming near-Gaussian nonlinear model equations and real turbulence 11 p2039 A70-26533
- Velocity circulation in laminar motion of fluid in cylindrical tube, assuming equilibrium under dissipative forces 14 p2564 A70-30164
- Equilibrium forms of prolonged rectangular plate in gas flow in terms of nonlinear boundary problem, emphasizing plate with hinged supports 15 p2671 A70-31471
- Steady state one dimensional nozzle flow of reacting inviscid gas mixtures, giving numerical solution procedure for hydrogen-oxygen reactions 15 p2694 A70-32269
- Equilibrium air boundary layer flows at three dimensional stagnation points, discussing flow characteristics and real gas heat transfer parameters [AIAA PAPER 70-806] 17 p3005 A70-34455
- Near equilibrium shock layers nonequilibrium radiant emission calculation, noting application to Mars entry conditions [AIAA PAPER 70-773] 17 p3007 A70-34481
- Mean electron density profiles and fluctuations in equilibrium high speed turbulent boundary layers, calculating temperature effects [AIAA PAPER 70-743] 17 p3066 A70-34500
- Reacting gas relaxation with particle sink removing products from system calculating relaxation processes during equilibrium state approach 18 p3292 A70-36291
- One dimensional unsteady equilibrium flow stability of relaxing two phase medium consisting of perfect gas and incompressible liquid 20 p3613 A70-40295
- Equilibrium sonic velocity in reacting gas mixture in nozzle flow for unlimited species and independent chemical reactions 22 p4074 A70-42753
- Equilibrium performance of closed Stirling cycle with chemically reactive gas as working fluid, discussing power density and thermal efficiency 22 p3982 A70-42756
- EQUILIBRIUM METHODS**
- Nonequilibrium and equilibrium schemes studies of nuclear symmetry energy of finite nuclei, discussing binding energy of nuclei with neutron excess 01 p0148 A70-11106
- Astatic equilibrium in Saint Venant principle applied to surface of linear elastic body, discussing stress field produced by boundary loading 08 p1591 A70-21463

Approximations implicit in Cayrel statistical equilibrium or non-LTE analysis of ionic hydrogen bound free continuum in sun

10 p1947 A70-24989

Optimal control theory applied to oligopoly, considering economic problems and Nash equilibrium solutions

15 p2831 A70-32552

Equilibrium theory of finite deformation of elastic solids, discussing applications and approximate solution methods

18 p3335 A70-35975

Brittle bodies with sharp pointed defects, constructing limiting equilibrium diagrams by stress concentration factor representations

20 p3733 A70-40393

Laminar circular cylindrical shells supersonic flutter characteristics determination by dynamic equilibrium boundary value problem eigenvalues analysis, obtaining critical flutter speeds

24 p4424 A70-45588

EQUINOXES

Diurnal and seasonal variations of sporadic E layer observed at ionospheric station

14 p2568 A70-30134

EQUIPMENT

Soviet collection of papers on equipment working with alkali metals covering turbines, level meters, hydraulic coupling, etc

14 p2534 A70-31007

EQUIPMENT SPECIFICATIONS

Respiratory mass spectrometer design specifications, considering sampling and vacuum systems

01 p0041 A70-11649

Airborne instrument landing systems and ground facilities analysis and specifications, examining future use of microwave frequencies

02 p0333 A70-11982

ELDO-PAS apogee motor prequalification test to determine specifications for constructing units for qualification testing

03 p0581 A70-13854

Electrical and mechanical characteristics and specifications of second parabolic reflector antenna at Pleumeur-Bodou space communications center

05 p0819 A70-15982

Microwave transistor amplifier design and specifications, discussing applications and economy in design, production and use

06 p1018 A70-17358

Selection criteria for nonturbobcharged air or liquid cooled reciprocating type prime movers used in aircraft ground support equipment

07 p1248 A70-18801

Civil air transport passenger escape devices design and installation criteria

07 p1191 A70-18805

Propellant transfer unit for weapon or space vehicle systems, specifying aerospace ground equipment criteria

07 p1248 A70-18806

International air traffic jurisdictional area of German aeronautical law regarding aircraft equipment regulations and residents

07 p1427 A70-18886

Specification of minimum performance standards and test procedures for automatic pressure altitude digitizer equipment

07 p1279 A70-18901

Air-land demountable cargo containers specifications, establishing dimensional, structural and environmental requirements

07 p1249 A70-19599

High precision strain gage installation, discussing specifications and errors caused by oblique load action, natural frequency and deformation

08 p1493 A70-20585

U.S. cryogenic refrigerators specifications in tabular form

09 p1655 A70-22291

Quality information equipment engineering including specifying, development, design, procurement, construction, installation, checkout, etc

09 p1792 A70-22569

Specifications nomographs for earth resources IR radiometers, considering ground resolution, aperture diameters, detector arrays, etc

09 p1677 A70-22870

Radio marker beacon-receiver design, tabulating technical data

09 p1684 A70-23574

Tolerance limits for equipment periodic field checkout, considering performance failure effects on system accuracy, costs and availability

10 p1896 A70-24911

Flight test instrumentation specifications for V/STOL aircraft, considering design, installation and accuracy

10 p1892 A70-24927

Computerized data communication system /CDCS/ equipment unit capacities and topology specified with aid of vertex weighted linear graph

11 p2009 A70-26253

Equipment specifications and design for creep testing at variable load and temperature under uniaxial tension, emphasizing test environment control

13 p2509 A70-28537

Automatic test equipment third generation specifications and design

13 p2525 A70-29682

Sequential circuit specification in terms of input/output pair strings, allowing programmed translation algorithm for automation of flow table construction

15 p2711 A70-32605

Practical electronic components criteria accommodating reliability engineer and circuit designer

15 p2832 A70-32653

Microwave transistors parameters measurement by scattering /S/ parameter method for characterizing noise, gain and dynamic range, reading input and output impedances from Smith chart

19 p3386 A70-37692

Collision avoidance system flight test and evaluation program for airline industry CAS specification

19 p3466 A70-38240

Portable telescope for river and ocean vessels, discussing design and operation thermal stability and hermetization

20 p3629 A70-39311

Thermal radiation detectors operation principles, design, specifications and applications

20 p3632 A70-39626

Silicon solar cell specifications and cost reduction without output or reliability loss

21 p3756 A70-41008

Power conditioning requirements and specifications for spacecraft electric propulsion ion thruster

21 p3758 A70-41209

High power gas lasers constructed in Poland, describing structural design and operational specifications

22 p4051 A70-43441

Apparatus characteristics determination for ultrasonic inspection, recommending calibration block

22 p4041 A70-43622

Specification sheets for fluidics clarified by demonstrating step-by-step solutions for typical problems involving flip-flop and OR/NOR gate

24 p4293 A70-45431

EQUIPOTENTIALS

Large spacecraft in circular earth orbit calculated for internal gravitational field

05 p0924 A70-16637

Theory for describing rotating fluid planets external geometry in state of hydrostatic equilibrium, noting role of equipotential surfaces

06 p1153 A70-18559

EQUIVALENCE

Equivalent linear dynamic systems obtained by analog computers for determining equivalence equations coefficients and by Chebyshev functional to assess discrepancy

01 p0052 A70-10193

Equivalence class technique to compute measure of similitude between two vehicles based on radar signature in terms of scattering matrix elements

04 p0648 A70-14656

Nonlinear differential equations approximate periodic solutions generation by finding equivalent system in sense of minimum mean square difference

09 p1712 A70-22666

Time-invariant linear dynamical systems transfer equivalence leading to algorithm for minimal realizations of transfer function matrices

11 p2072 A70-26161

Kinetic synthesis for multivariable system by asymptotic equivalence method

16 p2944 A70-34279

Functional equivalence between FS expression and programs

17 p3130 A70-35139

Rank permutation codes equivalence to binary code class capable of generation and detection through direct and inverse transformations respectively

20 p3594 A70-39975

EQUIVALENT CIRCUITS

Equivalent circuit for trapped energy resonators and calculations of capacitances ratios for straight crested waves

01 p0088 A70-10777

Nonlinear vibrations in mechanical systems of elastic components having equivalent circuits represented by finite number of discrete masses interconnected by weightless infinite rod

01 p0143 A70-11027

Polar geomagnetic disturbances global current systems representation by prototypes of equivalent current systems

01 p0084 A70-11557

Equivalent circuit for acoustoelectric oscillator providing practical device analog, discussing oscillation suppression and resonant frequency changes under reactive load

04 p0656 A70-14719

Mathematical model based on equivalent electrical circuit for transient radiation analysis by computer

/TRAC/ family of circuit analysis programs, simulating semiconductor devices

04 p0657 A70-14737

Equivalent conductances and resistances vs pumping oscillation modes of p-n junction in parallel and series-connected three-frequency parametric circuits

04 p0659 A70-15209

Sensitivity functions of nonlinear circuits obtained by calculation of dependent linear model responses, topologically equivalent to original circuit

05 p0824 A70-16125

Equivalent circuit for fluidic transmission line used for studying behavior of lines with circular and rectangular cross sections

06 p0988 A70-17439

Acoustic scattering parameters for interdigital transducer as function of electrical loading and frequency using equivalent circuit model

06 p1062 A70-17485

Parasitic elements influence on stability of linear equivalent circuits with tunnel diodes

06 p1022 A70-17674

Rectangular waveguides broad wall longitudinal slot equivalent networks, noting series/parallel function dependence on slot length

07 p1240 A70-19221

Equivalent scheme for tunnel diode oscillator operating mode and parameters effect on LF modulating signal phase correlations

07 p1241 A70-19287

Equivalent transformations method for minimizing electronic equipment sensitivity to circuit components value variations during operation

08 p1474 A70-21221

TRAPATT oscillator circuit characteristics determined from measurements and equivalent circuit calculations

08 p1475 A70-21277

Three dimensional RC network simulating temperature fields in IC at different heat source power dissipation laws, discussing harmonic heat source field

09 p1643 A70-22128

Equivalent circuit for radiation admittance of infinite planar array of phased rectangular waveguide apertures

09 p1646 A70-22692

Electrical narrowband noise model for laser speckle pattern, obtaining image intensity statistical properties

09 p1638 A70-23370

Integrated image sensor matrix array derived from equivalent circuit to minimize sneak path effects

10 p1854 A70-23879

Avalanche diodes properties, establishing equivalent circuit accounting for static electricity, carriers transit time and thermal effects

10 p1850 A70-24625

Varactor diode equivalent circuit determination for application to cooled parametric amplifiers design

11 p2017 A70-25573

Cochlear microphonics in guinea pigs using analog equivalent electrical circuit

11 p1992 A70-26494

Sound generation and detection by distributed piezoelectric sources using frequency response and equivalent circuit

11 p2085 A70-26701

Equivalent circuits for transistors in class A amplification over wide frequency band

11 p2021 A70-26831

Piezoelectric effects in ferroelectric ceramics using equivalent circuits and admittance matrices

12 p2283 A70-27005

Impedance in coaxial line generated by tee-fed waveguide slot antenna, using equivalent circuit

12 p2198 A70-27966

Plane parallel perfectly conducting grating by integral equation procedure, presenting equivalent network under multimode propagation conditions

14 p2562 A70-31317

IMPATT microwave diodes small signal characterization by equivalent circuit using iterative computer procedure

15 p2708 A70-31971

Equivalent circuits and general formulas for small hole coupling of resonant cavities and waveguides

15 p2714 A70-32817

Fluid amplifiers equivalent circuit with stagnation pressure source in series with orifice and load, discussing applications to small signal circuit analysis

16 p2844 A70-33446

Microwave receiving antenna, discussing directivity, cross section, power gain, equivalent circuit, etc

17 p3044 A70-35054

Interdigital Rayleigh wave transducers piezoelectric coupling coefficient from bulk constants, permitting equivalent circuit parameters prediction

17 p3055 A70-35875

Equivalent radioelectric plan of ammoniac maser marginal type oscillator

18 p3265 A70-35946

Electronic circuits design by discrete equivalent transformations for selecting components parameters within given limits

18 p3231 A70-36239

Equivalent circuit of Gunn oscillators for quenched domain mode operation, noting optimal working conditions 18 p3229 A70-36668

Positive ions energy dispersion effused from RF plasma, presenting ion extraction model for plasma sheath system and equivalent circuit 20 p3678 A70-39608

Heat conduction problems solved allowing for radiation on electrical models, using nonlinear resistance and composite circuit methods 20 p3738 A70-40178

State space method for small signal lumped IM-PATT diode model predicting small signal impedance 22 p3998 A70-43251

Thermospheric density variations as equivalent oscillator circuit system, applying to atmospheric tides 22 p4023 A70-43297

Equivalent circuits for charge storage varactor diode in frequency multiplier mode 23 p4169 A70-43782

Microwave p-i-n diode RLC equivalent circuit parameters experimental determination 23 p4171 A70-43956

Packaged microwave junction diodes in reduced-height waveguide, discussing parasitics and equivalent circuit parameters measurement technique 24 p4318 A70-45220

ERGODIC PROCESS

Ergodic steady random functions measurement and analysis in terms of statistical properties [ONERA-TP-720] 07 p1411 A70-19825

Linear system under ergodic random processes, determining optimal dynamic characteristics by approximation of spectral density by Laguerre series 16 p2944 A70-34280

Sufficient condition for asymptotic stability of ergodic coefficient linear stochastic systems 17 p3129 A70-34982

Random ergodic process extremal behavior, determining mean time to reach maximum or minimum for first time 22 p3985 A70-42400

ERGOMETERS

Standardized bicycle ergometer training effects at sea level and simulated altitudes, indicating hypoxia potentiating role 05 p0807 A70-16674

Veloergometric assembly using two bicycles for simultaneously measuring muscular motor activity of persons in competition 07 p1221 A70-19525

Cycloergometer with powder type electromagnetic brake for respiratory and circulatory measurements and functional rehabilitation 14 p2541 A70-30379

Oxygen uptake capacity, ventilation, heart rate and acid base values during bicycle ergometer exercise 17 p3036 A70-34594

Hand held device for finger /thumb/ strength measurements 24 p4309 A70-46121

ERGONOMICS

U HUMAN FACTORS ENGINEERING

EROSION

NT WATER EROSION

Graphite rocket engine nozzles chemical erosion at various temperatures, comparing reaction and diffusion rates 03 p0516 A70-13619

Graphite sphere mass erosion in low temperature hypersonic air plasma shock flow, determining breakdown temperature and mass entrainment rates 03 p0517 A70-13741

Air plasma pulsed discharge jets erosive effects on metals, semiconductors and dielectrics, noting role of thermal effect 03 p0532 A70-13742

Materials science experimental and diagnostic phases in mechanisms of metal erosion by impacting dust particles [ASME PAPER 69-WA/MET-8] 04 p0704 A70-14760

Erosion characteristics similarities and differences of brittle and ductile materials, noting dependence on particle velocity and diameter [ASME PAPER 69-WA/MET-7] 04 p0704 A70-14761

Metals, plastics and ceramic materials under erosion by irregular quartz particles, using vacuum whirling [ASME PAPER 69-WA/MET-6] 04 p0704 A70-14762

Laser induced alloys erosion under various focusing conditions, determining optimal conditions for spectral studies 06 p1089 A70-17762

Discharge circuit parameters and heat physical constants of electrode material effects on electrical erosion of metals 07 p1294 A70-19351

Sand erosion of metals and plastics, discussing effects of impact conditions and impacting particles and target surface properties 07 p1314 A70-20004

Metal erosion under liquid drop impingement attack, investigating damage from microplastic deformation to surface material removal using wheel and jet apparatus 08 p1519 A70-21354

Hypersonic wind tunnel for erosion test of multiple particle impacts, considering dust on cork, carbazole and silicone rubber [AIAA PAPER 69-341] 09 p1656 A70-23240

Lunar cratering and erosion from Orbiter 5 photographs, observing crater densities, highland and maria regions, etc 10 p1942 A70-24643

Electrode erosion or entrainment in MPD arcs due to excess current density, considering inner cathode and outer ring anode with axial magnetic field 10 p1925 A70-25040

Electrode erosion during high voltage vacuum breakdown measured by neutron activation analysis and gamma ray spectrometry, noting plasma formation from electrode material 10 p1854 A70-25317

Quasi-steady analysis of material under ablation-erosion heat transfer for hypersonic vehicles 11 p2149 A70-26144

Slope failure erosional and mass wastage forms identification, characteristics and distribution based on large scale aerial photography depicted by remote sensor returns 12 p2217 A70-26913

Pulsed plasma jet radiant heat flux effect on celophane film coated, polished and etched metals, noting erosion destruction 12 p2282 A70-28287

Surface erosion of sublimating graphite and naphthalene due to inequilibrium mass transfer in gas flows 13 p2437 A70-28580

Proton and electron irradiation producing oxygen vacancies in silicates, minerals and rocks, indicating similar processes in lunar surface materials erosion and transport 13 p2395 A70-28908

Circulated air natural and technical impurities effects on gas turbine time dependent performance emphasizing erosion, deposits and overheating 13 p2475 A70-29713

Lunar surface erosion model by small projectiles impact for analytic representation of crater shape change as function of time 14 p2637 A70-30494

Erosion damage of porous sintered Fe in water or oil in test device with disk rotating near sample surface, noting relationship to metal fatigue 14 p2592 A70-31272

Friction theory, discussing surface mechanics, wear and erosion control 15 p2743 A70-31699

Laminar Cu-W electrode erosion resistivity in single chamber electric arc hydrogen plasmatrons with gas vortex stabilization 15 p2780 A70-32130

Alloys resistance against erosion-corrosion attack via abrasive slurries in corrosive media in pulp and paper industry 15 p2763 A70-32774

Lunar dimple craters formation by meteoritic erosion of concentric impact craters 15 p2807 A70-32850

Mechanical erosion concomitant with thermochemical erosion in mass and energy transfer at interface of boundary layer and ablating nylon-silica-phenol material [AIAA PAPER 70-824] 16 p2941 A70-33942

Compressor erosion correlation with aerodynamic parameters in gas turbine engines 17 p3147 A70-34711

Erosion by solid particles, discussing impacting velocity effects, natural sand quartz particle size distribution and composition, artificial industrial abrasives, etc 17 p3126 A70-35600

CH-54A helicopter gas turbine engine air particle separator /EAPS/ field service in Vietnam, noting time before engine removal for erosion [ASME PAPER 70-GT-97] 18 p3303 A70-36844

Lunar surface erosion due to Apollo 11 descent engine 18 p3316 A70-36960

Materials jet-like ejection from metal surfaces under high density laser radiation action, investigating erosion and plasma spectrum 19 p3448 A70-38734

Eroding surface transient heat conduction problem, considering temperature dependent surface properties, ablation, convective heating, etc 20 p3738 A70-40279

Nuclear space power three stage potassium turbine erosion testing in stainless steel loop with various contamination levels 21 p3756 A70-41005

Fe-group cosmic ray exposure tracks in Apollo 11 lunar rock interior, erosion rate and solar flare paleontology 21 p3917 A70-41673

Helicopter gas turbine engine protection against sand and dust erosion using particle separators, screens and coatings 22 p4090 A70-42671

Sand and dust erosion reduction in gas turbine engines by coatings, sleeves and inserts [SAE PAPER 700706] 22 p4090 A70-42672

Laser and flash X ray shadowgraph techniques in hypervelocity ablation/erosion investigations in hyperballistics range [SMPT PREPRINT 28] 22 p4034 A70-43047

Water drop-solid surface collision experiments to study rain impact erosion process, using gas gun projectiles, high speed photography, photomicrography and profilometry techniques 22 p4116 A70-43096

Short-term creep and erosion resistance testing of Ti alloy in high speed air flows under aerodynamic vibrations 24 p4360 A70-45826

ERROR ANALYSIS

Resonant cavity method for measuring varactor diodes cut-off frequency, avoiding errors from circuit losses and parasitic effects 01 p0048 A70-10049

Error estimation during application of Cauchy approximate integral formulas to numerical differentiation of analytic functions by quadrature 01 p0131 A70-10543

Right ascension screw error effects on observations of stellar image passage through meridian, evaluating effect 01 p0181 A70-10662

Radiometric method for calibrating loss of multimode antenna-feed components with linear or circular polarization, deriving calibration and error analysis equations 01 p0050 A70-10711

Digital filters output error due to roundoff accumulation and input quantization calculated by floating point arithmetic 01 p0050 A70-10778

Reentry trajectory dispersions due to atmospheric uncertainties determined using continuous differential equations based on atmospheric random processes method 01 p0183 A70-10846

Bit-slippage errors due to onboard tape recording of PCM/FM telemetry data for Apollo Telescope Mount, noting roles of S/N ratio, data characteristics, etc 01 p0044 A70-10940

Runge-Kutta method with position dependent optimal parameter alpha for initial value problem solution to minimize total error 01 p0134 A70-11364

Spacecraft trajectory optimal determination without knowing measurements error distribution function, examining computer solution properties of linear programming 01 p0192 A70-11477

Optimal moments for trajectory parameters measurements determined by linear analysis to minimize error for initial conditions 01 p0094 A70-11478

Rms error for reproduction of satellite signal transmitted through continuous Gaussian channel assessed by numerical calculation 01 p0046 A70-11513

Error estimates of stress concentration at free hole determined by two dimensional elasticity theory of thick plates 01 p0212 A70-11564

Rb-75 adapted reconnaissance cameras error sources on basis of processed Echo 2 satellite photographs 02 p0294 A70-11772

Error probability, signal to noise ratio and average signal level for coherent heterodyne and photon limited laser communication systems, using Poisson distributions 02 p0255 A70-11914

Coronal emission lines wide slit photometry systematic error analysis and suggested error elimination by varying observation method 02 p0373 A70-12375

Far field radiation pattern determination particularly suitable for large parabolic antennas, detailing measurement errors 02 p0267 A70-12399

Transient response role in limiter-discriminator detection of binary FSK signals, comparing resulting and optimum error probabilities 02 p0258 A70-12421

Total electron content /TEC/, time delay and polarization errors on one way path through ionosphere, discussing measurements and predictions 02 p0293 A70-12568

Airplane navigation based on VHF ranging between aircraft and geostationary satellite, examining errors by unknown propagation characteristics of signal in ionosphere 02 p0262 A70-12594

- Earth satellites optical observations accuracy for geodetic purposes based on errors in station position determinations 03 p0445 A70-13183
- Earth satellite tracking data reduction for determining geodetic ground nets, examining errors in triangulation procedures 03 p0445 A70-13184
- Simultaneous ground and space triangulation procedures, recommending use of satellite photographic observations for error reduction 03 p0445 A70-13185
- Gyrocompass composed of angular velocity integrators and interconnected by correction amplifiers, analyzing behavior during roll on vessel, determining error components 03 p0484 A70-13371
- Inertial navigation system with gyrocompass sensor, deriving equations for continuous orientation determination within gimbal system, estimating errors 03 p0522 A70-13372
- Nonlinear gyroscopic navigation system intrinsic error derived as function of linear operator 03 p0522 A70-13373
- Shallow flexible shells similarity conditions derived in dimensionless form, assessing error 03 p0592 A70-13450
- Rapid fading intensity distribution formula for analysis of aperture phase and amplitude errors in front on antenna arrays directional characteristics 03 p0456 A70-13463
- Axial geometry deformations of laser resonator due to fabrication errors and misalignment during operation 03 p0502 A70-13748
- Venusian cloud layer radius, discussing error in determination of occultation level height of regulus by venus 03 p0574 A70-13881
- Transistor admittance and diffusion parameters in indirect measurement with varying frequency, evaluating reliability 03 p0459 A70-14285
- Recursive nonlinear system state estimation for arbitrary path magnetic navigation tested on simplified model by Monte Carlo simulation, considering derived error expression 04 p0715 A70-14627
- Prediction accuracies of atmospheric models investigated for medium altitude satellites during disturbed geomagnetic conditions, discussing solar flux and geomagnetic indices as input data [AAS PAPER 69-617] 04 p0677 A70-14647
- Soviet book on nonsearching gradient self adjusting system for determining error function gradient, using Liapunov method to study stability 04 p0661 A70-14677
- Poisson ratio of elastomers determination for defining compliant surface fluid film thrust bearings behavior, considering method and error analysis [ASME PAPER 69-WA/LUB-7] 04 p0712 A70-14751
- Algorithm for optimal decoding of convolutional codes confirmed using error probability upper bound 04 p0654 A70-15067
- Atmospheric density measurements from Explorer 17 satellite by density gage and drag techniques resolved for difference by calibration and systematic errors considerations 04 p0691 A70-15120
- Error sources affecting data comparison accuracy between gyro measurements and reference solutions and due to gyro axes misalignment and gimbal angular movement 04 p0692 A70-15327
- Radar signals optimal synthesis characterized by ambiguity surfaces minimized over predetermined regions of ambiguity plane, noting weighted error criterion role 04 p0651 A70-15328
- Prediction errors lower bound for accuracy in predicting future position of randomly accelerating target 04 p0652 A70-15342
- Reconnaissance uncertainty effect on precision of return to fixed point applied to circular error probable, drms calculations and Loran 04 p0652 A70-15345
- Differential screw gauge for determining micrometer screw periodic errors and error components in level triers, using Rydberg method 04 p0693 A70-15488
- Miniaturized proportional counter to measure radioactive Ar 37 ultramicroquantities, assessing errors 05 p0898 A70-15930
- Z term from astronomical latitude data compared with catalog error corrections, showing nearness to absolute star system 05 p0907 A70-16030
- Numerical integration of linearized two level forecast model to analyze behavior of accumulated error 05 p0878 A70-16153
- Error analysis of resonant orbits for geodesy, discussing high order geopotential coefficient recovery by resonance and gravity model errors 05 p0909 A70-16341
- Critique of solar system resonant structure hypothesis based on planetary orbital frequencies errors 05 p0910 A70-16394
- Statistical analysis for personal variations contribution to total mean square error in time determinations 05 p0914 A70-16649
- Periodic observation errors in air temperature, relative humidity, vapor and air pressure 05 p0879 A70-16665
- Integral equations for interpolation process remainder estimation, including convergence of functions interpolation and error analysis 05 p0877 A70-16970
- Error resulting from elasticity modulus and linear thermal field coefficient removal from integral in Burger formula for turbine blade thermal stresses 05 p0954 A70-17061
- Probability distributions and error estimates for Monte Carlo solutions of radiation heat transfer problems, considering wavelength and direction of emitted photon bundles 06 p1175 A70-17683
- Flow parameters measured in low density hypersonic nozzle, estimating error of all relevant parameters 06 p1030 A70-18302
- Measurement error associated with heat conduction in temperature sensor, using mathematical model 06 p1070 A70-18443
- Photometric error analysis and optimum use of photomultipliers, discussing pulse-height spectra, detection and weighting systems 06 p1071 A70-18517
- Capacity and error bounds derived for nonsynchronized channel, discussing binary coding strategy 06 p1012 A70-18623
- Optimal signal detection with random phase on Gaussian noise background, estimating error probabilities 07 p1226 A70-18685
- Error analysis for pendulum type gyrocompass with indirect correction during irregular rolling, taking into account second infinitesimal order terms of equations of motion 07 p1278 A70-18735
- Size and shape error distribution law for cross sections of cylindrical components, discussing probability characteristics 07 p1290 A70-18740
- Equations for deep hole drilling errors calculations ensuring accuracy 07 p1291 A70-18826
- OMEGA frequencies propagation characteristics measured to estimate navigation errors from multiple waveguide propagation modes close to transmitter, comparing day and night errors 07 p1330 A70-19222
- Nonstationary correlation function for cross correlation of sample records from random processes, discussing minimum mean square error and weighting method 07 p1238 A70-19250
- Ion counter circuit using second equivalent condenser for compensating background radiation current, assessing error 07 p1281 A70-19526
- Explicit expressions for inertial navigation system errors analysis derived as function of plant coordinates, gyrocompass fluctuations, external moments and initial conditions 07 p1331 A70-19541
- Interagency chemical rocket propulsion group method of treating measurement error for liquid rocket engine performance parameters, using uncertainty model [AIAA PAPER 69-734] 07 p1365 A70-19723
- Bending tests for characterizing off-axis unidirectional composite beams, discussing errors due to lift off from supports 07 p1412 A70-19963
- Inertial navigation system design principles, deriving error equations and equations of ideal operation 07 p1332 A70-20177
- Error propagation in linear first order difference equations studied to improve accuracy of derivative recursive computation 07 p1328 A70-20249
- Nova Delphini 1967 brightness visual evaluations by amateurs, discussing effect of personal factors and instruments on accuracy 08 p1568 A70-20634
- Soviet collection of papers on apparatus for meteorological measurements covering error analysis, reliability engineering, use of computers, etc 08 p1494 A70-20771
- Communication channel average binary error and stationary Markov chain state probabilities relationship, using mathematical model and HF ionospheric FSK error sequence measurement 08 p1458 A70-20793
- Viterbi decoding error probability for convolutional codes using finite Markov chain modeling 08 p1458 A70-20794
- Fading effect on error probability of multi-hop PCM radio system, noting domination by worst hop 08 p1458 A70-20797
- Extremal statistics for signal and noise error probabilities estimation and computer simulation of digital feedback communication systems 08 p1459 A70-20800
- Error statistics recording for digital communications channel performance by extreme value technique 08 p1459 A70-20801
- Artificial crystallization zones width measurement error during time intervals after cloud seeding by aircraft and solar reflection methods 08 p1538 A70-21110
- Soviet collection of papers on astrometric observations including error analysis 08 p1573 A70-21151
- Catalog systems orientation based on major and minor planets observation, discussing zero points corrections 08 p1574 A70-21152
- Instantaneous latitudes observations during stellar transit at Poltava, describing error correction procedure 08 p1488 A70-21153
- Clock corrections smoothing by linear transformation operator, calculating operator transfer function and averaged errors deviations 08 p1574 A70-21155
- Moon rotational constants determination allowing for crater Moesting A coordinate errors 08 p1574 A70-21156
- Lunar latitude evaluation investigated for origin of discrepancy between two methods 08 p1577 A70-21494
- Positions measurement for 4C radio sources between declinations of 4 and 20 degrees, noting RMS errors 08 p1577 A70-21533
- Heart dipole moment calculation error due to deletion of individual electrode contributions to surface potential map, analyzing multielectrode grids 08 p1453 A70-21753
- Error analysis of Barakat-Clark explicit heat diffusion equations for thermally insulated surface 08 p1600 A70-21831
- Reliability estimations precision evaluated by Monte Carlo simulation, analyzing causes of data inaccuracy 09 p1689 A70-22019
- Sewage water flowmeter calibration, analyzing error propagation and tolerance 09 p1672 A70-22027
- Quantum mechanical form of Cramer-Rao inequality used to determined error lower bound for radiating object parameter observed by quantum-limited optical system 09 p1694 A70-22072
- Hyperbolic navigation systems circular fixes derivation error analysis 09 p1719 A70-22191
- Loran in range-range mode for computing user position based on remote clock synchronization, evaluating accuracy 09 p1719 A70-22192
- Piezoelectric quartz and tourmaline pressure gages static calibration, evaluating errors 09 p1675 A70-22599
- Error analysis in calculating periodic limiting state of rotor motion 09 p1727 A70-22624
- ELDO rocket tracking error, considering guidance antenna angular precision and UHF circuit performance in signal comparison 09 p1720 A70-22649
- Laminar boundary layer in adverse pressure gradient calculated for momentum thickness from approximate equation, analyzing error 09 p1660 A70-22832
- Relaxation time influence on mass output calculation errors for gases in small diameter sonic nozzles 09 p1604 A70-22841
- Tracking station clock synchronization error measurement using Deep Space Network Mark I ranging system, discussing system theory, design, operation, economy and versatility 09 p1656 A70-23038
- Error analysis of position finding techniques using analytical model composed of equations describing position error differential relationships 09 p1724 A70-23045
- Error sensitivity to measurement uncertainties and satellite geometry of satellite linked hyperbolic navigation systems 09 p1724 A70-23046
- Static error of varactor-controlled tuning-locked discriminator using computer 09 p1638 A70-23323
- Errors in aerial stereo photogrammetry, deriving equation to account for lens distortion and internal orientation 09 p1682 A70-23394

Radio and automatic control electronic equipment reliability estimation by vibration testing, determining test stand simulation accuracy
09 p1650 A70-23632

Plasma electron density errors in measurement by microwave interferometers, noting effects of inaccurate phase shift determination
09 p1738 A70-23634

Pulse duration, time and amplitude of pulse modulation, discussing device, detection circuit and statistical error analysis
09 p1639 A70-23697

Asymmetric deformation of spherical shell by solving homogeneous differential equation in spherical functions, assessing approximation error
09 p1786 A70-23719

Electro-optical autocollimating focus sensor for optical systems of high angular resolution, analyzing defocus detection and errors
09 p1687 A70-23764

Eye spherical, cylindrical and spherocylindrical refractive errors incidence at various visual acuity levels, tabulating standards
10 p1810 A70-24035

Pulsating flow mean total pressure measurement accuracy in high turbulence regions, discussing standing and traveling acoustic waves produced at measuring system entrance
10 p1867 A70-24160

SNR and system error rate prediction for coherent nonlinear satellite channels based on bounding techniques
10 p1836 A70-24341

Error probability degradation for digital satellite communication systems, employing multiphase signal sets distorted by bandlimited filtering
10 p1836 A70-24342

Error propagation in flowmeter calibration on model using empirical model-transmission equation
10 p1888 A70-24391

Error analysis and monotone convergence of finite difference approximations to linear one dimensional singular boundary value problems
10 p1909 A70-24406

Nonlinear operational equation iteration solution error estimation, discussing Banach space nonlinear operator equation
10 p1909 A70-24508

Statistical estimation of aeromagnetic survey data errors due to diurnal variations, navigational inaccuracies and instrument drift
10 p1914 A70-24646

Photogrammetric map compilation from orbital satellite photographs, with fictitious and ground coordinates generated by electronic computer, discussing error sources
10 p1890 A70-24728

Gravity gradient satellites equilibrium attitude error analysis showing relative effects of error sources
10 p1951 A70-24825

Solar outer corona brightness distribution from rocket observation with scanning devices during solar eclipse, estimating error
11 p2107 A70-25397

Errors estimation arising in inertial navigation equations solution while neglecting terms dependent on earth asphericity and gravitational field
11 p2077 A70-25558

Plane tension in elastic infinite strip covered by elastic plate, considering applicability to strain measurement errors calculation
11 p2129 A70-25565

ATC procedures based on system error and aircraft accident probabilities, traffic flow and navigation control and controller manpower
11 p2078 A70-25721

Error propagation in rectangular grid leveling networks assuming fixed height of center of mass
11 p2045 A70-25798

Electronic circuits automated endurance tests by follow-up scanning method, describing error sources in proper operation region cross section determination
11 p2013 A70-25922

Transfer functions estimation by taking Fourier transform ratio of finite length samples of input and response measurements, considering error term probability density
11 p2071 A70-25954

Systematic errors of reference star catalogs in satellite geodesy, discussing influence on orbit predictability
11 p2045 A70-26180

Quadratic error of semiautomatic measuring apparatus for photographic plates, noting operator contribution
11 p2051 A70-26182

Classical astronomical photographic methods for reducing satellite photographs taking into account linear and nonlinear methods, analyzing random errors
11 p2006 A70-26184

Error analysis algorithms for reducing computational load in stochastic estimation and control problems in hybrid navigation systems
11 p2025 A70-26208

Tracking of goal seeking attack vehicles, discussing error improvement and destination estimating by tracking station observer
11 p2080 A70-26243

Switched self balancing comparison radiometer with coupling between channels, showing measurement errors due to coupling correctable by phase switching
11 p2018 A70-26269

Geometric and predictive methods for developing bounds on epsilon-entropy for infinity error norm constraint
11 p2014 A70-26306

Digital filters response errors due to signal amplitude quantization, resulting from analog-to-digital conversion and arithmetic operations
11 p2029 A70-26333

Steady state surface temperature measurement errors by thermistors, thinistors and thermocouples, discussing sources
11 p2052 A70-26361

Arithmetic mean, least squares method and standard deviation concepts in random error analysis of measurement data
11 p2117 A70-26674

Finite element method solutions for plate bending, improving convergence based on error analysis
11 p2144 A70-26676

Errors in determining controlled satellite rotation periods, proposing scheme for corrected trajectory calculation of small eccentricity orbits
11 p2118 A70-26779

Satellite trajectory parameters estimation by maximum likelihood method applied to continuous satellite observations assuming random Gaussian process as measurement error
11 p2081 A70-26780

Cross sensitivity errors effect on stress determination by free-filament wire strain gages used at high temperature
11 p2058 A70-26838

Batch program testing, developing standards for various computer installations by daily work error case examples
12 p2191 A70-27012

Frequency-time coded multichannel communication system error probability bounds to investigate frequency selective fading effect on performance
12 p2184 A70-27416

Upper bound on system errors caused by quantization in multirate digital control system
12 p2204 A70-27841

Performance characteristics of quadriphase PSK communication system with noisy reference signal, formulating error probability
12 p2187 A70-27907

Statistical analysis of control system with nonlinear zero-memory element evaluated for error using Fokker-Planck equation
12 p2204 A70-27985

Linear and nonlinear parabolic boundary value problems with first boundary conditions solved by method of lines, estimating error
12 p2262 A70-28031

Atmospheric refractivity role in range errors from ground station to stationary satellite and in range rate measurement
12 p2189 A70-28058

Local heat sink thermal processes on convectively cooled solid surface, noting applications to temperature measurement errors
12 p2333 A70-28112

Manual spacecraft rendezvous system based on handheld instruments and manual computations, considering error analysis and simulation
13 p2357 A70-28392

Navigation satellite systems, analyzing error sources in signal processing and propagation developing computer programs
13 p2447 A70-28429

Preston tube errors in pipe flow wall shear stress determination due to velocity distribution deviations
13 p2387 A70-28848

Spaceborne logarithmic variable prescaling counters for automatic compression of particle measurement data, discussing statistical error
13 p2406 A70-28931

Shape and location error separation in deterministic predictions of meteorological scalar fields, considering air pressure system forecasting
13 p2445 A70-28995

Range of ground station to stationary satellite and range rate measurement errors induced by atmospheric refractive index fluctuation
13 p2365 A70-29095

Jeans escape rate error for atmospheric H and He attributed to perturbed velocity distribution function, using realistic atom-atom elastic scattering cross sections
13 p2398 A70-29226

Refraction errors and anomalies effects on satellite observation, using atmospheric model
13 p2449 A70-29275

Plane multielement antenna field statistics as function of correlated phase-amplitude aperture errors
13 p2378 A70-29306

Satellite time and position observations mean square error analysis using calculus of variations
13 p2367 A70-29528

Doppler radar aircraft navigation system with gyroscopic reference platform and computer, showing error propagation dependence on velocity and latitude
13 p2449 A70-29621

Black body design for radiometry, discussing error sources in calibration
13 p2410 A70-29658

Computer techniques for rounding error analysis, stability in linear algebra, matrices factorization, Jacobi rotation method and iteration procedures
13 p2443 A70-29768

True height of reflection determination for oblique sounding data interpretation, considering method error
14 p2547 A70-30230

Errors estimation in wind velocity values by radio echo observations in meteor trails of different densities
14 p2572 A70-30330

Viper Dart Robin System high altitude data reduction program accuracy, discussing winds and density errors
14 p2606 A70-30566

Inter-Range Instrumentation Group /IRIG/ document regarding meteorological data reliability, defining measuring process accuracy and errors
14 p2606 A70-30567

Quasi-linear elliptic boundary value problem approximate solution and error bounds, considering linear programming for computation
14 p2599 A70-30646

Human error as function of variability, considering frequency, effects and controllability
14 p2543 A70-31115

Open loop TV image motion compensation by image transducer with gyro demodulator analyzing errors in rate and rate-integrating gyros and AC pick-offs
14 p2588 A70-31190

Damped vibrations logarithmic decrement determination during automatic recording of number of cycles, emphasizing error analysis
15 p2733 A70-31531

Aluminum alloys endurance limit determination by accelerated methods, evaluating errors by comparison with conventional tests
15 p2755 A70-31539

Ionospheric electron concentration and temperature measurements by cylindrical Langmuir probe on rockets and satellites, emphasizing error sources
15 p2723 A70-31657

Vertical gravity gradient effect on calculations accuracy of earth figure, deriving corrections for anomalies
15 p2731 A70-32149

Charpy impact test accuracy for model machine certification, discussing erroneously high test values
15 p2820 A70-32236

Redundant variable errors in weather prediction, specifying initial conditions for time integration of hydrothermodynamic equations for atmospheric motion
15 p2771 A70-32368

Sampling error origin and magnitude during soil temperature measurements, noting dependence on weather character and season
15 p2731 A70-32459

Cascade digital filter computerized design with favorable signal to noise ratio, considering round-off errors
15 p2709 A70-32465

Statistical error analysis of autonomous manned spacecraft navigation in long duration eccentric Mars orbits
15 p2773 A70-32503

Error probability bounds for M-ary pattern recognition, proposing adaptive feature extraction criteria
15 p2703 A70-32564

Software reliability program development, functional analysis and error sources
15 p2742 A70-32667

Criteria for estimating errors in quadratic approximations to asymptotic stability involving Popov condition based on existence of quadratic Liapunov functions
16 p2941 A70-33045

Hall generator measurement of impulse currents, noting error sources and compensation
16 p2900 A70-33072

Laser ranging and tracking for high velocity targets, discussing SNR considerations, ambiguity resolution, error analysis, measurement centroid and target acquisition
16 p2862 A70-33165

Upper bound determination for errors due to signal quantization in multirate digital control system through state variable or z transform formulations
16 p2867 A70-33306

Linearization error bound analysis in solution of equations of motion of reentry vehicle
16 p2974 A70-33319

- Fifty percent coverage problem /Circular Error Probable/ of general bivariate Gaussian distribution from viewpoint of navigation systems error analysis 16 p2948 A70-33451
- Observational errors effects on surface waves resolution, describing shear velocity determination in crust and mantle from observed waves 16 p2897 A70-33647
- Automatic tracking antenna aiming errors, discussing remedies, design, motion compensation and mechanical resonance damping 16 p2880 A70-34268
- Adaptive linear estimator for stationary time series, evaluating asymptotic mean square error bound 17 p3128 A70-34852
- Discrete Fourier transform method for factoring spectral density functions, calculating absolute error 17 p3129 A70-34855
- Inner code concatenation with outer code to yield error probability uniform bound with exponential decrease 17 p3049 A70-34858
- Upper atmosphere temperatures from vapor cloud diffusion, eliminating errors from bright sky background at twilight 17 p3076 A70-34940
- Sine wave discrete components detection from complex spectrum with random noise, evaluating errors 17 p3059 A70-35168
- Ground test noise measurements accuracy and repeatability on JT8D turbojet engine 17 p3060 A70-35183
- Systematic errors in rotating mirror framing cameras and film records for quantitative high speed motion analysis 17 p3095 A70-35632
- Conical expansion nozzles manufacturing errors effect on flow expansion considered for large Mach numbers 17 p3011 A70-35662
- Error correcting decoders, investigating lower bounds on three complexity measures to meet error probability requirement 18 p3230 A70-35942
- Micropolar elasticity theory, discussing difficulties from erroneous thermodynamic inequality 18 p3335 A70-36061
- Error analysis of Corcos hypothesis concerning cross spectra of pseudoacoustic LF turbulent pressure pulsations on flat plate 18 p3241 A70-36305
- Linear differential equation integration method, using Eulerian technique for error reduction 18 p3282 A70-36358
- Chebyshev method for Banach spaces, discussing location theorem for reducing error bounds 18 p3282 A70-36359
- Eigenvalues and errors in asymptotic approximation of ordinary differential equations of second and fourth order 18 p3283 A70-36365
- Wideband analog signal data transmission, evaluating messages accuracy in terms of error probability 18 p3228 A70-36623
- Implementation delay error reduction in discrete Kalman filter, noting application to inertial navigation systems analysis 18 p3236 A70-36712
- Vertical deflections errors statistical analysis by gravity anomaly measurements, determining autocorrelation functions 18 p3248 A70-36771
- Satellite orbit theory error bounds and initialization, investigating first order von Zeipel method in axisymmetric force field 18 p3320 A70-37067
- P Cygni line profiles emission and absorption components rectification procedure, considering errors 18 p3321 A70-37123
- Observation classification /image identification/ for two normal sets with common covariance matrix, investigating error probability asymptotic behavior 19 p3375 A70-37283
- Poisson ratio of elastomers determination for defining compliant surface fluid film thrust bearings behavior, considering method and error analysis [ASME PAPER 69-WA/LUB-7] 19 p3434 A70-37602
- Differential time division multiplexing system, discussing errors due to imperfections of field effect transistor as multiplexer switch 19 p3388 A70-37906
- Nonlinear two point boundary value problem, examining quadrature error effects in approximate numerical solutions by variational techniques 19 p3458 A70-37979
- Neptune position errors by meridian observations compared with photoelectric observation of stellar occultation 19 p3518 A70-38008
- Thermal error in temperature differences between actual and simulated space environment 19 p3401 A70-38301
- Preliminary taxonomy for errors in serial, self-paced choice reaction time experiments, discussing speed-error tradeoff 19 p3362 A70-38313
- Control error effect on performance index in Pontryagin principle calculation of optimum control 19 p3394 A70-38501
- Mean square error for measurement series with unknown error distribution law, specifying necessary number of terms 19 p3390 A70-38583
- Navigation errors and time delays in prediction techniques for air traffic control 19 p3468 A70-38642
- Power spectrum analysis of division errors of graduated circles associated with meridian astronomy 19 p3523 A70-38686
- Random values statistical characteristics by digital methods, deriving errors as function of quantization parameters 19 p3432 A70-38705
- Low resistance multirange potentiometers, performing error analysis 19 p3432 A70-38706
- Galactic rotation law parameters determination, considering effect of random and systematic errors on accuracy 19 p3525 A70-38774
- Kalman filter set for state vector and observation error variance estimation in discrete time linear system, using empirical Bayes techniques [AIAA PAPER 70-1058] 19 p3395 A70-38873
- Multiconic method space flight trajectories analysis, discussing computation time and circumlunar flight altitude and velocity errors 19 p3529 A70-38876
- Artificial satellite position visual estimates based on geometric relationship to reference stars pair accuracy 19 p3531 A70-38946
- Light characteristics and geometry of photoelectric photometer system measuring light attenuated by atmosphere, discussing error sources 20 p3625 A70-39030
- Strapdown inertial guidance systems critical dynamic errors mathematical modeling and verification [AIAA PAPER 70-1029] 20 p3666 A70-39508
- Missile systems accuracy determination, analyzing pertinent errors statistical properties [AIAA PAPER 70-1007] 20 p3657 A70-39525
- Aircraft and rocket guidance systems navigation error analysis, discussing numerical integration techniques and computer program [AIAA PAPER 70-1004] 20 p3667 A70-39527
- Automatic control system stability error analysis, discussing sensitivity and statistical dispersion analysis [AIAA PAPER 70-985] 20 p3668 A70-39544
- Discrete Kalman-Bucy linear filtering with inaccurate noise covariances, considering optimal and sub-optimal systems, error analysis, probability theory, etc [AIAA PAPER 70-955] 20 p3601 A70-39573
- Voltage-to-frequency transducers with negative feedback, analyzing errors and conversion transconductance 20 p3601 A70-39789
- Velocity measurement by Doppler effect in two-point direction finding, calculating error dependence on angular coordinates and distance 20 p3587 A70-39792
- Controlled systems characteristics multistep statistical evaluation by extrapolation, analyzing prediction errors 20 p3593 A70-39904
- Controlled nonstationary plant dynamic characteristics determination by model, evaluating accuracy 20 p3673 A70-39906
- Nonstationary inhomogeneous random vector fields linear prediction, determining minimum mean square approximation error 20 p3604 A70-39911
- Digital correlator errors due to quantization by levels, designing analyzer of slow processes 20 p3594 A70-39922
- Preflight error statistics of earth based Doppler tracking for Mariner navigation concerning Mars 1971 and Venus-Mercury 1973 missions [AIAA PAPER 70-1077] 20 p3670 A70-40023
- Solar orbit corona brightness distribution from rocket observation with scanning devices during solar eclipse, estimating error 20 p3710 A70-40089
- Human mass exchange parameters permissible errors for manned space vehicles life support systems design 20 p3581 A70-40200
- Aperture antennas admittance calculation, considering upper bound on error involved in approximating finite ground plane conductivity by perfect conductivity 20 p3599 A70-40316
- Circular rib reinforced cylindrical shells, analyzing error due to Kirchhoff-Love hypothesis 20 p3734 A70-40435
- Structural vibration tests, analyzing errors due to couplings and dampers addition 20 p3734 A70-40439
- Donnell-Vlasov shallow shell equations error analysis 20 p3734 A70-40441
- Mutual impedance of interacting dipoles at wedge tip, determining errors for short spacing distances 21 p3796 A70-40638
- Human error as factor in aircraft accidents, considering man machine incompatibility and prevention measures 21 p3771 A70-41723
- Optical communication in turbulent media, investigating error rate for binary single path fading channels by photocount detection 21 p3837 A70-41935
- Wideband detection of frequency uncertain M-ary frequency shift-keyed /MFSK/ transmission in Gaussian noise, deriving symbol error rate for limiting SNR cases 21 p3792 A70-42177
- Linear elasticity problem approximation by elastic energy expression modification, deriving upper bounds for errors 22 p4113 A70-42537
- Ultrasonic absorption in gaseous molecular relaxation processes, considering error due to neglecting thermal conductivity effect on frequency dependence 22 p4073 A70-42649
- Integrated air navigation by least square adjustment, analyzing Doppler navigation errors 22 p4067 A70-42655
- Optimal self adaptive control systems with incomplete input information, ensuring minimum error dispersion 22 p4004 A70-42890
- Horizontal passpoint error in block analytic aerotriangulations with dense perimeter ground control 22 p4031 A70-42964
- Gyro misalignment and encoder quantization effects for strapdown attitude error sources 22 p4040 A70-43588
- Error sources and magnitudes in dynamic gradiometer using inertial grade pendulous accelerometer, discussing compensating modifications 22 p4042 A70-43658
- Gravity error propagation in dynamic gravimetry associated with navigation and gradient measurement errors, emphasizing standard error limits in navigation data 22 p4068 A70-43660
- Stochastic processes for probabilistic error analysis in airborne gravimetry, using gravity sensing instruments 22 p4025 A70-43666
- Radio signal source encoding, investigating error exponent 23 p4159 A70-43755
- Multilevel FSK system with limiter discriminator followed by low pass filter as demodulator, calculating error rates for comparison with other analyses 23 p4161 A70-44003
- Fundamental error in Galerkin method application to bending problem of elastic rods 23 p4268 A70-44172
- Optimal algorithm for searching extremum of single variable unimodal function satisfying Lipschitz condition based on maximum possible error criteria 23 p4177 A70-44305
- Discrete radio sources absolute spectra in 10-5000 MHz range, discussing data disagreement and measurement errors 23 p4247 A70-44795
- Cross correlation measurement errors for fluid pipe flow with pseudorandom sequence generated temperature fluctuations, considering transport time, impulse response and laminar flow 24 p4333 A70-45111
- Satellite orbital elements determination by differential correction procedure, considering observation stations distribution influence on accuracy 24 p4406 A70-45530
- Short period lunar perturbation on satellites by computer program with Fortran statements, considering errors, program output and table driven algebraic processors 24 p4406 A70-45532
- GEOS A and OGO-4 satellite orbits and trajectory analysis using Definitive Orbit Determination System, discussing tracking stations error role 24 p4407 A70-45536
- Error analysis of satellite orbits obtained by synchronous satellites range and range rate measurements 24 p4407 A70-45539
- Satellite motion deviations from reference orbit by generalized Fourier analysis, discussing earth gravitational field parameters determination and errors 24 p4408 A70-45546
- Optimum finite memory model for sequential minimum-mean-square-error estimation of random variable in added noise 24 p4317 A70-46052

Weak noise and threshold effects on estimation error for nonlinear PM systems 24 p4312 A70-46053

Estimation errors of multilevel modified digital correlator using auxiliary random noise for unbiased output 24 p4312 A70-46054

Electron density and collision frequency distributions in lower ionosphere, deriving error limits from VLF and LF sounder data 24 p4314 A70-46127

True height of reflection determination for oblique sounding data interpretation, considering method error 24 p4316 A70-46305

Dynamic errors of digital converter for digit-to-digit compensation estimated by probability and information characteristics methods 24 p4340 A70-46404

ERROR BAND

U ACCURACY

ERROR CORRECTING DEVICES

Dual frequency ranging within narrow bandwidth of VHF communications satellite repeater for transmitted signals correction of ionospheric refraction error 01 p0043 A70-10781

Refraction-induced range and tracking errors estimation in exponential model atmosphere by closed functions 01 p0044 A70-11087

Remote data processing and wideband data transmission between France and U.S. via telecommunication satellites, discussing error detection and correction 02 p0263 A70-12612

Stereocomparator and electronic computer used to determine aerial photographs relative orientation elements, discussing measurement error elimination 03 p0482 A70-13108

Generalized approach for optimal corrector in mean squared sense for predictor-corrector filter structure, illustrating signal modes with nonlinear and linear dynamics 03 p0520 A70-14170

Differential correction procedures, using residuals to obtain celestial body orbital elements by linear programming 04 p0751 A70-14943

Error correction for previous derivation of radio propagation of wave-hop series for anisotropic ionosphere resulting in improved nighttime field strength accuracy 04 p0649 A70-14967

Controlled vehicle disturbed trajectory multiple correction, considering constrained control or limited accessible coordinates for observations 04 p0716 A70-15007

VTOL aircraft fly by wire system eliminating errors automatically, discussing electronic and electrohydraulic control components, flight test model design, prototype, etc [DGLR-69-41] 04 p0623 A70-15149

Correction method for single frequency search in extremal control of continuous quick response multivariable plants 04 p0662 A70-15434

Blockage and wall corrections proposed for obtaining uniform results from low speed wind tunnel models 05 p0789 A70-15812

Block diagram for eliminating counting errors and spurious coincidences in telescope used at cosmic ray stations 05 p0845 A70-15931

Spatial resonance capture rates for U-238 thick slabs to correct gamma ray attenuation errors in broad group shielding calculations 05 p0884 A70-16169

Error correction training procedures convergence for committee solution to pattern recognition problem 05 p0817 A70-16175

Correction factors required for estimating influence of pupil area reduction on retinal illumination at oblique angles 05 p0801 A70-16449

Charged particle concentration emitted by inhomogeneous plasma determinable from emission spectral lines broadening, suggesting error correction procedure 05 p0889 A70-16541

Error correction for correlation coefficient between satellite data of earth radiation intensity and satellite vision field shift 05 p0841 A70-16729

Two degrees of freedom differentiating gyroscope response time decrease and phase and amplitude error reduction, using differential feedback 05 p0853 A70-17003

Distribution function distortions produced in counting devices due to simultaneous arrival of particles, correcting errors 06 p1064 A70-17830

Low speed wind tunnel test results correction program, considering solid, wake blockage, lift, static pressure gradient and wall interference effects 06 p0968 A70-17934

Apollo onboard computers tracking data state-vector corrections covariance matrix, considering initial estimate, noise and tracking geometry errors [AIAA PAPER 70-162] 06 p1015 A70-18072

Thermomolecular pressure corrections in tubes and at orifices for errors in gaseous pressure measurements by temperature gradients 06 p1113 A70-18371

Arithmetical divisible codes with error correction in single digit for nonbinary positional number systems, using comparison and group theories 07 p1246 A70-19645

Inertial navigation systems errors determined by geometric method, obtaining object coordinates 07 p1332 A70-20145

Rocket sounding to obtain thermistor temperature profiles of 30-65 km atmospheric region, discussing error correction equation 07 p1288 A70-20261

Temperature measurement in stratospheric circulation by meteorological rocketsonde wire sensor, presenting error correction technique 07 p1289 A70-20264

Arithmetic codes rate upper bound derived by combinatorial analysis, discussing decoding method for multiple error correction 08 p1465 A70-20792

Aerodynamic coefficients for axisymmetric bodies moving in rarefied plasma, calculating corrections for thermal ion velocities 08 p1432 A70-21089

Precision frequency analog converter using crystal oscillator and transistor switch reducing errors 09 p1653 A70-23698

Atmospheric refractive corrections in high accuracy radio interferometry 10 p1890 A70-24649

Multiplicity recorder for cosmic rays neutron component studies, reducing star redistribution errors by coincidence effect compensation 11 p2103 A70-25527

Fighter aircraft firing accuracy improved by high pass filter to automatically compensate sideslip induced by rudder through follow up slippage by aileron 11 p1979 A70-25820

Bit error probability after decoding for binary perfect single error correcting codes 11 p2014 A70-26247

Cyclic codes for error correction noting connection with exponential sum theorems 11 p2074 A70-26312

Time response deviation correction in hybrid computer control systems with digital feedback elements containing quantized coefficients 11 p2029 A70-26334

Vibrational motion sensors amplitude-frequency characteristics correction by passive electrical filters, deriving spectral transmittances 11 p2055 A70-26444

Aircraft pilot ability tests validity, applying correction methods in decision making regarding applicant acceptance [DFVLR-SONDDR-32] 12 p2176 A70-27031

Reference systems for two dimensional visual indications as correction device for pilot guidance errors associated with rotation effects 12 p2177 A70-27036

Correction factor for finite span effect on unsteady wing lift or moment during sinusoidal gusts or vertical oscillations 12 p2155 A70-27200

Data sampling system compensation based on bending frequency filtering through information obtained by varying sample rate, using saturn 5 launch vehicle simulation 12 p2192 A70-27411

Sounding rockets impact dispersion associated with wind measurement errors and thrust misalignments, discussing correction via reduced aerodynamic stability and initial rocket spin 13 p2503 A70-28677

Navigation correction systems for space missions, discussing prelaunch analysis, design and mission operations, hardware, etc 13 p2448 A70-28705

Tektites age from fission track method, discussing elimination technique for strain caused spurious tracks 13 p2488 A70-28721

Temperature-dependent physical properties effects on turbulent heat transfer, determining corrective factor for semiempirical equations 13 p2520 A70-28847

Error correcting algorithms for pattern classification, finding optimal approximation to unknown optimal decision function 13 p2374 A70-29579

Biresidue error-correcting codes for digital computers involving use of residue check circuitry working with arithmetic unit 13 p2375 A70-29938

Redundant threshold logic elements synthesis based on von Neumann multiplexing principle for automatic error correction 13 p2376 A70-29940

Correction factor for free stream Reynolds number errors resulting from low temperature viscosity in He wind tunnels 13 p2385 A70-29985

Electric resistance type strain gages, eliminating errors due to device length 14 p2582 A70-30174

Wind velocity determination by radar tracking of meteor trails, investigating errors 14 p2572 A70-30328

Multivariable feedback control system, minimizing mean squared error and error sensitivity to random perturbations 14 p2560 A70-30622

Convergence corrections for absorption coefficient measurements by far IR Michelson interferometer 14 p2586 A70-30988

Optimum interleavers realization procedure for reordering contiguous symbols sequence to satisfy minimum distance requirement for improving communication system performance 14 p2554 A70-31121

Combined radio and physical navigation systems, considering noise rejection and corrections of position and speed 15 p2772 A70-31623

Null and fixed correction methods for pressure and/or velocity gradient error in flow direction measurement 15 p2736 A70-31898

Correction method for near field antenna measurements made with measuring antenna of arbitrary but known characteristics 15 p2698 A70-31954

Dynamic fracture toughness measurement of low strength steels via instrumented Charpy impact test with correction factor for inertia loading effects 15 p2820 A70-32237

Optimal open loop controller and suboptimal feedback law to minimize terminal error of entry vehicle 16 p2947 A70-33439

Kinetic energy correction factor for nonuniform flow at Vena Contracta, using experimental data and modified Bernoulli equation [ASME PAPER 70-FE-34] 16 p2892 A70-33639

Correction techniques for thermal network lumped parameter inaccuracies with conduction and radiation coupling, considering temperature control system [AIAA PAPER 70-821] 16 p3002 A70-33943

Error correcting decoders, investigating lower bounds on three complexity measures to meet error probability requirement 18 p3230 A70-35942

Autoignition, ignition and surface temperatures of M-2 double base propellant at low pressure, correcting thermocouple measurements by theoretical model 18 p3299 A70-36697

Clock corrections determinations by stars pairs situated symmetrically around zenith, obtaining formulas by various methods 18 p3324 A70-37146

Error reduction methods for linear acceleration gyrointegrators measuring linear velocities 19 p3420 A70-37257

SUREFIRE /system for utilization of remote equipment for failure investigation and reliability evaluation/ monitoring reliability in closed loop failure reporting and corrective action system 19 p3555 A70-38834

Correction procedures for measurement errors in actinometers and pyrohelimeters caused by circumsolar radiation 20 p3625 A70-39029

Aerosol correction for atmospheric ozone content measurements using direct sunlight 20 p3615 A70-39032

Multiplicity recorder for cosmic rays neutron component studies, reducing star redistribution errors by coincidence effect compensation 21 p3882 A70-41277

Lense-Thirring effect in test masses approaching in same orbit around rotating body, noting correction dependence on central body geometry and angular velocity 21 p3926 A70-42240

Nonbinary redundant error correcting codes for improving TV transmission speed and fidelity 22 p3985 A70-42493

One dimensional cellular logic arrays fault circumvention by bypass switching out defective cells in cascade 22 p4004 A70-43073

Automatic control systems small oscillations suppression by nonlinear correcting elements 22 p4005 A70-43564

Inertial Navigation System /INS/, geodetic reference and optimal data smoothing for estimating vertical deflection and ocean currents 22 p4069 A70-43665

Unit distance redundant counting code for single error correction or double error detection with digital equipment simplicity advantages

24 p4316 A70-45104

Suboptimum sequential algorithm for recovery decoding errors in convolutional codes, using Hamming distance criterion

24 p4314 A70-46066

Circuit design providing thermal compensation for atmospheric pressure sensor, using mercury barometer

24 p4340 A70-46403

ERROR DETECTION CODES

Arithmetical divisible codes with error correction in single digit for nonbinary positional number systems, using comparison and group theories

07 p1246 A70-19645

Lunar daily variation in geophysical data determined by Chapman-Miller method, improving probable error determination method and giving computer program in FORTRAN

09 p1764 A70-23701

Digital sampled-data loop of phase lock control containing digital zone error detector and digital frequency regulator with reversible counter as memory unit

10 p1833 A70-24085

Fixed information bit rate approach to coding over space channel introducing redundancy and check digits for error probability

11 p2014 A70-26223

Biresidue error-correcting codes for digital computers involving use of residue check circuitry working with arithmetic unit

13 p2375 A70-29938

Spacecraft onboard computer for prelaunch targeting constants verification through checksum equation and error detection scheme, using generated number sequence

[AIAA PAPER 69-946]

14 p2599 A70-30769

Q-ary /n, k/ cyclic code and subcode generations and weight distributions relationship

14 p2554 A70-31123

Fibonacci codes polarized and partial error detection and correction capabilities

15 p2707 A70-32702

Majority logic decodability of product of two majority logic decodable cyclic codes

17 p3049 A70-34853

Convolutional code decoder modeled as autonomous stochastic sequential machine, considering finite Markov chain theory for error probability

17 p3049 A70-34854

Cyclic block code structures for generating binary sequences with good autocorrelation properties

19 p3375 A70-37284

Existence theorem concerning arbitrarily long good binary block /nonlinear/ codes preserved under large permutation groups

20 p3594 A70-39974

Rank permutation codes equivalence to binary code class capable of generation and detection through direct and inverse transformations respectively

20 p3594 A70-39975

Binary codes linear metric properties description reduced to finite set determination by convex programming procedure

22 p3993 A70-42494

Unit distance redundant counting code for single error correction or double error detection with digital equipment simplicity advantages

24 p4316 A70-45104

Information theory in physics and engineering, considering data processing, error correction codes, space communication, optical data transmission, noise effects and holography

24 p4379 A70-45616

Communication channel modeling with feedback for small error probability compared to unfolding capacity

24 p4313 A70-46056

Single-error nongroup binary codes with maximum codewords, including quadratic residue, Reed-Muller and tripple-error constructions

24 p4313 A70-46057

Algebraic structure convolutional codes using minimal encoders with feedback-free delay-free inverses

24 p4313 A70-46058

ERROR FUNCTIONS

Refraction-induced range and tracking errors estimation in exponential model atmosphere by closed functions

01 p0044 A70-11087

Soviet book on nonsearching gradient self adjusting system for determining error function gradient, using Liapunov method to study stability

04 p0661 A70-14677

Aircraft lift, thrust and drag coefficients inaccuracies expressed as errors in measured flight performance characteristics

04 p0624 A70-15386

Error probability upper and lower bounds determined for self synchronized binary PSK communications systems, presenting maximum-likelihood and Monte Carlo computer simulation

08 p1463 A70-21777

Narrow width pulse-position modulated optical communication system design, determining performance in terms of error probability and information rates

08 p1463 A70-21778

Error functional minimization in class of current distribution relay functions noting applications to linear antennas and FM signals synthesis

09 p1637 A70-23154

Error probability bounds for systematic convolutional codes

12 p2192 A70-27422

Learning self learning relationship in image recognition, analyzing resolving function with minimum probability for erroneous recognition

14 p2553 A70-30420

Complex error function computation using approximation method with single algorithm

14 p2599 A70-30648

Noise rejection and spurious reception probability in optimal channel for continuous sequenced signal with undetermined arrival and overlapping spectra

15 p2696 A70-31509

Gyroscopic navigation systems errors as function of sensor errors in terms of arbitrary operators requiring optimization

15 p2773 A70-32155

Numerical quadrature of singular functional equations, tabulating integral functions, Cauchy principle values and integral transformations for optimal error function

18 p3280 A70-36219

Distribution functions of errors in earth and moon horizon sighting due to planetary surface unevenness

21 p3884 A70-40840

ERROR SIGNALS

Carbon dioxide laser frequency stabilization, using plasma tube impedance variations generating error signal

10 p1901 A70-24946

False signal in scanning interferometer for helium-neon lasers in single and simultaneous TEM modes

15 p2749 A70-31557

Self alignment for gimballess inertial navigation system fixed base by generating computer programs from error signals derived from inertial sensors

16 p2946 A70-33302

Optimum pulse radar signal-receiver design, considering implementation errors for maximum target detectability in clutter

24 p4313 A70-46055

ERRORS

NT INSTRUMENT ERRORS

NT PHASE ERROR

NT PILOT ERROR

NT POSITION ERRORS

NT RANDOM ERRORS

NT RANGE ERRORS

NT ROOT-MEAN-SQUARE ERRORS

NT TRUNCATION ERRORS

NT VELOCITY ERRORS

ERYTHROCYTES

Hypoxic stimulation effect on erythropoiesis in vivo bone marrow

01 p0017 A70-10464

Hemoglobin concentration in red blood cells in men of various ages as function of altitude, discussing correlations with body weight and plasma protein

01 p0024 A70-10978

Biomechanics of microcirculation, discussing rheological characteristics of blood, erythrocyte and vessel wall, hydrodynamics of erythrocyte-shaped bodies mathematical models, etc

01 p0039 A70-11160

Erythropoietic response in anesthetized dogs subjected to sublethal whole-body proton irradiation followed by hypoxic hypoxia, discussing test procedure and results

01 p0027 A70-11300

Erythrocyte sedimentation rate in chicken blood predictable by Stokes equation

02 p0238 A70-12547

Radiation protective action of aminoalkylthiols, aminoalkyl disulfides, isothioureas, thiazolidine etc, in mouse tissues, erythrocytes and yeast cells exposed to X ray doses

03 p0419 A70-13307

Red blood cell mechanical fragility independence from cell age in rats

06 p0989 A70-17221

High altitude and sea level erythropoietic and somatic development in chick embryos indicating optimal physiological adaption with prolonged exposure

07 p1202 A70-18864

Increased blood flow resistance caused by red cell membrane shrinking due to plasma surface tension alteration

07 p1203 A70-18999

Hyperoxia effects on red blood cell /RBC/ survival in rats on normal diets, noting relatively normal erythropoiesis after long term exposure

07 p1214 A70-19935

Plasma viscosity and aggregation effects on whole-blood viscosity investigated in observation chamber for erythrocyte aggregation

09 p1622 A70-23546

Mountain climbing and prolonged stays at high altitudes effects on blood composition

13 p2352 A70-29355

Serologic comparisons of carbonic anhydrases in human and other primate erythrocytes

13 p2355 A70-29805

Erythropoiesis inhibitor in blood from rabbit kidney vein during hyperoxia in nitrogen-oxygen atmosphere

14 p2535 A70-30155

Red cell deformability and flow resistance and blood electrical resistance under low centrifugation

15 p2680 A70-31700

Prolonged hyperoxia effect on red blood cell survival and hemolysis in rats on normal diet

15 p2681 A70-31786

Blood plasma and red cell volumes simultaneous measurement in native group living at high altitude

15 p2684 A70-32537

Oxygen-hemoglobin reaction rate constants in red cells obtained by applying in vitro blood data to solutions of differential equations describing intracellular oxygen transport

15 p2686 A70-32846

Organic solutes diffusion in stagnant blood plasma and red cell suspensions, using models from transport theory

15 p2686 A70-32847

Antigens existence shared by human blood serum and proteins of erythrocyte stroma established through RAHS absorption by stroma and subsequent microimmunoelectrophoresis of serum

15 p2687 A70-32900

Chloride ion shift of respiration occurring between plasma and erythrocytes as function of carbon dioxide, using rapid filtration method

19 p3364 A70-38366

Erythrocyte suspension subjected to gas bubble ultrasonic oscillation, investigating hemolysis mechanism

20 p3573 A70-39981

ESAKI DIODES

U TUNNEL DIODES

ESCAPE (ABANDONMENT)

Marine safety aspects of helicopters with flotation equipment, considering effects of severe winds and waves, aircraft abandonment procedure, etc

01 p0007 A70-11316

Escape and survivability rates in various aircraft flight envelope regimes, using existing escape statistics and mission profiles

23 p4141 A70-44492

ESCAPE CAPSULES

Spacecraft or escape capsule rescue, discussing design, recovery planning, forces and sites

17 p3180 A70-35301

F-111 aircraft crew cockpit escape module design for maximum efficiency, including survival equipment after ejection

23 p4141 A70-44491

Helicopter personnel escape capsule system feasibility by UH-25B helicopter, discussing incorporation into CH-46 and UH-1

[SAE PAPER 700832]

24 p4290 A70-45890

ESCAPE ROCKETS

Tractor rocket powered escape system of 600 knot extraction capability using drogue parachute and barometric time delay device

[AIAA PAPER 70-1209]

21 p3751 A70-41809

ESCAPE SYSTEMS

Aircrew escape/rescue capability /AERCAB/ flying ejection seat design and test programs, noting rotary wing, fixed wing and parawing feasibility

01 p0035 A70-10714

Three man space escape system, describing emergency situations, parachute descent, life raft design, rescue operations and engineering tests

[AIAA PAPER 68-936]

04 p0763 A70-15403

YANKEE escape system adapted for helicopters using tractor rocket, noting modular concept advantages

06 p0986 A70-17719

RAPIDJET escape, recovery and survival system providing rapid escape for large aircrew complement by manual bailout system utilizing semiautomatic escape slide

06 p0986 A70-17720

Solid propellant cool gas generating systems applications to inflating emergency escape slides, rafts, pontoons and flotation bags

06 p0986 A70-17721

Cool gas inflation systems for evacuation equipment on large aircraft with size and weight fitting into aircraft doors

06 p0986 A70-17722

Emergency in-flight evacuation concepts adapted from military experience considered for application to commercial aircraft

06 p0986 A70-17723

Rocket catapult design, development and qualification for Advanced Concept Ejection Seat System /ACES/

06 p0987 A70-17724

Civil air transport passenger escape devices design and installation criteria

[SAE-ARP-495A]

07 p1191 A70-18805

Aircrew parachute with low speed-low altitude capability, considering static on-the-deck recovery, pack volume, weight, escape envelope spectrum, etc
07 p1191 A70-19014

Flying ejection seat providing capability for leaving hostile area before vertical descent by parachute, using Princeton Sailing and bypass fanjet
07 p1192 A70-19020

Combat and noncombat ejection/extraion fatalities and major injuries to USAF crewmen
07 p1192 A70-19023

Aircraft escape systems, discussing F-111 system capabilities and development
13 p2345 A70-28969

Concorde aircraft design for emergency passenger evacuation, emphasizing overwing inflatable escape slides and kinetic heating effects
15 p2675 A70-32222

Side access hatch system for Apollo command module
16 p2986 A70-34153

Manned space station safety, discussing hazards identification and elimination, rescue/escape systems, etc
[AAS PAPER 70-056] 17 p3016 A70-34792

Combat and noncombat ejection/extraion fatalities and major injuries to USAF crewmen
17 p3039 A70-35576

F-111 crew escape module, describing main parachute and pyrotechnics severance improvements, parachute deployment and inflation, etc
[AIAA PAPER 70-1210] 21 p3751 A70-41807

SIIS-3 ejection seat escape system design, considering minimum weight, cost and maximum performance
[AIAA PAPER 70-1211] 21 p3751 A70-41808

Tractor rocket powered escape system of 600 knot extraction capability using drogue parachute and barometric time delay device
[AIAA PAPER 70-1209] 21 p3751 A70-41809

Hi-glide personnel canopy /Para-Foil, Parawing, Sailing, Volplane/ technology capability requirements identification from performance parameters tradeoffs
[AIAA PAPER 70-1194] 21 p3753 A70-41822

In-flight escape systems and survival equipment reliability in U.S. Navy ejections
23 p4143 A70-44460

High energy emergency exit systems for passenger survival in aircraft accidents
23 p4140 A70-44466

Stretch fabric materials for personnel high speed escape parachute systems
23 p4141 A70-44482

Modularized multiple use SIIS-3 ejection seat escape system, discussing weight, envelope and low cost
23 p4143 A70-44499

Space vehicle personnel escape/rescue/ survivability capabilities, considering on board, prepositioned aid and earth launched concepts
23 p4260 A70-44620

Aerospace pyrotechnics applications, considering pressure controlled propellant actuated device for escape systems
[SAE PAPER 700831] 24 p4295 A70-45889

Helicopter personnel escape capsule system feasibility by UH-25B helicopter, discussing incorporation into CH-46 and UH-1
[SAE PAPER 700832] 24 p4290 A70-45890

ESCAPE VELOCITY

Spacecraft range control algorithm during reentry at parabolic velocity into atmosphere with varying parameter distributions
01 p0197 A70-11498

Kinetic theory applied to free flow in spherical geometry to study collisionless thermal escape of particles from planetary atmospheres
06 p1147 A70-18293

Parking orbit optimal orientation for minimal impulsive maneuvers total velocity increment in three dimensional capture-escape mission
[AIAA PAPER 69-918] 17 p3172 A70-35649

Nonperturbability conditions and equations of motion of bigyroscopic vertical below escape velocity
18 p3259 A70-36592

ESCHERICHIA

Chemostat culture method for studying control mechanisms during utilization of glucose/lactose and glucose/L-aspartic acid by populations of Escherichia coli
01 p0021 A70-10787

Hydrostatic pressure effects on DNA, RNA and protein synthesis and division in Escherichia coli cultures
04 p0637 A70-15475

Nontoxic method of immobilizing protozoan Tetrahymena pyriformis and bacterium Escherichia coli in acrylamide polymers, discussing microorganism viability
05 p0802 A70-16477

X and UV radiation effects on Escherichia coli B/r in vacuum, noting irradiated cell inactivation and radiation sensitivity increases
06 p0995 A70-17750

Vacuum and radiation effects on Escherichia coli, noting role of cells water desorption in vacuum damage
07 p1203 A70-18962

Density gradient sedimentation of Escherichia coli populations irradiated with Co 60 gamma rays, showing correlation between DNA degradation and cell death
08 p1441 A70-20680

Escherichia coli cell division patterns, discussing generation times spread, gamma ray irradiation in nutrient broth, DNA damage and growing points, etc
08 p1441 A70-20681

DNA enzymatic breakdown in Escherichia coli as function of ionizing radiation and temperature
08 p1445 A70-20775

Extraterrestrial gravitational effects on microorganisms, describing impetus-applied high g study of freeze dried Escherichia coli
11 p1987 A70-26028

Monograph on ionizing radiation effects on molecular biology of Escherichia coli, discussing cellular damage, DNA degradation and synthesis, incorporating radioactivity, mutations, etc
16 p2848 A70-33098

ESG [GYROSCOPES]**U ELECTROSTATIC GYROSCOPES****ESOPHAGUS**

Human atrial flutter studies using electrocardiographic electrodes placed within esophagus and right atrium
03 p0424 A70-13773

Human esophagus physiology, studying sphincter function from data on healthy and afflicted subjects
07 p1214 A70-19793

Position dependent variations in intrapericardial, pleural and esophageal pressures and cardiac output in thorax of dogs
13 p2356 A70-29946

Pressure recording site localization in esophagus, discussing cardiac artifacts morphology and localization over esophagus length
21 p3765 A70-42152

Esophageal swallowing pattern of longitudinal and circular muscular layer contraction, using intraluminal pressure recordings
24 p4300 A70-45844

ESRO SATELLITES

NT ESRO 1 SATELLITE

NT ESRO 2 SATELLITE

NT HEOS A SATELLITE

NT HEOS SATELLITES

ESRO 4 satellite as ESRO 2 design modification, describing experiments involving topside ionosphere ions, mass spectrometry, auroral particles distribution, solar and trapped particle fluxes
02 p0381 A70-12503

European Ultra-Violet Astronomical Satellite /U-VAS/ to replace Large Astronomical satellite /LAS/ to reduce cost while maintaining scientific objectives
03 p0582 A70-14343

Wide field stellar astronomical ESRO project, reviewing application of earth orbiting spin stabilized satellites and OAO
09 p1767 A70-23435

ESRO 4 satellite design, listing basic requirements of experiments in terms of orbital maneuvers and sensor locations
09 p1767 A70-23700

ESRO satellite projects, studying interplanetary magnetic field, ionosphere, relations between sun and earth, gamma radiation sources, particle flow, electric fields, etc
10 p1951 A70-24867

ESRO-1 satellite attitude stabilization and thermal balance
13 p2505 A70-28842

ESRO organization, program, locations, establishments and operational and future scientific satellites
17 p3200 A70-35204

ESRO applied research program, discussing IR technology, onboard computers, electric propulsion, etc
19 p3553 A70-37870

Automated data handling system for satellite environmental testing used by ESRO
21 p3805 A70-42258

ESRO 1 satellites attitude reconstruction, describing torque determination from known attitude
23 p4259 A70-44614

FSRO satellites missions and payloads, emphasizing studies of earth magnetic and electric field environment and of polar region particle measurements
23 p4191 A70-44663

ESRO 1 SATELLITE

ESRO 1 thermal behavior, discussing trajectory effects, onboard temperature measurement, data storage, data transmission, telemetered data and data comparison
04 p0762 A70-15164

ESRO 1 satellite attitude stabilization in launching, transition and stabilized phases
[DGLR-69-14] 04 p0762 A70-15168

ESRO 1, ESRO 2 and HEOS 1 satellites solar arrays orbital performance
09 p1765 A70-22648

ESRO-1, ESRO-2 and HEOS-1 simultaneous observation of solar event of 25 February 1969, describing satellite and experiments
19 p3531 A70-37496

Ionospheric electron density and temperature variation measurements after solar proton event of 25 February 1969, using ESRO 1 satellite
19 p3411 A70-37514

Trapped and precipitated electron observations at northern high latitudes in 45-450 keV range, using ESRO-1 satellite
19 p3496 A70-37515

Low energy electron and proton measurements by ESRO 1 satellite, discussing electron spectra, auroral zones and proton precipitation
19 p3412 A70-37516

ESRO satellite projects IRIS/ESRO 2, Aurorae/ESRO 1, HEOS-A1 and future TD-1 and HEOS-A2
23 p4264 A70-45004

ESRO 2 SATELLITE

ESRO 1, ESRO 2 and HEOS 1 satellites solar arrays orbital performance
09 p1765 A70-22648

ESRO-1, ESRO-2 and HEOS-1 simultaneous observation of solar event of 25 February 1969, describing satellite and experiments
19 p3531 A70-37496

High energy primary electron flux measurements by Cerenkov counter onboard ESRO 2 satellite
19 p3504 A70-38107

ESRO satellite projects IRIS/ESRO 2, Aurorae/ESRO 1, HEOS-A1 and future TD-1 and HEOS-A2
23 p4264 A70-45004

ESSA SATELLITES**NT ESSA 9 SATELLITE**

ESSA system operation, describing applications of satellite meteorological data
03 p0454 A70-13667

TIROS, Nimbus, ESSA and ATS weather satellites configurations, onboard equipment and cloud photographs
09 p1765 A70-22227

TIROS weather satellite TV system providing observations to ground stations via ESSA satellites
14 p2654 A70-31148

ESSA 9 SATELLITE

Automated Weather Network and Environmental Survey Satellite /ESSA 9/ global weather sensing systems
11 p2033 A70-26505

ESTERS

NT ACRYLATES

NT CELLULOSE NITRATE

NT GLUTAMATES

NT GLYCERIDES

NT ISOCYANATES

NT LACTATES

NT ORGANIC NITRATES

NT PHTHALATES

NT POLYCARBONATES

NT POLYESTERS

NT URETHANES

Hydroxy fatty acid methyl esters gas chromatography and mass spectrometry, noting trimethylsilylation usefulness for locating double bond
02 p0252 A70-12515

Peptides removal from Merrifield solid phase by transesterification with anion exchange resin
06 p1003 A70-17154

Cyclization of alkoxyl radicals, investigating 4-pentenoxyl radical and entropy factors effect
08 p1455 A70-20975

Helical twisting power of steroidal solutes in cholesteric mesophases, discussing nematic temperature shift dependence on ester chain
08 p1455 A70-21524

Gas-liquid chromatographic separation applied in derivatization chemistry of protein amino acids as N-trimethylsilyl/TMS/esters
09 p1629 A70-22337

Butyl esters separation from protein amino acids, using acid washed Chromosorb W of various mesh sizes
10 p1828 A70-24397

Aliphatic diesters as high temperature lubricants, discussing viscosity range extension, oxidation inhibition and thermal stability
13 p2438 A70-29125

Synthetic fluids as lubricants, examining physicochemical properties of polyglycols, silicones and esters
[ASME PAPER 70-DE-13] 16 p2917 A70-33421

Optically active alpha-amino acids synthesis from esters of alpha-keto acids by hydrogenolytic asymmetric transamination
17 p3041 A70-34749

P32 labeled organic phosphate esters in water extracts of soil
20 p3615 A70-38979

Gas-liquid chromatography studies of direct esterification of protein amino acids to n-butyl esters
22 p3984 A70-43525

ESTIMATES

NT COST ESTIMATES

Interior estimates for second order elliptic differential or finite difference equations, applying maximum principle

01 p0131 A70-10375

Bias-free estimation of linear process in recursive filtering, avoiding numerical inaccuracies introduced by computations with vectors and matrices

02 p0273 A70-12730

Minimal deviation estimates for linear approximations by seminorms for space defined by differential equations

23 p4210 A70-44018

ESTIMATING

Optimum estimation equations as simple averaging extension, considering application to Kalman filtering in integrated space navigation system

03 p0522 A70-13608

Bit transition time/bit synchronization/estimation, developing bit synchronizer from Bayes estimation and optimization theories

04 p0647 A70-14655

Optimal iterative weighted least squares estimation of rotation-coupled flexural oscillations of boom stabilized satellites in earth orbits

04 p0763 A70-15413

Identification algorithm for estimating parameters in constant coefficient linear system independent of prior estimates

06 p1015 A70-18164

Cup and vane anemometers theory, determining overestimation errors of differential equation for mean values in sinusoidally fluctuating winds

08 p1501 A70-21975

Statistical estimation of aeromagnetic survey data errors due to diurnal variations, navigational inaccuracies and instrument drift

10 p1914 A70-24646

Suboptimal nonlinear state estimation from noise corrupted measurements in ballistic trajectory, using simplified extended Kalman filter

11 p2028 A70-26303

Nonlinear estimation with quantized measurements, applying algorithms to PCM, predictive quantization and data compression

12 p2192 A70-27420

Waveform estimation by adaptive combination of analog and hardlimited sensor signals

12 p2187 A70-27906

Dynamic nonlinear estimation, deriving general algorithms for filtering, smoothing and prediction for continuous and discrete systems

14 p2562 A70-31366

Semiwideband and adaptive noise variance recursive estimation techniques applicable to spacecraft trajectory analysis

15 p2803 A70-32586

Monograph on state variable approach to continuous estimation of random processes with applications to analog communication theory

17 p3045 A70-35189

Continuous time nonlinear filter for space vehicle attitude determination, using estimation theory

17 p3130 A70-35291

Monograph on estimation and optimal control with quantized measurements covering linear, nonlinear and time varying systems

20 p3658 A70-40024

Steady random process intensity estimation, using iterative probability algorithm

22 p3987 A70-42559

ESTIMATORS

Multivariate linear model and robust estimators of parameters based on rank tests

07 p1323 A70-19027

Distributional results pertaining to complex Wishart processes and time varying spectral estimators on null hypothesis of stationary Gaussian time series

07 p1323 A70-19028

Quasi-linear estimator algorithms to achieve both optimal nonlinear filtration and signal interpolation resulting in significant gain of estimate accuracy

09 p1633 A70-22408

Hybrid computer for decision-directed estimators of two-class decision boundary, noting applications to medical diagnosis, communications and pattern recognition

09 p1641 A70-22965

Cramer-Rao efficiencies of best linear invariant estimators, using Weibull distribution in model for survival populations connected with life testing

10 p1910 A70-24604

Optimal linear estimation and control theory application to high precision optical spacecraft tracking systems design

11 p2028 A70-26302

Stochastic linearized state estimator for nonlinear dynamic systems with Markovian noise, using digital simulation

15 p2715 A70-31975

State estimation for nonlinear discrete time systems with quantized measurements, obtaining recursive algorithm through boundary value problem linearization

16 p2867 A70-33305

Adaptive linear estimator for stationary time series, evaluating asymptotic mean square error bound

17 p3128 A70-34852

Weak noise and threshold effects on estimation error for nonlinear PM systems

24 p4312 A70-46053

Estimation errors of multilevel modified digital correlator using auxiliary random noise for unbiased output

24 p4312 A70-46054

Optimal noiseless linear information feedback estimation for additive white Gaussian noise channels, applicable to digital transmission

24 p4313 A70-46064

Multidimensional integral Monte Carlo evaluation applying regression analysis to linear unbiased estimators

24 p4370 A70-46100

ESTUARIES

Fraunhofer line discriminator/FLD/ used for airborne fluorometer applicable to marine and estuarine studies

09 p1681 A70-23350

ETCHING

Single crystal Ge surface etching characteristics using laser beam reflection pattern

05 p0860 A70-16656

Tracks shape associated with dislocation motion during etching of Mo single crystals

07 p1309 A70-19639

Nb and Nb alloys activation in polarized light by etching technique, observing grain contrast improvement

10 p1906 A70-25229

Holographic projection to print etching patterns on semiconductor wafers, discussing development, basic principles and uses

18 p3233 A70-36773

Etching effects on mesa profiles and edge breakdown of silicon avalanche diodes at high power and temperatures, using scanning electron microscope

19 p3389 A70-37971

Fossil nuclear particle tracks in extraterrestrial matter using high voltage electron microscope and chemical etching

19 p3519 A70-38031

Printing, electro etching and vacuum deposition stencil methods for preparing moire grids

19 p3432 A70-38721

Chemical etching for revealing structure of carbon-graphite materials subjected to different graphitization stages

23 p4209 A70-44045

ETHANE

Methane and ethane released from Apollo 11 lunar samples by crushing or acid treatment, suggesting carbides hydrolysis as main source

12 p2304 A70-27719

Methane and ethane hydrate number measurement, alleviating liquid water occlusion and evaluating pressure effect

13 p2362 A70-29212

ETHERS

NT POLYPHENYL ETHER

Aliphatic ethers low resolution mass spectra interpretation using computer program heuristic

09 p1631 A70-23400

Polyvinyl alkyl ethers multiple transitions at low temperatures, using linear variable differential transformer

21 p3844 A70-42137

ETHYL ALCOHOL

Altitude effects on Borkenstein Breathalyzer accuracy determined from alveolar ethanol analysis

06 p1000 A70-17303

Ethanol ingestion effect on human response to submaximal and maximal exercise, measuring cardiac output and intraarterial pressure

21 p3761 A70-41135

ETHYL COMPOUNDS

Silicon organic binding materials properties, assessing ethyl silicate-50 perspectives in fabrication of precision castings

08 p1506 A70-21144

Self heating accompanying exothermic decomposition of gaseous diethyl peroxide in spherical vessel measured positionally by thermocouple

12 p2330 A70-27223

Thermal testing of decomposition and spontaneous ignition of diethyl peroxide before explosion

12 p2330 A70-27224

Ethyl nitrate positive and negative ion-molecule chemistry investigated by ion cyclotron single/double resonance techniques

16 p2855 A70-33090

Combustion products of 280-400 C oxidation of ethyl acetate, methyl propionate and i-propyl acetate

21 p3864 A70-40882

ETHYLENE

Molecular beam carbon dioxide laser Q switching by ethylene as saturating filter, reducing pulse duration by varying ethylene pressure and active mixture composition

12 p2248 A70-27509

EULER EQUATIONS OF MOTION

Ethylene-propylene elastomers compatibility with hydrazine determined under ambient conditions from gas evolution rate by catalytic decomposition

13 p2472 A70-28669

Ignition and combustion in ducted turbulent supersonic flow, discussing premixed and unpremixed ethylene

[AIAA PAPER 70-720] 16 p2997 A70-33488

Ethylene and ethylene-acetylene mixtures ion-molecule reaction product distributions calculation using quasi-equilibrium theory of unimolecular reactions

16 p2858 A70-34012

Auxin downward transport by gravity in leaves, examining ethylene inhibition

20 p3570 A70-39234

Ion-molecule reactions in mixtures of hydrogen sulfide with ethylene and acetylene from deuterium labeling studies via ion cyclotron resonance spectroscopy

21 p3773 A70-41200

ETTINGSHAUSEN COOLERS

U THERMOELECTRIC COOLING

EUCLIDEAN GEOMETRY

NT ANGLES [GEOMETRY]

NT BRAGG ANGLE

NT BREWSTER ANGLE

NT CARTESIAN COORDINATES

NT CATENARIES

NT CIRCLES [GEOMETRY]

NT CONICS

NT GREAT CIRCLES

NT HYPERBOLAS

NT INFLECTION POINTS

NT LINES [GEOMETRY]

NT LOCI

NT OBLATE SPHEROIDS

NT OCTAHEDRONS

NT PARABOLAS

NT PARALLELEPIPEDS

NT PARALLELOGRAMS

NT POINTS [MATHEMATICS]

NT POLYGONS

NT POLYHEDRONS

NT PROJECTIVE GEOMETRY

NT PROLATE SPHEROIDS

NT RADII

NT RECTANGLES

NT SPHEROIDS

NT TANGENTS

NT TORUSES

NT TRAPEZOIDS

NT TRIANGLES

NT TRIGONOMETRY

Regular C cubed space curve bending in Euclidean 3-space into piecewise helix, considering torsion and curvature

12 p2260 A70-26973

Linear differential evasion game termination with phase vector approaching given subspace in Euclidean coordinates

13 p2443 A70-29755

Optimal control problems solution using Cartesian product of space of right-hand sides of differential equations with Euclidean n space

17 p3129 A70-34868

Weak compactness of set of measures in functional space corresponding to stochastic differential equations solutions for n-dimensional Euclidean space

23 p4212 A70-44341

EUCLIDEAN SPACE

U EUCLIDEAN GEOMETRY

EUGLENA

Temperature-synchronized semicontinuous culture and monitoring system for autotrophically growing Euglenas

04 p0633 A70-15453

Streptomycin effects on euglena gracilis chloroplasts, comparing effects on chloroplastic ribosomal system to cytoplasmic ribosomal system

09 p1616 A70-22302

EULER BUCKLING

Column end fixity using Euler load and maximum flexibility coefficient for span point lateral load

17 p3188 A70-35226

Euler buckling of inflated toroidal gas bodies, including packaging and load deflection tests for Mylar, dacron-neoprene and stainless steel-silicone fabrics

[AIAA PAPER 70-198] 21 p3938 A70-41818

EULER EQUATIONS OF MOTION

Euler-Poisson equations application to motion of heavy solid body about fixed point to determine kinetic momentum vector relative to fixed reference system

01 p0145 A70-11434

Strain rate tensor coincidence in Lagrangian and Eulerian descriptions of turbulence demonstrated for homogeneous flow of incompressible fluid

07 p1252 A70-18672

Strain rate tensor coincidence in Lagrangian and Eulerian descriptions of turbulence demonstrated for homogeneous flow of incompressible fluid

15 p2718 A70-31464

Kinetic energy and pressure distribution of three dimensional compressible fluid flow, using invariant transformation of Euler motion equation

16 p2890 A70-33073

Gasdynamics equations in Euler variables, constructing completely conservative difference schemes with first and second orders of approximation

18 p3241 A70-36288

Rigid body with external torque acting along one principal axis, deriving Euler equations of motion

23 p4221 A70-44572

Rigid body rotation about fixed point under oscillatory precession and nutation due to noncentral attractive force, showing errors in Euler equations

23 p2427 A70-44792

EULER-LAGRANGE EQUATION

Lagrange solution to differential equations of motion of body with fixed point, deriving directrices of mobile and fixed hodograph

01 p0144 A70-11429

Lagrange and Hamilton equations of motion of mass point in physical space of general theory of relativity based on least action principle

01 p0146 A70-11444

Euler-Lagrange linear operators in variational embedding with one dependent function

05 p0881 A70-16058

Stationarization problems involving nonlocal and null class Euler-Lagrange operators, considering vector spaces of function spaces

05 p0881 A70-16059

Solutions existence for differential, integral and integrodifferential equations proved by variational imbedding of nonlocal linear Euler-Lagrange operator functioning as automatic adjoint calculator

05 p0881 A70-16060

Momentum-energy complex obtained for nonlocalized fields in variational mechanics, deriving integrodifferential identities for Euler equations quadratures

05 p0881 A70-16078

Nonlocal variational mechanics with one field variable, developing algorithm for Euler-Lagrange operator calculation

05 p0882 A70-16137

Nonlocal Euler-Lagrange operator nature and characteristics, discussing operation of class of all Lagrangian functions

05 p0882 A70-16138

Lagrange rotational motion stability of heavy symmetrical body attached at point to platform moving forward using Liapunov theorem

07 p1334 A70-19641

Kantorovich theorem application as weak Newton method used in boundary value problems containing Euler-Lagrange equation for variational problems and ordinary differential equations

12 p2260 A70-27002

Optimal control problem solution methods, comparing Euler-Lagrange equations, Pontryagin principle, dynamic programming and invariant imbedding

17 p3057 A70-35589

Lagrange equations for translational motion and diameter variation of bubble system moving in hydrostatic field, taking into account dissipative forces

18 p3240 A70-36270

Motion and stability of rotating connected two body space station satellite system, developing Lagrangian equations of motion and optimizing damping system parameters

[ALAA PAPER 69-919]

20 p3716 A70-39678

Perforated solid body moving in ideal incompressible fluid, deriving equations of motion in Lagrangian form

20 p3610 A70-39732

EUROPA LAUNCH VEHICLES

NT EUROPA 1 LAUNCH VEHICLE

NT EUROPA 2 LAUNCH VEHICLE

NT EUROPA 3 LAUNCH VEHICLE

Europa satellite launch vehicle inertial guidance and navigation system, discussing program of environmental, system integration and performance tests

05 p0879 A70-15816

Radio and inertial guidance of Europa 1 and 2 ELDO launch vehicles

08 p1542 A70-21870

Europa Launch Assembly installations covering liquid oxygen and nitrogen factories and CECLES program telemetry equipment

09 p1656 A70-23064

EUROPA 1 LAUNCH VEHICLE

Altitude simulation equipment for third stage Europa 1 booster rocket

04 p0664 A70-15302

Vibration tests on Europa 1 launch vehicle third stage, describing multipoint measuring and servocontrolled excitation systems and data connection to EDP

10 p1951 A70-24864

Optimum filtering techniques for radio guidance of third stage of Europa 1 booster compared for effectiveness

13 p2381 A70-28437

Flight behavior of pyrotechnic circuits in ELDO-EUROPA 1 booster for separating stages and autodestruction

15 p2709 A70-32288

ELDO Europa 1 and 2 launchers configurations tendencies, discussing use of liquid propellant boosters, chemical, electrostatic or thermonuclear propulsion system, etc

23 p4263 A70-45002

EUROPA 2 LAUNCH VEHICLE

Monte Carlo methods for calculating simple and multiple integrals and random variables characteristics, noting applications to Europa 2 booster

03 p0454 A70-15355

Orbit mechanical investigations for increasing Europa 2 booster rocket payload to place German-French communications satellite Symphonie into 24 hr orbit

04 p0754 A70-15153

Europa 2 launcher fourth/perigee stage, describing trajectories, propulsion system design and performance, separation systems, etc

19 p3532 A70-37871

Europa 2 booster perigee stage engine design, discussing total and propellant masses, spin stabilization, materials, etc

23 p4234 A70-44672

ELDO Europa 1 and 2 launchers configurations tendencies, discussing use of liquid propellant boosters, chemical, electrostatic or thermonuclear propulsion system, etc

23 p4263 A70-45002

Gyroscopically stabilized solid propellant apogee motor for experimental satellite of CECLES/ELDO Europa 2 program

23 p4235 A70-45018

EUROPA 3 LAUNCH VEHICLE

Europa 3 satellite carrier system configurations, discussing rocket design, propellant composition, etc

13 p2502 A70-28445

Europa 3D carrier rocket design and operational data, discussing communication satellites

13 p2502 A70-28446

Europa 3 launch vehicle liquid propellant engine design and performance data, discussing West German research in high pressure rocket engines

13 p2473 A70-28447

European launcher for geostationary orbit (ELGO)/program, describing Europa 3 payload, propulsion unit, propellant transfer, etc

13 p2502 A70-28449

Europa III SLV payload for geostationary equatorial orbit, describing engine thrust and propellant capacity for high energy second stage

24 p4414 A70-46357

EUROPE

Life styles of engineering, comparing U.S. and European attitudes to aircraft development and design

06 p1184 A70-17198

European air transport navigation, discussing air traffic control and planned VHF omnirange/distance measuring equipment network (VOR/DME)

07 p1332 A70-20226

Monograph on hypersonic flow boundary layers research conducted by European countries, determining pressures, velocity and temperature profiles, skin friction, heat transfer, displacements, etc

08 p1601 A70-21844

International aircraft engine industry management in Europe, discussing cooperation, corporations, U.S. competition and structural changes

09 p1792 A70-22339

Corporate aircraft operations in Europe, discussing meteorological conditions, flight planning, airport arrival and departure procedures and language differences

16 p2842 A70-33820

Aerospace industry in Europe, discussing role in electronics, international cooperation and projects allocation

19 p3554 A70-38493

EUROPEAN SPACE PROGRAMS

European Space Operations Center activities in observing HEOS 1 satellite, discussing launch, data processing and S-11 experiment involving ionized Ba cloud creation

01 p0197 A70-11118

Future phase of satellite TV programs distribution in Europe

02 p0403 A70-12645

Intelsat 4 communications satellite design and manufacture, discussing European participation with emphasis on British involvement

02 p0383 A70-12649

Digital onboard telecommunications and tracking equipment based on Dioscures two satellite system for L band operation

03 p0442 A70-12990

Flight test results of attitude control device for TACTTE rocket probe to explore solar disk and neighborhood

[ONERA-TP-762]

German-French communication satellite project Symphonie for radio, TV, telephone, teletype and data

transmission, discussing objectives, organization and technical problems

[DVL-910] 03 p0580 A70-13796

Global and European geodetic satellite network, discussing San Marco equatorial satellite and observation stations

03 p0581 A70-13829

European application satellite systems operation by administrative organizations dealing with communications, earth resources determination and industry participation

03 p0609 A70-13839

Italian space satellite booster programs for launching satellite payloads into low orbit

03 p0609 A70-13846

Solar power system of ELDO F-9 satellite boosted into polar orbit by EUROPA 1, discussing cell placement

03 p0573 A70-13847

Space activities cooperation of European organizations including CERS/ESRO, CECLES/ELDO and CETES, discussing European Space Conference

03 p0611 A70-14259

European Ultra-Violet Astronomical Satellite (U-VAS) to replace Large Astronomical Satellite (LAS) to reduce cost while maintaining scientific objectives

03 p0582 A70-14343

Guiana Space Center for French space programs, describing launch complexes, measurement and control methods, safety methods, launch operation planning, etc

04 p0663 A70-14939

German Space Research Association reliability and testing function, using failure analysis for space projects components and structures

[DGLR-69-30] 04 p0698 A70-15137

TD-1 satellite design and scientific payload

[DGLR-69-11] 04 p0762 A70-15142

Orbit mechanical investigations for increasing Europa 2 booster rocket payload to place German-French communications satellite Symphonie into 24 hr orbit

04 p0754 A70-15153

Mercury flyby mission feasibility study for ESRO considering payload, picture transmitting TV system, orbits, etc

[DGLR-69-12] 04 p0754 A70-15157

ASTRID two axis stabilization system for rocket payloads, aligning optical axis of experiment with star

[DGLR-69-42] 04 p0762 A70-15161

German developments in electric propulsion and energy supply systems for commercial satellites in geostationary orbits

[DGLR-69-20] 04 p0735 A70-15169

European space research - Conference, Dusseldorf, West Germany, December 1968

04 p0664 A70-15301

Mission objectives and technical realization of AZUR research satellite and Symphonie communication satellite

04 p0763 A70-15303

Ground station location, equipment and function for radio communication with German research satellites, noting NASA and ESRO cooperation

04 p0664 A70-15304

Reliability engineering related to general and professional levels, discussing space program methods and Concerto program for electronic components

05 p0853 A70-15810

Europa satellite launch vehicle inertial guidance and navigation system, discussing program of environmental, system integration and performance tests

05 p0879 A70-15816

Transmission equipment of Pleumeur-Bodou space communication installation including modulators, converters and amplifiers for telephone and TV carriers

05 p0819 A70-15986

Artemis I and II telemetering antennas at Guiana Space Center for spacecraft tracking

05 p0819 A70-15987

ELDO launch vehicle achievements, potential and use, showing relationship to possible satellite payloads

05 p0924 A70-16896

Nuclear and electric propulsion systems performance, considering applications in future European space activities

05 p0897 A70-16898

European role in future INTELSAT Organization operational rules and principles covering proprietary, financial and voting procedures

06 p1184 A70-17579

ESRO aims, structure and achievements in space technology improvement by research involving satellites, interplanetary probes and sounding rockets

06 p1185 A70-18395

Azur satellite program, describing NASA-German cooperative effort

[DGLR-69-052] 07 p1391 A70-18815

Dioscures project satellites design, considering use of rotation stabilization

07 p1392 A70-18989

Analog-numerical measurements on French liquid oxygen and hydrogen motor

07 p1364 A70-19129

- West German space research programs, discussing ESRO and ELDO, industry participation, ground support facilities, personnel recruitment and training, etc
08 p1568 A70-20607
- German satellite ground station system central station design, discussing cooperation between aerospace institute and electronic company
08 p1481 A70-21368
- French geodetic satellites Diademe I and II experiments in navigation, noting laser and Doppler devices
09 p1725 A70-23049
- Europa Launch Assembly installations covering liquid oxygen and nitrogen factories and CECLES program telemetry equipment
09 p1656 A70-23064
- Mercury flyby mission feasibility study for ESRO considering payload, picture transmitting TV system, orbits, etc
09 p1763 A70-23426
- TD-1 satellite design and scientific payload
09 p1767 A70-23429
- European space and communication satellite programs priority considerations, noting operational hardware
10 p1970 A70-25458
- Franco-German telecommunication satellite Symphonie mission objectives and system design [AIAA PAPER 70-406]
11 p1996 A70-25401
- UK UHF telemetry command station capabilities for Skynet satellites control, discussing equipment [AIAA PAPER 70-415]
11 p2030 A70-25420
- Italian SIRIO SHF experiment for study of atmospheric effects on satellite link, discussing system design and performance [AIAA PAPER 70-502]
11 p1999 A70-25442
- Symphonic satellite telecommunication network for multiple access telephone, telegraph, data transmission, radio and TV dissemination
11 p2005 A70-26008
- Italian polyvalent data acquisition system for ground space tests, discussing electronic instrumentation system
11 p2032 A70-26293
- Italian Sirio project, describing SHF propagation and communication, cosmic ray and confined plasma experiments
11 p2011 A70-26604
- European company for providing and operating European application satellite systems [EUROSAT], discussing organization, tasks and financial structure
12 p2335 A70-27469
- Symphonic communication satellite orbit and attitude stabilization systems components, operation and accuracy requirements
13 p2502 A70-28432
- Cost optimal carrier rocket system for European satellite TV, communication, navigation and earth survey networks
13 p2502 A70-28448
- European launcher for geostationary orbit [ELGO/program, describing Europa 3 payload, propulsion unit, propellant transfer, etc
13 p2502 A70-28449
- Cost optimal booster stage for European satellite launchers, comparing liquid and solid propellant rockets
13 p2502 A70-28450
- British national and Commonwealth collaborative sounding rocket programs, discussing organization, scope and range facilities
13 p2523 A70-28685
- INTA-255 ionospheric sounding rocket, describing vehicle and launcher design, test firings, ground facilities, etc
13 p2504 A70-28686
- ESRange-high altitude sounding rocket range for European space research, discussing location, safety, equipment, instrumentation, staff and programs
13 p2523 A70-28690
- Azur satellite flight results, noting trajectory accuracy telemetry reception, yo-yo triggering and attitude control
13 p2505 A70-28766
- Aeros aerodynamic satellite mission, orbit and design for upper atmosphere observations, noting braking field analyzer for ion and electron speed measurement
13 p2505 A70-28767
- ELGO launcher system with apogee booster for placing payload in geostationary orbit
13 p2505 A70-28768
- European information retrieval network for interconnecting NASA master file on space literature using computer terminals
14 p2670 A70-31174
- Report to COSPAR on Belgian National Committee for Space Research, discussing efforts of various universities and institutions
15 p2829 A70-31703
- Report to COSPAR on ESRO space research /1969/ covering ESRO 1 second flight model, sounding rockets, and sun- and star-pointing rockets development, etc
15 p2829 A70-31705
- Report to COSPAR on Austrian space research covering picture transmissions, solar activity, satellite observation, etc
15 p2829 A70-31707
- Report to COSPAR on Czechoslovakian space research /1969/ covering satellite telemetry and tracking, proton flares, aeronomy, etc
15 p2829 A70-31710
- Report to COSPAR on East German space research including Intercosmos satellites scientific apparatus preparation, meteorological and ionospheric research, etc
15 p2830 A70-31712
- Report to COSPAR on Hungarian space research including satellite observations, upper atmosphere, geomagnetic effect, geodesy, cosmic rays, etc
15 p2830 A70-31713
- Report to COSPAR on Greek space research /1969/ covering big planets observations, solar activity, ionospheric propagation, airglow measurements, satellite trackings, etc
15 p2830 A70-31714
- Report to COSPAR on Italian space programs, discussing cosmic ray physics, EM propagation, international research efforts, etc
15 p2830 A70-31717
- Report to COSPAR on Netherlands space research /1969/ including solar and stellar X radiation and UV spectrophotometry, cosmic ray measurements, satellite geodesy, etc
15 p2830 A70-31719
- Report to COSPAR on space exploration research in Poland including satellite tracking, geodesy, meteorology and aerospace medicine
15 p2830 A70-31721
- Report to COSPAR on Swedish space research /1969/ including rocket-borne auroral particle experiments, plasma physics, atmospheric, solar, cosmic radiation, etc
15 p2830 A70-31722
- COSPAR report on UK space research /1969/ covering neutral atmosphere, ionosphere, solar radiation, etc
15 p2831 A70-31723
- Europa 3 configurations for launching payloads into geostationary orbit using various rocket stage combinations
15 p2789 A70-32254
- Europa 3C light alloy space booster powered by Rolls-Royce engines using kerosene and LOX
15 p2810 A70-32257
- Repeater and antennas for space telecommunications onboard ELDO STV-F9 satellite, describing tests and measurements
15 p2811 A70-32282
- SIRIO mission algorithm and computer program, determining spacecraft position, ground trace and tracking station visibility
15 p2811 A70-32286
- Counterrotating antenna onboard Italian satellite in synchronous equatorial orbit for microwave propagation experiment
15 p2709 A70-32287
- Modular launch vehicle system for European commercial satellites using Eldo-A/1 Astris and French rocket stages
16 p2987 A70-34342
- PCM telemetry transmitters, command receiver and ground control for German research satellite Azur
16 p2890 A70-34349
- ESRO organization, program, locations, establishments and operational and future scientific satellites
17 p3200 A70-35204
- UK space program, describing scientific satellites, Black Arrow launch vehicle and sounding rockets
17 p3167 A70-35206
- British X 3 satellite for investigating thermal control surface finishes stability, ultrathin solar cells, electronic systems reliability and micrometeoroid flux measurement
18 p3333 A70-36511
- European participation in American space program, considering space station, shuttle and tug
19 p3531 A70-37379
- ESRO applied research program, discussing IR technology, onboard computers, electric propulsion, etc
19 p3553 A70-37870
- Signal measurement and processing in thermal vacuum and space simulation tests of Azur and Dial satellites
19 p3400 A70-38298
- ELDO project planning and progress monitoring system for management provided by Central Planning and Progress Monitoring Service
21 p3956 A70-41497
- Discosure satellite navigation system for aircraft and ships, discussing coverage, radio links, project costs, etc
22 p4067 A70-42657
- U.S. and European space program costs and resources with particular reference to telecommunication satellites
22 p4126 A70-43247
- European participation in U.S. space projects, discussing economics, space shuttles and tugs and earth orbital space station
22 p4126 A70-43407
- European avionics role in Post Apollo program, noting space shuttles, space tugs, space stations and modules
22 p3999 A70-43501
- Management organization of European operational application satellite systems, concerning interurban telecommunication and air traffic control
22 p4127 A70-43502
- European wind tunnels suitable for Post Apollo Program aerodynamic testing, presenting detailed tabulated information on available facilities
22 p4007 A70-43503
- Eurospace Symphonie satellite communication system and ground facilities, discussing international and regional coverage
22 p4111 A70-43504
- U.S. aerospace industry participation in European Application Satellites Program
22 p4127 A70-43506
- European-U.S. cooperation in shuttle and space station program, noting experience in unmanned systems
22 p4127 A70-43508
- European rocket engine technology, discussing liquid rockets, reliability, restart capability, performance, cryogenic engine, components, facilities and U.S. cooperation
22 p4092 A70-43509
- European cooperation possibilities in future NASA space programs
22 p4127 A70-43510
- European participation in small space shuttle development, discussing design, test vehicle program and European applications
22 p4111 A70-43511
- European space applications program, discussing communication and meteorological satellites
22 p4111 A70-43515
- European Space Research Organization programs, stressing international cooperation
22 p4128 A70-43633
- International space program cooperation, discussing NASA projects, Apollo 11 flight and European and Soviet programs
22 p4129 A70-43655
- European space policy decisions regarding continuation of existing programs and participation in U.S. post-Apollo programs
23 p4285 A70-44325
- European space organization as intergovernmental agency developing industry, scientific and technological research, application satellites and boosters
23 p4285 A70-44652
- Project AZUR organizational structure and post-launch problems, discussing onboard experiments
23 p4262 A70-44685
- ESRO satellite projects IRIS/ESRO 2, Aurorae/ESRO 1, HEOS-A1 and future TD-1 and HEOS-A2
23 p4264 A70-45004
- British National and Commonwealth collaborative sound rocket programs, discussing organization, scope and range facilities
24 p4431 A70-46124
- European Space Research and Technology Center space science department, examining cosmic ray, ionospheric and surface physics divisions
24 p4323 A70-46356
- EUROPEAN SPACE RESEARCH ORGANIZATION**
SAT
NT ESRO 1 SATELLITE
NT ESRO 2 SATELLITE
EUROPIUM
Spectral broadening mechanisms for trivalent Eu ions in glass, considering fluorescence and absorption spectra measurements
06 p1127 A70-18640
- EUROPIUM ISOTOPES**
Europium isotope ratio in solar atmosphere equal to terrestrial using spectral line profiles analysis
09 p1757 A70-22727
- EUTECTIC ALLOYS**
Microstructural interfacial stability and property retention after elevated temperature exposure of eutectic composites, discussing coarsening rate relationship to interfacial area and energy
01 p0117 A70-10485
- Phase changes in Ni/Ti alloys with equiatomic composition, resolving discrepancy on nonMartensitic eutectoid decomposition of B2 structure and intermediate precipitate
01 p0121 A70-11232
- Semicoherent interface dislocations in directionally solidified Ni-Al-Cr eutectic, discussing lattice mismatch
01 p0123 A70-11247
- Mechanical properties of eutectic superalloys compared with commercial superalloys, noting thermal stability applicability to gas turbine engines [SAE PAPER 690689]
05 p0861 A70-15827
- Al-Si and Cu-Ti eutectic alloys showing good ohmic contacts to SiC
10 p1927 A70-23990

Stainless steel fiber reinforced Sn-Pb eutectic alloy composite mechanical properties, noting tensile strength and rupture behavior

13 p2436 A70-29625

Eutectic NiAl-Cr structure and high temperature tensile strength as function of solidification rate

15 p2755 A70-31560

Al-Zn eutectoid alloys defect structures and interactions in superplastic deformation process

15 p2756 A70-31567

Cellular precipitation in laminar eutectic and cast Ni-Cr alloys

15 p2761 A70-32383

Metallic superplasticity and superplastic alloys in simple tension, forming tubes and sheets of superplastic Sn-Pb eutectic alloy by pressure forming techniques

16 p2916 A70-32916

Massive eutectic and fine gamma phases precipitation in cast nimonic 100 alloy at 900 C aging

16 p2930 A70-33083

Microstructural changes of Ni-Cr lamellar eutectic alloy during creep deformation at 625 and 760 C

18 p3272 A70-36034

Aligned composite materials preparation by unidirectional lamellar eutectoid decomposition in Co-Si, Cu-Al, Ni-In and in supersaturated solid solution Sn in Pb

18 p3274 A70-36052

Isothermal phase equilibria in Ti rich ternary Ti-Al-Fe alloys, noting eutectoidal transformation

18 p3275 A70-36123

Ti-Si eutectic alloys unidirectional solidification by zone melting

19 p3450 A70-37375

Duplex eutectic with Ni-Be fibers embedded in Ni-Cr solid solution matrix, discussing solidification conditions, optimum composition, heat treatment, mechanical properties and oxidation

20 p3647 A70-39107

Composites made by unidirectional solidification of eutectics with transition metal carbide fibers embedded in metal matrix, discussing tensile tests [ONERA-TP-853]

22 p4057 A70-43457

Al-Be eutectic alloys structure, using laue X ray method and electron microscopy in studying fibrous morphology due to unidirectional solidification

24 p4356 A70-45143

Ternary Co-Cr-C alloys unidirectional solidification with metal matrix and carbide simultaneous freezing at eutectic liquidus line

24 p4358 A70-45235

Unidirectionally solidified carbide reinforced Co-Cr eutectic alloy, examining tensile strength and creep behavior

24 p4358 A70-45236

Eutectic NiAl-Cr alloys, investigating quaternary additions effect on rod-plate transition to faceted microstructure

24 p4359 A70-45244

Prestraining effect on cellular precipitation in Ni-Cr lamellar eutectic during creep testing

24 p4359 A70-45247

Eutectic and hypereutectic Al-Si alloy quench modification by rapid solidification, investigating microstructure and mechanical properties

24 p4362 A70-46183

EUTECTIC DIAGRAMS

U PHASE DIAGRAMS

EUTECTICS

NT EUTECTIC ALLOYS

Subsolidus state multicomponent eutectics systems temperature range based on number and melting points ratios of individual components

24 p4367 A70-45476

EVACUATING (TRANSPORTATION)

Ground and ditching emergency evacuation tests of C-9A aeromedical aircraft under worst possible simulated crash conditions

01 p0035 A70-10716

DC-8 aircraft ditching in San Francisco Bay on 22 November 1968, discussing accident sequence, evacuation operations, life raft stowage and deployment, etc

06 p0985 A70-17705

Aeromedical Evacuation System in overall treatment process for seriously ill patient

09 p1628 A70-23467

Emergency evacuation on land of passengers and crew of airliners, discussing training, equipment, standardization, communication and protective fabrics

15 p2675 A70-32220

High energy chemical systems for postcrash emergency evacuation of commercial passenger aircraft, discussing exit opening via explosive methods

15 p2675 A70-32221

Passenger survival and evacuation of civil jet transport aircraft after ditching at sea

15 p2676 A70-32223

Presentation styles of passenger emergency evacuation briefing cards, noting preference for sequential action graphic displays with minimum key wording

23 p4141 A70-44486

EVACUATING (VACUUM)

Spontaneous ignition dependence on transient temperature variations accompanying gas entry to evacuated vessel

12 p2330 A70-27222

Gas pressure differential across multilayer insulation blanket during rapid evacuation predicted, using one dimensional flow theory

[AIAA PAPER 69-608] 23 p4282 A70-44522

EVALUATION

Apollo Program mission evaluation and flight anomalies team to identify and understand unforeseen peculiarities and systems problems during spacecraft mission

09 p1768 A70-23708

Evaluation technique for astrophysics subsystems in automated spacecraft designed for interplanetary missions, considering operation times, navigation updating and midcourse correction

[AIAA PAPER 69-882] 11 p2079 A70-26118

Project economic evaluation, discussing value analysis from market research recommendations

19 p3555 A70-38620

Pilot assessment aspects of flight simulation in terms of experiment planning, facility and results reporting and analysis

23 p4153 A70-44546

EVANESCENCE

Holographic recording of information contained in evanescent wave fields in high resolution photographic emulsions

07 p1281 A70-19367

EVAPORATION

NT PROPELLANT EVAPORATION

NT TRANSPIRATION

Liquid nitrogen evaporation in PSB foam polystyrene vessels compared with glass vessels for cryogenic application

02 p0305 A70-11875

Velocity distribution of atoms evaporating from superfluid He II at low temperatures, noting roton shifting and multiexcitation processes

06 p1108 A70-18639

Linear kinetic theory for condensation and evaporation at small Knudsen numbers, considering extrapolated temperature jump determination

07 p1422 A70-19656

Capillary grooves effect on surface wetting and evaporation using heat transfer coefficients for grooves with triangular, semicircular and square cross sections

[ASME PAPER 69-HT-19] 09 p1790 A70-23559

Heat and mass transfer during liquid surface evaporation in vacuum, calculating temperature field on basis of heat balance level

09 p1791 A70-23717

Solar radiation effects on evaporation of dust with high latent heat of vaporization, considering particles in comets and zodiacal cloud

11 p2117 A70-26648

Molten lithium sodium carbonate electrolyte decomposition and evaporation at high temperatures in various atmospheres, noting water and carbon dioxide additives effects

12 p2166 A70-27763

Electromagnetic theory of forces for coalescence in granular layers during thermal evaporation of thin films, calculating interaction between instantaneous dipoles

13 p2471 A70-29640

Evaporography at room temperature, showing necessity of recording images on color films

14 p2583 A70-30362

Linear kinetic theory for condensation and evaporation at small Knudsen numbers, considering extrapolated temperature jump determination

15 p2828 A70-32693

Fog dissipation on aircraft runways, using aircraft jet engine exhaust heat and mixing properties

17 p3133 A70-35929

Meteoric masses evaporation during flare, showing discrepancies for luminosity factors

18 p3315 A70-36604

Laser beam alignment system for monitoring dielectric film evaporation

19 p3445 A70-37686

Heat transfer mechanism during fluid evaporation in porous wick structure contacting heat pipe surface

21 p3946 A70-41042

Green function theory of evaporation of He 3 atoms from liquid He 3/He 4 mixtures, determining energy distribution

24 p4377 A70-45255

EVAPORATION RATE

Vasopressin antidiuretic hormone effects on evaporative body weight loss during heat exposure

01 p0020 A70-10516

Mass loss rate of evaporating liquid droplet with vapor reacting with oxygen of atmosphere in combustion front

[DFVLR-SONDDR-16] 01 p0216 A70-10932

Quasi-equilibrium treatment of heterogeneous reactions applied to evaporation rate /desorption/ compu-

tation for volatile species formed in oxygen reactions with W, Mo and graphite

06 p1004 A70-17330

Evaporation rate from spherical drop into vacuum influenced by molecular collisions occurring in gas cloud formed by emitted particles

06 p1113 A70-18283

One dimensional cumulus convection model modified by incorporating rain evaporation rate and temperature changes from downdrafts

06 p1099 A70-18568

Adhesive joint failure, studying adhesive, cohesive and adherend ruptures by evaporative rate analysis

07 p1292 A70-18931

Isothermal reaction rate determination at given temperature from nonisothermal data illustrated on Knudsen cell vaporizations

07 p1424 A70-19901

Evaporation rates from rotating planet, showing augmentation over stationary planet

07 p1390 A70-20290

Flow parameters behind shock waves calculated, determining amount of condensate evaporation and error in pressure measurements due to evaporation

09 p1607 A70-23711

Permalloy evaporation rates from resistance heated W boat, revealing departure from free molecular flow

13 p2452 A70-29203

Evaporation and combustion kinetics of droplets and particles in hot air stream, observing luminous trace

14 p2664 A70-30392

Lubrication system components behavior in vacuum environment, investigating evaporation, friction, adhesion, wear, etc

16 p2923 A70-34156

Liquid nitrogen drops anomalous behavior in film boiling, resolving vaporization time discrepancies

17 p3194 A70-34741

Gas velocity and static pressure effects on evaporation rate of moving liquid fuel droplets

21 p3953 A70-42094

EVAPORATIVE COOLING

NT FILM COOLING

NT SWEAT COOLING

Thunderstorm downdraft trajectories and temperatures, discussing evaluation of cooling due to evaporation

02 p0325 A70-12256

EVAPORATORS

Heat exchange unit for low thrust attitude control propulsion system evaporator designed for converting liquid propellants to gas

[AICHE PREPRINT 25] 01 p0216 A70-10969

Vacuum cleavage device for producing small area evaporated metal semiconductor contacts free from oxygen or other contamination

02 p0304 A70-12748

EVASIVE ACTIONS

Humanoid unmanned reconnaissance and assault vehicle maneuvers, describing cover-seeking and obstacle-avoidance functions from physiological and engineering viewpoint

01 p0033 A70-10495

Policies and controller design for pursuing vehicle developed in terms of pursuit-evasion differential games

06 p1025 A70-17955

Search and rescue /SAR/ concepts behind advanced Navy systems, emphasizing flying ejection seat /AER-CAB/ for air to air self rescue

07 p1192 A70-19024

Fixed target pursuit-evasion differential game based on pursuer-evader proximity as termination condition

11 p2073 A70-26242

Pursuit game problems with pursuer and target described by k-dimensional phase vectors, discussing evasion problems

13 p2452 A70-29276

Linear differential evasion game termination with phase vector approaching given subspace in Euclidean coordinates

13 p2443 A70-29755

Pursuit evasion game with uncertain state-dependent measurements, modifying Brown-Robinson algorithm for behavior strategies computation

20 p3660 A70-40384

Unilateral and minimax control with functional restrictions, including pursuit and evasion games

23 p4177 A70-44906

EVECTION

U LUNAR ORBITS

U ORBIT PERTURBATION

U SOLAR GRAVITATION

EVEN-EVEN NUCLEI

Hartree-Fock method to study doubly even nuclei in 2s-1d shell, generating basis functions by Wood-Saxon well

04 p0722 A70-15318

EVENING

Direction and time variations of O I 4368 A emission following evening twilight

18 p3245 A70-36026

EVOLUTION (DEVELOPMENT)

NT ABIOTIC GENESIS

NT BIOLOGICAL EVOLUTION
 NT GALACTIC EVOLUTION
 NT LUNAR EVOLUTION
 NT PLANETARY EVOLUTION
 NT STELLAR EVOLUTION
 Magnetic susceptibility of synthetic australite and
 pillowite-like tektites measured in 77-560 K range,
 discussing origin 05 p0916 A70-16836
 Cosmic evolution of radio sources, discussing ob-
 servations and data interpretation 07 p1374 A70-18746
 Evolutionary effects associated with quasars listed
 in 3CR catalog using Schmidt method 07 p1389 A70-20209
 Inertial navigation evolution, considering Reich
 studies [DFVLR-SONDDR-1] 08 p1540 A70-20683
 Extragalactic radio sources evolution, discussing
 energy requirements of hollow-shell models 12 p2299 A70-27377
 Jacobi ellipsoid quasi-static evolution by gravita-
 tional radiation, discussing direction of increasing an-
 gular velocity toward nonradiating state at bifurcation
 point with Maclaurin sequence 20 p3702 A70-39018
 Cosmic evolution of radio sources, discussing ob-
 servations and data interpretation 21 p3890 A70-41171
 Aircraft handling qualities specifications and defini-
 tions evolution based on test pilot rating correlation
 with engineering data and piloting ease evaluation with
 transfer functions [ICAS PAPER 70-19] 23 p4138 A70-44114
 Scientific satellites evolution during past decade and
 future development possibilities in conjunction with
 space shuttles and stations 23 p4260 A70-44621

EVOLUTION (LIBERATION)
 NT GAS EVOLUTION

EXAMINATION
 NT EYE EXAMINATIONS

EXCHANGING
 NT CHARGE EXCHANGE
 NT GAS EXCHANGE
 NT ION EXCHANGING
 NT RESONANCE CHARGE EXCHANGE

EXCITATION
 NT ACOUSTIC EXCITATION
 NT ATOMIC EXCITATIONS
 NT HARMONIC EXCITATION
 NT SELF EXCITATION
 NT WAVE EXCITATION
 Semiconductor laser excitation by bremsstrahlung
 from electrons and gamma radiation from nuclear
 reactor 01 p0107 A70-10187
 Periodic potential and residual Coulomb interaction
 effect on inelastic light scattering from electronic ex-
 citations in semiconductors, using diagrammatic per-
 turbation theory 01 p0156 A70-10280
 Multistate impact parameter treatment of hydrogen-
 helium excitation collisions, considering distortion,
 back- and rotational-coupling and virtual transition
 sequence 01 p0147 A70-10285
 Total cross section for electron impact excitation
 and ionization in He, CO, nitrogen, oxygen, carbon
 dioxide, ethylene and benzene, emphasizing threshold
 values 01 p0147 A70-10489
 Driving point admittance of infinite cylindrical an-
 tenna excited by uniform gap and immersed in lossy
 compressible isotropic plasma, discussing propagation
 constants 01 p0051 A70-11102
 Nonlinear system under random excitation,
 discussing analytic solution method and statistical pro-
 perties 01 p0206 A70-11149
 Nitrogen, oxygen and air luminescence spectra
 excited by fast electrons at low gas pressures in IR
 spectral region compared with polar auroral spectra 01 p0083 A70-11536
 Excited terminal states emission in bound exciton-
 donor materials to determine donor ionization ener-
 gies, electron effective masses and electron G values 02 p0350 A70-11847
 Cavity resonator linear excitation by Gunn diode,
 considering external circuit effects on oscillation con-
 ditions and GaAs single crystal parameters 03 p0457 A70-13965
 Vertical profiles of atomic and excited molecular
 oxygen concentration in upper atmosphere calculated
 from spectral band intensity, determining excitation
 reaction rates 04 p0682 A70-15733
 Absolute values of emission cross sections for
 vibrational Meinel bands of molecular nitrogen ions
 excited by electron impact 05 p0901 A70-16279
 Excitation emission of diatomic nitrogen molecule
 for first negative band broadening, considering high
 energy primary beam with secondary electrons 06 p1124 A70-18305

Equivalent excited-state temperature of high pres-
 sure plasma calculated for unequal electron and gas
 temperature, considering ion and electron recombina-
 tion 06 p1114 A70-18634
 Rotating and oscillating spectra in diatomic
 molecule excited by slow and fast electrons,
 discussing Boltzmann distribution of excited
 molecules 07 p1337 A70-19044
 IR spectra excited by fast electrons in nitrogen, ox-
 ygen, carbon monoxide, carbon dioxide, nitrogen ox-
 ide, methane, ammonia and water molecules 07 p1337 A70-19045
 Geometrical model of human cardiac excitation
 stages based on normal heart anatomy, discussing ap-
 plication to study of QRS loop in vectorcardiogram 07 p1211 A70-19592
 Solid state laser kinetic regime as function of diffu-
 sive and directional motions of active medium excita-
 tions 07 p1299 A70-19860
 Antenna exciter of crossed radio telescope,
 discussing design, performance and increased wide
 band sensitivity 08 p1473 A70-21069
 Heavy particle collisions impact parameter and
 wave equations for direct excitation and electron cap-
 ture processes 08 p1548 A70-21502
 Chemically formed carbon monoxide lasing in fast
 flow system, discussing reaction and excitation
 mechanisms 09 p1697 A70-22922
 Ionospheric plasma lower hybrid resonance mea-
 surement and excitation via rocket-borne probe 09 p1670 A70-23319
 Nonlinear system with piecewise linear spring
 characteristic response to stochastic excitation of
 white noise type process, discussing technical stability 10 p1918 A70-25323
 Nonlinear panel flutter for random excitation and
 linear/nonlinear aerodynamic loading, using Rayleigh-
 Ritz approximation to Hamilton variational principle 12 p2316 A70-27105
 Low pressure nitrogen and air spectra excitation by
 low energy proton bombardment, using spectroscopic,
 photometric and microphotometric analyses 14 p2619 A70-30653
 Vertical profiles of atomic and excited molecular
 oxygen concentration in upper atmosphere calculated
 from spectral band intensity, determining excitation
 reaction rates 14 p2575 A70-30817
 Semiclassical collision theory for computing fine
 structure proton impact excitation rates and cross sec-
 tions for positive ions, presenting excitation rate ta-
 bles 14 p2652 A70-31383
 Hybrid solid state image detectors, discussing in-
 tegration and excitation storage operation modes 17 p3053 A70-35122
 Metallic core shielded squirrel cage waveguide ex-
 citation by charged filament, giving equations for
 Fourier coefficients of electromagnetic fields 19 p3386 A70-37732
 Metastable excitation levels in np/4 configuration
 for population inversion, discussing free electron col-
 lisions, forbidden line intensity and flow density pres-
 sure 20 p3642 A70-39751
 Resonance excitation of oscillations in diatomic
 molecules by slow electrons, calculating scattering on
 spherical potential well 20 p3642 A70-39753
 Electron impact excitation and ionization cross sec-
 tions, describing various approximation methods 20 p3675 A70-39937
 Strip array excitation by field with large phase shift
 per period, deriving approximate solution from
 averaged boundary conditions 21 p3784 A70-40627
 Nitrogen photoelectron excitation in dayglow, ex-
 amining 3371 A band intensity, energy spectrum and
 flux in ionosphere 21 p3882 A70-41093
 Excited state complexes laser action in coumarin
 dyes indicated from stimulated fluorescence time de-
 pendence 22 p4048 A70-42328
 Atomic or molecular gases excited state lifetime
 measurements, using time to amplitude conversion
 and multichannel analyzer 23 p4198 A70-44946

EXCITED STATES
 U EXCITATION

EXCITONS
 Hydrogen type exciton model applied to analysis of
 intermediate exciton state role in two quantum absorp-
 tion in semiconductors 01 p0153 A70-10068
 Excited terminal states emission in bound exciton-
 donor materials to determine donor ionization ener-
 gies, electron effective masses and electron G values 02 p0350 A70-11847

Exciton spectrum in semiconductor laser emission,
 investigating location in Brillouin zone and tempera-
 ture dependence 07 p1298 A70-19478
 Crystals nonlinear permittivity related to tempera-
 ture-time Green function for electromagnetic radia-
 tion, determining crystal polarizability by light-exciton
 method 07 p1335 A70-19868
 Coulomb interaction during optical transitions
 between Landau subbands of Ge semiconductor
 valence and conduction bands in magnetic field, ob-
 serving diamagnetic excitons 10 p1928 A70-25029
 Second quantization exciton theory in amorphous
 disordered materials, discussing hamiltonian, boson
 annihilation operators and electronic polarization 14 p2627 A70-30693
 Formation and radiative recombination of free ex-
 citonic molecules in CuCl single crystals via Q
 switched ruby laser excitation 24 p4353 A70-45604

EXCRETION
 Ambient temperature effects on rats excretion of
 epinephrine, norepinephrine and major metabolites 02 p0232 A70-11714
 Excretion and balance of K, Ca, Mg, P, S and N
 during prolonged use of dehydrated food diets 03 p0435 A70-13713
 Excretion and balance of K, Ca, Mg, P, S and N
 during prolonged use of dehydrated food diets 11 p1989 A70-25513
 Daily electrolyte excretion dynamics of subjects
 with shifted work-rest schedule, noting disagreement
 with Scharp results 13 p2358 A70-29343
 Transmeridian flights effect on diurnal urinary
 excretion of unconjugated 17-hydroxycorticosteroids
 in males, evaluating time shift effects 21 p3770 A70-41477

EXECUTIVE AIRCRAFT
 U GENERAL AVIATION AIRCRAFT
 U PASSENGER AIRCRAFT

EXERCISE (PHYSIOLOGY)
 Comfort and thermal sensations and associated
 physiological responses during exercise at various am-
 bient temperatures, noting effects on sensory esti-
 mates 01 p0031 A70-11648
 Oxygen consumption, lactic acid production and
 mechanical performance of anesthetized dog gastroc-
 nemius muscle with increased blood flow 02 p0235 A70-12090
 Physiological load of exercise at altitude evaluated
 by heart rate and recovery rate measurements 04 p0631 A70-14984
 Pulmonary extravascular /PEV/ and intravascular
 /PBV/ fluid volumes measured at rest and exercise 07 p1211 A70-19595
 Cardiac output and coronary blood flow during
 steady state recumbent exercise, discussing CO and
 Rb 84 measurements in human subjects 08 p1453 A70-21936
 Energy consumption in male subjects during walk-
 ing and running in erect and supine position under
 simulated gravity 13 p2351 A70-29335
 Exercise and rest of humans under hypoxia and
 hyperoxia, determining blood acid-base state, ventila-
 tion and carbon dioxide partial pressure 16 p2849 A70-34256
 Heart rate-time curves before, during and after step-
 up exercise in relation to physical fitness 22 p3978 A70-42873
 Human ventilatory response to resistance unloading
 during muscular exercise 23 p4144 A70-43823
 Four channel FM radio telemetry for exercise
 physiology, measuring EKG, respiration rate and pul-
 monary ventilation 23 p4151 A70-44380
 Electrolyte changes after marathon running noting
 increase in serum sodium and serum potassium 24 p4302 A70-46108
 Oxygen breathing effects in exercise on respiration,
 circulation and metabolism during high altitude accli-
 matization 24 p4303 A70-46110

EXERTION
 U PHYSICAL WORK

EXHAUST DIFFUSERS
 High hub/tip ratio centrifugal compressor with pipe
 and vane cascade diffusers for turbofan engines,
 determining impeller performance [ASME PAPER 69-WA/FE-28] 04 p0733 A70-14774
 Tailpipe effects on gas turbine diffuser performance
 with fully developed inlet conditions [ASME PAPER 70-GT-86] 18 p3210 A70-36881

EXHAUST FLOW SIMULATION
 NT ATMOSPHERIC ENTRY SIMULATION
 NT FLIGHT SIMULATION
 Wind tunnel tests for engine jet plume effect on
 boattail pressure drag [AIAA PAPER 70-132] 06 p1038 A70-18050

Multiple jet flow exhausting into arbitrary crossflow in ground effect, solving continuity and momentum equations for jet path and induced velocity field
13 p2387 A70-29011

Powered nacelles simulating exhaust flow for propulsion and airframe problems in subsonic flow
[AIAA PAPER 70-636] 16 p2888 A70-33594

Liquid propane turbojet exhaust simulator for wind tunnel propulsion testing, emphasizing nozzle jet properties
[AIAA PAPER 70-634] 16 p2888 A70-33595

Radar backscattering from turbulent rocket exhaust plumes
[AIAA PAPER 69-71] 21 p3791 A70-41730

EXHAUST GASES

Turbojet engines air pollution emissions processes resulting from combustor primary and secondary zone conditions, discussing engine design modifications
[AIAA PAPER 69-1040] 01 p0162 A70-10602

Apollo lunar module descent engine exhaust organic combustion products, estimating ion intensities of various species in all mass spectra
02 p0356 A70-12693

Aircraft engine exhaust emissions air pollution role in air terminal area and adjacent communities
[ASME PAPER 69-WA/APC-4] 04 p0733 A70-14788

Exhaust gas ejectors for engine cooling, discussing ejector design, flow rates, fuel consumption, etc
06 p1129 A70-17144

Heat transfer boundary conditions determination in studying heat protective coatings effectiveness, discussing measurement methods for stagnation temperatures and heat fluxes from exhaust gases
06 p1173 A70-17662

Wind tunnel tests for engine jet plume effect on boatall pressure drag
[AIAA PAPER 70-132] 06 p1038 A70-18050

Jet aircraft air pollutant production and dispersion of nitric oxide and soot, discussing mixing process
[AIAA PAPER 70-115] 06 p1131 A70-18070

Atmospheric contamination due to Be solid propellant exhaust products, discussing pollution levels, governmental restrictions on testing, etc
[AIAA PAPER 70-117] 06 p0997 A70-18085

Titan 3C launch environmental hazards including noise and exhaust cloud content
07 p1393 A70-19225

Fluorocarbon fluid Rankine cycle system utilizing gas turbine exhaust heat for environmental control
[SAE PAPER 7001-60] 11 p1982 A70-25371

Aircraft turbine engines gaseous emission measurements, discussing instrumentation for continuous pollutant concentration monitoring
[SAE PAPER 7002-49] 12 p2290 A70-27428

Standard method for aircraft engine exhaust smoke measurement for air pollution control
[SAE PAPER 7002-50] 12 p2290 A70-27429

Jet engine pollution reduction for airport areas, discussing chemical equilibrium failure in exhaust gases and combustor design
12 p2291 A70-27993

Aircraft smoke emission reduction and elimination by engine modifications
14 p2628 A70-30190

Rolls-Royce RB 211 turbofan engine, discussing fuel consumption, specific weight, noise and smoke level, reliability and maintainability
15 p2787 A70-31948

Rocket exhaust gases radiant heat transfer prediction, using band models with computer program
[AIAA PAPER 70-841] 16 p3000 A70-33924

Titan 3C solid rocket motor exhaust plumes thermal radiation analysis for designing Stage I engines and components thermal protection
[AIAA PAPER 70-842] 16 p3000 A70-33925

ATS-C satellite rocket exhaust plume convective heating measurements of VHF whip antennas, discussing nozzle flow and heating rate
[AIAA PAPER 70-843] 16 p3000 A70-33926

Nonequilibrium combustion products and condensables containing reactive multiphase rocket nozzle flows and exhaust plumes characterization using generalized kinetics streamtube program /MGKS/
[AIAA PAPER 70-845] 16 p3001 A70-33928

Community air pollution from airports, discussing exhaust emissions, pollutant dispersion, etc
17 p3200 A70-35177

Hunting phenomena of hydrogen gas plastic balloon at ceiling altitude, considering exhaust duct, extra volume and shape
17 p3018 A70-35317

Optimum adaptation of propulsion gas generators to power jet driven rotors with blown flap control, considering jet engine, fanjet and engine driven compressor
17 p3024 A70-35661

Fog dissipation on aircraft runways, using aircraft jet engine exhaust heat and mixing properties
17 p3133 A70-35929

Aircraft turbine engines emission sampling, handling and measurement, evaluating various instruments and techniques
[SAE PAPER 7003-38] 18 p3226 A70-36810

Gas turbine emissions analysis for air pollutants, determining species distribution and concentration
[ASME PAPER 70-GT-81] 18 p3226 A70-36883

Exhaust gas ingestion suppression model tests for VTOL lift engines, measuring inlet thermal environment
[AIAA PAPER 70-905] 19 p3490 A70-37396

Aircraft gas turbine engine smoke emission measurement, discussing test equipment and procedure standardization
20 p3689 A70-39720

SERT 2 spacecraft surface contamination by Hg ion thruster effluents, using solar cell sensors
[AIAA PAPER 70-1128] 20 p3690 A70-40217

Aircraft condensation trails formation by interactions of exhaust emission, vorticity of wing induced downwash and ambient atmosphere
22 p3958 A70-42684

Jet engine air pollution in U.S., discussing fuel types, additives and burner design for smoke emission reduction
23 p4233 A70-44200

Warm gas reaction control thrusters via solid propellant exhaust products for ballistic missiles attitude control
[SAE PAPER 7007-80] 24 p4295 A70-45863

EXHAUST JETS

U EXHAUST GASES

EXHAUST NOZZLES

NT CONVERGENT-DIVERGENT NOZZLES

NT PLUG NOZZLES

NT TURBINE EXHAUST NOZZLES

Exit geometry effects on peripheral jet device lift, considering operating height, curtain thickness, base extension, etc
04 p0619 A70-15388

Gross thrust coefficient for turbofan engines thrust estimates, discussing full scale nozzle simulation
04 p0736 A70-15390

Nozzle exit turbulence and excess fuel combustion as low and high speed jet noise source using Lighthill theory
05 p0834 A70-16782

Shot delivery per second per unit area from ejector nozzle during shot peening, determining ideal delivery rates for shot of various sizes
07 p1291 A70-18830

Single and twin jet afterbody configuration models, describing drag and interference characteristics at subsonic speeds
14 p2528 A70-30862

Exhaust nozzle model tests at high subsonic Mach numbers, investigating differences in nozzle drag in contrast to engine conditions
[AIAA PAPER 70-668] 16 p2967 A70-33573

Liquid propane turbojet exhaust simulator for wind tunnel propulsion testing, emphasizing nozzle jet properties
[AIAA PAPER 70-634] 16 p2888 A70-33595

C-5A turbofan engine thrust determination using pressure and temperature values in exhaust nozzles
[AIAA PAPER 70-611] 16 p2969 A70-33606

Computerized design for radial flow splitters in three dimensional fan exhaust nozzles
18 p3207 A70-36462

Exhaust nozzle/airframe interference test evaluation for twin engine supersonic fighter
[AIAA PAPER 69-430] 22 p3958 A70-42702

Hydrogen and air nonequilibrium chemical recombination effects in two dimensional exhaust nozzles, using Bray freezing criterion
22 p3982 A70-42760

Airframe installation effects at transonic speeds on underlying supersonic cruise exhaust nozzles, using flight and wind tunnel tests
22 p3960 A70-43274

Two stream ejector type propelling nozzles for supersonic aircraft, investigating various configuration effects over range of secondary/primary air flow ratios
[ICAS PAPER 70-48] 23 p4133 A70-44145

EXHAUST SYSTEMS

Exhaust gas ejectors for engine cooling, discussing ejector design, flow rates, fuel consumption, etc
06 p1129 A70-17144

Air backflow in nuclear exhaust system duct for ground testing of NERVA engines, noting overpressure effect
[AIAA PAPER 69-325] 06 p1027 A70-17174

Acoustically treated inlet and fan exhaust duct configurations for JT3D turbofan engine on DC 8 aircraft
22 p4090 A70-42533

Optimum manifold and injector hole area of pulsed exhaust systems of two cycle engine with turbosupercharger
22 p4091 A70-42809

EXHAUST VELOCITY

Multistage rocket optimum ascent regime obtained by height function of engine gas outlet velocity
06 p1155 A70-17585

Axisymmetric nozzles flow regimes with subsonic ejection velocities analyzed by stabilization method, noting role of pressure in nozzle exit section
09 p1660 A70-22440

Thrust measurements on pulsed vacuum-arc thruster, comparing specific impulse and efficiency with exhaust velocity measurements by ion collecting double probes
[AIAA PAPER 70-1146] 20 p3567 A70-40207

Alfvén critical velocity concept in MPD arcs analysis, obtaining exhaust velocity relationship from one dimensional flow model
[AIAA PAPER 70-1096] 20 p3683 A70-40240

Exhaust velocity, electron density and temperature of pulsed megawatt nitrogen MPD-ARC thruster, using Thomson scattering of pulsed laser light
[AIAA PAPER 70-1081] 20 p3694 A70-40254

Rocket motion and space propulsion systems, discussing exhaust velocity effect on payload
21 p3869 A70-42039

Spacecraft electric propulsion system performance, discussing exhaust velocity optimization
21 p3869 A70-42043

EXHAUSTION

Blood lactate changes during prolonged exhaustive running at varied intensities and durations
10 p1809 A70-24001

EXISTENCE THEOREMS

Existence theorem used for proof of asymptotic methods in nonlinear stability of laminar flow
[ONERA-TP-750] 01 p0061 A70-10298

Solution existence of linear unsteady Boltzmann equation for single space variable in Hilbert space defined by scalar product
01 p0143 A70-10673

Conditionally periodic orbits existence in restricted problem of three bodies, using similarity transformation
02 p0369 A70-11997

Numerically stable solutions existence for one dimensional monochromatic radiative transfer, using linear algebra including vector and matrix norms, convergence, etc
02 p0340 A70-12643

Elasticity theory contact type problems, proving solutions existence and uniqueness
03 p0589 A70-13346

Differential equations system under side condition, examining solutions existence
03 p0519 A70-14073

Existence theorems for optimal control problems with multiple integrals
03 p0460 A70-14075

Existence conditions of conjugate points for non-trivial solution of fourth order differential equation
03 p0519 A70-14079

Plane static boundary value problems solutions in zero moment elasticity theory, proving solutions existence and uniqueness
04 p0775 A70-15214

Stefan free boundary problems with prescribed flux reduced to form solvable by numerical methods, proving existence and uniqueness theorems
05 p0956 A70-15783

Solutions existence for differential, integral and integrodifferential equations proved by variational imbedding of nonlocal linear Euler-Lagrange operator functioning as automatic adjoint calculator
05 p0881 A70-16060

Existence and uniqueness of nonlinear boundary value problem solutions formulated by fixed point theorem and Green function
05 p0876 A70-16562

Existence and uniqueness, stability and asymptotic stability of nonlinear operator differential equation
05 p0878 A70-17098

Existence and stability problems of nonlinear operator differential equations containing linear operator with domain and range contained in real Hilbert space
05 p0878 A70-17099

Existence results for Cauchy problem for linear variable coefficient hyperbolic operators with multiple characteristics
06 p1094 A70-17898

Linear Boltzmann equation in bounded domain, studying solutions existence, uniqueness and structure
06 p1047 A70-18317

Growth conditions used in existence theorem for calculus of variations in optimal control problems
06 p1027 A70-18506

Existence and uniqueness theorem for boundary value problem solution for parabolic equation in domain with singular points on boundary
07 p1322 A70-18853

Dynamic discrete systems unsteady motions stability, formulating theorem for finite characteristic numbers existence
08 p1543 A70-20493

Existence theorem for linear stochastic systems optimal control described by differential equation with random coefficients, providing rms stabilization
08 p1480 A70-21637

Existence and uniqueness of mixed problem solution for Tricomi equation proved by a priori estimates
10 p1908 A70-23925

Existence theorem for periodic solutions of nonlinear differential equations with deviating arguments
10 p1910 A70-24605

Periodic solution existence theorem using harmonic linearization method
11 p2023 A70-25725

Nonlinear differential equations systems, deriving periodic solutions existence conditions
13 p2440 A70-29049

Existence and uniqueness theorem for boundary value problem solutions to nonlinear canonical ordinary differential equations
17 p3131 A70-35339

Existence theorem for piecewise-continuous solutions of waves and shocks in relativistic MHD, using Riemann manifold
19 p3477 A70-37579

Nonrigorous hyperbolic systems, discussing existence and uniqueness theorems contradiction in linear equations and proof of Cauchy problem
19 p3478 A70-37582

Equivalent interferometer existence theorem in holography
19 p3423 A70-37830

Existence theorem for finite integral matrix extended to infinite matrices, prescribing upper and lower bounds for row and column deficiencies
20 p3657 A70-39445

Existence theorem concerning arbitrarily long good binary block /nonlinear/ codes preserved under large permutation groups
20 p3594 A70-39974

Existence theorem for boundary layer problems, including swirling flow between coaxial rotating disks
22 p4009 A70-42844

Quasi-linear higher order differential equations, examining periodic solutions existence and stability
22 p4062 A70-42698

Linear discrete feedback systems uniqueness, existence and stability under various input-output conditions
22 p4004 A70-43024

Einstein-Maxwell fields in presence of matter and pressure, expressing existence conditions in terms of eigenvalues and eigenvectors of Ricci tensor
22 p4074 A70-43206

Cauchy problem for singular parabolic equation, establishing existence, uniqueness and representation theorem by integral operator techniques in conjunction with function-theoretic methods
23 p4212 A70-44895

Linear elasticity with constraint couples, establishing existence theorems by variational methods
24 p4420 A70-45267

Pre-Maxwellian electromagnetic equations application to MHD, investigating existence theorems generalization from system at rest to system with motion
24 p4386 A70-45593

Nonlinear boundary value problems, deriving existence theorems
24 p4369 A70-46022

One-phase Stefan problem of heat conduction with melting, proving existence and uniqueness theorems for solid and free boundary temperature determination
24 p4429 A70-46036

EXITS (DOORS)
U DOORS
EXOBIOLOGY

Martian hypothetical organisms biological model, describing nonchlorophyllic photosynthesis, epithelial hydrochrome pigments, scale insect morphology, etc
03 p0422 A70-13702

Biological experiment on Zond 5 automatic station in earth-moon-earth trajectory determining cosmic radiation absorption and effects on plant seeds, turtles, larvae, etc
03 p0428 A70-14066

Physical and life supporting properties of hypothetical Martian biosphere, considering organism adaptation theories
05 p0803 A70-17109

Biological performance studies under extreme environmental stresses for gaining insight into potential of earth-type life here and in universe
09 p1623 A70-23699

Martian hypothetical organisms biological model, describing nonchlorophyllic photosynthesis, epithelial hydrochrome pigments, scale insect morphology, etc
11 p1985 A70-25502

Photoelectric device for recording plant rhythmic leaf movements in space
16 p2849 A70-33998

Life detection for unmanned planetary exploration from extraterrestrial sample involving growth, gas changes and carbon dioxide fixation
21 p3769 A70-41003

Extraterrestrial life development and evolution in solar system, describing Mars suitability
22 p3975 A70-43692

Life support systems for biological flight experiments on Biosatellite project and Skylab A mission
23 p4154 A70-44665

EXOSPHERE

Exospheric temperature variations by Thompson scatter technique, considering solar and geomagnetic activity effects
01 p0078 A70-11209

Polar ionic exosphere electric field polarization, considering positive and negative charges escape fluxes, electric potential, mean ion velocity, etc
02 p0289 A70-12108

Dynamic electric field in solar coronal exosphere on basis of kinetic and hydrodynamic theories, giving estimate of solar wind
02 p0359 A70-12609

Ion and electron concentrations far field disturbances caused by satellite motion in ionosphere and lower exosphere, deriving plasma drag
04 p0762 A70-14935

Lyman alpha transition line in exosphere deuterium line implying enrichment factor ratio to earth surface deuterium
04 p0742 A70-15129

Polar ion-exosphere model with open geomagnetic field lines, calculating electrostatic field for region
07 p1270 A70-20077

Simultaneous Thomson scatter measurements for middle and low latitudes, comparing electron density and temperature and exospheric and global temperature distributions
10 p1872 A70-23821

Exospheric density from Echo 2 orbit, observing 27 day variations associated with sun rotation and correlation with geomagnetic disturbances
11 p2046 A70-26566

Wave dispersion in lower exospheric multicomponent plasma, investigating mode group velocity frequency dependence at various altitudes
13 p2395 A70-28940

Upper atmospheric temperature-gravitational potential relationship for sun, earth and several planets
13 p2495 A70-29765

Exospheric density at opposite hemispheres, showing variations from winter helium bulge
15 p2724 A70-31679

Solar wind models based on exospheric theory assuming collisionless particles
15 p2794 A70-32613

Ballistical transport in collisionless exosphere, discussing heat flux of ballistical oxygen and model temperatures for day and night conditions
17 p3080 A70-35765

Electron temperature in 500-1000 km range during minimum solar activity based on Alouette satellite data and atmospheric model, observing latitudinal variation
18 p3254 A70-37029

Earth exospheric plasma distribution, relating solar eclipses effects to geophysical phenomenon
19 p3418 A70-38904

Maximum to minimum exospheric temperature ratio determination, concluding solar wind dependence of diurnal variation in thermosphere
20 p3621 A70-39345

Upper atmospheric temperature-gravitational potential relationship for sun, earth and several planets
20 p3710 A70-40090

Exospheric neutral hydrogen temperature diurnal variation from satellite resonance filter data, suggesting Lyman alpha source external to geocorona
23 p4186 A70-43852

EXOTHERMIC REACTIONS

Exothermic reaction front propagation in condensed phase, analyzing Novozhilov system of equations
01 p0217 A70-11009

Thermal conditions and graph-analytic solution of laminar boundary layer combustion of disk rotating in free atmosphere and plate in Couette flow
01 p0218 A70-11017

Adiabatic calorimeter for exothermic chemical reactions determining heats of polymerization, curing rate and thermal decomposition rates as temperature function for high energy propellants
04 p0688 A70-14711

Solid rocket motor ignition system based on exothermic alloying of bimetallic wire constituents [AIAA PAPER 69-425]
06 p1128 A70-17179

Preignition heat release rate profile in ethylene-air mixture flow against hot surface, determining temperature and velocity distribution optically
07 p1420 A70-19263

Thermal explosion criterion for explosion/ignition delay of exothermic material surrounding heated wire as function of time
07 p1424 A70-20005

Thermal conditions and graph-analytic solution of laminar boundary layer combustion of disk rotating in free atmosphere and plate in a Couette flow
09 p1787 A70-22266

Self heating accompanying exothermic decomposition of gaseous diethyl peroxide in spherical vessel measured positionally by thermocouple
12 p2330 A70-27223

Optimal startup control of jacketed tubular reactor with first order reversible exothermic reaction, presenting distributed maximum principle for diffusional parameter system
16 p2885 A70-33330

Ammonium perchlorate pyrolysis, investigating exothermic surface reactions and gasification rates
16 p2963 A70-33873

Premature exothermic decomposition suppression in propellant grade ammonium perchlorate, using differential thermal analysis
18 p3300 A70-36699

Ammonium and magnesium perchlorate mixture thermal stability study with differential scanning calorimetry, noting exothermic decomposition of AP
20 p3688 A70-40272

Solid rocket propellants linear and nonlinear pressure coupled combustion instability behavior relationship to exothermic surface processes
20 p3694 A70-40274

Titanium powder compacts exothermic solid phase reaction ignition by focused laser pulse, obtaining temperature profile from mathematical model based on energy transport
20 p3639 A70-40473

Laser kinetics based on exothermal chemical reactions for electron transition stimulation, emphasizing single mode operation
24 p4354 A70-45656

EXPANDABLE STRUCTURES

NT BALLOONS
NT BALLUTES
NT BEACON SATELLITES
NT BELLWS
NT EXPLORER 22 SATELLITE
NT HIGH ALTITUDE BALLOONS
NT INFLATABLE STRUCTURES
NT METEOROLOGICAL BALLOONS
NT ROBIN BALLOONS
NT TETHERED BALLOONS

Expandable space hangar with composite wall for orbiting maintenance shelter, providing radiation and meteoroid protection for occupants
02 p380 A70-11934

Deployable STEM /storable tubular extendible member/ booms for aerospace gravity gradient stabilization, noting interlocked BI-STEM
04 p0761 A70-14725

Expandable rigidizable solar shields operational, structural and thermal performance tests conducted with spherical models for cryogenically fueled space vehicles
12 p2312 A70-27131

Optimum overlap design of thin walled tubular extendible spacecraft structures under solar heating in zero-g environment
14 p2657 A70-30762

Storable tubular extendible member /STEM/, discussing advantages of BI-STEM for erecting unfurlable structures in space
16 p2846 A70-34141

Expandable and modular structures technology for manned and unmanned space missions, discussing expandable air lock experiment
17 p3177 A70-35230

Deployable meteoroid shield for Saturn I workshop, describing design and hardware kinematics
23 p4257 A70-44386

Saturn Orbital Workshop experiment for testing chemically rigidized expandable materials and structures for space applications, discussing resin impregnated glass fiber cloth
23 p4264 A70-45012

EXPANSION

NT GAS EXPANSION
NT THERMAL BUCKLING

Self adjoint operator generated by differential expression and pseudodifferential boundary conditions, using Berezanskii procedure for operator eigenfunction expansion
07 p1327 A70-19809

Vertical and horizontal expansion rate of crystallization of dry-ice seeded internal stratus clouds
08 p1538 A70-21109

Hubble expansion constant and expansion deceleration value roles in cosmological model testing
08 p1581 A70-21752

Milky Way expansion, explaining Weber gravitation signals by collisions between neutron and normal star
10 p1943 A70-24698

Algorithm for transfer matrix Heaviside expansion, using Krylov and Vandermonde transformations for multiple eigenvalue case
10 p1910 A70-24705

Slow and fast coronal expansion phenomena associated with solar flares
17 p3152 A70-35869

Expansion motions in inner Galaxy, discussing lower velocity absorption features, mass estimation method and model
19 p3522 A70-38602

EXPANSION WAVES

U ELASTIC WAVES

EXPECTATION

Expected values optimal measurement, given auxiliary conditions between measured value number and quantization
02 p0299 A70-12400

EXPERIMENTAL DESIGN

NT FACTORIAL DESIGN

Experimentation in fluid mechanics research, discussing equilibrium flows, relaxation processes, turbulence structure and digital techniques
02 p0286 A70-12355

Wideband satellites bandwidth and aperture limits direct measurement based on ground monitoring of CW signals, taking into account ionospheric dispersion

02 p0261 A70-12577

Mathematical planning of experiments applied to biological mineralization of human wastes, using continuous microorganism cultivation

03 p0435 A70-13715

Reaction time task to examine relationship between preparatory intervals and auditory stimulus intensity in experimental designs

03 p0424 A70-13764

Experiment design and data acquisition for V/STOL aircraft flying qualities simulations, emphasizing pilot rating and comment data and control usage information

[SAE PAPER 690695] 05 p0825 A70-15860

Experimental procedure for investigating radioprotective effectiveness of chemical compounds against X ray irradiation, discussing Cysteamine protection for golden hamsters and fetuses

06 p0993 A70-17429

Identification experiments and computational algorithms allowing synthesis of adaptive optimization process for real dynamic plants

06 p1023 A70-17634

Solar activity model for simulating scheduling of observation experiments for Apollo Telescope Mount missions

[AIAA PAPER 70-32] 06 p1145 A70-18121

Electron diffusion in magnetosphere, describing experimental model

07 p1367 A70-19494

Man-computer interactions in experiment design analysis, discussing applications to computer simulation

08 p1464 A70-20606

IR spectral absorption coefficients determined for water vapor at high temperatures, describing experimental details including data acquisition and reduction

09 p1725 A70-22069

Equipment design for burst synchronization control in TDMA experiment system

10 p1836 A70-24339

Photogrammetry methods for experimental structural mechanics, describing Balplex 525 Plotter camera system, image measurement and displacement vector computation

10 p1827 A70-24736

Navigational satellite communication experimental design emphasizing mobile, ship or aircraft station technical characteristics

[AIAA PAPER 70-407] 11 p2001 A70-25469

Mathematical planning of experiments applied to biological mineralization of human wastes, using continuous microorganism cultivation

11 p1990 A70-25515

Differential thermal analysis-effluent gas analysis /DTA-EGA/ experiment for lightweight Martian landed capsule

11 p2050 A70-25802

Cloud model development and computer simulation uses, noting applications to aerospace experiment design

14 p2608 A70-30597

ALSEP component configuration and deployment environment, describing passive thermal control system for data processing equipment

14 p2651 A70-31340

Electron diffusion in magnetosphere, describing experimental model

15 p2795 A70-32739

Nonlinear regression techniques for statistical simultaneous measurement of thermal properties including convergence criterion

16 p2998 A70-33859

Mariner Mars 1971 scientific experiments, describing onboard equipment, mission objectives, etc

16 p2983 A70-34026

ALSEP magnetometer mission and environmental requirements and mechanical design

16 p2914 A70-34152

Ten year NASA manned space station in low earth orbit, grouping experiments in functional program elements /FPE/

[AAS PAPER 70-033] 17 p3156 A70-34802

Alouette and ISIS experiments programs and design

17 p3180 A70-35305

Manned space station design, discussing durations of scientific experiments and crew operation

19 p3532 A70-37752

Attention theory experimental design logic, discussing quantitative theory

19 p3362 A70-38315

Auditory direction finding ability, discussing experimental arrangement, white noise production, test conduction and statistical evaluation

20 p3582 A70-40538

Apollo lunar surface experiment package-SNAP 27 program, discussing mission profile, design and performance characteristics

22 p4071 A70-43194

Sequential experiments design and model discrimination, comparing Chernoff and Box-Hill approaches

22 p4064 A70-43527

EXPERIMENTATION

Automatic control systems for scientific experiments, considering algorithms, mathematical models and system designs

13 p2524 A70-28887

ATS 6 and 7 satellite design features, operational characteristics and experiments objectives

[AIAA PAPER 70-1307] 24 p4415 A70-45375

EXPIRATION

Gravity dependent lung region emptying sequence effects on alveolar Xe 133 and nitrogen plateaus in pivoted subjects

13 p2356 A70-29944

Intermittent forced inspirations or expirations effects on venous tone and blood flow in human skin vessels

17 p3024 A70-34595

Expiratory gas flow oscillations during forced vital capacity maneuvers in atmospheres of various composition and pressure

22 p3981 A70-43702

EXPIRED AIR

Radiology instrument for examining pulmonary functions during deep inspiration, expiration and rest, describing material, components and assembly, mounting and radiogram development

01 p0040 A70-11401

Respiratory flow rate effect on emptying of lung regions, assessing regional and end-expiratory volumes

03 p0428 A70-14155

Human exhaled air contaminants analysis role in disease diagnosis, metabolism study and spacecraft cabin atmosphere changes

07 p1220 A70-19514

Cardiac output in humans by analog computer program using mass spectrometer analysis of expired air

08 p1454 A70-21948

Human exhaled air contaminants analysis role in disease diagnosis, metabolism study and spacecraft cabin atmosphere changes

11 p1991 A70-26113

Exhaled alveolar air data acquisition using mass spectrometer and multichannel analyzer

19 p3367 A70-37356

Uncoated quartz twin crystal microbalance for monitoring water vapor content of respiratory gases

19 p3368 A70-37844

EXPLODING CONDUCTOR CIRCUITS

U CIRCUITS

U EXPLODING WIRES

EXPLODING CONDUCTORS

U EXPLODING WIRES

EXPLODING WIRES

Electrical exploding wire experiments at constant current with inductive energy storage system, discussing experiments with various cross sectioned copper wires

02 p0338 A70-11870

CW and radar type RF signal effects on electroexplosive devices sensitivity in bridgewire heating mode

03 p0550 A70-14142

Exploding bridgewire detonator electrical input requirements, discussing waveform, peak current and time to peak

03 p0550 A70-14143

Exploding wire discharges in high vacuum, discussing particle emission MHD instabilities, plasma temperature and electron density

05 p0890 A70-16820

Facility for studying energy characteristics of electrohydraulic stamping, discussing copper wire exploding in water

06 p1077 A70-17869

Refractory metals electrical resistivity as function of density near critical point, using exploding wire

07 p1335 A70-19899

Thermal explosion criterion for explosion/ignition delay of exothermic material surrounding heated wire as function of time

07 p1424 A70-20005

LC circuit with time dependent resistance containing wire explosion physics, solving differential equation of discharge circuit

09 p1726 A70-22492

Exploding tungsten wires in air and vacuum, describing visible and X-ray spectrum characteristics

10 p1915 A70-23994

Operation characteristics of flash, arc, incandescent and explosion type laser pump lamps

13 p2431 A70-29874

Chemical reactor using successive rapid multiple electrical explosions of metal wires

15 p2717 A70-32436

Hypervelocity gas, electromagnetic, explosive drive and exploding wire accelerometers and high explosive, shaped charge, plasma drag and electrostatic accelerators for projectile impact studies

15 p2718 A70-32783

Tungsten exploding wires electron emission during vacuum melting

17 p3137 A70-35726

Plasma vortices during electrodynamic distortion of curved copper wire exploding in atmospheric air, using shadowgraphs

22 p4081 A70-42807

Striations due to mechanical oscillations in fast wire explosions, using dispersion for elastic waves in solid cylinders

22 p4074 A70-43002

Exploding wire light source modification by immersing in transparent fluid to increase intensity, measuring spectral characteristics

[SMPT PREPRINT 64] 22 p4032 A70-43037

Volt-ampere characteristics of exploding Cu, Nichrome, Al and Ni wires during explosions induced by pulsed current in air

24 p4378 A70-45466

EXPLOITATION

Plasticity and superplasticity exploitation - Conference, Eastbourne, Sussex, England October 1969

12 p2327 A70-28143

EXPLORATION

NT LUNAR EXPLORATION

NT SPACE EXPLORATION

Gravity and magnetic geophysical prospecting methods, discussing data acquisition, reduction and analysis in terms of underground geologic anomalies

22 p4018 A70-43086

EXPLORER SATELLITES

NT EXPLORER 33 SATELLITE

NT EXPLORER 38 SATELLITE

NT EXPLORER 40 SATELLITE

EXPLORER SATELLITES

NT EXPLORER 1 SATELLITE

NT EXPLORER 4 SATELLITE

NT EXPLORER 17 SATELLITE

NT EXPLORER 19 SATELLITE

NT EXPLORER 20 SATELLITE

NT EXPLORER 21 SATELLITE

NT EXPLORER 32 SATELLITE

NT EXPLORER 33 SATELLITE

NT EXPLORER 38 SATELLITE

NT EXPLORER 40 SATELLITE

NT OUTER PLANETS EXPLORERS

NT RADIO ASTRONOMY EXPLORER SATELLITE

EXPLORER 1 SATELLITE

Extraterrestrial sources radiation including galactic, solar and magnetospheric radio emissions observed by RAE-I satellite at long wavelengths

[AIAA PAPER 69-1049] 01 p0170 A70-10603

Solar activity indices and upper atmospheric density interrelationship from Explorer 1 satellite observations, showing statistical variations

02 p0356 A70-11762

EXPLORER 4 SATELLITE

Explorer 4 magnetic coordinates recalculation using spherical harmonic representation and modified B-L package

12 p2222 A70-27191

EXPLORER 17 SATELLITE

Atmospheric density measurements from Explorer 17 satellite by density gage and drag techniques resolved for difference by calibration and systematic errors considerations

04 p0691 A70-15120

EXPLORER 19 SATELLITE

Period changes of satellite 1963 53 A due to accelerations from atmospheric drag and solar radiation pressure

02 p0362 A70-11764

EXPLORER 20 SATELLITE

Spin decay from telemetered flight data of Explorer 20 compared with calculation based on solar influence theory

07 p1394 A70-19721

EXPLORER 22 SATELLITE

Faraday rotation observations on Explorer 22 signals at two receiving stations, discussing comparative evaluation procedures and results

03 p0472 A70-12874

Troposphere effects on low incident Explorer 22 satellite signal amplitude, noting role of diffraction

03 p0449 A70-13611

EXPLORER 31 SATELLITE

Positive ionospheric ion species concentration measurements using magnetic deflection mass spectrometer on Explorer 31 satellite

21 p3815 A70-40999

EXPLORER 32 SATELLITE

Ionosphere atmospheric densities from Explorer 32 drag data including semiannual variations

01 p0077 A70-11206

EXPLORER 33 SATELLITE

Solar-magnetospheric neutral sheet reconnection and noise in geomagnetic tail from Explorer 33 Ames magnetometer

22 p4013 A70-42471

EXPLORER 38 SATELLITE

Explorer 38 critical component equilibrium temperature tests in thermal vacuum chamber using modified solar simulator, noting agreement with model

[AIAA PAPER 69-999] 02 p0275 A70-12527

EXPLORER 40 SATELLITE

Ion cyclotron whistler in Injun 5 satellite VHF radio noise data
09 p1638 A70-23499

EXPLOSIONS

NT AERIAL EXPLOSIONS
NT CHEMICAL EXPLOSIONS
NT GAS EXPLOSIONS
NT NUCLEAR EXPLOSIONS
NT THERMONUCLEAR EXPLOSIONS
NT UNDERGROUND EXPLOSIONS
NT UNDERWATER EXPLOSIONS

Expansion isentropes of TNT/hexogen melts explosion products from measured shock wave parameters in Al, organic glass, foam polystyrene, argon and air
01 p0216 A70-11003
Blast wave model for galaxy M82 explosion using Sedov self similar solutions, indicating line excitation mechanism origin in shock wave heating and compression
02 p0372 A70-12247

Explosion analogy to study hypersonic flow region behind shock wave including boundary layer at blunt body surface
03 p0406 A70-13332

Gas dynamics analysis of explosion phenomena based on unsteady flow fields and thermodynamic properties of chemically reacting substance
03 p0607 A70-13922

Graphite-polyester plastic material with electrical resistance for eliminating static charges leading to explosions
07 p1295 A70-19764

Shock propagation from point explosion energy source into cold exponential atmosphere with radiative heat transfer in rear of shock front
10 p1869 A70-24525

Expansion isentropes of TNT/hexogen melts explosion products from measured shock wave parameters in Al, organic glass, foam polystyrene, argon and air
10 p1960 A70-25008

Tapered resonance tubes matching supersonic air jet geometries considered for explosion hazards created by pneumatic system seals failure
11 p2035 A70-25981

Dissection techniques for measuring dynamic parameters of debris clouds expanding from energetic events
14 p2584 A70-30510

Explosion analogy to study hypersonic flow region behind shock wave including boundary layer at blunt body surface
14 p2528 A70-30711

Pentolite spherical charge gaseous explosion products expansion into vacuum, using Taylor similarity solution for flow in detonation wave
15 p2774 A70-31764

Hydrogen solubility in electrically exploded metals
15 p2762 A70-32747

Vacuum effect on explosive coupling seismic energy considered in lunar geophysical experiment
16 p2896 A70-33092

Gas dynamics of explosions and reacting systems - Conference, Novosibirsk, U.S.S.R., August 1969
17 p3074 A70-35882

Nonlinear interactions of plasma waves with positive and negative energies producing explosive instability
18 p3295 A70-36420

Porous matrix explosions during sublimation of dusty ice with nonvolatile particles
19 p3471 A70-37659

Explosive phase of solar flares in nonuniform atmosphere, determining explosion energy and shock wave front shape for various times
20 p3699 A70-39463

Radiative propagation nondiffusive effects of thermal pulse in explosion, obtaining solutions for plane and spherical case by asymptotic expansion and numerical integration
21 p3950 A70-41379

Spherical shock from point explosion in medium with varying density, obtaining exact similarity solution for propagation
21 p3808 A70-41448

Short pulse length X ray flash electro-optical recording equipment for explosive processes, describing technique, experimental setup, optical characteristics and information retrieval
[SMPT PREPRINT 69]
22 p4037 A70-43071

EXPLOSIVE DECOMPRESSION

Thoracic cage, heart and extirpated lung dimensions measurement for dogs before and after explosive decompression and after ground level recompression
08 p1448 A70-21793

EXPLOSIVE DEVICES

NT BOMBS [ORDNANCE]
NT DETONATORS
NT INITIATORS [EXPLOSIVES]
NT SHAPED CHARGES

Electrical and thermal factors in mathematical characterization of electroexplosive devices, including heuristic predictions
03 p0548 A70-14119

Fixed gap electrostatic spark discharge apparatus for booster type explosive sensitivity tests, discussing construction of two models, safety features and results
03 p0548 A70-14120

Nondestructive testing of Apollo CSM /Command and Service Module/ spacecraft ordnance explosive devices by indirect and direct neutron radiography
03 p0494 A70-14123

Electroexplosive devices /EED/ in electromagnetic environments, discussing principles of warship safety
03 p0549 A70-14129

Test setup to determine safe limits of atmospheric potential gradients in electroexplosive device initiation
03 p0549 A70-14136

Reduced ambient pressure effects on hot wire sensitivity of initiating materials of electroexplosive devices used in missiles
03 p0549 A70-14139

Performance characteristics of RDX-metal sheath systems, using high speed motion picture photography for missile design applications
03 p0550 A70-14141

Sonic bang simulation by linearly distributed explosives, creating blast waves with wide range of shapes and durations
05 p0796 A70-16796

Explosive driver development with hypervelocity gas in thin walled tube surrounded by concentric cylinder of high explosive, discussing detonation wavefront propagation
07 p1248 A70-19098

Remote controlled diaphragm exploding device associated with shock tube for MHD generator
11 p2090 A70-26170

Nonmagnetic explosive actuated indexing device permitting precise 180 deg rotation of magnetometer sensor on Pioneer 6 spacecraft
16 p2914 A70-34124

Explosively actuated /pyromechanical/ devices for spacecraft, discussing guidelines for design, testing, application and cost efficiency
16 p2963 A70-34125

Agenda D vehicle self destruct charge ordnance component, discussing design, performance and tests
16 p2963 A70-34126

Shock wave and surface velocity measurements in exploding foil testing by streak photography with image converter camera
21 p3824 A70-40863

Emergency life saving instant exits for transport aircraft, using electromechanical confined transfer shaped explosive device
23 p4141 A70-44487

EXPLOSIVE FORMING

Displacement rate measurement in initial portion of blank subjected to explosive forming by capacitance pickup
06 p1076 A70-17868

Explosive forming of large domes from flat blanks with full scale trial-and-error elimination [ASTME PAPER MF-69-186]
12 p2240 A70-27079

Ti explosive bonding and forming, examining peel and shear strengths on Ti clad steel plate
17 p3098 A70-34446

Elastoplastic deformations during explosive extrusion of pipes of different materials with linear strain hardening law
18 p3335 A70-36132

EXPLOSIVE GASES

U FLAMMABLE GASES

EXPLOSIVE WELDING

Modified explosive bonding process for welding wire reinforced Al composite materials
03 p0497 A70-13120

Cover plates unsteady motion during explosive welding of metals, discussing edge damage
13 p2416 A70-28484

Explosive bonding applications, safety, detonation velocity, cost and handling
13 p2419 A70-29119

Weld transition joints from explosive bonded Al-steel and Al-Cu composite plates, discussing mechanical and electrical properties
17 p3102 A70-35551

Explosive metal bonding in electronics, noting explosive strength and initial surface angle effects on bond physical and chemical properties
19 p3438 A70-38752

EXPLOSIVES

NT CELLULOSE NITRATE

NT PENTOLITE

NT RDX

NT TRINITROTOLUENE

Critical diameter and detonation parameters of nitromethane and tetranitromethane as function of powder content
01 p0217 A70-11004

Smoked-foil technique for transverse wave quantitative study in condensed-phase explosives
03 p0606 A70-13814

Explosives and pyrotechnics information sources including government manuals, commercial publications, symposium proceeding, R and D programs
03 p0610 A70-14127

Laboratory bench technique assessing performance of explosives, using brass small arms cartridge cases as witness vessels
05 p0894 A70-16323

Al powder explosive compacting processing, equipment and tests noting heat treatment effect
05 p0894 A70-16324

Shock wave amplitude found strongest influence in explosives initiation to detonation by shock
07 p1359 A70-19675

Detonation model, discussing combustion gases from solid explosives detonation
13 p2520 A70-28803

Impulsive loading of structures via light-initiated sprayed explosives
17 p3059 A70-35162

Combustion rate as function of oxidizer molecular refractivity in perchlorates and nitrates of aliphatic and aromatic mono- and polyamines explosives
21 p3783 A70-42241

Solid propellant ingredients and explosives differential thermal analyses, discussing thermogravimetry, isothermal or adiabatic constant volume decomposition, crystallographic phase changes, etc
21 p3865 A70-42263

EXPONENTIAL FUNCTIONS

NT LOGARITHMS

Leonid meteoroids mass distribution law exponent evaluation based on unstable meteoric radio echo durations integral distribution
03 p0574 A70-13884

Time-varying loads effect on linear elastically hereditary media described by generalized fractional-order exponential functions and Rzhantitsyn type viscoelastic kernels
05 p0946 A70-16954

Cyclic codes for error correction noting connection with exponential sum theorems
11 p2074 A70-26312

Characteristic exponents for periodic orbits of infinitesimal body attracted according to Newtonian law by two finite bodies revolving in ellipses about mass center
13 p2498 A70-30005

Nonlinear discrete systems absolute stability exponential property proved by modified frequency condition, applying analog transformation to Szego-Kalman equations
16 p2882 A70-33044

Incompressible laminar boundary layer, vortex and axisymmetric wake/jet flow parabolic equations solution by weighted residuals method, describing use of exponentials
17 p3074 A70-35883

Distribution functions of cosmic ray path length, obtaining exponential type for high and low energy data
19 p3509 A70-38146

Exponential kernel approximation effect on radiative energy transfer in high temperature hydrogen plasma
20 p3684 A70-40278

EXPONENTS

Leonid meteoroids mass distribution law exponent evaluation based on unstable meteoric radio echo durations integral distribution
03 p0574 A70-13884

EXPORTS

U INTERNATIONAL TRADE

EXPLOSURE

Optical performance of image intensifier system with good resolution for exposure times down to 1 nsec
04 p0695 A70-15568

Automatic exposure control system for airborne cameras, providing iris and shutter control through taking lens for sudden light changes
05 p0844 A70-15771

Noontime ground surface temperature relationship to exposure and slope angle for meadows and woodland, using airborne IR pyrheliometer
06 p1054 A70-17415

Photoelectric exposure meter for meridian circle readings photographic recording
08 p1496 A70-21159

Exposure duration effect on luminance requirements for hue perception and identification
17 p3040 A70-35724

Automatic shutter for recording holograms with laser light, controlling exposure time by photoconductor cell
23 p4197 A70-44472

Aerial survey cameras exposure time automatic control circuits for high quality photographs with constant integral density
24 p4334 A70-45497

Exposed photographic layers blackening phenomenon energy spectrum and mean square
24 p4336 A70-45655

Industrial radiography for nondestructive control of products quality, discussing exposure time determination method
24 p4337 A70-45712

EXPRESSIONS [MATHEMATICS]

U FORMULAS [MATHEMATICS]

EXTENSOMETERS

- High temperature vacuum dilatometer for continuous photographic recording of expansion curves for refractory materials, determining thermal expansion coefficient 09 p1675 A70-22565
- Automatic dilatometers for volume variations in steel and Co-W alloy during aging and heat treatment, noting microstructural changes 18 p3257 A70-36202

EXTERNAL STORES

NT PODS [EXTERNAL STORES]

- Flight tests to investigate external munitions carriage effect on aircraft stability and control 08 p1437 A70-21733

EXTINCTION

- Statistical analysis of Zwicky catalog of galaxies and clusters of galaxies, interpreting very distant clusters in terms of intergalactic extinction 05 p0915 A70-16697

- Ignition and extinction of diffusion flames predicted from studying forced convection in boundary layers [WSCIPAPER 69-36] 06 p1178 A70-17976
- Ignition and extinction in opposed jet diffusion flame for flow of compressible fluid with competitive/chain reactions 07 p1422 A70-19578

- Propellant extinction near powder-metal contact to study nonsteady combustion mechanism 09 p1742 A70-23228

- Bend /near 4300 A/ in Nandy interstellar extinction rules effect on Geneva Observatory photometric index in seven colors 13 p2498 A70-30014

- Extinction pressures of polyurethane propellants increased by presence of AP, AP coated with silane and KP [AIAA PAPER 70-657] 16 p2963 A70-33619

- Extinction model of composite solid propellant combustion including wall and flame heat release zones 17 p3147 A70-34511

- UV interstellar extinction from comparison of epsilon and zeta Persei, noting graphite features 17 p3159 A70-34877

- Extinction condition for diffusion flame formed from opposing coaxial gas jets 20 p3739 A70-40399

EXTINGUISHERS

U FIRE EXTINGUISHERS

EXTINGUISHING

- Motor design parameters effects on solid propellant extinguishment predicted from mathematical combustion model 16 p2962 A70-33571

- Solid propellant extinguishment by rapid depressurization, investigating motor configuration effect, binder, burning rate catalyst, oxidizer, metal loading and exhaust pressure levels 16 p2962 A70-33572

- Combustion extinguishment of composite solid propellant motors by fluid injection, considering binder, curing agent and burning rate catalyst [AIAA PAPER 70-641] 16 p2968 A70-33599

- Oxygen atom catalytic recombination and flame inhibition mechanism literature survey 23 p4157 A70-44002

EXTRACTION

NT ION EXTRACTION

- Morphological box for extracting chemical elements and compounds from lunar materials for manned operations on moon 14 p2634 A70-30200

EXTRAGALACTIC LIGHT

U EXTRATERRESTRIAL RADIATION

U LIGHT [VISIBLE RADIATION]

EXTRAPOLATION

- Monograph on integral calculation method for disk problems with mixed boundary conditions covering two dimensional stress-strain state, extrapolation methods, etc 11 p2140 A70-26474

- Differential equations in two point boundary value problems solved by combining Newton-Raphson iterative method with parameter variation extrapolation 12 p2260 A70-27003

- Controlled systems characteristics multistep statistical evaluation by extrapolation, analyzing prediction errors 20 p3593 A70-39904

EXTRATERRESTRIAL ENVIRONMENTS

- NT CHROMOSPHERE
- NT CISLUNAR SPACE
- NT DEEP SPACE
- NT INTERPLANETARY SPACE
- NT INTERSTELLAR SPACE
- NT JUPITER ATMOSPHERE
- NT LUNAR ATMOSPHERES
- NT LUNAR ENVIRONMENT
- NT MARS ATMOSPHERE
- NT MARS ENVIRONMENT
- NT PLANETARY ATMOSPHERES
- NT PLANETARY ENVIRONMENTS
- NT SOLAR ATMOSPHERE
- NT STELLAR ATMOSPHERES

- Signal reception possibly due to gravitational radiation of cosmic origin, estimating energy 07 p1387 A70-19699

- Line of demarcation of national sovereignty between air space and free space 12 p2334 A70-27009

- Astronomical observations from outside terrestrial atmosphere, discussing vehicles and equipment for solar and stellar research, rocket and balloon data, etc 23 p4257 A70-45043

EXTRATERRESTRIAL LIFE

- Martian hypothetical organisms biological model, describing nonchlorophyll photosynthesis, epithelial hydrochrome pigments, scale insect morphology, etc 03 p0422 A70-13702

- Physical and life supporting properties of hypothetical Martian biosphere, considering organism adaptation theories 05 p0803 A70-17109

- Space law by analogy with earth legal concepts, considering possible relations with extraterrestrial life 07 p1427 A70-18887

- Soviet book on extraterrestrial civilizations and problems of interstellar communication 08 p1457 A70-20766

- Conditions for life in universe, analyzing evolutionary stages of matter to determine steps producing complex organic compounds 09 p1762 A70-23121

- Biological performance studies under extreme environmental stresses for gaining insight into potential of earth-type life here and in universe 09 p1623 A70-23699

- Mars biological activity suggested from metabolic energy cycle based on oxidation of carbon monoxide [NGL-07-004-043] 09 p1765 A70-23798

- Martian hypothetical organisms biological model, describing nonchlorophyll photosynthesis, epithelial hydrochrome pigments, scale insect morphology, etc 11 p1985 A70-25502

- Differential thermal analysis capabilities in mineralogy for determining present/past planetary environmental parameters having significance for biological experiment 11 p1994 A70-25811

- Cryobiological data for life mechanisms on planets in solar system emphasizing Mars 14 p2536 A70-30344

- Replicating molecules on primordial earth, suggesting chemical evolution on Jupiter via demonstrable alpha-aminonitriles synthesis 14 p2536 A70-30364

- Venus water presence from Venera 4 and Mariner 5 data suggesting polar seas and oceans saturated with hydrochloride and carbon dioxide as plant life source 14 p2637 A70-30365

- Organic compounds detection and identification on Mars surface for living systems existence or evolution 16 p2857 A70-33977

- Scanning UV spectrometer for Mariner Mars 1971 orbital mission, investigating atmospheric composition for biological activity 16 p2978 A70-34030

- Hydrogen flame ionization detector /HYFID/ for life-derived organic matter in Martian/Lunar soil 19 p3426 A70-37896

- Life detection for unmanned planetary exploration from extraterrestrial sample involving growth, gas changes and carbon dioxide fixation 21 p3769 A70-41003

- Apollo 11 lunar dust and microbeicri microscale biological examination, discussing biological morphology 21 p3778 A70-41620

- Apollo 11 lunar fines carbon compounds, examining chemical state of porphyrins, fatty and amino acids, purines, pyrimidines and carbohydrates, etc 21 p3779 A70-41625

- Viable organisms in Apollo 11 lunar fines, discussing tests, laboratory and sterile biological barrier system 21 p3911 A70-41634

- Lunar soil sample preparation and monitoring for viable microorganisms presence 22 p3978 A70-42973

- Hydrogen, N, O, Kr methane and carbon dioxide gas chromatographic examination, discussing life detection device for Mars landing 22 p3983 A70-43094

- Apollo 11 lunar rock samples examined for clues to moon life 22 p3972 A70-43425

- Extraterrestrial life development and evolution in solar system, describing Mars suitability 22 p3975 A70-43692

- Venus vegetative life suggested from algae growth under pure carbon dioxide in hot acid media at high pressures 23 p4253 A70-44836

- Space biological exploration for determining life origin on earth, emphasizing extraterrestrial life possibilities on other planets 24 p4301 A70-46000

EXTRATERRESTRIAL MATTER

- NT COSMIC GASES
- NT COSMIC PLASMA
- NT INTERPLANETARY GAS

NT INTERSTELLAR GAS

- Chemical analysis of Australasian tektites inferring extraterrestrial igneous origin, noting similarity to preimpact parent rock 05 p0916 A70-16832

- Tektite field studies in China concerning stratigraphic occurrence and chemistry 06 p1148 A70-18393

- Single parameter photometric analysis for density distribution of matter in comets atmospheres 07 p1374 A70-18707

- Color and black-and-white photomicrographs and photomicrographs of Apollo 11 moon rock sample consisting of spongy gray mass of pumice-like material 07 p1288 A70-20224

- High energy neutron activation method for remote extraterrestrial in situ rock surface constituents analysis 10 p1932 A70-24614

- Recovered extraterrestrial material, considering activation analysis, mass spectroscopy, emission spectroscopy, flame photometry, etc 10 p1942 A70-24615

- Extraterrestrial magnetic spherules concentration in relation to meteor shower activity and rainfall probability 14 p2640 A70-30740

- Fossil nuclear particle tracks in extraterrestrial matter using high voltage electron microscope and chemical etching 19 p3519 A70-38031

EXTRATERRESTRIAL RADIATION

NT EXTRATERRESTRIAL RADIO WAVES

NT GALACTIC RADIATION

NT GALACTIC RADIO WAVES

NT INTERSTELLAR RADIATION

NT LUNAR RADIATION

NT PLANETARY RADIATION

NT PRIMARY COSMIC RAYS

NT SOLAR CORPUSCULAR RADIATION

NT SOLAR COSMIC RAYS

NT SOLAR PROTONS

NT SOLAR RADIATION

NT SOLAR RADIO BURSTS

NT SOLAR RADIO EMISSION

NT SOLAR WIND

NT SOLAR X-RAYS

NT STELLAR RADIATION

NT STELLAR WINDS

NT SUNLIGHT

NT TYPE 2 BURSTS

NT TYPE 3 BURSTS

NT TYPE 4 BURSTS

NT TYPE 5 BURSTS

NT ZODIACAL LIGHT

- Extrastellar far IR background radiation observed with liquid He cooled telescope carried by Aerobee rocket 02 p0358 A70-12197

- Nuclear and space radiation effects - IEEE Conference, Pennsylvania State University, July 1969 04 p0656 A70-14726

- Particle flux and dose rates in Jupiter Van Allen belts based on assumed synchrotron radiation from trapped electrons in dipole magnetic field [AIAA PAPER 69-18] 04 p0742 A70-15543

- Scientific equipment on Cosmos 237 satellite for recording extraterrestrial radiation data, discussing specifications, operation and mission purpose 05 p0851 A70-16733

- Space radiation environment, discussing characteristics and measurement techniques of various radiation types and sources 06 p1134 A70-17260

- Dose calculation by space radiation dose evaluation codes /SPARDEC/ for various space radiation environments 06 p0990 A70-17261

- Space environment radiation dose monitoring systems requirements and implementation, discussing material distribution, dose equivalence, parameters accuracy, etc 06 p0990 A70-17262

- Radiation dose measurements from satellite and space probe experiments, considering radiation and shielding characteristics, sensor orientation effects, etc 06 p0990 A70-17266

- Space radiation doses in inner Van Allen belt, comparing calculated and satellite measured rates 06 p0991 A70-17272

- Spacecraft radiation environment, dosage and shielding problems, discussing high energy protons and electrons exposure hazards for astronauts and mission planning computer codes 06 p0991 A70-17273

- Universal X ray background as superposition of nascent pulsars in various galaxies, using Crab Nebula pulsar as guide 09 p1748 A70-23792

- Extragalactic objects polarization due to synchrotron radiation superimposed on stellar radiation, discussing Seyfert galaxies nuclei 12 p2307 A70-27869

Catalog in tabular form of discrete celestial X ray sources in energy region above 2 keV
13 p2489 A70-28903

Scorpio X-1 and Taurus X-1 /Crab/ X ray flux effects on nighttime ionospheric radio transmission, discussing ion production and resulting electron density
14 p2631 A70-30541

Space radiation effects on secondary electron conduction /SEC/ image tube performance, observing temporary degradation and permanent damage
16 p2878 A70-33433

High energy electrons in near space excess radiation from high altitude balloon and satellite data
18 p3307 A70-36170

EXTRATERRESTRIAL RADIO WAVES
NT GALACTIC RADIO WAVES
NT SOLAR RADIO BURSTS
NT SOLAR RADIO EMISSION
NT TYPE 2 BURSTS
NT TYPE 3 BURSTS
NT TYPE 4 BURSTS
NT TYPE 5 BURSTS

Cosmic radio absorption nightly variations, considering ionospheric structure and composition and various scattering mechanisms
07 p1367 A70-19456

Cosmic microwave radiation origin based on discrete source models
13 p2479 A70-29787

Cosmic radio absorption nightly variations, considering ionospheric structure and composition and various scattering mechanisms
18 p3309 A70-36930

Extended extragalactic bright radio sources with complex structure, comparing radio to optical field
21 p3892 A70-41189

Extragalactic radio source optical identifications showing association with quasars or Seyfert galaxies nuclei
24 p4413 A70-46168

EXTRATERRESTRIAL RESOURCES
Applied sciences research and utilization of lunar resources - Conference, New York, October 1968
14 p2633 A70-30192

Lunar resources classified as rocket fuel, construction and life support materials, discussing implications for manned surface exploration missions
14 p2634 A70-30198

Extraterrestrial resources for space flight maintenance and human life support in space and on extraterrestrial bodies
14 p2634 A70-30199

Morphological box for extracting chemical elements and compounds from lunar materials for manned operations on moon
14 p2634 A70-30200

Treaty on principles governing activities of states in exploration and use of outer space, appraising various provisions
17 p3173 A70-35792

Lunar and other celestial bodies natural resources, discussing need for international Space Resources Agreement
17 p3203 A70-35794

Legal status of natural resources of celestial bodies, discussing limitations of Space Treaty of 27 January 1967
17 p3203 A70-35796

Regulations existence and application to exploitation of resources in celestial bodies
17 p3203 A70-35798

EXTRAVEHICULAR ACTIVITY
Water immersion technique to simulate zero and partial gravity conditions for investigation of astronaut capability to execute extravehicular work procedures
01 p0038 A70-10963

Dynamic characteristics of model of spacecraft-astronaut-tether system during approach, deriving kinetic potential
01 p0192 A70-11587

Physiological effects on men of 10 hr exposure to nitrogen-oxygen mixture followed by pure oxygen 4 hr exposure, simulating conditions during Eva
03 p0436 A70-13899

Apollo Telescope Mount Extra Vehicular Activity system for Apollo Applications Program [ASME PAPER 69-WA/BHF-16]
04 p0761 A70-14857

Space suit meteoroid protection for extravehicular activity, discussing Gemini and lunar surface EVA suits and bumper concept
04 p0645 A70-15402

Apollo extravehicular mobility unit /EMU/ system developed from Gemini EVA system with improved thermal control and mobility to support contingency extravehicular transfer in emergency
04 p0645 A70-15665

Relative motion of two bodies linked by flexible weightless tether in artificial earth satellite orbit, simulating extravehicular walk
06 p1142 A70-17882

Extravehicular activity space suits evolution emphasizing appropriate body temperature control under various conditions and work loads
10 p1824 A70-24412

Cooling system control system for astronaut thermal equilibrium and work output maximization during extravehicular space missions
13 p2357 A70-28526

Astronaut maneuvering research vehicle /AMRV/ subsystems, including automatic stabilization, attitude control, propulsion and displays
16 p2853 A70-33707

Extravehicular activity maneuvering devices, describing design and performance of Gemini project unit
21 p3929 A70-41075

Water immersion facility training for extravehicular activities and man physical movements in spacecraft, utilizing buoyancy-gravitation balance
21 p3804 A70-41191

Apollo spacecraft tests in Space Environment Simulation Laboratory, discussing thermal data, astronaut training, extravehicular activity, reaction control system, etc
21 p3805 A70-41271

EXTREMA
U RANGE [EXTREMES]
EXTREMELY HIGH FREQUENCIES
Lightweight Ka band magnetron for radar system use in missile fusing and airborne applications, discussing fixed frequency operation, anode and cathode, etc
04 p0655 A70-14622

Atmospheric effects on passive microwave sensing in EHF region under all-weather conditions on global scale using satellites
06 p1010 A70-18099

K band imagery of New England for evaluating size, shape and distribution of built-up areas
12 p2216 A70-26912

Atmospheric effects on passive microwave sensing in EHF region under all-weather conditions on global scale using satellites
20 p3586 A70-39703

SHF and EHF waves simultaneous propagation over slant line-of-sight overwater path, comparing phase variations and fading for signal coherence
20 p3588 A70-40301

SHF-EHF region uses, discussing microwave radiometry and applications to radio astronomy and meteorology
21 p3799 A70-41421

Millimeter wave radio systems for relieving crowding at lower frequencies, discussing technology, atmosphere effects and applications
22 p3990 A70-43418

EXTREMELY LOW RADIO FREQUENCIES
VLF and ELF EM wave propagation in earth-ionosphere cavity during solar flares
12 p2183 A70-27189

Ultra low frequency waves features in magnetosphere, considering geomagnetic pulsations, magnetic data from Explorer 33 and bounce resonance
12 p2223 A70-27573

Ionospheric probing with LF/VLF/ELF radio waves, discussing measurement techniques and temporal and spatial resolutions
12 p2224 A70-27731

Terrestrial ELF waves F layer nighttime reflections, discussing effects of electron density, geomagnetic field radial component and absorption by ions
13 p2365 A70-29190

Automatic audio frequency spectrometer for ELF and VLF amplitude spectrum of atmospherics, discussing attenuation band near 3 kHz
15 p2725 A70-31856

Electromagnetic ELF radiation model for multiple return strokes of cloud to ground lightning discharges, considering channel length
15 p2726 A70-31864

Transient excitation of Schumann earth-ionosphere cavity resonances by large ELF atmospherics, using propagation model
15 p2726 A70-31865

VLF and ELF radio wave propagation with mode coupling in inhomogeneous stratified ionosphere
17 p3047 A70-35402

Terrestrial ELF electromagnetic wave fields strength variation with distance over earth surface, using residue series zero-order term
19 p3380 A70-38405

ELF and VLF propagation for perturbed ionosphere models, discussing effects of ion collision frequencies and molecular weights
20 p3585 A70-39454

Diurnal variations of sudden enhancements and decreases of ELF atmospherics, using mode theory
21 p3814 A70-40939

Lightning discharge characteristics contributing to electromagnetic background noise at ELF determined from slow tail waveform measurements
22 p4015 A70-42777

ELF and VLF waves in waveguide propagation mode, calculating lower ionosphere effect on attenuation and phase velocity
22 p3989 A70-42960

ELF emissions dependence on plasmapause location in magnetosphere indicated from OV-3 observations
23 p4186 A70-43847

Earth-ionosphere cavity ELF electromagnetic pulse propagation from atmospheric source, considering transient field as frequency and time functions
24 p4314 A70-46130

EXTREMUM VALUES
NT LIMITS [MATHEMATICS]
NT MAXIMA
NT MINIMA

Noise variance extreme value estimator for biorthogonally block coded high rate telemetry system for Mariner missions
08 p1459 A70-20799

Extremal statistics for signal and noise error probabilities estimation and computer simulation of digital feedback communication systems
08 p1459 A70-20800

Mathematical programming and conditional extremum problems solution in analytic functions based on Chebyshev function systems and Stieltjes moments
08 p1534 A70-21451

Probability of given configuration and statistical distribution of peaks between mean crossings of broad-band locally stationary and Gaussian processes [ONERA-TP-806]
10 p1805 A70-24546

Circuit for analog computing system to determine function extremum of many variables in presence of constraints
11 p2023 A70-25927

Associative analog designed for decision making by man searching for extremum in form of multilayer stochastic automaton
11 p1990 A70-25928

Momentum transport bounds in turbulent shear flow using variational methods
11 p2039 A70-26535

Upper bound on system errors caused by quantization in multirate digital control system
12 p2204 A70-27841

Extremum criterion for singular solutions to optimal trajectory equations in calculus of variations
13 p2443 A70-29747

Extremum conditions for optimal control with operator constraints using gradient algorithms
14 p2559 A70-30181

Book on extremum principles covering energy methods of static and dynamic structural analysis
19 p3541 A70-37976

Mode clamping theorems for eigenvalues upper and lower bounds
20 p3657 A70-39232

Heterogeneous materials statistical theory, evaluating bounds for effective elastic constants by cell model using variational principles and perturbation solution
20 p3729 A70-40033

Linear feedback control system with quadratic penalty function, deriving lower bound on optimal performance for suboptimality evaluation
20 p3604 A70-40116

Random ergodic process extremal behavior, determining mean time to reach maximum or minimum for first time
22 p3985 A70-42400

Optimal design of electronic circuits, using mathematical methods for solving nonlinear multivariable function extremum
23 p4171 A70-43951

Radar echo superrefraction and subrefraction concepts used with atmospheric waveguide model explaining extremal behavior and relations to atmospheric stratification
23 p4163 A70-44233

Bang-Bang principle and vector functions at extreme points, considering Lebesgue measure and Liapunov theorem
23 p4176 A70-44237

Optimal algorithm for searching extremum of single variable unimodal function satisfying Lipschitz condition based on maximum possible error criteria
23 p4177 A70-44305

Rarefied gas plane Couette flow, calculating upper and lower bounds on shear stress
24 p4325 A70-45600

EXTRUDING
Al extrusions, discussing tooling, controls, indirect extrusion, drawn tubing and painted extrusions
03 p0512 A70-13777

Extrusion forces required for metals and alloys determined by mathematical equations correlating extrusion pressures with process variables, discussing lubrication systems effectiveness
04 p0697 A70-14767

Ceramic fibers formation by particles mechanical deformation by extrusion in W matrix, describing grain structure of various extruded metal oxides
04 p0699 A70-15643

- Kinematic characteristics of annular-blank elements extruded by pulsed magnetic fields, noting proportionality to energy stored in capacitor bank
05 p0857 A70-17018
- Superplastic nickel superalloys fabrication by controlled densification during direct extrusion
12 p2257 A70-28020
- Extrusion forces required for metals and alloys determined by mathematical equations correlating extrusion pressures with process variables, discussing lubrication systems effectiveness
[ASME PAPER 69-WA/LUB-6] 19 p3435 A70-37604
- Mo alloys strengthening by hydrostatic extrusion, combining dynamic strain aging with low temperature strain hardening
24 p4341 A70-45251
- Al and Al alloys cold extrusion, discussing die entry angle, lubrication control, ingot preparation, etc
24 p4349 A70-46217
- EYE [ANATOMY]**
- NT CHOROID MEMBRANES
- NT CORNEA
- NT FOVEA
- NT NYSTAGMUS
- NT OCULOMOTOR NERVES
- NT PUPILS
- NT RETINA
- Human eye integration of short monochromatic light flashes at TV frame frequencies
02 p0238 A70-12463
- Scaling and refractoriness effect in neutral-pulse train transmission on eye incremental sensitivity, discussing applicability as intraretinal mechanism concept
02 p0247 A70-12466
- Human eye image accumulation effect and meteor brightness estimation dependence on angular velocity based on visual and telescopic observations
03 p0569 A70-13358
- Color vision mechanisms spectral sensitivities measured by increment threshold technique for normal and deutan observers
03 p0427 A70-13947
- Human saccadic system properties, discussing eye movements and correction saccades with and without visual fixation points
03 p0427 A70-13949
- Efference role in eye tracking of moving targets, discussing oculomotor system role
03 p0439 A70-14345
- Human eye contribution to visual evoked responses under different color stimuli during all possible monocular and binocular combinations
05 p0801 A70-16382
- Observed objects physical properties influence on boundary conditions of visibility perception by human eye
06 p0994 A70-17631
- Modulation transfer function /MTF/ of eye-visual system as spatial frequency filter
07 p1216 A70-18870
- Photoconductivity detected in pigmented epithelium of eye during illumination by visible light
08 p1444 A70-20738
- Biological effects of laser radiation on human eye, discussing damage caused by long term exposure to visible, IR and UV wavelengths
08 p1451 A70-21043
- Retinal damage thresholds by exposing rhesus monkey and human eyes to laser radiation, testing rabbit eyes for corneal thresholds
08 p1451 A70-21044
- Microwave irradiation effects on rabbit eye lenses, noting injury dependence on frequency
[IMPI PAPER DA-4] 08 p1452 A70-21273
- Dark adaptation correlated with in vivo visual pigments regeneration as function of bleaching during monomolecular time course
08 p1447 A70-21722
- Human eye sensitization and dark adaptation, noting annular surrounding light addition effect on rod threshold
08 p1447 A70-21723
- Microwave radiation exposure control program for biological hazards, particularly to eye lens
09 p1623 A70-22221
- Differential luminance sensitivity of human eye using signal detection theory, correlating discrimination and detection results with electrophysiological data
10 p1812 A70-24599
- Human eye image accumulation effect and meteor brightness estimation dependence on angular velocity based on visual and telescopic observations
11 p2118 A70-26723
- Human blinking reflex recorded by electromyography, studying latent period in response to stimulation by air stream
12 p2168 A70-27346
- Servocontrolled IR optometer providing electrical signal proportional to refractive power of human eye
12 p2237 A70-28123

- Ocular fixation index and vestibular stimulation by caloric tests, discussing central processes for nystagmic rhythm regulation
14 p2538 A70-30912
- Book on visual perception space covering biological optics, eye model, monocular vision, etc
14 p2539 A70-31349
- Electrophysiological characteristics of rabbit eye muscles tonic fibers, measuring postsynaptic and membrane rest potentials
15 p2679 A70-31604
- Hand-eye coordination in altered gravitational fields, using mirror viewed target in reaching test
15 p2689 A70-31886
- Noise bursts response of positive and inhibitory conditioned eyelid reflexes in cats brain, discussing auditory system function
15 p2687 A70-32871
- Human eye early receptor potential, investigating contributions of rods and cones
17 p3034 A70-35896
- Cat lens motion in response to ciliary ganglion step and sinusoidal stimulation, indicating damped accommodative system
19 p3366 A70-38925
- Ruby laser radiation injury relationship to position and number of energy absorbing pigment particles in iris
20 p3579 A70-39425
- Laser radiation effects on lens lipid content in adult Rana temporaria frogs during cataract development
22 p3978 A70-43139
- Human eye components as image forming system from model based on Gaussian optics, discussing pupil size and influences on visual acuity
23 p4144 A70-43818
- Light flashes observed by Apollo astronauts, proposing Cerenkov radiation or direct excitation of eye retina by cosmic rays
24 p4307 A70-45403
- Ox, calf, pig, rabbit, guinea pig and human eye measurements, determining wet and dry weight of iris, ciliary body and choroid
24 p4305 A70-46346

EYE DISEASES

- NT ASTIGMATISM
- NT CATARACTS
- Space or atmospheric flight caused or aggravated ophthalmic lesions, noting retinal and conjunctival hemorrhages from barometric pressure fall and rapid acceleration and deceleration
01 p0022 A70-10858
- Biological hazards of laser radiation, noting eye injuries and cataract from transscleral exposure on rabbits
03 p0434 A70-13679
- Polarized light study of fundus oculi facilitating early diagnosis of various optical nerve and yellow spot diseases
08 p1445 A70-20749
- Ophthalmological treatment of severe thermomechanical eye injuries investigated on radiant-energy burned rabbit eyelids
09 p1617 A70-22473
- Optic chiasm damage effects on human depth perception implying interhemispheric link for binocular integration in central vision
09 p1618 A70-22669
- Corpus callosum damage effects on human depth perception implying interhemispheric link for binocular integration in central vision
09 p1618 A70-22670
- Human retinal detachment treatment by centrifugation
22 p3975 A70-43699
- EYE DOMINANCE**
- Superior recognition of right visual field of left eye with monocular viewing of letters as interaction of visual acuity and right superiority
02 p0239 A70-12623
- Visually evoked cortical potentials /VECP/ to different probe stimuli to suppressed human eye in binocular rivalry experiments, discussing eye dominance problems
09 p1618 A70-22674

EYE EXAMINATIONS

- Temporary or permanent visual field injury in test parachutists compared to control group
07 p1223 A70-19943
- Fundus oculi in polarized light, investigating light intensity variations and polarization pattern in yellow spot
08 p1444 A70-20748
- Polarized light study of fundus oculi facilitating early diagnosis of various optical nerve and yellow spot diseases
08 p1445 A70-20749
- Flight personnel color perception requirements and hereditary and acquired anomalies detection
09 p1627 A70-23115

EYE MOVEMENTS**NT NYSTAGMUS**

- Mathematical model for vestibular nystagmus adaptation to subjective sensation of rotation, noting time constants
01 p0032 A70-10362
- Visual attention testing, considering perception focusing on stimulus object and eyelid blinking recording, measuring eye distance to work plane
01 p0023 A70-10861
- Mathematical model formulated in terms of feedback controller for simulation of horizontal eye movement for positioning upon objects of interest
02 p0243 A70-12098
- Vestibular reactions in rats under hypothermal conditions by measuring postrotatory nystagmus beats number and duration, respiration rates and rectal temperature
03 p0425 A70-13893
- Eye movements during two dimensional tracking tasks, showing oculomotor system transfer characteristics function of target motion spectral content
03 p0427 A70-13948
- Human saccadic system properties, discussing eye movements and correction saccades with and without visual fixation points
03 p0427 A70-13949
- Time delay between ocular movement and retinal input by yoking visual target to eye movement using real time computer systems
05 p0805 A70-16094
- Human macrosaccadic eye movements related to four dial display conditioned by concurrent variable interval schedules of signals
05 p0800 A70-16127
- Helmholtz proprioceptive theory of apparent visual direction for predicting displacement of egocentric straight ahead as aftereffect of eyes deviation from normal position
05 p0801 A70-16142
- Nonlinearity of human eye movement control system in two dimensional tracking tasks, explaining visual axis lags as time delays dependent on target motion
08 p1447 A70-21724
- Monograph on systematically disturbed sensorimotor coordination, studying various parameters effects on eye-hand system recorelation
09 p1618 A70-22529
- Visual search activity decrease observed as function of time-on-task for skilled and unskilled helicopter pilots, recording eye movements and blinks
09 p1628 A70-23463
- IR electro-optical tracker Oculometer using human eye motions for pointing and tracking
11 p1989 A70-25352
- Stimuli eliciting vergence eye movements and stereopsis, discussing retinal disparity locations and limits due to form, spatial position, luminance, contrast and onset
12 p2171 A70-28034
- Two dimensional eye position control in dark over prolonged periods, noting role of conjunctiva cues, drifts and saccades
12 p2171 A70-28037
- Visual acuity determination by tape with staggered squares rotating behind screen with window
13 p2350 A70-29298
- Suprathreshold angular acceleration effects on oculogyral illusion, obtaining magnitude estimates during and after acceleration
14 p2543 A70-30897
- Eye movements effects on apparent /beta/ movement perception tested by display with ambiguous illusory movement
15 p2683 A70-32454
- Eye movements direction during perceptual errors related to stimulus location
15 p2683 A70-32456
- Eye movements during visual search and meaningless pattern discrimination
19 p3361 A70-38054
- Retinal images smearing during voluntary saccadic eye movements, obtaining thresholds for horizontal and vertical stimuli bands
19 p3366 A70-38927
- Visual suppression linear dependence on angular size of voluntary saccadic eye movements, observing percentage of trials for stimulus perception
19 p3367 A70-38928
- Temporal and spatial distribution of visual suppression during voluntary saccadic eye movement on different places of retina
19 p3367 A70-38929
- Pilot scanning dwell times and control workload in simulated instrument approach, using eye-point-of-regard /EPR/ measurements
[AIAA PAPER 70-999] 20 p3580 A70-39532
- Spectral sensitivity of freely moving human eye by determining threshold energy for correct choice between two monochromatically illuminated stimulus patches
22 p3972 A70-43412
- Visual target tracking with active head rotation, indicating independent eye response due to vestibulo-ocular reflex
22 p3979 A70-43492

- Visual acuity during ocular tracking movements as function of field illumination density
23 p4147 A70-44777
- Retinal image tracking movement effect on discriminatory perceptibility of orifice orientations of Landolt ring
23 p4147 A70-44778
- Perceptual suppression of retinal emissive afterimages by rapid eye movements
23 p4147 A70-44780
- Human compensatory two dimensional visual display tracking performance with superimposed apparent vertical vibration, studying frequency dependent eye pursuit movements
24 p4309 A70-46078
- EYE PROTECTION**
- Annotated bibliography of laser eye hazards
03 p0434 A70-13680
- Laboratory and field laser hazards control, noting beam termination in outdoor environment and optical density marking on protective eyewear
03 p0434 A70-13681
- Photochromic aminotriaryl methane filter solutions for flash blindness protection, noting stability against xenon flash UV exposure
04 p0690 A70-15028
- Laser eye and skin hazard evaluation from views of threshold effect levels and worst case assumptions
07 p1219 A70-19224
- Laser radiation protective goggle design, investigating retinal energy density levels and attenuation
08 p1451 A70-21046
- Accident prevention in laser operation emphasizing eye protection
13 p2361 A70-30018
- Safety factor estimation by nomographic techniques for eye protection against direct viewing of laser beam
21 p3768 A70-40761

F

- F CENTERS**
- U COLOR CENTERS
- F DISPLAYS**
- U F REGION
- F LAYER**
- U F REGION
- F REGION**
- NT F 1 REGION
- NT F 2 REGION
- Oxygen collisional quenching rate in F region determined by comparing nightglow intensities with intensities calculated from electron density profiles
01 p0070 A70-10403
- Ionsospheric F layer in equatorial, mid and high latitude regions for various major phenomena including anomalies, neutral air winds, photoelectrons, etc
01 p0073 A70-10585
- F region ionized and neutral atmospheric movements interactions, discussing ion drag forces, electromagnetism drift, wind effects, etc
01 p0074 A70-10587
- Nighttime F layer thickness relations to atmospheric temperature
01 p0078 A70-11211
- F region ion velocity measurements by Thompson scatter probe, deducing neutral winds diurnal and seasonal variations in thermosphere
01 p0078 A70-11214
- Atmospheric gravity waves in F region, discussing neutral gas-ionization interaction and detection by electron density profile measurements
01 p0079 A70-11216
- Ionsospheric slopes and range frequency characteristics obtained from oblique incidence sounding of horizontally nonuniform ionosphere
01 p0083 A70-11534
- Hourly N/h/ profiles of F region calculated from nomograms by normal integral method during magnetic disturbance, measuring region temperature
01 p0083 A70-11548
- Solar eclipse effects in equatorial F region electron density, noting data analysis method for reexamining existing measurements
02 p0290 A70-12157
- Seasonal effect on F region midlatitude slab thickness diurnal variations during magnetic disturbances using monitoring VHF signals from geostationary satellites
02 p0290 A70-12160
- F region irregularity drift, morphology and generation in magnetosphere, discussing ionospheric structure at different latitudes and solar activity association
02 p0293 A70-12572
- Secular variation in F region ionization response to sunspot number, noting dominant component as cosine term equal to four sunspot cycles
04 p0678 A70-14972
- F region ionograms processing with correction for ionization effects between E and F layers
04 p0684 A70-15748

- Vertical motion of ionized formations in ionospheric F region related to sporadic E layer
05 p0842 A70-16760
- Corpuscular radiation as F region ionization source, solving time dependent ionospheric continuity equation
06 p1054 A70-17588
- Seasonal variations of maximum electron concentration in stratified E-F region, including E 2 layer recombination coefficient and F layer characteristics probability
06 p1057 A70-17842
- Backscatter observations of F region field-aligned irregularities during IQSY, discussing diurnal variations of echoes
06 p1059 A70-18539
- Aspect sensitivity of HF backscatter auroral echoes in F layer, utilizing F supported ground scatter echo to account for ionospheric refraction
06 p1012 A70-18541
- LUF for F layer propagation modes, discussing mode cut-off significance using computer ray tracing program
07 p1229 A70-19159
- Diurnal variations of lower F region ion composition and recombination coefficient based on numerical modeling of continuity equations for electrons and molecular species
07 p1265 A70-19431
- Ionized formations motion direction and velocity in F region from triangular ionospheric sounding
07 p1267 A70-19451
- F region electron and ion concentration vertical distribution, discussing various ionization reactions
07 p1276 A70-20430
- Nighttime ionospheric F region velocity component and recombination coefficient computer calculation
07 p1277 A70-20449
- Photoelectrons entry into F region detected at conjugate point during winter night by Thomson scatter observations of plasma lines appearing in signal spectrum
08 p1489 A70-21386
- Vertical incidence /VI/ F layer ionograms, magnetograms and signal amplitude data obtained during annular eclipse of 23 November 1965
09 p1671 A70-23494
- F region vertical electron drift velocity determined from Thomson scatter observations
09 p1671 A70-23665
- F region ion-molecule reaction rate constants laboratory measurements, observing reactions energy dependence
10 p1872 A70-23825
- F region electrons collision frequency from short radio waves amplitude and group path relationship
10 p1876 A70-24535
- Ionsospheric F and E layers collision frequency estimates, comparing pulse absorption and cosmic radio noise measurements
10 p1880 A70-24804
- F region irregularity model to include field-aligned columns and sheets and frontal irregularity shapes effect on radio star and satellite scintillations
10 p1841 A70-24805
- Gravity wave attenuation in F region investigated for role of ohmic losses
10 p1885 A70-25264
- Nocturnal F layer electron density profile and temperature dependence on solar activity
10 p1885 A70-25266
- F region magnetic disturbances due to low energy solar plasma penetration during proton bursts
11 p2104 A70-25535
- Ion component drift displacing components from E and F layers ascribed to vertical electric field presence in hydrogen arc
11 p2104 A70-25541
- E and F layer ion chemistry dependence on ion-neutral reactions and dissociative recombination
12 p2223 A70-27220
- Experimental IR earth horizon profiles measured by satellite in F region, discussing spectral channels and attitude control
12 p2225 A70-27751
- Three-point simultaneous observations for ionospheric drift characteristics in E and F regions
13 p2396 A70-29097
- Terrestrial ELF waves F layer nighttime reflections, discussing effects of electron density, geomagnetic field radial component and absorption by ions
13 p2365 A70-29190
- F region nightglow emissions rocket data, discussing rate coefficient for oxygen atoms quenching by molecular nitrogen
13 p2398 A70-29200
- Interlayer ionization valley depth influence on F region heights, calculating N/h/ profiles from ionograms
14 p2571 A70-30229
- Neutral winds effect on F region vertical ion drifts derived from continuity equation, noting diurnal and seasonal variations
14 p2574 A70-30738

- F region horizontal drift velocity height and diurnal variations, using ionograms
14 p2574 A70-30751
- F region ionograms processing with correction for ionization effects between E and F layers
14 p2576 A70-30832
- Electron and ion temperature and electron density relationship in F region during sunspot maximum, using incoherent scatter experiment
14 p2581 A70-31271
- Correlated daily variations of ionospheric drift and anisotropy parameters in E and F regions at Thumba, India
15 p2725 A70-31858
- F region electron and ion densities, temperatures and plasma velocities computed for eclipse at Wallops Island on 7 March 1970
15 p2726 A70-31866
- Polar peak F layer electron density around magnetic noon related to dayside aurora flux, comparing with soft particle precipitation
15 p2727 A70-31872
- Neutral particle and electron density measurements by Explorer 32 proving thermospheric gravity waves association with wave-like structure in F region electron density
15 p2727 A70-31907
- Planetary distribution of F region disturbances and related vertical electron concentration using satellite and ground data
15 p2729 A70-32079
- Ionization-neutralization processes and recombination coefficient in F and E regions, using radiophysical measurements
15 p2730 A70-32083
- Electron-ion gas ionization, neutralization and ambipolar diffusion effects on F region vertical profile
15 p2730 A70-32090
- F region electron density profiles interpretation by electron balance equation facilitating comparison of aeronomical and ionospheric data
15 p2731 A70-32091
- F region electron content and recombination times during solar eclipse of 7 March 1970, using Faraday rotation technique
16 p2897 A70-33829
- F region integrated electron density response during solar eclipse of 7 March 1970, using Faraday rotation of linearly polarized signals from ATS 3
16 p2898 A70-33835
- Ionsospheric vertical base selection for recording discontinuities motion of F region
16 p3246 A70-36085
- F region small scale ionization discontinuities parameters observational data concerning anisotropy, dimensions, velocity and lifetime
16 p3246 A70-36088
- Diurnal variations of lower F region ion composition and recombination coefficient based on numerical modeling of continuity equations for electrons and molecular species
18 p3249 A70-36905
- Ionized formations motion direction and velocity in F region from triangular ionospheric sounding
18 p3249 A70-36925
- Electrons and ions diffusion effect on vertical distribution in F region, discussing diurnal variations at various heights
18 p3254 A70-37027
- Ion composition and charged particle vertical distribution in F region and protonosphere from satellite and ground based observations
18 p3254 A70-37028
- F region photoionization rate vs height twin peak profile in presence of temperature maximum, taking into account ionization of atmospheric gases by quasi-monochromatic radiation
18 p3254 A70-37031
- Magnetosphere dynamics relationship with inhomogeneous electron density formation in F region, discussing scattering diurnal variations and intensity in magnetically conjugate points
18 p3255 A70-37035
- F layer scattering and earth electromagnetic field short period oscillations, relating electron density with pearl micropulsations amplitude and occurrence
18 p3255 A70-37036
- Chemical reactions neutralizing electron-ion gas in F region
18 p3255 A70-37044
- F layer absence and nonuniform horizontal electron concentration of nighttime ionosphere at high latitudes, using Alouette 1 sounding
19 p3408 A70-37308
- Solar eclipse effects on E and F layers, discussing photoionization rate, electron density and temperature, plasma diffusion, electric fields, etc
19 p3418 A70-38903
- E and F region electron density response to incident radiation intensity on upper atmosphere during solar eclipses
19 p3419 A70-38916

Vertical electron concentrations in upper F region during solar eclipses in South Atlantic from satellite observation

19 p3419 A70-38920

Ionized magnetospheric tubes electron content, determining ionization interchange between F region and protonosphere by whistler observations

20 p3584 A70-39332

Equatorial F layer irregularity extent from propagation path observations to synchronous satellites

20 p3624 A70-40485

Low latitude F region irregularities from scintillations of beacon satellite signals

20 p3624 A70-40486

High latitude F region irregularity structure during magnetic storm from multistation scintillation observations of ATS 3 transmission

20 p3624 A70-40490

Multistation observations of long range field aligned backscatter irregularities in F layer, using ray path calculations

21 p3814 A70-40940

F region synoptic electron densities and electron and ion temperatures from Thomson scatter radar data

21 p3816 A70-41065

Midlatitude F region electron and ion temperatures during magnetic storms, examining Thomson scattering, density and time dependence

21 p3817 A70-41094

F region heating by magnetic storms, discussing electron temperature, ring current conduction and red arcs

21 p3817 A70-41095

Atomic oxygen density and temperature diurnal variation determination by F region incoherent scatter measurements, using nonlinear regression analysis

21 p3817 A70-41096

Universal time control of south polar F layer during IGY attributed to low energy electron precipitation, comparing IGY and recent satellite data

21 p3818 A70-41101

F region radar and optical temperature measurements, discussing Doppler and backscatter ion temperature

21 p3818 A70-41103

F region magnetic disturbances due to low energy solar plasma penetration during proton bursts

21 p3882 A70-41285

Ion component drift displacing components from E and F layers ascribed to vertical electric field presence in hydrogen arc

21 p3882 A70-41291

F region electron density measurement during magnetic storm by incoherent scatter technique

22 p4019 A70-43157

F region electron content day-to-day changes observation by Early Bird satellite, determining cross correlation with magnetic indices

22 p4020 A70-43161

Upper atmosphere ionization balance, examining metastable species in E and F regions

22 p4106 A70-43306

Polar cap ionization processes in F region, discussing effects of particle precipitation, solar radiation, electromagnetic field drifts, atmospheric winds and magnetospheric tail distortion

22 p4024 A70-43309

F region night airglow in equatorial and midlatitudes, discussing red and blue emission origins

23 p4185 A70-43839

F region equatorial anomaly formation, investigating vertical EM drift effect

23 p4187 A70-43857

F region ionospheric disturbances size and shape from radio amplitude and phase scintillations in satellite transmission to ground stations

23 p4187 A70-43879

Short radio wave propagation over single jump lines in F sub zero F 2 gradient presence, examining maximum usable frequency increase

23 p4162 A70-44076

Neutral air winds in ionospheric F region for asymmetric global pressure system, including ion velocity correction

24 p4329 A70-45356

Interlayer ionization valley depth influence on F region heights, calculating N/h profiles from ionograms

24 p4331 A70-46304

F 1 REGION

Needle-shaped filament artificial ion cloud drift and diffusion in F 1 region plasma in presence of neutral wind and uniform electric field

01 p0070 A70-10401

F 1 layer nonlinear ionospheric continuity equation to investigate role of diurnal variations of loss and production processes in electron density midday biteout effect

01 p0079 A70-11221

Cosine dependence of F 1 critical characteristics on solar zenith angle discriminating alpha neutralization and mixed alpha-beta deionization

06 p1057 A70-17841

Seasonal variation of F 1 region ion composition measured by rocket-borne mass spectrometer, noting altitude dependence of electron and ion temperatures

06 p1059 A70-18540

F 1 region ion structure diurnal variations, calculating photoionization rates

14 p2571 A70-30227

F 1 layer occurrence and geometrical parameters relating to critical frequencies of F1/F2 layers

14 p2571 A70-30228

F 1 layer formation and ion production rates related to F layer stratification, atomic oxygen, zenith angle and solar activity periods

15 p2730 A70-32086

F 1 layer occurrence probability as function of mean monthly Wolf numbers at midlatitudes, noting solar activity effect

18 p3254 A70-37032

F 1 region unsteady model, examining vertical distribution profile of electron concentration on summer day

19 p3409 A70-37323

F 1 region positive nitric oxide and oxygen ions concentrations ratio and conversion rates from rocket data and theoretical formulas

23 p4189 A70-44075

F 1 region ion structure diurnal variations, calculating photoionization rates

24 p4331 A70-46302

F 1 layer occurrence and geometrical parameters relating to critical frequencies of F1/F2 layers

24 p4331 A70-46303

F 2 REGION

Ionization variations and correlation coefficients of F 2 critical frequency variations, using airborne ionospheric sounder over Sogra and Kerguelen Island conjugate areas

01 p0080 A70-11224

F 2 layer state prediction as function of solar activity by series expansion for describing space-time variations of monthly F 2 medians critical frequencies

01 p0083 A70-11547

F 2 region acoustic waves over Kansas and Nebraska attributed to local storms in troposphere

02 p0290 A70-12158

Electromagnetic drifts and neutral air winds effects on F 2 region derived from electron continuity equation, using Jacchia model atmosphere

04 p0677 A70-14966

Lunar tides in midday critical frequency of F 2 layer, determining phase reversal location

04 p0651 A70-15309

Anomalous ionization variations of F 2 layer at northern geomagnetic pole during winter coincident with decrease in solar plasma density

04 p0682 A70-15726

Positive correlation between normal ionizations at magnetically conjugate regions in ionospheric F 2 layer from aircraft vertical soundings

04 p0683 A70-15741

Magnetic declination effect on F 2 layer behavior determined from critical frequencies at two magnetically conjugate points

04 p0683 A70-15742

Diurnal fluctuations of quiet F 2 region intensity at midlatitude based on vertical probe observations during solar activity minimum

04 p0684 A70-15745

Cosmic ray intensity decreases in relation to geomagnetic and F 2 region disturbances characterized by Forbush decreases from vertical sounding data

05 p0898 A70-15940

F 2 layer electron density changes during geomagnetic storms linked to DS current and electromagnetic disturbances

05 p0838 A70-16280

F 2 region critical frequency conjugacy latitudinal variations observation at conjugate stations compared with results from nonconjugate stations

05 p0839 A70-16286

Nighttime F 2 region temperature distribution under geomagnetically calm and disturbed conditions calculated from Alouette 1 satellite data

06 p1057 A70-17887

Height scale of loss coefficient in F 2 region under geomagnetic perturbation at midnight based on electron number profiles, estimating thermosphere temperature

07 p1265 A70-19433

Midlatitude F 2 perturbations from vertical sounding stations data during solar activity minimum, discussing F 2 region critical frequency variation

07 p1266 A70-19450

F 2 small scale inhomogeneities drift relation to current systems of dynamo region, discussing solar activity effects on ionospheric conductivity

07 p1267 A70-19452

Positive and negative correlations in F 2 layer perturbations by network of paired conjugate ionospheric stations at low latitude

07 p1277 A70-20450

Global distribution of F 2 layer critical frequencies by expanding empirical function of diurnal variations into natural orthogonal components

07 p1277 A70-20451

Critical sunspot dependence of F 2 region noon biteout phenomenon at various equatorial latitudes, observing magnetic dip

08 p1492 A70-21837

Lunar daily and monthly tidal variations in horizontal magnetic field and F 2 region maximum electron density and peak ionization height at Puerto Rico

10 p1872 A70-23823

Field-aligned plasma velocity dependence on plasma diffusion and wind velocity illustrated with model of night F 2 layer

10 p1881 A70-24814

F 2 field-aligned ion velocity measurement compared with theoretical results, discussing difference at sunspot minimum and daytime ion velocity-plasma loss relation

10 p1881 A70-24815

F 2 layer midday ionization level annual variation gradient, noting gradient latitudinal distribution dependence on solar activity level

11 p2042 A70-25532

F 2 layer midday ionization equatorial anomaly during summer and winter solstices, using calculated mean critical frequencies

11 p2042 A70-25533

Polarization regularities of Pc 1 oscillations interpreted from propagation along ionospheric waveguide centered at F 2 layer

11 p2043 A70-25543

F 2 layer critical frequencies rms deviations approximate dependences on latitude and solar activity for computer calculation of long-range ionospheric forecasts

11 p2043 A70-25549

Ionospheric plasma drift vertical and meridional velocity components latitudinal distributions in F 2 region, considering wind effects in upper atmosphere

11 p2045 A70-25931

Electron density decrease in F 2 layer ascribed to 9 July 1962 thermonuclear explosion, noting dissociative recombination role

11 p2047 A70-26791

F 2 region critical frequency from Alouette 2 satellite data compared with ground based measurement

12 p2226 A70-28066

F 2 critical frequencies from Alouette 2 satellite ionogram data compared with ground-based sounding results

13 p2396 A70-29094

Thermal diffusion effects on F 2 region ion densities, deriving diffusion coefficients for partially ionized atomic oxygen plasma

13 p2398 A70-29232

F 2 layer ionization asymmetry for Northern and Southern Hemispheres during solstice periods due to electron density variations and aeronomic conditions

14 p2569 A70-30206

Solar activity variations effects on equation parameters, describing nighttime F2 ionization levels dependence on geographical latitude

14 p2570 A70-30224

Geomagnetic field influence on annual F 2 layer longitudinal ionization at midlatitudes, relating solar activity level

14 p2570 A70-30225

Quasi-periodic influence of traveling disturbances on ionospheric F 2 layer small scale drift discontinuities

14 p2570 A70-30226

F 1 layer occurrence and geometrical parameters relating to critical frequencies of F1/F2 layers

14 p2571 A70-30228

F 2 layer effects on ionospheric short wave scattering lines for operating frequencies above MUF

14 p2547 A70-30231

Anomalous ionization variations of F 2 layer at northern geomagnetic pole during winter coincident with decrease in solar plasma density

14 p2575 A70-30810

Positive correlation between normal ionizations at magnetically conjugate regions in ionospheric F 2 layer from aircraft vertical soundings

14 p2575 A70-30825

Magnetic declination effect on F 2 layer behavior determined from critical frequencies at two magnetically conjugate points

14 p2575 A70-30826

Diurnal fluctuations of quiet F 2 region intensity at midlatitude based on vertical probe observations during solar activity minimum

14 p2576 A70-30829

Daytime seasonal anomaly in electron density of topside F 2 region near sunspot minimum, using Alouette 1 data

15 p2726 A70-31863

F 2 layer heating by photoelectrons reconsidered in terms of electron inelastic collisions effect on temperature

15 p2727 A70-31870

- Diurnal, seasonal and latitudinal variations of maximum electron concentration in F 2 region, using global network observations
15 p2729 A70-32077
- F 2 layer afternoon and evening ionization maxima dependence on season, zenith angle and solar activity
15 p2730 A70-32084
- Equatorial F 2 region response during solar eclipse of 7 March 1970, emphasizing ionization production and loss, transport processes and electron temperature
16 p2897 A70-33826
- Night F 2 layer underside morphology for magnetically quiet period at sunspot minimum
17 p3076 A70-34937
- F2 region disturbance development during magnetic storm, discussing layer height increases
17 p3080 A70-35772
- Ionospheric small scale ionization discontinuities vertical drift effect on diurnal variations of F 2 layer critical frequency
18 p3246 A70-36086
- Short wave propagation above F2 maximum usable frequency, observing field intensity and SNR seasonal and diurnal variations
18 p3226 A70-36092
- Vertical drift contribution to daytime N/h electron profiles in F 2 region, taking into account ionization-recombination processes and ambipolar diffusion
18 p3247 A70-36292
- Height scale of loss coefficient in F 2 region under geomagnetic perturbation at midnight based on electron number profiles, estimating thermosphere temperature
18 p3249 A70-36907
- Midlatitude F 2 perturbations from vertical sounding stations data during solar activity minimum, discussing F 2 region critical frequency variation
18 p3249 A70-36924
- F 2 small scale inhomogeneities drift relation to current systems of dynamo region, discussing solar activity effects on ionospheric conductivity
18 p3249 A70-36926
- Ionization-recombination parameters based on diurnal variations of electron concentration in F 2 layer maximum, discussing latitudinal variations
18 p3254 A70-37033
- Ionization-recombination parameters variation as function of season and solar activity, using diurnal changes of F 2 layer maximum electron concentration
18 p3254 A70-37034
- F 2 layer maximum electron concentration diurnal variations dependence on ionization intensity and dissociative recombination and ion-molecular reactions rate coefficients
18 p3255 A70-37039
- Electron concentration disturbances in outer ionosphere and F 2 maximum on daylight side during magnetic storm
19 p3408 A70-37307
- Global diurnal variations in F 2 layer seasonal anomaly during high and low solar activity, noting coronal radiation role
19 p3491 A70-37326
- F 2 region critical frequency diurnal variation forecasting, using series expansion of natural orthogonal components
19 p3409 A70-37327
- Lunar perturbations in horizontal geomagnetic field, F 2 layer thickness and electron density, discussing tidal variations
20 p3617 A70-39141
- Solar eclipse effects on equatorial F 2 layer by transient solutions of time dependent continuity equation, calculating electron concentrations
20 p3622 A70-39453
- Neutral atmosphere continuity equation of ionization and equation of motion in F 2 region for different seasons in various solar activity epochs
20 p3623 A70-40478
- Earth magnetic field effects on midlatitude F 2 layer deviative absorption
21 p3812 A70-40727
- Midlatitude F 2 layer electron density structure using theoretical model, accounting for atmospheric physical and chemical processes
21 p3815 A70-41062
- F 2 region critical frequency cross correlation coefficients for magnetically conjugate stations, considering magnetic disturbances effects
21 p3816 A70-41069
- F 2 layer midday ionization level annual variation gradient, noting gradient latitudinal distribution dependence on solar activity level
21 p3819 A70-41282
- F 2 layer midday ionization equatorial anomaly during summer and winter solstices, using calculated mean critical frequencies
21 p3819 A70-41283
- Polarization regularities of Pcl oscillations interpreted from propagation along ionospheric waveguide centered at F 2 layer
21 p3819 A70-41293
- F 2 layer critical frequencies rms deviations approximate dependences on latitude and solar activity for computer calculation of long-range ionospheric forecasts
21 p3819 A70-41299
- Minor ion diffusion coefficients in F 2 region, noting Coulomb collisions role in ion density sensitivity to ionospheric fluxes
22 p4019 A70-43109
- Electron density profiles calculation from model atmosphere, deriving F 2 layer ionization vertical distribution
22 p4023 A70-43303
- Meteoric metallic ions above F 2 peak, discussing current density and transport mechanisms
23 p4239 A70-43841
- F 2 region anisotropic response to individual internal gravity waves as function of propagation azimuth
23 p4185 A70-43844
- F 2 layer nighttime ionization at mid-latitudes, investigating conjugate point effects on observation point
23 p4188 A70-44055
- F 2 layer critical frequency and maximum electron concentration statistical characteristics for predicting SW propagation conditions
23 p4188 A70-44056
- Diurnal variations of photoelectron heat fluxes and energy production by thermal coupling between upper F 2 region and magnetosphere
24 p4328 A70-45354
- F 2 layer ionization asymmetry for Northern and Southern Hemispheres during solstice periods due to electron density variations and aeronomic conditions
24 p4330 A70-46281
- Solar activity variations effects on equation parameters, describing noontime F 2 ionization levels dependence on geographical latitude
24 p4331 A70-46299
- Geomagnetic field influence on annual F 2 layer longitudinal ionization at midlatitudes, relating solar activity level
24 p4331 A70-46300
- Quasi-periodic influence of traveling disturbances on ionospheric F 2 layer small scale drift discontinuities
24 p4331 A70-46301
- F 1 layer occurrence and geometrical parameters relative to critical frequencies of F 1/F 2 layers
24 p4331 A70-46303
- F 2 layer effects on ionospheric short wave scattering lines for operating frequencies above MUF
24 p4316 A70-46306
- F-1 ROCKET ENGINE**
F-1 rocket engine acoustic liner, reevaluating damping data for combustion stability improvement
16 p2968 A70-33588
- F-4 AIRCRAFT**
Wind tunnel and flight test methods for determining transonic buffet characteristics on model F-4 aircraft [AIAA PAPER 70-584]
13 p2348 A70-29886
- F-4 Be rudders design and tests compared to Al structure [ASM PAPER W70-12.4]
15 p2676 A70-32336
- F-5 AIRCRAFT**
Digital data acquisition system for CF-5A flight test program, discussing recording system design
19 p3384 A70-38532
- F-8 AIRCRAFT**
F-8 wing service life extension design techniques, emphasizing fatigue design curves and procedures
02 p0386 A70-11939
- F-8D aircraft transonic flight and wind tunnel tests for buffet onset prediction, considering effects of g level and fluctuation amplitude and frequency [AIAA PAPER 70-341]
09 p1611 A70-23020
- F-14 AIRCRAFT**
Air inlet and exhaust nozzle form and location effect in afterburning turbofan engines, discussing stalling, afterburner blowouts and thrust losses prevention
05 p0895 A70-15807
- F-14A engine air inlet control, describing variable geometry system open loop design [AIAA PAPER 70-697]
16 p2841 A70-33560
- F-14 carrier based fighter development program requirements, inherent difficulties and variable geometry configuration
21 p3750 A70-41264
- F-28 HELICOPTER**
Noise reduction design of Enstrom F-28A helicopter, noting operation at lower tip speeds and blade loading
12 p2162 A70-28096
- F-28 TRANSPORT AIRCRAFT**
Fokker F-28 wing flap, lift dumpers and aileron development, including wind tunnel and flight tests
08 p1438 A70-21864
- Data collection system for prototype flight tests of Fokker F-28 based on DC-8 aircraft digital system
19 p3384 A70-38546
- F-80 AIRCRAFT**
U T-33 AIRCRAFT
- F-104 AIRCRAFT**
Servoactuator simulating vertical acceleration in F-104 simulator, duplicating other forces conventionally
02 p0229 A70-12864
- F-104 jet windshield components research concerning plate glass optical deviation problems to meet quality standards
09 p1691 A70-22571
- F-106 AIRCRAFT**
F-106B aircraft in-flight study of airframes installation effects on propulsion system performance at transonic speeds
08 p1437 A70-21732
- Aluminum-boron composite material applications to structural components of F-106 aircraft, noting weight saving and mechanical properties [AIAA PAPER 68-975]
12 p2257 A70-28082
- Variable stability trainer modification of F-106 to reproduce flight characteristics of aircraft for pilot training in potentially dangerous situations
16 p2842 A70-33815
- F-110 AIRCRAFT**
U F-4 AIRCRAFT
- F-111 AIRCRAFT**
Crushable honeycomb regulating operating pressure of propellant actuated devices applied to recovery parachute catapult in F-111 crew module
03 p0546 A70-14108
- Transverse and shear strengths of Al-B composite materials used in F-111 aircraft components, investigating cold work, thermal treatments and steel wire addition effects
08 p1509 A70-21857
- F-111 aircraft wings unstable fore and aft oscillations in swept forward position ascribed to actuator motor drive rate variations
12 p2160 A70-27112
- Aircraft escape systems, discussing F-111 system capabilities and development
13 p2345 A70-28969
- F-111A reliability levels achieved via high reliable hardware and redundancy and alternate mode capability requirements in contract
15 p2676 A70-32638
- F-111A airplane in-flight inlet pressure fluctuations for engine compressor surge, discussing average turbulence factor [AIAA PAPER 70-624]
16 p2840 A70-33543
- F-111 high strength steel design experience concerning wing, fuselage and empennage support structure [AIAA PAPER 70-884]
17 p3018 A70-35803
- F-111 crew escape module, describing main parachute and pyrotechnics severance improvements, parachute deployment and inflation, etc [AIAA PAPER 70-1210]
21 p3751 A70-41807
- F-111 aircraft crew cockpit escape module design for maximum efficiency, including survival equipment after ejection
23 p4141 A70-44491
- FAB [PROGRAMMING LANGUAGE]**
U FORTRAN
- FABRICATION**
Fiber reinforced composites emphasizing refractory fibers, preparation methods, properties and fabrication
01 p0129 A70-10939
- Solar cell array fabrication methods extending operating temperature by pulsed spot welding techniques and deletion of adhesives
02 p0228 A70-12080
- Epitaxial GaAs FET using evaporated Au-Ge-Ni contacts and Ni Schottky barrier, describing fabrication and electrical properties measurement
04 p0660 A70-15367
- Fragment fabrication of hybrid propellant solid grain emphasizing spherical shape and diameter uniformity
04 p0737 A70-15673
- Flight type pressure vessels fabricated with quenched and tempered Ni-Cr-Mo-V structural steel, discussing fracture toughness, design, fabrication techniques [SAE PAPER 690680]
05 p0853 A70-15866
- Carbon fiber-reinforced plastics fabrication, discussing leaky mold, prepreg and filament winding methods
05 p0855 A70-16581
- Fabrication and electrical properties of p-ZnTe/n-InAs heterojunctions obtained by interface alloying, suggesting p-i-n structure from characteristics and capacitance behavior
06 p1125 A70-17123
- Small penetration axial rocket motors fabrication, discussing axial- and tangential-thrust integral assembly, impulse levels, delay line convection for igniters, production evolution, etc [AIAA PAPER 69-520]
07 p1295 A70-19714
- Fabrication and properties of carbon fibers and carbon fiber reinforced epoxy resins
07 p1318 A70-19772
- Strength, corrosion resistance and fabricating qualities future improvements in metals and alloys, discussing chemical composition approach, dispersion hardening, superplasticity, etc
08 p1518 A70-21267
- Engineering use of filament reinforced metal matrix composites dependent on fabrication cost reduction, consistent properties and form flexibility
08 p1509 A70-21851

Fabrication effects on current instability during injection and breakdown of p-n junctions in GaAs oscillators

09 p1740 A70-23351

Microwave surface acoustic delay lines properties, advantages, electron beam fabrication, optical probing for propagation loss measurement, etc

11 p2005 A70-26166

Composite materials fabrication with glass, boron and graphite fibers reinforcement, discussing matrix and binder materials

12 p2253 A70-27267

Superplastic nickel superalloys fabrication by controlled densification during direct extrusion

12 p2257 A70-28020

Borsic-aluminum composite materials fabrication, properties and applications to aircraft parts

13 p2420 A70-29246

He-Cd laser construction with quartz tube manufactured separately, describing flow-through processing

14 p2594 A70-30509

Filament reinforced metal matrix composites fabrication and engineering uses

14 p2590 A70-30542

Nd laser drilling and welding tool for microminiature electronic device fabrication

14 p2594 A70-30639

Filament orientation and fabrication variables effect on Ag matrix-W fiber composite mechanical properties

15 p2756 A70-31569

Al alloy matrix-boron fiber-stainless steel wire composites fabrication into various shapes with desired mechanical properties for aerospace structural components applications

18 p3263 A70-36837

Carbon fiber/carbon matrix composites fabrication by isotropic casting, flock and spray lay-up and pulp molding, describing physical and mechanical properties

20 p3636 A70-39208

Matrix condenser for tuning hybrid thin film self excited quartz oscillator with common base transistor configuration, discussing electrical properties and fabrication

20 p3597 A70-39257

Soviet book on glass staple fibers covering classification, properties, composition, production, tests and industrial applications

20 p3655 A70-39399

Filament wound composites, investigating interaction of fabrication variables and outward environments by delineating effect of each on structural performance

20 p3731 A70-40055

Ceramic fiber technology, forming processes and matrix composites fabrication, discussing chemical and physical compatibility factors, plastic forming, slip casting, cold pressing, etc

22 p4045 A70-42477

Papers on plastics, volume 1 covering materials, design, fabrication, applications, etc

24 p4368 A70-46223

High temperature coatings of high melting point alloys on graphite, determining optimum fabrication conditions

24 p4368 A70-46339

W, Ta and Mo composites economical fabrication by plasma spraying for rocket nozzles, susceptors and crucibles

24 p4350 A70-46355

FABRICS

NT DACRON [TRADEMARK]

NT PARACHUTE FABRICS

NT WOOL

Thermal protection rating systems for clothing fabrics based on pain and blister effects in human skin

03 p0438 A70-14064

Polyamide fabric burning rates in oxygen-inert gas mixtures, studying damping effects of density, thermal conductivity, molecular constants and mass flow

06 p1090 A70-17284

Carbon fabrics and filaments, resin carbonizing and carbon-carbon composites, discussing processing parameters, initial carbonizing resin binder and reinforcement effects on laminate properties

07 p1316 A70-18932

Fireproof fabrics tested for flame retarding and protection capabilities, discussing applications to aircraft interiors, escape parachutes, flight coveralls and protective clothing

07 p1219 A70-19017

Polymers industrial applications in textiles, building materials, furniture, aviation, automobile industry and packaging

19 p3455 A70-38700

High strength graphite fabrics evaluation for flexible structures, discussing temperature effects, fabrication, mechanical properties, oxidation and protective coatings

[AIAA PAPER 70-1183]

21 p3842 A70-41830

Aerial retrieval webbing performance characteristics, discussing structure, type of material, finishing and strength levels

[AIAA PAPER 70-1181]

21 p3843 A70-41832

Basket weave fabrics for gliding descent decelerators with polyurethane and nylon coatings for tearing strength and pressure packing

[AIAA PAPER 70-1180] 21 p3843 A70-41833

Decelerator fabric elastic constants for structural analyses using generalized Hooke's law

[AIAA PAPER 70-1179] 21 p3843 A70-41834

FABRY-PEROT INTERFEROMETERS

Solar Mg II doublet and XUV images obtained by Fabry-Perot interferometer mounted in Skylark spectrograph

01 p0177 A70-10339

Laser optoelectronic and spectroscopic methods using fixed gap spherical mirror confocal Fabry-Perot interferometer and multiple beam image tube framing camera

01 p0112 A70-10901

Q switching of continuously pumped Nd/YAG using double Fabry-Perot etalons to replace laser resonator output mirror

01 p0112 A70-10903

Crossed Fabry-Perot etalons and spectrographs for studying atmospheric solar absorption spectra

02 p0299 A70-12438

Helium-neon laser wavelength calculations from spectral observations by Fabry-Perot etalon, proposing formulas to enhance accuracy

02 p0299 A70-12439

Ruby laser light wavelength temperature dependence measurement using Fabry-Perot etalon

02 p0313 A70-12440

Slitless system using interference filter, fixed Fabry-Perot etalon and automatically controlled etalon for recording spectral information for efficient light detection

04 p0685 A70-14523

Laser Doppler velocimeter directly measuring detected frequency with passive confocal Fabry-Perot interferometer

05 p0860 A70-16658

Anomalous dispersion measurements in IR range with multibeam sequential Fabry-Perot interferometers using photoelectric method

06 p1064 A70-17811

Fabry-Perot interferometer application to photometric analysis of solar line profiles

09 p1756 A70-22652

Pressure chamber with inserted holder for adjusting Fabry-Perot interferometer

09 p1681 A70-23337

Scanning spherical mirror interferometer for carbon dioxide lasers radiation spectrum analysis, discussing instrument errors in mode and wavenumber studies

09 p1683 A70-23519

He-Ne laser Q factor modulator based on Fabry-Perot interferometer with alternating absorption

10 p1899 A70-24255

Supersonic gas flow past sphere investigated for characteristics using Fabry-Perot etalon

10 p1888 A70-24258

Scanning Fabry-Perot interferometer for plasma diagnostics, determining kinetic temperatures

12 p2231 A70-27215

Differentiating Fabry-Perot interferometer, obtaining emission spectrum derivatives respecting frequency in millimeter range

12 p2238 A70-28177

Spectral line width and shift measured by spectrograph crossed with Fabry-Perot interferometer in pressure chamber, measuring magnetic field in solenoid

12 p2238 A70-28178

Optical resonator longitudinal modes selection, comparing Michelson interferometer, internal slanted Fabry-Perot interferometer and absorbing film methods

12 p2251 A70-28290

Fabry-Perot resonator mirrors with local reflecting inhomogeneities within perimeter of single crystal wafer for application in optically coupled semiconductor lasers

13 p2427 A70-28884

Fabry-Perot resonator higher modes excitation by external TEM wave, discussing optimal mismatch for maximum intensity

13 p2408 A70-29358

Reflecting surface nonplane parallelism effects on Fabry-Perot interferometers superposition bands contrast and multiplied length measurement accuracy

13 p2408 A70-29366

Fabry resonator X band model with step or slope rimmed mirrors, noting periodical trend of power losses

14 p2558 A70-31320

FM optical signals detection, using Fabry-Perot interferometer with air gap between mirrors

15 p2733 A70-31523

Concentric polarization Fabry-Perot duochromator for spectral line displacement measurements applied to ion drifts in hollow cathode plasma

15 p2737 A70-32042

Diagram extracting Lorentzian line widths from Fabry-Perot interferometer profiles

15 p2737 A70-32050

Fabry-Perot interferometry of solar Mg II resonance lines

17 p3162 A70-34897

Fabry-Perot interferometer series as tunable optical narrow passband filter with high spectral and angular resolution, discussing performance in solar magnetograph

17 p3097 A70-35872

Fabry-Perot microwave interferometer, examining resonant system electrodynamic properties by matrix method

19 p3422 A70-37722

Light modulator design based on Fabry-Perot interferometer controlled by electro-optical effect

22 p4026 A70-42507

Reflection echelon and Fabry-Perot interferometer with surface imperfections, comparing spectral resolution limit with Rayleigh limit

22 p4040 A70-43612

Confocal microwave Fabry-Perot interferometer resonator diffraction loss and field configuration measurements, noting agreement with theory

24 p4381 A70-46242

FABRY-PEROT LASERS

U LASERS

FABRY-PEROT SPECTROMETERS

Dispersion function and measured line profile distortion by rectangular detector slit of order scanning Fabry-Perot spectrometer

06 p1063 A70-17622

FACE [ANATOMY]

Algorithms based on continuous-group pattern recognition, distinguishing human faces, speech and handwritten characters

09 p1640 A70-22143

FACE CENTERED CUBIC LATTICES

Martensite transformation with fcc lattice in Ti alloys containing 5.9 percent Fe as function of cooling rate, using X ray analysis

01 p0124 A70-11590

Two phase theory of ordered to disordered state transition in ternary alloys with fcc lattice, constructing phase diagrams

03 p0505 A70-13103

Austenitic fcc Cr-Mn-N stainless steels ductile-to-brittle transition behavior noting role of deformation faulting

03 p0506 A70-13133

Fcc metals surface changes following adhesion using low energy electron diffraction (LEED), relating intersurface metal transfer to applied adhesive force

07 p1305 A70-18920

Molecular beam interactions with solid crystalline surface with fcc lattice elementary cell, investigating intensity distribution of scattered particles

07 p1342 A70-20119

Electron elastic scattering from surface plane of Au and W fcc lattices using quantum mechanics

07 p1343 A70-20120

Deformation amplitude effects on dislocation structure and strengthening mechanism of fcc aluminum under cyclic loading

08 p1516 A70-20985

Lennard-Jones atom interaction potential, calculating adsorption energy of atom onto surface structure of fcc substrate, tabulating adsorption and surface diffusion activation energies

10 p1927 A70-24078

Irreversible yield stress component of aluminum, Armco iron and tantalum with fcc lattice, showing temperature dependence

13 p2436 A70-29500

Superconductivity in noble metal rich hexagonal close packed phases and fcc solid solutions ascribed to Fermi surface-Brillouin zone interaction

15 p2785 A70-32398

Fcc metals surface self diffusion temperature dependence, using model based on complex defects contribution to diffusion flux at high temperatures

19 p3483 A70-37545

Elastic-plastic behavior of fine grained fcc polycrystals based on single crystal slip data, satisfying displacement compatibility, equilibrium condition, etc

19 p3538 A70-37792

Neutron irradiation effect on elevated temperature fracture of various fcc alloys

22 p4054 A70-42957

FACETS

U FLAT SURFACES

FACSIMILE COMMUNICATION

NT AUTOMATIC PICTURE TRANSMISSION

FACTOR ANALYSIS

Textbook reissue on diffraction of electromagnetic and acoustic waves at open end of waveguide, using Wiener-Hopf-Fock factorization method

13 p2363 A70-28724

Generalized spectral analysis method implementing orthogonal transformations through Kronecker product representation and matrix factorization

15 p2767 A70-32099

Discrete Fourier transform method for factoring spectral density functions, calculating absolute error

17 p3129 A70-34855

FACTORY DESIGN

Chain pooling tests for two level factorial replication-free experiments using Monte Carlo methods
06 p1093 A70-17305

FACTORS

U INDUSTRIAL PLANTS

FACTORS

U VARIABLE

FACULAE

Solar wind acceleration and coronal plasma heating above plane regions from spectra of solar radio echoes, computing temperature rise and energy input
04 p0740 A70-15049

Solar activity centers life history in terms of radio emission and Ca plane intensity, noting radio emission decay faster than plane intensity
05 p0911 A70-16440

Turbulent velocities of convective motions in active and unperturbed photospheric faculae based on spectral observations
07 p1384 A70-19415

Faculae and flocculi intensity relationship to orientation of magnetic fields in solar photosphere and magnetosphere
08 p1560 A70-20837

Darkening and brightening of disturbed spot on sun surface determined by abnormal stress in seen layers due to magnetic and velocity fields
08 p1570 A70-20903

Circular polarization time dependent reversals during simultaneous microwave solar bursts at different plages, considering relations to coincident flares
10 p1932 A70-24626

Solar radio spectrum and history of McMath 607 plane region during eclipse of 7 March 1970, considering residual emission
16 p2977 A70-33845

H alpha filtergrams of sun during solar eclipse of 7 March 1970, showing bright plane area
16 p2980 A70-34226

Fe II line behavior in plages near solar limb
17 p3174 A70-35866

H alpha flares occurrence in plages with little or no spots
21 p3880 A70-40964

FADING

NT SELECTIVE FADING

NT SIGNAL FADING

FAHRENHEIT TEMPERATURE SCALE

U TEMPERATURE SCALES

FAIL-SAFE SYSTEMS

Safe-life and fail-safe structural design philosophies in fatigue damage and operating lifetime control
02 p0389 A70-12615

V/STOL fatigue design parameters, balancing fail-safe and safe-life design procedures
[AHS PAPER 376] 02 p0228 A70-12764

Transmitting-receiving latching ferrite switch with 180 degree differential phase shift toroids for temperature stability and receiver protection in case of driver failure
03 p0458 A70-14036

Twinjet helicopter design for business transport, emphasizing redundant systems for safety and bad weather flight capability
07 p1191 A70-18844

Built-in test equipment for automatic flight control systems, discussing testing programs and fail safe hybrid circuitry
08 p1471 A70-20670

Fail-operational fail-safe redundant yaw damper system, comparing reliability requirements with reliability prediction, development and production testing and field usage data
10 p1896 A70-24913

Digital fail-operative flight control computers for automatic landings, describing system requirements and problems and flight test program
[AIAA PAPER 70-1032] 20 p3591 A70-39505

FAILURE

NT ENGINE FAILURE

NT FAILURE ANALYSIS

NT STRUCTURAL FAILURE

NT SYSTEM FAILURES

FAILURE ANALYSIS

Acoustic emission to monitor metal structures, pipes, pressure vessels and graphite shapes to detect structural deterioration before failure, emphasizing nuclear reactor pressure systems
01 p0054 A70-10015

Hazards due to nonohmic materials responsible for electrostatic failures in missile and space programs and ground equipment
01 p0141 A70-10088

Life-test sampling plan for electron tubes based on exponential failure distribution for reliability demand of military specifications
01 p0099 A70-10112

Failure mode evaluation techniques application to system design and product assurance activities, with examples of performance evaluation of components, circuits and systems
01 p0049 A70-10116

Laboratory tests to determine KC-135 air conditioning failure due to turbine wheel icing by flight condition simulation
01 p0005 A70-10694

Stress rupture strength dependence on specimen geometry /scale effect/ from analyzing metals failure under prolonged loads
02 p0383 A70-11655

Product reliability using statistical probability technology with product failure studies, discussing performance prediction accuracy
02 p0309 A70-12301

Product reliability engineering, discussing product life cycle, operational reliability, failure analysis and design
02 p0309 A70-12303

Mechanical strength and breakdown metallography of plate shaped structural steel and Al alloy specimen under various HF elastic vibrations
02 p0318 A70-12398

Optimal use of adaptive renewal capability determined for first order time varying linear systems with quadratic performance index by exponential model of component failure
02 p0273 A70-12729

Periodic biharmonic stress cycling determination of load influence of fatigue failure used for random load serviceability tests
02 p0391 A70-12855

Failure mechanisms in notched or damaged fiber reinforced composite materials determined from analysis of axial tensile strength and broken fibers
03 p0515 A70-13124

Failure and defect formation in gas turbine engine disks made of steel alloys, stressing fabrication methods effect on reliability
03 p0588 A70-13251

Project management systems failure analysis, discussing cost, products quality and project objectives
03 p0610 A70-13963

Digital network reliability with redundancy to mask logic modules failure for asymmetric failure modes
03 p0454 A70-14022

Neutron radiography for visual nondestructive failure analysis and production inspection of ordnance components compared with X ray radiography
03 p0494 A70-14122

Reliability analysis formulation for statically indeterminate structures, using modified transition probabilities and computer program for systematic failure paths counting
04 p0768 A70-14747

German Space Research Association reliability and testing function, using failure analysis for space projects components and structures
[DGLR-69-30] 04 p0698 A70-15137

Inertial navigation system reliability indices and improvement, discussing mission success, mean time between failure and automatic monitoring
04 p0716 A70-15166

Gas turbine rotating disks failure analysis, studying strength as function of material properties, thermal stresses and hole dimensions
04 p0775 A70-15260

Performance degradation in cadmium sulfide solar cells, discussing cause identification technique, I-V curve parameter changes, etc
04 p0628 A70-15329

Overstress cycles sensitivity for welded specimens on basis of French fatigue damage line and Wohler S-N line
05 p0941 A70-16520

Failure prediction for arbitrary shape flawed pressurized vessels using structural geometry, crack length, ultimate and yield stresses and fracture toughness
05 p0942 A70-16803

Refractory materials deformation and failure analysis based on relations between stresses, strains and irreversible energy absorption per cycle in thermal cyclic fatigue testing
05 p0867 A70-17042

E1617 alloy breakdown resistance tests under multiple alternating static tension-compression and vibrational loads at 800 C
05 p0867 A70-17044

Monograph on models of failure covering mathematical system reliability determination and relationship to physical nature of failures
06 p1171 A70-18394

Material inhomogeneity during high temperature fatigue tests taking into account probability density of random failure coordinate distribution
07 p1401 A70-18839

Adhesive joint failure, studying adhesive, cohesive and adherend ruptures by evaporative rate analysis
07 p1292 A70-18931

Materials selection and simulated service testing to preclude failure, considering roles of design, fabrication and maintenance
07 p1248 A70-19235

Transverse stress failure analysis of reinforced extruded plastic laminates taking into account cohesive and adhesive failure
07 p1410 A70-19768

Computerized generation of cost optimal decision logic for malfunction analysis
08 p1470 A70-20659

Sealed cells failure analysis procedures analogous to medical examination in external and internal inspection and diagnosis
08 p1440 A70-20713

Geometry effect on short beam tests for interlaminar shear strength of composite materials
08 p1529 A70-21882

Failure criteria application to quasi-homogeneous anisotropic materials, discussing material constants
08 p1595 A70-21890

Unidirectional filamentary composites failure theory for uniaxial and combined stress, considering constituent material properties and fabrication processes
08 p1532 A70-21902

Failure mode in shear loaded graphite filament reinforced epoxy composites dependent on interfacial bond strength
08 p1533 A70-21915

Polybutadiene-ammonium perchlorate solid propellant microscopic failure analysis under uniaxial tension
09 p1741 A70-22424

Failure analysis of unidirectionally reinforced fiberglass composites due to winding, using critical stress distribution function
09 p1710 A70-22462

Variational principle application to stability in failure mechanics of arbitrary linearly elastic bodies, discussing inertia effect on steady state vibrations of cracked bodies
09 p1771 A70-22465

Inertia effect in failure mechanics for steadily developing equilibrium cracks in dynamic system with time dependent periodically variable load
09 p1771 A70-22466

Alloy equivalent susceptibility to damage at intermediary service periods and different stress levels under creep conditions at 750 C
09 p1701 A70-22470

Damage model for materials failure prediction under cyclic loading developed for strain controlled cycle with hold time
09 p1774 A70-22588

Creep failure fatigue life prediction methods involving hold period effects on high temperature fatigue properties
09 p1775 A70-22594

Fatigue life and limit distribution obtained from analysis of crack formation start and final failure in notched and smooth specimens
09 p1776 A70-22619

Machine parts fatigue strength calculated from failure probability parameter during unsteady loading
09 p1776 A70-22622

Fault finding strategy optimization in systems with single defective element
09 p1693 A70-22974

Aircraft maintenance, discussing trend toward increased use of quantified methods, failures reclassification, control techniques and check frequencies
09 p1693 A70-23371

Soviet book on control and search for defects in complex systems, presenting statistical optimization methods, programmings for assumed Markov processes, etc
09 p1693 A70-23540

Optimization of controlled systems with allowance for failures of parallel connected elements dependent on control inputs and phase coordinates
10 p1854 A70-24279

Cramer-Rao efficiencies of best linear invariant estimators, using Weibull distribution in model for survival populations connected with life testing
10 p1910 A70-24604

Corrosive wear due to oxygen and/or moisture in air indicated as major failure mode in lubricated gears
10 p1895 A70-24852

Automatic Malfunction Analysis /AMA/ digital computer software system supporting checkout and testing, defining normal system status by computer simulation
[AIAA PAPER 70-383] 10 p1861 A70-24922

Interplanetary space systems, analyzing failure factors to assure reliability
11 p2112 A70-26051

Test pattern generation algorithm and program for failure detection in asynchronous sequential logic circuits, using combinational method
11 p2024 A70-26205

High temperature fatigue tests of materials under uniaxial controlled strain, describing equipment, failure interpretation and data reduction
11 p2033 A70-26613

Viscoelastic polymeric materials tensile failure under multiaxial loading
12 p2321 A70-27205

Transparent polymeric materials failure under neodymium-glass laser radiation in free generation mode 13 p2427 A70-29300

Reliability relation to mean time between failures /MTBF/ relation for long life repairable equipment with limited life components 13 p2421 A70-29567

Automatic Failure Rate Assessment Machine /FRAM/ for subjecting guided weapons electronic modules to cyclic stresses inducing failure of inherent weakness 13 p2379 A70-29686

Failure prediction testing and elements replacement at field maintenance level for increasing equipment reliability 13 p2423 A70-29697

Guidance system cost and reliability by Monte Carlo analysis of failure statistics 14 p2614 A70-30462

SST system safety program, discussing federal office structure, planning and control, design support, integration and evaluation, requirement analysis and failure recurrence control 15 p2675 A70-32214

C-5 aircraft failures and system safety program, noting landing gear, pressure equalization, visor nose, crosswind computer, nacelle separation and propulsion design 15 p2675 A70-32215

Numerically controlled /N/C/ machines reliability program based on organized failure reporting and analysis system for cost effectiveness and downtime reduction 15 p2747 A70-32635

Decreasing failure rate /DFR/ with time in electronic systems operating in avionics applications 15 p2712 A70-32646

Failure mode and mechanism in dielectrically isolated IC attributed to metal bridging under planar oxide 15 p2713 A70-32648

Integrated circuits failures due to electromigration in thin films, discussing hole formation and circuit reliability prediction 15 p2713 A70-32649

High usage military system integrated circuit failure modes analysis for reliability improvement 15 p2713 A70-32650

Electronic components prefailure analysis resulting in reduced failure rates, scrap and rework 15 p2832 A70-32652

System failure rate estimation as function of age using incomplete field reliability data 15 p2748 A70-32660

Reliability physics role in kinetic studies of physical and chemical degradation and failure mechanisms in semiconductor devices 15 p2713 A70-32661

Failure analysis in third generation reliability approach to IC product quality improvement, investigating Si-Al contact irregularity cause and effect 15 p2713 A70-32663

Microscopic data importance in recognizing IC semiconductor failure characteristic traits, revealing current direction, voltage magnitude, microsurface temperature excursion and approximate transient duration 15 p2693 A70-32664

Nonparametric reliability application to numerical data involving failure distribution, using mathematical model 15 p2748 A70-32669

Logic circuits reliability with series and parallel connected elements during random malfunctions, obtaining failure formulas for trigger 15 p2716 A70-32901

Structural fatigue failure analysis and design, applying local stress-strain approach [ASME PAPER 70-DE-24] 16 p2989 A70-33424

Algebraic computation of diagnostic tests for combinational digital circuits single gate failure detection and location 16 p2868 A70-33455

Secondary effect signatures for potential failure detection in jet aircraft engine compressor blades [ASME PAPER 70-DE-58] 16 p2918 A70-33517

Hazard plotting methods for analyzing service life data with different failure modes 16 p2921 A70-34024

Linear stress based cumulative damage law for structural component failures 17 p3186 A70-34987

Cost effective reliability apportionment in spacecraft subsystems, allocating failure-risk goals by mathematical model 17 p3101 A70-35160

System with N independently failing subsystems minimum cost solution mathematical model based on opportunistic preventive replacement policy 19 p3437 A70-38400

Stress rupture strength dependence on specimen geometry /scale effect/ from analyzing metals failure under prolonged loads 19 p3547 A70-38428

Failure and defect formation in gas turbine engine disks made of steel alloys, stressing fabrication methods effect on reliability 19 p3548 A70-38469

Military electronic equipment reliability limitations in terms of mean time to failure, considering quality control of components 19 p3390 A70-38596

Project risk or cost estimation for antipollution, moon mining, tooling, burn-in test and warranties by theory of Takacs processes and correlated queues 19 p3554 A70-38598

Soviet book on statistical algorithms for reliability covering repairable and first failure systems with ideal and imperfect switching 19 p3395 A70-38798

SUREFIRE /system for utilization of remote equipment for failure investigation and reliability evaluation/ monitoring reliability in closed loop failure reporting and corrective action system 19 p3555 A70-38834

Economics of reliability relating risks of failure and cost of failure prevention 19 p3555 A70-38841

Airborne electronic equipment guarantees, discussing USAF experience with full life, maximum failure rate and failure free plans 19 p3391 A70-38843

Integrated microcircuits reliability prediction models based on failure mode and mechanism knowledge 19 p3391 A70-38846

Large scale array /LSA/ MOS devices failure rate prediction model, determining reliability 19 p3391 A70-38847

Classical reliability concept generalization for subjective and objective factors in structural engineering design, obtaining risk of failure 19 p3443 A70-38849

Fatigue strength distributions at specific cycles of finite life with given cycles-to-failure, calculating reliability 19 p3550 A70-38851

Sequential Bayes procedure for demonstrating mean time to failure beyond minimum acceptable value 20 p3658 A70-39642

Failure probability from finite sampling characteristics, emphasizing statistical safety factors to characterize structures strength reliability 20 p3724 A70-39856

Brittle failure under creep during slow cyclic loading, discussing damage accumulation assumptions 20 p3725 A70-39868

Materials viscous failure at various temperatures and stresses, discussing damage accumulation 20 p3725 A70-39870

Corrosion failures diagnosis, describing visual, electron microscope, metallographic and chemical analysis techniques 20 p3650 A70-39968

Uniaxial fiber composites tensile strength models, including failure analysis 20 p3731 A70-40046

Wire reinforced solid rocket propellant grains mechanical properties and failure modes 20 p3689 A70-40050

Failure rate and MTBF in reliability engineering, clarifying ambiguous terminology 20 p3638 A70-40061

Welding failure case histories, discussing design, materials and processes, fabrication and quality control integration 21 p3832 A70-40787

Accelerated failure tests of ammonia-Al-stainless steel heat pipes for fluid loss or energy transport degradation 21 p3947 A70-41049

Finite element analysis of critical stress distribution in canopy of deployed twin keel parawing, predicting failure stress levels 21 p3753 A70-41820

[AIAA PAPER 70-1196] Carbon fiber reinforced polymer /CFRP/ failure mechanism, discussing nondestructive testing, destructive and cyclic loads 22 p4058 A70-42476

Optimal burn-in testing of repairable equipment, improving reliability by decreasing failure rate with age under operating conditions 23 p4199 A70-43923

Failure analysis - IEEE Conference, University of Pennsylvania, May 1970 23 p4174 A70-44743

Failure reporting, analysis and correcting system for effective management 23 p4200 A70-44745

Electrical and electronic semiconductor device failures from metallurgical viewpoint 23 p4175 A70-44746

RF power transistors failure analysis, describing IR radiometer technique 23 p4175 A70-44747

Failure analysis, surveying roles of design, manufacturing processes, random variables, etc 23 p4200 A70-44748

Integrated circuits failure analysis techniques, including electrical diagnostics, visual inspection, surface examination, shorts location, etc 23 p4175 A70-44749

Failure analysis methods for connectors and interconnections, discussing visual inspection, X ray vidicon analysis, electrical evaluation, etc 24 p4320 A70-46249

FAINTING

U SYNCOPE

FAIRCHILD MILITARY AIRCRAFT

U MILITARY AIRCRAFT

FALKNER-SKAN EQUATION

Flow about blunted wedge with laminar boundary layer at stagnation point and approaching Falkner-Skan flow at infinity, discussing asymptotic behavior 01 p0061 A70-10540

Sturm-Liouville problem associated with Falkner-Skan equation, obtaining asymptotic solutions 03 p0520 A70-14080

Linear spatial stability of two dimensional laminar wake- and jet-like similarity solution of Falkner-Skan equation 04 p0613 A70-14455

Nonsimilar energy and species equations for flow velocities described by Falkner-Skan equation 07 p256 A70-19307

Boundary layer retarded flow past porous surface with suction, using Runge-Kutta computerized integration of Falkner-Skan equation 15 p2720 A70-31586

Falkner-Skan type boundary value problem of three dimensional flow near stagnation point 20 p3658 A70-40103

FALLING SPHERES

Upper atmosphere density and temperature height profiles perturbations in falling sphere probe 15 p2723 A70-31663

FALLOUT

Atmospheric dust natural radioactivity effect on tropospheric Pb 210 mean residence time determination for Pb210 and Ra226 fallout in rain near Moscow 14 p2630 A70-30131

Atmospheric radon concentration ratios diurnal and vertical variations used for turbulent exchange and washout study 17 p3132 A70-34611

FAN IN WING AIRCRAFT

NT XV-5 AIRCRAFT

Noise radiated from VTOL lifting fan in wing inlet under static inflow conditions, attributing discrete tones to spacing between rotor and stator blades [ASME PAPER 69-WA/GT-6] 04 p0734 A70-14889

FANLIFT DEVICES

U LIFT FANS

FANS Single stage experimental front fan designed for aircraft engines, measuring overall and blade element performances 02 p0355 A70-12258

Fan rotors aerodynamic noise tonal annoyance reduction by blade unequal circumferential spacing, noting sound-pressure wave shape determination [ASME PAPER 69-WA/FE-23] 04 p0614 A70-14776

Aircraft engine support system dynamic loads induced by fan unbalance analyzed by coupling pylon and engine vibration modes [SAE PAPER 690613] 05 p0895 A70-15850

Wind tunnel experiments for apparent reverse transition during expansion fan and turbulent boundary layer interaction, discussing Reynolds stresses 07 p1257 A70-19345

Casing and suction cone effects on fans with cambered forward curved blading 11 p1975 A70-25796

Nonfree vortex flow in contrarotating axial flow fans under radial equilibrium assumption, discussing pressure rise coefficient and static efficiency 12 p2156 A70-27600

Axial flow fans performance dependence on aspect ratio from empirical relationships, plotting various component losses and stage efficiency 14 p2529 A70-31418

Computerized design for radial flow splitters in three dimensional fan exhaust nozzles 18 p3207 A70-36462

Forced vortex impeller in axial flow fan without inlet vanes, presenting lift and drag coefficients of blade sections, loss of head, etc 19 p3352 A70-38222

Three dimensional flow through rotor of axial vortex flow fan, using airflow method for design 19 p3352 A70-38248

FAR FIELDS

Linearized potential theory application in aerodynamic design and analysis of supersonic aircraft emphasizing far field viewpoint [AIAA PAPER 69-1132] 01 p0002 A70-10608

Far field radiation pattern determination particularly suitable for large parabolic antennas, detailing measurement errors 02 p0267 A70-12399

Plane electromagnetic wave diffraction at conducting stripline, calculating surface current density and 02 p0267 A70-12399

far field scattering using edge wave and factorization methods

03 p0451 A70-13755

Ion and electron concentrations far field disturbances caused by satellite motion in ionosphere and lower exosphere, deriving plasma drag

04 p0762 A70-14935

Simultaneous recording of near and far field diffraction patterns at several exposures for single laser pulse

04 p0701 A70-15022

Electromagnetic scattering from perfect conductors by numerical analysis, presenting far field pattern calculation for plane wave scattering from square cylinder

04 p0652 A70-15363

Cartographic radiation patterns far field characteristics of aperture antenna arrays obtained by optical simulation method

05 p0820 A70-16254

Antenna far field noise effect on monopulse type and conical scanning radar angle meters performance

05 p0813 A70-16256

Gabor holography producing interference phenomena, discussing far field fringes, circular fringes, diffuser, etc

05 p0849 A70-16529

Far field synthesis for calculating excitation pattern of waveguide-excited aperture antenna arrays

07 p1243 A70-20325

News function relation with far fields of sources obtained in linear approximation for axisymmetric case in integrating Einstein field equation

08 p1543 A70-20721

Far field directionality and acoustic power of noise radiated by axial flow fans and compressors using fluctuating forces model

08 p1547 A70-21860

Ground reflection effect on plane uniform sound source distribution applicable to compressor and fan noise under far field conditions

09 p1726 A70-22240

Edge smear in far field holography as function of interference orders, using short-cut trace technique

09 p1684 A70-23532

Plane electromagnetic waves scattering from radially inhomogeneous cylindrical structure, deriving expressions for far field and cross section for both polarizations

10 p1841 A70-24856

Plane electromagnetic wave diffraction at conducting stripline, calculating surface current density and far field scattering using edge wave and factorization methods

10 p1842 A70-25002

Microwave illuminated aperture near radiation field mapped and processed for microwave hologram suitable for optical imaging for far field pattern simulation

11 p2051 A70-26025

Radiation from electric dipole in moving isotropic plasma analyzed for plasma velocity effect on pattern and far fields

11 p2091 A70-26178

Far field radiation patterns of Cassegrain, offset paraboloid and horn reflector antennas by stationary phase approximation method

11 p2019 A70-26659

Thermally self induced laser beam phase modulation resulting in far field aberrational rings, describing structure and profile

13 p2431 A70-29834

Microwave axicon with dielectric cone at aperture of focused antenna to reduce far-field radiation pattern beamwidth

14 p2549 A70-30512

Gyrosynchrotron from accelerated electron, discussing effects of cold and collisionless magnetoplasma on far field and frequency spectra

15 p2728 A70-31989

Optical images from microwave far field/Fourier transform/ holograms, noting carrier fringe dependence

16 p2913 A70-34043

Far field antenna patterns synthesis and steering for optical heterodyne receivers

16 p2866 A70-34261

Simple antenna sources, deriving far zone radiation field from arbitrary current distribution

17 p3043 A70-35052

Uniformly spaced antenna arrays along curve, determining far field as product of element and array factors

17 p3044 A70-35055

Log periodic antennas, discussing dipole array and planar sheath spiral structures, base current and far field pattern calculations, etc

17 p3052 A70-35073

Shadow current method for asymptotic solution to two dimensional problem of electromagnetic wave far diffraction field on ideally conducting plane with infinite rectilinear slot

18 p3227 A70-36142

Power flow patterns of near to far field transition of scalar wave pencil beam without reference to specific radiating structure

19 p3536 A70-37703

Far field diffraction, radiation and gain of wide flare angle corrugated conical horns

19 p3389 A70-37970

Reflectors group mean effective scattering cross section measurement by far field criterion

22 p3995 A70-42387

Elastic wave diffraction by rigid inclusion, calculating far field displacement and cross section by integral equation method

22 p4073 A70-42636

Antenna far/near field correlation, noting measurement accuracy role

23 p4160 A70-43769

Far field diffraction spreading of surface acoustic waves on cut Li-niobate in two directions

23 p4230 A70-44199

Far field power of coherent Cerenkov radio emission from cosmic ray showers in turbulent atmosphere, using radio telescopes

23 p4247 A70-44791

Two dimensional electromagnetic scattering body geometry reconstruction from given incident and scattered far field distributions

23 p4165 A70-44958

FAR INFRARED RADIATION

Far IR night sky emission above 120 km over millimeter range, using rocket-borne telescope

01 p0069 A70-10040

Ge bolometer cooled by liquid helium 3 to near absolute zero to achieve high sensitivity for far IR detection

01 p0091 A70-10910

Extrasolar far IR background radiation observed with liquid He cooled telescope carried by Aerobee rocket

02 p0358 A70-12197

Far IR spectra of liquid hydrogen at para concentrations, noting absorption coefficient variation consistent with composition

04 p0718 A70-14696

Far IR extrinsic photoconductive detectors for rocket-borne liquid He-cooled IR telescope, discussing limiting noise factor

04 p0689 A70-15018

Solar and sky far IR radiation in upper atmosphere, estimating precipitable water quantities and low absorption regions

04 p0681 A70-15521

Far IR measurement of solar minimum temperature with Michelson interferometer carried on NASA research aircraft

06 p1143 A70-17997

Far IR radiation transmission through bismuth and gallium normal and superconducting thin films, considering transition temperature role

09 p1739 A70-22323

Far IR radiation at galactic center suggested as thermal emission by dust particles

09 p1744 A70-22502

Far IR airborne spectroscopy for measuring solar brightness temperature, emphasizing scanning Michelson interferometer and radiometric calibration

09 p1683 A70-23525

Iostropic background radiation measured in ozone sphere with balloon-borne far IR radiometer

10 p1917 A70-24630

IR luminosity of galactic nucleus from far IR observations, noting considerations favoring nonthermal model consisting of multiple sources

10 p1947 A70-24996

Plasma self Q switching in pulsed far IR lasers, discussing lens effect of plasma electrons delaying laser pulses

11 p2062 A70-25634

HCN laser far IR line phase locked to absolute frequency standard

13 p2426 A70-28810

Bibliography of far IR spectroscopy with subject index

14 p2586 A70-30987

Convergence corrections for absorption coefficient measurements by far IR Michelson interferometer

14 p2586 A70-30988

Quasi-optical filters with bandpass and pseudohigh pass structures for millimeter wave and far IR frequencies

14 p2558 A70-31318

Far IR second harmonic generation and frequency mixing in CdTe using pulsed water vapor laser

15 p2751 A70-31983

Complex dielectric constant of alpha-AgI measured in microwave region and far IR, noting sample positioning

16 p2960 A70-33225

Spectrophotometric solar brightness temperature measurements in far IR, discussing collision type spectral variation of absorption coefficient

18 p3319 A70-37056

Diffuse cosmic X rays produced by Compton scattering of far IR radiation on cosmic ray electrons

19 p3505 A70-38113

Optical emission conversion from solid state lasers into far IR region by nonlinear polarization with difference frequency generation

19 p3448 A70-38741

Submillimeter gas lasers with low noise and CW operation for far IR spectroscopy, noting emission lines multiplicity

20 p3641 A70-39423

Universe cold matter structure and distribution from far IR data

22 p4096 A70-43395

Rate equation study of multiwavelength far IR laser oscillations in water vapor, taking into account molecular rotation-vibration interaction

24 p4354 A70-45812

Double beam diffraction grating spectrometer for vacuum operation over far IR from 40 microns to 1 mm

24 p4339 A70-46323

FAR ULTRAVIOLET RADIATION

NT LYMAN ALPHA RADIATION

Solar Mg II doublet and XUV images obtained by Fabry-Perot interferometer mounted in Skylark spectrograph

01 p0177 A70-10339

Far UV spectroscopy of Jupiter by rocket-borne spectrograph

01 p0179 A70-10528

Intensity distribution determination in spectrum of solar XUV fluxes incident upon upper atmosphere, considering quantitative model construction

01 p0170 A70-10593

Atmospheric density variations during solar maximum and minimum, discussing solar corpuscular stream and EUV radiation

01 p0075 A70-10594

Monk-Gillieson convergent beam dispersion method applied to rocket-borne photoelectric spectrophotometer for far UV stellar spectra observation

01 p0090 A70-10904

Absorption of EUV sunlight by Jupiter upper atmosphere, discussing photoelectron energy loss, thermal equilibrium and heating efficiencies

02 p0367 A70-11816

Constricted DC Ar arc with N or O additions calibrated as vacuum UV radiation standard for photon flux measurements

02 p0343 A70-11905

Extreme UV spectral line intensity enhancement during class 3 flare related to abundance of radiating element

02 p0358 A70-12205

Lifetimes of upper levels of N II and N III UV multiplets determined from radiative deexcitation of excited ions

03 p0527 A70-13074

Semitransparent Pt film reflectance in vacuum UV evaporated on glass, quartz, Al, Au and Cr on glass compared with opaque films

04 p0731 A70-15023

Diffuse far UV radiation analysis in connection with stars and dust grains distribution and grains optical properties

05 p0903 A70-16571

Reflectance of clean and fluoride coated aluminum surfaces in vacuum UV

05 p0883 A70-16590

Extreme UV flashes of solar flare observed by sudden ionospheric frequency deviations compared with energetic X rays observations

05 p0905 A70-16981

Photodissociation of diatomic O and N molecules in far UV

07 p1338 A70-20052

Vacuum UV spectrum interferometer with grazing incidence reflections between plane parallel mirrors to obtain coherent beams, discussing fringe patterns

07 p1286 A70-20081

Altitude profiles and absolute intensities of far UV emission features in aurora measured by filterwheel photometer in Aerobee rocket, determining molecular oxygen densities

08 p1489 A70-21384

Interplanetary density distribution of cold interstellar origin hydrogen dependent on solar EUV flux, considering interaction with solar wind protons

08 p1562 A70-21401

Vacuum UV atomic nitrogen and oxygen lines contribution to energy transfer in high density plasma, noting f values and Stark half widths

09 p1730 A70-22229

Vacuum UV photons production during ground state neutral argon atomic collisions, measuring relative cross sections energy dependence

09 p1731 A70-22333

Narrow band detector for polarized light in far UV based on plasma resonance

09 p1676 A70-22650

Auroral arcs far UV observations by OGO 4, discussing luminosity, morphology, position, etc

09 p1670 A70-23493

Diffraction filters characteristics used in XUV spectroscopy involving solar, stellar and laboratory experiments

09 p1729 A70-23526

Fluorescent integrating sphere for absolute hemispherical reflectance measurements on imperfectly

diffuse surfaces in vacuum UV, eliminating erroneous signals by filtering

09 p1729 A70-23527

Solar limb brightening of XUV lines of carbon, nitrogen, oxygen and silicon ions in chromospheric-coronal transition region

11 p2108 A70-25740

Solar active regions in chromosphere and corona observed by EUV spectrophotometer aboard OSO-4 spacecraft, discussing ion formation and temperatures

12 p2303 A70-27705

Far UV emission spectrum of plasma produced by laser beam impact on Al target observed as function of time, determining electron temperature

13 p2460 A70-28729

Solar extreme UV radiation measurements over rotation period onboard satellite OSO-3, using atmospheric absorption correction

15 p2792 A70-31666

Time controllable continuous photon emission from plasma produced by pulsed laser vacuum spark applied to absorption spectroscopy in vacuum UV

15 p2734 A70-31757

Daily amplitude variability of equatorial electrojet current related to solar extreme ultraviolet radiation /XUV/influx

15 p2727 A70-31873

Absolute quantum efficiency of phosphor calcium tungstate-lead under monochromatic far UV illumination

15 p2729 A70-32017

EUV solar spectrometer in orbiting solar observatory /OSO-1/, describing satellite, optics and detector, data coding, etc

15 p2736 A70-32027

Glancing incidence extreme UV telescopes optical design in solar physics applications, employing surfaces of revolution

15 p2736 A70-32029

Photometric calibration changes in EUV solar satellite instruments during orbital operation

15 p2737 A70-32045

Single beam grazing incidence spectrophotometer with concave diffraction grating for far UV region, emphasizing instrument adjustment

16 p2915 A70-34218

Orion stars far UV intensities, considering photometric data and spectrographic spectra from rocket sounding

17 p3160 A70-34882

Far UV photometer for space research, isolating specific bands by combining spectral response of individual solar blind photocathodes with thin metallic films transmission qualities

17 p3096 A70-35766

Atomic hydrogen population distribution in far UV of comets

19 p3526 A70-38782

Formaldehyde absorption coefficients measured photoelectrically in vacuum UV range

20 p3703 A70-39165

Emission cross sections of nitrogen in vacuum UV by electron impact

20 p3675 A70-39617

Vacuum UV laser action in molecular hydrogen Lyman bands, examining stimulated emission in P branch lines and light pulse duration

20 p3643 A70-40496

Decay lifetimes and electron impact cross sections of vacuum UV O I and O II emission multiplets, using pulsed electron beam in low pressure gases

21 p3852 A70-40718

Absorption diffuse band systems of diatomic argon molecule in vacuum UV region

21 p3853 A70-41395

Extreme UV spectroscopy with synchrotron radiation storage ring light sources in 40-400 A range, including thin film photoabsorption measurements

21 p3826 A70-41451

Atomic Ar absorption spectrum in vacuum UV region, observing Rydberg series interactions as perturbations and autoionizations

21 p3781 A70-41933

Solar equatorial limb brightening of far UV resonance lines of lithium-like N V, O VI, Ne VIII, Mg X and Si XIII ions, interpreting osso-4 data with coronal model

21 p3924 A70-42185

Solar far UV limb brightening of C III, N III, N IV, O III, O IV and Si IV lines in chromospheric-corona transition region, correcting coronal model for spicule effects

21 p3925 A70-42186

Oso-4 far UV observations of solar chromosphere and corona active regions

21 p3925 A70-42187

NO molecule gamma system in emission spectra of polar auroras in far UV by monochromator aboard Skylark rocket

21 p3821 A70-42261

EUV solar spectral intensity distribution and cyclic variations

22 p4106 A70-43299

Upper atmosphere photoionization by extreme UV solar radiation compared with ionization by charged particles collisions

22 p4096 A70-43302

Spectral filtration methods in diffraction instruments at vacuum UV region, discussing ambient storage conditions and fabrication effects

23 p4219 A70-44412

Solar XUV and soft X ray photometry, describing sounding rocket and satellite grazing incidence spectrometers

24 p4339 A70-45822

FARADAY EFFECT

Frequency locking of flashlamp pumped Rhodamine 6G dye lasers to D lines of Na vapor by Faraday rotation, noting doublet splitting

01 p0110 A70-10568

Upper atmospheric contribution to Faraday rotation angle above 5000 km determined from beacon frequencies of geostationary satellite, noting geomagnetism weighting and electron content decrement role

01 p0076 A70-10874

Transient Faraday rotation of S-band telemetry carrier observed during Pioneer 6 occultation by solar corona, correlating with decametric solar radio bursts

02 p0369 A70-12059

Dispersive Doppler shift and Faraday rotation second order theory for curved earth-ionosphere geometry, calculating phase path differences

02 p0260 A70-12574

Faraday rotation observations on Explorer 22 signals at two receiving stations, discussing comparative evaluation procedures and results

03 p0472 A70-12874

Phase distortion and Faraday rotation of wideband radio waves propagating through ionosphere

03 p0449 A70-13584

Traveling ionospheric disturbances from signatures left in columnar electron content records obtained by measuring signal Faraday rotation angle from geostationary satellite

03 p0477 A70-13991

Faraday type open circuit MPD generator model obtained with allowance for temperature and pressure losses and gas transport properties dependence on static parameters

04 p0725 A70-14530

Electron density profiles alongOGO 1 orbit portions calculated by measuring harmonic radio beacon transmissions differential Doppler frequencies and Faraday polarization rotation angle

04 p0741 A70-15118

Faraday modulator for polarized laser radiation, eliminating analyzer by oblique magneto-optical active element, converting angular modulation into amplitude modulation

05 p0858 A70-16251

Ionospheric electron content, virtual height and profile measured by Faraday effect of satellite radio emissions compared with radar soundings

05 p0839 A70-16288

Rate of change of radio ray path length for transionospheric satellite VHF signals determined from Doppler and Faraday effect analyses

06 p1008 A70-17578

Winter midlatitude electron density trough from length fluctuation of Faraday signal fading period of satellite Explorer 22, noting characteristic seasonal variation

07 p1270 A70-20034

Closely spaced frequencies method of determining ionospheric electron content from Faraday rotation measurements

07 p1271 A70-20156

Ionospheric electron content and concentration variations analysis based on data of radio waves propagating from satellite, considering Doppler shift and Faraday effect

07 p1237 A70-20427

Faraday rotation in pulsars and in interstellar medium, discussing position angle drift, polarization changes and pulse fine structure

08 p1564 A70-20553

Ionospheric electron content estimated from measurements of Faraday rotation of VHF signals from geostationary satellite

08 p1489 A70-21388

Galactic latitude dependence of polarization and Faraday rotation of extragalactic radio sources at centimeter wavelengths

08 p1577 A70-21534

Ionospheric electron content diurnal, latitudinal variations and equivalent slab thickness determined from observing satellite signals Faraday fading

10 p1874 A70-24426

He-Ne laser amplifier in axial magnetic field, measuring Faraday rotation and gain for various input signal intensity values

10 p1901 A70-24945

Ionospheric electron content from Doppler data and from Faraday observations of satellite S-66

10 p1884 A70-25256

Ionospheric electron content calculations based on satellite measurements of Faraday rotation and phase path length variations

12 p2294 A70-27739

Solar flares responsible for Faraday rotation events observed in passage of Pioneer 6 radio signal through solar corona

12 p2295 A70-28023

Interband Faraday effect in doped semiconductors by quasi-classical approximation

13 p2469 A70-28878

Vertical ionospheric electron concentration profiles, horizontal gradients and integral component from Doppler and Faraday signal recording on geophysical rockets, using diversity reception

14 p2569 A70-30205

Faraday type MHD generators, investigating gas velocity and temperature profiles effect on electrical performance by equivalent circuits simulation

14 p2534 A70-30537

Ionospheric total electron content measurements by Faraday method and bottom and topside soundings

14 p2580 A70-31258

Prolonged upper ionospheric observations from Sputnik 3, Transit 4A and Explorer 22 signals Faraday fading and phase shifts, showing electron content dependence on solar activity

15 p2731 A70-32093

Faraday rotation in pulsars and in interstellar medium, discussing position angle drift, polarization changes and pulse fine structure

15 p2805 A70-32708

Ionospheric electron density during solar eclipse of 7 March 1970, using Faraday rotation measurements of geostationary satellites VHF transmissions

16 p2898 A70-33831

F region integrated electron density response during solar eclipse of 7 March 1970, using Faraday rotation of linearly polarized signals from ATS 3

16 p2898 A70-33835

Gravity wave generation during solar eclipse confirmed by satellite observation on Faraday rotation angle of ionospheric VHF transmissions

16 p2898 A70-33836

Magneto-optics of semiconductors, taking into account intraband and interband effects with Faraday and Voigt field configurations

18 p3297 A70-35951

Ionospheric refraction during radio wave propagation using space diversity recordings of Faraday and Doppler effects for coherent signals from geophysical rockets

19 p3407 A70-37306

Faraday rotation of radio beacon satellite signals during traveling ionospheric disturbances simulated for spaced ground stations

20 p3590 A70-40481

Ionosphere and magnetosphere total electron content from beacon method of measuring difference-differential-doppler /DDD/ and Faraday effects via synchronous satellite signal frequencies

20 p3590 A70-40484

Magneto-optic rotation and hysteresis recording instrument for thin magnetic films as function of temperature and wavelength, using Faraday effect

21 p3826 A70-41452

Magnetic holography, considering Faraday and polar Kerr effect reconstructions and potential as computer storage

22 p3994 A70-43608

Ionospheric electron content measurement from Faraday effect of troposphere on beacon satellite Explorer 22 radio signals

23 p4163 A70-44231

Radar astronomical polarization measurements for lunar echoes by exploiting ionospheric Faraday rotation with linearly polarized antenna

23 p4165 A70-44964

Vertical ionospheric electron concentration profiles, horizontal gradients and integral component from Doppler and Faraday signal recording on geophysical rockets, using diversity reception

24 p4330 A70-46280

Hot electrons Faraday effect in many-valley semiconductors, considering constant energy surface ellipsoidal form

24 p4392 A70-46360

FARADAY ROTATION

U FARADAY EFFECT

FARM CROPS

NT POTATOES

Aerial color IR photography for crop disease identification by tonal and geographic patterns, discussing cameras, films, filters and exposure procedures

05 p0837 A70-16144

Automated crop surveys from integrating observations made at different times /time dimensioning/ during growing season, noting earth resources satellites role

09 p1666 A70-22263

Crop species and soil conditions identification from space by comparison of multivase and multiemulsion

photography, assigning standard signature to optical fields
10 p1879 A70-24745

Methodology for machine processing for identification of individual crop types, discussing discriminant photoanalysis
12 p2227 A70-28108

Agricultural crop identification, using optical Stokes parameters such as wavelength, geometry, and bidirectional photometric and polarization factors
22 p4014 A70-42769

FAST NEUTRONS

Millimeter and nanosecond resolution of fast neutrons in pulse dense high temperature deuterium plasma discharge with polyethylene collimators and photomultipliers
02 p0303 A70-12739

Superconducting properties of polycrystalline disordered cold worked Nb-Ti-V alloys showing unexpected sensitivity to fast neutron irradiation
03 p0508 A70-13144

High energy neutron accelerator as fast neutron radiography source, comparing contrasts with gamma and X radiography
05 p0844 A70-15779

Fast neutron transport characteristics of helical ducts using Monte Carlo code FASTER, computing neutron fluxes and attenuation
05 p0884 A70-16163

High energy neutrons searched for during solar flares by balloon flights, giving upper limits for gamma ray and neutron fluxes
06 p1136 A70-18008

Polarized Co59 target using He3-He4 dilution refrigerator, analyzing fast neutron scattering
14 p2584 A70-30508

Void formation and creep during fast neutron irradiation of austenitic stainless steel based on thermodynamic approach, calculating nucleation and growth rates
17 p3123 A70-34626

Mitotic activity and aberrant mitoses frequency in mice corneal and duodenal epithelium cells under fast fission neutron irradiation
17 p3026 A70-35319

Flexible shallow shell with plastic inhomogeneity due to yield point-fast neutron flux relation, examining stability under uniform load
20 p3734 A70-40437

Fast neutron radiography, considering sources and transfer and scintillator-film detectors
24 p4376 A70-45749

Fast neutrons for radiogenic nondestructive material testing, describing defectoscope performance, sensitivity and cost efficiency
24 p4377 A70-45851

FASTENERS

NT BOLTS
NT LOCKS [FASTENERS]
NT NUTS [FASTENERS]
NT RIVETS
NT SCREWS

Eddy current inspection method for detecting fatigue cracks location and depth in fastener holes
01 p0097 A70-10008

Al fasteners design guidelines including material forming capabilities, cost consideration, applications, etc
04 p0697 A70-14722

Mechanical fastening, adhesive bonding and machining methods for laminated fiberglass reinforced plastic materials
05 p0856 A70-16618

Design concept, materials application and performance characteristics of high temperature fasteners [AIME PAPER F-69-6]
07 p1290 A70-18811

Ti alloy suitability for fastener applications noting cold workability, high strength and stress corrosion resistance [ASM PAPER W70-17.3]
15 p2760 A70-32338

Fastener standardization for airline maintenance requirements [AIAA PAPER 70-894]
17 p3102 A70-35811

Beta III Ti alloy for aircraft fasteners, describing microstructure and mechanical properties
20 p3650 A70-39966

Ultrasonic crack detection in fastener holes in C-5A wings
24 p4341 A70-45571

Thrust parameters effect on steel and Ti high strength fasteners fatigue life [SAE PAPER 700831]
24 p4425 A70-45881

Bonded honeycomb sandwich structure fastening techniques in aerospace design, noting application to aircraft and spacecraft structures [SAE PAPER 700850]
24 p4425 A70-45882

FAT EMBOLISMS

Lung lipid embolization effect in decompression sickness on obese mice, showing no relationship to dysbaric syndrome
01 p0015 A70-10361

Fat embolism and decompression sickness similarities, studying lipid stability changes resulting from liver tissue injury by nitrogen bubbles
07 p1222 A70-19936

FATIGUE [BIOLOGY]

NT FLIGHT FATIGUE
NT MUSCULAR FATIGUE

Visual fatigue symptoms, causes, relation to general fatigue and psychological aspects, discussing testing for sensory and visual fatigue
01 p0022 A70-10857

Cortical cells fatigue and performance in subjects doing mental work, using motion picture signal perception method
04 p0639 A70-15509

Agricultural pilots fatigue based on flight and environmental effects
11 p1993 A70-26522

Collection of articles on fatigue, sleep and dreams covering mechanisms, biochemistry, pathological physiology, etc
15 p2680 A70-31739

Fatigue phenomena at spinal motor synapses, investigating role of accompanying vegetative phenomena as source of fatigue
15 p2680 A70-31740

Mechanical and morphological characteristics of overload and fatigue in dog ulnas, showing elastic and plastic deformation zones
15 p2682 A70-31935

Fatigue effects on relationship between oxygen consumption, electromyographic activity and isometric contraction in human leg muscles
21 p3766 A70-42159

FATIGUE [MATERIALS]

NT BENDING FATIGUE
NT METAL FATIGUE
NT THERMAL FATIGUE

Materials strength characteristics with respect to breakdown probability parameter by statistical fatigue stability analysis under unsteady loads and various distribution laws
01 p0211 A70-11424

Optimum prism angles and ultrasonic frequencies for detecting fatigue cracks
02 p0301 A70-12487

Fatigue testing facilities and methods with emphasis on consumable load, randomized serviceability and random process tests, examining closed loop control servohydraulic appliances
02 p0276 A70-12853

Swenson shear fatigue crack model expanded to include mean stress effect on cyclic shear crack growth [ASME PAPER 69-WA/APM-8]
04 p0772 A70-14918

Test rig for load controlled strain fatigue, describing main structure, pin joint bearings and hydraulic specimen clamps
04 p0773 A70-15040

Fiberglass reinforced plastics energy dissipation during fatigue failure phases, studying mechanical-to-thermal energy transformation under cyclic strain
04 p0713 A70-15263

Fatigue crack propagation and fracture toughness in pressurized thin walled cylindrical tubes, basing analysis on shallow shell bending theory
05 p0942 A70-16802

Creep rupture effect on fatigue damage of structural material, constructing nondimensional stress range diagrams
05 p0943 A70-16806

Collection of papers on strength at small number of load cycles, problems of mechanical fatigue
06 p1160 A70-17382

Fatigue breakdown criteria for elastoplastic materials under cyclic loads, deriving equations as functions of stress-strain states kinetic behavior
06 p1162 A70-17390

Glass fiber reinforced thermoplastics fatigue behavior during and after cyclic loading
06 p1091 A70-17600

Materials fatigue failure ultrasonic early detection by continuous surface wave irradiation
06 p1077 A70-17920

Epoxy-fenolic coatings effect on fatigue durability of bent steel samples
08 p1587 A70-21075

Composite materials fatigue determinations providing curves of stress-strain magnitude vs usable life or time to failure, considering environmental effects in service for design criteria
08 p1531 A70-21895

Tensile, fatigue, creep and stress-rupture behavior of unidirectional, unidirectional off-axis and cross-ply composites of B filaments in Al alloy matrix
08 p1531 A70-21896

Thermal and high strain fatigue covering cyclic tests, crack initiation and propagation, stress-strain behavior, structural design, frequency and temperature effects, etc
09 p1773 A70-22576

Damage model for materials failure prediction under cyclic loading developed for strain controlled cycle with hold time
09 p1774 A70-22588

Soviet collection of papers on mechanical fatigue from statistical standpoint
09 p1775 A70-22614

Stress concentration effect, surface states and similarity conditions in fatigue ruptures in machine construction, considering statistical analysis
09 p1776 A70-22615

Machine parts fatigue strength calculated from failure probability parameter during unsteady loading
09 p1776 A70-22622

Aviation and space industry metallic and nonmetallic materials testing, discussing corrosion and ultimate fatigue due to impurities
10 p1861 A70-24664

Energy methods applied to fatigue crack propagation rate under tensile mean stress
10 p1963 A70-25090

Fatigue crack propagation rate in sheet alloys with holes as stress concentrators related to duration of various development phases
10 p1965 A70-25290

Quasi-brittle materials limit surface, approximating curve in deviator plane by second order curves leading to strength criteria
10 p1965 A70-25292

Low cycle fatigue problems, environmental influence of operational differences on component life, life limits and controls for safe operation of jet engines [SAE PAPER 700207]
11 p2102 A70-25879

Continually changing residual stress patterns effect defined for predicting cumulative damage in structural fatigue
11 p2137 A70-26090

Fatigue behavior prediction for complex parts and structures using laboratory tests of small specimens
11 p2137 A70-26091

Airframe structures fatigue crack propagation with and without strain hardening during variable amplitude loading
12 p2315 A70-27014

Polycarbonate fatigue fracture surfaces and striation feature
12 p2259 A70-27168

Stress measurements for eye beams forming of high fatigue strength based on brittle lacquer studies of isotropic material models
13 p2507 A70-28482

Moisture effect on fatigue crack propagation and fracture path through microstructure of 300-grade maraging steel
13 p2432 A70-28607

Transparent polymeric materials failure under neodymium-glass laser radiation in free generation mode
13 p2427 A70-29300

Fatigue damage accumulation deterministic models for predicting longevity
14 p2656 A70-30300

Cumulative creep strain and damage based on stress amplitude coefficients, considering continuous single step system of loads
15 p2821 A70-32339

Glass reinforced laminates fatigue characteristics, discussing differences from metals due to composites anisotropic structure
16 p2989 A70-33420

Structural fatigue failure analysis and design, applying local stress-strain approach [ASME PAPER 70-DE-24]
16 p2989 A70-33424

Kinetic theory of fatigue crack propagation, discussing stochastic nucleation process and power exponent relation
16 p2992 A70-33968

CH-47 cruise guide indicator for displaying fatigue loading to pilots, discussing design and operation
17 p3082 A70-34705

Fatigue crack propagation in solids in terms of nucleation theory, explaining temperature dependence of fatigue strength and size effect
17 p3191 A70-35464

Failure of materials under multicycle fatigue, deriving general theory of defects
18 p3341 A70-36586

Rotating mechanical components reliability under complex fatigue, presenting design data
19 p3442 A70-38845

Structural fatigue design loads computation for fighter aircraft using multivariable load environment model from oscillograph recorded multichannel aircraft response data [AIAA PAPER 70-948]
20 p3719 A70-39579

Fatigue phenomena based on solid body model, establishing breaking stress dependence on time or load cycles number
20 p3724 A70-39854

Fatigue crack growth detection by acoustic emission techniques
23 p4194 A70-44214

Miner rule for cumulative fatigue damage, obtaining upper and lower bounds on load cycle number to failure
24 p4426 A70-46024

FATIGUE DIAGRAMS
U S-N DIAGRAMS

FATIGUE LIFE

- S/N fatigue life gage for nondestructive evaluation of cumulative damage, discussing calibration and two step, block and random tests 01 p0053 A70-10009
- Nondestructive testing and fatigue life analysis of cyclically loaded mechanism, determining dynamic responses to velocity shocks by computer techniques 01 p0053 A70-10010
- Loads effects on refractory alloy fatigue strength and life at high temperatures, describing aircraft turbine blade tests 01 p0115 A70-10069
- Loading frequency effects on Duralumin endurance limit in air and in water, noting stress level role 01 p0115 A70-10070
- Roller bearing endurance dependence on shaft speed, surface finish and elastohydrodynamic lubricants temperature, viscosity and film thickness [ASME PAPER 69-LUB-18] 01 p0101 A70-10387
- Boron fiber reinforced epoxy fatigue life dependence on reinforcing fibers aspect ratio 01 p0129 A70-11082
- Fretting corrosion effect on structural steel fatigue strength under asymmetric load cycles 01 p0207 A70-11155
- Turbine blades durability and fatigue characteristics, plotting fatigue diagram from statistical tests 01 p0105 A70-11418
- Chromium-nickel steel fatigue strength under repeated thermal cycles, showing dependence on long term fatigue buildup and single cycle fatigue damage effects 02 p0383 A70-11653
- Machine parts fatigue behavior and service life, studying endurance margin under load cycles spectra below initial endurance limit 02 p0383 A70-11657
- Safe-life and fail-safe structural design philosophies in fatigue damage and operating lifetime control 02 p0389 A70-12615
- V/STOL fatigue design parameters, balancing fail-safe and safe-life design procedures [AHS PAPER 376] 02 p0228 A70-12764
- Cr diffusion coating influence on fatigue life of Fe and steel, discussing residual stress measurement technique 02 p0320 A70-12848
- Fatigue life of rocket nozzle coolant tubes under thermal cycling environmental conditions, considering design formulas for thermal buckling prediction 03 p0579 A70-12963
- Light alloys cold hardening effect and fatigue strength estimation, considering residual stress variability with time 03 p0587 A70-13239
- Metals fatigue strength prediction by hysteresis loop method, presenting results for irreversible energy dissipation rules during cyclic loading 03 p0587 A70-13240
- Model gas turbine engine blades fatigue strength under stress conditions, considering tensile stresses reproducibility from centrifugal loads 03 p0587 A70-13241
- Al alloy and structural steel fatigue strength under superelastic cyclic axial stresses, describing observed plastic deformation patterns 03 p0509 A70-13271
- Fatigue life of stiffened skin panels under acoustic loading of wideband frequencies to achieve structural resistance optimization [DGLR-69-63] 04 p0774 A70-15140
- Surface work hardening and stress concentrations effects on fatigue strength of alloy under asymmetric tension and compression load cycles at high temperatures 04 p0707 A70-15270
- Stress analysis split method for determining residual strength and fatigue crack life of damaged or initially cracked VTOL structures [AIAA PAPER 69-214] 04 p0624 A70-15395
- Three dimensional photoelastic model for structural analysis of aircraft bulkhead to improve fatigue life 05 p0937 A70-16376
- Gas turbine blade material properties change effect on thermal fatigue strength after long term heating 05 p0864 A70-16700
- Nickel-based alloys small cycle thermal and mechanical fatigue limit during tensile stresses and operational temperatures, analyzing fatigue curves 05 p0867 A70-17046
- Fatigue life tests for heat resistant gas turbine blade alloys under power and thermal loads simulating aircraft flight 05 p0953 A70-17051
- Rotor blades structural fatigue strength tested on gas dynamic test stand under cyclic thermal loading and static tensile load 05 p0954 A70-17058
- Heating influence on circular bending fatigue strength of refractory steel and alloys, using radiative and HF inductive heating 05 p0868 A70-17059
- Fatigue strength of T-shaped blade roots of steam turbine regulating stages subjected to combined static tension and cyclic bending 05 p0954 A70-17060
- Stress kinetics and breakdown time of hardening Al alloys and steels under cyclic loads, noting dependence on plastic deformation 06 p1162 A70-17391
- Temperature cycle duration effects on heat resistant alloys thermal fatigue resistance, noting stress relaxation occurrence 06 p1085 A70-17398
- Low cycle fatigue life of various structural steels and alloys, studying stress cycle number relations 06 p1085 A70-17402
- Structures elastic-plastic behavior under changing cyclic heating, calculating long time strength from linear damage accumulation assumptions 06 p1164 A70-17405
- Machines selection for determining low cycle fatigue life, emphasizing automatic control system for regulating load and strain regimes 06 p1164 A70-17407
- Fatigue life of unidirectionally glass fiber reinforced composites subjected to low cycle loading, using linear elastic body model for cyclic deformation process 06 p1091 A70-17408
- Adverse effects of temperature and strain rate on low cycle fatigue resistance of austenitic stainless steels at elevated temperatures compared with tension tests 06 p1086 A70-17452
- Mean cyclic stress effect on stress concentration and fatigue strength of smooth and notched steel specimens at normal and high temperatures with superimposed bending 06 p1088 A70-17653
- Cyclic plastic deformation changes with load increase under uniform stress with normal loading and nonuniform stress with impact loading, considering fatigue limit 06 p1168 A70-17923
- Ultrasonic surface waves detection of transverse fatigue crack initiation in rails under load, applying results to fatigue life determination 06 p1168 A70-17924
- Spiral gears bearing disks contact fatigue endurance process, deriving critical points cyclic stability from stress distribution considerations 07 p1291 A70-18819
- Steels fatigue strength under biaxial tension, considering complex stress-strain state 07 p1304 A70-18823
- Gas turbine engine blades grinding and polishing procedures, considering fatigue life increase and physical properties stabilization 07 p1292 A70-18833
- Mechanical and electrochemical polishing effect on turbine blade alloy fatigue strength, discussing surface strain hardening as function of temperature in mechanical polishing 07 p1304 A70-18838
- Fatigue strength of sintered aluminum powder at room and elevated temperatures, discussing sensitivity to tensile loads misalignment 07 p1304 A70-18840
- Miniature resistance strain gage performance in low cycle fatigue, discussing zero drift and gage sensitivity changes 07 p1281 A70-19241
- Fatigue crack growth in polycrystalline Mo at room temperature under cyclic loads observed along grain boundaries 07 p1314 A70-20013
- Duraluminum sheets fatigue life and corrosion fatigue strength decrease with corrosion damage area increase 08 p1515 A70-20921
- Creep strain effect on cyclic fatigue life of duralumin at room temperature 08 p1516 A70-20988
- Gas turbine blades design and exploitation processes, discussing long time fatigue strength, static durability and heating effects at elevated temperatures 09 p1772 A70-22469
- Bearing materials rolling contact fatigue life, describing three ball-cone test machine 09 p1702 A70-22555
- High strength stress corrosion resistant aluminum alloy die forgings, evaluating tensile, tensile fatigue and fracture toughness properties 09 p1702 A70-22556
- High-strain fatigue life temperature dependence of austenitic and ferritic power plant materials compared to creep-rupture life 09 p1773 A70-22577
- Creep failure fatigue life prediction methods involving hold period effects on high temperature fatigue properties 09 p1775 A70-22594
- Fatigue limits distribution functions of full-scale machine parts estimated by rupture similarity criterion, discussing stress concentration and scale factor effects 09 p1776 A70-22616
- Stress concentration effect on fatigue strength of Al- and Mg-base structural alloy specimens of different sizes analyzed statistically 09 p1703 A70-22617
- Fatigue life cyclic sensitivity threshold with random nature statistically estimated on basis of maximum likelihood principle 09 p1776 A70-22618
- Fatigue life and limit distribution obtained from analysis of crack formation start and final failure in notched and smooth specimens 09 p1776 A70-22619
- Fatigue strength tests of alloy during static and programmed loading at high temperatures from statistical standpoint 09 p1703 A70-22620
- Machine parts lifetime dispersion determined by fatigue limits distribution during cyclic loading 09 p1776 A70-22623
- Endurance limit of momentless shells of revolution under uniform internal pressure, deriving differential equations based on aging and creep theories 09 p1779 A70-23096
- High intensity ultrasonics for changing solids properties, discussing effects on metal powder sintering, yield strength, fatigue life, crystallization rate, etc 09 p1728 A70-23348
- Expansion bellows fatigue strength based on load and displacement measurements performed during low cycle model tests 10 p1965 A70-25299
- Design mean stress and ground-air cycles minimum stress effect on fatigue behavior of titanium alloy in supersonic transport operating environment [SAE PAPER 700033] 11 p1218 A70-25370
- Aircraft structures fatigue durability estimations, studying crack propagation rates under cyclic loadings by fail-safe method 11 p2132 A70-25624
- High fatigue life resulting from titanium spot welding realized by preweld and postweld treatment 11 p2059 A70-25662
- Fatigue properties of electron beam welded precipitation hardening stainless steels 11 p2059 A70-25664
- Aircraft structures fatigue, discussing prediction of response to fatigue environment, load distribution, fatigue life, crack propagation rates and residual strength 11 p2132 A70-25677
- Environment and complex load effects on fatigue life - ASTM Conference, Atlanta, September-October 1968 11 p2137 A70-26088
- Stress ratio effects on Al alloy during crack propagation and fatigue, introducing notch stress and strain approximations 11 p2066 A70-26089
- Prestrain and mean stress effects on fatigue life using cumulative damage procedure based on Al alloy and aircraft quality steel tests 11 p2137 A70-26092
- Stress peak distribution effects on fatigue life of test specimen excited to bending by Gaussian random vibrations 11 p2137 A70-26093
- Stress level, block size and constant and variable loading sequence effect on fatigue life of Al alloy box beams 11 p2138 A70-26094
- Fatigue life tests of Al alloy under narrow and broad band random loads based on number of peaks to failure 11 p2066 A70-26095
- Programmed and randomized loading flight-by-flight tests for fatigue life, noting stress cycles 11 p2138 A70-26096
- Fatigue life of Ni vibrated in reversed bending at 300 C in oxygen and in water vapor at various pressures 11 p2067 A70-26098
- Metals low cycle fatigue resistance, discussing repeated plastic straining effect on mechanical properties 11 p2141 A70-26609
- Materials fatigue lifetime estimation under irregular loads by simultaneous use of random programming for testing machines and computing equipment 12 p2315 A70-26873
- Experimental stress analyses for aircraft design enhancing structural fatigue strength, using S-N diagrams and photoelastic models 12 p2318 A70-27128
- Materials fatigue life dependence on statistical characteristics of random loads obtained from energy balance equation solution 12 p2323 A70-27339
- Gas turbine blade materials investigated for effect of prolonged heating on mechanical properties and thermal fatigue strength 13 p2434 A70-28994

Ni-based heat resisting alloy /Inconel 700/ investigated for hot corrosive environment effect on stress rupture and fatigue strengths

13 p2434 A70-29157
Fatigue life and long term strength of polycarbonate components in pneumatic pulsating pressure equipment described by power and exponential equations

13 p2440 A70-29784
Fatigue damage accumulation deterministic models for predicting longevity

14 p2656 A70-30300
Thermoplastics fatigue strength, considering stress variations with time in constant strain tests

14 p2598 A70-31425
Alloy high temperature creep and long term strength, determining exponential relations between stress, strain rate and durability

15 p2755 A70-31529
Aluminum alloys endurance limit determination by accelerated methods, evaluating errors by comparison with conventional tests

15 p2755 A70-31539
Plastic deformation and aging effects on fatigue characteristics of steels until rupture under cyclic loads

15 p2755 A70-31540
Passenger aircraft structures accelerated testing for safety and fatigue durability under operational conditions, describing tests planning and evaluation

15 p2673 A70-31541
Transient overloads effect on long term fatigue strength of notches and smooth steel samples, emphasizing heat treatment effect on notch sensitivity at high temperatures

15 p2814 A70-31546
Ultrasonics for steel cleanliness rating, considering advantages and fatigue life

15 p2743 A70-31768
Fibre reinforced polymers fatigue life under cyclic stresses, obtaining data from rotary cantilever tests

15 p2764 A70-31933
Pure iron and low carbon steel macroscopic stress measurements, determining correlation between residual stress, fatigue damage and fatigue life

15 p2759 A70-32322
Computerized statistical analysis programs finding plastic stress and acoustic emission as predictors of annealed steel fatigue life

15 p2760 A70-32326
Delayed rupture and relaxation in Ti alloys during cyclic deformation, comparing fatigue tests results for continuous and discontinuous cyclic loadings

16 p2931 A70-33209
Carbon fiber reinforced plastics potential as fatigue resistant materials

16 p2936 A70-33367
Rolling element bearings fatigue life prediction and extension, using elastohydrodynamic lubrication theory

16 p2917 A70-33423
Fatigue life estimation from fracture mechanics data, discussing flaw geometry and propagation, mechanical properties, damage accumulation, etc

16 p2989 A70-33601
Randomized load sequence simulating narrow band Gaussian process for predicting fatigue strength, assuming crack propagation mechanism

17 p3183 A70-34660
Fatigue life prediction under irregular stress conditions, considering material characteristics determination by standard tests

17 p3187 A70-34990
Fiber reinforced composite with ductile matrix, discussing fatigue life prediction from strain hardening characteristics

17 p3128 A70-35465
Working fluid /Ar/ purity and stability effects on fatigue life and creep of Nb and Mo alloys using gas analysis, microstructure and microhardness data

17 p3126 A70-35715
Flight loads spectrum data for army CH-47A, UB-1B and CH-54A helicopters components compared with fatigue life spectra

18 p3210 A70-35955
Stainless steel load-strain characteristics and cumulative damage in cyclic fatigue life

18 p3273 A70-36048
Ti alloy prior plastic deformation effect on fatigue strength under bending, tension, torsion and rolling

18 p3275 A70-36141
Fatigue resistance of high yield strength steel weldments under uniaxial loading, describing cyclic behavior by S-N curve

18 p3278 A70-37114
Inconel 713 alloy, investigating chromaluminization treatment effect on fatigue strength at 700°C

18 p3278 A70-37211
Fatigue strength in pulsed tension of butt-welded tubular joints, evaluating test results statistically

19 p3433 A70-37357
Chromium-nickel steel fatigue strength under repeated thermal cycles, showing dependence on long term fatigue buildup and single cycle fatigue damage effects

Machine parts fatigue behavior and service life, studying endurance margin under load cycles spectra below initial endurance limit

19 p3547 A70-38430
Light alloys cold hardening effect and fatigue strength estimation, considering residual stress variability with time

19 p3548 A70-38457
Metal fatigue strength prediction by hysteresis loop method, presenting results for irreversible energy dissipation rules during cyclic loading

19 p3548 A70-38458
Model gas turbine engine blades fatigue strength under stress conditions, considering tensile stresses reproducibility from centrifugal loads

19 p3548 A70-38459
Fatigue strength distributions at specific cycles of finite life with given cycles-to-failure, calculating reliability

19 p3550 A70-38851
Ternary Al-Cu-Mg alloys, considering aged structure relationship to fatigue strength

19 p3454 A70-38955
Aluminum alloys subjected to random loading, comparing fatigue life with predictions based on linear accumulation of damage hypothesis

20 p3647 A70-39157
Hot corrosive environment effect on stress rupture and fatigue strength of Ni heat resistant alloy used in gas turbine rotating blade

20 p3647 A70-39241
Structural Ti, investigating effect of surface strain hardening by cold rolling on fatigue strength

20 p3648 A70-39250
Aircraft design fatigue life and cumulation damage problems, discussing information value of programmed load and random tests

20 p3720 A70-39622
Fiberglass reinforced plastics fatigue life, analyzing structural factors role

20 p3655 A70-39891
Electron beam welded hollow balls for high speed ball bearings, comparing fatigue life with solid balls

22 p4055 A70-43103
Helicopter parts and assemblies fatigue life estimation and testing, discussing loading spectra, service conditions, etc

22 p4046 A70-43119
Fatigue limits of Ti alloy by Wohler and Locati loading methods

22 p4055 A70-43103
Fatigue strength of stiffened aircraft panels subjected to repeated buckling by compression loads

22 p4044 A70-42444
Bcc metals, measuring correlation between residual stress level and fatigue damage by X ray diffraction analysis

22 p4207 A70-44422
Fluttering isotropic rectangular flat plate fatigue life estimation, taking into account stress, dynamic pressure, frequency, Mach number and plate thickness

23 p4207 A70-44577
Vibration loads in turbomachinery blading, examining blade detuning effects on resonant response levels and fatigue life

24 p4392 A70-45157
German monograph on fatigue crack propagation in thin notched plate, considering microscopic element fracture probability

24 p4422 A70-45574
Defect effects on welds fatigue properties in low carbon steel plates estimated, using radiograms

24 p4347 A70-45733
Thread parameters effect on steel and Ti high strength fasteners fatigue life

24 p4425 A70-45881
Heat resistant alloys with metal coatings applied by diffusion in vacuum, investigating structure and fatigue strength at high temperatures

24 p4364 A70-46342
FATIGUE TESTING MACHINES

Prototype inspection equipment for automatic detection of fatigue damage in helicopter transmission gears teeth by magnetic perturbation method

01 p0097 A70-10011
Cyclic loading test apparatus for studying ferromagnetic metals structural changes due to fatigue

01 p0116 A70-10076
Fatigue testing facilities and methods with emphasis on consumable load, randomized serviceability and random process tests, examining closed loop control servohydraulic appliances

02 p0276 A70-12853
Equipment for cyclic biaxial stress states testing by simultaneous direct pressurization and axial loading of thin cylindrical specimens

03 p0462 A70-12966
Machine for refractory crystals creep testing in thermal vacuum or inert protective medium

Test rig for load controlled strain fatigue, describing main structure, pin joint bearings and hydraulic specimen clamps

04 p0773 A70-15040
Machines selection for determining low cycle fatigue life, emphasizing automatic control system for regulating load and strain regimes

06 p1164 A70-17407
Refractory Nb alloy low cycle fatigue characteristics in vacuum at high temperatures, describing testing machine

06 p1086 A70-17453
Ti alloy welded sheets bending fatigue test facility, discussing test stand calibration and optimal welding

07 p1291 A70-18824
Bearing materials rolling contact fatigue life, describing three ball-cone test machine

09 p1702 A70-22555
Low cycle fatigue testing facility and methods used at NASA Lewis Research Center

11 p2033 A70-26610
Procedures for conducting fatigue studies at high temperatures on servocontrolled testing machines using stress, axial, transverse or plastic strains

11 p2033 A70-26612
Fibre reinforced polymers fatigue life under cyclic stresses, obtaining data from rotary cantilever tests

15 p2764 A70-31933
Materials testing machine for tension, compression and flexure at constant strain rate and for fatigue

16 p2900 A70-33067
Automated programmed device for fatigue tests based on harmonic oscillator, presenting schematic diagram

16 p2900 A70-33068
Variable loads programming by semicomputers/semihardware method for 747 fatigue testing

17 p3050 A70-35511
High strain fatigue machine with axial loading and servocontrol for short endurance testing

17 p3063 A70-35586
Creep testing machine with constant load for HF thermal cycling under vacuum

17 p3063 A70-35587
Dynamic characteristics of hydraulic fatigue testing machines, using hydraulic activation efficiency factor

17 p3064 A70-35718
Programmed fatigue testing machine for specimens under cyclic axial loads, transforming angular into linear displacements

18 p3237 A70-36473
Strain multiplier for fatigue sensor in moderate amplitude cyclic strain applications

20 p3628 A70-39159
Steels thermal fatigue in testing machine, investigating strains and stresses due to nonuniform temperature distribution during thermal cycle

21 p3840 A70-41433
FATIGUE TESTS

Ultrasonic detection system for crack initiation and propagation in notched low cycle axial fatigue testing using surface and longitudinal waves

01 p0096 A70-10004
Welded flat plate specimen to evaluate low cycle crack initiation and propagation of butt welds under compressive loading, discussing design, fabrication and testing

01 p0199 A70-10452
Glass reinforced and unreinforced thermoplastics HF fatigue failure modes, discussing isothermal and nonisothermal test procedure

01 p0129 A70-11081
Continuous measurement and automatic recording of metals electrical resistance during fatigue testing in vacuum at elevated temperatures

01 p0092 A70-11108
Correlation between sustained-load and fatigue crack growth in high strength steels for aggressive environment effects

02 p0318 A70-12544
Fiberglass reinforced textile fatigue characteristics under impact tensile loads, noting different characteristics under cyclic sinusoidal loads

02 p0323 A70-12815
Fatigue testing facilities and methods with emphasis on consumable load, randomized serviceability and random process tests, examining closed loop control servohydraulic appliances

02 p0276 A70-12853
Aircraft structures service life estimation, comparing results of serviceability tests, solo flight tests, programmed random load tests and linear defect buildup hypothesis

02 p0391 A70-12854
Periodic biharmonic stress cycling determination of load influence of fatigue failure used for random load serviceability tests

02 p0391 A70-12855
Reversed bending fatigue tests on stainless steel fibermetal with porous structure to investigate effects of density, thickness, wire diameter, screen stiffening, etc

03 p0481 A70-12957

Fatigue tests results parametric representation for nickel base alloys tested at various temperatures and times to failure

04 p0707 A70-15264

Stroboscope lighting system for microstructural examination of fatigue test sample failure

05 p0845 A70-15882

Amsler Vibrophore machine modifications to permit narrow band random fatigue tests

05 p0826 A70-15887

Summation of cycle ratios for various loading programs to control cumulative damage concept based on French curve, using fatigue tests

05 p0939 A70-16485

Gas turbine blade material properties change effect on thermal fatigue strength after long term heating

05 p0864 A70-16700

Fatigue defects accumulation in aluminum alloy under impact tensile loads programmed to simulate loads encountered by aircraft in practice

05 p0947 A70-17009

Unsteady cyclic creep effect on stressed state and margin safety of elements, noting discrepancy of experimental and theoretical characteristics

05 p0866 A70-17030

Stress rupture strength and relaxation and time to failure of AMG-6M sheet under creep using energy dissipation method

05 p0952 A70-17034

Low cycle fatigue of alloy and steel materials under bending and cyclic heating, relating strains and number of cycles to failure

05 p0866 A70-17036

Test stand design and automatic recording of turbine blade fatigue test data, including statistical evaluation

05 p0953 A70-17054

Structural changes in polycrystalline Al subjected to HF fatigue, using transmission electron microscopy

06 p1084 A70-17127

Creep effects on structural failure under low cycle fatigue at high temperatures, noting role of plastic deformation

06 p1164 A70-17409

Gas turbine compensating bellows structural strength, discussing low cycle fatigue test under static loads

06 p1167 A70-17664

Test stand for endurance and creep testing of plastics, glazed ceramics and other brittle materials

06 p1028 A70-17665

Thermal fatigue resistance of steel to copper weldments under thermal cycling, noting intergranular crack growth accompanied by oxidation along crack boundaries

06 p1078 A70-18515

Laboratory Electronic Servo Controller for structural fatigue tests, aircraft material tests, model position and velocity control in wind tunnels

06 p0989 A70-18606

Material inhomogeneity during high temperature fatigue tests taking into account probability density of random failure coordinate distribution

07 p1401 A70-18839

Fatigue tests to relate boron-epoxy laminate fatigue behavior to thermal preconditioning environments

07 p1320 A70-19960

Stress and strain spatial distribution in notched steel plate under cyclic loading determined by finite element method

08 p1590 A70-21315

Static and dynamic low temperature crack toughness behavior of steels, determining strain rate effect

08 p1518 A70-21317

Rate sensitive materials dynamic fracture test concepts, considering crack speed, division, arrest, toughness, etc

08 p1590 A70-21318

Nonmetallic inclusions effect on steels cyclic strength dependence on inclusion composition and metallic matrix properties derived from fatigue tests

08 p1590 A70-21413

Collection of papers on aerospace technology covering Fokker F-28 aircraft design, airfoil computer graphics, helicopter rotor tuft analysis, aircraft fatigue, launch vehicle guidance, etc

08 p1438 A70-21863

Fatigue testing and thermal mechanical treatment effects on uni- and biaxial Al alloy-B composites tensile strength at room and elevated temperatures

08 p1523 A70-21893

Al alloys fatigue cracks propagation rate using electron microfractography

09 p1701 A70-22223

Coffin method for thermal fatigue testing noting deficiencies in determining plastic strain, temperature distribution and tubular specimens durability characteristics, etc

09 p1701 A70-22298

Cyclic heating and thermal stresses effect on fatigue strength and durability of turbine blade alloys and structural elements

09 p1771 A70-22463

Thermal fatigue cycle produced by cooled gas turbine blades, using stress-strain tests and thermal simulation

09 p1655 A70-22585

Fatigue limit and rupture stress distribution patterns of Al- and Mg-base structural alloys using accelerated Prot and Enomoto methods

09 p1703 A70-22621

Machine parts lifetime dispersion determined by fatigue limits distribution during cyclic loading

09 p1776 A70-22623

Lattice defects in Al-Zn alloy due to fatigue investigated for mechanism and effect on aging kinetics by resistivity measurement

09 p1707 A70-23326

Fatigue effects of incident illumination on area sensitivity, dynode gain stability and anode output for end-on photomultipliers

09 p1683 A70-23511

Ni-Cr austenitic steel bending, surface temperature variations, crack development and propagation under double fatigue tests

10 p1902 A70-23819

Mean stress effect on low cycle fatigue strength, deriving expression for completely reversed stress cycling

10 p1964 A70-25091

Materials bending fatigue strength calculations for biaxial tension compared with experiments showing agreement

10 p1964 A70-25289

VTOL aircraft metal fatigue examination by photoelasticity emphasizing stress reduction

11 p2132 A70-25622

Sinusoidal and random loading response of age hardening aluminum alloy determined by fatigue testing

11 p2133 A70-25732

Fatigue behavior prediction for complex parts and structures using laboratory tests of small specimens

11 p2137 A70-26091

Low cycle fatigue tests on stainless steel, discussing crack behavior dependence on temperature and plastic strain range

11 p2139 A70-26405

Collection of papers on low cycle fatigue testing covering mechanical properties and test facilities

11 p2033 A70-26608

Axial strain controlled fatigue tests at elevated temperature, discussing specimen gripping, alignment and break detection for mechanical and closed loop hydraulic test machines

11 p2033 A70-26611

High temperature fatigue tests of materials under uniaxial controlled strain, describing equipment, failure interpretation and data reduction

11 p2033 A70-26613

Low cycle fatigue tests advantages by reversed bending ascribed to simplicity, specimen stability at high strain levels and minimum equipment costs

11 p2034 A70-26614

Uniaxial low cycle thermal fatigue test procedure for ductile metals, describing strain measuring system allowing direct recording of load vs mechanical deformation

11 p2034 A70-26615

Fatigue crack initiation and propagation in steel using surface plastic replication method, determining propagation rate by stress intensity

12 p2321 A70-27207

Thermal metal fatigue testing, including resistance to cyclic temperature variation, operating conditions simulation and stress-strain determination

12 p2322 A70-27218

Phenomenological theory of crack propagation during fatigue experiments, noting role of work hardening

13 p2510 A70-28672

Polymer materials fatigue strength and deformability testing in vacuum, air and gas atmospheres at low and high temperatures, subjecting to cyclic loading

13 p2385 A70-29428

Light twin engined aircraft airframe fatigue evaluation program

[SAE PAPER 700219] 13 p2348 A70-29606

Weibull distribution as statistical method for interpreting fatigue test data

14 p2656 A70-30700

Thermoplastics fatigue strength, considering stress variations with time in constant strain tests

14 p2598 A70-31425

Dynamic fracture toughness test on heat treated precracked steel specimens under dynamic loading

15 p2759 A70-32243

High temperature metal fatigue crack growth monitoring by ultrasonic detection

[SESA PAPER 1622] 15 p2744 A70-32321

Analog/digital system for full scale airframe fatigue amplitude and phase signature measurements on CH-46D tandem rotor helicopter

15 p2739 A70-32323

Dislocation distribution in Ta foil following yield point fatigue testing, using thin film electron microscopy

15 p2761 A70-32385

Fractography of spall cavities and crack growth in ball rolling contact fatigue, using scanning electron microscope

15 p2745 A70-32444

Creep and tensile fatigue behavior of notched and unnotched graphite/epoxy composites

[ASME PAPER 70-DE-32] 16 p2938 A70-33503

Polycarbonate plate fatigue crack propagation, discussing length due to repetitions, striation number relationship to cycles, and stress intensity

16 p2941 A70-34335

Unalloyed polycrystalline Ti fatigue tests, observing cyclic stresses effect on twinning

17 p3116 A70-34393

Wear and fatigue of Ti-Mo-Al-Sn-Si /Hylite 50/ alloy with resistant Mo or Cr coatings

17 p3099 A70-34447

Polymeric materials fatigue tests, investigating correlation between crack propagation and stress intensity factor

17 p3127 A70-34624

Fiberglass reinforced plastics fatigue properties, describing electric model and nondestructive testing

17 p3183 A70-34658

Crack propagation, fatigue damage and interaction effects in aircraft structures and materials under flight simulation loading

17 p3185 A70-34924

Fatigue and surface crack detection using holographic techniques

17 p3086 A70-35015

Structural fatigue testing by computer control of random force cycles

17 p3062 A70-35505

Energy dissipation measurement in materials during fatigue testing by dynamic hysteresis loop method

17 p3096 A70-35712

Creep and failure tests for Ti alloys at 500 C, discussing work dissipation during creep process

17 p3126 A70-35714

Multidimensional discrete control for fatigue testing under random loads, discussing model

18 p3234 A70-36074

Glass fiber reinforced cross ply and quasi-isotropic plastics, considering notches effect on fatigue behavior for comparison with metals

19 p3455 A70-37951

Structural fatigue strength model tests for turbine blade root connections, using asymmetric load cycle and working temperature

19 p3547 A70-38433

Fatigue crack propagation under programmed loads, correlating crack growth rates and tip opening displacements

19 p3549 A70-38628

High temperature endurance strength of temper finished bolt connections under cyclic loads, using programmed fatigue testing machines

20 p3718 A70-39223

Hollow balls for high speed bearings by electron beam welding, describing full scale and rolling element fatigue tests

20 p3637 A70-39236

Reinforced materials endurance testing, discussing clamping and edge restraints effects

20 p3655 A70-39775

Fatigue crack growth tests on Al alloy sheets under variable amplitude loading

21 p3831 A70-40749

Statistical data for optimum fatigue reliability design for dynamic and rotary machinery, considering static strength, cycle-to-failure and stress-to-failure distributions

21 p3833 A70-41004

Turbocompressor disk materials selection by low cycle fatigue tests, discussing stop and start repetition and cracks in stress concentration zones

21 p3867 A70-41261

Book on fatigue crack propagation in pure Al covering tension and compression tests, single and polycrystalline materials, elastic stress, notched and smooth specimens, etc

22 p4057 A70-43740

Step-amplitude stress cycle program effects on durability of heat resistant alloy for turbine blades under cyclic loading

23 p4204 A70-43934

Load cycle sequences for full scale aircraft structures and components fatigue testing

[ICAS PAPER 70-32] 23 p4266 A70-44101

Aircraft structure fatigue load monitoring, discussing strain gage installation in critical areas

[ICAS PAPER 70-31] 23 p4267 A70-44102

Helicopter rotors fatigue testing using small scale models of full scale components

[ICAS PAPER 70-34] 23 p4267 A70-44131

Double linear damage rule applicability to dual type alloys from two-stress level rotating bending and axial fatigue tests

[ICAS PAPER 70-39] 23 p4267 A70-44137

Papers on plane strain fracture toughness testing covering metallic materials, steels and aluminum alloys

23 p4205 A70-44189

Fracture toughness testing of metallic materials including fatigue cracking, thickness limitations and crack detection

23 p4206 A70-44190

Plane strain fracture toughness testing of high strength Al alloys and steels, using fatigue cracked bend specimens

23 p4206 A70-44191

Crack length and bend specimen thickness effects in plane strain fracture toughness tests of high strength steels

23 p4268 A70-44192

Crack and thickness effects on fracture toughness tests of high strength steel in precracked sheet and bend specimens

23 p4206 A70-44193

Specimen size and mechanical factors in plane strain fracture toughness testing of metallic materials

23 p4206 A70-44195

Aircraft structures acoustic fatigue testing, discussing test facilities, environment simulation, etc

23 p4269 A70-44329

Commercial transport aircraft fatigue loading data from NASA VGH /airspeed-acceleration-altitude/program, discussing instrumentation, sample sizes, etc

23 p4270 A70-44548

Servo-hydraulic testing machine for measuring cyclic stress-strain behavior of materials subjected to fatigue and creep at elevated temperature

23 p4178 A70-44912

NDT for aircraft service life extension, discussing fatigue tests and crack detection

24 p4346 A70-45719

FATS

NT CHOLINE

Brown fat thermoregulatory function and physiological control in mammals, discussing heat production and biochemical stimulation

02 p0230 A70-11683

Chicken body mass and percentage body fat following 24 weeks chronic acceleration determined from fatty acid metabolism, liver citrate cleavage and malic enzyme activities

02 p0233 A70-11720

Altitude changes effect on brown fat content and metabolism in deer mice, noting oxygen consumption and heat production limitation by hypoxia

02 p0242 A70-12865

Flavor sweetening preference in high protein and high fat diets, basing human subjects experimental range on choice of formulas

07 p1216 A70-18948

FATTY ACIDS

NT OLEIC ACID

Gas chromatography study of fatty acids and polar lipids of thermophilic filamentous bacterial masses from hot Yellowstone Park springs

01 p0021 A70-10791

Gas chromatography and mass spectroscopy study of fatty acids and hydroxy acids in 5000 year sediment from English Lake District

02 p0252 A70-12507

Hydroxy fatty acid methyl esters gas chromatography and mass spectrometry, noting trimethylsilylation usefulness for locating double bond

02 p0252 A70-12515

Hydrocarbons and fatty acids distribution in living organisms, fossils, sediments and crude oils, discussing slow thermal maturation role and geological applications

02 p0252 A70-12520

Fatty acids and aliphatic hydrocarbons in 3.4 billion year old metamorphosed sediment, suggesting biological origin

03 p0475 A70-13820

Statistical data to demonstrate atherosclerotic diseases affected by cholesterol and saturated fatty acids in foods

03 p0430 A70-14277

Plasma free fatty acid level relationship to acute and chronic exposure to cold in rabbits, rats and humans

04 p0631 A70-14983

Unsaponifiable, molecular weight acids, alcohols and esters effect on rheological properties of lithium lubricants based on synthetic fatty acids

06 p1076 A70-17800

Free fatty acids, glycerol and triglyceride levels in arterial and femoral venous blood in humans before and after physical training

12 p2169 A70-27625

Rats myocardial contractility depression by free fatty acids during hypoxia or anoxia, noting mechanical performance improvement by glucose

12 p2170 A70-27898

Plasma free fatty acids and glucose relative role in contribution to metabolic state and energy production in partially hepatectomized rats

16 p2850 A70-34319

Glucose-free fatty acid interactions in working heart, noting increase in glucose uptake, oxidation and glycogenolysis with physiologic work increment

17 p3031 A70-35429

Precambrian cherts hydrocarbon and fatty acid concentrations and C and S stable isotope ratios, discussing biological evolution rate

18 p3244 A70-35969

FAULT MECHANICS

U FRACTURE MECHANICS

FBFM [MODULATION]

U FEEDBACK FREQUENCY MODULATION

FCC LATTICES

U FACE CENTERED CUBIC LATTICES

FEAR

NT FEAR OF FLYING

Conditioned fear reaction produced by electric stimulation of cat anterior hypothalamus, discussing effect of neocortex removal

03 p0420 A70-13425

Conditioned reflex type fear reaction by electric stimulation of hippocampus in cats

14 p2535 A70-30184

FEAR OF FLYING

Cliniconosographic criteria of flight phobia and differentiation from other psychopathologic syndromes, noting sociofamilial and operative factors

01 p0031 A70-10235

Psychological measures in RAF operational aircrew to obtain details for comparison of flying anxiety casualties from same population

07 p1214 A70-19941

FEASIBILITY

Electronic equipment optimal design variant selection method, based on relative characteristics of feasible versions, widening weighting coefficients determination basis

09 p1643 A70-22129

Unmanned Mars roving vehicle navigation subsystem feasibility study covering inertial and gyrocompass-odometer systems

11 p2080 A70-26211

Penalty function algorithm for linear/nonlinear programming optimization problems subject to equality/inequality constraints, discussing feasibility determination capability

13 p3273 A70-29462

FECES

Prototype space foods effects on humans, determining changes in bacterial fecal flora content

17 p3032 A70-35565

FEDERATIONS

NT TEAMS

FEED SYSTEMS

Parametric vibrations onset and resonance regions boundaries determined for feed line system with flexible compensator

07 p1403 A70-19114

Liquid fluorine feed system valves, seals and seats, discussing design criteria for flight weight components [AIAA PAPER 70-705]

16 p2844 A70-33564

Boeing 747 aircraft pressure fueling system, describing tanks, feed system, refueling and electrostatic charge minimization

18 p3214 A70-36816

Zero gravity liquid ammonia propellant feed system, describing regulator/capillary tube assembly for propellant delivery pressure control [AIAA PAPER 70-1151]

20 p3690 A70-40204

Parabolic antenna properties generated by dual band circularly polarized focused two channel monopulse feed system, discussing tracking data from helicopter, Apollo 8 and Cassiopeia A

20 p3589 A70-40323

FEEDBACK

NT NEGATIVE FEEDBACK

NT NONLINEAR FEEDBACK

NT SENSORY FEEDBACK

Electronic polarimeter using signal sampling technique and feedback to measure periodic retardation changes

02 p0297 A70-11918

Steady state operation and synchronization range of frequency dividers with complex feedback derived by symbolic abbreviated equations and modulation technique

05 p0813 A70-16263

Amplitude and frequency characteristics of gas ring laser with optical feedback between oppositely moving waves amplified by reflecting mirrors

06 p1081 A70-17497

Quasi-linear feedback effect of enhanced ion-wave fluctuations on average electron distribution in current-carrying plasma

07 p1338 A70-19822

Emission spectrum of He-Xe CW laser with non-resonant feedback mode achieved with scattering agent and various mirror schemes

12 p2246 A70-27354

Optimal constant output feedback gains for linear multivariable systems, noting control vector as time invariant function of output vector

13 p2382 A70-29064

Feedback delay effects on eye-hand synchronism in stimulus tracking and steering using self generated body movements

16 p2852 A70-33662

He-Ne laser emission wavelength, using laser interferometry based on feedback between moving mirror and resonator

17 p3104 A70-35088

Linear discrete feedback systems uniqueness, existence and stability under various input-output conditions

22 p4004 A70-43024

Emission spectrum of He-Xe CW laser with non-resonant feedback mode achieved with scattering agent and various mirror schemes

22 p4052 A70-43597

Communication channel modeling with feedback for small error probability compared to unfolding capacity

24 p4313 A70-46056

Algebraic structure convolutional codes using minimal encoders with feedback-free delay-free inverses

24 p4313 A70-46058

FEEDBACK AMPLIFIERS

Response characteristics of negative feedback galvanometer amplifier with inductive source impedance for geomagnetic micropulsation detection

07 p1242 A70-19998

Parasitic effects due to coupling of wideband regenerative amplifier with nonideal ferrite circulators to antenna feeder duct

08 p1468 A70-20575

Transistorized amplifiers synthesis with multiloop feedback

15 p2707 A70-31518

Intracellular myocardium potentials under vagus inhibition by electrometric DC amplifiers with positive and negative feedback

19 p3370 A70-38213

Selective inductorless amplifier design with four layered distributed RGC line in feedback loop, obtaining high Q factors in transfer function

19 p3390 A70-38674

Two-cascade amplifying circuits with current and voltage feedback for semiconductor precision devices

24 p4321 A70-46394

FEEDBACK CIRCUITS

Trigger scaling circuits with pulsed and blanking feedback analysis for minimizing number of couplings

01 p0047 A70-10984

Randomly sampled linear systems stability with linear or nonlinear feedback loops, using stochastic Liapunov function method

02 p0272 A70-12727

Pulse rate techniques for signal processing and computation, considering feedback circuits, discussing stochastic rates, sampled systems and digital differential analyzer

06 p1027 A70-18510

Digital data transmission over discrete time Gaussian channel with noisy feedback, investigating error-exponent/reliability/ and finite SNR

07 p1235 A70-19362

Unsaturable frequency discriminator influence in semiconductor laser feedback loop on laser emission spectrum

08 p1514 A70-21821

He-Ne laser memory, discussing induced oscillation excitation with radiation fed back to resonator by moving reflecting mirror

13 p2429 A70-29572

Amplifiers with selective feedback and clamping circuits for electrocardiology and electroencephalography

15 p2691 A70-31924

Feedback in electrical networks, discussing transient processes within cybernetics framework

15 p2716 A70-32362

Feedback system with combined pulse modulator incorporating pulse frequency and pulse width modulation laws

16 p2882 A70-33036

Adaptive system synthesized to compensate stochastic feedback or external disturbance, obtaining quasi-optimal compensation algorithms

17 p3056 A70-35368

Lower reliability estimates for block codes of binary channels with feedback noise

18 p3235 A70-36599

Low pass linear phase active feedback circuit synthesis using distributed RC networks to realize flat magnitude response

19 p3392 A70-37707

Asynchronous delta modulation channels with RLC integrators in feedback circuit, measuring articulation in presence and absence of noise

20 p3587 A70-40144

Fluid logic circuits with combined feedback input signals, describing synthesis procedure [ASME PAPER 70-FLCS-18]

22 p3963 A70-42409

FEEDBACK CONTROL

NT CASCADE CONTROL

Nonlinear closed-loop automatic control systems steady state characteristics calculation by graphic method

01 p0052 A70-10194

Position control of burning solid nonmetallized propellant strand in combustion bomb using closed loop servomechanism

01 p0215 A70-10830

Plasma arc wind tunnel gas velocity measurement with electron beam probe using closed-loop electronic controller to stabilize beam position

01 p0092 A70-11195

Mathematical model formulated in terms of feedback controller for simulation of horizontal eye movement for positioning upon objects of interest

02 p0243 A70-12098

Popov type nonlinear control systems from synthesis viewpoint, using state variable feedback results to insure absolute stability

02 p0271 A70-12194

Pneumatic fluidic oscillator consisting of bistable multivibrator, analyzing feedback loop operation based on electropneumatic analog system

02 p0229 A70-12673

Respiratory center functional organization established as automatism with negative feedback, based on experimental data of dogs and cats artificial respiration and hypocapnic apnea

03 p0417 A70-13069

Nonlinear feedback control system analysis and synthesis by parametric plane method, investigating frequency response by describing functions

03 p0460 A70-13970

Energetic stability theorems of dynamical feedback system, removing assumption concerning local square integrability

03 p0460 A70-13971

Closed loop nonlinear optimal control systems sensitivity to small parameter variations noting influence of feedback

03 p0461 A70-14171

Optimal control for thermionic nuclear reactor space power plant utilizing state variable feedback with limited input simplifying computation

03 p0461 A70-14342

Natural vibrations damping of holonomic mechanical systems with feedbacks not explicit function of time reduced to optimal stabilization problem

04 p0718 A70-14494

Feedback technique for frequency stability requirements of airborne radar systems, discussing non-coherent radar applications and cost comparison to power-amplifier approach

04 p0656 A70-14708

Closed loop frequency response analyzer with steepest descent computing procedure to obtain in-phase and quadrature signal components in linear or nonlinear systems

[ASME PAPER 69-WA/AUT-3] 04 p0688 A70-14830
Control system response improvement by state variable feedback illustrated by frequency and transient response tests data from analog model

04 p0662 A70-15331

Two degrees of freedom differentiating gyroscope response time decrease and phase and amplitude error reduction, using differential feedback

05 p0853 A70-17003

Absolute stability of automatic control systems with multiple rigid and tachometer feedbacks

06 p1024 A70-17812

Suboptimal control to minimize quadratic cost functional for nonlinear systems, using Taylor series representation for feedback gain matrix

06 p1025 A70-17961

M measurement optimal feedback control algorithm for stochastic discrete time systems, considering nonlinear plant, constrained controls, nonquadratic cost and simulations

06 p1025 A70-17962

Space-sampled feedback control of amplifying wave on infinite continuum, discussing system stability

06 p1025 A70-17963

Open and closed loop time optimal systems compared with respect to sensitivity measure represented by terminal error norm

06 p1026 A70-17969

Nonlinear feedback control systems frequency domain stability criterion obtained using gain-phase plot

06 p1026 A70-17972

Remote feedback suppression method for plasma collisional drift instability using modulated microwave irradiation, describing linear heating mechanism theory

06 p1122 A70-18014

Differential game analysis of dynamic systems feedback control, presenting extremal aiming for successful pursuit completion

07 p1332 A70-18681

Periodic motions and dynamic stability of nonlinear distributed sampled data system of closed loop of pulsed element governed by heat conduction equation

07 p1226 A70-18749

Entropy analysis of feedback control systems leading to separation theorem and feedback process information interpretation

07 p1245 A70-19095

Delay locked closed loop system with and without signal clipping in noisy /Gaussian/ environment applied to radar, sonar and seismic propagation

07 p1242 A70-19997

Adaptive control function technique for lateral stability augmentation system design for manned lifting body entry vehicle

07 p1247 A70-20404

Optimal feedback control synthesis for linear system with time delay through error criterion minimization

08 p1478 A70-20780

Feedback stabilization of surface instabilities of highly conducting plasma, discussing application to linear pinch with uniform axial static magnetic field

09 p1734 A70-22272

Feedback systems stability treated by functional analysis, describing procedures for generating instability criteria

09 p1654 A70-22348

Statistical linearization technique for nonlinear control systems with feedback and zero memory under random input excitation evaluated for output signal characteristics

09 p1654 A70-22960

Microwave sources power stabilization, control and noise reduction using feedback techniques

09 p1649 A70-23275

Human body homeostatic mechanisms autoregulation, discussing feedback control systems for blood pressure and flow regulation, bodily movements and postural control, etc

10 p1810 A70-24038

Closed loop control system design with preassigned eigenvalues based on multipoint linear stationary system synthesis with dynamic feedback

10 p1855 A70-24394

Root-locus approximation technique extended for complex plane analysis of equations with quadratic term in variable parameter for linear multivariable feedback systems

10 p1855 A70-24449

Linear control systems design with restricted number of feedbacks based on optimization criteria concerning responses to initial disturbance

10 p1855 A70-24703

Scalar measure of system sensitivity to plant parameter variations applied to design of linear lumped stationary multivariable feedback control systems

10 p1856 A70-25233

Optimal feedback control obtained for linear time-varying system with time delay, developing numerical method for solving performance differential equations

10 p1856 A70-25235

Delayed feedback for LF periodic conditions /auto-oscillations/ in relay systems of cosmic flying apparatus stabilization

11 p2119 A70-25342

Linear systems optimal control problems with sensitivity considerations for restriction to linear feedback of output variables

11 p2026 A70-26235

Feedback controller specific suboptimal estimation and control parameters determination using stochastic approximation algorithms

11 p2026 A70-26236

Air to air missile guidance to moving target via optimal feedback strategies

11 p2080 A70-26244

Nonlinear control systems on-off oscillations with instants of commutation determined by simultaneous equations, noting feedback control

11 p2027 A70-26254

Optimum transmitter strategy and receiver gain for linear feedback communication in nonstationary additive noise

11 p2011 A70-26328

Hydraulic driving system stick-slip prevention by acceleration and transient velocity feedback compensation techniques

11 p2060 A70-26407

Feedback stabilization and mode coupling of ionization waves in positive column discharges, noting dynamic stabilization of unstable bounded plasma systems

12 p2280 A70-27787

Optimal and suboptimal aircraft lateral directional stability augmentation applying optimal control and model-following techniques

12 p2162 A70-27812

Visual feedback delay effects on steering and tracking performance

12 p2179 A70-28147

Hydraulic piston-valve-type slave mechanism oscillations with rigid feedback and inertial load at actuated shaft, using harmonic linearization method

12 p2167 A70-28340

Man machine function distribution optimization in spacecraft closed-loop automatic control system

13 p2380 A70-28381

Admissible controls synthesis for closed loop system /satellite/ stability

13 p2500 A70-28410

Gauss-Newton nonlinear programming algorithm applications to optimization of optimal control law parameters and closed loop control system synthesis

13 p2381 A70-28435

Pilot-aircraft closed-loop characteristics, using pilot transfer functions for handling qualities prediction [AIAA PAPER 70-568]

13 p2346 A70-29033

Feedback control systems automatic testing by examining frequency response

13 p2423 A70-29696

Satellite orientation control and stabilization by gyro with statically and dynamically balanced rotors, showing steady motions and stability region augmentation

13 p2507 A70-29769

Terminal guidance by dynamic programming to obtain optimal feedback control law in nominal trajectory neighborhood for minimum energy consumption

13 p2449 A70-29963

Motion cue requirements in one and two axis closed loop compensatory control tracking tasks, discussing error rates

14 p2540 A70-30247

Closed loop MHD test facility ARGAS I, describing engineering performance and test measurements

14 p2533 A70-30532

Multivariable feedback control system, minimizing mean squared error and error sensitivity to random perturbations

14 p2560 A70-30622

VTOL aircraft stability augmentation system design based on control theory state variable methods, using minimum power levels

14 p2531 A70-30856

Quality information system consisting of closed loop input/feedback methods insuring design requirements of Saturn S-2 stage

14 p2654 A70-31116

Satellite feedback attitude control system resulting in high accuracy earth pointing motions in elliptic orbits

14 p2654 A70-31172

Time lag system performance index bounds determination and optimal feedback controller design based on min-max criteria

14 p2561 A70-31185

Riccati-like linear functional differential equation with quadratic cost, analyzing feedback control solution existence and uniqueness

14 p2600 A70-31204

Aircraft vertical channel landing condition autopilot using state variable feedback control techniques

15 p2773 A70-32553

Nonlinear feedback control systems forced asymptotic stability, using linear transformation of circle criterion

15 p2716 A70-32554

Phase locked loop damping characteristics optimization based on input rms error rate minimization and transient error integral square value limitation

15 p2704 A70-32604

Minimal time closed loop controller design for linear systems with bounded control amplitudes and rates using approximate functional expression

16 p2880 A70-32984

Feedback gains for repeated eigenvalues in Simon-Mitter pole allocation algorithm

16 p2941 A70-32986

Nonlinear systems stabilization with linear system estimator output state to provide feedback for asymptotic stability of overall system

16 p2881 A70-33033

Finite settling response for single input/output feedback control system obtained by dual rate sampled data control algorithm

16 p2882 A70-33037

Control strategy for linear system performance based on synthesis of optimal closed loop controller with both sensitivity and state feedback

16 p2882 A70-33042

Distributed sampled-data control systems with memoryless nonlinear feedback element, deriving frequency domain stability criterion

16 p2884 A70-33308

Pulse modulated feedback control system, deriving sufficient condition theorem for input-output stability

16 p2884 A70-33309

Minimum energy feedback control for electrically driven vehicles by dynamic programming

16 p2884 A70-33310

Conditionally stable feedback control systems with saturation, comparing large signal stabilization methods

16 p2884 A70-33313

Popov and circle criteria for stability of nonlinear feedback control systems, using parameter plane representation

16 p2884 A70-33314

Desensitized linear servo model following feedback control systems design using specific optimal control concepts

16 p2884 A70-33315

Linear multivariable feedback control systems design method based on transfer matrix, testing decoupling desirability

16 p2884 A70-33318

Controllability of nonlinear dynamic feedback systems based on Liapunov-like stability approach and optimal control theory

16 p2885 A70-33321

Output feedback control systems design, considering closed loop system sensitivity to plant parameters based on linear optimal control problem

16 p2885 A70-33324

Suboptimal nonlinear feedback control synthesis for linear time-invariant system with convex cost functional

16 p2886 A70-33334

Actuating signal at sampling instants determined in phase plane by Mullin-Jury method for sampled data feedback containing quantizer and zero order hold circuit

16 p2886 A70-33336

Distributed parameter feedback systems with quadratic cost criteria, obtaining optimal controls characterization

16 p2886 A70-33339

Aircraft stability augmentation systems design by parameter optimization techniques and feedback selection

16 p2840 A70-33342

Nonlinear digital programming techniques for airplane stability augmentation systems design

16 p2840 A70-33343

Neighboring optimum feedback control scheme for aerospace vehicles to handle small disturbances from nominal trajectory with unspecified final time

16 p2887 A70-33438

Optimal open loop controller and suboptimal feedback law to minimize terminal error of entry vehicle

16 p2947 A70-33439

Feedback analysis of learning and performance in hand-yoked, steering and stimulus tracking control of breath-produced visual target

16 p2852 A70-33660

Continuous time nonlinear feedback control systems, using modified gradient procedure for parameters adaptation

17 p3056 A70-34952

Feedback control systems synthesis by three parameter space, using two dimensional graphic techniques

17 p3130 A70-35296

Neural pulse frequency modulation system stability, using feedback control model

17 p3056 A70-35553

Single input control system design for specified roots using output feedback

17 p3057 A70-35554

Linear control systems stability range with delay time examined by digital computer, discussing critical loop gain

18 p3235 A70-36501

Discrete automatic control theories, including linear, nonlinear, feedback, optimal and adaptive systems and bibliographies

18 p3235 A70-36626

Nd-YAG Q switched laser using feedback loss control to increase switching speed for digital scanning

18 p3270 A70-36744

Linear continuous feedback control system with dead time compensated by proportional plus integral controller, considering stability region variations

18 p3236 A70-36943

Linear feedback control system with dead time compensated by proportional integral derivative action controller, evaluating stability by digital computer

18 p3236 A70-36944

Linear stochastic continuous feedback system with white noise and control input, investigating combined problem of filtering and optimal control

19 p3393 A70-37850

Quasi-optimal feedback control method for minimum time intercept of target in central force field

19 p3393 A70-37865

Feedback regulator synthesis for linear time invariant dynamic system with quadratic performance index, using computer algorithm for algebraic Riccati matrix equation

19 p3395 A70-38937

Electrochemical dimensional machining of complex profile components, using servosystem with feedback for interelectrode gap control

20 p3636 A70-39196

Pilot/vehicle feedback systems with flight director computer for transport aircraft longitudinal control during landing, discussing design by manual control displays theory

[AIAA PAPER 70-1001] 20 p3560 A70-39530

Nutational stability and closed loop position control of dual spin spacecraft with despun platform

[AIAA PAPER 70-975] 20 p3715 A70-39554

Multiphase relaxation oscillator with inductive coupling and common base resistor in feedback loop, determining circuit parameters effect on pulse length

20 p3598 A70-39791

Controlled variable perturbation effects on system with internal positive feedback

20 p3602 A70-39829

Closed loop automatic speed control system for working shaft of two stage alternating current electric servomotor, using invariance principle

20 p3564 A70-39849

Automatic stabilization of random noise mathematical expectancy and mean square deviation by feedback control system

20 p3593 A70-39916

NASA Lewis closed loop MHD generator subsonic tests, discussing ducts, purge and Cs injection systems, electrode coating, etc

20 p3566 A70-40011

Linear feedback control system with quadratic penalty function, deriving lower bound on optimal performance for suboptimality evaluation

20 p3604 A70-40116

Linear multivariable feedback control system, deriving conditions for existence of triangular decoupling transfer function matrices

20 p3605 A70-40118

High performance aircraft self adaptive feedback control system, using airborne digital computer with inputs of elevator deflection and pitch rate for effectiveness identification

20 p3605 A70-40119

Feedback control system characteristic equation generalized root locus following technique using straight line approximation

20 p3659 A70-40121

Nonlinear closed loop systems frequency response determination by graphical method

20 p3605 A70-40122

Optimal and conventional good control systems relationships, considering open and closed loop characteristics, cost functions, etc

21 p3926 A70-40781

Conventional closed loop controller design treated as particular formulation of optimal control problem through gain and integration derivations

21 p3927 A70-40783

Feedback control systems stability over range of parameter changes, determining criterion satisfied by loop gain of rated system

21 p3801 A70-40795

Solar cell array maximum power point in scientific satellites via closed loop conductance matching regulator

21 p3758 A70-41220

Local control loop model of multiphase rectifier used as power amplifier, considering extension to nonautonomous and discontinuous conduction systems

21 p3802 A70-42267

Hybrid fluidic heading reference system with negative feedback servo loop around vortex rate sensor [ASME PAPER 70-FLCS-10]

22 p3963 A70-42417

Input-output stability of feedback systems, using inverse operator model

22 p4004 A70-43490

Stability augmentation in aircraft design for handling and operation benefits, discussing control techniques, autopilot modes and load limitations [ICAS PAPER 70-24]

23 p4138 A70-44109

Cryogenic fluid heat exchanger flow oscillation automatic feedback control, discussing design and simulation

23 p4280 A70-44370

Computerized algorithm facilitating automatic synthesis of time invariant linear compensation for highly complex multiloop control systems

[AIAA PAPER 69-941] 23 p4177 A70-44561

Closed loop life support system employing algae and bacteria cultures to recycle water in addition to atmospheric regeneration

23 p4156 A70-45024

Jet interaction type proportional fluid amplifier as feedback oscillators, measuring frequency response

24 p4292 A70-45291

Hypogravic skeletal atrophy model, considering bone maintenance as feedback control system

24 p4296 A70-45328

Hybrid fluidic damper control for yaw axis stability augmentation of commercial jet aircraft

[SAE PAPER 700794] 24 p4294 A70-45853

Hydrofluidics flight controls for aircraft stability augmentation systems, noting component performance, transfer functions and operation

[SAE PAPER 700793] 24 p4294 A70-45854

Closed loop synthesis algorithm and comparison to sensitivity of open loop system, noting applicability to optimal control

24 p4322 A70-46013

FEEDBACK FREQUENCY MODULATION

Higher order frequency demodulators with feedback in canonical form and with baseband filter

08 p1479 A70-20809

FM feedback demodulator performance model using mixer-correlator, showing cross correlation receiver design

08 p1479 A70-20810

Threshold extension capabilities of phase lock loop and FM feedback demodulators, calculating output SNR for broadband systems

18 p3229 A70-36784

FEEDFORWARD CONTROL

Adaptive pattern recognition systems design based on notions of convergence and feedforward interconnection of two systems

21 p3794 A70-41499

FEEDING (SUPPLYING)

Stiffness of multipad externally pressurized journal bearings with incompressible fluid feeding, comparing hydrodynamic and rolling bearings

15 p2745 A70-32445

Load bearing capacity of radial gas bearing with annular injection line, discussing gas feeding methods

20 p3637 A70-39816

FEEDING DEVICES

U ANTENNA FEEDS

FEEL

U SENSORY FEEDBACK

FELDSPARS

Dating method for stone meteorites feldspar phase based on time interval between solar nebula Al 26 production and decay into Mg 26

06 p1150 A70-18479

He, Ne, Ar and Xe in plagioclase concentrate separated from Serra de Mage meteorite feldspar

13 p2497 A70-29855

FELLOWSHIP AIRCRAFT

U F-28 TRANSPORT AIRCRAFT

FELSITE

U IGNEOUS ROCKS

FEMALES

Orthostatic tilt tolerances in young men and women noting heart rates and blood pressure

09 p1627 A70-23454

FEMUR

Human femur junctions load actions and stresses during walking calculated from measurements

15 p2692 A70-32327

FERMENTATION

Continuous Chlorella production as function of total illumination in high intensity light system incorporating aerobic fermenter for heterotrophic cells

04 p0645 A70-15454

FERMI STATISTICS

U QUANTUM STATISTICS

FERMI SURFACES

Possible pairing without superconductivity at low carrier concentrations in bulk and thin film superconducting semiconductors

06 p1127 A70-18641

Absorption and luminescence in complex molecules and semiconductors, describing particle distribution and Fermi quasi-levels dependence on temperature and excitation intensity

08 p1555 A70-20510

Fermi triplet resonance between fundamental molecular vibrations possible in presence of harmonic or composite tone of same symmetry

12 p2275 A70-27502

Emission field and Fermi quasi-levels distribution in injection laser with n-p heterojunction, determining frequency and threshold current temperature dependence

13 p2426 A70-28876

Ferromagnetic Ni band structure and Fermi surface including spin-orbit and exchange interactions obtained by Mueller interpolation scheme

14 p2626 A70-30479

Semiconductor surfaces electrical equilibrium, considering statistical occupation of surface energy and Fermi levels for given doping of bulk material

15 p2786 A70-32766

Fermi level for crystal with slowly changing impurity determinable by solving Poisson equation and by condition of electroneutrality

15 p2786 A70-32899

Fermi energy and bandtail parameters in heavily doped and degenerate n-type GaAs, calculating conduction band density of states by screened Coulomb potential

21 p3864 A70-42018

Single crystal and pyrolytic graphite, examining spin split Landau levels, Fermi energy changes and anomalous g shifts

21 p3854 A70-42110

Short range order and Fermi surface effects in copper-rich Cu-Al alloys single crystals from X ray scattering measurements

23 p4204 A70-43886

Thermoelectric power and Hall effect quantum resonances in graphite for locating majority carrier electron and hole Fermi Surfaces in Brillouin zone

24 p4389 A70-45597

FERMI-DIRAC STATISTICS

U QUANTUM STATISTICS

FERMIONS

NT ANTINEUTRINOS

NT BARYON RESONANCES

NT FAST NEUTRONS

NT HYPERONS

NT LEPTONS

NT MESON RESONANCES

NT MESONS
NT NEUTRONS
NT PHOTONEUTRONS
NT PROTONS
NT SOLAR PROTONS
NT THERMAL NEUTRONS

Self gravitating bosons or fermions equilibrium configuration in ground state, confirming Oppenheimer-Volkoff treatment approximation

08 p1581 A70-21741

Rarita-Schwinger fields in general relativity, extending equations for Fermion motion in linearized gravitational field to higher spin particles

24 p3480 A70-45818

FERRIMAGNETIC MATERIALS

Microwave phase shifter with rectangular ferrimagnetic toroid in waveguide longitudinal center, discussing impedance matching, phased array applications, etc

10 p1852 A70-24891

Antiferro-, ferri- and ferromagnetic semiconductors properties, discussing narrow band electron correlation, electrostatic and magnetic polarons formation, etc

21 p3864 A70-42254

FERRIMAGNETISM

Semistatic acceleration sensor, using ferrite rod magnetostriction effects to convert acceleration stress to microwave resonant frequency shift

03 p0495 A70-14191

Ferrimagnetically tunable transistor oscillator in common collector configuration

09 p1645 A70-22603

FERRITES

Ferrite and martensite precipitation hardening in Fe-Ni-Mo alloy, studying dislocation structure and aging kinetics

01 p0123 A70-11243

Long range order formation kinetics in lithium ferrite octahedral sublattice after stepwise annealing and quenching in water, using X ray analysis

03 p0537 A70-12867

Magnetoelastic surface wave propagation properties in ferrites at UHF wavelengths, using numerical calculations for gallium-YIG

03 p0540 A70-13700

Transmitting-receiving latching ferrite switch with 180 degree differential phase shift toroids for temperature stability and receiver protection in case of driver failure

03 p0458 A70-14036

Semistatic acceleration sensor, using ferrite rod magnetostriction effects to convert acceleration stress to microwave resonant frequency shift

03 p0495 A70-14191

Surface interactions in incompressible dynamics and stability of ferrofluid with nonlinear magnetization properties

04 p0665 A70-14451

Residual free energy effects on ferrites density and structure after sintering, using powders obtained by thermal decomposition of solid solutions of salts

07 p1355 A70-18703

UHF and VHF stacked ferrite loaded junction circulators construction, improving cost to power performance

08 p1476 A70-21292

Rectangular waveguides filled with magnetized ferrite with/without dielectric, calculating phase shift and attenuation by Ritz method

09 p1645 A70-22548

High-strain fatigue life temperature dependence of austenitic and ferritic power plant materials compared to creep-rupture life

09 p1773 A70-22577

Alloying Ni, Cu and Nb effects on grain and strengthening of low carbon precipitation-hardenable ferritic steels

09 p1705 A70-22804

Ferrite Y-circulator, studying effects of attenuation in ferrite on mean frequency, admittance, forward and reverse losses, etc

09 p1648 A70-23157

Optimal construction of microwave filters with TWT and ferrite direct gain receivers

09 p1648 A70-23166

Reliability testing of waveguide ferrite devices based on quantitative technique using circular charts with filled in endurance test results

09 p1652 A70-23661

Surface wave reflection during propagation along transversely magnetized ferrite plate on metal backing, using perturbation theory to find cylindrical wave field

10 p1844 A70-25163

Single bit latching reciprocal ferrite phase shifter design, operation and performance, noting linear phase response and low phase nonreciprocity

10 p1853 A70-25243

HF energy nonresonance dissipation in polycrystalline yttrium-garnet ferrites subjected to constant magnetizing field

11 p2097 A70-25384

Microwave lines dispersion equations for ferrite cylinder and spiral and circular waveguides

11 p2012 A70-26803

Ferritic and martensitic Fe-Ni alloys lattice parameter determined by standard X-ray techniques

12 p2256 A70-27613

Power ferrite modulator and switch for SHF band based on Faraday rotation principle

12 p2199 A70-28000

C band latching ring-and-post ferrite waveguide circulator for radar transmitting-receiving functions, presenting performance and design parameters

12 p2202 A70-28166

Ferrites as harmonic generators, discussing physical reasons for generation of double frequency magnetization

14 p2549 A70-30439

French monograph on microwave ferrite devices, discussing paramagnetism, ferromagnetism, ferrimagnetism, gyromagnetic resonance and nonreciprocal effects, isolators, attenuators, phase shifters, etc

16 p2873 A70-33267

Spinel lithium ferrite magnetic and crystallographic properties, considering effects of Li and oxygen losses, sintering temperature and cooling rate

16 p2961 A70-33272

C band radar antenna with pencil beam steered in plane by ferrite phase shifters

16 p2875 A70-33394

Ni-Fe ferrites resistivity and thermoelectric power as function of temperature, proposing two energy level model for Fe ions

17 p3143 A70-35604

Two phase stainless steels with microduplex structures, taking into account martensite and ferrite effects on mechanical properties

18 p3272 A70-36038

Microstructure effects on magnetic properties of polycrystalline MnZn ferrites with high permeability

19 p3484 A70-37565

Crystal dislocations and microstructure effects on magnetic properties of polycrystalline MnZn ferrites with high permeability, noting eddy currents role

19 p3484 A70-37566

Ferrite single crystals physical properties - Conference, Krasnoyarsk, U.S.S.R., June-July 1969

19 p3484 A70-37621

Ion magnetic moments in crystallographically nonequivalent lattice regions in ferrites

19 p3484 A70-37622

Neel temperature of thermally stable garnet orthoferrites of YFeAlMn composition

19 p3484 A70-37623

Multiquantum combination effects in ferrites at UHF frequencies

19 p3484 A70-37624

Ferrite single crystals physical properties - Conference, Krasnoyarsk, U.S.S.R., June-July 1969

19 p3485 A70-37626

Magnetite and ferrite spinels Hall effect, magnetoresistance and electrical conductivity over wide temperature range

19 p3485 A70-37627

Single crystal ferrite thin film microwave parameters measurement, examining susceptibility in weak magnetic fields and ferromagnetic resonance

19 p3485 A70-37628

Ferrite reactive modulation amplifier design, using yttrium garnet for noise reduction

19 p3386 A70-37629

Single crystal yttrium ferrite garnet intrinsic electromagnetic radiation as function of coupling coefficient between specimen and waveguide

19 p3485 A70-37630

Automatic meteor station jamming protection using ferrite diode logical elements

19 p3422 A70-37652

Ferrite phase shifter for array antennas, discussing design trends, production, performance characteristics and future developments

19 p3388 A70-37864

Semiconductors, ferrites and semiconductors automatic temperature stabilization problem based on heat source energy conversion

20 p3597 A70-39255

Thermal decomposition of fine-dispersion iron sulfate powders under continuous heating during ferrites manufacture

23 p4205 A70-44041

Microwave lines dispersion equations for ferrite cylinder and spiral and circular waveguides

24 p4317 A70-45178

Ferrite junction microwave circulator bibliography (1956-1969) covering stripline and waveguide versions theory, designs, constructions and applications

24 p4318 A70-45210

Magnetostrictive Ni-Mn-Co ferrites and Al-Fe alloys, measuring magnetic field effect on piezomagnetic coefficients at room temperature

24 p4389 A70-45400

FERROCENES

Acetylferrocene preparation by reacting ferrocene with acetic anhydride in phosphoric acid and reducing acetylferrocene to alpha-hydroxyethyl ferrocene by potassium borohydride in methanol

02 p0249 A70-11678

FERROELECTRICITY

Ferroelectric sodium nitrite single crystals LF linear electro-optical coefficients as function of temperature

01 p0154 A70-10104

Metal/ferroelectric work functions in short circuited capacitor, noting effect of electrodes presence

01 p0156 A70-10186

AsSbSI crystal production technology concerning substitution-type solid solution structure and photoconducting ferroelectric properties

04 p0729 A70-14409

Ferroelectric control circuits controlling electroluminescent cells in matrix, pointer, bargraph, alphanumeric and other displays

05 p0827 A70-16187

Electro-optic effects in ferroelectric ceramics with electrically variable coefficients of piezoelectricity and birefringence, discussing applications

09 p1739 A70-22633

Photographs of ferroelectric tungsten oxide crystal domains obtained with photoemission microscope, noting memory effect after electron beam sweeping

11 p2099 A70-26463

Wave propagation in solid state plasma with ferroelectric and ferromagnetic properties, deriving matrix equation allowing for nonlinearity of dielectric constant and magnetic permeability

12 p2283 A70-26970

Piezoelectric effects in ferroelectric ceramics using equivalent circuits and admittance matrices

12 p2283 A70-27005

Magnetically ordered ferroelectric materials properties for various compounds and solid solutions

15 p2785 A70-32749

Ferroelectric radiation detectors theory and applications, considering polarization changes due to temperature increase from absorbed radiation

17 p3082 A70-34649

Integrated ferroelectric photoconductor device for hologram storage, discussing improved phase readout technique for reconstruction

22 p3994 A70-43609

FERROMAGNETIC FILMS

Narrow Curie point switching transfer in Mn-Bi films by controlling magnetization direction within preselected areas

11 p2098 A70-26069

Ni-Fe thin films flux reversal with transverse bias field from dynamic magnetization configuration photographs

12 p2284 A70-27242

Normal and unconstrained vacuum-deposited Permalloy films composition dependence of magnetization-induced uniaxial anisotropy, noting agreement with magnetostrictive constraint theory

12 p2284 A70-27244

Thin ferromagnetic film sensitive elements for detection of weak magnetic fields

13 p2415 A70-30041

Uniaxial magnetic anisotropy in electrodeposited Permalloy films in terms of magnetostrictive mechanism

20 p3687 A70-40160

FERROMAGNETIC MATERIALS

NT FERROMAGNETIC FILMS

NT MAGNETITE

NT PERMALLOYS [TRADEMARK]

Cyclic loading test apparatus for studying ferromagnetic metals structural changes due to fatigue

01 p0116 A70-10076

Textolites and ferromagnetodielectric wedges mechanical strengths compared for use in open grooves of compound winding

01 p0008 A70-10195

Plane electromagnetic wave penetration into ferromagnetic half space solved for nonlinear parabolic equations using difference method

07 p1227 A70-18992

Ferromagnetic domain wall-dislocations magnetoelastic interaction in Fe and Ni computed as function of relative separation, discussing effects on magnetic properties

09 p1705 A70-22811

Ferromagnetic crystal weakly coupled spin Green and correlation functions calculated for wide temperature range

09 p1740 A70-23193

Temperature effects on energy dissipation during vibration in ferromagnetic and nonferromagnetic metals, comparing damping capabilities for homologous temperatures

10 p1903 A70-24245

Static tensile stresses effect on magnetized ferromagnetic materials damping properties explained by anisotropic microplastic strains dissipating energy during bending vibration

10 p1904 A70-24246

Thin n-type Ge film electrical conductivity effect on ferromagnetic barium titanate single crystals as function of magnitude and sign of polarizing field

11 p2097 A70-25383

Ni-Fe alloy sheets magnetic shielding effectiveness correlated with DC magnetic properties at various frequencies
12 p2201 A70-28127

Ferromagnetic cubic sulfide of Fe easy axis by electron diffraction pattern, aligning sulfide particles along magnetic field
13 p2472 A70-29712

Ferromagnetic Ni band structure and Fermi surface including spin-orbit and exchange interactions obtained by Mueller interpolation scheme
14 p2626 A70-30479

Magnetically ordered ferroelectric materials properties for various compounds and solid solutions
15 p2785 A70-32749

Micromagnetic theory of ferromagnets based on vector magnetization as continuous function of position, discussing free energy
19 p3471 A70-37953

Apollo 11 lunar fines glass spherules magnetic properties, considering soft and hard ferromagnetic components
21 p3918 A70-41681

Antiferro-, ferri- and ferromagnetic semiconductors expansions, discussing narrow band electron correlation, electrostatic and magnetic polarons formation, etc
21 p3864 A70-42254

Ferromagnetic microwave amplifiers operation, describing longitudinal pumping amplifier using YIG
23 p4170 A70-43825

Optical permittivity and dielectric permeability of electron gas in magnetic field, considering application to ferromagnetic materials
23 p4221 A70-45051

Field emission from narrow 3d bands of ferromagnetic nickel, calculating 3d and free electron transmission coefficients ratio, using triangular surface barrier model
24 p4391 A70-45671

Ferromagnetic cylindrical specimens eddy current density distribution under influence of field strength dependent permeability corresponding to Rayleigh law
24 p4344 A70-45695

Spin waves amplification in ferromagnetic conductor crystals, taking into account arbitrary external electric field and propagation vector orientations and space charge
24 p4392 A70-46363

FERROMAGNETIC RESONANCE
Shift in nuclear paramagnetic resonance frequency of ligand nuclei in ferromagnets above Neel temperature
10 p1928 A70-24826

Single crystal ferrite thin film microwave parameters measurement, examining susceptibility in weak magnetic fields and ferromagnetic resonance
19 p3485 A70-37628

FERROMAGNETISM
Generalized Watson sums evaluation without series expansions or extensive computer summations, calculating magnetization of anisotropic Heisenberg ferromagnet for cubic, bcc and fcc lattices
04 p0730 A70-14689

Disordered ferromagnetic binary alloys of transition metals magnetic moment distributions based on thermal neutron scattering experiments
05 p0893 A70-16950

Landau Orbital Ferromagnetism in electron gas as magnetic field source for neutron stars
07 p1380 A70-19279

Magnetic display devices covering magneto-optical displays, magnetic-electrostatic technique combinations and ferromagnetography
08 p1499 A70-21685

Co-Fe core ability to adjust roll spacing in model rolling mill determined from magnetostrictive properties
10 p1905 A70-25175

Wave propagation in solid state plasma with ferroelectric and ferromagnetic properties, deriving matrix equation allowing for nonlinearity of dielectric constant and magnetic permeability
12 p2283 A70-26970

Ni and Ni alloys elastic properties relationship with ferromagnetic and magnetostriction effects, determining modulus of elasticity for wide temperatures and heat treatment
13 p2432 A70-28760

Single phase static ferromagnetic frequency multiplier with odd multiplication factor
14 p2559 A70-31357

Magnetically ordered ferroelectric materials properties for various compounds and solid solutions
15 p2785 A70-32749

Magnetization oscillation in single crystal yttrium-iron garnet under fluctuating SHF magnetic field
19 p3484 A70-37625

Magnetoelastic ferromagnet linear theory, considering spin-elastic microwaves propagation in ferromagnetic crystal subjected to pulsed magnetic fields
19 p3487 A70-37947

Weak itinerant ferromagnetism theory for Ni-Ga and Ni-Al intermetallics, allowing for molecular field parameter magnetization dependence
22 p4087 A70-43197

Antiferromagnetic and ferrimagnetic resonance frequencies, determining temperature dependence by spin wave theory
24 p4388 A70-45132

FERRY SPACECRAFT
Space station-logistics vehicle docking and men-material transfer problem
[AIAA PAPER 69-1118]
01 p0193 A70-10612

Reusable airbreathing launcher for manned space station ferry operations, considering nozzles, intakes, thrust, acceleration, flight plan, weight analysis, etc
02 p0381 A70-12502

Reusable space shuttle employing two stages resembling subsonic aircraft for carrying passengers and cargo between earth surface and orbit
07 p1392 A70-18873

Strap-on ferry package for reusable spacecraft and launch vehicles subsonic lift/drag increase
[AIAA PAPER 70-259]
07 p1397 A70-20390

Reusable ferry spacecraft program, discussing space shuttles, cost reduction and nuclear propulsion for deep space missions
15 p2791 A70-32300

Strap-on ferry package for reusable spacecraft and launch vehicles subsonic lift/drag increase
[AIAA PAPER 70-259]
21 p3931 A70-41867

FERTILIZATION
Map making for Soviet soil fertilization, discussing map symbols and scale
19 p3407 A70-37275

Altered gravitational field effects on frog eggs centrifuged under various conditions after fertilization, noting time dependence of induced abnormalities
24 p4298 A70-45619

FET [TRANSISTORS]
U FIELD EFFECT TRANSISTORS

FEYNMAN DIAGRAMS
Asymptotic high energy behavior of Feynman integrals in scalar field theory models for elastic scattering
19 p3457 A70-37549

FIAT AIRCRAFT
NT G-91 AIRCRAFT
NT G-222 AIRCRAFT
FIAT G-91 AIRCRAFT
U G-91 AIRCRAFT
FIAT G-222 AIRCRAFT
U G-222 AIRCRAFT

FIBER OPTICS
Fiber optics theory and applications, discussing geometric optics, cladding, contrast enhancement, numerical aperture, collection and transmission efficiency, depth of focus, resolution, etc
01 p0142 A70-10419

Laser communication system for outer space, beam guiding and fiber optical guiding systems
04 p0649 A70-15038

Optical effects in parallel glass fibers irradiated by He-Ne laser beam, studying resonance tunneling and periodic power repumping between fibers
04 p0702 A70-15215

Linked and fiber optic components, describing applications as punched card and tape reading, geometrical converters and sensing and scanning probes
16 p2904 A70-33145

HE sub 11 mode launching in optical communication system, considering fiber tapering effect on excitation efficiency
16 p2875 A70-33400

Fiber optics lens for transferring specimen image to camera during vibration tests
17 p3095 A70-35633

Fiber optics in functional electronic circuits, considering multichannel optical communication
18 p3290 A70-36235

Coupled fiber lasers maximum energy transfer between passive conductors, determining minimum pulse duration
19 p3443 A70-37286

Arbitrary mode launching on fiber-optical dielectric waveguides by spatial filtering technique
21 p3829 A70-41930

Fiber optic components quality control by image transmission intensity distribution measurement
22 p4045 A70-42513

Optical waveguides and resonators propagation modes detection and discrimination techniques evaluated for circular cylinder dielectrics /optical fibers/
22 p4030 A70-42949

FIBER STRENGTH
Fiber breakage during powder metallurgy fabrication of compact Al-B composites as function of density
01 p0104 A70-10741

High strength high modulus carbon fibers for use in structural reinforced plastics, describing carbonizing and pyrolysis processes
02 p0320 A70-11856

Composite materials possible applications, considering metal matrices reinforced by high strength metallic or nonmetallic fibers
03 p0512 A70-13857

Composite materials use in nonload bearing and heavily stressed materials, considering applications in aircraft industry and high strength fibers role
05 p0870 A70-16576

High modulus fibers as reinforcing fillers in thermoplastic matrices, discussing cost compensation in low fiber loadings
05 p0870 A70-16578

Composite strength and stiffness prediction from fiber and matrix properties using computer
05 p0870 A70-16579

Tensile strength test and clamping of epoxy impregnated fiber strands
07 p1250 A70-19959

Compatibility of single metal coated carbon fibers, discussing structural recrystallization in contact with Ni or Co matrix by dissociation/ diffusion/precipitation mechanism
07 p1315 A70-20048

Fiber reinforcement of metals, considering strength of boron, alumina, graphite, silicon carbide and silica glass fibers
08 p1514 A70-20471

Composite material tensile strength, discussing statistical scatter in fiber strength and local fiber overstress caused by fiber discontinuities
08 p1532 A70-21914

Longitudinal strength characteristics of filament reinforced composites, discussing bond strength effect on filament fracture
08 p1533 A70-21918

Processing temperature effects on breaking strength-modulus relation for carbonized acrylic fibers
10 p1907 A70-24533

High strength glassy carbon fibers obtained by carbonizing extruded phenol hexamine polymers
11 p2071 A70-26672

High modulus graphite fiber structure using electron beam
11 p2071 A70-26845

High modulus carbon fibers low angle X ray diffraction correlation to physical properties
12 p2259 A70-28050

Work to fracture measurements on brittle fiber ductile-matrix metal composites, using Charpy test
15 p2763 A70-32832

Boron, silicon carbide and graphite fibers surface properties
16 p2937 A70-33376

High strength graphite fiber reinforced polyimide resin composites fabrication
17 p3127 A70-34560

Brittle fibers strand strength as function of statistical distribution of limiting stresses
18 p3342 A70-36648

High modulus graphite fiber tensile strength and structure, using X ray diffraction
20 p3653 A70-39205

High strength and modulus continuous graphite fibers from pitch, describing production process from asphalt and specifications
21 p3842 A70-40732

Composites reinforced with weakened fibers, investigating weak points effect on fracture toughness by fiber pullout and tensile tests
21 p3843 A70-41889

High modulus carbon fibers production and properties describing polymer chains intermolecular structuring by pyrolysis and strength increase by fibers stretching at 2700 C
24 p4366 A70-45166

Composite materials tensile strength dependence on reinforced fibers with dispersed tensile strength, using model to predict crack propagation from fiber rupture
24 p4427 A70-46270

FIBERGLASS
U GLASS FIBERS

FIBERS
NT COTTON FIBERS
NT DACRON [TRADEMARK]
NT GLASS FIBERS
NT HAIR
NT MICROFIBERS
NT RAYON
NT REINFORCING FIBERS
NT SYNTHETIC FIBERS
NT WOOL

Fibrous filter materials filtering capability, comparing extruded and drawn metallic filters
01 p0007 A70-10159

Physiological significance of myocardial fibers curvature in left ventricle wall determined by numerical solutions based on mathematical description
01 p0039 A70-11368

Mathematical model for ejection fraction of human left ventricle incorporated with fiber orientation and ventricular geometry, showing consistent results with biplane angiocardigraphic films
03 p0433 A70-12975

- Porosity in graphitized polyacrylonitrile-based carbon fibers determined from surface area increase during heat treatment in vacuum
04 p0711 A70-14400
- Filamentary casting technique for nonequilibrium alloy structures to produce continuous specimens by rapid solidification
04 p0698 A70-15135
- Carbon fiber structural model agreeing with experimental results
06 p1092 A70-18025
- Connection character of rubrospinal tract fibers with various neuron groups of spinal cord on basis of electrophysiological and morphological investigations
07 p1206 A70-19468
- Design allowables and factors of safety for filamentary composite materials, discussing reliability
08 p1595 A70-21900
- Plastic bodies plane flow Lagrangian description applied for prescribed deformation path of material fibers
09 p1769 A70-22251
- Myocardial individual fibers length calculation based on ellipsoidal model of left ventricle and fibers helicoidal course, noting distension nonuniform effect
12 p2174 A70-27020
- Recrystallization effect on 3-D graphite orientation in carbon fibers under high temperature heat treatment
12 p2259 A70-27720
- Tensile properties of fibrous materials at high rates of strain and subambient temperatures, considering nylon, Dacron, Nomex, Beta Fiberglass and Karma metal yarns
14 p2598 A70-30928
- Limit surface behavior equations for structural membrane elements in terms of number, orientation and limit load of constituent fibers by limit theorems
21 p3934 A70-40778
- Dry and water-saturated sintered fiber metal wick thermal conductivity, obtaining semipirical correlations for solid and fluid phases and void fraction
21 p3945 A70-41041
- Strong fibrous solids - Conference, London, January 1970
24 p4366 A70-45165
- High modulus carbon fibers production and properties describing polymer chains intermolecular structuring by pyrolysis and strength increase by fibers stretching at 2700 C
24 p4366 A70-45166
- Fibrous composites use in compressor blades, discussing materials characteristics requirements relative to environmental and stress conditions in aircraft operational service
24 p4392 A70-45169
- Fibrous composites thermomechanical properties derivation by theoretical analysis from basic constituents characteristics, presenting comparisons with experimental results
24 p4366 A70-45170
- Fibrous composite interface effects and fracture work, discussing tip stresses of crack normal to fiber, energy dissipation by pullout and debonding in brittle fiber composites, etc
24 p4419 A70-45171
- Fibrous composites design for mechanical properties improvement, discussing interfacial properties conflicting requirements as to interlaminar shear, transverse tensile strength, high work of fracture values, etc
24 p4419 A70-45172
- FIBRILLATION**
- Atrioventricular conduction in atrial fibrillation and flutter in man, using His bundle recordings
03 p0415 A70-12887
- Hypokinesia effects on transversostriated muscle fibers of mice, noting changes in myofibrillar apparatus, mitochondria and sarcoplasm
04 p0629 A70-14569
- Oxygen transport after cardiopulmonary resuscitation from asystole and ventricular fibrillation in dogs
10 p1822 A70-25085
- Multifocal atrial tachycardia, discussing arrhythmia progression to atrial fibrillation and association with acute and chronic diseases
21 p3761 A70-41134
- FIBRIN**
- Flight stress in Starfighter aircraft pilots related to fibrinolysis activity in blood
09 p1625 A70-23003
- X ray structural and electrophoretic investigation of donor and fibrinolytic blood protein components, observing crystalline to amorphous transition in blood serum and plasma lyophilization
09 p1621 A70-23149
- FIBRINOGEN**
- Resting concentrations of fibrinogen, plasminogen and levels of euglobulin fibrinolytic activity, plasmin inhibitors and urokinase in blood in inactive and exercising men
13 p2356 A70-29942

FIBROSIS

- Radial and tangential stress distribution through annulus fibrosis dependence on material inhomogeneity for human intervertebral disk
15 p2692 A70-32328
- Repeated decelerations effects on mice and rats, noting fibrotic changes in liver
17 p3025 A70-35133

FIBROUS MATERIALS

U FIBERS

FIDELITY

U ACCURACY

FIELD COILS

- Nonlinear characteristics of electromagnetic actuating mechanism induced by magnetic field of coil
07 p1281 A70-19529

FIELD EFFECT TRANSISTORS

- Metal-nitride-oxide semiconductor /MNOS/ FET load devices by changing from enhancement to depletion through polarizing voltage
01 p0051 A70-10785

- Junction gate and MOS field effect transistors thermal noise calculations, using circuit analysis based on equivalent circuits
02 p0258 A70-12424

- MOSFET uses in spacecraft electronic subsystems, describing digital control unit and typical logic circuitry
03 p0456 A70-13534

- Field effect transistors with controlled p-n junction and metal-dielectric-semiconductor transistors investigated for radiation effects on physical and electrical properties
04 p0730 A70-14500

- Chromium doping effect on ionizing radiation damage in MOS field effect transistors
04 p0658 A70-14744

- Schottky barrier FET fabrication using epitaxial growth of single crystal GaAs on insulating sapphire substrate
04 p0660 A70-15364

- Epitaxial GaAs FET using evaporated Au-Ge-Ni contacts and Ni Schottky barrier, describing fabrication and electrical properties measurement
04 p0660 A70-15367

- VHF field effect transistors thermal noise characteristics and effects of feedback and parasitic impedance
05 p0814 A70-16420

- Cross modulation due to nonlinearity and linear cross modulation due to local oscillator pulling in FET FM receiver, discussing mixer operating points
08 p1460 A70-20818

- Two dimensional numerical analysis of current saturation mechanism for junction field effect transistors with small and large length-to-width ratio values
09 p1740 A70-23110

- Steady state large signal computer model for junction-gate field effect transistors below pitch-off
11 p2019 A70-26711

- MOS-FET HF noise quantities computed in terms of substrate doping, angular frequency and gain-bandwidth product
12 p2196 A70-27672

- Neutron irradiation effect on n-channel GaAs junction FET performance, considering transconductance, drain current, pinch-off voltage and cut-off frequency
13 p2376 A70-28932

- Surface field effect, contact potential and photoconductivity measurements on p- and n-type heteroepitaxial single crystal silicon films on sapphire
13 p2470 A70-29372

- MOSFET integrated circuits radiation resistance measurements under electron irradiation, determining changes in threshold voltage, transconductance and on-resistance for applications in spacecraft
14 p2559 A70-31372

- Junction FET potential field and carrier distribution in channel investigated for current saturation mechanism
15 p2708 A70-31841

- MAGFET devices for integrated circuits, calculating magnetic sensitivity as function of channel aspect ratio and Hall electrode position
15 p2710 A70-32572

- Junction and MOSFET transistors thermal noise characteristics at cryogenic temperatures
15 p2710 A70-32585

- Large signal junction FET model involving piecewise linear approximation for ECAP circuit analysis program
15 p2711 A70-32596

- S band GaAs FET fabrication technology and frequency response
16 p2877 A70-33414

- Differential time division multiplexing system, discussing errors due to imperfections of field effect transistor as multiplexer switch
19 p3388 A70-37906

- Electrical conductivity of thin semiconductor films for FETs, investigating excessive conductivity scattering
19 p3389 A70-38067

- Low noise FET amplifier for satellite magnetometer, measuring interplanetary fields
21 p3799 A70-41923

- MOS field effect transistor, measuring electrons and holes thermal emission rates and activation energies at gold centers in Si
22 p3997 A70-43016

- Surface density, charge and field effect mobilities for electrons and holes on MIS insulator-semiconductor structure on narrow bandgap HgCdTe
22 p4086 A70-43018

FIELD EMISSION

- Field emission mechanism of hot electrons from semiconductors, discussing experiments with n-Si of high resistivity
06 p1126 A70-17749

- Electrohydrodynamic /EHD/ technique for generating ions from liquid metals by using electrostatic forces to overcome surface tension forces for field emission of ions
06 p1125 A70-18610

- Silicon carbide whiskers end structure using field emission patterns
08 p1528 A70-21551

- Molecular vibration spectra from inelastic interaction between electrons and adsorbed molecules at metal-vacuum interface
09 p1732 A70-22904

- Cerenkov radiation field in infinite parallel dielectric layer by sinusoidally bunched beam of electric charges moving with constant velocity along surface
10 p1916 A70-24408

- Avalanche diodes in presence of microwave instabilities related to field emission and charge transfer across depleted zone, discussing positive and negative resistance
10 p1850 A70-24621

- Field ionization from hydrogen layers adsorbed at 4.2 K on W emitters in sealed-off tubes
12 p2274 A70-26858

- Corona discharges from fine W points in liquid He initiated by field ionization or emission, noting anomalous characteristics
23 p4421 A70-44889

- Strong magnetic fields effect on field emission currents in Bi, Zn, Ta and W
24 p4379 A70-45621

- Field emission from narrow 3d bands of ferromagnetic nickel, calculating 3d and free electron transmission coefficients ratio, using triangular surface barrier model
24 p4391 A70-45671

FIELD INTENSITY METERS

- Narrow band atmospheric noise peak field strength measurement, describing design and calibration of noise meter output unit
10 p1832 A70-23998

- Rocket-borne double probe electric field detector design and operation, discussing error sources
22 p4030 A70-42793

FIELD STRENGTH

NT ELECTRIC FIELD STRENGTH

NT MAGNETIC FLUX

- Meter wave type 3 solar radio waves associated with solar X ray flares, discussing sudden enhancements of LF field strength due to D layer ionization enhancement
01 p0168 A70-10257

- Lagrangian gravitational field density related to contraction to expansion transition in terms of cosmological model, discussing quadratic corrections and singularity
03 p0524 A70-13412

- Method of characteristic calculation of field amplitude of electromagnetic waves propagating in inhomogeneous nonlinear medium applicable for computer
03 p0448 A70-13461

- Error correction for previous derivation of radio propagation of wave-hop series for anisotropic ionosphere resulting in improved nighttime field strength accuracy
04 p0649 A70-14967

- He and Ne adsorption and desorption on field ion microscope tip, determining minimum required field strengths of gas films at different temperatures
05 p0891 A70-15975

- Field strength predictions for expected returns from backscatter ionospheric soundings, predicting ionospheric propagation modes and losses during sunspot minimum
07 p1229 A70-19161

- Ionospheric radio transmission field strength calculation for given electron density and collision frequency profiles, considering electron variations along transmission path
07 p1230 A70-19165

- Mathematical models of vertical antennas of finite length and height, discussing signal strength and LUF determinations
07 p1240 A70-19167

- Field strength prediction for vertical horizontal broadside and horizontal end-on HF antennas, noting necessary polarization corrections
07 p1232 A70-19177

Graphic method of calculating radio wave absorption in ionosphere and field strength at reception point with aid of vertical sounding data

07 p1235 A70-19437

Radio wave refraction and field strength in model Venus atmosphere for various spacecraft trajectories

07 p1235 A70-19492

Field strength determination at reception point for long range short wave paths, taking into account multiple ray paths and antenna radiation patterns

07 p1237 A70-20435

Electrodynamic plasma accelerators fast particle generation mechanism during entrainment, studying polarization field potential structure

08 p1549 A70-20506

Field strength and interferential structure at different cross sections of inhomogeneous ionospheric channel calculated during bounce mode propagation of radio waves

08 p1461 A70-20969

Magnetic field measurements in geomagnetic tail from Explorers 33 and 35 indicating depressed field region centered on neutral sheet

08 p1488 A70-21379

Linear antenna array synthesis by variational calculus, minimizing sidelobe level for fixed input powers and field strengths

09 p1644 A70-22404

Loran C radio wave field intensity diurnal variations measurements, investigating ionospheric waves characteristics

10 p1832 A70-23921

Narrow band atmospheric noise peak field strength measurement, describing design and calibration of noise meter output unit

10 p1832 A70-23998

SID effects during recording of long wave transmitter field strength, indicating relation between solar X-ray flares and field anomalies

10 p1932 A70-24485

Long wave transmitter field strength calculation to 1000 km based on optical beam method and ionosphere model to account for radio wave reflection

10 p1840 A70-24495

Field strength correlation with micropressure variations caused by internal gravity waves propagating in lower troposphere

10 p1883 A70-25252

Short wave signal field strength measurement errors by frame antenna, outlining correction procedure

11 p2003 A70-25552

Second order self conjugate elliptical differential equation for modulus of gravitational field strength, giving geometrical interpretation of coefficient

12 p2223 A70-27349

Fluxgate and Ru vapor magnetometers for space measurements over wide field intensities, reducing electronic phase shift and experiment weight

13 p2415 A70-30045

Radio wave field intensity in middle frequency range, determining propagation curves for large distances

14 p2547 A70-30208

Single mode gas laser theory for arbitrary field intensities in terms of ensemble averaged form of density-matrix equations of motion

14 p1594 A70-31361

Radio wave refraction and field strength in model Venus atmosphere for various spacecraft trajectories

15 p2705 A70-32737

Electromagnetic field intensity measurements in focal region of wide angle spherical reflector antenna illuminated by polarized plane wave

16 p2872 A70-32976

Natural fluctuations sources intensity in annular lasers taking into account field strength dependence

16 p2927 A70-33197

Q switched laser turn-on nonlinear dynamics, deriving field intensity distribution function

18 p3270 A70-36743

Graphic method of calculating radio wave absorption in ionosphere and field strength at reception point with aid of vertical sounding data

18 p3229 A70-36911

Wave diffraction by finite dimension grating, determining EM field strength distribution by approximate method

19 p3377 A70-37716

Terrestrial ELF electromagnetic wave fields strength variation with distance over earth surface, using residue series zero-order term

19 p3380 A70-38405

X ray star effects on ionospheric LF radio wave field strength, examining absorption and ionization in D region

21 p3873 A70-40668

Short wave signal field strength measurement errors by frame antenna, outlining correction procedure

21 p3786 A70-41302

Helicon/magnetoacoustic waves/ effect on plasma instabilities, examining HF field amplitudes and magnetic fields

22 p4084 A70-43475

Electroreflectance at CdS-electrolyte interface, noting field strength effect on relaxation time

23 p4230 A70-43930

Geomagnetic perturbation effects on conduction along field lines and short period fluctuations associated with plasma turbulization in magnetosphere

23 p4189 A70-44065

VHF and UHF radio field strength changes due to tropospheric reflecting layers disintegration during anticyclonic weather, using ray tracing technique

24 p4315 A70-46153

Radio wave field intensity in middle frequency range, determining propagation curves for large distances

24 p4316 A70-46283

FIELD THEORY [ALGEBRA]

NT CUBIC EQUATIONS

NT QUADRATIC EQUATIONS

Numerical method for field problems analysis using algorithm based on generalized Betti-Maxwell theorem

06 p1094 A70-17942

FIELD THEORY [PHYSICS]

Gravitational theories scheme combining tetrad field with bimetric theories, including general relativity, space-time dependent Lorentz rotations, red shift and light deflection

01 p0141 A70-10232

Field equations in particle neighborhood for spherically symmetric metric in conformal gravitation theory, considering particle inertial mass as function of position

01 p0142 A70-10492

Linear field theory of gravitation by considering gravitational field functions decomposition into spin components

01 p0143 A70-10712

Nonlinear modification of Maxwell equations, discussing conformal invariance and nonsingular solutions to neutral and charged states with zero mass

02 p0339 A70-12067

Element relations of phase transformation matrix for scattering, relating radiation field vector to scattered field vector

02 p0339 A70-12283

Discrete space theory for radiative transfer in one dimensional scattering media of arbitrary constitution

02 p0340 A70-12642

Quasi-classical theory of solid state lasers generation and amplification, describing radiation by Maxwell equations and atoms in external fields by Schroedinger equation

02 p0315 A70-12832

Radiation transfer problem in waveguide with statistically uneven walls reduced to Dyson and Bethe-Salpeter equations in quantum field theory

03 p0524 A70-13066

Close spaced material points motion stability in gravitational field of attractive center using Liapunov theorem, assuming nongravitational forces action on points

03 p0524 A70-13369

Tension field theory describing buckling of membranes or thin plates with boundaries subjected to excessive planar displacements

03 p0599 A70-14246

Dipole shielding tensor of atom in arbitrary time dependent field, giving conditions for general variational calculations yielding results

04 p0721 A70-14389

Stationary solutions of Einstein-Maxwell equations constructed from Einstein-Maxwell or vacuum fields

06 p1106 A70-17748

Field theory of moving dislocations in Cosserat continuum considered incomplete regarding constitutive equations, basing analysis on Mic-developed mathematical analogy to electrodynamics

07 p1334 A70-19564

Axial-vector current divergence in external gravitational field, using perturbation approach in Minkowski space

07 p1336 A70-20167

News function relation with far fields of sources obtained in linear approximation for axisymmetric case in integrating Einstein field equation

08 p1543 A70-20721

Einstein power transfer theory used for demonstrating energy transfer rate by gravitational radiation from emitter to absorber

08 p1546 A70-21742

Total optical field in inhomogeneous medium, questioning uniqueness of division into direct and reversed wave propagation

08 p1546 A70-21785

Unified geometric description of gravitational and electromagnetic fields, determining electromagnetic field influence on geometry from dimensionless constant

08 p1546 A70-21811

Multipole analysis applied to 1965 International Geomagnetic Reference Field, separating secular variation field into drifting and nondrifting components

09 p1666 A70-22065

Cosmological solutions of Jordan-Dicke relativistic scalar-tensor theory, giving qualitative analysis of homogeneous isotropic problem at zero pressure

09 p1754 A70-22459

Material elasticity effects on librational motion of arbitrary shaped satellite

10 p1950 A70-24177

Cosmic rays, particles and fields physics in relation to radio and X ray astronomy

10 p1931 A70-24410

Different gravitational force fields effecting optimal rocket trajectories and queried validity of Newtonian law

10 p1943 A70-24820

Fields in wave interaction region during spatial trapping of parametrically amplified waves by radiation of pumping, using Laplace transformation

10 p1844 A70-25157

Soviet book on physical fields in general relativity theory

10 p1917 A70-25200

Stability conditions of rotational motions of symmetrical solid body on vibrating base in potential force field

11 p2098 A70-25916

Field equations in conformal theory of gravitation, noting invariance

11 p2084 A70-26552

Terrestrial external gravitational field approximation using sphere and ellipsoid attraction, showing mass, angular velocity and size dependence

12 p2300 A70-27477

Magnetic field equation for gyrotropic and anisotropic turbulence, observing large scale magnetic field generation

12 p2210 A70-27546

Aperture field modal decomposition of optical system in terms of integral equation eigenfunctions during detection and estimation of incoherent objects

12 p2273 A70-28121

Book on electromagnetic fields and waves covering electrostatic and magnetic fluids, relativity, vectors, Maxwell equations and propagation

12 p2273 A70-28150

Gravitational force equation solution, using Levi scheme

13 p2394 A70-28851

Yagi antenna field theory derived from Maxwell equations by solving in cylindrical coordinates and satisfying boundary conditions

13 p2364 A70-28898

Euler potentials for magnetic fields field-line structure representation, discussing cross products of gradients of scalars in plasma physics

13 p2451 A70-29123

Quantum noises in laser systems, deriving kinetic equation for traveling wave generation field density matrix

13 p2428 A70-29360

Particles and fields in magnetosphere - Conference, Santa Barbara, August 1969

13 p2479 A70-30058

Solar cosmic rays entry into magnetosphere, showing entrance on smoothly connected field lines

13 p2480 A70-30059

Microscopic particle mass spectra in six dimensional scalar, spinor and vector fields, noting cosmological implications and eight dimensional theory

14 p2616 A70-30342

Frequency dependence of gravitational-electromagnetic fields interaction assumption inconsistent with general relativity and consistent with data on deflection of radiation by massive bodies

14 p2573 A70-30616

Ellipsoidal plasmodium equilibrium in external HF field, calculating rotation rate and potential energy

15 p2779 A70-32113

Stochastic medium mathematical model for loose medium motion in potential field of forces

15 p2821 A70-32342

Thermal EM field as function of coherent states, outlining quantum theory for thermal radiation and solar energy

15 p2678 A70-32423

HF electrical communication based on Kelvin transmission line and Maxwell field theories, noting linear arrays

16 p2860 A70-32951

Collection of papers on antenna theory, part I covering EM fields, radiation sources and patterns, etc

17 p3043 A70-35051

Potential calculation from given source distribution, including direct and iterative methods, error analysis, convergence, computer programs and applications in plasma physics

18 p3284 A70-36790

Lunar magnetic monopole charge effects on nearby magnetic field configuration

18 p3316 A70-36898

Motion stability in periodic cubic force field, using nonlinear differential equation integration with time periodic square wave function and Jacobian table

18 p3284 A70-37065

Satellite orbit theory error bounds and initialization, investigating first order von Zeipel method in axisymmetric force field

18 p3320 A70-37067

- Nondipole geomagnetic field effect on magnetosphere boundary, presenting graphs for distance dependence on polar angle 19 p3409 A70-37321
- Strain gradient theory for random media, considering equations for response to forcing field 19 p3456 A70-37382
- Earth magnetic field, discussing origin, field absence on planets and moon and MHD theory 19 p3410 A70-37399
- Maxwell field quantization theory for case of interaction with Dirac field, calculating S matrix for interacting electrons 19 p3473 A70-37413
- Vertical gravimetric deflections calculation based on linear interpolated gravity anomalies 19 p3410 A70-37461
- Asymptotic high energy behavior of Feynman integrals in scalar field theory models for elastic scattering 19 p3457 A70-37549
- Plane polarized electromagnetic wave diffraction by dielectric grating, obtaining linear algebraic equations for field coefficients 19 p3376 A70-37713
- Diffraction-field structure on two-element gratings in near zone, calculating amplitude, phase and energy flux for normal and slant incidence of EM fields 19 p3377 A70-37720
- Elastic materials consisting of particles with rotary inertia, long range force and dipole interactions, deriving constitutive relations 19 p3538 A70-37794
- Piezoelectric force and moment measurement by quartz multicomponent devices 19 p3426 A70-37937
- Pulsar radiation mechanisms, discussing magnetic field topology and current distribution estimation 19 p3518 A70-38022
- Correction to Wu theory of microstrip leading to exponentially increasing fields 21 p3784 A70-40558
- Antenna radiation pattern analysis by application of Kirchhoff and Weber integrals, noting choice of complex radial wavenumber consistent with radial field decay 21 p3796 A70-40560
- External field perturbations by local inhomogeneities in elastic medium, deriving expressions for interaction energy and forces between defects 21 p3933 A70-40604
- Variable mass body rotational motion stability in central Newtonian field with gyroscope on symmetry axis 21 p3849 A70-40616
- Structures of linear field theories concerning constitutive equations and operators dual relationship 21 p3851 A70-42098
- Chronometrically invariant formulation of Petrov gravitational fields algebraic classification at spacetime fixed point in general relativity 21 p3851 A70-42239
- Einstein-Maxwell fields in presence of matter and pressure, expressing existence conditions in terms of eigenvalues and eigenvectors of Ricci tensor 22 p4074 A70-43206
- Conservation laws in theory of field with group invariance properties, examining infinitesimal transformations method 22 p4075 A70-43400
- Antenna far/near field correlation, noting measurement accuracy role 23 p4160 A70-43769
- Magnetic declination data, using spherical harmonics to examine global and secular geomagnetic field variations 23 p4189 A70-44067
- Two particles relative motion in elliptical orbits in inverse square central force field 23 p4244 A70-44576
- Maxwell electromagnetism and Einstein gravitation analogy in vacuum field equations, showing metric analytical for inverse distance parameter r 24 p4377 A70-45142
- Nonlinear Lagrangians in relativistic cosmology of open oscillating world model 24 p4404 A70-45409
- Hermitian symmetry in Einstein unified field theory in terms of pseudotensor 24 p4380 A70-45819
- FIGHTER AIRCRAFT**
- NT JAGUAR AIRCRAFT**
- Sonic boom pressure signatures for uniform and maneuvering flight conditions determined for fighter and SST aircraft [AIAA PAPER 69-1134] 01 p0005 A70-10606
- Harrier close-support fighter aircraft with short or zero takeoff run capability, discussing design, cruise efficiency, maneuverability and navigation-attack system 02 p0225 A70-12310
- Banked position and angle of attack changes in fighter aircraft sighting and attacking target, determining spatial zone of possible attack 02 p0227 A70-12406

- V/STOL supersonic fighter VJ 101, transport Do 31 and VTOL fighter/reconnaissance VAK 191 development in West Germany, discussing control and stabilization during hovering 03 p0413 A70-13794
- Air combat model /AIRCOM/ to evaluate close-in air-to-air fighter aircraft combat capability, determining relative changes in kill probability per firing pass 03 p0413 A70-13958
- Fighter aircraft design combining optimal qualities with economy 05 p0793 A70-15902
- Harrier G.R. Mk 1 VTOL vectored thrust aircraft for attacking targets at conventional strike aircraft speed, discussing design and combat effectiveness 06 p0985 A70-17157
- Supersonic aircraft aerodynamic properties and control systems performance, considering piloting of delta wing fighters 07 p1194 A70-19640
- Procurement problems for U.S. Defense Department taking into account fighter F-15 development for USAF 07 p1428 A70-19672
- Hawker Siddeley Harrier structural design, power plant, rear fuselage, wing tail unit structures, undercarriage features, weight control, fatigue testing, etc 08 p1435 A70-20620
- Electronic displays and flight control system of Multi-Role Combat Aircraft developed by Germany, Italy and UK 08 p1493 A70-20631
- Fighter aircraft inflight thrust control using thrust reverser technology to improve operational capability [AIAA PAPER 70-513] 09 p1610 A70-23019
- Fighter flight control design criteria for providing maximum combat effectiveness, safety and survivability without excessive cost or risk 09 p1611 A70-23021
- Air combat simulator with attacker and evader pilots control capability, comparing simulated interceptions with flight test maneuvers 09 p1656 A70-23023
- Computer aided design programs as decision-making tool for fighter development projects technical management 09 p1611 A70-23024
- Mirage F1 fighter aircraft, describing aerodynamic characteristics, fuselage construction, wing edges, etc 10 p1807 A70-24975
- Fighter aircraft firing accuracy improved by high pass filter to automatically compensate sideslip induced by rudder through follow up slideslipping by aileron 11 p1979 A70-25820
- Fighter-missile launch and control using direct radar information for guidance to reduce computation time and computer storage space 11 p2015 A70-26332
- Systems engineering study of sensors in fighter aircraft avionics 11 p2081 A70-26501
- Fighter pilot selection and training in Royal Netherlands Air Force 12 p2176 A70-27029
- Elementary flight training study in Royal Netherlands Air Force for improving pilot selection, discussing instructor and social science roles 12 p2176 A70-27030
- Harrier short takeoff fighter aircraft cockpit design, describing layout, lighting, warning and escape systems, etc 12 p2162 A70-27888
- Harrier fighter aircraft hydraulic systems and flying controls 12 p2166 A70-27889
- Gust response calculations compared with flight measurements for two fighter aircraft and jet transport to determine accuracy 12 p2162 A70-28077
- Wind tunnel tests, analytical methods and fixed base simulation for predicting fighter aircraft spin characteristics 13 p2346 A70-29030
- Tactical fighter requirements and designs, considering operational environment and weapon characteristics with emphasis on turning performance 13 p2346 A70-29035
- European Panavia 100/200 two engine variable wing military aircraft, noting prototype design, use and production sharing 13 p2347 A70-29051
- Fighter engine capabilities in Mach 3 to 7 speed range, discussing propulsion system configurations [AIAA PAPER 70-943] 16 p2965 A70-33542
- Medical and professional disadaptation in fighter pilots, considering fatigue, digestive disorders, anxiety, absenteeism, efficiency loss and accident proneness 16 p2850 A70-34347
- VAK 191 B VTOL aircraft fitting NATO Basic Military Requirements for low level reconnaissance-fighter operations developed from Fiat G-91 17 p3017 A70-34992

- Flying qualities criterion for fighter flight control systems design 17 p3020 A70-35837
- [AIAA PAPER 70-927]
- Fighter aircraft design for spin resistance and recovery using analytical approach, wind tunnel and flight tests 17 p3020 A70-35838
- [AIAA PAPER 70-928]
- Air superiority fighter design philosophy, including tradeoffs between armament, detection capability, thrust, speed and load factor 17 p3021 A70-35840
- [AIAA PAPER 70-930]
- Airframe-inlet integration for supersonic tactical fighters, testing wind tunnel models 17 p3149 A70-35843
- [AIAA PAPER 70-933]
- Computerized air combat simulation with comparison of analog and digital approaches, noting Air to Air Combat Fort Worth 18 p3230 A70-36453
- Structural fatigue design loads computation for fighter aircraft using multivariable load environment model from oscillograph recorded multichannel aircraft response data 20 p3719 A70-39579
- [AIAA PAPER 70-948]
- Fighter aircraft higher order control system dynamics effects on longitudinal handling qualities evaluated by in-flight simulator for role of pilot induced oscillations tendencies 22 p3961 A70-42711
- [AIAA PAPER 69-768]
- Strike fighter aircraft fuselage side air intakes, measuring external drag as function of design at subsonic and supersonic speeds 23 p4133 A70-44146
- [ICAS PAPER 70-49]
- Avionics system for fighter aircraft, discussing weapons design, navigation-attack systems integration, etc 23 p4173 A70-44413
- FIGURE OF MERIT**
- Cascaded thermoelements with high figure of merit for increasing solar thermoelectric generator efficiency, noting high temperature materials effect 01 p0158 A70-10754
- Operational figure of merit of high performance antennas in communication satellite earth stations as function of design 08 p1471 A70-20825
- Figure of merit for thermoelectric generator determined experimentally, assuming temperature difference between heated and cooled junctions 10 p1808 A70-25035
- Acoustooptics materials selection guidelines, estimating lead molybdate figure of merit on basis of chemical composition and density 13 p2469 A70-28796
- Phased arrays universal figure of merit, including aperture efficiency, sidelobe level, scanning frequency and noise temperature 16 p2864 A70-33482
- Microwave power transistors, considering figure of merit, performance and packaging 19 p3886 A70-37691
- Reliability figure of merit variations for predicted microwave radio system outages, using computer method 20 p3583 A70-38987
- Merit factor for evaluation of aircraft types and missions, matching aircraft characteristics to mission load, range and speed 20 p3562 A70-40360
- [SAWE PAPER 842]
- Image forming performance in photographic system design, considering Cobb chart resolution as figure of merit 24 p4334 A70-45449
- FILAMENT WINDING**
- Carrying capacity of shells of revolution obtained with threads spun around metallic shell, including stresses during spinning process 01 p0210 A70-11414
- Elasticity theory of orthotropic materials applied to steady rotation of long cylindrical tubes of filament reinforced plastics 03 p0602 A70-14331
- Filament winding methods of aerospace industry based on motor case winding, emphasizing reinforcing materials, winding geometry and finished composite evaluation methods 05 p0856 A70-16615
- Metal lined glass filament-wound pressure vessel performance at cryogenic temperatures, discussing fibers, resins and liners 06 p1091 A70-17615
- Stress analysis of multiaxially loaded tubes of fiberglass reinforced composite wound in three directions 07 p1318 A70-19755
- Filament wound bodies of revolution manufacture with consideration for linear and nonlinear winding, analyzing mechanically and electronically controlled machines 07 p1295 A70-19765
- Air bubble free glass fiber-plastic laminates fabricated by wet-winding method using vacuum, noting void free filament wounppipes 07 p1295 A70-19766

Stress analysis of composite materials reinforced with glass ribbons embedded in epoxy matrix by photoelastic technique, discussing perturbation effect 08 p1594 A70-21862

Filament tensile strengths and pressure strain characteristics of high modulus boron filament wound/resin composite pressure vessels for cryogenic applications 08 p1509 A70-21909

Failure analysis of unidirectionally reinforced fiberglass composites due to winding, using critical stress distribution function 09 p1710 A70-22462

Open pattern winding technique for composite materials, laying fibers without weaving around pillars at edge of table and to stiff beam 11 p2060 A70-26344

Filament winding process for boron modified phenolic resin tape used in high temperature applications 12 p2242 A70-27204

Filament winding reinforcement and resin noting production equipment and costs 15 p2744 A70-31932

Mechanical properties prediction analysis of boron filament wound reinforced composite structures verified by structural tests 16 p2937 A70-33370

Failure prediction for interlaminar shear stress in filament wound rectangular plate 17 p3188 A70-35228

Strain measurement on filament-wound structural members, incorporating electric resistance wire as strain gage within windings 19 p3550 A70-38719

Shaping methods for filament wound carbon structures, emphasizing matrix building by chemical vapor deposition 20 p3636 A70-39209

Filament wound composites, investigating interaction of fabrication variables and outward environments by delineating effect of each on structural performance 20 p3731 A70-40055

FILAMENTS

Optically trapped filaments in liquid carbon disulfide by side illumination and crossed polarizers using glass laser, noting birefringence and duration time 04 p0703 A70-15619

C-axis single crystalline sapphire filament tensile and fracture tests 08 p1514 A70-20647

Crab Nebula filametary system, examining excitation conditions in terms of ionization and heating by HF radiation 20 p3702 A70-39011

Ceramic whisker and continuous filaments reinforced metals, discussing processing, properties, matrices selection of reinforced composites, etc 20 p3650 A70-39948

Flow parameters radial dependence of thin solar wind filament corotating with sun 21 p3881 A70-40972

Filamentary composites stress wave amplitude distribution calculation and plotting 22 p4114 A70-42645

Dynamic deformation in thin walled axisymmetric plastic shells and filaments under time variable loads applied to high energy rate forming techniques 23 p4200 A70-44235

Whiskers and filaments properties compared for fiber reinforcement applications in composite materials production 24 p4356 A70-45167

FILLERS

Ta-V-Cb and Ta-V-Ti alloys used as brazing fillers for refractory metals bonding, noting wetting and flow characteristics, shear strength, remelt temperatures, etc 02 p0319 A70-12753

Interactions between adhesive polymers and fillers, emphasizing reinforced plastics composites properties [ONERA-TP-733] 03 p0516 A70-13644

Commercial Ni-Co gas tungsten arc filler metal with mechanical properties stable following stress relief 04 p0710 A70-15653

Thin walled cylindrical shell stability with hollow filler under distributed external loads, determining critical loads 07 p1399 A70-18663

Stability equations of three layer panels with allowance for rigid filler transverse deformations 07 p1415 A70-20186

Natural axisymmetric vibrations of cylindrical shell with hollow filler, analyzing motion by shallow shell and elasticity theory dynamic equations 07 p1415 A70-20191

Dynamic mechanical properties of filled polymers as function of filler concentration, particle agglomeration and ratio of particle to polymer modulus 08 p1527 A70-21335

Energy dissipation in free oscillations of multilayer shells consisting of alternating rigid elastic layers and soft fillers, deriving equations of motion 10 p1956 A70-24249

Syntactic foam material of hollow carbon micro-sphere fillers embedded in high compression strength epoxy resin matrix 13 p2437 A70-28780

Colloidal filler /carbon black/ reinforced rubber for various applications, noting fabrication into composite material 15 p2764 A70-31930

Flight vehicle dynamic response prediction from elastic filler stiffness contained between rigid sphere and ellipsoidal shell 16 p2991 A70-33878

Teflon crosshatched ablation patterns elimination by grooving or glass filler addition [AIAA PAPER 70-769] 17 p3193 A70-34483

Natural oscillations of cylindrical shell with elastic filler, using simple load distribution model 22 p4119 A70-43572

FILLETS

Photoelastic stress analysis of shouldered shafts with keyways in shanks under direct loading and torsion, including keyway and shoulder fillet stresses 02 p0388 A70-12496

Nonuniform stress distribution along side fillet welds and in welded plates of lap joint, discussing tangential stresses and plate width 11 p2058 A70-25598

Orthotropic plates bending with shallow and sharp fillets, determining normal stresses 12 p2325 A70-27533

Thick plate titanium alloy welds using filler wire to regulate chemical composition and plate phase constitution 13 p2435 A70-29456

FILLING

Controlled filling of container with compressed gas through time-variable cross section inlet, using variable mass thermodynamics 23 p4180 A70-44160

FILM BOILING

HF pressure oscillations during heat transfer to n-heptane at various flow rates and pressures, studying film or bubble boiling associated with oscillations 03 p0605 A70-13516

Liquid fuel film vaporizing combustor for gas turbines, considering combustion efficiency and flame intensity 03 p0552 A70-14324

Gravity and size effects on film boiling from horizontal cylinders, recommending formulas for wavelength and minimum heat flux predictions [ASME PAPER 69-WA/HT-12] 04 p0784 A70-14821

Time dependent pressure fluctuations effect on laminar film pool boiling on vertical flat plate by perturbation method to predict heat transfer 06 p1177 A70-17696

Radiation effect on heat transfer during film boiling in forced convection boundary layer of liquid flow past plate, noting vaporization temperature 07 p1423 A70-19812

Boiling heat transfer enhancement inside tubes using integral fins, discussing water film retention on walls 08 p1599 A70-21825

Film heat transfer coefficients and thicknesses for condensation and evaporation and two phase flow inside circular tubes [ASME PAPER 67-HT-1] 08 p1599 A70-21827

Meteor ablation, investigating removal rate of molten film and droplet evaporation 09 p1754 A70-22476

Critical thermal flux and heat transfer coefficients dependence on simulated gravity during bubble and film boiling in inclined flat containers 12 p2331 A70-27325

Cryogenic single tubes transient cool-down by liquid hydrogen, deriving film boiling heat transfer correlation [AIAA PAPER 70-660] 16 p2998 A70-33621

Film boiling heat transfer from horizontal wires to water, using Nusselt condensation model 16 p3003 A70-34198

Liquid nitrogen drops anomalous behavior in film boiling, resolving vaporization time discrepancies 17 p3194 A70-34741

Pressure, subcooling and diameter effects on liquid nitrogen film boiling on thin horizontal wires, using high speed movies 17 p3194 A70-34742

Liquid or solid Leidenfrost film boiling on saturated cryogenic liquid surface, discussing hydrodynamic model similar to propellant spillage accidents 17 p3194 A70-34744

Buoyancy effects on liquid nitrogen film boiling in vertical flow, using resistance heated test apparatus 17 p3195 A70-34745

Film boiling covering drops and puddles, pool boiling for various geometries and forced convective film boiling 17 p3195 A70-34747

Radiation effect on heat transfer during film boiling in forced convection boundary layer of liquid flow past plate, noting vaporization temperature 20 p3736 A70-39259

Vapor volume entrained in liquid bulk from boundary layer boiling on vertical plate in low gravity field 21 p3947 A70-41055

Interfacial instability effect on heat transfer to liquid nitrogen drops undergoing film boiling on flat Al surface, obtaining vaporization rates and times 21 p3948 A70-41203

Pool film boiling heat transfer data from small spheres, noting curvature effects and similarities of flat plate, cylinder and sphere theoretical analyses 21 p3949 A70-41310

Critical thermal flux and heat transfer coefficients dependence on simulated gravity during bubble and film boiling in inclined flat containers 21 p3952 A70-42066

Heat transfer measurement from Pt wire to carbon dioxide near critical pressure, discussing film boiling and free convection flows 21 p3953 A70-42167

Natural convection film boiling heat transfer literature, data sources for specific substances, photographic studies, mathematical models, etc 22 p4121 A70-42305

Comparative analytic and experimental film boiling heat transfer for horizontal cylinders in helium II [ASME PAPER 70-HT-3] 22 p4122 A70-42441

Heat and mass transfer for liquid film evaporation during two phase two component flow in vertical steel tube under adiabatic and nonadiabatic conditions 23 p4276 A70-44215

Capillary boiling and heat transfer for coolant fluids, using motion photography and visual observations 23 p4277 A70-44320

Liquid nitrogen drops undergoing film boiling on Al surface, measuring heat transfer coefficient 23 p4279 A70-44360

Cylindrical heaters in corresponding-states fluids, estimating film boiling heat transfer coefficients by correlation procedure using least squares expression 23 p4279 A70-44361

Liquid nitrogen saturated film boiling from wire at pressures up to critical, discussing liquid-vapor interface configuration 23 p4279 A70-44362

Liquid He II, determining correlation of depth effect on film boiling heat transfer with vapor film geometry from motion pictures 23 p4279 A70-44363

FILM CONDENSATION

Film heat transfer coefficients and thicknesses for condensation and evaporation and two phase flow inside circular tubes 08 p1599 A70-21827

Film condensation in tubes, considering liquid-vapor interface, zero gravity and electrostatic field conditions 15 p2828 A70-32541

Film condensation rates of vaporized substance in shock tube during passage of shock wave, formulating quasi-one dimensional problem 18 p3239 A70-36244

Three dimensional laminar boundary layer equations for film condensation on curved surface in quiescent vapor, investigating flow at stagnation point 21 p3954 A70-42168

FILM COOLING

Foreign gas injection and slot geometry influencing film cooling effectiveness 01 p0219 A70-11182

Interaction between surface liquid film and hot gaseous turbulent boundary layer analyzed for hypersonic vehicle surface thermal protection design problems 04 p0669 A70-14927

Prandtl mixing length and effective Schmidt number distributions from wall jet and wake data to predict film cooling 06 p1035 A70-17688

Porous matrix flow, surface liquid layer and hot gaseous boundary layer interactions at nose tip of reentry vehicle 06 p1037 A70-18028

Transpiration and film cooling systems comparison for high speed flows with foreign gas injection effects [AIAA PAPER 70-153] 06 p1179 A70-18073

Velocity and concentration profiles for mixing of two dimensional foreign gas jet injected into parallel air mainstream, emphasizing film cooling applications 10 p1801 A70-24155

Film cooling effectiveness measured following air injection through discrete holes into turbulent boundary layer of air on flat plate 11 p2146 A70-25690

Two dimensional film cooled turbine blade aerodynamics, investigating massive blowing effect through discrete holes in single blade test facility [AIAA PAPER 70-713] 16 p2834 A70-33537

Transpiration and film cooling effects on aerodynamic characteristics of slender cone in hypersonic flow tested in hypervelocity wind tunnel using mass injection 16 p2837 A70-33857

Two dimensional turbulent film cooling, predicting initial region temperature distribution by solving finite difference form of thermal energy equation 18 p3346 A70-36497

Film cooling protecting axisymmetric nozzle slot surface exposed to high temperature Mach 6 air injection 18 p3242 A70-36695

Heat transfer between wall and liquid and vapor films in internal regenerative cooling of thrust chambers 21 p3867 A70-41027

Gaseous film cooling effect on adiabatic wall temperature distribution in rocket nozzle with gas injection 21 p3867 A70-41028

Injection slot geometry effect on gas film cooling, discussing effect of secondary stream acceleration 21 p3952 A70-42084

Gas turbine combustion chamber convective and radiant heat transmission, examining steam film cooling of flame tube 22 p4092 A70-43199

Convection, transpiration and full coverage film cooling methods for various local turbine inlet temperatures, gas pressures and cooling air temperatures 22 p4092 A70-43275

Gas coolant slot injection into hypersonic laminar boundary layer, comparing experimental results to boundary layer equations numerical integration 23 p4282 A70-44694

Film cooling efficiency for flat plate behind tangential slot at blowing coefficients below unity 23 p4282 A70-44727

Flat plate film cooling efficiency behind tangential slot at blown-main flow velocity ratio over three 23 p4283 A70-44741

FILM THICKNESS

Synchronous dynamic response of gaseous double squeeze film thrust plate with very high frequencies, showing increased load capacity and stiffness [ASME PAPER 69-LUB-8] 01 p0102 A70-10395

Squeeze film investigation between rotating plane annuli, considering inertia due to centrifugal effect [ASME PAPER 69-LUB-6] 01 p0102 A70-10396

Bonded solid lubricant films wear life equation for low contact stress conditions, determining optimal film thickness [ASME PAPER 69-LUB-5] 01 p0102 A70-10397

Rayleigh step journal bearings, considering pressure distribution, load capacity and attitude angle and optimal film thickness ratio for incompressible fluid lubrication 02 p0307 A70-12167

Load support and leakage from microasperity lubricated face seals, developing hydrodynamic lubricant films [ASLE FICFS PREPRINT 21] 02 p0308 A70-12174

Eccentric face seal with tangentially varying film thickness, analyzing leakage flow proportional to eccentricity and surface waviness [ASLE FICFS PREPRINT 15B] 02 p0308 A70-12176

Molybdenum disulfide surface and bulk properties, comparing endurance of fractions and grades with synthetic chalcogenides at same layer thickness in dry atmospheres [ASLE PREPRINT 69-LC-7] 02 p0322 A70-12538

Thickness measurement of nonmagnetic coatings on magnetic substrates taking into account surface roughness effect 02 p0302 A70-12672

Sputter machining thickness reduction methods for VHF resonant piezoelectric transducers 03 p0496 A70-14207

Oxide layers on metal substrate noting emittance dependence on thickness in aluminum-aluminum oxide and Cu-CuO systems [ASME PAPER 69-WA/HT-4] 04 p0705 A70-14825

Calorimetric measurements determining total hemispheric emittance of thin gold films as function of temperature, demonstrating film thickness effect [AIAA PAPER 70-63] 06 p1180 A70-18140

Nusselt theory of laminar liquid films movement on vertical smooth solid surface, attributing thickness variation to gas movement and surface active agents in liquid 07 p1251 A70-18656

Rheology applied to motor oil viscosity, elastohydrodynamic/EHD/ and extremely thin film lubrication, examining viscosity relationship to film thickness 07 p1293 A70-18954

Film heat transfer coefficients and thicknesses for condensation and evaporation and two phase flow inside circular tubes [ASME PAPER 67-HT-1] 08 p1599 A70-21827

Compound semioaque thin films quality control for thickness uniformity by observing fringe patterns generated by optical data processing techniques 09 p1687 A70-23765

Residual stress measurement in anodic film on duraluminum as function of film thickness and cyclic loadings in air and corrosive media 15 p2757 A70-31635

Thickness measurement for thin films in inaccessible locations using scanning electron microscope, comparing accuracy with interferometric techniques 15 p2741 A70-32435

Coating thickness measurement and analysis by radioisotope techniques including beta-particle, X or gamma ray backscatter and X ray fluorescence and absorption 15 p2742 A70-32780

X ray fluorescence determination of thickness and composition of Permalloy films deposited on wire surface 18 p3258 A70-36466

Squeeze film investigation between rotating plane annuli, considering inertia due to centrifugal effect [ASME PAPER 69-LUB-6] 19 p3435 A70-37608

Optimum one dimensional journal bearing for maximum load with minimum film thickness, using Pontryagin principle [ASME PAPER 69-LUB-9] 19 p3435 A70-37614

Hydrodynamic lubrication film breakdown in cold strip rolling, showing thickness consistency with critical value of modified Sommerfeld number 21 p3833 A70-41256

Thin film microwave acoustic transducers, calculating top electrode thickness effect on frequencies of infinite conversion loss 24 p4333 A70-45218

FILMS

Sliding steel specimens anomalous friction behavior in vacuum, noting friction-time plot dependence on oxide film rupture, load, environmental pressure, etc 02 p0321 A70-12534

Two dimensional irrotational incompressible fluid motion bounded by flexible stretched and unstretched film, noting hydrodynamic shock for closed film 12 p2213 A70-28238

Oxide film and liquid effects on friction coefficient, surface relief and dislocation density along depth related to plastic deformation 15 p2743 A70-31638

X ray and neutron propagation in multilayer film composite, discussing boundary conditions in interferential systems 24 p4380 A70-46095

Stainless steel oxide films structures and chemical compositions, examining oxidation time, polishing conditions, vapor humidity and temperature effects 24 p4362 A70-46191

FILTERING

U FILTRATION

FILTERS

Fibrous filter materials filtering capability, comparing extruded and drawn metallic fibers 01 p0007 A70-10159

Square root filters algorithms based on covariance and invariance matrices extended to include process noise effects 01 p0144 A70-11193

Clutter symmetry as indication of matching optimum signal filter pair, comparing mismatched and matched systems 06 p1013 A70-18626

Sampled analog waveforms transmission, deriving optimum pre- and postfilters 15 p2703 A70-32557

Filter parameter estimation in serially correlated measurement noise, using recursive least squares analysis 15 p2704 A70-32591

Nondiverging filter with single additional multiplication by fixed scalar s at each observation time, proposing algorithm 16 p2887 A70-33872

Vibration transducer systems design, using active filter networks to tailor phase and frequency responses 17 p3095 A70-35527

Water separation index modified /WSIM/ test for jet fuel surface active materials in relation to filter/separators performance [SAE PAPER 700279] 18 p3300 A70-36815

Thor launch vehicles steering filters design using automated method of optimizing large order linear stochastic systems control [AIAA PAPER 70-986] 20 p3600 A70-39543

Discretization interval in discrete analog filters for optimal processing of complex radar signals, estimating systematic errors 22 p3984 A70-42393

FILTRATION

NT SPATIAL FILTERING

Fibrous filter materials filtering capability, comparing extruded and drawn metallic fibers 01 p0007 A70-10159

Spectrophotometric facility for measuring spectral characteristics of color filters, photomultipliers and photographic plates as function of temperature 02 p0301 A70-12494

Photochromic aminotriarymethane filter solutions for flash blindness protection, noting stability against xenon flash UV exposure 04 p0690 A70-15028

Slowly varying component filtration from multiplicative mixture of two random processes by statistical analysis 06 p1009 A70-17670

Magnetic field filtration into time-variable and constant parts, using signal to noise analogies 07 p1266 A70-19440

Platelet aggregation in whole blood, basing measurement method on filtration pressure with added adenosine diphosphate /ADP/ 07 p1210 A70-19591

Carbon-bearing materials for modification of Mg-Al-Zn-Mn alloys filtration processes 08 p1505 A70-21132

Kalman-Bucy filtering for nonlinear system consisting of missile in flight, discussing state variables values selected by estimator 11 p2025 A70-26221

Book on stochastic processes and filtering theory covering probability theory, Markov processes, linear and nonlinear filters, etc 13 p2442 A70-29575

Magnetic field filtration into time-variable and constant parts, using signal to noise analogies 18 p3249 A70-36914

FIN STABILIZERS

U FINIS

U STABILIZERS [FLUID DYNAMICS]

FINANCE

European airbuses designs, considering potential market and financial problems 19 p3357 A70-38952

Financing methods for airport redevelopment and expansion, discussing economic and political framework of operations [AIAA PAPER 70-1267] 24 p4430 A70-45920

FINANCIAL MANAGEMENT

Incentive earnings and payments in CPIF /cost plus incentive fee/ contracts, considering legal principles 14 p2668 A70-30523

Value engineering for British aerospace industry management planning 19 p3555 A70-38619

FINE STRUCTURE

Steel crystal lattice fine structure and mechanical properties during annealing using X rays as function of temperature 03 p0511 A70-13422

Tropospheric fine structure influence on radio wave propagation, including atmospheric gases and precipitation effects and radar, navigation and TV applications 03 p0449 A70-13612

Alouette 2 Langmuir probe measurements analyzed for size and amplitude of electron concentration fine structure irregularities in topside ionosphere, discussing F spread 04 p0679 A70-15111

Chromospheric fine structure photographed at H alpha line center, discussing size, lifetimes and relationship between dark and bright mottles 05 p0910 A70-16428

High resolution observations of low chromosphere beyond limb at H-alpha line center revealing fine structures, identifying chromospheric spicules with dark mottles 05 p0910 A70-16429

Rapid fine structure in hard solar X ray bursts observed by OSO-5, explaining time structure by mechanism based on repetitive production of monoenergetic electrons 05 p0904 A70-16980

Absorption transition fine structure measurements for bulk rare earth garnets single crystals using reflectivity techniques [IEEE PAPER 19.6] 05 p0894 A70-16998

Age mixtures and physical heterogeneity of G-M cold stars emphasized in study of galactic fine structure and evolution 06 p1140 A70-17640

Magnetic and velocity fields in unipolar sunspot, discussing fluctuations associated with penumbral and umbral fine structures 06 p1144 A70-18002

Fine structure of excited P states of Li measured for magnetic fields in proton NMR frequency using level crossing and Zeeman effect 07 p1346 A70-20239

Low field and high field hyperfine structure and lifetimes of excited P states of Li using level crossing spectroscopy 07 p1346 A70-20240

Resonant and foreign gas broadening using Schrodinger equations for collision problems 07 p1346 A70-20244

Modulation lanes in fine structure of dynamic spectra of Jovian I bursts possibly due to ionosphere or magnetosphere 08 p1576 A70-21394

Fine structure morphology in dynamic spectra of Jupiter decametric radiation determined from spectral recordings 08 p1562 A70-21514

Tropospheric elevated layers fine structure characteristics by balloon-borne spaced cavity refractometer 09 p1714 A70-22353

Atmospheric fine-scale structure determination from forward scatter radio wave propagation, considering refractive index role 09 p1715 A70-22362

Intermittency characteristics associated with fine scale structure and motion of atmosphere from data pertaining to various atmospheric layers 09 p1717 A70-22375

White Leghorn laying hens parathyroid glands fine structure from electron microscopic studies, noting electron dense membrane bound mature secretory granules in cytoplasm 09 p1619 A70-22800

Coherent optical beam propagation measurement of fine scale turbulent atmosphere structure, inferring microscale size and permittivity spectra 09 p1635 A70-22963

Quadratic Stark shifts of absorption lines hyperfine components in cesium atom beam measured using optical spectroscopy 10 p1887 A70-24033

Absorption strengths of j-manifolds in R branch of Jupiter atmosphere methane band, discussing fine structure blending 10 p1919 A70-24473

Ionospheric fine structure from ionograms, discussing probe and half automatic digital evaluation method 10 p1884 A70-25257

Ionospheric fine structure from signal broadening measurements on ionograms, including scattering region algorithm 11 p2044 A70-25553

Gravitational field signatures for planetary fine structure analysis, describing lunar orbiter, selenodesy experiment and gravity field and earth gravity field satellite observation 11 p2111 A70-26029

Merope /IC 349/ nebula, noting luminescence and continuous spectrum fine structure 12 p2307 A70-27867

Pulsed Ne laser superradiation spectrum fine structure, using Fabry-Perot interferometer 13 p2428 A70-29362

Solar chromospheric fine structure from high resolution photographs 13 p2497 A70-29849

Satellite plasma diagnostics for electric and magnetic fields and fine structure of collisionless shocks in solar wind plasma flows and interplanetary shocks 13 p2481 A70-30069

Fine grained structure effect on steels and Ni alloys short term heat resistance at high temperatures 14 p1594 A70-30168

Isomer shift, Mossbauer recoil free fraction and nuclear quadrupole splitting for Fe57 in iron fluoride measured for lattice dynamics, fine and hyperfine structure 14 p2626 A70-30484

Lunar surface fine structure and geological analysis from Ranger 7, 8 and 9 photographs 14 p2644 A70-31052

Semiclassical collision theory for computing fine structure proton impact excitation rates and cross sections for positive ions, presenting excitation rate tables 14 p2652 A70-31383

Fine structure in Ca II K line core, determining reduced high dispersion spectra at solar disk center 15 p2804 A70-32618

Nitric oxide gas IR radiation properties at high temperatures, determining spectral mean fine structure and total band absorptance correlations 16 p3003 A70-34253

Pulse structure, polarization, time varying features and tight beam emission by pulsar model using finite thickness interfaces 17 p3153 A70-34532

Pulsar RF spectral fine structure in decimeter wave range 17 p3163 A70-35050

Fine structure of hydromagnetic ULF emissions on spectrograms of whistlers, periodic emissions, choruses and sweepers 17 p3047 A70-35640

Chromospheric spicules fine structure recorded on H alpha spectrograms and filtergrams from high altitude coronagraph 17 p3174 A70-35863

Fine structure of geomagnetic Pc 1 micropulsations by cyclotron instability due to anisotropic energetic proton velocity 19 p3410 A70-37334

Closed coupled partial wave calculation of cross section for fine structure transitions in Na in collisions with He 19 p3372 A70-37541

Lifetimes and fine structure of differentially metastable autoionizing states of negative He ion in axial magnetic field, using time of flight techniques 19 p3473 A70-37746

Semiannual oscillation and fine structure of earth magnetic field horizontal intensity during March and September 19 p3413 A70-38004

High Reynolds number isotropic homogeneous turbulence fine scale structure heuristic model, relating spatial intermittency to vorticity generation 20 p3609 A70-39665

Pulsar observational data and theories, discussing main pulse shape, wavelength, polarization, fine structure distance estimates, intensity and scintillations 20 p3706 A70-39935

Ionospheric fine structure from signal broadening measurements on ionograms, including scattering region algorithm 21 p3819 A70-41303

Nickel surface layer fine structure changes in supersonic air flows at various temperatures and times 22 p4056 A70-43341

Gravity gradiometry for fine structure of gravity influenced by local anomalies 22 p4108 A70-43659

Gravitational field fine structure representation near earth surface as sum of global model in spherical harmonics and local model in harmonic B functions 24 p4328 A70-45287

Li doublet in 21 March 1969 sunspot, examining fine structure caused by self reversal in line core 24 p4400 A70-45309

Pulsar intensity variations, showing fine frequency structure by interstellar scintillation model 24 p4404 A70-45416

High resolution cylindrical capacitor observation of fine structure of distribution function of electron beam interacting with plasma 24 p4387 A70-45820

FINENESS RATIO

Minimal interference thin metal strap support system for dynamic stability tests of high fineness ratio wind tunnel models [AIAA PAPER 69-350] 17 p3063 A70-35657

FINES

Apollo 11 lunar rocks and fines, examining clinopyroxenes augite and pigeonite by single crystal X ray diffraction microprobe optical and electron optical techniques 21 p3902 A70-41549

Apollo 11 lunar rock and fines shock induced and melting microstructural mineral damage, discussing meteorite bombardment, phases without melting and microbreccia 21 p3902 A70-41550

Elemental composition and structure of metallic iron particles in lunar fines compared to meteorites, using neutron activation technique 21 p3774 A70-41556

Apollo 11 fines gas evolution and physical changes via heat treatment, discussing Ar 40 anomaly, lava structure origin and oxidation rate 21 p3907 A70-41577

Chemical composition and reducing capacity of Apollo 11 igneous rocks, breccia and soil fines, using semimicro X ray fluorescence 21 p3777 A70-41602

Apollo 11 fines and rocks major and trace elements data obtained by combined instrumental and neutron activation analysis 21 p3910 A70-41615

Volatilizable C compounds in lunar fines from Mare Tranquillitatis, investigating pyrolysis and acid hydrolysis products by mass spectroscopy and gas chromatography 21 p3779 A70-41628

Apollo 11 fines and rocks analysis by chromatography, mass spectrometry and light and scanning electron microscopy 21 p3779 A70-41631

Organic solvent extracts of Apollo 11 bulk fine sample examined for porphyrins using spectrofluometry 21 p3780 A70-41635

Micro-breccia, igneous rocks and lunar fines elastic properties at ambient conditions and as function of pressure, discussing near surface mare region models 21 p3913 A70-41640

Directional, spectral and total reflectance for Apollo 11 fines and rock chips, observing dependence on illumination angle 21 p3913 A70-41643

Apollo 11 fines thermal conductivity under vacuum, using line heat source technique 21 p3913 A70-41647

Apollo 11 fines, breccias and crystalline rocks thermoluminescence, observing temperature dependence of glow curve peaks 21 p3914 A70-41649

Apollo 11 bulk and core tube fines and rock cosmic ray tracks, discussing material history and corpuscular radiation flux and energy spectra near moon 21 p3916 A70-41667

Apollo 11 rock and fines magnetic resonance, examining line shapes, temperature dependences and electron spin 21 p3917 A70-41670

Apollo 11 lunar fine thermal conductivity measurement under vacuum conditions and lunar temperature range, using line heat source method 23 p4243 A70-44442

Apollo 11 lunar fines glassy particles, investigating morphology, optical properties and chemical composition 24 p4403 A70-45401

FINGERS

Human finger tips skin temperature periodical variations process and influencing factors using electronic analog model 10 p1823 A70-25306

Hand held device for finger /thumb/ strength measurements 24 p4309 A70-46121

FINISHES

NT ENAMELS

NT GLAZES

FINITE DIFFERENCE THEORY

Boundary layer around blunted cone solved numerically by finite difference method 01 p0001 A70-10297

Interior estimates for second order elliptic differential or finite difference equations, applying maximum principle 01 p0131 A70-10375

Finite difference scheme for linear second order third boundary value problem in ordinary differential equations 01 p0131 A70-10455

Finite difference schemes compared for numerical weather prediction by application to shallow water equations on hemisphere, noting mesh spacing 01 p0135 A70-11064

Conservation equations for mass, mean momentum and kinetic energy for incompressible turbulent boundary layer, using finite difference procedure 02 p0284 A70-12347

Hydrodynamic turbulent boundary layer on smooth wall, using finite difference theory 02 p0285 A70-12351

Finite difference solution of compressible turbulent boundary layer equations of motion, using eddy viscosity concept 02 p0286 A70-12353

Electromagnetic pulse scattering in time varying inhomogeneous medium, applying finite difference method to Maxwell equations 02 p0261 A70-12588

Flow development in conical diffusers, delaying stall with high velocity air injection through annular slot at diffuser inlet predicted by finite difference method 02 p0224 A70-12866

Summary representations method to analyze finite difference schemes for integrating parabolic equations with constant coefficients, solving boundary value problems 03 p0518 A70-13078

Summary representations method to determine eigenfrequencies of finite difference Laplace operator for boundary conditions 03 p0518 A70-13079

Finite difference method applied to solving equations of motion for computing natural torsional vibration frequencies of pretwisted cantilever beams 03 p0595 A70-13811

Finite difference method for obtaining free vibrations natural frequencies and mode shapes for rectangular plates of varying stiffnesses 03 p0595 A70-13812

Finite difference theory applied to numerical analysis of laminar equilibrium MHD flow in circular tube [ASME PAPER 69-WA/HT-55] 04 p0727 A70-14794

Heat conduction equation solutions, comparing finite element and finite difference methods [ASME PAPER 69-WA/HT-35] 04 p0781 A70-14805

Method of integral relations, finite differences and method of characteristics applied to numerical solution of steady state problems of gas dynamics 04 p0670 A70-14961

Integral relations and finite difference methods application to problems of boundary layer equations in gas dynamics 04 p0670 A70-14962

Spherical caps axisymmetric static and dynamic buckling under load, using axisymmetric nonlinear elastic shell theory approximation and finite difference equations [AIAA PAPER 69-89] 04 p0778 A70-15587

Finite difference wave equation to obtain asymptotic estimate for magnitude of precursor effects 05 p0875 A70-16310

Finite difference solution of time dependent Navier-Stokes equations for two and three dimensional laminar incompressible flow, discussing results for flat plates [AIAA PAPER 70-46] 06 p1041 A70-18170

Time dependent inviscid gas flow on infinite domain computed by finite difference method [AIAA PAPER 70-45] 06 p1042 A70-18188

Finite difference analysis of partial differential equations derived from Navier-Stokes equations in

hypersonic leading edge problem in merged gas flow-layer regime

06 p0980 A70-18349

Flexural elastic behavior of rectangular plates with boundary restraint acting on same side using finite differences method

07 p1406 A70-19348

Partial differential equations hyperbolic systems solutions by finite difference methods, considering schemes stability and viscosity from first differential approximation standpoint

07 p1326 A70-19559

Interstellar gas clouds collapse using finite difference numerical methods in solving hydrodynamic equations involving gravitation

07 p1390 A70-20288

Nonlinear difference approximating scheme and iterative method for Stefan problem with several unknown fronts

08 p1534 A70-20851

Laminar boundary layer equations solution by approximation compared with results from finite difference method

08 p1483 A70-21033

Biharmonic equation in polar coordinates solved for circular plates and plate sectors with various boundary conditions, using finite difference approximations

08 p1589 A70-21246

Steady state finite difference solution of equations governing arbitrarily biased bipolar transistor action in two dimensions

08 p1477 A70-21641

Survey of papers on computer calculation of two and three dimensional gas flows, emphasizing method of characteristics and finite difference techniques

09 p1603 A70-22265

Biharmonic boundary value problems with re-entrant boundaries, comparing Motz and Woods finite difference solution methods

09 p1711 A70-22285

Boundary layer equations for multicomponent flow with finite chemical reactions solved by finite difference method

09 p1605 A70-23201

Finite difference methods stability for time dependent Navier-Stokes equations coupled to energy equation with quadratic terms in velocity gradients

10 p1866 A70-24106

Error analysis and monotone convergence of finite difference approximations to linear one dimensional singular boundary value problems

10 p1909 A70-24406

Moving mass effects on Euler beam analysis extended to Timoshenko beam, obtaining numerical solutions by finite difference method

10 p1963 A70-25073

Axissymmetrically loaded shells of revolution with displacement behavior defined by fourth order differential equations, discussing finite difference method suitability for solution

11 p2144 A70-26679

Coefficients for finite difference methods of numerical integration of products of Fourier and ordinary polynomials

11 p2074 A70-26848

Finite difference methods for approximating first order nonlinear hyperbolic differential equations, considering convergence

13 p2441 A70-29098

Discontinuous hydrodynamic flows derived for stability condition using three dimensional second-order difference schemes

13 p2441 A70-29099

Boundary layer flow between nodal and saddle points of attachment, comparing matched series and finite difference methods

14 p2565 A70-30281

Biharmonic equation numerical solution by finite differences, discussing outer and inner iteration schemes

14 p2599 A70-30647

Finite difference algorithm for supersonic three dimensional steady flow past blunt bodies with generating line bends, allowing for gas equilibrium and frozen states

15 p2671 A70-31495

Boundary value problems of biharmonic finite difference equation in rectangular domain, deriving calculation formulas for summary representations solution method

15 p2814 A70-31583

Stress analysis for plate with large displacements by multicamera photogrammetry, comparing results with numerical solution by finite differences

15 p2821 A70-32313

Supersonic and hypersonic gas flow past blunt bodies, using finite difference and integral relation methods

16 p2890 A70-33244

Finite difference schemes for systems of elliptic and parabolic equations, using brute force algorithm

16 p2941 A70-33246

Singular perturbations of boundary value problems, investigating asymptotic solutions to finite difference equations

17 p1328 A70-34613

Finite difference scheme for solving continuum mechanics problems in two space dimensions and time

17 p1313 A70-35885

Supersonic axisymmetric flows past bell-shaped bodies of varying bluntness, using Godunov finite difference method

17 p3012 A70-35887

Two dimensional free boundary problems approximate solution by finite difference method, deriving algorithms for computer program implementation

18 p3230 A70-35941

Explicit differences scheme for heat and mass transfer differential equations

18 p3345 A70-36114

Finite difference theory applied to first boundary value problem of elasticity theory for Lamé equation

18 p3280 A70-36158

Steady incompressible flow past circular cylinder at Reynolds numbers up to 100, using finite difference solutions of motion equations

18 p3238 A70-36191

Matrix filtering method for stability solutions of shells and plates by finite difference method

18 p3341 A70-36580

Elastic systems impact buckling approximate solution by finite difference method

18 p3342 A70-36591

Thermoelasticity boundary value problems by finite difference method, determining thermal, displacement and stress fields in continuous medium

18 p3342 A70-36671

Finite difference methods for collisionless plasma models, taking into account Eulerian form of Vlasov equation in phase space

18 p3296 A70-36792

Finite difference time integration method for computing seismic ray intensities

19 p3412 A70-37837

Numerical integration of finite difference analogs of nonlinear partial differential equations, investigating data smoothing, filtering and boundary effects on computational instability

19 p3459 A70-38417

Book on structural analysis by finite difference calculus covering elastic and elastoplastic states, vibration and buckling of beams, gridworks, plates and shells

19 p3548 A70-38599

Time harmonic waveguide scattering involving metallic obstacles, obtaining numerical solution by finite difference Green function method

20 p3586 A70-39469

Optimal control problems with moving ends in presence of phase constraints, deriving difference approximation stability condition

20 p3601 A70-39730

Steady sub and supersonic flow calculations behind receding shock wave, using finite difference scheme

20 p3611 A70-39803

Parametric boundary layer theory numerical solution in two parameter approximation, solving partial differential equation by finite difference method

20 p3611 A70-39807

Transonic flow past bodies of revolution, using finite difference scheme

21 p3743 A70-40611

Finite difference numerical integration method for melting and freezing problems extended to free convection in liquid and unequal densities for phases

21 p3953 A70-42093

Coanda effect in bistable fluid amplifier, using finite difference method for computer programmed solution of flow equations

[ASME PAPER 70-FLCS-12]

22 p4008 A70-42415

Finite difference method for initial value problems of fokker-Planck equations

22 p4080 A70-42743

Finite difference method for stress wave propagation and multiple reflection in elastic bar with discontinuities

22 p4115 A70-42744

Plane transonic flow around airfoils, using hodograph based methods for shock free flow and finite difference methods for flow with shock waves

[ICAS PAPER 70-12]

23 p4132 A70-44123

Steady irrotational gas flow characteristics calculation from finite difference scheme for three dimensional method of characteristics, considering supersonic nozzle flow

23 p4133 A70-44308

Rectangular and triangular grids with variably sized mesh elements for finite difference analysis of shell structures

23 p4272 A70-44709

Arbitrary shells large deflection transient response, using finite difference computer program

23 p4272 A70-44710

Shell analysis based on discretization into one, two and three dimensional configurations, comparing

finite difference, numerical integration and finite element methods

23 p4272 A70-44715

Nonlinear shell analysis by finite difference energy method, using BOSOR3 and STAGS computer programs

23 p4273 A70-44723

Microwave transmission systems, determining electric potential functions in inhomogeneous dielectrics by Earnshaw theorem and finite difference computation

24 p4318 A70-45217

FINITE ELEMENT METHOD

Finite element solution of incompressible lubrication problem by minimum principle for transient incompressible Reynolds equation with boundary conditions

[ASME PAPER 69-LUB-A]

01 p0100 A70-10378

Direct and incremental variational formulations for steady compressible lubrication based on finite element method, noting limitations of numerical techniques

[ASME PAPER 69-LUB-12]

01 p0102 A70-10393

Steady state heat conduction problems solved by finite element method, with examples involving internal heat generation and various boundary conditions

01 p0215 A70-10558

Finite element method for thin shells using specialized form of Reissner variational principle for stresses and displacements

01 p0208 A70-11184

Finite element method for postbuckling analysis of thin elastic plates, using iterative method to obtain equilibrium configurations

03 p0583 A70-12917

Finite element technique extended for plastic buckling of flat plates, using Stowell theory

[RM-460]

03 p0584 A70-12923

Triangular conforming plate bending element applied to static and dynamic problems, investigating convergence rates of finite element approximations

03 p0584 A70-12924

Frozen stress techniques for photoelastic analysis of orthotropic plate on nonlinear foundation, providing results to compare with future finite element analysis

03 p0480 A70-12952

Homogeneous waveguide solutions by finite element method using matrix operator and function minimization to assure rapid convergence to eigenvalue

03 p0457 A70-13936

Transient heat conduction solution by finite element methods application to nonlinear boundary condition problems

[ASME PAPER 69-WA/HT-36]

04 p0781 A70-14804

Heat conduction equation solutions, comparing finite element and finite difference methods

[ASME PAPER 69-WA/HT-35]

04 p0781 A70-14805

Finite element method applied to heat conduction in solids with temperature dependent thermal conductivity, using nonlinear constitutive equation for heat flux

[ASME PAPER 69-WA/HT-34]

04 p0782 A70-14806

Finite element method applied to finite dimensional state variable formulation of transient heat conduction with surface diffusion of thin circular rotating disk

[ASME PAPER 69-DE-B]

04 p0785 A70-14874

Saint Venant torsion problem using finite element method, establishing direct matrix relation between forces and displacements

04 p0778 A70-15527

NASTRAN digital computer program for static and dynamic structural analysis using finite element method

[SAE PAPER 690612]

05 p0816 A70-15851

Finite element discretization and linear programming methods for shakedown theory in perfect elastoplasticity with associated and nonassociated flow laws

05 p0925 A70-15873

Continuum, harmonic and finite element perturbation studies of elastica to yield postbuckling path derivatives from nonlinear energy formulation

05 p0927 A70-16011

Two and three dimensional flow using TRIC and TRIM-like triangular finite elements

05 p0832 A70-16115

Finite element method for large displacement elastic-plastic analysis of plates and shells, using geometric stiffness matrices and stress-strain relationships

05 p0943 A70-16809

Finite element method analysis of axisymmetrically loaded thin shells of revolution, considering nonlinearity due to material properties and shell geometry changes

05 p0944 A70-16812

Finite element analysis of elastic thin shells, approximating shell surface by network of triangular plate elements

05 p0944 A70-16813

Finite element method applied to potential distribution and stress analysis in earth sciences, determining

- elastic response of rock layer using structural matrix analysis 06 p1055 A70-17606
- Finite elements of time dependent phenomena using Hamilton variational principle for time integration 06 p1165 A70-17645
- Frontal solution program for symmetric positive definite equations met in finite element applications 06 p1014 A70-17936
- Heat conduction transient field problems in two and three dimensional isoparametric finite element solutions using Galerkin method 06 p1178 A70-17938
- Displacement hybrid finite element models for analyzing shells with distributed loads 06 p1168 A70-17939
- Eigenvalue solutions convergence rates using two finite plate multidegrees of freedom bending elements 06 p1169 A70-17941
- Hybrid finite element analysis for combination of axisymmetric shell and linear displacement triangular ring elements [AIAA PAPER 70-137] 06 p1169 A70-18052
- Triangular plate bending elements with enforced compatibility, using cubic interpolation polynomial to describe element displacement [AIAA PAPER 70-136] 06 p1171 A70-18169
- Structural element for discrete element idealization missile and liquid propellant as one composite structure [AIAA PAPER 70-123] 06 p1042 A70-18182
- Finite element method using cubic polynomials over triangle as trial functions for solving second order boundary value problems in linear theory of elasticity 07 p1324 A70-19075
- Finite element method applied to two dimensional variational first order problems in plane elasticity of triangular or rectangular elements 07 p1409 A70-19562
- Three dimensional finite element method for quasi-homogeneous laminate moduli, discussing interlaminar and in-plane shear properties 07 p1321 A70-19966
- Automatic system of kinematic analysis /ASKA/, based on matrix displacement finite element method, applied to structural strains calculations 07 p1417 A70-20362
- Finite element models for nonlinear problems analysis in coupled thermoelasticity dynamical theory, deriving heat conduction equations from energy balance considerations 07 p1417 A70-20363
- Finite bending elements for static deflections of angular and circular plates loaded by concentrated forces, calculating free vibrations 08 p1588 A70-21243
- Rectangular plate girder webs buckling under partial edge loadings, using finite element method for flange-web interaction 08 p1589 A70-21247
- Transient heat conduction and stationary temperature distribution calculation in curvilinear coordinates using finite element method 08 p1590 A70-21362
- Cylindrical shell vibration modal characteristics finite element solutions accuracy compared with exact solutions 08 p1596 A70-21979
- Elastic solution and finite element method applied to heat conduction and thermal stress in temperature field determination 09 p1774 A70-22587
- Plate bending triangular finite element for shell structure analysis, considering displacement functions, stiffness matrix and load vector 10 p1957 A70-24482
- Finite element matrix structural analysis by direct stiffness method and use of computers, considering thin wall box beams [SAE PAPER 700218] 11 p2134 A70-25890
- Finite element method using shallow shell stiffness matrix extended to cylindrical shell solution 11 p2138 A70-26159
- Discrete models for boundary value problems analysis in first strain-gradient elasticity theory, using extended finite element method 11 p2142 A70-26637
- Finite element solution procedures for inextensible beams elastica problem, using galerkin method for element stiffness matrices 11 p2143 A70-26640
- Finite element bending stress analysis of thin rectangular and skew plates, discussing computational procedure generating stiffness matrices 11 p2143 A70-26641
- Conforming plate bending solution with third degree polynomial deflection functions in triangular finite elements, using Lagrange multipliers as stress parameters 11 p2143 A70-26642
- Finite element method solutions for plate bending, improving convergence based on error analysis 11 p2144 A70-26676
- Asymmetric stiffened shell structure analysis by finite element method, introducing constant transverse shear model concept 11 p2144 A70-26677
- Automatic input data generation for finite element method using algorithm based on complex geometrical configurations topological classification in terms of natural coordinates [JPL-TR-32-1486] 11 p2144 A70-26678
- Two and three dimensional flow analysis using various versions of finite element techniques 11 p2042 A70-26680
- Two and three dimensional potential flow analysis using finite element technique based on method of singularities 11 p2042 A70-26681
- Finite element computer code /AXICRP/ for creep analysis of plane stress, plane strain and axisymmetric bodies of revolution 11 p2015 A70-26682
- Finite element methods applications to linear fracture mechanics and crack propagation theory, computing stress intensity 11 p2144 A70-26685
- Stress analysis of plane, shell and three dimensional structures using finite element method 12 p2315 A70-26886
- Finite element method application, origin, development and relation to other mathematical methods, comparing with finite difference discretization processes 12 p2315 A70-26965
- Two dimensional structures large strain elastoplastic analysis by finite element method, using variational principles to derive equilibrium equations 12 p2320 A70-27148
- Elastic-plastic plane stress analysis of two dimensional structures based on Tresca yield criterion, using finite element technique 12 p2326 A70-27795
- Circular arch finite element solutions compared for convergence rates 12 p2327 A70-27838
- Finite element method applications to finite axisymmetric deformations of incompressible elastic solids of revolution 13 p2510 A70-28734
- Elastoplastic thermal stress analysis using finite element matrix method exemplified by cylindrical bar induction quenching 13 p2513 A70-28992
- Minimum weight design for complex structures subject to frequency constraint using finite element method and computer program 13 p2517 A70-29965
- Finite element methods application in civil engineering - Conference, Vanderbilt University, November 1969 14 p2658 A70-31126
- Stiffness matrices of three dimensional finite elements, considering tetrahedron, hexahedron and nodal configurations 14 p2659 A70-31127
- Finite elements for three dimensional compressible and incompressible solid continua based on minimum potential energy and variational principles 14 p2659 A70-31128
- Thin shells stiffness matrix and shear by finite curved triangular elements based on discrete Kirchhoff hypothesis 14 p2659 A70-31129
- Curved finite element for shells of revolution based on minimum potential energy principle, discussing stiffness and equilibrium of domed and branched shells 14 p2659 A70-31130
- Axisymmetric postyielded tongue and groove cylindrical joint stress analysis using finite element method 14 p2659 A70-31131
- Finite element method applications to structural analysis problems involving geometric and material nonlinearities 14 p2660 A70-31134
- Stress-strain relationships model for nonlinear restrained cylinders, using compression tests and finite element method 14 p2660 A70-31135
- Finite element displacement method for elastoplastic bilinear strain hardening orthotropic plates and shells, comparing initial and tangent stiffness 14 p2660 A70-31136
- Plane frames with and without shear walls, determining dynamic response under vibration by finite element method 14 p2660 A70-31137
- Arbitrary shaped shell structures analysis by finite element method, using curved shell elements approach 16 p2988 A70-33289
- Closed form difference equations for finite element models in structural mechanics, noting plate and grid applications 16 p2990 A70-33672
- Structural incompressible liquid element for discrete linear idealization of missile and propellant vibration analysis 16 p2991 A70-33852
- Shells of revolution nonlinear finite element analysis by matrix displacement method, including higher order strain energy terms 16 p2991 A70-33885
- Finite element formulation for large strain and displacement problems with emphasis on elastic-plastic behavior in metals 17 p3184 A70-34905
- Shallow shell finite element of triangular shape, noting application to static problems 17 p3184 A70-34908
- Curved finite elements for shell calculations, obtaining potential energy of internal forces 18 p3337 A70-36369
- Inverse variational principles of thin plate, dividing into subregions /finite elements/ for optimal thickness distribution, sectional forces and displacement values 18 p3339 A70-36481
- Finite element procedure convergence for fourth order boundary value problems solution 18 p3283 A70-36493
- Structure of flexural members, analyzing torsional and lateral stability by finite element method and matrix formulation 18 p3339 A70-36494
- Axisymmetric structure with elastic contact, analyzing stresses by finite element method with differential displacements 18 p3339 A70-36496
- Direct and incremental variational formulations for steady compressible lubrication based on finite element method, noting limitations of numerical techniques [ASME PAPER 69-LUB-12] 19 p3436 A70-37616
- Stress and displacement within internally pressurized composite cylinders having continuous fiber reinforcement in circumferential direction, using finite element method 19 p3538 A70-37797
- Discrete finite element models for nonlinear viscoelastic continua 19 p3458 A70-38358
- Finite element method with first order displacement functions to compute crack tip stress intensity factor in various shapes under different loading conditions 19 p3548 A70-38623
- Compressible and incompressible Stokesian fluids motion described by finite element analog of Navier-Stokes equation 20 p3607 A70-38999
- Finite element stiffness matrix technique for composite structures, discussing airplane component design program 20 p3730 A70-40040
- Plate structural analysis by finite element method, obtaining geometric continuity by additional displacements and forces at corner nodes 21 p3932 A70-40553
- Boundary value problems for elliptic equations with discontinuous coefficients, using finite element method 21 p3845 A70-40734
- Swing tail cargo aircraft fuselage section stress analysis by finite element method, discussing displacement models, deformation modes and economics 21 p3935 A70-41260
- Finite element analysis of critical stress distribution in canopy of deployed twin keel parawing, predicting failure stress levels [AIAA PAPER 70-1196] 21 p3753 A70-41820
- Spacecraft parachute stress analysis, using finite elements with nonlinear elastic properties to obtain shape and load distribution [AIAA PAPER 70-1195] 21 p3753 A70-41821
- Stress intensity factors for complicated crack configurations in finite plates, using finite element method with cracked elements 21 p3940 A70-42034
- Curved finite element for thin elastic shells satisfying rigid body motions and energy convergence 22 p4116 A70-43202
- Bounds to direct influence coefficient derived by hybrid stress finite element method 22 p4116 A70-43203
- Systematic approach to construction of finite elements, discussing choice of generalized coordinates useful in problems involving singularities 22 p4116 A70-43208
- Finite element method for bending-extensional coupling in angle-ply laminates deformation behavior 22 p4061 A70-43685
- Cantilever plate random vibration response, calculating eigenvectors and natural frequencies by finite element method 23 p4270 A70-44591
- Digital computer codes for production finite element structural analysis, discussing input, output and engineering details 23 p4270 A70-44701

Gradient minimization and higher order discrete elements application to shell buckling and vibration eigenproblems, using 48 degree of freedom Bogner cylindrical panel element

23 p4271 A70-44705

Thin shell structural analysis by doubly curved arbitrary quadrilateral finite element, using Kirchhoff theory and cubic polynomial for membrane displacements

23 p4272 A70-44711

Mixed formulations for finite element shell analysis based on flat and curved elements

23 p4272 A70-44713

Shell analysis based on discretization into one, two and three dimensional configurations, comparing finite difference, numerical integration and finite element methods

23 p4272 A70-44715

Finite element structural analysis /FESTRAN/ computer program predicting static structural response of plate and shell structures

23 p4272 A70-44717

Thin shells static and dynamic finite element analysis

23 p4273 A70-44721

Complex structures component modal dynamic analysis technique, describing investigations with combination of finite element and composite modes computer program

23 p4273 A70-44722

Finite beam element in bending, deriving shear deflection terms in stiffness matrix based on stress assumption

23 p4274 A70-44909

Large element method for stiffness matrix order reduction in two-dimensional continua problems

23 p4275 A70-44940

Linear algebraic system stability and monotony, investigating plane structures by finite element method

23 p4213 A70-44996

Curved element approximation of orthotropic axisymmetric thin shells under axial loads

24 p4419 A70-45152

Gradient iterative solution of large algebraic systems arising from finite element discretization, using computer methods

24 p4419 A70-45153

Kinematically unsteady aerodynamic coefficients consistent with stiffness and inertia properties of lifting surface in supersonic flow by finite element method

24 p4287 A70-45154

German monograph on deformations and tensile stresses calculation in axisymmetric bodies via finite element method involving matrix displacement method

24 p4420 A70-45225

Numerical integration of equations of motion from finite element analysis in structural mechanics, using computer program

24 p4420 A70-45278

Discrete element idealization of missile and liquid propellant for vibration analysis, deriving sloshing theory

24 p4326 A70-45885

FINITE-STATE MACHINES

U TURING MACHINES

FINLAND

Report to COSPAR on space research covering satellite tracking telemetry, Apt, meteorology, cosmic rays, solar activity and international cooperative programs, etc

15 p2829 A70-31709

FINNED BODIES

Dynamic instability of finned missiles occurring as angle of attack undamping and caused by differential lift from windward and leeward fins

[AIAA PAPER 70-206] 06 p1158 A70-18178

Finned tube radiators with constant longitudinal specific heat flow, determining thermal efficiency and optimal thermal and structural parameters

06 p1184 A70-18556

Natural frequencies and modes of tapered swept back rudder fin of aircraft using vibration analysis

07 p1417 A70-20417

Circumferential wall temperature gradients in spacecraft radiator tubes as function of tube wall fins

09 p1789 A70-23261

Flutter suppression in elastic finned beams in supersonic flow controlled automatically by rudder deflection according to flexural strain

09 p1785 A70-23615

Nonlinear rolling motion of four-finned missile, investigating function of angle of attack and cubic damping

13 p2503 A70-28531

Freely spinning finned stabilizer static wind tunnel tests on free fall research store, determining Magnus effect, body flow interference and static stability

[AIAA PAPER 70-559] 13 p2340 A70-29024

Finned configurations with nonlinear aerodynamic properties, obtaining solutions for angular motion at and near resonance

[AIAA PAPER 70-535] 13 p2506 A70-29026

Counter current heat exchanger with spiral finned tubing and solid core

14 p2617 A70-31019

Cruciform-finned missiles dynamic stability investigation by nonlinear differential equations of motion, considering roll lock-in, resonance instability and catastrophic yaw

[AIAA PAPER 70-969] 20 p3715 A70-39560

FINS

NT COOLING FINS

Radiative heat transfer from longitudinal rectangular conducting fins on plane wall involving mutual irradiation, using iterative method

[ASME PAPER 69-WA/HT-22] 04 p0782 A70-14812

Flow phenomena about beating plates, fins and wings, discussing biological and engineering applications

05 p0790 A70-16155

Spread fin design as antisuperstar and antispin auxiliary device, discussing wind tunnel and simulation tests

06 p0967 A70-17258

Boiling heat transfer enhancement inside tubes using integral fins, discussing water film retention on walls

08 p1599 A70-21825

Thermal design of counter current cryogenic heat exchangers employing spiral finned tubing

14 p2617 A70-31018

Hovercraft wind directional stability and control by cam operated fin-tab assembly

19 p3357 A70-38942

Fin slots and tabs effect on dynamic stability characteristics of low drag bomb, discussing free rolling and pitching tests

21 p3747 A70-41880

FIRE CONTROL

Integrated display for crowded tactical aircraft cockpits, presenting multisensor information for weapons and fire control systems

08 p1500 A70-21760

Airborne computer design for short range attack missile /SRAM/ to perform aircraft navigation and missile fire control

12 p2192 A70-27800

Attack helicopter fire control system with day and night detection, recognition and kill capabilities, discussing system components, operation and reliability

17 p3043 A70-34732

OV-10A forward air control and light attack aircraft design, specifications and performance

[SAE PAPER 700837] 24 p4290 A70-45883

FIRE CONTROL CIRCUITS

Fighter aircraft firing accuracy improved by high pass filter to automatically compensate sideslip induced by rudder through follow up slideslipping by aileron

11 p1979 A70-25820

FIRE EXTINGUISHERS

Materials selection and Apollo command module atmosphere design considerations, discussing fire extinguisher system, equipment design changes, etc

03 p0437 A70-14058

Water or bromotrifluoromethane content required in propellant Aerozine-50 /A-50/ spill to inert against ignition in air, considering fire extinguishment

04 p0732 A70-15408

Crash fire protection at Los Angeles International Airport, discussing protein foam and light water usage

06 p1028 A70-17707

Fire extinguisher compounds /bromochloromethane and bromotrifluoromethane/ pyrolysis products inhalation toxicities for rats

07 p1219 A70-19223

FIRE FIGHTING

Fire safety in hyperbaric systems isolated from environment by gas tight barrier

[ASME PAPER 69-WA/SAF-2] 04 p0784 A70-14836

Fire performance of spray applied rigid urethane foam applied as storage vessel insulation, noting continued functioning until destruction

09 p1710 A70-23345

Aircraft crash fire fighting equipment and tactics for future airport needs

[SAE PAPER 700262] 12 p2160 A70-27433

FIRE POINT

Atmosphere classification according to fire hazard based on heat capacity per mole of oxygen, noting exponential growth rate

03 p0607 A70-14054

FIRE PREVENTION

Aircraft/aerospace fluid systems flexible hose and rigid tube assemblies fire resistance and test requirements

01 p0011 A70-11459

Fire prevention problems in closed oxygen-rich environments, discussing ignition temperature and flame propagation rate

03 p0607 A70-13961

Atmosphere classification according to fire hazard based on heat capacity per mole of oxygen, noting exponential growth rate

03 p0607 A70-14054

Nonflammable material development program for Apollo spacecraft, noting requirements imposed by high oxygen environments, toxic offgassing and temperature range

03 p0436 A70-14055

Fire and explosion suppression technology for aircraft and hypobaric and hyperbaric oxygen-rich atmospheres, discussing time available for suppression action

03 p0437 A70-14056

Cabin interior materials studied and tested for greater fire resistance, lower smoke and toxic gas by-products and flash fire possibility lessening

03 p0437 A70-14057

Fire safety in hyperbaric systems isolated from environment by gas tight barrier

[ASME PAPER 69-WA/SAF-2] 04 p0784 A70-14836

Water or bromotrifluoromethane content required in propellant Aerozine-50 /A-50/ spill to inert against ignition in air, considering fire extinguishment

04 p0732 A70-15408

Flammability control requirements and related hazards in avionics systems materials and components, using systems approach

[SAE PAPER 690712] 05 p0956 A70-15854

Tetrabromophthalic anhydride /TBPA/ in polyester and epoxy resins, studying fire retardant capabilities by comparative combustion tests

05 p0811 A70-16584

N-substituted tetrabromophthalimides prepared as fire retardant additives to PVC, polyester and epoxy resins

05 p0811 A70-16585

Fire resistant protective flight clothing program for USN aircrewmembers, presenting accident case histories

07 p1218 A70-19013

Electrostatic ignition discharge prevention on fiberglass reinforced depot tanks, noting ground connection safeguard

07 p1295 A70-19763

Preventive measures against fire and blast hazards in high oxygen concentration chambers

08 p1599 A70-21795

Rigid fire-retardant polyurethane foams obtained from phosphonopropionate polyols, discussing physical properties and shelf stability tests

10 p1907 A70-24063

Flame-resistant trichloromethyl-containing polyester-styrene system, describing curing characteristics at room and higher temperatures

10 p1907 A70-24066

Flammability resistance and smoke emission characteristics of aircraft interior fire retardant materials under ambient and increased temperature and zero ventilation conditions

10 p1908 A70-24905

Gelled and emulsified fuels for jet transport aircraft, testing rheological and physical properties regarding fire hazard reduction in crashes

[SAE PAPER 700251] 12 p2160 A70-27430

Hydraulic seals for fire resistant fluids in hydraulic equipment, describing computerized designs

13 p2416 A70-28610

Centrifugal pumps of various metals for liquid oxygen, describing fire and explosion tests

14 p2617 A70-31020

Aircraft in-flight and post crash fire protection developments, considering controlled flammability fuel systems and fire fighting methods

[ASME PAPER 70-GT-109] 18 p3215 A70-36847

Fire and overheat detection system design for turbine powered vehicles

[ASME PAPER 70-GT-125] 18 p3260 A70-36891

Fire and fire test scope and meaning limitations for consumer awareness

23 p4208 A70-43871

Catalytic combustion fuel tank inerting techniques for fire protection in military and civilian aircraft

23 p4141 A70-44485

FIREBALLS

Interacting meson systems effective masses with/without secondary proton measured, detecting heavy boson resonances and fireballs, considering proton nuclear interactions

03 p0472 A70-13031

Meteorite fireball track projected on earth surface determined from nearly overhead observations

07 p1387 A70-19629

Fireball detection and discovery, investigating angular distribution of secondary particles using Van Hove and Amati theory

09 p1747 A70-23729

Bright sporadic fireballs and faint photographic meteors orbits, discussing clustering in diagram of geocentric velocity vs inclination

13 p2490 A70-29040

Fireball of 25 April 1969 crossing England, Wales, Irish Sea and northern Ireland, recovering meteorites in northern Ireland

16 p2973 A70-33117

Fireballs atmospheric debris collection by high altitude filtration, describing analysis results

18 p3311 A70-35971

Fireball end point height as indication of meteoroid existence likelihood 24 p4411 A70-45787

FIREPROOFING
 Fireproof fabrics tested for flame retarding and protection capabilities, discussing applications to aircraft interiors, escape parachutes, flight coveralls and protective clothing 07 p1219 A70-19017
 Fibrous, cellulosic, elastomeric and plastic materials with improved flame resistant properties for space applications 23 p4152 A70-44461
 Manned spacecraft nonmetallic construction materials selection criteria, testing and configuration control, considering flammability hazard 23 p4152 A70-44462
 Aircraft passengers and crew fire protection in crashes via insulating air-carrying foam ejected into compartment from fuselage 23 p4140 A70-44465
 Nonflammable fibrous textile materials for injury and personnel loss prevention in fires by aircraft accidents 23 p4153 A70-44481
 Fireproof nonmetallic materials for spacecraft and aircraft, discussing functional utility, durability and aesthetic requirements relative to environmental conditions 23 p4210 A70-44610

FIRES
 Vertical plume velocity and temperature measurements by hot wire probe on turbulent free convection zones over model fires 07 p1282 A70-19582
 USAF aviation accidents diagnostic patterns of injury and death, noting increase in fire and/or associated complications 17 p3039 A70-35574
 Closed compartment fire mathematical model to analyze combustion parameter effects, atmosphere pressure and temperature during fire 17 p3198 A70-35646

FIREWORKS
 U PYROTECHNICS
FIRING [IGNITING]
 NT RETROFIRING
 NT ROCKET FIRING
 NT STATIC FIRING
 NT TEST FIRING
 Nomogram solution of electroexplosive device firing time equation permitting firing data prediction from blueprint data 03 p0548 A70-14117
 Computerized approximations for quantitative predictions of EED firing characteristics based on header geometry and electrical leads 03 p0548 A70-14118
 Engine firing rate measurement from acoustic waveform autocorrelation analysis 12 p2290 A70-27161

FIRING TIME
 U BURNING TIME

FIRST AID
 Helicopters for injured or sick persons transportation as compared with ambulance use based on West Germany experience 03 p0436 A70-13822
 Medical kit utility for colds, sore throats, scrapes, cuts and bruises 07 p1219 A70-19021

FISH
 U FISHES

FISHES
 Remote sensors application to direct and indirect fish detection in fishery research, using aerial and Gemini photography 07 p1262 A70-18957
 Pesinogens A, C and D from stomach mucosae of smooth dogfish separated by chromatography on DEAE cellulose 11 p1987 A70-26007
 Biological tests of fish and invertebrates exposed to Apollo 11 lunar surface material, noting absence of pathological effects 19 p3513 A70-37409

FISHTAILING
 U YAW

FISSILE MATERIALS
 U FISSIONABLE MATERIALS

FISSION
 Erasure fission tracks in soda-lime glass, tektite, biotite and apatite by shock loading, determining dynamic pressure and associated temperature effects 19 p3414 A70-38035

FISSION ELECTRIC CELLS
 NT SNAP 8

FISSION PRODUCTS
 Atmospheric ionization by beta particles due to fission product decay, showing diagram for magnetic shell parameters and postfission periods 04 p0743 A70-15739

Fission gases trapped in fuel particles, cladding and matrix of irradiated refractory metal-uranium oxide cermet determined by gamma counting 07 p1332 A70-19851
 Angra dos Reis stone meteorite containing cosmogenic and fissionogenic xenon 10 p1935 A70-23850
 Atmospheric ionization by beta particles due to fission product decay, showing diagram for magnetic shell parameters and postfission periods 14 p2632 A70-30823
 Mitotic activity and aberrant mitoses frequency in mice corneal and duodenal epithelium cells under fast fission neutron irradiation 17 p3026 A70-35319
 Cosmic ray track sources in meteoritic minerals, considering heavy primaries, secondary spallation and fission products 19 p3508 A70-38142

FISSIONABLE MATERIALS
 Electromotive force appearance in fissionable material semiconductor during thermal neutrons irradiation 13 p2469 A70-28879

FITNESS
 NT FLIGHT FITNESS
 NT PHYSICAL FITNESS

FITTINGS
 Attachment loads and beam bending moments design curves for linear and right angle fittings on honeycomb inserts to determine internal loading 02 p0386 A70-11949
 Protruding, stepped and conical end fittings for confined detonating fuse, discussing assembly procedures effect on characteristics based on statistical scanning test 03 p0547 A70-14115
 Tubing, fitting and flexible line designs and testing for production aircraft hydraulic distribution systems [SAE PAPER 700789] 24 p4294 A70-45856

FITZGERALD-LORENTZ CONTRACTION
 U LORENTZ CONTRACTION

FIXED POINTS [MATHEMATICS]
 Table lookup/interpolation function generation for fixed point digital computations, illustrating sine-cosine generator 01 p0047 A70-10459
 Geometrical interpretation of motion of body about fixed point in Hess case based on Kharlamov kinematic equations, using special coordinates system 01 p0144 A70-11428
 Lagrange solution to differential equations of motion of body with fixed point, deriving directrices of mobile and fixed hodograph 01 p0144 A70-11429
 Mobile hodograph in problem of gyrostat motion about fixed point 01 p0094 A70-11430
 Kharlamova motion equations solution for solid body with fixed point in potential force field, assuming fixed center of gravity 01 p0145 A70-11432
 Kharlamov motion equations solution for solid body with fixed point subjected to zero-potential forces 01 p0145 A70-11433
 Euler-Poisson equations application to motion of heavy solid body about fixed point to determine kinetic momentum vector relative to fixed reference system 01 p0145 A70-11434
 Kharlamov conditions for existence of linear and quadratic invariant relationships between equations of motion of body about fixed point 01 p0145 A70-11435
 Canonic equations of motion of heavy solid body with fixed point 01 p0145 A70-11436
 Motion of body with fixed point reduced to single second-order differential equation, analyzing special cases of gyrostatic motion 01 p0145 A70-11437
 Bifurcation and stability analysis of point mappings with polynomial succession function, using parametric diagrams 13 p2383 A70-29751

FIXED WINGS
 Helicopter engineering covering structure, rotor systems, aerodynamics, vibration and applicability to fixed wing aircraft 02 p0225 A70-12309
 Blended wing-body design concept for F-15 air superiority fighter, providing fixed wing planform for maneuverability at transonic speed 04 p0622 A70-14395
 Pitching moment coefficient changes due to ground effect in fixed wing aircraft flight test method, considering constant angle of attack approach 04 p0619 A70-15394
 V/STOL and fixed wing tactical transport aircraft survivability while supporting forward area logistics bases, noting V/STOL advantage 05 p0792 A70-15857
 V/STOL fixed wing aircraft design parameters evaluation by digital variable stability system [SAE PAPER 690696] 05 p0792 A70-15859

DO-231 fixed wing V/STOL airliner project based on DO-31 development, construction and flight tests, considering design problems, controls, safety, performance targets, etc 05 p0793 A70-15901
 High speed helicopter with fixed wings and longitudinal axis tail rotor 05 p0794 A70-16349
 Stability derivatives from flight data of fixed-wing aircraft determined by modified Newton-Raphson method 07 p1194 A70-19272
 Fixed wing aircraft and associated subsystems simulation by digital computer, having full FORTRAN capability [AIAA PAPER 70-572] 13 p2385 A70-29897
 Fixed and variable sweep wing structure computerized design optimization [ASME PAPER 70-DE-41] 16 p2869 A70-33506
 Fixed wing and VTOL aircraft all-weather landing guidance and control philosophy 19 p3466 A70-38365
 AERCAB /Aircrew Escape/Rescue Capability/ flying ejection seat, considering rotary wings, fixed wings and parawings [AIAA PAPER 70-1213] 21 p3751 A70-41806

FIXED-WING AIRCRAFT
 U AIRCRAFT CONFIGURATIONS
 U FIXED WINGS

FIXTURES
 Test fixture for determining mechanical properties of metals and steels at moderate strain rates, detailing design and instrumentation 03 p0462 A70-12883

FIZEAU EFFECT
 Holographic two beam real-time Fizeau interferometer for recording and reconstructing reflected light waves in silvered flat surfaces measurement 01 p0090 A70-10905

FLAKES
 Viscosity anisotropy in fluid matrix suspensions of parallel rigid flakes as function of flake content and width-to-thickness ratio 03 p0515 A70-13122

FLAME FRONTS
 U FLAME PROPAGATION

FLAME HOLDERS
 Free recirculation areas in wake of flame holders used for flame stabilization at bluff bodies in supersonic flow 06 p0965 A70-17244
 Aerodynamic holder stabilized smoke flames to avoid intermittent flaming and thick puffs for incinerator air pollution reduction 21 p3942 A70-40887
 Turbofan engines afterburner flame stabilization at low inlet temperature, noting flame holder geometry role 22 p4088 A70-42336

FLAME INTERACTION
 U CHEMICAL REACTIONS
 U FLAME PROPAGATION

FLAME IONIZATION
 Flame positive ion concentration measurements with Langmuir probes with mean free path smaller than probe diameter 02 p0397 A70-12019
 Ionization studies in collision dominated high pressure flame plasma using electrostatic probes 03 p0534 A70-14212
 OH, NH and amine radicals concentrations in flame gases from flat ammonia-oxygen-nitrogen flames measured as function of distance from burner surface 09 p1788 A70-22343
 Flame ionization, extra-equilibrium excitation and electronic temperature resulting from electron collisions with gas molecules 14 p2666 A70-31096
 Electron temperatures and electron and negative ion concentrations in low pressure hydrocarbon flames 14 p2666 A70-31098
 Book on electrical aspects of combustion processes covering formation, behavior in fields, diagnostics, uses of ions, electrons and charged particles, flame ionization, etc 16 p2996 A70-33030
 Potassium salts thermal and chemical ionization in flames of hydrogen-oxygen-helium and hydrogen-air mixtures in constant volume vessels 18 p3345 A70-36243
 Hydrogen flame ionization detector /HYFID/ for life-derived organic matter in Martian/Lunar soil 19 p3426 A70-37896
 Ion concentrations in premixed propane-air two dimensional laminar nozzle burner flames with seeding, discussing dependence on temperature and equivalence ratio 21 p3772 A70-40880
 Book on stationary flame structure, radiation and temperature covering flow visualization, burning velocity, propagation, ionization, etc 22 p4121 A70-42325

FLAME PROBES

- Powder and solid propellant combustion, discussing heterogeneous and homogeneous systems, characteristics of foam, fizz and flame zones, etc
03 p0544 A70-13860
- Vertical plume velocity and temperature measurements by hot wire probe on turbulent free convection zones over model fires
07 p1282 A70-19582
- Optically dense high temperature flame pyrometric diagnostics based on modified Kirchhoff formula
10 p1967 A70-24251
- Oscillator strengths relative values determined from flame atom absorption line sensitivity measurements
10 p1828 A70-24259
- FLAME PROPAGATION**
- Flame propagation rate calculation methods, considering mass burning rate values
01 p0217 A70-11008
- Exothermic reaction front propagation in condensed phase, analyzing Novozhilov system of equations
01 p0217 A70-11009
- Flame propagation in gases with two chemical phases, studying phase interaction effects on burning rate
01 p0217 A70-11010
- Tetrafluorodibromomethane combustion inhibitor effects on aircraft hydrocarbon fuels flame propagation rate and explosion pressure
01 p0160 A70-11011
- Electric field effects on flame structure and propagation rate in methane-air mixture
01 p0217 A70-11013
- Pressure oscillograms and schlieren photographs of shock wave amplification during interaction of cellular flame of gas mixtures in cylindrical combustion chamber
01 p0217 A70-11014
- Liquid diethylcyclohexane /DECH/ sprays detonation propagation in gaseous oxygen, studying drop size effect on steady state development
02 p0351 A70-12003
- Aluminum additives effects on stoichiometric ammonium perchlorate/polyformaldehyde mixtures deflagration, determining temperature distribution, burning rate dependence on pressure and heat flow due to radiation
02 p0351 A70-12004
- Flame spreading mechanism over surface of igniting condensed phase materials in quiescent gaseous environment with chemically reacting component
02 p0396 A70-12014
- Flame spreading theory for plastic fuels surfaces in nitrogen-oxygen mixtures, considering initial fuel temperature, pressure and mixture composition effects
02 p0396 A70-12015
- Laminar diffusion flame spread against air stream over solid or liquid fuel bed, noting influence of stoichiometric and thermal properties and data inconsistency
02 p0396 A70-12016
- Supersonic diffusion flames produced by subsonic and supersonic free jet injection of hydrogen into high enthalpy airstream
02 p0399 A70-12042
- Internal structure of ideal explosive waves at Chapman-Jouguet point, discussing coupling between flow and chemical reactions
02 p0279 A70-12103
- U-shaped combustion chamber two dimensional model for studying factors influencing flame spread and stabilization and heat transfer in gas turbines
02 p0355 A70-12257
- Flat flames in stationary gas in tubes useful for flame speed measurements without correction procedure
03 p0607 A70-13917
- Burning velocity of methane-air flames inhibited by methyl bromide, using schlieren cone-nozzle burner method involving unburnt gas velocity measurement
03 p0607 A70-13918
- Computerized stepwise construction of Hugoniot curve for detonation waves and Chapman-Jouguet detonation and deflagration points
03 p0607 A70-13920
- Fire prevention problems in closed oxygen-rich environments, discussing ignition temperature and flame propagation rate
03 p0607 A70-13961
- Atmosphere classification according to fire hazard based on heat capacity per mole of oxygen, noting exponential growth rate
03 p0607 A70-14054
- Temperature evolution of detonation products of Na seeded propane-oxygen mixtures, observing periodic variation for helicoidal cases
03 p0608 A70-14356
- Calor-electric voltage calculation for stoichiometric flame burning in air introducing allowance for charged particle densities
04 p0780 A70-14706
- Dynamic response of solid propellant flame to oscillating pressure field using T-tube rocket motor,

- discussing entropy waves produced in oscillatory combustion
[AIAA PAPER 68-499] 04 p0737 A70-15580
- Unbranched chain reaction in hydrogen bromide for studying laminar one dimensional flame propagation, determining temperature dependence, velocity and concentrations at fixed time
06 p1177 A70-17797
- Flame spreading velocity characteristics over solid fuel surfaces, discussing environmental pressure, chemical reactivity, pyrolysis, forced convection, etc
[WSCI PAPER 69-33] 06 p1178 A70-17979
- Hydrogen-oxygen difluoride flame burning velocity, diffusion coefficient and light output
[WSCI PAPER 69-49] 06 p1178 A70-17982
- HF periodic velocity oscillations effect on axisymmetric wake diffusion flames
[AIAA PAPER 70-10] 06 p1182 A70-18179
- Flame propagation rate and combustion zone extension dependence on chamber dimensions for turbulent flow of homogeneous mixtures
08 p1597 A70-21187
- Slot burner laminar flame front stability loss ascribed to increased slot dimensions and angles between velocity vector and flame front
08 p1598 A70-21208
- Partial statistical description of turbulent flame interior and turbulent flame speed determination for effects of turbulence on flame propagation
08 p1485 A70-21607
- Steady flame propagation attainment for chemical reaction initiation in gaseous fuel by heated surface with various wall temperatures
09 p1787 A70-22115
- Flame spread rate across surface of liquid fuels, discussing effects of ignition mode, fuel purity and temperature, fuel container dimensions and material
10 p1929 A70-24090
- Liquid phase convective heat transfer as rate controlling mechanism for flame propagation, analyzing surface tension driven liquid flow induced by temperature profile
10 p1929 A70-24091
- Wall heat transfer effect on expansion following Chapman-Jouguet detonation wave, calculating pressure and gas velocity profiles from friction coefficient
10 p1869 A70-24423
- Velocity and pressure distribution and flame front shape of confined flame in constant section duct
10 p1969 A70-24786
- Gas dynamic processes insufficiency for triggering transition to detonation obtained from laser schlieren records of nonsteady flow field ahead of accelerating turbulent flame
11 p2150 A70-26378
- Flame propagation in slowly combustng fuel-air mixtures using gas chromatography and flame speed
11 p2151 A70-26381
- Perfluoropropene, -cyclobutene and -cyclobutane mixing with atmospheric pressure oxygen to determine burning velocities
11 p2100 A70-26383
- Methane and propane flames in rotating air flow fields generated by cylindrical rotating wire mesh screen, discussing flame lengths and blowoff velocities
14 p2666 A70-31090
- Hydrazine decomposition in low pressure flame, investigating isotopic substitution effect on flame speed
14 p2628 A70-31094
- Gas phase chemicals synthesis via AC diffuse discharge superimposed on propane-air flame seeded with potassium carbonate in electrically augmented flame burner
14 p2546 A70-31097
- Diffusion flame development in homologous turbulent shear flow, investigating flame structure and chemical reaction by statistical theory
[AIAA PAPER 70-722] 16 p2997 A70-33499
- Uniform two dimensional turbulent boundary layer with hydrogen-nitrogen mixture injection and combustion at flame front, obtaining velocity distribution by kinetic energy equation
16 p2894 A70-33880
- Pressure histories of burning modes in combustion driven shock tube using ignition of stoichiometric hydrogen-oxygen mixture with He dilution
17 p3195 A70-34922
- Wave-periodic acceleration feedback during vibrational flame propagation in tubes, testing carbon monoxide-air mixture
17 p3196 A70-35350
- Tetrafluorodibromo-ethane and bromomethyl inhibiting effects on explosion development in constant volume container and flame expansion rates in hydrogen-air mixtures
18 p3345 A70-36241
- Flame propagation in narrow slit and fine hole of solid propellant grain
18 p3300 A70-36698
- Nonsteady combustion analysis, using method of flame front penetration through fine metal layer in solid propellant
18 p3300 A70-36704

- Flame propagation velocity of gasoline-air mixture during two stage combustion process in laminar and turbulent flows, discussing combustion products effect
19 p3550 A70-37253
- Low speed air-propane flame stability, examining holder diameter effects on vibration cutoff wavelength
20 p3738 A70-40281
- Hydrogen-oxygen and hydrogen-nitrous oxide systems combustion, measuring isotopic substitution effect on flame speed by schlieren technique with rotating drum camera
20 p3583 A70-40472
- Electric field control of oscillatory acetylene flame combustion for chemical rocket engines
21 p3942 A70-40885
- Book on stationary flame structure, radiation and temperature covering flow visualization, burning velocity, propagation, ionization, etc
22 p4121 A70-42325
- Real time holographic interferometry for flame propagation research, using high speed camera
[SMPT PREPRINT 9] 22 p4035 A70-43053
- Solid phase energy role in flame spreading over solid fuel bed surface in oxidant-containing environment
23 p4281 A70-44424
- Flame propagation limits and damping mechanism in gases under convection, determining boundary and initial conditions
24 p4428 A70-45492
- FLAME QUENCHING**
- U EXTINGUISHING
U QUENCHING [COOLING]
- FLAME STABILITY**
- Monograph on angular momentum effects on swirling flames stability, considering premixed and unpremixed flames with and without baffle barriers
01 p0214 A70-10309
- Chlorine dioxide-methane mixture flame stabilized in low pressure burner, determining emission spectra, burning velocity, activation energy, etc
02 p0251 A70-12033
- Turbulence detection and velocity fluctuations in jets and flames based on equations of motion and impact probes
02 p0398 A70-12037
- U-shaped combustion chamber two dimensional model for studying factors influencing flame spread and stabilization and heat transfer in gas turbines
02 p0355 A70-12257
- Ammonia/chlorine dioxide and ammonia/chlorine dioxide/methane flames burner stabilization and burst velocities
02 p0400 A70-12670
- Structure of hydrogen-oxygen diffusion flame in equilibrium using iterative solution
02 p0352 A70-12796
- Free recirculation areas in wake of flame holders used for flame stabilization at bluff bodies in supersonic flow
06 p0965 A70-17244
- Laminar flow mixing stability and diffusion flame flow field measurements revealing role of Tollmien-Schlichting waves in enclosed flames vibrations
[WSCI PAPER 69-46] 06 p1179 A70-17985
- Main stream interaction with flame stabilizing jets in combustion chambers and afterburners using gas dynamic models
07 p1419 A70-18754
- Slot burner laminar flame front stability loss ascribed to increased slot dimensions and angles between velocity vector and flame front
08 p1598 A70-21208
- Turbulent flames bluff-body stabilization model, measuring recirculation zone concentrations and temperatures for methane and propane-air mixtures
10 p1967 A70-24092
- Mixture composition and airflow rate dependence of combustion efficiency in turbojet afterburner chamber with air-fuel flame stabilizer
10 p1929 A70-24282
- Ammonia-chlorine dioxide flame stabilization for simulating ammonium perchlorate combustion at high pressures
11 p2099 A70-25994
- Combustion research prospects, considering turbulence and flame stabilization, pollution control, flame self acceleration, subsonic/ supersonic flow combustion and flame dynamics
11 p2150 A70-26376
- Methane-air inverted flames blowoff at thin stabilization plates of twin slit inverted flame burner, determining critical values of Karlovitz flame stretch factor
14 p2666 A70-31092
- Flame ionization, extra-equilibrium excitation and electronic temperature resulting from electron collisions with gas molecules
14 p2666 A70-31096
- Flame stabilization in boundary layer during mixing of cold homogeneous fuel mixture and hot gas based on combustion and turbulent jets theories
20 p3736 A70-39267

Low speed air-propane flame stability, examining holder diameter effects on vibration cutoff wavelength 20 p3738 A70-40281

Aerodynamic holder stabilized smoke flames to avoid intermittent flaming and thick puffs for incinerator air pollution reduction 21 p3942 A70-40887

Gravitational effects on laminar gas jet diffusion flame stability, including zero gravity environment 21 p3949 A70-41316

Turbofan engines afterburner flame stabilization at low inlet temperature, noting flame holder geometry role 22 p4088 A70-42336

Oxygen atom catalytic recombination and flame inhibition mechanism literature survey 23 p4157 A70-44002

FLAME TEMPERATURE

Light scattering from thermally stable magnesium oxide particles in premixed turbulent flames used for measuring mean and fluctuating temperature values 02 p0398 A70-12039

High pressure tests of primary zone flame radiation, flame and tube metal temperatures in aircraft combustion chambers, including oxygen and vitiated inlet air effects 02 p0355 A70-12051

Flame structure of liquid methanol burning spheres, discussing temperature and composition profiles 03 p0544 A70-13924

Electron temperature of hydrogen-oxygen flame plasma obtained by floating probe method compared to spectroscopic method results 03 p0608 A70-14380

LF nonacoustic instability of solid propellant rocket motors, using combustion model allowing flame temperature oscillations with chamber pressure [AIAA PAPER 68-179] 07 p1421 A70-19319

Analog computing spectral photometer for high temperature measurements in gas flames 07 p1285 A70-19896

Turbulent flames bluff-body stabilization model, measuring recirculation zone concentrations and temperatures for methane and propane-air mixtures 10 p1967 A70-24092

Optically dense high temperature flame pyrometric diagnostics based on modified Kirchhoff formula 10 p1967 A70-24251

Graphite IR radiator for radiative capacity and flame temperature measurements investigated for life time dependence on ambient pressure and temperature 10 p1888 A70-24257

Cyanogen-nitrous oxide flame temperature determination for different concentrations of mixture in flat stainless steel diffusion flame burner 11 p2101 A70-26386

Combustion gases compositions and adiabatic flame temperatures of potassium seeded propane-air mixtures calculated at various equivalence ratios and temperatures assuming thermal equilibrium 12 p2330 A70-27227

Book on chemical propellants performance covering properties and parameters effects, rocket performance, chemical thermodynamics, flame temperature, etc 12 p2289 A70-27350

Flame temperatures simultaneous measurement in two spectral regions, using photoelectric IR pyrometer 12 p2237 A70-28158

Ignition transients in solid propellant rocket engines, taking into consideration flame temperature changes with pressure and igniter secondary mass addition 14 p2628 A70-30778

Temperature estimation of micro hydrogen-air diffusion flame from hydrogen content of unburned gas mixture 14 p2666 A70-31095

Rocket engine propellants flame temperature measurement by spectral line intensity comparison method 15 p2786 A70-32270

Propellant flame temperature and emission spectra during depressurization by rarefaction waves, using rapid scanning spectrometer [AIAA PAPER 70-663] 16 p2962 A70-33570

Extinction model of composite solid propellant combustion including wall and flame heat release zones 17 p3147 A70-34511

Free convection in air and water above horizontal wire heated by DC current, measuring flame temperature distribution by diffraction interferometer 17 p3198 A70-35743

Combustion products of 280-400 C oxidation of ethyl acetate, methyl propionate and i-propyl acetate 21 p3864 A70-40882

Book on stationary flame structure, radiation and temperature covering flow visualization, burning velocity, propagation, ionization, etc 22 p4121 A70-42325

Chemical equilibrium premixed flame composition at given temperature, pressure and mixture strength, using Newton-Raphson iteration technique for simultaneous nonlinear equations 23 p4157 A70-43892

FLAMEOUT

Flameout from burning liquid fuel droplet within reduced film theory 14 p2664 A70-30394

Flameout and ignition correlation for diffusion fuel burnup behind angled stabilizers in annular turbine combustion chamber 18 p3300 A70-36127

FLAMES

NT DIFFUSION FLAMES

NT PREMIXED FLAMES

Book on turbulent diffusive flames in combustion of gaseous fuels covering mass, heat, flame exchange and stabilization processes, etc 01 p0219 A70-11377

Reaction analysis of acetylene-oxygen flames with known concentrations and temperature profiles, integrating one dimensional flame equations numerically 02 p0251 A70-12035

Radiation from flames in gas turbines and rocket engines, discussing effects of soot formation fuel chemical composition, combustor operating conditions, etc 02 p0354 A70-12050

Liquid fuel combustion luminous flame monochromatic radiation distribution, considering soot particle clouds effective emission thickness 06 p1172 A70-17142

Emission flame spectrometer based on double diffraction monochromator, describing design features and operating characteristics 08 p1493 A70-20545

Electron affinity and compound formation in hydrogen/nitrogen/oxygen flames containing potassium and boron using mass spectrometry 10 p1832 A70-25150

Monograph on stability of laminar boundary layer separation at free jets and turbulent free jet flames, considering effects of velocity gradients and temperature 11 p2146 A70-25499

Low cost flame retardant high service temperature glass reinforced electrical grade laminate tested for continuous use 16 p2935 A70-33355

Hydrogen-oxygen flames recombination rates measurements analysis, taking into account reverse reaction rates 20 p3583 A70-40470

Cool flame isothermal theory with oscillatory features accounting for damping time evolution and thermic reaction nature 21 p3942 A70-40886

Shock tube measurements of bimolecular reaction rates in branched chain hydrogen-carbon monoxide-oxygen system, monitoring flame band emission 21 p3773 A70-41314

FLAMMABILITY

Fiber glass reinforcement effect on flammability properties of thermoplastics 01 p0128 A70-10771

Nonflammable material development program for Apollo spacecraft, noting requirements imposed by high oxygen environments, toxic offgassing and temperature range 03 p0436 A70-14055

Flammability control requirements and related hazards in avionics systems materials and components, using systems approach [SAE PAPER 690712] 05 p0956 A70-15854

Oxygen index flammability test for polymeric materials, showing general applicability in quality control and research 09 p1710 A70-23346

Flammability resistance and smoke emission characteristics of aircraft interior fire retardant materials under ambient and increased temperature and zero ventilation conditions [AIAA PAPER 70-400] 10 p1908 A70-24905

Hyperbaric environment combustion, discussing burning rate data and fire resistance scale 14 p2665 A70-30626

Space suit thermal insulation properties, wear durability and nonflammability improvements, reflecting techniques in fabricating cryogenic multilayer insulation systems [AIAA PAPER 70-851] 16 p2939 A70-33918

NRL research in flammability and combustion, discussing oxygen concentration effects on ignition and combustion, chemi-ion formation, etc 16 p3002 A70-33967

Manned spacecraft nonmetallic construction materials selection criteria, testing and configuration control, considering flammability hazard 23 p4152 A70-44462

FLAMMABLE GASES

Aerodynamic gas flame theory and computations, discussing diffusion burning, turbulent flow burning rate, Reynolds number effects, etc 01 p0217 A70-11006

Unmixed gases diffusion burning calculations, discussing turbulent flame burning aerodynamics in jet flows 01 p0217 A70-11007

Flame propagation in gases with two chemical phases, studying phase interaction effects on burning rate 01 p0217 A70-11010

Gas ignition and burning processes calculation with allowance for hydrodynamics, discussing time saving finite difference solution of differential equations system 01 p0218 A70-11020

Preignition heat release rate profile in ethylene-air mixture flow against hot surface, determining temperature and velocity distribution optically 07 p1420 A70-19263

Minimal initial size of explosion reaction center used to explain ignition process in flammable mixtures, noting dependence on pressure, temperature and composition 07 p1422 A70-19586

Electron affinity and compound formation in hydrogen/nitrogen/oxygen flames containing potassium and boron using mass spectrometry 10 p1832 A70-25150

Flame propagation limits and damping mechanism in gases under convection, determining boundary and initial conditions 24 p4428 A70-45492

FLANGE WRINKLING

Local buckling and failure of thin walled compression column with supported flanges, analyzing strength reduction by eccentricity 03 p0600 A70-14254

Horizontally curved I beams flanges elastic buckling, determining prebuckling flange stresses in longitudinal and radial directions 07 p1413 A70-20001

FLAP CONTROL

U AIRCRAFT CONTROL

U FLAPS [CONTROL SURFACES]

FLAPPING

Lifting rotor blades flapping response to atmospheric turbulence, discussing time averaging and perturbation schemes [AIAA PAPER 69-206] 04 p0624 A70-15378

Blade torsional degree of freedom effects on stability and flapping response of rotors operating at high advance ratios 13 p2507 A70-28444

Flapping wing unsteady periodic motion relationship to forces effect on wing profile and vortex street in wake, determining propeller thrust by potential theory 13 p2337 A70-28479

FLAPS [CONTROL SURFACES]

NT JET FLAPS

NT TRAILING-EDGE FLAPS

NT WING FLAPS

Boeing 707 B-epoxy composite foreflap design, analysis, fabrication and flight testing 02 p0307 A70-11955

Lifting reentry dynamic stability of flare stabilizers and flap controls 09 p1766 A70-23242

Supersonic flows over flaps and backward facing steps, using steady state heat transfer measurement technique involving uniform heat flux dissipation at model surface 10 p1798 A70-24120

Control efficiency of flaps at hypersonic speeds, considering thick turbulent boundary layer compression process 16 p2836 A70-33751

High lift flaps for sailplane cross country speed improvement by cruise-climb tradeoffs [AIAA PAPER 70-878] 17 p3016 A70-34814

Optimum adaptation of propulsion gas generators to power jet driven rotors with blown flap control, considering jet engine, fanjet and engine driven compressor 17 p3024 A70-35661

FLARED BODIES

Blunt nose effects on drag of flared conical body in supersonic flow, considering pressure loss through shock wave and vorticity 17 p3196 A70-35237

FLARES

UV Ceti type flare stars observational and theoretical results related to nebular or chromospheric flare models 03 p0566 A70-13316

Multicolor photometry of Orion flare stars in U, B, V and R, constructing diagrams confirming flare stars scattering about main sequence 03 p0567 A70-13317

Young flare stars in solar vicinity, considering spatial density, kinematic properties and luminosities 03 p0567 A70-13318

Nebular variables and flare stars in Orion aggregate 03 p0567 A70-13319

Meteorite flakes nature and statistics obtained from meteorites characterized by irregular brightness curve 03 p0574 A70-13883

Mayeda flare observed on Mars 4 June 1937, suggesting oriented reflection of solar rays from ice crystals cloud or Martian surface feature 05 p0918 A70-16916

Correlation function prediction of rapid brightness variations in quasar based on variable optical emission model including flares

07 p1383 A70-19403

Qualitative analysis and comparison of hypothesis versions of Martian point flare observed by Maeda, considering solar ray reflection from ice cloud or vertical surface object

07 p1385 A70-19420

Sco X-1 simultaneous X ray and optical flares correlation and X ray enhancements

08 p1561 A70-20900

Meteor flare photographs statistical analysis, noting duration and weight distribution dependence on meteor velocity

08 p1574 A70-21214

Orion Nebula region search, giving characteristics and locations of flare type variable stars

10 p1949 A70-25249

Short period hypothetical orbits distribution formed by flaring on Jovian satellites

11 p2109 A70-25925

Flare stars distribution in Pleiades, discussing flare visual magnitude and frequency

15 p2807 A70-32876

RW Aur type variable stars percentage with photographically observable flares

15 p2807 A70-32877

Comet Alcock flareup on 27-29 May 1969, noting visible rays in coma, dust grains expulsion from nucleus, tail structure, etc

16 p2980 A70-34304

Meteoric masses evaporation during flare, showing discrepancies for luminosity factors

18 p3315 A70-36604

Soviet book on red dwarf star flares covering data acquisition, flare frequency, mechanisms and nebular model

20 p3705 A70-39722

Magnesium-sodium nitrate porotechnic flare spectral radiant energy comparison with radiative transfer theory data, considering Na resonance continuum formation

21 p3850 A70-41937

Star flare HD 160202 in M6, discussing luminosity, time duration, magnitude and temperature

22 p4102 A70-42971

Optimal color hierarchy for pyrotechnic markers and signals indicating red, violet and amber hues on top

23 p4146 A70-44459

Smoke, chaff and flare distress signals design and operation for search and rescue operations

23 p4143 A70-44494

FLASH

Background luminance effect on flash brightness in eyes, measuring increment threshold and luminances required for various brightnesses

01 p0025 A70-11052

Critical duration for pupillary light reflexes measured with IR scanning pupillometer using various flash duration stimuli

02 p0237 A70-12458

Human eye integration of short monochromatic light flashes at TV frame frequencies

02 p0238 A70-12463

Cats visual analyzer functional rearrangement mechanisms under prolonged light stimulation, considering evoked potential dependence on pulse duration and intensity

07 p1198 A70-18699

Rabbits visual cortex evoked potential changes due to light flashes under different conditions

07 p1198 A70-18716

Onset, mass motion and flash phase in 2b solar flares observed in filtergrams spanning H alpha line

11 p2105 A70-25748

Transistorized differed synchronizer for delaying photoflash initiation in scientific photography

12 p2228 A70-26879

FLASH BLINDNESS

Flash blindness of cats using Q switched laser beam, discussing ERG response and retina changes

01 p0113 A70-10920

Photochromic aminotriarylmethane filter solutions for flash blindness protection, noting stability against xenon flash UV exposure

04 p0690 A70-15028

Time requirement determined for visual acuity restoration after illumination with short duration bright light flash

08 p1450 A70-20746

Light sensitivity restoration in humans exposed to bright flashes, studying photonic afferent system braking effect on scotopic system

08 p1450 A70-20747

FLASH LAMPS

Spectral efficiency of coaxial flash lamp pumping gas laser, noting dependence on geometrical and physical parameters of source and active body

01 p0106 A70-10061

High intensity short pulse flash lamps using quartz envelopes and wire electrodes for pumping high energy organic dye lasers

02 p0314 A70-12741

Flash lamp-pumped organic dye scintillator lasers using coaxial Xe-filled lamp, tabulating blue-violet organic liquid lasers characteristics

03 p0499 A70-13161

Flash lamp pumped tunable organic dye laser, using capacitor bank for reliable operation

05 p0861 A70-16845

Flashtube photostimulators for examining human physiological response, discussing design and calibration

09 p1624 A70-22673

Atmospheric particles photographed in situ by cameras using microsecond flash lamps, discussing required mechanical motion compensation at aircraft speed

10 p1886 A70-23930

Operation characteristics of flash, arc, incandescent and explosion type laser pump lamps

13 p2431 A70-29874

Electronically modified stroboscope as light source for multiflash photography of transient events, noting mechanical switches elimination

18 p3262 A70-37095

High speed X ray flash motion picture installation for ballistic photography

22 p4037 A70-43068

Ultrabright nanosecond flash light generation technique, using superradiant light sources for shadowgraph photography in high resolution hypervelocity field

22 p4037 A70-43070

FLASH TUBES

U FLASH LAMPS

FLASH WELDING

Al alloys flash welding for rings used in Poseidon program

06 p1078 A70-18502

Flash, gas-pressure and electron-beam welding of airframe steels

12 p2239 A70-26987

FLASHING (VAPORIZING)

Quasi-steady radially symmetric theory of liquid drop vaporization and homogeneous combustion extended to burning of solid carbon spheres gasified by chemical attack

07 p1419 A70-18915

Gaseous pyrolysis products detection and identification during eruption from polymeric surfaces subjected to flash heating by time of flight mass spectrometer

07 p1319 A70-19887

Single component two phase pipe flow choking and shock phenomena, including flashing flow vibratory effects

13 p3286 A70-28846

FLAT CONDUCTORS

Electromagnetic propagation in flat waveguide with local gyrotropic filling and transverse magnetization, using Galerkin method

19 p3470 A70-37430

Plane EM wave diffraction by conducting strip, using algorithm for reducing integral to linear algebraic equations

19 p3376 A70-37433

Regularizing algorithm for Fredholm integral equation used in diffraction by ideally conducting strip

19 p3376 A70-37434

Thin two phase film conductivity, noting conditions for equality with geometric mean and for metal-to-dielectric transition

22 p4088 A70-43466

Current and vector potential in thin superconducting film in HF field, considering high and low temperatures

22 p4088 A70-43467

Stripline bandstop filter design method, discussing response shape and resonator number determination, reactance calculation, etc

22 p3999 A70-43488

FLAT LAYERS

Elastoplastic thick layer with disk-shaped crack analyzed for stress and strain, determining width of plastic zone

05 p0939 A70-16482

Transient heat transfer combining conduction and radiation in absorbing plane layer analyzed by differential approximation

12 p2332 A70-27801

Planar absorbing and emitting layer exposed to monochromatic collimated radiation, analyzing line or band shape effect on radiative transfer

13 p2451 A70-29135

FLAT PLATES

Thin flat plates effective width under axial edge compression slightly beyond buckling limit, solving von Karman differential equations

01 p0198 A70-10094

Welded flat plate specimen to evaluate low cycle crack initiation and propagation of butt welds under compressive loading, discussing design, fabrication and testing

01 p0199 A70-10452

Hot-wire probe support orientation to minimize flat plate turbulent boundary layer mean velocity determination errors

01 p0087 A70-10665

High speed hail impact damage on flat Al alloy plates observed for effects of impact angle and velocity, plate material properties and thickness

01 p0056 A70-10690

Viscous fluid flow due to long flat plate moving rectilinearly inside cylinder, assuming zero pressure gradient

01 p0062 A70-10801

Free convection to rotating central plate in synchronously rotating surroundings with and without consideration of Coriolis forces

[AICHE PREPRINT 9] 01 p0216 A70-10968

Transient thermal stress concentration at small thickness change of plate obtained by photoelastic studies

01 p0207 A70-11157

Surface catalysis and variable transport properties effects on chemically frozen dissociated hypersonic air flow boundary layers enveloping flat plates and slender wedges

01 p0067 A70-11179

Unsteady heat transfer from porous flat plate with impulsive motion and rising temperature, analyzing compressible boundary layer equations using Laplace transform

01 p0067 A70-11390

Diffuse isotropic light interaction with compact corn leaf, using transparent plate model with rough plane-parallel surfaces

02 p0338 A70-11893

Navier-Stokes difference equations numerically integrated by computer for viscous fluid flow along parallel flat plate at low Reynolds number

02 p0277 A70-11909

Static and cyclic stress distributions in buckling shear panel comprising flat plate of clad Cu-Al alloy

02 p0388 A70-12497

Finite element technique extended for plastic buckling of flat plates, using Stowell theory

[RM-460J] 03 p0584 A70-12923

Eddy viscosity equation derived from flat plate turbulent boundary layer velocity data, considering shear stresses and mixing length profiles

03 p0464 A70-12943

Thermoelastic stresses in plate due to arbitrary temperature variations of heat transfer agent calculated in second approximation, allowing for transfer coefficient time dependence

03 p0590 A70-13400

Energy equation for thermal turbulent boundary layer on adiabatic flat plate

03 p0466 A70-13421

Heat transfer under conditions of forced convection from flat plate in laminar flow, considering plate surface temperature arbitrary variation in time

03 p0605 A70-13518

Hall current effect on steady boundary layer flow of incompressible viscous electrically conducting fluid past semiinfinite flat plate in transverse magnetic field

03 p0469 A70-14183

Aerodynamic velocity field induced by plate in motion correlated with ideal gas flow at specific Reynolds number, discussing wake formation

03 p0410 A70-14270

Sound attenuation rate of rectangular flat steel plates contact and branch point relation to velocity difference and absorption length

03 p0526 A70-14353

Free convective flows above flat horizontal plate demonstrating laminar boundary layer existence at intermediate Grashof numbers, using semifocusing color schlieren photography

04 p0780 A70-14456

Laminar compressible wake behind thin flat plate at zero angle of attack, solving boundary layer equations in von Mises coordinate plane

[ASME PAPER 69-WA/FE-6] 04 p0614 A70-14783

Convective heat transfer rates measured on cooled sharp leading edge flat plates at various angles of attack in hypersonic merged flow

[ASME PAPER 69-WA/HT-21] 04 p0614 A70-14813

Discrete frequency noise generation associated with wakes due to fluid flow over turbomachine blades, supporting spokes, flat plates, etc

[ASME PAPER 69-WA/GT-13] 04 p0733 A70-14883

Heat transfer from two dimensional hypersonic low density stream to wedges and sharp flat plates at expansion angles of attack

04 p0615 A70-14944

Boundary layer along flat plate at zero incidence with homogeneous suction using momentum and kinetic energy integral equations through boundary layer velocity profile

04 p0615 A70-15052

Flat plates thermal buckling calculations with allowance for transverse shear deformation effect, using Riessner variational principle

04 p0773 A70-15091

Hydromagnetic flow of viscous incompressible electrically conducting fluid near accelerated infinite porous flat plate with variable suction or injection

04 p0672 A70-15095

Boundary layer transition limits at high Mach numbers, discussing transition on flat plate and bodies of rotation and Reynolds number

04 p0672 A70-15177

Values measured on sharp flat plate in 10.4 Mach boundary layer induced pressure gradient, discussing effects of wall pressure and temperature gradients

04 p0621 A70-15609

Model flow studied for viscous flow near trailing edge of semiinfinite flat plate in middle of moving channel, noting Couette flow tendencies

05 p0831 A70-15879

Computational procedures for matrix analysis of stability and vibration of thin flat rectangular plates in longitudinal compression

05 p0927 A70-16010

Photoelastic and photorheological analysis of time-dependent variation of stress distribution in long strip compressed oppositely with elastic flat punches

05 p0928 A70-16012

Spin-up of electrically conducting fluid between infinite flat plates under axial magnetic field, considering Ekman-Hartmann boundary layer on single plate

05 p0832 A70-16017

Natural vibrational frequencies of trapezoidal, triangular, circular and elliptical isotropic flat plates with different edge conditions tabulated

05 p0936 A70-16319

Unsteady laminar free convection caused by heating semiinfinite flat vertical plate, obtaining velocity and temperature distributions

05 p0957 A70-16370

Inviscid gas injection through flat plate in supersonic flow, obtaining self similar solution by integrating differential equation for stream function

05 p0791 A70-16963

Unsteady laminar gas flow near infinite flat plate using Laplace transforms, obtaining closed form solutions for plate velocity and temperature

05 p0836 A70-17106

Buoyancy effects in laminar forced convection on vertical flat plate, obtaining heat transfer coefficient

06 p1172 A70-17141

Pressure distribution and drag measurements at flat triangular bodies and rectangular plates with blunt trailing edge in compressible flow

06 p0965 A70-17243

Boundary layer on sharp flat plate in low density flow computed by continuum approach, obtaining parabolic partial differential equation system [DVL-914]

06 p1034 A70-17250

Natural convection heat transfer from vertical plate immersed in thermally stratified fluid

06 p1175 A70-17685

Skin friction and heat transfer on flat plate in high velocity laminar motion with mass transfer for any free stream and injected gas combination

06 p1176 A70-17689

Unheated solid starting length effect on skin friction and heat transfer characteristics in incompressible transpired laminar boundary layer on flat plate

06 p1035 A70-17691

Time dependent pressure fluctuations effect on laminar film pool boiling on vertical flat plate by perturbation method to predict heat transfer

06 p1177 A70-17696

Blowing intensity influence on turbulent boundary layer of incompressible fluid and friction drag of flat plate

06 p1036 A70-17852

Kinetic flow regime in hypersonic flow past flat plate leading edge, using Boltzmann equation [AIAA PAPER 70-181]

06 p0970 A70-18094

Boundary layer-induced pressures on flat plate in unsteady hypersonic flight calculated using tangent wedge approximation [AIAA PAPER 70-184]

06 p1039 A70-18095

Finite difference solution of time dependent Navier-Stokes equations for two and three dimensional laminar incompressible flow, discussing results for flat plates

[AIAA PAPER 70-46]

06 p1041 A70-18170

Flat plate boundary layer flow of partially ionized gas, measuring charged particle density, electron temperature and plasma potential distributions with Langmuir probe

[AIAA PAPER 70-86]

06 p1041 A70-18174

Meksyn asymptotic method of integrating boundary layer equations applied to ordinary differential equations for slip flow past semiinfinite flat plate

06 p0979 A70-18348

Density field around leading edge of blunted flat plate, using electron beam measurements in low density hypersonic wind tunnel

06 p0980 A70-18351

Sharp hypersonic flat plates inclined at various angles, obtaining flow field and merged region details

06 p0980 A70-18353

Hypersonic rarefied argon and nitrogen flows over flat plate, investigating flow field and surface measurements from merged layer into transition regime

06 p0981 A70-18355

Kinetic theory of rarefied supersonic flow over finite plate, calculating molecular velocity distribution functions for flowfield

06 p0981 A70-18356

Free molecular drag for flat plate with normal protuberance, determining flowfield distribution functions and stress components

06 p0981 A70-18357

Aerodynamic forces and heat transfer on shielded flat plates in free molecular flow calculated by Monte Carlo technique

06 p0981 A70-18358

Surface pressures and shock wave shapes on sharp flat plates and wedges in rarefied hypersonic transition flow with emphasis on merged layer regime

06 p0982 A70-18362

Continuum to free molecule hypersonic flow near flat plate sharp leading edge, studying Knudsen, Reynolds and Mach numbers effects

06 p0982 A70-18365

Orifice effect investigated for sharp flat plate in hypersonic rarefied flow, measuring surface pressure

06 p0982 A70-18366

Wind tunnel study of heat transfer on smooth plate surfaces in longitudinal air flow using intermittently insulated calorimeter

07 p1279 A70-19065

Trailing edge region of flat plate in laminar incompressible flow examined for high Reynolds numbers limit using Navier-Stokes reduced equations

07 p1255 A70-19213

Downstream distribution of trace element injected into boundary layer of flat plate or cone with self similar mass transfer

[SAMSO-TR-69-56]

07 p1256 A70-19313

Flat plate boundary layer induced pressures in unsteady hypersonic flight

07 p1257 A70-19327

Unsteady boundary layer in compressible fluid laminar flow over accelerating semiinfinite flat plate

07 p1258 A70-19566

Hole reinforcement in flat plate under uniaxial load with high stress region at boundary, resulting in weight savings

07 p1414 A70-20174

Circular turbulent air jet from flat plate into deflecting stream using potential flow model, noting applicability to V/STOL aircraft technology

[AIAA PAPER 69-223]

07 p1190 A70-20406

Pressure distribution on flat plate resulting from potential incompressible flow interaction between secondary jet and subsonic mainstream

07 p1190 A70-20415

Symmetrical laminar distorted velocity profiles between flat parallel plates, analyzing decay using integral method

08 p1433 A70-21325

Two dimensional natural convection boundary layer on finite isothermal horizontal plate, examining upward facing cold plate and downward facing hot plate

08 p1598 A70-21580

Thermal boundary layer thickness and Nusselt number approximations for heat transfer in laminar flow along flat plate with power law heat flux distribution

08 p1599 A70-21583

Finite disturbance effect on laminar incompressible wake behind flat plate determined by interaction between two dimensional fluctuation amplitude and mean flow

08 p1433 A70-21605

Counterrotating vertical vortices produced by corona discharge on heated flat plate under free convection conditions

08 p1599 A70-21828

Nonuniqueness theorems for von Karman equations governing thin flat elastic plate deflections clamped at edges and subjected to normal and edge loading

09 p1768 A70-22063

Plane flow of electrically conducting fluids around oscillating plate, using equations linearized by Oseen method

09 p1734 A70-22316

Temperature field in infinite plate with disk shaped inclusion and stationary point heat source determined, allowing for heat transfer conditions

09 p1778 A70-23082

Stress-strain state analysis of transversely isotropic plates with inclusions under bending loads

09 p1782 A70-23298

Failure compression tests of flat rectangular Al alloy panels presented in unitary form, adopting structural load index for solution from weight standpoint

09 p1782 A70-23376

Incompressible anisotropic fluid flow around semiinfinite plate at large Reynolds numbers, using interlocked asymptotic expansions and deformed coordinates to obtain boundary layer equations

09 p1663 A70-23390

Laminar viscous flow past semiinfinite flat plate parallel to uniform stream, solving Navier-Stokes equation to determine local skin friction coefficient

09 p1663 A70-23581

Flat plate laminar boundary layer blowoff due to wall injection analyzed by parameter matched asymptotic expansion

10 p1862 A70-23844

Boundary layer flow near flat plate trailing edge taking into account pressure gradient induced locally in external flow

10 p1862 A70-23846

Motion and continuity equations for unsteady two dimensional flow of incompressible viscous fluid along infinite flat plate with time dependent suction

10 p1862 A70-23877

Skin friction near flat plate trailing edge at high Reynolds number by linearizing velocity profile

10 p1801 A70-24159

Navier-Stokes solution to laminar flow past semiinfinite flat plate valid for any Reynolds number, discussing skin friction, displacement thickness, etc

10 p1869 A70-24415

Unsteady compressible laminar boundary layer flow around flat plate influenced by compressibility as function of Mach number

10 p1869 A70-24543

Wind tunnel study of heat transfer on smooth plate surfaces in longitudinal air flow using intermittently insulated calorimeter

10 p1970 A70-25216

Molecular reflection effects on aerodynamic characteristics of rarefied gas flow past plate

11 p1973 A70-25386

Grid shadow moire method to measure displacement contours of large plates, discussing sensitivity changes

11 p2131 A70-25589

Film cooling effectiveness measured following air injection through discrete holes into turbulent boundary layer of air on flat plate

11 p2146 A70-25690

Panel flutter theory applied to aeroelastic stability of flat unloaded plates and cylindrical shells

11 p2134 A70-25951

Flow near leading edge of sharp insulated and cooled flat plates, using Monte Carlo direct molecular simulation

11 p1975 A70-25968

Boundary layer transition detection at supersonic speeds using thin film gages to infer local laminar and turbulent supersonic skin friction

11 p2035 A70-25970

Uncooled leading edge effect on cooled-wall hypersonic flat plate boundary layer transition, discussing leading edge bluntness effects

11 p1976 A70-25984

Buckled plates flutter at zero dynamic pressure, considering initial plate imperfections, including aerodynamic damping in quasi-steady supersonic approximation

11 p2135 A70-25988

Ideal fluid flow containing small spherical particles past cylinder and flat plate normal to stream using small perturbations method

11 p1976 A70-26012

Flat plate flowfield for freestream/jet interaction wrap-around on bodies of revolution, using separation shock model and blast wave analogy

11 p1976 A70-26135

Flat plate normal to two dimensional impinging air jet, investigating heat/mass/transfer structure using naphthalene method

11 p1977 A70-26411

Wall pressure fluctuations beneath turbulent boundary layers on flat plate and cylinder

11 p2038 A70-26529

Parallel isotropic flat plates vibration and flutter in supersonic/subsonic flow over one surface, observing plane loadings and elastic medium stiffness effects

12 p2316 A70-27104

Newtonian fluid laminar boundary layer flow over flat plate with nonNewtonian fluid injection

12 p2209 A70-27212

Superlayer structure in turbulent boundary layer on flat plate obtained by statistical processing of signals from hot-wire probes

12 p2209 A70-27226

Axisymmetrical stress tensor singularity convergence of rigidly clamped circular plate, showing identity of plane stressed state transcendental equations

12 p2325 A70-27558

Radiation profiles in ablating flat plate air-Teflon laminar boundary layer, discussing visible, UV and IR wavelengths

12 p2211 A70-27803

Pressure buckling values of rod and plate profiles with thicknesses graduated across pressure direction in presence of uniform and nonuniform stress distributions

13 p2507 A70-28477

Residual stress determination in flat strip elastoplastically deformed by finite bending

13 p2508 A70-28485

Free flow field from underexpanded rocket motor nozzle and impingement effects of pressure and heat transfer to flat plate

[AIAA PAPER 69-568] 13 p2473 A70-28510

Stress concentration factors determined for u-shaped and semielliptical edge notches in semifinite sheet under uniaxial tension parallel to edge

13 p2509 A70-28535

MHD boundary layer flow past yawed flat plate in presence of pressure gradient, determining skin friction expansion terms

13 p2461 A70-28804

Heat transfer increase near stagnation point for turbulent jet impinging on paraffin coated plates used for flow visualization

13 p2521 A70-28866

Viscous and compressible fluid flow in presence of plane plate

13 p2389 A70-29489

Free convection flow and heat transfer from semiinfinite horizontal flat plate with time-oscillating temperature, using successive approximations process

13 p2522 A70-29537

Plane plate motion in weightless fluid flow with free upper boundary, showing lifting capacity increment by underlying solid surface

13 p2390 A70-29644

Plane cavity geometry behind plate in incompressible potential flow, deriving geometrical functions to obtain desirable shapes

13 p2390 A70-29645

Transient free convection flow due to arbitrary motion of vertical plate, linearizing equations of boundary layer flow and heat transfer

13 p2523 A70-30009

Postbuckling of flat variable thickness rectangular plates with unloaded transverse edges, using dynamic relaxation method

13 p2518 A70-30024

Flat plate and cylinder with periodic Joulian heating from time dependent heat source, analyzing transient temperature distribution

14 p2664 A70-30269

Laminar flow of suspension over flat plate, analyzing particulate velocity and concentration profiles relationships to drag and lift forces

14 p2565 A70-30270

Steady laminar heat transfer in open circuit aligned field MHD flow past flat plate, using parametric differentiation

14 p2664 A70-30272

Supersonic rarefied flow over sharp flat plate with merged shock layer and free molecular-continuum transition, using electron beam fluorescence

14 p2529 A70-31028

Synthetic array radar flying past flat plate, analyzing image relationship to flight path

14 p2552 A70-31193

Turbulent boundary layer correlations on flat plate, noting inadequate Spalding-Chi predictions

14 p2567 A70-31396

Subsonic and transonic gas flow in wake behind finite thickness plate based on Navier-Stokes equations

15 p2719 A70-31484

Incompressible turbulent boundary layer calculation based on shearing stress hypothesis, considering layer at flat plate, boundary conditions and velocity profiles

15 p2719 A70-31490

Curvilinear cracks development in flat brittle body under asymmetrical loads using small parameter method

15 p2817 A70-32165

Plane rectangular plate in acoustic field of jet engine exhaust, calculating surface stresses

15 p2819 A70-32186

Stress concentration in flat rectangular and skew panels with circular holes from photoelastic verification of direct stiffness method

[SESA PAPER 1633] 15 p2820 A70-32303

Hypersonic near free molecule flow over flat plate with sharp leading edge, using linearized kinetic B-K-G equation for small thermal accommodation coefficient

15 p2673 A70-32796

High voltage photoelectric generator containing semiconductor plates with series- and parallel-connected p-n junctions forming solid circuit for super-high light flux concentrations

16 p2843 A70-33201

Laminar compressible flat plate boundary layer dependence on Prandtl number and viscosity-temperature relations

16 p2893 A70-33673

Boundary value problem of two dimensional Poisson equation solution procedure with Hockney formulas, applying to unsteady viscous incompressible flow past flat plate

16 p2943 A70-33737

Radiatively interacting adjacent plates in presence of collimated solar flux, considering surface roughness effects on equilibrium temperature distribution

[AIAA PAPER 70-817] 16 p3002 A70-33946

Plane harmonic sound wave reflection and transmission in flowing medium by infinite set of arbitrary spaced and staggered flat plates

16 p2971 A70-34016

Stress, strain and acceleration spatial variation in structures subject to broad frequency band vibration excitation, considering simply supported flat plate

16 p2992 A70-34017

Radiative heat transfer between opaque interacting surfaces for equal temperature adjacent plates with one dimensional surface roughness profile

16 p3002 A70-34196

Turbulent flow in stratified fluids over flat plate, relating density profile curvature and heat transfer

16 p2895 A70-34242

Two dimensional supersonic wake behind heated slender flat plate, considering flow properties in transition zone

17 p3006 A70-34466

Low density hypersonic flow over finite width flat plate at zero incidence

17 p3007 A70-34473

Transitional flow separation upstream of compression corner at trailing edge of sharp leading edge flat plate

[AIAA PAPER 70-764] 17 p3007 A70-34487

Rarefied binary gas mixture transient Couette flow, considering nonlinear case of plate with equal temperature accelerated impulsively

17 p3067 A70-34546

Steady two dimensional MHD boundary layer flow with uniform suction or injection past semiinfinite flat plate in cross fields

17 p3067 A70-34618

Two dimensional solidification of forced viscous flow over flat plate with constant heat removal

17 p3194 A70-34634

Hypersonic rarefied gas flow around flat plate with sharp leading edge and circular cylinder in transition region

17 p3011 A70-35241

Laminar free convection boundary layer on vertical heated plate near discontinuity in plate temperature, discussing velocity field

17 p3198 A70-35593

Vortex sheet instability leaving semiinfinite flat plate, considering boundary effects

17 p3073 A70-35601

Heat and gas curtain efficiency in turbulent boundary layer on flat plate, including heat transfer data

17 p3198 A70-35731

Turbulent boundary layer of flat plate, investigating superlayer structure by hot wire anemometer

18 p3238 A70-36066

Angular dependence of instability and Rayleigh number of natural convection flow on inclined flat plates, using electrochemical flow visualization

18 p3345 A70-36190

Horizontal boundary layers development on flat plate in nondiffusive stratified flow characterized by Reynolds and Russell numbers

18 p3239 A70-36192

Airfoil trailing edge stall in laminar flow, investigating circulation around flat plate

18 p3205 A70-36194

Wake behind trailing edge of flat plate in constant velocity impulsively started stream, using boundary layer theory

18 p3206 A70-36196

Viscous incompressible liquid two dimensional flow around flat plate, discussing visualization techniques and velocity distribution measurement

18 p3239 A70-36218

Magnetohydrodynamic flow of electrically conducting viscous incompressible fluid past nonconducting semiinfinite flat plate under transverse magnetic field

18 p3295 A70-36431

Mathematical model of three dimensional separated flows with applications to small aspect ratio delta wing and flat plate

18 p3207 A70-36438

Stress concentration in notched flat samples under plane plastic deformation

18 p3340 A70-36570

Finite plate length effect on two dimensional supersonic turbulent boundary layer with large distributed surface injection

18 p3242 A70-36688

Radiant heat transfer at vertex of adjacent flat plates separated by vacuum

18 p3243 A70-36711

Turbulence in supersonic wake behind flat plate at zero incidence and heat transfer rate, using hot-wire anemometer

19 p3403 A70-37528

Turbulent boundary layer characteristics on unblown flat plate at low Reynolds numbers, extending to cases with blowing and suction

19 p3405 A70-38020

Clamped edge thin flat elliptic plate subject to elliptic paraboloidal loading, determining middle surface deformations for nonlinear large deflections

19 p3547 A70-38359

Suction velocity effects on Rayleigh problem in MHD of flat nonmagnetic nonconducting plate, solving for velocity distribution and skin friction

19 p3481 A70-38448

Sound wave radiation and excitation in plane infinite plate by vortices

19 p3354 A70-38722

Bearing force and moment produced by motion of inclined plate supported by compressed air in ground effect machines with small angle of attack

20 p3557 A70-39140

Natural convection problem solution along nonuniformly heated vertical plate with variable transverse magnetic field

20 p3735 A70-39144

Unsteady incompressible flow in laminar boundary layer with homogeneous suction during longitudinal flow past flat plates, investigating boundary layer stability

20 p3614 A70-40391

Laminar convective flow from linear heat source along vertical plate, solving numerically for incompressible fluid by boundary layer approximation

20 p3614 A70-40403

Flat plate boundary layer flow with surface blowing and suction /mass transfer/, investigating stability by numerical techniques

20 p3615 A70-40507

Flat plate compressible laminar boundary layer flow with variable fluid properties, using series solution by splitting up flow variables into sets of universal functions

21 p3806 A70-40825

NonNewtonian fluids flow and heat transfer characteristics past flat plate, determining velocity and temperature distributions

21 p3806 A70-40900

Forced convection heat transfer from flat plate and cylinder in cross flow to simulated Mars atmosphere

21 p3945 A70-41026

Two dimensional compressible laminar MHD boundary layer flow across flat plate with heat transfer, considering continuity, momentum and energy equations

21 p3856 A70-41039

Boundary layer transition region of flat plate in incompressible flow by subsonic wind tunnel tests, demonstrating harmonic wall perturbation effect

21 p3808 A70-41440

Two dimensional unsteady viscous incompressible MHD flow past infinite flat plate with uniform suction, considering Hartmann and Reynolds numbers

21 p3858 A70-41450

Steady viscous flow past oblique flat plate at high Reynolds number, using Oseen linearized approximation

21 p3809 A70-41714

Combined effects of flow unsteadiness and surface mass transfer on displacement thickness of boundary layer, using flat plate geometry

21 p3811 A70-42092

Karman-Polhausen method applied to unsteady thermal boundary layer on isothermal flat plate

21 p3954 A70-42208

Subsonic channel incompressible gas flow past semiinfinite flat plate base, using flow pattern for cavitation flow

21 p3748 A70-42213

Flat plate airfoil unsteady lift due to chordwise velocity perturbations, using Horlock frozen gust pattern theory

22 p3957 A70-42303

Fluid flow around plane plate system, basing model on potential flow theory and variational principle

22 p4009 A70-42606

Unsteady hydromagnetic boundary layer flow past semiinfinite flat plate under steady magnetic field and small free stream perturbation

22 p4080 A70-42631

Hypersonic viscous interaction between laminar boundary layer growing over flat plate and external flow field extended to curved surfaces

22 p3958 A70-42688

Variable thickness flexible plates thermoelastic flexure and buckling, obtaining nonlinear differential matrix equations by difference-differential method

22 p4115 A70-42811

Radiation forces on flat plate in ecliptic earth orbit applicable to satellite attitude dynamics during pitching libration

22 p4125 A70-43437

Electrically conducting fluid hydromagnetic spin-up between infinite flat insulating plates in uniform magnetic field normal to boundaries

23 p4223 A70-43972

Numerical integration of Orr-Sommerfeld equation for flat plate Blasius boundary layer transition

23 p4179 A70-43973

Neutral stability curve for flat plate boundary layer in zero pressure gradient with increasing thickness, giving critical Reynolds number

23 p4179 A70-43974

Tollmein-Schlichting waves in flat plate Blasius boundary layer, comparing experimental and theoretical critical Reynolds number 23 p4179 A70-43975

EM induction in flat plates with two dimensional conductivity distribution, describing approximation method 23 p4217 A70-44054

Laminar to turbulent boundary layer flow transition over flat plate, using space amplified numerical solutions of Orr-Sommerfeld equation 23 p4181 A70-44234

Hall effect on incompressible electroconducting viscous fluid motion past finite conducting flat plate, discussing boundary conditions 23 p4225 A70-44247

Heat transfer from turbulent axisymmetric jet to normal flat wall at critical point with small Reynolds numbers 23 p4181 A70-44321

Conducting viscoelastic fluid flow near harmonically oscillating nonconducting flat plate under uniform transverse magnetic field, considering stress-strain rate relationship 23 p4226 A70-44375

Two phase plume at various incidence angles on flat plate, determining impinging particle mass flux, forces and damage 23 p4134 A70-44566

Fluttering isotropic rectangular flat plate fatigue life estimation, taking into account stress, dynamic pressure, frequency, Mach number and plate thickness 23 p4270 A70-44577

Dissociative nonequilibrium hypersonic flow of low density gas mixtures over flat plate in free stream, noting catalytic wall effect on flow field 23 p4135 A70-44604

Film cooling efficiency for flat plate behind tangential slot at blowing coefficients below unity 23 p4282 A70-44727

Heat exchange during flat plate transverse vibrations in water, discussing frequency and amplitude effects and natural convection role 23 p4282 A70-44728

Powdered flat steel plates cooling by air blown through pores, determining internal heat exchange coefficients 23 p4283 A70-44731

Flat plate film cooling efficiency behind tangential slot at blown-main flow velocity ratio over three 23 p4283 A70-44741

Partially cavitating flow past plate, calculating characteristics by Riabushinskii scheme 24 p4325 A70-45642

Heat flux exchange by natural convection along flat vertical isothermal plate in laminar, transition and turbulent flows, using fluxmeters 24 p4429 A70-46207

FLAT SURFACES

Holographic two beam real-time Fizeau interferometer for recording and reconstructing reflected light waves in silvered flat surfaces measurement 01 p0090 A70-10905

Propagation of turbulent jet impinging on flat surface at certain incidence angle analyzed for application to V/STOL aircraft, ventilation equipment, etc 03 p0468 A70-13878

Potential axisymmetric vortex flow interaction with stationary flat surface, using existing numerical analysis by transforming boundary value problem to Volterra integral equations [ASME PAPER 69-APM-R] 04 p0668 A70-14864

Electromagnetic plane wave oblique reflection from flat surface with spatially modulated surface impedance, computing wave spectrum 13 p2367 A70-29527

Heat transfer at flat melting surface under forced convection and laminar boundary layer solved by Karman-Pohlhausen method 18 p3347 A70-36502

FLAW DETECTION

U NONDESTRUCTIVE TESTS

FLAWS

U DEFECTS

FLEXIBILITY

Mechanical vibration of beams analyzed by partial differential equations of beam vibration involving mass concentration and flexibility 07 p1411 A70-19786

Flexible nickel cadmium secondary battery as nocturnal power supply for meteorological balloons transceiver and measuring instruments 08 p1440 A70-20711

Derivation procedure for dynamic flexibility matrix including material damping for triangular plate in bending, twisting and shear 13 p2509 A70-28540

Red cell deformability and flow resistance and blood electrical resistance under low g centrifugation 15 p2680 A70-31700

Twisted uniform beam element flexibility and stiffness matrices, using continuous bending theory 16 p2894 A70-33887

Column end fixity using Euler load and maximum flexibility coefficient for span point lateral load 17 p3188 A70-35226

Dual spin spacecraft bearing assembly flexibility effects on attitude stability [AIAA PAPER 70-1043] 19 p3533 A70-38858

Solar panel flexibility effect on attitude control of solar electric spacecraft for deep space mission [AIAA PAPER 70-1140] 20 p3716 A70-40209

Parachute flexibility as performance parameter, discussing stiffness-weight index, inflation process, squidding, etc [AIAA PAPER 70-1166] 21 p3755 A70-41845

FLEXIBLE BODIES

Dynamic stability of flexible aircraft fuselage in controlled supersonic flight at zero angle of attack, basing analysis on elastic oscillation equations 03 p0579 A70-13418

Complex Young modulus of plastics during flexural vibration, discussing deformation of viscoelastic bodies and test results of various plastics [ONERA-TP-715] 03 p0487 A70-13645

Motion stability and time dependent deflections of thin flexible cylinder with zero bending rigidity in viscous stream 03 p0595 A70-13783

Flexible flight vehicles longitudinal stability with tandem lifting surfaces, studying aerodynamic time delay effects by root locus technique 03 p0408 A70-13802

Flexible spacecraft equations of motion derived by modeling as rigid central body with arbitrary subsidiary flexible bodies [AIAA PAPER 70-19] 06 p1157 A70-18116

Hybrid coordinate formulation for flexible space vehicle attitude control system design [AIAA PAPER 70-20] 06 p1158 A70-18180

Parametric vibrations onset and resonance regions boundaries determined for feed line system with flexible compensator 07 p1403 A70-19114

Aeroelasticity problems, discussing unrestrained flexible structures design, nonconservative systems stability, biomechanics, etc 09 p1777 A70-22972

Dynamical characteristics of variable-mass flexible spinning rocket with internal flow, investigating rigid body motion, elastic displacements and vibrations 09 p1767 A70-23252

Two-disk flexible rotor balancing method based on shaft vibration and bearing forces analysis 10 p1896 A70-25093

Oriented flexible rolled-up solar array /FRUSA/ for spacecraft electric power generation, describing orientation and deployment mechanisms, solar panel, system operation, etc [AIAA PAPER 70-738] 11 p2119 A70-25434

Flexible vehicle control, using cybernetic model for system design and response [AIAA PAPER 69-115] 12 p2314 A70-27811

Geometrical theory of nonlinearly elastic inhomogeneous flexible shells, deriving variational equation in terms of displacement component and stress function 13 p2514 A70-29288

Optimal control surface location for flexible aircraft determined by matrix minimum principle and calculus of variations 16 p2840 A70-33316

Random vibration test for quasi-flexible specimens with each mounting point subjected to different vibration levels and spectrum shapes 16 p2889 A70-34022

Flexural pivots for space structures, describing design, fabrication and applications 16 p2924 A70-34170

Flexible space vehicles dynamics and control covering free vibration analysis, thermal flutter and structural deflection effect on attitude control 17 p3177 A70-35233

Dual spin satellites considered as deformable flexible gyrostats, obtaining stability criteria 17 p3177 A70-35234

Flexible channel multiplier for particle counting with electron conductive polymer composition, discussing secondary electron emission, gain distribution and degradation 17 p3054 A70-35279

Matricial group representation theory for constructing elastic vibration equations of symmetric flexible mobile controlled members 17 p3180 A70-35293

Dynamic flexible artificial earth satellites with mass distribution, considering control systems design principles 17 p3180 A70-35294

Nonrigid satellites dynamical equations derivation in modeling by generalized coordinates 18 p3333 A70-36702

Torque free spinning satellite with flexible appendages, investigating design parameters effects on nutational stability [AIAA PAPER 70-1046] 19 p3534 A70-38861

Flexible shallow shell with plastic inhomogeneity due to yield-point-fast neutron flux relation, examining stability under uniform load 20 p3734 A70-40437

Aircraft, rocket or other rigid or flexible structure, computing inertial constants based on measurements of generalized masses of natural modes 21 p3935 A70-41408

All-flexible parawings aerodynamic performance prediction based on slender wing theory and circular arc approximations for canopy shape [AIAA PAPER 70-1188] 21 p3754 A70-41827

High strength graphite fabrics evaluation for flexible structures, discussing temperature effects, fabrication, mechanical properties, oxidation and protective coatings [AIAA PAPER 70-1183] 21 p3842 A70-41830

Aerodynamic forces on flexible launch vehicles and missiles in supersonic flight based on first order method, solving boundary value problem for surface velocities 21 p3746 A70-41853

Flexible antennas and solar panels effect on dynamic behavior and control system response of dual spin spacecraft 21 p3931 A70-41855

Variable thickness flexible plates thermoelastic flexure and buckling, obtaining nonlinear differential matrix equations by difference-differential method 22 p4115 A70-42811

Earth gravity deforming effect on flexible crossed-dipole satellite configuration, considering dynamic stability and spin stabilization 22 p4110 A70-43434

Earth gravity effect on spin vector attitude stability of flexible crossed dipole satellite configuration 22 p4110 A70-43435

Soviet bibliography on flexible plates covering elastic bending, elastoplastic state under transverse load and bending beyond elastic limit 22 p4119 A70-43710

Rotating flexible cable-connected space station dynamic scale model, describing suspension system and artificial gravity generation 23 p4258 A70-44528

FLEXIBLE WINGS

NT PARAWINGS

Lift and drag characteristics of flexible parawings at subsonic speeds, predicting angle of attack for trailing edge flutter commencement 12 p2157 A70-28079

Packable near weightless nylon cloth wings without rigid members for improved aeronautical efficiency in cargo delivery, powered flight and rocket and spacecraft recovery [AIAA PAPER 70-880] 17 p3017 A70-34815

Wings flexural deformability influence on longitudinal stability of glider, using small perturbation theory 17 p3017 A70-35190

FLEXING

Moments and shear forces in plate flexure represented by single valued stress functions of position, stating variational principle for compatibility 01 p2021 A70-10931

Flexural wave propagation in infinitely long circular bimaterial cylinders based on equations of linear elasticity, noting dispersion characteristics different from homogeneous cylinders 01 p2028 A70-11188

Exact polynomial solution Saint Venant flexure of twisted rectangular plate treated as shallow hyperbolic paraboloidal shell 05 p0928 A70-16056

Flexural elastic behavior of rectangular plates with boundary restraint acting on same side using finite differences method 07 p1406 A70-19348

Autocollimation technique for determining flexure of tube of Wanschaff vertical circle 08 p1496 A70-21158

Curved thin rods torsional and flexural waves propagation equations, considering geometry and shear and Young moduli 08 p1588 A70-21201

Life and confidence tests of miniature self contained flexure pivots in critical mechanisms [ASME PAPER 70-DE-76] 16 p2918 A70-33552

Arbitrary cross sections center of flexure formula, transforming surface integral to line integral dependent on boundary conditions 18 p3343 A70-36716

Triboelectric noise in mechanically flexed low level signal cables for piezoelectric transducers with high gain amplifiers 21 p3825 A70-40866

Elastic bar attached to free edge of infinite length cantilever plate, calculating free flexural vibration for comparison with experiment 22 p4114 A70-42648

Flexural vibrations of clamped circular plate with nonlinear elasticity for small strains and displacements, using variational principle 22 p4120 A70-43719

FLEXORS

Heterochronism of coordinated cophasal flexor and extensor movements during acrobatic leap in human subjects

12 p2168 A70-27344

FLEXURE

U FLEXING

FLICKER

Monocular and interocular threshold luminance changes during flicker stimulation, noting interflash duration effects

08 p1453 A70-21792

Thermal feedback theory of flicker noise generation in transistors and temperature fluctuations effect in vicinity of recombination centers

12 p2196 A70-27687

Flickerless regeneration rates for CRT displays as function of scan order and phosphor persistence, using computer experiment

24 p4298 A70-45511

FLICKER FUSION FREQUENCY

U CRITICAL FLICKER FUSION

FLIGHT ALTITUDE

Fluoric altitude insensitive thruster based on two way gas flow diversion valve developed for VTOL aircraft and missile hot gas attitude control systems [ASME PAPER 69-WA/FLCS-10]

04 p0626 A70-14843

Pulse radar altimeter for measuring meteorological balloon altitude, using superregenerative RF stage

05 p0845 A70-15805

Midaltitude satellite system for continuous three dimensional navigation, considering elevation angles, constellations and orbits

12 p2270 A70-27923

Aircraft altimeter measurement for vertical separation based on atmospheric pressure unit changes /Cayleys/ compared with linear measurements in meters and feet

13 p2411 A70-29778

Hunting phenomena of hydrogen gas plastic balloon at ceiling altitude, considering exhaust duct, extra volume and shape

17 p3018 A70-35317

Supersonic flight altitude stability, studying effects of velocity, lift-drag ratio, thrust law, wind direction, engine unstarts, etc

22 p3961 A70-42712

FLIGHT CHARACTERISTICS

Flight recorder survey to determine combat operating environments of instrumented CH-46D Sea Knight helicopters

01 p0006 A70-10702

Meteorological data provision for supersonic civil transport operations, considering various flight phases

02 p0325 A70-12221

VTOL transport aircraft stability and maneuverability compared with conventional aircraft

02 p0228 A70-12759

Flight characteristics differences between VTOL and conventional transport aircraft, recommending differences consideration in regulations

03 p0414 A70-14095

Flying qualities criteria and piloted simulator studies during development and flight testing of stability augmentation system for B-52 aircraft [AIAA PAPER 68-1066]

04 p0624 A70-15380

Aircraft lift, thrust and drag coefficients inaccuracies expressed as errors in measured flight performance characteristics

04 p0624 A70-15386

Experiment design and data acquisition for V/STOL aircraft flying qualities simulations, emphasizing pilot rating and comment data and control usage information [SAE PAPER 690695]

05 p0825 A70-15860

Flow phenomena about beating plates, fins and wings, discussing biological and engineering applications

05 p0790 A70-16155

VTOL aircraft control and stability with emphasis on flight characteristics and man machine interaction

05 p0809 A70-17089

Flight performance prediction for throttling bipropellant rocket engine utilizing ablative combustion chamber throat, discussing lunar module descent engine

06 p1130 A70-17176

Aerodynamic flight characteristics of lifting reentry bodies in subsonic to hypersonic range in wind tunnel tests

06 p1154 A70-17249

Rotation and forward flight effects on separation line of laminar incompressible boundary layer along helicopter blade of airfoil shape [AIAA PAPER 70-49]

06 p0973 A70-18151

Enhanced real time operational impact and casualty analysis /ERIOCA/ for range safety, discussing computer-driven CRT display and missile flight parameters selection

07 p1251 A70-20371

Soviet monograph on inertial methods of flight vehicle motions parameters measurement

08 p1540 A70-20692

Dual inertial navigation transpolar flight to North Pole aboard KC-135 airplane, discussing performance, installation, etc

09 p1719 A70-22189

Chemical rocket propulsion systems approximate calculation for characteristic velocity dependence on mixture ratio and pressure in combustion chamber [DFVLR-SONDDR-24]

10 p1929 A70-23842

Super sonic booms occurrence and propagation, discussing aircraft operating conditions for prevention of effect on ground

10 p0000 A70-24130

Helicopter blade flapping torsion flutter behavior analysis showing stabilization effect in forward flight

10 p1958 A70-24559

Statistical methods for flying quality research concerning sailplane dynamic stability, maneuverability, sensitivity, rolling and pilot induced oscillations

10 p1805 A70-24582

Military specification revision of Flying Qualities of Piloted Airplanes evaluated by flight test including Flight Path Stability and Roll Rate Oscillation techniques

10 p1806 A70-24930

Circumplanetary aircraft design for solo nonstop great circle around world flight without refueling, noting application to sport, transportation, surveillance, photography, etc

11 p1981 A70-26046

Aircraft flight characteristics simulated on trainer with automatic control system and measuring system

11 p2056 A70-26455

Aviation equipment and systems operational durability, formulating physical model to construct functions for analysis

12 p2240 A70-27015

Glider longitudinal stability and control in symmetrical flight positions, determining flight characteristics

12 p2161 A70-27723

Wind-launch vehicle interaction in flight, using equations of motion for aerodynamic loads [AGARDGRAPH-115]

13 p2504 A70-28756

Azur satellite flight results, noting trajectory accuracy telemetry reception, yo-yo triggering and attitude control

13 p2505 A70-28766

Soviet book on aerodynamics of Tu 134 aircraft, covering 30 turbojet engines, flight characteristics, etc

13 p2344 A70-28875

Dual controlled elastically twisting rotor blade performance during flight with azimuthal and collective variations compared to direct control rotor

13 p2345 A70-29012

Longitudinal short-period flying qualities as closed-loop pilot-airplane system, noting acceptance values [AIAA PAPER 70-569]

13 p2346 A70-29034

German-French jet aircraft trainers, discussing Alpha Jet TA 501, E 650 Eurotrainer and VF T 291 flight characteristics

13 p2347 A70-29052

Sailplanes flight characteristics concerning longitudinal stability and control position gradient

14 p2531 A70-30634

Soviet book on practical aerodynamics of Mi 6 helicopter covering engine/rotor power balance, control, flight characteristics and solutions to in-flight emergencies

14 p2532 A70-31414

Rumanian book on flight stability and control covering Liapunov general stability theory, control systems, stability models, etc

15 p2673 A70-31695

L-1011 aircraft payload, range, configuration, engine selection, design features, equipment systems, flight characteristics, internal arrangement, maintenance and performance

15 p2673 A70-31947

Flight behavior of pyrotechnic circuits in ELDO-EUROPA 1 booster for separating stages and autodestruction

15 p2709 A70-32288

Auxiliary inlet ejector and plug nozzle flight performance, describing design variation effects for high supersonic speeds

16 p2841 A70-33563

Flight performance of Apollo LM descent-ascent propulsion systems, considering telemetry data, prediction correlation and modifications

16 p2967 A70-33577

Variable stability trainer modification of F-106 to reproduce flight characteristics of aircraft for pilot training in potentially dangerous situations

16 p2842 A70-33815

CAT shear spectra above ground frictional layer in jet stream flight conditions, using aircraft measurements

16 p2946 A70-33825

UH-1C, AH-1G and UH-1H helicopters combat operational flight profiles, considering airspeed, altitude, rotor speed, load factor, etc

17 p3014 A70-34717

Tilt-fold-proporator VTOL aircraft characteristics, stability and control, emphasizing flying qualities

17 p3014 A70-34722

SST flight efficiency trends, discussing breakthrough and development method and Concorde aerodynamic, propulsion and structural history

17 p3016 A70-34811

Flying qualities criterion for fighter flight control systems design

17 p3020 A70-35837

Fighter aircraft design for spin resistance and recovery using analytical approach, wind tunnel and flight tests

17 p3020 A70-35838

Soviet book on VTOL design covering aerodynamic and weight characteristics, turboprop and turbojet engines, flight regimes, etc

19 p3354 A70-37233

MBB Bo-209 Monsun travel, commuter and acrobatics aircraft, discussing configurations, specifications, structure and handling characteristics

19 p3355 A70-37388

Soviet book on helicopter aerodynamics covering main rotor operation, types classification and various flight characteristics

19 p3355 A70-37390

Flight data acquisition methods standardization, discussing digital recording modes and formats and hardware rationalization

19 p3429 A70-38515

Bobweights effects on pilot induced oscillations, noting role in flying qualities and control system design

20 p3560 A70-39529

Flight characteristics and performance calculation of single rotor helicopters by digital computers, considering wobble plate steering margin, compressibility, ground effects, separation and autorotation

20 p3561 A70-39716

German book on principal characteristics of flight mechanics and ballistics covering mirror symmetric aircraft and axisymmetric bodies such as projectiles and missiles

21 p3749 A70-40738

Yak-40 business jet design and flight characteristics

21 p3755 A70-42174

SN 600 Corvette business jet design and performance

21 p3755 A70-42175

Para-foil application programs and test results, discussing flight and glide performance, turn control, deployment inflation, etc

22 p3961 A70-42706

Downwash angle behind straight wing for unsteady aperiodic flight at subsonic speeds, using vorticity model

22 p3959 A70-42802

Canadair CL-84 V/STOL aircraft flight characteristics and structural design

23 p4137 A70-44017

Small airplane unsteady motion downwash angle at low speeds, comparing results from rectilinear steady flights

23 p4138 A70-44108

Harrier aircraft development history, discussing V/STOL constraints on transonic flight properties [ICAS PAPER 70-51]

23 p4139 A70-44148

Enhanced real time operational impact and casualty analysis for range safety, discussing computer-driven CRT display and missile flight parameters selection

23 p4178 A70-44517

Aircraft geometry effects on longitudinal flight characteristics calculations, noting wing aspect ratio and horizontal tail changes

24 p4289 A70-45437

Stationary aeroelastic cases studied in subsonic flow range, providing criteria for aircraft design with required flight characteristics

24 p4422 A70-45443

Commercial STOL aircraft takeoff and landing physical parameters relationships based on wind tunnel and flight tests

24 p4292 A70-45959

Viggen aircraft testing for flight properties, discussing measuring instruments, analog and digital recording, preprogrammed control, etc

24 p4317 A70-46228

FLIGHT CLOTHING

Flight safety, survival and personal equipment - Conference, Las Vegas, October 1969, Volume 2

07 p1217 A70-19003

Fire resistant protective flight clothing program for USN aircrewmembers, presenting accident case histories

07 p1218 A70-19013

Pilot helmets, discussing sound attenuation, noise protection and speech intelligibility

12 p2177 A70-27040

Testing laboratory for safety, survival and life support equipment concerning parachutes, aircrew protective helmets and maintenance manuals

23 p4141 A70-44488

FLIGHT CONDITIONS

Atmospheric effects on SST, discussing turbulence, temperature, wind, cloud cover, hail, toxic gases, etc

02 p0325 A70-12218

- Streamlining design for high altitude hypersonic flight vehicles based on drag minimization at flight condition 07 p1189 A70-19717
- Jet transport aircraft turbine engine performance monitoring by flight data, discussing historical highlights and future prospects [SAE PAPER 700314] 18 p3301 A70-36801
- FLIGHT CONTROL**
 - NT AUTOMATIC FLIGHT CONTROL
 - NT AUTOMATIC LANDING CONTROL
 - NT FLY BY WIRE CONTROL
 - NT POINTING CONTROL SYSTEMS
 - NT THRUST VECTOR CONTROL
- Civil aviation electronics - Conference, London, September 1969, Part 1, Electronics in flight control 02 p0329 A70-11831
- Projected and head-up flight information displays using cathode ray tubes, discussing optical system, lens design and landing aid application 02 p0330 A70-11843
- Flight vehicles intrinsic vibration frequency spectra for controllable flight determined by graph-analytical method 02 p0227 A70-12415
- Optimum automatic system for controlling helicopter formation flight, stressing transient response Q factor and transmission ratios 03 p0413 A70-13859
- Cockpit information transfer between pilot and flight control information displays improved by on-board data processing system 03 p0436 A70-14021
- Aircraft visual flight control displays development, considering liquid crystals in alpha numeric data output devices and holograms for three dimensional structures reproduction 05 p0853 A70-17090
- Flight deck controls and instrument disposition in business aircraft emphasizing size 06 p1061 A70-17318
- Electronic displays and flight control system of Multi-Role Combat Aircraft developed by Germany, Italy and UK 08 p1493 A70-20631
- Carrier-based attack aircraft avionics, describing optimal large scale analysis procedure for flight control, communications and radar subsystems 08 p1470 A70-20660
- Astronomical sounding balloon to study interplanetary scattered light, discussing actuating and control, structure, onboard and ground electronics 08 p1497 A70-21349
- Pilot systems for controlling aircraft in flight, considering direct lift control, displays, simulators, tests, etc 08 p1437 A70-21734
- Soviet book on flight dynamics in turbulent atmosphere covering air motion, aircraft lateral and longitudinal motion, gust loads, autopilot flight, takeoff and landing 09 p1610 A70-22598
- Fighter aircraft inflight thrust control using thrust reverser technology to improve operational capability. [AIAA PAPER 70-513] 09 p1610 A70-23019
- Fighter flight control design criteria for providing maximum combat effectiveness, safety and survivability without excessive cost or risk 09 p1611 A70-23021
- Alpine dependability on basis of improvements in jet engine, avionics, pilot seat cushions and flight control systems 09 p1611 A70-23453
- Apollo Program flight control operations personnel premission planning and training, discussing resolution of launch problems and emergencies 09 p1768 A70-23707
- Degenerate variational problem of optimum gliding along zero proximity line, determining number of control switchings and deviation during perturbed motion 10 p1854 A70-24277
- Control theory, Volume 2, Analysis and design of space vehicle flight control systems 11 p2122 A70-25772
- Area navigation system advantages for pilots, flight control systems and improved accuracy through rejection of VOR course scalloping [SAE PAPER 700214] 11 p2079 A70-25885
- Low cost lightweight flight control systems for business aircraft providing equivalent performance to larger equipment [SAE PAPER 700213] 11 p2079 A70-25886
- Integral relay operations effectiveness based on random spatial distribution of aircraft under control of Army flight operations center 11 p2080 A70-26265
- Psychic stress at simulated flight vehicle guidance tasks evaluated quantitatively 12 p2177 A70-27037
- Hydraulic systems for Boeing 747 aircraft flight control 12 p2167 A70-28019
- Wind load aerodynamics effects on launch vehicle flight control systems design [AGARDOGRAPH-115] 13 p2504 A70-28753
- Soviet book on dynamics of rockets covering solid and liquid fuel rocket stability, controllability and transfer functions 13 p2505 A70-28799
- Airline flight crews training need, emphasizing pilot flight maneuver capabilities for emergencies 13 p2345 A70-28974
- Flight control and human role in avionics system, discussing stabilization, autopilot and ILS systems 13 p2450 A70-29997
- Temperature rate flight control system/TRFCS/ for lifting reentry vehicles control and guidance 14 p2614 A70-30464
- Rumanian book on flight stability and control covering Liapunov general stability theory, control systems, stability models, etc 15 p2673 A70-31695
- Airplane performance improvement by flight control system design, discussing ride quality, flutter margin, maneuver load, etc [AIAA PAPER 70-875] 17 p3017 A70-34816
- Structural weight reduction and increased aerodynamic efficiency in aircraft design by including flight control technology early in configuration development phase [AIAA PAPER 70-874] 17 p3017 A70-34817
- Apollo lunar landing flight control functions, organization, disciplines and activities at Mission Control Center 17 p3134 A70-35292
- Integrated flight management system for commercial aircraft pilot using computer [AIAA PAPER 70-908] 17 p3134 A70-35820
- Flying qualities criterion for fighter flight control systems design [AIAA PAPER 70-927] 17 p3020 A70-35837
- Commercial aircraft flight deck systems controls and time sharing displays, emphasizing crew management [AIAA PAPER 70-938] 17 p3021 A70-35847
- Heat-up display /HUD/ system, discussing development, production, commercial aircraft applications and flight sequences uses 18 p3223 A70-36210
- Recursive digital filters for flight control system airborne computer, considering quantization effects and eigenvalue sensitivity 20 p3601 A70-39575
- Aerospace electronics covering fly-by-wire aircraft flight control, ATC, star trackers for spacecraft attitude control, etc 20 p3669 A70-39668
- Airborne integrated computerized ASW system, describing navigation, flight control, display and sensor subsystems 21 p3821 A70-40575
- Papers on aerospace vehicle flight control systems covering controller design, flow difference sensors, etc 21 p3926 A70-40780
- UpSTAGE interceptor missile flight control system, discussing command logic to capitalize on lifting body advantages to enhance roll maneuver 21 p3927 A70-40782
- Liquid metal hydraulic servoactuation packages for flight control in high temperature environments without coolant systems 21 p3750 A70-40785
- Pilot hand-held and leg-mounted controllers for precision tracking from aircraft under buffeting tested in static and dynamic motion simulator 24 p4308 A70-45513
- Hydrofluidics flight controls for aircraft stability augmentation systems, noting component performance, transfer functions and operation [SAE PAPER 700793] 24 p4294 A70-45854
- Formation flight stability in dynamic environment, using stationkeeping geometry simulation [AIAA PAPER 70-1337] 24 p4373 A70-45931
- FLIGHT CREWS**
 - Syncope occurrence among flight crews 01 p0033 A70-10371
 - Aircrew escape/rescue capability /AERCAB/ flying ejection seat design and test programs, noting rotary wing, fixed wing and parawing feasibility 01 p0035 A70-10714
 - Diurnal periodicity of physiological functions of flight crews flying through several time zones found to correspond to time zone of permanent residence 03 p0425 A70-13894
 - Airline stewards cardiovascular and ischaemic heart disease statistics compared with civilian pilots and general population 03 p0438 A70-14070
 - Aircraft crews in-flight medically controlled feeding, discussing physiological and nutritive value of foods 06 p1001 A70-17669
 - Commercial flight crew oxygen system using mask mounted diluter demand regulator 06 p1002 A70-17715
 - Fire resistant protective flight clothing program for USN aircrewmembers, presenting accident case histories 07 p1218 A70-19013
- Aircrew parachute with low speed-low altitude capability, considering static on-the-deck recovery, pack volume, weight, escape envelope spectrum, etc 07 p1191 A70-19014
- Psychiatric disorder in civil aircrew leading to suspension or loss of licence, discussing physicians role and complications of treatments 07 p1223 A70-19940
- Flight crews spatial vision, estimating absolute distance perception of pilots and navigators with emmetropic refraction 08 p1450 A70-20742
- Postinfectious noncoronogenic afflictions of myocardium in flight personnel, discussing clinical record, arteriosclerotic differentiation and ECG variation 09 p1617 A70-22474
- Apollo 11 mission crew observation of operational and scientific phenomena associated with lunar landings, discussing preflight geologic training and briefings 11 p2109 A70-25847
- Aircrew equipment assemblies taking into account altitude, flight acceleration, environment, escape and survival 13 p2345 A70-28971
- Medical wastage of professional aviators in military and civil aviation, discussing reasons for preventing flying license revalidation 13 p2359 A70-29440
- Fatigue and aircraft environment effects on physical and mental state of airline flight attendants during prolonged cruises 15 p2692 A70-32211
- Emergency evacuation on land of passengers and crew of airliners, discussing training, equipment, standardization, communication and protective fabrics 15 p2675 A70-32220
- Human factors in aircraft accidents, noting cockpit crew members overconfidence and carelessness 15 p2692 A70-32228
- Aircraft crew oral temperature related to work-rest schedules, discussing hypothermia, flight stress and in-flight depression 17 p3032 A70-35563
- Wolff-Parkinson and White syndrome applicability in aeromedical appraisal for aircrew selection, noting effects of paroxysmal tachycardia 17 p3040 A70-35916
- Renal lithiasis frequency among flight crews during aeronautical activity, noting role of rich food intake 17 p3040 A70-35917
- Medicopsychological and labyrinthic exploration of flight crew candidates aeronautical adaptation, using electronystagmographic method of swinging chair 17 p3041 A70-35918
- Aircrewmembers work credit under Flying Time system to determine rank order for mission scheduling, noting legitimate functions performance 21 p3771 A70-41483
- Statistical data on waivers granted to airline flight crew members by French Civil Aviation Medical Board based on ICAO medical standards 21 p3771 A70-41491
- Flight crews with aortic insufficiency, observing hermodynamically insignificant valvular defect 21 p3771 A70-41492
- F-111 crew escape module, describing main parachute and pyrotechnics severance improvements, parachute deployment and inflation, etc [AIAA PAPER 70-1210] 21 p3751 A70-41807
- Atherosclerosis and latent coronary insufficiency diagnosis in flight crews, evaluating various tests 22 p3975 A70-43696
- Aircraft crew and pilot in-flight work load measurement and simulator [ICAS PAPER 70-43] 23 p4138 A70-44141
- F-111 aircraft crew cockpit escape module design for maximum efficiency, including survival equipment after ejection 23 p4141 A70-44491
- Sleep patterns during double aircrew continuous flying operations, suggesting 3-day maximum mission duration 24 p4306 A70-45327
- Concorde thrust control by employment of variable area nozzle and reheat system, discussing crew work load [SAE PAPER 700817] 24 p4394 A70-45900
- FLIGHT FATIGUE**
 - Flight fatigue syndrome origin, therapy and prevention, noting cortical adrenal hormones tests 01 p0031 A70-10234
 - Fatigue and aircraft environment effects on physical and mental state of airline flight attendants during prolonged cruises 15 p2692 A70-32211
 - Medical and professional disadaptation in fighter pilots, considering fatigue, digestive disorders, anxiety, absenteeism, efficiency loss and accident proneness 16 p2850 A70-34347

FLIGHT FITNESS

Astronaut vestibular fitness determined from threshold labyrinthine tests on isolated horizontal and vertical semicircular canals

03 p0437 A70-14059

Astronauts physical training for space flight requirements

04 p0629 A70-14564

Flight personnel psychological fitness appraisal techniques, reviewing literature concerning test methods

06 p0995 A70-17668

Vital capacity measurements made preflight and postflight on jet fighter aircrew breathing pure oxygen at various G forces

07 p1222 A70-19934

Asymptomatic pilot with idiopathic paralysis of hemidiaphragm, discussing clinical picture and aeromedical significance

07 p1215 A70-19942

Aviation medicine, discussing pilots physical fitness and training, spatial orientation, ground crew, data flow, etc

08 p1451 A70-20977

Aircraft pilots fitness under flight stress, discussing smoking, overweight, lack of exercise, etc, leading to coronary afflictions

09 p1620 A70-23013

Aircraft pilots physical exercise program to maintain optimal state of fitness, discussing harmful effects caused by nervous and psychic strains

09 p1626 A70-23014

Body training type and amount effect on physiological functions and physical fitness of pilots, discussing pulse frequency

09 p1626 A70-23015

High risk factors for posttraumatic epilepsy /head injury complicated by subdural hematoma and spike EEG abnormality/ precluding return to flying

09 p1622 A70-23470

Psychological fitness capacity of students in pilot training, determining unfavorable traits for flight

11 p1985 A70-25670

Preflight medical examination of flying personnel, describing portable device for recording systolic/diastolic pressure, body temperature and pulse rates

13 p2357 A70-29296

Flying personnel fitness, discussing Wolff- Parkinson-White syndrome

22 p3975 A70-43695

FLIGHT HAZARDS

NT METEOROID HAZARDS

Hazards due to nonohmic materials responsible for electrostatic failures in missile and space programs and ground equipment

01 p0141 A70-10088

Bird impact damage effect on aircraft structural design, considering forward facing areas and minimum weight

01 p0200 A70-10687

Bird deflection grill device for turboprop engine inlet ducts, noting effects on inlet flow characteristics, engine performance, etc

01 p0165 A70-10688

Space or atmospheric flight caused or aggravated ophthalmic lesions, noting retinal and conjunctival hemorrhages from barometric pressure fall and rapid acceleration and deceleration

01 p0022 A70-10858

Forward sounding sensors /weather radar/ development for aiding human eye in detecting flight hazards /storms and CAT/

02 p0297 A70-11989

Crash control for reduction of operational hazards and flight accidents to survivable level, discussing pilot training for emergencies

07 p1191 A70-19008

Seismic measurements of sonic boom induced ground vibrations for hazard to structures

12 p2227 A70-28078

Conditions leading to lightning as triggered by Apollo 12 and suggestions for minimizing such hazards

13 p2394 A70-28838

Infectious disease hazards on space flight, discussing internal environmental factors including resistance and etiologic agents transmission

14 p2537 A70-30366

Flight Impact Simulator for simulating bird strikes and bird-proofing of aircraft

16 p2888 A70-33290

Netherlands Air Force bird strike problem and warning system

18 p3211 A70-35977

U.S. Air Force bird-aircraft collisions problem and bird control research

18 p3211 A70-35984

Soviet monograph on collision hazards between aircraft and birds covering accidents, damage and preventive measures

23 p4137 A70-44099

FLIGHT INSTRUMENTS

NT APPROACH INDICATORS

NT ATTITUDE INDICATORS

NT AUTOMATIC PILOTS

NT FLIGHT TEST INSTRUMENTS

NT GYRO HORIZONS

NT HORIZON SCANNERS

NT RADIO ALTIMETERS

Visual flight displays technological and human engineering development

01 p0039 A70-11259

Projected and head-up flight information displays using cathode ray tubes, discussing optical system, lens design and landing aid application

02 p0330 A70-11843

Precision and accuracy evaluation of convergence angles for measuring vertical and horizontal components of space position applicable to geodesy and flight measurement

[AAS PAPER 69-605] 04 p0676 A70-14634

Flight deck controls and instrument disposition in business aircraft emphasizing size

06 p1061 A70-17318

Flight deck displays based on digital computer providing signals for CRT and instrumentation

06 p1061 A70-17319

Flight configured single sideband telemetry accuracy determined by digitally computed frequency response

06 p1012 A70-18600

Book on aircraft flight and engine instruments covering fuel gages, altitude and speed indicators, altimeters, magnetic compasses, gyroscopes, tachometers, pressure, gages, flowmeters etc

11 p2048 A70-25574

Japanese jet aircraft pilots instrument reading and checking procedures during landing operation under contact flight rules

11 p2078 A70-25667

Capacitive pressure transducer with linearly coupled armatures for aerospace use

11 p2051 A70-26294

Low cost headup displays /HUD/ for pilot error reduction during takeoff, approach and landing, discussing displayed functions vs cost tradeoffs

16 p2911 A70-33818

Commercial aircraft flight deck systems controls and time sharing displays, emphasizing crew management

[AIAA PAPER 70-938] 17 p3021 A70-35847

Heat-up display /HUD/ system, discussing development, production, commercial aircraft applications and flight sequences uses

18 p3223 A70-36210

Soviet book on man in aircraft control system covering engineering psychology, complex flight problems, human factors and instrument panels

19 p3367 A70-37236

Jaguar flight test instrumentation methods, discussing Anglo-French participation

19 p3356 A70-38534

Concorde prototype 002 flight test data recording instrumentation, emphasizing digital system for quasi-static parameters

19 p3432 A70-38545

VTOL aircraft instrument flight in terminal area, defining requirements and operating characteristics for vertical and low speed capabilities

[AIAA PAPER 70-1333] 24 p4291 A70-45935

FLIGHT LOAD RECORDERS

AH-1G helicopters combat flight loads from on-board oscillograph data recording, defining performance in terms of critical variables

17 p3013 A70-34706

Structural fatigue design loads computation for fighter aircraft using multivariable load environment model from oscillograph recorded multichannel aircraft response data

[AIAA PAPER 70-948] 20 p3719 A70-39579

FLIGHT MECHANICS

Soviet papers on flight dynamics, Number 2, covering satellite orbit stabilization, flight vehicle optimal control, optimal pursuit, fighter attack on target, etc

02 p0226 A70-12401

Optimal control synthesis in flight dynamics, solving Hamilton-Jacobi-Bellman equation by finite difference technique

02 p0336 A70-12403

Soviet book on flight vehicle trajectories covering equations of motion, flight mechanics, reference systems, etc, for rockets and spacecraft

03 p0410 A70-12871

Computer program /TACTICS/ for simulating three vehicles simultaneous motion in space, considering intercepter-target guidance and intercept trajectories

07 p1239 A70-20414

Soviet book on new methods of variational calculus in aerospace vehicle flight dynamics covering controlled processes optimization theory analysis

09 p1767 A70-23473

Ordnance flight dynamics, considering trajectory analysis and inaccuracies due to projectile wobble

[AIAA PAPER 70-533] 13 p2506 A70-29001

Reentry vehicles development, discussing systems analysis and design, vehicle aerodynamics, aerodynamic heating and shielding, and flight mechanics and control

13 p2506 A70-29055

Book on aerodynamics and flight mechanics, discussing aircraft parts, subsonic, transonic and supersonic flows, level ascending and descending flights, landing and takeoff, etc

15 p2672 A70-32075

Analytic theory of unsteady separated flow effects on dynamics of heat sink type reentry bodies and elastic launch vehicles

[AIAA PAPER 70-762] 17 p3008 A70-34489

German book on principal characteristics of flight mechanics and ballistics covering mirror symmetric aircraft and axisymmetric bodies such as projectiles and missiles

21 p3749 A70-40738

FLIGHT OPTIMIZATION

Optimal control synthesis in flight dynamics, solving Hamilton-Jacobi-Bellman equation by finite difference technique

02 p0336 A70-12403

Sufficient conditions for relative extremum in flight dynamics optimization determined by variational method

02 p0381 A70-12417

Jet aircraft long range flight planning using computer for wind and temperature forecasts, path altitude profile computation and optimization

02 p0403 A70-12841

Shooting method for real time optimization of multiple burn rocket flights, presenting analysis, algorithm and test results

04 p0761 A70-14932

Flight plans monitoring in real time with on-line computer for optimal route, fuel consumption and speed

05 p0817 A70-16362

Optimum rocket climbing regime in dense atmospheric layers, including gravitational acceleration investigation in outside layers

06 p1155 A70-17626

Optimality criteria for selecting flight conditions for civil aviation helicopters, considering scheduled speed and efficiency, commercial load factor, wind rose, vertical separation, etc

06 p1185 A70-17874

Economic flight conditions for civil aviation VTOL aircraft selected by graph-analytical method concerning phases of ascent, cruising and descent

06 p0987 A70-17875

Vehicles optimal flights with controlled or boundary level thrust in circular orbit neighborhood, using linearized equations of motion

06 p1142 A70-17876

Level flight optimization in horizontal wind varying with altitude, using glider concept and induced drag correction

[ONERA-TP-700] 07 p1193 A70-19131

Interplanetary midcourse velocity correction schedules optimization, discussing timing equations modifications, mission simulation and role of earth based radar

09 p1759 A70-22760

Favorable air mass type and season for long cross country soaring flights over eastern U.S. determined from record analysis

09 p1718 A70-23062

Soviet book on new methods of variational calculus in aerospace vehicle flight dynamics covering controlled processes optimization theory analysis

09 p1767 A70-23473

Spacecraft optimal flight from earth orbit to outer planet orbit with ideally controlled engine using differential motion equations

10 p1941 A70-24512

Computing optimum flight profiles by Balakrishnan epsilon method, including equations of motion constraint in cost function to be minimized

[AIAA PAPER 69-75] 12 p2162 A70-28088

Optimal distance flight, discussing glider polar performance data

16 p2842 A70-34174

Aircraft optimal operating procedure development by integral-variational performance analysis methods, discussing flight paths, fuel consumption, mission requirements, etc

[AIAA PAPER 70-876] 17 p3016 A70-34812

Rocket vehicle flight optimization for model including rigid body degrees of freedom in boundary layer approximation to attitude transients

17 p3180 A70-35664

Weight growth factor in aircraft design, discussing fixed and variable weight, payload, performance, flight quality, structural criteria and life expectancy

[SAWE PAPER 839] 20 p3562 A70-40363

Optimal flight route selection with respect to meteorological prediction errors, using decision under risk and Monte Carlo method

22 p4067 A70-42656

FLIGHT PATHS

NT GLIDE PATHS

Monograph on future air traffic control concerning radio navigation, color display and computer determined flight paths

01 p0136 A70-10090

Optimum flight paths of energy and power limited rockets with generalized thrust characteristic, con-

sidering vertical, horizontal, rectilinear, zero drag and vacuum trajectories

01 p0193 A70-10425

Air traffic control inadequacy and restrictive regulations influence on aviation growth, implying need of airport-airways system improvements

[AIAA PAPER 69-1052] 01 p0138 A70-10642

Interurban air transportation network structure contribution to airport and airways congestion, considering addition of nonstop links

[AIAA PAPER 69-1037] 01 p0005 A70-10647

Air cargo transport routes and geographical distribution, examining development in African countries

02 p0402 A70-12225

Ground-airborne steep descent VTOL automatic flight control and vertical path selection using hover augmentation system /HAS/ and remote area terminal system /RATS/

02 p0337 A70-12769

Jet aircraft long range flight planning using computer for wind and temperature forecasts, path altitude profile computation and optimization

02 p0403 A70-12841

Meteors spectral intensity variations along flight path noting color dependence on brightness

08 p1572 A70-20946

Range, block speed and fuel-weight ratio formulas for hypervelocity, boost glide and ballistic vehicles

08 p1582 A70-21871

Course deviation indicator /CDI/ display applicability to tracking Omega lines of position, providing reduction in weight, volume, cost and complexity

12 p2269 A70-27920

Computing optimum flight profiles by Balakrishnan epsilon method, including equations of motion constraint in cost function to be minimized

12 p2162 A70-28088

Aeronautical navigation under various wind velocity conditions, studying flight times for closed flight paths

13 p2448 A70-28750

Minimum fuel takeoff and landing paths for VTOL aircraft with constraints on state and control, determining optimal trajectories

13 p2345 A70-29015

Frequency and amplitude during longitudinal control surface pumping by pilots in precise flight path handling for aircraft design

13 p2346 A70-29032

Pictorial display area navigation system for air traffic control in terms of cockpit utilization, interface with ground navigation aids, parallel multiple routes, etc

13 p2449 A70-29171

Fine scale temperature variability along flight path during smooth and turbulent conditions

14 p2609 A70-30605

Climatology of safe threshold Mach number and airplane ground speed for boomless supersonic cruise, considering San Francisco-New York route

14 p2530 A70-30606

Northern Hemisphere temperature atlas for SST cruise altitudes, estimating probabilities of enroute temperatures and risk increase

14 p2609 A70-30609

Synthetic array radar flying past flat plate, analyzing image relationship to flight path

14 p2552 A70-31193

Meteors spectral intensity variations along flight path noting color dependence on brightness

15 p2806 A70-32758

Optimum approach and departure paths for VTOL aircraft simulated by hybrid computer under constraints

18 p3213 A70-36452

Area navigation system charting, discussing effect on flight information publications

19 p3465 A70-38231

Highly localized clear air turbulence at aircraft flight level over Mediterranean, noting simultaneous temperature rise

19 p3463 A70-38948

Aircraft trajectory postflight reconstruction involving photographic starfield and landmark referenced to inertial navigator output, discussing optimal data smoothing technique

20 p3666 A70-39512

Aircraft flying at constant speed in circular orbits, calculating flight path under effect of uniform velocity wind

21 p3750 A70-40920

Airborne data acquisition equipment for accident flight path and engine performance recording

21 p3796 A70-41922

Optimal flight route selection with respect to meteorological prediction errors, using decision under risk and Monte Carlo method

22 p4067 A70-42656

FLIGHT PERFORMANCE

U FLIGHT CHARACTERISTICS

FLIGHT PLANS

Air cargo transport routes and geographical distribution, examining development in African countries

02 p0402 A70-12225

Flights best day pair and weekly leg schedules concept based on decision making model for traffic volume estimation in airline operations

02 p0403 A70-12787

Jet aircraft long range flight planning using computer for wind and temperature forecasts, path altitude profile computation and optimization

02 p0403 A70-12841

Flight plans monitoring in real time with on-line computer for optimal route, fuel consumption and speed

05 p0817 A70-16362

Apollo mission planning process, discussing flight schedule evolution from panels, meetings and working groups

09 p1768 A70-23710

Equipment and subsystems application to flight management avionics in military and commercial aircraft, noting role of ground-air information transfer

16 p2878 A70-33724

Corporate aircraft operations in Europe, discussing meteorological conditions, flight planning, airport arrival and departure procedures and language differences

16 p2842 A70-33820

Commercial air transport mission payload and range capability analysis, noting on-line flight planning computers

[AIAA PAPER 70-899] 17 p3204 A70-35815

Automatic ATC with feedback, describing information processing and flight plan algorithm

19 p3464 A70-38161

Signal automatic air traffic control system /SATCO/ for flight plan processing, using multi-processing real time computer, electronic displays and software facilities

19 p3469 A70-38646

Meteorological wind and temperature distributions on selected routes at Concorde cruising level, noting computer use for flight planning

24 p4374 A70-46204

FLIGHT RECORDERS

Flight recorder survey to determine combat operating environments of instrumented CH-46D Sea Knight helicopters

01 p0006 A70-10702

Flight data recorders, examining present systems and planned improvements

02 p0302 A70-12621

Pilot/vehicle dynamics from flight test records, discussing close-loop attitude control tasks

10 p1824 A70-23897

Transport aircraft flight recorders for parameters essential for operation and aircraft maintenance

11 p2050 A70-25818

Airborne data acquisition and flight recorder systems, comparing civil and military aircraft requirements

17 p3094 A70-35515

Flight data recorders and system integration, discussing data replay system backing flight recording

18 p3258 A70-36340

Flight data recording systems for accident investigation and operational purposes, discussing U.S., British and French regulations

18 p3258 A70-36341

Flight/accident data recorders and associated equipment for civil and military aircraft requirements

18 p3258 A70-36342

Underwater recovery requirements for flight data recorders, suggesting compressed air instead of explosive charges for ejection force

18 p3258 A70-36343

Digital flight data recording, considering aircraft integrated data systems /AIDS/

19 p3426 A70-37892

Flight data recording system /FDRS/ for crashes expanded to aircraft integrated data system /AIDS/ for airlines

19 p3426 A70-37893

Airborne crash recorders objectives, design and features ensuring crash survival of recordings

19 p3429 A70-38518

Flight recorder role in aircraft accident investigation and prevention, noting audio instruments and data recovery

19 p3356 A70-38613

FLIGHT RULES

NT INSTRUMENT FLIGHT RULES

Air traffic control procedures pertaining to personnel, hardware and regulations

11 p2078 A70-25720

FLIGHT SAFETY

Aeronautical satellite system for civil flight safety, discussing operational, technical and economic aspects

03 p0522 A70-13610

Readaption times of eyes adapted to darkness using night vision training device in relation to helicopter flight safety conditions

03 p0436 A70-13823

Pilot visual information display systems influence on flight safety, discussing aircraft accidents and human error factors

04 p0691 A70-15143

Flight safety, survival and personal equipment - Conference, Las Vegas, October 1969, Volume 1

06 p1001 A70-17702

Flight safety, survival and personal equipment - Conference, Las Vegas, October 1969, Volume 2

07 p1217 A70-19003

Fireproof fabrics tested for flame retarding and protection capabilities, discussing applications to aircraft interiors, escape parachutes, flight coveralls and protective clothing

07 p1219 A70-19017

Concorde electronics systems for testing and flight safety, controlling center of gravity, braking, kinetic heating, air conditioning, fuel flow and inertial navigation

07 p1194 A70-19741

Computer program /SAFETE/ for evaluating missile launch risk on near real time basis

[AIAA PAPER 70-248] 07 p1250 A70-20370

Missile and space vehicle range safety policies and practices using past statistical performance data and cost consideration

[AIAA PAPER 70-246] 07 p1251 A70-20372

Human factors responsibility for aircraft accidents, discussing cooperation between air safety service and flight surgeons

09 p1626 A70-23016

Apollo lunar module manned testing in thermal vacuum, emphasizing safety aspects of hardware, procedures and training

10 p1859 A70-24389

Clear air turbulence effect on supersonic aircraft safety and comfort, noting shallow zones and effects of topography and thunderstorms

10 p1912 A70-24506

Flight safety evaluation based on ICAC and German flight accident data indicating pilot role and tabulating statistical analysis

11 p1981 A70-25948

Urban airport runway capacity increase via reduced aircraft separation, additional parallels and improved terminal traffic control, discussing design for acceptable safety levels

12 p2207 A70-27627

Flight safety - Conference, Montreux, Switzerland, October 1969

15 p2674 A70-32206

Fatal accidents involving airline aircraft /1968- 69/

15 p2674 A70-32208

Accident/incident information exchange in aviation community, noting Flight Safety Foundation

15 p2674 A70-32209

Flight safety standards, criteria and requirements, stressing accident prevention shift from accident investigation

15 p2831 A70-32212

Aircraft accidents during descent, approach and landing, discussing B 747, C5A and SST

15 p2675 A70-32216

Management role in flight operations safety, stressing need for confidence and discipline

15 p2831 A70-32218

Human factors in aircraft accidents, noting cockpit crew members overconfidence and carelessness

15 p2692 A70-32228

Airport safety standards for overall system including aircraft, ATC, navigation, runways, etc

15 p2717 A70-32229

Flight safety - Conference, Washington, D.C., May 1969

16 p2841 A70-33813

Aircraft design, construction, operation and maintenance improvement efforts by FAA, discussing airworthiness requirements, audit team visits to factories, etc

16 p2842 A70-33824

Evolution and current status of Apollo crew safety, discussing hazard aspects, program approach and measures and activities incorporated in project

[AAS PAPER 70-051] 17 p3176 A70-34790

Space shuttle safety program for low risk passenger transportation, combining large aircraft experience with spacecraft technology

[AAS PAPER 70-055] 17 p3176 A70-34793

Air transportation growth with regularity and safety - Conference, London, November 1969

17 p3021 A70-35851

Data acquisition system applications philosophy, discussing data integrity, expansion facility, flight safety, etc

18 p3258 A70-36339

Aeronautical satellite system for civil flight safety, discussing operational, technical and economic aspects

21 p3848 A70-41131

Automated aircraft flight safety, concerning probabilities and onboard elimination of servomotor failures in hydraulic system due to fuel contamination

22 p3961 A70-42804

Survival and flight equipment - Conference, Las Vegas, September-October 1970, Volume 1

23 p4151 A70-44453

NASA safety related research programs based on technology transfer involving information summariz-

ing, indexing and storage from global aerospace research and development

23 p4285 A70-44457

Aircraft passengers and crew fire protection in crashes via insulating air-carrying foam ejected into compartment from fuselage

23 p4140 A70-44465

Operational requirements for NASA space shuttle Survival and Flight Equipment, discussing protection during launch and ascent

23 p4258 A70-44484

FLIGHT SIMULATION

USAF visual flight simulation devices from engineering and psychological standpoints, discussing human factors considerations

01 p0057 A70-10808

Flying spot scanner design and performance to generate images for visual flight simulation

01 p0089 A70-10816

Hardware CRT display system based on digital computer for dynamic flight simulation of moving spatial objects

01 p0089 A70-10818

Flight training simulators recording, playback, demonstration and instructor facilities and six degrees of freedom motion system

02 p0273 A70-11840

Air combat model (AIRCOM) to evaluate close-in air-to-air fighter aircraft combat capability, determining relative changes in kill probability per firing pass

03 p0413 A70-13958

Free flight ranges for hypersonic simulation from Mach 1 to Mach 30, noting onboard high-g telemetry instrumentation

04 p0663 A70-14723

Experiment design and data acquisition for V/STOL aircraft flying qualities simulations, emphasizing pilot rating and comment data and control usage information

05 p0825 A70-15860

Adaptive training applied to simulated pilot training system, discussing methods for variables selection, error measurement, trainee feedback, etc

05 p0805 A70-16007

Fatigue life tests for heat resistant gas turbine blade alloys under power and thermal loads simulating aircraft flight

05 p0953 A70-17051

Transposition and lunar docking simulation tests for Apollo 9 and subsequent missions using test vehicles equipped with flight type hardware

06 p1030 A70-18209

Laboratory electronics role in Concorde aircraft structural and acoustical fatigue analysis, flight simulation and flight studies

07 p1250 A70-19745

Astronauts celestial training, using Mercury capsule simulator and Zeiss planetarium projector for flight simulation

08 p1481 A70-21275

Boeing 747 pretesting work including wind tunnel, components, engines and static structural tests, flight simulation, etc

08 p1437 A70-21730

Trisonic high pressure wind tunnel simulating flow conditions on large transonic aircraft, noting high Reynolds number capability

09 p1655 A70-22023

ATC and SST operations in terminal area simulation study involving airline crews and controllers in real time traffic situation

09 p1721 A70-22946

Digital computer impact on aerospace sciences and technologies in terms of computerized design, interactive graphics, flight simulation, Apollo systems checkout, etc

09 p1642 A70-23277

Apollo crew procedures, simulation and flight planning, discussing navigation, guidance and control procedures

09 p1657 A70-23706

Color closed circuit TV visual cues in flight simulation during flare and touchdown, including ATA requirements and acuity limits

10 p1857 A70-24201

Dual cockpit wide angle visual cue simulator design, discussing sky-earth-sun projector with four axis gimbal drive

10 p1857 A70-24204

Visual threshold effect on closed loop control of aircraft of poor resolution studied by flight simulation of approach and flare, showing degraded control accuracy

10 p1858 A70-24206

V/STOL cockpit three degree of freedom multicrew research simulator, utilizing visual display and digital computer

10 p1858 A70-24207

Ground-based and in-flight simulation using variable stability aircraft, investigating pilot rating

10 p1858 A70-24209

Flight simulation data on motion cues effects in controlling compensatory tracking tasks

10 p1859 A70-24211

Human response to angular acceleration, discussing implications for motion capability in flight simulator

[AIAA PAPER 70-350] 10 p1824 A70-24212

Ground based simulation for hypersonic reusable lifting reentry vehicle design with pilot-in-loop, discussing six degree of freedom simulation

[AIAA PAPER 70-385] 10 p1861 A70-24920

Launch load simulation on scaled vibration model concerning Saturn 5 structural integrity and flight failure

10 p1953 A70-25072

Three axis motion simulator for in-orbit spacecraft attitude control evaluation using earth, sun and star sensor references

[AIAA PAPER 69-1029] 11 p2031 A70-26147

Aircraft pilot candidates reactions under simulated flight conditions tested using precision coordination analyzer /PCA II/ and instrument coordination analyzer /ICA/

12 p2176 A70-27034

Psychic stress at simulated flight vehicle guidance tasks evaluated quantitatively

12 p2177 A70-27037

High temperature, electrically heated convective gas heating system for high velocity atmospheric flight simulation using air-nitrogen working fluids

12 p2205 A70-27100

Plenum-chamber air-bearing and labyrinth-seal types air cushion lifting mechanisms performance in simulated hovering flight

12 p2162 A70-27981

Low thrust mission simulation dependence on hardware definition, discussing power plant characteristics, jet velocity and thruster efficiency

13 p2486 A70-28517

Supersonic flight simulation in hypersonic wind tunnels for developing hypersonic air breathing propulsion, describing ceramic storage heaters

13 p2384 A70-28666

Hypersonic test equipment, describing flight simulating hypervelocity wind tunnels, firing tunnels and shock wave tubes

13 p2384 A70-28927

Wind tunnel tests, analytical methods and fixed base simulation for predicting fighter aircraft spin characteristics

[AIAA PAPER 70-565] 13 p2346 A70-29030

Ionospheric spacecraft flight conditions simulation in vacuum chamber, discussing low energy ion sources

15 p2717 A70-31814

Mission simulation testing in thermal vacuum environment for Apollo Lunar Module, noting conformal skin heaters

[AIAA PAPER 69-991] 15 p2718 A70-32515

Large scale hydrogen fueled supersonic combustor test at simulated Mach 8 flight, describing fuel injector design

[AIAA PAPER 70-715] 16 p2965 A70-33539

Crack propagation, fatigue damage and interaction effects in aircraft structures and materials under flight simulation loading

17 p3185 A70-34924

Humidity resistance test method involving flight simulation for airborne equipment in tropical environment

17 p3058 A70-35159

Real time hybrid computer simulation of guided and controlled rocket flight, noting correlation with digital simulation

17 p3060 A70-35285

C-5 flight simulation program for design of basic aircraft, flight control and guidance subsystems

[AIAA PAPER 70-922] 17 p3064 A70-35833

Runway test vehicle for lifting rotor performance in simulated forward flight, comparing with wind tunnel tests

19 p3402 A70-38611

Pilot scanning dwell times and control workload in simulated instrument approach, using eye-point-of-regard /EPR/ measurements

[AIAA PAPER 70-999] 20 p3580 A70-39532

Transposition and lunar docking simulation tests for Apollo 9 and subsequent missions using test vehicles equipped with flight type hardware

20 p3606 A70-39685

Gust field in lowest atmospheric layer over homogeneous terrain, deriving statistical models and simulating effects on XV-5 V/STOL aircraft

21 p3750 A70-40784

Mission analysis and trajectory simulation /MATSP/ program, discussing computer controls, modular design, integration evaluation

[AIAA PAPER 69-939] 21 p3920 A70-41872

Flight simulation as aircraft design tool, discussing ground and in-flight simulation techniques

[ICAS PAPER 70-41] 23 p4178 A70-44139

Flight simulation in SAAB A37 aircraft development, describing analog and digital computers, cockpit simulators, automatic pilots, control and display devices

[ICAS PAPER 70-42] 23 p4178 A70-44140

Pilot assessment aspects of flight simulation in terms of experiment planning, facility and results reporting and analysis

23 p4153 A70-44546

Decompression sickness relationship to physical exercise during simulated Apollo flight

24 p4307 A70-45336

Visual air-to-ground target recognition simulation, comparing predictions from Autonetics Detection Model in low altitude flight

24 p4308 A70-45507

FLIGHT SIMULATORS

NT COCKPIT SIMULATORS

Concorde aircraft flight simulator, describing piloting system refinement and pilot training

01 p0057 A70-10797

Airborne sensor simulator using recorded imagery for target detection and recognition problems, discussing closed circuit TV

01 p0088 A70-10810

Trainers and simulators based on digital computers, eliminating system sensitivity to ambient conditions, power fluctuations, circuit imperfections and digital to analog conversion

02 p0274 A70-11841

Servoactuator simulating vertical acceleration in F-104 simulator, duplicating other forces conventionally

02 p0229 A70-12864

Visual spaceflight simulators for spacemen and aircraft pilot training

04 p0663 A70-14691

Variable anamorphic motion picture system to produce visual display for use with flight simulator

[ASME PAPER 69-WA/BHF-8] 04 p0642 A70-14852

French guided satellite space flight simulator developed in search for suitable three axial onboard guidance systems

06 p1028 A70-17933

Pilot systems for controlling aircraft in flight, considering direct lift control, displays, simulators, tests, etc

08 p1437 A70-21734

Air transport total in-flight simulator /AT/TIFS/ equipped with six degree of freedom variable stability system for aircraft development and pilot training

08 p1437 A70-21736

Flight simulators for pilot training, discussing need for aircraft motion cues

09 p1655 A70-22296

Air combat simulator with attacker and evader pilots control capability, comparing simulated interceptions with flight test maneuvers

[AIAA PAPER 70-340] 09 p1656 A70-23023

Airborne simulator program for evaluation of motion and visual cue effects on pilot performance in roll, using compensatory tracking tasks

[AIAA PAPER 70-351] 10 p1857 A70-24202

Real time wide angle multicolor scanned laser display for visual flight simulators, utilizing flying-spot camera and rotating optical polygons

[AIAA PAPER 70-361] 10 p1857 A70-24203

Flight simulator for advanced aircraft /FSA/ featuring six degrees of freedom and 100 ft lateral travel

[AIAA PAPER 70-359] 10 p1858 A70-24205

Simulator servo drive system dynamic requirements for single-axis manual control task using pilot models and computer

[AIAA PAPER 70-355] 10 p1858 A70-24208

Amplitude and Rotational 3-Axis Flight Simulators for handling qualities research, outlining physical constraints and methodology for driving visual display and motion systems

[AIAA PAPER 70-353] 10 p1858 A70-24210

Ground based moving-base aircraft flight simulator using computer program to establish motion requirements

[AIAA PAPER 70-348] 10 p1859 A70-24213

Civil VTOL transport aircraft handling and performance qualities using fixed base simulator with electronically generated display

[AIAA PAPER 70-345] 10 p1859 A70-24214

Aircraft flight displays, simulating low altitude high speed mission by four degree of freedom Dynamic Flight Simulator

[AIAA PAPER 70-343] 10 p1859 A70-24216

Hybrid simulation, determining vehicle and performance parameters on longitudinal flying qualities of STOL transport in power approach configuration

[AIAA PAPER 70-387] 10 p1806 A70-24918

General aviation aircraft fixed-base engineering flight simulator involving use of analog computer, discussing equations of motion and aircraft cockpit

[SAE PAPER 700235] 11 p2031 A70-25904

Aircraft flight characteristics simulated on trainer with automatic control system and measuring system

11 p2056 A70-26455

Test techniques for X-22A VTOL research aircraft during ground simulator work and actual flight test, describing stability and control characteristics

[AIAA PAPER 69-319] 12 p2162 A70-28086

Book on space flight simulation systems examining real time and real performance requirements, mathematical models and various simulation programs

14 p2563 A70-30955

Digital computer six degree of freedom wind tunnel separation simulator for air launched missile trajectory analysis

17 p3063 A70-35509

- Spacecraft wide angle attitude control system stability analysis, using air bearing table simulation
17 p3134 A70-35651
- Concorde aircraft man machine simulation and handling using fixed cabin, variable stability and ground based simulators
[AIAA PAPER 70-923] 17 p3064 A70-35834
- Ground simulations data of jet lift V/STOL compared with visual flight results, noting hover, lateral quick start and stop maneuver
18 p3236 A70-35954
- Aircraft crew and pilot in-flight work load measurement and simulator
[ICAS PAPER 70-43] 23 p4138 A70-44141
- Pilot navigation efficiency in low altitude terrain following flight, using synchronized TV and simulator with inertial guidance
24 p4307 A70-45506
- FLIGHT STABILITY TESTS**
- VTOL transport aircraft stability and maneuverability compared with conventional aircraft
02 p0228 A70-12759
- Full scale R/V flight test base pressure data for slender cones with ablative heat shields, considering mass flow and addition effects
[AIAA PAPER 70-109] 06 p0973 A70-18148
- Stability derivatives from flight data of fixed-wing aircraft determined by modified Newton-Raphson method
07 p1194 A70-19272
- F-8D aircraft transonic flight and wind tunnel tests for buffet onset prediction, considering effects of g level and fluctuation amplitude and frequency
[AIAA PAPER 70-341] 09 p1611 A70-23020
- Rumanian book on flight stability and control covering Liapunov general stability theory, control systems, stability models, etc
15 p2673 A70-31695
- Blade flexibility effects on static stability derivatives of prop/rotors in propeller flight mode
17 p3013 A70-34701
- AH-1G Hueycobra helicopter stability, control, performance, vibration and structural loads characteristics during controlled steady state maneuvers
17 p3014 A70-34716
- Full scale R/V flight test base pressure data for slender cones with ablative heat shields, considering mass flow and addition effects
[AIAA PAPER 70-109] 21 p3745 A70-41753
- FLIGHT STRESS**
- German collection of papers on flight stress and medicine
09 p1624 A70-23002
- Flight stress in Starfighter aircraft pilots related to fibrinolysis activity in blood
09 p1625 A70-23003
- Eosinophilic leukocytes behavior in blood of Starfighter aircraft pilots due to flight stress
09 p1625 A70-23004
- Flight stress effect on blood clotting stabilization of Starfighter aircraft pilots, observing no change in thrombocytes number
09 p1625 A70-23005
- Aircraft pilots psychic and flight stress admissible degree not resulting in hazardous consequences, suggesting measures to increase resistance
09 p1625 A70-23006
- Physiological reactions detection, transmission and data evaluation of aircraft pilots subjected to various stress environments, using radio telemetry
09 p1626 A70-23009
- Blood pressure variations resulting in permanent irreversible hypertonia in air force pilots subjected to repeated stress situations and emotional irritations
09 p1626 A70-23011
- Aircraft pilots fitness under flight stress, discussing smoking, overweight, lack of exercise, etc, leading to coronary afflictions
09 p1620 A70-23013
- Launch load simulation on scaled vibration model concerning Saturn 5 structural integrity and flight failure
10 p1953 A70-25072
- FLIGHT STRESS (BIOLOGY)**
- NT SPACE FLIGHT STRESS**
- French book on aeronautical and astronautical physiopathology and pathology covering stress factors of flying, high speed and altitude including hypoxia, atmospheric vacuum, etc
01 p0029 A70-11380
- Cardiology role in aviation medicine, evaluating jumbo jet and SST flight stress effects on pilots and passengers in age factor study of arteriosclerosis
05 p0803 A70-16721
- Pilot emotional state during stressful situations from tape recorded vocal utterances of air to ground radio communications using spectrographic analysis
06 p1000 A70-12797
- Physiological mechanism and differentiation of alt-ernobaric vertigo in flyers
08 p1449 A70-21947
- Pilot electroencephalograms during F-104 flights recorded by telemetering noting alpha, beta and theta activities
11 p1990 A70-25668
- Civil airlines training captains heart rate response to simulator stress, base conversion and line training
11 p1992 A70-26519
- Short duration high workload effects in pilot interval and finger tremor during Boeing 747 aircraft let-down, approach and landing
11 p1993 A70-26521
- Agricultural pilots fatigue based on flight and environmental effects
11 p1993 A70-26522
- Psychic stress at simulated flight vehicle guidance tasks evaluated quantitatively
12 p2177 A70-27037
- Pilots psychophysiological reactions to various aircraft types and flight maneuvers, considering recorded comments, blood pressure and heart rate
12 p2177 A70-27042
- Civilian pilot trainee stress level dependence on individual flying instructors, detecting psychophysiological variables by inflight recording
12 p2178 A70-27044
- Respiratory syncope with cardiac ineffectiveness and numerous complications during and after flight at high altitude clinically observed for causes
12 p2171 A70-28040
- Soviet book on flight stress covering physiological bases, prediction and prevention methods, physical training, etc
13 p2357 A70-28775
- Pilots energy expenditure during jet, propeller and helicopter cargo aircraft flight, using expired air samples
15 p2689 A70-31876
- Rest periods assignment on long distance air travel of passengers based on physiological stress factor
15 p2690 A70-31892
- Airsickness frequency, pathogenesis and prevention, discussing cadet selection
17 p3037 A70-35129
- Aircraft crew oral temperature related to work-rest schedules, discussing hypothermia, flight stress and in-flight depression
17 p3032 A70-35563
- Etiopathogenesis of auditory disorders in flying personnel and aircraft engineers resulting from exposure to acoustic stresses
17 p3034 A70-35677
- Transmeridian flights effect on diurnal urinary excretion of unconjugated 17-hydroxycorticosteroids in males, evaluating time shift effects
21 p3770 A70-41477
- Sleep patterns during double aircrew continuous flying operations, suggesting 3-day maximum mission duration
24 p4306 A70-45327
- FLIGHT SURGEONS**
- Flight doctor-pilot relationship, studying personal motivation
12 p2178 A70-27049
- Aerospace medicine approach to medical investigator training for aircraft accidents, noting flight surgeon role as life support specialists chief
23 p4152 A70-44454
- FLIGHT TEST INSTRUMENTS**
- Flight test instrumentation specifications for V/STOL aircraft, considering design, installation and accuracy
[AIAA PAPER 70-376] 10 p1892 A70-24927
- Telemetry instrumentation for free flight wind tunnel models, discussing system component characteristics
17 p3047 A70-35495
- DC-10 airborne flight test PCM data system, discussing capability, onboard operating characteristics and test results
17 p3093 A70-35498
- Flight test instrumentation for V/STOL stability derivatives extraction, noting instrument errors and required compensation
17 p3094 A70-35502
- Airborne magnetic recording flight test instrumentation of Anglo-French Jaguar aircraft
19 p3431 A70-38535
- Seismic fluid suspended triaxial angular accelerometer for high performance aerospace vehicle flight test application
19 p3431 A70-38540
- Viggen aircraft testing for flight properties, discussing measuring instruments, analog and digital recording, preprogrammed control, etc
24 p4317 A70-46228
- FLIGHT TEST VEHICLES**
- Growth test vehicle /GTV/ flight test program for development of hypersonic flight to orbital speeds, discussing design, costs, capabilities, etc
03 p0582 A70-14188
- Lifting reentry flight test vehicle aerodynamic configuration development, emphasizing lateral stability and maneuverability
[ICAS PAPER 70-02] 23 p4257 A70-44118
- FLIGHT TESTS**
- NT FLIGHT STABILITY TESTS**
- Mark III airborne Omega system designed as receiver-computer to demonstrate real time operation, discussing flight test results
01 p0136 A70-10302
- Flight test experiments for H-19 helicopter to evaluate aided inertial system performance for terminal guidance
01 p0136 A70-10303
- Flight tests conducted in artificial and natural icing conditions, using CH-3C helicopter with rotor blades equipped with polyethylene antiicing tape
01 p0006 A70-10695
- TV system for controlling QF-9 drone aircraft landing, takeoff and BQM-34A target drone in-flight test operations
01 p0058 A70-10815
- Thermal and pressure environments analysis in Saturn S-1C stage base during flight tests, noting base gas flowfield and heating
[AIAA PAPER 69-318] 01 p0195 A70-10833
- Electronic head-up display experience in transport aircraft flight tests including human factor, installation, operational applications, etc
02 p0224 A70-11836
- Boeing 747 nacelle development programs involving outdoor and ground test rigs, flying test bed, flight tests, etc
[SAE PAPER 690389] 03 p0550 A70-12894
- Flight evaluation of direct lift control /DLC/ on modified B-52 aircraft, noting controllability improvement during ILS approaches and aerial refueling
[SAE PAPER 690406] 03 p0411 A70-12896
- Hawker Siddeley/Smith Trident Autoland Program, discussing flight test data for Smith autopilot and autothrottle certification
03 p0522 A70-13349
- LF wave propagation using Ioran C radio navigation system flight performance tests
03 p0523 A70-13615
- Flight test results of attitude control device for TACITE rocket probe to explore solar disk and neighborhood
[ONERA-TP-762] 03 p0523 A70-13626
- Artillery type projectiles field photography in flight in connection with service integrity evaluation of weapon components under real environment conditions
03 p0490 A70-13658
- Stability characteristics from flight test results using regression analysis
04 p0623 A70-15155
- Flying qualities criteria and piloted simulator studies during development and flight testing of stability augmentation system for B-52 aircraft
[AIAA PAPER 68-1066] 04 p0624 A70-15380
- Power spectral density functions of vertical gust velocities, comparing theoretical results and C-141A flight test measurements
04 p0624 A70-15384
- Pitching moment coefficient changes due to ground effect in fixed wing aircraft flight test method, considering constant angle of attack approach
04 p0619 A70-15394
- Flight tests with mounted and unmounted SG 1262 hovering test rig in Germany to determine optimal control and stability characteristics for VTOL VAK 191B
04 p0624 A70-15704
- Reusable lifting entry vehicle flight tests, investigating handling qualities and subsonic-transonic aerodynamics of M2-F2/M2-F3, HL-10 and X-24A
[SAE PAPER 690662] 05 p0792 A70-15840
- Net thrust determination for high bypass ratio engines in cruise, suggesting performance evaluation in actual flight tests
[SAE PAPER 690652] 05 p0895 A70-15841
- Integrated flight test data acquisition and processing system with real time graphic display, discussing ground station function
[SAE PAPER 690678] 05 p0793 A70-15867
- Helicopters usefulness in rescue service via test flights, discussing rescue cars and centers for emergency patients
05 p0806 A70-16325
- Flight test results of avionics in aircraft
05 p0822 A70-16699
- Radio astronomy spacecraft /RAS/ engineering design, technology and flight results
06 p1153 A70-17151
- Pre-space flight tests effects on Macaca nemestrina monkeys spermatogenesis, considering immobilization and exposure time effects
06 p0991 A70-17287
- Space transportation system booster and orbiter development ground and flight tests, considering vehicle size and reusability requirements
[AIAA PAPER 70-276] 07 p1397 A70-20385
- Silicide-coated columbium alloys reuse capabilities under flight conditions, considering coating local damage and emittance
[AIAA PAPER 70-279] 07 p1315 A70-20388
- Flight test evaluation program for airborne multisensor electro-optical display systems performance in TV mode under variety of optical conditions
07 p1289 A70-20403
- Aircraft roll rate response and aileron step input matching in terms of modal parameters with flight test records by analog computer program
08 p1465 A70-20781

Experimental test pilots - Conference, Beverly Hills, September 1969

08 p1436 A70-21726

Concorde flight testing program, discussing results on prototype, preproduction and production aircraft

08 p1436 A70-21727

Concorde aircraft test flight results, considering ground handling, takeoff, approach and landing, low speed flight, aeroelasticity, stability, power plant, etc

08 p1437 A70-21728

C-5A aircraft testing program covering ground handling, towing, cargo handling, takeoff and landing, cold weather testing, etc

08 p1437 A70-21729

Boeing 747 pretesting work including wind tunnel, components, engines and static structural tests, flight simulation, etc

08 p1437 A70-21730

Bolkow BO-105 twin turbine rigid rotor helicopter flight tests

08 p1437 A70-21731

F-106B aircraft in-flight study of airframes installation effects on propulsion system performance at transonic speeds

08 p1437 A70-21732

Flight tests to investigate external munitions carriage effect on aircraft stability and control

08 p1437 A70-21733

Pilot systems for controlling aircraft in flight, considering direct lift control, displays, simulators, tests, etc

08 p1437 A70-21734

Aircraft flight testing techniques modification to cover maximum performance values

08 p1437 A70-21735

In-flight investigation to determine effect of variations in bank angle control parameters on cruise flight handling qualities

08 p1437 A70-21738

Program, test equipment and data reduction of aircraft prototype flight tests

08 p1438 A70-21865

Onboard measurements of single engine propeller-driven aircraft performance, stability and control in nonsteady symmetric flight

08 p1438 A70-21869

LSI Mark 3 airborne Omega system with computerized signal processing for navigation parameters, discussing system features and flight test results

09 p1719 A70-22190

Airborne EROS collision avoidance system, discussing flight performance, range and closing rate measurements

09 p1720 A70-22241

Boundary layer transition measurements on flight tests of experimental 22 degree conical reentry vehicle with Be heat shield and graphite nose

[AIAA PAPER 68-1152]

09 p1606 A70-23243

Pilot/vehicle dynamics from flight test records, discussing close-loop attitude control tasks

10 p1824 A70-23897

Ground and flight tests in aeronautical system development process as transfer of basic technology into cost effective operational systems

[AIAA PAPER 70-381]

10 p1857 A70-24172

Aircraft ground and flight tests effectiveness planning, preparation and conduct for operational safety, noting Flight Controls Development Test Stand

[AIAA PAPER 70-371]

10 p1806 A70-24843

Biosatellite Primate Mission Program for component qualification levels validated by flight tests data, performing vibration tests on prime structure spacecraft

[AIAA PAPER 70-403]

10 p1951 A70-24902

Flight test programs site selection method using computer program analysis of magnetic tape weather records

[AIAA PAPER 70-397]

10 p1806 A70-24908

Space station program development requirements, describing ground and flight tests synthesis

[AIAA PAPER 70-377]

10 p1952 A70-24926

Helicopter flight test and evaluation tools including data processing facilities to improve test validity

[AIAA PAPER 70-373]

10 p1806 A70-24929

Military specification revision of Flying Qualities of Piloted Airplanes evaluated by flight test including Flight Path Stability and Roll Rate Oscillation techniques

[AIAA PAPER 70-372]

10 p1806 A70-24930

Integrated Test Program for S-3A Weapon System, detailing test sequence flow and interfaces to assure vehicle and avionics systems reliability and maintainability

[AIAA PAPER 70-370]

10 p1959 A70-24931

Space shuttle program, considering vehicle configurations mission capabilities and cost estimates with emphasis on ground and flight tests

[AIAA PAPER 70-739]

10 p1953 A70-25074

Small turboprop engine development, flight tests, performance and weight reduction

[SAE PAPER 700206]

11 p2102 A70-25878

Aircraft performance, stability and control testing from nonsteady flight measurements, ascertaining repeatability of results

[SAE PAPER 700236]

11 p1980 A70-25905

Small scale and full scale wind tunnel and flight test data correlated for Lear jet aircraft

[SAE PAPER 700237]

11 p1981 A70-25906

Programmed and randomized loading flight-by-flight tests for fatigue life, noting stress cycles

11 p2138 A70-26096

Kalman filtering and differential correction techniques applied to T-33 flight test data for aircraft system parameters identification

11 p1982 A70-26233

Mechanical parameters measurement by radio telemetry during aircraft and motor vehicles tests, noting onboard recording methods

11 p2056 A70-26452

IR remote temperature gradient sensor as clear air turbulence detector, presenting inflight test results

12 p2229 A70-26947

Test techniques for X-22A VTOL research aircraft during ground simulator work and actual flight test, describing stability and control characteristics

[AIAA PAPER 69-319]

12 p2162 A70-28086

Rocket-borne flight testing of sensitive accelerometer developed to measure small forces applied to satellite or space probe surface

13 p2403 A70-28433

Harrier aircraft flight test program considering instrumentation, data acquisition, airframe, avionics, systems engineering, etc

13 p2344 A70-28922

XB-70 aircraft flight tests in cruise and landing approach to evaluate handling qualities criteria

[AIAA PAPER 70-566]

13 p2346 A70-29031

Integrated computerized data acquisition and reduction system for aircraft flight and wind tunnel tests

13 p2373 A70-29156

Flight test experiments for H-19 helicopter to evaluate aided inertial system performance for terminal guidance

13 p2449 A70-29622

Wind tunnel and flight test methods for determining transonic buffet characteristics on model F-4 aircraft

[AIAA PAPER 70-584]

13 p2348 A70-29886

Flight testing of high sensitivity Cactus accelerometer, measuring deceleration components due to sphere drag

15 p2735 A70-31813

Head up display /HUD/ flight tests, examining effects decreasing quality of manually handled instrument approach, discussing space myopia and disorientation

16 p2912 A70-33819

Single stage /rigid/, two stage and stretch yo-yo despin mechanisms, discussing advantages, disadvantages and flight tests

16 p2985 A70-34114

Airborne flight test data acquisition and ground based automatic bulk data processing system for helicopter test and development programs

17 p3014 A70-34713

Two-point suspension system with longitudinally displaced cargo hooks for handling helicopter loads, discussing wind tunnel and flight tests

17 p3014 A70-34714

Spacecraft waste management system zero-gravity flight tests, describing components and functions

17 p3036 A70-34751

Small rocket systems research programs, discussing Apollo-Pacemaker and planetary entry parachute flight tests

17 p3177 A70-35203

DC 8 Super 63 aircraft direct lift control flight evaluation

17 p3018 A70-35496

Flight test program for helicopter gas turbine engines, considering engine-airframe-control systems integration and environmental tests

[ASME PAPER 70-GT-38]

18 p3303 A70-36836

Data acquisition and processing system for electronic countermeasure aircraft tests

19 p3383 A70-37900

C-5A engineering flight test /EFT/ computer controlled data processing system operation, illustrating capability, performance and limitations

19 p3355 A70-37917

Collision avoidance system flight test and evaluation program for airline industry CAS specification

19 p3466 A70-38240

Instrumentation magnetic recorders in aerospace industry in relation to new components and techniques development, investigating airborne recorder as flight test tool

19 p3429 A70-38516

Data processing systems functions and composition for random data reduction during aircraft flight tests based on analog and digital techniques

19 p3430 A70-38524

Multiaircraft flight test program time compression by management techniques, discussing program length and costs

19 p3355 A70-38530

Boeing 747 transport airplane flight test data system, discussing recording media, major PCM and FM tape systems, etc

19 p3431 A70-38531

Digital data acquisition system for CF-5A flight test program, discussing recording system design

19 p3384 A70-38532

Jaguar flight test instrumentation methods, discussing Anglo-French participation

19 p3356 A70-38534

Jaguar flight test data processing system, discussing airborne digital computer

19 p3384 A70-38536

Digital computer magnetic tape recording system for flight tests of Jaguar aircraft, discussing data treatment

19 p3384 A70-38537

ONERA accelerometer flight test of performance in zero gravity environment, using Vesta sounding rocket for simulation

19 p3431 A70-38541

Concorde prototype 002 flight test data recording instrumentation, emphasizing digital system for quasi-static parameters

19 p3432 A70-38545

Data collection system for prototype flight tests of Fokker F-28 based on DC-8 aircraft digital system

19 p3384 A70-38546

Emmanual magnetic recording system used with airborne digital computers for aircraft in-flight tests

19 p3432 A70-38547

Magnetic tape instrumentation system installed aboard Hawker Siddeley Harrier for flight development, discussing digital format recording system

19 p3384 A70-38549

Ground station to retrieve and process data recorded on airborne digital magnetic tape instrumentation system for Hawker Siddeley Harrier flight development

19 p3384 A70-38550

Mariner 1969 test and operations program evaluated by ground tests and flight results, giving flight acceptable spacecraft recommendations

19 p3533 A70-38819

Apollo Lunar Module strapdown Abort Guidance system, correlating performance prediction with flight test results

[AIAA PAPER 70-1028]

20 p3666 A70-39509

SERT 2 spacecraft ion thruster ground tests and flight operation, tabulating performance data

[AIAA PAPER 70-1125]

20 p3691 A70-40220

Concorde aircraft flight test program for verifying design features of wing vortices, fuel transfer, longitudinal stability, etc

21 p3749 A70-40580

High speed track facility for V/STOL aircraft tests, discussing characteristics and design

21 p3803 A70-40581

Flow difference sensor for aircraft hydraulic systems damage vulnerability reduction, discussing design, operation and flight tests results

21 p3750 A70-40786

Parafol flight performance predictions and test results based on wind tunnel data and manned free flight

[AIAA PAPER 70-1190]

21 p3754 A70-41826

Glide and landing performance of twin-keel parawings, discussing wind tunnel, radio flight and simulator tests

[AIAA PAPER 70-1186]

21 p3754 A70-41829

Parachutes for low density atmospheres, describing low and high altitude test results

[AIAA PAPER 70-1164]

21 p3755 A70-41846

Radar inertial system flight evaluation, discussing V/STOL program for approach and landing by use of ground based radar for updating onboard inertial navigator

22 p4066 A70-42651

Harrier flight testing in terms of V/STOL capability compared with conventional aircraft

22 p3962 A70-42975

Flight simulation as aircraft design tool, discussing ground and inflight simulation techniques

[ICAS PAPER 70-41]

23 p4178 A70-44139

Cactus high sensitivity accelerometer flight tests, discussing operation and experimental conditions

[ONERA-TP-875]

23 p4198 A70-44660

NACA/NASA rotary wing aircraft research history 1915-1970, Part 3, covering rotor and helicopter theory, related flight and wind tunnel testing, etc

23 p4142 A70-44853

Iantar 1 automatic ionospheric laboratory flight tests results, investigating Ar ion engine performance

23 p4264 A70-45009

Boeing 747 flight test certification program, describing methods, data systems, inertial navigation, engines, flutter, etc

[SAE PAPER 700828]

24 p4290 A70-45891

Sapuc-Salut system for evaluating test data measured onboard Viggen aircraft

24 p4339 A70-46229

FLIGHT TIME

Synchronization of ground stations clocks by time scale comparison with overflying aircraft

[ONERA-TP-759]

03 p0487 A70-13642

- Circadian rhythm of pilot efficiency and multiple time zone travel effects
[DFVLR-SONDDR-29] 08 p1451 A70-21935
- Circumplanetary aircraft design for solo nonstop great circle around world flight without refueling, noting application to sport, transportation, surveillance, photography, etc 11 p1981 A70-26046
- Metastable time-of-flight technique for measuring free molecular flow velocity distribution 12 p2231 A70-27555
- Aeronautical navigation under various wind velocity conditions, studying flight times for closed flight paths 13 p2448 A70-28750
- Rest periods assignment on long distance air travel of passengers based on physiological stress factor 15 p2690 A70-31892
- Astronaut weight loss relation to flight duration during manned space missions 20 p3574 A70-40125
- Time-of-flight mass flow rate and thrust stand data comparison for two 100 micropound colloid thrusters [AIAA PAPER 70-1114] 20 p3691 A70-40229
- Aircrewmen work credit under Flying Time system to determine rank order for mission scheduling, noting legitimate functions performance 21 p3771 A70-41483
- Travel time for trips to Neptune, calculating earth gravitational field escape hyperbola and waiting time before return 23 p4245 A70-44653
- Sleep patterns during double aircrew continuous flying operations, suggesting 3-day maximum mission duration 24 p4306 A70-45327
- FLIGHT TRAINING**
- NT SPACE FLIGHT TRAINING**
- Flight training simulators recording, playback, demonstration and instructor facilities and six degrees of freedom motion system 02 p0273 A70-11840
- Trainers and simulators based on digital computers, eliminating system sensitivity to ambient conditions, power fluctuations, circuit imperfections and digital to analog conversion 02 p0274 A70-11841
- Soviet book on air navigation covering civil navigator training, geographic concepts, navigation means, flight and meteorological conditions, instrument errors, etc 06 p1103 A70-17642
- Aviation medicine, discussing pilots physical fitness and training, spatial orientation, ground crew, data flow, etc 08 p1451 A70-20977
- Elementary flight training study in Royal Netherlands Air Force for improving pilot selection, discussing instructor and social science roles 12 p2176 A70-27030
- Minnesota Multiphasic Personality Inventory scores compared with various pilot training proficiency levels, noting low correlation 12 p2176 A70-27032
- Vestibular habituation among pilots and flying staff from training and seniority standpoint 14 p2538 A70-30914
- Flight training quality prediction by multidimensional regression analysis, discussing relationship to candidates psychophysiological examinations 20 p3578 A70-38964
- FLIGHT VEHICLES**
- Flight vehicles intrinsic vibration frequency spectra for controllable flight determined by graph-analytical method 02 p0227 A70-12415
- Soviet book on flight vehicle trajectories covering equations of motion, flight mechanics, reference systems, etc, for rockets and spacecraft 03 p0410 A70-12871
- Explosive blast wave effects on flight vehicle in supersonic flow, using conical blast generator and short duration supersonic wind tunnel [AIAA PAPER 70-221] 06 p0972 A70-18127
- Soviet monograph on inertial methods of flight vehicle motions parameters measurement 08 p1540 A70-20692
- Soviet book on practical aerodynamics and flight vehicles covering supersonic aircraft, sweptback wings, military aviation and satellites 08 p1435 A70-20765
- Optimal control synthesis for flight vehicle in vertical plane involving digital and analog computers 08 p1479 A70-20997
- Pilot/vehicle dynamics from flight test records, discussing close-loop attitude control tasks 10 p1824 A70-23897
- Noise-flutter interrelation in flight vehicle flexible plate and shell configurations immersed in fluid flow 11 p2132 A70-25726
- Quasi-steady devices design to investigate high Reynolds number flows for flight vehicles, noting test time 11 p2041 A70-26573
- Relay stabilization system for flight vehicle motion about center of mass, using point transformations method and bifurcations theory 15 p2674 A70-32151
- Flight vehicle dynamic response prediction from elastic filler stiffness contained between rigid sphere and ellipsoidal shell 16 p2991 A70-33878
- Soviet book on vibrations in flight vehicle engines covering linear and nonlinear systems, computer methods, etc 18 p3305 A70-37229
- Computer aided laboratory testing of flight vehicles in real environmental conditions, illustrating vertical stabilizer subject to gust loads 19 p3396 A70-37874
- German book on principal characteristics of flight mechanics and ballistics covering mirror symmetric aircraft and axisymmetric bodies such as projectiles and missiles 21 p3749 A70-40738
- FLIP-FLOPS**
- Supersonic fluid bistable amplifier used as air motor, converting supply air flow energy into reciprocating piston motion 10 p1807 A70-24791
- Bistable fluid amplifier elements static characteristics, considering control flow and pressure variation domain 10 p1808 A70-24971
- Proportional and flip-flop elements in hydraulic circuits using oils, noting cavitation effect on switching stability in digital elements 14 p2534 A70-30677
- CW GaAs junction lasers bistable operation above delay transition temperature based on double acceptor trap theory 18 p3268 A70-36729
- Flip-flops switching time reduction, using equivalent amplifier circuit with positive feedback 19 p3390 A70-38580
- Coanda effect in bistable fluid amplifier, using finite difference method for computer programmed solution of flow equations [ASME PAPER 70-FLCS-12] 22 p4008 A70-42415
- Specification sheets for fluidics clarified by demonstrating step-by-step solutions for typical problems involving flip-flop and OR/NOR gate 24 p4293 A70-45431
- FLOATING**
- Seadrome advantages and structural design concepts, describing floating runways, breakwaters, noise reduction, building costs, etc 09 p1655 A70-22243
- Critical Levitation Loci for floating spheres on cryogenic fluids 17 p3136 A70-34743
- FLOATING POINT ARITHMETIC**
- Digital filters output error due to roundoff accumulation and input quantization calculated by floating point arithmetic 01 p0050 A70-10778
- FLOATS**
- Flotation dummy to simulate unconscious survivors characteristics analyzed for life jacket design 07 p1218 A70-19004
- Flotation device for infants and small children incorporating life support and survival capabilities for aviation and marine applications 23 p4153 A70-44480
- FLOODS**
- Flood plain boundaries delineation by panchromatic and color airphoto interpretation 24 p4329 A70-45362
- FLOQUET THEOREM**
- Floquet-Liapunov theorem matrix representation derivation, improving accuracy of Liapunov classical representation 15 p2774 A70-31643
- Lifting rotor blade motions stability computation using Floquet transition matrix 17 p3009 A70-34726
- Multidimensional linear differential equations with periodic coefficients, proving analog of Floquet-Liapunov theorem 20 p3659 A70-40170
- FLORA**
- U PLANTS [BOTANY]**
- FLOTATION**
- Modeling techniques based on Froude scaling laws for helicopter ditching and flotation stability characteristics 17 p3016 A70-34738
- FLOTATION SYSTEMS**
- U FLOATS**
- FLOW CHARACTERISTICS**
- NT BOUNDARY LAYER STABILITY**
- NT FLAME STABILITY**
- NT FLOW DISTRIBUTION**
- NT FLOW STABILITY**
- NT FLOW VELOCITY**
- NT MAGNETOHYDRODYNAMIC STABILITY**
- Vortex street parameters in free wake behind body in plane fluid flow, deriving equations for vortex frequency, circulation and interspacing 01 p0060 A70-10146
- Laminar boundary layer analysis of heat and mass transfer in dispersed two phase flow over heated surface 01 p0214 A70-10293
- Airport terminal configurations payload flow-through characteristics and space allocations, discussing passenger processing, baggage systems, etc [AIAA PAPER 69-1088] 01 p0000 A70-10622
- MHD entrance region compressible flow characteristics, determining velocity pressure and temperature distributions, friction and heat transfer coefficients, etc 01 p0067 A70-11136
- Incompressible viscous fluid flow in contact with infinite plate and rotating in perpendicular magnetic field, obtaining flow characteristics by Laplace transform 01 p0067 A70-11138
- Pressure waves propagation velocity dependence on flow regime in gas-liquid mixtures 01 p0067 A70-11302
- Turbulent viscous fluid flow characteristics obtained from integrating Navier-Stokes equation for unsteady flow with periodic momentum variation 01 p0069 A70-11626
- Turbulence constant for flows near walls, analyzing viscosity dependence on wall distance by utilizing maximum stability principle 01 p0069 A70-11627
- Internal structure of ideal explosive waves at Chapman-Jouguet point, discussing coupling between flow and chemical reactions 02 p0279 A70-12103
- Conservation equations for mass, mean momentum and kinetic energy for incompressible turbulent boundary layer, using finite difference procedure 02 p0284 A70-12347
- Mean velocity and mean turbulent energy field methods of calculating boundary layer behavior based on numerical solutions of equations of motions 02 p0285 A70-12349
- Turbulence characteristics in liquids measured by hot film anemometry, discussing calibration methods selecting criteria as temperature control, drift influence and relative speed determination 02 p0303 A70-12687
- Two phase flow visualization by various photographic and optical methods, describing equipment and lighting used and types of data obtainable 02 p0305 A70-12834
- Hypersonic flow characteristics on yawed circular cone surface at moderate angle of attack, applying results to inviscid and boundary layer flow computations 03 p0406 A70-12944
- Walljet in crossflow, discussing characteristics and pressure field on plate, using flow visualization methods 03 p0465 A70-13004
- Supersonic flow in dihedral angle between intersecting wings and in space between parallel wings, using integrating wave equation by Volterra method 03 p0407 A70-13492
- Incompressible gas turbulent jet flow characteristics in subsonic wind tunnel, stressing pressure distribution in recirculation region for interpreting heat transfer in separated flows 03 p0593 A70-13495
- Flow parameters of two interacting submerged turbulent jets from rectangular nozzles, determining total pressure profiles of coincident flow 03 p0466 A70-13504
- Ionizing shock wave propagation into magnetic field from Ar gas flow characteristics in electromagnetic shock tube 03 p0532 A70-13548
- MGD finite flow regions surrounded by nonconducting gas, considering wave behavior at boundary of conducting region and magnetic field influence 03 p0533 A70-13803
- Flow characteristics of compressible fluid in compressor or turbine stage, determining radial distribution of downstream Mach number 03 p0410 A70-14271
- Statistical model equations to predict discharge coefficients for concentric orifice plates as function of line size, diameter ratio and Reynolds number [ASME PAPER 69-WA/FM-6] 04 p0667 A70-14837
- Ideal fluid motion characteristics near variable volume spheres with radial mass transfer through surfaces 04 p0672 A70-15198
- Structural characteristics of supersonic twisting underexpanded air jet, using filming and schlieren photography 04 p0618 A70-15246
- Cold flow-porous plate simulation of swirling flow-field in spinning end-burning rocket chamber, noting vortex generation and flow characteristics 04 p0764 A70-15541

Hypersonic far wake mean flow properties behind two dimensional slender body wind tunnel models at zero angle of attack

[AIAA PAPER 68-700] 04 p0621 A70-15578

Strong radiating shock wave structure and reflection at rigid wall, investigating flow velocity, density and temperature changes

05 p0956 A70-15788

Radial outflow effect on fluid motion between rotating and stationary plane disks associated with rotor cooling in turbomachinery

05 p0833 A70-16503

Laminar flow in circular pipe with arbitrary axial variation of wall temperature or heat flux, using integral type approximation

05 p0957 A70-16519

Steady state boundary layer of anisotropic Erickson fluid incident obliquely on infinite cylinder, obtaining differential equations for dynamic behavior

05 p0835 A70-16860

Flow characteristics of curved porous wall gas core reactors for nuclear rocket engines, visualizing simulated fuel flow with air-smoke combination

06 p1104 A70-17509

Liquid flow through cylindrical slot of constant and variable thickness, calculating flow variations

06 p1034 A70-17630

Axial profile characteristics of hypersonic near wake of slender circular cone based on pitot pressure, static pressure and stagnation temperature measurements

06 p0968 A70-17916

Helmholtz resonator associated flow field analysis in nonlinear regime, considering external pressure, mean flow, velocity fluctuations and orifice flow

06 p1038 A70-18065

Supersonic flow separation over rearward facing step, measuring upstream boundary layer, lip shock and shear layer formation by pitot probe and surface pressure survey

[AIAA PAPER 70-106] 06 p0973 A70-18153

Time mean flow property measurements for homogeneous and nonhomogeneous free turbulent jets

[AIAA PAPER 70-130] 06 p1041 A70-18159

Combustion and flow characteristics associated with direct injection of liquid hydrocarbons into high speed air stream

[AIAA PAPER 70-88] 06 p1182 A70-18198

Flow parameters measured in low density hypersonic nozzle, estimating error of all relevant parameters

06 p1030 A70-18302

Nitrogen hypersonic transitional flow at adiabatic sharp flat plate leading edge, presenting density, flow-field shape and local rotational temperature for various regions

06 p0982 A70-18361

Flow properties and heat transfer of wall jet spreading over permeable surface with suction and blowing

07 p1258 A70-19720

Turbulent shear flow kinematic characteristics determined by photographic method and flow visualization using vortex model

07 p1259 A70-19827

Damped turbulent whirling tube flow friction characteristics and heat exchange, solving equation of maximum tangential flow rate

07 p1261 A70-20464

Three dimensional gas flow calculated by direct method of characteristics

08 p1431 A70-20860

Flow turbulence in wind tunnel model tests, observing generation methods effect on aerodynamic flow characteristics distribution

08 p1483 A70-21074

Flow structure in rectangular cavity in lower wall of two dimensional channel for various aspect ratios and Reynolds numbers

08 p1484 A70-21313

Shock ionized Ar flow properties estimation using alignment charts

08 p1551 A70-21324

Prandtl-Kolmogoroff model of turbulence with inclusion of second order terms for stress and velocity gradient not to vanish coincidentally

08 p1484 A70-21458

Tape-generated swirl flow of single phase water investigated for heat transfer and pressure drop characteristics

[ASME PAPER 68-WA/HT-3] 08 p1600 A70-21829

Flow characteristics behind sphere suspended in vertical axisymmetric jet dependent on ratio of specific parameter

09 p1658 A70-22118

Plastic bodies plane flow Lagrangian description applied for prescribed deformation path of material fibers

09 p1769 A70-22251

Axisymmetric nozzles flow regimes with subsonic ejection velocities analyzed by stabilization method, noting role of pressure in nozzle exit section

09 p1660 A70-22440

Macroscopic properties of thermal molecular flow between coaxial cylinders and concentric spheres, using transpiration theory in Knudsen gas

09 p1788 A70-22906

Arc driven shock tunnel operation with expansive area change at main diaphragm, evaluating flow characteristics

09 p1657 A70-23279

Hypersonic laminar boundary layer in strong viscous interaction region on wedge, determining velocity and enthalpy profiles, displacement thickness and induced pressure distributions, etc

09 p1606 A70-23294

Supersonic flow behind cone, studying bottom pressure and stagnation zone dependence on incident flow parameters and static pressure distribution

09 p1663 A70-23623

Flow field around and drag on sphere rising axially through rotating viscous fluid

09 p1663 A70-23676

Wake source model for two dimensional incompressible potential flow past bluff body, considering pressure distribution, flow separation, wake width, etc

09 p1607 A70-23681

Fluid system control valve gain dependence on flow characteristics slope due to series resistance or centrifugal pump

09 p1613 A70-23685

Laminar boundary layer parameters on porous surface in presence of pressure gradient obtained for inner/wall/ and outer regions

09 p1664 A70-23712

Fluid microstructure effects on velocity, boundary layer and shear stress in nonsteady parallel flows, including accelerated plane wall equation

10 p1863 A70-23955

Plane steady flows characteristics of incompressible viscous fluids in rigid walled rectangular channels found asymptotic to Poiseuille and Couette flows

10 p1866 A70-24112

Strong shock wave reflection from rigid wall at high shock velocities, studying effect on flow structure

10 p1922 A70-24152

Supersonic gas flow past sphere investigated for characteristics using Fabry-Perot etalon

10 p1888 A70-24258

Unsteady compressible laminar boundary layer flow around flat plate influenced by compressibility as function of Mach number

[ONERA-TP-803] 10 p1869 A70-24543

Closed streamline low Mach number compressible fluid flow without temperature restrictions, noting incompressible flow behavior

10 p1869 A70-24547

Bistable fluid amplifier elements static characteristics, considering control flow and pressure variation domain

10 p1808 A70-24971

Grid turbulence unified analysis, estimating turbulence intensity, dissipation length and integral scale for any grid flow

10 p1871 A70-24976

Laminar boundary layer characteristics in axisymmetric hypersonic nozzle calculated by finite difference method

10 p1804 A70-25187

Characteristics and calibration of flow in gas induction driven close return transonic wind tunnel

11 p2030 A70-25687

Flow characteristics of airfoil rotating cascades in variable width channel in incompressible liquid

11 p1975 A70-25789

Heat conduction and viscosity effects on compressible fluids characteristics

11 p2037 A70-26399

Homogeneous viscous fluid steady state parallel Stokes flow in annular region between concentric cylinders at low Reynolds numbers

11 p2038 A70-26478

Nonturbulent fluid entrainment into turbulent flow dependent on flow properties controlling energy balance

11 p2038 A70-26528

Quasi-steady devices design to investigate high Reynolds number flows for flight vehicles, noting test time

11 p2041 A70-26573

Flow dynamics effects on characteristics of high temperature plasmatron, describing plasma burner design and HF discharge plasma experiment

11 p1984 A70-26740

Turbulent boundary layer in axisymmetric channel having interactions with flow core, calculating flow characteristics and separation point

12 p2209 A70-27289

Portable low cost shearing interferometer for plasma and flow analysis and instruction aid

12 p2235 A70-27754

Flush-mounted electrostatic probes behavior in shock tube over wide range of freestream conditions and bias voltage

12 p2236 A70-27810

Mathematical model for flow within external target type thrust reverser, assuming inviscid incompressible two dimensional flow

[AIAA PAPER 69-3] 12 p2291 A70-28085

Supersonic and hypersonic motion past circular cone at angle of attack, analyzing for velocity and pressure distributions by linearizing conical motion equations

12 p2158 A70-28213

Longitudinal gravitational field effect on cavitation wedge flow, investigating characteristics by Zhukovskii-Roshko method

13 p2390 A70-29646

Ideal weightless fluid plane potential flow in channel with permeable wall, deriving expressions for dynamic characteristics

13 p2390 A70-29648

Turbulent boundary layer characteristics on simple shapes in hypersonic flow, using mixing length theory and eddy exchange coefficient

14 p2564 A70-30262

Solar wind interaction with planetary ionosphere, considering flow behavior across bow MHD shock

14 p2647 A70-31073

Hypersonic gas flow characteristics incident on elliptic paraboloid and triaxial ellipsoid at arbitrary angles of attack

15 p2672 A70-31647

Pressure-flow relation for fluid in pipe obeying Casson equation, considering applicability to human blood

15 p2690 A70-31917

Water and blood flow characteristics in converging-diverging plastic tube, considering implications in occlusive vascular disease

15 p2691 A70-31937

One flow influence on another at two plane jets interaction zone, applying to proportional fluid amplifier inlet impedance calculation

15 p2720 A70-32020

Flow nonuniformity effects on heat exchangers efficiency

15 p2827 A70-32140

Periodic flow structure between gas turbine blades, using asymptotic representation

[ONERA-TP-790] 16 p2833 A70-33102

Aerodynamic wake structure of cylinders and spheres in hypersonic rarefied gas flow as function of Mach and Knudsen numbers

16 p2836 A70-33756

Axial compressor aerodynamics investigation methods concerning compressor flow for efficiency improvement

16 p2836 A70-33757

Helicopter rotors flow conditions by digital computer, investigating slipstream configuration

16 p2836 A70-33761

Equilibrium air boundary layer flows at three dimensional stagnation points, discussing flow characteristics and real gas heat transfer parameters

[AIAA PAPER 70-806] 17 p3005 A70-34455

Axisymmetric blunt base cylindrical body with turbulent initial boundary layer, investigating flow structure in annular nozzle wind tunnel

[AIAA PAPER 70-796] 17 p3006 A70-34464

Two dimensional supersonic wake behind heated slender flat plate, considering flow properties in transition zone

17 p3006 A70-34466

Stratified-rotating fluids mathematical analogy, examining flow constraints, parameters and variables

17 p3068 A70-34664

Turbulent boundary layer structure, considering flow properties prediction, wakelike behavior, bursts, compressibility, transport properties, etc

17 p3068 A70-34665

Continuous variation measurements of wind tunnel parameters minimizing testing time, discussing flow characteristics measurements during angle of attack variation

17 p3057 A70-34775

Flow velocity and pressure on thin wing of small span width near sonic speed, using parabolic type linear equation

18 p3207 A70-36374

Compression and expansion characteristics of steady supersonic flow passing along yawing slender body of rotation, linearizing differential equations

18 p3207 A70-36382

Fuel cell cavities, analyzing fluid motion purge dynamics based on anisotropic porous media model

18 p3216 A70-36766

Heat transfer characteristics of flows between high speed rotating disk and parallel stationary shroud, discussing experimental facility and procedures

[ASME PAPER 70-GT-20] 18 p3349 A70-36865

Weak stratification and geometry effect on steady mechanically driven motion of contained rotating viscous fluid

20 p3608 A70-39357

Turbulent boundary layer in axisymmetric channel having interactions with flow core, calculating flow characteristics and separation point

20 p3613 A70-40339

Flat plate compressible laminar boundary layer flow with variable fluid properties, using series solution by splitting up flow variables into sets of universal functions

21 p3806 A70-40825

NonNewtonian fluids flow and heat transfer characteristics past flat plate, determining velocity and temperature distributions

21 p3806 A70-40900

Mass force fields effects on flow phenomena from heat transfer and hydraulic resistance analyses

21 p3951 A70-41764

Heat transfer and friction effects on flow parameters in nozzle with independent cooling

21 p3951 A70-41769

Flow structure in plane submerged turbulent jet, determining velocity, friction stress and correlation coefficients distributions

21 p3749 A70-42221

Newtonian fluid turbulent flow development characteristics in inlet region of smooth concentric annulus from momentum integral equations

22 p3957 A70-42304

Transonic turbine cascades exit flow parameters taking into account blade profile

22 p4088 A70-42346

Thermoelasticity theory concerning Navier-Stokes-Fourier type fluid universal motion characterization in absence of body forces and external heat supply

22 p4010 A70-42637

Buoyant hot two dimensional laminar vertical jet in quiescent colder fluid, calculating temperature and velocity distributions by integral method

22 p4010 A70-42639

MHD channel flow of suspension for prescribed wall heat flux and temperature, determining flow and heat transfer characteristics

22 p4080 A70-42670

Nonuniform flow parameters for maximum thrust in nozzle, discussing specific impulse determination

22 p3960 A70-43366

Fluidic networks nonlinear component AC and DC behavior, discussing Bernoulli equation, nonlinear resistances, transmission lines and various flows

23 p4142 A70-44296

Steady irrotational gas flow characteristics calculation from finite difference scheme for three dimensional method of characteristics, considering supersonic nozzle flow

23 p4133 A70-44308

Subsonic Ludwig /simple expansion/ tube as shock tube for aerodynamic testing, examining flow characteristics

23 p4182 A70-44578

German monograph on flow phenomena in gas containing fluids, covering pressure and ultrasonic induced cavitation in steady and unsteady flow

24 p4324 A70-45098

Jet-ambient air mixing effect on flow characteristics around thin airfoil with jet flap

24 p4288 A70-45439

Axisymmetric laminar compressible jet flow characteristics, allowing for compressibility effects due to temperature dependent density and viscosity variations

24 p4325 A70-45584

Partially cavitating flow past plate, calculating characteristics by Riabushinskii scheme

24 p4325 A70-45642

Sonic boom, discussing characteristic flow phenomena, intensity, effects on buildings and animals, human reactions, etc

24 p4289 A70-45786

FLOW CHARTS

Meteorological parameters measuring instruments optimal design, presenting formalized procedure flow chart and examples

14 p2607 A70-30568

Signal flow graphs for selectively invariant autonomous multichannel control systems design

24 p4321 A70-45641

FLOW COEFFICIENTS

NT DISCHARGE COEFFICIENT

Turbulent viscosity and thermal conductivity coefficients for entire cross section of fluid flow including wall boundary layers

01 p0069 A70-11624

Turbulent boundary layer calculations by integral dissipation method, using various dissipation coefficient laws

02 p0283 A70-12340

Very small diameter laminar flow orifice coefficient calculation as function of Reynolds number

08 p1484 A70-21321

Adiabatic flow coefficient in supersonic nozzle with choked flow conducted over throat Reynolds number range

11 p1976 A70-25999

Rarefied gas slip flow coefficients calculations at nonuniformly heated surface, demonstrating relationship between temperature and isothermal slip coefficients

15 p2776 A70-31478

FLOW DEFLECTION

Monograph on weak interactions on cones in supersonic and hypersonic flows, discussing flow divergence, measurement errors and data reliability

04 p0615 A70-15141

Hypersonic viscous gas flow past power law bodies under viscous interaction between boundary layer and inviscid flow extended to slender bodies

04 p0618 A70-15240

Fundamental matrix asymptotic forms obtained for supersonic and subsonic three dimensional steady flows past body in uniform stream of viscous thermally conducting fluid

04 p0673 A70-15320

Fluid boundary at curved wall under pressure

05 p0834 A70-16680

Steady state boundary layer of anisotropic Ericksen fluid incident obliquely on infinite cylinder, obtaining differential equations for dynamic behavior

05 p0835 A70-16860

Three dimensional supersonic flow around delta wings, considering lifting and thickness problems, leading edge characteristics, separated and non-separated shock waves, etc

06 p0964 A70-17241

Frictionless hypersonic flow around blunt bodies of revolution, taking into account real gas effects in equilibrium and frozen flow calculations

06 p0965 A70-17242

Combustion kinetics in supersonic gas flows past various bodies, assuming exothermal and inverse recombination reactions behind adiabatic shock wave after induction period

08 p1596 A70-20855

Mangler displacement thickness correction for slender cones

08 p1590 A70-21320

Plane flow of electrically conducting fluids around oscillating plate, using equations linearized by Oseen method

09 p1734 A70-22316

Circulating flow around elliptical cylinder in inviscid liquid vortex

09 p1659 A70-22435

Shock wavefront configurations before inclined obstacles in supersonic flow, studying inclination angle role

09 p1604 A70-22443

Stokes flow around sphere moving along axis of cylinder with near-unity diameters relationship

09 p1661 A70-22839

Atmospheric model for flow crossing ground obstacle using nonlinear differential equation

09 p1718 A70-22848

Rarefied gas flow past arbitrary three dimensional body using variational principles based on linearized BGK equation, considering constant and adiabatic wall temperature

09 p1605 A70-23178

Shear flow of inviscid incompressible fluid past sphere, calculating secondary vorticity and upstream velocity distribution

09 p1664 A70-23680

Wake source model for two dimensional incompressible potential flow past bluff body, considering pressure distribution, flow separation, wake width, etc

09 p1607 A70-23681

Symmetrical, asymmetrical and three dimensional sonic flows past finite obstacle, investigating regions upstream and downstream from shock waves for airfoil

10 p1800 A70-24134

Viscosity and heat conductivity effects in compressible fluid flow past finite body showing dependence on spatial dimensions

10 p1800 A70-24135

Suction force increase resulting from turbulent jet interaction with transverse flow

10 p1868 A70-24166

Unsteady supersonic flow past tail-body system with harmonic oscillatory motions

10 p1803 A70-24789

Supersonic flow around slender polygonal wings with nonsymmetrically distributed incidence using method for circular flow around angular wings

10 p1803 A70-24797

Hydraulic loss and secondary circulation of fluid flow in three dimensional bend commercial conduits, discussing relationship to velocity distribution

10 p1871 A70-25094

Monograph on Beltrami steady state, frictionless flow of incompressible medium past spherical surfaces, assuming vortex and stream lines argument

11 p2034 A70-25498

Lee wave flow disturbances due to mountains by midtroposphere balloon and aircraft observation, noting flow features nonstationarity

12 p2262 A70-26883

Three dimensional oblique incidence liquid jet impinging on solid surface, evaluating flow force by applying mass and momentum conservation

13 p2389 A70-29540

Reverse flow in plasma generated in conical electromagnetic shock tube and reflected from downstream bulkhead, noting stabilization effects

13 p2469 A70-29974

Two phase convex corner flows of particle imbedded inviscid incompressible fluid using small perturbations method

14 p2565 A70-30279

Ventilating flowmeter tests with jet deflection for respiration measurement in patient

14 p2541 A70-30380

Transonic flow past bodies of revolution, using finite difference scheme

21 p3743 A70-40611

Asymptotic behavior of boundary layer equations solution for viscous incompressible flow past curvilinear obstacle

21 p3806 A70-40613

Micropolar incompressible fluid slow stationary flow past sphere

21 p3812 A70-42252

Flow past streamlined obstacles under nonNewtonian fluid injection into hydrodynamic laminar and turbulent boundary layer

21 p3812 A70-42266

Jet-deflection proportional amplifier design and performance, discussing pressure and momentum control, static and dynamic characteristics aspect ratio, geometry effects, etc

[ASME PAPER 70-FLCS-17] 22 p3963 A70-42410

Fluid flow around plane plate system, basing model on potential flow theory and variational principle

22 p4009 A70-42606

Perfect gas circular subsonic flow around convex obstacle, using hodographic method for boundary problem

22 p3958 A70-42608

Conducting fluid supersonic flow past slender body of revolution in circular wind tunnel under inclined magnetic field, investigating MHD interference problem

22 p3958 A70-42669

Radial flow microturbines deflection and wave losses in circular nozzle ring oblique exit section

22 p3965 A70-43359

Shock curvature at wedge or cone tip in radiating gas flow, noting differences between radiative and chemically coupled gas dynamics

23 p4135 A70-44638

Rocket engine nozzle with wall-mounted obstacle, examining shock front shape, pressure distribution and side force characteristics

23 p4234 A70-44684

Channel vs deflection flow in boundary layer theory, considering Navier-Stokes equations

23 p4183 A70-44736

Perturbation of steady MHD Stokes flow past hollow sphere assuming small Hartmann and Reynolds numbers

24 p4384 A70-45262

Numerical analysis of fuel combustion in supersonic stationary flows of hydrogen air mixture past bodies by two-component reaction kinetics model

[ICAS PAPER 70-52] 24 p4428 A70-45500

Two dimensional incompressible air flow past circular cylindrical body, investigating separation point control by suction and jet injection

24 p4288 A70-46010

Jet momentum for flow separation control of air past circular cylindrical surface

24 p4288 A70-46011

FLOW DIRECTION INDICATORS

NT WIND VANES

Flow direction and velocity measurement in three dimensional boundary layer, discussing instrument and restrictions

02 p0299 A70-12312

Null and fixed correction methods for pressure and/or velocity gradient error in flow direction measurement

15 p2736 A70-31898

FLOW DISTORTION

Cavitation initial phase flow model, analyzing flow past stepped obstacle in plane channel

01 p0064 A70-11002

Incompressible turbulent boundary layer and separation flow into forward facing normal step, considering step heights and boundary layer thickness

01 p0066 A70-11133

Transient plane disturbance of stream angular to applied magnetic field, discussing relationship to airfoil and Alfvén waves

04 p0615 A70-15093

Supersonic flow past elliptic cone of small eccentricity treated as axisymmetric conical flow perturbation

05 p0790 A70-16506

Inviscid flow through staggered airfoil cascades in oscillatory and distorted flow simulating axial flow compressor

[AIAA PAPER 70-131] 06 p0969 A70-18049

Disturbances of air flow originating from small scale mountains using numerical model

07 p1330 A70-19799

Large axisymmetric disturbances generated in laminar pipe flow by sleeve oscillating at wall, measuring flow with laser-Doppler velocimeter
07 p1286 A70-19995

Straight-walled two dimensional diffusers with incompressible steady flow, noting effects of inlet blockage and aspect ratio on performance
08 p1433 A70-21322

Symmetrical laminar distorted velocity profiles between flat parallel plates, analyzing decay using integral method
08 p1433 A70-21325

Air intake distortions effect on compressor performance, discussing radial and peripheral gradients
15 p2787 A70-32248

Laminar vortex flow interaction with stationary surface, considering flow field, velocity, Reynolds number, etc
19 p3405 A70-38348

Shock wave nonlinear refraction by upstream disturbances in two dimensional steady nonuniform flow
20 p3608 A70-39354

Free stream disturbances influence on hypersonic boundary layer transition Reynolds number in heated and unheated flows
[AIAA PAPER 69-704] 21 p3809 A70-41744

Upstream disturbances propagation during hypersonic flow boundary layer interaction
21 p3748 A70-42205

FLOW DISTRIBUTION

Density distribution measurements in flow field using interference methods, including laser light sources
01 p0085 A70-10268

Airframe flow field effects on propulsion system performance in transonic flight, studying case of underwing aft mounted turbojet engine nacelles
01 p0004 A70-10321

Gas-particle primary and pure gas secondary streams turbulent mixing, solving for various mixing zone flow field parameters
01 p0061 A70-10337

Flow profiles in models of human bronchial tree typical junctions, visualizing inspiration and expiration patterns for various Reynolds numbers
01 p0034 A70-10653

Analog time delay device for returning respiratory flow signal to correct time
01 p0035 A70-10654

Flow patterns in circular ducts with circumferential roughness variation, determining axial turbulence, Reynolds number effect and applications as two phase flow analog
01 p0066 A70-11132

Heat transfer, three dimensional boundary layers and high speed flow calculations, utilizing original entrainment equation
02 p0284 A70-12341

Flow development in conical diffusers, delaying stall with high velocity air injection through annular slot at diffuser inlet predicted by finite difference method
02 p0224 A70-12866

Boundary layer equations describing flow field in turbulent swirling jet diffusion flame solved in von Mises plane
03 p0603 A70-12911

Holographic interferometry with pulsed ruby laser hologram for examining flow distribution in supersonic free jet wind tunnel
03 p0480 A70-12948

Circumferential contour shape influence on three dimensional flow pattern of fan shaped annular turbine stages
03 p0407 A70-13417

Turbulent submerged plasma jet boundaries calculated theoretically and compared with experimental results from dynamic head profiles
03 p0532 A70-13515

Annular nozzle shapes established via method of straight line characteristics, noting flow patterns at various regions
03 p0409 A70-13872

Flow field of jet spoilers downstream from nozzle, accounting for main stream and secondary jet mixing and fuel injection problems during supersonic combustion
03 p0608 A70-14098

Torque and flow patterns in supercritical Taylor instability regime of circular Couette flow
03 p0470 A70-14235

Entrainment rate of ambient medium by MPD arc jet, discussing flow field in and around jet and pressure distribution along vacuum tank wall
03 p0553 A70-14373

Flow field calculation for axisymmetrical gas flow in axial compressor cascade applicable to optimal blade design
04 p0617 A70-15191

Vortex separation effects on elliptic bodies lift distribution, analyzing separated flow pattern
04 p0619 A70-15385

Flow fields construction for normal shock waves with nonequilibrium chemical reactions reflected from shock tube end wall
[AIAA PAPER 68-732] 04 p0674 A70-15537

Cold flow-porous plate simulation of swirling flow-field in spinning end-burning rocket chamber, noting vortex generation and flow characteristics
04 p0764 A70-15541

Flow distribution inside triangular shaped cavities of variable depth resembling liquid propellant rocket motor baffle cavities, simulating radial and tangential oscillation modes
04 p0674 A70-15566

Flow field between infinitely massive wall and rigid piston accelerated by detonation products, comparing analytical results to finite difference numerical integration
05 p0830 A70-15782

Hydrodynamic fields of revolution around sphere in unbounded fluid governed by Oseen equation, emphasizing streamlines and attached vortex
05 p0832 A70-16157

Numerical results for perturbed downstream flow field resulting from entropy wave interaction with normal shock and oblique shock generated by wedge flow
05 p0835 A70-16788

Sliding tube assembly for diverting carrier gas from flow pattern of Verneuil apparatus for flame fusion crystal growth
05 p0829 A70-16849

Flow distribution for short isentropic supersonic inlet diffusers, using method of characteristics and Oswatich and Connors procedures
06 p0963 A70-17234

Self similar flow patterns arising during cylindrical shock and detonation waves propagation in gas at rest, considering MGD shock waves
06 p1119 A70-17516

Laminar hypersonic blunt cone wakes, discussing flow fields and axial static pressure distributions
06 p0968 A70-17553

Rotta differential equation for turbulent boundary layer flow with fixed profiles of length scale, shear stress and kinetic energy
06 p1035 A70-17694

Helmholtz resonator associated flow field analysis in nonlinear regime, considering external pressure, mean flow, velocity fluctuations and orifice flow
[AIAA PAPER 70-128] 06 p1038 A70-18065

One dimensional compressible flow analysis for near field aerodynamics of tube-vehicles, showing drag coefficient dependence
[AIAA PAPER 70-140] 06 p1038 A70-18077

Viscous radiating flowfield coupled with ablation for computations on blunt body entering earth atmosphere at interplanetary return velocities
[AIAA PAPER 70-128] 06 p0970 A70-18090

Flow model for steady asymmetric vortex system shed from slender body of revolution in coning motion
[AIAA PAPER 70-52] 06 p0971 A70-18118

Inviscid transonic approximation theory, calculating mixed flow field around nonlifting slender ogive body, accounting for shock wave generation, strength and location
[AIAA PAPER 70-189] 06 p0972 A70-18132

Time mean flow property measurements for homogeneous and nonhomogeneous free turbulent jets
[AIAA PAPER 70-130] 06 p1041 A70-18159

Multiphase two dimensional mixing and combustion of flow fields suspended in gaseous medium for propulsion systems problems, obtaining governing equations
[AIAA PAPER 70-145] 06 p1181 A70-18175

Mach disk in underexpanded exhaust plume predicted by dividing flow field into subregions
[AIAA PAPER 70-231] 06 p0974 A70-18176

Unified model for transverse gaseous jet penetration into supersonic stream agreeing with measured flow field properties
[AIAA PAPER 70-93] 06 p0976 A70-18201

Rotational and vibrational temperatures measured in hypersonic nonequilibrium rarefied gas flow field of cooled circular cylinder by electron beam technique
06 p1123 A70-18304

Sharp hypersonic flat plates inclined at various angles, obtaining flow field and merged region details
06 p0980 A70-18353

Hypersonic rarefied argon and nitrogen flows over flat plate, investigating flow field and surface measurements from merged layer into transition regime
06 p0981 A70-18355

Kinetic theory of rarefied supersonic flow over finite plate, calculating molecular velocity distribution functions for flowfield
06 p0981 A70-18356

Free molecular drag for flat plate with normal protuberance, determining flowfield distribution functions and stress components
06 p0981 A70-18357

Flow field measurements upstream of axisymmetrical blunt body in rarefied hypersonic flow used to investigate merging between bow shock and boundary layer
06 p0983 A70-18372

Drag and heat transfer predicted by kinetic theory for rarefied gas flow over sphere at low Mach numbers, analyzing flow field
06 p0984 A70-18381

Pressure-time history in spherical shock waves flow field at low ambient pressures recorded with piezoelectric transducers, showing shock strength decrease
06 p1052 A70-18385

Body surface curvature effect on surrounding laminar flow field, investigating oblate spheroids of various thicknesses
07 p1259 A70-19977

Stable flow distribution of sonic jet exhausting counter to low density supersonic airstream
07 p1189 A70-19982

Two dimensional flow field behind shock wave resulting from boundary layer growth in driven gas of shock tube
07 p1260 A70-19983

Flowfields in lifting-line approximation for finite bladed, lightly loaded propellers in axial cruise and heavily loaded propellers in static operation
07 p1190 A70-20411

Holography for visualization and analysis of aerodynamic flow fields in wind tunnel experiments, recreating events in space and time
08 p1493 A70-20650

Polymeric materials flow at tube entrance, discussing pressure drop and flow birefringent patterns at tapered and sharp entrances
08 p1486 A70-21861

Supersonic air jet structure in central shock wave region affected by both Mach number and flow rarefaction
09 p1734 A70-22185

Interaction between bodies and spherical detonation wave, measuring force pulse transfer to immobile cylinder and flow patterns past flying blunt body
09 p1659 A70-22186

Finite plates impact flow field analysis from isentropic one dimensional flow equations solution through hodograph transformation
09 p1776 A70-22721

One dimensional flow field behind ionizing detonation wave in magnetic field using Chapman-Jouguet hypothesis, accounting for Alfvén speed
09 p1660 A70-22722

Turbulent three dimensional incompressible wall jets issuing into quiescent air ambient, tangent to and at surface of flat plate, investigating shear stress and flow field
09 p1661 A70-23215

Rocket exhaust plume flow fields studied for vehicle effects taking into account nozzle boundary layer, coalescence shock and nonisentropic flow
[AIAA PAPER 69-569] 09 p1743 A70-23246

Three dimensional flow field codes for spheres cones at nonzero angles of attack, comparing numerical and experimental results
09 p1606 A70-23254

Flow field around and drag on sphere rising axially through rotating viscous fluid
09 p1663 A70-23676

Pressure and velocity distribution within radial flow gas turbine rotor computed by two dimensional streamline curvature method
09 p1608 A70-23737

Pressure waves of varying amplitude effect on flow through turbomachine blade passages, discussing interaction with curved diffusers geometry
09 p1608 A70-23743

Subsonic compressible or incompressible inviscid flow field through turbomachine blade row determined by matrix and streamline curvature methods
09 p1608 A70-23745

Sodium balance effect on intrarenal distribution of blood flow in normal man determined with Xe washout method
10 p1810 A70-24005

Gas flow from nozzle into duct with enlarged cross section investigated for flow pattern and boundary conditions, noting oscillation behavior
10 p1799 A70-24123

Flow structure around incurved lateral jet issuing from narrow orifices, determining interaction zone geometry with main current by hot wire technique
10 p1868 A70-24165

Electrostatic cylindrical probes applicability to hypersonic flow field diagnostics
11 p2086 A70-25684

Flow pattern of axial flow of turbine stage calculated from cascade characteristics
11 p1975 A70-25794

Axisymmetric or two dimensional incompressible laminar boundary layer flow field numerical analysis using quasi-linearization and Chebyshev series
11 p2072 A70-25965

Laminar boundary layer behind normal shock wave with vaporization and combustion, obtaining profiles on analog computer
11 p2148 A70-25967

Two dimensional unsteady fluid flow in square cavity numerically analyzed from continuity and Navier-

Stokes equations and recorded as computer-generated motion picture

11 p2035 A70-25971

Pulsed laser holographic interferometry of density field created by high speed projectile motion in air [AIAA PAPER 69-347]

11 p2051 A70-25987

Flat plate flowfield for freestream/jet interaction wrap-around on bodies of revolution, using separation shock model and blast wave analogy

11 p1976 A70-26135

Gas dynamic processes insufficiency for triggering transition to detonation obtained from laser schlieren records of nonsteady flow field ahead of accelerating turbulent flame

11 p2150 A70-26378

Nearly homogeneous turbulent shear flow for flow field structure, determining pressure/velocity tensor using wind tunnel

11 p2039 A70-26530

Nonlinear orographic waves in atmosphere, investigating influence of meteorological parameters, temperature jump, incident flow and ridge geometry on flow patterns

12 p2263 A70-27517

Blood flow redistribution during sustained high skin temperatures of men in supine position

12 p2169 A70-27654

Time or space decay of turbulent parameters along flow direction in jets, wakes or grid-generated turbulence, illustrating time variation of wave number spectrum

12 p2211 A70-27831

Shock wave reflection into ideal gas flow with linear density variation analyzed for flow field

12 p2211 A70-27832

Supersonic flow in inner and outer regions of annular wings by method of singularities, obtaining Abel type integral equations for every step [DFVLR-SONDDR-37]

12 p2158 A70-28207

Nonstationary pressure pulse acting on body in liquid or gas, discussing flow with unperturbed parameters at infinity

12 p2213 A70-28239

Supersonic jet spoilers flow fields with various nozzle shapes to determine secondary jets penetration depth and mixing in wake

13 p2338 A70-28480

Free flow field from underexpanded rocket motor nozzle and impingement effects of pressure and heat transfer to flat plate

[AIAA PAPER 69-568]

13 p2473 A70-28510

Numerical method of characteristics for three dimensional supersonic nozzle flow field calculations

13 p2338 A70-28512

Multiple jet flow exhausting into arbitrary crossflow in ground effect, solving continuity and momentum equations for jet path and induced velocity field

13 p2387 A70-29011

Gaseous injection into supersonic flow, investigating secondary Mach number and injection angle effects on flowfield in supersonic wind tunnel

[AIAA PAPER 70-552]

13 p2339 A70-29017

Unsteady fluid flow around circular cylinder with sudden acceleration using flow pattern photographs

13 p2387 A70-29056

Basic flow convergence or divergence effect on steady flow pattern around circular cylinder using fluid motion visualization

13 p2387 A70-29058

Tidal forces effect on wind system in lower ionosphere, using Navier-Stokes equation for lower layer and Euler equations for upper layer

14 p2571 A70-30232

Radiating gas flow about pointed bodies, investigating shock curvature at wedge or cone tip and straight shock waves flow field downstream

14 p2663 A70-30267

Linearized gas mixture nonequilibrium flow fields, analyzing consequences of multiplicity of principal relaxation frequencies

14 p2566 A70-30474

Thunderstorm bottom wind profile model, analyzing flow distribution, isotach, isogon and isotherm characteristics

14 p2607 A70-30584

Marginal fluid flow stability in porous media taking into account inhomogeneity created by temperature

14 p2577 A70-31000

Statistical transport, energy and chemical reaction rate in turbulent flow field with uniform velocity gradient, using Brownian motion theory

14 p2566 A70-31029

Methane and propane flames in rotating air flow fields generated by cylindrical rotating wire mesh screen, discussing flame lengths and blowoff velocities

14 p2666 A70-31090

Aerodynamic characteristics of wing with tip clearance within uniform flow, investigating main stream flow pattern effect

14 p2529 A70-31331

Isolated convective plumes immersed in return flow turbulent downdraft

15 p2769 A70-31440

Internal shock waves in axisymmetric flowfield of perfect gas past blunt cone, noting roles of Mach number and cone half angle

15 p2672 A70-31592

Boltzmann equation for Knudsen layer and outer region of weakly rarefied gas flow

15 p2777 A70-32131

Hemisphere model flow field investigations in low density plasma wind tunnel, considering flow regimes of transition and shock formation

15 p2673 A70-32838

Aerodynamic performance of axisymmetric body traveling at transonic Mach numbers for predicting installed nozzle flow fields and efficiency

[AIAA PAPER 70-700]

16 p2835 A70-33562

Turbulent boundary layer response in flow field downstream of upstanding step change in surface roughness

[ASME PAPER 70-FE-17]

16 p2891 A70-33630

Flow equations for flow field in entry to radial or mixed flow impellers of turbomachines

[ASME PAPER 70-FE-36]

16 p2892 A70-33640

Flow structure in wake of blunt bodies placed perpendicular in parallel airstream determined from hot-wire anemometry

[AIAA PAPER 69-746]

16 p2838 A70-33876

Time asymptotic solutions for hypervelocity blunt body flow field with coupled nongray radiation, treating shock as discrete surface

[AIAA PAPER 70-865]

16 p2999 A70-33908

Liquid rocket propellant engine exhaust plume flow field, discussing mathematical models for combustion chamber, throat region and nozzle

[AIAA PAPER 70-844]

16 p3001 A70-33927

Graphite oxidation on exposure to high temperature flow field based on surface coupled model

[AIAA PAPER 70-823]

16 p2940 A70-33941

Pressurized gas bearing flow field, discussing velocity transversal component, pressure distribution and profile

16 p2924 A70-34237

Collisionless monatomic gas flow density and velocity distribution on axis of diffusely reflecting circular cone at zero attack angle with free stream

16 p2839 A70-34273

Weightlessness and gravitational effects on human pulmonary blood flow distribution, considering optimal gas exchange efficiency

[AIAA PAPER 70-785]

17 p3035 A70-34472

Flowfields behind reflected shock waves, predicting end-wall radiating heat transfer and radiative gas dynamic coupling effects

[AIAA PAPER 70-774]

17 p3065 A70-34480

Hypersonic flow field around yawed half angle cone from wind tunnel measurements including surface pressure distributions and flow visualization photographs

17 p3007 A70-34485

Plasma diagnostic data from onboard Langmuir probes, reflectometers, antenna VSWR and beacon and telemetry attenuation for blunt body reentry flow field

[AIAA PAPER 70-756]

17 p3008 A70-34495

Adiabatic and chemically inactive hypersonic continuum flow around blunt body, analyzing flow field

17 p3010 A70-35036

Radiation gas dynamics, investigating thermal radiation effects on flow field of high temperature gas

17 p3195 A70-35038

Method of characteristics for nonequilibrium flow fields analysis, reviewing theory, numerical methods and examples

17 p3071 A70-35470

Flow field on suction side of slender body of revolution with/without wings, investigating by directional probe in wind tunnel

17 p3013 A70-35924

Compressible flow of two component two phase mixtures through convergent nozzles and orifices, determining initially or annular dispersed flow patterns

18 p3239 A70-36231

Flow field about leading edges of tapered wings set at incident angle of attack, using gas dynamic and Monge equations

18 p3207 A70-36376

Computerized design for radial flow splitters in three dimensional fan exhaust nozzles

18 p3207 A70-36462

Pressure balanced rotor flow path design for mixed flow centrifugal compressors, calculating losses in rotor and diffuser section

[ASME PAPER 70-GT-12]

18 p3209 A70-36863

Transonic high turning low aspect ratio stator cascades flow field performance prediction, reducing secondary flows by partial slots

[ASME PAPER 70-GT-63]

18 p3209 A70-36875

Unsteady incompressible planar gas jets with stable vortex street, investigating near flow field region to establish oscillatory component

19 p3404 A70-37799

Holographic flow and sound visualization, determining three dimensional density distributions in aerodynamic flows

19 p3425 A70-37888

Incompressible axisymmetric flow through turbomachines, developing flowfield for given velocity distribution along arbitrary streamline

19 p3354 A70-38933

Relativistic high temperature gas asymptotic solutions with or without body force, comparing flow field with photon gas

20 p3673 A70-39654

Three dimensional supersonic and hypersonic gas flow by Oseen equations, obtaining asymptotic flow field

20 p3609 A70-39656

Gas dynamic functions of point explosions, determining flow parameters for instantaneous energy release in quiescent, inviscid, nonheat conducting perfect gas

20 p3612 A70-39821

Flow field model for large surface blowing problem accounting for upstream and downstream effects with large rate normal injection near trailing edge

20 p3559 A70-40110

Hypersonic flow pattern past windward side of triangular wing with supersonic leading edges, joining potential and vortex regions behind shock wave

21 p3743 A70-40609

Transport model for flow field and convective heat transport in planar turbulent supersonic base flow

21 p3744 A70-41030

Flow field, heat transfer rates and reattachment surface wall temperature of planar supersonic turbulent flow

21 p3744 A70-41036

Nonlinear orographic waves in atmosphere, investigating influence of meteorological parameters, temperature jump, incident flow and ridge geometry on flow patterns

21 p3846 A70-41165

Liquid droplet shape effect flow field velocity and pressure distribution over windward surface in high speed gas streams

21 p3809 A70-41762

Nonuniform free stream supersonic flow past aerodynamic decelerators, calculating inviscid flow fields by method of characteristics

[AIAA PAPER 70-1176]

21 p3746 A70-41837

Earth upper mantle phase change instability, discussing temperature gradient, transformation influence on fluid, olivine-spinel phase flow patterns and tectonics

21 p3820 A70-41895

Centrifugal compressor losses as function of suction chamber exit nonuniform flow field delivered to impeller

21 p3747 A70-41954

Interface interaction of colliding plates of different materials, reducing flow problem to differential equation via hodograph transformation

21 p3747 A70-41962

Two dimensional peripheral turbulent jet curtain structure, determining curved and impinging jet flow field by pressure and velocity measurements

22 p3957 A70-42277

Unsteady aerodynamic forces at stall flutter, applying vortex sheet theory to separated flow field around thin airfoil at high angle of attack

22 p3957 A70-42284

Hypersonic viscous interaction between laminar boundary layer growing over flat plate and external flow field extended to curved surfaces

22 p3958 A70-42688

Induced voltage electromagnetic flowmeter, assessing performance in terms of weight vector to obtain conditions for ideal flow patterns

22 p4029 A70-42692

Shear flow distribution equations in prismatic shells under constant shear loading

23 p4265 A70-43891

Near field flow effects on sonic boom for incident triangular wing with constant lift distribution

[ICAS PAPER 70-20]

23 p4138 A70-44113

Iterative method based on slender body approximation applied to axisymmetric sonic flow fields, splitting differential equation into coupled parabolic equations

[ICAS PAPER 70-13]

23 p4132 A70-44124

Internal shock waves in axisymmetric flow field of perfect gas past blunt cone, noting poles of Mach number and cone half angle

23 p4133 A70-44276

Spinning cold-flow rocket motor, studying rotation effects on chamber flow velocity field

23 p4233 A70-44579

Two dimensional laminar near wake of slender body in supersonic flow at high Reynolds number

23 p4135 A70-44693

Pointed ogival body of revolution in supersonic flow field, investigating local pressure distributed by variational methods

23 p4136 A70-44992

Average isobaric air flow field divergence calculation of vertical motion by two dimensional Gaussian integral theorem

24 p4371 A70-45134

Lighthill aerodynamic noise theory fundamental equation for acoustic field density distribution, deter-

- mining flow fields for surfaces in uniform translational motion 24 p4324 A70-45268
- NonNewtonian fluids injection into boundary layer, comparing flow and pressure effects with water injection 24 p4324 A70-45364
- Combustion chamber flow visualization, obtaining information on pressure loss, velocity field, flow pattern and temperature gradients 24 p4393 A70-45444
- Narrow capillary supermolecular flow density relation to vapor molecule specular reflection, considering Knudsen flow conditions 24 p4381 A70-45491
- Cascade flow field analysis from given blade geometry, deriving expressions for numerical solution of inverse turbine design problem 24 p4288 A70-45501
- Sphere rotating in viscous fluid at rest, investigating surrounding flow field from creeping flow to turbulent boundary layer 24 p4326 A70-45989
- Inviscid hypersonic flow fields past lower/compression/ surface of delta wing calculated by one strip approximation of integral relations method 24 p4289 A70-46245
- Tidal forces effect on wind system in lower ionosphere, using Navier-Stokes equation for lower layer and Euler equations for upper layer 24 p4331 A70-46307

FLOW EQUATIONS

- NT HELMHOLTZ VORTICITY EQUATION
- NT VON KARMAN EQUATION
- NT VORTICITY EQUATIONS
- Boundary layer equations for plane steady incompressible flow, studying given velocity profiles effects on equations solutions 01 p0060 A70-10144
- Turbulent boundary layer computations for flows with various pressure distributions 01 p0063 A70-10928
- Boundary value problem for quasi-linear equation of unsteady transonic gas flow, including linear model and operators for group of transformations 01 p0069 A70-11628
- Supersaturated vapor condensation in supersonic nozzles, obtaining flow and droplet growth equations for local equilibrium condition 02 p0279 A70-12049
- Method of weighted residuals [MWR] applied to turbulent boundary layer equations, describing two parameter prediction technique 02 p0282 A70-12330
- Momentum integral method using auxiliary equation for two and three dimensional flow problems 02 p0284 A70-12344
- Governing equations determined for turbulent boundary layer and quasi-parallel turbulent shear flows, taking into account effects of convection, diffusion, pressure, etc 02 p0285 A70-12348
- Evaluation of performance of prediction methods for mandatory flows 02 p0286 A70-12359
- Small parameter method for reducing self similar viscous flow problems to ordinary third order differential equations with boundary conditions at wall and infinity 02 p0288 A70-12821
- Swirling flow equations in converging nozzles, comparing analytical and experimental data 03 p0405 A70-12929
- Eddy viscosity equation derived from flat plate turbulent boundary layer velocity data, considering shear stresses and mixing length profiles 03 p0464 A70-12943
- Energy equation for thermal turbulent boundary layer on adiabatic flat plate 03 p0466 A70-13421
- Martin method for reducing determination of steady plane MHD flow to Bernoulli and direct functions satisfying quasi-linear partial differential equations 03 p0533 A70-14200
- Asymptotic form of axisymmetric solution with Dirichlet integral for Navier-Stokes equations applied to flow past bodies of revolution with smooth surfaces 03 p0471 A70-14303
- Sonic throat formation from two dimensional viscous layer interaction with supersonic inviscid outer stream, using boundary layer equations 04 p0665 A70-14452
- Jet pump cavitation prediction and elimination using limiting-flow equation based on selected index [ASME PAPER 69-WA/FE-29] 04 p0666 A70-14773
- Boundary value problems of Cauchy-Riemann differential equations using solution to derive integral equation for stationary infrasonic flow 04 p0671 A70-15094
- Plane and axisymmetric transonic vortex flow approximate equations of inviscid nonheat conducting gas for point on sonic line with entropy having extremal value 04 p0617 A70-15234

- Dissimilar coaxial axisymmetric jets confined laminar mixing obtained from numerical solution of boundary layer equations, considering binary, isothermal and nonreacting system 04 p0621 A70-15579
- Incompressible two dimensional time dependent Navier-Stokes equations for oscillating body with rectangular boundaries 04 p0779 A70-15616
- Unsteady flow equations for periodic axisymmetric laminar flow of second order fluids in circular cylindrical pipes 05 p0831 A70-15871
- Singularity method applied to two and three dimensional potential flow described by Poisson, Helmholtz or related partial differential equations 05 p0832 A70-16114
- Rarefied H, He, air, carbon dioxide and water vapor flow rates between parallel optically flat glass surfaces measured, giving flow equation describing channel flow 05 p0833 A70-16525
- Incompressible two dimensional turbulent boundary layer equations with arbitrary pressure distribution solved by weighted residual method 06 p1032 A70-17214
- Velocity, magnetic field and drag equations for steady incompressible viscous conducting fluid flow around spherical hollow shell 06 p1122 A70-17917
- Closed form solution of modified inviscid transonic equation embodying character of viscous- transonic equation applied to shockless transonic airfoils [AIAA PAPER 70-187] 06 p0970 A70-18096
- Multiphase fluid continuum model and hydrothermodynamic equations under phase transformations, including dimensionless and similarity parameters 07 p1254 A70-19085
- Nonsimilar energy and species equations for flow velocities described by Falkner-Skan equation 07 p1256 A70-19307
- Book on mathematical theory of viscous incompressible flow covering stationary and nonstationary boundary value problems for linearized and nonlinear Navier-Stokes equations 07 p1258 A70-19697
- Axisymmetric swirling jet ejection from semiinfinite tube into free space filled by fluid, solving flow equation by Wiener-Hopf method 09 p1658 A70-22153
- Plane flow of electrically conducting fluids around oscillating plate, using equations linearized by Oseen method 09 p1734 A70-22316
- Steady turbulent perfect compressible gas flow in axisymmetrical or plane channel, using equations governing channel height and static pressure variations 09 p1659 A70-22429
- Nonlinear equations for large fluid oscillations in axisymmetric rotating cavities with radial partitions 09 p1660 A70-22438
- Second order boundary layer equations for incompressible flow, presenting simplified integral momentum equation for two dimensional and axisymmetric flow 09 p1660 A70-22681
- Two dimensional equations of boundary layer with arbitrary pressure gradient solved using successive approximations for numerical integration 09 p1605 A70-23168
- Boundary layer equations for multicomponent flow with finite chemical reactions solved by finite difference method 09 p1605 A70-23201
- Unsteady flow equations and thermodynamics for studying homogeneous fluidic transmission in circular and rectangular cross section lines 09 p1613 A70-23403
- Streamline curvature technique for two dimensional flow equations, deriving optimal damping factor for quasi-orthogonal method to test stability, convergence and accuracy 09 p1609 A70-23749
- Laminar boundary layer with blowing through wedge surface, solving linearized motion equation analytically 10 p1862 A70-23868
- Fluid microstructure effects on velocity, boundary layer and shear stress in nonsteady parallel flows, including accelerated plane wall equation 10 p1863 A70-23955
- Perturbed equations solutions for plane supersonic steady and nonsteady gas flows, considering propagation of perturbations in initially nonstationary main flow 10 p1866 A70-24107
- MHD boundary layer flow equations solution by initial value method to eliminate iteration process 10 p1924 A70-24563
- MHD exact solutions class, observing conducting flow intensification by magnetic field application 10 p1924 A70-24573

- Asymptotic eigensolutions for equations governing flow between oppositely rotating infinite plane disks in inviscid limit 10 p1870 A70-24607
- Turbulent flow downstream from abrupt widening of circular jet, using flow and momentum equations 10 p1870 A70-24782
- Compressible flow equations of motion applied to incompressible fluid flow through nozzle with eddies and springs 10 p1871 A70-24796
- Regional growth functions of turbulent wakes at small Mach numbers using regression equations 11 p1976 A70-25998
- Equilibrium properties of nearly normal turbulence assuming near-Gaussian nonlinear model equations and real turbulence 11 p2039 A70-26533
- Numerical solution for steady supersonic inviscid flow around smooth conical bodies by solving elliptic partial differential equations for conical flow 12 p2155 A70-27202
- Sonic surface and Cauchy problem of Monge-Ampere equations in plane unsteady transonic channel flow solved by hodographic analysis 12 p2156 A70-27299
- Incompressible fluid turbulent motion statistical equations, considering Lagrangian distributions of fluid particles coordinates and velocities 12 p2212 A70-28190
- Three dimensional laminar boundary layer equations for body of revolution at angle of attack in supersonic gas flow derived for equations 12 p2158 A70-28198
- Boundary layer equations with pressure gradient for revolving slender body, examining transverse curvature influence on layer separation and integral characteristics 12 p2214 A70-28249
- Flow equations for curvilinear boundary layer based on laminar incompressible boundary layer in streamwise corner 13 p2386 A70-28541
- Compressible fluids steady state equations invariant transformation, establishing sound speed-Mach number relation 13 p2389 A70-29458
- Turbulent shear flow direct interaction equations simplification to differential equations amenable to computation 13 p2389 A70-29463
- Viscous shock layer equations of laminar hypersonic flow past blunt body at moderate to high Reynolds numbers 13 p2343 A70-29952
- Flow dynamic lubrication equation for porous bearings under radial load with undefined axial dimension 15 p2745 A70-32442
- Viscid-inviscid equations solution, describing flows with coupled mixing, combustion and lateral pressure gradients 15 p2718 A70-32516
- Boundary layer equations for laminar flow, drag and heat transfer of gas in circular tube, considering parabolic and uniform entrance velocity profiles 15 p2722 A70-32692
- Flow equations for flow field in entry to radial or mixed flow impellers of turbomachines [ASME PAPER 70-FE-36] 16 p2892 A70-33640
- Outer boundary conditions derivation from asymptotic form of similar boundary layer equations with unit Prandtl number 16 p2894 A70-33874
- Laminar hypersonic boundary layer interaction with corner expansion wave, presenting numerical solutions to viscous-inviscid equations for small turning angles [AIAA PAPER 70-807] 17 p3065 A70-34457
- Vibrational nonequilibrium nozzle flow problems, obtaining similar solutions for various initial conditions and nozzle geometries [AIAA PAPER 70-804] 17 p3065 A70-34459
- Interior ideal liquid flow of vertical jet under gravity, using differential equation to relate flow plane to unit half disk 17 p3069 A70-34979
- Semiempirical theory of anisotropic turbulent transport, deriving closed system of flow equations 17 p3073 A70-35736
- Incompressible laminar boundary layer, vortex and axisymmetric wake/jet flow parabolic equations solution by weighted residuals method, describing use of exponentials 17 p3074 A70-35883
- Incompressible laminar boundary layer equations approximate solution by Galerkin-Kantorovich technique 18 p3238 A70-35972
- Similarity equations for rotating flow near disk, using Navier-Stokes equations for case of complicated boundary conditions 18 p3239 A70-36223

Gasdynamic equations in Euler variables, constructing completely conservative difference schemes with first and second orders of approximation

18 p3241 A70-36288

German book on continuum theory of flowing media covering tensor analysis, equations for kinematics, mechanics, thermodynamics and electrodynamics

18 p3243 A70-37226

WKB method for asymptotic oscillatory solutions of nonlinear equations of relativistic fluid mechanics

19 p3403 A70-37587

Canonical coordinates for numerical computation of free surface flows, considering steady motion and elliptic partial differential equations

19 p3457 A70-37679

Two dimensional equations of boundary layer with arbitrary pressure gradient solved using successive approximations for numerical integration

19 p3406 A70-38390

Compressible viscous fluid steady plane flow in laminar boundary layer on impermeable isothermal surface, describing parametric method of integrating flow equations

20 p3611 A70-39806

Turbulent flow asymmetrical mechanics equations derivation from conservation laws, discussing Navier-Stokes equation, angular momentum and transport theory

21 p3806 A70-40612

Compressible boundary layer equations with second order surface curvature and displacement effects

21 p3809 A70-41751

Closing method for turbulence equations of velocity field quantities joint probability distributions

21 p3811 A70-42075

Coanda effect in bistable fluid amplifier, using finite difference method for computer programmed solution of flow equations

[ASME PAPER 70-FLCS-12] 22 p4008 A70-42415

Equations for unsteady frozen nonequilibrium flow of dissociating and relaxing gas, using Lighthill ideal dissociating diatomic gas for aerothermochemical model

22 p4124 A70-42754

Incompressible fluid turbulent motion statistical equations, considering Lagrangian distributions of fluid particles coordinates and velocities

22 p4012 A70-43315

Three dimensional laminar boundary layer equations for body of revolution at angle of attack in supersonic gas flow derived for equations

22 p3960 A70-43323

Magnetic fields and electrically conducting fluids interaction with emphasis on magnetodynamics equations, investigating rectilinear flows in pipes and nozzles, shock waves, etc

23 p4223 A70-44098

MHD equations for one dimensional plane steady flow, considering conservative difference schemes for approximation

23 p4226 A70-44307

Gas coolant slot injection into hypersonic laminar boundary layer, comparing experimental results to boundary layer equations numerical integration

23 p4282 A70-44694

MHD nonstationary three dimensional problems, describing difference method

23 p4227 A70-44738

Plane flow of incompressible elastic perfectly plastic solid, deriving hyperbolic stress and velocity equations

24 p4427 A70-46043

FLOW FIELDS

U FLOW DISTRIBUTION

FLOW GEOMETRY

Ducted turbulent mixing and burning of coaxial streams, presenting experimental results for rocket-air mixing system

[AIAA PAPER 69-85] 06 p1130 A70-17171

Correlation functions for resistance to heat and momentum transfer in viscous sublayer at rough walls defined for varied geometry flows

[ASME PAPER 69-HT-2] 08 p1486 A70-21833

Geometric, cinematic and dynamic conditions of ideal fluid adiabatic nonstationary movement expressed by differential external system /s/

09 p1659 A70-22254

Local Nusselt numbers beyond abrupt circular channel expansion tested for Reynolds numbers with air as working fluid

09 p1790 A70-23554

Hydrodynamic entrance length in channels and tubes of varying cross section with arbitrary initial velocity profile

[DFVLR-SONDDR-39] 12 p2212 A70-28210

Basic flow convergence or divergence effect on steady flow pattern around circular cylinder using fluid motion visualization

13 p2387 A70-29058

Jet flow past arc curve approximation using successive conformal mapping on circle and wedge

13 p2391 A70-29746

Rotovale induced flow angle variations associated with data repeatability and scatter in blow down wind tunnels at transonic speed

[AIAA PAPER 70-582] 13 p2385 A70-29888

Two phase convex corner flows of particle imbedded inviscid incompressible fluid using small perturbations method

14 p2565 A70-30279

Forced convective heat transfer in annular passage with axially varying cross section, noting role of acceleration parameter

17 p3195 A70-34999

Velocity profiles of laminar flow through rectangular duct with moving wall and arbitrary cross section under nonslip boundary condition

19 p3405 A70-38043

Homopolar device electric arc dynamics dependence on gas type, noting flow geometry-Hall effect competition

20 p3681 A70-40009

Jet flow reattachment to walls of various shapes, measuring undeveloped velocity profiles at nozzle exit

[ASME PAPER 70-FLCS-2] 22 p4008 A70-42429

Jeffery-Hamel flows in symmetric divergent channels with small wall curvature, calculating eigenvalues and nonlinear stability limits

22 p4010 A70-42638

German monograph on supersonic strongly deflecting retardation cascades covering flow geometry and application to axial flow compressor stage

24 p4287 A70-45095

FLOW GRAPHS

Matrix graph concept to unify signal-flow, flow- and N-graph technique approaches to representation and evaluation of matrices and linear algebraic equations

07 p1238 A70-19676

FLOW MEASUREMENT

Cascade tests to investigate nature of flow in rotor blade channels of axial flow turbines with partial admission

01 p0162 A70-10329

Polarographic probe for wall studies of turbulent flow velocity and direction by measuring maximum reduction current on redox compound microelectrode

01 p0062 A70-10664

X array hot-wire anemometer measurements in flows with changing mean velocity direction during traverse

01 p0088 A70-10710

Pitot tube measurements of mixing zone of turbulent shear flow, discussing velocity gradient effects

01 p0066 A70-11134

Speed ratio of rarefied gas flows by molecular miniature pressure probes with orifice at thin cylindrical tube side, discussing LTE deviation regions

02 p0296 A70-11871

Two phase flow instrumentation - Conference, Minneapolis, August 1969

02 p0304 A70-12833

Hot-wire and hot-film anemometry in two phase air-water and steam-water flow, discussing bubble passage, signal processing and measurements

02 p0305 A70-12836

Electronic spray analyzers and conductance and capacitance probes for two phase flow studies, describing operation, characteristics and types of data obtainable

02 p0305 A70-12837

Pitot boundary layer probes with position indicators using extensometric gages for boundary layers on wind tunnel test models

03 p0487 A70-13628

[ONERA-TP-754] Turbulent fluctuation rates of temperature and velocity on basis of measurements in boundary layer with wall heat transfer

03 p0470 A70-14237

Ultrasonic beam scanning measurements in high temperature axisymmetric gas flow, discussing errors and use of numerical transformation methods

04 p0685 A70-14536

Turbine flowmeter theoretical model

[ASME PAPER 69-WA/FM-2] 04 p0689 A70-14841

Schlieren recorder and Erdmann field absorption methods applied to qualitative and quantitative flow process studies in high velocity wind tunnel

04 p0689 A70-14925

Blood flow sensors based on electrical conductivity dependence on flow rate, discussing system instrumentation and experimental results

04 p0644 A70-15295

Razor blade calibration and measurement of wall jet flow shear stress in turbulent boundary layer with secondary injection

05 p0833 A70-16504

Probe geometry effects on hot film anemometer probe performance during turbulence measurements in liquids

06 p1032 A70-17213

Calibration for five hole spherical pitot probe plotting data for velocity, inclination and static pressure factors

06 p1063 A70-17621

Air floated skin friction balance adaptable for cylindrical and plane surfaces

06 p1076 A70-17625

Laminar ablation testing under turbulent boundary layer heating conditions, obtaining recession rate and heat of ablation for turbulent ablation of Teflon

[AIAA PAPER 70-226] 06 p1179 A70-18071

Hypersonic corner flow in He investigated by heat transfer, surface pressure, pitot surveys, oil and electron beam flow measurements

[AIAA PAPER 70-227] 06 p1039 A70-18110

Time mean flow property measurements for homogeneous and nonhomogeneous free turbulent jets

[AIAA PAPER 70-130] 06 p1041 A70-18159

Intensity measurements of molecular beams skimmed from nearly inviscid nitrogen and Ar free jets, interpreting beam attenuation in terms of collisional models

06 p1043 A70-18254

Electron gun onboard reentering spacecraft to measure densities and temperatures in flowing gases

06 p1078 A70-18286

Flow parameters measured in low density hypersonic nozzle, estimating error of all relevant parameters

06 p1030 A70-18302

Impact tube test to find empirical equation for correcting effect of shear in displacing effective pressure center in viscous flow

06 p1052 A70-18383

Lasers industrial application to distance and flow rate measurement, automated machining and tunneling, inspection, die hole punching, welding, etc

06 p1078 A70-18431

Liquid and slush hydrogen gravimetric flow calibration system for research in slush generation, slush fluid mechanics and flow instrumentation

06 p1031 A70-18449

Haematocrit variations effect on electromagnetic blood flowmeter sensitivity, discussing blood specific impedance changes

07 p1217 A70-18951

Electromagnetic induction blood flowmeter measuring blood velocity as function of voltage in pick-up electrodes

07 p1217 A70-18952

Lower limbs circulation of peripheral vascular diseased patients transcatheterously assessed with ultrasonic flow detector, comparing results with arteriograms

07 p1217 A70-18956

Laminar to turbulent boundary layer transition and separation on circular cylinder measured by heated end-window film sensor applicable to water flow

07 p1259 A70-19831

Large axisymmetric disturbances generated in laminar pipe flow by sleeve oscillating at wall, measuring flow with laser-Doppler velocimeter

07 p1286 A70-19995

Aerodynamic subsonic and supersonic wind tunnels parameter measurement methods including static and total pressure, current direction, velocity, density, etc

09 p1674 A70-22314

Heat, moisture and momentum fluxes measurement in atmospheric boundary layer, discussing instrumental accuracy necessary for various measuring techniques

09 p1717 A70-22379

Flow noise measurement for boundary layer pressure fluctuations at rigid wall, analyzing effect of transducer size, shape and orientation on resolution

09 p1675 A70-22387

Holographic flow visualization system retaining all information in light wave passing through flow field, noting reconstruction as shadowgram, schlierens or interferograms

09 p1689 A70-23781

Whirl effect on heat exchanger efficiency and reliability, discussing tests with transparent models and defective filling of circuits by feeding system

[ONERA-TP-768] 10 p1968 A70-24400

Turbulent water flow velocity distribution measurement using laser light intensity fluctuation spectroscopy

10 p1869 A70-24600

Gas flow rate measurement by repeated spark method suitable for stationary and nonstationary flows past surfaces of complex shape

10 p1892 A70-25119

Naphthalene rotating disk with confronting stationary disk, investigating heat and mass transfer dependence on shroud dimensions, measuring flow types

11 p2060 A70-26410

Nearly homogeneous turbulent shear flow for flow field structure, determining pressure/velocity tensor using wind tunnel

11 p2039 A70-26530

Electromagnetic blood flow determination by catheter in external magnetic field, discussing intravascular EM flow sensor capable of percutaneous introduction into vascular system

11 p1993 A70-26663

Turbulent wakes in Canadian Armament Research and Development Establishment free flight ranges measured for mean and fluctuating properties

11 p1978 A70-26774

Ultrasonic flowmeter with electronic components, discussing flow rate parameters and wave propagation relative to flow

12 p2236 A70-28074

Apparent mass measurements of supersonic jet in incalculable flow regimes, determining dependence on Mach number at nozzle and on distance from exit

13 p2387 A70-28859

Axial-flow compressors stall characteristics measurement using water as working fluid

13 p2341 A70-29446

Plane turbulent wall jet from small slot, investigating velocity distribution dependence on slot inclination

13 p2388 A70-29448

Strongly accelerated turbulent boundary layer, investigating free stream turbulence effect on heat transfer

14 p2564 A70-30252

Maximum velocity decay in wall jets calculated for comparison with experimental velocity profile

14 p2566 A70-30777

Radial static pressure distribution of turbulent jet flow over rotating cylinder with constant curvature

14 p2567 A70-31399

Wind tunnel tests of flow past oblate ellipsoid of revolution incident on major axis, measuring pressure distribution

15 p2671 A70-31494

Inductive flow measurement history, considering Maxwell, material and Poisson equations

15 p2735 A70-31823

Null and fixed correction methods for pressure and/or velocity gradient error in flow direction measurement

15 p2736 A70-31898

Laser anemometer for fluid flow measurements, noting sample size restraint, frequency response and velocity range

16 p2926 A70-33141

Gaseous flows and local droplet velocity measurement in dense gas/liquid sprayfields, using noninterference technique

[AIAA PAPER 70-728] 16 p2910 A70-33491

Flow and diffusion phenomena in rarefied gas mixtures associated with separation nozzle process, using molecular pressure probe and mass spectrometer

16 p2893 A70-33699

Argon plasma viscosity measurements at one atmosphere and 10-13,000 K, using discharge with laminar flow as plasma source

[AIAA PAPER 70-775] 17 p3139 A70-34479

Nozzle wall hypersonic turbulent boundary layers at free stream Mach number using pitot, hot wire, and wall fluctuation and static pressure measurements

[AIAA PAPER 70-746] 17 p3065 A70-34497

Fluctuation measurements at wall and across laminar, transitional and turbulent compressible boundary layers on flat plate, using hot film probes

[AIAA PAPER 70-745] 17 p3066 A70-34498

Turbulent boundary layer velocity, temperature and concentration instantaneous measurements, describing automatic circuit procedure

17 p3088 A70-35041

Turbulent boundary layer of flat plate, investigating superlayer structure by hot wire anemometer

18 p3238 A70-36066

Velocity pulsation spectra in subsonic wakes behind circular disks and sphere, using thermoanemometer with constant filament temperature

18 p3207 A70-36279

Thermal electronic instrumentation applied to biological flows including blood flow, cardiac outputs and volumes

19 p3368 A70-37843

High temperature gas boundary layer flows with or without magnetic fields, discussing measurement by X ray absorption technique

19 p3405 A70-38192

Classical invariant characteristic of quantification conditions for flow quantifiers

20 p3671 A70-39122

Radio-telemetry measurements of blood pressure and flow in unrestrained animals

20 p3579 A70-39370

Gas flow rate measurement by repeated spark method suitable for stationary and nonstationary flows past surfaces of complex shape

20 p3635 A70-40512

MHD measurements of gas flow velocity and boundary layer in oxyhydrogen explosions in detonation tube

21 p3942 A70-40876

Interaction zone between gas flow and injected air jets, measuring turbulence characteristics by thermoanemometer

21 p3809 A70-41773

Large fluid-amplifier-type jets, measuring upstream flow disturbances effects on spreading velocity profiles

[ASME PAPER 70-FLCS-A] 22 p3964 A70-42431

Pure Ni plastic flow threshold measurement under combined ultrasonic and static loadings, noting annealing

22 p4053 A70-42644

Induced voltage electromagnetic flowmeter, assessing performance in terms of weight vector to obtain conditions for ideal flow patterns

22 p4029 A70-42692

Ultrasonic measurements of flow velocity and fluid rate, using high speed switching and synchronous demodulator

22 p4041 A70-43619

Sunyah-Mathieu intermittence measuring method applied to turbulent flow boundary studies, discussing flow transition line definition

23 p4180 A70-44201

Oscillatory flow measurements by directionally sensitive laser velocimeter, discussing concept, design and construction

23 p4197 A70-44473

Wave rider aerodynamic properties at small Reynolds numbers, using non-Weiler wing for flow field, pressure and force measurements at rarefied flow conditions

[AVA-FB-7029] 23 p4135 A70-44668

Metal vapor flow measurement by quadrupole mass spectrometer for control of thin film depositions by evaporation

23 p4198 A70-44872

Regional cerebral cortical blood flow measurement, using heat clearance thermistor probe

23 p4157 A70-45082

Cross correlation measurement errors for fluid pipe flow with pseudorandom sequence generated temperature fluctuations, considering transport time, impulse response and laminar flow

24 p4333 A70-45111

Boundary layer instantaneous velocity distributions theoretical and experimental determination

24 p4288 A70-45583

HF pulsating air flow measuring technique with sharp edged orifice meter, discussing experimental setup and pulsation frequency and intensity effects

24 p4335 A70-45591

Flow visualization measuring liquid flow velocity, using flow dichroism

24 p4338 A70-45816

Laser Doppler shift theory and applications to vibration and flow velocity field measurements

24 p4340 A70-46351

FLOW PATTERNS

U FLOW DISTRIBUTION

FLOW RATE

U FLOW VELOCITY

FLOW REGULATORS

NT FUEL FLOW REGULATORS

Spiral grooved turbulent screw seal (viscoseal) analysis, combining results of spiral grooved journal bearing study with turbulent fluid film theory

[ASLE FICFS PREPRINT 32] 02 p0308 A70-12169

Conscious dogs temporary local hypoxia effect on coronary blood flow regulation

09 p1623 A70-23585

Thermal choking of channel flow by radiative transfer from upstream and application to shock waves generation

17 p3195 A70-35039

FLOW RESISTANCE

NT AERODYNAMIC DRAG

NT FRICTION DRAG

NT SUPERSONIC DRAG

NT VISCOUS DRAG

Perfusion pressure and flow effects on coronary resistance, noting venous blood perfusion

01 p0026 A70-11075

Compressible swirling inviscid nozzle flows approximate solution showing changed choking at throat, axial velocity distributions and reversing in subsonic region

01 p0003 A70-11128

Airway resistance effect on ventilation and gas exchange during exercise, discussing minute volume and work of breathing response

03 p0429 A70-14157

Acute coronary occlusion effects on adjacent unoccluded artery resistance, discussing responsible mechanisms in ischemic heart

04 p0637 A70-15473

Breathing valve with reduced air resistances based on aerodynamic principles

06 p1000 A70-17433

Flow separation angle and loss coefficient in cascades with small aspect ratio blades under secondary vortex pair expansion over channel

06 p1130 A70-17858

Pipe orifice conductance for rarefied gas flow measured for specific Knudsen numbers and pressure ratios

06 p1052 A70-18370

Increased blood flow resistance caused by red cell membrane shrinking due to plasma surface tension alteration

07 p1203 A70-18999

Electronic measurement of bronchial flow resistance in pulmonary function to determine impediment in inhaled and exhaled air passage

08 p1449 A70-20676

Dissolved macromolecules effect on flow resistance due to turbulent friction in nonNewtonian liquids, considering physical parameters and hydrodynamic conditions

08 p1483 A70-21228

Human nostril airflow resistance during supported sitting and lateral recumbency and crutch pressure, discussing ipsilateral nasal congestion mechanisms

08 p1448 A70-21874

Turbulent MHD channel flow velocity profiles and hydraulic resistance relations for various Reynolds numbers, using two layer model

09 p1658 A70-22175

Secondary losses in axial turbine cascades without end clearance noting correlation with blade loading

09 p1743 A70-22980

MHD flow turbulence suppression at small magnetic Reynolds numbers, considering MHD interaction parameter role

10 p1924 A70-24575

Potential flow resistance theory, deriving monoparameter wake formula for circular cylinder moving through viscous fluid

10 p1870 A70-24788

Viscous fluid dynamics for reducing hydrodynamic resistance, discussing aquatic animals speeds, vortex flows, etc

10 p1871 A70-25193

Tribonucleation emphasizing viscosity-velocity product in gas nuclei formation and cavitation

12 p2170 A70-27661

Fluidic components downstream impedance calculation, using measured/monitored pressure ratio

14 p2534 A70-30680

Low Reynolds number laminar flow gas turbine regenerators, investigating manufacturing tolerances effects on heat transfer and flow friction behavior

14 p2629 A70-31022

Model for hydraulic resistance reduction for turbulent fluid flows by injecting suspended impurities

15 p2719 A70-31489

Red cell deformability and flow resistance and blood electrical resistance under low g centrifugation

15 p2680 A70-31700

Rheological calculation of plate resistance and heat transfer in laminar flow of structurally viscous fluids

15 p2827 A70-32126

Admittance calibration of short HF through flow pneumatic lines, using hot-wire anemometer

[ASME PAPER 70-FE-10] 16 p2891 A70-33628

Real gas effects in blowdown analysis of leakage through choked nozzle in air flask

17 p3073 A70-35670

Steady two dimensional incompressible shear flow, correlating velocity profiles with resistance distribution

19 p3406 A70-38350

Mass force fields effects on flow phenomena from heat transfer and hydraulic resistance analyses

21 p3951 A70-41764

Turbulent flow velocity profile in constant transverse magnetic field, determining resistance coefficient

21 p3861 A70-42235

Viscous compressible gas flows in pipe initial section, calculating friction and heat transfer coefficients

23 p4135 A70-44734

Resistance to two phase gas-liquid flow in airways simulating human bronchial tree

24 p4303 A70-46111

FLOW SEPARATION

U BOUNDARY LAYER SEPARATION

U SEPARATED FLOW

FLOW STABILITY

NT BOUNDARY LAYER STABILITY

NT FLAME STABILITY

NT MAGNETOHYDRODYNAMIC STABILITY

Existence theorem used for proof of asymptotic methods in nonlinear stability of laminar flow

[ONERA-TP-750] 01 p0061 A70-10298

Goertler vortices effect on boundary layer transition on concave surface, discussing instability oscillations breakdown leading to turbulent motion

01 p0061 A70-10539

Hydrodynamic stability of high purity insulating incompressible fluid subjected to unipolar ion injection

01 p0151 A70-10669

Critical conditions for hydrodynamic stability of incompressible nonconducting fluids subjected to unipolar injection, establishing variational principle leading to characteristic relation

01 p0152 A70-10672

Three dimensional instability of perturbed conducting fluid laminar boundary layer flow on concave walls in transverse magnetic field, analyzing various Hartmann numbers

01 p0152 A70-10934

Flow stability criterion in rough pipes, deriving laminar to turbulent flow transition characteristics and drag as function of Reynolds number

01 p0064 A70-10998

Petrov proof of plane Couette and Poiseuille flow stability with respect to infinitesimal disturbances, rejecting validity of proof

01 p0064 A70-11071

Dynamic behavior of dissociating homonuclear diatomic gas, deriving instability equations, proposing stability loss in transonic region 01 p0068 A70-11584

Liquid film stability relation to angle of attack oscillations during reentry body deceleration 03 p0406 A70-12939

Laminar capillary jet of viscoelastic fluid, discussing breakup, nonNewtonian jet stability and elastic properties 03 p0468 A70-13782

Incompressible inviscid free shear layer stability with respect to spatially growing three and two dimensional disturbances, considering hyperbolic tangent velocity profile [DFVLR-SONDDR-10] 03 p0468 A70-13786

Fourier expansion method applied to hydrodynamic stability of plane jet, testing boundary conditions 03 p0469 A70-14180

Navier-Stokes boundary value problem describing viscous incompressible fluid flow between coaxial fixed and rotating cylinders, emphasizing stability analysis 03 p0470 A70-14242

Electrical and mechanical instability of jets, threads and sheets of viscous fluid, noting role of deceleration 03 p0471 A70-14253

Linear spatial stability of two dimensional laminar wake- and jet-like similarity solution of Falkner-Skan equation 04 p0613 A70-14455

Difference methods application to supersonic gas flow past blunt body and unsteady axisymmetric flow past body of unspecified configuration, analyzing stability 04 p0670 A70-14957

Instability of viscous laminar plane jet of incompressible fluid, finding minimum critical Reynolds number for various assumptions of parallelism 04 p0670 A70-14990

Mixed nozzle flows solution complex boundary value problem reducible to Cauchy problem for hyperbolic system with three dependent variables by applying flow stabilization method 04 p0617 A70-15236

Flow stability of plane channel formed by incompressible viscous fluid injection through porous parallel walls 04 p0673 A70-15238

Plane Poiseuille flow stability as function of periodic disturbances of finite amplitude in channel axis direction 05 p0832 A70-16018

Laminar flow stability along flexible boundary on basis of Orr-Sommerfeld equation 05 p0836 A70-16923

Wind tunnel investigated flow stabilization at horizontal control surfaces by vortex BCL technique, considering angles of attack, elevator deflection and shape 06 p0968 A70-17853

Stability theory for pair of trailing vortices, investigating induced field convection, modes, amplification, cut-off distance, etc [AIAA PAPER 70-53] 06 p0969 A70-18055

Stable two phase water flow system for transpiration cooling in thermal protection of SST noise suppressor situated in afterburning engine exhaust gas stream [AIAA PAPER 70-151] 06 p1181 A70-18146

Dynamic instability of motion of rigid and elastic bodies with liquid filled cavities associated with practical problems of rocket technology 06 p1107 A70-18415

Free steady convective flow stability relative to three dimensional disturbances between parallel planes reduced to equivalent plane disturbances problem 07 p1252 A70-18669

Turbulent friction in gas flow core determined on basis of maximum stability principle 07 p1253 A70-18719

Unsteady hydrodynamic coefficients of supercavitating hydrofoil in harmonic oscillation in Helmholtz flow with free surface, investigating frequency, angle of attack and submergence depth 07 p1255 A70-19134

Time dependent stability of viscous rotational Couette flow induced by impulsively started rotating inner cylinder, using dye injection and motion pictures 07 p1255 A70-19209

Nonlinear stability of plane Couette flow, computing stream function, vorticity distribution and Reynolds stresses 07 p1255 A70-19211

Conducting fluids flow instabilities characterized by incipience at critical electric Hartmann number and convection rate proportional to electric Reynolds number 07 p1348 A70-19265

Current sheet pattern and gas flow stabilization in pulsed plasma accelerators [AIAA PAPER 69-112] 07 p1348 A70-19322

Instability of plane Couette flow of three superposed layers of fluids of different viscosity between two horizontal planes 07 p1260 A70-19978

Supersonic molecular beam source operation, discussing dominant degradation factors and nozzle beam generation intensities and energies improvement 07 p1341 A70-20104

Shock front stability under free flow in electromagnetically driven shock tubes, determining critical hydrodynamic Reynolds number 08 p1482 A70-21529

Quasi-geostrophic baroclinic instability in non-separable parallel flow, using perturbation theory 08 p1539 A70-21604

Finite disturbance effect on laminar incompressible wake behind flat plate determined by interaction between two dimensional fluctuation amplitude and mean flow 08 p1433 A70-21605

Plane Couette flow stability numerical analysis, predicting eigenvalue behavior for arbitrary Reynolds and wave numbers 09 p1658 A70-22124

Plane shock wave stability propagating in external magnetic field determined by temperature dependence of medium electrical conductivity 09 p1658 A70-22168

Blasius flow stability on deformable surface of membrane using Orr-Sommerfeld equation to calculate amplitude of function for perturbation flow 09 p1658 A70-22182

Aerodynamic characteristics of plane straight walled diffusers initial and stabilized flow segments, assuming incompressible fluid and turbulent boundary layer 09 p1659 A70-22430

Irreversible radiative energy transfer effect on stability of flow with two dimensional stationary infinite contact discontinuity 09 p1731 A70-22431

Radiation effects on polytropic atmosphere convective instability using method of disturbances 09 p1753 A70-22456

Two dimensional Poiseuille flow stability at deformable walls, assuming pressure proportionality to displacement and rate 09 p1660 A70-22533

Hydrodynamic stability criterion of isolating incompressible fluids subjected to unipolar space charge injection 09 p1737 A70-23311

Plane Poiseuille flow with nonlinear temperature distribution, studying vortex type secondary flow onset due to buoyant forces [ASME PAPER 69-HT-37] 09 p1790 A70-23555

Vertical liquid jets capillary instability under audio frequency disturbances, measuring disturbance growth rates for various wavelengths and fluid viscosities 09 p1664 A70-23678

Steady and unsteady viscous incompressible one dimensional flows parameters in deformable cylindrical tube determined, solving continuity and motion equations by Galerkin method 09 p1664 A70-23715

Asymmetry and vorticity effects on linear instability of channel flow with one parameter velocities and inflection points, proving wave speed theorem 10 p1862 A70-23951

Landau damping and stability of low density crossed field electron beams using analogy with inviscid shear flows 10 p1918 A70-23964

Elasticity stratification stabilization effect on two layer flows down inclined plane found dependent on time response difference between layers 10 p1863 A70-24009

Self similar and steady state flows near singularities, studying flow stability by partial differential equations 10 p1863 A70-24071

Nonlinear stability problem posed by Navier-Stokes equations in case of laminar flows stability using semigroups theory [ONERA-TP-775] 10 p1863 A70-24094

Small linear disturbance and stability of potential unsteady motion of finite mass of liquid with free boundary 10 p1866 A70-24111

Orr-Sommerfeld equation of hydrodynamic stability theory solved for incompressible two dimensional boundary layer flow on basis of reduction to integral equation 10 p1867 A70-24161

Plane Couette oscillating flow stability to small disturbances under composed unsteady velocity at high Reynolds number 10 p1868 A70-24197

Viscous incompressible flows nonlinear stability theory, considering perturbed flows tending toward stationary or flow periodic in time [ONERA-TP-802] 10 p1869 A70-24542

Nonlinear disturbance decay in unbounded viscous fluid calculated by iterative solution of Navier-Stokes equations 10 p1871 A70-24854

Two fluid hydrodynamic model of heat conductivity and viscosity effects on drift laminar flow stability of dense inhomogeneous plasma 10 p1926 A70-25125

One dimensional compressible constant entropy flows stability, noting unstable regions with fluid particles undergoing compression 11 p2034 A70-25679

Stability analysis using energy method applied to Navier-Stokes equations for unsteady viscous flow 11 p2042 A70-26849

Flow stability of electrically conducting inviscid fluid in coaxial cylindrical annular space under influence of axial magnetic field 12 p2210 A70-27799

Convergent-divergent nozzle operation at low pressure ratios causing separation of internal flow, discussing stability and flow field 12 p2157 A70-28084

Transverse flow convective instability spectrum in vertical channel with porous walls, noting Peclet number effects 12 p2333 A70-28199

Heat transfer and flow stabilization dependence on initial shock wave reflection from conducting wall 12 p2213 A70-28228

Swirling flow between concentric cylinders, studying helical instability modes 13 p2386 A70-28805

Discontinuous hydrodynamic flows derived for stability condition using three dimensional second-order difference schemes 13 p2441 A70-29099

Joseph theorem on parallel flow linear stability, allowing stronger limitation on amplification velocity of perturbation by using simple inequalities 13 p2464 A70-29543

Reverse flow in plasma generated in conical electromagnetic shock tube and reflected from downstream bulkhead, noting stabilization effects 13 p2469 A70-29974

Mean field approximations to Couette flow stability between fixed and coaxial rotating inner cylinder, using Roberts preferred mode method 13 p2392 A70-30007

Inviscid, incompressible superposed fluids stability in presence of inhomogeneous porous media, noting motion with decaying amplitude 14 p2577 A70-30993

Marginal fluid flow stability in porous media taking into account inhomogeneity created by temperature 14 p2577 A70-31000

Interfacial and free surface mode instabilities of time periodic flows of viscosity and density stratified fluids at various Froude numbers 14 p2566 A70-31026

Two dimensional jet velocity profile evolution under symmetrical and antisymmetrical perturbations 14 p2567 A70-31200

Free steady convective flow stability relative to three dimensional disturbances between parallel planes reduced to equivalent plane disturbances problem 15 p2718 A70-31461

Linearized two dimensional double vortex sheet model of inviscid compressible jet instabilities over all Mach numbers 15 p2722 A70-32375

Convective flow stability in rotating fluid layer under rigid boundary conditions, calculating critical Taylor number as function of Prandtl number 16 p2893 A70-33686

Far wake linear stability behind circular cylinders at hypersonic speed, comparing experiments and predictions 16 p2838 A70-33898

Shear flow perturbations in inviscid incompressible stratified fluid of given density, comparing stability characteristics with jet flow 16 p2895 A70-34243

Wedge and cylinder high supersonic wakes stability and transition at various Reynolds numbers 17 p3006 A70-34465

Absolute stability and turbulent transport upper bounds in Couette flow, using variational analysis 17 p3066 A70-34543

Micropolar fluids turbulent flow, investigating microstress couples, stability, inviscid flow, etc 17 p3071 A70-35435

Vortex sheet instability leaving semiinfinite flat plate, considering boundary effects 17 p3073 A70-35601

Couette flow stability between coaxial rotating cylinders, calculating eigenvector in first approximation small perturbation equations 17 p3073 A70-35695

Hydrodynamic flow stability, formulating localizability properties for short wave perturbation 17 p3073 A70-35735

Angular dependence of instability and Rayleigh number of natural convection flow on inclined flat plates, using electrochemical flow visualization 18 p3345 A70-36190

Incompressible heavy fluid film stability during flow along inclined plane constituting crystallization front, analyzing linearized equations of perturbed flow 18 p3240 A70-36271

Flow stability of incompressible heavy viscous fluid along wall of vertical circular cylindrical pipes, relating flow parameters to stability 18 p3240 A70-36278

Lumped parameter pipeline and hydraulic systems stability, deriving equations of motion for closed and open cycle control systems 18 p3216 A70-36946

Laminar two dimensional wall jet with small natural disturbances, examining flow stability at various Reynolds numbers 19 p3402 A70-37526

Viscoelastic fluids stratified flow down inclined plane, examining liquids elasticity role in stability 19 p3403 A70-37531

Stability of thermal and inertial perturbations superimposed on unstably stratified plane parallel flow with variable vertical shear 19 p3462 A70-37753

Viscous dielectric incompressible fluid cylinder capillary stability under small axisymmetric disturbances and axial electric field, deriving perturbed fluid flow equations 19 p3406 A70-38351

Maclaurin spheroid secular stability, examining energy dissipation of gravitational radiation 20 p3702 A70-39017

Time varying flow properties effects on hypersonic wind tunnel spectroscopic measurements, considering direct emission and electron beam techniques 20 p3607 A70-40271

One dimensional unsteady equilibrium flow stability of relaxing two phase medium consisting of perfect gas and incompressible liquid 20 p3613 A70-40295

Plane parallel viscous conducting fluid flows stability in transverse magnetic field, considering small perturbation spectrum, Hartmann and Reynolds numbers 20 p3684 A70-40397

Laminar fluid flow in pipes of rectangular cross section, determining critical Reynolds numbers and maximum instability locations 20 p3614 A70-40400

Flat plate boundary layer flow with surface blowing and suction/mass transfer, investigating stability by numerical techniques 20 p3615 A70-40507

Two fluid hydrodynamic model of heat conductivity and viscosity effects on diffusive laminar flow stability of dense inhomogeneous plasma 20 p3685 A70-40518

Plane horizontal fluid film convective stability with free boundaries in vertical circular cylinder for periodic modulation of vertical temperature gradient or gravitational field 21 p3941 A70-40608

Poiseuille pipe flow instability, considering asymptotic analysis for small wave number disturbances 21 p3807 A70-41241

Self similar flow instability behind collapsing cavity boundary, examining perfect gas adiabatic equation of state 21 p3808 A70-41500

Plane Poiseuille flow in second order Rivlin-Ericksen fluids with small viscoelastic parameters, calculating three dimensional disturbance stability 21 p3810 A70-42030

Cellular convection in fluid layers with parabolic temperature distribution, calculating stability effects of gravity and surface tension gradients 21 p3952 A70-42078

Nonparallel viscous incompressible fluid flows in channel between parallel porous plates with suction and blowing respectively, calculating stability by numerical solution 21 p3811 A70-42216

Viscous incompressible fluid flow between two rotating concentric spheres, calculating stability 21 p3811 A70-42217

Jeffery-Hamel flows in symmetric divergent channels with small wall curvature, calculating eigenvalues and nonlinear stability limits 22 p4010 A70-42638

Poiseuille-Couette spiral flow stability between concentric rotating cylinders 22 p4010 A70-42691

Liquid jet breakup in supersonic airstream, using high speed photographic techniques [SMPTE PREPRINT 90] 22 p4036 A70-43063

Viscoelastic strip in gas flow, analyzing stability conditions 22 p4117 A70-43353

MHD flow universal stability, investigating nonlinear system by energy methods 23 p4223 A70-43967

Miles-Howard theorem extension to gravitationally stratified compressible fluid containing parallel shear flow, considering stability against adiabatic perturbations 23 p4179 A70-43976

Linear stability of fluid flow, proving equivalence of slow and rapid asymptotic solutions of Orr-Sommerfeld equations 23 p4180 A70-43994

Ladyzhenskaia-type fluids linear flow stability criteria for two dimensional case 23 p4218 A70-44238

Temperature gradient effect on Couette flow heat transfer and stability 23 p4181 A70-44250

Solar chromosphere model convective instability, considering temperature and magnetic field effects 24 p4399 A70-45303

Incompressible viscous fluid two dimensional flow in absence of mass forces, considering Tollmien-Schlichting wave perturbation effect on flow stability 24 p4324 A70-45365

Velocity profile in viscous sublayer at wall based on maximum stability principle applied to Karman constant for turbulent channel flow 24 p4325 A70-45495

Stability of self-similar flows of second kind near critical point 24 p4327 A70-46004

Viscous flow stability between two concentric rotating porous cylinders, calculating critical Taylor numbers for wave numbers and velocity ratios 24 p4328 A70-46366

FLOW THEORY

NT MIXING LENGTH FLOW THEORY

Linear small disturbance theories applied to two component gas mixture with fluid motion accompanied by nonequilibrium effects, discussing linear convection and reaction processes 01 p0062 A70-10803

Interplanetary plasma flow simulation around earth magnetosphere and planets not considering initial conditions influence 01 p0172 A70-11488

Modified shock layer theory for predicting hypersonic internal flow in axisymmetric converging duct with attached shock at leading edge 02 p0276 A70-11854

Mean velocity and mean turbulent energy field methods of calculating boundary layer behavior based on numerical solutions of equations of motions 02 p0285 A70-12349

Evaluation of performance of prediction methods for mandatory flows 02 p0286 A70-12359

Wave packet dynamics recapitulation and tentative application to turbulent shear flow 02 p0287 A70-12362

Shock wave shapes over axisymmetric power law bodies in hypersonic flow, noting asymptotic flow theory implications 03 p0406 A70-12946

Propagation of turbulent jet impinging on flat surface at certain incidence angle analyzed for application to V/STOL aircraft, ventilation equipment, etc 03 p0468 A70-13878

Turbulent boundary layer model using two region characterization for eddy viscosity and similarity solution taking into account interfacial conditions [ASME PAPER 69-WA/APM-27] 04 p0668 A70-14905

Inviscid flow problems solution by partial differential equations, considering propagation processes, stratified media, potential, subsonic and three dimensional flows [DGLR-69-2] 04 p0672 A70-15170

Couette problem for Krook kinetic equation solution, considering shear stress variation at high plate velocities 04 p0672 A70-15228

One dimensional unsteady gas flows formation theories extended to include viscosity, heat conductivity, diffusion and chemical reactions effects 04 p0672 A70-15230

Model flow studied for viscous flow near trailing edge of semiinfinite flat plate in middle of moving channel, noting Couette flow tendencies 05 p0831 A70-15879

Two and three dimensional flow using TRIC and TRIM-like triangular finite elements 05 p0832 A70-16115

Flow phenomena about beating plates, fins and wings, discussing biological and engineering applications 05 p0790 A70-16155

Transonic flow theory, investigating thin three dimensional lifting wings, similarity for lift and drag, plane flow past airfoil, far field and hodograph solutions [D1-82-0878] 05 p0834 A70-16693

Two dimensional laminar and turbulent boundary layer flow theory covering heat and mass transfer, compressibility, turbulence, roughness, chemical reactions and axial symmetry 06 p1032 A70-17227

Flow disturbance calculation for heat transfer between boundary layer flows and adjacent walls modified to allow for wall attachment of thermal boundary layer 06 p1032 A70-17228

Aircraft wing load calculations using aerodynamic influence coefficients based on linear subsonic or supersonic flow theory 06 p0967 A70-17255

Plastic flow theory applied to cyclic deformation of metals under complex cyclic loads 06 p1162 A70-17385

Non-Newtonian fluids in continuum mechanics, classical Navier-Stokes theory limitations and theory of incompressible fluids for viscometric flows 06 p1037 A70-17926

Small disturbance theory for internal conical inlet hypersonic flows, using method of characteristics for similarity law verification 06 p0969 A70-18048

Navier-Stokes equations numerical integration in Eulerian coordinates, applying results to compressible and incompressible fluids steady flow 06 p1040 A70-18113

Thermal molecular flow kinetic theory, discussing anisotropic distribution function, thermal transpiration, thermal conduction, entropy production, etc 06 p1113 A70-18369

Nusselt theory of laminar liquid films movement on vertical smooth solid surface, attributing thickness variation to gas movement and surface active agents in liquid 07 p1251 A70-18656

Unsteady boundary layer flow with suction, deriving equations for circular cylinder impulsive motion 07 p1253 A70-18862

Free piston compression with sonic flow outlet for determining orifice size by matching with bounce parameters 07 p1249 A70-19334

Rigid viscoplastic incompressible fluid flow governed by system of variational inequalities involving Navier-Stokes equations 08 p1482 A70-20590

Laminar boundary layer equations solution by approximation compared with results from finite difference method 08 p1483 A70-21033

Gas flow in arc heaters, discussing dissociation, ionization, swirl flow, arc discharge, gas temperature/pressure ratio, gas composition, etc 08 p1554 A70-21925

Elastoplastic stress state of variable thickness disk under combined effect of nonuniform heating and centrifugal forces, applying flow theory to stress component determination 09 p1779 A70-23095

Fluid microstructure effects on velocity, boundary layer and shear stress in nonsteady parallel flows, including accelerated plane wall equation 10 p1863 A70-23955

Supersonic leading edge problem solved by ellipsoidal model using discrete ordinate method compared with BGK model solution 10 p1797 A70-23957

Flow rule for viscoplastic symmetric cylindrical shells, using constitutive equations for strain rate sensitive materials based on Huber-Mises yield condition 10 p1954 A70-24020

Potential flow resistance theory, deriving monoparameter wake formula for circular cylinder moving through viscous fluid 10 p1870 A70-24788

Book on plasma dynamics covering charged particle orbit theory, macroscopic equations, hydromagnetics, hot and cold plasma waves, kinetic theory and plasma radiation 11 p2087 A70-25500

Linear viscous theory of steady rotating fluid flows with nonlinear modification of boundary layers, considering inertial modifications 11 p2036 A70-26011

Turbulence theory based on Wiener-Hermite expansion of velocity distribution to predict energy decay rate for Reynolds numbers greater than two 11 p2040 A70-26542

Two and three dimensional flow analysis using various versions of finite element techniques 11 p2042 A70-26680

Pressure distribution in two dimensional incompressible potential flow on Joukowski airfoils with normal upper surface spoilers, emphasizing potential flow theory [AIAA PAPER 67-737] 12 p2155 A70-27193

Inviscid flow theory for ACV high speed peripheral jets, considering component inefficiencies, pressure losses, nozzle geometry, etc 12 p2156 A70-27211

Transient flow of viscous incompressible fluids with free surfaces calculated using Lagrangian coordinates 12 p2210 A70-27425

Book on aerodynamics covering flow theory, boundary layers, shock waves, wing design, etc 12 p2157 A70-28148

Perfect gas supersonic flow with constant velocity, pressure and density around finite nonaxisymmetric body at small angles of attack

12 p2158 A70-28197

Transonic flow theory for two and three dimensional streamlined bodies in steady irrotational flow of inviscid perfect gas

12 p2158 A70-28201

Mathematical model for describing flow in Hele-Shaw cell, predicting attached viscous shear layers in lifting body wake

13 p2338 A70-28818

Steady diabatic complex lamellar gas flow, obtaining parameters by extending geometric theory of surfaces and curves in fluid flow theory

13 p2387 A70-29122

Joseph theorem on parallel flow linear stability, allowing stronger limitation on amplification velocity of perturbation by using simple inequalities

13 p2464 A70-29543

Boundary conditions and initial value lines for unsteady homentropic flow, performing straight pipe calculations

13 p2392 A70-30023

Two dimensional incompressible steady turbulent flows based on Prandtl hypothesis relating eddy viscosity to kinetic energy and scale

14 p2564 A70-30259

Turbulent boundary layer correlations on flat plate, noting inadequate Spalding-Chi predictions

14 p2567 A70-31396

Nonself similar problem of plane submerged fluid jet expelled from annular nozzle, obtaining asymptotic expansion for stream function

15 p2719 A70-31485

Turbulent flow theory of dilute linear polymer solutions in smooth and rough tubes based on Reynolds equation

15 p2719 A70-31491

Book on aerodynamics for engineering students covering hydro- and aerostatics, flow theory, propulsion principles, aerofoil theories, aircraft performance and stability, etc

16 p2838 A70-33953

Transport and relaxation processes prediction for turbulent fluid, noting similarities to Fourier integral representation of flow field

16 p2895 A70-33969

Turbulent flows calculation based on two parameter turbulence model, considering model application to free jets

16 p2895 A70-34199

Turbulent shear flow asymptotic theory, discussing channel, pipe and two dimensional boundary layers

16 p2895 A70-34244

Steady state laminar flow model for near wake of slender body in supersonic flow

17 p3006 A70-34467

Laminar incompressible separating and reattaching flows, correlating finite difference solutions with experimentation

[AIAA PAPER 70-763]

17 p3008 A70-34488

Analytic theory of unsteady separated flow effects on dynamics of heat sink type reentry bodies and elastic launch vehicles

[AIAA PAPER 70-762]

17 p3008 A70-34489

Boundary layer theory development in U.S.S.R., surveying findings and papers

17 p3067 A70-34662

Continuum plasma dynamics with electromagnetic forces of same order of magnitude as gas dynamic forces, discussing various flow problems

17 p3141 A70-35040

Materials deformational flow theory, relating dislocation motions in solids to fluid viscosity concept

17 p3190 A70-35452

Turbulence theory from Liouville equation for Navier-Stokes velocity field distribution

17 p3073 A70-35629

Fluid turbulence unified heuristic model, defining determinate solutions for Navier-Stokes equations numerical integration at high Reynolds numbers

17 p3074 A70-35884

Axisymmetric one dimensional compressible flow theory applications to compressible fluids ducted flow

[ASME PAPER 70-GT-82]

18 p3243 A70-36882

Quasi-two dimensional supersonic cascade flow, taking into account transverse stream contraction effect

18 p3210 A70-37206

Eringen theory of micropolar fluids for hydrodynamic turbulence

19 p3404 A70-37783

Eringen theory of microfluids with nonhomogeneous micromotion, discussing eccentricity, stress moments, microinertia, etc

19 p3404 A70-37784

Stratford prediction method of separation position for compressible boundary layer flow

19 p3406 A70-38617

One dimensional channel flow theory for ram wings, deriving lift and drag laws for comparison with wind tunnel and free flight tests results

[AIAA PAPER 70-971]

20 p3558 A70-39558

Modified linearized transonic flow theory application to pressure coefficient distribution on circular arc bodies of revolution

20 p3608 A70-39614

Axial pressure, electric current and potential distribution in two-phase particulate electrogasdynamic flow, discussing space charge electric field effect

20 p3683 A70-40257

Wall jet turbulent flow regions with shear stress and mean velocity gradient of opposite sign, considering theoretical explanation

20 p3615 A70-40501

Two dimensional turbulent boundary layer computation using two parameter family of velocity profiles and skin friction law

21 p3806 A70-40921

Unsteady flow in rectangular cavity with moving wall, using iterative solution of Navier-Stokes equations

21 p3807 A70-41317

Rarefied gas flow over plane wall, considering boundary layer thickness of order of mean free path

21 p3809 A70-41715

Viscous laminar parallel flow along cylindrical surfaces, discussing boundaries described by algebraic polynomials

21 p3810 A70-41959

Plane parallel transonic flow with curved compression shock discontinuity in supersonic region, obtaining solution by indeterminate coefficients and hypergeometric functions

21 p3748 A70-42212

Existence theorem for boundary layer problems, including swirling flow between coaxial rotating disks

22 p4009 A70-42484

Time dependent shock wave structure, considering shock tube flow as initial and boundary value problem

22 p4009 A70-42516

Buoyant hot two dimensional laminar vertical jet in quiescent colder fluid, calculating temperature and velocity distributions by integral method

22 p4010 A70-42639

Cylindrical afterbodies base pressure drag under powered supersonic flight, modifying Korst flow model recompression criterion

22 p3959 A70-42713

Perfect gas supersonic flow with constant velocity, pressure and density around finite nonaxisymmetric body at small angles of attack

22 p3960 A70-43322

Free jet stream effect on thin jet-flapped airfoil with fully developed wake, using linear theory

22 p3960 A70-43737

NonNewtonian fluids variational problems, discussing generalized solutions existence and uniqueness

23 p4179 A70-43987

German book on propeller theory covering airfoil theory, propeller flow and pressure fields, propeller vibrations, shrouded and tilted propellers, helicopter rotors, etc

23 p4180 A70-44097

Navier-Stokes equations for discrete flows of viscous fluids, using grid cell representation

23 p4181 A70-44220

Gas pressure differential across multilayer insulation blanket during rapid evacuation predicted, using one dimensional flow theory

[AIAA PAPER 69-608]

23 p4282 A70-44522

Three dimensional hypersonic laminar boundary layer subdivided into inner and outer regions, obtaining flow description by matching inner and outer solutions

[AIAA PAPER 69-710]

23 p4182 A70-44565

Two dimensional turbulent wake theory, considering shear stress and velocity distribution behind flat plate and circular cylinder

23 p4134 A70-44575

German monograph on flow phenomena in gas containing fluids, covering pressure and ultrasonic induced cavitation in steady and unsteady flow

24 p4324 A70-45098

Boundary layer instantaneous velocity distributions theoretical and experimental determination

24 p4288 A70-45583

Pulsatile flow in circular rigid tube with and without longitudinal vibration, obtaining momentum integral solution

24 p4325 A70-45623

FLOW VELOCITY

Output power and gain saturation characteristics for high speed flowing gas molecular lasers, discussing electrically excited fluid mixing carbon dioxide laser

01 p0107 A70-10103

Polarographic probe for wall studies of turbulent flow velocity and direction by measuring maximum reduction current on redox compound microelectrode

01 p0062 A70-10664

X array hot-wire anemometer measurements in flows with changing mean velocity direction during traverse

01 p0088 A70-10710

Flow velocity pulsations effect on frequency spectrum of flow optical fluctuations, discussing methods for separating turbulence characteristics

01 p0092 A70-10996

Plasma arc wind tunnel gas velocity measurement with electron beam probe using closed-loop electronic controller to stabilize beam position

01 p0092 A70-11195

Pressure drops in turbulent flow through circular or plane parallel section pipes, obtaining mean velocity expressions suitable for application to lubrication

02 p0277 A70-11912

Flow direction and velocity measurement in three dimensional boundary layer, discussing instrument and restrictions

02 p0299 A70-12312

Plasma velocity, electron temperature and density and ion density determined by two mutually perpendicular probes

03 p0529 A70-12940

Eddy viscosity equation derived from flat plate turbulent boundary layer velocity data, considering shear stresses and mixing length profiles

03 p0464 A70-12943

Book on flow and thermal boundary layers covering laminar and turbulent flow velocity profiles, Prandtl equation, heat transfer problems, etc

03 p0465 A70-13015

Contactless asynchronous flowmeter for measuring liquid metal coolant small flow rates, describing design and characteristics

03 p0483 A70-13211

HF pressure oscillations during heat transfer to n-heptane at various flow rates and pressures, studying film or bubble boiling associated with oscillations

03 p0605 A70-13516

Time varying blood flow in pulmonary capillaries affecting overall diffusing capacity and alveolar-arterial oxygen tension gradient

03 p0421 A70-13570

Velocity structure associated with motion of interface between turbulent and nonturbulent fluid at turbulent boundary layer edge, considering shear flows

03 p0470 A70-14240

Secondary velocities analysis in turbulent boundary layer in dihedron interior based on turbulence anisotropy and effects on wall pressure gradient

03 p0471 A70-14354

Volumetric flow rate of rare gases, hydrogen and deuterium between parallel plates at various pressures and Knudsen numbers

04 p0665 A70-14414

Turbulent flow velocity and stress components simultaneous measurement by single hot wire, discussing equations and computer program

04 p0685 A70-14447

Transverse magnetic fields effects on velocity perturbations and vortices behind circular cylinder in electrolyte flow at various Reynolds and Stewart numbers

04 p0726 A70-14543

Rarefied gas flow through ultrafine porous filtering media used to predict flow rate

[ASME PAPER 69-WA/PID-8]

04 p0666 A70-14755

Circular tube entrance upstream and downstream velocity profiles at small axial distances measured by laser Doppler flowmeter

[ASME PAPER 69-WA/FE-13]

04 p0667 A70-14780

Mean flow velocity distribution calculated from momentum deficit superposed behind single cylinders in finite array of arbitrarily spaced parallel cylinders

[ASME PAPER 69-WA/FE-11]

04 p0614 A70-14781

Similarity of velocity profiles and pressure distribution of turbulent jet over inclined wall, indicating limitations of Glauert analysis

[ASME PAPER 69-WA/FLCS-1]

04 p0668 A70-14849

Viscous inlet flow into straight channels, studying velocity profiles at low Reynolds numbers

[ASME PAPER 69-APM-Q]

04 p0668 A70-14863

Steady, ambipolar, low and high speed plasma transport equations developed for terrestrial ionosphere, discussing boundary conditions for supersonic and subsonic flows

04 p0679 A70-15112

Optimal orbit velocities of charged particles for spacecraft electrostatic thrusters

[DFVLR-SONDDR-28]

04 p0735 A70-15173

Transonic flow about slender profiles computed for flow velocities slightly below and above Mach 1

04 p0616 A70-15185

Pressure pulsations and velocity measurements in turbulent boundary layer without longitudinal gradient, analyzing Reynolds numbers, self similarity and structural characteristics

04 p0673 A70-15250

Blood flow sensors based on electrical conductivity dependence on flow rate, discussing system instrumentation and experimental results

04 p0644 A70-15295

Blood flow velocity and pressure measurements on conscious man with catheter-tip velocity probe

04 p0645 A70-15439

Rarefied H, He, air, carbon dioxide and water vapor flow rates between parallel optically flat glass surfaces measured, giving flow equation describing channel flow

05 p0833 A70-16525

Compressible fluid flow velocity profile in turbine stage evaluated by streamline correlation and actuator disk method

06 p0967 A70-17469

Repetitive scanner for wave velocity measurements in annular two phase gas or liquid flow using pivoted mirror

06 p1062 A70-17618

Hot air breather test facility design to increase flowrate range at maximum pressure level

06 p1028 A70-17981

Thermal slip velocity of gas in infinite temperature gradient tangential to solid wall, basing calculation on linearized Boltzmann kinetic equation

06 p1049 A70-18332

Surface diffusion slip velocity in binary gas mixture above solid surface, basing calculation on distribution functions determined from Boltzmann equation

06 p1049 A70-18333

Velocity profile at entrance of two dimensional channel immersed in rarefied slow moving uniform flow with slip at walls

06 p1052 A70-18384

Wall roughness effects on model heat transfer in high Reynolds number shock tunnel milliseconds flow using thick film fast response calorimeter

06 p1070 A70-18446

Turbine flowmeter in-place calibration for measuring cryogenic propellant flow rates in rocket engine testing

06 p1071 A70-18448

Three dimensional boundary layer on body in external harmonic flow with HF velocity fluctuations

07 p1252 A70-18711

Electromagnetic induction blood flowmeter measuring blood velocity as function of voltage in pick-up electrodes

07 p1217 A70-18952

Turbulence effect on heat transfer in flow carrying section of turbine engines, considering flow velocity pulsations frequency characteristics

07 p1362 A70-19067

Nonsimilar energy and species equations for flow velocities described by Falkner-Skan equation

07 p1256 A70-19307

Flow mean velocity measurement using probe submerged in moving electrolyte and not requiring external power source

07 p1257 A70-19377

Flow velocity distribution near boundaries of model of plates of parallel faces, obtaining Laplace equation solution

07 p1258 A70-19378

Unsteady boundary layer in compressible fluid laminar flow over accelerating semiinfinite flat plate

07 p1258 A70-19566

High electrical conductivity effects on alignment between magnetic field and flow velocity vector in two dimensional plasma flow

07 p1349 A70-19568

Spectral functions of airflow velocity pulsations in circular pipe at various Reynolds numbers, considering laminar, transition and turbulent regimes

07 p1259 A70-19826

Velocity pulsations of hypersonic working flow in wind tunnel using miniature pressure transducers, discussing rms error

07 p1259 A70-19828

Wall proximity and velocity gradient effects on thermocouple readings in turbulent boundary layer

07 p1285 A70-19834

Viscoelasticity in shearing and accelerative flows by integral theory, discussing stress distribution and pressure drop

07 p1412 A70-20000

Molten Al alloys flow rate and behavior in various casting systems, considering gate geometry and casting temperature effects

08 p1505 A70-21133

Dynamic behavior of subcritical fluid flow past airfoils, expanding flow potential to obtain formulas for velocities, local Mach numbers and pressure

08 p1433 A70-21173

Turbulent-laminar transition in divergent radial flow between disks, relating velocity fluctuations to Reynolds number

08 p1483 A70-21235

Unsteady flow in circular tube of constant section with time dependent discharge, determining pressure gradient and velocity distribution

08 p1484 A70-21477

Transverse oscillation periods of cylinder containing flowing fluid obtained by solving nonlinear partial differential equations describing transverse and longitudinal motion

08 p1592 A70-21480

Harmonics generated in hot-wire anemometers responses by wires thermal lag and amplitude of flow velocity fluctuations using computerized simulation

08 p1498 A70-21586

De Laval nozzle behavior in vacuo, discussing flow rate parameters, viscosity and real gas effects, thermal effects, turbulent jet separation and reattachment, etc [AGARDGRAPH-120]

08 p1434 A70-21932

Instantaneous velocities measured for wall region of smooth duct during turbulent fluid flow by chronophotography of particles

09 p1658 A70-22046

Small-scale local flow velocity measurements with laser using differential Doppler method

09 p1694 A70-22125

Turbulent jet injection from circular opening into unbounded transverse shear flow, determining velocity distribution along axis

09 p1659 A70-22427

Average velocities profile measurement in wall region of turbulent fluid flow in smooth duct

09 p1661 A70-22838

Karman trail vortices tangential velocity decay measurement by hot film anemometer experiments

09 p1661 A70-22961

Optimal outlet velocities of charged particles for spacecraft electrostatic thrusters

09 p1744 A70-23428

Velocity and friction stress profiles of semibounded plane turbulent jets discharging from finite slit along smooth plate into moving medium

09 p1663 A70-23617

Charged particles velocity profile across shock determined by induction velocimetry, considering eddy currents effects on induced potential gradient

09 p1738 A70-23677

Blade inter-row distances upstream and downstream related to potential flow velocity disturbances created by cascade in turbomachines

09 p1607 A70-23734

Pressure and velocity ratios and energy requirements dependence on flow parameters of cylindrical capsule in horizontal pipeline

09 p1665 A70-23747

Compressor blade performance dependence on Reynolds number, turbulence intensity and axial velocity ratio, considering wind tunnel tests with porous side walls

09 p1609 A70-23748

Heat sources effect on pressure and velocity of supersonic flow, discussing iteration procedure and asymptotic expansion

10 p1799 A70-24125

Flow past yawed delta wing at supersonic flight velocities, obtaining real velocity near singular surface and replacing Mach number by perturbed parameter

10 p1799 A70-24126

Small flow rate flowmeter design and application to nonreactive liquids and liquid gases with low viscosity

10 p1888 A70-24392

Statistical chance characteristics of velocity profiles and friction for flow along infinite plane wall with constant suction

10 p1869 A70-24519

Gas flow rate measurement by repeated spark method suitable for stationary and nonstationary flows past surfaces of complex shape

10 p1892 A70-25119

Turbulence effect on heat transfer in flow carrying section of turbine engines, considering flow velocity pulsations frequency characteristics

10 p1930 A70-25218

Velocity distribution of plane airfoil cascade given by geometry, using method of least squares

11 p1974 A70-25785

Airfoil cascades flow for given profile shape by singularity method, obtaining velocities

11 p1975 A70-25790

Homogeneous turbulence multipoint multitime correlations for fluctuating velocity

11 p2036 A70-26014

Velocity profile and volume flow rate for rarefied gas flowing isothermally parallel plates, solving linearized Boltzmann equation by BGK model

11 p2037 A70-26168

Laminar boundary layer flow with exponential velocity distribution in outer flow described by differential equations, studying slip velocity at wall

11 p2037 A70-26350

Plasma density and velocity required for simulating solar wind flow over magnetosphere /bow shock/ in plasma wind tunnel

11 p2032 A70-26372

Hydrogen-air turbulent diffusion flame structure at differing air and hydrogen velocities

11 p2151 A70-26387

Cavity pressure and velocities distributions of interfering two dimensional dual jets from parallel slot nozzles

11 p2037 A70-26419

Steady state two dimensional flow velocity profiles at low Reynolds numbers of homogeneous incompressible viscous liquid in straight channel inlet region

11 p2037 A70-26476

Incompressible boundary layers velocity distributions on cylinders rotating in axial flow, considering centrifugal force effects, momentum thicknesses, local shearing stress, etc

11 p2038 A70-26477

Monograph on axially symmetric tandem grids for supersonic flow deceleration to subsonic speeds, using schlieren optical tests and pressure measurements

11 p1977 A70-26525

Atmospheric turbulent boundary layer velocity signals correlation with lognormal distribution

11 p2076 A70-26531

Turbulence theory based on Wiener-Hermite expansion of velocity distribution to predict energy decay rate for Reynolds numbers greater than two

11 p2040 A70-26542

Incompressible homogeneous isotropic turbulence velocity expanded in Hermite functionals of Gaussian white noise random function advected by fluid

11 p2040 A70-26543

Homogeneous turbulent velocity effect on magnetic field distribution in electrically conducting fluid with no external source, observing dynamo action

11 p2091 A70-26545

Velocity fluctuations measurements in conducting fluids flowing through tubes

12 p2230 A70-27091

Ultrasonic flowmeter with electronic components, discussing flow rate parameters and wave propagation relative to flow

12 p2236 A70-28074

Turbulent diffusion coefficients and time dependent velocity pulsations in air flow, considering relation between Eulerian and Lagrangian turbulence characteristics

12 p2213 A70-28235

Turbulent flow of incompressible fluid, obtaining closed system of approximate equations for probability distribution of velocities

12 p2213 A70-28237

River bed channel flow instantaneous velocities described by logarithmic law, determining turbulent energy dissipation

12 p2265 A70-28336

Eulerian space-time correlations of velocity and pressure for universal homogeneous turbulence by separating kinematic convection effects of large eddies from velocity assumption

13 p2386 A70-28645

Lateral motions of vertical uniform tubular cantilever conveying fluid, considering oscillatory instability at high flow velocities

13 p2511 A70-28741

Air velocities measurement with heated thermistors probe, discussing calibration and reliability dependence on flow velocity range

13 p2405 A70-28841

Asynchronous liquid metal MHD generator parameters, assuming constant vertical distribution of working fluid velocity

13 p2349 A70-28968

Fixed end nonprismatic bar stability in fluid flow, studying form influence on critical flow velocity

13 p2512 A70-28982

Oxygen motion velocity effect at various pressures on heatproof and heat resistant steels and alloys ignition, noting minimum ignition temperature

13 p2434 A70-29168

Earth core flow velocity field to construct kinematic model of hydromagnetic dynamo, discussing magnetic field development

13 p2398 A70-29209

Excess pressure in pulsed fluid jet with different emergent velocities from water hammer, discussing interaction between discrete sections

13 p2388 A70-29425

Turbulent boundary layer formation in upstream wake of accelerated flow indicated from boundary layer profile and wall static pressure measurements

13 p2392 A70-29996

Velocity circulation in laminar motion of fluid in cylindrical tube, assuming equilibrium under dissipative forces

14 p2564 A70-30164

Flow velocity distributions in laminar boundary layer by perturbation methods

14 p2566 A70-30850

Two dimensional incompressible laminar boundary layers asymptotic structure with injection, obtaining velocity profiles

14 p2566 A70-30995

Low aspect ratio wing aerodynamic characteristics in shear flow, noting forces dependence on flow velocity gradients

14 p2529 A70-31274

Karman vortex shedding phenomenon for flow rate measurement in channel or pipe

14 p2588 A70-31333

Screw flows in fluid dynamics, showing helicoidal type flow for constant flow velocity on stream lines

15 p2718 A70-31447

Constant temperature hot split film anemometer sensors based on velocity and heat flux distribution about probe, measuring flow rates

15 p2734 A70-31691

Miniaturized electromagnetic catheter flowmeter for measuring volume flow rate by potential difference between electrodes

15 p2689 A70-31747

- Automatic numerical analysis of velocity information from Doppler effect ultrasonic blood flow meter 15 p2691 A70-31920
- Vortex streets characteristics determination for plane jet having uniform initial velocity profile 16 p2890 A70-33108
- Liquid hydrogen axial flow pump under, describing suction pressure measurements, fluid conditions and flow rate [AIAA PAPER 70-627] 16 p2919 A70-33592
- Additional inertia introduced by velocity profile gradient in flow direction effects on externally pressurized gas bearing 16 p2924 A70-34233
- Transonic flow around perpendicular plate, determining front side velocity and pressure from known stagnation point and transonic region 16 p2839 A70-34236
- MHD flow velocity and magnetic flux profiles in rectangular ducts for secondary boundary layer 16 p2959 A70-34239
- Arterial wall nonlinear distensibility effects on blood flow velocity profiles, considering various mathematical and physical artery models 17 p3035 A70-34468
- Upper pulmonary airways plastic conduit model, measuring laminar and turbulent flow velocity profiles by hot-wire anemometer 17 p3035 A70-34469
- Gas flow velocity measurement using hot foil probes 17 p3082 A70-34680
- Shock tube orifice effect on gas flow velocity and pressure drop, using pressure probes and Jenny friction formula 17 p3069 A70-34699
- Helicopter blade sections dynamic stall characteristics, considering accelerated flow generation by nonzero pitch rate 17 p3014 A70-34718
- Low speed rarefied slip flow over wedge by asymptotic method of boundary layer equations integration, obtaining velocity profiles for various angles 17 p3010 A70-34973
- Turbulent mixing of axisymmetrical supersonic air jet into hot air, investigating Mach number and temperature difference effects on axial decay of velocity 17 p3072 A70-35546
- Aerofoil section characteristics in shear flows of arbitrary velocity profile calculated by Glauert image method 18 p3205 A70-35957
- Wake behind trailing edge of flat plate in constant velocity impulsively started stream, using boundary layer theory 18 p3206 A70-36196
- Turbulent velocity pulsations characteristics determination by diffusion measurements 18 p3240 A70-36265
- Turbulent shear flow velocity and kinetic energy distributions in tunnel 18 p3241 A70-36383
- Wall cooling effects on turbulent boundary layer in low speed air flow, using smooth tube and thermocouple measurements 18 p3347 A70-36505
- Gas particle mixtures nozzle flow at high loading ratios 18 p3208 A70-36693
- Three dimensional boundary layer flow on rotating axial flow turbine buckets, determining velocity profiles [ASME PAPER 70-GT-59] 18 p3243 A70-36874
- Steady state nonlinear dynamics of low latitude atmospheric global boundary layer, indicating inverse relation between air flow vertical velocity and distance from equator 19 p3460 A70-37417
- Velocity profiles in steady and unsteady rotating flows for impulsive slow down and acceleration in cylindrical chamber 19 p3403 A70-37527
- Turbulent velocity correlation function computation in Burger fluid model, using functional integral expression 19 p3403 A70-37530
- Ionized argon supersonic flow velocity and local electron density by optical methods 19 p3480 A70-38173
- Pressure and velocity distribution inside casing and around impeller of volute pumps, discussing flow at exit and in wedge shape space 19 p3437 A70-38225
- Suction velocity effects on Rayleigh problem in MHD of flat nonmagnetic nonconducting plate, solving for velocity distribution and skin friction 19 p3481 A70-38448
- Two dimensional steady inviscid incompressible flow past profiles in parallel flow with nonuniform velocity distribution 19 p3354 A70-38676
- NonNewtonian boundary layer flow having arbitrary potential velocities from methods for Newtonian fluids 19 p3407 A70-38932
- Turbine blade profiles calculation by hodographs, obtaining compatibility with continuous flow velocity distribution and improved boundary layer stability 19 p3491 A70-38949
- MHD flow in channel of arbitrary cross section, deriving velocity and electric potential distribution by variational principle 20 p3677 A70-39360
- Flow velocity and pressure profiles due to vortex ring confined in cylindrical channel, using electromagnetic analogy 20 p3609 A70-39651
- Prototype synchronizing valves for maintaining identical flow velocities of two hydraulic actuating elements, noting unbalanced hydrodynamic forces and orifices asymmetry effects 20 p3564 A70-39717
- High velocity gas motion in laminar boundary layer, describing universal motion equations two parameter solution 20 p3611 A70-39805
- One wavelength MHD induction generator, discussing field pressure gradients, fluid velocities, excitation and electrical output power 20 p3566 A70-40015
- Wall proximity and velocity gradient effects on thermocouple readings in turbulent boundary layer 20 p3634 A70-40341
- Longitudinal averaged and pulsating turbulent flow velocities in rectangular channel with one-sided air injection through porous wall 20 p3614 A70-40346
- Steady plane conducting gas flow across magnetic field in channel, calculating flow rate effect on current density distribution 20 p3684 A70-40386
- Gas flow rate measurement by repeated spark method suitable for stationary and nonstationary flows past surfaces of complex shape 20 p3635 A70-40512
- Turbulent boundary layers calculation with and without mass addition based on eddy viscosity concept, including accelerating flows 21 p3807 A70-41029
- Accelerated self similar compressible laminar boundary layer flows with and without mass transfer, obtaining numerical solutions 21 p3807 A70-41031
- ULF ballistocardiogram amplitudes relationship to blood flow velocity for cardiovascular disease diagnosis 21 p3763 A70-41234
- Blood velocity in ascending aorta in man by transcutaneous ultrasonic Doppler technique, investigating heart hemodynamic performance and systemic perfusion 21 p3770 A70-41235
- Heat transfer in laminar channel flow with random velocity variations, using Monte Carlo technique 21 p3949 A70-41312
- Turbulent energy balance and spectra of axisymmetric wake behind sphere in incompressible fluid, measuring flow velocity 21 p3745 A70-41376
- Shock wave extinction point within plane steady upstream flow with uniform entropy and limit velocity 21 p3808 A70-41441
- Constant temperature linearized hot-wire anemometer for low velocity high turbulence flow 21 p3827 A70-41455
- Eddy currents in Hall generator with conducting side wall, studying velocity and temperature effects for turbulent boundary layer and laminar flows 21 p3859 A70-41733
- Transformation theory for compressible turbulent boundary layer with arbitrary pressure gradient [AIAA PAPER 69-160] 21 p3809 A70-41741
- Liquid droplet shape effect flow field velocity and pressure distribution over windward surface in high speed gas streams 21 p3809 A70-41762
- Viscous gas flow through Laval nozzle, calculating velocity coefficient and pressure recovery in contracting and expanding parts 21 p3746 A70-41774
- Interactions between components of turbulent flow velocity correlation tensor due to pressure fluctuations 21 p3810 A70-41956
- Wave number spectral correlation of temperature and longitudinal velocity fluctuations in fully developed pipe flow 21 p3811 A70-42090
- Gas velocity and static pressure effects on evaporation rate of moving liquid fuel droplets 21 p3953 A70-42094
- Turbulent incompressible conducting fluid jets velocity and temperature characteristics in presence of longitudinal and transverse magnetic fields 21 p3860 A70-42226
- Thermoanemometric velocity measurements in nonstationary MHD Hg flows by insulated Pt sensors 21 p3831 A70-42229
- Microplanar incompressible fluid slow stationary flow past sphere 21 p3812 A70-42252
- Elastic plate response to boundary layer pressure fluctuations, estimating vibration modes dependence on fluctuation convection velocity and response magnification as function of flow direction 22 p4007 A70-42283
- High power plasma flow generation at variable pressure and rates, describing device characteristics and performance 22 p4079 A70-42367
- Isothermal steady laminar flow through tube with change in wall temperature, examining velocity profile relationship to temperature profile [ASME PAPER 70-HT-C] 22 p4008 A70-42421
- Time-mean velocity and skin friction of laminar boundary layer near two dimensional stagnation point with oscillating oncoming flow 22 p4010 A70-42686
- High velocity isothermal viscous compressible steam flow in circular tubes, measuring pressure drops 22 p4011 A70-42845
- Nb-Zr alloy and yttria corrosion by high velocity Li flow, discussing material removal depth 22 p4055 A70-43100
- Cavitation characteristics of jet nozzles, formulating relationship between pressure differential and fluid flow rate 22 p3965 A70-43369
- Turbojet engines noise-suppressing nozzles flow rate and thrust characteristics calculation 22 p4092 A70-43371
- Flowing medium turbulent velocity measurement using laser Doppler device 22 p4040 A70-43615
- Ultrasonic measurements of flow velocity and fluid rate, using high speed switching and synchronous demodulator 22 p4041 A70-43619
- Twisted incompressible viscous fluid flow in conical diffuser described by differential equation system, considering flow velocity field and separation point 23 p4133 A70-44159
- Cryogenic pipelines cooldown to operating temperature, calculating cryogen flow rate limits due to thermal stresses in steel and Al flanges 23 p4280 A70-44368
- Nitrogen plasma viscosity measurements as function of velocity and axial static pressure gradient 23 p4226 A70-44439
- Laminar boundary layer wall shear and velocity profiles by N parameter integral method, using exponentials 23 p4182 A70-44567
- Gas turbine engines flow velocity fields, comparing various calculation methods 23 p4136 A70-44735
- Flat plate film cooling efficiency behind tangential slot at blow-main flow velocity ratio over three 23 p4283 A70-44741
- Reynolds stress measurement, using laser flowmeter with cylindrical lenses and square aperture mask 23 p4202 A70-44945
- Jet engine combustion chamber pressure loss, flow velocity through flare tube holes and air supply calculation, noting adaptation for computer use 24 p4393 A70-45446
- Beam laser operational efficiency relation to molecule /atom/ interaction in focusing system, explaining lasing power drop at large flow rates 24 p4351 A70-45457
- Magnetized conducting sphere steady rotation in viscous conducting liquid, solving for fluid velocity and induced magnetic field 24 p4386 A70-45609
- Flow visualization measuring liquid flow velocity, using flow dichroism 24 p4338 A70-45816

FLOW VISUALIZATION

- Flow profiles in models of human bronchial tree typical junctions, visualizing inspiration and expiration patterns for various Reynolds numbers 01 p0034 A70-10653
- Holographic color schlieren flow visualization system for three dimensional photography, variable focus shadowgraph, knife edge schlieren, etc 01 p0091 A70-10908
- Flow visualization of boundary layer transition downstream of Gortler vortices, distinguishing successive instability modes by Te method 01 p0065 A70-11094
- Two phase flow visualization by various photographic and optical methods, describing equipment and lighting used and types of data obtainable 07 p3035 A70-12834
- Dogs left ventricle areas supplied by coronary arterial branches visualized utilizing scintillation photography and radioactive Xe 03 p0432 A70-12892
- Schlieren photograph intensity variations correlated with statistical parameters for turbulent flow density variations 03 p0464 A70-12941
- CW laser light sources for Mach-Zehnder interferometer, obtaining results for carbon dioxide injected through porous bottom wall into air flow 03 p0484 A70-13397

Fluid flow visualization in closed channels, using spherules of pulverized fusible materials prepared in swirl injector

03 p0485 A70-13473

Transillumination holography in environmental tests, discussing camera design, particle field and applications, including flow visualization in wind tunnel tests

03 p0486 A70-13539

Striated plasma flow in MHD duct of conducting rings using Ar with K vapor detected by high speed camera

04 p0725 A70-14533

Lumped model formulated for dynamics of proportional fluidic amplifiers, describing flow visualization experiments for resonances and instabilities mechanisms [ASME PAPER 69-WA/FLCS-3]

04 p0627 A70-14848

Semifocusing color schlieren systems for quantitative investigations of flows in fluid mechanics and heat transfer, including photographs of boundary layers

04 p0690 A70-15029

Supersonic wake flow visualization, obtaining direct photographs of various smoke streamlines [AIAA PAPER 69-346]

04 p0621 A70-15595

Schlieren system modification using diffraction grating to produce color applied to airflow flowfield analysis [AIAA PAPER 70-223]

06 p1029 A70-18165

Turbulent shear flow kinematic characteristics determined by photographic method and flow visualization using vortex model

07 p1259 A70-19827

Holography for visualization and analysis of aerodynamic flow fields in wind tunnel experiments, recreating events in space and time

08 p1493 A70-20650

Static tank visualizations obtained in two dimensional flow and on rotors hovering or in transition in ONERA hydrodynamic tunnel

[ONERA-TP-777]

08 p1434 A70-21846

Unsteady aerodynamic forces on helicopter rotors using pressure measurements and wind tunnel visualizations of smoke emission

[ONERA-TP-777]

08 p1434 A70-21847

Holographic flow visualization system retaining all information in light wave passing through flow field, noting reconstruction as shadowgram, schlierens or interferograms

09 p1689 A70-23781

Electron beam probe applied to flow visualization in rarefied gas wind tunnels

10 p1860 A70-24549

Turbulent boundary layer vortex structures using hydrogen bubble technique

11 p2035 A70-25864

Gasdynamic flows strong and weak density discontinuity surfaces determination, using shadowgraphs and interference patterns

12 p2238 A70-28248

Heaving airfoil wakes visualization with jet flap augmented lift, measuring vortex street parameters

13 p2338 A70-28821

Heat transfer increase near stagnation point for turbulent jet impinging on paraffin coated plates used for flow visualization

13 p2521 A70-28866

Unsteady fluid flow around circular cylinder with sudden acceleration using flow pattern photographs

13 p2387 A70-29056

Ground effect visualization at low speed flow around aircraft models, discussing airbus, VTOL aircraft and Concorde

14 p2528 A70-30291

Rotor wakes and diffuser blades interactions visualization using hydraulic setup

14 p2528 A70-30297

Unsteady relative flow in centrifugal impeller passage running at part capacity and zero flow observed by hydrogen bubble flow visualization method [ASME PAPER 69-GT-35]

14 p2529 A70-31024

Flow structure in wake of blunt bodies placed perpendicular in parallel airstream determined from hot-wire anemometry

[AIAA PAPER 69-746]

16 p2838 A70-33876

High Reynolds number flow in moving corner, observing vortex motion at piston and cylinder wall interface by flow visualization techniques

16 p2895 A70-34240

Vortex visualization applications in helicopter noise research, using smoke generator in rotor blade tip

17 p3057 A70-34712

Air jets from sonic orifice, investigating three zones of isochor families by visualization and density measurement

17 p3070 A70-35046

Shock waves in supersonic conical nozzle flow due to secondary gas injection, using conical lens for flow visualization

17 p3011 A70-35236

Subsonic flow visualization, using steam and cold nitrogen gas mixture and normal tunnel lighting

18 p3237 A70-36460

Turbulent flows shadowgraph analysis, solving electromagnetic equations for optical response

18 p3242 A70-36692

ONERA low pressure wind tunnel equipped with electron beam probing device to visualize flows too rarefied for optical methods

18 p3210 A70-37208

Turbulent mixing in supersonic cone near wake, using laser planogram technique for flow visualization

19 p3351 A70-37529

Holographic flow and sound visualization, determining three dimensional density distributions in aerodynamic flows

19 p3425 A70-37888

Subsonic air flow around airfoil in wind tunnel, detecting density gradients by pulsed ruby laser holographic visualization

21 p3822 A70-40809

Jet curtain flow recirculation model based on air-bubble flow visualization technique, determining minimum power for air cushion vehicle

22 p3957 A70-42278

Spark tracing in gaseous flows in flames, wind tunnels, nozzles and pneumatic valves, using pulse transformer [SMPTE PREPRINT 41]

22 p4033 A70-43041

Supersonic wakes visualization and photographic measurement by schlieren techniques, using amplitude subtraction and He-Ne laser

[SMPTE PREPRINT 94]

22 p4036 A70-43061

Color filter schlieren photography for visualization of wind tunnel shock and pressures, liquid mixing and convection currents

22 p4036 A70-43065

Combustion chamber flow visualization, obtaining information on pressure loss, velocity field, flow pattern and temperature gradients

24 p4393 A70-45444

Flow visualization measuring liquid flow velocity, using flow dichroism

24 p4338 A70-45816

Seeding particles motion recording in fluid flow by holographic velocimetry, using optical matched spatial filtering to determine particle location

24 p4340 A70-46350

FLOWMETERS

NT HOT-WIRE FLOWMETERS

NT RHEOMETERS

Transcutaneous Doppler-shift flowmeter for arterial blood velocity measurement by ultrasound

01 p0037 A70-10880

Flowmeter errors caused by nuclear magnetic relaxation decreased with increasing magnetic field strength of NMR sensor

01 p0091 A70-10981

Doppler flowmeter-catheter system to record aortic flow velocity in man during cardiac arrhythmias, considering atrial fibrillation, heart block, etc

02 p0241 A70-12697

Contactless asynchronous flowmeter for measuring liquid metal coolant small flow rates, describing design and characteristics

03 p0483 A70-13211

Laser velocimeter measurements on drag reducing polyacrylamide solution compared to water

03 p0502 A70-13821

Circular tube entrance upstream and downstream velocity profiles at small axial distances measured by laser Doppler flowmeter

[ASME PAPER 69-WA/FE-13]

04 p0667 A70-14780

Multiple array critical flow venturi air flow metering system constructed for gas turbine engines, developing pressure control valve

[ASME PAPER 69-WA/FM-5]

04 p0688 A70-14838

Fluidic oscillator use as volume flowmeter, discussing effects of setback, aspect ratio, splitter distance and feedback location on oscillation frequency

[ASME PAPER 69-WA/FM-3]

04 p0688 A70-14840

Turbine flowmeter with hydraulic bearings operation based on photosensitive recording of light beam interruptions, discussing test results

06 p1065 A70-17911

Linear momentum mass flowmeter, discussing operation, damping torque-mass flow rate relationship, operation and advantages

06 p1067 A70-18427

Turbine flowmeter in-place calibration for measuring cryogenic propellant flow rates in rocket engine testing

06 p1071 A70-18448

Haematocrit variations effect on electromagnetic blood flowmeter sensitivity, discussing blood specific impedance changes

07 p1217 A70-18951

Orifice diameter for low Reynolds number flowmeter dependent on pipeline diameter tolerances

08 p1482 A70-20684

Sewage water flowmeter calibration, analyzing error propagation and tolerance

09 p1672 A70-22027

Electromagnetic flowmeter for cardiac output changes in unanesthetized rats, discussing construction, form and associated electronic equipment of implanted probe

09 p1627 A70-23267

Error propagation in flowmeter calibration on model using empirical model-transmission equation

10 p1888 A70-24391

Small flow rate flowmeter design and application to nonreactive liquids and liquid gases with low viscosity

10 p1888 A70-24392

Turbine flowmeter dynamic characteristics dependence on individual parameters, deriving equations of motion and time constant

11 p2055 A70-26450

Electromagnetic differential flowmeter design and performance, considering SNR

12 p2231 A70-27162

Turbine flow meters dynamic calibration employing sinusoidally perturbed orifice flow

12 p2236 A70-28033

Ultrasonic flowmeter with electronic components, discussing flow rate parameters and wave propagation relative to flow

12 p2236 A70-28074

Ventilating flowmeter tests with jet deflection for respiration measurement in patient

14 p2541 A70-30380

Implantable EM blood flowmeter errors due to nonsymmetrical blood flow velocity distribution and nonuniform magnetic flux density

14 p2542 A70-30797

Karman vortex shedding phenomenon for flow rate measurement in channel or pipe

14 p2588 A70-31333

Circulation meter using parallel yawmeters linked to manometer, showing sensitivity in lateral velocity

14 p2589 A70-31397

Miniaturized electromagnetic catheter flowmeter for measuring volume flow rate by potential difference between electrodes

15 p2689 A70-31747

Doppler effect pulsed ultrasonic blood flowmeter using transducer alternating as transmitter and receiver

15 p2690 A70-31919

Automatic numerical analysis of velocity information from Doppler effect ultrasonic blood flow meter

15 p2691 A70-31920

Phase shift ultrasonic flowmeter measuring transit time between oppositely propagating waves in blood vessels

15 p2691 A70-31921

Induction flowmeters operation, emphasizing various factors effects on induced voltage

19 p3426 A70-37396

Heat flowmeters calibration by conductive method, reducing error due to radiative, conductive and convective losses

19 p3430 A70-38522

Classical invariant characteristic of quantification conditions for flow quantifiers

20 p3671 A70-39122

Electromagnetic blood flowmeters for circulatory research

20 p3579 A70-39371

Aircraft capacitive fuel gage improvement by integration with flowmeter system, DC torque display and digital techniques, considering other measurement principles

21 p3821 A70-40619

Induced voltage electromagnetic flowmeter, assessing performance in terms of weight vector to obtain conditions for ideal flow patterns

22 p4029 A70-42692

Oscillatory flow measurements by directionally sensitive laser velocimeter, discussing concept, design and construction

23 p4197 A70-44473

Reynolds stress measurement, using laser flowmeter with cylindrical lenses and square aperture mask

23 p4202 A70-44945

HF pulsating air flow measuring technique with sharp edged orifice meter, discussing experimental setup and pulsation frequency and intensity effects

24 p4335 A70-45591

FLOX

Oxygen and fluorine-based liquid fuels and oxidizers development, considering chemical rocket propulsion reaction principles

07 p1361 A70-19917

FLOX methane propellant rocket engines, describing operating conditions, injectors, thrust chambers fabrication and cooling, engine cycles, turbomachinery, etc [AIAA PAPER 70-718]

16 p2965 A70-33540

FLUCTUATION THEORY

Finite disturbance effect on laminar incompressible wake behind flat plate determined by interaction between two dimensional fluctuation amplitude and mean flow

08 p1433 A70-21605

Homogeneous turbulence multipoint multitime correlations for fluctuating velocity

11 p2036 A70-26014

Nonequilibrium self gravitating medium unified thermodynamics theory based on propagators, describing spatial and temporal fluctuations and coupling for galactic formation

12 p2310 A70-27978

Magnetic moment fluctuations of arbitrary solid body by fluctuation-dissipation theorem for thermal equilibrium

13 p2454 A70-30033

Solar wind energies spherical surface average and fluctuations from integration of conservation equations

14 p2630 A70-30357

FLUERIC

Flueric altitude insensitive thruster based on two way gas flow diversion valve developed for VTOL aircraft and missile hot gas attitude control systems [ASME PAPER 69-WA/FLCS-10]

04 p0626 A70-14843

Pressure and temperature sensitivity tests of flueric oscillator for timer application, testing fluid relaxation oscillators using R-C-R feedback loops [ASME PAPER 69-WA/FLCS-9]

04 p0626 A70-14844

Flueric sensor for RF induced currents providing alternative to bridge wires as initiators of explosive charges

14 p2534 A70-30681

Flueric position and distance sensor characteristics

24 p4293 A70-45427

FLUID AMPLIFICATION

U FLUID AMPLIFIERS

FLUID AMPLIFIERS

NT JET AMPLIFIERS

Gas jets collision flowing from parallel wall channels, applying solution to calculating geometrical characteristics or fluid jet amplifiers

01 p0011 A70-11569

Fluidic oscillator use as volume flowmeter, discussing effects of setback, aspect ratio, splitter distance and feedback location on oscillation frequency [ASME PAPER 69-WA/FM-3]

04 p0688 A70-14840

Supersonic fluid amplifier performance and design for use as power amplifier and high outlet leg differentials in vacuum environments [ASME PAPER 69-WA/FLCS-7]

04 p0626 A70-14846

Fluidic component linearized characteristics in coupled or uncoupled environment determined for wide frequency range, discussing application to proportional fluidic amplifier [ASME PAPER 69-WA/FLCS-2]

04 p0626 A70-14847

Lumped model formulated for dynamics of proportional fluidic amplifiers, describing flow visualization experiments for resonances and instabilities mechanisms [ASME PAPER 69-WA/FLCS-3]

04 p0627 A70-14848

Plane jet velocity profiles determination applied to calculating gain of proportional fluid amplifier

08 p1485 A70-21670

Acoustic fluidic amplifiers, considering receiver, transmitter and operating mode

09 p1672 A70-22012

Fluidic operational amplifier design and applications

09 p1614 A70-23687

Self contained remote sense remote control pressure regulator using pure fluid amplifiers, controlling large or small flow over wide pressure range

09 p1614 A70-23688

Fluidic digital position sensor consisting of fluid monostable amplifier, analyzing operation by characteristics method

09 p1614 A70-23689

Supersonic fluid bistable amplifier used as air motor, converting supply air flow energy into reciprocating piston motion

10 p1807 A70-24791

Bistable fluid amplifier elements static characteristics, considering control flow and pressure variation domain

10 p1808 A70-24971

Proportional fluid amplifiers noise and instability sources related to geometry and power jet flow, considering noise reduction methods

12 p2164 A70-27071

Analog fluidic elements /operational amplifiers/ with beam deflector proportional amplifiers incorporated into close coupled circuit

12 p2164 A70-27072

Bonding and sealing of fluid amplifiers with epoxy resin dry-film adhesive, noting low rejects rate

12 p2164 A70-27075

Fluidic elements construction, behavior and applications, considering vortex and turbulence amplifiers, input and output elements, etc

12 p2164 A70-27221

One flow influence on another at two plane jets interaction zone, applying to proportional fluid amplifier inlet impedance calculation

15 p2720 A70-32020

Fluidic devices theory and operation including flow control mechanisms, modulators, logic circuits, amplifier types, etc

16 p2843 A70-33444

Fluid amplifiers equivalent circuit with stagnation pressure source in series with orifice and load, discussing applications to small signal circuit analysis

16 p2844 A70-33446

Coanda effect in bistable fluid amplifier, using finite difference method for computer programmed solution of flow equations

[ASME PAPER 70-FLCS-12] 22 p4008 A70-42415

Fluidic amplifier with axisymmetric jets, deriving approximate mathematical model for static no-load operation

[ASME PAPER 70-FLCS-4] 22 p3964 A70-42427

Bistable wall attachment fluid amplifier, calculating unsteady end wall switching transient based on turbulent jet entrainment properties

[ASME PAPER 70-FLCS-3] 22 p3964 A70-42428

Large fluid-amplifier-type jets, measuring upstream flow disturbances effects on spreading velocity profiles

[ASME PAPER 70-FLCS-A] 22 p3964 A70-42431

Fluidic amplifiers in measurement technology including turbulence, pulse, Coanda, induction, vortex, arc and focusing amplifiers

23 p4142 A70-44246

Jet interaction type proportional fluid amplifier as feedback oscillators, measuring frequency response

24 p4292 A70-45291

FLUID BOUNDARIES

NT GAS-SOLID INTERFACES

NT JET BOUNDARIES

NT LIQUID-LIQUID INTERFACES

NT LIQUID-SOLID INTERFACES

NT LIQUID-VAPOR INTERFACES

Stability conditions for helical motions of body bounded by multiply connected surface in fluid

01 p0145 A70-11439

Steady convective motions in horizontal fluid layer bounded by porous walls of various temperatures at supercritical Rayleigh numbers, noting nonlinear convection equations

04 p0673 A70-15237

Interface instability between gases due to shock wave increased linearly with time

04 p0673 A70-15245

Boundary layer development on body accelerating in viscous incompressible fluid, using straight lines approximation and asymptotic expansions

08 p1485 A70-21631

Ultrasonic wave propagation guided by fluid layer between two elastic solids, plotting normalized velocities and layer thicknesses

12 p2273 A70-28097

Plasma sheath boundary as closed Mach surface, demonstrating Bohm criterion application to ion velocity component normal to sheath edge

13 p2464 A70-29465

Plane plate motion in weightless fluid flow with free upper boundary, showing lifting capacity increment by underlying solid surface

13 p2390 A70-29644

Aerodynamic characteristics of supercavitating airfoil, investigating effect of free surface of unsteady fluid flow with stream separation, solving boundary value problem

13 p2391 A70-29650

Plane normal shock front diffraction along free interface between half planes of homogeneous fluids at rest, using method of characteristics and Whitham technique

17 p3074 A70-35886

Heat transfer across boundary between two stationary fluids, applying elastic wave theory in isotropic media

18 p3345 A70-36118

Equilibrium form shapes of fluid free surface in vessel under gravitational and magnetic field with tension

18 p3240 A70-36269

Capillary ball game phenomenon under weightlessness, showing photographs of mercury droplet reflection from fluid boundary

18 p3242 A70-36638

Plasma-air junction problem in parallel plate waveguide, obtaining discontinuity admittance expression

22 p3994 A70-42350

Sunyach-Mathieu intermittence measuring method applied to turbulent flow boundary studies, discussing flow transition line definition

23 p4180 A70-44201

Unsteady radiating nongray gas diffuse boundary conditions, emphasizing monochromatic radiation slip and one dimensional radiant flux

23 p4282 A70-44593

FLUID DYNAMICS

NT AERODYNAMICS

NT AEROTHERMODYNAMICS

NT ELASTOHYDRODYNAMICS

NT ELECTROHYDRODYNAMICS

NT GAS DYNAMICS

NT HYDRODYNAMICS

NT HYPERSONICS

NT MAGNETOHYDRODYNAMICS

NT RAREFIED GAS DYNAMICS

NT ROTONS

NT ROTOR AERODYNAMICS

Boundary layer and singular inviscid stagnation point reacting flow matching, corrections structure and decay and ranking comparison with second order effects in fluid mechanics

01 p0065 A70-10996

Unsteady incompressible laminar flow under time dependent body force solved for rectangular and circular conduit and plane and cylindrical Couette flows

01 p0066 A70-11130

Nongeostrophic baroclinic stability theory predictions test experiment with vertical heating provision, describing fluid motions

02 p0289 A70-11830

Noncontacting minimum leakage dynamic seals requiring liquid-vapor interface with leakage tolerance [ASLE FICFS PREPRINT 40] 02 p0308 A70-12175

Absolute ULF ballistocardiogram /BCG/ values as pulsatile fluid pumping values in cardiodynamic function before and after exercise

02 p0248 A70-12677

Surface interactions in incompressible dynamics and stability of ferrofluid with nonlinear magnetization properties

04 p0665 A70-14451

Liquid sheet and jet breakup in supersonic gas stream, characterizing breakup mechanism by gross jet fracture

06 p1039 A70-18109

German book on fluid dynamics for nonideal fluids covering viscosity effects, Prandtl boundary layer, turbulence and aerodynamics

08 p1431 A70-20751

Fluids equilibrium stability within medium at constant temperature and pressure, discussing time behavior of thermodynamic processes

09 p1786 A70-22062

Advanced fluid dynamics - Conference, Tarda, Poland, September 1967

10 p1863 A70-24101

Numerical methods of viscous fluid dynamics, considering unsteady flow in simply and multiply connected regions

10 p1866 A70-24110

Turbulent flow criterion for negligible initial boundary layer case, introducing corrections regarding Korst criterion as function of geometric and aerodynamic flow

10 p1799 A70-24128

Fluid dynamics literature, considering single and two phase flows, cavitation phenomena, liquid films and stratified flows, bubble dynamics, drop formation, etc

11 p2037 A70-26473

Turbulence of fluids and plasmas - Conference, New York, April 1968

11 p2093 A70-26751

SAE aerospace applied thermodynamics manual covering aerodynamics, fluid dynamics, heat transfer, materials properties, aerospace application engineering, etc

12 p2329 A70-26872

Fluid motion in cylindrical tank with arbitrary sector annular cross section subjected to harmonic longitudinal excitation

12 p2211 A70-27818

Screw flows in fluid dynamics, showing helicoidal type flow for constant flow velocity on stream lines

15 p2718 A70-31447

Classical single fluid dynamics theory derived from unitary formulation of two fluid theory

15 p2827 A70-32261

Nonlinear dynamic stability of fluid layer heated from below in time dependent bounded domain

16 p2943 A70-34249

Lagrangian invariants of inviscid compressible fluid dynamics applied to hydrodynamic equations

17 p3070 A70-35333

Micropolar fluids turbulent flow, investigating microstress couples, stability, inviscid flow, etc

17 p3071 A70-35435

Collection of papers on nonequilibrium flows, Part 2, covering relaxation gas dynamics, nozzle flow, method of characteristics, etc

17 p3071 A70-35466

Collection of papers on transport phenomena in fluids covering hydrodynamics, thermodynamics, kinetic theory, thermal diffusion, etc

17 p3072 A70-35528

Isotropic fluid systems in nonequilibrium, investigating thermodynamic characteristics of transport phenomena

17 p3072 A70-35529

Nonequilibrium fluid system with two subsystems in local equilibrium, investigating thermodynamic properties including entropy creation

17 p3196 A70-35530

Statistical theory of irreversible transport processes in fluids, considering deviation from equilibrium as stochastic process

17 p3131 A70-35532

Time correlation functions approach to calculation of properties of nonequilibrium ensembles in fluid molecular motions

17 p3197 A70-35535

Nonlinearized exact solution of Navier-Stokes equations for fluid motion between two coaxial circular disks rotating at equal velocity

18 p3241 A70-36381

Fluid dynamics of pulsed plasma accelerators, discussing energy transfer and losses limitations

18 p3301 A70-36660

Gas turbine shrouded rotating disk system with radial outflow of air coolant, investigating fluid dynamics, pressure distribution and frictional moment [ASME PAPER 70-GT-6]

18 p3208 A70-36862

Relativistic and nonrelativistic fluid dynamic equations, deriving limiting procedure leading to fluid magnetodynamic Lundquist equations

19 p3478 A70-37590

Fluid inertia and compressibility effects considered in equations for foil over lubricating film [ASME PAPER 69-WA/LUB-10]

19 p3435 A70-37615

Collisionless plasmas fluid dynamical equations in presence of strong magnetic field, discussing Larmor and electron plasma frequencies

20 p3678 A70-39609

Flow parameters radial dependence of thin solar wind filament corotating with sun

21 p3881 A70-40972

Resonance tube fluid dynamics, examining oscillation start and growth by wave diagram and gas-speed/sound-speed diagram

21 p3807 A70-41244

Sufficient conditions for confined fluids stability, defining critical and modified Rayleigh numbers

21 p3810 A70-41952

Fluid dynamics nonlinear equations for thermally driven motions in compressible, isothermal gravitational solar atmosphere, considering flow discontinuities and heat conduction

21 p3925 A70-42191

Electron mass evaluation, using fluid dynamic flow process

22 p4076 A70-43672

German book on propeller theory covering airfoil theory, propeller flow and pressure fields, propeller vibrations, shrouded and tilted propellers, helicopter rotors, etc

23 p4180 A70-44097

Principle pressure vector components for liquid in moving V-shaped and U-shaped cross section tanks

23 p4180 A70-44164

Boundary geometry of region with fluid motions harmonic functions obeying Bernoulli law containing free surface curvature

23 p4218 A70-44337

Boundary value problems of fluid dynamics in dynamic cavities reduced to integral equations system

23 p4182 A70-44347

Constitutive equations in fluid dynamics, discussing Newtonian, Oldroyd and Walter, Reiner-Rivlin, Rivlin-Ericksen, Noll, Bingham and oriented fluids

24 p4327 A70-46149

FLUID FILMS

Gravitational instability of finitely conducting incompressible fluid layer of finite thickness surrounded by nonconducting medium

05 p0915 A70-16696

Nusselt theory of laminar liquid films movement on vertical smooth solid surface, attributing thickness variation to gas movement and surface active agents in liquid

07 p1251 A70-18656

Hydrostatic journal bearing dynamic rigidity for compressible and incompressible fluids, describing fluid film elasticity and damping characteristics

07 p1293 A70-19121

Gas flow influence on wave characteristics of thin viscous liquid layers pulled by gravity vertical surface compared with water layer experiments

08 p1482 A70-20917

Suction effect on thin film laminar flow past vertical wall, obtaining approximate solution for small porosity in accelerated region

08 p1484 A70-21309

Horizontal fluid layer heated from above or below analyzed for gravitational field sinusoidal modulation effects on stability

10 p1968 A70-24523

Viscosity variation factor at film inlet in fluid square taper pad bearing investigated by modified Reynolds equation

13 p2418 A70-28746

Inviscid film flow by fluid injection through bounding surface, considering porous plate inclination and power law injection rates

16 p2895 A70-34241

Interface stability of thin liquid film adjacent to supersonic air flow, using sphere-cone and blunt wedge test configurations

[AIAA PAPER 70-801]

17 p3005 A70-34461

Cumulative jets during shock induced collapse of air cavities in thin fluid layers, using high speed motion picture photography

17 p3074 A70-35742

Incompressible heavy fluid film stability during flow along inclined plane constituting crystallization front, analyzing linearized equations of perturbed flow

18 p3240 A70-36271

Plane horizontal fluid film convective stability with free boundaries in vertical circular cylinder for periodic modulation of vertical temperature gradient or gravitational field

21 p3941 A70-40608

Heat transfer between wall and liquid and vapor films in internal regenerative cooling of thrust chambers

21 p3867 A70-41027

Three-lobe fluid film bearing configuration for gas turbine concentric rotating shafts/spool shafts/

[ASME PAPER 70-LUBS-10]

22 p4045 A70-42450

Parallel circular squeeze film bearing, calculating Newtonian fluid inertia effect on lubrication by perturbation solution

[ASME PAPER 70-LUBS-9]

22 p4045 A70-42451

Fluid film lubricated, thrust loaded, angular contact ball bearing high speed performance, predicting skidding by isothermal Newtonian behavior in ball to raceway contact

[ASME PAPER 70-LUBS-7]

22 p4045 A70-42452

Monograph on MHD, covering fluid layer stability under adverse temperature gradient, geomagnetic field origin, vector relations, etc

22 p4084 A70-43448

Full and half journal bearings in axial magnetic field, discussing hydromagnetic noncyclic squeeze fluid films

24 p4349 A70-45995

FLUID FILTERS

NT AIR FILTERS

Static and centrifugal filters merits for turbine engine lubrication systems, considering mechanical reliability, efficiency, dirt capacity and maintenance

01 p0164 A70-10686

Physical and chemical phenomena and critical factors underlying, furthering or impeding water droplets coalescence in glass-fiber bed of filter-separator

04 p0625 A70-14709

Rarefied gas flow through ultrafine porous filtering media used to predict flow rate

[ASME PAPER 69-WA/PID-8]

04 p0666 A70-14755

Jet aircraft fuel systems icing prevention, considering fuel filters

05 p0796 A70-17020

Fuel filter icing prevention by injecting antifreeze into filter instead of fuel

06 p0988 A70-17873

Liquids particulate contamination sizing and counting by membrane filtration, specifying procedures and apparatus used

[SAE-ARP-598A]

07 p1195 A70-18804

FLUID FLOW

NT ADIABATIC FLOW

NT AIR CURRENTS

NT AIR FLOW

NT AIR JETS

NT ANNULAR FLOW

NT AXIAL FLOW

NT AXISYMMETRIC FLOW

NT BAROTROPIC FLOW

NT BASE FLOW

NT BELTRAMI FLOW

NT BLASIUS FLOW

NT BLOOD FLOW

NT BOUNDARY LAYER FLOW

NT BOUNDARY LAYER SEPARATION

NT CAPILLARY FLOW

NT CASCADE FLOW

NT CAVITATION FLOW

NT CHANNEL FLOW

NT COAXIAL FLOW

NT COMBUSTIBLE FLOW

NT COMPRESSIBLE FLOW

NT CONTINUUM FLOW

NT CONVECTIVE FLOW

NT CORE FLOW

NT COUETTE FLOW

NT COUNTERFLOW

NT CRITICAL FLOW

NT DUCTED FLOW

NT EQUILIBRIUM FLOW

NT EQUIPOTENTIALS

NT FREE FLOW

NT FREE MOLECULAR FLOW

NT FROZEN EQUILIBRIUM FLOW

NT FUEL FLOW

NT GAS FLOW

NT HARTMANN FLOW

NT HELICAL FLOW

NT HYPERVELOCITY FLOW

NT INCOMPRESSIBLE FLOW

NT INLET FLOW

NT INVISCID FLOW

NT ISOTHERMAL FLOW

NT JET FLOW

NT JET MIXING FLOW

NT JET STREAMS [METEOROLOGY]

NT KNUDSEN FLOW

NT LAMINAR FLOW

NT LIQUID FLOW

NT MAGNETOHYDRODYNAMIC FLOW

NT MASS FLOW

NT MERIDIONAL FLOW

NT MOLECULAR FLOW

NT MULTIPHASE FLOW

NT NONEQUILIBRIUM FLOW

NT NONNEWTONIAN FLOW

NT NONUNIFORM FLOW

NT NOZZLE FLOW

NT ONE DIMENSIONAL FLOW

NT ORIFICE FLOW

NT OSCILLATING FLOW

NT PERIPHERAL JET FLOW

NT PIPE FLOW

NT PLASTIC FLOW

NT POTENTIAL FLOW

NT PROPELLANT TRANSFER

NT RADIAL FLOW

NT REATTACHED FLOW

NT RECIRCULATIVE FLUID FLOW

NT REVERSED FLOW

NT SECONDARY FLOW

NT SEPARATED FLOW

NT SHEAR FLOW

NT SINGLE-PHASE FLOW

NT SLIP FLOW

NT STAGNATION FLOW

NT STEADY FLOW

NT STEAM FLOW

NT STOKES FLOW

NT STRATIFIED FLOW

NT SUBCRITICAL FLOW

NT SUPERCavitating FLOW

NT SUPERCRITICAL FLOW

NT SUPERSONIC JET FLOW

NT THREE DIMENSIONAL FLOW

NT TRANSITION FLOW

NT TRESCA FLOW

NT TURBULENT FLOW

NT TWO DIMENSIONAL FLOW

NT TWO PHASE FLOW

NT UNIFORM FLOW

NT UNSTEADY FLOW

NT VERTICAL AIR CURRENTS

NT VISCOUS FLOW

NT WALL FLOW

NT WATER FLOW

NT WEDGE FLOW

Vorticity number derivation for rotational flows, discussing reciprocal of kinematic Rossby number and vorticity measures

01 p0061 A70-10541

Turbulence constant for flows near walls, analyzing viscosity dependence on wall distance by utilizing maximum stability principle

01 p0069 A70-11627

Navier-Stokes difference equations numerically integrated by computer for viscous fluid flow along parallel flat plate at low Reynolds number

02 p0277 A70-11909

Incompressible viscous fluid plane flow using series expansion

02 p0277 A70-11910

Soviet book on boundary value problems involving motion of ideal fluids in unsteady cavities of various geometries, determining attached fluid masses and oscillation frequencies

04 p0666 A70-14678

Fluid flow at pneumatic network junction, considering junction pressure determination as boundary condition for all transmission lines meeting at junction

[ASME PAPER 69-APM-N]

04 p0627 A70-14862

Discrete frequency noise generation associated with wakes due to fluid flow over turbomachine blades, supporting spokes, flat plates, etc

[ASME PAPER 69-WA/GT-13]

04 p0733 A70-14883

Computer program to calculate ideal rotating fluid flow in arbitrary airfoil lattice on axisymmetric stream surface in variable thickness layer

04 p0617 A70-15239

Self similar problems of anisotropic fluid boundary layer involving infinite disk rotation and fluid flow near stagnation point

05 p0835 A70-16857

Steady gravitational waves produced by variable pressure in fluid channel flow assuming small perturbed flow velocity components

05 p0836 A70-16969

Numerical analysis of low-g fluid flow and heating problems encountered with liquid propellant storage and supply

[AIAA PAPER 69-567]

07 p1394 A70-19719

Integrodifferential equation derived for energy balance in laminar boundary layer of fluid flow, taking into account viscous energy dissipation, radiative energy transfer, etc

07 p1423 A70-19813

Functions describing spatial-temporal temperature distribution in hyperbolic partial differential equations for nonstationary heat exchange between fluid flow and boundary wall

07 p1423 A70-19839

Dynamic behavior of subcritical fluid flow past airfoils, expanding flow potential to obtain formulas for velocities, local Mach numbers and pressure

08 p1433 A70-21173

Loading effects in measurements involving electrical and nonelectrical systems used in determining gas pressure and fluid flow

09 p1672 A70-22011

Lunar sinuous rilles formation by fluid flow mechanisms, discussing evidence for lava and rille formation by lava tube collapse

09 p1759 A70-22799

Turbulent heat and mass transfer from wall to plane-parallel fluid flow at large Reynolds and Peclet numbers, developing universal law

09 p1789 A70-23169

Incompressible anisotropic fluid flow around semiinfinite plate at large Reynolds numbers, using interlocked asymptotic expansions and deformed coordinates to obtain boundary layer equations

09 p1663 A70-23390

Direct digital control valves in fluid flow process evaluated for performance by analog computer simulation

09 p1613 A70-23684

Self contained remote sense remote control pressure regulator using pure fluid amplifiers, controlling large or small flow over wide pressure range

09 p1614 A70-23688

Fluid microstructure effects on velocity, boundary layer and shear stress in nonsteady parallel flows, including accelerated plane wall equation

10 p1863 A70-23955

Hydraulic loss and secondary circulation of fluid flow in three dimensional bend commercial conduits, discussing relationship to velocity distribution

10 p1871 A70-25094

Noise-flutter interrelation in flight vehicle flexible plate and shell configurations immersed in fluid flow

11 p2132 A70-25726

Spatial correlation effect of unsteady sectional loads in axial direction on average or apparent loads over finite region of circular cylinder immersed in moving fluid

11 p2036 A70-26148

Waves and mean currents excitation in stratified fluid due to moving heat source, studying effect on mean motion

11 p2036 A70-26167

Variational analysis of fluid flow in hydrodynamic, thermal and diffusional boundary layers including viscous effects, heat and mass transfer and chemical reactions

11 p2041 A70-26652

Fixed end nonprismatic bar stability in fluid flow, studying form influence on critical flow velocity

13 p2512 A70-28982

Coaxial fluid streams mixing within finite length tube based on dimensional analysis of aerodynamic noise generation, discussing subsonic and supersonic flows within ejector

13 p2474 A70-29080

Plane plate motion in weightless fluid flow with free upper boundary, showing lifting capacity increment by underlying solid surface

13 p2390 A70-29644

Turbulent boundary layer formation in upstream wake of accelerated flow indicated from boundary layer profile and wall static pressure measurements

13 p2392 A70-29996

Motion equation derivation for incompressible fluid flow in baroclinic ocean, allowing for horizontal macro turbulent exchange

14 p2601 A70-30136

Conductive rubber pressure transducers for fluid flow measurement

14 p2584 A70-30503

Marginal fluid flow stability in porous media taking into account inhomogeneity created by temperature

14 p2577 A70-31000

Error measurements of shaped edged circular static pressure hole normal to moving fluid boundary using flush transducers

15 p2722 A70-32374

Swirling flow in unbounded space, investigating swirl intensity effect on heat transfer

15 p2828 A70-32857

Periodic flow structure between gas turbine blades, using asymptotic representation

[ONERA-TP-790] 16 p2833 A70-33102

Laser Doppler velocimeter for measuring turbulence in gas and fluid flows

16 p2926 A70-33140

Laser anemometer for fluid flow measurements, noting sample size restraint, frequency response and velocity range

16 p2926 A70-33141

Heat and mass transfer in flowing fluid, deriving conservation and constitutive equations, with application to boundary layer flow of gases

17 p3069 A70-35033

Fluid flow longitudinal temperature profiles for inclusion in heat transfer computer program

17 p3198 A70-35659

Fuel cell cavities, analyzing fluid motion purge dynamics based on anisotropic porous media model

18 p3216 A70-36766

Thin plates and thin walled cylinders aeroelastic stability in fluid flow, analyzing panel flutter

19 p3546 A70-38342

Turbulent heat and mass transfer from wall to plane-parallel fluid flow at large Reynolds and Peclet numbers, developing universal law

19 p3552 A70-38392

Power law fluid flow past suddenly accelerated wall, applying group theory to similarity solutions

19 p3406 A70-38444

Flow noise mechanisms, considering discharge, propeller, ventilator, jet engine, boundary layer, water pipe and supersonic aircraft sources

19 p3406 A70-38474

Sound field produced in uniform moving ideal fluid stream by nonuniform oscillating elastic wall

19 p3353 A70-38657

Integrodifferential equation derived for energy balance in laminar boundary layer of fluid flow, taking into account viscous energy dissipation, radiative energy transfer, etc

20 p3736 A70-39261

Electrokinetic model for semicircular canal transduction, focusing IR beam on exposed ampullae from posterior canals of Rana pipiens

21 p3765 A70-41696

Axially reciprocating pump, calculating fluid over-flow effect on working cell pressure change

21 p3759 A70-41775

Unsteady compressible boundary layer formation on rotating disk, assuming uniform fluid rotation

22 p4009 A70-42616

Thermoelasticity theory concerning Navier-Stokes-Fourier type fluid universal motion characterization in absence of body forces and external heat supply

22 p4010 A70-42637

Sea surface temperature relationship with ocean currents, using bathythermograph data

22 p4014 A70-42768

Ultrasonic measurements of flow velocity and fluid rate, using high speed switching and synchronous demodulator

22 p4041 A70-43619

Liquid droplet breakup by aerodynamic forces, obtaining solutions for fluid flow inside droplet and in coupled liquid-gaseous boundary layer

22 p4012 A70-43741

Linear stability of fluid flow, proving equivalence of slow and rapid asymptotic solutions of Orr-Sommerfeld equations

23 p4180 A70-43994

Hall effect on incompressible electroconducting viscous fluid motion past finite conducting flat plate, discussing boundary conditions

23 p4225 A70-44247

Single component fluid behavior in liquid-vapor critical point vicinity, using LF acoustic resonant cavity technique for isochoric measurements

23 p4222 A70-44432

Cross correlation measurement errors for fluid pipe flow with pseudorandom sequence generated temperature fluctuations, considering transport time, impulse response and laminar flow

24 p4333 A70-45111

Two spherical particles rotation and slow motion about axis of circular cylinder in direction perpendicular to line of centers, considering fluid flow characteristics

24 p4325 A70-45781

FLUID INJECTION

NT GAS INJECTION

NT LIQUID INJECTION

NT WATER INJECTION

Flow and pressure distribution for large normal injection along surface in supersonic stream solved numerically for two dimensional or axisymmetric body and wedge

01 p0001 A70-10336

Laminar and turbulent boundary layer equations with or without wall injection over two dimensional or axisymmetric bodies solved by finite difference techniques

02 p0287 A70-12370

Flow stability of plane channel formed by incompressible viscous fluid injection through porous parallel walls

04 p0673 A70-15238

Inert, oxidizing or reducing fluids wall injection into combustion gas boundary layer of variable composition noting effects on wall temperature

05 p0956 A70-15919

Base bleed fluid injection effect on steady separated flow past two dimensional bluff body, studying streamline pattern near object

06 p0967 A70-17518

Viscous hypersonic flow past sphere in presence of strong injection through front surface at large Reynolds numbers using asymptotic method

07 p1189 A70-20146

Incompressible conducting fluid MHD flow at infinite plane wall forward stagnation point, considering suction or injection effects

07 p1354 A70-20237

Flat plate laminar boundary layer blowoff due to wall injection analyzed by parameter matched asymptotic expansion

10 p1862 A70-23844

Swirl velocity and cavity stability in rotating container filled radially through porous cylindrical wall at constant and applied pressure

10 p1868 A70-24195

Hypersonic viscous interactions on insulated slender cone with mass injection assuming perfect gas flow and negligible transverse curvature effects

10 p1803 A70-24821

Newtonian fluid laminar boundary layer flow over flat plate with nonNewtonian fluid injection

12 p2209 A70-27212

Oscillatory flow in porous channel with suction and injection, using Laplace transform technique

13 p2389 A70-29538

Orbital refueling techniques, discussing vapor-liquid interface stability, pressurant requirements, transfer line chillover, propellant transfer dynamics, dielectrophoresis, suction speed estimating and system tradeoffs

[AIAA PAPER 69-564] 14 p2653 A70-30752

Two dimensional incompressible laminar boundary layers asymptotic structure with injection, obtaining velocity profiles

14 p2566 A70-30995

Incompressible viscous fluid steady flow admission into bounded space from cylindrical tube, demonstrating solvability of plane and three dimensional versions

15 p2720 A70-31642

Combustion extinguishment of composite solid propellant motors by fluid injection, considering binder, curing agent and burning rate catalyst

[AIAA PAPER 70-641] 16 p2968 A70-33599

Experimental and theoretical investigation of mass injection effect on high current MPD arc

[AIAA PAPER 69-266] 16 p2959 A70-33869

Inviscid film flow by fluid injection through bounding surface, considering porous plate inclination and power law injection rates

16 p2895 A70-34241

Steady two dimensional MHD boundary layer flow with uniform suction or injection past semiinfinite flat plate in cross fields

17 p3067 A70-34618

Turbulent boundary layer on porous surface with fluid injection into layer reexamined for causes of discrepancy with experimental results

17 p3072 A70-35547

Laminar flows with surface injection, calculating thermal boundary layer-porous wall coupling effects

[ASME PAPER 70-GT-1] 18 p3243 A70-36860

Vestibular thermal stimulation method using distilled water injected into ear, discussing nystagmus appearance and duration

19 p3367 A70-37355

Two phase flows and atomization jet during fluid injection into supersonic flow, determining vaporization range

20 p3736 A70-39268

Flow field model for large surface blowing problem accounting for upstream and downstream effects with large rate normal injection near trailing edge

20 p3559 A70-40110

Flow past streamlined obstacles under nonNewtonian fluid injection into hydrodynamic laminar and turbulent boundary layer

21 p3812 A70-42266

Turbulent boundary layer control by uniform fluid injection and suction, discussing velocity profiles, wall and wake laws, skin friction and shear stress transport equation

[ICAS PAPER 70-10] 23 p4180 A70-44121

NonNewtonian fluids injection into boundary layer, comparing flow and pressure effects with water injection

24 p4324 A70-45364

Porous tube inlet region, calculating fluid injection effect on laminar flow from integral form boundary layer equations

24 p4326 A70-45782

FLUID JET AMPLIFIERS

U FLUID AMPLIFIERS

U JET AMPLIFIERS

FLUID JETS

NT AIR JETS

NT FREE JETS

NT GAS JETS

NT HYDRAULIC JETS

NT VAPOR JETS

Electrical and mechanical instability of jets, threads and sheets of viscous fluid, noting role of deceleration

03 p0471 A70-14253

Critical load and instability of smooth and mesh surface mechanical systems subjected to impinging fluid jet, noting static buckling and flutter effects

[ASME PAPER 69-WA/AFM-10] 04 p0772 A70-14917

Bottom topography effect on jets stability in baroclinic fluid, discussing two layer model 04 p0715 A70-15518

Electrically driven jets of slightly conducting viscous fluids drawn from conducting tubes, discussing cylindrical soap film instability under radial electric field 05 p0831 A70-15917

Free incompressible oil jet interaction with mobile plate, discussing plate configuration, oil feed pressure and nozzle diameter, applications to electrohydraulic converter design, etc 09 p1613 A70-22825

Vertical liquid jets capillary instability under audio frequency disturbances, measuring disturbance growth rates for various wavelengths and fluid viscosities 09 p1664 A70-23678

Plane incompressible conducting fluid laminar jets analysis in magnetic field, using boundary layer equations for zero electric field 13 p2461 A70-28964

Excess pressure in pulsed fluid jet with different emergent velocities from water hammer, discussing interaction between discrete sections 13 p2388 A70-29425

Three dimensional oblique incidence liquid jet impinging on solid surface, evaluating flow force by applying mass and momentum conservation 13 p2389 A70-29540

Nonself similar problem of plane submerged fluid jet expelled from annular nozzle, obtaining asymptotic expansion for stream function 15 p2719 A70-31485

Cumulative jets during shock induced collapse of air cavities in thin fluid layers, using high speed motion picture photography 17 p3074 A70-35742

Two phase flows and atomization jet during fluid injection into supersonic flow, determining vaporization range 20 p3736 A70-39268

Liquid jets aerodynamic atomization at orifice exit in reentry vehicle into gaseous crossflow, investigating critical Weber number variation with Knudsen number 20 p3610 A70-39701

Turbulent incompressible conducting fluid jets velocity and temperature characteristics in presence of longitudinal and transverse magnetic fields 21 p3860 A70-42226

Fluidic amplifier with axisymmetric jets, deriving approximate mathematical model for static no-load operation [ASME PAPER 70-FLCS-4] 22 p3964 A70-42427

Short wing lift investigated via lateral fluid jets fired in wind tunnel for various lengths 22 p3958 A70-42614

Liquid jet breakup in supersonic airstream, using high speed photographic techniques [SMPT PREPRINT 90] 22 p4036 A70-43063

FLUID LOGIC

Fluidic devices for systems engineering, discussing design and applications of logic simulator, element tester and three mode controller 06 p1015 A70-18428

Fluidic display, discussing applications for fluidic computers and control systems 08 p1441 A70-21684

Fluidic logic elements to control firing and extinction of plasma matrix display system cells with constant electrical power supply 09 p1673 A70-22032

Fluidic logic components for automatic data processing, describing circuits designed to solve specific problems 09 p1612 A70-22771

Fluidic devices theory and operation including flow control mechanisms, modulators, logic circuits, amplifier types, etc 16 p2843 A70-33444

Fluid logic systems synthesis by computer aided design programs, proposing referee system [ASME PAPER 70-DE-47] 16 p2844 A70-33510

Fluid logic sequential circuits with optional input signals, describing synthesis procedure [ASME PAPER 70-FLCS-19] 22 p3963 A70-42408

Fluid logic circuits with combined feedback input signals, describing synthesis procedure [ASME PAPER 70-FLCS-18] 22 p3963 A70-42409

Fluidic applications in missile components production, discussing various types of fluidic control and logic in relation to functional requirements [ASME PAPER 70-FLCS-11] 22 p3963 A70-42416

Fluidic logic devices compared with electric relay and hydraulic/pneumatic valve equivalents 24 p4293 A70-45429

Hydraulic and pneumatic components for logic circuits of automatic controls, considering amplifiers, interlocked systems and use of fluidics 24 p4293 A70-45418

FLUID MECHANICS
NT AERODYNAMICS
NT AEROTHERMODYNAMICS
NT ELASTOHYDRODYNAMICS

NT ELECTROHYDRODYNAMICS
NT FLUID DYNAMICS
NT GAS DYNAMICS
NT HYDRODYNAMICS
NT HYDROMECHANICS
NT HYDROSTATICS
NT HYPERSONICS
NT MAGNETOHYDRODYNAMICS
NT PNEUMATICS
NT RAREFIED GAS DYNAMICS
NT ROTONS
NT ROTOR AERODYNAMICS

Experimentation in fluid mechanics research, discussing equilibrium flows, relaxation processes, turbulence structure and digital techniques 02 p0286 A70-12355

Prediction criteria regarding turbulent separation in fluid mechanical devices and systems, emphasizing vanishing wall shear stress 02 p0286 A70-12358

Evaluation of performance of prediction methods for mandatory flows 02 p0286 A70-12359

Wave drag in stratified flow lee waves without upstream influence calculated for cylindrical and three dimensional obstacles 03 p0479 A70-14229

Collapse of homogeneous fluid mass in stratified fluid with initially slender interface and ineffective internal wave motion, discussing internal wave generation 03 p0470 A70-14247

Initial value method for solution of nonlinear two point boundary value problems in fluid mechanics, considering Blasius equation and unsteady gas flow [ASME PAPER 69-WA/FE-8] 04 p0667 A70-14782

Semifocusing color schlieren systems for quantitative investigations of flows in fluid mechanics and heat transfer, including photographs of boundary layers 04 p0690 A70-15029

Fluid mechanical problems with pressure distribution determined by interaction between external supersonic inviscid flow and inner laminar viscous layer 04 p0674 A70-15529

German research institutes activities in fluid mechanics, structural materials, propulsion, flight control and electronics, space physics and medicine 05 p0829 A70-16374

Book on mechanics of continuous medium, discussing constitutive equations, fluid mechanics, linearized elasticity, vectors and tensors, stress, strain and deformation, etc 06 p1104 A70-17420

Liquid and slush hydrogen gravimetric flow calibration system for research in slush generation, slush fluid mechanics and flow instrumentation 06 p1031 A70-18449

Peristaltic motion of viscous incompressible fluid, applying long wave approximation to two dimensional urine flow model 07 p1219 A70-19247

Transient phenomena accompanying heating of fluid situated between heat conducting plane horizontal plates, using interferometry and streak photography 08 p1596 A70-20592

Fluid system control valve gain dependence on flow characteristics slope due to series resistance or centrifugal pump 09 p1613 A70-23685

Thermodynamics and fluid mechanics - Conference, Glasgow, March 1970 09 p1607 A70-23733

Fluid mechanics and fluid machinery - Conference, Budapest, September 1969 11 p1973 A70-25776

Fluid material line growth in grid-generated isotropic turbulent flow measured by tagging lines with hydrogen bubbles 11 p2035 A70-25843

Algebraic method for role of part inversion in fluid structure problems with mixed variables 11 p2135 A70-25979

Book on quasi-linearization and nonlinear fluid and orbital mechanics covering ablating wall, electrostatic probe, laminar boundary stability, pipe flow and optimum bang-bang transfer 11 p2072 A70-26225

Fluid mechanics of jet engine turbomachinery, considering supersonic compressor and blade rows flows and airframe propulsion system compatibility 11 p1977 A70-26574

Light storage by Venus machine using refractive properties of gas and involving fluid mechanical optics 11 p2114 A70-26575

Nonviscous relativistic fluid energy momentum tensor modification to rule out sound wave propagation velocities above speed of light 13 p2454 A70-29900

Heat transfer and fluid mechanics - Conference, Stanford, California, June 1970 14 p2662 A70-30251

Nonlinear branching point problems in fluid mechanics using perturbation technique 14 p2565 A70-30471

Cardiovascular and circulatory phenomena fluid mechanical aspects emphasizing pulsatile blood flow 15 p2720 A70-31789

Hypervelocity impact generated shock propagation based on governing differential equations, using fluid mechanical model for perfect gas and real fluid 15 p2824 A70-32788

Fluid mechanics and engine dynamics and start-up experiments simulating thermal environment in nuclear light bulb engine 16 p2949 A70-33552

Collection of papers on fluid mechanics, Volume 2, covering boundary layers, numerical modeling, wave propagation, etc 17 p3067 A70-34661

Fluid mechanics phenomena numerical modeling, considering present methods three dimensional problems, turbulence treatment, etc 17 p3068 A70-34663

Boundary layer momentum thickness growth in channels with adverse pressure gradients by stepwise integration of Truckenbrodt equation and extending Gruschwitz-Schmidbauer separation criterion [ASME PAPER 70-GT-12] 18 p3243 A70-36864

Energy and impulse tensor of nonviscous relativistic fluid, excluding sound velocity greater than light velocity 19 p3404 A70-37593

Eringen theory of microfluids with nonhomogeneous micromotion, discussing eccentricity, stress moments, microinertia, etc 19 p3404 A70-37784

Turbulent flow asymmetrical mechanics equations derivation from conservation laws, discussing Navier-Stokes equation, angular momentum and transport theory 21 p3806 A70-40612

French book on compressible fluid mechanics covering adiabatic, one and two dimensional flows, linear equations, friction factor, heat exchanges, supersonic, subsonic flows, etc 21 p3743 A70-40624

Gravitating sphere high speed rotation in monatomic gas, discussing viscous and thermal boundary layers, velocity fields, temperature effects and fluid motion 23 p4131 A70-43944

Ureter fluid mechanical model from lubrication theory viewpoint, discussing waveforms, pressure distribution, etc 23 p4179 A70-43966

Particle motion in constant density dynamic viscosity random translational velocity fluid 24 p4324 A70-45139

Transverse and longitudinal current correlations in fluids from modeled kinetic equations, noting inelastic neutron scattering from liquids 24 p4378 A70-45261

Three dimensional laminar boundary layer in unsteady incompressible flow, presenting solution by successive approximations method 24 p4325 A70-45594

Turbulent flow mechanics heuristic exposition, discussing random processes, instability, nonlinear interactions, energy exchange, intermittency dependence on Reynolds number, fluid properties and boundary conditions effects, etc [AIAA PAPER 70-1308] 24 p4326 A70-45948

FLUID POWER

Si fluid thermal actuator as temperature sensor and prime mover for active thermal controller in spacecraft 05 p0806 A70-16124

Fluids for aerospace power technology, tabulating properties of hydraulic, damper and heat transfer fluids, fuels, oils, etc 07 p1316 A70-18807

Fluid power systems computer aided design and optimization, describing modeling and simulation, parameter sensitivity, systems stability, etc [ASME PAPER 70-DE-44] 16 p2869 A70-33508

FLUID SWITCHING ELEMENTS

Fluidic devices for systems engineering, discussing design and applications of logic simulator, element tester and three mode controller 06 p1015 A70-18428

Fluidics elements construction, behavior and applications, considering vortex and turbulence amplifiers, input and output elements, etc 12 p2164 A70-27221

Proportional and flip-flop elements in hydraulic circuits using oils, noting cavitation effect on switching stability in digital elements 14 p2534 A70-30677

Fluidic membrane pressure wave switch with air control-action release, noting use in light signal control, conveyor belt counting, storage vessel level control, etc 21 p3759 A70-41425

Bistable wall attachment fluid amplifier, calculating unsteady end wall switching transient based on turbulent jet entrainment properties [ASME PAPER 70-FLCS-3] 22 p3964 A70-42428

Hydraulic and pneumatic components for logic circuits of automatic controls, considering amplifiers, interlocked systems and use of fluidics 24 p4293 A70-45618

FLUID TRANSMISSION LINES

Fluid flow at pneumatic network junction, considering junction pressure determination as boundary condition for all transmission lines meeting at junction [ASME PAPER 69-APM-N] 04 p0627 A70-14862
Equivalent circuit for fluidic transmission line used for studying behavior of lines with circular and rectangular cross sections 06 p0988 A70-17439

Unsteady flow equations and thermodynamics for studying homogeneous fluidic transmission in circular and rectangular cross section lines 09 p1613 A70-23403

Fluidic circular and rectangular transmission lines characteristics noting frequency dependence 13 p2349 A70-29477

No-inertia line, lumped parameter and distributed parameter models for dynamic characteristics of fluid transmission lines 15 p2678 A70-32526

FLUID TRANSPIRATION

U TRANSPARATION

FLUIDICS

NT FLUIDICS

Pneumatic fluidic oscillator consisting of bistable multivibrator, analyzing feedback loop operation based on electropneumatic analog system 02 p0229 A70-12673

Fluid oscillators for sensing and missile control, discussing performance, design, frequency variation and applications [ASME PAPER 69-WA/FLCS-8] 04 p0626 A70-14845

Fluidic sun sensor design and breadboard test for spacecraft and missile attitude control systems 04 p0716 A70-15415

Fluidics application in sounding rocket guidance control circuits used in space boosters 05 p0797 A70-15809

Fluidics background, operational principles, constituent elements, system assemblies and applications, discussing integrated and multiple function circuits, cost and reliability advantages, etc 05 p0798 A70-16146

Equivalent circuit for fluidic transmission line used for studying behavior of lines with circular and rectangular cross sections 06 p0988 A70-17439

Fluidic accelerometer utilizing seismic mass nulled by feedback loop and independent of supply pressure variations 06 p1068 A70-18429

Fluidic air gauge back pressure signal frequency response as function of time [ASME PAPER 68-WA/FE-16] 08 p1441 A70-21316

Fluidic display, discussing applications for fluidic computers and control systems 08 p1441 A70-21684

Fluidic devices and applications to gas turbine control, discussing beam deflection amplifiers design parameters [AGARDOGRAPH-120] 08 p1559 A70-19133

Acoustic fluidic amplifiers, considering receiver, transmitter and operating mode 09 p1672 A70-22012

Optimizing control system design using fluidic digital circuitry and FM type transducers 09 p1614 A70-23690

Fluidic logic elements for controlling selected cells extinction in hybrid plasma-fluidic display 09 p1738 A70-23758

Semifluidic proportional industrial control systems using diaphragm summing junction including applications to temperature control, remote sensing and drill bit adaptive measurement 12 p2164 A70-27073

Fluidic gas turbine controls, discussing high temperature operation, hybrid sensors and logic in hostile environment applications 12 p2164 A70-27074

Fluidics elements construction, behavior and applications, considering vortex and turbulence amplifiers, input and output elements, etc 12 p2164 A70-27221

Fluidic circular and rectangular transmission lines characteristics noting frequency dependence 13 p2349 A70-29477

Proportional and flip-flop elements in hydraulic circuits using oils, noting cavitation effect on switching stability in digital elements 14 p2534 A70-30677

Fluidic components downstream impedance calculation, using measured/monitored pressure ratio 14 p2534 A70-30680

Fluidic systems linear lumped components design with allowance for energy factor Q, investigating capacitance and inductance 15 p2678 A70-32675

Fluidic devices theory and operation including flow control mechanisms, modulators, logic circuits, amplifier types, etc 16 p2843 A70-33444

Fluidic technology for avionics systems, considering potential cost reduction and reliability improvement 16 p2843 A70-33445

Fluidic attitude control for boost phase of tactical surface to surface missile 16 p2844 A70-33447

Solid propellant rocket motor combustion control by fluidic vortex valve, considering thrust variation [AIAA PAPER 70-643] 16 p2965 A70-33535

Reentry vehicles fluidically controlled hydrazine rocket engine modules for roll rate control [AIAA PAPER 70-650] 16 p2970 A70-33617

NERVA engine chamber pressure control, investigating replacement of TPCV with fluidic vortex valve [AIAA PAPER 70-658] 16 p2970 A70-33620

Fluidic technology applications to space and oceanography, discussing control, monitoring, sequencing and signal processing 16 p2845 A70-33714

Fluidic oscillator molecular weight of flowing mono- and polyatomic gases, discussing frequency dependence on pressure drop and temperature 17 p3081 A70-34515

Fluidic parallel flow low airspeed indicator for V/STOL instrumentation tested in wind tunnel [AIAA PAPER 70-906] 17 p3096 A70-35818

Soviet book on fluidic theory covering jet elements, pneumatic throttles, chambers, communication channels, etc 19 p3357 A70-37469

Dynamic pressure transducer calibration system using fluidic pressure generators 19 p3358 A70-37897

Hydraulic and pneumatic controls construction and use in machine tools 19 p3359 A70-38725

Fluidic inertial platform feasibility model for air to surface missile line-of-sight guidance, noting cost, reliability and environmental advantages [AIAA PAPER 70-1009] 20 p3667 A70-39523

Fluidic gyro compatible with PDM missile guidance system, discussing spherical gas bearing design [AIAA PAPER 70-1008] 20 p3631 A70-39524

Nuclear rocket engine fluidic chamber pressure control, discussing design concepts for static and dynamic subsystems [AIAA PAPER 70-1010] 20 p3688 A70-39585

Fluidic oscillators frequency stability evaluation, noting analog circuits superiority over digital [ASME PAPER 70-FLCS-20] 22 p3963 A70-42407

Fluidic control devices and systems, discussing turbulence amplifiers, impact modulators, logic gates, active and passive elements, etc [ASME PAPER 70-FLCS-15] 22 p3963 A70-42412

Impact configuration fluidic amplifier, investigating modulation of power jet formed by impacting plane wall jets in bounded region [ASME PAPER 70-FLCS-14] 22 p3963 A70-42413

Fluidic applications in missile components production, discussing various types of fluidic control and logic in relation to functional requirements [ASME PAPER 70-FLCS-11] 22 p3963 A70-42416

Vortex pressure regulator with adjustable settings, discussing design, operation and test results [ASME PAPER 70-FLCS-9] 22 p3964 A70-42418

Fluidic controls for propulsion engines, describing optimum fabrication techniques [ASME PAPER 70-FLCS-7] 22 p3964 A70-42420

Fluidic amplifier with axisymmetric jets, deriving approximate mathematical model for static no-load operation [ASME PAPER 70-FLCS-4] 22 p3964 A70-42427

Bistable wall attachment fluid amplifier, calculating unsteady end wall switching transient based on turbulent jet entrainment properties [ASME PAPER 70-FLCS-3] 22 p3964 A70-42428

Working medium excess and absolute pressure effects on pneumatic elements characteristics 22 p3967 A70-43566

Fluidic amplifiers in measurement technology including turbulence, pulse, Coanda, induction, vortex, arc and focusing amplifiers 23 p4142 A70-44246

Fluidic networks nonlinear component AC and DC behavior, discussing Bernoulli equation, nonlinear resistances, transmission lines and various flows 23 p4142 A70-44296

Fluidics - Conference, Chicago, November 1968 24 p4293 A70-45426

Fluidics in naval avionics, discussing CH-46A helicopter stability augmentation and approach power compensator for carrier-based aircraft 24 p4293 A70-45428

Fluidic logic devices compared with electric relay and hydraulic/pneumatic valve equivalents 24 p4293 A70-45429

Fluidic elements operation and performance, considering wall attachment, jet interaction, turbulence, gain load, operating ranges, etc 24 p4293 A70-45430

Specification sheets for fluidics clarified by demonstrating step-by-step solutions for typical problems involving flip-flop and OR/NOR gate 24 p4293 A70-45431

Semifluidic proportional control systems for industrial controls involving oven temperature, remote hydraulic pressure regulation, drill bit pressure 24 p4293 A70-45432

Two dimensional aperture flow with downstream asymmetric pressure distribution due to jet reattachment to boundary, simulating flows in hydraulic spool valves and fluidic devices 24 p4325 A70-45582

Hybrid fluidic damper control for yaw axis stability augmentation of commercial jet aircraft [SAE PAPER 700794] 24 p4294 A70-45853

Hydrofluidics flight controls for aircraft stability augmentation systems, noting component performance, transfer functions and operation [SAE PAPER 700793] 24 p4294 A70-45854

High pressure hydraulic fluidic vortex rate sensor feasibility, considering variable geometry sensor design, fabrication and tests [SAE PAPER 700788] 24 p4294 A70-45857

Fluidically controlled aircraft fuel transfer system three-tank model construction, noting maintenance and fail safe operation [SAE PAPER 700786] 24 p4294 A70-45858

Fluidically augmented artificial feel system for fighter and attack aircraft control, discussing improved handling qualities [SAE PAPER 700785] 24 p4294 A70-45859

Fluidics for aircraft high pressure hydraulic systems, discussing circuit breaker, feel computer and landing gear sequencing circuit [SAE PAPER 700784] 24 p4295 A70-45860

Spacecraft fluid mechanical system design, considering environments, materials, lubrication, zero gravity and inflight maintenance [SAE PAPER 700781] 24 p4295 A70-45862

Turbojet and turbofan engine control evolution, noting increased complexity and adoption of hybrid fluidics and computer technologies [SAE PAPER 700825] 24 p4394 A70-45894

FLUIDIZED BED PROCESSORS

Lunar craters origin by study of slowly collapsing fluidized beds 05 p0906 A70-15920

FLUIDS

Fluid sealing - ASLE-ASME Conference, Philadelphia, May 1969 13 p2416 A70-28609

Fluid quantum corrections to viscosity, thermal conductivity and diffusion, expanding Wigner operator in Planck constant 14 p2665 A70-30655

Gravitational instability and collapse of thin spherical shell of charged fluid, using energy conservation law 16 p2952 A70-33787

Ultrasonic pulses velocity and attenuation in fluids by coherent detection technique, measuring delay and decrease in amplitude due to transmission path length increase 16 p2913 A70-34084

Fluid intermolecular potential and virial calculation, noting relationships to Boyle and Joule-Thompson inversion temperatures 20 p3671 A70-38988

FLUORESCENCE

NT PHOSPHORESCENCE

NT X RAY FLUORESCENCE

Dispersed fluorescence spectra from vacuum UV photon impact on COS, noting absence of emission from higher vibrational levels 01 p0148 A70-11353

High speed fluorescent cell sorting system for sorting mouse spleen cells from Chinese hamster ovarian tumor cells 02 p0240 A70-12695

Rapid photoprocesses decay kinetics, using CW Ar ion laser beam interrupted periodically by electro-optical shutter 02 p0314 A70-12742

Superfluorescence losses in large aperture disk laser systems using Monte Carlo method, determining maximum population inversion from enhanced photon flux density considerations 03 p0503 A70-14209

Transient hologram recording with fluorescein-boric acid glass organophosphor, noting effects of dye concentration, sample thickness, laser power and excited state lifetime 04 p0690 A70-15027

Molecular fluorescence emission rate factors for strong bands of nitric oxide gamma systems, noting day airglow temperature dependence 05 p0886 A70-17085

Electron beam fluorescence in rarefied air flow at low static temperature used to study influence of 05 p0886 A70-17085

secondary electron emission on rotational temperature measurements

06 p1123 A70-18300

Spectral broadening mechanisms for trivalent Eu ions in glass, considering fluorescence and absorption spectra measurements

06 p1127 A70-18640

Biological fluorescent substances passage in rabbit central nervous system as indicators of blood supply to cells

07 p1197 A70-18657

Rotational temperature of molecular beam by electron excited fluorescence method, discussing signal level, background light and scattering effects

07 p1345 A70-20140

Polarization of interacting atoms resonance fluorescence and coherence transfer due to excitation exchange, considering electrostatic dipole-dipole and electromagnetic radiative interactions

08 p1548 A70-21341

Supernova fluorescent light excited by radiation impingement on material surrounding explosion site, assuming explosion time and UV energy

09 p1749 A70-21997

Fluorescence produced by resonant coherent light pulse passing through medium assuming infinite relaxation times and negligible pulse attenuation

09 p1726 A70-22321

Potassium iodide and paratoluidine fluorescent quenching effect on lasing threshold in rhodamine 6G alcohol solutions

09 p1696 A70-22487

Fraunhofer line discriminator (FLD) used for airborne fluorometer applicable to marine and estuarine studies

09 p1681 A70-23350

Two photon fluorescence and second harmonic generation methods for studying picosecond structure of laser output signals

09 p1699 A70-23362

Fluorescent integrating sphere for absolute hemispherical reflectance measurements on imperfectly diffuse surfaces in vacuum UV, eliminating erroneous signals by filtering

09 p1729 A70-23527

Electron beam fluorescence probes for rarefied gas flow, describing local density and temperature measurement methods

10 p1888 A70-24399

Vapor phase fluorescence spectra from benzene and deuterated benzene at zero point vibrational level

15 p2694 A70-31731

Photodissociation and fluorescence cross sections for hydrogen by Lyman-alpha photons emission from collisional quenching

16 p2953 A70-33006

Nitrogen and air bombardment by relativistic electrons, determining absolute fluorescence intensity of nitrogen molecular ion first negative band

16 p2954 A70-33279

Manganese deficiency effect on chlorophyll fluorescence in algae adapted to hydrogen, determining electron transport mechanism

16 p2848 A70-33291

Symbiotic stars UV spectrum, discussing molecular fluorescence phenomena

17 p3161 A70-34891

Fluorescence method of determining solid state laser parameters using spontaneous and stimulated emission observations

17 p3106 A70-35101

Simultaneity in optical photon pairs parametric production, verifying quantum mechanical description of fluorescence

17 p3143 A70-35187

Two photon absorption-fluorescence measurement of laser pulse width, using three level model of absorber

19 p3422 A70-37671

Atmospheric fluorescence observation of super-nova energetic photon short pulse burst, using photomultiplier

19 p3500 A70-38079

Pulsar NP 0535 X rays detection by ground based observations of upper air fluorescence

21 p3871 A70-40654

Spatial energy loss and ionization deposition distributions of fluorescent radiation emission induced by electron beam in nitrogen gas

21 p3853 A70-41913

Rotational quantum numbers from iodine molecule resonance fluorescence measurements during laser excitation using Fabry-Perot interferometer

23 p4202 A70-44938

Fluorescent penetrants vs magnetic powder test for individual and continuous material inspection, discussing sensitivity and surface finish influence

24 p4338 A70-45741

Commercial fluorescent penetrants for natural and artificial cracks, considering indication characteristics

24 p4348 A70-45742

UV excited powdery fluorescent products, describing crystal for photo and thermoluminescence at various temperatures

24 p4339 A70-46097

Fluorescent probes inserted into biological membranes for molecular structural and dynamic facets

24 p4304 A70-46231

FLUORESCENT EMISSION U FLUORESCENCE FLUORIDES

NT BARIUM FLUORIDES
NT BERYLLIUM FLUORIDES
NT BORON FLUORIDES
NT CADMIUM FLUORIDES
NT CALCIUM FLUORIDES
NT CHLORINE FLUORIDES
NT DIFLUORIDES
NT HYDROFLUORIC ACID
NT LITHIUM FLUORIDES
NT MAGNESIUM FLUORIDES
NT OXYFLUORIDES
NT OXYGEN FLUORIDES
NT STRONTIUM FLUORIDES
NT SULFUR FLUORIDES

Reduced Nd ion absorption in matrices of fluorides, fluoride mixtures or oxygen-containing compounds with various ion concentrations, analyzing optical centers statistical properties

01 p0107 A70-10210

Friction and wear tests on solid lubricant graphite fluoride compared with molybdenum disulfide at specific temperatures, considering friction coefficient

[ASLE PREPRINT 69-LC-9] 02 p0321 A70-12536

Group 4A difluorides vaporization thermodynamics and bond dissociation energies, tabulating mass spectra, vapor composition, reaction enthalpies, heats of polymerization and thermodynamic functions

07 p1319 A70-19889

Chemical kinetics of carbonyl fluoride thermal decomposition in argon and nitrogen diluent behind shock waves, using IR monitoring method

11 p1995 A70-25824

Methyl fluoride calculated for ion-molecule reaction rate constants from ion cyclotron resonance spectra

12 p2180 A70-26862

Antifriction and wear properties of iron fluoride materials and white cast iron under sliding friction in air and vacuum

15 p2743 A70-31637

Antiferromagnetic resonance measurement in manganese difluoride as function of microwave frequency, sample size and shape

21 p3850 A70-41908

FLUORINATION

Silver fluorination kinetics, taking temperature and pressure effects into account

22 p3983 A70-43416

FLUORINE

Fluorine injectors for main tank injection of space vehicle liquid hydrogen tank, including study of hypergolicity and reaction product freezing

[AIAA PAPER 69-528] 04 p0736 A70-15406

Limits of self ignition in reaction of F with H detected photoelectrically

05 p0956 A70-16156

Atomic F reaction with hydrogen studied for vibrational, rotational and translational energy distribution, using IR chemiluminescence method

07 p1225 A70-20055

Analytical model for liquid fluorine no-vent loading operations noting application to flightweight upper stage systems

[AIAA PAPER 69-579] 09 p1662 A70-23251

Fluorine toxicity, discussing fluorine reactions with animal proteins and lipids, short-term exposure toxicity data, emergency tolerance limits, threshold limit, etc

10 p1824 A70-24060

Enthalpy-entropy, enthalpy-pressure and composition diagrams of fluorine-hydrogen system, noting possible applications to rocket propulsion systems

10 p1929 A70-25100

CW chemical laser performance using molecular hydrogen diffused into supersonic fluorine atoms streams

11 p2063 A70-26067

Liquid fluorine feed system valves, seals and seats, discussing design criteria for flight weight components

[AIAA PAPER 70-705] 16 p2844 A70-33564

Fluorine-compatible apparatus for measuring temperature PVT properties of gaseous and liquid fluorine

20 p3630 A70-39485

Diatomic fluorine dissociation energy by mass spectrometry

20 p3582 A70-39615

Electron collisional detachment from negative fluorine ions in shock tube following nonequilibrium ion overshoot in CsF dissociation in argon, noting correlation with temperature

21 p3853 A70-41705

Gaseous and liquid fluorine exposure effects on nitroso rubbers at ambient and cryogenic temperatures, using impact tests and IR spectroscopy

21 p3844 A70-42140

Fluorine specific heat derived from measurements on two phase liquid vapor system at constant volume by PVT properties at coexistence

23 p4157 A70-44001

FLUORINE COMPOUNDS

NT BARIUM FLUORIDES

NT BERYLLIUM FLUORIDES
NT BORON FLUORIDES
NT CADMIUM FLUORIDES
NT CALCIUM FLUORIDES
NT CHLORINE FLUORIDES
NT DIFLUORIDES
NT DIFLUORO COMPOUNDS
NT FLUORIDES
NT FLUORINE ORGANIC COMPOUNDS
NT FLUORO COMPOUNDS
NT FLUOROCARBONS
NT FLUOROHYDROCARBONS
NT HYDROFLUORIC ACID
NT LITHIUM FLUORIDES
NT MAGNESIUM FLUORIDES
NT OXYFLUORIDES
NT OXYGEN FLUORIDES
NT POLYTETRAFLUOROETHYLENE
NT STRONTIUM FLUORIDES
NT SULFUR FLUORIDES

High temperature reaction kinetics between oxygen difluoride and CO in shock tube, discussing carbon dioxide formation

16 p2855 A70-33010

Laser oscillation in atomic fluorine from electrically pulsed discharge of fluoride compounds-helium mixtures, identifying as 3p-2P and 3s-2P transitions in fluorine I

17 p3108 A70-35910

Apollo 11 lunar rock fluorapatite and trace minerals, examining pressure and oxidizing conditions of formation, grain and crystallization

21 p3898 A70-41527

FLUORINE ORGANIC COMPOUNDS

NT FLUOROCARBONS
NT FLUOROHYDROCARBONS
Chlorotrifluoroethylene and difluorodichloromethane saturable absorbers for wavelength extensions of passively Q switched carbon dioxide lasers

03 p0502 A70-13816

Fluorinated lubricating oils and greases for use as liquid oxygen compatible lubricants, correlating stability and hydrogen substitution

10 p1907 A70-24064

Reaction kinetics of gas phase pyrolysis of polydifluoroaminomethanes in various reactors, obtaining C-N bond cleavage as rate determining step

16 p2856 A70-33652

Temperature and long term effects on volatility of perfluoroalkyl ether and polysiloxane greases

[ASME PAPER 70-HT-31] 22 p4058 A70-42435

HF chemical laser emission in fluorine-containing organic compounds via arc discharges, noting molecular hydrogen effect on p sub 10 and p sub 21 transitions

24 p4355 A70-46046

FLUORINE-LIQUID OXYGEN

U FLOX

FLUORO COMPOUNDS
NT DIFLUORO COMPOUNDS
NT FLUORINE ORGANIC COMPOUNDS
NT FLUOROCARBONS
NT FLUOROHYDROCARBONS
NT POLYTETRAFLUOROETHYLENE
Solid and liquid lithium tetrafluoroborate enthalpy relative to 273 K measured at temperatures between 323-873 K, deriving thermodynamic properties

04 p0646 A70-14583

Teflon and fluoropolymers relative toxicity due to thermal degradation at 370 C, testing carboxy nitroso rubber, Kapton polyimide film, perfluorated polymers, etc

13 p2439 A70-29260

Nine-alpha-fluorohydrocortisone preventing bedrest induced orthostatism, considering plasma volume decrease effects on cardiovascular performance

13 p2358 A70-29433

FLUOROCARBONS

Fluorocarbon polymer coatings, discussing role of fluorine content and carbon bond in chemical inertness, degradation resistance, thermal stability and low surface friction

[SAE PAPER 690645] 05 p0868 A70-15842

Fluorel spectral reflectance, transmittance and absorbance under monochromatic irradiation, considering thermal analysis and surface finish

09 p1710 A70-22794

Perfluoropropene, -cyclobutene and -cyclobutane mixing with atmospheric pressure oxygen to determine burning velocities

11 p2100 A70-26383

FLUOROHYDROCARBONS

Tetrafluorodibromomethane combustion inhibitor effects on aircraft hydrocarbon fuels flame propagation rate and explosion pressure

01 p0160 A70-11011

Water or bromotrifluoromethane content required in propellant Aerazine-50 (A-50) spill to inert against ignition in air, considering fire extinguishment

04 p0732 A70-15408

Photoelectron spectra of methane, silane, germane, methyl fluoride, difluoromethane and

- trifluoromethane, describing electron spectrometer with double focusing electrostatic plates
19 p3374 A70-38269
- FLUOROMICA
- U MICA
- FLUOROSCOPY
- Fluoroscopes for radiographic examination of materials and products with X ray and hard bremsstrahlung radiation
24 p4348 A70-45847
- FLUTING
- U GROOVING
- FLUTTER
- NT PANEL FLUTTER
- NT SUBSONIC FLUTTER
- NT SUPERSONIC FLUTTER
- NT TRANSONIC FLUTTER
- Mitral stenosis and atrial flutter with atrial sounds heard and recorded, discussing sound generating mechanism
01 p0013 A70-10271
- Arrhythmia resembling atrial flutter simulated in dogs by coronary sinus and left atrial pacing and in man by coronary sinus pacing
02 p0240 A70-12696
- Diastolic and equivocal fluttering of mitral valve in aortic insufficiency by echocardiography
09 p1615 A70-22209
- Noise-flutter interrelation in flight vehicle flexible plate and shell configurations immersed in fluid flow
11 p2132 A70-25726
- Computer applications in aerospace research involving flutter, supersonic flow, unsteady wing flow, etc
12 p2191 A70-27025
- Space shuttle structural dynamic problems, discussing stall flutter due to transition from high angle of attack to normal aircraft flying attitude
[AIAA PAPER 70-740] 12 p2312 A70-27150
- FLUTTER ANALYSIS
- Flutter investigation on model designed and constructed for tail unit of HFB 320 Hansa jet aircraft, discussing classical and statistical methods
04 p0775 A70-15180
- Aerodynamic forces for boundary layer profiles of flexible plate under transient motion in shear flow using computer programs
[AIAA PAPER 70-76] 06 p0972 A70-18122
- Variable sweep aircraft aeroelastic stability, considering wing-tail interaction flutter
[AIAA PAPER 70-80] 06 p1170 A70-18162
- Aircraft flutter equations solution by reduced frequency scanning method
[ONERA-TP-786] 06 p1171 A70-18470
- Thermomechanical coupling effect on stability of elastic continuous systems subjected to nonconservative forces, reducing flutter load by thermal damping
08 p1589 A70-21245
- Nonlinear flutter of three dimensional simply supported curved plates, employing quasi-steady supersonic aerodynamic theory
09 p1780 A70-23212
- Asymptotic method for aeromagnetic flutter of plane MGD nozzle, discussing conditions of MGD nozzle stability
10 p1800 A70-24129
- Helicopter blade flapping torsion flutter behavior analysis showing stabilization effect in forward flight
10 p1958 A70-24559
- Flutter characteristics of uniform cantilever wing with concentrated inertias using Direct Matrix method
10 p1963 A70-25071
- Buckled plates flutter at zero dynamic pressure, considering initial plate imperfections, including aerodynamic damping in quasi-steady supersonic approximation
11 p2135 A70-25988
- Flutter instability critical velocity and frequency for thin cantilevered plate with follower jet determined by Galerkin and computer simulation
12 p2316 A70-27106
- Two dimensional circular cylinder vortex excitation in uniform flow using linear binary system for flutter analysis
13 p2341 A70-29057
- Compressor cascade flutter phenomenon, investigating factors affecting aerodynamic damping force on annular cascade blades
13 p2341 A70-29447
- Flutter analysis, criteria and experiments emphasizing aircraft applications
15 p2815 A70-31798
- Thin cylindrical shells flutter analysis in supersonic flow, using linearized potential theory
15 p2815 A70-31916
- Magnetic field effect on critical flutter speed and frequency of elastic plate in ionized gas flow, deriving dispersion equation
15 p2818 A70-32173
- Low aspect ratio plates flutter analysis for subsonic and supersonic models
16 p2991 A70-33888
- Circular cylindrical shells with clamped ends, investigating supersonic panel flutter by two mode approach and Galerkin method
17 p3184 A70-34695
- Rotor blade flutter in forward flight accounting for wake unsteady aerodynamic effect
17 p3184 A70-34727
- Helicopter rotor blade stall flutter response prediction based on NACA 0012 airfoil aerodynamic data
17 p3009 A70-34734
- Nonlinear balance mass solutions for tab-aileron flutter free operation of jet trainer for arbitrary store configuration
17 p3185 A70-34923
- Flexible space vehicles dynamics and control covering free vibration analysis, thermal flutter and structural deflection effect on attitude control
17 p3177 A70-35233
- Critical flutter behavior of variable geometry aircraft with wing of 70 degree leading edge sweep, noting wing-tail interference
18 p3338 A70-36445
- Flutter design charts for isotropic panels stressed to verge of buckling for tropical values of structural damping
18 p3338 A70-36446
- Ground vibration testing for aircraft and missile flutter prevention
[ONERA-TP-816] 18 p3339 A70-36508
- Flutter analysis of n degrees of freedom system, basing stability criteria on energy balance considerations
19 p3542 A70-38244
- Sweptback thin cantilever wing transonic flutter characteristics, investigating concentrated mass spanwise location effects
22 p4112 A70-42274
- Circular cylindrical shell supersonic panel flutter nonlinear analysis, using averaging and numerical integration methods
22 p4112 A70-42275
- Low aspect ratio cantilever plate wings supersonic bending torsion flutter speed calculation, using spanwise and chordwise variables and potential energy principle
22 p4112 A70-42276
- Unsteady aerodynamic forces at stall flutter, applying vortex sheet theory to separated flow field around thin airfoil at high angle of attack
22 p3957 A70-42284
- Flutter of elastic current-carrying shell containing incompressible inviscid nonconducting fluid flow
22 p4117 A70-43383
- Elastic coupling and dynamic equations for flight elastomechanical vibration systems, including tiptanks on aircraft wings
23 p4274 A70-44767
- Thin cylindrical shell flutter in linearized supersonic potential theory, considering Mach number, aspect ratio and pressure effects on critical wave number
24 p4420 A70-45263
- Laminar circular cylindrical shells supersonic flutter characteristics determination by dynamic equilibrium boundary value problem eigenvalues analysis, obtaining critical flutter speeds
24 p4424 A70-45588
- FLUX [RATE PER UNIT AREA]
- U FLUX DENSITY
- FLUX [RATE]
- NT HEAT FLUX
- NT MAGNETIC FLUX
- NT SOLAR FLUX
- Electron flux parameters determination from ionograms and reflected signal amplitudes between 120-130 km, considering electron collision frequencies
01 p0084 A70-11551
- Electron flux interaction with electromagnetic field in comb type waves via linear approximation assuming small space charge
03 p0447 A70-13291
- Leonid meteor shower radar observation data, analyzing flux rates and particle size distribution
13 p2487 A70-28694
- Flat emission spectra of quasars in 3CP catalog attributed to anisotropic relativistic electron fluxes
13 p2493 A70-29387
- Solar wind observations by Pioneer 6, considering particle density, flux and kinetic energy
16 p2972 A70-32949
- Flux emissivity tables for water vapor, carbon dioxide and ozone based on wavelength dependent absorption coefficients and flux transmissivities
17 p3081 A70-35927
- Homogeneous opaque reactive solid heating and ignition by constant energy flux, examining physical and chemical parameters at critical conditions
20 p3738 A70-40078
- Magnetic field and electron flux observations near magnetopause via magnetometer and triaxial electron spectrometer on OGO-E
24 p4328 A70-45350
- FLUX DENSITY
- NT CURRENT DENSITY
- NT ELECTRON FLUX DENSITY
- NT ILLUMINANCE
- NT IRRADIANCE
- NT LUMINANCE
- NT LUMINOUS INTENSITY
- NT NEUTRON FLUX DENSITY
- NT PARTICLE FLUX DENSITY
- NT PHOTON DENSITY
- NT PROTON FLUX DENSITY
- NT RADIANCE
- NT RADIANT FLUX DENSITY
- NT SOLAR CONSTANT
- NT SOLAR FLUX DENSITY
- NT SOUND INTENSITY
- NT ZERO SOUND
- Density distribution measurements in flow field using interference methods, including laser light sources
01 p0085 A70-10268
- Electromagnetic propagation in linear dispersive media, discussing energy transport velocities of total stored energy density and electromagnetic energy
01 p0043 A70-10779
- Minimum weight sandwich plates complying with von Mises criterion, providing constant dissipated energy density
01 p0202 A70-10947
- Corpuscular radiation contributions to D layer ionization determined from intensity measurements
01 p0172 A70-11490
- Heat transfer and flux density during bubble boiling of liquid oxygen employing simulated weak gravitational fields
03 p0605 A70-13393
- Photoelectric intensity measurements on emission bands of oxygen Herzberg I system excited in argon-oxygen afterglow
03 p0528 A70-14350
- Mo/Mo cylindrical thermionic converter steady state performance, measuring efficiency and power density at various low emitter and collector temperatures
04 p0627 A70-14947
- Backscattered signal power density distribution along equivalent propagation path of delayed components, determining reflecting layers characteristics from echo signal phase
04 p0654 A70-15728
- Riometric data processing method for radio wave absorption measurement, considering nighttime cosmic radio emission intensity
05 p0842 A70-16742
- Solar X-ray flux from Explorer 33 and 35 observations, presenting catalog of tabular and graphical data
06 p1135 A70-18006
- Empirical method for calculating critical thermal flux density during boiling of underheated liquid-vapor systems
07 p1420 A70-19068
- Transverse particle and energy fluxes in toroidal magnetic traps magnetic fields with ionized plasmas, discussing particle diffusion coefficient and thermal conductivity
08 p1554 A70-21807
- Heat, moisture and momentum fluxes measurement in atmospheric boundary layer, discussing instrumental accuracy necessary for various measuring techniques
09 p1717 A70-22379
- Equatorial electrojet diurnal variability in intensity, position and width obtained from H records of magnetometers
09 p1747 A70-23495
- Varying flux density values measured at SHF for radio galaxy PK 0048-09 indicating recent origin of radio source
09 p1764 A70-23790
- Daily horizontal intensity spectrum for equatorial observatories, computing power densities near 27 day variation during high, moderate and low solar activity
10 p1875 A70-24440
- Empirical method for calculating critical thermal flux density during boiling of underheated liquid-vapor systems
10 p1970 A70-25219
- Solid state laser optical pumping energy density calculations for case of circular cylindrical image of pumping lamp formed in rod
13 p2429 A70-29476
- Vertical flux densities of momentum and sensible heat dependence on displacement height and surface roughness
14 p2602 A70-30371
- Backscattered signal power density distribution along equivalent propagation path of delayed components, determining reflecting layers characteristics from echo signal phase
14 p2550 A70-30812
- Critical heat flux density during annular channel internal heating, examining transfer crisis under forced motion of unheated water
18 p3345 A70-36111
- Variable radio source linear polarization at 8 GHz, examining degree, position angle and flux density
18 p3317 A70-37001

- Meteoroid flux density from radar measurements, noting detectability dependence on initial ionized trail radius 19 p3515 A70-37660
- High energy gamma ray flux enhancement towards galactic plane from OSO-3 particle telescope observations 19 p3501 A70-38089
- Solar spectral intensity distribution and ionizing radiation spatial emission patterns during eclipse, discussing effects on ionosphere 19 p3418 A70-38908
- Radio sources flux density and variability at microwave wavelengths 20 p3703 A70-39025
- Radio source master catalog giving name, coordinates, flux density and frequency of observation 20 p3713 A70-40539
- Defect detection by measurement of magnetic field leakage around flaw 24 p4346 A70-45727
- Spallation limits on low energy cosmic and nuclear gamma rays interstellar fluxes, evaluating fast particle effects on interstellar medium 24 p4397 A70-45758
- FLUX MAPPING**
U FLUX DENSITY
U MAPPING
- FLUX QUANTIZATION**
Photospheric magnetic flux quantization away from sunspots, studying nonsunspot field strength distribution 06 p1142 A70-17992
- Maxwell field quantization theory for case of interaction with Dirac field, calculating S matrix for interacting electrons 19 p3473 A70-37413
- High energy solar neutron flux via balloon measurement of flux difference from solar direction and from symmetrical direction about zenith 23 p4236 A70-43881
- FLUXMETERS**
U MAGNETIC MEASUREMENT
U MEASURING INSTRUMENTS
- FLY BY WIRE CONTROL**
VTOL aircraft fly by wire system eliminating errors automatically, discussing electronic and electrohydraulic control components, flight test model design, prototype, etc 04 p0623 A70-15149
- FLYBY MISSIONS**
NT GRAND TOURS
NT MARINER-MERCURY 1973
IR spectrometer on Mariner 7 Mars flyby recording sharp absorption near 3 microns at Martian southern polar cap 01 p0182 A70-10823
- Structural design experience in developing large area Be solar array for Mars flyby mission, describing configurations, requirements, material and manufacturing 02 p0228 A70-11935
- Mercury flyby mission feasibility study for ESRO considering payload, picture transmitting TV system, orbits, etc 04 p0754 A70-15157
- High energy propulsion module utilizing F/H fuels for planet flyby, orbiter mission and injection of 24-hr satellites, discussing design and equipment 04 p0736 A70-15176
- Ground-based and onboard guidance and navigation systems for outer planet flyby missions concerning direct, Jupiter swingby and Grand Tour trajectories [AIAA PAPER 70-71] 06 p1104 A70-18194
- Mercury flyby mission feasibility study for ESRO considering payload, picture transmitting TV system, orbits, etc 09 p1763 A70-23426
- Manned Mars flyby/orbiter mission, discussing cost, scientific returns, technology advances, popular support, etc 12 p2304 A70-27749
- Radio command guidance system for Mars probe ascent from surface to rendezvous with flyby vehicle on escape trajectory 13 p2447 A70-28421
- Operational and environmental factors constraining onboard navigation system design for outer planet flyby missions 14 p2614 A70-30467
- Unmanned flyby missions to Mercury in 1973-1990, discussing scientific objectives and payloads [AAS PAPER 70-027] 17 p3155 A70-34798
- Spinning symmetric satellite attitude stability in hyperbolic orbit on flyby mission, examining by numerical integrations of equations of motion 17 p3181 A70-35753
- Perturbative effects of Jupiter moons on spacecraft flyby and postencounter heliocentric trajectories, noting precision targeting [AIAA PAPER 69-932] 18 p3316 A70-36680
- Comet de Arrest 1976 opportunity mission analysis, considering flyby and rendezvous trajectories and guidance problems [AIAA PAPER 70-1073] 19 p3513 A70-37426
- Mission planning for 1973 Mariner Venus/Mercury flyby, discussing trajectory and navigation aspects [AIAA PAPER 70-1049] 19 p3528 A70-38864
- Pioneer-F Jupiter flyby mission planning, considering use of optimum broken plane trajectories to increase launch opportunity and/or payload capability [AIAA PAPER 70-1050] 19 p3528 A70-38865
- Jupiter swingby trajectory analysis for comet flyby and rendezvous missions, discussing approach velocity and payloads [AIAA PAPER 70-1074] 19 p3530 A70-38886
- Solar arrays for Venus-Mercury flyby, evaluating temperature and power performance 21 p3756 A70-41010
- RF requirements of deep space-outer planet spacecraft communications for Jupiter, Saturn, Uranus and Neptune flyby missions 21 p3791 A70-41369
- Solar probe trajectory optimization, using Venus gravitational field for braking 23 p4243 A70-44506
- Interplanetary periodic orbits and flyby dates for multiple earth-Venus swingby missions, describing various iterative solutions for trajectory [AIAA PAPER 69-931] 23 p4243 A70-44508
- Automated mission requirements for outer planets, discussing flyby spacecraft, orbiters, atmospheric entry and grand tour missions [AIAA PAPER 70-1246] 24 p4411 A70-45919
- FLYING BEDSTEAD AIRCRAFT**
U FLYING PLATFORMS
- FLYING PERSONNEL**
NT AIRCRAFT PILOTS
NT ASTRONAUTS
NT COSMONAUTS
NT FLIGHT CREWS
NT ORBITAL WORKERS
NT PILOTS [PERSONNEL]
NT SPACECREWS
NT TEST PILOTS
- Civil aviation personnel cardiovascular rehabilitation using single-lead electrocardiographic telemetry for monitoring and assessing cardiovascular status during supervised exercise 03 p0438 A70-14069
- Peripheral arterial piezography for cardiological screening tests and checkups of flying personnel 05 p0807 A70-16495
- Flying disability period due to coccidioidomycosis in southwestern U.S., giving recommendations for earlier return to flying duty 06 p1000 A70-17300
- Electroencephalographic study of flying personnel utilizing nasopharyngeal electrodes to determine neurological disorders 06 p1000 A70-17302
- Flight personnel psychological fitness appraisal techniques, reviewing literature concerning test methods 06 p0995 A70-17668
- Psychological measures in RAF operational aircrew to obtain details for comparison of flying anxiety casualties from same population 07 p1214 A70-19941
- Flying safety and human factors from job dissatisfaction in Japan Air Self Defense Force 08 p1453 A70-21794
- Flight personnel color perception requirements and hereditary and acquired anomalies detection 09 p1627 A70-23115
- Human engineering in weapon systems development, considering flying and ground personnel training plans 12 p2177 A70-27038
- Psychovegetative and neurovegetative stress syndromes in flying personnel removed prematurely from active service as result of psychophysiological complementary diagnostics [DFVLR-SONDDR-31] 12 p2177 A70-27041
- Heart rhythm disorders among flying personnel, noting occurrence frequency of sinus bradycardia and arrhythmia 12 p2180 A70-28362
- Preflight medical examination of flying personnel, describing portable device for recording systolic/diastolic pressure, body temperature and pulse rates 13 p2357 A70-29296
- Vestibular habituation among pilots and flying staff from training and seniority standpoint 14 p2538 A70-30914
- Motion sickness among USAF flying personnel, examining organic and psychiatric factors 15 p2690 A70-31890
- Etiopathogenesis of auditory disorders in flying personnel and aircraft engineers resulting from exposure to acoustic stresses 17 p3034 A70-35677
- Darkness adaptation of flight personnel in polar regions, discussing effects of physical and nervous strain, sickness and alcoholic intoxication 20 p3576 A70-40290
- Cardiological examination of flying personnel, taking ECG anomalies and artery wall elasticity into account 22 p3981 A70-43694

Flying personnel fitness, discussing Wolff-Parkinson-White syndrome 22 p3975 A70-43695

Solid cloth personnel parachutes opening forces, discussing loading conditions, flight path shock parameters, mass ratio variations and elasticity of system [AIAA PAPER 70-1167] 23 p4137 A70-43992

Pitch illusion in flight personnel under centripetal acceleration 24 p4306 A70-45330

Occipital migraine in flying personnel, discussing diagnosis and flight status disposition 24 p4297 A70-45344

FLYING PLATFORM STABILITY **U AERODYNAMIC STABILITY** **U FLYING PLATFORMS** **FLYING PLATFORMS**

AERCAB/Aircrew Escape/Rescue Capability/ flying ejection seat, considering rotary wings, fixed wings and parawings [AIAA PAPER 70-1213] 21 p3751 A70-41806

Aircraft capabilities as scientific observation platform in astronomy and geophysics, including instrument adaptation and IR absorber problems 22 p4019 A70-43146

Plastic balloon platforms for atmospheric research and engineering applications, discussing design and use of unreinforced polyethylene and reinforced Mylar types 22 p3962 A70-43650

FLYING QUALITIES **U FLIGHT CHARACTERISTICS** **FLYING WING AIRCRAFT** **U TAILLESS AIRCRAFT** **FLYWHEELS**

Hydrodynamic journal-thrust bearing system for satellite attitude control flywheel, discussing bearing stability, grease lubricant seal, power consumption, etc [ASLE PREPRINT 69-LC-22] 02 p0309 A70-12532

Optimal stabilization of free solid body equilibrium state with gyroscope, using solution of three flywheel system stabilization 03 p0484 A70-13364

Satellites gravity-gradient stabilization by flywheels in elliptical orbits, designing control system for orientation and optimal motion damping 03 p0582 A70-14321

Flywheel stabilization for communication satellites, considering stabilization by reaction wheels, gyros, gas jets, etc [DGLR-69-058] 07 p1392 A70-18817

DODGE satellite gravity gradient stabilization at synchronous altitude by flywheel and magnetic sample-and-hold damping, noting boom bending 13 p2503 A70-28527

Simultaneous satellite attitude control and flywheel desaturation using external torque 13 p2503 A70-28527

Hydrodynamic journal-thrust bearing system for satellite attitude control flywheel, discussing bearing stability, grease lubricant seal, power consumption, etc 17 p3099 A70-34630

FM/PM [MODULATION]

Ternary data transmission systems characteristics for modulated codes with known parameters or random initial phases 05 p0816 A70-17006

FOAMS

Liquid nitrogen evaporation in PSB foam polystyrene vessels compared with glass vessels for cryogenic application 02 p0305 A70-11875

Crash fire protection at Los Angeles International Airport, discussing protein foam and light water usage 06 p1028 A70-17707

Dynamic compressive properties of polypropylene, polystyrene bead and extruded polystyrene foams tested at given strain rate under room temperature 08 p1527 A70-21329

Synthetic foam material of hollow carbon microsphere fillers embedded in high compression strength epoxy resin matrix 13 p2437 A70-28780

Rigid one component epoxy foam system mechanical, electrical and thermal properties for foamed-in-place electronic potting and encapsulation 13 p2439 A70-29263

Fluid flow damping in flexible liquid filled foams at various frequencies and temperatures 15 p2765 A70-31967

Synthetic foams of high filler content, low density, high compression strength and hydrolytic stability using hollow carbon microspheres in epoxy resin matrix 16 p2936 A70-33365

Foamed in place epoxy resins in aircraft composite structures 16 p2937 A70-33369

One-component rigid epoxy foam system suitable for lightweight electronic potting determining mechanical, electrical and thermal properties 20 p3652 A70-39167

Dynamic elastic moduli of model two phase continuous composites, using polymer and metallic foams 22 p4059 A70-43077

Aircraft passengers and crew fire protection in crashes via insulating air-carrying foam ejected into compartment from fuselage 23 p4140 A70-44465

FOCI

Optical systems for coude focus spectroscopic telescopes, discussing advantages over Newtonian and Cassegrain foci 04 p0685 A70-14522

Reflector focus location for variable profile antenna of radio telescope determined by modified Hartmann method in optics field 09 p1648 A70-23164

Paraboloidal and spherical reflectors focal region fields matching over corrugated waveguide open end propagating hybrid modes 16 p2861 A70-32966

FOCUSING

NT DEFOCUSING

NT SELF FOCUSING

Hyperbolic type gas lens design and focusing characteristics for use in laser light beam waveguide 01 p0106 A70-10033

Focusing factor dependence on range in spherically stratified medium with linearly varying refractive index profile, including earth atmosphere 01 p0142 A70-10490

Maximum power transfer theorem, discussing rotation symmetry with respect to optic axis and confocal optical resonators 02 p0339 A70-12454

Field pattern near paraboloid reflectors focus for low f/D ratios, considering vectorial character of electromagnetic field 02 p0268 A70-12474

Light spark and rapid nonlinear effects in focusing powerful light by longitudinal beam 04 p0718 A70-14405

Pulse position modulation focused TWT for airborne electronic countermeasure broadband jamming, considering output power and thermal design 04 p0653 A70-15656

Wave focusing along static magnetic field from radiating VLF source immersed in cold magnetoplasma 06 p1120 A70-17577

Sonic boom focalization, considering linear propagation for real atmosphere with wind and Jericho experiments 07 p1193 A70-19130

Radiation focusing properties of gravitational bodies associated with curving light trajectories analyzed by geometrical and waveguide optics approximations 07 p1384 A70-19411

Detector for focus assessment of laser on target, scanning image by fiber optics 07 p1302 A70-20089

Perturbed ionospheric regions acting as radio wave focusing lens, discussing frequency, power and pattern selection 07 p1237 A70-20448

Radial self focusing of low density electron beam by interaction with plasma in presence of beam plasma instability 08 p1554 A70-21818

Turbulent medium refractive index fluctuations effect on parameters of focused plane light wave, calculating diffraction patterns center of gravity 09 p1636 A70-23138

Aluminized epoxy integrating hemiellipsoidal reflector, discussing fabrication, focusing properties and selection of detector size 09 p1683 A70-23530

Electro-optical autocollimating focus sensor for optical systems of high angular resolution, analyzing defocus detection and errors 09 p1687 A70-23764

Ocular focus stimulator with provision for optical distance change between object and observer without brightness and visual angle variation 12 p2237 A70-28125

Gas laser radiation focusing with spherical mirrors, calculating field distribution and beam path 13 p2424 A70-28592

Electrostatically focused klystron design, discussing gain, bandwidth, efficiency, noise and reliability 13 p2379 A70-29666

Temporal dependence of photoelectron multiplier output waveform and focusing under photocathode alternating modulation, noting thresholds for optical reception 15 p2696 A70-31505

Charged particles focusing and sorting in bispiral systems, deriving differential equations for relativistic trajectories 15 p2707 A70-31520

Fourth order aberration in gas lens used as focusing element in light beam waveguide systems 15 p2697 A70-31829

Highly directive radio telescope antenna parameters in near zone, using focusing at minimum distance 17 p3055 A70-35679

Time dependence of laser rod focal length, measuring thermal lensing effects 18 p3270 A70-36756

Low elevation angle focusing of oblique radio waves after reflection from E and F layers 19 p3379 A70-37965

Prime focus feeds performance for radiotelescopes, using one- or two-hybrid modes in circumferentially corrugated waveguides 19 p3388 A70-37967

High power neodymium laser with aspherical lenses to focus photon beam for nuclear fusion experiments 19 p3447 A70-38165

Magnetically focused two and four stage cascade picture amplifiers for astronomy and nuclear physics applications 20 p3630 A70-39426

Monograph on optimum focusing of laser light with nonideal lenses having spherical aberration 22 p4052 A70-43739

Microwave holography coherent radar with improved focusing, applying to side-looking, bistatic, passive and pulse compression radars 23 p4161 A70-43874

Molecular jet velocity distribution, investigating adiabatic focalization conditions 24 p4351 A70-45370

Beam laser operational efficiency relation to molecule /atom/ interaction in focusing system, explaining laser power drop at large flow rates 24 p4351 A70-45457

FOG

Visibility improvement in fog at airports, discussing fog-seeding and warm fog modification operations 01 p0135 A70-11320

Temperature limit of efficiency threshold for ground based liquid propane sprayer for supercooled fog dispersal at Orly airport 02 p0324 A70-11872

Italian fog distribution charts compiled by Italian Air Force and Istituto Centrale di Statistica compared and criticized 02 p0328 A70-12397

Bouguer single-scatter theory applicability dependence on angular aperture of receiver and laser beam parameters in water mists 03 p0451 A70-13756

Numerical solution of physical equations describing temperature changes near ground fog-free air and in radiation fog 03 p0521 A70-13910

Airport fog attenuation systems design and operation consisting of power and communication cables linking diffusers to central control and command 05 p0830 A70-17092

He-Ne laser emission attenuation coefficient relation to water content of artificial fogs for 0.63, 1.15 and 3.39 microns 06 p1079 A70-17209

Electrostatic methods considered for using earth electric field in smog dispersion in polluted areas and for airport fog clearing 06 p1058 A70-18217

Laser radiation attenuation coefficient in artificial fog related to water droplet concentration, suggesting single scattering for given optical thickness 07 p1296 A70-18725

Bouguer single-scatter theory applicability dependence on angular aperture of receiver and laser beam parameters in water mists 10 p1842 A70-25005

Fog visibility improvement by optical range gating, increasing image contrast by background radiance reduction 11 p2064 A70-26719

Airport runway to fog radiative heat transfer analysis by Monte Carlo method 12 p2333 A70-28115

Fog droplet size growth time dependence and spectral variations during simulated cloud formation by water vapor condensation in chamber 14 p2601 A70-30128

Sound propagation in atmospheric fog, considering mass, momentum and energy transfer mechanisms between particles and gas 15 p2769 A70-31443

Warm fog clearing effectiveness by seeding with hygroscopic nuclei as function of fog droplet and seeding nuclei distribution 17 p3132 A70-35928

Fog dissipation on aircraft runways, using aircraft jet engine exhaust heat and mixing properties 17 p3133 A70-35929

Solar and IR radiation distribution in multiple scattering and absorbing ground fog, obtaining intensities, fluxes and vertical divergence 18 p3284 A70-35943

Thick plane fog layers reflection and transmission properties, using emerging light angular distribution for Milne problem 18 p3284 A70-35944

Atmospheric aerosols, fog and rain effects on signal transmittance and backscatter at 3400-10600 A 18 p3248 A70-36751

Hygroscopic materials warm fog clearing capabilities comparison, recommending urea and ammonium nitrate 20 p3664 A70-40065

Airport fog layers repetition frequency after low visibility periods 22 p4065 A70-43246

High power pulsed laser fog dispersal, calculating vaporization regimes of droplet interaction with laser radiation 23 p4201 A70-44592

FOIL BEARINGS

High speed rotor supported by air lubricated foil bearings subjected to periodic unidirectional excitation by vibrator, noting stability at high speeds [ASME PAPER 69-LUB-E] 01 p0099 A70-10376

Air lubricated foil bearing support design with external pressurization for high speed rotor in high temperature turbomachinery [ASME PAPER 69-LUB-D] 01 p0100 A70-10377

Gas lubricated three-foil bearing for high speed rotor support, considering dynamic and static behavior in zero gravity environment [ASME PAPER 70-LUBS-18] 22 p4044 A70-42443

Gas lubricated foil bearing performance as support for turborotor simulator, examining heating and thermal gradient effects [ASME PAPER 70-LUBS-12] 22 p4044 A70-42448

Dynamic characteristics of turborotor simulator supported on gas lubricated foil bearings, considering rotor response to imbalance [ASME PAPER 70-LUBS-11] 22 p4044 A70-42449

FOILS [MATERIALS]

NT METAL FOILS

Foil type resistance strain gages /tensometers/, studying measurement current effects on readings 11 p2053 A70-26428

Uranium ion impact ejection and electronic excitation of thin foil particles, observing optical spectra of Be, carbon and Al atoms and ions 20 p3674 A70-39135

Shock wave and surface velocity measurements in exploding foil testing by streak photography with image converter camera 21 p3824 A70-40863

Resistance strain foil gage response to dynamic plastic strain 22 p4039 A70-43451

FOKKER AIRCRAFT

NT F-28 TRANSPORT AIRCRAFT

FOKKER BOND TESTERS

U ADHESION TESTS

FOKKER F 28 AIRCRAFT

U F-28 TRANSPORT AIRCRAFT

FOKKER-PLANCK EQUATION

Tracking systems synthesis and performance analysis based on continuous Markov processes theory, particularly Fokker-Planck equation 01 p0043 A70-10776

Fokker-Planck Coulomb collisions effect on plasma wave echoes 09 p1736 A70-23181

Differential Pulse Code Modulation (DPCM)/ system with quantizer separating slope overload and granular noise, using Fokker-Planck-Kolmogorov equation 10 p1844 A70-25204

Fokker-Planck equation solution for electron scattering and energy loss in mirror confined hot electron plasma 11 p2090 A70-26022

Brownian motion for large viscosity, deriving modified Fokker-Planck equation based on quasi-Huygens relation 11 p2084 A70-26398

Statistical analysis of control system with nonlinear zero-memory element evaluated for error using Fokker-Planck equation 12 p2204 A70-27985

Aerosol particle convective diffusion from gas medium into obstacle, solving Fokker-Planck equation for particle distribution 15 p2774 A70-31493

Stochastic systems technical stability problem solution by Fokker-Planck equation 16 p2944 A70-34294

Magnetic mirror confined plasmas, solving Fokker-Planck equation 18 p3296 A70-36795

Thermoviscoelasticity stochastic problems for bar with temperature independent viscosity, discussing Fokker-Planck equation for two temperature processes 21 p3937 A70-41435

Transient behavior of first order phase locked loop in presence of noise, solving Fokker-Planck equation for loop dynamics by numerical integration 21 p3802 A70-42181

Finite difference method for initial value problems of Fokker-Planck equations 22 p4080 A70-42743

- Reefing systems for Parawings, Sailwings, Para-Flyers, Paraplanes and Volplanes, discussing performance tests
[AIAA PAPER 70-1192] 21 p3753 A70-41824
- FOLIC ACID**
Hematologic changes in rats under hypergravity, effects of vitamin B12, folic acid and return to 1 g
06 p0991 A70-17283
- FOOD**
Prolonged dehydrated food diet effect on metabolism of humans, noting complete adaptation after three or four months
04 p0630 A70-14577
Image memory in Papio hamadryas monkeys reacting to visual and flavor food stimuli
04 p0632 A70-15219
Airline passenger food service, discussing public health measures, low temperature and cryogenic galley cooling
[SAE PAPER 690674] 05 p0804 A70-15833
Aircraft crews in-flight medically controlled feeding, discussing physiological and nutritive value of foods
06 p1001 A70-17669
Research diets cost analysis including labor, ingredients, preparation and storage
07 p1217 A70-18949
- FOOD INTAKE**
Protein metabolism of mice exposed to compression of air-oxygen mixture containing 27 percent oxygen, showing relationship to food intake
01 p0028 A70-11363
Diet and feeding method effects on food intake and plasma amino acid concentrations of rats fed low protein diet with amino acid imbalance
02 p0231 A70-11707
Starvation effect on intestinal amino acid absorption of rats, noting protein synthesis reduction
02 p0234 A70-11731
Atrophic changes in tortoises during roundtrip to moon on Zond 5 ascribed to hunger and space flight factors
07 p1207 A70-19496
Fasting and postprandial serum amino acid patterns of human males fed protein-free or protein-sufficient diets
09 p1621 A70-23399
Rehydratable food consumption in zero-gravity environments with spoons and forks, observing interfacial tensions between water and food, containers and utensils
09 p1628 A70-23464
Antidiuresis associated with oral cavity stimulation during food ingestion by rats
13 p2355 A70-29813
Atrophic changes in tortoises during roundtrip to moon on Zond 5 ascribed to hunger and space flight factors
15 p2685 A70-32741
Renal lithiasis frequency among flight crews during aeronautical activity, noting role of rich food intake
17 p3040 A70-35917
Food-water deprivation influence on alveolar surface activity of rat lungs
24 p4303 A70-46115
- FORBIDDEN BANDS**
Dipole magnetosphere model with cylindrical or spherical forbidden band for studying plasma motion in quasi-hydrodynamic approximation
01 p0082 A70-11521
Forbidden Fe II lines and AlO band intensities in long period variable stars confirming stratified models of emitting layers
05 p0907 A70-16031
Forbidden bandwidth in Brillouin zone and valence band spin-orbital splitting degree determined for mixed gallium-phosphide-arsenide
06 p1126 A70-17815
Ca II 7323 forbidden line in solar Fraunhofer spectrum, estimating center-limb variation of equivalent width of transition
06 p1143 A70-17994
Transparent semiconductor crystals breakdown under intense ruby laser radiation, noting threshold power correlation with forbidden region and pulse duration
07 p1357 A70-19856
Predawn enhancement of emission rate of 6300 Å forbidden O I line in nightglow spectrum, discussing onset time
07 p1275 A70-20286
Celestial emission bodies forbidden line analysis for physical conditions determination using formulas and graphs
08 p1569 A70-20831
Metastable level populated by dissociative recombination mechanism, estimating efficiencies of various processes
09 p1745 A70-23438
Resonance, intercombination and forbidden lines observed in solar He isoelectronic sequence of oxygen, Ne, Al, Si and sulfur with Bragg crystal spectrometer
10 p1944 A70-24954

- Doped semiconductors electronic state density in forbidden band, assuming fluctuations in impurities in form of homogeneous spheres with varying charges and radii
12 p2286 A70-27363
- Forbidden Ne iv lines intensity in high excitation gaseous nebulae based on upper level-j populations
12 p2277 A70-28215
- Predawn forbidden OI 6300 Å airglow seasonal variations by isophoto maps, discussing photoelectrons precipitation
13 p2395 A70-28944
Postdusk and predawn seasonal variations of forbidden OI 6300 Å airglow, discussing photoelectron precipitation
13 p2395 A70-28945
Forbidden lines of OI, NI, Cl, Fe II, Ni II, Si I, Si and Ca II in solar absorption, investigating effects on element abundance and gaps in thermodynamic equilibrium
14 p2637 A70-30339
Interstellar hot low density intercloud medium in H I region, estimating diffuse emission in forbidden lines O I at 6300 Å and N I at 5200 Å
18 p3310 A70-37020
Plasma satellites near He I forbidden lines during turbulent heating
19 p3475 A70-37441
Solar photospheric spectrum Ni II forbidden lines analysis, determining abundance of Ni for comparison with coronal and meteoritic data
20 p3711 A70-40405
Solar coronal and photospheric iron abundances from absorption forbidden lines, discussing discrepancy with permitted lines
21 p3925 A70-42195
Orion nebula H alpha/forbidden N II ratio measurement using wide field multislit spectrograph
22 p4101 A70-42857
Forbidden iron emission lines excitation in Seyfert galaxies, discussing various mechanisms
22 p4102 A70-42977
Orion Nebula and 32 other planetary nebulae spectra in yellow-green obtained with electronic camera, discussing forbidden N I and II lines
22 p4103 A70-42983
- FORBIDDEN TRANSITIONS**
Reply to Swings comments on validity of forbidden S I lines in solar spectrum communicated by Swenson
01 p0175 A70-10240
Satellite lines of forbidden transition in laser-produced He plasma attributed to longitudinal plasma oscillations
02 p0379 A70-12717
Nickel IV forbidden lines suggested from spectrum study of slow nova RR Telescopii
05 p0905 A70-15758
Variational and Z-expansion calculations for magnetic quadrupole transitions decay rates of He sequence
05 p0920 A70-16942
Allowed and forbidden transitions probability in isoelectron sequences of solar corona, using scale factor method and variational wave functions
09 p1751 A70-22155
Perturbation rotational levels in triplet states of CO emission spectra attributed to resonance fluorescence process involving optically forbidden transitions
09 p1731 A70-22282
Electron and proton excitation of forbidden transition lines in Ca XV ground configuration determined for coronal densities and temperature
11 p2109 A70-25742
Gaseous nebulae electron densities based on interpretation of forbidden Cl III lines using collisional strengths and transition probabilities
15 p2798 A70-31746
Helium-like resonance, intercombination and forbidden transitions of Ca, Si and S lines during 3b solar flare decay
20 p3700 A70-40420
Solar iron abundance from forbidden Fe II magnetic dipole transition probabilities
21 p3888 A70-41118
Electron impact induced transitions in ions with configurations 3p/q responsible for forbidden lines in gaseous nebulae
22 p4105 A70-43234
Negative hydrogen ion forbidden bound-free continuum absorption cross section recalculation, deriving 10 to 8th power smaller than previous value
24 p4404 A70-45410
- FORBUSH DECREASES**
Cosmic ray increases during Forbush decrease onset stage in terms of transient spatial anisotropy
03 p0559 A70-13914
Forbush decrease recorded on 26-27 January 1968 showing large anisotropies in cosmic ray flux after SC magnetic storm
03 p0560 A70-13979
Cosmic ray energy spectrum variations possible effect on ray intensity amplitude intensity increases preceding Forbush decreases
04 p0743 A70-15719

- Lower ionospheric cosmic layer state during Forbush decreases from radio absorption observations interpreted on basis of electron production rate analysis
04 p0743 A70-15720
Forbush effect on intensity of neutron component of cosmic rays during quiet sun period
05 p0897 A70-15795
Cosmic ray intensity decreases in relation to geomagnetic and F 2 region disturbances characterized by Forbush decreases from vertical sounding data
05 p0898 A70-15940
Cosmic ray intensity preceding Forbush effects as function of chromospheric flares solar longitude and solar wind velocity
05 p0903 A70-16730
Cosmic ray intensity increase preceding Forbush effect using statistical correlation method
07 p1367 A70-19444
Forbush decreases of cosmic rays calculated assuming semitransparent magnetic piston action with free particle exchange
07 p1372 A70-20340
Forbush effects influence on cosmic layer state in lower ionosphere using long radio waves
12 p2295 A70-28220
Cosmic ray energy spectrum variations possible effect on amplitude of intensity increases preceding Forbush decreases
14 p2632 A70-30803
Lower ionospheric cosmic layer state during Forbush decreases from radio absorption observations interpreted on basis of electron production rate analysis
14 p2632 A70-30804
Cosmic ray variations during PCA absorption, relating Forbush decreases to lower ionosphere ionization intensity increase
18 p3306 A70-36096
Cosmic ray intensity increase preceding Forbush effect using statistical correlation method
18 p3309 A70-36918
Long term variations of cosmic ray electron spectrum above 500 MeV from balloon and satellite observations, noting reduction during Forbush decreases
19 p3503 A70-38105
Cosmic ray intensity decreases and Forbush effects energy spectra during various solar activity periods
20 p3696 A70-39281
Forbush effects influence on cosmic layer state in lower ionosphere using long radio waves
20 p3700 A70-40095
- FORBUSH EFFECT**
U FORBUSH DECREASES
FORCE
Simulated zero gravity tests of force application by subjects in Apollo suits, varying worksite geometry, personnel restraints and force type and direction
01 p0038 A70-10964
Separable potential with hard core effects, treating short range repulsion in nucleon-nucleon interaction, generating T matrix for existing data
09 p1725 A70-22042
Dynamic force measurement, evaluating hybrid system with reaction force summation and operational compensation subsystems
10 p1889 A70-24580
Delayed moment of force relativistic definition within reference of inertia, discussing lever bent at right angles
13 p2452 A70-29635
Magnetoelastic sensors for small force measurement, describing instrument error reduction
15 p2733 A70-31577
Relativistic static force transformation showing no contraction in static conditions
17 p3136 A70-34823
Elastic crack structure, discussing formalism for force law between faces of brittle and semibrittle fractures
17 p3191 A70-35461
Piezoelectric sensors for multicomponent force and moment measurement
20 p3635 A70-40533
- FORCE DISTRIBUTION**
Three machine parts problem with relative motion and given active forces distribution and time variation, determining entrainment motion
01 p0142 A70-10554
Current stream function, Hall current density, force densities and pressure distribution for typical MPD thruster
03 p0552 A70-14372
Elastic spherical shell excited by point force, analyzing HF response in terms of near field and flexural wave field
[ASME PAPER 69-WA/APM-18]
04 p0771 A70-14912
Mean acoustic force on small spherical and nonspherical inclusions in standing acoustic field, discussing equilibrium orientations of body
04 p0720 A70-15085
Stress distribution in vicinity of stress-free Griffith crack in elastic solid acted upon by symmetric distribution of body forces
05 p0930 A70-16084

Compressive forces eccentricity influence on circular cylindrical shell stability noting relation to bending moments
05 p0936 A70-16239

Transient stress waves generated by spatially uniform distribution of transverse forces in laminated medium, using modal analysis
05 p0938 A70-16409

Simply supported beams large deflection analysis in bending under symmetrical pair of forces, based on integration of elastic line differential equation
05 p0941 A70-16521

Normal force component distribution and aerodynamic pressure position on rocket bodies at supersonic and hypersonic velocities
06 p0964 A70-17238

Electromagnetic torsion balance measurement of forces exerted on clean Au surfaces by monoenergetic steady state Ar and Kr beams, calculating thermal accommodation coefficients
06 p1066 A70-18258

Shallow spherical sandwich shells under concentrated forces, obtaining inhomogeneous equations solution by integral Hankel transforms
07 p1402 A70-19053

Disturbances in infinite aeolotropic inhomogeneous medium due to transient forces and twists on elastic cylindrical source surface
07 p1407 A70-19382

Molecular beam and pure surface interactions on background of external forces field
08 p1547 A70-21080

Linearization of elastic forces in vibration system with percussion
10 p1958 A70-24516

Supersonic jet force acting on target investigated for air and argon using dimensional analysis
10 p1804 A70-25122

Eccentric cylinders with outer cylinder rotating measured for eccentricity and clearance ratios effects on pressure distribution and force on inner cylinder
11 p2060 A70-26409

Elastic system stability with two degrees of freedom under action of retarded follower forces
11 p2142 A70-26631

Sound radiation from rigid flow spoilers correlated with fluctuating forces, measuring jet-pipe drag and lift components with transducers
11 p2085 A70-26699

Electromagnetic single-coil suspension for cryogenic gyroscope with superconducting sphere rotor, calculating suspension force characteristics
12 p2234 A70-27565

Elastic beam vibration under constant amplitude and varying frequency periodic forces during passage through resonance
12 p2326 A70-27798

Laser radiation interaction with hot nonuniform plasma, determining thermal and electromagnetic forces for various temperatures and densities
13 p2460 A70-28643

Concentrated force action inside transversely isotropic half space analyzed by mirror image method
13 p2512 A70-28865

Vortex- and Doublet-Lattice methods for calculating aerodynamic lift distributions on surfaces in steady and oscillatory motion at subsonic speeds
13 p2339 A70-29006

Slope deflection method for computing spatial trusses and plane frameworks under dynamic aperiodic forces
13 p2516 A70-29532

Unsteady nonlinear aerodynamic loads measurements in wind tunnel, using linearized mathematical analog
13 p2343 A70-29896

Radial clearance, pressure and piston length and diameter dependence of friction force at rest in piston type hydraulic devices
14 p2534 A70-30872

Force acting on cylinder in ideal incompressible fluid plane flow with steady vorticity
15 p2719 A70-31498

Closed spherical shell, demonstrating effects of concentrated forces at poles
15 p2818 A70-32170

Deformation formulas for simply connected micropolar isotropic homogeneous centrosymmetric elastic body under external forces and heating
16 p2990 A70-33742

Generalized Lagrange kinetic potentials, discussing force systems with ideal holonomic constraints
16 p2944 A70-34292

Continuum plasma dynamics with electromagnetic forces of same order of magnitude as gas dynamic forces, discussing various flow problems
17 p3141 A70-35040

Parallel edge dislocations in elastically isotropic crystals, discussing climb and glide forces
17 p3126 A70-35454

Lifting and side force distributions acting on body in transonic flow
17 p3012 A70-35696

Sonic boom minimization through airstream alteration by force or heat fields and aircraft body shaping
17 p3019 A70-35817

Shallow conical shell stability under uniformly distributed pressure and concentrated force at apex for rigid and free clamping boundary conditions
18 p3341 A70-36589

Motion stability in periodic cubic force field, using nonlinear differential equation integration with time periodic square wave function and Jacobian table
18 p3284 A70-37065

Granular medium particles contact forces distribution measurement by absolute retardation method using photoelastic techniques
19 p3427 A70-38344

Bearing force and moment produced by motion of inclined plate supported by compressed air in ground effect machines with small angle of attack
20 p3557 A70-39140

Supersonic jet force acting on target investigated for air and argon using dimensional analysis
20 p3560 A70-40515

Mass force fields effects on flow phenomena from heat transfer and hydraulic resistance analyses
21 p3951 A70-41764

Steady vibrations of mechanical system with asymmetrical restoring force, reviewing formulas for mean angular frequency and Fourier expansion coefficients
22 p4113 A70-42544

Solid particles interactions during entrainment by viscous incompressible fluid in pipe, calculating interaction force as function of radius, distance and Reynolds number
23 p4181 A70-44310

Rubber mount vibration and shock isolation problems, discussing dynamic response to reaction forces and force concentration
23 p4269 A70-44330

Rocket engine nozzle with wall-mounted obstacle, examining shock front shape, pressure distribution and side force characteristics
23 p4234 A70-44684

FORCE FIELDS
U FIELD THEORY (PHYSICS)
FORCED CONVECTION

Forced convection of hot wire in hypersonic flow, determining Nusselt-Reynolds number relationship for hot-wire anemometers
02 p0223 A70-12101

Transient heat transfer in forced convection flow over curved wall with zero Prandtl number, applying to laminar boundary layer with variable free stream velocity
02 p0400 A70-12857

Heat transfer under conditions of forced convection from flat plate in laminar flow, considering plate surface temperature arbitrary variation in time
03 p0605 A70-13518

Heat transfer to absorbing fluid by coupled thermal radiation and laminar forced convection at pipe entry region, considering gray and nongray absorption
04 p0783 A70-14818

Buoyancy effects in laminar forced convection on vertical flat plate, obtaining heat transfer coefficient
06 p1172 A70-17141

Ignition and extinction of diffusion flames predicted from studying forced convection in boundary layers
06 p1178 A70-17976

Laminar flow forced convection heat transfer in circular pipe entrance region for constant wall temperature and constant wall heat flux
07 p1420 A70-19215

Radiation effect on heat transfer during film boiling in forced convection boundary layer of liquid flow past plate, noting vaporization temperature
07 p1423 A70-19812

Thermal entrance region effect on Nusselt number determination in asymmetrically heated rectangular duct with uniform heat flux
07 p1425 A70-20223

Forced convection heat transfer between two parallel plates analyzed numerically for effect of constant heat transfer coefficient boundary condition
08 p1598 A70-21425

Laminar boundary layer equations solved for mass and energy transfer in binary gas mixture, investigating forced and free convection
11 p2151 A70-26558

Mixed forced and natural convection with low speed air flow over horizontal electrically heated cylinders
15 p2740 A70-32373

Forced convective heat transfer in annular passage with axially varying cross section, noting role of acceleration parameter
17 p3195 A70-34999

Fluid transpiration arc radiation source based on forced convection effect on electric arc
17 p3023 A70-35153

Heat transfer at flat melting surface under forced convection and laminar boundary layer solved by Kármán-Pohlhausen method
18 p3347 A70-36502

Radiation effect on heat transfer during film boiling in forced convection boundary layer of liquid flow past plate, noting vaporization temperature
20 p3736 A70-39259

Forced convection heat transfer from flat plate and cylinder in cross flow to simulated Mars atmosphere
21 p3945 A70-41026

Free and forced convection of supercritical carbon dioxide normal to heated cylinder at constant temperature, measuring heat transfer rates
21 p3945 A70-41034

Heat transfer by laminar forced convection of viscous fluid in noncircular cylindrical channel with internal heat source and varying wall temperature
23 p4276 A70-44236

Forced convection heat transfer to liquid nitrogen near critical point, determining coefficients from given wall temperature and heat flux
23 p4279 A70-44358

Thermal-acoustic oscillations in forced convection, giving time delay analog for perturbation feedback
23 p4280 A70-44369

Static pressure effects on heat flux critical density for free convection and forced flow in circular pipes
23 p4282 A70-44726

FORCED OSCILLATION
U FORCED VIBRATION
FORCED VIBRATION

Transversely isotropic circular cylinder acted upon by transient shearing force at one end, noting forced torsional oscillation using cylindrical coordinates
01 p0200 A70-10550

Stability analysis of rotors consisting of disks on massless shaft mounted in unsymmetrical flexible bearings, considering free and forced vibrations with damping neglected
03 p0599 A70-14248

Spectrum deductions from profile excited random vibration response, considering single profile imposed displacements
03 p0600 A70-14250

Forced vertical oscillations in viscous stratified fluid, showing phase angle dependence on amplitude and relation to Brunt-Väisälä frequency
04 p0666 A70-14611

Solid viscoelastic cylinder bonded to thin elastic casing, analyzing normal and tangential stresses for stress and displacement frequency responses in forced transverse vibration
04 p0771 A70-14911

Complex uncoupled modes to analyze forced vibrations of three layer damped sandwich beam with arbitrary boundary conditions, discussing orthogonality
04 p0773 A70-15076

Inertial damping of soft rubber under forced torsional vibrations, discussing viscoelastic body linear model
04 p0712 A70-15100

Periodic drag of vibrating cylinders as function of excitation amplitude and frequency, noting similarity to nonlinear oscillator subjected to forced vibration
04 p0691 A70-15148

Bifurcation frequency and nonlinear distortions determined in nonlinear semiconductor circuit with series-opposed connections of p-n junctions operating in forced oscillation mode
04 p0659 A70-15206

Amplitude and phase frequency characteristics relations established by analyzing forced resonant oscillations in nonlinear circuit operating at power source frequency
04 p0662 A70-15207

Forced torsional vibration of elastic stratum produced by rigid circular disk approximated by Fredholm equations
04 p0777 A70-15497

Secondary vortex generation in near wake of circular cylinders under forced oscillation, analyzing motion dependent transition regimes using hydrogen bubbles flow visualization
06 p1032 A70-17212

Prismatic pendularly supported beam load-forced vertical vibrations, critical load amplitude and force pulsation in case of stability loss
06 p1165 A70-17586

Approximate linearization of nonlinear automatic control systems with two frequency forced oscillations
07 p1243 A70-18687

Absolute stability ranges of forced motions and damping in nonlinear systems determined by Sturm theorem
07 p1243 A70-18688

Forced and free vibrations of shaft carrying unsymmetrical rotor, studying effects of distributed shaft mass and nonlinear shaft stiffness
07 p1401 A70-18976

Shallow orthotropic shell of rectangular platform with edges under dynamic load, studying forced vibrations by anisotropic shell theory
07 p1403 A70-19057

Motion of second order autonomous quasi-linear system with disturbances, obtaining criterion for recognition of random forced and self oscillations
07 p1247 A70-20180

Steady oscillations under random forces of nonlinear system described by stochastic partial differential difference equations with distributed parameters and delayed argument
08 p1542 A70-20486

Nonlinear quasi-harmonic systems forced vibrations using one degree of freedom system as example
08 p1543 A70-20700

Forced vibrations amplitude of rotor mounted on elastically damping supports
08 p1588 A70-21181

Cyclic bending stresses in web of precessing disk-type gyroscope rotor, considering fatigue failure and forced vibration response
09 p1770 A70-22270

Free and forced vibrations of three layer freely suspended plate with allowance for energy dissipation
09 p1772 A70-22468

Forced vibrations of trusses calculated by dynamic rigidities method allowing for friction forces
09 p1773 A70-22540

Longitudinal vibration of finite viscoelastic rod with changing boundaries under time-variant force, analyzing impulse response by transform calculus
09 p1777 A70-22833

Rotating cantilever beams mounted on disk periphery, analyzing forced and free vibrations characteristics
09 p1781 A70-23283

Forced inertial oscillations in rotating processing fluid-filled cylindrical cylinder
09 p1664 A70-23682

Nonlinear many degrees of freedom systems steady state forced vibrations analysis, expressing response in nonlinear normal coordinates
10 p1954 A70-24010

Numerical analysis of forced parametrically excited plate vibration in plane supersonic flow, using digital computer
10 p1958 A70-24527

Forced vibrations of cylindrically curved multispan shell structures, using transfer matrix methods
10 p1962 A70-25062

Forced vibration of rib-skin structures under random pressure and heavy damping using wave group theory
10 p1963 A70-25066

Forced oscillations of oscillator matched to transistor as active element, obtaining stability conditions by Liapunov first method
11 p2018 A70-25945

Self-synchronization of forced frictional mechanical vibrators assuming simple harmonic combination
11 p2139 A70-26417

Force controlled vibration for shock tests, discussing feasibility and merits for simulation testing
12 p2205 A70-27099

Elastic moduli and damping coefficients for glass- and boron-epoxy beams determined from resonant frequencies and bandwidths during lateral forced vibrations
12 p2253 A70-27120

Pressurized orthotropic cylindrical membrane shells free and forced vibration, considering dynamic response dependence on internal pressure
12 p2326 A70-27815

Clamped beams steady state free and forced response and stability for large amplitude motion, discussing multimode analytical and numerical technique
12 p2327 A70-27821

Force input and thoraco-abdominal strain due to sinusoidal motion of electrohydraulic shake table over 2-14 Hz range imposed on human body
13 p2359 A70-29438

Book on vibrations covering natural oscillations, damped and undamped oscillations, energy sources, forced vibrations, resonance and multiple degree of freedom systems
13 p2515 A70-29452

Slope deflection method for computing spatial trusses and plane frameworks under dynamic aperiodic forces
13 p2516 A70-29532

He-Ne laser memory, discussing induced oscillation excitation with radiation fed back to resonator by moving reflecting mirror
13 p2429 A70-29572

Free and forced motion characteristics in absolutely stable nonstationary nonlinear system analysis by variational approach
13 p2453 A70-29716

Forced vibration in taxiing aircraft interaction with ground structure
14 p2563 A70-30699

Vibrational motion equations of interconnected bodies based on Newtonian approach, investigating gyroscopic vibration absorber
16 p2992 A70-34020

Free and forced vibrations of linear systems, dissipative systems with nonlinear friction, aeroelastic vibrations, rotor vibrations, mode locking, random vibrations, etc
16 p3004 A70-34277

Nonlinear systems excitation by two harmonic forces, analyzing vibration by linearization of differential equation of motion
16 p2995 A70-34286

Disk forced vibration mounted on rotating shaft with ball bearings, assuming nonlinear elastic characteristic of system
16 p2996 A70-34293

Elastic plate vibration with damping under random load, calculating linear response by harmonic analysis
18 p3334 A70-35958

Forced vibration in Cartesian half space filled with elastic medium, investigating uniqueness conditions
18 p3337 A70-36289

Pilot induced oscillation rating regression analysis, examining time delay, slope after and time to first peak and stick force per g
18 p3213 A70-36444

Laser emission intensity oscillations during resonator Q sinusoidal variations
18 p3267 A70-36617

Vibrations induced by frictional moving force in viscoelastic beam with free ends on elastic base, showing critical load dependence on damping
18 p3343 A70-36720

One dimensional magnetostrictive bar electromagnetically forced vibration, using Lagrange equations and normal mode analysis
19 p3472 A70-37959

Forced torsional vibrations of thin elastic spherical and hemispherical shells with free or restrained edge, using Gegenbauer transform
19 p3541 A70-38037

Forced vibrations of rotor with variable rotating speed, investigating inertia terms effect
19 p3542 A70-38221

Rectangular plates free and forced vibrations, including rotatory inertia and shear deformation effects in dynamic response analysis
19 p3544 A70-38327

Undamped forced two degree of freedom system with one linear and one nonlinear spring, analyzing subharmonic vibrations by Ritz averaging method
19 p3544 A70-38329

Harmonic forced transverse vibrations effects on rectangular plates with cross braces, deriving motion stability equations
20 p3725 A70-39867

Elastic body steady forced oscillations under monoharmonic excitation, investigating hereditary nonlinearity effects on systems dynamic characteristics
20 p3733 A70-40395

Ideal fluid-cylindrical tank elastic bottom coupled forced oscillations, determining hydrodynamic pressure for tank reverse translational motion
20 p3615 A70-40444

Helicopter dynamic tests for aeroelastic and mechanical instabilities and forced vibration problems
21 p3749 A70-40583

Kinetic friction and friction induced vibration measurements by pin-on-disk tribometer
22 p4044 A70-42446

Forced harmonic vibrations of clamped circular plate in inviscid fluid, calculating radiation pressure and power distributions
22 p4073 A70-42646

Cantilevered tube conveying fluid, calculating forced vibration under time dependent loading and arbitrary initial conditions
22 p4010 A70-42650

Free and forced oscillations of dynamic system with linear hysteretic damping, using nonlinear model
22 p4114 A70-42700

Forced longitudinal oscillations of cylinder with given surface displacements, using Lamé equations
22 p4118 A70-43571

FORCED VIBRATORY MOTION EQUATIONS

U EQUATIONS

U FORCED VIBRATION

FOREARM

Posture change effects on vasodilator responses in humans, studying reactive, postexercise and local heat hyperaemia in forearms of subjects lying and standing
07 p1211 A70-19596

Human forearm motion control mechanism, examining mechanogram, instantaneous velocity, acceleration and biopotentials of biceps and triceps brachii
12 p2173 A70-28314

Muscular group response to sinusoidal and trapezoidal force applied to forearm, discussing frequency dependent limb oscillations and neuromuscular effects
21 p3767 A70-42161

FOREBODIES

NT ABLATIVE NOSE CONES

NT NOSE CONES

NT NOSES [FOREBODIES]

NT ROCKET NOSE CONES

FORECASTING

NT LONG RANGE WEATHER FORECASTING

NT NUMERICAL WEATHER FORECASTING

NT PERFORMANCE PREDICTION

NT PREDICTION ANALYSIS TECHNIQUES

NT STATISTICAL WEATHER FORECASTING

NT WEATHER FORECASTING

Book on technological forecasting covering philosophical basis, Federal Government activity, R

and D management resource allocation, correlation and regression analysis, etc
01 p0221 A70-11307

Long range solar flare forecasting noting correlation between planetary conjunctions and proton events
[AAS PAPER 69-624] 04 p0740 A70-14658

Space forecasting system to predict solar radiation bursts and effects on earth
06 p1136 A70-18023

Technological forecasting for management planning, discussing structuring, prediction techniques, personnel selection, quantification, etc
09 p1794 A70-23413

Long range army budget forecasting model based on research projects cost distributions and parameters, describing computer program
09 p1794 A70-23415

Technological forecasting for R and D planning including project selection and resource allocation decision making
09 p1794 A70-23416

Forecasting necessity and limitations in management decision making process
15 p2829 A70-31574

Technological forecasting as management concept in decision making process
17 p3199 A70-34679

Solar particle events forecasting based on classification scheme, discussing proton active regions
19 p3493 A70-37476

Transport aircraft noise at three major airports by noise exposure forecast /NEF/ contours methodology
21 p3750 A70-40896

FORECASTS

U FORECASTING

FOREIGN POLICY

NT INTERNATIONAL COOPERATION

NT INTERNATIONAL RELATIONS

FOREST FIRE DETECTION

Airborne IR line scanning systems for forest fire surveillance, determining size and characteristics during smoke or darkness
09 p1686 A70-23753

Satellite use for forest fire detection in Italy, discussing forest distribution and measuring instruments
18 p3248 A70-36669

FORESTS

Remote sensing application to agriculture, forestry and range resources in terms of human priority over monetary benefits, noting high altitude aircraft use
[AAS PAPER 69-583] 04 p0788 A70-14638

Airborne remote sensing automatic data processing for forest identification through pattern discrimination, utilizing power spectrum analysis
10 p1878 A70-24734

Aerial photography applications to timber management programs of forest industries
10 p1879 A70-24746

Seasonal variations in radio signal propagation from aircraft navigation system antenna located in dense forest, solving problem with Doppler-VOR installation
10 p1854 A70-25254

Mixed hardwoods and pine area forest cover types identification by aerial photography
14 p2577 A70-30981

Day/night thermal IR imagery detection of moisture stress of girdled trees in upland forest
16 p2898 A70-34047

Large scale aerial color photography over spruce fir stands during 10 year period for assessing damage caused by budworm epidemic
17 p3078 A70-35614

Data acquisition by earth resources technology satellite /ERTS/ for user needs in forestry and agriculture
20 p3616 A70-39062

FORGING

Grain size, forging parameter and microstructure effect on stress-rupture properties of wrought Ni-base alloy
03 p0511 A70-13567

Alloy EI 602 ingots low ductility during forging ascribed to nonferrous metal atoms, decreasing iron diffusion and forming brittle nitride and carbide compounds
05 p0863 A70-16545

Powder metallurgy all-inert processing method for producing nickel base superalloys forgings, discussing microstructure, reproducibility, mechanical properties, etc
09 p1701 A70-22553

Saturn booster Ti alloy pressure vessel forging, heat treatment and welding, discussing machining, cleaning and tooling
[SME PAPER AD-70-733] 12 p2241 A70-27085

Diffusion and electron beam welding combined with forging for cost reduction and production enhancement of titanium structural components
[SME PAPER AD-70-735] 12 p2241 A70-27087

Ti alloy forgings for aircraft industry, utilizing high strength/weight ratio
17 p3097 A70-34357

Ti alloys beta forging effect on physical properties and tensile ductility

17 p3097 A70-34358

Ti alloy aircraft parts heavy press forging, considering mechanical properties, temperature effects, cost factors, etc

17 p3097 A70-34360

Forged alpha/beta Ti alloys, investigating relationship between mechanical properties and microstructures produced by heating

17 p3120 A70-34427

Fatigue characteristics of Ti alloy forgings for rotary wing vehicles, discussing effects of welding, annealing, reduction, surface finish and shot peening

17 p3122 A70-34441

FORM

U SHAPES

FORM FACTORS

Potential gradient radiosonde field distortion formula, deriving form factors

09 p1671 A70-23602

German monograph on form factors and torsion at shafts with longitudinal keyways under pure torsion

17 p3189 A70-35374

FORM PERCEPTION

U SPACE PERCEPTION

FORMALDEHYDE

Aluminum additives effects on stoichiometric ammonium perchlorate/polyformaldehyde mixtures deflagration, determining temperature distribution, burning rate dependence on pressure and heat flow due to radiation

02 p0351 A70-12004

Interstellar formaldehyde absorption from radio observations with parametric amplifier

04 p0747 A70-14515

Microwave absorption by rotational transition of interstellar formaldehyde in direction of Sgr B2, Sgr A and W51

08 p1570 A70-20896

Physicochemical methods of producing formaldehyde for carbohydrate synthesis in life support systems

09 p1623 A70-22080

Formaldehyde absorption profile in direction of Milky Way center observed using lunar occultation

10 p1936 A70-23905

Temperature, solvent, catalyst and formaldehyde concentration effects on monosaccharide synthesis from formaldehyde condensation

13 p2362 A70-29327

Rotational transition of interstellar formaldehyde in absorption in direction of galactic and extragalactic objects

14 p2641 A70-30878

Absorption spectrum of terrestrial atmosphere with sun as source, obtaining formaldehyde line with rotating grid spectrometer

14 p2579 A70-31256

Physicochemical methods of producing formaldehyde for carbohydrate synthesis in life support systems

15 p2693 A70-32676

Formose sugars production from formaldehyde, discussing economic conversion by catalytic reactions

16 p2855 A70-33063

Cosmic microwaves anomalous absorption by interstellar IR-pumped formaldehyde in dust clouds shocked heated layer

17 p3154 A70-34535

Al particles fusion during combustion of stoichiometric mixtures of ammonium and potassium perchlorate and polyformaldehyde

18 p3299 A70-36246

Formaldehyde rotational transition hyperfine components measured by molecular beam maser

20 p3702 A70-39008

Thioformaldehyde isotopic species reversible transition in interstellar clouds

20 p3703 A70-39164

Formaldehyde absorption coefficients measured photoelectrically in vacuum UV range

20 p3703 A70-39165

Radio search for formaldehyde rotational transition and H 109 alpha recombination line in comet Bennett during perihelion passage

21 p3921 A70-41976

FORMALISM

Dubovitskii and Milyutin formalism applied to optimization problems involving equality and operator constraints via mathematical programming in normed linear space

22 p4061 A70-42462

FORMAT

Delta preprocessing operating system /DEPOS/ for high speed telemetry format-independent deconvolution and data compression

11 p2010 A70-26307

Computer simulation model documentation exemplified by cardiovascular simulation using Continuous Systems Modeling Program /CSMP/ and emphasizing format uniformity

15 p2689 A70-31774

Flight test and airborne data recovery and processing, discussing data format, recorder characteristics, ground equipment and time requirement

19 p3429 A70-38517

FORMATION HEAT

U HEAT OF FORMATION

FORMATIONS

Formation flight stability in dynamic environment, using stationkeeping geometry simulation

[AIAA PAPER 70-1357] 24 p4373 A70-45931

FORMING TECHNIQUES

NT CASTING

NT COLD ROLLING

NT COLD WORKING

NT ELECTROHYDRAULIC FORMING

NT EXPLOSIVE FORMING

NT EXTRUDING

NT FORGING

NT HOT WORKING

NT HYDROSPINNING

NT INVESTMENT CASTING

NT MAGNETIC FORMING

NT METAL DRAWING

NT PRESSING [FORMING]

NT PROPELLANT CASTING

NT ROLL FORMING

NT STAMPING

Forming techniques to overcome pressing behavior of maraging steels, noting tendency to thin during stretching and reluctance to stretch

03 p0497 A70-13620

Ni dispersion-strengthened composites from ultrafine comminuted powders, describing forming techniques and test results

04 p0709 A70-15629

Terminal mechanical characteristics of metals after ambient-temperature high energy rate forming compared with low rate processes

08 p1520 A70-21554

Cost effectiveness in Ti forming, discussing materials, tooling and fabrication cost ratios

10 p1970 A70-23852

Creep forming application in producing aircraft parts from metal sheets, plates and extrusions, discussing blank forming and drawing

10 p1893 A70-23854

Metal matrix composites forming processes, describing liquid-metal infiltration, vapor deposition, electroforming, mechanical compaction and unidirectional solidification

11 p2060 A70-26343

Nickel base alloy as die material for creep forming titanium

11 p2060 A70-26424

Deep shells formation by high pressure methods, discussing fluid, mechanical edge pressure and friction aided extrusion techniques

[SME PAPER MF-69-147] 12 p2240 A70-27080

Engineering development role in metal forming industry expansion, discussing metals ductility or plasticity increase for extending processes

12 p2244 A70-28146

Stresses in cylindrical pressure vessels with heads formed by internal fluid pressure

13 p2509 A70-28532

Thermal stresses and curing in electronic modules transfer molding, discussing various design test models

13 p2420 A70-29252

Transfer molding process in fabrication of electronic modules components, emphasizing criticality and unfavorable characteristics

13 p2420 A70-29253

Internal stresses in transfer molding of electronic modules by photoelastic technique, discussing component failure

13 p2420 A70-29254

Transfer molding of electronic modules, discussing materials for evaluating selection and processing guidelines

13 p2421 A70-29255

Al-B composites forming and machining, discussing tooling, methods and filament orientation

[ASM PAPER W70-5.2] 15 p2744 A70-32334

Metallic superplasticity and superplastic alloys in simple tension, forming tubes and sheets of superplastic Sn-Pb eutectic alloy by pressure forming techniques

16 p2916 A70-32916

Pressure forming Ti sheet alloy blanks in superplastic condition under controlled temperature and strain rate

17 p3117 A70-34402

Forming Ti-Al-V sheet metal in heat treated conditions, showing mechanical properties improvement over mill annealed parts

17 p3098 A70-34445

High magnetic fields applications, emphasizing metal forming and superconducting rings levitation

19 p3471 A70-37948

Long structural shape production for titanium and super alloys, discussing rolling, extrusion, drawing, frictionless forming and filler techniques

19 p3437 A70-38420

Dynamic deformation in thin walled axisymmetric plastic shells and filaments under time variable loads applied to high energy rate forming techniques

23 p4200 A70-44235

Metal matrix composite structures tooling and fabrication processes, considering forming, joining, welding, machining joining, etc

[SAE PAPER 700752] 24 p4348 A70-45873

FORMULAS [MATHEMATICS]

Prime formulas for studying perfect relativistic fluids with spin

09 p1728 A70-22840

FORSTERITE

Adiabatic elastic stiffness constants of single crystal forsterite measured as function of hydrostatic pressure and temperature, using pulse superposition technique

04 p0678 A70-15055

Electron paramagnetic resonance of Mn ions in single crystal and powder forsterite, testing heat treatment and proton irradiation effect on ordering

16 p2960 A70-33008

FORTRAN

Computer aided network design course using FORTRAN 4 emphasizing modeling of semiconductor devices

06 p1015 A70-18419

NASAP program FORTRAN subroutine LOOPS for loop detection in circuit analysis, discussing automatic instrumentation process for computation time reduction

06 p1015 A70-18421

Computerized FORTRAN equations simulation of linear and nonlinear circuits for symbolic analysis and transient response

06 p1026 A70-18424

Three dimensional ray tracing computer program in Fortran for determining radio paths in ionosphere

07 p1230 A70-19163

Cardiovascular control system mathematical model incorporating fundamental properties of heart muscle for digital simulation using FORTRAN program

08 p1453 A70-21513

Computer programs for calculating spectral lines oscillator strength in Coulomb approximation, proposing Fortran program

12 p2192 A70-27595

Fixed wing aircraft and associated subsystems simulation by digital computer, having full FORTRAN capability

[AIAA PAPER 70-572] 13 p2385 A70-29897

NTWO Fortran IV family of subsystems for thermodynamic and transport properties of nitrogen

17 p3195 A70-34746

Interactive man computer systems evaluation considering speech communication, SKETCHPAD and graphics capabilities, FORTRAN and programming languages and future manned space missions

24 p4317 A70-45928

FORWARD SCATTERING

Forward scattering by nonergodic system of identical particles, relating temporal correlation function of scattered radiation and intensity moments

02 p0255 A70-11919

Parachute-borne densitometer using forward scattering of low energy beta particles for direct measurement of atmospheric density at 30-60 km

[AAS PAPER 69-570] 04 p0687 A70-14654

Forward angle microwave scattering by plasma covered magnetized metallic sphere, calculating radial electron density distribution

06 p1008 A70-17576

Atmospheric fine-scale structure determination from forward scatter radio wave propagation, considering refractive index role

09 p1715 A70-22362

Astronomical, geometrical and physical selectivity factors of forward scattering radar observation concerning meteor weight

14 p2635 A70-30310

Three-reception-point radar system for radiant and speed measurement of individual meteors in stream, using forward scattering

14 p2582 A70-30311

Forward scattered radar reflections from various depths of rain volume, employing ultrasonic simulation

15 p2704 A70-32599

Water droplet size measurement by forward light scatter holography, evaluating reconstructed wave front by Fresnel transform

20 p3628 A70-39132

Fuel nozzle sprays mean droplet diameter based on computerized analysis of small angle forward scattered light profile

21 p3806 A70-40805

FOSSIL METEORITE CRATERS

U FOSSILS

U METEORITE CRATERS

FOSSILS

Porphyry in Fig Tree shale and Onverwacht chert from Swaziland System sediments, noting age of three billion years and importance in abiogenesis research

01 p0070 A70-10327

- Meteorites fossil tracks due to cosmic radiation heavy nuclei
02 p0361 A70-11748
- Hydrocarbons and fatty acids distribution in living organisms, fossils, sediments and crude oils, discussing slow thermal maturation role and geological applications
02 p0252 A70-12520
- Phenolic aldehydes generated from lignin in fossil woods and carbonaceous sediments by oxidative degradation
13 p2361 A70-28911
- Biology of fossil genus *Kakabekia* and living species *Kakabekia barghoorniana* Siegel cultured from Alaskan soil samples
24 p4304 A70-46232

FOUNDATIONS

- Impulsive and transient load disturbances in thin elastic finite circular plate on Pasternak type viscoelastic foundation
03 p0595 A70-13905
- Static buckling load for beam with pinned ends and Wiegardt-type elastic foundation, considering shear stresses effect
05 p0955 A70-17105
- Dynamic response of free-free beams on viscoelastic Winkler foundation using complex foundation modulus based on antivibration isolator
06 p1165 A70-17627
- Asymptotic buckling analyses of imperfect columns on nonlinear elastic foundations by perturbation expansions, equivalent linearization and truncated hierarchy approximations
21 p3934 A70-40777

FOUNDRIES

- Foundry facilities for high strength nodular, pearlitic malleable and Cr-Mo gray iron and Al castings
13 p2420 A70-29250

FOUR BODY PROBLEM

- Solar attraction effects on zero-mass body planar motion near triangular earth-moon libration points, obtaining variational equations of motion
09 p1754 A70-22477
- Periodic solutions of restricted three body libration point perturbation due to fourth body gravitational and radiative influence using Huang model
09 p1761 A70-23053
- Perturbation of body motion in vicinity of smallest primary according to Huang model of restricted four body problem, discussing near lunar satellite application
21 p3884 A70-40874

FOURIER ANALYSIS

- NT FOURIER SERIES
- Conducted interference on input power lines of AC to DC power supplies with diode rectification and smoothing capacitors predicted by Fourier analysis
01 p0049 A70-10089
- Energy inequality solutions properties pertaining to mixed boundary value problem of partial differential equations, using Fourier method
01 p0130 A70-10154
- Fields and power transfer for electromagnetic waves in hot plasma calculated using Fourier integral and Fourier series methods
05 p0888 A70-16165
- Fourier spectra of Pi 1 pulsations during magnetic field sudden disturbances derived from amplitude analysis
05 p0840 A70-16641
- Large scale atmospheric turbulence using wave number frequency Fourier analysis of velocity distributions on latitude circles
11 p2076 A70-26498
- Interaction between turbulent air flow and water surface based on Fourier analysis of finite intervals of field
11 p2042 A70-26775
- Speckle patterns Fourier transform analysis for diffraction limited resolution attainment in large telescopes
14 p2589 A70-31382
- Shock function response and Fourier spectra relationship, using Fourier transform for equation of motion solution
19 p3456 A70-37381
- Astronomical Fourier spectroscopy, discussing techniques, improvements, advantages and mode of use
20 p3706 A70-39933
- Ideal limiter with polyharmonic signal input, calculating output spectral composition by Fourier series expansion
20 p3587 A70-40143
- Satellite motion deviations from reference orbit by generalized Fourier analysis, discussing earth gravitational field parameters determination and errors
24 p4408 A70-45546

FOURIER LAW

- Thermoelectricity generalization from physically motivated modification of Fourier heat conduction law, postulating constitutive equations valid for finite deformations and temperature variations
05 p0929 A70-16062

FOURIER SERIES

- Left ventricular muscle time varying elastic properties, using dynamic model and Fourier series representations
01 p0040 A70-11371
- Periodic process analysis method based on trigonometric Fourier series, noting applications to heat conduction problems
03 p0606 A70-13519
- Fourier expansion method applied to hydrodynamic stability of plane jet, testing boundary conditions
03 p4469 A70-14180
- Simply supported skew plates calculated for buckling loads by Rayleigh-Ritz method using double Fourier series
05 p0940 A70-16514
- Fourier series localization conditions for fundamental system of Beltrami operator functions in arbitrary n -dimensional space
05 p0877 A70-16972
- Container fluid viscosity effect on container-obstacle interaction solved in Fourier series form
07 p1252 A70-18676
- Semiinfinite elastic strip supporting thin heavy beam using Airy stress function and Laplace transform, with boundary conditions expressed as Fourier series
08 p1594 A70-21768
- Fourier spectrum of chopped bivariate normal intensity distribution with coefficients calculated numerically by computer, verifying by chopped laser beam signal analysis
09 p1729 A70-23520
- Bending of homogeneous orthotropic rectangular plate of variable thickness supported on opposite edges, obtaining solution as Fourier series
10 p1955 A70-24083
- Antenna pattern synthesis with circular distributed current source, analyzing directivity characteristics through Fourier series n th order mode concept
10 p1849 A70-24616
- Coefficients for finite difference methods of numerical integration of products of Fourier and ordinary polynomials
11 p2074 A70-26848
- Rotating shaft model with slight curvature for estimating maximum bending moment through Fourier series analysis
13 p2416 A70-28372
- Nonlinear Vlasov equation treatment by Fourier-Hermite expansion techniques for plasma problems
13 p2457 A70-28556
- Nonsteady coupled MHD Couette flow, presenting solution by Fourier series expansion method
14 p2621 A70-30549
- Cesaro Fourier series summation method for boundary value problems in electrostatics
14 p2600 A70-31419
- Container fluid viscosity effect on container-obstacle interaction solved in Fourier series form
15 p2719 A70-31468
- Fast Fourier transformation algorithm for Fourier series rapid computation
19 p3383 A70-38039
- Soviet book on conjugate functions and trigonometric series covering Hilbert transform, Fourier series properties, Cesaro methods, etc
19 p3459 A70-38799
- First order linear distributed systems with two point boundary values, obtaining eigenfunction expansion by generalized Fourier method
21 p3846 A70-41949
- Integral equations solution by Kupradze-Aleksidze general Fourier series method
23 p4211 A70-44094
- Fourier hologram synthesis using laser point source and Wollaston birefringent prism
24 p4336 A70-45667
- FOURIER TRANSFORMATION
- Fourier transform applied to power spectral distribution determination for two dimensional Fraunhofer holographic data of thin spherical lenses
01 p0090 A70-10907
- Sampled signal and associated sequence with identical Fourier transforms, noting applications to digital spectral analysis onboard spacecraft
03 p0449 A70-13538
- Soviet collection of papers on boundary problems for differential equations covering variational problems in half space, polynomial behavior at infinity, function spaces, Fourier transformation, etc
07 p1322 A70-18851
- ALGOL program modification for Fast Fourier Transform to eliminate computation time difference with Fortran
07 p1238 A70-19677
- Optical data processing systems with spatial filters for two dimensional signals detection, using film nonlinearities to record Fourier transform hologram
07 p1287 A70-20094
- Stress-strain state of shells with positive Gaussian curvature under concentrated tangential loads, basing fundamental solution on two dimensional Fourier transform
08 p1587 A70-21169

- Radar target short pulse transient scattering response computation using fast Fourier transform algorithm
08 p1463 A70-21597

- Optical image processor using Fourier transform corrective function for image restoration
09 p1688 A70-23774
- Velocity synchronized Fourier transform hologram camera system for recording hypervelocity particles
09 p1688 A70-23775
- Modified fast Fourier transform for hybrid computer program data processing of human operator describing functions
10 p1824 A70-23900
- Integrated circuits involving long-strip heat source surrounded by multiple layers, expressing temperature distribution by Fourier transformation obtained integrals
10 p1850 A70-24620
- Pattern recognition model simulating human physiology based on two dimensional Fourier transform of input images
10 p1827 A70-24770
- Collection of papers on digital signal processing covering digital filter synthesis, Fourier transforms, algorithms, etc
11 p2003 A70-25575
- Real nonnegative function representing transmittance of computer synthesized Fourier transform hologram displayed on flying spot scanner and recorded on film
11 p2049 A70-25631
- Random phase mask for Fourier Transform hologram recording of data mask, noting minimum space bandwidth required
11 p2049 A70-25637
- Transfer functions estimation by taking Fourier transform ratio of finite length samples of input and response measurements, considering error term probability density
11 p2071 A70-25954
- Algorithm for Fast Two Dimensional Fourier Transform requiring logarithm additions and multiplication
11 p2073 A70-26250
- Computer texture analysis for two dimensional scenery pictures involving periodicity invariance under Fourier transform
11 p2014 A70-26251
- BBGKY hierarchy state functional formalism in nonequilibrium statistical mechanics for many particle system using Fourier transformation
11 p2087 A70-26548
- Fourier transform calculations on finite Abelian groups
12 p2261 A70-27423
- Pipeline fast Fourier transform signal processor for digital spectrum analysis of wideband radars
12 p2186 A70-27904
- Automatic image interpretation and classification using two dimensional digital Fourier transforms
12 p2193 A70-28106
- Propagation characteristics of instabilities represented by multidimensional Fourier integrals
13 p2454 A70-28640
- Numerical integration or quadrature technique for evaluating Fourier integrals in theory of infinite cylindrical antenna
13 p2440 A70-29088
- Coherent or spatially incoherent light recordings of Fourier transform holograms, investigating resolution cells film grain and signal to noise ratio
14 p2588 A70-31207
- Hologram camera system recording hypervelocity particles by velocity synchronized Fourier transform method, employing interferometer
15 p2737 A70-32039
- Algorithm for inverse Laplace transformation of irrational transfer function via fast Fourier transform
15 p2768 A70-32577
- Superdirective small linear antennas computer aided design using Fourier integral and transform techniques
15 p2711 A70-32601
- IR reflectometer system using Fourier transform spectrometer and ellipsoidal mirror, describing design, construction and performance
16 p2905 A70-33171
- Automatic speech recognition using spatial filtering and Fourier transforms
16 p2869 A70-33462
- Fast Fourier digital processor for real time filtering of radar signals, discussing applications as Fourier transform system
16 p2870 A70-33738
- Scattered radiation from plane parallel Mie atmosphere containing spherical particles by Fourier transform method
16 p2952 A70-33983
- Discrete Fourier transform method for factoring spectral density functions, calculating absolute error
17 p3129 A70-34855
- Integral equation for three dimensional Fourier transform applied to isotropic scattering of radiation from point source in finite spheroidal atmosphere
17 p3137 A70-35599

Dynamic system modeling pulse test data reduction by digital computer and functional approximation for Fourier transform calculations 18 p3230 A70-36458

Fourier and Hermite transform methods for Vlasov equation solutions in plasma physics 18 p3296 A70-36789

Shock function response and Fourier spectra relationship, using Fourier transform for equation of motion solution 19 p3456 A70-37381

Automatic control system impulse response points identification by fast Fourier transform 19 p3393 A70-37852

Fast Fourier transformation algorithm for Fourier series rapid computation 19 p3383 A70-38039

Spectra and cross-spectra estimation by fast Fourier transform algorithm 19 p3384 A70-38040

Random signal nonlinear transformations using relations between Laplace and Fourier transforms 20 p3583 A70-39123

Axisymmetric contact problem of hollow semi-infinite elastic cylinder subjected to stresses on lower end face, solving by Fourier integral transform 20 p3720 A70-39734

Venus spectrum from high resolution Michelson interferometers with Fourier transform and digital computation, discussing Venus atmospheric models 22 p4099 A70-42721

Recording of inhomogeneous mutual coherence functions in one hologram by combining image with Fourier/Fresnel/holography 22 p4038 A70-43151

Sideband Fresnel and lensless Fourier transform holographic images elongation and contraction 24 p4339 A70-45817

FOVEA

Human foveal color vision in terms of tetrachromatic hypothesis, citing supporting evidence 01 p0026 A70-11054

Central fovea dichromacy tests, using color naming technique 22 p3972 A70-43410

Foveal threshold measurements, using small flash of light at center of bright white disk on black background 22 p3972 A70-43411

FRACTIONATION

Chondrites elements fractionation in solar nebula starting from carbonaceous material 10 p1949 A70-25329

Gold and iridium distribution in stony meteorites, discussing metal silicate fractionation process during chondrite formation 13 p2497 A70-29862

Electron radiation damaged Si, investigating p type defect concentration effect on isochronal temperature in annealing by fractionation experiment 23 p4231 A70-44887

Basalt heating with IR carbon dioxide laser, investigating vapor fractionation for inert atmospheres, very high temperatures and silicon dioxide poor materials 24 p4409 A70-45673

FRACTOGRAPHY

Crack propagation mode in laminated steel-Ni composites, analyzing softer layer effect using impact tests and C replica fractographs 01 p0120 A70-10743

Fractography utility to stress analyst, discussing fracture causes 06 p1085 A70-17438

Fractography of Al-B metal matrix composites to study micromechanical behavior, using scanning electron microscopy 08 p1524 A70-21913

Microtopography of fracture surfaces by stereo electron fractography, using large angle tilting of specimens 13 p2431 A70-28605

Fractography of spall cavities and crack growth in ball rolling contact fatigue, using scanning electron microscopy 15 p2745 A70-32444

Fractography of fatigue and delayed fracture of hydrogenated, unplated and Cd-plated ultrahigh strength steel 17 p3124 A70-34654

Fatigue crack closure in flat sheet specimens under zero-to-peak tension cyclic loading, analyzing stress distribution from fractographic striation patterns 19 p3549 A70-38625

Low energy fracture of high strength Al alloys with void nucleating particles, using microprobe fractography 23 p4206 A70-44194

FRACTURE MECHANICS

Nimonic Ni-Cr based alloys fracture characteristics used to determine temperature and time effects on equicohesive points positions 01 p0116 A70-10073

Spherical pressure vessel fracture initiation and propagation from long flaws considered from theoretical and experimental approaches 01 p0199 A70-10264

Fracture predictions in engineering structures based on small scale tests, materials microstructure, crack initiation and propagation 01 p0121 A70-11159

Quasi-brittle fracture of plastic materials based on Griffith theory and crack propagation, analyzing real surface energy and work of plastic strain 01 p0212 A70-11562

Variational principle for admissible functions particular solution in elasticity theory involving solid bodies with cracks 01 p0212 A70-11608

Fracture and degree of material removal of glassy body in hypersonic gas flow, considering radiant heat conduction inside body 03 p0516 A70-13391

Brittle fracture in neutron irradiated and nonirradiated Mo specimens tested in tension and compression at low temperature 03 p0513 A70-14013

Polysiloxanes morphology crystallized isothermally from melt using electron microscopy, noting fracture ease increment with molecular weight decrease 03 p0517 A70-14203

Fracture mechanical theory for crack propagation in brittle ceramics subjected to thermal shock, deriving crack stability criteria 04 p0767 A70-14505

Internal pressure deformed cruciform crack energy and stress intensity factor determined by linear equations 04 p0777 A70-15499

High speed photographic study of breakdown, crack formation, thermal explosions and molecular weight of transparent plastic dielectrics under laser beam 05 p0869 A70-16210

Statistical stress distribution of breakdown during scaling of wound fiberglass reinforced plastics, noting relation between critical stress and defects 05 p0870 A70-16214

Micromechanisms of fracture in metals and polymers before plastic deformation onset, discussing macroscopic polymer properties from microstructure and molecular structure 05 p0937 A70-16365

Stress gradient theory interpreted in terms of time dependent failure criterion to study critical stress vs impulse theory of spall fracture 05 p0938 A70-16481

Differential equation for crack propagation applied to threshold conditions for brittle fracture caused by impulsive load 05 p0939 A70-16486

Crack behavior of Al alloy as cryogenic tankage material, establishing relationship of temperature effects and basic crack size to failure stress 07 p1279 A70-18997

Metal adhesive joints under cyclic stresses, studying stress distribution and fracture occurrence by high speed cameras 08 p1504 A70-20889

Dugdale crack model extended to include effects of linearly varying tensile loading, noting plastic zone length sensitivity 08 p1593 A70-21512

Fracture processes in homogeneous anisotropic fiber composite materials, describing microcrack initiation, growth and unstable propagation at critical stress level 08 p1532 A70-21912

Austenitic stainless steel hydrogen damage noting role of martensite plastic deformation 08 p1525 A70-21965

Linear and nonlinear rupture mechanics applied to thick walled pressure vessels of high strength materials 09 p1769 A70-22184

Particle fracture in oxide dispersed stainless steels during plastic deformation at room temperature 09 p1706 A70-22813

Fracture mechanics model for stress corrosion cracking of Al alloys, discussing bond strength lessening by adsorption of damaging species 09 p1706 A70-22941

Fracture mechanics applications in stress analysis and structural design, considering rocket motor case failure 09 p1786 A70-23799

Subcritical cracking rate behavior estimation in metallic service structures by linear elastic fracture mechanics 10 p1960 A70-24977

Hypercritical crack growth resistance and notch toughness of aluminum alloys derived from fracture tests 11 p2064 A70-25331

Finite element methods applications to linear fracture mechanics and crack propagation theory, computing stress intensity 11 p2144 A70-26685

Binary and ternary Mg alloys ductile fracture mechanism, studying coherent/noncoherent particles effects 12 p2256 A70-27612

Thin cut plate quasi-brittle breakdown under tensile stress, considering elastoplastic equilibrium under Tresca-St. Venant yield conditions 12 p2329 A70-28325

Polymer-metal adhesive joints rupture characteristics, considering polymer in solid or structurally fluid/elastic/state during tests 12 p2244 A70-28341

Plastic deformation in brittle and ductile fracture, discussing elastoplastic stress analysis of cracked bodies, plane strain deformation near cracks, etc 13 p2509 A70-28601

Dynamic analysis involving crack extension force for two dimensional multiple radial crack division 13 p2510 A70-28602

Crack extension by alternating shear indicated from slip line flow field comparison at sharp crack tip and blunted crack 13 p2432 A70-28606

Moisture effect on fatigue crack propagation and fracture path through microstructure of 300-grade maraging steel 13 p2432 A70-28607

Width corrections in calculation of stress intensity factor for sheet with central crack in uniform uniaxial tension 13 p2510 A70-28608

Fracture kinetics model for polymers emphasizing quantum effects even at room temperature 13 p2510 A70-28670

Ductile fracture in Al matrix composite reinforced with unidirectional stainless steel fibers described by critical crack tip displacement and fracture strain criteria 13 p2512 A70-28917

Thin walled duralumin cylinders catastrophic fracture analysis by linear elastic fracture mechanics noting fatigue crack propagation 13 p2434 A70-29173

Brittle rupture cracks theory, discussing unstable/Griffith/crack, stress intensity coefficient, propagation criterion, etc 13 p2517 A70-29715

Fracture mechanics and stress analyses comparison for fatigue cracked steel cantilever beam stress corrosion specimens 15 p2755 A70-31473

Plain strain fracture toughness index measurement, discussing application to metal fatigue and stress corrosion 15 p2757 A70-31927

Precrack Charpy slow rate straining sensitivity of high strength steel at increased temperatures, comparing fracture energy of impact tests 15 p2758 A70-32238

Instrumented Charpy impact test evaluating strain rate, alloying and irradiation effects on ductile-brittle transition temperature and fracture of pressure vessel steels 15 p2820 A70-32239

Drop-weight tear test evaluation taking into account operator, test machine, specimen thickness, notch type and strength level effects 15 p2759 A70-32241

Inconel 600 high temperature high strain rate fracture process by hot torsion tester, noting temperature effects 15 p2762 A70-32389

Fracture of failed tensile impact and compression test pieces of hardened SAE 52100 steel, using scanning electron microscope 15 p2745 A70-32443

Laminated multioriented filamentary composites strength and fracture characteristics under longitudinal tension and compression [ASME PAPER 70-DE-31] 16 p2989 A70-33502

Fatigue life estimation from fracture mechanics data, discussing flaw geometry and propagation, mechanical properties, damage accumulation, etc [ATAA PAPER 70-601] 16 p2989 A70-33601

Microscopic and macroscopic viewpoints of low temperature brittle fracture, noting Inglis, Griffith and Barenblatt theories 16 p2989 A70-33671

Alpha Ti-hydrogen alloys, discussing fracture behavior temperature dependence 17 p3117 A70-34396

Viscoelastic materials cut growth, discussing strain, fracture and modulus of elasticity dependence on temperature variations 17 p3146 A70-35220

Elastic field near moving antiplane crack tip to determine energy release rate 17 p3191 A70-35462

Metal surface through and part through cracks, investigating dimensions and material properties effects on fracture stresses 18 p3278 A70-36565

- Three dimensional stress fracture criterion for initial microcracking derived by generalizing Griffith flaw theory 19 p3540 A70-37955
- Finite element method with first order displacement functions to compute crack tip stress intensity factor in various shapes under different loading conditions 19 p3548 A70-38623
- Pop-in fractures analyzed by semiquantitative model, establishing relationship between pop-in length, stress intensity factor and crack-front plastic deformation 19 p3549 A70-38626
- Deformable bodies rupture condition formulation by melting analogy, comparing results to experimental data 20 p3733 A70-40394
- Anisotropic material two dimensional crack propagation under deforming stress at infinity, examining fracture criterion, dislocation distributions and crack nucleation 21 p3936 A70-41413
- Metal cracking and fracture mechanics under creep conditions at elevated temperatures, discussing notch rupture testing 21 p3937 A70-41437
- Fracture mechanics application to fusion weld [ASME PAPER 70-MET-2] 22 p4043 A70-42424
- Slip, fracture and rupture in sintered and cast ductile and brittle polycrystalline Mo under tension, using optical and electron microscopy 23 p4204 A70-43884
- Fracture mechanics of craze growth of stressed polymethyl methacrylate in methanol 24 p4368 A70-45778
- ### FRACTURE RESISTANCE
- #### U FRACTURE STRENGTH
- #### FRACTURE STRENGTH
- Inconel 718 and Al 2219 alloys surface flawed specimens fracture toughness and flaw growth comparison for high pressure hydrogen vessel 01 p0114 A70-10029
- Weak interfaces effects in laminates under triaxial tensions at crack tip, analyzing delamination during crack propagation and fracture resistance 01 p0127 A70-10482
- Fiber breakage during powder metallurgy fabrication of compact Al-B composites as function of density 01 p0104 A70-10741
- Numerical solution of bending stresses in internally pressurized elliptical tubular or ring specimens for testing uniaxial and multiaxial fracture strength 01 p0203 A70-11061
- Materials strength characteristics with respect to breakdown probability parameter by statistical fatigue stability analysis under unsteady loads and various distribution laws 01 p0211 A70-11424
- Ingot and powder metallurgy polycrystalline Be flow and fracture behavior and microstructure pressure dependence at room temperature 02 p0317 A70-12318
- Ductile-brittle fracture transition in steel pressure vessels suppressed by utilizing thin laminations 03 p0583 A70-12903
- Microdeformation resistance in Ni alloys with ordered phase diagrams related to strain level, analyzing Bauschinger effect 03 p0505 A70-13106
- WC-Co alloys noting polishing and grinding effects on residual stress and crack resistance 03 p0508 A70-13145
- Hammer forces and specimen bending moment-time responses and fracture resistance during notched beam impact test 05 p0938 A70-16479
- Fatigue crack propagation and fracture toughness in pressurized thin walled cylindrical tubes, basing analysis on shallow shell bending theory 05 p0942 A70-16802
- Crack behavior of Al alloy as cryogenic tankage material, establishing relationship of temperature effects and basic crack size to failure stress 07 p1279 A70-18997
- Creep and stress relaxation tests to investigate time dependent fracture strength of unidirectional glass fiber reinforced epoxy composites 07 p1321 A70-19962
- Polycarbonate ductile fracture measured for strain energy release rates and plastic zone size and shapes to correlate with existing theories and experimental data 07 p1321 A70-20041
- C-axis single crystalline sapphire filament tensile and fracture tests 08 p1514 A70-20647
- Quenched and tempered steels ductile fracture with respect to plasticity, structure and crack development conditions using microfractography 08 p1515 A70-20922
- Static and dynamic low temperature crack toughness behavior of steels, determining strain rate effect 08 p1518 A70-21317
- Rate sensitive materials dynamic fracture test concepts, considering crack speed, division, arrest, toughness, etc 08 p1590 A70-21318
- Impact forces and specimen bending moments generated during dynamic test interpreted in terms of system dynamics and material fracture characteristics 08 p1518 A70-21319
- Mechanical properties and fracture behavior of chemically bonded glass matrix-metal composites 08 p1521 A70-21699
- Ultrahigh strength Ni steels fracture toughness analysis, studying effects of chemical composition, yield strength, air melting, vacuum melting, etc 09 p1701 A70-22552
- High strength stress corrosion resistant aluminum alloy die forgings, evaluating tensile, tensile fatigue and fracture toughness properties 09 p1702 A70-22556
- Fracture toughness and deformation kinetics dependence on compositional, microstructural and textural variations of alpha and alpha-beta Ti alloys at low temperatures 09 p1704 A70-22801
- Plane disks and turbine disks of complex profile made of heat resistant Cr-Ni alloys studied for rupture strength under various temperature conditions 09 p1785 A70-23599
- Heat resistant materials strength characteristics with long service periods, formulating equation for time dependence of rupture resistance 10 p1903 A70-24237
- Long time strength and creep rectilinear diagrams constructed for heat resistant alloys to obtain extrapolation values 10 p1903 A70-24239
- Test results extrapolation for heat resistant alloys long time strength using exponential relation between time to rupture and value for initial stress decrease 10 p1903 A70-24240
- Aluminum alloy deformations and rupture strength under complex stress at low temperatures, observing anisotropy decrease with temperature 10 p1903 A70-24243
- Residual stresses effect on strength and hardness of tungsten carbide-cobalt alloy by application of small plastic deformations, observing crack formation anisotropy 10 p1904 A70-25168
- Strain tempering effects on upper and lower bainite, discussing strengthening and fracture toughness as function of temperature 10 p1905 A70-25173
- Quartz and alkaline glasses fracture stability in water vapor and aqueous solutions with enhanced surface activity as function of time 11 p2068 A70-25379
- Brittle fracture strength of welded joints in high strength steels 11 p2059 A70-25663
- Interstitial and substitutional impurity effects on fracture strength, plastic properties and ductile-brittle transition temperature of vanadium determined from impact and tensile tests 11 p2066 A70-25913
- Elastic-plastic shear cracks propagation in two phase composite materials using dislocation model, determining critical fracture strength 11 p2136 A70-26081
- Filament reinforced composites tested under dynamic compression loads for determining relations among strain rate, constituent properties, stress-strain behavior, fracture energy and mode 12 p2253 A70-27119
- Fracture toughness and cyclic crack propagation of surface cracked high strength aircraft structure steels 12 p2254 A70-27467
- Annealed stainless steel low cycle fatigue data analysis leading to method of characteristic slopes approach for correlating plastic strain range to fracture time 12 p2255 A70-27604
- Stress measurements for eye beams forming of high fatigue strength based on brittle lacquer studies of isotropic material models 13 p2507 A70-28482
- Ductile fractures analysis using critical strain near crack tip as criterion 13 p2432 A70-28673
- Griffith flaws limitation effect on glass matrix-tungsten composites strength, considering dispersed phase with wide particle size distribution 13 p2437 A70-28827
- Hot torsion test for Al alloys workability assessment, noting test temperature and specimen geometry effects on fracture strain values 13 p2436 A70-29816
- Austenization temperature, cooling rate and tempering conditions effect on steel castings structure, strength and impact properties 14 p2596 A70-30875
- Charpy V notch and dynamic tear tests compared for fracture toughness characterization of Ni-Cr-Mo-V steel 14 p2596 A70-30931
- Plain strain fracture toughness index measurement, discussing application to metal fatigue and stress corrosion 15 p2757 A70-31927
- Impact loaded Griffith-Irwin, Charpy and drop weight tear tests of fracture toughness for design, screening and materials acceptance 15 p2819 A70-32233
- Dynamic fracture toughness measurement of low strength steels via instrumented Charpy impact test with correction factor for inertia loading effects 15 p2820 A70-32237
- Inertial load-time effects in instrumented impact tests, showing corrections for bending stress and dynamic fracture toughness measurements 15 p2820 A70-32240
- Impact test machines, specimen design and energy measurement in dynamic tear test method for steel fracture strength 15 p2759 A70-32242
- Dynamic fracture toughness test on heat treated precracked steel specimens under dynamic loading 15 p2759 A70-32243
- Bend formability and fracture toughness tests on Be ingot and cross-rolled powdered sheet and brake grade block materials 15 p2760 A70-32337
- [ASME PAPER W70-15.3] Heat treatment effect on maraging steel fracture toughness and subcritical crack growth loaded at slow strain rate in laboratory air 15 p2760 A70-32377
- Work to fracture measurements on brittle fiber ductile-matrix metal composites, using Charpy test 15 p2763 A70-32832
- High yield strength alpha-beta Ti alloys ductility control, observing fracture strength dependence on morphology, grain location and size for constant heat treatment 17 p3119 A70-34417
- High strength Ti alloy for cryogenic applications, comparing plane strain fracture toughness 17 p3122 A70-34438
- Viscoelastic materials fracture strength as function of cut length, defect size and temperature 17 p3146 A70-35221
- Impact transition behavior and strength-toughness relation of high purity Ni maraging steels, noting intergranular fracture at grain boundaries 18 p3273 A70-36043
- Sapphire and ruby plastic deformation and fracture properties at room temperature, discussing sapphire base ceramics 18 p3278 A70-36046
- Papers on cracking during postweld heat treatment of Ni alloys covering Rene 41 mechanical properties and resistance to strain age cracking 18 p3277 A70-36522
- Rene 41 resistance to strain-age cracking during postweld heat treatment 18 p3277 A70-36523
- Rene 41 ductility reduction by environmental oxygen promoting intergranular cracking at high temperatures 18 p3277 A70-36524
- Energy balance criterion for continuum mechanics analysis of fracture threshold for blistered adhesive elastic layer between elastic material and rigid substrate 19 p3536 A70-37774
- Notched sheet failure prediction based on Dugdale crack model, including work hardening and finite width effects, strain fracture criterion and yield failure mechanism 19 p3548 A70-38624
- Nb effects on steel susceptibility to brittle fracture at various temperatures, discussing impact strength and nucleation energy of crack formation 19 p3453 A70-38709
- High temperature endurance strength of temper finished bolt connections under cyclic loads, using programmed fatigue testing machines 20 p3718 A70-39223
- Tungsten wire reinforced copper matrix composite, determining fibers pull-out contribution to fracture work 20 p3651 A70-40047
- Composites reinforced with weakened fibers, investigating weak points effect on fracture toughness by fiber pullout and tensile tests 21 p3843 A70-41889
- Fracture toughness and surface energy of fibrous reinforced composites as function of fiber content, strength, diameter, modulus and matrix flow stress 21 p3843 A70-41890
- Butt joined epoxy Al plates tensile strength, observing fracture strength dependence on stress concentration at bond edges below characteristic crack length 21 p3939 A70-42032
- Ti and Al alloy weldments plane strain fracture toughness and mechanical properties for cryogenic applications, using gas metal arc and gas tungsten arc welding [ASME PAPER 70-MET-4] 22 p4043 A70-42423

Fracture behavior and tempered martensite embrittlement relationship in steel, using V- notched and fatigue precracked Charpy specimens 22 p4054 A70-42736

Weightlessness and immobilization effects on mechanical tolerance of bone compressive and breaking strength in monkeys 22 p3973 A70-43648

Crack propagation resistance-cyclic fracture strength relation for Mn-Cr-V steels, considering thermomechanical working effects 23 p4204 A70-43935

Scale factor effect on brittle fracture resistance for Ti and Al alloys and high strength steels 23 p4265 A70-43936

Papers on plane strain fracture toughness testing covering metallic materials, steels and aluminum alloys 23 p4205 A70-44189

Fracture toughness testing of metallic materials including fatigue cracking, thickness limitations and crack detection 23 p4206 A70-44190

Plane strain fracture toughness testing of high strength Al alloys and steels, using fatigue cracked bend specimens 23 p4206 A70-44191

Crack length and bend specimen thickness effects in plane strain fracture toughness tests of high strength steels 23 p4268 A70-44192

Crack and thickness effects on fracture toughness tests of high strength steel in precracked sheet and bend specimens 23 p4206 A70-44193

Low energy fracture of high strength Al alloys with void nucleating particles, using microprobe fractography 23 p4206 A70-44194

Specimen size and mechanical factors in plane strain fracture toughness testing of metallic materials 23 p4206 A70-44195

Moire technique application to fracture toughness tests on Zr alloys, measuring crack opening displacements and plastic flow beneath notch 23 p4208 A70-44914

Brittle fracture of welded notched steels with different stress concentrations, using subzero tensile tests 24 p4347 A70-45732

Heat treatable beta Ti alloys cold workability, fracture toughness, tensile ductility and applications [SAE PAPER 700856] 24 p4361 A70-45880

FRACTURE TOUGHNESS

U FRACTURE STRENGTH

FRACTURES [MATERIALS]

Stress criterion for unstable crack propagation from Al alloy sheet tests, examining fracture data for vessels of various geometries and materials [ASME PAPER 69-SESA-2] 01 p0117 A70-10451

Fiber-composite materials fracture, noting interface mechanical strength effects on composite properties under tension and shear 01 p0127 A70-10481

Honeycomb structure fracture initiation flaw detection method using liquid crystal determination of stress concentration sites, noting absence of external heat source 03 p0515 A70-13121

Damage tolerance as design consideration for aircraft safety and reliability, discussing application of failed single principal member concept to airframe construction [AIAA PAPER 69-212] 07 p1417 A70-20401

Cleavage fracture of Ta-Mo bcc alloys, investigating short range ordering and size effects by X ray diffraction 09 p1708 A70-23573

Polycarbonate fatigue fracture surfaces and striation feature 12 p2259 A70-27168

Viscoelastic-plastic solid delayed fracture associated with wedge formation of crazed material at crack tip 15 p2816 A70-32010

Fractography of fatigue and delayed fracture of hydrogenated, unplated and Cd-plated ultrahigh strength steel 17 p3124 A70-34654

Elastic crack structure, discussing formalism for force law between faces of brittle and semibrittle fractures 17 p3191 A70-35461

Polymeric materials yielding and fracture behavior under uniaxial and multiaxial fields, plotting octahedral shear stress 20 p3656 A70-39949

Ti alpha alloy fracture characteristics at high temperatures, discussing strain rates, deformation resistance and grain growth 22 p4056 A70-43343

Boron-Al composite filament fracture behavior and postimpact tensile strength, examining shock loading and impact velocity effects 22 p4060 A70-43682

Hydrogen effect on deformation and fracture of polycrystalline nickel 24 p4365 A70-46372

FRACTURING

Bursting speed and mode of high speed rotating disk with rim, boss and blades, noting influence of boss thickness 06 p1129 A70-17129

Neutron irradiation effect on elevated temperature fracture of various fcc alloys 22 p4054 A70-42957

FRAGMENTATION

Meteorite falls statistics correlations for fragmentation relationships with mass, time of fall and class 05 p0912 A70-16447

Meteor fragmentation in flares, determining fragments mass, time and special parameters for plotting flare brightness curves 06 p1140 A70-17734

Meteoroids structure, composition and fragmentation, summarizing existing evidence for photographic and radio meteors and meteor luminous and ionizing efficiency 06 p1153 A70-18551

Electron impact induced fragmentation of androstane using deuterium labeling 08 p1454 A70-20524

Cyclohexene oxide mass spectral fragmentation by means of deuterium labeled analogs 09 p1630 A70-23397

Mass distribution of Sikhote Alin meteorite fragmentation, noting similarity to terrestrial rocks 13 p2490 A70-28916

Liquid metallic particles fragmentation in two phase flow injected into vacuum, noting atomization enhancement by sodium nitrate 13 p2391 A70-29994

Oxadiazolone pyrolytic and photolytic fragmentation, noting intramolecular cyclizations and intermediate azomethine nitrene production 17 p3041 A70-34771

Mathematical model of asteroidal evolution and meteoric mass distributions under collisional fragmentation using power law 18 p3312 A70-36213

Primary cosmic rays nuclear transitions, determining fragmentation parameters 20 p3696 A70-39284

Geometrical figure fragmentation produced by intermittent illumination, examining dependence on presentation frequency and temporal factors 20 p3580 A70-39491

FRAGMENTS

Meteor fragments motion and vaporization based on photographs 06 p1140 A70-17733

High speed photographic recording of bursting rotor in fragment control device 17 p3063 A70-35523

FRAME PHOTOGRAPHY

Photoobjective and camera resolution tests regarding entire frame using two dimensional azimuth mark 05 p0852 A70-16864

Initial vapor bubble growth on horizontal heated wall during saturated nucleate boiling using combined streak and high speed frame photography 08 p1542 A70-21584

High speed three-frame electronic camera with storage tube, slow scanning and magnetic recording [SMPT PREPRINT 55] 22 p4033 A70-43038

High resolution ultrahigh speed continuous-writing framing camera with extended spectral range [SMPT PREPRINT 36] 22 p4033 A70-43042

Stereo laser framing camera for miniature surface cracks and perturbations produced in materials by explosively induced shock waves [SMPT PREPRINT 21] 22 p4035 A70-43052

FRAMES

NT AIRFRAMES

NT UNDERCARRIAGES

Minimum weight beams and frames calculation for random loads taking into account material carrying capacity 07 p1400 A70-18821

Minimum weight reliable beams and frames calculation for random loads, using one degree of freedom system to obtain closed form solution 07 p1401 A70-18825

Reinforced plastics underframe design based on hooks law, noting middle layer loaded laminates and shell advantages 07 p1410 A70-19762

Slope deflection method for computing spatial trusses and plane frameworks under dynamic aperiodic forces 13 p2516 A70-29532

Plane frames with and without shear walls, determining dynamic response under vibration by finite element method 14 p2660 A70-31137

Frame synchronization in biorthogonal coded multiplex communication system, describing PCM, pattern insertion and double encoding methods 17 p3045 A70-35266

Frames nonlinear elastic postbuckling behavior, using static perturbation technique 19 p3542 A70-38058

Elastic-plastic equilibrium bifurcation in geometrically simple frame model with symmetrically loaded beam, comparing characteristics with Shanley uniformly stressed column model 19 p3549 A70-38671

Tracking elevation/azimuth errors due to frame misalignment, presenting least squares procedure for determining true bias and misalignment angle and axis 23 p4215 A70-44518

FRAMING CAMERAS

Laser optoelectronic and spectroscopic methods using fixed gap spherical mirror confocal Fabry-Perot interferometer and multiple beam image tube framing camera 01 p0112 A70-10901

Metal film graded filter fabrication for schlieren photographic system with laser light source and framing camera, using vacuum evaporation 01 p0113 A70-10921

Drum-type, high-speed, frame or streak photographic camera, discussing film mounting and operating specifications 03 p0485 A70-13531

High speed camera synchronization by frame reference pulses for strobe triggering 06 p1060 A70-17147

Systematic errors in rotating mirror framing cameras and film records for quantitative high speed motion analysis 17 p3095 A70-35632

Ultrahigh speed ballistic-synchrophotography, using Imacon image converter camera for framing and streak modes 22 p4031 A70-43028

High resolution ultrahigh speed continuous-writing framing camera with extended spectral range [SMPT PREPRINT 36] 22 p4033 A70-43042

Orthogonal multistreak recording by framing camera applied to arrival of detonation wave at front surface of explosive charge [SMPT PREPRINT 32] 22 p4034 A70-43045

Stereo laser framing camera for miniature surface cracks and perturbations produced in materials by explosively induced shock waves [SMPT PREPRINT 21] 22 p4035 A70-43052

FRANCE

Guiana Space Center for French space programs, describing launch complexes, measurement and control methods, safety methods, launch operation planning, etc 04 p0663 A70-14939

Second antenna at Pleumeur-Bodou /France/ for satellite transmissions reception in Intelsat network program 05 p0826 A70-15981

Electrical and mechanical characteristics and specifications of second parabolic reflector antenna at Pleumeur-Bodou space communications center 05 p0819 A70-15982

Electrical and hydraulic units controlling second antenna at Pleumeur-Bodou space communication center 05 p0819 A70-15984

Antenna-central building connecting equipment at Pleumeur-Bodou space telecommunication center, discussing frequency compression demodulators 05 p0819 A70-15985

Transmission equipment of Pleumeur-Bodou space communication installation including modulators, converters and amplifiers for telephone and TV carriers 05 p0819 A70-15986

Artemis I and II telemetering antennas at Guiana Space Center for spacecraft tracking 05 p0819 A70-15987

French guided satellite space flight simulator developed in search for suitable three axial onboard guidance systems 06 p1028 A70-17933

Dioscures project satellites design, considering use of rotation stabilization 07 p1392 A70-18989

Analog-numerical measurements on French liquid oxygen and hydrogen motor 07 p1364 A70-19129

French microwave semiconductor technology in terms of basic research, technology studies, reliability and integrated circuits 09 p1739 A70-22602

French geodetic satellites Diademe I and II experiments in navigation, noting laser and Doppler devices 09 p1725 A70-23049

Aeronautical construction complexes in France 10 p1895 A70-24862

Composite and double base solid rocket propellants manufactured by French factory for ballistic missiles, discussing plant installations 11 p2030 A70-25520

Photographic reduction techniques at Meudon Observatory, discussing computation of standard and measured coordinates 11 p2007 A70-26197

French jet engines, outlining various models built by SNECMA and Turbomeca 13 p2474 A70-29144

French photographic observations of Apollo 12 trans lunar trajectory 15 p2697 A70-31676

French airline pilots training program at Montpellier and St-Yan, considering selection, licensing and simulators 16 p2853 A70-33675

FRANCK-CONDON PRINCIPLE

Polyatomic molecules radiationless transition rate statistical analysis, suggesting role of Franck-Condon principle in determination of nonradiative decay rates 16 p2858 A70-34014

FRAUNHOFER LINE DISCRIMINATORS

Fraunhofer line discriminator (FLD) used for airborne fluorometer applicable to marine and estuarine studies 09 p1681 A70-23350

Luminescing materials remote sensing during daylight by Fraunhofer line depth method with sun as excitation source 12 p2221 A70-26958

Solar stimulated terrestrial materials luminescence remote detection by Fraunhofer line depth method using UV grating spectrometer 23 p4199 A70-45007

FRAUNHOFER LINES

Simultaneous filtergrams of velocity and intensity field of central solar disk obtained in blue and red wings of Fraunhofer line 01 p0175 A70-10242

Interference fringe in Fraunhofer hologram reconstruction of tapered glass fibers related to fiber profiles 01 p0090 A70-10906

Fourier transform applied to power spectral distribution determination for two dimensional Fraunhofer holographic data of thin spherical lenses 01 p0090 A70-10907

Diffraction plates for classroom demonstrations of Fraunhofer patterns, Babinet principle and Rayleigh resolution by computer generation 01 p0093 A70-11292

Zeeman-split Fraunhofer line profiles for pure absorption lines determined taking into account solar atmosphere elliptical birefringence 03 p0570 A70-13595

Schwerd color drawings of amplitude and intensity distributions of Fraunhofer diffraction patterns, verifying accuracy with computer generated diffraction plate photographs 04 p0719 A70-15014

Limb effect of solar Fraunhofer lines determined by telescope equipped with autocollimated type diffraction spectrograph 05 p0918 A70-16912

Radiative transfer equations for Zeeman multiplets of electric and magnetic dipoles and quadrupole radiation in solar Fraunhofer spectrum 06 p1142 A70-17991

Ca II 7323 forbidden line in solar Fraunhofer spectrum, estimating center-limb variation of equivalent width of transition 06 p1143 A70-17994

Solar radiation flux observation-prediction discrepancies due to Fraunhofer line absorption, studying Balmer continuum as atmospheric model criterion 06 p1148 A70-18451

Solar IR Fraunhofer line damping constants empirical values and variation with optical depth, noting discrepancy with theoretical constants 09 p1757 A70-22726

Day sky Fraunhofer lines filling-in /Ring effect/ considered from analogous effects in surface albedo, suggesting role of Rayleigh wings 10 p1947 A70-24992

Table of Fraunhofer solar lines without Zeeman splitting 13 p2496 A70-29843

Solar disk center to limb variation of Fraunhofer lines, comparing measurements to predictions by BCA, Elste and Holweger models 16 p2980 A70-34307

Fraunhofer holography for recording small particles to determine size distribution without disturbing sample 17 p3086 A70-35016

Fraunhofer line equivalent widths differences between pole and equator spectra of solar disk 17 p3173 A70-35734

Solar search for neutral rhenium lines using low noise, high resolution photometric tracings of Fraunhofer spectrum 20 p3711 A70-40406

FRAUNHOFER REGION

U FAR FIELDS

FREDHOLM EQUATIONS

Elastic contact between bodies in presence of friction or adhesion by reducing singular integral equations to Fredholm equation 08 p1585 A70-20958

Plane E-polarized wave diffraction by slit in conducting screen using Fredholm integral equations of second kind 08 p1461 A70-21004

Prolate spheroidal wave functions applied to detection Fredholm equation for band-limited noise and signals 09 p1640 A70-23803

Temperature distribution in shadowed lunar craters formulated in Fredholm integral equations, showing constant temperature and correction for soil thermal inertia [ALAA PAPER 69-595] 11 p2112 A70-26155

Linearized Fredholm equation solution, describing temperature field for energy transport by radiation and heat conduction 13 p2521 A70-28860

Algorithm for Fredholm integral equation in inverse problems of satellite meteorology 14 p2603 A70-30405

Electromagnetic wave diffraction by heterogeneous planar dielectric structures, showing field distributions by single variable Fredholm equations 15 p2695 A70-31436

Thermal atmospheric sounding from satellites based on Fredholm integral equations, obtaining vertical temperature profiles 16 p2896 A70-33257

Regularizing algorithm for Fredholm integral equation used in diffraction by ideally conducting strip 19 p3376 A70-37434

Electromagnetic wave diffraction by inhomogeneous anisotropic body, applying Fredholm integral equations 19 p3376 A70-37436

Compressible fluids flow with conductivity tensor in presence of thin wing under orthogonal fields, reducing integral equation to Fredholm equation 19 p3351 A70-37599

Elastic contact between bodies in presence of friction or adhesion by reducing singular integral equations to Fredholm equation 20 p3719 A70-39381

Book on state variable solution techniques for homogeneous and inhomogeneous Fredholm integral equations in communication theory, discussing application to linear estimation theory 21 p3846 A70-41791

Linear methods for approximate solutions of ordinary differential equations and Fredholm integral equations by polynomials 23 p4211 A70-44249

Successive iterative solution for large matrix equations reduced from Fredholm integral equations of second kind 24 p4369 A70-45164

FREDHOLM OPERATORS

U FREDHOLM EQUATIONS

U OPERATORS [MATHEMATICS]

FREE ATMOSPHERE

Earth model based on free air gravity anomaly with condensed topography for eliminating gravity reduction difficulties, noting use in Vening-Meins formula 05 p0840 A70-16640

Sheared frontal zones structure and stability, studying Richardson number limiting role in free atmosphere 08 p1492 A70-21971

Free atmosphere clear air turbulence, discussing velocity and temperature spectra, Kelvin-Helmholtz instability, isentropic cross sections, energy budget, etc 09 p1714 A70-22354

Friction and orography influence on wave motions in real atmosphere, discussing planetary boundary layer and propagation in free atmosphere 09 p1718 A70-23331

Kinetic energy turbulence spectrum in free atmosphere from rawinsonde and aircraft data 15 p0000 A70-32369

CAT shear spectra above ground frictional layer in jet stream flight conditions, using aircraft measurements 16 p2946 A70-33825

Significant terms in equations of motion for parachutes inflating in free air and in wind tunnel experiments [ALAA PAPER 68-924] 18 p3213 A70-36449

Free atmosphere turbulent diffusion coefficient determination, releasing dipole reflectors from helicopter for radio echo observation 19 p3461 A70-37423

Free air temperature by onboard satellite IR spectrometer /SIRS/, measuring earth spectral radiance in carbon dioxide 15 micrometer band 20 p3660 A70-39077

FREE BOUNDARIES

Radio wave propagation in linear, isotropic homogeneous medium with irregular boundaries solved by expanding Helmholtz integral 04 p0648 A70-14965

Stefan free boundary problems with prescribed flux reduced to form solvable by numerical methods, proving existence and uniqueness theorems 05 p0956 A70-15783

Continuous dependence theorem and differentiability properties of free boundary problem solution for heat equation 09 p1788 A70-22609

Small linear disturbance and stability of potential unsteady motion of finite mass of liquid with free boundary 10 p1866 A70-24111

Plane EM wave reflection and transmission at moving boundary, discussing frequency disparity with incident wave 15 p2697 A70-31834

Soviet book on hydrodynamics of flows with free boundaries, covering fluids penetration by solid body, hydrofoil motion, cavitation flow, etc 16 p2890 A70-32912

Circular free boundary problem associated with phase transformation by first order perturbation solution, discussing radial solidification and melting of fluid over cylindrical rod 16 p2941 A70-33003

Perturbation complex potential and aerodynamic forces determined for rectilinear profile motion under free surface, using linear theory 16 p2837 A70-33848

Two dimensional free boundary problems approximate solution by finite difference method, deriving algorithms for computer program implementation 18 p3230 A70-35941

Equilibrium form shapes of fluid free surface in vessel under gravitational and magnetic field with tension 18 p3240 A70-36269

Nonlinear free boundary problem for hyperbolic one dimensional gas dynamics equations 20 p3658 A70-40105

Nonlinear free boundary value problems involving region bounded by curvilinear ring consisting of smooth curves, reducing problem to nonlinear equations in Banach space 23 p4212 A70-44342

Ducted propeller subsonic rotational flow with free boundaries, presenting second-order partial differential equation solution without linearizing assumptions 24 p4287 A70-45269

FREE CONVECTION

Free convection to rotating central plate in synchronously rotating surroundings with and without consideration of Coriolis forces [AICHE PREPRINT 9] 01 p0216 A70-10968

Horizontal and vertical sound fields local effects on natural convection from heated horizontal circular cylinder, using shadowgraphy 01 p0219 A70-11198

Invariant group study of free atmospheric convection equations at combination of Grashof numbers, Prandtl numbers and boundary conditions, noting infinite flux velocity 02 p0328 A70-12387

Pseudoboiling heat transfer from platinum wire to carbon dioxide during free convection 03 p0604 A70-13209

Boundary layer approximation for natural convection in flat vertical symmetrically heated channel with stabilized laminar flow for local and mean Nusselt numbers 03 p0605 A70-13395

Free convective flows above flat horizontal plate demonstrating laminar boundary layer existence at intermediate Grashof numbers, using semifocusing color schlieren photography 04 p0780 A70-14456

Instantaneous heat transfer from oscillating wire in free convection in still air as function of time [ASME PAPER 69-WA/HT-15] 04 p0783 A70-14819

Heat and momentum transfer efficiency of the thermal convection, calculating eddy coefficients for vertical transfer 05 p0831 A70-15876

Unsteady laminar free convection caused by heating semiinfinite flat vertical plate, obtaining velocity and temperature distributions 05 p0957 A70-16370

Steady free convection over point and horizontal line heat sources in vertical magnetic field 06 p1120 A70-17519

Bulk and wall temperature measurements for natural fluid convection in container with and without baffles for various heat flux and aspect ratios 06 p1175 A70-17684

Natural convection heat transfer from vertical plate immersed in thermally stratified fluid 06 p1175 A70-17685

Laminar natural convection boundary layer stability over vertical uniform flux surface, measuring disturbance temperature and velocity distributions 06 p1035 A70-17686

Free steady convective flow stability relative to three dimensional disturbances between parallel planes reduced to equivalent plane disturbances problem 07 p1252 A70-18669

MHD free convection of electrically conducting fluid in strong cross field using perturbation technique, considering liquid metals and ionized gases 07 p1348 A70-19208

Vertical plume velocity and temperature measurements by hot wire probe on turbulent free convection zones over model fires

07 p1282 A70-19582

Temperature fields and hydrodynamics in laminar flow of vertical liquid layers during free convection

07 p1422 A70-19655

Natural convection heat transfer from horizontal finned circular cylinder noting effect of distance between fins

07 p1425 A70-20169

Thermal convection determination in earth, Venus, Mars and moon interiors based on thermal stability analysis, obtaining viscosity depth profiles

07 p1272 A70-20203

Finite amplitude effects on MHD thermal convection in rotating layer of conducting fluid, discussing subcritical instability

08 p1563 A70-20472

Two dimensional natural convection boundary layer on finite isothermal horizontal plate, examining upward facing cold plate and downward facing hot plate

08 p1598 A70-21580

Natural heat convection measurements in vertical annular spaces, noting importance of local density and velocity product

08 p1433 A70-21671

Unsteady free convection laminar power-law fluid flow past porous vertical wall, studying similarity solution dependence on wall temperature and suction

08 p1486 A70-21765

Counterrotating natural vortices produced by corona discharge on heated flat plate under free convection conditions

08 p1599 A70-21828

Natural heat convection in vertical annular space taking into account variations of volumetric mass, viscosity and thermal conductivity of air with temperature

09 p1786 A70-22047

Heat and mass transfer coefficients in binary laminar boundary layer convection obtained with integral equations and Karman-Pohlhausen method

09 p1787 A70-22264

Heat and mass transfer in binary turbulent boundary layer during natural convection on vertical surface, allowing for diffusional heat conduction

09 p1787 A70-22267

Magnetic field effect on free convection in laminar boundary layer formed by laminar flow of viscous conducting fluid along vertical wall

09 p1737 A70-23308

Rectangular fins arrangement on horizontal surfaces for optimum free convection heat transfer coefficient, considering fin weight, height and spacing effects [ASME PAPER 69-HT-44]

09 p1789 A70-23551

Unsteady laminar free convection on heated axially symmetric body under stepwise surface temperature variations and unity Prandtl number

10 p1967 A70-23875

Laminar boundary layer equations solved for mass and energy transfer in binary gas mixture, investigating forced and free convection

11 p2151 A70-26558

Simultaneous heat and mass transfer coefficients in laminar free convection boundary layers on horizontal cylinders or vertical axisymmetric bodies

11 p2151 A70-26559

Laminar boundary layer transition to quasi-cellular flow in natural convection above horizontal heated plates and disks

12 p2155 A70-27197

Laminar natural convection plumes behavior above energy sources calculated by simplest variables, indicating optimum formulation of boundary value problem

12 p2332 A70-27700

Free convection flow and heat transfer from semi-infinite horizontal flat plate with time-oscillating temperature, using successive approximations process

13 p2522 A70-29537

Transient free convection flow due to arbitrary motion of vertical plate, linearizing equations of boundary layer flow and heat transfer

13 p2523 A70-30009

Convective heat transfer from rotating Al spheres in air at rest, investigating structure and boundary layer changes by schlieren method

14 p2665 A70-30398

Free steady convective flow stability relative to three dimensional disturbances between parallel planes reduced to equivalent plane disturbances problem

15 p2718 A70-31461

Free convection and heat transfer in square region bounded by solid impermeable walls heated from above, using two dimensional model

15 p2824 A70-31492

Thermal convection formation in viscous fluid plane horizontal layer from measurements of unsteady temperature field

15 p2824 A70-31591

Natural convection wake from heated horizontal line source in liquids and in air, determining temperature field in plume above wires

15 p2825 A70-31817

Electric space charge pulse density measurements near ground in sunny weather related to free convection

15 p2726 A70-31868

Thermal boundary layer and heat and mass transfer at porous horizontal heated surface in presence of free convection, considering blowing and suction effects

15 p2827 A70-32133

Mixed forced and natural convection with low speed air flow over horizontal electrically heated cylinders

15 p2740 A70-32373

Natural convection heat transfer from vertical cylinder outer surface to liquids, discussing apparatus design and measurements

17 p3197 A70-35540

Laminar free convection boundary layer on vertical heated plate near discontinuity in plate temperature, discussing velocity field

17 p3198 A70-35593

Free convection in compressible viscous heat conducting fluid, determining parameters leading to onset

17 p3198 A70-35697

Free convection in air and water above horizontal wire heated by DC current, measuring flame temperature distribution by diffraction interferometer

17 p3198 A70-35743

Laminar free convection near two dimensional and axisymmetric nonisothermal bodies, examining surface temperature distribution and heat flux

18 p3345 A70-35999

Angular dependence of instability and Rayleigh number of natural convection flow on inclined flat plates, using electrochemical flow visualization

18 p3345 A70-36190

Free convection boundary layer on two dimensional or axisymmetric body with sudden temperature increase, determining skin friction and heat transfer coefficients

18 p3346 A70-36487

Natural convection problem solution along nonuniformly heated vertical plate with variable transverse magnetic field

20 p3735 A70-39144

Transient and steady state free convection heat transfer with mercury in vertical rectangular channel, measuring temperature distributions

21 p3941 A70-40773

Free and forced convection of supercritical carbon dioxide normal to heated cylinder at constant temperature, measuring heat transfer rates

21 p3945 A70-41034

Natural convection boundary layer stability on isothermal flat vertical wall or subjected to linear temperature distribution

21 p3950 A70-41443

Finite difference numerical integration method for melting and freezing problems extended to free convection in liquid and unequal densities for phases

21 p3953 A70-42093

Dynamic nonstationary thermal convection in closed region with heat input from lateral surface for high Rayleigh and Fourier numbers

21 p3954 A70-42214

Nonstationary axisymmetric thermal convection in spherical cavity with boundary heat flux proportional to temperature, using difference scheme and networks method

21 p3954 A70-42215

Natural convection film boiling heat transfer literature, data sources for specific substances, photographic studies, mathematical models, etc

22 p4121 A70-42305

Buoyancy effects on transient free convection heat transfer in revolving tube for zero to 100 g centrifugal acceleration

[ASME PAPER 70-HT-10]

22 p4122 A70-42437

Thermal convection formation in viscous fluid plane horizontal layer from measurements of unsteady temperature field

23 p4277 A70-44278

Static pressure effects on heat flux critical density for free convection and forced flow in circular pipes

23 p4282 A70-44726

Viscous fluid two dimensional steady natural convection between horizontal concentric cylinders for low Grashof numbers

24 p4429 A70-46007

Heat flux exchange by natural convection along flat vertical isothermal plate in laminar, transition and turbulent flows, using fluxmeters

24 p4429 A70-46207

FREE ELECTRONS

Thunderstorm lightning discharge formation mechanism, investigating electric charge concentration and motion of free electrons

01 p0134 A70-10169

High intensity pulsed laser radiation scattering by free electrons, studying linearly polarized incident radiation

02 p0312 A70-12276

Free carrier light absorption in n-type GaAs, InAs and Ge semiconductors with mechanically polished surfaces as function of thickness and crystal structure

03 p0538 A70-13057

Electron momentum distributions from Compton profiles of Li-Mg polycrystalline samples, exhibiting discontinuity at free electron value of Fermi momentum

05 p0892 A70-16471

Free current carriers activity in indirect magnetooptical junctions in quantized magnetic field

06 p1126 A70-17817

Free electron formation ahead of strong shock waves traveling into nitrogen-oxygen mixtures in shock tube, observing electron densities

06 p1065 A70-18029

Light scattering from free electrons in laboratory plasma, showing frequency spectrum equal to electron density fluctuations

07 p1347 A70-18899

Nonlinear parameter of two intersecting laser beams in interaction with free electrons plane wave external field coupling

09 p1695 A70-22213

Free-free opacity of stellar interiors by ion correlations applied to red giant degenerate cores

09 p1755 A70-22510

Coupled Boltzmann and rate equations for free electron distribution function and level populations in monatomic partially ionized gas including nonelastic collisions

10 p1918 A70-23958

Impurity centers thermal and autoionization and effective capture cross section dependent on free carrier concentration in GaAs under electric field, allowing for plasma shielding

12 p2285 A70-27361

Free carriers effective mass and relaxation time in semiconductors determined from IR spectra of light reflection

12 p2285 A70-27362

Free electrons non-Maxwellian equilibrium kinetic energy distribution function, considering partially ionized hydrogen-like plasma in thermal equilibrium

13 p2459 A70-28634

Free carriers mobility and concentration in microwave semiconductors measurable by two mode resonator over temperature ranges and magnetic fluxes

13 p2470 A70-28881

Semiconductor laser emission at band-band transitions with free carriers participation under quantizing magnetic field, using kinetic equations

15 p2749 A70-31627

Laser beam scattering by free electrons in terms of classical electrodynamics, discussing radiation damping effects

15 p2752 A70-32451

Laser beam scattering by free electrons in semiclassical radiation theory, discussing intensity dependent frequency shift

15 p2753 A70-32452

Radiative transfer in spherical stellar atmosphere, considering free electrons density gradient and thermal motions, atmospheric layer curvature, optical thickness, etc

15 p2732 A70-32905

Ethyl alcohol fuel diffusion flame, examining thermal decomposition pyrolysis and free electron concentration distribution

18 p3345 A70-36113

Total cross sections for production of free electrons in collisions of low energy negative atomic oxygen ions with molecular nitrogen

18 p3292 A70-36188

Thomson theory of arbitrarily intense elliptically polarized plane electromagnetic wave scattering by free electrons, solving electron equations of motion

18 p3267 A70-36649

Radiation transfer in plane parallel layers consisting of two atomic energy levels, assuming free electrons Maxwellian energy distribution

19 p3525 A70-38764

Particulate matter interaction with ionized gas in external magnetic field and nonequilibrium state, examining free electron density

20 p3677 A70-39324

D region free electron temperatures at northern auroral zone by dual polarized antenna, observing incident noise radio fluxes

20 p3622 A70-39452

Metastable excitation levels in np/4 configuration for population inversion, discussing free electron collisions, forbidden line intensity and flow density pressure

20 p3642 A70-39751

Solar wind free electron number density measurement by Pioneer 6 spacecraft after solar proton flare, constructing plasma cloud models

21 p3881 A70-41079

Light generation by free electrons interaction with metallic diffraction grating, devising experiments for explaining incompatibility with simple electrostatic image theory

22 p4074 A70-42943

FREE ENERGY NT GIBBS FREE ENERGY

- Free energies of formation determined for tantalum silicides from EMF measurements on cells with solid thorium-yttria electrolytes 01 p0041 A70-10084
- Residual free energy effects on ferrites density and structure after sintering, using powders obtained by thermal decomposition of solid solutions of salts 07 p1355 A70-18703
- Interfacial energy and free energy estimation by quasi-continuum approximation for two component water-organic or organic-organic liquid systems 10 p1915 A70-23843
- Ternary phase diagrams and quaternary excess free energy prediction using binary data, applied to Pb-Sn-Zn, Ag-Pd-Cu and Pb-Sn-Cd-Bi systems 12 p2254 A70-27475
- Gaseous monoxides dissociation energies and free energy functions tabulation for calculating partial pressures 14 p2545 A70-30902
- Free energy and enthalpy of single ion solvation in water and propylene carbonate, using electrostatic model 15 p2695 A70-32829
- Micromagnetic theory of ferromagnets based on vector magnetization as continuous function of position, discussing free energy 19 p3471 A70-37953
- Heats of combustion and free isomerization energies of exo- and endo-isomers of 2- and 1-methylbicyclo heptane 22 p3982 A70-42680
- Al-Mg alloys solid phases free energy, entropies and formation heats determination by electromotive force measurement 24 p4357 A70-45230
- FREE FALL**
- Ignition of freely falling single fuel droplets, considering initial size, oxidizer temperature, fuel composition, droplet spacing, etc 04 p0733 A70-15540
- Drop sondes dynamic and aerodynamic design for lower Venus atmosphere based on solution for free fall of body in atmosphere with constant temperature gradient 09 p1766 A70-22935
- Free fall vehicle dynamics for wind tunnel measurements of research shapes used in computer simulation of vehicle trajectories [AIAA PAPER 69-229] 12 p2157 A70-28081
- Freely spinning finned stabilizer static wind tunnel tests on free fall research store, determining Magnus effect, body flow interference and static stability [AIAA PAPER 70-559] 13 p2340 A70-29024
- Blunt planetary entry body free fall drop tests determining low speed stability and base pressure characteristics [AIAA PAPER 70-577] 13 p2342 A70-29892
- Free fall sport jumping with parachute, discussing exercises for changing positions 16 p2842 A70-34175
- FREE FLIGHT**
- Nonlinear aerodynamic moments for arbitrary motions of bodies of revolution in free flight [AIAA PAPER 70-205] 06 p0971 A70-18102
- Free flight static, dynamic stability and drag data for 10 degree semiangle cone obtained at 8-16 Mach numbers [AIAA PAPER 69-133] 09 p1605 A70-23218
- Aerodynamic effects of bluntness on slender cones in free flight tests at Mach 17 [AIAA PAPER 70-554] 13 p2340 A70-29019
- Parawing canopy behavior during deployment in free flight at specific altitudes and dynamic pressures [AIAA PAPER 70-1189] 21 p3751 A70-41804
- Heat transfer measurements compared in free flight and in hypersonic wind tunnel at similar Reynolds number and temperature ratios [ICAS PAPER 70-06] 23 p4275 A70-44115
- FREE FLIGHT TEST APPARATUS**
- Free flight ranges for hypersonic simulation from Mach 1 to Mach 30, noting onboard high-g telemetry instrumentation 04 p0663 A70-14723
- Free flight wind tunnel test for feasibility of hypersonic drogue deployment into reentry vehicle wake [AIAA PAPER 70-587] 17 p3060 A70-35195
- Telemetry instrumentation for free flight wind tunnel models, discussing system component characteristics 17 p3047 A70-35495
- FREE FLOW**
- Two dimensional plane and axisymmetric free streamline flow problems solved by finite difference methods for supercavitating wedge in potential flows 01 p0065 A70-11127
- Incompressible slow viscous non-Newtonian flow with free surface solved by finite element method, showing computerized results for squeezed fluid between two plates 01 p0066 A70-11131
- Pressure gradient required for self preserving of turbulent jets and wakes with small mean velocity variations compared with free stream velocity 02 p0223 A70-11860

- Free stream turbulence effect on heat transfer in circular cylinder stagnation region 03 p0469 A70-14216
- Free stream turbulence effect on drag coefficient of bluff sharp edged cylinders with small square section 05 p0789 A70-15923
- Skin friction and heat transfer on flat plate in high velocity laminar motion with mass transfer for any free stream and injected gas combination 06 p1176 A70-17689
- Melting ablation for two dimensional and axisymmetric blunt bodies with body force, predicting gas-liquid interface temperature for free stream conditions 06 p1176 A70-17690
- Kinetic theory applied to free flow in spherical geometry to study collisionless thermal escape of particles from planetary atmospheres 06 p1147 A70-18293
- Conducting fluid incompressible flow in entrance of MHD channel by momentum integral method, permitting edge stress existence at boundary layer free stream interface [AIAA PAPER 69-724] 11 p2035 A70-25977
- Flat plate flowfield for freestream/jet interaction wrap-around on bodies of revolution, using separation shock model and blast wave analogy 11 p1976 A70-26135
- Intermittency role in free turbulent flow and EM wave scattering by hypersonic wakes 11 p1978 A70-26776
- Flush-mounted electrostatic probes behavior in shock tube over wide range of freestream conditions and bias voltage 12 p2236 A70-27810
- Subsonic kernel function applicability limited to surfaces with small inclinations to freestream, considering wing with deflected control surface 12 p2212 A70-28089
- Free flow field from underexpanded rocket motor nozzle and impingement effects of pressure and heat transfer to flat plate [AIAA PAPER 69-568] 13 p2473 A70-28510
- Strongly accelerated turbulent boundary layer, investigating free stream turbulence effect on heat transfer 14 p2564 A70-30252
- Heat transfer from acceleration induced boundary layer reverse transition, considering free stream turbulence effects 14 p2667 A70-31169
- Laminar near wake of cylinder at free stream Mach 6, using modified Lees-Reeves method 16 p2836 A70-33762
- Turbulent kinetic energy equation for determining turbulent flow fields applied to free mixing problem of constant density streams 16 p2894 A70-33856
- Collisionless monatomic gas flow density and velocity distribution on axis of diffusely reflecting circular cone at zero attack angle with free stream 16 p2839 A70-34273
- Annoyance assessment for sonic boom series exposure near airport 16 p2843 A70-34325
- Nozzle wall hypersonic turbulent boundary layers at free stream Mach number using pitot, hot wire, and wall fluctuation and static pressure measurements [AIAA PAPER 70-746] 17 p3065 A70-34497
- Model diffusion equation for inhomogeneous incompressible turbulent flow, applying to free turbulent flows 17 p3069 A70-34825
- Canonical coordinates for numerical computation of free surface flows, considering steady motion and elliptic partial differential equations 19 p3457 A70-37679
- Hypersonic test flow in arc heated wind tunnel, measuring freestream Pitot pressure, mass flux, stagnation point heat transfer rate and wall pressure 20 p3607 A70-40270
- Laminar incompressible free shear layers by method of weighted residuals for turbulent jets, obtaining velocity profiles for similarity and physical planes 20 p3613 A70-40286
- Elastoviscous incompressible electrically conducting oscillating free stream flow along infinite porous plate with suction in transverse magnetic field 20 p3685 A70-40508
- Free stream disturbances influence on hypersonic boundary layer transition Reynolds number in heated and unheated flows [AIAA PAPER 69-704] 21 p3809 A70-41744
- Nonuniform free stream supersonic flow past aerodynamic decelerators, calculating inviscid flow fields by method of characteristics [AIAA PAPER 70-1176] 21 p3746 A70-41837
- Free stream turbulence effect on heat transfer to stagnation point of sphere 21 p3953 A70-42095
- Unsteady hydromagnetic boundary layer flow past semiinfinite flat plate under steady magnetic field and small free stream perturbation 22 p4080 A70-42631

- Two dimensional steady flow around slender profiles at free transonic stream with curved compression shocks, approximating by hodographic method 23 p4131 A70-44023
- FREE JETS**
- Turbulence intensity and fluctuation rates in isothermal swirling free jets, using constant temperature hot wire anemometer method 01 p0059 A70-10031
- Radiation effect on enthalpy and velocity distributions of laminar compressible planar free jet 01 p0061 A70-10295
- Supersonic diffusion flames produced by subsonic and supersonic free jet injection of hydrogen into high enthalpy airstream 02 p0399 A70-12042
- Pulsation energy distribution in free turbulent incompressible jets, noting role of mean velocity distribution 03 p0466 A70-13384
- Laminar-turbulent transition in free axisymmetric viscous incompressible jet from shaped nozzle and long cylindrical tube 03 p0466 A70-13396
- Radiation-convection interaction in plasma free jet, using two-thermal-domain model for enthalpy distribution determination [ASME PAPER 69-WA/HT-50] 04 p0781 A70-14798
- Free plane turbulent jet virtual origin using tests determining influence of upstream conditions and nozzle shape 04 p0674 A70-15554
- Time mean flow property measurements for homogeneous and nonhomogeneous free turbulent jets [AIAA PAPER 70-130] 06 p1041 A70-18159
- Species concentration, jet structure and diatomic nitrogen rotational temperature measured for diffusive separation of nitrogen-helium mixture free jets, using electron beam 06 p1043 A70-18253
- Intensity measurements of molecular beams skimmed from nearly inviscid nitrogen and Ar free jets, interpreting beam attenuation in terms of collisional models 06 p1043 A70-18254
- Translational relaxation in low density axisymmetric hypersonic free gas jet, describing transition from isentropic to free molecular flow 06 p1043 A70-18277
- Rotational relaxation times for low density hypersonic nitrogen free jet, comparing measured and predicted impact pressures 06 p1043 A70-18279
- Nitric oxide free jet expansion, studying molecular cluster formation, inhibition and chemiluminescence 06 p1044 A70-18281
- Supersonic free jets condensation, examining kinetics of reactions in mono- or diatomic gases 06 p1044 A70-18282
- Supersonic molecular free jets using electron diffraction technique, discussing vibrational and condensation states 06 p1044 A70-18301
- Helium and argon atoms number densities radial profiles in supersonic free jets of binary gas mixtures by molecular beam sampling 07 p1341 A70-20105
- Radicals in low pressure supersonic free jets, investigating production by flash photolysis 07 p1343 A70-20126
- Monograph on convective heat flow in stagnation points of turbulent partly premixed free jet flames at cooled plates 08 p1598 A70-21343
- Shallow water waves simulation method for studying aerodynamic noise of free jet emitted from nozzle with variable wall roughness 08 p1485 A70-21608
- Free incompressible oil jet interaction with mobile plate, discussing plate configuration, oil feed pressure and nozzle diameter, applications to electrohydraulic converter design, etc 09 p1613 A70-22825
- Ar and nitric oxide free jets dimmer and cluster abundance dependence on nozzle diameter and reservoir temperature and pressure 09 p1733 A70-22907
- Monograph on stability of laminar boundary layer separation at free jets and turbulent free jet flames, considering effects of velocity gradients and temperature 11 p2146 A70-25499
- C-4 supersonic free jet test cell, discussing Concorde development contribution and model tests on full scale cell nozzle 11 p2031 A70-25853
- Free jet test facility for supersonic engine/ intake combination testing, discussing benefits to aircraft flying hours, development costs and safety 11 p2101 A70-25854
- Stick-slip problem for motion of free jet at low Reynolds numbers by Wiener-Hopf technique, con-

sidering two dimensional Newtonian jet without gravity

11 p2041 A70-26554

Free jet expansions in molecular beam sampling systems, using Sherman equations and chemical kinetic equations

13 p2389 A70-29608

Incompressible free jet characteristics determination from unique differential equation in laminar and turbulent flow regimes by unitary method

16 p2893 A70-33750

Combustion effects on mixing of axisymmetric supersonic and turbulent free jets to obtain species concentrations, pitot pressures and temperatures

16 p2998 A70-33860

Nonequilibrium vibrational energy and relaxation equation for carbon dioxide-nitrogen molecular gas mixtures in supersonic free jet exhausting into vacuum [AIAA PAPER 70-867]

16 p2895 A70-33910

Turbulent flows calculation based on two parameter turbulence model, considering model application to free jets

16 p2895 A70-34199

Mach disk structure in free low density expanding supersonic jet from static pressure probe measurements

17 p3068 A70-34696

Underexpanded carbon dioxide free jet expanding into vacuum from conical nozzles

17 p3070 A70-35246

Free turbulent incompressible jet, analyzing pulsating characteristics and energy balance with Reynolds stress equations

18 p3240 A70-36264

Discrete components of noise frequency spectrum of free supersonic jet

19 p3354 A70-38661

Plane symmetrical and axisymmetrical laminar and turbulent free jets, interpreting statistical character of boundary layer profiles

19 p3407 A70-38684

Irrational incompressible free falling jet, using asymptotic expansion solution for mixed boundary value potential problems

22 p4012 A70-42938

Free jet flow axial gradient effects on drag coefficient measurement of slender blunted cones at zero attack angle

23 p4135 A70-44584

Two dimensional incompressible laminar free jet, analyzing higher order viscous interactions with surrounding fluid by matched asymptotic expansions method

24 p4326 A70-45944

FREE MOLECULAR FLOW

Free molecular mass flow rate through vacuum seal separating two rarefied gas environments, using coupled integral equations formulated on kinetic theory [ASME PAPER 69-WA/FE-18]

04 p0625 A70-14779

Actively participating bounding surfaces effect on free molecular flow through slit or annular orifice situated in wall separating different pressure regions [ASME PAPER 69-WA/APM-26]

04 p0668 A70-14906

Circular cylinder drag in hypersonic transverse flows between continuum and free molecular flow, measuring drag and pressure distribution

04 p0615 A70-15089

Free molecular flow through long circular tube rotating with constant angular velocity about axis, discussing rotation speed effect on mass flow

05 p0836 A70-16994

Modified Maxwellian models for particle reflection in free molecular flow, correlating model parameters with gas-surface properties

06 p1110 A70-18259

Lift and drag forces measured on metal surfaces inclined to Ar ion stream above and below earth-satellite speeds in free molecular flow

06 p1111 A70-18269

Translational relaxation in low density axisymmetric hypersonic free gas jet, describing transition from isentropic to free molecular flow

06 p1043 A70-18277

Knudsen iteration for predicting cooled blunt body near free molecular drag in hypersonic stream, using BGK model for collisions

06 p0979 A70-18313

Free molecular drag for flat plate with normal protuberance, determining flowfield distribution functions and stress components

06 p0981 A70-18357

Aerodynamic forces and heat transfer on shielded flat plates in free molecular flow calculated by Monte Carlo technique

06 p0981 A70-18358

Continuum to free molecule hypersonic flow near flat plate sharp leading edge, studying Knudsen, Reynolds and Mach numbers effects

06 p0982 A70-18365

Monte Carlo analysis of free and near free molecular flow through circular tubes for mass, momentum and energy transfer

06 p1051 A70-18367

Sphere drag measurements in low density hypersonic transition and near free molecular flow

06 p1124 A70-18373

Dynamic simulation parameters for sphere drag coefficient data correlation in near free molecular flow

06 p0983 A70-18374

Free molecular heat transfer from sphere at rest in rarefied monatomic gas solved for Krook model of Boltzmann equation

06 p1183 A70-18375

Circular cylinders drag and pressure distribution in hypersonic range between continuum and free molecular flow

06 p0983 A70-18376

Sphere drag in near free supersonic molecular flow

06 p0983 A70-18377

Free flight ballistic range method for measuring average drag coefficients for microscopic spherical iron particles in free molecular flow

06 p0983 A70-18378

First collision Monte Carlo method for calculating aerodynamic drag on hard sphere and Maxwell molecular models in near-free molecular flow

06 p0983 A70-18379

Drag on infinite cylinder in hypersonic nearly free molecular flow for various angles of attack, using kinetic approach

06 p0983 A70-18380

Density profiles of sphere wake in rarefied hypersonic flow compared to free molecular flow calculations

08 p1431 A70-20591

Aerodynamic characteristics of nonconvex bodies in free molecular flow of monatomic gas

08 p1547 A70-21081

Transverse free molecular flow past broken plate of infinite span, determining aerodynamic coefficients

08 p1432 A70-21082

Aerodynamic characteristics of cylinder with wings in free molecular hypersonic flow of monoatomic gas at various angles of attack and slip

08 p1432 A70-21083

Aerodynamic coefficients of nonconvex bodies in free molecular flow of monatomic gases based on delta representation of flow velocity distribution function

08 p1432 A70-21084

Drag on cylinder in transverse rarefied gas flow varying from free molecular to almost continuum

09 p1604 A70-22448

Near-free molecular flow through orifice measured for velocity distribution dependence on Knudsen number and angular position using time-of-flight technique

10 p1918 A70-23969

Metastable time-of-flight technique for measuring free molecular flow velocity distribution

12 p2231 A70-27255

Permalloy evaporation rates from resistance heated W boat, revealing departure from free molecular flow

13 p2452 A70-29203

Supersonic rarefied flow over sharp flat plate with merged shock layer and free molecular-continuum transition, using electron beam fluorescence

14 p2529 A70-31028

Hypersonic near free molecule flow over flat plate with sharp leading edge, using linearized kinetic B-K-G equation for small thermal accommodation coefficient

15 p2673 A70-32796

Thin wire Langmuir probe measurements of electron temperature and density in transition and free molecular nozzle flow of short duration reflected shock tunnel

16 p2912 A70-33864

Rarefied gas dynamics at different Knudsen numbers, discussing elements of kinetic theory and analyzing free molecular and slip flows

17 p3070 A70-35037

Thermophoresis of aerosol particles in nearly free molecular nonuniformly heated gas, using linearized Boltzmann equation

18 p3292 A70-36254

Knudsen effusion in free molecular flows in supersonic jet during expansion through circular orifice, discussing power and heat transmission

18 p3346 A70-36379

Monoenergetic nitrogen free molecule beam impingement on solid surface, calculating satellite drag coefficients from momentum transfer measurements

21 p3745 A70-41743

Planar resonance probe in free molecular arc heated flowing plasma, examining shift nature in measured frequency position of minimum drawn current

22 p4081 A70-43013

FREE OSCILLATIONS

U FREE VIBRATION

FREE RADICALS

Postirradiation free radical processes in cellular organelles of rat liver exposed to gamma irradiation detected by graft copolymerization method

03 p0418 A70-13302

Photodynamic damage in biological cells, discussing free radical originators and protective action of thiourea, mono and polyvinylpyrrolidone, cysteine and antibiotics

03 p0419 A70-13306

Free radical antioxidation reactions in lipids from blood, liver, spleen, brain and intestines of rats exposed to ionizing radiation

03 p0419 A70-13309

Atomic oxygen and chlorine attack on refractory materials studied for kinetics of chemical reactions of free radicals and atoms

07 p1313 A70-19903

Free radical destruction by gamma irradiation in organic solids at low temperature measured by electron spin resonance spectroscopy, noting dosage relationship

07 p1225 A70-20324

Free radical formation in irradiated pyrimidines from ESR spectrum analysis of gamma irradiated single crystals of alloxantin, confirming radical stability

08 p1455 A70-20774

Free radicals role in high temperature surface reactions of solid metal oxide particles interacting with unburned flame gases

09 p1629 A70-22320

OH, NH and amine radicals concentrations in flame gases from flat ammonia-oxygen-nitrogen flames measured as function of distance from burner surface

09 p1788 A70-22343

Free radicals role in astrophysics, considering diatomic or triatomic radicals in atmospheres of earth, sun, planets, comets, stars and interstellar space

10 p1943 A70-24839

Free radical content changes in mice organs under hyperoxia and hypoxia

11 p1986 A70-25941

Microwave lines due to hydroxyl radical in interstellar medium, discussing emission from excited OH states

13 p2484 A70-28371

Kinetics for two free radical conversion processes in electron irradiated D, L-valine, measuring activation energies by electron spin spectroscopy

14 p2544 A70-30111

Disproportionation to combination ratio of hydrazyl radicals generated in absence of hydrazine direct decomposition

14 p2544 A70-30120

Spectrophotometry of comet Honda 1968c, showing free cation and radical emissions and head asymmetry

14 p2635 A70-30304

Radiation induced free radicals in thymidine single crystals, attributing electron spin resonance spectral observations to nature of various radicals

22 p3981 A70-42348

FREE STREAM EFFECTS

U FREE FLOW

FREE STREAMS

U FREE FLOW

FREE VIBRATION

Semidiscrete approximation of equation for free vibrations of beam with nonuniform cross section, using method of straight lines

01 p0213 A70-11636

Acoustical resonators free oscillations and pressure effects on damping, amplification, decay decrement and relaxation time

02 p0304 A70-12772

Free oscillations and surface wave dispersions from lunar models based on Orbiter data and corresponding pressure region of earth crust

02 p0379 A70-12777

Centrally clamped spinning circular disk free transverse vibration analysis within accuracy of numerical computations

03 p0584 A70-12931

Finite difference method for obtaining free vibrations natural frequencies and mode shapes for rectangular plates of varying stiffnesses

03 p0595 A70-13812

Stability analysis of rotors consisting of disks on massless shaft mounted in unsymmetrical flexible bearings, considering free and forced vibrations with damping neglected

03 p0599 A70-14248

Natural oscillations and flutter of three layer cylindrical shell in supersonic gas flow analyzed by semimomentless theory, discussing boundary value problems, damping effects, etc

03 p0600 A70-14301

Natural vibrations damping of holonomic mechanical systems with feedbacks not explicit function of time reduced to optimal stabilization problem

04 p0718 A70-14494

Thin elastic revolving shells free axisymmetric oscillations by determining differential equations eigenvalues and eigenfunctions

04 p0768 A70-14604

Free vibrations of reinforced elastic shell structures subject to constraints imposed by reinforcing elements, utilizing equivalent models without reinforcing elements

[ASME PAPER 69-WA/APM-25]

04 p0770 A70-14907

Orthogonality of aircraft natural vibration modes by calculating complete matrix of generalized masses [DGLR-69-59] 04 p0774 A70-15150

Free vibrations of layer of micropolar continuum, analyzing displacements, microrotations and frequencies as wave number power series 04 p0777 A70-15498

Stiffness and mass matrices of free-free vibration structure reduced to eliminate zero frequencies 04 p0778 A70-15553

Eigenvalues upper and lower bounds of vibrating anisotropic material with multiple elastic constants, predicting free vibration frequencies by bounding isotropic moduli 05 p0937 A70-16408

Electrical network models simulating initial and boundary value problems of applied mechanics, exemplifying with string free vibrations and thin plate bending 06 p1094 A70-17928

Forced and free vibrations of shaft carrying unsymmetrical rotor, studying effects of distributed shaft mass and nonlinear shaft stiffness 07 p1401 A70-18976

Human head model for craniocerebral trauma analysis, studying fluid filled spherical shell free vibrations axisymmetric response 07 p1219 A70-19243

Circular plates with optimal natural frequency of transverse vibrations, discussing boundary conditions 07 p1405 A70-19256

Geomagnetic tail natural oscillations, studying magnetospheric substorms role 07 p1268 A70-19499

Bladed wheels stability in centrifugal compressors, calculating natural vibration frequencies of rotors 07 p1364 A70-19634

Hard alloy mixture shaping by free vibrational compacting of powders 07 p1296 A70-19801

Natural vibration frequencies and mode shapes for laminated orthotropic shells of revolution using finite element method 07 p1411 A70-19951

Natural axisymmetric vibrations of cylindrical shell with hollow filler, analyzing motion by shallow shell and elasticity theory dynamic equations 07 p1415 A70-20191

Natural frequencies and modes of tapered swept back rudder fin of aircraft using vibration analysis 07 p1417 A70-20417

Natural oscillation frequencies determined for shallow shells with hinged and clamped edges 08 p1583 A70-20484

Natural oscillations of three dimensional bundle of parallel strapped rods with variable elastic mass parameters determined by Hamilton-Ostogradskii variational principle 08 p1583 A70-20485

Natural oscillation frequencies of three layer plates with rectangular planar form determined by integrated representations method 08 p1583 A70-20495

Laser resonator with concave mirrors and ring aperture as radiation outlet, calculating natural oscillations by wave equation 08 p1510 A70-20508

Variable coefficient equations for free oscillations of shallow shells of variable thickness in Vlasov moment theory 08 p1586 A70-21011

Earth free diurnal nutation parameters determination from latitude observations, establishing amplitude and phase time-independent variations 08 p1488 A70-21154

Finite bending elements for static deflections of annular and circular plates loaded by concentrated forces, calculating free vibrations 08 p1588 A70-21243

Free in-plane flexural vibrations of circular rings, developing equation of motion to include shear deformation and rotatory inertia effects 08 p1592 A70-21473

Free vibrations and dynamic buckling of hinged extensible beam under axial force 09 p1768 A70-22061

Natural oscillation frequencies of subsonic gas flow past plate array, solving eigenvalue problem by splicing method 09 p1603 A70-22117

Free and forced vibrations of three layer freely suspended plate with allowance for energy dissipation 09 p1772 A70-22468

Free vibrations of plates and beams of pyrolytic graphite type materials, analyzing transverse shear deformation and rotatory inertia [AIAA PAPER 69-55] 09 p1780 A70-23210

Free vibration of rib stiffened freely supported circular cylindrical shells, verifying rib eccentricity importance to natural frequencies by numerical solutions 09 p1780 A70-23211

Rotating cantilever beams mounted on disk periphery, analyzing forced and free vibrations characteristics 09 p1781 A70-23283

Natural bending vibrations of circular plates with allowance for stress tensor asymmetry, deriving transcendental frequency equation 09 p1782 A70-23292

Elastic chain systems stability and natural vibrations using parameter coupling method permitting integral equation construction 09 p1784 A70-23596

Axisymmetric free vibrations of orthotropic cylindrical shell loaded on ends by constant axial force, investigating nonlinear elasticity 09 p1785 A70-23625

Natural oscillation mode in symmetrically graded p-n junction using Missawa small signal equations for avalanche diode 09 p1653 A70-23804

Energy dissipation in free oscillations of multilayer shells consisting of alternating rigid elastic layers and soft fillers, deriving equations of motion 10 p1956 A70-24249

Small natural vibrations effect of solar sail-propelled system on heliocentric orbit motion 10 p1950 A70-24319

Large amplitude free vibration of rectangular plates subjected to aerodynamic heating with different boundaries and temperature distribution, deriving Duffing nonlinear differential equation 10 p1957 A70-24417

Large amplitude free vibration of heated circular plates, analyzing energy equations by successive approximation method and elliptic integrals 10 p1957 A70-24480

Free vibration analysis of elastic structures using Rayleigh-Ritz method and finite element methods 10 p1961 A70-25055

Natural vibration analysis of uniform cylindrical and cantilever rectangular tubes with cutouts 10 p1961 A70-25057

Nonaxisymmetric free oscillations of self gravitating disk reduced to eigenvalue problem to investigate galactic spiral structures 10 p1917 A70-25207

ARAVA aircraft free-free vibrational characteristics evaluation by integral-aircraft lumped mass analytical method verified by ground resonance test 11 p1979 A70-25688

Inplane and rotary inertia effects on free vibration frequencies of circular cylindrical shells eccentrically stiffened by orthogonal set of stringers and/or rings 11 p2135 A70-25993

Free vibration characteristics of circular cylindrical shells of finite length, utilizing Flugge equations 11 p2135 A70-25997

Axisymmetric and unsymmetric free vibrational modes of right-circular conical or cylindrical sandwich shells with free edges, discussing Rayleigh-Ritz solution 11 p2145 A70-26700

Kane-Mindlin equations and frequency spectra determined for free extensional vibrations in isotropic elastic plate strips 11 p2146 A70-26703

Pressurized orthotropic cylindrical membrane shells free and forced vibration, considering dynamic response dependence on internal pressure 12 p2326 A70-27815

Clamped beams steady state free and forced response and stability for large amplitude motion, discussing multimode analytical and numerical technique 12 p2327 A70-27821

Aerofoil free vibrations with fixed center of gravity in incompressible potential flow under representative previous histories effect 12 p2328 A70-28214

Book on vibrations covering natural oscillations, damped and undamped oscillations, energy sources, forced vibrations, resonance and multiple degree of freedom systems 13 p2515 A70-29452

Free and forced motion characteristics in absolutely stable nonstationary nonlinear system analysis by variational approach 13 p2453 A70-29716

Complex plates free transverse oscillation modes and frequencies using Ritz method 15 p2818 A70-32183

Geomagnetic tail natural oscillations, studying magnetospheric substorms role 15 p2732 A70-32744

Displacements and stresses in freely vibrating aeolotropic deep spherical shells, including effects of shear deformation, rotary inertia and transverse normal strain 16 p2993 A70-34091

Free oscillations of Euler-Bernoulli and Timoshenko cantilever beams of variable cross section, obtaining approximate modes and natural frequencies bounds 16 p2994 A70-34234

Free and forced vibrations of linear systems, dissipative systems with nonlinear friction, aeroelastic vibrations, rotor vibrations, mode locking, random vibrations, etc 16 p3004 A70-34277

Mechanical models of single speed gears for torsional vibrations, taking into account nodes of first free vibration mode 16 p2995 A70-34289

Free vibration of thin circular cylindrical shells, comparing experimental results to Egle-Sewall analysis 17 p3181 A70-34520

Three dimensional linear small deformation theory of elasticity solution for free vibration of simply supported homogeneous isotropic thick laminated rectangular plates 17 p3181 A70-34522

Natural frequencies and corresponding mode shapes for free flexural vibrations of circular plates, extending to elastic support cases 17 p3186 A70-34980

Flexible space vehicles dynamics and control covering free vibration analysis, thermal flutter and structural deflection effect on attitude control 17 p3177 A70-35233

Single axis gyroscopic stabilizer with floating-type integrating gyro, describing natural oscillations by differential equations of motion 17 p3096 A70-35701

Damping characteristics /absorption coefficient/ of dissipative systems, defining authentic value of energy dissipation characteristic determination from natural vibrations damping 17 p3192 A70-35711

Nonlinear differential solutions for free isochronous oscillations of conservative one degree of freedom oscillators 18 p3283 A70-36386

Mechanical systems spontaneous oscillation due to different critical velocities with and without arbitrarily small damping 18 p3338 A70-36430

Natural vibrations of free autonomous system of carried and carrier solid bodies connected by elastic couplings 18 p3342 A70-36594

Unidirectional composites subjected to free vibration and axial end loading, considering longitudinal stress wave propagation in fiber direction 19 p3540 A70-37954

Rectangular plates free and forced vibrations, including rotatory inertia and shear deformation effects in dynamic response analysis 19 p3544 A70-38327

Rectangular plate with three clamped edges, analyzing free vibration by Ritz method with deflection functions 19 p3544 A70-38328

Thin elastic conical shell axisymmetric solution for free vibration in terms of power series 19 p3545 A70-38335

Surface waves free period partial derivative correlation and relation to resolution of gross earth data 19 p3414 A70-38374

Elastic panel nonlinear free vibrations, analyzing small amplitude phenomena 20 p3672 A70-39493

Thin elastic shell natural vibrations, examining orthogonality of form shapes 20 p3724 A70-39862

Viscosity and vessel geometry effects on fluids natural and forced oscillation, taking surface tension into account 20 p3614 A70-40438

Free vibration optimization analysis by reducing stiffness and mass matrices 21 p3933 A70-40587

Complementary variational principles applied to free oscillations of incompressible fluid in container, using linearized hydrodynamic equations 21 p3807 A70-41323

Fluid filled elastic spherical shell, calculating free vibration axisymmetric response and fundamental mode 21 p3940 A70-42053

Elastic wave propagation in isotropic homogeneous bodies, considering free vibrations and propagation velocity 21 p3940 A70-42099

Kinetic friction and friction induced vibration measurements by pin-on-disk tribometer [ASME PAPER 70-LUBS-15] 22 p4044 A70-42446

Elastic bar attached to free edge of infinite length cantilever plate, calculating free flexural vibration for comparison with experiment 22 p4114 A70-42648

Free and forced oscillations of dynamic system with linear hysteretic damping, using nonlinear model 22 p4114 A70-42700

Natural oscillations of cylindrical shell with elastic filler, using simple load distribution model 22 p4119 A70-43572

Rectangular plates natural vibration problem, using straight line method with approximate separation of variables 23 p4265 A70-43982

Thin circular cylindrical shells with clamped-clamped and fixed-fixed edges, calculating natural frequencies of nonsymmetrical free vibrations 23 p4266 A70-43997

Iterative Rayleigh-Ritz method for eigenvalue determination in natural vibration problems
23 p4270 A70-44580

Thick isotropic rectangular laminates free vibration and buckling, applying three dimensional linear small deformation theory of elasticity
24 p4422 A70-45296

Frequency equations derived for cylindrical panels with surface loading, comparing free vibration natural frequencies of panels with attached mass at centers
24 p4422 A70-45297

Elastic orthotropic plates vibration analysis by finite strip method via eigenvalue matrix, obtaining natural frequencies and modal vectors by small computer
24 p4423 A70-45579

Ring-stiffened thin circular cylindrical shells, calculating free vibration natural frequencies and mode shapes by finite element method
24 p4427 A70-46067

Periodically supported beams and plates free vibration, calculating natural frequency spectrum distribution and normal modes
24 p4427 A70-46070

FREEDOM FIGHTER AIRCRAFT
U F-5 AIRCRAFT

FREEZING
Growth rate and spatial distribution of solid deposit freezing onto vertical surface in presence of convective heat transfer at moving phase interface
12 p2331 A70-27696

Radiation effects on dihydrothymine in frozen sulfuric acid solutions, detecting thymine after melting via low temperature UV absorption measurements
20 p3583 A70-40454

Freezing and melting of warm water flow at stagnation point over cooled plate for convective condition at solid-liquid interface
21 p3949 A70-41311

Finite difference numerical integration method for melting and freezing problems extended to free convection in liquid and unequal densities for phases
21 p3953 A70-42093

FREEZING POINTS
U MELTING POINTS

FREIGHT COSTS
Aircraft transport tariffs used to determine economic approach to design
07 p1426 A70-18841

Air freight transportation economics, rate reductions and comparison with passenger aircraft
09 p1792 A70-22244

Air cargo transport growth, considering deterrents of high freight rates, ground movement time and customs clearance
17 p3204 A70-35853

Air freight containers in continuous air/land transportation chain, discussing weight, performance, cost, technical concepts and inter and nonintermodal prototypes
22 p4007 A70-43273

FRENCH GUIANA
Guiana Space Center for French space programs, describing launch complexes, measurement and control methods, safety methods, launch operation planning, etc
04 p0663 A70-14939

French rocket launching base at French Guiana, discussing launch pads, tracking stations, control centers and storage areas
11 p2030 A70-25519

FRENCH SATELLITE
NT DIADEME SATELLITE

FRENCH SPACE PROGRAMS
Liquid propulsion studies at CNES
10 p1930 A70-24374

Valois motor with nitrogen peroxide oxidizer for Diamant B first stage, describing design and assembly problems
10 p1930 A70-24375

French rocket launching base at French Guiana, discussing launch pads, tracking stations, control centers and storage areas
11 p2030 A70-25519

Plumeur-Bodou satellite telecommunications center, discussing antennas
11 p2031 A70-26009

Protective clothing for personnel handling toxic and corrosive liquid propellants in hot climatic conditions at Guyana Space Center
12 p2179 A70-28043

Diamant B satellite launcher testing and construction, discussing DIAL/WIKA scientific satellite launch
12 p2314 A70-28299

Report to COSPAR on French space program, discussing rocket sounding, satellite data, scientific experiments, etc
15 p2829 A70-31711

Rockets trajectories recording on real time at Guiana Space Center using IR pointing deviation meter
15 p2698 A70-31960

Stabilized platform stellar detector for French probe balloons, using semicircular light modulator
15 p2738 A70-32249

Low, medium and high specific impulse microthrusters development in France, using cold gases, subliming solids, hydrazine, ammonia and cesium ions
16 p2969 A70-33613

[AIAA PAPER 70-617]
Combustion chamber, turbopump and combustion control system for French turbopump-fed booster rocket motor
20 p3688 A70-39649

Dioscours project for ATC over Atlantic Ocean, describing distance measurement by simultaneous use of two geostationary satellites
21 p3848 A70-41258

FRENKEL DEFECTS
Frenkel pairs and interstitial hydrogen atoms observed in thin silver films after proton bombardment
12 p2253 A70-27209

Upper critical field dependence on s- and p-wave scattering of Frenkel effects in electron irradiated niobium
13 p2471 A70-29535

FREON
N-heptane and Freon-13 droplets vaporizing size and temperature at supercritical pressures in heated air stream
06 p1182 A70-18204

[AIAA PAPER 70-6]
Stress corrosion cracking in Ti-Al-V alloy exposed to Freon environments
17 p3114 A70-34373

Heated surface orientation and reduced gravity effects on Freon 113 nucleate
21 p3948 A70-41204

FREQUENCIES
NT AUDIO FREQUENCIES
NT BEAT FREQUENCIES
NT BROADBAND
NT C BAND
NT CARRIER FREQUENCIES
NT CRITICAL FREQUENCIES
NT CYCLOTRON FREQUENCY
NT EXTREMELY HIGH FREQUENCIES
NT EXTREMELY LOW RADIO FREQUENCIES
NT HIGH FREQUENCIES
NT INFRASONIC FREQUENCIES
NT INTERMEDIATE FREQUENCIES
NT IONIZATION FREQUENCIES
NT LOW FREQUENCIES
NT MAXIMUM USABLE FREQUENCY
NT MICROWAVE FREQUENCIES
NT NYQUIST FREQUENCIES
NT PLASMA FREQUENCIES
NT RADIO FREQUENCIES
NT RESONANT FREQUENCIES
NT SUPERHIGH FREQUENCIES
NT SWEEP FREQUENCY
NT ULTRAHIGH FREQUENCIES
NT VERY HIGH FREQUENCIES
NT VERY LOW FREQUENCIES

Frequency bandwidth reduction for geophysical data transmission from satellites or lunar stations by time correlation of signal and transmission channel band changes
05 p0847 A70-15968

Frequency dependence of impedance of p-n-n diode with short base in presence of large forward current densities
20 p3598 A70-40021

FREQUENCY AMPLIFIERS
U AMPLIFIERS

FREQUENCY ANALYZERS
Ionospheric probe for simultaneous measurement of radio signal reflection coefficient and amplitude-frequency characteristics
04 p0684 A70-15746

Closely spaced frequencies method of determining ionospheric electron content from Faraday rotation measurements
07 p1271 A70-20156

Pulsed microwave spectrum analyzer using holography and Fourier spectroscopy compared with frequency methods
09 p1675 A70-22485

Microwave Gunn oscillators loaded Q factors determined on basis of frequency changes resulting from constant-depth probe movement along output line
09 p1645 A70-22601

Ultrasonic pulse frequency spectrum analyzer, describing electronic components, transducer type and positioning, beam collimation, applications in testing, etc
10 p1895 A70-24830

Ionospheric probe for simultaneous measurement of radio signal reflection coefficient and amplitude-frequency characteristics
14 p2576 A70-30830

Doppler radar frequency tracker with servomechanism applicable to velocity computation of aircraft for self contained navigation
18 p3226 A70-36063

Amplitude-phase data from gathering receiving antenna array, obtaining Doppler frequency spectrum as arrival angle function
20 p3599 A70-40319

Statistical confidence levels for frequency analysis, detecting peak sinusoid for desired signal to noise ratio
21 p3825 A70-40867

FREQUENCY ASSIGNMENT
Channels demand assignment between earth terminals of international satellite communication systems, examining multiple access problems
03 p0453 A70-14323

Adaptive frequency selection of optimum channels for radio communication on noninterference basis, discussing implementation and compatibility problems with nonadaptive systems
05 p0814 A70-16347

LUF /lowest useful frequency/ prediction for HF sky wave communication, emphasizing prediction methods using computers
07 p1229 A70-19156

Mathematical models of vertical antennas of finite length and height, discussing signal strength and LUF determinations
07 p1240 A70-19167

Signaling system for communication satellites demand assignment, considering error control, unit negative acknowledgement, system parameters selection, control signals, etc
10 p1837 A70-24347

Demand assignment /DAMA/ and preassignment /PAMA/ Multiple Access Systems mix for cost minimization, developing algorithm for satellite high usage groups and overflow facilities
10 p1838 A70-24357

Demand assignment economics relative to ground stations in satellite telecommunication systems
10 p1838 A70-24360

Digital transmission techniques optimal utilization of assigned frequency spectrum for phase modulation of frequency carriers
10 p1839 A70-24365

Message traffic problems in satellite telephone network, considering traffic distribution characteristics, interarrival mean time, bidirectional traffic, etc
10 p1839 A70-24367

Geostationary satellite communication bandwidth increase by reusing same frequency band in multiple independent earthward beams, discussing modulation and interference noise allocation effects
11 p1996 A70-25405

[AIAA PAPER 70-442]
COMSAT measurement of precipitation scatter effects on propagation for frequency sharing with terrestrial radio relay terminals
11 p1997 A70-25413

[AIAA PAPER 70-499]
Multiple-access and demand-assignment techniques, discussing compatibility of PCM-FDMA /SPADEF/, PCM-TDMA, ATIC and INTEL SAT 4 systems
11 p1997 A70-25415

Orbit utilization, discussing sharing of satellite communication frequency bands and use of multiple earthward antenna beams
11 p1999 A70-25428

Frequency sharing between satellite-transmitted FM TV signals and terrestrially transmitted AM-VSB TV signals
11 p2001 A70-25467

[AIAA PAPER 70-438]
Report on Spectrum Utilization and System Constraints session of Intelsat/IEE International Conference on Digital Satellite Communication, London, November 1969
11 p2002 A70-25486

[AIAA PAPER 70-465]
Channel assignment, considering low cost solution and co-channel interference
11 p2010 A70-26310

Optimal pulse allocation for radar array in simultaneous tracking of multiple targets, suggesting algorithms
13 p2365 A70-29068

Demand assigned domestic satellite communications system with capability of single hierarchy switching and serving terrestrial common carriers and direct users
14 p2552 A70-31351

Lx band characteristics and utilization, describing evolutionary systems based on TACAN and IFF
16 p2948 A70-33452

Frequency allocation in EM environment of 1970s based on interference compatibility analysis
17 p3045 A70-35158

Satellite broadcasting frequency resources, discussing interference, frequency sharing, antenna transmitting and receiving patterns, etc
17 p3046 A70-35271

UN space committee discussion on rules governing direct TV broadcasting by satellite, taking into account frequency allocation, geostationary orbits, etc
17 p3201 A70-35779

International Telecommunication Union /ITU/ legal recommendations on radio spectrum use, interference and frequency assignment problems
20 p3585 A70-39411

Millimeter wave space-to-space and space-to-ground satellite communication links frequency allocation problems
21 p3787 A70-41335

Single channel per carrier PCM FDMA demand assignment satellite communication system, discussing digital encoding, quadrature PSK modulation, etc 21 p3791 A70-41367

FREQUENCY BANDS U FREQUENCIES

FREQUENCY COMPRESSION DEMODULATORS

Antenna-central building connecting equipment at Pleumeur-Bodou space telecommunication center, discussing frequency compression demodulators 05 p0819 A70-15985
Threshold characteristics of compression line demodulator obtained from output SNR 09 p1631 A70-22017

FREQUENCY CONTROL

NT AUTOMATIC FREQUENCY CONTROL

Frequency control of ruby laser pumped lithium niobate singly resonant parametric oscillator by radiation injection of CW Nd-YAG laser 01 p0110 A70-10566

Frequency locking of flashlamp pumped Rhodamine 6G dye lasers to D lines of Na vapor by Faraday rotation, noting doublet splitting 01 p0110 A70-10568

Gas laser frequency stabilization by employing Zeeman splitting in external discharge tube containing He-Ne mixture in alternating magnetic field 03 p0498 A70-13090

Frequency selection systems synthesis with digital AND type logical elements, noting basic design relations 04 p0647 A70-14404

Minimum time frequency transitions in phase locked loops with phase and frequency controls using Pontryagin principle, obtaining switchless control strategies 04 p0652 A70-15339

Steady state operation and synchronization range of frequency dividers with complex feedback derived by symbolic abbreviated equations and modulation technique 05 p0813 A70-16263

Polarization interference filter as laser resonator frequency selector, showing Q factor measurable within spontaneous emission line 06 p1082 A70-17771

Dispersive resonator for near IR frequency control of neodymium-silicate glass laser 08 p1512 A70-20850

Natural frequency of paramagnetic amplifier retuned by coupling Cr ions doped silver coated ruby resonator to passive resonator 10 p1901 A70-25138

Dual conversion receiver for remote frequency control in satellite TV distribution system [AIAA PAPER 70-414] 11 p2002 A70-25482

Data sampling system compensation based on bending frequency filtering through information obtained by varying sample rate, using saturn 5 launch vehicle simulation 12 p2192 A70-27411

Tapered Gunn effect microwave oscillators frequency tuning by resistive quenching of high field domain 12 p2199 A70-27986

Shielded-cathode mode Gunn oscillators to eliminate constraints on operating frequency 12 p2200 A70-28056

Active RC bandpass filter with independent linear control of Q peak gain and frequency 13 p2376 A70-28801

Frequency selection in telemetry taking into account systems for minimum interference and crosstalk 13 p2366 A70-29216

Ruby laser radiation frequency control by birefringent calcite plate and KDP electro-optical Q switch 13 p2428 A70-29363

Pulsed noise stability of discrete data transmission system having multipositional frequency manipulation as compared to binary system 14 p2547 A70-30148

Binary varactor diode microwave device, displaying two capacitance values in reverse bias operation for application in phased array systems and frequency control 14 p2556 A70-30919

Frequency locked noise effect on beat frequency measurement of angular velocity with ring laser, comparing gyroscope and phase methods 15 p2749 A70-31551

Gunn oscillator external negative differential/END/conductance broadband measurement noting effect of cavity control 16 p2875 A70-33398

Frequency discrimination circuits for multiple remote control receiver systems with high harmonic noise levels 18 p3235 A70-36428

Frequency dependent reversible switching characteristics of glass semiconductors, assuming current control 19 p3389 A70-38070

Crystal controlled digital frequency setting for microwave oscillators in mobile FM radio links with remote handling 20 p3596 A70-39162

Mutual synchronization of oscillators at multiple frequencies, analyzing effect of tuning on frequency and phase 20 p3597 A70-39252

Homing radar tracking accuracy improvement by glint reduction using frequency diversity [AIAA PAPER 70-992] 20 p3586 A70-39538

Invariance conditions in two parameter frequency control unit for electric power generator driven by variable speed motor 20 p3565 A70-39850

Frequency locking and control of autodyne oscillating NMR detector for signal averaging 21 p3827 A70-41454

Digital frequency and phase flip-flop comparator for slave oscillators fine control by master frequency 22 p3996 A70-42819

Current oscillations produced in finite-length electron hole semiconductors by strong electric and magnetic fields, discussing HF stabilization 22 p4084 A70-43469

Controlled self excited quartz triode oscillator, calculating flicker noise effect on frequency stability 23 p4171 A70-43959

FREQUENCY CONVERSION

U FREQUENCY CONVERTERS

FREQUENCY CONVERTERS

NT FREQUENCY DIVIDERS

NT FREQUENCY MULTIPLIERS

NT FREQUENCY SYNTHESIZERS

NT PARAMETRIC FREQUENCY CONVERTERS

Light signals frequency converters and amplifiers applied to detection problems 05 p0813 A70-16264

Circuit and operation of transistorized linear voltage-to-frequency converter performing current integration proportional to input signal 06 p1022 A70-17779

Second harmonic generation and frequency conversion efficiencies for laser beam shaping in nonlinear medium 08 p1514 A70-21984

Vacuum tube signal frequency converters for meteorological telemetry measurements including blocking oscillators, multivibrator and fantastron 09 p1718 A70-23332

Precision frequency analog converter using crystal oscillator and transistor switch reducing errors 09 p1653 A70-23698

Ground frequency converters for reception of NTSC color TV transmission from synchronous communication satellites, tabulating cost estimates [AIAA PAPER 70-440] 11 p2002 A70-25490

KDP crystal single cut for laser beam frequency conversion and tuning 12 p2245 A70-27302

Frequency conversion during multiple phase modulation of supply voltage by pulse width technique 14 p2548 A70-30372

Voltage-frequency conversion technique using FM principle and RF oscillator beating with crystal oscillator output 15 p2705 A70-32705

Optical emission conversion from solid state lasers into far IR region by nonlinear polarization with difference frequency generation 19 p3448 A70-38741

Voltage-to-frequency transducers with negative feedback, analyzing errors and conversion transconductance 20 p3601 A70-39789

Soviet book on modulation-type frequency converters based on electromagnetic and semiconductor elements covering modulators static and dynamic characteristics, optimal operating conditions, etc 24 p4319 A70-45626

FREQUENCY DISTRIBUTION

Langmuir oscillations excited by electron beam in plasma during instability development investigated for temporal and spatial structure, using visualization 01 p0150 A70-10174

Flow velocity pulsations effect on frequency spectrum of flow optical fluctuations, discussing methods for separating turbulence characteristics 01 p0092 A70-10996

Geomagnetic field pulsations frequency changes in relation to geomagnetic and solar activity level 01 p0084 A70-11559

Tangential force applied to column end by jet reaction from nozzle clamped to column end, obtaining critical load and oscillation frequency 02 p389 A70-12644

Frequency amplitude-threshold EEG analyzer with automatic distribution of filter signals over recording levels 03 p0434 A70-13695

Three dimensional elasticity theory of generalized continua developed from atomic lattice theory model, 03 p0525 A70-14232

discussing frequency spectra, specific heat and applications to crystal defects 03 p0525 A70-14232

Variable RF signals in pulsed radar, examining circuits design for required functions 03 p0452 A70-14281

Frequency distribution of apparent visual magnitudes of meteors observed from November 1960 to January 1967 04 p0750 A70-14707

Discrete frequency noise generation from axial flow compressor blade row, using experiments in small scale Freon loop [ASME PAPER 69-WA/FE-22] 04 p0733 A70-14777

Periodic drag of vibrating cylinders as function of excitation amplitude and frequency, noting similarity to nonlinear oscillator subjected to forced vibration 04 p0691 A70-15148

Statistical ionospheric model of sporadic E layer frequency characteristics dependence on equipment parameters, determining permissible variation of transmitter power and receiver gain 04 p0682 A70-15727

Inhomogeneity and water vapor absorption influence on frequency spectrum of amplitude fluctuations of plane wave propagating in turbulent atmosphere 05 p0813 A70-16252

Radio wave scattering and brightness on uneven interface, determining frequency spectrum of signal reflected from surface assuming uniformly moving receiver 05 p0813 A70-16261

Random vibrations of linear system with viscous damping excited by stochastically acting force with monotonically varying frequency, using correlation method 05 p0882 A70-16372

Automatic formant-frequency extraction using vowel-type spectrum, inverse filtering, moment calculation and evaluation by synthesized speech 06 p1009 A70-17909

Frequency analysis of arterial sounds used in studying atherosclerosis, correlating spectra with jet flow turbulence past occlusion [AIAA PAPER 70-144] 06 p1003 A70-18220

Phonon spectrum of mixed semiconductor crystals based on AIII-BV and AII-BVI compounds, studying frequency spectrum as function of crystal composition 07 p1300 A70-19867

Frequency characteristics deviation of discrete cosmic radio emission sources from exponential law, analyzing radio wave absorption in galactic and intergalactic media and ionized hydrogen 07 p1370 A70-20315

Frequency spectra of Pi 2 geomagnetic field pulsations, noting effects of aural zone location, configuration and structure 07 p1277 A70-20438

Frequency characteristics optimization of symmetrical octupole bridge networks based on relationships between electrical parameters functions and impedance matrices eigenvalues 08 p1468 A70-20572

Resonator system frequency spectrum in coaxial inverted magnetron with stepped interaction space 09 p1651 A70-23643

Spatial frequency spectra of three dimensional phase object and three dimensional hologram, discussing interaction characteristic for monochromatic illumination 10 p1888 A70-24263

Langmuir oscillations excited by electron beam in plasma during instability development, investigating temporal and spatial structure using visualization 10 p1925 A70-25019

Vibrational motion sensors amplitude-frequency characteristics correction by passive electrical filters, deriving spectral transmittances 11 p2055 A70-26444

Frequency spectrum determination of hydrodynamic instability excited in fast large amplitude magnetosonic wave 12 p2278 A70-27542

Central sidelobes of multifrequency radar signals ambiguity functions, discussing code composition and auxiliary modulations 12 p2185 A70-27686

Frequency spectra of log amplitude fluctuations of electromagnetic wave propagating in turbulent atmosphere, using geometrical optics approximation 12 p2190 A70-28173

Differentiating Fabry-Perot interferometer, obtaining emission spectrum derivatives respecting frequency in millimeter range 12 p2238 A70-28177

Comparative passband of optimal and fixed frequency systems in ionospheric scatter communications during nighttime 14 p2547 A70-30239

Linearized gas mixture nonequilibrium flow fields, analyzing consequences of multiplicity of principal relaxation frequencies 14 p2566 A70-30474

Statistical ionospheric model of sporadic E layer frequency characteristics dependence on equipment parameters, determining permissible variation of transmitter power and receiver gain

14 p2575 A70-30811

Spectral line formation, assuming frequency redistribution for plane parallel stellar atmosphere containing nonuniform distribution of internal emission sources

14 p2651 A70-31289

Gyrosynchrotron from accelerated electron, discussing effects of cold and collisionless magnetoplasma on far field and frequency spectra

15 p2728 A70-31989

Radiometer employing frequency domain coding of noise-like signal spectrum, comparing with Dicke system

16 p2871 A70-32926

Frequency spectra of gravitational waves radiated from celestial phenomena, suggesting mass exchange in binary containing neutron star

17 p3067 A70-34619

Pc 1 pulsations occurrence frequency diurnal annual and 11 year variations at midlatitudes, relating distribution with carrier frequencies of perturbation

19 p3408 A70-37316

PCM data transmission, considering baseband code and modulated carrier formats and spectral distributions

19 p3379 A70-37905

Resonance radiation transport in optically thick media, investigating complete frequency redistribution mathematical assumption

20 p3671 A70-39021

He-Xe laser with pure Xe-136 gain cell inside cavity, observing enhanced Lamb dip in power output vs frequency curve

20 p3640 A70-39154

Bubble frequencies random distribution during boiling of pure liquids and binary liquid mixtures by optical measurement

21 p3941 A70-40775

Energy losses frequency distributions for fast charged particles in small pathlengths in equimolar He-carbon dioxide mixture

21 p3852 A70-40973

Amplitude and phase frequency characteristics of open and closed multiloop nonlinear automatic control systems by graphical methods

22 p4000 A70-42830

Steady state frequency spectra for Alfvén waves and MHD turbulence in collisionless plasma with nonlinear interaction by particle scattering

24 p4383 A70-45114

Periodically supported beams and plates free vibration, calculating natural frequency spectrum distribution and normal modes

24 p4427 A70-46070

Comparative passband of optimal and fixed frequency systems in ionospheric scatter communications during nighttime

24 p4316 A70-46314

FREQUENCY DIVIDERS

Low loss low sidelobe N-way microwave optical power divider for single plane electronically steerable Ku band phased array antenna

04 p0655 A70-14624

Sound propagation along cylindrical duct of wind tunnel, discussing fluid flow effect on modal cut-off frequencies

04 p0719 A70-15078

Pulse counting frequency divider with discrete phasing device for use with quartz clock and electron beam chronoscope

04 p0694 A70-15492

Steady state operation and synchronization range of frequency dividers with complex feedback derived by symbolic abbreviated equations and modulation technique

05 p0813 A70-16263

Numerical analysis of magnetic frequency divider operation

09 p1649 A70-23338

Analog simulation of frequency multipliers and dividers with step recovery diodes

15 p2709 A70-32467

Varied-frequency signals separation using bridge circuits for splitting process resulting in unchanged phase ratio and changed amplitude ratio

23 p4159 A70-43759

Digital frequency filter for data processing

24 p4318 A70-45435

Multivibrators with improved stability and frequency-division capacity, using distributed R-C-NR structures

24 p4321 A70-46396

FREQUENCY DIVISION MULTIPLEXING

Tandem link multichannel LOS FDM-FM communication system cost optimization by computer-aided design

08 p1459 A70-20798

Intermodulation noise performance of FM FDM trunk radio systems in two path fading situations, calculating noise/power ratio and baseband enhancements

09 p1632 A70-22237

FDMA and TDMA systems for demand assignment of satellite circuits noting PCM/TDM operation trends in satellite and ground communications

10 p1838 A70-24355

Adaptive multiple access satellite communication system at millimeter wavelengths in time- and frequency-division modes, compensating rainfall attenuation

10 p1838 A70-24358

PSK distortion spectra generated in satellite transponders by interactions of FDMA PSK modulated carriers, developing computer programs for multichannel FDMA PSK modulated systems

10 p1839 A70-24364

TDMA communication satellite system compared favorably with FDMA or CDMA systems in efficiency, flexibility and feasibility for commercial and military uses

10 p1842 A70-24884

Frequency stability characteristics and control in SSB-FDMA/PhM multiple access system tested by ATS

[AIAA PAPER 70-411] 11 p2000 A70-25460

Threshold extension demodulator /TED/ using bandpass filter without oscillator for FM multiplex

12 p2197 A70-27908

Frequency division multiple access satellite communication system, calculating bandwidth variations effects on intermodulation distortion

21 p3787 A70-41328

Single channel per carrier PCM FDMA demand assignment satellite communication system, discussing digital encoding, quadrature PSK modulation, etc

21 p3791 A70-41367

Directional microwave transmitter for 300 frequency division multiplexed telephone channels, discussing transmission quality, reliability, design and operation

23 p4172 A70-44298

FREQUENCY MEASUREMENT

Resonant cavity method for measuring varactor diodes cut-off frequency, avoiding errors from circuit losses and parasitic effects

01 p0048 A70-10049

Frequency measurement for HCN laser at 0.357 and 0.311 mm wavelength by mixing signal with backward wave tube harmonics

03 p0500 A70-13464

Laser Doppler velocimeter directly measuring detected frequency with passive confocal Fabry-Perot interferometer

05 p0860 A70-16658

Frequency calculation and measurement for acoustic waves produced by carbon dioxide Q switched lasers

06 p1084 A70-18620

Lowest usable frequency /LUF/ measurement and prediction through synchronized oblique ionospheric sounding

07 p1233 A70-19181

Level differences measured at 300 Hz to 200 MHz frequency range, discussing methods and measuring circuits and components

07 p1234 A70-19354

CW water vapor laser line frequency measurements by beating with radiations from HCN laser in metal-on-metal point contact diode

09 p1697 A70-22925

Laser frequency measurement and active and passive stabilization techniques, emphasizing HCN laser phase locking to frequency standard output

09 p1697 A70-22951

Frequency measurement in millimeter and submillimeter ranges, using high quality Fabry-Perot resonator

09 p1680 A70-23141

F region electrons collision frequency from short radio waves amplitude and group path relationship

10 p1876 A70-24535

Absolute frequency wideband high resolution determination, using frequency synthesizer as phase locked loop local oscillator

10 p1854 A70-25316

CW carbon dioxide laser absolute frequency measurements at 28 THz by beating lines with water vapor laser and klystron in tungsten on nickel point contact diode

11 p2063 A70-26070

Device for measuring turbine blades natural frequencies by converting vibrations to electric current at same frequency

11 p2033 A70-26443

Frequency equation for harmonic waves propagating in composite circular-cylindrical rods consisting of circular core and circular casing of different material

11 p2145 A70-26693

Thermonuclear explosion Operation Starfish effect on ionospheric state from recording in central Kazakhstan, studying frequency characteristics

11 p2047 A70-26790

Optical processing for measuring frequency spectrum of PM wave induced by turbulent medium in laser beam

12 p2249 A70-27756

Automatic narrow band meter for continuous readout of frequency characteristics of radiation detectors

13 p2412 A70-29867

Earth frequency sounding based on geomagnetic field variations spherical analysis, tabulating nonconducting shell thickness, nucleus resistivity, etc

14 p2572 A70-30243

Time-frequency national airspace system, using distributed sensors and closed loop control to meet safety and traffic handling requirements

16 p2948 A70-33478

Frequency and stability measurements of IF signals generated between laser far IR radiations and conventional oscillators

17 p3104 A70-35084

He-Ne laser emission wavelength, using laser interferometry based on feedback between moving mirror and resonator

17 p3104 A70-35088

Photodetector frequency response measurement, using beat light signals from mixed single mode He-Ne lasers

17 p3108 A70-35688

Picosecond pulse frequency sweep measurement using time resolved spectroscopy

17 p3108 A70-35904

Frequency and time information transmission, discussing frequency and time measurement equipment at Czechoslovak facility

18 p3257 A70-36199

Synchronous measurements of reflection coefficient and frequency characteristics of sporadic E layer by ionospheric sounding

18 p3247 A70-36293

Hydrogen maser wall shift measurement, using flexible storage bulb for accuracy improvement

19 p3445 A70-37759

Gunn effect devices with concentric cylindrical electrodes, examining oscillation natural frequency-applied voltage relation

19 p3392 A70-38900

He/Ne laser amplifier and oscillator threshold bandwidth measurement by double laser device

20 p3643 A70-40126

Threshold SNR for signal frequency meter based on zero number count method, determining reliability

22 p3985 A70-42401

Italian Sirio satellite with local and foreign ground stations network measuring SHF wave propagation variables

23 p4158 A70-43753

S band tunable free running high Q triode oscillator phase and frequency instability measurement based on delay lines applications

23 p4170 A70-43796

Frequency measurement extension to 5 micron region by IR laser harmonic frequency mixing in point contact diode as multiplier chain

23 p4201 A70-44917

Hydrogen I region anomalous alpha lines recombination in Orion B spectrum, identifying carbon emitter by measured frequency separation

24 p4410 A70-45773

Earth frequency sounding based on geomagnetic field variations spherical analysis, tabulating nonconducting shell thickness, nucleus resistivity, etc

24 p4332 A70-46318

FREQUENCY MODULATION

NT FEEDBACK FREQUENCY MODULATION

NT FM/PM [MODULATION]

NT FREQUENCY SHIFT KEYING

NT PULSE FREQUENCY MODULATION

NT PULSE FREQUENCY MODULATION

TELEMETRY

Microwave circuit for increasing Gunn oscillators injection locking capabilities and reducing FM resulting from bias-voltage fluctuations

01 p0050 A70-10783

FM/FM telemetry systems waveform distortion measurement technique based on minimum rms error between input and output signals

01 p0044 A70-10941

IF optimum bandwidth for maximizing output SNR in FM receiver with barrier to noise ratio below discriminator threshold

01 p0051 A70-11119

FM data and telegraph signal transmission over PCM system analog channel, discussing adaptability to digital modulated signals

01 p0046 A70-11318

Dispersive compression of plane frequency modulated waves in inhomogeneous plasma based on generalizing geometric optics approximation to unsteady quasi-harmonic processes

03 p0447 A70-13287

Narrow bandwidth FM signal distortion during multiplication in lossless varactor multiplier calculated, using equivalent circuit of frequency doubler

03 p0452 A70-14040

Linear phase detection using FM demodulation for Apollo S band communication system eliminating baseband voice interference with telemetry

04 p0648 A70-14659

Saturation induced wave front distortions effect on beam divergence and frequency modulation in laser amplifiers, discussing refractive index changes 04 p0703 A70-15620

Spectral and lasing characteristics of microwave frequency modulated He-Ne laser operating at 0.63 micron wavelength 05 p0858 A70-16257

Modulation properties of stabilizing frequency standard for gas laser with signal control by separate absorption cells 06 p1079 A70-17440

Optical harmonic generation by doubling picosecond laser pulse frequency under nonstationary conditions 06 p1080 A70-17494

Amplitude and frequency characteristics of gas ring laser with optical feedback between oppositely moving waves amplified by reflecting mirrors 06 p1081 A70-17497

Analytical expressions for amplitude and frequency modulation characteristics of bias modulated tunnel diode oscillator on steady state mode 06 p1022 A70-17836

CW, pulsed and frequency modulated radar scattering, discussing flight, system, terrain and data processing parameters 06 p1012 A70-18594

Modulation transfer function (MTF) of eye-visual system as spatial frequency filter 07 p1216 A70-18870

Narrow band limiter influence on SNR at FM reception output by computer simulation using threshold pulse model 07 p1227 A70-19124

Oblique ionospheric pulse sounding records improvement by use of linear FM chirp transmission, discussing time delay resolution, transmitter power and RF interference rejection 07 p1233 A70-19184

Size reduction and low noise temperature in receiving antennas obtained by transistor integration and resonance frequency modulation 07 p1241 A70-19353

Ionospheric distortion of linearly FM radio signals used for sounding, considering signal characteristics in distortion equations 07 p1268 A70-19459

Radar coherent linear FM microwave generation with 14 microsecond pulse length and 1000 MHz bandwidth, discussing phase error and coherency 07 p1236 A70-20064

Matched filter rectangular pulse compression non-linear FM waveform design with low time sidelobes and zero mismatch loss due to spectral weighting 07 p1242 A70-20065

FM spectral density model with applications to radio transmitter bandwidth estimation and interference analysis 08 p1456 A70-20473

Tandem link multichannel LOS FDM-FM communication system cost optimization by computer-aided design 08 p1459 A70-20798

Phase locked loop method for waveshaping rectangular wave frequency modulation signals in phase coherent VLF-FSK systems, reducing transient effects and adjacent channel interference 08 p1459 A70-20803

Frequency locked loop optimization, showing advantages in frequency shift keying detection and FM signal demodulation 08 p1460 A70-20808

Multichannel performance measurement of threshold extension FM demodulators using click suppression techniques 08 p1460 A70-20812

Cross modulation due to nonlinearity and linear cross modulation due to local oscillator pulling in FET FM receiver, discussing mixer operating points 08 p1460 A70-20818

Large carrier to noise ratios in FM receivers as function of correlation between Gaussian and impulse shot noise /clicks/ 08 p1463 A70-21776

Double resonator ruby maser dynamic and static characteristics for centimeter band improved by pumping frequency modulation 09 p1695 A70-22188

Distortion-compensation circuit theory, considering voltage-frequency characteristics and varactor controlled oscillator nonlinearities of frequency modulators 09 p1632 A70-22235

Intermodulation noise performance of FM FDM trunk radio systems in two path fading situations, calculating noise/power ratio and baseband enhancements 09 p1632 A70-22237

Correlation function of oscillation modulated in amplitude, phase and frequency by random processes causing spectral density maximum shift away from carrier frequency 09 p1633 A70-22409

Optimizing control system design using fluidic digital circuitry and FM type transducers 09 p1614 A70-23690

Gunn oscillator current noise correlation with frequency modulation noise 10 p1848 A70-24230

FM noise threshold reduction achieved through narrow bandwidth of self synchronized N-path filter tracking incoming FM carrier 10 p1833 A70-24233

Geostationary orbit capacity based on multichannel telephony, comparing digital and analog modulation techniques 10 p1836 A70-24343

Communication commercial satellite systems capacity in terms of telephone channels, using frequency modulation and digital methods 10 p1836 A70-24344

AM and FM CW Doppler radar by combined AM-FM waveform, noting automatic track while scan radar application 10 p1840 A70-24445

Microwave devices excess AM and FM noise levels measurement by carrier suppression methods 10 p1841 A70-24579

Frequency sharing between satellite-transmitted FM TV signals and terrestrially transmitted AM-VSB TV signals [AIAA PAPER 70-438] 11 p2001 A70-25467

Probability density function of click duration in FM discriminator 11 p2018 A70-26270

FM/FM telemetry threshold carrier SNR and receiver IF bandwidth optimization through computer program 11 p2014 A70-26272

Telemetric systems for moving machine elements tests, discussing seven channel PFM and FM/FM systems 11 p2056 A70-26451

Narrow band FM noise suggested for masking studies application, discussing noise properties 11 p2011 A70-26496

PAM-FM modulation system optimal receiver derivation, assessing threshold performance assuming uniformly distributed modulating signal 12 p2183 A70-27155

Large capacity long distance transmission by circular waveguides, describing artery frequency modulation and equipment for multiplexed telephone messages transmission 12 p2194 A70-27233

Time constant, steady state and tracking error of AGC loops at input/output of FM link in AM-FM telemetry system 12 p2184 A70-27250

Threshold extension demodulator /TED/ using bandpass filter without oscillator for FM multiplex 12 p2197 A70-27908

Radar transmitter waveforms for multifunction operation, emphasizing phase and frequency modulation for CW radars 12 p2188 A70-27939

Frequency modulated RF pulses compression with dispersive property of lossless, isotropic and homogeneous plasma used to enhance receiver transmission resolution 12 p2282 A70-27960

Dynamic tracking filter response analysis for FM reception using equivalent circuit method 12 p2200 A70-28054

Wideband FM signals transionospheric propagation, calculating output spectrum, signal to distortion ratios and signal to noise ratios 13 p2367 A70-29588

FM detector without normalization useful for low S/N reception of FSK and PSK in telemetry systems 13 p2367 A70-29589

FM limiter-discriminator followed with ideal bandpass filter, deriving output signal to noise ratio 14 p2558 A70-31189

Wideband PCM/FM discriminator detection, predicting effects of predetection and postdetection filtering on system performance 14 p2558 A70-31192

Two signal selectivity and permissible noise level of FM receiver with linear cascades and detector non-linearity effects 15 p2696 A70-31506

FM optical signals detection, using Fabry-Perot interferometer with air gap between mirrors 15 p2733 A70-31523

Noise effect on modulation transfer function of visual channel by threshold measurements 15 p2698 A70-32013

FM/FM radio telemetry system for transmitting strain and temperature data from rotating parts 15 p2739 A70-32330

Delta modulation threshold extension technique for phase lock loop FM demodulator 15 p2703 A70-32559

Phase lock loop acquisition and tracking of carrier frequency modulated by single sinusoid, obtaining

parameter values through mathematical model and digital simulation 15 p2703 A70-32578

Voltage-frequency conversion technique using FM principle and RF oscillator beating with crystal oscillator output 15 p2705 A70-32705

Weak narrow band noise measurements using FM radiometer insensitive to gain fluctuations 17 p3053 A70-35278

Semiconductor laser frequency modulation by ultrasonic waves, noting pressure variation effect on sideband resolution 18 p3269 A70-36736

Ionospheric distortion of linear FM radio signals used for sounding, considering signal characteristics in distortion equations 18 p3250 A70-36933

IMPATT diode microwave oscillator with modulated bias current, discussing amplitude and frequency modulation sensitivity, thermal effects and load parameters 19 p3390 A70-38363

FM demodulation threshold extension by correlation detection implemented in impulse noise cancellation system 19 p3382 A70-38893

Sideband frequency disturbances at analog data magnetic storage using frequency modulation 20 p3586 A70-39706

FM transmission of multiplex telephone signals by communication satellites, deriving impulse noise due to adjacent channel interference 21 p3787 A70-41330

FM threshold extension for system performance improvement, comparing impulse noise elimination, correlation detection and delta modulation signal processing techniques implemented at demodulator output 21 p3787 A70-41334

Multicarrier FM communication system, calculating adjacent channel interference due to impulse noise 21 p3789 A70-41343

Optico-acoustic autocorrelator for linear FM signals spatial compression, discussing design and performance 22 p3984 A70-42398

Frequency modulated gas laser communication system, discussing Raman-Nath effect, Doppler shifting phase grating, monochromatic light, pseudostanding wave, optical heterodyne detector, etc 22 p3989 A70-42966

Linear differential equation solution associated with FM signal generation, presenting analytical methods for FM and AM components 22 p4063 A70-43209

Cuprous chloride /CuCl/ as low-loss electro-optic material modulating 10.6 micron laser radiation 22 p4051 A70-43334

Linear FM radar pulse compression matched filter response calculated by computer evaluation of cross ambiguity function for design tradeoff between resolution and performance 22 p3992 A70-43589

P-n junction dependent FM noise spectrum of UHF transistor power oscillator at transit frequency 23 p4161 A70-43789

Optical FM system with laser interferometer and sideband carrier circuit for measuring mechanical shock by Doppler shift 23 p4193 A70-43964

Four channel FM radio telemetry for exercise physiology, measuring EKG, respiration rate and pulmonary ventilation 23 p4151 A70-44380

Threshold output characteristic of FM signals, generalizing Gaussian baseband modulation solution to obtain autocorrelation function of output signal plus FM discriminator noise 24 p4313 A70-46063

FREQUENCY MULTIPLIERS

Narrow bandwidth FM signal distortion during multiplication in lossless varactor multiplier calculated, using equivalent circuit of frequency doubler 03 p0452 A70-14040

Imaging properties of parametric image converters, taking into account frequency doubling of brilliant object by self interaction within nonlinear material 05 p0852 A70-16991

Laser harmonic-frequency mixing techniques extended into IR with IR metal-metal point contact diode 06 p1083 A70-17944

Neodymium laser frequency doubling based on nonlinear functional relation between polarization and electric vector in matter 08 p1512 A70-20677

Five resonator broadband frequency doubler design using charge storage diodes 08 p1475 A70-21280

Deformed grating frequency multiplication by filtering in Fourier plane of lens, forming moire pattern in image plane by mechanical interference 10 p1890 A70-24592

UHF frequency doubler with series-parallel array of eight punch-through diodes, preventing spurious oscillations 12 p2196 A70-27650

Statistical output characteristics of harmonic cosine and sinusoidal inertialess phase periodic converters in two channel system with frequency multiplication 13 p2370 A70-29741

Harmonic generation in gas discharge by frequency multipliers, assessing multipliers capabilities for millimeter wavelength operation 14 p2549 A70-30437

Broadband frequency multipliers optimum efficiency solutions, realizing linear charge-voltage characteristics with MIS varactors 14 p2557 A70-31159

Single phase static ferromagnetic frequency multiplier with odd multiplication factor 14 p2559 A70-31357

Analog simulation of frequency multipliers and dividers with step recovery diodes 15 p2709 A70-32467

Wideband varactor multipliers with flat output as microwave sources in radar systems 16 p2877 A70-33412

Frequency multipliers with charge storage diodes, examining recombination and hysteresis effects on performance 17 p3050 A70-34588

Radar tracking of meteors with slow drift velocity, improving accuracy via echo frequency multiplication 19 p3514 A70-37644

Fundamental microwave oscillator subharmonic phase locking for stable power, comparing with varactor frequency multipliers 19 p3386 A70-37689

Frequency multipliers with charge storage diode, analyzing turn-off transient effect on performance by charge control model 19 p3391 A70-38748

Frequency multipliers with charge controlled junction diode model, predicting operational behavior 22 p3998 A70-43421

Spectrum generator with step recovery diode multiplier, discussing line spacing, energy and phase coherence 22 p3990 A70-43485

Equivalent circuits for charge storage varactor diode in frequency multiplier mode 23 p4169 A70-43782

Transistorized power amplifiers, frequency multipliers and parametric multipliers design for VHF and UHF ranges 23 p4170 A70-43876

Cascaded varactor frequency multiplier design for microwave range 23 p4170 A70-43877

Semiconductor microwave generator design for maser simulator using transistorized amplifier, varactor frequency multiplier and diode multiplier 23 p4171 A70-43878

Nd-glass mode-locked laser with KDP crystal frequency doubling and pulse selection with Pockels cell 23 p4201 A70-44476

Frequency measurement extension to 5 micron region by IR laser harmonic frequency mixing in point contact diode as multiplier chain 23 p4201 A70-44917

FREQUENCY RANGES

NT RADIO RANGE

Dual frequency ranging within narrow bandwidth of VHF communications satellite repeater for transmitted signals correction of ionospheric refraction error 01 p0043 A70-10781

Ionospheric reflection coefficients calculations by two full wave theory, using related monoenergetic and collisional frequency profiles and 10-100 kHz frequencies 01 p0076 A70-10870

Ionospheric slopes and range frequency characteristics obtained from oblique incidence sounding of horizontally nonuniform ionosphere 01 p0083 A70-11534

Optimum prism angles and ultrasonic frequencies for detecting fatigue cracks 02 p0301 A70-12487

Natural oscillation frequencies lower bounds of orthotropic plates determined as coupled elastic systems 03 p0592 A70-13451

Quasi-optical propagation in frequency wave range above 100 MHz as user problem in VOR, ILS, navigation satellite and CAT detection and warning systems 03 p0523 A70-13613

Constant temperature hot-wire anemometer to compensate for thermal lag of wire/film resistance thermometer within useful frequency range 03 p0492 A70-13761

Sky background brightness temperature measurement at 408 MHz by pyramidal horn antenna 03 p0496 A70-14344

Fluidic component linearized characteristics in coupled or uncoupled environment determined for wide frequency range, discussing application to proportional fluidic amplifier [ASME PAPER 69-WA/FLCS-2] 04 p0626 A70-14847

Informative filter automatic selection for describing visual object with aid of frequency spectrum, taking filter output voltage mean square value as criterion 04 p0662 A70-15438

Level differences measured at 300 Hz to 200 MHz frequency range, discussing methods and measuring circuits and components 07 p1234 A70-19354

Microwave mixer design to increase dynamic range applied to communications and video systems 07 p1243 A70-20216

Resonance radiation transport in optically thick layer, obtaining conservative light scattering solution 09 p1753 A70-22451

Ruby lasers simultaneous Q switching by single rotating prism, discussing possible differential frequency ranges 09 p1697 A70-22989

Rectangular waveguide with cross shaped slot as polarizer ensuring circular polarization over wide frequency range 09 p1652 A70-23649

Pulsars dynamic spectra in 110-420 MHz range, observing emission bandwidths to formulate power law 10 p1938 A70-24099

Type 3 burst sources velocity calculated by frequency drift and Newkirk model of electron density, discussing frequency range extension of Weissenau radiospectrograph 10 p1934 A70-25274

Vibration meter coupled with electrodynamic transducers for measurements in 3-2000 Hz range 11 p2055 A70-26448

Waveguide slot array operation in different frequency bands generating independent radiation patterns, utilizing orthogonal dominant modes propagation 12 p2199 A70-27967

Vibration effects on receptors in frog toe muscles at various frequencies 12 p2179 A70-28344

Ionospherically reflected HF radio signal frequency spread measurement involving phase difference crossings counting between antennas 14 p2550 A70-30743

Multipurpose pulse generator design for 1 Hz-100 MHz frequency range and adjustable rise and fall times 14 p2557 A70-31162

Atomic collision effect on frequency range of opposing traveling wave modes in gas ring laser, using density matrix equation 15 p2749 A70-31553

Classical and modern approaches to tracking problem, discussing optimal control in frequency domain and time domain terms 16 p2882 A70-33039

Phase shift direct and balance measurement procedures between signals over wide frequency range classified by conversion schemes 19 p3391 A70-38702

Passive microwave sensors based on brightness temperature vs frequency model for various atmospheric conditions, presenting vegetation pictures 20 p3626 A70-39054

Source antenna range length and aperture diameter, discussing length, frequency, aperture size and free space conditions 21 p3784 A70-40563

Wide frequency range dielectric spectrometer for insulating materials permittivity and loss factor measurement and display 21 p3830 A70-41950

Acoustoelectric domain spectra in n-GaAs by microwave emission, comparing results with parametric conversions theory 21 p3863 A70-42002

Shock waves strength and frequency in solar atmosphere heating deduced by empirical model, integrating radiative losses over height 21 p3925 A70-42188

Frequency dependence of Gunn oscillator maximum negative conductance 23 p4172 A70-44198

Light velocity frequency dependence in variable stars gravitational fields suggested from yellow and UV NP 0532 observations 24 p4405 A70-45488

Human EEG alpha rhythm during surface-tapping test with rod at time-limited maximum frequency, noting slowdown to preferred frequency 24 p4301 A70-45987

FREQUENCY REGULATION

U FREQUENCY CONTROL

FREQUENCY RESPONSE

Approximate determination of termination hydraulic servomotors frequency characteristics with four way valves using piecewise straight lines on Bode diagram 01 p0007 A70-10034

Frequency characteristics of air, water and blood filled pressure transducer systems using various needle and connecting tubing sizes 01 p0031 A70-10275

CRT resolution measurements by double slit method, relating light spot response to slit width 01 p0093 A70-11278

Optical and radio pulses from pulsars as test of light speed variation with frequency and photon mass possible existence 02 p0373 A70-12394

Wideband parametric and tunnel diode amplifiers synthesizing method for obtaining maximum flat amplitude frequency response 03 p0457 A70-13727

Nonlinear feedback control system analysis and synthesis by parametric plane method, investigating frequency response by describing functions 03 p0460 A70-13970

Closed loop frequency response analyzer with steepest descent computing procedure to obtain in-phase and quadrature signal components in linear or nonlinear systems [ASME PAPER 69-WA/AUT-3] 04 p0688 A70-14830

Solid viscoelastic cylinder bonded to thin elastic casing, analyzing normal and tangential stresses for stress and displacement frequency responses in forced transverse vibration [ASME PAPER 69-WA/APM-20] 04 p0771 A70-14911

Elastic spherical shell excited by point force, analyzing HF response in terms of near field and flexural wave field [ASME PAPER 69-WA/APM-18] 04 p0771 A70-14912

Control system response improvement by state variable feedback illustrated by frequency and transient response tests data from analog model 04 p0662 A70-15331

Optical resonator reaction to coupled laser frequency, attributing differences between theory and experiment to errors in mirror reflection efficiency measurement 05 p0859 A70-16354

Frequency reaction of optical resonator to coupled laser in mismatch case, measuring laser and resonator axes displacements 05 p0859 A70-16355

Frequency responses bounds of nonnormalized low pass and bandpass filters 05 p0820 A70-16360

Frequency response linearity for self excited microwave oscillators with complementary cavity derived, proposing parameters selection for widening voltage tunable frequency range 05 p0824 A70-16891

Frequency response of 6328 A He-Ne laser interferometer analyzed for multimode oscillations noting plasma diagnostics applications 05 p0861 A70-16989

Klystron amplifier output circuit large signal frequency response, showing dependence on distance between cavities 06 p1021 A70-17672

Ring laser frequency characteristics at two longitudinal modes emphasizing intermodal pulse frequencies 06 p1081 A70-17769

Microwave transistors frequency and power characteristics and tradeoffs in relation to thermal and packaging design 06 p1023 A70-18390

Flight configured single sideband telemetry accuracy determined by digitally computed frequency response 06 p1012 A70-18600

Electrocorticograms frequency spectra from different visual cortex layers of rabbits during exposure to rhythmic light pulses 07 p1198 A70-18698

Plane rigid airfoil frequency response in incompressible potential flow using simple equivalent oscillator based on Theodorsen function 07 p1404 A70-19232

Response characteristics of negative feedback galvanometer amplifier with inductive source impedance for geomagnetic micropulsation detection 07 p1242 A70-19998

Bernoulli-Euler beam equation describing natural frequencies and mode shapes for vibrating beam immersed in fluid 07 p1413 A70-20043

Fluidic air gauge back pressure signal frequency response as function of time [ASME PAPER 68-WA/FE-16] 08 p1441 A70-21316

May 1966 solar eclipse effects on sporadic E layer, including ionizing radiation decrease relation to boundary and blanketing frequencies decrease 08 p1490 A70-21432

Popping pressure of relief valve with helical spring under dynamic load noting frequency dependence [ASME PAPER 69-VIBR-48] 08 p1441 A70-21479

Single mode He-Ne ring laser lock-in threshold and output power relationships to frequency 08 p1514 A70-21692

Frequency function of sound localization in median plane measured psychoacoustically at both ears with narrow band signals

09 p1624 A70-22762

Linear high order aircraft and missile control systems design using Horowitz frequency response method

09 p1654 A70-22835

Integrated lunar disk wavelength dependence of polarization using photoelectric polarimeter, tabulating results

09 p1759 A70-22910

Open cut-off rectangular resonator calculated for frequency dependence on reflection coefficient and relative length

09 p1648 A70-23165

Standing wave ratio frequency dependence in miniature stripline power dividers and ring structure hybrid junction

09 p1652 A70-23653

Equivalent oscillatory model defined from asymptotes of frequency response amplitude and cut-off frequency amplitude value of plane rigid airfoil in incompressible potential flow

10 p1953 A70-23841

Broad band power amplification with Gunn effect diodes, describing frequency response and saturation characteristics and FM/AM noise spectrum measurements for reflection amplifier in X band

10 p1847 A70-23886

Waveguides consisting of three concentric regions suitable for plasma experiments, showing dispersion characteristics and cut-off frequencies

10 p1850 A70-24835

Vibration damping theory validity, discussing response curve for frequency dependence of energy dissipation

11 p2133 A70-25733

Maxima increases without limit in damped linear oscillator response to random wideband excitation interpreted by heuristic explanation

11 p2085 A70-26694

Sound generation and detection by distributed piezoelectric sources using frequency response and equivalent circuit

11 p2085 A70-26701

Log-periodic dipole /LPD/ antennas compressed along transmission-line axis, considering frequency dependent behavior in narrow bands and radiation pattern

12 p2198 A70-27955

Dynamic tracking filter response analysis for FM reception using equivalent circuit method

12 p2200 A70-28054

LF electrostatic waves oblique to magnetic field in plasma, evaluating dispersion relation near ion cyclotron frequency

13 p2363 A70-28641

Maximum frequency response of reactive modulation amplifier using parametrically excited oscillator circuit

13 p2377 A70-29304

Fluidic circular and rectangular transmission lines characteristics noting frequency dependence

13 p2349 A70-29477

Double diffused epitaxial silicon bipolar microwave transistor design, fabrication and performance evaluation, including scattering parameters vs frequency for common-emitter amplifier

13 p2379 A70-29592

Feedback control systems automatic testing by examining frequency response

13 p2423 A70-29696

Solar spectral line source function frequency dependence

13 p2496 A70-29842

Frequency sampling adjustable equalizer design and operation, describing coaxial cable system tests

14 p2547 A70-30282

Microwave avalanche diode emission frequency dependence on charge transfer across drift region, considering varactor diode output, negative resistance and noise factor

14 p2555 A70-30354

Linear control systems identification and synthesis from data containing modulus and phase information as frequency functions

14 p2559 A70-30520

SCAMP 4 program for electronic circuits statistical analysis in frequency domain, obtaining mathematical models and transfer functions

14 p2561 A70-30667

Extrinsic photoconductor with reduced background under uniform illumination, describing frequency response as function of recombination and dielectric relaxation times and load resistances

14 p2586 A70-30989

Low pass filter synthesis with transfer function having frequency response boost in pass band

15 p2708 A70-31833

Optical quantum amplifier frequency characteristics dependence on broad spectral composition amplified signal intensity and resonator parameters

15 p2754 A70-32862

Linear continuous vibratory system unknown parameters identification from frequency response data

16 p2988 A70-33337

S band GaAs FET fabrication technology and frequency response

16 p2877 A70-33414

Vibration transducer systems design, using active filter networks to tailor phase and frequency responses

17 p3095 A70-35527

Beat and synchronization modes of opposed waves in rotating gas ring laser, examining frequency response asymptotic behavior

17 p3108 A70-35683

Ionospheric scatter channel amplitude frequency characteristics recording equipment, discussing design

18 p3256 A70-36090

Ionospheric scatter communications channel phase frequency characteristics measuring method, considering probability density function

18 p3256 A70-36091

Radio wave absorption dependence on ionospheric sounding frequency at vertical incidence, using pulse method

18 p3255 A70-37038

Low pass linear phase active feedback circuit synthesis using distributed RC networks to realize flat magnitude response

19 p3392 A70-37707

Digital filter synthesis, discussing transfer function determination based on prescriptions for frequency or time response properties

19 p3391 A70-38746

Nonlinear acoustic absorbers behavior analysis, discussing spectral and temporal computation methods

20 p3672 A70-39237

Frequency discriminators output voltages under action of fluctuating signal and noise with arbitrary energy spectrum

20 p3584 A70-39254

Transistor amplifier with back coupled emitter and parallel inductive correction, calculating optimal frequency and phase characteristics under complex load

20 p3598 A70-39790

Nonlinear closed loop systems frequency response determination by graphical method

20 p3605 A70-40122

Rat neuron impulsive reactions and frequency response differences to varying sound signals, discussing time constant, signal intensity and frequencies

20 p3574 A70-40172

Nonlinear automatic control systems transient response by frequency response curves of amplitude and phase characteristics

22 p4001 A70-42831

Semiconductor luminescence and photodetector diodes near IR region transmission, describing frequency response measurements

22 p4087 A70-43445

Radio electronic circuits precision, deriving relationship between frequency response and component variations solvable by linear programming

23 p4171 A70-43958

Transistorized LF RC filter circuit design for desired frequency response characteristics

23 p4171 A70-43962

He-Ne laser with absorbing cell in magnetic field, investigating nonlinear effect in frequency dependence of output power

23 p4203 A70-45070

Microwave propagation in hollow conducting elliptical pipe waveguide, calculating successive modes cut-off wavelengths by numerical analysis

24 p4318 A70-45212

Thin film microwave acoustic transducers, calculating top electrode thickness effect on frequencies of infinite conversion loss

24 p4333 A70-45218

Jet interaction type proportional fluid amplifier as feedback oscillators, measuring frequency response

24 p4292 A70-45291

Nitrogen laser pumped exciplex 4-Methylumbelliferone and rhodamine 6G dye laser amplifier, measuring single pass power gain vs wavelength

24 p4355 A70-46088

Microwave transmission in partially dielectric filled circular waveguide, deriving cutoff wavelength and phase velocity vs frequency

24 p4315 A70-46260

FREQUENCY SCANNING

Numerical solutions to determinantal equation for predicting properties of periodically modulated dielectrically filled frequency scanning waveguide as microwave antenna

03 p0457 A70-13696

Aircraft flutter equations solution by reduced frequency scanning method [ONERA-TP-786]

06 p1171 A70-18470

Signal frequency capture probability vs frequency search rates and AFC loop parameters determined in phase locked oscillator

11 p1996 A70-25349

Meteor trail angular dimensions determined by frequency scanning method involving minimum points on reflected signal characteristics

11 p2107 A70-25556

Mode controlled Q switched tuneable ruby laser, obtaining frequency scanning by temperature and pressure control

15 p2752 A70-32048

Real time swept sine wave spectrum analyzer using time compression to change filter bandwidth as function of control signal

17 p3059 A70-35166

Signal frequency capture probability vs frequency search rates and AFC loop parameters determined in phase locked oscillator

20 p3589 A70-40461

Meteor trail angular dimensions determined by frequency scanning method involving minimum points on reflected signal characteristics

21 p3892 A70-41306

Periodically modulated corrugated surface array for application as phase-frequency scanning array, deriving design equations for comparison with radiation characteristics measurements

21 p3800 A70-41944

Nd glass laser with smooth emission frequency scanning, giving block diagrams and radiation spectra

24 p4353 A70-45646

Eddy current magnetic probe with frequency scanning for signal-noise discrimination in nondestructive testing of tubes

24 p4336 A70-45698

FREQUENCY SHIFT

Chromospheric average velocity field near sunspots determined from M alpha line absorption elements wavelength shifts

01 p0176 A70-10247

Sudden frequency deviation /SFD/ correlation with solar radio bursts at different frequencies following inverse square law of intensity

01 p0171 A70-10871

Horizontal gradients below satellite orbit effect on reduced and minimum difference in Doppler frequency shifts of coherent radio waves from satellite in inhomogeneous ionosphere

01 p0046 A70-11517

Electrodynamic contactless method for ultrasonic nondestructive testing of materials based on natural frequencies shift with and without defects

02 p0301 A70-12483

Angular dependence of one dimensional first and second index matching for optical parametric mixing of laser and SRS Stokes beams for tunable laser source

03 p0498 A70-13157

Semistatic acceleration sensor, using ferrite rod magnetostriction effects to convert acceleration stress to microwave resonant frequency shift

03 p0495 A70-14191

Resonance frequency shift in motional field averaging system due to nonuniformities in static magnetic or electric field may cause unexpected systematic errors

04 p0721 A70-14665

Radiation effects on swept-synthetic quartz resonators and materials, discussing frequency shift measurements and defect studies

04 p0731 A70-14735

Nonducted VLF walking trace whistlers and Doppler shifts in fixed frequency transmissions identified on OGO midlatitude spectrographic records

04 p0649 A70-15116

Center frequency shift prediction model for nonlinear collector junction capacitance in transistor Class C amplifiers

04 p0660 A70-15343

Frequency shift in Rb-87 atomic frequency standards dependence on filter temperature interpreted for optical pumping radiation improvement

05 p0859 A70-16269

Length shifts measurement with single 2-mode laser by observing beat frequency, obtaining frequency shift proportional to length shifts

05 p0859 A70-16356

Laser-forced medium anisotropy effects on nonlinear optical frequency mixing and combined forced scattering

07 p1335 A70-19863

Atomic hydrogen maser wall shift determined by measurements on FEP Teflon coated storage bulbs, suggesting Teflon properties change as basis

07 p1301 A70-19973

Optical to IR conversion in circumstellar dust envelope with spherical symmetry based on optical radiation scattering and absorption by dust

08 p1573 A70-21047

Mode locked laser pulse chopping by interferometrically combined electro-optical frequency shifters

08 p1513 A70-21541

Frequency change for coupled vibrations of slender rotating beam due to hub radius change determined in centrifugal force field by perturbation method
08 p1594 A70-21772

He-Ne laser IR generation in three mirror mismatched resonator, using Fabry-Perot interferometer to study mode and lasing range frequency shift
10 p1900 A70-24265

Electromagnetic radiation frequency shift during passage by sun or earth not caused by electrostatic or magnetic fields
10 p1917 A70-24860

Pseudonoise phase shift keying /PN/PSK/ and frequency hopping /PN/FH/ modulation technique for low altitude satellite receiving /VHF/ transmissions [AIAA PAPER 70-496]
11 p1999 A70-25436

Length shifts measurement with two mode laser, noting frequency shift proportionality to mirror displacement
11 p2062 A70-25632

Optical modulation using rotating diffraction grating to obtain frequency shifts
11 p2049 A70-25633

Sun effect on anomalous frequency shift in 21 cm absorption spectrum in Taurus A
11 p2108 A70-25659

Nova Delphini brightness variations, observing absorption lines shift toward violet
12 p2306 A70-27860

Spectral line width and shift measured by spectrograph crossed with Fabry-Perot interferometer in pressure chamber, measuring magnetic field in solenoid
12 p2238 A70-28178

Annular gas laser, considering external periodic perturbation effect on difference frequency of oppositely moving waves
12 p2251 A70-28291

Midlatitude chorus frequency spectrum changes in relation to previous local magnetic conditions
13 p2365 A70-29187

LF signals phase determination during solar eclipse of 22 September 1968, noting frequency shift magnitude
14 p2547 A70-30238

Mariner 6 radio signals frequency changes analysis during occultation measurement for determining Mars surface pressure and temperature
14 p2646 A70-31071

Laser beam scattering by free electrons in semiclassical radiation theory, discussing intensity dependent frequency shift
15 p2753 A70-32452

Doppler shifted radiation production, using time and space dependent radiant energy sources
16 p2952 A70-34255

Sunspot spectrograms analysis, observing wavelength shift in Zeeman triplet circular components and magnetic splitting inequality under different circular polarizations
18 p3322 A70-37136

Radio wave holography with unequal reference to signal frequency, recording linear object with superheterodyne receiver
19 p3420 A70-37290

Hydrogen maser wall shift measurement, using flexible storage bulb for accuracy improvement
19 p3445 A70-37759

Aperture size effect on frequency shift and frequency width variation of beat signals observed with laser Doppler velocity meter
19 p3428 A70-38502

Hydrogen maser frequency shift due to atomic collisions with deformable storage bulb surface
21 p3836 A70-41453

Frequency shifted diffraction of monochromatic Gaussian light beam by reflection off ultrasonic surface wave
21 p3850 A70-41907

Doppler frequency shift of reflected radio waves for ionospheric disturbances, discussing solar flares, geomagnetic variations, etc
21 p3820 A70-42256

Nonlinear frequency shift for electronic and ionic cyclotron modes in magnetospheric whistler and hydrodynamic propagation, using Vlasov equation
23 p4187 A70-43880

Single frequency gas laser synchronization by small harmonic signal from second laser, deriving frequency shift dependence on power
23 p4200 A70-43929

LF signals phase determination during solar eclipse of 22 September 1968, noting frequency shift magnitude
24 p4316 A70-46313

FREQUENCY SHIFT KEYING

Transient response role in limiter-discriminator detection of binary FSK signals, comparing resulting and optimum error probabilities
02 p0258 A70-12421

Step recovery frequency shift keyed retimer using Gunn effect FSK pulse regenerator for microwave communication
07 p1237 A70-20285

Phase locked loop method for waveshaping rectangular wave frequency modulation signals in phase coherent VLF-FSK systems, reducing transient effects and adjacent channel interference
08 p1459 A70-20803

UHF satellite receiver for binary FSK data collection system using matched integrate and dump filter detectors
08 p1459 A70-20804

Frequency locked loop optimization, showing advantages in frequency shift keying detection and FM signal demodulation
08 p1460 A70-20808

X band Gunn oscillators for binary FSK regenerator operation employing signal injection triggering
12 p2199 A70-28015

Analog data transmission over PCM telemetry link, comparing noncoherent FSK vs PSK reception performance for waveform error
14 p2552 A70-31187

Probability density function of specularly fading signal plus noise for frequency shift keying and pulse radar systems
16 p2865 A70-34040

Incoherent Manchester coded FSK system performance based on optimal signal detection theory, plotting instantaneous frequency vs time
16 p2866 A70-34074

Communication satellite UHF link with FSK or PSK modulation, considering coded digital transmissions
16 p2867 A70-34331

Satellite communications performance improvement by use of multipath signal for channel models including noncoherent FSK
21 p3787 A70-41329

Wideband detection of FSK transmissions in three component two path channel, obtaining channel bit error probability
21 p3792 A70-42176

Wideband detection of frequency uncertain M-ary frequency shift-keyed /MFSK/ transmission in Gaussian noise, deriving symbol error rate for limiting SNR cases
21 p3792 A70-42177

Multilevel FSK system with limiter discriminator followed by low pass filter as demodulator, calculating error rates for comparison with other analyses
23 p4161 A70-44003

FREQUENCY STABILITY

Gas laser frequency stabilization by employing Zeeman splitting in external discharge tube containing He-Ne mixture in alternating magnetic field
03 p0498 A70-13090

Molecular beam laser short term frequency instability found dependent on laser and measuring device noise
03 p0455 A70-13091

Frequency pulling and pulse position modulation of CW GaAs injection lasers by locking signal frequency variation
03 p0502 A70-13815

Feedback technique for frequency stability requirements of airborne radar systems, discussing noncoherent radar applications and cost comparison to power-amplifier approach
04 p0656 A70-14708

Frequency shift and FM noise of uncontrolled Gunn effect diode and reflex klystron oscillators
05 p0818 A70-15774

Modulation properties of stabilizing frequency standard for gas laser with signal control by separate absorption cells
06 p1079 A70-17440

Self pulsation in He-Cd laser, noting decreasing number of modes effect on beat frequency stability
07 p1301 A70-20017

Optimal linear control system with multiple controls, determining stability margins with respect to phase, amplitude, oscillation index and cut-off frequency
08 p1480 A70-21015

Gain stabilization of transistorized LF selective amplifiers in radiometric receivers, discussing two-frequency resonance system
08 p1473 A70-21061

Laser frequency measurement and active and passive stabilization techniques, emphasizing HCN laser phase locking to frequency standard output
09 p1697 A70-22951

Transistorized pulse repetition frequency bandpass and band elimination filters, using trigger circuit to improve pulse-edge steepness and critical frequency stability
09 p1650 A70-23630

Frequency jumps and small amplitude wobble in pulsars
09 p1764 A70-23794

Ruby monopulse laser emission spectrum wavelength stabilization by frequency tuning of generated radiation using Fabry-Perot interferometer
10 p1898 A70-23970

Axial mode selection and frequency stabilization of Nd-YAG laser by optimally designed crystal quartz etalon
10 p1900 A70-24943

Carbon dioxide laser frequency stabilization, using plasma tube impedance variations generating error signal
10 p1901 A70-24946

Frequency stability characteristics and control in SSB-FDMA/PhM multiple access system tested by ATS [AIAA PAPER 70-411]
11 p2000 A70-25460

Gain-stabilization of SHF traveling wave maser radiometer, using thermal noise from neon discharge tube
12 p2228 A70-26881

Automatic frequency control of single frequency He-Ne laser, tuning cavity length to extremum output power with Lamb dip
12 p2250 A70-28181

Gunn oscillator voltage supply influence on domain capacity, considering frequency stability
13 p2377 A70-29302

Oscillators frequency instability and spectral purity relations [ONERA-TP-829]
13 p2383 A70-29637

Tunable and fixed frequency high power magnetrons parallel operation to achieve stable output
13 p2379 A70-29667

HF instabilities effect on magnetospheric drift waves, considering Alfvén mode in auroral plasma
13 p2482 A70-30084

High stability oscillators frequency check, using meteor trails and combined least squares and moving averages methods
14 p2583 A70-30320

Coaxial, inside-out and rising-sun magnetrons for millimeter waves generation under pulsed conditions, discussing tunability, frequency stability and weight
14 p2555 A70-30429

Interference free and frequency stable transistorized multivibrator circuits using High Level Logic /HLL/ units
14 p2561 A70-31163

S band transmitters frequency deviations optimization enabling designer to determine optimum value within constraints of associated receiving equipment
14 p2559 A70-31373

CW injection laser frequency stability, noting injection current influence on lasing frequency
15 p2750 A70-31629

Motion and small vibration frequency stability of correctable gyroscope with correction moment at arbitrary angle with mismatch plane
15 p2738 A70-32154

Frequency instability of oscillator perturbed by internal thermal noise [ONERA-TP-838]
16 p2872 A70-33105

Cycle slipping rate in first order phase locked loop, extending Viterbi analysis
16 p2865 A70-34058

Optical frequency standards research covering lasers application with superstable emission frequency
17 p3104 A70-35081

Frequency and stability measurements of IF signals generated between laser far IR radiations and conventional oscillators
17 p3104 A70-35084

Primary wavelength standard established via line produced with wavelength-stabilized laser
17 p3104 A70-35086

He-Ne laser emission wavelength long and short term stability for metrological applications
17 p3104 A70-35087

Canadian laser stabilization program involving metrology and absolute standard replacing international meter
17 p3105 A70-35089

Spectral densities of intensity and frequency fluctuations of single frequency He-Ne laser radiation
17 p3105 A70-35092

Single frequency Ar ion laser, discussing power and frequency stability
17 p3105 A70-35095

Oscillation frequency retuning and stabilization and loss factor determination in solid state lasers by dispersive resonators
17 p3106 A70-35100

Radio observation of Crab Nebula radio pulsar NP 0532, discussing main and subpulse stability at optical and radio frequencies
17 p3164 A70-35116

GaAs laser with inhomogeneous injection, noting instability of stimulated RF oscillations
17 p3108 A70-35631

Gas laser frequency stabilization using nonlinear effects of magnetic Lamb dip
17 p3109 A70-35911

Phase locked automatic frequency control system, estimating duration of stabilization by theory Markov processes
18 p3228 A70-36625

Self induced intensity pulsations frequency stabilization and narrowing in continuously operating GaAs injection lasers
18 p3269 A70-36734

Optimum stabilized variable frequency multiple input phase locked oscillator in mutually synchronized systems
19 p3389 A70-37969

Transistorized quartz oscillators, testing frequency and amplitude stabilities and functions of input and output capacitances, supply voltage and feedback

20 p3597 A70-39258

Wave particle resonances broadening by particles random motion in turbulent electric field, determining cyclotron instabilities saturation level from vanishing nonlinear growth rate

20 p3679 A70-39661

Fluidic oscillators frequency stability evaluation, noting analog circuits superiority over digital

[ASME PAPER 70-FLCS-20] 22 p3963 A70-42407

Oscillator stability of selective RF transistor amplifiers, using stage dimensioning and gain graphs

22 p3996 A70-42818

Automatic frequency control device for power klystron with two cavities, obtaining stabilization at natural frequency of crystal-containing cavity

22 p3998 A70-43236

High Q frequency stabilized cavity controlled microwave oscillator using Super Invar resonator

23 p4169 A70-43792

S band tunable free running high Q triode oscillator phase and frequency instability measurement based on delay lines applications

23 p4170 A70-43796

Controlled self excited quartz triode oscillator, calculating flicker noise effect on frequency stability

23 p4171 A70-43959

High stability phase locked Gunn microwave oscillator with internal crystal reference, discussing applications as signal generator, low noise Doppler radar sources, etc

23 p4172 A70-44013

Single-frequency oscillations mode in nonlinear catenary systems, considering factors promoting stabilization and uniformity

23 p4218 A70-44344

Ionospheric HF Doppler frequency dispersion at low latitudes under various geomagnetic disturbance conditions

24 p4314 A70-46129

FREQUENCY STANDARDS

Frequency shift in Rb-87 atomic frequency standards dependence on filter temperature interpreted for optical pumping radiation improvement

05 p0859 A70-16269

Secondary frequency standard obtained for Hg laser operating at microwave frequencies

05 p0859 A70-16271

Modulation properties of stabilizing frequency standard for gas laser with signal control by separate absorption cells

06 p1079 A70-17440

Monograph on time measurements covering time scales, intervals, natural and artificial clocks, frequency standards, time and time signal transmission

07 p1283 A70-19664

Phase comparisons between commercial cesium beam frequency standards and NASA experimental hydrogen maser NX-1

08 p1513 A70-21592

Ionospheric effects and transmitter characteristics observed on HF standard and time stations, discussing spurious emissions arising from frequency overcrowding

10 p1842 A70-25050

Atomic frequency standards for phase calibration of large aerial arrays applied to radiobroadcasting

11 p2019 A70-26300

HCN laser 890 GHz line phase locked to multiplied standard frequency with wide bandwidth loop, narrowing line widths

13 p2426 A70-28798

HCN laser far IR line phase locked to absolute frequency standard

13 p2426 A70-28810

Optical frequency standards research covering lasers application with superstable emission frequency

17 p3104 A70-35081

Primary wavelength standard established via line produced with wavelength-stabilized laser

17 p3104 A70-35086

Standards for measuring pulsed laser energy, CW laser power and HCN laser frequency

17 p3105 A70-35097

Timing systems using Cs frequency standard for satellite tracking

21 p3828 A70-41697

Short and long term stabilized optical frequency standard of gas laser, using two absorption cells

23 p4202 A70-45057

FREQUENCY SYNCHRONIZATION

Steady state operation and synchronization range of frequency dividers with complex feedback derived by symbolic abbreviated equations and modulation technique

05 p0813 A70-16263

Magnetron amplifiers with ferrite circulators for synchronizing natural frequency, obtaining I-V characteristics and gain vs bandwidth curves

05 p0823 A70-16886

Second and third harmonic simultaneous generation in ammonium oxalate crystals achieved by three frequency interactions

10 p1901 A70-25159

Frequency synchronization of far spaced high stability oscillators with aid of meteor trails, discussing signal retranslation and duplex methods

14 p2636 A70-30321

Discrete signals optimal reception by lowering synchronization requirements for communications or radar purposes

16 p2863 A70-33242

Unrestrained oscillator under action of external synchronous signal, deriving differential synchronization equation

17 p3051 A70-34614

ATA Collision Avoidance System based on time and frequency synchronization via ground stations or other aircraft

19 p3466 A70-38239

Mutual synchronization of oscillators at multiple frequencies, analyzing effect of tuning on frequency and phase

20 p3597 A70-39252

Frequency synchronization channel pulse fluctuations effect on noise stability of binary signal reception

20 p3587 A70-40145

Ring lasers loss lock-in, attributing frequency synchronization between oppositely directed traveling waves to mutual coupling

21 p3838 A70-42007

Single frequency gas laser synchronization by small harmonic signal from second laser, deriving frequency shift dependence on power

23 p4200 A70-43929

FREQUENCY SYNTHESIZERS

Monograph on normal frequency generator serving devices measuring differential Doppler effect, discussing generator design for ionospheric research satellites frequencies

09 p1645 A70-22531

Absolute frequency wideband high resolution determination, using frequency synthesizer as phase locked loop local oscillator

10 p1854 A70-25316

Two-photon transitions effect on two-frequency generation threshold in media with line broadening, considering laser radiation effect on amplification in second channel

12 p2251 A70-28289

Digital frequency synthesizer design, operation and stability

19 p3390 A70-38581

FREQUENCY TRANSLATION

U FREQUENCY CONVERTERS

Fresnel diffraction Laser beam intensity distribution determination from measuring Fresnel diffraction pattern at straight edge using photographic plate

12 p2249 A70-28032

Optical and quasi-optical transmission of EM wave beams of type in directional antennas Fresnel region, examining free space and waveguide modes

14 p2549 A70-30445

Transparent spherical rotor spin axis orientation by measuring Fresnel drag effect of optical beam inside ring laser cavity

19 p3445 A70-37669

Fresnel diffraction using He-Ne gas laser and opaque wire

21 p3834 A70-40549

FRESNEL REGION

Antenna calibration by measuring emission of absorbing black disk positioned in Fresnel region

07 p1239 A70-18759

Laser with telescopic resonator, examining characteristics at different Fresnel zones and emission losses with geometric optics approximation

13 p2427 A70-29280

Antenna calibration by measuring emission of absorbing black disk positioned in Fresnel region

18 p3233 A70-37103

Radio beam trajectory in Fresnel zones of isotropic laminarly inhomogeneous ionosphere, discussing point source field and wave propagation

19 p3381 A70-38569

Tracking of point object in Fresnel zone from observation of amplitude-phase pattern in aperture plane

22 p4026 A70-42555

Weak-scattering limit in thin screen model of interplanetary scintillations of radio sources involving solar wind fluctuations at Fresnel scale

22 p4104 A70-42996

Near field vector evaluation of Fresnel zone field for microwave reflector antennas

23 p4161 A70-43771

Ultrasonic pulse emitter with interference-free near field and sidelobe suppression for materials testing

24 p4343 A70-45685

FRETING

Hydrogen effects on ELI Ti-Al-Sn alloy, conducting tensile, fretting and abrasion tests on stressed and thermal cycled specimens

07 p1309 A70-19710

Fretting and fretting fatigue in metal-metal contacts, showing friction as important parameter

12 p2253 A70-27110

FRETING CORROSION

Fretting corrosion effect on structural steel fatigue strength under asymmetric load cycles

01 p0207 A70-11155

Dislocation structure during fretting corrosion in steel plates, analyzing via electron microscopy

12 p2258 A70-28318

Fretting corrosion zone steel, measuring transient temperature distribution during contact friction

20 p3647 A70-39243

FRICITION

NT AERODYNAMIC DRAG

NT DRY FRICTION

NT FLOW RESISTANCE

NT FRICTION DRAG

NT INTERNAL FRICTION

NT KINETIC FRICTION

NT SKIN FRICTION

NT SLIDING FRICTION

NT STATIC FRICTION

NT SUPERSONIC DRAG

NT VISCOUS DRAG

Difference method for calculating one dimensional nozzle flow and expansion with allowance for relaxation, friction and heat losses, discussing fluorine-hydrogen mixture application

03 p0408 A70-13804

Dissolved macromolecules effect on flow resistance due to turbulent friction in nonNewtonian liquids, considering physical parameters and hydrodynamic conditions

08 p1483 A70-21228

Friction, wear and surface evaluation of alloys as bearing materials in prosthetic devices

09 p1690 A70-22044

Nonlinear differential equations analysis based on weighted linear approximation applied to singular points and trajectories in phase plane in friction problems

09 p1727 A70-22665

Metal surfaces friction and wear processes dynamic equilibrium noting loading conditions effects

13 p2423 A70-29766

Friction theory, discussing surface mechanics, wear and erosion control

15 p2743 A70-31699

Friction properties of internally lubricated and glass-fortified thermoplastic resins for gears and bearings

16 p2935 A70-33354

Elasticity theory two dimensional contact problems, examining cohesion or friction in contact area

17 p3192 A70-35693

Spacecraft simulator using air bearing technique to simulate low friction aspect of environment, considering application to satellite attitude control

18 p3236 A70-36064

Friction and temperature fields in lubricant film of journal bearings, discussing friction torque and heat dissipation

19 p3434 A70-37601

Metal surfaces friction and wear processes dynamic equilibrium noting loading conditions effects

20 p3638 A70-40099

FRICITION COEFFICIENT

U COEFFICIENT OF FRICTION

FRICITION DRAG

NT AERODYNAMIC DRAG

NT SUPERSONIC DRAG

NT VISCOUS DRAG

Pressure changes associated with surface friction and geostrophic drag coefficient related, discussing mass inflow and outflow

05 p0837 A70-16151

Vorticity effects on drag friction and heat transfer near stagnation point of supersonic jet impinging on obstacle

05 p0833 A70-16290

Frictional drag reducing polymer solution injection into boundary for turbulent pipe flow, discussing Reynolds number, injection rate, injection points and concentration

06 p1032 A70-17215

Blowing intensity influence on turbulent boundary layer of incompressible fluid and friction drag of flat plate

06 p1036 A70-17852

Turbulent incompressible boundary layer on porous heat insulated plate with uniform suction, calculating ratio of friction drag coefficients

07 p1254 A70-19082

Elastic coatings effect on turbulent friction using turbulence flow theory based on mixing length concept

08 p1483 A70-21227

Friction drag on thin pyramidal lobed bodies in supersonic flow, analyzing detached shock region and body geometry function

09 p1606 A70-23612

Velocity distribution along cylindrical pipe in adiabatic flow with friction and known inlet parameters

09 p1607 A70-23616

Convergent-divergent nozzle flow under influence of friction drag, determining heat transfer rate as function of nozzle geometry

17 p3194 A70-34694

Heat transfer and friction drag calculation for turbulent boundary layer of gas with temperature dependent physical properties

17 p3012 A70-35729

German monograph on casing and hub wall friction effects on three dimensional flow in turbocompressors in subsonic compressible working fluids

24 p4287 A70-45096

Friction-originated ageostrophic mass flux in ground friction layer at nonaccelerated geotriptic boundary layer flow

24 p4370 A70-45133

FRICITION FACTOR

Pneumatic line losses due to friction in pneumatic control systems

04 p0628 A70-15399

Packing rub effect on rotating machinery produced by unstable vibration generated by friction and heat of rubbing rotor in sliding contact

05 p0854 A70-15908

Friction on fuselage surface layer under static and instantaneous loads without allowance for oscillation

05 p0856 A70-17015

Equations of motion for hypersonic friction layers integrated using quadrature procedures

06 p1033 A70-17230

Potential flow over rocket contour containing bends calculated by polygonal distribution of singularities on axis of body of revolution, determining friction effects

06 p0964 A70-17239

Turbulent friction in gas flow core determined on basis of maximum stability principle

07 p1253 A70-18719

Complex elastic system coupled flexural vibrations resonant frequencies determined with allowance for friction

07 p1363 A70-19111

Elastic contact between bodies in presence of friction or adhesion by reducing singular integral equations to Fredholm equation

08 p1585 A70-20958

Single fluid theory for plasma laminar flow in field-free region of circular tube, obtaining friction factor and Nusselt number correlations

08 p1552 A70-21585

Forced vibrations of trusses calculated by dynamic rigidities method allowing for friction forces

09 p1773 A70-22540

Frictional traction-sliding speed relation in elastohydrodynamic lubrication in Barlow-Lamb model of viscoelastic liquid, discussing oscillatory and continuous shear

09 p1691 A70-22600

Friction and orography influence on wave motions in real atmosphere, discussing planetary boundary layer and propagation in free atmosphere

09 p1718 A70-23331

Velocity and friction stress profiles of semibounded plane turbulent jets discharging from finite slit along smooth plate into moving medium

09 p1663 A70-23617

Statistical chance characteristics of velocity profiles and friction for flow along infinite plane wall with constant suction

10 p1869 A70-24519

Atmospheric pressure variations as function of vertical movements caused by friction and orography, considering numerical forecasting

11 p2076 A70-26073

Self-synchronization of forced frictional mechanical vibrators assuming simple harmonic combination

11 p2139 A70-26417

One dimensional compressible flow with heat addition in nonconstant area duct extended for friction addition, discussing critical thermal shocking

11 p2041 A70-26651

Monograph on acoustic theory for determining frictional pressure drop effect on gas state behind reflected wave in shock tube

12 p2209 A70-27000

Fretting and fretting fatigue in metal-metal contacts, showing friction as important parameter

12 p2253 A70-27110

Two component piezoelectric skin friction force transducer for hypersonic flow tunnel

13 p2405 A70-28815

Wear intensity of abrasives during fine grinding of Armco Fe, Ti and Ti alloys, comparing friction and chemical composition effects

15 p2743 A70-31640

Drag optimal stern section of plane body at supersonic flow, allowing for friction forces

18 p3206 A70-36261

Mathematical solutions validity in determining constant interface friction factor from ring compression tests

[ASME PAPER 69-WA/LUB-8] 19 p3434 A70-37603

Pure metals structure effect on friction and lubrication under steady slip in ultrahigh vacuum at low temperatures

19 p3438 A70-38729

Oil seals service life as function of friction horsepower

[ASLE PREPRINT 70AM 5C-1]

19 p3439 A70-38807

Elastic contact between bodies in presence of friction or adhesion by reducing singular integral equations to Fredholm equation

20 p3719 A70-39381

MHD induction generator design, considering electrical and friction loss measurement and control

20 p3565 A70-39988

Turbulent gas boundary layer at finite Reynolds numbers, investigating relative changes in friction and heat transfer coefficients and temperature factor

20 p3614 A70-40390

Heat transfer and friction effects on flow parameters in nozzle with independent cooling

21 p3951 A70-41769

Earth rotation rate deceleration due to lunar tidal friction taking into account fluctuations from internal processes, discussing moon retreat from earth

21 p3921 A70-41970

Tidal friction theories relating to earth rotation and lunar evolution

21 p3921 A70-41972

Downstream heat transfer and wall friction predictions for quasi-developed strongly heated turbulent pipe flow, using mixing length model

[ASME PAPER 70-HT-8] 22 p4008 A70-42439

Acoustic frequency spectra of transverse vibrations in bracketed bar caused by dry friction, using Lagrange method

22 p4073 A70-42612

Antifriction number characterizing friction coupling, distinguishing between elastic and plastic modes

22 p4047 A70-43348

Equations solution for turbine blade flexural vibration, considering internal friction

22 p4117 A70-43363

Low friction seal for axial loading piston in triaxial soil testing cells

23 p4199 A70-43873

Orography and friction effects on numerical forecast of atmospheric pressure variation

24 p4370 A70-45112

FRICITION LOSS COEFFICIENT

U FRICITION FACTOR

FRICITION MEASUREMENT

High temperature internal friction measurements on miniature torsional pendulum specimens from TD nickel bar, showing damping differences due to microstructural anisotropy

01 p0122 A70-11237

Local skin friction measurement on model in blow-down hypersonic wind tunnels using floating element transducer, giving results for flat plate and wedge

[ONERA-TP-756] 03 p0463 A70-13629

Sliding friction and wear of polytetrafluoroethylene ball bearing filled with graphite investigated for irradiation effects

06 p1077 A70-18404

Sliding rigid conical indenter friction experiments over work hardenable metal flats in high adhesion conditions, observing forces, stresses and deformation modes

13 p2421 A70-29548

Supersonic skin friction measurements in grit type boundary layer transition trips with zero heat transfer

13 p2343 A70-29969

Test stand based on Froude pendulum for measuring friction coefficients and oscillation parameters of porous bushings

16 p2924 A70-34298

Friction coefficient theory and measurement, considering definition and measuring equipment

16 p2924 A70-34332

Ball bearing materials for ultrahigh vacuum space environments, determining frictional and wear behavior

17 p3099 A70-34573

Metal-silicate rock friction in ultrahigh vacuum of lunar environment

17 p3101 A70-34760

Force-balance principle application to pressure and skin friction measuring instruments, discussing construction, operation and performance

17 p3089 A70-35171

Skin friction measurement in supersonic flows by thin film heated element method, describing thermal boundary layer properties

18 p3243 A70-36710

Ultrahigh precision microminiature bearing resistance moment measurement with inductive sensors

18 p3264 A70-37069

Mathematical solutions validity in determining constant interface friction factor from ring compression tests

[ASME PAPER 69-WA/LUB-8] 19 p3434 A70-37603

FRICITION PRESSURE DROP

U SKIN FRICITION

FRICITION REDUCTION

Low speed Ga lubricated sliding electrical contacts of Be in vacuum, discussing Ga film role in friction and contact resistance

01 p0099 A70-10325

Compression test for ductile materials based on Saint Venant principle of plasticity to reduce friction effects on deformation by lubricant pressurization

04 p0776 A70-15373

Antifriction reinforced plastics based on polyamide fibers in epoxy phenolic resins, determining optimum ratios to obtain desired mechanical properties

09 p1710 A70-23675

Friction reducing oxide layer effects on Ti alloys low temperature plastic and mechanical properties

19 p3450 A70-37458

Liquid-gas separator design with reduced friction loss for MHD generators using two phase convergent-divergent nozzles

20 p3612 A70-40014

Power loss reduction from disk friction and gas leakage through rotor seals of low speed centrifugal pumps in aircraft hydraulic systems and liquid propellant rocket engines

22 p4091 A70-42806

FRICITIONLESS ENVIRONMENTS

Steady and frictionless supersonic flow of ideal gas of constant heat capacity around slightly deformed cone, calculating force exerted by gas

06 p0964 A70-17240

FRINGE PATTERNS

U DIFFRACTION PATTERNS

FROGS

Relationships between frog vestibular afferents, cerebellum and efferent vestibular system, using electron microscopy and Nauta degeneration technique

01 p0014 A70-10351

Cerebello-otolith system represented by axons of Purkinje cells, studying inhibitory vestibular efferent system relation to cerebellum in frog

01 p0014 A70-10352

Termination mode of primary and secondary vestibular fibers in cerebellar cortex of frog and cat, measuring evoked field and unitary potentials

01 p0014 A70-10353

Frog sartorius muscle heat production and work effect measured under isotonic and isometric conditions, using gradient layer calorimetry

02 p0232 A70-11715

High strength magnetic fields effect on early embryonic development of frogs, relating growth abnormalities and paramagnetic ferritin motions

16 p2848 A70-33099

Auditory perception by neuroelectrical tests based on logic coincidence among several detectors, discussing bullfrog inner ear

21 p3765 A70-41991

Organism reactions to gravity forces, discussing experimental zero and hyper g simulation studies with frog and nematode eggs

23 p4146 A70-44630

Altered gravitational field effects on frog eggs centrifuged under various conditions after fertilization, noting time dependence of induced abnormalities

24 p4298 A70-45619

FRONTAL AREAS [METEOROLOGY]

U FRONTS [METEOROLOGY]

FRONTS [METEOROLOGY]

Ball lightning mechanism proposal based on mathematical model for electric discharge current in parabolic plasma shell forming vortex-type storm front

05 p0879 A70-17021

Upper frontal waves behind quasi-stationary surface cold front using mathematical model

08 p1540 A70-21924

Sheared frontal zones structure and stability, studying Richardson number limiting role in free atmosphere

08 p1492 A70-21971

Heavy squalls observations by satellite TV and radar, considering wave disturbances at cold front

13 p2444 A70-28585

Extratropical planetary high altitude frontal zones statistical analysis and position forecasting by eigenfunction expansion

13 p2445 A70-29673

Upper level frontal zones geostrophic approximation theory based on scale analysis and case study diagnosis

15 p2769 A70-31442

Radiation fields structural characteristics of fronts, intertropical convergence zones and cyclone formations from radiation charts based on meteorological satellite observations

15 p2770 A70-32068

Maximum up- and downdrafts altitude, using two dimensional model of lee wave disturbances for post-frontal subsidence modification

16 p2945 A70-32948

Meteorological observation on atmospheric boundary layer during winter, determining width and inclination of frontal zones

19 p3463 A70-38758

Midtropospheric frontogenesis, using three hourly rawinsonde data for isentropic trajectories to describe velocity field in space and time

20 p3664 A70-39374

FROST

- Near IR reflectance spectrometer integrated into environmental chamber to study frost spectral properties
06 p1072 A70-18522
- Spectral reflectance of carbon dioxide and water frosts at 0.8-3.2 microns, growing frosts in cold vacuum chamber from high purity gases
07 p1388 A70-19945
- Martian polar cap spectra interpreted with laboratory measurements of water-carbon dioxide frost spectral reflectance
07 p1388 A70-19946
- Saturn ring IR spectrum, discussing resemblance and discrepancies of ammonia and water frost spectra
10 p1935 A70-23813
- Thermal conductivity of frost, using imbedded hot-wire method
18 p3262 A70-37118

FROUDE NUMBER

- Large Froude number solution for nonseparative impact of elliptical cylinder floating on incompressible fluid surface in half space extended to small Froude numbers
07 p1253 A70-18770
- Interfacial and free surface mode instabilities of time periodic flows of viscosity and density stratified fluids at various Froude numbers
14 p2566 A70-31026

FROZEN EQUILIBRIUM FLOW

- Mach numbers, electron density and temperature in partially ionized frozen equilibrium flows of Ar in hypersonic nozzle
01 p0063 A70-10994
- Normal shock waves in frozen, partly frozen and equilibrium flow in gas-solid particle mixtures
01 p0065 A70-11100
- Frictionless hypersonic flow around blunt bodies of revolution, taking into account real gas effects in equilibrium and frozen flow calculations
06 p0965 A70-17242
- Frozen flow effect in hypersonic wind tunnel nozzle on parameters of nonequilibrium incident flow past wedge
09 p1604 A70-22446
- One dimensional sound propagation in reacting gas mixture near equilibrium, obtaining equilibrium and frozen sound speed
22 p4074 A70-42752

FRUSTUMS

- Axisymmetric vibration modal properties /frequencies and mode shapes/ of thin conical shell frustums, considering dimensional and boundary condition influences
23 p4270 A70-44501

FUEL CAPSULES

- Thermal mapping vacuum chamber tests of nuclear fuel capsules for lunar surface experiments, using remote IR radiometric microscope
15 p2718 A70-32800

FUEL CELL CATALYSTS

U ELECTROCATALYSTS

FUEL CELLS

NT HYDROGEN OXYGEN FUEL CELLS
NT REGENERATIVE FUEL CELLS

- Book on electrochemical processes in fuel cells covering mass transport processes, electrode reactions, anodic oxidation, etc
06 p0989 A70-18250
- Fuel cell assemblies as primary electrical source for Apollo command and service modules, discussing heat removal, water vapor control and transient performance
08 p1439 A70-20702
- Molten carbonate fuel cells power source for military applications, considering catalytic recycle reformer
08 p1439 A70-20703
- Fuel cells - Conference, Brussels, June 1969
10 p1828 A70-24451
- Silver/polytetrafluoroethylene water-repellant air-breathing cathodes for fuel cells with alkaline electrolytes, discussing pressure compatibility
10 p1829 A70-24454
- Fuel cells phase equilibria between carbonate melt and Li, Na and K solid aluminate electrolytes, analyzing thermal and electrical conductances
10 p1830 A70-24458
- High temperature fuel cell electrolytes, analyzing electrical conductivity of ternary systems of zirconium, cesium or tantalum and yttrium oxides in fluoride phase
10 p1830 A70-24460
- Solid electrolyte high temperature fuel cells electrode materials, investigating various metal oxides
10 p1830 A70-24461
- CO electrochemical oxidation at porous solid electrolyte fuel cell anodes under high temperature, noting current density role
10 p1830 A70-24462
- Electrodes oxidation processes involving fuel cell molecules or derived adsorbed intermediates reacting with anodically generated surface oxide, considering Pt electrochemical reduction
10 p1830 A70-24465

Raney alloy catalyst activity and stability in fuel cell anodes, noting properties of ternary phases of nickel, aluminum and iron, molybdenum or titanium
10 p1831 A70-24466

Catalytic load carrying capacity of porous carbon electrodes impregnated with nickel salt and nickel boride in anodic fuel cell hydrazine oxidation
10 p1831 A70-24469

Electrode structural parameters effect on polarization characteristics of air-hydrogen cells to obtain optimum performance, reliability and service life
10 p1831 A70-24471

Low temperature fuel cell materials impurity effects on catalyst poisoning, stressing sulfur elimination from rubber molding
10 p1832 A70-25043

Fuel cells with solid oxide electrolyte, principles, advantages and drawbacks
12 p2163 A70-26994

Medium temperature hydrogen fuel cells design, operational characteristics and performance
12 p2163 A70-26996

Fuel cell electrolytes, describing porous tungsten carbide as catalyst
12 p2164 A70-27068

Fuel cell systems - ACS Conference, Chicago, September 1967, Part II
12 p2165 A70-27757

Fuel cells power density improvement under pulsed loading at high current density and constant voltage
12 p2165 A70-27758

Liquid hydrocarbon-air battery with fuel transport operation, considering electrode structure, boiling range, carbon dioxide rejection, etc
12 p2166 A70-27764

Electrocatalysts, electrode structure and design of fuel cells using air at cathode, describing applications to hybrid systems
12 p2166 A70-27765

Natural gas-air fuel cell battery with sulfuric acid electrolyte for low temperature operation
12 p2166 A70-27766

Book on fuel cells electrochemistry covering direct energy conversion methods, electrode kinetics, electrocatalysis, organic substances, electrochemical combustion, research techniques, etc
14 p2532 A70-30100

LPG use in fuel cells, discussing efficiency, weight and size
18 p3216 A70-36657

Fuel cell cavities, analyzing fluid motion purge dynamics based on anisotropic porous media model
18 p3216 A70-36766

High temperature fuel cell with thin disk solid electrolyte, evaluating performance as function of electrolyte, electrode and current collector resistance ratio
22 p3966 A70-42499

Hydrazine-fueled battery low power consumption auxiliary system with voltage regulator and gas pumps
22 p3966 A70-43539

Hydrazine-oxygen fuel cell design and operation, discussing efficiency, electrolyte space, etc
22 p3966 A70-43541

Batteries and fuel cells as portable and transportable electrochemical power sources
24 p4295 A70-46399

FUEL COMBUSTION

Book on turbulent diffusive flames in combustion of gaseous fuels covering mass, heat, flame exchange and stabilization processes, etc
01 p0219 A70-11377

Fuel droplets burning at pressures sufficient to reach critical temperature under zero gravity conditions in free fall apparatus
02 p0351 A70-12002

Flame spreading theory for plastic fuels surfaces in nitrogen-oxygen mixtures, considering initial fuel temperature, pressure and mixture composition effects
02 p0396 A70-12015

Laminar diffusion flame spread against air stream over solid or liquid fuel bed, noting influence of stoichiometric and thermal properties and data inconsistency
02 p0396 A70-12016

Hydrogen reactions with nitrogen dioxide, oxygen and mixtures of oxygen and nitric oxide in adiabatic flow reactor measured as function of temperature and pressure
02 p0250 A70-12020

Chemical additives effect on H-Cl-N mixtures burning velocity in air and nitrogen
02 p0398 A70-12031

Ultrasonic atomizer system for liquid fuels combustion
02 p0356 A70-12470

Polymethyl methacrylate fuel for hypersonic air breathing propulsion systems, studying ablation, mixing and combustion processes
03 p0603 A70-12942

Burning constants prediction for suspended hydrocarbon fuel droplets based on modified theoretical equation
03 p0544 A70-13916

Liquid fuel film vaporizing combustor for gas turbines, considering combustion efficiency and flame intensity
03 p0552 A70-14324

Emulsified jet fuels combustion characteristics evaluation by laboratory technique, presenting data on emulsifiers and corrosion inhibitors effect
04 p0785 A70-14893

Ignition of freely falling single fuel droplets, considering initial size, oxidizer temperature, fuel composition, droplet spacing, etc
04 p0733 A70-15540

Nozzle exit turbulence and excess fuel combustion as low and high speed jet noise source using Lighthill theory
05 p0834 A70-16782

Liquid fuel combustion luminous flame monochromatic radiation distribution, considering soot particle clouds effective emission thickness
06 p1172 A70-17142

Ducted turbulent mixing and burning of coaxial streams, presenting experimental results for rocket-air mixing system
06 p1130 A70-17171

Combustion stability in air-liquid fuel zone of jet engine burner with burning rate controlled by droplet vaporization rate controlled mechanism
06 p1178 A70-17980

Ignition of cold premixed fuel by hot projectile, obtaining distance for ignition occurrence
06 p1180 A70-18133

Combustion and flow characteristics associated with direct injection of liquid hydrocarbons into high speed air stream
06 p1182 A70-18198

Gas phase ignition theory of evaporating fuel in stagnant hot oxidizing gas as function of temperature
07 p1421 A70-19317

Mathematical model for calculating radiative heat transfer from turbulent diffusion buoyant flame and predicting liquid fuel burning rate
07 p1425 A70-20008

Condensed fuel mixtures and oxidizers combustion rates as function of pressure and particle size
09 p1786 A70-22104

Steady flame propagation attainment for chemical reaction initiation in gaseous fuel by heated surface with various wall temperatures
09 p1787 A70-22115

Flame propagation in slowly combusting fuel-air mixtures using gas chromatography and flame speed
11 p2151 A70-26381

Temperature and metallic contact effects on composition and structure of solid phase deposits during reactive fuel oxidation
12 p2289 A70-27493

Solid fuel steady combustion regime stability dependence on heat generation in reaction zones and temperature and velocity fields inhomogeneity
13 p2522 A70-29423

Shock wave interaction with burning liquid fuel droplets in gaseous oxygen atmosphere, observing wave amplification due to mass combustion rate increase
13 p2522 A70-29424

Liquid fuel droplet ignition quasi-stationary theory occurring at maximum chemical reaction rate
14 p2664 A70-30393

Flameout from burning liquid fuel droplet within reduced film theory
14 p2664 A70-30394

High temperature combustion wind tunnels for investigating gas and liquid fuel combustion stabilized by shock waves in supersonic flow
16 p2996 A70-32991

Thermodynamic diagram indicating enthalpy and entropy of oil combustion gases for any state and air excess value
16 p2997 A70-33295

External burning fuels environmental temperature requirements from nonlinear droplet ignition model, emphasizing droplet size importance
16 p2997 A70-33604

Powder combustion on metal plate, investigating unburned layer thickness dependence on initial temperature
17 p3198 A70-35738

Chemical kinetics effect on combustion rates of fuel plate in turbulent oxidizer flow, deriving conservation equations in boundary layer and diffusion equation
18 p3346 A70-36245

Turbine engine combustion chambers with various frontal devices, investigating burnout mechanism and heat yield in secondary air flow injection zone
19 p3489 A70-37246

Gas turbine engine combustion chamber efficiency dependence on injector characteristics, temperature and fuel physicochemical properties
19 p3489 A70-37247

Flame propagation velocity of gasoline-air mixture during two stage combustion process in laminar and turbulent flows, discussing combustion products effect
19 p3550 A70-37253

Elementary chemical reaction kinetics effect on electrophysical parameters of low temperature plasma jets, calculating relaxation time for C fuels
19 p3481 A70-38184

Soviet papers on kinetics and aerodynamics of fuel combustion processes covering supersonic flow, flame stabilization, fluid atomization, nonequilibrium recombination, etc
20 p3736 A70-39265

Combustion of decomposition products of Mg based pyrotechnic fuel in supersonic flow, obtaining heating device characteristics
20 p3736 A70-39266

Flame stabilization in boundary layer during mixing of cold homogeneous fuel mixture and hot gas based on combustion and turbulent jets theories
20 p3736 A70-39267

Air to air missile launch range maximization for plane trajectories and nonmaneuvering targets, discussing optimal fuel burning rate
[AIAA PAPER 70-980] 20 p3668 A70-39549

Turbulent jet system with previously unmixed chemically active gases, calculating heat and mass transfers during diffusion combustion
20 p3737 A70-39813

Hydrogen-oxygen and hydrogen-nitrous oxide systems combustion, studying isotopic substitution effect on flame speed by schlieren technique with rotating drum camera
20 p3583 A70-40472

Methane and hydrogen consumption rates during slow reactions in mixtures of molecular hydrogen, oxygen and nitrogen
21 p3772 A70-40879

Multicomponent fuels combustion in air, deriving simplified flame sheet model
21 p3942 A70-40881

Oxygen-kerosene fuel combustion products thermodynamic properties, tabulating computed values
21 p3865 A70-41771

Particulate boron levitated electrostatically in air and ignited by pulsed laser to avoid contamination, investigating combustion by high speed photography [SMPT PREPRINT 100] 22 p4032 A70-43034

Numerical analysis of fuel combustion in supersonic stationary flows of hydrogen air mixture past bodies by two-component reaction kinetics model
[ICAS PAPER 70-52] 24 p4428 A70-45500

Photographic measurement of droplets size, velocity and number during sprayed liquid fuel combustion, using Xe flash bulbs
24 p4429 A70-46008

FUEL CONSUMPTION

Optimal rendezvous maneuver of two spacecraft in circular orbits with minimum fuel consumption, taking into account propelled vehicle control program and flight path
01 p0193 A70-10424

Minimum propellant rendezvous maneuver of space vehicles in neighboring circular orbits
01 p0193 A70-10555

Minimum fuel consumption criteria applied to design of manned spacecraft attitude control system, using reaction jets for lateral and directional controls
01 p0196 A70-10950

Optimal fuel consumption for climbing, cruising and landing flight conditions for medium range subsonic, high supersonic and hypersonic aircraft
02 p0227 A70-12404

Minimum propellant maneuver during docking of elliptical orbit rendezvous between propelled and passive target vehicles, analyzing as variational problems
02 p0380 A70-12784

Turbojet engine controls and control devices design, considering fuel properties and fuel consumption
03 p0552 A70-13806

Optimal control of thrust limited minimum- propellant rocket-powered vehicle using expansion about optimal trajectory
04 p0750 A70-14928

Analytic guidance and control for minimum fuel expenditure and optimal guidance corrections for low thrust vehicle in Martian orbit
[AIAA PAPER 68-862] 04 p0716 A70-15544

Satellite circular orbital plane rotation by jet thrust, minimizing fuel for fixed time
07 p1393 A70-19497

Soviet helicopter and aircraft engines characteristics covering designer, power, rpm limits, fuel consumption, weight, geometry and applications
08 p1559 A70-21366

Composite programming of vertical ascending rocket with constant thrust phase followed by acceleration and coasting phases, discussing burnout altitude and fuel consumption
08 p1582 A70-21775

Range, block speed and fuel-weight ratio formulas for hypervelocity, boost glide and ballistic vehicles
08 p1582 A70-21871

Fourth order differential equation system with complex conjugate eigenvalues, deriving optimal control for fuel minimum
09 p1759 A70-22831

Linearized theory for minimum fuel guidance in neighborhood of minimum fuel space trajectory, unrestricted thrust magnitude and allowances for mid-course impulses
[AIAA PAPER 69-74] 11 p2079 A70-25957

Minimum fuel continuous thrust elliptical orbit transfer problem, obtaining optimal steering function for departure and arrival points
11 p2124 A70-26214

Accelerated gradient projection method applied to rocket trajectory optimization for minimizing fuel required for placing payload in circular orbits
13 p2485 A70-28395

Spacecraft rendezvous control at minimal propellant consumption, deriving algorithm
13 p2499 A70-28400

Minimum fuel takeoff and landing paths for VTOL aircraft with constraints on state and control, determining optimal trajectories
[AIAA PAPER 70-550] 13 p2345 A70-29015

Rolls-Royce RB 211 turbofan engine, discussing fuel consumption, specific weight, noise and smoke level, reliability and maintainability
15 p2787 A70-31948

Satellite circular orbital plane rotation by jet thrust, minimizing fuel for fixed time
15 p2813 A70-32742

Minimum impulse transfer between two neighboring low eccentricity orbits, discussing fuel consumption and transfer time
17 p3167 A70-35231

Linear time invariant plant driven by scalar control, deriving second variation algorithm for minimum fuel problems
17 p3057 A70-35555

Steady state off-on attitude control strategy for minimizing propellant consumption and thrust ignitions of satellite in presence of environmental disturbance torques
17 p3180 A70-35556

Optimum approach and departure paths for VTOL aircraft simulated by hybrid computer under constraints
[AIAA PAPER 69-209] 18 p3213 A70-36452

Integrals of motion for minimum fuel rocket trajectories in inverse square field calculated for constant power and constant exhaust rockets
18 p3316 A70-36678

Closed form solution for minimum fuel constant thrust trajectories for vehicle transfer in vacuum between arbitrary boundary conditions
18 p3316 A70-36683

Spacecraft fuel optimal controls for out-of-plane motion about translunar libration point based on phase plane methods
[AIAA PAPER 70-1079] 19 p3530 A70-38890

Optimum switching in minimum fuel, time-free impulsive planar transfer problem by primer vector concept
20 p3709 A70-40074

Fuel optimal orbital transfer trajectories by linear programming
20 p3711 A70-40337

Fuel consumption related to aircraft performance and engine type
22 p4090 A70-42602

Analytic approximation for initial adjoint vector for optimal/minimum propellant/ space trajectories
[AIAA PAPER 69-916] 23 p4243 A70-44509

Minimum fuel thrust limited transfer trajectories computation for coplanar elliptic orbits
[AIAA PAPER 69-914] 23 p4244 A70-44558

Interplanetary mission propellant reduction by using earth-moon-sun gravity field properties, discussing swingby techniques, low energy trajectories, etc
23 p4244 A70-44607

Two shaft bypass jet engine analog simulation, determining angular acceleration dependence on angular velocity and fuel consumption
24 p4393 A70-45442

TSCP700 aircraft auxiliary power unit design, fuel consumption and maintainability
[SAE PAPER 700815] 24 p4395 A70-45902

FUEL CONTAMINATION

Contaminants formation during pulse mode operation of liquid bipropellant attitude control rocket engine, discussing exhaust plume effects
[AIAA PAPER 69-574] 07 p1394 A70-19708

Field test for microbiological contamination of jet fuel, discussing phosphates detection
18 p3299 A70-36344

Water separation index modified /WSIM/ test for jet fuel surface active materials in relation to filter/separators performance
[SAE PAPER 700279] 18 p3300 A70-36815

Aircraft and engine fuel systems deposit formation and microstructure in various test rigs, using electron microscopy
[SAE PAPER 700258] 18 p3214 A70-36823

Automated aircraft flight safety, concerning probabilities and onboard elimination of servomotor failures in hydraulic system due to fuel contamination
22 p3961 A70-42804

FUEL CONTROL

RB.211 aircraft engine control, describing fuel and electronic control systems design and operation
[SAE PAPER 690404] 03 p0551 A70-12895

Turbojet engine controls and control devices design, considering fuel properties and fuel consumption
03 p0552 A70-13806

Concorde microelectronic power plant control system, noting overfueling prevention by throttle actuator during startup and speed governor function
05 p0896 A70-16003

Fuel suboptimal attitude control of spin stabilized axisymmetric spacecraft
10 p1953 A70-25237

Business aircraft fuel management system using capacitance and mass flow rate measurements, displaying fuel quantity and flow rate and flight time remaining
[SAE PAPER 700225] 11 p1983 A70-25896

Minimum fuel control for discrete time Gaussian processes, applying results to spacecraft midcourse guidance for earth-Mars mission
11 p2079 A70-25958

Capillary barriers to provide propellant positioning, expulsion capability and slosh dampening for spacecraft propulsion systems during rotational maneuvers
[AIAA PAPER 69-529] 11 p2123 A70-26119

Fuel-optimal retrothrust control in state dependent retarding force fields, taking into consideration synthesis for vertical trajectory system configuration
11 p2126 A70-26321

Hydrostatic stability and damping characteristics of perforated plates and screens for passive propellant control schemes from drop tower tests
[AIAA PAPER 69-531] 15 p2787 A70-32510

Dual bellows ball seat valve design for colloid thruster coupled to pressurized feed system, demonstrating thrust decay and flow regulation
[AIAA PAPER 70-615] 16 p2919 A70-33610

VTOL 5000 hp engine design optimization, considering component arrangements, rotor design, blade cooling method and fuel control
17 p3147 A70-34709

Fluidically controlled aircraft fuel transfer system three-tank model construction, noting maintenance and fail safe operation
[SAE PAPER 700786] 24 p4294 A70-45858

FUEL CORROSION

Temperature and metallic contact effects on composition and structure of solid phase deposits during reactive fuel oxidation
12 p2289 A70-27493

Solid tar deposits from hydrocarbon fuels oxidation during prolonged storage
12 p2289 A70-27494

Jet fuel system deposits measurement, noting reliability of oxygen combustion and beta ray backscattering techniques
[SAE PAPER 700257] 18 p3214 A70-36824

FUEL ECONOMY

U FUEL CONSUMPTION

FUEL ELEMENTS [NUCLEAR REACTORS]

U NUCLEAR FUEL ELEMENTS

FUEL FLOW

NT PROPELLANT TRANSFER

Flow characteristics of curved porous wall gas core reactors for nuclear rocket engines, visualizing simulated fuel flow with air-smoke combination
06 p1104 A70-17509

Fuel delivery and speed control systems for aircraft gas turbine engines, discussing control circuit transfers and block diagrams
22 p4091 A70-43116

FUEL FLOW REGULATORS

Fluidic vortex valve to modulate solid propellant generated hot gas flow
[AIAA PAPER 69-424] 09 p1743 A70-23249

FUEL GAGES

NT CAPACITIVE FUEL GAGES

Gaging system utilizing nuclear radiation to obtain mass measurement of fuel quantity
[SAE PAPER 690673] 05 p0880 A70-15832

FUEL INJECTION

Diffusion flame structure in boundary layer with fuel injection from wall, analyzing expansions with single step reversible chemical kinetics, including nonequilibrium case
01 p0214 A70-10334

Supersonic diffusion flames produced by subsonic and supersonic free jet injection of hydrogen into high enthalpy airstream
02 p0399 A70-12042

Fuel injections into supersonic air stream through isolated normal ports and porous wall, using interferometry, schlieren and high speed photography
02 p0354 A70-12044

Fuel injection and mixing and piloted ignition in supersonic flow design principles for scramjet engine, evaluating eddy viscosity model for parallel injection
02 p0354 A70-12047

Flow field of jet spoilers downstream from nozzle, accounting for main stream and secondary jet mixing

and fuel injection problems during supersonic combustion

03 p0608 A70-14098

Chemical composition of scale formation in jet engine injectors for various fuel types tabulated, noting buildup levels in transport aircraft and subsonic jets

07 p1362 A70-18651

Combustion of pure crystalline boron single particles injected into hot oxidizing gases streams at atmospheric pressure

[AIAA PAPER 69-562] 07 p1359 A70-19583

Pressure peaks control in hydrazine propulsion system during static tests by controlling initial hydrazine injection

11 p2101 A70-25691

Monopropellant rocket combustion one dimensional theory with uniform velocity and size droplets injection, obtaining chamber length

14 p2629 A70-30773

Large scale hydrogen fueled supersonic combustor test at simulated Mach 8 flight, describing fuel injector design

[AIAA PAPER 70-715] 16 p2965 A70-33539

Oxygen difluoride/diborane propellant thrust chamber and injector technology, discussing engine duty cycles and performance

[AIAA PAPER 70-717] 16 p2962 A70-33550

Liquid rocket engine injector elements design criteria, using noncircular orifice geometry to predict efficiency

[AIAA PAPER 70-704] 16 p2967 A70-33565

Hydraulic characteristics of flow through miniature slot orifices for rocket engine injectors, observing stability of effluent liquid streams

[AIAA PAPER 70-706] 16 p2891 A70-33566

Particle penetration of solid or liquid combustible additives injected into air breathing combustors airstreams

17 p3073 A70-35665

Liquid propellant rocket engines, investigating fuel injection effect on formation of fuel mixture

18 p3300 A70-36252

Air-mechanical fuel injection effect on gas turbine engine combustion chamber working process, investigating heat generation coefficient, temperature field nonuniformity and combustion efficiency

19 p3489 A70-37248

Integrated double oblique shock scramjet for supersonic combustion tests and instrumentation development, discussing fuel injection through sonic orifices, combustion data, etc

[AIAA PAPER 69-827] 21 p3867 A70-41752

Fuel atomization drop size calculation for mechanical swirl injectors with and without air input

21 p3867 A70-41770

FUEL SPRAYS

Ultrasonic atomizer system for liquid fuels combustion

02 p0356 A70-12470

Combustion chamber design for engines, considering atomization by rotating disk vs nozzle atomization

03 p0552 A70-14031

Fuel nozzle sprays mean droplet diameter based on computerized analysis of small angle forward scattered light profile

21 p3806 A70-40805

Photographic measurement of droplets size, velocity and number during sprayed liquid fuel combustion, using Xe flash bulbs

24 p4429 A70-46008

FUEL SYSTEMS

NT AIRCRAFT FUEL SYSTEMS

Gaseous He bubbles injection into liquid propellant launch vehicle fuel lines to reduce vehicle pogo oscillations by lowering feed system natural frequencies

01 p0196 A70-10851

Fuel filter icing prevention by injecting antifreeze into filter instead of fuel

06 p0988 A70-17873

Spacecraft stochastic optimal control, discussing design of least upper bound fuel optimal system with measurement uncertainty

11 p2025 A70-26222

Liquid rocket technology for chemical engineers, discussing propellant tanks, lines and valves, tank pressurization, turbopumps and combustion chamber problems

12 p2291 A70-27664

Saturn 5 S-2 stage propellant feedlines and J-2 engines simulating structural longitudinal oscillation by analog computer

[AIAA PAPER 70-626] 16 p2968 A70-33591

Jet fuels ground handling at airfields, describing flow monitors, filters, fueling techniques, etc

22 p4006 A70-43093

FUEL TANK PRESSURIZATION

Gas solubilities investigated for gaseous pressurization of propellants

01 p0160 A70-10840

Gas bubble formation and equilibrium conditions in air supersaturated fuel stored under atmospheric pressure after injection into evacuated tank

03 p0605 A70-13394

Fluorine injectors for main tank injection of space vehicle liquid hydrogen tank, including study of hypergolicity and reaction product freezing

[AIAA PAPER 69-528] 04 p0736 A70-15406

Helium properties and utilization in NASA projects, discussing pressurization of fuel tanks cooling of superconducting magnets

04 p0720 A70-15633

Helium low temperature applications to fuel tank pressurization, superconducting magnet cooling and cryopumping of solar space simulators

11 p2083 A70-25620

Vapor fraction dependence on liquid hydrogen propellant outflow during NERVA operation under stored gas or autogenous pressurization, using computer simulation

[AIAA PAPER 70-677] 16 p2950 A70-33578

Gas-wall heat losses reduced and heated gas pressurization systems performance improved by ullage mixing by gas flow from pressurant injectors

[AIAA PAPER 70-681] 16 p2962 A70-33581

Boeing 747 aircraft pressure fueling system, describing tanks, feed system, refueling and electrostatic charge minimization

[SAE PAPER 700276] 18 p3214 A70-36816

FUEL TANKS

NT WING TANKS

Spontaneous ignition temperature as function of surface-to-volume ratio in static systems for fuels

11 p2151 A70-26384

Jet A kerosene deposit accumulation problem and proposed SST fuel tank design

[SAE PAPER 700256] 18 p3214 A70-36825

Liquid fuel behavior in right circular cylindrical tank inclined to earth gravitational field, computing fundamental sloshing frequency

20 p3610 A70-39694

Automatic calculations for fuel volume mass properties in tanks at various angles of attack, considering total weight, gravity center moment and inertia product

[SAE PAPER 850] 20 p3563 A70-40376

Catalytic combustion fuel tank inerting techniques for fire protection in military and civilian aircraft

23 p4141 A70-44485

Low gravity fuel sloshing in axisymmetric rigid tank, calculating oscillations by modified Galerkin method

24 p4324 A70-45292

Fluidically controlled aircraft fuel transfer system three-tank model construction, noting maintenance and fail safe operation

[SAE PAPER 700786] 24 p4294 A70-45858

FUEL TESTS

Carbon deposit formation in gas turbine engines with various fuels, studying thermal insulation properties

09 p1742 A70-22472

Flame spread rate across surface of liquid fuels, discussing effects of ignition mode, fuel purity and temperature, fuel container dimensions and material

10 p1929 A70-24090

Gelled and emulsified fuels for jet transport aircraft, testing rheological and physical properties regarding fire hazard reduction in crashes

[SAE PAPER 700251] 12 p2160 A70-27430

Electrostatic charging hazard and flight evaluation of aviation fuels with static dissipator additive

[SAE PAPER 700278] 12 p2289 A70-27439

Toxic fuel test site selection, evaluating meteorological factors in Gypsum Canyon, California

14 p2563 A70-30613

Ethyl alcohol fuel diffusion flame, examining thermal decomposition pyrolysis and free electron concentration distribution

18 p3345 A70-36113

FUEL VALVES

Fluidic vortex valve to modulate solid propellant generated hot gas flow

[AIAA PAPER 69-424] 09 p1743 A70-23249

FUEL-AIR RATIO

Ducted turbulent mixing and burning of coaxial streams, presenting experimental results for rocket-air mixing system

[AIAA PAPER 69-85] 06 p1130 A70-17171

Unsensitized gaseous fuel-air mixtures photochemical ignition due to molecular oxygen photodissociation by radiant energy absorption

[AIAA PAPER 70-149] 06 p1183 A70-18225

Cold combustible mixture ignition at forward stagnation region of hot projectile, calculating temperatures for propane-air mixture

07 p1422 A70-19577

Mixture composition and airflow rate dependence of combustion efficiency in turbo-prop afterburner chamber with air-fuel flame stabilizer

10 p1929 A70-24282

Excess air ratio and heat release efficiency in combustion of kerosene mixture determined by volumetric gas analysis

10 p1968 A70-24283

Nozzle fuel and air system geometrical parameters to determine mean diameter of fuel droplets, dispersion angle and spectrum and flame jet shape

10 p1930 A70-24295

Flame propagation in slowly combusting fuel-air mixtures using gas chromatography and flame speed

11 p2151 A70-26381

Combustion gases compositions and adiabatic flame temperatures of potassium seeded propane-air mixtures calculated at various equivalence ratios and temperatures assuming thermal equilibrium

12 p2330 A70-27227

Open cycle MHD generator operation, comparing below stoichiometric air-fuel ratios to excess air level

14 p2533 A70-30534

Burning velocities for methane-air mixtures with water cooled porous metal flat flame burner, discussing surrounding ambient atmospheres effects

14 p2666 A70-31093

High temperature gas turbine aircraft engine control system requirements, noting stoichiometric fuel-air ratio

[SAE PAPER 700823] 24 p4394 A70-45895

FUELING

U REFUELING

FUELS

NT AEROZINE

NT AIRCRAFT FUELS

NT CRYOGENIC ROCKET PROPELLANTS

NT DOUBLE BASE ROCKET PROPELLANTS

NT GASOLINE

NT GELLED ROCKET PROPELLANTS

NT HYDROCARBON FUELS

NT HYDROGEN FUELS

NT HYPERGOLIC ROCKET PROPELLANTS

NT JET ENGINE FUELS

NT LIQUID ROCKET PROPELLANTS

NT METAL FUELS

NT METAL PROPELLANTS

NT MONOPROPELLANTS

NT NUCLEAR FUELS

NT SLURRY PROPELLANTS

NT SOLID ROCKET PROPELLANTS

FULL SCALE FATIGUE TESTS

U FATIGUE TESTS

U FULL SCALE TESTS

FULL SCALE TESTS

Full scale R/V flight test base pressure data for slender cones with ablative heat shields, considering mass flow and addition effects

[AIAA PAPER 70-109] 06 p0973 A70-18148

Aircraft design structural development and substantiation utilizing computer analysis and testing

[SAE PAPER 700216] 11 p2134 A70-25888

Full scale R/V flight test base pressure data for slender cones with ablative heat shields, considering mass flow and addition effects

[AIAA PAPER 70-109] 21 p3745 A70-41753

FUNCTION GENERATORS

Table lookup/interpolation function generation for fixed point digital computations, illustrating sine-cosine generator

01 p0047 A70-10459

Rotator and symmetrizer negative resistance circuits application in electronic function generator

05 p0824 A70-15991

Functions generation to determine probabilistic parameters of automatic air traffic control system

08 p1541 A70-20873

Separable potential with hard core effects, treating short range repulsion in nucleon-nucleon interaction, generating T matrix for existing data

09 p1725 A70-22042

Output and frequency limitations of functional converter using photopotentiometer with shaped resistor

09 p1682 A70-23358

Random process represented in canonical expansion form simulated by method of prognosis of reliability

11 p2022 A70-25344

Autonomous control system for moving plant based on logic threshold networks and multivariable functional converter

11 p2023 A70-25612

Walsh functions electrical generation with small orthogonality error based on multiplication theory, presenting circuit diagram for 32 channel analyzer

13 p2364 A70-28900

Logic cells for multiple arithmetic functions suitable for LSI

13 p2377 A70-29145

NaI scintillation spectrometer response function matrices semiautomatic generation, using standard source spectra to obtain normalized Compton continua

14 p2587 A70-31006

Liapunov functions direct generation by state space system vector matrix transformation

15 p2768 A70-32555

Digital computer generation of system stability Liapunov functions for ninth order spacecraft attitude control

16 p2867 A70-33043

Simultaneous generation of sensitivity functions for linear automatic control system with known characteristic differential equation

19 p3394 A70-37867

Generator for modeling random processes with given statistical parameters

20 p3593 A70-39915

Fast pseudorandom number generators for digital computers 21 p3793 A70-40851

Spherical Bessel functions fast generation recurrence technique, presenting real or complex arguments 22 p4062 A70-42920

FUNCTION SPACE

NT BANACH SPACE

NT HILBERT SPACE

Optimal control problems concerning vector determination and trajectory of point motion toward target in n-dimensional phase space 01 p0053 A70-11028

Linear functionals over Sobolev spaces and elliptical boundary value problems generated by theorems on homeomorphisms 03 p0519 A70-13505

Stronger locally convex topology on space C/S/ of bounded continuous functions proved in nonagreement with strict topology on norm bounded sets 05 p0875 A70-16050

Stationarization problems involving nonlocal and null class Euler-Lagrange operators, considering vector spaces of function spaces 05 p0881 A70-16059

Fourier series localization conditions for fundamental system of Beltrami operator functions in arbitrary n-dimensional space 05 p0877 A70-16972

Numerical solution of control optimization problems by systematic search in initial costate space, using Newton-Raphson method 06 p1025 A70-17964

Constraint optimization on phase coordinates and controls noting extension to functional spaces 07 p1330 A70-18683

Soviet collection of papers on boundary problems for differential equations covering variational problems in half space, polynomial behavior at infinity, function spaces, Fourier transformation, etc 07 p1322 A70-18851

Electromagnetic and gravitational fields classification methods using spinor techniques, introducing five dimensional complex linear space with Weyl tensors elements 07 p1337 A70-20302

Class of spaces containing class of order totally paracompact spaces, deriving invariance theorem 09 p1712 A70-22774

Regular C cubed space curve bending in Euclidean 3-space into piecewise helix, considering torsion and curvature 12 p2260 A70-26973

Linear time dependent stochastic optimal control with nonquadratic performance indices using function space approach 12 p2204 A70-27668

Diffusion processes on multidimensional cylindrical phase space for studying stochastic processes for physical systems with angular measurements, developing model for satellite under torque 12 p2273 A70-28067

Optimal control problems solution using Cartesian product of space of right-hand sides of differential equations with Euclidean n space 17 p3129 A70-34868

Feedback control systems synthesis by three parameter space, using two dimensional graphic techniques 17 p3130 A70-35296

Parameter analysis of dynamical systems by matrix approach, using n-dimensional parameter space 17 p3130 A70-35300

Nonlinear approximation under auxiliary conditions in normed space involving minimum solution 18 p3282 A70-36363

Antenna radiation patterns dependence on functional spaces in inverse problem of linear antenna theory, using calculus of variations 19 p3386 A70-37439

Soviet book on dynamic systems with cylindrical phase space covering differential equations with angular coordinates, parameter estimation, multidimensional and discontinuous systems, pendulums, etc 19 p3470 A70-37468

Inequality constrained optimal control problems by function space method, using integral equation representation of second variation 21 p3802 A70-41266

Minimal deviation estimates for linear approximations by seminorms for space defined by differential equations 23 p4210 A70-44018

Weak compactness of set of measures in functional space corresponding to stochastic differential equations solutions for n-dimensional Euclidean space 23 p4212 A70-44341

Isotropic transformation of tensor space, proving theorem for reducing hemitropic function to N invariants of rotations and single vector 24 p4378 A70-45271

FUNCTION TESTS
U TESTS

FUNCTIONAL ANALYSIS

NT BANACH SPACE

NT CONVOLUTION INTEGRALS

NT FOURIER TRANSFORMATION

NT FREDHOLM EQUATIONS

NT HARMONIC ANALYSIS

NT HILBERT SPACE

NT HILBERT TRANSFORMATION

NT INTEGRAL EQUATIONS

NT INTEGRAL TRANSFORMATIONS

NT LAPLACE TRANSFORMATION

NT SINGULAR INTEGRAL EQUATIONS

NT TESSERAL HARMONICS

NT VOLTERRA EQUATIONS

NT WIENER HOPF EQUATIONS

NT ZONAL HARMONICS

Nonlocal continuity and correctness of principle for comparing functions with Liapunov vector function, demonstrating continuous dependence of principle on certain parameters 01 p0130 A70-10151

Autonomous functional differential equations with finite time lag using Liapunov functionals, discussing stability and instability 01 p0132 A70-11070

Book on function theoretic methods for partial differential equations covering complex variables, harmonic functions, envelope method for singularities, operators, etc 01 p0133 A70-11325

Optimization potential selection in control system design by analytical method 02 p0272 A70-12412

R function method for solving plate bending problem by satisfying differential equations coordinates 04 p0767 A70-14489

Monograph on functional analysis and time optimal control as application of mathematics 07 p1322 A70-18857

Optimal control of linear distributed parameter systems using functional analysis 07 p1245 A70-19096

Neumann problem reformulation for regions having boundaries with limited rotation 07 p1325 A70-19538

Sufficient condition for calculus of variations problem, applying results to integrands without partial derivatives 07 p1327 A70-20022

Shallow shells of variable thickness and curvature calculated using small parameter method based on functional analysis 07 p1416 A70-20193

Feedback systems stability treated by functional analysis, describing procedures for generating instability criteria 09 p1654 A70-22348

Analytic systems theory using Volterra calculus of functionals applied to nonlinear differential equations 10 p1908 A70-23845

Continuous media geometry with given discrete structure reduced to analyzing relations between functions in denumerable set of points, presenting selected points of subregions 10 p1954 A70-24016

Narrow throat problems of linear dynamic programming concerning maximum linear functional determination in set of vector functions, giving algorithm for solution 10 p1855 A70-24393

Discrete calculus of variations for optimal control involving use of discrete time sequence and functionals 10 p1910 A70-24702

Mixed boundary value problem for linear parabolic equations with discontinuous coefficients, proving solution existence and uniqueness by functional method 10 p1911 A70-25304

Method of ascent for general representation in boundary value problems associated with differential equation of n variables 14 p2599 A70-30636

Sequential and combined gradient restoration algorithms for functional minimization in control theory 15 p2716 A70-32574

Software reliability program development, functional analysis and error sources 15 p2742 A70-32667

Jacobi conditions for singular optimization problems by transforming singular accessory minimum problem into nonclassical nonsingular form, considering optimal control theory applicability 16 p2885 A70-33331

Unified variational theory of quadratic forms, considering linear functional on real linear space and bilinear and quadratic functionals 17 p3129 A70-34867

Multistage rockets terminal control synthesis based on linear functionals 18 p3333 A70-36163

Book on abstract methods in partial differential equations, covering functional analysis and distribu-

tions, elliptic theory, linear and nonlinear problems, evolution equations, etc 18 p3284 A70-36782

German book on functional theory, Volume 6, tabulating theta and elliptic functions for application to applied physics, potential theory, fluid dynamics and oscillation theory 19 p3459 A70-38600

Characteristic functions for frequency analysis of fringes obtained by time-average holographic interferometry of generalized time dependent optical phase function 20 p3628 A70-39133

Optimal control of distributed parameter systems via functional analysis 20 p3600 A70-39136

Lissajous figures for phase response of N-path signal filter transfer functions, using switched modulators 22 p3998 A70-43256

Non-Chebyshevian moments induced by system of linearly independent functions expanding to semi-infinite programs 23 p4211 A70-44243

Limiting distribution of additive nonnegative continuous functional of homogeneous Markovian process with conditional transfer function 23 p4212 A70-44346

Cauchy problem for singular parabolic equation, establishing existence, uniqueness and representation theorem by integral operator techniques in conjunction with function-theoretic methods 23 p4212 A70-44895

Parameter methods generalization and D decomposition, using function minimization methods 24 p4322 A70-46155

Automatic weather station cost effectiveness criteria based on concepts of loss and error functions 24 p4323 A70-46405

FUNCTIONAL INTEGRATION

Functionally integrated superheterodyne receivers design by applying microwave IC technology, providing weight reduction, interconnecting cables elimination and circuit interface problems minimization 02 p0267 A70-12055

FUNCTIONS [MATHEMATICS]

NT ABEL FUNCTION

NT AIRY FUNCTION

NT ANALYTIC FUNCTIONS

NT APERIODIC FUNCTIONS

NT ASYMPTOTES

NT BOOLEAN FUNCTIONS

NT CONFORMAL MAPPING

NT COORDINATE TRANSFORMATIONS

NT DELTA FUNCTION

NT DISCRETE FUNCTIONS

NT DISTRIBUTION FUNCTIONS

NT DISTURBING FUNCTIONS

NT ELLIPTIC FUNCTIONS

NT ENTIRE FUNCTIONS

NT ERROR FUNCTIONS

NT EXPONENTIAL FUNCTIONS

NT FOURIER TRANSFORMATION

NT GREEN FUNCTION

NT HAMILTONIAN FUNCTIONS

NT HANKEL FUNCTIONS

NT HARMONIC FUNCTIONS

NT HYPERBOLIC FUNCTIONS

NT HYPERGEOMETRIC FUNCTIONS

NT KERNEL FUNCTIONS

NT LAGUERRE FUNCTIONS

NT LAME FUNCTIONS

NT LAPLACE TRANSFORMATION

NT LEGENDRE FUNCTIONS

NT LIAPUNOV FUNCTIONS

NT LINEAR TRANSFORMATIONS

NT LOGARITHMS

NT LORENTZ TRANSFORMATIONS

NT MATHIEU FUNCTION

NT MAXWELL-BOLTZMANN DENSITY FUNCTION

NT MELLIN TRANSFORMS

NT MEROMORPHIC FUNCTIONS

NT MONOTONE FUNCTIONS

NT NORMAL DENSITY FUNCTIONS

NT ORTHOGONAL FUNCTIONS

NT ORTHONORMAL FUNCTIONS

NT PERIODIC FUNCTIONS

NT POISSON DENSITY FUNCTIONS

NT PROBABILITY DENSITY FUNCTIONS

NT PROBABILITY DISTRIBUTION FUNCTIONS

NT RAMP FUNCTIONS

NT RATIONAL FUNCTIONS

NT RAYLEIGH DISTRIBUTION

NT RECURSIVE FUNCTIONS

NT SCHWARZ-CHRISTOFFEL TRANSFORMATION

NT SPACE-TIME FUNCTIONS

NT SPHERICAL HARMONICS

NT SPLINE FUNCTIONS

NT STEP FUNCTIONS

NT STRESS FUNCTIONS

NT TANGENTS

NT TIME FUNCTIONS

NT TRIGONOMETRIC FUNCTIONS
 NT WEIBULL DENSITY FUNCTIONS
 NT WEIGHTING FUNCTIONS
 NT WHITTAKER FUNCTIONS
 Functional optimization within partial differential equation solutions class by choosing optimum boundary values
 01 p0131 A70-10922
 Collection of papers on boundary value problems of mathematical physics and related aspects of function theory, Part I
 01 p0131 A70-11066
 Differential properties of class of functions of many real variables
 01 p0132 A70-11067
 Accelerated memory gradient method for minimization of functions with unconstrained variables, investigating generalization of Fletcher-Reeves algorithm
 01 p0132 A70-11194
 Material functions mathematical forms for Green-Rivlin constitutive equations of nonlinear viscoelasticity
 03 p0585 A70-12970
 Laplace transform of piecewise continuous function derivative for application to differential equations
 06 p1164 A70-17428
 Sequential gradient-restoration algorithm for minimization of function subject to constraint
 07 p1325 A70-19355
 Ergodic steady random functions measurement and analysis in terms of statistical properties
 [ONERA-TP-720]
 07 p1411 A70-19825
 Two point boundary value problems of quasi-differential equations, discussing conditions for continuous and increasing lower bounds of functions
 07 p1328 A70-20349
 Conjugate direction procedures for function minimization compared for convergence, recommending modified conjugate gradient procedure
 08 p1535 A70-21875
 Differential calculus for multifunctions using Rastrom embedding theorem for convex sets
 09 p1710 A70-22060
 Iterative technique for determining zero of differentiable function
 09 p1641 A70-22287
 H-function integrals for noncoherent isotropic scattering for two level atom, tabulating numerical values for Lorentz scattering profile
 09 p1727 A70-22506
 Circuit for analog computing system to determine function extremum of many variables in presence of constraints
 11 p2023 A70-25927
 Generalized inverse algorithm for solving linear inequalities from Ho-Kashyap algorithm
 11 p2013 A70-26207
 Relaxation function of linear viscoelastic body, defining mechanical deformation process using Stieltjes integral
 12 p2327 A70-28046
 Elsasser and statistical band models in single parameter functions representing mean absorption in given spectral range
 12 p2191 A70-28295
 Elliptic equations solved by projection network methods noting estimate derivation for convergence rates
 13 p2440 A70-28962
 Random-input describing function as linear approximation to instantaneous nonlinearity in terms of minimum mean-squared error
 13 p2382 A70-29070
 Extrema of functions of many variables in presence of constraints from modified simplex method with variable search step
 13 p2382 A70-29277
 Arbitrary function expansion into series of Legendre functions by generalizing Weyl-Lebedev-Skalaia integral transform
 13 p2441 A70-29312
 Stochastic analog approximation method minimizing criterion functions and for recovering functions from noisy measurements of values in learning systems
 13 p2442 A70-29585
 Uniform function defined throughout plane with isolated singularities at finite distance, obtaining solution uniqueness proof
 13 p2389 A70-29626
 Deflection function for annular plate simply supported and loaded with eccentric concentrated force
 13 p2518 A70-29981
 Penalty functions for state-space constraints elimination in continuous optimal control problems
 14 p2562 A70-31353
 Asymptotic expansion of contour integrals involving analytic functions of complex variable, using steepest descent method
 15 p2767 A70-31696
 Addition theorems for cylindrical functions, discussing applications to shell stress analysis and three dimensional elasticity theory
 15 p2819 A70-32187

Walsh functions and spectrum for signal processing, discussing computer compatibility
 16 p2864 A70-33483

Book on stochastic tools in turbulence covering generalized functions, probability, moments, characteristic functions, Gaussian distribution, random functions and multidimensional fields
 17 p3128 A70-34601

Functional equivalence between FS expression and programs
 17 p3130 A70-35139

Program for function computation replaced by notion of flow algorithm
 17 p3130 A70-35140

Quadratically convergent algorithms for function minimization, discussing unified method and applications to quadratic and nonquadratic functions
 19 p3458 A70-38302

Simultaneous approximation of function and product with given operator, applying to boundary value problems of partial differential equations
 19 p3459 A70-38682

Optimal variable shell thickness, describing numerical solution as function of forces, moments and thickness
 20 p3725 A70-39865

Asymptotic equivalent functions for integral Laplace transformation transition to original in continuous media mechanics
 20 p3726 A70-39873

Polynomial tensor functions generated by vector functions in space of invariants, noting applicability to isotropic media
 20 p3728 A70-39895

Chandrasekhar H function approximation for isotropic scattering, calculating absorption line contours
 22 p4109 A70-43750

Schedule theory problem with redundancy and technological constraints reduced to optimal control problem by penalty function, making maximum principle applicable
 23 p4177 A70-44304

Optimal algorithm for searching extremum of single variable unimodal function satisfying Lipschitz condition based on maximum possible error criteria
 23 p4177 A70-44305

Functions of two variables, using digital method for curve family modeling
 23 p4166 A70-44350

Real functions and sets representation theorems derivation and application to nonlinear programming, using Bellman quasi-linearization technique
 24 p4370 A70-46099

FUNGUS

NT SACCHAROMYCES

NT SPORES

NT YEAST

Flying disability period due to coccidioidomycosis in southwestern U.S., giving recommendations for earlier return to flying duty
 06 p1000 A70-17300

Penicillium mutant chemical stress tolerance in boric acid and potassium chloride selective media, studying carbohydrate and inosine-5-phosphate effects on growth rate
 10 p1811 A70-24325

FUNGICIDES

NT CAFFEINE

NT URIC ACID

NT XANTHINES

FURAN RESINS

NT POLYAMIDE RESINS

FURFURYL ALCOHOL

Ignition delay-reducing catalyst for furfuryl alcohol-red fuming nitric acid hypergolic bipropellant
 13 p2473 A70-29992

FURNACES

NT SOLAR FURNACES

NT VACUUM FURNACES

Small high temperature rotary plasma-heated furnace for refractory material high purity processing, discussing design and operation
 22 p4005 A70-42368

FUSELAGE MOUNTING

U AIRCRAFT PRODUCTION

FUSELAGES

Boron-polyimide composite reinforced Ti fuselage stringers design and test program for SST
 02 p0387 A70-11950

Dynamic stability of flexible aircraft fuselage in controlled supersonic flight at zero angle of attack, basing analysis on elastic oscillation equations
 03 p0579 A70-13418

Three dimensional flow separations on upswept rear fuselages, using flow visualization and pressure measurement
 05 p0790 A70-16097

Friction on fuselage surface layer under static and instantaneous loads without allowance for oscillation
 05 p0856 A70-17015

Pressure distribution and drag for inviscid flow past slender sharp-nosed fuselages and afterbodies at arbitrary transonic Mach numbers
 [AIAA PAPER 70-556]
 13 p2340 A70-29021

Airliner fuselage shape design and effect on manufacturing and flight operation economics
 14 p2532 A70-31369

Ti sheet welded construction for transport aircraft fuselages, assuming use of electron beam and plasma arc equipment
 17 p3198 A70-34452

Fuselage frames minimum weight analysis by automatic iterative method
 [SAWE PAPER 826]
 20 p3733 A70-40370

Swing tail cargo aircraft fuselage section stress analysis by finite element method, discussing displacement models, deformation modes and economics
 21 p3935 A70-41260

Elastic fuselage flight vehicle dynamic stability at supersonic speeds, using automatic pilot stabilization
 23 p4139 A70-44157

FUSES [ORDNANCE]

Protuding, stepped and conical end fittings for confined detonating fuse, discussing assembly procedures effect on characteristics based on statistical scanning test
 03 p0547 A70-14115

FUSIBILITY

Fluid flow visualization in closed channels, using spherules of pulverized fusible materials prepared in swirl injector
 03 p0485 A70-13473

Sodium-titanium-boron-silicate glass opacity and fusibility increase during partial substitution of K for Na, noting phase composition changes
 05 p0871 A70-16598

PbTe-based Sn, Se and Ge alloys lattice constant, thermal EMF and resistance, fusibility and microstructure
 08 p1555 A70-21117

FUSIFORM SHAPES

U CONES

FUSION [MELTING]

Geometrical analysis of partial fusion in earth crust and mantle formation, discussing solid solution and boundaries in MgO-iron oxide-silicon dioxide system
 09 p1670 A70-23398

Plasma torch for increasing material fusion temperatures in metallization methods
 12 p2244 A70-28072

Corrosion resistance of molybdenum coatings on steel and Pb-Bi eutectic alloy obtained by vacuum contact fusion method
 12 p2258 A70-28320

Electron beam welding, explaining high fusion zone homogeneity and weld defect formation by dynamic model
 17 p3100 A70-34637

Al particles fusion during combustion of stoichiometric mixtures of ammonium and potassium perchlorate and polyformaldehyde
 18 p3299 A70-36246

Thermal control through fusible materials for missile S band transmitter package, using computer analysis
 18 p3231 A70-36349

Installed system calibration thermocouples using temperature plateaus due to pure metals melting and freezing heat of fusion
 21 p3823 A70-40857

Linear aliphatic polyesters, calculating conformational contribution to heats and entropies of fusion
 22 p3981 A70-42501

Linear aliphatic polyesters melting point, fusion heat and entropy correlations to molecular parameters
 22 p3982 A70-42502

Al and W specific heat and Al heat of fusion by quasi-adiabatic calorimetry, estimating anharmonic lattice vibrations role via atomic thermodynamic analysis
 23 p4208 A70-44931

FUSION WELDING

NT ARC WELDING

NT BRAZING

NT ELECTRON BEAM WELDING

NT GAS TUNGSTEN ARC WELDING

NT GAS WELDING

NT LOW TEMPERATURE BRAZING

NT PLASMA ARC WELDING

NT ULTRASONIC SOLDERING

Computer program predicting thermal response of fusion welding tooling chill bars and holding fixtures, simulating moving heat source and contact
 08 p1508 A70-21487

Metal matrix fiber reinforced materials bonding, discussing brazing and fusion and diffusion welding
 [ASM PAPER W9-23.2]
 09 p1690 A70-22557

Porosity and intergranular crack formation in tungsten fusion welds using electron fractography
 11 p2059 A70-25666

Fusion welding cooling rates, peak temperatures and heating duration relationships to distance from fusion line predicted by theory for comparison with experiment
 21 p3832 A70-40791

Fracture mechanics application to fusion weld
 [ASME PAPER 70-MET-2]
 22 p4043 A70-42424

Gas porosity in fusion welds of chemical vapor deposited W, noting formation of microfissures due to pore linkup 22 p4046 A70-43149

F4H AIRCRAFT
U F-4 AIRCRAFT
F8U AIRCRAFT
U F-8 AIRCRAFT

G

G FORCE
U ACCELERATION [PHYSICS]
G-91 AIRCRAFT
VAK 191 B VTOL aircraft fitting NATO Basic Military Requirements for low level reconnaissance-fighter operations developed from Fiat G-91 17 p3017 A70-34992

G-222 AIRCRAFT
Fiat G-222 aircraft featuring high wing twin engine retractable landing gear for military cargo transport 10 p1805 A70-24381

GADOLINIUM
Zeeman interaction for super 8S term in ESR Hamiltonian determined, using trivalent GD magnetic spectrum at eightfold coordinated cubic sites of thorium 02 p0340 A70-12718
Gadolinium ions in zinc tungstate single crystals, studying low symmetry effects on EPR spectrum 08 p1556 A70-21120
Gadolinium II solar lines classification from photographic IR observations 10 p1947 A70-24990

Neutron capture effects in Gd from Norton County meteorite by isotopic composition analysis 12 p2300 A70-27524
Lunar rocks isotopic composition for Gd and variations due to low energy neutron capture produced by cosmic ray interactions 13 p2485 A70-28473

Thermogravimetric analysis (TGA) of gadolinium-doped silver carbonate decomposition, obtaining activation energy, preexponential factor and reaction order 15 p2694 A70-32074

Gadolinium surface work function from contact potential difference against platinum 20 p3687 A70-39996

Electron exchange coupling of Gd and Gd-Y alloy dihydrides from ESR indicating negative hydrogen ion entry 21 p3862 A70-41703

GAGES
U MEASURING INSTRUMENTS

GAIN (AMPLIFICATION)
U AMPLIFICATION

GALACTIC EVOLUTION

Statistical relation between radiation power of radio source and distance of center from radio-galactic nucleus, investigating evolution of radio galaxies 01 p0174 A70-10196

Three mode galactic age model for nucleosynthesis of solar radioisotopic material produced by r-processes 01 p0182 A70-10720

Computer model for evolution investigation of disks of stars, discussing methods to obtain gravitational potential 01 p0185 A70-11065

Lemaître universe and galaxy formation effect on stability of quasi-static epoch, deriving limits for red shift, cosmic ray and electromagnetic fluxes 02 p0363 A70-11779

Particle-antiparticle creation in galactic nuclei, expelling particles while retaining antiparticles 02 p0371 A70-12195

Stellar systems evolutionary stages, considering gravitational instability in rotating expanding gas, relaxation, viscosity, transition to metastable state and drift effect on geometry 02 p0376 A70-12445

T and L spiral waves existence in disk galaxies, noting helical and ring structures formation near center from standing waves onset 03 p0564 A70-13223

Magnetic cosmological nonuniformity hypothesis leading to galaxies and clusters isolation 03 p0564 A70-13224

Electron and positron flux steady state in interstellar space relationship to differential energy spectrum exponent in cosmic rays, discussing galactic halo and age 03 p0561 A70-14151

Hydrogen molecule formation relation to galaxy formation, discussing cosmic plasma neutralization role 03 p0577 A70-14152

Protogalaxy formation and molecular processes in primeval hydrogen gas, discussing cold gas cloud cooling mechanism and contraction 03 p0577 A70-14153

Brans-Dicke cosmological gravitational instability using Lagrangian gage for galaxy formation, discussing density contrast growth in time 03 p0577 A70-14154

Protogalaxy mass limits determined for galactic formation by thermal instability due to radiative cooling and followed by nonlinear gravitational contraction 04 p0744 A70-14469

Galactic mass loss by gravitational radiation, discussing galactic expansion and nucleus mass 04 p0752 A70-15068

Mass-energy content of universe, discussing galactic formation in positive energy systems and missing mass problems 04 p0753 A70-15073

Stellar systems dynamics, discussing dynamic interactions of point masses, forces in gravitational field, galactic model construction, etc 04 p0754 A70-15353

Radio galaxy evolution in terms of analysis of relation to superluminous elliptical systems, deriving radio emission duration upper limits 04 p0759 A70-15715

Physical conditions required to explain observations of radio galaxies through electrons of secondary origin, considering spectral characteristics and evolution 04 p0742 A70-15716

Elliptical cosmology, discussing evolutionary geometry, Sygne distribution, galactic age and distance from earth, Friedman equations and independence of constants 05 p0905 A70-15794

Primordial cosmic ray sources evidence suggesting galaxies and quasars in initial stages of formation 05 p0897 A70-15921

Galactic expansion due to mass energy loss by gravitational radiation 05 p0913 A70-16557

Statistical analysis of Zwicky catalog of galaxies and clusters of galaxies, interpreting very distant clusters in terms of intergalactic extinction 05 p0915 A70-16697

Galaxy mass loss on billion year time scale, discussing possibility on basis of bound stellar orbits 06 p1139 A70-17472

Age mixtures and physical heterogeneity of G-M cold stars emphasized in study of galactic fine structure and evolution 06 p1140 A70-17640

Galactic groups age considered in studying radio emission occurrence frequency 07 p1376 A70-18908

Model for gaseous proto-galaxy collapse and formation of spherical galaxy 07 p1390 A70-20287

Age dating of earth and universe emphasizing methods based on radioactivity, discussing stellar evolution, galactic age and assessment of cosmic time 08 p1568 A70-20633

T and L spiral waves existence in disk galaxies, noting helical and ring structures formation near center from standing waves onset 08 p1580 A70-21656

Gravitating bodies quasi-stationary rotating systems, giving equations of state and evolution 09 p1753 A70-22457

Galactic halo origin and evolution postulated from chemical evolution assuming stellar evolution details 09 p1758 A70-22742

Spherically symmetric galaxies dynamic evolution analysis, emphasizing irregular motions description using fluctuating gravitational field hypothesis to construct Markov process 09 p1758 A70-22747

Varying flux density values measured at SHF for radio galaxy PK 0048-09 indicating recent origin of radio source 09 p1764 A70-23790

Gas cloud expulsion from galactic nucleus indicated in 21 cm survey of neutral hydrogen 10 p1937 A70-23948

Gravitational instability theory for large density perturbations growth during expansion of matter without pressure 10 p1945 A70-24961

Nonaxisymmetric free oscillations of self gravitating disk reduced to eigenvalue problem to investigate galactic spiral structures 10 p1917 A70-25207

Soviet literature on galactic origins and physics including radio emission, star formation, quasars, nuclei activity, etc 12 p2307 A70-27868

Nonequilibrium self gravitating medium unified thermodynamics theory based on propagators, describing spatial and temporal fluctuations and coupling for galactic formation 12 p2310 A70-27978

Rotating spherical galaxy evolution, using equations of motion for mass points representing mass distribution 13 p2492 A70-29385

Gas injection model in galactic nuclei from evolving stars, producing high temperature, low density, thermally unstable medium 14 p2639 A70-30730

Galactic formation by spinning core theory, determining core properties by mass, energy and spin fluctuation parameters 14 p2640 A70-30734

Adiabatic relation between initial plasma density perturbations and radiation temperature fluctuations during galaxies formation, discussing relic radiation fluctuations 14 p2632 A70-31286

Dynamic spectrum of density fluctuations and galaxy clustering in Einstein universe, considering self gravitation of medium 14 p2652 A70-31389

Intergalactic gas condensation rates in galactic nuclei, considering recurrent magnetoplasma cores and quasar-like phenomena 15 p2801 A70-32479

Trail formation due to tidal effect in interacting galaxies during close approaches, considering mass flow hydrodynamics 15 p2801 A70-32481

Quasars as protoclusters of galaxies, discussing hypothesis of dense matter cascading fragmentation with subsequent scattering in form dispersing stellar systems 15 p2808 A70-32881

Arp hypothesis regarding radio source ejection from galaxies tested for quasars 15 p2808 A70-32887

Equations of motion and continuity for early and later stages of expanding universe, explaining matter concentration process of galaxy formation 16 p2976 A70-33783

Galactic evolution, reviewing Hubble theory of distances and red shift, Friedman model of expanding universe, big bang model, etc 17 p3168 A70-35328

Spiral galaxies structure, considering maintenance problem and effect of possible gas inflow from intergalactic space 18 p3326 A70-37152

Spiral galaxies pattern statistics, examining morphological type of Milky Way galaxy 18 p3326 A70-37155

Spiral structure gravitational theory, discussing separation between linear and nonlinear effects 18 p3330 A70-37189

Large scale spiral galaxy structure interpretation, examining density wave theory, Milky Way System and spiral form origin 18 p3331 A70-37196

Galactic spiral structure, discussing gravitational theory, pattern origin, radio and optical structure and magnetic field effects 18 p3332 A70-37201

Expansion motions in inner Galaxy, discussing lower velocity absorption features, mass estimation method and model 19 p3522 A70-38602

Galaxies systems dynamic evolution and instability in terms of nuclei division process model, comparing with observational data 19 p3525 A70-38765

Black hole objects in elliptical galaxies, using stellar light and velocity dispersion distribution in nuclear regions for mass limits 20 p3702 A70-39010

Galactic nuclei activity effect on galactic evolution and cosmology, discussing stellar and gaseous components 20 p3707 A70-39938

Supernova remnants catalog based on radio surface brightness, deriving galactic distribution and testing theories for nonthermal radio sources evolution 20 p3709 A70-40077

High velocity intergalactic hydrogen origin, examining galactic evolution by gas infall 21 p3887 A70-41112

Universe density estimation by galaxy formation theory, discussing spiral galaxies intergalactic gas thermal radiation and soft X rays 21 p3887 A70-41113

Total energies of stars with velocities perpendicular to galactic plane, examining absolute luminosities, galaxy size and local gravitational potential 21 p3890 A70-41162

Galactic distribution of supernova remnants and association with pulsars and X ray sources 21 p3892 A70-41188

Galactic evolution and secular variations of cosmic rays, magnetic fields and turbulence, assuming stellar birth rate dependence on gas density and temperature 21 p3919 A70-41700

Stellar system statistical mechanics, discussing collisionless gas in gravitational field, galaxy formation, stellar dynamics, double stars and bounded isothermal spheres 22 p4098 A70-42577

Computer model of self gravitating gas-stars system with spiral structure surviving galactic rotations 22 p4103 A70-42982

Interstellar molecules from stellar and galactic evolution viewpoint, emphasizing OH emission spectrum characteristics 23 p4238 A70-43801

Intergalactic gas condensation rates in galactic nuclei, considering recurrent magnetoplasma cores and quasar-like phenomena 23 p4240 A70-43904

Trail formation due to tidal effect in interacting galaxies during close approaches, considering mass flow hydrodynamics 23 p4240 A70-43906

Statistical estimates of precessional corrections, solar motion and galactic rotation from proper motions 23 p4246 A70-44752

Big bang temperature problem, discussing galactic masses determination possibility by gravity-strong interactions interplay in early stages 24 p4403 A70-45402

Galactic evolutionary models using disklike Riemann ellipsoids with internal motions and gravitational gas equilibria 24 p4410 A70-45759

High luminosity M type star photometry, determining supergiant intrinsic properties, interstellar extinction mean law and galactic evolution 24 p4410 A70-45764

Atmospheric composition of cool stars in relation to nucleosynthesis and galactic evolution 24 p4414 A70-46227

GALACTIC MAGNETIC FIELDS

U INTERSTELLAR MAGNETIC FIELDS

GALACTIC RADIATION

NT GALACTIC RADIO WAVES

Galactic water vapor line emission observations indicating short term variability in spectra of several sources 01 p0182 A70-10722

Cosmic ray gas galactic effects, discussing galactic magnetic field, hydromagnetic wave propagation, etc 02 p0361 A70-11749

Galactic interstellar absorption lower limit in selected Area 19 determined from Stellar spectra densities, using Schmidt camera 02 p0370 A70-12073

IR observations for position of hypothetical Seyfert-like nucleus explaining M82 polarization pattern 02 p0372 A70-12246

Galaxy model formulated in cylindrical coordinate system using Fokker-Planck equation for cosmic radiation particles propagation, discussing trajectories of high energy particles 03 p0553 A70-12880

IR flux variations from Seyfert galaxy NGC 4151 nucleus, using telescope 03 p0562 A70-14221

Long term behavior of blue photographic luminosity of Seyfert galaxy 3C 120 nucleus, considering similarity to quasar 3C 273B 04 p0748 A70-14589

Galactic cosmic rays scattering by solar wind magnetic field fluctuations, considering energy and momentum transfer 04 p0739 A70-14596

Galactic cosmic ray origins, discussing supernovae and galactic nucleus cosmic ray production 04 p0740 A70-15071

Gamma rays due to cosmic ray electrons bremsstrahlung in interstellar medium, predicting diffuse galactic X ray flux 04 p0742 A70-15713

Galactic X rays and high energy gamma rays in terms of cosmic ray electrons Compton scattering by submillimeter radiation 05 p0900 A70-16100

Galactic synchrotron emission and diffuse X ray background, noting correspondence between spectral indices of radio and X ray emissions in polar directions 05 p0913 A70-16472

Radio emission distribution from supernova remnants and galactic magnetic field 06 p1139 A70-17323

Galactic cluster A 262 luminosity function constructed from integral magnitudes of component galaxies obtained from continuous observations 07 p1376 A70-18904

Solar wind, using data on solar and galactic cosmic rays in interplanetary space 07 p1366 A70-19030

Solar wind effects on galactic cosmic rays isotropic diffusion and density distribution in interplanetary space in presence of azimuthal asymmetry 07 p1366 A70-19429

Galactic cosmic rays intensity long term modulation, studying roles of solar corona, solar wind and interplanetary electromagnetic field 07 p1369 A70-20075

Solar wind interaction with galactic cosmic radiation resulting in wind radial motion braking, discussing possible solar wind focusing 07 p1373 A70-20343

Ultrahigh energy primary cosmic rays model, considering galactic origin and energy spectrum 08 p1560 A70-20479

Solar modulation of low energy galactic cosmic ray protons, proposing diffusion-convection model with time dependent diffusion coefficient 08 p1561 A70-20906

Anomalous microwave recombination line at 11 cm detected in NGC 2024, Orion A, and IC 1795, discussing peak antenna temperature 08 p1576 A70-21399

Far IR radiation at galactic center suggested as thermal emission by dust particles 09 p1744 A70-22502

Angular size measurement for galactic X ray sources in Sagittarius region using modulation collimator aboard sounding rocket 09 p1744 A70-22521

Low energy positrons and gamma rays from large fluxes of galactic cosmic rays 09 p1746 A70-23477

Optically variable compact galaxy with broad emission lines similar to Seyfert and N-type galaxies, noting no stellar contribution in continuous spectrum 09 p1765 A70-23808

Hydrogen 109 alpha recombination line emission in galactic H II regions surveyed at National Radio Astronomy Observatory 10 p1936 A70-23942

Galactic radio source W 31 distance from sun determined from measurements of OH, H I and formaldehyde absorption lines 10 p1937 A70-23949

Gamma ray astronomy above 10 Mev, investigating intensity dependence on galactic latitude and radiation detection technology 10 p1931 A70-24067

Spectral lines and radial velocities of paired galaxies, noting red shift difference between emission and absorption lines 10 p1946 A70-24978

Alpha recombination line emission from galactic center detected, discussing possible origins in continuum source or interstellar medium 10 p1947 A70-24995

IR luminosity of galactic nucleus from far IR observations, noting considerations favoring nonthermal model consisting of multiple sources 10 p1947 A70-24996

Continuum spectra of well-resolved thermal and nonthermal galactic sources compared with H-alpha recombination line 12 p2296 A70-26898

X ray source from Coma cluster of galaxies, interpreting observed flux on basis of missing mass suggested by Virial theorem 12 p2293 A70-27388

Diffuse galactic radiation and absorbing clouds luminance illuminated by integral stellar radiation in Milky Way 12 p2307 A70-27866

Integral color indices relation to spectral type on NGC 3077 and M82 galaxies 12 p2308 A70-27871

Cosmic rays origin, discussing choice between galactic halo and radio disk models for trapping region 12 p2295 A70-27883

Absolute sky brightness temperatures measured with horn antennas and Dicke receivers, indicating spectrum change due to galactic nonthermal radiation 12 p2309 A70-27893

Compton electron scattering generated galactic gamma ray flux effects on diffuse IR 13 p2476 A70-28630

Cosmic rays and cosmic X rays, considering galactic and extragalactic sources, diffuse background, detection devices, etc 13 p2477 A70-29160

Galactic X ray stars and X ray sources positions, appearance frequency and intensities 13 p2495 A70-29818

Cosmic ray energy spectrum in absence of solar activity from eleven year ray variations, noting coincidence with galactic rays 14 p2630 A70-30204

Diffusion loss model for cosmic ray electron propagation in galaxy, considering direct and radio observations 14 p2631 A70-30538

Galactic cosmic ray actions on interstellar medium for origin of Li, Be and boron in stellar atmospheres and solar system 14 p2640 A70-30786

Cosmic IR radiation sources, discussing galactic and stellar masses 14 p2632 A70-30882

M31 continuum radio emission produced by magnetic field aligned along arms, discussing field turbulence effects 14 p2642 A70-30891

Galactic cosmic rays high altitude measurements by balloon-borne Sparmu type multidirectional detectors, revealing azimuthal anisotropy 14 p2632 A70-31309

Galactic cosmic rays origin in terms of statistical mechanical model of supernova explosions 15 p2799 A70-31793

Galactic abundances and cosmic ray spectra by IMP-4 satellite, obtaining He ratio 15 p2793 A70-31794

Book on nonthermal processes in galactic and extragalactic radio sources covering plasma behavior in magnetic field, energy redistribution in spectrum by electron scattering, etc 15 p2799 A70-31999

Galactic gamma rays from OSO-3 observations attributed to decay of neutral pions produced by cosmic rays interaction with interstellar gas nucleons 17 p3150 A70-34567

Galactic cosmic rays eleven year modulation, determining modulating region L depth from dynamical phase lag between changes in cosmic ray intensity and solar activity 17 p3150 A70-34833

Galactic UV emission attributed to solar radiation scattered by hydrogen atoms, using Mariner 5 measurements 17 p3163 A70-34902

UV background radiation observed above atmosphere for intergalactic gas, Galaxy and subcosmic ray components 17 p3163 A70-34903

Large anisotropy observed for gravitational radiation detector intensity as function of sidereal time, suggesting source from galactic center 17 p3137 A70-35725

Galactic center region lunar occultations in 21 cm neutral hydrogen line 18 p3313 A70-36328

Diffuse cosmic X ray background galactic component, using model to predict angular spread 18 p3308 A70-36484

Solar wind effects on galactic cosmic rays isotropic diffusion and density distribution in interplanetary space in presence of azimuthal asymmetry 18 p3309 A70-36903

Extragalactic objects 3C 273 NGC 5128 and M87 X ray emission detection, using proportional counters on Aerobee 150 rocket 18 p3310 A70-37016

Galactic 21 cm line emission motion picture film, discussing contour maps on neutral hydrogen distribution 18 p3327 A70-37163

Neutral hydrogen distribution in galactic region surveyed with radiotelescope 18 p3328 A70-37169

Integrated Milky Way spectrum, examining composition and galactic structure in solar neighborhood 18 p3329 A70-37182

Carina spiral feature progress report covering O and B star distribution, optical and radio H 2 and H I sources and cosmic dust 18 p3330 A70-37185

Low energy solar and galactic cosmic rays propagation in interplanetary medium observed by Zond and Venus space probes, discussing shock waves retardation 19 p3493 A70-37475

Water vapor and OH spectra overlap, investigating association of galactic OH masers and water emission sources with IR stars 19 p3444 A70-37571

Galactic plane hard X ray emission measurements, considering gamma and X ray origin from Compton scattering of photons by galactic electrons 19 p3497 A70-38023

Metagalactic and galactic sources of cosmic rays, including composition, electron spectra and radio emission 19 p3500 A70-38077

Extraterrestrial gamma radiation from Cygnus region of galactic disk, using OGO-5 observations 19 p3501 A70-38087

High energy gamma ray flux enhancement towards galactic plane from OSO-3 particle telescope observations 19 p3501 A70-38089

Galactic low energy cosmic ray positrons and gamma rays, considering production mechanism in interstellar space 19 p3503 A70-38099

High energy galactic gamma ray and X ray flux explained by cosmic ray electron scattering 19 p3504 A70-38112

High energy galactic gamma rays photons, suggesting two-component cosmic ray source model 19 p3505 A70-38115

Traversed matter thickness and charge composition for high energy galactic cosmic rays with various propagation modes 19 p3506 A70-38123

Galactic cosmic ray energy spectra of light and medium nuclei from IMP-4 satellite measurements, investigating L/M ratio 19 p3506 A70-38124

Low energy galactic cosmic radiation energy spectra and charge composition in 2-14 Z range by OGO-5, suggesting two component model for origin 19 p3507 A70-38127

Galactic cosmic rays temporal and spatial variations in solar system, discussing nuclear active particles and spallation products depth distribution in meteorites 19 p3509 A70-38143

Cosmic ray lifetime, investigating radioactive Be 10 nuclei decay effects on intensity ratios Be/B and Be/Li, suggesting nuclei confinement to galactic disk 19 p3509 A70-38148

Sideral daily variation in cosmic ray muon intensity at 60 mwe depth, indicating extragalactic origin 19 p3509 A70-38149

Galactic cosmic ray anisotropy, discussing amplitude and phase values of daily sidereal variation 19 p3510 A70-38152

Galactic disk model for confinement of cosmic ray electrons, assuming isotropic background radiation 19 p3510 A70-38156

Cosmic rays propagation and production in Milky Way galaxy, using equilibrium model 19 p3510 A70-38157

Cosmic rays relationship to cosmological parameters and galactic radiation source evolution 19 p3511 A70-38160

Sbc galaxy NGC 7320 radio emission and neutral H observations, showing improbability of physical association with Stephan Quintet by distance measurement 19 p3524 A70-38699

Galactic cosmic rays lifetime based on nuclei and matter interactions, discussing ionization losses effect 20 p3695 A70-38965

X ray emission mechanisms in galactic sources, considering black body, supernova remnants, synchrotron radiation, etc 21 p3874 A70-40679

Diffuse cosmic X rays, discussing energy spectrum and contribution of galactic integration 21 p3875 A70-40686

Galactic or extragalactic origin of diffuse X ray background, reporting sky survey results 21 p3875 A70-40688

High energy galactic gamma rays search onboard OGO-5, tabulating results 21 p3876 A70-40690

Galactic gamma ray intensity near Cygnus by OGO-5 spacecraft-borne telescope with acoustic spark chamber, discussing source intensity 21 p3876 A70-40691

Soft X ray background galactic absorption and intensity measurements indicating inverse relation to columnar atomic hydrogen density 21 p3877 A70-40698

Galactic gamma ray sources model with magnetic fields concentration in expanding shell, suggesting production by neutral pion decays in supernova remnants 21 p3877 A70-40701

Galactic K series emission at 1-10 kev by low energy cosmic rays and diffuse X rays interaction with H I region heavy ions 21 p3877 A70-40704

Soft X ray flux emanation from galactic disk, discussing latitude dependence, interstellar H, maps and discrete sources nature and properties 21 p3878 A70-40707

Gamma ray background anisotropy effects of Sgr A flux arising from Compton scattering and neutral pion decay, discussing complex radio and IR structure 21 p3878 A70-40926

M87 radio observations at 5 GHz, examining central region components, optical nucleus and jet and X ray emission 21 p3923 A70-42103

Galactic X ray background due to inner bremsstrahlung associated with suprathermal particles, taking into account interstellar gas self absorption and ionization rate 22 p4093 A70-42465

Galactic center region gamma radiation observations, discussing intensities, energy spectrum and decay 22 p4093 A70-42927

Forbidden iron emission lines excitation in Seyfert galaxies, discussing various mechanisms 22 p4102 A70-42977

Alpha hydrogen recombination lines 156, 166, 167 and 168 from galactic center, using radio telescope 22 p4103 A70-42980

Galactic soft X ray and subcosmic ray heating and ionizing of interstellar H I regions 22 p4094 A70-42985

Extragalactic variable radio sources as clue for quasars and galactic nuclei energy, using long baseline interferometry 22 p4105 A70-43226

Cosmic rays galactic propagation and confinement, discussing matter and star distributions, magnetic fields, positron flux and energy spectrum, etc 22 p4096 A70-43396

Outer space galactic cosmic rays energy spectrum and modulation region boundary determination, using meteorite observations 23 p4236 A70-44050

Interplanetary magnetic field inhomogeneities structure from galactic cosmic rays intensity fluctuations observation 23 p4237 A70-44053

Radio astronomy research covering solar radio emission, Milky Way radiation, molecular radio line spectra, etc 23 p4256 A70-45041

Excess galactic X rays, discussing synchrotron emission of high energy cosmic ray electrons 24 p4398 A70-46161

Discrete source interpretation of isotropic component of diffuse gamma radiation in Milky Way galaxy 24 p4398 A70-46166

Cosmic ray energy spectrum in absence of solar activity from eleven year ray variations, noting coincidence with galactic rays 24 p4398 A70-46279

GALACTIC RADIO WAVES

Extraterrestrial sources radiation including galactic, solar and magnetospheric radio emissions observed by RAE-I satellite at long wavelengths [AIAA PAPER 69-1049] 01 p0170 A70-10603

Galactic water vapor radio sources spectral observation suggesting correlation between time variation and polarization 04 p0747 A70-14547

Galactic clusters analyzed for identifying possible relationship between cluster configuration, type of component galaxies and radio emission 07 p1376 A70-18907

Galactic groups age considered in studying radio emission occurrence frequency 07 p1376 A70-18908

Mass to luminosity relations in RF region derived from data for nearest galaxies 07 p1383 A70-19404

Zero radiospectrometer for spectral observations of radio emission of excited galactic hydrogen at centimeter wavelength, noting Omega nebula detection 08 p1495 A70-21063

Cosmic electron detection and measurement techniques, considering presence in solar system, interstellar space and metagalaxy and galactic continuum radio emission 12 p2293 A70-27572

Galactic noise and solar type 3 bursts using Alouette 2 satellite HF receiver voltage recordings 12 p2226 A70-28065

Galactic noise spectrum and solar radio bursts in hecto-decimeter wave region observed by Alouette 2 satellite 13 p2491 A70-29093

Galactic continuum surveys at 8000 MHz by radio telescope, noting North American nebula and Cyg X region 13 p2491 A70-29096

Galactic hydroxyl emission sources right ascensions, presenting coordinates and antenna temperature measurements 15 p2796 A70-31594

Galactic radio radiation observations at 610 MHz, using corner reflector antenna 18 p3313 A70-36331

Physical processes in galactic and extragalactic sources of nonthermal radio emission, assuming pulsars as principal magnetic field and cosmic rays sources 18 p3321 A70-37126

Galactic radio corona existence, measuring northern galactic hemisphere sky brightness and cosmic ray distributions 18 p3322 A70-37129

Milky Way galaxy continuous background radio emission observed at various longitude intervals 18 p3322 A70-37130

Galactic hydroxyl emission sources right ascensions, presenting coordinates and antenna temperature measurements 23 p4242 A70-44277

GALACTOSE

Retention times and gas chromatographic conditions for resolution of galactonic and gluconic acid derivatives 16 p2855 A70-33064

GALAXIES

NT ANDROMEDA GALAXIES

NT MILKY WAY GALAXY

NT RADIO GALAXIES

NT SPIRAL GALAXIES

Velocity field measurements in NGC 5128 galaxy, discussing relative motion between gas and stars and correspondence of emission and absorption lines 01 p0184 A70-10898

Quasars radio emission tabulated, showing quasar B264 as member of galactic cluster 02 p0372 A70-12244

IR observations for position of hypothetical Seyfert-like nucleus explaining M82 polarization pattern 02 p0372 A70-12246

Blast wave model for galaxy M82 explosion using Sedov self similar solutions, indicating line excitation

mechanism origin in shock wave heating and compression 02 p0372 A70-12247

Soviet collection of articles on structure and dynamics of stellar systems, Part 2 02 p0375 A70-12442

Discrete statistical stellar system relation existence with continuous model proved by introducing unique volume concept for discrete systems 02 p0376 A70-12443

Self gravitating galaxies theoretical properties, including structural and dynamic characteristics of interacting and colliding galaxies 02 p0376 A70-12444

Statistical analysis of position angles of Berenice cluster galaxies, estimating mass, expansion, rotation period and age 02 p0376 A70-12448

Isophote flattening functions of elliptical galaxies including identification of giant and dwarf galaxies 02 p0377 A70-12449

T and L spiral waves existence in disk galaxies, noting helical and ring structures formation near center from standing waves onset 03 p0564 A70-13223

IR flux variations from Seyfert galaxy NGC 4151 nucleus, using telescope 03 p0562 A70-14221

Correlation function for spatial distribution of galaxies determined as function of inverse distance between galaxies 04 p0744 A70-14470

Double galaxy systems hypothesis with tidal interaction, presenting data from galaxy internal motion studies 04 p0747 A70-14519

Compact radio source in M87 nucleus observed with long base line interferometer composed of two telescopes, suggesting diameter 04 p0747 A70-14546

Models of partially relaxed stellar disks in galaxies, discussing gravitational instability and stellar velocities 04 p0748 A70-14588

Neutral H study of binary galaxies showing departures from circular symmetry, suggesting model involving hydromagnetic interaction 04 p0759 A70-15709

Tabular results of Galaxy mean and angular diameters and smallest/largest ratios measured on Palomar Atlas 05 p0906 A70-15797

Group velocity of spiral density waves propagating in disk galaxies implying self destruction, discussing possible replenishment sources 05 p0919 A70-16929

Galaxies statistical distribution studied to determine superclusters existence, correlating results with random distribution expectations 07 p1375 A70-18868

Galactic cluster A 262 luminosity function constructed from integral magnitudes of component galaxies obtained from continuous observations 07 p1376 A70-18904

Hydromagnetic self gravitating galactic slab embedded in halo, deriving stability criteria using models of magnetic field 07 p1390 A70-20293

Galactic longitude interval region radio telescope observations, obtaining isophotes of brightness distribution of RF spectral line of neutral H and continuous spectrum 08 p1564 A70-20551

T and L spiral waves existence in disk galaxies, noting helical and ring structures formation near center from standing waves onset 08 p1580 A70-21656

M87 jet, using theoretical model and observed emission lines for heating, cooling, ionization, cosmic ray proton regeneration of optical electrons, X radiation, etc 09 p1754 A70-22501

Quasar sky distribution as function of apparent magnitude for identification with galaxies of origin 09 p1759 A70-22909

Oscillations stability along symmetrical axis in galaxies analyzed by Jacobi and Lagrange equations, obtaining cylindrical coordinates upper and lower limits 09 p1761 A70-23052

Compact galaxies, discussing distribution, integral photometry and isophotometry, brightness outbursts, etc 09 p1763 A70-23373

Optically variable compact galaxy with broad emission lines similar to Seyfert and N-type galaxies, noting no stellar contribution in continuous spectrum 09 p1765 A70-23808

Interstellar flights, discussing human limitations, star systems with habitable planets and possible galactic communities 10 p1943 A70-24759

Noncircular ionized gas motions in NGC 253 central region observed in velocity field analysis, indicating outflow from center

10 p1946 A70-24979

Coma cluster of galaxies morphological and statistical characteristics, determining major and minor axes

10 p1948 A70-25194

Faint violet stars in southern galactic latitudes found during scanning of two color plates including halo stars, subdwarfs, white dwarfs and quasi-stellar galaxies

10 p1949 A70-25248

Stellar hydrodynamic equations for thin disk galaxy derived from collisionless Boltzmann equation moments

11 p2117 A70-26688

X ray source from Coma cluster of galaxies, interpreting observed flux on basis of missing mass suggested by Virial theorem

12 p2293 A70-27388

Nonthermal radiation effects on emission line spectra of Seyfert galaxies and quasars determined from ionization equilibrium of gas envelope

12 p2293 A70-27585

Soviet literature on galactic origins and physics including radio emission, star formation, quasars, nuclei activity, etc

12 p2307 A70-27868

Integral color indices relation to spectral type on NGC 3077 and M82 galaxies

12 p2308 A70-27871

Self gravitating collisionless particles instability related to anisotropic random velocity distribution function in presence of disk-galaxy type spiral wave perturbations

13 p2492 A70-29299

Galaxies rotation, applying optical and radio data to statistical analysis of angular velocities and periods

13 p2492 A70-29386

Absolute magnitudes of first brightest galaxies in rich clusters from luminosity model, allowing for mass variation

13 p2495 A70-29795

Gas injection model in galactic nuclei from evolving stars, producing high temperature, low density, thermally unstable medium

14 p2639 A70-30730

Radio sources spectroscopy, discussing central density and mass of elliptical galaxy NGC 3998 and red shifts of radio galaxies

14 p2642 A70-30893

Third integral of stellar dynamics, considering Contopoulos galactic system model separability

14 p2651 A70-31288

Cosmogenic phenomena instability, discussing red shift, expanding universe, galactic nuclei and quasars

15 p2800 A70-32144

Galactic masses and mass-luminescence ratios from motions data

15 p2801 A70-32480

Galactic longitude interval region radio telescope observations, obtaining isophotes of brightness distribution of RF spectral line of neutral H and continuous spectrum

15 p2805 A70-32706

Galactic composition differences, considering stellar and galactic nucleosynthesis

16 p2976 A70-33791

Red shift absorption systems ions related to intergalactic medium properties in clusters of galaxies

17 p3153 A70-34526

Disturbances rotational alignment in variable galaxies nuclei, using interstellar gas motions model

17 p3153 A70-34527

Giant E and SO galaxies, discussing radio spectra, emission characteristics and brightness distributions

18 p3313 A70-36332

Galaxies and globular clusters, obtaining data by measurements with intermediate bandpass photometry

18 p3321 A70-37121

Galaxies pairs motions, considering disintegrating, rotational and oscillatory types for comparison with observational data

18 p3322 A70-37133

Stellar magnitude equation from corrected catalog data to determine absolute proper motions relative to galaxies

18 p3323 A70-37145

Kinematics of M 33, M 51 and large Magellanic cloud (LMC)

18 p3326 A70-37157

Stellar velocity field in M 51 from image tube spectra

18 p3327 A70-37158

Flat model galaxy stability, examining unstable two armed density wave by numerical methods

18 p3330 A70-37190

Large scale galactic oscillations, discussing observational evidence and theoretical modal calculations

18 p3330 A70-37191

Galactic rotation law parameters determination, considering effect of random and systematic errors on accuracy

19 p3525 A70-38774

Black hole objects in elliptical galaxies, using stellar light and velocity dispersion distribution in nuclear regions for mass limits

20 p3702 A70-39010

Image tube observations of Large and Small Magellanic Clouds and southern planetary nebulae at Cerro Tololo Observatory

20 p3705 A70-39480

Oscillation stability of stars moving along axis of symmetry in galaxy, discussing first order orbit perturbations in general resonance case

21 p3884 A70-40873

Stellar polarization measurements in Magellanic Clouds, tabulating position, magnitude, spectral type, percentage polarization and electric vector position angle

21 p3922 A70-41979

Preferential galactic orientation based on inclination statistics of predominantly elliptical clustered nebulae

22 p4099 A70-42627

Star content in Small Magellanic Cloud wing counted to determine detachability from tidal arm and main body

22 p4099 A70-42628

Galactic noncircular velocity fields, discussing statistical correlation with radio luminosity, nuclear brightness and total mass

22 p4100 A70-42844

Galactic rotation model derived from radial velocities and spectrophotometric distances of H II regions

22 p4101 A70-42864

Galactic masses and mass-luminescence ratios from motions data

23 p4240 A70-43905

High velocity stars in Large Magellanic Cloud from spectroscopic observations, including A dwarfs and G-K giants

23 p4240 A70-44212

Extragalactic astronomy research covering quasars, Seyfert and related galaxies, cosmology, Magellanic Clouds, supernovae, etc

23 p4256 A70-45040

Extragalactic radio source optical identifications showing association with quasars or Seyfert galaxies nuclei

24 p4413 A70-46168

GALAXY AIRCRAFT U C-5 AIRCRAFT GALERKIN METHOD

Galerkin method applied to boundary layer flows, considering transport problems in unbounded domains

01 p0066 A70-11129

Bubnov-Galerkin approximations convergence in problem of thin plate nonlinear vibrations, allowing for inertial forces due to rotation

03 p0593 A70-13470

Galerkin method to formulate buckling problem of homogeneous and fiber reinforced anisotropic plates simply supported under uniform membrane loads

06 p1160 A70-17313

Buckling behavior of elliptical cylinders under normal pressure using linear thin shell theory and Galerkin method, compared with test results

06 p1169 A70-18038

Buckling of clamped skew plates under uniform system of applied stress using Galerkin method

07 p1406 A70-19339

Finite element solution procedures for inextensible beams elastica problem, using galerkin method for element stiffness matrices

11 p2143 A70-26640

Coordinate function selection for boundary value problems solution by Galerkin method demonstrated for heat conduction equation of anisotropic parallelepiped with internal source

12 p2271 A70-27291

Nonlinear equations boundary value problem solution by Galerkin method in integrodifferential equations form, determining Lipschitz conditions constant and proving existence and uniqueness

13 p2442 A70-29513

Incompressible solid propellant rocket charges axisymmetric problems, using Galerkin stress functions

14 p2657 A70-30772

Circular cylindrical shells with clamped ends, investigating supersonic panel flutter by two mode approach and Galerkin method

17 p3184 A70-34695

Incompressible laminar boundary layer equations approximate solution by Galerkin-Kantorovich technique

18 p3238 A70-35972

Elasticity theory for circular cylinder weakened by cavities, discussing boundary conditions on butt ends and Galerkin solutions

23 p4265 A70-43983

Fundamental error in Galerkin method application to bending problem of elastic rods

23 p4268 A70-44172

Rectangular cable networks covered by or embedded in membrane matrix, calculating vibration response under load by Galerkin method

24 p4421 A70-45279

Cylindrical shells dynamic thermoelastic response to sudden rotating thermal inputs, using Galerkin method

24 p4421 A70-45285

Low gravity fuel sloshing in axisymmetric rigid tank, calculating oscillations by modified Galerkin method

24 p4324 A70-45292

GALLIUM

Gallium found suitable for doping cadmium/tin arsenide semiconductor, exhibiting hole-type conductivity

01 p0156 A70-10214

Low speed Ga lubricated sliding electrical contacts of Be in vacuum, discussing Ga film role in friction and contact resistance

01 p0099 A70-10325

Brittleness of joints using Ga solders prevention by high temperature annealing noting application to aluminum alloys

05 p0855 A70-16199

Far IR radiation transmission through bismuth and gallium normal and superconducting thin films, considering transition temperature role

09 p1739 A70-22323

Al, Ga and In effects on creep and rupture stress of Ti at 500 C

17 p3120 A70-34425

Solar Ga abundance from spectral synthesis of region around 4172 A line

18 p3316 A70-36894

Fe meteorites with high Ge content, tabulating concentrations of Ni, Ga, Ge and Ir

23 p4241 A70-44259

GALLIUM ANTIMONIDES

Miniature electromechanical gallium antimonide tunnel diode transducer theory fabrication and performance

12 p2236 A70-28055

N-type Te-doped gallium antimonide conversion to p-type by electron irradiation, noting thermal conductivity variations

13 p2470 A70-29167

Ternary phase diagram of liquid epitaxially grown gallium arsenide antimonide, considering use as high quantum efficiency long wavelength photoemitter

15 p2782 A70-31758

GALLIUM ARSENIDE LASERS

GaAs injection laser operated with external optical resonator for diffraction-limited radiation, considering peak power and quantum efficiency

02 p0311 A70-11920

IR light beam modulation in Gunn oscillator near fundamental edge of GaAs, investigating mechanism

03 p0539 A70-13160

Frequency pulling and pulse position modulation of CW GaAs injection lasers by locking signal frequency variation

03 p0502 A70-13815

Simple approximations for threshold current, gain and lasing frequency of GaAs injection laser at room temperature

03 p0503 A70-14085

UHF self modulation in GaAs laser coupled to external cavity, focusing convergent beam on external mirror

04 p0701 A70-14718

Rate equation analysis of steady state behavior of double cavity GaAs diode laser, noting solution stability by perturbation method

04 p0703 A70-15618

Self induced light pulses from GaAs injection lasers in pulse driven diodes at liquid nitrogen temperatures, noting pulse width and frequency

04 p0703 A70-15623

Collection of papers on GaAs lasers covering injection lasers, p-n junction lasers, GaAs preparation and properties, laser applications, etc

07 p1297 A70-19394

GaAs p-n junction lasers operating properties under ideal and thermal conditions

07 p1298 A70-19396

GaAs lasers fabrication, discussing p-n junctions formation, laser die mounting, low resistance electrical contacts, optical cavities, etc

07 p1298 A70-19398

GaAs diode amplifiers and switching devices behavior, describing optical coupling between two GaAs lasers

07 p1241 A70-19399

GaAs laser and laser array applications, discussing pulse generators, laser cooling, laser optics, detectors, etc

07 p1298 A70-19400

CW GaAs junction laser bistable operation due to saturable absorbing centers in active medium

08 p1513 A70-21598

GaAs-Ge platelet laser output, observing absorption edge dynamic Burstein shift

09 p1697 A70-22920

Self stabilization and narrowing of optical pulses from GaAs junction lasers by regenerative feedback of oscillations in injection current

09 p1697 A70-22921

CRT laser with gallium arsenide crystal excited by electron gun, describing output characteristics

09 p1698 A70-23161

Second harmonic emission from GaAs injection laser and from stimulated KDP crystal at room temperature

12 p2245 A70-27306

Waveguide optical properties effect on injection GaAs laser threshold lasing and field distribution in near/far zones for various parameters of active region

12 p2246 A70-27365

Gallium arsenide laser with external mirror excited by electron beam, measuring radiation patterns

12 p2247 A70-27482

Laser tracking system for space guidance, describing equipment and operations

[ALAA PAPER 69-870] P-type GaAs laser diodes spontaneous emission power temperature dependence, considering radiative recombination mechanism

13 p2447 A70-28529

Modulation phase distribution over emitting surface of p-n junction GaAs laser at micron wavelength

13 p2431 A70-29866

GaAs junction lasers output oscillations, analyzing time dependent equations for low temperatures

13 p2378 A70-29545

Injection semiconductor lasers emission characteristics, discussing gallium arsenide diodes, nonlinear losses in pulsed mode, laser interactions, etc

15 p2749 A70-31453

Lasers and GaAs diode emitters near IR radiation intensity distributions, using IR films and IR display phosphors

15 p2753 A70-32607

GaAs injection lasers for optical communication, synthesizing high bit rate data link between synchronous relay satellites

16 p2865 A70-33710

Gallium arsenide laser ranging system for helicopters obstacle warning

17 p3103 A70-34720

GaAs laser with inhomogeneous injection, noting instability of stimulated RF oscillations

17 p3108 A70-35631

Close-confinement LPE /AlGaAs junction laser properties, examining range of alloy direct bandgap transition

18 p3268 A70-36727

Gain and loss processes in GaAlAs-GaAs heterostructure lasers as functions of current and cavity length

18 p3268 A70-36728

CW GaAs junction lasers bistable operation above delay transition temperature based on double acceptor trap theory

18 p3268 A70-36729

Spontaneous emission spectra and band tailing from GaAs laser diodes fabricated by vapor phase epitaxy with compensation in p-type side of junction

18 p3268 A70-36730

Reflectivity effect on external quantum efficiency of Fabry-Perot type GaAs injection lasers

18 p3268 A70-36731

Resonant modes of GaAs junction laser beams with Hermite-Gaussian rectangular symmetry, using stripe geometry with lens-slit combination

18 p3268 A70-36732

Microwave self modulating GaAs diode laser, showing coupled external cavity resonator influence on intrinsic resonance frequency

18 p3269 A70-36733

Self induced intensity pulsations frequency stabilization and narrowing in continuously operating GaAs injection lasers

18 p3269 A70-36734

Self induced sustained light pulsations from GaAs injection lasers with tandem double section stripe geometry based on repetitively Q switched model

18 p3269 A70-36735

Pulsed GaAs injection lasers second harmonic generation with nonlinear crystal alpha iodic acid phase matched by angular tuning

18 p3269 A70-36737

GaAs lasers with light propagation along curved junctions, discussing threshold current density variation with radius of curvature

18 p3269 A70-36738

Electron energy effect on output power and beam divergence of electron beam pumped GaAs lasers

18 p3269 A70-36740

CW multifilament GaAs laser diodes measurement, showing cross correlation between light and current noises

18 p3270 A70-36742

GaAs laser diodes thermal degradation, observing nature, extent and occurrence of permanent damage

19 p3446 A70-37818

Gallium aluminum arsenide-GaAs laser diodes properties and applications for CW operation, discussing p-GaAs layer thickness effects

19 p3447 A70-38454

Recombination lifetime /laser/ states in Si doped GaAs light emitting diodes on p-type thin platelets

21 p3838 A70-42016

GaAs laser and noncoherent IR emitting diodes fabrication and design, discussing card readers, encoders, alarms, range finders, bomb fuses and night vision systems

22 p4050 A70-43248

GaAs injection lasers, calculating effect of active region displacement from p-n junction waveguide on wave generation

23 p4203 A70-45074

CW GaAs semiconductor laser fabrication by liquid epitaxy, noting Ag plating role in output power

24 p4352 A70-45468

High efficiency gallium arsenide IR illuminators, comparing dome diodes fabricated from diffused or Si doped solution grown materials

24 p4319 A70-45784

GALLIUM ARSENIDES

Scanned laser microscope producing shadowgraph displays of IR transmittance variations attributed to defects in polished Si and GaAs semiconductor wafers

01 p1015 A70-10025

Edge luminescence effect in doped p-GaAs single crystals with various hole concentrations, determining band structure at liquid nitrogen and room temperature

01 p0154 A70-10097

Plane harmonic Rayleigh wave propagation in piezoelectric semiconductor GaAs crystals, using successive approximation procedure

01 p0154 A70-10131

Electrical properties of Si-doped GaAs p-n structures obtained by liquid phase epitaxy, considering charge buildup

01 p0155 A70-10132

Current dependence of integral brightness and electroluminescence spectrum of ZnS-GaAs heterojunctions obtained by I vapor reaction in H flow

01 p0155 A70-10142

Electric characteristics and impurity distribution in GaAs-Ge heterojunctions obtained by deposition on p-type Ge

01 p0155 A70-10143

Second phase formation in Czochralski grown Cr-doped GaAs crystals by metallography, radioactive indicators and X ray analysis

01 p0156 A70-10189

Iron behavior in GaAs during crystallization, studying Fe distribution ratio, impurity migration and diffusion coefficient

01 p0156 A70-10219

Planar Gunn effect devices using various surface electrode configurations, discussing limitations by breakdown on Ga arsenide exposed surface

01 p0049 A70-10287

GaAs - Conference, Dallas, October 1968

01 p0157 A70-10515

Negative resistance light emitting lateral GaAs diode, analyzing oscillation frequency, I-V characteristics, temperature and magnetic effects

01 p0050 A70-10565

Laser transitions to valence band or acceptor in low loss uniformly pumped crystal structure p-type GaAs at 77 K

01 p0113 A70-11168

Alloying additions effect on plastic deformation anisotropy in GaAs single crystals, determining dislocation activation energies from creep tests

01 p0160 A70-11606

Book on GaAs components technology covering properties, fabrication and applications of GaAs semiconductor elements in electronics

02 p0350 A70-11734

Semiconductor laser quantum mechanical rate equations derivation to determine temperature and current dependences of light output properties, indicating numerical calculations for GaAs

02 p0311 A70-11884

Autoelectron and autophotocurrent emission from Fe-doped p-type GaAs cathodes in vacuum, noting I-V and emission characteristics dependence on light flux

03 p0538 A70-13067

N-GaAs pulsed Gunn effect oscillators for decimeter band, discussing synchronization by external sinusoidal current

03 p0499 A70-13204

GaAs nonlinear I-V characteristics and negative differential conductivity associated with electron heating by electric field

03 p0540 A70-13720

GaAs n-type single crystals thermoreflectance spectra at various energies

03 p0541 A70-13721

Optical inhomogeneity of GaAs associated with current carrier distribution analyzed quantitatively using magnetooptical Faraday effect and transmittance method

03 p0541 A70-13726

Electrical properties of Cu-diffused GaAs, studying temperature effects on acceptor concentration and electron population growth

03 p0541 A70-13730

Cavity resonator linear excitation by Gunn diode, considering external circuit effects on oscillation conditions and GaAs single crystal parameters

03 p0457 A70-13965

GaAs microwave diode Gunn oscillator subharmonically injection phase locked at low frequency ratios

03 p0459 A70-14041

Carrier concentration profiles and surface resistance of Ohmic contacts to solution epitaxial n-type GaAs wafers measured by Schottky barrier capacitance

03 p0543 A70-14213

InAs-GaAs solid solutions microhardness and brittleness, studying chemical composition effects

04 p0730 A70-14464

GaAs tunnel diodes excess current nature and voltage dependence, considering thermal current measurements, depletion layer processes, electron barrier height, etc

04 p0656 A70-14713

Schottky barrier FET fabrication using epitaxial growth of single crystal GaAs on insulating sapphire substrate

04 p0660 A70-15364

Epitaxial GaAs FET using evaporated Au-Ge-Ni contacts and Ni Schottky barrier, describing fabrication and electrical properties measurement

04 p0660 A70-15367

Velocity field characteristic for electrons in GaAs in negative differential mobility region by method involving probe measurements

04 p0732 A70-15690

Doped n-type GaAs electrophysical parameters determinable from IR reflection spectra

05 p0892 A70-16540

Fabrication and electrical properties of p-ZnTe/n-InAs heterojunctions: obtained by interface alloying, suggesting p-n structure from characteristics and capacitance behavior

06 p1125 A70-17123

Bulk GaAs devices and avalanche /IMPATT and TRAPATT/ diodes compared as microwave sources

06 p1018 A70-17357

Forbidden bandwidth in Brillouin zone and valence band spin-orbital splitting degree determined for mixed gallium-phosphide-arsenide

06 p1126 A70-17815

Minority current carriers diffusion in heterojunctions and p-n junctions in AlAs-GaAs, using X ray microanalyzer performing electron beam scanning

06 p1126 A70-17816

GaAs preparation techniques, crystal structure, electrical and physical properties, single crystal growth, impurities properties and distribution, thermal and optical properties, etc

07 p1356 A70-19397

Magnetoresistance effects in impurity conduction mode of n-type GaAs crystals below 6 K, giving electron concentration

07 p1356 A70-19796

Semiconsulating GaAs doped with Cr, discussing negative resistance segment in current-voltage curves of S diodes

07 p1242 A70-19798

Polarized light electroreflection from GaAs single crystal, noting useful signal linear dependence on electric field

08 p1556 A70-21124

Gunn diode parallel combinations fabricated for X band with n-type GaAs crystals, discussing output power at CW operation

08 p1477 A70-21296

Negative differential conductivity effects in Gunn domain GaAs semiconductors, discussing physical properties and microwave applications

08 p1556 A70-21303

Plane harmonic Rayleigh wave propagation in piezoelectric semiconductor GaAs crystals, using successive approximation procedure

08 p1556 A70-21407

Electrical properties of Si-doped GaAs p-n structures obtained by liquid phase epitaxy, considering charge buildup

08 p1556 A70-21408

GaAs solar cells performance as function of doping levels, ascribing poor efficiencies to surface recombinations

08 p1557 A70-21721

Absorption spectra of n-type GaAs before and after proton irradiation, discussing dependence on wavelength

09 p1739 A70-22753

Microwave conductivity and limiting frequency in Gunn effect GaAs using drifted Maxwellian

09 p1739 A70-22849

Fabrication effects on current instability during injection and breakdown of p-n junctions in GaAs oscillators

09 p1740 A70-23351

Electrical, physical and technological requirements and methods of preparation of ohmic contacts on GaAs, noting use of Au-Ge-Ni alloy

10 p1927 A70-24225

Resistive parametric mixing in GaAs oscillators at microwave frequencies resulting in negative mobility at signal frequency

10 p1849 A70-24231

Gallium arsenide phosphide epitaxial films electroluminescence spectra noting composition effect
10 p1928 A70-24833

GaAs light amplifier p-n junction gain and output noise determination for wide photon energy ranges, studying input noise levels effects on sensitivity
10 p1928 A70-25167

Ion-implanted GaAs junction diodes anneal behavior and defect nature
11 p2098 A70-26391

Epitaxial surface morphology layer electrical properties and autoping at GaAs-Ge heterojunctions as function of substrate temperature, orientation and HCl concentration
11 p2098 A70-26392

Nucleation and heteroepitaxial GaAs film growth on sapphire using electrical measurements, reflection diffraction and electron microscopy
11 p2098 A70-26393

Temperature effects on width of current-voltage characteristics of GaAs Gunn oscillators
11 p2020 A70-26819

GaAs vapor phase epitaxial growth characteristics noting applications to Gunn diodes
11 p2020 A70-26826

GaAs relaxation and hybrid modes properties and formation conditions
11 p2099 A70-26827

Epitaxial or bulk GaAs for Gunn diodes in high power microwave oscillators
11 p2021 A70-26828

GaAs-Au surface barrier n-type photodiode structure, electrical parameters and response characteristics
12 p2194 A70-26969

Electron amplification and phase velocity of plane harmonic Rayleigh wave in gallium arsenide crystals under constant electric field
12 p2285 A70-27294

Impurity centers thermal and autoionization and effective capture cross section dependent on free carrier concentration in GaAs under electric field, allowing for plasma shielding
12 p2285 A70-27361

Low resistivity films synthesized on seminsulating GaAs by xenon, krypton, selenium and zinc ions bombardment
12 p2286 A70-27364

Chromium doped GaAs photoconductivity spectral distribution at various temperatures, determining temperature dependence of impurity maximum
12 p2286 A70-27366

Electroluminescence recombination emission spectra during avalanche breakdown in AlGaAs n-p and p-n heterojunctions
12 p2286 A70-27367

Electric field heating effect on edge photoluminescence of n-type GaAs, noting increase in electron energy
12 p2286 A70-27368

Iron impurity energy level behavior in seminsulating GaAs from determining temperature dependences of Hall coefficient, resistivity, optical absorption and steady spectral photoconductivity
12 p2286 A70-27370

Electron-hole transitions in GaAs obtained by sulfur diffusion, noting capacitance dependence on voltage at 293 and 77 K at various frequencies
12 p2287 A70-27481

Electroacoustic conversion in low resistivity GaAs crystal surface layer, applying external magnetic field to tune converter in wide frequency range
12 p2287 A70-27483

Radiation defects distribution in GaAs during proton irradiation, noting distribution dependence on proton energy and integral flux
12 p2287 A70-27488

Fe and Ni doped GaAs photoconductivity at various temperatures, determining activation energy level
12 p2287 A70-27489

Cu doped GaAs n- to p-type transition after fast reactor neutron irradiation, measuring Hall effect and photoconductivity to determine Cu electrical activation
12 p2287 A70-27490

Absorption spectra of seminsulating gallium arsenide in IR region, investigating transmittance and absorption coefficient at room and low temperatures
12 p2287 A70-27492

Sum and difference frequency signals generated and propagated by mixing carbon dioxide laser and millimeter wave klystron outputs in GaAs loaded waveguide
12 p2250 A70-28098

Ohmic contacts for gallium arsenide single crystals, describing fabrication technique and IV characteristics
12 p2202 A70-28187

Metallic contacts deposition on p- or n-GaAs using vacuum evaporation by electron bombardment
12 p2202 A70-28188

Lattice defect influence on EPR spectral and luminescent characteristics of annealed Fe doped gallium arsenide crystals
12 p2288 A70-28330

N-type GaAs carrier mobility and concentrations increased slow cooling after heat treatment
12 p2289 A70-28343

Solid solutions of GaAs with 2B or 6A intermetallic compounds, using metallographic and X ray methods
13 p2469 A70-28856

Optical charge exchange and thermal stimulation effects in Fe doped GaAs crystals, determining iron content role by EPR method
13 p2469 A70-28880

Photon lifetime dependence on hole and electron concentration in GaAs from IR reflection spectra analysis
13 p2470 A70-28882

Neutron irradiation effect on n-channel GaAs junction FET performance, considering transconductance, drain current, pinch-off voltage and cut-off frequency
13 p2376 A70-28932

High power L- and S-band transferred-electron oscillators from epitaxial GaAs
13 p2377 A70-28978

Parallel and perpendicular negative magnetoresistance measurements as function of magnetic field in p-type GaAs at 77 K
13 p2471 A70-29374

Microwave oscillator providing transition to stable emission at harmonics with power levels comparable to fundamental frequency, considering gallium arsenide oscillation mode
13 p2471 A70-29413

Undoped GaAs lattice constants and electrical properties before and after heat treatment
13 p2471 A70-29504

Iodide concentration effects on epitaxial GaAs p-n junctions growth characteristics
14 p2625 A70-30171

GaAs epitaxial layered wafer natural CW R band oscillations in LSA mode
14 p2550 A70-30688

Vaporization characteristics of solids for relationship between chemical bonding and sublimation mechanism emphasizing NaCl, CdS and GaAs
14 p2545 A70-30906

GaAs-Ge heterojunction transistors with microwave planar geometry, calculating performance for comparison with Ge homojunction transistor
14 p2556 A70-30925

GaAs Gunn devices oscillatory modes under various operating conditions
14 p2557 A70-31158

Gamma radiation effects on GaAs Gunn diodes, measuring Hall effect, low field resistance, output power and FM noise in X band cavity
14 p2558 A70-31322

Spectral distribution of GaAs photoconductivity, allowing for coordinate dependence of minority carrier lifetime in surface space charge region
15 p2782 A70-31626

Acceptor level formation kinetics from measuring Hall constant as function of temperature after diffusion of copper into n-type GaAs
15 p2782 A70-31633

Ternary phase diagram of liquid epitaxially grown gallium arsenide antimonide, considering use as high quantum efficiency long wavelength photoemitter
15 p2782 A70-31758

Surface photovoltage regeneration mechanism in GaAs dependent on free carrier concentration, space charge density and minority carriers
15 p2783 A70-31951

GaAs slices efficiency as transferred electron devices, correlating impurity profiles with microwave performance
15 p2708 A70-31957

Semiconducting gallium arsenide LF oscillations, considering domain behavior and illumination effects
15 p2783 A70-31972

Solar cells based on homogeneous diffusion p-n junctions in epitaxial GaAs films grown on Ge single crystal substrate
16 p2843 A70-33202

GaAs microwave devices including diffused varactor, Schottky barrier and Gunn diode, discussing single crystals preparation and epitaxial growth layers
16 p2873 A70-33293

High power microwave pulse generation in SHF region, discussing use of boat-grown and epitaxial GaAs diodes
16 p2875 A70-33396

SHF pulsed Gunn effect GaAs oscillators for nsec pulse length radar applications
16 p2875 A70-33397

Millimeter wave amplification by pumped n-type gallium arsenide oscillating in limited space charge accumulation mode
16 p2875 A70-33399

S band GaAs FET fabrication technology and frequency response
16 p2877 A70-33414

Transverse magnetic field influence on Gunn effect characteristics of n-type GaAs
17 p3142 A70-34622

Electron bombardment effect on volt-ampere, voltage-capacitance and pulse characteristics of GaAs point contact pulse diodes
17 p3055 A70-35675

Wideband UHF amplification in bulk n-type GaAs during domain generation, comparing cut-off and Gunn frequency
17 p3143 A70-35684

Hysteresis effects during retuning of n-type GaAs Gunn oscillator with bias source and LCR circuit, showing range of domain damping by low field
17 p3055 A70-35689

Shallow acceptor level in Au-doped n-type GaAs, using photoconductivity temperature dependence
17 p3143 A70-35702

Photoconductivity relaxation kinetics of low resistivity n- and p-type GaAs, showing nonradiative recombination
17 p3143 A70-35703

Electrical properties of n-type GaAs epitaxial films grown by gas transport method
17 p3144 A70-35706

Photosensitivity and electroluminescence spectra of GaAs-indium gallium arsenide p-n heterojunctions at room temperature
17 p3144 A70-35708

IV characteristics of high resistivity Ti-doped GaAs single crystals and S-diodes, using Hall constant and conductivity measurements
17 p3144 A70-35709

Gunn phenomenon, discussing GaAs Gunn diodes preparation and applications
18 p3231 A70-36198

GaAs diodes electroluminescence dependence on temperature and injection current
18 p3297 A70-36234

High resistance space charge region formation near crystal cathode in GaAs due to limited contact emissive capacity
18 p3297 A70-36417

Electrical conductivity, Hall constant and differential thermal emf n-type GaAs-CdS solid solutions
18 p3298 A70-36596

Epitaxial growth of GaAs thin films in vapor phase using hydrogen, gallium and arsenic trichloride as sources
19 p3488 A70-38200

In-Au contacts for GaAs, discussing fabrication and performance tests on transverse Gunn mode oscillator
20 p3686 A70-39118

Surface damage of GaAs crystals by mechanical handling and polishing with hard abrasive lapping materials
20 p3686 A70-39119

Microwave emission from GaAs due to EM wave amplification within biased sample
20 p3686 A70-39397

Epitaxial GaAs films growth from solid solutions of InAs-GaAs system deposited on GaAs substrates, noting electron mobility and temperature effect
20 p3686 A70-39629

Ga-as Gunn diodes small signal admittance in dipole oscillation mode, analyzing RC model
20 p3598 A70-40062

GaAs Gunn diodes design and fabrication, discussing material selection and operating heat removal
21 p3799 A70-41424

High energy electron irradiation generated defect centers in GaAs p-n electroluminescent diodes, using capacitance and thermally stimulated current measurements
21 p3863 A70-41914

Acoustoelectric domain spectra in n-GaAs by microwave emission, comparing results with parametric conversions theory
21 p3863 A70-42002

Transmission electron microscopy observation of thermal annihilation of stacking faults in epitaxial layers of GaAs grown from liquid phase
21 p3863 A70-42004

Electron tunneling through p-type GaAs point contacts on Pb single crystals at liquid He temperatures
21 p3864 A70-42017

Fermi energy and bandtail parameters in heavily doped and degenerate n-type GaAs, calculating conduction band density of states by screened Coulomb potential
21 p3864 A70-42018

Microwave output power and impedance for InP and GaAs bulk negative resistance oscillators, using velocity/field characteristics
21 p3800 A70-42049

Picosecond large amplitude pulse generating GaAs diode with nu-n structure
21 p3800 A70-42116

Thermally induced oscillations and negative resistance in seminsulating oxygen-doped GaAs double injection devices via heating beyond critical temperature
22 p4084 A70-42326

GaAs point contact diodes quick response performance with glass-metal or metal-ceramic bases, obtaining Schottky-type rectifying barriers by half period currents
22 p3995 A70-42406

GaAs stripline domains and guided EM waves, discussing velocity, conductivity, drift and transmission amplification gain
22 p3996 A70-42917

- Lattice parameter and thermal expansion of AlAs as function of temperature, indicating lattice match at 900 C with GaAs 22 p4086 A70-43004
- High purity surface-free GaAs epitaxial layer carrier lifetime measurement by optical transmission and excitation technique 22 p4086 A70-43017
- Photocurrent multiplication in single crystal n-type epitaxial GaAs due to impact ionization of shallow donors 22 p4087 A70-43218
- Low noise GaAs Schottky barrier beam lead mixer and chip style diodes, discussing fabrication and performance 22 p3998 A70-43333
- Millimeter band electromagnetic scattering from weakly doped GaAs, calculating reflection coefficient and phase angle 23 p4229 A70-43926
- N-type GaAs samples doped with Ag, Se, and Te respectively, measuring absorption coefficient spectral dependences at room temperature 23 p4229 A70-43928
- N type GaAs doped with Si, conductivity anisotropy observed from measurement and explanation in terms of electron distribution 23 p4231 A70-44890
- Irradiation influence on emission power of GaAs laser excited by high energy electron beam 23 p4203 A70-45060
- Terminal compensation influence on radiative recombination in n- and p-type GaAs, observing emission band in photoluminescence and electroluminescence spectra 23 p4231 A70-45063
- Threshold characteristics of injection and electron excitation semiconductor lasers having photoluminescence properties of n-type GaAs single crystals 23 p4203 A70-45065
- Intraband absorption in p-type GaAs associated with carrier transitions between heavy and light hole in valence band 23 p4232 A70-45066
- Spectral and threshold emission from optically pumped semiconductor lasers as function of carrier type and concentration in GaAs single crystals 23 p4203 A70-45069
- Temperature effects on width of current-voltage characteristics of GaAs Gunn oscillators 24 p4318 A70-45191
- Czochralski thermal probe for current carrier concentration in strip shaped area of n-type GaAs single crystals active growth 24 p4389 A70-45481
- Solid solution of GaAs with CdSe and CdS compounds, investigating intrinsic absorption edge dependence on temperature 24 p4390 A70-45663
- Internal Q switching deviation in gallium aluminum arsenides-GaAs single heterojunction lasers attributed to loss reduction at current pulse end 24 p4354 A70-45815
- GaAs crystal surface Raman scattering from phosphorus impurities localized modes, using Ar ion laser line 24 p4391 A70-46255
- GALLIUM COMPOUNDS**
- NT GALLIUM ANTIMONIDES
- NT GALLIUM ARSENIDES
- NT GALLIUM PHOSPHIDES
- NT GALLIUM SELENIDES
- Vapor deposited GaN single crystals tested for electrical and optical properties, determining band gap energy, electron concentration, etc 04 p0732 A70-15688
- Gallium trichloride and aqueous solution of lithium chloride as solar neutrino detectors 05 p0899 A70-15956
- GALLIUM PHOSPHIDES**
- Solution crystallization method to obtain gallium indium phosphide semiconductor alloys, discussing optical absorption thresholds and transitions 01 p0158 A70-10661
- Forbidden bandwidth in Brillouin zone and valence band spin-orbital splitting degree determined for mixed gallium-phosphide-arsenide 06 p1126 A70-17815
- Gallium arsenide phosphide epitaxial films electroluminescence spectra noting composition effect 10 p1928 A70-24833
- GALLIUM SELENIDES**
- Electrical conductivity of GaSe thin films developed in vacuum by electron bombardment as function of temperature 03 p0540 A70-13686
- GALVANIC CELLS**
- U ELECTROLYTIC CELLS
- GALVANIC SKIN RESPONSE**
- Noise effects on tracking performance, electroencephalography /EEG/ and galvanic skin resistance /GSR/ 04 p0643 A70-14977
- Human motor reactions rhythmic system, relating reaction-skin-galvanic reflex to formation of successive conditioned connections 07 p1197 A70-18697
- Skin galvanic reaction manifestation degree correlated to EEG changes accompanying injuries of human brain limbic structures 11 p1985 A70-25400
- GALVANIZING**
- U ZINC COATINGS
- GALVANOMAGNETIC EFFECTS**
- Relaxation time approximation formulas for galvanomagnetic effects in graphite based on energy spectrum model 01 p0126 A70-10181
- Transient response analysis in isotropic material under thermal galvanomagnetic effects involving interaction electric and thermal conductions in applied magnetic field [AIAA PAPER 70-17] 06 p1107 A70-18213
- Transport equation relation between irreducible tensorial sets, examining geometrical symmetry influence and thermomagnetic and galvanomagnetic effects 24 p4428 A70-45520
- GALVANOMAGNETISM**
- U GALVANOMAGNETIC EFFECTS
- GALVANOMETERS**
- Response characteristics of negative feedback galvanometer amplifier with inductive source impedance for geomagnetic micropulsation detection 07 p1242 A70-19998
- Ballistic pulsed photometer calibration without etalon light pulse using radiation sensitivity, oscillation period and galvanometer damping 12 p2338 A70-28179
- Electrochemical oxidation of p-type boron anode in aqueous solutions, using galvanostatic technique 17 p3041 A70-34514
- Quartz astatic galvanometer resistant to geomagnetic field variations, vibrations or microseismic noise 19 p3421 A70-37337
- GAME THEORY**
- NT MINIMAX TECHNIQUE
- NT SADDLE POINTS [GAME THEORY]
- Optimal strategies for controlled plant guidance into convex space assuming linear differential equations of motion 03 p0459 A70-13339
- Stochastic differential games with constrained state estimators, involving linear system, quadratic cost functional and white Gaussian noises corrupting output measurements 06 p1024 A70-17954
- Policies and controller design for pursuing vehicle developed in terms of pursuit-evasion differential games 06 p1025 A70-17955
- Linear-quadratic pursuit-evasion game with dynamics perturbed by additive white Gaussian noise, obtaining linear minimax solutions 06 p1025 A70-17957
- Differential game analysis of dynamic systems feedback control, presenting extremal aiming for successful pursuit completion 07 p1332 A70-18681
- Differential game with opponent receiving information on phase coordinates of adversary with delay caused by reception and processing procedures 07 p1244 A70-18718
- Pursuit games theory with bounded accelerations, using differential equations 07 p1323 A70-18947
- Risk-reducing information role in decision making using Marschak bidding procedure 07 p1203 A70-18964
- Sufficient conditions of optimality for strategic couple in theory of quantitative differential games 07 p1245 A70-19379
- Minimization of motion deviation from prescribed motion as differential game of converging motions using equations of motion 08 p1546 A70-21626
- Nonzero sum differential games with cost criteria minimized by inputs control to single dynamic system, emphasizing application to economic competition 11 p2072 A70-26227
- Cooperative differential game with cost functional minimized by each player, discussing problems with linear combinations of state variables final values 11 p2073 A70-26228
- Optimal strategies for game with nature and two-automata zero sum game under finite memory constraints 11 p2073 A70-26241
- Fixed target pursuit-evasion differential game based on pursuer-evader proximity as termination condition 11 p2073 A70-26242
- Pursuit game problems with pursuer and target described by k-dimensional phase vectors, discussing evasion problems 13 p2452 A70-29276
- Linear differential evasion game termination with phase vector approaching given subspace in Euclidean coordinates 13 p2443 A70-29755
- Soviet collection of papers on automation theory and biological systems simulation covering game theory and mathematical models 14 p2542 A70-30630
- Discrete approximation of differential game of navigation, considering control of object transfer to given set by finite time 15 p2775 A70-32472
- Pursuit-evasion differential games involving two linear dynamic systems with state and control dependent thermal noise 16 p2881 A70-32985
- Differential game theory, discussing two player zero sum situation 20 p3659 A70-40108
- Linear multiplayer differential games absolutely cooperative solution, discussing control variables assumption of interior values 20 p3660 A70-40383
- Pursuit evasion game with uncertain state-dependent measurements, modifying Brown-Robinson algorithm for behavior strategies computation 20 p3660 A70-40384
- Deorbiting target intercept energy optimization by game theory approach [AIAA PAPER 70-1019] 21 p3848 A70-41778
- Control space properties of pareto-optimal and cooperative solutions for static continuous and differential games involving vector cost criteria 22 p4061 A70-42460
- Differential rendezvous game theory with non-separated control inputs on right side of equations of motion applied to guidance problem 22 p4063 A70-43346
- GAMMA GLOBULIN**
- Human gamma globulin and binary/ternary protein structures conformation transitions studied by UV difference spectra 12 p2173 A70-28346
- GAMMA RADIATION**
- U GAMMA RAYS
- GAMMA RAY BEAMS**
- Gamma ray beam inspection of opposed arc weld with nugget penetration in Al-Cu alloy, including averaging circuit reducing counting statistics variation 01 p0054 A70-10020
- GAMMA RAYS**
- Local gamma irradiation effect on number of chromosome aberrations in lymphocytes of human blood of oncological patients after hysterectomy 01 p0013 A70-10137
- Semiconductor laser excitation by bremsstrahlung from electrons and gamma radiation from nuclear reactor 01 p0107 A70-10187
- PbSe and GeTe cast and pressed samples thermoelectric properties before and after high energy gamma ray irradiation, using scintillation counter with photomultiplier 01 p0159 A70-10756
- High altitude balloon measurements of secondary gamma quanta intensity vertical distribution, using scintillation counter with CsI/Tl crystal 01 p0172 A70-11544
- Gamma ray astronomy using balloon-borne telescope with digitized spark chamber 02 p0364 A70-11785
- Gamma ray background near proton synchrocyclotron beam degrader at NASA-LRC Space Radiation Effects Laboratory 02 p0275 A70-12268
- Discrete galactic and extragalactic X ray and gamma ray sources observation, discussing energy spectra, emission mechanisms, properties and suggested models 02 p0360 A70-12791
- Radiation hardened fiberglass reinforced plastics rupture, bending, compression and tensile strength and elastic modulus, considering gamma ray doses effect 02 p0323 A70-12811
- Two phase density and void fraction measurement using beta, gamma and X ray radiation, considering optical accuracy and beam collimation 02 p0305 A70-12835
- Electron and hard photon /X and gamma ray/ production and propagation in expanding metagalaxy, deducing universe matter density, cosmic ray sources, etc 03 p0557 A70-13225
- Postirradiation free radical processes in cellular organelles of rat liver exposed to gamma irradiation detected by graft copolymerization method 03 p0418 A70-13302
- Radioprotective action of pyridine derivatives in monkey heart and human epithelium cells exposed to gamma radiation evaluated by dioxyphenyl alpha-alanine oxidation 03 p0418 A70-13303
- Ultraweak luminescence intensity, radiation damage kinetics and spectral properties of cellular organelles of rat liver exposed to gamma radiation 03 p0419 A70-13304

Graft copolymerization and chemiluminescence analysis of lipids complexes in animal and plant tissue homogenates exposed to gamma radiation
03 p0419 A70-13305

Correlation between atmospheric meteor entry and gamma and neutron radiation intensity verifying micrometeor antimatter hypothesis
03 p0454 A70-13528

Peripheral blood, neutrophil myeloid hematopoiesis, phagocytic activity and serotonin level in gamma irradiated dogs
03 p0423 A70-13706

Gamma ray astronomy experiments, discussing likelihood method for analyzing and reporting results
03 p0559 A70-13810

Balloon-borne experiments with directional scintillators to measure low energy gamma radiation spectrum in midlatitude atmosphere for photons origin and gamma albedos investigation
03 p0561 A70-13996

Pulsed gamma radiation from pulsars searched for by Cerenkov air shower detection method
04 p0738 A70-14518

Four layer semiconductor device triggering by X or gamma radiation calculated by transport equations for electron and hole distribution motion and electric field distribution
04 p0657 A70-14731

Reactor gamma in-pile effects on thermionic diodes simulated in electron accelerator, noting ion production insufficient to support saturation currents
04 p0717 A70-14948

Allende carbonaceous chondrite radionuclide composition and concentration determined by nondestructive gamma ray spectrometry
04 p0754 A70-15275

Gamma rays due to cosmic ray electrons bremsstrahlung in interstellar medium, predicting diffuse galactic X ray flux
04 p0742 A70-15713

High energy neutron accelerator as fast neutron radiography source, comparing contrasts with gamma and X radiography
05 p0844 A70-15779

Gamma radiation integral fluxes and production rate evaluation from ground and neutron production in Plexiglas and Fe to calculate optimum recoil electron threshold
05 p0899 A70-15955

Spectral intensity recording facility design for high energy electrons and hard gamma quanta in upper layer and beyond atmosphere
05 p0846 A70-15959

Galactic X rays and high energy gamma rays in terms of cosmic ray electrons Compton scattering by submillimeter radiation
05 p0900 A70-16100

Spatial resonance capture rates for U-238 thick slabs to correct gamma ray attenuation errors in broad group shielding calculations
05 p0884 A70-16169

Transistor circuit design with junction compensation techniques to reduce transient gamma radiation effects
05 p0821 A70-16418

Environmental control underground low level radiation counting facility of Lunar Receiving Laboratory for gamma ray spectrometry, including radon adsorption system
05 p0829 A70-16707

Cosmic gamma radiation sources above 50 Mev investigated by high altitude balloons in Northern Hemisphere with spark chamber system
05 p0904 A70-16930

Molecular fluorescence emission rate factors for strong bands of nitric oxide gamma systems, noting day airglow temperature dependence
05 p0886 A70-17085

Survival rates of continuously cultivated *Chlorella* plants in air-carbon dioxide atmosphere after single exposure to gamma radiation, using microcolony counting technique
05 p0803 A70-17113

Positive effect of shielding and cystamin administration on tonic and evacuator functions of rats gastrointestinal tract after gamma irradiation
05 p0804 A70-17122

Acid soluble nucleotides content in normal and gamma irradiated rat spleens, presenting table
06 p0995 A70-17799

Geomagnetic field amplification near gamma radiation steady source, describing field displacement
07 p1367 A70-19446

Monograph on balloon and satellite borne spark chambers for cosmic gamma radiation energy and direction determination, discussing relativistic electrons multiple scattering
07 p1368 A70-19617

Calf thymus DNA structural and functional changes following exposure to hydrogen atoms and gamma radiation
07 p1215 A70-20050

Free radical destruction by gamma irradiation in organic solids at low temperature measured by electron

spin resonance spectroscopy, noting dosage relationship
07 p1225 A70-20324

Satellite recording of electron-positron annihilation gamma emission on Cosmos 135 artificial earth satellite relating to meteors antimatter nature
07 p1371 A70-20334

Electron and gamma quanta concentrations measurements by high altitude balloon, noting fluctuations at various altitudes
07 p1374 A70-20446

Density gradient sedimentation of *Escherichia coli* populations irradiated with Co 60 gamma rays, showing correlation between DNA degradation and cell death
08 p1441 A70-20680

Escherichia coli cell division patterns, discussing generation times spread, gamma ray irradiation in nutrient broth, DNA damage and growing points, etc
08 p1441 A70-20681

Gamma radiation effects on emission time, excitation threshold and efficiency of four level Nd glass laser under multimode operation
08 p1512 A70-21209

Electron and hard photon /X and gamma ray/ production and propagation in expanding metagalaxy, deducing universe matter density, cosmic ray sources, etc
08 p1563 A70-21658

Chronic gamma irradiation effects on bone marrow mitotic activity and chromosome aberrations in dogs
09 p1614 A70-22083

Nuclear landing roll aid based on gamma radiation field built along approach line, runway and taxiways
09 p1721 A70-22662

Gamma radiation effects on higher mammals nerve activity after chronic total body exposure
09 p1619 A70-22790

Trapped Ag atoms production in silver nitrate ice by gamma irradiation, discussing reaction enhancement by fluoride ion
09 p1631 A70-23445

Gamma-neutron irradiation effect on miniature pig, observing incapacitation with severe convulsions and performance decrement
09 p1622 A70-23461

Low energy positrons and gamma rays from large fluxes of galactic cosmic rays
09 p1746 A70-23477

High energy electron and gamma quanta flux measurement in atmosphere at different heights by high altitude balloons
09 p1747 A70-23728

High energy pulsed gamma rays detection method for pulsars based on search for nanosecond duration Cerenkov light signals
09 p1748 A70-23795

Radiation transport calculations based on approximate method restricted to X ray and low energy gamma ray region of electromagnetic spectrum
10 p1915 A70-23977

Gamma ray astronomy above 10 Mev, investigating intensity dependence on galactic latitude and radiation detection technology
10 p1931 A70-24067

Primary cosmic gamma-quanta fluxes measured using telescope consisting of Cerenkov counters
10 p1931 A70-24316

Peripheral blood, neutrophil myeloid hematopoiesis, phagocytic activity and serotonin level in gamma irradiated dogs
11 p1985 A70-25506

Cosmic gamma ray spectrum from secondary neutral pion production in p-p interactions, discussing delta isobar, fireball and nuclear interactions effects
11 p2106 A70-26707

High energy break in isotropic gamma ray spectrum predicted from critical test of cosmological pion-decay hypothesis
11 p2106 A70-26844

Gamma irradiation effects on thermal stability and decomposition of ammonium perchlorate
12 p2289 A70-26870

Solar gamma ray lines search with high resolution balloon-borne directional spectrometer based on lithium-drifted germanium detector
12 p2292 A70-27178

Cosmic gamma rays observation by balloon flight and satellite with scintillation detector, tabulating counting rates in pulse height channels relative to Crab Nebula
12 p2292 A70-27387

Diffuse cosmic X and gamma ray background radiation isotropic component
12 p2295 A70-27887

Sgr gamma-1 source, determining upper limit on soft X rays intensity
13 p2475 A70-28615

Compton electron scattering generated galactic gamma ray flux effects on diffuse IR
13 p2476 A70-28630

X- and gamma-ray detectors design based on combination of solar batteries with scintillators, noting stability requirements
13 p2404 A70-28657

Radioactive Mn 54 with high specific activity for short distance gamma radiography
13 p2404 A70-28658

Combined neutron and gamma ray irradiation effects on piezoresistive accelerometers
13 p2405 A70-28814

Pulsed gamma ray emission from Crab Nebula pulsar NP 0532 investigated by balloon-borne spark chamber detector
13 p2492 A70-29271

Marrow granulocyte reserve restoration in dogs exposed to chronic gamma radiation, discussing leukocyte reaction to pyrogenic agent
13 p2351 A70-29326

Total Absorption Shower Cascade (TASC) detector for gamma ray astronomy space, discussing energy and angular resolution
14 p2587 A70-31004

Gamma radiation effects on GaAs Gunn diodes, measuring Hall effect, low field resistance, output power and FM noise in X band cavity
14 p2558 A70-31322

Cosmic X ray and gamma ray spectral energy distribution slope change explained by measurement process involving photon spectrum
15 p2792 A70-31431

Planetary gamma and X radiation by remote sensing and passive observation for gross chemical composition
15 p2793 A70-31749

Chronic gamma irradiation effects on bone marrow mitotic activity and chromosome aberrations in dogs
15 p2685 A70-32679

Neutron stars gamma and radio emission in gas accretion state, determining surface gravitational potential
15 p2808 A70-32883

X and gamma ray astronomy instrumentation, point sources, continuum emission, line spectra, etc
16 p2976 A70-33721

Mars evolution observation by gamma ray spectrometer in Martian orbit, transmitting information to earth as pulse height distribution
16 p2912 A70-33978

Omnidirectional cosmic gamma ray flux in 1-6 MeV range observed by ERS-18 satellite
17 p3149 A70-34539

Critique of paper on Crab Nebula pulsar pulsed gamma ray emission, considering photon flux and statistical data analysis
17 p3149 A70-34565

Critique of paper on pulsed gamma rays detection from Crab Nebula pulsar by balloon flights, attributing pulsations to random fluctuations
17 p3149 A70-34566

Galactic gamma rays from OSO-3 observations attributed to decay of neutral pions produced by cosmic rays interaction with interstellar gas nucleons
17 p3150 A70-34567

Nonpenetrative reentry vehicle nose thickness ablation sensor using gamma radiation backscatter
17 p3094 A70-35519

Gamma ray pulse height spectra during active and quiet solar periods from midlatitude balloon flights
17 p3152 A70-35774

Vertical secondary cosmic gamma spectra from primary nucleon and electron spectra, discussing effects of solar cycle and geomagnetic cut-off
18 p3308 A70-36500

Geomagnetic field amplification near gamma radiation steady source, describing field displacement
18 p3309 A70-36920

Depleted uranium for gamma radiation shielding, discussing properties, alloys, fabrication and applications
19 p3469 A70-37834

Galactic plane hard X ray emission measurements, considering gamma and X ray origin from Compton scattering of photons by galactic electrons
19 p3497 A70-38023

High energy cosmic gamma radiation detection from point source in Sagittarius, using balloon mounted spark chamber with Cerenkov telescope
19 p3500 A70-38078

High energy gamma rays detection from pulsars by fast night sky Cerenkov counter
19 p3500 A70-38083

Periodic high energy gamma rays from pulsars, using night sky Cerenkov light receiver for proton showers
19 p3500 A70-38084

Cygnus constellation energetic gamma ray emission by nuclear emulsion and spark chamber telescope on high altitude balloon
19 p3501 A70-38086

Extraterrestrial gamma radiation from Cygnus region of galactic disk, using OGO-5 observations
19 p3501 A70-38087

Astronomical gamma ray emission measurement by balloon-borne spark chamber, presenting results for discrete and diffuse sources and albedo intensities
19 p3501 A70-38088

High energy gamma ray flux enhancement towards galactic plane from OSO-3 particle telescope observations
19 p3501 A70-38089

Periodic cosmic gamma radiation from pulsars, using reflector detection of shower generated Cerenkov light

19 p3501 A70-38090

Cosmic gamma ray sources detection in 100-1000 GeV range by atmospheric Cerenkov radiation from energetic particle showers

19 p3501 A70-38091

High energy primary gamma quanta intensity limits from Proton-2 and Cosmos-208 measurements

19 p3502 A70-38092

Energetic primary gamma ray fluxes by satellite-borne spark chamber, isolating galactic radiation

19 p3502 A70-38093

Galactic low energy cosmic ray positrons and gamma rays, considering production mechanism in interstellar space

19 p3503 A70-38099

High energy galactic gamma ray and X ray flux explained by cosmic ray electron scattering

19 p3504 A70-38112

High energy galactic gamma rays photons, suggesting two-component cosmic ray source model

19 p3505 A70-38115

ESR spectrum of gamma irradiated cycloheptatriene silver perchlorate, indicating free radicals and trapped electrons

19 p3374 A70-38272

Diffuse cosmic X and gamma ray spectrum analysis, considering implications for Compton scattering models in intergalactic space

20 p3695 A70-39049

Atmospheric gamma rays vertical intensity dependence on spectrum and altitude from high altitude balloon studies

20 p3697 A70-39286

Recording device for gamma quanta in primary cosmic radiation

20 p3629 A70-39316

Stony meteorites radionuclides gamma emission measurement, determining specific activity ratios

20 p3703 A70-39322

Human body radioactive nuclides in vivo quantitative analysis by gamma ray spectra, considering matrix method accuracy

20 p3582 A70-40449

Nonsolar X and gamma ray astronomy - Conference, Rome, May 1969

21 p3870 A70-40651

Optical photometric observations of nonsolar gamma and X ray sources WX Cen, NGC 5189 and GX3 plus 1

21 p3873 A70-40669

Pulsed hard X and gamma rays from NP0532 pulsar in Crab Nebula, comparing with extrapolated optical data

21 p3874 A70-40675

Cosmic gamma radiation from pulsars, examining atmospheric Cerenkov light generated by energetic particle showers

21 p3874 A70-40676

Discrete X ray and gamma ray sources theories, considering binary and gas stream models

21 p3874 A70-40680

Magnetic field lower limit in Crab Nebula from cosmic gamma ray studies using optical reflector to detect atmospheric Cerenkov radiation

21 p3875 A70-40684

Extragalactic gamma ray and X ray intensity with power law spectrum, comparing galactic plane and high latitude spectra

21 p3875 A70-40687

High energy galactic gamma rays search onboard OGO-5, tabulating results

21 p3876 A70-40690

Galactic gamma ray intensity near Cygnus by OGO-5 spacecraft-borne telescope with acoustic spark chamber, discussing source intensity

21 p3876 A70-40691

Gamma ray astronomical point sources by balloon flight and satellite observation, discussing detector system and telescope for flux and energy spectrum

21 p3821 A70-40694

High energy gamma rays detection by balloon flights, investigating flux and energy spectrum

21 p3876 A70-40696

Omnidirectional cosmic gamma ray flux near one MeV observed by ERS-18 satellite, plotting spectral energy distribution

21 p3876 A70-40697

Galactic gamma ray sources model with magnetic fields concentration in expanding shell, suggesting production by neutral pion decays in supernova remnants

21 p3877 A70-40701

Background gamma ray observations attributed to decay of pi-mesons produced by extragalactic cosmic ray protons collisions, noting radiation sources age

21 p3877 A70-40703

Pulsars and other discrete sources celestial gamma rays flux distribution calculation

21 p3878 A70-40745

Gamma ray background anisotropy effects of Sgr A flux arising from Compton scattering and neutral pion decay, discussing complex radio and IR structure

21 p3878 A70-40926

Dosso stony meteorite gamma emitters radioactivity by nondestructive spectroscopy, obtaining quantitative analysis by least squares method

21 p3893 A70-41446

Galactic center region gamma radiation observations, discussing intensities, energy spectrum and decay

22 p4093 A70-42927

Pulse height distributions due to terrestrial gamma rays, using NaI/Tl scintillation counter

23 p4187 A70-43899

High Energy Astronomy Observatory for space X rays, gamma and cosmic rays research via unmanned spacecraft

23 p4261 A70-44680

Temperature effect on radiation tolerance of mice exposed to low dose rate gamma radiation, noting mortality delay in low temperature environment

23 p4148 A70-44789

WC radiation damage by resonant absorption following Coulomb excitation observed from gamma ray spectra

23 p4231 A70-44888

Gamma ray nondestructive tests for materials defects, discussing cinematic, geometric and radiological factors effects on detection

24 p4337 A70-45711

Aircraft structures service life estimation, using Ir-192 and Tm-170 gamma ray radiography

24 p4346 A70-45725

Spallation limits on low energy cosmic and nuclear gamma rays interstellar fluxes, evaluating fast particle effects on interstellar medium

24 p4397 A70-45758

Radiative flow detection problems, calculating gamma radiation scattering

24 p4348 A70-45848

Liquid compensators for gamma ray flow detection of complex metal product configurations, considering radiation source energy spectrum and specimen density

24 p4348 A70-45849

Discrete source interpretation of isotropic component of diffuse gamma radiation in Milky Way galaxy

24 p4398 A70-46166

Gamma ray inspection of opposed-arc weld-nugget penetration in Al-Cu alloy

24 p4350 A70-46384

GANGLIA

NT NERVES

NT NEURONS

Local stress effect on immunocompetent cells differentiation in guinea pigs lymphatic ganglia, noting increase in number of antibody producing cells

05 p0803 A70-17114

GAPS

NT SPARK GAPS

Anisotropic superconducting energy gap of pure Zn from microwave absorption measurements

16 p2961 A70-33776

Anisotropic energy gap model in superconducting Zn to describe microwave absorption measurements

16 p2961 A70-33777

Scattering and radiation from circumferential gap in circular dielectric-loaded waveguide, using integral equations

23 p4167 A70-43765

GARNETS

NT YTTRIUM-ALUMINUM GARNET

NT YTTRIUM-IRON GARNET

Abundance levels of K, Rb, Sr and Ba in pyroxenes, olivines and garnets of ultramafic rocks for upper mantle composition

03 p0472 A70-13149

Absorption transition fine structure measurements for bulk rare earth garnets single crystals using reflectivity techniques

[IEEE PAPER 19.6] 05 p0894 A70-16998

Absorption spectra of single crystals TbAlG and DyAlG garnets, investigating Verdet constant dependence on ion concentration

07 p1355 A70-18705

Magneto-optical birefringence anisotropy and light propagation in terbium ferrite garnet in presence of Faraday and Cotton-Mouton effects

11 p2097 A70-25377

HF energy nonresonance dissipation in polycrystalline yttrium-garnet ferrites subjected to constant magnetizing field

11 p2097 A70-25384

Majorite garnet in veinlet of Coorara meteorite suggesting transformation from pyroxene

13 p2492 A70-29267

Spectral emission in trivalent Ho doped Yb-Al garnet single crystals grown by optical zone melting

15 p2784 A70-32198

Lunar rocks almandine-rich garnet chemical composition and crystallography, noting cell edge and refractive index

21 p3883 A70-40711

GAS ANALYSIS

NT OZONOMETRY

Bimolecular transfer reactions activation energies for multivalent gaseous compounds estimated by bond energy method avoiding use of adjustable parameters

03 p0441 A70-14045

Computerized mass spectrometer for monitoring atmosphere in astronauts suits and cabin

[AIAA PAPER 69-1016] 07 p1249 A70-19730

Portable unit for collection and analysis of toxic gas contaminants in enclosed aircraft and spacecraft cabin atmospheres

07 p1224 A70-20222

Multicomponent gas absorption analysis to illustrate interactions of coupled fluxes in ammonia-water system

08 p1597 A70-21028

Oxygen uptake by brain as function of oxygen tension in rats using venous outflow method and blood gas analysis

08 p1446 A70-21436

Simultaneous titration of gases, metalloids and metals in steels and refractory alloys by far UV vacuum spectrometry

[ONERA-TP-765] 08 p1455 A70-21842

Modified apparatus for volumetric determination of alveolar carbon dioxide as indicator of pilot hypernea

10 p1825 A70-24503

Hydrogen, oxygen and carbon dioxide in off-gas stream from nuclear reactor experiment using on-line gas chromatography

11 p1994 A70-25615

Differential thermal analysis-effluent gas analysis /DTA-EGA/ experiment for lightweight Martian landed capsule

11 p2050 A70-25802

Atmospheric hydrogen content continuous recording method based on absorption line analysis of mercury vapor from mercuric oxide reduction

11 p2052 A70-26389

Aircraft turbine engines gaseous emission measurements, discussing instrumentation for continuous pollutant concentration monitoring

[SAE PAPER 700249] 12 p2290 A70-27428

Liquid hydrazine decomposition by Shell 405 catalyst, determining gaseous products by gas chromatography and titrometric analysis

[AIAA PAPER 70-606] 16 p2856 A70-33603

Aircraft turbine engines emission sampling, handling and measurement, evaluating various instruments and techniques

[SAE PAPER 700338] 18 p3226 A70-36810

Gas turbine emissions analysis for air pollutants, determining species distribution and concentration

[ASME PAPER 70-GT-81] 18 p3226 A70-36883

Residual atmosphere analysis and application to ion pumping on Al alloy high pressure chamber of differential vacuum system

19 p3434 A70-37464

Ultrahigh vacuum pressure measurement by improved residual gas analysis mass spectroscopy with magnetic section

19 p3396 A70-37465

Evolved gas analysis by mass spectrometry /EGA-MS/, discussing filament heating system and data processing

19 p3374 A70-38495

Fluorine-compatible apparatus for measuring temperature PVT properties of gaseous and liquid fluorine

20 p3630 A70-39485

Rare gas analysis of Apollo 11 lunar soil and breccia for surface layer history

21 p3906 A70-41571

GAS BEARINGS

Two axis spherical gas bearing gyro for accurate measurements of space vehicle position and attitude rates while maintaining compatibility with exotic environments

01 p0086 A70-10308

Air lubricated foil bearing support design with external pressurization for high speed rotor in high temperature turbomachinery

[ASME PAPER 69-LUB-D] 01 p0100 A70-10377

Externally pressurized air journal bearings load capacity, film stiffness, attitude-eccentricity locus and mass flow, studying supply pressure and shaft rotation effects

[ASME PAPER 69-LUB-29] 01 p0100 A70-10380

Externally pressurized gas lubricated journal bearings zero load rotating stability, using digital computer

[ASME PAPER 69-LUB-27] 01 p0100 A70-10382

Synchronous dynamic response of gaseous double squeeze film thrust plate with very high frequencies, showing increased load capacity and stiffness

[ASME PAPER 69-LUB-8] 01 p0102 A70-10395

Inertia forces effect in turbulent and laminar, self acting and infinitely long film bearings, considering compressible and incompressible lubricants

[ASME PAPER 69-LUB-2] 01 p0103 A70-10400

Step thrust self acting gas bearing without feed grooves for two directions of shaft rotation, determining geometric, gas and speed parameter characteristics

02 p0307 A70-12164

Book on gas lubrication covering general equations, externally pressurized journal and thrust bearings, etc

02 p0310 A70-12651

Carrying capacity and moment of friction calculated for cylindrical MHD bearing for small magnitude of radial clearance

03 p0497 A70-13877

Time transient and step-jump dynamic analyses of gas lubricated bearing, illustrating hybrid journal and Rayleigh-Step thrust bearings

[ASME PAPER 69-WA/LUB-5] 04 p0697 A70-14768
Pendulous integrating gyro accelerometer gas bearing wheel characteristics at high slow rates monitored by differential varmeter

[ASME PAPER 69-WA/LUB-3] 04 p0698 A70-14770
Optimum one dimensional Rayleigh gas slider bearing, calculating step location, pressure and load capacity for range of bearing numbers

[ASME PAPER 69-WA/LUB-1] 04 p0698 A70-14772
Molecular mean free path influence on gas lubricated thrust bearings performance, discussing slip flow effect and load capacity

05 p0854 A70-15909
Self acting, hydrostatic and squeeze-film gas lubricated bearings applications to gyroscopes, accelerometers, torque testers, etc

05 p0855 A70-16446
Load capacity of rotating field MHD hydrostatic thrust bearing increased by rotating axial magnetic field

06 p1076 A70-17527
Dynamic response of gas lubricated radial sliding bearing from transfer function derived from pH linearized mathematical model of gas lubrication

07 p1290 A70-18739
Oil vapor lubricated bearing for compensated antenna of spin stabilized spacecraft, discussing service life, power and storage in sintered porous material [DGLR-69-062] 07 p1391 A70-18775

Spherical gas bearings static characteristics and performance, discussing materials selection, optimum clearances and surface hardness

07 p1294 A70-19122
Equilibrium state instability of radial gas bearing accompanied by oscillations, examining bearing dynamics and nonlinear film reaction characteristics

07 p1295 A70-19536
Central equilibrium position stability of gas bearing supported rotor allowing for inertia and lubricant compressibility

08 p1502 A70-20695
Air brake with compressed air fed bearings for testing small turbines, determining power and friction moment

08 p1481 A70-21188
Spherical radial bearing with gas lubricant, solving Reynolds equation by small parameter method

09 p1690 A70-22450
Stable equilibrium of rotor in pressurized gas bearing, considering perturbed rotor motion equation together with Reynolds equations for pressures in lubricant layer

09 p1690 A70-22544
Pressurized gas bearing analysis, using finite difference method for solving Reynolds equation for pressures in lubricant layer

09 p1690 A70-22545
Load parameters of externally pressurized gas journal bearing with multiple supply holes

09 p1693 A70-22977
Externally pressurized porous journal gas bearings with solid sleeve parts for reducing porous media waviness and roughness effects

10 p1896 A70-25097
Balanced rotor with radial sliding bearing bushings, studying lubricant gas restoring force effect on stability with allowance for bushings translational movements

11 p2058 A70-25581
Externally pressurized bearing with electrically-conducting gas lubricant under axial magnetic field, considering load capacity

12 p2244 A70-28018
Externally pressurized air journal bearing performance prediction, obtaining pressure distribution by numerical solution of Reynolds equation

13 p2418 A70-28743
Oil-vapor lubricated ball bearing system for deployable spin-free antenna of spin stabilized spacecraft

13 p2349 A70-28843
Free rotor air bearing gyros active damping evaluated through experimental studies

[AIAA PAPER 67-590] 15 p2741 A70-32506
Additional inertia introduced by velocity profile gradient in flow direction effects on externally pressurized gas bearing

16 p2924 A70-34233
Pressurized gas bearing flow field, discussing velocity transversal component, pressure distribution and profile

16 p2924 A70-34237
Spacecraft simulator using air bearing technique to simulate low friction aspect of environment, considering application to satellite attitude control

18 p3236 A70-36064
Spherical gas lubricated sliding bearing with forced injection, determining pressure distribution by numerical integration

18 p3262 A70-36273

Pneumatic instability, capacity and rigidity of thrust and journal gas bearings with external air injection

18 p3264 A70-37072

Inertia forces effect in turbulent and laminar, self acting and infinitely long film bearings, considering compressible and incompressible lubricants

[ASME PAPER 69-LUB-2] 19 p3435 A70-37613
Optimum one dimensional Rayleigh gas slider bearing, calculating step location, pressure and load capacity for range of bearing numbers

[ASME PAPER 69-WA/LUB-1] 19 p3436 A70-37617
Pendulous integrating gyro accelerometer gas bearing wheel characteristics at high slow rates monitored by differential varmeter

[ASME PAPER 69-WA/LUB-3] 19 p3436 A70-37618
Time transient and step-jump dynamic analyses of gas lubricated bearing, illustrating hybrid journal and Rayleigh-Step thrust bearings

[ASME PAPER 69-WA/LUB-5] 19 p3436 A70-37619
Aerostatic journal bearings with double plane admission feeder holes, determining maximum load and stiffness by numerical method

19 p3443 A70-38898
Fluidic gyro compatible with PDM missile guidance system, discussing spherical gas bearing design

[AIAA PAPER 70-1008] 20 p3631 A70-39524
Load bearing capacity of radial gas bearing with annular injection line, discussing gas feeding methods

20 p3637 A70-39816
Cylindrical gas suspension lubricating layer pressure distribution calculation by perturbation method, determining angular rigidity

20 p3637 A70-39818
Unsteadiness effect on load bearing capacity of cylindrical sectoral gas bearing

20 p3637 A70-39819
Heat generation effects in air hydrostatic journal bearing, including shaft and housing thermal deformation and lubricant viscosity changes

[ASME PAPER 70-LUBS-19] 22 p4044 A70-42442
Gas lubricated three-foil bearing for high speed rotor support, considering dynamic and static behavior in zero gravity environment

[ASME PAPER 70-LUBS-18] 22 p4044 A70-42443
Dynamic characteristics of turborotor simulator supported on gas lubricated foil bearings, considering rotor response to imbalance

[ASME PAPER 70-LUBS-11] 22 p4044 A70-42449

GAS CHROMATOGRAPHY

Gas chromatography and mass spectroscopy study of fatty acids and hydroxy acids in 5000 year sediment from English Lake District

02 p0252 A70-12507

Gas chromatography and mass spectrometry applied to porphyrin microanalysis, studying homologous porphyrin series in ancient sediments and oils

02 p0252 A70-12516

Palladium alloy transmodulator for gas chromatograph, demonstrating sensitivity gain for thermal conductivity and ionization cross section detectors

03 p0442 A70-14325

Gas chromatography based on sampling gas-vapor phase at liquid surface for determining volatile oxygen containing compounds in biological media

04 p0646 A70-14580

Butyl esters separation from protein amino acids, using acid washed Chromosorb W of various mesh sizes

10 p1828 A70-24397

Carbonaceous chondrites composition by gas chromatography for light hydrocarbons and carbon, discussing origin of organic matter

10 p1949 A70-25327

Propylene carbonate applications in nonaqueous electrolyte batteries, describing impurities identification by gas-liquid chromatographic analysis

12 p2164 A70-27069

Retention times and gas chromatographic conditions for resolution of galactonic and gluconic acid derivatives

16 p2855 A70-33064

Digital logic control of chromatographic system for measuring instrumental contributions to band broadening

16 p2855 A70-33120

Chromatographic analysis of organic matter in Pueblito de Allende meteorite

17 p3173 A70-35754

Quantitative and qualitative analysis of biochemically and radiobiologically important thiols and disulfides via gas-liquid chromatography

19 p3373 A70-37836

Hydrogen, N, O, Kr methane and carbon dioxide gas chromatographic examination, discussing life detection device for Mars landing

22 p3983 A70-43094

Quantitative gas-liquid chromatography of histidine, using N-TFA n-butyl ester derivatives and histidine converted trimethylsilyl derivative

22 p3983 A70-43524

Gas-liquid chromatography studies of direct esterification of protein amino acids to n-butyl esters

22 p3984 A70-43525

GAS COMPOSITION

NT CARBON DIOXIDE CONCENTRATION

Chemical and physical adsorption of gaseous oxygen contaminants to maintain purity for respiratory purposes, noting trichlorethylene and carbon tetrachloride

01 p0031 A70-10236

Acoustic and shock waves propagation in multicomponent media, assuming uniform speed for components and complex density dependence of media on pressure

03 p0465 A70-13329

Al alloys crack growth effects due to gaseous environment and fatigue frequencies, suggesting role of gas adsorption

05 p0938 A70-16478

Inhaled air intrapulmonary distribution uniformity and alveolar N concentration using single breath method

05 p0802 A70-16496

EKG, EEG, pneumograms and X ray pictures showed no pathological effect after prolonged confinement in sealed chamber having artificial atmosphere with variable gas composition

05 p0810 A70-17121

Kinetic relaxation and Boltzmann equations for studying shock waves propagating in gas composed of rigid ideally elastic spherical molecules without internal degrees of freedom

06 p1036 A70-17756

Vertical profile of angular mass distribution of atmospheric water vapor and ozone as gas proportion function

06 p1097 A70-17794

Statistical models in kinetic theory for describing gases ranging from gas with no internal degrees of freedom to multicomponent reacting mixtures

06 p1047 A70-18312

Zr, Ti, Nb and Ta carbides deposition from metal chloride, methane, hydrogen and argon mixture, studying gas concentration and temperature effects on deposition rate

08 p1517 A70-21147

Gas turbine engines contribution to air pollution, using model combustor to study burned gas composition, emphasizing nitric oxide concentration

08 p1559 A70-21481

Power output of sealed carbon dioxide-nitrogen-helium laser as function of gas composition and pressure

08 p1514 A70-21751

Gaseous species in equilibrium with Apollo 11 holocrystalline rocks during crystallization

09 p1758 A70-22744

Dynamics of multicomponent plasma involving charged or neutral gases with transport phenomena for case of no magnetic field

09 p1738 A70-23580

Vertical profile of angular mass distribution of atmospheric water vapor and ozone as gas proportion function

10 p1913 A70-25025

Combustion gases compositions and adiabatic flame temperatures of potassium seeded propane-air mixtures calculated at various equivalence ratios and temperatures assuming thermal equilibrium

12 p2330 A70-27227

Resonance radiation transport in optically thick plane gas layer with two-level atoms

12 p2305 A70-27853

Metals purity, gas content and porosity effects on nature and size of material zone affected by laser beam treatment

12 p2250 A70-28219

Acoustic and shock waves propagation in multicomponent media, assuming uniform speed for components and complex density dependence of media on pressure

14 p2566 A70-30709

Navier-Stokes equations derivation for multicomponent gas with internal nonrotary degrees of freedom, using moment equations

15 p2672 A70-31649

Metals purity, gas content and porosity effects on nature and size of material zone affected by laser beam treatment

20 p3643 A70-40094

Premixed laminar flames of hydrogen, oxygen and nitrogen burned on Meker burner, investigating diffusional effects on gas composition changes

20 p3739 A70-40469

Atmospheric pressure hydrocarbon-air mixtures confined by thin plastic membrane, obtaining composition range for detonation initiation limits

21 p3865 A70-40884

Dynamic spacecraft cabin atmospheres for extended operation, discussing gas composition, weightlessness and various stress factors

22 p3980 A70-43643

Limit analysis for ionization potential reduction effect on ionized gas atomic composition, considering temperature and electron density

23 p4220 A70-44435

Flow-through carbon dioxide lasers population inversion relation to individual gas components and electron velocity distribution functions

24 p4352 A70-45458

GAS COOLED REACTORS

NT HIGH TEMPERATURE NUCLEAR REACTORS

Nuclear light bulb reactor and coaxial flow reactor for gas core nuclear rocket engines [AIAA PAPER 70-708] 16 p2949 A70-33532

GAS COOLING

Foreign gas injection and slot geometry influencing film cooling effectiveness 01 p0219 A70-11182

Brazed plate-fin superalloy panels suitable for hydrogen-cooled structures, discussing fabrication techniques, performance tests and pressure containment and fatigue characteristics 02 p0306 A70-11930

Subsonic, transonic and supersonic laminar boundary layers acceleration and cooling effects, discussing heat transfer and gas enthalpy 12 p2211 A70-27830

Injection slot geometry effect on gas film cooling, discussing effect of secondary stream acceleration 21 p3952 A70-42084

GAS DENSITY

Hydrodynamics, mass and energy transfer equations for moderately dense gases multicomponent mixtures, using Bogoliubov theory 01 p1146 A70-10129

Thermospheric structure and variations obtained from satellite drag data analysis, discussing gas density, temperature and atmospheric composition 01 p0077 A70-11203

Interstellar neutral hydrogen flux effects on atmospheric hydrogen density, considering annual and semiannual density variations 01 p0186 A70-11207

Particle velocity distributions in low density supersonic jets measured by molecular beam sampling technique and multidisk velocity analyzer 02 p0276 A70-11849

Recombination instabilities in plasmas and gases undergoing density changes through volumetric processes, solving linearized and nonlinear cases by simplified fluid mechanics equations 02 p0348 A70-12238

Acoustic and shock waves propagation in multicomponent media, assuming uniform speed for components and complex density dependence of media on pressure 03 p0465 A70-13329

Supernova light emitted from surrounding gas layer, describing gas density role in type I and type II events 04 p0748 A70-14590

Equation of state for neutron, proton and electron gas mixture associated with cold matter above white dwarf densities and below nuclear density 05 p0905 A70-15756

Neutrinos production by primary cosmic rays in rarefied and dense media, calculating spectra 05 p0899 A70-15963

Density effects on rotational temperature measurements in nitrogen by electron beam excitation, discussing emission intensity distribution 06 p1067 A70-18306

Density field around leading edge of blunted flat plate, using electron beam measurements in low density hypersonic wind tunnel 06 p0980 A70-18351

Nonlinear relativistic wave velocity distribution within spherical nucleus bounded by shock wave in superdense gas determined by Cauchy problem 08 p1484 A70-21403

Hydrodynamics, mass and energy transfer equations for moderately dense gases multicomponent mixtures using Bogoliubov theory 08 p1548 A70-21405

Simple molecules viscosity as function of temperature and density using empirical equation 09 p1731 A70-22292

Electrostatic shielding of nuclei Coulomb field during thermonuclear reactions in degenerate gases of arbitrary densities 11 p2087 A70-26578

Gas and electron density fluctuations in weakly ionized turbulent wake behind hypersonic spheres and cones 11 p1978 A70-26773

Mesosphere payload to measure neutral gas density, positive and negative ions concentration and mobility in D region 13 p2393 A70-28682

Interstellar hydrogen density around solar system from calibrated Lyman-alpha intensity measurements of Vela 7 13 p2489 A70-28894

Elastic scattering formation and decay of unstable particle gases, discussing density and corrections to chemical and nuclear statistical equilibrium equations 13 p2455 A70-29223

Acoustic and shock waves propagation in multicomponent media, assuming uniform speed for components and complex density dependence of media on pressure 14 p2566 A70-30709

Electroless traveling wave accelerator for wind tunnel use, determining gas stream density for subsonic and supersonic operation 16 p2889 A70-33868

Low Reynolds number flow inside Delaval nozzle, examining gas density and rotational temperatures by electron beam techniques [AIAA PAPER 70-810] 17 p3065 A70-34454

Kinetic theory of moderately dense gases, obtaining generalized Boltzmann equation 17 p3072 A70-35534

Earth Lyman alpha emission rates as function of atomic hydrogen column density in outer atmosphere, using Mariner 5 measurements 18 p3244 A70-36007

Kinetic effects of Barnett equations and slip conditions for continuous dense gas flows at small Knudsen numbers 18 p3239 A70-36256

Pulsar AP 2015 21 cm line absorption profile, indicating uniform density and temperature neutral H model invalid 19 p3518 A70-38026

Atomic hydrogen population distribution in far UV of comets 19 p3526 A70-38782

Cosmic ray superhigh energy electrons and neutrinos propagation in degenerate neutrino gas universe, considering gas density in cosmological models 20 p3700 A70-39593

Combustion driven Hall configuration MHD generator, discussing boundary layer analysis, gas density nonuniformity and electrode drop 20 p3566 A70-40003

Hydrogen emanation and distribution in metals and alloys by Nd hydrogen metal detection method 20 p3651 A70-40071

Schlieren method application in plasma diagnostics, obtaining density change of neutral, ion and electron gases 21 p3825 A70-40950

Molecular oxygen density and vibrational distribution in lower atmosphere, observing solar UV radiation absorption by satellite OSO-4 21 p3816 A70-41066

Mean density and temperature measurements in hypersonic Ti spheres wakes in nitrogen atmosphere, using electron beam fluorescence probes 21 p3745 A70-41754

Neutral interplanetary particle impact ionization of atmosphere, discussing density of neutral interstellar media near solar system 22 p4106 A70-43291

H II regions density-size relationship, using emission measurements and radio data 22 p4109 A70-43746

Binary gas mixture separation effects by centrifugation in cylindrical tube, calculating maximum radial concentration difference between wall and axis by numerical integration 23 p4181 A70-44206

Compressibility, viscosity and thermal conductivity of dense gases, examining high temperature and pressure effects 23 p4222 A70-44431

Oscillating vane and rotating disk pressure gauge theory, considering gas damping and density variations 23 p4198 A70-44948

GAS DETECTORS

Hydrocarbon gas detection using He-Ne laser radiation absorption, discussing detector electronics 17 p3107 A70-35520

GAS DISCHARGE COUNTERS

U COUNTERS

U GAS DISCHARGE TUBES

GAS DISCHARGE TUBES

Ceramic plasma containers construction by soldered seal technique for ion lasers, noting moly-manganese process 02 p0314 A70-12746

Gas laser frequency stabilization by employing Zeeman splitting in external discharge tube containing He-Ne mixture in alternating magnetic field 03 p0498 A70-13090

Discharge tube rotation effects on ring laser polarization, Q factor and radiation frequency 03 p0501 A70-13744

Cadmium vapor density distribution by cataphoresis in He-Cd laser discharge tube determined by side light measurements 06 p1084 A70-18613

Argon ion laser output powers dependence on discharge tube design and mirror reflection coefficient in emission line 08 p1511 A70-20541

Aircraft gas discharge displays, discussing segmented alphanumeric annunciator devices with field effect electroluminescent elements and incandescent lamps 08 p1493 A70-20671

Carbon dioxide molecules dissociation along tube length, measuring temperature drop behind shock front at various pressures and 4300 K 09 p1730 A70-22172

Ar ion laser performance improvement by using beryllia for sealed-off discharge tube 09 p1699 A70-23443

Carbon dioxide-neon-helium flowing lasers gain characteristics determined by transverse-discharge configuration 10 p1901 A70-24944

He-Ne laser noise caused by discharge current fluctuation and moving striation in long capillary tubes 12 p2245 A70-27272

He-Cd laser construction with quartz tube manufactured separately, describing flow-through processing 14 p2594 A70-30509

Ar ion laser gas discharge tube construction, using anodically oxidized directly cooled aluminum segments 19 p3444 A70-37567

Sealed-off carbon dioxide laser discharge deposits analyzed by mass spectroscopy 19 p3445 A70-37670

He-Ne laser with conical discharge tube, investigating transverse cross section geometry influence on power gain 19 p3449 A70-37845

Ionic and molecular gas lasers, discussing pumping, transitions, emission, discharge tube dimensions, cooling, pressures, optical elements and applications 19 p3449 A70-37851

Triangular ring laser polarization, using discharge tube with Brewster angle windows in optical circuit 20 p3639 A70-39084

Carbon dioxide-helium laser hollow cathode negative glow discharge amplifier, discussing construction and advantages compared to other excitation media and discharge structures 21 p3834 A70-40568

Low voltage slotted hollow cathode laser tube design with transverse discharge operation and uniform axial distribution of laser media, including metal vapors 21 p3834 A70-40571

Stable ellipsoidal plasma configurations in alternating electrode annular system, considering longitudinal magnetic field strength, electrode voltage and gas discharge chamber pressure 24 p4385 A70-45456

GAS DISCHARGES

NT RING DISCHARGE

NT TOROIDAL DISCHARGE

LF longitudinal waves propagation in DC gas discharge plasma, obtaining wave dispersion equation for various limiting gases 01 p0149 A70-10162

Critical magnetic fields, frequencies and spatial structure of ion-acoustic instability of HF induction discharge plasmas in hydrogen, Ar, He and Hg vapor 02 p0348 A70-12261

Static breakdown voltage of air and nitrogen measured under uniform field conditions for specific gas number densities, comparing results with Paschen law 03 p0528 A70-14086

Laser cavity structure for homogeneous transverse discharge in carbon dioxide-nitrogen-helium mixtures, discussing energy and power increase per unit volume 03 p0503 A70-14357

Ionization study of gas discharge parameters behind shock wave front produced by moving plasma pulse interaction with immovable gas discharge plasma 03 p0535 A70-14361

Electric discharges in low pressure Ar in external magnetic fields, studying charge in transport coefficients and drift due to MHD forces 04 p0724 A70-14529

Discharges in Ar flow in membrane shock tube at Mach 5, discussing plasma compression, shock wave position and effect on electrode region 04 p0725 A70-14534

Longitudinal pressure gradient measurement for DC discharges in He, Ne and Ar, investigating effects of gas purity, tube geometry, etc 04 p0671 A70-14995

Pulsed high current arc burning in hydrogen at pressures to 400 atm, discussing stability and discharge plasma parameters 04 p0729 A70-15224

Gas discharge avalanche breakdown in Si semiconductors, analyzing micropasmas, ionization coefficients, p-n junction voltage, electron and light emissions 04 p0731 A70-15494

Steady state plasma generation in metallic waveguide without dielectric container by cold cathode discharge in He 05 p0819 A70-15803

Charge carriers recombination and diffusion coefficients for confined gas discharge plasma obtained from data on radial particle distribution profile 05 p0888 A70-16330

Physical theory of ball lightning based on cooling air spheres models, calculating equilibrium composition,

GAS DISSOCIATION

temperature profiles, output radiation and mass density

05 p0843 A70-17102

Collective interactions and low density plasma instability in high current gas discharge showing influence on neutral gas breakdown in interelectrode space

07 p1354 A70-20317

Intense quasi-steady He plasma discharge stability in magnetic field measured by Langmuir and optical techniques

07 p1354 A70-20321

Anodic precursors of convergent cylindrical shock wave of z-pinch discharges in He and Ar

07 p1261 A70-20357

Transformed thermodynamics equations derived automatically by substitution codes, noting exceptions for real gas and discharge flow

08 p1597 A70-20918

Plasma display system characteristics and history, discussing gas discharge cell construction and behavioral mechanisms

08 p1499 A70-21688

Anodic electric layer in self sustaining discharge in transverse magnetic field with neutral gas burnout, studying neutral atom ionization probability

09 p1734 A70-22110

Inert gas glow discharge current change under laser radiation, investigating dependence on discharge region, gas and electrode material and configuration

09 p1696 A70-22484

Time delay between pulses of discharge current and ionized argon laser power as function of current and discharge pressure

09 p1697 A70-22847

Coherent radiation amplification factor for 0.63 micron wavelength in He-Ne mixture, noting dependence on discharge current for various pressures

09 p1698 A70-23304

Transient laser phenomenon /observations and evanescent localized glows/ related to dust raised by degassing and electrostatic glow discharges in gas phase

10 p1938 A70-24069

LF longitudinal waves propagation in DC gas discharge plasma, obtaining wave dispersion equation for various limiting gases

10 p1925 A70-25010

Carbon dioxide dissociation in flowing carbon dioxide nitrogen helium laser and effects of carbon monoxide on discharge properties

11 p2063 A70-26068

Microscopic behavior and excitational processes found similar in argon ion lasers with hollow cathode or conventional heated oxide cathode discharge

11 p2063 A70-26370

Gas mixture plasma ionized and heated by discharge and ejected into vacuum, considering nonequilibrium ionization calculation with gap between electron and heavy particle temperatures

11 p2092 A70-26732

Waveguide gas discharge indicator of transmitted microwave power, investigating sensitivity, discharge conditions, filler gas and pressure effects

11 p2020 A70-26807

Laser emission generation on sodium lines, studying pulsed discharge mechanism involving ion-ion recombination in sodium vapor and hydrogen mixture

13 p2425 A70-28600

Gas discharge gap preionization by thin preheated tungsten wire ignition without explosion, resulting in plasma turbulence prevention and radiation density increase

13 p2462 A70-28986

Shock waves in partially ionized gas discharge argon plasma, recording potential jump at wavefront

13 p2388 A70-29419

AC and DC driven gas discharge aircraft displays, discussing capabilities and applications

13 p2412 A70-29875

Hot-wire probe measuring He-air mixture velocity and concentration following He discharge from circular orifice, noting calibration method

13 p2412 A70-29990

Harmonic generation in gas discharge by frequency multipliers, assessing multipliers capabilities for millimeter wavelength operation

14 p2549 A70-30437

Shock wave propagation during moving pulsed plasma interaction with stationary gas discharge plasma

15 p2780 A70-32197

Electron energy loss per collision in Cs vapor discharge, measuring electric field and electron temperature by Langmuir probes

16 p2954 A70-33281

Electrothermal instability in nonequilibrium plasma interpreted in terms of generalized instability in gas discharge

17 p3139 A70-34550

Spacecraft flight systems voltage breakdown due to DC gas discharge, discussing occurrence and preventive techniques

17 p3053 A70-35164

Nonequilibrium plasma from pulsed discharge in crossed electric and magnetic fields

17 p3142 A70-35727

Gas discharge in longitudinal magnetic field, investigating instability of diffusion dominated positive column

20 p3677 A70-39112

Fugacities of HCl and HF compared with abundance in volcanic fumarolic emanations, indicating magma undersaturation

20 p3619 A70-39321

Homopolar device electric arc dynamics dependence on gas type, noting flow geometry-Hall effect competition

20 p3681 A70-40009

Dense plasma jet kinetic instabilities and heating in strong magnetic field

20 p3682 A70-40138

Gaseous neon plasma positive column electrons density and drift velocities measurements by Langmuir probe technique

20 p3683 A70-40163

Microwave propagation in circular waveguide containing inhomogeneous gas discharge plasma

21 p3785 A70-40630

Two probe electron energy distribution measurements in gaseous discharges with random and coherent oscillations, giving xenon results at low pressures

21 p3828 A70-41471

Apollo 11 fines gas evolution and physical changes via heat treatment, discussing Ar 40 anomaly, lava structure origin and oxidation rate

21 p3907 A70-41577

Carbon dioxide-He-nitrogen gas mixture pulsed discharge system afterglow gain measurements up to one atmosphere, using CW laser

21 p3837 A70-41719

Gas discharges - IEE Conference, London, September 1970

22 p4077 A70-42351

Carbon dioxide-nitrogen He discharge gas temperature measurements involving plasma refractivity determination by interferometer

22 p4049 A70-42366

Gas discharge positive column finite length effect on wave dispersion and instability, indicating critical magnetic field

22 p4079 A70-42374

Cs seeded Ar discharges electron energy distribution, discussing drift velocities, electrons elastic and inelastic collisions with ions and molecules, etc

22 p4081 A70-43198

Microwave characteristics in plasma of short discharges in low pressure cesium and mercury vapors, noting spectral and spatial distribution of microwave power and intensities

22 p4083 A70-43392

Hydrogen cluster beam discharges, determining transient plasma ion density from Stark broadening measurements of H beta line

23 p4228 A70-44939

Waveguide gas discharge indicator of transmitted microwave power, investigating sensitivity, discharge conditions, filler gas and pressure effects

24 p4317 A70-45179

GAS DISSOCIATION

Collision induced dissociations of 2000 eV diatomic O, N, CO and NO positive molecular ions as function of reactant ion internal energy

01 p0148 A70-11354

Dynamic behavior of dissociating homonuclear diatomic gas, deriving instability equations, proposing stability loss in transonic region

01 p0068 A70-11584

Carbon dioxide temperature distribution, absorption and concentration as functions of molecular dissociation behind shock wave determined by measuring IR bands intensity

01 p0069 A70-11623

Oscillations and decomposition of diatomic gas molecules at high temperatures during atom-molecule collisions, deriving kinetic equations for energy level changes

01 p0148 A70-11630

Oxygen molecules dissociation by molecular and atomic collisions in shock tube from measuring molecular O concentration behind shock wave front

01 p0149 A70-11632

Nimbus 3 satellite observations of near UV solar flux intensity and variability, describing instrumentation and measurement of radiation producing molecular oxygen photodissociation

02 p0291 A70-12295

Hypersonic flow in thermodynamic equilibrium of diatomic dissociating gas with power law shock, investigating self similar solutions of Van Dyke small disturbance equations

03 p0405 A70-12925

Atomic oxygen reaction with carbon dioxide and carbon dioxide dissociation in shock waves, using nitrous oxide decomposition for oxygen source

03 p0440 A70-13578

Molecular hydrogen destruction by reaction with carbon dioxide ion in Martian ionosphere, discussing conversion into atomic hydrogen

03 p0575 A70-13997

Dissociative attachment of low energy electrons in nitrous oxide as function of gas temperature

03 p0441 A70-14006

Equilibrium composition and thermodynamic functions calculated for mixtures of dissociating and ionizing high temperature gases from standard data

04 p0780 A70-14538

Equivalent pressure concept for breakdown processes and sparking voltage of gas moving at angle to electric field across uniformly stressed gap

05 p0881 A70-16000

Nitrous oxide molecular beam reflection and dissociation on tungsten surface at high temperatures from angular distribution measurements

06 p1004 A70-17493

Slope and shape of blood-gas dissociation curve as factor influencing pulmonary gas exchange in presence of ventilation-perfusion inequality

06 p0994 A70-17522

Attractive potential effects on free and bound particles distribution in dissociating gas, studying recombination reaction effects on gas kinetic structure

06 p1044 A70-18280

Kinetics of attack of SiC in monoatomic mixtures of N and O generated by microwave discharge dissociation

07 p1421 A70-19332

Dissociating hydrogen transport coefficients analysis compared with data calculated as function of temperature and pressure without allowance for ionization

07 p1338 A70-19654

Photodissociation of diatomic O and N molecules in far UV

07 p1338 A70-20052

Water vapor dissociation in dilute mixtures with Ar behind shock waves, studying OH concentrations using flash-absorption technique

08 p1548 A70-21355

Comet brightness outbursts monochromatic measurements for lifetime of parent gaseous molecules in solar radiation fields

08 p1575 A70-21373

Numerical solutions of one dimensional expanding flow of dissociating gas initially in frozen state for variations in recombination rate

08 p1484 A70-21531

Carbon dioxide molecules dissociation along tube length, measuring temperature drop behind shock front at various pressures and 4300 K

09 p1730 A70-22172

Forward and backward rate constants for diatomic recombination and dissociation in dilute gas

09 p1730 A70-22231

Water vapor high temperature dissociation kinetics in dilute mixtures with argon in shock waves

09 p1629 A70-22319

Shock heated molecular beams of argon, oxygen and mixtures with helium, measuring particle velocities and gas dissociation

09 p1733 A70-23180

State equation for entropy of dissociated air with enthalpy and pressure as independent variables for calculating gas dynamic processes on computers

10 p1966 A70-23839

Vibrational and dissociation relaxation effects on plane shock wave structure and supersonic flow around blunt bodies

10 p1801 A70-24150

Carbon dioxide dissociation effects on refractive index gradients and decay rates in pulsed carbon dioxide-nitrogen laser mixture

10 p1900 A70-24602

Thermal dissociation kinetics in chlorine pentafluoride over high temperature range

11 p1994 A70-25823

Carbon dioxide dissociation in flowing carbon dioxide nitrogen helium laser and effects of carbon monoxide on discharge properties

11 p2063 A70-26068

CO dissociation kinetics in Ar and mixtures of O in Ar by shock tube study using vacuum UV absorption

12 p2180 A70-26857

Coupled relaxation dependence on translational and vibrational temperature and number of modes in polyatomic gases, noting molecular dissociation

12 p2276 A70-27797

Oxygen cation electron dissociative recombination rate coefficient measurement during expanding oxygen flow in nozzle

12 p2276 A70-27802

Vibrational dissociation relaxation effects on chemical reactions, molecular energy and thermal quanta in air flow behind direct shock wave

12 p2213 A70-28232

Pseudo one dimensional dissociational nonequilibrium nozzle flows, obtaining equilibrium and nonequilibrium solution through similar transformation of governing equations

14 p2527 A70-30264

Molecular gases ionization and dissociation by low energy atoms, using mass spectroscopy on secondary ionic products of collisions

14 p2619 A70-30723

Gaseous monoxides dissociation energies and free energy functions tabulation for calculating partial pressures

14 p2545 A70-30902

Nonequilibrium dissociation effect on supersonic oxygen flow past inverted blunted cones at angle of attack, considering thermal fluxes and aerodynamic forces

15 p2671 A70-31496

Dissociating hydrogen transport coefficients analysis comparison with data calculation as function of temperature and pressure without allowance for ionization

15 p2828 A70-32691

Dissociation energy of gaseous TiN molecule at high temperature

15 p2695 A70-32748

Thermodynamic equations of state for dissociating and ionizing air in equilibrium, noting applications to vertical and oblique compression shocks [DGLR-70-026]

15 p2828 A70-32840

Fragment ion products velocity vector distribution for dissociative collisions of molecular ions with He

16 p2953 A70-33005

Gas breakdown produced by long wave IR pulsed radiation of carbon dioxide laser

16 p2928 A70-33655

Rocket chambers combustion products isentropic expansion effects within nozzle on dissociation degree, assuming shifting and frozen equilibria

16 p2963 A70-34341

Shock tube flow of dissociating oxygen with chemical relaxation using Lax method

17 p3070 A70-35243

Carbon dioxide electric discharge dissociation producing oxygen molecules

17 p3138 A70-35588

Perfect and dissociating gas nonstationary supersonic flow around sharp profile of finite thickness analyzed by linearization and method of characteristics

19 p3351 A70-37242

Carbon dioxide initial dissociation rates in glow discharges and gas mixtures at low pressures, using mass spectrometric sampling and plasma diagnostic methods

20 p3674 A70-39235

Diatomic fluorine dissociation energy by mass spectrometry

20 p3582 A70-39615

Self focusing schlieren observation in gas breakdown, discussing cubic polarizability of excited atoms in electron cascade due to laser pulses

21 p3835 A70-40594

Titanium dicarbide and tetracarbide vaporization at high temperatures, using Knudsen effusion method with mass spectroscopy, determining dissociation energies

21 p3773 A70-41274

Collision induced dissociation of nitric oxide and molecular oxygen ions at low kinetic energies, noting internal ionic excitation effects

21 p3773 A70-41398

Electron collisional detachment from negative fluorine ions in shock tube following nonequilibrium ion overshoot in CsF dissociation in argon, noting correlation with temperature

21 p3853 A70-41705

Equations for unsteady frozen nonequilibrium flow of dissociating and relaxing gas, using Lighthill ideal dissociating diatomic gas for aerothermochemical model

22 p4124 A70-42754

Threshold parameters of liquid and gaseous helium breakdown caused by ruby laser beam, noting Mandelstam-Brillouin scattering in liquid phase

22 p4051 A70-43465

Three body recombination and dissociation rate coefficients of nitrogen in Ar atoms heat bath, using modified phase-space theory

23 p4221 A70-44008

Dissociative nonequilibrium hypersonic flow of low density gas mixtures over flat plate in free stream, noting catalytic wall effect on flow field

23 p4135 A70-44604

GAS DYNAMICS

NT AERODYNAMICS

NT AEROTHERMODYNAMICS

NT HYPERSONICS

NT RAREFIED GAS DYNAMICS

NT ROTOR AERODYNAMICS

Moving gas with thermodynamic relaxation process, discussing bulk viscosity and application to shock structure calculations

01 p0063 A70-10927

Aerodynamic gas flame theory and computations, discussing diffusion burning, turbulent flow burning rate, Reynolds number effects, etc

01 p0217 A70-11006

Gas motion and heating by radiation behind shock wave front, noting ionization and radiation absorption occurrence

01 p0068 A70-11570

Soviet book on gas thermodynamics of solid propellant rocket engines covering combustion products equilibrium in nozzle and chamber, engine design, etc

02 p0353 A70-11690

Arc phenomena for producing interaction effects, discussing reflected shocks rarefaction waves and gas dynamics

02 p0345 A70-11863

Gas detonation dynamics associated with shock tube self ignition kinetics, noting chemokinetic factors role

02 p0397 A70-12024

Book on gas kinetics, treating experimental methods, reaction theories, transition state theories, complex processes, etc

02 p0251 A70-12058

Gas-stabilized electric arc heater electrical and gas dynamic parameters, studying velocity and enthalpy radial distributions and IV characteristics

03 p0531 A70-13386

Galactic bending dynamics, discussing omega and zeta motions coupling of neutral hydrogen in outer region

03 p0570 A70-13553

Formation of Maxwell and nonMaxwellian energy distribution in gases, noting reduction of time reversible to time irreversible equations

03 p0606 A70-13861

Gas dynamics analysis of explosion phenomena based on unsteady flow fields and thermodynamic properties of chemically reacting substance

03 p0607 A70-13922

Applied MHD and high temperature gas dynamics - Conference, Prague, May 1968

04 p0724 A70-14526

Ultrasonic beam scanning measurements in high temperature axisymmetric gas flow, discussing errors and use of numerical transformation methods

04 p0685 A70-14536

Difference methods application to supersonic gas flow past blunt body and unsteady axisymmetric flow past body of unspecified configuration, analyzing stability

04 p0670 A70-14957

Unsteady problems of gas dynamics solved by method of characteristics, Godunov method, difference methods, etc

04 p0670 A70-14958

Method of integral relations, finite differences and method of characteristics applied to numerical solution of steady state problems of gas dynamics

04 p0670 A70-14961

Integral relations and finite difference methods application to problems of boundary layer equations in gas dynamics

04 p0670 A70-14962

Temperature distribution around radiating sphere in homogeneous gas medium with molecular heat transfer, solving energy transport equation

04 p0785 A70-15012

Gas dynamics of intense explosion with expanding inner contact surface in Newtonian limit, discussing shock layer reattachment

04 p0619 A70-15322

Nonlinear wave propagation in relaxing gas with internal energy characterized by translational and internal temperature, using model equation for piston induced motion

04 p0786 A70-15324

Real gas properties effect on base pressure of blunt nosed vehicle flying through atmosphere at high velocities

04 p0764 A70-15556

Gas dynamics theory with nonequilibrium radiative and collisional ionization applied to strong normal shock wave structure

05 p0831 A70-15870

Thermal and gas dynamic characteristics of aircraft turbine engine annular vaporizing combustion chamber determined from air distribution ratio

05 p0895 A70-15897

Thermal and dynamical evolution of gas clouds in transparent and opaque stages by comparing rates of cooling, heating, contraction and expansion

05 p0907 A70-16041

Gas dynamic functions using critical velocity and Laval number

06 p1033 A70-17237

Numerical methods for solving Boltzmann gas kinetics equation, assessing various methods effectiveness

06 p1036 A70-17752

Approximate solution to Boltzmann gas kinetics equation, using moment relations of collision integral and reverse collision operator

06 p1036 A70-17758

Motion of gaseous medium with uniform deformation with respect to three dimensional Cartesian coordinates

06 p1036 A70-17854

Gas dynamic effects of reaction center in explosive gas mixture analyzed by model and numerical computation

[AIAA PAPER 70-147] 06 p1181 A70-18144

Collision cross sections direct measurement for determining macroscopic reaction rates in inelastic molecular collision processes in gas dynamics

06 p1113 A70-18276

Boltzmann equation at arbitrary Knudsen numbers and kinetics of polyatomic molecule gases

06 p1047 A70-18310

Monte Carlo method applied to solving nonlinear Boltzmann equation for plane shock waves in elastic sphere gases

06 p1050 A70-18335

Density field around leading edge of blunted flat plate, using electron beam measurements in low density hypersonic wind tunnel

06 p0980 A70-18351

Explosive driver development with hypervelocity gas in thin walled tube surrounded by concentric cylinder of high explosive, discussing detonation wavefront propagation

07 p1248 A70-19098

Numerical method of characteristics for unsteady radiation gas dynamics, discussing surface pressures and heat transfer rates

[AIAA PAPER 68-163] 07 p1256 A70-19314

Carbon dioxide gas dynamic layer in shock tube facility, measuring shape, time, output energy, beam diameter, etc

07 p1301 A70-20021

Model for gaseous proto-galaxy collapse and formation of spherical galaxy

07 p1390 A70-20287

One dimensional difference scheme for gas dynamics with heat conduction

08 p1482 A70-20859

Two temperature gasdynamics for binary gas mixtures of differing molecular weight components, analyzing ultrasound and shock wave propagation

08 p1486 A70-21808

Kramer problem in kinetic gas theory and gas dynamics applied to Boltzmann equation, discussing uniqueness theorem [ONERA-TP-776]

08 p1486 A70-21845

Transparent gas radiation behind strong shock wave front with small pressure gradient due to energy losses

08 p1486 A70-21986

Plane one dimensional motion of shock wave with moving inner boundary investigated for given shock wave front position and gas mass and energy

09 p1659 A70-22432

Aircraft turbine engines strength and gas dynamic characteristics improved by vibration decrease using elastic elements

09 p1742 A70-22471

Nonlinear stellar density waves in galaxy using gas dynamic equations, assuming one dimensional and steady waves

09 p1762 A70-23073

Uniaxial strain pulse propagation through various materials loaded uniformly with step function pressure by gas dynamic shock wave reflection

09 p1783 A70-23449

Discontinuous weak solutions of differential equations of gas dynamics as limits in topology of functions

10 p1866 A70-24109

One dimensional fluid flows with shock waves described by constructing discontinuous solution for gas dynamic equations, using successive approximation

10 p1866 A70-24113

Excited gas kinetic state determination from observed spectral profiles during interaction with radiation

10 p1919 A70-24147

Plane exponential reactive shock waves following piston impact on gamma-law gas solved by similarity method, including Whitham conditions and shock acceleration

10 p1967 A70-24194

Gas dynamics regarding velocity field excited by vibrations propagating over elastic wing surface at finite velocity

10 p1803 A70-24779

Noncircular ionized gas motions in NGC 253 central region observed in velocity field analysis, indicating outflow from center

10 p1946 A70-24979

Electrostatic dynamic energy converter load current analysis, deriving expression for space charge electric field with axially varying or constant charge distribution

10 p1808 A70-25036

Gasdynamic test stand analyzing elastoplastic strains in aircraft gas turbine disks and liquid-propellant rocket engines turbopumps under alternating nonisothermal loads

10 p1862 A70-25298

Gasdynamic functions of supersonic flow past spherically and ellipsoidally blunted inverted cones

11 p1973 A70-25522

Gas passing through shock wave, investigating constitutive relations for stress and heat flux using Maxwell moment method

11 p2036 A70-26015

Gas dynamic processes insufficiency for triggering transition to detonation obtained from laser schlieren records of nonsteady flow field ahead of accelerating turbulent flame

11 p2150 A70-26378

Monograph on relaxation processes at high temperatures for thrust nozzle calculation and optimization covering real gas effects, reaction kinetics, heat transfer, etc

11 p2103 A70-26475

Reduced second virial gas coefficients calculations by modified Lennard-Jones intermolecular potential function

12 p2180 A70-26860

Acoustic and gas dynamic characteristics of jet noise muffler using adapters at outlet section of exhaust nozzle

12 p2160 A70-27295

Spectra, luminescence and gas dynamic effects in variable stars, discussing nonthermal theory to explain continuous emission

12 p2306 A70-27857

Gas with large radial velocity in radio galaxy NGC 1275, suggesting constitution of separate galaxy

12 p2308 A70-27870

Piston formed weak steady shock wave propagation in relaxing gases, investigating via characteristics method

[DFVLR-SONDDR-38]

12 p2212 A70-28206

Kinetic theory of gas composed of identical particles with discrete velocity distribution, using Chapman-Enskog method

12 p2213 A70-28211

Nonstationary pressure pulse acting on body in liquid or gas, discussing flow with unperturbed parameters at infinity

12 p2213 A70-28239

Stagnation point position as function of gas thermodynamic state behind detached shock for spherical segment at incidence in three dimensional hypersonic flow

12 p2159 A70-28247

One dimensional steady state flows and discontinuities in radiation gas dynamics, neglecting radiation pressure, viscosity and heat conduction

13 p2387 A70-28937

Book on interstellar medium covering gas dynamics, dust, magnetic fields and nonthermal radio emission, cosmic ray diffusion in galaxy, gravitational instability theory, etc

13 p2490 A70-28996

Jeans escape rate error for atmospheric H and He attributed to perturbed velocity distribution function, using realistic atom-atom elastic scattering cross sections

13 p2398 A70-29226

EGD energy converter system geometries for maximum power efficiencies, comparing slender conversion channels, abrupt expansion, free jet and divergent for operating characteristics

14 p2534 A70-30536

Periodic shock waves amplitudes and profiles, investigating longitudinal nonlinear oscillations of gas excited in closed tube

15 p2719 A70-31482

Gravitational compression of spherical cloud, determining asymptotic features of gas motion near center

15 p2808 A70-32882

Gas dynamic molecular laser with electrons in ground state, using incoherent optical pumping from stationary shock wave

16 p2927 A70-33255

Vibrational relaxation and energy transfer processes in gas dynamic flows, discussing cross sections, atom-molecule interactions, molecular rotation, kinetic equations, etc

17 p3068 A70-34670

Dusty gas dynamics, examining shock wave structure, boundary layers stability, flow equations, acoustic damping, velocity and density perturbations, etc

17 p3068 A70-34671

Collection of papers on gas dynamics covering hypersonic flow, rarefied gas and plasma dynamics, heat and mass transfer, etc

17 p3069 A70-35031

Steady and unsteady gas dynamics analogies with two dimensional water flow, taking into account energy and continuity equations

17 p3069 A70-35032

Hypersonic flow past slender bodies, discussing inviscid flows, outer edge singularity of boundary layer and three dimensional interaction on needle-like bodies

17 p3010 A70-35035

Adiabatic and chemically inactive hypersonic continuum flow around blunt body, analyzing flow field

17 p3010 A70-35036

Radiation gas dynamics, investigating thermal radiation effects on flow field of high temperature gas

17 p3195 A70-35038

Relaxation gas dynamics with chemical reactions, emphasizing differences and similarities with classical gas dynamics behavior

17 p3071 A70-35467

Gas dynamics of explosions and reacting systems - Conference, Novosibirsk, U.S.S.R., August 1969

17 p3074 A70-35882

Gasdynamic equations in Euler variables, constructing completely conservative difference schemes with first and second orders of approximation

18 p3241 A70-36288

Gas turbines dynamics and control system requirements, discussing equipment design and reliability [ASME PAPER 70-GT-76]

18 p3305 A70-36887

Neutral H concentrations far from galactic plane associated with spiral arms

18 p3327 A70-37166

Radial velocities of neutral hydrogen in anticenter region of Galaxy

18 p3328 A70-37170

Boltzmann equation for relativistic gas, adapting Grad solution method

19 p3403 A70-37584

Boltzmann equation for relativistic gas without dissipation, solving for relaxation time and elastic collisions

19 p3403 A70-37586

Relativistic kinetic theory of gases, considering phase space quantum statistics, Liouville equation, Boltzmann equation, conservation laws, kinematics, equilibrium distributions, etc

19 p3404 A70-37594

Soviet monograph on gas dynamics one dimensional problems in variable networks, discussing difference schemes, boundary conditions and discontinuities

19 p3407 A70-38930

Radiative gas dynamic equations similarity representation with spherical symmetry, constructing numerical examples for strong explosions and implosions

20 p3609 A70-39657

Gas dynamic functions of point explosions, determining flow parameters for instantaneous energy release in quiescent, inviscid, nonheat conducting perfect gas

20 p3612 A70-39821

Nonlinear free boundary problem for hyperbolic one dimensional gas dynamics equations

20 p3658 A70-40105

Book on nonuniform gas theory covering viscosity, thermal conduction, diffusion, Maxwell-Boltzmann equations, density, quantum theory, transport phenomena, mixtures, electric fields, etc

20 p3673 A70-40135

Axial pressure, electric current and potential distribution in two-phase particulate electrodynamic flow, discussing space charge electric field effect

20 p3683 A70-40257

Gas dynamic quantum amplifier improvement, discussing power utilization, photon distribution and radiation transport

21 p3836 A70-41418

Computerized evaluation of Krook kinetic relaxation equation approximating Boltzmann nonlinear integral equation for rarefied gas motion

21 p3851 A70-42201

Decelerated channel flow dynamics of ideal gas with supersonic velocity closed by compression shock, using finite difference method

21 p3747 A70-42203

Laser torch plasma dispersion gas dynamics from motion and kinetics of ionization processes

21 p3839 A70-42238

Perfect gas acyclic and cyclic, steady and irrotational motions in subsonic regime around convex profile with constant curvature variation by Chaplygin method

21 p3846 A70-42259

Relaxation gas dynamics, discussing vorticity and drag generation by relaxation, linearized theory and shock waves structure

23 p4178 A70-43889

Plane shock wave decay by interaction with simple wave, solving nonisentropic equations of gas dynamics

23 p4179 A70-43969

Gas dynamic molecular laser with electrons in ground state, using incoherent optical pumping from stationary shock wave

23 p4201 A70-44284

Shock curvature at wedge or cone tip in radiating gas flow, noting differences between radiative and chemically coupled gas dynamics

23 p4135 A70-44638

Relativistic gas bulk motion nonrelativistic equations, demonstrating spatially random fluctuations damp suprathermal hydromagnetic perpendicular propagation mode to interstellar magnetic field

24 p4397 A70-45761

GAS EVACUATING U. EVACUATING [VACUUM]

GAS EVOLUTION

Free gas formation in propellant systems and effects on attitude control systems

[AIAA PAPER 69-434]

04 p0763 A70-15418

Tribonucleation emphasizing viscosity-velocity product in gas nuclei formation and cavitation

12 p2170 A70-27661

Ethylene-propylene elastomers compatibility with hydrazine determined under ambient conditions from gas evolution rate by catalytic decomposition

13 p2472 A70-28669

Gases adsorption on water snows in cometary nucleus, noting sublimation rate role as regulating mechanism in gas production

14 p2650 A70-31244

Gas formation by sliding friction of self lubricating Teflon with carbon black on steel in ultrahigh vacuum, using mass spectrometry [DFVLR-SONDDR-54]

15 p2745 A70-32446

Ammonium perchlorate pyrolysis, investigating exothermic surface reactions and gasification rates

16 p2963 A70-33873

Photosystem II and oxygen evolution kinetics

24 p4305 A70-46411

GAS EXCHANGE

Pulmonary artery blood sampled before or during rebreathing of carbon dioxide in nitrogen mixtures, at rest and during exercise, discussing oxygen pressure changes

01 p0020 A70-10652

Airway resistance effect on ventilation and gas exchange during exercise, discussing minute volume and work of breathing response

03 p0429 A70-14157

Alveolar ventilation difference in nasal and oral breathing in hyperventilation due to work

05 p0802 A70-16492

Slope and shape of blood-gas dissociation curve as factor influencing pulmonary gas exchange in presence of ventilation-perfusion inequality

06 p0994 A70-17522

Prolonged hypodynamia effect on human external respiration, arterial blood oxygenation, circulation rate and gas exchange under various physical stress conditions

10 p1814 A70-24674

Pursed lips breathing effects on ventilation and blood gas exchange in patients with chronic airway obstruction

15 p2684 A70-32538

Human muscular function in conditioned and unconditioned thermoregulatory reflex changes of gaseous metabolism during repeated cooling

18 p3218 A70-36528

Gas exchange adaptation to heat and cold in rats with different ecological backgrounds

18 p3218 A70-36533

Gas metabolism in passerine birds adaptation to ambient temperature

18 p3219 A70-36536

Gas metabolism, chemical thermoregulation, body temperature and weight of rats during adaptation to repeated high temperature exposure

18 p3219 A70-36538

High temperature adaptation, gas exchange and thermoregulation in dogs during repeated overheatings in open sunshine

18 p3219 A70-36539

Gas exchange, body temperature and electrical activity of neck and back muscles of cold-acclimated white rats subjected to various temperatures

18 p3219 A70-36540

Repeated local spine cooling effect on gas exchange and electrical activity of white rats skeletal muscles

18 p3219 A70-36541

Adaptive recession of gas metabolism in rats during multiple high temperature exposures

18 p3220 A70-36545

Altered respiratory pattern effect on alveolar gas exchange in mechanically ventilated dogs after introducing end-inspiratory pause

21 p3766 A70-42156

GAS EXPANSION

Nonequilibrium effect of expanding water vapor condensation on supersonic nozzle flows with or without inert carrier gas

01 p0063 A70-10806

Transient energy transfer during expansion of plane layer of radiating gas bounded by strong shock, assuming LTE and perfect inviscid nonconducting gas

02 p0279 A70-12230

Difference method for calculating one dimensional nozzle flow and expansion with allowance for relaxation, friction and heat losses, discussing fluorine-hydrogen mixture application

03 p0408 A70-13804

Monatomic gas steady expansion into cylindrical vacuum, considering Maxwell molecules with cylindrical symmetry

04 p0674 A70-15557

Plasma gas jets high velocity propagation, studying radiation precursor and divergence and expansion chamber effects

04 p0675 A70-15594

Time dependent expansions into vacuum of monatomic gases with spherical symmetry, obtaining moments expressions for Maxwellian molecules

05 p0831 A70-16015

- Temperature at end of admission process and exhaust gas temperature in cylinder of internal combustion engine using reversible adiabatic hypothesis
06 p1173 A70-17629
- Exhaust plume from underexpanded sonic and supersonic nozzles including boundary mixing analyzed by approximate model to predict Mach disk location [AIAA PAPER 70-229]
06 p0972 A70-18135
- Isentropic model for time behavior of steady spherical source expanding into arbitrary ambient gas [AIAA PAPER 70-232]
06 p1042 A70-18215
- Species spatial distribution measured for He-Ar gas mixtures expanding in supersonic jets, compared to measurements with skimmer-nozzle arrangement
06 p1066 A70-18256
- Nitric oxide free jet expansion, studying molecular cluster formation, inhibition and chemiluminescence
06 p1044 A70-18281
- Boltzmann equation fourth moment numerically solved to study distribution function characteristics during monatomic gases spherical expansions into vacuum
06 p1048 A70-18320
- Shock wave profiles in rarefied gas expansion flows, using static and impact pressure probes
06 p1052 A70-18386
- Numerical solutions of one dimensional expanding flow of dissociating gas initially in frozen state for variations in recombination rate
08 p1484 A70-21531
- Hypersonic spherical gas expansion into finite pressure region with transition from supersonic to subsonic flow in shock wave, discussing structure and pressure effects
09 p1658 A70-22116
- Arc driven shock tunnel operation with expansive area change at main diaphragm, evaluating flow characteristics
09 p1657 A70-23279
- External supersonic potential flow effects on turbojet engine ring and needle nozzle performance, considering gas overexpansion operation
10 p1930 A70-24286
- Comets ionized shells, studying plasma expansion in corpuscular solar wind magnetic field
10 p1940 A70-24372
- Wall heat transfer effect on expansion following Chapman-Jouguet detonation wave, calculating pressure and gas velocity profiles from friction coefficient
10 p1869 A70-24423
- Deuterium plasma expansion resulting from thermal shock produced by laser impulse
10 p1923 A70-24526
- Chemiluminescence from NO adiabatically expanded against supersonic H atoms stream in inert carrier
10 p1831 A70-24566
- Conducting gas unsteady efflux from plane tube into vacuum, determining time dependent position of expanding rarefaction wave fronts
10 p1924 A70-24569
- Tapered resonance tubes matching supersonic air jet geometries considered for explosion hazards created by pneumatic system seals failure
11 p2035 A70-25981
- Population inversions in rapidly expanded flows of nonequilibrium gases, discussing kinetic processes in cooled mixtures of shock heated nitrogen and carbon dioxide
11 p2041 A70-26572
- Oxygen cation electron dissociative recombination rate coefficient measurement during expanding oxygen flow in nozzle
12 p2276 A70-27802
- Steady expansion flows at three dimensional supersonic edges with small corner angles using analytical method of characteristics
13 p2338 A70-28491
- Time and spatial evolution of shock and expansion wave evolution from density discontinuity for gas with repulsive delta function interaction between particles
13 p2388 A70-29224
- Variable temperature plasma with two ion species, noting rarefaction wave propagation during one dimensional expansion into vacuum
13 p2464 A70-29415
- Spherically symmetric state of slightly ionized gas of unbounded expanse about catalytic conductor by nonequilibrium continuum theory, analyzing Debye number limit for electrostatic probes
14 p2665 A70-30946
- Pentolite spherical charge gaseous explosion products expansion into vacuum, using Taylor similarity solution for flow in detonation wave
15 p2774 A70-31764
- Inviscid air nonequilibrium shock layer properties correlation based on plenum entropy, predicting composition of downstream converging-diverging nozzle expanding air flow
16 p2838 A70-33909
- Rocket chambers combustion products isentropic expansion effects within nozzle on dissociation degree, assuming shifting and frozen equilibria
16 p2963 A70-34341
- Underexpanded carbon dioxide free jet expanding into vacuum from conical nozzles
17 p3070 A70-35246
- Conical expansion nozzles manufacturing errors effect on flow expansion considered for large Mach numbers
17 p3011 A70-35662
- Magnetic storms development via initial asymmetric inflation of evening magnetosphere, using Explorer 26 and ground observatory data
18 p3311 A70-36008
- Knudsen effusion in free molecular flows in supersonic jet during expansion through circular orifice, discussing power and heat transmission
18 p3346 A70-36379
- Convergent-divergent nonequilibrium nozzle flow numerical solution by time dependent technique, investigating rapid vibrational nonequilibrium supersonic expansion of gas mixture with population inversion
20 p3609 A70-39655
- Moist air expansion through supersonic nozzle, investigating small ions role in water condensation
22 p4011 A70-42774
- Mathematical model for plasma expansion resulting from short energy pulse absorption
24 p4387 A70-45799
- ### GAS EXPLOSIONS
- Gas dynamics of intense explosion with expanding inner contact surface in Newtonian limit, discussing shock layer reattachment
04 p0619 A70-15322
- Gas dynamic effects of reaction center in explosive gas mixture analyzed by model and numerical computation [AIAA PAPER 70-147]
06 p1181 A70-18144
- Gaseous detonation transverse wave propagation and measurement from smoked foil records
07 p1424 A70-20006
- Projectile acceleration under gas explosion calculated for velocity
09 p1777 A70-22723
- High electron density plasma generation by ionized gaseous filament explosion, noting plasma frequency effect on spectral brightness
10 p1915 A70-23961
- Detonation in nonuniformly heated gas capable of chemical reaction, obtaining numerical solution
17 p3198 A70-35737
- Tetrafluorodibromo-ethane and bromethyl inhibiting effects on explosion development in constant volume container and flame expansion rates in hydrogen-air mixtures
18 p3345 A70-36241
- Gas dynamic functions of point explosions, determining flow parameters for instantaneous energy release in quiescent, inviscid, nonheat conducting perfect gas
20 p3612 A70-39821
- MHD measurements of gas flow velocity and boundary layer in oxyhydrogen explosions in detonation tube
21 p3942 A70-40876
- Atmospheric pressure hydrocarbon-air mixtures confined by thin plastic membrane, obtaining composition range for detonation initiation limits
21 p3865 A70-40884
- ### GAS FLOW
- NT AIR CURRENTS
- NT AIR FLOW
- NT CONTINUUM FLOW
- NT EQUILIBRIUM FLOW
- NT FREE MOLECULAR FLOW
- NT FROZEN EQUILIBRIUM FLOW
- NT JET STREAMS [METEOROLOGY]
- NT KNUDSEN FLOW
- NT MERIDIONAL FLOW
- NT MOLECULAR FLOW
- NT NONEQUILIBRIUM FLOW
- NT SLIP FLOW
- NT TRANSITION FLOW
- NT VERTICAL AIR CURRENTS
- Plastic deformation of wedge shaped model asperities influencing gas leakage between contacting surfaces, discussing critical contact pressure
01 p0060 A70-10267
- Heat and mass transfer in Couette flow of partially ionized symmetric diatomic gas for chemical equilibrium and chemically frozen flow cases
01 p0060 A70-10290
- Normal shock waves in frozen, partly frozen and equilibrium flow in gas-solid particle mixtures
01 p0065 A70-11100
- Plasma arc wind tunnel gas velocity measurement with electron beam probe using closed-loop electronic controller to stabilize beam position
01 p0092 A70-11195
- Rumanian book on shock tubes covering facility construction, gas flow, electronic measuring equipment, etc
01 p0059 A70-11379
- Compressible gas flow problem in point body gravitational field solved with reference to sun and interstellar gas
01 p0172 A70-11489
- Navier-Stokes equations for compressible gas, generalizing viscous channel flow of heat conducting gas to slip flow of rarefied gas
01 p0068 A70-11579
- Potential triple traveling space waves in barotropic gas with arbitrary equation of state, analyzing adjacent and three dimensional self similar flows
01 p0068 A70-11582
- Dynamic behavior of dissociating homonuclear diatomic gas, deriving instability equations, proposing stability loss in transonic region
01 p0068 A70-11584
- Hydrodynamic approximation to interplanetary gas motion influenced by solar flare caused perturbations
01 p0192 A70-11586
- Speed ratio of rarefied gas flows by molecular miniature pressure probes with orifice at thin cylindrical tube side, discussing LTE deviation regions
02 p0296 A70-11871
- Self similar wave solutions of continuity and momentum equations for two dimensional unsteady isentropic motion of polytropic gas
02 p0278 A70-11998
- Optical density measurements in high speed confined air vortex, discussing light deflection mapping of vortex density field at off axis positions [AIAA PAPER 68-694]
03 p0480 A70-12906
- Heat resistant coatings in high temperature gas flow, studying external layer deformation kinetics during shrinkage
03 p0483 A70-13250
- Fracture and degree of material removal of glassy body in hypersonic gas flow, considering radiant heat conduction inside body
03 p0516 A70-13391
- Mean volume heat transfer coefficient, mean thermal head and coolant temperature determined for gas flowing through porous wall with internal heat source
03 p0605 A70-13474
- Turbulence in hypersonic nozzle due to two phase flow of ideal gas and solid spherical particles, discussing thermal and dynamic differences
03 p0407 A70-13494
- Incompressible gas turbulent jet flow characteristics in subsonic wind tunnel, stressing pressure distribution in recirculation region for interpreting heat transfer in separated flows
03 p0593 A70-13495
- Rib-reinforced rectangular plate flutter in gas flow, considering shell stability, rib torsional rigidity, etc
03 p0593 A70-13498
- Carbon dioxide supersonic flows, describing numerical integration procedure for chemical and vibrational relaxation
03 p0440 A70-13743
- Supersonic unsteady gas flow around bodies at low Strouhal numbers, noting angle of attack amplitude and leading edge shock wave
03 p0409 A70-13865
- AD Herculis components as Algol system with gas flow based on observed absorption effects
03 p0577 A70-14100
- Boundary value problems for partial differential equations representing steady gas flow hydrodynamic problems
03 p0469 A70-14228
- Axisymmetric and three dimensional gas flow around blunt bodies using numerical methods, discussing finite difference algorithms for gas dynamic equations
03 p0410 A70-14251
- Natural oscillations and flutter of three layer cylindrical shell in supersonic gas flow analyzed by semimomentless theory, discussing boundary value problems, damping effects, etc
03 p0600 A70-14301
- Viscous compressible heat conducting laminar perfect gas flow in slender axisymmetric channels with adiabatic walls, using equations of motion
03 p0471 A70-14383
- Discharges in Ar flow in membrane shock tube at Mach 5, discussing plasma compression, shock wave position and effect on electrode region
04 p0725 A70-14534
- Nonlinear rarefied Couette flow with heat transfer in polyatomic gases, using kinetic theory of gases [ASME PAPER 69-WA/HT-39]
04 p0781 A70-14803
- Mass flow rate calculation of methane and natural gas mixtures through critical flow nozzles [ASME PAPER 69-WA/FM-4]
04 p0667 A70-14839
- One dimensional unsteady gas flows formation theories extended to include viscosity, heat conductivity, diffusion and chemical reactions effects
04 p0672 A70-15230
- Viscous gas self similar channel flow with heat transfer at wall corresponding to fixed Mach number profile in all channel cross sections
04 p0673 A70-15231
- Hypersonic viscous gas flow past power law bodies under viscous interaction between boundary layer and inviscid flow extended to slender bodies
04 p0618 A70-15240
- One dimensional steady adiabatic source nonisentropic flow of thermally and calorically perfect gas in

conical nozzle, considering exit divergence and nonuniform flow effects

04 p0619 A70-15427

Gas core nuclear reactors feasibility based on gas core hydrodynamics, heat transfer and neutronics development, noting spacecraft weight and trip time reduction potential

04 p0717 A70-15639

Ideal equivalent gas method for studying thermodynamic properties in supersonic gas flows behind shock wave

05 p0831 A70-15872

Equivalent pressure concept for breakdown processes and sparking voltage of gas moving at angle to electric field across uniformly stressed gap

05 p0881 A70-16000

Low Reynolds number flow of variable property gas past infinite heated circular cylinder at large temperature differences, measuring drag on cylinder

05 p0789 A70-16014

Sliding tube assembly for diverting carrier gas from flow pattern of Verneuil apparatus for flame fusion crystal growth

05 p0829 A70-16849

Unsteady laminar gas flow near infinite flat plate using Laplace transforms, obtaining closed form solutions for plate velocity and temperature

05 p0836 A70-17106

DC electric arc with superimposed axial subsonic gas flow breakdown voltage and anode heat transfer using high speed photography

06 p1177 A70-17697

Spatially homogeneous distribution function describing uniform gas motion derived to permit computer calculations in obtaining numerical solutions to kinetic equation

06 p1036 A70-17753

Water flow with solid particles, obtaining predictions for two component two phase gas flow

06 p1037 A70-17899

Cold ducted supersonic flow of premixed ethylene and air ignition by hot turbulent jet

[AIAA PAPER 70-148]

06 p1131 A70-18057

Time dependent inviscid gas flow on infinite domain computed by finite difference method

[AIAA PAPER 70-45]

06 p1042 A70-18188

Electron gun onboard reentering spacecraft to measure densities and temperatures in flowing gases

06 p1066 A70-18286

Interactions between hypersonic neutral gas beam and orificed pressure gauge in spinning satellite noting dependence on angle of attack

06 p1159 A70-18290

Monte Carlo method for modeling gas flow by simulated molecules concurrently followed through collisions and boundary interactions in simulated physical space within computer

06 p1113 A70-18314

Monatomic gas flow past moderate curvature body, obtaining approximate solutions to Boltzmann equation under form of matched asymptotic expansions

06 p0979 A70-18316

Transition regime gas flows using Navier-Stokes equations and boundary conditions set, considering heat transfer, torque and drag in spherical geometry

06 p1049 A70-18331

Thermal slip velocity of gas in infinite temperature gradient tangential to solid wall, basing calculation on linearized Boltzmann kinetic equation

06 p1049 A70-18332

Finite difference analysis of partial differential equations derived from Navier-Stokes equations in hypersonic leading edge problem in merged gas flow-layer regime

06 p0980 A70-18349

Shock wave profiles in rarefied gas expansion flows, using static and impact pressure probes

06 p1052 A70-18386

Radiating gas flows during hypersonic planetary reentry, discussing atmospheric composition, shock layer characteristics, nonequilibrium flows, etc

06 p0985 A70-18558

Nonequilibrium processes behind shock wave in shock tube supersonic air and nitrogen flow, using photoelectrical shadow method

06 p1053 A70-18562

Rarefied gas flow past sphere, using integral iteration method for Krook equation

07 p1187 A70-18675

Equilibrium forms of prolonged rectangular plate in gas flow in terms of nonlinear boundary problem, emphasizing plate with hinged supports

07 p1187 A70-18679

Turbulent friction in gas flow core determined on basis of maximum stability principle

07 p1253 A70-18719

Three dimensional hypersonic flow past body solved assuming developable surface head shock wave

07 p1187 A70-18767

Laminar flow of compressible gas in axisymmetrical channel in absence of wall insulation using velocity profiles, heat transfer, etc

07 p1253 A70-19062

Velocity fields and turbulent pulsations effects on heat transfer in gas flow past plate with rectangular protrusion using wind tunnel tests

07 p1254 A70-19063

Low density hypersonic flow over slender cone using air and He test gases

07 p1188 A70-19309

Asymptotic behavior of inviscid radiating gas flow near stagnation point of blunt body

07 p1188 A70-19315

Gas phase ignition theory of evaporating fuel in stagnant hot oxidizing gas as function of temperature

07 p1421 A70-19317

Current sheet pattern and gas flow stabilization in pulsed plasma accelerators

[AIAA PAPER 69-112]

07 p1348 A70-19322

Real gas behavior effect on shock tube temperature and pressure flow nonuniformity for range of Mach numbers

07 p1257 A70-19337

Sound waves dispersion and attenuation produced in gas flow by relaxation effects of solid particles presence

07 p1258 A70-19567

HF arc anemometer for subsonic and supersonic gas flow turbulence measurement

07 p1285 A70-19837

Earth ionosphere and magnetosphere electrodynamic state as function of neutral gas small scale motions, considering magnetic disturbances and ionospheric discontinuities

07 p1276 A70-20426

Boundary value problem solution in study of axisymmetric viscous heat conducting gas flow past body of revolution

08 p1431 A70-20854

Combustion kinetics in supersonic gas flows past various bodies, assuming exothermal and inverse recombination reactions behind adiabatic shock wave after induction period

08 p1596 A70-20855

Three dimensional gas flow calculated by direct method of characteristics

08 p1431 A70-20860

Gas flow influence on wave characteristics of thin viscous liquid layers pulled by gravity vertical surface compared with water layer experiments

08 p1482 A70-20917

Aerodynamic characteristics of nonconvex bodies in free molecular flow of monatomic gas

08 p1547 A70-21081

Infinitely wide plate bending at small angle of attack in supersonic gas flow, obtaining critical flow rate equal to divergence rate

08 p1588 A70-21175

Variational problem of determining optimal heat transfer from gas flow to porous plate boundary layer

08 p1597 A70-21176

Shock ionized Ar flow properties estimation using alignment charts

08 p1551 A70-21324

Dominant radiation field interaction with gas flow field using matched asymptotic expansion method

08 p1598 A70-21579

Navier-Stokes equations exact solutions for two dimensional steady flow of compressible viscous heat conducting perfect gas

08 p1485 A70-21638

Gas flow in pipe with uniform wall heat flux, analyzing turbulent heat transfer using heat balance equation

[ASME PAPER 69-HT-H]

08 p1486 A70-21834

Aerothermochemistry of two phase flow in gaseous media of solid or liquid particles or spherical gas pockets

[ONERA-TP-691]

08 p1600 A70-21848

Gas flow in arc heaters, discussing dissociation, ionization, swirl flow, arc discharge, gas temperature/pressure ratio, gas composition, etc

08 p1554 A70-21925

Continuous generation of gas trace component quantities into carrier gas flow using dosage device

09 p1672 A70-22028

Natural oscillation frequencies of subsonic gas flow past plate array, solving eigenvalue problem by splicing method

09 p1603 A70-22117

Local heat transfer to gas mixed with graphite particles described for variable temperature differences and wall temperatures

09 p1787 A70-22174

Survey of papers on computer calculation of two and three dimensional gas flows, emphasizing method of characteristics and finite difference techniques

09 p1603 A70-22265

Steady laminar gas flow on duct wall boundary layer considering external swirling flow and wall heat transfer

09 p1659 A70-22428

Steady turbulent perfect compressible gas flow in axisymmetrical or plane channel, using equations governing channel height and static pressure variations

09 p1659 A70-22429

Energy losses in gas turbine flows ascribed to combined exhaust and internal losses, noting usefulness of entropy loss concept

09 p1743 A70-22659

Magnetic field and gas thermal conductivity effects in analysis of solar wind as one dimensional, steady and spherically symmetric flow

09 p1745 A70-22687

Relaxation time influence on mass output calculation errors for gases in small diameter sonic nozzles

09 p1604 A70-22841

Macroscopic properties of thermal molecular flow between coaxial cylinders and concentric spheres, using transpiration theory in Knudsen gas

09 p1788 A70-22906

Dissociative-recombination rate coefficient measured for dissociative recombination reaction in inviscid nozzle flow of reflected shock tunnel, using high temperature and pressure nitrogen

09 p1737 A70-23225

Fluidic vortex valve to modulate solid propellant generated hot gas flow

[AIAA PAPER 69-424]

09 p1743 A70-23249

Laminar boundary layers behavior in shock tube flows behind primary moving shock wave using perturbation method

09 p1662 A70-23281

Population inversion generation through gaseous oxides mixing with nitrogen flow thermally excited

09 p1700 A70-23569

Heat transfer from circular cylinder in rarefied gas flow at low Mach number, using B-G-K model of Boltzmann equation

09 p1791 A70-23582

Hydrogen 21 cm emission line in Pegasus region observed for motion of neutral hydrogen connected with II Per, discussing stellar radial velocity

10 p1937 A70-23944

One dimensional Navier-Stokes equations solution for viscous heat conducting gas flow involving spherical sink for finite pressure at infinity

10 p1865 A70-24104

Perturbed equations solutions for plane supersonic steady and nonsteady gas flows, considering propagation of perturbations in initially nonstationary main flow

10 p1866 A70-24107

Inverse blunt body problem using integral relations method assuming inviscid axisymmetric hypersonic gas flow

10 p1798 A70-24116

Three dimensional supersonic gas flow solution by numerical method of characteristics, discussing direct and inverse tetrahedral and semicharacteristic schemes

10 p1798 A70-24117

Gas flow from nozzle into duct with enlarged cross section investigated for flow pattern and boundary conditions, noting oscillation behavior

10 p1799 A70-24123

Shock wave and gas flow structure at constant Mach number past three dimensional blunt bodies, applying method for unsteady flow

10 p1799 A70-24127

Transonic aerodynamics problems concerning plane and spatial rotational flows of perfect gas, discussing analytical and numerical methods

10 p1800 A70-24132

Supersonic gas flow past sphere investigated for characteristics using Fabry-Perot etalon

10 p1888 A70-24258

Molecular, viscomolecular and laminar gas flows in tubes and porous bodies at low pressures

10 p1869 A70-24287

Chaplygin function approximation in subsonic steady gas flow analysis

10 p1909 A70-24293

Model testing gas flow calculation in system emitting electron beam into atmosphere through supersonic gas seal

10 p1895 A70-24590

Hypersonic viscous interactions on insulated slender cone with mass injection assuming perfect gas flow and negligible transverse curvature effects

10 p1803 A70-24821

Gas flow rate measurement by repeated spark method suitable for stationary and nonstationary flows past surfaces of complex shape

10 p1892 A70-25119

Laminar flow of compressible gas in axisymmetrical channel in absence of wall insulation using velocity profiles, heat transfer, etc

10 p1871 A70-25213

Velocity fields and turbulent pulsations effects on heat transfer in gas flow past plate with rectangular protrusion using wind tunnel tests

10 p1871 A70-25214

Population inversions in rapidly expanded flows of nonequilibrium gases, discussing kinetic processes in cooled mixtures of shock heated nitrogen and carbon dioxide

11 p2041 A70-26572

- Electric arc column properties in channel gas flow, including electric fields distribution of potential and heat conduction function 11 p2092 A70-26729
- Electric arc in cylindrical channel gas flow described by boundary layer equations, assuming equilibrium and quasi-neutral media 11 p2151 A70-26730
- Heat exchange in linear vortex plasmatron with bilateral ejection, noting dependence on electrodes geometry and gas flow rates 11 p1984 A70-26737
- Carrier gas effect on homogeneous condensation in supersonic nozzle using liquid drop theory 12 p2211 A70-27829
- Shock wave reflection into ideal gas flow with linear density variation analyzed for flow field 12 p2211 A70-27832
- Carbon dioxide laser electrical discharge stabilization against transverse gas flow by cross magnetic field 12 p2250 A70-28099
- Turbulent and laminar heat transfer to gases in circular ducts entry region, considering various gas properties 12 p2212 A70-28114
- One dimensional perfect gas motion under spatial pressure distribution, investigating self similar solutions 12 p2212 A70-28189
- Vortex layer and entropy of supersonic gas flow past circular cones at incidence using surface velocity corrections 12 p2159 A70-28230
- Gasdynamic flows strong and weak density discontinuity surfaces determination, using shadowgraphs and interference patterns 12 p2238 A70-28248
- Monge equation in small perturbation method of characteristics applied to propagation phenomena in three dimensional supersonic gas flow 13 p2386 A70-28490
- Pressure measurements and gas flow analysis during thermal vacuum tests of manned spacecraft indicating adequate space vacuum simulation [AIAA PAPER 69-1033] 13 p2384 A70-28518
- Graphite mass removal rates under ohmic heating in reacting gas turbulent flows 13 p2519 A70-28579
- DC plasma arc jet excitation and emission characteristics for solution analysis with economical inert gas flow rates 13 p2362 A70-29107
- Steady diabatic complex lamellar gas flow, obtaining parameters by extending geometric theory of surfaces and curves in fluid flow theory 13 p2387 A70-29122
- Inviscid thermally nonconducting gas unsteady and steady motions in Laval nozzle of known geometry, obtaining solutions for subsonic, transonic and supersonic regions 13 p2391 A70-29756
- Rarefied gas flow in slip regime through cylindrical tube assuming parabolic velocity profile 14 p2565 A70-30263
- Radiating gas flow about pointed bodies, investigating shock curvature at wedge or cone tip and straight shock waves flow field downstream 14 p2663 A70-30267
- Gas transfer through silicone elastomer capillaries wall in variable pressure chamber 14 p2541 A70-30386
- He-Cd laser construction with quartz tube manufactured separately, describing flow-through processing 14 p2594 A70-30509
- Gas flow calculations application to gas turbines simulations, considering engine dynamics, one dimensional flow and program structure 14 p2629 A70-30990
- High temperature inviscid flow of ideal radiating gas, analyzing effects of radiation pressure and energy on flow field 14 p2666 A70-30999
- Rarefied gas flow past sphere, using integral iteration method for Krook equation 15 p2671 A70-31467
- Equilibrium forms of prolonged rectangular plate in gas flow in terms of nonlinear boundary problem, emphasizing plate with hinged supports 15 p2671 A70-31471
- Viscous gas hypersonic flow past blunt nosed bodies based on Navier-Stokes equation 15 p2671 A70-31481
- Subsonic and transonic gas flow in wake behind finite thickness plate based on Navier-Stokes equations 15 p2719 A70-31484
- Reinforced shells of revolution carrying capacity upper limit subjected to internal adiabatic ideal gas flow 15 p2814 A70-31534
- Internal shock waves in axisymmetric flowfield of perfect gas past blunt cone, noting roles of Mach number and cone half angle 15 p2672 A70-31592
- Hypersonic gas flow characteristics incident on elliptic paraboloid and triaxial ellipsoid at arbitrary angles of attack 15 p2672 A70-31647
- Superradiant pulsed 5401 A neon laser for interferograms of gas flow through nozzles in shock tunnel 15 p2750 A70-31763
- Aerothermopressor experiment in subsonic and supersonic gas flow compared with numerical solutions of equations 15 p2720 A70-31900
- Gas flow velocity measurement by coherent detection of scattered laser radiation from small particles suspended in fluid, using Doppler effect 15 p2751 A70-32030
- Electric arc in unbounded axisymmetric steady gas flow, solving energy equation 15 p2780 A70-32129
- Boundary layer equations for laminar flow, drag and heat transfer of gas in circular tube, considering parabolic and uniform entrance velocity profiles 15 p2722 A70-32692
- Laser Doppler velocimeter for measuring turbulence in gas and fluid flows 16 p2926 A70-33140
- Supersonic and hypersonic gas flow past blunt bodies, using finite difference and integral relation methods 16 p2890 A70-33244
- Stationary hydrodynamic equations of gas channel and nozzle flow with inlet tangential discontinuities 16 p2833 A70-33247
- Monograph on steady shock waves in one dimensional frictionless gas flows with thermodynamic relaxation, using continuum mechanics 16 p2891 A70-33294
- Gaseous flows and local droplet velocity measurement in dense gas/liquid sprayfields, using noninterference technique 16 p2910 A70-33491
- [AIAA PAPER 70-728] Maximum thrust nozzles design for rotational or nonequilibrium simple dissociating gas flows, including boundary layer effects 16 p2891 A70-33567
- [AIAA PAPER 70-707] Gas-wall heat losses reduced and heated gas pressurization systems performance improved by ullage mixing by gas flow from pressurant injectors 16 p2962 A70-33581
- [AIAA PAPER 70-681] Flow and diffusion phenomena in rarefied gas mixtures associated with separation nozzle process, using molecular pressure probe and mass spectrometer 16 p2893 A70-33699
- Experimental and numerical nonequilibrium shock layer around cones in hypersonic pure oxygen flows with simultaneous rotational, vibrational and dissociation relaxation [AIAA PAPER 69-136] 16 p2894 A70-33858
- German monograph on temperature distribution and motion of free burning arcs in transversal magnetic fields and gas flows, covering aerodynamic model concept 16 p2959 A70-34077
- Gas flow velocity measurement using hot foil probes 17 p3082 A70-34680
- Shock tube orifice effect on gas flow velocity and pressure drop, using pressure probes and Jenny friction formula 17 p3069 A70-34699
- Shock tube flow of dissociating oxygen with chemical relaxation using Lax method 17 p3070 A70-35243
- Supersonic electrically conducting gas flow in flat channel with dielectric walls in inhomogeneous magnetic field 17 p3141 A70-35334
- Heat transfer and friction drag calculation for turbulent boundary layer of gas with temperature dependent physical properties 17 p3012 A70-35729
- Heat and gas curtain efficiency in turbulent boundary layer on flat plate, including heat transfer data 17 p3198 A70-35731
- Viscous heat-conducting one dimensional piston driven gas flow, assuming sharp shock discontinuity 17 p3075 A70-35890
- Plane nonconducting elastic plate with one side impinged upon by supersonic conducting gas flow, determining magnetic field effect on flutter vibrations 18 p3336 A70-36135
- Hypersonic gas flow around blown plane of segmentally blunted cones at large angle of attack, using two dimensional model 18 p3206 A70-36258
- Laminar gas flow enthalpy determination in stagnation regions based on energy balance equation across separation streamline 18 p3240 A70-36266
- Unsteady two dimensional gas flow calculation axisymmetric shock tube of variable cross section, using numerical method 18 p3240 A70-36275
- One dimensional steady gas flow, deriving algorithm for iterative solution of Boltzmann kinetic equation by statistical approach 18 p3241 A70-36285
- Soviet book on passenger aircraft aerodynamics covering motions of gases and immersed bodies, similarity laws, boundary layer theory, finite span wing, etc 18 p3208 A70-36507
- Turbulent coaxial flow analysis predicting fuel volume fraction in gas core nuclear rocket reactor cavity, using free-jet computer code and eddy viscosity equation 18 p3290 A70-36560
- Radiative energy loss and wall sublimation effects on gas flow parameters behind reflected strong plane shock wave, taking into account small disturbances 18 p3348 A70-36673
- Method of characteristics for two dimensional steady supersonic gas flows with foreign particles in plane and axisymmetric nozzles 18 p3210 A70-37228
- Optimal control for one dimensional compressible gas flow, combustion and heat exchange, described by first order partial differential hyperbolic equations 19 p3402 A70-37240
- Conducting gas channel and jet flow in electric and magnetic fields, using linearizing equations of motion under assumption of small magnetic Reynolds number 19 p3479 A70-37598
- Multicomponent chemically unstable nonequilibrium gas flow past body, taking into account boundary layer behavior 19 p3373 A70-38182
- Heat transfer behind shock wave in air, oxygen or carbon dioxide flow past wedge, determining thermal fluxes vs wave velocity 19 p3405 A70-38188
- Heat resistant coatings in high temperature gas flow, studying external layer deformation kinetics during shrinkage 19 p3428 A70-38468
- Gas flow velocity measurement by thermal signal emitted from thin wire fed with modulated known frequency current 19 p3406 A70-38673
- Pressure and temperature distribution in constant volume viscous Poiseuille gas flow velocity profile 20 p3608 A70-39121
- Electrically conducting gas flow past slender body of arbitrary cross section in presence of crossed magnetic field by MHD Stokes approximation 20 p3558 A70-39613
- Three dimensional supersonic and hypersonic gas flow by Oseen equations, obtaining asymptotic flow field 20 p3609 A70-39656
- Optical image hologram production, investigating gas flows around body by means of Mach-Zehnder interferometer 20 p3633 A70-39761
- Laminar boundary layer equations on plate with arbitrary catalytic properties in diatomic gas flow undergoing vibrational dissociative relaxation 20 p3611 A70-39802
- High velocity gas motion in laminar boundary layer, describing universal motion equations two parameter solution 20 p3611 A70-39805
- Radiation field multidimensionality effect on radiating gas jet flow, taking into account radiative energy transfer by differential approximation 20 p3611 A70-39808
- Chemically active surface decomposition in dissociated gas flow with turbulent boundary layer, determining diffusion fluxes in laminar sublayer 20 p3612 A70-39812
- Flow rate, momentum and energy perturbations during gas motions through shock wave, discussing acoustic waves impinging from supersonic region 20 p3612 A70-39815
- Shock tube with diffuser in low shock wave Mach number range, considering gas flow models to relate wave intensity to initial conditions in chambers 20 p3606 A70-39820
- Heat fluxes from shock-heated gas to shock tube wall and wedge surface as function of Mach number, using platinum resistance thermometers 20 p3613 A70-40343
- Local variables in boundary layer of high temperature ionized gas flowing in magnetic field, using X ray absorption 20 p3613 A70-40344
- Turbulent gas boundary layer at finite Reynolds numbers, investigating relative changes in friction and heat transfer coefficients and temperature factor 20 p3614 A70-40390
- Gas flow rate measurement by repeated spark method suitable for stationary and nonstationary flows past surfaces of complex shape 20 p3635 A70-40512
- Axisymmetric detached shock before blunt body in hypersonic monatomic gas flow, obtaining radiative ionization patterns in cold precursor 21 p3950 A70-41731
- Interaction zone between gas flow and injected air jets, measuring turbulence characteristics by thermocanemometer 21 p3809 A70-41773

Viscous gas flow through Laval nozzle, calculating velocity coefficient and pressure recovery in contracting and expanding parts

21 p3746 A70-41774

Inviscid thermally nonconducting gas unsteady and steady motions in Laval nozzle of known geometry, obtaining solutions for subsonic, transonic and supersonic regions

21 p3811 A70-42074

Heat transfer from thin plate in compressible gas flow, considering interface temperature as nonanalytic function

21 p3953 A70-42086

Gas velocity and static pressure effects on evaporation rate of moving liquid fuel droplets

21 p3953 A70-42094

Self similar formulations for motion of radiating-absorbing perfect gas symmetric flow

21 p3954 A70-42202

Linear corrections formulas for shear stress and heat transfer coefficients associated with boundary layer blowing in binary gas mixture

21 p3748 A70-42207

Two layer gas flows in supersonic axisymmetric nozzles, using method of characteristics

21 p3748 A70-42210

Subsonic channel incompressible gas flow past semiinfinite flat plate base, using flow pattern for cavitation flow

21 p3748 A70-42213

One dimensional supersonic flow of ideal conducting gas in linear channel under transverse magnetic field

21 p3861 A70-42228

Perfect gas circular subsonic flow around convex obstacle, using hodographic method for boundary problem

22 p3958 A70-42608

Shock wave damping by perforated walls in gas channel, visualizing curved fronts with 24-spark HF camera

[SMPTE PREPRINT 104] 22 p4032 A70-43031

Spark tracing in gaseous flows in flames, wind tunnels, nozzles and pneumatic valves, using pulse transformer

[SMPTE PREPRINT 41] 22 p4033 A70-43041

Gas velocity measurement by high speed schlieren observation of laser induced breakdown phenomena

[SMPTE PREPRINT 27] 22 p4034 A70-43048

One dimensional perfect gas motion under spatial pressure distribution, investigating self similar solutions

22 p4012 A70-43314

Viscoelastic strip in gas flow, analyzing stability conditions

22 p4117 A70-43353

Potential flow around oscillating shell-plate structure subjected to supersonic gas flow at zero angle of attack, solving nonlinear aerelasticity problem

22 p4117 A70-43362

Isentropic gas two dimensional unsteady flow through channel contraction, using hydraulic analogy

22 p4012 A70-43438

Expiratory gas flow oscillations during forced vital capacity maneuvers in atmospheres of various composition and pressure

22 p3981 A70-43702

Controlled filling of container with compressed gas through time-variable cross section inlet, using variable mass thermodynamics

23 p4180 A70-44160

Internal shock waves in axisymmetric flow field of perfect gas past blunt cone, noting poles of Mach number and cone half angle

23 p4133 A70-44276

Steady irrotational gas flow characteristics calculation from finite difference scheme for three dimensional method of characteristics, considering supersonic nozzle flow

23 p4133 A70-44308

Reacting gas supersonic flow over two dimensional base, examining reaction rate effects on base pressure

23 p4135 A70-44626

Viscous compressible gas flows in pipe initial section, calculating friction and heat transfer coefficients

23 p4135 A70-44734

Turbulent nonadiabatic flow of compressible gas at inlet and main sections of variable cross section plane channel

23 p4183 A70-44739

Low Reynolds number gas flow past heated circular cylinder, considering Stokes region transport properties

23 p4284 A70-44978

Non-LTE radiative gas flow conservation equations

24 p4325 A70-45610

Simple wave functions solutions in multidimensional nonviscous polytropic gas unsteady and steady flow

24 p4327 A70-46030

Diabatic steady gas flow vorticity, examining various kinematic and kinetic properties

24 p4328 A70-46365

GAS GENERATOR ENGINES

U ENGINES

U GAS GENERATORS

GAS GENERATORS

Strong shocks and high temperature gases production using multistage gaseous detonation driven shock tube

02 p0274 A70-11855

Solid propellant cool gas generating systems applications to inflating emergency escape slides, rafts, pontoons and flotation bags

06 p0986 A70-17720

Cool gas inflation systems for evacuation equipment on large aircraft with size and weight fitting into aircraft doors

06 p0986 A70-17721

Continuous generation of gas trace component quantities into carrier gas flow using dosage device

09 p1672 A70-22028

Electrodynamic generator channel electric field model, evaluating electric body forces on ionized working fluid flow

10 p1807 A70-24571

Electrodynamic generator with spatial charge neutralization for direct thermal-to-electrical energy conversion at high gas pressures

12 p2165 A70-27330

Pressurization system for nitrogen generation based on hydrazine catalytic decomposition, describing metal membrane configuration, fuel additives, etc [AIAA PAPER 70-682]

16 p2962 A70-33583

High temperature and pressure hot gas source for testing fluidic temperature sensor used in gas turbine engine inlet simulation

17 p3058 A70-35157

Optimum adaptation of propulsion gas generators to power jet driven rotors with blown flap control, considering jet engine, fanjet and engine driven compressor

17 p3024 A70-35661

Solid oxygen generator for oxygen gas production from sodium chlorate decomposition, discussing reliability, safety and maintenance

18 p3225 A70-36211

Electrodynamic generator with spatial charge neutralization for direct thermal-to-electrical energy conversion at high gas pressures

21 p3760 A70-42071

Solid propellant cool gas generating systems, discussing development history, general capabilities and applications

22 p3962 A70-42297

GAS GUNS

Hypervelocity gas, electromagnetic, explosive drive and exploding wire accelerometers and high explosive, shaped charge, plasma drag and electrostatic accelerators for projectile impact studies

15 p2718 A70-32783

Gas gun and instrumentation for impact tests

18 p3238 A70-37090

Ames Hypervelocity Free Flight Facility, discussing aerodynamic tunnel, radiation tunnel and light gas gun for reentry simulation

22 p4006 A70-42764

GAS HEATING

Gas motion and heating by radiation behind shock wave front, noting ionization and radiation absorption occurrence

01 p0068 A70-11570

Thermal properties of neutral interstellar gas heated by low energy cosmic rays, noting role of electrons in heating processes

02 p0364 A70-11783

Electrical and thermal characteristics of stabilized gas heating by electric arc at high pressures calculated by successive approximation

07 p1350 A70-19840

Intense laser radiation effect on light absorption, gas breakdown and formation of spark at focus

10 p1899 A70-24154

Gas heating and ionization by Q switched laser beam, discussing electron collisions, density, etc

12 p2277 A70-27007

High temperature, electrically heated convective gas heating system for high velocity atmospheric flight simulation using air-nitrogen working fluids

12 p2205 A70-27100

Self heating accompanying exothermic decomposition of gaseous diethyl peroxide in spherical vessel measured positionally by thermocouple

12 p2330 A70-27223

Pulsed CO₂ laser calculating upper level lifetime of carbon dioxide molecule with allowance for gas heating at relaxation

12 p2251 A70-28296

Radiant gas heater for Brayton cycle space power system

[ASME PAPER 70-GT-36] 18 p3303 A70-36834

Interstellar gas thermal instability under cosmic ray heating, investigating perturbations causing transition to dense cool phase in pressure equilibrium with intercloud phase

18 p3309 A70-37003

Crab Nebula filamentary system, examining excitation conditions in terms of ionization and heating by HF radiation

20 p3702 A70-39011

GAS INJECTION

Hydrogen-oxygen variable length combustor longitudinal instability, studying hydrogen injection temperature effects on pressure interaction index and pressure sensitive time lag

01 p0214 A70-10324

Rocket engines gas/liquid injectors atomization characteristics using molten wax technique, considering drop sizes and gas streams velocity, density and pressure

01 p0161 A70-10326

Gaseous He bubbles injection into liquid propellant launch vehicle fuel lines to reduce vehicle pogo oscillations by lowering feed system natural frequencies

01 p0196 A70-10851

Foreign gas injection and slot geometry influencing film cooling effectiveness

01 p0219 A70-11182

Laminar isothermal entrance flows in circular cross section ducts with uniform mass injection at wall from boundary layer equations, discussing molecular weight effects

02 p0288 A70-12859

Porous wall material entrainment in turbulent boundary layer during supplementary inert gas injection, including nonisothermicity effects in heat and mass transfer equations

03 p0440 A70-13385

Optimization of control forces in rocket nozzles produced by multipoint secondary gaseous injection

05 p0923 A70-15889

Heat and mass transfer in reacting laminar boundary layer over porous cylinder with propane injection in wind tunnel experiments

05 p0956 A70-16289

Inviscid gas injection through flat plate in supersonic flow, obtaining self similar solution by integrating differential equation for stream function

05 p0791 A70-16963

Skin friction and heat transfer on flat plate in high velocity laminar motion with mass transfer for any free stream and injected gas combination

06 p1176 A70-17689

Residence time of foreign gas injected into recirculation region of wake behind slender body in axisymmetric supersonic flow

[AIAA PAPER 70-111] 06 p0968 A70-18040

Transpiration and film cooling systems comparison for high speed flows with foreign gas injection effects

[AIAA PAPER 70-153] 06 p1179 A70-18073

Base mass injection effects of various gases on slender body supersonic near wake stability, diffusion and cooling

[AIAA PAPER 70-110] 06 p0970 A70-18075

Helium injection Mach number effect on supersonic jet penetration into Mach 2 air stream from flat plate determined from concentration measurements

[AIAA PAPER 70-92] 06 p0975 A70-18200

Heat protection effectiveness of rectangular channel plane wall with flow by air injection through aperture on wall

07 p1420 A70-19066

Injectant stagnation temperature and molecular weight variation effect on flow field generated from secondary gas injection into supersonic stream

[AIAA PAPER 69-1] 09 p1733 A70-23217

Interaction shock shape prediction for gaseous and liquid injection in supersonic flow, using solid body and complementary models

09 p1662 A70-23244

Injection induced swirl effect on thrust and mass flow through nozzle in spinning rocket, discussing internal and exhaust flow measurements and visualization

09 p1606 A70-23247

Relative transition probabilities of Si I and II determined from emission spectra obtained by injecting SiCl₄ vapor into argon plasma jet

09 p1737 A70-23315

Velocity and concentration profiles for mixing of two dimensional foreign gas jet injected into parallel air mainstream, emphasizing film cooling applications

10 p1801 A70-24155

Heat protection effectiveness of rectangular channel plane wall with flow by air injection through aperture on wall

10 p1970 A70-25217

Characteristics and calibration of flow in gas induction driven close return transonic wind tunnel

11 p2030 A70-25687

Film cooling effectiveness measured following air injection through discrete holes into turbulent boundary layer of air on flat plate

11 p2146 A70-25690

Injectant stagnation temperature and molecular weight effects in jet interaction flowfield

11 p2036 A70-25989

Laminar multicomponent boundary layer for large injection and heat transfer, with particular reference to vehicle entry into planetary atmosphere

12 p2159 A70-28234

Gaseous injection into supersonic flow, investigating secondary Mach number and injection angle effects on flowfield in supersonic wind tunnel

[AIAA PAPER 70-552] 13 p2339 A70-29017

Cone boundary layer transition location and Reynolds number as function of nose bluntness combined effect with Ar, air and He mass injection [AIAA PAPER 69-706] 13 p2343 A70-29954

Surface pressure and heat transfer over blunt conical body in hypersonic flow with uniform mass addition of various gases [AIAA PAPER 69-716] 13 p2523 A70-29977

Chemically reacting stagnation point boundary layers with wall injection of gas, comparing multicomponent solution with binary approximation and chemical simplifications 14 p2565 A70-30265

Flow disturbances and side forces in supersonic rocket nozzle with O to gaseous secondary injection analyzed by semiempirical models 14 p2629 A70-30756

High velocity gas jet injection into subsonic and supersonic air streams from wall injectors [AIAA PAPER 70-714] 16 p2834 A70-33538

Uniform two dimensional turbulent boundary layer with hydrogen-nitrogen mixture injection and combustion at flame front, obtaining velocity distribution by kinetic energy equation 16 p2894 A70-33880

Numerical solutions for velocity and concentration profiles to nonsimilar isothermal diffusion laminar boundary layer equations for uniform injection of foreign gas 17 p3069 A70-34824

Shock waves in supersonic conical nozzle flow due to secondary gas injection, using conical lens for flow visualization 17 p3011 A70-35236

Heat exchange in dissociating partly ionized gas flow over critical point on permeable surface with injection into laminar boundary layer 17 p3011 A70-35347

Finite plate length effect on two dimensional supersonic turbulent boundary layer with large distributed surface injection 18 p3242 A70-36688

Film cooling protecting axisymmetric nozzle slot surface exposed to high temperature Mach 6 air injection 18 p3242 A70-36695

Helium injection Mach number effect on supersonic jet penetration into Mach 2 air stream from flat plate determined from concentration measurements 20 p3558 A70-39690

Pressure vessels charging procedure efficiency analysis 20 p3606 A70-39692

Load bearing capacity of radial gas bearing with annular injection line, discussing gas feeding methods 20 p3637 A70-39816

Gas lubrication with injection at large compressibility numbers, deriving asymptotic solution 20 p3637 A70-39817

Longitudinal averaged and pulsating turbulent flow velocities in rectangular channel with one-sided air injection through porous wall 20 p3614 A70-40346

Gaseous film cooling effect on adiabatic wall temperature distribution in rocket nozzle with gas injection 21 p3867 A70-41028

Reentry vehicle with multicomponent gas mixture injection, calculating heat and mass transfer correlations for stagnation point flow 21 p3945 A70-41033

Rocket roll control by secondary compressed air injection via slender fins inserted into nozzle convergent 21 p3931 A70-41953

Injection slot geometry effect on gas film cooling, discussing effect of secondary stream acceleration 21 p3952 A70-42084

Analytical evaluation of secondary flow injection effects on rocket engine performance including cold flow and simulated hot flow data [AIAA PAPER 69-473] 23 p4233 A70-44516

Gas coolant slot injection into hypersonic laminar boundary layer, comparing experimental results to boundary layer equations numerical integration 23 p4282 A70-44694

Coaxial plasma deflagration gun for accelerating particles to high velocities at low thermal energy for plasma injection experiments 24 p4383 A70-45120

GAS IONIZATION

NT ATMOSPHERIC IONIZATION

NT AURORAL IONIZATION

NT FLAME IONIZATION

Low voltage arc discharge in thermionic converter at low Ce pressures measured for current-voltage characteristics, showing degree of ionization 01 p0150 A70-10173

Total cross section for electron impact excitation and ionization in He, CO, nitrogen, oxygen, carbon dioxide, ethylene and benzene, emphasizing threshold values 01 p0147 A70-10489

Threshold laser power density-atom density relation in cesium vapor optical breakdown, suggesting two photon ionization process 01 p0110 A70-10569

Electron gas heating at E region altitudes as function of ionization of atmospheric gases, noting rocket experiments during solar eclipse 01 p0082 A70-11492

Gas motion and heating by radiation behind shock wave front, noting ionization and radiation absorption occurrence 01 p0068 A70-11570

Cross sections determined for formation of secondary positive molecular and atomic hydrogen ions during 1.4-46 keV positive molecular hydrogen passing through hydrogen 02 p0344 A70-12704

Ionizing shock wave propagation into magnetic field from Ar gas flow characteristics in electromagnetic shock tube 03 p0532 A70-13548

Ionization spatial growth similarity with Paschen law in air and nitrogen for specific electric field/gas number density values, discussing ionization coefficients 03 p0528 A70-14087

Shock tube measurements of ionization relaxation times behind shock waves in air at shock Mach numbers from 8 to 17 03 p0471 A70-14360

Hydromagnetic normal ionizing shock wave properties in H and D mixtures and pure gases in SUPPER 2 shock wave tube 03 p0536 A70-14365

Reflected shock wave velocity, boundary layer disturbance and wall ionization measurements using thin film resistance thermometers 04 p0666 A70-14537

Equilibrium composition and thermodynamic functions calculated for mixtures of dissociating and ionizing high temperature gases from standard data 04 p0780 A70-14538

Neutral gas ionization and ion recombination effect on electrodynamic plasma acceleration in coaxial and flat electrode accelerators 04 p0728 A70-15222

Nitrogen ionization rate increase by admixing neutral molecules of electronically excited nitrogen, noting nitrogen decay controlled by spontaneous radiation and wall collisions 05 p0884 A70-15918

Slow electron attachment to O molecules forming stable O-ions, discussing formation rate constant 06 p1109 A70-17488

Equivalent excited-state temperature of high pressure plasma calculated for unequal electron and gas temperature, considering ion and electron recombination 06 p1114 A70-18634

Interstellar gas ionization and heating by background X radiation, studying neutral hydrogen density distribution between spiral arms and at galactic peripheries 07 p1383 A70-19401

Excitation, ionization and recombination rates for charged ions during collisions with electrons in solar corona assuming Maxwellian electron distribution 07 p1384 A70-19409

Hydromagnetic ionizing shock wave structure in electromagnetic fields, using model composed of strong adiabatic shock to translational equilibrium followed by ionization initiation 07 p1351 A70-19985

Note on Bell-Kington paper on Born total and differential cross sections for proton impact ionization of He 08 p1548 A70-21501

Electron ion recombination role in atomic collision process in rare gases ionization path, considering scintillation mechanism 08 p1549 A70-21815

Anodic electric layer in self sustaining discharge in transverse magnetic field with neutral gas burnout, studying neutral atom ionization probability 09 p1734 A70-22110

One dimensional flow field behind ionizing detonation wave in magnetic field using Chapman-Jouguet hypothesis, accounting for Alfvén speed 09 p1660 A70-22722

Intense laser radiation effect on light absorption, gas breakdown and formation of spark at focus 10 p1899 A70-24154

Laser beam ionization of gases, using proportional ionization counter 10 p1890 A70-24588

Quasars photoionization of intergalactic high density hydrogen gas to interpret absorption features absence, noting gas temperature 10 p1942 A70-24628

Low voltage arc discharge in thermionic converter at low Ce pressures measured for current-voltage characteristics, showing degree of ionization 10 p1925 A70-25018

Small parameter structure and propagation velocity of ionization front in gas, applying nonequilibrium plasma model and electron equation 10 p1926 A70-25191

Book on engineering aspects of MHD power generation, discussing working gas ionization and electrical

conductivity, incompressible conducting fluid motion in magnetic field, etc 11 p1982 A70-25525

Shock-heated noble gases total ionization times, considering recombination and atom-atom and atom-electron collisions 12 p2274 A70-26856

Gas heating and ionization by Q switched laser beam, discussing electron collisions, densities, etc 12 p2277 A70-27007

N and O ions electron impact ionization rates calculated from approximate cross sections 12 p2275 A70-27173

Ionization kinetics of Ar, Xe and Hg monatomic gas behind shock wave front at high temperatures 12 p2210 A70-27319

Gas discharge gap preionization by thin preheated tungsten wire ignition without explosion, resulting in plasma turbulence prevention and radiation density increase 13 p2462 A70-28986

Shock wave multiple ionization in hydrogen with impurities, discussing intensity and duration effects on electron temperature profile and ion concentrations 13 p2388 A70-29369

Inert gas ionization behind shock wave at high Mach numbers, using electrical conductivity and continuum emission measurements 13 p2388 A70-29380

Interstellar electron gas distribution and temperature, suggesting cosmic ray heating as main ionization source 13 p2495 A70-29796

Shock slip analysis of merged layer stagnation point air ionization, clarifying effects of reaction rates, species diffusion, etc 13 p2343 A70-29987

Ionization and metastable excitation in low energy collisions of ground state argon atoms formed by charge transfer 14 p2618 A70-30121

Molecular gases ionization and dissociation by low energy atoms, using mass spectroscopy on secondary ion products of collisions 14 p2619 A70-30723

Spherically symmetric state of slightly ionized gas of unbounded expanse about catalytic conductor by nonequilibrium continuum theory, analyzing Debye number limit for electrostatic probes 14 p2665 A70-30946

Gas ionization with hydrogen atoms in gravitational equilibrium at constant temperature in upper half space by instantaneous radiation burst in lower space 15 p2775 A70-31477

Electron-ion gas ionization, neutralization and ambipolar diffusion effects on F region vertical profile 15 p2730 A70-32090

Thermodynamic equations of state for dissociating and ionizing air in equilibrium, noting applications to vertical and oblique compression shocks [DGLR-70-026] 15 p2828 A70-32840

Axially symmetric detached shock preceding blunt body immersed in hypersonic monatomic gas flow, considering radiative ionization in cold precursor by differential approximation 16 p2839 A70-34252

Plasma diagnostic data from onboard Langmuir probes, reflectometers, antenna VSWR and beacon and telemetry attenuation for blunt body reentry flow field [AIAA PAPER 70-756] 17 p3008 A70-34495

Nonequilibrium air ionization in hypersonic viscous shock layers in flow about axisymmetric blunt bodies 17 p3008 A70-34501

Channeling and guidance of electrical breakdown streamer via laser induced gas ionization trail 17 p3108 A70-35905

Argon and helium breakdown induced by ruby laser 50-picosec pulse at various pressures 18 p3267 A70-36616

Interstellar H I gas physical conditions, discussing ionization ratio average values and temperature conditions 18 p3328 A70-37175

Stepwise ionization effect on electron distribution, transport and balance coefficients in low voltage low pressure neon plasma 19 p3476 A70-37555

Ionization relaxation behind reflected luminous shock front in argon plasma flow interaction with magnetic fields, using spectroscopic and streak interferometric observations 19 p3479 A70-37814

P autoionization states of helium and hydrogen negative ions, calculating widths and shifts 19 p3474 A70-38307

Crab Nebula filamentary system, examining excitation conditions in terms of ionization and heating by HF radiation 20 p3702 A70-39011

Preionization in Cs seeded Ar nonequilibrium plasma for MHD generators, examining discharge characteristics, recombination reactions, etc 20 p3680 A70-39991

- Hydrogen ionization and second quantum level excitation by collision with H atoms in ground state
21 p3852 A70-40596
- Nitrogen, hydrogen, oxygen and He total ionization cross sections due to electron impact
21 p3852 A70-40597
- X ray emission of hot dense intergalactic plasma, discussing evolution equation for temperature and degree of gas ionization vs red shift
21 p3877 A70-40702
- Axisymmetric detached shock before blunt body in hypersonic monatomic gas flow, obtaining radiative ionization patterns in cold precursor
21 p3950 A70-41731
- Spatial energy loss and ionization deposition distributions of fluorescent radiation emission induced by electron beam in nitrogen gas
21 p3853 A70-41913
- Ionization kinetics of Ar, Xe and Hg monatomic gas behind shock wave front at high temperatures
21 p3854 A70-42061
- Laser torch plasma dispersion gas dynamics from motion and kinetics of ionization processes
21 p3839 A70-42238
- Prebreakdown ionization growth in gases based on initial photocurrents production from high voltage uniform field electrodes
22 p4026 A70-42353
- Intense high ionization degree discharge plasma initiation at low gas pressures, using auxiliary discharge
22 p4078 A70-42356
- Molecular vibrational temperature dependence on electron and neutral gas temperatures and degree of ionization for plasma excitation in nitrogen
22 p4078 A70-42358
- Dissociated and ionized hypersonic flows of hydrogen heated by electric arc techniques, investigating flows in wind tunnel nozzles
22 p4011 A70-42759
- Optically thin plasma population and ionization equilibrium, taking into account heavy particle collisions
22 p4082 A70-43219
- Plasma generation by pulsed laser heating, investigating ionization effects on temperature
22 p4082 A70-43224
- Laser induced gas breakdown, considering plasma generation and properties
23 p4225 A70-44185
- Multiphoton gas ionization by coherent radiation, showing electron transitions role with gas ionization model
23 p4201 A70-44205
- Upstream gas photoionization caused precursor ionization effects on MHD switch-on shock structure
24 p4382 A70-45106
- Gas ionization with Q switched carbon dioxide laser radiation, determining breakdown threshold or minimum power density requirement
24 p4355 A70-46261
- GAS JETS**
- IR radiation absorption from carbon dioxide laser in supersonic gas jet, applying results to nitrogen-carbon dioxide gas dynamic laser action
01 p0148 A70-11123
- Gas jets collision flowing from parallel wall channels, applying solution to calculating geometrical characteristics or fluid jet amplifiers
01 p0011 A70-11569
- Structural characteristics of supersonic twisting underexpanded air jet, using filming and schlieren photography
04 p0618 A70-15246
- Sound vibrations effect on pulsation characteristics of turbulent gas jet
04 p0618 A70-15248
- Plasma gas jets high velocity propagation, studying radiation precursor and divergence and expansion chamber effects
04 p0675 A70-15594
- Unsteady calorimetric sensor for measurement of heat transfer between gas jets and solid targets
06 p1064 A70-17857
- Unified model for transverse gaseous jet penetration into supersonic stream agreeing with measured flow field properties
06 p0976 A70-18201
- [AIAA PAPER 70-93] Species spatial distribution measured for He-Ar gas mixtures expanding in supersonic jets, compared to measurements with skimmer-nozzle arrangement
06 p1066 A70-18256
- Translational relaxation in low density axisymmetric hypersonic free gas jet, describing transition from isentropic to free molecular flow
06 p1043 A70-18277
- Supersonic free jets condensation, examining kinetics of reactions in mono- or diatomic gases
06 p1044 A70-18282
- Roshko model cavity solution based on Falkovich method application to two dimensional permanent irrotational flow of subsonic gas jet
07 p1258 A70-19571
- Heat transfer from impinging gas jets on enclosed concave surface, noting self recirculation currents within cavity
07 p1425 A70-20413
- Metal cutting by gas jet lasers, discussing single and multimode lasers, carbon dioxide lasers, power and power density requirements, etc
08 p1501 A70-20470
- Supersonic gas jets applicability as vacuum locks for molecular fluxes at thermal velocity in magnetic trap
08 p1549 A70-20509
- Axisymmetric helium jet transition to turbulent flow in air slipstream, measuring temperature and velocity profiles
09 p1660 A70-22439
- M87 jet, using theoretical model and observed emission lines for heating, cooling, ionization, cosmic ray proton regeneration of optical electrons, X radiation, etc
09 p1754 A70-22501
- Velocity and concentration profiles for mixing of two dimensional foreign gas jet injected into parallel air mainstream, emphasizing film coating applications
10 p1801 A70-24155
- Coaxial plasmatron pulsation on intensity of heat exchange between high temperature nitrogen jet and axisymmetric body near critical point region of spherical bluntness
11 p1984 A70-26739
- Gas jet bounding of Ar arc column, providing high power/intensity light source
12 p2237 A70-28159
- Solid particles or liquid drops admixture effect on propagation of inhomogeneous turbulent gas jet, using Prandtl mixing length theory to estimate pulsation velocities
12 p2213 A70-28218
- Carbon dioxide jet plumes condensation on model nozzle in vacuum chamber, noting particle size and growth rate
13 p2523 A70-29983
- Gas kinetic pressure profile and mass density of propagating current sheet in argon pinch discharge, using piezoelectric transducer
14 p2624 A70-31041
- Schlieren optical method for measuring He jet penetration into supersonic flow
15 p2741 A70-32520
- High velocity gas jet injection into subsonic and supersonic air streams from wall injectors
16 p2834 A70-33538
- [AIAA PAPER 70-714] Unsteady incompressible planar gas jets with stable vortex street, investigating near flow field region to establish oscillatory component
19 p3404 A70-37799
- Sound vibrations resonant frequency relation to jet internal structure in gas jet stem radiator
19 p3354 A70-38658
- Solid particles or liquid drops admixture effect on propagation of inhomogeneous turbulent gas jet, using Prandtl mixing length theory to estimate pulsation velocities
20 p3612 A70-40091
- Extinction condition for diffusion flame formed from opposing coaxial gas jets
20 p3739 A70-40399
- Gravitational effects on laminar gas jet diffusion flame stability, including zero gravity environment
21 p3949 A70-41316
- Stagnation temperature of two phase nozzle gas jet containing solid particles on particle density and velocity
21 p3748 A70-42220
- Supersonic air flow interaction with transverse gas jet from plate orifice
21 p3749 A70-42222
- Computerized integral treatment of turbulent constant pressure mixing of two dimensional gas jet with atmosphere having different temperature and composition
22 p4011 A70-42755
- Trajectory equations for plane and three dimensional gas jets with arbitrary injection hole shapes in subsonic shear flow
22 p3960 A70-43365
- Low density gas jet from short circular cylindrical tube, calculating molecular flux radial density variation
22 p4076 A70-43430
- Space vehicle attitude control by cold gas jets, examining principles of operation, optimal conditions for gas consumption and gravitational and gyroscopic effects
23 p4261 A70-44662
- [MBB-UR-37-70-0]
- GAS LASERS**
- Population inversion induced in middle channel of cascade gas laser, using probability method
01 p0106 A70-10059
- Spectral efficiency of coaxial flash lamp pumping gas laser, noting dependence on geometrical and physical parameters of source and active body
01 p0106 A70-10061
- Gas laser beams divergence at various laser power levels vs resonator nonconfocality
01 p0106 A70-10062
- Ar ion laser with high discharge current density observed for working level populations by simultaneously measuring power gain and spontaneous emission lines intensity
01 p0106 A70-10063
- He-Ne laser heterodyne system evaluating dispersive effect in He-Ne laser, measuring dispersion as function of cavity loss, excitation level, etc
01 p0107 A70-10102
- Output power and gain saturation characteristics for high speed flowing gas molecular lasers, discussing electrically excited fluid mixing carbon dioxide laser
01 p0107 A70-10103
- Coherent short wave and UV radiation generation using continuous ion gas laser, discussing efficiency, stability and feedback effects
01 p0108 A70-10356
- Gas laser beams short time constant and thermal self defocusing following small spot focusing on thin dye sample
01 p0109 A70-10431
- Critique of double resonance theory in gaseous lasers, including correction regarding saturation parameter for small RF perturbations and line width dependence
01 p0109 A70-10432
- He-Ne gas laser simultaneous oscillation detection based on output power modulation due to variable path length element placed in cavity
01 p0109 A70-10434
- Critical impurity concentrations of He-Ne laser quenching determined with mass spectrometer, giving impurities molecular weight and ionization potential for input powers
01 p0110 A70-10491
- Helium-cadmium laser operation, using DC cathaphoresis to maintain spatially uniform optimal Cd vapor concentration
01 p0110 A70-10562
- Sulfur compound effects on carbon monoxide-nitrogen laser emission stability, obtaining continuous operation independently of tube quality
01 p0111 A70-10660
- Noise power spectrum characteristics for He-Ne laser as function of discharge characteristics, measuring effect of cold vs hot cathodes
01 p0111 A70-10745
- Gas laser technology, discussing light emission and absorption by gas discharges and basic properties of He-Ne, Ar ion and carbon dioxide lasers
01 p0112 A70-10875
- IR spectrometer scanning function measurement by gas laser
01 p0092 A70-10989
- He-Ne laser amplifier photon density, bandwidth and gain as functions of inversion and excited Ne atoms density
01 p0114 A70-11357
- High resolution silver halide photoemulsions by holographic resolvemetry using He-Ne laser to obtain interference patterns
01 p0095 A70-11633
- He-Ne ring lasers with plane mirrors investigated for amplitude and frequency characteristics at high gain operation at 3.39 microns
02 p0312 A70-12099
- Gas pressure differences and diffusion rates recording using He-Ne laser interferometer, discussing aerodynamic applications and avionic instrumentation problems
02 p0299 A70-12272
- Helium-neon laser wavelength calculations from spectral observations by Fabry-Perot etalon, proposing formulas to enhance accuracy
02 p0299 A70-12439
- Partial coherence in spontaneous Raman effect, using He-Ne laser source
02 p0313 A70-12465
- Brillouin scattering of hypersonic waves produced in liquid medium, using He-Ne laser light source
02 p0313 A70-12471
- Ceramic plasma containers construction by soldered seal technique for ion lasers, noting moly- manganese process
02 p0314 A70-12746
- Interferential picture visibility in turbulent atmosphere measured at large path differences with Michelson-Twyman-Green interferometer using He-Ne laser radiation source
03 p0498 A70-12869
- Pulse peak width of He-Ne laser with Ne filled absorbing cell in resonator found dependent on saturating field and Ne pressure in cell
03 p0498 A70-13089
- Gas laser frequency stabilization by employing Zeeman splitting in external discharge tube containing He-Ne mixture in alternating magnetic field
03 p0498 A70-13090
- Transverse mode controlled hydrogen Stokes laser oscillator optically pumped by pulsed ruby laser
03 p0498 A70-13153

- Frequency measurement for HCN laser at 0.357 and 0.311 μ m wavelength by mixing signal with backward wave tube harmonics 03 p0500 A70-13464
- Complex profile aspherical mirrors used in He-Ne gas laser to obtain single mode emission 03 p0500 A70-13465
- Sealed-off He-Cd laser construction, describing life test, noise, Cd transport characteristics and transverse magnetic field effect 03 p0501 A70-13582
- He-Ne laser using K-activated alumina cold cathode and coaxial construction, discussing output, low noise applications, construction and testing 03 p0501 A70-13583
- Nonlinear differential equations for determining radiation density of three level pulsed gas laser as function of power losses, active medium parameters and time 03 p0502 A70-13745
- Fabry-Perot resonator misalignment effect on TEM wave transmission coefficient in gas laser 03 p0492 A70-13749
- Gain interaction among oscillating modes of gas laser analyzed from rate equations viewpoint 03 p0503 A70-14208
- Measurement method for second and third order photon intensity correlation functions, using optical field produced by gas laser operating near oscillation threshold 04 p0700 A70-14686
- Optical effects in parallel glass fibers irradiated by He-Ne laser beam, studying resonance tunneling and periodic power repumping between fibers 04 p0702 A70-15215
- Polarization effects of helium-neon laser emission at 3.39 micron wavelength investigated in longitudinal and transverse magnetic fields 04 p0702 A70-15227
- He-Ne-Cd II laser operation modes for optimum pressure fill, obtaining red to blue outputs by varying current and/or temperature 04 p0702 A70-15366
- Ar laser as suitable source for LF heterodyne anemometry experiments through noise spectrum suppression under optimum conditions 04 p0702 A70-15569
- Pulsed Ar ion lasers at high currents, measuring plasma parameters, electrical conductivity, electron temperature and density for inversion mechanism 04 p0703 A70-15617
- Spectral and lasing characteristics of microwave frequency modulated He-Ne laser operating at 0.63 micron wavelength 05 p0858 A70-16257
- Power output of gas laser pumped by laser contained in single resonator 05 p0858 A70-16259
- Gain measurement in He-Ne laser based on small modulation of discharge current 05 p0859 A70-16267
- Secondary frequency standard obtained for Hg laser operating at microwave frequencies 05 p0859 A70-16271
- Monograph on He-Ne laser beam noise properties and intensity fluctuations during single mode operation 05 p0860 A70-16559
- Frequency response of 6328 A He-Ne laser interferometer analyzed for multimode oscillations noting plasma diagnostics applications 05 p0861 A70-16989
- Laser signal modulation at RF by subjecting emitting atoms of Xe-He laser amplifier to simultaneous DC and RF magnetic fields 06 p1079 A70-17191
- He-Ne laser emission attenuation coefficient relation to water content of artificial fogs for 0.63, 1.15 and 3.39 microns 06 p1079 A70-17209
- Modulation properties of stabilizing frequency standard for gas laser with signal control by separate absorption cells 06 p1079 A70-17440
- Amplitude and frequency characteristics of gas ring laser with optical feedback between oppositely moving waves amplified by reflecting mirrors 06 p1081 A70-17497
- Two cavity mode locking of He-Ne laser using electro-optic phase modulator 06 p1083 A70-17947
- Radiation from nonlinear polarization sideband in Ar lasers, discussing anomalous beat notes and mode locking phenomena 06 p1083 A70-17949
- Operational characteristics, spectroscopy and inversion mechanisms of noble gas ion lasers in light of plasma theories and atomic data [AIAA PAPER 70-82] 06 p1083 A70-18236
- Cadmium vapor density distribution by cataphoresis in He-Cd laser discharge tube determined by side light measurements 06 p1084 A70-18613
- He-Cd laser output improved by transverse magnetic field application 06 p1084 A70-18619
- Two mode gas laser behavior under external signal action showing mode locking possibility by combination frequencies due to medium nonlinearity 07 p1296 A70-18764
- Optical polygon calibration by interferometric method using He-Ne laser light source 07 p1297 A70-19227
- Self pulsation in He-Cd laser, noting decreasing number of modes effect on beat frequency stability 07 p1301 A70-20017
- He-Ne single frequency laser output characteristics at various active medium pressures noting emission polarization 08 p1511 A70-20517
- Longitudinal modes competition in He-Ne laser, studying effects of active medium isotopic composition and pressure 08 p1511 A70-20518
- He-Ne laser plasma vibrations and radiation power during active medium discharge excitation by DC current, noting characteristic energy hysteresis 08 p1511 A70-20519
- Radiation field photon density matrix for gas laser with ring resonator determined from double level atomic model, considering photon dispersion and wave reflection feedback 08 p1513 A70-21420
- CW laser operation at 10.6 microns in DF-carbon dioxide and HF-carbon dioxide molecular systems achieved by purely chemical means 08 p1513 A70-21539
- Pulsed nitrogen gas laser to obtain continuously tunable dye laser action to 3550 A with output at 3771 A in UV 08 p1513 A70-21553
- Single mode He-Ne ring laser lock-in threshold and output power relationships to frequency 08 p1514 A70-21692
- Statistical characteristics of Q switched He-Ne laser emission gain during transient process from subthreshold to superthreshold value 08 p1514 A70-21814
- He-Ne laser investigated for He and Ne population inversion as function of discharge parameters 09 p1694 A70-22006
- He-Ne laser emission in transverse oscillation mode, analyzing spatial and temporal coherence characteristics 09 p1694 A70-22135
- Collision effects on saturation of He line transition in He-Ne laser, determining power output dependence on cavity tuning and gas pressure 09 p1695 A70-22322
- He-Ne and argon lasers for measuring radar scattering cross sections of plane and three dimensional targets 09 p1632 A70-22405
- He-Ne laser emission modulation by varying discharge current, studying gas pressure effect and role of ballast resistor 09 p1695 A70-22411
- Microwave in-cavity modulation of helium-neon laser, obtaining frequency dependence of modulation depth 09 p1696 A70-22628
- Solid state and gas lasers industrial applications in machining and nonmachining areas, discussing limiting factors 09 p1692 A70-22706
- Pulse train transition in Nd-YAG and He-Ne lasers mode-locked by intracavity phase modulator 09 p1697 A70-22919
- CW water vapor laser line frequency measurements by beating with radiations from HCN laser in metal-on-metal point contact diode 09 p1697 A70-22925
- Laser frequency measurement and active and passive stabilization techniques, emphasizing HCN laser phase locking to frequency standard output 09 p1697 A70-22951
- Single mode output power at 6328 A spectral line during He-Ne laser oscillation simultaneously at 6328 A and 3.39 microns 09 p1697 A70-22957
- LEPR spectrometer with sample cavity as part of HCN laser for experiments with gases, noting improved sensitivity 09 p1698 A70-22991
- Axial mode gas laser radiation intensity fluctuations for plane and spherical light waves in turbulent atmosphere 09 p1636 A70-23137
- He-Ne CW and pulsed lasers operation, design and technology, describing measurement methods for output, beam divergence and radiation spectrum distribution 09 p1698 A70-23303
- Coherent radiation amplification factor for 0.63 micron wavelength in He-Ne mixture, noting dependence on discharge current for various pressures 09 p1698 A70-23304
- Mode coupling and intensity pulsations observed between two 6328 A He-Ne lasers through nonlinear gain characteristics of inverted population 09 p1699 A70-23363
- Laser action in 5d-6p electron transitions of neutral atomic iodine, measuring electron temperature and density 09 p1699 A70-23517
- Atmospheric phase jitter for He-Ne locked laser measured by retroreflector for half mile round trip 09 p1699 A70-23539
- Population inversion generation through gaseous oxides mixing with nitrogen flow thermally excited 09 p1700 A70-23569
- He-Ne laser Q factor modulator based on Fabry-Perot interferometer with alternating absorption 10 p1899 A70-24255
- He-Ne laser emission electro-optical modulation by three mirror optical cavity, considering structural and thermal stability and coupled resonators geometry effects 10 p1899 A70-24260
- He-Ne laser IR generation in three mirror mismatched resonator, using Fabry-Perot interferometer to study mode and lasing range frequency shift 10 p1900 A70-24265
- Carbon dioxide dissociation effects on refractive index gradients and decay rates in pulsed carbon dioxide-nitrogen laser mixture 10 p1900 A70-24602
- He-Ne laser amplifier in axial magnetic field, measuring Faraday rotation and gain for various input signal intensity values 10 p1901 A70-24945
- Doppler beat spectrum and modulation depth of He-Ne laser emission with backward beam reflected from moving mirror into resonator 10 p1901 A70-25123
- Tunable nitrous oxide laser cavity losses and absorption by carbon dioxide determined spectroscopically 11 p2061 A70-25361
- Mirror adjustment effect on transverse structure, time dependence and spatial coherence of pulsed UV molecular nitrogen laser emission 11 p2062 A70-25394
- Scanned beam holography reducing system stability time for hologram production with CW gas laser 11 p2050 A70-25639
- Cyanide gas lasers design for submillimetric region of electromagnetic spectra 11 p2062 A70-25735
- Foreign gases effects on He-Ne lasers IR emission, describing quenching due to positive column electron temperature decrease 11 p2062 A70-25826
- He-Ne optical laser CW operation under DC excitation, considering output power, discharge current, total pressure, mixture ratio, etc 11 p2062 A70-25827
- Auto-oscillatory regimes in annular gas laser under coupling due to scattering, considering mode competition 11 p2064 A70-26811
- Multiplicative modulation noise of helium-neon traveling wave laser amplifier at micron wavelength 11 p2020 A70-26816
- He-Ne laser noise caused by discharge current fluctuation and moving striation in long capillary tubes 12 p2245 A70-27272
- He-Ne lasers mode locking by self beat feedback between cavity modes, achieving nonlinearity control by circuit adjustment 12 p2245 A70-27273
- Emission spectrum of neon-helium laser receiving Doppler shifted signal from moving mirror, showing memory effect due to beat harmonics 12 p2246 A70-27352
- Emission spectrum of He-Xe CW laser with non-resonant feedback mode achieved with scattering agent and various mirror schemes 12 p2246 A70-27354
- Photoelectric receiver and light beam alignment in gas laser aerial photography, considering directrix rectilinearity verification 12 p2247 A70-27476
- Transient process statistical characteristics in He-Ne laser operating near excitation threshold with pronounced rise time oscillations of light wave field 12 p2247 A70-27507
- Saturation homogeneity ascribed to resonant photon capture in emission of neon laser 12 p2247 A70-27508
- Local losses distribution effect on intensity and opposing waves generation in ring gas laser analyzed in approximation of noninteracting modes 12 p2248 A70-27510
- Carbon monoxide, carbon dioxide and oxygen impurities effects on threshold current and output power of HCN laser 12 p2249 A70-27648
- Raman scattering by oxygen and nitrogen in atmosphere observed by using pulsed nitrogen UV laser 12 p2189 A70-28093

Submillimeter range HCN gas laser design and characteristics, noting single mode, linear polarization and output power

12 p2250 A70-28180

Automatic frequency control of single frequency He-Ne laser, tuning cavity length to extremum output power with Lamb dip

12 p2250 A70-28181

Maximum mode selection tuning of scanning interferometer with spherical mirrors applied to He-Ne laser spectrum analysis

12 p2250 A70-28182

Analog information transmission device using He-Ne laser radiation, discussing optical telemetric channel transfer characteristics for pulsed nanosecond analog signals

12 p2250 A70-28184

Annular gas laser, considering external periodic perturbation effect on difference frequency of oppositely moving waves

12 p2251 A70-28291

He-Ne laser optimal mixture component ratio for generating IR radiation at two wavelengths

12 p2251 A70-28293

Ruby and He-Ne laser radiation attenuation found due to scattering by gas molecules and aerosols from atmospheric spectral transparency fine structure studies

12 p2191 A70-28294

Q switched CO-HE laser IR fluorescence, considering population inversion recovery by vibrational energy transfer

13 p2423 A70-28496

Soviet collection of articles on gas laser physics, covering focusing, spectra, modes, resonators etc

13 p2424 A70-28591

Gas laser radiation focusing with spherical mirrors, calculating field distribution and beam path

13 p2424 A70-28592

Operator representing anisotropic element in gas laser resonator, considering phase crystalline and rotating plates

13 p2424 A70-28593

Anisotropic two phase plates gas laser resonator spectrum, analyzing zero or 90 degree angles between plates

13 p2424 A70-28594

Three mirror resonator He-Ne laser output spectra, studying frequencies and intensities of generated modes

13 p2424 A70-28595

Hanle effect in single mode He-Ne laser, observing spontaneous emission on different spectral lines and estimating lifetimes of Ne excited states

13 p2424 A70-28598

Spontaneous emission modulation, interference beat and level crossings observable in gas laser operating at two output frequencies

13 p2425 A70-28599

Power output dependence on cavity configuration of He-Ne laser in TEM mode operation

13 p2425 A70-28625

HCN laser 890 GHz line phase locked to multiplied standard frequency with wide bandwidth loop, narrowing line widths

13 p2426 A70-28798

High power CO lasers, discussing UV and visible sidelight, gas mixtures, spectral output, gas pressure, etc

13 p2426 A70-28807

HCN laser far IR line phase locked to absolute frequency standard

13 p2426 A70-28810

Dye laser small signal gain via pumping by UV nitrogen laser

13 p2426 A70-28811

He-Ne laser beam transmission through atmosphere, investigating intensity, spot size, polarization and power spectrum fluctuations

13 p2427 A70-29103

Gas laser active medium nonlinear polarizability calculations with allowance for resonance emission capture effect on atomic velocity and population distributions

13 p2427 A70-29284

Pulsed Ne laser superradiation spectrum fine structure, using Fabry-Perot interferometer

13 p2428 A70-29362

Homogeneous absorption line and peak power widths relationship in high resolution gas laser with internal absorbing cell

13 p2428 A70-29365

Electronic heterodyne astronomical spectroscopy, using lasers for absolute monochromatic flux and polarization measurements on star-like objects

13 p2408 A70-29473

He-Ne laser focused beam effect on negative Si diodes base I-V characteristics

13 p2378 A70-29517

He-Ne laser memory, discussing induced oscillation excitation with radiation fed back to resonator by moving reflecting mirror

13 p2429 A70-29572

Crossed field nitrogen laser operation in second positive band to obtain high UV pulse output

13 p2429 A70-29669

Laser acoustooptic quartz modulators inserted inside He-Ne and argon cavities for internal power extraction

13 p2430 A70-29705

He-Ne laser radiation absorption in dense Li plasma, calculating absorptivity for bremsstrahlung and photoionization

13 p2465 A70-29710

Continuous operation He-Ne lasers, discussing excitation, structural and optical design, mode selection and performance specifications

14 p2593 A70-30353

Pulsed molecular and atomic gas laser sources design for submillimeter region

14 p2593 A70-30433

He-Cd laser construction with quartz tube manufactured separately, describing flow-through processing

14 p2594 A70-30509

High voltage gas laser trigger pulse generators featuring high pulse rate with semiconductor controlled rectifier

14 p2594 A70-31181

Single mode gas laser theory for arbitrary field intensities in terms of ensemble averaged form of density-matrix equations of motion

14 p1594 A70-31361

Gas ring lasers, discussing optimal parameters, colliding waves interference, nonmutual effect and radiation polarization

15 p2749 A70-31451

Atomic collision effect on frequency range of opposing traveling wave modes in gas ring laser, using density matrix equation

15 p2749 A70-31553

False signal in scanning interferometer for helium-neon lasers in single and simultaneous TEM modes

15 p2749 A70-31557

Carbon dioxide-nitrogen and nitrous oxide-nitrogen laser systems, substituting diatomic N 15 for N 14 to investigate radiation intensity

15 p2750 A70-31761

Superradiant pulsed 5401 A neon laser for interferograms of gas flow through nozzles in shock tunnel

15 p2750 A70-31763

High power CW CO laser operation at room temperature by introducing mercury vapor into discharge

15 p2751 A70-31979

He-Cd laser with cathapboretic transport and diffusion return path, noting condenser critical temperature for radiation noise reduction

15 p2751 A70-31987

White light laser construction using Ar-Kr laser with suitable mixture and pressure of gases to provide equal output intensities of red, yellow, green and blue

15 p2752 A70-32046

Single mode gas laser with large saturation and dispersion effects, discussing resonator alignment to spectral line frequency

15 p2752 A70-32196

Plasma concentration measurement in coaxial accelerator, using gas laser and multiple wave interferometer in vacuum chamber

15 p2781 A70-32858

Bleachable dye filters selection for periodic undamped output power oscillations in laser

15 p2753 A70-32859

Gas dynamic molecular laser with electrons in ground state, using incoherent optical pumping from stationary shock wave

16 p2927 A70-33255

Gas laser amplitude, competition, self locking, beat frequency and modes time development, using Kutta-Merson integration method

16 p2928 A70-33284

He-Ne laser geodimeter for Coast and Geodetic Survey length measurements on continental traverses

16 p2928 A70-33525

Coaxial gas laser generating high intensity pulses at constant pulse repetition rate, using singly ionized Ar and molecular nitrogen as active media

16 p2928 A70-33698

Mode locked He-Ne laser nsec pulses propagation along multimode clad glass fibers

16 p2865 A70-34039

Light velocity from frequency and wavelength differences between gas laser lines, using precision long path interferometry

17 p3104 A70-35085

He-Ne laser emission wavelength long and short term stability for metrological applications

17 p3104 A70-35087

He-Ne laser emission wavelength, using laser interferometry based on feedback between moving mirror and resonator

17 p3104 A70-35088

Canadian laser stabilization program involving metrology and absolute standard replacing international meter

17 p3105 A70-35089

Spectral densities of intensity and frequency fluctuations of single frequency He-Ne laser radiation

17 p3105 A70-35092

Excited atoms transfer mechanism in helium plasma, using He-Ne laser

17 p3106 A70-35102

Gas laser components optical properties determination, describing measuring apparatus and techniques

17 p3106 A70-35104

Plasma opacity measurements using CW He-Ne and Ar lasers as light sources

17 p3106 A70-35107

He-Ne CW laser emission line width measurement, describing apparatus and technique

17 p3106 A70-35108

Pulsed plasmas refractive index measurement by two-wavelength He-Ne laser interferometry, estimating effects of heavy atoms and neutral gas density

17 p3107 A70-35110

Gas laser phase locking due to loss modulation with double mode spacing

17 p3107 A70-35474

Internally loss modulated multimode ring gas laser, showing pulse peak intensity with detuning for phase locking

17 p3107 A70-35475

Hydrocarbon gas detection using He-Ne laser radiation absorption, discussing detector electronics

17 p3107 A70-35520

Beat and synchronization modes of opposed waves in rotating gas ring laser, examining frequency response asymptotic behavior

17 p3108 A70-35683

Photodetector frequency response measurement, using beat light signals from mixed single mode He-Ne lasers

17 p3108 A70-35688

He-Cd laser discharge, determining population densities and lifetimes for levels of Cd ion excited by He metastables

17 p3108 A70-35903

Gas laser frequency stabilization using nonlinear effects of magnetic Lamb dip

17 p3109 A70-35911

Transverse flow CO chemical laser using atomic oxygen reaction with carbon disulfide, comparing output with longitudinal flow devices

18 p3266 A70-36313

Two mode gas laser behavior under external signal action showing mode locking possibility by combination frequencies due to medium nonlinearity

18 p3271 A70-37108

Gas laser radiation depolarization coefficient as function of radiation energy, cavity anisotropy and operating transition type

19 p3444 A70-37445

Gas lasers intensity expression derived by theory of double resonance spectroscopy, comparing results with He-Ne laser experimental data

19 p3445 A70-37672

Helium to electron excitation ratios for population inversion in helium-neon laser

19 p3445 A70-37758

Three level gas laser amplifier theory, considering quantum mechanical atomic system in interaction with two monochromatic EM waves

19 p3446 A70-37829

Plasma lasers, investigating striation oscillations and excess noise phenomena and generation mechanisms

19 p3446 A70-37858

Gas laser iterative alignment of Mach-Zehnder interferometer for monochromatic and white light fringes

19 p3424 A70-37880

Monograph on gas laser dynamics, emphasizing single mode intensity measurement as function of cavity loss in He-Ne laser

19 p3446 A70-37978

He-Ne laser beam hazard to human retina

19 p3371 A70-38309

Low noise He-Ne laser with capillary elements, measuring current threshold of noise free operation as function of design parameters

19 p3448 A70-38512

Transverse magnetic field effect on emission spectrum of He-Ne laser, using scanning interferometer

19 p3448 A70-38735

Pulsed laser emission at IR transitions of xenon and neon under electron beam pumping

19 p3449 A70-38743

He-Ne laser with conical discharge tube, investigating transverse cross section geometry influence on power gain

19 p3449 A70-38745

Ionic and molecular gas lasers, discussing pumping, transitions, emission, discharge tube dimensions, cooling, pressures, optical elements and applications

19 p3449 A70-38751

CW second harmonic He-Ne laser light second order intensity correlation function measurements

20 p3640 A70-39153

He-Xe laser with pure Xe-136 gain cell inside cavity, observing enhanced Lamb dip in power output vs frequency curve

20 p3640 A70-39154

He-Ne laser profile-tracing system for contour measurement, suggesting steps for error reduction

20 p3640 A70-39417

Submillimeter gas lasers with low noise and CW operation for far IR spectroscopy, noting emission lines multiplicity

20 p3641 A70-39423

Light He isotope effect on He-Ne laser power output

20 p3641 A70-39737

Pulsed composite laser performance with He-Ne active section and neodymium-glass power gain section

20 p3641 A70-39740

Radiation divergence from gas laser resonator with coupling aperture

20 p3642 A70-39752

He/Ne laser amplifier and oscillator threshold bandwidth measurement by double laser device

20 p3643 A70-40126

Doppler beat spectrum and modulation depth of He-Ne laser emission with backward beam reflected from moving mirror into resonator

20 p3643 A70-40516

Gas and semiconductor diode lasers construction and operation principles, discussing terminology, Boltzmann distribution function, excitation methods, population inversion, etc

20 p3643 A70-40535

Fresnel diffraction using He-Ne gas laser and opaque wire

21 p3834 A70-40549

Q switching of nitrous oxide laser with Freon 12 and sulfurhexafluoride absorbers, comparing wavelengths with carbon dioxide laser outputs

21 p3834 A70-40567

Continuous wave laser action in chlorine, Ar and He gas mixtures, observing energy transfer between Ar and chlorine by pumping action

21 p3834 A70-40570

Low voltage slotted hollow cathode laser tube design with transverse discharge operation and uniform axial distribution of laser media, including metal vapors

21 p3834 A70-40571

Carbon monoxide laser efficiency increase through addition of Xe, noting change in laser output spectral intensity distribution

21 p3835 A70-40572

Methane IR filter for monochromatizing He-Ne laser

21 p3823 A70-40823

Optical properties of off-axis multimode resonators with spherical mirrors, discussing application to He-Ne lasers

21 p3836 A70-40914

Optimum tube diameter for maximum radiation output of single and multimode He-Ne lasers

21 p3836 A70-40916

Wideband high speed PCM/AM optical communication system using mode locked He-Ne laser, noting simultaneous signal transmission and bit rate

21 p3789 A70-41354

CW gas laser improvement, discussing optimum efficiency and photon beam spatial distribution

21 p3836 A70-41419

Carbon monoxide-nitrogen laser mechanism vibrational populations, discussing operational characteristics and walls condition and nature

21 p3837 A70-41716

Carbon monoxide-nitrogen laser luminescent phenomena by electronic spectroscopy

21 p3837 A70-41717

Mode intensity fluctuations in unlocked multiple mode He-Ne laser related to LF noise

21 p3837 A70-41918

Laser torch plasma dispersion gas dynamics from motion and kinetics of ionization processes

21 p3839 A70-42238

Water cooled carbon monoxide-He-nitrogen-oxygen laser CW output at room temperature

22 p4048 A70-42327

Ne absorption cell and He-Ne gain cell pulse velocities compared with free space light velocity

22 p4048 A70-42329

Lasing transitions time delay in carbon monoxide laser under pulsed electrical excitation, attributing inversion to anharmonic decoupling

22 p4048 A70-42330

Multifrequency autooscillatory systems, comparing reflex klystron with He-Ne laser

22 p3995 A70-42404

He-Ne gas laser, construction, operation and characteristic mode patterns

22 p4049 A70-42959

Saturated absorption spectroscopy of various molecules using emission spectra of carbon dioxide and nitrous oxide lasers

22 p4050 A70-43239

Longitudinal, transverse and simultaneous longitudinal-transverse gas laser mode locking

22 p4051 A70-43329

High power gas lasers constructed in Poland, describing structural design and operational specifications

22 p4051 A70-43441

Emission spectrum of neon-helium laser receiving Doppler shifted signal from moving mirror, showing memory effect due to beat harmonics

22 p4052 A70-43596

Emission spectrum of He-Xe CW laser with non-resonant feedback mode achieved with scattering agent and various mirror schemes

22 p4052 A70-43597

Single frequency gas laser synchronization by small harmonic signal from second laser, deriving frequency shift dependence on power

23 p4200 A70-43929

Gas dynamic molecular laser with electrons in ground state, using incoherent optical pumping from stationary shock wave

23 p4201 A70-44284

High gain Xe laser effects on longitudinal mode splitting, noting increased frequency of radiation propagation through highly dispersive medium

23 p4201 A70-44918

Magnetic flux dependent interference beats in spontaneous emission of gas discharge of He-Ne laser, estimating Hertzian coherence duration

23 p4202 A70-45052

Axial modes interaction in He-Ne laser with atomic collisions in active medium, computing intensities and emission frequencies

23 p4202 A70-45053

Carrier frequency transfer of amplitude modulated signal at two coupled transitions in traveling wave gas laser

23 p4202 A70-45055

Short and long term stabilized optical frequency standard of gas laser, using two absorption cells

23 p4202 A70-45057

He-Ne laser with absorbing cell in magnetic field, investigating nonlinear effect in frequency dependence of output power

23 p4203 A70-45070

Auto-oscillatory regimes in annular gas laser under coupling due to scattering, considering mode competition

24 p4351 A70-45183

Multiplicative modulation noise of helium-neon traveling wave laser amplifier at micron wavelength

24 p4317 A70-45188

Electro-optical light speed measurements with interference comparator using He-Ne lasers with light modulators

24 p4353 A70-45562

Rate equation study of multiwavelength far IR laser oscillations in water vapor, taking into account molecular rotation-vibration interaction

24 p4354 A70-45812

High pressure pulsed Xe laser obtained with transversely excited He-Xe discharge

24 p4355 A70-46087

Thermonuclear spacecraft propulsion, comparing X ray pumped gas laser and ion drive systems

24 p4377 A70-46211

Interference fringes on gas laser beam reflected by total reflection prism

24 p4356 A70-46272

GAS LIQUEFACTION U CONDENSING GAS LUBRICANTS

High speed rotor supported by air lubricated foil bearings subjected to periodic unidirectional excitation by vibrator, noting stability at high speeds

[ASME PAPER 69-LUB-E] 01 p0099 A70-10376

Direct and incremental variational formulations for steady compressible lubrication based on finite element method, noting limitations of numerical techniques

[ASME PAPER 69-LUB-12] 01 p0102 A70-10393

Book on gas lubrication covering general equations, externally pressurized journal and thrust bearings, etc

02 p0310 A70-12651

Hydrostatic thrust bearing with electrically conducting gas lubricant under axial current induced MGD pinch

03 p0497 A70-13780

Augmented small parameter gas film equation for squeeze film journal bearing solved in terms of radial displacement

[ASME PAPER 69-WA/LUB-9] 04 p0697 A70-14766

Self acting, hydrostatic and squeeze-film gas lubricated bearings applications to gyroscopes, accelerometers, torque testers, etc

05 p0855 A70-16446

Balanced rotor with radial sliding bearing bushings, studying lubricant gas restoring force effect on stability with allowance for bushings translational movements

11 p2058 A70-25581

Externally pressurized bearing with electrically-conducting gas lubricant under axial magnetic field, considering load capacity

12 p2244 A70-28018

Spherical gas lubricated sliding bearing with forced injection, determining pressure distribution by numerical integration

18 p3262 A70-36273

Augmented small parameter gas film equation for squeeze film journal bearing solved in terms of radial displacement

[ASME PAPER 69-WA/LUB-9] 19 p3435 A70-37609

Direct and incremental variational formulations for steady compressible lubrication based on finite element method, noting limitations of numerical techniques

[ASME PAPER 69-LUB-12] 19 p3436 A70-37616

Gas lubrication with injection at large compressibility numbers, deriving asymptotic solution

20 p3637 A70-39817

Cylindrical gas suspension lubricating layer pressure distribution calculation by perturbation method, determining angular rigidity

20 p3637 A70-39818

Externally pressurized air lubricated journal bearings with multiple supply holes, predicting load carrying capacity, flow requirement and stiffness

20 p3639 A70-40505

Spiral grooved gas lubricated thrust bearings, calculating self heating induced thermal distortion effects on load capacity

[ASME PAPER 70-LUBS-14] 22 p4044 A70-42447

Gas lubricated foil bearing performance as support for turborotor simulator, examining heating and thermal gradient effects

[ASME PAPER 70-LUBS-12] 22 p4044 A70-42448

GAS LUBRICATED BEARINGS U GAS BEARINGS

GAS MASERS

Dynamic time constants for specific transition and relaxation times of hydrogen maser, noting coupling between hyperfine differences and atomic polarization

03 p4498 A70-13007

Ammonia maser transient spiking effects under periodic oscillation condition modulation, noting frequency sweep width role

07 p1299 A70-19685

Atomic hydrogen maser wall shift determined by measurements on FEP Teflon coated storage bulbs, suggesting Teflon properties change as basis

07 p1301 A70-19973

Phase comparisons between commercial cesium beam frequency standards and NASA experimental hydrogen maser NX-1

08 p1513 A70-21592

Orbiting clock experiment for measuring gravitational red shift of earth by comparing ground based and satellite-borne hydrogen maser clocks

08 p1501 A70-21950

Submillimeter wave applications in measurement and communication, developing submillimeter gas maser sources

09 p1676 A70-22784

Cavity and storage temperature effects on hydrogen maser oscillation in 77-293 K range

13 p2425 A70-28713

Hydrogen maser wall shift measurement, using flexible storage bulb for accuracy improvement

19 p3445 A70-37759

Hydrogen maser frequency shift due to atomic collisions with deformable storage bulb surface

21 p3836 A70-41453

GAS MIXTURES

NT DETONABLE GAS MIXTURES

Hydrodynamics, mass and energy transfer equations for moderately dense gases multicomponent mixtures, using Bogoliubov theory

01 p1146 A70-10129

Gas-particle primary and pure gas secondary streams turbulent mixing, solving for various mixing zone flow field parameters

01 p0061 A70-10337

Pulmonary artery blood sampled before or during rebreathing of carbon dioxide in nitrogen mixtures, at rest and during exercise, discussing oxygen pressure changes

01 p0020 A70-10652

Linear small disturbance theories applied to two component gas mixture with fluid motion accompanied by nonequilibrium effects, discussing linear convection and reaction processes

01 p0062 A70-10803

Relaxation in gas-particle flow, analyzing thermodynamic properties, interactions, single particles and one dimensional flow equations

01 p0062 A70-10805

Molecular sieve mixed gas adsorption and vacuum desorption of carbon dioxide in Apollo spacecraft cabin

01 p0040 A70-11450

Diffusion coefficients for laminar multicomponent dissociating boundary layer at surfaces of thermally decomposing protective coatings

01 p0042 A70-11583

Chemical kinetics in reaction zone of shock heated hydrogen-carbon monoxide-oxygen mixtures, measuring density field behind normal shock wave by optical interferometry

02 p0250 A70-12022

Detonation of gaseous systems with marginal compositions, showing sensitivity to physicochemical factors

02 p0251 A70-12025

Premixed methane-oxygen-nitrogen combustion in conical reactor fed by choked sonic flow jet, analyzing reaction products chromatographically

02 p0397 A70-12030

Structure of hydrogen-oxygen diffusion flame in equilibrium using iterative solution

02 p0352 A70-12796

Density effects on transport coefficients of gaseous mixtures, solving modified Boltzmann equation including collisional transfer and three-particle collision effects

03 p0606 A70-13576

Numerical analysis of near equilibrium flow regions in chemically relaxing gas mixtures past blunt bodies at supersonic speeds

04 p0666 A70-14603

Ionic collision processes in nitrogen and oxygen mixtures in mass spectrometer ion source

04 p0646 A70-14700

Gas diffusion coefficients for He-N and nitrogen-carbon dioxide systems in diffusion cell utilizing porous stainless steel barrier

04 p0780 A70-14710

Thermal recovery factors at hemispheric probe stagnation point in low density supersonic jets of He-Ar and H-N mixtures

[ASME PAPER 69-WA/HT-27] 04 p0782 A70-14810

Mass flow rate calculation of methane and natural gas mixtures through critical flow nozzles

[ASME PAPER 69-WA/FM-4] 04 p0667 A70-14839

Admixtures effect of chloroform, diethyl ether and acetone vapors on carbon dioxide laser output power

04 p0702 A70-15202

Shock wave width and temperature expressions for argon-helium mixture

04 p0672 A70-15223

Diatomic oxygen-nitrogen collisions in mixtures with CO, determining vibration-vibration energy exchange probabilities

04 p0723 A70-15562

Equation of state for neutron, proton and electron gas mixture associated with cold matter above white dwarf densities and below nuclear density

05 p0905 A70-15756

Initial disturbances propagation in gas mixtures by asymptotic analysis, observing diffusely and viscously damped modes

05 p0833 A70-16404

Polyamide fabric burning rates in oxygen-inert gas mixtures, studying damping effects of density, thermal conductivity, molecular constants and mass flow

06 p1090 A70-17284

Vigilance time degradation, studying effects of breathing gas mixtures with varying oxygen and carbon dioxide content

06 p1000 A70-17293

Kinetic analysis of ion-molecule reactions in Ar-N mixtures with H, deuterium and HD using ion ejection mode of ion-cyclotron-resonance spectroscopy

06 p1108 A70-17332

Chemical laser action in spark excited CS₂-O₂ mixtures, attributing emission to combustion product CO

06 p1080 A70-17445

Chemical laser CW operation achieved by mixing gases, obtaining pumping energy from chemical reactions

06 p1080 A70-17492

Inviscid hypersonic blunt body flow of hydrogen-oxygen mixtures in shock layer stagnation region

06 p0968 A70-17555

Gas mixture internal energy in internal combustion engine cylinder calculated with allowance for thermal discontinuity

06 p1130 A70-17628

Viscosity, thermal conductivity, specific heat and Prandtl number of hydrogen, methane and hydrogen-methane mixtures calculated for variation with temperature neglecting dissociation effects

06 p1177 A70-17700

Kinetic Boltzmann equations for spatially uniform two component gas mixture solved with allowance for relaxation processes, assuming differing temperatures

06 p1109 A70-17754

Energy and mass transfer during elastic and inelastic molecular collisions in reacting gas mixtures, using Enskog and variational methods in solving Boltzmann equations

06 p1110 A70-17760

Maxwellian distribution perturbation in chemically reacting gas mixtures with lower inelastic collision frequency than elastic

06 p1110 A70-17761

Laser induced Raman scattering as diagnostic technique for measuring specie concentrations in gas mixtures

[AIAA PAPER 70-224] 06 p1066 A70-18214

Unsensitized gaseous fuel-air mixtures photochemical ignition due to molecular oxygen photodissociation by radiant energy absorption

[AIAA PAPER 70-149] 06 p1183 A70-18225

Species concentration, jet structure and diatomic nitrogen rotational temperature measured for diffusive separation of nitrogen-helium mixture free jets, using electron beam

06 p1043 A70-18253

Species spatial distribution measured for He-Ar gas mixtures expanding in supersonic jets, compared to measurements with skimmer-nozzle arrangement

06 p1066 A70-18256

Boltzmann equation for binary mixtures of rarefied gases solution involving specific expansion of distribution functions

06 p1047 A70-18311

Surface diffusion slip velocity in binary gas mixture above solid surface, basing calculation on distribution functions determined from Boltzmann equation

06 p1049 A70-18333

Moment methods for calculating modeled diffusion gas mixture shock waves using Monte Carlo method, discussing distribution function and flow pattern

06 p1050 A70-18336

Normal shock wave structure in binary gas mixtures of chemically inert monatomic molecules, using kinetic theory moment method

06 p1051 A70-18343

Shock structure in binary gas mixture, discussing governing equations and Chapman-Enskog procedure

06 p1051 A70-18344

Shock wave structure in He-Ar mixture velocity and temperature profiles based on kinetic model equations

06 p1051 A70-18346

Thermal conductivity calculation for chemically reacting multicomponent gas mixture, comparing results from Brokaw method and simplified formula

06 p1184 A70-18554

Thermodynamic properties of nonequilibrium multicomponent gas mixtures including Fermi-Dirac statistics effect, discussing internal partition function for free and confined atoms

06 p1184 A70-18637

Stainless steels case hardening in hydrogen, nitrogen, propane and butane mixture, showing temperature and process duration effects

07 p1291 A70-18831

P-v-T-x relationships determination method for gaseous mixtures at high pressures and temperatures, studying He-nitrogen mixtures compressibility

07 p1420 A70-19205

Preignition heat release rate profile in ethylene-air mixture flow against hot surface, determining temperature and velocity distribution optically

07 p1420 A70-19263

Kinetics of attack of SiC in monoatomic mixtures of N and O generated by microwave discharge dissociation

07 p1421 A70-19332

Coupled vibrational relaxation in mixtures of diatomic gases, showing energy pumping phenomenon between species

07 p1338 A70-19627

Cesium plasma composition as equilibrium mixture of ideal gases assuming chemical equilibrium attainable by specified reactions

07 p1349 A70-19660

Helium and argon atoms number densities radial profiles in supersonic free jets of binary gas mixtures by molecular beam sampling

07 p1341 A70-20105

Photochemical calculations on mesospheric ozone for oxygen only, oxygen-hydrogen and oxygen-hydrogen-nitrogen atmospheres

07 p1273 A70-20268

Diffusive separation of Ar 36 and 40 and He in axisymmetric supersonic jet taking into account pressure diffusion

08 p1431 A70-21027

Multicomponent gas absorption analysis to illustrate interactions of coupled fluxes in ammonia-water system

08 p1597 A70-21028

Oscillatory relaxation of binary system of heat conducting viscous gases composed of nonspherical molecules

08 p1547 A70-21085

Shock wave structure in binary mixture of monoatomic gases based on integral kinetic equations, using iteration process

08 p1483 A70-21086

Bromine monoxide formation by atomic oxygen-bromine reaction in flash photolysis of bromine-nitrous oxide and bromine-nitrogen dioxide mixtures

08 p1455 A70-21342

Hydrodynamics, mass and energy transfer equations for moderately dense gases multicomponent mixtures using Bogoliubov theory

08 p1548 A70-21405

Thermal conductivity of multicomponent gas mixtures obtained in higher approximations

09 p1788 A70-22317

Ti tetrachloride, Si tetrachloride and hydrogen gas mixtures flow over heated graphite substrates, describing Ti silicides formation

09 p1703 A70-22646

Ni-Cr superalloys hot corrosion, studying sulfidation-oxidation in various synthetic controlled gas mixtures

09 p1706 A70-22944

Shock heated molecular beams of argon, oxygen and mixtures with helium, measuring particle velocities and gas dissociation

09 p1733 A70-23180

Coherent radiation amplification factor for 0.63 micron wavelength in He-Ne mixture, noting dependence on discharge current for various pressures

09 p1698 A70-23304

Electric discharge reactions in mixtures of phosphine with methane, ammonia and water, obtaining biologically significant inorganic and organic phosphorus compounds

09 p1630 A70-23396

Population inversion generation through gaseous oxides mixing with nitrogen flow thermally excited

09 p1700 A70-23569

Near equilibrium transonic flows of reacting gas mixtures based on linearization of thermodynamic and kinetic quantities

10 p1867 A70-24133

Solar radiation energy distribution simulated using vacuum monochromator, discussing Ar-Kr-Xe-methane mixture

10 p1931 A70-24317

Specific intensity production from photolysis of ozone-oxygen mixtures at 2537 Å, investigating mechanism

10 p1831 A70-24565

Perfect gas mixtures thermodynamic functions at high temperatures with correction for Debye-type electrostatic interaction effects

10 p1968 A70-24707

Molecular densities and population inversion pulse shape in working gas in mixture with thermally excited auxiliary gas

10 p1920 A70-25112

Thermal conductivity of monatomic binary gas mixtures at moderately low temperatures and pressures, considering various Ar-He mixtures

11 p2147 A70-25755

Gas mixture composition effect on bacteria growth oxidizing methane and propane, establishing proportional biomass concentration to hydrogen and oxygen in mixture

11 p1991 A70-25938

Carbon dioxide fixation in hydrogenomonas eutropha determined from titrating liquid culture with carbon dioxide, showing dependence on oxygen content in gas mixture

11 p1991 A70-25940

Hypoxia tolerance of albino rats in He-oxygen and Ar-oxygen environments in heat-pressure chamber, discussing He-oxygen mixture cooling effect

11 p1987 A70-26103

Recombination in hydrogen-oxygen reaction studied by monitoring IR emission from water vapor formed by shock initiated combustion

11 p1995 A70-26377

Hydrogen-air turbulent diffusion flame structure at differing air and hydrogen velocities

11 p2151 A70-26387

Laminar boundary layer equations solved for mass and energy transfer in binary gas mixture, investigating forced and free convection

11 p2151 A70-26558

Gas mixture plasma ionized and heated by discharge and ejected into vacuum, considering nonequilibrium ionization calculation with gap between electron and heavy particle temperatures

11 p2092 A70-26732

Reaction rate constants in heated mixture of hydrogen, carbon dioxide and Ar behind shock waves measured by IR spectroscopy

12 p2274 A70-26891

Radiative intensity calculations for carbon dioxide and carbon dioxide-nitrogen plasmas for various temperatures, densities and path lengths, computing UV and continuum spectra

12 p2275 A70-27170

Primitive earth prebiological organic synthesis via amino acids shock heating in atmosphere: simulating gas mixture, suggesting energy sources from atmospheric entry

12 p2167 A70-27269

He-Ne laser optimal mixture composition ratio for generating IR radiation at two wavelengths

12 p2251 A70-28293

Quenching efficiency of molecular oxygen relative to nitrogen, carbon monoxide, carbon dioxide and argon, involving photolysis of gas mixtures

13 p2361 A70-28498

Reaction rates temperature dependence for artificial carbographites of various densities in oxidizing gas media

13 p2519 A70-28577

Electron radiation temperature measurements in sealed-off carbon dioxide laser, determining gas mixture effect on discharge properties

13 p2426 A70-28808

Ar ion lasers investigated for effect of added He on pulse output intensity

13 p2426 A70-28809

- Human respiratory responses to gas mixtures with different oxygen content under rarefied atmospheric conditions 13 p2353 A70-29521
- Hot-wire probe measuring He-air mixture velocity and concentration following He discharge from circular orifice, noting calibration method 13 p2412 A70-29990
- Linearized gas mixture nonequilibrium flow fields, analyzing consequences of multiplicity of principal relaxation frequencies 14 p2566 A70-30474
- Transport cross sections for isotopic methane and mixtures, considering inelastic and thermal diffusion effects 14 p2665 A70-30652
- Turbulent mixing at contact surface in driven shock wave in shock tube with bursting diaphragm for He-Ar test gas mixtures 14 p2566 A70-31030
- Methane-air inverted flames blowoff at thin stabilization plates of twin slit inverted flame burner, determining critical values of Karlovitz flame stretch factor 14 p2666 A70-31092
- Temperature estimation of micro hydrogen-air diffusion flame from hydrogen content of unburned gas mixture 14 p2666 A70-31095
- Nitrogen dioxide continuum in green-white afterglow of molecular oxygen and nitrogen, using spectrometry and photometry 14 p2579 A70-31254
- Supersonic nonequilibrium gas mixture flow past segmental bodies nose areas to simulate Venusian atmosphere, determining temperature, pressure and concentration distributions 15 p2796 A70-31483
- White light laser construction using Ar-Kr laser with suitable mixture and pressure of gases to provide equal output intensities of red, yellow, green and blue 15 p2752 A70-32046
- Heat conductivity of Xe-He binary gas mixtures, allowing for molecular transfer and polarity effects 15 p2827 A70-32107
- Rarefied gas mixtures efflux from opening at various pressures, calculating component discharge coefficients for molecular flow conditions 15 p2721 A70-32137
- Cesium plasma composition as equilibrium mixture of ideal gases, assuming chemical equilibrium attainable by specified reactions 15 p2781 A70-32697
- Approximate formula for viscosity of binary polar gas mixtures confirmed for unlike cross sections 16 p2996 A70-33055
- Spacecraft attitude control microthrusters utilizing catalytically reactive gas mixtures during pulse mode and steady state operation [AIAA PAPER 70-614] 16 p2969 A70-33611
- Flow and diffusion phenomena in rarefied gas mixtures associated with separation nozzle process, using molecular pressure probe and mass spectrometer 16 p2893 A70-33699
- Nonequilibrium vibrational energy and relaxation equation for carbon dioxide-nitrogen molecular gas mixtures in supersonic free jet exhausting into vacuum [AIAA PAPER 70-867] 16 p2895 A70-33910
- High temperature plasmas of mixtures of nitrogen with rare gases, calculating equilibrium thermodynamic properties 17 p3195 A70-34932
- Aluminum spherical particles nonautonomous and autonomous combustion in O with N or Ar initiated by HF induction heating 17 p3145 A70-35042
- Coulomb interaction Fermi gas mixture collision integral, obtaining formula from Boltzmann equations and Taylor series expansion 17 p3070 A70-35043
- Thermal diffusion of isotropic, nonisotropic and multicomponent mixtures with monatomic and polyatomic molecules, considering kinetic theory and experimental results 17 p3197 A70-35537
- Orifice length-to-diameter ratio effect on spray mixture uniformity from unlike impinging jets 17 p3073 A70-35671
- Potassium salts thermal and chemical ionization in flames of hydrogen-oxygen-helium and hydrogen-air mixtures in constant volume vessels 18 p3345 A70-36243
- Gas particle mixtures nozzle flow at high loading ratios 18 p3208 A70-36693
- Heat transfer coefficient of chemically reacting gas mixture as function of Lewis-Semenov number, discussing nitrogen dioxide decomposition 19 p3550 A70-37251
- Pulsed argon ion laser output properties from electron temperatures and densities produced by He-Ar gas mixture 20 p3640 A70-39137
- Carbon dioxide initial dissociation rates in glow discharges and gas mixtures at low pressures, using mass spectrometric sampling and plasma diagnostic methods 20 p3674 A70-39235
- Noble gas mixture large shock tunnel driven linear MHD generator, examining electron density, operating characteristics and electrical properties 20 p3682 A70-40012
- Orthostatic tolerance increase in animals by application of hyperoxic and hypercapnic gas mixtures 20 p3574 A70-40185
- Weak steady shock waves formation in relaxing binary gas mixture, discussing vibrational specific heat temperature dependence 20 p3614 A70-40350
- Premixed laminar flames of hydrogen, oxygen and nitrogen burned on Meker burner, investigating diffusional effects on gas composition changes 20 p3739 A70-40469
- Hydrogen-oxygen and hydrogen-nitrous oxide systems combustion, measuring isotopic substitution effect on flame speed by schlieren technique with rotating drum camera 20 p3583 A70-40472
- Continuous wave laser action in chlorine, Ar and He gas mixtures, observing energy transfer between Ar and chlorine by pumping action 21 p3834 A70-40570
- Methane and hydrogen consumption rates during slow reactions in mixtures of molecular hydrogen, oxygen and nitrogen 21 p3772 A70-40879
- Ion-molecule reactions in mixtures of hydrogen sulfide with ethylene and acetylene from deuterium labeling studies via ion cyclotron resonance spectroscopy 21 p3773 A70-41200
- Shock tube measurements of bimolecular reaction rates in branched chain hydrogen-carbon monoxide-oxygen system, monitoring flame band emission 21 p3773 A70-41314
- Carbon dioxide-He-nitrogen gas mixture pulsed discharge system afterglow gain measurements up to one atmosphere, using CW laser 21 p3837 A70-41719
- Helium and nitrogen role in carbon dioxide laser excitation, discussing optimum gas mixture 21 p3837 A70-41919
- Carbon dioxide-nitrogen He discharge gas temperature measurements involving plasma refractivity determination by interferometer 22 p4049 A70-42366
- One dimensional sound propagation in reacting gas mixture near equilibrium, obtaining equilibrium and frozen sound speed 22 p4074 A70-42752
- Equilibrium sonic velocity in reacting gas mixture in nozzle flow for unlimited species and independent chemical reactions 22 p4074 A70-42753
- Nonequilibrium gasdynamic and thermodynamic properties of chemically reacting gas mixtures in high expansion subsonic and supersonic nozzles for selected rocket propellants 22 p3982 A70-42761
- Interdiffusion coefficients for hydrogen-carbon dioxide and oxygen-carbon dioxide systems at low temperatures 22 p4076 A70-43393
- Binary gas mixture separation effects by centrifugation in cylindrical tube, calculating maximum radial concentration difference between wall and axis by numerical integration 23 p4181 A70-44206
- Kinetic transport theory for mixed dilute gases consisting of linear rotating diamagnetic molecules in external homogeneous magnetic field 23 p4223 A70-44927
- Rarefied binary gas mixture, determining temperature gradient effect under various pressures 23 p4284 A70-44984
- Heat transfer in chemically reacting gases boundary layers, obtaining approximate solution by film theory 24 p4428 A70-45101
- Numerical analysis of fuel combustion in supersonic stationary flows of hydrogen air mixture past bodies by two-component reaction kinetics model [ICAS PAPER 70-52] 24 p4428 A70-45500
- GAS PHASES**
- U VAPOR PHASES**
- GAS PIPES**
- Comparative load capacity of disk models of natural gas blowers of different designs under plastic strain 23 p4232 A70-43941
- GAS POCKETS**
- Roshko model cavity solution based on Falkovich method application to two dimensional permanent irrotational flow of subsonic gas jet 07 p1258 A70-19571
- GAS PRESSURE**
- Pulsed arcs in argon and helium at superhigh pressures, noting plasma ionization and temperature and charged particle density 01 p0149 A70-10168
- Coronal gas pressure boundary conditions on model upper chromosphere, determining temperature and hydrogen density assuming hydrostatic equilibrium 01 p0175 A70-10243
- Pulmonary artery blood sampled before or during rebreathing of carbon dioxide in nitrogen mixtures, at rest and during exercise, discussing oxygen pressure changes 01 p0020 A70-10652
- Gas solubilities investigated for gaseous pressurization of propellants 01 p0160 A70-10840
- Nitrogen, oxygen and air luminescence spectra excited by fast electrons at low gas pressures in IR spectral region compared with polar auroral spectra 01 p0083 A70-11536
- Leakage in mechanical face seals with hydrodynamic films, noting misaligned seal theories for pumping with cavities and two fluids [ASLE FICFS PREPRINT 19] 02 p0308 A70-12170
- Longitudinal pressure gradient measurement for DC discharges in He, Ne and Ar, investigating effects of gas purity, tube geometry, etc 04 p0671 A70-14995
- Axial neutral gas pressure gradient calculated in cylindrical positive column of DC discharge due to driving volume force 04 p0671 A70-15003
- Pulsed high current arc burning in hydrogen at pressures to 400 atm, discussing stability and discharge plasma parameters 04 p0729 A70-15224
- Spectroscopic determination of radial temperature distribution at various currents in negative glow of hollow cathode discharge, analyzing influence of gas pressure 05 p0888 A70-16358
- Gas pressure and pressure stratification in sunspot, using curve of growth analysis 05 p0911 A70-16432
- Hypersonic rarefied merged layer flow over sharp slender cones, using strong interaction theory and free molecular flow to analyze surface pressures 06 p0982 A70-18363
- Orifice effect investigated for sharp flat plate in hypersonic rarefied flow, measuring surface pressure 06 p0982 A70-18366
- Dense gas effects in free piston hypersonic wind tunnel, discussing Longshot facility, free piston cycle, reservoir conditions decay and hypersonic nozzle flow [AIAA PAPER 69-169] 07 p1249 A70-19310
- Loading effects in measurements involving electrical and nonelectrical systems used in determining gas pressure and fluid flow 09 p1672 A70-22011
- He-Ne laser emission modulation by varying discharge current, studying gas pressure effect and role of ballast resistor 09 p1695 A70-22411
- Stable equilibrium of rotor in pressurized gas bearing, considering perturbed rotor motion equation together with Reynolds equations for pressures in lubricant layer 09 p1690 A70-22544
- Pressurized gas bearing analysis, using finite difference method for solving Reynolds equation for pressures in lubricant layer 09 p1690 A70-22545
- Fast neutral particles produced in electron-ion oscillation discharge as function of gas pressure and magnetic field 09 p1736 A70-23190
- Turbulent gas nonresonant pressure pulsations effects on local convective heat transfer in tube flow 10 p1968 A70-24288
- Helium ions diffusion perpendicular to magnetic field in He gas, measuring coefficients as function of field strength and for various gas pressures 10 p1925 A70-25108
- Gas effect on natural frequency of electrostatically excited string vibrating between flat electrodes at medium pressures 11 p2048 A70-25582
- Thermodynamic and transport properties of high temperature and pressure gases measured with ultrasonic pulse technique 11 p2147 A70-25753
- Effusion steady state pressures time dependence of carbon monoxide and calcium vapors generated during calcium oxide-graphite interaction 11 p1995 A70-26602
- Isotropic Be billet fabrication by gas pressure consolidation and pressureless sintering techniques 12 p2252 A70-26888
- Monograph on acoustic theory for determining frictional pressure drop effect on gas state behind reflected wave in shock tube 12 p2209 A70-27000
- EHF microwave absorption in compressed carbon dioxide, measuring dielectric loss as function of gas density 12 p2273 A70-27571
- Electron density determination, establishing gas pressure relation to discharge current 13 p2460 A70-28710

- Gas pressure effects on visible and UV laser action in small argon Z-pinch plasma discharge, using streak photographs 15 p2750 A70-31968
- White light laser construction using Ar-Kr laser with suitable mixture and pressure of gases to provide equal output intensities of red, yellow, green and blue. 15 p2752 A70-32046
- Current-voltage relation for ion collection spherical DC probe at high ambient gas pressure 16 p2899 A70-32929
- Nonabsorbing gas effect in radiation-conduction heat transfer interaction, predicting magnitude and pressure trends by wideband gas model [AIAA PAPER 70-836] 16 p3001 A70-33931
- Hunting phenomena of hydrogen gas plastic balloon at ceiling altitude, considering exhaust duct, extra volume and shape 17 p3018 A70-35317
- Vibrating diaphragm gas pressure measuring system based on membrane damping, applying to prototype atmospheric entry probes 17 p3095 A70-35524
- Oxygen pressure effect on stainless steel cyclic hardening during vibration tests at resonant frequency 18 p3273 A70-36042
- Reliability tests of blood carbon dioxide pressure measurement methods, indicating carbon dioxide-electrode method superiority 19 p3365 A70-38371
- Argon hydrostatic pressure effect on self diffusion coefficients and activation energy of Al and Be single crystals 20 p3644 A70-38961
- Transversely excited atmospheric pressure TEA/carbon dioxide laser, noting power output and cost 20 p3641 A70-39424
- Hypersonic sound speeds measured in methane at moderate pressures by spontaneous Brillouin light scattering experiments 21 p3830 A70-41938
- Intense high ionization degree discharge plasma initiation at low gas pressures, using auxiliary discharge 22 p4078 A70-42356
- Gaseous substances thermodynamic functions and chemical equilibrium constants logarithms dependence on temperature and pressure, deriving internally self consistent formulas 22 p4124 A70-42682
- Combustion driven shock tunnel applied to tailored interface operating conditions, controlling mass flow into tube by throttling plates 22 p4006 A70-42765
- Gas pressure differential across multilayer insulation blanket during rapid evacuation predicted, using one dimensional flow theory [AIAA PAPER 69-608] 23 p4282 A70-44522
- Oxygen pressure effects on Ni oxidation kinetics at high temperatures 23 p4408 A70-44920
- One dimensional gas pressure as function of activity, using Poisson-type partition function for perturbation calculation of thermodynamic limit 24 p4430 A70-46269
- GAS REACTORS**
- Flow characteristics of curved porous wall gas core reactors for nuclear rocket engines, visualizing simulated fuel flow with air-smoke combination 06 p1104 A70-17509
- GAS SPECTROSCOPY**
- Dispersed fluorescence spectra from vacuum UV photon impact on COS, noting absence of emission from higher vibrational levels 01 p0148 A70-11353
- Spectral absorption and transparency of water vapor, carbon dioxide, carbon monoxide, methane and nitrous oxide bands in IR region 04 p0715 A70-15255
- Tunable nitrous oxide laser cavity losses and absorption by carbon dioxide determined spectroscopically 11 p2061 A70-25361
- Ion cyclotron resonance spectroscopy technique for determining electrons photodetachment energy from negative ions in gas phase 11 p1995 A70-26001
- Average rotational temperature of Venus atmosphere above cloud tops from carbon dioxide band spectroscopy 14 p2650 A70-31219
- Gaseous Al oxide bond bending frequency in Ne and Ar matrices at liquid He temperatures, investigating IR spectrum 15 p2695 A70-32830
- Turbulent and reacting flows temperature and mixing rates determination, using gaseous HF tracer spectroscopy [AIAA PAPER 70-726] 16 p2856 A70-33497
- Ar plasma generation by focused Q switched ruby laser beam, measuring density and temperature by electro-optical spectroscopy 17 p3107 A70-35111
- Secondary combustion products of air augmented boron loaded solid propellant rocket ramjet, measuring properties by spectroscopy 17 p3196 A70-35196

- Optimal separation height of instrument container in atmospheric gas composition mass spectrometric studies 18 p3260 A70-36996
- Excitation transfer by spontaneous emission in atomic gas, investigating static magnetic field effect on radioactive cascade 19 p3443 A70-37363
- Transition probabilities of visible and near-IR neon lines, using gas-driven shock tube spectroscopy 20 p3674 A70-39134
- Level relaxation constants measurements by three-level laser spectroscopy, using line shape of stimulated shifted resonance scattering in gas 24 p4354 A70-45821
- GAS STREAMS**
- Gas-particle primary and pure gas secondary streams turbulent mixing, solving for various mixing zone flow field parameters 01 p0061 A70-10337
- Injected B particles burning in hot gas stream of oxidant mixture with Ar and H, observing trace widening by motion picture technique 01 p0218 A70-11016
- Circulation gas lens temperature distribution, considering effects of gravity, wall thermal conductivity, glass interlayer, etc 03 p0604 A70-13387
- Optimum radiation shield quantity assuring gas temperature measurement accuracy, using radiation transfer equations and shield-to-shield temperature estimations 03 p0486 A70-13556
- Axisymmetric radiating flow behind paraboloidal shock in ideal inviscid gas hypersonic stream, using differential approximation method for blunt body solution 04 p0669 A70-14937
- Breakthrough curve shape prediction during adsorption from gas stream in fixed bed adsorbers for trace contaminant control applied to activated charcoal 04 p0786 A70-15317
- Liquid sheet and jet breakup in supersonic gas stream, characterizing breakup mechanism by gross jet fracture [AIAA PAPER 70-89] 06 p1039 A70-18109
- Combustion of pure crystalline boron single particles injected into hot oxidizing gases streams at atmospheric pressure 07 p1359 A70-19583
- Brightness curves for eclipsing binary V448 Cygni indicating gas stream flows in system 08 p1577 A70-21441
- Current diffusion from magnetic piston into postshock gas upstream observed in electromagnetic shock tube 09 p1736 A70-23185
- Gas stream velocity field produced by shock wave impinging against wing moving at supersonic speed 10 p1799 A70-24124
- Rarefied gas stream density measurements with electron beam fluorescence experiment, determining pressures and densities behind plane shock wave and in supersonic nozzles 11 p2087 A70-26743
- Plane, steady, irrotational flow of gaseous subsonic stream bounded by two infinite parallel walls, discussing application to incompressible fluids 13 p2389 A70-29631
- Carbon dioxide absorption from gas streams by weak base ion exchange resins 18 p3226 A70-36767
- Gas dynamics turbulence of controlled properties effect on electrical discharge across plasma stream, preventing filamentary nature 20 p3681 A70-40008
- High velocity intergalactic hydrogen origin, examining galactic evolution by gas inflall 21 p3887 A70-41112
- Liquid droplet shape effect flow field velocity and pressure distribution over windward surface in high speed gas streams 21 p3809 A70-41762
- GAS TRANSPORT**
- Monte Carlo method applied to Boltzmann collision integral in solving heat transfer between plates at different temperatures in elastic spheres gas 06 p1183 A70-18324
- Step profile decay of initial perturbations of radiating gas as function of optical depth and Boltzmann number 07 p1255 A70-19212
- Transport properties of high temperature gases compared with room temperature differences, considering chemical equilibria, heat conduction and atom-free radical forces 07 p1424 A70-19880
- Downward ozone transport from troposphere to atmospheric boundary layer by turbulent diffusion calculated by model, estimating annihilation rate 10 p1875 A70-24486
- Physiology of oxygen transport in human organism and genesis of tissue hypoxia, discussing pulmonary functions, blood transport properties and tissue blood flow and diffusion 10 p1821 A70-25077

- Physiology and pathophysiology of oxygen transport in human blood, discussing fluctuations in O₂ capacity and affinity 10 p1821 A70-25079
- Critical oxygen supply of cerebral mitochondria and intercapillary oxygen transport 10 p1821 A70-25080
- Oxygen transport after cardiopulmonary resuscitation from asystole and ventricular fibrillation in dogs 10 p1822 A70-25085
- External respiration, hemodynamics, oxygen transport and consumption in lungs during static load tests 10 p1822 A70-25176
- Nitrogen transport properties to 26,000 degrees K, measuring current-field intensity properties and radial temperature distributions in molecular nitrogen cascade 11 p2151 A70-26841
- Open circuit gas washout test of lungs under inspiration-expiration transmission symmetry, using Hilbert-Schmidt operators 12 p2175 A70-27021
- Spontaneous ignition dependence on transient temperature variations accompanying gas entry to evacuated vessel 12 p2330 A70-27222
- Hydrogen oxygen fuel cell investigated for oxygen transfer to Pt cathode surface 12 p2166 A70-27848
- Resonance radiation transport in optically thick plane gas layer with two-level atoms 12 p2305 A70-27853
- Dilute gas transport properties calculation, investigating numerical techniques to minimize computation time to prescribed accuracy 13 p2441 A70-29089
- Kinetic gas theory mathematical models, analyzing system of N particles in cube 14 p2601 A70-31422
- Hybrid computer simulation of steady state oxygen transport and consumption in capillary-tissue system 15 p2694 A70-32845
- Oxygen-hemoglobin reaction rate constants in red cells obtained by applying in vitro blood data to solutions of differential equations describing intracellular oxygen transport 15 p2686 A70-32846
- Electrical properties of n-type GaAs epitaxial films grown by gas transport method 17 p3144 A70-35706
- Nitrogen and nitric oxide production and diffusion, examining photochemistry and transport at high altitudes 20 p3620 A70-39339
- Hyperbaric oxygen exposure produced hypertension and pulmonary edema, discussing carbon dioxide transport mechanism in blood 20 p3572 A70-39430
- Lower thermosphere minor gaseous constituents vertical transport by nonlinear gravity wave process, showing density scale height decrease from diffusive equilibrium 21 p3818 A70-41098
- Approximate calculations of thermal and viscous transport in high temperature air based on empirical transport equations 21 p3951 A70-41750
- Perturbation method with small parameter applied to turbulent transfer equation in lower atmosphere, solving longitudinal diffusion effect on evaporation 22 p4065 A70-42911
- Nitrogen transport coefficients as function of high temperature in stationary plasma produced in cascade arc chamber 22 p4082 A70-43373
- Enskog theory extended to three particle collisions for gas transport properties 23 p4222 A70-44427
- Gas transport properties at high temperatures and pressures, discussing Ar plasma arc characteristics 23 p4226 A70-44433
- GAS TUBES**
- Gas tube isolator circuit for arcing amplifier in phased arrays, using, programmed charge of capacitance bank during interpulse 16 p2879 A70-34072
- GAS TUNGSTEN ARC WELDING**
- Commercial Ni-Co gas tungsten arc filler metal with mechanical properties stable following stress relief 04 p0710 A70-15653
- Weld porosity in TIG welding of technical Ni in ternary mixtures of Ar with H, O and N 08 p1518 A70-21345
- Low cost programming system for gas tungsten arc welding process for Ti taper and stepped joint designs 08 p1507 A70-21484
- Gas tungsten arc welding application broadened by introducing controlled droplet transfer process 10 p1896 A70-25308
- Electrode shape and background resistance effects on power rationing between gas tungsten arc and electrode 10 p1897 A70-25314

- Numerically controlled gas tungsten arc welding, discussing tape programming, fixture design and fabrication for various welded metal joint configurations
11 p2058 A70-25661
- Pulsed current gas tungsten arc welding in inert gas atmosphere and applications
12 p2238 A70-26853
- Gas tungsten arc hot wire welding operational characteristics and applications
14 p2590 A70-30929
- In-place gas tungsten arc fusion welding for joining small diameter precipitation hardenable aluminum tubing
14 p2590 A70-30930
- Argon-arc welds porosity mechanism in Ti welding
17 p3098 A70-34443
- Al-Si welding rods tests with various surface finishes, considering oxide coatings effect on gas tungsten arc weld quality
18 p3264 A70-37113
- Porosity effects on mechanical properties of Al alloy gas tungsten arc welds, noting strength loss proportional to cross sectional area loss
18 p3265 A70-37205
- Tungsten-helium arc atmospheric contaminants spectral monitoring parameters under welding conditions, using rotating circular wedge to oscillate emission lines across exit slits
21 p3831 A70-40725
- Stainless steel gas tungsten arc welding, considering anode spot size variation and current density
22 p4042 A70-42377
- Repair weld procedures effects on annealed Ti-Al-V weldments mechanical properties, examining defects in inert gas shielded arc welded joints
[ASME PAPER 70-MET-1] 22 p4043 A70-42425
- GAS TURBINE ENGINES**
- NT DUCTED FAN ENGINES
- NT JET ENGINES
- NT RAMJET ENGINES
- NT SUPERSONIC COMBUSTION RAMJET ENGINES
- NT T-56 ENGINE
- NT TURBOFAN ENGINES
- NT TURBOJET ENGINES
- NT TURBOPROP ENGINES
- NT TURBORAMJET ENGINES
- Gas turbine engines vibration characteristics, discussing statistical analysis obtained through condensed vibration overload control program
01 p0166 A70-11420
- Model gas turbine engine blades fatigue strength under stress conditions, considering tensile stresses reproducibility from centrifugal loads
03 p0587 A70-13241
- Failure and defect formation in gas turbine engine disks made of steel alloys, stressing fabrication methods effect on reliability
03 p0588 A70-13251
- Multiple array critical flow venturi air flow metering system constructed for gas turbine engines, developing pressure control valve
[ASME PAPER 69-WA/FM-5] 04 p0688 A70-14838
- Nickel base alloy, WAZ-20 with improved strength in 2000-2200 F range for application to gas turbine engine starter vanes
04 p0706 A70-15097
- Inertia bonded and electron beam welded joints of Waspaloy compared for suitability in aircraft gas turbine engines
04 p0700 A70-15655
- Thermal and gas dynamic characteristics of aircraft turbine engine annular vaporizing combustion chamber determined from air distribution ratio
05 p0895 A70-15897
- Moisture absorptivity and hydrolytic stability effects on operational parameters of gas turbine engine lubricants
06 p1075 A70-17222
- Gas turbine engine blades grinding and polishing procedures, considering fatigue life increase and physical properties stabilization
07 p1292 A70-18833
- Coating and coating processes for superalloys in hot section components of gas turbine engines for aircraft, industrial, marine and vehicular applications
07 p1362 A70-18929
- Centrifugal force induced stressed state in gas turbine blades using photoelastic analysis, emphasizing stress distribution at shroud holes
07 p1403 A70-19118
- Aerodynamic and mechanic design of gas turbine for light helicopters, including flight tests and program objectives
08 p1558 A70-20686
- Gas turbine engines contribution to air pollution, using model combustor to study burned gas composition, emphasizing nitric oxide concentration
08 p1559 A70-21481
- Tubing materials for gas turbine engines covering fabrication, selection, etc
08 p1559 A70-21854
- Aircraft turbine engines strength and gas dynamic characteristics improved by vibration decrease using elastic elements
09 p1742 A70-22471
- Carbon deposit formation in gas turbine engines with various fuels, studying thermal insulation properties
09 p1742 A70-22472
- Energy losses in gas turbine flows ascribed to combined exhaust and internal losses, noting usefulness of entropy loss concept
09 p1743 A70-22659
- Gas turbine components, discussing material selection, fabrication and assembly with emphasis on combustion and turbine sections, turbine coatings, shafts, bearings and seals
10 p1929 A70-23851
- Fluorocarbon fluid Rankine cycle system utilizing gas turbine exhaust heat for environmental control
[SAE PAPER 700160] 11 p1982 A70-25371
- Gas turbine engine technology for military and commercial aircraft, discussing operations economy, design matching to missions and fabrication methods
11 p2101 A70-25873
- Gas turbine engine performance prediction with water-methanol injection, describing analytical method
[SAE PAPER 700208] 11 p2102 A70-25881
- Fluidic gas turbine controls, discussing high temperature operation, hybrid sensors and logic in hostile environment applications
12 p2164 A70-27074
- Tubular gas turbine combustors design by analytical model, summarizing theories of combustor analysis, turbulent flame speed, microvolume burning and stirred reactors
[WSCI PAPER 70-2] 13 p2474 A70-29613
- Soviet book on gas turbine engines for helicopters covering aircraft design and flight dynamics
15 p2787 A70-32199
- Aircraft fan and turbine noise reduction, discussing blade wake interaction, jet mixing and duct acoustic linings
16 p2963 A70-32946
- Weight-dimensions correlation for gas turbine engine/airplane optimization analyses, determining tradeoffs among performance, noise, drag characteristics, etc
[AIAA PAPER 70-669] 16 p2967 A70-33575
- High strength Ti alloys for aircraft gas turbine engines, determining critical properties for compressor fan blades
17 p3122 A70-34436
- Compressor erosion correlation with aerodynamic parameters in gas turbine engines
17 p3147 A70-34711
- Aircraft gas turbine propulsion, discussing engine performance characteristics, thermodynamics, noise and installation
[AIAA PAPER 70-873] 17 p3147 A70-34810
- High temperature and pressure hot gas source for testing fluidic temperature sensor used in gas turbine engine inlet simulation
17 p3058 A70-35157
- Aircraft design minimizing damage by bird strikes to gas turbine engine components, discussing service experience, airworthiness demonstration tests and research programs
18 p3300 A70-35994
- Gas turbine aero engines damage due to bird strikes, emphasizing rig testing and simulation at first stage rotor blading
18 p3236 A70-35995
- Flameout and ignition correlation for diffusion fuel burnup behind angled stabilizers in annular turbine combustion chamber
18 p3300 A70-36127
- High temperature radial turbine design for small gas turbine engines, discussing aerodynamic, structure and thermal analyses
18 p3301 A70-36450
- Gas turbine engine dynamic performance simulation, using analog and digital techniques
[ASME PAPER 70-GT-23] 18 p3327 A70-36830
- Ni superalloys for gas turbine engines, discussing chemical composition, microstructure, strength, solidification, etc
[ASME PAPER 70-GT-24] 18 p3278 A70-36831
- Helicopter gas turbine governor systems for engine and rotor speed control, minimizing pilot activity
[ASME PAPER 70-GT-37] 18 p3214 A70-36835
- Flight test program for helicopter gas turbine engines, considering engine-airframe-control systems integration and environmental tests
[ASME PAPER 70-GT-38] 18 p3303 A70-36836
- Critical aviation gas turbine rotating component life limit determination, describing statistical, maintenance, inspection and life evaluation computer program (SMILE)
[ASME PAPER 70-GT-66] 18 p3303 A70-36841
- Helicopter gas turbine engines protection against salt spray, dust, sand, ice, cut grass, etc
[ASME PAPER 70-GT-96] 18 p3263 A70-36843
- Electronic gas turbine diagnostic systems, discussing engine parameters and analysis system
[ASME PAPER 70-GT-131] 18 p3259 A70-36857
- Control system considerations for small shaft-type aircraft gas turbines providing torque, temperature, load sharing and overspeed limiting functions
[ASME PAPER 70-GT-132] 18 p3304 A70-36858
- Aerodynamic stability of branched diffuser systems used in annular combustors of gas turbine engines
[ASME PAPER 70-GT-27] 18 p3209 A70-36868
- Aero gas turbine engines digital computer control, discussing special properties, design and safety problems
[ASME PAPER 70-GT-40] 18 p3304 A70-36870
- Gas turbine emissions analysis for air pollutants, determining species distribution and concentration
[ASME PAPER 70-GT-81] 18 p3226 A70-36883
- Surface alterations by machining processes for gas turbine engine materials, emphasizing effects of milling on Ti and grinding on high strength steels
[ASME PAPER 70-GT-100] 18 p3264 A70-36888
- Ceramic materials for low cost high inlet temperature gas turbine engine components
[ASME PAPER 70-GT-105] 18 p3279 A70-36889
- Gas turbines, dust and air cleaners interrelationship in preventing failure due to air contaminants
[ASME PAPER 70-GT-104] 18 p3305 A70-36890
- Aircraft gas turbine engine development, considering gas dynamic and structural parameters
19 p3489 A70-37238
- Gas turbine engine combustion chamber efficiency dependence on injector characteristics, temperature and fuel physicochemical properties
19 p3489 A70-37247
- Air-mechanical fuel injection effect on gas turbine engine combustion chamber working process, investigating heat generation coefficient, temperature field nonuniformity and combustion efficiency
19 p3489 A70-37248
- Model gas turbine engine blades fatigue strength under stress conditions, considering tensile stresses reproducibility from centrifugal loads
19 p3548 A70-38459
- Failure and defect formation in gas turbine engine disks made of steel alloys, stressing fabrication methods effect on reliability
19 p3548 A70-38469
- Aircraft gas turbine engine smoke emission measurement, discussing test equipment and procedure standardization
20 p3689 A70-39720
- Angular contact bearing balls track position on aero gas turbine engines shaft measurement in test rig at high speeds
20 p3638 A70-40141
- Gas turbine engine compressor rotor roller bearing operation conditions analysis by computer calculation of thermal regime
21 p3834 A70-41777
- Helicopter gas turbine engine protection against sand and dust erosion using particle separators, screens and coatings
[SAE PAPER 700705] 22 p4090 A70-42671
- Sand and dust erosion reduction in gas turbine engines by coatings, sleeves and inserts
[SAE PAPER 700706] 22 p4090 A70-42672
- Fuel delivery and speed control systems for aircraft gas turbine engines, discussing control circuit transfers and block diagrams
22 p4091 A70-43116
- Gas turbine combustion chamber convective and radiant heat transmission, examining steam film cooling of flame tube
22 p4092 A70-43199
- Convection, transpiration and full coverage film cooling methods for various local turbine inlet temperatures, gas pressures and cooling air temperatures
22 p4092 A70-43275
- Gas turbine engine combustion chamber starting, discussing effects of temperature, nozzle characteristics and fuel physicochemical properties
22 p4092 A70-43356
- Two stage gas turbine engine optimal tuning for RPM, thrust, fuel rate and gas temperature, describing automated bench tests
22 p4092 A70-43361
- Stepwise heat removal for increased continuous combustion gas turbine engine cycle efficiency, deriving equations describing cycles
22 p4092 A70-43372
- Computerized calculation of gas turbine cycles thermal efficiency, using hydrocarbon fuel, considering fuel composition and heat of combustion changes
22 p4125 A70-43439
- Aircraft flight propulsion systems performance improvement via materials technology for gas turbine engine components
22 p4057 A70-43573
- Surface degradation by oxidation, temperature fluctuations and hot corrosion of Ni- and Co-base superalloys in gas turbine engines
22 p4057 A70-43574

- Statistical analysis of durability data of heat resistant alloys for gas turbine engines, using long term strength tests of melts in mass production
23 p4204 A70-43940
- Gas turbine engines flow velocity fields, comparing various calculation methods
23 p4136 A70-44735
- Heat transfer at air cooled gas turbine blade trailing edges at various wall temperatures and Reynolds numbers
23 p4283 A70-44737
- Columnar grain and Ni alloy single crystal gas turbine engine components resistant to high temperatures produced by precision casting, using directional solidification
23 p4207 A70-44857
- High temperature gas turbine aircraft engine control system requirements, noting stoichiometric fuel-air ratio [SAE PAPER 700823]
24 p4394 A70-45895
- Turbofan, turbojet and turboprop engine development in aircraft gas turbine evolution, discussing VTOL propulsion, centrifugal and axial compressor engines
24 p4396 A70-46251
- GAS TURBINES**
- Heat transfer coefficients in transpiration cooled gas turbine blades, using two dimensional theory covering porous wall and internal cooling passages
01 p0166 A70-11392
- Chemical composition of cermet material for radial sealing of high temperature gas turbines, ensuring structural stability and oxidation resistance
01 p0124 A70-11621
- Combustion instability in gas turbine main combustors, noting heat release and inlet air flow rates coupling
02 p0353 A70-12012
- Radiation from flames in gas turbines and rocket engines, discussing effects of soot formation fuel chemical composition, combustor operating conditions, etc
02 p0354 A70-12050
- U-shaped combustion chamber two dimensional model for studying factors influencing flame spread and stabilization and heat transfer in gas turbines
02 p0355 A70-12257
- Aerodynamic performance of cascade of porous gas turbine blades with cooling air effusion compared with solid noneffusing blades
02 p0355 A70-12311
- Monograph on application of semiclosed thermosiphon system to gas turbine blade cooling, covering heat transfer and temperature distribution analysis, etc
03 p0551 A70-12992
- Air cooling with radial and jet blowing on gas turbine stage, discussing influence on aerodynamic characteristics
03 p0551 A70-13486
- Liquid fuel film vaporizing combustor for gas turbines, considering combustion efficiency and flame intensity
03 p0552 A70-14324
- Gas turbine rotating disks failure analysis, studying strength as function of material properties, thermal stresses and hole dimensions
04 p0775 A70-15260
- Gas turbine blade material properties change effect on thermal fatigue strength after long term heating
05 p0864 A70-16700
- Gas turbine blades thermal fatigue strength under simultaneous temperature cycles and static tensile loads, analyzing temperature and stress fields
05 p0953 A70-17053
- Temperature field in internally cooled gas turbine blades determined, using integrator combined with coordinating device
05 p0954 A70-17057
- Steady state and dynamic performance of variable geometry free gas turbine using nomogram and analog simulation
06 p1129 A70-17143
- Thin gas turbine disk strength under axisymmetric flexural vibrations, noting agreement of calculated and experimental rotor rpm danger zone
06 p1166 A70-17654
- Gas turbine compensating bellows structural strength, discussing low cycle fatigue test under static loads
06 p1167 A70-17664
- Fluidic devices and applications to gas turbine control, discussing beam deflection amplifiers design parameters [AGARDOGRAPH-120]
08 p1559 A70-21933
- Gas turbine blades design and exploitation processes, discussing long time fatigue strength, static durability and heating effects at elevated temperatures
09 p1772 A70-22469
- Thermal fatigue cycle produced by cooled gas turbine blades, using stress-strain tests and thermal simulation
09 p1655 A70-22585

- Thermal stresses in gas turbine blade calculated, showing role of initial temperature increase of blade cooling air
09 p1775 A70-22596
- Pressure and velocity distribution within radial flow gas turbine rotor computed by two dimensional streamline curvature method
09 p1608 A70-23737
- Balancing method for correcting mathematical model discrepancy with gas turbine based on test data
10 p1930 A70-24289
- Heat transfer from gas to gas turbine buckets, determining angle of attack and rotation influences by extending transfer equation
10 p1930 A70-25140
- Gasdynamic test stand analyzing elastoplastic strains in aircraft gas turbine disks and liquid-propellant rocket engines turbopumps under alternating nonisothermal loads
10 p1862 A70-25298
- Gas turbine blade materials investigated for effect of prolonged heating on mechanical properties and thermal fatigue strength
13 p2434 A70-28994
- Circulated air natural and technical impurities effects on gas turbine time dependent performance emphasizing erosion, deposits and overheating
13 p2475 A70-29713
- Gas flow calculations application to gas turbines simulations, considering engine dynamics, one dimensional flow and program structure
14 p2629 A70-30990
- Gas turbine performance dynamic modeling by analog and digital computer simulation providing clear picture of transient behavior
14 p2629 A70-30991
- Low Reynolds number laminar flow gas turbine regenerators, investigating manufacturing tolerances effects on heat transfer and flow friction behavior
14 p2629 A70-31022
- Periodic flow structure between gas turbine blades, using asymptotic representation [ONERA-TP-790]
16 p2833 A70-33102
- Emergency auxiliary electric and/or hydraulic power for commercial and military aircraft using self contained monofueled gas turbine system
16 p2964 A70-33472
- German monograph on gas turbine combustion chambers part-load behavior improvement by load controlled change of flame tube air cross section
17 p3148 A70-35373
- High temperature radial turbine design for small gas turbine engines, discussing aerodynamic, structure and thermal analyses
18 p3301 A70-36450
- Fiber-metal matrix composites for gas turbine blades, discussing stress rupture strength, modulus of elasticity, fabrication, etc [ASME PAPER 70-GT-133]
18 p3302 A70-36827
- Transpiration cooling for high temperature gas turbines, investigating effects on aerodynamic and thermodynamic performance [ASME PAPER 70-GT-56]
18 p3303 A70-36839
- Brayton cycles in gas turbines, investigating intercooling or reheat and pressure ratio proportioning influence on efficiency and specific work [ASME PAPER 70-GT-130]
18 p3304 A70-36856
- Axial gas turbine performance prediction method improvements based on comparison with tests [ASME PAPER 70-GT-2]
18 p3304 A70-36859
- Gas turbine shrouded rotating disk system with radial outflow of air coolant, investigating fluid dynamics, pressure distribution and frictional moment [ASME PAPER 70-GT-6]
18 p3208 A70-36862
- High speed combustion chambers for gas turbine applications, using finite rate chemistry and turbulent mixing computer program for burner design [ASME PAPER 70-GT-25]
18 p3304 A70-36866
- Tailpipe effects on gas turbine diffuser performance with fully developed inlet conditions [ASME PAPER 70-GT-86]
18 p3210 A70-36881
- Gas turbines dynamics and control system requirements, discussing equipment design and reliability [ASME PAPER 70-GT-76]
18 p3305 A70-36887
- Thermal fatigue cracking of gas turbine blades in fuel combustion product flow, investigating surface composition, microhardness and structure under simulated loads
19 p3490 A70-37338
- Gas turbine propulsion systems design, performance and applications for industrial and military uses, discussing sensors for measurement and control of critical engine parameters
19 p3424 A70-37881
- Monograph on radial flow between air cooled gas turbine rotating and stationary disk near stator covering turbulent boundary layer, velocity distribution, etc
19 p3404 A70-38007
- Critical rotation rates of gas turbine rotors disk-drum designs, describing initial parameters of model in matrix form
20 p3721 A70-39782

- High temperature Ni, Co and Fe alloys for gas turbines, examining sulfidation-oxidation corrosion test methods
20 p3651 A70-39971
- Heat transfer from gas to gas turbine buckets, determining angle of attack and rotation influences by extending transfer equation
20 p3694 A70-40345
- Nozzle geometry effects on turbine gas ejector characteristics
21 p3867 A70-41765
- Single stage gas turbines rational design based on minimum diametric dimensions
21 p3867 A70-41768
- Gas turbine ball bearings, measuring effect of rolling elements shape on hydrodynamic power losses
21 p3834 A70-41776
- Three-lobe fluid film bearing configuration for gas turbine concentric rotating shafts/spool shafts/ [ASME PAPER 70-LUBS-10]
22 p4045 A70-42450
- Ni base superalloy for gas turbines, describing heat treatment for precipitation hardening
22 p4055 A70-43099
- Gas turbine design by nomograms with minimal preliminary calculations
22 p3960 A70-43368
- High temperature gas turbine blades cooling by liquid Na-K alloy [ONERA-TP-872]
22 p4125 A70-43458
- Nonsteady temperature and thermal stress distribution in gas turbine blades, using plastic model and photothermoelastic method
22 p4093 A70-43743
- Gas turbine controller design by inverse Nyquist method compared to conventional multivariable design methods
24 p4396 A70-46157
- GAS VALVES**
- Electroexplosively powered release valve for high pressure N stored in hermetically sealed container of missile, discussing design and performance tests
03 p0546 A70-14106
- Fluoric altitude insensitive thruster based on two way gas flow diversion valve developed for VTOL aircraft and missile hot gas attitude control systems [ASME PAPER 69-WA/FLCS-10]
04 p0626 A70-14843
- Breathing valve with reduced air resistances based on aerodynamic principles
06 p1000 A70-17433
- Comet tail simulation by using fast acting gas valve to produce gas cloud for interaction with plasma stream
12 p2298 A70-27190
- Thin high vacuum gate valve design for use with UV grating spectrograph
19 p3357 A70-37687
- Magnetic pressure fast opening gas puff valve for hydrogen bursts in conical theta pinch plasma source
21 p3833 A70-41472
- Gas reducers transient processes, analyzing valve equations of motion
22 p3965 A70-43357
- Single stage warm gas directed jet valve for missile attitude control, noting servovalve and auxiliary power unit control applications [SAE PAPER 700778]
24 p4295 A70-45864
- GAS VISCOSITY**
- Moving gas with thermodynamic relaxation process, discussing bulk viscosity and application to shock structure calculations
01 p0063 A70-10927
- Viscosity of nitrogen, hydrogen, Ar and He at high pressures measured by capillary flow viscometer with range extended to minus 100 C
04 p0718 A70-14697
- Steady circulation and temperature perturbations in stratified nonrotating ideal gas atmosphere with viscosity and heat conduction
04 p0681 A70-15517
- Temperature dependence of viscosity coefficient determined for hydrogen, helium, argon and nitrogen at atmospheric pressure using capillary viscometry
07 p1424 A70-19980
- Inert gases and nitrogen determined at high temperature, discussing revision of existing functions representing intermolecular energy
08 p1598 A70-21525
- Simple molecules viscosity as function of temperature and density using empirical equation
09 p1731 A70-22292
- Gas viscosity high temperature measurement method in shock tube using boundary layer equations for velocity and static temperature distributions
10 p1867 A70-24151
- Correction factor for free stream Reynolds number errors resulting from low temperature viscosity in He wind tunnels
13 p2385 A70-29985
- Viscous gas hypersonic flow past blunt nosed bodies based on Navier-Stokes equation
15 p2671 A70-31481
- Approximate formula for viscosity of binary polar gas mixtures confirmed for unlike cross sections
16 p2996 A70-33055

Argon plasma viscosity measurements at one atmosphere and 10-13,000 K, using discharge with laminar flow as plasma source
[AIAA PAPER 70-775] 17 p3139 A70-34479

Viscosity and thermal conductivity of dilute gaseous para and normal hydrogen at various temperatures
19 p3551 A70-37710

Polar gas rotational relaxation time calculation, comparing volume viscosity and energy equation definitions
19 p3473 A70-38266

Shock tube high temperature air viscosity from laminar boundary layer heat exchange data
20 p3608 A70-39633

Book on nonuniform gas theory covering viscosity, thermal conduction, diffusion, Maxwell-Boltzmann equations, density, quantum theory, transport phenomena, mixtures, electric fields, etc
20 p3673 A70-40135

Nitrogen viscosity coefficient at high pressure, describing viscosimeter operation and kinetic theory calculations
20 p3738 A70-40140

Solar photosphere negative viscosity phenomenon, examining Rossby wave on differentially rotating isothermal spherical shell of nonconducting inviscid ideal gas
22 p4109 A70-43748

Compressibility, viscosity and thermal conductivity of dense gases, examining high temperature and pressure effects
23 p4222 A70-44431

Nitrogen plasma viscosity measurements as function of velocity and axial static pressure gradient
23 p4226 A70-44439

Atmospheric pressure Ar plasma viscosity measured over heavy particle temperature range 3500-8500 K, using DC wall stabilized cylindrical arc
23 p4229 A70-44983

GAS WELDING
NT BRAZING
NT LOW TEMPERATURE BRAZING
NT ULTRASONIC SOLDERING
Flash, gas-pressure and electron-beam welding of airframe steels
[ASTM PAPER MR-69-712] 12 p2239 A70-26987

Pressure role in inert gas shielded metal arc welding, discussing voltage-pressure relation, weld head profile, metal transfer, etc
22 p4043 A70-42383

GAS-GAS INTERACTIONS
Cavitating flow in converging channels of hydraulic system, calculating energy distribution at gas-vapor phase using Borda-Carnot theorem
03 p0466 A70-13513

Helium injection Mach number effect on supersonic jet penetration into Mach 2 air stream from flat plate determined from concentration measurements
[AIAA PAPER 70-92] 06 p0975 A70-18200

Interactions between hypersonic neutral gas beam and orificed pressure gauge in spinning satellite noting dependence on angle of attack
06 p1159 A70-18290

Atmospheric gases atomic and molecular binary short range repulsive forces, determining interaction potentials from elastic scattering cross sections
07 p1345 A70-20141

Circular turbulent air jet from flat plate into deflecting stream using potential flow model, noting applicability to V-STOL aircraft technology
[AIAA PAPER 69-223] 07 p1190 A70-20406

Nonequilibrium interaction of radiative and vibrational rate processes in IR-active diatomic gas using macroscopic equations
08 p1549 A70-21574

Wave number, intensity and half width of vibrational-rotational lines pertaining to transition of carbon monoxide perturbed by argon
09 p1733 A70-23316

Kinetic theory applied to model of interaction between two gas flows colliding at sharp leading edge at different hypersonic speeds
10 p1800 A70-24139

Perfect gas mixtures thermodynamic functions at high temperatures with correction for Debye-type electrostatic interaction effects
10 p1968 A70-24707

Turbulent flow generation by interacting principal stream with transverse jets, obtaining flow domains in test chamber of two dimensional wind tunnel
10 p1870 A70-24785

Injectant stagnation temperature and molecular weight effects in jet interaction flowfield
11 p2036 A70-25989

Turbulent mixing at contact surface in driven shock wave in shock tube with bursting diaphragm for He-Ar test gas mixtures
14 p2566 A70-31030

Krook gas particle collision model for relaxation from nonequilibrium to equilibrium Boltzmann distribution in spatially uniform gases
17 p3068 A70-34697

Energy and momentum exchange between gases in elastic collisions at different temperatures and velocities
19 p3551 A70-37538

Helium injection Mach number effect on supersonic jet penetration into Mach 2 air stream from flat plate determined from concentration measurements
20 p3558 A70-39690

Nonequilibrium radiation from stagnation region of high velocity spherical gas cap traveling through air
22 p4124 A70-42758

EPR method for elementary reaction kinetics of vapor phase oxygen atoms interacting with molecular hydrogen
22 p3983 A70-43349

Three body recombination and dissociation rate coefficients of nitrogen in Ar atoms heat bath, using modified phase-space theory
23 p4221 A70-44008

CO vibrational relaxation measurements in shock tube expansion wave generated in argon heat bath
23 p4180 A70-44009

GAS-ION INTERACTIONS
F region ionized and neutral atmospheric movements interactions, discussing ion drag forces, electromagnetic drift, wind effects, etc
01 p0074 A70-10587

Atmospheric gravity waves in F region, discussing neutral gas-ionization interaction and detection by electron density profile measurements
01 p0079 A70-11216

Dissociative charge-transfer reactions of positive He ions with molecular N and O measured in drift tube-mass spectrometer
06 p1109 A70-17490

Resonant and foreign gas broadening using Schroedinger equations for collision problems
07 p1346 A70-20244

Elementary processes cross sections in charged states changes during proton-hydrogen molecule interactions
08 p1549 A70-21817

Hydromagnetic coupling between neutral and ionized atmosphere perturbations, noting role of gravity waves
13 p2397 A70-29191

Hydromagnetic fluid model of solar wind for interpreting discontinuities in plasma and magnetic field, interaction with atmosphere, heating mechanism and chemical composition
13 p2481 A70-30067

Rare gas diatomic ions reactions with molecules and rare gas atoms, measuring rate coefficients and product channels by flowing afterglow technique
15 p2776 A70-31726

Rare gas diatomic and hydride ions reactions with hydrogen, determining rate coefficients and product channels by flowing afterglow technique
15 p2776 A70-31727

Positive atomic oxygen ion reactions with carbon dioxide detected using ion cyclotron and double resonance methods
18 p3225 A70-36189

Fully ionized magnetized rotating plasma interaction with neutral gas blanket, discussing plasma decay and velocity field
19 p3481 A70-38489

Chemical reactions of ions and neutral particles in D region, discussing photochemistry of atomic oxygen and ozone and reaction rate constants
19 p3418 A70-38905

Mass spectroscopy analysis of neutral and ionic population of plasma in carbon dioxide laser gas mixture, discussing collision processes
21 p3838 A70-42006

GAS-LIQUID INTERACTIONS
Two phase flow in cylindrical channel, formulating maximum momentum flow variational principle for laminated adiabatic vapor- and gas-liquid flows
01 p0213 A70-10216

Gas bubble formation and equilibrium conditions in air supersaturated fuel stored under atmospheric pressure after injection into evacuated tank
03 p0605 A70-13394

Porous matrix flow, surface liquid layer and hot gaseous boundary layer interactions at nose tip of reentry vehicle
[AIAA PAPER 70-152] 06 p1037 A70-18028

Interaction between turbulent air flow and water surface based on Fourier analysis of finite intervals of field
11 p2042 A70-26775

Gas mass diffusivity measurements in plasma and reaction velocity constant in human and dog blood
15 p2692 A70-32311

Resistance to two phase gas-liquid flow in airways simulating human bronchial tree
24 p4303 A70-46111

GAS-METAL INTERACTIONS
Effects of solidification conditions and gas content in melt on continuously cast Al ingots as-cast structure
02 p0316 A70-12297

Hydrogen, oxygen and nitrogen effects on gas shielded arc weld porosity of Ni, comparing MIG and TIG processes
02 p0310 A70-12543

Pseudoboiling heat transfer from platinum wire to carbon dioxide during free convection
03 p0604 A70-13209

Energy accommodation coefficients for He3-W and He4-W, comparing results with classical gas-solid interaction theory
04 p0721 A70-14388

Hydrogen diffusion in pure Ti and beta Ti alloy VT15, determining diffusion coefficient for various temperatures
04 p0707 A70-15190

Polymorphic transformation effects on oxygen diffusion rate in alpha and beta phases of Ti, considering temperature effects and activation energy
04 p0707 A70-15211

Ti-hydrogen reaction at ambient temperatures, investigating factors favoring reaction and preventive measures
05 p0863 A70-16524

Quasi-equilibrium treatment of heterogeneous reactions applied to evaporation rate /desorption/ computation for volatile species formed in oxygen reactions with W, Mo and graphite
06 p1004 A70-17330

Quasi-equilibrium treatment of heterogeneous reactions applied to flash desorption data for oxygen reaction with tungsten surface, discussing species desorption dependence on adsorption temperature
06 p1004 A70-17331

Mo-nitrogen interaction, studying nitriding influence at various temperatures on Mo alloys properties
06 p1089 A70-17741

Cold molecular beam of helium impinging on LiF or Si crystals investigated for gas-surface interactions, using time of flight method
06 p1043 A70-18255

Nitrogen molecule-tungsten surface interactions, computing trajectories and accommodation coefficients for various temperatures by equations of motion
06 p1110 A70-18262

Particle, momentum and energy flux spatial distributions of molecules scattered in collisions of low energy Ar atoms with mica and Ag surfaces
06 p1111 A70-18268

Lift and drag forces measured on metal surfaces inclined to Ar ion stream above and below earth-satellite speeds in free molecular flow
06 p1111 A70-18269

Angular distributions of fast scattered particles resulting from noble gases collision with metal surfaces
06 p1112 A70-18271

Rare gas scattering from Ag surfaces calculated up to earth satellite energy values
06 p1112 A70-18275

Weld porosity in TIG welding of technical Ni in ternary mixtures of Ar with H, O and N
08 p1518 A70-21345

Gas saturation and inhomogeneity in surface layer of Ti alloys with alpha and beta stabilizers after high temperature heating
09 p1700 A70-22078

Rhenium single crystals basal plane surface properties using LEED and Auger electron spectroscopy, describing gas adsorption studies
09 p1739 A70-22526

Propellant extinction near powder-metal contact to study nonsteady combustion mechanism
09 p1742 A70-23228

Oxygen reduction reaction mechanism and catalysis, considering metal electrode surfaces and substrates, hydrogen peroxide role, adsorption, metal-oxygen bonds, etc
10 p1829 A70-24452

Al and B particles combustion in methane-oxygen system, considering reaction zone models, energy release rate, particle kinetics, instabilities, etc
11 p2149 A70-26284

Oxygen adsorption on W(110) surface determined for coverage as function of exposure by Auger electron spectroscopy
12 p2180 A70-27253

High temperature gaseous molecular beams impingement on Cu surfaces at cryogenic temperatures measured for condensation rates
12 p2271 A70-27265

Oxygen interaction on rhenium filament, considering sticking probability as function of temperature
12 p2181 A70-27677

Nitrous oxide chemisorption by rhenium filament at low pressures at various temperatures, determining sticking probability
12 p2181 A70-27678

CO adsorption on smooth polycrystalline platinum and rhodium electrodes at various potentials
12 p2182 A70-27761

Hydrogen solubility in electrically exploded metals
15 p2762 A70-32747

Electron energy losses at interface of helium inclusions in aluminum irradiated by radioactive lithium
15 p2785 A70-32764

Scattering cross sections for monoenergetic Ar beams on epitaxial Ag films
16 p2956 A70-34013

Hydrogen embrittlement of Ti and Ti alloys under plastic deformation and critical hydrogen concentration 17 p3117 A70-34397

Ti alloys thermomdiffusion impregnation with rarefied nitrogen and oxygen plasma, determining optimal gas pressure and temperature conditions and magnetic field frequency effects 17 p3101 A70-35391

Relaxation peaks associated with interaction clusters of Zr and N dissolved in Nb 18 p3274 A70-36056

Depth measurement of gas-saturated surface layer in Ti alloys, using microhardness method 18 p3277 A70-36472

Alloying elements effect on diffusion coefficient of hydrogen in low-alloyed alpha titanium 19 p3449 A70-37274

Clean Ru/0001/ and Rh/111/ surface properties by LEED and Auger electron spectroscopy, discussing gas adsorption 19 p3483 A70-37546

Monatomic inert gas molecules interaction with continuous elastic solid of alkaline and nonalkaline metals, calculating energy exchange 19 p3373 A70-37816

Niobium yield stress at room temperature for various nitrogen and oxygen concentrations 19 p3454 A70-38814

Particulate matter interaction with ionized gas in external magnetic field and nonequilibrium state, examining free electron density 20 p3677 A70-39324

Interactions between moving alkali-metal seeded dense plasma and metallic thermionically emitting electrode with surface properties influenced by seed particle absorption 20 p3681 A70-40007

Clean iron /011/ surfaces, determining sulfur, oxygen and hydrogen sulfide films effects on adhesion behavior 21 p3831 A70-40748

Thermodynamic equilibrium analysis of metal oxidation and thermal dissociation of oxides in vacuum, noting decreased affinity by evaporation 24 p4361 A70-45835

Oxygen and nitrogen adsorption on thin tantalum films, measuring pressure, electrical resistivity and temperature 24 p3463 A70-46219

Diffusing element deposition on metal surface during saturation from gas phase based on calculation of equilibrium composition of reaction mixture 24 p4364 A70-46333

GAS-SOLID INTERFACES

Equilibrium existing at gaseous-condensed phases interface inferred as mechanism for dissociative sublimation of ammonium perchlorate 05 p0894 A70-17079

Gas phase reactions near solid-gas interface of deflagrating double base propellant causing abrupt changes in burning rate-pressure curve [AIAA PAPER 70-124] 06 p1179 A70-18046

Velocity distributions of incident and reflected Ar beams, determining partial energy accommodation coefficients for reflection from copper and carbon dioxide deposited surfaces 06 p1111 A70-18264

Gas stream-elastic solid surface scattering characteristics, calculating trajectories, particle flux angular distributions, velocities, transfer coefficients, etc 06 p1111 A70-18265

Momentum transfer from neutral nitrogen molecules to solid surfaces measured for various incident beam molecule energies 06 p1112 A70-18272

Nonlinear Knudsen layer gas flow using BGK model for Boltzmann equation 06 p1048 A70-18322

Pressure effects in predicting ablation velocities for gas-solid systems, assuming reactions and gaseous products reversible adsorption on solid surfaces 07 p1422 A70-19373

Low and moderate energy gas molecule-solid surface interactions using molecular beams 07 p1328 A70-20116

Molecular beam interactions with solid crystalline surface with fcc lattice elementary cell, investigating intensity distribution of scattered particles 07 p1342 A70-20119

Reflected molecular beam intensity distribution interpreted in terms of disturbances in boundary layer between gas and solid 07 p1343 A70-20122

Gas molecules scattering by solid surface for monoenergetic and Maxwellian beams, discussing model with different values for magnitude and velocity direction 07 p1343 A70-20124

Atomic gas particles interactions with self and solid surfaces based on rarefied gas dynamics and classical mechanics 08 p1547 A70-21077

Molecular beams and particle adsorbing surfaces interactions in state of relaxation, determining reflection parameters as function of gas characteristics 08 p1547 A70-21078

Molecular beams and particle adsorbing surfaces interaction with allowance for deposited atoms relaxation, determining reflected flux 08 p1547 A70-21079

Molecular beam and pure surface interactions on background of external forces field 08 p1547 A70-21080

Aerodynamic characteristics of nonconvex bodies in free molecular flow of monatomic gas 08 p1547 A70-21081

Aerodynamic coefficients of nonconvex bodies in free molecular flow of monatomic gases based on delta representation of flow velocity distribution function 08 p1432 A70-21084

Free radicals role in high temperature surface reactions of solid metal oxide particles interacting with unburned flame gases 09 p1629 A70-22320

Monograph on ionosphere-satellite interactions, discussing ionosphere layers, plasma sheaths and wakes, electromagnetic wave propagation, spacecraft antennas, etc 10 p1944 A70-24900

Heat transfer from gas to gas turbine buckets, determining angle of attack and rotation influences by extending transfer equation 10 p1930 A70-25140

Gas-filled composites under impact loading, studying thermal damping due to heat transfer between compressed gas and solid structure 11 p2140 A70-26480

Solid-gas phase equilibria of binary systems related to cryogenics 12 p2329 A70-27023

Neutral molecule-solid surface interactions mass spectrometric techniques for measuring molecular flux and mean thermal energy after interaction 12 p2181 A70-27257

Graphite-carbon dioxide interaction at high temperatures in presence of solid phase diffusion from bulk to reacting surface 13 p2520 A70-28581

Heat exchange measurements between solid body and high enthalpy gas flow at stagnation point using electric arc heater 15 p2826 A70-32102

Gas-particle efflux from nozzle at critical velocities, noting particle size and concentration effects on inlet pressure 15 p2721 A70-32136

Gas-wall heat losses reduced and heated gas pressurization systems performance improved by ullage mixing by gas flow from pressurant injectors [AIAA PAPER 70-681] 16 p2962 A70-33581

Dusty gas dynamics, examining shock wave structure, boundary layers stability, flow equations, acoustic damping, velocity and density perturbations, etc 17 p3068 A70-34671

Light gas atoms adsorption on solid surfaces, calculating wave function, energy, mobility, sticking coefficient, etc 18 p3225 A70-36186

Plane wall surface sublimation under radiation from shock wave heated gas 18 p3348 A70-36721

Heat transfer from gas to gas turbine buckets, determining angle of attack and rotation influences by extending transfer equation 20 p3694 A70-40345

Piston problem numerical solution by Boltzmann collision integral, considering shock waves and thermal disturbances evolution at gas-solid interfaces 21 p3808 A70-41378

Phase velocity and attenuation of shear waves in gases from sampled-CW ultrasonic crystal resonator reflection measurement 21 p3827 A70-41457

Gases interaction with ablator and components during thermal conductivity, measuring nitrogen, helium, carbon dioxide and water sorption 21 p3951 A70-41873

Heat transfer from thin plate in compressible gas flow, considering interface temperature as nonanalytic function 21 p3953 A70-42086

Radiative energy transfer during interaction between blunt body and hypersonic gas flow, noting effect on flow temperature, shock wave separation, etc 23 p4136 A70-45020

Contact region structure with viscosity, conduction and radiative transfer effects applied to plane shock wave reflection from heat conducting wall 24 p4326 A70-46001

GASEOUS CAVITATION

U CAVITATION FLOW

U GAS FLOW

GASEOUS DIFFUSION

Metal surface microscopic defects detection and display using diffused radioactive Kr-85 gaseous penetrant for anodized flaws, bearing porosity and turbine blade cracks 01 p0096 A70-10006

Human pulmonary gas mixing between large airways and alveolar spaces, using argon bolus inhalation 01 p0024 A70-10976

Structure of hydrogen-oxygen diffusion flame in equilibrium using iterative solution 02 p0352 A70-12796

Diffusivities of argon, krypton and xenon determined in olive oil by curve-fitting analysis of sorption curves 03 p0429 A70-14159

Gas diffusion coefficients for He-N and nitrogen-carbon dioxide systems in diffusion cell utilizing porous stainless steel barrier 04 p0780 A70-14710

Hydrogen diffusion in pure Ti and beta Ti alloy VT15, determining diffusion coefficient for various temperatures 04 p0707 A70-15190

Polymorphic transformation effects on oxygen diffusion rate in alpha and beta phases of Ti, considering temperature effects and activation energy 04 p0707 A70-15211

Initial disturbances propagation in gas mixtures by asymptotic analysis, observing diffusely and viscously damped modes 05 p0833 A70-16404

Pulmonary CO diffusing capacity in young men during muscular exercise 06 p0993 A70-17432

Species concentration, jet structure and diatomic nitrogen rotational temperature measured for diffusive separation of nitrogen-helium mixture free jets, using electron beam 06 p1043 A70-18253

Turbulent heat and mass diffusion in catalytic reactors for hydrazine decomposition, developing computer program to calculate temperature and reactant concentration distributions [AIAA PAPER 69-421] 07 p1365 A70-19706

Hydrogen supply rate by solar wind found comparable to hydrogen losses from earth by diffusion into space 08 p1487 A70-20637

Hydrogen penetrability in heat resistant steels subjected to high temperature creep, observing activation energy decrease with increased stress 08 p1515 A70-20923

Austenitic Fe-Cr-Ni-Ti alloys at high temperature to determine activation energy for nitrogen diffusion, noting oxygen role 08 p1522 A70-21707

Oxygen diffusion time into nitrogen in dichotomously branched human lung model calculated by finite difference technique, discussing alveolar plateau 10 p1809 A70-24003

Teflon-bonded gas diffusion electrode flooded agglomerate model, determining porosity, surface area, IR drop, etc 10 p1829 A70-24455

Oxygen diffusion in presence of hemoglobin taking into account chemical kinetics, showing approximate and computer solutions 10 p1819 A70-24772

Air pollution measured from high altitude balloons and satellites by remote sensing of diffused atmospheric gases, using solar illumination 12 p2221 A70-26950

Oxygen and hydrogen diffusion coefficients in aqueous potassium hydroxide electrolyte solutions at various temperatures and concentrations 12 p2181 A70-27575

Oxygen diffusion facilitation in vivo and nonsteady state conditions under physiological circumstances, emphasizing hemoglobin in red cells and myoglobin in muscle 12 p2171 A70-28024

Self diffusion coefficient for gaseous ammonia at specific temperature range, applying polar gases theory 13 p2453 A70-29800

Soviet monograph on gas laws in aviation medicine for reduced oxygen pressure pathology, discussing kinetic theory, temperature effects, solubility, diffusion, etc 15 p2682 A70-31925

Gas mass diffusivity measurements in plasma and reaction velocity constant in human and dog blood 15 p2692 A70-32311

Internal friction in hydrogenated Ti-Mn alloys, observing relaxation peak formation under stress induced hydrogen diffusion in beta phase 16 p2930 A70-33082

Flow and diffusion phenomena in rarefied gas mixtures associated with separation nozzle process, using molecular pressure probe and mass spectrometer 16 p2893 A70-33699

- Intrapulmonary distribution of gases inhaled during positive and transverse accelerations
17 p3037 A70-35130
- Lung diffusing capacity for CO in Caucasians native to 3100 m noting membrane diffusing capacity, lung capillary volume and age effects
17 p3031 A70-35427
- Thermodynamic effects and transport phenomena in discontinuous system of gas filled containers connected by membrane, deriving entropy production and diffusion flux in membrane
17 p3197 A70-35531
- Time and altitude dependences between 340-1000 km of delta parameter for height scale ratio of neutral and electron-ion gases, discussing diffusion coefficient
18 p3254 A70-37030
- Binary Nb vapor systems mutual diffusion coefficients concentration and temperature dependences, discussing interatomic bonds and melting point of alloys
19 p3454 A70-38715
- Turbulent jet system with previously unmixed chemically active gases, calculating heat and mass transfers during diffusion combustion
20 p3737 A70-39813
- Book on nonuniform gas theory covering viscosity, thermal conduction, diffusion, Maxwell-Boltzmann equations, density, quantum theory, transport phenomena, mixtures, electric fields, etc
20 p3673 A70-40135
- Premixed laminar flames of hydrogen, oxygen and nitrogen burned on Meker burner, investigating diffusional effects on gas composition changes
20 p3739 A70-40469
- Oxygen diffusion coefficient of alpha-Ti from oxidation of saturated and unsaturated beta phase in 932-1142 C range
22 p4053 A70-42731
- Interdiffusion coefficients for hydrogen-carbon dioxide and oxygen-carbon dioxide systems at low temperatures
22 p4076 A70-43393
- Carbon dioxide molecular vibration excitation by Q switched carbon dioxide laser, obtaining accommodation and diffusion coefficients by relaxation measurements
24 p4351 A70-45369
- GASEOUS FISSION REACTORS**
Engine weight estimation for showing effect on thrust, specific impulse and uranium loss rate for open cycle gas fueled nuclear rocket engine
[ALAA PAPER 70-690] 16 p2949 A70-33553
- Gas-core nuclear rocket engine simulation by induction coupled plasma torch, determining gas flow patterns
[ALAA PAPER 70-691] 16 p2950 A70-33555
- Gas core nuclear rocket engine light and heavy species centrifugal separation by MHD-driven rotating flow, discussing fluid dynamic simulation results
20 p3671 A70-40256
- GASEOUS ROCKET PROPELLANTS**
Book on turbulent diffusive flames in combustion of gaseous fuels covering mass, heat, flame exchange and stabilization processes, etc
01 p0219 A70-11377
- Long term life test and vacuum tests of high temperature resistors using ammonia and hydrogen propellants
[ALAA PAPER 70-1136] 20 p3567 A70-40212
- Nuclear light bulb and coaxial flow gaseous core nuclear rocket reactors based on energy transfer via thermal radiation
22 p4070 A70-43182
- GASES**
NT AIR
NT ARGON
NT ARGON ISOTOPES
NT CARBON DIOXIDE
NT CARBON MONOXIDE
NT COLD GAS
NT COSMIC GASES
NT DETONABLE GAS MIXTURES
NT DEUTERIUM
NT DEUTERIUM PLASMA
NT DIATOMIC GASES
NT EXHAUST GASES
NT FLAMMABLE GASES
NT GAS MIXTURES
NT GAS STREAMS
NT GRAY GAS
NT HELIUM
NT HELIUM ATOMS
NT HELIUM FILM
NT HELIUM ISOTOPES
NT HIGH TEMPERATURE AIR
NT HIGH TEMPERATURE GASES
NT HYDROGEN
NT HYDROGEN ATOMS
NT HYDROGEN IONS
NT HYDROGEN ISOTOPES
NT HYDROGEN PLASMA
NT IDEAL GAS
NT INTERPLANETARY GAS
NT INTERSTELLAR GAS
- NT IONIZED GASES
NT LIQUEFIED GASES
NT LIQUID AMMONIA
NT LIQUID HELIUM
NT LIQUID HYDROGEN
NT LIQUID NITROGEN
NT LIQUID OXYGEN
NT LORENTZ GAS
NT MOLECULAR GASES
NT MONATOMIC GASES
NT NEON
NT NEON ISOTOPES
NT NITROGEN
NT ORTHO HYDROGEN
NT OXYGEN
NT PARA HYDROGEN
NT PHOSGENE
NT POLAR GASES
NT POLYATOMIC GASES
NT RADON
NT RARE GASES
NT RAREFIED GASES
NT REAL GASES
NT RESIDUAL GAS
NT SOLIDIFIED GASES
NT TRITIUM
NT XENON
NT XENON ISOTOPES
NT XENON 129
NT XENON 133
- Steady state thermal defocusing of carbon dioxide laser radiation in gases as function of beam power, gas absorption coefficient and pathlength
06 p1079 A70-17190
- Light inductions and echo intensities in liquids and gases, investigating thermal vibrations, translational Brownian motion, particle collisions and laser diffusion effects
06 p1082 A70-17809
- Thermal conductivity for organic compound gases at atmospheric pressure
08 p1597 A70-21026
- Gaseous media absorption coefficient and refractive index in field of two nonmonochromatic radiation streams quasi-resonant with neighboring atoms and molecules transitions
19 p3448 A70-38740
- GASOLINE**
Acute gasoline poisoning toxicology and prophylaxis, manner of ingestion and effects on organs and systems
08 p1451 A70-20976
- Commercial aviation gasoline inspection data tabulated and compared for 1969 and 1964
[SAE PAPER 700228] 11 p2099 A70-25897
- GASTROINTESTINAL SYSTEM**
NT INTESTINES
NT RECTUM
NT STOMACH
- Stainless steel micropipettes implantation in rat amygdala to study role in gastric secretion
02 p0234 A70-11729
- Starvation effect on intestinal amino acid absorption of rats, noting protein synthesis reduction
02 p0234 A70-11731
- Positive effect of shielding and cystamin administration on tonic and evacuator functions of rats gastrointestinal tract after gamma irradiation
05 p0804 A70-17122
- Radioactive isotopes removal from respiratory tract, lungs and gastrointestinal tract by ion dilution and antagonism, blood transfusion and hemodialysis, etc
06 p0994 A70-17666
- Low ambient temperature exposure effect on hamster intestinal absorption capacity, using glucose test compound
19 p3360 A70-37772
- Cardiac rhythm, respiration and rhythmical processes of alimentary tract, using digital data device
19 p3370 A70-38214
- GATES [CIRCUITS]**
NT THRESHOLD GATES
- Picosecond on-off light gate based on Kerr cell design, using optical pulses to induce birefringence in liquids
01 p0111 A70-10571
- Burst noise in forward biased silicon diodes and transistors, discussing measurements on gate controlled devices
03 p0458 A70-14029
- Preamplifier-discriminator-gate generator in printed circuit for use with photomultipliers, noting pulse sensitivity and cost
09 p1679 A70-22997
- Hysteresis in MOS transistors attributed to trapped charge carriers on oxide near silicon oxide interface
14 p2555 A70-30338
- Binary division by logic gates cellular arrays, noting accuracy and operating speed
14 p2556 A70-30517
- Algebraic computation of diagnostic tests for combinational digital circuits single gate failure detection and location
16 p2868 A70-33455
- Interference free high speed monolithic digital integrated gate, determining current swing, lead inductances and switching times
17 p3048 A70-34587
- DC transistorized Nor logic gates design based on graphic analytic method permitting influence of circuit parameters variations for reliability improvement
21 p3793 A70-40765
- Specification sheets for fluidics clarified by demonstrating step-by-step solutions for typical problems involving flip-flop and OR/NOR gate
24 p4293 A70-45431
- GATES [OPENINGS]**
Night vision systems with integrated pulse gated viewing and laser ranging, analyzing transmitter and viewer
12 p2236 A70-27902
- Non Q switched Nd laser light intensity correlation function measurement, using optical gate for producing second harmonic light
13 p2430 A70-29706
- GAUSS EQUATION**
Stationary Gaussian stochastic processes sample functions properties and local times
02 p0324 A70-12504
- Gaussian approximation of parameters of arbitrarily oriented magnetic dipole representing geomagnetic field
07 p1266 A70-19441
- Gaussian approximation of parameters of arbitrarily oriented magnetic dipole representing geomagnetic field
18 p3249 A70-36915
- GAUSS FUNCTION**
U GAUSS EQUATION
- GAUSS-MARKOV THEOREM**
Probability of given configuration and statistical distribution of peaks between mean crossings of broadband locally stationary and Gaussian processes
[ONERA-TP-806] 10 p1805 A70-24546
- GAUSSIAN DISTRIBUTIONS**
U NORMAL DENSITY FUNCTIONS
- GAUSSIAN NOISE**
U RANDOM NOISE
- GAUSSMETERS**
U MAGNETOMETERS
- GCR [REACTORS]**
U GAS COOLED REACTORS
- GEAR TEETH**
Prototype inspection equipment for automatic detection of fatigue damage in helicopter transmission gears teeth by magnetic perturbation method
01 p0097 A70-10011
- Dynamic loads calculation on teeth of cylindrical straight tooth gears under engaged and disengaged conditions, performing strength analysis
01 p0105 A70-11421
- Overcut phenomenon in early stage of cutting developed as theory for tip interference in internal gears
05 p0854 A70-15885
- Gear ratios series determination for planetary reduction gear having positive and negative difference between number of gear teeth
05 p0856 A70-17007
- Discrete mechanical models of single speed gearings in torsional vibrations without teeth deformation and damping resistance
16 p2995 A70-34288
- GEARS**
Vacuum evaluation of lubricants and techniques applicable to miniature ball bearings and instrument gearing for space systems
[ASME PAPER 69-LUB-30] 01 p0100 A70-10379
- Gear materials evaluation program for space environment application with unlubricated or solid film lubricated operation mode
[ASLE PREPRINT 69-LC-6] 02 p0309 A70-12539
- Structural design of boron/epoxy front housing for T-56 turboprop reduction gear case achieving reduced weight and increased stiffness
[SAE PAPER 690666] 05 p0853 A70-15837
- Self stopping in involute gear mechanisms with external and internal gearing
07 p1290 A70-18818
- Spiral gears bearing disks contact fatigue endurance process, deriving critical points cyclic stability from stress distribution considerations
07 p1291 A70-18819
- Gear materials evaluation program for space environment application with unlubricated or solid film lubricated operation mode
10 p1893 A70-23837
- Corrosive wear due to oxygen and/or moisture in air indicated as major failure mode in lubricated gears
10 p1895 A70-24852
- Vacuum evaluation of lubricants and techniques applicable to miniature ball bearings and instrument ball bearings and instrument gearing for space systems
13 p2419 A70-29120
- Gear pumps for hydraulic systems, discussing costs, types and applications
14 p2590 A70-30302

Swinging gear drive, breather cartridge and hypocyclid timer mechanisms for reliable aerospace applications

16 p2921 A70-34104

Discrete mechanical models of single speed gearings in torsional vibrations without teeth deformation and damping resistance

16 p2995 A70-34288

Mechanical models of single speed gearings for torsional vibrations, taking into account nodes of first free vibration mode

16 p2995 A70-34289

GEIGER COUNTERS

Density spectrum exponent of penetrating muon component of extensive air showers determined for hodoscopic assembly of Geiger-Muller counters with lead absorber

03 p0556 A70-13043

Cosmos-261 satellite-borne scintillation electron proton spectrometers and lead shielded Geiger counter, measuring electron and proton energy spectra, pitch distributions, etc

08 p1501 A70-21799

Charged particle albedo latitude dependence estimated from balloon-borne Geiger telescopes

09 p1746 A70-23481

ESRO 1 satellite and ground observations of energetic auroral electrons angular distribution during solar event, using Geiger counters

19 p3412 A70-37519

Soft X ray astronomical instrumentation for space experiments, discussing Geiger tubes, gas counters, modulation collimators, telescopes, etc

23 p4196 A70-44416

GEIGER-MUELLER TUBES

U GEIGER COUNTERS

GELATINS

Dichromated gelatin holographic films preparation, sensitization, exposure and development, giving diffraction efficiencies and reconstruction SNR

04 p0691 A70-15031

Calcium phosphate crystals precipitation from nutrient gel to determine role of gelatinous ground substance in calcification

10 p1832 A70-25075

GELLED PROPELLANTS

NT GELLED ROCKET PROPELLANTS

GELLED ROCKET PROPELLANTS

Gelled space-storable oxygen difluoride and diborane analysis, including particle preparation, yield stresses, viscosities and storability

16 p2962 A70-33607

GELS

NT DOUBLE BASE ROCKET PROPELLANTS

Calcium phosphate crystals precipitation from nutrient gel to determine role of gelatinous ground substance in calcification

10 p1832 A70-25075

Gelled and emulsified fuels for jet transport aircraft, testing rheological and physical properties regarding fire hazard reduction in crashes

12 p2160 A70-27430

Dispersion/peak broadening/ in gel chromatography measured with nonporous and porous column packings, suggesting diffusion controlled separation with linear permeation isotherm

12 p2181 A70-27474

Gel permeation chromatography peak broadening, discussing liquid dispersion factors and column efficiency

24 p4310 A70-46349

GEMINI FLIGHTS

NT GEMINI 4 FLIGHT

NT GEMINI 6 FLIGHT

NT GEMINI 11 FLIGHT

NT GEMINI 12 FLIGHT

Space suit meteoroid protection for extravehicular activity, discussing Gemini and lunar surface EVA suits and bumper concept

04 p0645 A70-15402

Cardiac cycle and phases shortening observations from analyzing electro- and phonocardiographic data recorded during Gemini flights

13 p2359 A70-29437

GEMINI PROJECT

Extravehicular activity maneuvering devices, describing design and performance of Gemini project unit

21 p3929 A70-41075

GEMINI SPACECRAFT

Gemini spacecraft shielding configuration and radiation detectors, describing cabin radiation distributions

06 p0990 A70-17269

Meteoroid impacts on Gemini spacecraft windows, calculating flux-mass relation

19 p3520 A70-38376

Space shuttle electronics requirements, considering systems in Mercury and Gemini spacecraft and Apollo lunar and command service modules

23 p4259 A70-44612

GEMINI 4 FLIGHT

Accumulated dose and dose rate during Gemini 4 and 6 flights measured as function of elapsed time and position within spacecraft

06 p0990 A70-17270

GEMINI 6 FLIGHT

Accumulated dose and dose rate during Gemini 4 and 6 flights measured as function of elapsed time and position within spacecraft

06 p0990 A70-17270

GEMINI 11 FLIGHT

Supergiant alpha Car UV spectrophotometry from Gemini 11, comparing with model atmosphere

17 p3161 A70-34888

GEMINI 12 FLIGHT

Gemini 12 photographs examined for urban and transportation data content

12 p2228 A70-26909

GEMINID METEORIODS

Geminid and Quadrantid meteor shower densities observed on wave-channel-antenna radar

14 p2635 A70-30305

GENERAL AVIATION AIRCRAFT

NT DH 125 AIRCRAFT

Unstable spiral precursor to jet upset /Mach tucks/ in executive jet transports

06 p0987 A70-18248

STOL touring aircraft propeller design and aerodynamics, discussing takeoff runs, landing runs, high lift, downwash, ground effects, etc

08 p1435 A70-20628

General aviation urban airport capacity problem, suggesting diversion of training portion of peak-hour traffic

08 p1481 A70-21306

Light aircraft-airliner collision avoidance, discussing Time-Frequency Collision Avoidance System cost restriction, Pilot Warning Instruments, etc

11 p2079 A70-25872

Operating characteristics and performance of business aircraft jet engines compared with piston engine handling

11 p2102 A70-25880

CRT displays for business aircraft emphasizing EADI/electronic attitude director indicator/

11 p2079 A70-25882

Low cost lightweight flight control systems for business aircraft providing equivalent performance to larger equipment

11 p2079 A70-25886

Adhesive bonding for structural efficiency, lower weight, reduced production costs and improved appearance in general aviation industry

11 p2134 A70-25893

Air conditioning systems design for turboprop commuter and business aircraft

11 p1980 A70-25895

Business aircraft fuel management system using capacitance and mass flow rate measurements, displaying fuel quantity and flow rate and flight time remaining

11 p1983 A70-25896

FAA recommendations on general aviation airports and heliport design standards, explaining standards establishment or modification procedures

11 p2031 A70-25900

General aviation aircraft styling and interior developments, describing seat construction role in personalized aircraft production costs

11 p1980 A70-25901

General aviation aircraft fixed-base engineering flight simulator involving use of analog computer, discussing equations of motion and aircraft cockpit

11 p2031 A70-25904

Cessna CITATION aircraft design, considering engineering, marketing and corporate cooperation

11 p1981 A70-25910

Light general aviation aircraft production cost reduction, considering adhesive bonding, production certification, etc

11 p1981 A70-25911

General aviation requirements for national aviation system of 1970s including use of airspace and airports under all conditions

12 p2335 A70-27446

Optical IR system as low cost pilot warning indicator providing audible and visual collision warnings to general aviation aircraft

12 p2234 A70-27647

Twin turboprop executive aircraft /Falcon/ development, describing modifications and antinoise features

12 p2162 A70-28026

Falcon 10 economical executive aircraft development involving dimensions of cabin, powerplant and range

12 p2162 A70-28027

General aviation demands on Pilot Warning Indicator systems for collision avoidance

14 p2615 A70-31176

General aviation growth forecast during next decade, considering economic importance, air traffic control, collision avoidance, etc

16 p3003 A70-33469

Antenna design for single engine light general aviation aircraft weather radar, reviewing attenuation and terrain return problems

16 p2864 A70-33471

Corporate aircraft accident statistics, causes and prevention, noting pilot errors, mechanical failures, etc

16 p2842 A70-33814

Corporate aircraft operations in Europe, discussing meteorological conditions, flight planning, airport arrival and departure procedures and language differences

16 p2842 A70-33820

Reliability maintenance problems in corporate aircraft operations, discussing equipment calibration, aircraft systems analysis and repair facility selection

16 p2921 A70-33821

Aircraft utilization rate vs invested money as factor determining financial justification of corporate aircraft operations, discussing maintenance engineering

16 p2921 A70-33822

Fatal general aviation accidents examined by pathologists, determining pilot incapacity, accident sequence, aircraft design modification and crash protection performance

17 p3033 A70-35567

General aviation aircraft accident investigation toxicological findings, describing methods of examination for drugs and toxic agents

17 p3033 A70-35569

General aviation aircraft accident post mortem findings, emphasizing standardization of format and terminology

17 p3040 A70-35579

Corporate-executive market for helicopters related to fixed wing business air transportation problems

18 p3350 A70-36814

MBB Bo-209 Monsun travel, commuter and acrobatics aircraft, discussing configurations, specifications, structure and handling characteristics

19 p3355 A70-37388

Air conditioning in piston-powered light general aviation aircraft, comparing vapor cycle and cryogenic systems

19 p3359 A70-38500

ATC and general aviation growth, considering airport capacity, radars, navigation, National Airspace System, etc

19 p3467 A70-38631

Yak-40 business jet design and flight characteristics

21 p3755 A70-42174

SN 600 Corvette business jet design and performance

21 p3755 A70-42175

General aviation traffic control, discussing limitations of present system and improvements of position information and area navigation approach procedures

22 p4066 A70-42385

Pilot heart rate during in-flight simulated ILS approaches in general aviation aircraft

24 p4306 A70-45333

General aviation aircraft influences on federal airways systems, considering area and Omega navigation examples

24 p4373 A70-45929

General aviation expansion and competitive position dependence on safety and utility improvements and simultaneous cost reductions

24 p4291 A70-45953

General dynamics aircraft

NT CANADIAN AIRCRAFT

NT CL-84 AIRCRAFT

NT F-106 AIRCRAFT

NT F-111 AIRCRAFT

GENERAL DYNAMICS MILITARY AIRCRAFT

U MILITARY AIRCRAFT

GENERALIZATION (PSYCHOLOGY)

Attention and cue-producing responses in response-mediated stimulus generalization

09 p1617 A70-22342

GENETIC CODE

Biophysics research, discussing supramolecular biological structures, synthesis of proteins, nucleic acids and genetic codes, biological membranes, coding in nervous system, etc

03 p0420 A70-13491

Nucleated organisms divergence from bacteria compared to nucleated organisms divergence into separate kingdoms by analysis of genetic changes in cytochrome c and transfer RNA

16 p2846 A70-32990

GENETICS

NT GENETIC CODE

NT MUTATIONS

Space environment and radiation on Biosatellite 2 enhancing radiation effects in developing flour beetle *Tribolium confusum*

02 p0238 A70-12517

Soviet book on radiation genetics problems covering radiation damage of chromosomes, sexual and somatic cells, postradiation cell recovery, etc

08 p1445 A70-20761

Genetic theory application to selection of partial descriptions for algorithms group handling

08 p1466 A70-20875

Partial nucleotide sequences for fragments isolated from ribonuclease digests of tobacco mosaic virus RNA, suggesting genetic duplication possibility

13 p2363 A70-29798

Space travel genetic effects, discussing radiation, weightlessness, vibration and acceleration
21 p3761 A70-40842

Lunar rocks petrography, mineralogy and petrogenesis from Apollo 11 samples
21 p3902 A70-41554

Mammalian tissues metabolic and genetic alteration during weightlessness, relating rats liver regeneration delay to centrifuging intensity following hepatectomy
23 p4146 A70-44617

Inherited hypertension genetic and autonomic factors, discussing rats crossbreeding for genetic contribution ratio in males vs females, age effects, etc
24 p4299 A70-45806

GENTOURINARY SYSTEM
NT BLADDER
NT OVARIES
NT TESTES

GEOASTROPHYSICS
U ASTROPHYSICS
U GEOPHYSICS

GEOCENTRIC COORDINATES
Geocentric coordinate system definition by earth mass center and rotation axis and Greenwich meridian plane
01 p0082 A70-11456

Ground station geocentric coordinates from intersection of spatial directions in Baker- Nunn network determined by satellites
02 p0254 A70-11758

Earth poles motion influence on latitude, longitude, azimuth and geocentric rectangular coordinates of points determinations on earth surface
03 p0473 A70-13187

Great circle vector formula in space triangulation, discussing topocentric and geocentric position of satellite and tracking stations and absolute distance determination
03 p0445 A70-13193

North American datum related to geocentric satellite reference system, using Lambeck method for geodetic parameters
05 p0841 A70-16644

Astronomical and physical geodesy, discussing geometrical methods involving triangulation and trilateration and geocentric coordinates method in navigation
07 p1265 A70-19370

Three vector coplanarity equations for space geodetic triangulation grid, discussing role of satellite photographic observation
09 p1667 A70-22488

Equations for converting satellite geodetic latitude and altitude into geocentric Cartesian system
20 p3669 A70-39691

Electron densities between inner edge plasma sheet and plasmasphere as function of geocentric radial distance from OGO-3 electrostatic measurements
23 p4236 A70-43834

GEOCHEMISTRY
NT BIOGEOCHEMISTRY
Hydrocarbon content of coorongite derived from algae analyzed by IR spectrometry, gas chromatography and mass spectrometry, discussing alkanes and alkenes occurrence
01 p0041 A70-10037

Hydrocarbon contents of two sediments from Scottish Carboniferous Formation, examining isoprenoid alkanes abiogenesis
01 p0041 A70-10038

Steranes and triterpanes identification from Green River shale by capillary gas liquid chromatography and mass spectrometry
02 p0252 A70-12514

Hydrocarbons and fatty acids distribution in living organisms, fossils, sediments and crude oils, discussing slow thermal maturation role and geological applications
02 p0252 A70-12520

Gas chromatographic-mass spectrometric identification of aliphatic hydroxy acids in plants and sediments
02 p0252 A70-12521

Amino acid stability in pyrolyzed Pleistocene Mercenaria shells, comparing decomposition rates for aqueous solution
03 p0472 A70-13150

Electron microprobe determinations of Si concentrations in metal of iron meteorites, showing weak evidence for Si presence in earth core
05 p0921 A70-17094

Earth central region chemical exploration using antineutrino flux produced by natural radioactive isotopes
09 p1761 A70-22985

Phenolic aldehydes generated from lignin in fossil woods and carbonaceous sediments by oxidative degradation
13 p2361 A70-28911

Geochemistry of venus volatile elements identifying cloud forming species as Hg compounds
14 p2650 A70-31217

Mobile geochemical laboratory for in situ radiation measurement and elemental analyses in lunar exploration
15 p2717 A70-31801

Carbonaceous complex use as indicators of geothermal history and high temperature organic geochemistry
17 p3042 A70-35331

Sulphur in earth core composition, considering volatile element abundances and iron melt in thermal models
18 p3256 A70-37078

Apollo 11 lunar rock and soil elemental abundances, discussing composition, volatile element depletion, rare earths, basalt and geochemical processes
21 p3909 A70-41593

GEOCHRONOLOGY
Age dating of earth and universe emphasizing methods based on radioactivity, discussing stellar evolution, galactic age and assessment of cosmic time
08 p1568 A70-20633

Australite fall age determination from in situ radioactive carbon and standard geological dating methods
09 p1750 A70-22055

GEOCORONAL EMISSIONS
D-2 experiments measuring atomic oxygen emission from terrestrial atmosphere and polarization rate and emission intensity from geocoronal hydrogen
03 p0559 A70-13828

Solar Lyman-alpha radiation observed by OGO 4 spacecraft showing short term fluctuations superposed with monthly variation
04 p0741 A70-15128

Geocoronal glow as resonant scattering of solar Lyman-alpha-radiation by H atoms in upper atmosphere
07 p1270 A70-20032

Hydrogen UV geocorona photoionizing effect on nighttime E region electron density in low and midlatitudes, comparing with ionosonde data
14 p2581 A70-31270

Lyman alpha geocoronal emission rate as function of altitude at midnight during solar minimum, solving radiative transfer equations
20 p3619 A70-39329

Lunar based vs orbiting astronomical observatories, discussing limitations imposed by geocorona
22 p4108 A70-43630

Exospheric neutral hydrogen temperature diurnal variation from satellite resonance filter data, suggesting Lyman alpha source external to geocorona
23 p4186 A70-43852

GEODESY
Oblate earth gravitational field effect on ballistic missile trajectories, including body range determination and quadratures expressed by elementary functions
01 p0178 A70-10423

Core convection consequences with regard to earth figure and continental drift, indicating no changes in magnitude of magnetization
01 p0076 A70-10899

Gyrotheodolites application to azimuth determination, discussing use for directional control, photogrammetry in geodetic measurements, etc
02 p0295 A70-11800

Geodetic treatment of satellite observation - Conference, Tashkent, Uzbek SSR, November 1968
03 p0444 A70-13182

Earth satellite tracking data reduction for determining geodetic ground nets, examining errors in triangulation procedures
03 p0445 A70-13184

Satellite observations for determining earth shape and gravitational field zonal harmonics, using dynamic methods
03 p0473 A70-13188

Earth external gravitational potential expressed as infinite series of spherical harmonics, using transformation property on coefficients
03 p0478 A70-14178

Precision and accuracy evaluation of convergence angles for measuring vertical and horizontal components of space position applicable to geodesy and flight measurement
04 p0676 A70-14634

De Sitter hydrostatic equations solution possible with help of boundary condition from external potential theory with/without assumed equilibrium in earth interior
04 p0678 A70-15051

Variational methods in semigeodesic projections of analytic surfaces on plane surface, determining projections impossible by classical cartography
05 p0839 A70-16368

Earth figure parameters from satellite orbit dynamics, including potential on geoidal surface and scale factor for lengths
05 p0840 A70-16638

Geodetic vertical and geoidal height deflection calculated by gravimetric method, considering satellite orbits data
05 p0841 A70-16643

North American datum related to geocentric satellite reference system, using Lambeck method for geodetic parameters
05 p0841 A70-16644

Laser interferometer for earth strain study, measuring Michelson arm length changes by counting fringes in interference pattern
05 p0861 A70-16843

Earth axis position and displacements measured by earth-moon laser telemetry
06 p1058 A70-18452

Astronomical and physical geodesy, discussing geometrical methods involving triangulation and trilateration and geocentric coordinates method in navigation
07 p1265 A70-19370

Earth shape formulas reduction to Taylor series, considering Molodenskii solution method for simple layer density integral equation
09 p1670 A70-23343

Earth surface mapping and shape and internal constitution determination by satellite geodesy
10 p1876 A70-24642

Quaternion representation of general relativity applied to geodesic equation and planetary motion, noting difference from Einstein formulation
10 p1944 A70-24859

Errors estimation arising in inertial navigation equations solution while neglecting terms dependent on earth asphericity and gravitational field
11 p2077 A70-25558

ALGOL modified Gaussian algorithm for geodetic calculations, combining matrices for storage place economy
11 p2013 A70-25797

Systematic errors of reference star catalogs in satellite geodesy, discussing influence on orbit predictability
11 p2045 A70-26180

Plate measurement on comparators in satellite geodesy, discussing optics, magnification, mark selection and error elimination
11 p2051 A70-26181

Spatial geodesy calculations based on photographs of satellites against star background, recommending ECHO type satellites
11 p2046 A70-26191

Radiotelescope measurements for geodetic purposes, applying interferometric principles to quasars
13 p2396 A70-29163

Triaxial earth ellipsoid best fitting parameters for geoidal surface radius vector by spherical harmonics with coefficients computed from satellite observations
13 p2398 A70-29207

Harmonic functions defining geopotential and gravity derived from satellite orbit dynamics, applying to earth shape parameters
13 p2398 A70-29208

Decreasing gravitational constant effects on secular earth figure and dimension changes using Clairaut equation
14 p2568 A70-30143

Gravitational field representation in satellite geodesy by simple layer potential, comparing with geopotential expansion in spherical harmonics
15 p2722 A70-31548

Spacecraft tracking methods applied to solid earth and ocean physics
15 p2809 A70-31685

Report to COSPAR on Hungarian space research including satellite observations, upper atmosphere, geomagnetic effect, geodesy, cosmic rays, etc
15 p2830 A70-31713

Report to COSPAR on space exploration research in Poland including satellite tracking, geodesy, meteorology and aerospace medicine
15 p2830 A70-31721

Reduction constants simultaneous determination in earth figure theory based on astronomical, geodetic and gravimetric data
15 p2731 A70-32147

Triaxial earth attraction potential from expanding certain elliptical functions into series, noting consistency with concepts of astronomy and geodesy
15 p2731 A70-32148

Vertical gravity gradient effect on calculations accuracy of earth figure, deriving corrections for anomalies
15 p2731 A70-32149

Laser interferometry strain gage for measuring earth strain, taking into account wavelength stabilization
16 p2925 A70-33023

Vacuum interferometer strain gage for absolute earth strain measurement via length change comparison with wavelength standard
16 p2925 A70-33024

Geodesic Luneberg lens Q band antenna design, construction and evaluation, noting point feeding and energy collimation
16 p2876 A70-33408

Physical geodesy - Conference, Prague, September 1969
20 p3617 A70-39068

Fundamental equations of physical geodesy for earth figure by oceanic and continental parts via external gravity field
20 p3617 A70-39069

- Stokes earth constants from gravity anomalies
20 p3617 A70-39070
- Curvilinear orthogonal coordinates for gravimetric deduction related to Cartesian coordinates as solvability condition for Molodenskii problem
20 p3617 A70-39071
- Integral equations for gravity field and plumb line deflections solved by Neumann and Molodenskii methods
20 p3617 A70-39073
- Earth ellipticity in past, using hydrostatic equations based on density distribution and angular velocity to obtain oblateness
21 p3820 A70-41973
- Spatial aerotriangulation by analytical method based on independent models matched with geodesic grid
22 p4013 A70-42597
- Earth curvature effects on position of terrain points on planar aerial photographs for various survey altitudes
24 p4333 A70-45197
- Resonant satellites geodesy, determining orbit perturbation and gravity constant via mean Kepler elements high speed analysis
24 p4408 A70-45540
- Laser measurements in semidynamic space geodesy on D1-D satellite using Mediterranean stations
24 p4352 A70-45541
- Doppler satellite measurements in semidynamic geodesy using data from Mediterranean ground stations
24 p4312 A70-45543
- Dynamical and geometrical geodesy on European datum, comparing data from Doppler, laser and photographic satellite measurements
24 p4312 A70-45544
- Geodetic parameters estimated from satellite dynamic and geometric solutions and Mariner 4 and 5 missions
24 p4312 A70-45545

GEODETIC COORDINATES

- Satellite triangulations scale and orientation control, describing terrestrial methods of geodetic bases determination
02 p0254 A70-11755
- Receiving station geodetic coordinates computed from Doppler curves of artificial satellite, using method of differential corrections
02 p0254 A70-11757
- Geodetic coordinate system referred to center of mass and earth rotation axis constructible from satellite observations
03 p0472 A70-13186
- Satellite surveys and astronomic-geodetic nets for joint terrestrial, space triangulation and gravimetric measurements, including laser distance determination
03 p0445 A70-13191
- Satellite observations used to construct coordinate system referred to earth center of mass and axis of rotation
03 p0474 A70-13733
- Book on methods of geodetic astronomy for intertropical zone covering azimuth, latitude and time determination, spherical geometry and geographical coordinate reduction
04 p0677 A70-14750
- Simultaneous maximum likelihood estimation and coordinate conversion for redundant hyperbolic lines of position in radio navigation
04 p0717 A70-15545
- Astronomical and physical geodesy, discussing geometrical methods involving triangulation and trilateration and geocentric coordinates method in navigation
07 p1265 A70-19370
- Vacuum metrics with null geodesic expanding shear-free congruences using holomorphic solution
07 p1334 A70-19600
- Three vector coplanarity equations for space geodetic triangulation grid, discussing role of satellite photographic observation
09 p1667 A70-22488
- Geographic coordinates of intersection points determined directly on sphere, noting reduction on ellipsoid and adjustment for surplus intersections
09 p1670 A70-23441
- Geodetic systems relative positions determination based on satellite synchronous observation
13 p2400 A70-29529
- Equations for converting satellite geodetic latitude and altitude into geocentric Cartesian system
20 p3669 A70-39691
- Tesseral harmonics of geopotential and station coordinates from combined Baker-Nunn, laser and range data from satellites
24 p4407 A70-45538

GEODETIC SATELLITES

- NT GEOS 1 SATELLITE
- NT GEOS 2 SATELLITE
- NT PAGEOS SATELLITE
- Satellite surveys and astronomic-geodetic nets for joint terrestrial, space triangulation and gravimetric measurements, including laser distance determination
03 p0445 A70-13191

- Great circle vector formula in space triangulation, discussing topocentric and geocentric position of satellite and tracking stations and absolute distance determination
03 p0445 A70-13193
- Satellite optical tracking data in space geodesy, determining stations position from minimum number of stations and observations with time errors
03 p0446 A70-13195
- Ranger, Surveyor and Lunar Orbiter televised and reconstructed picture quality, suggesting improvements in existing photographic systems
03 p0490 A70-13656
- Global and European geodetic satellite network, discussing San Marco equatorial satellite and observation stations
03 p0581 A70-13829
- Artificial satellites for geodetic, topographic and cartographic purposes, outlining photographic and distance measuring equipment
03 p0475 A70-13831
- Tradeoff methodology establishing evaluation criteria for comparing radar and laser systems to meet geodetic satellite altimeter performance requirements [AAS PAPER 69-604]
04 p0686 A70-14648
- Laser ranging systems used with retroreflecting satellites in geodetic and geophysical applications
05 p0815 A70-16691
- Data reduction from D1A satellite VHF and UHF Doppler measurements to attempt geodetic link between Nice and Beirut
07 p1262 A70-18941
- Geodetic satellite positional problems taking into account parallax refraction
09 p1765 A70-22653
- NASA Geodetic Satellite Program applications to long range navigation, spacecraft orbit prediction, navigation experiments calibration, etc
09 p1724 A70-23048
- French geodetic satellites Diademe I and II experiments in navigation, noting laser and Doppler devices
09 p1725 A70-23049
- Earth surface mapping and shape and internal constitution determination by satellite geodesy
10 p1876 A70-24642
- Mathematical-physical parametric model of satellite geodetic laser range accuracy, false alarm and count probabilities, correlating with retroreflector signal strength
16 p2863 A70-33166
- Pulse compression for geodesy satellite radar altimeter, considering tradeoff based on system accuracy, power and life
16 p2911 A70-33715
- Position and velocity of geodetic drag free satellite in near circular orbit, including lunar- solar gravitational effects and zonal and tesseral harmonics [AIAA PAPER 70-1054]
19 p3528 A70-38869
- GEODETIC SURVEYS
- Geodetic air mapping and surveying system, describing cartographic camera and system operation
03 p0489 A70-13655
- Error analysis of resonant orbits for geodesy, discussing high order geopotential coefficient recovery by resonance and gravity model errors
05 p0909 A70-16341
- Data reduction from D1A satellite VHF and UHF Doppler measurements to attempt geodetic link between Nice and Beirut
07 p1262 A70-18941
- U.S. Coast and Geodetic Survey satellite triangulation data reduction methods, discussing data acquisition system, plate preparation, etc
11 p2046 A70-26190
- Geodetic systems relative positions determination based on satellite synchronous observation
13 p2400 A70-29529
- He-Ne laser geodimeter for Coast and Geodetic Survey length measurements on continental traverses
16 p2928 A70-33525
- Geodetic boundary value problem reformulation based on geometric satellite geodesy involving gravity measurements
22 p4025 A70-43667
- GEOS 1 satellite short arc optical observations over North American network to improve survey coordinates of tracking stations
24 p4312 A70-45542
- GEODIMETERS
- He-Ne laser geodimeter for Coast and Geodetic Survey length measurements on continental traverses
16 p2928 A70-33525
- GEOELECTRICITY
- NT TELLURIC CURRENTS
- Electrostatic methods considered for using earth electric field in smog dispersion in polluted areas and for airport fog clearing [AIAA PAPER 70-118]
06 p1058 A70-18217
- Magnetic and electric field changes across earth bow shock and magnetosheath, discussing Pioneer 8 andOGO-5 data
19 p3494 A70-37483

GEOGRAPHY

NT OROGRAPHY

GEIDS

- Earth figure parameters from satellite orbit dynamics, including potential on geoidal surface and scale factor for lengths
05 p0840 A70-16638
- Geodetic vertical and geoidal height deflection calculated by gravimetric method, considering satellite orbits data
05 p0841 A70-16643
- Triaxial earth ellipsoid best fitting parameters for geoidal surface radius vector by spherical harmonics with coefficients computed from satellite observations
13 p2398 A70-29207
- Second approximations of deflection of vertical and quasi-geoid height dependence on difference between unknown earth surface and known hypsometric surface
20 p3617 A70-39072
- Global geoid sections determined by satellite orbit dynamics, using best fitting ellipses
21 p3812 A70-40591
- Lunar effects on vertical and shape of geoid in universal time
22 p4100 A70-42852
- Gravity measurement errors in high speed aircraft parallel to undulating geoid attributed to associated vertical accelerations
22 p4025 A70-43662
- GEOLOGICAL FAULTS
- Gas volcanic activity, meteoric impact and geological faults as origin of lunar craters, cracks, maria, etc
03 p0563 A70-13169
- Topographic shadow linears image enhancement by low angle illumination, describing pseudoradar technique for subcontinental sized fracture systems detection
12 p2221 A70-26960
- Vredfort Ring origin, discussing paleomagnetic evidence to choose between meteorite impact or terrestrial cause
16 p2899 A70-34050
- GEOLOGY
- NT GEOCHRONOLOGY
- NT GEOMORPHOLOGY
- NT GLACIOLOGY
- NT LUNAR GEOLOGY
- NT OROGRAPHY
- NT PETROGRAPHY
- NT PETROLOGY
- NT PHOTOGEOLOGY
- NT TECTONICS
- NT VOLCANOLOGY
- Hydrocarbon contents of two sediments from Scottish Carboniferous Formation, examining isoprenoid alkanes abiogenesis
01 p0041 A70-10038
- Lherzolite, anorthosite, Gabbro and basalt dredged from Mid-Indian Ocean Ridge noting geological and geophysical features
04 p0675 A70-14422
- Geological contribution of satellite photography, discussing synoptic surveyability of vast areas and reduced scale maps of little known remote territories
05 p0837 A70-16073
- IR imagery by InSb detectors applied to mapping earth surface thermal distribution
05 p0840 A70-16498
- Geology from air covering aerial and space photography, nonvisible spectrum utilization, photograph transmission from Mars and moon, balloon flights, etc
07 p1272 A70-20225
- Lunar dimple /drainage/ craters formation mechanisms, considering analogous earth drainage craters associated with lava tubes
09 p1666 A70-22311
- Continental migration role in lunar maria formation, suggesting similarity with geological formation of earth ocean floor
09 p1765 A70-23797
- Radiophase and induced pulse transient /input/ remote sensor systems for geological mapping, describing data acquisition and reduction techniques
12 p2221 A70-26961
- Mars geology, discussing polar caps phenomena, diurnal variations, orbital eccentricity, seasonal meteorology, volcanism, erosion, etc
15 p2800 A70-32059
- Geological and cartographical data acquisition and processing, considering aircraft and satellite-borne photography of earth surface
20 p3616 A70-39061
- GEOMAGNETIC ANOMALIES
- U MAGNETIC ANOMALIES
- GEOMAGNETIC CROTCHETS
- U SUDDEN IONOSPHERIC DISTURBANCES
- GEOMAGNETIC EFFECTS
- U MAGNETIC EFFECTS
- GEOMAGNETIC EQUATOR
- U MAGNETIC EQUATOR
- GEOMAGNETIC FIELD
- U GEOMAGNETISM
- GEOMAGNETIC HOLLOW
- Steady state tangential drag by solar wind on geomagnetic cavity, describing unipolar induction
22 p4013 A70-42469

GEOMAGNETIC LATITUDE

Geographically smoothed geomagnetic cut-offs for eliminating discontinuity in neutron monitor latitude variation in Mexico City vicinity

01 p0167 A70-10229

Spatial distribution of Pi 2 micropulsations over specific distances and geomagnetic latitudes, noting coastline and geological effects

02 p0290 A70-12154

Geomagnetic latitude survey by neutron multiplicity monitor covering threshold rigidity ranges at various elevations, relating data to primary cosmic ray rigidity spectrum

04 p0741 A70-15125

Evening time latitudinal distribution of polar magnetic field perturbations compared with nighttime distribution, indicating evening electrojets

04 p0684 A70-15751

Magnetic activity effect on ionospheric drift speeds variation with latitude, observing correlation with electron density

05 p0837 A70-15922

F 2 region critical frequency conjugacy latitudinal variations observation at conjugate stations compared with results from nonconjugate stations

05 p0839 A70-16286

Latitudinal dependence of period and amplitude of steady Pc 3-4 pulsations observed at group of widely spaced stations

07 p1268 A70-19464

Critical sunspot dependence of F 2 region noon observed phenomenon at various equatorial latitudes, observing magnetic dip

08 p1492 A70-21837

Charged particle albedo latitude dependence estimated from balloon-borne Geiger telescopes

09 p1746 A70-23481

Pi2-type pulsations in and near auroral zone observed for amplitude variation dependence on geomagnetic latitude and local time

10 p1885 A70-25280

F 2 layer critical frequencies rms deviations approximate dependences on latitude and solar activity for computer calculation of long-range ionospheric forecasts

11 p2043 A70-25549

Low momentum muon intensity dependence on geomagnetic latitude

13 p2476 A70-28919

Pc-periods dependence on geomagnetic latitude during active sun years, using IGY data

13 p2395 A70-28943

Evening time latitudinal distribution of polar magnetic field perturbations compared with nighttime distribution, indicating evening electrojets

14 p2576 A70-30835

Latitude profiles made of low energy solar electrons over polar cap, finding latitude knee position

18 p3306 A70-36020

Geomagnetic latitudinal variations in Sq/H and Sq/Z in equatorial region, using electric simulation

18 p3246 A70-36099

Latitudinal dependence of period and amplitude of steady Pc 3-4 pulsations observed at group of widely spaced stations

18 p3250 A70-36938

Low energy solar protons penetration, examining geomagnetic cutoff latitude during magnetically disturbed period

21 p3881 A70-41077

F 2 layer critical frequencies rms deviations approximate dependences on latitude and solar activity for computer calculation of long-range ionospheric forecasts

21 p3819 A70-41299

Corrected geomagnetic midnight local time calculations, using nomogram

23 p4187 A70-43862

Pitch-angle distribution of electron fluxes in auroral zone as function of geomagnetic latitude

23 p4192 A70-44878

GEOMAGNETIC MICROPULSATIONS

Geomagnetic micropulsations relation to magnetospheric boundary location on sun-earth line, noting influence of solar wind pressure variations

01 p0071 A70-10412

Regular/irregular micropulsations variations during solar cycle, noting possible magnetospheric contraction and solar wind velocity influence

01 p0075 A70-10600

Amplitude modulated pearl type geomagnetic micropulsations connected with auroral X ray emission variations

01 p0171 A70-11228

Geomagnetic micropulsations fluctuations during solar activity cycle showing changes in excitation frequency with change in corpuscular fluxes parameters

01 p0083 A70-11539

Spatial distribution of Pi 2 micropulsations over specific distances and geomagnetic latitudes, noting coastline and geological effects

02 p0290 A70-12154

Dynamic spectra of quasi-periodic VLF emissions noting association with geomagnetic micropulsations

03 p0477 A70-13985

Latitude-period relation existence in geomagnetic micropulsations, discussing coupling between components of geomagnetic field fluctuations

05 p0838 A70-16278

Numerical analysis of cyclotron amplification of geomagnetic micropulsations in magnetosphere based on dispersion relation for three component cold plasma beam system

05 p0838 A70-16284

Stably trapped magnetospheric plasma distribution determined from Pi2 micropulsations and auroral electrojet index AE

05 p0839 A70-16285

Oscillations intervals with diminishing period during magnetic storms, noting relationship to midlatitude disturbances in F region

05 p0842 A70-16746

Pc 2-4 geomagnetic pulsations abrupt disappearance on global scale ascribed to magnetosphere boundary stabilization, noting interplanetary magnetic field role

05 p0843 A70-16766

Magnetosphere and interplanetary space diagnostics by micropulsations analysis, discussing geomagnetic cavity boundary, cold plasma density, energetic particles, etc

07 p1264 A70-19191

Geomagnetic micropulsation amplitudes and polarization along meridional profile analyzed from simultaneous ground station recording

07 p1268 A70-19463

Pc micropulsations with periods of 4-12 sec, discussing occurrence probability and diurnal characteristics

07 p1268 A70-19465

Response characteristics of negative feedback galvanometer amplifier with inductive source impedance for geomagnetic micropulsation detection

07 p1242 A70-19998

Polar cap magnetic field micropulsations simultaneous recordings at Greenland, Alaska, and Finland, noting seasonal variations

07 p1270 A70-20152

Alfvén wave structure mechanism of geomagnetic micropulsation type in cometary tails, assuming Kelvin-Helmholtz instability at comet plasma-solar wind interface

08 p1565 A70-20567

Longitude and latitude dependence of pc geomagnetic micropulsations related to local time, using analog spectral analysis

09 p1666 A70-22064

Electron precipitation modulation exponential dependence on micropulsation amplitude derived from idealized model

09 p1747 A70-23492

Equatorial geomagnetic micropulsations using earth current technique, discussing night and diurnal variations

10 p1875 A70-24435

Geomagnetic pulsations /pc 4/ characteristics from analyzing magnetosphere model yielding plasma densities consistent with experimental data

10 p1875 A70-24483

Drift instability of Alfvén waves at electron plasma sheet edge as source of auroral micropulsation instability

12 p2222 A70-27184

Geomagnetic micropulsations recording by transistorized saturated core magnetometers noting sensitivity

13 p2416 A70-30055

Book on geomagnetic micropulsations covering dynamic processes of magnetically trapped particles and micropulsations usability in remote sensing of magnetosphere

14 p2581 A70-31325

Geomagnetic micropulsations horizontal polarization characteristics relationship between stations in southern and northern auroral zones

15 p2725 A70-31859

Alfvén wave structure mechanism of geomagnetic micropulsation type in cometary tails, assuming Kelvin-Helmholtz instability at comet plasma-solar wind interface

15 p2805 A70-32722

Earth magnetic field Pc 1 micropulsations polarization characteristics examined in narrow frequency bands

[AFCL-70-0247]

16 p2897 A70-33299

Fine structure of hydromagnetic ULF emissions on spectrograms of whistlers, periodic emissions, choruses and sweepers

17 p3047 A70-35640

Geomagnetic micropulsation amplitudes and polarization along meridional profile analyzed from simultaneous ground station recording

18 p3250 A70-36937

Pc micropulsations with periods of 4-12 sec, discussing occurrence probability and diurnal characteristics

18 p3250 A70-36939

F layer scattering and earth electromagnetic field short period oscillations, relating electron density with pearl micropulsations amplitude and occurrence

18 p3255 A70-37036

Fine structure of geomagnetic Pc 1 micropulsations by cyclotron instability due to anisotropic energetic proton velocity

19 p3410 A70-37334

LF geomagnetic micropulsations recordings by two component induction magnetometer, relating diurnal frequency and occurrence variations to local K-index changes

19 p3412 A70-37995

HF geomagnetic micropulsations recordings by two component induction magnetometer, relating diurnal frequency and occurrence variations to local K-index

19 p3412 A70-37996

Pc 1 geomagnetic micropulsation statistics for middle latitudes, discussing solar cycle and annual variations in occurrence rates

21 p3817 A70-41088

Substorm aspects of magnetic pulsations, discussing classification micropulsations, generation and propagation effects

22 p4019 A70-43145

Micropulsation Pc-1 phase and polarization comparisons concerning L to R wave coupling in ionosphere

22 p4024 A70-43313

Micropulsations polarization characteristics from statistical spectrum analysis

23 p4185 A70-43837

Polarization of short period oscillations Pc2-Pc4 dependence on time of day, oscillation type and geoelectromagnetic field activity

23 p4190 A70-44086

Pi geomagnetic micropulsations relation to magnetotail energetic electron bursts, from ground based midlatitude magnetic observatories and IMP-1 data

23 p4193 A70-44924

GEOMAGNETIC PULSATIONS

NT GEOMAGNETIC MICROPULSATIONS

Short irregular geomagnetic pulsations repetitive characteristics relationship with magnetospheric cavity dimensions

01 p0081 A70-11229

Stable geomagnetic pulsations related to plasma density shock position in magnetosphere and to magnitude of diurnal variations

01 p0082 A70-11508

Electrical phenomena in upper atmosphere and solar wind may control geomagnetic disturbances and aurorae

01 p0082 A70-11523

Geomagnetic field pulsations frequency changes in relation to geomagnetic and solar activity level

01 p0084 A70-11559

Pc 1 range geomagnetic pulsation sweepers /MHD waves/ event in evening sector, considering delay time between sweepers appearance and polar magnetic substorms onset

02 p0290 A70-12121

Postbreakup pulsating aurora association with conjugate absorption bays, indicating hard electron precipitation source location

02 p0290 A70-12161

Fourier spectra of Pi 1 pulsations during magnetic field sudden disturbances derived from amplitude analysis

05 p0840 A70-16641

Geomagnetic field secular variations relation to variations of magnetic field of optimum dipoles, noting earth core role

05 p0842 A70-16747

Latitudinal dependence of period and amplitude of steady Pc 3-4 pulsations observed at group of widely spaced stations

07 p1268 A70-19464

Frequency spectra of Pi 2 geomagnetic field pulsations, noting effects of aural zone location, configuration and structure

07 p1277 A70-20438

PPi bursts interpreted as proton beams cyclotron instability in geomagnetic field

07 p1277 A70-20439

Plasma concentration in nondipole magnetosphere model from Pc 5 pulsations periods for high geomagnetic latitudes, noting solar winds effect

07 p1277 A70-20443

Geomagnetic pulsations with intensity maximum at midlatitudes, noting north to south decreasing trend

07 p1278 A70-20459

Geomagnetic pulsations, discussing giant pulsations and pulsations associated with nuclear detonations, meteor showers, ionospheric pressure waves, ocean waves and earthquakes

08 p1487 A70-20641

Lunar daily and monthly tidal variations in horizontal magnetic field and F 2 region maximum electron density and peak ionization height at Puerto Rico

10 p1872 A70-23823

Pi2-type pulsations in and near auroral zone observed for amplitude variation dependence on geomagnetic latitude and local time

10 p1885 A70-25280

Polarization regularities of Pc 1 oscillations interpreted from propagation along ionospheric waveguide centered at F 2 layer

11 p2043 A70-25543

Geomagnetic damped type pulsations associated with storms interpreted as interaction between hydromagnetic oscillations and magnetospheric motions caused by solar wind

11 p2047 A70-26567

Quasi-sinusoidal fluctuations of magnetic field during geomagnetic storms measured by ATS 1 in synchronous equatorial orbit

12 p2223 A70-27192

Ultra low frequency waves features in magnetosphere, considering geomagnetic pulsations, magnetic data from Explorer 33 and bounce resonance

12 p2223 A70-27573

Solar and lunar daily geomagnetic variations, correcting harmonic components calculated values

12 p2303 A70-27673

Low latitude atmospheric vertical density variations, comparing solar and geomagnetic activities effects

12 p2227 A70-28264

Pc-periods dependence on geomagnetic latitude during active sun years, using IGY data

13 p2395 A70-28943

Auroral electron precipitation and ground based magnetic field pulsations correlation for magnetic storms inception

13 p2401 A70-30053

Solar wind parameters time variations influence on geomagnetic activity from measurements by electrostatic analyzers on Vela satellites

13 p2481 A70-30065

Earth hydromagnetic dynamo spectrum fluctuation related to secular geomagnetic field variations, using unsteady kinematic models

14 p2568 A70-30202

Earth frequency sounding based on geomagnetic field variations spherical analysis, tabulating nonconducting shell thickness, nucleus resistivity, etc

14 p2572 A70-30243

Geomagnetic pulsations and hydromagnetic wave propagation in magnetosphere, using geometric optics approximation

15 p2722 A70-31452

Lunar tidal diurnal and semidiurnal variations in equatorial sporadic E layer related to H geomagnetic field and sunspot period

15 p2726 A70-31862

Superposed effects in solar quiet daily variations of geomagnetic horizontal component, using Lerwick and Eskdalemuir data

15 p2728 A70-31991

Geomagnetic disturbances temporal behavior and spatial scales

15 p2732 A70-32543

Pi 2 pulsation power spectra change with magnetospheric substorm development, relating pulsations and electron precipitation

17 p3080 A70-35641

Long term geomagnetic pulsations /PCS/ with sinusoidal waveforms, using IGY data

17 p3080 A70-35642

Latitudinal dependence of period and amplitude of steady Pc 3-4 pulsations observed at group of widely spaced stations

18 p3250 A70-36938

Pc 1 pulsations occurrence frequency diurnal annual and 11 year variations at midlatitudes, relating distribution with carrier frequencies of perturbation

19 p3408 A70-37316

Magnetospheric plasma concentration from geomagnetic pulsations periods

19 p3409 A70-37320

Diurnal variations in polarization axis direction of Pc 1 pulsations

19 p3410 A70-37333

Geomagnetic storms at ATS 1 in 1967, discussing storm-time disturbance field and associated pulsations

19 p3410 A70-37488

Earth EM field short period pulsations distribution within magnetic storms

19 p3416 A70-38585

Pc-1 pulsations during solar activity maximum and minimum, discussing diurnal, seasonal and cyclic variations

19 p3416 A70-38586

Geomagnetic field pulsations prior to polar magnetic disturbance onset, discussing solar wind role

19 p3416 A70-38588

Geomagnetic pulsations propagation through horizontally inhomogeneous ionosphere, solving EM wave diffraction problem

19 p3416 A70-38589

Pc-1 pulsation production by Cerenkov emission of proton beam oscillating along magnetic field line

19 p3417 A70-38590

Short period Pc-1 pulsations frequency spectra relationship to magnetospheric He ion concentration

19 p3417 A70-38591

Geomagnetic fluctuations relationship to magnetospheric ring current and plasmapause during magnetic storm

20 p3619 A70-39328

Mechanical analogies of magnetodynamic oscillations in homogeneous density column subject to material body impact, relating to earth magnetic field

21 p3854 A70-40593

Polarization regularities of Pc1 oscillations interpreted from propagation along ionospheric waveguide centered at F 2 layer

21 p3819 A70-41293

Dual satellite magnetic field and plasma measurements of earth bow shock pulsation shock by Vela 3A and Explorer 33

22 p4013 A70-42470

Worldwide geomagnetic fluctuations during disturbed conditions computed from spectrum analysis, considering long period oscillation caused by solar wind structure changes

22 p4019 A70-43114

Pc-1 and IPDP pulsations propagation characteristics from ground based measurements, discussing spectral structure, waveforms, polarization, time delay between different observation stations, etc

22 p4021 A70-43277

Solar wind intensity and direction correlated with intensity of earth surface magnetic disturbances and geomagnetic pi-2 type pulsations

22 p4022 A70-43284

Virial theorem for magnetospheric dynamics, discussing boundary and ring currents and densities and geomagnetic sudden impulses and commencement

23 p4184 A70-43830

Global geomagnetic field fluctuations of internal and external origins, analyzing HF spectrum based on monthly mean plots

23 p4187 A70-43861

Solar wind flux correlation with earth EM field pulsations, noting flare-generated shock front effects on magnetosphere

23 p4236 A70-44051

Geomagnetic perturbation effects on conduction along field lines and short period fluctuations associated with plasma turbulence in magnetosphere

23 p4189 A70-44065

Pi 2 type geomagnetic pulsations relationship to auroral zone morphological features

23 p4190 A70-44085

Earth surface magnetic field variations due to magnetopause current system

24 p4329 A70-45355

Earth hydromagnetic dynamo spectrum fluctuation related to secular geomagnetic field variations, using unsteady kinematic models

24 p4330 A70-46277

Earth frequency sounding based on geomagnetic field variations spherical analysis, tabulating nonconducting shell thickness, nucleus resistivity, etc

24 p4332 A70-46318

GEOMAGNETIC STORMS

U MAGNETIC STORMS

GEOMAGNETIC TAIL

Geomagnetic bays produced by neutral sheet plasma earthward movement resulting from solar wind enlargement of geomagnetic tail

01 p0071 A70-10409

Geomagnetic perturbation coincidences observed at conjugate Polar Cap observatories, suggesting magnetospheric tail field lines convergence with plasma neutral layer

03 p0565 A70-13232

Geomagnetic tail observations by Pioneer 8 probe

03 p0475 A70-13851

Geomagnetic tail observations by Pioneer 8 at 500 earth radii, analyzing time-averaged magnetic field data

03 p0575 A70-13983

Magnetopause shape determination model allowing for solar wind direction obliquely toward geomagnetic dipole axis

03 p0560 A70-13984

Resonant compression waves in geomagnetic tail estimated for frequency and spatial distribution by single layered two dimensional model

04 p0680 A70-15127

Magnetic storm /14 September 1966/ observation by Explorer 33 in geomagnetic tail and by polar stations, studying relation in magnetosphere and on earth

05 p0843 A70-16764

Electric field in earth magnetotail via Explorer 33 and 35 satellite observation of solar electrons above 50 kev energy

06 p1058 A70-18528

Geomagnetic tail natural oscillations, studying magnetospheric substorms role

07 p1268 A70-19499

Magnetic field measurements in geomagnetic tail from Explorers 33 and 35 indicating depressed field region centered on neutral sheet

08 p1488 A70-21379

Geomagnetic perturbation coincidences observed at conjugate Polar Cap observatories, suggesting magnetospheric tail field lines convergence with plasma neutral layer

08 p1580 A70-21665

Magnetopause boundary between shocked streaming solar plasma and geomagnetic tail observed at lunar orbit by magnetometer on Explorer 35

10 p1941 A70-24436

Plasmapause form in equatorial plane in presence of magnetospheric tail subsonic potential convective flow

11 p2047 A70-26796

Geomagnetic tail structure and magnetic field fluctuations from IMP 3 satellite measurements, showing enhancement during/after SSC and sudden impulses /SI/

13 p2396 A70-29182

LF MHD waves propagation model through earth magnetic tail, considering analogy with hydromagnetic plasma waveguide

13 p2398 A70-29210

Geomagnetic tail formation, cross section and length and auroral irradiation, discussing observations, models, vacuum magnetic merging and field aligned currents processes

13 p2402 A70-30060

Magnetotail plasma sheet temporal variations during substorms and plasma pressure as related to dynamic pressure of solar wind from Vela satellites observation

13 p2480 A70-30061

Energetic particles measurements in geomagnetic tail by Explorer 33/35 for determining gross magnetic topology of distant tail and electric fields

13 p2481 A70-30070

Spatial distribution and directional anisotropies of tail plasma sheet energetic electrons from measurements by electrostatic analyzer and energetic particle experiments on Vela 4

13 p2482 A70-30071

Geomagnetic tail structure and shape from Explorer 33 and 35 and Pioneer 8 observation data, examining field lines divergence with distance from earth

13 p2402 A70-30075

Magnetospheric tail neutral layer magnetic field distribution, comparing satellite data with theory

14 p2570 A70-30222

Pioneer 8 wave and particle observations correlation showing broadband wave levels reduction during extended geomagnetic tail crossings

15 p2727 A70-31904

Geomagnetic tail natural oscillations, studying magnetospheric substorms role

15 p2732 A70-32744

Solar protons penetration into magnetosphere and magnetotail

18 p3306 A70-36004

Interplanetary plasma observations by Vela satellites in solar wind and plasma sheet of magnetotail during magnetic storm

19 p3410 A70-37490

Magnetotail magnetic field perturbations associated with polar magnetic substorms, using IMP-A and B satellite observations

21 p3882 A70-41720

Solar-magnetospheric neutral sheet reconnection and noise in geomagnetic tail from Explorer 33 Ames magnetometer

22 p4013 A70-42471

Magnetospheric tail magnetic field and particle motion calculation, assuming constant radius cylinder with current sheet bisecting center

22 p4019 A70-43111

Geomagnetic wake in solar wind at 500 earth radii, correlating Explorer 35 and Pioneer 8 data

23 p4184 A70-43828

Geomagnetic tail and plasma sheet hydromagnetic oscillations, deriving dispersion equations and stability conditions

23 p4184 A70-43829

Pi geomagnetic micropulsations relation to magnetotail energetic electron bursts, from ground based midlatitude magnetic observatories and IMP-1 data

23 p4193 A70-44924

Magnetospheric tail neutral layer magnetic field distribution, comparing satellite data with theory

24 p4331 A70-46297

GEOMAGNETICALLY TRAPPED PARTICLES

U RADIATION BELTS

GEOMAGNETISM

Cosmic rays nucleon component measurements interpretation in terms of geomagnetic field model

01 p0169 A70-10354

Spatial characteristics of magnetosheath magnetic field observed simultaneously by Explorer satellites, showing zero order agreement with prediction of MGD theory

01 p0071 A70-10410

Ionospheric auroral oval, proton aurora and midlatitude trough relationship to magnetospheric structure, trapping outer boundary, storm time belt and plasmapause

01 p0073 A70-10586

Earth satellites magnetic survey contributions to World Magnetic Survey project /WMS/, discussing international reference standards and magnetic mapping

01 p0075 A70-10595

Rocket and satellite studies of geomagnetic field during IQSY, confirming ionospheric currents responsible for magnetic diurnal variations

01 p0075 A70-10596

Physical processes responsible for conjugate point phenomena involving particles and waves in magnetosphere and IQSY observations

01 p0075 A70-10598

Magnetic bay microstructures occurrences at low latitude not restricted to day or night hemisphere

01 p0076 A70-10668

Upper atmospheric contribution to Faraday rotation angle above 5000 km determined from beacon frequencies of geostationary satellite, noting geomagnetism weighting and electron content decrement role

01 p0076 A70-10874

Core convection consequences with regard to earth figure and continental drift, indicating no changes in magnitude of magnetization

01 p0076 A70-10899

Jacchia 1965 model discrepancies in solar and geomagnetic activity and semiannual effects observed in satellite drag measurements at 150-200 km and 700-1500 km

01 p0077 A70-11204

Geomagnetic potential optimal representation in frame of reference of eccentric inclined dipole using conversion formulas to determine harmonic coefficients

01 p0081 A70-11230

Real configuration effect of magnetic field in moderately perturbed magnetosphere on whistlers dynamic spectra, stressing geomagnetic perturbation detection

01 p0082 A70-11486

Mariner 2 measurements of geomagnetic field and interplanetary plasma parameters, analyzing interaction between interplanetary medium and magnetosphere during decreased solar activity

01 p0192 A70-11520

Magnetosphere boundary configuration calculated with allowance for geomagnetic dipole inclination to geographic axis and nondipole section of geomagnetic field

01 p0082 A70-11522

Interplanetary magnetic field sectoral structure effect on diurnal cosmic ray intensity and geomagnetic field, noting field direction influence

01 p0172 A70-11525

Lunar diurnal variation parameters at Irkutsk determined from IGY data concerning geomagnetic components

01 p0083 A70-11538

Secular variations distribution on earth surface, plotting isopore charts from mean annual values of magnetic elements /1960-1965/

01 p0083 A70-11540

Polar geomagnetic disturbances global current systems representation by prototypes of equivalent current systems

01 p0084 A70-11557

Harmonic analysis of magnetic storms initial phases having steep leading edges and distinct steady portions, showing homogeneity in first approximation

01 p0084 A70-11558

Geomagnetic field pulsations frequency changes in relation to geomagnetic and solar activity level

01 p0084 A70-11559

Multipole analysis for earth magnetic field allowing secular variation to be illustrated by time trends in multipole parameters

02 p0288 A70-11742

Data collection for ionospheric disturbances, geomagnetic field, radio wave intensity, cosmic rays and solar activity

02 p0290 A70-12125

Geomagnetic activity effect on ionospheric electron content from statistical analysis of data obtained during three year period

02 p0293 A70-12576

Geomagnetic field influence on satellite motion for various angles between field vector and satellite angular velocity vector

03 p0563 A70-13180

Geomagnetic field representation in terms of spherical harmonics, analyzing data for spherical and oblate models of earth

03 p0476 A70-13906

Electron temperature anisotropy in ionospheric plasma for case of ionizing sunlight propagating along geomagnetic field

03 p0479 A70-14376

Geomagnetic conjugate point problems involving temporal displacement field line tracing, display, etc

03 p0479 A70-14385

Cyclonic convective cell fluctuation and nonuniform core rotation effects on reversal of geomagnetic field, investigating fossil magnetism

04 p0676 A70-14600

Satellite observation of energetic particles and magnetic fields, discussing radiation belts, magnetosphere, galactic cosmic rays, etc

04 p0740 A70-14620

Recursive nonlinear system state estimation for arbitrary path magnetic navigation tested on simplified model by Monte Carlo simulation, considering derived error expression

04 p0715 A70-14627

Explorer 31 Langmuir probe data for electron temperature at conjugate point, tracing magnetic field line passing through spacecraft to earth

04 p0000 A70-14971

Intermediate ionospheric layer at high latitudes, discussing relationship to geomagnetic and auroral activity and F region continuity

04 p0678 A70-14974

Ionosphere beacon satellites BeB and BeC transits for field alignment of small ionospheric irregularities

04 p0678 A70-14975

Temporal behavior of energy injection into geomagnetic ring current found burst-like and similar to Dp at all magnetic levels

04 p0679 A70-15108

Solar and geomagnetic effects on variations in physiological tests using alimentary reflex of dogs

04 p0639 A70-15512

Geomagnetic field lines inclination effect on hydromagnetic waves propagation in lower ionosphere, using atmospheric model in plane form with integral conductivity tensor

04 p0683 A70-15737

Positive correlation between normal ionizations at magnetically conjugate regions in ionospheric F 2 layer from aircraft vertical soundings

04 p0683 A70-15741

Coordinates computation method using spherical harmonic expansion of geomagnetic field, discussing direct computations by perturbation method

05 p0837 A70-15820

Solar and geomagnetic activity daily parameters persistence, discussing autocorrelation function, variance spectra, sunspot numbers, radiation flux, etc

05 p0906 A70-15877

Solar magnetic discontinuity fluxes analyzed by studying 27-day cosmic ray and geomagnetic activity variations using linear filtration method

05 p0900 A70-15969

Low energy charged particle motion parallel with magnetic force lines analyzed in magnetosphere model with constant electric field

05 p0903 A70-16726

Polar auroral region displacement ascribed to distant magnetic field disturbances, proposing calculation method

05 p0842 A70-16745

Statistical description of geomagnetic field as random vector field, presenting correlation functions from empirical estimates from geomagnetic charts

05 p0842 A70-16748

Geomagnetic normal fields determination using spherical harmonic analysis, including extension to local fields

05 p0842 A70-16749

Magnetic damping of homogeneous cylindrical satellite rotation about transverse axis

05 p0924 A70-16751

Magnetic torquers consisting of permanent magnets or coils for attitude stabilization of earth satellites in geomagnetic field

[IEEE PAPER 27.1]

05 p0924 A70-17000

Ionospheric storms north-south asymmetry, discussing effects of horizontal and vertical movements of ionization controlled by asymmetric geomagnetic field

06 p1055 A70-17594

Geomagnetic center position determined by coordinate system referred to dipole approximating geomagnetic field

06 p1057 A70-17844

Electrically charged earth satellite motion under action of Lorentz force produced by geomagnetic field interaction, relating field trajectories to acceleration

06 p1142 A70-17879

Nighttime F 2 region temperature distribution under geomagnetically calm and disturbed conditions calculated from Alouette 1 satellite data

06 p1057 A70-17887

Book on ionospheric physics covering neutral atmosphere, ionospheric measurements, photochemical processes, morphology, phenomena, geomagnetism, storms, etc

07 p1262 A70-18856

Gaussian approximation of parameters of arbitrarily oriented magnetic dipole representing geomagnetic field

07 p1266 A70-19441

Geomagnetic field variations represented by optimal electric current loops or dipoles, noting advantages over spherical polynomials

07 p1266 A70-19442

Geomagnetic field amplification near gamma radiation steady source, describing field displacement

07 p1367 A70-19446

Ionospheric radio wave absorption and geomagnetic perturbations correlated with solar activity variations

07 p1267 A70-19457

Quartz magnetometer design to measure horizontal component of geomagnetic field, observing stability of H/zero/ constant

07 p1281 A70-19467

Polar ion-exosphere model with open geomagnetic field lines, calculating electrostatic field for region

07 p1270 A70-20077

Radar measurements of magnetic dip in E region compared with surface values and spherical harmonic models for dip angles

07 p1271 A70-20163

27-day variations in ionization layer created by galactic cosmic rays, discussing association with 27-day cosmic ray and geomagnetic field variations

07 p1373 A70-20345

Earth magnetic field transition recorded in basaltic lavas in southeastern Oregon

07 p1276 A70-20351

Lower ionosphere geomagnetic field local gradients determination by partial reflection method

07 p1277 A70-20455

Terrestrial electrical conductivity measurement from electromagnetic field variations determination by geomagnetic sounding

07 p1277 A70-20458

Geomagnetic field lines coordinates calculation based on coefficients obtained in spherical harmonic analysis

07 p1278 A70-20460

Geomagnetic field total vector modulus secular variations from airborne measurements

07 p1278 A70-20461

Near zero magnetic fields effect on biological systems studied to determine terrestrial magnetic field absence effect on astronauts

08 p1449 A70-20724

Magnetosphere model for quasi-circular precipitation zones of energetic particles based on geomagnetic activity distribution patterns

08 p1489 A70-21385

Mapping of normal distribution of geomagnetic elements in Bulgaria

08 p1490 A70-21433

Multipole analysis applied to 1965 International Geomagnetic Reference Field, separating secular variation field into drifting and nondrifting components

09 p1666 A70-22065

Geogravitational field correlations to geomagnetic fields emphasizing displacements in longitude

09 p1667 A70-22381

Solar cosmic rays development, discussing corpuscular radiation of flare origin, radio noise, geomagnetic activity and intensity measurements

09 p1745 A70-23128

Solar wind magnitude and variability effects on geomagnetic activity and cosmic ray intensity modulation from satellite observations

09 p1745 A70-23272

Algorithm for inversion of geomagnetic induction problem, determining earth radial conductivity distribution

09 p1669 A70-23305

Gravity and vertical magnetic anomalies interpretation to infer magnetization direction

09 p1729 A70-23601

Asymptotic method for aeromagnetic flutter of plane MGD nozzle, discussing conditions of MGD nozzle stability

10 p1800 A70-24129

Ionospheric current flow past circular inhomogeneous spot with Pedersen and Hall conductivities, calculating earth surface magnetic field by Lipshits-Hankel integral

10 p1873 A70-24309

Hydrogen ion flux detected along earth magnetic force lines in Northern Hemisphere midlatitudes, determining flux magnitude

10 p1874 A70-24321

Solar wind-geomagnetic field interactions, considering day and night hemispheres, satellite observations, shock and magnetopause motion, shock structure, etc

10 p1932 A70-24553

Vertical gradient of total geomagnetic field using curves based on continuous records of magnetic variations

10 p1876 A70-24589

Statistical estimation of aeromagnetic survey data errors due to diurnal variations, navigational inaccuracies and instrument drift

10 p1914 A70-24646

Geomagnetic field secular variation and cyclic components amplitudes separation by digital filters, observing seasonal and solar activity effects

10 p1880 A70-24808

Magnetosphere large-scale motions dependence on earth magnetic axis inclination against rotational axis

10 p1885 A70-25279

Dawn chorus frequency relation to solar activity, showing correlation to mean geomagnetic activity

10 p1886 A70-25282

Geomagnetic field upward calculation in lower ionosphere, discussing accurate data acquisition difficulties in Dirichlet problem solution

11 p2043 A70-25544

Sporadic E formation correlation to geomagnetic activity from ionospheric radio absorption observed at midlatitude and polar zone stations

11 p2044 A70-25554

Solar wind correlation with geomagnetic activity, comparing Vela 3 and 4 observations with Mariner 2 measurements

11 p2105 A70-26075

Lunar tides relationship with equatorial electrojet currents using daily variations at fixed lunar ages and monthly variations at solar hours of horizontal magnetic field

11 p2114 A70-26564

Ion temperature gradient along magnetic field lines in outer plasmasphere by thermal diffusion equations compared with electron temperature observations

11 p2047 A70-26568

Explorer 4 magnetic coordinates recalculation using spherical harmonic representation and modified B-L package

12 p2222 A70-27191

Moving object angles of rotation averaging during single measurement of geomagnetic field vector components by quantum magnetometer

12 p2234 A70-27566

Adiabatic drawing of quasi-captured charged particles by geomagnetic trap field during phase recovery period of magnetic storm

12 p2295 A70-28258

Plasmasphere ion concentration measurements on-board Elektron 2 and 4 satellites, observing dependence on geomagnetic activity

12 p2295 A70-28260

Interplanetary magnetic field intensity and geomagnetic activity level correlation with 27-day solar activity cycle based on Venera 4 and Mariner 5 data comparison

12 p2310 A70-28263

Satellite stabilization one-axis control system using earth magnetic torque

13 p2500 A70-28405

Geogravity-geomagnetic fields correlation due to lateral temperature variations in upper mantle

13 p2393 A70-28620

Auroral oval position with trapping region ϕ s boundary compared with closed geomagnetic field lines ϕ c, using Alouette 2 satellite data

13 p2398 A70-29229

Magnetometer for geomagnetic field declination measurement, eliminating thermal drift by light modulation method

13 p2415 A70-30042

Digital recording of geomagnetic field variations, using IBM or international telex code for radio transmission

13 p2415 A70-30043

Automatic cancelling devices with compensating coils for terrestrial magnetic field vector

13 p2401 A70-30044

Magnetic induction sensors sensitivity for magnetotelluric surveying in geophysics

13 p2415 A70-30048

Stability requirements for precision magnetic field measurements on ground and in space, discussing magnetic balances and fluxgate magnetometers for geomagnetic variations and spacecraft attitude

13 p2415 A70-30050

Constant and alternating magnetic field characteristics effects on magnetometric measurements in space near to and far from earth

13 p2401 A70-30052

Geomagnetic noise constraints on weak field measurements in upper magnetosphere

13 p2401 A70-30056

Horizontal geomagnetic force variations, considering ionospheric wind effects on ions in transition layer

13 p2402 A70-30057

Geomagnetic field distortion in high beta magnetospheric regions fromOGO observations for quiet and slightly disturbed conditions

13 p2402 A70-30076

Geomagnetic field distant fluctuations during substorm from ATS 1 magnetometer data on abrupt recoveries of H component

13 p2482 A70-30077

Satellite observation of alpha particles trapped geomagnetically in radiation belts, including Injun 5 results

13 p2484 A70-30092

Outer belt electron intensity variations related to geomagnetic activity indices, using Elektron measurements

14 p2630 A70-30201

Polar auroral hydrogen emission intensity dependence on K index of geomagnetic activity

14 p2569 A70-30213

Polar storm simultaneous onset and development, using observational data for geomagnetic field and aurora

14 p2570 A70-30214

Polar cap elementary magnetic disturbance relationship to auroral electrojet

14 p2570 A70-30215

Magnetosphere boundary altitude dependence on longitude, considering role of electric current density along geomagnetic lines of force

14 p2570 A70-30217

Geoactive ionizing radiation emitted by solar flares having metallic spectral lines of various brightness intensities

14 p2630 A70-30219

Geomagnetic field influence on annual F 2 layer longitudinal ionization at midlatitudes, relating solar activity level

14 p2570 A70-30225

Geomagnetism-sporadic E layer relationship, discussing critical frequencies and H component variations

14 p2571 A70-30236

Geomagnetic storm intensity nonuniform relationship to 27 day and 11 year cycles

14 p2571 A70-30240

Geomagnetic short period oscillations occurrence frequency during IQSY, discussing dependence on magnetic activity and time of day

14 p2572 A70-30242

Errors magnitude in quartz variometer readings resulting from variations of geomagnetic field perpendicular component

14 p2582 A70-30244

Earth dipole field disk dynamo model, studying connection between polarity intervals and precession effects

14 p2638 A70-30619

Mathematical model for interaction of solar wind with geomagnetic field, predicting magnetosphere shape

14 p2574 A70-30736

Daily variations of geomagnetic field horizontal component at dip equator associated with ionospheric current

14 p2575 A70-30792

Geomagnetic field lines inclination effect on hydrodynamic waves propagation in lower ionosphere, using atmospheric model in plane form with integral conductivity tensor

14 p2575 A70-30821

Positive correlation between normal ionizations at magnetically conjugate regions in ionospheric F 2 layer from aircraft vertical soundings

14 p2575 A70-30825

Magnetic activity intensity comparison in Northern and Southern hemispheres, noting correlation with solstices and equinoxes

14 p2580 A70-31260

Geomagnetic dipole field disturbances by trapped particles, calculating self consistent equilibrium configuration for ring current dipole moments

15 p2727 A70-31905

Spherical harmonic analysis of geomagnetic secular variation, applying to regional effects

15 p2799 A70-31992

Terrestrial magnetosphere dynamics in magnetospheric disturbances, analyzing solar wind-geomagnetic field interaction and storm development

15 p2729 A70-32080

Geomagnetic conjugacy variations observed via riometry in Northern and Southern Hemispheres

16 p2897 A70-33792

Spin stabilized satellite reorientation, using magnetic dipole interaction with geomagnetic field

17 p3179 A70-35287

High energy electrons in near space excess radiation from high altitude balloon and satellite data

18 p3307 A70-36170

Temporal and spatial covariation of high latitude geophysical phenomena, using unified mechanism of solar plasma stream interaction with geomagnetic field

18 p3247 A70-36404

Gaussian approximation of parameters of arbitrarily oriented magnetic dipole representing geomagnetic field

18 p3249 A70-36915

Geomagnetic field variations represented by optimal electric current loops or dipoles, noting advantages over spherical polynomials

18 p3249 A70-36916

Geomagnetic field amplification near gamma radiation steady source, describing field displacement

18 p3309 A70-36920

Ionospheric radio wave absorption and geomagnetic perturbations correlated with solar activity variations

18 p3250 A70-36931

Quartz magnetometer design to measure horizontal component of geomagnetic field, observing stability of H/zero/constant

18 p3260 A70-36941

Geomagnetic activity relation to large scale variations in interplanetary magnetic field and solar wind deformation velocity, using satellite and space probe observations

19 p3491 A70-37304

Spherical harmonic analysis of geomagnetic field strength for global magnetic anomaly charts

19 p3408 A70-37317

Nondipole geomagnetic field effect on magnetosphere boundary, presenting graphs for distance dependence on polar angle

19 p3409 A70-37321

Geomagnetic field variations recording by two variometers, correcting for variation components effects by instruments orientation

19 p3420 A70-37335

Earth magnetic field, discussing origin, field absence on planets and moon and MHD theory

19 p3410 A70-37399

Solar wind disturbances associated with solar activity observed by spacecraft probing interplanetary space, considering geomagnetic activity classes

19 p3494 A70-37478

Magnetic and electric field changes across earth bow shock and magnetosheath, discussing Pioneer 8 andOGO-5 data

19 p3494 A70-37483

Auroral phenomena interdisciplinary investigations, discussing electron precipitation and conjugate point drift due to geomagnetic axis position variations

19 p3411 A70-37493

Geomagnetic activity effect on potential gradient and air-earth conduction current density

19 p3413 A70-38000

Semiannual oscillation and fine structure of earth magnetic field horizontal intensity during March and September

19 p3413 A70-38004

Cretaceous rock paleomagnetism from Israel lava fields, determining original magnetization directions

19 p3413 A70-38034

Night airglow oxygen red lines predawn enhancement calculations, confirming role of photoelectrons from magnetic conjugate ionospheric

19 p3414 A70-38380

Lunar perturbations in horizontal geomagnetic field, F 2 layer thickness and electron density, discussing tidal variations

20 p3617 A70-39141

Soviet papers on relations between earth troposphere phenomena and solar activity covering geomagnetic and stratosphere perturbations, warmings and circulation, solar cycles, etc

20 p3618 A70-39181

Geomagnetic perturbation indices indicating different solar corpuscular streams and heliogeophysical properties

20 p3618 A70-39182

H sub 500 field features during natural synoptic seasons in Northern Hemisphere, including circulation characteristics

20 p3663 A70-39271

Geomagnetic field configuration and magnetic drift envelopes of particles with various pitch angles at equator calculated from two-dipole model of magnetosphere

20 p3619 A70-39299

Plasmapause motion in equatorial plane under sudden dawn-dusk field with constant solar wind-magnetosphere interaction

20 p3620 A70-39341

Adiabatic bounce periods of particle gyrophase coherence in earth field for cyclotron echo and triggered emission analyses

20 p3621 A70-39343

Inner magnetosphere magnetic field mapping, deriving Pogo model

20 p3621 A70-39349

Computer program transforming spherical harmonic coefficients into arbitrarily tilted coordinate systems, tabulating coefficients of International Geomagnetic Reference Field 1965 in dipole coordinate system

20 p3621 A70-39353

Steady state magnetic and electric fields in magnetosheath by linear superposition of field vectors, using axisymmetric velocity function from gas dynamics

21 p3815 A70-41063

Low latitude observations of spread F echoes and stationary satellite scintillations, correlating with ionospheric disturbances and geomagnetic activity

21 p3818 A70-41097

Geomagnetic field upward calculation in lower ionosphere, discussing accurate data acquisition difficulties in Dirichlet problem solution

21 p3819 A70-41294

Sporadic E formation correlation to geomagnetic activity from ionospheric radio absorption observed at midlatitude and polar zone stations

21 p3819 A70-41304

Spherical harmonic analysis of declination and secular geomagnetic variation

21 p3820 A70-41884

Earth magnetic dipole represented by Rikitake two-disk MHD dynamo system

22 p4013 A70-42633

Nighttime and daytime midlatitude magnetic bays statistical correlations with riometer-auroral absorption, suggesting precipitating particles role

22 p4018 A70-43107

F region electron content day-to-day changes observation by Early Bird satellite, determining cross correlation with magnetic indices

22 p4020 A70-43161

Geomagnetic axial dipole deviation from true north associated with earth core asymmetric motion, discussing geomagnetic reversal

22 p4020 A70-43231

Geomagnetic daily variations analysis in terms of universal time components, considering solar wind-magnetosphere interactions, auroral zone effects, etc

22 p4021 A70-43278

Lunar tidal effects on horizontal magnetic field compared at equatorial and midlatitude stations

22 p4021 A70-43279

Interplanetary magnetic field directional variation effect on polar caps geomagnetic field, discussing polarity reversals

22 p4022 A70-43285

Geomagnetic variations origin from satellite space probe data, correlating DP 1 activities to interplanetary magnetic field variations

22 p4022 A70-43286

Solar wind properties correlated with geomagnetic activity, discussing interplanetary discontinuities, shock waves, flare associated disturbances and geomagnetic activity sequences

22 p4022 A70-43288

Solar and geomagnetic events for maximum solar activity year 1968, correlating magnetic storms

22 p4022 A70-43290

Monograph on MHD, covering fluid layer stability under adverse temperature gradient, geomagnetic field origin, vector relations, etc

22 p4084 A70-43448

Proton energy angular distribution measurement by OV2-5 research satellite confirming model of shell splitting in geomagnetic field

23 p4236 A70-43832

E region winds response to solar radiation variations, including geomagnetism role

23 p4186 A70-43848

Ionospheric electron trough and magnetospheric plasmopause movements from satellite observations, showing statistical correlation with geomagnetic field

23 p4186 A70-43854

Geomagnetic Sq variation examination, using field expansion into natural orthogonal component series

23 p4188 A70-44063

Laminar geoelectromagnetic field excited by coaxial circular current, determining impedance and magnetic field ratios of spherical harmonics

23 p4189 A70-44064

Magnetic declination data, using spherical harmonics to examine global and secular geomagnetic field variations

23 p4189 A70-44067

Geomagnetic field behavior prediction based on extrapolation of magnetic data collected by observatories and dipole model approximation

23 p4189 A70-44068

Lower ionosphere electromagnetic induction effect on geomagnetic field guided MHD wave propagation, considering Hall effect

23 p4189 A70-44072

Particle motions in magnetic field, demonstrating existence of adiabatic region in particle phase space for Van Allen belt region

23 p4238 A70-44898

Magnetic field and electron flux observations near magnetopause via magnetometer and triaxial electron spectrometer onOGO-E

24 p4328 A70-45350

Geomagnetic activity dependence on angle between earth-sun and hourly averaged vectors of interplanetary magnetic field

24 p4405 A70-45523

Solar corpuscular flux and visible solar spot area correlation with geomagnetic planetary index for 27-day intervals, considering relationship to earth satellites motion

24 p4408 A70-45547

Outer belt electron intensity variations related to geomagnetic activity indices, using Elektron measurements

24 p4398 A70-46276

Polar auroral hydrogen emission intensity dependence on K index of geomagnetic activity

24 p4331 A70-46288

Polar storm simultaneous onset and development, using observational data for geomagnetic field and aurorae

24 p4331 A70-46289

Polar cap elementary magnetic disturbance relationship to auroral electrojet

24 p4331 A70-46290

Magnetosphere boundary altitude dependence on longitude, considering role of electric current density along geomagnetic lines of force

24 p4331 A70-46292

Geoactive ionizing radiation emitted by solar flares having metallic spectral lines of various brightness intensities

24 p4398 A70-46294

Geomagnetic field influence on annual F 2 layer longitudinal ionization at midlatitudes, relating solar activity level

24 p4331 A70-46300

Geomagnetism-sporadic E layer relationship, discussing critical frequencies and H component variations

24 p4332 A70-46311

Geomagnetic storm intensity nonuniform relationship to 27 day and 11 year cycles

24 p4332 A70-46315

Geomagnetic short period oscillations occurrence frequency during IQSY, discussing dependence on magnetic activity and time of day

24 p4332 A70-46317

Errors magnitude in quartz variometer readings resulting from variations of geomagnetic field perpendicular component

24 p4339 A70-46319

GEOMETRICAL HYDROMAGNETICS **U MAGNETOHYDRODYNAMICS** **GEOMETRICAL OPTICS** **U OPTICS** **GEOMETRODYNAMICS** **U RELATIVITY** **GEOMETRY**

NT ANGLES [GEOMETRY]

NT BRAGG ANGLE

NT BREWSTER ANGLE

NT CARTESIAN COORDINATES

NT CATENARIES

NT CIRCLES [GEOMETRY]

NT CONICS

NT COPLANARITY

NT CURVATURE

NT CURVES [GEOMETRY]

NT CUSPS [MATHEMATICS]

NT DIFFERENTIAL GEOMETRY

NT DOUBLE CUSPS

NT EUCLIDEAN GEOMETRY

NT FIXED POINTS [MATHEMATICS]

NT FLOW GEOMETRY

NT GREAT CIRCLES

NT HOMOTOPY THEORY

NT HYPERBOLAS

NT IMBEDDINGS [MATHEMATICS]

NT INFLECTION POINTS

NT INVARIANT IMBEDDINGS

NT LIE GROUPS

NT LINES [GEOMETRY]

NT LOCI

NT METRIC SPACE

NT NOZZLE GEOMETRY

NT OBLATE SPHEROIDS

NT OCTAHEDRONS

NT PARABOLAS

NT PARALLELEPIPEDS

NT PARALLOGRAMS

NT POINTS [MATHEMATICS]

NT POLYGONS

NT POLYHEDRONS

NT PROJECTIVE GEOMETRY

NT PROLATE SPHEROIDS

NT RADII

NT RECTANGLES

NT RIEMANN MANIFOLD

NT SPHEROIDS

NT SPINOR GROUPS

NT TANGENTS

NT TANK GEOMETRY

NT TENSOR ANALYSIS

NT TOPOLOGY

NT TORUSES

NT TRAPEZOIDS

NT TRIANGLES

NT TRIGONOMETRY

NT VECTOR ANALYSIS

NT VORTICITY

High temperature solar energy converter cavity absorbers geometry, considering absorption parameters of radiation reflected by concentrator

01 p0010 A70-10761

Foreign gas injection and slot geometry influencing film cooling effectiveness

01 p0219 A70-11182

Geometrical interpretation of motion of body about fixed point in Hess case based on Kharlamov kinematic equations, using special coordinates system

01 p0144 A70-11428

Focal length-to-aperture ratio for maximizing collection of scattered light at right angles to illuminating laser beam used in Raman spectroscopy

02 p0311 A70-11888

Geometrical determination of real roots of equations applied to linear oscillator and gyroscope in gimbal suspension

03 p0484 A70-13374

Axial geometry deformations of laser resonator due to fabrication errors and misalignment during operation

03 p0502 A70-13748

Two dimensional plasma modes involving geometry and velocity spaces, discussing Vlasov equation

05 p0890 A70-17025

Eigenvalue corresponding to decaying modes for wave equation in exterior of obstacle investigated for dependence on obstacle geometry

06 p1095 A70-18474

Theory for describing rotating fluid planets external geometry in state of hydrostatic equilibrium, noting role of equipotential surfaces

06 p1153 A70-18559

Geometrical-mechanical properties in terms of interlaminar shear stress of composite cantilever beams under end load

07 p1412 A70-19965

Radiation detector geometrical factor approximation for cylindrical bodies, observing convergence for right square and circular cylinders

07 p1286 A70-19971

GEOPHYSICAL OBSERVATORIES

Unified geometric description of gravitational and electromagnetic fields, determining electromagnetic field influence on geometry from dimensional constant

08 p1546 A70-21811

Geometry effect on short beam tests for interlaminar shear strength of composite materials

08 p1529 A70-21882

Glass fiber reinforced epoxy laminate specimens tests in tension and flexure at various strain rates to determine geometry effect on strength

08 p1532 A70-21898

Continuous media geometry with given discrete structure reduced to analyzing relations between functions in denumerable set of points, presenting selected points of subregions

10 p1954 A70-24016

Plane cavity geometry behind plate in incompressible potential flow, deriving geometrical functions to obtain desirable shapes

13 p2390 A70-29645

Geomagnetic tail formation, cross section and length and auroral irradiation, discussing observations, models, vacuum magnetic merging and field aligned currents processes

13 p2402 A70-30060

Deformed parabolic mirror antenna equivalent geometrical parameters based on known points coordinates on real profile of reflector

14 p2563 A70-30147

Plasticity limit theorems applicability extended without geometry change requirement, discussing load elastic buckling and fiber pullout from composite materials

17 p3186 A70-34977

Geometrical interpretation of controlled evolution of optical systems with mixed state constraints, using Pontryagin and variational methods

19 p3542 A70-38056

Coordinate sequences for regions with complex geometries and various boundary conditions, using linear operators

19 p3460 A70-38940

GEOMORPHOLOGY

Earth photographs for geotectonic research from manned orbiting spacecraft, describing Apollo and Gemini belts

[AAS PAPER 69-579]

04 p0677 A70-14663

Geometrical analysis of partial fusion in earth crust and mantle formation, discussing solid solution and boundaries in MgO-iron oxide-silicon dioxide system

09 p1670 A70-23398

Morphology of thermal and energetic particles in inner magnetosphere during geomagnetic disturbances and solar cycles

14 p2630 A70-30358

Soviet papers on morphology of quiet and perturbed ionosphere covering electromagnetic phenomena, measurements, etc

18 p3245 A70-36084

Lunar geomorphological map technique, discussing lunar rock formation classifications

19 p3516 A70-37981

Lunar geomorphological charts of Mare Imbrium southern region, emphasizing crater and maria formations

19 p3516 A70-37983

Lunar geomorphological charts of Mare Nubium northern part, considering structural features in equatorial band

19 p3517 A70-37984

Lunar geomorphological charts of Theophilus and Ptolemaeus walled plains, investigating central region tectonics

19 p3517 A70-37985

Lunar geomorphological charts in Archimedes crater and Appenine and Haemus mountain region, examining duration and stages in Mare Imbrium depression development

19 p3517 A70-37986

Soviet collection of lunar geological and morphological maps and relief tracings, showing tectonic features, craters and surface characteristics

19 p3518 A70-38011

Lunar geomorphic features and mass wasting relation, discussing landslides, rockfalls, debris slides, slump and creep play

22 p4102 A70-42972

Pi 2 type geomagnetic pulsations relationship to auroral zone morphological features

23 p4190 A70-44085

New Mexico Bandera lava tube systems, noting similarities with lunar surface sinuous rilles

23 p4254 A70-44884

GEON [TRADEMARK]

U POLYVINYL CHLORIDE

GEOPHYSICAL OBSERVATORIES

NT OGO

NT OGO-A

NT OGO-B

NT OGO-D

NT OGO-E

NT OGO-F

Hydromagnetic emissions recordings at two Australian stations indicating simultaneous occurrence

10 p1875 A70-24441

Aircraft capabilities as scientific observation platform in astronomy and geophysics, including instrument adaptation and IR absorber problems
22 p4019 A70-43146

GEOPHYSICAL SATELLITES

NT OGO
NT OGO-A
NT OGO-B
NT OGO-D
NT OGO-E
NT OGO-F

Digital telemetry systems for geophysical satellites, describing onboard and ground systems design criteria and experimental results
03 p0451 A70-13837

Laser ranging systems used with retroreflecting satellites in geodetic and geophysical applications
05 p0815 A70-16691

Geophysical parameters of atmosphere and underlying surfaces from outgoing thermal radio emission measurements on Cosmos 243 satellite
07 p1261 A70-18724

Spacecraft and boosters for earth resources surveys, discussing design, payloads, orbits, etc
10 p1950 A70-24641

Space technology applications to earth survey, discussing use of automatic satellites and manned space laboratories for meteorological, geophysical and related purposes
23 p4191 A70-44634

GEOPHYSICS

Solar-terrestrial physics, Terrestrial aspects - IQSY and COSPAR Conference, London, July 1967
01 p0071 A70-10577

Geoscience electronics - IEEE Conference, Washington, D.C., April 1969
05 p0849 A70-16683

Finite element method applied to potential distribution and stress analysis in earth sciences, determining elastic response of rock layer using structural matrix analysis
06 p1055 A70-17606

Geophysical-solar phenomenological interrelationships, considering earth rotation and nutation, sunspot area, earthquake energy, etc
06 p1056 A70-17636

International data exchange guide for solar-terrestrial physics, including listing of stations active during International Years of Active Sun
07 p1377 A70-18937

Earth central region chemical exploration using antineutrino flux produced by natural radioactive isotopes
09 p1761 A70-22985

Geophysical measurement curves mechanical transformation by digitizing curve on punched tape followed by processing in computer
10 p1845 A70-24494

Earth interior structure models using geophysical data in Monte Carlo inversion procedure
11 p2042 A70-25332

Crystal-chemical and geophysical implications concerning earth mantle phase transitions from beta magnesium silicate crystal structure
11 p1994 A70-25333

Project HARP gun-launched projectiles as vertical sounding probes for upper atmospheric meteorological and geophysical measurements, discussing payloads development for high acceleration
11 p2122 A70-26047

Book on statistical processing of geophysical and meteorological data covering independent and autocorrelated data, random processes, check tests, stochastic functions, filtering, etc
11 p2046 A70-26425

Book on space physics covering earth radiation belts, atmosphere, ionosphere, and magnetosphere, solar structure and composition, interplanetary space, etc
12 p2309 A70-27973

Weak magnetic fields in geo- and space physics - Conference, Paris, May 1969
13 p2413 A70-30026

Magnetic induction sensors sensitivity for magnetotelluric surveying in geophysics
13 p2415 A70-30048

Laser applications in geosciences - Conference, Huntington Beach, California, June-July 1969
16 p2925 A70-33013

Atmospheric turbulence effects on optical communication systems in geosciences
16 p2900 A70-33019

Algebraic manipulation of empirical relationships between geophysical parameters, discussing invalid results
17 p3080 A70-35760

Temporal and spatial covariation of high latitude geophysical phenomena, using unified mechanism of solar plasma stream interaction with geomagnetic field
18 p3247 A70-36404

Airborne IR scanner as geophysical research tool depicting surface emission and heat mass transfer
18 p3259 A70-36558

Soviet book on aerial photo plotting of aerogeophysical routes and anomalies covering techniques, equipment, low altitude surveys, etc
19 p3410 A70-37408

Surface waves free period partial derivative correlation and relation to resolution of gross earth data
19 p3414 A70-38374

Earth exospheric plasma distribution, relating solar eclipses effects to geophysical phenomenon
19 p3418 A70-38904

Geomagnetic perturbation indices indicating different solar corpuscular streams and heliogeophysical properties
20 p3618 A70-39182

Geophysical environment, discussing vibrations, foundation conditions, local gravity vector and atmospheric conditions in relation to precision instruments tests and operation
20 p3622 A70-39570

Precise sensing systems and instruments calibration with respect to inertial frame of reference for geokinetics
20 p3622 A70-39571

Palaeogeophysics - Conference, University of Newcastle-upon-Tyne, England, April 1968
21 p3921 A70-41969

Gravity and magnetic geophysical prospecting methods, discussing data acquisition, reduction and analysis in terms of underground geologic anomalies
22 p4018 A70-43086

Space and astronomic methods applied to solid earth and ocean physics
22 p4025 A70-43669

Collisionless plasma shock wave structures from geophysical and astrophysical phenomena standpoint, describing tarantula experiment
23 p4225 A70-44184

GEOPOENTIAL

NT GEOPOENTIAL HEIGHT

Earth potential errors from gravity and satellite motion measurements, discussing sectoral, tesseral and zonal harmonics with large and small second indices
03 p0473 A70-13190

Coefficients of Legendre polynomial expansion of earth gravitational potential, using Stokes problem solution
03 p0474 A70-13344

Earth external gravitational potential expressed as infinite series of spherical harmonics, using transformation property on coefficients
03 p0478 A70-14178

Spherical harmonics expansion for earth surface and outer space geopotential by mapping earth surface onto sphere
05 p0837 A70-15926

Resonance effects on satellite orbits due to tesseral harmonics in potential field
05 p0908 A70-16335

Error analysis of resonant orbits for geodesy, discussing high order geopotential coefficient recovery by resonance and gravity model errors
05 p0909 A70-16341

Earth figure parameters from satellite orbit dynamics, including potential on geoidal surface and scale factor for lengths
05 p0840 A70-16638

Geopotential zonal harmonic coefficients determined from satellite orbit perturbations, using spherical harmonics orthogonality
05 p0840 A70-16639

Prognostic maps of geopotential and wind in middle troposphere derived from hydrodynamic equations
07 p1330 A70-20307

Numerical procedure for determining horizontal wind from geopotential height in barotropic model, discussing solutions for resultant simultaneous equations
08 p1540 A70-21968

Geopotential resonance effects on low altitude satellites orbit determination, analyzing GEOS 2 orbit variations to determine even-degree coefficients
10 p1939 A70-24189

Simple layer model of geopotential from satellite-borne Baker-Nunn camera observations
10 p1876 A70-24645

Harmonic functions defining geopotential and gravity derived from satellite orbit dynamics, applying to earth shape parameters
13 p2398 A70-29208

Geopotential fields seasonal statistical analysis over first natural synoptic region, using expansion into orthogonal eigenfunctions
13 p2446 A70-29674

First order node to node satellite orbital elements perturbations due to arbitrary zonal geopotential harmonic, determining computation methods and time
14 p2638 A70-30703

Coefficients of Legendre polynomial expansion of earth gravitational potential, using Stokes problem solution
14 p2573 A70-30719

Gravitational field representation in satellite geodesy by simple layer potential, comparing with geopotential expansion in spherical harmonics
15 p2722 A70-31548

Triaxial earth attraction potential from expanding certain elliptical functions into series, noting consistency with concepts of astronomy and geodesy
15 p2731 A70-32148

Earth gravity field from successive satellite passages, introducing direction and range observations of first passage
17 p3154 A70-34683

Geopotential fields forecasting on isobaric surfaces over Northern Hemisphere by linear four level nonadiabatic model, discussing eddy transport and heat flux equations
20 p3662 A70-39179

Resonant and nonresonant satellite eccentric orbits for determination of high order terms in geopotential
20 p3709 A70-40073

Statistical interpolation for numerical analysis of middle troposphere AT potential based on geopotential and wind observations
24 p4371 A70-45135

Satellite orbital elements calculation using ellipsoidal harmonics for geopotential representation
24 p4406 A70-45531

Geopotential zonal spherical harmonics coefficients revised values determined from reduced Baker-Nunn observations for satellites
24 p4407 A70-45538

Tesseral harmonics of geopotential and station coordinates from combined Baker-Nunn, laser and range data from satellites
24 p4407 A70-45538

GEOPOENTIAL HEIGHT

Geopotential fields expansion on 500 mb surface for hemisphere in terms of Chebyshev polynomials along meridian and trigonometric polynomials along latitude
07 p1329 A70-19648

Real time global temperature and geopotential height profiles acquisition from satellite spectrometer measurements by least squares regression method
21 p3820 A70-42121

GEOS 1 SATELLITE

GEOS A and OGO-4 satellite orbits and trajectory analysis using Definitive Orbit Determination System, discussing tracking stations error role
24 p4407 A70-45536

GEOS 1 satellite short arc optical observations over North American network to improve survey coordinates of tracking stations
24 p4312 A70-45542

GEOS 2 SATELLITE

Attitude performance of GEOS 2 gravity gradient spacecraft, discussing prelaunch design and post-launch analyses
06 p1154 A70-17162

Geopotential resonance effects on low altitude satellites orbit determination, analyzing GEOS 2 orbit variations to determine even-degree coefficients
10 p1939 A70-24189

GEOSTROPHIC WIND

Jupiter upper atmosphere cloud bands zonal motion velocities, examining barotropic stability criterion and geostrophic balance hypothesis
02 p0368 A70-11828

Nongeostrophic baroclinic stability theory predictions test experiment with vertical heating provision, describing fluid motions
02 p0289 A70-11830

Geostrophic baroclinic flow with zonal magnetic field in beta plane channel, analyzing instability, phase velocities, Alfvén-Rossby waves and Eady problem
02 p0291 A70-11284

Cyclone waves development during stationary long wave basic state two dimensional quasi-geostrophic two layer model
03 p0521 A70-14288

Hydromagnetodynamic equations of two dimensional unsteady geostrophic wind field in turbulent ionosphere
04 p0680 A70-15254

Pressure changes associated with surface friction and geostrophic drag coefficient related, discussing mass inflow and outflow
05 p0837 A70-16151

Jupiter geostrophy indicated by circulation, vorticity and Rossby number determined from Great Red Spot observations
08 p1580 A70-21573

Geostrophic wind vector rotation correlated with precipitation and circulation in vertical solenoid field
11 p2076 A70-26074

Lower atmospheric layer temperature and wind vertical distribution effect on wind velocity ratio to geostrophic wind at earth surface
13 p2444 A70-28586

Barotropy, baroclinity and baroclinity induced variations of geostrophic wind vector with altitude within planetary boundary layer
14 p2604 A70-30546

Upper level frontal zones geostrophic approximation theory based on scale analysis and case study diagnosis
15 p2769 A70-31442

Winter stratospheric circulation quasi-geostrophic model based on joint radiative-photochemical equilibrium, investigating ozone cycle and warming
16 p2945 A70-33250

Thermotropic quasi-geostrophic atmospheric model, deriving linear and quadratic integral invariants 19 p3463 A70-38754

Atmospheric circulation two level quasi-geostrophic model, examining dynamic large scale features of baroclinic wave blocking by high latitude cold anticyclonic cells 20 p3621 A70-39372

Coriolis parameter effects on stream and pressure functions in geostrophic wind equation 22 p4065 A70-43167

GEP TELESCOPES
U PARTICLE TELESCOPES

GERDIEN ARC HEATERS
U ARC HEATING
U HEATING EQUIPMENT

GERMANIUM
NT SILICON
NT TELLURIUM
NT TELLURIUM ISOTOPES

Photoconductivity and photomagnetic effect measurements in Ge for determining nonequilibrium current carrier concentration produced by Q switched neodymium laser 01 p0107 A70-10099

Electric characteristics and impurity distribution in GaAs-Ge heterojunctions obtained by deposition on p-type Ge 01 p0155 A70-10143

Ge bolometer cooled by liquid helium 3 to near absolute zero to achieve high sensitivity for far IR detection 01 p0091 A70-10910

HF admittance and noise in forward-biased majority carrier Ge-Si n-n heterojunctions and Schottky barrier 03 p0539 A70-13159

Ge films crystallinity deposited on Ge substrates in vacuum as function of deposition rate, substrate temperature and thermal treatment and background O pressure 03 p0543 A70-14204

Single crystal Ge surface etching characteristics using laser beam reflection pattern 05 p0860 A70-16656

Reactive scattering from solid surfaces, discussing atom beam reaction of O with heated Ge and Si single crystals 07 p1342 A70-20117

LEED pattern and germanium surface conductivity during oxidation indicating electron states annihilation 09 p1738 A70-22215

Electron tunneling into amorphous Ge films using Al-aluminum sesquioxide-germanium tunnel junctions, observing conductance dependence on bias voltage 09 p1739 A70-22918

Transverse Dember effect in elastically bent Ge single crystal illuminated by light beam, considering EMF distribution and photocell application 09 p1740 A70-23191

Ruby laser illuminated Ge recombination radiation intensity measured at room temperature 12 p2286 A70-27369

Radiation defects in Ge single crystals surface layers caused by low energy bombardment with He ions 12 p2287 A70-27486

Cryogenic Ge bolometers sensitivity variation and noise, noting radiation absorption by sensor and by coating 12 p2237 A70-28151

Epitaxial Ge deposits on Si control by Kikuchi pseudolines, considering surface polish, crystallinity and substrate orientation 13 p2470 A70-28957

Metal-Ge n-type semiconductor tunnel junctions, discussing Sb and As doped units and conductance and barrier heights air cleavage effects 14 p2626 A70-30482

GaAs-Ge heterojunction transistors with microwave planar geometry, calculating performance for comparison with Ge homojunction transistor 14 p2556 A70-30925

Nickel-doped p- and n-type Ge hot electrons recombination characteristics in strong electric fields, examining electron capture cross section 15 p2782 A70-31628

Ge and Si hemispherical emittance, showing doping and temperature effects 15 p2784 A70-32055

Growth mechanism and crystal structure of Ge films deposited from molecular beam onto GaAs, Si and Ge substrates 18 p3297 A70-36415

Ge and Si surface electrical properties, discussing conductivity, field effect, work function, current carriers, photoconductivity, photocurrent carrier capture, etc 19 p3483 A70-37297

Fe meteorites with high Ge content, tabulating concentrations of Ni, Ga, Ge and Ir 23 p4241 A70-44259

GERMANIUM ALLOYS

Si-Ge air-vacuum thermocouples for thermoelectric conversion, describing construction materials,

mechanical and electrical properties, radiative heat transfer operation, etc 10 p1807 A70-24896

Thermoelectric generators design, discussing Si-Ge air-vac thermocouple configurations, compression modules, thermal losses, etc 10 p1808 A70-24897

German monograph on use of Ge as oxidation resistant refractory materials alloy component covering base materials, test samples processing methods and apparatus, etc 24 p4367 A70-45525

GERMANIUM COMPOUNDS

GeTe thermoelectric power, electrical/thermal conductivity and expansion coefficient measured at 20-600 C, determining suitability as thermoelectric material 01 p0158 A70-10755

Nonstoichiometric GeTe defects nature from band structure analysis based on two carrier model 02 p0350 A70-11698

GERMANIUM DIODES

Ge IMPATT diodes under pulsed operation to produce LF high efficiency oscillations, recording current and voltage waveforms 05 p0821 A70-16417

Germanium p-n-p-m transistor frequency oscillation dependence on emitter current, noting forced air cooling effect 09 p1741 A70-23354

Planar Ge and Si diodes application in pulsed bridge elements, investigating current-voltage and resistance-voltage characteristics 11 p2015 A70-25350

Planar Ge and Si diodes application in pulsed bridge elements, investigating current-voltage and resistance-voltage characteristics 20 p3600 A70-40462

Low temperature Ge diode thermometer with computer circuit transforming voltage to temperature readout 21 p3828 A70-41473

GERMANIUM RECTIFIERS

U GERMANIUM DIODES

GERMANY

German society of aeronautics and astronautics, yearbook 1968 03 p0411 A70-13789

German light aircraft construction industry situation and prospects regarding manufacture of gliders, sport-ing and touring aircraft and motor gliders 03 p0413 A70-13791

Rotor propelled aircraft development in West Germany, analyzing military and civil demand for rotor aircraft, light helicopters and V/STOL transports 03 p0413 A70-13793

V/STOL supersonic fighter VJ 101, transport Do 31 and VTOL fighter/reconnaissance VAK 191 development in West Germany, discussing control and stabilization during hovering 03 p0413 A70-13794

German VTOL transport aircraft projects, discussing Dornier 231/lift by turbojets/ and Bolkow 140/swiveling wing with gas turbine propellers/ 04 p0623 A70-14955

German developments in electric propulsion and energy supply systems for commercial satellites in geostationary orbits [DGLR-69-20] 04 p0735 A70-15169

German transport VTOL projects, discussing VC-500 swiveling wings with turbine powered propellers and HFB-600 blade cascade flow deflectors for vertical takeoff 04 p0623 A70-15349

Electronic search and rescue system developed for West German Air Force, consisting of personal transceiver and automatic distress signal transmitter unit, etc 05 p0793 A70-15904

German research institutes activities in fluid mechanics, structural materials, propulsion, flight control and electronics, space physics and medicine 05 p0829 A70-16374

German aeroballistic hypersonic test facility with moving model and rest atmosphere, describing acceleration mechanism and several tests 06 p0965 A70-17246

Max Planck Institute of Astronomy /Germany/ installations and equipment planned 06 p1029 A70-18024

Azur satellite program, describing NASA- German cooperative effort 07 p1391 A70-18815

International air traffic jurisdictional area of German aeronautical law regarding aircraft equipment regulations and residents 07 p1427 A70-18886

German Research Establishment for Air and Space Navigation covering aerodynamics, aircraft design, flight mechanics, guidance and jet propulsion 07 p1249 A70-19671

West German space research programs, discussing ESRO and ELDO, industry participation, ground support facilities, personnel recruitment and training, etc 08 p1568 A70-20607

German satellite ground station system central station design, discussing cooperation between aerospace institute and electronic company 08 p1481 A70-21368

Digital data display system designed for central station of German ground station system 08 p1462 A70-21369

Regional air traffic in Germany, discussing aircraft, airports, growth rate and control 10 p1970 A70-24199

Photographic satellite plates reduction by astrometric method at geodetic institute at Potsdam, discussing star coordinates, astronomical refraction, etc 11 p2008 A70-26200

Azur satellite flight results, noting trajectory accuracy telemetry reception, yo-yo triggering and attitude control 13 p2505 A70-28766

Aeros aeronomic satellite mission, orbit and design for upper atmosphere observations, noting braking field analyzer for ion and electron speed measurement 13 p2505 A70-28767

Report to COSPAR on East German space research including Intercosmos satellites scientific apparatus preparation, meteorological and ionospheric research, etc 15 p2830 A70-31712

West German aircraft bird hazards problems, discussing research activities and recommendations for strike avoidance 18 p3349 A70-35980

Hypersonic wind tunnel facility for hypersonic aircraft and recoverable booster systems development [DFVLR-SONDDR-19] 23 p4178 A70-44799

GERMICIDES

U BACTERICIDES

GERMINATION

Spore and vegetative cell adenylate kinases of Bacillus subtilis proved indistinguishable by polyacrylamide gel electrophoresis DEAE cellulose chromatography 01 p0021 A70-10789

Seed germination in simulated planetary atmospheres, considering biological responses of various organisms 14 p2537 A70-30692

Parental termini-daughter strand linkage in initiation of DNA replication in Bacillus subtilis after thymine-less germination 16 p2847 A70-33060

GETTERS

High sensitivity photomultiplier TWT microwave photodetector with internal lowered secondary electron multiplier and spiral HF getter 09 p1645 A70-22413

Titanium monoxide thin film as low temperature getter, measuring activity coefficient and capacity under ultra high vacuum 15 p2783 A70-31844

GIANT STARS

Isophote flattening functions of elliptical galaxies including identification of giant and dwarf galaxies 02 p0377 A70-12449

Hypotheses for symbiotic stars nature, emphasizing binary with late type giant and hot small star components 03 p0568 A70-13325

Horizontal branch and red giant stars ratio estimated in globular clusters for He abundance 05 p0906 A70-15894

Neutrino emission, mass loss and giant branch termination in young clusters with giants originating from intermediate mass main sequence stars 06 p1138 A70-17277

Red giants age and mass estimation based on K-line luminosities, noting role of metal abundance 06 p1139 A70-17416

Red giants and supergiants intrinsic radiation polarization characteristics 08 p1569 A70-20826

Gravitational radiation detection from pulsating neutron star, considering asymmetries in gravitational collapse of massive stars as origin 09 p1749 A70-21996

Metal-poor stars evolution during hydrogen and helium burning from main sequence to giant branch, estimating relative cluster ages 09 p1755 A70-22507

Free-free opacity of stellar interiors by ion correlations applied to red giant degenerate cores 09 p1755 A70-22510

Low mass star evolution from helium burning to white dwarf, describing red giant and mass loss stages in model 10 p1946 A70-24982

OH radio emission from IR stars, discussing spectra, polarization properties and red giant star model with expanding atmosphere 14 p2641 A70-30881

Red giant model, investigating inclusion of semirelativistic partially degenerate gas characteristics by perturbatory technique 14 p2651 A70-31290

Shock wave propagation through giant star atmosphere, using approximate analytical method 16 p2980 A70-34305

- Red giant star chromospheric activity, discussing Balmer absorption lines and emission lines
17 p3161 A70-34889
- Horizontal branch stars evolution based on mass distributions from comparison with giant branch, investigating evolutionary track characteristics during core helium burning
20 p3702 A70-39019
- Hyades giant stars epsilon and gamma Tau strong line profile analysis, obtaining effective temperatures
21 p3885 A70-40931
- Circumstellar dust cloud model of spectral distribution and anomalous excess emissions in IR T Tauri and red giant stars coincident with photometric measurements
23 p4239 A70-43868
- High velocity stars in Large Magellanic Cloud from spectroscopic observations, including A dwarfs and G-K giants
23 p4240 A70-44212
- Single normal main sequence stars rotational velocities compared with giant, supergiant, Be, A and metallic line stars and Population II objects
23 p4248 A70-44802
- Nitrogen abundance of subgiant nu Indi from observed and computed stellar spectra of CN violet bands
24 p4404 A70-45411
- Old open clusters red giant observations comparison with stellar evolution calculations, discussing proper motions, magnitudes, data acquisition and analysis, etc
24 p4404 A70-45418
- Massive star pulsational stability in He burning phase, investigating opacity variation effects on flux dissipation in outer layers
24 p4405 A70-45419
- Main sequence and giant stars atmospheric structure models, noting metal deficiency effects
24 p4413 A70-46159
- GIBBS FREE ENERGY**
Alloys stacking faults thermodynamics based on Gibbs treatment of interfacial free energy
22 p4124 A70-42726
- GIMBALLESS INERTIAL NAVIGATION**
Stable, soup-can size, field replaceable, plug in/out gyro unit strapped to vehicle body without gimbals
13 p2409 A70-29480
- Self alignment for gimballess inertial navigation system fixed base by generating computer programs from error signals derived from inertial sensors
16 p2946 A70-33302
- GIMBALS**
Flip-flop type intergimbal compensation system for gyroscopic integrators error reduction, obtaining natural oscillations constant amplitude
01 p0092 A70-10987
- Probability theory for gimbal errors in directional gyroscopes upon irregular rocking, using linearization of functions of random arguments
04 p0692 A70-15281
- Axial misalignment control of gimbal pivots and rotors in gyroscopes
04 p0692 A70-15282
- Dual cockpit wide angle visual cue simulator design, discussing sky-earth-sun projector with four axis gimbal drive
10 p1857 A70-24204
- [AIAA PAPER 70-360]
Gimbal influence on three axis gyro stabilized platform in spacecraft guidance during maneuvers
13 p2446 A70-28388
- Viscous friction force moments effect on gyroscope drift in gimbal suspension during base angular vibrations, obtaining drift velocity
15 p2738 A70-32153
- Mariner Mars 1971 gimbal actuator design and life test for autopilot system using hypergolic bipropellant rocket engine
17 p3022 A70-34758
- Gyroscope in gimbal suspension on free base of four solid bodies connected by flat hinges
18 p3259 A70-36593
- Control moment gyro /CMG/ for spacecraft attitude control, determining optimal gimbal angle rate for desired torque
19 p3433 A70-38857
- [AIAA PAPER 70-1042]
Freely spinning satellites gimbal and momentum wheel system, determining stable equilibrium states by analog computer simulations
20 p3714 A70-39547
- [AIAA PAPER 70-982]
Precision gimbaled sensor pointing system calibration data errors due to misalignments and inaccuracies in transducer readout
22 p4040 A70-43587
- GIRDER WEBS**
Rectangular plate girder webs buckling under partial edge loadings, using finite element method for flange-web interaction
08 p1589 A70-21247
- GLACIOLOGY**
Oxygen 18 concentration in Greenland ice core correlation to solar activity index, indicating earth temperature control by solar activity
13 p2489 A70-28909
- GLANDS [ANATOMY]**
NT ADRENAL GLAND

- NT ENDOCRINE GLANDS
NT GONADS
NT OVARIES
NT PARATHYROID GLAND
NT PINEAL GLAND
NT PITUITARY GLAND
NT SALIVARY GLANDS
NT TESTES
NT THYMUS GLAND
NT THYROID GLAND
- GLASS**
NT GLASS FIBERS
NT OBSIDIAN GLASS
NT PYROCERAM [TRADEMARK]
NT S GLASS
NT SILICA GLASS
- Stannic or cobalt oxide film coated glasses optical and energy characteristics determined for potential use in solar energy engineering
01 p0159 A70-10766
- Fracture and degree of material removal of glassy body in hypersonic gas flow, considering radiant heat conduction inside body
03 p0516 A70-13391
- Bivalent cations effect on crystallization and viscosity of glazed glass
05 p0871 A70-16592
- Glass filled thermoplastics fabrication techniques and composites, discussing molding compounds and processes, reinforced thermoplastics properties and applications
05 p0873 A70-16605
- Glassy drops identity and moldavites sculpturing origin in Pannonian sediments in southern Moravia
05 p0916 A70-16838
- Silane coupling agents glass-catalyzed hydrolysis without presence of acid, discussing reaction kinetics
06 p1091 A70-17599
- Ar beam scattering and UV radiation from glass target surface with adsorbed gas layer
06 p1112 A70-18274
- Spectral broadening mechanisms for trivalent Eu ions in glass, considering fluorescence and absorption spectra measurements
06 p1127 A70-18640
- Laser pulse power effect on edge absorption of glass filter used for Q switching applications
07 p1299 A70-19855
- Thermal conductivities of glass reinforced polystyrene and polyethylene plastics measured over range of glass concentrations and sizes
07 p1320 A70-19958
- Thermoluminescent glass X ray dosimeter sensitivity tested as function of rigidity of gamma and X radiation, noting compensating filters for incident radiation
08 p1496 A70-21217
- Switching and memory phenomena in semiconductor glasses, thin films and variable threshold metal-oxide-nitride-semiconductor MNOS transistor
08 p1556 A70-21304
- Allende meteorite showing presence of Ca-Al-rich glasses associated with other crystalline phases
08 p1579 A70-21562
- Photolytic reactions mechanism in photochromic glass with silver halide crystals formed during glass manufacture, discussing properties and applications
08 p1499 A70-21683
- Mechanical properties and fracture behavior of chemically bonded glass matrix-metal composites
08 p1521 A70-21699
- Excitation energy transfer processes in oxide glasses containing trivalent Tb ions in combination with other rare earth activators
09 p1738 A70-22137
- F-104 jet windshield components research concerning plate glass optical deviation problems to meet quality standards
09 p1691 A70-22571
- Neodymium spectral line widths in various glasses, studying role of inhomogeneous broadening
10 p1900 A70-24266
- Quartz and alkaline glasses fracture stability in water vapor and aqueous solutions with enhanced surface activity as function of time
11 p2068 A70-25379
- Thermo-optical constant of laser neodymium glasses measured with interferometer
13 p2430 A70-29761
- Lasing characteristics of Nd glass, measuring efficiency, pump threshold energy and absorption under test conditions instability
13 p2431 A70-29873
- Tektite glass in lunar sample from Apollo 12, discussing chemical composition and possible volcanic origin
14 p2642 A70-30983
- Electric conductivity, thermal emf and EPR spectra of oxide semiconductor glasses based on vanadium and phosphorus oxides, correlating unpaired electron and charge carrier concentrations
15 p2784 A70-32201
- Glass bonding techniques for semiconductor strain gages, discussing outgassing minimization, hysteresis and repeatability and operational temperature range extension
15 p2739 A70-32325

- Radioisotopic and complementary surface chemical analysis of coupling agent films on glass surfaces
16 p2917 A70-33375
- Cone crack closure in brittle solids, discussing optical and X ray studies on glass and silicon during unloading
17 p3183 A70-34621
- Glass laser materials characteristics, discussing refractive index thermal coefficient, stress optical coefficients, spontaneous emission, etc
17 p3105 A70-35091
- Surface destruction of glass dielectric by pulsed laser beam, considering plasma clouds, shock waves, ablation and crack formation
18 p3266 A70-36153
- Spaceborne lightweight mirror blanks made from ceramics fabricated from glass crystallization
18 p3263 A70-36559
- Glass switching /Ovshinsky effect/, discussing various theoretical explanations
18 p3298 A70-36956
- Iron phosphate semiconducting glasses, determining electrical and magnetic properties dependence on thermal treatment
19 p3487 A70-37861
- Erasure fission tracks in soda-lime glass, tektite, biotite and apatite by shock loading, determining dynamic pressure and associated temperature effects
19 p3414 A70-38035
- Frequency dependent reversible switching characteristics of glass semiconductors, assuming current control
19 p3389 A70-38070
- Giant pulse neodymium glass laser emission spectrum structure, showing cavity geometry effect on fine structure
20 p3641 A70-39450
- Solid state laser glass filters for absorbing UV light emitted by pumping tubes
20 p3641 A70-39739
- Glass plastic composite electrically heated windshields for aircraft, discussing design, fabrication, qualification testing and service experience
21 p3750 A70-41137
- Petrologic analyses of minerals and glass spherules in Apollo 11 lunar rocks, indicating little fractionation and shallow-level differentiation
21 p3897 A70-41521
- Petrography and shock vaporization origin of Apollo 11 lunar breccias and glasses compared to terrestrial impactites and chondrites
21 p3898 A70-41524
- Compositions of lunar fines, crystalline rock and glass spherules, showing high normative anorthite
21 p3899 A70-41531
- Apollo 11 lunar igneous rocks minerals and glassy phases characteristics, using electron probe microanalysis
21 p3900 A70-41538
- Glass spherule lunar particles and breccia from Apollo 11 site, showing passage through impact generated cloud of hot fragmental material
21 p3901 A70-41541
- Microprobe analysis of glassy spherules from Apollo 11 lunar regolith, discussing zoning, composition and hypervelocity impact formation
21 p3903 A70-41558
- Apollo 11 lunar fines glass spherules magnetic properties, considering soft and hard ferromagnetic components
21 p3918 A70-41681
- Apollo 11 lunar dust small glassy spherules and cylinders examination by interferometry, discussing specular reflection, microcracking, chipping and origin
21 p3919 A70-41682
- High strength glass for aircraft structures, discussing applications to passenger cabin windows
21 p3843 A70-41891
- Optical glasses photoelastic constants measurement, tabulating results
22 p4072 A70-42509
- Particle size, shape and absorptivity effects on inclusion damage of Nd-doped barium crown laser glass
22 p4050 A70-43007
- Materials for glass-metal compressed joints, tabulating stress and thermal expansion coefficients
22 p3999 A70-43447
- Tektite glass absence in Apollo 12 lunar sample
23 p4238 A70-43806
- Apollo 11 lunar fines glassy particles, investigating morphology, optical properties and chemical composition
24 p4403 A70-45401
- GLASS COATINGS**
Selective glass coatings applications in solar thermoelectric generators working without radiation concentrators
01 p0011 A70-10767
- Semitransparent Pt film reflectance in vacuum UV evaporated on glass, quartz, Al, Au and Cr on glass compared with opaque films
04 p0731 A70-15023

- Specular reflectivity measurement method for optical thin film coating in 10.6 micron IR region using carbon dioxide laser source 07 p1302 A70-20084
- GLASS FIBERS**
- Zinc and resin coated alkaline glass fibers tensile strength, describing test procedure 01 p0126 A70-10220
- Water effect on glass fiber-resin bonds in interphase region, discussing initial stiffening and long term effects 01 p0127 A70-10484
- Interfacial equilibrium free surface energies between glass fibers, coupling agent and resin matrix, considering wetting, absorption and bonding 01 p0128 A70-10486
- Glass fiber-fortified thermoplastics development, properties and applications, considering ionomer, polyimide, chlorinated trifluoroethylene polymer, polymethylpentene, polybutylene, polyaryl ether and nylon 01 p0128 A70-10770
- Fiber glass reinforcement effect on flammability properties of thermoplastics 01 p0128 A70-10771
- Solid glass sphere reinforced nylon resins properties, processing and applications, noting tensile and impact strength and heat distortion 01 p0128 A70-10772
- Glass-reinforced polypropylene for structural applications, investigating time/temperature dependent creep characteristics 01 p0128 A70-10773
- Glass fiber-reinforcing techniques of polymers, discussing coating and compounding processes 01 p0104 A70-10775
- Interference fringe in Fraunhofer hologram reconstruction of tapered glass fibers related to fiber profiles 01 p0090 A70-10906
- Glass reinforced and unreinforced thermoplastics HF fatigue failure modes, discussing isothermal and nonisothermal test procedure 01 p0129 A70-11081
- Fortified thermoplastic compounds for increased flame retardancy, environmental resistance and toughness 02 p0320 A70-11865
- Chemically coupled glass-reinforced polypropylene, studying short term physical properties, creep rupture and deformation, dynamic failure, etc 02 p0322 A70-12605
- Mechanical losses in fiberglass reinforced textolite converted into thermal energy during cyclic tension and compression 02 p0323 A70-12807
- Fiberglass reinforced plastic shells stability analysis, assuming weak shear resistance of shell material 02 p0390 A70-12808
- Radiation hardened fiberglass reinforced plastics rupture, bending, compression and tensile strength and elastic modulus, considering gamma ray doses effect 02 p0323 A70-12811
- Stress concentration in optically active fiberglass reinforced plastics during static loading determined by optical polarization method 02 p0390 A70-12812
- Component proportion and porosity effect on fiberglass reinforced plastics properties, establishing relation between bending strength and thermal conductivity coefficient 02 p0323 A70-12814
- Fiberglass reinforced textolite fatigue characteristics under impact tensile loads, noting different characteristics under cyclic sinusoidal loads 02 p0323 A70-12815
- Compression failure of unidirectional fiberglass reinforced plastics 04 p0712 A70-14487
- Damping factor of fiberglass-reinforced cylindrical shells, concerning dependence on wave number and energy losses due to medium resistance and acoustic radiation 04 p0712 A70-14488
- Physical and chemical phenomena and critical factors underlying, furthering or impeding water droplets coalescence in glass-fiber bed of filter-separator 04 p0625 A70-14709
- Optical effects in parallel glass fibers irradiated by He-Ne laser beam, studying resonance tunneling and periodic power repumping between fibers 04 p0702 A70-15215
- Fiberglass reinforced plastics energy dissipation during fatigue failure phases, studying mechanical-to-thermal energy transformation under cyclic strain 04 p0713 A70-15263
- Statistical stress distribution of breakdown during scaling of wound fiberglass reinforced plastics, noting relation between critical stress and defects 05 p0870 A70-16214
- Statistical stability of cylindrical fiberglass reinforced plastic shells under axial compression, showing breakdown loads vs radius/thickness ratio 05 p0933 A70-16215
- Residual stress variations in ring shaped fiberglass reinforced plastic shells produced by winding due to elastic modulus decrease and filler/binder contraction 05 p0934 A70-16216
- Fiberglass reinforced rectilinear plastic plates bending under various edge loads, noting shear pliability 05 p0934 A70-16220
- Axial and nonlinear bending performance compared for compression moldings laminated from random glass fiber mat 05 p0870 A70-16577
- Handbook on fiberglass and advanced plastics composites covering raw materials, processing methods, design and applications 05 p0872 A70-16601
- Glass fibers performance characteristics and applications, discussing fiber production, glass composition, fiber reinforced plastics surface treatment, etc 05 p0873 A70-16606
- Mechanical fastening, adhesive bonding and machining methods for laminated fiberglass reinforced plastic materials 05 p0856 A70-16618
- Bubbles elimination in glass filament wound parts involving total or partial placement of production equipment and process in vacuum 05 p0856 A70-16825
- External hydrostatic pressure effect on fiberglass-reinforced plastics strength under unilateral heating, analyzing stress distribution 05 p0875 A70-17067
- Thermoplastic polymers adhesion to glass fibers determined by measuring force necessary to pull fiber from flat film of polymer 06 p1091 A70-17317
- Fatigue life of unidirectionally glass fiber reinforced composites subjected to low cycle loading, using linear elastic body model for cyclic deformation process 06 p1091 A70-17408
- Glass fiber reinforced thermoplastics fatigue behavior during and after cyclic loading 06 p1091 A70-17600
- Anisotropic fiberglass reinforced plastics creep properties under biaxial compression, showing compressive to tensile strain elimination or change 07 p1316 A70-19546
- Arbeitsgemeinschaft Verstärkte Kunststoffe - Conference, Freudenstadt, West Germany, September-October 1969 07 p1316 A70-19753
- Crack formation in resin matrix and effect on fiberglass reinforced composites behavior under loading 07 p1318 A70-19754
- Stress analysis of multiaxially loaded tubes of fiberglass reinforced composite wound in three directions 07 p1318 A70-19755
- Buckling stress calculation and measurement in cylindrical fiberglass reinforced composite shells under axial pressure 07 p1409 A70-19756
- Sizing and design of large vessels of fiberglass reinforced composites based on minimum cost 07 p1409 A70-19757
- Fiberglass reinforced materials characteristics under stress evaluated by ring test in form of split disk or hydraulic tests 07 p1410 A70-19758
- Fiberglass reinforced plastics bonding, discussing structure fabrication and use as material 07 p1295 A70-19759
- Rupture safety in fiberglass reinforced plastics using variation coefficient illustrated in vessel design 07 p1410 A70-19760
- Fiberglass plastics structure safety design using time dependent limiting states with wear allowance 07 p1410 A70-19761
- Electrostatic ignition discharge prevention on fiberglass reinforced depot tanks, noting ground connection safeguard 07 p1295 A70-19763
- Air bubble free glass fiber-plastic laminates fabricated by wet-winding method using vacuum, noting void free filament wounpipes 07 p1295 A70-19766
- Interlaminar shear strength determination methods taking into account plastics composition, considering polyester and epoxy plastics, glass and graphite fiber reinforcing materials 07 p1410 A70-19767
- Tensile and compressive stress cycles effect on short term strength of glass fiber plastic laminates 07 p1411 A70-19769
- Boron and carbon fiber reinforced composites mechanical properties compared with fiberglass reinforced composites 07 p1318 A70-19770
- Creep and stress relaxation tests to investigate time dependent fracture strength of unidirectional glass fiber reinforced epoxy composites 07 p1321 A70-19962
- Glass fiber reinforced polyether composites long time strength under plane stress 07 p1321 A70-20187
- Elastic and optical properties anisotropy in fiberglass reinforced epoxy plates using photoelastic method 07 p1416 A70-20295
- Modulus of elasticity of fiber glass reinforced plastic under transverse bending as function of length-to-height ratio in laminates 08 p1526 A70-20532
- Glass filament reinforced plastics characteristics, considering filament protection during manufacture 08 p1526 A70-20717
- Thermoelastic characteristics of glass fiber reinforced plastic materials, determining temperature dependent deformation of composite plate 08 p1526 A70-21164
- Adhesion characteristics in composites, investigating correlation between short beam and torsion shear tests in glass and graphite reinforced epoxy materials 08 p1531 A70-21892
- Glass fiber reinforced epoxy laminate specimens tests in tension and flexure at various strain rates to determine geometry effect on strength 08 p1532 A70-21898
- Fiberglass-epoxy laminates mechanical behavior under biaxial loading, describing test equipment and procedures 08 p1532 A70-21904
- Fiberglass reinforced plastic laminates shear characteristics determination, giving expressions for shear modulus and tangential stress 09 p1709 A70-22300
- Failure analysis of unidirectionally reinforced fiberglass composites due to winding, using critical stress distribution function 09 p1710 A70-22462
- Single and clad glass fibers radii and refractive indices measurements on basis of laser light scattering 09 p1699 A70-23444
- Temperature fields and thermal stresses in FN fiberglass reinforced textolite under nonstationary unilateral heating, determining stress as function of time and heating rate 09 p1710 A70-23724
- Fiberglass reinforced textolite creep strains as function of stress, temperature and time, noting correlation with theory to 200 C 09 p1710 A70-23725
- Epoxy glass fiber composites pyrolyzates IR spectra as function of time, observing changes in fingerprint region 10 p1828 A70-24065
- Glass-epoxy composites failure mode dependence on matrix characteristics and fiber orientation, observing flexural strength increase with strain rate 10 p1908 A70-25174
- Glass epoxy cross ply laminates with brittle or ductile epoxy matrices tensile tested, comparing mechanical performance 11 p2068 A70-25686
- Heat flow comparator for nondestructive testing of resin-impregnated fiber glass, detecting nonuniformities leading to thermal properties variation 11 p2059 A70-25764
- Radiative heat transfer due to radiation conductivity and transmission in low density glass fiber insulations by heat flowmeter for hot and cold surfaces 11 p2148 A70-25769
- Thermoplastics reinforcement with glass and asbestos fibers taking into account fiber properties 11 p2070 A70-25825
- High strength glassy carbon fibers obtained by carbonizing extruded phenol hexamine polymers 11 p2071 A70-26672
- Elastic stiffness of unidirectional glass reinforced epoxy fiber composite determined from ultrasonic velocity measurements 11 p2071 A70-26692
- Residual stresses levels in glass fiber reinforced plastic components after production by compression or winding 12 p2325 A70-27534
- Orthotropic fiberglass reinforced plastic deformation during stretching with allowance for binder breakdown in transverse layer 12 p2259 A70-28283
- Fiberglass plastic reinforced high pressure balloons design and fabrication with oblated ellipsoid of revolution, discussing deformability, strength and cyclic loadings resistance 12 p2328 A70-28285
- Fiberglass content effects on reinforced polycarbonates long term dimensional stability during compression and tension creep tests 12 p2259 A70-28298
- Glass fiber reinforced resin structures and equipment quality and physical/mechanical conditions determined by plastographic analysis 13 p2404 A70-28665
- Fiberglass reinforcement effects on injection molded thermoplastics physical properties, noting role of binder and glass content 13 p2438 A70-29204
- S glass fibers strength characteristics at quasi-static strain rates, considering temperature effects on elastic modulus 13 p2439 A70-29707

Cutting speed, feed parameters and tool tip curvature effects on machined surface roughness of turned fiberglass reinforced epoxy laminates

14 p2590 A70-30873

Heat transfer through axially symmetric boundary layer on moving circular fiber at uniform temperature

15 p2825 A70-31819

Stress distribution in fiberglass unidirectionally reinforced composite material under uniaxial tension

15 p2765 A70-32180

Dangerous plane stressed state surfaces for fiberglass reinforced plastic pipes, using fourth degree polynomial

15 p2766 A70-32852

Stress rupture shear strength of fiberglass reinforced plastics under monotonic, prolonged and cyclic loading

15 p2766 A70-32853

Anisotropic glass fiber reinforced plastics strength and deformability under cyclic axial loads

15 p2766 A70-32897

Fiberglass reinforced anisotropic plastics heating during cyclic axial loading

16 p2934 A70-33215

Diluent resins properties for blending with glass fiber reinforced high density polyethylene concentrate

16 p2935 A70-33353

Friction properties of internally lubricated and glass-fortified thermoplastic resins for gears and bearings

16 p2935 A70-33354

Low cost flame retardant high service temperature glass reinforced electrical grade laminate tested for continuous use

16 p2935 A70-33355

High service temperature glass reinforced premix compound on Glastic grade electrical laminate, discussing optimum molding and applications

16 p2936 A70-33356

Glass fiber reinforced resin structures evaluation by plastographic analysis using visual, macrographic, stereomicroscopic, and scanning electron microscope methods

16 p2908 A70-33361

Moisture induced failure of glass-resin composites at interface, discussing water adsorption, crack propagation, wet strength and nonsilicate reinforcements

16 p2937 A70-33373

Interfacial chemistry of glass fiber reinforced thermoplastics, discussing matrix resin-reinforcement bond

16 p2937 A70-33378

Polymeric binders adhesion to glass fibers as function of type and chemical structure

16 p2938 A70-33379

Fiber reinforced prepreg properties measurements in high modulus graphite/epoxy and fiberglass/ epoxy prepreg sheets and tapes

16 p2938 A70-33386

Glass reinforced laminates fatigue characteristics, discussing differences from metals due to composites anisotropic structure

16 p2989 A70-33420

Joint design for fiberglass reinforced plastic aircraft composites regarding minimum weight and reliability [ASME PAPER 70-DE-56]

16 p2989 A70-33516

Mode locked He-Ne laser nsec pulses propagation along multimode clad glass fibers

16 p2865 A70-34039

Flexural creep deflections of glass fiber reinforced polycarbonate and Nylon thermoplastics

17 p3127 A70-34657

Fiberglass reinforced plastics fatigue properties, describing electric model and nondestructive testing

17 p3183 A70-34658

CH-47C helicopter fiberglass main rotor blade, discussing composite materials impact on design

17 p3013 A70-34702

Temperature and constant compressive loading effects on mechanical characteristics of fiberglass reinforced plastics

17 p3127 A70-35341

Composite wing section design and fabrication utilizing unidirectional glass reinforcement [AIAA PAPER 70-919]

17 p3193 A70-35813

Gliders made of glass fiber reinforced plastics, investigating thermodynamic properties under solar irradiation and surrounding warm air

19 p3454 A70-37370

Glass fiber reinforced cross ply and quasi-isotropic plastics, considering notches effect on fatigue behavior for comparison with metals

19 p3455 A70-37951

Light focusing glass fiber with variable refractive index using ion exchange process, discussing applications to laser communications and data processing

20 p3671 A70-39129

Soviet book on glass staple fibers covering classification, properties, composition, production, tests and industrial applications

20 p3655 A70-39399

Shearing strain in oriented fiberglass reinforced plastics under torsion, obtaining creep curves

20 p3655 A70-39768

Fiberglass reinforced plastics fatigue life, analyzing structural factors role

20 p3655 A70-39891

Glass reinforced plastics /GRP/ mechanical properties degradation by water, discussing effects of temperature, pressure, environment, etc

20 p3656 A70-40056

Contact shaped fiberglass-reinforced plastic tensile creep tests, showing strain property linearity dependence on direction

21 p3841 A70-40642

Multilayer three dimensionally woven fiberglass-reinforced materials, measuring strength and deformation under tension, compression, bending, torsion and shear tests

21 p3841 A70-40646

Unidirectional fiberglass-reinforced plastic, investigating binder content and porosity effects on strength

21 p3841 A70-40647

Thin walled fiberglass-reinforced plastic cylinders in torsion, calculating load carrying capacity as function of temperature

21 p3841 A70-40648

Orthotropic fiberglass-reinforced plastic cylindrical shell with allowance for material creep, calculating stress-strain state during bending under external pressure

21 p3842 A70-40649

Textolite and fiberglass-reinforced plastics relaxation parameters tabulation for viscoelasticity boundary value problems solution

21 p3842 A70-40650

Deformational characteristics of unidirectional glass epoxy composites with ductile and brittle matrices evaluated in flexure

22 p4059 A70-43101

Internal friction and shear modulus of thin glass fibers of sodium silicate, aluminosodium silicate and nonalkaline aluminoborosilicate

22 p4059 A70-43135

Clad glass fibers axial stress measurement by photoelastic techniques

22 p4060 A70-43415

Glass-epoxy composites, measuring embedding filaments effect on time-temperature relationship under ultimate stress conditions

22 p4118 A70-43549

Transverse bending of orthotropic glass fiber reinforced plastic plates under uniformly distributed loads

22 p4120 A70-43720

Mechanical properties and internal stress fields in composite materials reinforced by glass fibrous filler under transverse shear

22 p4061 A70-43724

Prestressed loadings on two layer fiberglass-reinforced plastic cylindrical shell under internal pressure

23 p4265 A70-43937

Stress-strain diagrams for oriented fiberglass-reinforced plastic under tension taking into account temperature and anisotropy effects

23 p4209 A70-43938

Fiberglass reinforced plastic strength and deformation properties under creep and stress relaxation, investigating temperature effects and load duration

23 p4209 A70-43980

Saturn Orbital Workshop experiment for testing chemically rigidized expandable materials and structures for space applications, discussing resin impregnated glass fiber cloth

23 p4264 A70-45012

German monograph on fiberglass, matrix and filler effect on service life of composites with low fiberglass content

24 p4365 A70-45084

German monograph on glass fiber reinforcement effect on soft thermoplastics strength, adhesion and slip properties

24 p4366 A70-45088

Natural dispersion effect on bandwidth of glass fiber transmission line using optical glasses

24 p4319 A70-46079

Thermosetting glass reinforced plastics fabrication and use for pressure vessels, vacuum vessels and pipes

24 p4350 A70-46388

GLASSWARE

Glass drainline development and marketing, describing technology transfer role

20 p3740 A70-39100

GLAUBER THEORY

Hydrogen atom excitation at various energy levels by electron impact, applying Glauber theory

16 p2954 A70-33287

GLAUERT COEFFICIENT

U AERODYNAMIC FORCES

U MACH NUMBER

GLAZES

Bivalent cations effect on crystallization and viscosity of glazed glass

05 p0871 A70-16592

Criticism of hypothesis regarding solar flash heating mechanism creating glaze within lunar craterlets at Apollo 11 landing site

13 p2489 A70-28912

GLIDE ANGLES

U GLIDE PATHS

GLIDE LANDINGS

Subsonic glide landing approach guidance for unpowered lifting vehicles, using perturbation feedback and approximation of heading and position coordinates

[AIAA PAPER 69-865] 09 p1725 A70-23253

Gliding parachute air cargo systems using nonproportional and proportional automatic manual control, estimating wind effects on ground track and impact computer simulation

[AIAA PAPER 70-1193] 21 p3753 A70-41823

Static and dynamic longitudinal stability of semirigid parafoil gliding descent system in pitching motion

[AIAA PAPER 70-1191] 21 p3753 A70-41825

Glide and landing performance of twin-keel parawings, discussing wind tunnel, radio flight and simulator tests

[AIAA PAPER 70-1186] 21 p3754 A70-41829

GLIDE PATHS

Geometrical model for characterizing instrument landing system /ILS/ null reference glide path utilizing CW measuring system

04 p0716 A70-15330

Planetary atmospheric entry optimal three dimensional glide paths, considering polar curve altitude dependence, flight path changes, braking maneuvers, etc

07 p1378 A70-18985

Integrated glide path localizer system for landing, takeoff and enroute guidance through rugged country, minimizing spurious reflection, required information bits, etc

09 p1720 A70-22222

Terminal area guidance for unpowered aircraft instrument approach relevant to manned space shuttle effort

14 p2614 A70-30465

Planetary atmospheric entry optimal three dimensional glide paths, considering polar curve altitude dependence, flight path changes, braking maneuvers, etc [DFVLR-SONDDR-49]

16 p2982 A70-33771

Airborne vertical glide path guidance computer for aircraft landing, using barometric altitude and DME data

16 p2871 A70-34053

ILS glide slope calibration using optically projected digital codes as reference

19 p3464 A70-37912

GLIDE SLOPES

U GLIDE PATHS

GLIDERS

NT BOOSTGLIDE VEHICLES

NT FLEXIBLE WINGS

NT HYPERSONIC GLIDERS

NT PARAGLIDERS

NT PARAWINGS

Wind tunnel comparative performance tests of glider laminar wing profile with fixed and flexible trailing-edge flap

02 p0304 A70-12800

German light aircraft construction industry situation and prospects regarding manufacture of gliders, sporting and touring aircraft and motor gliders

03 p0413 A70-13791

Sigma glider design for high cruising speed, using extensible wing to double area in flight

04 p0622 A70-14625

Schleicher AS-W15 glider wing span, weight, wing loading capacity and speed range, noting performance in international competition

05 p0793 A70-15905

Two place sport gliders development, design reliability and competition requirements

05 p0794 A70-16352

Level flight optimization in horizontal wind varying with altitude, using glider concept and induced drag correction

[ONERA-TP-700] 07 p1193 A70-19131

Favorable air mass type and season for long cross country soaring flights over eastern U.S. determined from record analysis

09 p1718 A70-23062

Motion equations and dynamic lateral stability of towed glider in steady horizontal flight treated by small perturbations method, including design and handling influence

09 p1611 A70-23063

Sailplane design standards concerning retractable undercarriage and trailing-edge flaps revised to achieve better performance

09 p1612 A70-23575

Statistical methods for flying quality research concerning sailplane dynamic stability, maneuverability, sensitivity, rolling and pilot induced oscillations

10 p1805 A70-24582

Glider pilots flight above cloudstreets in clear sky, discussing situation for wave soaring over flat ground

10 p1805 A70-24583

Spanwise distribution of aerodynamic torsion on sailplane wings in vertical dive, discussing wing twist and lift effects

12 p2156 A70-27721

- Glider longitudinal stability and control in symmetrical flight positions, determining flight characteristics 12 p2161 A70-27723
- Sailplanes flight characteristics concerning longitudinal stability and control position gradient 14 p2531 A70-30634
- Optimal distance flight, discussing glider polar performance data 16 p2842 A70-34174
- Rotary piston engine for powered gliders and light aircraft power source by modifying industrial Wankel engine 17 p3147 A70-34690
- High lift flaps for sailplane cross country speed improvement by cruise-climb tradeoffs [AIAA PAPER 70-878] 17 p3016 A70-34814
- Wings flexural deformability influence on longitudinal stability of glider, using small perturbation theory 17 p3017 A70-35190
- Water ballast effect on glider loads, using concept of characteristic velocities 18 p3213 A70-36253
- Gliders made of glass fiber reinforced plastics, investigating thermodynamic properties under solar irradiation and surrounding warm air 19 p3454 A70-37370
- Reefing systems for Parawings, Sailwings, Para-Flyers, Paraplanes and Volplanes, discussing performance tests [AIAA PAPER 70-1192] 21 p3753 A70-41824
- Optimum light construction design of glider wings, considering spar weight, aluminum honeycomb structure and repair 22 p3962 A70-42961
- Water ballast loadings on sailplane Cobra 17, considering wing, aileron, tailplane, fuselage and landing gear 22 p3962 A70-42962
- GLIDING**
- Biphasic nature of pilot error in gliding, suggesting means of reducing aircraft accidents 03 p0433 A70-13261
- Degenerate variational problem of optimum gliding along zero proximity line, determining number of control switchings and deviation during perturbed motion 10 p1854 A70-24277
- Basket weave fabrics for gliding descent decelerators with polyurethane and nylon coatings for tearing strength and pressure packing [AIAA PAPER 70-1180] 21 p3843 A70-41833
- GLINT**
- Sea surface sunglint pattern irregularities in earth orbiting satellite photographs, observing dark patches 05 p0838 A70-16152
- Anomalous dark areas in sunglint patterns from ATS photographs, considering water temperature effect on ocean surface conditions 16 p2897 A70-33725
- Homing radar tracking accuracy improvement by glint reduction using frequency diversity [AIAA PAPER 70-992] 20 p3586 A70-39538
- GLOBULINS**
- NT GAMMA GLOBULIN**
- Separate gamma irradiation effect of enzyme and hemoglobin-albumin-globulin substrates on proteolysis dynamics 03 p0419 A70-13308
- Amino acids changes distribution in specificity regions of light polypeptide chains of immunoglobulins showing correspondence with Poisson distribution 14 p2536 A70-30349
- Albumin and IgG degradation, studying high altitude effect on hepatic function in man 15 p2683 A70-32532
- GLOW**
- U LUMINESCENCE**
- GLOW DISCHARGES**
- Spectroscopic determination of radial temperature distribution at various currents in negative glow of hollow cathode discharge, analyzing influence of gas pressure 05 p0888 A70-16358
- Inert gas glow discharge current change under laser radiation, investigating dependence on discharge region, gas and electrode material and configuration 09 p1696 A70-22484
- Transient lunar phenomenon /obscurations and evanescent localized glows/ related to dust raised by degassing and electrostatic glow discharges in gas phase 10 p1938 A70-24069
- Thin wire glow during corona discharge in metal cylinders analyzed by photomultiplier 11 p2083 A70-25924
- Acoustic wave propagation through positive column of glow discharge of three component plasma, noting amplitudes dependence on excitation wave amplitude 17 p3140 A70-34872
- Molybdenum carbide in methane-based plasma glow discharge, considering possible pyrocarbon layer formation and temperature effects 19 p3434 A70-37456
- Carbon dioxide initial dissociation rates in glow discharges and gas mixtures at low pressures, using mass spectrometric sampling and plasma diagnostic methods 20 p3674 A70-39235
- Surface contaminated Langmuir probe measurements in glow discharge plasmas, discussing errors 20 p3633 A70-40161
- Carbon dioxide-helium laser hollow cathode negative glow discharge amplifier, discussing construction and advantages compared to other excitation media and discharge structures 21 p3834 A70-40568
- Hollow cathode shape effect on glow discharge parameters and potential jump in cathode region, investigating I-V curves 22 p4078 A70-42357
- Glow discharge electron guns for welding and heating, discussing beam current and energy balance 22 p4042 A70-42376
- GLUCOSE**
- Chemostat culture method for studying control mechanisms during utilization of glucose/lactose and glucose/L-aspartic acid by populations of *Escherichia coli* 01 p0021 A70-10787
- Growth rate effect on glucose utilization rate using sporogenic strain of *Bacillus subtilis* during N and L-tryptophan limitation 01 p0021 A70-10790
- Retention times and gas chromatographic conditions for resolution of galactonic and gluconic acid derivatives 16 p2855 A70-33064
- Plasma free fatty acids and glucose relative role in contribution to metabolic state and energy production in partially hepatectomized rats 16 p2850 A70-34319
- Blood glucose and plasma immunoreactive insulin concentrations before, during and after intermittent short duration maximal exercise and glucose infusion 17 p3030 A70-35420
- Mathematical model of human pituitary gland mechanism controlling secretions of serum growth hormone in response to glucose deficiency 20 p3569 A70-38995
- Human gluco-regulatory hormone reserve depressions following acute and chronic acceleration exposure 20 p3572 A70-39436
- Fasting plasma glucose concentration in rats after chronic hypoxia 20 p3577 A70-40542
- Glucose metabolism in chickens under chronic centrifugal acceleration, meeting increased energy requirements 23 p4147 A70-44786
- GLUCOSIDES**
- Ca ion reversible effects of hydrochloric acid and ammonia water on betacyanin leakage from beetroot sections 19 p3365 A70-38375
- Cardiac glycosides and beta receptor blocking agent effect on ULF displacement ballistocardiogram in healthy young men, measuring heart rate and blood pressure 21 p3763 A70-41227
- GLUES**
- Vinoflex glue for constant strain gauges in low temperature tensometry, showing satisfactory recording at single and multiple loadings 08 p1495 A70-20984
- GLUTAMATES**
- Amino acids L-glutamate and gamma-aminobutyric acid as communication agents in brain 23 p4148 A70-44864
- GLUTAMIC ACID**
- Glutamic and aspartic acid concentrations in brain tissue and incubation medium after adding gamma-aminobutyric acid 01 p0018 A70-10507
- GLUTAMINE**
- Glutamine deamidation enhancement by N-acetyl-L-aspartic acid addition to mitochondrial preparations of rabbit brain incubated in Tris buffer 01 p0018 A70-10508
- Renal and hepatic glutamine synthetase distribution in mammals, studying relation between glutaminase and urinary activities /ammonia metabolism/ 02 p0232 A70-11710
- GLYCERIDES**
- Free fatty acids, glycerol and triglyceride levels in arterial and femoral venous blood in humans before and after physical training 12 p2169 A70-27625
- Coronary heart disease prediction based on clinical suspicion, age, total cholesterol and triglyceride, using relationships established by cinearteriographic studies 23 p4145 A70-43947
- Lipoprotein lipase activation on emulsified triglycerides by specific glycopeptides of human serum lipoproteins 24 p4298 A70-45802
- GLYCERINS**
- U GLYCEROLS**
- GLYCEROLS**
- Mechanized glycerine process for fibers and whiskers alignment on large scale at low cost 05 p0855 A70-16580
- Free fatty acids, glycerol and triglyceride levels in arterial and femoral venous blood in humans before and after physical training 12 p2169 A70-27625
- Hibernation and glycerol production in wasps *Ichneumonidea*, discussing possible physiological cryoprotective function 24 p4304 A70-46140
- GLYCINE**
- Peptide formation during glycine reaction with linear polyphosphates and cyclic metaphosphates, considering prebiotic synthesis 09 p1630 A70-23395
- Acute hypoxia effects on C14-tagged glycine absorption, distribution and discharge in rats organs and tissues 17 p3030 A70-35360
- Trichroic IR absorption lines of triglycine selenate, computing optical and dielectric constants from transmission and reflection data 19 p3470 A70-37366
- GLYCOGENS**
- Glycogen accumulation in astroglia following brain trauma caused by partial transection of cerebral hemisphere in rats 09 p1620 A70-22898
- GLYCOLS**
- Synthetic fluids as lubricants, examining physicochemical properties of polyglycols, silicones and esters [ASME PAPER 70-DE-13] 16 p2917 A70-33421
- Thermal stability of glycolytic enzymes from thermophilic clostridia 17 p3042 A70-35327
- GLYCOLYSIS**
- Glycolysis and glycolytic enzymes activity increase in tissues observed during training of rats to hypoxia, discussing adaptive reactions at cellular level 12 p2167 A70-26975
- GLYCOSIDES**
- U GLUCOSIDES**
- GNOTOBIOTICS**
- Germ-free biology experimental and clinical aspects - Conference, Buffalo, June 1968 01 p0027 A70-11309
- Gnotobiotic techniques for human hematopoietic cell culture establishment and maintenance, considering culture transfer 01 p0027 A70-11311
- Gnotobiotic mice with orally inoculated microorganisms observed for quantitation and fate of bacteria in intestinal tract 01 p0027 A70-11312
- GOATS**
- Spinal cord blood flow response to carbon dioxide partial pressure in anesthetized goats 02 p0232 A70-11713
- Ventilatory response to carbon dioxide in goats during acute and chronic hypoxia 15 p2684 A70-32539
- GODDARD EXPERIMENT PACKAGE TELESCOPE**
- U PARTICLE TELESCOPES**
- GOGGLES**
- Laser radiation protective goggle design, investigating retinal energy density levels and attenuation 08 p1451 A70-21046
- GOLD**
- Calorimetric measurements determining total hemispheric emittance of thin gold films as function of temperature, demonstrating film thickness effect [AIAA PAPER 70-63] 06 p1180 A70-18140
- Crystalline structure effect on molecular beam reflection from rough polycrystalline Au surfaces 07 p1343 A70-20123
- Gold and iridium distribution in stony meteorites, discussing metal silicate fractionation process during chondrite formation 13 p2497 A70-29862
- Photoemission from evaporated gold films, measuring quantum yield, photoelectric energy distribution curves and optical density states 14 p2626 A70-30481
- Gold impurity photovoltaic effect in silicon, determining optical cross section for transition 14 p2627 A70-30528
- Au-Pd films boundary structure during diffusion annealing, noting polymerized oil vapor effect originating from vacuum pump 15 p2758 A70-32121
- Thermoelectric power measurement of thin Au films, relating results to transport parameters and internal stresses 15 p2785 A70-32582
- Lattice planes and interplanar spacings of small vapor deposited gold crystals, using transmission electron microscopy 16 p2961 A70-33644
- Shallow acceptor level in Au-doped n-type GaAs, using photoconductivity temperature dependence 17 p3143 A70-35702

- Gold foil surface thermal contact resistance, investigating temperature and pressure effects and elastic and plastic deformation of surface structure
21 p3953 A70-42166
- Crystal growth in polycrystalline Au, Ag and Au-Ag thin films annealing, observing by electron microscopy and electron diffraction
24 p4391 A70-45672
- GOLD ALLOYS**
Gold alloys electrocatalytic activity in cathodic reduction of oxygen in potassium hydroxide
12 p2182 A70-27760
- Specific heat measurements on disordered and ordered phases of Cu-Au alloys at low temperatures
14 p2626 A70-30497
- GOLD COATINGS**
GaAs-Au surface barrier n-type photodiode structure, electrical parameters and response characteristics
12 p2194 A70-26969
- Au films nucleation and growth on single crystal graphite substrates in ultrahigh vacuum, using transmission electron microscopy for examination
14 p2627 A70-30499
- GOLD PLATE**
U GOLD COATINGS
- GONADS**
Brain norepinephrine synthesis rate in gonadectomized and control rats treated with alpha-methyl paratyrosine
03 p0416 A70-12987
- GONDOLAS**
Balloon gondola azimuthal angle control by twisting suspension rope
17 p3090 A70-35315
- Reaction jet azimuth control system for balloon-borne gondola
17 p3018 A70-35316
- GONIOMETERS**
Ultrasonic methods for materials evaluation, discussing goniometry, measuring techniques and acoustic wave propagation in various materials
01 p0104 A70-10878
- GOSS [SUPPORT SYSTEM]**
U GROUND OPERATIONAL SUPPORT SYSTEM
- GOVERNMENTS**
DOD procurement practices for advanced weapon systems, discussing government errors in contracting policies
07 p1428 A70-19678
- Government environment challenges to government sponsored big technology management illustrated by space nuclear engine research program
09 p1792 A70-22494
- Data management functions of National Space Science Data Center (NSSDC), discussing data processing and information system for secondary usage
[AIAA PAPER 70-320] 09 p1641 A70-22866
- Data management functions of National Space Science Data Center (NSSDC), discussing data processing and information system for secondary usage
[AIAA PAPER 70-320] 23 p4285 A70-44514
- GOVERNORS**
U SPEED REGULATORS
- GRADIENTS**
NT ELECTRON DENSITY PROFILES
NT POTENTIAL GRADIENTS
NT PRESSURE GRADIENTS
NT TEMPERATURE GRADIENTS
Multiplier and gradient methods in computing variational and optimal control problems
07 p1325 A70-19267
- Gradient algorithm for sequential identification of features in dynamic linear systems
13 p2383 A70-29582
- High speed dynamic systems synthesis with optimal damping of elastic vibrations, using gradient method
14 p2617 A70-31354
- Sequential and combined gradient restoration algorithms for functional minimization in control theory
15 p2716 A70-32574
- Strain gradient theory for random media, considering equations for response to forcing field
19 p3456 A70-37382
- GRADIOMETERS**
U MAGNETOMETERS
- GRADUATION**
U CALIBRATING
- GRAIN BOUNDARIES**
Martensitic steel (AFC 77) austenite grain size refinement process, noting effects on yield strength, toughness, stress corrosion resistance and fatigue crack growth rate
01 p0120 A70-10739
- FeCo V plastic deformation and fracture, noting temperature and grain size effects on yield and flow stresses, ductile to brittle transition, etc
01 p0123 A70-11244
- TD-Ni low cycle fatigue properties at high temperature, discussing grain morphology, theta particles role and oxidation resistant coating effect
01 p0123 A70-11245

- Backreflection X ray microbeam camera with arrangement for positioning preselected area to study grain boundary during creep by Laue method
03 p0492 A70-13759
- Ductile-brittle transition temperature relation with grain size in polycrystalline Mo as function of annealing temperature
05 p0862 A70-15907
- Impurities effect on grain boundaries composition and brittle fracture of metals
06 p1087 A70-17608
- Ni-Cr alloys effects of grain size and surface deformation on oxidation properties at high temperature
06 p1088 A70-17610
- High melting point oxides effects on niobium alloys recrystallization temperature and grain growth
07 p1303 A70-18741
- Prestrain effect on cavity formation at grain boundaries causing creep strength decrease
07 p1307 A70-19392
- Heat resistant alloys creep ductility, considering grain boundary cavitation, sliding and migration
09 p1701 A70-22554
- Creep behavior transition analysis, considering activation energies and creep rate dependence on temperature, stress and grain size
09 p1704 A70-22720
- Cellular structure and grain size effects on mechanical properties of strained and recrystallized chromium
10 p1902 A70-23862
- Grain boundary grooves growth kinetics in pure CoO at high temperatures, determining diffusion species and mechanisms
12 p2255 A70-27603
- Al-aluminum oxide composite steady state creep due to grain boundary sliding, accounting for activation energy level
12 p2258 A70-28348
- Ceramics microcrack propagation control through small slab with simultaneous microscopic observation of path and force changes, considering grain boundaries effects
15 p2741 A70-32434
- Grain boundary sliding model subjected to shear strain, discussing effect on mechanical properties
16 p2932 A70-33789
- Elastic interactions between anisotropic crystal dislocations and twin and grain boundaries in Ti
17 p3115 A70-34386
- Unalloyed alpha titanium mechanical properties, emphasizing grain size and interstitial content effects on strain hardening and deformation dynamics
17 p3116 A70-34391
- Grain boundary allotriomorphs growth mechanisms in Al-Cu alloy at high temperatures, indicating interfacial and direct volume diffusion
18 p3271 A70-36027
- Ti-Al binary and Ti-Al-X ternary alloys grain boundary precipitation kinetics and correlation with mechanical properties
18 p3272 A70-36035
- Carbide precipitation and grain boundary migration in solution annealed duplex stainless steel as function of aging time
18 p3274 A70-36050
- Al-Zn-Mg alloys structural transformations by diffraction electron microscopy, investigating grain boundary and dislocation structure as function of heat treatment and chemical composition
20 p3646 A70-39044
- Al alloy stress corrosion susceptibility, examining grain size and anisotropy role
20 p3651 A70-40070
- Ti mechanical properties dependence on grain boundary size and hydride precipitation characteristics, considering transcrystalline and intercrystalline fracture
20 p3652 A70-40179
- Strain component determination for grain boundary sliding influence in creep of alpha iron
20 p3735 A70-40446
- Grain boundary damping characteristics of Cu-Ni alloys solid solutions, discussing height, temperature and activation energy of solute peak
22 p4053 A70-42729
- Intergranular brittleness in powder metallurgy W by Auger Electron Emission Spectroscopy for fracture surfaces chemical analysis
22 p4053 A70-42733
- Steady state creep behavior during multiple deformation process, developing grain boundary sliding relation to grain size
23 p4207 A70-44759
- Maraging steel grain size and externally applied shear stress effects on morphology of martensite formation
24 p4357 A70-45231
- 18-8 stainless steels pitting corrosion, examining grain boundaries influence
24 p4362 A70-46184
- Pure Ni recrystallization, noting stacking faults and parallel sided and thin annealed twins formation during boundary migration
24 p4363 A70-46192

- Grain growth abnormality in Al-Mg ingots with small amounts of Mn and Cr during secondary recrystallization
24 p4363 A70-46197
- Superplasticity, discussing strain rate-flow stress relationship and grain boundary sliding
24 p4363 A70-46218
- GRAINS**
Grain size, forging parameter and microstructure effect on stress-rupture properties of wrought Ni-base alloy
03 p0511 A70-13567
- GRAINS [FOOD]**
Wheat culture continuous subirrigation for life support system applications in spacecraft, discussing harvest yields
17 p3026 A70-35321
- GRAMMARS**
Descriptive pattern analysis methods, considering grammar formalism for broad application
12 p2193 A70-28102
- GRAND TOURS**
Ground-based and onboard guidance and navigation systems for outer planet flyby missions concerning direct, Jupiter swingby and Grand Tour trajectories [AIAA PAPER 70-71] 06 p1104 A70-18194
- Outer solar system exploration, discussing swingby and junction missions, Jovian satellite grand tours, mission energy requirements, etc [AIAA PAPER 70-58] 06 p1147 A70-18229
- Thermoelectric outer planet spacecraft (TOPS) project incorporating adaptable data handling system and self testing and repairing computer with triple redundancy subsystems
11 p1996 A70-25368
- Course correction requirements for ballistic grand tours and outer planet missions, considering trajectory disturbances by random nongravitational forces
13 p2448 A70-28707
- Deep space microwave and optical communications, describing grand tour requirements
21 p3784 A70-40546
- Grand tours navigation system consisting of deep space network radio and onboard TV for future TOPS/Thermoelectric Outer Planet Spacecraft applications
21 p3849 A70-41799
- Automated mission requirements for outer planets, discussing flyby spacecraft, orbiters, atmospheric entry and grand tour missions [AIAA PAPER 70-1246] 24 p4411 A70-45919
- Long life spacecraft design and reliability based on marine practices and advanced system technology project, considering grand tour outer planets mission [AIAA PAPER 70-1247] 24 p4412 A70-45964
- GRANULAR MATERIALS**
Thermal stability of graphite core-solid hydrogen mantle grains determined from temperature and evaporation rates calculated for interstellar space
04 p0743 A70-14398
- Metals, plastics and ceramic materials under erosion by irregular quartz particles, using vacuum whirling [ASME PAPER 69-WA/MET-6] 04 p0704 A70-14762
- Temperature dependence of thermal conductivity of granulated borazon powders measured in He and vacuum
07 p1319 A70-19803
- Decomposition of supersaturated solid solutions in granulated Al alloys with Mn, Cr, Zr, Ti, V and Mo, studying microhardness and electrical resistivity
12 p2258 A70-28274
- Grains impurities effect on interstellar extinction curve from graphite grain model, discussing dirty ice coatings
13 p2489 A70-28915
- Lunar anorthosites Ni-Fe grains from Mare Tranquillitatis, discussing contamination by meteoritic metal, magnetic fractionation and fractional crystallization
19 p3519 A70-38032
- Granular medium particles contact forces distribution measurement by absolute retardation method using photoelastic techniques
19 p3427 A70-38344
- H II region dust grains thermal emission, examining effect on diffuse nebulae
24 p4413 A70-46158
- GRAPHIC ARTS**
Graphic method for classifying EM waves directed by open waveguides, obtaining wave numbers from dispersion equation
05 p0812 A70-16245
- Digital and analog computers applicability to graphic arts noting lack of aesthetic theories
10 p1845 A70-24235
- Symbols design for machine displays based on Gestalt pattern perception theory, considering symbol learning, perceptibility, detail, boundaries, etc
10 p1827 A70-24771
- Regular and irregular line-drawing data processing, discussing quantization and encoding methods
12 p2193 A70-28104

Photographic patterns from brittle coatings, grids, photoelasticity and moire, considering variability, association with other images and esthetic value
19 p3546 A70-38343

Presentation styles of passenger emergency evacuation briefing cards, noting preference for sequential action graphic displays with minimum key wording
23 p4141 A70-44486

GRAPHITE

NT PYROLYTIC GRAPHITE

Relaxation time approximation formulas for galvanomagnetic effects in graphite based on energy spectrum model
01 p0126 A70-10181

Graphite fiber-epoxy resin composites interfacial bonding, describing various surface treatments for increased interlaminar shear strength
01 p0127 A70-10477

Liquid metals contact effect on mechanical strength of T shaped graphite specimens at high temperatures in argon atmosphere
01 p0129 A70-11038

Design allowable curves based on laminate test data for high modulus graphite fiber and resin systems, considering Wagner cantilever beam specimens
02 p0387 A70-11954

Friction and wear tests on solid lubricant graphite fluoride compared with molybdenum disulfide at specific temperatures, considering friction coefficient [ASLE PREPRINT 69-LC-9]
02 p0321 A70-12536

Interlaminar shear stress and fabrication of high modulus graphite-reinforced epoxy matrix composites
03 p0515 A70-13119

Graphite fiber content determination technique for plastic composites based on epoxy, polyimide and phenolic resins, using concentrated sulfuric acid
03 p0515 A70-13123

Graphite rocket engine nozzles chemical erosion at various temperatures, comparing reaction and diffusion rates
03 p0516 A70-13619

Graphite sphere mass erosion in low temperature hypersonic air plasma shock flow, determining breakdown temperature and mass entrainment rates
03 p0517 A70-13741

X ray diffraction method to determine degree of orientation of crystallites in extruded graphite
03 p0517 A70-13964

Rate and heat of vaporization of graphite filaments in 2500-3400 K range in vacuum and in He, using pulse heating techniques
03 p0517 A70-14004

Interstellar polarization by graphite-silicate grain mixtures, observing variability in wavelength dependence of polarization for various models
03 p0577 A70-14218

Thermal stability of graphite core-solid hydrogen mantle grains determined from temperature and evaporation rates calculated for interstellar space
04 p0743 A70-14398

Particle removal in ablation of artificial graphite linked to oxidation, using high speed motion pictures in analysis
04 p0787 A70-15610

Graphite yarn, cloth and fiber composites physical properties tabulated, discussing multiply laminates for graphite-epoxy composites
05 p0873 A70-16610

Creep, ductility and short term tensile and compression strength test facility for graphite in 300-3500 K temperature range
05 p0875 A70-17068

Graphite microstructure effect on ablation performance, discussing grain size, porosity and degree of graphitization
[AIAA PAPER 70-155]
06 p1092 A70-18147

Dynamic elastic modulus of graphites and composites measured as function of temperature using thin rod resonance method
06 p1070 A70-18447

Thermoelectric characteristics of graphite and titanium carbide compared with platinum after prolonged annealing at 2300 C
07 p1316 A70-19661

Interlaminar shear strength determination methods taking into account plastics composition, considering polyester and epoxy plastics, glass and graphite fiber reinforcing materials
07 p1410 A70-19767

Graphite shell molds for Al castings mass production
08 p1505 A70-21135

Solidification thermal conditions during Ti casting by melting out patterns in graphite molds, investigating heat accumulation coefficients in molds
08 p1506 A70-21142

Dynamic tensile properties of monolithic and pyrolytic graphite compared with static tensile strength
08 p1527 A70-21334

Microphotometric spectral reflectivity correlation to static Young moduli of carbon and graphite yarn filaments as optical testing method
08 p1497 A70-21350

Graphite crystals surface ribbed growth in Ni-C solutions due to B content observed by scanning electron microscope
08 p1520 A70-21552

Adhesion characteristics in composites, investigating correlation between short beam and torsion shear tests in glass and graphite reinforced epoxy materials
08 p1531 A70-21892

Creep and rupture of graphite-epoxy composites under unidirectional state of stress and controlled temperature environment, extrapolating long term loading behavior
08 p1531 A70-21897

Graphite fiber/resin matrix composites for airframe structures, studying tensile, compressive and in-plane shear strengths
08 p1532 A70-21901

Local heat transfer to gas mixed with graphite particles described for variable temperature differences and wall temperatures
09 p1787 A70-22174

Energy storage in creep deformed graphite from stress reduction tests, discussing negative creep, test procedures and results
09 p1709 A70-22386

Graphite IR radiator for radiative capacity and flame temperature measurements investigated for life time dependence on ambient pressure and temperature
10 p1888 A70-24257

High modulus graphite fiber structure using electron beam
11 p2071 A70-26845

Nonisothermal burn-up rates of graphite surfaces in turbulent air flow under neutral gas shield estimated by measuring channel diameter
12 p2331 A70-27323

Recrystallization effect on 3-D graphite orientation in carbon fibers under high temperature heat treatment
12 p2259 A70-27720

Reaction rates temperature dependence for artificial carbographites of various densities in oxidizing gas media
13 p2519 A70-28577

Artificial carbographites surface combustion processes using mercury porosimetry analysis
13 p2519 A70-28578

Graphite mass removal rates under ohmic heating in reacting gas turbulent flows
13 p2519 A70-28579

Surface erosion of sublimating graphite and naphthalene due to inequilibrium mass transfer in gas flows
13 p2437 A70-28580

Graphite-carbon dioxide interaction at high temperatures in presence of solid phase diffusion from bulk to reacting surface
13 p2520 A70-28581

Wool felt based carbon and graphite composite materials for orthogonally isotropic high shear strength compared with rayon felt based composites
13 p2437 A70-28776

Phosphorus compounds inhibition effect on oxidation and wear of graphite lubricants
13 p2437 A70-28854

Grains impurities effect on interstellar extinction curve from graphite grain model, discussing dirty ice coatings
13 p2489 A70-28915

Protective coatings with Si-Zr alloys for graphite, discussing wettability, spreading kinetics and impregnation
13 p2439 A70-29503

Nonsimilar ablation of graphite sphere cones under ballistic entry conditions, predicting steady state rate and surface temperature
13 p2523 A70-29975

Au films nucleation and growth on single crystal graphite substrates in ultrahigh vacuum, using transmission electron microscopy for examination
14 p2627 A70-30499

Ca atom-graphite grain model for interstellar absorption at 4430 A, calculating resonant line shift and width as functions of atom-surface distance
14 p2639 A70-30729

WC as densification aid for NbC-C composites, examining fabrication temperature, mechanical properties, solid solution composition, etc
15 p2757 A70-31797

Graphite Shore hardness measurement at high temperature on Joule heated specimens, describing apparatus and procedure
15 p2764 A70-31944

Graphite surface Debye temperature calculation based on crystal lattice dynamics
15 p2765 A70-32024

Carbon-graphite porous materials thermal conductivity at various temperatures
15 p2765 A70-32141

Rocket motor combustion chamber lining thickness distribution matching to effusor by designing effusor as multiple nozzle made of circular graphite plate
15 p2790 A70-32271

Chemical structure and room temperature tensile, flexural and compressive properties of metaphen-

ylene-diamine cured castings for graphite fiber reinforced epoxy resin matrices
16 p2936 A70-33358

Boron, silicon carbide and graphite fibers surface properties
16 p2937 A70-33376

Graphite fiber reinforced polyimide composites with low void content, high strength and modulus
16 p2938 A70-33384

Fiber reinforced prepreg properties measurements in high modulus graphite/epoxy and fiberglass/ epoxy prepreg sheets and tapes
16 p2938 A70-33386

Creep and tensile fatigue behavior of notched and unnotched graphite/epoxy composites
[ASME PAPER 70-DE-32]
16 p2938 A70-33503

Graphite oxidation on exposure to high temperature flow field based on surface coupled model
[AIAA PAPER 70-823]
16 p2940 A70-33941

High pressure ablation of plastic composites and graphites in arc heater, measuring erosion rate, shape change, surface roughness and physical characterization
[AIAA PAPER 70-770]
17 p3193 A70-34482

High strength graphite fiber reinforced polyimide resin composites fabrication
17 p3127 A70-34560

UV interstellar extinction from comparison of epsilon and zeta Persei, noting graphite features
17 p3159 A70-34877

Graphite fibers made from polyacrylonitrile yarn examining density-Young modulus relationship
17 p3127 A70-35149

Graphite modulus of elasticity as function of temperature, considering effects of moisture content in pores
18 p3278 A70-36470

Graphite-epoxy resin cross-plyed composites fabrication, analyzing residual thermal stresses role in cracking
[ASME PAPER 70-GT-84]
18 p3279 A70-36828

Graphite-polyimide composites development for high temperature environments, discussing mechanical properties
19 p3455 A70-38425

Dry face mechanical shaft seal operating on self generated graphitic film without boundary fluid lubrication
[ASLE PREPRINT 70AM 3C-2]
19 p3439 A70-38809

Graphite fiber reinforced polycarbonate composites interfacial adhesion improvement by controlled thermal treatment
20 p3652 A70-39168

High modulus graphite fiber tensile strength and structure, using X ray diffraction
20 p3653 A70-39205

Graphite filament composite structure shear strength decrease with modulus increase, examining fiber microstructure effect on interlaminar properties by short beam shear test
20 p3654 A70-39206

Carbons and graphites ablation tests for predicting performance under reentry conditions, considering microstructure effects
20 p3735 A70-39214

Short graphite fiber classification and orientation control in matrix by electrostatic methods
20 p3654 A70-39215

Graphites erosion by water and carbon dioxide at high temperatures, using liquid rocket simulator for kinetics study
[AIAA PAPER 70-638]
20 p3736 A70-39587

Quartz- and silicate-graphite mixtures carbothermal reduction in vacuum at 1400 C
20 p3583 A70-40425

High strength and modulus continuous graphite fibers from pitch, describing production process from asphalt and specifications
21 p3842 A70-40732

Magnetoresistance nonlinearity and Hall effect in graphite in magnetic field, observing temperature dependence below 4.2 K
21 p3862 A70-40945

High strength graphite fabrics evaluation for flexible structures, discussing temperature effects, fabrication, mechanical properties, oxidation and protective coatings
[AIAA PAPER 70-1183]
21 p3842 A70-41830

Direct electrical heating for high temperature thermal conductivity measurements of pure W, giving results for graphite
21 p3850 A70-42057

Nonisothermal burn-up rates of graphite surfaces in turbulent air flow under neutral gas shield estimated by measuring channel diameter
21 p3952 A70-42064

Ni-Cu-C solid solutions, measuring temperature dependence of graphite solubility by vapor transport method
21 p3841 A70-42149

Thermal variation of diamagnetism and susceptibility of rhombohedral graphite
21 p3845 A70-42268

Graphite fiber oxidation prevention in metal matrix composites, examining various thermodynamic parameters

22 p4126 A70-43676

Graphite and carbon fiber surfaces, correlating Raman spectrum and shear strength of composite

22 p4060 A70-43680

Chemical etching for revealing structure of carbon-graphite materials subjected to different graphitization stages

23 p4209 A70-44045

Interstellar dust clouds, discussing graphite, iron and silicate mixture, solid carbon material, starlight extinction and astrophysical processes

24 p4403 A70-45408

Thermoelectric power and Hall effect quantum resonances in graphite for locating majority carrier electron and hole Fermi Surfaces in Brillouin zone

24 p4389 A70-45597

Graphite dielectric constant as function of frequency, considering electron energy loss anisotropy in UV

24 p4380 A70-45668

Cool star atmospheric structure, discussing models with and without graphite particle inclusion opacity

24 p4410 A70-45765

High temperature coatings of high melting point alloys on graphite, determining optimum fabrication conditions

24 p4368 A70-46339

GRAPHITIZATION

Structural orientation and defects in graphitized coke crystallites, establishing relation between thermal expansion coefficient and macrostructure

03 p0514 A70-12868

Porosity in graphitized polyacrylonitrile-based carbon fibers determined from surface area increase during heat treatment in vacuum

04 p0711 A70-14400

Vacuum condensed thin carbon films graphitization stages using electron diffraction

11 p2068 A70-25381

GRAPHS [CHARTS]

NT PATTERSON MAP

Graphical method for determining sounding rocket altitudes from optical sensor and flux gate magnetometer data

01 p0196 A70-10841

Graphical display of diverse methods of flow predictions by various authors for turbulent boundary layers

02 p0287 A70-12363

Electron multiple scattering theory graphic approximation showing angular distribution in electron beam

03 p0527 A70-13053

Linear functionals over Sobolev spaces and elliptical boundary value problems generated by theorems on homeomorphisms

03 p0519 A70-13505

Graphical solution of optimum trajectories for third order systems depending on single control function, including maximum error and switching time

[ASME PAPER 69-WA/AUT-6] 04 p0661 A70-14828

Dynamical systems with three degrees of freedom, presenting slice cutting and stereoscopic views graphical techniques for restricted three body problem with perturbations

06 p1149 A70-18462

Thermal tolerance and comfort graph for air conditioned spaces with low air velocity, considering fighter plane cockpits

08 p1454 A70-21949

Periodic orbits in highly perturbed dynamical systems, studying characteristic curves of various families in galactic-type potential

09 p1760 A70-22916

Time-temperature charts for one dimensional unsteady conduction with uniform internal heat generation

09 p1791 A70-23567

Transistor bistable multivibrator design by graphic analytic method, considering effects of loading and supply voltages, temperature and component values on circuit performance

10 p1848 A70-23995

Geophysical measurement curves mechanical transformation by digitizing curve on punched tape followed by processing in computer

10 p1845 A70-24494

Optimal directed circuit and cycle elimination in weighted diagraphs by edge reversal orientation

11 p2072 A70-26219

Theorem formulation and proof for maximal length cycle classification by weight

11 p2073 A70-26309

Stratospheric clear air turbulence (CAT) vertical extent above thunderstorm graphically represented

12 p2265 A70-28095

Curve approximation quality by method of informative evaluation for determining minimum required number of measured points on ST interval of electrocardiogram

13 p2360 A70-29775

Graphical plotting of critical Preston tube diameter, allowing for Mach and Reynolds numbers effects and introducing limiting line

14 p2586 A70-30871

Auroral orientation curves evaluation, testing parameters by numerical integration and revised geomagnetic coordinate system

14 p2576 A70-30918

Graph theory in Soviet literature, applications and bibliographies

14 p2600 A70-31421

Euler graphs with special properties, discussing Hamiltonian lines existence and derivatives

14 p2601 A70-31424

Graphical data conversion into code for storage in computer memory

15 p2705 A70-31576

Nonlinear systems absolute stability by graphic methods, noting use of Nichol chart and analog computer

15 p2715 A70-31974

Thermodynamic diagram indicating enthalpy and entropy of oil combustion gases for any state and air excess value

16 p2997 A70-33295

Hazard plotting methods for analyzing service life data with different failure modes

16 p2921 A70-34024

Plane wave reflection decay rate representation by slowness diagrams

16 p2952 A70-34089

Hologram image construction by graphical method

16 p2915 A70-34216

Bulk negative resistance microwave oscillators efficiency calculation by graphical method

17 p3056 A70-35876

Graphical stability for linear systems in parameter plane with time delay

18 p3235 A70-36479

Cassegrain antennas design parameters using graphs for minimum blockage condition

19 p3376 A70-37690

Lunar crater number and density vs diameter graph, showing rhythmical deviations from mean asymmetrical cosine curve

19 p3517 A70-37990

Differential equations approximate solution by interval differential equations, obtaining graphs with analog computer

19 p3459 A70-38931

Nonlinear closed loop systems frequency response determination by graphical method

20 p3605 A70-40122

Functions of two variables, using digital method for curve family modeling

23 p4166 A70-44350

Image forming performance in photographic system design, considering Cobb chart resolution as figure of merit

24 p4334 A70-45449

Cobb chart resolution in photographic system including independent sources of image spread and single source of granularity

24 p4334 A70-45450

Defect size estimation, using ultrasonic angle beam probes and distance-gain-size (DGS) diagram

24 p4343 A70-45689

Ni/sulfuric acid AC voltage polarization curves for anodic dissolution region

24 p4364 A70-46220

Psychrometric chart for physiological research involving moist air thermodynamic properties

24 p4304 A70-46275

Galactic neutral hydrogen velocity distributions from 21 cm line profiles analysis

24 p4414 A70-46382

GRASHOF NUMBER

Free convective flows above flat horizontal plate demonstrating laminar boundary layer existence at intermediate Grashof numbers, using semifocusing color schlieren photography

04 p0780 A70-14456

Heat transfer at low Reynolds and Grashof numbers determined using constant temperature anemometric wire

13 p2521 A70-28952

GRASSES

Remote photometric and spectrometric measurements for plant structure and productivity of grass and shrub vegetation in desert environments

12 p2218 A70-26923

GRASSMANN ALGEBRA

U VECTOR SPACES

GRATINGS [SPECTRA]

NT ECHELETTE GRATINGS

Diffraction plates for classroom demonstrations of Fraunhofer patterns, Babinet principle and Rayleigh resolution by computer generation

01 p0093 A70-11292

Bleached diffraction gratings produced holographically on spectroscopic plates, describing processing and quality

02 p0297 A70-11929

Schlieren system converted into Kraushaar diffraction grating interferometer with isolated optical platform, considering applications to supersonic flow over airfoil shapes

04 p0689 A70-15016

Satellite lines from diffraction grating observed by densitometer tracings of plates connected with optical mixing in stimulated Brillouin scattering

04 p0701 A70-15030

Correctness of Meixner assumption of scattered light field singularity near grating edge due to diffraction

05 p0816 A70-16879

Displacement measurement using single reflecting phase grating

06 p1060 A70-17148

Schlieren system modification using diffraction grating to produce color applied to airfoil flowfield analysis

[AIAA PAPER 70-223] 06 p1029 A70-18165

Diffraction gratings produced by holographic techniques and vacuum metallization to provide high performance

07 p1279 A70-19049

Long wave IR spectrometer with two diffraction gratings for various micron ranges

08 p1493 A70-20544

Permittivity of thin films in millimeter and submillimeter wavelengths measured by diffraction grating method

08 p1464 A70-21985

Mirror-grating system optical properties emphasizing coma-type aberration elimination

09 p1729 A70-23528

Grate spectrometer with high resolution for 20-45 micron range, describing water vapor transmission spectrum

[ONERA-TP-782] 10 p1886 A70-23912

Optical modulation using rotating diffraction grating to obtain frequency shifts

11 p2049 A70-25633

Holographic dielectric gratings analyzed by Raman-Nath formalism modified for losses

11 p2050 A70-25640

Solar horizontal telescope performance improvement by adding birefringent monochromator and diffraction grating

11 p2057 A70-26590

Transmission diffraction grating for astronomical applications constructed holographically with laser light and photoresist films

12 p2234 A70-27589

Grating spectrometer performance in measuring earth IR radiance determined from balloon flights

12 p2235 A70-27752

Plane electromagnetic waves anomalous reflections from diffraction grating with periodic array of rectangular holes in dielectric layer, observing resonant character

12 p2191 A70-28175

Large diffraction gratings by interferometrically controlled commercial measuring machine

13 p2412 A70-29821

Plane parallel perfectly conducting grating by integral equation procedure, presenting equivalent network under multimode propagation conditions

14 p2562 A70-31317

Laser Doppler heterodyning system for velocity measurements without directional ambiguity, employing incident beams of different frequencies through rotating diffraction grating or Bragg cell application

15 p2751 A70-31986

Single beam grazing incidence spectrophotometer with concave diffraction grating for far UV region, emphasizing instrument adjustment

16 p2915 A70-34218

Holographic techniques, investigating ultrasonic fields in transparent media based on light separation by grating into optical moments

16 p2915 A70-34330

Visual contrast sensitivity adaptation to temporal frequencies using high modulation sinusoidal grating

17 p3034 A70-35898

Plane wave diffraction by periodic grating reduced to waveguide problem, determining asymptotic behavior of integral solution

18 p3291 A70-36286

Plane electromagnetic waves diffraction by periodic structure of infinite system of parallel strips, reducing problem to solution of linear algebraic equations

18 p3227 A70-36287

Hemispherical open resonators with plane mirror partially coated by reflecting diffraction grating

18 p3231 A70-36411

Efficiency of holographic gratings in instrumental spectroscopy

19 p3421 A70-37360

Plane electromagnetic wave diffraction by thin metal gratings, using mathematical method of elasticity theory

19 p3376 A70-37712

Plane polarized electromagnetic wave diffraction by dielectric grating, obtaining linear algebraic equations for field coefficients

19 p3376 A70-37713

Polarized plane EM wave diffraction by inclined half plane grating, obtaining transformation matrices coefficients
19 p3376 A70-37714

Wave diffraction by finite dimension grating, determining EM field strength distribution by approximate method
19 p3377 A70-37716

Diffraction grating systems resonance properties, obtaining transcendental equations for natural slow wave and radiation modes
19 p3377 A70-37717

Plane EM wave diffraction by ribbon periodic grating, determining diffraction spectrum wave amplitudes
19 p3377 A70-37718

Plane EM wave diffraction by bounded and unbounded periodic gratings
19 p3377 A70-37719

Diffraction-field structure on two-element gratings in near zone, calculating amplitude, phase and energy flux for normal and slant incidence of EM fields
19 p3377 A70-37720

Plane monochromatic EM wave diffraction by rectangular metal bar tapered grating, examining amplitude and polarization parameters
19 p3377 A70-37721

Ponderomotive forces of plane electromagnetic wave incident at arbitrary angle on metal grating, based on diffraction results
19 p3377 A70-37723

Strain transducer /optical diffraction grating/ for plastic wave propagation measurement along specimens subjected to impact
19 p3425 A70-37884

Strain analysis by moire technique, using triangular and square root of 2 gratings
19 p3432 A70-38720

Printing, electro etching and vacuum deposition stencil methods for preparing moire grids
19 p3432 A70-38721

Gratings as laser wavelength-selective end reflectors, noting application to carbon dioxide and dye lasers
20 p3639 A70-39083

Pulsed ruby free emission mode laser spectrum narrowing, using diffraction lattice adjusted in resonator transversely to beam axis
20 p3643 A70-39757

Electromagnetic wave diffraction at multilayer wire grating, discussing computer program for diffraction field calculation
22 p3985 A70-42399

Light generation by free electrons interaction with metallic diffraction grating, devising experiments for explaining incompatibility with simple electrostatic image theory
22 p4074 A70-42943

Time resolving X ray grating polychromator, discussing photoelectric attachment with surface barrier semiconductor detectors
[SMPT PREPRINT 75] 22 p4037 A70-43069

Wavelength selective carbon dioxide laser using stationary grating to correlate pulses for high J values and line number
22 p4050 A70-43153

Compression of laser pulses reflected from periodic and zone plate gratings
22 p3990 A70-43337

Transparent objects holographic interferometry with illumination derived from phase gratings to eliminate laser speckle
22 p4040 A70-43611

Optical transmission and reflection gratings formed by standing light waves evaporation of thin metallic films in ruby laser cavity
23 p4200 A70-43817

Soft X ray slitless spectrometer with gold-shadowed transmission gratings for rapid astronomical spectral surveys
23 p4196 A70-44418

Double beam diffraction grating spectrometer for vacuum operation over far IR from 40 microns to 1 mm
24 p4339 A70-46323

GRAVIMETERS

Microtopography effects on measuring horizontal gravity gradients by gravimeters
02 p0295 A70-11799

Stochastic processes for probabilistic error analysis in airborne gravimetry, using gravity sensing instruments
22 p4025 A70-43666

GRAVIMETRY

Earth gravity field intensity variations measured by orbiting two geometrically identical satellites, discussing sensitivity and cost
01 p0087 A70-10445

Gravimetric and satellite tracking data reduction for determining coefficients in mathematical expansion representing earth gravitational field
03 p0473 A70-13189

Earth potential errors from gravity and satellite motion measurements, discussing sectoral, tesseral and zonal harmonics with large and small second indices
03 p0473 A70-13190

Satellite surveys and astronomic-geodetic nets for joint terrestrial, space triangulation and gravimetric measurements, including laser distance determination
03 p0445 A70-13191

Geodetic vertical and geoidal height deflection calculated by gravimetric method, considering satellite orbits data
05 p0841 A70-16643

Vertical deflections errors statistical analysis by gravity anomaly measurements, determining autocorrelation functions
18 p3248 A70-36771

Vertical gravimetric deflections calculation based on linear interpolated gravity anomalies
19 p3410 A70-37461

Curvilinear orthogonal coordinates for gravimetric deduction related to Cartesian coordinates as solvability condition for Molodenskii problem
20 p3617 A70-39071

Gravitational experiments in manned spaceflight employing Eotvos balance in orbit and direct force technique
21 p3929 A70-41002

Dynamic gravimetry - Conference, Fort Worth, March 1970
22 p4024 A70-43656

Gravity error propagation in dynamic gravimetry associated with navigation and gradient measurement errors, emphasizing standard error limits in navigation data
22 p4068 A70-43660

DR-S Raydist radio location system in fixed wing aircraft for dynamic gravimetry
22 p4068 A70-43661

Gravity measurement errors in high speed aircraft parallel to undulating geoid attributed to associated vertical accelerations
22 p4025 A70-43662

Integrated helicopter gravity measuring system for various terrains, describing instrumentation and recording monitors
22 p4042 A70-43663

Airborne and surface downward continuation of gravity, discussing integral equations solutions and data filtering of noise interference
22 p4025 A70-43664

Stochastic processes for probabilistic error analysis in airborne gravimetry, using gravity sensing instruments
22 p4025 A70-43666

Gravity measurements and adjustments of First Order Gravity Network /FOGN/ in Iran
24 p4332 A70-46409

GRAVIRECEPTORS

NT OTOLITH ORGANS

GRAVITATION

NT ARTIFICIAL GRAVITY
NT GRAVITY ANOMALIES
NT HIGH GRAVITY ENVIRONMENTS
NT LUNAR GRAVITATION
NT PLANETARY GRAVITATION
NT REDUCED GRAVITY
NT SOLAR GRAVITATION

Air pressure, air density and gravity tables, including corrections for mercury barometer measurements
12 p2222 A70-27008

Gravitational force equation solution, using Levi scheme
13 p2394 A70-28851

Self gravitating three dimensional particles system evolution using water bag model
13 p2498 A70-30012

Gravitating sphere high speed rotation in monatomic gas, discussing viscous and thermal boundary layers, velocity fields, temperature effects and fluid motion
23 p4131 A70-43944

GRAVITATION THEORY

Gravitational theories scheme combining tetrad field with bimetric theories, including general relativity, space-time dependent Lorentz rotations, red shift and light deflection
01 p0141 A70-10232

Field equations in particle neighborhood for spherically symmetric metric in conformal gravitation theory, considering particle inertial mass as function of position
01 p0142 A70-10492

Linear field theory of gravitation by considering gravitational field functions decomposition into spin components
01 p0143 A70-10712

Solar motion effects on planetary orbits, discussing preferred coordinate systems of scalar theory of gravitation
01 p0186 A70-11104

Neutrino in nonquantum and quantum gravitation theories, neutrino sea, etc, discussing classical neutrino dynamics
02 p0341 A70-11669

PostNewtonian equations of Brans-Dicke scalar-tensor theory for n gravitating point masses, using obtained equations of motion for radar tracking
02 p0337 A70-11777

Gravitational theory for disk galaxies, considering radial velocity variations, spiral structure, heat equation verification, etc
02 p0378 A70-12688

Coefficients of Legendre polynomial expansion of earth gravitational potential, using Stokes problem solution
03 p0474 A70-13344

Relativistic tensor theories of gravitation in flat space with Neumann and Newton forms of gravitational potential, deriving expressions to estimate differences perceived by observer
03 p0526 A70-14305

Relativistic stellar structure equations for spherically symmetric configurations in slow motion, using Einstein gravitational field and conservation equations
05 p0912 A70-16454

Hydrostatic equilibrium in self gravitating core of rotating relativistic star, considering Newton and Einstein gravitation theories
05 p0914 A70-16648

Stellar configurations of cold static neutral plasma consisting of nuclei and degenerate electron gas, calculating integral parameters by Newton gravitation theory
07 p1376 A70-18912

Cosmological solution of Einstein gravitational equations with singularity in time
07 p1381 A70-19361

Cosmological gravitation theory for uniformly expanding universe model providing fundamental reference frame and acceleration field
08 p1563 A70-20497

General relativity equations of gravitation consistent with empirical data, discussing curvature tensor, scalar gravitational waves and solar mass difference
08 p1577 A70-21419

Einstein gravitational equations general solution having physical singularity with respect to time
08 p1546 A70-21424

Relativistic gravity theories testing, discussing experimental tools and relativistic effects in solar system
09 p1750 A70-22059

Baryon configurations in relativistic generalized theory of gravitation, discussing field equation transformations, mass distribution, central pressure, etc
09 p1753 A70-22454

Gravitating bodies quasi-stationary rotating systems, giving equations of state and evolution
09 p1753 A70-22457

Relativistic generalized gravity theory, studying polytropic models
09 p1754 A70-22458

Vortex and potential motions interactions in relativistic hydrodynamics, noting effects of gravitation equations nonlinearity
09 p1754 A70-22461

Nongravitational effects, systematic residuals and close Jupiter approach problems in motions of comets
09 p1759 A70-22913

Incompressible homogeneous fluid model in non-relativistic generalized gravitation theory using analytical solution
09 p1762 A70-23118

Maxwell electromagnetism analogy to Einstein gravitation inferred from asymptotic studies of electromagnetic and gravitational radiation
10 p1915 A70-24029

Particle escape from Newtonian gravitational system of positive energy
10 p1938 A70-24183

Physical singularity reduced to imaginary by introducing arbitrary function in form of perturbation into gravitational equations general solution
10 p1917 A70-25032

Milne special relativistic cosmology consistency with Birkhoff flat space gravitation theory, calculating red shift correction in galactic light
11 p2114 A70-26549

Field equations in conformal theory of gravitation, noting invariance
11 p2084 A70-26552

Rotation effect on singularities in general relativity from local observer standpoint, inquiring into gravitational collapse in ideal fluid
12 p2271 A70-26978

Coefficients of Legendre polynomial expansion of earth gravitational potential, using Stokes problem solution
14 p2573 A70-30719

Relativistic gravitation theory and experimentation, surveying literature on gravity waves, EM propagation, gyroscopic precession, etc
16 p2973 A70-33230

Newtonian gravity law in light of relativistic theories, considering deviations of quasars and red shift deviations from Newton theory
16 p2976 A70-33722

Cosmic time varying gravitational constant effects on stellar age determination
16 p2978 A70-33966

Gravitational force and potential within static metric spaces
17 p3136 A70-35597

- Spiral structure gravitational theory, discussing separation between linear and nonlinear effects
18 p3330 A70-37189
- Galactic spiral structure, discussing gravitational theory, pattern origin, radio and optical structure and magnetic field effects
18 p3332 A70-37201
- Gravitational experiments in manned spaceflight employing Eotvos balance in orbit and direct force technique
21 p3929 A70-41002
- Space-time Riemann metric for scalar-tensor gravitational theories with arbitrary omega parameter
22 p4104 A70-42991
- Einstein gravitational equations solution for expanding universe, discussing possible sudden collapse into zero volume with infinite density
22 p4105 A70-43215
- Gravitational equations with oscillatory physical singularity, noting Bianchi type IX homogeneous metric
22 p4063 A70-43477
- Static spherically symmetric charged mass distribution exact solutions derived for electrons in scalar tensor theory of gravity by Hamilton-Jacobi method
23 p4222 A70-44403
- Maxwell electromagnetism and Einstein gravitation analogy in vacuum field equations, showing metric analytical for inverse distance parameter r
24 p4377 A70-45142
- Hoyle-Narlikar gravitation theory, considering Bohr quantization of direct interparticle action over all pairs
24 p4403 A70-45405
- Newton and Einstein gravitation theories applied to light velocity in gravitational field
24 p4379 A70-45487
- Gravitational relativistic theory tests using tracking data from interplanetary spacecraft, orbiters and landers
[AIAA PAPER 70-1317] 24 p4414 A70-46326
- ### GRAVITATIONAL COLLAPSE
- White dwarf mass changes during cooling, describing white dwarf collapse-type I supernova outbursts relationship
01 p0174 A70-10197
- Faint, metal poor, subluminescent and red degenerate stars occurrence and properties, considering spectra of candidate degenerates
01 p0188 A70-11338
- Low mass protostar evolution in dynamic collapse, investigating opacity laws
01 p0190 A70-11345
- Two armed spiral galactic shock waves as triggering mechanism for gravitational collapse leading to star formation, considering gaseous disk motion using Schmidt model
02 p0363 A70-11781
- Protogalaxy formation and molecular processes in primeval hydrogen gas, discussing cold gas cloud cooling mechanism and contraction
03 p0577 A70-14153
- Brans-Dicke cosmological gravitational instability using Lagrangian gauge for galaxy formation, discussing density contrast growth in time
03 p0577 A70-14154
- Collapse of homogeneous fluid mass in stratified fluid with initially slender interface and ineffective internal wave motion, discussing internal wave generation
03 p0470 A70-14247
- Protogalaxy mass limits determined for galactic formation by thermal instability due to radiative cooling and followed by nonlinear gravitational contraction
04 p0744 A70-14469
- Envelope stars evaporation effects on star cluster contraction, discussing energy inflow from envelope to nucleus
04 p0745 A70-14475
- Light emission from collapsing nonrotating gas in general relativity, noting restrictions on range and frequency shift
04 p0719 A70-14702
- Experimental observations of neutrino in collapsing stars in Galaxy, showing detector capability of recording positrons or electrons from antineutrino-neutrino flux induced reactions
05 p0900 A70-15966
- Galactic expansion due to mass energy loss by gravitational radiation
05 p0913 A70-16557
- Statistical analysis of Zwicky catalog of galaxies and clusters of galaxies, interpreting very distant clusters in terms of intergalactic extinction
05 p0915 A70-16697
- NonJeans gravitational instability of stars and interstellar gas in Galaxy due to wave interaction with stars having velocity near wave phase velocity
05 p0917 A70-16906
- Stellar mass loss in gravitational contraction and variation of rotation law during transition to main sequence
05 p0917 A70-16909
- Cosmological theories taking into consideration gravitational collapse, discussing pulsars, quasars and X ray stars evolution
06 p1140 A70-17584
- Dense pulsating stellar core structure model for pulsars, discussing catastrophic collapse mechanism
07 p1380 A70-19278
- Collapse-anticollapse transition near Schwarzschild radius in multimode universe with arbitrary number of time-similar dimensions
07 p1381 A70-19286
- Model for gaseous proto-galaxy collapse and formation of spherical galaxy
07 p1390 A70-20287
- Interstellar gas clouds collapse using finite difference numerical methods in solving hydrodynamic equations involving gravitation
07 p1390 A70-20288
- Interstellar cloud models to investigate heating, cooling and density distribution effects on collapse and to suggest theory of stellar evolution
07 p1390 A70-20292
- Earth observations of collapsing star neutrinos and neutrino oscillations in Milky Way galaxy
07 p1371 A70-20331
- Space-time singularities of gravitational collapse and cosmology indicated by timelike or null geodesic incompleteness
08 p1575 A70-21353
- Relativistic gravitational stellar collapse calculations for stars exceeding neutron star limit, discussing results in terms of supernovae or neutrinos
09 p1749 A70-21991
- Late stage stellar evolution association with supernovae in terms of gravitational collapse and exploding light emission using evolutionary model
09 p1749 A70-21993
- Gravitational radiation detection from pulsating neutron star, considering asymmetries in gravitational collapse of massive stars as origin
09 p1749 A70-21996
- Gravitational collapse models with magnetic dipole and gravitational quadrupole, treating asymmetries as small perturbations
09 p1752 A70-22274
- Neutrino emission effect on collapse of supermassive stars, estimating energy radiated, discussing envelope explosion
10 p1938 A70-24022
- Pulsars nature based on hypothesis for main energy of novae and supernovae bursts equaling gravitational energy of collapse
11 p2117 A70-26708
- Gravitational collapse of star and general relativity role, considering Schwarzschild solution to Einstein vacuum equations
12 p2298 A70-27058
- State equations of matter at high density and zero temperature, considering neutron stars relationship to supernova explosions and collapse
12 p2298 A70-27059
- Gravitational forces accompanying radiation bursts of metric outside collapsing supernova core
12 p2300 A70-27393
- Collapsed spherical bodies equilibrium structure, considering density-pressure state equations for cold neutron gas and gas-radiation mixture
12 p2300 A70-27395
- Gravitational collapse of slightly spherical body with axial symmetry characteristics, taking linear approximation of equation for additions to metric in empty space
12 p2310 A70-28223
- Pulsar formation mechanism, showing core collapse to neutron star state
15 p2806 A70-32773
- Gravitational instability and collapse of thin spherical shell of charged fluid, using energy conservation law
16 p2952 A70-33787
- Disk shaped galaxy stationary spiral shock pattern, examining gas cloud gravitational collapse for star formation
18 p3331 A70-37198
- Gravitational collapse of slightly spherical body with axial symmetry characteristics, taking linear approximation of equation for additions to metric in empty space
20 p3710 A70-40098
- Gravitational collapse for astrophysical matter distributions, discussing differential geometry, relativity, Schwarzschild metric, static equilibrium and space-time geometries
22 p4098 A70-42579
- Einstein gravitational equations solution for expanding universe, discussing possible sudden collapse into zero volume with infinite density
22 p4105 A70-43215
- ### GRAVITATIONAL CONSTANT
- Geogravitational constants and mass determination, discussing Cavendish constant and measurement theory and technique
03 p0473 A70-13236
- Einstein equations for five dimensional spherically symmetric space solved using gravitational constant without singularities on Schwarzschild sphere
05 p0880 A70-15793
- Time variation of gravitational constant on structure of central solar region and neutrino luminosity
05 p0899 A70-15952
- Torsion balance for measuring gravitational constant based on Langevin resonance method
08 p1543 A70-20593
- Soviet monograph on constant of gravitation, mass and density of earth covering torsion balance, weight experiments and nonlinear vibration techniques
08 p1487 A70-20764
- Geogravitational constants and mass determination, discussing Cavendish constant and measurement theory and technique
08 p1491 A70-21669
- Decreasing gravitational constant effects on secular earth figure and dimension changes using Clairaut equation
14 p2568 A70-30143
- Cosmic time varying gravitational constant effects on stellar age determination
16 p2978 A70-33966
- Gravitational variable constant in celestial mechanics, considering theories based on vacuum Jordan Lagrangian
18 p3320 A70-37066
- Stokes earth constants from gravity anomalies
20 p3617 A70-39070
- Resonant satellites geodesy, determining orbit perturbation and gravity constant via mean Kepler elements high speed analysis
24 p4408 A70-45540
- ### GRAVITATIONAL EFFECTS
- Body motions containing cavity filled with viscous fluid under influence of gravity, formulating motion equations for fluid and body
01 p0068 A70-11576
- Lower bounds of Stekloff and free membrane eigenvalues for sloshing of incompressible inviscid fluid, subject to gravity in rigid tank with free surface
02 p0278 A70-11999
- Self gravitating galaxies theoretical properties, including structural and dynamic characteristics of interacting and colliding galaxies
02 p0376 A70-12444
- Stellar systems evolutionary stages, considering gravitational instability in rotating expanding gas, relaxation, viscosity, transition to metastable state and drift effect on geometry
02 p0376 A70-12445
- Stellar clusters equilibrium state in gravitational field, discussing dispersed clusters formation by gravitational instability in gas containing stars of various ages
02 p0376 A70-12446
- Gravitational finite propagation velocity effects in celestial mechanics, describing binary star motion studies
02 p0380 A70-12783
- Gravity effect on atoms, neutrons, electrons and photons, measurement techniques and comparison with macroscopic bodies
03 p0524 A70-13172
- Secular increase in pulsar periods attributed to gravitational emission, velocity effects and galactic escape
03 p0564 A70-13219
- Kinetic equation describing variation of distribution function of stellar residual velocities under action of gravitational field, discussing stellar diffusion in velocity field
03 p0564 A70-13227
- Multiple periodicities in beta Canis Majoris Star 16 Lacertae attributed to tidal perturbation effects on pulsation mode of structural changes
03 p0567 A70-13320
- Close spaced material points motion stability in gravitational field of attractive center using Liapunov theorem, assuming nongravitational forces action on points
03 p0524 A70-13369
- Circulation gas lens temperature distribution, considering effects of gravity, wall thermal conductivity, glass interlayer, etc
03 p0604 A70-13387
- Human motion coordination under acceleration followed by weightlessness during jet flights along Keplerian orbits, discussing initial disturbance and subsequent subsiding
03 p0425 A70-13897
- Stellar model surface convective zone using diffusion equation taking into account transport due to gravitational separation, noting role of turbulent diffusion
03 p0574 A70-13932
- Satellite motion in earth gravitational field under additional forces using Stockel theorem
04 p0760 A70-14432
- Thermal instability of uniformly rotating self gravitating homogeneous medium with perturbations in plane perpendicular to rotation axis
04 p0745 A70-14471
- Hypokinesia and nutrition deficiency effect on blood coagulation, noting combination with accelerations may lead to hypocoagulation
04 p0630 A70-14578
- Models of partially relaxed stellar disks in galaxies, discussing gravitational instability and stellar velocities
04 p0748 A70-14588

Gravity and size effects on film boiling from horizontal cylinders, recommending formulas for wavelength and minimum heat flux predictions [ASME PAPER 69-WA/HT-12] 04 p0784 A70-14821

Gravitational effects on heat transfer during evaporation and condensation processes in heat pipe, discussing conditions in Na filled heat pipe [DGLR-69-44] 04 p0785 A70-15171

Gravity influence on constitutive equations of elasticity for crystals treated as continuous body and particle system, taking into account lattice structure 05 p0925 A70-15869

Gravitational radiation damping effect on motion of two bodies, evaluating field components in approximation by Einstein-Infeld-Hoffman method 05 p0882 A70-16308

Hydrostatic equilibrium in self gravitating core of rotating relativistic star, considering Newton and Einstein gravitation theories 05 p0914 A70-16648

Gravitational instability of finitely conducting incompressible fluid layer of finite thickness surrounded by nonconducting medium 05 p0915 A70-16696

Hot star photogravitational acceleration determined from difference between apex and antipeak brightness, noting constant magnitude and direction of principal component of apex force 05 p0918 A70-16914

Hematologic changes in rats under hypergravity, effects of vitamin B12, folic acid and return to 1 g 06 p0991 A70-17283

Spacecraft level vibrations and gravity effects on blue-green algae Plectonema Boryanum proposed as gas exchange medium 06 p0999 A70-17292

Homogeneous gravitating sphere deformation by internal dislocations determined using Green dyad 06 p1055 A70-17605

Phase growth of free vapor bubbles in water, ethanol and isopropanol at uniform superheats under normal and zero gravity 07 p1418 A70-18646

Gravitational effects on organisms - Conference, Warsaw, March 1969 07 p1200 A70-18784

Dust growth, density distribution and collisions in interior of cometary head atmosphere, considering gravitational attraction to nucleus 07 p1379 A70-19039

Telescopic paraboloid mirrors optical distortion from surface deformation due to gravity loads 07 p1281 A70-19254

Radiation focusing properties of gravitational bodies associated with curving light trajectories analyzed by geometrical and waveguide optics approximations 07 p1384 A70-19411

Approximate method for celestial mechanics problems, considering particle motion under gravitation from central body in cylindrical coordinate system 07 p1387 A70-19626

Back reflection of zero-mass scalar or vector waves in gravitational fields produced by non-Lorentz part of spatial metric components 07 p1387 A70-19923

Photoelastic stress analysis of composite structures subjected to gravitational forces using immersion analogy, considering constant acceleration stresses 07 p1413 A70-20038

Hydromagnetic self gravitating galactic slab embedded in halo, deriving stability criteria using models of magnetic field 07 p1390 A70-20293

O star red shift considering gravitation interpretation effects on stellar masses 07 p1391 A70-20465

Visual analyser physiology under effects of gravitation, atmospheric pressure, mechanical vibrations, etc 08 p1444 A70-20740

Ideal fluid in lightly filled spherical vessel under gravitational force investigated for surface tension effect on vibration frequencies 08 p1482 A70-20853

Solar oblateness and gravitational quadrupole moment related under assumption of magnetic and velocity fields absence in surface layers, including rotation effects 08 p1570 A70-20902

Gas flow influence on wave characteristics of thin viscous liquid layers pulled by gravity vertical surface compared with water layer experiments 08 p1482 A70-20917

Steady motions and stability of gravitating gyrost and spheroid, considering dynamically asymmetrical and symmetrical conditions 08 p1544 A70-20965

Static deflection effect on harmonic vibration of system with restoring forces of hardening nonlinear spring, considering gravity effect 08 p1586 A70-21035

Momentum vector and spin tensor definitions for extended body moving in arbitrary gravitational and

electromagnetic fields, considering test body in de Sitter universe 08 p1545 A70-21352

Stresses and displacements in largely deflected cantilever beams subjected to gravity using photoelasticity 08 p1593 A70-21619

Secular increase in pulsar periods attributed to gravitational emission, velocity effects and galactic escape 08 p1580 A70-21652

Kinetic equation describing variation of distribution function of stellar residual velocities under action of gravitational field, discussing stellar diffusion in velocity field 08 p1580 A70-21660

Orbiting clock experiment for measuring gravitational red shift of earth by comparing ground based and satellite-borne hydrogen maser clocks 08 p1501 A70-21950

Optimal transfer ellipse obtained by complete rotation in gravitational field of axisymmetric planet 09 p1751 A70-22161

Uniformly rotating gas disk large scale spiral structure analysis, studying density waves due to gravitational disturbance by supersonic particle 09 p1755 A70-22503

Lunar surface luminescence considered for correlation with tidal forces of earth 09 p1758 A70-22748

Periodic solutions of restricted three body libration point perturbation due to fourth body gravitational and radiative influence using Huang model 09 p1761 A70-23053

Gravitational effects on heat transfer during evaporation and condensation processes in heat pipe, discussing conditions in Na filled heat pipe 09 p1789 A70-23427

Gravity and vertical magnetic anomalies interpretation to infer magnetization direction 09 p1729 A70-23601

Cavitational symmetric flow around wedge taking into account gravity and surface tension 10 p1868 A70-24162

Elongated rotating configuration evolution by gravitational radiation and secular instability using homogeneous figures of Maclaurin and Jacobi 10 p1916 A70-24404

Solar wind model with electrons, protons and alpha particles coupled by electric field and expanding due to pressure gradient and solar gravitation 10 p1931 A70-24433

Horizontal fluid layer heated from above or below analyzed for gravitational field sinusoidal modulation effects on stability 10 p1968 A70-24523

Gravitational instability theory for large density perturbations growth during expansion of matter without pressure 10 p1945 A70-24961

Dynamic orbital mixing in self gravitating spherical stellar system using water bag model 10 p1945 A70-24965

Luminous hot stars mass loss attributed to negative effective gravities in outer parts of reversing layers from ionic UV resonance lines 10 p1946 A70-24981

Reduced gravity effect on nucleate boiling using drop tower method with high speed motion pictures and telemetry 10 p1969 A70-25096

Rotating degenerate gravitating fluid cylinders equilibrium configuration 10 p1917 A70-25208

Solid body acceleration by ideally conducting gas in constant gravity field under magnetic field, considering rarefaction, reflected waves, motion equation, wall pressure, etc 11 p2082 A70-25389

Extraterrestrial gravitational effects on microorganisms, describing impulse-applied high g study of freeze dried Escherichia coli 11 p1987 A70-26028

Gravitational disturbance by exterior planets, considering Brown transformation of longitudinal perturbation problem in relation to planet Neptune discovery 11 p2117 A70-26658

Swirling and meridional flow induced by steady rotation of gravitating sphere in compressible monatomic gas, considering compressibility effects and surface layer [ASTM PAPER MR-69-714] 11 p1978 A70-26690

Critical thermal flux and heat transfer coefficients dependence on simulated gravity during bubble and film boiling in inclined flat containers 12 p2331 A70-27325

Inertial and gravitational mass equivalence related to observation of anomalous K-meson decay 12 p2272 A70-27391

Nonequilibrium self gravitating medium unified thermodynamics theory based on propagators, describing spatial and temporal fluctuations and coupling for galactic formation 12 p2310 A70-27978

Dynamics of gravity stabilized satellite having maximum damping rate 13 p2499 A70-28391

Satellite motion in earth gravitational field under additional forces using Stockel theorem 13 p2503 A70-28457

Gravity effect on positional alcohol nystagmus in man and rabbits, observing threshold value in weightless state 13 p2359 A70-29442

Longitudinal gravitational field effect on cavitational wedge flow, investigating characteristics by Zhukovskii-Roshko method 13 p2390 A70-29646

Density wave theory and spiral gravitational field effects in migrating stars orbits and origins in Milky Way spiral arm, using Schmidt model 13 p2495 A70-29801

Gravity dependent lung region emptying sequence effects on alveolar Xe 133 and nitrogen plateaus in pivoted subjects 13 p2356 A70-29944

Gravity effect on conical vortex separator, predicting body force effect on heavy fluid boundary layer flow for limiting condition determination 13 p2391 A70-29978

Book on thermal and gravitational atmospheric tides covering solar oscillations, lunar air tides, upper air data, ozone radiation absorption, etc 14 p2573 A70-30633

Thermal tidal friction and gravitation effects on Mercury libration after solidification, noting equilibrium with orbital and rotational periods locked in 3/2 resonant state 14 p2638 A70-30701

Interplanetary low thrust orbit transfer optimization by dynamic programming, including gravitational perturbation effects from earth, Mars and Jupiter 14 p2640 A70-30759

Vestibular threshold dependence on gravity, considering linear accelerations effect on canals sensitivity 14 p2539 A70-30916

Compressible plasma gravitational instability taking into account Hall effect 14 p2624 A70-31225

Synchronous satellite orbits determination using mathematical model for simulating gravitational perturbations induced by terrestrial globe and foreign bodies 14 p2651 A70-31279

Orbiting gyrostats equilibrium orientations under gravitational torques, considering internal angular momentum effects 14 p2655 A70-31364

Dynamic spectrum of density fluctuations and galaxy clustering in Einstein universe, considering self gravitation of medium 14 p2652 A70-31389

Elementary particles gravitational interactions, identifying tensor field with local gravitation 15 p2776 A70-31732

Hand-eye coordination in altered gravitational fields, using mirror viewed target in reaching test 15 p2689 A70-31886

Trail formation due to tidal effect in interacting galaxies during close approaches, considering mass flow hydrodynamics 15 p2801 A70-32481

Translational-rotational motion of axisymmetrical moon in earth gravitational field 15 p2803 A70-32496

Gravitational atmosphere thermally driven motions, noting expansion towards lower density regions in solar chromosphere 15 p2804 A70-32619

Gravitational compression of spherical cloud, determining asymptotic features of gas motion near center 15 p2808 A70-32882

Heterogeneous conducting fluid stability between fixed rigid cylinders with radiant gravitational force and magnetic field 16 p2894 A70-33784

Solar system Eotvos experiments for measuring gravitational to inertial mass ratio of celestial bodies 16 p2978 A70-34033

Fluid analog for lung tissue response to gravitational acceleration, examining lung density, transpulmonary pressure, expansion, etc 16 p2850 A70-34257

Weightlessness and gravitational effects on human pulmonary blood flow distribution, considering optimal gas exchange efficiency [AIAA PAPER 70-785] 17 p3035 A70-34472

Gravitational bremsstrahlung for small mass with relativistic velocity passing large mass in unbound trajectory, calculating energy flux of emitted waves 17 p3136 A70-34596

Artificial planetary satellites long term orbital evolution under strong perturbations, considering solar and lunar gravitational effects [AAS PAPER 70-038] 17 p3155 A70-34779

Interior ideal liquid flow of vertical jet under gravity, using differential equation to relate flow plane to unit half disk

17 p3069 A70-34979

Intermediate orbit calculation, allowing for spacecraft large gravitational perturbation during motion near planetary sphere of influence

18 p3312 A70-36166

Mascon effects on close lunar orbit, using short arc perturbation technique

18 p3314 A70-36518

Relativistic thermal equilibrium conditions in external gravitational field, considering heat with inertial and gravitational mass

18 p3291 A70-36552

Nomograms for meteor geocentric velocity and trajectory with correction for zenith attraction and radiant

18 p3315 A70-36605

Gravitational field effect on natural frequencies of rotating ring laser, using general relativity and electromagnetic fields theories in continuous media

18 p3267 A70-36622

Large planets mass determination based on Kepler law and gravitational effects

18 p3318 A70-37045

Lateral compression of rocks and global shells multilayers, using equations for buckling of single free stratum

18 p3255 A70-37076

Tightly wound spiral nonlinear density waves in pressureless self gravitating disk with external gravitational field, examining solid body and differential rotation

18 p3331 A70-37192

Gravitationally induced (Machian) magnetic field by rotating mass-shell with centrally located stationary charged sphere, using linearized relativity theory

19 p3471 A70-37815

Lunar basalt lava bed formations, examining vacuum and gravity effects during cooling

19 p3517 A70-37988

Many body gravitational problem, computing evolution of two groups by numerical integration with two different computers

19 p3523 A70-38692

Near parabolic trajectories between moon and cislunar libration point, considering earth perturbative influence

[AIAA PAPER 70-1059]

19 p3529 A70-38874

Gravity effects on impact damper performance, investigating dynamic stability and kinematic viability of various steady state motion solutions

20 p3717 A70-38974

Gravitational effects on impact damper performance, discussing dynamic stability and kinematically viable periodic motion and resonant conditions

20 p3717 A70-38975

Solid and hollow spheres gravitational and surface load stresses determination by freezing method of photoelasticity and mercury immersion

20 p3717 A70-38998

Maclaurin spheroid secular stability, examining energy dissipation of gravitational radiation

20 p3702 A70-39017

Auxin downward transport by gravity in leaves, examining ethylene inhibition

20 p3570 A70-39234

Steady motions and stability of gravitating gyrost and spheroid, considering dynamically asymmetrical and symmetrical conditions

20 p3672 A70-39387

Accelerometer calibration in low g range by mass attraction as equivalent acceleration input

[AIAA PAPER 70-1030]

20 p3631 A70-39507

Spinning missile gravity induced angular motion for various trajectory portions, considering quasi-steady state assumption validity

[AIAA PAPER 70-968]

20 p3715 A70-39561

Periodic collision orbits in plane elliptic three body problem of infinitesimal mass under gravitational field of two finite masses

20 p3705 A70-39603

Liquid fuel behavior in right circular cylindrical tank inclined to earth gravitational field, computing fundamental sloshing frequency

20 p3610 A70-39694

Stellar wind theory and related steady radial flows, discussing gravitating point mass, heat conduction, shocks, viscosity, outflows and inflows

20 p3706 A70-39928

Artificial earth satellite orbit perigee motion, calculating perturbation effect due to gravitational and magnetic fields on orientation and rotation

21 p3884 A70-40843

Optimum cryogenic heat pipe design, considering gravitational effects for spacecraft applications

21 p3946 A70-41044

Vapor volume entrained in liquid bulk from boundary layer boiling on vertical plate in low gravity field

21 p3947 A70-41055

Pluto space probe using swingby technique with Jupiter, Saturn and Uranus gravitation fields for acceleration

21 p3886 A70-41073

Gravity darkening of tidally and nonuniformly rotating Roche components of close binary systems, calculating surface temperature and spectral distributions

21 p3888 A70-41120

Heated surface orientation and reduced gravity effects on Freon 113 nucleate

21 p3948 A70-41204

Gravitational effects on laminar gas jet diffusion flame stability, including zero gravity environment

21 p3949 A70-41316

Critical thermal flux and heat transfer coefficients dependence on simulated gravity during bubble and film boiling in inclined flat containers

21 p3952 A70-42066

Cellular convection in fluid layers with parabolic temperature distribution, calculating stability effects of gravity and surface tension gradients

21 p3952 A70-42078

Fluid dynamics nonlinear equations for thermally driven motions in compressible, isothermal gravitational solar atmosphere, considering flow discontinuities and heat conduction

21 p3925 A70-42191

Lense-Thirring effect in test masses approaching in same orbit around rotating body, noting correction dependence on central body geometry and angular velocity

21 p3926 A70-42240

Stellar evolution, rotation and atmospheric motion, discussing gravity darkening, spectral lines, angular momentum, braking mechanisms and late stars

22 p4102 A70-42970

Computer model of self gravitating gas-stars system with spiral structure surviving galactic rotations

22 p4103 A70-42982

Earth gravity deforming effect on flexible crossed-dipole satellite configuration, considering dynamic stability and spin stabilization

22 p4110 A70-43434

Earth gravity effect on spin vector attitude stability of flexible crossed dipole satellite configuration

22 p4110 A70-43435

Earth quadrupole moment indirect effect on satellite gyroscope precession

23 p4217 A70-43799

Vertical force exertion on mass at ends of elongated rotating nonspherical asteroids calculated for man safety and mobility

23 p4239 A70-43849

Xanthine dehydrogenase activity in *Drosophila* and *Habrobracon* under hypogravity conditions onboard Biosatellite

23 p4144 A70-43863

Trail formation due to tidal effect in interacting galaxies during close approaches, considering mass flow hydrodynamics

23 p4240 A70-43906

Translational-rotational motion of axisymmetrical moon in earth gravitational field

23 p4240 A70-43917

Miles-Howard theorem extension to gravitationally stratified compressible fluid containing parallel shear flow, considering stability against adiabatic perturbations

23 p4179 A70-43976

Solar probe trajectory optimization, using Venus gravitational field for braking

23 p4243 A70-44506

Organism reactions to gravity forces, discussing experimental zero and hyper g simulation studies with frog and nematode eggs

23 p4146 A70-44630

Lawden intermediate rocket thrust arcs numerical integration and Kelley-Contensou optimality in Newton central force field

23 p4245 A70-44657

Artificial liquid satellite orbited to verify tidal theory

23 p4183 A70-44659

Ion acoustic wave propagation in collisionless gravity-supported plasma in static magnetic field calculated from linearized Vlasov equation

24 p4382 A70-45109

Gravity effects on perinatal organ growth in chicks

24 p4297 A70-45342

G-suit hazards in lower extremity thrombophlebitis in pilots

24 p4307 A70-45347

Big bang temperature problem, discussing galactic masses determination possibility by gravity-strong interactions interplay in early stages

24 p4403 A70-45402

Newton and Einstein gravitation theories applied to light velocity in gravitational field

24 p4379 A70-45487

Light velocity frequency dependence in variable stars gravitational fields suggested from yellow and UV NP 0532 observations

24 p4405 A70-45488

Artificial satellite motion theory, discussing gravitational and nongravitational force effects

24 p4406 A70-45527

Altered gravitational field effects on frog eggs centrifuged under various conditions after fertilization, noting time dependence of induced abnormalities

24 p4298 A70-45619

Galactic evolutionary models using disklike Riemann ellipsoids with internal motions and gravitational gas equilibria

24 p4410 A70-45759

Ionized matter stability in intense radiation field opposed to gravitation, explaining quasar properties

24 p4398 A70-46162

Peak pool boiling heat flux on horizontal cylinders, describing interactions of gravity and heater size effects

24 p4429 A70-46176

GRAVITATIONAL FIELDS

Elliptic integrals for plane motion of stars, assuming stationary gravitational potential of stellar system

01 p0174 A70-10138

Inertial gravitational fields described by Maxwell equations, showing potentials defining four vector velocity field of test particles

01 p0141 A70-10140

Gravitational field equations in flat space, using quaternion representation of general relativity Riemannian space time in terms of spinors

01 p0141 A70-10279

Oblate earth gravitational field effect on ballistic missile trajectories, including body range determination and quadratures expressed by elementary functions

01 p0178 A70-10423

Earth gravity field intensity variations measured by orbiting two geometrically identical satellites, discussing sensitivity and cost

01 p0087 A70-10445

Linear field theory of gravitation by considering gravitational field functions decomposition into spin components

01 p0143 A70-10712

Computer model for evolution investigation of disks of stars, discussing methods to obtain gravitational potential

01 p0185 A70-11065

Compressible gas flow problem in point body gravitational field solved with reference to sun and interstellar gas

01 p0172 A70-11489

Spacecraft horizontal maneuvers in homogeneous gravitational field to achieve soft landing on planetary surface, including optimal liftoff and orbital transfer

01 p0197 A70-11501

Gyrostabilized satellite steady state motions in Newtonian force field having displaced satellite center of mass orbital plane relative to center of attraction

01 p0198 A70-11577

Conformally plane solutions to Einstein equations derived with energy momentum tensor characteristics of pulverized material representing gravitational fields

01 p0193 A70-11629

Microtopography effects on measuring horizontal gravity gradients by gravimeters

02 p0295 A70-11799

Two step optimal motion of target and pursuer with thrust vector control in vacuum under arbitrary gravitational field, determining distance strategy

02 p0272 A70-12405

Stellar clusters equilibrium state in gravitational field, discussing dispersed clusters formation by gravitational instability in gas containing stars of various ages

02 p0376 A70-12446

Lunar gravitational field determination from analysis of Lunar Orbiter spacecraft tracking data

03 p0562 A70-12915

Satellite observations for determining earth shape and gravitational field zonal harmonics, using dynamic methods

03 p0473 A70-13188

Gravimetric and satellite tracking data reduction for determining coefficients in mathematical expansion representing earth gravitational field

03 p0473 A70-13189

Steady motions stability of gyrost satellite in central Newtonian gravitational field

03 p0579 A70-13343

Close spaced material points motion stability in gravitational field of attractive center using Liapunov theorem, assuming nongravitational forces action on points

03 p0524 A70-13369

Heat transfer and flux density during bubble boiling of liquid oxygen employing simulated weak gravitational fields

03 p0605 A70-13393

Lagrangian gravitational field density related to contraction to expansion transition in terms of cosmological model, discussing quadratic corrections and singularity

03 p0524 A70-13412

Energy analysis of unstable gravitational oscillations in galaxies, using two component model for normal spiral galaxies

03 p0570 A70-13532

Relativistic tensor theories of gravitation in flat space with Neumann and Newton forms of gravitational potential, deriving expressions to estimate differences perceived by observer

03 p0526 A70-14305

Gravitational wave propagation velocity determined by laboratory measurement of spin-spin coupling of two rotating masses

04 p0718 A70-14397

Translational-rotational motion of long dumbbell in Newtonian central force field, analyzing plane center of mass trajectory with perpendicular kinetic moment vector

04 p0744 A70-14427

Optimal impulse orbital transfer in ring between coplanar orbits intersecting ring boundaries in central Newtonian force field

04 p0744 A70-14429

Galactic mass loss by gravitational radiation, discussing galactic expansion and nucleus mass

04 p0752 A70-15068

Stellar systems dynamics, discussing dynamic interactions of point masses, forces in gravitational field, galactic model construction, etc

04 p0754 A70-15353

Formula for energy radiated from particles system applied to electromagnetic and gravitational radiation and illustrated by charged particle motion in magnetic field

05 p0882 A70-16309

Large spacecraft in circular earth orbit calculated for internal gravitational field

05 p0924 A70-16637

Geodetic vertical and geoidal height deflection calculated by gravimetric method, considering satellite orbits data

05 p0841 A70-16643

Gravitational-repulsion forces of interstellar vacuum, investigating relations between magnitudes and red shift of galactic objects and quasars

05 p0920 A70-16968

Pulsed gravitational radiation emitted by dense star clusters

05 p0921 A70-16977

Shear-free gravitational radiation described by Einstein equations, analyzing physical properties including energy, angular momentum, radiation flux and trapped surfaces

06 p1104 A70-17185

Second vertical derivative of gravity field, using formulas based on Taylor series expansion method

06 p1055 A70-17604

Time-similar and isotropic geodetic curves simulating paths of test bodies in Riemann space corresponding to gravitational field

06 p1107 A70-18564

Hypothesis concerning initial spectrum of metric perturbations in Friedman model, discussing long wavelength gravitational waves energy

07 p1383 A70-19406

Gaseous spheres gravitational stability in proper field, considering convection and radial perturbations effects

07 p1383 A70-19408

Radiation focusing properties of gravitational bodies associated with curving light trajectories analyzed by geometrical and waveguide optics approximations

07 p1384 A70-19411

Potential and gravity distributions on lunar surface, showing presence of harmonics of all orders

07 p1385 A70-19425

Meteorological satellites motion parameters long term prediction, using final analytic relationships with allowance for zonal harmonics of gravitational field

07 p1329 A70-19650

Signal reception possibly due to gravitational radiation of cosmic origin, estimating energy

07 p1387 A70-19699

Axial-vector current divergence in external gravitational field, using perturbation approach in Minkowski space

07 p1336 A70-20167

Gravitating particles systems equilibrium states, solving kinetic equations for sphere and cylinder in isotropic and anisotropic cases

07 p1389 A70-20207

Electromagnetic and gravitational fields classification methods using spinor techniques, introducing five dimensional complex linear space with Weyl tensors elements

07 p1337 A70-20302

Cosmological gravitation theory for uniformly expanding universe model providing fundamental reference frame and acceleration field

08 p1563 A70-20497

Matter distribution and motion in conformally flat gravitational fields, analyzing Friedmann solution to Einstein equations

08 p1544 A70-20991

Gravitational waves in general relativity theory, discussing Kaigorodov exact solution to Einstein equations

08 p1545 A70-20993

Gravity long wave variations correlation with crust and upper mantle geological activity, describing anomaly distribution

08 p1488 A70-21014

Statistics and coincidences of Argonne-Maryland gravitational radiation detector array with and without time delays

08 p1545 A70-21271

Schwarzschild metric properties in synchronous reference system, using succession of Schwarzschild interval holonomic transformations as function of gravitational radius

08 p1545 A70-21406

Magnetothermal instability and radiative effects on incipient fragmentation of rotating gravitating interstellar fluid forming condensations

08 p1578 A70-21545

Einstein power transfer theory used for demonstrating energy transfer rate by gravitational radiation from emitter to absorber

08 p1546 A70-21742

Unified geometric description of gravitational and electromagnetic fields, determining electromagnetic field influence on geometry from dimensional constant

08 p1546 A70-21811

Gravitational radiation detection from pulsating neutron star, considering asymmetries in gravitational collapse of massive stars as origin

09 p1749 A70-21996

Geogravitational field correlations to geomagnetic fields emphasizing displacements in longitude

09 p1667 A70-22381

Spherically symmetric galaxies dynamic evolution analysis, emphasizing irregular motions description using fluctuating gravitational field hypothesis to construct Markov process

09 p1758 A70-22747

Static gravitation field of spherical mass immersed in cosmological gas, using combined model of Einstein and de Sitter static universes and Schwarzschild solutions

09 p1763 A70-23312

Stellar wind theory based on spherically symmetric isothermal and stationary stellar atmosphere with non-negligible gravitational potential

09 p1747 A70-23605

Maxwell electromagnetism analogy to Einstein gravitation inferred from asymptotic studies of electromagnetic and gravitational radiation

10 p1915 A70-24029

Eclipsing binary beta Aurigae effective temperature and surface gravity determination from photoelectric spectrum and abundance analyses

10 p1938 A70-24100

Gravitational waves and radiation study based on relativity theory, discussing outer space sources and antenna recording design and properties

10 p1916 A70-24384

Milky Way expansion, explaining Weber gravitation signals by collisions between neutron and normal star

10 p1943 A70-24698

Different gravitational force fields effecting optimal rocket trajectories and queried validity of Newtonian law

10 p1943 A70-24820

Errors estimation arising in inertial navigation equations solution while neglecting terms dependent on earth asphericity and gravitational field

11 p2077 A70-25558

Gravitational field and ellipsoidal gravitational waves anisotropy, deriving gravitistics results from electrostatics

11 p2083 A70-25944

Asymptotic model for stationary radiative stationary transitions using Newman-Penrose spin coefficient approach to gravitational radiation for Riemann spacetime

11 p2084 A70-26547

Optimal pulsed orbital transfer between close nearly circular orbits in central field of gravity realized by geometrical solution

11 p2118 A70-26778

Gravitational and magnetic anomaly interpretation by regression analysis including geological field discrimination, inverse gravimetry and magnetometry, etc

12 p2223 A70-27318

Second order self conjugate elliptical differential equation for modulus of gravitational field strength, giving geometrical interpretation of coefficient

12 p2223 A70-27349

Terrestrial external gravitational field approximation using sphere and ellipsoid attraction, showing mass, angular velocity and size dependence

12 p2300 A70-27477

Orbital perturbations earth satellite due to zonal and tesseral earth gravitational harmonics and external body fields

12 p2302 A70-27671

Einstein equations derivation in comoving reference frame for spatially homogeneous gravitational fields

12 p2310 A70-28221

Coplanar transfer orbits optimal trajectories in central Newtonian gravitational field, using Krotov sufficient criteria

12 p2310 A70-28252

Rendezvous trajectory control problems solution by regularization techniques, emphasizing equations of motion in gravitational field

13 p2446 A70-28380

Translational-rotational motion of long dumbbell in Newtonian central force field, analyzing plane center of mass trajectory with perpendicular kinetic moment vector

13 p2485 A70-28452

Optimal impulse orbital transfer in ring between coplanar orbits intersecting ring boundaries in central Newtonian force field

13 p2485 A70-28454

Geogravity-geomagnetic fields correlation due to lateral temperature variations in upper mantle

13 p2393 A70-28620

Convection effects in mantle on earth gravitational field using hydrodynamic model

13 p2488 A70-28764

Gravity radiation detector insensitivity to cosmic rays

13 p2405 A70-28835

Einstein-Maxwell equations for monopolar point electrical charge, calculating proper energy for electromagnetic and gravitational fields

13 p2451 A70-28956

Stellar light pressure and gravitational force ratios for spherical water, quartz and graphite particles in interstellar space, considering refractive dependence on wavelength

13 p2493 A70-29396

Two body system with Newtonian force interaction, calculating gravitational wave energy losses and spectral decomposition

13 p2453 A70-29668

Upper atmospheric temperature-gravitational potential relationship for sun, earth and several planets

13 p2495 A70-29765

Frequency dependence of gravitational-electromagnetic fields interaction assumption inconsistent with general relativity and consistent with data on deflection of radiation by massive bodies

14 p2573 A70-30616

Steady motions stability of gyrostat satellite in central Newtonian gravitational field

14 p2653 A70-30718

Gravitational field representation in satellite geodesy by simple layer potential, comparing with geopotential expansion in spherical harmonics

15 p2722 A70-31548

Triaxial earth attraction potential from expanding certain elliptical functions into series, noting consistency with concepts of astronomy and geodesy

15 p2731 A70-32148

Vertical gravity gradient effect on calculations accuracy of earth figure, deriving corrections for anomalies

15 p2731 A70-32149

Electrodynamical-gravitational model of radio galaxies and quasars accounting for complex field, particle acceleration, angular momentum, luminosity and line emission

15 p2807 A70-32811

Neutron stars gamma and radio emission in gas accretion state, determining surface gravitational potential

15 p2808 A70-32883

Secular variations in osculating orbital elements of particle in Saturn ring gravitational field, considering motion in both external and internal space

16 p2973 A70-33226

Pulsar gravitational waves detection by lunar mascons, discussing resonant standing vibrations

16 p2980 A70-34306

Frequency spectra of gravitational waves radiated from celestial phenomena, suggesting mass exchange in binary containing neutron star

17 p3067 A70-34619

Horizontal gravity gradient components in outer space from Stokes function expansion, using sphere as model

17 p3154 A70-34682

Earth gravity field from successive satellite passages, introducing direction and range observations of first passage

17 p3154 A70-34683

Large anisotropy observed for gravitational radiation detector intensity as function of sidereal time, suggesting source from galactic center

17 p3137 A70-35725

Energy transfer in convective envelope of rotating star and solar differential rotation, using Lucy gravity-darkening law

18 p3313 A70-36214

Equilibrium form shapes of fluid free surface in vessel under gravitational and magnetic field with tension

18 p3240 A70-36269

Parametric representation of brachistochrones of mass point in centrosymmetrical gravitational field

18 p3283 A70-36387

Self interaction of nonsingular sourceless first order pulse of gravitational radiation imploding from infinity to focus point and exploding to infinity

18 p3291 A70-36475

Relativistic thermal equilibrium conditions in external gravitational field, considering heat with inertial and gravitational mass

18 p3291 A70-36552

Near earth motion equations for electrically charged dust particles in gravitating dipole magnetic fields, using zero-relative-velocity surfaces and energy integral

18 p3315 A70-36606

Artificial satellite orbital motion numerical integration, computing spherical harmonic terms for earth gravitational potential

18 p3334 A70-37063

Gravitational field on Liapunov surface approximating earth relief, using double sphere solution

19 p3407 A70-37299

Autocorrelation functions of anomalous gravitational and magnetic fields for ocean lines, relating Mohorovičić boundary and Curie isotherm

19 p3408 A70-37318

Insular system energy and momentum definition in external gravitational field, using dynamic equations and Einstein theory

19 p3513 A70-37412

Stress energy tensor equal time commutation, observing metric dependence inability to satisfy relations for linearized gravitational fields

19 p3536 A70-37550

Quantum gravity and UV infinities in quantum electrodynamics, describing constant gravitational length from nonperturbative calculations for self mass and self charge

19 p3473 A70-37575

Fundamental equations of physical geodesy for earth figure by oceanic and continental parts via external gravity field

20 p3617 A70-39069

Integral equations for gravity field and plumb line deflections solved by Neumann and Molodenskii methods

20 p3617 A70-39073

Gaussian gravity field structure, calculating gravity correlation function using differential equation from density correlation function

20 p3617 A70-39075

Upper atmospheric temperature-gravitational potential relationship for sun, earth and several planets

20 p3710 A70-40090

Einstein equations derivation in comoving reference frame for spatially homogeneous gravitational fields

20 p3710 A70-40096

Plane horizontal fluid film convective stability with free boundaries in vertical circular cylinder for periodic modulation of vertical temperature gradient or gravitational field

21 p3941 A70-40608

Gravitational radiation scattering by Schwarzschild horizon, discussing odd parity waves of angular momentum

21 p3878 A70-40731

Emission and escape of light from inside spherically symmetric gravitational mass, examining escape cone

21 p3923 A70-42106

Chronometrically invariant formulation of Petrov gravitational fields algebraic classification at spacetime fixed point in general relativity

21 p3851 A70-42239

Stellar system statistical mechanics, discussing collisionless gas in gravitational field, galaxy formation, stellar dynamics, double stars and bounded isothermal spheres

22 p4098 A70-42577

Quasi-Maxwellian equations of inertial-gravitational fields

22 p4075 A70-43223

Airborne and surface downward continuation of gravity, discussing integral equations solutions and data filtering of noise interference

22 p4025 A70-43664

Geodetic boundary value problem reformulation based on geometric satellite geodesy involving gravity measurements

22 p4025 A70-43667

Interplanetary mission propellant reduction by using earth-moon-sun gravity field properties, discussing swingby techniques, low energy trajectories, etc

23 p4244 A70-44607

Doppler effect simplification to classical Laplacian orbit determination, deriving equations in perturbed gravity field for initial point determination

23 p4246 A70-44697

Gravitational radiation detectors design and components, discussing background noise and thermal fluctuations

23 p4198 A70-44850

Gravitational field fine structure representation near earth surface as sum of global model in spherical harmonics and local model in harmonic B functions

24 p4328 A70-45287

Satellite motion deviations from reference orbit by generalized Fourier analysis, discussing earth gravitational field parameters determination and errors

24 p4408 A70-45546

Interorbital optimum trajectories with specified transfer angle in inverse square gravitational field, examining minimum velocity increment

24 p4412 A70-46003

Gravitational wave associated radio pulse observations using long baseline spaced receivers

24 p4412 A70-46136

GRAVITATIONAL POTENTIAL

U GRAVITATIONAL FIELDS

GRAVITATIONAL RADIATION

U GRAVITATIONAL FIELDS

GRAVITONS

Photon pair annihilation process in graviton pair, examining IR emission in two scalar particle collision

19 p3472 A70-38172

GRAVITY

U GRAVITATION

GRAVITY ANOMALIES

Mare Orientale positive gravity anomaly

17 p3158 A70-34865

Cylindrical body with gravitational and magnetic anomalies, selecting point coordinates for body parameters

19 p3407 A70-37298

Vertical gravimetric deflections calculation based on linear interpolated gravity anomalies

19 p3410 A70-37461

Stokes earth constants from gravity anomalies

20 p3617 A70-39070

Gravity and magnetic geophysical prospecting methods, discussing data acquisition, reduction and analysis in terms of underground geologic anomalies

22 p4018 A70-43086

Gravity gradiometer in moving vehicle for gravity anomaly surveying

22 p4041 A70-43657

Gravity gradiometry for fine structure of gravity influenced by local anomalies

22 p4108 A70-43659

Gravity measurement errors in high speed aircraft parallel to undulating geoid attributed to associated vertical accelerations

22 p4025 A70-43662

Gravity measurements and adjustments of First Order Gravity Network /FOGN/ in Iran

24 p4332 A70-46409

GRAVITY GRADIENT SATELLITES

NT APPLICATIONS TECHNOLOGY SATELLITES

NT ATS 1

NT ATS 3

NT ATS 5

NT ORBITAL SATELLITE

Satellite attitude control, discussing passive, active and hybrid stabilization methods including spin, gravity gradient and magnetic stabilization

01 p0197 A70-11264

Three-body gravity gradient satellite orbital plane motion analysis, studying transient damping of proposed tethered orbiting interferometer /TOI/

02 p0383 A70-12781

Satellites gravity-gradient stabilization by flywheels in elliptical orbits, designing control system for orientation and optimal motion damping

03 p0582 A70-14321

Deployable STEM /storable tubular extendible member/ booms for aerospace gravity gradient stabilization, noting interlocked BI-STEM

04 p0761 A70-14725

Optimal iterative weighted least squares estimation of rotation-coupled flexural oscillations of boom stabilized satellites in earth orbits

04 p0763 A70-15413

Semiactive gravity gradient attitude stabilization system /SAGS/ providing active pitch control and semipassive roll/yaw control, discussing design, development and testing

05 p0923 A70-15863

Attitude performance of GEOS 2 gravity gradient spacecraft, discussing prelaunch design and post-launch analyses

06 p1154 A70-17162

Capture and gravity gradient stabilization of LIDOS satellite in eccentric orbit

06 p1154 A70-17175

Stochastic Liapunov stability of satellite motion influenced by aerodynamic and gravity gradient torques, considering atmospheric density uncertainty

06 p1159 A70-18185

DODGE satellite launched into near-synchronous orbit to demonstrate gravity-gradient stabilization at high altitude and to experiment with damping techniques

06 p1159 A70-18218

Gravity gradient satellites equilibrium attitude error analysis showing relative effects of error sources

10 p1951 A70-24825

Orbit eccentricity effect on gravity gradient system with single damping boom, investigating optimum steady state and transient response conditions

11 p2123 A70-26129

Librational motion of damped gravity oriented satellite in circular orbit

12 p2313 A70-27201

Attitude-translation motion coupling effect on stability of gravity-stabilized drag-free satellites

13 p2501 A70-28424

DODGE satellite gravity gradient stabilization at synchronous altitude by flywheel and magnetic sample-and-hold damping, noting boom bending

13 p2501 A70-28425

Gravity gradient stabilization systems for earth-pointing satellites, noting long term reliability and accuracy

13 p2507 A70-29828

Gravity gradient ATS program experiments including spin scan cloud cover and stabilization research

14 p2654 A70-31145

Attitude dynamics of slowly spinning axisymmetric satellites under influence of gravity gradient torques, using analytical and numerical techniques

15 p2809 A70-31778

Book on passive gravity gradient libration dampers covering design, flight experience, evaluation criteria, performance monitoring, failure prevention, etc

16 p2983 A70-33954

Spacecraft gravity gradient stabilization by damping out oscillatory motions by energy dissipation, using combined eddy current and hysteresis dampers /Combination Passive Damper/

16 p2985 A70-34133

Torsion wire libration damper for satellite gravity-gradient stabilization at near synchronous altitudes

16 p2985 A70-34134

Two axis eddy current and single axis gravity gradient dampers for satellite stabilization

16 p2985 A70-34135

Low thrust station keeping guidance scheme for gravity gradient stabilized 24-hour satellite, solving equations of motion for near circular equatorial orbit

18 p3289 A70-36676

Gravity stabilized gyrostat satellite attitude motion stability, using three dimensional diagram and Liapunov functions

18 p3334 A70-37061

Gravity gradient attitude control for satellites near lunar far side libration point

19 p3528 A70-38868

Gravity stabilized drag free satellites attitude instabilities due to coupling between attitude and translational motions

20 p3714 A70-39535

Magnetic compensation for attitude control of gravity gradient stabilized satellite using environmental torques and moment gyro damping

20 p3668 A70-39537

Radio Astronomy Explorer satellite boom deployment method resulting in gravity gradient capture, emphasizing role of predeployment attitude and antenna Vee angle

21 p3931 A70-41856

Sliding mass and damper boom damping mechanisms for gravity-oriented satellites, using method of characteristic roots coalescence

22 p4110 A70-43436

Aerodynamic and gravitational torque effects on orbiting satellites attitude stability, applying Liapunov direct method in case of conservative aerodynamic torque

23 p4258 A70-44559

Structure and systems design of large gravity gradient stabilized orbiting tethered satellites structure for radio astronomy

23 p4259 A70-44603

Parameter optimization of gravity gradient stabilized satellite in circular orbit, considering minimum transition time and eccentricity oscillation

23 p4264 A70-45014

GRAVITY GRADIOMETERS

Microtopography effects on measuring horizontal gravity gradients by gravimeters

02 p0295 A70-11799

Dynamic gravimetry - Conference, Fort Worth, March 1970

22 p4024 A70-43656

Gravity gradiometer in moving vehicle for gravity anomaly surveying

22 p4041 A70-43657

Error sources and magnitudes in dynamic gradiometer using inertial grade pendulous accelerometer, discussing compensating modifications

22 p4042 A70-43658

Gravity gradiometry for fine structure of gravity influenced by local anomalies

22 p4108 A70-43659

Rotating gravity gradiometer for simulated terrain mapping with subsurface density fluctuations

22 p4007 A70-43668

GRAVITY WAVES

NT BAROCLINIC WAVES

Vertical wind observations during lower ionosphere wind measurements by Na release method, discussing gravity effects and standing waves

01 p0078 A70-11213

Internal gravity waves theory to interpret large amplitude oscillations in electron density and temperature and ion temperature and velocity observed in thermosphere

01 p0079 A70-11215

- Atmospheric gravity waves in F region, discussing neutral gas-ionization interaction and detection by electron density profile measurements
01 p0079 A70-11216
- Resonance amplification theory of standing interfacial gravity waves in viscous fluids applied to obtain wavelengths prediction of atmospheric bow waves
01 p0081 A70-11299
- Dispersion relation governing hydromagnetic gravity waves propagation in rotating nonisotropic medium, discussing effects of constant entropy gradient
04 p0745 A70-14473
- Steady gravitational waves produced by variable pressure in fluid channel flow assuming small perturbed flow velocity components
05 p0836 A70-16969
- Signal reception possibly due to gravitational radiation of cosmic origin, estimating energy
07 p1387 A70-19699
- Atmospheric gravity wave generation, propagation and dissipation, considering stratospheric tides
07 p1275 A70-20276
- Gravity waves generated by heating in auroral regions and propagating toward lower latitudes possibly causing thermospheric heating
08 p1491 A70-21675
- Stratified atmosphere boundary layer motions, studying turbulence and internal gravity waves characteristics
09 p1716 A70-22369
- Acoustic gravity waves horizontal ducting in atmosphere with spatially periodic wind shears
09 p1671 A70-23498
- Nonlinear oscillations averaging method applied to resonant interactions of acoustic gravity waves
09 p1729 A70-23666
- Field strength correlation with micropressure variations caused by internal gravity waves propagating in lower troposphere
10 p1883 A70-25252
- Gravity wave attenuation in F region investigated for role of ohmic losses
10 p1885 A70-25264
- Gravitational field and ellipsoidal gravitational waves anisotropy, deriving gravistatics results from electrostatics
11 p2083 A70-25944
- Gravity waves structure simultaneous determination from airborne ozone and temperature sensors and satellite observations data
11 p2076 A70-26072
- Gravity radiation detector insensitivity to cosmic rays
13 p2405 A70-28835
- Hydromagnetic coupling between neutral and ionized atmosphere perturbations, noting role of gravity waves
13 p2397 A70-29191
- Auroral currents as source of atmospheric gravity waves and associated traveling ionospheric disturbances
13 p2399 A70-29234
- Vertical momentum flux correction for planetary scale gravity waves in equatorial lower stratosphere
13 p2445 A70-29623
- Two body system with Newtonian force interaction, calculating gravitational wave energy losses and spectral decomposition
13 p2453 A70-29668
- Lower stratosphere temperature and wind periodic variations associated with shear flow gravity waves
14 p2601 A70-30124
- Nonlinear diurnal tide and gravity wave interactions at meteor heights below mesopause
14 p2579 A70-31251
- Atmospheric turbulence effects on acoustic-gravity waves propagation, deriving dispersion relation for phase velocity and propagation constants
14 p2579 A70-31252
- Neutral particle and electron density measurements by Explorer 32 proving thermospheric gravity waves association with wave-like structure in F region electron density
15 p2727 A70-31907
- Gravity wave generation during solar eclipse confirmed by satellite observation on Faraday rotation angle of ionospheric VHF transmissions
16 p2898 A70-33836
- Pulsar gravitational waves detection by lunar mascons, discussing resonant standing vibrations
16 p2980 A70-34306
- Long and short period internal gravity waves in atmosphere observed by high resolution radar, investigating generation mechanisms
17 p3075 A70-34609
- Frequency spectra of gravitational waves radiated from celestial phenomena, suggesting mass exchange in binary containing neutron star
17 p3067 A70-34619
- Zonal wind component in lower ionosphere observed for gravity waves partial reflections by temperature discontinuities, using least mean square method for reflection coefficient
17 p3077 A70-34946
- Self interaction of nonsingular sourceless first order pulse of gravitational radiation imploding from infinity to focus point and exploding to infinity
18 p3291 A70-36475
- Internal gravity waves reflection, inspecting differential equations for behavior of two wave parameters
19 p3471 A70-37779
- Maclaurin spheroid secular stability, examining energy dissipation of gravitational radiation
20 p3702 A70-39017
- Jacobi ellipsoid quasi-static evolution by gravitational radiation, discussing direction of increasing angular velocity toward nonradiating state at bifurcation point with Maclaurin sequence
20 p3702 A70-39018
- Gravitational radiation scattering by Schwarzschild horizon, discussing odd parity waves of angular momentum
21 p3878 A70-40731
- Geostationary beacon satellite recording of gravity wave influence on ionospheric electron content
21 p3815 A70-40943
- Lower thermosphere minor gaseous constituents vertical transport by nonlinear gravity wave process, showing density scale height decrease from diffusive equilibrium
21 p3818 A70-41098
- Internal gravity waves mathematical model for atmosphere with arbitrary distributions of temperature, molecular weight, viscosity and conductivity, deriving wave propagation into thermosphere
21 p3821 A70-42257
- F 2 region anisotropic response to individual internal gravity waves as function of propagation azimuth
23 p4185 A70-43844
- Lower atmosphere gravity wave motions due to cooling by solar eclipse shadow
23 p4185 A70-43845
- ELF acoustic gravity wave arrival from Apollo launches recorded by Doppler shift ionospheric sounder channeled near mesopause and lower thermosphere
23 p4187 A70-43859
- CAT origin in unstable atmospheric shear and gravity waves, using ultrahigh resolution radar for observation of transition process
23 p4214 A70-44032
- Internal gravity wave shape at temperature inversion in lower atmosphere from high resolution vertically pointing FM/CW radar sounding
23 p4162 A70-44038
- Gravity waves produced in liquid electric conductor by piston subjected to sinusoidal pulsation, calculating magnetic field effect on amplitude and phase velocity
23 p4225 A70-44208
- Gravitational acoustic wave emission in isothermal stellar atmosphere with mass sources
23 p4242 A70-44267
- GRAY GAS**
- Differential equation with associated boundary conditions constructed for radiative transfer with spherical symmetry, applying to gray gas between concentric black spheres
03 p0603 A70-12904
- Two dimensional approximate formulation for radiant heat flux applied to radiative equilibrium in gray gas
03 p0603 A70-12905
- Thermal radiation shield influence on stationary radiative heat transfer in closed arbitrarily shaped two gray surface system
10 p1966 A70-23865
- Radiative transfer effect on thermal instability and critical Rayleigh number in gray transparent fluid layer heated from below
10 p1967 A70-23952
- Radiative heat transfer through gray gas in equilibrium between concentric spheres, using variational method
13 p2521 A70-29137
- Radiative heat transfer in optically thick gas between concentric spheres treated by matched asymptotic expansions, comparing results with Rosseland approximation and numerical solution
14 p2663 A70-30266
- Nomogram for true and apparent radiometric temperatures of remote graybodies in presence of atmosphere
14 p2577 A70-31231
- Temperature distributions and heat flux for gray gas in radiative equilibrium bounded by walls with different temperatures, using differential approximation [AIAA PAPER 70-834]
16 p3001 A70-33929
- Nonadiabatic self absorbing radiative flow of gray gas around sharp cornered blunt body at hyperbolic speed by integral relations method
17 p3010 A70-34974
- Steady state radiative heat transfer through gray gas in spherical cavity, solving transport equation by singular integral equations for uniform heat generation
23 p4283 A70-44784
- GREASES**
- Thermal conductivity temperature dependence measured in greases bulk and thin layers at liquid helium temperature
05 p0874 A70-16842
- Thickening of fluids with tetrafluoroethylene polymer to provide physically and chemically stable grease type lubricants for military applications
07 p1292 A70-18863
- Liquid and solid lubricants, discussing properties, temperature ranges, costs, environmental effects and outlook
07 p1316 A70-18953
- Apiezon N grease thermal conductivity at liquid helium temperatures noting behavior as insulator
12 p2258 A70-27024
- Temperature and long term effects on volatility of perfluoroalkyl ether and polysiloxane greases [ASME PAPER 70-HT-31]
22 p4058 A70-42435
- GREAT BRITAIN**
- UK aeronautics R and D, attributing competitive technology lag in military and subsonic civil fields to failure in aims and targets and program cost justification
02 p0402 A70-12306
- Intelsat 4 communications satellite design and manufacture, discussing European participation with emphasis on British involvement
02 p0383 A70-12649
- Royal Air Force air reconnaissance function, discussing cameras, films, processing and printing, photointerpretation, etc
03 p0495 A70-14144
- British military and civilian aircraft and flying between World War I and II, discussing weapons systems and accidents
05 p0794 A70-16113
- Guided weapons management techniques applied to Rapier light weight anti-aircraft weapon system
08 p1601 A70-21037
- Aviation maintenance in Britain, discussing continuing airworthiness techniques, development and international aspects
08 p1436 A70-21256
- UK UHF telemetry command station capabilities for Skyenet satellites control, discussing equipment [AIAA PAPER 70-415]
11 p2030 A70-25420
- Edwards Inquiry Report into British Civil Air Transport based on cost effective economic study, involving airlines and regulatory system
11 p2153 A70-25855
- Edwards Report on UK domestic air services, considering unprofitability, trunk route competition and V/STOL development exploitation
11 p2153 A70-25860
- British air transport from aircraft manufacturing industry viewpoint, discussing governmental organization of air industries and aircraft design negotiation atmosphere
11 p2153 A70-25861
- British national and Commonwealth collaborative sounding rocket programs, discussing organization, scope and range facilities
13 p2523 A70-28685
- Air traffic in 1980s in UK, considering domestic services, V/STOL operation and private and executive aviation
14 p2667 A70-30102
- Commercial aircraft manufacturing industry in UK, discussing SST, wide cabin aircraft, turboprop replacement, engine influence on airframe industry, etc
14 p2668 A70-30936
- Military aviation economics in UK emphasizing aircraft industry and government cooperation in meeting RAF requirements
14 p2668 A70-30938
- COSPAR report on UK space research /1969/ covering neutral atmosphere, ionosphere, solar radiation, etc
15 p2831 A70-31723
- RAF aircraft damage due to bird strikes in U.K., discussing preventive measures at airfields
18 p3211 A70-35978
- British government technological partnership with domestic industry and other countries
21 p3956 A70-41892
- British National and Commonwealth collaborative sound rocket programs, discussing organization, scope and range facilities
24 p4431 A70-46124
- GREAT CIRCLES**
- Great circle vector formula in space triangulation, discussing topocentric and geocentric position of satellite and tracking stations and absolute distance determination
03 p0445 A70-13193
- Rayleigh and Love wave phase velocities for great circle paths from ordinary seismograms of World Wide Standard Seismographic Network /WWSSN/ stations
09 p1672 A70-23702
- GREAT POLAR CAPS**
U POLAR CAPS

GREECE

Report to COSPAR on Greek space research /1969/ covering big planets observations, solar activity, ionospheric propagation, airglow measurements, satellite trackings, etc

15 p2830 A70-31714

GREEN FUNCTION

Energy spectrum of electrons and holes in semiconductors under strong electromagnetic wave field, calculating electron-phonon interaction Green function

01 p0155 A70-10184

Green function type solutions of shell equations by small parameter technique for case of free terms consisting of Dirac delta function

01 p0212 A70-11565

Premature saturation in strongly magnetic systems explained by model with nonuniform magnon modes, applying time dependent Green functions

02 p0338 A70-11886

Rectangular anisotropic beam torsion using Green function combined with wide step network method

03 p0593 A70-13471

Reflection coefficients of circular posts in rectangular waveguides computed by Green function and method of moments

05 p0820 A70-16384

Existence and uniqueness of nonlinear boundary value problem solutions formulated by fixed point theorem and Green function

05 p0876 A70-16562

Green operator structure and eigenvalue approximation of boundary value problems regarding vibrations and buckling of clamped plates using orthogonal invariants

05 p0876 A70-16563

Homogeneous gravitating sphere deformation by internal dislocations determined using Green dyad

06 p1055 A70-17605

Boundary value problems in nonlocal elasticity, considering two one dimensional media coupling with microstructure by Green function analog

07 p1399 A70-18665

Green function of region near circle approximation by matrix method, considering Laplace differential equation solution, conjugate harmonic function and conformal transformation

07 p1253 A70-18924

Crystals nonlinear permittivity related to temperature-time Green function for electromagnetic radiation, determining crystal polarizability by light-excitation method

07 p1335 A70-19868

Green matrices construction for joint shells by method of arbitrary constants variation, considering strained state symmetrical with joint lines

07 p1413 A70-20144

Quadrature solution for elastic sphere deformation by axisymmetric normal loads, writing Green function of boundary value problem in finite form

08 p1585 A70-20956

Boundary value problems in one speed transport theory, applying Green function technique to neutrons with spherical symmetry

08 p1542 A70-21253

Asymptotic distribution of operator eigenvalues for self adjoint elliptic boundary value problem in unbounded region using Green function

09 p1711 A70-22148

Ferromagnetic crystal weakly coupled spin Green and correlation functions calculated for wide temperature range

09 p1740 A70-23193

Mixed boundary value problems with radiation-type boundary conditions solved by complex Green function, discussing water waves in irrotational motion

13 p2452 A70-29536

Monograph on nonlinear oscillation equations resonance solutions and solution stability, considering Green matrix, differential equations reduction to integrodifferential equations, etc

14 p2618 A70-31417

Electromagnetic field determination from oscillating vertical and horizontal electric dipoles above flat earth, demonstrating Sommerfeld formulation and dyadic Green function technique equivalence

16 p2861 A70-32974

Transient heat and mass transfer in adiabatic regenerator, solving mathematical model in terms of Green functions

17 p3197 A70-35542

Quadrature solution for elastic sphere deformation by axisymmetric normal loads, writing Green function of boundary value problem in finite form

20 p3719 A70-39379

Time harmonic waveguide scattering involving metallic obstacles, obtaining numerical solution by finite difference Green function method

20 p3586 A70-39469

Periodic boundary value problems with cyclic totally positive Green functions, considering applications in vibrating physical systems and spline theory

23 p4213 A70-44899

Green function theory of evaporation of He 3 atoms from liquid He 3/He 4 mixtures, determining energy distribution

24 p4377 A70-45255

GREEN THEOREM

U GREEN FUNCTION

GREENHOUSE EFFECT

Greenhouse effect in Venusian atmosphere, discussing cause of vertical temperature distribution established by Venera 4 probe

01 p0192 A70-11506

Radiative-convective equilibrium model to investigate photodissociation of water in Venus atmosphere, considering greenhouse effect

04 p0757 A70-15516

IR absorption properties of CO, HCl and sulfur dioxide measured for role in Venus greenhouse effect

08 p1579 A70-21567

Venus atmosphere and surface conditions, describing temperature, accumulation of carbon dioxide and runaway greenhouse effect

15 p2806 A70-32771

GREENLAND

Oxygen 18 concentration in Greenland ice core correlation to solar activity index, indicating earth temperature control by solar activity

13 p2489 A70-28909

GRIDS

Precision machining and repair of radioactive Plum Brook Reactor core fuel grid

01 p0140 A70-10322

Spectral energy transfer measurements in isotropic grid turbulence to determine validity of dynamical equation

03 p0468 A70-13785

Pulsed grid modulation for ion cyclotron resonance spectrometer

07 p1286 A70-19974

Ion-burst excited by pulsed mesh grid in plasma in connection with sheath structure

10 p1922 A70-23989

Grid turbulence unified analysis, estimating turbulence intensity, dissipation length and integral scale for any grid flow

10 p1871 A70-24976

Error propagation in rectangular grid leveling networks assuming fixed height of center of mass

11 p2045 A70-25798

Monograph on axially symmetric tandem grids for supersonic flow deceleration to subsonic speeds, using schlieren optical tests and pressure measurements

11 p1977 A70-26525

Alouette plasma resonance stimulated perpendicularly to magnetic field by planar dipole charge sheet and permeable grids

13 p2467 A70-29907

Dynamic stiffness, natural frequencies and mode shapes of prismatic and thin walled open grids, including warping and shear flange deformation

14 p2659 A70-31132

Closed form difference equations for finite element models in structural mechanics, noting plate and grid applications

16 p2990 A70-33672

Transonic compression grid functions, considering shock wave configurations

16 p2836 A70-33752

Plane diffuser grid profiles for subcritical velocities of oncoming flow, using wind tunnel test data

18 p3205 A70-36129

Plane electromagnetic wave diffraction by infinite grid above finite dielectric layer, calculating field distribution

19 p3375 A70-37281

Sheaths effect on capacitance of plane grid capacitor in plasma, discussing satellite aerials admittance

21 p3792 A70-42046

Rectangular and triangular grids with variably sized mesh elements for finite difference analysis of shell structures

23 p4272 A70-44709

GRIFFITH CRACK

Quasi-brittle fracture of plastic materials based on Griffith theory and crack propagation, analyzing real surface energy and work of plastic strain

01 p0212 A70-11562

Vacancies influence on macrodefect nucleus formation in single metal crystals under uniaxial strain explaining Griffith crack initiation

05 p0861 A70-15784

Stress distribution in vicinity of stress-free Griffith crack in elastic solid acted upon by symmetric distribution of body forces

05 p0930 A70-16084

Surface stress distribution to maintain Griffith crack in prescribed shape, using theorems of Fourier transforms and dual integral equations

05 p0930 A70-16086

Mixed boundary value problems of plane elasticity, solving stress field of central Griffith crack in wedge using singular integral equations

05 p0932 A70-16173

Equilibrium cracks in elastic bodies on basis of atomic interaction law, using Griffith problem to estimate bearing capacity

07 p1400 A70-18666

Elastic equilibrium of semiinfinite two dimensional medium with Griffith crack under axisymmetric load and free and rigidly clamped edges

08 p1594 A70-21771

Viscoelastic plate crack growth analysis within continuum mechanics framework as analog to Griffith problem

13 p2510 A70-28671

Griffith flaws limitation effect on glass matrix-tungsten composites strength, considering dispersed phase with wide particle size distribution

13 p2437 A70-28827

Brittle rupture cracks theory, discussing unstable /Griffith/ crack, stress intensity coefficient, propagation criterion, etc

13 p2517 A70-29715

Impact loaded Griffith-Irwin, Charpy and drop weight tear tests of fracture toughness for design, screening and materials acceptance

15 p2819 A70-32233

Rigid inclusion effect on stress distribution in isotropic infinite solid with Griffith crack under plane strain

16 p2994 A70-34250

Three dimensional stress fracture criterion for initial microcracking derived by generalizing Griffith flow theory

19 p3540 A70-37955

GRINDING [COMMINUTION]

Pulverization effects on lunar rocks albedo under full moon conditions for different grain sizes, noting inverse relation to absorption coefficient

14 p2649 A70-31214

GRINDING [MATERIAL REMOVAL]

NT METAL GRINDING

Temperature field in work piece generated by grinding wheel face investigated for cylindrical and surface grinding

10 p1894 A70-24291

Wear intensity of abrasives during fine grinding of Armo Fe, Ti and Ti alloys, comparing friction and chemical composition effects

15 p2743 A70-31640

Grinding by abrasive tape, superimposing transverse vibrations to improve performance and life

22 p4046 A70-42816

Automatic TV radioscopic X ray control for mass NDT of refractories and grinding wheels

24 p3468 A70-45723

GRINDING MACHINES

Tangential cutting force measurements during Ti grinding by microtools, noting properties of W, aluminum boride and zirconium carbide

04 p0697 A70-14466

Roller bearings convex conical surfaces grinding using centerless grinder

08 p1506 A70-21192

GROOVES

Radiant heat exchange for rectangular groove represented by integral equations using rapid iteration method

08 p1600 A70-21835

Capillary grooves effect on surface wetting and evaporation using heat transfer coefficients for grooves with triangular, semicircular and square cross sections

09 p1790 A70-23559

[ASME PAPER 69-HT-19] LF plane wave scattering from semielliptic groove in conducting ground plane noting validity for arbitrary polarization, incidence, directions and eccentricity

13 p2453 A70-29822

GROOVING

Teflon crosshatched ablation patterns elimination by grooving or glass filler addition

17 p3193 A70-34483

GROUND BASED CONTROL

NT AIR TRAFFIC CONTROL

NT RADAR APPROACH CONTROL

Terminal area approach control sequencing, using digital computer to allocate identification mode and landing time slot

02 p0332 A70-11971

Display/control system and key technical decisions at Manned Space Mission Control Center, discussing command consoles

05 p0829 A70-16194

Air traffic control system using ground controlled satellite-borne phased array antenna to overcome UHF downlink path loss

11 p2077 A70-25421

[AIAA PAPER 70-497] Ground ATC facilities, discussing landing, automation, surveillance, communication and navigation

11 p2079 A70-25723

V/STOL aircraft ground guidance systems using microwave instruments for approach and landing

12 p2266 A70-27458

[SAE PAPER 700322] Intermittent positive control system for issuing commands to normally uncontrolled aircraft for midair collision avoidance, discussing aircraft and conflict detection

12 p2267 A70-27634

Intermittent positive control (IPC) role in midair collision avoidance, using mathematical model to determine command frequency and implementation 12 p2269 A70-27913

Ground controlled remote manipulator spacecraft system through wideband radio link for satellite maintenance and repair 15 p2810 A70-31780

Apollo lunar landing flight control functions, organization, disciplines and activities at Mission Control Center 17 p3134 A70-35292

Computerized automatic ground equipment (CAGE) as intelligence system for checkout and control of launch vehicles and spacecraft 19 p3397 A70-37915

Lunik 16 lunar soft landing technique, discussing automatic and ground controlled mission phases 22 p4110 A70-43210

Upper Air Space Control Center Automatic Data Processing and Display System for air traffic control 24 p4323 A70-46238

GROUND CREWS

Aviation medicine, discussing pilots physical fitness and training, spatial orientation, ground crew, data flow, etc 08 p1451 A70-20977

Flying safety and human factors from job dissatisfaction in Japan Air Self Defense Force 08 p1453 A70-21794

Human engineering in weapon systems development, considering flying and ground personnel training plans 12 p2177 A70-27038

GROUND EFFECT

Ground proximity effect on rectangular wing, studying lift and pitching coefficients dependence on angle of attack 03 p0407 A70-13493

Pitching moment coefficient changes due to ground effect in fixed wing aircraft flight test method, considering constant angle of attack approach 04 p0619 A70-15394

Ram wing vehicles aerodynamics application to high speed ground transportation, studying effect on passenger ride quality [AIAA PAPER 70-142] 06 p0973 A70-18145

Ground reflection effect on plane uniform sound source distribution applicable to compressor and fan noise under far field conditions 09 p1726 A70-22240

Atmospheric model for flow crossing ground obstacle using nonlinear differential equation 09 p1718 A70-22848

Integral equation for radiation patterns from vertical antenna over variable impedance surface [AFCRRL-69-0315] 09 p1639 A70-23670

Super sonic booms occurrence and propagation, discussing aircraft operating conditions for prevention of effect on ground 10 p0000 A70-24130

Numerical solutions of thick cambered jet flap in ground effect for flat plate and diamond shaped airfoil [AIAA PAPER 69-738] 12 p2155 A70-27199

Ground effect for increasing lift during aircraft landing 13 p2345 A70-28973

Multiple jet flow exhausting into arbitrary crossflow in ground effect, solving continuity and momentum equations for jet path and induced velocity field 13 p2387 A70-29011

Lifting surface problem for finite span wing in ground effect using matched asymptotic expansions method 14 p2527 A70-30280

Ground effect visualization at low speed flow around aircraft models, discussing airbus, VTOL aircraft and Concorde 14 p2528 A70-30291

Aperture antennas admittance calculation, considering upper bound on error involved in approximating finite ground plane conductivity by perfect conductivity 20 p3599 A70-40316

Planar wing with end plates in ground effect, calculating minimum induced drag by approximation theory 21 p3743 A70-40919

GROUND EFFECT MACHINES

NT HOVERCRAFT GROUND EFFECT MACHINES

International agreement to govern hovercraft use covering application range, registry, rights, owner or user responsibility, leasing and goods transportation 01 p0220 A70-10373

Forward air cushion performance of tracked hovercraft entering tunnel, determining arrival of reflected expansion wave at vehicle front 02 p0226 A70-12313

Two seater hovercraft development, considering lift system, fan, transmission and structural designs and construction steps to keep within automobile cost range 03 p0414 A70-14148

NASA research studies supporting tracked air cushion vehicle (TACV) program illustrating

aerospace technology application to ground transportation [AAS PAPER 69-565] 04 p0622 A70-14639

Multiple skirt air cushion vehicle (ACV) pitch and heave dynamic characteristics, describing mathematical modeling and analog computer simulation 04 p0624 A70-15389

Water tests with N 300 Naviplanes confirming flexible skirt concept regarding speeds and stability 08 p1435 A70-20622

Wave resistance of pressure field of hovercraft drifting over water surface determined as definite integral based on Wehausen expression 09 p1609 A70-22219

Camber and twist distributions for closed ground effect wing optimum design for zero induced drag, employing linearized theory 10 p1801 A70-24158

Inviscid flow theory for ACV high speed peripheral jets, considering component inefficiencies, pressure losses, nozzle geometry, etc 12 p2156 A70-27211

Plenum-chamber air-bearing and labyrinth-seal types air cushion lifting mechanisms performance in simulated hovering flight 12 p2162 A70-27981

High speed commercial transport hovercraft economic factors, considering traffic needs, fares, service frequency, reliability, etc 13 p2347 A70-29158

Pneumatic suspension systems for air cushion skirts 16 p2841 A70-33759

Ground effect machine, discussing tactical transport support role 16 p2843 A70-34265

External aerodynamics role in handling qualities of amphibious hovercraft, discussing tests of hull shape, air cushion efflux and hollow models 17 p3017 A70-34919

Tracked air cushion vehicle dynamic heave response, examining flow characteristics, active lip control, guideway contact, acceleration response, etc 17 p3017 A70-35178

Hydrofoil and hovering craft design by fiber technology, discussing composite materials, whisker mechanical properties, polycrystalline fibers, matrix materials, etc 19 p3456 A70-38941

Hovercraft wind directional stability and control by cam operated fin-tab assembly 19 p3357 A70-38942

Bearing force and moment produced by motion of inclined plate supported by compressed air in ground effect machines with small angle of attack 20 p3557 A70-39140

Static and dynamic spring constants of peripheral jet air cushion vehicle in heaving motion, obtaining sinusoidal input response characteristics 22 p3960 A70-42279

Nonlinear heaving motion of plenum-chamber air cushion vehicles induced by sinusoidal ground irregularity 22 p3961 A70-42280

Peripheral jet ground effect machine model heaving motion, investigating static hover and forced and free vibration characteristics 22 p3961 A70-42281

Ground Effect Takeoff and Landing (GETOL) aircraft, evaluating energy absorption capability of air cushion landing gear in touch-down condition 22 p3961 A70-42282

Horizontal flight speed effects on aerodynamic characteristics of air cushion vehicles with elliptical planform 22 p3959 A70-42801

Hovercraft operational advantages and legal status 22 p4127 A70-43499

GROUND HANDLING

AIRLORD system consisting of central data processing and I/O units for predeparture handling of passengers and freight at airports 11 p2013 A70-25365

Performance standards for intra-airport batch type people-moving systems, discussing seating requirements, platforms and stations, communications and power systems, etc [SAE PAPER 700260] 12 p2206 A70-27432

Air terminal and ground transfer design to provide improved access to aircraft and total transportation time reduction 12 p2208 A70-27992

Aircraft ground damage during maintenance and servicing 15 p2675 A70-32210

Mobile lounges and airport productivity concepts for optimal handling of passengers at airport terminal [AIAA PAPER 70-918] 17 p3064 A70-35830

C-5 aircraft cargo loading system for terminals minimizing ground time 17 p3064 A70-35831

Airport terminal design, describing electromechanical baggage handling and sorting systems [SAE PAPER 700261] 18 p3237 A70-36822

Jet fuels ground handling at airfields, describing flow monitors, filters, fueling techniques, etc 22 p4006 A70-43093

Air cargo management problems, discussing economics, ground handling, Jumbo jets, terminal facilities, mechanization, document handling, information flow, data systems, etc 22 p4006 A70-43269

Centralized terminal air cargo handling capacity, discussing Jumbo aircraft, airside ramp system, container movement, computer control and automation 22 p4006 A70-43270

Automated air cargo and data flow system with on-line computers, discussing handling, document management, load planning, information transmission, storage and mechanized freight systems 22 p3994 A70-43271

Computerized air cargo clearing, discussing London Airport Cargo Electronic-data-processing Scheme 22 p4007 A70-43272

GROUND OPERATIONAL SUPPORT SYSTEM

Integrated logistic support for cost effectiveness of ground communication system 01 p0220 A70-10114

GROUND RESONANCE

U GROUND EFFECT

U RESONANCE

GROUND RUN-UP

U ENGINE TESTS

U GROUND TESTS

GROUND SPEED

Doppler memory mode of ground speed and drift angle calculations analyzed by operators for possible errors 04 p0716 A70-14629

GROUND SQUIRRELS

Carbohydrate-phosphorus metabolites content in gophers brains under normal conditions during hypothermia and spontaneous warming at room temperature 01 p0012 A70-10055

GROUND STATE

Adiabatic and distortion approximations to two state treatment of ground state H atoms collisions at low energies 01 p1146 A70-10284

Ammonia spectral lines positions, intensities and half widths under Jovian conditions calculated, including ground state rotation and rotation inversion bands 02 p0368 A70-11820

Quadrupole moment matrix elements in adiabatic approximation for transition bands of hydrogen, HD and deuterium molecules in ground electronic state 02 p0342 A70-11822

Rotation-vibration matrix elements of quadrupole moments and absorption coefficients of ground electronic states of hydrogen, HD and deuterium 02 p0902 A70-11823

Excitation of ground configuration of Fe XIII for density and temperature range in solar corona, using proton collisions, electron collision strengths, etc 05 p0902 A70-16434

Radiative lifetimes of transitions to ground state for CS, SO and diatomic sulfur, showing relationship to absolute transition probabilities in terms of physiochemical applications 05 p0885 A70-16456

Self gravitating bosons or fermions equilibrium configuration in ground state, confirming Oppenheimer-Volkoff treatment approximation 08 p1581 A70-21741

Quasi-bound levels determination method for molecular hydrogen ground state 10 p1919 A70-24395

Molecular I ground state dissociation energy value, proposing spectroscopic reassignment 12 p2180 A70-26861

Quantum mechanical model of electron scattering by homonuclear diatomic molecule at ground state, calculating differential and integral cross sections for elastic scattering 14 p2618 A70-30113

Vibrational energies, rotational constants and inter-nuclear potential of ground state molecular iodine, using reanalyzed spectroscopic data 16 p2954 A70-33056

Carbon ground state correlation energy calculation, emphasizing assessment of truncation error sources 16 p2954 A70-33277

Li ion elastic scattering by He, calculating ground state interaction potential 16 p2956 A70-34310

Nitrogen deactivation by ground state atomic oxygen resulting in metastable oxygen atom as auroral green line source 17 p3080 A70-35770

Steepest descent method for determining lowest ground state eigenvectors for molecular wave configurations 22 p4062 A70-42747

GROUND STATIONS

NT DEEP SPACE FACILITY

NT INTEGRATED MISSION CONTROL CENTER

Gain, noise temperature and gain to noise temperature ratio measurement techniques for electrically large earth station antenna, recommending radar star technique

01 p0051 A70-11121

Automatic picture transmission (APT) ground station design for reception of weather satellite cloud cover photographs, discussing SNR

01 p0059 A70-11451

Receiving station geodetic coordinates computed from Doppler curves of artificial satellite, using method of differential corrections

02 p0254 A70-11757

Ground station geocentric coordinates from intersection of spatial directions in Baker-Nunn network determined by satellites

02 p0254 A70-11758

Automatic camera theodolite at Sophia satellite tracking station, discussing instrument constants

02 p0273 A70-11774

Azimuth between two stations of triangulation net determined by simultaneous observation of two satellites, discussing mathematical principles and applications in Europe

02 p0289 A70-11797

Satellite international system chain consisting of down path, receiving earth station and domestic receiver for Europe, North Africa and Middle East TV distribution

02 p0258 A70-12420

Intelsat satellites telemetry and telecontrol (TTC), describing Fucino plant design and operation

02 p0263 A70-12647

Small read-out stations for automatic picture reception from meteorological satellites, detailing design

02 p0382 A70-12648

Faraday rotation observations on Explorer 22 signals at two receiving stations, discussing comparative evaluation procedures and results

03 p0472 A70-12874

Synchronization of ground stations clocks by time scale comparison with overflying aircraft

[ONERA-TP-759] 03 p0487 A70-13642

Ground stations and low orbiting satellite system for automatic collection of meteorological data over Italy

03 p0581 A70-13832

Channels demand assignment between earth terminals of international satellite communication systems, examining multiple access problems

03 p0453 A70-14323

Data transmission from automatic space stations on Mars and Venus, considering relaying via artificial planet satellite or direct transmission to ground station

04 p0648 A70-14931

Ground station location, equipment and function for radio communication with German research satellites, noting NASA and ESRO cooperation

04 p0664 A70-15304

Second antenna at Pleumeur-Bodou /France/ for satellite transmissions reception in Intelsat network program

05 p0826 A70-15981

Antenna-central building connecting equipment at Pleumeur-Bodou space telecommunication center, discussing frequency compression demodulators

05 p0819 A70-15985

Satellite communications influence on ground stations design, describing steerable antenna and receive and transmit configurations for domestic station

05 p0811 A70-16095

Spacecraft telecommunication and tracking systems in Gemini, Mercury and Apollo programs, emphasizing Apollo command and lunar modules equipment and mission ground stations

05 p0813 A70-16326

Earth resources survey aircraft system producing optical spectrum imagery of continental U.S. with photometric and photogrammetric fidelity

05 p0850 A70-16686

Magnetic storm /14 September 1966/ observation by Explorer 33 in geomagnetic tail and by polar stations, studying relation in magnetosphere and on earth

05 p0843 A70-16764

Microelectronic L-band phase-lock loop receiver for data transmission between earth stations and satellites

06 p1017 A70-17338

Simultaneity circle for calculating spatial direction of straight line joining satellite observation stations, noting time factor role

06 p1139 A70-17548

Spatial direction Riga-Cairo determined using simultaneous photographic observations of Pageos A satellite

06 p1054 A70-17550

Airborne and ground based radar data on thunderstorm echoes compared within framework of storm reflectivity model and radar theory

06 p1010 A70-18246

Gokhberg magnetovariational sounding method for single location analysis of magnetic storms early phases, comparing ground station network observations

07 p1277 A70-20440

Positive and negative correlations in F 2 layer perturbations by network of paired conjugate ionospheric stations at low latitude

07 p1277 A70-20450

Optimal distance between satellite communication system ground stations for surface network cost equivalent, analyzing economic efficiency for various cases

08 p1456 A70-20569

Optimal satellite communication system design concerning station spectrum and interference limits

08 p1459 A70-20805

Operational figure of merit of high performance antennas in communication satellite earth stations as function of design

08 p1471 A70-20825

German satellite ground station system central station design, discussing cooperation between aerospace institute and electronic company

08 p1481 A70-21368

Digital data display system designed for central station of German ground station system

08 p1462 A70-21369

ARCOM earth terminal for Domestic Satellite Communication System bringing telephone, TV and data service to northern Canada

09 p1656 A70-22945

Digital record message communication satellite network system involving synchronous satellites and small earth terminals

10 p1834 A70-24327

Satellite communication system using delta modulation for telephone service to large number single channel earth stations

10 p1834 A70-24329

Demand assignment economics relative to ground stations in satellite telecommunication systems

10 p1838 A70-24360

Intermeshed TDMA systems efficiency in interconnecting ground stations in communications satellite systems, discussing rigid and variable burst lengths

10 p1839 A70-24363

Satellite capacity utilization for mixed earth stations network using SPADE concept/digital satellite communication system employing demand assignment and voice-activated carrier techniques

[AIAA PAPER 70-420] 11 p1996 A70-25404

Earth station antenna radiation diagrams with respect to interference isolation capability

11 p2015 A70-25414

UK UHF telemetry command station capabilities for Skynet satellites control, discussing equipment

[AIAA PAPER 70-415] 11 p2030 A70-25420

Low cost earth station and antenna for Canadian domestic satellite, bringing color TV to northern territories

[AIAA PAPER 70-432] 11 p2000 A70-25458

Plumeur-Bodou satellite telecommunications center, discussing antennas

11 p2031 A70-26009

SHF tactical satellite communications ground terminals, discussing system concepts, relationship to satellites and design problems

11 p2031 A70-26259

Cassegrain antenna feed system for satellite communication earth stations, noting low noise characteristics

11 p2011 A70-26716

Earth resources satellite ground data handling system providing initial processing, reproduction, indexing, storage, retrieval and dissemination functions

12 p2191 A70-26943

Atmospheric refractivity role in range errors from ground station to stationary satellite and in range rate measurement

12 p2189 A70-28058

Ground stationed automatic orbital operations system /AOOSY/ for satellites and space probes, discussing flow diagram and Siemens computer programming

13 p2372 A70-28398

Wind measurement with two spaced coherent-pulse radar stations for probing same region of meteor zone

14 p2582 A70-30317

Meteor observation station design and operation, describing calibration difficulties and reflecting points coordinates determination

14 p2583 A70-30331

Space-surface path loss due to atmospheric gases, rain and clouds, considering military ground site location for space communication

14 p2608 A70-30596

Lidar for cloud height measurements from ground and meteorological satellites

14 p2611 A70-31155

Electronically tracking antenna system for satellite reception in VHF range suitable for unmanned receiving stations

14 p2558 A70-31196

Cosmic rays geomagnetic bending and effective angles of approach for various ground stations

14 p2633 A70-31313

Ground sounding of ionization variations and vertical distribution using model, integral and normal laminar methods

15 p2729 A70-32078

Sirio satellite SHF transponder for experiments in atmospheric propagation and communication between ground stations

15 p2709 A70-32285

Spatial vectors determination by two laser measurements and one optical observation of artificial satellite

16 p2926 A70-33118

Low noise wideband amplifier design for Intelsat 3 satellite ground stations

16 p2877 A70-33415

Ground based photographic experiments using portable equipment during 7 March 1970 solar eclipse in North Carolina

16 p2977 A70-33840

Luminous emissions related to Apollo 12 mission observed in Belgium, discussing flight chronology, gas ejection, stage separation, etc

16 p2981 A70-34318

High power TWT for satellite communications ground stations, including Intelsat experience

17 p3054 A70-35282

Radar receiving station equipment for studying upper atmosphere by radio meteor echoes

17 p3047 A70-35605

Navigation aids evolution and trends, noting ground stations, Intelsat 3 and navigation satellites

17 p3048 A70-35879

Loran C principles, ground station operation and navigation equipment

17 p3135 A70-35881

Small earth stations to link isolated areas with Intelsat network, discussing costs

18 p3229 A70-36957

Solar flare of 25 February 1969 ground observations comparison to satellite data, measuring magnetic fields, radio emission, sunspots, ionospheric effects, etc

19 p3513 A70-37497

Ground station to retrieve and process data recorded on airborne digital magnetic tape instrumentation system for Hawker Siddeley Harrier flight development

19 p3384 A70-38550

Earth resources ground data processing in image formats from sensors in aerospace platforms, discussing collection control, image storage, retrieval, etc

20 p3591 A70-39058

Communication satellites systems for civil application, considering ground stations design, regional communication, ATC and maritime communications and navigation

20 p3585 A70-39409

SKYNET PCM telemetry and command station, discussing system design, pseudomonopulse feed, command and computer subsystems, etc

20 p3589 A70-40322

Small ground stations in communication satellite systems involving regional telecommunication, TV distribution, air traffic and maritime applications, data exchange, weather and education service

21 p3785 A70-40764

Multistation observations of long range field aligned backscatter irregularities in F layer, using ray path calculations

21 p3814 A70-40940

Fences and pits effectiveness for shielding satellite earth stations from local terrestrial facilities interference

21 p3789 A70-41342

Transportable earth station for satellite communications system, describing antenna design and transportation modes

21 p3798 A70-41344

Ground station requirements for transition to multitransponder INTELSAT 4 satellite, discussing interference filtering, group delay distortion, etc

21 p3789 A70-41346

Multiple beam earth station torus microware antenna for satellite communication with nonplanar field of view over geostationary arc

21 p3798 A70-41357

Interference coupling between satellite ground station and radio relay station due to rain scattering at SHF

22 p3990 A70-43201

Pc-1 and IPDP pulsations propagation characteristics from ground based measurements, discussing spectral structure, waveforms, polarization, time delay between different observation stations, etc

22 p4021 A70-43277

Eurospace Symphonie satellite communication system and ground facilities, discussing international and regional coverage

22 p4111 A70-43504

Communications satellites for offshore systems, noting development of small earth station

22 p3991 A70-43576

Electromagnetic interference reduction between communication satellite earth stations and microwave radio relay stations by pit shielding
22 p3991 A70-43577

Ground TV station network operating with communication satellites in remote areas
23 p4159 A70-43758

Low noise dual receiver system for satellite communication earth station using parametric and transistor amplifiers
23 p4169 A70-43791

Satellite orbital elements determination by differential correction procedure, considering observation stations distribution influence on accuracy
24 p4406 A70-45530

Doppler satellite measurements in semidynamic geodesy using data from Mediterranean ground stations
24 p4312 A70-45543

GROUND SUPPORT EQUIPMENT
NT GROUND OPERATIONAL SUPPORT SYSTEM

Power supply equipment with automatic control for category 2 airport lighting, discussing reliability and economic efficiency
01 p0055 A70-10300

Orbital space station operations requirements and interactions, considering experimentation, support vehicles, ground support and follow-on growth [AIAA PAPER 69-1062]
01 p0195 A70-10636

Airborne instrument landing systems and ground facilities analysis and specifications, examining future use of microwave frequencies
02 p0333 A70-11982

Large aircraft servicing, describing equipment and procedures
02 p0276 A70-12762

Superjets demands on airport fuel handling facilities [SAE PAPER 690559]
03 p0463 A70-13263

Digital telemetry systems for geophysical satellites, describing onboard and ground systems design criteria and experimental results
03 p0451 A70-13837

Airport fog attenuation systems design and operation consisting of power and communication cables linking diffusers to central control and command
05 p0830 A70-17092

Selection criteria for nonturbocharged air or liquid cooled reciprocating type prime movers used in aircraft ground support equipment [SAE-ARP-1052]
07 p1248 A70-18801

Propellant transfer unit for weapon or space vehicle systems, specifying aerospace ground equipment criteria [SAE-AIR-1129]
07 p1248 A70-18806

Aerospace ground air conditioning design, discussing ground support equipment, manuals, manufacturer catalogs, etc
07 p1248 A70-18808

Onboard and ground checkout systems for space station and space shuttle operations [AIAA PAPER 70-245]
07 p1251 A70-20373

Ground and onboard electronics systems for space shuttle vehicles, discussing role in equipment reliability and maintainability, life cycle costs, management control, etc [AIAA PAPER 70-261]
07 p1398 A70-20391

Real time simulation of space vehicle and ground support equipment by digital computer for launch programs checkout
16 p2870 A70-33733

PCM telemetry transmitters, command receiver and ground control for German research satellite Azur
16 p2890 A70-34349

Boeing 747 ground operations and airport services, discussing computerized check-in, baggage handling equipment, etc
17 p3019 A70-35808

Flight test and airborne data recovery and processing, discussing data format, recorder characteristics, ground equipment and time requirement
19 p3429 A70-38517

GROUND SUPPORT SYSTEMS
Aircraft ground support system analysis from airplane designers viewpoint [SAE PAPER 690561]
03 p0463 A70-13265

Exit geometry effects on peripheral jet device lift, considering operating height, curtain thickness, base extension, etc
04 p0619 A70-15388

Ground truth calibration for aircraft and spacecraft earth resource sensors, discussing ground truth instrumentation, procurement procedures, reduction techniques, etc [AIAA PAPER 70-296]
09 p1678 A70-22887

Space navigation for Apollo 11 mission, emphasizing ground and onboard systems, interfaces with guidance and use in phases of lunar landing
13 p2447 A70-28547

Ground support real time operating system 360 for manned spaceflight, discussing system features and performance
13 p2375 A70-29937

Real time computer complex /RTCC/ supporting role in Project Apollo, describing mission control center data interfaces, equipment configuration, software, etc
17 p3060 A70-35295

Space vehicle and mission control center telecommunications networks for Apollo lunar landing program, considering NASCOM relay system
17 p3047 A70-35585

Radio astronomy Explorer A attitude determination via disk-oriented programming ground support system for reducing and calibrating telemetry data, attitude prediction and command, etc [AIAA PAPER 69-983]
21 p3795 A70-41857

GROUND TESTS
NT COLD FLOW TESTS
NT PRELAUNCH TESTS
NT STATIC FIRING

Ground based space simulation of arc-type electrothermal propulsion systems, discussing test facilities
01 p0161 A70-10225

Shock tunnel type differential sensor for low range base pressure measurements on full scale flight reentry vehicles, discussing ground tests
01 p0089 A70-10843

Ground-based biological experiments on insects and frog eggs to investigate effects of space flight weightlessness and radiation on mitosis and meiosis
04 p0631 A70-14942

Altitude simulation equipment for third stage Europa 1 booster rocket
04 p0664 A70-15302

Design and qualification test criteria for components derived by enveloping peaks of shock response spectra in ground tests of missile stages explosive separation [SAE PAPER 690616]
05 p0922 A70-15849

Vitiated contamination effect on airbreathing engine ground testing, considering equilibrium, vibrational and chemical relaxation, condensation, combustion, mixing and engine performance [AIAA PAPER 69-456]
06 p1172 A70-17172

Air backflow in nuclear exhaust system duct for ground testing of NERVA engines, noting overpressure effect [AIAA PAPER 69-325]
06 p1027 A70-17174

Noise field from ground testing of nuclear rocket engines operated at various reactor power levels
06 p1133 A70-18234

Simulated Concorde kinetic heating system for ground studies of thermal stresses
07 p1250 A70-19744

Space transportation system booster and orbiter development ground and flight tests, considering vehicle size and reusability requirements [AIAA PAPER 70-276]
07 p1397 A70-20385

Ground and flight tests in aeronautical system development process as transfer of basic technology into cost effective operational systems [AIAA PAPER 70-381]
10 p1857 A70-24172

Ground-based and in-flight simulation using variable stability aircraft, investigating pilot rating [AIAA PAPER 70-354]
10 p1858 A70-24209

Aircraft ground and flight tests effectiveness planning, preparation and conduct for operational safety, noting Flight Controls Development Test Stand [AIAA PAPER 70-371]
10 p1806 A70-24843

Rocket plume effects impulsive ground test technique under simulated high altitude pressure conditions, discussing hardware simplifications [AIAA PAPER 70-399]
10 p1951 A70-24906

Ground based simulation for hypersonic reusable lifting reentry vehicle design with pilot-in-loop, discussing six degree of freedom simulation [AIAA PAPER 70-385]
10 p1861 A70-24920

Space station program development requirements, describing ground and flight tests synthesis [AIAA PAPER 70-377]
10 p1952 A70-24926

Integrated Test Program for S-3A Weapon System, detailing test sequence flow and interfaces to assure vehicle and avionics systems reliability and maintainability [AIAA PAPER 70-370]
10 p1959 A70-24931

Space shuttle program, considering vehicle configurations mission capabilities and cost estimates with emphasis on ground and flight tests [AIAA PAPER 70-739]
10 p1953 A70-25074

Optimum sequence integration and ground testing of Defense Communication System Phase II Satellite, considering vibration, shock, space simulation, spin/despin, RF and acoustic requirements [AIAA PAPER 70-447]
11 p2030 A70-25444

Ground testing apparatus with three degrees of freedom for artificial satellites attitude control systems, establishing mathematical model by digital and analog techniques
11 p2031 A70-26290

Italian polyvalent data acquisition system for ground space tests, discussing electronic instrumentation system
11 p2032 A70-26293

Aircraft equipment automatic test methods, comparing in-flight, on ground and second line testings
13 p2348 A70-29681

Mission simulation testing in thermal vacuum environment for Apollo Lunar Module, noting conformal skin heaters [AIAA PAPER 69-991]
15 p2718 A70-32515

Ground test reactor design based on colloid fueled reactor concept [AIAA PAPER 70-688]
16 p2950 A70-33587

Ground environmental simulation test for captive carrying cycling of air launched missiles
17 p3060 A70-35182

Ground test noise measurements accuracy and repeatability on JT8D turbojet engine
17 p3060 A70-35183

Ground vibration testing for aircraft and missile flutter prevention [ONERA-TP-816]
18 p3339 A70-36508

Mariner 1969 test and operations program evaluated by ground tests and flight results, giving flight acceptable spacecraft recommendations
19 p3533 A70-38819

Noise field from ground testing of nuclear rocket engines operated at various reactor power levels
20 p3689 A70-39688

SERT 2 spacecraft ion thruster ground tests and flight operation, tabulating performance data [AIAA PAPER 70-1125]
20 p3691 A70-40220

Flight simulation as aircraft design tool, discussing ground and in-flight simulation techniques [ICAS PAPER 70-41]
23 p4178 A70-44139

GROUND TRACKS
Baseline length and orientation of closely co-orbiting satellites estimated by combined onboard sensor and ground tracking data [AIAA PAPER 70-39]
06 p1146 A70-18186

High speed track facility for V/STOL aircraft tests, discussing characteristics and design
21 p3803 A70-40581

Baseline length and orientation of closely co-orbiting satellites estimated by combined onboard sensor and ground tracking data [AIAA PAPER 70-39]
23 p4243 A70-44505

GROUND TRUTH
Coastal areas remote sensing instrumentation and techniques, discussing data handling and analysis and ground verification of color and multispectral imagery [AIAA PAPER 70-299]
09 p1669 A70-22885

Nonimaging remote sensor data display in spatial registration with ground scene to determine sensor bore-sight position accuracy
12 p2229 A70-26940

GROUND WAVE PROPAGATION
Self contained and ground referenced radio systems combination for tactical air navigation, including Loran D and hybrid Loran /HYLO/
04 p0716 A70-14628

Ground wave electric field intensity prediction model in EMC applications, discussing soil conditions and polarization effects
07 p1336 A70-20217

Electromagnetic ground wave propagation, deriving exact solution from two dimensional cylindrical earth model with any number of homogeneous sections
23 p4164 A70-44405

GROUND-AIR-GROUND COMMUNICATIONS
Transistorized lightning protected VHF ground antenna for air traffic communication providing high operational safety standards
03 p0459 A70-14297

Pilot emotional state during stressful situations from tape recorded vocal utterances of air to ground radio communications using spectrographic analysis
06 p1000 A70-17297

Spot III satellite-supported system for transoceanic aircraft navigation, traffic control, voice and data communication, etc
07 p1331 A70-19291

Secondary radar application to assist ATC achieving air to ground communications reduction
08 p1541 A70-21020

Independent burst and burst coherent TDMA methods compared for ground station-satellite communication
10 p1836 A70-24340

Position location and aircraft communication equipment concept and Experimental PLACE System providing ATC two-way voice and digital data communications via geostationary satellites
12 p2269 A70-27921

Ground stationed automatic orbital operations system /AOOSY/ for satellites and space probes, discussing flow diagram and Siemens computer programming
13 p2372 A70-28398

Pictorial display area navigation system for air traffic control in terms of cockpit utilization, interface with ground navigation aids, parallel multiple routes, etc [AIAA PAPER 69-798]
13 p2449 A70-29171

Multifunctional multimode avionics design integrating communications, navigations and identification subsystems /ICNI/
13 p2368 A70-29619

- Space-to-ground link wideband digital laser communications system design and performance tests
21 p3787 A70-41331
- Millimeter wave space-to-space and space-to-ground satellite communication links frequency allocation problems
21 p3787 A70-41335
- Ground station requirements for transition to multitransponder INTELSAT 4 satellite, discussing interference filtering, group delay distortion, etc
21 p3789 A70-41346
- ATC data link communications system speeding information flow between controller and pilot
21 p3789 A70-41348

GROUND-TO-AIR MISSILES U SURFACE TO AIR MISSILES

GROUP THEORY

NT HOMOMORPHISMS

- Explicit spinor basis states for irreducible unitary representations of spinor covering group of deSitter group $SO(4,1)$
02 p0344 A70-12282

- Invariant group study of free atmospheric convection equations at combination of Grashof numbers, Prandtl numbers and boundary conditions, noting infinite flux velocity
02 p0328 A70-12387

- Poincare invariance compatibility with general relativity, discussing Brandt groupoid, decomposition and local groups
06 p1106 A70-17540

- Group theory investigation of three photon light scattering tensor for all vibration modes of specific crystal classes
07 p1299 A70-19861

- Genetic theory application to selection of partial descriptions for algorithms group handling
08 p1466 A70-20875

- Locally compact topologies on group G and corresponding continuous irreducible unitary representations, noting existence of subgroup
08 p1534 A70-21276

- Zeta-Kleinian functions derived from Abelian functions
[ONERA-TP-800] 09 p1712 A70-22837

- Maximum principle optimality for nonlinear two group parameter control applicable to plants described by integrodifferential and delay equations
10 p1911 A70-25184

- Multidimensionality in complex control systems, discussing circuit and oscillation theory, decomposition, variational problems, finite automata and group theory
11 p2023 A70-25602

- Fourier transform calculations on finite Abelian groups
12 p2261 A70-27423

- Tensor and torsion functors on Abelian semigroups
13 p2440 A70-29076

- Boundedness of solutions and higher derivatives for degenerate matrices, showing dependence on characteristic numbers and linear groups
13 p2443 A70-29744

- Semigroup B , uniquely divisible range space for compact divisible commutative semigroups
16 p2941 A70-33095

- Matricial group representation theory for constructing elastic vibration equations of symmetric flexible mobile controlled members
17 p3180 A70-35293

- Linear representations of symmetry groups and use in discrete automatic control systems
18 p3290 A70-36070

- Group variational procedure for first integrals of nonconservative dynamical systems
19 p3458 A70-38060

- Power law fluid flow past suddenly accelerated wall, applying group theory to similarity solutions
19 p3406 A70-38444

- Cyclic q -ary codes invariant under linear group substitutions using polynomial method
24 p4313 A70-46062

GROUP VELOCITY

- Group delay characteristics of C band nondegenerative parametric amplifier determined by Nyquist method and compared to phase frequency derivative measurement
03 p0458 A70-14037

- Radially nonsymmetric stress wave propagation from tip of moving crack in infinite plates, deriving minimal group velocity
05 p0941 A70-16516

- Group velocity of spiral density waves propagating in disk galaxies implying self destruction, discussing possible replenishment sources
05 p0919 A70-16929

- Electromagnetic waves phase modulation index during propagation in nonlinear media found dependent on mismatch between interacting waves group velocities, relaxation time and losses
07 p1227 A70-18763

- Group velocity and propagation of hydromagnetic waves in ionospheric duct, comparing calculations and measured values
10 p1875 A70-24442

- Refractive index and group velocity in moving dispersive half space/cold plasma or dielectric/ under incident wave from vacuum
16 p2859 A70-32936

- Wave propagation and group velocity in warm magnetoplasma, using adiabatic theory for ionosphere and far magnetosphere models
16 p2859 A70-32937

- Electromagnetic waves phase modulation index during propagation in nonlinear media found dependent on mismatch between interacting waves group velocities, relaxation time and losses
18 p3229 A70-37107

- Electrostatic ion waves in uniform magnetic field, calculating phase and group velocities as function of propagation angle for comparison with dispersion measurements
20 p3678 A70-39659

- Transmission factors of microwave filters with prescribed attenuation and group delay
22 p3997 A70-43173

- Phase and group velocity variations of LF transmission compared against crystal oscillator
23 p4163 A70-44228

GROUP 1A COMPOUNDS

U ALKALI METAL COMPOUNDS

GROUP 2A COMPOUNDS

U ALKALINE EARTH COMPOUNDS

GROUP 4A COMPOUNDS

- Group 4A difluorides vaporization thermodynamics and bond dissociation energies, tabulating mass spectra, vapor composition, reaction enthalpies, heats of polymerization and thermodynamic functions
07 p1319 A70-19889

- Combined solubility of group IVA metals and carbon in solid state molybdenum at various temperatures
09 p1704 A70-22754

- Preferred disorder and shock histories of chemical group 4A meteorites from metallographic and X ray diffraction, discussing preterrestrial shock loading
21 p3920 A70-41940

GROUP 6A COMPOUNDS

- Laser induced vaporization of Bi compounds with group VIA elements, analyzing vapor species, condensed phase and molecular configurations by mass spectroscopy
08 p1455 A70-21338

- Vapor composition and condensed phase structure of As and Sb compounds with group VIA elements analyzed by laser mass spectrometer
08 p1455 A70-21339

GROUP 7A COMPOUNDS

U HALOGEN COMPOUNDS

GROWTH

- NT CROP GROWTH
NT CRYSTAL GROWTH
NT CZOCHRALSKI METHOD
NT EPTAXY

- Single and combined hypoxia and hypercapnia effects on growing rats, discussing body weights, blood and histological measurements
13 p2357 A70-29948

- Involuntary vectorcardiographic signs of right ventricular hypertrophy
17 p3025 A70-34859

- Serum growth hormone response to hypoglycemia in man following insulin administration, reviewing lumped parameter model
19 p3360 A70-38006

- Unicellular hot spring acidophilic alga *Cyanidium cadarium* cultured in pure carbon dioxide, examining packed cell volume, oxygen production and growth rate
20 p3572 A70-39492

- Microgram 2-nitro-1-butyl pyridinium sulfate /NBPS/ inhibition of growth of *Bacillus subtilis* by blocking thymidylate synthetase
23 p4158 A70-44998

- Homogeneous magnetic fields effects on growth rate of *Saccharomyces cerevisiae* and *Micrococcus denitrificans*
24 p4306 A70-45102

GRUMMAN AIRCRAFT

- NT F-111 AIRCRAFT
GRUMMAN MILITARY AIRCRAFT
U MILITARY AIRCRAFT

GRUNEISEN CONSTANT

- Gruneisen parameter for metal and semiconductor single crystals obtained from measuring one dimensional thermoelastic response during exposure to pulsed electron beam
07 p1357 A70-20020

- Gruneisen ratios for polymeric materials, comparing values determined by ultrasonic and thermal studies
11 p2069 A70-25805

- Hydrostatic pressure derivatives of adiabatic elastic moduli of single crystal zirconium, noting high temperature Gruneisen-thermal expansion deviation
19 p3486 A70-37763

GUANIDINES

- Metabolism and biological activity of urea, citrulline, argininosuccinic acid in organism ornithine cycle, discussing role in brain and liver
01 p0019 A70-10513

- NN dimethylguanidine for prevention of arterial lesions induced by cholesterol in rabbits
01 p0020 A70-10707

- Methylating agents and nitrosoguanidine actions on polynucleotides, including ribonucleic acid
03 p0440 A70-13550

GUIDANCE [MOTION]

- NT AIRCRAFT GUIDANCE
NT COMMAND GUIDANCE
NT INERTIAL GUIDANCE
NT INJECTION GUIDANCE
NT MIDCOURSE GUIDANCE
NT REENTRY GUIDANCE
NT RENDEZVOUS GUIDANCE
NT SATELLITE GUIDANCE
NT SPACECRAFT GUIDANCE
NT STRAPDOWN INERTIAL GUIDANCE
NT TERMINAL GUIDANCE

- Book on optimal control and guidance theory covering state and transition equations and canonical forms of linear systems, systems stability, servo loops, etc
07 p1246 A70-19668

- Rapid guiding system for high resolution astronomical observations using thermal expansion of electrically conducting wires
09 p1721 A70-22741

- Dual flow turbojet engines automatic control and guidance characteristics
17 p3147 A70-34687

- Satellite launching rocket guidance and control based on implicit measurement
17 p3133 A70-35283

- Guidance and control and propulsion technology, discussing fluidic systems, digital computers and structural materials, solid and liquid propellant engines
17 p3179 A70-35284

- Second order approximations to velocity required concept for boundary value problems in guidance, deriving Riccati equation and position required concept
20 p3666 A70-39518

- [AIAA PAPER 70-1015] ACRA supersonic antitank missile with IR laser beam guidance system
22 p4110 A70-43212

GUIDANCE SENSORS

- Inertial navigation system with gyrocompass sensor, deriving equations for continuous orientation determination within gimbal system, estimating errors
03 p0522 A70-13372

- Flight test evaluation program for airborne multisensor electro-optical display systems performance in TV mode under variety of optical conditions
07 p1289 A70-20403

- Strapdown redundant experimental sensor inertial navigation package containing gyros and accelerometers, discussing signal real time processing by digital computer
21 p3849 A70-41858

GUIDANCE STABILITY

- U CONTROL STABILITY
U GUIDANCE [MOTION]

GUIDE VANES

NT JET VANES

- Two stage axial flow compressor with variable pitch guide vanes, discussing HF vibration reduction of rotor blades
01 p0166 A70-11419

- Axial flow compressor off-design performance optimization by adjustable inlet guide vanes with variable trailing edge flaps
18 p3304 A70-36846

GUIDED MISSILES

U MISSILES

GUINEA PIGS

- Guinea pig cochlear hair cell damage after exposure to impulse noise
02 p0236 A70-12322

- Local stress effect on immunocompetent cells differentiation in guinea pigs lymphatic ganglia, noting increase in number of antibody producing cells
05 p0803 A70-17114

- Sinusoidal vertical vibration effect on adrenocortical function in guinea pigs
06 p0992 A70-17424

- Quantitative characteristics of central compensatory process, investigating nystagmus responses in guinea pigs subjected to bilateral labyrinthectomy
06 p0995 A70-17806

- Z axis acceleration and high temperature effects on guinea pig carbohydrate metabolism, discussing blood and muscle tissues composition
07 p1202 A70-18798

- Cochlear microphonics in guinea pigs using analog equivalent electrical circuit
11 p1992 A70-26494

GULF STREAM

- Satellite IR measurements of surface horizontal temperature structure of Gulf Stream compared with ship and aircraft data
05 p0844 A70-17104

GUMBEL THEORY

U RANGE [EXTREMES]

GUN LAUNCHERS

Global meteorological sounding network requirements, restraints and sensors, considering gun launched meteorological probe role

01 p0054 A70-10082

Meteorological guns for synoptic sounding of stratospheric circulation, discussing system characteristics and operations

07 p1250 A70-20280

Optimum drogue gun firing angle of stabilization times for MEW [Minimal Envelope and Weight] ejection seat system, considering zero and high velocities [AIAA PAPER 70-1208]

21 p3751 A70-41810

GUNFIRE

Protection methods for increasing ground fire survivability of military aircraft hydraulic systems classified by cost, system and component design criteria

05 p0797 A70-15777

GUNN EFFECT

Planar Gunn effect devices using various surface electrode configurations, discussing limitations by breakdown on Ga arsenide exposed surface

01 p0049 A70-10287

Delay times elimination in pulse operated X band Gunn effect oscillators, using RF power injection

01 p0050 A70-10463

Microwave circuit for increasing Gunn oscillators injection locking capabilities and reducing FM resulting from bias-voltage fluctuations

01 p0050 A70-10783

Gunn effect bibliography supplement [1960-1968/]

01 p0159 A70-10799

Microwave generation and amplification using Gunn effect semiconductor devices

01 p0160 A70-11289

IR light beam modulation in Gunn oscillator near fundamental edge of GaAs, investigating mechanism

03 p0539 A70-13160

N-GaAs pulsed Gunn effect oscillators for decimeter band, discussing synchronization by external sinusoidal current

03 p0499 A70-13204

Cavity resonator linear excitation by Gunn diode, considering external circuit effects on oscillation conditions and GaAs single crystal parameters

03 p0457 A70-13965

GaAs microwave diode Gunn oscillator subharmonically injection phase locked at low frequency ratios

03 p0459 A70-14041

Frequency shift and FM noise of uncontrolled Gunn effect diode and reflex klystron oscillators

05 p0818 A70-15774

Self excited microwave mixer and transmitting oscillator using Gunn diode applied to short distance Doppler radar

05 p0822 A70-16678

Step recovery frequency shift keyed retimer using Gunn effect FSK pulse regenerator for microwave communication

07 p1237 A70-20285

Millimeter wave CW Gunn oscillators construction by packaging free from spurious resonance, using sapphire ring and Au cap

08 p1468 A70-20482

Wideband tunable CW Gunn effect oscillator design, discussing microwave circuit effects on performance

08 p1471 A70-20788

Gunn diode parallel combinations fabricated for X band with n-type GaAs crystals, discussing output power at CW operation

08 p1477 A70-21296

Negative differential conductivity effects in Gunn domain GaAs semiconductors, discussing physical properties and microwave applications

08 p1556 A70-21303

P-n junction avalanche and bulk Gunn effect microwave oscillators, analyzing IMPATT and TRAPATT modes

09 p1644 A70-22224

Microwave Gunn oscillators loaded Q factors determined on basis of frequency changes resulting from constant-depth probe movement along output line

09 p1645 A70-22601

X band Gunn oscillators amplitude modulation by pulse signals from another Gunn diode

09 p1646 A70-22707

Microwave conductivity and limiting frequency in Gunn effect GaAs using drifted Maxwellian

09 p1739 A70-22849

Broad band power amplification with Gunn effect diodes, describing frequency response and saturation characteristics and FM/AM noise spectrum measurements for reflection amplifier in X band

10 p1847 A70-23886

Gunn oscillator current noise correlation with frequency modulation noise

10 p1848 A70-24230

Impact ionization effects in electric field domain on stability of current-voltage characteristics of Gunn diodes

11 p2020 A70-26813

Temperature effects on width of current-voltage characteristics of GaAs Gunn oscillators

11 p2020 A70-26819

GaAs vapor phase epitaxial growth characteristics noting applications to Gunn diodes

11 p2020 A70-26826

Epitaxial or bulk GaAs for Gunn diodes in high power microwave oscillators

11 p2021 A70-26828

Dispersion relation derived for space-charge waves propagating in thick Gunn diode, showing validity limit of one dimensional approach

12 p2194 A70-27164

Tapered Gunn effect microwave oscillators frequency tuning by resistive quenching of high field domain

12 p2199 A70-27986

X band Gunn oscillators for binary FSK regenerator operation employing signal injection triggering

12 p2199 A70-28015

High speed linear phase and amplitude modulation of X band Gunn oscillators

12 p2199 A70-28016

Shielded-cathode mode Gunn oscillators to eliminate constraints on operating frequency

12 p2200 A70-28056

HF quenched-domain mode [Q mode] Gunn effect oscillator in single frequency operation using signal analysis, obtaining instantaneous I-V transfer characteristics

12 p2202 A70-28162

Gunn oscillator voltage supply influence on domain capacity, considering frequency stability

13 p2377 A70-29302

Gunn diodes I-V characteristics with as function of carrier concentration/mobility and diode length, noting role of impact ionization in strong electric field

13 p2378 A70-29408

Millimeter waves generation by tunnel, Gunn and avalanche diodes, tabulating frequency, efficiency and power data

14 p2548 A70-30435

GaAs Gunn devices oscillatory modes under various operating conditions

14 p2557 A70-31158

Gamma radiation effects on GaAs Gunn diodes, measuring Hall effect, low field resistance, output power and FM noise in X band cavity

14 p2558 A70-31322

Gunn diode simulation with variable cross section, showing subthreshold and mode oscillograms

15 p2707 A70-31510

High pulse repetition rate digital systems signal processing using Gunn effect diodes

15 p2710 A70-32583

GaAs microwave devices including diffused varactor, Schottky barrier and Gunn diode, discussing single crystals preparation and epitaxial growth layers

16 p2873 A70-33293

SHF pulsed Gunn effect GaAs oscillators for nsec pulse length radar applications

16 p2875 A70-33398

Gunn oscillator external negative differential [END]/conductance broadband measurement noting effect of cavity control

16 p2875 A70-33398

Terminal negative resistance of X band Gunn diodes, discussing frequency conditions for modulation and parametric amplification

16 p2877 A70-33417

Doped Gunn diode domain field width, nucleation and annihilation dependence on electron drift velocity

16 p2879 A70-34044

Transverse magnetic field influence on Gunn effect characteristics of n-type GaAs

17 p3142 A70-34622

Phase control of locked negative resistance [Gunn]/oscillator under operational conditions, noting coupled varactor diode use

17 p3055 A70-35630

Wideband UHF amplification in bulk n-type GaAs during domain generation, comparing cut-off and Gunn frequency

17 p3143 A70-35684

Hysteresis effects during retuning of n-type GaAs Gunn oscillator with bias source and LCR circuit, showing range of domain damping by low field

17 p3055 A70-35689

Current oscillations of GaAs Gunn diodes over wide voltage range, discussing diode behavior dependence on polarity and applied voltage

18 p3230 A70-36197

Gunn phenomenon, discussing GaAs Gunn diodes preparation and applications

18 p3231 A70-36198

Equivalent circuit of Gunn oscillators for quenched domain mode operation, noting optimal working conditions

18 p3229 A70-36668

Magnetic surface loading of Gunn oscillators domain state for use as logic gates, pulse function generator, etc

19 p3387 A70-37819

Gunn effect pulse regenerators, describing random domain triggering rate voltage dependence comparison with Johnson noise predictions

19 p3387 A70-37820

Gunn effect devices with concentric cylindrical electrodes, examining oscillation natural frequency-applied voltage relation

19 p3392 A70-38900

Gunn effect in two-valley semiconductors with traps explained by model, assuming field-dependent trapping times and field-independent carrier generation rates

20 p3686 A70-39116

In-Au contacts for GaAs, discussing fabrication and performance tests on transverse Gunn mode oscillator

20 p3686 A70-39118

Ga-as Gunn diodes small signal admittance in dipole oscillation mode, analyzing RC model

20 p3598 A70-40062

Semiconductor diodes, discussing characteristics and applications of Schottky barrier, varactor, tunnel, Gunn and field effect diodes, etc

20 p3600 A70-40500

GaAs Gunn diodes design and fabrication, discussing material selection and operating heat removal

21 p3799 A70-41424

Microwave frequency marginal oscillator for electron spin resonance spectrometer, using Gunn diode in sample cavity

21 p3827 A70-41460

Microwave parameters for Gunn devices with low electric field, obtaining data on characteristics and operating mode

21 p3863 A70-41989

Gunn diode oscillators in domain suppression mode, showing dynamic I-V curve shape relationship to donor concentration and crystal thickness

22 p3997 A70-43128

Gunn microwave oscillators I-V characteristics in quenched and retarded modes, using piecewise linear approximation

23 p4168 A70-43778

Gunn effect, comparing intervalley scattering model to diffusion model for dynamic domain equilibrium

23 p4229 A70-43794

High stability phase locked Gunn microwave oscillator with internal crystal reference, discussing applications as signal generator, low noise Doppler radar sources, etc

23 p4172 A70-44013

Gunn oscillation stabilization in layered semiconductors based on space charge growth reduction via two-stream interaction between GaAs diode and passive bias semiconductor

23 p4230 A70-44196

Frequency dependence of Gunn oscillator maximum negative conductance

23 p4172 A70-44198

Impact ionization effects in electric field domain on stability of current-voltage characteristics of Gunn diodes

24 p4317 A70-45185

Temperature effects on width of current-voltage characteristics of GaAs Gunn oscillators

24 p4318 A70-45191

Carrier injection-limited Gunn diode wideband performance, deriving expression for admittance

24 p4319 A70-46081

GUNS [ORDNANCE]

NT ARTILLERY

GUST ALLEVIATORS

Free wing aircraft dynamic characteristics, discussing gust alleviation and handling qualities

[AIAA PAPER 70-947] 20 p3561 A70-39580

Self adjusting autopilot system based on invariance principle for stabilization against wind gusts

20 p3670 A70-39840

GUST LOADS

Slender delta wing aircraft dynamic behavior under vertical and lateral gusts, particularly during landing approach

[DGLR-69-52] 04 p0623 A70-15145

Incompressible flow past airfoils with oscillating jet flaps used as rapid lift and momentum generators in aircraft gust load alleviation and mode stabilization

[AIAA PAPER 70-79] 06 p0975 A70-18196

Empennage loads on T tail transport determined for combined vertical and lateral gust loads using real time analog-digital computer simulation

12 p2160 A70-27113

Gust response calculations compared with flight measurements for two fighter aircraft and jet transport to determine accuracy

[AIAA PAPER 68-892] 12 p2162 A70-28077

Load generation on two dimensional thin airfoil by yawed sinusoidal gust in incompressible flow, using lifting surface theory

13 p2344 A70-30025

Preliminary aircraft wing design for gusts or landing impacts inducing vibrations, inertia effects and dynamic overloads

14 p2655 A70-30177

- Wind gust data analysis for spacecraft design using power spectrum approach 14 p2607 A70-30580
- Helicopter gust response at high forward speed for various rotor loads noting effects of gust shape, gradual penetration, nonsteady aerodynamics and blade aerelasticity [AIAA PAPER 68-981] 14 p2531 A70-30855
- Sears function and lifting surface theory for harmonic gust fields in incompressible flow, modifying function for accurate interpolation of large numbers 14 p2528 A70-30860
- Flat plate airfoil unsteady lift due to chordwise velocity perturbations, using Horlock frozen gust pattern theory 22 p3957 A70-42303
- Similarity rules for sinusoidal gust loads on thin two dimensional wing in nonstationary subsonic flows 23 p4131 A70-43970

GUSTATORY PERCEPTION

U TASTE

GUSTS

- Numerical method for calculating gust effect on wing of complex platform at subsonic speeds by converting continuous to discrete processes 04 p0618 A70-15242
- Power spectral density functions of vertical gust velocities, comparing theoretical results and C-141A flight test measurements 04 p0624 A70-15384
- Maximum gust correlation with gust mean distribution within given hour determined from high speed anemometer 06 p1096 A70-17414
- Aircraft design formulas for equivalent gust velocity compared with vertical acceleration form, discussing design problems for large jets and T-tailed configurations 06 p0988 A70-18589
- Time averaging and length of record effects on horizontal wind speed variance, determining maximum wind gusts as function of height and averaging time 10 p1909 A70-23928
- Wind field statistical properties using model incorporating quasi-steady state speed, shear, gusts and small scale motions [AGARDGRAPH-115] 13 p2444 A70-28752
- Deformable and rigid wings aerodynamic characteristics with subsonic leading and trailing edges, calculating action of gust 15 p2671 A70-31486
- Radiosonde technique for locating atmospheric turbulence regions and estimating vertical air movement component in associated gusts 19 p3427 A70-38246
- Gust field in lowest atmospheric layer over homogeneous terrain, deriving statistical models and simulating effects on XV-5 V/STOL aircraft 21 p3750 A70-40784
- Mathematical modeling of atmospheric gusts in stratosphere, mountain wave and thunderstorm conditions relevant to aircraft design 24 p4371 A70-45420

GUTENBERG ZONE

- Gutenberg-Bullen interior model applied to fading of earth spheroidal oscillations 14 p2568 A70-30153

GYMNASTICS

U EXERCISE [PHYSIOLOGY]

GYRATION

- NT AUTOROTATION
- NT EARTH ROTATION
- NT LARMOR PRECESSION
- NT MOLECULAR ROTATION
- NT PRECESSION
- NT ROTATION
- NT SATELLITE ROTATION
- NT SOLAR ROTATION
- NT STELLAR ROTATION

GYRATORS

- NT MICROWAVE FILTERS
- Integrated directly coupled gyrator operating mode via comparison with switching elements, considering behavior under capacitance load and high pass filter application 21 p3797 A70-40793

GYRO HORIZONS

- Exact solutions class of nonlinearized equations of motion of adjustable two rotor gyrohorizon compass 07 p1288 A70-20176
- Drift of two platform gyroazimuth with stabilized base under harmonic or random vibrations 15 p2734 A70-31622
- Independent integrals of perturbed motion equations of spatial gyrohorizon compass 17 p3090 A70-35344

GYROCOMPASSES

- Gyrocompass composed of angular velocity integrators and interconnected by correction amplifiers, analyzing behavior during roll on vessel, determining error components 03 p0484 A70-13371

- Inertial navigation system with gyrocompass sensor, deriving equations for continuous orientation determination within gimbal system, estimating errors 03 p0522 A70-13372

- Dead zone initial disturbance of sensitive element dynamic coordinate in two rotor gyrocompass determined using method of averages 03 p0484 A70-13419

- Optimal damping time required for gyrocompass oscillations, allowing for maximum initial deflections 04 p0692 A70-15280

- North seeking declination gyrocompass design and operation with directing moment induced through bifilar suspension 05 p0844 A70-15775

- Drift error of correctable three degree of freedom free-floating astatic gyrocompass mounted on aircraft flying straight course at uniform speed 05 p0848 A70-16224

- Error analysis for pendulum type gyrocompass with indirect correction during irregular rolling, taking into account second infinitesimal order terms of equations of motion 07 p1278 A70-18735

- Rectilinear oblique harmonic vibration effect on gyrocompass with torsional suspension 07 p1278 A70-18737

- Gyrocompass with sensitive element mounted on horizontally stabilized platform and aligned with meridian by applied correcting moments, deriving equations of motion 07 p1282 A70-19532

- Differential equations of motion for sensitive element of gyrocompass with torsional suspension under small amplitude spatial vibrations, taking into account torsional and flexural rigidities 07 p1282 A70-19534

- Exact solutions class of nonlinearized equations of motion of adjustable two rotor gyrohorizon compass 07 p1288 A70-20176

- Two rotor gyrocompass unperturbed motion nonasymptotic stability as function of vessel speed and cruising latitudes 09 p1681 A70-23299

- Torsional vibration effect on gyrocompass with torsion suspension from studying sensing element forced motion, determining dynamic equilibrium position of sensor 11 p2048 A70-25578

- Unmanned Mars roving vehicle navigation subsystem feasibility study covering inertial and gyrocompass-odometer systems 11 p2080 A70-26211

- Time optimal control synthesis of fast acting gyrocompass mounted on fixed foundation and with hydraulic damper and torsional suspension of sensor 12 p2233 A70-27564

- Energy dissipation effect on complex parametric resonance and stability of two rotor gyrocompass on ship in motion 13 p2408 A70-29295

- Independent integrals of perturbed motion equations of spatial gyrohorizon compass 17 p3090 A70-35344

- Gyrocompassing for self contained lunar surface vehicles navigation, proposing local vertical determination method [AIAA PAPER 70-1003] 20 p3667 A70-39528
- Guidance and navigation systems precision azimuth measurement by star sighting and gyrocompass techniques 22 p4067 A70-42663

GYROFREQUENCY

- Electron gyrofrequencies computed from split pair bursts in 1966 compared with results from type II bursts in 1967 04 p0738 A70-14510

- Magnetospheric VLF emissions properties at frequencies below electron gyrofrequency 06 p1117 A70-17374

- Plasma instabilities in solar wind for frequencies near proton gyrofrequency, driving instabilities by electron and proton thermal anisotropies 08 p1561 A70-21261

- Whistler instability examined on gyrating electron beam interaction with cold background plasma propagating parallel to magnetic field 13 p2468 A70-29932

- Adiabatic bounce periods of particle gyrophase coherence in earth field for cyclotron echo and triggered emission analyses 20 p3621 A70-39343

GYROINTERACTION

U MAGNETIC RIGIDITY

GYROMAGNETISM

- NT GYROFREQUENCY
- Electromagnetic wave propagation in gyromagnetic medium, solving for field vectors in degenerate hypergeometric form 09 p1637 A70-23158
- Gyrotron efficiency increment at fundamental gyroresonance by applying magnetostatic field variable along length of interaction space 12 p2233 A70-27535

GYROPLANES

U HELICOPTERS

GYROS

U GYROSCOPES

GYROSCOPES

- NT ATTITUDE GYROS
- NT CONTROL MOMENT GYROSCOPES
- NT CRYOGENIC GYROSCOPES
- NT ELECTROSTATIC GYROSCOPES
- NT GYRO HORIZONS
- NT GYROCOMPASSES
- NT GYROSCOPIC PENDULUMS
- NT GYROSTABILIZERS
- NT NUCLEAR GYROSCOPES
- NT OPTICAL GYROSCOPES
- NT ROTARY GYROSCOPES
- NT TUNING FORK GYROSCOPES

- Two axis spherical gas bearing gyro for accurate measurements of space vehicle position and attitude rates while maintaining compatibility with exotic environments 01 p0086 A70-10308

- Conventional inertial gyro modified to provide specification performance for aircraft environments 01 p0086 A70-10312

- Floated single degree of freedom gyroscope and pendulous integrating gyroscope accelerometer, discussing design features as inertial sensors for future space missions 01 p0086 A70-10313

- Gyroscope bearing cross-torque control techniques, noting ball-group misalignment coupling [ASME PAPER 69-LUB-17] 01 p0101 A70-10388

- Solid state ring laser properties as oscillator, waveguide, interferometer and mechanical gyro considered for potential as rate gyro 01 p0108 A70-10417

- Flip-flop type intergimbal compensation system for gyroscopic integrators error reduction, obtaining natural oscillations constant amplitude 01 p0092 A70-10987

- Book on gyroscopic theory, design and instrumentation covering reference frames, Coriolis theorem, mechanical laws, etc 02 p0294 A70-11692

- Gyrotheodolites application to azimuth determination, discussing use for directional control, photogrammetry in geodetic measurements, etc 02 p0295 A70-11800

- Nonlinear gyroscopic navigation system intrinsic error derived as function of linear operator 03 p0522 A70-13373

- Probability theory for gimbal errors in directional gyroscopes under irregular rocking, using linearization of functions of random arguments 04 p0692 A70-15281

- Axial misalignment control of gimbal pivots and rotors in gyroscopes 04 p0692 A70-15282

- Optimal stabilization of spinning body motion about dynamic symmetry axis by controllable gyroscope 05 p0923 A70-16221

- Vertical gyroscope with nonlinear compensation circuit under random distortion of signal spectral composition 05 p0880 A70-16223

- Self acting, hydrostatic and squeeze-film gas lubricated bearings applications to gyroscopes, accelerometers, torque testers, etc 05 p0855 A70-16446

- Precession of aircraft mounted astatic gyroscope under constant and periodic moments of external forces, discussing roll angle and rotor axis deviations from inertia axes 07 p1282 A70-19533

- Finite structural rigidity of statically unbalanced three degree of freedom gyroscope influence on operation, discussing instrument error 07 p1282 A70-19535

- Steady motions and stability of gravitating gyrostat and spheroid, considering dynamically asymmetrical and symmetrical conditions 08 p1544 A70-20965

- Differential equations of motion for body with stationary point, allowing for Kovalevskaya conditions and assuming nonzero gyrostatic moment 09 p1726 A70-22149

- Combined gyromotors optimal starting and operating conditions, considering size and weight characteristics 09 p1680 A70-23146

- Three degrees of freedom astatic gyroscopes dynamic characteristics determination by vibration tests 09 p1681 A70-23300

- Fluid sphere gyro satellite nutation sensor 11 p2057 A70-26504

- Oscillating gyroscopes in satellite testing general relativity and earth gravitational field relation to stars 11 p2057 A70-26706

- Helicopter rotor, discussing conventional, semirigid, gyro and ABC systems in relation to roll balance and control 13 p2344 A70-28849

Stable, soupcan size, field replaceable, plug in/out gyro unit strapped to vehicle body without gimbals 13 p2409 A70-29480

Cost effective reliability prediction techniques, discussing precision gyros procurement by NASA 15 p2736 A70-31964

Motion and small vibration frequency stability of correctable gyroscope with correction moment at arbitrary angle with mismatch plane 15 p2738 A70-32154

Gyroscopic navigation systems errors as function of sensor errors in terms of arbitrary operators requiring optimization 15 p2773 A70-32155

Wearout life and reliability of rate gyros from field service test data 15 p2748 A70-32668

Apollo lunar module rendezvous radar redundant gyro system for reliability enhancement, discussing principles and logic 16 p2983 A70-34066

Gyroscopic drifts associated with angular support motions 17 p3133 A70-34960

Small swing angle detector for balloon payloads, using rate gyro principle 17 p3090 A70-35314

Satellite optimal guidance, discussing gyroscope application for stabilization and orientation control 17 p3181 A70-35691

Astatic gyroscope subjected to steady random translational vibration, optimizing parameters by mathematical model 18 p3257 A70-36136

Gyroscope in gimbal suspension on free base of four solid bodies connected by flat hinges 18 p3259 A70-36593

Gravity stabilized gyrostatt satellite attitude motion stability, using three dimensional diagram and Liapunov functions 18 p3334 A70-37061

Gyroscope dissipative function, using quasi-elastic gyroscope model and forced oscillation method 19 p3420 A70-37260

Test data interpretation by design margin techniques in poststorage reliability of high quality gyro assemblies 19 p3441 A70-38822

Reliability enforcement in design by competition and test program, using gyroscope example 19 p3433 A70-38842

Steady motions and stability of gravitating gyrostatt and spheroid, considering dynamically asymmetrical and symmetrical conditions 20 p3672 A70-39387

Ring laser gyro angular rate sensor for strapdown inertial systems [AIAA PAPER 70-1025] 20 p3631 A70-39510

Self calibrating TRIM gyromonitor inertial platform with gyroflex gyro, describing operation and performance [AIAA PAPER 70-1012] 20 p3667 A70-39521

Small low angular momentum /SLAM/ gyro for inertial guidance systems, discussing drift performance, float suspension, signal generator, flex leads, etc [AIAA PAPER 70-1011] 20 p3631 A70-39522

Fluidic gyro compatible with PDM missile guidance system, discussing spherical gas bearing design [AIAA PAPER 70-1008] 20 p3631 A70-39524

Seismic measurements at inertial test facilities, considering vibration environment relevant to single degree of freedom gyroscope performance tests [AIAA PAPER 70-951] 20 p3606 A70-39576

Hollow test platform for gyros and accelerometers used in inertial navigation [AIAA PAPER 70-952] 20 p3606 A70-39577

Beryllium use in inertial navigation as stable platform structure and control gyro, discussing physical properties, design concept, fabrication, service, cost and tradeoffs 20 p3639 A70-40451

Single degree of freedom gyroscope design factors applicable to strapdown guidance system, discussing torque-to-balance loop, multiple pulse bursting and error sources [AIAA PAPER 69-848] 21 p3849 A70-41859

Gyro drift rate mathematical modeling based on stationary and nonstationary time series analysis techniques with random process reduction to white noise residuals [AIAA PAPER 69-838] 23 p4197 A70-44557

Freely spinning gyrostatt satellites with dissipation, deriving rotational motion equations by osculating elements method 23 p4261 A70-44681

Gyroscope system steady states, showing dynamic couplings centering in finite angular precession rate case 24 p4335 A70-45630

GYROSCOPIC COUPLING

Gyroscopes orientation cross coupling effect on dynamic drift of three axis gyrostabilizer solved by method of successive approximation 07 p1278 A70-18736

Book on gyroscope couple stabilizing role on ships, satellites and stabilized platforms, discussing kinetic motion, gyroscopic precession, degrees of freedom, etc 07 p1283 A70-19665

Gyro system determining aerodynamic moment integral vector in wind measurements 24 p4340 A70-46402

GYROSCOPIC DRIFT

U GYROSCOPES
U GYROSCOPIC STABILITY
GYROSCOPIC PENDULUMS

Floated single degree of freedom gyroscope and pendulous integrating gyroscope accelerometer, discussing design features as inertial sensors for future space missions 01 p0086 A70-10313

Pendulous integrating gyro accelerometer float bearing wheel characteristics at high slew rates monitored by differential varmeter [ASME PAPER 69-WA/LUB-3] 04 p0698 A70-14770

Sectional gyroscopic pendulum stability in space of system parameters reduced to determining periodic motions regions by Hamiltonian equations 08 p1496 A70-21206

Vertical position stability of gyropendulum mounted on vibrating platform, showing foundation induced gimbal rotor parametric vibrations 12 p2233 A70-27563

Pendulous integrating gyro accelerometer float excursions minimization in random vibration environment /Saturn 5 launch/ by statistical technique 14 p2589 A70-31344

Nonperturbability conditions and equations of motion of bigyroscopic vertical below escape velocity 18 p3259 A70-36592

Pendulous integrating gyro accelerometer gas bearing wheel characteristics at high slew rates monitored by differential varmeter [ASME PAPER 69-WA/LUB-3] 19 p3436 A70-37618

Gyro pendulum mounted on randomly vibrating platform, calculating stability of rotor axis vertical position 22 p4039 A70-43557

GYROSCOPIC STABILITY

Single axis gyrostabilizer drifting motion mounted on aircraft subjected simultaneously to roll, pitch and yaw, deriving motion equations 01 p0091 A70-10986

Mobile hodograph in problem of gyrostatt motion about fixed point 01 p0094 A70-11430

Motion of body with fixed point reduced to single second-order differential equation, analyzing special cases of gyrostatic motion 01 p0145 A70-11437

Kirchhoff kinematic analogy applied to solution of gyrostatt motion, noting elastic rod deformation under torsion, using Kharlamov equations 01 p0094 A70-11441

Two degree of freedom gyroscopes stability with hydrodynamic grooved rotor bearings, describing parallel and conical whirling rotor oscillations 02 p0307 A70-12163

Steady motions stability of gyrostatt satellite in central Newtonian gravitational field 03 p0579 A70-13343

Optimal nonlinear correcting of vertical gyro obtainable with correction containing nonlinear elements with variable linearized coefficients 03 p0483 A70-13363

Power gyrostabilizer stability with dry friction at bearings, using point mapping to obtain system phase image 03 p0484 A70-13365

Gyrostatt motion stabilization with respect to unperturbed circular orbit vector radius, considering gravitational, aerodynamic, perturbation moments action and zero dry friction moment 03 p0484 A70-13370

Stability characteristics of two degree of freedom gyroscope having hydrodynamic grooved journal rotor bearings, discussing frequency of self excited oscillation [ASME PAPER 69-LUB-H] 04 p0689 A70-14872

Randomly oriented vibration effect on noncompensated three degree of freedom gyroscope with displaced center of gravity 04 p0692 A70-15278

Two degree of freedom gyroscope sensitivity threshold during gimbal vibration with respect to casing 04 p0692 A70-15279

Error sources affecting data comparison accuracy between gyro measurements and reference solutions and due to gyro axes misalignment and gimbal angular movement 04 p0692 A70-15327

Rotor-driven vibrational gyroscopic device dynamic characteristics, stability, transient delta function, signal response and sensitivity assessment 05 p0848 A70-16222

Drift error of correctable three degree of freedom free-floating astatic gyrocompass mounted on aircraft flying straight course at uniform speed 05 p0848 A70-16224

Weighting function of optimal correctable gyroscopic servosystem in random narrow band noise 05 p0880 A70-16225

Dynamic characteristics from equations of motion of gyroscope with allowance for structural damping forces between inner gimbal and rotor 05 p0852 A70-16961

Two degrees of freedom differentiating gyroscope response time decrease and phase and amplitude error reduction, using differential feedback 05 p0853 A70-17003

Closed form variational synthesis of optimally fast acting stabilization systems for rigid single axis gyroscopic platforms using integrating nonanalytic equations 06 p1103 A70-17860

Gyrostatt satellite equilibrium positions in circular equatorial orbit under action of gravitational magnetic and aerodynamic moments based on gyrostabilized satellite equations of motion 06 p1155 A70-17884

Rectilinear oblique harmonic vibration effect on gyrocompass with torsional suspension 07 p1278 A70-18737

Linear vibrations in gimbal suspension rotor and base, estimating gyroscope drift during base and rotor vibrational coincidence 07 p1279 A70-18738

Precession of aircraft mounted astatic gyroscope under constant and periodic moments of external forces, discussing roll angle and rotor axis deviations from inertia axes 07 p1282 A70-19533

Book on gyroscope couple stabilizing role on ships, satellites and stabilized platforms, discussing kinetic motion, gyroscopic precession, degrees of freedom, etc 07 p1283 A70-19665

Phase shift effect on astatic gyro axis drift and stability during periodic perturbations, describing motion by nonlinear differential equations 08 p1493 A70-20489

Sectional gyroscopic pendulum stability in space of system parameters reduced to determining periodic motions regions by Hamiltonian equations 08 p1496 A70-21206

Perturbed gyroscopic system consisting of disk hinged by rigid weightless rod, investigating stability condition at axial and equatorial inertia moments 08 p1496 A70-21210

Cyclic bending stresses in web of precessing disk-type gyroscope rotor, considering fatigue failure and forced vibration response 09 p1770 A70-22270

Directional gyroscopes with accelerated rotors on moving bases, deriving gyro errors as base motion functions 09 p1680 A70-23145

Two rotor gyrocompass unperturbed motion nonasymptotic stability as function of vessel speed and cruising latitudes 09 p1681 A70-23299

Space vehicle attitude stabilization by passive control moment gyros, discussing viscous and Coulomb friction effects 10 p1950 A70-24054

Moments equations for electrostatic gyroscope drift caused by rotor asphericity 11 p2048 A70-25559

Torsional vibration effect on gyrocompass with torsion suspension from studying sensing element forced motion, determining dynamic equilibrium position of sensor 11 p2048 A70-25578

Three degrees of freedom astatic gyroscope drift due to base vibrations according to harmonic law 11 p2048 A70-25579

Adjustable gyroscope errors under compensating-loop linearity zone limitation, showing saturation filtering influence on sensing element 12 p2233 A70-27562

Vertical position stability of gyropendulum mounted on vibrating platform, showing foundation induced gimbal rotor parametric vibrations 12 p2233 A70-27563

Quasi-linear elastic gyroscopic systems with distributed and lumped parameters, studying periodic solutions stability 12 p2238 A70-28194

Energy dissipation effect on complex parametric resonance and stability of two rotor gyrocompass on ship in motion 13 p2408 A70-29295

Doppler radar aircraft navigation system with gyroscopic reference platform and computer, showing error propagation dependence on velocity and latitude 13 p2449 A70-29621

Steady motions stability of gyrostatt satellite in central Newtonian gravitational field 14 p2653 A70-30718

- Open loop TV image motion compensation by image transducer with gyro demodulator analyzing errors in rate and rate-integrating gyros and AC pick-offs
14 p2588 A70-31190
- Pendulous integrating gyro accelerometer float excursions minimization in random vibration environment /Saturn 5 launch/ by statistical technique
14 p2589 A70-31344
- Orbiting gyrostats equilibrium orientations under gravitational torques, considering internal angular momentum effects
14 p2655 A70-31364
- Viscous friction force moments effect on gyroscope drift in gimbal suspension during base angular vibrations, obtaining drift velocity
15 p2738 A70-32153
- Optimal distributed feedback surface temperature control of inertial grade floated rate integrating gyroscope, minimizing instrument degradation
16 p2908 A70-33347
- Vibrational motion equations of interconnected bodies based on Newtonian approach, investigating gyroscopic vibration absorber
16 p2992 A70-34020
- Gyroscopic drifts associated with angular support motions
17 p3133 A70-34960
- Dual spin satellites considered as deformable flexible gyrostats, obtaining stability criteria
17 p3177 A70-35234
- Single axis gyroscopic stabilizer with floating-type integrating gyro, describing natural oscillations by differential equations of motion
17 p3096 A70-35701
- Error reduction methods for linear acceleration gyrointegrators measuring linear velocities
19 p3420 A70-37257
- Strapdown inertial guidance systems critical dynamic errors mathematical modeling and verification [AIAA PAPER 70-1029]
20 p3666 A70-39508
- Quasi-linear elastic gyroscopic systems with distributed and lumped parameters, studying periodic solutions stability
22 p4038 A70-43319
- Correctable gyroscope stability estimation by energy method taking into account nutation and precession motions
22 p4039 A70-43556
- Gyro pendulum mounted on randomly vibrating platform, calculating stability of rotor axis vertical position
22 p4039 A70-43557
- Earth quadrupole moment indirect effect on satellite gyroscope precession
23 p4217 A70-43799
- Gyro drift rate mathematical modeling based on stationary and nonstationary time series analysis techniques with random process reduction to white noise residuals [AIAA PAPER 69-838]
23 p4197 A70-44557
- ### GYROSTABILIZERS
- Inertial damper optimum parameter selection for achieving maximum nutation damping factor for gyroscopic stabilizer
01 p0091 A70-10985
- Single axis gyrostabilizer drifting motion mounted on aircraft subjected simultaneously to roll, pitch and yaw, deriving motion equations
01 p0091 A70-10986
- Airborne cartographic azimuthal instrument with reflecting prism type optomechanical assembly and trihedral pyramid gyroscope for stabilization
01 p0093 A70-11269
- Gyrostabilized satellite steady state motions in Newtonian force field having displaced satellite center of mass orbital plane relative to center of attraction
01 p0198 A70-11577
- Navigation system with twin gyro platform and Doppler sensor, discussing performance and cost advantage over inertial systems
02 p0334 A70-11987
- Optimal stabilization of free solid body equilibrium state with gyroscope, using solution of three flywheel system stabilization
03 p0484 A70-13364
- Power gyrostabilizer stability with dry friction at bearings, using point mapping to obtain system phase image
03 p0484 A70-13365
- Gyroplatform angular position with respect to reference stars from solving nonlinear differential equations, applying Liapunov method
03 p0524 A70-13366
- Gyrostabilized attitude reference platform for high altitude rotating research rocket payload alignment with preselected star
03 p0579 A70-13606
- Gyrostat satellite equilibrium positions in circular equatorial orbit under action of gravitational magnetic and aerodynamic moments based on gyrostabilized satellite equations of motion
06 p1155 A70-17884
- Gyroscopes orientation cross coupling effect on dynamic drift of three axis gyrostabilizer solved by method of successive approximation
07 p1278 A70-18736
- Kinematic drifts of three axis gyrostabilizer platform associated with angular oscillations using theory of finite rotations
07 p1282 A70-19531
- Stability of three axis indicator gyrostabilizer system consisting of stabilized platform mounted in three degree of freedom Cardan suspension
07 p1288 A70-20179
- Double axis gyrostabilizer with auxiliary tracking system of subtracking ring, analyzing system stability and operation
09 p1676 A70-22629
- Nutation damping in gyrostabilization for multispin satellites in terms of energy momentum and damping torque arguments
11 p2119 A70-25357
- Low sensitivity optimal controls synthesis for gyrostabilizer stabilization circuit using variable structure systems theory
11 p2048 A70-25580
- Gyroscopic platform stabilizers /GPS/ dynamic properties improved by compensation of perturbing torques
12 p2237 A70-28155
- Molniya 1 communication satellite attitude control involving automatic solar panel and antenna orientation, using powered gyroscopic stabilizers
13 p2499 A70-28387
- Gimbal influence on three axis gyrostabilized platform in spacecraft guidance during maneuvers
13 p2446 A70-28388
- Gyrostabilized platforms for astronomical observations, minimizing position errors
13 p2403 A70-28441
- Satellite orientation control and stabilization by gyro with statically and dynamically balanced rotors, showing steady motions and stability region augmentation
13 p2507 A70-29769
- Gravity stabilized gyrostat satellites internal angular momentum effect on nonlinear resonant attitude motions
15 p2810 A70-31785
- Gyroplatform for controlling rocket motion during rotation about longitudinal axis
19 p3420 A70-37258
- Small parameter effects on absolutely invariant systems under transient perturbation, analyzing gyrostabilizer performance
20 p3603 A70-39831
- Invariance conditions for inertial gyrostabilizer with powered stabilization system in presence of dynamic imbalance, noting improvement via compensating loop
20 p3670 A70-39846
- Satellite steady state motion and relative equilibrium position optimal stabilization by additional forces application
21 p3849 A70-40606
- Gyrostabilizer design based on composite optimal controls with respect to different regional criteria
22 p4040 A70-43559
- ### GYROSTATS
- ### U GYROSCOPES
- ### GYROTROPISM
- Direction fluctuations in radio wave scattering in turbulent gyrotropic medium using Einstein-Fokker-Kolmogoroff equation
04 p0653 A70-15722
- Magnetic field equation for gyrotropic and anisotropic turbulence, observing large scale magnetic field generation
12 p2210 A70-27546
- Direction fluctuations in radio wave scattering in turbulent gyrotropic medium using Einstein-Fokker-Kolmogoroff equation
14 p2550 A70-30806
- Gyrotropic waveguides parameters computer calculation based on inhomogeneous isotropic region, taking into account discontinuities
19 p3378 A70-37736
- Electromagnetic scattering by homogeneous gyrotropic cylinder, discussing matrix equations formulation and solution by reciprocity theorem
23 p4165 A70-44959
- ## H
- ### H ALPHA LINE
- Chromospheric average velocity field near sunspots determined from M alpha line absorption elements wavelength shifts
01 p0176 A70-10247
- High reflectivity mirror construction for H Lyman alpha line using vacuum deposited Al layer coated by magnesium fluoride
02 p0299 A70-12367
- Night airglow emission intensities during IQSY concerning Na, OH and H alpha lines compared with intensities during IGY
02 p0292 A70-12433
- Classical path methods for treating Stark spectral line broadening in plasmas illustrated by Lyman alpha line of hydrogen calculations
04 p0726 A70-14670
- Excitation of H-alpha and H-beta lines in night sky, calculating solar L radiations variation with altitude
04 p0679 A70-15075
- Chromospheric fine structure photographed at H alpha line center, discussing size, lifetimes and relationship between dark and bright mottles
05 p0910 A70-16428
- High resolution observations of low chromosphere beyond limb at H-alpha line center revealing fine structures, identifying chromospheric spicules with dark mottles
05 p0910 A70-16429
- H alpha line for emission nebulae analyzed by Fabry-Perot etalon, noting Doppler profile
05 p0917 A70-16907
- Transition probability and Stark profile of H alpha standards for absolute intensity calibration of spectroscopic data from thermal shock tube plasma
05 p0853 A70-17083
- Solar flare H alpha brightness measurement from photograph taken through birefringent filter, deriving flare morphological changes from isophotes
06 p1135 A70-18004
- X ray and H alpha emissions associated with solar proton flares, correlating rise time with solar cosmic rays
06 p1137 A70-18547
- H alpha brightening areas related to sunspot magnetic fields configuration and solar proton flares
07 p1369 A70-20072
- Spectral line intensities in hydrogen plasma, calculating relative intensities and Balmer line width for various electron temperatures and optical thicknesses in H alpha line
07 p1389 A70-20205
- Longitudinal magnetic field measurement along H alpha line of solar prominence
08 p1560 A70-20838
- Hydrogen 109 alpha recombination line emission in galactic H II regions surveyed at National Radio Astronomy Observatory
10 p1936 A70-23942
- Cygnus X region surveyed with NRAO radio telescope, estimating visual absorption by comparing radio and H alpha emission
10 p1937 A70-23943
- Alpha recombination line emission from galactic center detected, discussing possible origins in continuum source or interstellar medium
10 p1947 A70-24995
- Supergranules /convective cells/ development shown in quiet sun filtergrams of H alpha chromospheric network taken above Arctic Circle
11 p2109 A70-25741
- Onset, mass motion and flash phase in B2 solar flares observed in filtergrams spanning H alpha line
11 p2105 A70-25748
- Continuum spectra of well-resolved thermal and nonthermal galactic sources compared with H-alpha recombination line
12 p2296 A70-26898
- Absorption at solar H Lyman alpha line by earth hydrogen atmosphere measured as function of altitude from Aerobee flight spectrograms
12 p2222 A70-27182
- Dark band in H alpha solar chromosphere above photospheric limb, outlining approaches to obtain spectrally pure observational results
13 p2486 A70-28627
- Stark broadening calculations of H alpha and H gamma hydrogen lineshapes
14 p2620 A70-31303
- Cygnus loop nebula H alpha line halfwidths and radial velocities
15 p2802 A70-32482
- H alpha and H beta lines electrodynamic broadening with linear Stark effect, calculating relative intensity
15 p2777 A70-32490
- H alpha and Fe I lines, calculating velocity effects on profiles for differentially moving atmosphere
15 p2804 A70-32616
- Orion Nebula photographed at H alpha line with half angstrom filter
15 p2807 A70-32805
- Orbiting solar telescope design for solar disturbances location and monitoring in H alpha line
16 p2907 A70-33188
- Coronal structures relationship to chromospheric features in H alpha and Ca II K
16 p2977 A70-33843
- H alpha filtergrams of sun during solar eclipse of 7 March 1970, showing bright plage area
16 p2980 A70-34226
- Luminosity effects in Balmer lines of early type stars, noting H alpha equivalent width decrease
17 p3170 A70-35388

- Solar atmosphere vortex ring observation in H alpha light / 2 December 1969/ 20 p3703 A70-39022
- Particle ejections in solar atmosphere and chromosphere structure, discussing dark halo exhibited by H alpha line in active region 20 p3699 A70-39464
- H alpha chromospheric network lifetime from time lapse photographs 20 p3711 A70-40409
- H alpha flares occurrence in plages with little or no spots 21 p3880 A70-40964
- Solar X-ray bursts correlation with H alpha flares and microwave bursts observed by Explorer 34 experiment 21 p3880 A70-40970
- Particle acceleration phase in solar flare development, discussing H alpha maximum, hard X ray burst and bremsstrahlung 21 p3880 A70-40971
- Carina nebula NGC 3372 continuum map at 5 GHz compared to optical photographs, discussing H alpha lines 21 p3887 A70-41109
- Radio search for formaldehyde rotational transition and H 109 alpha recombination line in comet Bennett during perihelion passage 21 p3921 A70-41976
- Instrumental and atmospheric observational problems regarding dark mottles, fibrils and H alpha solar limb photographic interpretations 21 p3926 A70-42199
- Orion nebula H alpha/forbidden N II ratio measurement using wide field multislit spectrograph 22 p4101 A70-42857
- H alpha emission objects in Southern Milky Way, discussing positions, photometric data and relation to galactic structure 22 p4101 A70-42865
- Alpha hydrogen recombination lines 156, 166, 167 and 168 from galactic center, using radio telescope 22 p4103 A70-42980
- H alpha and H beta lines electrodynamic broadening with linear Stark effect, calculating relative intensity 23 p4221 A70-43912
- UV Cet type flare star rotational velocity upper limits from H alpha emission line width in chromospheres 23 p4251 A70-44824
- Coherent motion effects on brightness of clouds moving above photosphere, describing H alpha Doppler brightening and Lyman alpha Doppler dimming in solar prominences 24 p4400 A70-45313
- H alpha solar spray-like prominence ejected in association with bright limb flare, determining knots trajectories and velocities from coronagraph observations 24 p4396 A70-45323
- Hydrogen I region anomalous alpha lines recombination in Orion B spectrum, identifying carbon emitter by measured frequency separation 24 p4410 A70-45773
- H BETA LINE**
- Solar radiation pressure effects on zodiacal dust particle orbital velocity, computing Doppler shift of H-beta absorption line as function of elongation 01 p0070 A70-10348
- Photoelectric line photometry used to study H beta/gamma and He I 4471 absorption line intensities of early B stars, determining projected rotational velocity 02 p0369 A70-12072
- Plasma jet temperature and density determination from intensity ratio of H beta line and continuous spectrum 04 p0725 A70-14535
- Excitation of H-alpha and H-beta lines in night sky, calculating solar L radiations variation with altitude 04 p0679 A70-15075
- Intensity and altitude profile of H beta light emission and energetic hydrogen fluxes during auroral breakup using rocket soundings 08 p1489 A70-21383
- Stark effect He II and H beta on lines observed for transverse and longitudinal fields, using beam-foil light source 09 p1731 A70-22779
- Stark broadening of neutral helium line in plasmas for electron densities measurements accuracy, comparing to H beta determined densities 13 p2456 A70-29225
- H alpha and H beta lines electrodynamic broadening with linear Stark effect, calculating relative intensity 15 p2777 A70-32490
- Luminous nebulae near Sco X-1 indicating H beta emission 17 p3156 A70-34829
- Delta Scuti stars, determining consistent absolute magnitudes by Stromgren intermediate band colors and Crawford photoelectric H beta indices 17 p3171 A70-35443
- Open star h and chi Persei cluster four color and H beta photoelectric photometry, discussing interstellar reddening, ages and distances 21 p3922 A70-41982
- H alpha and H beta lines electrodynamic broadening with linear Stark effect, calculating relative intensity 23 p4221 A70-43912
- Hydrogen cluster beam discharges, determining transient plasma ion density from Stark broadening measurements of H beta line 23 p4228 A70-44939
- H GAMMA LINE**
- Photoelectric line photometry used to study H beta/gamma and He I 4471 absorption line intensities of early B stars, determining projected rotational velocity 02 p0369 A70-12072
- Stark broadening calculations of H alpha and H gamma hydrogen lineshapes 14 p2620 A70-31303
- H gamma profiles of B type supergiants, discussing electron density levels, Stark effect, Balmer and Paschen series breaks, etc 14 p2652 A70-31385
- H LINES**
- NT H ALPHA LINE
- NT H BETA LINE
- NT H GAMMA LINE
- NT K LINES
- NT LYMAN SPECTRA
- NT PASCHEN SERIES
- NT RYDBERG SERIES
- NT TELLURIC LINES
- Slitless spectrograms of chromosphere obtained during 1962 eclipse to determine H level populations decrements, self absorption in Balmer lines and chromosphere model 01 p0175 A70-10245
- Intermediate band four color photometry of white dwarfs, considering hydrogen line blocking and H delta line 01 p0188 A70-11335
- Two layer model of Jovian clouds including clear space, showing computed and measured equivalent widths of H quadrupole lines 02 p0367 A70-11813
- Collision-narrowed growth curves for interpreting hydrogen quadrupole lines applied to photoelectric observations of Jupiter vibration-rotation bands 02 p0368 A70-11824
- Ionized matter complex at galactic periphery deduced from neutral hydrogen line and continuous spectrum observations 03 p0564 A70-13222
- Lyman alpha transition line in exosphere deuterium line implying enrichment factor ratio to earth surface deuterium 04 p0742 A70-15129
- Hydrogen atoms van der Waal dispersion interaction effects on H lines broadening in neutral medium, taking into account resonance interaction 04 p0723 A70-15714
- SS Cygni outburst origin in G type star indicated from radial velocity variations of hydrogen absorption lines during rising light 05 p0915 A70-16695
- Double radio source W 49 hydrogen line absorption measurements revealing two H I clouds with different radial velocities 06 p1149 A70-18461
- Hydrogen and helium emissions in upper atmosphere, observing amplifications towards geomagnetic poles and in winter hemisphere 07 p1266 A70-19439
- Galactic longitude interval region radio telescope observations, obtaining isophotes of brightness distribution of RF spectral line of neutral H and continuous spectrum 08 p1564 A70-20551
- Seyfert galaxy NGC 4151 nucleus relation to quasars, discussing cloud structure and velocity and H line properties 08 p1568 A70-20617
- Spectral radiometer for observing excited hydrogen radio frequency lines using paramagnetic traveling wave quantum amplifier 08 p1495 A70-21052
- Parametric amplifier for spectral radiometer of U.S.S.R. astronomical telescope, showing improved sensitivity observations of neutral H emission 08 p1473 A70-21066
- Pulsar clusters and associations within 1 kpc of sun and hot O-stars and supergiants, calculating radius of surrounding H II regions 08 p1577 A70-21493
- Ionized matter complex at galactic periphery deduced from neutral hydrogen line and continuous spectrum observations 08 p1580 A70-21655
- Numerical calculation of S matrices for Stark broadening of Lyman-alpha line based on straight line classical path model 09 p1730 A70-22228
- Measured and theoretical stark-broadened line profiles and asymptotic wing approximation of hydrogen Balmer lines at specific electron density and temperature 09 p1732 A70-22782
- Hydrogen 21 cm emission line in Perseus region observed for motion of neutral hydrogen connected with II Per, discussing stellar radial velocity 10 p1937 A70-23944
- Elongated neutral-hydrogen emission feature in Sco-Oph region, comparing with interstellar sodium lines for distance from sun 10 p1945 A70-24966
- Violet K2 emission in H and K line cores of solar calcium ions using atmospheric model in state of motion 12 p2303 A70-27701
- Calcium H and K lines core residual intensities in stars with quiet and active chromosphere, suggesting activity due to thermal gradient 12 p2303 A70-27702
- Solar Ca II H and K lines formation, discussing double reversal, limb darkening, plage and spot lines and anomalous line ratios 13 p2494 A70-29481
- Molonglo pulsars H line absorption and dispersion in interstellar medium 13 p2495 A70-29788
- Polar auroral hydrogen emission intensity dependence on K index of geomagnetic activity 14 p2569 A70-30213
- Galactic longitude interval region radio telescope observations, obtaining isophotes of brightness distribution of RF spectral line of neutral H and continuous spectrum 15 p2805 A70-32706
- Hyades stars between F4 and K5, measuring chromospheric H and K emission lines dependence on bolometric luminosity 17 p3157 A70-34832
- Solar chromosphere resonance lines, observing H and K line profiles of Mg ions 17 p3161 A70-34893
- Auroral protons and resonant concept of substorm, eliminating discrepancy between hydrogen emission spectroscopic and direct measurements 18 p3307 A70-36177
- Galactic center region lunar occultations in 21 cm neutral hydrogen line 18 p3313 A70-36328
- Hydrogen and helium emissions in upper atmosphere, observing amplifications towards geomagnetic poles and in winter hemisphere 18 p3249 A70-36913
- Hydrogen line absorption at 21 cm from Centaurus A / NGC 5128/ radio galaxy 18 p3318 A70-37017
- Galactic spiral structure from atomic hydrogen line intensity longitudinal distribution 18 p3328 A70-37168
- Neutral hydrogen distribution in galactic region surveyed with radiotelescope 18 p3328 A70-37169
- Radial velocities of neutral hydrogen in anticenter region of Galaxy 18 p3328 A70-37170
- O type stellar clusters hydrogen line observation revealing associated gas clouds 18 p3328 A70-37172
- Galactic spiral structure from optical radial velocities of H II regions 18 p3329 A70-37179
- Near collisions approximation in Stark broadening of hydrogen Lyman alpha line 18 p3296 A70-37227
- Vacuum UV laser action in molecular hydrogen Lyman bands, examining stimulated emission in P branch lines and light pulse duration 20 p3643 A70-40496
- Atomic hydrogen 21 cm line intensity distribution in Carina arm of Milky Way galaxy 22 p4100 A70-42851
- Be stars hydrogen emission lines widths measurement 22 p4101 A70-42867
- Microwave recombination H lines, deriving electron temperature, electron density and emission measure sequentially 24 p4402 A70-45388
- Polar auroral hydrogen emission intensity dependence on K index of geomagnetic activity 24 p4331 A70-46288
- Neutral hydrogen 21 cm line profiles in galactic plane, tabulating terminal positive velocity and brightness temperatures 24 p4414 A70-46381
- Galactic neutral hydrogen velocity distributions from 21 cm line profiles analysis 24 p4414 A70-46382
- H WAVES**
- Anomalous H wave absorption in circular waveguide by dense collisionless plasma, connecting to instability excitation with subsequent plasma heating 03 p0537 A70-14379

- Eigenvalue and eigenfunction of H01 wave in bend of cross shaped waveguide, determining field components and propagation constant change
04 p0651 A70-15291
- Symmetrical H mode wave propagation in inhomogeneous plasma filled circular waveguide solved by hypergeometric functions, noting use for microwave diagnostics and computer programs verification
06 p1009 A70-17825
- HE sub 11 mode launching in optical communication system, considering fiber tapering effect on excitation efficiency
16 p2875 A70-33400
- H and E waves diffraction in circular waveguide by diaphragm thickness, using linear equations and Fourier-Bessel series for representation
19 p3378 A70-37731
- H-56 HELICOPTER**
Electron beam welding of AH-56A helicopter rotor hubs outside of vacuum chamber, discussing modifications of machine
04 p0699 A70-15651
- HABITABILITY**
Underwater saturation habitats application as behavioral workshops for mission planning and human engineering of manned space flight, discussing Project Teklite
[AIAA PAPER 69-1120] 01 p0034 A70-10611
- Habitability factors in space station crew quarter design, discussing hygiene and dining facilities
17 p3036 A70-34803
- Long term space flight crew habitation emphasizing food management, station housekeeping, personal hygiene and waste handling
23 p4154 A70-44622
- HABITUATION [LEARNING]**
Vestibular nystagmic and electrical responses facilitation, inhibition and habituation, noting modulation by subcortical and cortical systems
14 p2538 A70-30909
- Pattern center hypothesis for habituation to centrifugal and linear accelerations in man, investigating aftereffects by nystagmography
14 p2538 A70-30913
- Vestibular habituation among pilots and flying staff from training and seniority standpoint
14 p2538 A70-30914
- Vestibular habituation acquisition, retention and transfer correlation with stimulation, discussing alertness and arousal effects
14 p2539 A70-30915
- Habituation and dishabituation in semimaintained Aplysia preparation with central nervous system removed
18 p3217 A70-36517
- HADRONS**
Cosmic ray muon source implied from hadrons X pairs produced in primary cosmic ray collisions
02 p0360 A70-12845
- Muonic and hadronic component arrival time distribution in EAS measured under rock compared to Monte Carlo computation
03 p0562 A70-14187
- Electromagnetic component of extensive air showers to three dimensional Monte Carlo simulations of hadronic component using electromagnetic cascade theory
07 p1368 A70-19967
- Extensive air shower simulation for determining inelasticity effect on electrons, hadrons and muons variation at sea level
08 p1563 A70-21674
- Equation of state for cold matter at neutron star densities, deriving equilibrium equations for nuclear interactions among hadrons
09 p1764 A70-23606
- Hadron energy levels description by Lorentz invariant wave equation in form of supermultiplets
15 p2776 A70-31736
- Deep inelastic lepton-hadron scattering cross sections universality properties based on Wilson theory
20 p3674 A70-39150
- Three dimensional Monte Carlo simulation of extensive air shower processes, comparing with hadrons and electrons energy spectra
20 p3699 A70-39442
- Ionization spectrometer for hadron energy measurement, analyzing instrument accuracy by Monte Carlo model for nuclear-EM cascade in iron absorber
20 p3635 A70-40456
- Friedmann universe evolution after big bang via Hagedorn hadronic equation of state, noting primordial He abundance criterion
21 p3888 A70-41122
- HAFNIIUM**
High temperature Hf oxidation in air and oxygen using thermogravimetry, X ray diffraction and electron microscopy
05 p0863 A70-16522
- Chondritic and achondritic meteorites Zr and Hf abundances, distributions and ratios, using thermal and neutron activation analyses
18 p3310 A70-35968

HAFNIIUM ALLOYS

- Internal nitriding kinetics of W-base alloys containing Hf, investigating morphology of resulting Hf nitride dispersion
02 p0317 A70-12319
- Omega transformation in Hf-Nb alloys, investigating aging at various temperatures
18 p3273 A70-36044
- Oxygen solubility in Nb-Hf alloys at elevated temperatures, using isothermal sections for Nb-rich part
19 p3453 A70-38708

HAFNIIUM CARBIDES

- Temperature dependence of Vickers pyramid hardness for Ti, Zr and Hf carbides at wide temperature range in vacuum
08 p1516 A70-20986

HAFNIIUM COMPOUNDS

- NT HAFNIUM OXIDES**
Ti, Zr and Hf diborides electrophysical properties, discussing temperature effects and electronic structures
23 p4205 A70-43991
- Thermal and electrical conductivities of zirconium and hafnium diborides polycrystalline powders at 300-1300 K
23 p4209 A70-44443

HAFNIIUM OXIDES

- Microstructure and composition of hafnium dioxide stabilized with Ca, Y and Mg oxides using metallographic, X ray and microprobe
20 p3654 A70-39242

HAIL

- High speed hail impact damage on flat Al alloy plates observed for effects of impact angle and velocity, plate material properties and thickness
01 p0056 A70-10690
- Aircraft structural damage due to high speed hailstone impact, considering aircraft design modifications
02 p0386 A70-11938
- Reliability of Doppler radar hail detection, discussing corrupting effects of turbulence and shear, size-sorting and vertical air motions
03 p0443 A70-13167
- Cloud base updraft field, three dimensional reflectivity pattern and rain and hailfall pattern for thunderstorms in Alberta, discussing shear
06 p1099 A70-18569
- Radar model of shower and hail clouds as two phase system of independently scattering spherical particles, stressing radar properties dependence on particle properties
08 p1536 A70-21097
- Electric field effects on electrification of colliding ice spheres, discussing relaxation time of sphere charges and charge exchange
08 p1538 A70-21114

HAILSTONES

- U HAIL**
Guinea pig cochlear hair cell damage after exposure to impulse noise
02 p0236 A70-12322
- Chemically treated rolled hair properties following long term use in hair hygrometers
24 p4333 A70-45138
- Sonic boom effects on guinea pigs Corti organ, comparing auditory damage in cochlea with hair cell damage
24 p4305 A70-46374

HALF CONES

- Transonic dynamic stability of free flight half angle cones in wind tunnel for high drag planetary entry vehicles, discussing Mars entry trajectories
[AIAA PAPER 69-105] 06 p1154 A70-17164

HALF LIFE

- Half life of Mn53 calculated from measured activity in sample from Fe meteorite and isotopic ratio Mn53/Mn55
07 p1337 A70-19226

HALF PLANES

- Fourier transform applied to Riemann boundary value solution to biharmonic equation governing elastic theory for half plane with circular protrusion or indentation
01 p0199 A70-10155
- Boundary value problems for orthotropic half plane and infinite orthotropic plane with cuts, considering loads at various points
03 p0593 A70-13497
- Stress distribution in anisotropic half plane with reinforced circular hole under external loads applied at plane infinity and ring edge
04 p0765 A70-14417
- Displacements and stresses obtained for elastic half plane with variable Poisson ratio under certain traction boundary conditions, using Fourier transform method
05 p0940 A70-16512
- Contact stresses between elastic half planes and elastic cover plates determined by integrodifferential equation with Hilbert kernel
07 p1400 A70-18667
- Isotropic elastic body occupying half plane assuming elasticity coefficients of certain class
07 p1407 A70-19376

- Singular part of half plane stress field solution using Cosserat elasticity theory
07 p1409 A70-19570

- Steady temperature field and stresses produced by thermal sources in infinite elastic plane containing insulated rectilinear crack, determining thermoelastic state of half plane
08 p1587 A70-21172

- Thermoelasticity problem for plane with rectilinear cut with constant temperature at initial moment of time, using approximating kernel of integral equation
10 p1965 A70-25296

- Contact stresses in elastic half plane with boundary connected to rod and moment applied at arbitrary point
10 p1965 A70-25324

- Viscoelastic half plane creep under discontinuous boundary conditions, obtaining exact closed-form solution based on Fourier transforms and distribution theory
10 p1965 A70-25325

- Plane electromagnetic wave diffraction by perfectly reflecting half plane calculated by elementary method
12 p2184 A70-27234

- Closed form solutions of boundary value problems for Burger equation within half plane from zero to infinity
14 p2598 A70-30492

- Elastic half plane with crack perpendicular to free surface and under arbitrary pressure distribution, obtaining exact solution for stress and displacement fields
15 p2767 A70-31854

- Wave diffraction by half plane limit of parabolic cylinder and wedge, using Fresnel integral and Heaviside step function
15 p2700 A70-32409

- Plane wave diffraction by cylinder tipped half plane, demonstrating localized behavior by geometrical theory
16 p2872 A70-32975

- Monochromatic electromagnetic wave diffraction on moving ideally conducting half plane, deriving parameters and spectral composition after diffraction
16 p2863 A70-33216

- Elastic Cosserat half plane, analyzing wave propagation of small amplitude thermoelastic disturbances and uniform motion of concentrated line load along surface
18 p3338 A70-36434

- Polarized plane EM wave diffraction by inclined half plane grating, obtaining transformation matrices coefficients
19 p3376 A70-37714

- Half plane with stress-free surface deformed by protrusions or notches, deriving edge force or screw dislocation by linear elastic analysis
21 p3939 A70-42028

HALF SPACES

- Time dependence of contact zone radius of rigid sphere pressed against viscoelastic half space by normal force
02 p0384 A70-11738

- Stress distribution in half space of inhomogeneous media, studying scale and edge effects relation for elastic and ideally plastic media
03 p0590 A70-13376

- Elastokinetic three dimensional boundary value vibration problem, involving rectangular area on surface of elastic half space under periodic normal stress
03 p0601 A70-14319

- Linear nonaxisymmetric bending of infinite plate coupled to elastic half space under concentrated loads using double Fourier transforms
04 p0766 A70-14480

- Plane Lamb problem in semiinfinite micropolar elastic body solved by transformation to one dimensional wave propagation problem in elastic half space
05 p0925 A70-15785

- Unloading wave in elastic-plastic half space with rigid unloading for two parameter loads, discussing deformation body model
05 p0925 A70-15825

- Axial compression of elastic circular cylinder in contact with identical elastic half spaces, determining interfacial surface stresses for frictionless and adhesive contacts
05 p0930 A70-16082

- Adhesive rocking and parallel translation contact for circular cylindrical punch indenting elastic half space solved using simultaneous equations
05 p0932 A70-16139

- Mixed boundary value problems of isotropic elastic half space with ring shaped separation region
05 p0935 A70-16232

- Plane and cylindrical elastic waves dynamic characteristics propagating in half space with holes, reducing boundary value problem and deriving formulas for interacting waves
05 p0946 A70-16858

- Model for impact behavior of elastic body at elastic half space, measuring gas molecule impulse exchange at metal surfaces
06 p1171 A70-18260

Large Froude number solution for nonseparative impact of elliptical cylinder floating on incompressible fluid surface in half space extended to small Froude numbers

07 p1253 A70-18770

Plane electromagnetic wave penetration into ferromagnetic half space solved for nonlinear parabolic equations using difference method

07 p1227 A70-18992

Torsion of elastic half space containing circular crack with symmetry axis coinciding with annular stamp rigidly coupled to half space

07 p1414 A70-20183

Inhomogeneous elastic half space surface response to moving line loads

08 p1584 A70-20645

Half space elasticity problems solved by operator method

08 p1586 A70-21013

Dynamic response of joined elastic quarter spaces of solids to time varying free surface shear tractions parallel to plane of juncture

[ASME PAPER 69-APMW-16] 08 p1591 A70-21467

Transient waves propagation in homogeneous isotropic linearly elastic half space excited by traveling normal point load on surface, deriving displacements

[ASME PAPER 69-APMW-12] 08 p1592 A70-21468

Monochromatic plane electromagnetic wave incident from vacuum on plane boundary of plasma half space, discussing specular reflection and diffuse scattering boundary conditions

08 p1553 A70-21611

Steady harmonic oscillations of half space with circular holes, deriving algebraic equations for boundary value problems

09 p1782 A70-23296

Reissner-Sagoci transient mixed boundary value problem concerning displacement of infinite half space of isotropic elastic material, deriving surface displacement and reactive torque

09 p1784 A70-23571

Point electric dipole EM radiation in presence of moving dispersive dielectric half space

09 p1639 A70-23669

Nonstationary thermoelasticity in half space with moving boundary condition described in Cartesian rectilinear coordinates allowing for time term in heat conduction equation

10 p1954 A70-24012

Vertical tubular dipole antenna input admittance and current distribution above infinite dissipative half space

12 p2197 A70-27953

Coherent wave reflection from random half space, solving scalar Dyson equation in bilocal approximation for oblique incidence

12 p2189 A70-27972

Concentrated force action inside transversely isotropic half space analyzed by mirror image method

13 p2512 A70-28865

Plane harmonic wave steady state diffraction at cylinder in elastic half space, applying method of images

13 p2366 A70-29320

Nonlinear wave propagation in continuous media involving stress-strain state of half space under pressure or load expanding over boundary

13 p2517 A70-29770

Time harmonic waves propagation in elastic half-space with submerged cylindrical cavity, assuming linear plane strain conditions

13 p2518 A70-30010

Elastoviscoplastic medium filled half space motion under pressure front moving along surface with time varying velocity, analyzing penetrating wave fronts form

16 p2990 A70-33780

Wave propagation from two dimensional expanding load on liquid half space with load fronts decelerating monotonically from initial supersonic speed

17 p3069 A70-34976

Ideal fluid contained in half space with circular or strip-like aperture, formulating mathematical model to determine sloshing frequencies

18 p3238 A70-36057

Forced vibration in Cartesian half space filled with elastic medium, investigating uniqueness conditions

18 p3337 A70-36289

Half space nonstationary temperature field with mobile heating at edges, using integral transformations

18 p3348 A70-36725

Dipole antenna radiation in compressible anisotropic electron plasma overlying imperfectly conducting half space, solving for lunar environment

19 p3381 A70-38407

Dipole antenna radiation in compressible anisotropic electron plasma overlying imperfectly conducting half space, evaluating Fourier-Bessel integrals for lunar environment

19 p3381 A70-38408

Skin effect for unsteady radio waves emitted into homogeneous nonmagnetic isotropic half space, calculating electric field

19 p3381 A70-38571

Pair correlations effect in equilibrium and nonequilibrium theory, taking Coulomb collisions into account for ionized plasmas confined to half space by reflecting boundary

20 p3679 A70-39662

HALIDES

NT ALUMINUM CHLORIDES
NT AMMONIUM CHLORIDES
NT BARIUM FLUORIDES
NT BERYLLIUM FLUORIDES
NT BORON CHLORIDES
NT BORON FLUORIDES
NT CADMIUM FLUORIDES
NT CALCIUM FLUORIDES
NT CARBON TETRACHLORIDE
NT CHLORIDES
NT CHLORINE FLUORIDES
NT COPPER CHLORIDES
NT DIBROMIDES
NT DIFLUORIDES
NT HYDROBROMIDES
NT HYDROCHLORIC ACID
NT HYDROCHLORIDES
NT HYDROFLUORIC ACID
NT IRON CHLORIDES
NT LITHIUM CHLORIDES
NT LITHIUM FLUORIDES
NT MAGNESIUM FLUORIDES
NT METAL HALIDES
NT NITROSYL CHLORIDES
NT OXYFLUORIDES
NT OXYGEN FLUORIDES
NT PHOSGENE
NT POTASSIUM CHLORIDES
NT SILVER HALIDES
NT SILVER IODIDES
NT SODIUM CHLORIDES
NT SODIUM IODIDES
NT STRONTIUM FLUORIDES
NT SULFUR CHLORIDES
NT SULFUR FLUORIDES
NT TITANIUM CHLORIDES

Thermodynamics of LiBr in anhydrous dimethyl sulfoxide determined at several temperatures using EMF method

06 p1003 A70-17219

Thermal decomposition of acetate ion in potassium halide matrices, using IR spectroscopy

22 p3981 A70-42453

Al purification by subhalide reaction, discussing contamination sources and thermodynamics

24 p4349 A70-46187

HALL ACCELERATORS

Coaxial electrodes with electric and magnetic fields to study instability in MPD arcs
[AIAA PAPER 69-230] 04 p0737 A70-15542
Low density Hall ion thruster with application to Van Allen probe and orbit-to-orbit transfer
[AIAA PAPER 69-281] 13 p2475 A70-29957
Electrical characteristics of high current two stage DC Hall accelerator for use in controlled thermonuclear fusion 24 p4383 A70-45117

HALL COEFFICIENT

U HALL EFFECT

HALL CURRENTS

U ELECTRIC CURRENT

U HALL EFFECT

HALL EFFECT

Electrothermal instability and critical Hall parameter growth rates in closed cycle linear plasma generators with variable electron mobility, discussing perturbation effects

01 p0151 A70-10655

Geomagnetic field directed hydromagnetic waves propagation in lower ionosphere noting inhomogeneous conductivity, Hall effect and lines of forces role

01 p0083 A70-11546

Hall current effect on steady boundary layer flow of incompressible viscous electrically conducting fluid past semiinfinite flat plate in transverse magnetic field

03 p0469 A70-14183

Current stream function, Hall current density, force densities and pressure distribution for typical MPD thruster

03 p0552 A70-14372

Electron temperature and particle density measurements in annular MHD duct, demonstrating Hall effect existence

04 p0725 A70-14532

Plasma acceleration by induced Hall currents, discussing Hall-to-current ratio maximum at critical magnetic field

04 p0729 A70-15596

Compressible fluid flow satisfying perfect gas equation in presence of thin foil, developing operators characterizing incompressible and compressible flows without Hall effect

05 p0790 A70-16158

Hall voltage measurements on Ta thin films using square wave generator current, discussing parasitic effects and suppression possibilities

05 p0863 A70-16366

Hall effect measurements in liquid semiconductors and metals

06 p1127 A70-17919

Critical Hall parameter indicating instability in alkali-seeded noble gases in nonequilibrium MHD generators

[AIAA PAPER 70-40] 06 p1122 A70-18107

Hall voltage and electric conductivity measurements in alternating magnetic field and current by narrow band amplifier with synchronous detector

07 p1279 A70-18944

Hall current effects on anisotropic plasma magnetogravitational instability under uniform magnetic field, considering electron inertia role and plasma perturbations

07 p1348 A70-19228

Hall effect and electric conductivity of cadmium arsenide at high temperatures as function of carrier concentration dependence on temperature and phase transformation

07 p1357 A70-20314

Tensor conductivity, magnetic field and electric field effect on heat transfer in MHD channel flow, solving for temperature and Nusselt number

08 p1554 A70-21773

Hall effect on MGD flow past axisymmetric body by studying incompressible inviscid fluid past body of revolution at zero incidence

09 p1661 A70-23074

Boundary layer of MGD flow past axisymmetric insulator body analyzed to determine torque due to Hall effect

09 p1663 A70-23579

Ionospheric current flow past circular inhomogeneous spot with Pedersen and Hall conductivities, calculating earth surface magnetic field by Lipschitz-Hankel integral

10 p1873 A70-24309

Nonequilibrium plasma MHD generator critical pressures determination, applying electron energy balance equation and relation between plasma conductivity and Hall parameters

10 p1809 A70-25142

Thermoelectric power and Hall effect quantum resonances in pressure annealed pyrolytic graphite crystals for carrier locations evidence

11 p2097 A70-25616

Hall effect influence on HF traveling magnetic field penetration into solid cylinder plasma device compared to magnetically contained plasma

11 p2088 A70-25712

Hall constant and carrier mobility in semiconductor diamond films doped by boron ion injection, observing temperature dependence of mobility

12 p2287 A70-27480

Compressible fluids Alfvén flow with Hall effect presence of thin foils, reducing problem to Fourier integral equation

13 p2442 A70-29484

Hall, polarization and Pedersen charged particle drift velocities in static magnetic and time dependent electric field

14 p2624 A70-31046

Compressible plasma gravitational instability taking into account Hall effect

14 p2624 A70-31225

Acceptor level formation kinetics from measuring Hall constant as function of temperature after diffusion of copper into n-type GaAs

15 p2782 A70-31633

Equilibrium and steady state Hall and thermoelectric effects in inhomogeneous semiconductor materials

15 p2783 A70-31760

Coaxial electrode arc discharge plasma accelerators at reduced pressure under crossed fields, employing Hall effect

15 p2779 A70-32104

Continuously working plasma thrusters, describing operating principles of Hall current and self magnetic acceleration systems

15 p2790 A70-32277

MAGFET devices for integrated circuits, calculating magnetic sensitivity as function of channel aspect ratio and Hall electrode position

15 p2710 A70-32572

Micro-Hall device as tool for evaluating epitaxial silicon in integrated circuit processing

15 p2710 A70-32573

Near cathode magnetic field effect on instability in linear Hall current accelerators, using geometry of field extending from anode to cathode region

[AIAA PAPER 69-381] 16 p2959 A70-33870

Electrical conductivity, Hall constant and differential thermal emf n-type GaAs-CdS solid solutions

18 p3298 A70-36596

Magnetite and ferrite spinels Hall effect, magnetoresistance and electrical conductivity over wide temperature range

19 p3485 A70-37627

Helicon electromagnetic wave attenuation control by steady current of uniform density in propagation direction, considering Hall effect role

20 p3585 A70-39396

Homopolar device electric arc dynamics dependence on gas type, noting flow geometry-Hall effect competition

20 p3681 A70-40009

Nonequilibrium plasma stability, conductivity and Hall parameter influenced by current flow parallel to magnetic field, discussing Ar-Cs and He-Cs plasma data

20 p3682 A70-40019

Magnetoresistance nonlinearity and Hall effect in graphite in magnetic field, observing temperature dependence below 4.2 K

21 p3862 A70-40945

Drift reducing NMR stabilization of Hall regulated electromagnet, applying error signal to bias coil

21 p3827 A70-41456

Rb and Cs ions implanted Si analyzed by Hall effect and sheet resistivity measurements and channeling techniques

22 p4087 A70-43143

Hall effect on incompressible electroconducting viscous fluid motion past finite conducting flat plate, discussing boundary conditions

23 p4225 A70-44247

Critical Hall parameter for linear development of MHD electrothermal instability in bounded nonequilibrium plasma

23 p4227 A70-44555

Analog three dimensional electrical signal multiplier circuit based on Hall effect, considering division and square root extraction

24 p4319 A70-45484

Thermoelectric power and Hall effect quantum resonances in graphite for locating majority carrier electron and hole Fermi Surfaces in Brillouin zone

24 p4389 A70-45597

Inviscid conducting incompressible fluid steady motion past thin airfoils, presenting crossed and aligned fields and Alfvén motion with Hall effect

24 p4289 A70-46033

HALL GENERATORS

Hall generator DC brushless motor operation and applications, obtaining motor action by rotor and stator magnetic fields interaction

02 p0228 A70-12053

Hall MHD generator with supersonic flow instability to magnetoacoustic waves propagating antiparallel to steady electric current in dense weakly ionized gas

12 p2281 A70-27805

Hall generator measurement of impulse currents, noting error sources and compensation

16 p2900 A70-33072

Combustion driven Hall configuration MHD generator, discussing boundary layer analysis, gas density nonuniformity and electrode drop

20 p3566 A70-40003

Performance comparison of diagonal conducting wall MHD generator and Hall generator of equal dimensions, investigating wall temperature effect

20 p3566 A70-40004

Eddy currents in Hall generator with conducting side wall, studying velocity and temperature effects for turbulent boundary layer and laminar flows

21 p3859 A70-41733

Optimal load circuits number for maximum power extraction from Hall MHD generator with nonuniform gas flow along channel

23 p4143 A70-44900

HALO PARACHUTING

U PARACHUTE DESCENT

HALOGEN COMPOUNDS

NT ALUMINUM CHLORIDES
NT AMMONIUM CHLORIDES
NT AMMONIUM PERCHLORATES
NT BARIUM FLUORIDES
NT BERYLLIUM FLUORIDES
NT BORON CHLORIDES
NT BORON FLUORIDES
NT BROMINE COMPOUNDS
NT CADMIUM FLUORIDES
NT CALCIUM FLUORIDES
NT CARBON TETRACHLORIDE
NT CHLORATES
NT CHLORIDES
NT CHLORINE COMPOUNDS
NT CHLORINE FLUORIDES
NT CHLORINE OXIDES
NT COPPER CHLORIDES
NT DIBROMIDES
NT DIFLUORIDES
NT DIFLUORO COMPOUNDS
NT FLUORINE ORGANIC COMPOUNDS
NT FLUORO COMPOUNDS
NT FLUOROCARBONS
NT FLUOROHYDROCARBONS
NT HALIDES
NT HYDROBROMIDES
NT HYDROCHLORIC ACID
NT HYDROCHLORIDES
NT HYDROFLUORIC ACID
NT IODATES
NT IODIDES
NT IODINE COMPOUNDS
NT IRON CHLORIDES
NT LITHIUM CHLORIDES
NT LITHIUM FLUORIDES
NT MAGNESIUM FLUORIDES
NT MAGNESIUM PERCHLORATES
NT METAL HALIDES

NT NITROSYL CHLORIDES
NT OXYFLUORIDES
NT OXYGEN FLUORIDES
NT PERCHLORATES
NT PHOSGENE
NT POLYTETRAFLUOROETHYLENE
NT POTASSIUM CHLORIDES
NT POTASSIUM PERCHLORATES
NT SILVER HALIDES
NT SILVER IODIDES
NT SODIUM CHLORIDES
NT SODIUM IODIDES
NT STRONTIUM FLUORIDES
NT SULFUR CHLORIDES
NT SULFUR FLUORIDES
NT TITANIUM CHLORIDES

Chemiluminescence in alkali metals and halogenated methanes diffusion flames, studying diatomic Cs spectral bands

02 p0250 A70-12018

Fire extinguisher compounds/bromochloromethane and bromotrifluoromethane/pyrolysis products inhalation toxicities for rats

07 p1219 A70-19223

Tetrafluorodibromo-ethane and bromomethyl inhibiting effects on explosion development in constant volume container and flame expansion rates in hydrogen-air mixtures

18 p3345 A70-36241

HALOGENATION

NT CHLORINATION

NT FLUORINATION

HALOGENS

NT BROMINE

Work function measurement for adsorption of diatomic I, Br and Cl on W crystal using electron beam retarding potential method

05 p0891 A70-15973

HALOPHILES

Purification and reversible inactivation of isocitrate dehydrogenase /ICDH/ of Halobacterium cutirubrum, overcoming difficulties in purifying halophilic enzymes

01 p0021 A70-10792

Nicotinamide adenine dinucleotide phosphate /NADP/ specific isocitrate dehydrogenase /ICDH/ inactivation from obligate halophile at low NaCl levels

15 p2685 A70-32671

Halophilic bacteria electron transport chain, examining hydrophobic forces role in menadiene reductase structure

21 p3772 A70-40574

HALOS

Ice crystal density in Martian atmosphere from brightness of Martian polaric halo

08 p1564 A70-20547

Galactic halo origin and evolution postulated from chemical evolution assuming stellar evolution details

09 p1758 A70-22742

Scattering particle distribution relation to halo formation in polydisperse clouds, using Kirchhoff approximation for halos theory construction

12 p2264 A70-27522

Cosmic rays origin, discussing choice between galactic halo and radio disk models for trapping region

12 p2295 A70-27883

Halo rings at hexagonal ice crystals in Martian atmosphere, analyzing via bright formations with respect to planetary phase angles

13 p2493 A70-29397

Angular distribution of diffusely reflected solar rays over spherical shell planetary atmosphere, determining halo brightness

14 p2632 A70-31222

Ice crystal density in Martian atmosphere from brightness of Martian polaric halo

15 p2796 A70-31456

HAMBURGER AIRCRAFT

NT HFB-320 AIRCRAFT

Monograph on HFB 600 V/STOL transport for civil and military air traffic, discussing intercity travel, military dispersal requirements, systems performance, cockpit layout, etc

07 p1194 A70-19605

Hansa 330 fan jet design for executive and commuter market, discussing forward-swept wing concept and standardized structures and systems

07 p1194 A70-19619

HAMBURGER HFB-320 AIRCRAFT

U HFB-320 AIRCRAFT

HAMILTON-JACOBI EQUATION

MHD wave propagation through plasma in magnetic field of current filament, developing Hamilton-Jacobi equation by geometrical optics

01 p0151 A70-10466

Optimal control synthesis in flight dynamics, solving Hamilton-Jacobi-Bellman equation by finite difference technique

02 p0336 A70-12403

Spherical pendulum equations of motion solved using Hamilton-Jacobi theory

08 p1546 A70-21465

Collisionless plasmas strong turbulence in terms of mixing length and Hamilton-Jacobi theories

13 p2458 A70-28562

Optimal control in nonlinear systems, discussing conditions for analytical solutions for Hamilton-Jacobi equations

16 p2886 A70-33335

Classical approach to quantum mechanics, emphasizing Schroedinger equations and starting from Hamilton-Jacobi equations

16 p2990 A70-33778

Optimal trajectories analysis by canonical transformation for obtaining solution to Hamilton-Jacobi equation without quadratures

16 p2943 A70-33899

Hamilton-Jacobi theorem for nonlinear dynamic system moving with holonomic Cetaev constraints, investigating necessary and sufficient conditions

23 p4210 A70-44024

Static spherically symmetric charged mass distribution exact solutions derived for electrons in scalar tensor theory of gravity by Hamilton-Jacobi method

23 p4222 A70-44403

HAMILTONIAN FUNCTIONS

Lagrange and Hamilton equations of motion of mass point in physical space of general theory of relativity based on least action principle

01 p0146 A70-11444

Final motions of Hamiltonian conservative systems, analyzing Liouville type, homogeneous and similar systems

01 p0146 A70-11561

Autonomous two degrees of freedom Hamiltonian system triangular libration points found stable for all mass ratios in circular restricted three body problem

01 p0192 A70-11575

Bounded operator functionals used for deriving nonlocal interaction Hamiltonian of quantum electrodynamics corresponding to converging series for scattering matrix in perturbation theory

05 p0883 A70-16876

Bounded nonlocal operator used in deriving series of subtracting Hamiltonians representing S matrix in perturbation theory after transition to local limit

05 p0883 A70-16877

Magnetoelastic spin Hamiltonians applied to magnetostriiction of Yb in YIG

06 p1128 A70-18642

Hamiltonian methods applied to homogeneous cosmological models, obtaining Einstein equations, passing to quantum theory by imposing canonical commutation relations

07 p1336 A70-19921

Periodic orbits for reduced problem of conservative Hamiltonian system with two degrees of freedom, discussing emergence from resonant equilibrium

10 p1939 A70-24187

Euler graphs with special properties, discussing Hamiltonian lines existence and derivatives

14 p2601 A70-31424

Bilinear scalar spin Hamiltonian inadequacy to describe electron exchange in systems containing orbitally degenerate ions, considering cobalt magnon spectra

15 p2777 A70-32399

Gaseous diatomic molecules quantum mechanical treatment, calculating Hamiltonian matrix elements for interpretation of electron resonance spectra

16 p2955 A70-33799

Delaunay reduced Hamiltonian verification in lunar ephemeris theory based on Lie transforms

16 p2978 A70-33972

Perturbation theories based on canonical transformations, examining von Zeipel theory and Hamiltonian functions

22 p4109 A70-43749

Three body problem periodic solutions, considering near equilibrium conservative Hamiltonian system consisting of two harmonic oscillators with rationally related frequencies

23 p4213 A70-44897

German monograph on Hamilton principle and Hermetian polynomials for solving linear and nonlinear differential equations via computer method

24 p4369 A70-45091

Lunar theory literal solution for average node and perigee movements compared with Delaunay results, using Lie transforms for Hamiltonian function

24 p4399 A70-45141

HAMSTERS

Mice and hamster infection resistance following short term acceleration stress, eliminating low hydrocortisone level as protective agent

03 p0428 A70-14067

Experimental procedure for investigating radioprotective effectiveness of chemical compounds against X ray irradiation, discussing Cysteamine protection for golden hamsters and fetuses

06 p0993 A70-17429

HAND (ANATOMY)

Monograph on systematically disturbed sensorimotor coordination, studying various parameters effects on eye-hand system recorelation

09 p1618 A70-22529

Hand-eye coordination in altered gravitational fields, using mirror viewed target in reaching test

15 p2689 A70-31886

Hand held device for finger /thumb/ strength measurements
24 p4309 A70-46121

HANDBOOKS
Planetary trajectory handbooks for mission and system analysis covering opportunities for Mercury, outer planets and Mars, contour charts, etc
13 p2486 A70-28525

HANDLING
U MATERIALS HANDLING
HANDLING EQUIPMENT
NT CRANES
Personnel/cargo lowering and retrieval system requirements, design approach and effects on performance for CH-47 helicopter, discussing fabrication and testing on mockup
06 p0985 A70-17711
Pressure chamber with inserted holder for adjusting Fabry-Perot interferometer
09 p1681 A70-23337
Automated baggage handling and processing, requiring total aviation community participation [AIAA PAPER 70-917]
17 p3204 A70-35829

HANDLING QUALITIES
U CONTROLLABILITY
HANGARS
Equation for disturbance of ILS localizer signals by reflection from flat hangar wall, discussing computer program
04 p0652 A70-15344

HANKEL FUNCTIONS
Radial vibration of cylindrical shell of transversely isotropic material determined using finite Hankel transform
03 p0595 A70-13904
Hankel integral transforms of half orders for solving boundary value problems in terms of spherical coordinates
09 p1712 A70-22834
Influence coefficients for toroidal shells under axisymmetric edge loads, taking one term in asymptotic expansion of Hankel function
11 p2132 A70-25693

HANSEN LUNAR THEORY
Iterative Hansen method of general perturbations programmed for digital computer, evaluating major and minor planetary theory
18 p3320 A70-37060

HARDENERS
Ternary Al-Mn alloys precipitation hardening with Cr, V and Ti, investigating ferro and ferrimagnetic phases
07 p1307 A70-19390
Gamma-gamma prime mismatch effects on stress rupture of Ni and Fe-Ni based alloys with Al and Ti hardeners
08 p1521 A70-21701

HARDENING [MATERIALS]
NT CARBURIZING
NT COLD HARDENING
NT HOT PRESSING
NT NITRIDING
NT PRECIPITATION HARDENING
NT PULSE HEATING
NT SHOT PEENING
NT SILICONIZING
NT STRAIN HARDENING
NT WORK HARDENING
Calorimetric analysis and hardness test to investigate low temperature aging behavior of maraging stainless steels
01 p0125 A70-11642
Radiation hardened fiberglass reinforced plastics rupture, bending, compression and tensile strength and elastic modulus, considering gamma ray doses effect
02 p0323 A70-12811
Mechanical properties of ordered Ni-Cr alloys, establishing hardening effect of annealing
03 p0505 A70-13105
Case hardened steels structure and properties, intermetallic phases, hardness variation with depth and hardening techniques by Be and B
03 p0510 A70-13351
Titanium alloys case hardened by diffusion of various metals at high temperatures, measuring increase in wear resistance
03 p0513 A70-13858
Elastic interaction energy involved in Ti solution hardening by oxygen determined using anisotropic elasticity, presenting atomistic calculations and chemical bonds breaking role
05 p0862 A70-15906
Stress kinetics and breakdown time of hardening Al alloys and steels under cyclic loads, noting dependence on plastic deformation
06 p1162 A70-17391
Thin walled tubular aluminum specimens hardening by temporary reduction of temperature during creep under torsion
06 p1089 A70-17795
Alloying elements effects on vanadium alloys case hardening by boronizing
07 p1303 A70-18742

Stainless steels case hardening in hydrogen, nitrogen, propane and butane mixture, showing temperature and process duration effects
07 p1291 A70-18831
Ni-Cr alloys hardened by complex alloying with Ti-Al or Ti-Zr-C additions, improving strength at elevated temperatures in oxidizing atmosphere
10 p1904 A70-24836
Ta solid solution hardening by nitrogen and oxygen, noting yield stress variation with interstitial gas concentration
13 p2434 A70-29084
Alloying elements and austenization conditions effects on hardenability of steels, investigating critical cooling rates based on TTT diagrams
15 p2744 A70-31929
Axisymmetric elastoplastic deformation of compressible plate with arbitrary hardening under uniform load, solving in quadratures
15 p2817 A70-32167
Ti-Al-V-Sn hardenability, using high temperature solution treated Jominy bars tests
15 p2762 A70-32393
Fracture of failed tensile impact and compression test pieces of hardened SAE 52100 steel, using scanning electron microscope
15 p2745 A70-32443
Quench hardening and Ni content relationship in Ti-Ni intermetallic compounds, investigating heat treatment effect on mechanical properties
16 p2930 A70-33084
High strength Ti alloys depth hardenability, discussing mechanical properties and use in aircraft components
17 p3121 A70-34434
Al single crystals hardening under low temperature reactor irradiation, emphasizing yield phenomenon associated with Luders bands
17 p3123 A70-34647
Strain rate effect on cyclic behavior of materials with hardening and softening characteristics
17 p3187 A70-34988
Structural hardening of nickel maraging steels related to Portevin-Le Chatelier effect in necking zone of stress-strain curves
17 p3124 A70-35141
Mn and Ti effects on hardening of Fe-Ni-Mn-Ti and Fe-Ni-Mn maraging martensitic steels
17 p3125 A70-35145
Alloy hardening statistical theory, applying flow stress to second phase randomly dispersed particles
17 p3191 A70-35458
Oxygen pressure effect on stainless steel cyclic hardening during vibration tests at resonant frequency
18 p3273 A70-36042
Ultrasonic irradiation effects on steel hardenability and carbon diffusion rate during annealing, noting microstructure
18 p3273 A70-36049
Deformable Al alloys hardening, emphasizing heat treatment in solid state
18 p3276 A70-36308
Maraging steels heat treatment, measuring hardness as function of temperature for various heating rates
19 p3452 A70-37807
Metallurgical changes induced by planar shock wave propagation through metals and alloys, describing shock-hardened metals macro and substructure
20 p3652 A70-40142
Ta single crystal inherent lattice and interstitial solution hardening, discussing impurity doping effect on flow stress thermal component
21 p3839 A70-40902
Maraging steels hardening mechanisms, discussing dislocations density and distribution and Ni, Mo and Co additives effects
23 p4208 A70-44919

HARDENING (SYSTEMS)
Nuclear environments determination methodology for ground military equipment hardening, considering personnel and equipment responses to detonation in atmosphere
12 p2271 A70-27097

HARDNESS
NT KNOOP HARDNESS
NT MICROHARDNESS
NT ROCKWELL HARDNESS
Carbon effect on high temperature elasticity modulus and long term hardness of Nb, indicating diffusion enhancement and counteractive Zr addition
03 p0509 A70-13252
Al and Ti single additions effects on recrystallization of Ni-Cr alloys, noting phase transformation and hardness variations
03 p0513 A70-14300
Titanium carbide based cermets with steel matrices, studying heat treatment effects on hardness
04 p0696 A70-14462
Hard alloy mixture shaping by free vibrational compacting of powders
07 p1296 A70-19801
Temperature dependence of Vickers pyramid hardness for Ti, Zr and Hf carbides at wide temperature range in vacuum
08 p1516 A70-20986

Metal and alloys hardness measuring devices at high temperatures in ultrahigh vacuum based on use of synthetic sapphire pyramidal indenter
09 p1675 A70-22566
Isomorphous beta type Ti-Mo alloy omega phase transformations and morphology by electron microscopy, relating hardness to aging
10 p1902 A70-23817
Microconstituents effect on wear behavior of high hardness steels on basis of crossed-cylinder testing, discussing intermetallic compounds influence
10 p1895 A70-24853
Residual stresses effect on strength and hardness of tungsten carbide-cobalt alloy by application of small plastic deformations, observing crack formation anisotropy
10 p1904 A70-25168
Fe-Mo-C and Fe-Ti-C alloys microstructure and hardness after rapid cooling from melt, considering phase dispersion and particle size, spacing and shape
11 p2065 A70-25774
Titanium alloys quench hardenabilities, determining variations with distance from end of Jominy bars after annealing
17 p3119 A70-34415
Friction coefficient dependence on hardness of softer element of friction pair determined at constant values of shear strength, using external friction concepts
17 p3102 A70-35672
Carbon effect on high temperature elasticity modulus and long term hardness of Nb, indicating diffusion enhancement and counteractive Zr addition
19 p3453 A70-38470
W-Mo-Nb-Ta system with constant 30 percent W, discussing specific weight and hardness
19 p3453 A70-38714
Heating conditions effect on microstructure, hardness, transformation temperatures and dimensional anisotropy of maraging steel
20 p3649 A70-39941

HARDNESS TESTS
Rockwell hardness tester attachment design for studying temperature dependence in various multiphase alloys at high temperature
01 p0121 A70-11110
Hardness measuring instrument by dynamic method at high temperatures in vacuum, using magnetic or nonmagnetic indenter balls
01 p0092 A70-11111
Steel objects microstructure and hardness tested by continuous magnetic technique, describing experimental apparatus model
02 p0300 A70-12479
Ferroprobe coercimeter with attached electromagnets for nondestructive hardness testing, describing components and mounting
02 p0301 A70-12489
Aged Al-Cu alloys hardness test data normalized and correlated for interpretation in terms of physical metallurgy
08 p1525 A70-21967
Graphite Shore hardness measurement at high temperature on Joule heated specimens, describing apparatus and procedure
15 p2764 A70-31944
Ti-Al-V-Sn hardenability, using high temperature solution treated Jominy bars tests
15 p2762 A70-32393
Pure Fe and Ta hot hardness using ultrahigh temperature hardness tester
17 p3124 A70-34659
Pure Fe and Ta hot hardness tests by ultrahigh temperature tester involving use of electron microscope
21 p3840 A70-41900

HARDWARE
Large wall display system for USAF command and control with central computer and seven color projector, discussing hardware and operational features
05 p0828 A70-16193
Hardware and system testing mathematical model assuming stochastic design and manufacturing defects detection and nondetection probability equations analogous to reliability function
10 p1896 A70-24915
Air traffic control procedures pertaining to personnel, hardware and regulations
11 p2078 A70-25720
ATC ground hardware technology implementation, considering national air space system, airports, cost estimates and capacity increase
11 p2078 A70-25722
Manufacturing error rate and inspection efficiency relevance to hardware product reliability
12 p2244 A70-28014
Low thrust mission simulation dependence on hardware definition, discussing power plant characteristics, jet velocity and thrustor efficiency
13 p2486 A70-28517
Navigation correction systems for space missions, discussing prelaunch analysis, design and mission operations, hardware, etc
13 p2448 A70-28705

Interactive computer graphics applied to continuous system modeling program /CSMP/, describing hardware system configuration

16 p2870 A70-33727

Apollo J mission hardware modification for lunar exploration, describing systems engineering role

21 p3928 A70-40979

Aerospace digital computer family structural commonality, considering architecture, hardware and support software

21 p3794 A70-41687

HARMONIC ANALYSIS

NT TESSERAL HARMONICS

NT ZONAL HARMONICS

Harmonic analysis of upper atmospheric wind periodic data from radar sounding of meteor trails, defining principal diurnal wind variations

01 p0134 A70-10201

Underground and surface telescope measurements of second harmonic of primary cosmic ray daily variation and upper solar modulation limit

01 p0170 A70-10405

Geomagnetic potential optimal representation in frame of reference of eccentric inclined dipole using conversion formulas to determine harmonic coefficients

01 p0081 A70-11230

Harmonic analysis of magnetic storms initial phases having steep leading edges and distinct steady portions, showing homogeneity in first approximation

01 p0084 A70-11558

Geomagnetic field representation in terms of spherical harmonics, analyzing data for spherical and oblate models of earth

03 p0476 A70-13906

Harmonic equilibrium method applied in dynamic problems analysis of autopilot electrohydraulic servomechanisms stability

03 p0415 A70-13930

HF expansions of harmonic solutions concentrated at waves propagating in inhomogeneous medium to dynamic equations in elasticity theory

04 p0767 A70-14499

Modified harmonic balance method applied to critical values determination of nonlinear automatic control system parameters

04 p0661 A70-14555

Continuum, harmonic and finite element perturbation studies of elastica to yield postbuckling path derivatives from nonlinear energy formulation

05 p0927 A70-16011

Geomagnetic normal fields determination using spherical harmonic analysis, including extension to local fields

05 p0842 A70-16749

Three dimensional boundary layer on body in external harmonic flow with HF velocity fluctuations

07 p1252 A70-18711

Potential and gravity distributions on lunar surface, showing presence of harmonics of all orders

07 p1385 A70-19425

Harmonic analysis of ionospheric electron density oscillation spectra, noting density fluctuations classes due to internal gravity wave propagation and N/h profiles calculation errors

07 p1266 A70-19449

Magnetic storms effect on cosmic ray neutron component diurnal variation, determining amplitudes and phases of harmonics by harmonic analysis

07 p1372 A70-20341

Geomagnetic field lines coordinates calculation based on coefficients obtained in spherical harmonic analysis

07 p1278 A70-20460

Dispersion equation harmonic analysis for three dimensional periodic structure

09 p1637 A70-23156

Periodic solution existence theorem using harmonic linearization method

11 p2023 A70-25725

First harmonic of diurnal variation in pressure corrected cosmic ray neutron monitor rate, discussing amplitude variation with height and observed time dependence

12 p2291 A70-27177

Sinusoidal signal harmonics measurement to determine nonlinear resistance junction I-V equation, discussing applications to circuit analysis

12 p2204 A70-28132

Cosmic radiation periodic variations measurements noting second harmonic importance of daily variations

13 p2478 A70-29230

Harmonic analysis of digital data from satellite measurements of periodic phenomena with unknown periodicity

14 p2554 A70-31415

Controlled libration point satellite limit cycle motion, deriving solution in infinite series by harmonic analysis

17 p3181 A70-35752

Elastic plate vibration with damping under random load, calculating linear response by harmonic analysis

18 p3334 A70-35958

Harmonic analysis of ionospheric electron density oscillation spectra, noting density fluctuations classes due to internal gravity wave propagation and N/h profiles calculation errors

18 p3249 A70-36923

DC-to-sinusoidal inverter employing PWM waveform, analyzing circuit parameters effect on harmonic content

19 p3358 A70-37854

Low temperature anharmonicity in thorium dioxide with Co 57 impurities, using Mossbauer effect of Fe 57

21 p3862 A70-40975

Spherical harmonic analysis of declination and secular geomagnetic variation

21 p3820 A70-41884

Soviet papers on harmonic linearization method in design of nonlinear automatic control systems

22 p3999 A70-42826

Harmonic linearization method for nonlinear automatic control systems, describing theoretical fundamentals

22 p4000 A70-42827

Harmonic linearization of nonlinear hysteretic elements in automatic control systems

22 p4000 A70-42828

Harmonic linearization method for periodic regimes in nonlinear control systems based on periodic solution sensitivity to higher harmonics and small parameters

22 p4000 A70-42829

Harmonic linearization equations for frequency and amplitude of self oscillations in nonlinear automatic control systems

22 p4001 A70-42832

Harmonic linearization method for periodic regimes in discrete nonlinear automatic control systems performing signal quantization with respect to level or time

22 p4001 A70-42833

Harmonic linearization for nonsearching self adaptive automatic control systems described by nonlinear differential equations

22 p4001 A70-42835

Harmonic linearization method for nonlinear automatic control systems with finite automata, discussing self oscillating modes of operation

22 p4001 A70-42836

Satellite orbital elements calculation using ellipsoidal harmonics for geopotential representation

24 p4406 A70-45531

Virtual work equations steady state subharmonic solutions by Newton-Raphson method, developing generalized iterative procedure for nonlinear differential equations

24 p4423 A70-45577

HARMONIC EXCITATION

Flexural vibrations of rotor resting on nonlinear elastic bearings under action of exciting forces harmonics using variational method based on Hamilton principle

07 p1403 A70-19112

Laser emission from organic molecules under neodymium laser harmonics excitation, describing absorption and photochemical inversions effects and emission spectra characteristics

07 p1300 A70-19866

Selective harmonic excitation in one dimensional collisionless plasma conforming to Vlasov equation by counterstreaming electron beams, noting velocity distribution conditions

07 p1353 A70-20202

Hysteretic linear damping theory applied to representation of structural damping under harmonic excitation

10 p1961 A70-25060

Fluid motion in cylindrical tank with arbitrary sector annular cross section subjected to harmonic longitudinal excitation

12 p2211 A70-27818

Floating resonance spike on Alouette 2 ionograms after sounder pulse transmission at half upper hybrid frequency, noting harmonic excitation role

13 p2370 A70-29905

Time decay of higher order cyclotron harmonic resonances with decreasing perpendicular wave number

13 p2467 A70-29908

Linear dynamic systems under nonconservative and harmonic forces, examining stability conditions

16 p2952 A70-33896

Nonlinear systems excitation by two harmonic forces, analyzing vibration by linearization of differential equation of motion

16 p2995 A70-34286

Aeroelastic test equipment for Concorde SST using harmonic method and electromagnetic shakers

19 p3402 A70-38548

Organic laser spectral and energy characteristics, discussing practical operation principles, low generation threshold and harmonic energy

20 p3642 A70-39754

Ideal limiter with polyharmonic signal input, calculating output spectral composition by Fourier series expansion

20 p3587 A70-40143

Elastic body steady forced oscillations under monoharmonic excitation, investigating hereditary nonlinearity effects on systems dynamic characteristics

20 p3733 A70-40395

Dynamic response of simply supported non-homogeneous beam and triangular pulse loads

21 p3933 A70-40584

Linear elastomechanical systems natural vibration parameters by harmonic excitation method

22 p4116 A70-43200

Nonlinear systems subharmonic oscillations under polyharmonic disturbance and viscous damping

24 p4427 A70-46378

HARMONIC FUNCTIONS

Zero crossings of signal harmonic function with normal phase distribution, deriving relations with spectrum and modulating process parameters

03 p0447 A70-13289

Soviet monograph on method of functional equations for solving boundary value problems, discussing computer programs and various applications

09 p1712 A70-23548

Thin airfoil theory, discussing harmonic Dirichlet problem for complex plane

10 p1798 A70-24105

Harmonic functions defining geopotential and gravity derived from satellite orbit dynamics, applying to earth shape parameters

13 p2398 A70-29208

Boundary geometry of region with fluid motions harmonic functions obeying Bernoulli law containing free surface curvature

23 p4218 A70-44337

Homotopic classification of boundary value problems with directional derivatives for harmonic functions

23 p4212 A70-44348

Gravitational field fine structure representation near earth surface as sum of global model in spherical harmonics and local model in harmonic B functions

24 p4328 A70-45287

HARMONIC GENERATIONS

Harmonic generation in scattering of electromagnetic waves by anharmonically bound electrons, noting light source intensity

01 p0141 A70-10278

Nonlinear optical properties of lithium niobate single crystals, considering optically induced index inhomogeneity and second harmonic generation

01 p0157 A70-10422

Third harmonic generation detection for strongly absorbing media in reflection with neodymium-glass mode-locked laser, measuring nonlinear susceptibilities of semiconductors and metals

03 p0501 A70-13649

Laser emission intensity fluctuations influence on optical second and higher harmonic production and optical mixing arising from multimode oscillation

04 p0701 A70-14688

Time dependent variation of first and second harmonics amplitudes of diurnal cosmic ray variations during SC magnetic storms

05 p0898 A70-15942

High power giant pulse YAG laser using nonlinear material to achieve complete second harmonic conversion in intracavity experiment

05 p0859 A70-16470

Optical harmonic generation by doubling picosecond laser pulse frequency under nonstationary conditions

06 p1080 A70-17494

Optical third harmonic generation in ADP crystals using mode locked and nonmode locked lasers

06 p1082 A70-17943

Harmonics generated in hot-wire anemometers responses by wires thermal lag and amplitude of flow velocity fluctuations using computerized simulation

08 p1498 A70-21586

Second harmonic generation and frequency conversion efficiencies for laser beam shaping in nonlinear medium

08 p1514 A70-21984

Two photon fluorescence and second harmonic generation methods for studying picosecond structure of laser output signals

09 p1699 A70-23362

Q switched laser pulses lengthened using internal second harmonic generator

10 p1898 A70-23981

Neodymium glass laser fundamental frequency spatial structure effects on KDP crystal second harmonic generation efficiency, describing optimal system for laser beam shaping

10 p1899 A70-24262

Molecular-statistical theory of second-harmonic light generation by isotropic bodies immersed in external AC or DC electric field

10 p1916 A70-24379

Synchronous harmonics generation of sinusoidal signal with given frequency for vibration analysis of linear and nonlinear structures

10 p1860 A70-24550

Second and third harmonic simultaneous generation in ammonium oxalate crystals achieved by three frequency interactions

10 p1901 A70-25159

Intensity and photocounts statistical distribution of harmonic generated in nonlinear crystal by laser and thermal radiation

12 p2248 A70-27547

Alternating electric field effect on weakly ionized gases, analyzing electronic temperature and harmonics generation

13 p2458 A70-28560

Optical second harmonic generation internal to laser cavity, discussing nonlinearity magnitude for optimum coupling for all power levels

13 p2425 A70-28795

Cosmic radiation periodic variations measurements noting second harmonic importance of daily variations

13 p2478 A70-29230

Microwave oscillator providing transition to stable emission at harmonics with power levels comparable to fundamental frequency, considering gallium arsenide oscillation mode

13 p2471 A70-29413

Boltzmann equation in circular magnetic field solved by Fourier series and Legendre polynomials, correcting distribution function due to free electron harmonics

13 p2464 A70-29485

Non Q switched Nd laser light intensity correlation function measurement, using optical gate for producing second harmonic light

13 p2430 A70-29706

Microwave harmonic generation by nonlinear plasma-metal junctions noting calcium, gallium, molybdenum, gold, copper and platinum cathodes

14 p2549 A70-30438

Third harmonic generation using hot electron nonlinearity characteristics of semiconductors, considering plane-polarized electromagnetic wave nonlinear interaction with sample

15 p2783 A70-31970

Far IR second harmonic generation and frequency mixing in CdTe using pulsed water vapor laser

15 p2751 A70-31983

Intensity correlations in optical parametric noise and second harmonic generation measured by two photon delayed coincidence counting

15 p2753 A70-32603

Ruby laser second harmonic radiation generation efficiency, using cylindrical lens beam forming optical system

16 p2929 A70-34212

Pulsed GaAs injection lasers second harmonic generation with nonlinear crystal alpha iodine acid phase matched by angular tuning

18 p3269 A70-36737

Nonlinear effects of harmonic generation and mixing in lithium niobate microwave acoustic surface wave delay lines measured using laser light deflection

19 p3485 A70-37698

CW second harmonic He-Ne laser light second order intensity correlation function measurements

20 p3640 A70-39153

Harmonic generation and small signal mixing in thin magnetic films subjected to static and time varying fields, generating output voltage expressions

21 p3864 A70-42012

EM wave second harmonic generation by plasma wave, discussing decay processes in inhomogeneous plasma layer

22 p4083 A70-43381

Laser light pulse interaction with solid targets, observing second harmonic generation in induced plasma from time resolved spectra

22 p4084 A70-43673

Ruby laser second harmonics generation in low loss lithium iodate crystal with high conversion efficiency

24 p4355 A70-46085

HARMONIC GENERATORS

Repetitively Q switched Nd-YAG laser operated with interactivity second harmonic generator to produce one watt average power

13 p2340 A70-29831

Nonlinear resistance and reactance type harmonic generator diodes performance with output in millimeter wave decade

14 p2548 A70-30436

Harmonic generation in gas discharge by frequency multipliers, assessing multipliers capabilities for millimeter wavelength operation

14 p2549 A70-30437

Ferrites as harmonic generators, discussing physical reasons for generation of double frequency magnetization

14 p2549 A70-30439

Multiple remote control systems effectiveness increased via controlled rectifier as even voltage harmonics generator

18 p3235 A70-36427

HARMONIC MOTION

Frequency equation for harmonic waves propagating in fluid filled circular cylindrical cavity in infinite isotropic solid medium

07 p1253 A70-18846

Longitudinal vibrations propagation in nonlinear elastic beam under harmonic kinematic disturbance solved by harmonic linearization method

09 p1773 A70-22541

Elastic harmonic waves propagation in cylinder with longitudinal cavities and in space with cylindrical cavities solved using series method

09 p1783 A70-23387

Membrane theory for thin single layer orthotropic cylindrical shells experiencing harmonic axisymmetric motion

11 p2136 A70-26084

Harmonic fields with boundary flow losses, discussing similarity on basis of dimensional analysis and pi theorem

12 p2271 A70-26877

Artificial satellite orbital motion numerical integration, computing spherical harmonic terms for earth gravitational potential

18 p3334 A70-37063

Linear damping theory, discussing simple harmonic motion model extension to transient motion

19 p3472 A70-38041

HARMONIC OSCILLATION

Optimal dynamic design of system consisting of elastic cantilever rod with two concentrated masses subjected to harmonic vibrations under force at free end

02 p0384 A70-11739

Two dimensional wing model with harmonically oscillating control surface in transonic range, comparing theoretical with experimental results on unsteady pressure distribution

06 p0966 A70-17252

Rectilinear oblique harmonic vibration effect on gyrocompass with torsional suspension

07 p1278 A70-18737

Pressure drop at slender profile performing harmonic vibrations near interface between two media of different density solved by numerical method

07 p1254 A70-19079

Quasi-biennial, annual and semiannual zonal wind and temperature harmonic amplitudes and phases in tropical and extratropical latitudes in stratosphere and low mesosphere

07 p1269 A70-19949

Interference kernel discontinuities in integral equations relating amplitude of angle of attack and pressure distribution on T tail harmonically oscillating in subsonic flow

07 p1416 A70-20210

Integral equation for time development of harmonic oscillations in finite one dimensional chain of elastically coupled discrete elements, using Bessel functions for solution

08 p1547 A70-20535

Static deflection effect on harmonic vibration of system with restoring forces of hardening nonlinear spring, considering gravity effect

08 p1586 A70-21035

Steady harmonic oscillations of half space with circular holes, deriving algebraic equations for boundary value problems

09 p1782 A70-23296

Steady state analysis of harmonic oscillations in HF synchronized transistor autooscillators, considering transistor inertial properties

09 p1649 A70-23341

Unsteady supersonic flow past tail-body system with harmonic oscillatory motions

10 p1803 A70-24789

Monograph on numerical treatment method for harmonically oscillating wings covering pressure distributions, logarithmic singularity, etc

11 p2129 A70-25497

Automatic phase control of demodulating signal in one dimensional extremal system with harmonic tracking oscillations

12 p2205 A70-28338

Drift of two platform gyroazimuth with stabilized base under harmonic or random vibrations

15 p2734 A70-31622

Monograph on harmonic and random vibrations filtering, discussing objects protection from ground vibrations produced by mechanical source

15 p2774 A70-31693

Dynamic response of simply supported elastic bodies due to oscillating point mass executing longitudinal harmonic motion based on linear theory

16 p2993 A70-34092

Nonlinear vibrations of beam harmonically excited by periodic motion of supporting base, using Galerkin method

17 p3185 A70-34962

Heat pipe performance tests under longitudinal harmonic vibration

17 p3193 A70-35751

Steady state ultraharmonic oscillations of first and third order in yielding systems with linear work hardening law

19 p3542 A70-38059

Undamped forced two degree of freedom system with one linear and one nonlinear spring, analyzing subharmonic vibrations by Ritz averaging method

19 p3544 A70-38329

Oscillation harmonics in rods under loads, giving inequalities to obtain algorithm for determination of overtones

20 p3721 A70-39781

Quasi-harmonic friction induced near sinusoidal form vibration, calculating amplitude dependence on sliding velocity

22 p4044 A70-42445

Harmonic linearization method for automatic control systems having hydraulic or pneumatic actuating device with two nonlinear elements

22 p4002 A70-42841

Harmonically oscillating wing linearized motion in subsonic flow, calculating generalized aerodynamic forces

22 p4105 A70-43118

Conducting viscoelastic fluid flow near harmonically oscillating nonconducting flat plate under uniform transverse magnetic field, considering stress-strain rate relationship

23 p4226 A70-44375

Thick wedge large amplitude harmonic oscillations in hypersonic flow

23 p4270 A70-44609

Aerodynamic interferences of lifting surfaces harmonically vibrating in subsonic flow

23 p4136 A70-44765

Pressure measurements on harmonically vibrating sweptback wing with two control surfaces in incompressible flow

23 p4274 A70-44768

Harmonic oscillations recurrence in linear systems with lumped and distributed parameters, obtaining amplitudes by least squares estimator

24 p4379 A70-45483

Oscillatory motion of triangular wing with conical body of arbitrary cross section in supersonic flow, considering wing-body interference effects

24 p4288 A70-45592

Nonlinear systems subharmonic oscillations under polyharmonic disturbance and viscous damping

24 p4427 A70-46378

HARMONIC OSCILLATORS

Coulomb, Gaussian and harmonic oscillator potentials for particle pairs in three body system, using S wave expansion

01 p0147 A70-10519

Linear physical chains with Sturm-Liouville characteristic polynomials used for natural frequency determination of coupled harmonic oscillators or electrical analog

01 p0142 A70-10520

Vibrational energy exchange between colliding diatomic molecules modulated by harmonic oscillators with insignificant frequency difference

01 p0147 A70-11035

Simple harmonic oscillator vibrations due to local random processes in spacecraft launching, calculating oscillator displacement variance

04 p0774 A70-15102

Basis functions with harmonic oscillator radial dependence in Hartree-Fock calculations for light deformed nuclei

04 p0723 A70-15635

High efficiency oscillator using avalanche square wave diode, considering case of silicon p-i-n diode

05 p0819 A70-15815

Vibrational energy exchange between colliding diatomic molecules modulated by harmonic oscillators with insignificant frequency difference

10 p1920 A70-25004

Simple harmonic scotch yoke mechanical oscillator for strain gauge accelerometer calibration in VLF range

16 p2900 A70-32995

Automated programmed device for fatigue tests based on harmonic oscillator, presenting schematic diagram

16 p2900 A70-33068

Coupled simple harmonic oscillators with almost degenerate energy levels, comparing partitioning perturbation techniques with Rayleigh-Schrodinger approach

16 p2955 A70-34002

Harmonic oscillator with exponentially decreasing spring constant, obtaining closed form solution for equation of motion

17 p3137 A70-35602

Reduced dissipation of biharmonic oscillations, examining dynamic model under force and kinematic harmonic perturbation

18 p3344 A70-37070

Three body problem periodic solutions, considering near equilibrium conservative Hamiltonian system consisting of two harmonic oscillators with rationally related frequencies

23 p4213 A70-44897

Harmonic radiation

P-n structure dynamic I-V characteristics at high injection levels mathematically determined, showing rectifying capability decrease with increasing harmonic signal frequency

05 p0892 A70-16196

Single mode neodymium laser second harmonic radiation self focusing resulting in filamentary fractures in solid dielectrics

06 p1080 A70-17496

Frequency equation for harmonic waves propagating in composite circular-cylindrical rods consisting of circular core and circular casing of different material

11 p2145 A70-26693

Second harmonic emission from GaAs injection laser and from stimulated KDP crystal at room temperature

12 p2245 A70-27306

Interference holograms of low temperature nitrogen plasma jet using fundamental and second harmonic ruby laser emissions

13 p2464 A70-29384

Microwave oscillator providing transition to stable emission at harmonics with power levels comparable to fundamental frequency, considering gallium arsenide oscillation mode

13 p2471 A70-29413

Time harmonic waves propagation in elastic half-space with submerged cylindrical cavity, assuming linear plane strain conditions

13 p2518 A70-30010

Circular cylindrical cavity in elastic space, calculating stresses due to incident plane harmonic compression wave

15 p2819 A70-32204

Plane harmonic sound wave reflection and transmission in flowing medium by infinite set of arbitrary spaced and staggered flat plates

16 p2971 A70-34016

Two dimensional positions of fundamental and harmonic type 2 solar bursts, using coronal streamer plasma and backward refracted radiation model

21 p3891 A70-41179

Two dimensional position measurements of harmonic type 2 solar bursts, using 80 MHz observations

21 p3891 A70-41180

Electron beam interaction with external harmonic microwave field in planar diode gap, calculating electric field current and voltage distribution functions

22 p3995 A70-42396

Forced harmonic vibrations of clamped circular plate in inviscid fluid, calculating radiation pressure and power distributions

22 p4073 A70-42646

HARMONICS

NT HARMONIC EXCITATION
NT HARMONIC GENERATIONS
NT HARMONIC OSCILLATION
NT SPHERICAL HARMONICS
NT SUPERHARMONICS
NT TESSERAL HARMONICS
NT ZONAL HARMONICS

Diurnal cosmic ray intensity variations first and second harmonics amplitudes during sudden phase variations diagrammed from neutron monitor data during IGY

05 p0898 A70-15936

Relation between Fourier harmonics equilibrium distribution and bulk viscosity and second thermal conductivity established in critical regions of liquid-vapor condensation and mixing

05 p0958 A70-16550

Parametric coupling between space-time harmonics of electromagnetic wave propagating in dielectrics modulated by pump wave

05 p0815 A70-16660

First harmonic precision improvement of dual input describing function, applying to self oscillation of nonlinear systems

14 p2560 A70-30625

Periodically strip loaded dielectric slab guided electromagnetic waves, discussing attenuation and space harmonics amplitudes relationship

16 p2861 A70-32960

Nd glass laser ultrashort light impulse optical rectification, presenting lower harmonics angular dependence

19 p3443 A70-37287

Harmonic mixed boundary value problem with singularity, deriving approximate solution by dual series technique with conformal transformation and finite difference method

22 p4062 A70-42642

HARRIER AIRCRAFT

Harrier navigation/attack system to provide successful single pass attack for close support and strike roles, noting target finding optimization

10 p1914 A70-24847

Harrier armament system design for ordnance carriage to full combat load factors, describing Weapon Control Panel

10 p1807 A70-24848

Harrier communications and radio navigation aid VLF/UHF and TAC/VHF equipment

10 p1841 A70-24849

Harrier maintainability for reliability with minimum down-time and man hours, discussing servicing, turn-round, role change, inspection and engine changes

10 p1806 A70-24850

Harrier short takeoff fighter aircraft cockpit design, describing layout, lighting, warning and escape systems, etc

12 p2162 A70-27888

Harrier fighter aircraft hydraulic systems and flying controls

12 p2166 A70-27889

Harrier fighter aircraft cabin air conditioning and pressurization system

12 p2166 A70-27890

Harrier fighter aircraft electrical supply system, considering generator design and installation

12 p2166 A70-27891

Harrier aircraft flight test program considering instrumentation, data acquisition, airframe, avionics, systems engineering, etc

13 p2344 A70-28922

Harrier V/STOL trainer aircraft design features including fuselage, cockpit, power plant, etc

13 p2345 A70-28923

Harrier aircraft in Marine Corps close air support role

[AIAA PAPER 70-885] 17 p3018 A70-35804

Magnetic tape instrumentation system installed aboard Hawker Siddeley Harrier for flight development, discussing digital format recording system

19 p3384 A70-38549

Ground station to retrieve and process data recorded on airborne digital magnetic tape instrumentation system for Hawker Siddeley Harrier flight development

19 p3384 A70-38550

Harrier flight testing in terms of V/STOL capability compared with conventional aircraft

22 p3962 A70-42975

Harrier aircraft development history, discussing V/STOL constraints on transonic flight properties

[ICAS PAPER 70-51] 23 p4139 A70-44148

Harrier aircraft operation in Marine Corps for fast reaction close support based near maneuver units

[SAE PAPER 700835] 24 p4290 A70-45887

HARTMANN FLOW
Heat transfer to insulator wall of linear MGD accelerator attached to shock tube, comparing measurements with Hartmann boundary layer analysis

[ASME PAPER 69-WA/HT-53] 04 p0781 A70-14796

Electrical conductivity variations effects in subsonic Hartmann plasma flow under transverse magnetic field in channel with cooled walls

07 p1352 A70-19986

HARTMANN NUMBER
Magnetohypersonic boundary layer interactions, discussing boundary layer thickness relationship to Hartmann and Reynolds numbers

04 p0729 A70-15564

Conducting fluids flow instabilities characterized by incipience at critical electric Hartmann number and convection rate proportional to electric Reynolds number

07 p1348 A70-19265

MHD flow in rectangular duct with arbitrary conductivity via modified Fourier method, obtaining magnetic induction and current for various Hartmann numbers

[ASME PAPER 69-WA/APM-17] 08 p1551 A70-21308

HARTREE APPROXIMATION
Electromagnetic wave propagation in homogeneous plasma waveguide satisfying Appleton-Hartree approximation without collisions in presence of longitudinal magnetic induction

02 p0349 A70-12724

Hartree-Fock method to study doubly even nuclei in 2s-1d shell, generating basis functions by Wood-Saxon well

04 p0722 A70-15318

Basis functions with harmonic oscillator radial dependence in Hartree-Fock calculations for light deformed nuclei

04 p0723 A70-15635

Hartree model to study superfluid He film bound to uniform substrate

05 p0883 A70-16469

Scattering matrix noniterative integral solutions applied to singlet and triplet s-wave Hartree-Fock phase shifts for electron-H-atom scattering

06 p1108 A70-17486

Localized one electron states in perfect crystals of widely separated atoms, using thermal single determinant/Hartree-Fock/ approximation

14 p2626 A70-30488

Coupled channel calculation of inelastic proton scattering from Ne 20 using Hartree-Fock wave functions

17 p3137 A70-34517

HARTREE-APPLETON APPROXIMATION
U HARTREE APPROXIMATION

HARTREE-FOCK APPROXIMATION

U HARTREE APPROXIMATION

HASTELLOY (TRADEMARK)

Elevated isothermal and low cycle thermal fatigue of Hastelloy X, investigating test temperature, cycle frequency and stress temperature effects

06 p1087 A70-17457

HATCHES

Side access hatch system for Apollo command module

16 p2986 A70-34153

HAWAII

Cosmic ray latitude survey in western U.S. and Hawaii in summer 1966 using neutron and muon monitors

01 p0167 A70-10228

HAWK MISSILE

Beaded-doubler reinforced skin design concept for Improved HAWK Missile wing, considering compression stress, weight, cost and field service characteristics

02 p0380 A70-11946

HAWKER SIDDELEY AIRCRAFT

NT AVRO 707 AIRCRAFT
NT BUCCANEER AIRCRAFT
NT DH 121 AIRCRAFT
NT DH 125 AIRCRAFT
NT VULCAN AIRCRAFT

Hawker Siddeley/Smith Trident Autoland Program, discussing flight test data for Smith autopilot and autothrottle certification

03 p0522 A70-13349

Harrier G.R. Mk 1 VTOL vectored thrust aircraft for attacking targets at conventional strike aircraft speed, discussing design and combat effectiveness

06 p0985 A70-17157

Hawker Siddeley Harrier structural design, power plant, rear fuselage, wing tail unit structures, undercarriage features, weight control, fatigue testing, etc

08 p1435 A70-20620

Harrier engine nozzle actuation system role in short ground takeoff run facility, discussing pneumatic system, air motor servo unit and pilot control

09 p1610 A70-22606

HAZARDS

NT AIRCRAFT HAZARDS
NT FLIGHT HAZARDS
NT METEOROID HAZARDS
NT OPERATIONAL HAZARDS
NT RADIATION HAZARDS
NT TOXIC HAZARDS

Occupational and medicative hazards in ophthalmology - Conference, Amsterdam, June 1968

01 p0022 A70-10855

Static electricity hazards and problems in electronics and aerospace industries

07 p1333 A70-18930

Graphite-polyester plastic material with electrical resistance for eliminating static charges leading to explosions

07 p1295 A70-19764

Hazards in manufacturing solid propellants evaluated to design tests and suggest process conditions

07 p1361 A70-19915

HAZE

Venusian atmosphere low reflectivity reinterpretation based on spectrophotometric data indicating constituents of yellow and upper UV haze layers

02 p0377 A70-12555

Haze model atmospheres scattering characteristics by computer simulation concerning optical contrast reduction by aerosols for direct and diffuse radiation

06 p1057 A70-18156

Absorption lines in hazy planetary atmosphere with isotropic scattering, examining phase variations of equivalent width

08 p1571 A70-20910

Critique of blue haze negative hypothesis in preliminary Mariner 6 data report

08 p1578 A70-21556

Blue haze hypothesis of Martian atmosphere using Mariner 6 and 7 blue filter photographs, reviewing topographic observations

10 p1943 A70-24841

Surface haze and vertical aerosol attenuation for various meteorological ranges within 1.2-15 km, tabulating for UV, visible and IR wavelengths

20 p3661 A70-39082

Refractive index complex part effect on polarization and radiance of reflected and transmitted light for continental haze and nimbostratus cloud models

21 p3847 A70-41724

HC-1 HELICOPTER

U CH-47 HELICOPTER

HD-1 GROUND EFFECT MACHINES

U HOVERCRAFT GROUND EFFECT MACHINES

HEAD [ANATOMY]

NT CRANIUM

NT OCCIPITAL LOBES

NT SKULL

Helmet loss and failure role in major and fatal head injuries of USAF ejections

01 p0032 A70-10370

Human head model for craniocerebral trauma analysis, studying fluid filled spherical shell free vibrations axisymmetric response

07 p1219 A70-19243

High risk factors for posttraumatic epilepsy /head injury complicated by subdural hematoma and spike EEG abnormality/ precluding return to flying
09 p1622 A70-23470

Carbohydrate metabolism disorders in head injury cases, comparing incidence with EEG abnormalities
10 p1810 A70-24037

Squid head cartilage properties in terms of light and electron microscopic appearance, amino acid composition and X ray diffraction
24 p4305 A70-46348

HEAD (PRESSURE)
U PRESSURE HEADS
HEAD MOVEMENT
Vestibular sensing system role in providing information concerning vertical, linear and angular head movements to central organs
02 p0246 A70-12191

Mathematical elastodynamic model for parametric dynamic study of forced resonance solution of motion equations during head trauma
02 p0238 A70-12548

Visual vertical related to head tilts, observing location of gravitational vertical
04 p0645 A70-15445

Head movement effect on accuracy of visual and kinesthetic localization for free and fixed head conditions
05 p0803 A70-16669

Monograph on directional hearing in meridian plane with head in fixed position, noting extended concept of sound
08 p1452 A70-21299

Human head-up tilt circulatory stress effects on left ventricular systolic time intervals
10 p1820 A70-24937

Vibration mode response and impact time sensitivity of mechanical impedance of human skull, relating head injury factors
15 p2682 A70-31934

Psychophysical adjustment methods effect on visual vertical orientation during head tilt
15 p2683 A70-32455

Nystagmic response to directional inert shift of endolymph in semicircular canals in frontal plane head subject rotation
18 p3220 A70-36635

Visual target tracking with active head rotation, indicating independent eye response due to vestibulo-ocular reflex
22 p3979 A70-43492

Head movement role in motion sickness as function of angular velocity, discussing prediction of human tolerance in space station
24 p4297 A70-45341

HEADACHE
Headache and personality traits related to visual acuity and brightness sensitivity increases from sea level to high altitude
04 p0633 A70-15444

Nocturnal headache relationship to REM sleep stage from EEG, EOG and EMG data
20 p3569 A70-38994

Occipital migraine in flying personnel, discussing diagnosis and flight status disposition
24 p4297 A70-45344

HEADERS
Oblique flow headers design for heat exchangers based on one dimensional momentum and continuity
08 p1598 A70-21482

HEALTH
NT HEALTH PHYSICS
Health conditions and operational efficiency of Italian military paratroopers during air transportation analyzed from questionnaire data
05 p0807 A70-16494

HEALTH PHYSICS
Health hazards and physiological effects of atmospheric infrasonic waves, discussing sources, ear protecting devices and electrochemical detectors
02 p0247 A70-12467

Infectious disease hazards on space flight, discussing internal environmental factors including resistance and etiologic agents transmission
14 p2537 A70-30366

HEARING
NT ACOUSTIC FATIGUE
NT BINAURAL HEARING
Pilots hearing level based on pure tone threshold audiograms compared with personnel not exposed to job noise
04 p0631 A70-14982

Hearing threshold and ear canal pressure levels, using circumaural enclosure with varying acoustic field
06 p0994 A70-17598

Collection of papers on human hearing, source book in psychoacoustics
06 p0995 A70-17822

Temporary and permanent threshold shifts in hearing of guinea pigs exposed to intense rocket booster engine noise
07 p1214 A70-19931

Auditory averaged evoked potentials to clicks in man subjected to selective listening task, comparing effect on attended and rejected ear
07 p1215 A70-20213

Monograph on directional hearing in meridian plane with head in fixed position, noting extended concept of sound
08 p1452 A70-21299

Functional model of signal analysis and pulse sequence conversion in nervous system at periphery of hearing
10 p1827 A70-25127

Pulse duration dependent threshold intensity difference for sine tones related to dynamic properties of hearing
23 p4155 A70-44699

Information theory of hearing, considering subjective properties of nonsteady sound signals and discernibility relations
23 p4155 A70-44700

HEARING LOSS
U AUDITORY DEFECTS
HEART
NT CARDIAC AURICLES
NT CARDIAC VENTRICLES
NT EPICARDIUM
NT MYOCARDIUM
Piezoelectric ultrasonic crystal on cardiac catheter tip measuring cardiac diameter in vitro and in excised canine hearts
01 p0038 A70-11025

Model for simulating normal/abnormal depolarization and repolarization of heart and to reproduce electrocardiograms, describing design and programming
03 p0432 A70-12889

Book on engineering in heart and blood vessels stressing technological aspects of artificial internal organs
06 p1001 A70-17649

Nucleic acid and protein synthesis dynamics in rat brain and heart during adaptation to high altitude hypoxia
07 p1209 A70-19518

Geometrical model of human cardiac excitation stages based on normal heart anatomy, discussing application to study of QRS loop in vectorcardiogram
07 p1211 A70-19592

P wave and P loop changes during transvenous pacing of specific locations in coronary sinus and left atrium in dogs and man
08 p1445 A70-21266

Biochemical and histoenzymochromic parallels of enzymatic activity in blood, cardiac muscle and liver under hypoxia
08 p1446 A70-21445

Heart dipole moment calculation error due to deletion of individual electrode contributions to surface potential map, analyzing multielectrode grids
08 p1453 A70-21753

Diastolic and equivocal fluttering of mitral valve in aortic insufficiency by echocardiography
09 p1615 A70-22209

Heart dimension measurement by miniature implantable ultrasonic sonomicrometer, describing system design and operation
12 p2174 A70-26897

Chronic hypoxia effects on heart size and hematocrit ratios tested in pigeons
12 p2172 A70-28075

Electrocardiography electrical bridge type leads system based on potential quenching phenomenon, determining electric dipole displacement of heart in transverse plane of body
19 p3369 A70-38208

Electric dipole displacement of heart estimation by supplementing orthogonal with precordial lead, discussing stationary and moving point dipole hypotheses
19 p3369 A70-38209

HEART DISEASES
Mitral stenosis and atrial flutter with atrial sounds heard and recorded, discussing sound generating mechanism
01 p0013 A70-10271

Vascular anatomy correlation with human heart conduction tissue structures to study coronary artery disease cases exhibiting major conduction disturbances by ECG
01 p0013 A70-10273

Oral potassium chloride usefulness and toxicity in EKG nonspecific T wave abnormality evaluation
01 p0014 A70-10274

Serologic evidence of immune mechanisms, including heart muscle antibodies in patients with idiopathic cardiomyopathy, showing no autoimmune disease in majority
01 p0014 A70-10276

Atrial and ventricular gallops incidence during acute myocardial infarction by serial auscultation and phonocardiograms
01 p0014 A70-10277

Intermittent left anterior hemiblock as natural experiments for changes induced by conduction disturbance on human electrocardiograms
01 p0015 A70-10435

Atrial high gain and HF recordings on three plane vector cardiograms for magnitude and direction for normal and heart diseased patients
01 p0015 A70-10436

Right and left atrial polarization time sequence as guide to p wave origin in heart diseased patients following electrical stimulation of atria and ventricles
01 p0015 A70-10437

Autoimmunity to heart tissues in cardiac diseases, reviewing immune mechanisms in rheumatic fever, postcardiomy and postinfarction syndromes
01 p0016 A70-10438

Patients with/without coronary heart disease inhaled various gas mixtures to induce arterial hypoxemia and hyperoxia, noting O availability for myocardial metabolism
01 p0016 A70-10440

Lipid and carbohydrate behavioral abnormalities in patients with angiographically documented coronary artery disease observed by glucose tolerance tests
01 p0016 A70-10441

Reciprocal rhythm occurring with impulses of atrial or atrioventricular (A-V/ nodal or ventricular origin, noting role of A-V nodal pathways
01 p0016 A70-10442

Prospective epidemiological recognition of clinical coronary heart disease, discussing effects of habitual physical inactivity, excessive dietary fat, socioeconomic stresses, etc
01 p0023 A70-10865

External environmental factors, life habits and personality structure effects on development of coronary artery disease, discussing psychosomatic aspects of myocardial infarction
01 p0023 A70-10866

Radio telemetry of athlete hearts, noting strenuous physical stress induction of transient serum potassium increase, metabolic acidosis, T-wave amplitudes, etc
02 p0230 A70-11694

Left ventricular function during paired pulse and single pulse stimulation in dogs, sheep, goats and calves before and after induced heart failure
02 p0233 A70-11719

Valvular aortic stenosis severity estimation using digital computer program and tape recorder for determining valve area
02 p0243 A70-12094

Left ventricle wall forces and dimensional measurements during cardiac cycle based on stress-strain terms, including results for mitral, aortic and myocardial disease
02 p0238 A70-12512

Readers interpretation and applications of Starr criteria for ULF ballistocardiograms, showing uniformity for patients with coronary heart disease
02 p0248 A70-12680

Chronological age correlations with ballistocardiographic modalities /stroke volume and minute volume indices/ for patients with no cardiovascular disease
02 p0248 A70-12682

Intermittent EKG recordings during hypoxia test for detection and diagnosis of heart disorders in airmen
02 p0242 A70-12850

Phonocardiographic and ultrasound observations of acute rejection following cardiac transplantation, considering rejection treatment at early stage
03 p0415 A70-12888

Electrocardiographic criteria for left ventricular hypertrophy diagnosis, using chamber dissection technique
03 p0432 A70-12890

Electrocardiac events observed in cardiac transplant recipient emphasizing unique finding
03 p0433 A70-12893

Functional and organic systolic murmur differentiation using phonocardiography test
03 p0420 A70-13478

Hypercholesterolemia chemotherapy experimental results with five hypocholesterolemic drugs /nicotinic acid, triparanol, aluminum nicotinate, Atromid and nonfenimizing estrogen/
03 p0426 A70-13937

Coronary thromboses age estimation based on comparison of blood cells, fibrin, collagenous tissue and neocapillaries quantitative changes
03 p0426 A70-13938

Pathological Q waves in various diseases in absence of myocardial infarction, discussing electrophysiological mechanism
03 p0426 A70-13941

Pathologic findings of left ventricular papillary muscle related to electrocardiogram, discussing papillary muscle dysfunction syndrome
03 p0426 A70-13942

Phonocardiographic and mechanocardiographic features of patients with nonejection clicks and mid- or late-systolic murmurs
03 p0427 A70-13944

Airline stewards cardiovascular and ischaemic heart disease statistics compared with civilian pilots and general population
03 p0438 A70-14070

QRS and ST-T areas in multiple bipolar chest leads during normal and abnormal activation in patient measured for checking ventricular gradient concept
04 p0632 A70-15307

Hemodynamic determinants of gallop sounds in patients with aortic valve disease based on clinical, hemodynamic and angiographic observations

04 p0633 A70-15308

Ejection click of valvular pulmonic stenosis by external phonocardiograms and intracardiac pressure recordings during successive respiratory cycles

04 p0633 A70-15440

Pathological manifestations of acute myocardial ischemia without acute myocardial necrosis and myocardial infarction, discussing subjects with chronic occlusive coronary atherosclerosis

04 p0634 A70-15456

Platelet function in coronary artery disease and myocardial infarction, considering thrombosis, atherosclerosis, emboli in microcirculation, etc

04 p0635 A70-15458

Myocardial infarction therapeutic prevention possibilities on basis of epidemiologic and dietary studies involving hypercholesterolemia and hyperlipemia in coronary disease

04 p0635 A70-15463

Heparin role in anticoagulant therapy for myocardial infarction based on proved application to other venous thrombotic diseases, noting hemorrhagic complications controllability

04 p0636 A70-15465

Exercise relation to acute myocardial infarction, coronary thrombosis, stenosis and obstruction, discussing prevention value of physical reconditioning in heart patients

04 p0636 A70-15466

Familial aggregation for coronary artery disease and familial similarities in coronary anatomy, considering possible genetic analysis of myocardial infarction

04 p0636 A70-15467

Myocardial metabolism in ischemic heart disease using arterial and coronary sinus catheterization

04 p0636 A70-15469

Sudden and early death in acute myocardial infarction, discussing prophylactic measures

04 p0637 A70-15472

Cardiac echography applied to diagnosis and therapy evaluation in idiopathic hypertrophic subaortic stenosis

05 p0800 A70-16103

Myocardial scarring sites localized in human subjects by HF ECG components

05 p0800 A70-16104

Computer program for on-line analysis of exercise ECG considered for improved diagnosis of ischemic heart disease

05 p0805 A70-16105

Diurnal and seasonal variations of mortality due to cardiac and regulatory failure using model representing daylight regulation of human organism

05 p0802 A70-16663

Hemodynamics in cardiosclerosis patients and healthy subjects under hypoxia, investigating heart activity and blood circulation

06 p0994 A70-17667

Acute myocardial ischemic injury and infarction in dogs related to changes in man using oxygraph tracings

06 p0997 A70-18405

Ventricular ectopic beats and bradyarrhythmia associated with myocardial infarction, discussing enhanced automaticity, reentry activity, drugs and heart pacing

06 p0998 A70-18407

Bradycardic rhythms in acute myocardial infarction, investigating pathophysiologic, hemodynamic and electrophysiologic aspects and ECG interpretation

06 p0998 A70-18408

Arrhythmia monitor for cardiac distress prediction, using small hybrid computer for detection of abnormal rhythm and ECG complex comparison

07 p1221 A70-19604

Exercise habits and environmental emotional stresses role in origin and prevention of degenerative heart disease

07 p1212 A70-19692

Physical activity and epidemiology of coronary heart disease

07 p1212 A70-19694

Epidemiologic investigation of physical activity and fitness effect on prevention of premature clinical coronary heart disease

07 p1212 A70-19695

Myocardium, endocardium and/or epicardium disease characteristics, discussing primary and secondary cardiomyopathy groups

09 p1616 A70-22277

Postinfarction noncoronarygenic afflictions of myocardium in flight personnel, discussing clinical record, atherosclerotic differentiation and ECG variation

09 p1617 A70-22474

Idiopathic myocardial disease patients investigated for serological anomalies and markers of immunopathology

09 p1621 A70-23301

Vectorcardiographic diagnosis of left ventricular hypertrophy based on changes in MQV magnitude and other QRS vectors

09 p1629 A70-23626

Ischemic heart disease /IHD/ prognosis using abnormal electrocardiographic stress test

10 p1820 A70-24940

Cardiovascular model for closed loop analog simulation of congenital heart defects hemodynamics

11 p1990 A70-25705

Arteriographic determination of severe coronary artery disease in presence of normal resting electrocardiogram

12 p2170 A70-27775

Air transport of cardiac patients with auriculoventricular blocks, noting feasibility due to portable surveillance and treatment apparatus

12 p2172 A70-28041

Heart rhythm disorders among flying personnel, noting occurrence frequency of sinus bradycardia and arrhythmia

12 p2180 A70-28362

Intrinsic heart rate /IHR/ range and variability in healthy subjects measured showing age as important determinant in absence of heart disease

15 p2678 A70-31433

Asymptomatic myocardial infarction in USAF flyers detected by annual electrocardiograms

15 p2690 A70-31889

Primary myocardial disease, describing hemodynamic and angiographic observation of left ventricular volume and wall changes

16 p2848 A70-33110

Coxsackie B virus as cause of myopericarditis in adults

17 p3025 A70-34860

Hemodynamic response to dopamine before and after myocardial infarction in dogs

17 p3026 A70-35200

Single ventricle and hypoplastic left and right heart syndromes, investigating with reflected ultrasound

17 p3032 A70-35472

Continuous murmur due to combination of rheumatic mitral stenosis and rare type of partial anomalous pulmonary venous drainage

17 p3032 A70-35473

In-flight coronary occlusions role in aircraft accidents, discussing need for full autopsies, Double Masters ECG and full medical histories

17 p3033 A70-35570

Focal myocarditis associated with aircraft accidents, discussing difficulties in diagnosis and assessment

17 p3033 A70-35571

Electrocardiograms amplitude probability densities, noting variations for different heart diseases

17 p3034 A70-35877

Cutaneous liquid crystal temperature sensors for thermographic patterns of angina pectoris induced by treadmill exercise

19 p3364 A70-38361

Circadian rhythms from electrocardiogram and cardiostachogram of patient with human heart transplant, noting P waves relationship between donor and recipient tissues

20 p3570 A70-39166

Pathophysiology of congenital heart disease - Conference, University of California, Los Angeles, July 1967

20 p3570 A70-39361

Pulmonary hypertension in congenital heart diseases as function of blood flow

20 p3571 A70-39367

Multifocal atrial tachycardia, discussing arrhythmia progression to atrial fibrillation and association with acute and chronic diseases

21 p3761 A70-41134

ULF ballistocardiogram amplitudes relationship to blood flow velocity for cardiovascular disease diagnosis

21 p3763 A70-41234

Postexercise electrocardiogram detection of latent coronary heart disease in flyers prior to myocardial infarction

21 p3771 A70-41494

Epidemiological investigations of coronary disease in Finland, relating customary loads and working capacity

22 p3969 A70-42903

Coronary heart disease risk factors and prevention, discussing blood pressure, cholesterol, body weight, smoking, etc

22 p3975 A70-43693

Flying personnel fitness, discussing Wolff-Parkinson-White syndrome

22 p3975 A70-43695

Indirect serial determination of left ventricular systolic ejection time changes in human patients with acute transmural and nontransmural myocardial infarctions

23 p4144 A70-43946

Coronary heart disease prediction based on clinical suspicion, age, total cholesterol and triglyceride, using relationships established by cinearteriographic studies

23 p4145 A70-43947

Cinecoronary arteriographic investigation of chest pain patients, establishing correlations of clinical symptoms, coronary artery narrowing, arterial lesions, serum cholesterol levels, etc

23 p4145 A70-43948

Optimum bed rest time schedules for cardiovascular patients from neurological, dynamometric, electromyographic and myogenic-tonus tests

23 p4149 A70-45077

Human atrial systole timing influence on mitral valve closure and on first renewed heart sound following blockage

24 p4302 A70-46077

HEART FUNCTION

NT HEART MINUTE VOLUME

Cardiac activity temperature coefficients in dogs, specifying physical and chemical cardiac functions

01 p0012 A70-10052

Bioelectrically controlled system for indirect heart massage, noting dynamic simulation of system on digital computers using block oriented programming languages

01 p0047 A70-10261

Artificially induced heart rate changes effect on atrial circumference and pressure in anesthetized cats, showing increase with tachycardia and bradycardia

01 p0017 A70-10473

Physiological interpretation of blood velocity curves recorded in right heart cavities of dogs by ultrasonic directional probe, using Doppler effect

01 p0035 A70-10709

Canine aortic flow as function of simultaneous mean aortic and mean right atrial pressures

02 p0233 A70-11723

Physiological signals of cardiovascular system transducing methods applied to vector ECG, heart sounds, peripheral pulse waves, chest microphone and plethysmography

02 p0243 A70-12095

Absolute ULF ballistocardiogram /BCG/ values as pulsatile fluid pumping values in cardiodynamic function before and after exercise

02 p0248 A70-12677

Stroke volume formula depending on blood density and viscosity, indicating Hagen-Poiseuille law nonapplicability to ballistocardiography

02 p0248 A70-12681

Release-recovery and dynamic stiffness phenomenon in frog heart muscle at various Ca ion concentrations and temperatures

02 p0241 A70-12771

Controlled premature atrial stimulation effects on atrioventricular conduction in man, using electrode catheter technique to record electrical activity of specialized conducting fibers

03 p0415 A70-12886

Arterial counterpulsation effect on mechanics of left ventricular contraction and myocardial oxygen consumption in normal and abnormal animals

03 p0416 A70-13009

Myocardial changes in rabbits after general chronic ionizing irradiation attributed to lower cardiac activity, hypotrophy and dystrophy

03 p0425 A70-13888

External work and energy expenditure relations of heart, including myocardial oxygen consumption

03 p0426 A70-13940

Cardiac output and coronary blood flow changes in patients at rest and during peak exertion, stating correlation coefficients

03 p0428 A70-14065

Acidosis effects on anoxic rat heart cardiac performance and anaerobic energy generation

04 p0635 A70-15461

Ventricular performance as function of infarcting myocardium, discussing dynamic characteristics

04 p0637 A70-15470

Glucagon infusion effect on human coronary circulation, relating changes in cardiac dynamics to myocardial oxygen consumption and blood flow

05 p0800 A70-16101

Propranolol effects on human cardiac conduction and intraventricular conduction in dogs studied by recording His bundle electrograms, noting P-H interval prolongation

05 p0800 A70-16102

Cardiac work limiting factors during exercise under hypoxia, studying cardiac output and coronary blood flow capacities

06 p0991 A70-17282

Alpha-methyl-DOPA inhibitor effect on catecholamines and cardiac spontaneous activity in pacemaker fibers in rabbits

06 p0992 A70-17422

Cranioerebral hypothermia effects on phase structure of cardiac thrust in dogs

07 p1204 A70-19140

Left ventricular function myocardial infarction induced acute depression and subsequent recovery in intact conscious dogs

07 p1211 A70-19615

Exercise influence on cardiac output and coronary blood flow during hypoxia, correlating CO and systolic pressure with blood flow changes

07 p1214 A70-19928

Cardiovascular control system mathematical model incorporating fundamental properties of heart muscle for digital simulation using FORTRAN program

08 p1453 A70-21513

- Strong magnetic field effects on squirrel monkeys electrical and mechanical cardiac functions determined from vectorcardiogram and aortic blood flow characteristics 09 p1617 A70-22524
- Hyperbaric oxygen effect on heart muscle contractions in mammals, considering cells enzymatic activity and substrate utilization 09 p1623 A70-23586
- Left ventricle pressure rise rate as function of heart contractility and hemodynamics 09 p1623 A70-23587
- Soviet book on nervous stress and cardiac activity covering hypothalamus and cardiovascular reactions and cardiac component of complex conditioned reflexes and emotional reactions 10 p1809 A70-23873
- EKG and cardiac rhythm changes during prolonged hypodynamia /bed rest/ with restricted physical activity 10 p1814 A70-24669
- Prolonged hypodynamia effect on human cardiac cycle phases using poly- and kinetocardiographic data 10 p1814 A70-24672
- Prolonged hypodynamia effect on heart size and myocardium function obtained from human chest X ray studies 10 p1814 A70-24673
- Electrocardiac activity, myocardium and hemodynamic disorders in subjects after prolonged hypodynamia with or without physical exercises and during orthostatic test 10 p1817 A70-24692
- Human head-up tilt circulatory stress effects on left ventricular systolic time intervals 10 p1820 A70-24937
- Ultrasonic echography for ventricular size determination, calculating stroke volume and valvular regurgitation severity 10 p1820 A70-24938
- Oxygen transport after cardiopulmonary resuscitation from asystole and ventricular fibrillation in dogs 10 p1822 A70-25085
- Cardio-respiratory functions preceding syncope induced by combined lower body negative pressure and head-up tilt 11 p1988 A70-26510
- Respiratory syncope with cardiac ineffectiveness and numerous complications during and after flight at high altitude clinically observed for causes 12 p2171 A70-28040
- Microwave radiation effects on radar operators myocardium functions 12 p2180 A70-28358
- Periodic high temperature effects on human systolic phase dynamics 12 p2174 A70-28359
- X ray irradiation effects on phonocardiograms, EKGs, cardiac activity phases and Kunos-Garan mechano-electric coefficient in dogs 13 p2350 A70-28890
- Intrinsic heart rate /IHR/ range and variability in healthy subjects measured showing age as important determinant in absence of heart disease 15 p2678 A70-31433
- Comparative cardiac output measurements in dogs using left/right heart dye injections and pulmonary/aortic electromagnetic flow probes 15 p2688 A70-31434
- Isolated human heart measurements for time course and instantaneous distribution of normal heart excitatory process 15 p2683 A70-32471
- Cardiac structure-functional relations, discussing muscle strand continuum, basal fibrous skeleton, epicardial, endocardial and myocardial layers 15 p2685 A70-32834
- Contractile mechanics of cat papillary muscle during hypoxia and reoxygenation recovery 15 p2686 A70-32836
- Autonomic drugs induced contractures of cardiac muscle of frogs, relating inotropic action with Ca influx during low membrane potential 15 p2686 A70-32837
- Oxygen uptake and cardiac output in males during submaximal and maximal treadmill and bicycle exercise 17 p3039 A70-35428
- Glucose-free fatty acid interactions in working heart, noting increase in glucose uptake, oxidation and glycogenolysis with physiologic work increment 17 p3031 A70-35429
- Minnesota Impedance Cardiograph method evaluated by applying to cardiac output measurements in postural stress studies 17 p3031 A70-35431
- Human cardiac flow during acceleration as function of time with and without anti-g suit, using electric plethysmograph 17 p3040 A70-35915
- Left ventricle pumping function self regulation mathematical model, obtaining transfer function 18 p3217 A70-36080
- Soviet book on isolated animal heart autoregulation, considering cardio-pulmonary preparations, functional capacity, biometrics and computer technology for heart activity simulation models 19 p3359 A70-37404
- Cardiac rhythm, respiration and rhythmical processes of alimentary tract, using digital data device 19 p3370 A70-38214
- Cardiac contraction rhythm autocorrelation and spectral analysis in healthy subjects and patients with disturbed sinus node functional states 20 p3578 A70-38963
- Mechanical analysis involving clamping apparatus for cardiac muscle contractile response 20 p3570 A70-39362
- Muscular mechanics of intact heart contraction, discussing effects of altered fiber length, afterload and inotropic state 20 p3571 A70-39363
- Cardiac ventricular function in compression pump terms, relating mechanical activity to end-diastolic fiber length 20 p3571 A70-39364
- Ultrasonic nonsearch Doppler cardiography for cycle phase analysis, recording single functions 20 p3581 A70-40199
- Heart stroke volume estimation at submaximal exercise using blood hemoglobin content and heart rate 20 p3576 A70-40328
- Ethanol ingestion effect on human response to submaximal and maximal exercise, measuring cardiac output and intraarterial pressure 21 p3761 A70-41135
- Hypoxia and hyperoxia effect on ballistocardiogram of healthy males, determining systolic and minute cardiac forces 21 p3763 A70-41231
- Ballistocardiogram relationship to cardiac performance index in hypoxia and hyperoxia conditions, investigating systolic and minute cardiac forces 21 p3770 A70-41232
- Blood velocity in ascending aorta in man by transcutaneous ultrasonic Doppler technique, investigating heart hemodynamic performance and systemic perfusion 21 p3770 A70-41235
- Contractive function of myocardium in middle and advanced age individuals under high physical loads during prolonged periods 22 p3970 A70-42907
- Atrioventricular conduction in the human heart, analyzing electrocardiogram response patterns recorded by electrode catheter in unanesthetized man 22 p3970 A70-42942
- Space flight effects on dogs cardiac activity, brain circulation and systemic-tissue circulation interactions 22 p3972 A70-43635
- Atherosclerosis and latent coronary insufficiency diagnosis in flight crews, evaluating various tests 22 p3975 A70-43696
- Human atrial systole timing influence on mitral valve closure and on first renewed heart sound following blockage 24 p4302 A70-46077
- HEART MINUTE VOLUME**
- Chronological age correlations with ballistocardiographic modalities /stroke volume and minute volume indices/ for patients with no cardiovascular disease 02 p0248 A70-12682
- Computer evaluation of photographic imagery of left ventricle volume obtained by cineangiography, including densitometric measurements 03 p0434 A70-13678
- Automatic photo-optical technique for processing of cineangiograms to find time-course history of left ventricular volume 04 p0641 A70-14559
- Circulating blood volume and heart minute and stroke volumes in rabbits, using isotope-labeled albumin 19 p3366 A70-38724
- Sea sickness symptoms in relation to reduced minute blood volumes in human after Coriolis acceleration 23 p4149 A70-45079
- Human cardiovascular compensatory responses to environmental cold stress, relating heart stroke to increased oxygen consumption 24 p4302 A70-46103
- Cardiovascular dimensions changes and heart volume in physically trained young men, comparing with response in old age 24 p4303 A70-46109
- Electronic simulation of indicator-dilution curves for comparative evaluation of cardiac output computers 24 p4309 A70-46120
- HEART RATE**
- NT ARRHYTHMIA
- NT BRADYCARDIA
- NT SYSTOLE
- NT TACHYCARDIA
- Computer analysis and comparison of ST segment on Frank and bipolar lead electrocardiograms of healthy persons and cardiac patients during exercise, noting physiological responses 01 p0013 A70-10270
- On-line electronic integration of aortic flow during systole to provide beat by beat readout of stroke volume 01 p0038 A70-11044
- Heart rate and skin conductance measurements during attention-direction tasks involving proprioceptive stimuli position on environmental acceptance and rejection continuum 01 p0026 A70-11166
- Heart rate change effect on myocardial oxygen consumption and nutritional circulation with constant coronary blood flow suggesting oxygen extraction independence of capillary surface 02 p0235 A70-11991
- Life support system model using heart rate to monitor man doing physical work in space suits under simulated space environment 02 p0245 A70-12146
- Accelerative and decelerative heart rate responses in human subjects given differential conditioning trials by auditory and electric shock stimuli under paced respiration 02 p0239 A70-12628
- Atrioventricular conduction in atrial fibrillation and flutter in man, using His bundle recordings 03 p0415 A70-12887
- Ultrasonic Doppler method for timing mitral and aortic valves rapid movements, using filter to eliminate LF signals due to heart walls 03 p0432 A70-12891
- Conditioned reflexes, respiration and heart beat rates changes in white rats under hypothermia 03 p0424 A70-13717
- External work and energy expenditure relations of heart, including myocardial oxygen consumption 03 p0426 A70-13940
- Heart rate augmentation during constant performance in excess of endurance limit, considering muscle fatigue 03 p0431 A70-14292
- Diurnal variations of phase coupling between heart beat and respiration under resting conditions and modification by quantitatively regulated physical effort 03 p0431 A70-14294
- Physiological load of exercise at altitude evaluated by heart rate and recovery rate measurements 04 p0631 A70-14984
- Bed rest effects on whole leg venous distensibility, discussing heart rate and leg volume measurements 06 p0999 A70-17288
- Heart rate-body temperature relationship during walking in hot environment 06 p0993 A70-17431
- Heart rate and circulatory load as ergonomic criteria based on muscular work, environment temperature, mental stress, etc 06 p0997 A70-18017
- Statistical methods for characterizing interval sequences of ECG, treating interval distribution and joint probability density function of adjacent interval pairs 07 p1211 A70-19593
- Energy cost and heart rate responses to single state, nonsteady state submaximal exercise procedures used in diagnostic and functional testing 07 p1211 A70-19690
- Physical training effects on sedentary men with stable activity pattern, recording heart rates and oxygen uptake 07 p1215 A70-20171
- Heart frequency profiles of persons during parachute jumps measured by electrocardiograms recorded directly and telemetrically to investigate psychical and physical stresses 09 p1626 A70-23010
- Electromagnetic flowmeter for cardiac output changes in unanesthetized rats, discussing construction, form and associated electronic equipment of implanted probe 09 p1627 A70-23267
- Metabolic and heart rates determined in experienced and inexperienced pilots during Hiller 12-E and 12-EL helicopters flight through standard maneuvers 09 p1627 A70-23455
- Heat accumulation, oral temperature and heart rate recovery of subjects in various thermal environments 10 p1810 A70-24034
- Ballistographic psychological evaluation of heart and circulatory system by recording displacement, velocity, acceleration and total forces imparted during each beat 10 p1810 A70-24039
- Arterial oscillograms, pressure and heart beat rate during prolonged hypodynamia, noting neurocirculatory dystonia 10 p1817 A70-24693
- Left ventricular volumes, pressure and heart rate in patients and dogs after diagnostic coronary arteriography 10 p1820 A70-24939

Conditioned reflexes, respiration and heart beat rate changes in white rats under hypothermia

11 p1985 A70-25517

Rats heart rate change during running at simulated altitude, discussing respiratory-circulatory training effect

11 p1985 A70-25671

Rhesus monkeys tolerance to graded increase in closed environment carbon dioxide, examining heart rate and cardiac rhythm

11 p1988 A70-26517

Civil airlines training captains heart rate response to simulator stress, base conversion and line training

11 p1992 A70-26519

Canoe paddlers physical training effect on cardiac output and local blood flow and metabolism at and during exercise and recovery

12 p2169 A70-27653

Respiratory gas exchange, heart rate, arterial acidemia and hypoxemia responses to physical work in hyperbaric environments and hyperoxia conditions

12 p2169 A70-27655

Autonomic effects on heart rate, portal, renal, cutaneous and muscle blood flows during arterial hypoxia in unanesthetized sham operated thalamic and pontine rabbits

12 p2170 A70-27899

Paced respiration and selective attention effects on heart rate and finger pulse amplitude in adult females subjected to visual stimuli

13 p2350 A70-29241

Cardiac cycle and phases shortening observations from analyzing electro- and phonocardiographic data recorded during Gemini flights

13 p2359 A70-29437

2000 meter race for endurance testing, using heart rate radiotelemetry before, during and after

14 p2543 A70-31173

Actoballistocardiography based on piezoelectricity for biorythmic activity, respiratory movements and heart rate of small animals

14 p2543 A70-31321

Intrinsic heart rate /IHR/ range and variability in healthy subjects measured showing age as important determinant in absence of heart disease

15 p2678 A70-31433

Sleep intensity and stages from EEG studies concerning rapid eye movements, vegetative nervous system, heart/respiration rate, blood pressure, body temperature and stomach motility

15 p2680 A70-31743

Heart rate elicitation and blood pressure increase, considering parasympathetic and sympathetic nervous outflows adjustments of initial cardiovascular response to muscular contraction

15 p2684 A70-32535

Heart rate variations due to influence of body position rapid changes, emphasizing oxygen consumption in crouching position

17 p3024 A70-34591

Oxygen uptake capacity, ventilation, heart rate and acid base values during bicycle ergometer exercise

17 p3036 A70-34594

Centrifugation effects on human peripheral arterial pulse behavior

17 p3037 A70-35126

Serum calcium-digitalis synergism effect on dogs heart excitability, noting hypoxia role in arrhythmia production

17 p3026 A70-35325

Aldosterone effects on hemodynamics of dogs under restricted motor activity, observing cardiac activity stimulation

17 p3030 A70-35358

Sheep cardiac rate, respiration rate, hematocrit, erythrocytes per cubic mm and hemoglobin concentration responses to elevated ambient carbon dioxide

17 p3030 A70-35421

Intact femoral artery pressure-diameter relationship in man, discussing noradrenaline infusions effects

18 p3222 A70-37222

Heart stroke volume estimation at submaximal exercise using blood hemoglobin content and heart rate

20 p3576 A70-40328

Athletes ventilation and heart rate dynamic responses to supine leg exercise with sinusoidal work load

20 p3576 A70-40329

Myocardial blood flow response to cardioacceleration by right atrial pacing in normal subjects, using coincidence counting

21 p3760 A70-40576

Cardiac glycosides and beta receptor blocking agent effect on ULF displacement ballistocardiogram in healthy young men, measuring heart rate and blood pressure

21 p3763 A70-41227

Heart rate-time curves before, during and after step-up exercise in relation to physical fitness

22 p3978 A70-42873

Mathematical model of heart beat control during muscular activity in aging individuals, reflecting neural and hormonal control circuits

22 p3969 A70-42901

Valsalva maneuver beat-to-beat effects on systolic cardiac intervals compared with time based measurements

22 p3972 A70-43484

Safety standards and biological effects of microwave radiation, investigating cataractogenesis and heart rate in rabbits

23 p4144 A70-43790

Real time contourgraphic electrocardiographic display determining heart rate from CRT face on beat-by-beat basis

23 p4150 A70-44377

Pilot heart rate during in-flight simulated ILS approaches in general aviation aircraft

24 p4306 A70-45333

HEAT

NT DRY HEAT

Systematization of thermodynamic cycles from elementary reversible evolutions concerning exchange of work, heat and combined relations

06 p1173 A70-17470

HEAT ACCLIMATIZATION

U ACCLIMATIZATION

U HEAT TOLERANCE

HEAT BALANCE

Gas flow in pipe with uniform wall heat flux, analyzing turbulent heat transfer using heat balance equation [ASME PAPER 69-HT-11]

08 p1486 A70-21834

Hydrogen-oxygen fuel cell reaction water removal and heat loss using reconcentration device

12 p2163 A70-27066

ESRO-I satellite attitude stabilization and thermal balance

13 p2505 A70-28842

Earth radiation balance climatological characteristics based on satellite and published data, analyzing earth-atmosphere albedo on global scale

14 p2603 A70-30402

Matter and heat balance of cosmic grains surrounded by plasma and neutral gas under radiation

22 p4097 A70-42473

HEAT BUDGET

NT ATMOSPHERIC HEAT BUDGET

HEAT CAPACITY

U SPECIFIC HEAT

HEAT CONDUCTION

U CONDUCTIVE HEAT TRANSFER

HEAT CONTENT

U ENTHALPY

HEAT DISSIPATION

U COOLING

HEAT DISSIPATION CHILLING

U COOLING

HEAT EFFECTS

U TEMPERATURE EFFECTS

HEAT ENGINES

U ENGINES

HEAT EQUATIONS

U THERMODYNAMICS

HEAT EXCHANGERS

NT TUBE HEAT EXCHANGERS

CH-54 engine air inlet antice system design, manufacture and testing, solving heat balance equations describing tapered gap heat exchanger

01 p0165 A70-10693

Length calculation method for nonadiabatic imaginary tip extension of heat exchanger fins, predicting heat conduction rate

01 p0215 A70-10842

Heat exchange unit for low thrust attitude control propulsion system evaporator designed for converting liquid propellants to gas

01 p0216 A70-10969

Monograph on laminar flow heat transfer in thermal entrance region of flat and profiled ducts, treating construction and efficiency of plate heat exchangers

03 p0603 A70-12988

Heat exchangers efficiency taking into account surface, weight and cost

05 p0958 A70-16551

Heat transfer coefficients for heat exchangers rotating in air at various velocities computed from skin friction coefficients in laminar and turbulent flow regime

06 p1177 A70-17701

Oblique flow headers design for heat exchangers based on one dimensional momentum and continuity

08 p1598 A70-21482

Whirl effect on heat exchanger efficiency and reliability, discussing tests with transparent models and defective filling of circuits by feeding system

10 p1968 A70-24400

Heat transfer in Z shaped regenerative heat exchangers with/without air mixing, determining parameters defining thermal efficiency

13 p2520 A70-28857

Flow nonuniformity effects on heat exchangers efficiency

15 p2827 A70-32140

Book on heat transfer covering conduction, convection, thermal radiation and heat exchange equipment

19 p3550 A70-37231

Diathermic heat exchange cooling systems, analyzing volume boiling in terms of separation into convective and radiative components

19 p3550 A70-37239

Pin fin coldplate heat exchanger for cooling Apollo spacecraft electronic equipment, calculating forced convection heat transfer and fluid pressure drop

21 p3797 A70-41025

Thermal efficiency of ceramic and metal heat exchangers for biowaste resistojet thrusters

[AIAA PAPER 70-1135] 21 p3868 A70-41779

Aerobee rocket-borne cryogenic air samplers heat exchanger design by mathematical model and computer solution

23 p4280 A70-44365

Cryogenic fluid heat exchanger flow oscillation automatic feedback control, discussing design and simulation

23 p4280 A70-44370

HEAT FLOW

U HEAT TRANSMISSION

HEAT FLUX

Solid bodies unsteady thermal conductivity in presence of quasi-steady heat transfer under combined radiant and thermal fluxes, presenting thermodynamic nomograms

01 p0213 A70-10215

Hot junctions nonuniform heating influence on thermoelectric generator efficiency, taking into account temperature dependence of thermoelement materials properties

01 p0009 A70-10753

Power and location prediction at critical heat flux onset under nonuniform axial heating conditions, using local approach method

01 p0219 A70-11303

Diffuse soft X ray photoionization and heating of H I regions compared to cosmic ray heating

02 p0364 A70-11784

Radiative transfer in nongray gas between parallel walls, solving heat flux and temperature distribution

02 p0392 A70-11907

Nonsteady thermal decomposition of plastics subjected to large heat flows, introducing equations governing char layers and pyrolysis zones

02 p0397 A70-12021

Low temperature high sensitivity temperature compensated heat flux transducers to measure conductive, convective and radiative heat transfer

02 p0303 A70-12740

Periodic shock fronted longitudinal pressure wave effect on instantaneous heat flux rates at tube end wall

02 p0400 A70-12860

Two dimensional approximate formulation for radiant heat flux applied to radiative equilibrium in gray gas

03 p0603 A70-12905

Transverse magnetic field effects on electrode heat fluxes in heavy-current discharge, discussing anodic space thermal ionization

03 p0531 A70-13205

Extrapolation formulas to calculate temperature gradients and heat fluxes in solid heated by variable heat flux, estimating errors

03 p0606 A70-13521

Measured heat flux conversion into average radiation incident on convex satellite surfaces in test chambers

03 p0606 A70-13536

Transient and steady state radiation heat flux sensors calibration by developing and evaluating heat flux source

03 p0606 A70-13558

Turbulent reattachment of supersonic axisymmetric jet on cylindrical wall in air, investigating wall temperature effect on cavity pressure and heat flux

03 p0467 A70-13643

Radiative heat flux between two parallel copper disks at cryogenic temperature, showing dependence on emitter temperature and spacing

04 p0784 A70-14823

Matrix analysis of steady state temperature field and heat flux through multilayer, plane, cylindrical or spherical partitions with internal heat sources

04 p0785 A70-14924

Heat fluxes, shear stresses and pressures distribution at spike on body in supersonic flow from asymptotic solutions of Navier-Stokes equations

04 p0673 A70-15232

Response characteristics of asymptotic or Gardon type thin foil heat flux transducer, discussing heat transfer coefficient effect on response time and curve

04 p0694 A70-15548

Laminar flow in circular pipe with arbitrary axial variation of wall temperature or heat flux, using integral type approximation

05 p0957 A70-16519

Heat transfer boundary conditions determination in studying heat protective coatings effectiveness, discussing measurement methods for stagnation temperatures and heat fluxes from exhaust gases

06 p1173 A70-17662

Bulk and wall temperature measurements for natural fluid convection in container with and without baffles for various heat flux and aspect ratios

06 p1175 A70-17684

Heat radiation effect on set-up and scale of cellular convection in atmosphere

06 p1097 A70-17789

- Unsteady inverse heat conduction of semibounded body solved by least squares method 06 p1178 A70-17856
- Convective and radiative heat fluxes measurement on charring ablative materials surface in rocket nozzle environment 06 p1070 A70-18444
- Microsecond-response bolometer for measuring thermal fluxes as function of time in high explosion driven shock tubes and plasma jets 06 p1070 A70-18445
- Heat flux, electrical and thermal conductivity of H measured on plasma in cascade arc chamber of high power load at 1 atm pressure 06 p1107 A70-18525
- Time dependent relaxation model for heat flux in metals from quantum mechanical form of Boltzmann transport equation, yielding damped wave equation for temperature 06 p1090 A70-18612
- Electrically heated wire diameter and orientation on heat flux in saturated pool and surface boilings of water and aqueous binary mixtures 07 p1417 A70-18643
- Empirical method for calculating critical thermal flux density during boiling of underheated liquid-vapor systems 07 p1420 A70-19068
- Heat exchange in laminar and turbulent boundary layers on plate for arbitrary heat flux distribution allowing for initial unheated plate segment 07 p1423 A70-19657
- Specific radiant heat flow and spectral blackness degree of tungsten with different surface finish 07 p1309 A70-19662
- Steady temperature field of two dimensional periodic contact surface in vacuum, using conjugate harmonic functions for thermal flux lines, isotherms and thermal resistance 07 p1423 A70-19820
- Turbulent thermal flux in Venus atmosphere estimated from amplitude fluctuation dispersion of Venera 4 and Mariner 5 radio signals 07 p1390 A70-20305
- Gas flow in pipe with uniform wall heat flux, analyzing turbulent heat transfer using heat balance equation [ASME PAPER 69-HT-H] 08 p1486 A70-21834
- Atmospheric momentum and heat flux height variations in surface boundary layer, stressing instrument performance and measurement techniques 09 p1715 A70-22359
- Heat, moisture and momentum fluxes measurement in atmospheric boundary layer, discussing instrumental accuracy necessary for various measuring techniques 09 p1717 A70-22379
- Temperature distribution in infinite and finite circular hollow cylinders, considering surface heat flux and linear heat transfer 09 p1788 A70-22595
- Anode energy transfer model for measurement of circumferential current and heat flux distributions of MPD arc thruster 09 p1736 A70-23203
- Flux equations of single velocity Boltzmann type for unsteady transport problems applied to concentration discontinuity propagation through plane layer 10 p1966 A70-23871
- Heat radiation effect on set-up and scale of cellular convection in atmosphere 10 p1882 A70-25021
- Empirical method for calculating critical thermal flux density during boiling of underheated liquid-vapor systems 10 p1970 A70-25219
- Temperature and heat flux in plane, cylindrical and spherical multilayer diaphragms with boundary conditions, assuming harmonic temperature variation 10 p1970 A70-25321
- Energy equations solved for step change of wall temperature and heat flux, determining turbulent heat transfer in tube, discussing asymptotic solutions validity 11 p2146 A70-25334
- Transient heat flux measurement with surface thermocouples, thin film resistance thermometers and mathematical computation programs 11 p2065 A70-25768
- Gas passing through shock wave, investigating constitutive relations for stress and heat flux using Maxwell moment method 11 p2036 A70-26015
- Remote monitoring of atmospheric wind and turbulence by cross correlation passive techniques, measuring heat and humidity fluxes 12 p2230 A70-26948
- Laminar boundary layer and heat flux at forward stagnation point of indestructible body in partially ionized air flow calculated as function of enthalpy 12 p2156 A70-27287
- Critical thermal flux and heat transfer coefficients dependence on simulated gravity during bubble and film boiling in inclined flat containers 12 p2331 A70-27325
- Turbulent heat transfer in concentric annuli entrance region with uniform wall heat flux 12 p2333 A70-28117
- Pulsed plasma jet radiant heat flux effect on cellophane film coated, polished and etched metals, noting erosion destruction 12 p2282 A70-28287
- Nucleate pool boiling, calculating sinusoidal and square wave pressure variations effect on heat flux for comparison with measurements 14 p2616 A70-30254
- Surface temperature fluctuations during dropwise condensation at various heat fluxes 14 p2663 A70-30256
- Atmospheric airflow model above changes in surface roughness, temperature and heat flux, using boundary layer approximations and Businger-Dyer and mixing length hypotheses 14 p2602 A70-30368
- Radiant heat flux for standard model, dry and humid atmosphere, calculating temperature variations with altitude for entire IR spectrum 14 p2603 A70-30401
- Heat transfer coefficient from circular cylinder subjected to uniform surface heat flux and cooled by ring of holes 14 p2667 A70-31427
- Heating rate effect on parameters of resistance wire strain gages subjected to temperature gradients 15 p2733 A70-31536
- Heat flux measurements in hypersonic rarefied gas flow by thin film surface thermometer 15 p2825 A70-31820
- Heat stress levels in cockpit of AH-1G Hueycobra helicopter parked in sunlight with closed canopy, using sweating copper mannikin 15 p2689 A70-31881
- Atmospheric radiation and heat fluxes calculations comparison with satellite and ground station actinometric measurements 15 p2770 A70-32067
- Heat exchange in laminar and turbulent boundary layers on plate for arbitrary heat flux distribution taking into account initial unheated plate segment 15 p2828 A70-32694
- Ablative materials performance in high radiative heat flux environments produced by CW carbon dioxide laser [AIAA PAPER 70-864] 16 p2939 A70-33907
- Temperature distributions and heat flux for gray gas in radiative equilibrium bounded by walls with different temperatures, using differential approximation [AIAA PAPER 70-834] 16 p3001 A70-33929
- Mathematical model of heat flux absorbed by heated part in radiant heating reflector systems, considering shape, spectral, directional and polarizing effects [AIAA PAPER 70-818] 16 p3002 A70-33945
- Surface temperature or heat flux density estimation for nonlinear inverse heat conduction problem involving temperature dependent thermal properties 16 p3002 A70-34195
- Heat exchange in dissociating partly ionized gas flow over critical point on permeable surface with injection into laminar boundary layer 17 p3011 A70-35347
- Nonaxisymmetric thermal stress distribution in infinite elastic solid containing external stress-free crack with prescribed heat flux 17 p3196 A70-35437
- Ballistical transport in collisionless exosphere, discussing heat flux of ballistical oxygen and model temperatures for day and night conditions 17 p3080 A70-35765
- Laminar free convection near two dimensional and axisymmetric nonisothermal bodies, examining surface temperature distribution and heat flux 18 p3345 A70-35999
- Critical heat flux density during annular channel internal heating, examining transfer crisis under forced motion of unheated water 18 p3345 A70-36111
- Adiabatic calorimeter for heat flux sensor contact calibration, describing operational principles and design 18 p3257 A70-36115
- Error sources in carbon black coating on thin foil heat flux sensors accounting for false altitude effects in vacuum calibration 18 p3262 A70-37100
- Heat transfer behind shock wave in air, oxygen or carbon dioxide flow past wedge, determining thermal fluxes vs wave velocity 19 p3405 A70-38188
- Mode-generated average variables of atmospheric horizontal heat flux by transient cyclonic eddies used in mean motion circulation model 20 p3664 A70-40063
- Isoperibol calorimetry for laser power and energy measurements, discussing boundary value problem for heat flow 21 p3838 A70-42021
- Critical thermal flux and heat transfer coefficients dependence on simulated gravity during bubble and film boiling in inclined flat containers 21 p3952 A70-42066
- Turbulent air flow measurements through heated pipe, determining local heat flux from simultaneous velocity and temperature fluctuation 21 p3811 A70-42091
- Dynamic nonstationary thermal convection in closed region with heat input from lateral surface for high Rayleigh and Fourier numbers 21 p3954 A70-42214
- Nonstationary axisymmetric thermal convection in spherical cavity with boundary heat flux proportional to temperature, using difference scheme and networks method 21 p3954 A70-42215
- Sphere and axisymmetric body with spherical blunting in low density gas flow, measuring local heat transfer flux 21 p3748 A70-42218
- Stationary turbine blades heat flux measurements, considering heat exchange coefficients and turbulent boundary layer [ONERA-TP-871] 22 p4126 A70-43459
- Static pressure effects on heat flux critical density for free convection and forced flow in circular pipes 23 p4282 A70-44726
- Critical heat flux during forced pipe flow of boiling ethanol-water and acetone-water binary mixtures 23 p4283 A70-44730
- Thermal flux surface distribution lifting bodies, discussing aerodynamic efficiency dependence on drag and zero angle of attack Mach number 23 p4136 A70-45019
- Plate temperature jump and heat flux in Knudsen layer using Bhatnagar-Gross-Krook model 24 p4429 A70-45997
- Controllable states with prescribed heat flux for incompressible isotropic thermoelastic bodies with temperature dependent response functions 24 p4426 A70-46041
- Peak pool boiling heat flux on horizontal cylinders, describing interactions of gravity and heater size effects 24 p4429 A70-46176
- Heat flux exchange by natural convection along flat vertical isothermal plate in laminar, transition and turbulent flows, using fluxmeters 24 p4429 A70-46207

HEAT GAIN U HEATING HEAT GENERATION

- Steady state heat conduction problems solved by finite element method, with examples involving internal heat generation and various boundary conditions 01 p0215 A70-10558
- Esthesiometric analysis of cutaneous thermoreceptors reaction dependence on heat production rates of human organisms 07 p1206 A70-19472
- Transient temperature distribution in flow through channel with arbitrary cross section, taking into account internal heat generation and viscous dissipation 08 p1599 A70-21767
- Time-temperature charts for one dimensional unsteady conduction with uniform internal heat generation 09 p1791 A70-23567
- Temperature field in work piece generated by grinding wheel face investigated for cylindrical and surface grinding 10 p1894 A70-24291
- Insulators, ablators, reflectors and computer analyses for aerodynamic and engine heat for aerospace thermal design 11 p1980 A70-25874
- Solid fuel steady combustion regime stability dependence on heat generation in reaction zones and temperature and velocity fields inhomogeneity 13 p2522 A70-29423
- High argon plasma temperatures via pulsing constricted electric arc 14 p2621 A70-30504
- Thermal degradation of anhydride-cured epoxy resin by carbon dioxide laser heating through platinum crucible 15 p2695 A70-32828
- Plastic deformation zones at crack tip considered as distributed heat sources, using stress and strain distribution solutions 17 p3191 A70-35463
- Localization and functional topology of thermosensible central nervous structures in rats cervical spinal cord, discussing role in generating heat to avert coldness 22 p3967 A70-42316
- Heat generation effects in air hydrostatic journal bearing, including shaft and housing thermal deformation and lubricant viscosity changes [ASME PAPER 70-LUBS-19] 22 p4044 A70-42442
- Human body heat production and transfer through convection, radiation and evaporation under normal and reduced atmospheric pressure 23 p4154 A70-44654

- Steady state radiative heat transfer through gray gas in spherical cavity, solving transport equation by singular integral equations for uniform heat generation 23 p4283 A70-44784
- Ruby laser in repetitive pulse operation, determining temperature, heat generation and transfer coefficient from spectrum shift measurement 23 p4203 A70-45071
- Surface temperature distribution of heat generating solid body in contact with parallel viscous fluid flow 24 p4430 A70-46368

HEAT MEASUREMENT

- Cycloheptane and mixture of exo- and endo-cycloheptene heats of combustion and formation, isomerization and hydrogenation 01 p0213 A70-10134
- Calorimetric measurement of electron temperature in collisionless shock wave propagating in plasma column, discussing role of H beta line Stark broadening 01 p0153 A70-11589
- Calorimetric analysis and hardness test to investigate low temperature aging behavior of maraging stainless steels 01 p0125 A70-11642
- Frog sartorius muscle heat production and work effect measured under isotonic and isometric conditions, using gradient layer calorimetry 02 p0232 A70-11715
- Kinetic energy of atomic motions for vitreous and crystalline high polymers measured by differential scanning calorimetry and thermal analysis 02 p0253 A70-12522
- Thin film heat gauge for measuring thermal transport from plasma to end wall of shock tube, discussing measurements in high temperature Ar 03 p0496 A70-14381
- Alpha beryllium nitride enthalpy and thermodynamic properties measured between 273-1173 K using drop calorimetric method 04 p0646 A70-14582
- Radiative heat transfer through dust clouds in radiative equilibrium and isothermal clouds between parallel plates measured with heat flowmeter [ASME PAPER 69-WA/HT-41] 04 p0781 A70-14802
- Sweeping W wire probe in rotational high temperature plasmas for local heat transfer measurement 06 p1120 A70-17699
- Reaction heat for flameless combustion of double-base propellant using differential scanning calorimetry and thermogravimetric analysis, noting pressure effects [AIAA PAPER 70-125] 06 p1179 A70-18045
- Measurement error associated with heat conduction in temperature sensor, using mathematical model 06 p1070 A70-18443
- Convective and radiative heat fluxes measurement on charring ablative materials surface in rocket nozzle environment 06 p1070 A70-18444
- Liquid nitrogen tetroxide enthalpy measured by indirect heating techniques, obtaining data at supercritical temperatures 06 p1005 A70-18560
- Wind tunnel study of heat transfer on smooth plate surfaces in longitudinal air flow using intermittently insulated calorimeter 07 p1279 A70-19065
- Caloric data determining saturated vapor pressure of nitrogen tetroxide and heat of sublimation for sublimation curve 07 p1358 A70-19206
- Enthalpy of nitrogen tetroxide in liquid phase using direct heating of test substance in calorimeter 07 p1358 A70-19207
- Heat transfer from composite propellant burning zone to regressing surface measured using multimirjet burner 07 p1359 A70-19587
- Natural heat convection measurements in vertical annular spaces, noting importance of local density and velocity product 08 p1433 A70-21671
- Segmented anode current and heat distribution in MPD engine measured with current shunts and calorimetric methods [AIAA PAPER 69-244] 09 p1613 A70-23238
- Wind tunnel study of heat transfer on smooth plate surfaces in longitudinal air flow using intermittently insulated calorimeter 10 p1970 A70-25216
- Guarded disk type emissometer for hemispherical emittance measurements of sample materials in 88 to 420 K range based on steady state calorimetry [AIAA PAPER 69-600] 13 p2404 A70-28524
- Linear high polymers heat capacity measurements theory emphasizing simple mechanical systems and contribution of lattice vibrations 13 p2438 A70-28997
- Nucleate pool boiling, calculating sinusoidal and square wave pressure variations effect on heat flux for comparison with measurements 14 p2616 A70-30254

Calorimetric measurements for Re specific heat in normal and superconducting states, comparing to theoretical calculation 14 p2626 A70-30478

Specific heat measurements on disordered and ordered phases of Cu-Au alloys at low temperatures 14 p2626 A70-30497

Specific heat, thermal pressure and molar volume of liquid krypton measured with adiabatic calorimeter, discussing thermal expansion coefficients 14 p2617 A70-31016

Heat exchange measurements between solid body and high enthalpy gas flow at stagnation point using electric arc heater 15 p2826 A70-32102

Steady state temperature dependence of heat conduction coefficient using arc approximation 15 p2826 A70-32106

Heat flow measurement, discussing operation principles, heat conduction and stationary and transient temperature conditions 17 p3082 A70-34681

Measurement methods for forces, pressure and heat flow in hotshot hypersonic wind tunnels 17 p3057 A70-34773

Natural convection heat transfer from vertical cylinder outer surface to liquids, discussing apparatus design and measurements 17 p3197 A70-35540

Turbine engine combustion chambers with various frontal devices, investigating burnout mechanism and heat yield in secondary air flow injection zone 19 p3489 A70-37246

Convective and radiative heat flux measurement incident on ablative surface in solid rocket nozzles 21 p3824 A70-40858

Microsecond response bolometer for measuring thermal radiation fluxes in shock tube, discussing design, calibration and performance 21 p3824 A70-40859

Thick film thermocouple gages for roughened solid surface heat flux measurements in high Reynolds number shock tunnel 21 p3824 A70-40860

Turbulent air flow measurements through heated pipe, determining local heat flux from simultaneous velocity and temperature fluctuation 21 p3811 A70-42091

Fluorine specific heat derived from measurements on two phase liquid vapor system at constant volume by PVT properties at coexistence 23 p4157 A70-44001

Differential scanning calorimetry and thermogravimetric analysis combination for thermochemical kinetic measurements, matching analytical and experimental curves for data accuracy 23 p4196 A70-44429

Al and W specific heat and Al heat of fusion by quasi-adiabatic calorimetry, estimating anharmonic lattice vibrations role via atomic thermodynamic analysis 23 p4208 A70-44931

HEAT OF COMBUSTION

Reaction heat for flameless combustion of double-base propellant using differential scanning calorimetry and thermogravimetric analysis, noting pressure effects [AIAA PAPER 70-125] 06 p1179 A70-18045

Two body collisions reaction mechanisms with small heats of reaction for Be and Al gaseous oxidation, noting low free energy properties of polymerization 10 p1928 A70-24089

Excess air ratio and heat release efficiency in combustion of kerosene mixture determined by volumetric gas analysis 10 p1968 A70-24283

Turbine engine combustion chambers with various frontal devices, investigating burnout mechanism and heat yield in secondary air flow injection zone 19 p3489 A70-37246

Physicochemical properties of monomer and associated aluminokalks, determining heats of combustion 22 p4124 A70-42677

Heats of combustion and free isomerization energies of exo- and endo-isomers of 2- and 1-methylbicyclo heptane 22 p3982 A70-42680

Computerized calculation of gas turbine cycles thermal efficiency, using hydrocarbon fuel, considering fuel composition and heat of combustion changes 22 p4125 A70-43439

HEAT OF DISSOCIATION

Diatomic fluorine dissociation energy by mass spectrometry 20 p3582 A70-39615

HEAT OF FORMATION

Polymerization reaction kinetics investigated with differential scanning calorimeter at isothermal conditions, determining heat of polymerization 11 p1994 A70-25810

Gas phase stabilities of bicyclic cations, establishing heats of formation limits by ion- molecule reactions identification 16 p2848 A70-33091

Titanium base binary systems phase diagrams, describing component activity and compound phases heat of formation 17 p3114 A70-34379

Oxygen isotope fractionation and formation temperature of minerals from Apollo 11 rocks, including plagioclase-clinopyroxene-magnetite concordancy diagram 21 p3776 A70-41597

Oxides compounds heats of formation isocomponent and primary product composition relationship in binary systems 22 p3982 A70-42679

Al-Mg alloys solid phases free energy, entropies and formation heats determination by electromotive force measurement 24 p4357 A70-45230

HEAT OF SOLUTION

Solubilities and heats of solutions of Mo, W, V, Ti and Zr in liquid K 04 p0710 A70-15632

HEAT OF VAPORIZATION

Rate and heat of vaporization of graphite filaments in 2500-3400 K range in vacuum and in He, using pulse heating techniques 03 p0517 A70-14004

Solar radiation effects on evaporation of dust with high latent heat of vaporization, considering particles in comets and zodiacal cloud 11 p2117 A70-26648

Heat of evaporation of sweat measured in human calorimeter at various air and dew-point temperatures, finding value 7 percent above water 17 p3031 A70-35423

HEAT PIPES

Na heat pipe with wick structure consisting of wire rods observed for ease of wick rewetting, dryout limit reproducibility, etc [AICHE PREPRINT 7] 01 p0216 A70-10967

Unsteady heat transfer equations for laminar fluid flow in pipe with varying wall temperature 03 p0604 A70-13207

Gravitational effects on heat transfer during evaporation and condensation processes in heat pipe, discussing conditions in Na filled heat pipe [DGLR-69-44] 04 p0785 A70-15171

Heat pipe structural alloys compatibility with different working fluids using capsule tests at high temperatures, noting corrosion behavior [AIME PAPER F-69-2] 07 p1304 A70-18812

Heat pipes to cool electronic circuitry, discussing design and operation 09 p1786 A70-22015

Gravitational effects on heat transfer during evaporation and condensation processes in heat pipe, discussing conditions in Na filled heat pipe 09 p1789 A70-23427

Unidirectional heat pipe system design to control temperature of high power traveling wave tubes in synchronous orbit communication satellite, dissipating waste heat 11 p2127 A70-26362

Quasi-isothermal heat transfer pipe design and operation 12 p2330 A70-27275

Radiative heat transfer in channel with unsteady radiating medium temperature, assuming absolutely black walls with zero temperature 13 p2522 A70-29725

Lithium vapor fueled applied field MPD arc jet performance using open end heat pipe vaporizer and hollow cathode [AIAA PAPER 69-241] 13 p2475 A70-29959

Heat pipes design for rocket engines cooling, discussing connections to space radiator and to heat rejection device and heat transfer capability [AIAA PAPER 69-582] 15 p2791 A70-32517

Heat pipe cooled thrust chambers for space storable propellants, discussing design feasibility for radiation and regeneratively cooled concepts [AIAA PAPER 70-942] 16 p2965 A70-33541

Heat pipes in nuclear aircraft propulsion system, describing core, heat exchangers, and reactor to jet engine heat transport system [AIAA PAPER 70-662] 16 p2950 A70-33623

Liquid metal corrosion of heat pipe refractory alloys at high temperatures, noting oxygen role 16 p2933 A70-34208

Heat pipe performance tests under longitudinal harmonic vibration 17 p3193 A70-35751

Aircraft electronic equipment cooling techniques, discussing natural and forced convection, phase change and heat pipes 18 p3232 A70-36763

Flexible heat pipe test for heat flux and wick pumping capacity under vibration and evaporator-condenser modification 21 p3945 A70-41040

Heat transfer mechanism during fluid evaporation in porous wick structure contacting heat pipe surface 21 p3946 A70-41042

Working fluids liquid property variations effects on cryogenic heat pipe performance 21 p3946 A70-41043

Optimum cryogenic heat pipe design, considering gravitational effects for spacecraft applications 21 p3946 A70-41044

Heat pipes in OAO 3 spacecraft for minimizing structural temperature gradients and validating thermal control approach 21 p3946 A70-41045

Liquid metal heat pipes in magnetic fields of controlled fusion reactors, considering geometry, compound wick structure and vapor flow 21 p3946 A70-41046

Liquid or vapor phase working fluids penetration effects on steady state and transient performance of hot reservoir gas controlled heat pipes 21 p3946 A70-41047

Thermal scale modeling of heat pipe in deep space, using material and heat flux preservation techniques 21 p3946 A70-41048

Accelerated failure tests of ammonia-Al-stainless steel heat pipes for fluid loss or energy transport degradation 21 p3947 A70-41049

Heat pipe performance map with ammonia as working fluid, comparing thermal transport efficiency with water pipe 21 p3947 A70-41050

Mercury as stainless steel heat pipe working fluid, determining wetting characteristics and heat transfer capability 21 p3947 A70-41051

Static pressure effects on heat flux critical density for free convection and forced flow in circular pipes 23 p4282 A70-44726

Critical heat flux during forced pipe flow of boiling ethanol-water and acetone-water binary mixtures 23 p4283 A70-44730

HEAT RADIATORS

NT SPACECRAFT RADIATORS

Thermal efficiency of modified transtage of Titan 3C spacecraft, discussing environmental simulation, heat rejection system and test firing [AIAA PAPER 70-171] 06 p1156 A70-18027

Finned tube radiators with constant longitudinal specific heat flow, determining thermal efficiency and optimal thermal and structural parameters 06 p1184 A70-18556

Solar energy exchange with radiator surface recessed within specular axisymmetric cylindrical spinning cavity, using deterministic ray tracing scheme 11 p2150 A70-26353

Variable reproducible black radiator of resistance heated carbon tube designed for temperatures between carbon glowing and sublimation point 12 p2329 A70-27090

Conical heat radiator system for cooling short cylinders 15 p2827 A70-32142

Al radiator with thin stainless steel tube liner using liquid metal coolant tested for heat rejection system of SNAP-8 Rankine cycle power system [AIAA PAPER 70-855] 16 p3000 A70-33922

HEAT REGULATION

U TEMPERATURE CONTROL

HEAT REJECTION DEVICES

U HEAT RADIATORS

HEAT RESISTANCE

U THERMAL RESISTANCE

HEAT RESISTANT ALLOYS

NT MOLYBDENUM ALLOYS

NT NIMONIC ALLOYS

NT NIOBIUM ALLOYS

NT REFRACTORY METAL ALLOYS

NT RENE 41

NT RHENIUM ALLOYS

NT TANTALUM ALLOYS

NT TUNGSTEN ALLOYS

NT UDIMET ALLOYS

NT WAPALLOY

Heat resistant alloys for gas turbine blades observed for long term heating effects on changes of hardness, tensile, impact and stress-rupture properties and microstructure 01 p0116 A70-10149

Transmission electron microscope study of deformation mode during rapid tensile testing of Ni-base superalloy, discussing twinning and stacking fault modes 01 p0118 A70-10705

Tungsten effect on phase transformations and carbide reactions to attain equilibrium at 850 C in Ni-base superalloys 01 p0118 A70-10727

Precipitation in Ni-base superalloy analysis with dark field electron microscopy and electron and X ray diffraction 01 p0119 A70-10730

Ni-based superalloys microstructure, describing composition, formation and characteristics of various phases 01 p0124 A70-11448

Mo coated with Ni-base Nimonic and Co-base heat resistant alloys, for working degree effect on creep rupture strength 01 p0126 A70-11646

Carrying capacity of heat resistant steel turbomachine elements, discussing plastic deformation and cyclic load effects, breakdown load determination, stress analysis, etc 02 p0352 A70-11659

Brazed plate-fin superalloy panels suitable for hydrogen-cooled structures, discussing fabrication techniques, performance tests and pressure containment and fatigue characteristics 02 p0306 A70-11930

Heat and creep resistant Ni- and Fe-base alloys application in gas turbines, superheaters, steam pipes, chemical and petrochemical plants and heat treatment equipment 02 p0319 A70-12711

Chromium refractory alloys, discussing production difficulties, mechanical properties, engineering applications, etc 02 p0320 A70-12760

Oxidation and sulfidation resistant diffusion coatings for superalloys, discussing processing methods, composition, properties and application [SAE PAPER 690479] 03 p0509 A70-13266

Carbide phase in Cr-Mn heat resistant steels at annealing temperatures, isolating gamma, chromium carbide and niobium carbide phases 03 p0509 A70-13279

Heat treatment effects on phase components of Cr-Mn-B alloys with W and Nb additions, discussing heat resistance 03 p0510 A70-13280

Cr alloys applications in high temperature environments, describing alloying elements effects on strength and ductility 03 p0511 A70-13566

Heat resistant alloys densities calculated from chemical composition, estimating error 03 p0512 A70-13778

Prealloyed powders of Ni base alloys, made by inert gas atomization for improved strength and ductility 04 p0706 A70-14951

Nickel base alloy, WAZ-20 with improved strength in 2000-2200 F range for application to gas turbine engine stator vanes 04 p0706 A70-15097

Ni addition effects on Mg-Nd and Mg-Nd-Mn alloys structure and heat resistance 04 p0706 A70-15189

Chromoluminizing process protecting alloys for gas turbines against oxidation at high temperatures by diffusion mechanism 04 p0711 A70-15683

High temperature properties mechanisms in aluminate coated vacuum cast nickel base superalloys 04 p0711 A70-15705

Mechanical properties of eutectic superalloys compared with commercial superalloys, noting thermal stability applicability to gas turbine engines [SAE PAPER 690689] 05 p0861 A70-15827

Internal friction method for studying dislocation, stacking points and strengthening processes in steels and heat resisting austenitic steel behavior at high temperatures 05 p0864 A70-16870

E1617 alloy breakdown resistance tests under multiple alternating static tension-compression and vibrational loads at 800 C 05 p0867 A70-17044

Heat resistant steel and nickel alloys stress rupture strength at operating temperatures, discussing endurance diagrams under cyclic bending loads 05 p0868 A70-17047

Fatigue life tests for heat resistant gas turbine blade alloys under power and thermal loads simulating aircraft flight 05 p0953 A70-17051

Cylindrical Al, high strength pig iron and heat resistant steels elastoplastic deformation diagrams for cyclic compression tension loads 06 p1084 A70-17387

Temperature cycle duration effects on heat resistant alloys thermal fatigue resistance, noting stress relaxation occurrence 06 p1085 A70-17398

Coating and coating processes for superalloys in hot section components of gas turbine engines for aircraft, industrial, marine and vehicular applications 07 p1362 A70-18929

Fe-Cr-Ni alloys for use in high temperature oxidizing environments 07 p1305 A70-18966

Oxidation, hot corrosion resistance and mechanical properties of aluminate coated superalloys, discussing failure analysis instruments and methods 07 p1305 A70-18969

Alloying elements effect on polymorphic alpha-beta transformation temperature of Ti systems, discussing heat resistance 07 p1307 A70-19555

Soviet book on mechanical properties of heat resistant steels and alloys at room and elevated temperatures 08 p1515 A70-20691

Hydrogen penetrability in heat resistant steels subjected to high temperature creep, observing activation energy decrease with increased stress 08 p1515 A70-20923

Energy dissipation in heat resistant Ni steels under cyclic tension and compression at room temperature 08 p1516 A70-20981

Cyclic creep and relaxation of heat resistant alloys at high temperatures, showing inapplicability of static load conditions 08 p1516 A70-20982

Carburization resistance of refractory steels, emphasizing chemical composition effect on corrosion rate 08 p1519 A70-21434

Tungsten alloy fiber reinforced Ni-base superalloy composites evaluated for high temperature turbojet engine applications, considering stress-rupture strength, oxidation and impact resistance 08 p1523 A70-21907

Plasma beam welding of light metal and heat resistant alloys, discussing weld characteristics, beam I-V characteristics, etc 09 p1690 A70-22077

Sigma and mu phase formations in Ni heat resistant alloys x ray analysis using phase isolation by anodic dissolution 09 p1700 A70-22079

Cyclic heating and thermal stresses effect on fatigue strength and durability of turbine blade alloys and structural elements 09 p1771 A70-22463

Powder metallurgy all-inert processing method for producing nickel base superalloys forgings, discussing microstructure, reproducibility, mechanical properties, etc 09 p1701 A70-22553

Heat resistant alloys creep ductility, considering grain boundary cavitation, sliding and migration 09 p1701 A70-22554

Heat resistant cast alloys creep strength reporting criteria, comparing U.S. and European practices [ASM PAPER P9-15.2] 09 p1702 A70-22558

Internal nitridation temperature effect on dispersion hardening of austenitic stainless Fe-Cr-Ni-Ti steels, investigating interparticle spacing and layer thickness effects 09 p1705 A70-22810

Ni-Cr superalloys hot corrosion, studying sulfidation-oxidation in various synthetic controlled gas mixtures 09 p1706 A70-22944

Plane disks and turbine disks of complex profile made of heat resistant Cr-Ni alloys studied for rupture strength under various temperature conditions 09 p1785 A70-23599

Heat resistant materials strength characteristics with long service periods, formulating equation for time dependence of rupture resistance 10 p1903 A70-24237

Long time static strength, durability and thermal stability relations determined for heat resistant alloys at operational temperatures 10 p1903 A70-24238

Long time strength and creep rectilinear diagrams constructed for heat resistant alloys to obtain extrapolation values 10 p1903 A70-24239

Test results extrapolation for heat resistant alloys long time strength using exponential relation between time to rupture and value for initial stress decrease 10 p1903 A70-24240

Yield point temperature dependence in heat resistant austenitic alloys, showing tendency to brittle failure under short term overloads 10 p1906 A70-25291

Heat resistant alloys low cycle fatigue tests between 20-800 C, establishing residual strain change patterns as function of stress and temperature 10 p1906 A70-25294

Powder base superalloy with superplastic behavior, ascribing mechanism to migration of second phase gamma prime particles 12 p2252 A70-26889

Short time tensile properties of thermomechanically treated astrolloy showing improvement due to refined gamma precipitate and grain boundary carbides 12 p2256 A70-27610

Superplastic nickel superalloys fabrication by controlled densification during direct extrusion 12 p2257 A70-28020

Structural stability of friction welded joint between high temperature low alloy weld metal from CrMoV electrode and high temperature Cr steel 12 p2244 A70-28349

Ni alloys hardening by solid solution precipitation and insoluble particles dispersion, emphasizing heat resistant alloys and mechanical properties

13 p2433 A70-28762

Ni-based heat resisting alloy /Inconel 700/ investigated for hot corrosive environment effect on stress rupture and fatigue strengths

13 p2434 A70-29157

Oxygen motion velocity effect at various pressures on heatproof and heat resistant steels and alloys ignition, noting minimum ignition temperature

13 p2434 A70-29168

Ni-Fe base superalloy notch and rupture properties as function of thermal and chemical changes, using electron microscopy

13 p2437 A70-29829

Superalloys commercial development, investigating strength, heat resistance and weldability of Fe- and Ni-based alloys

[ASM PAPER W70-9.4]

15 p2760 A70-32335

Glass bead blast induced residual stress and surface cold work effects on Ni base superalloy fatigue crack initiation and propagation

15 p2761 A70-32381

Co base superalloys for aircraft structures and parts, discussing temperature stability, corrosion resistance, creep, fatigue and strength

16 p2932 A70-33705

Al effects on B and Cr diffusion in protective coating on Cr-Ni heat resistance alloy, noting thermochemical kinetics for homogeneous layers

17 p3125 A70-35405

Sodium sulfate induced accelerated oxidation of Ni and superalloys, investigating thermodynamics and reaction mechanism

18 p3272 A70-36037

Ni-Al-Nb superalloy, determining temperature effect on phase relationships in Ni-rich portion of phase diagram

18 p3273 A70-36041

Heat resistant alloys technology, surveying various metals, mechanisms and characteristics

18 p3276 A70-36307

Ni superalloys for gas turbine engines, discussing chemical composition, microstructure, strength, solidification, etc

[ASME PAPER 70-GT-24]

18 p3278 A70-36831

Fluxless paste for thermomodification calorizing stainless and heat resistant steels and alloys

19 p3434 A70-37459

High vacuum effects on creep properties of single crystal low carbon nickel base superalloy

19 p3451 A70-37705

Long structural shape production for titanium and super alloys, discussing rolling, extrusion, drawing, frictionless forming and filler techniques

19 p3437 A70-38420

Carrying capacity of heat resistant steel turbomachine elements, discussing plastic deformation and cyclic load effects, breakdown load determination, stress analysis, etc

19 p3547 A70-38432

Soviet papers on heat resistant alloys and steels structure by electron microscopes

20 p3644 A70-39036

Ni-Cr heat resistant alloys structural transformation kinetics under aging, creep and operational conditions, discussing solid solution decomposition, hardening phases coagulation and dissolution, etc

20 p3645 A70-39037

Solidification and composition model of macroscopic freckles in nickel base superalloys single crystals

20 p3646 A70-39101

Optimum conditions and methods for vacuum diffusion welding of heat resistant alloys, removing thermodynamically stable surface oxide films by gaseous reaction products

20 p3636 A70-39197

Hot corrosive environment effect on stress rupture and fatigue strength of Ni heat resistant alloy used in gas turbine rotating blade

20 p3647 A70-39241

High temperature Ni base superalloy stress-rupture life dependence on casting variables and section size

20 p3648 A70-39413

Creep resistant Ni-base superalloys ductility and thermal shock resistance improvement by precision casting technique, producing columnar grain and single crystal structures

20 p3648 A70-39415

High temperature Ni, Co and Fe alloys for gas turbines, examining sulfidation-oxidation corrosion test methods

20 p3651 A70-39971

Cold metal working techniques, describing electromagnetic, explosive, ultrasonic, high velocity hammering, stretch forming, deep drawing and superalloy shaping

20 p3639 A70-40445

Stacking faults in gamma prime precipitation hardened high temperature Ni base alloys, relating fault energy to strength

22 p4053 A70-42728

Ni base superalloy for gas turbines, describing heat treatment for precipitation hardening

22 p4055 A70-43099

Surface degradation by oxidation, temperature fluctuations and hot corrosion of Ni- and Co- base superalloys in gas turbine engines

22 p4057 A70-43574

Light rare earth metals improving Mg alloys, Al alloys, Cu alloys and superalloys

22 p4057 A70-43575

Step-amplitude stress cycle program effects on durability of heat resistant alloy for turbine blades under cyclic loading

23 p4204 A70-43934

Statistical analysis of durability data of heat resistant alloys for gas turbine engines, using long term strength tests of melts in mass production

23 p4204 A70-43940

Ni base superalloys gamma prime phase long range order parameter measured by X ray diffraction

23 p4207 A70-44423

Superalloys dispersion strengthening and age hardening by mechanical alloying

24 p4341 A70-45246

Notch sensitivity dependence on plastic strain in Al alloy, heat resistant steels and Ni alloys under tensile tests at room temperature

24 p4360 A70-45827

High purity Cr-Ni heat resisting steels, investigating phase transformations with microhardness measurements magnetic analysis, X ray diffraction and microstructure examination

24 p4362 A70-46181

High temperature coatings of high melting point alloys on graphite, determining optimum fabrication conditions

24 p4368 A70-46339

Heat resistant alloys with metal coatings applied by diffusion in vacuum, investigating structure and fatigue strength at high temperatures

24 p4364 A70-46342

HEAT SHIELDING

NT REENTRY SHIELDING

Ultrasonics inspection applied to reentry vehicle heat shields and composite materials, verifying anomalies by microscopic area examination

01 p0097 A70-10016

Blunt and conical body optimum heat shield shapes for Jupiter atmospheric entry, noting shallow flight path

[AIAA PAPER 68-1150]

01 p0195 A70-10827

Quartz-Fiberfrax heat shield tests for Thor booster at high radiative heating rates, noting optimum material performance dependence on loose stitching

01 p0129 A70-10850

Energy partitioning process under strong shielding with debris acting as energy sink

06 p1130 A70-17181

Elastomeric silicone ablator reinforced by carbon cloth or fibers for Venus entry heat protection

[AIAA PAPER 70-201]

06 p1157 A70-18086

Ablation of heat shielding materials subjected to superorbital reentry conditions, noting dependence on heating rate to surface

[AIAA PAPER 70-202]

06 p0970 A70-18100

Massive blowing effect on stagnation point radiative energy transfer of ablative heat shield during planetary entry at hypersonic velocities

[AIAA PAPER 70-203]

06 p0971 A70-18101

Full scale R/V flight test base pressure data for slender cones with ablative heat shields, considering mass flow and addition effects

[AIAA PAPER 70-109]

06 p0973 A70-18148

Ablation, transmission transparency and embrittlement of heat shield materials for Voyager tested under simulated Mars entry conditions

07 p1395 A70-19885

Refurbishable ablative thermal protection for reusable lifting reentry vehicles

[AIAA PAPER 70-277]

07 p1397 A70-20386

Thermal control coatings as solar reflectors for spacecraft heat dissipation

08 p1527 A70-21357

Thermal radiation shield influence on stationary radiative heat transfer in closed arbitrarily shaped two gray surface system

10 p1966 A70-23865

Line source technique for ablative heat shield materials thermal conductivity measurements, comparing vacuum and atmospheric test results

[AIAA PAPER 69-1013]

11 p2051 A70-26142

Nonisothermal burn-up rates of graphite surfaces in turbulent air flow under neutral gas shield estimated by measuring channel diameter

12 p2331 A70-27323

Blunt heat shield effectiveness for trailing payload in reentry capsules, discussing dynamic instability effect

[AIAA PAPER 70-563]

13 p2341 A70-29028

Boundary value problem of nonlinear one dimensional conduction in radiating heat shields, using perturbation and numerical methods

15 p2824 A70-31450

Heat shield analysis covering high temperature ablation interactions in conical anisotropic structure immersed in hypersonic environment

20 p3738 A70-40054

Dynamic response of distended carbon materials to shock loading defined by measuring equation of state, unloading behavior and spallation strength

20 p3657 A70-40263

Full scale R/V flight test base pressure data for slender cones with ablative heat shields, considering mass flow and addition effects

[AIAA PAPER 70-109]

21 p3745 A70-41753

Nonisothermal burn-up rates of graphite surfaces in turbulent air flow under neutral gas shield estimated by measuring channel diameter

21 p3952 A70-42064

Nonlinear one dimensional conduction in radiating heat shields, solving two point boundary value problem by asymptotic and numerical solutions

[ASME PAPER 70-HT-E]

22 p4121 A70-42422

Cracked Teflon heat shields ablative behavior for laminar and turbulent boundary layers in supersonic flow, describing heat transfer to substructure

23 p2827 A70-44585

Space shuttle structural design concepts and fabrication, tabulating structural and heat shield materials

[SAE PAPER 700768]

24 p4415 A70-45867

Environmental heat shielding for various sized Jupiter atmospheric entry probes

[AIAA PAPER 70-1324]

24 p4429 A70-45941

Heat transport conduction mode and earth as heat sink in solar atmosphere, discussing mesopause coldest region, turbulence and solar plasma-earth electromagnetic interactions

[AAS PAPER 69-622]

04 p0677 A70-14644

One dimensional Navier-Stokes equations solution for viscous heat conducting gas flow involving spherical sink for finite pressure at infinity

10 p1865 A70-24104

Local heat sink thermal processes on convectively cooled solid surface, noting applications to temperature measurement errors

12 p2333 A70-28112

Thermal anchoring of wire or rod components to heat sinks in cryogenic equipment in vacuum

14 p2584 A70-30501

Finned tube-sheet spacecraft radiator transient response for perturbations caused by power supply and heat sink temperature changes

22 p4123 A70-42519

Hypersonic airbreathers aerodynamic, structural and propulsive system interactions, discussing hydrogen fuel heat sink, airframe and engine cooling and airframe materials

[ICAS PAPER 70-16]

23 p4138 A70-44127

Thermal preconditioning using radioisotope heat source to eliminate inertial sensor warmup time by maintaining aircraft navigation system at constant temperature

01 p0140 A70-10310

Heat sources in E region from electron temperature data analysis recorded by rockets during eclipses in July 1963

01 p0082 A70-11491

Aeronomy of Jovian upper atmosphere at pressures below 25 mb, discussing stratospheric heat sources, thermal emissivity, photochemistry of methane, ammonia, etc

02 p0366 A70-11804

Mean volume heat transfer coefficient, mean thermal head and coolant temperature determined for gas flowing through porous wall with internal heat source

03 p0605 A70-13474

Transient and steady state radiation heat flux sensors calibration by developing and evaluating heat flux source

03 p0606 A70-13558

Thermal model for Venus ionosphere, considering photoionization and solar wind influx for possible heat sources

03 p0575 A70-13981

Transient temperature distribution, thermal stresses and deformations in thin finite circular disk due to continuous point heat source, using linear thermoelasticity

[ASME PAPER 69-WA/PVP-6]

04 p0768 A70-14789

Chemical heat source combined with metals ignition properties considered for spacecraft heating during Mars nighttime landing

04 p0628 A70-15426

One dimensional stress waves propagation in elastoplastic medium, determining stress and velocity fields due to heat sources motion by characteristics method

04 p0776 A70-15447

Heat source temperature distribution on surface of infinite cylinder with zero temperature, presenting solution to boundary value problem

05 p0957 A70-16296

Heat conduction in anisotropic materials to measure thermophysical parameters, using pulsed point or line heat source

05 p0957 A70-16457

Temperature of contact surface between two homogeneous isotropic solid bodies determined by calculating plane heat source of steady three dimensional temperature field
05 p0958 A70-17014

Steady free convection over point and horizontal line heat sources in vertical magnetic field
06 p1120 A70-17519

Temperature distribution law for semiinfinite and infinite solid bodies under steady heat conduction in presence of concentrated heat source
06 p1178 A70-17872

Workpiece temperature during asymmetrical plane polishing by wheel face, deriving temperature distribution formulas for maximum heat source intensity
07 p1291 A70-18828

Reinforced graphite cloth composite for reentry heat shielding of SNAP 27 isotopic heat sources, describing structure, thermal and mechanical properties and ablative characteristics
07 p1332 A70-18933

Temperature stress in ring-like plate caused by point heat source, discussing thermoelastic problem
07 p1413 A70-20147

Thermoelastic state of plate near foreign circular inclusion, assuming heating by uniformly distributed sources and ideal plate-inclusion thermal contact
08 p1587 A70-21171

Transient thermal stresses in plates with distributed heat source and heat exchange with arbitrary time dependent surroundings
08 p1593 A70-21623

Solar wind heating, determining roles of various energy sources from Explorer 34 observations
09 p1755 A70-22511

Temperature field in infinite plate with disk shaped inclusion and stationary point heat source determined, allowing for heat transfer conditions
09 p1778 A70-23082

Temperature field distribution in long thin narrow plate composed of materials differing in thermophysical characteristics, creating field by moving heat source on plate
09 p1791 A70-23723

High power CW carbon dioxide laser design and operation for use as heat source in metal fusing, welding and cutting
10 p1897 A70-23816

Heat sources effect on pressure and velocity of supersonic flow, discussing iteration procedure and asymptotic expansion
10 p1799 A70-24125

Integrated circuits involving long-strip heat source surrounded by multiple layers, expressing temperature distribution by Fourier transformation obtained in integrals
10 p1850 A70-24620

Venus clouds self consistent radiative-convective model with sun as heat source
11 p2107 A70-25647

Waves and mean currents excitation in stratified fluid due to moving heat source, studying effect on mean motion
11 p2036 A70-26167

Semiinfinite elastic body with instantaneous heat source on surface, analyzing temperature and thermal stress distributions
11 p2139 A70-26406

Two dimensional dynamic thermoelastic problem for thin plates with internal heat sources solved by integral Laplace and Fourier transforms
12 p2323 A70-27337

Radiative energy transfer in hydrogen plasma having uniform heat source and bounded by parallel black plates
12 p2278 A70-27695

Radiating drop unsteady vaporization or growth for uniformly distributed internal heat sources, discussing gas temperature distribution and diffusion thermal effect
13 p2521 A70-29417

Real time Apollo lunar module thermal mission data analysis using computer programs
14 p2653 A70-30774

Natural convection wake from heated horizontal line source in liquids and in air, determining temperature field in plume above wires
15 p2825 A70-31817

Positive/negative curvature shells local stresses due to concentrated loads and heat sources, deriving approximate solutions
15 p2817 A70-32161

Point heat source generation of thermal stresses in elliptical plate with circular hole, using functions of complex variable for stress field determination
15 p2818 A70-32182

Plastic deformation zones at crack tip considered as distributed heat sources, using stress and strain distribution solutions
17 p3191 A70-35463

Stationary heat conduction model of two cylinders abutting at ends with internal nonuniform temperature distribution
18 p3345 A70-36128

Venus atmospheric visible clouds circulation, determining zonal flow induced by moving heat sources
19 p3519 A70-38252

Unsteady temperature field in cylinder surrounded by thin shell under uniformly distributed heat sources
20 p3737 A70-39640

Thermal preconditioning unit using radioactive isotope heat source for temperature control of inertial navigation system
20 p3671 A70-40059

Radiative heat transfer between concentric spheres separated by absorbing-emitting medium with heat sources, deriving approximate solution
20 p3739 A70-40294

Laminar convective flow from linear heat source along vertical plate, solving numerically for incompressible fluid by boundary layer approximation
20 p3614 A70-40403

Apollo 11 fines thermal conductivity under vacuum, using line heat source technique
21 p3913 A70-41647

Reentry protection for radioisotope heat sources, using thermal switch of composite ceramic foam with metal impregnants
22 p4054 A70-42958

Nonlinear distributed sources induced diffusion, calculating relationship between source intensity and maximum temperature or mass concentration field
24 p4380 A70-46034

HEAT STORAGE
Orbital mission solar energy power conversion system, discussing heat transfer processes for storage feasibility
21 p3951 A70-41852

HEAT TESTS
U HIGH TEMPERATURE TESTS
HEAT TOLERANCE
Vasopressin antidiuretic hormone effects on evaporative body weight loss during heat exposure
01 p0020 A70-10516

Gas chromatography study of fatty acids and polar lipids of thermophilic filamentous bacterial masses from hot Yellowstone Park springs
01 p0021 A70-10791

Cross adaptations of physiological functions, discussing results for heat, altitude and cold adapted animals
02 p0242 A70-12824

Cardiovascular responses to sustained high skin temperature in resting men noting dizziness, impaired vision and extracutaneous vasodilatation
03 p0429 A70-14162

Evaporative weight losses by sweating in man exposed to warm environment as function of time, including graphical method for heat storage prediction
03 p0430 A70-14164

High temperature effects on pilots psychomotor performance and physiological function, discussing measurements taken during complex tasks
06 p0999 A70-17290

Heat accumulation, oral temperature and heart rate recovery of subjects in various thermal environments
10 p1810 A70-24034

Physiological reactions of humans to orthostatic heat tolerance and natural acclimatization in summer and winter using tilt-table test and bicycle ergometer
12 p2169 A70-27656

Thermostability and survival rates of white mice in ambient medium with temperature variations
13 p2351 A70-29332

Physiological indices criteria for human thermal stress tolerance, discussing rectal temperature, body surface condition, body temperature and local cooling effects
13 p2351 A70-29332

Solid state laser active element lateral surface microprofile effect on heat endurance
16 p2929 A70-34220

Soviet papers on physiological adaptation to heat and cold covering thermoregulatory reflexes, bionics, temperature gradients, hypothalamus, gas exchange, heat generation, etc
18 p3217 A70-36526

Extreme heating effects on polypnea reaction in aquatic birds
18 p3219 A70-36537

Respiratory activity of internal organs and skeletal muscles in rats exposed to long term heat and cold
18 p3220 A70-36546

Thermal thermesthesiometer for skin heat sensitivity studies
19 p3368 A70-37806

Heat stress effects on serial reaction time in subjects performing visual tasks
19 p3361 A70-38053

Astronauts medical examination, using thermal load as functional and diagnostic test
20 p3575 A70-40195

Intracellular shifts in body fluids and dehydration tolerance in burro, comparing water content of desert animals
21 p3766 A70-42157

Syncope prevention in orthostatic heat test by inflating cuffs around legs and lower abdomen
24 p4306 A70-45331

HEAT TRANSFER
NT AERODYNAMIC HEAT TRANSFER
NT CONDUCTIVE HEAT TRANSFER
NT CONVECTIVE HEAT TRANSFER
NT HYPERSONIC HEAT TRANSFER
NT LAMINAR HEAT TRANSFER
NT RADIATIVE HEAT TRANSFER
NT SUPERSONIC HEAT TRANSFER
NT TURBULENT HEAT TRANSFER
Heat and mass transfer in Couette flow of partially ionized symmetric diatomic gas for chemical equilibrium and chemically frozen flow cases
01 p0060 A70-10290

Laminar boundary layer analysis of heat and mass transfer in dispersed two phase flow over heated surface
01 p0214 A70-10293

Wet vapor flow with/without inert diluent, assuming momentum and heat transfer between phases according to Stokes law and Nusselt number of unity
01 p0061 A70-10332

Transient heat transfer near two dimensional stagnation point in viscous incompressible fluid steady flow
01 p0002 A70-10457

Hypersonic dissociated laminar boundary layers with/without heat transfer calculated by integral method for case of thermodynamic equilibrium
01 p0003 A70-10933

Aerodynamics, heat and mass transfer in vapor condensation from humid air on flat plate in longitudinal flow in asymmetrically cooled slot
01 p0004 A70-11178

Organic liquid nucleate pool boiling experiments determining stresses, surface tension, viscosity and gravitation relationships to bubble shape and microlayer formation
01 p0218 A70-11180

Unsteady heat transfer from porous flat plate with impulsive motion and rising temperature, analyzing compressible boundary layer equations using Laplace transform
01 p0067 A70-11390

Weak shock waves relaxation time and amplitude and acoustic velocity as functions of thermorelaxing media
01 p0068 A70-11588

Structural support strut design for cryogenic propellant tanks to optimize load carrying capability and heat transfer characteristics
02 p0306 A70-11942

U-shaped combustion chamber two dimensional model for studying factors influencing flame spread and stabilization and heat transfer in gas turbines
02 p0355 A70-12257

Heat transfer, three dimensional boundary layers and high speed flow calculations, utilizing original entrainment equation
02 p0284 A70-12341

Low temperature high sensitivity temperature compensated heat flux transducers to measure conductive, convective and radiative heat transfer
02 p0303 A70-12740

Monograph on application of semiclosed thermopion system to gas turbine blade cooling, covering heat transfer and temperature distribution analysis, etc
03 p0551 A70-12992

Book on flow and thermal boundary layers covering laminar and turbulent flow velocity profiles, Prandtl equation, heat transfer problems, etc
03 p0465 A70-13015

Heat transfer effects on corrosion behavior of stainless steel in boiling water, noting stress corrosion cracking increase with chloride ion contamination
03 p0507 A70-13137

Soviet bibliography on heat and mass transfer covering thermodynamics, heat conduction, convection and radiation, phase and chemical transitions, aerodynamics, geophysics, etc
03 p0605 A70-13392

Heat transfer and flux density during bubble boiling of liquid oxygen employing simulated weak gravitational fields
03 p0605 A70-13393

Unsteady heat transfer theories reviewed to assess steady state heat transfer relations applicability
03 p0605 A70-13401

Incompressible gas turbulent jet flow characteristics in subsonic wind tunnel, stressing pressure distribution in recirculation region for interpreting heat transfer in separated flows
03 p0593 A70-13495

HF pressure oscillations during heat transfer to n-heptane at various flow rates and pressures, studying film or bubble boiling associated with oscillations
03 p0605 A70-13516

Heat transfer under conditions of forced convection from flat plate in laminar flow, considering plate surface temperature arbitrary variation in time
03 p0605 A70-13518

Integral method for studying wall heat transfer influence on compressible boundary layer on cone at angle of attack in supersonic flow
03 p0409 A70-13953

Free stream turbulence effect on heat transfer in circular cylinder stagnation region 03 p0469 A70-14216

Heat transfer in steady state flow of electrically conducting incompressible viscous fluid in annular channel between coaxial circular cylinders under magnetic field 03 p0608 A70-14335

Ablative throat nozzle performance, plotting change in thrust, exit pressure and Mach number as function of ablated to initial area ratio 03 p0410 A70-14336

Thermochemical relaxation influence on shock heated plasma gases via heat transfer experiments on ionized Ar, molecular nitrogen and carbon dioxide 03 p0536 A70-14366

Thin film heat gauge for measuring thermal transport from plasma to end wall of shock tube, discussing measurements in high temperature Ar 03 p0496 A70-14381

Electron heat transfer to spherical body in nonequilibrium quiescent plasma by asymptotic solution [ASME PAPER 69-WA/HT-56] 04 p0727 A70-14793

Heat transfer in partially ionized argon plasma flowing in water cooled circular tube as function of temperature, Reynolds number and tube entrance diameters [ASME PAPER 69-WA/HT-54] 04 p0780 A70-14795

Heat transfer to insulator wall of linear MGD accelerator attached to shock tube, comparing measurements with Hartmann boundary layer analysis [ASME PAPER 69-WA/HT-53] 04 p0781 A70-14796

Heat transfer rates to stagnation point of hemisphere in supersonic high enthalpy low density nitrogen plasma flow [ASME PAPER 69-WA/HT-49] 04 p0614 A70-14799

Nonlinear rarefied Couette flow with heat transfer in polyatomic gases, using kinetic theory of gases [ASME PAPER 69-WA/HT-39] 04 p0781 A70-14803

Transient heat conduction solution by finite element methods application to nonlinear boundary condition problems [ASME PAPER 69-WA/HT-36] 04 p0781 A70-14804

Interpolation method for predicting and correlating heat transfer in rarefied gases, yielding correct limiting results in free molecular and continuum regimes [ASME PAPER 69-WA/HT-30] 04 p0782 A70-14808

Hypersonic blunt body heat transfer prediction, including coupled effects of real gas behavior and slip boundary conditions [ASME PAPER 69-WA/HT-28] 04 p0614 A70-14809

Nonlinear boltzmann equation for heat transfer in rarefied gases between parallel plates at different temperatures using Monte Carlo method [ASME PAPER 69-WA/HT-23] 04 p0782 A70-14811

Heat transfer to absorbing fluid by coupled thermal radiation and laminar forced convection at pipe entry region, considering gray and nongray absorption [ASME PAPER 69-WA/HT-16] 04 p0783 A70-14818

Thermal damping in gas-filled composite materials during impact loading due to heat transport, discussing role in impact energy dissipation [ASME PAPER 69-APM-V] 04 p0712 A70-14867

Thermal steady state characterization of isotopic radioisotope thermoelectric generator, discussing design features and heat transfer models for operating temperatures and output performance [ASME PAPER 69-WA/ENER-12] 04 p0717 A70-14897

Heat transfer from two dimensional hypersonic low density stream to wedges and sharp flat plates at expansion angles of attack 04 p0615 A70-14944

Semifocusing color schlieren systems for quantitative investigations of flows in fluid mechanics and heat transfer, including photographs of boundary layers 04 p0690 A70-15029

Gravitational effects on heat transfer during evaporation and condensation processes in heat pipe, discussing conditions in Na filled heat pipe [DGLR-69-44] 04 p0785 A70-15171

Viscous gas self similar channel flow with heat transfer at wall corresponding to fixed Mach number profile in all channel cross sections 04 p0673 A70-15231

Circulation model of joint ocean-atmosphere system constructed with ocean and atmospheric models, discussing heat transfer by ocean currents 04 p0680 A70-15297

Equations and techniques to analyze transient heat and mass transfer characteristics of packed adsorption beds for spacecraft life support systems 04 p0786 A70-15316

Transient one dimensional heat transfer analysis demonstrating infiltrant melting effect on self heat-retarding porous metal composite during surface melt layer formation 04 p0709 A70-15414

High temperature thermal transport and ionization relaxation in Ar from measurements by thin film surface thermometer in high pressure shock tube end wall 04 p0787 A70-15607

Heat transfer in MHD Couette flow influenced by wall electrical conductances with suction 05 p0886 A70-15823

Heat and momentum transfer efficiency of thermal convection, calculating eddy coefficients for vertical transfer 05 p0831 A70-15876

Heat and mass transfer in reacting laminar boundary layer over porous cylinder with propane injection in wind tunnel experiments 05 p0956 A70-16289

Vorticity effects on drag friction and heat transfer near stagnation point of supersonic jet impinging on obstacle 05 p0833 A70-16290

Soviet bibliography on heat and mass transfer covering thermodynamics, heat conduction, convective and radiant heat transfer, phase and chemical transformations, combustion, etc. 05 p0957 A70-16297

Heat transfer data for rotary piston and conventional piston engines, studying compression energy losses due to working fluid leakage 05 p0897 A70-17002

Flow disturbance calculation for heat transfer between boundary layer flows and adjacent walls modified to allow for wall attachment of thermal boundary layer 05 p1032 A70-17228

Skin friction law for compressible boundary layer allowing calculation of coefficient of friction for isothermal walls with heat transfer 06 p1033 A70-17232

Heat transfer boundary conditions determination in studying heat protective coatings effectiveness, discussing measurement methods for stagnation temperatures and heat fluxes from exhaust gases 06 p1173 A70-17662

Collection of papers on heat and mass transfer theories, measurements and applications 06 p1174 A70-17676

Heat transfer to hydrogen calculated with reference to design of cooled rocket nozzles and combustion chambers 06 p1174 A70-17677

Laminar sublayer resistance to momentum and heat transfer, noting effects of Prandtl number and surface roughness using mathematical model and experiments 06 p1034 A70-17680

Collection of papers on heat and mass transfer, Volume 2, covering free convection, forced fluid flow, nozzle flow, boundary value problems, etc. 06 p1174 A70-17682

Heat transfer from constant temperature and heat flux surfaces to viscous fluids with high Prandtl numbers, considering transient and steady state flow 06 p1176 A70-17687

Skin friction and heat transfer on flat plate in high velocity laminar motion with mass transfer for any free stream and injected gas combination 06 p1176 A70-17689

Unheated solid starting length effect on skin friction and heat transfer characteristics in incompressible transpired laminar boundary layer on flat plate 06 p1035 A70-17691

Heat and mass transfer in passive transpiration cooling system with two moving boundaries, observing porosities and radius of curvature effects 06 p1176 A70-17692

Heat and mass transfer across laminar boundary layer around stagnation line of cylinder in crossflow affected by free stream turbulence intensity 06 p1176 A70-17693

Heat transfer during nucleate boiling, discussing transfer from heated surface to superheated liquid layer and exchange on gas-liquid interface 06 p1176 A70-17695

DC electric arc with superimposed axial subsonic gas flow breakdown voltage and anode heat transfer using high speed photography 06 p1177 A70-17697

Sweeping W wire probe in rotational high temperature plasmas for local heat transfer measurement 06 p1120 A70-17699

Heat transfer in dense high temperature plasma due to drift waves instability at trapped electrons 06 p1121 A70-17802

Melting zone evolution in thermal history of earth, investigating upper mantle heat transfer effect on layer motion due to radioactive decay 06 p1056 A70-17804

Unsteady calorimetric sensor for measurement of heat transfer between gas jets and solid targets 06 p1064 A70-17857

Ignition of single particles of light metal hydrides, considering combustion stages and heat transfer [WSCIPAPER 69-47] 06 p1179 A70-17984

Static pressure, temperature profiles, heat transfer and optical data for turbulent boundary layer-shock interaction with/without injection [AIAA PAPER 70-91] 06 p1042 A70-18210

Unsteady nonlinear molecular flow problems concerning plane Couette flow, heat transfer between parallel plates and density discontinuity propagation solved by Monte Carlo method 06 p1113 A70-18321

Plane Couette flow and heat transfer between parallel plates problems treated by generalizing BGK model and applying variational principle to linearized Boltzmann equation 06 p1048 A70-18323

Monte Carlo method applied to Boltzmann collision integral in solving heat transfer between plates at different temperatures in elastic spheres gas 06 p1183 A70-18324

Plane Couette flow and heat transfer problem numerical solution, using Krook kinetic equation and Maxwell boundary condition 06 p1048 A70-18326

Rarefied gas flows and heat transfer between parallel plates, concentric cylinders and spheres in presence of fractionally accommodating boundaries 06 p1049 A70-18330

Transition regime gas flows using Navier-Stokes equations and boundary conditions set, considering heat transfer, torque and drag in spherical geometry 06 p1049 A70-18331

Aerodynamic forces and heat transfer on shielded flat plates in free molecular flow calculated by Monte Carlo technique 06 p0981 A70-18358

Free molecular heat transfer from sphere at rest in rarefied monatomic gas solved for Krook model of Boltzmann equation 06 p1183 A70-18375

Drag and heat transfer predicted by kinetic theory for rarefied gas flow over sphere at low Mach numbers, analyzing flow field 06 p0984 A70-18381

Wall roughness effects on model heat transfer in high Reynolds number shock tunnel milliseconds flow using thick film fast response calorimeter 06 p1070 A70-18446

Heat transfer effects during solidification on mechanical properties of Al alloy castings compared with sand castings [ASM PAPER W9-7.2] 07 p1293 A70-18998

Heat transfer at inlet edge of turbine blade based on wind tunnel study of cylinder in air flow 07 p1362 A70-19061

Velocity fields and turbulent pulsations effects on heat transfer in gas flow past plate with rectangular protrusion using wind tunnel tests 07 p1254 A70-19063

Wind tunnel study of heat transfer on smooth plate surfaces in longitudinal air flow using intermittently insulated calorimeter 07 p1279 A70-19065

Turbulence effect on heat transfer in flow carrying section of turbine engines, considering flow velocity pulsations frequency characteristics 07 p1362 A70-19067

Heat transfer from composite propellant burning zone to regressing surface measured using microjet burner 07 p1359 A70-19587

Heat exchange in laminar and turbulent boundary layers on plate for arbitrary heat flux distribution allowing for initial unheated plate segment 07 p1423 A70-19657

Heat transfer measurement in ionized high temperature gas flows with discharge shock tube and thermal sensors 07 p1283 A70-19663

Flow properties and heat transfer of wall jet spreading over permeable surface with suction and blowing 07 p1258 A70-19720

Streamwise directed vortices and crosshatched surface roles in heat transfer and ablation processes of reentry vehicles 07 p1394 A70-19729

Heat transfer during plane air jet impact into concave surface with parabolic profile, determining specific thermal fluxes by electrocalorimetry 07 p1189 A70-19810

Radiation effect on heat transfer during film boiling in forced convection boundary layer of liquid flow past plate, noting vaporization temperature 07 p1423 A70-19812

Functions describing spatial-temporal temperature distribution in hyperbolic partial differential equations for nonstationary heat exchange between fluid flow and boundary wall 07 p1423 A70-19839

Heat transfer from impinging gas jets on enclosed concave surface, noting self recirculation currents within cavity 07 p1425 A70-20413

Heat transfer from inner wall of annular ducted cylindrical body cooled by liquid nitrogen, discussing effects of Teflon, asbestos and vaseline coating and thickness effects 08 p1596 A70-20577

Multiple pass tube heat exchangers efficiency, solving energy and heat transfer equations from fluids homogeneity and constant thermal capacity considerations 08 p1596 A70-20613

Heat exchange at stagnation point of subsonic and supersonic axisymmetric jets interacting with perpendicular plane partition, allowing for turbulence 08 p1482 A70-20919

Time dependent height of lower boundary of subinversion stratus clouds using atmospheric moisture and heat transport equations 08 p1537 A70-21102

Vertical motions and turbulent exchange influence on height variation of stratus clouds based on atmospheric moisture and heat transport equations 08 p1537 A70-21103

Heat exchange during solidification of castings in molds, studying thermal properties effect for achieving constant mold surface temperature 08 p1506 A70-21141

Variational problem of determining optimal heat transfer from gas flow to porous plate boundary layer 08 p1597 A70-21176

Computer program predicting thermal response of fusion welding tooling chill bars and holding fixtures, simulating moving heat source and contact 08 p1508 A70-21487

Thermal boundary layer thickness and Nusselt number approximations for heat transfer in laminar flow along flat plate with power law heat flux distribution 08 p1599 A70-21583

Transient thermal stresses in plates with distributed heat source and heat exchange with arbitrary time dependent surroundings 08 p1593 A70-21623

Heat transfer in axially symmetric laminar viscous boundary layer flow due to rotating bodies of revolution, obtaining temperature distribution 08 p1485 A70-21698

Heat transfer in MHD channel flow of viscous incompressible rarefied gas with slip flow and temperature jump boundary conditions 08 p1554 A70-21769

Tensor conductivity, magnetic field and electric field effect on heat transfer in MHD channel flow, solving for temperature and Nusselt number 08 p1554 A70-21773

Boiling heat transfer enhancement inside tubes using integral fins, discussing water film retention on walls 08 p1599 A70-21825

Tape-generated swirl flow of single phase water investigated for heat transfer and pressure drop characteristics [ASME PAPER 68-WA/HT-3] 08 p1600 A70-21829

Heat transfer augmentation in tubes by surface roughness and twisted tape generated swirl flow 08 p1600 A70-21830

Correlation functions for resistance to heat and momentum transfer in viscous sublayer at rough walls defined for varied geometry flows [ASME PAPER 69-HT-2] 08 p1486 A70-21833

Diabatic mean profile forms in atmospheric surface layer, establishing profile relationships based on log-linear analysis 08 p1540 A70-21973

Local heat transfer to gas mixed with graphite particles described for variable temperature differences and wall temperatures 09 p1787 A70-22174

Heat and mass transfer in binary turbulent boundary layer during natural convection on vertical surface, allowing for diffusive heat conduction 09 p1787 A70-22267

Two dimensional supersonic wake transition characteristics noting effect of heat transfer from vehicle or model body 09 p1605 A70-23184

Gravitational effects on heat transfer during evaporation and condensation processes in heat pipe, discussing conditions in Na filled heat pipe 09 p1789 A70-23427

Taylor-Goertler vortex formation effect on heat transfer through boundary layer on concave wall [ASME PAPER 69-HT-3] 09 p1790 A70-23556

Boundary layer equations with heat transfer for laminar and turbulent incompressible flows about two dimensional and axisymmetric flows, using finite difference method [ASME PAPER 69-HT-7] 09 p1663 A70-23560

Heat transfer from circular cylinder in rarefied gas flow at low Mach number, using B-G-K model of Boltzmann equation 09 p1791 A70-23582

Heat and mass transfer during liquid surface evaporation in vacuum, calculating temperature field on basis of heat balance level 09 p1791 A70-23717

Unsteady heat transfer on electronic analog model, using installation prescribing variable boundary conditions of third kind 10 p1966 A70-23872

Air flow turbulence intensity and plug effect influence on local heat exchange on cylinder surface 10 p1797 A70-24028

Supersonic flows over flaps and backward facing steps, using steady state heat transfer measurement

technique involving uniform heat flux dissipation at model surface 10 p1798 A70-24120

Wall heat transfer effect on expansion following Chapman-Jouget detonation wave, calculating pressure and gas velocity profiles from friction coefficient 10 p1869 A70-24423

Heat transfer influence on three dimensional boundary layer separation on walled ellipsoid of revolution 10 p1870 A70-24781

Heat transfer from gas to gas turbine buckets, determining angle of attack and rotation influences by extending transfer equation 10 p1930 A70-25140

Heat transfer at inlet edge of turbine blade based on wind tunnel study of cylinder in air flow 10 p1930 A70-25212

Velocity fields and turbulent pulsations effects on heat transfer in gas flow past plate with rectangular protrusion using wind tunnel tests 10 p1871 A70-25214

Wind tunnel study of heat transfer on smooth plate surfaces in longitudinal air flow using intermittently insulated calorimeter 10 p1970 A70-25216

Turbulence effect on heat transfer in flow carrying section of turbine engines, considering flow velocity pulsations frequency characteristics 10 p1930 A70-25218

Naphthalene rotating disk with confronting stationary disk, investigating heat and mass transfer dependence on shroud dimensions, measuring flow types 11 p2060 A70-26410

Flat plate normal to two dimensional impinging air jet, investigating heat /mass/ transfer structure using naphthalene method 11 p1977 A70-26411

Gas-filled composites under impact loading, studying thermal damping due to heat transfer between compressed gas and solid structure 11 p2140 A70-26480

Dimensionless parameters associated with heat transport within living tissues using biothermal model 11 p1992 A70-26513

Heat exchange in linear vortex plasmatron with bilateral ejection, noting dependence on electrodes geometry and gas flow rates 11 p1984 A70-26737

Coaxial plasmatron pulsation on intensity of heat exchange between high temperature nitrogen jet and axisymmetric body near critical point region of spherical bluntness 11 p1984 A70-26739

SAE aerospace applied thermodynamics manual covering aerodynamics, fluid dynamics, heat transfer, materials properties, aerospace application engineering, etc 12 p2329 A70-26872

Quasi-isothermal heat transfer pipe design and operation 12 p2330 A70-27275

Electromagnetic effects on separation of turbulent MHD boundary layers allowing for heat transfer 12 p2278 A70-27324

Compressible turbulent plane Couette flow solution with variable heat transfer based on von Karman model extended to arbitrary wall temperature 12 p2211 A70-27839

Three-nodes analysis for thermal design of spinning spherical satellite using heat transfer equations in mathematical model 12 p2332 A70-28061

Heat transfer research /1968/ literature covering channel flow, boundary layer flow, separated flow, transfer mechanisms, convection, measurement techniques, etc 12 p2333 A70-28109

Unsteady heat or mass transfer to translating fluid sphere thermal boundary layer, determining analytical solution method accuracy 12 p2333 A70-28116

Heat transfer and flow stabilization dependence on initial shock wave reflection from conducting wall 12 p2213 A70-28228

Laminar multicomponent boundary layer for large injection and heat transfer, with particular reference to vehicle entry into planetary atmosphere 12 p2159 A70-28234

Transient heat transfer considered for thermal boundary layer over rotating disk following temperature change 13 p2519 A70-28493

Increased heat transfer for thermal coupling by interleaving fins in space applications 13 p2519 A70-28522

Mechanical seals ringing sound relationship with heat transfer and interfacial conditions, noting sliding surfaces temperature effect 13 p2417 A70-28611

Heat transfer in dense high temperature plasma due to drift waves instability at trapped electrons 13 p2460 A70-28653

Heat transfer in Z shaped regenerative heat exchangers with/without air mixing, determining parameters defining thermal efficiency 13 p2520 A70-28857

Heat energy transport mechanism in metallic plasma deposited coating, investigating role of elastic crystal lattice vibrations, electrons, molecules, etc 13 p2419 A70-28858

Heat transfer mechanism in foil-vacuum insulations, analyzing factors responsible for point of inflection on experimental temperature field curves 13 p2521 A70-28861

Heat transfer increase near stagnation point for turbulent jet impinging on paraffin coated plates used for flow visualization 13 p2521 A70-28866

Heat transfer at low Reynolds and Grashof numbers determined using constant temperature anemometric wire 13 p2521 A70-28952

Pressure distributions and heat transfer at wall calculated to investigate supersonic laminar reattachment 13 p2338 A70-28953

Steady diabatic complex lamellar gas flow, obtaining parameters by extending geometric theory of surfaces and curves in fluid flow theory 13 p2387 A70-29122

Free convection flow and heat transfer from semi-finite horizontal flat plate with time-oscillating temperature, using successive approximations process 13 p2522 A70-29537

Heat transfer and fluid mechanics - Conference, Stanford, California, June 1970 14 p2662 A70-30251

Strongly accelerated turbulent boundary layer, investigating free stream turbulence effect on heat transfer 14 p2564 A70-30252

Two dimensional incompressible turbulent boundary layer with mass addition and heat transfer, calculating temperature and velocity profiles by marching integration 14 p2564 A70-30261

Radiation effects on heat transfer in turbulent channel flow for small optical depths and optically thin limit 14 p2665 A70-30548

Heat transfer from acceleration induced boundary layer reverse transition, considering free stream turbulence effects 14 p2667 A70-31169

Supercritical pressure system heat transfer characteristics for cryogenic space oxygen storage and supply 14 p2667 A70-31342

Surface, volume and body center temperature of convex polyhedrons under steady heat transfer 15 p2825 A70-31624

Monograph on momentum, heat and mass transfer rates to vertical continuous cylinder moving through quiet fluid in forced and free convection 15 p2825 A70-31694

Heat transfer through axially symmetric boundary layer on moving circular fiber at uniform temperature 15 p2825 A70-31819

Heat exchange measurements between solid body and high enthalpy gas flow at stagnation point using electric arc heater 15 p2826 A70-32102

Rheological calculation of plate resistance and heat transfer in laminar flow of structurally viscous fluids 15 p2827 A70-32126

Heat transfer between incompressible fluid flow and insulated walls with time varying temperature at channel inlet, applying Laplace transforms 15 p2827 A70-32175

Heat exchange in laminar and turbulent boundary layers on plate for arbitrary heat flux distribution taking into account initial unheated plate segment 15 p2828 A70-32694

Swirling flow in unbounded space, investigating swirl intensity effect on heat transfer 15 p2828 A70-32857

Gas-particle mixture cascade flow over turbine blades, considering momentum/heat transfer and particle trajectories [AIAA PAPER 70-712] 16 p2835 A70-33569

Cryogenic single tubes transient cool-down by liquid hydrogen, deriving film boiling heat transfer correlation 16 p2998 A70-33621

Nuclear rocket nozzle cooling passages, discussing heat transfer and friction correlations for single-phase hydrogen turbulent flow [AIAA PAPER 70-661] 16 p2950 A70-33622

Gas phase chemical reactions effect on heat transfer to charring ablator, deriving numerical solution for multicomponent stagnation point flow [AIAA PAPER 70-869] 16 p2999 A70-33912

Lateral heat transfer along parallel conducting and radiating plates spaced by absorbing and isotropically scattering dielectric [AIAA PAPER 70-849] 16 p2939 A70-33916

Heat transfer in tungsten-tungsten and Armo Iron-Armo Iron specimens, confirming Bowden-Tabor model of elastoplastic events during cyclic engagement of surfaces
[AIAA PAPER 70-853] 16 p3000 A70-33920

Heat transfer and pressure drag of axisymmetric body in hypersonic flow, obtaining minimum energy nose and leading edge shapes by Pontryagin principle
[AIAA PAPER 70-825] 16 p3001 A70-33940

Instantaneous burning rates prediction methods based on flame structure model and steady state burning rate data as pressure and initial temperature functions
[AIAA PAPER 70-667] 16 p2971 A70-33949

Film boiling heat transfer from horizontal wires to water, using Nusselt condensation model
16 p3003 A70-34198

Turbulent flow in stratified fluids over flat plate, relating density profile curvature and heat transfer
16 p2895 A70-34242

Equilibrium air boundary layer flows at three dimensional stagnation points, discussing flow characteristics and real gas heat transfer parameters
[AIAA PAPER 70-806] 17 p3002 A70-34455

Two dimensional solidification of forced viscous flow over flat plate with constant heat removal
17 p3194 A70-34634

Convergent-divergent nozzle flow under influence of friction drag, determining heat transfer rate as function of nozzle geometry
17 p3194 A70-34694

Heat and mass transfer in flowing fluid, deriving conservation and constitutive equations, with application to boundary layer flow of gases
17 p3069 A70-35033

Anodes heat transfer in xenon short arc lamps
17 p3023 A70-35154

Atmospheric reentry nosetip shape changes supersonic flow, considering rough surface effects on heat transfer
[AIAA PAPER 70-827] 17 p3196 A70-35193

Optimum nozzle geometry for minimum heat transfer to convergent-divergent nozzle wall from high enthalpy flow
17 p3196 A70-35238

Nonstationary temperature fields and stresses in wedge shaped strip and thin plates with heat transfer for discontinuous boundary conditions
17 p3189 A70-35342

Transient heat and mass transfer in adiabatic regenerator, solving mathematical model in terms of Green functions
17 p3197 A70-35542

Fluid flow longitudinal temperature profiles for inclusion in heat transfer computer program
17 p3198 A70-35659

Sonic boom minimization through airstream alteration by force or heat fields and aircraft body shaping
[AIAA PAPER 70-903] 17 p3019 A70-35817

Critical heat flux density during annular channel internal heating, examining transfer crisis under forced motion of unheated water
18 p3345 A70-36111

Explicit differences scheme for heat and mass transfer differential equations
18 p3345 A70-36114

Steam-water jet discharge heat transfer features, examining critical region parameters from nozzle into submerged space with large counterpressure
18 p3345 A70-36117

Heat transfer across boundary between two stationary fluids, applying elastic wave theory in isotropic media
18 p3345 A70-36118

Heat transfer at flat melting surface under forced convection and laminar boundary layer solved by Karman-Pohlhausen method
18 p3347 A70-36502

Biophysical model of heat transfer from organism, describing adaptation to ambient temperature
18 p3218 A70-36531

Prolonged cold adaptation effect on heat transfer during recovery period after hypothermia in white rats
18 p3220 A70-36543

Repeated snow cooling effect on heat transfer in white rats during temperature homeostasis recovery after hypothermia
18 p3220 A70-36544

Ideal relativistic fluids adiabatic flow, investigating heat exchange effects within framework of special relativity
18 p3347 A70-36554

Heat transfer rates in short flow duration facilities /shock tubes/ from surface temperature measurement of solid exposed to flow
18 p3348 A70-36715

Heat transfer characteristics of flows between high speed rotating disk and parallel stationary shroud, discussing experimental facility and procedures
[ASME PAPER 70-GT-20] 18 p3349 A70-36865

Optimal control for one dimensional compressible gas flow, combustion and heat exchange, described by first order partial differential hyperbolic equations
19 p3402 A70-37240

Soviet papers on transfer phenomena in low temperature plasmas
19 p3480 A70-38180

Heat transfer in plasma flow incident normally on cylinder, examining laminar boundary layers in presence of turbulence
19 p3552 A70-38187

Heat transfer behind shock wave in air, oxygen or carbon dioxide flow past wedge, determining thermal fluxes vs wave velocity
19 p3405 A70-38188

DC plasma generator with Ar stabilized arc, investigating heat and mass transfer in jet discharge channel
19 p3481 A70-38189

Unsteady flow and heat transfer in viscous incompressible fluid due to infinite porous cylinder oscillations about axis with suction at surface
19 p3406 A70-38445

Heat transfer in boiling liquid from temperature field and temporal changes in liquid above heating surface, determining isotherms by laser interferometry
19 p3447 A70-38455

Radiation effect on heat transfer during film boiling in forced convection boundary layer of liquid flow past plate, noting vaporization temperature
20 p3736 A70-39259

Heat transfer during plane air jet impact into concave surface with parabolic profile, determining specific thermal fluxes by electrocalorimetry
20 p3736 A70-39260

Heat transfer from cylinder in axial air flow with induced turbulence of incident boundary layer, noting temperature effects
20 p3736 A70-39264

Heat exchange and temperature distribution between two liquids divided by plate, discussing possible errors
20 p3737 A70-39634

Heat fluxes from shock-heated gas to shock tube wall and wedge surface as function of Mach number, using platinum resistance thermometers
20 p3613 A70-40343

Heat transfer from gas to gas turbine buckets, determining angle of attack and rotation influences by extending transfer equation
20 p3694 A70-40345

Ducted laminar and turbulent diffusion flames, examining electric fields effect on heat transfer, geometry and velocity field
20 p3739 A70-40471

Stagnation point heat transfer of spherical cylinder in argon and air, developing electrically insulated calorimeter gage theory
21 p3941 A70-40774

Fusion welding cooling rates, peak temperatures and heating duration relationships to distance from fusion line predicted by theory for comparison with experiment
21 p3832 A70-40791

NonNewtonian fluids flow and heat transfer characteristics past flat plate, determining velocity and temperature distributions
21 p3806 A70-40900

Space technology and heat transfer - ASME Conference, Los Angeles, June 1970, Part I
21 p3927 A70-40976

Wall heat transfer for partially ionized argon laminar flow within square channel conducting walls with and without transverse magnetic field
21 p3856 A70-41032

Reentry vehicle with multicomponent gas mixture injection, calculating heat and mass transfer correlations for stagnation point flow
21 p3945 A70-41033

Local heat transfer between heated circular cylinder and air in transverse slip flow at low Reynolds and Mach numbers
21 p3945 A70-41035

Two dimensional compressible laminar MHD boundary layer flow across flat plate with heat transfer, considering continuity, momentum and energy equations
21 p3856 A70-41039

Heat transfer mechanism during fluid evaporation in porous wick structure contacting heat pipe surface
21 p3946 A70-41042

Pt and Ag surface effects on LOX nucleate boiling heat transfer, considering embedded abrasives relationship to hysteresis
21 p3947 A70-41056

Interfacial instability effect on heat transfer to liquid nitrogen drops undergoing film boiling on flat Al surface, obtaining vaporization rates and times
21 p3948 A70-41203

Nucleation phenomena associated with boiling heat transfer in pure liquids at solid heating surfaces
21 p3948 A70-41205

Water and alkali metal boilers, predicting helical-flow-promoting inserts effect on pressure drop penalties by constant slip model
21 p3949 A70-41308

Pool film boiling heat transfer data from small spheres, noting curvature effects and similarities of flat plate, cylinder and sphere theoretical analyses
21 p3949 A70-41310

Tube heat transfer augmentation by helical vane inserts, noting Reynolds number and mass flow rate effects
21 p3949 A70-41318

Book on heat transfer covering supersonic flows with imbedded separated regions, unsteady convection and thermodynamics in channels, friction in turbulent pipe flow, etc
21 p3949 A70-41371

Heat transfer measurements based on optical methods with temperature dependence of refractive index making temperature field visible
21 p3826 A70-41373

Heat transfer and skin friction in quasi-steady axisymmetric turbulent pipe flow of incompressible fluid with variable physical properties
21 p3808 A70-41375

Mass force fields effects on flow phenomena from heat transfer and hydraulic resistance analyses
21 p3951 A70-41764

Heat transfer and friction effects on flow parameters in nozzle with independent cooling
21 p3951 A70-41769

Orbital mission solar energy power conversion system, discussing heat transfer processes for storage feasibility
21 p3951 A70-41852

Arc ignition and cathode spot movement dynamics of thermionically emitting cathode surfaces in heat feedback plasma
21 p3859 A70-41903

Electromagnetic effects on separation of turbulent MHD boundary layers allowing for heat transfer
21 p3860 A70-42065

Thermal design of high altitude balloons and instrument packages, analyzing vertical motion dependence on heat transfer and radiation environment
21 p3755 A70-42077

Upstream mass injection effects on downstream heat transfer of supersonic reacting boundary layer
21 p3952 A70-42079

Charge separated and quasi-neutral solutions of electron heat transfer to spherical body in quiescent nonequilibrium plasma, noting diagnostic applications
21 p3860 A70-42080

Heat transfer in closed partially liquid filled steady state porous systems, testing linear flux force equation validity
21 p3952 A70-42081

Wall recombination heat transfer in rarefied flow with velocity slip near leading edge
21 p3952 A70-42083

Surfaces separated by radiatively nonparticipating medium, determining absorptivities and heat transfer boundary conditions in gray surface problems by irradiation factor method
21 p3953 A70-42085

Heat transfer from thin plate in compressible gas flow, considering interface temperature as nonanalytic function
21 p3953 A70-42086

Free stream turbulence effect on heat transfer to stagnation point of sphere
21 p3953 A70-42095

Heat and mass transfer in plane inductionless and dissipationless incompressible MHD boundary layer with longitudinal pressure gradient
21 p3861 A70-42231

Downstream heat transfer and wall friction predictions for quasi-developed strongly heated turbulent pipe flow, using mixing length model
[ASME PAPER 70-HT-8] 22 p4008 A70-42439

Comparative analytic and experimental film boiling heat transfer for horizontal cylinders in helium II
[ASME PAPER 70-HT-3] 22 p4122 A70-42441

MHD channel flow of suspension for prescribed wall heat flux and temperature, determining flow and heat transfer characteristics
22 p4080 A70-42670

Effective pressure ratio nomographs for mechanical energy conversion and heat transfer of closed regenerative Stirling engines, using isothermal theory
22 p4091 A70-42757

Heat transfer in heated wire in supersonic flow near molecular transition zone, estimating anemometer sensitivity to motion fluctuations
22 p3959 A70-43240

Stepwise heat removal for increased continuous combustion gas turbine engine cycle efficiency, deriving equations describing cycles
22 p4092 A70-43372

Ablative heat transfer to nonstagnation surfaces of high speed rocket vehicle in continuum atmosphere, using finite difference theory
22 p4125 A70-43433

Heat transfer measurements compared in free flight and in hypersonic wind tunnel at similar Reynolds number and temperature ratios
[ICAS PAPER 70-06] 23 p4275 A70-44115

Pressure distribution, force and heat transfer measurements on varied-configurations of lifting reentry vehicles in hypersonic flow [ICAS PAPER 70-03] 23 p4132 A70-44117

Wave-riders aerodynamics and heat transfer, investigating lift to drag ratios for supersonic and hypersonic vehicles [ICAS PAPER 70-18] 23 p4276 A70-44129

Sandwich multilayer structures temperature fields and heat transfer characteristics at high temperature [ICAS PAPER 70-38-BIS] 23 p4277 A70-44136

Heat and mass transfer for liquid film evaporation during two phase two component flow in vertical steel tube under adiabatic and nonadiabatic conditions 23 p4276 A70-44215

Temperature gradient effect on Couette flow heat transfer and stability 23 p4181 A70-44250

Time optimal problems involving parabolic equations in heating of rod with piecewise continuous thermophysical characteristics and temperature distribution constraints, deriving iterative solution 23 p4277 A70-44306

Capillary boiling and heat transfer for coolant fluids, using motion photography and visual observations 23 p4277 A70-44320

Near critical heat transfer in cryogenic fluids, discussing thermodynamic and transport properties 23 p4279 A70-44357

Liquid He II, determining correlation of depth effect on film boiling heat transfer with vapor film geometry from motion pictures 23 p4279 A70-44363

Cracked Teflon heat shields ablative behavior for laminar and turbulent boundary layers in supersonic flow, describing heat transfer to substructure 23 p4282 A70-44585

Heat transfer and viscous flow pedagogy, discussing classroom use of remote time sharing computer terminals 23 p4166 A70-44642

Human body heat production and transfer through convection, radiation and evaporation under normal and reduced atmospheric pressure 23 p4154 A70-44654

Heat exchange during flat plate transverse vibrations in water, discussing frequency and amplitude effects and natural convection role 23 p4282 A70-44728

Transition zone heat exchange during air mixed flow in pipes with conical duct or Vitoshinski nozzle inlets 23 p4283 A70-44729

Heat exchange on turbine blade profiles, examining boundary layer flow transition region coordinates 23 p4283 A70-44732

Heat transfer at air cooled gas turbine blade trailing edges at various wall temperatures and Reynolds numbers 23 p4283 A70-44737

Bodies of revolution optimal configuration, considering minimum head drag coefficient and low heat transfer at hypersonic speeds, using modified Newtonian and hypersonic flow theories 23 p4136 A70-45021

Heat transfer in chemically reacting gases boundary layers, obtaining approximate solution by film theory 24 p4428 A70-45101

Local or surface boiling phenomenon under triangular channel laminar flow conditions, investigating heat transfer with and without phase change 24 p4429 A70-46089

Diabatic steady gas flow vorticity, examining various kinematic and kinetic properties 24 p4328 A70-46365

HEAT TRANSFER COEFFICIENTS

Heat transfer coefficients for mesh simulating porous parachute cloth, measuring Nusselt number as function of sonic Reynolds number 01 p0004 A70-10292

Conductive heat transfer coefficients of densely packed electronic subassemblies 01 p0051 A70-10990

Electronic wafer packages heat transfer coefficients determined analytically, considering roles of geometrical and physical parameters 01 p0051 A70-10991

MHD entrance region compressible flow characteristics, determining velocity pressure and temperature distributions, friction and heat transfer coefficients, etc 01 p0067 A70-11136

Heat transfer coefficients in transpiration cooled gas turbine blades, using two dimensional theory covering porous wall and internal cooling passages 01 p0166 A70-11392

Wall temperatures and heat transfer coefficients for solid-vapor mixtures of para hydrogen and nitrogen flowing in heated tube 03 p0604 A70-13018

Thermoelastic stresses in plate due to arbitrary temperature variations of heat transfer agent calculated in second approximation, allowing for transfer coefficient time dependence 03 p0590 A70-13400

Mean volume heat transfer coefficient, mean thermal head and coolant temperature determined for gas flowing through porous wall with internal heat source 03 p0605 A70-13474

Equilibrium temperature and heat transfer of sphere in supersonic flow of rarefied air 03 p0409 A70-13874

Heat transfer coefficient in turbulent duct flow of fine particles suspension, using coupled similar equations 03 p0608 A70-14382

Plume-induced flow separation effect on thermal environment using Saturn 5 film and instrument data, attributing heating rate increase to recirculated exhaust gases [ASME PAPER 69-WA/HT-18] 04 p0761 A70-14815

Dominant and small parameters determination through sensitivity coefficients in heat transfer problem [ASME PAPER 69-WA/AUT-4] 04 p0713 A70-14829

Response characteristics of asymptotic or Gardon type thin foil heat flux transducer, discussing heat transfer coefficient effect on response time and curve 04 p0694 A70-15548

Heat exchanges between man and environment due to incidents or accidents during aircraft operation evaluated by combined heat transfer coefficient 05 p0799 A70-15764

Heat transfer coefficients for heat exchangers rotating in air at various velocities computed from skin friction coefficients in laminar and turbulent flow regime 06 p1177 A70-17701

Local heat transfer coefficients determined from temperature distribution on porous walls, deriving mathematical expressions for various surface geometries and transfer modes 06 p1184 A70-18555

Meteoroids atmospheric drag and heat transfer coefficients, considering weak shielding by repelled and vaporized molecules 08 p1572 A70-20945

Heat exchange coefficient during Ti melting in lined arc furnace, determining relation between heat flows to side walls and bottom of graphite crucible 08 p1506 A70-21140

Local heat transfer coefficients for unsteady conditions in tube determined by gradient method, noting use in reacting flow and jet nozzle protection 08 p1598 A70-21189

Forced convection heat transfer between two parallel plates analyzed numerically for effect of constant heat transfer coefficient boundary condition 08 p1598 A70-21425

External convective heat transfer coefficients from quartz-coated cylindrical hot film anemometer probes in mercury 08 p1599 A70-21582

Film heat transfer coefficients and thicknesses for condensation and evaporation and two phase flow inside circular tubes [ASME PAPER 67-HT-1] 08 p1599 A70-21827

Local heat transfer coefficients determination for unilaterally heated rectangular coolant duct by approximation and experiment applicable to circular tubes 09 p1787 A70-22170

Heat transfer coefficient to gas in tube under unsteady heat flow conditions, studying Nusselt number dependence on Reynolds and Prandtl numbers 09 p1787 A70-22173

Heat and mass transfer coefficients in binary laminar boundary layer convection obtained with integral equations and Karman-Polhausen method 09 p1787 A70-22264

Rectangular fins arrangement on horizontal surfaces for optimum free convection heat transfer coefficient, considering fin weight, height and spacing effects [ASME PAPER 69-HT-44] 09 p1789 A70-23551

Turbulent pipe flow with wall suction, calculating friction factor, pressure gradient, heat and mass transfer coefficients, velocity and temperature profiles [ASME PAPER 69-HT-4] 09 p1790 A70-23558

Capillary grooves effect on surface wetting and evaporation using heat transfer coefficients for grooves with triangular, semicircular and square cross sections [ASME PAPER 69-HT-19] 09 p1790 A70-23559

Fluid boiling heated nonuniformly in pipe, deriving formulas for unsteady temperature field by integrating energy equation 09 p1791 A70-23716

Heat conduction analysis for plane body with boundary condition and time variable heat exchange coefficient, applying automatic control technique 10 p1966 A70-23869

Temperature gradient method for determining local heat transfer coefficients in variable cross section channel 10 p1968 A70-24290

Transient thermal stresses in restrained-in-bending slab with surfaces heated and cooled with finite heat transfer coefficients 10 p1964 A70-25095

Radiant heat exchange local and angular coefficients determined allowing for absorbing and scattering medium between bodies 10 p1969 A70-25141

Simultaneous heat and mass transfer coefficients in laminar free convection boundary layers on horizontal cylinders or vertical axisymmetric bodies 11 p2151 A70-26559

Nusselt numbers of nonstationary and stationary heat transfer between metal spheres and liquid flow, showing bulk heat and geometry dependence 12 p2330 A70-27288

Critical thermal flux and heat transfer coefficients dependence on simulated gravity during bubble and film boiling in inclined flat containers 12 p2331 A70-27325

Iron and stony iron meteorite cooling rates and thermal models, showing melting, radioactive heat source redistribution and surface heating effects 13 p2497 A70-29861

Surface heat transfer coefficients under perforated plate of multiple square array round impinging air jets [ASME PAPER 69-GT-4] 14 p2666 A70-31025

Heat transfer coefficient from circular cylinder subjected to uniform surface heat flux and cooled by ring of holes 14 p2667 A70-31427

Laminar natural convective heat transfer along outer surface of vertical cylinder, giving coefficients nondimensionally by approximate formulas 15 p2826 A70-31821

Laminar boundary conditions for heat transfer in gradient flow region for plane turbulent jet impingement on plate normal to flow 15 p2721 A70-32134

Meteoroids atmospheric drag and heat transfer coefficients, considering weak shielding by repelled and vaporized molecules 15 p2806 A70-32757

Thin cylinder longitudinal two phase dispersed flow, examining heat transfer coefficient 18 p3345 A70-36112

Environmental heat stress indices of human subjects in bicycle ergometer experiment 18 p3224 A70-36226

Free convection boundary layer on two dimensional or axisymmetric body with sudden temperature increase, determining skin friction and heat transfer coefficients 18 p3346 A70-36487

Burning rate theory applied to heat and mass transfer rates of monopropellant droplets in heat-up and steady burning at wet bulb temperature 18 p3348 A70-36696

Heat transfer coefficient of chemically reacting gas mixture as function of Lewis-Semenov number, discussing nitrogen dioxide decomposition 19 p3550 A70-37251

Cooling rate effect on Al-Mg equilibrium state during heat treatment after annealing 20 p3644 A70-38959

Stagnation point heat transfer coefficient to elliptical model taking into account pressure, model blunting and diameter, Mach number, etc 20 p3737 A70-39699

Uniqueness theorem for first boundary value problem of heat conduction equation with discontinuous coefficient 20 p3737 A70-39710

Dimensionless heat transfer and resistance coefficients during stabilized nonNewtonian fluid flow in circular pipe 20 p3613 A70-40176

Temperature gradient method for determining local heat transfer coefficients in variable cross section channel 20 p3739 A70-40348

Turbulent gas boundary layer at finite Reynolds numbers, investigating relative changes in friction and heat transfer coefficients and temperature factor 20 p3614 A70-40390

Heat transfer between wall and liquid and vapor films in internal regenerative cooling of thrust chambers 21 p3867 A70-41027

Flow field, heat transfer rates and reattachment surface wall temperature of planar supersonic turbulent flow 21 p3744 A70-41036

Critical thermal flux and heat transfer coefficients dependence on simulated gravity during bubble and film boiling in inclined flat containers 21 p3952 A70-42066

Linear corrections formulas for shear stress and heat transfer coefficients associated with boundary layer blowing in binary gas mixture 21 p3748 A70-42207

Cylindrical wall nonstationary heat conductivity for time variable heat transfer coefficient 22 p4125 A70-43358

Tube heat exchangers operation at low transfer coefficient, calculating unsteady temperature field in wall and heat transfer agent 22 p4125 A70-43364

Heat exchange coefficients on side surfaces of constant thickness gas turbine disk, using temperature distribution method and integral transformations

22 p4125 A70-43367

Stationary turbine blades heat flux measurements, considering heat exchange coefficients and turbulent boundary layer

[ONERA-TP-871]

22 p4126 A70-43459

Thermal conductivity coefficient calculation by multiple temperature measurements of plate-shaped sample, using iteration process

23 p4276 A70-44166

Forced convection heat transfer to liquid nitrogen near critical point, determining coefficients from given wall temperature and heat flux

23 p4279 A70-44358

Liquid nitrogen drops undergoing film boiling on Al surface, measuring heat transfer coefficient

23 p4279 A70-44360

Cylindrical heaters in corresponding-states fluids, estimating film boiling heat transfer coefficients by correlation procedure using least squares expression

23 p4279 A70-44361

Saturated nitrogen vapors condensing coefficients measurement by cryostat, comparing results with theoretical prediction

23 p4218 A70-44364

Powdered flat steel plates cooling by air blown through pores, determining internal heat exchange coefficients

23 p4283 A70-44731

Viscous compressible gas flows in pipe initial section, calculating friction and heat transfer coefficients

23 p4135 A70-44734

Turbulent heat exchange coefficient and Prandtl number in turbulent air flow through heated pipe with constant heat flux

23 p4183 A70-44740

Ruby laser in repetitive pulse operation, determining temperature, heat generation and transfer coefficient from spectrum shift measurement

23 p4203 A70-45071

HEAT TRANSMISSION

NT AERODYNAMIC HEAT TRANSFER

NT CONDUCTIVE HEAT TRANSFER

NT CONVECTIVE HEAT TRANSFER

NT HEAT TRANSFER

NT HYPERSONIC HEAT TRANSFER

NT LAMINAR HEAT TRANSFER

NT RADIATIVE HEAT TRANSFER

NT SUPERSONIC HEAT TRANSFER

NT TURBULENT HEAT TRANSFER

Combustion instability in gas turbine main combustors, noting heat release and inlet air flow rates coupling

02 p0353 A70-12012

Diffusive transport term in hydrodynamic equations describing flow over strongly ablating entry objects, discussing charge separation and pressure diffusion

03 p0405 A70-12926

Thermal stresses of semiinfinite plate with circular hole filled with elastic inclusion and subjected to uniform heat flow

03 p0601 A70-14317

Heat transmission by current carriers to cryogenic region, ascribing heat flux to Joule effect in conductor

05 p0881 A70-16025

Crack stability under tension and thermal stresses caused by uniform disturbed heat flow, using Barenblatt fracture criterion

05 p0939 A70-16483

Negative pressure gradients effects on wall heat flow and characteristic patterns for turbulent boundary layer profiles

06 p1033 A70-17231

Transient heat flow in three dimensional rectangular panels, developing criterion for problem dimensionality

[AIAA PAPER 70-16]

06 p1182 A70-18212

Thermal molecular flow kinetic theory, discussing anisotropic distribution function, thermal transpiration, thermal conduction, entropy production, etc

06 p1113 A70-18369

Thermal conductivity of arbitrarily inhomogeneous bodies, considering vectorial field isotropy and temperature gradients dispersion

09 p1789 A70-23103

Partial differential equation describing one dimensional heat transmission problems solved by eigenvalues for initial and boundary conditions

10 p1969 A70-25098

Linear heat propagation in rarefied and non-homogeneous atmospheres, considering Green function behavior and various boundary and initial value problems

11 p2107 A70-25542

Heat flow comparator for nondestructive testing of resin-impregnated fiber glass, detecting nonuniformities leading to thermal properties variation

11 p2059 A70-25764

Apollo 13 lunar surface heat flow experiment to measure vertical temperature gradients as function of time and soil thermal conductivity

11 p2118 A70-26747

Heat removal influence on dynamic errors of cylindrical temperature sensors using electric models

14 p2662 A70-30183

Quasi-stationary analysis of thermophysical characteristics of materials, considering cylinder and plate samples under unsteady heating

15 p2826 A70-32105

Thermodynamically perfect fluids in general relativity, considering heat transmission paradox and wave propagation velocities

16 p2997 A70-33103

Heat flow measurement, discussing operation principles, heat conduction and stationary and transient temperature conditions

17 p3082 A70-34681

Heat conduction from sliding solids, discussing restrictions effect on temperature field near interface

17 p3197 A70-35543

Knudsen effusion in free molecular flows in supersonic jet during expansion through circular orifice, discussing power and heat transmission

18 p3346 A70-36379

Heat flowmeters calibration by conductive method, reducing error due to radiative, conductive and convective losses

19 p3430 A70-38522

Linear heat propagation in rarefied and non-homogeneous atmospheres, considering Green function behavior and various boundary and initial value problems

21 p3892 A70-41292

Temperature distribution and thermal constriction resistance due to steady heat flow in laminated composite

22 p4126 A70-43689

Closed cell polyurethane foam for cryogenic insulation, determining thermal conductivity and net heat flow by analytical model and test

23 p4280 A70-44367

Temperature dependent materials heat flow analysis using perturbation method for nonlinear boundary value problems

23 p4282 A70-44589

HEAT TREATMENT

NT ANNEALING

NT NITRIDING

NT PULSE HEATING

NT STRESS RELIEVING

NT TEMPERING

Nimonic Ni-Cr based alloys fracture characteristics used to determine temperature and time effects on equicohesive points positions

01 p0116 A70-10073

High temperature heat treatment effects on Mo, W, Ta and Re crystal surface order and faceting observed by electron diffraction, noting contamination role

03 p0538 A70-13097

Heat treatment effects on phase components of Cr-Mn-B alloys with W and Nb additions, discussing heat resistance

03 p0510 A70-13280

Residual stresses in cylindrical shells eliminated by local heat treatment, determining temperature field in elastic strain regions

03 p0497 A70-13739

Beta III Ti alloy cold formability, mechanical properties and heat treatment noting use for fasteners, sheet metal parts, honeycomb sandwich sections and metal matrix composites

03 p0512 A70-13776

Heat treatment effects on mechanical properties of Ti-Fe and Ti-Fe-Al alloys

03 p0512 A70-13855

Electro-pyrotechnic initiators for space applications subjected to dry heat sterilization cycles and to post-sterilization mechanical and electrical environments

03 p0495 A70-14131

Titanium carbide based cermets with steel matrices, studying heat treatment effects on hardness

04 p0696 A70-14462

Induction furnace for thermal treatments and melting of solid and liquid metals, alloys and sintering and degassing ceramic and metallic systems in vacuum

04 p0664 A70-15371

Cold working with subsequent heat treatment increased creep rupture and creep behavior of V alloys

04 p0708 A70-15372

Cobalt alloys physical properties and heat treatment, discussing service conditions and critical problems

04 p0711 A70-15684

Maraging steel mechanical properties with Mn, Mo and Co additions in heat treated condition

05 p0865 A70-16874

Mechanical properties of nickel steels with carbon after suitable heat treatment found similar to high strength nickel steels properties without carbon

05 p0865 A70-16875

Thermophysical characteristics of annealed Ta and Mo alloy welded joints under electron beam and ray heating, noting use for short term tests

05 p0865 A70-17028

Microstructure effects on smooth and notched fatigue and room temperature tensile properties of Ti-Al-V alloy using heat treatment combinations

06 p1087 A70-17458

Al-Zn-Mg alloys anodic corrosion behavior under various heat treatment regimes using potentiostatic method

06 p1090 A70-17922

Interrelation of precipitation state, mechanical properties and electrical conductivity of wrought aluminum age hardened alloy under varied heat treatment conditions

07 p1294 A70-19389

Optimal localized heat treatment of welded products, analyzing temperature fields and stresses during heating and cooling of ferromagnetic materials

07 p1294 A70-19477

Ti-based alloys with Al and Mo investigated for chemical composition and heat treatment effects on mechanical properties

08 p1518 A70-21200

High temperature thermomechanical treatment effects on stainless steels and Ti alloys microheterogeneity, noting corrosion resistance improvement

08 p1519 A70-21444

Martensitic transformations during quenching and tempering of maraging steels

08 p1520 A70-21495

Softening of cold worked alloy by high speed electrical heating, noting supersaturation before natural aging

08 p1520 A70-21496

Cobalt modified Ti-6Al-4V plate and billet, testing effects on heat treatment response, microstructure, tensile and fatigue properties, fracture toughness, etc

08 p1523 A70-21852

Silicon containing alpha matrix Ti alloy with high creep strength and stability at elevated temperatures, studying processing and heat treatment effects on properties

08 p1509 A70-21853

Fatigue testing and thermal mechanical treatment effects on uni- and biaxial Al alloy-B composites tensile strength at room and elevated temperatures

08 p1523 A70-21893

Vacuum melting and heat treating equipment for high melting point metals from phase equilibria studies viewpoint

09 p1655 A70-22562

Heat treatment effects on hardened steels acoustic constants, calculating sound velocity in liquid metals

09 p1692 A70-22643

Thermal treatment function of austenitic grain size and mechanical properties of 18 pct Ni maraging steels

09 p1704 A70-22803

Internal stresses and substructures dependence on thermomechanical histories of stainless steel during creep, noting subgrain orientation

09 p1705 A70-22805

Saturn booster Ti alloy pressure vessel forging, heat treatment and welding, discussing machining, cleaning and tooling

[SME PAPER AD-70-733]

12 p2241 A70-27085

Ti alloys tensile properties correlated with microstructure for multiple heat treatment cycle variations for high strength and adequate ductility

12 p2252 A70-27107

Resistivity anomalies of nickel-chromium alloy with Al additions subjected to deformation and heating, studying K-state

12 p2254 A70-27496

Short time tensile properties of thermomechanically treated astroloy showing improvement due to refined gamma precipitate and grain boundary carbides

12 p2256 A70-27610

Undoped GaAs lattice constants and electrical properties before and after heat treatment

13 p2471 A70-29504

Heat treatment induced shape distortions measurements in maraging steel bars, plates and sheets, noting dependence on number of anneals and product form

14 p2595 A70-30544

Al heat treatable alloys for welded structures, considering stress corrosion resistance, aging effects, brittle and delayed rupture resistance, etc

14 p2596 A70-30961

Al-Mg-Zn alloy composition, mechanical properties and structure for various heat treatments, discussing welded structures stability, stress relief, corrosion resistance and tensile strength

14 p2597 A70-30966

Transient overloads effect on long term fatigue strength of notched and smooth steel samples, emphasizing heat treatment effect on notch sensitivity at high temperatures

15 p2814 A70-31546

Heat treatment effect on maraging steel fracture toughness and subcritical crack growth loaded at slow strain rate in laboratory air

15 p2760 A70-32377

Thermal-mechanically treated stainless steels structure and properties, discussing stress relief aging effects

15 p2761 A70-32380

- Electron paramagnetic resonance of Mn ions in single crystal and powder forsterite, testing heat treatment and proton irradiation effect on ordering
16 p2960 A70-33008
- Composition and heat treatment effects on Fe-Ni alloys structure, using micrographic, autoradiographic and potentiokinetic methods
16 p2916 A70-33080
- Quench hardening and Ni content relationship in Ti-Ni intermetallic compounds, investigating heat treatment effect on mechanical properties
16 p2930 A70-33084
- Al-Mg alloys creep characteristics dependence on Ag, Si and Zn additions during aging heat treatments, establishing activation energy and stress exponents
16 p2930 A70-33086
- Heating effect above beta transus at intermediate and final stages of processing on Ti alloys properties
17 p3097 A70-34359
- Solution heat treatment temperature effects on strength and age hardening of Ti alloys
17 p3120 A70-34419
- Heat treatment effect on strength and ductility of Ti-Al-V-Sn alloy by optical and electron microscopy and X ray diffraction
17 p3122 A70-34437
- Heat treatment and composition effect on mechanical properties of alpha Ti-base alloy, discussing creep resistance, tensile strength, etc
17 p3122 A70-34439
- Forming Ti-Al-V sheet metal in heat treated conditions, showing mechanical properties improvement over mill annealed parts
17 p3098 A70-34445
- Pyrolyzed tetraethoxysilane for carburizing steels and Ti alloys at 850-1050 C
17 p3102 A70-35409
- Cobalt addition to Ti-Al-V alloys, examining yield strength, heat treatment, ductility and microstructure
18 p3271 A70-35964
- Binary Co-Cr alloy open circuit potential and microstructure, examining effects of composition, heat treatment, allotropic transformation and precipitation
18 p3271 A70-35966
- Automatic dilatometers for volume variations in steel and Co-W alloy during aging and heat treatment, noting microstructural changes
18 p3257 A70-36202
- Fe-Ni alloy alpha-gamma phase transformation after heating, noting deformation planes and directions in martensite
18 p3275 A70-36204
- Deformable Al alloys hardening, emphasizing heat treatment in solid state
18 p3276 A70-36308
- Papers on cracking during postweld heat treatment of Ni alloys covering Rene 41 mechanical properties and resistance to strain age cracking
18 p3277 A70-36522
- Rene 41 resistance to strain-age cracking during postweld heat treatment
18 p3277 A70-36523
- Rene 41 ductility reduction by environmental oxygen promoting intergranular cracking at high temperatures
18 p3277 A70-36524
- Oxygen role in crack initiation and growth in Ni alloys postwelding heat treatment
18 p3277 A70-36525
- Plates and rods tendency to warp and form nonsymmetrical stress systems during heat treatment
19 p3433 A70-37272
- Soviet monograph on bimetal and refractory metals production by rolling in vacuum or inert media
19 p3433 A70-37402
- Wear resistant titanium carbide based cermet material production by impregnation techniques, discussing grain size and heat treatment effects
19 p3450 A70-37453
- Maraging steels heat treatment, measuring hardness as function of temperature for various heating rates
19 p3452 A70-37807
- Low temperature electrical resistivities of Al, Ni, Cu, Ti and Fe alloys for different heat treated conditions
19 p3452 A70-37825
- Iron phosphate semiconducting glasses, determining electrical and magnetic properties dependence on thermal treatment
19 p3487 A70-37861
- Cooling rate effect on Al-Mg equilibrium state during heat treatment after annealing
20 p3644 A70-38959
- Heat treatment and alloying element influence on phase and structure transformations in Ti alloys, investigating mechanical properties and creep resistance
20 p3645 A70-39039
- Ti alloys fine structure, mechanical properties and alloying elements diffusion mobility during heat treatment, observing chemical and structural inhomogeneities
20 p3645 A70-39040
- Ti alpha alloys subjected to heating in beta region, investigating plate-like precipitates by electron transmission microscopy
20 p3645 A70-39042
- Graphite fiber reinforced polycarbonate composites interfacial adhesion improvement by controlled thermal treatment
20 p3652 A70-39168
- Ti alloy bolts mechanical properties improvement by beta heat treatment
20 p3650 A70-39965
- Al alloy products heat treatment, using synthetic quenchant for distortion control
20 p3650 A70-39967
- Lithium-diffused silicon, investigating heat treatment and electron irradiation effects on electrical resistivity at high temperatures
20 p3687 A70-40164
- Al alloys heat treatment methods and equipment, discussing quenching, stress relief, incubation, postquench working and aging
21 p3834 A70-41722
- Heat treatment and photovoltaic properties of copper disulfide-cadmium sulfide heterojunctions, measuring I-V characteristics, capacitance and spectral response
21 p3862 A70-41911
- Ni base superalloy for gas turbines, describing heat treatment for precipitation hardening
22 p4055 A70-43099
- Silicon precipitation in nonrefined annealed Al, examining heat treatment effects
22 p4057 A70-43550
- Impurities and heat treatment effects on W internal friction at high temperatures, considering relaxation processes, recrystallization and microstructure
24 p4357 A70-45227
- Nondestructive thermal and thermochemical treatment penetration depth measurement in metal, examining magnetic test and ultrasonic techniques
24 p4346 A70-45721
- Metal and nonmetal thermal nondestructive tests based on surface temperature distribution produced by heat treatment
24 p4348 A70-45744
- Heat treatment effects on dispersion strengthening of Ni alloys, showing enhanced long term creep strength at 1100 C
24 p4360 A70-45828
- Nonequilibrium solidification and metastable phase transformation during heating of Al-Mo and Al-Cr alloys
24 p4360 A70-45829
- Heat treatable beta Ti alloys cold workability, fracture toughness, tensile ductility and applications [SAE PAPER 700856]
24 p4361 A70-45880
- ### HEATING
- NT AERODYNAMIC HEATING
NT ARC HEATING
NT ATMOSPHERIC HEATING
NT BASE HEATING
NT GAS HEATING
NT INDUCTION HEATING
NT IONOSPHERIC HEATING
NT KINETIC HEATING
NT LASER HEATING
NT PLASMA HEATING
NT PULSE HEATING
NT RADIANT HEATING
NT RADIO FREQUENCY HEATING
NT RESISTANCE HEATING
NT SHOCK HEATING
NT SOLAR HEATING
NT SUPERHEATING
NT TRANSIENT HEATING
- Liquid heating in thin walled porous shells under various boundary conditions, deriving formulas for temperature fields
03 p0604 A70-13208
- Numerical analysis of low-g fluid flow and heating problems encountered with liquid propellant storage and supply
07 p1394 A70-19719
- Temperature fields in cylindrical shell under axisymmetric heating, ensuring optimal stressed state
09 p1778 A70-23081
- Heating rate effect on Ti-V martensite decomposition, discussing elastic properties effects of partial tempering
16 p2931 A70-33256
- Brayton cycles in gas turbines, investigating intercooling or reheat and pressure ratio proportioning influence on efficiency and specific work
18 p3304 A70-36856
- Al-Mg alloys recrystallization, investigating heating rate and annealing time effects on sheet grain size
19 p3450 A70-37372
- Heating rate effect on Ti-V martensite decomposition, discussing elastic properties effects of partial tempering
23 p4206 A70-44285
- ### HEATING EQUIPMENT
- NT BOILERS
NT EVAPORATORS
NT FURNACES
- NT SOLAR FURNACES
NT VACUUM FURNACES
- MHD high temperature heating equipment, describing power generation and conversion and magnetic field-working fluid interactions
02 p0348 A70-12418
- Natural convection flow interactions from individual surfaces in closely spaced array of heated elements, discussing effect on heat transfer, induced flow and temperature field
07 p1418 A70-18644
- High temperature, electrically heated convective gas heating system for high velocity atmospheric flight simulation using air-nitrogen working fluids
12 p2205 A70-27100
- Supersonic flight simulation in hypersonic wind tunnels for developing hypersonic air breathing propulsion, describing ceramic storage heaters
13 p2384 A70-28666
- Electrothermal helicopter rotor blade deicing system, discussing design, operation and solutions for mechanical and reliability problems
13 p2348 A70-29552
- Microwave feeding system for heating and cooking prepackaged meals during extended space missions
19 p3368 A70-37747
- Al alloys heat treatment methods and equipment, discussing quenching, stress relief, incubation, postquench working and aging
21 p3834 A70-41722
- Direct electrical heating for high temperature thermal conductivity measurements of pure W, giving results for graphite
21 p3850 A70-42057
- Cylindrical heaters in corresponding-states fluids, estimating film boiling heat transfer coefficients by correlation procedure using least squares expression
23 p4279 A70-44361
- ### HEAVING
- Multiple skirt air cushion vehicle [ACV] pitch and heave dynamic characteristics, describing mathematical modeling and analog computer simulation
04 p0624 A70-15389
- Tracked air cushion vehicle dynamic heave response, examining flow characteristics, active lip control, guideway contact, acceleration response, etc
17 p3017 A70-35178
- Static and dynamic spring constants of peripheral jet air cushion vehicle in heaving motion, obtaining sinusoidal input response characteristics
22 p3960 A70-42279
- Nonlinear heaving motion of plenum-chamber air cushion vehicles induced by sinusoidal ground irregularity
22 p3961 A70-42280
- Peripheral jet ground effect machine model heaving motion, investigating static hover and forced and free vibration characteristics
22 p3961 A70-42281
- ### HEAVY COSMIC RAY PRIMARIES
- U HEAVY NUCLEI
U PRIMARY COSMIC RAYS
- ### HEAVY ELEMENTS
- NT PLUTONIUM ISOTOPES
- Electromagnetic showers fluctuations produced by electrons and photons in heavy materials, determining moments of particle numbers and bremsstrahlung differential cross sections
01 p0171 A70-11026
- Theoretical and experimental cascade curves comparison for heavy materials used for particle absorption in tracking experiments, discussing Coulomb scattering
03 p0527 A70-13051
- Globular clusters in M31, discussing metallicity and heavy element enrichment in Andromeda
06 p1138 A70-17306
- Solar core opacity, investigating individual heavy elements influence and effect of changes in abundances
18 p3317 A70-37005
- Heavy elements critical energy calculation, taking into account low energy electrons effects on losses in electromagnetic cascade
20 p3674 A70-39303
- Heavy elements diffusive separation as explanation of metallic and magnetic A stars abundance anomalies at outer convective envelope bases
24 p4410 A70-45775
- ### HEAVY IONS
- Heavy positive ions pulse counting by spiral-type continuous channel electron multiplier, noting long pulse rise time composed of numerous after pulsing
07 p1286 A70-19970
- VHF wave interference from heavy ion layers in lower ionosphere
14 p2574 A70-30737
- Heavy ions traces in crystals of lunar rocks, discussing applications as detectors
18 p3321 A70-37084
- Uranium ion impact ejection and electronic excitation of thin foil particles, observing optical spectra of Be, carbon and Al atoms and ions
20 p3674 A70-39135

HEAVY NUCLEI

Iron group nuclei abundance relative to oxygen determined for solar cosmic ray event of 2 September 1966

01 p0167 A70-10042

Meteorites fossil tracks due to cosmic radiation heavy nuclei

02 p0361 A70-11748

Heavy nuclei survival in cosmic rays Colgate supernova acceleration model, assuming plasma wave instability in shock wave

02 p0357 A70-11788

Electron loss in heavy body collisions from free scattering model and Born approximation

02 p0342 A70-11879

Ionization losses effect on energy spectra of cosmic ray heavy nuclei with Fermi acceleration, using transfer equation

04 p0742 A70-15201

Interstellar propagation effect on spectra and charge ratios due to ionization energy loss and nuclear spallation during traversal of matter

05 p0897 A70-15762

Pulsars as possible sources of superheavy nuclei in primary cosmic radiation, evaluating flux and mean power

05 p0901 A70-16314

Cosmic protons and high energy heavy nuclei interaction with radiation in expanding universe, including estimates of light radiation influence on cosmic ray spectra

05 p0904 A70-16903

Iron peak nuclei synthesis by charged particles under supernova mechanism conditions predicted by hydrodynamic conditions

09 p1749 A70-21994

Energy spectra and composition of heavy nuclei in primary cosmic rays during low solar activity by nuclear emulsion stacks exposure in balloon flights

11 p2105 A70-26295

Charge spectrum of heavy relativistic cosmic ray nuclei, using tracks from balloon-borne photographic emulsions

18 p3308 A70-36781

Charge spectrum of high and low energy heavy cosmic ray nuclei, using balloon-borne nuclear emulsions

19 p3507 A70-38130

Heavy cosmic ray abundance attributed to thermal nucleosynthesis during silicon burning at high temperature and density

19 p3507 A70-38132

Cosmic ray heavy nuclei charge composition from satellite-borne emulsion stacks exposure

19 p3507 A70-38134

Highly charged cosmic ray heavy nuclei primaries, examining charge spectra and solar elements abundances

19 p3508 A70-38136

Super heavy cosmic ray nuclei charge composition and track identification, using LEXAN polycarbonate, cellulose triacetate /CTA/ and nuclear emulsion

19 p3508 A70-38137

Primary cosmic ray particles with Z greater than 40 identified by tracks in balloon-borne nuclear emulsions and plastic detectors

19 p3508 A70-38138

Very heavy primary cosmic ray particles propagation calculation, using fragmentation parameters

19 p3508 A70-38139

Heavy and super heavy nuclei steady state spectra, comparing propagation parameters of light and medium nuclei

19 p3508 A70-38140

Cosmic ray track sources in meteoritic minerals, considering heavy primaries, secondary spallation and fission products

19 p3508 A70-38142

Explosive nucleosynthesis as heavy nuclei source for stars

20 p3712 A70-40426

Low energy cosmic ray heavy primary particles composition from nuclear emulsion stack observation

21 p3879 A70-40930

Optically thin plasma population and ionization equilibrium, taking into account heavy particle collisions

22 p4082 A70-43219

HEAVY WATER REACTORS

Third body coefficients of water and heavy water reactions in KCl coated and aged boric acid coated vessels with vibrational-vibrational exchanges

14 p2546 A70-31091

HEIGHT

NT SCALE HEIGHT

Seasonal variations of sporadic E virtual height at middle latitudes attributed to homospheric expansion depending on ozone amount

03 p0476 A70-13907

Vertical motions and turbulent exchange influence on height variation of stratus clouds based on atmospheric moisture and heat transport equations

08 p1537 A70-21103

Erroneous height correlation coefficients in physical optics formulation of rough surface scatter

16 p2859 A70-32938

Ionospheric disturbances heights at subauroral latitude from Explorer 22 satellite beacon signals recorded at spaced receivers

20 p3624 A70-40492

Transition zone height in corona-chromosphere interface from high resolution disk spectra near limb

21 p3926 A70-42198

HEISENBERG THEORY

Laser with nonresonant feedback calculated for single mode and total radiation fields correlation functions from Heisenberg equations

03 p0503 A70-14175

Kolmogoroff constant determined by Heisenberg turbulence formula and model for transfer of turbulent energy between different wave numbers

06 p1034 A70-17467

Spin-spin correlation in Heisenberg magnet linear chain at infinite temperature, discussing non-monotonic frequency dependence

14 p2619 A70-30486

Heisenberg uncertainty principle in communications technology, discussing variance products deficiencies and limits in carrier frequency pulses application

20 p3584 A70-39160

Uncertainty principle in optimum communication theory, discussing existence and value of minimum product of pulse duration in terms of calculus of variations and differential equations

20 p3584 A70-39161

Anisotropic Heisenberg antiferromagnet theory, developing nonlinear spin-wave approximation

24 p4388 A70-45131

HELICAL ANTENNAS

Current distribution in finite length helical antenna in HF field, using cylindrical model of infinitely good conductivity

01 p0050 A70-10713

Antenna biasing with DC field to improve power handling capacity tested on U-slot and helical antennas

02 p0269 A70-12595

Normal mode helical antennas performance in medium and short wave regions, discussing advantage over log periodic antennas and maximum radiation angle achieved by phase shift

02 p0270 A70-12735

Helicone antenna /axial mode helix combined with conical horn/ compared to conical horn in pattern and polarization characteristics [AAS PAPER 69-623]

04 p0655 A70-14662

Spacecraft phased array antenna techniques, discussing tape helix radiators design for applications in navigation, TV broadcasting and data relay systems [AIAA PAPER 70-425]

11 p2015 A70-25452

Spacecraft high efficiency phased arrays with deployable helix radiating elements, considering gain and weight factors

12 p2197 A70-27930

Axial mode helical antenna design with built-in impedance transformer for airborne applications

21 p3796 A70-40758

Radar cross section and current distribution of dipole deformed into low pitch angle helix

23 p4166 A70-44974

HELICAL FLOW

Stability conditions for helical motions of body bounded by multiply connected surface in fluid

01 p0145 A70-11439

Kinetic equation of helicons interactions in electron-hole plasma, discussing turbulence spectrum and effect on current carrier drift velocity

03 p0531 A70-13407

Helicon wave dispersion in cold multicomponent plasma of n-type Si and Ge semiconductors in linear hydrodynamic approximation

10 p1928 A70-24832

Helical propagation in multivalley semiconductors of n-Ge type, obtaining polarization anisotropy

10 p1928 A70-24842

Helical vortex generation in rotating flow in straight tube having angular momentum flux sufficiently large relative to linear momentum flux

14 p2565 A70-30277

Screw flows in fluid dynamics, showing helicoidal type flow for constant flow velocity on stream lines

15 p2718 A70-31447

Plasma helix equilibrium and stability in transverse magnetic field, considering oscillation damping by ohmic heating

15 p2781 A70-32910

Galactic spiral arm helical magnetic fields related to interstellar gas flow, using magnetohydrodynamic models

18 p3331 A70-37200

HELICAL INDUCERS

Plasma equilibrium in stellarator type magnetic trap /vintatron/ with magnetic configuration created by strong longitudinal field

12 p2277 A70-27313

HELICAL WINDINGS

Axial stress pulse induced elastic waves propagation in thin anisotropic circular cylindrical shell of helical wrap construction allowing for shear coupling

03 p0587 A70-13118

Fast neutron transport characteristics of helical ducts using Monte Carlo code FASTER, computing neutron fluxes and attenuation

05 p0884 A70-16163

Plasma stabilizing effect of shear and magnetic flux minimum in asymmetric conductors and currents in helical stellarator winding

11 p2088 A70-25711

Helical engraving influence on aerodynamic stability of bullets at long range, discussing wind tunnel tests [AIAA PAPER 70-557]

13 p2340 A70-29022

HELICOPTER ATTITUDE INDICATORS

U ATTITUDE INDICATORS

U HELICOPTERS

HELICOPTER CONTROL

Automatic flight control and instrumentation in civil helicopters, examining military developments and Ferranti automatic stabilization system

02 p0329 A70-11834

Helicopter automatic hybrid navigation system for increased accuracy over unfamiliar terrain and above-human performance, comparing navigating pilot performance with machine

02 p0335 A70-12134

Simplified aircraft instrument landing system /SAILS/ employing lightweight helicopter-borne radar for tracking radio beacon at touchdown point

02 p0337 A70-12768

Optimum automatic system for controlling helicopter formation flight, stressing transient response Q factor and transmission ratios

03 p0413 A70-13859

Helicopter tail rotors aerodynamic characteristics, using statistical methods for planning experiments and interpreting results

05 p0793 A70-15900

Blind flight and helicopter navigation during prolonged maritime survival operations

07 p1193 A70-19132

Soviet book on control systems for single rotor helicopters covering automatic stabilization system design, autopilots, pilot operation within closed control circuit, etc

08 p1435 A70-20769

Helicopter rotor, discussing conventional, semirigid, gyro and ABC systems in relation to roll balance and control

13 p2344 A70-28849

Dual controlled elastically twisting rotor blade performance during flight with azimuthal and collective variations compared to direct control rotor

13 p2345 A70-29012

Soviet book on practical aerodynamics of Mi 6 helicopter covering engine/rotor power balance, control, flight characteristics and solutions to in-flight emergencies

14 p2532 A70-31414

Automatic flight control and instrumentation in civil helicopters, examining military developments and Ferranti automatic stabilization system

15 p2772 A70-31771

High powered high speed helicopters autorotation entry characteristics, noting capability of meeting control time delay requirement

17 p3014 A70-34715

Gallium arsenide laser ranging system for helicopters obstacle warning

17 p3103 A70-34720

Crane helicopter controllability, discussing load stabilization and precision hovering

17 p3015 A70-34723

Hingeless rotor helicopter airborne and ground resonance characteristics, noting feedback stability control interference with rotors aerodynamic damping

17 p3015 A70-34733

Dynamic control model of lift helicopters with two cable sling loads using multiple part motion equations [AIAA PAPER 70-929]

17 p3020 A70-35839

Helicopter gas turbine governor systems for engine and rotor speed control, minimizing pilot activity [ASME PAPER 70-GT-37]

18 p3214 A70-36835

Helicopter radar approach aid for serving oil rigs

19 p3466 A70-38621

Computer simulated decision hierarchical model of helicopter and VTOL pilot for multiloop closure and tracking characteristics of man-vehicle system

19 p3372 A70-38921

Comfort plane switch mounting design for helicopter collective controls, noting mock-up evaluation by test pilots

19 p3372 A70-38922

Helicopter stabilization systems design, synthesizing controllers by modal control theory [AIAA PAPER 70-1036]

20 p3560 A70-39501

Single and coaxial dual rotor helicopter piloting characteristics during turning flight, discussing operational problems in snow

22 p3962 A70-43530

Main rotor wake adverse effects on tail rotor directional control in low velocity wind
23 p4140 A70-44323

Tail rotor thrust increase for yaw control via increased blade area, higher tip speeds and cambered airfoils
23 p4140 A70-44324

Helicopter automatic approach and hover coupler systems, discussing cockpit display devices, handling qualities, pilot workload and fatigue and external load stabilization
23 p4140 A70-44464

HELICOPTER DESIGN

Composite fibrous materials applicability to V/STOL rotor blades design and fabrication confirmed by structural analysis
02 p0225 A70-11953

Helicopter avionics systems man machine capability estimation based on pilot workload, applying results to design evolution
02 p0244 A70-12136

Helicopter engineering covering structure, rotor systems, aerodynamics, vibration and applicability to fixed wing aircraft
02 p0225 A70-12309

Helicopters for injured or sick persons transportation as compared with ambulance use based on West Germany experience
03 p0436 A70-13822

Mil-10 Soviet giant helicopter cargo and altitude record, VTOL and STOL capability and weight design
03 p0414 A70-14286

Rotor noise reduction in helicopter design for increased blade loadings and higher tip speed
[SAE PAPER 690684] 05 p0792 A70-15865

High speed helicopter with fixed wings and longitudinal axis tail rotor
05 p0794 A70-16349

Sound radiated by fluctuating forces on helicopter rotor analyzed, predicting noise output variation as function of helicopter design parameters
05 p0796 A70-16792

Proximity Warning System/Pilot Warning Indicator for helicopters, discussing applications to fixed wing aircraft
06 p0985 A70-17710

YANKEE escape system adapted for helicopters using tractor rocket, noting modular concept advantages
06 p0986 A70-17712

Twinjet helicopter design for business transport, emphasizing redundant systems for safety and bad weather flight capability
07 p1191 A70-18844

Bolkow BO-105 twin turbine rigid rotor helicopter flight tests
08 p1437 A70-21731

Circulation-controlled lifting rotor built and tested on hovering rig, analyzing performance
09 p1611 A70-23284

Compound helicopter in civil aviation to alleviate air traffic congestion, discussing design and operative capacities of S-65-200
10 p1804 A70-24046

Bifilar pendulum vibration absorber for counteracting helicopter main motor vibratory forces
10 p1805 A70-24657

Crane helicopters characteristics, history and projected applications to petrochemical, shipping, construction and power transmission industries
[SAE PAPER 700284] 12 p2160 A70-27427

Noise reduction design of Enstrom F-28A helicopter, noting operation at lower tip speeds and blade loading
12 p2162 A70-28096

Rotorcraft design and aerodynamics, discussing structural vibrations and all-weather operation
13 p2344 A70-28545

SA-330 Puma tactical support helicopter design and performance
14 p2530 A70-30286

Analog/digital system for full scale airframe fatigue amplitude and phase signature measurements on CH-46D tandem rotor helicopter
15 p2739 A70-32323

Fatigue characteristics of Ti alloy forgings for rotary wing vehicles, discussing effects of welding, annealing, reduction, surface finish and shot peening
17 p3122 A70-34441

Aircraft, helicopters and rockets aviation systems design and components service life problems, emphasizing maintenance intervals
17 p3100 A70-34686

CH-47C helicopter fiberglass main rotor blade, discussing composite materials impact on design
17 p3013 A70-34702

Composite tail rotor driveshaft for next generation helicopter, discussing materials, fabrication and tests
[AHS PREPRINT 451] 17 p3100 A70-34703

Pressure jet helicopter with tipjet propelled rotor system, discussing power available calculation, mission performance, power management, etc
17 p3013 A70-34707

VTOL aircraft power plants optimization for future helicopter missions without restrictions of limited off-shelf inventory
17 p3147 A70-34708

Vortex visualization applications in helicopter noise research, using smoke generator in rotor blade tip
17 p3057 A70-34712

Helicopter structural weight statistical prediction and evaluation, discussing comparable fixed wing experience
17 p3015 A70-34728

Heavy lift helicopters cockpit display problems, describing photographic flight research program for data acquisition
17 p3082 A70-34731

Helicopter vibration reduction techniques, considering antivibration devices design and comfort crossover speed increase
17 p3015 A70-34735

Swept tip rotor blade design, discussing wind tunnel-whirl stand correlations
17 p3015 A70-34736

Second generation helicopter design, considering compound, convertible and electrically powered configurations
17 p3018 A70-35549

Convertible helicopter rotor technology, discussing materials, blade configurations and variable diameter concept
17 p3018 A70-35550

H3-E Sprinter semicompound helicopter with pneumatic rotor drive and side mounted fans for forward flight
17 p3018 A70-35626

Cross section deformation effect on helicopter rotor blade torsional vibration, using differential equations of vibrating beam
18 p3334 A70-35959

Helicopter engine rotor matching for tip propulsion efficiency, comparing with conventional shaft drive propulsion
[ASME PAPER 70-GT-68] 18 p3215 A70-36842

Soviet book on helicopter aerodynamics covering main rotor operation, types classification and various flight characteristics
19 p3355 A70-37390

Rotor drive systems for rotary wing aircraft, indicating mechanical hub drive advantages over reaction blade drive
21 p3755 A70-41850

Soviet helicopter development after World War II, discussing Mi-8, Mi-2, Ka-26 and MI-10K helicopters
23 p4137 A70-43895

Armor airframed helicopter for aerial armored reconnaissance vehicle, noting design, fabrication and weight
23 p4137 A70-44095

Fenestron shrouded tail rotor for SA 341 Gazelle helicopter eliminating ground contact during approach and landing
23 p4140 A70-44322

Tail rotor thrust increase for yaw control via increased blade area, higher tip speeds and cambered airfoils
23 p4140 A70-44324

NACA/NASA rotary wing aircraft research covering autogyro and helicopter development, noting flight safety
23 p4142 A70-44851

SA-341 Gazelle French military helicopter configuration, performance, flight characteristics, technological particulars and design
23 p4142 A70-44854

Helicopter personnel escape capsule system feasibility by UH-25B helicopter, discussing incorporation into CH-46 and UH-1
[SAE PAPER 700832] 24 p4290 A70-45890

Military helicopter test program application to commercial VTOL operations, discussing military-civil design and development relationships
[AIAA PAPER 70-1242] 24 p4292 A70-46327

Helicopter hazards elimination measures, considering crash resistant fuel systems, flotation devices, redesigned seats, in-flight escape, etc
24 p4292 A70-46383

HELICOPTER ENGINES

Boeing inertial separator system for eliminating air dust taken by CH-46 helicopter engines during takeoff and landing on unprepared areas
01 p0162 A70-10677

Inertial particle separator-type turbine engine air cleaner for OH-6A light observation helicopter, describing evolution
01 p0164 A70-10682

CH-54A engine air particle separator/EAPS/field experience, discussing engine removal times due to erosion, environment evaluation and design improvements
01 p0164 A70-10684

CH-54 engine air inlet antice system design, manufacture and testing, solving heat balance equations describing tapered gap heat exchanger
01 p0165 A70-10693

Helicopter turbine engine bleed air requirements obtained by compressor extraction for engine designers
01 p0167 A70-11462

U.S. rotorcraft research regarding materials and engine technologies of conventional and compounded helicopters
02 p0226 A70-12314

Development trends, design and gas dynamic characteristics of turbine engines for helicopter propulsion systems including pressure, turbofan and integral engines
05 p0896 A70-16350

Aerodynamic and mechanic design of gas turbine for light helicopters, including flight tests and performance objectives
08 p1558 A70-20686

Helicopter turboshaft engines design and performance
08 p1559 A70-21517

Soviet book on practical aerodynamics of Mi 6 helicopter covering engine/rotor power balance, control, flight characteristics and solutions to in-flight emergencies
14 p2532 A70-31414

Soviet book on gas turbine engines for helicopters covering aircraft design and flight dynamics
15 p2787 A70-32199

Pressure jet helicopter with tipjet propelled rotor system, discussing power available calculation, mission performance, power management, etc
17 p3013 A70-34707

VTOL aircraft power plants optimization for future helicopter missions without restrictions of limited off-shelf inventory
17 p3147 A70-34708

Helicopter gas turbine governor systems for engine and rotor speed control, minimizing pilot activity
[ASME PAPER 70-GT-37] 18 p3214 A70-36835

Flight test program for helicopter gas turbine engines, considering engine-airframe-control systems integration and environmental tests
[ASME PAPER 70-GT-38] 18 p3303 A70-36836

Helicopter engine rotor matching for tip propulsion efficiency, comparing with conventional shaft drive propulsion
[ASME PAPER 70-GT-68] 18 p3215 A70-36842

Helicopter gas turbine engines protection against salt spray, dust, sand, ice, cut grass, etc
[ASME PAPER 70-GT-96] 18 p3263 A70-36843

CH-54A helicopter gas turbine engine air particle separator/EAPS/field service in Vietnam, noting time before engine removal for erosion
[ASME PAPER 70-GT-97] 18 p3303 A70-36844

Helicopter gas turbine engine protection against sand and dust erosion using particle separators, screens and coatings
[SAE PAPER 700705] 22 p4090 A70-42671

HELICOPTER PERFORMANCE

Flight test experiments for H-19 helicopter to evaluate aided inertial system performance for terminal guidance
01 p0136 A70-10303

Marine safety aspects of helicopters with flotation equipment, considering effects of severe winds and waves, aircraft abandonment procedure, etc
01 p0007 A70-11316

Blade forces of helicopter rotor in forward flight calculated by unsteady lifting-line theory
01 p0004 A70-11366

Helicopter vibrations recording on magnetic tape for subsequent frequency analysis, describing frequency spectrogram
02 p0304 A70-12761

Helicopters for injured or sick persons transportation as compared with ambulance use based on West Germany experience
03 p0436 A70-13822

Mil-10 Soviet giant helicopter cargo and altitude record, VTOL and STOL capability and weight design
03 p0414 A70-14286

Helicopter tail rotors aerodynamic characteristics, using statistical methods for planning experiments and interpreting results
05 p0793 A70-15900

Helicopters usefulness in rescue service via test flights, discussing rescue cars and centers for emergency patients
05 p0806 A70-16325

High speed compound helicopters with rigid and hinged rotors noting features, advantages and construction
05 p0794 A70-16351

Personnel/cargo lowering and retrieval system requirements, design approach and effects on performance for CH-47 helicopter, discussing fabrication and testing on mockup
06 p0985 A70-17711

Optimality criteria for selecting flight conditions for civil aviation helicopters, considering scheduled speed and efficiency, commercial load factor, wind rose, vertical separation, etc
06 p1185 A70-17874

Rotation and forward flight effects on separation line of laminar incompressible boundary layer along helicopter blade of airfoil shape
[AIAA PAPER 70-49] 06 p0973 A70-18151

Tuft position on rotating helicopter blade in hovering and forward flight, calculating tip path plane and tuftlines 08 p1438 A70-21868

Helicopter hoist rescue system, considering helicopter power, cable length, pilot visibility, etc 09 p1610 A70-22341

Flight test experiments for H-19 helicopter to evaluate aided inertial system performance for terminal guidance 13 p2449 A70-29622

Patients emergency transportation by helicopter, discussing vehicle types and onboard medical treatment 14 p2540 A70-30191

Real time analog simulation of helicopter rotor, calculating lift and drag coefficients along blade 15 p2672 A70-31775

Helicopter aerodynamic problems, discussing rotor performance improvement for increased cruising speed 16 p2841 A70-33758

AH-1G helicopters combat flight loads from on-board oscillograph data recording, defining performance in terms of critical variables 17 p3013 A70-34706

Airborne flight test data acquisition and ground based automatic bulk data processing system for helicopter test and development programs 17 p3014 A70-34713

AH-1G Hueycobra helicopter stability, control, performance, vibration and structural loads characteristics during controlled steady state maneuvers 17 p3014 A70-34716

UH-1C, AH-1G and UH-1H helicopters combat operational flight profiles, considering airspeed, altitude, rotor speed, load factor, etc 17 p3014 A70-34717

Helicopter rotors noise intensity prediction for high tip Mach number, including compressibility and thickness effects 17 p3015 A70-34729

Modeling techniques based on Froude scaling laws for helicopter ditching and flotation stability characteristics 17 p3016 A70-34738

Helicopter rotor blade differential pressure and structural load characteristics in transient and steady state maneuvers 17 p3016 A70-34739

STOL takeoff trajectory optimization for heavily loaded helicopter, using optimal control theory 17 p3021 A70-35841

Aerodynamics theory for separated flow effects on helicopter lift-drag capability, taking into account three dimensional flow and blade aeroelasticity 18 p3205 A70-35956

Soviet book on helicopter aerodynamics covering main rotor operation, types classification and various flight characteristics 19 p3355 A70-37390

Model testing for helicopters, considering scaling, ditching and rotor performance 19 p3402 A70-38610

Structural reliability testing methods and loads prediction for rotary wing vehicle components, considering AH-56A compound helicopter 19 p3356 A70-38612

Flight characteristics and performance calculation of single rotor helicopters by digital computers, considering wobble plate steering margin, compressibility, ground effects, separation and autorotation 20 p3561 A70-39716

Helicopter parts and assemblies fatigue life estimation and testing, discussing loading spectra, service conditions, etc 22 p4046 A70-43119

Helicopter rotor tests in large wind tunnel for increased flight speed, noting pressure and noise measurements 23 p4132 A70-44142

[ICAS PAPER 70-44] SA-341 Gazelle French military helicopter configuration, performance, flight characteristics, technological particulars and design 23 p4142 A70-44854

HELICOPTER PROPELLER DRIVE

V/STOL power drive systems structural efficiency, comparing mechanical and pneumatic components from weight-optimal viewpoint 04 p0622 A70-14901

[ASME PAPER 69-WA/AV-7] Helicopter mechanical power transmission design, describing gearing, shaft bending, bearings, lubrication, weight factors, etc [SAWE PAPER 844] 20 p3563 A70-40367

HELICOPTER ROTORS

U ROTARY WINGS

HELICOPTER WAKES

Rotor blade flutter in forward flight accounting for wake unsteady aerodynamic effect 17 p3184 A70-34727

Main rotor wake adverse effects on tail rotor directional control in low velocity wind 23 p4140 A70-44323

HELICOPTERS

NT BO-105 HELICOPTER

NT CH-3 HELICOPTER

NT CH-46 HELICOPTER

NT CH-47 HELICOPTER

NT CH-54 HELICOPTER

NT COMPOUND HELICOPTERS

NT F-28 HELICOPTER

NT H-56 HELICOPTER

NT MILITARY HELICOPTERS

NT OH-6 HELICOPTER

NT RIGID ROTOR HELICOPTERS

NT SA-330 HELICOPTER

NT UH-1 HELICOPTER

Prototype inspection equipment for automatic detection of fatigue damage in helicopter transmission gears teeth by magnetic perturbation method 01 p0097 A70-10011

Helicopter all-visibility operation realized by using main rotor blade as scanning radar antenna 05 p0793 A70-16040

Collision safety standards in helicopter services for shore-to-ship transportation of pilots, stores and spares 06 p1103 A70-17639

Helicopter dynamics structural model extended to LF longitudinal motions by including stabilizing feedback loop representing forward velocity influence on main rotor 06 p0987 A70-17910

Helicopter utilization in emergency transportation of civilian patients, discussing questionnaire results from medical and police agencies 08 p1454 A70-21937

Metabolic and heart rates determined in experienced and inexperienced pilots during Hiller 12-E and 12-EL helicopters flight through standard maneuvers 09 p1627 A70-23455

Visual search activity decrease observed as function of time-on-task for skilled and unskilled helicopter pilots, recording eye movements and blinks 09 p1628 A70-23463

Helicopter blade flapping torsion flutter behavior analysis showing stabilization effect in forward flight 10 p1958 A70-24559

Helicopter flight test and evaluation tools including data processing facilities to improve test validity [AIAA PAPER 70-373] 10 p1806 A70-24929

Helicopters for short haul intercity transport, discussing power failure safety, weather factors and costs 12 p2161 A70-27596

Helicopter gust response at high forward speed for various rotor loads noting effects of gust shape, gradual penetration, nonsteady aerodynamics and blade aeroelasticity 14 p2531 A70-30855

[AIAA PAPER 68-981] Soviet book on practical aerodynamics of Mi 6 helicopter covering engine/rotor power balance, control, flight characteristics and solutions to in-flight emergencies 14 p2532 A70-31414

Heat stress levels in cockpit of AH-1G Hueycobra helicopter parked in sunlight with closed canopy, using sweating copper mannikin 15 p2689 A70-31881

Corporate-executive market for helicopters related to fixed wing business air transportation problems [SAE PAPER 700285] 18 p3350 A70-36814

Soviet book on helicopter aerodynamics covering main rotor operation, types classification and various flight characteristics 19 p3355 A70-37390

Helicopter operations integration into civil air traffic system, noting special requirements for mixed fixed and rotary wing terminal environments 19 p3465 A70-38230

Helicopter cost reduction by transmission overhaul frequency reduction, discussing savings with on-condition maintenance 19 p3441 A70-38824

Comparative demand forecasting for military helicopter spare parts, stressing exponential smoothing model 20 p3740 A70-39643

Helicopter vibration measurement techniques, discussing in-service fault diagnosis 21 p3749 A70-40582

Helicopter dynamic tests for aeroelastic and mechanical instabilities and forced vibration problems 21 p3749 A70-40583

Integrated helicopter gravity measuring system for various terrains, describing instrumentation and recording monitors 22 p4042 A70-43663

HELIOCENTRIC ORBITS

U SOLAR ORBITS

HELIOGRAPHS

U SPECTROHELIOGRAPHS

HELIOGRAPHY

U SPECTROHELIOGRAPHS

HELIOMAGNETISM

U SOLAR MAGNETIC FIELD

HELIOMETERS

NT PYROHELIOMETERS

Solar constant measurement by Eppley normal incidence pyrliometers on high altitude balloons 08 p1501 A70-21920

Circumsolar sky radiation effect on pyrliometric measurements, considering atmospheric scattering and turbidity 13 p2400 A70-29660

HELIOMETRY

U HELIOMETERS

U PYROHELIOMETERS

HELIUM

NT HELIUM ATOMS

NT HELIUM FILM

NT HELIUM ISOTOPES

NT LIQUID HELIUM

He camera with reduced linear absorption coefficient for contact microradiography, relating exposure, X ray wavelength and atmosphere 01 p0084 A70-10013

Multistate impact parameter treatment of hydrogen-helium excitation collisions, considering distortion, back- and rotational-coupling and virtual transition sequence 01 p0147 A70-10285

Helium-cadmium laser operation, using DC cathaporesis to maintain spatially uniform optimal Cd vapor concentration 01 p0110 A70-10562

Gaseous He bubbles injection into liquid propellant launch vehicle fuel lines to reduce vehicle pogo oscillations by lowering feed system natural frequencies 01 p0196 A70-10851

Ferritic stainless steel embrittlement caused by He injected into tensile samples by alpha particle cyclotron irradiation tested at elevated temperatures 01 p0122 A70-11235

High temperature ductility improvement in stainless steels containing He, analyzing lattice damage and interphase cavities after fast neutron irradiation 01 p0123 A70-11246

Photoelectric line photometry used to study H beta/gamma and He I 4471 absorption line intensities of early B stars, determining projected rotational velocity 02 p0369 A70-12072

Helium gas shaft seal for spacecraft electrically driven LOX pump, noting advantages of floating carbon face seal type [ASLE FICFS PREPRINT 24] 02 p0308 A70-12168

He isoelectronic sequence 3d-nf transitions, determining UV wavelengths and oscillator strengths 04 p0739 A70-14601

Stark broadening of ionized helium lines by collective electric fields in theta pinch 04 p0722 A70-14684

Helium properties and utilization in NASA projects, discussing pressurization of fuel tanks cooling of superconducting magnets 04 p0720 A70-15633

Al foil exposed to solar wind on moon during Apollo 11 mission examined for helium particles, finding lunar solar wind albedo 05 p0900 A70-16093

Transient emissions on He I wavelength during breakup phase of auroral events, discussing observational interference by OH bands 05 p0907 A70-16277

He excitation by low energy He ions giving support for Rosenthal-Foley postcollision-interaction model, testing model predictions 05 p0885 A70-16556

He to carbon fusion reaction rate enhancement in dense matter by inelastic scattering processes, discussing C 12 deexcitation to ground state 05 p0885 A70-16934

Variational and Z-expansion calculations for magnetic quadrupole transitions decay rates of He sequence 05 p0920 A70-16942

Gaseous He measured for thermal conductivity along isotherms to observe pressure dependence 06 p1174 A70-17678

Hypersonic corner flow in He investigated by heat transfer, surface pressure, pitot surveys, oil and electron beam flow measurements [AIAA PAPER 70-227] 06 p1039 A70-18110

Charged particles and He nuclei spatial distribution from recordings in cosmic ray equator region by Cerenkov counter mounted on Proton 2 satellite 07 p1367 A70-19490

Mean lives measurement for excited levels in singlet system of neutral He using beam foil technique 07 p1338 A70-19821

Energy dependence of elastic total collision cross section of identical He molecules, using velocity selected primary beams at low target temperature 07 p1345 A70-20137

Anodic precursors of convergent cylindrical shock wave of z-pinch discharges in He and Ar 07 p1261 A70-20357

O and B type stars neutral He lines, studying UV line blanketing effects on predicted departures from LTE

Note on Bell-Kingston paper on Born total and differential cross sections for proton impact ionization of He

Axisymmetric helium jet transition to turbulent flow in air slipstream, measuring temperature and velocity profiles

Solar wind properties and helium abundance determined from satellite-borne electrostatic analyzers

Electron and proton impact excitations of He using Born two and four state versions of impact parameter treatment

Energy dependence and threshold behavior of ion Ar lines excited in low-energy He ion-Ar collisions

Neutral helium line profiles for line-blanketed model atmospheres grid

Ar ion lasers investigated for effect of added He on pulse output intensity

Correction factor for free stream Reynolds number errors resulting from low temperature viscosity in He wind tunnels

Potential energy curves for diatomic He molecules constructed by Rydberg-Klein-Rees procedures

H and He intraatmospheric migration and dissipation, considering MHD waves, ionospheric plasma motions, chemical reactions, etc

Nuclear reactions and elementary particle reactions in Friedman universe with positive lepton abundance and degenerate electrons, discussing prestellar helium synthesis

Non-LTE and LTE line profiles and equivalent widths for transitions in singlet and triplet systems of neutral He in hot stars, explaining anomaly

Exospheric density at opposite hemispheres, showing variations from winter helium bulge

CW Cd vapor laser oscillation achieved with slotted hollow cathode discharge containing He carrier gas at pressures of several Torr

Solar disk 10830 A He absorption line, attributing depression at blue wing to triplet

Schlieren optical method for measuring He jet penetration into supersonic flow

Charged particles and He nuclei spatial distribution from recordings in cosmic ray equator region by Cerenkov counter mounted on Proton 2 satellite

Long term helium-oxygen atmosphere effects on rats and mice, investigating biochemical and metabolic changes

Li ion elastic scattering by He, calculating ground state interaction potential

Excitation cross sections for Ar I and He I spectral lines in low energy He ion-Ar collisions

Solar neutrino fluxes, calculating capture rates and primordial helium abundance

He-Cd laser discharge, determining population densities and lifetimes for levels of Cd ion excited by He metastables

Compressibility factors and virial coefficients for He-N mixture, He and nitrogen at low temperatures and high pressures

He-Cd pulsed laser mode locking at 4416 and 3250 A using intracavity acoustic loss modulator

Argon and helium breakdown induced by ruby laser 50-picosec pulse at various pressures

Na I 5889 A pressure broadening by high temperature neutral He, allowing damping constant direct measurements

Helium abundance in unevolved main sequence eclipsing binaries by comparing to homogeneous models in mass luminosity plane

Closed coupled partial wave calculation of cross section for fine structure transitions in Na in collisions with He

Helium to electron excitation ratios for population inversion in helium-neon laser

Primary cosmic ray He nuclei rigidity measurement with magnetic spectrograph

P autoionization states of helium and hydrogen negative ions, calculating widths and shifts

Stellar interiors and cosmic He abundance observations, discussing B stars, sun galactic and globular clusters, planetary nebulae, interstellar medium, novae, etc

Carbon dioxide-helium laser hollow cathode negative glow discharge amplifier, discussing construction and advantages compared to other excitation media and discharge structures

Methane IR filter for monochromatizing He-Ne laser

Optimum tube diameter for maximum radiation output of single and multimode He-Ne lasers

Southern objective prism plates B stars with strong neutral He I absorption lines

High transmission Mylar window He cryostat for Mossbauer measurements

Carbon dioxide-He-nitrogen gas mixture pulsed discharge system afterglow gain measurements up to one atmosphere, using CW laser

Helium and nitrogen role in carbon dioxide laser excitation, discussing optimum gas mixture

Corona and voltage breakdown for spacecraft electrical components in low pressure helium-oxygen atmospheres, measuring between parallel plates

He-Ne gas laser, construction, operation and characteristic mode patterns

Threshold parameters of liquid and gaseous helium breakdown caused by ruby laser beam, noting Mandelstam-B Brillouin scattering in liquid phase

Solar disk 10830 A He absorption line, attributing depression at blue wing to triplet

H and He intraatmospheric migration and dissipation, considering MHD waves, ionospheric plasma motions, chemical reactions, etc

HELIUM AFTERGLOW

Microwave transmission through afterglow of RF excited electrodeless He discharge approximating low collision frequency plasma slab of uniform electron density in magnetic field

Hydrogen and helium emissions in upper atmosphere, observing amplifications towards geomagnetic poles and in winter hemisphere

Flowing afterglow system below 300 K for rate constants of certain gases association with helium third body, investigating oxygen cluster ions formation and reactions

Hydrogen and helium emissions in upper atmosphere, observing amplifications towards geomagnetic poles and in winter hemisphere

Electron attachment rate to sulfur hexafluoride in He buffered flowing afterglow

HELIUM ATOMS

Upper atmospheric atomic H and He concentration height distribution, considering L alpha and H alpha emissions, He emission, light components and direct measurements

Inelastic He atom-ion collisions provide understanding of capture and excitation cross sections

Born wave for atom-atom inelastic cross sections, calculating He excitation from ground state to higher states by H atom collision

Population of P level He excitation in solar prominences in H luminescence regions, noting ionization-recombination mechanism by UV radiation

Three body atomic systems with He atom and H negative ion on basis of scattering experiments dealing with resonance and threshold behavior

Born approximation used in calculating wave functions of helium atom for determining generalized oscillator strengths in first ionized continuum of helium

Helium excitation from ground to excited state by electron impact, determining differential and integral scattering cross sections

Solar prominences monochromatic images in He I D3 and He II 4686 lines allowing for contamination in 4686 images

Population of P level He excitation in solar prominences in H luminescence regions, noting ionization-recombination mechanism by UV radiation

Mean lives of excited levels in neutral He by beam foil method testing calculations for radiative transition probabilities

Cosmic X rays interstellar absorption, giving atomic He total photoionization cross section

HELIUM FILM

Hartree model to study superfluid He film bound to uniform substrate

Liquid He II, determining correlation of depth effect on film boiling heat transfer with vapor film geometry from motion pictures

HELIUM IONS

Solar helium-like ion line intensities, determining electron densities and excitation rate ratios

Inelastic He atom-ion collisions provide understanding of capture and excitation cross sections

He excitation by low energy He ions giving support for Rosenthal-Foley postcollision-interaction model, testing model predictions

Dissociative charge-transfer reactions of positive He ions with molecular N and O measured in drift tube-mass spectrometer

Inelastic scattering of He ions by Ne as function of angle, initial energy and energy loss using collision spectroscopy

Binary star spectrum analysis establishing seasonal and season-to-season variations in He II emission band intensity and shift toward long wave region

Oxygen enhancement ratio and relative biological effectiveness of accelerated helium nuclei on mouse tumor cells, discussing applicability in radiation therapy

Stark effect He II and H beta on lines observed for transverse and longitudinal fields, using beam-foil light source

D-pattern changes of helium ions irradiated polycrystalline Mo and Ni specimens, observing line splitting

Born approximation used in calculating wave functions of helium atom for determining generalized oscillator strengths in first ionized continuum of helium

Helium ions diffusion perpendicular to magnetic field in He gas, measuring coefficients as function of field strength and for various gas pressures

Helium ion bombardment activated tungsten crystal surface migration using field emission microscopy

Cross sections for electron impact excitation of positive helium and hydrogen ions, using non-relativistic Coulomb-Born-Oppenheimer reactance matrices

Metastable He ion two photon decay, observing photon coincidence angular correlation in spectral distribution

He II 3s and 3d states mean lives and initial population as function of energy, analyzing emitted radiation intensity

Lifetimes and fine structure of differentially metastable autoionizing states of negative He ion in axial magnetic field, using time of flight techniques

Short period Pc-1 pulsations frequency spectra relationship to magnetospheric He ion concentration

Helium II line broadening in high temperature plasma, measuring profile for comparison with theoretical prediction

He/plus/-H/minus/ collisional charge exchange cross sections, using modulated inclined ion beams technique

He/plus/-H/minus/ collisional charge exchange cross sections, using modulated inclined ion beams technique

HELIUM ISOTOPES

Cosmic ray origin in high energy H and He isotropic abundances and energy spectra observed by IMP 4 satellite during solar quiet times

02 p0358 A70-12250

He 4 and Ar 40 abundance in lower Venus atmosphere, underlining He 4 dominance in upper atmosphere

03 p0575 A70-13982

Energy accommodation coefficients for He³-W and He⁴-W, comparing results with classical gas-solid interaction theory

04 p0721 A70-14388

Accommodation coefficients ratio of He 4 to He 3 measured on W and K clean surfaces

06 p1183 A70-18257

Velocity distribution of atoms evaporating from superfluid He II at low temperatures, noting roton shifting and multiscattering processes

06 p1108 A70-18639

Carbonaceous chondrites primordial He and Ne isotopes variations

07 p1388 A70-20037

Cross sections measured for symmetric $p, 2p$ reactions on deuterium and He, discussing nonsymmetric $p, 2p$ events in He

08 p1548 A70-21233

Helium melting pressure curve to calibrate cerium magnesium nitrate or NMR low temperature thermometers

09 p1728 A70-22999

High energy proton-He 3 elastic scattering cross section measurement, comparing result with Glauber model calculation

13 p2456 A70-29459

Thermonuclear reactions in interior of sun, discussing models for He isotope concentration and flow to interpret solar neutrino generation

13 p2494 A70-29573

Polarized Co⁵⁹ target using He³-He⁴ dilution refrigerator, analyzing fast neutron scattering

14 p2584 A70-30508

Galactic abundances and cosmic ray spectra by IMP-4 satellite, obtaining He ratio

15 p2793 A70-31794

Microscopic quantum theory of liquid He isotopes emphasizing method of correlated basis functions

16 p2951 A70-32997

Light He isotope effect on He-Ne laser power output

20 p3641 A70-39737

Friedmann universe evolution after big bang via Hagedorn hadronic equation of state, noting primordial He abundance criterion

21 p3888 A70-41122

Criticism of theory for cosmogenic tritium produced oceanic He 3 excess

21 p3920 A70-41883

Differential elastic cross sections of 42 MeV alpha particles scattering from He 3, using optical model with spin-orbit potential

22 p4076 A70-42722

Green function theory of evaporation of He 3 atoms from liquid He 3/He 4 mixtures, determining energy distribution

24 p4377 A70-45255

HELIUM PLASMA

Local thermodynamic equilibrium conditions in superhigh pressure He plasma produced by laser action, obtaining threshold electric field relationship with gas pressure and temperature

02 p0312 A70-12078

Satellite lines of forbidden transition in laser-produced He plasma attributed to longitudinal plasma oscillations

02 p0379 A70-12717

Acoustic wave excitation and damping in cryogenic He plasma produced by HF pulse discharge, considering nonadiabatic heating and dissipation during reflection

03 p0529 A70-13056

Solar flare induced interplanetary shock and helium enriched driver gas observed on 13 February 1967, discussing wind velocity and plasma acceleration

06 p1152 A70-18526

Intense quasi-steady He plasma discharge stability in magnetic field measured by Langmuir and optical techniques

07 p1354 A70-20321

Thermal properties associated with temperature gradients in He-K plasma, studying mass motions initiated by cold wall contact

09 p1735 A70-22844

Electron temperature and concentration in decaying He and Ar plasmas with cesium vapor additions

11 p2092 A70-26733

Magnetically constrained steady state plasma production by hot cathode DC arc discharge in He

13 p2465 A70-29819

Excited atoms transfer mechanism in helium plasma, using He-Ne laser

17 p3106 A70-35102

Plasma satellites near He I forbidden lines during turbulent heating

19 p3475 A70-37441

Helium plasma ionization rate in positive column with DC discharge, considering gas pressure, electron density, electric field strength and plasma radius

19 p3476 A70-37559

Stationary DC discharge positive column in helium, determining production balance and loss of charge carriers

19 p3476 A70-37560

Equilibrium compositions of helium-nitrogen, argon-nitrogen and xenon-nitrogen plasmas at atmospheric pressure between 5000 and 35,000 K

19 p3552 A70-37831

Homogeneous helium plasma column LF wave propagation in uniform magnetic field

22 p4082 A70-43216

Local thermal equilibrium validity for electron temperature and density determination in reflected shock waves in He plasma, comparing laser scattering and spectroscopic methods

23 p4229 A70-44986

Temperature, densities and electric field strength of cascaded arcs burning in He under normal pressure

24 p4384 A70-45425

Theta pinch He plasma stability using cusp coils added to mirror coil ends

24 p4386 A70-45611

Density correlation measurements for diffusion coefficient in magnetized He plasma

24 p4386 A70-45614

HELIUM 2

U HELIUM ISOTOPES

HELIUM 3

U HELIUM ISOTOPES

HELIUM 4

U HELIUM ISOTOPES

HELIXES

U CURVES [GEOMETRY]

HELLMANN-FEYNMAN THEOREM

Integral Hellmann-Feynman formula for dissociation energies in H, Li and LiH molecules, discussing transition densities and dissociation energy

12 p2275 A70-27569

Integral Hellmann-Feynman formula applied to binding energy of molecular H and LiH, using SCF wavefunctions for atomic states

12 p2276 A70-27570

HELMETS

Helmet loss and failure role in major and fatal head injuries of USAF ejections

01 p0032 A70-10370

Army aviation personnel ear protection, evaluating APH-5 and SPH-4 helmets

06 p1002 A70-17703

Fleet evaluation program of AOH-1 helmet for replacement of standard flight helmet, oxygen mask retainer kit and oxygen regulator

06 p1002 A70-17709

Foamed-in-place polyurethane for form fitting pilot helmet shock absorbing liner noting medical applications

07 p1218 A70-19015

Pilot helmets, discussing sound attenuation, noise protection and speech intelligibility

12 p2177 A70-27040

Testing laboratory for safety, survival and life support equipment concerning parachutes, aircrew protective helmets and maintenance manuals

23 p4141 A70-44488

HELLMOLTZ EQUATIONS

Summary representation formulas for solving boundary value problems for Helmholtz and Poisson equations in rectangle

03 p0518 A70-13076

Two dimensional wave diffraction problems involving discontinuity line, analyzing instability behavior of geometrically induced singularities by applying integral transform on Helmholtz equations

03 p0525 A70-14199

Helmholtz integral for radio waves scattering from surfaces expanded for reflection from terrain or atmospheric layers

04 p0648 A70-14964

Modified method of cross sections applied to solution of scalar Helmholtz equation in infinite symmetrical waveguides

12 p2272 A70-27296

Nonhomogeneous Helmholtz vibration equation for sectorial-annular membranes and plates under arbitrary load, using Fourier method

19 p3535 A70-37343

Helmholtz equation initial value problem solution by integral operators

19 p3459 A70-38680

Multidimensional correspondences between Helmholtz equation eigenfunctions and eigenvalues, including involutorial transformations

23 p4218 A70-44211

HELLMOLTZ VORTICITY EQUATION

Unsteady hydrodynamic coefficients of supercavitating hydrofoil in harmonic oscillation in Helmholtz flow with free surface, investigating frequency, angle of attack and submergence depth

07 p1255 A70-19134

First vorticity theorem of Helmholtz derived in general relativistic and covariant differential form, proving invariant kinematical identity

10 p1916 A70-24498

HEMATITE

Lamellae stresses and magnetostrictive effects on magnetic properties of titanomagnetite and ilmenohematite series minerals

15 p2728 A70-31993

HEMATOCRIT

Haematocrit variations effect on electromagnetic blood flowmeter sensitivity, discussing blood specific impedance changes

07 p1217 A70-18951

HEMATOCRIT RATIO

Chronic hypoxia effects on heart size and hematocrit ratios tested in pigeons

12 p2172 A70-28075

HEMATOLOGY

Hematologic changes in rats under hypergravity, effects of vitamin B12, folic acid and return to 1 g

06 p0991 A70-17283

Peripheral blood and structural changes in hemopoietic organs of rabbits and mice exposed to microwave radiation

07 p1216 A70-18730

Maximum isovolemic hemodilution by volume substitution determined by plasma expanders infusion in dogs

10 p1821 A70-25083

Hematologic responses of mice subjected to continuous hypoxia in subatmospheric pressure

11 p1989 A70-26666

Hematologic changes in mice associated with meningovirus infection and hypobaric hypoxia during barometric pressure changes

15 p2681 A70-31878

Hematology of sea level and high altitude native Sonoran deer mice, correlating hemoglobin electrophoretic patterns with oxygen affinity

15 p2686 A70-32835

Portable battery operated system for rapid measurements of blood plasma electrolytes during aeromedical evacuation

20 p3579 A70-39433

HEMATOPOIESIS

Peripheral blood, neutrophil myeloid hematopoiesis, phagocytic activity and serotonin level in gamma irradiated dogs

03 p0423 A70-13706

Peripheral blood, neutrophil myeloid hematopoiesis, phagocytic activity and serotonin level in gamma irradiated dogs

11 p1985 A70-25506

HEMATOPOIETIC SYSTEM

Gnotobiotic techniques for human hematopoietic cell culture establishment and maintenance, considering culture transfer

01 p0027 A70-11311

HEMISPHERE CYLINDER BODIES

Stagnation point velocity gradients for spherical segment models with bluntness ranging from hemisphere to flatnose cylinder in hypersonic flow

03 p0406 A70-12947

HEMISPHERES

Heat transfer rates to stagnation point of hemisphere in supersonic high enthalpy low density nitrogen plasma flow

[ASME PAPER 69-WA/HT-49] 04 p0614 A70-14799

HEMISPHERICAL SHELLS

Structural vibration of ring stiffened and mass-attached hemispherical shells

08 p1593 A70-21618

Thermal radiation absorption in hemispherical cavity, determining apparent absorptivity for diffuse and parallel irradiation

09 p1790 A70-23565

Hemisphere model flow field investigations in low density plasma wind tunnel, considering flow regimes of transition and shock formation

15 p2673 A70-32838

Metallic diaphragms design, fabrication and testing for cryogenic fluid and positive expulsion systems [AIAA PAPER 70-683]

16 p2918 A70-33582

Oscillations of rigidly clamped elastic liquid filled hemispherical shell with gas bubble

18 p3242 A70-36583

Hollow spheres and hemispheres nonlinear axisymmetric deformation, using shell theory reduced to two point boundary value problem for differential equations

22 p4112 A70-42288

HEMODYNAMIC RESPONSES

Acceleration component in pelvis to head direction found influencing hyperemia of brain at various g forces

04 p0630 A70-14579

Hemodynamic determinants of gallop sounds in patients with aortic valve disease based on clinical, hemodynamic and angiographic observations

04 p0633 A70-15308

Rat body fluids displacement during positive centripetal accelerations by radioisotope tracer com-

- pounds, freezing rates in liquid nitrogen to fix hemodynamic changes 07 p1202 A70-18796
- Prolonged hypodynamia effect on human blood serum mineral content and enzyme activity 10 p1815 A70-24677
- Electrocardiac activity, myocardium and hemodynamic disorders in subjects after prolonged hypodynamia with or without physical exercises and during orthostatic test 10 p1817 A70-24692
- Position dependent variations in intrapericardial, pleural and esophageal pressures and cardiac output in thorax of dogs 13 p2356 A70-29946
- Primary myocardial disease, describing hemodynamic and angiocardigraphic observation of left ventricular volume and wall changes 16 p2848 A70-33110
- Hemodynamic response to dopamine before and after myocardial infarction in dogs 17 p3026 A70-35200
- Blood platelets aggregation and release reaction in thromboembolic disease due to injury 17 p3032 A70-35471
- Atropine effects on circulatory responses to diminished effective blood volume and vasodepressor syncope, noting heart rate increase 17 p3032 A70-35562
- Hemodynamic changes in Andean native after two years at sea level, measuring intravascular pressures, cardiac output, heart rate and stroke index 20 p3571 A70-39427
- Renal hemodynamic response of unanesthetized dogs to positive accelerations within physiological tolerance range, measuring pressure and blood flow velocity 20 p3577 A70-40332
- Myocardial blood flow response to cardioacceleration by right atrial pacing in normal subjects, using coincidence counting 21 p3760 A70-40576
- Human elbow induced forearm and hand vessels tachyphylaxis to angiotensin, noradrenaline and acetylcholine compared to vascular response of vasopresin 21 p3761 A70-40577
- Hemodynamic indices of aged individuals engaging in physical exercises over long period of time 22 p3970 A70-42906
- Age determined hemodynamic reactions in men and women performing walking motions in lying position 22 p3970 A70-42908
- Hypothermia and body rewarming effects on renal hemodynamics in anesthetized dogs 24 p4301 A70-45998
- Dynamic response of peripheral blood flow to hypothalamic temperature waveforms in baboon, using implanted thermodes 24 p4303 A70-46116
- ### HEMODYNAMICS
- Renal hemodynamics and clearances alterations in owl monkey, using hemorrhagic shock procedure 02 p0234 A70-11732
- Hemodynamics in cardiosclerosis patients and healthy subjects under hypoxia, investigating heart activity and blood circulation 06 p0994 A70-17667
- Left ventricle pressure rise rate as function of heart contractility and hemodynamics 09 p1623 A70-23587
- Sodium balance effect on intrarenal distribution of blood flow in normal man determined with Xe washout method 10 p1810 A70-24005
- Human vascular tonus and hemodynamics during prolonged hypokinesia, observing changes in reaction to cold and reduced vascular tonicity 10 p1814 A70-24670
- Prolonged hypodynamia effects on hemodynamics using dye dilution method, noting adaptability in cardiovascular system 10 p1814 A70-24671
- Arterial oscillograms, pressure and heart beat rate during prolonged hypodynamia, noting neurocirculatory dystonia 10 p1817 A70-24693
- External respiration, hemodynamics, oxygen transport and consumption in lungs during static load tests 10 p1822 A70-25176
- Cardiovascular model for closed loop analog simulation of congenital heart defects hemodynamics 11 p1990 A70-25705
- Unanesthetized dogs renal hemodynamic response to negative centrifugal acceleration 15 p2681 A70-31883
- Aldosterone effects on hemodynamics of dogs under restricted motor activity, observing cardiac activity stimulation 17 p3030 A70-35358
- Hemodynamic effect of lidocaine given by infusion and bolus injections in myocardial infarction, examining cardiac output, heart rate, systolic left ventricular and aortic pressures 19 p3366 A70-38575
- Circulating blood volume and heart minute and stroke volumes in rabbits, using isotope-labeled albumin 19 p3366 A70-38724
- Human arterial hypertension, correlating ECG changes with systemic hemodynamics 20 p3573 A70-40069
- Continuous blood oxygen analyzer standardized with atmospheric air, demonstrating on dogs during occlusion of left anterior descending coronary artery 21 p3772 A70-42162
- Blood circulatory system and hemodynamic interdependencies simulation by analog computer, using Warner model 23 p4155 A70-44862
- Sea sickness symptoms in relation to reduced minute blood volumes in human after Coriolis acceleration 23 p4149 A70-45079
- Conduit arteries viscoelastic properties in normal and hypertensive dogs from recorded pressure and diameter waves 24 p4299 A70-45808
- Arterial hemodynamics in hypertension, discussing pulse changes mechanism as consequence of decreased arterial distensibility via disturbed relationship between ventricular ejection wave and impedance characteristics 24 p4299 A70-45809
- ### HEMOGLOBIN
- NT CARBOXYHEMOGLOBIN
NT OXYHEMOGLOBIN
- Hemoglobin concentration in red blood cells in men of various ages as function of altitude, discussing correlations with body weight and plasma protein 01 p0024 A70-10978
- Separate gamma irradiation effect of enzyme and hemoglobin-albumin-globulin substrates on proteolysis dynamics 03 p0419 A70-13308
- Temperature and hemoglobin concentration effect on oxygen solubility in blood, constructing table for Bunsen solubility coefficients 03 p0428 A70-14156
- Nomograms for correlation of dose to methemoglobinemia or plasma monomethylhydrazine /MMH/ concentration observed on dogs, considering human skin contact evaluation 06 p0992 A70-17298
- Oxygen diffusion in presence of hemoglobin taking into account chemical kinetics, showing approximate and computer solutions 10 p1819 A70-24772
- Oxygen diffusion facilitation in vivo and nonsteady state conditions under physiological circumstances, emphasizing hemoglobin in red cells and myoglobin in muscle 12 p2171 A70-28024
- Xenon absorption by myoglobin at various temperatures and pressures, presenting evidence for HpXe formation 14 p2545 A70-30927
- Hematology of sea level and high altitude native Sonoran deer mice, correlating hemoglobin electrophoretic patterns with oxygen affinity 15 p2686 A70-32835
- Oxygen-hemoglobin reaction rate constants in red cells obtained by applying in vitro blood data to solutions of differential equations describing intracellular oxygen transport 15 p2686 A70-32846
- Carbon dioxide content of dialyzed human hemoglobin measured at specific pressure and varying pH values as function of 2,3 diphosphoglycerate 19 p3364 A70-38367
- Heart stroke volume estimation at submaximal exercise using blood hemoglobin content and heart rate 20 p3576 A70-40328
- Human hemoglobin chain, noting zeta chain synthesis during embryonic development 24 p4297 A70-45406
- Temperature gradient spectra on complexes of met-myoglobin and methemoglobin with ligands, discussing boundary forms equilibria for various electron spin configurations 24 p4301 A70-45985
- ### HEMOLYSIS
- Prolonged hyperoxia effect on red blood cell survival and hemolysis in rats on normal diet 15 p2681 A70-31786
- Erythrocyte suspension subjected to gas bubble ultrasonic oscillation, investigating hemolysis mechanism 20 p3573 A70-39981
- ### HEMORRHAGES
- Renal hemodynamics and clearances alterations in owl monkey, using hemorrhagic shock procedure 02 p0234 A70-11732
- Blood pH effects on adrenomedullary response to hemorrhage, studying catecholamines release in anesthetized dogs 02 p0235 A70-11733
- Blood volume and circulation rate in dogs subjected to traumatic shock and hemorrhage under high mountain conditions 07 p1198 A70-18708
- Pneumatic compression effects on canine cardiovascular dynamics after hemorrhage tested in G-suit inflation 11 p1988 A70-26516
- G suit application to clinical therapeutics, noting intraabdominal bleeding control 21 p3767 A70-40737
- Oxygen transport, arterial resistance and consumption in normovolemic and hypovolemic dogs in hemorrhagic shock 24 p4302 A70-46106
- ### HEOS A SATELLITE
- HEOS 1 satellite project management, discussing costs, supervision problems and roles of experimenters, contractors, NASA and ESRO 01 p0221 A70-11112
- Interplanetary space investigation by HEOS 1 satellite during maximum solar activity, discussing orbital apogee, mission and technical requirements 01 p0186 A70-11113
- HEOS 1 satellite for interplanetary space exploration, describing eccentric orbit, structure, power supply, attitude measurement and control, spin rate control, telemetry and telecommand systems 01 p0196 A70-11114
- HEOS 1 satellite telemetry, telecommand and tracking systems, noting data transmission degradation due to high solar activity 01 p0045 A70-11115
- HEOS 1 launch operations, discussing test and checkout phase, mating with Thor Delta launch vehicle, countdown phase and launch 01 p0196 A70-11116
- Postlaunching operations putting HEOS 1 satellite into orbit, verifying subsystem functions, starting experiments and tracking for data recovery 01 p0197 A70-11117
- European Space Operations Center activities in observing HEOS 1 satellite, discussing launch, data processing and S-11 experiment involving ionized Ba cloud creation 01 p0197 A70-11118
- HEOS-1 satellite development for ESRO to investigate interplanetary magnetic fields, cosmic radiation, solar wind outside magnetosphere and earth shock wave 02 p0382 A70-12646
- ESRO German-built satellite HEOS 1 planned scientific space measurements, required orbit and technical concepts 03 p0580 A70-13798
- ESRO 1, ESRO 2 and HEOS 1 satellites solar arrays orbital performance 09 p1765 A70-22648
- HEOS 1 low energy proton measurements in interplanetary space, discussing particle direction during solar event and anisotropy time history 19 p3495 A70-37505
- High energy solar electrons observed by HEOS-A1 satellite, discussing semitransparent barrier existence at distance from sun 19 p3497 A70-37521
- Electron energy spectra range from HEOS A1 satellite mounted Cerenkov counter with shower telescope 19 p3503 A70-38103
- Heos 1 research satellite space simulation tests at ESTEC test facility 19 p3399 A70-38292
- ### HEOS SATELLITES
- NT HEOS A SATELLITE
- Test program preceding first German satellite experiment using HEOS satellite for Ba ion cloud injection into deep space 02 p0380 A70-12081
- Satellite HEOS-1 S 73 experiment launched during solar maximum to determine flux and energy distribution of solar wind positive component 05 p0900 A70-16077
- HEOS-A2 project development plan for investigating unexplored interplanetary space in eccentric orbit 05 p0923 A70-16588
- Reliability and environmental testing of residual magnetic field measurements of satellite HEOS-A1 electronic equipment, using Rb vapor magnetometers 13 p2380 A70-30031
- ESRO-1, ESRO-2 and HEOS-1 simultaneous observation of solar event of 25 February 1969, describing satellite and experiments 19 p3531 A70-37496
- ESRO satellite projects IRIS/ESRO 2, Aurorae/ESRO 1, HEOS-A1 and future TD-1 and HEOS-A2 23 p4264 A70-45004
- ### HEPARINS
- Heparin role in anticoagulant therapy for myocardial infarction based on proved application to other venous thrombotic diseases, noting hemorrhagic complications controllability 04 p0636 A70-15465
- ### HEPTANES
- Cycloheptane and mixture of exo- and endo-cycloheptene heats of combustion and formation, isomerization and hydrogenation 01 p0213 A70-10134

- HF pressure oscillations during heat transfer to n-heptane at various flow rates and pressures, studying film or bubble boiling associated with oscillations
03 p0605 A70-13516
- N-heptane and Freon-13 droplets vaporizing size and temperature at supercritical pressures in heated air stream
06 p1182 A70-18204
[AIAA PAPER 70-6]
- Heats of combustion and free isomerization energies of exo- and endo-isomers of 2- and 1-methylbicyclo heptane
22 p3982 A70-42680
- Specific heat and thermodynamic functions of endo- and exo-isomers of 2-methylbicyclo heptane in 12-310 K temperature range
22 p3982 A70-42681
- HERCULES NOVA**
Stellar system DQ Herculis photometry by synchronous signal averaging, indicating sinusoidal light curve with increasing binary period
02 p0373 A70-12392
- HEREDITY**
Familial aggregation for coronary artery disease and familial similarities in coronary anatomy, considering possible genetic analysis of myocardial infarction
04 p0636 A70-15467
- Long rhythms of periodic disparate heritable diseases in man
19 p3365 A70-38414
- HERMETIC SEALS**
Electroexplosively powered release valve for high pressure N stored in hermetically sealed container of missile, discussing design and performance tests
03 p0546 A70-14106
- Hermetically sealed miniature strain gages /tensometers/ design and testing, noting insensitivity to effects of fuels and oils
11 p2054 A70-26430
- Microcircuit packaging /primarily hermetic/ and assembly techniques, considering cost reduction
20 p3597 A70-39443
- HERMITIAN POLYNOMIAL**
Spatially homogeneous Boltzmann equation containing initial distribution functions expandable into Hermitean polynomials, using ordinary differential equations
03 p0526 A70-14302
- Multiplication theorem for Shtraus characteristic functions of quasi-Hermitean operators, including open systems coupling
05 p0877 A70-16880
- One dimensional steady neutral shock wave structure, using expanded Boltzmann equation distribution function in terms of Hermite polynomials
07 p1260 A70-19984
- Incompressible homogeneous isotropic turbulence velocity expanded in Hermite functionals of Gaussian white noise random function advected by fluid
11 p2040 A70-26543
- HERTZSPRUNG-RUSSELL DIAGRAM**
Red subluminescent stars and high UV excess stars in region between main sequence and white dwarfs, tabulating observations of stellar color and magnitude
01 p0182 A70-10795
- Horizontal branch and red giant stars ratio estimated in globular clusters for He abundance
05 p0906 A70-15894
- HR diagram calibration based on proper motions and radial velocities, deriving absolute magnitudes and statistical parallaxes
06 p1149 A70-18456
- Three color photometry of RW Auriga stars, discussing UVB curves, H-R diagram and UV emission excess
15 p2797 A70-31612
- Two dimensional quantitative spectral classification of F-G5 stars, using meniscus telescope with preobjective prism at Abastuman observatory
15 p2797 A70-31613
- Stellar evolution in globular clusters, considering H-R diagrams of age, He abundance and thermal instability
16 p2973 A70-33076
- H-R diagram stellar spectra interpretation using model atmospheres describing temperature, gravity and chemical composition
17 p3169 A70-35381
- Initial horizontal branch metal poor star models, examining opacities, luminosity and cluster ages of RR Lyrae stars
18 p3317 A70-37006
- Dispersed stellar clusters color excesses and distance moduli from color-magnitude diagram, considering evolutionary deviation from main sequence
18 p3323 A70-37138
- Stellar ring 373, comparing color-magnitude and color-color diagrams to adjacent star fields
21 p3888 A70-41121
- Globular cluster color-magnitude diagram parameters, examining giant branch and metal content
21 p3889 A70-41153
- Color-magnitude diagram of star cluster Kron 3 in Small Magellanic Cloud, using electronographic photometry
22 p4102 A70-42978
- Globular cluster M5 giant, asymptotic and horizontal branches, determining color-magnitude diagram and luminosity
22 p4109 A70-43745
- Red supergiants location in H-R diagram, discussing significance of mass loss, rotational mixing and neutrino emission as stellar model mechanisms
24 p4403 A70-45393
- HERZBERG BANDS**
Chemiluminescent reaction rates measurements for emission of diatomic oxygen molecules Herzberg bands in oxygen and oxygen-inert-gas afterglows
03 p0440 A70-13579
- Photoelectric intensity measurements on emission bands of oxygen Herzberg I system excited in argon-oxygen afterglow
03 p0528 A70-14350
- Excitation and layers heights for 5577 A and O2 bands of atmospheric and Herzberg systems in night airglow estimated, suggesting Chapman reaction for emission
08 p1492 A70-21755
- HETEROCYCLIC COMPOUNDS**
NT ACETAZOLAMIDE
NT ADENOSINE DIPHOSPHATE [ADP]
NT ADENOSINE TRIPHOSPHATE [ATP]
NT ADENOSINES
NT ASCORBIC ACID
NT ATROPINE
NT AZINES
NT AZOLES
NT AZULENE
NT CAFFEINE
NT CYANOCOBALAMIN
NT FOLIC ACID
NT INDOLES
NT MORPHINE
NT NICOTINAMIDE
NT OXAZOLE
NT PHTHALOCYANIN
NT PYRIDOXINE
NT PYRROLES
NT RDX
NT RETINENE
NT THYMININE
NT THYMIDINE
NT TOCOPHEROL
NT TRYPTOPHAN
NT URIC ACID
NT XANTHINES
- Cyclization of N-allylamides to disubstituted-2-oxazolines, giving melting points, yields, picrate melting points and NMR spectra
02 p0249 A70-11681
- Red bicyclic condensation product from reaction of acetone with sym-trinitrobenzene and diethylamine
02 p0251 A70-12278
- Protonation mechanism in acid catalyzed cyclization reactions of 2-acetamido 3-methylbicyclo-heptene
02 p0253 A70-12523
- Polymers with high temperature oxidation resistance, discussing problems caused by aromatic heterocyclic structures and manufacturing methods
05 p0873 A70-16604
- Ionene polymers, investigating cyclic and linear compounds and reaction products from tetramethyldiaminoalkanes and dibromoalkanes using NMR, IR and mass spectroscopy
06 p1004 A70-17511
- Photochromism of dihydroquinoline compounds and absorption spectra of color forms, noting color development upon UV light irradiation and thermal eradication
09 p1629 A70-22334
- IR Raman and vibrational spectra and structure of gaseous and liquid 1-pyrazoline
16 p2857 A70-34007
- Oxadiazolone pyrolytic and photolytic fragmentation, noting intramolecular cyclizations and intermediate azomethine nitrene production
17 p3041 A70-34771
- Photolysis of 3-phenyl-oxadiazol-5-one by UV irradiation, eliminating carbon dioxide
17 p3041 A70-34772
- Heterocyclic polymer BBB properties, discussing IR absorption studies of structure
21 p3783 A70-42131
- HETERODYNING**
NT OPTICAL HETERODYNING
- Three frequency heterodyne system for acquisition and tracking of radar and communications signals, noting applicability in optical and microwave ranges
06 p1010 A70-17948
- Relaying interferometer design consisting of heterodyne frequency diversity antennas with coherent mixer, relaying transmitter and receiver
08 p1495 A70-21071
- Heterodyne conversion transducer large signal internal parameters dependence on heterodyne, signal amplitudes and intermediate voltage
16 p2873 A70-33240
- Superheterodyne EPR spectrometer microwave bridge using single X band klystron
23 p4170 A70-43798
- HETEROGENEITY**
Composite orthotropic cylindrical shells linear thermoelastic equations solution for fixed end boundary conditions, noting heterogeneity effects on stress distribution
17 p3184 A70-34909
- Metalized solid propellant, calculating condensed phase distribution heterogeneity effect on performance
18 p3300 A70-37207
- Heterogeneous materials statistical theory, evaluating bounds for effective elastic constants by cell model using variational principles and perturbation solution
20 p3729 A70-40033
- Thin circular cylindrical panels in supersonic gas current parallel to generatrices, calculating heterogeneity effect on flutter
22 p4113 A70-42603
- HETEROTROPHS**
Biogeocenosis applicability to artificial closed ecological systems consisting of plants creating organic matter and heterotrophic organisms
13 p2353 A70-29501
- HEURISTIC METHODS**
Human performance evaluation and data acquisition as requirements for heuristic analytical models in systems engineering
05 p0805 A70-16008
- Heuristic principles for self organization algorithm of cognitive automation system with active learning strategy
08 p1466 A70-20874
- Group Method of Data Handling based on heuristic self organization for solving complex system problems, with applications to random processes prediction
10 p1845 A70-24869
- Heuristic programs and approaches in artificial intelligence
15 p2706 A70-32565
- Fluid turbulence unified heuristic model, defining determinate solutions for Navier-Stokes equations numerical integration at high Reynolds numbers
17 p3074 A70-35884
- Photoelimination reactions of macromolecules, emphasizing intermediate pathways heuristic description via energy level diagrams
23 p4157 A70-44391
- Heuristic self organizing systems role in technical cybernetics
24 p4321 A70-45645
- Turbulent flow mechanics heuristic exposition, discussing random processes, instability, nonlinear interactions, energy exchange, intermittency dependence on reynolds number, fluid properties and boundary conditions effects, etc
24 p4326 A70-45948
- HEUS ROCKET ENGINES**
HEUS solid rocket motor impulse control, describing liquid quench concept development through full scale test firing
[AIAA PAPER 70-1308]
16 p2969 A70-33600
- HEXAGONAL CELLS**
Extended chain crystals of hexagonal Se temporary superheating before final melting, presenting melting equation
01 p0126 A70-10222
- Surface energy data calculated for bcc and hcp metals and high melting point compounds
06 p1090 A70-17845
- Superconductivity in noble metal rich hexagonal close packed phases and fcc solid solutions ascribed to Fermi surface-Brillouin zone interaction
15 p2785 A70-32398
- Twinned hexagonal martensites crystallography in Ti alloys, discussing alpha-beta and beta-fcc transformations
17 p3118 A70-34405
- Hexagonal crystal dislocations treatment based on anisotropic elasticity theory, obtaining formulas for displacement and stress fields
19 p3454 A70-38954
- Crystallography of euhehedral single crystals from lunar troilite indicating hexagonal forms consistent with high temperature NiAs type structure
21 p3898 A70-41522
- HEXENES**
Cyclohexene oxide mass spectral fragmentation by means of deuterium labeled analogs
09 p1630 A70-23397
- HEXOGENES (TRADEMARK)**
Accelerating shock wave fronts by detonating passive troyl and hexogen using high speed photography
09 p1658 A70-22103
- HFB-320 AIRCRAFT**
Flutter investigation on model designed and constructed for tail unit of HFB 320 Hansa jet aircraft, discussing classical and statistical methods
04 p0775 A70-15180
- HIBERNATION**
Physiology of hibernation and hypothermia, noting potential use for metabolic need reduction during long interplanetary flight
10 p1943 A70-24757

Norepinephrine synthesis inhibition effect on arousal triggering and maintenance in hibernating golden hamsters, examining sympathetic activity
23 p4148 A70-44874

Hibernation and glycerol production in wasps *Ichneumonidea*, discussing possible physiological cryoprotective function
24 p4304 A70-46140

HIERARCHIES
NT DICHOTOMIES
Lines and letters identification and localization relationships to stimulus attributes in visual perception supporting hierarchical processing hypothesis
03 p0425 A70-13825

HIGH ACCELERATION
Human tolerance to short duration high acceleration in centrifuge concerning peripheral or central vision trouble or synopses
09 p1626 A70-23112

HIGH ALTITUDE
Mesoscale slope limits in constant pressure surfaces relation to g-forces on aircraft at SST altitude, using radiosonde measurements
14 p2530 A70-30607

High altitude neutron supermonitor investigation of cosmic ray microvariations
18 p3307 A70-36104

High altitude humidity from millimeter-band water vapor lines, using EHF atmospheric spectral transparency calculation
19 p3461 A70-37633

Atmospheric humidity measuring equipment and procedures for high altitudes, considering hygrometers, mass spectrometers, sondes, absorption spectra, etc
19 p3461 A70-37635

HIGH ALTITUDE BALLOONS
Twilight brightness measurements with balloons, scattering coefficient and indicatrix for high altitudes and comparison with Rayleigh-Cabann theory
01 p0079 A70-11218

Cosmic gamma radiation sources above 50 Mev investigated by high altitude balloons in Northern Hemisphere with spark chamber system
05 p0904 A70-16930

Cryostat design and performance for use with optical telescopes in high altitude balloons
09 p1674 A70-22294

Multiplexer-interface system for digital nuclear and position control data transfer from high altitude balloons to earth monitoring instruments
12 p2233 A70-27407

Galactic cosmic rays high altitude measurements by balloon-borne Sparmo type multidirectional detectors, revealing azimuthal anisotropy
14 p2632 A70-31309

Balloon systems characterized by day to night altitude variations for permanent atmospheric sounding
14 p2531 A70-31312

Constant altitude helium filled zero pressure polyethylene balloon for stratospheric meteorological data and atmospheric tides studies
17 p3075 A70-34607

Hypsometer design for accurate pressure measurements at high balloon altitudes
17 p3090 A70-35313

High energy electrons in near space excess radiation from high altitude balloon and satellite data
18 p3307 A70-36170

Cygnus constellation energetic gamma ray emission by nuclear emulsion and spark chamber telescope on high altitude balloon
19 p3501 A70-38086

PCM command control system for high altitude ballooning operations, discussing component equipment
20 p3587 A70-40085

Liquid hydrogen balloon inflation system for use at remote locations, discussing characteristics and economy
20 p3607 A70-40086

Thermal design of high altitude balloons and instrument packages, analyzing vertical motion dependence on heat transfer and radiation environment
21 p3755 A70-42077

HIGH ALTITUDE BREATHING
High altitude acclimatization effects on cardiovascular system, external respiration, blood composition, optical and vestibular analyzers in human subjected to various stresses
04 p0630 A70-14576

Dogs breathing air or oxygen during slow and rapid decompression, measuring intraocular and cardiovascular pressure changes and retinal responses
09 p1621 A70-23460

HIGH ALTITUDE ENVIRONMENTS
High altitude clear air turbulence /HICAT/ occurrence frequency, showing effects of altitude, wind and temperature fields, terrain features, etc
01 p0006 A70-10696

High altitude scale model experiment to evaluate rocket plume impingement effects on Manned Orbital Workshop pressures, heating rates, forces and moments
03 p0579 A70-13646

High altitude environmental effects on adrenal glands and hypothalamic neurosecretion in rats
04 p0629 A70-14568

Physiology of high altitude, studying animal and man adaptation and changes in body processes due to life stresses and hypoxia
08 p1441 A70-20469

Rocket plume effects impulsive ground test technique under simulated high altitude pressure conditions, discussing hardware simplifications
[AIAA PAPER 70-399] 10 p1951 A70-24906

Mountain climbing and prolonged stays at high altitudes effects on blood composition
13 p2352 A70-29355

Viper Dart Robin System high altitude data reduction program accuracy, discussing winds and density errors
14 p2606 A70-30566

Albumin and IgG degradation, studying high altitude effect on hepatic function in man
15 p2683 A70-32532

Blood plasma and red cell volumes simultaneous measurement in native group living at high altitude
15 p2684 A70-32537

Human bioclimatology at high altitude, discussing energy balance in terms of net solar and terrestrial radiation balance in mountain area
19 p3367 A70-37369

High altitude wind measurement during daytime using photometer for detection of Li trail
20 p3630 A70-39486

Acute mountain sickness symptomatology and cognitive performance, using standardized General High Altitude Questionnaire
20 p3581 A70-40025

Mice immunobiological reactivity at simulated high altitude
20 p3575 A70-40189

Myocardial Na and K content of rats exposed to high altitude, preparing isolated right ventricular strip
20 p3577 A70-40541

Velocity ballistocardiogram modifications during high altitude stay, observing amplitude and RJ and RI variations
21 p3763 A70-41228

Parachutes for low density atmospheres, describing low and high altitude test results
[AIAA PAPER 70-1164] 21 p3755 A70-41846

Growth and caloric intake of rats exposed to high altitude dependence on high carbohydrate, protein and fat diets
22 p3967 A70-42458

Protein catabolism increase during high altitude exposure to hypoxia in rats, noting amino acid incorporation into tissue proteins
22 p3967 A70-42459

High altitude outer radiation zone boundary region electron energy measurement by satellite Injun 3, noting angular distribution dependence on local time, latitude, etc
23 p4236 A70-43833

Atmosphere and earth-reflected solar radiation pressure effects on high altitude satellite orbits
24 p4408 A70-45555

HIGH ALTITUDE FLIGHT
U HIGH ALTITUDE
HIGH ALTITUDE TESTS
Net thrust determination for high bypass ratio engines in cruise, suggesting performance evaluation in actual flight tests
[SAE PAPER 690652] 05 p0895 A70-15841

Ionosphere disturbances due to high altitude thermonuclear explosions, discussing experimental proof by cosmos satellites short wave transmitter radio signal scintillation statistical evaluation
06 p1057 A70-17888

UV radiation effects on pea plant chloroplasts photosynthesis at high altitudes, noting disruption of electron-transport chain reactions and cyclic phosphorylation
08 p1445 A70-21216

Human sea-level natives physiological changes during high altitude physical exercise, considering carbon dioxide arterial pressure, plasma cortisol, adrenal function indexes, etc
08 p1453 A70-21873

Personnel protection against accidental decompression in transport aircraft at high altitudes, recommending flight stations with capsule to achieve ground level oxygen equivalent
09 p1627 A70-23459

High altitude liver function and blood flow, determining bromsulphophthalein transport maximum and storage capacity and galactose elimination
15 p2683 A70-32531

Nitrogen and nitric oxide production and diffusion, examining photochemistry and transport at high altitudes
20 p3620 A70-39339

HIGH ASPECT RATIO
Three dimensional turbulent boundary layers on high aspect ratio bodies /swept wings/, discussing shear stress direction determination
02 p0286 A70-12354

HIGH ASPECT RATIO WINGS
U SLENDER WINGS
HIGH EFFICIENCY
U EFFICIENCY
HIGH ENERGY
U ENERGY
HIGH ENERGY ELECTRONS
Normal and anomalous Doppler shifted cyclotron power radiated by energetic electrons spiralling along geomagnetic line considered as VLF source from magnetosphere
01 p0080 A70-11227

Explorer observations of large temporal variations of midlatitude outer zone energetic electron intensities interpreted as redistribution during geomagnetic disturbances
03 p0560 A70-13989

Spectral intensity recording facility design for high energy electrons and hard gamma quanta in upper layer and beyond atmosphere
05 p0846 A70-15959

Astrophysical plasmas radio emission interpreted as collective bremsstrahlung due to ultrarelativistic electron trails, discussing Crab Nebula, quasars and Jupiter
05 p0904 A70-16932

Cosmic ray electron spectrum above 200 Gev based on pure nuclear emulsion stack using horizontal sandwich assembly
06 p1135 A70-17473

Metric type I and decametric type III bursts relationship, suggesting common generation by high energy electron outward streams from photosphere or low chromosphere
06 p1150 A70-18466

IR spectra excited by fast electrons in nitrogen, oxygen, carbon monoxide, carbon dioxide, nitrogen oxide, methane, ammonia and water molecules
07 p1337 A70-19045

VLF and LF auroral or polar hiss as generated by incoherent Cerenkov radiation from high energy electrons
07 p1264 A70-19190

Outer radiation belt high energy electron fluxes correlated with VLF hiss ground observations
07 p1367 A70-19498

Inverse Compton collisions of relativistic electrons with universal black body photons for diffuse component of cosmic X rays
07 p1369 A70-20166

Contraction and expansion in solar region producing synchrotron emission of relativistic electrons to explain solar burst behavior
08 p1560 A70-20841

Fast electron ionization losses due to multiple scattering with atoms during passage through thin layer, calculating spatial energy distribution function
08 p1547 A70-20989

High energy electrons elastic scattering from 2s-1d shell nuclei based on Dirac equation solution in Glauber approximation
09 p1730 A70-22043

High energy electron and gamma quanta flux measurement in atmosphere at different heights by high altitude balloons
09 p1747 A70-23728

Primary cosmic rays electron-positron component, considering relative roles of collision-produced and directly accelerated electrons
12 p2292 A70-27382

Van Allen radiation belts energetic electrons injection and distribution due to magnetic storms, using satellite-borne spectrometers
13 p2483 A70-30090

High energy electron temperature in beam plasma discharge pulsed laser measured by bremsstrahlung X radiation spectrum
15 p2752 A70-32194

Outer radiation belt high energy electron fluxes correlated with VLF hiss ground observations
15 p2795 A70-32743

Acceleration and precipitation of Van Allen outer zone energetic electrons, using correlation experiment between magnetosphere and auroral zone
18 p3306 A70-36010

High energy electrons in near space excess radiation from high altitude balloon and satellite data
18 p3307 A70-36170

Degenerate relativistic electrons in intense magnetic field, computing transverse electrical conductivity
18 p3296 A70-36896

Cosmic ray high energy electron component intensity and spectra, using nuclear emulsion detector with counter triggered spark array
19 p3502 A70-38095

High energy primary electron flux measurements by Cerenkov counter onboard ESRO 2 satellite
19 p3504 A70-38107

Primary cosmic ray electron flux above 30 GeV, using nuclear emulsion plate chamber
19 p3504 A70-38110

Excess galactic X rays, discussing synchrotron emission of high energy cosmic ray electrons
24 p4398 A70-46161

High energy electron proton and heavy nuclei absorption in pulsar vicinity, discussing implications for cosmic rays 24 p4398 A70-46170

HIGH ENERGY INTERACTIONS

High energy nuclear interactions defined by computerized determination of sea level lateral distribution of muons from primary cosmic ray air showers 01 p0171 A70-10667

Cosmic ray nuclear interactions under paraffin and lead, using counter controlled multiple cloud chamber 03 p0553 A70-12877

Nucleons and high energy pions inelastic interactions with complex nuclei involving external diffraction production of pions 03 p0526 A70-13029

Charged particles distribution according to multiplicity during pion-nucleon and nucleon-nucleon interactions at high energies 03 p0555 A70-13033

High energy primary cosmic ray and proton spectra measurements from Proton satellites 03 p0555 A70-13036

High energy muon production and interaction, analyzing ionization burst spectra 03 p0555 A70-13037

Cosmic ray particles high energy interactions during extensive air showers, noting inelastic superhigh energy collisions 03 p0556 A70-13040

Light-gathering amplitude and intrinsic resolution of large-area flat scintillation detectors used for cosmic rays-nuclear interaction experiments at high energies 03 p0484 A70-13466

Electron-electron and electron-atom bremsstrahlung, giving graphical expressions for one and two electron atoms cross sections 04 p0721 A70-14667

Extensive air showers with nuclear particle interactions using ionization calorimeters, neutron monitor, scintillation and Cerenkov radiation counters 05 p0846 A70-15958

Cosmic protons and high energy heavy nuclei interaction with radiation in expanding universe, including estimates of light radiation influence on cosmic ray spectra 05 p0904 A70-16903

Three dimensional model for high energy scattering of inert gas atoms from solid surfaces, calculating trapping, accommodation and flux and velocity distributions 06 p1110 A70-18261

Quark search in cores of air showers with four million GeV mean energy, deducing rough production rate 07 p1368 A70-19925

Localized high energy flaring of active center monitored with time-associated radio bursts in spot umbrae 08 p1561 A70-20905

Cosmic ray air showers simulation, discussing high energy nuclear interaction and linear relation of primary particle energy to number 09 p1744 A70-22048

Pion and nucleon interactions, tabulating average multiplicity and inelasticity values for various primary cosmic ray energy levels 09 p1745 A70-22775

K-mesons role in high energy cosmic ray muons angular distribution and nuclear interaction 09 p1748 A70-23731

High energy oxygen positive-ion reaction with molecular nitrogen, presenting semiempirical model with assumed crossing of potential energy surfaces 10 p1920 A70-25146

Fireball role in N-N interactions at primary cosmic ray energies, using fireball model to explain particle production 13 p2476 A70-28913

High energy proton-He 3 elastic scattering cross section measurement, comparing result with Glauber model calculation 13 p2456 A70-29459

High energy proton flux variations in inner belt during solar cycle and magnetic storm, using satellite and balloon measurements 13 p2483 A70-30091

Primary cosmic ray flux and p-carbon cross sections measurements by satellites showing heavy particle production at high energies 15 p2792 A70-31733

Energy loss of high energy cosmic rays traversing isotropic radiation field of arbitrary energy spectrum in pair producing collisions with ambient photons 17 p3150 A70-34598

Electrons lateral distribution in large air showers determining inelasticity of high energy nuclear interactions 18 p3305 A70-35947

Asymptotic high energy behavior of Feynman integrals in scalar field theory models for elastic scattering 19 p3457 A70-37549

Syrovatkii mechanism of high energy particle production near neutral line of magnetic field, noting solar flares occurrence conditions 19 p3478 A70-37581

High energy electron and photon cascades in Metagalaxy, considering electromagnetic radiation density and cosmic ray origin estimation 19 p3500 A70-38081

Energy spectrum distortion of ultrahigh energy cosmic rays due to interactions with photons and neutrinos in universe 19 p3510 A70-38155

High energy cosmic ray-photon interactions, discussing ion production, nuclear fission, proton energy loss, red shift, etc 20 p3696 A70-39283

Secondary cosmic ray muon inelasticity in high energy neutrino interactions for deep mine experiments, using lepton current 21 p3845 A70-41139

Cosmic ray research role in high energy physics, discussing elementary particle interactions 22 p4096 A70-43398

HIGH ENERGY PROPELLANTS

Adiabatic calorimeter for exothermic chemical reactions determining heats of polymerization, curing rate and thermal decomposition rates as temperature function for high energy propellants 04 p0688 A70-14711

Analytical model for liquid fluorine no-vent loading operations noting application to lightweight upper stage systems [AIAA PAPER 69-579] 09 p1662 A70-23251

Chemical high energy rocket propellants, discussing metal combustion, hybrid and tribrid engines, combustion chambers, etc 11 p2100 A70-26282

HIGH EXPLOSIVES

U EXPLOSIVES

HIGH FIELD MAGNETS

Uniform bulk magnetization concept in superparamagnets related to physical statistics of magnetic first order phase transitions 15 p2785 A70-32400

High magnetic fields applications, emphasizing metal forming and superconducting rings levitation 19 p3471 A70-37948

HIGH FREQUENCIES

VLF phase disturbances and HF absorption during solar proton events of 28 August and 2 September 1966 related to proton intensities, energies and cut-off latitudes 04 p0741 A70-15124

Two frequency electron beam modes produced by O-type TWT at simultaneous input of HF signals of different amplitudes and frequencies 05 p0824 A70-16894

Aspect sensitivity of HF backscatter auroral echoes in F layer, utilizing F supported ground scatter echo to account for ionospheric refraction 06 p1012 A70-18541

Ray tracing in ionospheric HF communications, describing computational method for ray paths and ionospheric absorption 07 p1230 A70-19166

HF radio noise environment, discussing local storm effects, noise power estimation, noise measurement methods, etc 07 p1231 A70-19172

Field strength prediction for vertical horizontal broadside and horizontal end-on HF antennas, noting necessary polarization corrections 07 p1232 A70-19177

Oblique incidence HF pulse ionospheric sounding, discussing propagation modes, seasonal and diurnal effects, frequency spectra, etc 07 p1233 A70-19182

Ionospheric HF radio wave propagation, describing oblique backscatter sounding during IQSY 07 p1233 A70-19183

HF cylindrical waves propagation by line source in stratified medium, investigating refraction and diffraction at plane boundary using mathematical and ray methods 07 p1335 A70-19683

HF arc anemometer for subsonic and supersonic gas flow turbulence measurement 07 p1285 A70-19837

Surface oscillations of plasma in external HF field derived from hydrodynamics and Maxwell equations 07 p1355 A70-20367

Solar meter wave emissions enhancement or emission centers, comparing radio and optical coronal enhancements 08 p1576 A70-21402

Sinusoidal modulated HF pulse signal, deriving parametric envelope and power density function 10 p1833 A70-24086

Ionospheric effects and transmitter characteristics observed on HF standard and time stations, discussing spurious emissions arising from frequency overcrowding 10 p1842 A70-25050

HF energy nonresonance dissipation in polycrystalline yttrium-garnet ferrites subjected to constant magnetizing field 11 p2097 A70-25384

Spatial-temporal distribution of wind swell HF components measured by two dimensional antenna array fed by DC signals 12 p2263 A70-27516

MOS-FET HF noise quantities computed in terms of substrate doping, angular frequency and gain-bandwidth product 12 p2196 A70-27672

HF electrostatic waves generation by electrons in magnetosphere 13 p2482 A70-30083

Wave polarization effects on ionospheric HF radio wave transmission and reception in communication and broadcasting networks 14 p2550 A70-30650

Ionospherically reflected HF radio signal frequency spread measurement involving phase difference crossings counting between antennas 14 p2550 A70-30743

Ionospheric electron distribution by true height analysis of oblique incidence HF radio wave sounding data, applying to forward and ground backscatter 14 p2550 A70-30745

Noise sources and identification in low noise RF amplifiers via noise temperature or factors 15 p2708 A70-31952

HF geomagnetic micropulsations recordings by two component induction magnetometer, relating diurnal frequency and occurrence variations to local K-index 19 p3412 A70-37996

Canadian HF T array radio telescope at Dominion Radio Astrophysical Laboratory, discussing design and performance 19 p3397 A70-38275

Current and vector potential in thin superconducting film in HF field, considering high and low temperatures 22 p4088 A70-43467

Transistor circuit analysis at high frequencies and large signals, considering collector current, inertia and conductance conditioned by diffusion and recombination 23 p4161 A70-43779

VLF phase disturbances, HF absorption and solar protons in 1967 PCA events, using ionization model 24 p4314 A70-46128

HIGH GAIN

High gain Xe laser effects on longitudinal mode splitting, noting increased frequency of radiation propagation through highly dispersive medium 23 p4201 A70-44918

HIGH GRAVITY (ACCELERATION)

U HIGH GRAVITY ENVIRONMENTS

HIGH GRAVITY ENVIRONMENTS

Extraterrestrial gravitational effects on microorganisms, describing impulse-applied high g study of freeze dried *Escherichia coli* 11 p1987 A70-26028

HIGH IMPULSE

NERVA Xe-Prime test series, discussing computer simulation, full power and high specific impulse operation and startup under varying initial conditions [AIAA PAPER 70-709] 16 p2951 A70-33950

Low thrust high impulse nuclear and electric space propulsion systems, discussing performance capability for space missions 18 p3290 A70-36566

HIGH LATITUDES

U POLAR REGIONS

HIGH LIFT DEVICES

U LIFT DEVICES

HIGH MELTING COMPOUNDS

U REFRACTORY MATERIALS

HIGH PASS FILTERS

Fighter aircraft firing accuracy improved by high pass filter to automatically compensate sideslip induced by rudder through follow up slideslipping by aileron 11 p1979 A70-25820

Quasi-optical filters with bandpass and pseudohigh pass structures for millimeter wave and far IR frequencies 14 p2558 A70-31318

Integrated directly coupled gyrator operating mode via comparison with switching elements, considering behavior under capacitance load and high pass filter application 21 p3797 A70-40793

HIGH POLYMERS

Kinetic energy of atomic motions for vitreous and crystalline high polymers measured by differential scanning calorimetry and thermal analysis 02 p0253 A70-12522

Yield criteria for plastic deformation on glassy high polymers induced by stress field, noting crazing and shear yielding dependence on first stress invariant 15 p2764 A70-31787

Plasticized high polymers mechanical and optical properties, studying birefringence phenomena interrelation with applied external stresses 24 p4424 A70-45590

HIGH PRESSURE

- Liquid propellant spray injection into high pressure gaseous environment noting geometric, dynamic and thermal characteristics
[AIAA PAPER 70-8] 06 p1182 A70-18211
- Permittivity cell and encapsulation for liquids subjected to high pressures and temperature extremes
14 p2533 A70-30502
- Teflon bucket and Be-Cu cap seal against hydrostatic pressure, discussing applications for high pressure superconductivity measurements
18 p3262 A70-37097
- Nitrogen viscosity coefficient at high pressure, describing viscosimeter operation and kinetic theory calculations
20 p3738 A70-40140
- Gas transport properties at high temperatures and pressures, discussing Ar plasma arc characteristics
23 p4226 A70-44433

HIGH PRESSURE OXYGEN

- White rats parenchymatous organs morphological changes following convulsion-producing exposure to pure hyperbaric oxygen
07 p1207 A70-19503
- Vascular and dystrophic disturbances in rat parenchymatous organs in hyperbaric pure oxygen atmospheres, observing increased tissue eosinophilia
07 p1207 A70-19504
- Protective ability of various compounds against hyperoxia at 5, 7, 9 and 11 atmosphere of pure oxygen
08 p1441 A70-20629
- Preventive measures against fire and blast hazards in high oxygen concentration chambers
08 p1599 A70-21795
- Hyperbaric oxygenation treatment physiology and techniques, discussing limitations of equipment
09 p1620 A70-23017
- Hyperbaric oxygen effect on heart muscle contractions in mammals, considering cells enzymatic activity and substrate utilization
09 p1623 A70-23586
- White rats parenchymatous organs morphological changes following convulsion-producing exposure to pure hyperbaric oxygen
11 p1987 A70-26102
- Respiratory gas exchange, heart rate, arterial acidemia and hypoxemia responses to physical work in hyperbaric environments and hyperoxia conditions
12 p2169 A70-27655
- Altitude acclimatization protection against lung damage from exposure to oxygen at high partial pressures experimented on rats
12 p2170 A70-27659
- Rats cardiac aerobic and anaerobic pathways response to hyperbaric oxygen exposure
13 p2349 A70-28833
- High oxygen pressure effect on consumption rate constant for in vivo tissues
15 p2679 A70-31608
- Prolonged hyperbaric oxygen breathing effect on human physical performance at rest and during severe exercise
19 p3364 A70-38369
- Human and animal tolerances to hyperbaric oxygen, discussing response variation, toxicity modification, etc
22 p3976 A70-43701
- Hyperbaric oxygen effects on Coxsackievirus infection in mice
24 p4296 A70-45338

HIGH Q

U Q FACTORS

HIGH RESISTANCE

- Band model of switching effects between conducting and high resistance states of amorphous semiconductors
18 p3297 A70-35952

HIGH RESOLUTION

- High resolution silver halide photoemulsions by holographic resolvometry using Ne-He laser to obtain interference patterns
01 p0095 A70-11633
- Millimeter and nanosecond resolution of fast neutrons in pulse dense high temperature deuterium plasma discharge with polyethylene collimators and photomultipliers
02 p0303 A70-12739
- Optical performance of image intensifier system with good resolution for exposure times down to 1 nsec
04 p0695 A70-15568
- Return Beam Vidicon /RBV/ system compatibility with requirements for Earth Resources Observation Satellite /EROS/, featuring high resolution image sensor for decreasing signal noise
07 p1280 A70-19231
- Celestial X ray sources resolved against diffuse nearly isotropic background radiation by rocket and balloon experiments, noting brightness
09 p1745 A70-22895
- High resolution multiple spark photography, discussing facility
09 p1680 A70-23070

- Transmission diffraction grating for astronomical applications constructed holographically with laser light and photoresist films
12 p2234 A70-27589
- Two inch high resolution vidicon for TV line processing of printed documents
16 p2906 A70-33173
- High resolution electron return beam vidicon cameras, comparing transfer functions and SNR with photographic films
20 p3630 A70-39496
- High resolution electron beams application to electron spectroscopy, discussing elastic and inelastic scattering, resonances and atomic and diatomic molecular ionization
20 p3676 A70-40156
- High resolution observation of compact radio sources at 13 cm, using long baseline dual antenna interferometer
22 p4102 A70-42976
- High resolution ultrahigh speed continuous-writing framing camera with extended spectral range [SMPT PREPRINT 36]
22 p4033 A70-43042
- HIGH SENSITIVITY**
U SENSITIVITY
HIGH SPEED
Angular contact bearing balls track position on aero gas turbine engines shaft measurement in test rig at high speeds
20 p3638 A70-40141
- Stretch fabric materials for personnel high speed escape parachute systems
23 p4141 A70-44482
- HIGH SPEED CAMERAS**
NT FRAMING CAMERAS
Optimum procedure for high speed cinematography of holographic interferograms permitting microsecond exposures while retaining picture quality
02 p0298 A70-12213
- Drum-type, high-speed, frame or streak photographic camera, discussing film mounting and operating specifications
03 p0485 A70-13531
- High speed photography for instability onset and subsequent buckling process in photoelastic circular cylindrical shells under axial compression
03 p0594 A70-13659
- Development and characteristics of inexpensive and reliable detonator for precise synchronization with high speed photographic or electronic experiments
03 p0547 A70-14110
- Automatic measurement of frequency-contrast characteristics of photographic films using linear, photoelectric and high speed comparator devices
05 p0852 A70-16865
- High speed camera synchronization by frame reference pulses for strobe triggering
06 p1060 A70-17147
- Initial vapor bubble growth on horizontal heated wall during saturated nucleate boiling using combined streak and high speed frame photography
08 p1542 A70-21584
- Holographic recording of three dimensional rapid events, using Q switched laser pulses with sufficient coherence length for illumination
09 p1676 A70-22786
- High resolution multiple spark photography, discussing facility
09 p1680 A70-23070
- High speed instrumentation camera system for recording rapid motions during Apollo landing impact
09 p1688 A70-23770
- Atmospheric particles photographed in situ by cameras using microsecond flash lamps, discussing required mechanical motion compensation at aircraft speed
10 p1886 A70-23930
- Ultrahigh speed photographic equipment with electronic systems, investigating integral images and slit cameras
14 p2589 A70-31401
- Electronic systems for high speed photography, noting application to data processing and storage
14 p2589 A70-31402
- Microchannel electron multiplier and optical focusing output shutter tubes for high speed photography
14 p2589 A70-31403
- Photographic still and high speed cameras, using Kerr effect electro-optical shutters with transmission line structure
14 p2589 A70-31404
- High speed electron cameras with opening time below one nsec, discussing shutter types
14 p2589 A70-31405
- Electron camera with two stage image intensifier control electrode tube for rapidly evolving and slightly luminous phenomena, discussing exposure times
14 p2590 A70-31406
- Ultrahigh speed camera with high optical resolution for dense plasma diagnosis
14 p2590 A70-31407
- Hologram camera system recording hypervelocity particles by velocity synchronized Fourier transform method, employing interferometer
15 p2737 A70-32039

- Holographic interferometry combination with high speed photography, obtaining time resolved record of event
15 p2737 A70-32051
- Reactive stream separation high speed color photography for impinging streams of nitrogen tetroxide and hydrazine
16 p2998 A70-33605
- High speed pulsed ruby laser holography, discussing transmission-reflection holocameras and applications
17 p3085 A70-35007
- High speed photographic recording of bursting rotor in fragment control device
17 p3063 A70-35523
- Systematic errors in rotating mirror framing cameras and film records for quantitative high speed motion analysis
17 p3095 A70-35632
- Event-triggered high speed spectrograph shutter, studying shock tube plasmas
20 p3630 A70-39484
- Rapid exposure scanning camera for high speed cinematography, discussing optical system and operation principles
20 p3632 A70-39748
- High speed cameras for submicrosecond exposures in plasma research involving theta and zeta pinches
20 p3635 A70-40526
- High speed photographic systems for ballistic studies, describing high intensity lighting systems
20 p3635 A70-40527
- Superradiant light /SRL/ converted from electron beam energy by semiconductor targets applied to nanosecond photography
20 p3635 A70-40529
- Artificial rain erosion effects on missile and spacecraft recorded via high speed photography
20 p3635 A70-40531
- Ultrahigh speed ballistic-synchrophotography, using Imacon image converter camera for framing and streak modes
22 p4031 A70-43028
- High speed cinematographic recording of wake behind hypervelocity projectiles
22 p4032 A70-43033
- Spark photography of models in free flight in hypersonic shock tunnel
22 p4032 A70-43035
- Pulsating light source afterglow increasing high speed film information content, discussing streak image, tearing process and impact stress tests
22 p4032 A70-43036
- High speed three-frame electronic camera with storage tube, slow scanning and magnetic recording [SMPT PREPRINT 55]
22 p4033 A70-43038
- Electronographic camera for ultrahigh speed photography, using nuclear emulsion as recording medium [SMPT PREPRINT 54]
22 p4033 A70-43039
- High speed camera rotating mirror dynamic surface deformations, discussing reflected waves, astigmatism, gas turbulence and pressure effects [SMPT PREPRINT 34]
22 p4033 A70-43043
- Partial frame shutter for high speed rotating mirror camera, using explosively driven opaque dust cloud [SMPT PREPRINT 33]
22 p4033 A70-43044
- Phase locked solid state laser with picosecond pulses applied to high speed cinematography [SMPT PREPRINT 22]
22 p4034 A70-43051
- Real time holographic interferometry for flame propagation research, using high speed camera [SMPT PREPRINT 9]
22 p4035 A70-43053
- Rotating mirror hologram camera for high speed phenomena, using Q switched ruby laser pulses [SMPT PREPRINT 7]
22 p4035 A70-43054
- Acoustic Bragg diffraction for laser light deflection, solving high speed photography and holography motion problems [SMPT PREPRINT 5]
22 p4035 A70-43055
- High speed holographic recording of transient events by single shot ruby and Nd-doped pulsed lasers, applying to shock tubes and wind tunnels [SMPT PREPRINT 3]
22 p4035 A70-43056
- Shock wave propagation studies by grating spectrograph with high speed camera, computing equilibrium detonation gases temperature from emitted light [SMPT PREPRINT 98]
22 p4035 A70-43057
- Liquid jet breakup in supersonic airstream, using high speed photographic techniques [SMPT PREPRINT 90]
22 p4036 A70-43063
- High speed pic registered intermittent camera, discussing film transport, magazines operating speed, motor drive and boreighting provisions [SMPT PREPRINT 78]
22 p4036 A70-43066
- High speed X ray flash motion picture installation for ballistic photography [SMPT PREPRINT 76]
22 p4037 A70-43068
- Cantilever beam transient response measurement by stored beam /real time/ holographic interferometry combined with high speed motion picture photography
22 p4039 A70-43452
- Hologram rapid sequence recording, using scatter plate holographic system
23 p4198 A70-44947

- Highspeed raster motion picture cameras with high aperture ratios 24 p4335 A70-45651
- SFR high speed photochronograph for visible and UV raster, stereoscopic and spectral photography 24 p4335 A70-45652
- HIGH SPEED FLIGHT**
- U HIGH SPEED**
- HIGH STRENGTH**
- Solvents and chemicals resistant thermosetting resin producing high strength glass reinforced laminates based on polyanhydride crosslinked with monoepoxide 16 p2938 A70-33382
- High strength and modulus continuous graphite fibers from pitch, describing production process from asphalt and specifications 21 p3842 A70-40732
- High strength graphite fabrics evaluation for flexible structures, discussing temperature effects, fabrication, mechanical properties, oxidation and protective coatings [AIAA PAPER 70-1183] 21 p3842 A70-41830
- HIGH STRENGTH ALLOYS**
- NT HIGH STRENGTH STEELS**
- NT MARAGING STEELS**
- Thermal conductivity, electrical resistivity, Lorentz ratio and thermopower of aerospace alloys at cryogenic temperatures, considering Inconel, Hastelloy, Ti and Al alloys 03 p0512 A70-13807
- Nickel base alloy, WAZ-20 with improved strength in 2000-2200 F range for application to gas turbine engine stator vanes 04 p0706 A70-15097
- Cylindrical Al, high strength pig iron and heat resistant steels elastoplastic deformation diagrams for cyclic compression tension loads 06 p1084 A70-17387
- Mo effect on structure and properties of Ni-Al-Nb system alloys in gamma and gamma prime solid solutions range, discussing high temperature strength 08 p1514 A70-20549
- Wrought aluminum based high strength alloys structure and mechanical properties 08 p1522 A70-21708
- Linear and nonlinear rupture mechanics applied to thick walled pressure vessels of high strength materials 09 p1769 A70-22184
- High strength stress corrosion resistant aluminum alloy die forgings, evaluating tensile, tensile fatigue and fracture toughness properties 09 p1702 A70-22556
- Vacuum rolling of high strength hard-workable dispersion-hardened Nb base alloys excluding recrystallization 09 p1692 A70-22756
- Titanium high strength alloys, considering hardening by interstitials, precipitation, solid solution, etc 10 p1904 A70-24425
- Mechanical notches and saltwater corrosion effects on flexural fatigue behavior of high strength structural alloys, investigating yield strength to density ratio 11 p2066 A70-26097
- Carbide-strengthened Mo alloys dynamic strain aging processes 12 p2255 A70-27605
- Al-Zn-Mg high strength weldable alloys rupture characteristics, analyzing crack distribution, stress raisers and weld defects 14 p2591 A70-30971
- Ti alloy suitability for fastener applications noting cold workability, high strength and stress corrosion resistance [ASM PAPER W70-17.3] 15 p2760 A70-32338
- Phase diagrams of high strength metastable Ti beta alloys, showing minimum quantity of alloying elements for solid solution retention 17 p3119 A70-34418
- Ultrahigh strength alpha-beta titanium alloys, examining carbon and oxygen effects on mechanical properties 17 p3121 A70-34429
- High strength Ti alloys depth hardenability, discussing mechanical properties and use in aircraft components 17 p3121 A70-34434
- High strength Ti alloys for aircraft gas turbine engines, determining critical properties for compressor fan blades 17 p3122 A70-34436
- High strength Ti alloy for cryogenic applications, comparing plane strain fracture toughness 17 p3122 A70-34438
- High strength ferrous alloys susceptibility to stress corrosion in seawater environment, tension loading single edge notched and fatigue cracked specimens in NaCl solution 17 p3123 A70-34554
- Porosity effects on mechanical properties of high strength Al alloy weldments 18 p3265 A70-37204

- High strength and stress corrosion resistant materials, considering Ti, Ni, Al alloys, metal-matrix composites and polymers 20 p3655 A70-39666
- Double linear damage rule applicability to dual type alloys from two-stress level rotating bending and axial fatigue tests [ICAS PAPER 70-39] 23 p4267 A70-44137
- Low energy fracture of high strength Al alloys with void nucleating particles, using microprobe fractography 23 p4206 A70-44194
- HIGH STRENGTH STEELS**
- NT MARAGING STEELS**
- Thermomechanical processing of high strength low alloy steels to evaluate effects of composition, coiling temperature and cooling rate on mechanical properties and microstructures 01 p0118 A70-10726
- Fatigue crack growth rate for high strength steels from crack length during cyclic loading and striation spacings after fracture 01 p0119 A70-10732
- Correlation between sustained-load and fatigue crack growth in high strength steels for aggressive environment effects 02 p0318 A70-12544
- Ti alloys, high strength steels and plastics for aircraft and spacecraft constructions, including aging behavior of lap joints and prepreg laminates in vacuum [DGLR-69-58] 04 p0699 A70-15162
- Silicon effect on stress corrosion resistance of low alloy high strength steels in NaCl solution for different tensile strength ranges 04 p0707 A70-15272
- Delayed failure due to hydrogen embrittlement of structural high strength steels, discussing stress corrosion 04 p0710 A70-15678
- Hydrogen embrittlement as delayed rupture origin in high strength steels 04 p0711 A70-15682
- Flight type pressure vessels fabricated with quenched and tempered Ni-Cr-Mo-V structural steel, discussing fracture toughness, design, fabrication techniques [SAE PAPER 690680] 05 p0853 A70-15866
- Cryogenic temperature effect on short life torsional fatigue properties of Ni-Cr-Mo steel, discussing cyclic strain range effects 05 p0864 A70-16807
- Reverse-bend and tension-tension fatigue properties of high strength Cr-Mn-N stainless steel sheet in notched and unnotched conditions 07 p1305 A70-18993
- Stress corrosion-fatigue crack propagation in high strength structural steels, relating growth rates to crack tip stress intensity factor [ASME PAPER 69-MET-5] 08 p1519 A70-21452
- Recrystallization in austenite phases of vanadium and columbium HSLA steel alloys determined in high temperature deformation tests 08 p1521 A70-21704
- Ultrahigh strength Ni steels fracture toughness analysis, studying effects of chemical composition, yield strength, air melting, vacuum melting, etc 09 p1701 A70-22552
- Microconstituents effect on wear behavior of high hardness steels on basis of crossed-cylinder testing, discussing intermetallic compounds influence 10 p1895 A70-24853
- Brittle fracture strength of welded joints in high strength steels 11 p2059 A70-25663
- Fatigue crack propagation in high strength steels during fatigue cycling in dry and wet environment containing NaCl 11 p2067 A70-26100
- Fracture toughness and cyclic crack propagation of surface cracked high strength aircraft structure steels 12 p2254 A70-27467
- Fatigue crack growth dependence on load profile, temperature, test frequency and environment and stress in high strength Al and Ti alloys and steels 13 p2431 A70-28604
- Ultrahigh strength stainless steel for light gage springs and satellite antennas 13 p2420 A70-29248
- Hardened steel embrittlement in low pressure hydrogen caused by crack growth as function of temperature 13 p2436 A70-29804
- High temperature transformation of high speed steel low temper hardened in vacuum or atmosphere quench 15 p2756 A70-31568
- Precrack Charpy slow rate straining sensitivity of high strength steel at increased temperatures, comparing fracture energy of impact tests 15 p2758 A70-32238
- Stress corrosion cracking of high strength structural, tool and maraging steels due to hydride, diffusion controlled and mixed embrittlement 16 p2934 A70-34301

- Fractography of fatigue and delayed fracture of hydrogenated, unplated and Cd-plated ultrahigh strength steel 17 p3124 A70-34654
- Aircraft structural materials, considering high strength steels Al and Ti alloys 17 p3124 A70-34675
- F-111 high strength steel design experience concerning wing, fuselage and empennage support structure [AIAA PAPER 70-884] 17 p3018 A70-35803
- Transformation induced plasticity (TRIP)/TRIP high strength steels resistance to hydrogen embrittlement 18 p3273 A70-36047
- Fatigue resistance of high yield strength steel weldments under uniaxial loading, describing cyclic behavior by S-N curve 18 p3278 A70-37114
- Nondestructive ultrasonic measurements of crack depth in high strength steel plate weldments, studying low cycle fatigue 21 p3834 A70-41943
- Scale factor effect on brittle fracture resistance for Ti and Al alloys and high strength steels 23 p4265 A70-43936
- Papers on plane strain fracture toughness testing covering metallic materials, steels and aluminum alloys 23 p4205 A70-44189
- Crack length and bend specimen thickness effects in plane strain fracture toughness tests of high strength steels 23 p4268 A70-44192
- Crack and thickness effects on fracture toughness tests of high strength steel in precracked sheet and bend specimens 23 p4206 A70-44193
- High strength low-alloyed steel for solid propellant rocket engine case, discussing high temperature production and test methods 23 p4208 A70-45046
- High strength martensitic stainless steel stress corrosion resistance and fatigue crack growth rate, considering austenite content, strain aging and tempering temperatures 24 p4359 A70-45245
- Thread parameters effect on steel and Ti high strength fasteners fatigue life [SAE PAPER 700851] 24 p4425 A70-45881
- HIGH TEMPERATURE**
- Soviet book on creep of structural elements at high temperature noting metals, concrete and polymer materials, buckling, variety of structural elements and creep resistance 09 p1781 A70-23266
- Variable reproducible black radiator of resistance heated carbon tube designed for temperatures between carbon glowing and sublimation point 12 p2329 A70-27090
- High temperature dislocation model based on dislocation dynamics, rate theory and varying back stress ratio 13 p2436 A70-29563
- High temperature fuel cell with thin disk solid electrolyte, evaluating performance as function of electrolyte, electrode and current collector resistance ratio 22 p3964 A70-42499
- HIGH TEMPERATURE AIR**
- Compact 4 micron radiation band from high temperature air and gases measured on arc jet and shock tube, noting molecular O and N source 02 p0392 A70-11901
- State equation for entropy of dissociated air with enthalpy and pressure as independent variables for calculating gas dynamic processes on computers 10 p1966 A70-23839
- Film cooling protecting axisymmetric nozzle slot surface exposed to high temperature Mach 6 air injection 18 p3242 A70-36695
- Shock tube high temperature air viscosity from laminar boundary layer heat exchange data 20 p3608 A70-39633
- Approximate calculations of thermal and viscous transport in high temperature air based on empirical transport equations 21 p3951 A70-41750
- Hot air temperature decay, discussing relaxation process of lightning channel behavior 22 p4016 A70-42781
- HIGH TEMPERATURE ALLOYS**
- U HEAT RESISTANT ALLOYS**
- HIGH TEMPERATURE ENVIRONMENTS**
- Continuous measurement and automatic recording of metals electrical resistance during fatigue testing in vacuum at elevated temperatures 01 p0092 A70-11108
- Hardness measuring instrument by dynamic method at high temperatures in vacuum, using magnetic or nonmagnetic indenter balls 01 p0092 A70-11111
- Temperature measuring devices design for ultrahigh/ultralow temperatures, examining heat effects on gases, liquids and solids 02 p0295 A70-11864

High temperature thermometer using pulsed excitation ultrasonic resonance with ruthenium sensor, discussing resonator types, transmission lines and transducer

02 p0300 A70-12468

Cr alloys applications in high temperature environments, describing alloying elements effects on strength and ductility

03 p0511 A70-13566

Scout missile destruct charge system premature operational response to high temperature environment caused by combustion gas leak during stage separation

03 p0550 A70-14140

Material evaluation and selection for compact nuclear reactor control bearings operating at high temperature in vacuum

[ASME PAPER 69-WA/LUB-11]

04 p0697 A70-14765

Stress rupture strength of turbine blades fir tree type root joints under prolonged loads at high temperatures, studying disk teeth shearing

05 p0953 A70-17055

High temperature effects on pilots psychomotor performance and physiological function, discussing measurements taken during complex tasks

06 p0999 A70-17290

Heart rate-body temperature relationship during walking in hot environment

06 p0993 A70-17431

Heat pipe structural alloys compatibility with different working fluids using capsule tests at high temperatures, noting corrosion behavior

[AIME PAPER F-69-2]

07 p1304 A70-18812

Static loading effect at high temperatures in argon and liquid lithium on mechanical properties stability of steel

08 p1515 A70-20920

Matrix optimization of boron filament reinforced polymeric for short duration high temperature aerospace applications

08 p1530 A70-21891

High temperature, electrically heated convective gas heating system for high velocity atmospheric flight simulation using air-nitrogen working fluids

12 p2205 A70-27100

Thermal stresses in solid nonhomogeneous sphere in high periodic temperature field, assuming temperature dependent Young modulus and linear thermal expansion coefficient

13 p2512 A70-28979

Electropneumatic actuation systems for rocket engines in extreme environment applications involving high nuclear radiation levels and high and cryogenic temperatures

14 p2535 A70-31343

Beryllium fibers and Al matrix interactions at high temperatures and various durations, investigating diffusion by X ray diffraction, electron microscope and microprobe analysis

15 p2757 A70-31812

High temperature oxidation of Ni-Cr alloys and stainless steels in molten salt, observing grain boundary corrosion with electron probe

15 p2757 A70-31875

Inconel 600 high temperature high strain rate fracture process by hot torsion tester, noting temperature effects

15 p2762 A70-32389

Cooling hood effect on physiological responses to work in hot environment, discussing body temperature

17 p3031 A70-35422

Gas metabolism, chemical thermoregulation, body temperature and weight of rats during adaptation to repeated high temperature exposure

18 p3219 A70-36538

High temperature adaptation, gas exchange and thermoregulation in dogs during repeated overheatings in open sunshine

18 p3219 A70-36539

Adaptive recession of gas metabolism in rats during multiple high temperature exposures

18 p3220 A70-36545

White rats adaptation to multiple high temperature exposures, examining oxygen tension in skeletal muscles

18 p3220 A70-36549

Unsteady temperature fields in heat conduction problems associated with high temperature effects on abutted cylinders

18 p3348 A70-36572

Graphite-polyimide composites development for high temperature environments, discussing mechanical properties

19 p3455 A70-38425

Reinforced plastic composites thermal protection and ablative performance in high temperature environments for reentry vehicle applications

20 p3656 A70-40029

Hypoxia and high ambient temperature effects on altitude tolerance in animals

20 p3575 A70-40186

Liquid metal hydraulic servoactuation packages for flight control in high temperature environments without coolant systems

21 p3750 A70-40785

Titanium dicarbide and tetracarbide vaporization at high temperatures, using Knudsen effusion method with mass spectroscopy, determining dissociation energies

21 p3773 A70-41274

Sandwich multilayer structures temperature fields and heat transfer characteristics at high temperature [ICAS PAPER 70-38-BIS]

23 p4276 A70-44136

HIGH TEMPERATURE FLUIDS

NT HIGH TEMPERATURE AIR

NT HIGH TEMPERATURE GASES

End support cooling in hot-wire anemometry of low density high temperature flows

[AIAA PAPER 70-589]

13 p2412 A70-29882

Thermal radiative transfer and magnetic field effects on hydromagnetic stability of hot electrically conducting fluid

14 p2623 A70-30996

HIGH TEMPERATURE GASES

NT HIGH TEMPERATURE AIR

Injected B particles burning in hot gas stream of oxidant mixture with Ar and H, observing trace widening by motion picture technique

01 p0218 A70-11016

Characteristics method for calculating steady supersonic flow of burning gas mixture past wedge and rotating cones

01 p0218 A70-11018

Strong shocks and high temperature gases production using multistage gaseous detonation driven shock tube

02 p0274 A70-11855

Heat resistant coatings in high temperature gas flow, studying external layer deformation kinetics during shrinkage

03 p0483 A70-13250

Ultrasonic beam scanning measurements in high temperature axisymmetric gas flow, discussing errors and use of numerical transformation methods

04 p0685 A70-14536

Equilibrium composition and thermodynamic functions calculated for mixtures of dissociating and ionizing high temperature gases from standard data

04 p0780 A70-14538

Heat resistant silicate enamel coatings to protect steels and alloys against high temperature gas corrosion, studying properties by various methods

05 p0872 A70-16600

Phenolic nylon ablative thermal effectiveness in arc heated nitrogen, air and nitrogen-carbon dioxide streams

[AIAA PAPER 70-154]

06 p1183 A70-18233

Heavy particle impact ionization in hot gases analyzed for ionization rates relationships

06 p1113 A70-18278

Heat transfer measurement in ionized high temperature gas flows with discharge shock tube and thermal sensors

07 p1283 A70-19663

Transport properties of high temperature gases compared with room temperature differences, considering chemical equilibria, heat conduction and atom-free radical forces

07 p1424 A70-19880

Analog computing spectral photometer for high temperature measurements in gas flames

07 p1285 A70-19896

Water vapor high temperature dissociation kinetics in dilute mixtures with argon in shock waves

09 p1629 A70-22319

Fluidic vortex valve to modulate solid propellant generated hot gas flow

[AIAA PAPER 69-424]

09 p1743 A70-23249

Thermodynamic and transport properties of high temperature and pressure gases measured with ultrasonic pulse technique

11 p2147 A70-25753

Hydrogen, nitrogen and argon electrical and thermal conductivity measured at high temperature using electric arc as plasma source

11 p2148 A70-26016

Monograph on relaxation processes at high temperatures for thrust nozzle calculation and optimization covering real gas effects, reaction kinetics, heat transfer, etc

11 p2103 A70-26475

High temperature gaseous molecular beams impingement on Cu surfaces at cryogenic temperatures measured for condensation rates

12 p2271 A70-27265

Spectral absorption characteristics for C atom radiative processes in carbon dioxide-nitrogen mixtures at high temperatures corresponding to Venusian atmosphere

12 p2275 A70-27317

Ionization kinetics of Ar, Xe and Hg monatomic gas behind shock wave front at high temperatures

12 p2210 A70-27319

High temperature kinetics of pyrolytic silicon carbide oxidation and nitridation in dissociated gases

13 p2361 A70-29077

Simulated Venusian atmosphere effects on polymeric plastic and rubber materials, comparing with high temperature air and nitrogen exposures

14 p2640 A70-30781

HIGH TEMPERATURE LUBRICANTS

High temperature molecules matrix isolation in saturated vapor over refractory solids, discussing optical spectroscopy of VO, metal oxide and halide molecules

14 p2545 A70-30903

Molecular beams formation from high pressures, discussing detection, diagnosis and applications in high temperature chemistry

14 p2545 A70-30904

High temperature inviscid flow of ideal radiating gas, analyzing effects of radiation pressure and energy on flow field

14 p2666 A70-30999

Shock waves structure in radiating gases at high temperatures, taking into account radiation anisotropy in shock front

15 p2720 A70-31645

Graphite oxidation on exposure to high temperature flow field based on surface coupled model

[AIAA PAPER 70-823]

16 p2940 A70-33941

Nitric oxide gas IR radiation properties at high temperatures, determining spectral mean fine structure and total band absorbance correlations

16 p3003 A70-34253

Radiation gas dynamics, investigating thermal radiation effects on flow field of high temperature gas

17 p3195 A70-35038

High temperature and pressure hot gas source for testing fluidic temperature sensor used in gas turbine engine inlet simulation

17 p3058 A70-35157

High temperature radial turbine design for small gas turbine engines, discussing aerodynamic, structure and thermal analyses

18 p3301 A70-36450

Electronic excitation contribution to frozen properties and cut-off criteria of high temperature gas plasma

18 p3296 A70-36955

Vacuum brazed stainless steel hot gas actuators for guided weapons

18 p3265 A70-37202

High temperature gas boundary layer flows with or without magnetic fields, discussing measurement by X ray absorption technique

19 p3405 A70-38192

Heat resistant coatings in high temperature gas flow, studying external layer deformation kinetics during shrinkage

19 p3428 A70-38468

Hot gas pipe thermoelastic reduction factors, determining elastic support, material and dimensions

20 p3720 A70-39624

Metal vapors electrical conductivity and density measurement at high temperatures and supercritical pressures

20 p3648 A70-39637

Relativistic high temperature gas asymptotic solutions with or without body force, comparing flow field with photon gas

20 p3673 A70-39654

High temperature gases radiative heat exchange, evaluating approximation methods

20 p3739 A70-40293

Local variables in boundary layer of high temperature ionized gas flowing in magnetic field, using X ray absorption

20 p3613 A70-40344

Liquid or vapor phase working fluids penetration effects on steady state and transient performance of hot reservoir gas controlled heat pipes

21 p3946 A70-41047

Spectral absorption characteristics for C atom radiative processes in carbon dioxide-nitrogen mixtures at high temperatures corresponding to Venusian atmosphere

21 p3854 A70-42058

Ionization kinetics of Ar, Xe and Hg monatomic gas behind shock wave front at high temperatures

21 p3854 A70-42061

High temperature gas turbine blades cooling by liquid Na-K alloy

[ONERA-TP-872]

22 p4125 A70-43458

Intermolecular forces at close approach distances in calculating thermodynamic and transport properties of high temperature dilute gases, using molecular beam methods

23 p4222 A70-44430

Gas transport properties at high temperatures and pressures, discussing Ar plasma arc characteristics

23 p4226 A70-44433

Phenolic nylon ablative thermal effectiveness in arc heated nitrogen, air and nitrogen-carbon dioxide streams

[AIAA PAPER 70-154]

23 p4282 A70-44520

Warm gas reaction control thrusts via solid propellant exhaust products for ballistic missiles attitude control

[SAE PAPER 700780]

24 p4295 A70-45863

HIGH TEMPERATURE LUBRICANTS

Aliphatic diesters as high temperature lubricants, discussing viscosity range extension, oxidation inhibition and thermal stability

13 p2438 A70-29125

- High temperature organic resin binders and solid lubricant thermal and oxidative behavior examined by thermogravimetric analysis
[ASME PAPER 70-HT-30] 22 p4058 A70-42436
- HIGH TEMPERATURE MATERIALS**
- U REFRACTORY MATERIALS**
- HIGH TEMPERATURE NUCLEAR REACTORS**
- High temperature energy systems with plasma reactors and inductive MPD converters, discussing spacecraft propulsion and ground based pollution-free power generation
15 p2791 A70-32278
- High temperature liquid metal cooled nuclear reactor for military aircraft with long flight endurance and range
22 p4071 A70-43188
- HIGH TEMPERATURE PLASMA**
- Sweeping W wire probe in rotational high temperature plasmas for local heat transfer measurement
06 p1120 A70-17699
- Stationary collisionless shock waves in hot initial plasma produced by theta pinch discharge, discussing magnetic field, density and electron temperature profiles
10 p1924 A70-24697
- Plasma transport properties at temperatures up to 15000 K, considering electrical and thermal conductivity, radiation source strength and viscosity
11 p2089 A70-25759
- Stellar and nebular magnetic fields formation, considering role of high temperature plasma random charge and current fluctuations
12 p2307 A70-27864
- Laser radiation interaction with hot nonuniform plasma, determining thermal and electromagnetic forces for various temperatures and densities
13 p2460 A70-28643
- Circularly polarized emission from types I and 4 bursts and noise storms, considering mode coupling in warm plasma, gyroradiation and Cerenkov radiation
13 p2479 A70-29851
- Whistler mode wave packets propagation in hot inhomogeneous collisionless plasma immersed in nonuniform ambient magnetic field
13 p2468 A70-29931
- Helium II line broadening in high temperature plasma, measuring profile for comparison with theoretical prediction
20 p3677 A70-39115
- Passive corpuscular diagnostics of high temperature plasma based on charge exchange neutrals, calibrating stripping chamber
20 p3685 A70-40398
- HIGH TEMPERATURE PLASMAS**
- Electron quench additives electrophilic effects in high temperature air plasma flow, simulating reentry flight conditions
04 p0664 A70-15561
- NO ion dissociative recombination rate coefficient determined in high temperature air plasma from electron temperature and number density measurements
04 p0675 A70-15583
- Transpiration-cooled electric arcs for high temperature high density plasma generation, considering uncertainties in plasma transport properties and temperature distributions
04 p0729 A70-15591
- Plasma nature, properties and applications, discussing echoes, shocks, phase mixing and hot plasma containment
05 p0887 A70-16130
- Fields and power transfer for electromagnetic waves in hot plasma calculated using Fourier integral and Fourier series methods
05 p0888 A70-16165
- HF electromagnetic field penetration of plasma with finite conductivity and Hall constant for containment of hot plasmas, formulating nonlinear electrodynamic problem
05 p0889 A70-16490
- RF probe impedance variations with magnetic field strength in hot plasma for electron gyrofrequencies less than plasma frequency explained by model
06 p1117 A70-17371
- Heat transfer in dense high temperature plasma due to drift waves instability at trapped electrons
06 p1121 A70-17802
- Heat flux, electrical and thermal conductivity of H measured on plasma in cascade arc chamber of high power load at 1 atm pressure
06 p1107 A70-18525
- Electromagnetic wave scattering from charged particle in hot electron plasma in magnetic field, considering relativistic corrections for scattered radiation spectra
07 p1352 A70-19992
- Free plasma column discharge in HF field in high pressure deuterium atmosphere, discussing high plasma temperature inside column and reliable thermonuclear reaction achievement
08 p1551 A70-21417
- Stark broadening of singly ionized nitrogen lines measured in dense high temperature plasma behind reflected shock wave in T tube
09 p1731 A70-22776

- Continuum radiation of nitrogen plasma at atmospheric pressure at high temperatures
10 p1923 A70-24472
- Transfer impedance measurement for HF quadrupole probe immersed in hot magnetoplasma
10 p1877 A70-24709
- Thermally ionized cesium plasma viscosity at high temperatures in vacuum using capillary tube assembly
11 p2092 A70-26731
- Heat transfer in dense high temperature plasma due to drift waves instability at trapped electrons
13 p2460 A70-28653
- Alouette spikes decrease with time equivalent to antenna transient response during hot plasma immersion
13 p2371 A70-29921
- High argon plasma temperatures via pulsing constricted electric arc
14 p2621 A70-30504
- Convective or absolute electrostatic instability in weakly inhomogeneous hot magnetoplasma, determining density and frequency for onset
14 p2622 A70-30695
- Bounded hot plasmas with/without steady magnetic field, discussing ion-electron resonances
15 p2779 A70-31997
- High temperature plasmas of mixtures of nitrogen with rare gases, calculating equilibrium thermodynamic properties
17 p3195 A70-34932
- Vlasov high temperature plasmas numerical analysis, using Hamilton variational principle
18 p3296 A70-36793
- High radiation intensity neodymium glass laser, describing installation for heating plasmas to high temperatures
20 p3643 A70-39758
- Exponential kernel approximation effect on radiative energy transfer in high temperature hydrogen plasma
20 p3684 A70-40278
- Lagrange formulation for deriving energy-conserving numerical approximations for Vlasov plasmas
22 p4080 A70-42750
- Solar X-ray data from rocket and satellites, discussing hot dense plasmas and correlation with H alpha flares, calcium plages and microwave emission
22 p4096 A70-43300
- Hot plasmas physics - Conference, Newbattle Abbey, Scotland, July-August 1968
23 p4224 A70-44176
- Plane plasma waves in homogeneous conducting fluid with magnetic field, considering oscillations of two-fluid, cold and hot plasmas
23 p4224 A70-44179
- HIGH TEMPERATURE RESEARCH**
- Be oxidation in carbon dioxide at high temperatures, explaining observed kinetic discontinuity in terms of oxide morphology
01 p0124 A70-11638
- High temperature heat treatment effects on Mo, W, Ta and Re crystal surface order and faceting observed by electron diffraction, noting contamination role
03 p0538 A70-13097
- Temperature dependence of sputtering coefficient of quartz and chondrites at 2000 K and mass decrease prior to evaporation
03 p0569 A70-13357
- Applied MHD and high temperature gas dynamics - Conference, Prague, May 1968
04 p0724 A70-14526
- Torsion testing apparatus for refractory materials at 2400 C, measuring applied torsion moment, twisting angle and second order modulus of elasticity
05 p0825 A70-15881
- Collection of papers on high temperature physics and chemistry covering shock tube chemistry, plasmas, exploding wires, etc
06 p1063 A70-17726
- High temperature technology - Conference, Pacific Grove, California, September 1967
07 p1311 A70-19876
- High temperature techniques, measurement and data methodology noting refractory materials
07 p1312 A70-19877
- Reentry thermal protection materials technology, discussing thermophysical, thermomechanical and kinetic effects, noting interdisciplinary approach
07 p1319 A70-19878
- Laser characteristics and applications in high temperature research including metal heating, welding, machining, surface particle emission and plasma production
07 p1301 A70-19881
- Chemical bonding of high temperature molecular species, discussing ab initio calculations for diatomic atoms
07 p1225 A70-19882
- Temperature dependence of sputtering coefficient of quartz and chondrites at 2000 K and mass decrease prior to evaporation
11 p2118 A70-26722
- Alloy oxidation at high temperatures emphasizing binary and ternary alloys
12 p2257 A70-28005

- Collection of papers on high temperature chemistry covering gaseous dissociation, molecular beams, thermal plasmas, solids sublimation, solar furnace, etc
14 p2545 A70-30901
- High temperature solid-solid reactions and solid-liquid or condensed phase-gas equilibria, using solar furnace
14 p2545 A70-30907
- High temperature transformation of high speed steel low temper hardened in vacuum or atmosphere furnace
15 p2756 A70-31568
- Specific heat and enthalpy of body centered cubic refractory metals at high temperatures
15 p2757 A70-31943
- Soviet papers on high temperature thermophysics covering body-gas heat exchange, plasma jet breakdown of subliming materials, electric arc heaters, plasmatron regime, etc
15 p2826 A70-32101
- High temperature elastic moduli in polycrystalline Al rods from propagation velocity of elastic waves generated by Q switched laser
[SESA PAPER 1641] 15 p2759 A70-32304
- Compressibility factors and virial coefficients for He-N mixture, He and nitrogen at low temperatures and high pressures
18 p3290 A70-36250
- Product distribution of organic nitrogen compounds plasma sources computed by assuming high temperature limited thermodynamic equilibrium
18 p3226 A70-36764
- High temperature systems - Conference, Pasadena, December 1964, Volume 2
22 p4090 A70-42751
- High temperature specific heat terms for refractory metals and ceramics from room temperature to near-melting point
23 p4207 A70-44440
- HIGH TEMPERATURE TESTS**
- Loads effects on refractory alloy fatigue strength and life at high temperatures, describing aircraft turbine blade tests
01 p0115 A70-10069
- Refractory and heat resistant materials thermal diffusivity coefficient, discussing theoretical basis and technical implementation for measurement at high temperature
01 p0085 A70-10178
- Projector with paraboloid mirror solar radiation condensing lens for studying heat resistant materials mechanical properties at high temperatures
01 p0055 A70-10179
- Thermal diffusivity coefficient and conductivity of Cr at high temperatures determined by plane temperature wave method
01 p0117 A70-10190
- Air lubricated foil bearing support design with external pressurization for high speed rotor in high temperature turbomachinery
[ASME PAPER 69-LUB-D] 01 p0100 A70-10377
- Apparatus for continuous creep measurement at high temperature for fine wire and thin tubular samples with small cross sectional areas
01 p0088 A70-10746
- Quartz-Fiberfrax heat shield tests for Thor booster at high radiative heating rates, noting optimum material performance dependence on loose stitching
01 p0129 A70-10850
- Liquid metals contact effect on mechanical strength of T shaped graphite specimens at high temperatures in argon atmosphere
01 p0129 A70-10338
- Annular metal specimens protection against oxidation during high temperature relaxation testing by covering specimens with Al powder thinned with alcohol
01 p0121 A70-11109
- Rockwell hardness tester attachment design for studying temperature dependence in various multiphase alloys at high temperature
01 p0121 A70-11110
- TD-Ni low cycle fatigue properties at high temperature, discussing grain morphology, thoria particles role and oxidation resistant coating effect
01 p0123 A70-11245
- High temperature ductility improvement in stainless steels containing He, analyzing lattice damage and interphase cavities after fast neutron irradiation
01 p0123 A70-11246
- Reinforced metals properties and applications including fibers and lamination, notch sensitivity, brittle fracture, failure and heat resistance characteristics
01 p0124 A70-11619
- Co-Cr alloy oxidation behavior at high temperatures and various oxygen pressures
02 p0319 A70-12720
- Strain gauge data obtainable on rosettes used for measuring test component stresses at 550 F in inert atmosphere
03 p0482 A70-12965
- B-C alloys chemical composition effect on high temperature stability in pure oxygen
03 p0514 A70-12978

Oxidation resistance of mixed silicon nitride and silicon carbide refractory materials at high temperatures 03 p0514 A70-12979

Aluminum oxide solid state reaction with Ta at high temperatures using chemical analysis 03 p0511 A70-13487

Titanium carbide hemispherical and spectral emissivity and electrical resistivity measured at high temperature 03 p0512 A70-13752

Rate and heat of vaporization of graphite filaments in 2500-3400 K range in vacuum and in He, using pulse heating techniques 03 p0517 A70-14004

High temperature effects on mechanical properties of recrystallized Ta relating strength, hardness and yield point 04 p0707 A70-15267

Surface work hardening and stress concentrations effects on fatigue strength of alloy under asymmetric tension and compression load cycles at high temperatures 04 p0707 A70-15270

Binary system Mo-C determined in temperature range 1250-2270 C, using microscopical and thermal analyses and microhardness testing 05 p0862 A70-16198

Creep in single crystal and polycrystalline Nb between 1300-1900 C under stresses, showing stress independent activation energy 05 p0862 A70-16202

High temperature Hf oxidation in air and oxygen using thermogravimetry, X ray diffraction and electron microscopy 05 p0863 A70-16522

Deformation and failure of refractory metals at high temperatures under constant and variable thermal loads concerning turbomachine components 05 p0865 A70-17027

Strength and plasticity of Mo and Nb sheet in oxidizing medium at high temperatures and pressure range 05 p0865 A70-17029

Stress rupture tests with Nb-based alloys in 1273-1673 K temperature range 05 p0952 A70-17039

E1617 alloy breakdown resistance tests under multiple alternating static tension-compression and vibrational loads at 800 C 05 p0867 A70-17044

Heat resistant materials damping properties at high temperatures under distributed stresses measured in thin walled tubular specimens with vibrogram 05 p0952 A70-17049

Creep, ductility and short term tensile and compression strength test facility for graphite in 300-3500 K temperature range 05 p0875 A70-17068

Test facilities for studying materials thermophysical properties and stress relaxation, including dynamic hardness measurement and torsion tests up to 2500 K 05 p0830 A70-17074

Creep effects on structural failure under low cycle fatigue at high temperatures, noting role of plastic deformation 06 p1164 A70-17409

Fatigue at high temperatures - ASTM Conference, San Francisco, June 1968 06 p1086 A70-17451

Creep-low cycle fatigue interactions in Udimet alloy at elevated temperatures, investigating cumulative damage 06 p1086 A70-17455

Creep deformation resistance decrease in pure Al tubular specimens at high temperatures under multiple stress reversals 06 p1087 A70-17456

Elevated isothermal and low cycle thermal fatigue of Hastelloy X, investigating test temperature, cycle frequency and stress temperature effects 06 p1087 A70-17457

Book on optimization by variational methods covering use of differential equations, Pontryagin minimum principle, optimal and feedback control, dynamic programming, etc 06 p1093 A70-17650

Strain gage high temperature performance in rocket engines tested by spot welding to turbine manifold, noting installation and position influence 06 p1069 A70-18440

Material inhomogeneity during high temperature fatigue tests taking into account probability density of random failure coordinate distribution 07 p1401 A70-18839

Ni influence in high temperature oxidation of austenitic Fe-Cr-Ni alloys investigated thermogravimetrically, metallographically and by electron probe microanalysis 07 p1305 A70-18965

Soviet book on structures design for stability at high temperatures with large gradients, discussing thermoelasticity, thermoplasticity and creep equations for shells, plates, etc 07 p1409 A70-19601

Creep rupture and residual tensile strength tests to evaluate long time properties and structural stability of Inconel 718 alloy, performing phase analysis 07 p1310 A70-19731

Phase equilibria, crystallization and solidus surface in transition conode triangle of ternary system Mo-Ti-C at high temperatures 07 p1310 A70-19804

High temperature creep rupture tests of arc cast and powder metallurgy wrought unalloyed W sheets 07 p1313 A70-19884

Ablation, transmission transparency and embrittlement of heat shield materials for Voyager tested under simulated Mars entry conditions 07 p1395 A70-19885

Ablation products and high temperature boundary layer chemistry of polytetrafluoroethylene (Teflon) in arc jet streams using mass spectrometer 07 p1319 A70-19886

Gas phase thermal decomposition of ammonium perchlorate at elevated temperatures using mass spectrometer 07 p1362 A70-20009

Electrically conductive ablative materials rapidly heated to 7000 F in test facility, discussing heating method and high strain rate testing 07 p1250 A70-20042

Hall effect and electric conductivity of cadmium arsenide at high temperatures as function of carrier concentration dependence on temperature and phase transformation 07 p1357 A70-20314

Hydrogen penetrability in heat resistant steels subjected to high temperature creep, observing activation energy decrease with increased stress 08 p1515 A70-20923

Cyclic creep and relaxation of heat resistant alloys at high temperatures, showing inapplicability of static load conditions 08 p1516 A70-20982

Phase diagram of dysprosium oxide-chromium oxide system constructed by microstructural analysis in 1600-2400 C range in argon atmosphere 08 p1556 A70-21118

Nickel alloy based metal fiber reinforced composites long-time structural stability at high temperatures 08 p1517 A70-21150

Dynamic creep rupture of stainless steel tested at high stress levels and temperatures 08 p1518 A70-21333

Inert gases and nitrogen determined at high temperature, discussing revision of existing functions representing intermolecular energy 08 p1598 A70-21525

Metals thermal conductivity at high temperatures determined by direct electrical heating method, considering specimen geometry effects on radiation losses 08 p1497 A70-21526

Recrystallization in austenite phases of vanadium and columbium HSLA steel alloys determined in high temperature deformation tests 08 p1521 A70-21704

Microstructure of wrought arc-cast polycrystalline W sheet after high temperature creep deformation at various stress levels 08 p1525 A70-21962

Co-based alloy mechanical properties and physical parameters at high temperatures, discussing oxidation and hot corrosion resistance 09 p1700 A70-22025

Gas saturation and inhomogeneity in surface layer of Ti alloys with alpha and beta stabilizers after high temperature heating 09 p1700 A70-22078

Free radicals role in high temperature surface reactions of solid metal oxide particles interacting with unburned flame gases 09 p1629 A70-22320

Metal and alloys hardness measuring devices at high temperatures in ultrahigh vacuum based on use of synthetic sapphire pyramidal indenter 09 p1675 A70-22566

Magnesium solubility in titanium from X ray analysis of Mg distribution in diffusion zones at high temperature and pressures 09 p1703 A70-22567

Creep failure fatigue life prediction methods involving hold period effects on high temperature fatigue properties 09 p1775 A70-22594

Fatigue strength tests of alloy during static and programmed loading at high temperatures from statistical standpoint 09 p1703 A70-22620

High temperature fatigue crack growth in metal, suggesting condensation of vacancies at crack front after each loading cycle 09 p1776 A70-22644

Internal nitridation temperature effect on dispersion hardening of austenitic stainless Fe-Cr-Ni-Ti steels, investigating interparticle spacing and layer thickness effects 09 p1705 A70-22810

Molybdenum heat capacity, electrical resistivity and thermal radiation measurements at high temperatures with millisecond resolution 09 p1706 A70-22955

Gages for static strain measurements at high temperatures, discussing resistivity temperature coefficient compensation 09 p1680 A70-23109

Austenitic steels and alloys high temperature softening under conditions of stress relaxation and creep, noting hardening action of plastic deformation 09 p1709 A70-23785

High temperature creep of prestrained molybdenum single crystals as function of physical treatment and crystal orientation 10 p1902 A70-23860

Gas viscosity high temperature measurement method in shock tube using boundary layer equations for velocity and static temperature distributions 10 p1867 A70-24151

Bismuth oxide resistivity and structural characteristics at high temperature and during transformation from solid to liquid state 10 p1927 A70-24272

Thermal conductivity coefficient of metals and alloys above 1000 C by longitudinal heat flow method 11 p2065 A70-25761

Thermal diffusivity of opaque materials by phase shift method, using modulated radiation beam from carbon arc to heat material 11 p2068 A70-25767

Thermal dissociation kinetics in chlorine pentafluoride over high temperature range 11 p1994 A70-25823

Axial strain controlled fatigue tests at elevated temperature, discussing specimen gripping, alignment and break detection for mechanical and closed loop hydraulic test machines 11 p2033 A70-26611

Procedures for conducting fatigue studies at high temperatures on servocontrolled testing machines using stress, axial, transverse or plastic strains 11 p2033 A70-26612

High temperature fatigue tests of materials under uniaxial controlled strain, describing equipment, failure interpretation and data reduction 11 p2033 A70-26613

Cross sensitivity errors effect on stress determination by free-filament wire strain gages used at high temperature 11 p2058 A70-26838

Nitrogen transport properties to 26,000 degrees K, measuring current-field intensity properties and radial temperature distributions in molecular nitrogen cascade 11 p2151 A70-26841

Airframe structural tests in elevated temperature environment by applied load ratios and room temperature static results 12 p2205 A70-27134

High temperature compressive creep tests at constant stress, describing strain measurement techniques and servocontrolled compressive equipment 12 p2206 A70-27214

Metals thermal properties simultaneous determination at high temperatures, describing measuring equipment operation and circuitry 12 p2206 A70-27219

Materials absorption coefficients determination at high temperatures based on spectrophotometric analysis of emission from samples of different thicknesses 12 p2331 A70-27305

Congruent vaporization rates of niobium monocarbide phase at high temperatures in vacuum, using method of least squares 12 p2254 A70-27320

Grain boundary grooves growth kinetics in pure CoO at high temperatures, determining diffusion species and mechanisms 12 p2255 A70-27603

Molten lithium sodium carbonate electrolyte decomposition and evaporation at high temperatures in various atmospheres, noting water and carbon dioxide additives effects 12 p2166 A70-27763

Shock ionized xenon electrical conductivity measurement at high temperatures as function of Mach number, noting equilibrium effects 12 p2281 A70-27807

Vacuum annealing treatments effect on oxidation rate of Co-Cr alloy at high temperatures 12 p2257 A70-28007

Elastomeric seals and sealants selection for SST, describing tests in air, fuel vapors and hydraulic fluids at elevated temperatures 13 p2418 A70-28668

Phase transformations of molybdenum carbide under elevated temperature in vacuum, using X ray and differential thermographic analysis 13 p2433 A70-28852

Hot torsion test for Al alloys workability assessment, noting test temperature and specimen geometry effects on fracture strain values 13 p2436 A70-29816

Interatomic bond strength in solid solutions of Ti-Sn-O with respect to heat resistance at elevated temperatures 14 p2595 A70-30170

Creep properties of torsion-tension metal members subjected to nonproportionate loading at high temperatures 14 p2656 A70-30637

High temperature elastic moduli of slender polycrystalline aluminum rods with elastic waves generated by Q switched laser energy 14 p2595 A70-30638

Alloy high temperature creep and long term strength, determining exponential relations between stress, strain rate and durability 15 p2755 A70-31529

Measuring apparatus for cyclic plastic strains at high temperatures, discussing data processing techniques 15 p2733 A70-31538

Eutectic NiAl-Cr structure and high temperature tensile strength as function of solidification rate 15 p2755 A70-31560

Electrical conductors specific heat measurement at high temperatures, using optical techniques and digital systems 15 p2826 A70-31942

Graphite Shore hardness measurement at high temperature on Joule heated specimens, describing apparatus and procedure 15 p2764 A70-31944

High temperature metal fatigue crack growth monitoring by ultrasonic detection (SESA PAPER 1622) 15 p2744 A70-32321

Stainless steels creep behavior under long term tensile loads at high temperature 15 p2764 A70-32898

Massive eutectic and fine gamma phases precipitation in cast nimonic 100 alloy at 900 C aging 16 p2930 A70-33083

Al-Mg alloys creep characteristics dependence on Ag, Si and Zn additions during aging heat treatments, establishing activation energy and stress exponents 16 p2930 A70-33086

Polycrystalline NaCl-KCl solid solution alloy, considering high temperature creep under constant compression stress 16 p2961 A70-33275

Low cost flame retardant high service temperature glass reinforced electrical grade laminate tested for continuous use 16 p2935 A70-33355

Iron, Ni, Cr and Co corrosion and mass transfer in high temperature Na, examining properties of stainless steels and cobalt base alloys 16 p2933 A70-34209

Ti alloys embrittlement, investigating time temperature dependence of brittle subsurface layer formation during elevated temperature air exposure 17 p3112 A70-34365

Ti-Al-Sn-Zr system high temperature creep strength and ductility retention 17 p3120 A70-34424

Oxidation and atmospheric contamination protective coatings for high temperature materials, using burner ring tests 17 p3127 A70-34519

Pure Fe and Ta hot hardness using ultrahigh temperature hardness tester 17 p3124 A70-34659

Cyclic strain effects on creep for steel at elevated temperatures, discussing overload frequency effects on plastic strain buildup 17 p3127 A70-35719

Grain boundary allotriomorphs growth mechanisms in Al-Cu alloy at high temperatures, indicating interfacial and direct volume diffusion 18 p3271 A70-36027

High temperature reaging in Ni-Cr-Ti austenitic steel following reversion and interrupted quenching 18 p3274 A70-36054

Ceramic materials for low cost high inlet temperature gas turbine engine components [ASME PAPER 70-GT-105] 18 p3279 A70-36889

Welded Al plates high temperature bend tests, describing materials and procedures 18 p3278 A70-37115

Plastic deformation in Ni-Cr-Nb alloy precipitation hardened at different long terms of high temperature 19 p3451 A70-37706

Sulfidation kinetics and scale morphology of Cr and Cr-Mo alloys at high temperatures in hydrogen/hydrogen sulfide atmosphere 19 p3452 A70-37827

High temperature convective heat transfer in vortex chamber as function of Reynolds number and geometry, measuring pressure variations 19 p3552 A70-38186

High temperature transducer for engine vibration measurement, discussing piezoelectric accelerometers mechanical design, jet engines material evaluation, crystallographic considerations, etc 19 p3430 A70-38527

High temperature acoustic waves, examining solid and fluid properties, weld integrity nondestructive material tests and nondisruptive process measurement 20 p3628 A70-39170

High temperature endurance strength of temper finished bolt connections under cyclic loads, using programmed fatigue testing machines 20 p3718 A70-39223

Graphites erosion by water and carbon dioxide at high temperatures, using liquid rocket simulator for kinetics study [AIAA PAPER 70-638] 20 p3736 A70-39587

Nb single and polycrystalline thermal properties at high temperatures 20 p3648 A70-39639

Thermal stress and changes in modulus of elasticity and expansion coefficient effects on dynamical properties of turbine disks at high temperatures 20 p3721 A70-39783

Lithium-diffused silicon, investigating heat treatment and electron irradiation effects on electrical resistivity at high temperatures 20 p3687 A70-40164

Al yield surfaces in stress space at elevated temperatures for virgin and prestressed material in torsion 21 p3840 A70-41436

Metal cracking and fracture mechanics under creep conditions at elevated temperatures, discussing notch rupture testing 21 p3937 A70-41437

Surface ablation patterns in subliming materials tested in high temperature structures tunnel 21 p3951 A70-41755

Pure Fe and Ta hot hardness tests by ultrahigh temperature tester involving use of electron microscope 21 p3840 A70-41900

Recrystallized and nitrided Mo alloy microstructure under plastic deformation by tension at high temperatures 22 p4038 A70-43122

Mo microstructure changes at high temperatures, noting polygonization, grain migration and crack propagation during failure 22 p4055 A70-43125

Ti alpha alloy fracture characteristics at high temperatures, discussing strain rates, deformation resistance and grain growth 22 p4056 A70-43343

Strain gage stress measurement under elastic-plastic strain conditions at high temperature 22 p4117 A70-43454

German monograph on refractory materials softening under bending and compression at high temperatures 22 p4061 A70-43742

Mg high temperature creep mechanism in high and low stress regions, using isothermal tensile creep tests 23 p4204 A70-43885

Compressibility, viscosity and thermal conductivity of dense gases, examining high temperature and pressure effects 23 p4222 A70-44431

High speed photoelectric pyrometry of Ta heat capacity at high temperatures induced by pulse heating 23 p4207 A70-44441

Spectral absorption of 2.7 micron water vapor band under various high temperature and pressure conditions, using black body radiation 23 p4220 A70-44444

Boiling point method for alkali metals vapor pressure at high temperatures, estimating data accuracy 23 p4281 A70-44448

Cs high temperature vapor and critical pressure and temperature determination for predicting thermodynamic and transport properties, liquid phase nature and state relations 23 p4281 A70-44449

Cesium high temperature saturated liquid and vapor phase density and critical temperature and pressure 23 p4281 A70-44450

High temperature aluminum species in vapor over solid alumina, determining thermodynamic properties, composition and accommodation coefficient by Knudsen effusion and mass spectroscopy 23 p4281 A70-44451

Extremely high temperature deuterium examination, using coaxial plasma accelerators to determine neutron production and vorticity 23 p4227 A70-44452

Directional emissivity and thermal diffusivity of solids at 1000-3000 K by radiation comparison method, applying to sintered and plasma sprayed Mu, Ta and W 23 p4207 A70-44661

Zr-Cu alloys corrosion resistance in carbon dioxide at high temperatures, noting composition effect on behavior 23 p4208 A70-44875

Servo-hydraulic testing machine for measuring cyclic stress-strain behavior of materials subjected to fatigue and creep at elevated temperature 23 p4178 A70-44912

Atmospheric pressure Ar plasma viscosity measured over heavy particle temperature range 3500-8500 K, using DC wall stabilized cylindrical arc 23 p4229 A70-44983

Impurities and heat treatment effects on W internal friction at high temperatures, considering relaxation processes, recrystallization and microstructure 24 p4357 A70-45227

Ti single crystals plastic deformation in axial compression at high temperatures 24 p4358 A70-45239

Longitudinal phenomena and two phase structures effect on ductility of low carbon steel-chromium subjected to high temperature torsion 24 p4361 A70-46173

Al and liquid Al-Mg alloys oxidation at high temperatures, noting Mg content effect 24 p4361 A70-46174

High temperature solar furnace for investigating heat resistant protective coatings thermal stability 24 p4350 A70-46331

HIGH THRUST

Analytical method for design of supersonic flow and maximum thrust nozzles for chemically reacting gases, noting surface geometry [AIAA PAPER 70-129] 06 p0971 A70-18108

HIGH VACUUM

Thin high vacuum gate valve design for use with UV grating spectrograph 19 p3357 A70-37687

Arc welding in space under high vacuum weightless conditions, describing equipment design and Soyuz 6 experiments 19 p3436 A70-37803

HIGH VACUUM ORBITAL SIMULATOR

Thermal vacuum simulator for testing manned Lunar Module Test Vehicle, using conformal skin heaters to control heating rates and skin temperature 09 p1656 A70-23241

HIGH VOLTAGES

High sawtooth voltage generator with semiconductor triodes, giving circuit parameters and diagrams 16 p2873 A70-33212

High voltage MOST silicon integrated circuits, using dielectric isolation and field plate techniques 21 p3798 A70-41214

High voltage solar array with integral power conditioning, discussing weight factors, panel design and layout, mechanization, performance prediction, etc [AIAA PAPER 70-1158] 21 p3759 A70-41787

High voltage solar array operational problems in earth orbit environment, discussing conducting surfaces, power loss, plasma effects, leakage, etc 22 p3967 A70-43544

HIGHWAYS

Urban development detection by remote sensing imagery of highway and rail linkage 12 p2216 A70-26908

Spaceborne photography for detecting and identifying road networks, using color separation plates and photograph enlargement 12 p2216 A70-26910

Multipolarized radar imagery for detecting high return linear cultural features in geographic areas including channel markers, bridges, railroad and power-line networks, etc 12 p2228 A70-26911

Short haul transportation needs in multimodal transportation systems planning, discussing modeling in Northeast Corridor Project [AIAA PAPER 70-1265] 24 p4431 A70-45925

HIJACKING

U AIR PIRACY

HILBERT SPACE

NT BANACH SPACE

Solution existence of linear unsteady Boltzmann equation for single space variable in Hilbert space defined by scalar product 01 p0143 A70-10673

Residual stress determination in elastoplastic body with known plastic strains, using Hilbert space for symmetric tensor fields 01 p0209 A70-11399

Causality and analyticity related for case of separable complex Hilbert space, using algebra characterization of causal maps 03 p0461 A70-14168

Hilbert space stability theory over locally compact Abelian groups developed to obtain spectral theory and positivity conditions 03 p0461 A70-14169

Self adjoint boundary value problems with interior point boundary conditions using differential operator in Hilbert space 05 p0876 A70-16423

Multidimensional stochastic approximation theorems useful for infinite-dimensional Hilbert space or Banach space 07 p1324 A70-19029

Hilbert transform as operator in function space defined on harmonic analysis groups, noting application to noise stability, modulation and signal detection 07 p1235 A70-19644

Operator originated by Schroedinger equation having inhomogeneous boundary conditions on portion of boundary of Hilbert spaces orthogonal sum, defining region of self conjugation

13 p2442 A70-29514

Mixed boundary value problems for pseudoparabolic partial differential equations solved in Hilbert space, demonstrating solution existence and uniqueness

14 p2599 A70-30635

Radiation patterns Hilbert spaces for solving inverse problem of antenna theory

19 p3386 A70-37438

Approximate bounds for differential eigenvalues of self adjoint linear operators in Hilbert space

23 p4211 A70-44245

HILBERT TRANSFORMATION

Transverse nonrecursive digital filters for Hilbert transformation, investigating ideal quadrature filters with Chebyshev approximation errors

05 p0822 A70-16772

Hilbert transform as operator in function space defined on harmonic analysis groups, noting application to noise stability, modulation and signal detection

07 p1235 A70-19644

Computational load reduction in aircraft tracking, comparing sensitivity and Hilbert norm methods

11 p2025 A70-26212

Soviet book on conjugate functions and trigonometric series covering Hilbert transform, Fourier series properties, Cesaro methods, etc

19 p3459 A70-38799

HILL CURVES

U HILL METHOD

HILL DETERMINANT

Phase plane method for Hill equation in problems involving EM wave expansion in elliptical waveguides or single circuit parametric systems analysis

18 p3227 A70-36424

Dynamic systems stability with periodically varying parameters analyzed by Hill type infinite determinant, exemplifying helicopter rotor aeroelastic stability in forward flight

23 p4220 A70-44556

HILL METHOD

Polymers yield criterion determination using Hill method exemplified by polyvinyl chloride, discussing effects of transversal anisotropy and rheological properties

02 p0320 A70-11740

Planetary motion zero-rank effects numerical integration, using Hill secular perturbation method and trace of dyadics

14 p2639 A70-30704

HILLER MILITARY AIRCRAFT

U MILITARY AIRCRAFT

HILSCH TUBES

State and velocity distribution measurements for air in counterflow vortex tube to determine axial variation of flow quantities

05 p0831 A70-15884

Optimum low temperature two circuit vortex refrigerator using compressed air precooled in heat exchanger

22 p3965 A70-42808

HINDRANCE

U CONSTRAINTS

HINGE MOMENTS

U TORQUE

HINGED ROTOR BLADES

U HINGES

U ROTARY WINGS

HINGLESS ROTORS

U RIGID ROTORS

HINGES

Rotational stability of spacecraft with hinged inelastic rods determined in first approximation from motion equations

04 p0759 A70-14426

High speed compound helicopters with rigid and hinged rotors noting features, advantages and construction

05 p0794 A70-16351

Matrix method for calculating aerodynamic loads, shearing forces, bending moments, torques, etc, in hinged main rotor helicopter blades during hover and vertical flight

06 p1167 A70-17914

Dynamic synthesis of hinged four-element mechanism with respect to driven link position, transmission relations and allowance for transmission angle

11 p1983 A70-25934

Rotational stability of spacecraft with hinged inelastic rods determined in first approximation from motion equations

13 p2503 A70-28451

HIPPOCAMPUS

Direct links existence between rabbit temporal cortex neurons and neurons in each division of hippocampus, discussing topographic arrangement and axons quantity

03 p0417 A70-13071

Small amplitude discharges and neuron activity in dorsal hippocampus of cats recorded simultaneously with pyramid cell activity

04 p0632 A70-15221

Hypothalamus stimulation effect on electrical activity of hippocampus at threshold and super-threshold levels in cats

08 p1446 A70-21448

Hippocampus nerve cells protein fractions synthesis in rats, noting relation to learning process during transfer of handedness

12 p2172 A70-28217

Conditioned reflex type fear reaction by electric stimulation of hippocampus in cats

14 p2535 A70-30184

Sleep-wakefulness cycle electroencephalogram of auditory and visual portions of neocortex and hippocampus activity in cats, using spectral analysis and integration

14 p2536 A70-30185

Desynchronized sleep phase in cats, discussing activation and hippocampal theta and hippocampal delta rhythm predominance stages

20 p3574 A70-40171

Peripheral stimulations of various modalities effect on neurons impulse activity in hippocamp dorsal area of rabbits, noting excitation and latent periods

23 p4145 A70-44311

Mesencephalic reticular formation influence on threshold stimulation of cortex, hippocampus, amygdala, thalamic nuclei and caudatum in rabbits

24 p4300 A70-45839

HISS

VLF and LF auroral or polar hiss as generated by incoherent Cerenkov radiation from high energy electrons

07 p1264 A70-19190

Outer radiation belt high energy electron fluxes correlated with VLF hiss ground observations

07 p1367 A70-19498

Outer radiation belt high energy electron fluxes correlated with VLF hiss ground observations

15 p2795 A70-32743

VLF radiation observation at conjugate points, discussing hisses, choruses and geomagnetic effects

19 p3416 A70-38587

Lower hybrid resonance frequency propagation ducts in multiton upper ionosphere, showing association with VLF hiss bands

20 p3584 A70-39331

HISTAMINES

Cerebral histamine distribution in rat brains, noting highest concentrations in hypothalamus and thalamus

01 p0020 A70-10708

HISTIDINE

Quantitative gas-liquid chromatography of histidine, using N-TFA n-butyl ester derivatives and histidine converted trimethylsilyl derivative

22 p3983 A70-43524

HISTOGRAMS

Physiological data analyzer modification for simultaneously estimating scaled interval histograms /SIHs/ written in one memory subgroup

14 p2542 A70-30799

Radio sources angular dimensions estimation based on shifts in histograms of scintillation quasi-periods

19 p3525 A70-38766

Stellar axial rotational velocity statistical analysis to break-up limit, obtaining velocity distribution approximation from observed histogram

23 p4251 A70-44823

HISTOLOGY

Phosphopentomutase activity in rabbit tissue, reporting probable PG-mutase subsidiary function and activity of previously unrecognized enzyme

01 p0012 A70-10091

Vascular anatomy correlation with human heart conduction tissue structures to study coronary artery disease cases exhibiting major conduction disturbances by ECG

01 p0013 A70-10273

Coronary atheroma in hyperlipemic dog occurring in arterial tree at most intense physical stress exposure period, discussing interfacial tissue permeation

04 p0635 A70-15460

HISTORIES

NT CASE HISTORIES

HIVOS [SIMULATOR]

U HIGH VACUUM ORBITAL SIMULATOR

HO-6 HELICOPTER

U OH-6 HELICOPTER

HODOGRAPHS

Mobile hodograph in problem of gyrostat motion about fixed point

01 p0094 A70-11430

Kharlamova solution for solid body motion in Newtonian force field represented as rolling, without slipping, of mobile hodograph of angular velocity vector

01 p0145 A70-11431

Three dimensional picture of wave system of single headed spin detonation constructed by simultaneously considering wave mapping in real and hodograph planes

02 p0278 A70-12028

Compressible flows with circular sector hodographs, discussing Chaplygin equation for simple wedge flow and theorem on sonic jets

04 p0613 A70-14612

Chaplygin equation solution for wedge flows applied to Rethy flows, evaluating drag coefficient and approximate hodograph equations for subsonic and transonic regimes

04 p0614 A70-14613

Approximation for axisymmetric hodograph equation for nozzle calculation

07 p1188 A70-19347

Hodographic determination of required velocity changes for space vehicle transfer orbit, involving only launching point and trajectory plane

08 p1577 A70-21505

Hodograph or Riemann invariants method generalization for nonelliptic systems, discussing three dimensional potential supersonic flows

10 p1863 A70-24087

Riemann invariants, discussing method characteristics in physical and hodograph space applications and multidimensional hyperbolic systems

10 p1865 A70-24103

Chaplygin approximate hodograph method variants diagrams and tables with numerical values for proper application

13 p2442 A70-29486

Hodograph theory for family of almost vertical ballistic trajectories

14 p2617 A70-31355

Baecklund transformations applications to hodograph equations for steady two dimensional nondissipative MGD flows with aligned velocity and magnetic fields

15 p2781 A70-32453

Baecklund type matrix transformations application to hodograph equations system for aligned nondissipative MGD flows

16 p2958 A70-33747

Hodograph equations for relativistic irrotational steady plane flows, investigating transformation to physical plane

19 p3406 A70-38664

Turbine blade profiles calculation by hodographs, obtaining compatibility with continuous flow velocity distribution and improved boundary layer stability

19 p3491 A70-38949

Hodography of compressible fluids three dimensional irrotational isentropic flow

21 p3808 A70-41439

Perfect gas circular subsonic flow around convex obstacle, using hodographic method for boundary problem

22 p3958 A70-42608

Plane transonic flow around airfoils, using hodograph based methods for shock free flow and finite difference methods for flow with shock waves [ICAS PAPER 70-12]

23 p4132 A70-44123

Lifting quasi-elliptical airfoils with supercritical shock free flow, discussing Nieuwland hodograph theory to compute profile number [ICAS PAPER 70-15]

23 p4132 A70-44126

HODOSCOPES

Scintillation counters hodoscopic system for studying spatial distribution of muon and muon-number fluctuations in extensive air showers

03 p0482 A70-13042

Cosmic ray experiment for detecting quarks in low density showers, using hodoscope of wire proportional counters

16 p2972 A70-33048

Cosmic ray muon intensity deep underground vs depth measured with liquid scintillation detector hodoscope

18 p3308 A70-36897

HOHMANN TRAJECTORIES

U ELLIPTICAL ORBITS

U TRANSFER ORBITS

HOHMANN TRANSFER ORBITS

U ELLIPTICAL ORBITS

U TRANSFER ORBITS

HOLDERS

NT FLAME HOLDERS

Biplanar photocell in various holders noting intrinsic properties, emphasizing rise time characteristics

04 p0695 A70-15572

Specimen holder for 300 K/4.2 K resistance ratio measurement

09 p1655 A70-22645

Pressure chamber with inserted holder for adjusting Fabry-Perot interferometer

09 p1681 A70-23337

HOLE DISTRIBUTION [ELECTRONICS]

Edge luminescence effect in doped p-GaAs single crystals with various hole concentrations, determining band structure at liquid nitrogen and room temperature

01 p0154 A70-10097

Four layer semiconductor device triggering by X or gamma radiation calculated by transport equations for electron and hole distribution motion and electric field distribution

04 p0657 A70-14731

- Diffusion coefficient of charged particles in HF stabilization of current-convective instability measured in Ge semiconductor electron hole plasma
07 p1355 A70-20365
- SnTe of various nominal hole concentrations measured for longitudinal piezoresistance effect along different crystallographic directions
10 p1927 A70-23993
- Photon lifetime dependence on hole and electron concentration in GaAs from IR reflection spectra analysis
13 p2470 A70-28882
- Metallic state basic parameters determined by electron transfer technique, discussing ion charges, electron and hole concentrations current scattering cross sections, etc
13 p2433 A70-28886
- Electric field finite amplitude oscillations of electron hole plasma during pinch effect, considering impurities stabilizing effect
22 p4084 A70-43468
- Intraband absorption in p-type GaAs associated with carrier transitions between heavy and light hole in valence band
23 p4232 A70-45066
- HOLE DISTRIBUTION [MECHANICS]**
- Curvature and hole spacing effects on stress concentration of isotropic plate weakened by two curvilinear holes, applying small parameter method
01 p0212 A70-11447
- Two asymptotic dimensional moment theory of elasticity, analyzing stress concentration at curvilinear holes and fluctuating boundary loads
01 p0212 A70-11563
- Error estimates of stress concentration at free hole determined by two dimensional elasticity theory of thick plates
01 p0212 A70-11564
- Al alloy strips weakened by holes, analyzing limiting tensile load-carrying capacity
02 p0384 A70-11741
- Stress state of brittle alloy turbine disks with eccentric hole distributions, studying stress concentrations, hole number effects, etc
03 p0588 A70-13243
- Shells with holes using Neumann method, obtaining Fredholm alternative for singular integral equations
03 p0589 A70-13347
- Spherical shell elasticity having circular hole at apex using asymptotic method, calculating stress concentration at hole
03 p0590 A70-13381
- Stress-strain state of infinite isotropic perforated plate under cyclic symmetry, assuming finite strains and nonlinear material
03 p0592 A70-13445
- Membrane stress concentration near circular cutouts in uniaxially stressed sheets reduced by predeforming immediate surroundings of hole
05 p0940 A70-16515
- Plane and cylindrical elastic waves dynamic characteristics propagating in half space with holes, reducing boundary value problem and deriving formulas for interacting waves
05 p0946 A70-16858
- Stress concentration of circular cylindrical shell weakened by elliptic hole under torsion
05 p0947 A70-16965
- Effect of uniformly distributed circular holes in infinite double row on stress distribution in transversely bent strip, based on Kirchhoff bending theory
07 p1407 A70-19385
- Boundary value problems solution for infinite elastic isotropic plane weakened by arbitrarily distributed circular holes based on using series in Taylor functions
07 p1408 A70-19549
- Hole reinforcement in flat plate under uniaxial load with high stress region at boundary, resulting in weight savings
07 p1414 A70-20174
- Stressed state in region of strain raisers /round holes/ in plate subjected to two axial tension associated with plastic yield
09 p1771 A70-22464
- Thermal stress concentrations at arbitrary holes for nonlinearly elastic materials, developing small deformation theory for two dimensional problem
09 p1779 A70-23093
- Stress analysis for cylindrical shells with reinforced circular holes by collocation method
09 p1781 A70-23280
- Stress concentration at elliptical hole of arbitrary eccentricity in shallow sandwich shells with hard and soft fillers
09 p1783 A70-23385
- Stress distribution in strip with asymmetrically positioned infinite row of equal and equally spaced circular holes subjected to longitudinal tension or transverse bending
10 p1955 A70-24082
- Stresses in dynamically loaded struts with one or three holes by photoelasticity, using Fastax camera
12 p2315 A70-26878

- Plane periodic diffraction of elastic waves propagating in medium with infinite sequence of circular holes
12 p2325 A70-27557
- Stress concentration in fiberglass reinforced plastic composite cantilever cylindrical shell in round hole region subjected to concentrated load on free supported end
12 p2328 A70-28286
- Critical loads for brittle bodies weakened by sharp holes under combined diffuse thermal fluxes and crack crossing
12 p0000 A70-28321
- Stress concentrations and optimum shape minimum-weight reinforcement of circular holes in plates determined by polarization-optical technique
13 p2512 A70-28864
- Thermoelastic stresses in sphere with cylindrical cut under axisymmetric temperature field and constant surface temperature
14 p2655 A70-30135
- Shells with holes using Neumann method, obtaining Fredholm alternative for singular integral equations
14 p2657 A70-30721
- Surface heat transfer coefficients under perforated plate of multiple square array round impinging air jets [ASME PAPER 69-GT-4]
14 p2666 A70-31025
- Strength and critical load determination for spherical shells with reinforced hole under internal pressure based on stress-strain state analysis during deformations
15 p2814 A70-31543
- Stress analysis of polystyrene plate weakened by doubly periodic system of equal circular holes
15 p2817 A70-32166
- Stress concentration problems for partially strengthened circular hole in plate under uniaxial tension
15 p2819 A70-32185
- Elastic equilibrium of unbounded body with central hole and concentric cracks under symmetric load
15 p2819 A70-32188
- Stress distribution around oblique holes in uniaxially loaded plate using three dimensional photoelastic analysis
15 p2820 A70-32305
- [SESA PAPER 1618] Membrane and bending stresses at crack tip in cylindrical shell weakened by elliptic hole with major axis perpendicular to shell axis
17 p3186 A70-34981
- Shallow shell theory boundary value problems, calculating stress concentration for domes and shells with holes
17 p3192 A70-35694
- Circular cylindrical shell with round holes along generatrix subjected to internal pressure, determining stress concentration with aid of computer
18 p3335 A70-36131
- Elastic bending of perforated inhomogeneous plane with circular holes or inclusions
18 p3340 A70-36579
- Stress state of brittle alloy turbine disks with eccentric hole distributions, studying stress concentrations, hole number effects, etc
19 p3548 A70-38461
- Aerostatic journal bearings with double plane admission feeder holes, determining maximum load and stiffness by numerical method
19 p3443 A70-38898
- Infinite elastic plate with pair of insulated unequal circular holes, calculating thermal stresses
20 p3720 A70-39672
- Creep and breakdown of thin walled cylindrical shells with circular holes subjected to internal loads at high temperature, discussing time to failure
20 p3721 A70-39777
- Stress distribution at hole in orthotropic cylindrical sandwich shell under internal pressure
20 p3734 A70-40440
- Perforated steel strip axial tension load limit, considering various hole diameters and numbers
21 p3936 A70-41415
- Isotropic nonlinear elasticity problems of stress concentration near spherical cavity in field of triaxial tension, using small parameter method
22 p4120 A70-43714
- Free and supported curvilinear holes with random roughness, investigating stress concentration by conformal mapping
23 p4265 A70-43984
- Anisotropic media weakened by elliptical holes, using doubly periodic solution for stress concentration
23 p4266 A70-43986
- Stress concentration near holes in nonlinear viscoelastic plate, using elastic theory
23 p4266 A70-43989
- Steel and duralumin strips with circular holes tested under axial tension, determining relationship between strength weakening and ultimate stress
24 p4420 A70-45272

HOLE MOBILITY

- Hole mobility in n-type InSb semiconductors determined from solving kinetic equation for minority carriers allowing for scatterings
01 p0155 A70-10185

HOLES

- Spherical shell of variable thickness, calculating stress-strain state around reinforced circular hole during elastoplastic deformation
18 p3336 A70-36138
- Stresses around circular hole in shallow conical shell under torsional load, using perturbations in parameters for curvature and cone angle
21 p3934 A70-40779
- Circular cylindrical hole in uniaxial tension field of elastic media, solving plane strain problem for stress concentration factors
21 p3941 A70-42107
- Cylindrical boreholes as reference defects in ultrasonic inspection, discussing geometrical parameters effects on echo height
24 p4343 A70-45691
- Infinite plate perforated with rounded corner square hole under uniform partial loading, examining elasticity with conformal mapping
24 p4427 A70-46367
- HOLES [ELECTRON DEFICIENCIES]**
- Energy spectrum of electrons and holes in semiconductors under strong electromagnetic wave field, calculating electron-phonon interaction Green function
01 p0155 A70-10184
- Negative resistance mechanism model with larger electron accumulation in conduction band than free holes
03 p0539 A70-13212
- Kinetic equation of helicons interactions in electron-hole plasma, discussing turbulence spectrum and effect on current carrier drift velocity
03 p0531 A70-13407
- Photoconductivity growth and decay curves green edge emission and integral flux in optical flare of cadmium sulfide crystals due to hole trapping process
03 p0540 A70-13503
- Magnetic field effect on recombination radiation intensity under pinch effect in semiconductor non-degenerate electron hole plasma with recombination time exceeding carrier lifetime
03 p0540 A70-13508
- Electrical properties of Cu-diffused GaAs, studying temperature effects on acceptor concentration and electron population growth
03 p0541 A70-13730
- Electron-hole pair creation in semiconductors /Zener effect and impact ionization/ defined from qualitative study of electron-phonon collisions
10 p928 A70-24624
- Electron-hole transitions in GaAs obtained by sulfur diffusion, noting capacitance dependence on voltage at 293 and 77 K at various frequencies
12 p287 A70-27481
- Degenerate pinch in bipolar electron-hole plasma in semiconductors
13 p2472 A70-29760
- Photoemission of electrons and holes from Al into aluminum oxide, giving approximate energy band diagram of Al-aluminum oxide interface
15 p2783 A70-31759
- Average triton energy required to produce electron-hole pair in silicon measured, describing precision charge calibration of amplifier system
15 p2784 A70-32198
- Pinch effect in degenerate and nondegenerate electron hole plasma in semiconductors during bimolecular bulk recombination
18 p3298 A70-36620
- MOS field effect transistor, measuring electrons and holes thermal emission rates and activation energies at gold centers in Si
22 p3997 A70-43016

- HOLLAND**
U NETHERLANDS

- HOLMIUM**
- Spectral emission in trivalent Ho doped Yb-Al garnet single crystals grown by optical zone melting
15 p2784 A70-32198

- HOLOGRAPHY**
- Holographic interferometry as stress analysis technique for crack propagation studies, discussing advantages over classic interferometric and conventional photoelastic methods
01 p0198 A70-10002
- Holographic relationship of coherent optical processing applications to coherent or side-looking radar, discussing seismic holography concept
01 p0086 A70-10414
- Microwave holography, discussing zone plate lens design, coherent side-looking radar, large antennas, three dimensional radar display applications
01 p0086 A70-10415
- Optical reconstruction of microwave holograms recorded by liquid crystal detectors, emphasizing dependence on IR heat bias provided by incandescent bulb
01 p0086 A70-10421
- Holographic spectroscopy design and development, discussing components and recording yellow Na doublet
01 p0087 A70-10659

Holographic interferometry for determining optical path variations resulting from photographic plate emulsion thickness and refractive index changes during development
01 p0087 A70-10666

Ultrasonic holography in nondestructive testing, discussing metal block with simulated defects
01 p0089 A70-10882

Holographic techniques for extended high resolution images with resolved elements less than 0.5 micron in image field of 10 cm or more
01 p0090 A70-10886

Holographic two beam real-time Fizeau interferometer for recording and reconstructing reflected light waves in silvered flat surfaces measurement
01 p0090 A70-10905

Interference fringe in Fraunhofer hologram reconstruction of tapered glass fibers related to fiber profiles
01 p0090 A70-10906

Fourier transform applied to power spectral distribution determination for two dimensional Fraunhofer holographic data of thin spherical lenses
01 p0090 A70-10907

Holographic color schlieren flow visualization system for three dimensional photography, variable focus shadowgraph, knife edge schlieren, etc
01 p0091 A70-10908

Book on coherent optics and holography covering image restoration, holographic interferometry, lensless Fourier transform holography, etc
01 p0144 A70-11074

IR holography using thermochromic material and cuprous mercuric iodide to record on-axis interference pattern, reconstructing in visible range with He-Ne laser
01 p0092 A70-11170

High resolution silver halide photoemulsions by holographic resolvometry using Ne-He laser to obtain interference patterns
01 p0095 A70-11633

Holograms of light scattered by clouds of water droplets to determine drop size, noting agreement with Mie theory
02 p0296 A70-11890

Diffuse illumination in holography indicating spread increase dependence on product of phase mean-square value and spatial frequency bandwidth
02 p0296 A70-11891

Hologram image resolution, finding angular alignment of reconstruction wavefront as limiting factor
02 p0297 A70-11923

Bleached diffraction gratings produced holographically on spectroscopic plates, describing processing and quality
02 p0297 A70-11929

Anamorphic holograms in optical and radar holography and reconstruction, discussing formation and fundamentals
02 p0298 A70-12182

Optimum procedure for high speed cinematography of holographic interferograms permitting microsecond exposures while retaining picture quality
02 p0298 A70-12213

Sandwich structures nondestructive testing by holographic interferometry, discussing system operation, specimen stressing, acoustic vibration, etc
02 p0309 A70-12274

Photographic relief images with arbitrary profile produced by using image relief height as spatial frequency function
02 p0300 A70-12462

Quantitative interpretation of three dimensional weakly refractive phase objects using holographic interferometry, determining index of refraction
02 p0300 A70-12464

Microwave holography using probe scanning, analyzing causes of distortion and effects on image reconstruction
02 p0302 A70-12618

RF holographic vision through rain, fog or darkness, discussing cholesterol ester-coated Mylar sheets and pyroelectric hot plates detectors and antenna sensory matrix
02 p0305 A70-12843

Holographic interferometry with pulsed ruby laser holocamera for examining flow distribution in supersonic free jet wind tunnel
03 p0480 A70-12948

Holographic interferometry applications in experimental mechanics, illustrating nondestructive testing by flaw detection in bonded honeycomb
03 p0481 A70-12959

Hologram interferometry to study stresses in fixed two dimensional photoelastic models and three dimensional slice qualitative analysis
[SESA PAPER 1530] 03 p0482 A70-12964

Displacement interferograms and schlieren pictures of optical inhomogeneities in transparent media obtainable from single exposure hologram, using monochromatic and laser light for reconstruction
03 p0483 A70-13258

Double exposure holograms in diffuse radiation used to reconstruct in white light interferogram images localized in hologram plane
03 p0483 A70-13259

Interferogram contrast as spatial frequency function measured for photographic materials used in holography by He-Ne laser
03 p0485 A70-13530

Transillumination holography in environmental tests, discussing camera design, particle field and applications, including flow visualization in wind tunnel tests
03 p0486 A70-13539

Three dimensional structure determination for weakly scattering semitransparent objects from holographic data, discussing inverse scattering problem and refractive index calculation
03 p0487 A70-13647

Hologram interferometry accuracy, reliability, application to plate deformation and translation measurements, using moire method and correction factors
03 p0493 A70-13945

Holographic method for measuring optical instruments transfer function, using laser light source and beams interference
03 p0493 A70-13946

Image conversion scheme to obtain holograms of three dimensional objects illuminated with IR light, using nonlinear optics
04 p0685 A70-14406

Real image holography of complex organism or body organs as teaching aid and research tool in medicine and biology
04 p0685 A70-14558

Holographic wavefront reconstruction variants and applications to instrumentation, process engineering and information techniques
04 p0688 A70-14717

Hologram recording materials properties and limitations, discussing diffraction efficiency of thick and thin amplitude and phase holograms, silver and non-silver halide noise effects, etc
04 p0690 A70-15026

Transient hologram recording with fluorescein-boric acid glass organophosphor, noting effects of dye concentration, sample thickness, laser power and excited state lifetime
04 p0690 A70-15027

Dichromated gelatin holographic films preparation, sensitization, exposure and development, giving diffraction efficiencies and reconstruction SNR
04 p0691 A70-15031

Wave front reconstruction for perfectly bleached holograms not achievable by simple coherent illumination due to remaining amplitude variation
04 p0691 A70-15033

Holographic technique for transferring phase perturbation of subject waves onto spherical waves focusable through aperture and examinable by interferometric and schlieren methods
04 p0691 A70-15034

Image formation from wave front sampling in holography by spatial filtering, comparing Monte Carlo sampling to spaced sampling
04 p0692 A70-15365

Scaling and angular resolution for sequential type holographic stereogram, comparing results with conventional hologram
04 p0695 A70-15574

Information transmission capability of hologram without distortion, considering confocal resonator reconstructible transparencies for bounded hologram
05 p0848 A70-16265

Object visualization in phase contrast using nonlinear interferential holography by successive recording of intensities on photographic plate
05 p0848 A70-16273

Standing wave ratio of ultrasonic field determined by holographic method, using acoustic transmission lines with termination impedances
05 p0848 A70-16403

Gabor holography producing interference phenomena, discussing far field fringes, circular fringes, diffuser, etc
05 p0849 A70-16529

Hologram constructed with microwaves with image reconstruction at optical wavelengths using laser
05 p0849 A70-16659

Holography by fixing detector and scanning source based on reciprocity theorem for diffraction field
05 p0849 A70-16677

Optical wave front reconstruction principles applied to sonic and seismic wave holography for mapping earth subsurface structure
05 p0850 A70-16685

Double giant pulse ruby laser with 1.5 m coherence length for producing double exposure holograms of stress wave propagation in solids
05 p0861 A70-16850

Aircraft visual flight control displays development, considering liquid crystals in alpha numeric data output devices and holograms for three dimensional structures reproduction
05 p0853 A70-17090

Holographic method for reconstructing polarization of light emitted by photoelastic model, obtaining isochromatic and isoclinic fringe patterns
06 p1063 A70-17643

Image contrast in holographic reconstructions, discussing influence of given surface intensity recording and oblique reference wave on hemigram
06 p1067 A70-18398

Holographic interferometry applied to amplitude measurement of periodic mechanical surface vibration
06 p1069 A70-18436

Hologram storage and retrieval in photochromic SrTiO crystals at ruby laser wavelengths
06 p1072 A70-18519

Bleach process giving high efficiency low noise holograms using potassium ferricyanide, noting drying procedure and developer
06 p1072 A70-18520

Nonlinear system theory for optimal linearization in holography, discussing generalized method for photographic emulsion and first order amplitude transmittance
06 p1072 A70-18521

Optical properties of Gabor holograms with pure reference beam, discussing image reconstruction using He-Ne laser
06 p1072 A70-18565

Holography history and applications to interferometry, contour mapping and three dimensional photography
07 p1279 A70-18900

Diffraction gratings produced by holographic techniques and vacuum metallization to provide high performance
07 p1279 A70-19049

Body displacement and deformation measurement by fringe separation in holographic interferometry
07 p1280 A70-19143

Hologram interference fringes formation and location using grating model of diffusely reflecting surface
07 p1280 A70-19144

Multiple beam interferometer coherence analyzer for temporal and spatial study of laser beams, emphasizing application to pulsed lasers, holography and nonlinear optics
07 p1297 A70-19145

Holographic recording of information contained in evanescent wave fields in high resolution photographic emulsions
07 p1281 A70-19367

Book on lasers and holography covering coherence, wave diffraction, zone plates, etc
07 p1282 A70-19598

Book on holography principles and applications, discussing imaging properties, coherence, photographic emulsions, optical analog computers, etc
07 p1283 A70-19739

Holography without reference beam for two and three dimensional interferential wave front recording and reconstruction
07 p1285 A70-19858

Holographic recording and reconstruction for wide angle three dimensional displays noting limitations
07 p1287 A70-20085

Holo-diagrams for simplified evaluation of amplitude and direction displacement in double exposed holograms for interferometric measurements
07 p1287 A70-20086

Front lit holograms of transient events and live subjects obtained with reflected light pulsed laser system
07 p1287 A70-20087

Holograms produced with pulsed argon-ion lasers operating in singly oscillating transverse modes
07 p1287 A70-20088

Holograms in thick absorption recording media in terms of diffraction efficiency, angular orientation and wavelength sensitivities
07 p1287 A70-20093

Optical data processing systems with spatial filters for two dimensional signals detection, using film nonlinearities to record Fourier transform hologram
07 p1287 A70-20094

Holographic system to obtain time-bandwidth product improvement in spectral analysis without sacrificing multichannel processing capability
07 p1288 A70-20098

Zoom effect in magnification of reconstructed image in incoherent holography achieved by varying fringe scale via rotation of interferometer components
07 p1288 A70-20099

Word organized photodetector array design for holographic read-only optical memories
07 p1288 A70-20148

Laser focused hologram reconstruction in passing white light
07 p1289 A70-20320

Coherence improvement of ruby laser emission in free mode using corrective holograms in resonator
07 p1303 A70-20323

Holography for visualization and analysis of aerodynamic flow fields in wind tunnel experiments, recreating events in space and time
08 p1493 A70-20650

Light beam deflection for three dimensional fixed and time varying visual displays, discussing mechanical, acousto-optic, electro-optic, digital and holographic techniques

08 p1449 A70-20673

Holographic technique of coherent light field transformation with desirable phase distribution from laser light beams of arbitrary wavefront characteristics

08 p1497 A70-21410

Holographic pulse compression technique employing amplitude modulation to circumvent need of matched filter in chirp process

08 p1498 A70-21593

Laser display systems, discussing mechanical, diffractive and refractive beam deflection techniques, electro-optical polarization devices, holographic displays, etc

08 p1499 A70-21687

Scattered field amplitude and phase determined from hologram light intensity distribution, noting biological applications

08 p1500 A70-21786

Hologram data efficiency improvement by spatial offset removal, analyzing plane and spherical reference waves and plane and solid objects

08 p1500 A70-21787

Interferograms taken by phase difference amplification technique with nonlinear hologram, considering amplified image accuracy

08 p1500 A70-21788

Reconstructed holographic image complex amplitude expression derived, showing effects of film optical transfer function, size and shape

08 p1500 A70-21789

Holographic image reconstruction analysis based on two beam interferometry by spatially incoherent light source, obtaining optical transfer function

08 p1514 A70-21790

Hologram spatial bandwidth reduction by space-time multiplexing

09 p1673 A70-22074

Plasma discharge studies by holographic interferometry using ruby laser pulse for light source

09 p1674 A70-22171

Holography in terms of photogrammetry, reviewing interferometry role, wave construction and reconstruction, etc

09 p1674 A70-22260

Pulsed microwave spectrum analyzer using holography and Fourier spectroscopy compared with frequency methods

09 p1675 A70-22485

Photographic image reconstruction of spatially incoherent illuminated object using twofold holography

09 p1675 A70-22486

Real time hologram-interferometry application to optical aspheric surfaces testing explained by geometrical optics

09 p1676 A70-22717

Photographic emulsion nonlinear response effect on image quality, discussing holography for multiple exposures

09 p1676 A70-22718

Holographic recording of three dimensional rapid events, using Q switched laser pulses with sufficient coherence length for illumination

09 p1676 A70-22786

Inexpensive live stroboscopic holographic interferometry, discussing time averaged and stroboscopic methods

09 p1676 A70-22787

Holographic recording of Q switched neodymium laser beam achieved through lens testing on reconstituted beam

09 p1697 A70-22845

Two beam Fraunhofer holography noting effect of spatially coherent source

09 p1678 A70-22968

Stetson-Powell time fringe hologram technique of vibration analysis applied to nodal patterns in compressor blade and turbine disks

09 p1679 A70-22979

Rig using holographic techniques for vibration testing and aircraft engine components inspection

09 p1680 A70-23069

High resolution holography with pulsed radiation source, testing various emulsions for sensitivity and reciprocity behavior

09 p1681 A70-23175

Transient partially ionized plasmas observation by two wavelength holographic interferometry, describing electron density measurements

09 p1736 A70-23186

Sensitivity of nondiffuse double exposure holographic interferometry with transparent medium increased via multiple beam passage through medium placed in optical cavity

09 p1682 A70-23360

Computer-generated holography involving three dimensional object perspective projections computation for incremental rotations

09 p1683 A70-23529

Edge smear in far field holography as function of interference orders, using short-cut trace technique

09 p1684 A70-23532

Holographic 3D movie of front-lighted opaque objects, recording diffuse reflection with CW laser and high resolution film

09 p1684 A70-23533

IR holograms real time visual reconstruction by frequency stabilized carbon dioxide lasers

09 p1684 A70-23534

Velocity synchronized Fourier transform hologram camera system for recording hypervelocity particles

09 p1688 A70-23775

Holographic optical memory feasibility for digital data storage using Ar ion laser, acousto-optic beam deflector system, hologram storage plane and photodetector array

09 p1642 A70-23780

Holographic flow visualization system retaining all information in light wave passing through flow field, noting reconstruction as shadowgram, schlierens or interferograms

09 p1689 A70-23781

Motion picture holography using continuously pumped ruby laser illumination system in repetitive Q switched mode

09 p1689 A70-23782

Longitudinal distortion reduction in ultrasonic holograms

09 p1689 A70-23805

Holography application in engineering, discussing strains and distortions detection, vibration testing, design optimization, etc

10 p1887 A70-24198

Spatial frequency spectra of three dimensional phase object and three dimensional hologram, discussing interaction characteristic for monochromatic illumination

10 p1888 A70-24263

Lens aberrations compensations in partially coherent image holography

10 p1891 A70-24838

Hologram resolution and information storage along depth of reconstructed image related to maximum track density of bubble chamber

10 p1892 A70-25113

Holographic optical memory systems operational principles and potential advantages, discussing feasibility of 100 million bit memory capacity and one microsecond random access time

10 p1892 A70-25245

Image contrast and diffraction efficiency of dielectric hologram made from diffuse signal beam, bleaching photographic emulsions

11 p2048 A70-25359

Structural detail in transparent object through holographic measurement of scattered monochromatic light, noting similarity to crystal structure reconstruction in X ray diffraction experiments

11 p2048 A70-25360

Transient and steady state thermal stresses measured by holographic extension of photoelastic analysis

11 p2049 A70-25592

Photoelasticity stress analysis, determining principal stress differences and orientation, using holographic interferometry to obtain sum and separation

11 p2049 A70-25596

Real nonnegative function representing transmittance of computer synthesized Fourier transform hologram displayed on flying spot scanner and recorded on film

11 p2049 A70-25631

Random phase mask for Fourier Transform hologram recording of data mask, noting minimum space bandwidth required

11 p2049 A70-25637

Holographic compensation for atmospherically induced phase distortion of IR laser beam

11 p2049 A70-25638

Scanned beam holography reducing system stability time for hologram production with CW gas laser

11 p2050 A70-25639

Holographic dielectric gratings analyzed by Raman-Nath formalism modified for losses

11 p2050 A70-25640

Recording nonlinearities effect on image reconstruction from hologram of diffuse object

11 p2050 A70-25641

Modified holographic technique for three dimensional display of X ray pictures

11 p2050 A70-25644

Laser-light spatial-domain scanning function for deconvolution of blurred photographs using point-spread and holographic Fourier transform division filter

11 p2050 A70-25832

Pulsed laser holographic interferometry of density field created by high speed projectile motion in air [AIAA PAPER 69-347]

11 p2051 A70-25987

Microwave illuminated aperture near radiation field mapped and processed for microwave hologram suitable for optical imaging for far field pattern simulation

11 p2051 A70-26025

Moiré-holographic technique for deformed plane spatial displacements determination, describing diffraction patterns generation and stress analysis

11 p2140 A70-26487

Spatial domain deconvolution by laser scanning of blurred photographs, using holographic Fourier transform division filter and photoelectric integration

12 p2230 A70-26979

Blurred photographic image restoration by combining computer generated holographic phase and photographic amplitude filters

12 p2230 A70-26981

Holographic dynamic head-up display system for aircraft carrier deck landings in low visibility

12 p2232 A70-27371

Brightness distribution in hologram generated image modulated by square of temporal-spatial coherence modulus of laser emitting longitudinal and transverse modes

12 p2233 A70-27503

Wave fronts averaging by holographic technique to eliminate distortions arising in inhomogeneous media

12 p2233 A70-27504

Holograms formation without reference beam by illuminating transparency with coherent laser light

12 p2233 A70-27505

Transmission diffraction grating for astronomical applications constructed holographically with laser light and photoresist films

12 p2234 A70-27589

Plasma diagnostics by high sensitivity holographic interferometry

12 p2235 A70-27794

Coherent light holographic and incoherent interferometric imaging analogy, noting three dimensional image formation

12 p2236 A70-28120

Mutual coherence functions for quasi-monochromatic illumination measured by image holography

12 p2237 A70-28124

Holographic identification of similar two dimensional images by linear transformation of space by spherical lens using white light correlator

12 p2238 A70-28185

Holographic method for recovery of complete image/ghost/ from partial hologram and entire diffraction picture

12 p2238 A70-28186

Holographic achromatic reconstruction of laser holograms in transmitted white light using zonal plate

12 p2238 A70-28297

Holographic method for reconstructing polarization of light emitted by photoelastic model, obtaining isochromatic and isoclinic fringe patterns

13 p2405 A70-28726

Holographic memory devices design for information storage

13 p2405 A70-28792

Field distribution determination in holographic image space, obtaining ideal image and aberration terms

13 p2405 A70-28826

Laser beam photography utilization in engineering for optical pointers, interferometers and holographic visualization of surface strain and vibration

13 p2406 A70-28914

Wavefront reconstruction by holograms of focused images illuminated by white light, analyzing spatial coherence

13 p2408 A70-29364

Interference holograms of low temperature nitrogen plasma jet using fundamental and second harmonic ruby laser emissions

13 p2464 A70-29384

Microwave holography with artificial reference wave and receiver multiplier, improving linear resolution in image

13 p2408 A70-29407

Electronic heterodyne astronomical spectroscopy, using lasers for absolute monochromatic flux and polarization measurements on star-like objects

13 p2408 A70-29473

Hologram interferometry using moiré method to determine bending moments of object surface

13 p2409 A70-29474

Displacement component in chosen direction on deformed object surface, using hologram interferometry with double illumination

13 p2409 A70-29475

Heterogeneous combustion observation by motion picture holography, considering light source requirements and hologram separation at higher sampling rates [WSC1 PAPER 70-10]

13 p2409 A70-29610

Holography patents, books, conference reports and articles, discussing applications to interferometry, portraits, Cassette tv, computer storage, etc

13 p2411 A70-29782

Holographic display requirements anticipating applications to motion pictures and TV

13 p2411 A70-29791

Three dimensional images reconstruction with coherent light, facilitating transmission by holographic information volume reduction

14 p2581 A70-30146

Nondestructive bond inspection by interferometric holography of ultrasonically excited plates

14 p2588 A70-31166

- Off-axis nonlinear holograms, defining spurious distortion and SNR 14 p2588 A70-31206
- Coherent or spatially incoherent light recordings of Fourier transform holograms, investigating resolution cells film grain and signal to noise ratio 14 p2588 A70-31207
- Planar sandwich hologram recording 4 pi steradians with preservations of object spatial perspective by representing entire wave front 14 p2588 A70-31209
- Scattering function and image quality in sharp edge holography using single mode laser, analyzing coherent and diffuse light 15 p2733 A70-31556
- Three dimensional holographic optical imaging system, examining resolution factors 15 p2734 A70-31595
- Hologram superposition on photosensitive surface for multiimage successive recording, examining resolution, SNR, etc 15 p2734 A70-31596
- Photoelastic stress analysis, discussing holographic interferometry for main stresses separation and polyester resins application to birefringence pattern superposition elimination 15 p2815 A70-31809
- Wave front reconstruction from blazed holograms, noting wave front distortion for nonconstant amplitude case 15 p2736 A70-32011
- Holographic technique to record hypervelocity projectile with front light resolution, discussing image blurring 15 p2736 A70-32031
- Hologram camera system recording hypervelocity particles by velocity synchronized Fourier transform method, employing interferometer 15 p2737 A70-32039
- Plotter induced reconstruction errors minimization in computer generated binary Fourier transform holograms 15 p2737 A70-32044
- Holographic interferometry combination with high speed photography, obtaining time resolved record of event 15 p2737 A70-32051
- Scanning technique for allowing whole vibration cycles storage on one hologram 15 p2738 A70-32052
- Holography technique for dual real images reconstruction of transparent objects with all planes in focus 15 p2738 A70-32053
- Wave front multiplexing on spatially distinct area of single piece hologram 15 p2738 A70-32054
- Fringe interpretation in stress-holo- interferometry, emphasizing isopachic-isochromatic interaction effects in photoelastic analysis [SESA PAPER 1642] 15 p2739 A70-32309
- Photoplastic material thickness change from mechanical and holographic measurements, showing correlation with isochromatics during plastic yielding 15 p2821 A70-32314
- Semiclamped strut supported rectangular plate deflection determined holographically, mechanically and analytically [SESA PAPER 1650] 15 p2740 A70-32331
- Fringe visibility and localization in double exposure holographic interferometry of diffusely reflecting flat objects 15 p2740 A70-32340
- Rayleigh type holographic interferometer featuring production method for base pattern of variable fringe density 15 p2741 A70-32438
- Air cell optical phase shifter for holography based on refractive index variation with air pressure 15 p2741 A70-32439
- Holography for nondestructive testing, describing theory, equipment and applications 15 p2742 A70-32779
- Holography without reference waves, describing image characteristics of spherical waves from point source 15 p2743 A70-32893
- Aircraft turbine engine components vibrational testing by holographic interferometry methods 16 p2903 A70-33134
- Holographic data storage for random information display and retrieval in wide range consumer credit network 16 p2903 A70-33135
- Holographic recording of wideband pulsed carrier electric signals in Fourier transform, Fraunhofer, Fresnel and image formats 16 p2903 A70-33136
- Phase modulated holography for inherent noise reduction using thicker recording media, increasing signal beamwidth or beam ratio 16 p2904 A70-33137
- Holographic interferometry for evaluating bond between diaphragm and base in pressure transducer 16 p2904 A70-33138
- Holographic interferometry for moire strain analysis, discussing theory and applications 16 p2904 A70-33149
- Holographic device for satellite attitude determination, providing three axis reference information in analog or digital form from single star field sampling 16 p2946 A70-33158
- Holographic stereo model, comparing stereoscopic perception of phase and amplitude to model consisting of overlapping photos 16 p2908 A70-33228
- Book on holography covering principles, applications, spatial and temporal coherence, interference and diffraction theory and optical filtering 16 p2908 A70-33266
- Turbulent wakes density fluctuations measurement using pulsed laser holographic interferometry in ballistic range [AIAA PAPER 70-727] 16 p2834 A70-33494
- Holocamera holographic system for wide angle panoramic view, discussing dual laser beam illumination, side and top view diagrams, etc 16 p2913 A70-33984
- Optical images from microwave far field /Fourier transform/ holograms, noting carrier fringe dependence 16 p2913 A70-34043
- Hologram image construction by graphical method 16 p2915 A70-34216
- Image distortion in reconstructions from phase only holograms, noting savings in collection and processing of acoustic holographic data 16 p2915 A70-34324
- Holographic techniques, investigating ultrasonic fields in transparent media based on light separation by grating into optical moments 16 p2915 A70-34330
- Time-average holographic interferometry applied to HF transverse vibrations of uniform cantilever beam, noting correlation with Timoshenko beam theory 17 p3083 A70-34961
- Engineering uses of holography - Conference, University of Strathclyde, Glasgow, September 1968 17 p3083 A70-35001
- Holography techniques, discussing fringe pattern formation, various systems advantages and optical elements 17 p3084 A70-35002
- Photographic materials for holography, discussing spectral sensitivity, grain size, resolution, transfer functions, diffraction efficiency, etc 17 p3084 A70-35003
- Holodiagram for making and evaluating holograms for large objects dimension, deformation and vibration measurement 17 p3084 A70-35004
- Holographic interferometry measurements, including low frequency quartz vibration and relaxation effects in materials following strain or impacts 17 p3085 A70-35005
- Computer generated holograms, using binary transmittance for wave fronts and three dimensional images construction 17 p3085 A70-35006
- High speed pulsed ruby laser holography, discussing transmission-reflection holocameras and applications 17 p3085 A70-35007
- Holographic measurement of transient behavior of structures under unsteady or impulsive loading, using pulsed lasers 17 p3085 A70-35008
- Hologram interferometry for measuring surface deformation under force and anisotropy in transparent objects 17 p3085 A70-35009
- Pressure transducer diaphragms displacement measurement by holographic interferometry 17 p3085 A70-35010
- Normally loaded thin plate displacements, bending moments and stresses determined by hologram interferometry and indirect moire and superposition of grilles 17 p3085 A70-35011
- Axially loaded cylindrical shells prebuckling deformation behavior measurement by holographic interferometry 17 p3086 A70-35012
- Hologram interferometry with birefringent objects, showing advantages over polariscope and classical interferometers 17 p3086 A70-35013
- Fatigue and surface crack detection using holographic techniques 17 p3086 A70-35015
- Fraunhofer holography for recording small particles to determine size distribution without disturbing sample 17 p3086 A70-35016
- Vibration measurement by hologram interferometry, discussing wave front reconstruction and fringe theory based on Rayleigh integral formulation of light propagation 17 p3086 A70-35017
- Vibration amplitude measurement by holographic wave front reconstruction 17 p3087 A70-35018
- Engineering components vibration mode studies by time averaged holographic interferometry 17 p3087 A70-35019
- Zero order Bessel function fringe shape measurement for holographic sinusoidal vibration fringes 17 p3087 A70-35020
- Precision components engineering inspection and sonic transducer surface vibration modes analysis by hologram interferometry 17 p3087 A70-35021
- Holographic motion measurement verification of constant velocity, sinusoidal vibration and both, using interferometer 17 p3087 A70-35022
- Partial coherence theory in holography with photogrammetry applications, reconstructing images with fringes representing constant range contours 17 p3087 A70-35023
- Combined lens-hologram system for strain measurements by moire technique 17 p3087 A70-35024
- Shadow moire method for comparing diffusely reflecting component against holographically recorded master shape, noting turbine blade measurement 17 p3088 A70-35025
- Four dimensional recording using synchronous multiple pulse ruby laser holography 17 p3088 A70-35027
- Holographic projection for electronic microcircuit manufacture 17 p3088 A70-35028
- Optimum receiver for acoustical holography using discrete transducers arrays for image conversion 17 p3088 A70-35029
- Acoustical holography with single stationary point detector noting reciprocity between detector and point source illuminator 17 p3088 A70-35030
- Pulsed laser holography for liquid rocket combustion studies, describing apparatus and techniques 17 p3092 A70-35477
- Interferometric holograms of vibrating body via numerical analysis of oscillations amplitude and phases 18 p3258 A70-36303
- Real time holographic reconstruction by electro-optic light modulation through crystal 18 p3258 A70-36312
- Pulsed laser holographic nondestructive testing optimization technique, monitoring honeycomb panel surface temperature during thermal stressing 18 p3259 A70-36754
- Holographic projection to print etching patterns on semiconductor wafers, discussing development, basic principles and uses 18 p3233 A70-36773
- Holographic interferometry applications in stress analysis of photoelastic resins, describing holographic interferometry assembly 18 p3262 A70-37209
- Radio wave holography with unequal reference to signal frequency, recording linear object with superheterodyne receiver 19 p3420 A70-37290
- Efficiency of holographic gratings in instrumental spectroscopy 19 p3421 A70-37360
- Holographic registration of isochromatic and isopachous diffraction patterns of photoelastic birefringent objects, showing stress concentrations 19 p3422 A70-37649
- Holographic interferometry of rapid phase objects by two wavelengths from ruby laser and KDP crystal filter, noting application to dense plasmas 19 p3422 A70-37650
- Equivalent interferometer existence theorem in holography 19 p3423 A70-37830
- Holographic velocity data recording /velocimetry/, discussing axial resolution enhancement by spherical wave illumination 19 p3423 A70-37859
- Pulsed ruby laser holography with coherent light, discussing applications 19 p3425 A70-37886
- Acoustical holography forming optical wavefield analog for nondestructive testing, medical diagnosis, underwater and seismic imaging 19 p3425 A70-37887
- Holographic flow and sound visualization, determining three dimensional density distributions in aerodynamic flows 19 p3425 A70-37888
- Piezoelectric controlled device as standard for holographic interferometry, providing continuously variable subject plate displacement and/or rotation 19 p3425 A70-37890
- Holography, discussing light propagation, basic principles, skew reference wave, diffused illumination interferometry, character recognition, microscopy, high density information storage, etc 19 p3427 A70-38449
- Stress and vibration effects measurement by holographic interferometry, comparing results with direct measurements 19 p3427 A70-38450

Membrane attachment for pressure transducer with help of holographic interferometry, describing optical system 19 p3427 A70-38453

Bubble chamber photography and track image reconstruction by holography, discussing measurement apparatus, accuracy and tolerances 19 p3428 A70-38510

Holographic ultrasonic imager using liquid surface detector for real time imaging of test objects moving through viewfield, discussing nondestructive test applications 19 p3433 A70-38829

Holographic bandwidth reduction by periodic dispersion structures, noting large viewfield and compact data recording 20 p3627 A70-39096

Efficiency, low noise and photochromic effects suppression in bleached silver halide holography with various films 20 p3627 A70-39097

Computer generated holograms production, reducing memory size and plotter resolution 20 p3627 A70-39098

Diffraction-limited scalar image formation with large angle point reference hologram arrangement of arbitrary surface shape, point reference source and object 20 p3628 A70-39131

Water droplet size measurement by forward light scatter holography, evaluating reconstructed wave front by Fresnel transform 20 p3628 A70-39132

Characteristic functions for frequency analysis of fringes obtained by time-average holographic interferometry of generalized time dependent optical phase function 20 p3628 A70-39133

Microwave hologram recording for surface displacement, with laser beam illumination for optical reconstruction of image 20 p3628 A70-39152

Laser holography for nondestructive testing of C composite structures, reducing fringe patterns to radial deformation and surface strain for cylinders and cones 20 p3718 A70-39212

Spacecraft position determination by holographic approach involving single star formation 20 p3665 A70-39422

Double holography on phase objects in diffused light using pulsed ruby laser 20 p3630 A70-39499

Mach-Zehnder interferometer for holographic investigation of inhomogeneities in transparent media, discussing photointerpretation error reduction 20 p3633 A70-39749

Hologram line scattering function dependence on light source spatial coherence, presenting quantitative evaluation, theoretical and experimental data 20 p3633 A70-39760

Optical image hologram production, investigating gas flows around body by means of Mach-Zehnder interferometer 20 p3633 A70-39761

Holographic recording in transparent bodies with optical characteristics changeable under intensive light 20 p3633 A70-39999

Acoustic/microwave/ holography for large masses by crossed linear array of microphones, discussing computer simulation of virtual holograms and image reconstruction 21 p3822 A70-40715

Objective and subjective laser speckle noises in holography, discussing causes and methods of elimination 21 p3835 A70-40716

Two dimensional and volume diffuse signal beam dielectric holograms, calculating and measuring diffraction efficiency and signal to noise ratio 21 p3835 A70-40717

Subsonic air flow around airfoil in wind tunnel, detecting density gradients by pulsed ruby laser holographic visualization 21 p3822 A70-40809

Holographic measurement of general forms of motion based on reconstructed images dependence on coherence 21 p3822 A70-40810

Fraunhofer holography for small spherical particles three dimensional position and velocity measurements 21 p3822 A70-40811

Photographic emulsions and photosensitive materials for holography, measuring noise spectral power density at high spatial frequencies by scattered light method 21 p3822 A70-40812

Rigid cylinder rotation and flexible shaft torsion observation by holographic interferometry 21 p3822 A70-40813

Multiple wavelength desensitized hologram interferometry to extend displacement measurement range 21 p3822 A70-40814

Holography application to marine ecological studies, using laser beam reduction techniques for image recording and reconstruction of large areas and volumes 21 p3823 A70-40821

Holographic interferometry measurements of surface amplitudes distribution under periodic mechanical vibration 21 p3824 A70-40864

Holography application to high capacity permanent memory systems 21 p3825 A70-41125

Holographic photopolymer recording systems, discussing sensitivity, reconstruction, fixing, etc 21 p3829 A70-41926

Time average holographic interferometry of circular plate vibrating simultaneously in rationally related modes 21 p3829 A70-41927

High velocity source and receiver scanning effect on holographic image, observing rotation and distortion 21 p3829 A70-41928

Diffraction theory of sideband holography with transmission objects, discussing geometrical construction of image location and disappearance conditions 21 p3830 A70-41998

Microwave antenna array irregularity location from hologram by optical signal processing, using far field spatial filter 21 p3792 A70-42048

Passive and cooperative active hologram radar extended from stationary coherent radar, considering use in airport surveillance of aircraft 21 p3792 A70-42119

Photographic processing methods for high efficiency low noise phase holograms on silver halide emulsions 22 p4025 A70-42286

Combined hypersensitization and rapid in situ processing for time-average observation in real time hologram interferometry 22 p4025 A70-42321

Holographic recording on n-type Si single crystal surface by photoanodic engraving 22 p4026 A70-42332

Plasma diagnostics by two-beam optical interferometry and holographic techniques, discussing plasma parameter spatial distribution recording insensitivity to radiation and variable sensitivity interferometry 22 p4079 A70-42382

Three dimensional hologram diffractive efficiency measurement by spectrographic attachment 22 p4026 A70-42508

Ultrasonic holography for nondestructive testing, discussing reference beams and analogies to optical and electronic methods 22 p4028 A70-42586

Laser application to nondestructive testing via holography and hologram interferometry 22 p4028 A70-42587

Time average hologram interferometry, calculating light beam modulation effects on fringe loci and localization 22 p4030 A70-42950

Image holography nonlinearities analysis, using photographic film characteristics for phase deviation enhancement 22 p4031 A70-42951

Real time holographic interferometry for flame propagation research, using high speed camera [SMPT PREPRINT 9] 22 p4035 A70-43053

Rotating mirror hologram camera for high speed phenomena, using Q switched ruby laser pulses [SMPT PREPRINT 7] 22 p4035 A70-43054

Acoustic Bragg diffraction for laser light deflection, solving high speed photography and holography motion problems [SMPT PREPRINT 5] 22 p4035 A70-43055

High speed holographic recording of transient events by single shot ruby and Nd-doped pulsed lasers, applying to shock tubes and wind tunnels [SMPT PREPRINT 3] 22 p4035 A70-43056

High speed holographic methods for supersonic phase objects movement and replacement of conventional optical processes in shock tubes, firing tunnels, etc [SMPT PREPRINT 77] 22 p4037 A70-43067

Holographic interferometry sensitivity augmentation by use of nonlinear properties of photoemulsion 22 p4038 A70-43140

Recording of inhomogeneous mutual coherence functions in one hologram by combining image with Fourier/Fresnel/ holography 22 p4038 A70-43151

Doppler effect in interference fringe formation in holographic vibration analysis, discussing path length variation 22 p4038 A70-43152

Cantilever beam transient response measurement by stored beam/real time/ holographic interferometry combined with high speed motion picture photography 22 p4039 A70-43452

Holographic interferometry for study of transparent media, noting application to aerodynamic phenomena [ONERA-TP-851] 22 p4039 A70-43455

Holographic interferometry by backscattering, considering displacement and deformation problems [ONERA-TP-852] 22 p4039 A70-43456

Modulation transfer function applied to optimal holographic nondestructive testing systems, using edge gradient analysis 22 p4039 A70-43520

Nondestructive measurement of elastic and plastic deformation in soldered joints and printed circuit boards by holographic interferometry 22 p4047 A70-43521

Optical read-write mass memory based on holographic storage and light addressable matrix array, discussing significance to computer design and usage 22 p3994 A70-43606

Optical system for read-write holographic memory capable of high storage density 22 p3994 A70-43607

Magnetic holography, considering Faraday and polar Kerr effect reconstructions and potential as computer storage 22 p3994 A70-43608

Integrated ferroelectric photoconductor device for hologram storage, discussing improved phase readout technique for reconstruction 22 p3994 A70-43609

Holo-diagrams for predicting fringe patterns in hologram interferometry caused by translation motion and rotation 22 p4040 A70-43610

Transparent objects holographic interferometry with illumination derived from phase gratings to eliminate laser speckle 22 p4040 A70-43611

Holographic exposure and reconstruction processes, considering illumination beam polarization effects on image brightness 22 p4040 A70-43616

Acoustic and scanned holography for nondestructive testing, showing defects in metal samples 22 p4041 A70-43620

Photographic image deblurring method, using image forming holography and amplitude weighting transparency 22 p4042 A70-43670

Microwave holography coherent radar with improved focusing, applying to side-looking, bistatic, passive and pulse compression radars 23 p4161 A70-43874

Holographic primary and conjugate images properties, considering applications in moving scenes recording and multiple images storage and retrieval 23 p4193 A70-43924

Hologram interferometry as noncontact tool for vibration mode measurements of turbine blade groups 23 p4193 A70-43925

Laser applications in length measurement and holography, describing principles and techniques, modulated laser beams and pulse transit time 23 p4201 A70-43998

Soviet book on holography covering laser characteristics, scatterers for image enhancement, photoemulsion requirements, etc 23 p4194 A70-44100

Three dimensional holographic optical imaging system, examining resolution factors 23 p4195 A70-44279

Hologram superposition on photosensitive surface for multiimage successive recording, examining resolution, SNR, etc 23 p4195 A70-44280

Automatic shutter for recording holograms with laser light, controlling exposure time by photoconductor cell 23 p4197 A70-44472

Hologram rapid sequence recording, using scatter plate holographic system 23 p4198 A70-44947

Focused image holographic interferometry by double exposure with reconstruction in white light applied to flat rotating subject 23 p4199 A70-45058

Holographic interferometry of phase object by double exposure method, showing no effect of photographic emulsion compression on order of interference 24 p4334 A70-45368

Light scatterers use behind phase object in double exposure holography, determining laser radiation wave front dynamics effect on image quality 24 p4334 A70-45461

Turbine compressor blades vibration mode measurements by holographic interferometry 24 p4334 A70-45563

Information theory in physics and engineering, considering data processing, error correction codes, space communication, optical data transmission, noise effects and holography 24 p4379 A70-45616

Optical image reconstruction from holograms, discussing photographic materials resolution, response linearity, spatial noise, etc 24 p4335 A70-45654

Holographic interference pattern interpretation, measuring object rotation 24 p4336 A70-45666

Fourier hologram synthesis using laser point source and Wollaston birefringent prism 24 p4336 A70-45667

Holographic interferometry for NDT inspection of adhesive bonded honeycomb sandwich aerospace structures 24 p4338 A70-45754

Holographic nondestructive testing of laminate structures, honeycomb-bonded panels and rubber-to-metal bonds 24 p4338 A70-45755

Sideband Fresnel and lensless Fourier transform holographic images elongation and contraction 24 p4339 A70-45817

Acoustic holographic system producing two dimensional picture in real time, using stationary linear transducer arrays 24 p4339 A70-46080

Seeding particles motion recording in fluid flow by holographic velocimetry, using optical matched spatial filtering to determine particle location 24 p4340 A70-46350

HOMOMORPHISM

U ANALYTIC FUNCTIONS

HOMEOSTASIS

Compartmented physiological system dynamics by bilinear control model, relating homeostasis to system 15 p2693 A70-32571

Repeated snow cooling effect on heat transfer in white rats during temperature homeostasis recovery after hypothermia 18 p3220 A70-36544

Axiomatic approach to homeostasis, discussing living systems as oscillators with input-output and transit variables in duration and elongation 19 p3365 A70-38411

HOMING

Missile homing on moving target, assuming closing velocity vector angular rate proportional to line of sight 16 p2949 A70-34054

HOMING DEVICES

Design concept and operation of electronically lobed homing system providing commands to pilot for flying aircraft directly to transmitting emergency beacon 06 p0987 A70-17725

Roll induced cross coupling evaluation in two dimensional homing systems based on defining roll transfer matrix 11 p2122 A70-25681

Digital simulation of complex dynamic systems using homing missile as example, basing algorithm on I transforms for linear systems 11 p2013 A70-25692

Tracking of goal seeking attack vehicles, discussing error improvement and destination estimating by tracking station observer 11 p2080 A70-26243

Electronically lobed direction finder homing system for location and rescue of airmen downed on aircraft with emergency locator transmitter 13 p2449 A70-29170

Terminal kinematic variables prediction for missile homing, discussing line of sight angle, rate and acceleration 15 p2773 A70-32525

Homing radar tracking accuracy improvement by glint reduction using frequency diversity [AIAA PAPER 70-992] 20 p3586 A70-39538

HOMOGENEITY

Temperature fields and universal motions in homogeneous isotropic thermoelastic body in absence of body forces and external heat supply 02 p0387 A70-12000

Elastoplastic bending of rectangular plates by finite difference and variational methods assuming homogeneity in elastic region 05 p0946 A70-16962

Additive elements effect on structure and properties of sintered powdery Al-Cr and Al-Fe alloys obtained by atomization method, analyzing homogeneity 09 p1707 A70-23124

Wave propagation in bounded homogeneous elastic anisotropic media solved as sum of eigenvalue and static problems without transform calculus 10 p1915 A70-24058

Book on three dimensional problems of linear elasticity of homogeneous and isotropic solids, discussing prismatic bodies, bodies of revolution, notch effect, etc 12 p2326 A70-27669

Linear theory of homogeneous and anisotropic elastic media with microstructure, establishing reciprocity and variational theorems 13 p2512 A70-28951

Shell homogeneity theory, considering uniform states, spheres and circular cylinders 14 p2600 A70-31280

Homogeneity of commercially pure Ti and Ti-Al-V ingots, discussing oxygen distribution uniformity over cross section 17 p3112 A70-34353

Electron beam welding, explaining high fusion zone homogeneity and weld defect formation by dynamic model 17 p3100 A70-34637

Transient wave propagation in homogeneous anisotropic media, using hyperbolic equations and unitary operator 17 p3137 A70-35607

Homogeneity criteria for semiconductor materials, considering variation coefficient, goodness factor and overshoot density 18 p3298 A70-36468

Isomorphous mixed ammonium perchlorate and potassium perchlorate crystals structural homogeneity by X ray diffraction and differential thermal and thermogravimetric analyses 21 p3784 A70-42262

HOMOGENEOUS TURBULENCE

Burger one dimensional model equation for homogeneous turbulence treated by Fourier transform in space and time, using Bogoliubov expansion method 05 p0833 A70-16331

Anisotropic turbulent energy spectral distribution approximated assuming homogeneous and axisymmetric turbulence with vertical axis of symmetry 09 p1717 A70-22374

Turbulence model with level and scale functions for flows including homogeneous turbulence, logarithmic boundary layer, duct center flow, linear shear layer and viscous sublayer 11 p2035 A70-25685

Homogeneous turbulence multipoint multitime correlations for fluctuating velocity 11 p2036 A70-26014

Energy spectrum of homogeneous isotropic incompressible turbulence, discussing eddy relaxation and direct interaction approximation 11 p2040 A70-26541

Incompressible homogeneous isotropic turbulence velocity expanded in Hermite functionals of Gaussian white noise random function advection by fluid 11 p2040 A70-26543

Nonlinear viscoelastic turbulence model with monotone increasing time scale to predict behavior in homogeneous shear and in pure strain 11 p2040 A70-26544

Homogeneous turbulent velocity effect on magnetic field distribution in electrically conducting fluid with no external source, observing dynamo action 11 p2091 A70-26545

Eulerian space-time correlations of velocity and pressure for universal homogeneous turbulence by separating kinematic convection effects of large eddies from velocity assumption 13 p2386 A70-28645

Propeller in axial motion through homogeneous turbulence, studying forces and moments by statistical analysis [AIAA PAPER 70-549] 13 p2339 A70-29014

Homogeneous isotropic turbulence velocity field space-time variable correlation functions in fluid flow 15 p2719 A70-31487

Initial condition effects on weak homogeneous turbulence with uniform shear, studying energy transfer and dissipation 19 p3403 A70-37537

High Reynolds number isotropic homogeneous turbulence fine scale structure heuristic model, relating spatial intermittency to vorticity generation 20 p3609 A70-39665

HOMOGENIZATION

U HOMOGENIZING

HOMOGENIZING

Metal powder mixtures homogenization time calculation, using Fick equation and matrix model 13 p2433 A70-28845

HOMOLOGY

Optical and radio homologies of solar flares, studying correlation from astronomical telescope pictures 11 p2105 A70-25747

HOMOMORPHISMS

Homomorphic filters, discussing nonlinear filters for generalized linear system 15 p2710 A70-32580

HOMOTOPY THEORY

Homotopic classification of boundary value problems with directional derivatives for harmonic functions 23 p4212 A70-44348

Coupling components in homotopic classification of elliptic systems of second-order equations with independent variable 23 p4212 A70-44349

HONEYCOMB CORES

Attachment loads and beam bending moments design curves for linear and right angle fittings on honeycomb inserts to determine internal loading 02 p0386 A70-11949

Shear modulus of sandwich structure tubular core derived by virtual work principle and matrix approach, comparing results with honeycomb core [DGLR-69-64] 04 p0774 A70-15156

Rectangular waffle plates minimum-weight design efficiency with multiple rib sizes in stiffening direction compared to honeycomb core sandwich construction 04 p0777 A70-15526

Supersonic aerial target wing synthesis using sandwich construction with graphite-epoxy laminate skins bonded to Al honeycomb, achieving significant weight reduction 12 p2160 A70-27118

Potting material applicability to attaching honeycomb sandwich assemblies to structures, describing pre- and postpotting methods 13 p2418 A70-28667

HONEYCOMB STRUCTURES

NT HONEYCOMB CORES

Electrical discharge machining showing close tolerance sizing capability on honeycomb panels 02 p0310 A70-12665

Honeycomb structure fracture initiation flow detection method using liquid crystal determination of stress concentration sites, noting absence of external heat source 03 p0515 A70-13121

Crushable honeycomb regulating operating pressure of propellant actuated devices applied to recovery parachute catapult in F-111 crew module 03 p0546 A70-14108

Honeycomb and sandwich construction design, discussing optimal material selection, filament wound technology, panels fabrication, destructive and non-destructive test methods, etc 05 p0941 A70-16616

Adhesive joints design, considering layer type, pipe connections and honeycomb structures for application in aircraft and automotive industries 08 p1585 A70-20894

Nondestructive test procedures development and implementation for bond strength of honeycomb sandwich and metal-metal adhesive bonded structures of F-5 and T-38 aircraft 09 p1692 A70-22798

Honeycomb shock absorbers, noting landing gear applications 13 p2512 A70-28772

IR NDT bond inspection system for helicopter rotor blade honeycomb box assemblies, using closed circuit slow scan video system to detect bondline voids 17 p3101 A70-35184

Honeycomb panels with fiber reinforced facings, obtaining acoustic fatigue design criteria [AIAA PAPER 70-897] 17 p3064 A70-35814

Pulsed laser holographic nondestructive testing optimization technique, monitoring honeycomb panel surface temperature during thermal stressing 18 p3259 A70-36754

Simple high level shock machine producing trapezoidal and terminal peak sawtooth pulses with Al honeycomb impact material 19 p3396 A70-37832

Optimum light construction design of glider wings, considering spar weight, aluminum honeycomb structure and repair 22 p3962 A70-42961

Concorde downstream thrust reversal nozzle, noting weight saving by use of welded stainless steel honeycomb construction 22 p4092 A70-43213

Spacecraft landing gear shock attenuation systems using crushable honeycomb, draw-die tubes and retrorocket skirt jet 23 p4262 A70-44695

Thermal IR nondestructive testing of adhesively bonded boron composite/Al honeycomb structures, discussing surface, cross section and instrumentation sensitivity effects 24 p4341 A70-45570

Holographic interferometry for NDT inspection of adhesive bonded honeycomb sandwich aerospace structures 24 p4338 A70-45754

Holographic nondestructive testing of laminate structures, honeycomb-sandwich panels and rubber-to-metal bonds 24 p4338 A70-45755

Bonded honeycomb sandwich structure fastening techniques in aerospace design, noting application to aircraft and spacecraft structures [SAE PAPER 700850] 24 p4425 A70-45882

HOOKES LAW

Relativistic simple shear of slab of neo-Hookean material 05 p0929 A70-16067

Incremental stress distribution near circular crack with internal pressure in neo-Hookean solid under

deformation due to triaxial compression, illustrating initial stress effect

05 p0956 A70-17108

Fundamental integral for small deformations superposed on finite triaxial extension of neo-Hookean elastic material

07 p1409 A70-19563

Reinforced plastics underframe design based on hooks law, noting middle layer loaded laminates and shell advantages

07 p1410 A70-19762

Elastic waves propagation in finite thickness elastic plate under transient load, assuming material behavior in conformity with nonlinear Hooke's law

15 p2814 A70-31544

Decelerator fabric elastic constants for structural analyses using generalized Hooke's law

[AIAA PAPER 70-1179] 21 p3843 A70-41834

HOOKS

Aircraft arresting hook response to impact regarding beam flexibility and internal damping using numerical wave propagation methods

10 p1963 A70-25069

HORIZON

Horizon sky UV spectral radiance, noting solar position and cloud cover effects

18 p3248 A70-36752

HORIZON SCANNERS

Instrument error analysis for spacecraft orientation and positioning near planet from planet disk observations

01 p0094 A70-11511

Earth horizon signal sensors on spin stabilized satellites using micron filters for cloud signal rejection

09 p1686 A70-23757

Horizon sensor design with null operating capabilities for synchronous orbit 3-axis stabilized communication satellites, discussing operation and testing

[AIAA PAPER 70-476] 11 p2121 A70-25484

Experimental IR earth horizon profiles measured by satellite in F region, discussing spectral channels and attitude control

12 p2225 A70-27751

Earth IR horizon seasonal and longer variations for horizon sensing instruments design

12 p2226 A70-27931

Probe rocket Tacite 02 head attitude gyrorestoration for IR horizon analysis, using stellar sensor and signal measurements

13 p2500 A70-28408

Thermal interface between edge of planetary disk and space for providing attitude reference during orbiting of planet

13 p2403 A70-28442

Low altitude atmospheric effects on IR beam horizon sensors in carbon dioxide band, noting corrections for spacecraft attitude measurement

15 p2735 A70-31792

Satellite-borne conical IR scanner flight data hybrid simulation and error analysis, suggesting carbon dioxide horizon noise model

[AIAA PAPER 70-1021] 20 p3631 A70-39513

Distribution functions of errors in earth and moon horizon sighting due to planetary surface unevenness

21 p3884 A70-40840

HORIZON SENSING

U HORIZON SCANNERS

HORIZONTAL FINS

U FINS

HORIZONTAL FLIGHT

Blade forces of helicopter rotor in forward flight calculated by unsteady lifting-line theory

01 p0004 A70-11366

Level flight optimization in horizontal wind varying with altitude, using glider concept and induced drag correction

[ONERA-TP-700] 07 p1193 A70-19131

Motion equations and dynamic lateral stability of towed glider in steady horizontal flight treated by small perturbations method, including design and handling influence

09 p1611 A70-23063

Concorde SST horizontal navigation, discussing data sources, equipment specifications, flight rules, man-machine interaction, etc

22 p4067 A70-42660

Horizontal flight speed effects on aerodynamic characteristics of air cushion vehicles with elliptical planform

22 p3959 A70-42801

Rocket nose cone optimal turn into horizontal ballistic trajectory after separation from booster, using dynamic programming

22 p3962 A70-43351

HORIZONTAL STABILIZERS

U STABILIZERS [FLUID DYNAMICS]

HORIZONTAL TAIL SURFACES

Boeing 2707 SST horizontal tail multiple channel actuation system features

17 p3020 A70-35827

HORIZONTAL TAILS

U HORIZONTAL TAIL SURFACES

U TAIL ASSEMBLIES

HORMONE METABOLISMS

Dibutyltyl cyclic adenosine monophosphate stimulation of melatonin and serotonin synthesis from C-14 labeled tryptophan by rat pineals in organ culture

01 p0022 A70-10824

Thyrotropin /TSH/ effects on thyroidal iodine metabolism during hypoxia in rats

02 p0231 A70-11703

Ionizing radiation effects on endocrine system, studying ACTH metabolism in rats under X ray irradiation

19 p3372 A70-38723

Human gluco-regulatory hormone reserve depressions following acute and chronic acceleration exposure

20 p3572 A70-39436

Adrenocorticotrophic hormone effect on oxygen tension in rabbit kidney

24 p4301 A70-45845

HORMONES

Flight fatigue syndrome origin, therapy and prevention, noting cortical adrenal hormones tests

01 p0031 A70-10234

Thyroidin influence on RNA content and nucleotide composition in hypothalamus, cortex and phenolic fractions of cerebral hemispheres resulting in accelerated protein biosynthesis

01 p0019 A70-10511

Vasopressin antidiuretic hormone effects on evaporative body weight loss during heat exposure

01 p0020 A70-10516

Glucagon infusion effect on human coronary circulation, relating changes in cardiac dynamics to myocardial oxygen consumption and blood flow

05 p0800 A70-16101

Hormones excreted by adrenal cortex function in rhesus monkeys pathogenesis after irradiation by sublethal dose

09 p1620 A70-22822

Somatotropic hormone and esculamine injection effects on rat survival rates under acceleration, noting sex linked differences

13 p2352 A70-29345

Epinephrine uptake and metabolic disposition in rat brain, determining pathways and turnover of endogenous brain hormone and enzymatic synthesis

14 p2536 A70-30348

Serum growth hormone response to hypoglycemia in man following insulin administration, reviewing lumped parameter model

19 p3360 A70-38006

Mathematical model of human pituitary gland mechanism controlling secretions of serum growth hormone in response to glucose deficiency

20 p3569 A70-38995

Auxin downward transport by gravity in leaves, examining ethylene inhibition

20 p3570 A70-39234

HORN ANTENNAS

Multimode excitation of large aperture horn antennas to produce electronic deflections of directional pattern

01 p0046 A70-11454

E plane radiation patterns of E plane sectoral horns enhanced by metallic grills arranged in optimum positions

02 p0270 A70-12734

Sky background brightness temperature measurement at 408 MHz by pyramidal horn antenna

03 p0496 A70-14344

Helicone antenna /axial mode helix combined with conical horn/ compared to conical horn in pattern and polarization characteristics

[AAS PAPER 69-623] 04 p0655 A70-14662

Radiation pattern computation for lens corrected conical scalar horn, comparing patterns and beamwidths with uncorrected horn and waveguide

04 p0656 A70-14721

Surface waves excited by horn above dielectric disk backed by metallic disk, formulating characteristic wave equations and solving for attenuation and propagation constants

04 p0659 A70-15305

Spherical hybrid modes in corrugated antenna conical horns, obtaining radiation pattern and gain with small flare angle

07 p1243 A70-20284

Computer predicted horn antenna radiation patterns through aircraft radome compared with measured values

09 p1645 A70-22689

Antenna array circular polarization adjustment using reflections from horn radiator and mirror

09 p1650 A70-23633

Curvilinear horn antennas synthesis having smoothly changing cross sections, studying methods for solving Fourier integral equation

09 p1652 A70-23660

Two dimensional impedance horn antennas synthesis by aperture field distribution and radiation pattern configuration relationship, deriving energy balance equation

11 p2015 A70-25348

Corrugated waveguide structures for aperture type feeds for spherical and paraboloidal reflector antennas, discussing experiments on 2-hybrid mode horn

11 p2018 A70-26024

Far field radiation patterns of Cassegrain, offset paraboloid and horn reflector antennas by stationary phase approximation method

11 p2019 A70-26659

Absolute sky brightness temperatures measured with horn antennas and Dicke receivers, indicating spectrum change due to galactic nonthermal radiation

12 p2309 A70-27893

Surface wave antenna radiation pattern from finite aperture of corrugated horn antenna

12 p2199 A70-28017

Radiation characteristics of horn antennas loaded with curved transverse dielectric slabs and radial dielectric strips, discussing axial directivity and half-power beamwidth

13 p2370 A70-29836

Antenna pattern and power gain determination from near field measurements on electrically large horn lens, standard gain horn and measuring antenna duplicate

15 p2698 A70-31956

Multihorn array antenna performance improvement by shaping beam for optimum earth coverage from stabilized synchronous satellites

16 p2860 A70-32952

High speed millimetric horn antenna with small azimuth and elevation beamwidths for airfield radar

16 p2876 A70-33407

Open waveguides and small horns theory, using Wiener Hopf method for radiation calculation

17 p3051 A70-35065

Far field diffraction, radiation and gain of wide flare angle corrugated conical horns

19 p3389 A70-37970

Complex waveguides with diverging body of revolution shaped horn, solving equation by Frobenius-Latysheva method

20 p3587 A70-39765

X band electromagnetic horn antennas, measuring triangular shape dielectrics effects on radiation pattern

20 p3599 A70-40312

Two dimensional impedance horn antennas synthesis by aperture field distribution and radiation pattern configuration relationship, deriving energy balance equation

20 p3600 A70-40460

X band horn antennas precision phase center measurement technique for high resolution system applications

23 p4176 A70-44966

HOT AIR

U HIGH TEMPERATURE AIR

HOT CATHODES

Hot cathode reflex discharges investigated to improve ion generation efficiency in space ion thrusters

03 p0536 A70-14368

Microscopic behavior and excitational processes found similar in argon ion lasers with hollow cathode or conventional heated oxide cathode discharge

11 p2063 A70-26370

Radial distributions and escape of charged particles across magnetic field in hot cathode Penning discharge plasma with LF oscillations

15 p2780 A70-32191

Hot cathode magnetron ionization gauge design, discussing performance and sensitivity

19 p3421 A70-37467

HOT CYCLE PROPULSION SYSTEM

U TIP DRIVEN ROTORS

HOT ELECTRONS

Hot photoelectrons in semiconductors assuming short lived photoexcited current carriers, deriving expressions for energy distribution function of semiconductor current carriers

01 p0153 A70-10066

Nitrogen, oxygen and air luminescence spectra excited by fast electrons at low gas pressures in IR spectral region compared with polar auroral spectra

01 p0083 A70-11536

Electrical domain instability in homogeneous hot electron semiconductors, discussing boundary conditions application to fluctuations

02 p0350 A70-11697

Current density and electron concentration fluctuations in semiconductors under electric field, obtaining theory of light scattering at hot electrons

03 p0539 A70-13405

GaAs nonlinear I-V characteristics and negative differential conductivity associated with electron heating by electric field

03 p0540 A70-13720

Whistler mode instability due to anisotropic charged particle velocity distribution, establishing general onset conditions for variable density cold plasma containing hot electrons

03 p0537 A70-14378

Field emission mechanism of hot electrons from semiconductors, discussing experiments with n-Si of high resistivity

06 p1126 A70-17749

Kinetic equation describing dynamics of inhomogeneous cloud of fast electrons and ions trapped in earth magnetic field

07 p1276 A70-20429

Fokker-Planck equation solution for electron scattering and energy loss in mirror confined hot electron plasma

11 p2090 A70-26022

Nickel-doped p- and n-type Ge hot electrons recombination characteristics in strong electric fields, examining electron capture cross section

15 p2782 A70-31628

Third harmonic generation using hot electron nonlinearity characteristics of semiconductors, considering plane-polarized electromagnetic wave nonlinear interaction with sample

15 p2783 A70-31970

InSb semiconductor, measuring small signal microwave conductivity for hot electron region at 9.4 GHz in high electric DC fields

19 p3488 A70-38747

Hot electrons bunch spread deceleration in collisionless plasma, discussing stationary moving jump formation similar to shock wave

22 p4077 A70-42299

Hot electrons Faraday effect in many-valley semiconductors, considering constant energy surface ellipsoidal form

24 p4392 A70-46361

Franz-Keldysh and hot electron effects in interband absorption of semiconductors in external electric field

24 p4392 A70-46361

HOT EXTRUDING

U EXTRUDING

HOT FORMING

U HOT WORKING

HOT GAS SYSTEMS

U HIGH TEMPERATURE GASES

HOT GASES

U HIGH TEMPERATURE GASES

HOT JET EXHAUST

U HIGH TEMPERATURE GASES

U JET EXHAUST

HOT JETS

U JET FLOW

HOT MACHINING

Austenitic stainless steels high temperature machining with W arc heating, considering constant pressure feeding and chip breaking method

20 p3638 A70-39943

HOT PLASMAS

U HIGH TEMPERATURE PLASMAS

HOT PRESSING

Niobium powder hot pressing compaction in terms of porous body volume viscous flow, determining viscosity shift time dependence

04 p0696 A70-14461

Integrally stiffened structures made by hot isostatic pressing of metal powders followed by conventional rolling

12 p2242 A70-27109

Mo powder compacting by hot pressing, determining activation energy

16 p2931 A70-33222

Hot pressed zirconia-zirconia ceramic fiber reinforced ceramic matrix composites, discussing mechanical properties and failure modes

22 p4057 A70-42285

HOT STARS

NT A STARS

NT B STARS

NT O STARS

NT WHITE DWARF STARS

Hypotheses for symbiotic stars nature, emphasizing binary with late type giant and hot small star components

03 p0568 A70-13325

Hot star photogravitational acceleration determined from difference between apex and antipex brightness, noting constant magnitude and direction of principal component of apex force

05 p0918 A70-16914

Luminous hot stars mass loss attributed to negative effective gravities in outer parts of reversing layers from ionic UV resonance lines

10 p1946 A70-24981

F-type close stars residual spatial motions and rotational velocity relationship, discussing angular momentum loss

13 p2498 A70-30015

Non-LTE and LTE line profiles and equivalent widths for transitions in singlet and triplet systems of neutral He in hot stars, explaining anomaly

14 p2641 A70-30884

Hot small mass neutron stars cooling time and internal characteristics, discussing evolution based on H-R diagram

15 p2808 A70-32886

Wolf-Rayet associated nebulae, presenting radio observations and mass determinations

16 p2980 A70-34193

Effective temperature of star zeta Puppis from combined angular diameter measurement and model atmospheres, comparing hot stars

24 p4404 A70-45414

HOT SURFACES

Slab melting under hot spots, obtaining starting solutions

18 p3346 A70-36491

HOT WATER ROCKET ENGINES

Bora-Sond atmospheric probe providing two stage minimum cost high altitude sounding for supersonic transport /SST/, discussing hot water propulsion system

17 p3178 A70-35257

HOT WEATHER

Protective clothing for personnel handling toxic and corrosive liquid propellants in hot climatic conditions at Guyana Space Center

12 p2179 A70-28043

Hot environment and hyperthermy effects on oxygen consumption in subjects performing muscular exercise

13 p2360 A70-29947

HOT WORKING

Solution treating temperature and microstructure effects on hot rolled Ni base alloy properties

07 p1306 A70-18995

Chemical composition and heat treatment effects on deformation resistance of nonaging aluminum alloys during hot working, noting quenching effect on recrystallization

07 p1294 A70-19388

Cold and hot work deformation of aluminum alloys, discussing flow-stress dependence on strain rate, temperature and composition

09 p1692 A70-22642

Hot shortness of molybdenum alloys under tensile testing due to molybdenum carbide precipitation on grain boundaries

11 p2066 A70-25914

Hot torsion test for Al alloys workability assessment, noting test temperature and specimen geometry effects on fracture strain values

13 p2436 A70-29816

Gas tungsten arc hot wire welding operational characteristics and applications

14 p2590 A70-30929

Hot rolling and warm working effects on microstructure and mechanical properties of Ni-Cu-Cb steel, noting optimum austenite plus ferrite phase field

15 p2756 A70-31566

Hot plasticity elongation of cast and wrought Ti-Al-V alloy as function of temperature and strain rate

17 p3117 A70-34401

Ti-Cu alloy sheet material age hardening, considering cold and warm work effects at various stages in aging cycle

17 p3121 A70-34430

Ti hot forming, discussing sheet use as aircraft structural material

17 p3098 A70-34444

Hot work effect on properties and microstructure of wrought Waspaloy, observing temperature decrease effect on fracture ductility

22 p4054 A70-42739

Succession of passes in rolling and hot shaping of thin walled angle steel

22 p4045 A70-42813

Space shuttle structural technology for booster and orbiter, discussing hot and cold structure concepts, reentry bodies, military payloads, radiating protective coatings, refractory materials, etc

22 p4111 A70-43516

HOT-WIRE ANEMOMETERS

Hot-wire probe support orientation to minimize flat plate turbulent boundary layer mean velocity determination errors

01 p0087 A70-10665

X array hot-wire anemometer measurements in flows with changing mean velocity direction during traverse

01 p0088 A70-10710

Forced convection of hot wire in hypersonic flow, determining Nusselt-Reynolds number relationship for hot-wire anemometers

02 p0223 A70-12101

Turbulence characteristics in liquids measured by hot film anemometry, discussing calibration methods selecting criteria as temperature control, drift influence and relative speed determination

02 p0303 A70-12687

Hot-wire and hot-film anemometry in two phase air-water and steam-water flow, discussing bubble passage, signal processing and measurements

02 p0305 A70-12836

Spatial resolution analyses of vorticity meter and hot wire arrays for measuring velocity derivatives in isotropic turbulence

03 p0492 A70-13760

Constant temperature hot-wire anemometer to compensate for thermal lag of wire/film resistance thermometer within useful frequency range

03 p0492 A70-13761

Steady MHD shear layer velocity profiles using hot film anemometry

05 p0887 A70-15924

Probe geometry effects on hot film anemometer probe performance during turbulence measurements in liquids

06 p1032 A70-17213

Vertical plume velocity and temperature measurements by hot wire probe on turbulent free convection zones over model fires

07 p1282 A70-19582

Plasmatron generated rarefied helium plasma parameters in external magnetic field using hot-wire anemometer Langmuir probe

07 p1349 A70-19653

Wall proximity and velocity gradient effects on thermocouple readings in turbulent boundary layer

07 p1285 A70-19834

Hot-wire anemometry equation suitable for wide regions of velocity and temperature derived by computing thermal losses by supports

08 p1496 A70-21236

External convective heat transfer coefficients from quartz-coated cylindrical hot film anemometer probes in mercury

08 p1599 A70-21582

Harmonics generated in hot-wire anemometers responses by wires thermal lag and amplitude of flow velocity fluctuations using computerized simulation

08 p1498 A70-21586

Karman trail vortices tangential velocity decay measurement by hot film anemometer experiments

09 p1661 A70-22961

Hot-film anemometers for measuring storm turbulence in presence of heavy rain

10 p1887 A70-23940

Heat transfer at low Reynolds and Grashof numbers determined using constant temperature anemometric wire

13 p2521 A70-28952

End support cooling in hot-wire anemometry of low density high temperature flows

13 p2412 A70-29882

Hot-wire probe measuring He-air mixture velocity and concentration following He discharge from circular orifice, noting calibration method

13 p2412 A70-29990

Intraarterial hot film constant temperature anemometry for point blood velocity measurements, detecting flow reversal

15 p2688 A70-31435

Constant temperature hot split film anemometer sensors based on velocity and heat flux distribution about probe, measuring flow rates

15 p2734 A70-31691

Admittance calibration of short HF through flow pneumatic lines, using hot-wire anemometer

16 p2891 A70-33628

Gas flow velocity measurement using hot foil probes

17 p3082 A70-34680

Turbulent boundary layer of flat plate, investigating superlayer structure by hot wire anemometer

18 p3238 A70-36066

Temperature profile along hot-wire anemometer attached to wall and normal to parabolic velocity steady flow field, using singular perturbation techniques

18 p3242 A70-36488

Thermal conductivity of frost, using imbedded hot-wire method

18 p3262 A70-37118

Turbulent flow phase velocity fluctuations measurement by hot-wire anemometers, obtaining cross-spectral density by Fourier analysis digital techniques

19 p3404 A70-38019

Wall proximity and velocity gradient effects on thermocouple readings in turbulent boundary layer

20 p3634 A70-40341

Constant temperature linearized hot-wire anemometer for low velocity high turbulence flow

21 p3827 A70-41455

Reverse curvature silicon transistor linearizer for hot-wire and thin-film constant temperature anemometers for aorta blood flow velocity measurements

21 p3827 A70-41458

Calibration data correlation for constant temperature hot film anemometer for low speed nonisothermal laminar air flow, using modified King law

21 p3828 A70-41475

Heat transfer in heated wire in supersonic flow near molecular transition zone, estimating anemometer sensitivity to motion fluctuations

22 p3959 A70-43240

Displacement effect of hot-wire anemometric probes near wall as function of support orientation

22 p4038 A70-43241

Thermal and aerodynamic interactions between wires of velocity sensitive anemometric crossed-wire probe, showing reduction by correction of measurements and minimal gap

22 p4038 A70-43242

Thermal calibration errors and sensitivity equations for hot-wire anemometers

23 p4195 A70-44288

Low noise constant temperature hot-wire anemometer design with second order high-cut filter, determining system stability

23 p4199 A70-45050

HOT-WIRE FLOWMETERS

- Turbulent flow velocity and stress components simultaneous measurement by single hot wire, discussing equations and computer program
04 p0685 A70-14447
- Hot wire turbulence measurements of cylindrical wall jet compared to results from free circular and plane wall jets
06 p1034 A70-17526
- Yawed hot wire measurements of turbulence fluctuations, discussing calibration and mutual interference of adjacent wire and wire supporting prongs in X-ray wire case
06 p1071 A70-18487
- Thermal conductivity of nitrogen in 350-1500 K range using hot-wire diffusion columns
11 p2147 A70-25756
- Velocity fluctuations in temperature gradient turbulent jets and in turbulent flames, using hot wire in cooled pitot tube
17 p3096 A70-35749
- HOT-WIRE TURBULENCE METERS**
U HOT-WIRE FLOWMETERS
U TURBULENCE METERS
- HOTSHOT WIND TUNNELS**
Nozzle boundary layer displacement thickness at Mach 30-70 in helium using Langley hotshot tunnel tests
04 p0675 A70-15603
- Measurement methods for forces, pressure and heat flow in hotshot hypersonic wind tunnels
17 p3057 A70-34773
- Hotshot wind tunnel performance improvement by coating arc chamber with silastene to retard heat loss and metal pollution
17 p3057 A70-34774
- Integrated double oblique shock scramjet for supersonic combustion tests and instrumentation development, discussing fuel injection through sonic orifices, combustion data, etc
[AIAA PAPER 69-827] 21 p3867 A70-41752
- HOUSINGS**
NT COWLINGS
NT RADOMES
Numerical photogrammetric techniques application to cadastral surveys and mapping, discussing standard errors
10 p1880 A70-24753
- HOVERCRAFT**
U GROUND EFFECT MACHINES
HOVERCRAFT GROUND EFFECT MACHINES
State of sea definition for hovercraft performance purposes, recommending Hovercraft Coastal Wind Wave Code
13 p2347 A70-29126
- HOVERING**
Matrix method for calculating aerodynamic loads, shearing forces, bending moments, torques, etc, in hinged main rotor helicopter blades during hover and vertical flight
06 p1167 A70-17914
- Plenum-chamber air-bearing and labyrinth-seal types air cushion lifting mechanisms performance in simulated hovering flight
12 p2162 A70-27981
- Optimal fixed-form pilot model computer program for VTOL longitudinal control hover task evaluation
16 p2851 A70-33341
- Longitudinal dynamics of VTOL aircraft during hover-forward flight transition, using multiple time scale analysis
[AIAA PAPER 69-130] 18 p3213 A70-36681
- Helicopter automatic approach and hover coupler systems, discussing cockpit display devices, handling qualities, pilot workload and fatigue and external load stabilization
23 p4140 A70-44464
- Propeller blade aerodynamic characteristics at zero advance ratio, reducing singular integral equation to nonsingular form for computer solution
23 p4136 A70-44993
- HOVERING STABILITY**
Man machine interface in VTOL aircraft control and stabilization systems adaptation during manually controlled hovering flight
03 p0414 A70-14094
- Flight tests with mounted and unmounted SG 1262 hovering test rig in Germany to determine optimal control and stability characteristics for VTOL VAK 191B
04 p0624 A70-15704
- Wing vibration problems associated with roll attitude control in hovering autostabilized VTOL transport aircraft with wing-mounted jet lift engines
05 p0794 A70-16116
- Static tank visualizations obtained in two dimensional flow and on rotors hovering or in transition in ONERA hydrodynamic tunnel
[ONERA-TP-777] 08 p1434 A70-21846
- Model for pilots optimal manual control of hovering VTOL aircraft longitudinal position
14 p2543 A70-31409
- Crane helicopter controllability, discussing load stabilization and precision hovering
17 p3015 A70-34723

- Hingeless rotor helicopter airborne and ground resonance characteristics, noting feedback stability control interference with rotors aerodynamic damping
17 p3015 A70-34733
- HRB-1 HELICOPTER**
U CH-46 HELICOPTER
HS-125 AIRCRAFT
U DH 125 AIRCRAFT
HU-1 HELICOPTER
U UH-1 HELICOPTER
HUBS
Electron beam welding of AH-56A helicopter rotor hubs outside of vacuum chamber, discussing modifications of machine
04 p0699 A70-15651
- Frequency change for coupled vibrations of slender rotating beam due to hub radius change determined in centrifugal force field by perturbation method
08 p1594 A70-21772
- HUECKEL THEORY**
Plasma pi-electrons effects in annulene molecules, obtaining dispersion relation for plasma oscillations by Hueckel theory
14 p2621 A70-30116
- HUGHES AIRCRAFT**
NT OH-6 HELICOPTER
HUGHES MILITARY AIRCRAFT
U MILITARY AIRCRAFT
HUGONIOT ADIABAT
U HUGONIOT EQUATION OF STATE
HUGONIOT EQUATION OF STATE
Release adiabats and recentered Hugoniot curves determination by shock reverberation techniques for compressible nonlinear materials, presenting results for epoxy resin and porous tuff
01 p0198 A70-10106
- Computerized stepwise construction of Hugoniot curve for detonation waves and Chapman-Jouguet detonation and deflagration points
03 p0607 A70-13920
- High purity beryllium dynamic tests determining Hugoniot equation of state, shock profile and spall threshold/onset of microcracking/for elastic pulses
[AIAA PAPER 69-360] 11 p2066 A70-25964
- Thermodynamics and velocity of MHD shock waves in perfect conducting fluid, using compressibility conditions and relativistic Hugoniot equation
19 p3477 A70-37580
- Macroscopically homogeneous composites control volume approach, examining Hugoniot equation of state
22 p4060 A70-43683
- HUMAN BEHAVIOR**
Book on dynamics of complex systems represented by control and human operators and animals behavioral activities models
01 p0034 A70-10501
- Underwater saturation habitats application as behavioral workshops for mission planning and human engineering of manned space flight, discussing Project Tekite
[AIAA PAPER 69-1120] 01 p0034 A70-10611
- Human capacity to discriminate between poorly and well balanced diets and liability to select amino acid imbalanced mixtures for deficient nutrient
01 p0028 A70-11314
- Man and animals physiological adaptation and behavior under conditions of polar regions, highland and arid areas
01 p0030 A70-11465
- Human EEG relationship to verbal behavior, discussing separation of stressful from nonstressful verbal stimuli, semantics and question-answer sequences
02 p0236 A70-12119
- Restricted problem solving tasks /perceptual maze test/ formulated as multistage decision making, discussing use of dynamic programming and algorithms
02 p0246 A70-12321
- Somatic motor unit spikes human biceps during posture holding, obtaining Markov chain and random variable behavior patterns
03 p0416 A70-13011
- Crew requirements influence on systems design and operations criteria for long duration biomedical and behavioral measurement program in earth orbiting space laboratory
[ASME PAPER 69-WA/BHF-17] 04 p0643 A70-14858
- Research problems resulting from observational methods in social-psychological studies, discussing categorization systems and coding reliability
05 p0802 A70-16668
- Respiration behavior of men during inhalation of various gas mixtures, observing spontaneous changes in breathing rates
07 p1206 A70-19471
- Visual observation, free space traversal, accelerometry and telemetry for measuring and recording human behavior, discussing free space-time traversal data logging system
14 p2542 A70-30794

- People as conservative processors of fallible information, treating stationary data generating process as nonstationary
14 p2537 A70-30898
- Vestibular habituation acquisition, retention and transfer correlation with stimulation, discussing alertness and arousal effects
14 p2539 A70-30915
- Physiological tests of sampled data hypothesis in human motor control system
16 p2851 A70-33323
- Soviet monograph on secondary signaling system role in development of speech, thought, conditioned and unconditioned reflexes, human will and hypnosis, noting salivary gland function
19 p3359 A70-37407
- Human monitoring behavior, discussing display, task and organismic variables effects
19 p3363 A70-38323
- HUMAN BEINGS**
Mankind role in cosmos as function of self realization developed by science and technology
11 p2153 A70-26057
- Neurological differences in spinal projections of animals subjected to cordotomies compared with human material, using selective silver impregnation technique
13 p2350 A70-28998
- HUMAN BODY**
Somatic motor unit spikes human biceps during posture holding, obtaining Markov chain and random variable behavior patterns
03 p0416 A70-13011
- High altitude acclimatization effects on cardiovascular system, external respiration, blood composition, optical and vestibular analyzers in human subjected to various stresses
04 p0630 A70-14576
- Human body turning /orienting/ in unsupported /weightless/ position by own muscular forces, determining inertia moments of body and parts relative to various axes
07 p1207 A70-19495
- Screen filtration pressure of human blood, establishing time, anticoagulant, red cells, platelets and leucocytes as physical determinants
07 p1210 A70-19590
- Human esophagus physiology, studying sphincter function from data on healthy and afflicted subjects
07 p1214 A70-19793
- Whole body counters as standard measuring devices in nuclear medicine and radiation protection, using scintillation detector principles
09 p1624 A70-22819
- Human body homeostatic mechanisms autoregulation, discussing feedback control systems for blood pressure and flow regulation, bodily movements and postural control, etc
10 p1810 A70-24038
- Prolonged hypodynamia effect on heart size and myocardium function obtained from human chest X ray studies
10 p1814 A70-24673
- Human gamma globulin and binary/ternary protein structures conformation transitions studied by UV difference spectra
12 p2173 A70-28346
- Capillary details in lentiform nucleus region of human brains, measuring blood vessels diameters, lengths and densities
12 p2173 A70-28347
- Minimum ventilation volume requirement for space suit relation to air contaminants and body gas discharge intensities and locations
13 p2358 A70-29333
- Force input and thoraco-abdominal strain due to sinusoidal motion of electrohydraulic shake table over 2-14 Hz range imposed on human body
13 p2359 A70-29438
- Radial and tangential stress distribution through annulus fibrosus dependence on material inhomogeneity for human intervertebral disk
15 p2692 A70-32328
- Isolated human heart measurements for time course and instantaneous distribution of normal heart excitation process
15 p2683 A70-32471
- Human body turning /orienting/ in unsupported /weightless/ position by own muscular forces, determining inertia moments of body and parts relative to various axes
15 p2685 A70-32740
- Human body radiation shielding, describing development of computerized standing and seated model for space missions
[AAS PAPER 70-053] 17 p3036 A70-34794
- Human body core temperature control dependence during exercise on heat dissipation, noting sweating control
20 p3570 A70-38997
- Human body elastic properties effects on arterial pressure measurement by sphygmomanometer
20 p3581 A70-39879

Human body radioactive nuclides in vivo quantitative analysis by gamma ray spectra, considering matrix method accuracy

20 p3582 A70-40449

Elastic bounce of body resulting from falling to ground with calf muscles in sustained contraction and without knee bending

21 p3765 A70-42151

Circadian rhythm in human body temperature by Cosinor method, showing inapplicability for narrow time span

22 p3977 A70-42872

Mean skin temperatures of human body by 10 point method, using cold and hot exposure data

22 p3978 A70-42874

Human hemoglobin chain, noting zeta chain synthesis during embryonic development

24 p4297 A70-45406

Intact human forearms venous blood velocity measurements, using nuclear magnetic resonance techniques

24 p4309 A70-45675

HUMAN CENTRIFUGES

Human heart chronotropic reactions during centrifuge acceleration tests up to tolerance limit, establishing sinus tachycardia in various degrees

05 p0804 A70-17120

Cine recording ophthalmoscope with TV monitoring for retinal photography during centrifugation

06 p1061 A70-17286

Acceleration environment duplication difficulties, considering human physiological responses dependence on centrifuges performance characteristics and geometries

07 p1222 A70-19927

Acceleration training schedules performed with animals and test subjects, assessing schedules effectiveness in increasing tolerances to transverse acceleration

09 p1623 A70-22086

Acceleration training schedules performed with animals and test subjects, assessing schedules effectiveness in increasing tolerances to transverse acceleration

15 p2693 A70-32682

Human retinal detachment treatment by centrifugation

22 p3975 A70-43699

HUMAN ENGINEERING

U HUMAN FACTORS ENGINEERING

HUMAN FACTORS ENGINEERING

USAF visual flight simulation devices from engineering and psychological standpoints, discussing human factors considerations

01 p0057 A70-10808

Reduced gravity simulators for studies of human mobility in space and lunar missions

01 p0037 A70-10958

Simulated lunar environmental facility to investigate effects of high risk vacuum, lunar gravity and terrain characteristics and spacesuit encumbrances on astronaut performance

01 p0037 A70-10961

Human factors research with simulated reduced gravity conditions by parabolic flight technique with aircraft

[AMRL-TR-69-16] Visual flight displays technological and human engineering development

01 p0037 A70-10962

Digital computer display techniques relationship with man in modern environment, considering human engineering and educational problems and future impact on intellectual qualities

01 p0221 A70-11281

Electronic head-up display experience in transport aircraft flight tests including human factor, installation, operational applications, etc

02 p0224 A70-11836

Air traffic control system for intercity and metropolitan VTOL airway reducing pilot and air traffic controller workloads

02 p0335 A70-12135

Display system for Apollo Telescope Mount designed for unclouded sun view by orbiting astronaut-scientists, discussing human factors, film budgeting, etc

02 p0298 A70-12151

Static electricity generation and discharge in human beings due to clothing layers, analyzing body capacitance, resistance and inductance for ordnance and fuels safety

03 p0439 A70-14133

Management role in air traffic controllers stress reduction, considering human factors affecting ATC system capacity

03 p0439 A70-14316

Man-machine systems design emphasizing impedance matching exemplified by visual approach landing

[ASME PAPER 69-WA/GT-15] Pilot visual information display systems influence on flight safety, discussing aircraft accidents and human error factors

04 p0691 A70-15143

Radiography of spine in seated position, discussing aircraft seats, aeronautical ergonomics, etc

05 p0804 A70-15765

Physiological and environmental factors influencing oxygen breathing system design and use for passengers and aircrews of high flying aircraft

06 p1003 A70-17716

Heart rate and circulatory load as ergonomic criteria based on muscular work, environment temperature, mental stress, etc

06 p0997 A70-18017

Pilot limitations role in USAF midair collisions, discussing information systems for collision avoidance

07 p1192 A70-19022

Crew visibility requirements for rendezvous, docking and earth landing of reusable reentry vehicles [AIAA PAPER 70-262]

07 p1399 A70-20398

Display design for improved target detection performance taking into account human attention to display field areas

08 p1452 A70-21301

Human biological organism analysis based on physiological determination of regulating and control functions dependence on oscillatory properties

08 p1452 A70-21460

Control display requirements for manned spacecraft, integrating human operator with vehicle control system and determining man machine relations in stabilization, control and guidance

08 p1498 A70-21678

Workload relieving displays and controls for general aviation, discussing feasibility of digital computer driven integrated displays

08 p1601 A70-21679

Display media development and implementation from engineering psychology viewpoint for information transfer in form compatible to sensory-perceptual capabilities

08 p1447 A70-21690

C-5 design features for entire environment assuring human integration as crew member or troop passenger

09 p1609 A70-22021

Human factors data standardization in NASA Apollo Applications Program for computer data processing

09 p1623 A70-22295

Human factors responsibility for aircraft accidents, discussing cooperation between air safety service and flight surgeons

09 p1626 A70-23016

Human psychophysiological inability to avoid mid-air collisions investigated for aviation safety

09 p1611 A70-23465

Bibliography of literature on bioengineering, biocontrol, medical physics, biotechnology, safety and human factors in technology

09 p1629 A70-23692

Human reaction time study leading to promptness concept to embody quantitative and qualitative aspects of psychological behavior

10 p1818 A70-24716

IR electro-optical tracker Oculometer using human eye motions for pointing and tracking

11 p1989 A70-25352

Human reactions to confined interiors design, examining human-environment interactions present in aircraft

[SAE PAPER 700234]

11 p1990 A70-25903

Associative analog designed for decision making by man searching for extremum in form of multilayer stochastic automaton

11 p1990 A70-25928

Applied psychology role regarding human factors in man machine systems, considering boredom, skills application, age and experience, etc

12 p2176 A70-27035

Human engineering in weapon systems development, considering flying and ground personnel training plans

12 p2177 A70-27038

Man machine interface between operator and automatic testing equipment based on ergonomic design cost

13 p2360 A70-29687

Visual display reference system rotation effect on control quality and tracking error compensation using stick signal control

14 p2540 A70-30249

Human error as function of variability, considering frequency, effects and controllability

14 p2543 A70-31115

Human factors in aircraft accidents, noting cockpit crew members overconfidence and carelessness

15 p2692 A70-32228

Human skull porous dipole layer shear and compressive properties, measuring static and dynamic strain rates

15 p2683 A70-32308

Human element in system development to achieve optimum tradeoffs among reliability, cost and other system criteria

15 p2693 A70-32629

Workmen as environmental variables in design, introducing Human Factors Report during spacecraft components manufacture and testing

15 p2693 A70-32636

Dynamic systems control and guidance by man in light of anthropotechnics, treating approaches to man machine systems optimization

16 p2850 A70-33263

Human factors requirements for effective utilization of electronic reconnaissance displays, noting SNR and TV lines over target effects on performance

16 p2851 A70-33459

Discrete stochastic optimal control model of human operator for single loop compensatory/pursuit tracking situation, considering application to manual control system design

16 p2852 A70-33463

Field maintenance interface between human engineering and maintainability, discussing air defense system malfunction and troubleshooting deficiencies

16 p2852 A70-33665

Maintainability assessment techniques, discussing models in terms of utility, application, validity and human engineering data

16 p2853 A70-33667

Low cost headup displays /HUD/ for pilot error reduction during takeoff, approach and landing, discussing displayed functions vs cost tradeoffs

16 p2911 A70-33818

Head up display /HUD/ flight tests, examining effects decreasing quality of manually handled instrument approach, discussing space myopia and disorientation

16 p2912 A70-33819

Flight deck design since 1920, discussing ergonomics and avionic aspects

16 p2913 A70-34048

Ergonomic and medicomilitary aspects of human adaptation to cold environments, discussing metabolic and physical protective reactions, clothing and personnel selection

16 p2850 A70-34346

Human body radiation shielding, describing development of computerized standing and seated model for space missions

[AAS PAPER 70-053]

17 p0306 A70-34794

Habitability factors in space station crew quarter design, discussing hygiene and dining facilities

17 p0306 A70-34803

Heat-up display /HUD/ system, discussing development, production, commercial aircraft applications and flight sequences uses

18 p3223 A70-36210

Performance in monotonous work situations, discussing various factors affecting efficiency

18 p3224 A70-36317

Soviet book on man in aircraft control system covering engineering psychology, complex flight problems, human factors and instrument panels

19 p3367 A70-37236

Air traffic controller stress reduction, discussing work-rest intervals and various management and human factors

19 p3371 A70-38647

Human factors in ATC, discussing simulation trials and impending problems

19 p3371 A70-38648

Comfort plane switch mounting design for helicopter collective controls, noting mock-up evaluation by test pilots

19 p3372 A70-38922

Radar consoles with various display components under different illumination levels to determine optimal operator performance, discussing push-button design recommendations

20 p3580 A70-39713

Human mass exchange parameters permissible errors for manned space vehicles life support systems design

20 p3581 A70-40200

Advanced Integrated Life Support Systems, discussing subsystem requirements and mission parameters

21 p3768 A70-40988

Aerospace digital computer and avionics systems man machine relationship optimization, considering human information and control response requirements

21 p3794 A70-41688

Human error as factor in aircraft accidents, considering man machine incompatibility and prevention measures

21 p3771 A70-41723

Low cost and weight reliable microminiaturized IC automatic cockpit checklist systems for aircraft pilots

22 p3977 A70-42298

Book on environment and human efficiency covering stress mechanisms, experimentation, exposure to chemicals, radiation, noise, heat, cold, machines, etc

22 p3967 A70-42457

Pilot influence on dynamic aircraft design, taking into account physiological state during various operational tasks

[ICAS PAPER 70-37]

23 p4138 A70-44134

Man-rated chamber facilities at Manned Spacecraft Center /MSC/, discussing safety requirements and criteria, environmental test chamber design and test results

23 p4152 A70-44458

- Space station requirements and design, discussing space shuttles, operational personnel, long term effects, logistical systems, functions, etc
23 p4259 A70-44606
- Space transportation, discussing space shuttles, technological, commercial, human and philosophical aspects
23 p4245 A70-44641
- Biological life support system based on mutual equilibration of human metabolism and technically controlled algae culture, discussing experimental evaluation
23 p4156 A70-45026
- HUMAN PATHOLOGY**
- Local gamma irradiation effect on number of chromosome aberrations in lymphocytes of human blood of oncological patients after hysterectomy
01 p0013 A70-10137
- Vascular anatomy correlation with human heart conduction tissue structures to study coronary artery disease cases exhibiting major conduction disturbances by ECG
01 p0013 A70-10273
- Reciprocal rhythm occurring with impulses of atrial or atrioventricular (A-V) nodal or ventricular origin, noting role of A-V nodal pathways
01 p0016 A70-10442
- French book on aeronautical and astronautical physiopathology and pathology covering stress factors of flying, high speed and altitude including hypoxia, atmospheric vacuum, etc
01 p0029 A70-11380
- Postmortem coronary angiographies showing role of arterial hypertension in coronary pathology
03 p0426 A70-13939
- Pathologic findings of left ventricular papillary muscle related to electrocardiogram, discussing papillary muscle dysfunction syndrome
03 p0426 A70-13942
- Pathological manifestations of acute myocardial ischemia without acute myocardial necrosis and myocardial infarction, discussing subjects with chronic occlusive coronary atherosclerosis
04 p0634 A70-15456
- Primary and secondary pathological changes in small coronary arteries and role in acute myocardial infarction development, discussing coronary arteries distribution
04 p0635 A70-15457
- Clinicopathological studies of coronary artery occlusion and acute myocardial infarction, discussing coronary thrombosis
04 p0635 A70-15459
- Physiological and physiopathological effects of transverse accelerations on spacecraft crews, discussing cardiovascular and respiratory systems
05 p0799 A70-15763
- Victim examination, human factors and forensic problems in flight accident investigations
05 p0807 A70-16497
- Lower limbs circulation of peripheral vascular diseased patients transcatheterously assessed with ultrasonic flow detector, comparing results with arteriograms
07 p1217 A70-18956
- Spinal cord overstretching and circumscribed pathological tension mechanism, considering histological and radiological findings
07 p1204 A70-19242
- Human metabolic study showing effect of yeast RNA and allantoin on serum and urinary uric acid formation
08 p1454 A70-20679
- Idiopathic myocardial disease patients investigated for serological anomalies and markers of immunopathology
09 p1621 A70-23301
- Carbohydrate metabolism disorders in head injury cases, comparing incidence with EEG abnormalities
10 p1810 A70-24037
- Hypodynamia effects on humans during prolonged bed rest, investigating immunological resistance, psychic disorders, myocardium changes, responses to pharmaceuticals, etc
10 p1817 A70-24696
- Skin galvanic reaction manifestation degree correlated to EEG changes accompanying injuries of human brain limbic structures
11 p1985 A70-25400
- Long air voyage after exteriorization of Wallenberg syndrome, discussing case history of subject with cerebral vascular accident
12 p2172 A70-28044
- Stomatological diseases during prolonged space flights simulation, discussing gingivitis, stomatitis, dental caries, parodontitis and odontogenous inflammations
13 p2352 A70-29338
- Microbial flora in human subjects confined to long term Tekite 1 underwater habitat
15 p2681 A70-31879
- Fatal general aviation accidents examined by pathologists, determining pilot incapacity, accident

- sequence, aircraft design modification and crash protection performance
17 p3033 A70-35567
- Long rhythms of periodic disparate heritable diseases in man
19 p3365 A70-38414
- Mathematical model simulating human respiratory physiopathology, based on hypothetical stable auto-oscillations dependence on ventilation/pulmonary exchange system
23 p4155 A70-44859
- Obstructive lung diseases clinical, radiological and functional diagnosis in legal medicine
24 p4296 A70-45122

HUMAN PERFORMANCE

- NT ASTRONAUT PERFORMANCE**
- NT BLACKOUT PREVENTION**
- NT OPERATOR PERFORMANCE**
- NT PILOT PERFORMANCE**
- Equipment reliability data application in analytic techniques to predict human requirements for system, using in-space maintenance as reference frame
01 p0055 A70-10117
- Mathematical models for perception and skilled action in man or machine, noting sensorimotor theory
01 p0034 A70-10498
- Human subjects performances on fixed interval reinforcement schedules, emphasizing effects of instruction
01 p0035 A70-10793
- Image quality effects on human performance in simulation, discussing time sharing strategies and task difficulty factors
01 p0036 A70-10809
- Visual fatigue symptoms, causes, relation to general fatigue and psychological aspects, discussing testing for sensory and visual fatigue
01 p0022 A70-10857
- Visual attention testing, considering perception focusing on stimulus object and eyelid blinking recording, measuring eye distance to work plane
01 p0023 A70-10861
- Visual faculties testing to improve performances in visual inspection tasks, considering threshold line concept and visual performance relation to age
01 p0023 A70-10862
- Reduced traction effects on human work performance in weightless and lunar gravity environment
01 p0037 A70-10959
- Prototype lunar gravity simulator for studies of reduced gravity effects on human self locomotive capability, using magnetic air bearings and body support system
01 p0037 A70-10960
- Human activities inadvertent effects on planet earth, discussing catastrophic physical environment changes and compensation methods
01 p0077 A70-11045
- Voluntary control over velocity of smooth pursuits, discussing saccadic and saccade free modes and switching during tracking
01 p0026 A70-11056
- Intermittent vs continuous noise effects on signal detection measures during audio visual checking task performance
01 p0039 A70-11167
- Human and cat visual neuron properties, discussing encoding orientation and dimensions of retinal images
01 p0028 A70-11360
- Reactions to visual emergency signals in humans after administering adrenalin, aminazin, melipramine or andaxine to change control systems functional state of cerebrum
01 p0030 A70-11467
- Mathematical models construction for predicting and measuring air traffic controller workload, using synthetic and analytic methods
02 p0332 A70-11972
- Human decision making via man-computer interaction, noting skill role in nonoptimal performance handling of simultaneous factors
02 p0245 A70-12140
- Speed and accuracy of foot operation of controls tested by circular targets in rows within reach of right foot
02 p0245 A70-12144
- Correlations between organizational factors and individual engineer performance, analyzing stability of relationships and time lags in measurement
02 p0246 A70-12378
- Subjects trained in visual monitoring task with autoinstructional device, showing higher signal detection rate than group trained by practice alone
02 p0247 A70-12380
- Human feedback and response mode in performing Bayesian decision task
02 p0237 A70-12382
- Plethysmographic investigation of myogenic load influencing sportsmen central nervous systems state, tabulating short and long distance running results
03 p0420 A70-13403
- Diurnal rhythms of physiological functions and human adaptation to shifted sleep-wakefulness

- schedule on healthy pilots subjected to solitary confinement
03 p0423 A70-13711

- Relative slant judgments elicited by paired comparison methods from subjects viewing computer generated slides representing rotated regular dot patterns
03 p0435 A70-13769
- Monitoring behavior in three source visual task, studying selective attention by response observation method
03 p0435 A70-13770
- Event probability and cost effects on performance in continuous motor task
03 p0436 A70-13771
- Cardiovascular system, neuromuscular activity and mental fitness of subjects performing physical and mental assignments with prescribed work-rest schedule during confinement
03 p0425 A70-13895
- Prolonged hypokinesia effect on human resistance to physical stress, noting prophylactic influence of physical exercises
03 p0425 A70-13898
- Visual prediction accuracy in estimating point coincidence of two moving targets as function of viewing opportunity and length of period
03 p0428 A70-14084
- Heart rate augmentation during constant performance in excess of endurance limit, considering muscle fatigue
03 p0431 A70-14292
- Work and exercise conditions effect in early training stages of learning sensorimotor skill, considering different body positions
03 p0432 A70-14295
- Mathematical model building for temporal human motor responses /reaction, movement, manipulation/ by response surface technology and statistical experimental design
04 p0642 A70-14851
- Human controller decision in air traffic control, discussing manpower, on-line computer use and maximized systems
04 p0643 A70-14903
- Noise effects on tracking performance, electroencephalography (EEG) and galvanic skin resistance (GSR)
04 p0643 A70-14977
- Horizontal transverse vibration effects on manual tracking performance, relating tracking errors to frequency rather than acceleration
04 p0643 A70-14981
- Activity and rest alternation effect on fatigue and rehabilitation behavior of trained athletes, discussing muscle performance characteristics
04 p0639 A70-15510
- Time constant of man machine system as adaptive variable in training devices derived from combined vehicle properties and human control characteristics
05 p0805 A70-16005
- Human performance evaluation and data acquisition as requirements for heuristic analytical models in systems engineering
05 p0805 A70-16008
- Catecholamine excretion, cardiovascular functions and subjective effort in healthy male subjects under various physical work loads
05 p0801 A70-16141
- Acceleration cues removal effects on vehicular velocity perception, using movie technique to control visual cues
05 p0806 A70-16143
- Human controller in psychology and control engineering, discussing linear and nonlinear modeling of human behavior
05 p0807 A70-16487
- Health conditions and operational efficiency of Italian military paratroopers during air transportation analyzed from questionnaire data
05 p0807 A70-16494
- Statistical analysis for personal variations contribution to total mean square error in time determinations
05 p0914 A70-16649
- Postrest upswing or muscles warm-up in motor skill learning
05 p0803 A70-16671
- Hypoxia effect on self paced work behavior of humans
05 p0803 A70-16672
- Standardized bicycle ergometer training effects at sea level and simulated altitudes, indicating hypoxia potentiating role
05 p0807 A70-16674
- Prolonged wakefulness effect on human work capacity in isolated chamber, determining physical, intellectual and sensory capacities
05 p0809 A70-17117
- Vigilance time degradation, studying effects of breathing gas mixtures with varying oxygen and carbon dioxide content
06 p1000 A70-17293
- Time of useful function (TUF) determination for human exposure to toxic gas combinations due to fire
06 p1000 A70-17294

- Book on human factor in aircraft accidents covering desire to please, fatigue, diurnal rhythm, psychology, etc
06 p0987 A70-18249
- Neurophysiological vertical and horizontal visual coordinates localization in man
06 p0998 A70-18484
- Artificial effects on atmosphere and near-earth space caused by human activity, discussing occurrence altitude, means of action and consequences
07 p1262 A70-18778
- Surface and underwater swimming tests for statistical correlation to linear maximum accelerations effects
07 p1201 A70-18788
- Human visual performance, discussing effects of object size and exposure time
07 p1204 A70-19050
- Radiorheopneumographic study of external respiration of office workers during mental and physical activity
07 p1204 A70-19142
- Evoked potential /EP/ correlate of binocular depth perception in man, discussing responses to horizontal and vertical changes in retinal disparity
07 p1205 A70-19284
- Veloergometric assembly using two bicycles for simultaneously measuring muscular motor activity of persons in competition
07 p1221 A70-19525
- Symmetrical motor centers inequality significance in humans during interaction under conditions of successive innervations during exercise
07 p1213 A70-19790
- Human color vision simulation by mathematical and electronic analogs for photoelectric color measurement and eye resolution
08 p1450 A70-20727
- Weightlessness effects on human vision, studying color perception, field of vision and light sensitivity
08 p1444 A70-20743
- Cardiac output and coronary blood flow during steady state recumbent exercise, discussing CO and Rb 84 measurements in human subjects
08 p1453 A70-21936
- Solar simulation /SISS/ for evaluating human visual system performance in contrasting space environment
09 p1655 A70-22680
- ATC and SST operations in terminal area simulation study involving airline crews and controllers in real time traffic situation
09 p1721 A70-22946
- Various phases of human isometric left ventricle contraction, comparing results with previously published data
09 p1620 A70-23111
- Target velocity and approach angle effects on accuracy of moving targets intersection estimation tested on human subjects
09 p1628 A70-23578
- Observation noise model for human controller remnant
10 p1823 A70-23893
- Step tracking in normal human subjects, studying muscle system around ankle joint
10 p1824 A70-23898
- Environmental thermal stress effect on human performance under high mental and low physical workload
10 p1812 A70-24505
- Differential luminance sensitivity of human eye using signal detection theory, correlating discrimination and detection results with electrophysiological data
10 p1812 A70-24599
- Human movement speed and accuracy as function of age in pencil tapping between paper-drawn targets
10 p1817 A70-24711
- Speed-accuracy interrelationship in human performance as operating characteristic for reaction time under variety of task conditions
10 p1826 A70-24712
- Response times in deciding same or different between successive visual stimuli
10 p1826 A70-24722
- Perceptual selection and integration of sensory data conveyed to brain, explaining various optical illusions
10 p1827 A70-24766
- Functional visual field selective process, studying performance as function of display angle
10 p1827 A70-24769
- Diurnal rhythms of physiological functions and human adaptation to shifted sleep-wakefulness schedule on healthy pilots subjected to solitary confinement
11 p1985 A70-25511
- Nine degree of freedom pitch axis model of human postural control system, deriving kinetic and potential energy expressions
11 p1990 A70-25675
- Human performance as controller evaluated in man machine control system, considering pursuit or compensatory tracking tasks
12 p2177 A70-27039
- Thermal stress /high ambient and body temperatures/ effect on human performance in high mental and low physical activities
12 p2177 A70-27043
- Mental blocking /incidental long reaction times/ during continuous serial performance using perceptual-selection and response theories
12 p2178 A70-27045
- Continuous active work effects on human sensorimotor performance, comparing latency distributions in mass and spaced practice groups
12 p2178 A70-27046
- Pursuit tracking during disturbance signal as function of human performance in man machine system
12 p2266 A70-27198
- Heterochronism of coordinated cophasal flexor and extensor movements during acrobatic leap in human subjects
12 p2168 A70-27344
- Air controllers traffic capacity using automation, discussing airspace loading effect, area navigation and rerouting
12 p2267 A70-27637
- Anaerobic and aerobic oxidation efficiency in muscular work performance before and after achieving oxygen steady state consumption
12 p2169 A70-27658
- Human detection capability for objects on electro-optical imaging displays calculated as function of SNR, viewing distances and brightness levels
12 p2236 A70-27903
- Visual feedback delay effects on steering and tracking performance
12 p2179 A70-28147
- Human forearm motion control mechanism, examining mechanogram, instantaneous velocity, acceleration and biopotentials of biceps and triceps brachii
12 p2173 A70-28314
- Maximum oxygen uptake correlation to age of subjects performing physical and sedentary work
13 p2350 A70-29112
- Compensatory tracking task with tactile displays determining gains and body locations by describing function and error power analyses
13 p2354 A70-29599
- Human error as function of variability, considering frequency, effects and controllability
14 p2543 A70-31115
- Sensory function in multimodal signal detection forced choice experiment involving auditory, visual and auditory-visual stimuli
14 p2539 A70-31167
- Optimal manual control model of human compensatory tracking response
14 p2543 A70-31408
- Hand-eye coordination in altered gravitational fields, using mirror viewed target in reaching test
15 p2689 A70-31886
- Eye movements effects on apparent /beta/ movement perception tested by display with ambiguous illusory movement
15 p2683 A70-32454
- Personnel subsystem reliability through empirical approach, determining relations of man-hardware-procedure systems
15 p2804 A70-32665
- Human factors requirements for effective utilization of electronic reconnaissance displays, noting SNR and TV lines over target effects on performance
16 p2851 A70-33459
- Human and machine pattern discrimination correlated by statistical correlation method from pattern recognition task involving computer simulation and humans
16 p2852 A70-33461
- Electronic equipment maintainability in military environment, discussing myths for hardware and human performance conditions
16 p2852 A70-33664
- Human muscular strength capacity relationship to maximal or submaximal dynamic work performance
16 p2853 A70-33668
- Human power output dependence on muscle mechanical properties and kinematics of input motion, describing ergometer
16 p2853 A70-33669
- Displayed cursor velocity effect on radar target acquisition time for subjects in simulated air defense environment
16 p2853 A70-33670
- Human tracking performance in position, rate and acceleration control systems under short term psychological stress induced by electric shocks
16 p2853 A70-33689
- Human acceleration resistance and psychomotor behavior under emergency flight conditions, including high temperature exposure and remaining in clinical position
17 p3037 A70-35135
- Systems engineering approach to comparison by emphasis for employee performance evaluation
17 p3130 A70-35298
- Performance in monotonous work situations, discussing various factors affecting efficiency
18 p3224 A70-36317
- Equidistance effects on human size and distance perception in visual alley
19 p3368 A70-37771
- Heat stress effects on serial reaction time in subjects performing visual tasks
19 p3361 A70-38053
- Response bias of conservative human inference, using revised odds estimate experiments
19 p3361 A70-38055
- Stabilogram and support dynamograph based on amplitude modulation of carrier frequency for standing stability determination in humans
19 p3371 A70-38220
- Attention and performance - Conference, Soesterberg, Netherlands, August 1969
19 p3361 A70-38310
- Component decision logical and temporal arrangement in visual search, defining target by several attribute value combination
19 p3362 A70-38314
- Attention theory experimental design logic, discussing quantitative theory
19 p3362 A70-38315
- Optimum attention allocation, discussing distraction resistance and multiple task performance
19 p3362 A70-38316
- Performance and response organization as uncertainty and structure function in pursuit tracking tasks
19 p3363 A70-38320
- Human memory information structure, discussing pattern recognition, simultaneous attention, problem solving and logic
19 p3363 A70-38322
- Human vigilance paradigm and physiology, discussing relationships between vigilance, signal detection and animal discrimination
19 p3364 A70-38324
- Prolonged hyperbaric oxygen breathing effect on human physical performance at rest and during severe exercise
19 p3364 A70-38369
- Lighting and background effects on human binocular color vision of signal lights in industry
19 p3366 A70-38923
- Brightness contrast by human observer binocular matching, discussing neural networks models
19 p3366 A70-38924
- Choice reaction and movement time dependence on hypoxia induced by air pressure reduction inside decompression chamber, discussing adult human performance
20 p3573 A70-39714
- Acute mountain sickness symptomatology and cognitive performance, using standardized General High Altitude Questionnaire
20 p3581 A70-40025
- Mental performance changes due to extended exposure of man to sensory deprivation environment, discussing prevention and treatment methods
21 p3770 A70-41479
- Human error as factor in aircraft accidents, considering man machine incompatibility and prevention measures
21 p3771 A70-41723
- Book on environment and human efficiency covering stress mechanisms, experimentation, exposure to chemicals, radiation, noise, heat, cold, machines, etc
22 p3967 A70-42457
- Longitudinal vibration effects on human reaction time and motor performance involving toggle switch and manual knob control in different working positions
22 p3977 A70-42871
- Vestibular sinusoidal stimulation effects on compensatory tracking under various postures and display conditions
22 p3976 A70-43706
- Labyrinthine and sensory information role in driving, discussing car simulator, driver tests with impaired inputs, age factors, etc
22 p3976 A70-43708
- Integrated regenerative life support manned tests for space laboratory design and development
23 p4154 A70-44632
- Syncope prevention in orthostatic heat test by inflating cuffs around legs and lower abdomen
24 p4306 A70-45331
- Alcohol effects on human short term memory, discussing pathological intoxication from flying safety viewpoint
24 p4307 A70-45345
- Human tracking performance as function of information precision in electrocutaneous display
24 p4308 A70-45508
- Human mental stress evaluation through chemical analysis of 17-hydrocorticosteroid level in parotid fluid
24 p4308 A70-45509
- Human interpolation accuracy for pointer or index position between two scale graduations
24 p4308 A70-45512

Expert judgments validity of human task performance time against empirical measures for use in analytical modeling 24 p4308 A70-45515

Artificial gravity simulation effects on human performance in space base [AIAA PAPER 70-1329] 24 p4417 A70-45938
Human EEG alpha rhythm during surface-tapping test with rod at time-limited maximum frequency, noting slowdown to preferred frequency 24 p4301 A70-45987

Human compensatory two dimensional visual display tracking performance with superimposed apparent vertical vibration, studying frequency dependent eye pursuit movements 24 p4309 A70-46078

HUMAN REACTIONS

Book on subatmospheric decompression sickness in man, covering raised intrapulmonary pressure effects and compensating pressure applications [AGARDOGRAPH-125] 01 p0019 A70-10514

Acid base responses of arterial plasma of anesthetized man during acute carbon dioxide partial pressure changes, discussing anesthesia effects 01 p0020 A70-10651

Human thermoregulatory responses as function of peripheral thermoreceptors during imposed negative heat load in different ambient environments 01 p0024 A70-10977

Hemoglobin concentration in red blood cells in men of various ages as function of altitude, discussing correlations with body weight and plasma protein 01 p0024 A70-10978

Visual stimuli duration effect on saccades precision and reaction time in peripheral field in normal subjects 01 p0026 A70-11055

Jet aircraft flyovers annoyance relationship to physical parameters of sound evaluated, using psychophysical method of constant stimulus differences 01 p0006 A70-11199

Topically administered vitamin A radioprotective effect on postradiation skin reactions 01 p0029 A70-11402

EEG investigation of cerebral bio currents during polar night-day cycle, studying central nervous system nonspecific automatic control mechanism dependence on ecological factors 01 p0030 A70-11466

Time sense in human subjects kept in caisson or cave isolation determined as function of upper brain stem paraconsciousness 01 p0041 A70-11474

Thermal discomfort by changing operational temperature of human subjects environment found to follow power law 01 p0041 A70-11474

Human vibration test program for airline passenger reaction to vibration environments of large commercial aircraft 02 p0244 A70-12132

Propagation velocity relation with time delay in human visual system, using various sets of line stimuli having different spatial distance 02 p0237 A70-12457

Human perceptual and response biases in choice reaction time tasks involving visual and auditory stimuli 02 p0239 A70-12624

Mean signal response time relationship to nonaging foreperiod 02 p0239 A70-12627

Accelerative and decelerative heart rate responses in human subjects given differential conditioning trials by auditory and electric shock stimuli under paced respiration 02 p0239 A70-12628

Human response in Apollo flights emphasizing astronauts food, water, waste management, physical examination, preventive medicine problems, etc 02 p0239 A70-12669

Display devices for ballistocardiographic test data obtained from professional pilots free of cardiovascular disease subjected to displacement and acceleration 02 p0247 A70-12676

Effect of immersion in thermoindifferent water on circulatory control and work capacity in trained and untrained subjects 02 p0241 A70-12770

Sensor, vegetative, motor and vestibulosomatic reactions to brief weightlessness in fighter pilots and laymen, ascribing disorders absence to statokinetic stability of organism 02 p0241 A70-12799

Functional state changes in organism awaiting and performing parachute jump using orthostatic test, respiration retention and Howard step test 03 p0420 A70-13477

Vestibular analyzer stimulation effects on cerebral blood circulation in humans during angular acceleration using rheoencephalography 03 p0422 A70-13692

Dehydrated food effects on human functional state, noting published literature on food composition, preparation, caloric and nutritional values, digestibility, etc 03 p0435 A70-13703

Reaction time task to examine relationship between preparatory intervals and auditory stimulus intensity in experimental designs 03 p0424 A70-13764

Human oculogyral illusion thresholds determined on Ames Man-Carrying Rotation Device to establish stimulus duration effect on angular acceleration thresholds 03 p0424 A70-13765

Signal detection theory analysis indicating within-session changes in human willingness to respond in visual monitoring task, considering optimal decision behavior 03 p0435 A70-13766

Auditory and visual ready signal intensity effects on reaction time, considering roles of practice and individual differences 03 p0436 A70-13772

Human atrial flutter studies using electrocardiographic electrodes placed within esophagus and right atrium 03 p0424 A70-13773

Phagocytic activity and carbohydrate metabolism in peripheral blood neutrophils of men exposed to atmosphere with increased O content, noting neutrophil energy exchange disorder role 03 p0426 A70-13901

Cardiac output and coronary blood flow changes in patients at rest and during peak exertion, stating correlation coefficients 03 p0428 A70-14065

Mechanical vibrations effect on man including motor vehicle dynamic vibrations 03 p0439 A70-14097

Thermal comfort in disparate environments, discussing human subjects skin mean temperature and body water loss 03 p0429 A70-14158

Thin, fat and average men responses to cold during one year period in Antarctica, measuring metabolic rates, skin and rectal temperatures 03 p0429 A70-14163

Evaporative weight losses by sweating in man exposed to warm environment as function of time, including graphical method for heat storage prediction 03 p0430 A70-14164

Two loop control system model of human lens accommodative system derived on basis of muscle mechanics, optics and experiments 03 p0439 A70-14275

Oxygen consumption and body temperatures during acute hypoxia in man, based on low oxygen mixture breathing tests 03 p0439 A70-14291

Closed life support systems tests, describing effects of long term /one year/ confinement of three human subjects 04 p0641 A70-14565

Prolonged dehydrated food diet effect on metabolism of humans, noting complete adaptation after three or four months 04 p0630 A70-14577

Combined hypoxic hypoxia and high ambient temperature found relieving strain on humans by increasing heat release by evaporation 04 p0630 A70-14581

Nonextension lines characteristic to human skin utilized to provide natural mobility and minimal ballooning in full pressure suits noting mapping, testing, construction, etc [ASME PAPER 69-WA/AUT-22] 04 p0642 A70-14826

Reciprocating force measurement at shake table and subject interface and repetitive circumferential human torso deformation under sinusoidal input at various frequencies and intensities 04 p0631 A70-14850

Human functional changes in controlling C-8 trainer measured by flicker value, pulse rate, reaction time and instrument and control error before and after flight 04 p0643 A70-14976

Interindividual reaction time using target speed anticipation test and relationship with manifest anxiety scale 04 p0643 A70-14978

Aircraft pilots vertigo during flight using questionnaire and interviews, emphasizing bank directional disorientation 04 p0643 A70-14979

Human communication in pilots and in maintenance and administrative personnel, noting time factor influence 04 p0644 A70-14985

Classical human reaction time as function of high and low auditory signal rates in vigilance setting, supporting inhibition theory of vigilance decrement 04 p0640 A70-15646

Adaptive multiparameter experiment for iterative minimization of investigated data points, based on human response pattern to psychophysical inputs 05 p0805 A70-16006

Human macrosaccadic eye movements related to four dial display conditioned by concurrent variable interval schedules of signals 05 p0800 A70-16127

Book on sense of time covering psychological and physiological aspects and electrophysiological experimental results in man 05 p0800 A70-16129

Human eye contribution to visual evoked responses under different color stimuli during all possible monocular and binocular combinations 05 p0801 A70-16382

Electrocardiographic changes during positive headward acceleration of normal human subjects after oxygen breathing and propanolol administration 05 p0808 A70-16675

Recumbency effect on human heel bone density during bed rest using X rays 06 p0996 A70-17850

Human motor reactions rhythmic system, relating reaction-skin-galvanic reflex to formation of successive conditioned connections 07 p1197 A70-18697

Physiological effects of prolonged human motor activity restriction, discussing oxygen transport system, work capacity relationships, body fluids volume and distribution, metabolism, etc 07 p1200 A70-18786

Acceleration effects on chest organs by X ray studies noting heart shape changes, pulmonary areas, diaphragm position, etc 07 p1201 A70-18791

Flavor sweetening preference in high protein and high fat diets, basing human subjects experimental range on choice of formulas 07 p1216 A70-18948

Intracerebral, peripheral and central blood circulation relationship in humans during transverse accelerations 07 p1209 A70-19520

Periodic components distribution of human cardiac activity rhythm noting slow waves 07 p1210 A70-19556

Left ventricular wall motion in normal man at rest and after exercise using echocardiogram 07 p1210 A70-19573

Posture change effects on vasodilator responses in humans, studying reactive, postexercise and local heat hyperaemia in forearms of subjects lying and standing 07 p1211 A70-19596

Auditory averaged evoked potentials to clicks in man subjected to selective listening task, comparing effect on attended and rejected ear 07 p1215 A70-20213

Microinterval analysis of phased development of human visual color perception in presence of short stimuli 08 p1443 A70-20733

Constant periods method to eliminate human responses during threshold measurements by holding first threshold perception flash fixed 08 p1445 A70-20750

Multistage treadmill exercise tests on healthy business executives noting S-T-segment responses 08 p1445 A70-21265

Alveolar ventilation and pulmonary circulation during application of negative pressure to lower part of human body 09 p1615 A70-22090

Ego strength relationship to respiration in response to sound and light stimulation tested in subjects balanced for alertness-drowsiness by EEG criteria 09 p1616 A70-22331

Attention and cue-producing responses in response-mediated stimulus generalization 09 p1617 A70-22342

Human complex responses to noise, considering individual variations, social and psychological factors, adaptation, etc 09 p1617 A70-22392

Eosinophilic leukocytes behavior in blood of Starfighter aircraft pilots due to flight stress 09 p1625 A70-23004

Air traffic vibration effects on human organs and sensations, considering blood circulation, lungs, eyes and muscles 09 p1625 A70-23007

Physiological reactions detection, transmission and data evaluation of aircraft pilots subjected to various stress environments, using radio telemetry 09 p1626 A70-23009

Blood pressure variations resulting in permanent irreversible hypertonia in air force pilots subjected to repeated stress situations and emotional irritations 09 p1626 A70-23011

Psychic stress causing factors and reactions in aircraft pilots on duty, analyzing harmful effects on organism 09 p1620 A70-23012

- Discrete motor act short term retention measurement to investigate decay and interference effects
09 p1621 A70-23378
- Human sensory-motor adaptation and aftereffects of exposure to accelerative forces using hand-eye coordination measurements
09 p1628 A70-23466
- Startle auditory stimuli effects on motor performance and recovery characteristics from heart rate and skin conductance recordings
09 p1628 A70-23577
- Time variations in human spectral response, considering sequential gain and phase estimates formation by Gabor elementary signals theory
10 p1823 A70-23895
- Heat accumulation, oral temperature and heart rate recovery of subjects in various thermal environments
10 p1810 A70-24034
- Human response to angular acceleration, discussing implications for motion capability in flight simulator [AIAA PAPER 70-350]
10 p1824 A70-24212
- Soviet collection of papers on prolonged immobility and effects on human organism
10 p1812 A70-24665
- Relative value of prolonged bed confinement and hypodynamia in estimating biological effects of weightlessness
10 p1813 A70-24666
- Prolonged hypodynamia effect on human organism, describing organizational and methodological principles for conducting investigations
10 p1813 A70-24667
- Prolonged hypodynamia /bed rest/ clinical observations, noting psychological and physical effects
10 p1813 A70-24668
- EKG and cardiac rhythm changes during prolonged hypodynamia /bed rest/ with restricted physical activity
10 p1814 A70-24669
- Human vascular tonus and hemodynamics during prolonged hypokinesia, observing changes in reaction to cold and reduced vascular tonicity
10 p1814 A70-24670
- Mineral saturation in calcaneal bone and hand finger phalanx in humans under prolonged hypodynamia by X ray analysis, observing Ca salts reduction
10 p1815 A70-24676
- Prolonged hypodynamia effect on human blood serum mineral content and enzyme activity
10 p1815 A70-24677
- Prolonged hypodynamia effect on human blood coagulation, noting antihemophilic effect of physical exercise
10 p1815 A70-24678
- Immunity indices in humans subjected to hypodynamia, noting infection resistance lowering
10 p1815 A70-24679
- Human central nervous system changes during hypodynamia, noting unidirectional shifts in brain hemodynamics, rheographic wave propagation time reduction, etc
10 p1815 A70-24680
- Cardiovascular reactions and orthostatic stability during hypodynamia determined from ECG, seismocardiograms, phonocardiograms, sphygmograms and tachy-oscillograms
10 p1817 A70-24694
- Transverse g-force tolerance and stability after prolonged hypodynamia in bed rest, noting effects of pharmaceuticals, physical exercise and prophylactic measures
10 p1817 A70-24695
- Information hypothesis and repetition hypothesis concerning human reaction time to visual stimulus information
10 p1826 A70-24714
- Human reaction time study leading to promptness concept to embody quantitative and qualitative aspects of psychological behavior
10 p1818 A70-24716
- Human reactions to successive visual signals, studying response time in single and grouped reaction
10 p1826 A70-24720
- Visual stimuli intensity influence on delay in reaction to second of pair of visual stimuli
10 p1818 A70-24721
- Information processing stages by reaction time measurements permitting discovery, property assessment and separate testing of stage durations additivity and stochastic independence
10 p1826 A70-24723
- Neurophysiological mechanism of motor activity during simple reaction time situation performance
10 p1818 A70-24724
- Human finger tips skin temperature periodical variations process and influencing factors using electronic analog model
10 p1823 A70-25306
- Dehydrated food effects on human functional state, noting food composition, preparation, caloric and nutritional values, digestibility, etc
11 p1989 A70-25503
- Pilot electroencephalograms during F-104 flights recorded by telemetering noting alpha, beta and theta activities
11 p1990 A70-25668
- Physiological and psychological human reactions during space flight concerning hypokinesia, space kinetosis, isolation and limited room conditions
11 p1986 A70-25707
- Human reactions to confined interiors design, examining human-environment interactions present in aircraft
11 p1990 A70-25903
- Dietary protein and yeast RNA levels effect on uric acid metabolism in normal man
11 p1987 A70-26002
- Size effects on velocity threshold for real movement during narrow stimulus object length increase
11 p1989 A70-26662
- Psychic stress at simulated flight vehicle guidance tasks evaluated quantitatively
12 p2177 A70-27037
- Thermal stress /high ambient and body temperatures/ effect on human performance in high mental and low physical activities
12 p2177 A70-27043
- Cerebral circulatory reactions of smokers and non-smokers exposed to altitude, measuring vasomotor, blood flow and cardiac frequency indexes using scalp electrodes
12 p2172 A70-28042
- Minute hyperventilation of human lungs causing expiratory suppression of respiration
12 p2173 A70-28315
- Sensory afterdischarge of human brain under light stimuli during sleep and wakefulness
12 p2173 A70-28354
- Motor reactions and neural negative induction duration in male and female human subjects of different ages
12 p2174 A70-28356
- Periodic high temperature effects on human systolic phase dynamics
12 p2174 A70-28359
- Paced respiration and selective attention effects on heart rate and finger pulse amplitude in adult females subjected to visual stimuli
13 p2350 A70-29241
- Human proprioceptive reflexes fluctuations correlation with spontaneous respiration and cardiovascular rhythms
13 p2350 A70-29323
- Human proprioceptive reflexes fluctuations during controlled respiration and voluntary apnea
13 p2351 A70-29324
- Coriolis illusions amelioration during space flight, noting cross coupling effects minimization by reflex vestibular stabilization of head
13 p2358 A70-29432
- Human response in Apollo flights emphasizing astronaut food, water, waste management, physical examination, preventive medicine problems, etc
13 p2353 A70-29434
- Human respiratory responses to gas mixtures with different oxygen content under rarefied atmospheric conditions
13 p2353 A70-29521
- Motion sickness in man and animals as normal response with individual susceptibility dependent on motion duration
13 p2355 A70-29793
- Human temporal motor response models relating reaction, movement and manipulation time to stimulus, movement and manipulation information
14 p2540 A70-30248
- Human operator ocular tracking and decay time stimulation response measurements using information, statistical, point process and random analysis
14 p2537 A70-30388
- Arousal effects on vestibular nystagmus in man, discussing forced alertness in mental arithmetics form
14 p2538 A70-30911
- Closed circuit respiration studies on subjects at rest and work, demonstrating potassium superoxide as oxygen source in breathing apparatus
15 p2688 A70-31500
- Physiological examination of healthy human beings, considering repose situation abnormal
15 p2691 A70-31923
- Human renal response to various exercise rates, measuring endogenous creatinine clearance, urine volume, solutes, acid, elements and protein excretion
15 p2684 A70-32534
- Alveolar ventilation and pulmonary circulation during application of negative pressure to lower part of human body
15 p2685 A70-32686
- Human tracking performance in position, rate and acceleration control systems under short term psychological stress induced by electric shocks
16 p2853 A70-33689
- Human circadian coronary circulatory rhythms during space flight weightlessness or bedrest with and without exercise
16 p2854 A70-33991
- Annoyance assessment for sonic boom series exposure near airport
16 p2843 A70-34325
- Decision theory model evaluation based on experimental findings concerning relationship between stimulus intensity and reaction time
17 p3036 A70-34605
- Tracking error correction time and proprioceptive reaction time, suggesting role of central mechanism without sensory feedback
17 p3036 A70-34606
- Nonextension lines characteristic to human skin utilized to provide natural mobility and minimal ballooning in full pressure suits noting mapping, testing, construction, etc
17 p3036 A70-34951
- Centrifugation effects on human peripheral arterial pulse behavior
17 p3037 A70-35126
- Hypoxia and parotid secretion in humans exposed to angular accelerations
17 p3038 A70-35137
- Human operators psychological response to unforeseen information received during routine activity in prolonged solitary isolation
17 p3038 A70-35362
- Human water-salt metabolism following exposure to transverse accelerations, discussing diuresis and Cl-K excretion
17 p3038 A70-35364
- Cooling hood effect on physiological responses to work in hot environment, discussing body temperature
17 p3031 A70-35422
- Mountain climbing effects on urinary excretion of vanillylmandelic and homovanillic acids, discussing circulatory system acclimatization
17 p3039 A70-35425
- Oxygen uptake and cardiac output in males during submaximal and maximal treadmill and bicycle exercise
17 p3039 A70-35428
- Prototype space foods effects on humans, determining changes in bacterial fecal flora content
17 p3032 A70-35565
- Psychophysiological tests involving programmed memory device evaluating human memorization process and sensorimotor reactions to light signals
17 p3040 A70-35676
- Environmental heat stress indices of human subjects in bicycle ergometer experiment
18 p3224 A70-36226
- Cortical evoked potentials in human motor conditioning to photic stimulus
18 p3221 A70-37212
- Electrophysiological characteristics of man during disorders in rhythmic system of conditioned motor reactions
18 p3221 A70-37217
- Latent period of human motor reflex in telegraph key press testing in response to oral command
18 p3222 A70-37218
- Intact femoral artery pressure-diameter relationship in man, discussing noradrenaline infusions effects
18 p3222 A70-37222
- Decreased mental and physical performance of human beings due to T-oral and placebo vaccine reactions
19 p3359 A70-37389
- Human spatio-temporal visual evoked response characteristics, showing potential gradient rotation in same period as input stimulus
19 p3360 A70-37845
- Human brain LF activity in visual evoked response, determining relationship to stimulation
19 p3360 A70-37846
- Human response time to visual stimulus preceding or following auditory stimulus as function of interstimulus interval
19 p3362 A70-38311
- Reaction time intersensory facilitation relationship to single channel theories of attention and human performance
19 p3362 A70-38312
- Preliminary taxonomy for errors in serial, self-paced choice reaction time experiments, discussing speed-error tradeoff
19 p3362 A70-38313
- Human sleep pattern changes due to acute sleepwalking cycle reversal
20 p3569 A70-38990
- Airborne electronic equipment, collision avoidance systems, displays, instrumentation, human response and ground based control in air traffic control
20 p3665 A70-39198
- Frank orthogonal vectorcardiograms on humans during acceleration, using beat-by-beat real time analog-digital computer technique
20 p3572 A70-39435
- Human gluco-regulatory hormone reserve depressions following acute and chronic acceleration exposure
20 p3572 A70-39436

- Ship engineers cardiovascular system functional changes during HF internal combustion engine noise, investigating EKG recordings and arterial pressure 20 p3582 A70-40292
- Human peripheral blood flow rewarming in cold ambient temperature, examining skin, rectal and tympanic membrane and oxygen uptake 20 p3576 A70-40327
- Unitary and compound stimuli and role of response categories in decision time 21 p3767 A70-40751
- Line tilting aftereffects on central and peripheral vision following spatial coincidence of inspection and test contours 21 p3767 A70-40752
- Serum enzymes lactate dehydrogenase, creatine phosphokinase and isoenzymes in conditioned male after marathon run, noting little myocardium damage 21 p3766 A70-42158
- Lateral and angular acceleration effects on blood and urine contents in specific metabolic indices of healthy young men 22 p3971 A70-43136
- Visually evoked responses in man to different light stimuli intensities, noting marked increase in binocular over monocular visual response 22 p3972 A70-43408
- Spectral sensitivity of freely moving human eye by determining threshold energy for correct choice between two monochromatically illuminated stimulus patches 22 p3972 A70-43412
- Human postural control system response to mechanical torque disturbance, using second order differential equation with state dependent parameters for approximate analysis 22 p3979 A70-43494
- Normal human postural control system reflex response to tendon jerk disturbance 22 p3979 A70-43495
- Apollo program medical data contribution to knowledge of human response to space environment 22 p3980 A70-43651
- Human disturbance from SST overflight sonic booms, discussing overpressure, rise times and durations 23 p4137 A70-44016
- Passengers physiological and medical problems on subsonic and supersonic aircraft 23 p4150 A70-44223
- Aircraft noise reduction, discussing generation sources in propulsion system, noise levels and subjective responses 23 p4140 A70-44395
- Hypodynamic effects on human external respiratory function and cardiovascular state under various microclimatic conditions 23 p4149 A70-45078
- Mammal and human acoustic reflex for impulsive sound, investigating immunization effectiveness 24 p4297 A70-45373
- Sonic boom, discussing characteristic flow phenomena, intensity, effects on buildings and animals, human reactions, etc 24 p4289 A70-45786
- Desoxycorticosterone action on human kidneys and sweat glands as function of temperature tested with various DOCA and NaCl doses 24 p4301 A70-45988
- HUMAN TOLERANCES**
- Lipid and carbohydrate behavioral abnormalities in patients with angiographically documented coronary artery disease observed by glucose tolerance tests 01 p0016 A70-10441
- Pulsed noise biological effects on human organism, showing stimulation of auditory duct and baric and mechanical reception system causing neural functional shift 03 p0433 A70-13476
- Spine acceleration tolerance after prolonged human exposure to weightlessness, noting osseous apparatus tissue decalcination 03 p0423 A70-13712
- Thermal protection rating systems for clothing fabrics based on pain and blister effects in human skin 03 p0438 A70-14064
- Human alveolar-arterial oxygen differences during rest, sleep and exercise in initial hypoxia induced by simulated high altitude exposure 03 p0429 A70-14161
- Cardiovascular responses to sustained high skin temperature in resting men noting dizziness, impaired vision and extracutaneous vasodilatation 03 p0429 A70-14162
- Artificial gravitation parameters for manned compartments of spacecraft, analyzing permissible angular velocity and rotation radius regarding vestibular-vegetative disorders 04 p0760 A70-14446
- Autonomic nervous system role in controlling body functions after rapid decompression, increasing tolerance to pressure gradients by physical training 04 p0630 A70-14575

- Physiological limitations of air traffic controllers, considering stress factors connected with workload 04 p0716 A70-15314
- Human susceptibility to weak fluctuations in geomagnetic field intensity, showing frequency range 05 p0809 A70-16861
- Nonionizing radiation sources relationship to human targets, discussing damage threshold levels 06 p0998 A70-17201
- Hemodynamics in cardiosclerosis patients and healthy subjects under hypoxia, investigating heart activity and blood circulation 06 p0994 A70-17667
- Thorax potential resistivity at sea and high altitude levels measured in children and adults inferring relation to ECG differences 07 p1206 A70-19296
- Statistical analysis of pulmonary ventilation and gas exchange indices during orthostatic tests before and after water immersion 07 p1209 A70-19517
- Physiological responses during exercise recorded in patients with healed myocardial infarction, considering work tolerance 07 p1212 A70-19693
- Human physiological responses to lower body negative pressure (LBNP), studying presence or absence of change for orthostatic tolerance as function of time 07 p1222 A70-19933
- USAF permissible human exposure levels for laser irradiation established from monkey retina experiments 08 p1451 A70-21045
- Thermal tolerance and comfort graph for air conditioned spaces with low air velocity, considering fighter plane cockpits 08 p1454 A70-21949
- Acceleration training schedules performed with animals and test subjects, assessing schedules effectiveness in increasing tolerances to transverse acceleration 09 p1623 A70-22086
- Orthostatic tolerance in humans increased by lower limb muscles electrostimulation, correlating subjective feelings with heart and pulse rate measurements 09 p1615 A70-22089
- Hypercapnic atmosphere effect on human organisms found tolerable in state of rest or performing light labor 09 p1615 A70-22094
- Acute oxygen deficiency effects on blood electrolyte concentrations in altitude-adapted and nonadapted humans 09 p1616 A70-22217
- Flight stress in Starfighter aircraft pilots related to fibrinolysis activity in blood 09 p1625 A70-23003
- Aircraft pilots psychic and flight stress admissible degree not resulting in hazardous consequences, suggesting measures to increase resistance 09 p1625 A70-23006
- Aircraft pilots fitness under flight stress, discussing smoking, overweight, lack of exercise, etc, leading to coronary afflictions 09 p1620 A70-23013
- Human tolerance to short duration high acceleration in centrifuge concerning peripheral or central vision trouble or syncope 09 p1626 A70-23112
- Heat tolerance time extension due to prior body cooling observed in aircrew subjected to heat stresses 10 p1824 A70-24036
- Spine acceleration tolerance after prolonged human exposure to weightlessness, noting osseous apparatus tissue decalcination 11 p1985 A70-25512
- Statistical analysis of pulmonary ventilation and gas exchange indices during orthostatic tests before and after water immersion 11 p1988 A70-26116
- Incremental lower body negative pressure as assay method for human orthostatic tolerance 11 p1992 A70-26518
- Physiological reactions of humans to orthostatic heat tolerance and natural acclimatization in summer and winter using tilt-table test and bicycle ergometer 12 p2169 A70-27656
- Artificial gravitation parameters for manned compartments of spacecraft, analyzing permissible angular velocity and rotation radius regarding vestibular-vegetative disorders 13 p2503 A70-28471
- Physiological indices criteria for human thermal stress tolerance, discussing rectal temperature, body surface condition, body temperature and local cooling effects 13 p2351 A70-29332
- High intensity noise effects on auditory thresholds, blood pressure and time response to light stimuli, showing permissible levels during space flights 13 p2358 A70-29334
- Permissible radiation exposure levels during prolonged space flights based on clinical data 13 p2351 A70-29336

- Inspired carbon dioxide pressure effects on human response to physical exercise, noting dyspnea and intercostal muscle pain 13 p2360 A70-29949
- Pattern center hypothesis for habituation to centrifugal and linear accelerations in man, investigating aftereffects by nystagmography 14 p2538 A70-30913
- Acceleration training schedules performed with animals and test subjects, assessing schedules effectiveness in increasing tolerances to transverse acceleration 15 p2693 A70-32682
- Orthostatic tolerance in humans increased by lower limb muscles electrostimulation, correlating subjective feelings with heart and pulse rate measurements 15 p2685 A70-32685
- Hypercapnic atmosphere effect on human organisms found tolerable in state of rest or performing light labor 15 p2685 A70-32690
- Antimotion sickness drugs evaluated for effectiveness under standardized stress conditions in slow rotation room 20 p3572 A70-39439
- Temporal and spectra combination effects on aircraft sound judged noisiness, using human subjects in anechoic chamber 20 p3580 A70-39712
- Preliminary physical training for human water immersion resistance improvement 20 p3576 A70-40196
- Atmospheric composition cyclic changes effects on human basal metabolism under hypokinesia 20 p3576 A70-40197
- Hypokinesia and reduced diet effects on human tolerance to static loads, discussing acceleration tolerance prediction 20 p3576 A70-40198
- Acceleration effects on human organisms, describing centrifuge, rocket sleds and catapult simulators 22 p3979 A70-43528
- Low carbon dioxide concentration breathing effects on exercise tolerance, discussing aerobic capacity decrement and hypercapnia occurrence 22 p3973 A70-43637
- Decompression hazards in manned orbiting systems, considering consciousness time, survival, pathological response, water vapor and denitrogenation effects and recompression rates 22 p3973 A70-43638
- Human and animal tolerances to hyperbaric oxygen, discussing response variation, toxicity modification, etc 22 p3976 A70-43701
- Human tolerance and ventilatory response to inspiratory mechanical loads 23 p4144 A70-43822
- Human ventilatory response to resistance unloading during muscular exercise 23 p4144 A70-43823
- Optimum acceleration profile for minimum severity index in injuries sustained by human subject 23 p4150 A70-44376
- Human body heat production and transfer through convection, radiation and evaporation under normal and reduced atmospheric pressure 23 p4154 A70-44654
- Orthostatic stability reduction in experiments with simulated weightlessness, investigating functional compensation mechanisms 23 p4149 A70-45025
- Ear protection for persons exposed to various jet aircraft noise environments 24 p4306 A70-45121
- Head movement role in motion sickness as function of angular velocity, discussing prediction of human tolerance in space station 24 p4297 A70-45341
- Critical supersaturation vs phase equilibration of tissue in computing decompression schedules from depth and exposure time 24 p4301 A70-45983
- Human cardiovascular compensatory responses to environmental cold stress, relating heart stroke to increased oxygen consumption 24 p4302 A70-46103
- HUMAN WASTES**
- NT FECES
- NT URINE
- Mathematical planning of experiments applied to biological mineralization of human wastes, using continuous microorganism cultivation 03 p0435 A70-13715
- Ionol concentration variations in oncological patients blood, using liquid gas chromatography to determine removal by urine and feces 07 p1209 A70-19519
- Soviet monograph on toxicology of active human life gaseous products, noting implications for artificial atmosphere formation in pressurized compartments 09 p1624 A70-22549

- Mathematical planning of experiments applied to biological mineralization of human wastes, using continuous microorganism cultivation 11 p1990 A70-25515
- Minimum ventilation volume requirement for space suit relation to air contaminants and body gas discharge intensities and locations 13 p2358 A70-29333
- Spacecraft waste management system zero-gravity flight tests, describing components and functions 17 p3036 A70-34751
- Vacuum distillation vapor filtered catalytic oxidation for water reclamation from human waste, using radioisotopes for thermal energy 20 p3579 A70-39437
- Spacecraft wet oxidation for human waste processing, discussing temperature and gas pressure effects, catalyst types, pump requirements, etc 21 p3769 A70-40997
- Thermal efficiency of ceramic and metal heat exchangers for biowaste resistojet thrusters [AIAA PAPER 70-1135] 21 p3868 A70-41779
- HUMASON COMET**
- Humason 1960e-1959X comet hyperbolic orbit, indicating solar system permanent membership 19 p3516 A70-37934
- HUMIDITY**
- Turbojet aircraft engine performance correlation with relative humidity, noting air density effect on rotor performance resulting from moisture content 01 p0165 A70-10689
- Wave disturbances in tropical lower troposphere, discussing cross spectrum analysis of wind, temperature, relative humidity and surface pressure 07 p1275 A70-20304
- Precondensation visibility dependence on aerosol particle swelling due to increasing humidity 08 p1539 A70-21921
- Undried atmospheric air humidity effect on pressure and water vapor supercooling in supersonic wind tunnel nozzles 09 p1606 A70-23613
- Condensation start dependence on air humidity at inlet and nozzle geometry applied to supersonic wind tunnel using undried atmospheric air 09 p1606 A70-23614
- Monograph on troposphere pressure, temperature and humidity and satellite TV photographs interpretation 13 p2446 A70-29786
- Atmospheric optical thickness in visual spectrum region relationship to meteorological characteristics, plotting vertical profiles of humidity and aerosol attenuation coefficient 14 p2603 A70-30407
- Optimum alkali metal vapor humidity for turbine equipment estimated from energy output 14 p2535 A70-31008
- Water vapor abundance in Mars atmosphere from high resolution spectroscopy 14 p2649 A70-31211
- Electronic components environmental testing, examining temperature, humidity and vibration effects 14 p2558 A70-31295
- Clouds and precipitations radio brightness temperature contrasts taking into account underlying surface humidity 15 p2771 A70-32070
- Microwave propagation refractive index over India, showing influence of humidity and vapor pressure 15 p2701 A70-32470
- Unnatural environment behavior of leeches for long term biosatellite experiment, determining temperature, humidity, oxygen pressure, carbon dioxide concentration, calcium hydroxide limits, etc 16 p2854 A70-33994
- Humidity resistance test method involving flight simulation for airborne equipment in tropical environment 17 p3058 A70-35159
- Body temperature-maximum oxygen intake relations in hot humid air 17 p3038 A70-35424
- Aircraft air conditioning, discussing temperature and humidity control, cooling systems, etc 19 p3358 A70-37975
- Aerosol IR emission, discussing relative humidity, water droplet size and temperature effects on atmospheric radiance levels 21 p3846 A70-40804
- Integrated temperature and humidity control and water recovery subsystem for manned test in space station simulator 21 p3769 A70-40998
- Liquid rocket propellants tankage and components long term storage under extreme relative humidity and temperature conditions [SAE PAPER 700800] 24 p4392 A70-45911
- HUMIDITY MEASUREMENT**
- Remote monitoring of atmospheric wind and turbulence by cross correlation passive techniques, measuring heat and humidity fluxes 12 p2230 A70-26948
- Time constant equations for hair and film radiosonde hygrometers, allowing for inertial errors in humidity and cloud boundary measurements 14 p2603 A70-30412
- Humidity measurement for alkali metal vapor in turbines by electric calorimeter with two heaters 14 p2587 A70-31009
- Humidity calibration utilizing precision wide range optically controlled thermoelectrically cooled dew point hygrometer 14 p2587 A70-31165
- Humidity measurement and calibration systems, considering automatic optical dew point hygrometry 17 p3089 A70-35172
- High altitude humidity from millimeter-band water vapor lines, using EHF atmospheric spectral transparency calculation 19 p3461 A70-37633
- Atmospheric humidity measuring equipment and procedures for high altitudes, considering hygrometers, mass spectrometers, sondes, absorption spectra, etc 19 p3461 A70-37633
- Temperature induced humidity errors in military and Weather Bureau radiosondes carbon humidity element caused by solar irradiation 24 p4372 A70-46073
- Ruby laser application to air humidity measurement via hygrometric method 24 p4356 A70-46401
- HUMMINGBIRD AIRCRAFT**
- U XV-4 AIRCRAFT**
- HUNGARY**
- Report to COSPAR on Hungarian space research including satellite observations, upper atmosphere, geomagnetic effect, geodesy, cosmic rays, etc 15 p2830 A70-31713
- HURRICANES**
- Temperature and gust velocity turbulence at tropopause level over hurricane Beulah by instrumented U-2 aircraft 24 p4371 A70-45422
- HUYGENS PRINCIPLE**
- Kirchhoff theory of elastic wave diffraction in cylindrical case derived on modified Huygens principle, showing edge contribution 08 p1543 A70-20582
- Pulsar models distinguishing by Huygens principle in flat space-time, describing electromagnetic propagation in Riemann space 17 p3173 A70-35757
- Shadow photography applied to Mach reflections in argon, carbon dioxide and Freon 12 in shock tube, using Huygens principle for transfer mechanism 18 p3205 A70-36148
- Space three dimensionality compared with Huygens principle via quantum mechanics, discussing past and current theories and empirical arguments 24 p4380 A70-45643
- HYBRID COMBUSTION**
- HYBRID PROPELLANT ROCKET ENGINES**
- HYBRID COMPUTERS**
- One dimensional diffusion equation serial solution implementation by hybrid computation, using equivalence between differential and integral equations 02 p0324 A70-12259
- Automated modeling and structure optimization of linear dynamic systems and circuits, using hybrid computer techniques and time-domain test data 04 p0654 A70-15452
- Hybrid NASAP program module for direct design of linear dynamic circuits using simple optimization without sophisticated computer programming 06 p1015 A70-18422
- Arrhythmia monitor for cardiac distress prediction, using small hybrid computer for detection of abnormal rhythm and ECG complex comparison 07 p1221 A70-19604
- Random perturbation procedure for control variable functions optimization using hybrid computer method for analog solutions and digital storage 08 p1467 A70-21783
- Hybrid computers capabilities, programming and operation 09 p1640 A70-22212
- Hybrid computer for decision-directed estimators of two-class decision boundary, noting applications to medical diagnosis, communications and pattern recognition 09 p1641 A70-22965
- Hybrid computer applications in systems approach to engineering design, discussing design process and computer description 10 p1861 A70-24658
- Analog-digital real time data automatic acquisition and radar tracking system for air defense and air traffic control 11 p2014 A70-26313
- Time response deviation correction in hybrid computer control systems with digital feedback elements containing quantized coefficients 11 p2029 A70-26334
- Hybrid computing techniques for solving parabolic and hyperbolic partial differential equations, discussing serial method accuracy and use of parallel logic for integrator control 13 p2373 A70-29461
- Electron density profile calculation method using ionograms on analog-digital computer 14 p2569 A70-30209
- Analog/digital system for full scale airframe fatigue amplitude and phase signature measurements on CH-46D tandem rotor helicopter 15 p2739 A70-32323
- Speed convergence of hybrid vs digital computer synthesis of optimal boost vehicle controller, considering fuel consumption and pitch dynamics 16 p2981 A70-33442
- Optimal control solution for dynamic entry vehicle along planar trajectory, using hybrid computer simulation 16 p2981 A70-33443
- Variance reduction technique for hybrid computer generated random walk solutions of partial differential equations, comparing to analytical solution 16 p2942 A70-33731
- Design and reliability of digital systems for hard cores of fault tolerant computers /hybrid-redundant systems/, discussing advantages over multiplexed systems [JPL-TR-32-1490] 16 p2887 A70-33734
- Real time hybrid computer simulation of guided and controlled rocket flight, noting correlation with digital simulation 17 p3060 A70-35285
- Structural vibration test system, using hybrid computer for automatic control and data acquisition and reduction 17 p3061 A70-35488
- Small hybrid computer design, describing algorithms and subsystems for statistical studies 20 p3593 A70-39914
- Electron density profile calculation method using ionograms on analog-digital computer 24 p4330 A70-46284
- HYBRID NAVIGATION SYSTEMS**
- Helicopter automatic hybrid navigation system for increased accuracy over unfamiliar terrain and above-human performance, comparing navigating pilot performance with machine 02 p0335 A70-12134
- Error analysis algorithms for reducing computational load in stochastic estimation and control problems in hybrid navigation systems 11 p2025 A70-26208
- Inertial hybrid navigation system optimization, discussing performance curves and numerical filters synthesis and error elimination 13 p2448 A70-28747
- Digital self optimizing distortionless filter for hybrid navigation system 17 p3054 A70-35281
- HYBRID PROPELLANT ROCKET ENGINES**
- SR-1 hybrid propellant engine for sounding rockets, describing design and operating characteristics 13 p2474 A70-28689
- Delta launch vehicle for scientific and application satellites, describing three stage liquid and solid propulsion systems 15 p2810 A70-31783
- Hybrid rocket motor with solid oxidizer in ammonium nitrate additive, determining stable combustion conditions 15 p2790 A70-32274
- Hybrid rocket engine with solid oxidizer, noting applications as apogee or perigee motor 18 p3301 A70-36655
- High and low thrust hybrid rocket propulsion systems involving combinations of chemical, nuclear, thermal and electric propellants for interplanetary flights 21 p3869 A70-42042
- Quasi-hybrid rocket engines with solid propellant and liquid hydrogen injection, discussing performance in comparison with other propellant systems 22 p4089 A70-42498
- HYBRID PROPELLANTS**
- Hybrid propellant combustion mechanisms, connecting surface reactions to melting mechanism and subsequent liquid flow [ONERA-TP-736] 03 p0543 A70-13632
- Fragment fabrication of hybrid propellant solid grain emphasizing spherical shape and diameter uniformity 04 p0737 A70-15673
- Combustion and pyrolysis of carbonaceous solids considered for hybrid rocket fuels, using integrating factors in Caratheodory multiple entropies 06 p1172 A70-17468
- Tri- and bipropellants in spacecraft propulsion, discussing liquid and powder metals, hybrids, frozen tripropellants, etc 15 p2789 A70-32253
- Linear regression rate of spherical solid hybrid fuel grains oxidized in reducing gas flow 15 p2786 A70-32263

HYBRID PROPULSION

Hydrogen peroxide oxidizer for higher characteristic mixture ratio in hybrid propulsion systems with hypergolic reactions ignition [ONERA-TP-773] 02 p0352 A70-12209

Electrocatalysts, electrode structure and design of fuel cells using air at cathode, describing applications to hybrid systems 12 p2166 A70-27765

Energy transfer methods for hybrid air breathing ramjet propulsion systems with rocket motor S gas source [ICAS PAPER 70-61] 23 p4233 A70-44156

HYBRID ROCKET ENGINES

Chemical high energy rocket propellants, discussing metal combustion, hybrid and tribrid engines, combustion chambers, etc 11 p2100 A70-26282

Hybrid rocket engine with solid ammonium perchlorate oxidizer, discussing equilibrium conditions and engine performance 15 p2786 A70-32272

Hybrid rocket engine with solid oxidizer based on ammonium perchlorate and Al, studying performance with FORTRAN 5 program 15 p2787 A70-32273

Hybrid combustion ram rocket drives, discussing booster initial acceleration, exhaust gas use as fuel and payload gain [ICAS PAPER 70-50] 23 p4233 A70-44147

HYDRATES

Methane and ethane hydrate number measurement, alleviating liquid water occlusion and evaluating pressure effect 13 p2362 A70-29212

Thermodynamic stability of methane clathrate hydrate, building up ice grains halo within comets inner coma 14 p2650 A70-31243

HYDRATION

Tropospheric negative small ions formation reaction scheme, considering hydration degree 11 p2046 A70-26390

Hydration and lipid-protein ionic interaction in stearic acid monolayers during conformation of poly-L-lysine films 19 p3373 A70-37840

Space environment husbandry, examining chickens stress response to restraint and parental hydration 24 p4296 A70-45337

HYDRAULIC ACTUATORS

U ACTUATORS

U HYDRAULIC EQUIPMENT

HYDRAULIC ANALOGIES

Steady and unsteady gas dynamics analogies with two dimensional water flow, taking into account energy and continuity equations 17 p3069 A70-35032

Isentropic gas two dimensional unsteady flow through channel contraction, using hydraulic analogy 22 p4012 A70-43438

HYDRAULIC CONTROL

Triple mode control strategy to provide near optimal stable transient response in variably loaded electrohydraulic servomechanisms 02 p0272 A70-12728

Pulse width modulated /PWM/ electrohydraulic servo response characteristics from modulator transfer characteristic determination by Fourier series analysis of PWM signal [ASME PAPER 69-WA/AUT-2] 04 p0625 A70-14831

Static and dynamic characteristics of inertia load driving systems using electrohydraulic pressure and flow control servovalves [ASME PAPER 69-WA/FLCS-15] 04 p0626 A70-14842

Electrical and hydraulic units controlling second antenna at Pleumeur-Bodou space communication center 05 p0819 A70-15984

Hydrostatic synchronized steering of tow tractor for Boeing 747 and wide body jets compared to mechanical system 05 p0829 A70-16421

Fluid controlled solid rocket motors design for Mars mission with acceleration level as parameter, discussing mission specifications, system design and component considerations [AIAA PAPER 69-446] 07 p1365 A70-19707

Book on hydraulic and electrohydraulic mechanisms covering power transmission by fluids under pressure, data for designing and utilizing equipment, etc 09 p1612 A70-22636

Differential equation formulation for pipeline in hydraulic automatic control system considered as lumped or distributed parameter plant 09 p1612 A70-22823

Self contained remote sense remote control pressure regulator using pure fluid amplifiers, controlling large or small flow over wide pressure range 09 p1614 A70-23688

Fluidic logic elements for controlling selected cells extinction in hybrid plasma-fluidic display 09 p1738 A70-23758

Electrohydraulic fast response servosystem design and operation, describing nonlinear model based on component limitations 10 p1807 A70-24578

Pneumatically operated lifting mechanism and fluidic control system added to Izod impact testing machine for automatic impact repetition, counting and stopping 11 p2034 A70-26837

Time optimal control synthesis of fast acting gyrocompass mounted on fixed foundation and with hydraulic damper and torsional suspension of sensor 12 p2233 A70-27564

Electrohydraulic control system dynamics, examining executive component loading at low speeds and nonlinear resistances 13 p2349 A70-29720

Bang-bang control of electrohydraulic servomechanisms, approximating optimal control by quasi-optimal controls 16 p2887 A70-33685

SST electrohydraulic primary and standby brake control systems, discussing design and advantages [AIAA PAPER 70-913] 17 p3024 A70-35825

Three digit hydromechanical step type actuator drives with slide valve assembly for computer data sampling systems 18 p3216 A70-37071

Hydraulic and pneumatic controls construction and use in machine tools 19 p3359 A70-38725

Liquid metal hydraulic servoactuation packages for flight control in high temperature environments without coolant systems 21 p3750 A70-40785

Flow difference sensor for aircraft hydraulic systems damage vulnerability reduction, discussing design, operation and flight tests results 21 p3750 A70-40786

Fluidic controls for propulsion engines, describing optimum fabrication techniques [ASME PAPER 70-FLCS-7] 22 p3964 A70-42420

Fluidics for aircraft high pressure hydraulic systems, discussing circuit breaker, feel computer and landing gear sequencing circuit [SAE PAPER 700784] 24 p4295 A70-45860

HYDRAULIC EQUIPMENT

NT AIRCRAFT HYDRAULIC SYSTEMS

Approximate determination of termination hydraulic servomotors frequency characteristics with four way valves using piecewise straight lines on Bode diagram 01 p0007 A70-10034

Aircraft/aerospace fluid systems flexible hose and rigid tube assemblies fire resistance and test requirements 01 p0011 A70-11459

Quick-disconnect couplings selection guide for aerospace fluid systems, emphasizing functional and weight considerations [SAE-AIR-1047A] 01 p0197 A70-11461

Hydraulic drive mechanism for moving missile tower between launch pad and storage site 02 p0276 A70-12862

Slide and sleeve type servovalves used in Boeing aircraft possessing chip shearing capability of 200 pounds axial force 02 p0229 A70-12863

Cavitating flow in converging channels of hydraulic system, calculating energy distribution at gas-vapor phase using Borda-Carnot theorem 03 p0466 A70-13513

Small three stage hydraulic turbine for aerospace and commercial applications, discussing design and performance 04 p0628 A70-15640

Stability conditions for relief valves assumed to be part of closed hydraulic line simulating receiving part 05 p0797 A70-15899

Hydraulic jacks for Boeing 747 support during assembly, discussing operation, console, pressure system and safety features 05 p0798 A70-16422

Vibration damping of oil hydraulic system using bladder type accumulator composed of rubber, measuring frequency response of shock absorber 06 p0988 A70-17140

Book on hydraulic and electrohydraulic mechanisms covering power transmission by fluids under pressure, data for designing and utilizing equipment, etc 09 p1612 A70-22636

Stability region of hydraulic system containing centrifugal pump calculated from pressure head dependence on pump inlet pressure 09 p1607 A70-23622

Hydraulic regenerative servoamplifier system for electrohydraulic actuator design, discussing specifications and test results 09 p1614 A70-23686

Pressure loss in tubulature of oil-hydraulic drive mechanism, allowing for viscosity changes associated with oil temperature and pressure increases 10 p1809 A70-25209

Hydraulic driving system stick-slip prevention by acceleration and transient velocity feedback compensation techniques 11 p2060 A70-26407

Electrohydraulic vibrators and shakers for testing aircraft systems, diesel engines and structural joints, describing design and operation 11 p2032 A70-26442

Rotodynamic pumps energetic characteristics determination by pneumatic tests, describing air test results for various models 12 p2165 A70-27399

Hydraulic piston-valve-type slave mechanism oscillations with rigid feedback and inertial load at actuated shaft, using harmonic linearization method 12 p2167 A70-28340

Hydraulic seals for fire resistant fluids in hydraulic equipment, describing computerized designs 13 p2416 A70-28610

Hydraulic system pumps ratings, classification and selection 13 p2419 A70-29219

Gear pumps for hydraulic systems, discussing costs, types and applications 14 p2590 A70-30302

Adaptive hydraulic servomechanism control systems synthesis by Liapunov direct method, noting parameter compensation effect on state error reduction 14 p2534 A70-30621

Radial clearance, pressure and piston length and diameter dependence of friction force at rest in piston type hydraulic devices 14 p2534 A70-30872

Liquid metals pump with cylindrical hydraulic coupling for actuating axial wheel, investigating cavitation and pumping effects on performance 14 p2535 A70-31012

Emergency auxiliary electric and/or hydraulic power for commercial and military aircraft using self contained monofueled gas turbine system 16 p2964 A70-33472

Spacecraft hydraulic timers design and qualifications testing, discussing oil selection and temperature dependence 16 p2914 A70-34112

Automatic control system stability, allowing for position and velocity loads and compressibility of fluid in force cylinder of hydraulic actuating mechanism 17 p3024 A70-35367

Dynamic characteristics of hydraulic fatigue testing machines, using hydraulic activation efficiency factor 17 p3064 A70-35718

Supply valve influence on dynamic characteristics of volumetric hydraulic actuator 18 p3215 A70-36126

Lumped parameter pipeline and hydraulic systems stability, deriving equations of motion for closed and open cycle control systems 18 p3216 A70-36946

Nonlinear resistance element with square law I-V characteristics for electrical analogs of hydraulic systems 19 p3359 A70-38707

Prototype synchronizing valves for maintaining identical flow velocities of two hydraulic actuating elements, noting unbalanced hydrodynamic forces and orifices asymmetry effects 20 p3564 A70-39717

Aircraft vertical gyro with hydraulic damping device, calculating ballistic deviations limitation conditions 20 p3632 A70-39733

Hydraulic load loops with random force signal for aircraft structures endurance testing 20 p3593 A70-39913

Hydraulic synchronizers for motors and actuators speed equalization, describing operation and technical specifications 21 p3756 A70-40800

Servo-hydraulic testing machine for measuring cyclic stress-strain behavior of materials subjected to fatigue and creep at elevated temperature 23 p4178 A70-44912

Hydraulic servomechanism stability and step response, considering unequal oil volume on either side of jack 24 p4292 A70-45159

Fluidic logic devices compared with electric relay and hydraulic/pneumatic valve equivalents 24 p4293 A70-45429

Hydraulic and pneumatic components for logic circuits of automatic controls, considering amplifiers, interlocked systems and use of fluidics 24 p4293 A70-45618

High pressure hydraulic fluidic vortex rate sensor feasibility, considering variable geometry sensor design, fabrication and tests [SAE PAPER 700788] 24 p4294 A70-45857

Hydraulic and pneumatic dampers operation, analyzing force components 24 p4427 A70-46380

HYDRAULIC FLUIDS

Purity requirements for oil in hydraulic systems of modern aircraft, discussing filtering devices and Swedish Air Force and SAAB specifications

01 p0130 A70-11359

Hydraulic fluid cleanliness requirements for aircraft systems, filtering, servovalve life, solid particles effects on friction, etc

03 p0414 A70-12999

Ultrasonic testing of hydraulic liquids and aircraft and engine lubricating oils resistance to viscosity decrease, analyzing large molecule compounds disintegration

09 p1693 A70-23405

Pressure loss in tubulature of oil-hydraulic drive mechanism, allowing for viscosity changes associated with oil temperature and pressure increases

10 p1809 A70-25209

Hydraulic seals for fire resistant fluids in hydraulic equipment, describing computerized designs

13 p2416 A70-28610

Proportional and flip-flop elements in hydraulic circuits using oils, noting cavitation effect on switching stability in digital elements

14 p2534 A70-30677

Upstream wear of small metal orifices under large pressure drops in phosphate ester hydraulic fluids due to current driven electrochemical corrosion

[ASME PAPER 70-FE-15] 16 p2919 A70-33629

Hydraulic fluids and lubrication oils resistance to mechanical shear forces by ultrasonic method based on acoustically induced cavitation effects

20 p3655 A70-39718

HYDRAULIC HEATING SOURCES

U HEAT SOURCES

U HYDRAULIC EQUIPMENT

HYDRAULIC JETS

Disintegration of charged distilled water jets, discussing drops size, velocity distribution and instabilities

03 p0467 A70-13781

Core length of water jet from circular tube, considering wall roughness, tube diameter and water viscosity and surface tension

06 p1031 A70-17135

HYDRAULIC PUMPS

U HYDRAULIC EQUIPMENT

U PUMPS

HYDRAULIC SYSTEMS

U HYDRAULIC EQUIPMENT

HYDRAULIC TEST TUNNELS

Interference between body and porous walls of water tunnels by one dimensional solution for usable length of tunnel

07 p1248 A70-19078

Chemical reaction product fluctuations in reacting and nonreacting turbulent wake of sphere in water tunnel detected by injected salts conductimetric titration

[AIAA PAPER 68-686] 23 p4134 A70-44570

HYDRAULIC VALVES

U HYDRAULIC EQUIPMENT

U VALVES

HYDRAULICS

Resistance, capacitance and inductance in passive hydraulic circuits considered in analogy with electric circuits to determine dynamic characteristics

03 p0415 A70-13931

Hydraulic characteristics of flow through miniature slot orifices for rocket engine injectors, observing stability of effluent liquid streams

[AIAA PAPER 70-706] 16 p2891 A70-33566

HYDRAULIC ENGINES

Satellite attitude and orbit control systems based on electrically heated ammonia or hydrazine

09 p1767 A70-23432

ATS-3 hydrazine orbit control system efficiency evaluation statistical method, considering stationkeeping maneuvers

[AIAA PAPER 70-460] 11 p2121 A70-25464

Pressure peaks control in hydrazine propulsion system during static tests by controlling initial hydrazine injection

11 p2101 A70-25691

First pulse vacuum startup measurements of monopropellant hydrazine thrust reactors with sponaneous catalyst, simulating spacecraft control dynamics

14 p2628 A70-30753

Monopropellant hydrazine RCS rocket engine module, discussing operating conditions, development, thermal control and valve internal leakage

[AIAA PAPER 70-654] 16 p2965 A70-33544

Small rocket engines tailoff impulse and tailoff repeatability, comparing monopropellant hydrazine and storable bipropellant engines impulse data

[AIAA PAPER 70-674] 16 p2967 A70-33576

Reentry vehicles fluidically controlled hydrazine rocket engine modules for roll rate control

[AIAA PAPER 70-650] 16 p2970 A70-33617

HYDRAZINE NITRATE

Simultaneous mass spectrometric differential thermal analysis of low pressure decompositions of nitrate salts of monomethylhydrazine and methylamine

20 p3688 A70-40475

HYDRAZINES

NT DIMETHYLHYDRAZINES

NT METHYLHYDRAZINE

Hydrazine monopropellant performance and characteristics, describing various catalysts and propulsion systems

02 p0352 A70-12265

Nonequilibrium initial condition combustion effects on propellant performance for hydrazine/ chlorine pentafluoride and hydrogen/fluorine with equilibrium, kinetic and frozen nozzle flow

[AIAA PAPER 69-469] 04 p0732 A70-15423

Preignition products from hydrazine propellants at simulated high altitude conditions using IR spectrophotometry, mass spectrometry and differential thermal analysis

07 p1358 A70-19579

Turbulent heat and mass diffusion in catalytic reactors for hydrazine decomposition, developing computer program to calculate temperature and reactant concentration distributions

[AIAA PAPER 69-421] 07 p1365 A70-19706

Oxygen-hydrazine interactions on partially immersed metal electrodes, studying conjugated electrochemical reactions

10 p1830 A70-24457

Optimum penetration and separation mixing of unlike doublet injector element with hypergolic hydrazine and nitrogen tetroxide propellants

[JPL-TR-32-1487] 11 p2099 A70-25995

Combustion stability effects of additives on hydrazine/nitrogen tetroxide propellant combination by measuring droplet burning rates

11 p2100 A70-26283

Ethylene-propylene elastomers compatibility with hydrazine determined under ambient conditions from gas evolution rate by catalytic decomposition

13 p2472 A70-28669

Disproportionation to combination ratio of hydrazyl radicals generated in absence of hydrazine direct decomposition

14 p2544 A70-30120

Hydrazine decomposition in low pressure flame, investigating isotopic substitution effect on flame speed

14 p2628 A70-31094

Pressurization system for nitrogen generation based on hydrazine catalytic decomposition, describing metal membrane configuration, fuel additives, etc

[AIAA PAPER 70-682] 16 p2962 A70-33583

Liquid hydrazine decomposition by Shell 405 catalyst, determining gaseous products by gas chromatography and titrimetric analysis

[AIAA PAPER 70-606] 16 p2856 A70-33603

Reactive stream separation high speed color photography for impinging streams of nitrogen tetroxide and hydrazine

[AIAA PAPER 70-608] 16 p2998 A70-33605

Fuel cell development, discussing consumable electrode, hydrogen/oxygen, hydrazine/hydrogen superoxide, hydrazine/air and methanol/air cells

19 p3359 A70-38497

Hydrazine-fuelled battery low power consumption auxiliary system with voltage regulator and gas pumps

22 p3966 A70-43539

Hydrazine-oxygen fuel cell design and operation, discussing efficiency, electrolyte space, etc

22 p3966 A70-43541

Strontium nitride hydrolysis, investigating hydrazine presence among products

23 p4158 A70-44598

HYDRIDES

NT CARBORANE

NT DIBORANE

NT DIHYDRIDES

NT LITHIUM HYDRIDES

NT METAL HYDRIDES

NT PHOSPHINES

NT SILANES

NT ZIRCONIUM HYDRIDES

NH emission systems radiative lifetimes and SiH and SiH transition probabilities measured, noting effects of radiative cascading

05 p0885 A70-16424

SiH molecular absorption lines in solar disk spectrum, determining maximum equivalent widths and oscillator strength

06 p1143 A70-17996

Magnesium hydride absorption lines in sunspot spectrograms indicating heavy Mg enhancement in sun relative to earth

08 p1571 A70-20904

Hydrides precipitation in Ti-Al-Mo-V alloys using transmission electron microscopy, discussing crystal structure, activation energy, hydride-matrix phase interface, etc

08 p1525 A70-21964

Temperature and hydrogen concentration effect on microhardness of polycrystalline beta-vanadium hydride, obtaining photomicrographs of indentations

10 p1906 A70-25227

Hydride segregation in Ti alloy weldments made with unalloyed Ti filler metal, determining effect on mechanical properties

14 p2591 A70-30932

HYDROCARBON POISONING

Titanium hydride deformation assisted nucleation in alpha-beta titanium alloy, showing low strain rate embrittlement and stress corrosion crack propagation in aqueous environments

17 p3116 A70-34395

Ti mechanical properties dependence on grain boundary size and hydride precipitation characteristics, considering transcrystalline and intercrystalline fracture

20 p3652 A70-40179

HYDROACOUSTICS

U UNDERWATER ACOUSTICS

HYDROAEROMECHANICS

U AERODYNAMICS

HYDROBROMIDES

Unbranched chain reaction in hydrogen bromide for studying laminar one dimensional flame propagation, determining temperature dependence, velocity and concentrations at fixed time

06 p1177 A70-17797

HYDROCARBON COMBUSTION

Tetrafluorodibromoethane combustion inhibitor effects on aircraft hydrocarbon fuels flame propagation rate and explosion pressure

01 p0160 A70-11011

Electric field effects on flame structure and propagation rate in methane-air mixture

01 p0217 A70-11013

Premixed methane-oxygen-nitrogen combustion in conical reactor fed by choked sonic flow jet, analyzing reaction products chromatographically

02 p0397 A70-12030

Reaction analysis of acetylene-oxygen flames with known concentrations and temperature profiles, integrating one dimensional flame equations numerically

02 p0251 A70-12035

Noise generation in turbulent premixed flames, turbulent diffusion flames and liquid-spray combustion of hydrocarbon fuels, using optical method

02 p0399 A70-12040

Combustion and flow characteristics associated with direct injection of liquid hydrocarbons into high speed air stream

[AIAA PAPER 70-88] 06 p1182 A70-18198

Methane and propane flames in rotating air flow fields generated by cylindrical rotating wire mesh screen, discussing flame lengths and blowoff velocities

14 p2666 A70-31090

Methane-air inverted flames blowoff at thin stabilization plates of twin slit inverted flame burner, determining critical values of Karlovitz flame stretch factor

14 p2666 A70-31092

Gas phase chemicals synthesis via AC diffuse discharge superimposed on propane-air flame seeded with potassium carbonate in electrically augmented flame burner

14 p2546 A70-31097

Electron temperatures and electron and negative ion concentrations in low pressure hydrocarbon flames

14 p2666 A70-31098

Laminar hexane diffusion flame, investigating distribution of final and intermediate combustion products

22 p4123 A70-42522

HYDROCARBON FUELS

NT GASOLINE

NT JET ENGINE FUELS

Liquefied natural gas or liquefied methane as burning propulsion system for SST, examining storage volume, fuel-tank insulation and implosion danger

03 p0543 A70-12998

Burning constants prediction for suspended hydrocarbon fuel droplets based on modified theoretical equation

03 p0544 A70-13916

Solid tar deposits from hydrocarbon fuels oxidation during prolonged storage

12 p2289 A70-27494

Hydrocarbon fuel components relative reactivities in direct electrochemical oxidation on platinum black/Teflon electrodes in phosphoric acid

12 p2182 A70-27762

Liquid hydrocarbon-air battery with fuel transport operation, considering electrode structure, boiling range, carbon dioxide rejection, etc

12 p2166 A70-27764

Natural gas-air fuel cell battery with sulfuric acid electrolyte for low temperature operation

12 p2166 A70-27766

Atmospheric pressure hydrocarbon-air mixtures confined by thin plastic membrane, obtaining composition range for detonation initiation limits

21 p3865 A70-40884

Computerized calculation of gas turbine cycles thermal efficiency, using hydrocarbon fuel, considering fuel composition and heat of combustion changes

22 p4125 A70-43439

HYDROCARBON POISONING

Acute gasoline poisoning toxicology and prophylaxis, manner of ingestion and effects on organs and systems

08 p1451 A70-20976

HYDROCARBONS

NT ACETYLENE
 NT ALKANES
 NT ALKENES
 NT ANTHRACENE
 NT BENZENE
 NT BUTADIENE
 NT BUTANES
 NT CYCLIC HYDROCARBONS
 NT CYCLOBUTANE
 NT CYCLOPROPANE
 NT DIPHENYL COMPOUNDS
 NT ETHANE
 NT ETHYLENE
 NT HEPTANES
 NT HEXENES
 NT METHANE
 NT METHYLENE
 NT NAPHTHALENE
 NT NEOPENTANE
 NT PARAFFINS
 NT PROPANE
 NT PROPYLENE
 NT TOLUENE
 NT TRIPHENYLS

Hydrocarbon content of coorongite derived from algae analyzed by IR spectrometry, gas chromatography and mass spectrometry, discussing alkanes and alkenes occurrence

01 p0041 A70-10037

Hydrocarbon contents of two sediments from Scottish Carboniferous Formation, examining isoprenoid alkanes abiogenesis

01 p0041 A70-10038

Electron mobility in single component aromatic hydrocarbons, considering crystals structures and electrical properties, energy dissipation and fluctuation, etc

01 p0158 A70-10517

Hydrocarbon fraction examination of *Botryococcus braunii* growing in natural environment, discussing unsaturated isomeric hydrocarbons

02 p0249 A70-11679

CH and CD molecules UV absorption spectra, using flash photolysis of diazomethane

02 p0341 A70-11795

Hydrocarbons and fatty acids distribution in living organisms, fossils, sediments and crude oils, discussing slow thermal maturation role and geological applications

02 p0252 A70-12520

Hydrocarbon distribution of various algae and bacteria, discussing hydrocarbons diagenesis and biological transformations in sediments

06 p0997 A70-18401

Ozone formation in presence of nitrogen oxides and hydrocarbons during long wave UV irradiation, noting energy yield

09 p1629 A70-22328

CH, CD and CH ion excited states decay rates determined from phase shift and frequency data, discussing implications for astrophysics

09 p1731 A70-22513

Carbonaceous chondrites composition by gas chromatography for light hydrocarbons and carbon, discussing origin of organic matter

10 p1949 A70-25327

Hydrocarbon assimilating bacteria cultures selection, considering highest specific growth rate and maximum productivity

11 p1991 A70-25939

Early Precambrian chert porosity and permeability, investigating hydrocarbon content origin

13 p2400 A70-29863

Thermal product distributions and energy dependencies of ion-molecule reactions in allene and propyne, using ion cyclotron resonance

16 p2856 A70-33651

Hydrocarbon gas detection using He-Ne laser radiation absorption, discussing detector electronics

17 p3107 A70-35520

Precambrian cherts hydrocarbon and fatty acid concentrations and C and S stable isotope ratios, discussing biological evolution rate

18 p3244 A70-35969

Tetrafluorodibromo-ethane and bromethyl inhibiting effects on explosion development in constant volume container and flame expansion rates in hydrogen-air mixtures

18 p3345 A70-36241

Solid propellant binders of saturated aliphatic hydrocarbons, describing microstructure, performance contribution, etc

21 p3865 A70-42143

Saturated hydrocarbon prepolymers for solid propellant elastomeric binders

21 p3865 A70-42144

Abiotic synthesis of meteoritic aliphatic hydrocarbons produced by open flow Fischer-Tropsch processes for hydrogen and Co interactions

24 p4402 A70-45377

HYDROCHLORIC ACID

UV absorption cross sections of CO, HCl and ICN, analyzing reactions causing various spectral features

08 p1455 A70-21340

Criticism and reply to Venus cloud water drop HCl concentration preventing ice cloud formation

11 p2108 A70-25653

CW HCl chemical laser action via chlorine atoms reaction with hydrogen iodide in fast flowing mixing device

19 p3444 A70-37542

Ca ion reversible effects of hydrochloric acid and ammonia water on betacyanin leakage from beetroot sections

19 p3365 A70-38375

Hydrogen chloride self broadened fundamental vibration rotation band intensity variation with pressure investigated by absorption spectroscopy analysis

22 p3983 A70-42945

HYDROCHLORIDES

Fugacities of hCl and HF compared with abundance in volcanic fumarolic emanations, indicating magma undersaturation

20 p3619 A70-39321

HYDROCYANIC ACID

U HYDROGEN CYANIDES

HYDRODYNAMIC EQUATIONS

NT HELMHOLTZ VORTICITY EQUATION

Hydrodynamics, mass and energy transfer equations for moderately dense gases multicomponent mixtures, using Bogoliubov theory

01 p1146 A70-10129

Finite difference schemes compared for numerical weather prediction by application to shallow water equations on hemisphere, noting mesh spacing

01 p0135 A70-11064

Protostars rapid contraction and flare up evolutionary phases, solving hydrodynamic equations of motion

01 p0190 A70-11344

Hydrodynamic equations and Grad transport coefficients for nonequilibrium rarefied monatomic gases developed for molecular collisions

01 p0068 A70-11567

Hydrodynamic approximation to interplanetary gas motion influenced by solar flare caused perturbations

01 p0192 A70-11586

Equations of hydrodynamics governing perfect fluid in second postNewtonian approximation to general relativity, deriving energy momentum tensor equation

02 p0337 A70-11776

Static thermosphere model using hydrodynamic equations, assuming uniform temperature and non-existent Coriolis forces, viscous stresses, horizontal velocity vector and thermal fluxes

02 p0327 A70-12384

Diffusive transport term in hydrodynamic equations describing flow over strongly ablating entry objects, discussing charge separation and pressure diffusion

03 p0405 A70-12926

Linearized steady state hydrodynamic equations describing solar wind meridional motions used for studying zonal pressure perturbations

03 p0558 A70-13599

Boundary value problems for partial differential equations representing steady gas flow hydrodynamic problems

03 p0469 A70-14228

Hydrothermodynamic equations used in forecasting meteorological components solved by assuming equations of motion quasi-linear and reducing to ordinary differential equations

05 p0878 A70-16195

Hydrodynamic coefficients of algebraic equations for boundary value problems in disturbed motion of body with rib-reinforced liquid filled cavity

05 p0836 A70-16956

Linearized MHD equations for motion of solids in viscous and electrically conducting fluids

06 p1120 A70-17532

Primitive and balance hydrodynamics equations of meteorological fields noting computational viscosity

06 p1097 A70-17826

Short term weather forecast hydrodynamic equations reduced to solving nonlinear differential equations by introducing dependent variables

07 p1329 A70-19647

Interstellar gas clouds collapse using finite difference numerical methods in solving hydrodynamic equations involving gravitation

07 p1390 A70-20288

Prognostic maps of geopotential and wind in middle troposphere derived from hydrodynamic equations

07 p1330 A70-20307

Surface oscillations of plasma in external HF field derived from hydrodynamics and Maxwell equations

07 p1355 A70-20367

Hydrodynamics, mass and energy transfer equations for moderately dense gases multicomponent mixtures using Bogoliubov theory

08 p1548 A70-21405

Orr-Sommerfeld equation of hydrodynamic stability theory solved for incompressible two dimensional boundary layer flow on basis of reduction to integral equation

10 p1867 A70-24161

Hydrodynamic lubrication theory two dimensional problem, comparing numerical methods for elliptical nonlinear differential equations

10 p1893 A70-24164

Hydrodynamic equations for ions and electrons of ionized collisional plasma in inhomogeneous magnetic field based on Boltzmann kinetic equations

11 p2088 A70-25710

Stellar hydrodynamic equations for thin disk galaxy derived from collisionless Boltzmann equation moments

11 p2117 A70-26688

General relativistic hydrodynamics near equilibrium, discussing velocity and kinetic energy increase spherically symmetric large masses as function of radius change

12 p2300 A70-27392

Pressure field equation derivation for hydrodynamic journal bearing in superlaminar regime, using turbulent Couette and screw flow friction correlations

13 p2418 A70-28742

Convection effects in mantle on earth gravitational field using hydrodynamic model

13 p2488 A70-28764

Hydrodynamic equations to obtain transformation coefficient for HF weakly damped waves in magnetoactive plasma, applying to solar corona

13 p2463 A70-29227

Comparative sets of higher order adiabatic motion equations for plasmas in electric and magnetic fields with slow variations

14 p2624 A70-31043

Atmospheric cellular convection, reducing hydrodynamic equations to amplitude equations for vertical velocity

15 p2770 A70-32064

Redundant variable errors in weather prediction, specifying initial conditions for time integration of hydrothermodynamic equations for atmospheric motion

15 p2771 A70-32368

Stationary hydrodynamic equations of gas channel and nozzle flow with inlet tangential discontinuities

16 p2833 A70-33247

Post-Newtonian equations of hydrodynamics and radiation reaction in general relativity

17 p3156 A70-34828

Lagrangian invariants of inviscid compressible fluid dynamics applied to hydrodynamic equations

17 p3070 A70-35333

Gasdynamic equations in Euler variables, constructing completely conservative difference schemes with first and second orders of approximation

18 p3241 A70-36288

Acoustic turbulence spectrum in compressible fluid with potential motion, using complex traveling wave amplitudes in hydrodynamic equations

18 p3242 A70-36637

Complementary variational principles applied to free oscillations of incompressible fluid in container, using linearized hydrodynamic equations

21 p3807 A70-41323

Ion sound system one dimensional hydrodynamic equations, examining formation and interaction of nonlinear ion acoustic shock waves

21 p3857 A70-41384

Nonlinear properties of first order differential equations for axisymmetric velocity vector fields of ideal incompressible fluid, using nonlinear singular integral equation

23 p4181 A70-44343

Two point hydrodynamic equation for molecular fluctuations divergent growth in classical shear flow via B-B-G-K-Y procedure and double series moment expansion

24 p4382 A70-46254

HYDRODYNAMIC STABILITY

U FLOW STABILITY

HYDRODYNAMIC TUNNELS

U PLASMA JET WIND TUNNELS

HYDRODYNAMICS

NT ELASTOHYDRODYNAMICS

NT ELECTROHYDRODYNAMICS

NT MAGNETOHYDRODYNAMICS

Hydrodynamic explanation of upper atmosphere perturbation effects on tropospheric circulation, discussing experiments for solar activity effects on atmospheric dynamics

01 p0073 A70-10582

Gas ignition and burning processes calculation with allowance for hydrodynamics, discussing time saving finite difference solution of differential equations system

01 p0218 A70-11020

Organic liquid nucleate pool boiling experiments determining stresses, surface tension, viscosity and gravitation relationships to bubble shape and microlayer formation

01 p0218 A70-11180

Characteristics of dynamic mechanical systems including solid state and hydrodynamic analogs of ideal incompressible fluids, based on statistical theory of turbulence

01 p0068 A70-11594

Dynamics of turbulent motion of incompressible viscous fluid particles, using Lagrangian functions

01 p0068 A70-11603

Leakage in mechanical face seals with hydrodynamic films, noting misaligned seal theories for pumping with cavities and two fluids
[ASLE FICFS PREPRINT 19] 02 p0308 A70-12170

Hydrodynamic turbulent boundary layer on smooth wall, using finite difference theory
02 p0285 A70-12351

Dynamic electric field in solar coronal exosphere on basis of kinetic and hydrodynamic theories, giving estimate of solar wind
02 p0359 A70-12609

Star rotation and meridional circulation hydrodynamic theory, considering magnetic fields and internal friction
03 p0564 A70-13228

Hydromagnetic forces effects on tidal period hydrodynamic waves, explaining ionospheric tidal motion behavior
03 p0478 A70-13995

Polarohydrodynamics method applied to electrochemical kinetics of electrode cathodic or anodic current by coupling surface reaction with mass transfer
03 p0534 A70-14268

Weather prediction technique based on hydrodynamical equations, outlining atmospheric circulation models
[AAS PAPER 69-619] 04 p0714 A70-14646

Optimum one dimensional Rayleigh gas slider bearing, calculating step location, pressure and load capacity for range of bearing numbers
[ASME PAPER 69-WA/LUB-1] 04 p0698 A70-14772

Hydrodynamic theory of elastic-viscous liquid lubrication for journal bearings, assuming stress-strain relationship with unequal cross stresses
05 p0855 A70-16509

Hydrodynamic model of blood coagulation in stagnation point flow, analyzing platelet diffusion, white cell bonding stress and thrombus formation
[AIAA PAPER 70-143] 06 p1003 A70-18123

Temperature fields and hydrodynamics in laminar flow of vertical liquid layers during free convection
07 p1422 A70-19655

Lagrangian tensor formalism for hydrodynamic stretching of material line and surface elements under statistically isotropic incompressible turbulence
07 p1260 A70-19979

Plasma flow structure near frontal point in earth magnetosphere, using quasi-hydrodynamic two dimensional model to obtain power series solution
07 p1391 A70-20419

Direct and inverse problems of hydrodynamics of supercavitating lattices with leading and trailing edge caverns extending over upper surface of profile
08 p1482 A70-20534

Hydrodynamic sealing action resulting from helical grooving machined into shaft or lip of radial seal, describing pressure gradients role
08 p1507 A70-21268

Boltzmann systems dynamics, discussing excitation spectrum, momentum relaxation time, particle diffusion trajectory, macroscopic theory of quasi-collective processes, hydrodynamics, etc
08 p1545 A70-21421

Star rotation and meridional circulation hydrodynamic theory, considering magnetic fields and internal friction
08 p1580 A70-21661

Supernovae hydrodynamics, discussing early light curves energy requirements and shock wave dynamics in terms of neutrino diffusion
09 p1749 A70-21992

Hydrodynamic processes during focusing of monopulse ruby laser emission into water, determining photohydrodynamic coefficient
09 p1694 A70-22111

Vortex and potential motions interactions in relativistic hydrodynamics, studying mutual generation
09 p1754 A70-22460

Vortex and potential motions interactions in relativistic hydrodynamics, noting effects of gravitation equations nonlinearity
09 p1754 A70-22461

Hydrodynamic stability criterion of isolating incompressible fluids subjected to unipolar space charge injection
09 p1737 A70-23311

Hydrodynamic energy flow down horizontal tunnel from nuclear explosive detonated underground, recording shock front luminosity and time of arrival
10 p1857 A70-23985

Momentum-energy tensor and angular momentum for hydrodynamic and electrodynamic fields determined in transformations of m-parametric Lie group
10 p1922 A70-24098

Optimization in epihydrostatics and epihydrodynamics, discussing liquid in rectangular tank, electro-magneto-epi hydrodynamics and thermal instability
10 p1866 A70-24108

Cascade theory of turbulence, applying cascade decomposition resulting from Navier-Stokes applica-

tion to hydrodynamic turbulence to Riemann equation for atmospheric and plasma turbulence
10 p1868 A70-24167

Hydrodynamic analogy in restricted three body problem of celestial mechanics, discussing mass and momentum conservation and physical properties uniqueness
10 p1938 A70-24180

Viscous fluid dynamics for reducing hydrodynamic resistance, discussing aquatic animals speeds, vortex flows, etc
10 p1871 A70-25193

Optimal efficiency of axial turbomachines limit loading of blade root and hydrodynamical criteria
11 p1975 A70-25791

Shock wave formation and propagation analyzed by hydrodynamic model of two directional traffic flow based on continuity equations and velocity-density empirical relations
12 p2212 A70-28196

Hydrodynamic entrance length in channels and tubes of varying cross section with arbitrary initial velocity profile
[DFVLR-SONDDR-39] 12 p2212 A70-28210

Thermohydrodynamic seals design, properties and performance compared with standard mechanical seals
13 p2417 A70-28612

Hydrodynamically lubricated rectangular taper-land bearing pads, analyzing geometry, viscosity, load capacity, friction and operating temperature conditions
13 p2418 A70-28740

Discontinuous hydrodynamic flows derived for stability condition using three dimensional second-order difference schemes
13 p2441 A70-29099

Axisymmetric bodies slow rotation or rotary oscillation in hydrodynamics and MHD using boundary value problems solutions
14 p2527 A70-30276

Low amplitude waves and substantial frequencies interaction by averaging method for hydrodynamics of waves in collisionless plasmas
15 p2720 A70-32114

Trail formation due to tidal effect in interacting galaxies during close approaches, considering mass flow hydrodynamics
15 p2801 A70-32481

Hydrogen oxygen rocket engine two phase liquid hydrogen pump capability and hydrodynamic design, analyzing constant-quality flow, acoustic effects, compressible flow and cavitation
[AIAA PAPER 69-549] 15 p2791 A70-32511

Hypervelocity impact theory, discussing Euler hydrodynamic codes, projectile cratering dimensional analysis, self similar solutions, etc
15 p2823 A70-32785

Andromeda Galaxy M31 hydrodynamic model based on given mass distribution, determining kinematic functions
15 p2808 A70-32884

Soviet book on hydrodynamics of flows with free boundaries, covering fluids penetration by solid body, hydrofoil motion, cavitation flow, etc
16 p2890 A70-32912

Hydrodynamic internal streamline flow analysis for turboprop inducer blades under cavitating and non-cavitating conditions
[AIAA PAPER 70-629] 16 p2964 A70-33528

Liquid or solid Leidenfrost film boiling on saturated cryogenic liquid surface, discussing hydrodynamic model similar to propellant spillage accidents
17 p3194 A70-34744

Hydrodynamic entry length for laminar flow between parallel porous plates, using finite difference theory for flow equations
17 p3069 A70-34983

Hydrodynamic flow stability, formulating localization properties for short wave perturbation
17 p3073 A70-35735

Hydrodynamic model analogy to water bag/incompressible homogeneous fluid in phase space/, investigating nonlinear collisionless plasma oscillations
19 p3474 A70-37365

Optimum one dimensional Rayleigh gas slider bearing, calculating step location, pressure and load capacity for range of bearing numbers
[ASME PAPER 69-WA/LUB-1] 19 p3436 A70-37617

Eringen theory of micropolar fluids for hydrodynamic turbulence
19 p3404 A70-37783

Solar atmospheric hydrodynamic response to stationary random forces homogeneous over horizontal planes, discussing common energy argument, various models and photospheric oscillation
19 p3523 A70-38690

Two dimensional detonations structure by nonlinear theory for systems with hydrodynamically unstable steady state solutions, imposing periodic boundary conditions
20 p3609 A70-39658

Boundary conditions on vector and scalar potentials in viscous three dimensional hydrodynamics, investigating compressible flow problems
20 p3612 A70-40115

Unsteady convective heat transfer and hydrodynamics of laminar and turbulent channel flows
21 p3808 A70-41374

Turbulent hydrodynamic and thermal boundary layer development in internally heated annulus
[ASME PAPER 70-HT-9] 22 p4008 A70-42438

Shock wave formation and propagation analyzed by hydrodynamic model of two directional traffic flow based on continuity equations and velocity-density empirical relations
22 p4012 A70-43321

Newtonian hydrodynamic analogies for homogeneous anisotropic models in general relativity
22 p4075 A70-43472

Trail formation due to tidal effect in interacting galaxies during close approaches, considering mass flow hydrodynamics
23 p4240 A70-43906

HYDROELASTICITY
Hydroelastic sloshing of liquid in partially filled circular cylinder with rigid or elastic walls, including surface tension effect
04 p0671 A70-15092

Hydroelastic oscillations natural frequencies in incompressible and nonviscous liquid in circular cylinder with free surface, demonstrating wall elasticity effects
13 p2512 A70-28832

HYDROFLUORIC ACID
HF molecular vibration rotation band observed in sunspot spectra, carrying out model calculations for spots differing in temperature for fluorine abundance
04 p0751 A70-15048

Hydrogen fluoride fundamental vibration rotation band spectral line shift and broadening due to carbon dioxide
07 p1337 A70-19365

Fugacities of HCl and HF compared with abundance in volcanic fumarolic emanations, indicating magma undersaturation
20 p3619 A70-39321

HYDROFOIL BOATS
U HYDROFOIL CRAFT
HYDROFOIL CRAFT
Hydrofoil and hovering craft design by fiber technology, discussing composite materials, whisker mechanical properties, polycrystalline fibers, matrix materials, etc
19 p3456 A70-38941

HYDROFOIL OSCILLATIONS
Unsteady hydrodynamic coefficients of supercavitating hydrofoil in harmonic oscillation in Helmholtz flow with free surface, investigating frequency, angle of attack and submergence depth
07 p1255 A70-19134

Hydrodynamic forces by oscillating foils in ideal incompressible fluid turbulent flow with stream separation
13 p2390 A70-29649

HYDROFOILS
Sweep angle relationship to cavitation inception on hydrofoils and to hydrofoil performance deterioration due to cavitation
06 p1032 A70-17211

Off-design performance characteristics of supercavitating hydrofoils in cascade for various arrangements, flap angles and flap chord ratios
[ASME PAPER 70-FE-24] 16 p2892 A70-33633

HYDROFORMING
Molybdenum disulfide and phenol formaldehyde resin lubricants for hydroextrusion of steel
15 p2743 A70-31639

HYDROGEN
NT DEUTERIUM
NT DEUTERIUM PLASMA
NT HYDROGEN ATOMS
NT HYDROGEN IONS
NT HYDROGEN ISOTOPES
NT HYDROGEN PLASMA
NT LIQUID HYDROGEN
NT ORTHO HYDROGEN
NT PARA HYDROGEN
NT TRITIUM
Multistate impact parameter treatment of hydrogen-helium excitation collisions, considering distortion, back- and rotational-coupling and virtual transition sequence
01 p0147 A70-10285

Semiempirical potential energy surface generation for triatomic hydrogen from London equation by evaluating Coulomb and exchange integrals taking into account effective orbital overlap
01 p0147 A70-10469

Interstellar neutral hydrogen flux effects on atmospheric hydrogen density, considering annual and semiannual density variations
01 p0186 A70-11207

Galactic satellite interpretation for high velocity hydrogen clouds at high latitudes
02 p0363 A70-11780

Cosmic ray primaries and secondaries direct heating of thermal electrons for computation of H I regions electron densities and temperatures

02 p0363 A70-11782

Diffuse soft X ray photoionization and heating of H I regions compared to cosmic ray heating

02 p0364 A70-11784

Hydrogen pressure-induced IR absorption spectra, noting applications to planetary atmosphere studies

02 p0341 A70-11805

Mutual diffusion coefficient of hydrogen atoms and molecules in upper atmospheres of major planets calculated as function of temperature, using Chapman-Enskog theory

02 p0342 A70-11817

Differential elastic and rotational excitation cross sections for electron-hydrogen scattering in close coupling approximation with electron exchange neglected

02 p0342 A70-11880

Chemical additives effect on H-Cl-N mixtures burning velocity in air and nitrogen

02 p0398 A70-12031

Volumetric reaction rates and mass transport coefficients as function of position for ducted two dimensional turbulent hydrogen-air diffusion flame

02 p0398 A70-12036

Molecular hydrogen Lyman bands radiative transition probabilities, using electronic dipole moment functions

02 p0344 A70-12659

Nb-Mo alloys in various proportions prepared by vacuum casting, showing embrittlement under hydrogen atmosphere

02 p0318 A70-12671

Physiological equivalents of air with rare gases and H substitutes for nitrogen in inhaled gas mixtures providing normal oxygen intake

02 p0249 A70-12798

Free-bound and free-free continuous emission of hydrogen near Balmer jump in T Tauri star AS209

03 p0566 A70-13315

Galactic bending dynamics, discussing omega and zeta motions coupling of neutral hydrogen in outer region

03 p0570 A70-13553

Molecular hydrogen destruction by reaction with carbon dioxide ion in Martian ionosphere, discussing conversion into atomic hydrogen

03 p0575 A70-13997

Protogalaxy formation and molecular processes in primeval hydrogen gas, discussing cold gas cloud cooling mechanism and contraction

03 p0577 A70-14153

Slow electrons elastic scattering by diatomic hydrogen molecule, analyzing cross sections in two center prolate spheroidal coordinates emphasizing polarization effect

03 p0528 A70-14179

Ar plasma interaction with concentric cool hydrogen sheath for simulation study for gaseous core nuclear space propulsion system

03 p0536 A70-14375

Molecular and solid hydrogen in dense interstellar clouds suggested from underabundance of neutral atomic hydrogen, discussing grain temperature

04 p0747 A70-14585

L-alpha absorption equivalent width measurements in UV spectra of beta-one, delta and pi Scorpii for interstellar hydrogen densities

04 p0748 A70-14586

Pressure-volume-temperature measurements on H, calculating fugacity coefficients

04 p0719 A70-15057

Solar Lyman-alpha radiation observed by OGO 4 spacecraft showing short term fluctuations superposed with monthly variation

04 p0741 A70-15128

Tensile tests on alpha Ti containing oxygen and hydrogen at various temperatures and strain rates to determine deformation and fracture

04 p0706 A70-15133

Hydrogen diffusion in pure Ti and beta Ti alloy VT15, determining diffusion coefficient for various temperatures

04 p0707 A70-15190

Hydrogen embrittlement as delayed rupture origin in high strength steels

04 p0711 A70-15682

Limits of self ignition in reaction of F with H detected photoelectrically

05 p0956 A70-16156

Ti-hydrogen reaction at ambient temperatures, investigating factors favoring reaction and preventive measures

05 p0863 A70-16524

Density wave theory and Schmidt model applied to Milky Way spiral structure, considering systematic motion of interstellar neutral hydrogen

05 p0918 A70-16928

Heat transfer to hydrogen calculated with reference to design of cooled rocket nozzles and combustion chambers

06 p1174 A70-17677

Viscosity, thermal conductivity, specific heat and Prandtl number of hydrogen, methane and hydrogen-methane mixtures calculated for variation with temperature neglecting dissociation effects

06 p1177 A70-17700

H I gas and H II regions kinematics, comparing radial velocities near galactic center

06 p1149 A70-18459

Hydrogen concentration effect on self sustained detonation wave propagation in hydrogen-carbon monoxide-oxygen mixtures, using Q switched pulsed laser schlieren photography

07 p1420 A70-18918

Pressure-narrowing theory applied to calculating equivalent widths of lines in quadrupole rotation-vibration spectrum of molecular hydrogen

07 p1338 A70-19366

Dissociating hydrogen transport coefficients analysis compared with data calculated as function of temperature and pressure without allowance for ionization

07 p1338 A70-19654

Hydrogen effects on ELI Ti-Al-Sn alloy, conducting tensile, fretting and abrasion tests on stressed and thermal cycled specimens

07 p1309 A70-19710

Atomic F reaction with hydrogen studied for vibrational, rotational and translational energy distribution, using IR chemiluminescence method

07 p1225 A70-20055

Hydrogen triatomic molecules existence, stability and ionization in molecular beams

07 p1345 A70-20139

Jupiter conductive molten metallic hydrogen core of moderate temperature suggested from solids melting point temperature dependence on pressure

07 p1390 A70-20238

Population of P level He excitation in solar prominences in H luminescence regions, noting ionization-recombination mechanism by UV radiation

08 p1564 A70-20555

Hydrogen supply rate by solar wind found comparable to hydrogen losses from earth by diffusion into space

08 p1487 A70-20637

Hydrogen penetrability in heat resistant steels subjected to high temperature creep, observing activation energy decrease with increased stress

08 p1515 A70-20923

Zero radiospectrometer for spectral observations of radio emission of excited galactic hydrogen at centimeter wavelength, noting Omega nebula detection

08 p1495 A70-21063

Intensity and altitude profile of H beta light emission and energetic hydrogen fluxes during auroral breakup using rocket soundings

08 p1489 A70-21383

Interplanetary density distribution of cold interstellar origin hydrogen dependent on solar EUV flux, considering interaction with solar wind protons

08 p1562 A70-21401

Iron base and nickel base alloys susceptibilities to internal hydrogen and hydrogen environment embrittlements, studying crack initiation inside and at metal surface

08 p1520 A70-21515

Phase comparisons between commercial cesium beam frequency standards and NASA experimental hydrogen maser NX-1

08 p1513 A70-21592

Ionization of rare gases /H and N/ by nitrogen ions, determining cross sections of formation of slow ions and electrons

08 p1549 A70-21801

Austenitic stainless steel hydrogen damage noting role of martensitic plastic deformation

08 p1525 A70-21965

Sigma Orionis E hydrogen-deficient atmosphere, using grid of constant-flux model atmospheres to determine abundances of five elements

09 p1755 A70-22504

Ti tetrachloride, Si tetrachloride and hydrogen gas mixtures flow over heated graphite substrates, describing Ti silicides formation

09 p1703 A70-22646

Molecular hydrogen parallel and perpendicular dynamic polarizabilities calculated for frequency dependence, using many body perturbation theory

09 p1731 A70-22780

Equivalent widths for rotational lines to detect interstellar hydrogen gas, discussing absorption line

10 p1937 A70-23947

Gas cloud expulsion from galactic nucleus indicated in 21 cm survey of neutral hydrogen

10 p1937 A70-23948

Quasi-bound levels determination method for molecular hydrogen ground state

10 p1919 A70-24395

Electrocatalytic activity of oxides in redox reactions without adsorption, noting application to hydrogen oxidation in acid medium

10 p1831 A70-24470

Quasars photoionization of intergalactic high density hydrogen gas to interpret absorption features absence, noting gas temperature

10 p1942 A70-24628

Enthalpy-entropy, enthalpy-pressure and composition diagrams of fluorine-hydrogen system, noting possible applications to rocket propulsion systems

10 p1929 A70-25100

Deuterium atom reaction with hydrogen molecule yielding HD and H using modulated crossed beams, plotting angular distributions and reaction velocities

10 p1920 A70-25148

Hydrogen, oxygen and carbon dioxide in off-gas stream from nuclear reactor experiment using on-line gas chromatography

11 p1994 A70-25615

CW chemical laser performance using molecular hydrogen diffused into supersonic fluorine atoms streams

11 p2063 A70-26067

Hydrogen-air turbulent diffusion flame structure at differing air and hydrogen velocities

11 p2151 A70-26387

Atmospheric hydrogen content continuous recording method based on absorption line analysis of mercury vapor from mercuric oxide reduction

11 p2052 A70-26389

Hydrogen-air reaction by singular perturbation methods for temperature and pressure values of supersonic combustion, changing reaction velocity by initial stoichiometry

11 p1995 A70-26624

Field ionization from hydrogen layers adsorbed at 4.2 K on W emitters in sealed-off tubes

12 p2274 A70-26858

PdH system electrical resistivity, studying hydrogen concentration role

12 p2282 A70-26900

Lyman alpha intensity and hydrogen concentration at 5 to 19 earth radii determined from OGO 3 spacecraft measurements

12 p2222 A70-27181

Absorption at solar H Lyman alpha line by earth hydrogen atmosphere measured as function of altitude from Aerobee flight spectrograms

12 p2222 A70-27182

Oxygen and hydrogen diffusion coefficients in aqueous potassium hydroxide electrolyte solutions at various temperatures and concentrations

12 p2181 A70-27575

Rotation law and circulation velocities in solar hydrogen convection zone under anisotropic turbulent velocity

12 p2302 A70-27588

Porous hydrogen electrode performance with Ni skeleton catalyst, studying effects of temperature, active layer thickness, etc

12 p2182 A70-27759

Laser emission generation on sodium lines, studying pulsed discharge mechanism involving ion-ion recombination in sodium vapor and hydrogen mixture

13 p2425 A70-28600

Cavity and storage temperature effects on hydrogen maser oscillation in 77-293 K range

13 p2425 A70-28713

Interstellar hydrogen density around solar system from calibrated Lyman-alpha intensity measurements of Vela 7

13 p2489 A70-28894

Predissociation of excited molecules in molecular hydrogen and deuterium by electric field as linear function of field strength

13 p2362 A70-29479

Charge, hydrogen atom and ion transfer in collisions involving deuterium-labeled methanol- acetaldehyde system and molecular ions

14 p2543 A70-30110

Elastic scattering of electrons by hydrogen as function of vibrational excitation, discussing intensities and cross sections

14 p2618 A70-30114

Differential cross sections for electron scattering by hydrogen with and without vibrational excitation, discussing inelastic processes

14 p2618 A70-30115

H and He intraatmospheric migration and dissipation, considering MHD waves, ionospheric plasma motions, chemical reactions, etc

14 p2569 A70-30211

Plasma production by irradiating solid hydrogen foils with intense pulse ruby laser

14 p2622 A70-30659

Neptune data from photoelectric observations of 7 April 1968 occultation of BD-17 deg 4388, determining hydrogen dominance and molecular density

14 p2642 A70-30890

Hydrogen abundance in Jupiter atmosphere quadrupole line used in comparing jupiter and solar atmosphere C/H ratios

14 p2650 A70-31221

Metal to hydrogen ratio for sun, Hyades and F-G stars based on photoelectric measurements of weak metal lines

14 p2652 A70-31388

Hydrogen embrittlement of martensitic Fe-Ni alloys as function of temperature via slow strain rate tensile tests

15 p2755 A70-31559

- Titanium vacuum pump, discussing pumping speed, sticking factor and sorption coefficient for hydrogen 15 p2744 A70-31845
- Molecular hydrogen, methane, water vapor and tritium concentrations near stratopause from air samples collected on Aerobee flight with liquid hydrogen cooled cryocondenser 15 p2728 A70-31995
- Hydrogen effect on impurity redistribution in heteroepitaxial Si layers on sapphire substrate 15 p2785 A70-32529
- Dissociating hydrogen transport coefficients analysis comparison with data calculation as function of temperature and pressure without allowance for ionization 15 p2828 A70-32691
- Population of P level He excitation in solar prominences in H luminescence regions, noting ionization-recombination mechanism by UV radiation 15 p2805 A70-32710
- Hydrogen solubility in electrically exploded metals 15 p2762 A70-32747
- Hydrogen separation from supersaturated solid solution in Zn-Zr alloy, measuring at room temperature with eudiometer 15 p2764 A70-32856
- Photodissociation and fluorescence cross sections for hydrogen by Lyman-alpha photons emission from collisional quenching 16 p2953 A70-33006
- Pressure broadened line widths in electric field induced fundamental hydrogen spectral band, noting linear variation with density 16 p2954 A70-33276
- Waste hydrogen utilization in microthrusters for spacecraft attitude control involving mass expulsion of cold gas [AIAA PAPER 70-613] 16 p2969 A70-33609
- Nuclear rocket nozzle cooling passages, discussing heat transfer and friction correlations for single-phase hydrogen turbulent flow [AIAA PAPER 70-661] 16 p2950 A70-33622
- Real hydrogen driver performance, analyzing intermolecular forces effects under high compression and heat 16 p2998 A70-33889
- Alpha Ti and alpha Ti-hydrogen alloys fatigue behavior, emphasizing twin formation influence and hydrogen effects 17 p3116 A70-34394
- Alpha Ti-hydrogen alloys, discussing fracture behavior temperature dependence 17 p3117 A70-34396
- Hydrogen embrittlement of Ti and Ti alloys under plastic deformation and critical hydrogen concentration 17 p3117 A70-34397
- Interstellar Lyman alpha observations with OAO, providing upper limit to neutral hydrogen column density 17 p3162 A70-34899
- Lyman alpha radiation from gaseous hydrogen nebula model, taking into account absorption by dust and interstellar neutral hydrogen 17 p3163 A70-34904
- Hydrogen abundance in white dwarfs, discussing inconsistencies in mass and bolometric magnitude models for Sirius and Eri B 17 p3170 A70-35389
- High velocity neutral hydrogen cloud observations, presenting tabulated characteristics and maps 17 p3170 A70-35439
- OGO-4 observations of hydrogen Lyman-alpha airglow surrounding earth, measuring dependence on solar zenith angle 17 p3080 A70-35764
- Transformation induced plasticity /TRIP/ high strength steels resistance to hydrogen embrittlement 18 p3273 A70-36047
- Chemical composition selection for Ti alloys with low susceptibility to hydrogen induced brittleness 18 p3274 A70-36121
- Hydrogen line absorption at 21 cm from Centaurus A /NGC 5128/ radio galaxy 18 p3318 A70-37017
- Neutral H spiral structure in Milky Way galaxy, discussing map derivation, pattern interpretation, arm characteristics and kinematics 18 p3327 A70-37161
- Milky Way galaxy spiral structure analysis, using neutral H Hat Creek survey with southern observations 18 p3327 A70-37164
- Neutral H concentrations far from galactic plane associated with spiral arms 18 p3327 A70-37166
- Milky way galactic plane corrugation, discussing maximum hydrogen brightness temperature oscillating in sinusoidal pattern 18 p3328 A70-37167
- Radial velocities of neutral hydrogen in anticenter region of Galaxy 18 p3328 A70-37170
- Galactic spiral structure from optical radial velocities of H II regions 18 p3329 A70-37179
- Carina spiral feature progress report covering O and B star distribution, optical and radio H 2 and H 1 sources and cosmic dust 18 p3330 A70-37185
- Neutral hydrogen observations in Sagittarius and Scutum spiral arms, examining circular galactic rotation by density wave theory kinematic models 18 p3331 A70-37197
- Alloying elements effect on diffusion coefficient of hydrogen in low-alloyed alpha titanium 19 p3449 A70-37274
- Hydrogen maser wall shift measurement, using flexible storage bulb for accuracy improvement 19 p3445 A70-37759
- Hydrogen flame ionization detector /HYFID/ for life-derived organic matter in Martian/Lunar soil 19 p3426 A70-37896
- Pulsar AP 2015 21cm line absorption profile, indicating uniform density and temperature neutral H model invalid 19 p3518 A70-38026
- Sbc galaxy NGC 7320 radio emission and neutral H observations, showing improbability of physical association with Stephan Quintet by distance measurement 19 p3524 A70-38699
- Atomic hydrogen population distribution in far UV of comets 19 p3526 A70-38782
- Interstellar molecular H Lyman resonance-absorption bands in far UV spectrum using rocket observation 20 p3701 A70-39002
- Hydrogen molecules rotational excitation cross sections by electron impact in adiabatic excitation, discussing polarization and distortion effects 20 p3675 A70-39606
- Hydrogen emanation and distribution in metals and alloys by Nd hydrogen metal detection method 20 p3651 A70-40071
- Vibrationally adiabatic model for reaction dynamics of atomic and molecular hydrogen systems, using zero point energy path 21 p3773 A70-41397
- Hydrogen maser frequency shift due to atomic collisions with deformable storage bulb surface 21 p3836 A70-41453
- Apollo 11 lunar rocks and soil hydrogen, C and Si concentration and isotopic composition 21 p3774 A70-41568
- Barrier heights for hydrogen-iodine reaction from semiempirical four-electron valence bond calculation 21 p3780 A70-41709
- Hydrogen adsorption and coadsorption with oxygen on W single crystal surface measured by mass spectroscopy and low energy electron diffraction method 21 p3862 A70-41887
- Electron losses from avalanches in hydrogen in cylindrical tube with plane parallel end electrodes, assuming elastic electron collision 22 p4076 A70-42355
- Interstellar and intergalactic medium physics, examining H I and H II regions thermal and dynamic states 22 p4098 A70-42578
- Diffusion effect on hydrogen and oxygen constituents height distributions in atmosphere and lower thermosphere, solving diffusion and continuity equations 22 p4020 A70-43160
- EPR method for elementary reaction kinetics of vapor phase oxygen atoms interacting with molecular hydrogen 22 p3983 A70-43349
- Interdiffusion coefficients for hydrogen-carbon dioxide and oxygen-carbon dioxide systems at low temperatures 22 p4076 A70-43393
- Solar motion apex for neutral hydrogen concentrations at different velocities, suggesting relationship to galaxy 23 p4239 A70-43815
- Exospheric neutral hydrogen temperature diurnal variation from satellite resonance filter data, suggesting Lyman alpha source external to geocorona 23 p4186 A70-43852
- Hydrogen slush characteristics, discussing advantages of liquid-solid mixture over liquid hydrogen, production methods, aging effects, transfer and pumping losses, storage, instrumentation, etc 23 p4232 A70-45075
- Electronic energy collisional transfer between atomic and molecular hydrogen, measuring excited molecule vibrational distribution 24 p4381 A70-45650
- H and He intraatmospheric migration and dissipation, considering MHD waves, ionospheric plasma motions, chemical reactions, etc 24 p4331 A70-46286
- Hydrogen effect on deformation and fracture of polycrystalline nickel 24 p4365 A70-46372
- Neutral hydrogen 21 cm line profiles in galactic plane, tabulating terminal positive velocity and brightness temperatures 24 p4414 A70-46381
- Galactic neutral hydrogen velocity distributions from 21 cm line profiles analysis 24 p4414 A70-46382
- ### HYDROGEN ATOMS
- Adiabatic and distortion approximations to two state treatment of ground state H atoms collisions at low energies 01 p1146 A70-10284
- Upper atmospheric atomic H and He concentration height distribution, considering L alpha and H alpha emissions, He emission, light components and direct measurements 01 p0074 A70-10589
- Solid hydrogen condensation on interstellar grain surfaces at extremely low temperatures related to H atoms density 01 p0183 A70-10896
- Solar Lyman alpha line profile and atomic hydrogen vertical distribution measurement method for terrestrial atmosphere in 200-500 km range 01 p0078 A70-11208
- Cross section calculation for spin change in H atoms pair collision, discussing wave number and temperature effects 02 p0341 A70-11796
- Mutual diffusion coefficient of hydrogen atoms and molecules in upper atmospheres of major planets calculated as function of temperature, using Chapman-Enskog theory 02 p0342 A70-11817
- Stimulated emission of RF recombination lines from ionized atoms in H I regions 02 p0372 A70-12251
- Direct interaction between hydrogen atom and positive ion with one electron, using Born and two and four state impact parameter treatments 02 p0344 A70-12703
- Dynamic time constants for specific transition and relaxation times of hydrogen maser, noting coupling between hyperfine differences and atomic polarization 03 p0498 A70-13007
- Hydrogen molecule formation relation to galaxy formation, discussing cosmic plasma neutralization role 03 p0577 A70-14152
- Neutral atomic hydrogen in Virgo A cluster and between Galaxy and Virgo A, using emission and absorption measurements 04 p0758 A70-15707
- Hydrogen atoms van der Waal dispersion interaction effects on H lines broadening in neutral medium, taking into account resonance interaction 04 p0723 A70-15714
- Gray and colorless features of moon explained as atomic H imported by solar wind replacing lost H by photolytic decomposition of water vapor 05 p0908 A70-16303
- Scattering matrix noniterative integral solutions applied to singlet and triplet s-wave Hartree-Fock phase shifts for electron-H-atom scattering 06 p1108 A70-17486
- Electron scattering from diatomic molecular systems including coupling of partial waves in fixed-nuclei approximation 06 p1114 A70-18633
- Hydrogen atoms collisional excitation cross section expressed in terms of quantum numbers of levels and ratio of colliding electron energy to transition energy 07 p1338 A70-19410
- Atomic hydrogen maser wall shift determined by measurements on FEP Teflon coated storage bulbs, suggesting Teflon properties change as basis 07 p1301 A70-19973
- Geocoronal glow as resonant scattering of solar Lyman-alpha-radiation by H atoms in upper atmosphere 07 p1270 A70-20032
- Calf thymus DNA structural and functional changes following exposure to hydrogen atoms and gamma radiation 07 p1215 A70-20050
- Relaxation time calculation for ground and excited states of H atoms and H-like ions in optically thin and thick plasmas, considering electron density role 07 p1353 A70-20058
- Born wave for atom-atom inelastic cross sections, calculating He excitation from ground state to higher states by H atom collision 07 p1346 A70-20241
- Excitation cross sections for bound-bound transitions in optical levels in hydrogenlike atoms induced by fast charged particles 09 p1730 A70-22230
- Ionizer design for hydrogen atom beam ensuring storage of polarized protons, using electron beam for ionization 09 p1732 A70-22846
- Quadrupole coupling between single and double excitation channels in hydrogen-hydrogen collisions found ineffective due to energy defect between channels 09 p1733 A70-23268

Charge exchange probability in proton-hydrogen atom collisions computed with two state atomic orbital expansion

09 p1733 A70-23270

Associative and collisional detachment in H atom and negative ion collisions based on complex adiabatic potential

09 p1733 A70-23431

Hydrogen 21 cm emission line in Perseus region observed for motion of neutral hydrogen connected with II Per, discussing stellar radial velocity

10 p1937 A70-23944

Ionization front interactions in interstellar gas, investigating expanding planar H II region and contact discontinuity in H I region

10 p1937 A70-23975

Interstellar atomic and molecular hydrogen abundance and physical state using rocket observations of Lyman alpha absorption line and ground based observations

10 p1941 A70-24551

Chemiluminescence from NO adiabatically expanded against supersonic H atoms stream in inert carrier

10 p1831 A70-24566

Luminescence of powdered silica and basalt bombarded by atomic hydrogen, relating spectral distributions dependence on ion energy to lunar luminescence

10 p1942 A70-24647

Frenkel pairs and interstitial hydrogen atoms observed in thin silver films after proton bombardment

12 p2253 A70-27209

Hydrogen and inert gas atoms collisional excitation cross sections calculated by multistate impact parameter approximation

12 p2276 A70-27878

Polarized Lyman alpha radiation emitted in electron collisions with atomic and molecular hydrogen and by electric field quenching of metastable atom

13 p2455 A70-29221

Carbon and sulfur reactions with solar hydrogen atoms in Apollo 11 lunar samples accounting for isotopic composition of fine-grained basaltic rocks

14 p2545 A70-30791

Atomic emission in water vapor afterglow, revealing presence of Balmer series of H atom with sodium D line

14 p2579 A70-31255

Gas ionization with hydrogen atoms in gravitational equilibrium at constant temperature in upper half space by instantaneous radiation burst in lower space

15 p2775 A70-31477

Atomic hydrogen distribution in upper atmosphere and solar system obtained during spin operation of OGO 5 with Lyman alpha photometer

15 p2798 A70-31655

Atomic hydrogen escape effects on altitude distribution, discussing lateral flow limitations on thermospheric diurnal variation

15 p2725 A70-31796

Hydrogen atom excitation at various energy levels by electron impact, applying Glauber theory

16 p2954 A70-33287

Hydrogen behavior in Ti and alloys by internal friction measurement, attributing relaxation peaks to stress induced ordering of atoms

17 p3115 A70-34382

Galactic UV emission attributed to solar radiation scattered by hydrogen atoms, using Mariner 5 measurements

17 p3163 A70-34902

Metal surface ionization measurements for upper atmosphere and interplanetary space energetic neutral hydrogen analyzer design

17 p3138 A70-35309

UV absorption lines in H I regions heated by cosmic rays, discussing possible detection by rocket or satellite spectroscopic observations

17 p3152 A70-35748

Earth Lyman alpha emission rates as function of atomic hydrogen column density in outer atmosphere, using Mariner 5 measurements

18 p3244 A70-36007

Elastic energy transfer cross sections calculation of H-H scattering to estimate neutralized solar wind particles thermalization

18 p3309 A70-36951

Atomic H electron transition induced by H atom collisional-excitation rates at various thermal energies, explaining anomalous recombination lines in H I regions

18 p3253 A70-37021

Galactic spiral structure from atomic hydrogen line intensity longitudinal distribution

18 p3328 A70-37168

H I local spiral arm drift curves from radio telescope operation

18 p3328 A70-37171

Interstellar H I gas physical conditions, discussing ionization ratio average values and temperature conditions

18 p3328 A70-37175

Diurnal variations of thermospheric atomic hydrogen, investigating lateral flow effects on global distribution

19 p3415 A70-38419

Time and power dependent Lamb shift resonance shapes measurement with circular polarized RF field in beam foil excited H atoms

20 p3675 A70-39498

Positive ion and electron production in H atom collisions with atomic and molecular gases, deriving ionization cross sections

20 p3675 A70-39605

Hydrogen ionization and second quantum level excitation by collision with H atoms in ground state

21 p3852 A70-40596

Atomic hydrogen 2s and 2p excitations by proton and He ion impact, considering ion-multipole interactions effect

21 p3852 A70-40598

Soft X ray background galactic absorption and intensity measurements indicating inverse relation to columnar atomic hydrogen density

21 p3877 A70-40698

Ionization cross sections for excited H atom-ground state H atom collisions, using Born approximation

21 p3852 A70-40719

Atomic hydrogen emissions in dayglow, considering excitation by resonance absorption of solar radiation

21 p3812 A70-40728

Cold neutral atomic hydrogen in Taurus dust clouds from 21 cm line dips in radiotelescope observations

21 p3887 A70-41108

Atomic hydrogen 21 cm line intensity distribution in Carina arm of Milky Way galaxy

22 p4100 A70-42851

Silicon line collisional broadening by electrons and hydrogen atoms, discussing Stark effect and van der Waal interactions

22 p4076 A70-42861

Galactic soft X ray and subcosmic ray heating and ionizing of interstellar H I regions

22 p4094 A70-42985

Stark effect in hydrogen atoms for nonuniform electric fields, considering correction of energy eigenvalues of Schrodinger equation by WKB method

23 p4221 A70-44401

Heitler-London curves calculation for electron exchange in H-H collisions as function of internuclear distance and velocity

24 p4381 A70-45252

Interplanetary atomic hydrogen density distribution from Lyman alpha scattering calculation, explaining background radiation anisotropy detection by Vela 7 satellite

24 p4403 A70-45392

D2A satellite optical experiments, examining atmospheric atomic H and solar and extraterrestrial 1216 A emission

24 p4339 A70-46094

HYDROGEN BONDS

Polywater electronic structure model, proposing hydrogen bonds resembling short strong bonds in FHF⁻/ions

11 p1994 A70-25656

Ammonia gas phase IR intensity measurements for hydrogen bonding energy and related parameters

23 p4158 A70-44783

HYDROGEN CHLORIDE

U HYDROCHLORIC ACID

HYDROGEN COMPOUNDS

NT CARBORANE

NT DEUTERIUM COMPOUNDS

NT DIBORANE

NT DIHYDRIDES

NT HYDRIDES

NT HYDROBROMIDES

NT HYDROGEN CYANIDES

NT HYDROGEN PEROXIDE

NT HYDROGEN SULFIDE

NT LITHIUM HYDRIDES

NT METAL HYDRIDES

NT PHOSPHINES

NT SILANES

NT ZIRCONIUM HYDRIDES

Rare gas diatomic and hydride ions reactions with hydrogen, determining rate coefficients and product channels by flowing afterglow technique

15 p2776 A70-31727

HYDROGEN CYANIDES

Carbon monoxide, carbon dioxide and oxygen impurities effects on threshold current and output power of HCN laser

12 p2249 A70-27648

Submillimeter range HCN gas laser design and characteristics, noting single mode, linear polarization and output power

12 p2250 A70-28180

HCN laser 890 GHz line phase locked to multiplexed standard frequency with wide bandwidth loop, narrowing line widths

13 p2426 A70-28798

HCN laser far IR line phase locked to absolute frequency standard

13 p2426 A70-28810

HYDROGEN FLUORIDES

U HYDROFLUORIC ACID

HYDROGEN FUELS

Medium temperature hydrogen fuel cells design, operational characteristics and performance

12 p2163 A70-26996

Large scale hydrogen fueled supersonic combustor test at simulated Mach 8 flight, describing fuel injector design

[AIAA PAPER 70-715]

16 p2965 A70-33539

Nonequilibrium recombination in supersonic nozzle of dissociated combustion products of hydrogen in air, investigating initial system and rate constants effect

20 p3582 A70-39269

Hydrogen-oxygen and hydrogen-nitrous oxide systems combustion, measuring isotopic substitution effect on flame speed by schlieren technique with rotating drum camera

20 p3583 A70-40472

Low thrust trajectory transfer from low to synchronous orbit, examining hydrogen resistance jet and mercury bombardment ion thruster

22 p4089 A70-42487

HYDROGEN IONS

Electron pressure and negative H ion population in late type dwarfs atmospheres by Ca I resonance line observation, noting non-LTE mechanism

01 p0191 A70-11351

Cross sections determined for formation of secondary positive molecular and atomic hydrogen ions during 1.4-46 keV positive molecular hydrogen passing through hydrogen

02 p0344 A70-12704

Carbon atom RF recombination lines evaluated for conditions in H II regions and planetary nebulae

04 p0748 A70-14587

Exchange perturbation theories applied to delta function model of molecular hydrogen ion, discussing EL-HAV second order energy at large internuclear separations

05 p0884 A70-15878

Relaxation time calculation for ground and excited states of H atoms and H-like ions in optically thin and thick plasmas, considering electron density role

07 p1353 A70-20058

Charge exchange and electron loss measurements in steam target exposed to high energy hydrogen ions beam, using equilibrium fractions method

07 p1345 A70-20142

Pulsar clusters and associations within 1 kpc of sun and hot O-stars and supergiants, calculating radius of surrounding H II regions

08 p1577 A70-21493

Internal radial velocities of diffuse emission nebulae in H II region, using photographic Fabry-Perot interferometer

08 p1581 A70-21952

Three body atomic systems with He atom and H negative ion on basis of scattering experiments dealing with resonance and threshold behavior

09 p1731 A70-22247

Charged particle interaction influence on photoionization cross section of negative hydrogen ion, considering initial state polarization leading to free s wave electron

09 p1732 A70-22826

Charge exchange cross section of hydrogen position ion-negative ion collisions

09 p1733 A70-23269

Associative and collisional detachment in H atom and negative ion collisions based on complex adiabatic potential

09 p1733 A70-23431

Galactic radio sources examined for hydroxyl lines associated with H II regions, making observations in absorption and emission

10 p1936 A70-23904

Ionization front interactions in interstellar gas, investigating expanding planar H II region and contact discontinuity in H I region

10 p1937 A70-23975

Hydrogen ion flux detected along earth magnetic force lines in Northern Hemisphere midlatitudes, determining flux magnitude

10 p1874 A70-24321

H II region properties from non-LTE analysis of alpha, beta, gamma, delta and epsilon radio recombination line data, determining electron temperature and concentrations

10 p1945 A70-24959

Approximations implicit in Cayrel statistical equilibrium or non-LTE analysis of ionic hydrogen bound free continuum in sun

10 p1947 A70-24989

Dogs respiratory response to arterial hydrogen ions at different carbon dioxide pressure levels during hypoxia or hyperoxia, discussing acid-base balance effects

11 p1986 A70-25674

Triatomic hydrogen ion role in solar photosphere opacity implied from limb darkening and specific intensity data

11 p2104 A70-25739

- Population densities of levels of excited atoms and ions in nonthermal plasma including hydrogen-like ion partition function
11 p2086 A70-25835
- Ionization equilibrium of atoms and hydrogen-like ions in nonthermal plasma, transforming into Saha formula for high electron densities
11 p2086 A70-25836
- Cross sections for electron impact excitation of positive helium and hydrogen ions, using non-relativistic Coulomb-Born-Oppenheimer reactance matrices
13 p2455 A70-28988
- Shock wave multiple ionization in hydrogen with impurities, discussing intensity and duration effects on electron temperature profile and ion concentrations
13 p2388 A70-29369
- H II region stellar color anomaly attributed to interstellar extinction
14 p2641 A70-30879
- Negative hydrogen ion balance in high intensity plasma source, measuring flux as function of discharge current
15 p2780 A70-32195
- Triatomic hydrogen positive ion-yielding reactions, using EVA ion-molecule beam apparatus
16 p2855 A70-33012
- Effective cross sections for molecular hydrogen and hydrogen positive ion formation in collisions between He, Ne and Ar ions or atoms
16 p2954 A70-33193
- Hydrogen ion-molecule reactions analysis by flow-afterglow technique, noting application to proton affinity measurement
16 p2857 A70-34005
- Compact ionized hydrogen components inside galactic H II regions of lower electron density, explaining existence and evolution by various models
16 p2980 A70-34308
- Plasmasphere bulge region morphology from hydrogen ion concentration measurement by mass spectrometer on OGO 5 satellite
18 p3312 A70-36014
- H 2 regions in Sc galaxies NGC 628, 4254 and 5194
18 p3327 A70-37159
- H 2 region and neutral gas spiral structure and radial distribution, using optical observations and radio continuum surveys
18 p3327 A70-37162
- H 2 region galactic clusters and exciting stars, reevaluating distances by color magnitude diagrams
18 p3329 A70-37178
- Local spiral arm H 2 regions distribution in Cygnus direction, discussing symmetry due to magnetic field
18 p3329 A70-37180
- P autoionization states of helium and hydrogen negative ions, calculating widths and shifts
19 p3474 A70-38307
- Simultaneous hydrogen ion composition measurements by upper ionospheric polar orbiting OGO 4 and eccentric orbiting magnetospheric OGO 3 at midlatitude
19 p3520 A70-38377
- H II region radial velocity comparison to galactic spiral structure, using optical and radio investigations
19 p3524 A70-38698
- Hydrogen negative ion thermal energy reactions with oxygen, nitric oxide, carbon monoxide and nitrous oxide, determining rate constants
20 p3583 A70-39616
- He/plus-/H-/minus/ collisional charge exchange cross sections, using modulated inclined ion beams technique
21 p3852 A70-40599
- Galactic K series emission at 1-10 keV by low energy cosmic rays and diffuse X rays interaction with H I region heavy ions
21 p3877 A70-40704
- High velocity intergalactic hydrogen origin, examining galactic evolution by gas infall
21 p3887 A70-41112
- Galactic rotation model derived from radial velocities and spectrophotometric distances of H II regions
22 p4101 A70-42864
- Photoionization cross sections for atoms and ions of carbon, nitrogen, oxygen and neon as function of wavelength for H II regions and planetary nebulae
22 p4104 A70-42997
- H II regions density-size relationship, using emission measurements and radio data
22 p4109 A70-43746
- Negative hydrogen ion forbidden bound-free continuum absorption cross section recalculation, deriving 10 to 8th power smaller than previous value
24 p4404 A70-45410
- HYDROGEN ISOTOPES**
NT DEUTERIUM
NT TRITIUM
Cosmic ray origin in high energy H and He isotopic abundances and energy spectra observed by IMP 4 satellite during solar quiet times
02 p0358 A70-12250
- Binary transition metal hydrides consisting of single metal and single hydrogen isotope, discussing preparation and kinetic, thermodynamic and structural properties
05 p0863 A70-16523
- Hydrogen-oxygen and hydrogen-nitrous oxide systems combustion, measuring isotopic substitution effect on flame speed by schlieren technique with rotating drum camera
20 p3583 A70-40472
- Apollo 11 lunar matter rare gas, H and N concentrations and isotopic abundances, discussing solar wind, gas diffusion loss from silicates and spallation component
21 p3908 A70-41583
- HYDROGEN OXYGEN ENGINES**
NT J-2 ENGINE
Hydrogen-oxygen variable length combustor longitudinal instability, studying hydrogen injection temperature effects on pressure interaction index and pressure sensitive time lag
01 p0214 A70-10324
- Predicted and measured low density plume impingement effects on loads and heat transfer compared on orbiting Saturn 5 with oxygen-hydrogen burner engine
04 p0737 A70-15430
- Analog-numerical measurements on French liquid oxygen and hydrogen motor
07 p1364 A70-19129
- Resonance ignition technique for gaseous oxygen and hydrogen rocket propellants
14 p2627 A70-30776
- Steady state one dimensional nozzle flow of reacting inviscid gas mixtures, giving numerical solution procedure for hydrogen-oxygen reactions
15 p2694 A70-32269
- Hydrogen oxygen rocket engine two phase liquid hydrogen pump capability and hydrodynamic design, analyzing constant-quality flow, acoustic effects, compressible flow and cavitation
[AIAA PAPER 69-549]
15 p2791 A70-32511
- Space based reusable manned/unmanned tug, discussing potential missions, system requirements and auxiliary hydrogen oxygen propulsion system
[AIAA PAPER 70-719]
16 p2964 A70-33533
- Optical system measurement of density and rotational temperature in gaseous plume simulating auxiliary propulsion and oxygen hydrogen burner of S-4B
16 p2913 A70-34023
- Pressure histories of burning modes in combustion driven shock tube using ignition of stoichiometric hydrogen-oxygen mixture with He dilution
17 p3195 A70-34922
- Hydrogen oxygen engine designs for space vehicle auxiliary propulsion systems, considering long life thrust chamber performance with compatible heat transfer characteristics
[SAE PAPER 700803]
24 p4395 A70-45908
- HYDROGEN OXYGEN FUEL CELLS**
Materials for separator matrix of rechargeable hydrogen oxygen fuel cell, noting use of composite potassium titanate
09 p1612 A70-22045
- Silver cathodes and plasma-sprayed anodes for cost effective hydrogen/oxygen fuel cells with solid zirconium dioxide electrolyte, considering carbon precipitation avoidance
10 p1830 A70-24459
- Hydrogen oxygen fuel cells with porous electrodes based on Elofflux principle, discussing diaphragms, electrolyte flow and heat removal
10 p1830 A70-24464
- Raney catalyst preparation and continuous operation in molecular hydrogen and oxygen electrodes noting improved voltage, manipulation and energy yield
10 p1831 A70-24467
- Hydrogen peroxide fuel cell performance in acid and alkaline electrolytes, investigating cathodic reduction of oxygen on platinum
10 p1808 A70-25037
- Fuel cells with alkaline electrolyte consuming H and O and operating near ambient temperature, discussing electrodes composition and performance
12 p2163 A70-26993
- Hydrogen-air fuel cell with half kilowatt output, describing electrode construction, cell operation, porosity effects on polarization, etc
12 p2163 A70-26995
- Hydrogen-oxygen fuel cell reaction water removal and heat loss using reconcentration device
12 p2163 A70-27066
- Hydrogen oxygen fuel cell investigated for oxygen transfer to Pt cathode surface
12 p2166 A70-27848
- Hydrogen oxygen fuel cells, demonstrating matching of power source and load, charge transfer, porosity, Nernst equation and electrochemical water synthesis
14 p2533 A70-30533
- Fuel cell development, discussing consumable electrode, hydrogen/oxygen, hydrazine/hydrogen superoxide, hydrazine/air and methanol/air cells
19 p3359 A70-38497
- Regenerative hydrogen-oxygen secondary fuel cells as rechargeable battery for communication satellites
21 p3756 A70-41007
- HYDROGEN PEROXIDE**
Hydrogen peroxide oxidizer for higher characteristic mixture ratio in hybrid propulsion systems with hypergolic reactions ignition
[ONERA-TP-773]
02 p0352 A70-12209
- Hydrogen peroxide infusion effect on skin remission following exposure to ionizing radiation on rabbit legs
09 p1619 A70-22791
- Hydrogen peroxide fuel cell performance in acid and alkaline electrolytes, investigating cathodic reduction of oxygen on platinum
10 p1808 A70-25037
- Temperature measurement on thin steel shield subjected to hydrogen peroxide motor exhaust heating at cryogenic temperatures in space
23 p4280 A70-44389
- HYDROGEN PLASMA**
NT DEUTERIUM PLASMA
Cs seeding effect on bound-free UV photoabsorption of Cs-H plasma at constant electron density and energies below H ionization
02 p0343 A70-11904
- Radiative, conductive and convective combined heat transfer mechanism in nonisothermal atomic hydrogen plasma laminar flow
02 p0400 A70-12660
- Steady state deuterium-tritium fusion reactor approximate parameters prediction possibility based on interim assumptions of plasma confinement, model, etc
02 p0349 A70-12755
- Ionization and electron temperature dependence on shock wave structure in partially ionized hydrogen plasma allowing for luminescent energy losses
03 p0465 A70-13060
- Interstellar media under action of supernova or nova, solving Navier-Stokes equations of hydrogen plasma for motion during shock wave formation
03 p0564 A70-13221
- Hydromagnetic normal ionizing shock wave properties in H and D mixtures and pure gases in SUPPER 2 shock wave tube
03 p0536 A70-14365
- Pulsed high current arc burning in hydrogen at pressures to 400 atm, discussing stability and discharge plasma parameters
04 p0729 A70-15224
- Heat flux, electrical and thermal conductivity of H measured on plasma in cascade arc chamber of high power load at 1 atm pressure
06 p1107 A70-18525
- Spectral line intensities in hydrogen plasma, calculating relative intensities and Balmer line width for various electron temperatures and optical thicknesses in H alpha line
07 p1389 A70-20205
- Interstellar media under action of supernova or nova, solving Navier-Stokes equations of hydrogen plasma for motion during shock wave formation
08 p1580 A70-21654
- Variational model of collisional-radiative recombination of atomic ions in hydrogen and alkali plasmas
09 p1735 A70-22828
- Photon bremsstrahlung from relativistic hydrogen plasma determined by studying electron-positron pairing effect on plasma radiation intensity
09 p1735 A70-22986
- Velocity and temperature distribution behind shock waves in hydrogen plasma measured to determine factors responsible for discrepancies in Rankine-Hugoniot conditions
10 p1867 A70-24149
- Plasma production by solid hydrogen-giant pulse laser interaction, studying time dependent distributions of plasma density, temperature and velocity
10 p1902 A70-25222
- Radiative energy transfer in hydrogen plasma having uniform heat source and bounded by parallel black plates
12 p2278 A70-27695
- Statistical mechanics of partially ionized hydrogen plasma, deriving Saha equation to calculate ionization degree and potential for various electron densities and temperature
12 p2281 A70-27882
- Free electrons non-Maxwellian equilibrium kinetic energy distribution function, considering partially ionized hydrogen-like plasma in thermal equilibrium
13 p2459 A70-28634
- Surface emissivity effects on combined conduction, convection and radiation heat transfer in nonisothermal hydrogen plasma, discussing optically thin and thick solutions
13 p2521 A70-29134
- Coupled temperature and electric potential distribution in finite rotational symmetric hydrogen arc column in axial magnetic field
14 p2621 A70-30656
- Radial ion temperature distribution in hydrogen arc within axial magnetic field measured spectroscopically by thermal Doppler effect
14 p2621 A70-30657

Laminar Cu-W electrode erosion resistivity in single chamber electric arc hydrogen plasmatrons with gas vortex stabilization

15 p2780 A70-32130

Electrons, positrons and photon energy distribution inside hydrogen plasma injected with high energy electrons

15 p2781 A70-32429

Hydrogen plasma refractive index and absorption constant for laser radiation frequencies as functions of electron temperature and atomic density

16 p2959 A70-34338

Microwave diagnostics of electron density, temperature and light emission in self excited moving striations in hydrogen plasma

19 p3475 A70-37553

Exponential kernel approximation effect on radiative energy transfer in high temperature hydrogen plasma

20 p3684 A70-40278

Stationary hydrogen RF plasma, using quadrupole mass analyzer for ion composition and extraction study

22 p4078 A70-42363

Dissociated and ionized hypersonic flows of hydrogen heated by electric arc techniques, investigating flows in wind tunnel nozzles

22 p4011 A70-42759

Atomic hydrogen plasma slab, calculating thermodynamic equilibrium deviations effect on resonance radiation

23 p4223 A70-43824

Atomic levels occupation numbers and ionization degree for optically thin hydrogen plasma with self consistent electron velocity distribution

23 p4227 A70-44932

Electric field radial distribution measured for stationary hydrogen arc with axial magnetic field

23 p4227 A70-44933

Five-moments approximation calculation of magnetoplasmodynamic hydrogen arc radial pressure profile as function of ambient pressure and superimposed magnetic field

23 p4228 A70-44935

Magnetoplasmodynamic hydrogen arc radial pressure profile as function of ambient pressure and superimposed magnetic field, using thirteen-moments approximation

23 p4228 A70-44936

Hydrogen cluster beam discharges, determining transient plasma ion density from Stark broadening measurements of H beta line

23 p4228 A70-44939

Spatial potential measurements in magnetized non-Maxwellian hydrogen plasma, using Zaitsev-Mnev method

24 p4385 A70-45464

Pressure gradient induced drift waves in collisionless hydrogen plasma in homogeneous magnetic field

24 p4388 A70-46209

HYDROGEN RECOMBINATIONS

Stimulated emission of RF recombination lines from ionized atoms in H I regions

02 p0372 A70-12251

Hydrogen 109 alpha recombination line emission in galactic H II regions surveyed at National Radio Astronomy Observatory

10 p1936 A70-23942

H II region properties from non-LTE analysis of alpha, beta, gamma, delta and epsilon radio recombination line data, determining electron temperature and concentrations

10 p1945 A70-24959

Recombination in hydrogen-oxygen reaction studied by monitoring IR emission from water vapor formed by shock initiated combustion

11 p1995 A70-26377

Hydrogen recombination and hydrogen molecules formation may explain sharp brightness variations in later dwarf stars

11 p2115 A70-26581

Planetary nebula NGC 7027, discussing hydrogen recombination lines

13 p2486 A70-28629

Atomic H electron transition induced by H atom collisional-excitation rates at various thermal energies, explaining anomalous recombination lines in H I regions

18 p3253 A70-37021

Dwarf Me stars flare spectra, examining hydrogen recombination layer and impulse heating of photosphere

20 p3702 A70-39013

Hydrogen-oxygen flames recombination rates measurements analysis, taking into account reverse reaction rates

20 p3583 A70-40470

Alpha hydrogen recombination lines 156, 166, 167 and 168 from galactic center, using radio telescope

22 p4103 A70-42980

Microwave recombination H lines, deriving electron temperature, electron density and emission measure sequentially

24 p4402 A70-45388

Hydrogen I region anomalous alpha lines recombination in Orion B spectrum, identifying carbon emitter by measured frequency separation

24 p4410 A70-45773

HYDROGEN SULFIDE

Hydrogen sulfide participation in vinyl polymerization investigated for reaction mechanism

05 p0810 A70-16051

Clean iron /011/ surfaces, determining sulfur, oxygen and hydrogen sulfide films effects on adhesion behavior

21 p3831 A70-40748

Ion-molecule reactions in mixtures of hydrogen sulfide with ethylene and acetylene from deuterium labeling studies via ion cyclotron resonance spectroscopy

21 p3773 A70-41200

HYDROGEN 2

U DEUTERIUM

HYDROGEN 3

U TRITIUM

HYDROGENATION

Hydrogenated Ni activation energy difference for lower and higher critical temperatures due to hydride dislocations binding energy

08 p1522 A70-21705

Serrated yielding in hydrogenated nickel alloys, noting hydride stability role in Portevin-Le Chatelier effect

08 p1522 A70-21706

Weld quality relationship to aluminum surface contamination by hydrogen-containing compounds

13 p2407 A70-29108

Hydrogen impurities anelastic relaxation effect on internal friction alpha peak in cold worked tantalum and niobium

13 p2435 A70-29350

Hardened steel embrittlement in low pressure hydrogen caused by crack growth as function of temperature

13 p2436 A70-29804

Internal friction in hydrogenated Ti-Mn alloys, observing relaxation peak formation under stress induced hydrogen diffusion in beta phase

16 p2930 A70-33082

Cellulose ion exchanger palladium catalysts preparation and applications in asymmetric hydrogenation reactions

17 p3042 A70-35125

Addition and hydrogenation reactions of azomethines in chemistry of carbon-nitrogen bond, emphasizing Schiff bases

20 p3582 A70-38978

Hydrogenated Ni elastic limit discontinuity, discussing Portevin-Le Chatelier effect

23 p4208 A70-44921

HYDROGENOLYSIS

Optically active alpha-amino acids synthesis from esters of alpha-keto acids by hydrogenolytic asymmetric transamination

17 p3041 A70-34749

HYDROGENOMONAS

Organic substrates effects on Hydrogenomonas eutropha autotrophic and heterotrophic metabolism

10 p1817 A70-24700

Carbon dioxide fixation in hydrogenomonas eutropha determined from titrating liquid culture with carbon dioxide, showing dependence on oxygen content in gas mixture

11 p1991 A70-25940

Molar growth yields from chemostat cultures of Hydrogenomonas eutropha on succinate and on fumarate, noting equivalence to ATP via oxidation

13 p2350 A70-29113

Ammonia incorporation in chemolithotroph Hydrogenomonas eutropha, investigating responsible enzyme

15 p2682 A70-32000

Hydrogenomonas vs Chlorella spacecraft life support systems, discussing human requirements and equipment for balanced food supply on long duration space missions

16 p2855 A70-34315

Energy yield measurements of catabolic and anabolic activity in autotrophically growing Hydrogenomonas eutropha

23 p4149 A70-44997

HYDROGRAPHY

Airborne real time IR imagery of thermal anomalies for geophysical exploration of water resources

09 p1674 A70-22262

HYDROKINETICS

U HYDROMECHANICS

HYDROLOGY

Earth environmental satellite data for oceanography and hydrology, discussing sea surface temperature mapping, low level wind conditions, snow and ice mapping, etc

[AAS PAPER 69-596]

04 p0676 A70-14635

Earth surface hydrology effect incorporated into atmospheric circulation mathematical model for climate, considering ocean as atmospheric moisture reservoir

04 p0680 A70-15296

Remote sensing techniques for water resources evaluation and hydrobiological features mapping with multiband scanner imagery

10 p1879 A70-24742

Automatic search for data in hydrology and meteorology, describing information search language development

14 p2602 A70-30141

Venus water presence from Venera 4 and Mariner 5 data suggesting polar seas and oceans saturated with hydrochloric acid and carbon dioxide as plant life source

14 p2637 A70-30365

Space acquired hydrological cycle data relating to water occurrence and movement in atmosphere and earth surface mantle

20 p3616 A70-39063

HYDROLYSIS

Moisture absorptivity and hydrolytic stability effects on operational parameters of gas turbine engine lubricants

06 p1075 A70-17222

Silane coupling agents glass-catalyzed hydrolysis without presence of acid, discussing reaction kinetics

06 p1091 A70-17599

Synthesis of alpha-dichloro-seco-A-norcholestanol from diol monoacetate reaction with triphenylphosphine followed by hydrolysis and repeated chlorination

06 p1005 A70-17975

Refutation of Sylvén-Snellman report of catalysis of benzoylarginine beta-naphthylamide and leucine beta-naphthylamide hydrolysis by beef spleen cathepsin B

10 p1812 A70-24534

Adenosine phosphates hydrolysis in solutions containing Ca ions and in synthetic seawater, investigating living systems energy transfer and prebiological evolution

11 p1986 A70-25702

Stereospecificity and reaction rate of enzymatic hydrolysis of racemic substrate by pepsin determined by nuclear magnetic resonance spectroscopy

12 p2181 A70-27472

Methane and ethane released from Apollo 11 lunar samples by crushing or acid treatment, suggesting carbides hydrolysis as main source

12 p2304 A70-27719

Amino acids analysis of Apollo 11 lunar fines by hydrolysis of aqueous extracts

21 p3778 A70-41623

Lunar fines hydrochloric acid hydrolysates examination by gas-liquid chromatography indicating presence of organosiloxanes

21 p3779 A70-41627

Strontium nitride hydrolysis, investigating hydrazine presence among products

23 p4158 A70-44598

HYDROMAGNETIC FLOW

U MAGNETOHYDRODYNAMIC FLOW

HYDROMAGNETIC STABILITY

U MAGNETOHYDRODYNAMIC STABILITY

HYDROMAGNETIC WAVES

U MAGNETOHYDRODYNAMIC WAVES

HYDROMAGNETICS

U MAGNETOHYDRODYNAMICS

HYDROMAGNETISM

U MAGNETOHYDRODYNAMICS

HYDROMECHANICS

NT ELASTOHYDRODYNAMICS

NT ELECTROHYDRODYNAMICS

NT HYDRODYNAMICS

NT HYDROSTATICS

NT MAGNETOHYDRODYNAMICS

Hydromechanics and thermodynamics in mechanical radial face seal design

11 p2059 A70-25792

HYDROMETEOROLOGY

Grouping method estimation of statistical data during hydrometeorological information processing to calculate essential data for distribution curve judgement

06 p1096 A70-17786

Signal attenuation and bandwidth limitations imposed by atmospheric hydrometeors on communications satellite systems above 10 GHz, discussing Comsat measurement programs

[AIAA PAPER 70-500]

11 p1997 A70-25408

Short wave radiation fluxes inclusion in hydrodynamic model of general atmospheric circulation based on aircraft sounding data and aerostatic observations

12 p2263 A70-27512

Meteorological satellites TV pictures processing for hydrological information, emphasizing snow photographs interpretation

14 p2601 A70-30138

Hydrometeorological information processing using ALGOL-60 translator language

19 p3463 A70-38759

Multispectral hydrometeorological environment monitoring in Earth Resources Survey Program

23 p4191 A70-44664

Technological and economical characteristics of serviced and unserved automatic hydrometeorological stations and second class nonautomatic station

24 p4340 A70-46406

HYDROMETERS

Optical hydrometer measuring water vapor content in vertical atmosphere column, using interference filters and thermoelectric sensitive element
20 p3625 A70-39027

HYDRONIUM IONS

Hydronium ion formation mechanism for D region, obtaining experimental support from mass spectrometer observation of ion production in oxygen glow discharge
09 p1671 A70-23500

HYDROPLANING

Wet runway operations in air traffic control, discussing viscous, reverted rubber and dynamic hydroplaning
13 p2348 A70-29779

HYDROPONICS

Carrot plants growing during 374 days in conveyor type aeroponic assembly, noting yield and morphological features
03 p0436 A70-13902

Sweet potatoes productivity and nutritive value as carbohydrates source in manned space flights
04 p0641 A70-14572

Plant cultivation in closed biological cycles by hydroponic method using keramsit/alumoferrisilicate/substrate
13 p2358 A70-29328

HYDROSPHERE [EARTH]

U EARTH HYDROSPHERE

HYDROSPINNING

Electrically conducting fluid hydromagnetic spin-up between infinite flat insulating plates in uniform magnetic field normal to boundaries
23 p4223 A70-43972

HYDROSTATIC PRESSURE

Electrical lead sealing in hydrostatic high pressure systems with gaseous pressure transmitting medium, considering piston cone seals, frozen oil seals, epoxy seals, etc
01 p0104 A70-10744

Orthotropic cylindrical shell with initial deflection under long term effect of external hydrostatic pressure, solving bending problem
02 p0390 A70-12809

Polyethylene and polypropylene mechanical behavior under tensile and compressive loads and subject to hydrostatic pressure, obtaining tensile nominal stress-strain curves for various pressures
03 p0517 A70-14201

Inertia effects due to circumferential and radial velocity in MHD hydrostatic thrust bearing in axial magnetic field
04 p0698 A70-14871

Adiabatic elastic stiffness constants of single crystal forsterite measured as function of hydrostatic pressure and temperature, using pulse superposition technique
04 p0678 A70-15055

Hydrostatic pressure effects on DNA, RNA and protein synthesis and division in *Escherichia coli* cultures
04 p0637 A70-15475

Ultraminiature pressure sensor for continuous recording of hydrostatic pressure in renal tubules and blood capillaries
05 p0804 A70-15772

Resistance strain gauge load cell for measuring compressive loads under high hydrostatic pressure, discussing gauge bonding
05 p0848 A70-16377

External hydrostatic pressure effect on fiberglass-reinforced plastics strength under unilateral heating, analyzing stress distribution
05 p0875 A70-17067

Theory for describing rotating fluid planets external geometry in state of hydrostatic equilibrium, noting role of equipotential surfaces
06 p1153 A70-18559

Hydrostatic journal bearing calculation for case of shaft misalignment, deriving linear inhomogeneous equations with symmetrical matrix for pressure
07 p1293 A70-19119

Hydrostatic journal bearing dynamic rigidity for compressible and incompressible fluids, describing fluid film elasticity and damping characteristics
07 p1293 A70-19121

Zener diode used as hydrostatic pressure gauge, describing pressure effects on diode current/voltage characteristics
08 p1477 A70-21644

Circular membrane creep under one-sided hydrostatic pressure, using governing equations for finite deformation
10 p1959 A70-24828

Hydrostatic oil journal bearings performance with several supply holes and incompressible lubricant, analyzing Reynolds pressure equation by numerical method
10 p1895 A70-24851

Blunted spherical shells stability under hydrostatic pressure by reducing equilibrium equations to differential
12 p2322 A70-27333

Fiberglass plastic cylindrical shells stability against creep under prolonged hydrostatic pressure, obtaining critical loading times
12 p2328 A70-28278

Self energized hydrostatic shaft seal operating with incompressible fluid in laminar flow regime, using general lubrication theory
13 p2417 A70-28614

Plastic deformation of Be single crystals under hydrostatic pressure, considering resolved shear stresses on glide systems
14 p2595 A70-30334

Superplastic deformation of thin circular diaphragms subjected to one-sided hydrostatic pressure, emphasizing thickness variations in bulged shapes
16 p2916 A70-32917

Normally intersecting closed cylindrical shells subjected to internal hydrostatic pressure, using Donnell shell theory
16 p2990 A70-33678

Adhesive bond between steel wire and epoxy resin, investigating hydrostatic pressure effect on shear strength
17 p3123 A70-34623

Teflon bucket and Be-Cu cap seal against hydrostatic pressure, discussing applications for high pressure superconductivity measurements
18 p3262 A70-37097

Hydrostatic pressure dependences of second order elastic constants of ZnTe and ZnSe at 295 K, using ultrasonic pulse echo method
19 p3486 A70-37762

Hydrostatic pressure derivatives of adiabatic elastic moduli of single crystal zirconium, noting high temperature Gr₁₁ isen-thermal expansion deviation
19 p3486 A70-37763

Right-mov₁ thunderstorm characteristics from mesonet network rawinsonde updraft observations, considering hydrostatic pressure and cyclonic rotation
19 p3462 A70-38260

Argon hydrostatic pressure effect on self diffusion coefficients and activation energy of Al and Be single crystals
20 p3644 A70-38961

Stiffened thin walled circular cylinders buckling and postbuckling behavior under axial compression or external hydrostatic pressure
20 p3719 A70-39621

Working medium excess and absolute pressure effects on pneumatic elements characteristics
22 p3967 A70-43566

HYDROSTATICS

Static and centrifugal filters merits for turbine engine lubrication systems, considering mechanical reliability, efficiency, dirt capacity and maintenance
01 p0164 A70-10686

Hydrostatic equation nonequilibrium terms role in single and multicomponent atmospheres, deriving solutions to Boltzmann equation
02 p0328 A70-12386

Hydrostatic models of sunspot penumbra and umbra, analyzing spot transparency influence on Wilson effect
03 p0571 A70-13596

De Sitter hydrostatic equations solution possible with help of boundary condition from external potential theory with/without assumed equilibrium in earth interior
04 p0678 A70-15051

Hydrostatic equilibrium in self gravitating core of rotating relativistic star, considering Newton and Einstein gravitation theories
05 p0914 A70-16648

Hydrostatic equilibrium solutions of internal structure of neutron stars using Brueckner equation
06 p1139 A70-17541

Moon figure and gravitational field determination based on hydrostatic theory, libration observations, node and perigee motion, lunar satellite trajectories and visible topography
06 p1141 A70-17824

Hydrostatic bearings design for minimum power loss and leakage and maximum stiffness, using geometry- dependent operating parameter
08 p1508 A70-21600

Stellar evolution computations numerical instability due to coupling between hydrostatic equilibrium and thermal processes
09 p1755 A70-22508

Optimization in epiphydrostatics and epiphydrodynamics, discussing liquid in rectangular tank, electro-magneto-epiphydrodynamics and thermal instability
10 p1866 A70-24108

Dynamic instability of multirecess hydrostatic journal bearings at critical shaft rotation velocity
13 p2418 A70-28745

Lagrange equations for translational motion and diameter variation of bubble system moving in hydrostatic field, taking into account dissipative forces
18 p3240 A70-36270

Hyperelastic bodies stability subject to conservative configuration dependent forces, formulating surface potential for hydrostatic loading
22 p4114 A70-42695

HYDROX ENGINES

U HYDROGEN OXYGEN ENGINES

HYDROXIDES

NT LITHIUM HYDROXIDES

NT POTASSIUM HYDROXIDES

Water vapor dissociation in dilute mixtures with Ar behind shock waves, studying OH concentrations using flash-absorption technique
08 p1548 A70-21355

Spectroscopic technique measuring OH concentrations behind shock waves by measuring absorption of OH lines, using water cooled RF powered lamp
09 p1683 A70-23512

Airglow hydroxyl emissions diurnal variations as function of height, using digital computer for time dependent solution of equations for oxygen- hydrogen atmosphere
10 p1872 A70-23826

Transitions in interstellar OH observed at National Radio Astronomy Observatory
10 p1948 A70-25000

Balloon-borne photometer for collecting twilight and daytime OH intensity and rotational temperature variations data
13 p2399 A70-29240

Electrochemical properties of sintered and film nickel hydroxide electrodes
22 p3966 A70-43542

HYDROXYCORTICOSTEROID

Transmeridian flights effect on diurnal urinary excretion of unconjugated 17- hydroxycorticosteroids in males, evaluating time shift effects
21 p3770 A70-41477

HYDROXYL COMPOUNDS

NT ALCOHOLS

NT ETHYL ALCOHOL

NT GLYCOLS

NT METHYL ALCOHOLS

NT PHENOLS

Enzymatic hydroxylation mechanism of p- hydroxybenzoate hydroxylase from *Pseudomonas putida*, describing product separation and purification
02 p0236 A70-12100

Night airglow emission intensities during IQSY concerning Na, OH and H alpha lines compared with intensities during IGY
02 p0292 A70-12433

Gas chromatography and mass spectroscopy study of fatty acids and hydroxy acids in 5000 year sediment from English Lake District
02 p0252 A70-12507

Hydroxy fatty acid methyl esters gas chromatography and mass spectrometry, noting trimethylsilylation usefulness for locating double bond
02 p0252 A70-12515

Gas chromatographic-mass spectrometric identification of aliphatic hydroxy acids in plants and sediments
02 p0252 A70-12521

G values of hyperfine components of OH radical molecular vibrational-rotational levels determined using optical RF double resonance
02 p0345 A70-12822

Maser-like stimulated OH emission regions observed in interstellar rarefied gas
06 p1148 A70-18391

Hydroxyl emission during auroras, noting absence of correlation with O I brightness fluctuations for IBC II-III aurora of 1 November 1968
09 p1671 A70-23496

Galactic radio sources examined for hydroxyl lines associated with H II regions, making observations in absorption and emission
10 p1936 A70-23904

Sagittarius sources A and B2 O18H absorption lines measured at microwave frequencies, determining oxygen isotopes abundance ratios
10 p1936 A70-23907

Microwave lines due to hydroxyl radical in interstellar medium, discussing emission from excited OH states
13 p2484 A70-28371

OH radio emission from IR stars, discussing spectra, polarization properties and red giant star model with expanding atmosphere
14 p2641 A70-30881

Galactic hydroxyl emission sources right ascensions, presenting coordinates and antenna temperature measurements
15 p2796 A70-31594

Serotonin, 5-hydroxyindoleacetic acid /5-HIAA/ and monoamine oxidase in bovine pituitary organ and median eminence
21 p3761 A70-40850

Galactic hydroxyl emission sources right ascensions, presenting coordinates and antenna temperature measurements
23 p4242 A70-44277

HYDROXYL EMISSION

Spectrophotometric airglow intensity measurements of OH, O I 6300, hydrogen H alpha and oxygen Herzberg I bands by airborne laboratory

17 p3080 A70-35769

Water vapor and OH spectra overlap, investigating association of galactic OH masers and water emission sources with IR stars

19 p3444 A70-37571

Night airglow hydroxyl rotational brightness temperature determined from emission spectra

19 p3412 A70-37777

Weak predissociation effects of hydroxyl compounds electron state on radiative lifetime via phase shift method

19 p3374 A70-38270

Double resonator ruby maser for observing transitions of interstellar hydroxyl, noting incorporation in modulation radiometer of astronomical telescope

21 p3835 A70-40641

Hydroxyl atmospheric airglow secondary production processes, discussing vibrationally excited oxygen molecules and rapid quenching by atomic O and HO sub 2

21 p3816 A70-41068

Laboratory measurement and low noise search in W3/OH for microwave emission lines in excited rotational level of interstellar OH

21 p3922 A70-41977

Interstellar molecules from stellar and galactic evolution viewpoint, emphasizing OH emission spectrum characteristics

23 p4238 A70-43801

Airglow hydroxyl emission altitude profile observations by rocket-borne photometer

23 p4191 A70-44407

Polarized maser emission from interstellar hydroxyl and water related to nonlinear weak magnetoplasma

24 p4381 A70-45258

HYGIENE

Physiological and hygienic data on oxygen partial pressure in space cabin atmosphere analyzed for manned space flights

07 p1220 A70-19502

Physiological and hygienic data on oxygen partial pressure in space cabin atmosphere analyzed for manned space flights

11 p1991 A70-26101

HYGROMETERS

NT PSYCHROMETERS

Barium fluoride film hygrometer elements for radiosondes, discussing manufacturing and testing methods

13 p2408 A70-29470

Time constant equations for hair and film radiosonde hygrometers, allowing for inertial errors in humidity and cloud boundary measurements

14 p2603 A70-30412

Balloon-borne optical dew point hygrometer and radiosonde measurements of atmospheric range refractive index

14 p2585 A70-30573

Humidity calibration utilizing precision wide range optically controlled thermoelectrically cooled dew point hygrometer

14 p2587 A70-31165

Humidity measurement and calibration systems, considering automatic optical dew point hygrometry

17 p3089 A70-35172

Chemically treated rolled hair properties following long term use in hair hygrometers

24 p4333 A70-45138

HYGROSCOPICITY

Warm fog clearing effectiveness by seeding with hygroscopic nuclei as function of fog droplet and seeding nuclei distribution

17 p3132 A70-35928

Hygroscopic materials warm fog clearing capabilities comparison, recommending urea and ammonium nitrate

20 p3664 A70-40065

Cetyl alcohol and water vapor growth by absorption and condensation on hygroscopic nuclei population in atmosphere under cooling

20 p3664 A70-40066

HYLLERAAS COORDINATES

Quantum mechanical inverse problem of elastic scattering theory, discussing Hylleraas solution for determining potential energy function from phase shift

12 p2274 A70-26899

HYPERBARIC CHAMBERS

Pressor response to epinephrine in hyperbaric atmospheres measured in cats under change of sympathetic tone

17 p3032 A70-35566

Hyperbaric oxygen effects on Coxsackievirus infection in mice

24 p4296 A70-45338

HYPERBOLAS

Meteors hyperbolicity based on statistical considerations and radiant distribution, discussing orbits perturbation and observation from earth

13 p2490 A70-29041

Elastic two cavity hyperboloid of revolution under stress due to rotating rigid stamp, solving torsional problem numerically

15 p2819 A70-32189

Acoustic and EM scattering by hyperbolic cylinder, considering plane wave incidence and line sources

15 p2700 A70-32406

Hyperboloid of revolution acoustic scattering, using Bloom-type method for hard hyperbolic cylinder

15 p2701 A70-32416

HYPERBOLIC FUNCTIONS

Spatial amplification criteria for hyperbolic wave equations extended to include parabolic equations, discussing convective and absolute instabilities

03 p0519 A70-13522

Simultaneous maximum likelihood estimation and coordinate conversion for redundant hyperbolic lines of position in radio navigation

[AIAA PAPER 68-888] 04 p0717 A70-15545

Numerical solution of nonlinear hyperbolic systems of differential equations using methods of differences, applying results to invariant cross section gas flow

06 p0964 A70-17236

Existence results for Cauchy problem for linear variable coefficient hyperbolic operators with multiple characteristics

06 p1094 A70-17898

Mixed problems with linear homogeneous boundary conditions with time-independent coefficients for semihyperbolic equations, discussing constraints

08 p1534 A70-21005

Solvability of linear problems with minimal smoothness constraints and of mixed problems for quasi-linear hyperbolic equations with coefficients and boundary conditions nonlinearities

09 p1712 A70-23120

Maximum principle condition of optimal control of monodimensional system described by nonlinear hyperbolic equations with time delay

11 p2021 A70-25340

Multistep formulations of optimized Lax-Wendroff method for nonlinear hyperbolic systems in space variables

13 p2440 A70-29086

Finite difference methods for approximating first order nonlinear hyperbolic differential equations, considering convergence

13 p2441 A70-29098

Unique solvability of mixed semihyperbolic linear equations of higher order with respect to spatial variables and time

15 p2768 A70-32475

Second order hyperbolic partial differential equations solution by characteristic grid and continuous characteristic methods

15 p2768 A70-32818

Second order hyperbolic partial differential equations analog solution based on method of characteristics, showing advantage over digital computer solution

15 p2768 A70-32819

Class of third order difference methods for hyperbolic equations in one and two dimensions applicable to nonlinear initial value problems

17 p1313 A70-35893

Initial boundary value problems for hyperbolic partial differential equations, including Cauchy problem

19 p3457 A70-37678

Nonlinear free boundary problem for hyperbolic one dimensional gas dynamics equations

20 p3658 A70-40105

Wave front arbitrary curvature, examining integration of weak discontinuities growth equation in quasi-linear hyperbolic system

22 p4062 A70-42953

Cauchy-Dirichlet type mixed problems for hyperbolic equations in cylindrical domain, using Zygmund-Calderon approximate calculus

23 p4210 A70-43978

HYPERBOLIC NAVIGATION

NT DECCA NAVIGATION

NT LORAN

NT LORAN C

NT LORAN D

Hyperbolic navigation systems circular fixes derivation error analysis

09 p1719 A70-22191

Hyperbolic position finding with synchronous satellites having frequency conversion unit for operations at higher frequency satellite signals

09 p1724 A70-23044

Error sensitivity to measurement uncertainties and satellite geometry of satellite linked hyperbolic navigation systems

09 p1724 A70-23046

Eurocontrol evaluation of navigational aid systems air traffic control, examining HARCO and VORDAC systems

19 p3468 A70-38641

HYPERBOLIC SYSTEMS

Wave propagation in inhomogeneous media, reducing quasi-linear hyperbolic partial differential equations to single nonlinear equation integratable by method of characteristics

03 p0525 A70-14184

Partial differential equations hyperbolic systems solutions by finite difference methods, considering schemes stability and viscosity from first differential approximation standpoint

07 p1326 A70-19599

Riemann invariants, discussing method of characteristics in physical and hodograph space applications and multidimensional hyperbolic systems

10 p1865 A70-24103

Quasi-linear hyperbolic systems interactions for rarefaction waves, applying Glimm difference method

16 p2943 A70-33782

Nonrigorous hyperbolic systems, discussing existence and uniqueness theorems contradiction in linear equations and proof of Cauchy problem

19 p3478 A70-37582

HYPERBOLIC TRAJECTORIES

Optimal acceleration from earth orbit to hyperbolic velocities of low thrust space vehicle, constructing asymptotic expansions near and far from central field

10 p1940 A70-24305

Nonadiabatic self absorbing radiative flow of gray gas around sharp cornered blunt body at hyperbolic speed by integral relations method

17 p3010 A70-34974

Spinning symmetric satellite attitude stability in hyperbolic orbit on flyby mission, examining by numerical integrations of equations of motion

17 p3181 A70-35753

Humason 1960e-1959X comet hyperbolic orbit, indicating solar system permanent membership

19 p3516 A70-37934

Minimum impulse transfer between circular orbit and hyperbolic trajectory velocity vector, assuming fixed transfer times

19 p3527 A70-38853

Travel time for trips to Neptune, calculating earth gravitational field escape hyperbola and waiting time before return

23 p4245 A70-44653

HYPERCAPNIA

Acid base responses of arterial plasma of anesthetized man during acute carbon dioxide partial pressure changes, discussing anesthesia effects

01 p0020 A70-10651

Rodents hypoxia tolerance following adaptation to hypercapnia by recording time of useful consciousness /TUC/ in repeated sloped surface clinging tests

01 p0026 A70-11249

Polycythemia and hypercapnia effects on apparent oxygenation of rat brain during acute hypoxia by changes in creatine phosphate concentration and lactate/pyruvate ratio

02 p0232 A70-11717

Hypercapnic atmosphere effect on human organisms found tolerable in state of rest or performing light labor

09 p1615 A70-22094

Hypoxia tolerance in white rats after exposure in hypercapnic medium

13 p2355 A70-29757

Single and combined hypoxia and hypercapnia effects on growing rats, discussing body weights, blood and histological measurements

13 p2357 A70-29948

Inspired carbon dioxide pressure effects on human response to physical exercise, noting dyspnea and intercostal muscle pain

13 p2360 A70-29949

Hypercapnic atmosphere effect on human organisms found tolerable in state of rest or performing light labor

15 p2685 A70-32690

Ambient temperature effects on rats and white mice tolerance to hypoxia, asphyxia and hypercapnia in nitrogen-oxygen and He-oxygen atmospheres

17 p3030 A70-35353

Orthostatic tolerance increase in animals by application of hyperoxic and hypercapnic gas mixtures

20 p3574 A70-40185

Hypercapnia effect on oxygen tension in ischemic myocardium in dogs using polarographic method

24 p4300 A70-45843

HYPERFINE STRUCTURE

G values of hyperfine components of OH radical molecular vibrational-rotational levels determined using optical RF double resonance

02 p0345 A70-12822

Concentrated Fe-Co alloys, effects of local atomic configurational changes on hyperfine interaction using Mossbauer spectroscopy

12 p2284 A70-27245

Isomer shift, Mossbauer recoil free fraction and nuclear quadrupole splitting for Fe57 in iron fluoride measured for lattice dynamics, fine and hyperfine structure

14 p2626 A70-30484

Formaldehyde rotational transition hyperfine components measured by molecular beam maser

20 p3702 A70-39008

Magnetism in austenitic stainless steels, discussing Mossbauer measurements of temperature dependence of hyperfine field and single line width

22 p4055 A70-43012

HYPERGEOMETRIC FUNCTIONS

Structural synthesis of functional control systems represented by first order differential equations, determining hypersurface

08 p1479 A70-20871

Heat insulated plate compressible boundary layer energy equations approximate solutions in hypergeometric functions

10 p1966 A70-23867

Cylindrical shell of variable thickness, deriving axisymmetric thermal stresses in terms of hypergeometric functions

18 p3336 A70-36137

Confluent hypergeometric functions indefinite integrals analytic expressions and reduction formulas

22 p4062 A70-42572

HYPERGEOMETRY

U HYPERSPACES

HYPERGOLIC ROCKET PROPELLANTS

Hydrogen peroxide oxidizer for higher characteristic mixture ratio in hybrid propulsion systems with hypergolic reactions ignition

[ONERA-TP-773] 02 p0352 A70-12209

Fluorine injectors for main tank injection of space vehicle liquid hydrogen tank, including study of hypergolicity and reaction product freezing

[AIAA PAPER 69-528] 04 p0736 A70-15406

Optimum penetration and separation mixing of unlike doublet injector element with hypergolic hydrazine and nitrogen tetroxide propellants

[JPL-TR-32-1487] 11 p2099 A70-25995

Oxygen difluoride-diborane reaction measured for pressure-temperature relationships and gas composition dependence on time, noting possible applications as hypergolic rocket propellants

11 p1995 A70-26138

Solid propellant radiant and hypergolic ignition, examining radiation absorption and surface reaction between fuel and gaseous oxidizer

20 p3689 A70-40081

Solid phosphorus triamide derivatives as ignition aids in hypergolic propellant systems, testing characteristics in interaction with oxidizers

21 p3865 A70-41404

HYPERONS

Hyperon and resonance particle effects on neutron star vibration, discussing vibrational energy storage and atmospheric electromagnetic generation

02 p0379 A70-12699

Neutron stars properties, using static cold stellar model to examine relation between central density and mass, and cool hyperonic matter composition

09 p1749 A70-21995

Neutron core star models based on realistic nuclear matter calculations and hyperons equation of state

17 p3157 A70-34844

Equilibrium theory of white dwarfs, neutron and hyperon stars, deriving equations for nonrotating objects composed of degenerate cold electron or neutron gas

20 p3704 A70-39472

Stable hyperon star existence in general relativity, discussing state equations for baryon matter, radial pulsation and superlumina and ultrabaryon conditions

21 p3888 A70-41116

HYPEROXIA

Patients with/without coronary heart disease inhaled various gas mixtures to induce arterial hypoxemia and hyperoxia, noting O availability for myocardial metabolism

01 p0016 A70-10440

Retinal vessels of humans at 11-2.0 atmosphere oxygen partial pressures, noting arterioles and venules dilation response to hypoxia and vasoconstriction response to hyperoxia

01 p0023 A70-10863

Protein metabolism of mice exposed to compression of air-oxygen mixture containing 27 percent oxygen, showing relationship to food intake

01 p0028 A70-11363

Oxygen consumption and rectal temperature in male mice confined in nitrogen and helium diluted hyperoxic atmosphere at specific temperature and humidity ranges

03 p0425 A70-13891

Phagocytic activity and carbohydrate metabolism in peripheral blood neutrophils of men exposed to atmosphere with increased O content, noting neutrophil energy exchange disorder role

03 p0426 A70-13901

Low body temperature effects on convulsive activity elicited by hyperbaric oxygen in unrestrained unanesthetized rats

04 p0629 A70-14448

Hyperbaric oxygenation effects on metabolism, comparing protective agents for rats exposed to 5 absolute oxygen pressures

04 p0631 A70-14681

Fire safety in hyperbaric systems isolated from environment by gas tight barrier

[ASME PAPER 69-WA/SAF-2] 04 p0784 A70-14836

White rats parenchymatous organs morphological changes following convulsion-producing exposure to pure hyperbaric oxygen

07 p1207 A70-19503

Vascular and dystrophic disturbances in rat parenchymatous organs in hyperbaric pure oxygen atmospheres, observing increased tissue eosinophilia

07 p1207 A70-19504

Hyperoxia effects on red blood cell/RBC/survival in rats on normal diets, noting relatively normal erythropoiesis after long term exposure

07 p1214 A70-19935

Protective ability of various compounds against hyperoxia at 5, 7, 9 and 11 atmosphere of pure oxygen

08 p1441 A70-20629

Rats acute hypoxia and altitude tolerances after prolonged exposure to hyperoxic atmospheres

08 p1446 A70-21437

Hyperbaric oxygenation treatment physiology and techniques, discussing limitations of equipment

09 p1620 A70-23017

Hyperbaric oxygen effect on heart muscle contractions in mammals, considering cells enzymatic activity and substrate utilization

09 p1623 A70-23586

Dogs respiratory response to arterial hydrogen ions at different carbon dioxide pressure levels during hypoxia or hyperoxia, discussing acid-base balance effects

11 p1986 A70-25674

Free radical content changes in mice organs under hyperoxia and hypoxia

11 p1986 A70-25941

White rats parenchymatous organs morphological changes following convulsion-producing exposure to pure hyperbaric oxygen

11 p1987 A70-26102

Respiratory gas exchange, heart rate, arterial acidemia and hypocapnia responses to physical work in hyperbaric environments and hyperoxia conditions

12 p2169 A70-27655

Altitude acclimatization protection against lung damage from exposure to oxygen at high partial pressures experimented on rats

12 p2170 A70-27659

Erythropoiesis inhibitor in blood from rabbit kidney vein during hyperoxia in nitrogen-oxygen atmosphere

14 p2535 A70-30155

Prolonged hyperoxia effect on red blood cell survival and hemolysis in rats on normal diet

15 p2681 A70-31786

Exercise and rest of humans under hypoxia and hyperoxia, determining blood acid-base state, ventilation and carbon dioxide partial pressure

16 p2849 A70-34256

Hyperbaric oxygen exposure produced hypertension and pulmonary edema, discussing carbon dioxide transport mechanism in blood

20 p3572 A70-39430

Orthostatic tolerance increase in animals by application of hyperoxic and hypercapnic gas mixtures

20 p3574 A70-40185

Hypoxia and hyperoxia effect on ballistocardiogram of healthy males, determining systolic and minute cardiac forces

21 p3763 A70-41231

Ballistocardiogram relationship to cardiac performance index in hypoxia and hyperoxia conditions, investigating systolic and minute cardiac forces

21 p3770 A70-41232

Sodium pentobarbital effect on oxygen poisoned mice, observing respiratory depression coupled with lung failure

21 p3764 A70-41480

Dehydrogenases activities in rabbit retina homogenates exposed to oxygen at high partial pressure for various time periods

21 p3765 A70-41487

Human and animal tolerances to hyperbaric oxygen, discussing response variation, toxicity modification, etc

22 p3976 A70-43701

Oxidative phosphorylation and oxygen consumption during hyperoxia in mitochondria preparations and tissue homogenates from white rat liver

23 p4146 A70-44316

Hyperoxia effects on rats in vivo white blood cell counts

24 p4297 A70-45340

HYPERPLANES

Localized states reconstructed as superposition of canonical states, using hyperplane generalization

15 p2766 A70-31437

HYPERSONIC AIRCRAFT

NT HYPERSONIC GLIDERS

Airframe-propulsion system integration for Mach 6 transport and Mach 12 research airplane, examining off-design operation effects and interaction of aerodynamic forces

[AIAA PAPER 70-542] 13 p2345 A70-29009

Dicyclohexyl/DCH/ endothermic dehydrogenation to diphenyl/DP/ over platinum-alumina catalyst without added hydrogen considered for hypersonic aircraft engine cooling

14 p2546 A70-31175

Hyperonic aircraft technology, discussing long range transport, reusable launch vehicles and propulsion systems

15 p2673 A70-31851

HYPERSONIC BOUNDARY LAYER

Turboamjet powered hypersonic aircraft axisymmetric inlet systems using forward translating cowl and centerbody for various air flow characteristics

[AIAA PAPER 70-687] 16 p2835 A70-33586

Slender hypersonic airfoil shape optimization for maximum lift to drag ratio for given profile area, chord and free stream conditions

19 p3352 A70-38304

Hypersonic airbreathers aerodynamic, structural and propulsive system interactions, discussing hydrogen fuel heat sink, airframe and engine cooling and airframe materials

[ICAS PAPER 70-16] 23 p4138 A70-44127

Hypersonic aircraft stability and control problems, discussing bulky engines and air intake and exhaust geometry

[ICAS PAPER 70-17] 23 p4138 A70-44128

All-body configuration hypersonic transport aircraft performance by computer synthesis, considering sonic boom constraint, maximum payload ratio and optimal cruise speed

[AIAA PAPER 70-1224] 24 p4291 A70-45957

HYPERSONIC BOUNDARY LAYER

Hypersonic dissociated laminar boundary layers with/without heat transfer calculated by integral method for case of thermodynamic equilibrium

01 p0003 A70-10933

Surface catalysis and variable transport properties effects on chemically frozen dissociated hypersonic air flow boundary layers enveloping flat plates and slender wedges

01 p0067 A70-11179

Ablation effects on transition Reynolds number of hypersonic boundary layer on slender cones

03 p0465 A70-12945

Explosion analogy to study hypersonic flow region behind shock wave including boundary layer at blunt body surface

03 p0406 A70-13332

Boundary layer transition limits at high Mach numbers, discussing transition on flat plate and bodies of rotation and Reynolds number

04 p0672 A70-15177

Magnetohypersonic boundary layer interactions, discussing boundary layer thickness relationship to Hartmann and Reynolds numbers

04 p0729 A70-15564

Boundary layer-induced pressures on flat plate in unsteady hypersonic flight calculated using tangent wedge approximation

[AIAA PAPER 70-184] 06 p1039 A70-18095

Integral moment method for interactions between laminar boundary layer and external supersonic flow applied to hypersonic laminar boundary layer near sharp expansion corner

[AIAA PAPER 70-186] 06 p1039 A70-18111

Flat plate boundary layer induced pressures in unsteady hypersonic flight

07 p1257 A70-19327

Hypersonic laminar boundary layer in strong viscous interaction region on wedge, determining velocity and enthalpy profiles, displacement thickness and induced pressure distributions, etc

09 p1606 A70-23294

Uncooled leading edge effect on cooled-wall hypersonic flat plate boundary layer transition, discussing leading edge bluntness effects

11 p1976 A70-25984

Interaction of laminar hypersonic boundary layer and supersonic corner expansion wave, discussing upstream influence, transverse pressure gradients and external flow

[AIAA PAPER 69-137] 12 p2211 A70-27826

Discrete sonic jets as boundary layer trips producing turbulent hypersonic flows with negligible intrinsic drag and downstream distortions

13 p2523 A70-29973

Explosion analogy to study hypersonic flow region behind shock wave including boundary layer at blunt body surface

14 p2528 A70-30711

Prandtl number effects on adiabatic wall temperature and pressure gradient at separation point for hypersonic compressible laminar boundary layer

14 p2566 A70-31027

Laminar hypersonic boundary layer interaction with corner expansion wave, presenting numerical solutions to viscous-inviscid equations for small turning angles

[AIAA PAPER 70-807] 17 p3065 A70-34457

Shock wave and viscous layer structures ahead of blunt body in rarefied hypersonic flow, using continuum theory

17 p3009 A70-34698

Displacement interacting boundary layer in symmetry plane region of flat hypersonic delta wing by control volume balances for mass, momentum and energy

17 p3010 A70-34975

Space vehicle reentry hypersonic boundary layer characteristics, considering air components chemical reactions due to excessive heat

18 p3346 A70-36384

Compressible hypersonic turbulent boundary layers solution by finite difference method, relating mixing length to velocity profile shape factor
20 p3684 A70-40269

Free stream disturbances influence on hypersonic boundary layer transition Reynolds number in heated and unheated flows
[AIAA PAPER 69-704] 21 p3809 A70-41744

Three dimensional hypersonic laminar boundary layer subdivided into inner and outer regions, obtaining flow description by matching inner and outer solutions
[AIAA PAPER 69-710] 23 p4182 A70-44565

Gas coolant slot injection into hypersonic laminar boundary layer, comparing experimental results to boundary layer equations numerical integration
23 p4282 A70-44694

HYPERSONIC COMBUSTION

Polymethyl methacrylate fuel for hypersonic air breathing propulsion systems, studying ablation, mixing and combustion processes
03 p0603 A70-12942

HYPERSONIC FLIGHT

Deviation angle optimization for cruising hypersonic jet aircraft, noting effect of rotation losses on design
03 p0406 A70-13019

Growth test vehicle /GTV/ flight test program for development of hypersonic flight to orbital speeds, discussing design, costs, capabilities, etc
03 p0582 A70-14188

Normal force component distribution and aerodynamic pressure position on rocket bodies at supersonic and hypersonic velocities
06 p0964 A70-17238

Tail screens and spoiler rings aerodynamic braking effect in hypersonic range, discussing separated boundary layer periodic unsteady flow
06 p0965 A70-17247

Boundary layer-induced pressures on flat plate in unsteady hypersonic flight calculated using tangent wedge approximation
[AIAA PAPER 70-184] 06 p1039 A70-18095

Flat plate boundary layer induced pressures in unsteady hypersonic flight
07 p1257 A70-19327

Streamlining design for high altitude hypersonic flight vehicles based on drag minimization at flight condition
07 p1189 A70-19717

Quasi-steady analysis of material under ablation-erosion heat transfer for hypersonic vehicles
11 p2149 A70-26144

Hypersonic test equipment, describing flight simulating hypervelocity wind tunnels, firing tunnels and shock wave tubes
13 p2384 A70-28927

Control efficiency of flaps at hypersonic speeds, considering thick turbulent boundary layer compression process
16 p2836 A70-33751

Nonequilibrium gas states evolution in detached wave front of hypersonic blunt body, comparing vibrational relaxation in free flight and wind tunnel flow
18 p3335 A70-35962

Thermal protection system based on radiation cooling for high altitude cruising hypersonic flight, achieving zero net mass transfer
21 p3950 A70-41745

Newtonian hypersonic aerodynamic theory for arbitrary bodies, discussing computational difficulty for shadowed areas
21 p3747 A70-41866

HYPERSONIC FLOW

Inviscid surface pressures calculated on slender wedges and cones at low frequencies and large oscillation amplitudes in hypersonic flow
01 p0003 A70-10854

Navier-Stokes hypersonic weak interaction theory for viscous heat conducting compressible fluid flow past slender axisymmetric body
01 p0003 A70-11097

Modified shock layer theory for predicting hypersonic internal flow in axisymmetric converging duct with attached shock at leading edge
02 p0276 A70-11854

Shock wave shapes in hypersonic flow past blunt conical nosed circular cylinders, using analogy with Savic perturbed hypersonic blast wave theory
02 p0277 A70-11862

Forced convection of hot wire in hypersonic flow, determining Nusselt-Reynolds number relationship for hot-wire anemometers
02 p0223 A70-12101

Brillouin scattering of hypersonic waves produced in liquid medium, using He-Ne laser light source
02 p0313 A70-12471

Hypersonic flow in thermodynamic equilibrium of diatomic dissociating gas with power law shock, investigating self similar solutions of Van Dyke small disturbance equations
03 p0405 A70-12925

Hypersonic flow characteristics on yawed circular cone surface at moderate angle of attack, applying results to inviscid and boundary layer flow computations
03 p0406 A70-12944

Shock wave shapes over axisymmetric power law bodies in hypersonic flow, noting asymptotic flow theory implications
03 p0406 A70-12946

Stagnation point velocity gradients for spherical segment models with bluntness ranging from hemisphere to flatnose cylinder in hypersonic flow
03 p0406 A70-12947

Explosion analogy to study hypersonic flow region behind shock wave including boundary layer at blunt body surface
03 p0406 A70-13332

Fracture and degree of material removal of glassy body in hypersonic gas flow, considering radiant heat conduction inside body
03 p0516 A70-13391

Approximate solution for hypersonic inviscid flow around spherically blunted bodies at small angle of attack, noting stagnation problems
03 p0407 A70-13547

Boundary layer transition from laminar to turbulent in hypersonic wind tunnel, determining Reynolds and Mach number effects
[ONERA-TP-737D] 03 p0467 A70-13641

Similarity laws in hypersonic flow of real gas around slender blunted bodies, particularly bodies with rough lateral surface
03 p0409 A70-13866

Hypersonic flow over blunt bodies, discussing Mach number, specific heat and blast wave limits
04 p0613 A70-14454

Hypersonic blunt body heat transfer prediction, including coupled effects of real gas behavior and slip boundary conditions
[ASME PAPER 69-WA/HT-28] 04 p0614 A70-14809

Convective heat transfer rates measured on cooled sharp leading edge flat plates at various angles of attack in hypersonic merged flow
[ASME PAPER 69-WA/HT-21] 04 p0614 A70-14813

Heat transfer from two dimensional hypersonic low density stream to wedges and sharp flat plates at expansion angles of attack
04 p0615 A70-14944

Circular cylinder drag in hypersonic transverse flows between continuum and free molecular flow, measuring drag and pressure distribution
04 p0615 A70-15089

Monograph on weak interactions on cones in supersonic and hypersonic flows, discussing flow divergence, measurement errors and data reliability
04 p0615 A70-15141

Hypersonic flow region about ducted blunt bodies of revolution, assuming correspondent flow conditions to maximum intake through duct
04 p0617 A70-15233

Hypersonic viscous gas flow past power law bodies under viscous interaction between boundary layer and inviscid flow extended to slender bodies
04 p0618 A70-15240

Delta wing of given volume and planform with maximum lift-drag ratio in hypersonic flow
04 p0618 A70-15243

Unsteady pressure at slender blunt body surface in three dimensional hypersonic gas flow
04 p0618 A70-15244

Three dimensional viscous and inviscid hypersonic flow interaction at rectangular corner, measuring surface and Pitot pressures, heat transfer rates, shear stresses, etc
04 p0620 A70-15533

Mass transfer and viscous interaction combined effects on axisymmetric hypersonic flow of perfect gas over slender bodies
[AIAA PAPER 68-717] 04 p0675 A70-15576

Hypersonic laminar separation of slip flow on slender cone with attached compression flares, using surface pressure measurements and Pitot surveys
[DFVLR-SONDDR-26] 04 p0620 A70-15577

Hypersonic glider performance in mesosphere entry using models located in rarefied gas flow at Mach 8
05 p0789 A70-15811

Slender wing with blunted leading edge to reduce thermal stresses at supersonic speed studied for aerodynamic characteristics in hypersonic flow
05 p0791 A70-17001

Equations of motion for hypersonic friction layers integrated using quadrature procedures
[DVL-913] 06 p1033 A70-17230

Frictionless hypersonic flow around blunt bodies of revolution, taking into account real gas effects in equilibrium and frozen flow calculations
06 p0965 A70-17242

Longshot free-piston wind tunnel for very high Reynolds number hypersonic flows, describing piston cycle, supply conditions, real gas effects on nozzle flow, etc
06 p1027 A70-17245

Inviscid hypersonic blunt body flow of hydrogen-oxygen mixtures in shock layer stagnation region
06 p0968 A70-17555

Small disturbance theory for internal conical inlet hypersonic flows, using method of characteristics for similarity law verification
[AIAA PAPER 70-127] 06 p0969 A70-18048

Kinetic flow regime in hypersonic flow past flat plate leading edge, using Boltzmann equation
[AIAA PAPER 70-181] 06 p0970 A70-18094

Hypersonic corner flow in He investigated by heat transfer, surface pressure, pitot surveys, oil and electron beam flow measurements
[AIAA PAPER 70-227] 06 p1039 A70-18110

Pressure interaction with slender cone in hypersonic flow
[AIAA PAPER 70-183] 06 p0972 A70-18126

Hypersonic aerodynamic measurements on cone, investigating effects of oscillatory mass addition on stability
[AIAA PAPER 70-217] 06 p0974 A70-18171

Hyperboloids and paraboloids in flow of Reynolds number 22-65000 and Mach number 10, discussing viscous interactions effects on pressure, drag and skin friction
[AIAA PAPER 70-182] 06 p0976 A70-18240

Rotational relaxation times for low density hypersonic nitrogen free jet, comparing measured and predicted impact pressures
06 p1043 A70-18279

Interactions between hypersonic neutral gas beam and orificed pressure gauge in spinning satellite noting dependence on angle of attack
06 p1159 A70-18290

Rotational and vibrational temperatures measured in hypersonic nonequilibrium rarefied gas flow field of cooled circular cylinder by electron beam technique
06 p1123 A70-18304

Knudsen iteration for predicting cooled blunt body near free molecular drag in hypersonic stream, using BGK model for collisions
06 p0979 A70-18313

Finite difference analysis of partial differential equations derived from Navier-Stokes equations in hypersonic leading edge problem in merged gas flow-layer regime
06 p0980 A70-18349

Wall pressure distribution, drag and lift measured on flat plates and wedges at Mach 8 rarefied gas flow for various leading edges
06 p0980 A70-18350

Cone bluntness effect on merging onset and downstream flow in merged region at Mach 8 and various Reynolds numbers
06 p0980 A70-18352

Sharp hypersonic flat plates inclined at various angles, obtaining flow field and merged region details
06 p0980 A70-18353

Hypersonic leading edge problem solved, using merged layer theory to provide link between noncontinuum flow upstream of transition and boundary layer flow downstream
06 p0980 A70-18354

Hypersonic rarefied argon and nitrogen flows over flat plate, investigating flow field and surface measurements from merged layer into transition regime
06 p0981 A70-18355

Drag of diffusely reflecting and cool slender cone in hypersonic flow, using nonlinear Boltzmann equation for hard spheres
06 p0981 A70-18359

Nitrogen hypersonic transitional flow at adiabatic sharp flat plate leading edge, presenting density, flow-field shape and local rotational temperature for various regions
06 p0982 A70-18361

Surface pressures and shock wave shapes on sharp flat plates and wedges in rarefied hypersonic transition flow with emphasis on merged layer regime
06 p0982 A70-18362

Hypersonic rarefied merged layer flow over sharp slender cones, using strong interaction theory and free molecular flow to analyze surface pressures
06 p0982 A70-18363

Continuum to free molecule hypersonic flow near flat plate sharp leading edge, studying Knudsen, Reynolds and Mach numbers effects
06 p0982 A70-18365

Orifice effect investigated for sharp flat plate in hypersonic rarefied flow, measuring surface pressure
06 p0982 A70-18366

Flow field measurements upstream of axisymmetric blunt body in rarefied hypersonic flow used to investigate merging between bow shock and boundary layer
06 p0983 A70-18372

Sphere drag measurements in low density hypersonic transition and near free molecular flow
06 p1124 A70-18373

Circular cylinders drag and pressure distribution in hypersonic range between continuum and free molecular flow
06 p0983 A70-18376

Drag on infinite cylinder in hypersonic nearly free molecular flow for various angles of attack, using kinetic approach
06 p0983 A70-18380

Hypersonic rarefied gas flow near stagnation point investigated to predict drag on sphere in high speed gas stream with densities in transition regime

06 p0984 A70-18382

Sphere and sharp slender cone drag coefficients in hypersonic transitional flow measured by flow modulation technique

06 p0984 A70-18389

Laminar boundary layer in hypersonic flow calculated by integral method, including effects of entropy gradient and induced pressure gradient

[ONERA-TP-784] 06 p0984 A70-18468

Stagnation point heating in hypersonic gas flow past blunt bodies, considering radiative transfer effects on shock wave temperature and density distribution, wave separation, etc

06 p0985 A70-18557

Three dimensional hypersonic flow past body solved assuming developable surface head shock wave

07 p1187 A70-18767

Inviscid hypersonic flow analysis for chemically relaxing air about wedges and pointed circular cones using Dorodnitsyn integral method

[DGLR-69-037] 07 p1188 A70-18986

Low density hypersonic flow over slender cone using air and He test gases

07 p1188 A70-19309

Velocity pulsations of hypersonic working flow in wind tunnel using miniature pressure transducers, discussing rms error

07 p1259 A70-19828

Viscous hypersonic flow past sphere in presence of strong injection through front surface at large Reynolds numbers using asymptotic method

07 p1189 A70-20146

Hypersonic flow past blunted cylinder at Mach number of infinity, investigating real gas effect using Lighthill ideal dissociating gas model

08 p1431 A70-20646

Aerodynamic characteristics of cylinder with wings in free molecular hypersonic flow of monoatomic gas at various angles of attack and slip

08 p1432 A70-21083

Monograph on hypersonic flow boundary layers research conducted by European countries, determining pressures, velocity and temperature profiles, skin friction, heat transfer, displacements, etc

[ONERA-TP-770] 08 p1601 A70-21844

Aerodynamic heating of blunt bodies, investigating dependence of hypersonic limit distribution on Mach number

09 p1603 A70-22419

Numerical solutions of variational problems concerning symmetrical wings with minimum drag and optimal aerodynamic efficiency in hypersonic flow

09 p1603 A70-22433

Drag on sharp cones in hypersonic flow, studying effects of intense transverse mass injection through porous walls

09 p1603 A70-22441

Vibration of thin bodies subjected to large angle attack in hypersonic flow, discussing curved bodies method to reduce problem to steady state flows

09 p1771 A70-22445

Aerodynamic characteristics of cooled blunt spherical bodies in low density hypersonic gas flow, discussing heat flux representation for different body surface temperatures

09 p1604 A70-22447

Inviscid hypersonic small disturbance theory applied to flow behind concave and convex exponential shock waves, determining supporting two dimensional airfoil surfaces

09 p1605 A70-23220

Drag coefficients for spheres and sharp cones in rarefied hypersonic air flow obtained in shock tunnel using free flight technique

[AIAA PAPER 69-140] 09 p1605 A70-23221

Small disturbance and similitude applicability to internal hypersonic conical flows in edge shock and Busemann inlets

09 p1606 A70-23245

Wedges calculated for lift-drag ratios at hypersonic speeds to find optimum surface geometry

09 p1606 A70-23282

Blast wave eigenvalues in asymptotic expansions approximation for hypersonic flows past blunt bodies

10 p1797 A70-23953

Inverse blunt body problem using integral relations method assuming inviscid axisymmetric hypersonic gas flow

10 p1798 A70-24116

Kinetic theory applied to model of interaction between two gas flows colliding at sharp leading edge at different hypersonic speeds

10 p1800 A70-24139

Hypersonic viscous interactions on insulated slender cone with mass injection assuming perfect gas flow and negligible transverse curvature effects

10 p1803 A70-24821

Rarefied hypersonic axisymmetric blunt body, examining bow shock and viscous layer upstream merging

10 p1804 A70-24823

Electrostatic cylindrical probes applicability to hypersonic flow field diagnostics

11 p2086 A70-25684

Flow near leading edge of sharp insulated and cooled flat plates, using Monte Carlo direct molecular simulation

11 p1975 A70-25968

Three dimensional hypersonic steady flow around blunt and pointed cones at nonzero angles of attack calculated by method of characteristics

[AIAA PAPER 69-187] 11 p1975 A70-25969

Radiation effects on viscous hypersonic low density stagnation flow using two layer model, calculating flow field and heat transfer coefficient

12 p2158 A70-28204

Supersonic and hypersonic motion past circular cone at angle of attack, analyzing for velocity and pressure distributions by linearizing conical motion equations

12 p2158 A70-28213

Radiant shock layer in hypersonic air flow past blunt bodies, showing effects on temperature field and density

12 p2159 A70-28245

Stagnation point position as function of gas thermodynamic state behind detached shock for spherical segment at incidence in three dimensional hypersonic flow

12 p2159 A70-28247

Forward inclined two dimensional circular arc slot nozzle jet flaps at hypersonic speeds, considering amplification and interaction processes

[AIAA PAPER 70-553] 13 p2340 A70-29018

Viscous shock layer equations of laminar hypersonic flow past blunt body at moderate to high Reynolds numbers

13 p2343 A70-29952

Surface pressure and heat transfer over blunt conical body in hypersonic flow with uniform mass addition of various gases

[AIAA PAPER 69-716] 13 p2523 A70-29977

Turbulent boundary layer characteristics on simple shapes in hypersonic flow, using mixing length theory and eddy exchange coefficient

14 p2564 A70-30262

Solar wind interaction with earth, moon, planets and comets, using hypersonic fluid analog involving shock wave interactions

14 p2631 A70-30360

Explosion analogy to study hypersonic flow region behind shock wave including boundary layer at blunt body surface

14 p2528 A70-30711

Hypersonic low density transitional flow over slender conical vehicle, calculating drag coefficient and density profiles

14 p2529 A70-31365

Viscous gas hypersonic flow past blunt nosed bodies based on Navier-Stokes equation

15 p2671 A70-31481

Hypersonic gas flow characteristics incident on elliptic paraboloid and triaxial ellipsoid at arbitrary angles of attack

15 p2672 A70-31647

Heat flux measurements in hypersonic rarefied flow by thin film surface thermometer

15 p2825 A70-31820

Hypersonic near free molecule flow over flat plate with sharp leading edge, using linearized kinetic B-K-G equation for small thermal accommodation coefficient

15 p2673 A70-32796

Lifting body pressure and heat transfer measurements at various angles of attack in hypersonic flow

[DGLR-70-029] 15 p2828 A70-32841

Supersonic and hypersonic gas flow past blunt bodies, using finite difference and integral relation methods

16 p2890 A70-33244

Book on aerodynamics of bodies of revolution covering hypersonic flow parameters effects, method of characteristics, slender body drag, blunt bodies, rarefied gas aerodynamics, etc

16 p2834 A70-33271

Equations of supersonic and hypersonic motion past circular cone by linearized method based on small perturbations with respect to nearly incompressible flow

16 p2835 A70-33746

Far wake properties of reentry body in hypersonic air flow calculated with or without chemical kinetics, using finite difference method

16 p2836 A70-33753

Aerodynamic wake structure of cylinders and spheres in hypersonic rarefied gas flow as function of Mach and Knudsen numbers

16 p2836 A70-33756

Laminar near wake of cylinder at free stream Mach 6, using modified Lees-Reeves method

16 p2836 A70-33762

Longshot free piston gun tunnel for high Reynolds number hypersonic flow tests

16 p2889 A70-33855

Transpiration and film cooling effects on aerodynamic characteristics of slender cone in hyper-

sonic flow tested in hypervelocity wind tunnel using mass injection

16 p2837 A70-33857

Experimental and numerical nonequilibrium shock layer around cones in hypersonic pure oxygen flows with simultaneous rotational, vibrational and dissociation relaxation

[AIAA PAPER 69-136] 16 p2894 A70-33858

Hypersonic internal flow investigation by differential equation numerical integration, determining shock shape and surface pressure

16 p2838 A70-33881

Boundary layer to wake bleed venting for flare-induced separation prevention in hypersonic flow over blunt bodies

16 p2838 A70-33884

Heat transfer and pressure drag of axisymmetric body in hypersonic flow, obtaining minimum energy nose and leading edge shapes by Pontryagin principle

[AIAA PAPER 70-825] 16 p3001 A70-33940

Axisymmetric detached shock preceding blunt body immersed in hypersonic monatomic gas flow, considering radiative ionization in cold precursor by differential approximation

16 p2839 A70-34252

Hypersonic flow of chemically reacting binary mixture of oxygen atoms and molecules past blunt body, presenting viscous shock layer equations and slip boundary conditions

[AIAA PAPER 70-805] 17 p3005 A70-34458

Low density hypersonic flow over finite width flat plate at zero incidence

17 p3007 A70-34473

Hypersonic viscous interaction on curved surfaces, extending Cheng inclined flat plate analysis

[AIAA PAPER 70-782] 17 p3007 A70-34474

Hypersonic flow field around yawed half angle cone from wind tunnel measurements including surface pressure distributions and flow visualization photographs

17 p3007 A70-34485

Hypersonic flow of shock heated plasma past axisymmetric blunt body and onboard magnetic source, using numerical method

17 p3008 A70-34491

Nozzle wall hypersonic turbulent boundary layers at free stream Mach number using pitot, hot wire, and wall fluctuation and static pressure measurements

[AIAA PAPER 70-746] 17 p3065 A70-34497

Nonequilibrium air ionization in hypersonic viscous shock layers in flow about axisymmetric blunt bodies

17 p3008 A70-34501

Time dependent solution for inviscid hypersonic flow of chemically reacting gas mixture about blunt bodies

[AIAA PAPER 70-771] 17 p3009 A70-34502

Yawed two dimensional wedges in hypersonic stream, including leading edge bluntness, viscous interaction and angle of attack effects

[AIAA PAPER 70-783] 17 p3009 A70-34503

Collection of papers on gas dynamics covering hypersonic flow, rarefied gas and plasma dynamics, heat and mass transfer, etc

17 p3069 A70-35031

Two dimensional hypersonic viscous flow, analyzing viscosity and bluntness induced pressure effects

17 p3010 A70-35034

Hypersonic flow past slender bodies, discussing inviscid flows, outer edge singularity of boundary layer and three dimensional interaction on needle-like bodies

17 p3010 A70-35035

Adiabatic and chemically inactive hypersonic continuum flow around blunt body, analyzing flow field

17 p3010 A70-35036

Dihedra placed at angle of attack in hypersonic rarefied gas flow, investigating base flow and near wakes

17 p3010 A70-35047

Hypersonic rarefied gas flow around flat plate with sharp leading edge and circular cylinder in transition region

17 p3011 A70-35241

Hypersonic flow containing dust, investigating for cosmic dust collection and analysis, discussing conditions for collected particle size distribution correspondence to original distribution

17 p3012 A70-35921

Hypersonic gas flow around blown plane of segmentally blunted cones at large angle of attack, using two dimensional model

18 p3206 A70-36258

Viscous hypersonic flow around nonslender bodies with mass supply at small Reynolds numbers, using thin shock layer model

18 p3206 A70-36259

Hypersonic flow around delta wings of finite thickness with supersonic leading edges

18 p3206 A70-36260

Nonequilibrium ionized hypersonic flow over blunt body at low Reynolds number, using thin shock layer assumption in analysis

18 p3208 A70-36689

Ablating nose equilibrium shape in laminar hypersonic flow during reentry

18 p3208 A70-36707

- Hypersonic aerodynamic characteristics of sharp slender right circular cones at angles of attack, using Newtonian impact theory modified for flow separation effects
[AIAA PAPER 70-979] 20 p3558 A70-39550
- Three dimensional supersonic and hypersonic gas flow by Oseen equations, obtaining asymptotic flow field
20 p3609 A70-39656
- Hypersonic test flow in arc heated wind tunnel, measuring freestream Pitot pressure, mass flux, stagnation point heat transfer rate and wall pressure
20 p3607 A70-40270
- Laminar viscous effects over blunt cones at hypersonic conditions, taking into account first and second order boundary layer theories
20 p3559 A70-40285
- Wedge angle large amplitude slow oscillations in hypersonic and supersonic flows, examining attached bow shock
20 p3559 A70-40288
- Hypersonic flow pattern past windward side of triangular wing with supersonic leading edges, joining potential and vortex regions behind shock wave
21 p3743 A70-40609
- Entropy layer in hypersonic flows, determining body configuration from shock wave shape described by coordinates power function
21 p3743 A70-40610
- Axisymmetric detached shock before blunt body in hypersonic monatomic gas flow, obtaining radiative ionization patterns in cold precursor
21 p3950 A70-41731
- Upstream disturbances propagation during hypersonic flow boundary layer interaction
21 p3748 A70-42205
- Dust content effect on hypersonic wind tunnel flow test results, noting drag force on slender and blunt nosed models
21 p3749 A70-42224
- Hypersonic viscous interaction between laminar boundary layer growing over flat plate and external flow field extended to curved surfaces
22 p3958 A70-42688
- Dissociated and ionized hypersonic flows of hydrogen heated by electric arc techniques, investigating flows in wind tunnel nozzles
22 p4011 A70-42759
- Pressure distribution, force and heat transfer measurements on varied-configurations of lifting reentry vehicles in hypersonic flow
[ICAS PAPER 70-03] 23 p4132 A70-44117
- Heat transfer and shock wave shapes about blunt slender cones in viscous-inviscid coupling hypersonic flow
23 p4134 A70-44569
- Optimum thickness ratio and minimum drag of slender bodies in hypersonic viscous flow as function of altitude
23 p4134 A70-44571
- Dissociative nonequilibrium hypersonic flow of low density gas mixtures over flat plate in free stream, noting catalytic wall effect on flow field
23 p4135 A70-44604
- Thick wedge large amplitude harmonic oscillations in hypersonic flow
23 p4270 A70-44609
- Hypersonic three dimensional flow past elliptic cross section slender bodies, discussing disturbance equations, pressure, velocity and density distributions and shock shape
[DFVLR-70-27] 23 p4135 A70-44633
- Radiative energy transfer during interaction between blunt body and hypersonic gas flow, noting effect on flow temperature, shock wave separation, etc
23 p4136 A70-45020
- Inviscid hypersonic flow fields past lower/compression/ surface of delta wing calculated by one strip approximation of integral relations method
24 p4289 A70-46245
- HYPERSONIC FORCES**
- Scaling laws for nose bluntness effects on hypersonic aerodynamics of bodies of revolution
[AIAA PAPER 68-1158] 04 p0620 A70-15530
- Hypersonic cruise vehicle data to define temperature, load criteria and materials for air induction systems associated with two dimensional variable geometry inlet
[SAE PAPER 690664] 05 p0791 A70-15839
- HYPERSONIC GLIDERS**
- Hypersonic glider performance in mesosphere entry using models located in rarefied gas flow at Mach 8
05 p0789 A70-15811
- Wind tunnel tests for aerodynamic and thermal environment of hypersonic glider VERAS /Vehicle for Experimentation and Research in Aerothermodynamics and Structures/
[DGLR-69-042] 07 p1187 A70-18981
- Hypersonic orbital glider range maximization, analyzing optimal angle of attack by use of rectangular velocity components
07 p1393 A70-19341

- Hypersonic glider VERAS aerodynamic and thermal environments, noting wind tunnel tests by thermosensitive paint method
16 p2837 A70-33765
- Nonrolling lifting gliding vehicle hypersonic longitudinal dynamic stability, applying analysis to space shuttles
[AIAA PAPER 70-977] 20 p3715 A70-39552
- HYPERSONIC HEAT TRANSFER**
- Lifting body pressure and heat transfer measurements at various angles of attack in hypersonic flow
[DGLR-70-029] 15 p2828 A70-32841
- Heat transfer and shock wave shapes about blunt slender cones in viscous-inviscid coupling hypersonic flow
23 p4134 A70-44569
- HYPERSONIC INLETS**
- Hypersonic cruise vehicle data to define temperature, load criteria and materials for air induction systems associated with two dimensional variable geometry inlet
[SAE PAPER 690664] 05 p0791 A70-15839
- Starting criterion for hypersonic inlets with large turbulent boundary layers, considering total pressure recovery from all shock and viscous losses
14 p2529 A70-30865
- Turbofanjet powered hypersonic aircraft axisymmetric inlet systems using forward translating cowl and centerbody for various air flow characteristics
[AIAA PAPER 70-687] 16 p2835 A70-33586
- HYPERSONIC NOZZLES**
- Mach numbers, electron density and temperature in partially ionized frozen equilibrium flows of Ar in hypersonic nozzle
01 p0063 A70-10994
- Turbulence in hypersonic nozzle due to two phase flow of ideal gas and solid spherical particles, discussing thermal and dynamic differences
03 p0407 A70-13494
- Approximate solution for far downstream flow of condensation in hypersonic wind tunnels and nozzles for colloidal thrusters and EHD generators
04 p0621 A70-15600
- Nozzle boundary layer displacement thickness at Mach 30-70 in helium using Langley hotshot tunnel tests
04 p0675 A70-15603
- Flow parameters measured in low density hypersonic nozzle, estimating error of all relevant parameters
06 p1030 A70-18302
- Dense gas effects in free piston hypersonic wind tunnel, discussing Longshot facility, free piston cycle, reservoir conditions decay and hypersonic nozzle flow
[AIAA PAPER 69-169] 07 p1249 A70-19310
- Frozen flow effect in hypersonic wind tunnel nozzle on parameters of nonequilibrium incident flow past wedge
09 p1604 A70-22446
- Laminar boundary layer characteristics in axisymmetric hypersonic nozzle calculated by finite difference method
10 p1804 A70-25187
- Laminar boundary layers in low density supersonic and hypersonic conical and axisymmetric nozzles, treating displacement, transverse curvature, velocity slip and temperature jump
[AIAA PAPER 69-633] 13 p2386 A70-28513
- Film cooling protecting axisymmetric nozzle slot surface exposed to high temperature Mach 6 air injection
18 p3242 A70-36695
- Hypersonic nozzle ignition phenomenon in reflected shock wind tunnel
19 p3352 A70-38170
- HYPERSONIC REENTRY**
- Radiant heat transfer in hypersonic aerodynamic heating, discussing radiant flux and carbon dioxide concentration in reentry problems
01 p0219 A70-11625
- Acoustic technique for flow transition detection on hypersonic ablating reentry vehicles, presenting supersonic wind tunnel test results
04 p0620 A70-15531
- Massive blowing effect on stagnation point radiative energy transfer of ablative heat shield during planetary entry at hypersonic velocities
[AIAA PAPER 70-203] 06 p0971 A70-18101
- Radiating gas flows during hypersonic planetary reentry, discussing atmospheric composition, shock layer characteristics, nonequilibrium flows, etc
06 p0985 A70-18558
- Self contained optimal control synthesis for spacecraft entering atmosphere at first cosmic speed, considering landing spots dispersion component decrease
13 p2500 A70-28407
- Spacecraft trajectory control for hypersonic atmospheric entry
13 p2500 A70-28411
- Hypersonic viscous effects on space shuttle entry trajectory, measuring lift and drag in free flight regime
23 p4258 A70-44526

HYPERSONIC SHOCK

- Graphite sphere mass erosion in low temperature hypersonic air plasma shock flow, determining breakdown temperature and mass entrainment rates
03 p0517 A70-13741
- Shock tube measurements of ionization relaxation times behind shock waves in air at shock Mach numbers from 8 to 17
03 p0471 A70-14360
- Axisymmetric radiating flow behind paraboloidal shock in ideal inviscid gas hypersonic stream, using differential approximation method for blunt body solution
04 p0669 A70-14937
- Viscous shock layer at hypersonic blunt body stagnation point, applying finite difference and nonlinear overrelaxation methods to seven species air model
04 p0620 A70-15539
- Model sampling or Monte Carlo applied to normal shock, giving temperature and density profiles for Mach 10 shock
06 p1050 A70-18337
- Normal hypersonic shock wave structure in diatomic gas, measuring density by electron beam fluorescence technique
06 p1050 A70-18341
- Surface temperature effects on low Reynolds number hypersonic shock layer development over flat plate sharp leading edge
06 p0982 A70-18364
- Hypersonic spherical gas expansion into finite pressure region with transition from supersonic to subsonic flow in shock wave, discussing structure and pressure effects
09 p1658 A70-22116
- High intensity shock wave propagation and generation of high enthalpy hypersonic flow studied to determine IMF-2 hypersonic shock tube performance limit
10 p1871 A70-24795
- Solid particle motions in dusty gas in inviscid hypersonic shock layers of slender wedges and cones and stagnation regions of cylinders and spheres
12 p2156 A70-27827
- Nonuniform external flow near blunt body stagnation point in diverging hypersonic thin shock layer
18 p3206 A70-36267
- Spark photography of models in free flight in hypersonic shock tunnel
[SMPTE PREPRINT 99] 22 p4032 A70-43035
- HYPERSONIC SPEED**
- Aerodynamic flight characteristics of lifting reentry bodies in subsonic to hypersonic range in wind tunnel tests
06 p1154 A70-17249
- Velocity synchronized Fourier transform hologram camera system for recording hypervelocity particles
09 p1688 A70-23775
- Drag measurement for star-shaped body at hypersonic speeds, comparing results with cone-shaped model
10 p1799 A70-24122
- Compression process in turbulent boundary layer on control surface at hypersonic speeds, noting influence on surface effectiveness and heating
[ONERA-TP-814] 11 p1979 A70-25815
- Electric arc shape moving at hypersonic speed investigated by Newtonian pressure distribution for thin shock layer
11 p2090 A70-25992
- Flat-top airfoil determined for lower surface shape to maximize lift drag ratio at hypersonic speeds using calculus of variations
11 p1977 A70-26397
- Aerodynamic effects of bluntness on slender cones in free flight tests at Mach 17
[AIAA PAPER 70-554] 13 p2340 A70-29019
- Supersonic slot cooling for surface protection at hypersonic speeds using contoured axisymmetric nozzle with streamlined body
14 p2663 A70-30257
- Longitudinal and transverse hypersonic mm waves excitation in quartz single crystal at liquid helium temperature
16 p2952 A70-33258
- Fighter engine capabilities in Mach 3 to 7 speed range, discussing propulsion system configurations
[AIAA PAPER 70-943] 16 p2965 A70-33542
- Far wake linear stability behind circular cylinders at hypersonic speed, comparing experiments and predictions
16 p2838 A70-33898
- Unperturbed atmospheric parameters calculation from surface measurements of blunt body at hypersonic speeds under various aerodynamic conditions
18 p3247 A70-36181
- Hypersonic flat and biconvex conical wings, calculating yaw effects on shock shape and pressure distribution
21 p3761 A70-40918
- Hypersonic aerodynamic deceleration devices for axisymmetrical bodies with cylindrical main sections and various front sections, using gun tunnel techniques
[AIAA PAPER 70-1174] 21 p3746 A70-41839

- Continuous surface of revolution parachute for supersonic/hypersonic speeds, performing wind tunnel tests
[AIAA PAPER 70-1173] 21 p3754 A70-41840
- Hypersonic sound speeds measured in methane at moderate pressures by spontaneous Brillouin light scattering experiments
21 p3830 A70-41938
- Ultrabright nanosecond flash light generation technique, using superradiant light sources for shadowgraph photography in high resolution hypervelocity field
[SMPT PREPRINT 74] 22 p4037 A70-43070
- European hypersonic aerodynamic research activities, describing Eurohyp program
22 p4127 A70-43507
- Longitudinal and transverse hypersonic mm waves excitation in quartz single crystal at liquid helium temperature
23 p4218 A70-44281
- HYPERSONIC TEST APPARATUS**
- Free flight ranges for hypersonic simulation from Mach 1 to Mach 30, noting onboard high-g telemetry instrumentation
04 p0663 A70-14723
- Free flight static, dynamic stability and drag data for 10 degree semiangle cone obtained at 8-16 Mach numbers
[AIAA PAPER 69-133] 09 p1605 A70-23218
- Hypersonic test equipment, describing flight simulating hypervelocity wind tunnels, firing tunnels and shock wave tubes
13 p2384 A70-28927
- Hypersonic velocity and turbulence measurements in wind tunnels, using spectral analysis of Doppler shifted laser light
17 p3103 A70-34849
- HYPERSONIC VEHICLES**
- NT HYPERSONIC AIRCRAFT**
- NT HYPERSONIC GLIDERS**
- Structural design and fabrication of load bearing Ta alloy radiation cooled elevon control surface for high L/D hypersonic flight vehicle
02 p0306 A70-11941
- Interaction between surface liquid film and hot gaseous turbulent boundary layer analyzed for hypersonic vehicle surface thermal protection design problems
04 p0669 A70-14927
- Hypersonic cruise vehicle data to define temperature, load criteria and materials for air induction systems associated with two dimensional variable geometry inlet
[SAE PAPER 690664] 05 p0791 A70-15839
- Orbit-shuttle and SST craft hypersonic flight vehicles design, discussing aerodynamic heating, shock stresses and propulsion system requirements
05 p0797 A70-17087
- Air breathing launch vehicle for earth-orbit shuttle assessed in light of hypersonic propulsion and configuration development
[AIAA PAPER 70-269] 07 p1365 A70-20380
- Range, block speed and fuel-weight ratio formulas for hypervelocity, boost glide and ballistic vehicles
08 p1582 A70-21871
- Slender body approximation for shape determination of nonlender hypersonic body of revolution with minimum convective heat transfer rate
09 p1788 A70-22931
- Cone roll dynamics-ablation patterns coupling in hypersonic wind tunnels
[AIAA PAPER 70-562] 13 p2340 A70-29025
- Hypersonic cruise vehicles viscous interactions areas, examining compression corners, shock interactions, laminar and turbulent flow, boundary layer separation, etc
[AIAA PAPER 70-781] 17 p3007 A70-34475
- Aerospace thermophysics considerations in spacecraft and hypervelocity vehicles systems thermal design, discussing thermal control and control coatings optical and radiative properties
[AIAA PAPER 70-812] 17 p3194 A70-34509
- Laminar heating in hypersonic vehicles interior corners, analyzing helium tunnel heat transfer data for various intersecting wedge corners
20 p3737 A70-39700
- Wave-riders aerodynamics and heat transfer, investigating lift to drag ratios for supersonic and hypersonic vehicles
[ICAS PAPER 70-18] 23 p4276 A70-44129
- HYPERSONIC WAKES**
- Spectrum function in Booker scattering formula /first order Born approximation/ for dielectric constant fluctuations in hypersonic wake plasmas
03 p0529 A70-12908
- Hypersonic far wake mean flow properties behind two dimensional slender body wind tunnel models at zero angle of attack
[AIAA PAPER 68-700] 04 p0621 A70-15578
- Hypersonic near wake, discussing correlations from optical studies, laminar near wake, blunt body and turbulent wake measurements
05 p0790 A70-16120
- Laminar hypersonic blunt cone wakes, discussing flow fields and axial static pressure distributions
06 p0968 A70-17553
- Axial profile characteristics of hypersonic near wake of slender circular cone based on pitot pressure, static pressure and stagnation temperature measurements
06 p0968 A70-17916
- Cylinder wakes in rarefied gas flow at Mach 20, obtaining density profile data from electron gun, impact pressure and cooled film probe measurements
06 p0984 A70-18387
- Model for predicting laminar-turbulent transition point in hypersonic wake of two dimensional laminar viscous flow
06 p0985 A70-18499
- Anamorphic optics to focus luminous wakes of hypervelocity projectiles onto focal plane of slitless spectrograph in free flight ballistic range launching
07 p1287 A70-20082
- Density profiles of sphere wake in rarefied hypersonic flow compared to free molecular flow calculations
08 p1431 A70-20591
- Gas and electron density fluctuations in weakly ionized turbulent wake behind hypersonic spheres and cones
11 p1978 A70-26773
- Intermittency role in free turbulent flow and EM wave scattering by hypersonic wakes
11 p1978 A70-26776
- Laminar near wake flow field of two dimensional adiabatic circular cylinder with surface mass transfer
[AIAA PAPER 69-67] 13 p2343 A70-29951
- Electron density fluctuation measurements in wakes behind hypersonic sphere projectiles, using Langmuir probes
[AIAA PAPER 70-730] 16 p2834 A70-33489
- Chemiluminescent processes accounting for radiation from turbulent wake flows behind hypersonic spheres in air
[AIAA PAPER 70-729] 16 p2997 A70-33492
- Aerodynamic wake structure of cylinders and spheres in hypersonic rarefied gas flow as function of Mach and Knudsen numbers
16 p2836 A70-33756
- Steady state plasma wind tunnel for flow around ionospheric satellites, studying wakes of cylinders and spheres
16 p2837 A70-33866
- Far wake linear stability behind circular cylinders at hypersonic speed, comparing experiments and predictions
16 p2838 A70-33898
- Complex impedance measurements for monopole antenna for electron densities in/out of OGO satellite wake in upper ionosphere
17 p3080 A70-35771
- Shock wave attenuation and reflection effects on turbulent hypersonic wakes in ballistic ranges
18 p3237 A70-36708
- Hypersonic sphere turbulent wake velocity measurement by spark technique, determining distribution from least mean squares fits of Gaussian curves
20 p3559 A70-40283
- Mean density and temperature measurements in hypersonic Ti spheres wakes in nitrogen atmosphere, using electron beam fluorescence probes
21 p3745 A70-41754
- Hypersonic projectile turbulent wake measurements, discussing velocity, mass density and temperature determination
[ICAS PAPER 70-07] 23 p4132 A70-44130
- HYPERSONIC WIND TUNNELS**
- U HYPERVELOCITY WIND TUNNELS**
- HYPERSONICS**
- Nose bluntness, angle of attack and oscillation amplitude effect on hypersonic unsteady aerodynamics of slender cones
[AIAA PAPER 70-216] 06 p0969 A70-18059
- HYPERSPACES**
- Microscopic particle mass spectra in six dimensional scalar, spinor and vector fields, noting cosmological implications and eight dimensional theory
14 p2616 A70-30342
- HYPERTENSION**
- Cross adaptation criteria and modifications in physiologic and biochemical processes in man and mammals, demonstrating positive cross acclimation between hypertension and hypoxia exposure
02 p0242 A70-12825
- Postmortem coronary angiographies showing role of arterial hypertension in coronary pathology
03 p0426 A70-13939
- Pulmonary hypertension in congenital heart diseases as function of blood flow
20 p3571 A70-39367
- Hyperbaric oxygen exposure produced hypertension and pulmonary edema, discussing carbon dioxide transport mechanism in blood
20 p3572 A70-39430
- Human arterial hypertension, correlating ECG changes with systemic hemodynamics
20 p3573 A70-40069
- Ballistocardiograms hypertensive observations multivariate analysis, discussing factors for various groups discrimination
21 p3763 A70-41230
- Hypertensive mechanisms - Conference, Canberra, Australia, January 1970
24 p4298 A70-45803
- Inherited hypertension genetic and autonomic factors, discussing rats crossbreeding for genetic contribution ratio in males vs females, age effects, etc
24 p4299 A70-45806
- Conduit arteries viscoelastic properties in normal and hypertensive dogs from recorded pressure and diameter waves
24 p4299 A70-45808
- Arterial hemodynamics in hypertension, discussing pulse changes mechanism as consequence of decreased arterial distensibility via disturbed relationship between ventricular ejection wave and impedance characteristics
24 p4299 A70-45809
- HYPERTHERMIA**
- Hot environment and hyperthermy effects on oxygen consumption in subjects performing muscular exercise
13 p2360 A70-29947
- Extreme heating effects on polypnea reaction in aquatic birds
18 p3219 A70-36537
- HYPERTONIA**
- U OSMOSIS**
- HYPERTROPHY**
- U GROWTH**
- HYPERVELOCITY ACCELERATORS**
- U HYPERVELOCITY GUNS**
- HYPERVELOCITY CRATERING**
- U HYPERVELOCITY PROJECTILES**
- U PROJECTILE CRATERING**
- HYPERVELOCITY FLOW**
- Time asymptotic solutions for hypervelocity blunt body flow field with coupled nongray radiation, treating shock as discrete surface
[AIAA PAPER 70-865] 16 p2999 A70-33908
- HYPERVELOCITY GUNS**
- Hypervelocity gas, electromagnetic, explosive drive and exploding wire accelerometers and high explosive, shaped charge, plasma drag and electrostatic accelerators for projectile impact studies
15 p2718 A70-32783
- HYPERVELOCITY IMPACT**
- Hypervelocity impact of small different diameter right circular cylinders, describing launching method using light gas gun
03 p0583 A70-12918
- Penetration criterion for double walled structures subject to hypervelocity meteoroid impact providing choice of protective material properties
[AIAA PAPER 68-1058] 03 p0584 A70-12921
- Micrometeorite detection involving impact stress wave monitoring by strain gages embedded in viscoelastic plastic
03 p0487 A70-13573
- Hypervelocity impact craters formed in low and variable strength laboratory materials to provide insight into formation mechanics and resultant structures of meteorite craters
03 p0603 A70-14349
- Meteoroid impact mass loss and formation of planets, investigating projectile-ejecta ratio and dependence on escape speeds
05 p0910 A70-16393
- Bumper materials effect on two component hypervelocity impact shields performance, noting material density influence
[AIAA PAPER 69-379] 07 p1310 A70-19713
- Steel balls impact on polyurethane foam, porous rubber and fiber materials, noting effects on both pellets and targets
09 p1769 A70-22123
- Hypersonic wind tunnel for erosion test of multiple particle impacts, considering dust on cork, carbazole and silicone rubber
[AIAA PAPER 69-341] 09 p1656 A70-23240
- Two plate meteoroid shields effectiveness determined by analyzing debris cloud ejected behind front plate after hypervelocity impact
[AIAA PAPER 69-380] 11 p2138 A70-26132
- Impact crater cross section in fused silica, describing photomicrographic technique for distinguishing hypervelocity from low energy impacts
[AIAA PAPER 69-367] 11 p2138 A70-26133
- Filamentary crystal growth associated with hypervelocity microparticles impact upon Cu foil
13 p2513 A70-29264
- Hypervelocity impact dynamics on copper cube targets imbedded with nickel wires, discussing terminal positions, Vickers hardness, flow fields, etc
[AIAA PAPER 69-368] 14 p2657 A70-30765
- Collection of papers on high velocity impact phenomena covering strong shock waves, materials reaction, etc
15 p2823 A70-32782
- Hypervelocity impact theory, discussing Euler hydrodynamic codes, projectile cratering dimensional analysis, self similar solutions, etc
15 p2823 A70-32785

Damage mechanisms of hypervelocity projectile impact on thin targets and spacecraft shields

15 p2823 A70-32786
Hypervelocity impact computerized calculations, considering material response, laminated meteor bumper, hollowed projectiles and thick target cratering

15 p2823 A70-32787
Hypervelocity impact generated shock propagation based on governing differential equations, using fluid mechanical model for perfect gas and real fluid

15 p2824 A70-32788
Metal property effects on deformation and strain energy distribution during hypervelocity projectile cratering

15 p2824 A70-32790
Hypervelocity impact damage on complex targets, considering spacecraft and missile design

15 p2824 A70-32791
Hypervelocity impact of spheres on thin targets using numerical solutions utilizing STEEP code two dimensional technique based on hydrodynamic elastoplastic model

16 p2991 A70-33853
Pyrex spheres accelerated to 15 km/sec by plasma rail gun to study hypervelocity impact in twin stainless steel and Al targets

[ALAA PAPER 70-378] 18 p3342 A70-36685
Al spheres hypervelocity impact against dry quartz sand targets in light gas gun facility, discussing energy partitioning

18 p3344 A70-36769
Power loss due to cumulative meteoroid impacts on solar cells during extended planetary missions, investigating hypervelocity particle impacts into glass

[ALAA PAPER 70-1139] 20 p3567 A70-40210
Structural configurations effect on momentum imparted to spacecraft by hypervelocity meteoroid impact

21 p3938 A70-41879
Hypervelocity impact flash resolved into sub-microsecond continuum radiation pulse succeeded by slow rising long duration light pulse from neutral atomic line emission

HYPERVELOCITY LAUNCHERS

23 p4227 A70-44553
Hypervelocity impact of small different diameter right circular cylinders, describing launching method using light gas gun

HYPERVELOCITY PROJECTILES

03 p0583 A70-12918
Taylor model of elastoplastic wave interaction during cylindrical projectile impact

01 p0206 A70-11150
Hypervelocity projectile size and density effect on ballistic limit of dual sheet spacecraft meteoroid protection structures, considering penetration of low and high density particles

[ALAA PAPER 69-376] 04 p0776 A70-15422
Tekite damage caused by micrometeoroid impact, projectile firing at glass spheres and survival time estimation

05 p0916 A70-16834
Electrostatic probe measurements of radial distributions of mean ion density in N and air wakes behind hypervelocity spheres compared with electron microwave measurements

[ALAA PAPER 70-87] 06 p0975 A70-18197
Anamorphic optics to focus luminous wakes of hypervelocity projectiles onto focal plane of slitless spectrograph in free flight ballistic range launching

07 p1287 A70-20082
Spin requirement to limit projectile yawing oscillations in hyperballistic range

12 p2157 A70-27835
Holographic technique to record hypervelocity projectile with front light resolution, discussing image blurring

15 p2736 A70-32031
Hologram camera system recording hypervelocity particles by velocity synchronized Fourier transform method, employing interferometer

15 p2737 A70-32039
Damage mechanisms of hypervelocity projectile impact on thin targets and spacecraft shields

15 p2823 A70-32786
Electron density fluctuation measurements in wakes behind hypersonic sphere projectiles, using Langmuir probes

[ALAA PAPER 70-730] 16 p2834 A70-33489
Pyrex spheres accelerated to 15 km/sec by plasma rail gun to study hypervelocity impact in twin stainless steel and Al targets

[ALAA PAPER 69-378] 18 p3342 A70-36685
Mean density and temperature measurements in hypersonic Ti spheres wakes in nitrogen atmosphere, using electron beam fluorescence probes

21 p3745 A70-41754
High speed cinematographic recording of wake behind hypervelocity projectiles

[SMPT PREPRINT 102] 22 p4032 A70-43033
Laser and flash X ray shadowgraph techniques in hypervelocity ablation/erosion investigations in hyperballistics range

[SMPT PREPRINT 28] 22 p4034 A70-43047

Hypersonic projectile turbulent wake measurements, discussing velocity, mass density and temperature determination

[ICAS PAPER 70-07] 23 p4132 A70-44130

HYPERVELOCITY WIND TUNNELS

NT CASCADE WIND TUNNELS

NT HOTSHOT WIND TUNNELS

NT PLASMA JET WIND TUNNELS

NT SHOCK TUNNELS

Local skin friction measurement on model in blow-down hypersonic wind tunnels using floating element transducer, giving results for flat plate and wedge

[ONERA-TP-756] 03 p0463 A70-13629
Schlieren recorder and Erdmann field absorption methods applied to qualitative and quantitative flow process studies in high velocity wind tunnel

04 p0689 A70-14925
Wall and total temperature variations effects on transition Reynolds number in hypersonic He tunnel, noting sound mode dominance

04 p0620 A70-15560
Approximate solution for far downstream flow of condensation in hypersonic wind tunnels and nozzles for colloidal thrusters and EHD generators

04 p0621 A70-15600
Longshot free-piston wind tunnel for very high Reynolds number hypersonic flows, describing piston cycle, supply conditions, real gas effects on nozzle flow, etc

06 p1027 A70-17245
German aeroballistic hypersonic test facility with moving model and rest atmosphere, describing acceleration mechanism and several tests

06 p0965 A70-17246
Pressure distribution at circular slender cone with 10 deg semiapex angle in hypersonic vacuum wind tunnel

06 p0966 A70-17251
Crossed field plasma accelerator designed as element of hypersonic wind tunnel driver

06 p1119 A70-17471
Wind tunnel tests for aerodynamic and thermal environment of hypersonic glider VERAS /Vehicle for Experimentation and Research in Aerothermodynamics and Structures/

[DGLR-69-042] 07 p1187 A70-18981
Dense gas effects in free piston hypersonic wind tunnel, discussing Longshot facility, free piston cycle, reservoir conditions decay and hypersonic nozzle flow

[ALAA PAPER 69-169] 07 p1249 A70-19310
Velocity pulsations of hypersonic working flow in wind tunnel using miniature pressure transducers, discussing rms error

07 p1259 A70-19828
Frozen flow effect in hypersonic wind tunnel nozzle on parameters of nonequilibrium incident flow past wedge

09 p1604 A70-22446
Hypersonic wind tunnel for erosion test of multiple particle impacts, considering dust on cork, carborazole and silicone rubber

[ALAA PAPER 69-341] 09 p1656 A70-23240
Supersonic flight simulation in hypersonic wind tunnels for developing hypersonic air breathing propulsion, describing ceramic storage heaters

13 p2384 A70-28666
Hypersonic wind tunnel testing of Plexiglas and nylon hemispheres instrumented with strain gages and thermocouples, comparing with calculated strain, temperature and ablation

13 p2520 A70-28727
Two component piezoelectric skin friction force transducer for hypersonic flow tunnel

13 p2405 A70-28815
Hypersonic test equipment, describing flight simulating hypervelocity wind tunnels, firing tunnels and shock wave tubes

13 p2384 A70-28927
Spatial distribution of three dimensional laminar boundary layer transition zone on sharp half angle cone from hypersonic wind tunnel tests

[ALAA PAPER 69-112] 13 p2343 A70-29953
French H630 hypersonic wind tunnel operating at Mach 8, discussing test results and potential

15 p2718 A70-32839
Longshot free piston gun tunnel for high Reynolds number hypersonic flow tests

16 p2889 A70-33855
Free flight wind tunnel test for feasibility of hypersonic drogue deployment into reentry vehicle wake

[ALAA PAPER 70-587] 17 p3060 A70-35195
Low pressure measuring system for aerodynamic models tested in Mach 12-14 wind tunnel, discussing transducers and high speed digital recording and data processing system

17 p3062 A70-35493
Digital computer for high speed wind tunnel data acquisition, processing and operations control

19 p3397 A70-37923
Hypersonic test flow in arc heated wind tunnel, measuring freestream Pitot pressure, mass flux, stagnation point heat transfer rate and wall pressure

20 p3607 A70-40270

Time varying flow properties effects on hypersonic wind tunnel spectroscopic measurements, considering direct emission and electron beam techniques

20 p3607 A70-40271
Dust content effect on hypersonic wind tunnel flow test results, noting drag force on slender and blunt nosed models

21 p3749 A70-42224
Ames Hypervelocity Free Flight Facility, discussing aerodynamic tunnel, radiation tunnel and light gas gun for reentry simulation

22 p4006 A70-42764
Spark photography of models in free flight in hypersonic shock tunnel

[SMPT PREPRINT 99] 22 p4032 A70-43035
Heat transfer measurements compared in free flight and in hypersonic wind tunnel at similar Reynolds number and temperature ratios

[ICAS PAPER 70-06] 23 p4275 A70-44115
Hypersonic wind tunnel facility for hypersonic aircraft and recoverable booster systems development

[DFVLR-SONDDR-19] 23 p4178 A70-44799

HYPERVENTILATION

Alveolar ventilation difference in nasal and oral breathing in hyperventilation due to work

05 p0802 A70-16492
Oxygen uptake increase phenomena in passively hyperventilated anesthetized and paralyzed dogs

07 p1205 A70-19293
Carbon dioxide effect on oxygen uptake during hyperventilation in normal man

07 p1205 A70-19294
Minute hyperventilation of human lungs causing expiratory suppression of respiration

12 p2173 A70-28315
Forced hyperventilation effect in human subject based on indices regarding changes in respiration rhythm, EEG and finger plethysmogram

15 p2679 A70-31607
Rats brain oxygenation during hyperventilation with air or oxygen-nitrogen mixture, measuring creatine phosphate concentration and lactate/pyruvate ratio

21 p3762 A70-41225

HYPNOSIS

Differential effect of hypobaric hypoxia on depressant characteristics of sodium barbital, sodium pentobarbital and chloral hydrate in rats and mice

04 p0631 A70-14680
Tranquilizers and hypnotics from rats organs analyzed by thin layer chromatography

22 p3978 A70-42879

HYPOCAPNIA

Respiratory center functional organization established as automatism with negative feedback, based on experimental data of dogs and cats artificial respiration and hypocapnic apnea

03 p0417 A70-13069
Respiratory gas exchange, heart rate, arterial acidemia and hypocapnia responses to physical work in hyperbaric environments and hyperoxia conditions

12 p2169 A70-27655

HYPODYNAMIA

Prolonged hypokinesia effect on human resistance to physical stress, noting prophylactic influence of physical exercises

03 p0425 A70-13898
Hypokinesia and nutrition deficiency effect on blood coagulation, noting combination with accelerations may lead to hypocoagulation

04 p0630 A70-14578
Prolonged hypokinesia effect on dynamics of 5-ox-yindoleacetic acid elimination in rat urine, showing occurrence of shifts in serotonin metabolism

09 p1615 A70-22092
Soviet collection of papers on prolonged immobility and effects on human organism

10 p1812 A70-24665
Relative value of prolonged bed confinement and hypodynamia in estimating biological effects of weightlessness

10 p1813 A70-24666
Prolonged hypodynamia effect on human organism, describing organizational and methodological principles for conducting investigations

10 p1813 A70-24667
Prolonged hypodynamia /bed rest/ clinical observations, noting psychological and physical effects

10 p1813 A70-24668
EKG and cardiac rhythm changes during prolonged hypodynamia /bed rest/ with restricted physical activity

10 p1814 A70-24669
Human vascular tonus and hemodynamics during prolonged hypokinesia, observing changes in reaction to cold and reduced vascular tonicity

10 p1814 A70-24670
Prolonged hypodynamia effects on hemodynamics using dye dilution method, noting adaptability in cardiovascular system

10 p1814 A70-24671
Prolonged hypodynamia effect on human cardiac cycle phases using poly- and kinetocardiographic data

10 p1814 A70-24672

Prolonged hypodynamia effect on heart size and myocardium function obtained from human chest X ray studies

10 p1814 A70-24673

Prolonged hypodynamia effect on human external respiration, arterial blood oxygenation, circulation rate and gas exchange under various physical stress conditions

10 p1814 A70-24674

Prolonged hypodynamia effect on human nutritional habits and protein metabolism, noting decrease in energy requirement and body weight

10 p1814 A70-24675

Mineral saturation in calcaneal bone and hand finger phalanx in humans under prolonged hypodynamia by X ray analysis, observing Ca salts reduction

10 p1815 A70-24676

Prolonged hypodynamia effect on human blood serum mineral content and enzyme activity

10 p1815 A70-24677

Prolonged hypodynamia effect on human blood coagulation, noting antihemophilic effect of physical exercise

10 p1815 A70-24678

Immunity indices in humans subjected to hypodynamia, noting infection resistance lowering

10 p1815 A70-24679

Human central nervous system changes during hypodynamia, noting unidirectional shifts in brain hemodynamics, rheographic wave propagation time reduction, etc

10 p1815 A70-24680

Human nerve and muscle system changes under prolonged hypodynamia

10 p1815 A70-24681

Human motor functions changes following prolonged hypodynamia, including physical training and hypokinesia roles in standing and walking

10 p1815 A70-24682

Human locomotor performance before and after prolonged hypodynamia, discussing biochemical features and changes in step length, torso and extremity kinematics, etc

10 p1816 A70-24683

Psychic functions stability during prolonged hypodynamia, discussing memory, attention span, sensometer reactions, time estimating, etc

10 p1816 A70-24685

Vestibular analyzer and otolithic apparatus disturbances and normalization under prolonged hypodynamia, noting pathological effects of repeated caloric testing

10 p1816 A70-24686

Prolonged hypodynamia effects on visual analysis, investigating functional weakening, fundus oculi appearance change and restoration after normal activity resumption

10 p1816 A70-24687

Physical exercise effects on man during prolonged bed rest, investigating muscle performance, static endurance, walking coordination and psychomotor functions

10 p1816 A70-24688

Occlusion training during hypodynamia with inflatable thigh cuffs to prevent unfavorable effects on cardiovascular system

10 p1816 A70-24689

Amphetamine, caffeine and securinine effects on hypodynamic syndrome in subjects during orthostatic tests and transverse G-forces under prolonged hypokinesia

10 p1817 A70-24690

Hypodynamia aftereffects on nervous system, investigating organic microsymptoms, asthenia, vegetative-vascular instability and skin muscle aknetic hypotrophy

10 p1825 A70-24691

Electrocardiac activity, myocardium and hemodynamic disorders in subjects after prolonged hypodynamia with or without physical exercises and during orthostatic test

10 p1817 A70-24692

Arterial oscillograms, pressure and heart beat rate during prolonged hypodynamia, noting neurocirculatory dystonia

10 p1817 A70-24693

Cardiovascular reactions and orthostatic stability during hypodynamia determined from ECG, seismocardiograms, phonocardiograms, sphygmograms and tachy-oscillograms

10 p1817 A70-24694

Transverse g-force tolerance and stability after prolonged hypodynamia in bed rest, noting effects of pharmaceuticals, physical exercise and prophylactic measures

10 p1817 A70-24695

Hypodynamia effects on humans during prolonged bed rest, investigating immunological resistance, psychic disorders, myocardium changes, responses to pharmaceuticals, etc

10 p1817 A70-24696

Prolonged hypokinesia effect on dynamics of 5-oxindoleacetic acid elimination in rat urine, showing occurrence of shifts in serotonin metabolism

15 p2685 A70-32688

Hypodynamic effects on human external respiratory function and cardiovascular state under various microclimatic conditions

23 p4149 A70-45078

HYPOGLYCEMIA

Hypoglycemia role in air sickness, aggravating effects of hypoxia and acceleration

17 p3040 A70-35914

Serum growth hormone response to hypoglycemia in man following insulin administration, reviewing lumped parameter model

19 p3360 A70-38006

HYPOKINESIA

Skeletal muscle proteins fractional composition in white rats during hypokinesia, noting water content changes

17 p3030 A70-35356

Bone and muscle tissue morphological changes in caged and immobilized rodents and in myasthenic humans

17 p3030 A70-35357

Aldosterone effects on hemodynamics of dogs under restricted motor activity, observing cardiac activity stimulation

17 p3030 A70-35358

Hypokinesia effects on rats protein synthesis rates, determining body and organ weights, muscle tissue nitrogen content and transaminase activity

20 p3575 A70-40187

Atmospheric composition cyclic changes effects on human basal metabolism under hypokinesia

20 p3576 A70-40197

Hypokinesia and reduced diet effects on human tolerance to static loads, discussing acceleration tolerance prediction

20 p3576 A70-40198

Muscular activity in regulation of organism functions during aging, considering hypokinesia effects

22 p3968 A70-42894

Water and salt metabolism changes during prolonged hypokinesia of rabbits, noting blood plasma dilution, hematocrit number and hemoglobin concentration reduction, etc

23 p4146 A70-44656

HYPOTENSION

Hypotensive effects of chloridazepoxide, amobarbital and chlorpromazine on behaviorally induced elevated arterial blood pressure in squirrel monkey

24 p4298 A70-45620

HYPOTHALAMUS

Cortex functional interrelationships with hypothalamus and formatio reticularis, studying role of corticofugal effects in anesthetized cats

01 p0012 A70-10051

Corticofugal effects of various cortical regions on neuron activity in hypothalamus posterior lateral sections in cats

01 p0012 A70-10053

Thermoregulatory salivary responses of dog to various ambient temperatures, emphasizing hypothalamic temperature, threshold and proportionality constant

01 p0017 A70-10465

Cerebral histamine distribution in rat brains, noting highest concentrations in hypothalamus and thalamus

01 p0020 A70-10708

Skin and hypothalamic temperature inputs for behavioral regulation of hypothalamic temperature of rats

01 p0020 A70-10725

Appetitive behavior of rats following cessation of hypothalamic stimulation, observing eating and drinking inhibition

01 p0027 A70-11275

Object carrying behavior of rats, using electrical stimulation of hypothalamic structures

02 p0237 A70-12395

Physicochemical properties of hypothalamic secretions responsible for coronary dilatation in rats, cattle and pigs, using analytical techniques

03 p0417 A70-13215

Conditioned fear reaction produced by electric stimulation of cat anterior hypothalamus, discussing effect of neocortex removal

03 p0420 A70-13425

Degenerate retinal fibers in duck photoreceptor path connecting to supraoptical hypothalamic region detected following optic nerve dissection

03 p0427 A70-13955

High altitude environmental effects on adrenal glands and hypothalamic neurosecretion in rats

04 p0629 A70-14568

Hypothalamic stimulation effects on cardiac and vascular efferent components of baroreceptor reflexes in spinal cats

07 p1202 A70-18866

Hypothalamus influence on potentials and recovery cycles of mesencephalic reticular formation in response to sciatic nerve stimulation in anesthetized rabbits

07 p1204 A70-19138

Somato-vegetative and behavioral reactions of rabbits to electric stimulation of hypothalamus after injecting aminazine

07 p1209 A70-19521

Involvement reactions in dying and reanimated cats with nucleus reticular hypothalamicus stimulated by rectangular electric pulses

07 p1209 A70-19522

Midbrain reticular neurons activity in cats during response to individual and coincident cortical and hypothalamic stimulations

07 p1213 A70-19789

Direct anatomical couplings between retina and hypothalamus via centripetal and centrifugal fibers by investigating light evoked potentials in rabbits brains

08 p1444 A70-20737

Hypothalamus stimulation effect on electrical activity of hippocampus at threshold and super-threshold levels in cats

08 p1446 A70-21448

Hypothalamus stimulus effects on sympathetic nerve activity to heart, spleen, kidney and leg skeletal muscle in anesthetized cats

09 p1614 A70-22001

Soviet book on nervous stress and cardiac activity covering hypothalamus and cardiovascular reactions and cardiac component of complex conditioned reflexes and emotional reactions

10 p1809 A70-23873

Electrode placement ancillary technique for obtaining stereotaxic atlas of infant rat hypothalamus

13 p2350 A70-29322

Vegetative nervous system reactions of patients with diencephalic syndromes, investigating hypothalamo-hypophysial-adrenal system role

13 p2352 A70-29353

Electrical stimulation of dogs hypothalamus effect on blood and lymph circulation and composition

13 p2352 A70-29354

Hypothalamic motivation, presenting data supporting less anatomical specificity

13 p2355 A70-29794

Hypothalamic electric stimulation intensity effects on elicited behavior, considering possible neural circuit threshold reduction

13 p2355 A70-29807

Eating, drinking and gnawing motivation interchangeability under hypothalamic stimulation, noting role of neural substrate activation

13 p2356 A70-29814

Thyroxine stimuli transmission from posterior hypothalamus to cerebral cortex ascribed to dorsomedial nucleus of thalamus

16 p2848 A70-33261

Electrical stimulation in rostromedial hypothalamus effects on thermogenesis of juvenile rats, calculating heat transfer at trunk

16 p2849 A70-33696

Integrating influence of medio-rostral hypothalamic structures upon temperature regulation of juvenile rat based on Area praepoptica medialis stimulation

16 p2849 A70-33697

Positive pressure breathing effects on cerebral blood pressure and catecholamine content of hypothalamus and adrenal glands in dogs

16 p2849 A70-33997

Temperature change relation between anterior hypothalamus and concha auricularis in rabbits

18 p3218 A70-36532

Pathways of short latency reticulo-cortical responses to thalamic nuclei and hypothalamic destruction in cats

24 p4299 A70-45837

Dynamic response of peripheral blood flow to hypothalamic temperature waveforms in baboon, using implanted thermodes

24 p4303 A70-46116

Chronically implantable water perfused thermode system for hypothalamic temperature waveforms generation

24 p4309 A70-46117

Alpha and beta reciprocal hunger regulating systems localized in rats hypothalamus areas by varying injection sites of alpha and beta adrenergic drugs

24 p4304 A70-46233

HYPOTHERMIA

Carbohydrate-phosphorus metabolites content in gophers brains under normal conditions during hypothermia and spontaneous warming at room temperature

01 p0012 A70-10055

Physiological research on humans in hypothermia resulting from confinement to life raft on open sea, analyzing thermal conditions, thermoregulation and survival

01 p0013 A70-10233

Conditioned reflexes, respiration and heart beat rates changes in white rats under hypothermia

03 p0424 A70-13717

Vestibular reactions in rats under hypothermal conditions by measuring postrotatory nystagmus beats number and duration, respiration rates and rectal temperature

03 p0425 A70-13893

Temperature and hemoglobin concentration effect on oxygen solubility in blood, constructing table for Bunsen solubility coefficients

03 p0428 A70-14156

- Low body temperature effects on convulsive activity elicited by hyperbaric oxygen in unrestrained unanesthetized rats
04 p0629 A70-14448
- Hypothermia effect at various temperatures and durations on nervous activity and vegetative functions of rats, discussing pulse and respiratory rates
07 p1197 A70-18696
- Cranioerebral hypothermia effects on phase structure of cardiac thrust in dogs
07 p1204 A70-19140
- Cerebrum hyperemia of dogs subjected to cranioerebral hypothermia, recording rheoencephalograms by occipitofrontal needle electrodes
07 p1207 A70-19473
- Succinic dehydrogenase activity in white rats cerebrum and liver under hypothermia and after warming
07 p1207 A70-19475
- Physiology of hibernation and hypothermia, noting potential use for metabolic need reduction during long interplanetary flight
10 p1943 A70-24757
- Conditioned reflexes, respiration and heart beat rate changes in white rats under hypothermia
11 p1985 A70-25517
- Brain tussling respiration and oxygen consumption in rats during hypothermia
12 p2168 A70-27345
- Hypothermia and ionizing radiation effects on hamsters influenza immune response
13 p2349 A70-28834
- Aircraft crew oral temperature related to work-rest schedules, discussing hypothermia, flight stress and in-flight depression
17 p3032 A70-35563
- Prolonged cold adaptation effect on heat transfer during recovery period after hypothermia in white rats
18 p3220 A70-36543
- Repeated snow cooling effect on heat transfer in white rats during temperature homeostasis recovery after hypothermia
18 p3220 A70-36544
- Book on survival in cold water covering physiology and treatment of immersion hypothermia and drowning, thermoregulation, etc
19 p3360 A70-37977
- Blood oxygen, carbon dioxide and pN during hypothermia induced by He-oxygen mixture and cold exposure in hamsters, comparing with hibernation state
23 p4147 A70-44787
- Pulmonary arterial and venous response to cooling, discussing role of sympathetic nervous system alpha receptors in hypothermia induced pulmonary constrictions in dogs
23 p4148 A70-44788
- Hypothermia and body rewarming effects on renal hemodynamics in anesthetized dogs
24 p4301 A70-45998
- HYPOTHESES**
NT LAGRANGE SIMILARITY HYPOTHESIS
NT NULL HYPOTHESIS
NT VORTICITY TRANSPORT HYPOTHESIS
Hypotheses concerning optimal methods of solving mathematical physics problems, choosing algorithms employable in digital computers
18 p3291 A70-36284
- HYPOTONIA**
Emergency hypotonia regional control with/without blood circulation centralization, describing device consisting of inflatable balloon, extracorporeal shunt, electromagnetic valve, manometer and circuit
15 p2687 A70-32891
- HYPOXEMIA**
Patients with/without coronary heart disease inhaled various gas mixtures to induce arterial hypoxemia and hyperoxia, noting O availability for myocardial metabolism
01 p0016 A70-10440
- Hypoxemia and acidosis avoidance during respiration cessation in halothane anesthesia
10 p1822 A70-25086
- Partial oxygen pressure in hyperaemic earlobe capillary blood under hypoxemic conditions, noting correlation with age and body weight
10 p1822 A70-25088
- HYPOXIA**
Phospholipid metabolism intensity in brains of adrenalectomized and pseudo operated rats under hypoxia
01 p0012 A70-10054
- Cardiac output and coronary blood flow during steady state hypoxia, considering room air and different oxygen concentration breathings
01 p0014 A70-10360
- Hypoxic stimulation effect on erythropoiesis in vivo bone marrow
01 p0017 A70-10464
- Retinal vessels of humans at .11-2.0 atmosphere oxygen partial pressures, noting arterioles and venules dilation response to hypoxia and vasoconstriction response to hyperoxia
01 p0023 A70-10863

- Rodents hypoxia tolerance following adaptation to hypercapnia by recording time of useful consciousness /TUC/ in repeated sloped surface clinging tests
01 p0026 A70-11249
- Erythropoietic response in anesthetized dogs subjected to sublethal whole-body proton irradiation followed by hypoxic hypoxia, discussing test procedure and results
01 p0027 A70-11300
- Dogs coronary vasodilator responses to hypoxia and induced tachycardia before and after lidoflazine and adenosine
02 p0230 A70-11702
- Thyrotropin /TSH/ effects on thyroidal iodine metabolism during hypoxia in rats
02 p0231 A70-11703
- Polycythemia and hypercapnia effects on apparent oxygenation of rat brain during acute hypoxia by changes in creatine phosphate concentration and lactate/pyruvate ratio
02 p0232 A70-11717
- Lactate rise diminution in anesthetized paralyzed dogs subjected to hypoxia by gas mixtures before and after beta-adrenergic blockade
02 p0233 A70-11724
- Cross adaptation criteria and modifications in physiologic and biochemical processes in man and mammals, demonstrating positive cross acclimation between hypertension and hypoxia exposure
02 p0242 A70-12825
- Intermittent EKG recordings during hypoxia test for detection and diagnosis of heart disorders in airmen
02 p0242 A70-12850
- Altitude changes effect on brown fat content and metabolism in deer mice, noting oxygen consumption and heat production limitation by hypoxia
02 p0242 A70-12865
- White mice hypoxia tolerance enhancement after intraabdominal administration of dilute hydrochloric and lactic acids
03 p0424 A70-13718
- Antihypoxic preparations protective effect on white mice and rats subjected to gravitational accelerations
03 p0425 A70-13890
- Human alveolar-arterial oxygen differences during rest, sleep and exercise in initial hypoxia induced by simulated high altitude exposure
03 p0429 A70-14161
- Oxygen consumption and body temperatures during acute hypoxia in man, based on low oxygen mixture breathing tests
03 p0439 A70-14291
- Combined hypoxic hypoxia and high ambient temperature found relieving strain on humans by increasing heat release by evaporation
04 p0630 A70-14581
- Vascular resistance and constriction and muscle mass related in pulmonary arteries of mice subjected to alveolar hypoxia
04 p0630 A70-14679
- Differential effect of hypobaric hypoxia on depressant characteristics of sodium barbital, sodium pentobarbital and chloral hydrate in rats and mice
04 p0631 A70-14680
- Cats trained for visual form discrimination tested for retention and reversal performance, studying oxygen deprivation influence
04 p0633 A70-15443
- Hypoxia effect on self paced work behavior of humans
05 p0803 A70-16672
- Standardized bicycle ergometer training effects at sea level and simulated altitudes, indicating hypoxia potentiating role
05 p0807 A70-16674
- Cardiac work limiting factors during exercise under hypoxia, studying cardiac output and coronary blood flow capacities
06 p0991 A70-17282
- Hemodynamics in cardiosclerosis patients and healthy subjects under hypoxia, investigating heart activity and blood circulation
06 p0994 A70-17667
- Acute hypoxia effect on mono-, di- and triphosphonitrides metabolism and content in white rats cerebral tissues, using chromatographic analysis
07 p1199 A70-18721
- High altitude and sea level erythropoietic and somatic development in chick embryos indicating optimal physiological adaptation with prolonged exposure
07 p1202 A70-18864
- Posthypoxic vasodilation in extremities of anesthetized dogs preserved after carotid and aortic reflexogenic zones exclusion
07 p1204 A70-19139
- Resistance to decompression sickness increased and mortality rate decreased in mice after adaptation to hypoxia at normal barometric pressure
07 p1206 A70-19469
- Mathematical model for oxygen tension changes in dogs brain tissues under hypoxia during altitude simulation
07 p1208 A70-19505

- Motivation changes in rabbits exposed to increasing hypoxia in pressure chamber altitude simulation
07 p1208 A70-19506
- Adaptive reactions in thyroidectomized rats blood and brain during adaptation to hypoxia compared with intact animals
07 p1214 A70-19794
- Exercise influence on cardiac output and coronary blood flow during hypoxia, correlating CO and systolic pressure with blood flow changes
07 p1214 A70-19928
- Physiology of high altitude, studying animal and man adaptation and changes in body processes due to life stresses and hypoxia
08 p1441 A70-20469
- Hypoxia effect on retrograde amnesia /recent memory loss/ in albino rats subjected to shock and decompression treatments
08 p1441 A70-20477
- Parathyroidectomy effects on high altitude adaptation and adrenal cortex activity in rats exposed to chronic hypoxia
08 p1442 A70-20719
- Rats acute hypoxia and altitude tolerances after prolonged exposure to hyperoxic atmospheres
08 p1446 A70-21437
- Biochemical and histochemical parallels of enzymatic activity in blood, cardiac muscle and liver under hypoxia
08 p1446 A70-21445
- Drug-alcohol and hypoxia effects on multiple task operator performance tested at altitude and pressure chamber treatments
08 p1448 A70-21939
- Decompression rates effect on altitude tolerance of white rats, discussing hypoxia influence on cardiovascular, respiratory, circulatory, thermal control and central nervous systems
09 p1614 A70-22084
- Acute oxygen deficiency effects on blood electrolyte concentrations in altitude-adapted and nonadapted humans
09 p1616 A70-22217
- Conscious dogs temporary local hypoxia effect on coronary blood flow regulation
09 p1623 A70-23585
- Hypoxia fundamentals and clinical treatment - Conference, Mainz, Germany, October 1967
10 p1820 A70-25076
- Physiology of oxygen transport in human organism and genesis of tissue hypoxia, discussing pulmonary functions, blood transport properties and tissue blood flow and diffusion
10 p1821 A70-25077
- Pulmonary functions disturbances producing hypoxia, discussing alveolar hypoventilation, arterio-venous admixing, blood distribution and oxygen diffusion disturbances
10 p1821 A70-25078
- Hypoxia diagnosis based on excess lactate determination as indicator of oxidative metabolism changes
10 p1822 A70-25084
- White mice hypoxia tolerance enhancement after intraabdominal administration of dilute hydrochloric and lactic acids
11 p1985 A70-25518
- Dogs respiratory response to arterial hydrogen ions at different carbon dioxide pressure levels during hypoxia or hyperoxia, discussing acid-base balance effects
11 p1986 A70-25674
- Free radical content changes in mice organs under hyperoxia and hypoxia
11 p1986 A70-25941
- Hypoxia tolerance of albino rats in He-oxygen and Ar-oxygen environments in heat-pressure chamber, discussing He-oxygen mixture cooling effect
11 p1987 A70-26103
- Mathematical model for oxygen tension changes in dogs brain tissues under hypoxia during altitude simulation
11 p1987 A70-26104
- Motivation changes in rabbits exposed to increasing hypoxia in pressure chamber altitude simulation
11 p1987 A70-26105
- Hypoxia biphasic effect on adrenal catecholamine content of guinea pigs and rats during short and prolonged periods
11 p1989 A70-26665
- Hematologic responses of mice subjected to continuous hypoxia in subatmospheric pressure
11 p1989 A70-26666
- Glycolysis and glycolytic enzymes activity increase in tissues observed during training of rats to hypoxia, discussing adaptive reactions at cellular level
12 p2167 A70-26975
- Rats myocardial contractility depression by free fatty acids during hypoxia or anoxia, noting mechanical performance improvement by glucose
12 p2170 A70-27898
- Autonomic effects on heart rate, portal, renal, cutaneous and muscle blood flows during arterial hypoxia in unanesthetized sham operated thalamic and pontine rabbits
12 p2170 A70-27899

Chronic hypoxia effects on heart size and hematocrit ratios tested in pigeons

12 p2172 A70-28075

Acceleration and hypoxia resistance of mice and rats after injections of phenamine, sidnocarb, strychnine, securinine, aralesside, trioxazine, banactisine and chloridazepoxide

13 p2358 A70-29344

Systemic hypoxia effect on renal tubule sodium reabsorption in anesthetized mongrel dogs [AMRL-TR-69-135]

13 p2353 A70-29435

Oxygen effect on night vision tested in men at 5,000 ft above sea level, obtaining threshold curves of dark adaptation

13 p2359 A70-29443

Hypoxia tolerance in white rats after exposure in hypercapnic medium

13 p2355 A70-29757

Single and combined hypoxia and hypercapnia effects on growing rats, discussing body weights, blood and histological measurements

13 p2357 A70-29948

Chick embryogenesis during hypoxia at high altitude, noting metabolic repression effects, hypothermia and brain atrophy

14 p2536 A70-30188

Chronic hypoxia exposure effect on development and maintenance of renal hypertension in rats

14 p2539 A70-30956

Molecular respiratory reflex and fluorescent signal in rabbits during hypoxia, determining redox kinetics of intracellular pyridine nucleotides

14 p2539 A70-31346

Hematologic changes in mice associated with mengovirus infection and hypobaric hypoxia during barometric pressure changes

15 p2681 A70-31878

Soviet monograph on gas laws in aviation medicine for reduced oxygen pressure pathology, discussing kinetic theory, temperature effects, solubility, diffusion, etc

15 p2682 A70-31925

Hypoxia and acetazolamide effects on color sensitivity zones in visual field

15 p2684 A70-32533

Ventilatory response to carbon dioxide in goats during acute and chronic hypoxia

15 p2684 A70-32539

Decompression rates effect on altitude tolerance of white rats, discussing hypoxia influence on cardiovascular, respiratory, circulatory, thermal control and central nervous systems

15 p2685 A70-32680

Contractile mechanics of cat papillary muscle during hypoxia and reoxygenation recovery

15 p2686 A70-32836

Sodium oxybutyrate effects on brain tissue oxidation during hypoxia in mice

15 p2686 A70-32851

Exercise and rest of humans under hypoxia and hyperoxia, determining blood acid-base state, ventilation and carbon dioxide partial pressure

16 p2849 A70-34256

Hypoxia and parotid secretion in humans exposed to angular accelerations

17 p3038 A70-35137

Serum calcium-digitalis synergism effect on dogs heart excitability, noting hypoxia role in arrhythmia production

17 p3026 A70-35325

Ambient temperature effects on rats and white mice tolerance to hypoxia, asphyxia and hypercapnia in nitrogen-oxygen and He-oxygen atmospheres

17 p3030 A70-35353

Altitude hypoxia adaptation effects on brain protein and RNA synthesis in rats, noting increase in memory resistance to environmental stress effects

17 p3030 A70-35359

Acute hypoxia effects on C14-tagged glycine absorption, distribution and discharge in rats organs and tissues

17 p3030 A70-35360

Spinal reflex activity in normal and altitude exposed cats before, during and after acute hypoxia

17 p3031 A70-35430

Hypoglycemia role in air sickness, aggravating effects of hypoxia and acceleration

17 p3040 A70-35914

Myocardial contractile function in rats under acute overstrain, evaluating role of preliminary training to altitude hypoxia

19 p3360 A70-37805

Hypoxia effects on aviators visual accommodation, convergence and stereoacuity, noting myopia increase with altitude

20 p3569 A70-38996

Hypobaric hypoxia effects on MM virus infection resistance in mice

20 p3572 A70-39428

Hypoxia warning systems using polarographic sensor and miniaturized electronics for face-mask and cabin installation for aircraft and spacecraft

20 p3579 A70-39429

Choice reaction and movement time dependence on hypoxia induced by air pressure reduction inside

decompression chamber, discussing adult human performance

20 p3573 A70-39714

Hypoxia and high ambient temperature effects on altitude tolerance in animals

20 p3575 A70-40186

Hypoxia effects on cerebral blood flow in anesthetized dogs, considering acidosis and vasodilation

20 p3577 A70-40330

Fasting plasma glucose concentration in rats after chronic hypoxia

20 p3577 A70-40542

Hypoxia and hyperoxia effect on ballistocardiogram of healthy males, determining systolic and minute cardiac forces

21 p3763 A70-41231

Ballistocardiogram relationship to cardiac performance index in hypoxia and hyperoxia conditions, investigating systolic and minute cardiac forces

21 p3770 A70-41232

Activation energies of acceleration and hypoxia stress in man and rats, noting brain function survival

21 p3764 A70-41484

Bioelectric activity changes in rats lumbar neurons, membrane and postsynaptic potential and discharge frequency during and after asphyxiation

22 p3971 A70-43404

Rapid decompression due to pressure loss in space vehicle or suit, discussing fulminating hypoxia, mechanical trauma and ebullism

22 p3973 A70-43639

Sinus and diaphragmatic nerves impulse activity during hypoxia compared with normal respiration in cats

23 p4145 A70-44312

Oxidative phosphorylation and oxygen intake during circulatory hypoxia in mitochondria of liver and brain in rats subjected to acute ischemia

23 p4145 A70-44315

Hypoxia effects on voluntary response time to peripherally located visual stimuli

24 p4302 A70-46107

HYSOMETERS

Atmospheric pressure measuring device based on hypsometer and mercury barometer principles for automatic weather stations or remote readout

06 p1066 A70-18247

Hypsometric chart plot of visible lunar hemisphere with consideration of relief, obtaining isohypses

15 p2803 A70-32494

Hypsometer design for accurate pressure measurements at high balloon altitudes

17 p3090 A70-35313

Hypsometric chart plot of visible lunar hemisphere with consideration of relief, obtaining isohypses

23 p4240 A70-43916

HYSTERESIS

Dynamic unbalance effects in rigid body rotors, discussing lubricant temperature changes and instability hysteresis

[ASME PAPER 69-LUB-14] 01 p0101 A70-10391

Tunnel diode studied for oscillations initiation resulting in hysteresis involving supply voltage and load conductance variations

03 p0459 A70-14284

Structural metals hysteresis properties under cyclic plastic loading at room temperature, considering cycle dependent creep and stress relaxation

[ASME PAPER 69-WA-MET-4] 04 p0705 A70-14763

Cyclic hysteresis-loop stress-strain behavior of 1100 aluminum, deriving power function

[ASME PAPER 69-WA-MET-1] 04 p0705 A70-14764

Hysteresis effect on cosmic ray modulation and gradient ionization near solar minimum from measurements made near earth with OGO 1 and 3 ion chambers

04 p0740 A70-15106

Thermal conductivity and hysteresis measured in cylindrical In foil under magnetic fields at temperatures below 1 K

05 p0891 A70-15792

Bistable optical resonators with saturable absorbers, discussing hysteresis characteristics and Q switching applications

06 p1105 A70-17449

He-Ne laser plasma vibrations and radiation power during active medium discharge excitation by DC current, noting characteristic energy hysteresis

08 p1511 A70-20519

Elastic systems vibrations calculated with allowance for amplitude and frequency dependent energy dissipation using hysteresis loop contour expression

08 p1585 A70-20978

Martensitic stainless steels structure related to energy dissipation capability, obtaining damping mechanism as magnetomechanical hysteresis

08 p1515 A70-20979

Electronic recording of cyclic strain diagrams of metals in wide loading frequency range using dynamic hysteresis method

08 p1585 A70-20987

Missile oscillations in plane during pitching moment hysteresis, discussing test coefficients suitability for predicting motion

09 p1606 A70-23258

Hysteresis in MOS transistors attributed to trapped charge carriers on oxide near silicon oxide interface

14 p2555 A70-30338

Magnetic hysteresis dynamic model for digital simulation of stabilized satellite attitude motions

15 p2812 A70-32509

Hysteresis loop behavior under tension-compression cycle fatigue related to Meyer strain hardness values of cyclically strained metals

16 p2934 A70-34334

Frequency multipliers with charge storage diodes, examining recombination and hysteresis effects on performance

17 p3050 A70-34588

Hysteresis effects during retuning of n-type GaAs Gunn oscillator with bias source and LCR circuit, showing range of domain damping by low field

17 p3055 A70-35689

Pisarenko generalized equations for hysteresis loop contour applied to oscillations of one degree of freedom system

17 p3137 A70-35710

Energy dissipation measurement in materials during fatigue testing by dynamic hysteresis loop method

17 p3096 A70-35712

Dynamic hysteresis loop measurement of energy dissipation in materials, showing deformation effects on accuracy

19 p3535 A70-37346

Dynamic unbalance effects in rigid body rotors, discussing lubricant temperature changes and instability hysteresis

[ASME PAPER 69-LUB-14] 19 p3435 A70-37606

Interactive hybrid simulation of TRIAD satellite motions, describing attitude control system with magnetic hysteresis damping

[ALAA PAPER 70-994] 20 p3714 A70-39536

Magneto-optic rotation and hysteresis recording instrument for thin magnetic films as function of temperature and wavelength, using Faraday effect

21 p3826 A70-41452

Apollo 11 lunar dust hysteresis curves and thermomagnetic curves, discussing metallic Fe abundance, susceptibility, alpha-gamma transition, etc

21 p3918 A70-41676

Free and forced oscillations of dynamic system with linear hysteretic damping, using nonlinear model

22 p4114 A70-42700

Harmonic linearization of nonlinear hysteretic elements in automatic control systems

22 p4000 A70-42828

Air and liquid filled excised lungs P-V hysteresis curves, determining surface tension in situ

24 p4302 A70-46104

I

I BEAMS

Horizontally curved I beams flanges elastic buckling, determining prebuckling flange stresses in longitudinal and radial directions

07 p1413 A70-20001

IBM COMPUTERS

NT IBM 360 COMPUTER

IBM COMPUTERS

NT IBM 360 COMPUTER

IBM 360 COMPUTER

IBM System/360 Operating System submodel simulator for multiprogramming, discussing language and structure

02 p0266 A70-12281

Ground support real time operating system 360 for manned spaceflight, discussing system features and performance

13 p2375 A70-29937

ICARUS ASTEROID

Icarus radar and optical observations indicating surface smoothness differences between central and higher latitudes, radius size and radar reflectivity

01 p0180 A70-10534

Radar observations of Icarus, using detected echoes to determine radar cross section, radius size and reflectivity

01 p0180 A70-10535

Icarus asteroid rotation period and brightness variation values obtained from photometric observations at Cassegrain reflector focus

01 p0180 A70-10536

Icarus surface reflectivity estimated from reflected light polarization, combining estimate with inferred absolute magnitude to obtain radius

01 p0180 A70-10537

Icarus asteroidal nature and fragmentation origin suggested from inclusion in angular momentum density-mass diagram

01 p0180 A70-10538

Icarus asteroid positions, UVB magnitude, brightness, colors, light curves and polarization, noting stony-iron composition

11 p2113 A70-26470

Variational equations from Herrick variation of parameters method for Icarus encounter with earth

13 p2488 A70-28823

ICE

Spectral reflectance of carbon dioxide and water frosts at 0.8-3.2 microns, growing frosts in cold vacuum chamber from high purity gases

07 p1388 A70-19945

Refractive index variations effect on backscattering, scattering and attenuation cross sections of ice sphere at various low temperatures

08 p1536 A70-21098

Aircraft ice crystal counter for real-time measurement in cirriform clouds, using contact electrification detection

12 p2264 A70-28091

Halo rings at hexagonal ice crystals in Martian atmosphere, analyzing via bright formations with respect to planetary phase angles

13 p2493 A70-29397

Radio waves attenuation anisotropy in sea ice by comparing vertically and horizontally polarized signals

14 p2546 A70-30132

Ice radiation and reflection characteristics in IR spectral region at certain Brewster angles

14 p2568 A70-30133

Liquid water occurrence on Mars surface, considering ice melting, evaporative cooling, atmospheric moisture content, etc

14 p2651 A70-31298

Potential gradient effect on charge separation mechanism during interaction of polarized snow crystals with ice sphere

15 p2769 A70-31445

Porous matrix explosions during sublimation of dusty ice with nonvolatile particles

19 p3471 A70-37659

ICE FORMATION

NT CLOUD GLACIATION

Ice tunnel testing facility at Naval Air Propulsion Test Center (NAPTC), describing methods, systems, instrumentation and various turbofan and turbojet engine tests

01 p0056 A70-10691

Factors in icing mechanism and principal features of various ice detectors for aircraft and helicopters

01 p0056 A70-10692

Laboratory tests to determine KC-135 air conditioning failure due to turbine wheel icing by flight condition simulation

01 p0005 A70-10694

Flight tests conducted in artificial and natural icing conditions, using CH-3C helicopter with rotor blades equipped with polyethylene anti-icing tape

01 p0006 A70-10695

Venus atmosphere simulation at condensation level in uniform temperature mixing cloud chamber, studying artificial and natural ice nuclei nucleation

02 p0373 A70-12293

GHOST /Global Horizontal Sounding Technique/ balloon for meteorological observation over Southern Hemisphere emphasizing technique to overcome icing in clouds

04 p0622 A70-14550

Aircraft icing effects on conventional and jet aircraft and helicopters, discussing seasonal variations for main climatic regions

07 p1329 A70-18926

Ice crystal density in Martian atmosphere from brightness of Martian parhelic halo

08 p1564 A70-20547

Thermodynamic stability of methane clathrate hydrate, building up ice grains halo within comets inner coma

14 p2650 A70-31243

Growing ice crystals surface electric potentials during various stages of water vapor condensation

15 p2769 A70-31444

Ice crystal density in Martian atmosphere from brightness of Martian parhelic halo

15 p2796 A70-31456

Ice crystals growth rate in natural clouds over minus 2-mins 32 C range based on characteristic axial ratio

19 p3462 A70-38261

ICE NUCLEI

Ice nucleating properties of dust particles above 80 km compared with soil and AgI particles

01 p0081 A70-11296

Venus atmosphere simulation at condensation level in uniform temperature mixing cloud chamber, studying artificial and natural ice nuclei nucleation

02 p0373 A70-12293

ICE OBSERVATION

U ICE REPORTING

ICE PREVENTION

CH-54 engine air inlet anti-ice system design, manufacture and testing, solving heat balance equations describing tapered gap heat exchanger

01 p0165 A70-10693

Icing, bird collisions and static charge problems for jet aircraft, discussing protective devices

03 p0413 A70-13792

Jet aircraft fuel systems icing prevention, considering fuel filters

05 p0796 A70-17020

Criticism and reply to Venus cloud water drop HCl concentration preventing ice cloud formation

11 p2108 A70-25653

ICE REPORTING

Factors in icing mechanism and principal features of various ice detectors for aircraft and helicopters

01 p0056 A70-10692

Satellite high resolution IR imagery for arctic sea ice mapping, describing sensor design and day and nighttime operation in film-strip format

[AIAA PAPER 70-301] 09 p1669 A70-22884

Sea and sea ice remote sensing by four-frequency radar /4FR/ system in EC-121 aircraft

12 p2215 A70-26904

ICING

U ICE FORMATION

IDEAL FLUIDS

Irrational motions of relativistic ideal thermodynamic fluids fulfilling incompressibility conditions

01 p0063 A70-10948

Rayleigh method convergence for linear development of perturbations in unsteady plane parallel flow of ideal fluid, formulating and proving theorem

01 p0064 A70-11032

Spinning top motion stability in homogeneous incompressible ideal resting fluid, using stability derivative for body of revolution

01 p0145 A70-11438

Equations of hydrodynamics governing perfect fluid in second post-Newtonian approximation to general relativity, deriving energy momentum tensor equation

02 p0337 A70-11776

Two spheres moving in ideal incompressible fluid, studying velocity field, hydrodynamic forces, kinetic energy, etc

03 p0465 A70-13335

Ideal fluid flow past sphere in rectangular duct and slot solved in series form in spherical functions

04 p0666 A70-14605

Soviet book on boundary value problems involving motion of ideal fluids in unsteady cavities of various geometries, determining attached fluid masses and oscillation frequencies

04 p0666 A70-14678

Ideal fluid motion characteristics near variable volume spheres with radial mass transfer through surfaces

04 p0672 A70-15198

Computer program to calculate ideal rotating fluid flow in arbitrary airfoil lattice on axisymmetric stream surface in variable thickness layer

04 p0617 A70-15239

Structural element for discrete element idealization missile and liquid propellant as one composite structure

[AIAA PAPER 70-123] 06 p1042 A70-18182

Ideal fluid planar potential flow, approximating stream function and velocity potential by matrix method

07 p1253 A70-18925

Ideal fluid in lightly filled spherical vessel under gravitational force investigated for surface tension effect on vibration frequencies

08 p1482 A70-20853

Perfect fluid sonic flows around weakly lifting three dimensional bodies downstream of shock wave, proving existence of lifting boundary layer

08 p1433 A70-21238

Geometric, cinematic and dynamic conditions of ideal fluid adiabatic nonstationary movement expressed by differential external system /s/

09 p1659 A70-22254

Prime formulas for studying perfect relativistic fluids with spin

09 p1728 A70-22840

Circle theorem for potential flows extended to two dimensional steady incompressible ideal fluid flows of constant vorticity

09 p1664 A70-23714

Quasi-one dimensional motion of perfect compressible fluid through pipe, considering one dimensional schemes in aerodynamics

10 p1865 A70-24102

Rayleigh method convergence for linear development of perturbations in unsteady plane parallel flow of ideal fluid, formulating and proving theorem

10 p1871 A70-25001

Efficiency loss with tip clearance predicted for mixed and axial flow single stage turbomachines, using perfect fluid model

11 p1974 A70-25787

Ideal fluid flow containing small spherical particles past cylinder and flat plate normal to stream using small perturbations method

11 p1976 A70-26012

Ideal weightless fluid jet flow past supercavitating plate at incidence using Tulin scheme

12 p2214 A70-28241

Motion stability of variable mass solid body with ideal liquid filled cavities about stationary point using Liapunov theorem

13 p2452 A70-29310

Incompressible ideal plane fluid flow complex potential caused by profile motion in presence of fixed infinite wall

13 p2390 A70-29632

Ideal weightless fluid plane potential flow in channel with permeable wall, deriving expressions for dynamic characteristics

13 p2390 A70-29648

Hydrodynamic forces by oscillating foils in ideal incompressible fluid turbulent flow with stream separation

13 p2390 A70-29649

Chemically reacting ideal substance model, describing thermodynamic properties and application to energy conversion processes

14 p2533 A70-30529

Force acting on cylinder in ideal incompressible fluid plane flow with steady vorticity

15 p2719 A70-31498

Thermodynamically perfect fluids in general relativity, considering heat transmission paradox and wave propagation velocities

16 p2997 A70-33103

Incompressible ideal fluid plane laminar flows at large Reynolds numbers in region bounded by moving walls with closed concentric streamlines, establishing functional properties

16 p2893 A70-33749

Interior ideal liquid flow of vertical jet under gravity, using differential equation to relate flow plane to unit half disk

17 p3069 A70-34979

Ideal fluid contained in half space with circular or strip-like aperture, formulating mathematical model to determine sloshing frequencies

18 p3238 A70-36057

Axisymmetric ideal incompressible fluid jet outflow from cylindrical vessel with conical bottom, using small parameter technique and conformal mapping

18 p3240 A70-36272

Ideal relativistic fluids adiabatic flow, investigating heat exchange effects within framework of special relativity

18 p3347 A70-36554

General relativistic equations for stationary axially symmetric rotating perfect fluid in comoving coordinate system

18 p3292 A70-36900

Thermodynamics and velocity of MHD shock waves in perfect conducting fluid, using compressibility conditions and relativistic Hugoniot equation

19 p3477 A70-37580

Electrically conducting perfect compressible fluid flow in semiinfinite channel under electromagnetic field, using multiple scales method

19 p3479 A70-37595

Sound field produced in uniform moving ideal fluid stream by nonuniform oscillating elastic wall

19 p3353 A70-38657

Perforated solid body moving in ideal incompressible fluid, deriving equations of motion in Lagrangian form

20 p3610 A70-39732

Bubble motion in ideal incompressible fluid, deriving motion equation in low viscosity fluid

20 p3614 A70-40392

Ideal fluid-cylindrical tank elastic bottom coupled forced oscillations, determining hydrodynamic pressure for tank reverse translational motion

20 p3615 A70-40444

Relativistic observer in rotational motion relative to inertial observer, imposing velocity onto perfect relativistic fluid

21 p3851 A70-42096

Rotational two dimensional steady shear flows of perfect incompressible fluid, considering channel flow characteristics for various wave modes

23 p4181 A70-44202

IDEAL GAS

Two dimensional and axisymmetric bodies shapes providing minimum wave drag to supersonic flow of perfect gas, considering bodies around which flow causes bound shock waves

03 p0409 A70-13863

Viscous compressible heat conducting laminar perfect gas flow in slender axisymmetric channels with adiabatic walls, using equations of motion

03 p0471 A70-14383

Viscous ideal gas supersonic flow past spheres, using integral relations based on Navier-Stokes equations

04 p0613 A70-14606

One dimensional steady adiabatic source nonisentropic flow of thermally and calorically perfect gas in conical nozzle, considering exit divergence and nonuniform flow effects

04 p0619 A70-15427

Mass transfer and viscous interaction combined effects on axisymmetric hypersonic flow of perfect gas over slender bodies

[AIAA PAPER 68-717] 04 p0675 A70-15576

Ideal equivalent gas method for studying thermodynamic properties in supersonic gas flows behind shock wave

05 p0831 A70-15872

Compressible fluid flow satisfying perfect gas equation in presence of thin foil, developing operators characterizing incompressible and compressible flows without Hall effect

05 p0790 A70-16158

Steady and frictionless supersonic flow of ideal gas of constant heat capacity around slightly deformed cone, calculating force exerted by gas

06 p0964 A70-17240

Cesium plasma composition as equilibrium mixture of ideal gases assuming chemical equilibrium attainable by specified reactions

07 p1349 A70-19660

Steady turbulent perfect compressible gas flow in axisymmetrical or plane channel, using equations governing channel height and static pressure variations

09 p1659 A70-22429

Transonic aerodynamics problems concerning plane and spatial rotational flows of perfect gas, discussing analytical and numerical methods

10 p1800 A70-24132

Perfect gas mixtures thermodynamic functions at high temperatures with correction for Debye-type electrostatic interaction effects

10 p1968 A70-24707

Shock wave reflection into ideal gas flow with linear density variation analyzed for flow field

12 p2211 A70-27832

One dimensional perfect gas motion under spatial pressure distribution, investigating self similar solutions

12 p2212 A70-28189

Perfect gas supersonic flow with constant velocity, pressure and density around finite nonaxisymmetric body at small angles of attack

12 p2158 A70-28197

Stagnation point position and entropy at surfaces of supersonic paraboloids in perfect gas

12 p2160 A70-28250

Chemically reacting ideal substance model, describing thermodynamic properties and application to energy conversion processes

14 p2533 A70-30529

High temperature inviscid flow of ideal radiating gas, analyzing effects of radiation pressure and energy on flow field

14 p2666 A70-30999

Strong shock waves profiles in monatomic perfect gases by Monte Carlo simulation, obtaining maximum density slope thicknesses

14 p2567 A70-31031

Cesium plasma composition as equilibrium mixture of ideal gases, assuming chemical equilibrium attainable by specified reactions

15 p2781 A70-32697

Nonreacting and chemically reacting laminar flows, calculating equilibrium, nonequilibrium and ideal gas laminar boundary and viscous shock layers over hyperboloid

[AIAA PAPER 70-808]

17 p3005 A70-34456

Normal shock structure in thermally perfect gas, using perturbation methods

17 p3070 A70-35244

Perfect and dissociating gas nonstationary supersonic flow around sharp profile of finite thickness analyzed by linearization and method of characteristics

19 p3351 A70-37242

Perfect gas irrotational isentropic nozzle flow by solving partial differential equations set

21 p3744 A70-41240

Self similar flow instability behind collapsing cavity boundary, examining perfect gas adiabatic equation of state

21 p3808 A70-41500

Exhaust plume rarefaction from sonic orifice, considering continuum to transitional behavior for perfect gas

[AIAA PAPER 69-657]

21 p3745 A70-41742

Self similar formulations for motion of radiating-absorbing perfect gas symmetric flow

21 p3954 A70-42202

Decelerated channel flow dynamics of ideal gas with supersonic velocity closed by compression shock, using finite difference method

21 p3747 A70-42203

Perfect gas acyclic and cyclic, steady and irrotational motions in subsonic regime around convex profile with constant curvature variation by Chaplygin method

21 p3846 A70-42259

Perfect gas circular subsonic flow around convex obstacle, using hodographic method for boundary problem

22 p3958 A70-42608

Macroscopic equations of motion established by Maxwell transport equations for relativistic perfect gas

22 p4011 A70-42716

One dimensional perfect gas motion under spatial pressure distribution, investigating self similar solutions

22 p4012 A70-43314

Perfect gas supersonic flow with constant velocity, pressure and density around finite nonaxisymmetric body at small angles of attack

22 p3960 A70-43322

Perfect gas three dimensional boundary layer separation on circular cone at incidence, comparing numerical calculation and experimental results

23 p4133 A70-44207

Perfect nonrelativistic bounded gas thermodynamics and surface tension, assuming single particle energy level density dependence on external potential

23 p4284 A70-44928

Perfect gas statistical relations by perturbation form of state equation for atmosphere

24 p4372 A70-46071

IDENTIFYING

NT TIMBER IDENTIFICATION

Automatic control system identification with respect to optimality criteria, mathematical models, computing techniques and input signals

07 p1247 A70-20029

Differential correction algorithm for identifying air-plane parameters from flight test data, assuming differential equations

08 p1465 A70-20783

Quasi-linearization technique in computer program for aircraft parameters identification featuring efficient search for optimal parameters in algebraic or differential equations

08 p1465 A70-20784

Aircraft accidents victims identification, considering use of specialized laboratories

09 p1626 A70-23018

Maximum likelihood methods for aircraft identification problems, considering model types, flight disturbances and available data

16 p2885 A70-33326

Asteroid identification during different oppositions, using numbered planetoids and node catalog

16 p2974 A70-33657

Parameter variation effects on iterative identification of linear system by learning method

17 p3130 A70-35299

3-O-methyl-mannose neutral sugar identification as constituent of fungal polysaccharide

20 p3572 A70-39625

IFR (RULES)

U INSTRUMENT FLIGHT RULES

IGNEOUS ROCKS

NT ANORTHOSITE

NT BASALT

NT ENSTATITE

NT LAVA

NT MAGMA

NT MOLDAVITE

NT OLIVINE

NT PYROXENES

NT QUARTZ

Major and trace element concentration in contact zones of Precambrian diabase dikes from Wyoming ranges, showing dikes as continental tholeiites

03 p0472 A70-13148

Reflectance spectra obtained for igneous rocks and minerals, establishing correlation between reflectance and energy wavelength, composition and sample particle size

05 p0839 A70-16390

Chemical analysis of Australasian tektites inferring extraterrestrial igneous origin, noting similarity to preimpact parent rock

05 p0916 A70-16832

Apollo 10 and 11 photographs revealing probable igneous intrusions on lunar farside crater

06 p1137 A70-17195

Australasian microtektite compositional trends compared with critical plots enabling distinction between rocks formed by igneous sedimentary and vapor fractionation processes

06 p1150 A70-18477

Lunar surface samples characteristics correlation with terrestrial igneous rocks/basalts/ and eucrite meteorites based on alpha scattering analysis

07 p1380 A70-19203

Middle Miocene hiatus in volcanic activity of Western U.S., discussing K-Ar dates for Tertiary rock of Great Basin area

13 p2393 A70-28718

Apollo 11 lunar igneous rocks mineralogical, chemical and petrological features by optical and electron microscopy and X ray spectrometry

21 p3896 A70-41512

Opaque minerals in Apollo 11 lunar igneous and fragmental rocks, using reflecting microscope and electron microprobe

21 p3896 A70-41513

Fission track uranium distribution studies of Apollo 11 lunar volcanic rocks, using Lexan plastic print method

21 p3900 A70-41537

Apollo 11 lunar igneous rocks minerals and glassy phases characteristics, using electron probe microanalysis

21 p3900 A70-41538

Mineral chemistry of Apollo 11 igneous rocks, soil and breccia samples, comparing with meteorites

21 p3773 A70-41545

High crystallization temperatures for igneous rocks from Tranquility Base indicated from late formation of sulfide liquid forming complex troilite intergrowths and iron

21 p3902 A70-41553

Neutron activation analysis for Re and Os in Apollo 11 volcanic rocks, discussing possible meteoritic contamination of secondary rocks and fines

21 p3775 A70-41589

Chemical composition and reducing capacity of Apollo 11 igneous rocks, breccia and soil fines, using semimicro X ray fluorescence

21 p3777 A70-41602

Metallic Fe grains in Apollo 12 igneous rocks, discussing Ni and Co abundances

21 p3920 A70-41881

Terrestrial and synthetic lunar igneous rocks thermal conductivities in melting range, discussing thermal gradient

23 p4238 A70-43804

IGNIMBRITE

U LAVA

IGNITERS

NT DETONATORS

NT INITIATORS (EXPLOSIVES)

Ignition delay of uncompressed composite solid or hybrid propellant mixtures in rocket engine igniters

18 p3301 A70-36651

Aft-end igniter design and placement for solid propellant rocket motors avoiding overpressurization and nozzle pressure oscillations

21 p3866 A70-40892

IGNITION

NT ELECTRIC IGNITION

NT SOLID PROPELLANT IGNITION

NT SPARK IGNITION

Gas ignition and burning processes calculation with allowance for hydrodynamics, discussing time saving finite difference solution of differential equations system

01 p0218 A70-11020

Hydrogen peroxide oxidizer for higher characteristic mixture ratio in hybrid propulsion systems with hypergolic reactions ignition

[ONERA-TP-773]

02 p0352 A70-12209

Propane oxidation reaction and ignition delay times

[AIAA PAPER 68-633]

03 p0603 A70-12909

Ignition of freely falling single fuel droplets, considering initial size, oxidizer temperature, fuel composition, droplet spacing, etc

04 p0733 A70-15540

Combustion processes and ignition criteria in shock wave ignition of liquid fuel drop in oxidizing atmosphere

[AIAA PAPER 70-9]

06 p1180 A70-18142

Unsensitized gaseous fuel-air mixtures photochemical ignition due to molecular oxygen photodissociation by radiant energy absorption

[AIAA PAPER 70-149]

06 p1183 A70-18225

Preignition heat release rate profile in ethylene-air mixture flow against hot surface, determining temperature and velocity distribution optically

07 p1420 A70-19263

Gas phase ignition theory of evaporating fuel in stagnant hot oxidizing gas as function of temperature

07 p1421 A70-19317

Ignition and extinction in opposed jet diffusion flame for flow of compressible fluid with competitive/chain reactions

07 p1422 A70-19578

Liquid fuel droplet ignition quasi-stationary theory occurring at maximum chemical reaction rate

14 p2664 A70-30393

Preignition and combustion kinetics in airstream of Mg and Al suspensions in aviation kerosene and gasoline

14 p2664 A70-30395

Ignition and combustion in ducted turbulent supersonic flow, discussing premixed and unpremixed ethylene

16 p2997 A70-33488

Boron particles ignition and combustion in supersonic air stream, emphasizing axial and lateral two phase flow injection

[AIAA PAPER 70-720]

16 p2856 A70-33496

Pressure histories of burning modes in combustion driven shock tube using ignition of stoichiometric hydrogen-oxygen mixture with He dilution

17 p3195 A70-34922

Flameout and ignition correlation for diffusion fuel burnup behind angled stabilizers in annular turbine combustion chamber

18 p3300 A70-36127

Ignition surges role in combustion economics

18 p3348 A70-36652

Hypersonic nozzle ignition phenomenon in reflected shock wind tunnel

19 p3352 A70-38170

- Gas phase ignition theory with feedback of homogeneous propellant exposed to stagnant gas after shock reflection
[AIAA PAPER 69-559] 21 p3950 A70-41728
- IGNITION LIMITS**
Limits of self ignition in reaction of F with H detected photoelectrically
05 p0956 A70-16156
- Ignition and extinction of diffusion flames predicted from studying forced convection in boundary layers
[WSCJ PAPER 69-36] 06 p1178 A70-17976
- Cold ducted supersonic flow of premixed ethylene and air ignition by hot turbulent jet
[AIAA PAPER 70-148] 06 p1131 A70-18057
- Pregnation products from hydrazine propellants at simulated high altitude conditions using IR spectrophotometry, mass spectrometry and differential thermal analysis
07 p1358 A70-19579
- Minimal initial size of explosion reaction center used to explain ignition process in flammable mixtures, noting dependence on pressure, temperature and composition
07 p1422 A70-19586
- Gas discharge gap preionization by thin preheated tungsten wire ignition without explosion, resulting in plasma turbulence prevention and radiation density increase
13 p2462 A70-28986
- Low pressure deflagration, limit dependence on strand size in terms of cross section dimensions for composite ammonium chlorate propellant
[AIAA PAPER 69-144] 13 p2473 A70-29955
- Atmospheric pressure hydrocarbon-air mixtures confined by thin plastic membrane, obtaining composition range for detonation initiation limits
21 p3865 A70-40884
- IGNITION SYSTEMS**
Fuel injection and mixing and piloted ignition in supersonic flow design principles for scramjet engine, evaluating eddy viscosity model for parallel injection
02 p0354 A70-12047
- Solid rocket motor ignition system based on exothermic alloying of bimetallic wire constituents
[AIAA PAPER 69-425] 06 p1128 A70-17179
- Exothermic bimetallic ignition systems /EBIS/ design for solid propellant rocket motors of tactical missiles to reduce shock loadings
12 p2289 A70-27694
- Resonance ignition technique for gaseous oxygen and hydrogen rocket propellants
14 p2627 A70-30776
- Titanium powder compacts exothermic solid phase reaction ignition by focused laser pulse, obtaining temperature profile from mathematical model based on energy transport
20 p3639 A70-40473
- Composite solid propellant thermal ignition from hot wire tests and model
21 p3942 A70-40877
- Particulate boron levitated electrostatically in air and ignited by pulsed laser to avoid contamination, investigating combustion by high speed photography
[SMPE PREPRINT 100] 22 p4032 A70-43034
- IGNITION TEMPERATURE**
Fire prevention problems in closed oxygen-rich environments, discussing ignition temperature and flame propagation rate
03 p0607 A70-13961
- Ignition of cold premixed fuel by hot projectile, obtaining distance for ignition occurrence
[AIAA PAPER 70-150] 06 p1180 A70-18133
- Cold combustible mixture ignition at forward stagnation region of hot projectile, calculating temperatures for propane-air mixture
07 p1422 A70-19577
- Thermal explosion criterion for explosion/ignition delay of exothermic material surrounding heated wire as function of time
07 p1424 A70-20005
- Ammonium perchlorate-polymer mixtures combustion rates with/without cobalt oxide additions, studying ignition temperatures of stable flameless burning
09 p1787 A70-22108
- Stannic oxide-chromium oxide catalyst effects on thermal decomposition and ignition of ammonium perchlorate /AP/, calculating activation energy
11 p2100 A70-26281
- Spontaneous ignition temperature as function of surface-to-volume ratio in static systems for fuels
11 p2151 A70-26384
- Spontaneous ignition dependence on transient temperature variations accompanying gas entry to evacuated vessel
12 p2330 A70-27222
- Thermal testing of decomposition and spontaneous ignition of diethyl peroxide before explosion
12 p2330 A70-27224
- Oxygen motion velocity effect at various pressures on heatproof and heat resistant steels and alloys ignition, noting minimum ignition temperature
13 p2434 A70-29168

- External burning fuels environmental temperature requirements from nonlinear droplet ignition model, emphasizing droplet size importance
[AIAA PAPER 70-607] 16 p2997 A70-33604
- Autoignition, ignition and surface temperatures of M-2 double base propellant at low pressure, correcting thermocouple measurements by theoretical model
18 p3299 A70-36697

IGNITRONS

- Ignitron converters for feeding power plasmatrons and arc reactors, describing circuit and operation
11 p1984 A70-26742
- Semiconductors as igniter material for ignitrons, tabulating electrical characteristics
14 p2590 A70-30640

IGY [GEOPHYSICAL YEAR]**U INTERNATIONAL GEOPHYSICAL YEAR****ILLUMINANCE**

- Pupil diameter changes associated with constant change in accommodative stimulus as retinal illuminance varies
03 p0427 A70-13950

ILLUMINATING

- Illuminating conditions in deep layers of turbid plane-parallel medium for highly elongated scattering characteristic
04 p0745 A70-14497
- Spacecraft cabins illumination conditions selection based on cosmonaut visual perception of luminous objects
07 p1221 A70-19515
- Holographic 3D movie of front-lighted opaque objects, recording diffuse reflection with CW laser and high resolution film
09 p1684 A70-23533
- Motion picture holography using continuously pumped ruby laser illumination system in repetitive Q switched mode
09 p1689 A70-23782
- Spacecraft cabins illumination conditions selection based on cosmonaut visual perception of luminous objects
11 p1991 A70-26114
- Displacement component in chosen direction on deformed object surface, using hologram interferometry with double illumination
13 p2409 A70-29475
- Manual spectrograph for distant objects spectrophotometry under natural conditions and solar illumination
14 p2583 A70-30415
- Illumination level and contrast loss distribution in atmosphere to evaluate passive night vision equipment with image intensifier tubes
16 p2907 A70-33184
- Airborne illumination using argon vortex-stabilized arc lamp, noting applicability in near IR spectral range
17 p3023 A70-35152
- Lighting and background effects on human binocular color vision of signal lights in industry
19 p3366 A70-38923
- Object visibility limits when illuminated by laser beam with spatial selection method, discussing atmospheric conditions and light source radiation power
20 p3641 A70-39448

ILLUMINATION

- Diffuse illumination in holography indicating spread increase dependence on product of phase mean-square value and spatial frequency bandwidth
02 p0296 A70-11891
- Minimum altitudes for illumination levels of aerial color photographic film calculated for different landscapes
07 p1283 A70-19633
- Illumination of zenith region of sky before and during solar eclipse of September 1968 measured by luxometer
08 p1573 A70-20950
- Age and retinal illumination influence on human pupillary near reflex investigated by photographic measurements
12 p2171 A70-28036
- Si solar cell power output and spectral response as function of angle illumination, eliminating atmospheric influence
14 p2533 A70-30337
- Extrinsic photoconductor with reduced background under uniform illumination, describing frequency response as function of recombination and dielectric relaxation times and load resistances
14 p2586 A70-30989
- Illumination of zenith region of sky before and during solar eclipse of September 1968 measured by luxometer
15 p2806 A70-32762
- Illumination efficiency in shaped two reflector Cassegrain antenna system related to feed pattern deviation
16 p2861 A70-32968
- Geometrical figure fragmentation produced by intermittent illumination, examining dependence on presentation frequency and temporal factors
20 p3580 A70-39491

- Radar consoles with various display components under different illumination levels to determine optimal operator performance, discussing push-button design recommendations
20 p3580 A70-39713

- Visual acuity during ocular tracking movements as function of field illumination density
23 p4147 A70-44777

- Spatial aspects of sensitization effect properties compared to background light fields, lowering rod threshold at center by light addition to surrounding angular region
23 p4147 A70-44779

ILLUMINATORS

- Continuous Chlorella production as function of total illumination in high intensity light system incorporating aerobic fermenter for heterotrophic cells
04 p0645 A70-15454
- Monopulse ruby lasers for moving object illumination during shadow photography, noting applications to ballistic studies
09 p1698 A70-23173
- Acoustical holography with single stationary point detector noting reciprocity between detector and point source illuminator
17 p3088 A70-35030
- Thermoelectrically cooled GaAlAs injection laser illuminator, discussing optical-electronic interface problems and design and performance characteristics
22 p4052 A70-43603
- High efficiency gallium arsenide IR illuminators comparing dome diodes fabricated from diffused or Si doped solution grown materials
24 p4319 A70-45784

ILLUSIONS**NT MOON ILLUSION****NT OCULOGRAPHIC ILLUSIONS**

- Suprathreshold angular acceleration effects on oculographic illusion, obtaining magnitude estimates during and after acceleration
14 p2543 A70-30897
- Perceptual displacement of hashmark between detector and unequal squares, discussing contour repulsion and perspective interpretation
14 p2537 A70-30899
- Pitch and Coriolis illusions effects on pilot pitch angle adjustment in simulated takeoff
15 p2689 A70-31885
- Distorting and distorted components during geometrical illusions stereoscopic registration
19 p3366 A70-38926
- Imaginary axes effect of phenomenal space in contrast illusions of distance, discussing division of S field of vision by definite point fixation
20 p3573 A70-39764
- Stroboscopic stereophenomenon, investigating depth shift of oscillating target motion binocularly viewed for interocular luminance differences
23 p4147 A70-44781
- Pitch illusion in flight personnel under centripetal acceleration
24 p4306 A70-45330

ILMENITE

- Apollo 11 lunar rock clinopyroxene, plagioclase and ilmenite internal substructure, using high voltage transmission electron microscopy
21 p3901 A70-41544
- Apollo 11 ilmenite basalts petrology from regolith samples
23 p4239 A70-43898

ILS [LANDING SYSTEMS]**U INSTRUMENT LANDING SYSTEMS**

- ILYUSHIN AIRCRAFT**
Ilyushin 62 aircraft geometry, propulsion, structure, onboard equipment and performance
08 p1436 A70-21365

IMAGE CONTRAST

- Duty factor and contrast in scanned displays, discussing light modulator and emitting displays
01 p0043 A70-10780
- Simulation technique to evaluate TV contrast trackers standard scan performance using video tape recording
01 p0058 A70-10812
- Atmospheric water vapor effect on contrast between natural target and sky via spectrophotometric method, exploring target visibility and contrast relations
02 p0325 A70-11873
- Hologram image resolution, finding angular alignment of reconstruction wavefront as limiting factor
02 p0297 A70-11923
- Speckle pattern in image plane of laser illuminated diffuse object, calculating pattern intensity and contrast
02 p0312 A70-12106
- Photointerpreters information extraction, studying psychological effects of image contrast and resolution on accuracy of target detection
02 p0300 A70-12459
- Interferogram contrast as spatial frequency function measured for photographic materials used in holography by He-Ne laser
03 p0485 A70-13530

Photometry as aid for aerial photography, discussing resolution, mapping, etc 03 p0486 A70-13554

Object visualization in phase contrast using nonlinear interferential holography by successive recording of intensities on photographic plate 05 p0848 A70-16273

Automatic measurement of frequency-contrast characteristics of photographic films using linear, photoelectric and high speed comparator devices 05 p0852 A70-16865

Image contrast in holographic reconstructions, discussing influence of given surface intensity recording and oblique reference wave on hemigram 06 p1067 A70-18398

Photographic emulsions used for astronomical photography in U.S., discussing hypersensitization, exposure, processing and image evaluation methods 06 p1071 A70-18516

Threefold reduction of aerial negatives facilitating microfilming without impairing accuracy and clearness of image details 07 p1278 A70-18692

Visual and quantitative image definition, evaluating microdetail clarity in panchromatic, IR, color and color IR aerial photographs 07 p1281 A70-19369

Birefringence determination from contrast of interfering natural light beams 08 p1543 A70-20521

Resolution, contrast and gray scale performance of CRT displays compared to dot matrix displays 08 p1500 A70-21763

Small contrast objects detection by photographic technique, measuring gradients, granularity noise and density variations for emulsions 09 p1673 A70-22157

Photographic emulsion nonlinear response effect on image quality, discussing holography for multiple exposures 09 p1676 A70-22718

Object contrast effects on straight edge images in partially coherent illumination 10 p1898 A70-23910

Nb and Nb alloys activation in polarized light by etching technique, observing grain contrast improvement 10 p1906 A70-25229

Image contrast and diffraction efficiency of dielectric hologram made from diffuse signal beam, bleaching photographic emulsions 11 p2048 A70-25359

Fog visibility improvement by optical range gating, increasing image contrast by background radiance reduction 11 p2064 A70-26719

Quantitative analytic composite photography, performing image density point-to-point subtraction of two negatives 13 p2406 A70-28905

Microwave holography with artificial reference wave and receiver multiplier, improving linear resolution in image 13 p2408 A70-29407

Image coherence of object by laser illumination through moving diffuser related to diffuser autocorrelation 14 p2588 A70-31208

Scattering function and image quality in sharp edge holography using single mode laser, analyzing coherent and diffuse light 15 p2733 A70-31556

Radiograph images digital processing by linear and nonlinear position invariant techniques, obtaining contrast enhancement 15 p2706 A70-32569

Illumination level and contrast loss distribution in atmosphere to evaluate passive night vision equipment with image intensifier tubes 16 p2907 A70-33184

Modulation transfer function /MTF/ systems analysis with emphasis on target acquisition, relating image contrast characteristics of target and background 16 p2907 A70-33185

Optical system and light source imperfection effects interference image contrast lowering in laser interferometer for length measurements 16 p2928 A70-33292

Atmospheric optical inhomogeneity effect on image quality, investigating deflection angles for spherical light wave passage at various altitudes 16 p2915 A70-34215

INTIC tube memory image intensifier with contrast enhancement, describing design and performance 16 p2880 A70-34269

Metal grid capacitive memory for INTIC and direct view storage tubes, describing image contrast control 16 p2880 A70-34270

Meteor spectrosensitometric properties of panchromatic plates and films for aerial photos, investigating parametric conditions effect on image quality 19 p3422 A70-37653

Brightness contrast by human observer binocular matching, discussing neural networks models 19 p3366 A70-38924

Retinal images smearing during voluntary saccadic eye movements, obtaining thresholds for horizontal and vertical stimuli bands 19 p3366 A70-38927

Encircled energy calculation in optical systems with central obstruction, observing focus error, spherical aberration and central stop effects on image contrast 20 p3627 A70-39088

Sunspot umbras and penumbras magnetically nonsplit lines measured photographically by spot contrast discriminator 21 p3887 A70-41115

Optical telescope reflecting prism angle deviations effect on modulation transfer function and image quality 22 p4072 A70-42506

Pseudo three dimensional effect on monoscopic radar imagery for topographic relief differentiation, using offset superposition of transparencies 22 p4031 A70-42965

Cobb chart resolution in photographic system including independent sources of image spread and single source of granularity 24 p4334 A70-45450

Exposed photographic layers blackening phenomenon energy spectrum and mean square 24 p4336 A70-45655

Monochrome radiography for contrast strengthening to increase color images detectability by human eye 24 p4337 A70-45708

Radiography for nondestructive tests, considering image quality specification and choice of geometric progression for determining visibility 24 p4337 A70-45709

Wire and hole type penetrometers minimum perceptible image contrast level on radiograph, considering X ray quality and films effects 24 p4337 A70-45713

Photographic paper as emulsion film substitute in industrial radiography, evaluating sensitivity and image contrast 24 p4337 A70-45715

Radiography using photo-nuclear reaction emulsion to improve picture contrast by eliminating scattered photons in sample 24 p4337 A70-45716

Image contrast enhancement on neutron radiograph by energy tailored beams 24 p4376 A70-45748

IMAGE CONVERTERS

NT CELESCOPES

NT IMAGE TUBES

Image conversion scheme to obtain holograms of three dimensional objects illuminated with IR light, using nonlinear optics 04 p0685 A70-14406

Angular tolerance on IR radiation for phase matched image up-conversion in material with nonlinear susceptibility 04 p0703 A70-15621

Imaging properties of parametric image converters, taking into account frequency doubling of brilliant object by self interaction within nonlinear material 05 p0852 A70-16991

IR image conversion into visible using nonlinear KDP crystal 12 p2248 A70-27543

Acoustographic imaging system /AGIS/ using liquid crystal detection screen to provide color display of ultrasonic wave information 12 p2235 A70-27724

Retinal receptors physiology involved in transforming visible radiant energy into sensory message 12 p2172 A70-28105

Wide angle emitter images transformation into circular by reflecting cone and lens system, describing photographic and photoelectric methods 12 p2237 A70-28157

Holographic method for recovery of complete image /ghost/ from partial hologram and entire diffraction picture 12 p2238 A70-28186

Optical transformation of field ion micrographs providing orthographic, gnomonic projections and perspective images of hemispheric metal surface 14 p2584 A70-30506

Image processing and picture enhancement by computer, using fast binary log-antilog conversion 15 p2768 A70-32567

Optimal perturbation signal waveform linearizing nonlinear transfer characteristic of image sensing receptor array 15 p2705 A70-32725

Linked and fiber optic components, describing applications as punched card and tape reading, geometrical converters and sensing and scanning probes 16 p2904 A70-33145

Solid state IR to visible converter, using minority carriers stimulated tunnel injection into wide band gap phosphor 17 p3081 A70-34648

Optimum receiver for acoustical holography using discrete transducers arrays for image conversion 17 p3088 A70-35029

Apollo black and white TV scan converter design and operation 17 p3095 A70-35636

Ultrahigh speed ballistic-synchrophotography, using Imacon image converter camera for framing and streak modes [SMPT PREPRINT 113] 22 p4031 A70-43028

IMAGE CORRELATORS

Simultaneous recording of near and far field diffraction patterns at several exposures for single laser pulse 04 p0701 A70-15022

Stereo photographs conjugate image area matching, comparing automatic optical and electronic correlation techniques 09 p1680 A70-23067

Photoelectric devices for object position fixation and superposition of two images 09 p1684 A70-23635

Holographic identification of similar two dimensional images by linear transformation of space by spherical lens using white light correlator 12 p2238 A70-28185

Optical cross correlator with consecutive recording of mutual correlation function, using transparencies on different side of lens 13 p2412 A70-29865

Optical correlator for displacement measurements using laser produced speckle patterns of scattered coherent light 17 p3088 A70-35026

Image detection in pattern recognition through bipolar correlation, discussing reference generating algorithms and digital simulation results 20 p3633 A70-39972

IMAGE ENHANCEMENT

Aerial oceanographic photographic image enhancement by including blue spectral region, presenting Apollo 9 space photographs 12 p2217 A70-26917

Remote sensing techniques for earth resources inventory, describing image enhancement role in multiband space photography 12 p2220 A70-26936

Topographic shadow linears image enhancement by low angle illumination, describing pseudoradar technique for subcontinental sized fracture systems detection 12 p2221 A70-26960

Pilot midair collision warning instrument based on optical radar MTI, discussing target cross section enhancement by passive retroreflector 12 p2234 A70-27646

Image processing and picture enhancement by computer, using fast binary log-antilog conversion 15 p2768 A70-32567

Radiograph images digital processing by linear and nonlinear position invariant techniques, obtaining contrast enhancement 15 p2706 A70-32569

Apollo black and white TV scan converter design and operation 17 p3095 A70-35636

Interferometric holograms of vibrating body via numerical analysis of oscillations amplitude and phases 18 p3258 A70-36303

Holographic velocity data recording /velocimetry/, discussing axial resolution enhancement by spherical wave illumination 19 p3423 A70-37859

Photographic processing methods for high efficiency low noise phase holograms on silver halide emulsions 22 p4025 A70-42286

Holographic exposure and reconstruction processes, considering illumination beam polarization effects on image brightness 22 p4040 A70-43616

Photographic image deblurring method, using image forming holograph and amplitude weighting transparency 22 p4042 A70-43670

Picture transmitting systems noise rejection enhancement via redundancy, discussing video coding and decoding and signal filtration 23 p4159 A70-43760

Degraded photographic image enhancement limitations due to film grain noise 23 p4193 A70-43820

Light scatterers use behind phase object in double exposure holography, determining laser radiation wave front dynamics effect on image quality 24 p4334 A70-45461

Monochrome radiography for contrast strengthening to increase color images detectability by human eye 24 p4337 A70-45708

Image contrast enhancement on neutron radiograph by energy tailored beams 24 p4376 A70-45748

IMAGE FILTERS

Blurred photographic image restoration by combining computer generated holographic phase and photographic amplitude filters 12 p2230 A70-26981

Auxiliary minus-visual filters in high altitude IR aerial color photography, suggesting tests for film sensitometric properties

14 p2588 A70-31235

Orion Nebula photographed at H alpha line with half angstrom filter

15 p2807 A70-32805

International photographic planetary patrol network, discussing filmstrips of Mars and Jupiter using blue, green and red filters

23 p4242 A70-44262

IMAGE INTENSIFIERS

NT IMAGE ORTHICONS

Image intensifiers to improve telescope system sensitivity and spectral resolution in radiometric measurements of reentry vehicles

03 p0489 A70-13654

Automatic photo-optical technique for processing of cineangiograms to find time-course history of left ventricular volume

04 p0641 A70-14559

Optical performance of image intensifier system with good resolution for exposure times down to 1 nsec

04 p0695 A70-15568

Photographic film imagery, degraded by long term artificial atmospheric turbulence, restored by spatial filters placed in Fourier transform plane

07 p1336 A70-20090

Electron camera with two stage image intensifier control electrode tube for rapidly evolving and slightly luminous phenomena, discussing exposure times

14 p2590 A70-31406

Electronic zoom for low light level TV sensor employing electrostatic image intensifier coupled optically to SEC camera tube

16 p2903 A70-33128

INTIC tube memory image intensifier with contrast enhancement, describing design and performance

16 p2880 A70-34269

Image intensifier apparatus photographing nuclear electromagnetic cascades in ionization spectrometer

18 p3261 A70-37091

Magnetically focused two and four stage cascade picture amplifiers for astronomy and nuclear physics applications

20 p3630 A70-39426

Image intensifier systems for direct view radiological systems

22 p4028 A70-42589

Phosphor-output image intensifier response to single photon inputs in multichannel spectrophotometer for faint optical sources

23 p4195 A70-44291

IMAGE MOTION COMPENSATION

Image processing for motion blur removal, discussing methods for measuring degradation and filter design for image restoration

09 p1688 A70-23773

Open loop TV image motion compensation by image transducer with gyro demodulator analyzing errors in rate and rate-integrating gyros and AC pick-offs

14 p2588 A70-31190

Atmospheric ground layer temperature variations effect on astronomical telescope observations, discussing image motion character and origin

15 p2772 A70-32462

Spaceborne narrow band TV system with image memory tube and electronic shutter, noting variable exposure time, motion compensation and multimode scanning

17 p3089 A70-35267

Quantitative measurement of solar limb image motion and blurring, noting role of telescope aperture

20 p3634 A70-40424

IMAGE ORTHICONS

Optimum planetary image intensity at TV camera cathodes, exemplifying with Saturn orthicon image

04 p0688 A70-14694

Image orthicon in high precision astronomical camera, evaluating geometric accuracy and stability by distortion measurement

21 p3822 A70-40819

Meteorological TV imaging systems development in last decade, including low and synchronous altitude camera, sensors, orthicons, etc

23 p4193 A70-43963

Image orthicon detection and recording system adapted for spectroscopic measurements in shock tube emission studies

23 p4197 A70-44469

IMAGE TRANSDUCERS

Integrated image sensor matrix array derived from equivalent circuit to minimize sneak path effects

10 p1854 A70-23879

Thermal transducer for rapid nondestructive testing, discussing imaging of specimen bond defects and thermal property differences

10 p1894 A70-24173

High speed thermal transducer for imaging bond defects and thermal property differences within test specimens during nondestructive tests

13 p2420 A70-29244

Open loop TV image motion compensation by image transducer with gyro demodulator analyzing errors in rate and rate-integrating gyros and AC pick-offs

14 p2588 A70-31190

Semiconductor image detectors in photodiode and photoconductor forms, describing construction and operation modes

15 p2714 A70-32673

Optimal perturbation signal waveform linearizing nonlinear transfer characteristic of image sensing receptor array

15 p2705 A70-32725

Hybrid solid state image detectors, discussing integration and excitation storage operation modes

17 p3053 A70-35122

IMAGE TUBES

Electron image projection tube for fabricating integrated circuits of micron size transistors

03 p0458 A70-14027

Broadband image pick-up tube with high near IR sensitivity, comparing performance with other vidicons

16 p2907 A70-33186

Space radiation effects on secondary electron conduction /SEC/ image tube performance, observing temporary degradation and permanent damage

16 p2878 A70-33433

Metal grid capacitive memory for INTIC and direct view storage tubes, describing image contrast control

16 p2880 A70-34270

Image tube observations of Large and Small Magellanic Clouds and southern planetary nebulae at Cerro Tololo Observatory

20 p3705 A70-39480

Astronomical instrumentation and methods in different nations, emphasizing photoelectric image receivers

23 p4199 A70-45033

IMAGE VELOCITY SENSORS

Airborne electro-optical imaging sensor subsystems performance optimization, comparing mathematical and graphical methods for providing maximum SNR

16 p2906 A70-33172

IMAGERY

NT AERIAL PHOTOGRAPHY

NT ASTRONOMICAL PHOTOGRAPHY

NT AUTORADIOGRAPHY

NT CHRONOPHOTOGRAPHY

NT CINEMATOGRAPHY

NT CLOUD PHOTOGRAPHY

NT COLOR PHOTOGRAPHY

NT ELECTRO-OPTICAL PHOTOGRAPHY

NT HOLOGRAPHY

NT INFRARED IMAGERY

NT INFRARED PHOTOGRAPHY

NT LUNAR PHOTOGRAPHY

NT MICROWAVE PHOTOGRAPHY

NT PHOTOMICROGRAPHY

NT PHOTORECONNAISSANCE

NT RADAR IMAGERY

NT RADAR PHOTOGRAPHY

NT RADIOGRAPHY

NT REPRODUCTION [COPYING]

NT ROCKET-BORNE PHOTOGRAPHY

NT SATELLITE-BORNE PHOTOGRAPHY

NT SCHLIERN PHOTOGRAPHY

NT SHADOWGRAPH PHOTOGRAPHY

NT SPACEBORNE PHOTOGRAPHY

NT SPECTROHELIOGRAPHS

NT SPECTROPHOTOGRAPHY

NT STEREOGRAPHY

NT ULTRAVIOLET PHOTOMETRY

NT XEROGRAPHY

Diffraction limited resolution criteria for geoscene imagery

02 p0297 A70-11924

Imagery in medicine - Conference, Ann Arbor, May 1969

04 p0640 A70-14556

Earth resources satellite imagery processing techniques, discussing sensor and transmission link distortions, image quality and optical or digital approach

[ALAA PAPER 70-297] 09 p1677 A70-22852

Phobos image analysis on Mariner 7 frame 7F91, discussing surface darkness, limb profile and geometric albedo

13 p2492 A70-29266

Land use classification system of photointerpretation from remote sensor imagery

14 p2576 A70-30976

Human eye components as image forming system from model based on Gaussian optics, discussing pupil size and influences on visual acuity

23 p4144 A70-43818

IMAGES

NT AFTERIMAGES

NT IMAGE VELOCITY SENSORS

NT RETINAL IMAGES

Image memory in Papio hamadryas monkeys reacting to visual and flavor food stimuli

04 p0632 A70-15219

Photosensitivity and scanning of planar Si photodiode image detector arrays, using most ring counter and shift register

10 p1846 A70-23881

Automatic image interpretation and classification - Conference, Pisa-Tirrenia, Italy, August-September 1968

12 p2193 A70-28101

Automatic image interpretation and classification using two dimensional digital Fourier transforms

12 p2193 A70-28106

Image processing, considering sampled data methods applied to two dimensional data

12 p2193 A70-28107

Sufficient statistics for optimal correlation function in classifying optical images in pattern recognition, using permissible transformations

14 p2553 A70-30421

Close range atmospheric shape classification, using image recognition theory concepts

19 p3416 A70-38572

IMAGING TECHNIQUES

NT RADAR IMAGERY

Optical reconstruction of microwave holograms recorded by liquid crystal detectors, emphasizing dependence on IR heat bias provided by incandescent bulb

01 p0086 A70-10421

Dynamic shape recognition scheme with two dimensional image mapped by spatial integration onto one dimensional time varying function, discussing corner information preservation

01 p0033 A70-10496

Ultrasonic imaging of internal structure by Bragg diffraction, noting reflection and dark field extension and use for flaw detection and medical diagnostics

01 p0111 A70-10570

Real time recording and permanent display, using high power energy density focused Ar laser beam for ink transfer

01 p0111 A70-10782

Image quality effects on human performance in simulation, discussing time sharing strategies and task difficulty factors

01 p0036 A70-10809

Visual simulation limitations, discussing parallax error correction in display system, wraparound system, image generation, TV and motion picture film systems

01 p0036 A70-10813

Flying spot scanner design and performance to generate images for visual flight simulation

01 p0089 A70-10816

Flying spot scanners evaluation as image processing devices, discussing scan patterns effect on video signal

01 p0089 A70-10817

Ultrasonic imaging system for flaw detection, analyzing welds

01 p0104 A70-10881

Ultrasonic holography in nondestructive testing, discussing metal block with simulated defects

01 p0089 A70-10882

Holographic techniques for extended high resolution images with resolved elements less than 0.5 micron in image field of 10 cm or more

01 p0090 A70-10886

Birefringent lens producing spatially separated multiple images, discussing polarization control, thin crystalline lenses and electro-optic control

01 p0091 A70-10915

Optical spatial amplitude filtering techniques application to moire fringe patterns processing

01 p0058 A70-11060

Book on coherent optics and holography covering image restoration, holographic interferometry, lensless Fourier transform holography, etc

01 p0144 A70-11074

Ultrasonic image superposition technique for visualization of impact fractures in glass reinforced plastics

01 p0059 A70-11101

Diffraction limited resolution criteria for geoscene imagery

02 p0297 A70-11924

Alphanumeric label and vector scan converted bright display operation, characteristics and equipment, discussing line scanning method, visual storage, display phosphor problems, etc

02 p0256 A70-11974

Three dimensional picture of wave system of single headed spin detonation constructed by simultaneously considering wave mapping in real and hodograph planes

02 p0278 A70-12028

Man machine digital display low cost system for displaying black and white image data with gray levels, color image data and dot patterns

02 p0265 A70-12152

Photographic relief images with arbitrary profile produced by using image relief height as spatial frequency function

02 p0300 A70-12462

- Photographic negatives analysis, storage and reconstruction using facility permitting photography conditions simulation and computer image treatment
02 p0302 A70-12614
- Autostereoscopic display using vibrating vanifocal mirrors, including laboratory computer generated real time image and movie projection systems
02 p0302 A70-12631
- Image formation with partially coherent light, summarizing basic properties and diffraction theory of image formation
02 p0315 A70-12831
- RF holographic vision through rain, fog or darkness, discussing cholesterol ester-coated Mylar sheets and pyroelectric hot plates detectors and antenna sensory matrix
02 p0305 A70-12843
- Spatial registration of digitized multispectral video imagery obtained from multilens cameras, multichannel optical-mechanical line scanners and multiple TV camera systems
03 p0453 A70-13000
- Displacement interferograms and schlieren pictures of optical inhomogeneities in transparent media obtainable from single exposure hologram, using non-monochromatic and laser light for reconstruction
03 p0483 A70-13258
- Double exposure holograms in diffuse radiation used to reconstruct in white light interferogram images localized in hologram plane
03 p0483 A70-13259
- Rotating prism method for obtaining time correlation between streak photographs and characteristic waveforms of flash X ray discharges
03 p0492 A70-13762
- Real image holography of complex organism or body organs as teaching aid and research tool in medicine and biology
04 p0685 A70-14558
- Three dimensional X ray imaging technique from conventional radiograph set photoreduced and projected by special purpose imaging system
04 p0686 A70-14561
- Computer processing role in film scanning and digitizing for enhancing X ray and radioisotope scanner images in medical radiographs, discussing image noise reduction
04 p0654 A70-14562
- Computer method to combine autofluorescence data to produce three dimensional display of absorbed radioactive material from multiview images
04 p0686 A70-14563
- Holographic technique for transferring phase perturbation of subject waves onto spherical waves focusable through aperture and examinable by interferometric and schlieren methods
04 p0691 A70-15034
- Image formation from wave front sampling in holography by spatial filtering, comparing Monte Carlo sampling to spaced sampling
04 p0692 A70-15365
- Visual object images describable in terms of cross correlation functions without loss of information
04 p0662 A70-15437
- Optical, digital and hybrid image processing techniques with objectives of image enhancement and replacement
05 p0847 A70-16121
- Projection display methods using scanned and modulated multicolor laser beams, discussing beam generation, modulation and scanning
05 p0858 A70-16188
- Hologram constructed with microwaves with image reconstruction at optical wavelengths using laser
05 p0849 A70-16659
- Earth resources survey aircraft system producing optical spectrum imagery of continental U.S. with photometric and photogrammetric fidelity
05 p0850 A70-16686
- Imaging properties of parametric image converters, taking into account frequency doubling of brilliant object by self interaction within nonlinear material
05 p0852 A70-16991
- Image recognition problem analyzed by deterministic approach yielding criteria for operation of recognition algorithm
06 p1014 A70-17633
- Acoustic characteristics of high subsonic model cold jet using imaging technique and measurements of energy flux of flow, calculating energy flux from flow-field measurements
06 p1040 A70-18125
- Optical properties of Gabor holograms with pure reference beam, discussing image reconstruction using He-Ne laser
06 p1072 A70-18565
- Visual imaging systems for Mars orbiter compared for performance and interactions with mission and spacecraft design
07 p1280 A70-19230
- Book on holography principles and applications, discussing imaging properties, coherence, photographic emulsions, optical analog computers, etc
07 p1283 A70-19739
- Detector for focus assessment of laser on target, scanning image by fiber optics
07 p1302 A70-20089
- Aerial color photography, considering lens types, exposure, filters, films, etc
08 p1498 A70-21543
- Display devices using electrostatic forces, discussing electrostatic printing, magnetic display system, etc
08 p1499 A70-21686
- Interferograms taken by phase difference amplification technique with nonlinear hologram, considering amplified image accuracy
08 p1500 A70-21788
- Holographic image reconstruction analysis based on two beam interferometry by spatially incoherent light source, obtaining optical transfer function
08 p1514 A70-21790
- Small contrast objects detection by photographic technique, measuring gradients, granularity noise and density variations for emulsions
09 p1673 A70-22157
- Photographic image reconstruction of spatially incoherent illuminated object using twofold holography
09 p1675 A70-22486
- EROS program earth imaging models characteristics, describing airborne and spaceborne film return and global and geosynchronous space data transmission
09 p1678 A70-22889
- Parametric image transformation during sum frequency generation
09 p1636 A70-23134
- Digital image processing applied to picture generation, intensity and geometric manipulation, spatial frequency operations and image analysis
09 p1682 A70-23507
- Covert solid state imaging system applicability to totally dark laboratory environment
09 p1686 A70-23752
- Electro-optical autocollimating focus sensor for optical systems of high angular resolution, analyzing defocus detection and errors
09 p1687 A70-23764
- Duplex schlieren optical system with one channel for data recording and second channel for visual monitoring
09 p1687 A70-23766
- Textured gray-scale imagery by computer simulating lunar display
09 p1642 A70-23771
- Optical image processor using Fourier transform corrective function for image restoration
09 p1688 A70-23774
- Pulse-biased phototransistor imaging mosaics behavior measurement showing significant photovoltaic mode at high light levels
10 p1846 A70-23880
- Bragg diffraction imaging for sound fields visualization
10 p1893 A70-24170
- X ray laminography for nondestructive testing based on synchronous rotation of source, sample and image forming planes
10 p1895 A70-24577
- Swedish real time IR imaging system, discussing airborne applications in locating fresh water springs and defining irrigation patterns
10 p1879 A70-24743
- Lens aberrations compensations in partially coherent image holography
10 p1891 A70-24838
- Fisheye projection of undistorted images obtained by fisheye lenses onto spherical screen from spherical center for hemispheric display, minimal overhead occlusion, etc
10 p1892 A70-24951
- Hologram resolution and information storage along depth of reconstructed image related to maximum track density of bubble chamber
10 p1892 A70-25113
- Thermal imaging device adaptable to IR, microwave or ultrasound radiation, projecting image on heat sensitive surface
11 p2050 A70-25643
- Modified holographic technique for three dimensional display of X ray pictures
11 p2050 A70-25644
- Spatial and amplitude modulators for laser-photographic display system producing real time TV pictures or images
11 p2062 A70-25734
- Multispectral imaging from lander for Martian surface constituents discrimination
11 p2051 A70-26000
- Microwave illuminated aperture near radiation field mapped and processed for microwave hologram suitable for optical imaging for far field pattern simulation
11 p2051 A70-26025
- Satellite coherent side-looking imaging radars producing radar maps with photographic-type quality
11 p2005 A70-26038
- Photoelastic analysis using fringe multiplication instrument applied to two dimensional models under load and frozen stress slices
11 p2061 A70-26834
- Residential urban environment data extraction from high and low resolution images
12 p2216 A70-26907
- Urban development detection by remote sensing imagery of highway and rail linkage
12 p2216 A70-26908
- Blurred photographic image restoration by combining computer generated holographic phase and photographic amplitude filters
12 p2230 A70-26981
- Brightness distribution in hologram generated image modulated by square of temporal-spatial coherence modulus of laser emitting longitudinal and transverse modes
12 p2233 A70-27503
- Terrain spectral imagery from satellites for natural resources investigations
12 p2235 A70-27745
- Relative control data incorporation into sequential or simultaneous analytical triangulation systems, considering extraterrestrial photographs reduction
12 p2308 A70-27875
- Coherent light holographic and incoherent interferometric imaging analogy, noting three dimensional image formation
12 p2236 A70-28120
- Mutual coherence functions for quasi-monochromatic illumination measured by image holography
12 p2237 A70-28124
- Wavefront reconstruction by holograms of focused images illuminated by white light, analyzing spatial coherence
13 p2408 A70-29364
- Three dimensional images reconstruction with coherent light, facilitating transmission by holographic information volume reduction
14 p2581 A70-30146
- Soviet papers on image recognition covering sequential optimization, self learning processes, transformations statistics, spatial discretization, optical information processing, etc
14 p2552 A70-30418
- Maximum convergence function in image recognition using dynamic programming and sequential optimization
14 p2553 A70-30419
- Learning self learning relationship in image recognition, analyzing resolving function with minimum probability for erroneous recognition
14 p2553 A70-30420
- Standard pattern recognition with spatial discretization, concerning discrete cell or segment viewing
14 p2553 A70-30422
- Computerized control for beam scanning and optical data processing concerning symbols, letters and photographic images
14 p2553 A70-30424
- Essa 7, Surveyor 7 and Mariner 4 space TV systems geometric distortions analysis and potentials in analytic photogrammetry and topographical mapping
14 p2586 A70-30982
- Ultrahigh speed photographic equipment with electronic systems, investigating integral images and slit cameras
14 p2589 A70-31401
- Three dimensional holographic optical imaging system, examining resolution factors
15 p2734 A70-31595
- Hologram superposition on photosensitive surface for multiimage successive recording, examining resolution, SNR, etc
15 p2734 A70-31596
- Holographic technique to record hypervelocity projectile with front light resolution, discussing image blurring
15 p2736 A70-32031
- Solar catadioptric coronagraph design free from chromatic image defects
15 p2737 A70-32041
- Holography technique for dual real images reconstruction of transparent objects with all planes in focus
15 p2738 A70-32053
- Holography without reference waves, describing image characteristics of spherical waves from point source
15 p2743 A70-32893
- Imaging type electro-optical detection systems design for passive night surveillance, building camera system and testing in helicopters and fixed wing aircraft
16 p2903 A70-33127
- Surface temperature colour contour maps of objects undergoing aerodynamic testing, utilizing electro-optical and computer techniques
16 p2905 A70-33169
- Instrument for visualization of EM field in open resonators in mm range
16 p2908 A70-33213

TV experiment for Mariner Mars 1971 Project, providing fixed and variable feature imaging data

16 p2978 A70-34027

Optical images from microwave far field /Fourier transform/ holograms, noting carrier fringe dependence

16 p2913 A70-34043

Earth resources technology satellite /ERTS-A/ for Eros program, producing telemetric imagery spatially correlated to earth surface

16 p2898 A70-34046

TV photograph image instability of stars, developing discontinuity and variability criteria as elementary approximate method for comparing nonuniformities

16 p2979 A70-34177

Solar limb image vibrations, establishing quantitative comparisons between statistical characteristics of fluctuations and weather conditions on propagation path

16 p2979 A70-34179

Reflecting prism standards rotations effect on autocollimated images positions of optical instruments, investigating focusing method

16 p2915 A70-34214

Hologram image construction by graphical method

16 p2915 A70-34216

Image distortion in reconstructions from phase only holograms, noting savings in collection and processing of acoustic holographic data

16 p2915 A70-34324

Human lung internal surface area automated measurement by computerized image processing techniques, grading emphysema

17 p3035 A70-34578

Computer generated holograms, using binary transmittance for wave fronts and three dimensional images construction

17 p3085 A70-35006

Partial coherence theory in holography with photogrammetry applications, reconstructing images with fringes representing constant range contours

17 p3087 A70-35023

Photographic and multisensor imagery augmented by field survey for mapping vegetation boundaries and density differences within and between plant communities

17 p3079 A70-35616

Observation classification /image identification/ for two normal sets with common covariance matrix, investigating error probability asymptotic behavior

19 p3375 A70-37283

Acoustical holography forming optical wavefield analog for nondestructive testing, medical diagnosis, underwater and seismic imaging

19 p3425 A70-37887

Bubble chamber photography and track image reconstruction by holography, discussing measurement apparatus, accuracy and tolerances

19 p3428 A70-38510

Holographic ultrasonic imager using liquid surface detector for real time imaging of test objects moving through viewfield, discussing nondestructive test applications

19 p3433 A70-38829

Earth resources satellite orbits and imaging sensors, discussing multispectral spin scanner design

20 p3626 A70-39053

Earth resources ground data processing in image formats from sensors in aerospace platforms, discussing collection control, image storage, retrieval, etc

20 p3591 A70-39058

Holographic bandwidth reduction by periodic dispersion structures, noting large viewfield and compact data recording

20 p3627 A70-39096

Diffraction-limited scalar image formation with large angle point reference hologram arrangement of arbitrary surface shape, point reference source and object

20 p3628 A70-39131

Microwave hologram recording for surface displacement, with laser beam illumination for optical reconstruction of image

20 p3628 A70-39152

Photographic images formation mechanism, examining streaks resolving power and total densities

20 p3632 A70-39747

Optical image hologram production, investigating gas flows around body by means of Mach-Zehnder interferometer

20 p3633 A70-39761

Holographic recording in transparent bodies with optical characteristics changeable under intensive light

20 p3633 A70-39999

Lunar and earth surfaces imaging for astronaut training in LEM simulator

20 p3607 A70-40320

Holographic measurement of general forms of motion based on reconstructed images dependence on coherence

21 p3822 A70-40810

Holography application to marine ecological studies, using laser beam reduction techniques for image

recording and reconstruction of large areas and volumes

21 p3823 A70-40821

Field-ion microscope image formation, determining periodic surface potential variation effects on high field tunneling

21 p3862 A70-40974

Two dimensional data array contour tracing algorithm for reduction of image coding bits number

21 p3786 A70-41327

EROS program earth imaging models characteristics, describing airborne and spaceborne film return and global and geosynchronous space data transmission

[AIAA PAPER 70-294]

21 p3829 A70-41871

High velocity source and receiver scanning effect on holographic image, observing rotation and distortion

21 p3829 A70-41928

Diffraction theory of sideband holography with transmission objects, discussing geometrical construction of image location and disappearance conditions

21 p3830 A70-41998

Detonation front position determination in explosive by photoelectric technique

22 p4121 A70-42341

Ultrasonic imaging systems of nondestructive testing, discussing photographic and chemical systems, thermal, optical and mechanical methods and electronic systems

22 p4027 A70-42584

Neutron radiography in cold, resonance or epithermal, and fast neutron energy ranges, discussing converter materials for direct exposure or transfer method

22 p4028 A70-42590

Electron pulse generator for imaging of glass microspheres simulating meteorite flight and impact in evacuated vessel

[SMPT PREPRINT 96]

22 p4036 A70-43059

High speed holographic methods for supersonic phase objects movement and replacement of conventional optical processes in shock tubes, firing tunnels, etc

[SMPT PREPRINT 77]

22 p4037 A70-43067

Recording of inhomogeneous mutual coherence functions in one hologram by combining image with Fourier /Fresnel/ holography

22 p4038 A70-43151

Ultrashort time perceiving electron-optical conversion methods, discussing image quality and brightness, quantum yield and time resolution

22 p4038 A70-43424

Nondestructive testing by ultrasonic acousto-optical imaging in opaque objects

22 p4047 A70-43518

Material transfer image recording using focused laser beam, discussing experimental setup and test results

22 p4040 A70-43605

Transparent objects holographic interferometry with illumination derived from phase gratings to eliminate laser speckle

22 p4040 A70-43611

Photographic image deblurring method, using image forming holograph and amplitude weighting transparency

22 p4042 A70-43670

Line-by-line and two dimensional image processing performance, considering transmission rates and distortion

23 p4160 A70-43762

Holographic primary and conjugate images properties, considering applications in moving scenes recording and multiple images storage and retrieval

23 p4193 A70-43924

Three dimensional holographic optical imaging system, examining resolution factors

23 p4195 A70-44279

Hologram superposition on photosensitive surface for multiimage successive recording, examining resolution, SNR, etc

23 p4195 A70-44280

Automatic shutter for recording holograms with laser light, controlling exposure time by photoconductor cell

23 p4197 A70-44472

Focused image holographic interferometry by double exposure with reconstruction in white light applied to flat rotating subject

23 p4199 A70-45058

High resolution upper photosphere images obtained by slow raster scanning device and germanium bolometer, noting points around sunspots

24 p4400 A70-45307

Image forming performance in photographic system design, considering Cobb chart resolution as figure of merit

24 p4334 A70-45449

Optical image reconstruction from holograms, discussing photographic materials resolution, response linearity, spatial noise, etc

24 p4335 A70-45654

Sideband Fresnel and lensless Fourier transform holographic images elongation and contraction

24 p4339 A70-45817

Acoustic holographic system producing two dimensional picture in real time, using stationary linear transducer arrays

24 p4339 A70-46080

Microminiature solid state LSI imaging system design, construction and performance characteristics

24 p4320 A70-46216

IMBEDDINGS [MATHEMATICS]

NT INVARIANT IMBEDDINGS

Computer-aided circuit design by imbedding singular elements to transform network synthesis into analysis problem

10 p1855 A70-24762

IMCC [CONTROL CENTER]

U INTEGRATED MISSION CONTROL CENTER

IMIDES

N-substituted tetrabromophthalimides prepared as fire retardant additives to PVC, polyester and epoxy resins

05 p0811 A70-16585

Glutethimide and aminoglutethimide reversible inhibitory effect on rat pituitary adrenal system in response to stress

07 p1203 A70-18902

IMINES

Photoreaction produced N-cyclohexyldiphenylketenimine from cyclohexyl isocyanide and diphenyldiazomethane

17 p3042 A70-34820

Addition and hydrogenation reactions of azomethines in chemistry of carbon-nitrogen bond, emphasizing Schiff bases

20 p3582 A70-38978

IMMERSION

U SUBMERGING

IMMISCIBILITY

U SOLUBILITY

IMMITTANCE

U ELECTRICAL IMPEDANCE

IMMOBILIZATION

Hypokinesia effects on transversostriated muscle fibers of mice, noting changes in myofibrillar apparatus, mitochondria and sarcoplasm

04 p0629 A70-14569

Immobilization effects on alpha rhythm, locomotor coordination and visual alimentary motor reflexes of cats

04 p0629 A70-14570

Nontoxic method of immobilizing protozoan *Tetrahymena pyriformis* and bacterium *Escherichia coli* in acrylamide polymers, discussing microorganism viability

05 p0802 A70-16477

Physiological effects of prolonged human motor activity restriction, discussing oxygen transport system, work capacity relationships, body fluids volume and distribution, metabolism, etc

07 p1200 A70-18786

Hypokinesia effects on cellular and humoral indices of antibody formation in rats, noting exposure time role

07 p1208 A70-19509

Monograph on directional hearing in meridian plane with head in fixed position, noting extended concept of sound

08 p1452 A70-21299

Hypokinesia effects on cellular and humoral indices of antibody formation in rats, noting exposure time role

11 p1988 A70-26108

Blood serum enzyme activity in rats during prolonged hypokinesia, noting increase of aminotransferases

13 p2351 A70-29329

Macroscopic architectural changes of cancellous and cortical bone in Rhesus monkey following long term immobilization and chemical removal of calcium

20 p3569 A70-38983

Weightlessness and immobilization effects on mechanical tolerance of bone compressive and breaking strength in monkeys

22 p3973 A70-43648

IMMUNITY

Serologic evidence of immune mechanisms, including heart muscle antibodies in patients with idiopathic cardiomyopathy, showing no autoimmune disease in majority

01 p0014 A70-10276

Autoimmunity to heart tissues in cardiac diseases, reviewing immune mechanisms in rheumatic fever, postcardiotomy and postinfarction syndromes

01 p0016 A70-10438

Mice and hamster infection resistance following short term acceleration stress, eliminating low hydrocortisone level as protective agent

03 p0428 A70-14067

Immunity indices in humans subjected to hypodynamia, noting infection resistance lowering

10 p1815 A70-24679

Hypothermia and ionizing radiation effects on hamsters influenza immune response

13 p2349 A70-28834

Hypobaric hypoxia effects on MM virus infection resistance in mice

20 p3572 A70-39428

- Mammal and human acoustic reflex for impulsive sound, investigating immunization effectiveness 24 p4297 A70-45373
- IMMUNOLOGY**
- Postnatal increase of immunologic competence to sheep RBC antigen in germ free and conventionally reared mice 01 p0000 A70-11310
- Natural immunity characteristics in dogs after proton exposure, analyzing integumentary bactericidal activity, oral microflora and neutrophil phagocytic activity 03 p0423 A70-13707
- Space cabin atmosphere effects on primary and secondary immunological responses in mice relative to spleen weight and antibody titers following antigenic stimulation 03 p0437 A70-14062
- Spacecraft cabin atmosphere effects on mice primary and secondary immunological responses relative to spleen histochemical and biochemical changes in enzyme activity 03 p0437 A70-14063
- Local stress effect on immunocompetent cells differentiation in guinea pigs lymphatic ganglia, noting increase in number of antibody producing cells 05 p0803 A70-17114
- Radial immunodiffusion for serum proteins quantitation adapted to capillary blood and compared with results for venous blood 07 p1214 A70-19932
- Idiopathic myocardial disease patients investigated for serological anomalies and markers of immunopathology 09 p1621 A70-23301
- Natural immunity characteristics in dogs after proton exposure, analyzing integumentary bactericidal activity, oral microflora and neutrophil phagocytic activity 11 p1985 A70-25507
- Amino acids changes distribution in specificity regions of light polypeptide chains of immunoglobulins showing correspondence with Poisson distribution 14 p2536 A70-30349
- Infection resistance during extended space flights, discussing microfloral exchange, defense mechanisms, waste, etc 15 p2688 A70-31677
- Antigens immunological response during myocardial infarction 20 p3570 A70-39151
- Mice immunobiological reactivity at simulated high altitude 20 p3575 A70-40189
- Human elbow induced forearm and hand vessels tachyphylaxis to angiotensin, noradrenaline and acetylcholine compared to vascular response of vasopresin 21 p3761 A70-40577
- IMP**
- Interplanetary medium energetic electrons and isotopes measurement, discussing spectrometer electronics of IMP H and J 21 p3825 A70-41000
- IMP-D**
- U EXPLORER 33 SATELLITE
- IMP-E**
- U IMP
- IMPACT**
- NT ELECTRON IMPACT
- NT HYPERVELOCITY IMPACT
- NT ION IMPACT
- NT POINT IMPACT
- NT PROTON IMPACT
- Soviet monograph on theory and calculations of impact systems covering solid body collisions, elasticity, wave mechanics and nonflat rod applications 07 p1400 A70-18732
- Metal probes friction coefficient and impact temperature during impingement onto rotating chromium steel disk related to speed under various atmospheres 09 p1708 A70-23425
- Nonlunar origin of tektites indicated from molten glass dispersion generated by terrestrial crater-forming meteorite impact 12 p2302 A70-27584
- Dissection techniques for measuring dynamic parameters of debris clouds expanding from energetic events 14 p2584 A70-30510
- IMPACT ACCELERATION**
- Plane exponential reactive shock waves following piston impact on gamma-law gas solved by similarity method, including Whitham conditions and shock acceleration 10 p1967 A70-24194
- Impact accelerations measurement for shock pulse amplitude and duration, describing system for direct reading 11 p2055 A70-26447
- Maximum impact accelerations of spherical and conical bodies landing on water, using momentum theorem 15 p2722 A70-32524
- Point accelerations on semirigid body spacecraft from accelerometer data with structural vibration noise at landing 23 p4200 A70-44387
- IMPACT DAMAGE**
- NT METEORITIC DAMAGE
- NT RAIN IMPACT DAMAGE
- Slopes distribution over finite span on planetary surface excavated by primary impact craters, including typical lunar mare crater densities 01 p0178 A70-10443
- Bird impact damage effect on aircraft structural design, considering forward facing areas and minimum weight 01 p0200 A70-10687
- High speed hail impact damage on flat Al alloy plates observed for effects of impact angle and velocity, plate material properties and thickness 01 p0056 A70-10690
- Ultrasonic image superposition technique for visualization of impact fractures in glass reinforced plastics 01 p0059 A70-11011
- Aircraft structural damage due to high speed hail-stone impact, considering aircraft design modifications 02 p0386 A70-11938
- Angle of incidence effect on oblique impact crater formed by high speed solid spherical particles colliding with massive lead targets 03 p0592 A70-13449
- Materials science experimental and diagnostic phases in mechanisms of metal erosion by impacting dust particles 04 p0704 A70-14760
- [ASME PAPER 69-WA/MET-8] Metals, plastics and ceramic materials under erosion by irregular quartz particles, using vacuum whirling arm 04 p0704 A70-14762
- [ASME PAPER 69-WA/MET-6] Postdamage structural analysis based on Hardy-Cross method, describing mathematical techniques 04 p0776 A70-15391
- Single impact data considered ineffective in estimating target damage induced by micron-sized particle cloud impingement 04 p0737 A70-15425
- Solid surface-compressible liquid drop high speed impact damage, discussing contact pressure 06 p1053 A70-18611
- Sand erosion of metals and plastics, discussing effects of impact conditions and impacting particles and target surface properties 07 p1314 A70-20004
- Metal erosion under liquid drop impingement attack, investigating damage from microplastic deformation to surface material removal using wheel and jet apparatus 08 p1519 A70-21354
- Steel balls impact on polyurethane foam, porous rubber and fiber materials, noting effects on both pellets and targets 09 p1769 A70-22123
- Satellite impact interpretation of lunar maria surface distribution, discussing lava origins and mascon distribution 09 p1752 A70-22310
- Impact crater cross section in fused silica, describing photomicrographic technique for distinguishing hypervelocity from low energy impacts 11 p2138 A70-26133
- [AIAA PAPER 69-367] Aircraft impact against nuclear containment vessel and associated structures for dangers in aircraft-nuclear power station collisions 11 p2144 A70-26683
- Serra de Mage meteorite impact history from charge particle track analysis, noting feldspar content 13 p2497 A70-29854
- Hypervelocity impact dynamics on copper cube targets imbedded with nickel wires, discussing terminal positions, Vickers hardness, flow fields, etc 14 p2657 A70-30765
- [AIAA PAPER 69-368] Damage mechanisms of hypervelocity projectile impact on thin targets and spacecraft shields 15 p2823 A70-32786
- Hypervelocity impact damage on complex targets, considering spacecraft and missile design 15 p2824 A70-32791
- Lunar dimple craters formation by meteoritic erosion of concentric impact craters 15 p2807 A70-32850
- Flight loads data extraction and analysis from damaged magnetic tapes after aircraft crash 17 p3094 A70-35518
- Characteristic injuries from aircraft controls inflicted in fatal accidents, showing pilot position and hand location upon impact 17 p3039 A70-35573
- Erosion by solid particles, discussing impacting velocity effects, natural sand quartz particle size distribution and composition, artificial industrial abrasives, etc 17 p3126 A70-35600
- Natural thermoluminescence of limestone within/near Charlevoix meteorite impact structure, discussing impact effects on quartz-rich rocks 18 p3314 A70-36499
- Pyrex spheres accelerated to 15 km/sec by plasma rail gun to study hypervelocity impact in twin stainless steel and Al targets 18 p3342 A70-36685
- [AIAA PAPER 69-378] Meteoroid impacts on Gemini spacecraft windows, calculating flux-mass relation 19 p3520 A70-38376
- Apollo 12 lunar module impact laboratory simulation, investigating possible downrange ballistic effects and cratering process 20 p3709 A70-39976
- Apollo 11 lunar rock and fines shock induced and melting microstructural mineral damage, discussing meteorite bombardment, phases without melting and microbreccia 21 p3902 A70-41550
- Lunar surface impact cratering, comparing equilibrium size distributions 21 p3919 A70-41701
- Small craters number density in southern lunar highlands, supporting Tycho Association cometary impact origin 21 p3920 A70-41882
- Circular cylindrical orthotropic fiberglass-reinforced shell buckling under longitudinal impact, assuming initial surface imperfections 22 p4117 A70-43347
- Damage data comparison for vibratory cavitation and liquid impact on aluminum alloy, stainless steels and pure nickel 23 p4203 A70-43870
- Soviet monograph on collision hazards between aircraft and birds covering accidents, damage and preventive measures 23 p4137 A70-44099
- IMPACT DECELERATION**
- U DECELERATION
- U IMPACT ACCELERATION
- IMPACT LOADS**
- Mathematical pendulum oscillations under clockwise and counterclockwise impact impulse, deriving differential equations describing trajectories 01 p0141 A70-10153
- Taylor model of elastoplastic wave interaction during cylindrical projectile impact 01 p0206 A70-11150
- Metallographic examination of impact induced deformation textures of Campo del Cielo iron meteorite, analyzing phase homogeneity, microstructures and shock intensity 02 p0377 A70-12511
- Fiberglass reinforced textile fatigue characteristics under impact tensile loads, noting different characteristics under cyclic sinusoidal loads 02 p0323 A70-12815
- Simultaneous equations of longitudinal impact bending, introducing temporal and spatial transformations regarding dispersive wave characteristics in elastic rod 03 p0591 A70-13428
- Thermal damping in gas-filled composite materials during impact loading due to heat transport, discussing role in impact energy dissipation 04 p0712 A70-14867
- [ASME PAPER 69-APM-V] Structural strength under impact loading with allowance for shock waves, comparing various strength calculation methods 04 p0774 A70-15098
- Dynamic plastic response of finite bar subject to axial impact load noting reflected waves, stress-strain-time histories and residual strain 04 p0779 A70-15599
- Differential equation for crack propagation applied to threshold conditions for brittle fracture caused by impulsive load 05 p0939 A70-16486
- Cylindrical shell walls vibrations under impact loads, calculating damping factor in differential equation of motion of wall element 05 p0947 A70-17008
- Fatigue defects accumulation in aluminum alloy under impact tensile loads programmed to simulate loads encountered by aircraft in practice 05 p0947 A70-17009
- Impact against elastoplastic blank allowing for base and striker compressibility, giving solution in region of plane wave first reflection from base 05 p0947 A70-17016
- Thin walled cylindrical shells design for axisymmetric impulsive loads, calculating strains due to explosive forming in water 06 p1167 A70-17867
- Cyclic plastic deformation changes with load increase under uniform stress with normal loading and nonuniform stress with impact loading, considering fatigue limit 06 p1168 A70-17923
- Rotational relaxation times for low density hypersonic nitrogen free jet, comparing measured and predicted impact pressures 06 p1043 A70-18279

Large Froude number solution for nonseparative impact of elliptical cylinder floating on incompressible fluid surface in half space extended to small Froude numbers
07 p1253 A70-18770

Membrane stress in thin circular viscoelastic ring under impulsive loads and internal heat, using stress-strain relation for linear Maxwell material model
08 p1589 A70-21311

Impact forces and specimen bending moments generated during dynamic test interpreted in terms of system dynamics and material fracture characteristics
08 p1518 A70-21319

Elastic post stability under longitudinal impact on rigid support, considering loading/unloading phases for calculating shock half wave length and critical rate
08 p1591 A70-21443

Steady state motion of sinusoidally excited primary system with impact damper solved analytically by piecewise linear technique
08 p1546 A70-21858

Dynamic buckling of thin circular ring subjected to radially directed impulsive load, investigating in-plane and out-of-plane modes
08 p1596 A70-21978

Finite plates impact flow field analysis from isentropic one dimensional flow equations solution through hodograph transformation
09 p1776 A70-22721

Elastic beam stability, natural frequencies and critical forces under longitudinal impact with nonuniform compressing force
09 p1780 A70-23116

Transition of stress distribution on collision surface of seminfinitesimal elastic plane with rigid beam, using Fredholm integral equation
10 p1954 A70-23950

Aircraft arresting hook response to impact regarding beam flexibility and internal damping using numerical wave propagation methods
10 p1963 A70-25069

Gas-filled composites under impact loading, studying thermal damping due to heat transfer between compressed gas and solid structure
11 p2140 A70-26480

Reaction impulse during steel spheres impacts at lead surface in vacuum dependent on kinetic energy, velocity and spheres material
11 p2146 A70-26794

Seismic echo produced by jettisoned Apollo 12 S-4B stage impact at lunar surface analyzed by multiscatter scattering theory
12 p2298 A70-27280

Euler-Bernoulli and Timoshenko beam impact models compared for case of finite beam resting on spring supports
12 p2327 A70-27843

Missile impact and trajectory for water entry with zero angle of attack, including deceleration measuring instrumentation
[AIAA PAPER 70-531] 13 p2387 A70-29039

Jet collisions solutions for impact of pin at obstacle, solid body impact at surface, cylindrical shells longitudinal impact and jets interactions
13 p2453 A70-29771

Flight Impact Simulator for simulating bird strikes and bird-proofing of aircraft
16 p2888 A70-33290

One dimensional analysis of stress and strain concentration resulting from longitudinal impact of viscoelastic rods
17 p3185 A70-34965

Elastic and plastic cylindrical shells, investigating dynamic buckling under impulsive loads
18 p3338 A70-36436

Elastic systems impact buckling approximate solution by finite difference method
18 p3342 A70-36591

Strain transducer /optical diffraction grating/ for plastic wave propagation measurement along specimens subjected to impact
19 p3425 A70-37884

Nonlinear stress-strain model of unloading in symmetric longitudinal impact of two elastic-plastic bars, using numerical method
19 p3541 A70-38046

Passive shock isolation, describing environments, excitation types, equations of motion, etc
21 p3934 A70-40915

Bending stress at clamped support of impulsively loaded semiinfinite conical shell, obtaining formulas from perturbation theory
21 p3938 A70-41759

Seismic signal by Apollo 12 lunar module impact indicating deep layer of powder by signal propagation
21 p3920 A70-41894

Metal deforming machines permissible impact velocities determination
22 p4046 A70-42815

Transient elastic vibrations of air and liquid filled cylindrical shells under radial impact, using shadow-optical cinematography
[SMPT PREPRINT 107] 22 p4031 A70-43030

Rope transverse oscillations due to impact taking bending rigidity into account
24 p4424 A70-45627

IMPACT PREDICTION

Digital computer program /LANDIT/ for predicting structural impact response of axisymmetric landing vehicles consisting of rigid payload and crushable impact limiter system
02 p0380 A70-11945

Model for impact behavior of elastic body at elastic half space, measuring gas molecule impulse exchange at metal surfaces
06 p1171 A70-18260

Book on dynamics of mechanisms with elastic connections and impact systems covering differential and finite difference equations, equations of motion, friction effects, etc
08 p1502 A70-20753

Real time opto-triangulation by cinethedolites for data acquisition used in rocket impact prediction
09 p1640 A70-23779

Impact problems of slip clutch and beam scales dynamic characteristics simulation by 1130 CSMP /Continuous System Modeling Program/
10 p1860 A70-24653

Computational limitations of midcourse correction velocity for lunar impact trajectories, considering impact miss magnitude correction
11 p2109 A70-25955

Sounding rockets impact dispersion associated with wind measurement errors and thrust misalignments, discussing correction via reduced aerodynamic stability and initial rocket spin
13 p2503 A70-28677

Impact times measurement by photography, correlating projectile velocity with projectile-target distance
20 p3635 A70-40530

Apollo command module land impact capability, discussing impact dynamics, possible landing area, spacecraft structure, crew couch and strut attenuation system, etc
[AIAA PAPER 70-1165] 21 p3930 A70-41847

Spinal injury prediction during emergency ejection and crash impact protection research
23 p4153 A70-44489

Sounding rockets dispersion, considering deviations from predicted point of impact due to wind effects, thrust vector errors and manufacturing inaccuracies
23 p4262 A70-44845

Birdproofing aircraft research program using pneumatic cannon firing real and simulated bird carcasses
24 p4292 A70-46398

IMPACT PRESSURES

U IMPACT LOADS

IMPACT RESISTANCE

Digital computer program /LANDIT/ for predicting structural impact response of axisymmetric landing vehicles consisting of rigid payload and crushable impact limiter system
02 p0380 A70-11945

Bumper materials effect on two component hypervelocity impact shields performance, noting material density influence
[AIAA PAPER 69-379] 07 p1310 A70-19713

Austenization temperature, cooling rate and tempering conditions effect on steel castings structure, strength and impact properties
14 p2596 A70-30875

Conical pivot bearings for impact accelerations tolerance in space environments, discussing optimum dimensions and minimal torque design
16 p2923 A70-34164

Pressure distribution shock pattern and impact wave resistance in frictionless plane parallel and source shaped supersonic flow
18 p3207 A70-36385

High impact Ag-Zn cell design for space missions instrument package landing, considering heat sterilization and minimum operational capability
21 p3757 A70-41013

IMPACT SENSITIVITY

U IMPACT RESISTANCE

IMPACT STRENGTH

Microstructure and impact strength of welds of Cr-Mn steel containing nitrogen, observing grain growth dependence on nitrogen content
03 p0509 A70-13277

Structural strength under impact loading with allowance for shock waves, comparing various strength calculation methods
04 p0774 A70-15098

Matrix stiffened nickel-chromium welding products featuring high tensile strength at room and elevated temperatures and high impact strength at cryogenic temperatures
08 p1508 A70-21488

Cycloaliphatic epoxy resins tensile and impact strength improvement by modification with elastomeric materials, considering heat distortion temperature
16 p2936 A70-33359

Impact transition behavior and strength-toughness relation of high purity Ni maraging steels, noting intergranular fracture at grain boundaries
18 p3273 A70-36043

Boron-Al composite filament fracture behavior and postimpact tensile strength, examining shock loading and impact velocity effects
22 p4060 A70-43682

Full-swing and incremental Charpy impact and Izod tests for ceramic intrinsic impact strength
23 p4209 A70-43872

Mg addition effects on impact strength and micro structure of Al-Si-Cu alloys, using Charpy test and metallographic methods
24 p4363 A70-46196

IMPACT TESTING MACHINES

Shot delivery per second per unit area from ejector nozzle during shot peening, determining ideal delivery rates for shot of various sizes
07 p1291 A70-18830

Pneumatically operated lifting mechanism and fluidic control system added to Izod impact testing machine for automatic impact repetition, counting and stopping
11 p2034 A70-26837

Charpy impact test accuracy for model machine certification, discussing erroneously high test values
15 p2820 A70-32236

Drop-weight test machine evaluation taking into account operator, test machine, specimen thickness, notch type and strength level effects
15 p2759 A70-32241

Impact test machines, specimen design and energy measurement in dynamic test method for steel fracture strength
15 p2759 A70-32242

Gas gun and instrumentation for impact tests
18 p3238 A70-37090

Solid rocket fuels mechanical properties, using high speed pneumatic test machine and impact tensile tester
22 p4088 A70-42342

IMPACT TESTS

NT CHARPY IMPACT TEST

Hypervelocity impact of small different diameter right circular cylinders, describing launching method using light gas gun
03 p0583 A70-12918

Micrometeorite detection involving impact stress wave monitoring by strain gages embedded in viscoelastic plastic
03 p0487 A70-13573

Hypervelocity impact craters formed in low and variable strength laboratory materials to provide insight into formation mechanics and resultant structures of meteorite craters
03 p0603 A70-14349

Meteoroid impacts as sources of seismic energy on moon, using projectile impact coupling to seismic waves in vacuum chamber experiment
04 p0751 A70-15056

Plastic-viscoplastic bar wave propagation due to longitudinal impact, analyzing stress profiles to determine effect of strain rate
05 p0926 A70-15913

Hammer forces and specimen bending moment-time responses and fracture resistance during notched beam impact test
05 p0938 A70-16479

High velocity microparticle simulation techniques for studying properties, dynamics and origin of micrometeoroids, considering accelerators and impact results
[AIAA PAPER 70-30] 06 p1029 A70-18131

Diffused diaphragm pressure sensors in impact probes used in wind tunnel tests of dynamic response of supersonic air induction systems
06 p1074 A70-18605

Heat transfer during plane air jet impact into concave surface with parabolic profile, determining specific thermal fluxes by electrocalorimetry
07 p1189 A70-19810

Steel balls impact on polyurethane foam, porous rubber and fiber materials, noting effects on both pellets and targets
09 p1769 A70-22123

High speed instrumentation camera system for recording rapid motions during Apollo landing impact
09 p1688 A70-23770

Acoustic impact technique /AIT/ for aerospace structures nondestructive testing, describing theory, instrumentation and applications
10 p1894 A70-24175

Seismic analysis of lunar module impact and missile-earth impact, comparing recorded signal parameters
11 p2118 A70-26748

Maximum impact force and central deflection time function of transversely struck beam, assuming no reflected elastic wave effects on stresses
[DFVLR-SONDDR-48] 12 p2325 A70-27619

Penetration mechanics of multisheet structures based on discrete particle modeling of impact debris
[AIAA PAPER 69-371] 13 p2509 A70-28521

Hypervelocity impact dynamics on copper cube targets imbedded with nickel wires, discussing terminal positions, Vickers hardness, flow fields, etc
[AIAA PAPER 69-368] 14 p2657 A70-30765

- Severity comparisons of specified and actual impulse tests determining component reliability
14 p2563 A70-30867
- Microbial release from solid spacecraft materials after hard landings, testing survival during decontamination or terminal sterilization
15 p2688 A70-31664
- Vibration mode response and impact time sensitivity of mechanical impedance of human skull, relating head injury factors
15 p2682 A70-31934
- Impact testing of metals - ASTM Conference, Atlantic City, June 1969
15 p2758 A70-32232
- Inertial load-time effects in instrumented impact tests, showing corrections for bending stress and dynamic fracture toughness measurements
15 p2820 A70-32240
- Size effects on impact energy disposition in plastically deformed thick steel specimens at shelf temperature, using similitude laws
15 p2760 A70-32332
- Hypervelocity gas, electromagnetic, explosive drive and exploding wire accelerometers and high explosive, shaped charge, plasma drag and electrostatic accelerators for projectile impact studies
15 p2718 A70-32783
- Gas turbine aero engines damage due to bird strikes, emphasizing rig testing and simulation at first stage rotor blading
18 p3236 A70-35995
- Meteoritic dust collection in upper atmosphere by sounding rocket, discussing efficiency of sampling configurations for inertial impaction
18 p3316 A70-36768
- Heat transfer during plane air jet impact into concave surface with parabolic profile, determining specific thermal fluxes by electrocalorimetry
20 p3736 A70-39260
- Longitudinal tension impact tests on nylon tape and Apollo pilot parachute riser construction, determining wave propagation effects [AIAA PAPER 70-1182]
21 p3843 A70-41831
- High speed plasma jet propagation, obtaining time of arrival measurements, brightness temperature, pressure and impact data
22 p4012 A70-43014
- Birdproofing aircraft research program using pneumatic cannon firing real and simulated bird carcasses
24 p4292 A70-46398
- IMPACT TOLERANCES**
Analog simulation of elastic wave propagation in thick walled hollow circular cylinders to determine safe impact speed
17 p3185 A70-34964
- IMPACTORS**
Metal deforming machines permissible impact velocities determination
22 p4046 A70-42815
- IMPEDANCE**
NT ACOUSTIC IMPEDANCE
NT CONTACT RESISTANCE
NT ELECTRICAL IMPEDANCE
NT ELECTRICAL RESISTANCE
NT LC CIRCUITS
NT MECHANICAL IMPEDANCE
NT REACTANCE
NT RESPIRATORY IMPEDANCE
NT SKIN RESISTANCE
Open region waveguide radiation and scattering solved using impedance surfaces of related closed region convergence
09 p1640 A70-23807
- Electromagnetic plane wave oblique reflection from flat surface with spatially modulated surface impedance, computing wave spectrum
13 p2367 A70-29527
- One flow influence on another at two plane jets interaction zone, applying to proportional fluid amplifier inlet impedance calculation
15 p2720 A70-32020
- Dispersion equation for impedance elements periodic structures phase velocity calculation, discussing approximate solution methods
22 p3984 A70-42392
- Nonzero electron temperature effect on mutual impedance of quadrupole probe in hot isotropic plasma
22 p4080 A70-42720
- IMPEDANCE MATCHING**
Unconditional stability criterion of active two port in scattering and admittance matrix notation equivalent to conjugate matching for maximum power gain with part impedances
02 p0271 A70-12820
- Dispersion equation and coupling impedance of two dimensionally periodic slow wave structure of cellular cylinder type with parallel perpendicular diaphragms
03 p0456 A70-13438
- Man-machine systems design emphasizing impedance matching exemplified by visual approach landing [ASME PAPER 69-WA/GT-15]
04 p0642 A70-14856
- Multistage microwave transistor amplifiers design for 4 GHz band, describing poor input/output impedance matching solution
08 p1475 A70-21279
- Electric propulsion design, considering effects of weight, impedance matching, beam voltage regulation and operating point variations in formulating system mass and reliability
09 p1743 A70-23248
- Reactance filters for matching circuits design with optimum transforming performance
09 p1650 A70-23404
- Shock impedance definition consistent with acoustic limit, considering use of impedance mismatch to reduce sonic boom overpressure
10 p1805 A70-24522
- Mutual impedance coupling among minimum scattering antennas with electromagnetic properties expressed in terms of radiation patterns
12 p2198 A70-27956
- Mutual impedance between coplanar skew dipoles with arbitrary lengths and terminal positions, noting convenience for computer programming
16 p2861 A70-32970
- Wheatstone structure impedance bridges, describing balancing method in sinusoidal alternating regime
16 p2872 A70-33106
- Transmitter-antenna matching, using Pi-filter for resonance transformation
19 p3389 A70-38071
- Short cylindrical microwave antenna radiation directivity enhancement by optimum double impedance loading
20 p3599 A70-40318
- Mutual impedance of interacting dipoles at wedge tip, determining errors for short spacing distances
21 p3796 A70-40638
- Axial mode helical antenna design with built-in impedance transformer for airborne applications
21 p3796 A70-40758
- Transistorized IF amplifier output matching to long transmission line, deriving formulas for gain and pass-band over wide output impedance range
22 p3995 A70-42520
- Wideband TEM quarter wave microwave coupler with continuously variable coupling range, employing even and odd mode characteristic impedance levels change
24 p4318 A70-45215
- IMPEDANCE MEASUREMENTS**
Plasma density and electroacoustic resonance effects on coupled cylindrical antennas self and mutual impedances measured in Hg-arc discharge
01 p0050 A70-10461
- Probe impedance loss in cold magnetoplasma related to distribution of point charge potentials
02 p0346 A70-12124
- Transistor admittance and diffusion parameters in direct measurement with varying frequency, evaluating reliability
03 p0459 A70-14285
- Induced electromotive force method for determining impedance changes of monopole on base of large cone
06 p1019 A70-17558
- Slot line wavelength, impedance, transitions and tolerances measured at S band using different dielectric constant materials
08 p1475 A70-21282
- Reactive portion of mutual impedance of arbitrary antennas calculated from radiation patterns by interpolation method
09 p1648 A70-23162
- Electric bridge for measuring complex impedances and admittances in 60 kHz-30 MHz frequency range
09 p1650 A70-23402
- Transfer impedance measurement for HF quadrupole probe immersed in hot magnetoplasma
10 p1877 A70-24709
- Rectangular tolerancing of dipole impedance values scatter for random passive network samples
12 p2194 A70-26968
- Fluidic components downstream impedance calculation, using measured/monitored pressure ratio
14 p2534 A70-30680
- Phase errors of hydraulic input impedance of arterial bed due to proximal or distal pressure measurements
15 p2682 A70-31940
- Filter circuits composed of stripline resonators, determining input impedance and attenuation by digital computer
15 p2701 A70-32468
- Admittance measurements of rectangular or circular waveguide fed aperture antennas illuminating displaced metal plate
16 p2872 A70-32963
- Loaded resonant circular loop radiation field patterns table, determining load impedance for antenna design
16 p2872 A70-32971
- Avalanche diode transient temperature response, measuring thermal impedance under pulse bias conditions
16 p2878 A70-33695
- Transthoracic mutual impedance responses to lung ventilation, discussing spatial and temporal intravariability
17 p3035 A70-34576
- Complex impedance measurements for monopole antenna for electron densities in/out of OGO satellite wake in upper ionosphere
17 p3080 A70-35771
- Impedance measurements on microwave tripole antenna for circular polarization, including expressions for radiation pattern
19 p3388 A70-37868
- Antennas impedances in warm isotropic plasma, using hydrodynamic and kinetic /Vlasov/ equations
19 p3380 A70-38406
- Admittance matrix of microwave networks, referring to coaxial line-waveguide coupling through 3 kMc adapter
21 p3802 A70-42250
- Satellite-borne loop antenna resistive and reactive impedance measurements in topside ionosphere
22 p4019 A70-43112
- Automated high precision electrical resistance measuring system using digital computer control
24 p4334 A70-45384
- IMPEDANCE PROBES**
NT RADIO FREQUENCY IMPEDANCE PROBES
Collision and motion effect on rocket-borne quadrupole probe transfer impedance near lower hybrid resonance in ionosphere
13 p2371 A70-29919
- Electron density measurements in ionosphere along rocket trajectory, using sweep frequency RF impedance probe with guard ring
23 p4192 A70-44877
- IMPELLER BLADES**
U ROTOR BLADES (TURBOMACHINERY)
IMPELLERS
NT PUMP IMPELLERS
Axial flow turbine stator and impeller blade twist calculated from gas flow stage area diameter using continuity and vorticity equations
01 p0001 A70-10175
- Impeller elastic and elastoplastic strength of centrifugal supercharger with curved disks and radial blades, using variational method
01 p0211 A70-11417
- High hub/tip ratio centrifugal compressor with pipe and vane cascade diffusers for turbofan engines, determining impeller performance [ASME PAPER 69-WA/FE-28]
04 p0733 A70-14774
- Three dimensional incompressible turbulent boundary layer detachment on rotating blading of axial impellers
11 p1975 A70-25793
- Unsteady relative flow in centrifugal impeller passage running at part capacity and zero flow observed by hydrogen bubble flow visualization method [ASME PAPER 69-GT-35]
14 p2529 A70-31024
- Radial flow impellers design for maximum machine performance, using straight cascade characteristics
15 p2672 A70-31825
- Flow equations for flow field in entry to radial or mixed flow impellers of turbomachines [ASME PAPER 70-FE-36]
16 p2892 A70-33640
- Pure impulse principle applied to axial compressor impellers with high solidity high camber blades
18 p3301 A70-36647
- Forced vortex impeller in axial flow fan without inlet vanes, presenting lift and drag coefficients of blade sections, loss of head, etc
19 p3352 A70-38222
- Velocity distribution in boundary layer on thin rotating turbine blade of impeller driven at wind tunnel outlet, solving turbulent and laminar flows momentum equations
19 p3352 A70-38224
- IMPERFECTIONS**
U DEFECTS
IMPERMEABILITY
U PERMEABILITY
IMPINGEMENT
NT JET IMPINGEMENT
Single impact data considered ineffective in estimating target damage induced by micron-sized particle cloud impingement
04 p0737 A70-15425
- Predicted and measured low density plume impingement effects on loads and heat transfer compared on orbiting Saturn 5 with oxygen-hydrogen burner engine
04 p0737 A70-15430
- Free flow field from underexpanded rocket motor nozzle and impingement effects of pressure and heat transfer to flat plate [AIAA PAPER 69-568]
13 p2473 A70-28510
- IMPLANTATION**
Transducers for bioimplantable telemetry systems self used by nonhospitalized patients
13 p2357 A70-28816
- IMPLEMENTATION**
U PERFORMANCE
IMPREGNATING
Preimpregnated materials processing, discussing molding, resin-reinforcement, unidirectional materi-

als, ablative applications, mechanical data and air-frame uses

05 p0874 A70-16614

Low temperature oxide film effect on porous titanium carbide impregnation by liquid steel

07 p1311 A70-19805

Ti alloys thermoxidation impregnation with rarefied nitrogen and oxygen plasma, determining optimal gas pressure and temperature conditions and magnetic field frequency effects

17 p3101 A70-35391

Effective pores size, volume and surface area in refractory materials, using impregnation rate measurement

18 p3277 A70-36467

Wear resistant titanium carbide based cermet material production by impregnation techniques, discussing grain size and heat treatment effects

19 p3450 A70-37453

IMPULSE GENERATORS

Small rocket engines tailoff impulse and tailoff repeatability, comparing monopropellant hydrazine and storable bipropellant engines impulse data

[AIAA PAPER 70-674] 16 p2967 A70-33576

IMPULSE NOISE

U ELECTROMAGNETIC NOISE

IMPULSE TRANSFER ORBITS

U TRANSFER ORBITS

IMPULSES

Medium duration optimal rendezvous between near circular noncoplanar orbits with close orbital planes, analyzing six impulse solutions

[ONERA-TP-763] 03 p0571 A70-13639

Subjective measurement of sound level of impulses and pulses, investigating 1 kHz tone and selection of time length between sound events

05 p0882 A70-16344

Severity comparisons of specified and actual impulse tests determining component reliability

14 p2563 A70-30867

Hall generator measurement of impulse currents, noting error sources and compensation

16 p2900 A70-33072

Sandwich rings inplane transient response to concentrated radial impulsive loads based on Timoshenko type theory, noting dependence on extensional to shear stiffness ratio

16 p2993 A70-34093

Dynamical stresses in members and structures under impulsive loads, taking into account solid viscosities and frequencies effects

17 p3187 A70-34998

Energy and impulse tensor of nonviscous relativistic fluid, excluding sound velocity greater than light velocity

19 p3404 A70-37593

Automatic control system impulse response points identification by fast Fourier transform

19 p3393 A70-37852

IMPURITIES

Electric characteristics and impurity distribution in GaAs-Ge heterojunctions obtained by deposition on p-type Ge

01 p0155 A70-10143

Complex formation mechanisms and effects on impurity diffusion profiles in semiconductors

01 p0155 A70-10180

Critical impurity concentrations of He-Ne laser quenching determined with mass spectrometer, giving impurities molecular weight and ionization potential for input powers

01 p0110 A70-10491

Impurity diffusion in Ni using diffusion theory, considering activation energies for Mo and W

02 p0317 A70-12396

Phonon-photon scattering intensity and line shape used to study laser-excited impurity centers dynamic characteristics in stimulated induction regime

03 p0499 A70-13256

Contamination sources covering ball bearing contamination, relay contact failure, instrument window internal fogging, electronic circuit corrosion and air conditioning problems

05 p0809 A70-16712

Structure and interstitial impurities effects on Nb modulus of elasticity at normal and high temperatures, noting rolling

05 p0866 A70-17040

Impurities effect on grain boundaries composition and brittle fracture of metals

06 p1087 A70-17608

Kinetic theory of laser emission on band impurity transitions, noting spatial homogeneity effect on laser mode

07 p1299 A70-19852

Low temperature fuel cell materials impurity effects on catalyst poisoning, stressing sulfur elimination from rubber molding

10 p1832 A70-25043

Raman and IR spectrum analysis of polywater indicating impurities role in anomalous properties

11 p1994 A70-25655

Foreign gases effects on He-Ne lasers IR emission, describing quenching due to positive column electron temperature decrease

11 p2062 A70-25826

Interstitial and substitutional impurity effects on fracture strength, plastic properties and ductile-brittle transition temperature of vanadium determined from impact and tensile tests

11 p2066 A70-25913

Intense laser radiation effect on electrons interactions with acoustic and optical phonons and ionized impurities in semiconductors

12 p2246 A70-27360

Impurity centers thermal and autoionization and effective capture cross section dependent on free carrier concentration in GaAs under electric field, allowing for plasma shielding

12 p2285 A70-27361

Iron impurity energy level behavior in seminsulating GaAs from determining temperature dependences of Hall coefficient, resistivity, optical absorption and steady spectral photoconductivity

12 p2286 A70-27370

Carbon monoxide, carbon dioxide and oxygen impurities effects on threshold current and output power of HCN laser

12 p2249 A70-27648

Impurities and electrothermal instabilities effect on conductivity of two temperature nonequilibrium plasma

12 p2281 A70-27846

Energy resonances between laser levels of carbon dioxide and diatomic and triatomic molecular impurity species, discussing population inversion due to superelastic collisions

13 p2425 A70-28622

Grains impurities effect on interstellar extinction curve from graphite grain model, discussing dirty ice coatings

13 p2489 A70-28915

Hydrogen impurities anelastic relaxation effect on internal friction alpha peak in cold worked tantalum and niobium

13 p2435 A70-29350

Shock wave multiple ionization in hydrogen with impurities, discussing intensity and duration effects on electron temperature profile and ion concentrations

13 p2388 A70-29369

Impurities effects on UV absorption in semiconductors, deriving kinetic type equation for two particle Green function

13 p2471 A70-29511

Circulated air natural and technical impurities effects on gas turbine time dependent performance emphasizing erosion, deposits and overheating

13 p2475 A70-29713

Ionized impurity scattering in polar semiconductors by strong electric fields, using energy and momentum conservation equations in electron temperature approximation

13 p2472 A70-30017

Synthetic autoclave grown quartz crystals with W and Ga impurities, discussing spectral properties and weak absorption bands after irradiation

14 p2625 A70-30154

Gold impurity photovoltaic effect in silicon, determining optical cross section for transition

14 p2627 A70-30528

GaAs slices efficiency as transferred electron devices, correlating impurity profiles with microwave performance

15 p2708 A70-31957

Hydrogen effect on impurity redistribution in heteroepitaxial Si layers on sapphire substrate

15 p2785 A70-32529

Diffused p-n junction devices impurity profile from capacitance-voltage measurements

15 p2710 A70-32562

Fermi level for crystal with slowly changing impurity determinable by solving Poisson equation and by condition of electroneutrality

15 p2786 A70-32899

Heterodiffusion coefficients and activation energy for Cu, Ag and Au impurities in Al, using gamma spectrometry and X ray emission microanalysis

16 p2930 A70-33081

Impurities solubility in semiconducting indium telluride with stoichiometric vacancies, verifying thermodynamic model by phase diagrams

16 p2960 A70-33224

Fe and Al impurities in bis-ethylene chromium /BEC/ and in chromium films obtained by thermally induced decomposition of metal organic compound

18 p3297 A70-36463

Impurity distribution in diffused p-n junction in thin epitaxial film, calculating space charge region width and junction capacitance

20 p3685 A70-38967

Impurity dependent critical resolved shear stress of magnesium oxide single crystals, using compression testing

21 p3862 A70-41910

Impurities concentration estimate in metals by low temperature residual resistivity, investigating contact and contactless measurements

22 p4052 A70-42573

Stacking fault energy determination, discussing impurities influence in equilibrium dimensions distortion of extended nodes in titanium carbide

22 p4053 A70-42727

Boron impurities introduction into InP crystals grown by liquid encapsulation, detecting IR absorption bands due to localized lattice vibration

23 p4231 A70-44891

Monatomic crystal vibrational spectrum, noting quasi-local vibrations near high impurity concentrations

24 p4388 A70-45202

Mossbauer effect analysis of Fe impurity atoms in n- and p-type semiconductor compounds with wide and narrow forbidden gaps

24 p4388 A70-45204

Impurities and heat treatment effects on W internal friction at high temperatures, considering relaxation processes, recrystallization and microstructure

24 p4357 A70-45227

GaAs crystal surface Raman scattering from phosphorus impurities localized modes, using Ar ion laser line

24 p4391 A70-46255

IMPURITY

U PURITY

IN-FLIGHT MONITORING

In-flight compensation for space probe trajectory deviations, discussing attitude determination and control of triaxial and spin stabilized space probes

01 p0186 A70-11265

Integrity monitoring of redundant multiplex control systems for aircraft autoland operations, discussing Triplex autopilot

02 p0329 A70-11833

In-flight data acquisition systems to overcome manual methods limitations, discussing applications and system configuration

02 p0224 A70-11839

Radiation pyrometers development for in-flight measuring and controlling aircraft engine compressor blades temperature

03 p0480 A70-12900

In-flight radiometric calibration of low brightness OGO 4 airglow photometer

04 p0696 A70-15645

Automatic control of continuous medical monitoring in manned space flight

07 p1220 A70-19512

Self calibrating radiometer for in-flight measurement of earth surface thermal microwave radiation

07 p1282 A70-19616

Concorde electronics systems for testing and flight safety, controlling center of gravity, braking, kinetic heating, air conditioning, fuel flow and inertial navigation

07 p1194 A70-19741

MADAR onboard maintenance system designed for C-5 aircraft monitoring line replaceable units in electrical, avionics, environmental, mechanical and propulsion systems

07 p1195 A70-20375

Onboard integrated maintenance system for aircraft avionics in-flight subsystems monitoring

08 p1471 A70-20669

Onboard measurements of single engine propeller-driven aircraft performance, stability and control in nonsteady symmetric flight

08 p1438 A70-21869

Fighter aircraft inflight thrust control using thrust reverser technology to improve operational capability

09 p1610 A70-23019

Slip-ringless propeller blade mounted measurement system for steady state and vibratory stresses from multiple strain-gage locations during flight and ground tests

11 p2051 A70-25891

Aircraft performance, stability and control testing from nonsteady flight measurements, ascertaining repeatability of results

11 p1980 A70-25905

Automatic control of continuous medical monitoring in manned space flight

11 p1991 A70-26111

In-flight thrust measurement via internal gas generator and external traverse methods, discussing accuracy requirements, errors and aircraft design role

13 p2474 A70-28539

Aircraft equipment automatic test methods, comparing in-flight, on ground and second line testings

13 p2348 A70-29681

In-flight evaluation of selected aircraft pilots controllers, noting role in design

17 p3020 A70-35836

Avionics maintenance effectiveness logistics, discussing symptom pattern observation technique /SPOT/ for in-flight data

19 p3554 A70-38399

Aircraft landing maneuver optimization by in-flight monitoring of approach and landing phases, furnishing decision making display
[AIAA PAPER 70-1000] 20 p3560 A70-39531

In-flight thrust measurement methods on SERT 2 ion thrusters, using accelerometer, electrical parameters and orbit change
[AIAA PAPER 70-1126] 20 p3691 A70-40219

Airborne test computer for in-flight radar checkout featuring tape storage of computer program and cockpit mounted optical readout
22 p3993 A70-42320

Nondestructive tests for flaw detection during various aircraft production and operation phases
22 p4047 A70-43531

Astronaut biological parameters monitored under prolonged space flight conditions for rescue operations
23 p4146 A70-44678

IN-FLIGHT THRUST MEASUREMENT
U IN-FLIGHT MONITORING
U THRUST MEASUREMENT

INACTIVATION
U DEACTIVATION

INCANDESCENCE
Operation characteristics of flash, arc, incandescent and explosion type laser pump lamps
13 p2431 A70-29874

Electro-optical transducers based on photoconductive cells, phototransistors and microminiature incandescent and solid state light emitters
16 p2904 A70-33144

INCIDENCE
Angle of incidence effect on oblique impact crater formed by high speed solid spherical particles colliding with massive lead targets
03 p0592 A70-13449

Diffraction-field structure on two-element gratings in near zone, calculating amplitude, phase and energy flux for normal and slant incidence of EM fields
19 p3377 A70-37720

INCIDENT RADIATION
High intensity pulsed laser radiation scattering by free electrons, studying linearly polarized incident radiation
02 p0312 A70-12276

Measured heat flux conversion into average radiation incident on convex satellite surfaces in test chambers
03 p0606 A70-13536

Three dimensional characteristic of light scattered by lunar surface determined for various incidence angles and azimuths from Zond 3 photometric measurements
04 p0744 A70-14441

Azimuthal telescope for recording cosmic rays intensity, noting statistical error for vertical and oblique incident component
05 p0846 A70-15967

TEM wave reflection incident on conducting thin strips semiinfinite array in free space not accompanied by emission
05 p0812 A70-16243

Three dimensional electromagnetic scattering from thin walled conducting circular tube of finite length normally incident with E or H polarized plane wave
05 p0816 A70-16987

Transmission and reflection coefficients calculated for electromagnetic waves incident on inhomogeneous absorbing layer applicable to ionosphere, plasma and p-n junction
06 p1009 A70-17834

Ionospheric absorption at oblique incidence during IQSY, studying seasonal and diurnal variations as solar zenith angle function
06 p1009 A70-17905

Thermoluminescent glass X ray dosimeter sensitivity tested as function of rigidity of gamma and X radiation, noting compensating filters for incident radiation
08 p1496 A70-21217

Thermal radiation absorption in hemispherical cavity, determining apparent absorptivity for diffuse and parallel irradiation
09 p1790 A70-23565

Open region waveguide radiation and scattering solved using impedance surfaces of related closed region convergence
09 p1640 A70-23807

Energy spectra of electrons transmitted through Be, Al and Au targets measured for incident electron energy
10 p1918 A70-23984

Motion of incidence regions of X ray radiation in auroral zone using simultaneous balloon measurements
10 p1935 A70-25283

Topographic shadow linears image enhancement by low angle illumination, describing pseudoradar technique for subcontinental sized fracture systems detection
12 p2221 A70-26960

Radar look direction effects on geological features detectability, considering topographic relief and incidence angles roles in feature enhancement and suppression
12 p2221 A70-26962

Three dimensional characteristic of light scattered by lunar surface determined for various incidence angles and azimuths from Zond 3 photometric measurements
13 p2485 A70-28466

Meteor trail radiant, velocity and altitude measurement by obliquely incident radio waves
14 p2635 A70-30309

Sonic boom incident and ground reflected waves action on exterior wall, calculating arrival time as functions of aircraft speed and altitude and wall slope
14 p2566 A70-30861

Plane wave ray optical scattering by two spheres for arbitrary angle of incidence and observation, noting importance of first order interaction terms
14 p2551 A70-31157

Cosmic rays geomagnetic bending and effective angles of approach for various ground stations
14 p2633 A70-31313

Protective coatings for silicon photosensitive elements to reflect incident energy at wavelengths not participating in conversion into electricity
15 p2677 A70-31599

Backscattering, bistatic scattering and current distribution on thin wires during electromagnetic wave incidence
15 p2700 A70-32412

Plane wave random signals arrival angle maximum likelihood estimation for multiple antenna systems
15 p2704 A70-32594

Refractive index and group velocity in moving dispersive half space /cold plasma or dielectric/ under incident wave from vacuum
16 p2859 A70-32936

Attenuation, refraction and multiple reflection effects on light reflection from shock front at near grazing incidence
16 p2953 A70-34271

Optimum mounting angles for direct solar radiation flux on solar battery on circular orbit satellite
18 p3215 A70-36176

Crew radiation dosage from fission fragments in plume from gas core nuclear rocket
18 p3224 A70-36562

Ion temperatures and incident intensities in plasmas produced by solid target irradiation with Q switched laser beam
19 p3479 A70-37765

E and F region electron density response to incident radiation intensity on upper atmosphere during solar eclipses
19 p3419 A70-38916

Radiative transfer among surfaces forming long cavity exposed to collimated incident energy
21 p3944 A70-41022

Arbitrarily shaped cylindrical conducting structures with transient incident electromagnetic wave, calculating scattering from integral equation by digital computer
23 p4165 A70-44957

Two dimensional electromagnetic scattering body geometry reconstruction from given incident and scattered far field distributions
23 p4165 A70-44958

Two identical conducting thin cylinders illuminated by plane wave at arbitrary incidence angle, determining backscattering cross sections and induced current
24 p4314 A70-46133

INCINERATION
U INCINERATORS

INCINERATORS
Aerodynamic holder stabilized smoke flames to avoid intermittent flaming and thick puffs for incinerator air pollution reduction
21 p3942 A70-40887

INCLINATION
Critical inclination problem, discussing canonical variables and Bohlin Zeipel technique
14 p2639 A70-30707

INCLUSIONS
Thermal stresses of semiinfinite plate with circular hole filled with elastic inclusion and subjected to uniform heat flow
03 p0601 A70-14317

Mean acoustic force on small spherical and nonspherical inclusions in standing acoustic field, discussing equilibrium orientations of body
04 p0720 A70-15085

Stress distribution in long beams with circular annular inclusion under concentrated load solved in series form
05 p0928 A70-16024

Linear and nonlinear inelastic spherical inclusion in elastic and viscoelastic isotropic matrix with constant strain or stress fields at infinity
05 p0932 A70-16171

Three dimensional electrostriction theory for stress and displacement on penny-shaped crack in elastic dielectric with conducting oblate spheroidal inclusion
07 p1409 A70-19569

Thermoelastic state of plate near foreign circular inclusion, assuming heating by uniformly distributed sources and ideal plate-inclusion thermal contact
08 p1587 A70-21171

Nonmetallic inclusions effect on steels cyclic strength dependence on inclusion composition and metallic matrix properties derived from fatigue tests
08 p1590 A70-21413

Multiple scattering of plane time harmonic compressional elastic wave impinged on parallel circular cylindrical inclusions in finite domain, analyzing stress field
08 p1592 A70-21469

Carbonaceous material genesis in Tieschitz meteorite from electron microprobe analysis, discussing chondrule formation process residue likelihood
08 p1578 A70-21561

Temperature field in infinite plate with disk shaped inclusion and stationary point heat source determined, allowing for heat transfer conditions
09 p1778 A70-23082

Temperature fields and stress-strain state in elastic bodies with thin walled cylindrical shell inclusions during uniform heat flow at infinity
09 p1778 A70-23083

Stress-strain state analysis of transversely isotropic plates with inclusions under bending loads
09 p1782 A70-23298

Hyperelastic bodies containing finite number of inclusions and defects analyzed by continuous dynamic model
10 p1954 A70-24014

Elastic properties determined for reinforced composite material with hollow spherical inclusions embedded in matrix
11 p2136 A70-26083

Stress concentration around elastic spheroidal inclusions in isotropic elastic body under shear
11 p2140 A70-26483

Stress analysis of infinite elastic plate containing elastic rectangular inclusion subjected to uniform stress field
13 p2508 A70-28486

Weekeroo Station iron meteorite silicate inclusions chemical composition compared to chondrites
13 p2497 A70-29858

Isotropic slab with implanted elastic circular disk, analyzing stress-strain state due to torsional and bending moments
15 p2824 A70-32895

Rigid inclusion effect on stress distribution in isotropic infinite solid with Griffith crack under plane strain
16 p2994 A70-34250

Stress concentration around small elastic spherical inhomogeneous inclusion on circular cylinder in torsion
17 p3183 A70-34631

Bond stress distribution in elastic solid with axisymmetrical inclusions under uniform tension, using three function and point matching techniques
17 p3184 A70-34911

Circular inclusion interface separation in matrix under incident compressive waves interpreted for fiber reinforced composites
17 p3185 A70-34963

Quantitative analysis of nonmetallic inclusions in steels containing Ti after electrochemical anodic dissolution
18 p3277 A70-36464

Elastic bending of perforated inhomogeneous plane with circular holes or inclusions
18 p3340 A70-36579

Omnidirectional dynamic stress gauge as embedded elastic inclusion, discussing transient response to ground shock compression wave pressure
19 p3422 A70-37699

Elastic particulate composite solid with microinclusions, deriving dispersion relations governing plane longitudinal wave propagation modes by analogy with continuum theory
19 p3540 A70-37942

Stress concentrations due to cylindrical inclusions in homogeneous matrix, using stress function methods
20 p3656 A70-40045

Elastic and viscoelastic plates, calculating stress concentration and separation of embedded smooth circular inclusion under uniaxial tension
21 p3932 A70-40548

Lunar petrology of silicate melt inclusions from Apollo 11 rock samples, discussing heating experiments
21 p3902 A70-41548

Rigid circular cylindrical inclusion elastic bedding dynamic loading, calculating stresses in interface
22 p4112 A70-42345

Elastic wave diffraction by rigid inclusion, calculating far field displacement and cross section by integral equation method
22 p4073 A70-42636

Particle size, shape and absorptivity effects on inclusion damage of Nd-doped barium crown laser glass
22 p4050 A70-43007

Elastic plane equilibrium with thin walled flexible rectangular finite inclusion under symmetrical concentrated load, including computer calculated tangential stresses
22 p4118 A70-43569

INCOHERENCE

Photographic image reconstruction of spatially incoherent illuminated object using twofold holography
09 p1675 A70-22486

INCOHERENT SCATTERING

Pulse methods for measuring correlation function of incoherent scattered signal, calculating bit estimator errors for large and small SNR
01 p0045 A70-11088

Ionospheric measurements of electron density, electron and ion temperature profiles from strength of incoherent radio wave scattering
01 p0082 A70-11530

H-function integrals for noncoherent isotropic scattering for two level atom, tabulating numerical values for Lorentz scattering profile
09 p1727 A70-22506

Ionospheric parameters measurements by incoherent RF scattering, discussing current status of theory and observations
12 p2225 A70-27738

Incoherent scattering of radiation from collisionless plasma in quasi-stationary state, analyzing wave energy from spectral decomposition for given background distribution function
13 p2457 A70-28558

Electron beam interaction with plasma in absence of magnetic field, discussing microwave radiation emission and incoherent scattering and instability spatial growth
13 p2459 A70-28569

Incoherent scatter observations of atmospheric density and temperature in lower thermosphere, observing seasonal variations
14 p2578 A70-31246

Atomic oxygen density and temperature diurnal variation determination by F region incoherent scatter measurements, using nonlinear regression analysis
21 p3817 A70-41096

INCOMPRESSIBILITY

Nonlinear stress-strain equations for incompressible hyperelastic media developed for undeformed and deformed continuum states
01 p0201 A70-10892

Incompressible elastomer viscoelastic response to exponential extension ratio history in simple tension based on constitutive equations
01 p0201 A70-10893

Irrotational motions of relativistic ideal thermodynamic fluids fulfilling incompressibility conditions
01 p0063 A70-10948

Finite element method applications to finite axisymmetric deformations of incompressible elastic solids of revolution
13 p2510 A70-28734

Finite elements for three dimensional compressible and incompressible solid continua based on minimum potential energy and variational principles
14 p2659 A70-31128

Thermoelasticity of incompressible solids, integrating linearized equations using Helmholtz solution
14 p2660 A70-31224

Second order incompressible elastic torsion problems reduction to two dimensional classical linear elasticity problem without body force
17 p3189 A70-35434

Alfven waves synchrotron emission in incompressible medium, investigating generation by rotating DC current carrying circuit
21 p3861 A70-42227

Two incompressible isotropic nonlinear elastic solids mixture, investigating entropy production inequality effects
24 p4425 A70-45991

INCOMPRESSIBLE FLOW

NT STOKES FLOW

Boundary layer equations for plane steady incompressible flow, studying given velocity profiles effects on equations solutions
01 p0060 A70-10144

Finite element solution of incompressible lubrication problem by minimum principle for transient incompressible Reynolds equation with boundary conditions
[ASME PAPER 69-LUB-A] 01 p0100 A70-10378

Elongation and combined shear stresses in incompressible creeping plane flows of viscoelastic lubrication for squeeze-film bearings
[ASME PAPER 69-LUB-22] 01 p0101 A70-10385

Transient heat transfer near two dimensional stagnation point in viscous incompressible fluid steady flow
01 p0002 A70-10457

Parachute inflation dispersion studied by plotting dimensionless products characterizing incompressible flow process
01 p0006 A70-10849

Axisymmetric turbulent incompressible and isothermal self preserving jet investigation using linearized constant temperature hot-wire anemometers
01 p0065 A70-11099

Incompressible slow viscous nonNewtonian flow with free surface solved by finite element method,

showing computerized results for squeezed fluid between two plates
01 p0066 A70-11131

Incompressible turbulent boundary layer and separation flow into forward facing normal step, considering step heights and boundary layer thickness
01 p0066 A70-11133

Incompressible viscous fluid flow in contact with infinite plate and rotating in perpendicular magnetic field, obtaining flow characteristics by Laplace transform
01 p0067 A70-11138

Time dependent behavior of separated and unseparated unsteady flow of incompressible viscous and inviscid fluids without heat transfer
01 p0067 A70-11162

Parametric approximation method extended to incompressible laminar boundary layers with surface suction or injection
02 p0277 A70-11857

Isotropic incompressible three dimensional turbulence representation by wave vector scalar functions, discussing maximum functions number determination
02 p0277 A70-11878

Integral relations method efficiency and accuracy in solving incompressible turbulent boundary layer equations, noting acceptability for turbulent flows with small wake components
02 p0282 A70-12331

Extended mixing length method for computing turbulent shear stress distribution required in calculating two dimensional incompressible turbulent boundary layer
02 p0282 A70-12333

Boussinesq eddy viscosity concept solving equations of two dimensional incompressible turbulent boundary layer, using implicit five point finite difference method
02 p0285 A70-12350

Axial flow reversal in swirling incompressible tube flow, discussing static pressure, velocity profiles and turbulent Navier-Stokes equation
03 p0465 A70-13017

Axisymmetric incompressible fluid flow aerodynamic properties in flat vortex chamber, studying core and boundary layer interactions and velocity fields
03 p0551 A70-13731

Incompressible viscous fluid rectilinear flow along arbitrary cross section duct under pressure gradients oscillating at large frequencies
03 p0468 A70-14147

Surface singularities method for calculating incompressible potential flow about bodies of revolution with arbitrary thickness ratio and angle of attack
03 p0410 A70-14322

Boundary layer equations for axial laminar and turbulent incompressible flows over slender bodies of revolution solved by finite difference method
[ASME PAPER 69-WA/FE-2] 04 p0667 A70-14786

Incompressible laminar Falkner-Skan boundary layer suffering sudden acceleration by moving belt, noting boundary layer separation
[AIAA PAPER 69-40] 04 p0674 A70-15534

Incompressible two dimensional time dependent Navier-Stokes equations for oscillating body with rectangular boundaries
[AIAA PAPER 69-185] 04 p0779 A70-15616

Closed form solutions describing nonlinear motions of incompressible fluid flowing in thin walled tube buckled by uniform external pressure
05 p0832 A70-16090

Compressible fluid flow satisfying perfect gas equation in presence of thin foil, developing operators characterizing incompressible and compressible flows without Hall effect
05 p0790 A70-16158

Incompressible two dimensional turbulent boundary layer equations with arbitrary pressure distribution solved by weighted residual method
[AIAA PAPER 69-397] 06 p1032 A70-17214

Separated incompressible flow around wing profile, considering calculation of separated potential flow generation with given separation point
06 p0966 A70-17253

Lift and vortex drag due to flaps on thin sweptback tapered wings in inviscid incompressible flow, obtaining spanwise loadings
06 p0967 A70-17256

Viscous core of incompressible swirling flow through nozzle using momentum-integral equations
[AIAA PAPER 70-51] 06 p1038 A70-18079

Finite difference solution of time dependent Navier-Stokes equations for two and three dimensional laminar incompressible flow, discussing results for flat plates
[AIAA PAPER 70-46] 06 p1041 A70-18170

Tangent plane method and polar coordinates for lifting surfaces, calculating normal velocity at field point on surface carrying doublet distribution for incompressible flow
[AIAA PAPER 70-78] 06 p0975 A70-18195

Incompressible flow past airfoils with oscillating jet flaps used as rapid lift and momentum generators in aircraft gust load alleviation and mode stabilization
[AIAA PAPER 70-79] 06 p0975 A70-18196

Dynamic characteristics of systems consisting of train and air in tunnel using one dimensional incompressible fluid description
[AIAA PAPER 70-141] 06 p1042 A70-18216

Unsteady airfoil stall in incompressible flow, including pitch rate induced accelerated flow effect on leading edge and trailing edge stall
[AIAA PAPER 70-77] 06 p0976 A70-18237

Trailing edge region of flat plate in laminar incompressible flow examined for high Reynolds numbers limit using Navier-Stokes reduced equations
07 p1255 A70-19213

Plane rigid airfoil frequency response in incompressible potential flow using simple equivalent oscillator based on Theodorsen function
07 p1404 A70-19232

Navier-Stokes equations solved for unsteady incompressible three dimensional stagnation point flow, noting reduction to two dimensional and axisymmetric cases
07 p1188 A70-19343

Book on mathematical theory of viscous incompressible flow covering stationary and nonstationary boundary value problems for linearized and nonlinear Navier-Stokes equations
07 p1258 A70-19697

Pressure distribution on flat plate resulting from potential incompressible flow interaction between secondary jet and subsonic mainstream
07 p1190 A70-20415

Incompressible laminar boundary layer stability of incompressible fluid for nonparallel oncoming flow, deriving perturbed motion equation
08 p1483 A70-21179

Second order boundary layer equations for incompressible flow, presenting simplified integral momentum equation for two dimensional and axisymmetric flow
09 p1660 A70-22681

Laminar separation bubble in incompressible flow produced on flat plate by pressure gradients, correlating bursting with Reynolds number and pressure distribution
09 p1660 A70-22770

Boundary layer equations with heat transfer for laminar and turbulent incompressible flows about two dimensional and axisymmetric flows, using finite difference method
[ASME PAPER 69-HT-7] 09 p1663 A70-23560

Stress tensors in initial value problem for incompressible flow with nonlinear viscosity
09 p1663 A70-23570

Circle theorem for potential flows extended to two dimensional steady incompressible ideal fluid flows of constant vorticity
09 p1664 A70-23714

Steady and unsteady viscous incompressible one dimensional flows parameters in deformable cylindrical tube determined, solving continuity and motion equations by Galerkin method
09 p1664 A70-23715

Equivalent oscillatory model defined from asymptotes of frequency response amplitude and cut-off frequency amplitude value of plane rigid airfoil in incompressible potential flow
10 p1953 A70-23841

Orr-Sommerfeld equation of hydrodynamic stability theory solved for incompressible two dimensional boundary layer flow on basis of reduction to integral equation
10 p1867 A70-24161

Rigid body mode of viscous incompressible fluid flow response to small perturbations of rotating spherical container, applying torque interaction
10 p1868 A70-24196

Viscous incompressible flows nonlinear stability theory, considering perturbed flows tending toward stationary or flow periodic in time
[ONERA-TP-802] 10 p1869 A70-24542

Laminar flow into channel with symmetrical jets along walls, considering velocity profiles and flow establishment lengths
10 p1870 A70-24790

Monograph on Beltrami steady state, frictionless flow of incompressible medium past spherical surfaces, assuming vortex and stream lines agreement
11 p2034 A70-25498

Numerical techniques and solutions for compressible and incompressible laminar separated flows using time dependent finite difference equations
[AIAA PAPER 68-741] 11 p2035 A70-25972

Conducting fluid incompressible flow in entrance of MHD channel by momentum integral method, permitting edge stress existence at boundary layer free stream interface
[AIAA PAPER 69-724] 11 p2035 A70-25977

Incompressible inviscid fluid flow behind impeller blades, determining velocity profiles, flow-off angle and stable operation limits
11 p1977 A70-26349

Two dimensional incompressible mixing layer investigated by constant temperature linearized hot wire anemometers, discussing turbulent/nonturbulent interfaces

11 p2040 A70-26540

Energy spectrum of homogeneous isotropic incompressible turbulence, discussing eddy relaxation and direct interaction approximation

11 p2040 A70-26541

Incompressible homogeneous isotropic turbulence velocity expanded in Hermite functionals of Gaussian white noise random function advected by fluid

11 p2040 A70-26543

Inviscid incompressible conducting fluid flow past body in aligned magnetic field at low magnetic Reynolds number, discussing small perturbations evolution

11 p2041 A70-26623

Aerofoil free vibrations with fixed center of gravity in incompressible potential flow under representative previous histories effect

12 p2328 A70-28214

Two dimensional unsteady incompressible fluid flow through airfoil lattice

13 p2389 A70-29491

Incompressible ideal plane fluid flow complex potential caused by profile motion in presence of fixed infinite wall

13 p2390 A70-29632

Two dimensional incompressible steady turbulent flows based on Prandtl hypothesis relating eddy viscosity to kinetic energy and scale

14 p2564 A70-30259

Two dimensional incompressible turbulent boundary layer with mass addition and heat transfer, calculating temperature and velocity profiles by marching integration

14 p2564 A70-30261

DMC computer code for simulation of two dimensional viscous incompressible flow about arbitrarily shaped bodies

14 p2527 A70-30271

Unsteady incompressible laminar boundary layer equations solution after Crocco transformation by implicit finite difference scheme for flow around blunt body

14 p2528 A70-30290

Magnetoaerodynamic boundary layer of incompressible conducting fluid over right circular cylinder under magnetic field, showing flow separation

14 p2621 A70-30550

Sears function and lifting surface theory for harmonic gust fields in incompressible flow, modifying function for accurate interpolation of large numbers

14 p2528 A70-30860

Two dimensional incompressible laminar boundary layers asymptotic structure with injection, obtaining velocity profiles

14 p2566 A70-30995

Incompressible two dimensional potential flow analysis with compressibility effects for thick highly cambered multibodies in cascade, noting slotted compressor blade performance

14 p2529 A70-31023

Incompressible turbulent boundary layer calculation based on shearing stress hypothesis, considering layer at flat plate, boundary conditions and velocity profiles

15 p2719 A70-31490

Nonlinear bearing surface of symmetrical rectangular edge wings without slipping in incompressible flow, using oblique horseshoe vortex model

15 p2673 A70-32128

Book on flow separation covering steady/unsteady, turbulent and incompressible flows, base pressure, thermal effects, etc

16 p2833 A70-32913

Two dimensional incompressible isothermal laminar separation of Newtonian fluid in steady flow, obtaining velocity profiles

16 p2892 A70-33635

Laminar and turbulent boundary layer equations solutions for incompressible/compressible flows about two dimensional and axisymmetric bodies, using finite difference method

16 p2892 A70-33641

Equations of supersonic and hypersonic motion past circular cone by linearized method based on small perturbations with respect to nearly incompressible flow

16 p2835 A70-33746

Incompressible free jet characteristics determination from unique differential equation in laminar and turbulent flow regimes by unitary method

16 p2893 A70-33750

Incompressible flow interaction of perfect irrotational flow through two blade wheels in relative motion, observing pressure variations at nozzle profile

16 p2836 A70-33755

German monograph on planar straight cascades in incompressible frictionless potential flow, basing method on singularity method integral equation reversal

16 p2839 A70-34081

Annoyance assessment for sonic boom series exposure near airport

16 p2843 A70-34325

Laminar incompressible separating and reattaching flows, correlating finite difference solutions with experimentation

17 p3008 A70-34488

Model diffusion equation for inhomogeneous incompressible turbulent flow, applying to free turbulent flows

17 p3069 A70-34825

Incompressible laminar boundary layer, determining thermal conductivity gradient effect on temperature profiles

17 p3070 A70-35045

Incompressible laminar boundary layer along rectangular corner, obtaining similar solutions for velocity distribution

17 p3070 A70-35239

German monograph on oscillations of tandem wing without outgoing wake in plane incompressible flow, using numerical computations

17 p3011 A70-35372

Local skin friction law for turbulent boundary layers in incompressible flow, applying rule for compressible flow conditions

17 p3075 A70-35922

Incompressible laminar boundary layer equations approximate solution by Galerkin-Kantorovich technique

18 p3238 A70-35972

Steady incompressible flow past circular cylinder at Reynolds numbers up to 100, using finite difference solutions of motion equations

18 p3238 A70-36191

Free turbulent incompressible jet, analyzing pulsating characteristics and energy balance with Reynolds stress equations

18 p3240 A70-36264

Incompressible heavy fluid film stability during flow along inclined plane constituting crystallization front, analyzing linearized equations of perturbed flow

18 p3240 A70-36271

Axisymmetric ideal incompressible fluid jet outflow from cylindrical vessel with conical bottom, using small parameter technique and conformal mapping

18 p3240 A70-36272

Incompressible fluid flow past array of arbitrary profiles vibrating with arbitrary phase shift, taking into account blade displacement and vortex wake effect

18 p3206 A70-36277

Boundary value problem for Navier-Stokes equations of viscous incompressible fluid flow, discussing convergence of iterative solution

18 p3241 A70-36290

Magnetohydrodynamic flow of electrically conducting viscous incompressible fluid past nonconducting semiinfinite flat plate under transverse magnetic field

18 p3295 A70-36431

Laminar incompressible flow in arbitrary cross sectioned entrance region of ducts by numerical technique after transformation to boundary value problem

18 p3243 A70-36878

Two dimensional cascades for incompressible plane potential flows with given velocity distribution

18 p3209 A70-36880

Two dimensional steady inviscid incompressible flow past profiles in parallel flow with nonuniform velocity distribution

19 p3354 A70-38676

Incompressible axisymmetric flow through turbomachines, developing flowfield for given velocity distribution along arbitrary streamline

19 p3354 A70-38933

Perforated solid body moving in ideal incompressible fluid, deriving equations of motion in Lagrangian form

20 p3610 A70-39732

Boundary value problems in uniform incompressible inviscid flows past complex profile bodies by R functions method and variational technique

20 p3610 A70-39772

Laminar incompressible free shear layers by method of weighted residuals for turbulent jets, obtaining velocity profiles for similarity and physical planes

20 p3613 A70-40286

Unsteady incompressible flow in laminar boundary layer with homogeneous suction during longitudinal flow past flat plates, investigating boundary layer stability

20 p3614 A70-40391

Energy dissipation in laminar unsteady incompressible viscous fluid flows, discussing velocity fields, boundaries, tangential motion and entrainment

20 p3614 A70-40402

Asymptotic behavior of boundary layer equations solution for viscous incompressible flow past curvilinear obstacle

21 p3806 A70-40613

Incompressible MHD flow in entrance region of channel with electrically conducting walls, calculating interacted laminar heat transfer by integral method

21 p3856 A70-41038

Boundary layer transition region of flat plate in incompressible flow by subsonic wind tunnel tests, demonstrating harmonic wall perturbation effect

21 p3808 A70-41440

Two dimensional unsteady viscous incompressible MHD flow past infinite flat plate with uniform suction, considering Hartmann and Reynolds numbers

21 p3858 A70-41450

Irrotational incompressible flow through two dimensional channel with asymmetric contraction

21 p3809 A70-41757

Incompressible laminar boundary layers thermal response behavior in wedge flow, obtaining surface response, temperature fields, heat flux and steady state data

21 p3811 A70-42164

Subsonic channel incompressible gas flow past semiinfinite flat plate base, using flow pattern for cavitation flow

21 p3748 A70-42213

Nonparallel viscous incompressible fluid flows in channel between parallel porous plates with suction and blowing respectively, calculating stability by numerical solution

21 p3811 A70-42216

Viscous incompressible fluid flow between two rotating concentric spheres, calculating stability

21 p3811 A70-42217

Heat and mass transfer in plane inductionless and dissipationless incompressible MHD boundary layer with longitudinal pressure gradient

21 p3861 A70-42231

Micropolar incompressible fluid slow stationary flow past sphere

21 p3812 A70-42252

Incompressible Newtonian fluid laminar radial flow between parallel stationary disks, obtaining integral solution for Navier-Stokes equation

22 p4007 A70-42302

Laminar axisymmetric incompressible boundary layer calculation based on Mangler transformation

22 p4008 A70-42414

Two dimensional incompressible flow, calculating strong suction effects on laminar boundary layer separation by linear model

22 p4010 A70-42630

Thermal boundary layer near stagnation point in three dimensional fluctuating incompressible flow, using Lighthill method

22 p4124 A70-42685

Optimum pressure distribution and airfoil profiles for maximum lift without separation in incompressible flow determined by second order theory

22 p3959 A70-42704

Irrotational incompressible free falling jet, using asymptotic expansion solution for mixed boundary value potential problems

22 p4012 A70-42938

MHD incompressible viscous flow in nonconducting circular tube, determining pressure, flow rate and magnetic field level by continuum theory concepts

23 p4224 A70-44161

Incompressible laminar swirling jet flow, obtaining similarity solution for Navier-Stokes equations

23 p4184 A70-44982

Incompressible Newtonian fluid flow between closely spaced corotating disks, showing radial pressure distribution similar to laminar flow

24 p4324 A70-45293

Incompressible laminar flow in entrance region of rectangular duct allowing direct computation of eigenvalues

24 p4287 A70-45294

Unsteady incompressible thermal boundary layer flow past three dimensional obstacle for Prandtl numbers near unity

24 p4428 A70-45366

Three dimensional laminar boundary layer in unsteady incompressible flow, presenting solution by successive approximations method

24 p4325 A70-45594

Two dimensional incompressible air flow past circular cylindrical body, investigating separation point control by suction and jet injection

24 p4288 A70-46010

Inviscid conducting incompressible fluid steady motion past thin airfoils, presenting crossed and aligned fields and Alfvén motion with Hall effect

24 p4289 A70-46033

INCOMPRESSIBLE FLUIDS

Suffness values of externally pressurized incompressible fluid-film thrust bearings under turbulent Couette flow, discussing Reynolds number effects

01 p0100 A70-10383

Hydrodynamic stability of high purity insulating incompressible fluid subjected to unipolar ion injection

01 p0151 A70-10669

Critical conditions for hydrodynamic stability of incompressible nonconducting fluids subjected to unipolar injection, establishing variational principle leading to characteristic relation

01 p0152 A70-10672

Spinning top motion stability in homogeneous incompressible ideal resting fluid, using stability derivative for body of revolution

01 p0145 A70-11438

Characteristics of dynamic mechanical systems including solid state and hydrodynamic analogs of ideal incompressible fluids, based on statistical theory of turbulence

01 p0068 A70-11594

Dynamics of turbulent motion of incompressible viscous fluid particles, using Lagrangian functions

01 p0068 A70-11603

Incompressible viscous fluid plane flow using series expansion

02 p0277 A70-11910

Lower bounds of Stekloff and free membrane eigenvalues for sloshing of incompressible inviscid fluid, subject to gravity in rigid tank with free surface

02 p0278 A70-11999

Rayleigh step journal bearings, considering pressure distribution, load capacity and attitude angle and optimal film thickness ratio for incompressible fluid lubrication

02 p0307 A70-12167

Steady axially symmetric MHD flow of inviscid incompressible fluid of small conductivity in strong magnetic field past fixed axisymmetric bodies

02 p0347 A70-12234

Conservation equations for mass, mean momentum and kinetic energy for incompressible turbulent boundary layer, using finite difference procedure

02 p0284 A70-12347

Two spheres moving in ideal incompressible fluid, studying velocity field, hydrodynamic forces, kinetic energy, etc

03 p0465 A70-13335

Turbulent boundary layer of incompressible fluid flow in axisymmetric channels with swirl at inlet, considering components interaction, velocity, circulation profiles and resistance

03 p0466 A70-13389

Pulsation frequency affecting boundary layer separation from channel wall in incompressible fluid flow calculated by equation

03 p0466 A70-13399

Viscous incompressible laminar two dimensional flows using Navier-Stokes equations, emphasizing near wake and flow around leading edge

03 p0467 A70-13640

Unsteady state lift and moment action on lattice of profiles moving in incompressible fluid, determining suction originating at leading edges of profiles

03 p0409 A70-13868

Laminar boundary layer in incompressible liquid, noting effect of variation of kinematic viscosity and density on stability

03 p0468 A70-13870

Unsteady MHD flow of viscous incompressible electrically conducting fluid through rectangular duct under transverse magnetic field

03 p0471 A70-14333

Heat transfer in steady state flow of electrically conducting incompressible viscous fluid in annular channel between coaxial circular cylinders under magnetic field

03 p0608 A70-14335

Instability of viscous laminar plane jet of incompressible fluid, finding minimum critical Reynolds number for various assumptions of parallelism

04 p0670 A70-14990

Hydromagnetic flow of viscous incompressible electrically conducting fluid near accelerated infinite porous flat plate with variable suction or injection

04 p0672 A70-15095

Gravitational instability of finitely conducting incompressible fluid layer of finite thickness surrounded by nonconducting medium

05 p0915 A70-16696

Blowing intensity influence on turbulent boundary layer of incompressible fluid and friction drag of flat plate

06 p1036 A70-17852

Non-Newtonian fluids in continuum mechanics, classical Navier-Stokes theory limitations and theory of incompressible fluids for viscometric flows

06 p1037 A70-17926

Navier-Stokes equations numerical integration in Eulerian coordinates, applying results to compressible and incompressible fluids steady flow [AIAA PAPER 70-2]

06 p1040 A70-18113

Large Froude number solution for nonseparative impact of elliptical cylinder floating on incompressible fluid surface in half space extended to small Froude numbers

07 p1253 A70-18770

Approximate solution for heat transfer in incompressible fluid laminar flow in circular tube

07 p1253 A70-19060

Hydrostatic journal bearing dynamic rigidity for compressible and incompressible fluids, describing fluid film elasticity and damping characteristics

07 p1293 A70-19121

Turbulent wake behind plate due to confluence of two incompressible fluids with different densities

07 p1261 A70-20463

Rigid viscoplastic incompressible fluid flow governed by system of variational inequalities involving Navier-Stokes equations

08 p1482 A70-20590

Elastic body with incompressible fluid filled cavities, studying motion and stability by deriving motion equations starting from principle of least action

08 p1544 A70-20951

Propulsive and lifting motions of pointed profile in ideal incompressible fluid related to alternate vortices emission

08 p1433 A70-21234

Model for magnetic field-line reconnection in conducting incompressible fluid, determining maximum reconnection rate entirely by null point conditions

08 p1553 A70-21615

Boundary layer development on body accelerating in viscous incompressible fluid, using straight lines approximation and asymptotic expansions

08 p1485 A70-21631

Oscillations of highly viscous incompressible fluid in partially filled cavity of body moving about fixed point, solving Navier-Stokes equations by asymptotic method

08 p1485 A70-21632

Heat transfer in MHD channel flow of viscous incompressible rarefied gas with slip flow and temperature jump boundary conditions

08 p1554 A70-21769

Cauchy problem solution for linearized Navier-Stokes equations of incompressible rotating viscous fluid, discussing velocity and angular momentum effect on asymptotic behavior

09 p1659 A70-22326

Aerodynamic characteristics of plane straight walled diffusers initial and stabilized flow segments, assuming incompressible fluid and turbulent boundary layer

09 p1659 A70-22430

Free incompressible oil jet interaction with mobile plate, discussing plate configuration, oil free pressure and nozzle diameter, applications to electrohydraulic converter design, etc

09 p1613 A70-22825

Incompressible homogeneous fluid model in non-relativistic generalized gravitation theory using analytical solution

09 p1762 A70-23118

Hydrodynamic stability criterion of isolating incompressible fluids subjected to unipolar space charge injection

09 p1737 A70-23311

Incompressible anisotropic fluid flow around semiinfinite plate at large Reynolds numbers, using interlocked asymptotic expansions and deformed coordinates to obtain boundary layer equations

09 p1663 A70-23390

Motion and continuity equations for unsteady two dimensional flow of incompressible viscous fluid along infinite flat plate with time dependent suction

10 p1862 A70-23877

Transition from compressible to incompressible fluid assuming isothermal flows and finite stresses for density at or different from initial value

10 p1863 A70-24008

Alfven flow of dissipative conducting incompressible fluids in presence of thin airfoil in magnetic field, considering flow turbulence calculation

10 p1922 A70-24143

Laminar boundary layer flow of incompressible fluid in wake of symmetrical disturbance, deriving higher order approximations and introducing Euler transformation

10 p1802 A70-24420

Compressible flow equations of motion applied to incompressible fluid flow through nozzle with eddies and springs

10 p1871 A70-24796

Approximate solution for heat transfer in incompressible fluid laminar flow in circular tube

10 p1871 A70-25211

Viscous incompressible fluid secondary steady state flow due to rotating spheroid, considering acceleration terms in Stokes linear equation solution

11 p2034 A70-25390

Book on engineering aspects of MHD power generation, discussing working gas ionization and electrical conductivity, incompressible conducting fluid motion in magnetic field, etc

11 p1982 A70-25525

Velocity distribution around isolated and cascaded airfoils in plane potential flows of incompressible fluid determined by use of nonsingular integrals

11 p1974 A70-25781

Turbulent flow detachment in incompressible fluid around thick bodies, considering plate perpendicular to wind

11 p2037 A70-26466

Turbulence in incompressible electrically conducting fluid with uniform applied magnetic field, discussing nonlinear energy transfer mechanisms and magnetic effects

11 p2096 A70-26771

Two dimensional viscous incompressible conducting fluid flow between parallel porous walls in magnetic field, studying skin friction fluctuations

12 p2209 A70-27157

Wall shear stress distribution in noncircular ducts with steady incompressible fluid flow

12 p2209 A70-27217

Pulsation energy distribution in turbulent flow of incompressible fluid near tube wall, defining energy diffusion, production and dissipation terms in energy balance equation

12 p2210 A70-27321

Transient flow of viscous incompressible fluids with free surfaces calculated using Lagrangian coordinates

12 p2210 A70-27425

Incompressible fluid turbulent motion statistical equations, considering Lagrangian distributions of fluid particles coordinates and velocities

12 p2212 A70-28190

Turbulent flow of incompressible fluid, obtaining closed system of approximate equations for probability distribution of velocities

12 p2213 A70-28237

Two dimensional irrotational incompressible fluid motion bounded by flexible stretched and unstretched film, noting hydrodynamic shock for closed film

12 p2213 A70-28238

Homogeneous and stationary turbulence in incompressible fluid, proposing dynamic model for strong wave interactions during cascade process

13 p2457 A70-28557

Plane incompressible conducting fluid laminar jets analysis in magnetic field, using boundary layer equations for zero electric field

13 p2461 A70-28964

Viscous and inviscid incompressible fluids motion boundary value problems solutions with aid of kinetic stress functions

13 p2388 A70-29319

Unitary solution to incompressible and nonviscous fluids in presence of slender profile

13 p2464 A70-29542

Incompressible, viscous and electrically conducting fluid flow due to rotating disk in uniform magnetic field, discussing hydromagnetic interaction effect on velocity and friction

13 p2465 A70-29544

Plane, steady, irrotational flow of gaseous subsonic stream bounded by two infinite parallel walls, discussing application to incompressible fluids

13 p2389 A70-29631

Plane cavity geometry behind plate in incompressible potential flow, deriving geometrical functions to obtain desirable shapes

13 p2390 A70-29645

Hydrodynamic forces by oscillating foils in ideal incompressible fluid turbulent flow with stream separation

13 p2390 A70-29649

Motion equation derivation for incompressible fluid flow in baroclinic ocean, allowing for horizontal macroturbulent exchange

14 p2601 A70-30136

Incompressible turbulent fluid flow through ducts and pipes by integral boundary layer techniques, considering entrainment principles

14 p2564 A70-30258

Inviscid, incompressible superposed fluids stability in presence of inhomogeneous porous media, noting motion with decaying amplitude

14 p2577 A70-30993

Nonstationary MHD Couette flow of viscous incompressible fluid between two parallel walls caused by instantaneous fluctuations of applied transverse magnetic field

15 p2777 A70-31479

Force acting on cylinder in ideal incompressible fluid plane flow with steady vorticity

15 p2719 A70-31498

Incompressible viscous fluid steady flow admission into bounded space from cylindrical tube, demonstrating solvability of plane and three dimensional versions

15 p2720 A70-31642

Conducting incompressible fluid flow past sphere, examining effect on magnetic field for small magnetic Reynolds number

15 p2778 A70-31913

Conducting incompressible fluid laminar flow between rotating disks in transverse magnetic field with source at center

15 p2779 A70-31915

Steady flow of incompressible fluid through converging-diverging tube, considering implications in occlusive vascular disease

15 p2691 A70-31936

Computerized design of multipad and multirecess incompressible fluid film bearings

15 p2744 A70-31958

Heat transfer between incompressible fluid flow and insulated walls with time varying temperature at channel inlet, applying Laplace transforms

15 p2827 A70-32175

Viscous incompressible fluid nonstationary flow boundary layer extension around porous plate at Prandtl number equal to unity

15 p2722 A70-32873

Boundary value problem of two dimensional Poisson equation solution procedure with Hockney formulas, applying to unsteady viscous incompressible flow past flat plate

16 p2943 A70-33737

Incompressible ideal fluid plane laminar flows at large Reynolds numbers in region bounded by moving walls with closed concentric streamlines, establishing functional properties

16 p2893 A70-33749

Incompressible viscous fluid divergent turbulent flow detection in conical tube of revolution based on measuring wall pressure differences along tube generatrix

16 p2894 A70-33849

Structural incompressible liquid element for discrete linear idealization of missile and propellant vibration analysis

16 p2991 A70-33852

Wave propagation in infinite elastic plate in contact with inviscid incompressible liquid layer, deriving dispersion relation

16 p2993 A70-34094

Multistage solution algorithm for solving Navier-Stokes equations stationary problem, considering plane motion of incompressible fluid

18 p3239 A70-36216

Viscous incompressible liquid two dimensional flow around flat plate, discussing visualization techniques and velocity distribution measurement

18 p3239 A70-36218

Flow stability of incompressible heavy viscous fluid along wall of vertical circular cylindrical pipes, relating flow parameters to stability

18 p3240 A70-36278

Hydrodynamic model analogy to water bag/incompressible homogeneous fluid in phase space/, investigating nonlinear collisionless plasma oscillations

19 p3474 A70-37365

Stiffness values of externally pressurized incompressible fluid-film thrust bearings under turbulent Couette flow, discussing Reynolds number effects [ASME PAPER 69-LUB-25]

19 p3435 A70-37611

Unsteady incompressible planar gas jets with stable vortex street, investigating near flow field region to establish oscillatory component

19 p3404 A70-37799

Boundary layer equations for two dimensional flow of incompressible constant density micropolar fluid past plane wall, noting skin friction

19 p3404 A70-37962

Unsteady laminar incompressibles fluid flow in parallel plate channels and circular tubes, solving Navier-Stokes equations for prescribed discharge

19 p3405 A70-38347

Steady two dimensional incompressible shear flow, correlating velocity profiles with resistance distribution

19 p3406 A70-38350

Unsteady flow and heat transfer in viscous incompressible fluid due to infinite porous cylinder oscillations about axis with suction at surface

19 p3406 A70-38445

Viscous incompressible electrically conducting fluid steady flow between parallel coaxial rotating disks with transverse magnetic field

19 p3481 A70-38446

Compressible and incompressible Stokesian fluids motion described by finite element analog of Navier-Stokes equation

20 p3607 A70-38999

Turbulent wake behind plate due to confluence of two incompressible fluids with different densities

20 p3557 A70-39263

Elastic body with incompressible fluid filled cavities, studying motion and stability by deriving motion equations starting from principle of least action

20 p3672 A70-39376

Unsteady viscous flow of incompressible fluid through porous straight channel under time varying pressure gradient, determining suction and injection effects

20 p3609 A70-39670

Laminar boundary layer multidimensional universal equations solution for incompressible liquid using method of characteristics

20 p3611 A70-39804

Turbulent boundary layer calculation in incompressible fluid, using one parameter method

20 p3612 A70-39810

Thermal boundary layer theory for turbulent jets of incompressible fluids from relationship between velocity fluctuations and temperature

20 p3614 A70-40347

Bubble motion in ideal incompressible fluid, deriving motion equation in low viscosity fluid

20 p3614 A70-40392

Laminar convective flow from linear heat source along vertical plate, solving numerically for incompressible fluid by boundary layer approximation

20 p3614 A70-40403

Complementary variational principles applied to free oscillations of incompressible fluid in container, using linearized hydrodynamic equations

21 p3807 A70-41323

Heat transfer and skin friction in quasi-steady axisymmetric turbulent pipe flow of incompressible fluid with variable physical properties

21 p3808 A70-41375

Turbulent energy balance and spectra of axisymmetric wake behind sphere in incompressible fluid, measuring flow velocity

21 p3745 A70-41376

Pulsation energy distribution in turbulent flow of incompressible fluid near tube wall, defining energy diffusion, production and dissipation terms in energy balance equation

21 p3810 A70-42062

Incompressible fluid turbulent motion statistical equations, considering Lagrangian distributions of fluid particles coordinates and velocities

22 p4012 A70-43315

Lift determination of slender curved periodically recurring airfoils array in plane potential flow of inviscid incompressible fluid

23 p4133 A70-44158

Twisted incompressible viscous fluid flow in conical diffuser described by differential equation system, considering flow velocity field and separation point

23 p4133 A70-44159

Rotational two dimensional steady shear flows of perfect incompressible fluid, considering channel flow characteristics for various wave modes

23 p4181 A70-44202

Hall effect on incompressible electroconducting viscous fluid motion past finite conducting flat plate, discussing boundary conditions

23 p4225 A70-44247

Solid particles interactions during entrainment by viscous incompressible fluid in pipe, calculating interaction force as function of radius, distance and Reynolds number

23 p4181 A70-44310

Nonlinear properties of first order differential equations for axisymmetric velocity vector fields of ideal incompressible fluid, using nonlinear singular integral equation

23 p4181 A70-44343

Incompressible viscous fluid two dimensional flow in absence of mass forces, considering Tollmien-Schlichting wave perturbation effect on flow stability

24 p4324 A70-45365

Inertia effects and suspension rheology for incompressible Newtonian fluid shear flow around neutrally buoyant rigid sphere

24 p4327 A70-46243

INCONEL [TRADEMARK]

Inconel 718 and Al 2219 alloys surface flawed specimens fracture toughness and flaw growth comparison for high pressure hydrogen vessel

01 p0114 A70-10029

Ni-Cb intermetallics phase precipitation during aging of Inconel alloy 718, composition, stability and structure

01 p0116 A70-10093

Coherent precipitates effect on explosive shock hardening of pure nickel and Inconel alloy sandwich assemblies determined from simultaneous shock loading at specific pressures

01 p0116 A70-10107

Press load prediction for deep drawing Ti-Al-V alloy, stainless steel and Inconel X under various lubrication conditions at room temperature [ASME PAPER 69-WA/PROD-15]

04 p0698 A70-14835

Creep rupture and residual tensile strength tests to evaluate long time properties and structural stability of Inconel 718 alloy, performing phase analysis

07 p1310 A70-19731

Ni-based heat resisting alloy /Inconel 700/ investigated for hot corrosive environment effect on stress rupture and fatigue strengths

13 p2434 A70-29157

Diffusion layer microprobe analysis during chromaluminization of Inconel turbine blade

14 p2595 A70-30293

Inconel 600 high temperature high strain rate fracture process by hot torsion tester, noting temperature effects

15 p2762 A70-32389

Inconel 713 alloy, investigating chromaluminization treatment effect on fatigue strength at 700 C

18 p3278 A70-37211

Inconel short term creep properties measured for various temperature and stress levels, presenting results in polynomial and graph form

22 p4055 A70-43098

Low cycle notch fatigue tests on Inconel and low alloy steel, giving fatigue strength reduction factors for design

22 p4055 A70-43103

Metallurgical interaction phenomena in welding zone of heat treated Inconel 600, using hot ductility testing and metallographic methods

22 p4046 A70-43150

INDENTATION

Fourier transform applied to Riemann boundary value solution to biharmonic equation governing elastic theory for half plane with circular protrusion or indentation

01 p0199 A70-10155

Hardness measuring instrument by dynamic method at high temperatures in vacuum, using magnetic or nonmagnetic indenter balls

01 p0092 A70-11111

Adhesive rocking and parallel translation contact for circular cylindrical punch indenting elastic half space solved using simultaneous equations

05 p0932 A70-16139

Microhardness measurements of carbides, borides and nitrides in wide temperature range, considering indentation load selection

06 p1089 A70-17661

Surface mean deformation state under shot peening found equal to deformation under single indentation

07 p1292 A70-18835

Indentation pressures in rigid perfectly plastic solids correlated with ratio between indenter strain and material yield strain for various indenter geometries

12 p2322 A70-27232

INDEPENDENT VARIABLES

NT LATTICE PARAMETERS

Nonlocal continuity and correctness of principle for comparing functions with Liapunov vector function, demonstrating continuous dependence of principle on certain parameters

01 p0130 A70-10151

Dynamic programming for optimizing distributed parameter control systems described by parabolic linear integrodifferential equation with delayed argument

01 p0131 A70-10556

Dynamo theory of stellar and planetary magnetic fields, discussing mathematical analysis and electronic computation of eigenvalue problems and field parameters

01 p0185 A70-10957

Terminal state control systems efficiency from determining permissible range of control parameter variation for steady and unsteady linear dynamic systems

01 p0052 A70-10982

Inertial damper optimum parameter selection for achieving maximum nutation damping factor for gyroscopic stabilizer

01 p0091 A70-10985

Critical diameter and detonation parameters of nitromethane and tetranitromethane as function of powder content

01 p0217 A70-11004

Runge-Kutta method with position dependent optimal parameter alpha for initial value problem solution to minimize total error

01 p0134 A70-11364

Geomagnetic micropulsations fluctuations during solar activity cycle showing changes in excitation frequency with change in corpuscular fluxes parameters

01 p0083 A70-11539

Multipole analysis for earth magnetic field allowing secular variation to be illustrated by time trends in multipole parameters

02 p0288 A70-11742

Parametric approximation method extended to incompressible laminar boundary layers with surface suction or injection

02 p0277 A70-11857

Mixed boundary value problem for viscoelastic body with constant Poisson ratio solved by variables separation method, proving convergence

02 p0390 A70-12802

Small parameter method for reducing self similar viscous flow problems to ordinary third order differential equations with boundary conditions at wall and infinity

02 p0288 A70-12821

Single dispersion statistical analysis by simultaneous parameters tolerances application

03 p0518 A70-12937

Multielement active/passive antenna systems maximum SNR value obtained by determining conditions satisfied by parameters

03 p0456 A70-13092

Zero crossings of signal harmonic function with normal phase distribution, deriving relations with spectrum and modulating process parameters

03 p0447 A70-13289

Averaging over finite and infinite intervals derived for nonlinear integrodifferential equations with varying variables

03 p0594 A70-13507

Optimal synthesis and design of distributed parameter system for waveguides using gradient technique with devised algorithm to overcome convergence problem

03 p0449 A70-13563

Closed loop nonlinear optimal control systems sensitivity to small parameter variations noting influence of feedback

03 p0461 A70-14171

Ionization study of gas discharge parameters behind shock wave front produced by moving plasma pulse interaction with immovable gas discharge plasma

03 p0535 A70-14361

Relative satellite motion equations derived in generalized parameters, obtaining expressions for coefficients of correcting impulses sensitivity to measurement errors

04 p0760 A70-14430

Distributed parameter systems with arbitrarily many degrees of freedom, studying conditions for destabilization absence

04 p0767 A70-14483

Resonance oscillations onset by initial conditions in dynamic system described by hyperbolic equation containing independent time lag variable

04 p0718 A70-14485

Optimal control of multidimensional distributed parameters plants described by linear or nonlinear partial differential equations, considering boundary conditions

04 p0660 A70-14551

Modified harmonic balance method applied to critical values determination of nonlinear automatic control system parameters

04 p0661 A70-14555

Dynamic equilibrium prediction for creep and fatigue of various metals under various loading conditions, using time-temperature and cyclic stress-strain parameters

[ASME PAPER 69-WA/MET-9] 04 p0704 A70-14759

Dominant and small parameters determination through sensitivity coefficients in heat transfer problem

[ASME PAPER 69-WA/AUT-4] 04 p0713 A70-14829

Upper and lower bounds for eigenvalues of lumped parameter straight line torsional system determined by receptance synthesis based on Holzer method

04 p0773 A70-15083

Automated parameter search techniques applied to low thrust mission design, stressing trajectories and mission optimization

[AIAA PAPER 69-261] 04 p0736 A70-15404

Radar data parameter determination method, discussing false alarm calculation

05 p0811 A70-15988

Adaptive multiparameter experiment for iterative minimization of investigated data points, based on human response pattern to psychophysical inputs

05 p0805 A70-16006

Weighting coefficient matrix parameters for European satellite triangulation determined, considering sequence of separate points shown by photographs instead of single point

05 p0839 A70-16345

Slide rule for calculating electron number density, Debye length and Debye sphere particles in plasma parameters determination

05 p0852 A70-16847

Signal parameter quasi-optimal estimation during reception on background of normal noise with unknown correlation function

06 p1009 A70-17671

Identification algorithm for estimating parameters in constant coefficient linear system independent of prior estimates

[AIAA PAPER 70-34] 06 p1015 A70-18164

Roller machine adjustment parameters determination by analytical relations allowing for intermediary zone

07 p1292 A70-18837

Optimal control of linear distributed parameter systems using functional analysis

07 p1245 A70-19096

Parameters identification in nonlinear boundary value problems by successive approximations technique, using Lagrange multipliers and Newton-Raphson method

07 p1327 A70-20025

Shallow shells of variable thickness and curvature calculated using small parameter method based on functional analysis

07 p1416 A70-20193

Differential correction algorithm for identifying airplane parameters from flight test data, assuming differential equations

08 p1465 A70-20783

Quasi-linearization technique in computer program for aircraft parameters identification featuring efficient search for optimal parameters in algebraic or differential equations

08 p1465 A70-20784

Functions generation to determine probabilistic parameters of automatic air traffic control system

08 p1541 A70-20873

Model characteristics selection for dynamic system behavior simulation, studying characteristics variability extent without changing trajectory behavior dependence on parameter space

08 p1544 A70-20953

Optimization of control of oscillatory process with deviating argument in maximum principle form, reducing solution to boundary value problem

08 p1544 A70-20954

Automatic control system stability with restricted nonlinearity, investigating lumped and distributed parameter systems and unique and nonunique equilibrium positions

08 p1479 A70-20996

Sectional gyroscopic pendulum stability in space of system parameters reduced to determining periodic motions regions by Hamiltonian equations

08 p1496 A70-21206

Parameters defining elliptic vibration of light reflected from surface using photoelectric ellipsometer

08 p1546 A70-21673

Quantum mechanical form of Cramer-Rao inequality used to determined error lower bound for radiating object parameter observed by quantum-limited optical system

09 p1694 A70-22072

Flow characteristics behind sphere suspended in vertical axisymmetric jet dependent on ratio of specific parameter

09 p1658 A70-22118

Algorithm for controlled plant parameters determination based on sensitivity function calculation

09 p1653 A70-22145

Nonorthotropic pinched plates deflections solution, demonstrating asymptotic convergence of small parameter method

09 p1769 A70-22151

Nonlinear parameter of two intersecting laser beams in interaction with free electrons plane wave external field coupling

09 p1695 A70-22213

Parameter optimization of V and rhombic antennas with sloped wires, determining radiation angle from radiation pattern

09 p1649 A70-23336

Optimal control of distributed parameter systems, discussing necessary and sufficient optimality conditions based on functional analysis with emphasis on thermal processes

09 p1654 A70-23542

Wave propagation constants in electron wave TWT, studying nonuniformity parameter influence to determine relationships between beam and system parameters

09 p1652 A70-23655

Satellite orbit prediction formulas for Vinti dynamic model with three coordinates expressed in terms of independent variable

10 p1939 A70-24188

Numerical analysis of forced parametrically excited plate vibration in plane supersonic flow, using digital computer

10 p1958 A70-24527

Radial distribution of plasma parameters for thermionic converters with electrode shielding by plane sapphire rings, showing lateral surface effect

10 p1808 A70-25124

Pulsed system accuracy increment by increasing number of modulated signal parameters in addition to pulse duration modulation

10 p1843 A70-25137

Slowly varying parameters as engineering problem in nonlinear lumped systems

10 p1856 A70-25239

Digital control program parameters synthesis to realize time optimality with pure delay for ensuring absence of auto-oscillations under steady conditions

11 p2022 A70-25577

Algorithm for selective quadrupole parameter tolerance calculation, combining random search method with statistical testing

11 p2018 A70-25923

Multidimensional determined automatic control system structure and parameter synthesis by root method

11 p2023 A70-25926

Circuit for analog computing system to determine function extremum of many variables in presence of constraints

11 p2023 A70-25927

Constrained complex optimization method for synthesizing distributed-lumped-active networks

11 p2024 A70-26204

Kalman filtering and differential correction techniques applied to T-33 flight test data for aircraft system parameters identification

11 p1982 A70-26323

Dimensionless parameters associated with heat transport within living tissues using biothermal model

11 p1992 A70-26513

Satellite orientation by determining rotation parameters about centers of mass with respect to certain coordinates

11 p2128 A70-26782

Energy derivation for mechanics and thermodynamics with generalization to systems of more than two dynamic variables, considering transformations and Newton and Kepler laws

12 p2164 A70-27070

Lumped linear model parameters determined from dynamic test data on mode shapes and frequencies for approximating distributed elastic structure

12 p2317 A70-27122

Angular aberrations produced by airborne radomes calculated by computer, allowing optimal parameters selection and knowledge of radio properties

12 p2195 A70-27274

Design parameters for optimum heavily loaded single rotation ducted fan characterized by ultimate wake vortex system

[AIAA PAPER 69-222] 12 p2157 A70-28083

Optimal control for processes with parameters and state variable inequality constraints using gradient projection method and maximum principle

12 p2205 A70-28337

Space navigation procedures verification considering vehicle trajectory parameters, noting applicability to linear systems with estimable parameters

13 p2447 A70-28412

Relative satellite motion equations derived in generalized parameters, obtaining expressions for coefficients of correcting impulses sensitivity to measurements errors

13 p2503 A70-28455

Averaging over finite and infinite intervals derived for nonlinear integrodifferential equations with varying variables

13 p2440 A70-28656

Spacecraft parameters role in response to atmospheric disturbances, considering model design and control systems effects

[AGARDOGRAPH-115] 13 p2504 A70-28757

Linear distributed system with periodic parameters spectral characteristics based on multidimensional Fourier transforms with drift

13 p2383 A70-29718

Optimal policy for linearly distributed parameter control system, describing sufficient conditions

13 p2384 A70-29899

Parameters optimization of nonlinear electric servo actuator on basis of statistical criteria

14 p2559 A70-30157

Optimal control theory for system model dependence on state and control variables history

14 p2562 A70-31410

Gas ring lasers, discussing optimal parameters, colliding waves interference, nonmutual effect and radiation polarization

15 p2749 A70-31451

Relay control systems stability bound determination in nonphase variable form, assuming unknown system parameters

16 p2881 A70-33034

Pontryagin stability criterion interpretation for systems with time delay in parameter plane, using computer oriented method

16 p2882 A70-33046

Time optimal control for linear distributed parameter system using functional analysis with method of deepest descent

16 p2882 A70-33122

Heterodyne conversion transducer large signal internal parameters dependence on heterodyne, signal amplitudes and intermediate voltage

16 p2873 A70-33240

X-22 VTOL aircraft initial parameter, state and covariance matrix estimates by Kalman filter and smoothing algorithms

16 p2885 A70-33329

Linear continuous vibratory system unknown parameters identification from frequency response data

16 p2988 A70-33337

Parameter identification in distributed systems by method of characteristics, discussing noisy measurements and limited available transducers

16 p2942 A70-33338

Distributed parameter feedback systems with quadratic cost criteria, obtaining optimal controls characterization

16 p2886 A70-33339

Motor design parameters effects on solid propellant extinguishment predicted from mathematical combustion model

16 p2962 A70-33571

Mechanical system random excitation, evaluating parameters to satisfy conditions for statistical characteristics of steady state output processes

16 p2953 A70-34296

Binary data system parameters sudden change detection by noisy observation based on Bayes criterion

17 p3056 A70-34856

Control systems synthesis with parametric invariance for spacecraft boosters

17 p3177 A70-35219

Feedback control systems synthesis by three parameter space, using two dimensional graphic techniques

17 p3130 A70-35296

Parameter variation effects on iterative identification of linear system by learning method

17 p3130 A70-35299

Existence and uniqueness of optimal control for one dimensional linear system with distributed control

parameter using input-output integral with quadratic functional
17 p3057 A70-35627

Third order accuracy for nonlinear hyperbolic system of partial differential equations extended to equations with independent variables
17 p3131 A70-35891

F region small scale ionization discontinuities parameters observational data concerning anisotropy, dimensions, velocity and lifetime
18 p3246 A70-36088

Astatic gyroscope subjected to steady random translational vibration, optimizing parameters by mathematical model
18 p3257 A70-36136

Previous history effect on parameters relation in similar turbulent boundary layers under pressure distributions
18 p3241 A70-36375

Time and altitude dependences between 340-1000 km of delta parameter for height scale ratio of neutral and electron-ion gases, discussing diffusion coefficient
18 p3254 A70-37030

Cylindrical body with gravitational and magnetic anomalies, selecting point coordinates for body parameters
19 p3407 A70-37298

Cassegrain antennas design parameters using graphs for minimum blockage condition
19 p3376 A70-37690

Microwave transistors parameters measurement by scattering S_{11} parameter method for characterizing noise, gain and dynamic range, reading input and output impedances from Smith chart
19 p3386 A70-37692

Gyrotropic waveguides parameters computer calculation based on inhomogeneous isotropic region, taking into account discontinuities
19 p3378 A70-37736

Multiparameter systems with dominant complex roots constrained by degrees of freedom to construct reduced characteristic equation
19 p3392 A70-37824

Signal spectral parameters for reducing VLF atmospheric data from analyzer observations
19 p3412 A70-37998

Human monitoring behavior, discussing display, task and organismic variables effects
19 p3363 A70-38323

Electronic components mass production for automatic control equipment, determining parameters probabilistic scatter
19 p3390 A70-38578

Galactic rotation law parameters determination, considering effect of random and systematic errors on accuracy
19 p3525 A70-38774

Parameter S mean values measurement in Perseid meteor shower, discussing wind effects and accuracy
19 p3526 A70-38778

Optimal control of distributed parameter systems via functional analysis
20 p3600 A70-39136

Watts lunar limb correction charts parameters solution, using grazing and total stellar occultations by moon
20 p3705 A70-39478

Aircraft stability design by parameter plane technique, using for YO-3A aircraft
[AIAA PAPER 70-983] 20 p3560 A70-39546

Small parameter effects on absolutely invariant systems under transient perturbation, analyzing gyrostabilizer performance
20 p3603 A70-39831

Mode-generated average variables of atmospheric horizontal heat flux by transient cyclonic eddies used in mean motion circulation model
20 p3664 A70-40063

Discrete parameter stochastic optimization problems necessary conditions, deriving maximum principle
20 p3659 A70-40107

Parameters influence on mercury hollow cathode neutralizers for Kaufman ion thruster
[AIAA PAPER 70-1090] 20 p3693 A70-40245

Radial distribution of plasma parameters for thermionic converters with electrode shielding by plane sapphire rings, showing lateral surface effect
20 p3568 A70-40517

Optimal control problem for plant including dynamics and input constraints parameters treated by calculus of variations and Pontryagin maximum principle
21 p3801 A70-40899

Linear elastic structure with few degrees of freedom, discussing parameters experimental determination
21 p3935 A70-41409

Quasi-linearization relationship with Kalman filtering for nonlinear systems parameter estimation in process noise absence
21 p3845 A70-41749

Microwave parameters for Gunn devices with low electric field, obtaining data on characteristics and operating mode
21 p3863 A70-41989

System parameters identification from short-term signal observations, using Bayesian approach
21 p3802 A70-42253

Multiparameter eddy current test methods, describing test coil output signal amplification, demodulation and recombination
22 p4028 A70-42592

Spherical Bessel functions fast generation recurrence technique, presenting real or complex arguments
22 p4062 A70-42920

Magnetospheric plasma parameters from ground observation data of Pc-1 type micropulsations, assuming radiation belt plasma cyclotron instability
22 p4022 A70-43283

Coupling components in homotopic classification of elliptic systems of second-order equations with independent variable
23 p4212 A70-44349

Missiles aerodynamic coefficients parameter sensitivity from test data, using least squares analysis
23 p4133 A70-44525

Restricted osculating two body orbit with time derivative of eccentric anomalies difference position as independent variable in perturbation differential equations
23 p4244 A70-44635

Parameter optimization of gravity gradient stabilized satellite in circular orbit, considering minimum transition time and eccentricity oscillation
23 p4264 A70-45014

Bayesian identification of system parameters for observable and nonobservable input signals
24 p4316 A70-45474

Microwave oscillator design using Y-parameters from measured scattering parameter data at desired frequencies, applying negative resistance circuit theory
24 p4320 A70-46235

INDEXES [DOCUMENTATION]
Bibliography of far IR spectroscopy with subject index
14 p2586 A70-30987

Direct access on-line information retrieval system combining computer assisted instruction and bibliographic retrieval, using thesaurus for literature indexing
17 p3048 A70-34600

Graph theoretical cluster technique for producing index terms thesaurus for information retrieval system, discussing algorithms
24 p4316 A70-45161

INDEXES [RATIOS]
Angular dependence of one dimensional first and second index matching for optical parametric mixing of laser and SRS Stokes beams for tunable laser source
03 p0498 A70-13157

Oxygen index flammability test for polymeric materials, showing general applicability in quality control and research
09 p1710 A70-23346

Time lag system performance index bounds determination and optimal feedback controller design based on min-max criteria
14 p2561 A70-31185

Automated Readability Index for technical materials weighting word and sentence length in multiple regression equation
24 p4308 A70-45510

INDIA
Meghdoot program for satellite network communications technology applications to national goals in India
04 p0757 A70-15670

Civil air transportation in India, using mathematical models to estimate optimal development and efficiency of future air traffic potential
08 p1601 A70-21544

ACME hybrid airborne satellite TV and communications system for India, using airborne TV transmitters
[AIAA PAPER 70-472] 11 p1998 A70-25418

Report to COSPAR on Indian space research describing organizational structure, facilities, experiments and international cooperation
15 p2830 A70-31715

Microwave propagation refractive index over India, showing influence of humidity and vapor pressure
15 p2701 A70-32470

INDIAN OCEAN
Lherzolite, anorthosite, Gabbro and basalt dredged from Mid-Indian Ocean Ridge noting geological and geophysical features
04 p0675 A70-14422

Meteorological data from radiosonde and radar wind observations during Indian Ocean expedition of research vessel Meteor
07 p1329 A70-19350

INDICATING INSTRUMENTS
NT ANEMOMETERS

NT APPROACH INDICATORS
NT ATTITUDE INDICATORS
NT CLOUD HEIGHT INDICATORS
NT FLOW DIRECTION INDICATORS
NT GYRO HORIZONS
NT GYROCOMPASSES
NT HOT-WIRE ANEMOMETERS
NT MICROBALANCES
NT MICROWAVE SENSORS
NT PLAN POSITION INDICATORS
NT POSITION INDICATORS
NT RADIO DIRECTION FINDERS
NT SONIC ANEMOMETERS
NT SPACECRAFT POSITION INDICATORS
NT SPEED INDICATORS
NT TACHOMETERS
NT WEIGHT INDICATORS
NT WIND VANES

Radar visual indicator used with scan converter and as synthetic indicator with computer controlled flight safety system
02 p0263 A70-12700

Visual recordings of cardiac rhythm obtained from flashes of miniature indicator tube, describing circuit filter function
08 p1452 A70-21439

Coherent instrumentation radar for White Sands Missile Range, discussing system design emphasizing pulse Doppler capability
10 p1842 A70-24881

Short range aircraft collision pilot warning indicator for low altitude and closure speeds
11 p2078 A70-25706

Waveguide gas discharge indicator of transmitted microwave power, investigating sensitivity, discharge conditions, filler gas and pressure effects
11 p2020 A70-26807

Liquid metal level indicators and resistance type level meters for turbines using alkali metal as working media
14 p2587 A70-31010

CH-47 cruise guide indicator for displaying fatigue loading to pilots, discussing design and operation
17 p3082 A70-34705

Small swing angle detector for balloon payloads, using rate gyro principle
17 p3090 A70-35314

Fluidic parallel flow low airspeed indicator for V/STOL instrumentation tested in wind tunnel
[AIAA PAPER 70-906] 17 p3096 A70-35818

Two-axis electrolytic bubble level as precision vertical reference and tilt indicator for ballistic missiles inertial navigation systems
[AIAA PAPER 70-949] 20 p3631 A70-39578

Remote digital mean wind speed indicator with numerical display, using photoanemometer for airport application
21 p3831 A70-42247

Quartz Z-variometer for autonomous variation stations, describing construction and operation
23 p4194 A70-44089

Waveguide gas discharge indicator of transmitted microwave power, investigating sensitivity, discharge conditions, filler gas and pressure effects
24 p4317 A70-45179

INDICATORS
Search duration distribution of two stage lock-on indicator scanning signal search systems, using regenerative random process and integral recovery equation
15 p2696 A70-31501

INDIUM
DC electrical conduction in In and In-Pb alloy foils sandwich structures, discussing size effect and Pb diffusion rate
03 p0540 A70-13624

Thermal conductivity and hysteresis measured in cylindrical In foil under magnetic fields at temperatures below 1 K
05 p0891 A70-15792

Plastic deformation effects on superconductivity of wire specimens of high purity Pb, In and Ti cold worked at liquid He and annealed
06 p1127 A70-18614

Al, Ga and In effects on creep and rupture stress of Ti at 500 C
17 p3120 A70-34425

In thin film resistance thermometers fabrication by vapor deposition in vacuum, considering electrical properties dependence on temperature
22 p4039 A70-43446

Radiochemical neutron activation analysis of In, Cd, Y and rare earth elements in rocks
24 p4310 A70-46375

INDIUM ALLOYS
DC electrical conduction in In and In-Pb alloy foils sandwich structures, discussing size effect and Pb diffusion rate
03 p0540 A70-13624

Binary Co-In system thermal analysis, X ray diffraction and microscopy, discussing phase diagram
14 p2595 A70-30838

In-Au contacts for GaAs, discussing fabrication and performance tests on transverse Gunn mode oscillator
20 p3686 A70-39118

Direct gap conduction band and alloy composition monitoring InAlP, using electron microprobe cathodoluminescence and X ray emission
22 p4086 A70-43019

INDIUM ANTIMONIDES

Current carrier mobility in n-InSb calculated by Schwinger variational method over temperature range
01 p0154 A70-10098

Natural absorption band absorption coefficient frequency and temperature dependences in doped n-InSb
01 p0154 A70-10100

Hole mobility in n-type InSb semiconductors determined from solving kinetic equation for minority carriers allowing for scatterings
01 p0155 A70-10185

Plasma injection occurrence as function of temperature in n-InSb subjected to low electric field strengths and fitted with Ohmic contacts
01 p0159 A70-11176

Recombination emission of InSb semiconductor at low temperature during pinch effect with electron gas degeneration, calculating spectral distribution and effective temperature vs current
03 p0539 A70-13406

Coherent microwave generation mechanism in indium antimonide at high electric fields, formulating thin plasma layer double stream interaction theory
03 p0534 A70-14214

Active region characteristics of double injection laser employing electron-hole plasma in p-type indium antimonide
12 p2247 A70-27491

Electric field distribution in rectangular waveguide loaded with magnetized n-InSb at room temperature obtained by solving boundary value problem by variational method
12 p2202 A70-28163

Photovoltaic InSb IR detectors design and operation, emphasizing performance in restricted field of view
16 p2926 A70-33152

Submillimeter lasers radiation measurement with n-InSb detectors at liquid He temperature
17 p3107 A70-35109

High field noise emission from indium antimonide, suggesting electron-hole plasma as source
19 p3486 A70-37767

Sensing elements piezoresistive Si and indium antimonide film sensing elements for high sensitivity pressure transducers and accelerometers, discussing airborne telemetry applications
19 p3431 A70-38538

InSb semiconductor, measuring small signal microwave conductivity for hot electron region at 9.4 GHz in high electric DC fields
19 p3488 A70-38747

Circular waveguide with axially magnetized plasma, investigating twist mode propagation in InSb at 70 GHz
24 p4311 A70-45214

INDIUM ARSENIDES

Indium arsenide crystals conduction band structure with various electron concentrations, determining electron mass dependence on concentration and temperature
01 p0154 A70-10096

InAs-GaAs solid solutions microhardness and brittleness, studying chemical composition effects
04 p0730 A70-14464

N-type InAs single crystals optical properties with various carrier concentrations at 1-6 μ wavelengths and 300-78 K temperatures, studying absorption spectra
08 p1555 A70-20512

Microwave backward tunnel diodes in InAs, predicting reliability and sensitivity improvements over other materials
13 p2379 A70-29593

InAs thin films electrical properties and IR reflectance, determining thickness and substrate temperature effects on carrier concentration and mobility
15 p2783 A70-31965

Plasma reflection edge in thin film InAs semiconductors, calculating refractive index and extinction coefficient from free charge parameters
15 p2783 A70-31966

Indium arsenide role in IR image detectors, describing photoelectric threshold and quantum efficiency
17 p3143 A70-35118

Single and polycrystalline indium arsenide preparation methods and quality control
17 p3143 A70-35119

Indium arsenide p-n junctions fabrication and electrical and photoelectric properties
17 p3143 A70-35120

Absorption coefficient of n-type indium arsenide single crystals with varying electron and doping concentrations, investigating spectral dependence
17 p3144 A70-35705

Photosensitivity and electroluminescence spectra of GaAs-indium gallium arsenide p-n heterojunctions at room temperature
17 p3144 A70-35708

InAs p-n junction laser electrical and optical characteristics during spontaneous and stimulated radiative recombination
18 p3269 A70-36739

InAs pulsed injection laser at cryogenic temperature for measuring time constant of IR radiation detectors
20 p3630 A70-39449

Epitaxial GaAs films growth from solid solutions of InAs-GaAs system deposited on GaAs substrates, noting electron mobility and temperature effect
20 p3686 A70-39629

Highly alloyed indium arsenide reflection spectra and band structural characteristics
24 p4389 A70-45482

INDIUM COMPOUNDS

NT INDIUM ANTIMONIDES

NT INDIUM ARSENIDES

NT INDIUM PHOSPHIDES

NT INDIUM TELLURIDES

INDIUM PHOSPHIDES

Solution crystallization method to obtain gallium indium phosphide semiconductor alloys, discussing optical absorption thresholds and transitions
01 p0158 A70-10661

Bulk n-type InP single crystal transferred-electron oscillators, investigating current instabilities
14 p2556 A70-30686

Microwave oscillator performance of InP three level transferred electron devices
17 p3048 A70-35874

Microwave output power and impedance for InP and GaAs bulk negative resistance oscillators, using velocity/field characteristics
21 p3800 A70-42049

Boron impurities introduction into InP crystals grown by liquid encapsulation, detecting IR absorption bands due to localized lattice vibration
23 p4231 A70-44891

INDIUM TELLURIDES

Interband transitions and optical absorption edge analysis in indium telluride using dependence on photon energy
03 p0541 A70-13725

Impurities solubility in semiconducting indium telluride with stoichiometric vacancies, verifying thermodynamic model by phase diagrams
16 p2960 A70-33224

INDOLES

NT TRYPTOPHAN

Melatonin biosynthesis, discussing regulation by light and sympathetic nerves, daily pineal rhythms, estrous rhythms and ovarian hormones
03 p0424 A70-13809

Prolonged hypokinesia effect on dynamics of 5-oxyindoleacetic acid elimination in rat urine, showing occurrence of shifts in serotonin metabolism
09 p1615 A70-22092

Pineal C14-indoles synthesis in rats noting no direct effect of morphine
11 p1988 A70-26299

Prolonged hypokinesia effect on dynamics of 5-oxyindoleacetic acid elimination in rat urine, showing occurrence of shifts in serotonin metabolism
15 p2685 A70-32688

Serotonin, 5-hydroxyindoleacetic acid /5-HIAA/ and monoamine oxidase in bovine pituitary organ and median eminence
21 p3761 A70-40850

INDUCED FLUID FLOW

U FLUID FLOW

INDUCERS

U INTAKE SYSTEMS

INDUCTANCE

Impedance behavior of inductive posts with small capacitive gap in waveguide
08 p1468 A70-20644

Solid state device inductance by thermal effects, describing characteristics and applications in resonant circuits
15 p2783 A70-31839

Fluidic systems linear lumped components design with allowance for energy factor Q, investigating capacitance and inductance
15 p2678 A70-32675

Interference free high speed monolithic digital integrated gate, determining current swing, lead inductances and switching times
17 p3048 A70-34587

INDUCTION

Light inductions and echo intensities in liquids and gases, investigating thermal vibrations, translational Brownian motion, particle collisions and laser diffusion effects
06 p1082 A70-17809

Steady state tangential drag by solar wind on geomagnetic cavity, describing unipolar induction
22 p4013 A70-42469

INDUCTION HEATING

Induction furnace for thermal treatments and melting of solid and liquid metals, alloys and sintering and degassing ceramic and metallic systems in vacuum
04 p0664 A70-15371

Boundary value problems solutions estimated for heat conduction equation in unbounded domain, considering function satisfying heat induction equation
07 p1419 A70-18852

Powder metal parts induction sintering, comparing performance with conventional method
13 p2420 A70-29249

Induction plasmas in thermal equilibrium dominated by radial conduction losses, discussing energy balance equation and Ar plasmas at atmospheric pressure
13 p2465 A70-29701

Thermal induction plasma discharge characteristics, considering radiation and conduction losses
13 p2465 A70-29702

Asteroidal parent bodies heating by electrical induction during early solar evolution
18 p3310 A70-35938

INDUCTION SYSTEMS

U INTAKE SYSTEMS

INDUCTORS

Manganin piezoresistive shock gauge constant current supply using inductor and termination technique eliminating shunting
02 p0303 A70-12737

High speed homopolar inductor alternators with minimum leakage reactance, using geometric programming for objective function optimization
16 p2879 A70-34059

INDUSTRIAL MANAGEMENT

NT PERSONNEL MANAGEMENT

Quality control and reliability assurance in industrial supplier-customer relationship, emphasizing management role
24 p4431 A70-46386

INDUSTRIAL PLANTS

NT FOUNDRIES

Automatic multiple station test system for manufacturing plants, considering centrally controlled vs free standing and intelligent vs nonintelligent remote stations
08 p1470 A70-20655

Aeronautical construction complexes in France
10 p1895 A70-24862

Complex plants process control by experimental statistical methods, considering curves plotting, computer requirements, optimum method selection, etc
20 p3592 A70-39902

INDUSTRIAL SAFETY

Initiator desensitization process involving use of volatile inert liquid to increase safety during assembly operations
03 p0549 A70-14137

Static electricity hazards and problems in electronics and aerospace industries
07 p1333 A70-18930

Hazards in manufacturing solid propellants evaluated to design tests and suggest process conditions
07 p1361 A70-19915

Health hazards of laser operations, considering laser and laser area physical characteristics, operating procedures and controls
10 p1824 A70-24062

Commercial and industrial microwave hazards exposure criteria and survey techniques used in state and local governments
18 p3224 A70-36228

Safety program effectiveness based on evaluation activity for monitoring field installations
19 p3555 A70-38848

INDUSTRIES

NT AEROSPACE INDUSTRY

NT AIRCRAFT INDUSTRY

NT DEFENSE INDUSTRY

NT WEAPONS INDUSTRY

Engineering development role in metal forming industry expansion, discussing metals ductility or plasticity increase for extending processes
12 p2244 A70-28146

Soviet optical instrument industry development trend /1971-1975/, considering spectral, test, measuring, reading and microscopic equipment
13 p2412 A70-29864

Global weather prediction network economic benefits to key industries, discussing adverse weather effects on production schedules, fuel supplies, construction, harvesting, etc
14 p2610 A70-31143

INELASTIC BODIES

U RIGID STRUCTURES

INELASTIC COLLISIONS

Nucleons and high energy pions inelastic interactions with complex nuclei involving external diffraction production of pions
03 p0526 A70-13029

Cosmic ray particles inelastic nuclear interactions mean free path in iron measured in Wilson chamber and ionization calorimeter
03 p0554 A70-13030

Relativistic phase of stellar system evolution caused by inelastic stellar collisions, discussing thermal relaxation rate, obtaining distribution function
03 p0564 A70-13226

Electron density and temperature in ionized gas created by thermal collisions between neutral parti-

- cles, analyzing chemical ionization and inelastic collisions influence [ONERA-TP-752] 03 p0532 A70-13631
- Extensive air shower characteristics for inelasticity coefficient, nucleon-pion interaction cross sections and secondary particles, noting parameter interchangeability 05 p0898 A70-15946
- Inelastic He atom-ion collisions provide understanding of capture and excitation cross sections 05 p0885 A70-16555
- Maxwellian distribution perturbation in chemically reacting gas mixtures with lower inelastic collision frequency than elastic 06 p1110 A70-17761
- Collision cross sections direct measurement for determining macroscopic reaction rates in inelastic molecular collision processes in gas dynamics 06 p1113 A70-18276
- Energy distribution of positive Ar ions scattered from thermal diatomic D noting inelastic collisions 07 p1339 A70-20056
- Molecular beam research at low, intermediate and high energies, discussing inelastic processes, intermolecular potentials, etc 07 p1344 A70-20131
- Born wave for atom-atom inelastic cross sections, calculating He excitation from ground state to higher states by H atom collision 07 p1346 A70-20241
- Time dependent matrix elements for multistate impact-parameter calculations for atom-atom inelastic cross sections 07 p1346 A70-20242
- Relativistic phase of stellar system evolution caused by inelastic stellar collisions, discussing thermal relaxation rate, obtaining distribution function 08 p1580 A70-21659
- Extensive air shower simulation for determining inelasticity effect on electrons, hadrons and muons variation at sea level 08 p1563 A70-21674
- Transport cross sections for isotopic methane and mixtures, considering inelastic and thermal diffusion effects 14 p2665 A70-30652
- F 2 layer heating by photoelectrons reconsidered in terms of electron inelastic collisions effect on temperature 15 p2727 A70-31870
- Diatomic molecules inelastic collision cross sections for specific rotational transitions, discussing S matrix energy requirements for statistical analysis 19 p3474 A70-38268
- Low voltage arc nonequilibrium ionization rate, taking into account atom-electron collisions 20 p3684 A70-40389
- Secondary cosmic ray muon inelasticity in high energy neutrino interactions for deep mine experiments, using lepton current 21 p3845 A70-41139
- Interface interaction of colliding plates of different materials, reducing flow problem to differential equation via hodograph transformation 21 p3747 A70-41962
- INELASTIC SCATTERING**
- Periodic potential and residual Coulomb interaction effect on inelastic light scattering from electronic excitations in semiconductors, using diagrammatic perturbation theory 01 p0156 A70-10280
- Inelastic muon-nucleon scattering implications on cosmic rays, studying equation validity for absorption cross section 02 p0359 A70-12702
- Cosmic ray particles high energy interactions during extensive air showers, noting inelastic superhigh energy collisions 03 p0556 A70-13040
- Elastic and inelastic scattering of proton beams from magnesium and silicon isotopes, using optical model 04 p0723 A70-15637
- He to carbon fusion reaction rate enhancement in dense matter by inelastic scattering processes, discussing C 12 deexcitation to ground state 05 p0885 A70-16934
- Inelastic scattering of electrons by surface plasma oscillation for low energy electron diffraction and photoemission, interpreting surface plasmon excitation 07 p1337 A70-19359
- Inelastic scattering of He ions by Ne as function of angle, initial energy and energy loss using collision spectroscopy 07 p1346 A70-20243
- Pulsed electron beam irradiated dielectrics secondary electron emission in vacuum, emphasizing inelastic scattering 13 p2471 A70-29409
- Differential cross sections for electron scattering by hydrogen with and without vibrational excitation, discussing inelastic processes 14 p2618 A70-30115
- NO and oxygen ions vibrational excitation due to inelastic scattering from He, calculating scattering angle variation 16 p2955 A70-34010
- Inelastic energy losses in oxygen ion beams collisions with neutral molecules, determining vibrational transition probabilities 16 p2955 A70-34011
- Coupled channel calculation of inelastic proton scattering from Ne 20 using Hartree-Fock wave functions 17 p3137 A70-34517
- Deep inelastic lepton-hadron scattering cross sections universality properties based on Wilson theory 20 p3674 A70-39150
- Anomalous angular distribution and inelastic cross section of muon-nucleon interaction for penetrating underground cosmic ray particles 22 p4095 A70-43232
- Transverse and longitudinal current correlations in fluids from modeled kinetic equations, noting inelastic neutron scattering from liquids 24 p4378 A70-45261
- INEQUALITIES**
- U ELASTIC PROPERTIES**
- Differential and integral inequalities theory and applications, Volume 1, Ordinary differential and Volterra integral equations 01 p0133 A70-11324
- Constitutive inequalities for isotropic elastic solids under finite strain generated by introducing concept of conjugate pairs of stress 08 p1590 A70-21351
- Consistent and inconsistent linear inequalities evaluating speed and efficiency of algorithm for pattern recognition problems 08 p1467 A70-21782
- Nonlinear partial differential inequalities treated by comparison function mu associated with continuity and growth conditions 10 p1908 A70-23836
- Generalized inverse algorithm for solving linear inequalities from Ho-Kashyap algorithm 11 p2013 A70-26207
- Coerciveness /Korn/ inequalities role in boundary value problems for elliptic systems of partial differential equations, noting applications to three dimensional linear elasticity theory 12 p2260 A70-26974
- Generalized iterative inverse algorithm for linear inequalities set involved in pattern recognition and threshold logic requiring decision functions determination 16 p2870 A70-33739
- INERT ATMOSPHERE**
- Strain gauge data obtainable on rosettes used for measuring test component stresses at 550 F in inert atmosphere 03 p0482 A70-12965
- Powder metallurgy all-inert processing method for producing nickel base superalloys forgings, discussing microstructure, reproducibility, mechanical properties, etc 09 p1701 A70-22553
- Pulsed current gas tungsten arc welding in inert gas atmosphere and applications 12 p2238 A70-26853
- Soviet monograph on bimetal and refractory metals production by rolling in vacuum or inert media 19 p3433 A70-37402
- INERT GASES**
- U RARE GASES**
- INERTIA**
- NT INERTIA PRINCIPLE**
- NT MACH INERTIA PRINCIPLE**
- Inertial gravitational fields described by Maxwell equations, showing potentials defining four vector velocity field of test particles 01 p0141 A70-10140
- Squeeze film investigation between rotating plane annuli, considering inertia due to centrifugal effect [ASME PAPER 69-LUB-6] 01 p0102 A70-10396
- Aerosol particles Brownian motion under inertial forces in absence/presence of obstacle 01 p0143 A70-10997
- Inertia effects in squeeze film between two curved surfaces and in externally pressurized bearing with converging lubricant film 01 p0104 A70-11388
- Inertia effect of electrically conducting lubricant on load capacity of hydromagnetic inclined slider bearing under magnetic field 01 p0104 A70-11389
- Inertia effects on pressure distribution, load capacity and frictional torque in MHD hydrostatic thrust bearing lubrication flow 02 p0307 A70-12162
- Propulsion efficiency in air and in space measured according to relativity concepts, including electric field inertia explanation 02 p0355 A70-12364
- Vibrational response of simply supported and clamped circular plates subjected to gyroscopically induced inertia loads, using equations of motion 03 p0583 A70-12920
- Bubnov-Galerkin approximations convergence in problem of thin plate nonlinear vibrations, allowing for inertial forces due to rotation 03 p0593 A70-13470
- Static and dynamic characteristics of inertia load driving systems using electrohydraulic pressure and flow control servovalves [ASME PAPER 69-WA/FLCS-15] 04 p0626 A70-14842
- Inertia effects due to circumferential and radial velocity in MHD hydrostatic thrust bearing in axial magnetic field [ASME PAPER 69-LUB-F] 04 p0698 A70-14871
- Inertial damping of soft rubber under forced torsional vibrations, discussing viscoelastic body linear model 04 p0712 A70-15100
- Delay characteristics of narrow band double bridge amplifier used as inertial component of photoelectric star transit recorder 04 p0693 A70-15489
- Inertial parameters and functions of dissipative and restoring forces in quasi-linear oscillatory system determined from free motion characteristics 05 p0884 A70-16951
- Ballistic reentry vehicle roll related to trim angles caused by inertia asymmetries [AIAA PAPER 70-204] 06 p1156 A70-18074
- Nonlinear spinning shallow spherical shell equations solved for equilibrium stress and displacement distributions, discussing inertia loading 07 p1406 A70-19342
- Free in-plane flexural vibrations of circular rings, developing equation of motion to include shear deformation and rotatory inertia effects 08 p1592 A70-21473
- Inertia effect in failure mechanics for steadily developing equilibrium cracks in dynamic system with time dependent periodically variable load 09 p1771 A70-22466
- Forced inertial oscillations in rotating processing fluid-filled circular cylinder 09 p1664 A70-23682
- Flutter characteristics of uniform cantilever wing with concentrated inertias using Direct Matrix method 10 p1963 A70-25071
- Titan 3C boost phase inertia loads on payload estimated for satellite design, using frequency and interface acceleration methods [AIAA PAPER 70-485] 11 p2120 A70-25446
- Rockets angular motion due to thrust with ramp input, presenting graphs for different inputs and inertia ratios 11 p2123 A70-26125
- Inertial and gravitational mass equivalence related to observation of anomalous K-meson decay 12 p2272 A70-27391
- Hydraulic piston-valve-type slave mechanism oscillations with rigid feedback and inertial load at actuated shaft, using harmonic linearization method 12 p2167 A70-28340
- Delayed moment of force relativistic definition within reference of inertia, discussing lever bent at right angles 13 p2452 A70-29635
- Cloud droplets coagulation growth, calculating aerosols inertial capture coefficient by fine jet method 14 p2602 A70-30390
- Inertial load-time effects in instrumented impact tests, showing corrections for bending stress and dynamic fracture toughness measurements 15 p2820 A70-32240
- Solar system Eotvos experiments for measuring gravitational to inertial mass ratio of celestial bodies 16 p2978 A70-34033
- Additional inertia introduced by velocity profile gradient in flow direction effects on externally pressurized gas bearing 16 p2924 A70-34233
- Statistically indeterminate Timoshenko beams oscillations natural frequencies and modes by lumping properties of linear and rotary inertia at discrete points 16 p2994 A70-34235
- Human vision inertia and irradiation algorithm, satisfying Talbot law 18 p3217 A70-36082
- Squeeze film investigation between rotating plane annuli, considering inertia due to centrifugal effect [ASME PAPER 69-LUB-6] 19 p3435 A70-37608
- Fluid inertia and compressibility effects considered in equations for foil over lubricating film [ASME PAPER 69-WA/LUB-10] 19 p3435 A70-37615
- Elastic materials consisting of particles with rotary inertia, long range force and dipole interactions, deriving constitutive relations 19 p3538 A70-37794
- Forced vibrations of rotor with variable rotating speed, investigating inertia terms effect 19 p3542 A70-38221
- Aircraft, rocket or other rigid or flexible structure, computing inertial constants based on measurements of generalized masses of natural modes 21 p3935 A70-41408

- Apollo 11 lunar specimen thermal diffusivity, conductivity and inertia in breccias and crystalline igneous rocks measured over wide temperature range
21 p3916 A70-41663
- Parallel circular squeeze film bearing, calculating Newtonian fluid inertia effect on lubrication by perturbation solution
[ASME PAPER 70-LUBS-9] 22 p4045 A70-42451
- Quasi-Maxwellian equations of inertial-gravitational fields
22 p4075 A70-43223
- Inertia effect on low density plasma losses in toroidal MHD equilibrium in model stellarator field
24 p4383 A70-45115
- Inertia effects and suspension rheology for incompressible Newtonian fluid shear flow around neutrally buoyant rigid sphere
24 p4327 A70-46243
- INERTIA MOMENTS**
U MOMENTS OF INERTIA
INERTIA PRINCIPLE
NT MACH INERTIA PRINCIPLE
Numerical solution of satellite rotational damping by onboard motors using Euler equations, local variations and finite control time
13 p2505 A70-28963
- INERTIA WHEELS**
U REACTION WHEELS
INERTIAL ACCELEROMETERS
U ACCELEROMETERS
INERTIAL COORDINATES
Inertial acceleration in relative motion of two bodies subjected to external forces, basing equations of motion on rotating coordinates
07 p1375 A70-18890
- Relativistic observer in rotational motion relative to inertial observer, imposing velocity onto perfect relativistic fluid
21 p3851 A70-42096
- Moving object coordinates autonomous determination errors in accelerometers with dry friction, investigating inertial navigation system with integral horizon correction
23 p4193 A70-43981
- INERTIAL FORCES**
U INERTIA
INERTIAL GUIDANCE
NT STRAPDOWN INERTIAL GUIDANCE
Floated single degree of freedom gyroscope and pendulous integrating gyroscope accelerometer, discussing design features as inertial sensors for future space missions
01 p0086 A70-10313
- Step system of automatic extremal control algorithms for inertial plant in presence of noise
04 p0661 A70-15194
- Europa satellite launch vehicle inertial guidance and navigation system, discussing program of environmental, system integration and performance tests
05 p0879 A70-15816
- Digital computer interface for ELDO launcher inertial guidance system linking with platform, autopilots, telemetry equipment and rocket subsequenceurs
05 p0818 A70-16572
- Computer system for real time data acquisition and servicing of asynchronous inertial guidance system test stations
08 p1467 A70-21591
- Radio and inertial guidance of Europa 1 and 2 ELDO launch vehicles
08 p1542 A70-21870
- Digital guidance computer compatibility with analog attitude control loop in Digital Inertial Guidance System used in ELDO launch vehicle
11 p2080 A70-26280
- Aircraft lateral and longitudinal motion stability in steady rolling, deriving inertia cross coupled stability criterion
13 p2347 A70-29445
- Small low angular momentum (SLAM) gyro for inertial guidance systems, discussing drift performance, float suspension, signal generator, flex leads, etc
[AIAA PAPER 70-1011] 20 p3631 A70-39522
- Nonlinear programming for minimizing inertial guidance systems costs via optimal subsystem selection
20 p3740 A70-39645
- Low cost gimbaled inertial guidance platform providing medium accuracy in missile environment
[AIAA PAPER 70-1026] 20 p3669 A70-39721
- Inertial guidance technology applications for space navigation, considering instrument design tradeoff between accuracy and cost for performance and reliability improvements
21 p3848 A70-41128
- Programming and checkout of computer for ELDO inertial guidance system, including flight simulation and autopilot tests
[AIAA PAPER 69-961] 21 p3795 A70-41862
- Scientific satellite reentry guidance algorithms for inertial system, discussing controllability, onboard computer, gyros, accelerometers, jet actuators, terminal guidance, glide trajectory, etc
23 p4216 A70-44667

- Pilot navigation efficiency in low altitude terrain following flight, using synchronized TV and simulator with inertial guidance
24 p4307 A70-45506
- Satellite launch vehicle guidance equations for programmed optimization applied to Eldo inertial guidance system
24 p4375 A70-46359
- INERTIAL MEASURING UNITS**
U INERTIAL PLATFORMS
INERTIAL NAVIGATION
NT GIMBALESS INERTIAL NAVIGATION
Flight test experiments for H-19 helicopter to evaluate aided inertial system performance for terminal guidance
01 p0136 A70-10303
- Inertial navigation techniques application to commercial air traffic control, indicating decreased dependence on external navigation aids in oceanic operations
01 p0136 A70-10304
- Thermal preconditioning using radioisotope heat source to eliminate inertial sensor warmup time by maintaining aircraft navigation system at constant temperature
01 p0140 A70-10310
- Military inertial navigation technology applied to civil air transport aircraft
01 p0137 A70-10311
- Data analysis of inertial systems for commercial aircraft overseas operations, classifying systems error propagation as linear time drift or Foucault period oscillation
01 p0137 A70-10314
- Satellite navigation efficiency compared with inertial and Omega navigation techniques
01 p0139 A70-11263
- Inertial navigation systems, discussing role as flight control sensor with advent of all digital interface automatic flight control systems and cost and reliability
02 p0334 A70-11888
- Lateral separations using navigation error analysis, showing values for aircraft with or without Dioscures and inertial control under North Atlantic conditions
02 p0336 A70-12607
- Readjustment of aircraft navigation systems based on inertial platforms, discussing errors, corrections and damping stressing single platform
02 p0336 A70-12608
- Inertial navigation system with gyrocompass sensor, deriving equations for continuous orientation determination within gimbal system, estimating errors
03 p0522 A70-13372
- Recursive nonlinear system state estimation for arbitrary path magnetic navigation tested on simplified model by Monte Carlo simulation, considering derived error expression
04 p0715 A70-14627
- Inertial navigation system reliability indices and improvement, discussing mission success, mean time between failure and automatic monitoring
04 p0716 A70-15166
- Europa satellite launch vehicle inertial guidance and navigation system, discussing program of environmental, system integration and performance tests
05 p0879 A70-15816
- Onboard computer requirements for inertial navigation of spinning and maneuvering vehicle, determining design parameters
[AIAA PAPER 68-839] 06 p1013 A70-17161
- Optimum filter for aircraft inertial navigator and radio position fix data mixing using mathematical model of error propagation
[AIAA PAPER 70-35] 06 p1103 A70-18184
- Explicit expressions for inertial navigation system errors analysis derived as function of plant coordinates, gyrocompass fluctuations, external moments and initial conditions
07 p1331 A70-19541
- Inertial navigation systems errors determined by geometric method, obtaining object coordinates
07 p1332 A70-20145
- Inertial navigation system design principles, deriving error equations and equations of ideal operation
07 p1332 A70-20177
- Model of ideal accelerometer in form of mass point suspended within body of accelerometer mounted in spatial elastic weightless suspension on moving object
07 p1288 A70-20178
- Inertial navigation evolution, considering Reich studies
[DFVLR-SONDDR-1] 08 p1540 A70-20683
- Soviet monograph on inertial methods of flight vehicle motions parameters measurement
08 p1540 A70-20692
- Dual inertial navigation transpolar flight to North Pole aboard KC-135 airplane, discussing performance, installation, etc
09 p1719 A70-22189
- Commercial aircraft inertial navigation, examining gyroscope, accelerometer and electronic computer
10 p1914 A70-23848

- Inertial navigation systems, describing platform servos, computer, measurement devices, etc
10 p1914 A70-24861
- Errors estimation arising in inertial navigation equations solution while neglecting terms dependent on earth asphericity and gravitational field
11 p2077 A70-25558
- Self optimizing Kalman filter for hybrid inertial air navigation systems, noting implementation on airborne digital computer
11 p2078 A70-25682
- Unmanned Mars roving vehicle navigation subsystem feasibility study covering inertial and gyrocompass-odometer systems
11 p2080 A70-26211
- Inertial hybrid navigation system optimization, discussing performance curves and numerical filters synthesis and error elimination
13 p2448 A70-28747
- Nonlinear filtering methods for attitude computation in strapdown inertial navigation system
13 p2382 A70-29067
- Flight test experiments for H-19 helicopter to evaluate aided inertial system performance for terminal guidance
13 p2449 A70-29622
- Diurnal vibrations damping in inertial navigation system, demonstrating equations asymptotic stability for coordinates autonomous determination
15 p2775 A70-32156
- Commercial aircraft strapdown inertial navigation systems, examining initial self alignment techniques
18 p3289 A70-36442
- STOL navigation systems, evaluating Vector Analog Computer, Decca Omnitrac IIB and inertial system
18 p3289 A70-36513
- Implementation delay error reduction in discrete Kalman filter, noting application to inertial navigation systems analysis
18 p3236 A70-36712
- Inertial navigation platform system for long range flights, passing command through computer to automatic pilot
18 p3290 A70-36950
- Avionics hardware operational effectiveness assessment method, considering inertial navigation system LN-12D
19 p3442 A70-38837
- Aircraft trajectory postflight reconstruction involving photographic starfield and landmark referenced to inertial navigator output, discussing optimal data smoothing technique
[AIAA PAPER 70-1022] 20 p3666 A70-39512
- Hollow test platform for gyros and accelerometers used in inertial navigation
[AIAA PAPER 70-952] 20 p3606 A70-39577
- Two-axis electrolytic bubble level as precision vertical reference and tilt indicator for ballistic missiles inertial navigation systems
[AIAA PAPER 70-949] 20 p3631 A70-39578
- Thermal preconditioning unit using radioactive isotope heat source for temperature control of inertial navigation system
20 p3671 A70-40059
- Beryllium use in inertial navigation as stable platform structure and control gyro, discussing physical properties, design concept, fabrication, service, cost and tradeoffs
20 p3639 A70-40451
- Strapdown redundant experimental sensor inertial navigation package containing gyros and accelerometers, discussing signal real time processing by digital computer
[AIAA PAPER 69-851] 21 p3849 A70-41858
- Radar inertial system flight evaluation, discussing V/STOL program for approach and landing by use of ground based radar for updating onboard inertial navigator
22 p4066 A70-42651
- Inertial navigation system application to air transportation, discussing system mechanization and compatibility with ATC requirements
22 p4066 A70-42654
- Kalman filters for data mixing in optimally aided inertial navigation systems
22 p4067 A70-42661
- Inertial Navigation System (INS), geodetic reference and optimal data smoothing for estimating vertical deflection and ocean currents
22 p4069 A70-43665
- Moving object coordinates autonomous determination errors in accelerometers with dry friction, investigating inertial navigation system with integral horizon correction
23 p4193 A70-43981
- Stability solution of nonlinear differential equations in position determination on earth by inertial navigation
24 p4374 A70-46202
- INERTIAL PLATFORMS**
Readjustment of aircraft navigation systems based on inertial platforms, discussing errors, corrections and damping stressing single platform
02 p0336 A70-12608

- Optimal data filtering techniques and hardware for centrifuge testing of missile inertial platforms [AIAA PAPER 70-405] 10 p1861 A70-24901
- Initial quaternion for Cartesian time varying transformation matrix based on self alignment method of inertial analytic platform 11 p2072 A70-26150
- Attitude and heading reference system consisting of five-gimbal platform with two degree of freedom directional gyroscope 11 p2057 A70-26503
- Satellite attitude control via optical-inertial stabilization, using Bucy-Kalman linear statistical filtering 15 p2811 A70-32265
- Inertial navigation platform system for long range flights, passing command through computer to automatic pilot 18 p3290 A70-36950
- Inertial platform with integral dynamic self test and fault monitoring scheme, describing design and operation [AIAA PAPER 70-1013] 20 p3667 A70-39520
- Self calibrating TRIM gyromonitor inertial platform with gyroflex gyro, describing operation and performance [AIAA PAPER 70-1012] 20 p3667 A70-39521
- Fluidic inertial platform feasibility model for air to surface missile line-of-sight guidance, noting cost, reliability and environmental advantages [AIAA PAPER 70-1009] 20 p3667 A70-39523
- Low cost gimbaled inertial guidance platform providing medium accuracy in missile environment [AIAA PAPER 70-1026] 20 p3669 A70-39721
- Beryllium use in inertial navigation as stable platform structure and control gyro, discussing physical properties, design concept, fabrication, service, cost and tradeoffs 20 p3639 A70-40451
- Orbiting spacecraft angular velocities via inertial sensing platform consisting of linear accelerometers 24 p4372 A70-45475
- Aircraft navigation control system by digital computer combined with inertial platform, considering emergency backup, slow drift and system malfunctions 24 p4374 A70-46092
- INERTIAL REFERENCE SYSTEMS**
- Mass point motion in inertial reference system of special relativity, finding motion equations analogous to relative motion equations in classical mechanics 01 p0145 A70-11442
- Attitude and heading reference system consisting of five-gimbal platform with two degree of freedom directional gyroscope 11 p2057 A70-26503
- Star tracker rigidly connected to spacecraft frame for attitude determination by star field correlation 16 p2946 A70-33157
- Precise sensing systems and instruments calibration with respect to inertial frame of reference for geokinetics [AIAA PAPER 70-958] 20 p3622 A70-39571
- Two-axis electrolytic bubble level as precision vertical reference and tilt indicator for ballistic missiles inertial navigation systems [AIAA PAPER 70-949] 20 p3631 A70-39578
- INFARCTION**
- P wave changes in serial ECG in patients with acute myocardial infarction 01 p0013 A70-10272
- Atrial and ventricular gallops incidence during acute myocardial infarction by serial auscultation and phonocardiograms 01 p0014 A70-10277
- Myocardial infarct and other psychosomatic disturbances - Conference, Wiesbaden, West Germany, August 1967, Part 3 01 p0023 A70-10864
- External environmental factors, life habits and personality structure effects on development of coronary artery disease, discussing psychosomatic aspects of myocardial infarction 01 p0023 A70-10866
- Organic and psychological risk factors in myocardial infarction, presenting characteristic case history graphically 01 p0024 A70-10867
- Adrenal function in patients with acute myocardial infarction correlated with prognosis 01 p0029 A70-11405
- Acute myocardial infarction - Conference, Phoenix, March 1969 04 p0633 A70-15455
- Pathological manifestations of acute myocardial ischemia without acute myocardial necrosis and myocardial infarction, discussing subjects with chronic occlusive coronary atherosclerosis 04 p0634 A70-15456
- Primary and secondary pathological changes in small coronary arteries and role in acute myocardial infarction development, discussing coronary arteries distribution 04 p0635 A70-15457

- Platelet function in coronary artery disease and myocardial infarction, considering thrombosis, atherosclerosis, emboli in microcirculation, etc 04 p0635 A70-15458
- Clinicopathological studies of coronary artery occlusion and acute myocardial infarction, discussing coronary thrombosis 04 p0635 A70-15459
- Psychosocial factors in myocardial infarction and sudden death, considering possible causes of fatal cardiac arrhythmia 04 p0635 A70-15462
- Myocardial infarction therapeutic prevention possibilities on basis of epidemiologic and dietary studies involving hypercholesterolemia and hyperlipemia in coronary disease 04 p0635 A70-15463
- Plasma lipids and lipoprotein changes following myocardial infarction, discussing rise and normal return times of free fatty acids, cholesterol and beta lipoproteins 04 p0636 A70-15464
- Heparin role in anticoagulant therapy for myocardial infarction based on proved application to other venous thrombotic diseases, noting hemorrhagic complications controllability 04 p0636 A70-15465
- Familial aggregation for coronary artery disease and familial similarities in coronary anatomy, considering possible genetic analysis of myocardial infarction 04 p0636 A70-15467
- Myocardial blood flow in patients with acute myocardial infarction determined from measuring effective capillary flow /ECF/ by direct counting of rubidium 86 uptake 04 p0636 A70-15468
- Ventricular performance as function of infarcting myocardium, discussing dynamic characteristics 04 p0637 A70-15470
- Acute myocardial infarction clinical features, discussing gallop rhythm, ventricular arrhythmias, ventricular tachycardia, bradycardia, etc 04 p0637 A70-15471
- Sudden and early death in acute myocardial infarction, discussing prophylactic measures 04 p0637 A70-15472
- Myocardial scarring sites localized in human subjects by HF ECG components 05 p0800 A70-16104
- Acute myocardial ischemic injury and infarction in dogs related to changes in man using oxygraph tracings 06 p0997 A70-18405
- Ventricular ectopic beats and bradyarrhythmia associated with myocardial infarction, discussing enhanced automaticity, reentry activity, drugs and heart pacing 06 p0998 A70-18407
- Bradycardic rhythms in acute myocardial infarction, investigating pathophysiologic, hemodynamic and electrophysiologic aspects and ECG interpretation 06 p0998 A70-18408
- Left ventricular function myocardial infarction induced acute depression and subsequent recovery in intact conscious dogs 07 p1211 A70-19615
- Physiological responses during exercise recorded in patients with healed myocardial infarction, considering work tolerance 07 p1212 A70-19693
- Wolff-Parkinson-White syndrome simulation of myocardial infarction, indicating false positive tests for exercise electrocardiograms 09 p1622 A70-23468
- Asymptomatic myocardial infarction in USAF flyers detected by annual electrocardiograms 15 p2690 A70-31889
- Hemodynamic response to dopamine before and after myocardial infarction in dogs 17 p3026 A70-35200
- Electrocardiogram vs vectorcardiogram for myocardial infarction diagnosis 19 p3371 A70-38362
- Hemodynamic effect of lidocaine given by infusion and bolus injections in myocardial infarction, examining cardiac output, heart rate, systolic left ventricular and aortic pressures 19 p3366 A70-38575
- Antigens immunological response during myocardial infarction 20 p3570 A70-39151
- Postexercise electrocardiogram detection of latent coronary heart disease in flyers prior to myocardial infarction 21 p3771 A70-41494
- Indirect serial determination of left ventricular systolic ejection time changes in human patients with acute transmural and nontransmural myocardial infarctions 23 p4144 A70-43946

INFECTIONS

U INFECTIOUS DISEASES

INFECTIOUS DISEASES

NT AIRBORNE INFECTION

- Mice and hamster infection resistance following short term acceleration stress, eliminating low hydrocortisone level as protective agent 03 p0428 A70-14067
- Postinfectious noncoronogenic afflictions of myocardium in flight personnel, discussing clinical record, atherosclerotic differentiation and ECG variation 09 p1617 A70-22474
- Infectious disease hazards on space flight, discussing internal environmental factors including resistance and etiologic agents transmission 14 p2537 A70-30366
- Infection resistance during extended space flights, discussing microfloral exchange, defense mechanisms, waste, etc 15 p2688 A70-31677
- Hematologic changes in mice associated with meningovirus infection and hypobaric hypoxia during barometric pressure changes 15 p2681 A70-31878
- Hypobaric hypoxia effects on MM virus infection resistance in mice 20 p3572 A70-39428
- Systemic bacterial infection resistance in white mice exposed to simulated hypobaric normoxic space cabin environment 20 p3572 A70-39431
- Hyperbaric oxygen effects on Coxsackievirus infection in mice 24 p4296 A70-45338
- INFERENCE**
- Response bias of conservative human inference, using revised odds estimate experiments 19 p3361 A70-38055
- INFINITY**
- Asymptotic behavior at infinity of mixed boundary value problem analyzed for Sobolev equation involving operator 03 p0518 A70-13433
- Dynamic characteristics approximation in transfer functions class with singularity at infinity 07 p1327 A70-19806
- INFLATABLE DEVICES**
- U INFLATABLE STRUCTURES**
- INFLATABLE SPACECRAFT**
- NT BEACON SATELLITES
- NT EXPLORER 22 SATELLITE
- INFLATABLE STRUCTURES**
- NT BALLOONS
- NT BALLUTES
- NT BEACON SATELLITES
- NT EXPLORER 22 SATELLITE
- NT HIGH ALTITUDE BALLOONS
- NT METEOROLOGICAL BALLOONS
- NT ROBIN BALLOONS
- NT TETHERED BALLOONS
- Solid propellant cool gas generating systems applications to inflating emergency escape slides, rafts, pontoons and flotation bags 06 p0986 A70-17720
- Cool gas inflation systems for evacuation equipment on large aircraft with size and weight fitting into aircraft doors 06 p0986 A70-17721
- Occlusion training during hypodynamia with inflatable thigh cuffs to prevent unfavorable effects on cardiovascular system 10 p1816 A70-24689
- Concorde aircraft design for emergency passenger evacuation, emphasizing overwing inflatable escape slides and kinetic heating effects 15 p2675 A70-32222
- Thermal testing of inflatable solar shields for cryogenic space vehicles, discussing shield misalignment effects on propellant tank temperatures [AIAA PAPER 70-856] 16 p2982 A70-33901
- Ballistic trajectory, packageability, deployment and flight stability of attached ram air inflatable decelerator for high speed/low altitude store delivery [AIAA PAPER 70-1199] 21 p3752 A70-41817
- Euler buckling of inflated toroidal gas bodies, including packaging and load deflection tests for Mylar, dacron-neoprene and stainless steel-silicone fabrics [AIAA PAPER 70-1198] 21 p3938 A70-41818
- Energy methods for stability of linear inflatable pouch actuator based on energy change in pouch deflection 21 p3760 A70-41966
- Aircraft crash protection with preinflated air bag added to conventional seat/lap belt tested with human sled subjects 23 p4140 A70-44456
- INFLATING**
- Parachute inflation dispersion studied by plotting dimensionless products characterizing incompressible flow process 01 p0006 A70-10849
- Opening distance and inflation time prediction for parachutes deployed supersonically based on subsonic performance 07 p1394 A70-19725

Liquid hydrogen balloon inflation system for use at remote locations, discussing characteristics and economy 20 p3607 A70-40086

Stress distribution and shape in arbitrarily shaped gore parachute under unsteady pressure distribution during inflation and descent [AIAA PAPER 70-1197] 21 p3752 A70-41819

Three body problem for parachute system dynamics during inflation [AIAA PAPER 70-1170] 21 p3755 A70-41843

Parachute trajectory and opening load prediction based on inflation process and added mass, determining drag area as function of distance [AIAA PAPER 70-1168] 23 p4137 A70-43993

INFLECTION POINTS

Two dimensional wave front shapes induced in finitely strained elastic body by impulsive point body force, discussing normal and double inflection points 08 p1584 A70-20581

Heat transfer mechanism in foil-vacuum insulation, analyzing factors responsible for point of inflection on experimental temperature field curves 13 p2521 A70-28861

INFLUENCE COEFFICIENT

NT STRUCTURAL INFLUENCE COEFFICIENTS

Longitudinal stability derivatives prediction for rigid and elastic airplanes, using influence coefficient method [AIAA PAPER 69-131] 04 p0624 A70-15383

Aircraft wing load calculations using aerodynamic influence coefficients based on linear subsonic or supersonic flow theory 06 p0967 A70-17255

Influence coefficients for toroidal shells under axisymmetric edge loads, taking one term in asymptotic expansion of Hankel function 11 p2132 A70-25693

Unsteady aerodynamics prediction of supersonic elastic aircraft, discussing aerodynamics influence coefficients/AIC/method refinement [AIAA PAPER 70-944] 20 p3558 A70-39583

Bounds to direct influence coefficient derived by hybrid stress finite element method 22 p4116 A70-43203

INFORMATION

Electronic camera instrumental profile, information capacity and object recognition 14 p2583 A70-30363

INFORMATION DISSEMINATION

ELDO project planning and progress monitoring system for management provided by Central Planning and Progress Monitoring Service 21 p3956 A70-41497

Satellite data acquisition and dissemination functions of National Space Science Data Center (NSSDC) [AIAA PAPER 70-335] 24 p4322 A70-45615

INFORMATION PROCESSING

U DATA PROCESSING

INFORMATION RETRIEVAL

SPIRAL system for free-flowing text information storage and retrieval in machine readable library 02 p0264 A70-12129

Information storage and retrieval system development and operation for diversified crew/equipment task data, using general purpose digital computer 02 p0265 A70-12143

Explosives and pyrotechnics information sources including government manuals, commercial publications, symposium proceeding, R and D programs 03 p0610 A70-14127

Hologram storage and retrieval in photochromic SrTiO crystals at ruby laser wavelengths 06 p1072 A70-18519

Information extraction efforts using imaging sensors on earth resources satellites compared to data processing for environmental satellite imaging sensors [AIAA PAPER 70-284] 09 p1669 A70-22894

Verbal information recall latencies as function of time interval from initial memory storage and retrieval repetitions 10 p1818 A70-24718

European information retrieval network for interrogating NASA master file on space literature using computer terminals 14 p2670 A70-31174

Holographic data storage for random information display and retrieval in wide range consumer credit network 16 p2903 A70-33135

Direct access on-line information retrieval system combining computer assisted instruction and bibliographic retrieval, using thesaurus for literature indexing 17 p3048 A70-34600

Solid state display for on-line information retrieval using light emitting crystals, integrated circuits and hybrid packaging 17 p3063 A70-35514

Flight loads data extraction and analysis from damaged magnetic tapes after aircraft crash 17 p3094 A70-35518

Integrated data systems for aircraft maintenance, noting information retrieval role in maintenance management for cost reduction and safety 20 p3740 A70-39647

Papers on information science and technology covering computerized retrieval, automatic indexing, selective dissemination, etc 21 p3955 A70-40894

Scientific/technical information collection, retrieval and dissemination, discussing organization, employment of technical/scientific expert personnel and use of modern data processing equipment 23 p4286 A70-44670

Graph theoretical cluster technique for producing index terms thesaurus for information retrieval system, discussing algorithms 24 p4316 A70-45161

INFORMATION SYSTEMS

NT MANAGEMENT INFORMATION SYSTEMS

SPIRAL system for free-flowing text information storage and retrieval in machine readable library 02 p0264 A70-12129

Reliability optimization of information systems with discrete time resource output and measured efficiency control 04 p0661 A70-15195

Information display devices, discussing interactive graphic consoles, reusable film, magneto-optics, broadband laser, etc 05 p0851 A70-16725

Baseband transmission system information transmission rate improvement, using multivalued PCM signals 06 p1007 A70-17461

Stochastic model of information handling centers as typified by document storage and retrieval derived from integral equation to determine expected primary store size 06 p1016 A70-18450

Pilot limitations role in USAF midair collisions, discussing information systems for collision avoidance 07 p1192 A70-19022

Integrated display for crowded tactical aircraft cockpits, presenting multisensor information for weapons and fire control systems 08 p1500 A70-21760

Multidiscipline systems analysis of satellite assisted information system improving earth resource management, developing User Decision Models [AIAA PAPER 70-335] 09 p1792 A70-22855

Earth Resources Satellite Information Systems, discussing NASA Space Application Program relation to national goals, federal spending, cost effectiveness analysis, information sales, etc 09 p1793 A70-22860

Data management functions of National Space Science Data Center (NSSDC), discussing data processing and information system for secondary usage [AIAA PAPER 70-320] 09 p1641 A70-22866

Remote sensing data applications to agricultural statistics, discussing policy and standards for aggregate data release, confidentiality, error analysis, etc [AIAA PAPER 70-312] 09 p1793 A70-22868

User information traffic forecasting method for operational Earth Resource Satellite System, discussing user expectations [AIAA PAPER 70-293] 09 p1793 A70-22890

Soviet book on automatic scanning information systems, discussing equipment, system parameters, scanning methods, etc 10 p1840 A70-24376

Nonavionic Aircraft Integrated Data System configurations evaluation by computer model, showing cost effectiveness data in terms of aircraft maintenance and availability [AIAA PAPER 70-396] 10 p1808 A70-24909

AIRLORD system consisting of central data processing and I/O units for predeparture handling of passengers and freight at airports 11 p2013 A70-25365

Information transfer services potential demand including telephone, telegraph, videophone, electronic mail, etc [AIAA PAPER 70-443] 11 p2152 A70-25448

Earth resources satellite ground data handling system providing initial processing, reproduction, indexing, storage, retrieval and dissemination functions 12 p2191 A70-26943

Space information systems effectiveness evaluation based on generalized homomorphous model 13 p2372 A70-28377

Spaceborne information processing for manned missions, describing layered system with fault tolerance and onboard checkout 13 p2372 A70-28415

Onboard satellite information processing systems for bandwidth compression using digital filters and error correcting coding 13 p2381 A70-28431

Automatic search for data in hydrology and meteorology, describing information search language development 14 p2602 A70-30141

Price estimate elements interrelationship using three dimensional matrix for computerized cost data extraction 14 p2668 A70-30524

Memory systems in measurement and control equipment, describing applications to linearizing, compression and data refresh operations 14 p2554 A70-30676

Quality information system consisting of closed loop input/feedback methods insuring design requirements of Saturn S-2 stage 14 p2654 A70-31116

European information retrieval network for interrogating NASA master file on space literature using computer terminals 14 p2670 A70-31174

Accident/incident information exchange in aviation community, noting Flight Safety Foundation 15 p2674 A70-32209

Material data file and retrieval system for designers in automotive, equipment and appliance industries, discussing applications to other FRP markets 16 p2935 A70-33352

Airborne flight test data acquisition and ground based automatic bulk data processing system for helicopter test and development programs 17 p3014 A70-34713

Experiment information management, discussing data flow patterns, acquisition, processing, storage, etc 17 p3199 A70-34807

[AAS PAPER 70-057] Data acquisition system applications philosophy, discussing data integrity, expansion facility, flight safety, etc 18 p3258 A70-36339

Statistical properties of civil ATC system based on central processor, discussing system informational congestion 18 p3288 A70-36394

Optimization model for evaluating information management systems for handling control functions of long duration space station missions 19 p3532 A70-37851

Management information systems based on Apollo program experience, considering improvements in data accuracy, display, feedback, etc 19 p3553 A70-37862

Water management decision model using earth resources information system with satellite-based remote sensors, evaluating costs and benefits by systems analysis 20 p3616 A70-39066

Aircraft/spacelcraft assisted agricultural resource information system design concerning nongovernmental user and remote sensing needs 20 p3740 A70-39067

Digital optical storage for information system components 21 p3823 A70-40852

Papers on information science and technology covering computerized retrieval, automatic indexing, selective dissemination, etc 21 p3955 A70-40894

Automated airline communications system for collecting, analyzing, storing, transmitting, receiving and presenting information required by ATC and advisory services 21 p3789 A70-41347

Aircraft accident filing system data analysis using Fortran programs 22 p3962 A70-42880

Information handling for safety design concerning standards, criteria and requirements 23 p4153 A70-44493

Data management functions of National Space Science Data Center (NSSDC), discussing data processing and information system for secondary usage [AIAA PAPER 70-320] 23 p4285 A70-44514

Space station program information management system involving data acquisition and extended manned flight operation with minimum ground support [IBM-70-U60-0015] 23 p4164 A70-44637

Earth resources information systems using space, aerial and ground measurements, discussing Apollo 9 IR color photograph of Mississippi Valley and timber inventory applications 23 p4192 A70-44679

Graph theoretical cluster technique for producing index terms thesaurus for information retrieval system, discussing algorithms 24 p4316 A70-45161

Satellite based navigation/air traffic control information systems for short range STOL air carrier aircraft [AIAA PAPER 70-1338] 24 p4373 A70-45930

Upper Air Space Control Center Automatic Data Processing and Display System for air traffic control 24 p4323 A70-46238

INFORMATION THEORY

Book on communication and information theories application to fading dispersive communication channels, discussing tropospheric scatter, HF ionospheric links, moon bounds, etc 02 p0253 A70-11700

Rate distortion function for class of sources, proving positive and negative sides of Shannon encoding theorem for noisy channels 02 p0266 A70-12611

Visual object images describable in terms of cross correlation functions without loss of information 04 p0662 A70-15437

Informative filter automatic selection for describing visual object with aid of frequency spectrum, taking filter output voltage mean square value as criterion 04 p0662 A70-15438

Risk-reducing information role in decision making using Marschak bidding procedure 07 p1203 A70-18964

Entropy analysis of feedback control systems leading to separation theorem and feedback process information interpretation 07 p1245 A70-19095

Destructive and nondestructive tests optimum procedure for quality control based on information theory, decision statistics and cost optimization 09 p1691 A70-22573

Optimum coding of information for symmetric channel described by code word transformation probability 09 p1639 A70-23694

Information hypothesis and repetition hypothesis concerning human reaction time to visual stimulus information 10 p1826 A70-24714

Physical formula for information content in communication signals based on receiver observation concept, noting role of channel properties and encoding 10 p1844 A70-25223

Information theory, considering biological applications, coding and information content and transmission 10 p1846 A70-25284

Information theory as basis for statistical thermodynamics, discussing maximum entropy principle and probability as frequency in Gibbs ensemble 11 p2083 A70-25694

Optimum symbol sequence interleavers realization taking into account storage capacity and encoding delay 11 p2014 A70-26246

Random fields entropy estimation technique taking into account higher than immediately adjacent spatial dependencies 12 p2192 A70-27771

Practical codes in digital space communication systems, reviewing Shannon information theory theorems 15 p2698 A70-31963

Data transmission from information sources over communication channels with limit imposed on attainable reliability, discussing coding theorem of information theory 16 p2871 A70-34259

Book on random processes, communications and radar covering optimum filtering, detection, information theory, ergodic theory, probability and integration axioms, parameter estimation, coding, etc 17 p3043 A70-34602

General linear /Kalman/ sequential filter to account for finite correlated white noise without state vector augmentation or measurement differentiation 21 p3828 A70-41735

Information transmission and coding theory - Conference, Tashkent, Uzbek SSR, September-October 1969, Section 1, Data transmission theory, Methods of coding and decoding 22 p3985 A70-42490

Optimal reception of phase manipulated signal on noise background with unknown statistics and information parameter a priori probabilities 22 p3987 A70-42561

Recurrent adaptive methods for verification of multialternative hypotheses in stepwise signal processing 22 p3993 A70-42565

Suboptimum extraction of pattern features from continuous measurements, assuming different Gaussian random classes 22 p3991 A70-43493

Information theory of hearing, considering subjective properties of nonsteady sound signals and discernibility relations 23 p4155 A70-44700

Information theory in physics and engineering, considering data processing, error correction codes, space communication, optical data transmission, noise effects and holography 24 p4379 A70-45616

INFORMATION TRANSFER

U COMMUNICATING

INFORMATION TRANSMISSION

U DATA TRANSMISSION

INFRARED ASTRONOMY

Far IR night sky emission above 120 km over millimeter range, using rocket-borne telescope 01 p0069 A70-10040

Near limb solar IR brightness distribution observed during total solar eclipse of 12 November 1966 in Argentina by sounding rocket photometers 01 p0186 A70-11271

IR observations for position of hypothetical Seyfert-like nucleus explaining M82 polarization pattern 02 p0372 A70-12246

IR flux variations from Seyfert galaxy NGC 4151 nucleus, using telescope 03 p0562 A70-14221

Cassegrainian liquid He cooled IR telescope for rocket-borne IR astronomy, discussing optical, cryogenic and electronic designs 04 p0689 A70-15017

Far IR extrinsic photoconductive detectors for rocket-borne liquid He-cooled IR telescope, discussing limiting noise factor 04 p0689 A70-15018

Intensity and spectral distribution measurement techniques for nonvisible extraterrestrial radiation, discussing rocket spectroscopy results 04 p0757 A70-15648

SNR for IR photovoltaic semiconductor cell generalized for astronomical case, noting stars approximation to black body radiators 05 p0849 A70-16645

Unusual IR object IRC plus 10216 interpreted as galactic source surrounded by optically thick dust shells, noting resemblance to black body energy distribution 05 p0920 A70-16976

IR astronomy techniques and photometric standards, solar-lunar and planetary observations, cosmic background radiation, etc 06 p1153 A70-18549

IR luminosity of galactic nucleus from far IR observations, noting considerations favoring nonthermal model consisting of multiple sources 10 p1947 A70-24996

Submillimeter astronomy, discussing atmospheric absorption difficulties and principal areas of application 12 p2311 A70-28271

Spectrum of bright IR object VY Canis Majoris, noting absorption feature attributed to SiO molecules in stellar atmosphere 17 p3154 A70-34540

IR balloon observations of absolute solar brightness and stratosphere transparency, discussing BCA and HSRA models 17 p3078 A70-35580

Vesta diameter and albedo determination by IR emission measurements, allowing for roughness and rotation 17 p3173 A70-35758

Radio emission search from IR objects near IC 1805 18 p3318 A70-37018

Lunar and planetary laboratory communications, Volume 8 covering IR astronomy, Mercury, Mars, Uranus, comets, etc 19 p3515 A70-37929

Martian photographic map during 1967 opposition in red and near IR range 19 p3516 A70-37935

Nebula K3-50 IR radiation source observation, noting energy distribution resembling NGC 7027 and W51-IRS 2 20 p3701 A70-39003

Main sequence stars faint end IR observations for luminosities and temperatures 20 p3702 A70-39014

IR star types T-Tauri, B-emission and M supergiants observations using UVBRI photometry 21 p3890 A70-41163

IR observation of chromospheric Ca II K-line during total eclipse of 7 March 1970 24 p4401 A70-45314

INFRARED DETECTORS

CAT remote sensing for advance aircraft warning, using IR instrument to detect turbulence-associated temperature preceding aircraft 01 p0087 A70-10697

Ge bolometer cooled by liquid helium 3 to near absolute zero to achieve high sensitivity for far IR detection 01 p0091 A70-10910

IR systems in military intelligence and space research including aerospace and planetary investigations, discussing IR detection and IR and earth radiation 01 p0144 A70-11255

Intrinsic IR detectors photosaturation, studying performance degradation due to high background light levels 02 p0297 A70-11925

Resin bonding material suitable for IR detectors noting transmission properties 02 p0321 A70-11926

Mercury cadmium telluride alloy as photoconductive IR detector material noting properties, composition and temperature dependence of energy gap 03 p0543 A70-14196

Far IR extrinsic photoconductive detectors for rocket-borne liquid He-cooled IR telescope, discussing limiting noise factor 04 p0689 A70-15018

Nonlinear dielectric element /tandem/ for detecting IR radiation in contactless temperature measurement 05 p0848 A70-16363

Specifications nomographs for earth resources IR radiometers, considering ground resolution, aperture diameters, detector arrays, etc 09 p1677 A70-22870

Aircraft surface temperature measured with airborne IR TV system 09 p1686 A70-23754

Ge-Cu IR detector photoconducting characteristics and application to carbon dioxide laser mode pattern measurement 10 p1898 A70-23922

IR sensor for detecting clear air turbulence, discussing design, installation, supporting equipment and inflight test results 12 p2229 A70-26946

IR remote temperature gradient sensor as clear air turbulence detector, presenting inflight test results 12 p2229 A70-26947

Optical IR system as low cost pilot warning indicator providing audible and visual collision warnings to general aviation aircraft 12 p2234 A70-27647

Flame temperatures simultaneous measurement in two spectral regions, using photoelectric IR pyrometer 12 p2237 A70-28158

Photoconductive and thermal IR detectors development 13 p2410 A70-29656

IR radiating bodies angular displacement determination by vacuum evaporated thermocouple radiation detectors, describing stationary communication satellite altitude control 15 p2740 A70-32422

Photovoltaic InSb IR detectors design and operation, emphasizing performance in restricted field of view 16 p2926 A70-33152

Pyroelectric IR radiation detector based on materials polarization changes associated with temperature changes 16 p2905 A70-33154

Encapsulated liquid crystal screens for IR laser beam imaging detectors with high thermal sensitivity and real time viewing in bright light 16 p2927 A70-33167

Passive radiative coolers role in utilizing IR detector systems for low temperature spacecraft applications, describing staged radiator design, optimization and tests 16 p2983 A70-33921

[ALAA PAPER 70-854] Conical passive radiation coolers for quantum IR detectors on equatorial synchronous earth satellites, determining temperature excursions 16 p2915 A70-34314

Solid state IR to visible converter, using minority carriers stimulated tunnel injection into wide band gap phosphor 17 p3081 A70-34648

IR heterodyne signal statistics, discussing receiver characteristics and design 17 p3105 A70-35096

Indium arsenide role in IR image detectors, describing photoelectric threshold and quantum efficiency 17 p3143 A70-35118

Photoemitting cesium antimonide thin films for IR detectors 19 p3488 A70-38202

Cryogenically cooled photoconductive IR radiation detectors, determining wideband optical heterodyne performance 20 p3627 A70-39085

Optical thermal testing by IR radiation, reviewing thermistor bolometer, various detectors, radiometric microscopes, NDT equipment, etc 21 p3831 A70-40747

Cryogenic cooling of IR radiation sensors for increasing sensitivity, considering background radiation interference from sensor optical system and detector/preamplifier noise 21 p3825 A70-41052

IR radiation thermometry, discussing detector types, industrial applications and specialized instruments 21 p3828 A70-41698

IR radiation, transmission and detection in non-destructive testing, discussing atmospheric transmission, thermal and photon-type detectors, etc 22 p4029 A70-42595

Clear air turbulence detection by IR radiometry of thermal gradients, using staggered receivers for panoramic visualization 24 p4314 A70-46093

Semiramis IR angular deviation measuring unit, discussing operation theory and performance characteristics 24 p4339 A70-46322

INFRARED FILTERS

Methane IR filter for monochromatizing He-Ne laser 21 p3823 A70-40823

INFRARED HORIZON SCANNERS

U HORIZON SCANNERS

U INFRARED SCANNERS

INFRARED IMAGERY

Soil characteristics influence on soil thermal regime related to thermal IR imagery and subsurface soil conditions

03 p0474 A70-13555

Ground temperature effect on thermal resolution in IR line scan imagery, discussing equipment and operating procedures for temperature gradient detection

04 p0686 A70-14617

Angular tolerance on IR radiation for phase matched image up-conversion in material with nonlinear susceptibility

04 p0703 A70-15621

Line scanning IR imagery system for thermal mapping of fire, water and soil conditions

05 p0836 A70-15770

IR imagery by InSb detectors applied to mapping earth surface thermal distribution

05 p0840 A70-16498

Airborne real time IR imagery of thermal anomalies for geophysical exploration of water resources

09 p1674 A70-22262

Satellite high resolution IR imagery for arctic sea ice mapping, describing sensor design and day and nighttime operation in film-strip format [AIAA PAPER 70-301]

09 p1669 A70-22884

IR holograms real time visual reconstruction by frequency stabilized carbon dioxide lasers

09 p1684 A70-23534

Swedish real time IR imaging system, discussing airborne applications in locating fresh water springs and defining irrigation patterns

10 p1879 A70-24743

Thermal imaging device adaptable to IR, microwave or ultrasound radiation, projecting image on heat sensitive surface

11 p2050 A70-25643

IR image conversion into visible using nonlinear KDP crystal

12 p2248 A70-27543

System design for IR imaging radiometer from synchronous altitude satellite, considering spacecraft dynamics, detectors and cooling

14 p2586 A70-30974

Cloud formation and structure determination using aircraft-borne IR stereo imagery

15 p2769 A70-31687

Encapsulated liquid crystal screens for IR laser beam imaging detectors with high thermal sensitivity and real time viewing in bright light

16 p2927 A70-33167

Surface temperature measurement with airborne IR scanning imager for terrain analysis

16 p2905 A70-33170

Day/night thermal IR imagery detection of moisture stress of girdled trees in upland forest

16 p2898 A70-34047

Indium arsenide role in IR image detectors, describing photoelectric threshold and quantum efficiency

17 p3143 A70-35118

Remote multispectral sensing of environmental and vegetative gradients in Yellowstone National Park by intercomparison of thermal IR and visible band imagery

17 p3079 A70-35617

Day and night IR imagery compared for interpreting vegetation

17 p3079 A70-35618

Visible and IR imagery by meteorological satellites measuring surface temperature, atmospheric circulation and state parameters, storm development and tracking, cloud motions, etc

20 p3660 A70-39076

Ground temperature effects on thermal gradients resolution in IR line scan imagery

24 p4334 A70-45363

INFRARED INSPECTION

Composite window permitting visual or photographic observation and IR irradiation of test materials in ultrahigh vacuum system

09 p1698 A70-22994

IR NDT bond inspection system for helicopter rotor blade honeycomb box assemblies, using closed circuit slow scan video system to detect bondline voids

17 p3101 A70-35184

Thermal IR nondestructive testing of adhesively bonded boron composite/Al honeycomb structures, discussing surface, cross section and instrumentation sensitivity effects

24 p4341 A70-45570

INFRARED INSTRUMENTS

Meteorological spaceborne IR instruments associated with NASA satellites, discussing various Tiros and Nimbus instruments

03 p0491 A70-13666

Lidar and IR radiometer mobile laboratory for atmospheric optics research, including construction details and support equipment

03 p0463 A70-13677

IR equipment on Tiros and Nimbus 1 and 2 satellites, describing vertical atmospheric sounding

03 p0492 A70-13833

Microwave and IR distance measuring devices design and operational principles, discussing main circuits and reading displays

05 p0851 A70-16799

IR crossed beam system for direct density turbulence measurements in mixing region of subsonic air jet

[AIAA PAPER 70-235] 06 p1065 A70-18091

IR technology in aircraft, satellite and rocket electronics, discussing photography, scanners, search and pursuit devices, guided rockets, pilot warning devices, etc

08 p1494 A70-20687

IR thermometers in situ calibration, analyzing maximum error due to reflection effect

09 p1684 A70-23536

Sea surface temperature measurement over large areas using IR remote sensing system mounted on airborne platform

09 p1686 A70-23756

Graphite IR radiator for radiative capacity and flame temperature measurements investigated for life time dependence on ambient pressure and temperature

10 p1888 A70-24257

IR electro-optical tracker Oculometer using human eye motions for pointing and tracking

11 p1989 A70-25352

Servocontrolled IR optometer providing electrical signal proportional to refractive power of human eye

12 p2237 A70-28123

Temperature measurement of products in solar furnace by IR pyrometers, considering interference filters, reflections parasitic effects, etc

15 p2740 A70-32424

Visual IR laser beam display, using cathode ray tube phosphor with variable sensitivity and range control

15 p2752 A70-32441

IR optical radiometer for jet engine turbine blade temperature measurement, comparing with junction wire thermocouple

16 p2905 A70-33168

IR reflectometer system using Fourier transform spectrometer and ellipsoidal mirror, describing design, construction and performance

16 p2905 A70-33171

IR radiometer for Mariner Mars 1971 project providing surface brightness temperatures

16 p2913 A70-34028

Surveyor Canopus sensor and Project Scanner dual IR radiometer mechanical design

16 p2914 A70-34107

Global meteorological parameters measurement by satellites, discussing IR instruments

20 p3664 A70-39711

Thermocouple and IR temperature measurement techniques comparison for double base solid propellants at low pressures

20 p3694 A70-40275

Thermal emission spectra of earth and atmosphere from IR Michelson interferometer onboard Nimbus 3 satellite

24 p4330 A70-45977

INFRARED LASERS

Scanned laser microscope producing shadowgraph displays of IR transmittance variations attributed to defects in polished Si and GaAs semiconductor wafers

01 p0105 A70-10025

IR CW sum-frequency up-conversion of carbon dioxide laser radiation using phase matched proustite as nonlinear crystal

01 p0111 A70-10786

IR radiation absorption from carbon dioxide laser in supersonic gas jet, applying results to nitrogen-carbon dioxide gas dynamic laser action

01 p0148 A70-11123

Laser action observation on IR bands of first positive system of molecular nitrogen using pulsed excitation

04 p0704 A70-15625

IR laser giant pulses duration and power measured by photomultiplier and lithium metaniobate

06 p1082 A70-17770

CW laser operation at 10.6 microns in DF-carbon dioxide and HF-carbon dioxide molecular systems achieved by purely chemical means

08 p1513 A70-21539

Laser frequency measurement and active and passive stabilization techniques, emphasizing HCN laser phase locking to frequency standard output

09 p1697 A70-22951

He-Ne laser IR generation in three mirror mismatched resonator, using Fabry-Perot interferometer to study mode and lasing range frequency shift

10 p1900 A70-24265

Plasma self Q switching in pulsed far IR lasers, discussing lens effect of plasma electrons delaying laser pulses

11 p2062 A70-25634

Holographic compensation for atmospherically induced phase distortion of IR laser beam

11 p2049 A70-25638

Foreign gases effects on He-Ne lasers IR emission, describing quenching due to positive column electron temperature decrease

11 p2062 A70-25826

He-Ne laser optimal mixture component ratio for generating IR radiation at two wavelengths

12 p2251 A70-28293

IR spectroscopy and lasers for analysis of atmosphere in air pollution research and monitoring

13 p2407 A70-29106

Optically pumped cadmium phosphide laser, obtaining IR coherent oscillation from Q switched Nd doped YAG laser excitation

15 p2751 A70-31985

Lasers and GaAs diode emitters near IR radiation intensity distributions, using IR films and IR display phosphors

15 p2753 A70-32607

Encapsulated liquid crystal screens for IR laser beam imaging detectors with high thermal sensitivity and real time viewing in bright light

16 p2927 A70-33167

Carbon dioxide laser action at 10.6 micrometers at pressures up to atmospheric by transverse electrical discharges

16 p2928 A70-33643

Atomic spectroscopy of IR laser transitions in gases excited by HF pulsed discharges

17 p3105 A70-35093

Whisker diode coupling to polarized IR laser beam by orientation based on antenna theory

17 p3048 A70-35902

Carbon dioxide IR laser applications to manufacturing technology, discussing absorption, reflection and heat conduction characteristics of materials

19 p3447 A70-38452

Pulsed laser emission at IR transitions of xenon and neon under electron beam pumping

19 p3449 A70-38743

Thermal blooming of 10.6 micron laser beam in carbon dioxide absorption cell

22 p4049 A70-42335

ACRA supersonic antitank missile with IR laser beam guidance system

22 p4110 A70-43212

Frequency measurement extension to 5 micron region by IR laser harmonic frequency mixing in point contact diode as multiplier chain

23 p4201 A70-44917

Basalt heating with IR carbon dioxide laser, investigating vapor fractionation for inert atmospheres, very high temperatures and silicon dioxide poor materials

24 p4409 A70-45673

High efficiency gallium arsenide IR illuminators, comparing dome diodes fabricated from diffused or Si doped solution grown materials

24 p4319 A70-45784

Rate equation study of multiwavelength far IR laser oscillations in water vapor, taking into account molecular rotation-vibration interaction

24 p4354 A70-45812

INFRARED MASERS

U INFRARED LASERS

INFRARED PHOTOGRAPHY

IR holography using thermochromic material and cuprous mercuric iodide to record on-axis interference pattern, reconstructing in visible range with He-Ne laser

01 p0092 A70-11170

Aerial color IR photography for crop disease identification by tonal and geographic patterns, discussing cameras, films, filters and exposure procedures

05 p0837 A70-16144

Satellites for meteorological and geographical studies using information from TV and IR pictures

08 p1487 A70-20716

Color and color IR aerial photography, discussing effects of solar spectrum, films, filters, etc, in connection with terrain analysis

10 p1880 A70-24751

Aerial IR film optical density related to preharvest crop yield indicators in micro experiments with remote sensors

12 p2217 A70-26918

Aerial reconnaissance of soils, rocks, vegetation and streams, comparing color, IR color, and black-and-white photography

12 p2236 A70-27873

Soil characteristics determination from black and white, color and IR aerial photographs

14 p2577 A70-30980

Reflectance of single leaves and field plots of cotton, determining Cycocel treatment effects on aerial IR photography

14 p2577 A70-31233

Auxiliary minus-visual filters in high altitude IR aerial color photography, suggesting tests for film sensitometric properties

14 p2588 A70-31235

IR photography extension into long wave region of spectrum, discussing contact sensitized and electrically controlled semiconductor photographic systems

15 p2734 A70-31632

- False color aerial photography with IR film for distinguishing vegetation types and assessing plant vigor based on leaf reflectance 17 p3078 A70-35613
- Aerial IR surveys of surface temperature patterns of Hudson Bay during ice free seasons 17 p3079 A70-35621
- Background thermal radiation veiling effect on IR photography extension into long wave spectrum 18 p3257 A70-36282
- Aerial terrain analysis by color and color IR photography, analyzing physical factors affecting final image 22 p4018 A70-42963
- Photo copying in diapositive form, using ruby laser light on IR film 24 p4352 A70-45559
- INFRARED RADIATION**
- NT FAR INFRARED RADIATION
- NT NEAR INFRARED RADIATION
- IR emission from planetary nebulae, W-R, Of and symbiotic stars, discussing dust hypothesis for IR excess 01 p0173 A70-10039
- Mathematical model for saturable absorbers consisting of molecular gases for use in IR applied to carbon dioxide laser radiation absorption by sulfur hexafluoride 01 p0109 A70-10429
- Atmospheric IR radiation transmittance in 590 to 750 per cm interval, using balloon-borne spectrometer 02 p0256 A70-11928
- Two band Drude model validity for analysis of IR optical properties of transition metals obtained from experimental dielectric constant data 02 p0339 A70-12452
- IR light beam modulation in Gunn oscillator near fundamental edge of GaAs, investigating mechanism 03 p0539 A70-13160
- Image conversion scheme to obtain holograms of three dimensional objects illuminated with IR light, using nonlinear optics 04 p0685 A70-14406
- Angular tolerance on IR radiation for phase matched image up-conversion in material with nonlinear susceptibility 04 p0703 A70-15621
- Satellite IR measurements of surface horizontal temperature structure of Gulf Stream compared with ship and aircraft data 05 p0844 A70-17104
- Carbon dioxide and monoxide molecules IR emission in laser noting CO contribution to population of higher laser level 06 p1082 A70-17772
- Anomalous dispersion measurements in IR range with multibeam sequential Fabry-Perot interferometers using photoelectric method 06 p1064 A70-17811
- Laser harmonic-frequency mixing techniques extended into IR with IR metal-metal point contact diode 06 p1083 A70-17944
- Cloudy sky IR background radiation model for designing simulator of IR background for studying noise rejection characteristics of electro-optical automatic control systems 07 p1246 A70-19527
- Specular reflectivity measurement method for optical thin film coating in 10.6 micron IR region using carbon dioxide laser source 07 p1302 A70-20084
- Spectral band transmission functions of atmospheric water vapor, nitrogen, ozone, nitrous oxide and methane in IR region 07 p1330 A70-20306
- Optical to IR conversion in circumstellar dust envelope with spherical symmetry based on optical radiation scattering and absorption by dust 08 p1573 A70-21047
- Wall material diathermy effects on critical thermal load under radiant transfer, comparing results for quartz glass and stainless steel tubes 08 p1597 A70-21186
- Nonstellar 5 micron source in Orion nebula, noting intensity nonvariance and energy distribution calculation of temperature 08 p1575 A70-21375
- Center to limb variation of solar brightness measured at 5, 10 and 20 microns, discussing data collection and reduction and previous IR and UV measurements 08 p1562 A70-21396
- IR absorption properties of CO, HCl and sulfur dioxide measured for role in Venus greenhouse effect 08 p1579 A70-21567
- Temperature effects on IR absorption by water and carbon dioxide vapors measured in narrow spectral intervals 09 p1666 A70-22180
- IR energy interaction with earth atmosphere, determining multispectral scanner optimum wavelength intervals for earth resources applications [ALAA PAPER 70-289] 09 p1669 A70-22892
- IR light dispersion filters of compressed mixed powdered crystals, discussing optimal preparation procedures, passbands temperature dependence and stability 10 p1915 A70-24256
- Graphite IR radiator for radiative capacity and flame temperature measurements investigated for life time dependence on ambient pressure and temperature 10 p1888 A70-24257
- Atomic oxygen IR emission in earth atmospheric models, using reduction factor for comparison with optically thin atmosphere 10 p1875 A70-24439
- Carbon oxyfluoride IR radiation from boundary layer formed by arc-heated air passing over Teflon surface 10 p1968 A70-24475
- IR oxygen emission transmission characteristics in atmosphere compared with ground-based observation 10 p1876 A70-24538
- IR radiation sources /irtrons/ accounting for energy releases by continuous matter and antimatter creation 10 p1947 A70-24997
- Atmospheric absorption by ozone of solar radiation measured by balloon-borne spectrometer in 9-10 micron region 11 p2045 A70-25627
- Nimbus high resolution IR radiometer /HRIR/ data processed by color display enhancement system, demonstrating meteorological, oceanographic and geomorphological applications 11 p2049 A70-25636
- Corrugated skins solar absorbance and IR emittance computed for spacecraft thermal design, analyzing other nondiffusive radiative enclosures 11 p2150 A70-26352
- Recombination in hydrogen-oxygen reaction studied by monitoring IR emission from water vapor formed by shock initiated combustion 11 p1995 A70-26377
- IR radiation intensity distribution in solar neighborhood from grain models of dirty ice, graphite and graphite core-dirty ice mantle 11 p2106 A70-26710
- IR absorption in ozone band, including atmospheric inhomogeneity effects on accuracy of transmittance calculations 12 p2223 A70-27515
- Q switched CO-HE laser IR fluorescence, considering population inversion recovery by vibrational energy transfer 13 p2423 A70-28496
- Compton electron scattering generated galactic gamma ray flux effects on diffuse IR 13 p2476 A70-28630
- UV, visible and IR radiation measurement, discussing spectral distribution, thermopiles, monochromatic radiation and power measurements 13 p2410 A70-29653
- Lower and upper atmospheric IR fluxes and equivalent radiation temperatures measurements, describing two- and four-sphere mean radiation temperature /MRT/ meter 13 p2410 A70-29662
- Solar observations in intermediate IR, measuring continuum intensity of disk center in atmospheric water vapor window 13 p2498 A70-30006
- Atmospheric absorption, scattering and turbulence effect on visible and IR radiation propagation, discussing optical systems performance 14 p2583 A70-30399
- Cosmic IR radiation sources, discussing galactic and stellar masses 14 p2632 A70-30882
- Lunar IR radiation measurements for estimating thermophysical properties and small scale surface nature 14 p2645 A70-31057
- Balloon-borne midinfrared observations of lunar surface composition from interpreting peak emissivity differences 14 p2645 A70-31058
- Earth-space path attenuation measurements by 8-14 micrometer telescope appended to sun tracker 16 p2861 A70-32989
- Gas breakdown produced by long wave IR pulsed radiation of carbon dioxide laser 16 p2928 A70-33655
- Nitric oxide gas IR radiation properties at high temperatures, determining spectral mean fine structure and total band absorbance correlations 16 p3003 A70-34253
- Solar and IR radiation distribution in multiple scattering and absorbing ground fog, obtaining intensities, fluxes and vertical divergence 18 p3284 A70-35943
- IR radiation diffuse reflection, transmission and emission in water clouds 18 p3244 A70-35950
- Upper atmosphere IR emission model with reference to thermal excitation, chemical reactions and electron excitation 18 p3246 A70-36173
- IR absorption by water vapor in transmittance windows, considering continuous absorption coefficient dependence on window width 19 p3461 A70-37425
- Photon pair annihilation process in graviton pair, examining IR emission in two scalar particle collision 19 p3472 A70-38172
- Auroral enhancement of IR oxygen band, considering electric field excitation mechanisms 19 p3414 A70-38383
- Evening twilight airglow oxygen IR band ground based observation by two-channel photometric technique 19 p3415 A70-38385
- Nova Ser 1970 and Aql 1970 luminous IR emission, discussing stellar brightness, grain formation and optical decay 20 p3701 A70-39004
- CAT detection by IR radiation, remotely detecting atmospheric horizontal temperature gradients 20 p3626 A70-39080
- High speed electro-optic spectral scanning in UV, visible and IR regions, using monochromator deflection of dispersed light 20 p3671 A70-39090
- Anomalous IR auroral emission observation during rocket flight, indicating unknown energy sources of oxygen excitation 20 p3621 A70-39350
- InAs pulsed injection laser at cryogenic temperature for measuring time constant of IR radiation detectors 20 p3630 A70-39449
- Optical thermal testing by IR radiation, reviewing thermistor bolometer, various detectors, radiometric microscopes, NDT equipment, etc 21 p3831 A70-40747
- Apollo 11 rocks IR absorption properties, specific heat and thermal conductivity, discussing heat flow in surface layer 21 p3913 A70-41642
- IR radiation, transmission and detection in non-destructive testing, discussing atmospheric transmission, thermal and photon-type detectors, etc 22 p4029 A70-42595
- GaAs laser and noncoherent IR emitting diodes fabrication and design, discussing card readers, encoders, alarms, range finders, bomb fuses and night vision systems 22 p4050 A70-43248
- Stratosphere radiation measurements by Nimbus 3 infrared spectrometer for 15 micron frequency, considering temperature variations 24 p4330 A70-46074
- Ocean currents and sea surface temperature remote sensing by Nimbus 2 High Resolution IR Radiometer 24 p4332 A70-46400
- INFRARED REFLECTION**
- IR reflectance studies of lunar surface composition, showing absorption spectra suggestive of ferrous iron, olivines and orthopyroxenes 01 p0182 A70-10721
- Semiautomatic data collection system for IR reflectivity measurements, recording digitized output on punched cards for computer analysis 01 p0088 A70-10747
- Diamond-like glassy semiconductor compound of cadmium germanium arsenide, determining optical lattice vibrations from IR reflection spectra 01 p0160 A70-11599
- Solar IR light brightness distribution reflected by volcanic covers compared with lunar observation data 04 p0744 A70-14439
- Angular distribution measurements of visible and near IR radiation reflected from carbon dioxide cryodeposits formed on liquid nitrogen cooled surface in vacuum 04 p0720 A70-15538
- [ALAA PAPER 69-63] Doped n-type Ga-As electrophysical parameters determinable from IR reflection spectra 05 p0892 A70-16540
- Laboratory irradiation of rock samples for solar wind flux effects on IR reflectivity of lunar rocks 08 p1579 A70-21565
- Water depth determination by remote measurement of near IR reflectance of underwater plants, discussing effects of water path length changes 10 p1878 A70-24741
- IR reflectance of cirrostratus and cirrus clouds and jet contrail measured by spectrometer on high altitude aircraft 11 p2045 A70-25626
- Solar light brightness distribution reflected by volcanic covers compared with lunar observation data 13 p2485 A70-28464
- IR reflection spectrum of corundum compared for heating by reflecting furnace and laser radiation, discussing phonons statistical distribution 13 p2429 A70-29639
- InAs thin films electrical properties and IR reflectance, determining thickness and substrate temperature effects on carrier concentration and mobility 15 p2783 A70-31965
- IR radiation diffuse reflection, transmission and emission in water clouds 18 p3244 A70-35950

Lunar rocks mineralogy and visible and near IR reflectivity, discussing depression in telescopic curve
21 p3912 A70-41637

Visible and near IR radiation reflectance from vegetation, discussing incident solar radiation plant structures, leaf areas shadows and absorption by chlorophylls
22 p4014 A70-42767

INFRARED SCANNERS

NT MULTISPECTRAL BAND SCANNERS

IR microscope and digitally programmed mirror system for printed circuit inspection, allowing two dimensional scanning and magnetic tape reference
01 p0054 A70-10024

IR spectrometer scanning function measurement by gas laser
01 p0092 A70-10989

Aircraft multispectral IR scanning systems for earth resources remote sensing, discussing capabilities
03 p0491 A70-13670

Line scanning IR imagery system for thermal mapping of fire, water and soil conditions
05 p0836 A70-15770

IR energy interaction with earth atmosphere, determining multispectral scanner optimum wavelength intervals for earth resources applications
[AIAA PAPER 70-289] 09 p1669 A70-22892

Airborne IR line scanning systems for forest fire surveillance, determining size and characteristics during smoke or darkness
09 p1686 A70-23753

Earth IR horizon seasonal and longer variations for horizon sensing instruments design
12 p2226 A70-27931

Probe rocket Tacite 02 head attitude gyrorestoration for IR horizon analysis, using stellar sensor and signal measurements
13 p2500 A70-28408

Lunar surface brightness temperatures from IR observations, determining thermal emission directional characteristics to infer surface temperatures from Surveyor data
[AIAA PAPER 69-593] 13 p2486 A70-28501

Low altitude atmospheric effects on IR beam horizon sensors in carbon dioxide band, noting corrections for spacecraft attitude measurement
15 p2735 A70-31792

Airborne IR scanner as geophysical research tool depicting surface emission and heat mass transfer
18 p3259 A70-36558

Satellite-borne conical IR scanner flight data hybrid simulation and error analysis, suggesting carbon dioxide horizon noise model
[AIAA PAPER 70-1021] 20 p3631 A70-39513

Mechanical passive cone angle amplifier for spinning sounding rockets for IR sky scanning, solving equations of motion for system
21 p3931 A70-41905

Multispectral IR scanner system for earth resources survey programs
22 p4037 A70-43087

INFRARED SPECTRA

Atlas of near IR spectra of Venus, Mars, Jupiter and Saturn obtained by Fourier spectroscopy, discussing observational procedures, data recording and processing
01 p0173 A70-10078

Jupiter and Saturn near IR spectra for relative abundances of atmospheric constituents and distribution with altitude, noting rough solar composition
01 p0179 A70-10526

IR spectrometer on Mariner 7 Mars flyby recording sharp absorption near 3 microns at Martian southern polar cap
01 p0182 A70-10823

Double beam Michelson interferometer for middle IR with moving mirrors operating in constant velocity mode, applying method to atmospheric emission spectra
01 p0091 A70-10909

Near IR reflection spectra of artificial cumulus clouds with progressive droplet sizes
01 p0076 A70-10911

Stratospheric water vapor distribution from analyzing IR solar spectrum during sunset observed by balloon-borne spectrometer
01 p0081 A70-11295

Nitrogen, oxygen and air luminescence spectra excited by fast electrons at low gas pressures in IR spectral region compared with polar auroral spectra
01 p0083 A70-11536

Carbon dioxide temperature distribution, absorption and concentration as functions of molecular dissociation behind shock wave determined by measuring IR bands intensity
01 p0069 A70-11623

Hydrogen pressure-induced IR absorption spectra, noting applications to planetary atmosphere studies
02 p0341 A70-11805

Variable distribution of ammonia absorption on Jupiter deduced from IR spectra, indicating scattering in cloud layer
02 p0366 A70-11810

Atmospheric transmittance line by line calculations along variable pressure and mixing ratio paths from 1.7-20 microns
[AFCRL-70-0061] 02 p0289 A70-11908

IR spectra of four carbon stars and Sirius obtained with Michelson interferometer, indicating diatomic carbon and CO bands
02 p0372 A70-12252

IR spectrum of Jupiter with calibrations from laboratory studies of methane and ammonia bands
02 p0378 A70-12559

IR spectra of N isotopes adsorbed on nickel-on-Aerosil catalysts, investigating effects of intermolecular interaction and isotopic substitution
03 p0440 A70-13099

Eta Carinae IR region emission and absorption spectra characteristics in tabular form
03 p0565 A70-13269

IR spectra of M stars and alpha Tau obtained with Michelson interferometer, observing molecular features and water vapor absorption
04 p0747 A70-14548

Low resolution spectra of IR stars NML Tau, CIT 3, 6 and 13 considered inadequate for molecular band identification
04 p0748 A70-14591

IR colors and optical and IR spectra of irregular M variable star and bright OH source VY CMa indicating supergiant classification
04 p0749 A70-14592

Solar photospheric Fe abundance determined from IR supermultiplet line spectra, considering LTE effects
04 p0749 A70-14597

External optical phonon modes in ammonium and deuteroammonium halides phase transitions as function of temperature, using IR and Raman spectra
04 p0646 A70-14695

Integrated intensity measurements of carbon dioxide bands in micron regions, using self-broadening method
04 p0690 A70-15025

Spectral absorption and transparency of water vapor, carbon dioxide, carbon monoxide, methane and nitrous oxide bands in IR region
04 p0715 A70-15255

Identification of lines in Mohler photometric atlas of IR solar spectrum wavelengths
05 p0910 A70-16427

IR solar spectrum including water vapor, carbon dioxide and methane bands
05 p0913 A70-16566

Raman and IR spectra of unsymmetrical dimethylhydrazine and unsymmetrical dimethylhydrazine-d2 recorded in liquid and gaseous states
06 p1128 A70-17329

IR region spectral hemispherical emittance of surfaces measured by bihemispherical reflectometer
[AIAA PAPER 70-65] 06 p1107 A70-18205

Grating spectrometer with Ge-Cu detector used on balloon flights for studying variations of IR solar spectrum with altitude, emphasizing sunset features
06 p1152 A70-18523

Methylamine crystals lattice vibrations IR spectra recordings, making spectral band assignments according to translational and librational motions
07 p1356 A70-18958

IR spectra excited by fast electrons in nitrogen, oxygen, carbon monoxide, carbon dioxide, nitrogen oxide, methane, ammonia and water molecules
07 p1337 A70-19045

Nitrogen IR emission spectra from atomic and molecular excited electronic states transitions, studying DC discharges at various pressures
07 p1339 A70-20092

Jupiter and Saturn IR reflection spectra observed with Michelson interferometer-spectrometer, eliminating effects of terrestrial atmospheric absorption, solar spectral lines, etc
08 p1570 A70-20895

Threshold switching and thermal filaments in thick specimen of amorphous semiconductor using IR spectrum viewer
08 p1477 A70-21540

IR spectral absorption coefficients determined for water vapor at high temperatures, describing experimental details including data acquisition and reduction
09 p1725 A70-22069

IR absorption spectral curve interpretation using computer program for iterative solution
09 p1726 A70-22138

Hypersensitization of IR films for use in stellar photometry, discussing laboratory and astronomical tests
09 p1673 A70-22158

Seasonal measurements of atmospheric transmittance spectra for horizontal near-earth paths in IR region under haze and clear weather
09 p1666 A70-22179

Water vapor emission detection from IR stars, discussing radial velocities of microwave lines
09 p1756 A70-22523

Solar IR Fraunhofer line damping constants empirical values and variation with optical depth, noting discrepancy with theoretical constants
09 p1757 A70-22726

Photographic and IR multiband spectral discrimination for rock and soil mapping from orbiting ERTS satellites
[AIAA PAPER 70-303] 09 p1668 A70-22882

Binary collision-induced rotational far IR spectrum of tetrahedral molecular gas, using induced absorption theory
09 p1732 A70-22905

Saturn ring IR spectrum, discussing resemblance and discrepancies of ammonia and water frost spectra
10 p1935 A70-23813

Epoxy glass fiber composites pyrolyzates IR spectra as function of time, observing changes in fingerprint region
10 p1828 A70-24065

Gadolinium II solar lines classification from photographic IR observations
10 p1947 A70-24990

Stellar and planetary IR spectra from spectrometer with rotating circular variable thickness interference filter
11 p2113 A70-26468

Multichannel IR spectrophotometer to obtain albedo curves of Martian surface
12 p2229 A70-26927

Book on rotational structure of diatomic molecules spectra covering multiplets, intensity distributions and perturbations
12 p2274 A70-27094

Auroral enhancement of IR oxygen band at 1.27 micron compared with molecular nitrogen band intensity
12 p2222 A70-27185

Absorption spectra of semiinsulating gallium arsenide in IR region, investigating transmittance and absorption coefficient at room and low temperatures
12 p2287 A70-27492

Solar IR triplet of singly ionized Ca, suggesting limb darkening caused by chromospheric inhomogeneities for source function inequality
12 p2303 A70-27703

Solar rotational line positions due to red band in IR continuum region to resolve blue-violet ambiguity
12 p2303 A70-27704

Experimental IR earth horizon profiles measured by satellite in F region, discussing spectral channels and attitude control
12 p2225 A70-27751

Stark cell with high electric fields for studying inactive IR spectrum of homonuclear diatomic gas molecules
13 p2450 A70-28499

Nonoriented cadmium silicon arsenide single crystals optical properties, determining spectral distribution of IR absorptivity for various photon energies
13 p2470 A70-28883

IR reflection spectrum of corundum compared for heating by reflecting furnace and laser radiation, discussing phonons statistical distribution
13 p2429 A70-29639

Star HBV 475 emission spectra in near IR due to H, He I, OI and Ca II, confirming symbiotic character
13 p2495 A70-29641

Ice radiation and reflection characteristics in IR spectral region at certain Brewster angles
14 p2568 A70-30133

Radiant heat flux for standard model, dry and humid atmosphere, calculating temperature variations with altitude for entire IR spectrum
14 p2603 A70-30401

Water vapor absorption bands in solar IR spectrum, considering earth curvature and atmospheric inhomogeneity and refraction
14 p2572 A70-30404

Lunar surface thermal emission spectra, calculating IR emissivities
14 p2637 A70-30495

Bright IR stars observed using photometry and spectroscopy, suggesting protostars presence
14 p2641 A70-30880

OH radio emission from IR stars, discussing spectra, polarization properties and red giant star model with expanding atmosphere
14 p2641 A70-30881

IR photography extension into long wave region of spectrum, discussing contact sensitized and electrically controlled semiconductor photographic systems
15 p2734 A70-31632

Gaseous Al oxide bond bending frequency in Ne and Ar matrices at liquid He temperatures, investigating IR spectrum
15 p2695 A70-32830

Near IR electronic emission spectrum of positive column in flowing oxygen electric discharge, noting vibrational temperature
16 p2955 A70-33981

IR Raman and vibrational spectra and structure of gaseous and liquid 1-pyrazoline
16 p2857 A70-34007

IR and Raman spectra of gaseous and liquid germyl-cyclopentane, determining torsional barriers and skeletal ring atom symmetry

16 p2858 A70-34008
Interstellar silicate absorption in IR spectra, discussing existing observations

17 p3157 A70-34840
Approximate formulas for disperse attenuation and scattering coefficients for water drops in visible and IR spectrum

18 p3260 A70-36973
Trichroic IR absorption lines of triglycine selenate, computing optical and dielectric constants from transmission and reflection data

19 p3470 A70-37366
Electron temperature and concentration profiles behind shock front from IR emission and absorption simultaneous measurement, applying method to xenon ionization and recombination processes

19 p3402 A70-37443
Water vapor and OH spectra overlap, investigating association of galactic OH masers and water emission sources with IR stars

19 p3444 A70-37571
Pulsed emission in midinfrared region at neutral atomic transitions of inert gases and mixtures, tabulating wavelengths, intensity, component ratios and optimal pressure

19 p3448 A70-38736
Diatomic Cs 7667 A band vibrational spectrum analysis

20 p3676 A70-40349
Carbon dioxide and CO IR vibration-rotation spectral absorption coefficients, noting harmonic oscillator approximation

21 p3851 A70-40589
Aerosol IR emission, discussing relative humidity, water droplet size and temperature effects on atmospheric radiance levels

21 p3846 A70-40804
Atmospheric temperature profiles from terrestrial IR spectral radiances measured by balloon-borne grating spectrometer, discussing surface temperature variations

21 p3813 A70-40905
Auroral optical emission measurements, examining oxygen atmospheric and IR bands by rocket sounding

21 p3817 A70-41092
Solid para hydrogen IR and Raman spectra frequency analysis, examining lattice vibration effects

21 p3853 A70-41721
High resistivity single crystal silicon wafers induced IR absorption measurement, using Nd doped glass laser

21 p3837 A70-41916
Stellar IR spectra for types A0 to M7, using Mertz type Michelson interferometer as Fourier transform spectrometer

21 p3922 A70-41980
Planetary nebula NGC 7027 IR line spectra emission, examining S IV and AR III line intensities

22 p4094 A70-42933
Narrow band IR photometry of star alpha Orion, testing hypothetical correlation of emission peak with starlight-reflecting silicate dust

22 p4105 A70-43229
Circumstellar dust cloud model of spectral distribution and anomalous excess emissions in IR T Tauri and red giant stars coincident with photometric measurements

23 p4239 A70-43868
IR absorption bands absolute intensities determination method, giving special consideration to absorption band wings and precision

23 p4217 A70-44203
Ozone vertical distribution from satellite IR data, discussing Fredholm equations for radiation transfer

23 p4191 A70-44269
IR absorption spectra of high-cis forms of deuterated polyisoprenes

23 p4157 A70-44274
Spectral absorption of 2.7 micron water vapor band under various high temperature and pressure conditions, using black body radiation

23 p4220 A70-44444
Mars topography from Mariner 6 and 7 IR spectra, discussing geographical resolution, surface carbon dioxide pressure, depressions, ridges and valleys

24 p4399 A70-45128
Argon matrix isolated ammonia, examining IR spectra by carbon dioxide laser irradiation

24 p4354 A70-45648
Herculis 89 supergiant abnormal IR radiation flux originating in circumstellar shell of solid particles radiating at observed long wavelengths

24 p4410 A70-45772
Low temperature stars SiO IR spectral band identification based on rotation-vibration spectrum calculation

24 p4411 A70-45777

INFRARED SPECTROMETERS

Hydrocarbon content of coorongite derived from algae analyzed by IR spectrometry, gas chromatog-

raphy and mass spectrometry, discussing alkanes and alkenes occurrence

01 p0041 A70-10037
IR spectrometer scanning function measurement by gas laser

01 p0092 A70-10989
Grille spectrometer design for thermal IR measurements, discussing requirements to achieve optimum performance

02 p0296 A70-11917
Near IR reflectance spectrometer integrated into environmental chamber to study frost spectral properties

06 p1072 A70-18522
Long wave IR spectrometer with two diffraction gratings for various micron ranges

08 p1493 A70-20544
High resolution Fourier interference near IR spectrometer for aircraft, balloon and spacecraft remote sensing applications

09 p1683 A70-23508
Atmospheric temperature determination by satellite IR spectrometer (SIRS-A), describing data analysis and instrument design, calibration and performance

12 p2263 A70-26954
Grating spectrometer performance in measuring earth IR radiance determined from balloon flights

12 p2235 A70-27752
IR Michelson interferometer for Mariner Mars 1971 mission, investigating atmospheric and surface temperatures and atmospheric water vapor content

16 p2978 A70-34029
Nimbus 3 satellite-borne Michelson interferometer IR spectrometer for spectrum measurement, obtaining temperature, water vapor and ozone vertical distribution

18 p3257 A70-36175
Aircraft-borne spectrometer for atmospheric IR spectral transparency

18 p3260 A70-36972
Grille spectrometer design, fabrication and adjustments, noting increased IR sensitivity over slit devices

19 p3421 A70-37358
Atmospheric ozone remote sensing by high resolution IR interferometer spectrometer (IRIS) aboard Nimbus 3 satellite

19 p3414 A70-38262
Michelson IR interferometer spectrometer (IRIS) design calibration and performance onboard Nimbus 3 satellite, demonstrating data reduction and inflight calibration

20 p3626 A70-39078
Stellar IR spectra for types A0 to M7, using Mertz type Michelson interferometer as Fourier transform spectrometer

21 p3922 A70-41980
Temperature and height data for synoptic stratospheric evaluation, using Nimbus 3 satellite IR spectrometer

22 p4064 A70-42618
Double beam diffraction grating spectrometer for vacuum operation over far IR from 40 microns to 1 mm

24 p4339 A70-46323
INFRARED SPECTROPHOTOMETERS

Size and cost of Al mirror IR photometric telescopes optimized for scientific information acquisition

14 p2586 A70-30896

INFRARED SPECTROSCOPY

Nimbus 3 satellite carrying IR spectrometer to measure spectral radiances and retrieve atmospheric temperature profiles

04 p0675 A70-14393
Mariner 6 and 7 missions IR spectrometric records showing evidence of solid carbon dioxide in Martian upper atmosphere

06 p1137 A70-17194
Satellite determination of underlying surface temperature by IR spectroscopy, measuring emitted radiation in atmospheric windows

06 p1061 A70-17205
Reaction rate constants in heated mixture of hydrogen, carbon dioxide and Ar behind shock waves measured by IR spectroscopy

12 p2274 A70-26891
Airborne geological mapping by IR emission spectroscopy, describing instrumentation, materials discrimination capability, data processing, etc

12 p2230 A70-26957
IR spectroscopy and lasers for analysis of atmosphere in air pollution research and monitoring

13 p2407 A70-29106
IR spectroscopy, determining relative populations of carbon dioxide vibrational energy levels by comparing emission intensities

13 p2455 A70-29131
Tunable diode laser for high resolution IR spectroscopy of sulfur hexafluoride absorption near carbon dioxide laser lines

13 p2430 A70-29832
Bibliography of far IR spectroscopy with subject index

14 p2586 A70-30987

Mariner 6 and 7 TV camera pictures of Mars during approach and encounter, discussing IR spectroscopy, celestial mechanics experiment and Martian terrain

17 p3158 A70-34875
Atomic spectroscopy of IR laser transitions in gases excited by HF pulsed discharges

17 p3105 A70-35093
Submillimeter gas lasers with low noise and CW operation for far IR spectroscopy, noting emission lines multiplicity

20 p3641 A70-39423
Lunar environment diagnostic features enhancement on IR emission spectra, making moon excellent target for remote sensing

20 p3709 A70-39979
Peroxyacetyl nitrate decomposition products under continued and discontinued irradiations determined by IR spectral analysis

22 p3983 A70-42944
Ammonia gas phase IR intensity measurements for hydrogen bonding energy and related parameters

23 p4158 A70-44783
Boron impurities introduction into InP crystals grown by liquid encapsulation, detecting IR absorption bands due to localized lattice vibration

23 p4231 A70-44891

INFRARED TRACKING

Automatic IR control and tracking systems for aviation, space flights and military use, discussing sensor elements

01 p0139 A70-11262
Carbon dioxide laser radar system for studying radar techniques application to IR, discussing automatic tracking capability provision

03 p0450 A70-13676
Rockets trajectories recording on real time at Guiana Space Center using IR pointing deviation meter

15 p2698 A70-31960
Onboard IR receiver and ground photorecorder for Meteor satellite cloud tracking, using computer processed data

15 p2738 A70-32112

INFRASONIC FREQUENCIES

Two station simultaneous observations of auroral infrasonic wave substorms morphologies

01 p0071 A70-10411
Microbarographic oscillations associated with geomagnetic activity during observation of infrasonic waves on geomagnetically disturbed days

01 p0081 A70-11298
Health hazards and physiological effects of atmospheric infrasonic waves, discussing sources, ear protecting devices and electrochemical detectors

02 p0247 A70-12467
Auroral motions determined by absorption onsets pattern and infrasonic wave morphology

10 p1880 A70-24803
Infrasonic waves generated by pulsating aurora, using Joule heating and Lorentz force coupling

13 p2399 A70-29236
Infrasonic waves generation by supersonic translation of auroral electrojet currents

13 p2399 A70-29237
Long range infrasound from rockets, showing two wave groups generated by launch and first stage reentry

19 p3531 A70-37694

INGESTION [BIOLOGY]

NT DRINKING

NT EATING

Food ingestion initiation, investigating role of hyposmotic solutions from observation of rats under water deprivation

13 p2353 A70-29495
Antidiuresis associated with oral cavity stimulation during food ingestion by rats

13 p2355 A70-29813
Mongrel dogs pulmonary and systemic circulatory responses to dopamine infusion

20 p3569 A70-38986

INGESTION [ENGINES]

A-7 aircraft TF-41 engine tolerance to steam ingestion, discussing test program and results and engine modifications

01 p0165 A70-10700
Birdstrikes as aircraft hazard, discussing structural damage, engine ingestion and various countermeasures

18 p3213 A70-36319
Exhaust gas ingestion suppression model tests for VTOL lift engines, measuring inlet thermal environment

[AIAA PAPER 70-905] 19 p3490 A70-37396

INGOTS

Porosity formation in Al ingots made by semicontinuous casting, considering metal grade and purity, gas content and homogenization conditions

08 p1505 A70-21136
Homogeneity of commercially pure Ti and Ti-Al-V ingots, discussing oxygen distribution uniformity over cross section

17 p3112 A70-34353
Ti alloy ingot chemical macroinhomogeneity, investigating elimination by vacuum arc melting

17 p3112 A70-34355

INHABITANTS

NT MOUNTAIN INHABITANTS

INHALATION

U RESPIRATION

INHIBITION

Orientation detectors in human visual cortex, suggesting mutual lateral inhibition 23 p1414 A70-43813

INHIBITION (PSYCHOLOGY)

Retrospective and proactive inhibition in verbal discrimination learning, using paradigms characteristic of paired-associate retention studies 03 p0435 A70-13768

Efferent model to test inhibitory influence of inferotemporal cortex lesions on visual discrimination of monkeys, using paired flashes of light 04 p0629 A70-14449

Inhibitive stimulus control related to behavioral contrast during discriminative training 08 p1441 A70-20476

Vestibular nystagmic and electrical responses facilitation, inhibition and habituation, noting modulation by subcortical and cortical systems 14 p2538 A70-30909

Nervous inhibition effect on electroretinogram b wave during flash sequences 24 p4301 A70-45986

INHIBITORS

NT WEAR INHIBITORS

Burning velocity of methane-air flames inhibited by methyl bromide, using schlieren cone-nozzle burner method involving unburnt gas velocity measurement 03 p0607 A70-13918

Alpha-methyl-DOPA inhibitor effect on catecholamines and cardiac spontaneous activity in pacemaker fibers in rabbits 06 p0992 A70-17422

Cerebral biopotentials of rabbits exposed to RF weak electromagnetic field indicating cortex inhibition in EEGs 07 p1199 A70-18728

Glutethimide and aminoglutethimide reversible inhibitory effect on rat pituitary adrenal system in response to stress 07 p1203 A70-18902

Erythropoiesis inhibitor in blood from rabbit kidney vein during hyperoxia in nitrogen-oxygen atmosphere 14 p2535 A70-30155

Fast brittle crack slowing by mechanical twins in transformer steel and by slip bands in LiF and NaCl crystals 15 p2755 A70-31526

Tetrafluorodibromo-ethane and bromethyl inhibiting effects on explosion development in constant volume container and flame expansion rates in hydrogen-air mixtures 18 p3345 A70-36241

Auxin downward transport by gravity in leaves, examining ethylene inhibition 20 p3570 A70-39234

INHOMOGENEITY

Critical detonation diameter as function of concentration and dimensions of inhomogeneities in explosive, assuming chemical reaction generated behind detonation front 01 p0217 A70-11005

Stresses in plane elastic bodies analyzed by generalizing biharmonic stress function equation in polar coordinates, assuming constant Poisson ratio and nonhomogeneity 01 p0206 A70-11152

Transient temperature distribution in inhomogeneous material, using finite difference representation for temperature time derivative [ASME PAPER 69-WA/HT-33] 04 p0782 A70-14807

Fe diffusion coefficients measured at various temperatures above 1150 C to calculate homogenization times of Thailand tektite source 05 p0917 A70-16841

Disturbances in infinite aeolotropic inhomogeneous medium due to transient forces and twists on elastic cylindrical source surface 07 p1407 A70-19382

Nonlinear integral equations for inhomogeneous atmospheres derived from radiative transfer equations global form, noting relations to Ueno and Chandrasekhar equations 07 p1336 A70-20059

Torsional vibrations of nonhomogeneous anisotropic finite circular tube, computing natural frequencies for various parameters 07 p1414 A70-20173

Multibeam interferometer sensitivity restrictions due to diffraction effects on interference patterns near transparent inhomogeneities 08 p1493 A70-20540

Radio waveguides with random inhomogeneities, studying mathematical models by orthogonalization method 08 p1457 A70-20723

Total optical field in inhomogeneous medium, questioning uniqueness of division into direct and reversed wave propagation 08 p1546 A70-21785

Perseids time distribution, based on observations during meteor showers, contradicting appearance of homogeneous Poisson process 09 p1750 A70-22099

Active element inhomogeneity effects on semiconductor injection lasers emission spectra and radiation intensity distribution 09 p1695 A70-22481

Navier-Stokes equation approximation for nonhomogeneous case obtained by relating Burgers equation to Riccati equation through similarity transformation 09 p1711 A70-22613

Plane electromagnetic waves scattering from radially inhomogeneous cylindrical structure, deriving expressions for far field and cross section for both polarizations 10 p1841 A70-24856

Linear heat propagation in rarefied and nonhomogeneous atmospheres, considering Green function behavior and various boundary and initial value problems 11 p2107 A70-25542

Solar wind structure as function of corotating coronal inhomogeneities determined using perturbation equations for spherical polar coordinate system 12 p2292 A70-27179

Analytic expressions for concentration distribution functions in inhomogeneous solids within intermediate stages of homogenization process 12 p2253 A70-27282

Electromagnetic wave scattering on passively reflecting statistical clusters of inhomogeneities 12 p2184 A70-27498

Electromagnetic waves emission and propagation in chaotically inhomogeneous media, analyzing mean field and permittivity tensor for isotropic and anisotropic media 12 p2190 A70-28170

Geometrical theory of nonlinearly elastic inhomogeneous flexible shells, deriving variational equation in terms of displacement component and stress function 13 p2514 A70-29288

Anisotropic solar cosmic rays in inhomogeneous medium, investigating shell effect on pre-propagation by one dimensional model 15 p2795 A70-32624

Chemical and structural microinhomogeneity, diffusion and mechanical properties of Ti alloys in connection with phase transformation characteristics 17 p3112 A70-34354

Ti alloy ingot chemical macroinhomogeneity, investigating elimination by vacuum arc melting 17 p3112 A70-34355

Underlying surface inhomogeneity effect on radiation in presence of solid cloud cover 18 p3287 A70-36975

Planetary surface inhomogeneities detection by reflected and transmitted light polarimetry, using symmetry principles 18 p3319 A70-37057

Atmospheric inhomogeneity, comparing effective mass and Curtis-Godson approximation methods for transfer function of absorbing gas distribution 19 p3461 A70-37632

Gyrotropic waveguides parameters computer calculation based on inhomogeneous isotropic region, taking into account discontinuities 19 p3378 A70-37736

Safety factor limit analysis for anisotropic nonhomogeneous solids by variational method, exemplifying by four layer rectangular beam 19 p3547 A70-38355

Ti alloys fine structure, mechanical properties and alloying elements diffusion mobility during heat treatment, observing chemical and structural inhomogeneities 20 p3645 A70-39040

Nonhomogeneous shell theory, considering load carrying surfaces with constitutive equations independent of shell curvature 20 p3719 A70-39619

Plasma inhomogeneities effects on MHD generators I-V characteristics, energy conversion efficiency and optimum duct geometry 20 p3564 A70-39636

Mach-Zehnder interferometer for holographic investigation of inhomogeneities in transparent media, discussing photointerpretation error reduction 20 p3633 A70-39749

Statistically nonhomogeneous fields by variational principles of elasticity, obtaining bounds of average displacement for hollow sphere under pressure 20 p3732 A70-40112

External field perturbations by local inhomogeneities in elastic medium, deriving expressions for interaction energy and forces between defects 21 p3933 A70-40604

Electromagnetic wave propagation in inhomogeneous anisotropic linear media, discussing ray tracing, permittivity and relativistic electrodynamics 21 p3785 A70-40798

Linear heat propagation in rarefied and nonhomogeneous atmospheres, considering Green function behavior and various boundary and initial value problems 21 p3892 A70-41292

Beamguides with inhomogeneities regulated for constant radiation losses, systematizing broadening 22 p3984 A70-42389

Stationary saddle points phase method for wave diffraction problems in inhomogeneous medium, deriving asymptotic expansion for surface integrals 22 p3984 A70-42390

EM wave propagation in inhomogeneous media, examining permittivity and permeability 23 p4217 A70-43768

One dimensional radiation transfer equation in nonhomogeneous particle field, discussing spatial variations, particle number density, temperature, size distribution and optical properties 23 p4281 A70-44445

INITIAL VALUE PROBLEMS

U BOUNDARY VALUE PROBLEMS

INITIATION

Fatal ejections in USN, suggesting initiation delay as prime causal factor 07 p1191 A70-19006

Shock wave amplitude found strongest influence in explosives initiation to detonation by shock 07 p1359 A70-19675

INITIATORS (EXPLOSIVES)

NT DETONATORS

Electroexplosive devices - Conference, San Francisco, July 1969 03 p0544 A70-14101

Apollo spacecraft pyrotechnics on lunar landing mission, considering standard initiator, modular cartridges, noninterchangeability of special purpose devices, postmanufacture indexing and data system 03 p0582 A70-14102

Saturn 5 thru-bulkhead initiator for solid propellant rocket motor ignition, discussing transfer design, pressure output and postfire leakage 03 p0546 A70-14105

Electroexplosively powered release valve for high pressure N stored in hermetically sealed container of missile, discussing design and performance tests 03 p0546 A70-14106

Vacuum deposited thin film bridges in electroexplosive devices, discussing composition, surface conditions, substrate temperature, bell jar atmosphere and deposition rate 03 p0546 A70-14107

Detached electrode electroexplosive devices consisting of cylindrical column of explosive loaded into tube with thin closure disk at input end 03 p0547 A70-14109

Ordnance circuit RF filter in backshell of standard connector, discussing design, physical-electrical specifications and tests 03 p0494 A70-14113

Protuding, stepped and conical end fittings for confined detonating fuse, discussing assembly procedures effect on characteristics based on statistical scanning test 03 p0547 A70-14115

Nomographical solution of electroexplosive device firing time equation permitting firing data prediction from blueprint data 03 p0548 A70-14117

Computerized approximations for quantitative predictions of EED firing characteristics based on header geometry and electrical leads 03 p0548 A70-14118

Electrical and thermal factors in mathematical characterization of electroexplosive devices, including heuristic predictions 03 p0548 A70-14119

Electroexplosive devices output energy measurement through metal deformation by lead block and projectile penetration methods 03 p0548 A70-14121

Design reliability of through-bulkhead initiator explosive train using parametric test program data, discussing shock transmission and acceptor charge sensitivity energy balance 03 p0549 A70-14124

Test method for inertial impact sensor switches subjected to multiple and varied shock inputs, using high energy detonators 03 p0494 A70-14128

Electroexplosive devices (EED) in electromagnetic environments, discussing principles of warship safety 03 p0549 A70-14129

Broadband RF filter/attenuator plug to replace plastic type plugs for protecting wire bridge electroexplosive devices against RF energy 03 p0495 A70-14130

Electro-pyrotechnic initiators for space applications subjected to dry heat sterilization cycles and to post-sterilization mechanical and electrical environments 03 p0495 A70-14131

Electroexplosive devices protection from electrostatic discharge by creation of preferential discharge path, considering use of high intensity neon lamp 03 p0549 A70-14134

Philosophical, design, hardware or static sensitivity type myths refutation concerning electroexplosive devices 03 p0549 A70-14135

Test setup to determine safe limits of atmospheric potential gradients in electroexplosive device initiation 03 p0549 A70-14136

Initiator desensitization process involving use of volatile inert liquid to increase safety during assembly operations 03 p0549 A70-14137

Instrumentation concepts for electromagnetic compatibility measurements on electroexplosive devices, considering thin film thermocouple, electrical diode detector and microstrip transmission line techniques 03 p0495 A70-14138

Reduced ambient pressure effects on hot wire sensitivity of initiating materials of electroexplosive devices used in missiles 03 p0549 A70-14139

CW and radar type RF signal effects on electroexplosive devices sensitivity in bridgewire heating mode 03 p0550 A70-14142

Fluoric sensor for RF induced currents providing alternative to bridge wires as initiators of explosive charges 14 p2534 A70-30681

INJECTION

NT CARRIER INJECTION

NT FLUID INJECTION

NT FUEL INJECTION

NT GAS INJECTION

NT ION INJECTION

NT LIQUID INJECTION

NT SECONDARY INJECTION

NT WATER INJECTION

INJECTION CARBURETORS

U FUEL INJECTION

INJECTION GUIDANCE

Geostationary satellite payload-optimal injection trajectory from nonequatorial firing range, describing dog-logging maneuvers 03 p0573 A70-13845

Multiorbit injection earth departure technique for optimal thrust-weight ratio in manned interplanetary missions using NERVA engine [AAS PAPER 70-039] 17 p3175 A70-34780

Optimal explicit guidance equation using maximum principle for two stage vehicle injecting satellite into parking orbit 17 p3134 A70-35289

Parking orbit optimal orientation for minimal impulse maneuvers total velocity increment in three dimensional capture-escape mission [AIAA PAPER 69-918] 17 p3172 A70-35649

INJECTION LASERS

Frequency control of ruby laser pumped lithium niobate singly resonant parametric oscillator by radiation injection of CW Nd-YAG laser 01 p0110 A70-10566

Light emission by solids, discussing injection lasers, luminescence semiconductor diodes, group 2 and 6 compounds, etc 01 p0160 A70-11288

GaAs injection laser operated with external optical resonator for diffraction-limited radiation, considering peak power and quantum efficiency 02 p0311 A70-11920

Semiconductor injection laser modes, considering inhomogeneous lasing action levels over p-n junction area 03 p0499 A70-13410

Thermoelastic stresses in diode of pulsed and CW injection lasers, showing energy parameter limitation 03 p0499 A70-13437

Low threshold injection lasers in IR and visible spectrum at room temperature employing AlAs-GaAs heterojunctions, noting use for CW mode 03 p0501 A70-13723

Simple approximations for threshold current, gain and lasing frequency of GaAs injection laser at room temperature 03 p0503 A70-14085

Injection laser amplifier with emitting and amplifying diodes coupled by planar polyharmonic beam waveguide 04 p0702 A70-15292

Self induced light pulses from GaAs injection lasers in pulse driven diodes at liquid nitrogen temperatures, noting pulse width and frequency 04 p0703 A70-15623

Emission modulation in multifunctional injection laser-photodiode system used as optical memory, pulse generator, multivibrator and trigger 05 p0859 A70-16268

Semiconductor injection laser with large emitting area, discussing light absorption, waveguide channel formation as factors obstructing laser action 06 p1082 A70-17821

Injection laser theory taking into account radiative emission rates and spectral dependence, using two band semiconductor model 07 p1298 A70-19395

Thermoelastic stress degradation of injection lasers at high excitation levels, giving critical current densities for short pulse, CW and quasi-CW conditions 08 p1512 A70-20861

Semiconductor injection laser, analyzing light absorption by free carriers and gain characteristics 09 p1694 A70-22133

Active element inhomogeneity effects on semiconductor injection lasers emission spectra and radiation intensity distribution 09 p1695 A70-22481

Injection lasers for multichannel optical communication using composite cavities to improve spectral output 09 p1698 A70-23359

Second harmonic emission from GaAs injection laser and from stimulated KDP crystal at room temperature 12 p2245 A70-27306

Waveguide optical properties effect on injection GaAs laser threshold lasing and field distribution in near/far zones for various parameters of active region 12 p2246 A70-27365

Temperature effects on injection semiconductor lasers optical gain and threshold current using energy spectrum model 12 p2247 A70-27485

Active region characteristics of double injection laser employing electron-hole plasma in p-type indium antimonide 12 p2247 A70-27491

Emission field and Fermi quasi-levels distribution in injection laser with n-p heterojunction, determining frequency and threshold current temperature dependence 13 p2426 A70-28876

Injection lasers as logic elements in optical communication systems with time division multiplexing, examining optimal switching and pulse duration reduction 13 p2428 A70-29406

Injection semiconductor lasers emission characteristics, discussing gallium arsenide diodes, nonlinear losses in pulsed mode, laser interactions, etc 15 p2749 A70-31453

CW injection laser frequency stability, noting injection current influence on lasing frequency 15 p2750 A70-31629

Injection laser communication link for high data rate transmission, discussing design and construction of transmitter and receiver 16 p2862 A70-33139

GaAs laser with inhomogeneous injection, noting instability of stimulated RF oscillations 17 p3108 A70-35631

Reflectivity effect on external quantum efficiency of Fabry-Perot type GaAs injection lasers 18 p3268 A70-36731

Self induced intensity pulsations frequency stabilization and narrowing in continuously operating GaAs injection lasers 18 p3269 A70-36734

Self induced sustained light pulsations from GaAs injection lasers with tandem double section stripe geometry based on repetitively Q switched model 18 p3269 A70-36735

Pulsed GaAs injection lasers second harmonic generation with nonlinear crystal alpha iodic acid phase matched by angular tuning 18 p3269 A70-36737

InAs pulsed injection laser at cryogenic temperature for measuring time constant of IR radiation detectors 20 p3630 A70-39449

Thermoelectrically cooled GaAlAs injection laser illuminator, discussing optical-electronic interface problems and design and performance characteristics 22 p4052 A70-43603

GaAs injection lasers, calculating effect of active region displacement from p-n junction waveguide on wave generation 23 p4203 A70-45074

INJECTORS

Rocket engines gas/liquid injectors atomization characteristics using molten wax technique, considering drop sizes and gas streams velocity, density and pressure 01 p0161 A70-10326

Compression wave mechanism of supersonic combustion controlled by mixing, discussing multiple injector design, thermal compression and geometry effect 02 p0399 A70-12041

Fluorine injectors for main tank injection of space vehicle liquid hydrogen tank, including study of hypergolicity and reaction product freezing 04 p0736 A70-15406

Frozen wax measurement of droplet sizes and sprays from impinging injector elements, concerning like and unlike doublets and quintuplets 04 p0786 A70-15416

Optimum injector design for propellant spray mixing using nonreactive simulants and combustion efficiency model 04 p0737 A70-15419

Liquid rocket engine combustion processes determined by injector design using similarity principles 07 p1362 A70-19919

Optimum penetration and separation mixing of unlike doublet injector element with hypergolic hydrazine and nitrogen tetroxide propellants [JPL-TR-32-1487] 11 p2099 A70-25995

Solid state diffusion bonding applied to rocket engine injectors manufacture [AIAA PAPER 70-639] 16 p2968 A70-33597

Optimum manifold and injector hole area of pulsed exhaust systems of two cycle engine with turbosupercharger 22 p4091 A70-42809

INJUN 5 SATELLITE

U EXPLORER 40 SATELLITE

INJURIES

NT BACK INJURIES

NT BAROTRAUMA

NT BRAIN DAMAGE

NT BURNS [INJURIES]

NT CRASH INJURIES

NT EJECTION INJURIES

NT LESIONS

NT NOISE INJURIES

NT PARACHUTING INJURY

NT PARALYSIS

NT PULMONARY LESIONS

NT RADIATION INJURIES

Carbohydrate metabolism disorders in head injury cases, comparing incidence with EEG abnormalities 10 p1810 A70-24037

Monograph on measurement and regeneration of water vapor loss of human skin, studying protective qualities of horny layer 10 p1812 A70-24598

Blood platelets aggregation and release reaction in thromboembolic disease due to injury 17 p3032 A70-35471

Optimum acceleration profile for minimum severity index in injuries sustained by human subject 23 p4150 A70-44376

INLET FLOW

MHD entrance region compressible flow characteristics, determining velocity pressure and temperature distributions, friction and heat transfer coefficients, etc 01 p0067 A70-11136

Laminar isothermal entrance flows in circular cross section ducts with uniform mass injection at wall from boundary layer equations, discussing molecular weight effects 02 p0288 A70-12859

Monograph on laminar flow heat transfer in thermal entrance region of flat and profiled ducts, treating construction and efficiency of plate heat exchangers 03 p0603 A70-12988

Turbulent boundary layer of incompressible fluid flow in axisymmetric channels with swirl at inlet, considering components interaction, velocity, circulation profiles and resistance 03 p0466 A70-13389

MHD generators physical phenomena, discussing thermal efficiency, inlet parameters, operating principles, etc 04 p0625 A70-14716

Circular tube entrance upstream and downstream velocity profiles at small axial distances measured by laser Doppler flowmeter [ASME PAPER 69-WA/FE-13] 04 p0667 A70-14780

Heat transfer to absorbing fluid by coupled thermal radiation and laminar forced convection at pipe entry region, considering gray and nongray absorption [ASME PAPER 69-WA/HT-16] 04 p0783 A70-14818

Viscous inlet flow into straight channels, studying velocity profiles at low Reynolds numbers [ASME PAPER 69-APM-Q] 04 p0668 A70-14863

Noise radiated from VTOL lifting fan in wing inlet under static inflow conditions, attributing discrete tones to spacing between rotor and stator blades [ASME PAPER 69-WA/GT-6] 04 p0734 A70-14889

Settling length for turbulent air flow velocity profile in smooth concentric annuli with square-edged and bellmouth entrances [ASME PAPER 69-WA/APM-24] 04 p0669 A70-14908

Entrance length and pressure drop in MHD parallel plate channel flow using one parameter Pohlhausen method 05 p0887 A70-15978

Nonequilibrium models describing two phase critical discharge of initially saturated or subcooled liquid through sharp edged and smooth inlet geometries 05 p0956 A70-16162

Suddenly started laminar flow in circular tube entrance region, obtaining integral momentum equation for boundary layer thickness, entrance length, velocity profile, etc 06 p1034 A70-17528

Small disturbance theory for internal conical inlet hypersonic flows, using method of characteristics for similarity law verification [AIAA PAPER 70-127] 06 p0969 A70-18048

Velocity profile at entrance of two dimensional channel immersed in rarefied slow moving uniform flow with slip at walls

06 p1052 A70-18384

Heat transfer at inlet edge of turbine blade based on wind tunnel study of cylinder in air flow

07 p1362 A70-19061

Laminar flow forced convection heat transfer in circular pipe entrance region for constant wall temperature and constant wall heat flux

07 p1420 A70-19215

Cylindrical tubes steady axisymmetric inlet flow at lower Reynolds numbers, applying results to blood vessels entry flow

07 p1205 A70-19244

Blood-endothelial surface shear stress in artery inlet, considering asymmetric and radially symmetric plugging effects

07 p1220 A70-19248

Premixed compression initiated supersonic combustion, noting sensitivity to small perturbations in inlet flow variables

[AIAA PAPER 68-995] 07 p1421 A70-19318

Thermal entrance region effect on Nusselt number determination in asymmetrically heated rectangular duct with uniform heat flux

07 p1425 A70-20223

Straight-walled two dimensional diffusers with incompressible steady flow, noting effects of inlet blockage and aspect ratio on performance

08 p1433 A70-21322

Polymeric materials flow at tube entrance, discussing pressure drop and flow birefringent patterns at tapered and sharp entrances

08 p1486 A70-21861

Turbulent heat transfer in boundary layer at inlet of porous tube under nonisothermal conditions, studying velocity variations

09 p1787 A70-22169

Small disturbance and similitude applicability to internal hypersonic conical flows in edge shock and Busemann inlets

09 p1606 A70-23245

Velocity distribution along cylindrical pipe in adiabatic flow with friction and known inlet parameters

09 p1607 A70-23616

Laminar flow into channel with symmetrical jets along walls, considering velocity profiles and flow establishment lengths

10 p1870 A70-24790

Heat transfer at inlet edge of turbine blade based on wind tunnel study of cylinder in air flow

10 p1930 A70-25212

Conducting fluid incompressible flow in entrance of MHD channel by momentum integral method, permitting edge stress existence at boundary layer free steam interface

[AIAA PAPER 69-724] 11 p2035 A70-25977

Steady state two dimensional flow velocity profiles at low Reynolds numbers of homogeneous incompressible viscous liquid in straight channel inlet region

11 p2037 A70-26476

Turbulent and laminar heat transfer to gases in circular ducts entry region, considering various gas properties

12 p2212 A70-28114

Turbulent heat transfer in concentric annuli entrance region with uniform wall heat flux

12 p2333 A70-28117

Viscosity variation factor at film inlet in fluid square taper pad bearing investigated by modified Reynolds equation

13 p2418 A70-28746

Random data analysis application to aircraft inlet diagnostics

[AIAA PAPER 70-597] 13 p2375 A70-29878

Inflow and pressure difference for mean flow in straight suction duct with porous walls, using elementary momentum analysis

13 p2392 A70-30020

Steady and nonsteady engine/inlet flow field simulation for engine/compressor testing, determining feasibility of variable ramp aerodynamic device

[AIAA PAPER 70-591] 15 p2672 A70-31788

One flow influence on another at two plane jets interaction zone, applying to proportional fluid amplifier inlet impedance calculation

15 p2720 A70-32020

Heat transfer between incompressible fluid flow and insulated walls with time varying temperature at channel inlet, applying Laplace transforms

15 p2827 A70-32175

Inlet and engine control vector size and weight reduction, reliability, accuracy, etc

[AIAA PAPER 70-696] 16 p2967 A70-33559

Mathematical model of pulsatile viscous entrance flow in thick walled elastic tube, investigating flow development effects in large arteries

17 p3035 A70-34471

Hydrodynamic entry length for laminar flow between parallel porous plates, using finite difference theory for flow equations

17 p3069 A70-34983

Plane diffuser grid profiles for subcritical velocities of oncoming flow, using wind tunnel test data

18 p3205 A70-36129

Axial flow compressor off-design performance optimization by adjustable inlet guide vanes with variable trailing edge flaps

18 p3304 A70-36846

Axial flow compressor cascades, predicting total pressure losses for inlet relative Mach number greater than unity

[ASME PAPER 70-GT-57] 18 p3209 A70-36872

Tailpipe effects on gas turbine diffuser performance with fully developed inlet conditions

[ASME PAPER 70-GT-86] 18 p3210 A70-36881

Incompressible MHD flow in entrance region of channel with electrically conducting walls, calculating interacted laminar heat transfer by integral method

21 p3856 A70-41038

Constant property unsteady laminar flow thermal entrance problems, using variational formulation in Laplace transformed domain

21 p3954 A70-42169

Laminar-turbulent transition in magnetic field using Plexiglas model, observing inlet conditions effect on MHD flow stability

21 p3861 A70-42234

Newtonian fluid turbulent flow development characteristics in inlet region of smooth concentric annulus from momentum integral equations

22 p3957 A70-42304

Jet engine compressor noise analysis, noting inlet swirl role

22 p4090 A70-42725

Variable geometry radial inflow turbine performance estimation based on one dimensional flow theory

22 p3960 A70-43738

Controlled filling of container with compressed gas through time-variable cross section inlet, using variable mass thermodynamics

23 p4180 A70-44160

Turbulent nonadiabatic flow of compressible gas at inlet and main sections of variable cross section plane channel

23 p4183 A70-44739

Incompressible laminar flow in entrance region of rectangular duct allowing direct computation of eigenvalues

24 p4287 A70-45294

Porous tube inlet region, calculating fluid injection effect on laminar flow from integral form boundary layer equations

24 p4326 A70-45782

Radial inflow turbine optimum design geometry, calculating nozzle and rotor geometrical parameters efficiency

24 p4395 A70-46012

INLET NOZZLES

Entrance shape effects on tube rarefied flow in transition regime, noting role of Reynolds number in shape selection

04 p0675 A70-15593

Isentropic inlet diffusers of short design length at supersonic velocities

06 p0963 A70-17233

Flow distribution for short isentropic supersonic inlet diffusers, using method of characteristics and Oswatitch and Connors procedures

06 p0963 A70-17234

Wind tunnel tests of isentropic inlet diffusers, describing two dimensional model, test apparatus and modification and results

06 p0963 A70-17235

Inlet-engine compatibility testing for aircraft system development program

[AIAA PAPER 70-941] 16 p2965 A70-33534

Auxiliary inlet ejector and plug nozzle flight performance, describing design variation effects for high supersonic speeds

[AIAA PAPER 70-701] 16 p2841 A70-33563

Ejector maximum compression ratio calculation based on inlet nozzle gas flow model

21 p3746 A70-41767

Transition zone heat exchange during air mixed flow in pipes with conical duct or Vitoshinski nozzle inlets

23 p4283 A70-44729

INLET PRESSURE

Stability region of hydraulic system containing centrifugal pump calculated from pressure head dependence on pump inlet pressure

09 p1607 A70-23622

Aircraft turbojet engine/inlet compatibility, using data system for acquisition, identification and analysis of critical time variant pressure parameters

[AIAA PAPER 70-594] 13 p2375 A70-29877

Starting criterion for hypersonic inlets with large turbulent boundary layers, considering total pressure recovery from all shock and viscous losses

14 p2529 A70-30865

Gas-particle efflux from nozzle at critical velocities, noting particle size and concentration effects on inlet pressure

15 p2721 A70-32136

INLETS (DEVICES)

U INTAKE SYSTEMS

INNER RADIATION BELT

Satellite radiation dose rates in inner Van Allen belt, correlating calculated and measured rates with proton environment model

06 p1134 A70-17264

Space radiation doses in inner Van Allen belt, comparing calculated and satellite measured rates

06 p0991 A70-17272

Satellite observational data on time history of inner radiation belt /October 1963-December 1968/

09 p1746 A70-23488

Cosmos 137 proton spectra data obtained in inner radiation belt agreeing with Relay 1 data

11 p2106 A70-26786

Time comparative low energy proton measurements in inner radiation belt by Rubis rocket with detector telescopes and omnidirectional counters

13 p2475 A70-28572

Radio sounding of Van Allen inner belt from Antarctica, comparing American and Soviet deductions about magnetosphere structure

13 p2399 A70-29273

High energy proton flux variations in inner belt during solar cycle and magnetic storm, using satellite and balloon measurements

13 p2483 A70-30091

Book on dynamics of geomagnetically trapped radiation, covering radiation belts control, adiabatic theory, trapped particle diffusion, etc

16 p2972 A70-34300

Proton distribution in radiation belt inner zone from radial diffusion addition to cosmic ray produced albedo-neutron decay and atmospheric collision loss

17 p3150 A70-34644

INOCULATION

Radar measured precipitation increase from seeded cloud demonstrated by measurements, numerical cumulus model and physical reasoning

12 p2189 A70-28094

INORGANIC COATINGS

NT ANODIC COATINGS

NT CERAMIC COATINGS

Reflectance of clean and fluoride coated aluminum surfaces in vacuum UV

05 p0883 A70-16590

Soviet collection of papers on inorganic glassy coatings and materials

05 p0870 A70-16591

Metals mechanical properties with inorganic heat resistant coatings between 1900-2300 K in oxidizing medium, describing facility based on solar furnace

05 p0875 A70-17069

Dielectric coatings resistance to laser radiation, measuring rupture threshold of vacuum coatings consisting of zinc sulfide layers

10 p1901 A70-25111

Service life and friction coefficient of molybdenum disulfide-silicon lubricating coating as function of load, sliding rate and vacuum level

11 p2060 A70-25943

Boron and boron carbide coatings formation on graphite by vapor deposition, determining optimum parameters for reaction control

19 p3455 A70-38250

INORGANIC COMPOUNDS

NT AMMONIA

NT LIQUID AMMONIA

Thermal decomposition mechanism of inorganic oxidizers, discussing reactivity of alkali and alkali earth salts

18 p3299 A70-36240

Uridine phosphorylation by heating with inorganic orthophosphates achieved via nucleoside reactions

23 p4158 A70-44837

Inorganic liquid lasers, discussing Nd salts solution preparation and handling methods

23 p4201 A70-44929

INORGANIC MATERIALS

Inorganic liquid laser materials and use of circulating active medium

08 p1513 A70-21302

Inorganic ceramic materials in design and fabrication of microwave antennas, filters and stable resonators, discussing density and dielectric constant variability by ceramics foaming

09 p1689 A70-22007

Thermal analysis - Conference, Holy Cross College, August 1968, Volume 2, Inorganic materials and physical chemistry

11 p2070 A70-25808

INORGANIC NITRATES

NT AMMONIUM NITRATES

NT HYDRAZINE NITRATE

NT SILVER NITRATES

INORGANIC PEROXIDES

NT HYDROGEN PEROXIDE

Peroxides, superoxides and ozonides applications in industrial chemistry, semiconductors and rocket motor fuels, discussing chemical structure and properties and nomenclature

05 p0810 A70-15768

INORGANIC SULFIDES

NT CADMIUM SULFIDES

NT COPPER SULFIDES

NT HYDROGEN SULFIDE

NT MOLYBDENUM DISULFIDES

NT MOLYBDENUM SULFIDES
NT POLYSULFIDES
NT ZINC SULFIDES

INPUT
Rockets angular motion due to thrust with ramp input, presenting graphs for different inputs and inertia ratios
11 p2123 A70-26125
Random-input describing function as linear approximation to instantaneous nonlinearity in terms of minimum mean-squared error
13 p2382 A70-29070
Adaptive optimization methods involving minimization of unknown function, determining new input location via sequential search
13 p2383 A70-29583
High speed digital computer input device for reading data from magnetic tape, discussing design and operation principles
18 p3230 A70-36095
Real time analog display inputs for electronic computers and tracking in physiological control circuits, describing various manual controls
19 p3367 A70-37564
Bayesian identification of system parameters for observable and nonobservable input signals
24 p4316 A70-45474

INPUT/OUTPUT ROUTINES
State variable diagram for transfer function of single output/input linear stationary system obtained by parallel, direct and iterative methods
05 p0928 A70-16027
Autonomy and invariance conditions for control systems composed of multivariable components having same number of inputs and outputs
07 p1244 A70-18768
Pulse neurons random homogeneous networks macroscopic description, considering operation modes in terms of input frequencies and output pulse sequences
08 p1451 A70-21000
Real time sonic information input/output computer system for acoustic signals and speech synthesis, concerning man machine communication
14 p2553 A70-30425
Stable adaptive control design for linear time-invariant system with same number of inputs as outputs, considering disturbance effect
16 p2881 A70-33035
Finite settling response for single input/output feedback control system obtained by dual rate sampled data control algorithm
16 p2882 A70-33037
Digital computer input language with multiple access for engineering calculations
19 p3385 A70-38577
Linear discrete feedback systems uniqueness, existence and stability under various input-output conditions
22 p4004 A70-43024

INSECTICIDES
NT URETHANES

INSECTS
NT BEETLES
NT DROSOPHILA
NT MOTHS
Hibernation and glycerol production in wasps Ichneumonidae, discussing possible physiological cryoprotective function
24 p4304 A70-46140

INSENSITIVITY
U SENSITIVITY

INSERTION
Human mitral valve morphology, distinguishing chordae tendineae types by insertion mode
10 p1819 A70-24935

INSERTION LOSS
Microwave waveguide insertion-loss calibrations, comparing cavity Q and direct measurement methods
10 p1854 A70-25315

INSERTS
NT NOZZLE INSERTS
Infinite elastic plate with beam reinforced circular insert, using classical plate theory and Euler-Bernoulli hypothesis for beams
16 p2990 A70-33679
Water and alkali metal boilers, predicting helical-flow-promoting inserts effect on pressure drop penalties by constant slip model
21 p3949 A70-41308
Stress analysis of anisotropic circular ring with pressed-in solid disk, using sectionally holomorphic functions
22 p4119 A70-43686

INSPECTION
NT INFRARED INSPECTION
NT X RAY INSPECTION
Inspection penetrant systems reliability and performance predictability for nondestructive flaw detection
01 p0096 A70-10005
Automated inspection for defects and dimensions - Conference, Eastbourne, England, May 1969
01 p0105 A70-11394

Nondestructive inspection program for DC 10 aircraft maintenance
02 p0308 A70-12273
Automatic inspection data collecting and processing by human operator using display devices and computerized mathematical reduction for real time evaluation
02 p0266 A70-12469
Nondestructive test procedures for maintaining and determining serviceability of penetrant inspection materials during use
05 p0844 A70-15780
Lasers for optical inspection of components and calibration of machine tools
05 p0860 A70-16823
Liquid oxygen usage inspection penetrant systems combining nonreactivity with flaw detection sensitivity
08 p1508 A70-21745
Life support systems general inspection procedures, personal and survival equipment and accessories
11 p1990 A70-25673
Economical inspection of numerical-control produced parts through critical dimensions determination and dimension measurement reduction [SME PAPER IQ-70-710]
12 p2241 A70-27086
Computerized on-line industrial inspection involving automatic machine sequential control and product geometry error correction, discussing hardware and software requirements [SME PAPER IQ-70-712]
12 p2241 A70-27088
Manufacturing error rate and inspection efficiency relevance to hardware product reliability
12 p2244 A70-28014
Quality control goals for manufactured products translated into manufacturing process inspection and investment costs terms
13 p2421 A70-29675
Defect grouping role in MIL-STD-105D inspection techniques, discussing costs and acceptance probabilities
22 p4048 A70-43727
Ultrasonic crack detection in fastener holes in C-5A wings
24 p4341 A70-45571
Nondestructive testing technology, emphasizing component designer role in facilitating inspection of surface defects
24 p4342 A70-45679
Thickness measurement and internal defects inspection by ultrasonic resonance technique
24 p4343 A70-45683
Fluorescent penetrants vs magnetic powder test for individual and continuous material inspection, discussing sensitivity and surface finish influence
24 p4338 A70-45741
Inspection penetrant development for flaw detection, considering entrapment efficiency and dimensional sensitivity
24 p4348 A70-45743

INSPIRATION
Human tolerance and ventilatory response to inspiratory mechanical loads
23 p4144 A70-43822

INSTABILITY
U STABILITY

INSTALLATION
U INSTALLING

INSTALLING
Installation planning of electronic data processing unit using network and PERT program features
03 p0454 A70-13969
High precision strain gage installation, discussing specifications and errors caused by oblique load action, natural frequency and deformation
08 p1493 A70-20585
Accelerometer installation resonant frequency, discussing mounting methods, structure material, geometry and total mass
17 p3089 A70-35174

INSTITUTIONS
Launch facilities institutionalization for space shuttles launch cost minimization [AIAA PAPER 70-244]
07 p1251 A70-20374
Launch facilities institutionalization for space shuttles launch cost minimization [AIAA PAPER 70-244]
20 p3606 A70-39697

INSTRUCTIONS
U EDUCATION

INSTRUCTORS
Elementary flight training study in Royal Netherlands Air Force for improving pilot selection, discussing instructor and social science roles
12 p2176 A70-27030
Civilian pilot trainee stress level dependence on individual flying instructors, detecting psychophysiological variables by inflight recording
12 p2178 A70-27044

INSTRUMENT APPROACH
VTOL flight investigation to develop decelerating instrument approach capability with control-command information display for three degrees of freedom [SAE PAPER 690693]
05 p0792 A70-15862

INSTRUMENT COMPENSATION
Terminal area guidance for unpowered aircraft instrument approach relevant to manned space shuttle effort
14 p2614 A70-30465
Head up display /HUD/ flight tests, examining effects decreasing quality of manually handled instrument approach, discussing space myopia and disorientation
16 p2912 A70-33819
Pilot scanning dwell times and control workload in simulated instrument approach, using eye-point-of-regard/EPR/ measurements [AIAA PAPER 70-999]
20 p3580 A70-39532
Pilot heart rate during in-flight simulated ILS approaches in general aviation aircraft
24 p4306 A70-45333

INSTRUMENT COMPENSATION
NT TEMPERATURE COMPENSATION
One piece KDP and ADP reflector shutters used as laser Q switches, discussing compensation for working surfaces temperature displacement
01 p1016 A70-10060
Flip-flop type intergimbal compensation system for gyroscopic integrators error reduction, obtaining natural oscillations constant amplitude
01 p0092 A70-10987
Refraction-induced range and tracking errors estimation in exponential model atmosphere by closed functions
01 p0044 A70-11087
Low temperature high sensitivity temperature compensated heat flux transducers to measure conductive, convective and radiative heat transfer
02 p0303 A70-12740
Optimal nonlinear correcting of vertical gyro obtainable with correction containing nonlinear elements with variable linearized coefficients
03 p0483 A70-13363
Gyrostabil motion stabilization with respect to unperturbed circular orbit vector radius, considering gravitational, aerodynamic, perturbation moments action and zero dry friction moment
03 p0484 A70-13370
Constant temperature hot-wire anemometer to compensate for thermal lag of wire/film resistance thermometer within useful frequency range
03 p0492 A70-13761
Vertical gyroscope with nonlinear compensation circuit under random distortion of signal spectral composition
05 p0880 A70-16223
Ion counter circuit using second equivalent condenser for compensating background radiation current, assessing error
07 p1281 A70-19526
Solid state lasers thermal resonator buckling time dependence and compensation, graphing results of resonator field analysis
07 p1303 A70-20359
Dynamic force measurement methods, considering reaction force and operational compensation
09 p1672 A70-22013
Distortion-compensation circuit theory, considering voltage-frequency characteristics and varactor controlled oscillator nonlinearities of frequency modulators
09 p1632 A70-22235
Parabolic reflectors profile error compensation by means of multielement feed array with controllable phasing
09 p1644 A70-22236
Laser beam with small divergence angle kept in horizontal position by leveling instrument with automatic compensating device, discussing distortion effects on localization
09 p1699 A70-23442
Atmospheric particles photographed in situ by cameras using microsecond flash lamps, discussing required mechanical motion compensation at aircraft speed
10 p1886 A70-23930
Vacuum chamber for adjusting and calibrating spaceborne optical instruments used in studying UV radiations
10 p1860 A70-24479
Dynamic force measurement, evaluating hybrid system with reaction force summation and operational compensation subsystems
10 p1889 A70-24580
Microwave phase shift measurement errors caused by reflections from interference systems elements
10 p1853 A70-25130
Multiplicity recorder for cosmic rays neutron component studies, reducing star redistribution errors by coincidence effect compensation
11 p2103 A70-25527
Holographic compensation for atmospherically induced phase distortion of IR laser beam
11 p2049 A70-25638
Mechanical systems vibrations comprising tension couplings compensating misalignment between non-coaxial shafts
11 p2060 A70-26348

- Adjustable gyroscope errors under compensating-loop linearity zone limitation, showing saturation filtering influence on sensing element
12 p2233 A70-27562
- Gyroscopic platform stabilizers /GPS/ dynamic properties improved by compensation of perturbing torques
12 p2237 A70-28155
- Automatic cancelling devices with compensating coils for terrestrial magnetic field vector
13 p2401 A70-30044
- Motion and small vibration frequency stability of correctable gyroscope with correction moment at arbitrary angle with mismatch plane
15 p2738 A70-32154
- Adaptive radar beacon forming, using conjugate reflections for propagation path errors compensation
16 p2865 A70-34061
- Static weight tare compensation for V/STOL wind tunnel models, using accelerometer outputs
17 p3062 A70-35500
- Flight test instrumentation for V/STOL stability derivatives extraction, noting instrument errors and required compensation
17 p3094 A70-35502
- Magnetic compensation for attitude control of gravity gradient stabilized satellite using environmental torques and moment gyro damping
[ALAA PAPER 70-993]
20 p3668 A70-39537
- Strain gages for structural stress analysis in cryogenic environments, discussing correction factors for temperature dependent characteristics
21 p3932 A70-40545
- Multiplicity recorder for cosmic rays neutron component studies, reducing star redistribution errors by coincidence effect compensation
21 p3882 A70-41277
- Error sources and magnitudes in dynamic gradiometer using inertial grade pendulous accelerometer, discussing compensating modifications
22 p4042 A70-43658
- Ultrasonic inspection sensitivity loss, discussing depth compensation methods
24 p4343 A70-45690
- Circuit design providing thermal compensation for atmospheric pressure sensor, using mercury barometer
24 p4340 A70-46403
- INSTRUMENT DRIFT**
- Optimal nonlinear correcting of vertical gyro obtainable with correction containing nonlinear elements with variable linearized coefficients
03 p0483 A70-13363
- Transistorized photoelectric star transit recorder operable in ambient media with large temperature variations ensuring low zero point drift
04 p0694 A70-15490
- Drift error of correctable three degree of freedom free-floating astatic gyrocompass mounted on aircraft flying straight course at uniform speed
05 p0848 A70-16224
- INSTRUMENT ERRORS**
- Aeronautical satellites for monitoring positions of many commercial aircraft simultaneously crossing North Atlantic, discussing navigational error correction and atmospheric
01 p0178 A70-10454
- Right ascension screw error effects on observations of stellar image passage through meridian, evaluating effect
01 p0181 A70-10662
- Hot-wire probe support orientation to minimize flat plate turbulent boundary layer mean velocity determination errors
01 p0087 A70-10665
- Absorber positioning inaccuracy influence in concentrating solar unit mirror on unit energy parameters, discussing defocusing
01 p0010 A70-10763
- Flowmeter errors caused by nuclear magnetic relaxation decreased with increasing magnetic field strength of NMR sensor
01 p0091 A70-10981
- Flip-flop type intergimbal compensation system for gyroscopic integrators error reduction, obtaining natural oscillations constant amplitude
01 p0092 A70-10987
- X band electron paramagnetic resonance spectrometer with ruby maser preamplifier, correcting misinterpretation and noise figure analysis
01 p0114 A70-11196
- Instrument error analysis for spacecraft orientation and positioning near planet from planet disk observations
01 p0094 A70-11511
- Algorithm for determining readings dispersion during cosmic rays variability, statistical nature and instrument errors
01 p0172 A70-11526
- Rb-75 adapted reconnaissance cameras error sources on basis of processed Echo 2 satellite photographs
02 p0294 A70-11772

- Automatic landing systems research including VHF ILS accuracy, test equipment for servicing airborne equipment, etc
02 p0333 A70-11981
- Lateral separations using navigation error analysis, showing values for aircraft with or without Dioscures and inertial control under North Atlantic conditions
02 p0336 A70-12607
- Readjustment of aircraft navigation systems based on inertial platforms, discussing errors, corrections and damping stressing single platform
02 p0336 A70-12608
- Reliability of Doppler radar hail detection, discussing corrupting effects of turbulence and shear, size-sorting and vertical air motions
03 p0443 A70-13167
- UV radiation scattering and rocking instrument error source in vertical ozone profile determination with optical ozone probes
03 p0557 A70-13296
- Thermal balance of radiosonde thermometric elements and radiation errors in atmospheric temperature measurements using spectra of radiation fluxes reflected from cloud cover
03 p0557 A70-13297
- Gyrocompass composed of angular velocity integrators and interconnected by correction amplifiers, analyzing behavior during roll on vessel, determining error components
03 p0484 A70-13371
- Doppler memory mode of ground speed and drift angle calculations analyzed by operators for possible errors
04 p0716 A70-14629
- Corrections to observed thermistor temperature profiles presented for spherical bead thermistors with long lead or thin film mounting
[AAS PAPER 69-568]
04 p0687 A70-14664
- Probability theory for gimbal errors in directional gyroscopes under irregular rocking, using linearization of functions of random arguments
04 p0692 A70-15281
- Axial misalignment control of gimbal pivots and rotors in gyroscopes
04 p0692 A70-15282
- Error sources affecting data comparison accuracy between gyro measurements and reference solutions and due to gyro axes misalignment and gimbal angular movement
04 p0692 A70-15327
- Semidiurnal lunar tidal wave influence on clock corrections obtained by observations of stellar meridian passages at four localities
04 p0756 A70-15479
- Time measurement errors from astronomical observations resulting from thermal and refractive effects on instrument
04 p0756 A70-15482
- Transit instrument suspension improvement by isolating unloading mechanism from horizontal axis, reducing external observation errors
04 p0693 A70-15483
- Prismatic astrolabe errors, analyzing focal plane displacement due to temperature, micrometer motor adjustment, instrument and personal errors
04 p0693 A70-15485
- Differential screw gauge for determining micrometer screw periodic errors and error components in level triers, using Rydberg method
04 p0693 A70-15488
- Piezoelectric sensing diaphragm for detection of micrometeorites in space, noting vibration mode and effect of small beads contact time on calibration errors
04 p0695 A70-15567
- Block diagram for eliminating counting errors and spurious coincidences in telescope used at cosmic ray stations
05 p0845 A70-15931
- Neutron monitor calibration method to eliminate natural cosmic ray background, decreasing errors due to ray intensity variation
05 p0846 A70-15938
- Azimuthal telescope for recording cosmic rays intensity, noting statistical error for vertical and oblique incident component
05 p0846 A70-15967
- Aerological radio thermometers random and systematic errors compared to network radio probe
05 p0848 A70-16206
- Optical resonator reaction to coupled laser frequency, attributing differences between theory and experiment to errors in mirror reflection efficiency measurement
05 p0859 A70-16354
- Triaxial universal astrometric instrument for tracking artificial satellite path with eyepiece crosswire, considering instrument errors
05 p0851 A70-16698
- Network ozonometer compared to ozonometers with narrow interference filters, finding fictitious day lapse in data
06 p1064 A70-17791
- Errors arising in torsion-type ponderomotive wattmeter connected in homogeneous microwave trans-

- mission line with mismatched oscillator at input and mismatched load at output
06 p1024 A70-17861
- Photoelectric multislit micrometer for astronomical purposes, presenting stochastic variables mean error difference formula for arbitrary power spectrum
06 p1071 A70-18458
- Photometric error analysis and optimum use of photomultipliers, discussing pulse-height spectra, detection and weighting systems
06 p1071 A70-18517
- Flight configured single sideband telemetry accuracy determined by digitally computed frequency response
06 p1012 A70-18600
- Error analysis for pendulum type gyrocompass with indirect correction during irregular rolling, taking into account second infinitesimal order terms of equations of motion
07 p1278 A70-18735
- Linear vibrations in gimbal suspension rotor and base, estimating gyroscope drift during base and rotor vibrational coincidence
07 p1279 A70-18738
- Microscope objective effect on accuracy of optical systems modulation-transfer function based on corrected high speed lens measurements
07 p1334 A70-19147
- Optimal photometric data processing for planetary characteristics and surface details, considering errors due to image blurring in telescope
07 p1384 A70-19419
- Error estimation of gondola encased tugged undersea magnetometer as function of turbulence parameters
07 p1281 A70-19466
- Finite structural rigidity of statically unbalanced three degree of freedom gyroscope influence on operation, discussing instrument error
07 p1282 A70-19535
- Active and compensating sensors resistances, strain sensitivities, temperature gradients and lead resistances differences effect on accuracy of resistance strain gage measurements
07 p1283 A70-19747
- Inertial navigation system design principles, deriving error equations and equations of ideal operation
07 p1332 A70-20177
- High precision strain gage installation, discussing specifications and errors caused by oblique load action, natural frequency and deformation
08 p1493 A70-20585
- Soviet collection of papers on apparatus for meteorological measurements covering error analysis, reliability engineering, use of computers, etc
08 p1494 A70-20771
- Chromatic aberrations of Poltava observatory AVR-2 refractor
08 p1496 A70-21161
- Cup and vane anemometers theory, determining overestimation errors of differential equation for mean values in sinusoidally fluctuating winds
08 p1501 A70-21975
- Sewage water flowmeter calibration, analyzing error propagation and tolerance
09 p1672 A70-22027
- Stars photographic position determination errors with NAFA-3C/25 camera, comparing films and plates
09 p1673 A70-22164
- Atmospheric momentum and heat flux height variations in surface boundary layer, stressing instrument performance and measurement techniques
09 p1715 A70-22359
- Flow noise measurement for boundary layer pressure fluctuations at rigid wall, analyzing effect of transducer size, shape and orientation on resolution
09 p1675 A70-22387
- Strain gages for static deformation measurement of fiberglass reinforced plastics at room and higher temperatures, discussing error sources and gage-specimen adhesive bonding
09 p1780 A70-23107
- Tungsten-rhenium thermocouple for high temperature measurement of samples under unsteady heating processes, analyzing instrument error sources
09 p1789 A70-23108
- Directional gyroscopes with accelerated rotors on moving bases, deriving gyro errors as base motion functions
09 p1680 A70-23145
- Positional contact micrometer used to eliminate stars apparent oblique motion in astronomical universal instruments
09 p1681 A70-23342
- Dispersion effect on accuracy of measuring polycrystalline samples electronograms by comparator using statistical method
09 p1682 A70-23392
- Airborne monochromator and photoelectric filter radiometer for solar spectral irradiance measurements, estimating instrument errors
09 p1683 A70-23515

- Scanning spherical mirror interferometer for carbon dioxide lasers radiation spectrum analysis, discussing instrument errors in mode and wavenumber studies
09 p1683 A70-23519
- IR thermometers in situ calibration, analyzing maximum error due to reflection effect
09 p1684 A70-23536
- Large-base radio interferometer with separate heterodyne receivers and electrical length automatic control, studying causes of phase errors
09 p1650 A70-23631
- Constant temperature /phase transition/ calorimeter errors in measuring laser energy using ice as working medium
09 p1700 A70-23659
- Ambient temperature measurement by constant level balloon mounted thermistors, discussing errors from differential heating of thermistor support by solar radiation
10 p1886 A70-23935
- Network ozonometer compared to ozonometers with narrow interference filters, finding fictitious day lapse in data
10 p1892 A70-25023
- Microwave phase shift measurement errors caused by reflections from interference systems elements
10 p1853 A70-25130
- Extraterrestrial electron density precision measurement using HF impedance probe with guard ring to remove ion sheath effects
10 p1892 A70-25255
- FM telemetry channel noise effects on digital and analog accelerometer outputs accuracy, suggesting mean square error reduction methods
10 p1893 A70-25318
- Short wave signal field strength measurement errors by frame antenna, outlining correction procedure
11 p2003 A70-25552
- Plate measurement on comparators in satellite geodesy, discussing optics, magnification, mark selection and error elimination
11 p2051 A70-26181
- Quadratic error of semiautomatic measuring apparatus for photographic plates, noting operator contribution
11 p2051 A70-26182
- Steady state surface temperature measurement errors by thermistors, thinistors and thermocouples, discussing sources
11 p2052 A70-26361
- Dynamic errors of electric measurement devices during three dimensional polyharmonic vibrations of foundation
12 p2233 A70-27561
- Adjustable gyroscope errors under compensating-loop linearity zone limitation, showing saturation filtering influence on sensing element
12 p2233 A70-27562
- Polarization of extragalactic radio sources and supernova remnants emphasizing instrumental effects
12 p2309 A70-27894
- Probe rocket Tacite 02 head attitude gyrorestoration for IR horizon analysis, using stellar sensor and signal measurements
13 p2500 A70-28408
- Universal triaxial instrument with AT-1 telescope for visual observation of satellites, discussing applications and accuracy
13 p2408 A70-29274
- Reflecting surface nonplane parallelism effects on Fabry-Perot interferometers superposition bands contrast and multiplied length measurement accuracy
13 p2408 A70-29366
- Tungsten strip lamps spectral radiance calibration, discussing accuracy requirements for radiation constants, wavelength and black body temperature
13 p2410 A70-29655
- Black body design for radiometry, discussing error sources in calibration
13 p2410 A70-29658
- Superconducting bolometer operating temperature stabilization
13 p2412 A70-29868
- Electric resistance type strain gages, eliminating errors due to device length
14 p2582 A70-30174
- Heat removal influence on dynamic errors of cylindrical temperature sensors using electric models
14 p2662 A70-30183
- Errors magnitude in quartz vanometer readings resulting from variations of geomagnetic field perpendicular component
14 p2582 A70-30244
- Time constant equations for hair and film radiosonde hygrometers, allowing for inertial errors in humidity and cloud boundary measurements
14 p2603 A70-30412
- FPS-16/Jimsphere wind profiles measurement, discussing effect of data smoothing on accuracy and resolution
14 p2607 A70-30569
- Meteorological transponder rocketsonde instrumentation system evolution and data error analysis
14 p2585 A70-30579
- Implantable EM blood flowmeter errors due to nonsymmetrical blood flow velocity distribution and nonuniform magnetic flux density
14 p2542 A70-30797
- Convergence corrections for absorption coefficient measurements by far IR Michelson interferometer
14 p2586 A70-30988
- Photoelectric detector sensitivity variation effect on long term instability of servomagnet variometers
14 p2588 A70-31261
- Shifts method applicability to electronic camera for stellar magnitude photometry, studying instrument limitations and errors
14 p2589 A70-31379
- Asymmetrical transient attenuation effects of bridge circuit phase discriminator on accuracy of phase difference measurements
15 p2707 A70-31508
- Magnetoelastic sensors for small force measurement, describing instrument error reduction
15 p2733 A70-31577
- Discharged cleaned surface effect on accuracy and reliability of electron density and temperature measurements by Langmuir probes
15 p2778 A70-31765
- Null and fixed correction methods for pressure and/or velocity gradient error in flow direction measurement
15 p2736 A70-31898
- Plotter induced reconstruction errors minimization in computer generated binary Fourier transform holograms
15 p2737 A70-32044
- Ionospheric probe designs and measurement errors due to perturbations by satellite carriers
15 p2731 A70-32094
- Error measurements of sharpened edged circular static pressure hole normal to moving fluid boundary using flush transducers
15 p2722 A70-32374
- Thickness measurement for thin films in inaccessible locations using scanning electron microscope, comparing accuracy with interferometric techniques
15 p2741 A70-32435
- Thermoelectric force due to thermocouple inhomogeneities, showing relation to temperature gradient and measurement error
16 p2900 A70-33070
- Digital logic control of chromatographic system for measuring instrumental contributions to band broadening
16 p2855 A70-33120
- Ballistic missile instrument orientation optimization based on CEP criterion, considering acceleration induced errors
16 p2947 A70-33317
- Nonmagnetic explosive actuated indexing device permitting precise 180 deg rotation of magnetometer sensor on Pioneer 6 spacecraft
16 p2914 A70-34124
- Hypsometer design for accurate pressure measurements at high balloon altitudes
17 p3090 A70-35313
- Systematic errors in rotating mirror framing cameras and film records for quantitative high speed motion analysis
17 p3095 A70-35632
- Statistical analysis of cosmic radiation neutron component monitor error, taking into account generation multiplicity
18 p3307 A70-36097
- Recording instrumental noise resolution of standard algorithm for cosmic ray stations
18 p3307 A70-36100
- Statistical accuracy of standard muon azimuthal semicubic telescope for solar cosmic rays, discussing rms error
18 p3256 A70-36103
- Erroneous line of sight rates generation by radar radome refraction errors in aircraft tracking
18 p3231 A70-36457
- Error estimation of gondola encased tugged undersea magnetometer as function of turbulence parameters
18 p3260 A70-36940
- Mass spectrometer modified for use with X-Y recorder for accurate and reproducible ionization efficiency curves
18 p3262 A70-37099
- Error sources in carbon black coating on thin foil heat flux sensors accounting for false altitude effects in vacuum calibration
18 p3262 A70-37100
- Error reduction methods for linear acceleration gyrointegrators measuring linear velocities
19 p3420 A70-37257
- Ultrahigh vacuum gages absolute calibration by controllable conductance method, discussing accuracy
19 p3421 A70-37463
- Atmospheric aerosols optical and microphysical measurements comparison, evaluating sample collection equipment, errors, etc
19 p3421 A70-37637
- Hydrogen maser wall shift measurement, using flexible storage bulb for accuracy improvement
19 p3445 A70-37759
- Air total temperature measurement for jet powered aircraft, discussing subsonic and supersonic wind tunnel data for sensor thermal recovery characteristics
19 p3425 A70-37882
- High resolution successive approximation voltmeters using digital carry to improve speed and accuracy
19 p3427 A70-38049
- Bubble chamber photography and track image reconstruction by holography, discussing measurement apparatus, accuracy and tolerances
19 p3428 A70-38510
- Correction procedures for measurement errors in actinometers and pyroheliometers caused by circum-solar radiation
20 p3625 A70-39029
- Atmospheric ozone content during May 1966 solar eclipse, noting solar disk darkening effect on measurements
20 p3615 A70-39031
- Static pressure probes selection for measuring three dimensional flow at high velocities, considering sensitivity and errors
20 p3628 A70-39262
- Strapdown inertial guidance systems critical dynamic errors mathematical modeling and verification [AIAA PAPER 70-1029]
20 p3666 A70-39508
- Satellite-borne conical IR scanner flight data hybrid simulation and error analysis, suggesting carbon dioxide horizon noise model [AIAA PAPER 70-1021]
20 p3631 A70-39513
- Digital correlator errors due to quantization by levels, designing analyzer of slow processes
20 p3594 A70-39922
- Surface contaminated Langmuir probe measurements in glow discharge plasmas, discussing errors
20 p3633 A70-40161
- Electrostatic plasma probe inverse process I-V properties from current voltage characteristics, improving accuracy and reliability by theory in terms of new variables
20 p3683 A70-40162
- Optimum calibration intervals determination for obtaining instrument maintenance quality level at low cost
20 p3634 A70-40452
- Ionization spectrometer for hadron energy measurement, analyzing instrument accuracy by Monte Carlo model for nuclear-EM cascade in iron absorber
20 p3635 A70-40456
- Image orthicon in high precision astronomical camera, evaluating geometric accuracy and stability by distortion measurement
21 p3822 A70-40819
- Ion orientation technique based on counterflow sensing in earth upper atmosphere, discussing accuracy
21 p3927 A70-40844
- Heat conduction errors in immersion thermocouples and resistance temperature sensors, using mathematical model
21 p3823 A70-40856
- Inertial guidance technology applications for space navigation, considering instrument design tradeoff between accuracy and cost for performance and reliability improvements
21 p3848 A70-41128
- Short wave signal field strength measurement errors by frame antenna, outlining correction procedure
21 p3786 A70-41302
- Instrumental and atmospheric observational problems regarding dark mottles, fibrils and H alpha solar limb photographic interpretations
21 p3926 A70-42199
- Interference-polarization light filter, calculating phase shifter errors effects on transmittance by Poincare sphere method
22 p4072 A70-42505
- Optical telescope reflecting prism angle deviations effect on modulation transfer function and image quality
22 p4072 A70-42506
- Guidance and navigation systems precision azimuth measurement by star sighting and gyrocompass techniques
22 p4067 A70-42663
- Rocket-borne double probe electric field detector design and operation, discussing error sources
22 p4030 A70-42793
- Thermal and aerodynamic interactions between wires of velocity sensitive anemometric crossed-wire probe, showing reduction by correction of measurements and minimal gap
22 p4038 A70-43242
- Distance measurements by microwave tellurometers, discussing accuracy factors
22 p4039 A70-43426
- Precision gimbaled sensor pointing system calibration data errors due to misalignments and inaccuracies in transducer readout
22 p4040 A70-43587

- Gyro misalignment and encoder quantization effects for strapdown attitude error sources 22 p4040 A70-43588
- Error sources and magnitudes in dynamic gradiometer using inertial grade pendulous accelerometer, discussing compensating modifications 22 p4042 A70-43658
- Gravity error propagation in dynamic gravimetry associated with navigation and gradient measurement errors, emphasizing standard error limits in navigation data 22 p4068 A70-43660
- Gravity measurement errors in high speed aircraft parallel to undulating geoid attributed to associated vertical accelerations 22 p4025 A70-43662
- Stochastic processes for probabilistic error analysis in airborne gravimetry, using gravity sensing instruments 22 p4025 A70-43666
- Moving object coordinates autonomous determination errors in accelerometers with dry friction, investigating inertial navigation system with integral horizon correction 23 p4193 A70-43981
- Thermal calibration errors and sensitivity equations for hot-wire anemometers 23 p4195 A70-44288
- Guarded electrical cylindrical calorimeter measuring multilayer insulation thermal conductivity, discussing construction, test and error 23 p4195 A70-44366
- Isoclinic parameter determination from intersection points of secondary isochromatics lines in photoelastic analysis, discussing polariscope theory and imperfect quarter wave plates error effect 23 p4198 A70-44910
- X band horn antennas precision phase center measurement technique for high resolution system applications 23 p4176 A70-44966
- Laser sensors as alignment instrument for control and measurement of five degrees of freedom 24 p4351 A70-45383
- Radiosonde errors in temperature and pressure height determination using paired AN/GMD-1 probe flights 24 p4371 A70-46047
- Temperature induced humidity errors in military and Weather Bureau radiosondes carbon humidity element caused by solar irradiation 24 p4372 A70-46073
- Recording system errors for measuring pulmonary pressure-volume curves of excised lungs 24 p4309 A70-46122
- Errors magnitude in quartz vanometer readings resulting from variations of geomagnetic field perpendicular component 24 p4339 A70-46319
- ### INSTRUMENT FLIGHT RULES
- Low cost VHF and UHF navigation aids IFR procedures for low density airports [SAE PAPER 700230] 13 p2385 A70-29607
- Maximum throughput-rate capacity for runway and final approach path airspace involving multiple IFR landings 19 p3465 A70-38235
- ATC integration of SST, discussing en route and terminal projects of national airspace system, modular automation, instrument flight rules, etc 19 p3467 A70-38633
- VTOL aircraft instrument flight in terminal area, defining requirements and operating characteristics for vertical and low speed capabilities [AIAA PAPER 70-1333] 24 p4291 A70-45935
- ### INSTRUMENT LANDING SYSTEMS
- #### NT AUTOMATIC LANDING CONTROL
- Microwave ILS for difficult sites or conditions, detailing capabilities and operation principles 01 p0136 A70-10301
- Aircraft approach and guidance system radio components including localizer, glide path and marker systems and radio altimeters, discussing signal interference 02 p0333 A70-11980
- Automatic landing systems research including VHF ILS accuracy, test equipment for servicing airborne equipment, etc 02 p0333 A70-11981
- Airborne instrument landing systems and ground facilities analysis and specifications, examining future use of microwave frequencies 02 p0333 A70-11982
- VTOL steep descent beacon-guided landing systems 02 p0304 A70-12765
- Simplified aircraft instrument landing system /SAILS/ employing lightweight helicopter-borne radar for tracking radio beacon at touchdown point 02 p0337 A70-12768
- Geometrical model for characterizing instrument landing system /ILS/ null reference glide path utilizing CW measuring system 04 p0716 A70-15330
- Equation for disturbance of ILS localizer signals by reflection from flat hangar wall, discussing computer program 04 p0652 A70-15344
- Correlation protected instrument landing system proposed for international consideration to meet future aircraft traffic density 05 p0880 A70-16107
- Instrument landing system techniques based on hyperbolic geometry and correlation detection for terminal area traffic control, discussing applications 06 p1102 A70-17637
- ILS systems, considering possible improvements 08 p1541 A70-21021
- Pilot and copilot task distribution schedules adopted by European civil aviation for landing approaches under poor weather conditions 08 p1542 A70-21850
- Integrated glide path localizer system for landing, takeoff and enroute guidance through rugged country, minimizing spurious reflection, required information bits, etc 09 p1720 A70-22222
- Aircraft instrument landing system replacement requirements in terms of airports, aircraft, approach and landing paths, service classes, etc 12 p2269 A70-27917
- Air traffic control, discussing precision instrument landing, approach lighting, collision avoidance, navigation aids, etc 17 p3133 A70-35185
- Precision approach and landing guidance system selection by RTCA committee, discussing aircraft antennas, scan rates, international cooperation, etc [AIAA PAPER 70-937] 17 p3134 A70-35846
- ILS glide slope calibration using optically projected digital codes as reference 19 p3464 A70-37912
- Airport capacity and terminal area safety increase by scanning beam instrument landing system, discussing automatic guidance trajectory example 19 p3464 A70-37913
- ATC by scanning beam ILS and onboard control systems, increasing airport capacity and terminal area safety [AIAA PAPER 70-1033] 20 p3666 A70-39504
- Correlation detection methods providing information for ILS in terminal area congestion, discussing role in aircrew-ATC cooperation 22 p4068 A70-42667
- ### INSTRUMENT ORIENTATION
- Rocket telescope spectrometer precision pointing achieved by servocontrolling secondary mirror, discussing use for planetary atmospheres far UV spectrum studies 02 p0296 A70-11916
- Gyroplatform angular position with respect to reference stars from solving nonlinear differential equations, applying Liapunov method 03 p0524 A70-13366
- Transit instrument azimuthal stability, investigating horizontal axis support, screw controls and tube position during star observations 04 p0693 A70-15484
- Triaxial universal astrometric instrument for tracking artificial satellite path with eyepiece crosswire, considering instrument errors 05 p0851 A70-16698
- Errors in aerial stereo photogrammetry, deriving equation to account for lens distortion and internal orientation 09 p1682 A70-23394
- Molniya 1 communication satellite attitude control involving automatic solar panel and antenna orientation, using powered gyroscopic stabilizers 13 p2499 A70-28387
- Optically pumped He 4 magnetometers, investigating magnetic resonance signal dependence on orientation for nonresonance technique construction 13 p2414 A70-30036
- Upper atmospheric ion and neutral composition from rocketborne mass spectrometry, allowing for rocket velocity and analyzers orientation with respect to velocity vector 14 p2568 A70-30140
- Visual display reference system rotation effect on control quality and tracking error compensation using stick signal control 14 p2540 A70-30249
- Ballistic missile instrument orientation optimization based on CEP criterion, considering acceleration induced errors 16 p2947 A70-33317
- Thermal response of passive heliotrope solar array orientation device using rotating bimetallic helix, performing energy balance analysis for helix temperature distribution 17 p3082 A70-34761
- Whisker diode coupling to polarized IR laser beam by orientation based on antenna theory 17 p3048 A70-35902
- Geomagnetic field variations recording by two variometers, correcting for variation components effects by instruments orientation 19 p3420 A70-37335
- Quartz magnetic variometer allowing simultaneous recording of magnetic field variations and suspension axis inclination changes 19 p3420 A70-37336
- Transparent spherical rotor spin axis orientation by measuring Fresnel drag effect of optical beam inside ring laser cavity 19 p3445 A70-37669
- Ion orientation technique based on counterflow sensing in earth upper atmosphere, discussing accuracy 21 p3927 A70-40844
- Orientation system for pointing balloon-borne X ray detector using flux gate magnetometer, DC amplifier and motor control relay circuit 21 p3831 A70-42249
- Displacement effect of hot-wire anemometric probes near wall as function of support orientation 22 p4038 A70-43241
- Precision gimbaled sensor pointing system calibration data errors due to misalignments and inaccuracies in transducer readout 22 p4040 A70-43587
- Pointing systems for balloon-borne telescopes in astronomical investigations 22 p4041 A70-43649
- Internal and external orientation elements of aerial cameras from star photographs on clear dark sky 24 p4333 A70-45198
- ### INSTRUMENT PACKAGE
- #### NT APOLLO LUNAR SURFACE EXPERIMENTS PACKAGE
- ### INSTRUMENT PACKAGES
- #### NT APOLLO LUNAR SURFACE EXPERIMENTS PACKAGE
- Test program effectiveness for Saturn Instrument Unit /IU/, summarizing objectives, costs and results [AIAA PAPER 70-379] 10 p1891 A70-24924
- Upper atmospheric sounding rocket Skylark engine, attitude control and payload components modifications for increasing versatility and performance 13 p2503 A70-28678
- French EOLE tracking satellite-balloon network for global atmospheric data, describing satellite and electronic instrument package 14 p2611 A70-31154
- Gyro test package, dynamic test facility and real time attitude algorithm to investigate operational capabilities of strapdown inertial attitude package 17 p3134 A70-35652
- High impact Ag-Zn cell design for space missions instrument package landing, considering heat sterilization and minimum operational capability 21 p3757 A70-41013
- Scientific payloads integration with multimission electric propulsion interplanetary spacecraft, discussing possible contamination effects due to solar electric propulsion system [AIAA PAPER 70-1141] 21 p3930 A70-41781
- Strapdown redundant experimental sensor inertial navigation package containing gyros and accelerometers, discussing signal real time processing by digital computer [AIAA PAPER 69-851] 21 p3849 A70-41858
- Strapdown inertial system mechanization and modularized instrument packaging with self contained failure isolation, temperature control and redundant components [AIAA PAPER 70-1027] 22 p4066 A70-42315
- ### INSTRUMENT TRANSMITTERS
- Miniature temperature and strain telemetry transmitters developed for measurements in areas inaccessible to direct wire connections 06 p1069 A70-18433
- Rocket- and projectile-borne microwave miniature solid state transmitters, discussing transistor oscillator-multiplier, hybrid integrated circuits, bulk effect devices, etc 10 p1852 A70-24887
- Miniature wireless strain and temperature radio telemetry transmitters for measurements in areas inaccessible to direct wire connections 15 p2738 A70-32301
- ### INSTRUMENTAL ANALYSIS
- #### U AUTOMATION
- ### INSTRUMENTATION
- #### U INSTRUMENTS
- ### INSTRUMENTS
- #### NT LASER ALTIMETERS
- #### NT MICROWAVE SENSORS
- Two phase flow instrumentation - Conference, Minneapolis, August 1969 02 p0304 A70-12833
- Statistical control charts for evaluating instrumentation performance during ordnance devices testing, discussing evolution, interpretation and application 03 p0494 A70-14126
- Instruments and systems - Conference, San Francisco, August 1969 06 p1017 A70-17351
- Shock tube chemistry including ideal and nonideal behavior, instrumentation techniques, etc 06 p1005 A70-17727
- Instrumentation - ISA Conference, Houston, October 1969, Part 1 06 p1067 A70-18426

Instrumentation - ISA Conference, Houston, October 1969, Part 2
06 p1068 A70-18430

Instrumentation - ISA Conference, Houston, October 1969, Part 3
06 p1072 A70-18590

Instrumentation - ISA Conference, Houston, October 1969, Part 4
06 p1073 A70-18595

Instrumentation - ISA conference, New York, October 1968
09 p1613 A70-23683

Time shared computer system providing real time service to multiple laboratory instrumentation, discussing high speed channel, computer control and data abstracting techniques
13 p2375 A70-29830

Instrumentation in aerospace industry - Conference, Seattle, May 1970
19 p3423 A70-37873

Astronomical instrumentation and methods in different nations, emphasizing photoelectric image receivers
23 p4199 A70-45033

INSULATED STRUCTURES

Transient heat conduction in dual-layer insulated plate exposed to pulse heating, discussing temperature response
[AIAA PAPER 70-14] 06 p1180 A70-18120

INSULATING MATERIALS

U INSULATION

INSULATION

NT MULTILAYER INSULATION

NT THERMAL INSULATION

Solder mechanical contact strength to CdS insulating crystal platelets tested in liquid N, noting Ag epoxy
02 p0319 A70-12738

Insulating materials and apparatus evaluation in terms of thermal capability to effect competitive cost saving
05 p0869 A70-16033

Cable involving woven multiconductor arrangement and aromatic polyimide insulations to connect thermal moon probe with transmitter for temperature measurements on lunar surface
05 p0798 A70-16034

Portable megaohmmeter for measuring insulation resistance of strain gauge ceramic installations
05 p0848 A70-16378

Reusable booster rocket heat protection system design, discussing ablation and insulation methods
05 p0958 A70-16635

Radiative heat transfer along adjacent layers of multilayer insulation blanket determined as energy transport mode
09 p1789 A70-23265

Thermal conductivity of multilayer and mixed powder high temperature insulation systems over wide temperature range and vacuum conditions
[AIAA PAPER 70-637] 16 p2997 A70-33596

High voltage solar arrays for ion engines, discussing spacecraft propulsion, electric generation, insulation integrity, cell degradation and current leakage
[AIAA PAPER 70-1138] 20 p3567 A70-40211

INSULATORS

Electron surface states bands in insulators induced by image potential, determining lower limits for liquid and solid gases
02 p0345 A70-12823

Insulating materials and apparatus evaluation in terms of thermal capability to effect competitive cost saving
05 p0869 A70-16033

Diodes on cordwood module measured for stress during soldering, foaming and operation, describing methods for mounting semiconductor strain gages
05 p0854 A70-16036

Helium high energy molecular beams for insulating body heating and thermal constants determination
07 p1344 A70-20129

Strain gages moisture protection, deriving formula for calculating acceptable protection time of insulator
11 p2049 A70-25586

Linearized steady plane axisymmetric flows of inviscid finitely conducting incompressible fluid past insulator under magnetic induction with zero components
13 p2464 A70-29541

INSULIN

Blood glucose and plasma immunoreactive insulin concentrations before, during and after intermittent short duration maximal exercise and glucose infusion
17 p3030 A70-35420

Serum growth hormone response to hypoglycemia in man following insulin administration, reviewing lumped parameter model
19 p3360 A70-38006

INTAKE SYSTEMS

NT AIR INTAKES

NT CONICAL INLETS

NT ENGINE INLETS

NT HELICAL INDUCERS

NT HYPERSONIC INLETS

NT NOSE INLETS

NT SUPERSONIC INLETS

Pressure oscillations in LOX pump inducer of J-2 machine, using semianalytical first order model with retarded time mechanism
09 p1693 A70-23257

Hydrodynamic internal streamline flow analysis for turboprop inducer blades under cavitating and non-cavitating conditions
[AIAA PAPER 70-629] 16 p2964 A70-33528

Stress and vibration analysis of rocket engine turboprop inducer blades, using finite element method
[AIAA PAPER 70-630] 16 p2964 A70-33529

Bypass door control system for SST axisymmetric intake operation in external compression mode, obtaining dynamic performance
[AIAA PAPER 70-695] 16 p2966 A70-33558

S-IVB liquid rocket engine and propellant feed systems restart chilldown in orbital operations
[AIAA PAPER 70-672] 16 p2967 A70-33574

Turbofan engine compressor system performance dependence on circumferential extent, magnitude and rate of change of inlet temperature in altitude test facility
[AIAA PAPER 70-625] 16 p2968 A70-33590

Liquid hydrogen axial flow pump inducer, describing suction pressure measurements, fluid conditions and flow rate
[AIAA PAPER 70-627] 16 p2919 A70-33592

Prototype grill device for turboprop aircraft engine inlet protection against bird ingestion, discussing performance tests
18 p3212 A70-35996

Radial compressor diffusers design and technology
[ASME PAPER 70-GT-116] 18 p3304 A70-36850

M 3.5 two dimensional mixed compression inlet system with self restart using flexible variable ramp system
[AIAA PAPER 69-447] 22 p3959 A70-42707

Convection, transpiration and full coverage film cooling methods for various local turbine inlet temperatures, gas pressures and cooling air temperatures
22 p4092 A70-43275

INTEGERS

Equivalent linear programming in integer variables to solve production scheduling for N identical machines, minimizing changeover and inventory costs
10 p1895 A70-24662

INTEGRAL CALCULUS

Stochastic processes providing exposition of differential-integral calculus for Brownian motion paths, with applications to diffusion processes and related parabolic partial differential equations
01 p0133 A70-11322

Book on integrals and elliptic functions in real domain, solving fourth degree Hermitian equation and integral reduction
02 p0323 A70-11897

Integral dissipation method for predicting turbulent boundary layers, taking into account semiempirical past history
02 p0283 A70-12339

Boundary layer prediction methods criteria, discussing advantages and disadvantages of differential and integral methods for various flows
02 p0286 A70-12356

Energetic stability theorems of dynamical feedback system, removing assumption concerning local square integrability
03 p0460 A70-13971

One and two center Coulomb, hybrid and exchange integrals contributing to orbit-orbit interaction in diatomic molecules evaluated for Slater orbitals combinations
03 p0528 A70-14010

Inverse blunt body problem using integral relations method assuming inviscid axisymmetric hypersonic gas flow
10 p1798 A70-24116

Monograph on integral calculation method for disk problems with mixed boundary conditions covering two dimensional stress-strain state, extrapolation methods, etc
11 p2140 A70-26474

Keplerian integrals analogy to integrals of adjoint equations suggested by optimum space navigation trajectories considerations
12 p2261 A70-27834

Third integral of stellar dynamics, considering Centopoulous galactic system model separability
14 p2651 A70-31288

Confluent hypergeometric functions indefinite integrals analytic expressions and reduction formulas
22 p4062 A70-42572

INTEGRAL EQUATIONS

NT FREDHOLM EQUATIONS

NT SINGULAR INTEGRAL EQUATIONS

NT VOLTERRA EQUATIONS

NT WIENER HOPF EQUATIONS

Hydrodynamic and elasticity equations for squeeze films between elastic cylinders in normal approach reduced to integral equation
[ASME PAPER 69-LUB-13] 01 p0102 A70-10392

Optimization of distributed parameter control systems described by linear integro-partial differential

parabolic equation with delayed argument, using dynamic programming
01 p0131 A70-10548

Atomic variables elimination technique applied to Markovian laser master equation, resulting in integrodifferential equations for field statistical operator
01 p0112 A70-10884

Differential and integral inequalities theory and applications, Volume 1, Ordinary differential and Volterra integral equations
01 p0133 A70-11324

Time independent kernel integral equations in dynamic contact problems of elasticity and mathematical physics
01 p0146 A70-11571

Integral equation for emissivity inside uniform gray isothermal Lambertian cavity solved using successive approximations
02 p0323 A70-11889

Integral equation of first kind solution based on two dimensional boundary value problem solution
02 p0323 A70-11994

One dimensional diffusion equation serial solution implementation by hybrid computation, using equivalence between differential and integral equations
02 p0324 A70-12259

Prediction systems for turbulent boundary layers, noting momentum integral equation use in all integral methods
02 p0281 A70-12327

Integral method for turbulent shear flow based on momentum and moment-of-momentum equations and Cole velocity profile family, determining shear stress integral
02 p0282 A70-12329

Integral relations method efficiency and accuracy in solving incompressible turbulent boundary layer equations, noting acceptability for turbulent flows with small wake components
02 p0282 A70-12331

Turbulent boundary layers behavior prediction by strip integral momentum equation method, considering velocity profiles and shear stresses
02 p0282 A70-12332

Integral theory for two dimensional incompressible turbulent boundary layer in nonequilibrium flows, describing velocity profile in momentum and energy equations
02 p0283 A70-12335

Turbulent boundary layer development calculation by shear work integral method involving Reynolds number introduction procedure
02 p0283 A70-12336

Dissipation integral method for turbulent boundary layer problem based on nonequilibrium flow, analyzing inner and outer regions
02 p0283 A70-12338

Integral method for computing two dimensional incompressible turbulent boundary layer development, including entrainment process of irrotational fluid
02 p0284 A70-12343

Adiabatic invariance of action integral for motion in nonregular fields, explaining charged particles motion through magnetic shock front in interplanetary space
02 p0359 A70-12788

Integral equation solution in viscoelasticity theory based on creep tests with polymer containing elastic inclusion, improving convergence of approximations method
02 p0390 A70-12801

Integral formulas of thermoelasticity theory for calculating displacements and rotations caused by temperature field action in micropolar Cosserat and Hooke media
02 p0391 A70-12817

Shallow shell theory, discussing equation kernels, reduction of boundary value problems to integral equations, potential theory application and transformation into Fourier series
03 p0589 A70-13338

Integral equations for antisymmetric shallow shell stress-strain state with crack, obtaining asymptotic solution in form of power series
03 p0591 A70-13420

Laplace transform applied to ordinary differential equations with variable coefficients, obtaining representations of integral and integrodifferential equations
03 p0519 A70-13506

Averaging over finite and infinite intervals derived for nonlinear integrodifferential equations with varying variables
03 p0594 A70-13507

Existence theorems for optimal control problems with multiple integrals
03 p0460 A70-14075

Plane two body contact creep problem in presence of adhesive forces reduced to solving coupled integral equations with complex valued kernels
04 p0766 A70-14421

Method of integral relations, finite differences and method of characteristics applied to numerical solution of steady state problems of gas dynamics
04 p0670 A70-14961

Integral relations and finite difference methods application to problems of boundary layer equations in gas dynamics

04 p0670 A70-14962

Boundary value problems of Cauchy-Riemann differential equations using solution to derive integral equation for stationary infrasonic flow

04 p0671 A70-15094

Radiation view factor from differential area to conical surface determined using Stokes theorem and contour integration

04 p0787 A70-15598

Stress distributions in infinite elastic solids for shear loadings prescribed over coplanar circular regions, solving integral equations iteratively for coplanar penny-shaped cracks

05 p0928 A70-16057

Momentum-energy complex obtained for nonlocalized fields in variational mechanics, deriving integrodifferential identities for Euler equations quadratures

05 p0881 A70-16078

Integral constitutive relation representing incompressible viscoelastic materials and plane stress and strain conditions

05 p0930 A70-16087

Von Zeipel method applied to stellar three body problem, eliminating short period terms and establishing two integrals of motion

05 p0909 A70-16337

Integral equations for interpolation process remainder estimation, including convergence of functions interpolation and error analysis

05 p0877 A70-16970

Scattering matrix noniterative integral solutions applied to singlet and triplet s-wave Hartree-Fock phase shifts for electron-H-atom scattering

06 p1108 A70-17486

Noniterative integral solutions of scattering equations extended to coupled channels using matrix notation

06 p1108 A70-17487

Suddenly started laminar flow in circular tube entrance region, obtaining integral momentum equation for boundary layer thickness, entrance length, velocity profile, etc

06 p1034 A70-17528

Gaussian quadrature integration technique developed for collocation approach for integral equation of steady subsonic lifting surface theory

06 p0970 A70-18097

Stochastic model of information handling centers as typified by document storage and retrieval derived for integral equation to determine expected primary store size

06 p1016 A70-18450

Laminar boundary layer in hypersonic flow calculated by integral method, including effects of entropy gradient and induced pressure gradient

06 p0984 A70-18468

Cylindrical antennas immersed in arbitrary homogeneous isotropic media, solving integral equation for current

06 p1074 A70-18607

Optimal control of dynamical systems with transport lag determined using differential-integral equations

07 p1245 A70-19094

Simultaneous partial integrodifferential equations for transverse oscillations of uniform short beams

07 p1406 A70-19306

Integral methods for predicting two dimensional incompressible turbulent boundary layers development in arbitrary pressure gradients, using momentum integral equation and wall friction relation

07 p1256 A70-19308

Prandtl problem solution by reducing integrodifferential equation to linear differential equation in disk of complex variable, noting application to elliptical or rectangular wings

07 p1258 A70-19783

Integrodifferential equation derived for energy balance in laminar boundary layer of fluid flow, taking into account viscous energy dissipation, radiative energy transfer, etc

07 p1423 A70-19813

Plane anisotropic elastic bodies stress determination using Somigliana type integral formula to relate elastic displacement field to boundary traction and displacement vectors

07 p1412 A70-19953

Nonlinear integral equations for inhomogeneous atmospheres derived from radiative transfer equations global form, noting relations to Ueno and Chandrasekhar equations

07 p1336 A70-20059

Interference kernel discontinuities in integral equations relating amplitude of angle of attack and pressure distribution on T tail harmonically oscillating in subsonic flow

07 p1416 A70-20210

Integral equation for time development of harmonic oscillations in finite one dimensional chain of elastically coupled discrete elements, using Bessel functions for solution

08 p1547 A70-20535

Integral equations arising in contact problems of elasticity reduced to infinite linear algebraic equations

08 p1585 A70-20957

Paired integral equations of elasticity with kernels containing Legendre spherical harmonics, admitting exact solution in quadratures

08 p1544 A70-20960

Radiant heat exchange for rectangular groove represented by integral equations using rapid iteration method

08 p1600 A70-21835

Linear integral equations solutions using invariant functions

09 p1711 A70-22208

Heat and mass transfer coefficients in binary laminar boundary layer convection obtained with integral equations and Karman-Polhausen method

09 p1787 A70-22264

Integral equation perturbation technique, discussing applications to electrostatics, hydrodynamics, MHD, heat and mass transfer, etc

09 p1711 A70-22350

Earth shape formulas reduction to Taylor series, considering Molodenskii solution method for simple layer density integral equation

09 p1670 A70-23343

Radio wave propagation equations, applying stationary phase method for finite limits of dimensionless line integral

09 p1638 A70-23662

Integral equation for radiation patterns from vertical antenna over variable impedance surface

09 p1639 A70-23670

Time-bounded pulses with energy maximum in frequency band, solving integral equations for band-pass filters for maximum efficiency and optimum pulse shapes

11 p2004 A70-25799

Integral theorems on vorticity transport derived by Carstou method, suggesting need for redefining Truesdell concepts of convection and diffusion

11 p2037 A70-26175

Electromagnetic field singularities near sharp edge relating to geometry scatter used for treating singularities in current distribution integral equations

12 p2183 A70-26977

Integral manifolds of third order autonomous differential equations with unstable equilibrium point, investigating forward and negative asymptotic problems

12 p2261 A70-27375

Numerical quadratures application to integral equations for radiative heat transfer computations, discussing validity for parallel and adjoint plates

12 p2332 A70-27840

Nonlinear integral equations of radiation transfer of stellar and planetary atmospheres

12 p2305 A70-27852

Averaging over finite and infinite intervals derived for nonlinear integrodifferential equations with varying variables

13 p2440 A70-28656

Nonlinear integrodifferential equations of radiative transfer solved by invariant imbedding approach, discussing Rayleigh phase matrix

13 p2451 A70-29130

Shallow shell theory, discussing equation kernels, reduction of boundary value problems to integral equations, potential theory application and transformation into Fourier series

14 p2657 A70-30716

Monograph on nonlinear oscillation equations resonance solutions and solution stability, considering Green matrix, differential equations reduction to integrodifferential equations, etc

14 p2618 A70-31417

Asymptotic expansion of contour integrals involving analytic functions of complex variable, using steepest descent method

15 p2767 A70-31696

Linear integral equations for radiative transfer between parallel plates, using least squares method

15 p2826 A70-31822

Integral equation for transonic small disturbance flow applied to plane flows over lifting airfoils

15 p2673 A70-32768

Cylindrical and helical antennas impedance in cold magnetoplasma, using three dimensional integral involving Fourier transform and Green function

16 p2859 A70-32943

Electromagnetic field transmission through plasma slab with specified electron density-collision frequency profiles, using integral derived from transmission and reflection coefficients

16 p2957 A70-32979

German monograph on planar straight cascades in incompressible frictionless potential flow, basing method on singularity method integral equation reversal

16 p2839 A70-34081

Coupled integral equations for cutouts in shallow shells

17 p3186 A70-34970

Linear compressibility assumption incorporated into third order multiple integral representation of

nonlinear creep of polyurethane, reducing time independent kernel functions

17 p3186 A70-34972

Linear antennas theory using integral equations for current distributions

17 p3044 A70-35058

Elastic properties of complex screw dislocation arrays from equations for stress fields of dislocation segments

17 p3190 A70-35455

Integral equation for three dimensional Fourier transform applied to isotropic scattering of radiation from point source in finite spheroidal atmosphere

17 p3137 A70-35599

Boundary value problem approximation method for large numbers, using projective method applicable to linear integral, integrodifferential and differential equations

18 p3282 A70-36360

Spatial signal transmission through open resonator determination based on resonator integral equation, extending to dielectric lens with finite Fresnel diffraction number

18 p3259 A70-36480

Integrals of motion for minimum fuel rocket trajectories in inverse square field calculated for constant power and constant exhaust rockets

18 p3316 A70-36678

Satellite translational motion in circular problem of three bodies, discussing existence of equations integral

18 p3324 A70-37150

One dimensional integral equations for two dimensional problems of EM wave diffraction by cylindrical bodies

19 p3376 A70-37435

Asymptotic high energy behavior of Feynman integrals in scalar field theory models for elastic scattering

19 p3457 A70-37549

Nonlinear integral equations formal solution method, noting relationship to Fredholm solutions of linear integral equations

19 p3458 A70-38063

Subsonic wing theory calculation method, obtaining close solutions for integral expression constants for downward air currents

19 p3352 A70-38164

Noniterative homogeneous solutions of integral equations for coupled open channels and coupled eigenvalue scattering

19 p3473 A70-38264

Plane waveguide field with complex geometric inhomogeneity, describing perturbed section by integral equations

19 p3381 A70-38567

Integral equations for gravity field and plumb line deflections solved by Neumann and Molodenskii methods

20 p3617 A70-39073

Integral equations for plumb line deflections on earth surface model, considering Neumann, Molodenskii, Arnold methods, etc

20 p3617 A70-39074

Integrodifferential equation derived for energy balance in laminar boundary layer of fluid flow, taking into account viscous energy dissipation, radiative energy transfer, etc

20 p3736 A70-39261

Integral equations arising in contact problems of elasticity reduced to infinite linear algebraic equations

20 p3719 A70-39380

Paired integral equations of elasticity with kernels containing Legendre spherical harmonics, admitting exact solution in quadratures

20 p3672 A70-39382

Equations system for determining constants in Sedov integral for conformal mapping of polygonal airfoil lattice onto Riemann surface

20 p3658 A70-39767

Elasticity theory boundary value problems reduction to one dimensional integral equations

20 p3724 A70-39853

Asymptotic equivalent functions for integral Laplace transformation transition to original in continuous media mechanics

20 p3726 A70-39873

Asymmetric micropolar thermoelasticity, deriving integral expressions for strains, rotations and temperatures in finite body

20 p3726 A70-39878

Numerical methods, FORTRAN program and table form for complex integrals evaluation along unit circle in positive direction

20 p3605 A70-40120

Integral transforms applied to convective heat transfer during nonNewtonian fluid flow with power rheology in pipes and channels

20 p3613 A70-40177

Antenna radiation pattern analysis by application of Kirchhoff and Weber integrals, noting choice of complex radial wavenumber consistent with radial field decay

21 p3796 A70-40560

Integral equation of viscoelastic media with unstable properties, solving boundary value problems by approximation method 21 p3933 A70-40643

Circumstellar system crushing processes described by integrodifferential equations, deriving particle size distribution of fragments in interplanetary space 21 p3889 A70-41148

Linear control plant identification by solving integral equation obtained from input and output signals 22 p4005 A70-43565

Integral equations solution by Kupradze-Aleksidze general Fourier series method 23 p4211 A70-44094

Boundary value problems of fluid dynamics in dynamic cavities reduced to integral equations system 23 p4182 A70-44347

Unsteady aerodynamic loading of wings with control surfaces, discussing Kuessner integral equation of subsonic lifting theory 23 p4274 A70-44761

Relaxed minimax control with functional restrictions by Uryson integral financial equation 23 p4213 A70-44907

Dynamic structural stability analysis, describing integral equation matrix technique 24 p4419 A70-45156

Asymptotic properties of integral equations solutions for boundary value problems in theory of elasticity and mathematical physics 24 p4422 A70-45490

Multidimensional integral Monte Carlo evaluation applying regression analysis to linear unbiased estimators 24 p4370 A70-46100

INTEGRAL FUNCTIONS
U ENTIRE FUNCTIONS
INTEGRAL TRANSFORMATIONS
 NT CONVOLUTION INTEGRALS
 NT FOURIER TRANSFORMATION
 NT HILBERT TRANSFORMATION
 NT LAPLACE TRANSFORMATION

Integral theorems for wave-type heat conductivity equation 01 p0219 A70-11398

Integral methods for turbulent boundary layer solutions, emphasizing shape factor improvement in differential equations 02 p0286 A70-12357

Two dimensional wave diffraction problems involving discontinuity line, analyzing instability behavior of geometrically induced singularities by applying integral transform on Helmholtz equations 03 p0525 A70-14199

Conjugate points for simple integral problems in calculus of variations extended to multiple integral problems, using Jacobi equation 04 p0713 A70-14674

Hankel integral transforms of half orders for solving boundary value problems in terms of spherical coordinates 09 p1712 A70-22834

Systems identification in parameter estimation to acquire stability properties using integral transforms 11 p2028 A70-26311

Arbitrary function expansion into series of Legendre functions by generalizing Weyl-Lebedev-Skalskaia integral transform 13 p2441 A70-29312

Bipolar moment integral in celestial mechanics formed by product of particle kinetic moments for n body problem order reduction 13 p2494 A70-29399

First vector integral of planetary motion different from moment of momentum and Runge-Lenz integrals 15 p2806 A70-32797

Group variational procedure for first integrals of nonconservative dynamical systems 19 p3458 A70-38060

Successive iterative solution for large matrix equations reduced from Fredholm integral equations of second kind 24 p4369 A70-45164

INTEGRATED CIRCUITS
 NT LARGE SCALE INTEGRATION

Dielectric overcoatings effect on Al interconnections electromigration in IC metallization, noting longer intervals between failures 01 p0153 A70-10083

Integrated digital circuits for office type desk calculators based on machine concept 01 p0052 A70-11287

Ferrite-type phase shifter production by microstrip technique and integrated microwave system use in Gunn element Doppler radar 01 p0052 A70-11290

Miniaturized components in microstrips on low loss dielectric or magnetic substrates, noting suitability for microwave systems integration 01 p0052 A70-11313

Functionally integrated superheterodyne receivers design by applying microwave IC technology, providing weight reduction, interconnecting cables elimination and circuit interface problems minimization 02 p0267 A70-12055

Noise source model of Si planar diffused bipolar IC transistors in operational amplifiers, noting base-emitter junction burst noise 02 p0257 A70-12192

Electronic integration assembly/EIA/ incorporating modular electronic packaging design techniques to provide reliable mechanical configuration for spacecraft equipment 02 p0268 A70-12579

Beam-lead substrate package for six stage TTL shift register, discussing metallization systems for interconnections and beams 02 p0271 A70-12846

Device modeling for computer aided design and analysis of integrated circuits, discussing list of desirable properties and applications to transistor design 03 p0454 A70-14026

Electron image projection tube for fabricating integrated circuits of micron size transistors 03 p0458 A70-14027

Photocell uses in semiconductor integrated circuit, discussing scanned arrays applications and economics 03 p0459 A70-14265

Complementary symmetry MOS/CMOS/ integrated circuit transient response to electron irradiation 04 p0657 A70-14733

Computer modeling of operational amplifier integrated circuit in ionizing radiation environment, using RLC network and voltage transfer curve 04 p0658 A70-14740

Ionizing radiation response of integrated microcircuits with different circuit functions and manufactured by different methods 04 p0658 A70-14741

Integrated analog voltage regulator sensitivity to small signal transient radiation, discussing circuit hardening by diode compensation 04 p0658 A70-14742

Fluidics background, operational principles, constituent elements, system assemblies and applications, discussing integrated and multiple function circuits, cost and reliability advantages, etc 05 p0798 A70-16146

Microwave Si transistors with overlay and interdigital geometries and integrated circuit design considerations for power amplifiers, power oscillators and frequency multipliers 05 p0819 A70-16149

Thick film hybrid circuit technology providing higher packaging density and better cooling 06 p0106 A70-17276

Black box modeling of linear integrated circuits for computer analysis in frequency domain 06 p0106 A70-17276

Integrated circuit technology impact on electronic equipment designers and organization relationships within industry 07 p1239 A70-18800

Integrated switching circuits design optimization by ALGOL program, analyzing circuits transient behavior 07 p1242 A70-19752

Plastic symmetrical trough waveguides with metallized surfaces for hybrid millimeter-wave integrated circuit systems, discussing ferrite resonant isolator 07 p1243 A70-20151

Large scale integration /LSI/ in electronics, discussing high density microelectronic, memory and logic circuits, fabrication and computer aided design 08 p1468 A70-20468

Plastic semiconductor devices encapsulation materials and fabrication techniques, considering device performance in various environments and military applications 08 p1468 A70-20626

Radiation hardened ICs development, discussing problem of dielectric isolation 08 p1468 A70-20627

Monolithic, thick film, thin film and multichip integrated circuit techniques applied to communication equipment design 08 p1471 A70-20785

Monolithic zero crossing AC trigger IC for thyristor power control systems operating in on-off mode 08 p1478 A70-20786

Microstrip integrated circuit technology in development of microwave components, discussing fabrication, design, performance and applications 08 p1471 A70-20787

Interdigitated microstrip quadrature couplers suited for monolithic or hybrid thin film microwave integrated circuitry 08 p1476 A70-21291

Parallel multiplier design with carry-save scheme and constructed from series integrated circuits, discussing speed, complexity and cost 08 p1467 A70-21784

Solid state IC-compatible display devices optical, electrical, mechanical and thermal characteristics 09 p1642 A70-22018

Three dimensional RC network simulating temperature fields in IC at different heat source power dissipation laws, discussing harmonic heat source field 09 p1643 A70-22128

Hybrid microwave integrated circuits technology and design, discussing distributed and lumped-element structures and component properties 09 p1644 A70-22225

French microwave semiconductor technology in terms of basic research, technology studies, reliability and integrated circuits 09 p1739 A70-22602

Integrated circuit film and hybrid technologies in microelectronics, discussing role of monolithic Si arrays 09 p1645 A70-22632

Silicon monolithic integrated circuits technology for radiation environment near nuclear detonation 09 p1647 A70-23076

Light-emitting integrated circuit semiconductor display devices with inherent memory permitting logic and optical output functions performed on surface 10 p1846 A70-23883

Integrated CW UHF power amplifier modules using thin film lumped elements and UHF power transistor chips 10 p1846 A70-23884

S band CW high power broadband power source consisting of transistor amplifier-driven varactor doubler chains in hybrid integrated form 10 p1846 A70-23885

DICAP system to analyze digital sequential switching circuits, studying simulation technique range and limitations of applicability 10 p1845 A70-24236

Integrated TDMA switching/transmission system implementation into existing network 10 p1837 A70-24354

Flexible logical elements in integrated circuits with internal connections controllable from outside to realize variety of logical functions 10 p1850 A70-24618

Integrated circuits involving long-strip heat source surrounded by multiple layers, expressing temperature distribution by Fourier transformation obtained integrals 10 p1850 A70-24620

Integrated circuit microwave phased array radar antenna systems for multiple frequency bands and multifunction operations to save cost and space 10 p1851 A70-24878

Hybrid microwave integrated circuits application to phased array and Data Relay Satellite System space transponder 10 p1851 A70-24879

Integrated microwave systems development taking into account cost effectiveness and anticipating kilowatt and megawatt systems 10 p1851 A70-24880

Rocket- and projectile-borne microwave miniature solid state transmitters, discussing transistor oscillator-multiplier, hybrid integrated circuits, bulk effect devices, etc 10 p1852 A70-24887

Microwave IC-compatible resonators for communication systems filters, comparing microstrips, disks, waveguide cavities and dielectric-loaded cavities 10 p1852 A70-24892

Book on integrated electronic systems covering integrated circuit design, device and material properties, quality control, applications, etc 10 p1853 A70-25049

Integrated circuit failure analysis with scanning electron microscopy taking into account ball bond contamination and open metallization at contact windows 11 p2015 A70-25366

Integrated logic circuits, considering switching properties and medium and large scale integration 13 p2372 A70-29116

Digital correlator LSI circuits design, layout and mask considerations, diffusion, metallization and dielectric deposition 13 p2378 A70-29551

Ta thin film integrated circuit technology including resistor and capacitor elements, conductors, crossovers, etc 14 p2625 A70-30284

Integrated circuits design by combined automatic and manual system 14 p2554 A70-30670

Microwave integrated circuit lumped element approach, showing performance as function of geometry and frequency 14 p2561 A70-30920

Microstripline and balanced stripline, discussing parameters affecting maximum attainable Q in microwave integrated circuits 14 p2561 A70-30921

Microwaves in integrated military avionics systems, discussing CNI, ECM, component reliability, etc 14 p2551 A70-31177

MOSFET integrated circuits radiation resistance measurements under electron irradiation, determining changes in threshold voltage, transconductance and on-resistance for applications in spacecraft 14 p2559 A70-31372

Multiple wiring algorithm for automatic pattern design for AI interconnections and printed wiring in integrated circuits

15 p2715 A70-31842

Integrated tunnel diode amplifiers design using hybrid technique for communications satellites, noting stability and noise performance

15 p2710 A70-32469

MAGFET devices for integrated circuits, calculating magnetic sensitivity as function of channel aspect ratio and Hall electrode position

15 p2710 A70-32572

Micro-Hall device as tool for evaluating epitaxial silicon in integrated circuit processing

15 p2710 A70-32573

Monolithic linear IC building blocks for radar systems circuit design

15 p2704 A70-32581

Topology and component values in computerized design of distributed lumped active networks

15 p2711 A70-32595

Integrated analog shift register circuits computer aided design, using insulated gate field effect transistor /IGFET/

15 p2711 A70-32597

Computer aided design for microwave branch line couplers dimensions practical for integrated circuit microstrip fabrication

15 p2711 A70-32602

Failure mode and mechanism in dielectrically isolated IC attributed to metal bridging under planar oxide

15 p2713 A70-32648

Integrated circuits failures due to electromigration in thin films, discussing hole formation and circuit reliability prediction

15 p2713 A70-32649

High usage military system integrated circuit failure modes analysis for reliability improvement

15 p2713 A70-32650

Failure analysis in third generation reliability approach to IC product quality improvement, investigating Si-Al contact irregularity cause and effect

15 p2713 A70-32663

Microscopic data importance in recognizing IC semiconductor failure characteristic traits, revealing current direction, voltage magnitude, microsurface temperature excursion and approximate transient duration

15 p2693 A70-32664

Microwave IC methods applied to solid state signal sources design, using varactor tuned transistor oscillators, resistive isolation pads, amplifiers and frequency multipliers

16 p2872 A70-33069

Integrated X band superheterodyne receiver design using planar transmission lines as components

16 p2874 A70-33388

High Q reactance network realization for integrated microwave systems employing evanescent mode waveguide components

16 p2875 A70-33402

Solid state phased array radar employing MIC modules in radiating elements, achieving reliability by redundancy

16 p2877 A70-33411

Interference free high speed monolithic digital integrated gate, determining current swing, lead inductances and switching times

17 p3048 A70-34587

LSI circuits in space electronics, discussing packaging, reliability, applications, etc

17 p3053 A70-35274

Wideband microwave IC tunnel diode amplifier /TDA/ for artificial satellites, discussing noise, size and weight reduction

17 p3053 A70-35277

Complex control systems in integrated logic circuits and light laboratory materials production, discussing measurement equipment for quality control

17 p3090 A70-35416

Hybrid integrated microwave power amplifiers, using high-Q thin film lumped passive elements

18 p3232 A70-36760

Microelectronic systems radiation resistance, examining logic IC gates for reactor neutron irradiation

18 p3233 A70-36783

Aircraft digital interior communication systems, combining multiplexing techniques with solid state integrated circuits technology and systems integration [SAE PAPER 700302]

18 p3216 A70-36813

Thin films for semiconductor integrated circuits and solid state devices

19 p3389 A70-38195

Integrated microcircuits reliability prediction models based on failure mode and mechanism knowledge

19 p3391 A70-38846

Nonlinear LC circuit with p-n junction capacitance, examining relaxation vibrations during automatic biasing

20 p3596 A70-38970

Planar thin film optical waveguides for integrated circuits, utilizing information carrying potential of laser light in optical communication

20 p3598 A70-40129

Complementary metal oxide semiconductor and bipolar transistors fabrication on same integrated circuit chip by C-squared technology

20 p3598 A70-40130

Integrated directly coupled gyrator operating mode via comparison with switching elements, considering behavior under capacitance load and high pass filter application

21 p3797 A70-40793

Integrated circuit requirements for space power conditioning equipment for ion thrusters

21 p3797 A70-41211

Power IC fabrication methods covering monolithic chip, monobrid chips and IC driver with external power transistors

21 p3797 A70-41212

High power IC technical limits involving packaging, bonding wires, interconnect metal, power transistors

21 p3797 A70-41213

High voltage MOST silicon integrated circuits, using dielectric isolation and field plate techniques

21 p3798 A70-41214

Integrated circuits for control and telemetry functions in oxide cathode ion thruster power conditioning system operating from solar panel

21 p3798 A70-41216

Automatic and command multiple sequencer for spacecraft solar cell battery charger, providing switching logic by integrated circuits design

21 p3758 A70-41218

Semiconductor circuits large scale integration for aerospace computers, discussing fabrication and design

21 p3799 A70-41692

Aerospace microelectronic digital computer design, discussing optimal packaging by use of integrated circuits

21 p3795 A70-41694

Metal nitride oxide silicon /MNOS/ integrated circuit transistor, reviewing characteristics, operation mechanisms and applications

21 p3800 A70-42113

Monolithic precision castings using photoetched plastic and lost-wax investment techniques [ASME PAPER 70-FLCS-8]

22 p4043 A70-42419

Reprogrammable read-mostly memory /RMM/ using integrated circuit array of amorphous and crystalline semiconductor devices, discussing design and applications

22 p3996 A70-42772

Linear IC for RF applications including multistage amplifiers, simulating by actual units

22 p3999 A70-42821

Integrated 7 GHz small signal microwave balanced mixer, using microstrip transmission lines

23 p4168 A70-43777

Stripline and microstrip junction circulators analysis for microwave integrated circuits, based on clockwise and counterclockwise rotation modes

23 p4169 A70-43787

Klystron microwave signal generator power stabilization using compact low consumption integrated circuits

23 p4170 A70-43797

Metallization systems materials for IC, discussing environmental stability, metals electromigration, electrochemical corrosion tests, etc

23 p4173 A70-44533

Plastic encapsulated IC for military environments, discussing cooker, corrosion and thermal shock tests

23 p4173 A70-44534

High performance military aircraft missile command and control signal data processor microelectronics packaging, using integrated and printed circuit modules

23 p4174 A70-44542

Integrated circuits failure analysis techniques, including electrical diagnostics, visual inspection, surface examination, shorts location, etc

23 p4175 A70-44749

IC metallization systems in semiconductor devices fabrication and packaging, assessing metals alternate to Al for electromigration difficulties avoidance

24 p4319 A70-46075

Computer optimization program for solid state components and integrated circuits design with conversational system for man machine dialogues

24 p4317 A70-46321

INTEGRATED MISSION CONTROL CENTER

Intersite trunk elements design and usage in integrated mission control center /IMCC/ as interface equipment between internal voice communication and worldwide network

08 p1460 A70-20814

Mission Control Center and Apollo flight controller team, discussing personnel qualifications, equipment and individual evaluation

21 p3805 A70-41197

Computer real time Apollo simulation, checkout and training system duplicating actual mission for flight controllers in Mission Control Center

21 p3805 A70-41198

INTEGRATION [REAL VARIABLES]

U MEASURE AND INTEGRATION

INTEGRATORS

NT DIGITAL INTEGRATORS

Flip-flop type intergimbal compensation system for gyroscopic integrators error reduction, obtaining natural oscillations constant amplitude

01 p0092 A70-10987

Electronic transistorized harmonic signal integrator operating in connection with static-bridge

03 p0493 A70-13975

Meksyn asymptotic method of integrating boundary layer equations applied to ordinary differential equations for slip flow past seminfinit plate

06 p0979 A70-18348

Circuit analysis of pulse integrator and square-law receiver used as optimal filter during incoherent radio pulse reception on background fluctuating noise

08 p1461 A70-20865

Thermal stresses determination in turbine blades by making analogy between actual and electrical model, using EGDA integrator

09 p1785 A70-23598

Optimal distributed feedback surface temperature control of inertial grade floated rate integrating gyroscope, minimizing instrument degradation

16 p2908 A70-33347

Error reduction methods for linear acceleration gyrointegrators measuring linear velocities

19 p3420 A70-37257

Products integration of unit vector components over all solid angles

24 p4370 A70-46029

INTEGRODIFFERENTIAL EQUATIONS

U DIFFERENTIAL EQUATIONS

U INTEGRAL EQUATIONS

INTELLECT

Pilot training applicant test profiles, discussing difference between intelligent and intellectual candidates

12 p2176 A70-27028

INTELLIGENCE

NT ARTIFICIAL INTELLIGENCE

NT INTELLECT

Pilot training applicant test profiles, discussing difference between intelligent and intellectual candidates

12 p2176 A70-27028

Preparatory aviation training applicants intelligence correlated with number of brothers and sisters

12 p2178 A70-27050

INTELLIGIBILITY

NT SPEECH RECOGNITION

Fire and fire test scope and meaning limitations for consumer awareness

23 p4208 A70-43871

INTELSAT SATELLITES

Intelsat 4 communication system design and international cooperation, considering satellite design, TV and telephone channels capacity, etc

01 p0196 A70-10883

Intelsat satellites telemetry and telecontrol /TTC/, describing Fucino plant design and operation

02 p0263 A70-12647

Intelsat 4 communications satellite design and manufacture, discussing European participation with emphasis on British involvement

02 p0383 A70-12649

Intelsat satellite telecommunications system application for future long distance telephone communications

03 p0451 A70-13836

Intelsat communications /1963-1969/, discussing boosters, satellites, system characteristics and ground stations

03 p0451 A70-13840

Second antenna at Pleumeur-Bodou /France/ for satellite transmissions reception in Intelsat network program

05 p0826 A70-15981

European role in future INTELSAT Organization operational rules and principles covering proprietary, financial and voting procedures

06 p1184 A70-17579

Multichannel PCM/TDMA INTELSAT network with time preassignment and time assignment speech interpolation features for field test

10 p1835 A70-24332

TDMA demand-assigned satellite communication system developed for INTELSAT, discussing PCM, voice signals and channels, etc

10 p1839 A70-24362

Multiple-access and demand-assignment techniques, discussing compatibility of PCM-FDMA /SPADE/, PCM-TDMA, ATIC and INTELSAT 4 systems

11 p1997 A70-25415

Global commercial communications satellite system arrangements, considering evolutionary political, economic and technological developments within INTELSAT context

11 p2152 A70-25478

[AIAA PAPER 70-446]

Launch vehicle selection, utilization and mission planning and analysis in Comsat programs, discussing INTELSAT I-IV [AIAA PAPER 70-484] 11 p2002 A70-25489
 Atlas/Centaur and Titan/ Centaur launching of Intelsat 4 communication satellites, discussing booster, stage characteristics and payload [AIAA PAPER 70-483] 11 p2127 A70-26605
 Commercial satellite communications, discussing creation and objectives of Comsat and establishment of Intelsat 13 p2368 A70-29618
 Demodulators threshold performance for satisfying carrier to noise ratios requirement of Intelsat 4 system 14 p2552 A70-31352
 Low noise wideband amplifier design for Intelsat 3 satellite ground stations 16 p2877 A70-33415
 Intelsat IV command and control system, describing ground stations, control center, telemetry data handling and acquisition, etc 17 p3046 A70-35275
 Legal questions of satellites telecommunications at Washington Intelsat Conference 17 p3201 A70-35778
 Navigation aids evolution and trends, noting ground stations, Intelsat 3 and navigation satellites 17 p3048 A70-35879
 Worldwide communication satellite network cost optimization and application, discussing Intelsat role 18 p3228 A70-36510
 Small earth stations to link isolated areas with Intelsat network, discussing costs 18 p3229 A70-36957
 Monograph on communicating by satellite covering INTELSTAT system design, pricing, procurement, broadcasting, international community responsibilities, etc 21 p3955 A70-40739
 Power conditioning systems for INTELSTAT satellites, describing methods for battery charging, charge control, voltage regulation and power management 21 p3757 A70-41207
 Ground station requirements for transition to multitransponder INTELSTAT 4 satellite, discussing interference filtering, group delay distortion, etc 21 p3789 A70-41346
 Intelsat compatibility with independent regional telecommunication satellite systems 22 p4111 A70-43514

INTENSIFICATION
U AMPLIFICATION
INTENSIFIER TUBES
U IMAGE INTENSIFIERS
INTENSIFIERS
 NT IMAGE INTENSIFIERS
 NT IMAGE ORTHONICS
INTEPLANETARY SPACECRAFT
 NT MARINER-MERCURY 1973
INTERATOMIC FORCES
 Atmospheric gases atomic and molecular binary short range repulsive forces, determining interaction potentials from elastic scattering cross sections 07 p1345 A70-20141
 Inhomogeneous interatomic magnetic field effects on spectral line widening and shifts of emitting atoms in low temperature plasma 12 p2278 A70-27318
 Integral Hellman-Feynman formula applied to binding energy of molecular H and LiH, using SCF wavefunctions for atomic states 12 p2276 A70-27570
 Dissociation energy and long range interatomic potential of diatomic molecules from vibrational spacings of higher levels 13 p2454 A70-28495
 Interatomic bond strength in solid solutions of Ti-Sn-O with respect to heat resistance at elevated temperatures 14 p2595 A70-30170
 Adiabatic corrections to long range Born-Oppenheimer interatomic potentials from rotationally coupled Schroedinger equations 17 p3138 A70-35199
 Inhomogeneous interatomic magnetic field effects on spectral line widening and shifts of emitting atoms in low temperature plasma 21 p3860 A70-42059

INTERCEPTION
 Computer program /TACTICS/ for simulating three vehicles simultaneous motion in space, considering interceptor-target guidance and intercept trajectories 07 p1239 A70-20414
 Deorbiting target intercept energy optimization by game theory approach [AIAA PAPER 70-1019] 21 p3848 A70-41778

INTERCEPTOR AIRCRAFT
U FIGHTER AIRCRAFT
INTERCEPTORS
 Optimal interceptor-target allocation and guidance for linear interception and rendezvous using real time and storage computer 16 p2947 A70-33311

UpSTAGE interceptor missile flight control system, discussing command logic to capitalize on lifting body advantages to enhance roll maneuver 21 p3927 A70-40782

INTERCONTINENTAL BALLISTIC MISSILES
NT MINUTEMAN ICBM
INTERCRANIAL CIRCULATION
 Extradural sensor for continuous measurement and recording of human intracranial pressure in neurosurgical practice 19 p3367 A70-37353

INTERFACE STABILITY
 Fiber-polymer matrix interfacial tensile and shear strengths evaluation methods, including data correlation from various tests 01 p0087 A70-10478
 Fiber-matrix interface mechanics in composites, considering shear strength, stress distribution, fiber strength effects, etc 01 p0127 A70-10479
 Weak interfaces effects in laminates under triaxial tensions at crack tip, analyzing delamination during crack propagation and fracture resistance 01 p0127 A70-10482
 Microstructural interfacial stability and property retention after elevated temperature exposure of eutectic composites, discussing coarsening rate relationship to interfacial area and energy 01 p0117 A70-10485
 Shear moduli and lattice parameters effect on screw dislocation equilibrium in bimetallic medium of soft and hard phases 03 p0587 A70-13117
 Interface instability between gases due to shock wave increased linearly with time 04 p0673 A70-15245
 Elastic fields in bimaterial plate under uniform compressive and anti-plane shear loadings, finding stress distribution and induced interfacial shear stresses 07 p1412 A70-19957
 Internal waves breaking on sloping surface in two fluid system, studying interfacial shear instability by capacitance probe on-line computer system 09 p1717 A70-22371
 Orbital refueling techniques, discussing vapor-liquid interface stability, pressurant requirements, transfer line chillover, propellant transfer dynamics, dielectrophoresis, suction speed estimating and system tradeoffs [AIAA PAPER 69-564] 14 p2653 A70-30752
 Interfacial and free surface mode instabilities of time periodic flows of viscosity and density stratified fluids at various Froude numbers 14 p2566 A70-31026
 Hydrostatic stability and damping characteristics of perforated plates and screens for passive propellant control schemes from drop tower tests [AIAA PAPER 69-531] 15 p2787 A70-32510
 Shear and tensile joint strength measurements at fiber-polymer matrix interface, using pull-out test and debonding methods 16 p2937 A70-33372
 Moisture induced failure of glass-resin composites at interface, discussing water adsorption, crack propagation, wet strength and nonsilicate reinforcements 16 p2937 A70-33373
 Interface stability of thin liquid film adjacent to supersonic air flow, using sphere-cone and blunt wedge test configurations [AIAA PAPER 70-801] 17 p3005 A70-34461
 Circular inclusion interface separation in matrix under incident compressive waves interpreted for fiber reinforced composites 17 p3185 A70-34963
 Cracks and tensile failure of interface bonds in elastic composite hollow cylinder, deriving wave front propagation equations 18 p3283 A70-36388
 Composite laminates under uniform axial strain, determining interlaminar stresses and displacements by finite difference techniques 22 p4060 A70-43684

INTERFACES
NT FLUID BOUNDARIES
NT GAS-SOLID INTERFACES
NT JET BOUNDARIES
NT LIQUID-LIQUID INTERFACES
NT LIQUID-SOLID INTERFACES
NT LIQUID-VAPOR INTERFACES
NT SOLID-SOLID INTERFACES
 Interfaces in composites - ASTM Conference, San Francisco, June 1968 01 p0126 A70-10476
 Eccentric face seal with tangentially varying film thickness, analyzing leakage flow proportional to eccentricity and surface waviness [ASLE FICFS PREPRINT 15B] 02 p0308 A70-12176
 Radio wave scattering and brightness on uneven interface, determining frequency spectrum of signal reflected from surface assuming uniformly moving receiver 05 p0813 A70-16261

Saint Venant torsion and flexure of composite prismatic and cylindrical bars with circular and concentric interfaces 05 p0936 A70-16318
 Thermal and electric conductivities for interface separating two parts of system with different temperature and chemical and electrical potential 14 p2617 A70-31296

INTERFACIAL ENERGY
 Interfacial equilibrium free surface energies between glass fibers, coupling agent and resin matrix, considering wetting, absorption and bonding 01 p0128 A70-10486
 MOS structure electrical characteristics dependence on silicon/silicon dioxide interfacial energy and electric charges, considering fabrication difficulties 02 p0350 A70-12541
 Forces at boundary surface in solid phase in solids and adhesive film interactions, considering boundary surface energy 08 p1503 A70-20879
 Failure mode in shear loaded graphite filament reinforced epoxy composites dependent on interfacial bond strength 08 p1533 A70-21915
 Interfacial energy and free energy estimation by quasi-continuum approximation for two component water-organic or organic-organic liquid systems 10 p1915 A70-23843
 Adhesive debonding in case-bonded solid propellant rocket motors, describing stress analysis and interfacial surface energy measurement 17 p3146 A70-35222
 Energy balance criterion for continuum mechanics analysis of fracture threshold for blistered adhesive elastic layer between elastic material and rigid substrate 19 p3536 A70-37774
 Postmechanical interface separation in elastically supported rotary face seals under input excitation [ASLE PREPRINT 70AM 3C-3] 19 p3439 A70-38808
 Alloys stacking faults thermodynamics based on Gibbs treatment of interfacial free energy 22 p4124 A70-42726

INTERFACIAL STRAIN
U INTERFACIAL TENSION
INTERFACIAL TENSION
 Fiber-composite materials fracture, noting interface mechanical strength effects on composite properties under tension and shear 01 p0127 A70-10481
 Rigid plastic body of material insensitive to strain rate under time dependent surface tension and time independent body forces 02 p0391 A70-12816
 Plane elasticity solution for differential expansion stresses on interface of laminated elastic rectangular strip 03 p0586 A70-13114
 Stress intensity and strain energy release rate in elastic fiber-reinforced composites with different thermomechanical properties and imperfect bonding [ASME PAPER 69-WA/APM-15] 04 p0771 A70-14913
 Equilibrium shapes of rotating weightless fluid with surface tension in absence of external force field obtained by boundary layer theory 04 p0673 A70-15241
 Axial compression of elastic circular cylinder in contact with identical elastic half spaces, determining interfacial surface stresses for frictionless and adhesive contacts 05 p0930 A70-16082
 Adhesive or frictionless compression /or extension/ under axial load of elastic rectangle between two identical elastic half spaces in condition of plane strain 05 p0931 A70-16132
 Heat transfer during nucleate boiling, discussing transfer from heated surface to superheated liquid layer and exchange on gas-liquid interface 06 p1176 A70-17695
 Interface stresses in ceramic/metallic spherical shells for deep superelastic structures using hydrostatic testing and photoelastic analysis [AIAA PAPER 70-135] 06 p1170 A70-18089
 Surface tension plotted against density and temperature of hydrocarbon jet fuels, determining critical temperature 07 p1357 A70-18653
 Ideal fluid in lightly filled spherical vessel under gravitational force investigated for surface tension effect on vibration frequencies 08 p1482 A70-20853
 Rehydratable food consumption in zero-gravity environments with spoons and forks, observing interfacial tensions between water and food, containers and utensils 09 p1628 A70-23464
 Liquid phase convective heat transfer as rate controlling mechanism for flame propagation, analyzing surface tension driven liquid flow induced by temperature profile 10 p1929 A70-24091

- Cavitation flow around wedge taking into account gravity and surface tension 10 p1868 A70-24162
- Film cavitation between flat annular surfaces in face seal resulting from hydrodynamic pressure generated by misalignment and surface waviness 13 p2417 A70-28613
- Negative g Drone aircraft surface tension fuel system preventing air inclusion in turbojet engine fuel by tank filters/screens/ [AIAA PAPER 70-910] 17 p3019 A70-35822
- Mathematical solutions validity in determining constant interface friction factor from ring compression tests [ASME PAPER 69-WA/LUB-8] 19 p3434 A70-37603
- Viscosity and vessel geometry effects on fluids natural and forced oscillation, taking surface tension into account 20 p3614 A70-40438
- Cellular convection in fluid layers with parabolic temperature distribution, calculating stability effects of gravity and surface tension gradients 21 p3952 A70-42078
- Surface tension role in microliquid layer formation on solid surface with growing bubble in nucleate boiling, using optical method 21 p3953 A70-42089
- Perfect nonrelativistic bounded gas thermodynamics and surface tension, assuming single particle energy level density dependence on external potential 23 p4284 A70-44928
- Fibrous composite interface effects and fracture work, discussing tip stresses of crack normal to fiber, energy dissipation by pullout and debonding in brittle fiber composites, etc 24 p4419 A70-45171
- Fibrous composites design for mechanical properties improvement, discussing interfacial properties conflicting requirements as to interlaminar shear, transverse tensile strength, high work of fracture values, etc 24 p4419 A70-45172
- Intermaterial adhesion relation to association contact resistance-tension characteristics based on electric potential barrier model for Maxwell-Wagner effect 24 p4379 A70-45617
- Air and liquid filled excised lungs P-V hysteresis curves, determining surface tension in situ 24 p4302 A70-46104
- ### INTERFERENCE
- Interference fringe in Fraunhofer hologram reconstruction of tapered glass fibers related to fiber profiles 01 p0090 A70-10906
- Interference phenomenon observable by ultrasonic fields visualization in 1-10 MHz range, discussing beam stratification 13 p2404 A70-28646
- Doppler effect in interference fringe formation in holographic vibration analysis, discussing path length variation 22 p4038 A70-43152
- Wind tunnel wall interference effects for V/STOL aircraft with lift jets, using modified theoretical model for complex jet arrangements [ICAS PAPER 70-54] 23 p4139 A70-44150
- Oscillatory motion of triangular wing with conical body of arbitrary cross section in supersonic flow, considering wing-body interference effects 24 p4288 A70-45592
- ### INTERFERENCE DRAG
- Upwash interference on oscillating wing in slotted wall wind tunnels, analyzing acceleration and velocity potentials using small wing theory 04 p0621 A70-15605
- Transonic aircraft testing capabilities and limitations, considering tunnel wall interference and Reynolds number effects [AIAA PAPER 70-580] 13 p2348 A70-29876
- Single and twin jet afterbody configuration models, describing drag and interference characteristics at subsonic speeds 14 p2528 A70-30862
- Critical flutter behavior of variable geometry aircraft with wing of 70 degree leading edge sweep, noting wing-tail interference 18 p3338 A70-36445
- Transonic wind tunnel porous walls, investigating interference effects and aerodynamic characteristics 22 p3958 A70-42337
- Exhaust nozzle/airframe interference test evaluation for twin engine supersonic fighter [AIAA PAPER 69-430] 22 p3958 A70-42702
- ### INTERFERENCE GRATING
- Spatial distribution of field intensities of resonators, using diffraction gratings and prisms 04 p0651 A70-15289
- Holographic dielectric gratings analyzed by Raman-Nath formalism modified for losses 11 p2050 A70-25640
- Double asymmetric grating with thin ideally conducting strips, describing incident E-polarized electromagnetic wave diffraction 19 p3378 A70-37744
- Diffraction amplitudes in plane H-polarized electromagnetic wave incident obliquely on grating with closely spaced conducting rectangular bars, obtaining transmission coefficient 19 p3378 A70-37745
- Welded joint strain measurement by grating etching and moire fringe technique 19 p3428 A70-38513
- Plane electromagnetic waves diffraction by moving periodic metal strip grating, writing E polarized wave of unit amplitude by Lorentz transforms 22 p3984 A70-42388
- ### INTERFERENCE LIFT
- Wind tunnel boundary interference on V/STOL model calculated in test section with solid vertical and slotted horizontal walls, using image method and Fourier transforms [AIAA PAPER 70-575] 13 p2343 A70-29894
- Subsonic boundary lift interference in wind tunnels with perforated walls, using point matching method 14 p2563 A70-30869
- Aerodynamic interferences of lifting surfaces harmonically vibrating in subsonic flow 23 p4136 A70-44765
- ### INTERFERENCE MONOCHROMATIZATION
- #### U DIFFRACTION
- #### U MONOCHROMATIZATION
- ### INTERFEROGRAMS
- #### U INTERFEROMETRY
- ### INTERFEROMETERS
- NT FABRY-PEROT INTERFEROMETERS
- NT MACH-ZEHNDER INTERFEROMETERS
- NT MICHELSON INTERFEROMETERS
- NT MICROWAVE INTERFEROMETERS
- NT PHASE SWITCHING INTERFEROMETERS
- NT RADIO INTERFEROMETERS
- Density distribution measurements in flow field using interference methods, including laser light sources 01 p0085 A70-10268
- Interferometer for compressing linearly FM light pulses and analyzing spectra of picosecond pulses 01 p0111 A70-10670
- Holographic two beam real-time Fizeau interferometer for recording and reconstructing reflected light waves in silvered flat surfaces measurement 01 p0090 A70-10905
- Gas pressure differences and diffusion rates recording using He-Ne laser interferometer, discussing aerodynamic applications and avionic instrumentation problems 02 p0299 A70-12272
- Twin wave interferometer and strain gauge mechanism for press-fit measurements of contact deformation on metallic and polymer samples 03 p0484 A70-13426
- Schlieren system converted into Kraushaar diffraction grating interferometer with isolated optical platform, considering applications to supersonic flow over airfoil shapes 04 p0689 A70-15016
- Frequency response of 6328 A He-Ne laser interferometer analyzed for multimode oscillations noting plasma diagnostics applications 05 p0861 A70-16989
- Displacement measurement to fractions of micron using laser interferometer 06 p1060 A70-17149
- Multiple beam interferometer coherence analyzer for temporal and spatial study of laser beams, emphasizing application to pulsed lasers, holography and nonlinear optics 07 p1297 A70-19145
- Vacuum UV spectrum interferometer with grazing incidence reflections between plane parallel mirrors to obtain coherent beams, discussing fringe patterns 07 p1286 A70-20081
- Multibeam interferometer sensitivity restrictions due to diffraction effects on interference patterns near transparent inhomogeneities 08 p1493 A70-20540
- Stellar interferometer with superposed beams designed for measurements of close binaries, showing point light modulation convenient for photoelectric recording 08 p1493 A70-20564
- Laser interferometric technique involving use of unstable external resonator to facilitate electron density measurements in presence of transverse plasma density gradients 08 p1499 A70-21693
- Compact unequal-path radial shearing laser interferometer designed for small angular aperture wave front testing 09 p1696 A70-22719
- High resolution Fourier interference near IR spectrometer for aircraft, balloon and spacecraft remote sensing applications 09 p1683 A70-23508
- Axial mode selection and frequency stabilization of Nd-YAG laser by optimally designed crystal quartz etalon 10 p1900 A70-24943
- Electron concentration measurement range expansion in plasma by laser interferometer with optical signal phase modulation 12 p2278 A70-27328
- Portable low cost shearing interferometer for plasma and flow analysis and instruction aid 12 p2235 A70-27754
- Maximum mode selection tuning of scanning interferometer with spherical mirrors applied to He-Ne laser spectrum analysis 12 p2250 A70-28182
- Backward facing separated step boundary layer flow at Mach 2.25 investigated by diffraction grating interferometer and color schlieren technique [AIAA PAPER 70-571] 13 p2343 A70-29898
- Savart interferometer for high sensitivity measurements of refractive index gradients using double exposure technique 14 p2583 A70-30400
- Stellar intensity interferometer for close binaries and emission line stars, investigating gamma-two Velorum 14 p2640 A70-30733
- Water sources associated with W3, Orion Nebula, W49 and VY Canis Majoris observed with coherent interferometers having long baseline 14 p2642 A70-30892
- Venus radar mapping using fixed base line interferometer for hemispheric ambiguity resolution 14 p2647 A70-31078
- False signal in scanning interferometer for helium-neon lasers in single and simultaneous TEM modes 15 p2749 A70-31557
- Optical polarization, discussing radiation intensity and state measurement by two beam interferometer 15 p2736 A70-32035
- Rayleigh type holographic interferometer featuring production method for base pattern of variable fringe density 15 p2741 A70-32438
- Stellar interferometer with superposed beams designed for measurements of close binaries, showing point light modulation convenient for photoelectric recording 15 p2742 A70-32719
- Plasma concentration measurement in coaxial accelerator, using gas laser and multiple wave interferometer in vacuum chamber 15 p2781 A70-32858
- Optical resonator thermal deformations during pumping of circular cylindrical interferometer rods in illuminators, measuring thermo-optical constants of neodymium glass 15 p2754 A70-32863
- Vacuum interferometer strain gage for absolute earth strain measurement via length change comparison with wavelength standard 16 p2925 A70-33024
- Optical heterodyne interferometer for stellar diameter measurements 16 p2925 A70-33025
- Optical system and light source imperfection effects interference image contrast lowering in laser interferometer for length measurements 16 p2928 A70-33292
- Holographic motion measurement verification of constant velocity, sinusoidal vibration and both, using interferometer 17 p3087 A70-35022
- Intensity interferometer for weak noise-like signal power measurement in presence of additive Gaussian noise 17 p3089 A70-35265
- Equivalent interferometer existence theorem in holography 19 p3423 A70-37830
- High accuracy length measurement by fringe counting using laser interferometer 19 p3447 A70-38050
- Ronchi test interferometer for optical quality checking of laser crystals 20 p3627 A70-39094
- Power diffraction losses at mirrors of asymmetric confocal laser interferometers with output coupling apertures 20 p3628 A70-39130
- Laser interferometer system unwanted reflections elimination and intensities control in each arm by linear polarization method 21 p3823 A70-40820
- Acoustic interferometer for speed of sound measurement in pure gases, determining second virial coefficient for Ar and N 21 p3828 A70-41766
- Electron concentration measurement range expansion in plasma by laser interferometer with optical signal phase modulation 21 p3860 A70-42069
- Wollaston prism schlieren interferometer for quantitative density gradient measurements in air [SMPT PREPRINT 25] 22 p4034 A70-43050
- ### INTERFEROMETRY
- #### NT DIFFERENTIAL INTERFEROMETRY

Holographic interferometry as stress analysis technique for crack propagation studies, discussing advantages over classic interferometric and conventional photoelastic methods

01 p0198 A70-10002

Holographic interferometry for determining optical path variations resulting from photographic plate emulsion thickness and refractive index changes during development

01 p0087 A70-10666

Secondary surveillance radar and interferometry techniques to determine aircraft positions in real time and all weathers for air terminal approach control

02 p0331 A70-11965

Optimum procedure for high speed cinematography of holographic interferograms permitting microsecond exposures while retaining picture quality

02 p0298 A70-12213

Sandwich structures nondestructive testing by holographic interferometry, discussing system operation, specimen stressing, acoustic vibration, etc

02 p0309 A70-12274

Quantitative interpretation of three dimensional weakly refractive phase objects using holographic interferometry, determining index of refraction

02 p0300 A70-12464

Holographic interferometry with pulsed ruby laser holocamera for examining flow distribution in supersonic free jet wind tunnel

03 p0480 A70-12948

Holographic interferometry applications in experimental mechanics, illustrating nondestructive testing by flaw detection in bonded honeycomb

03 p0481 A70-12959

Hologram interferometry to study stresses in fixed two dimensional photoelastic models and three dimensional slice qualitative analysis [SESA PAPER 1530]

03 p0482 A70-12964

Displacement interferograms and schlieren pictures of optical inhomogeneities in transparent media obtainable from single exposure hologram, using non-monochromatic and laser light for reconstruction

03 p0483 A70-13258

Double exposure holograms in diffuse radiation used to reconstruct in white light interferogram images localized in hologram plane

03 p0483 A70-13259

Hologram interferometry accuracy, reliability, application to plate deformation and translation measurements, using moire method and correction factors

03 p0493 A70-13945

Holographic method for measuring optical instruments transfer function, using laser light source and beams interference

03 p0493 A70-13946

Surface roughness measurements by coherent optics and interferometry, including theory and experimental verification

04 p0689 A70-15015

Gabor holography producing interference phenomena, discussing far field fringes, circular fringes, diffuser, etc

05 p0849 A70-16529

Holographic interferometry applied to amplitude measurement of periodic mechanical surface vibration

06 p1069 A70-18436

Holography history and applications to interferometry, contour mapping and three dimensional photography

07 p1279 A70-18900

Body displacement and deformation measurement by fringe separation in holographic interferometry

07 p1280 A70-19143

Hologram interference fringes formation and location using grating model of diffusely reflecting surface

07 p1280 A70-19144

Holography without reference beam for two and three dimensional interferential wave front recording and reconstruction

07 p1285 A70-19858

Holo-diagrams for simplified evaluation of amplitude and direction displacement in double exposed holograms for interferometric measurements

07 p1287 A70-20086

Interferograms taken by phase difference amplification technique with nonlinear hologram, considering amplified image accuracy

08 p1500 A70-21788

Holography in terms of photogrammetry, reviewing interferometry role, wave construction and reconstruction, etc

09 p1674 A70-22260

Real time hologram-interferometry application to optical aspheric surfaces testing explained by geometrical optics

09 p1676 A70-22717

Inexpensive live stroboscopic holographic interferometry, discussing time averaged and stroboscopic methods

09 p1676 A70-22787

Transient partially ionized plasmas observation by two wavelength holographic interferometry, describing electron density measurements

09 p1736 A70-23186

Sensitivity of nondiffuse double exposure holographic interferometry with transparent medium increased via multiple beam passage through medium placed in optical cavity

09 p1682 A70-23360

Weak phase objects detection based on interferential and streak photography methods, noting fringe deformation role

10 p1916 A70-24587

Ambiguities during brightness temperature distributions reconstruction from intensity interferograms

11 p2048 A70-25335

Plastic strains at sharp notch roots in Perspex plates using interference patterns formed by gas laser monochromatic light beam for fracture initiation

11 p2131 A70-25594

Photoelasticity stress analysis, determining principal stress differences and orientation, using holographic interferometry to obtain sum and separation

11 p2049 A70-25596

Pulsed laser holographic interferometry of density field created by high speed projectile motion in air [ALAA PAPER 69-347]

11 p2051 A70-25987

Radar interferometry as diagnostic method for remote probing of turbulent plasma

11 p2096 A70-26766

Interferometric stress analysis in three dimensional photoelasticity, including practical measurements and analysis in terms of refractive index

12 p2326 A70-27621

Interferometric combinations of frequency-shifted mode-locked laser pulses achieved by optical modulation-demodulation methods

12 p2249 A70-27755

Plasma diagnostics by high sensitivity holographic interferometry

12 p2235 A70-27794

Coherent light holographic and incoherent interferometric imaging analogy, noting three dimensional image formation

12 p2236 A70-28120

Laser beam photography utilization in engineering for optical pointers, interferometers and holographic visualization of surface strain and vibration

13 p2406 A70-28914

Hologram interferometry using moire method to determine bending moments of object surface

13 p2409 A70-29474

Displacement component in chosen direction on deformed object surface, using hologram interferometry with double illumination

13 p2409 A70-29475

Large diffraction gratings by interferometrically controlled commercial measuring machine

13 p2412 A70-29821

Interferometric measurement of spatial correlation function of optical radiation fields propagating through turbulent atmosphere

13 p2454 A70-29825

Displacement sensor based on interference fringes counting by laser interferometry

14 p2594 A70-30683

Nondestructive bond inspection by interferometric holography of ultrasonically excited plates

14 p2588 A70-31166

Superradiant pulsed 5401 A neon laser for interferograms of gas flow through nozzles in shock tunnel

15 p2750 A70-31763

Photoelastic stress analysis, discussing holographic interferometry for main stresses separation and polyester resins application to birefringence pattern superposition elimination

15 p2815 A70-31809

Interferograms of window wave front deformations to measure angular deviations to line of sight

15 p2737 A70-32038

Laser beam shaping for streak interferometry, obtaining thin beam uniform over filling length

15 p2752 A70-32049

Holographic interferometry combination with high speed photography, obtaining time resolved record of event

15 p2737 A70-32051

Fringe interpretation in stress-holo- interferometry, emphasizing isopachic-isochromatic interaction effects in photoelastic analysis [SESA PAPER 1642]

15 p2739 A70-32309

Fringe visibility and localization in double exposure holographic interferometry of diffusely reflecting flat objects

15 p2740 A70-32430

Laser interferometry strain gage for measuring earth strain, taking into account wavelength stabilization

16 p2925 A70-33023

Aircraft turbine engine components vibrational testing by holographic interferometry methods

16 p2903 A70-33134

Holographic interferometry for evaluating bond between diaphragm and base in pressure transducer

16 p2904 A70-33138

Holographic interferometry for moire strain analysis, discussing theory and applications

16 p2904 A70-33149

Turbulent wakes density fluctuations measurement using pulsed laser holographic interferometry in ballistic range

[ALAA PAPER 70-727]

Time-average holographic interferometry applied to HF transverse vibrations of uniform cantilever beam, noting correlation with Timoshenko beam theory

16 p2834 A70-33494

Holographic interferometry measurements, including low frequency quartz vibration and relaxation effects in materials following strain or impacts

17 p3085 A70-35005

Hologram interferometry for measuring surface deformation under force and anisotropy in transparent objects

17 p3085 A70-35009

Pressure transducer diaphragms displacement measurement by holographic interferometry

17 p3085 A70-35010

Normally loaded thin plate displacements, bending moments and stresses determined by hologram interferometry and indirect moire and superposition of grilles

17 p3085 A70-35011

Axially loaded cylindrical shells prebuckling deformation behavior measurement by holographic interferometry

17 p3086 A70-35012

Hologram interferometry with birefringent objects, showing advantages over polariscope and classical interferometers

17 p3086 A70-35013

Vibration measurement by hologram interferometry, discussing wave front reconstruction and fringe theory based on Rayleigh integral formulation of light propagation

17 p3086 A70-35017

Engineering components vibration mode studies by time averaged holographic interferometry

17 p3087 A70-35019

Precision components engineering inspection and sonic transducer surface vibration modes analysis by hologram interferometry

17 p3087 A70-35021

Light velocity from frequency and wavelength differences between gas laser lines, using precision long path interferometry

17 p3104 A70-35085

He-Ne laser emission wavelength, using laser interferometry based on feedback between moving mirror and resonator

17 p3104 A70-35088

Pulsed plasmas refractive index measurement by two-wavelength He-Ne laser interferometry, estimating effects of heavy atoms and neutral gas density

17 p3107 A70-35110

Laser interferometry for accelerometer and dynamic pressure transducer calibration and vibration measurement

17 p3089 A70-35124

Electron concentration distribution over plasma discharge cross section, using interferometry

17 p3142 A70-35732

Interferometric holograms of vibrating body via numerical analysis of oscillations amplitude and phases

18 p3258 A70-36303

Holographic interferometry applications in stress analysis of photoelastic resins, describing holographic interferometry assembly

18 p3262 A70-37209

Holographic interferometry of rapid phase objects by two wavelengths from ruby laser and KDP crystal filter, noting application to dense plasmas

19 p3422 A70-37650

Piezoelectric controlled device as standard for holographic interferometry, providing continuously variable subject plate displacement and/or rotation

19 p3425 A70-37890

Holography, discussing light propagation, basic principles, skew reference wave, diffused illumination interferometry, character recognition, microscopy, high density information storage, etc

19 p3427 A70-38449

Stress and vibration effects measurement by holographic interferometry, comparing results with direct measurements

19 p3427 A70-38450

Membrane attachment for pressure transducer with help of holographic interferometry, describing optical system

19 p3427 A70-38453

Laser rod faces parallelism measurement by interferometric method for Brewster or square ended rods

20 p3640 A70-39095

Characteristic functions for frequency analysis of fringes obtained by time-average holographic interferometry of generalized time dependent optical phase function

20 p3628 A70-39133

Ring lasers design and performance, measuring angular velocity by interferometry

20 p3641 A70-39418

Laser interferometry with unstable external resonator, determining radial electron density distributions

during implosion phase of linear z-pinch discharge in argon 20 p3630 A70-39420

Optical interferometry device for large amplitude vibration measurement 20 p3630 A70-39488

Cathode spaces electron concentration, time dependence and axial distribution by laser beams interferometric method, noting accuracy and resolution 21 p3836 A70-40796

Rigid cylinder rotation and flexible shaft torsion observation by holographic interferometry 21 p3822 A70-40813

Multiple wavelength desensitized hologram interferometry to extend displacement measurement range 21 p3822 A70-40814

Holographic interferometry measurements of surface amplitudes distribution under periodic mechanical vibration 21 p3824 A70-40864

Apollo 11 lunar dust small glassy spherules and cylinders examination by interferometry, discussing specular reflection, microcracking, chipping and origin 21 p3919 A70-41682

Time average holographic interferometry of circular plate vibrating simultaneously in rationally related modes 21 p3829 A70-41927

Combined hypersensitization and rapid in situ processing for time-average observation in real time hologram interferometry 22 p4025 A70-42321

Plasma diagnostics by two-beam optical interferometry and holographic techniques, discussing plasma parameter spatial distribution recording insensitivity to radiation and variable-sensitivity interferometry 22 p4079 A70-42382

Laser application to nondestructive testing via holography and hologram interferometry 22 p4028 A70-42587

Interferometric investigation of rapidly variable frequency dependent phase objects, using ruby laser waves [SMPT PREPRINT 26] 22 p4034 A70-43049

Real time holographic interferometry for flame propagation research, using high speed camera [SMPT PREPRINT 9] 22 p4035 A70-43053

Holographic interferometry sensitivity augmentation by use of nonlinear properties of photoemulsion 22 p4038 A70-43140

Holographic interferometry for study of transparent media, noting application to aerodynamic phenomena [ONERA-TP-851] 22 p4039 A70-43455

Holographic interferometry by backscattering, considering displacement and deformation problems [ONERA-TP-852] 22 p4039 A70-43456

Nondestructive measurement of elastic and plastic deformation in soldered joints and printed circuit boards by holographic interferometry 22 p4047 A70-43521

Holo-diagrams for predicting fringe patterns in hologram interferometry caused by translation motion and rotation 22 p4040 A70-43610

Transparent objects holographic interferometry with illumination derived from phase gratings to eliminate laser speckle 22 p4040 A70-43611

Hologram interferometry as noncontact tool for vibration mode measurements of turbine blade groups 23 p4193 A70-43925

Laser applications in length measurement and holography, describing principles and techniques, modulated laser beams and pulse transit time 23 p4201 A70-43998

Focused image holographic interferometry by double exposure with reconstruction in white light applied to flat rotating subject 23 p4199 A70-45058

Holographic interferometry of phase object by double exposure method, showing no effect of photographic emulsion compression on order of interference 24 p4334 A70-45368

Electro-optical light speed measurements with interference comparator using He-Ne lasers with light modulators 24 p4353 A70-45562

Turbine compressor blades vibration mode measurements by holographic interferometry 24 p4334 A70-45563

Holographic interference pattern interpretation, measuring object rotation 24 p4336 A70-45666

Holographic interferometry for NDT inspection of adhesive bonded honeycomb sandwich aerospace structures 24 p4338 A70-45754

X ray and neutron propagation in multilayer film composite, discussing boundary conditions in interlateral systems 24 p4380 A70-46095

INTERGALACTIC MEDIA

Diffused X ray background in isotropic world models in terms of Compton radiation from cosmic ray electrons in intergalactic space 02 p0356 A70-11743

Galactic satellite interpretation for high velocity hydrogen clouds at high latitudes 02 p0363 A70-11780

Quasars photoionization of intergalactic high density hydrogen gas to interpret absorption features absence, noting gas temperature 10 p1942 A70-24628

Observational cosmology, discussing aspects of radio source and quasar counts, intergalactic medium and cosmic black body radiation 12 p2298 A70-27061

Intergalactic medium lukewarm models, considering physical state, cosmic photon spectrum and isothermal and adiabatic expansion 14 p2651 A70-31291

Intergalactic gas condensation rates in galactic nuclei, considering recurrent magnetoplasma cores and quasar-like phenomena 15 p2801 A70-32479

Red shift absorption systems ions related to intergalactic medium properties in clusters of galaxies 17 p1353 A70-34526

UV background radiation observed above atmosphere for intergalactic gas, Galaxy and subcosmic ray components 17 p1363 A70-34903

Spiral galaxies structure, considering maintenance problem and effect of possible gas inflow from intergalactic space 18 p3326 A70-37152

X ray emission of hot dense intergalactic plasma, discussing evolution equation for temperature and degree of gas ionization vs red shift 21 p3877 A70-40702

UV and nonthermal X ray interaction with intergalactic gas, considering photoionization and recoil associated with Compton X ray scattering 21 p3878 A70-40706

High velocity intergalactic hydrogen origin, examining galactic evolution by gas infall 21 p3887 A70-41112

Universe density estimation by galaxy formation theory, discussing spiral galaxies intergalactic gas thermal radiation and soft X rays 21 p3887 A70-41113

Interstellar and intergalactic medium physics, examining H I and H II regions thermal and dynamic states 22 p4098 A70-42578

Intergalactic gas condensation rates in galactic nuclei, considering recurrent magnetoplasma cores and quasar-like phenomena 23 p4240 A70-43904

Primeval cosmic magnetic fields origin, discussing galactic fields and limits on present intergalactic field 24 p4403 A70-45396

INTERGRANULAR CORROSION

Austenitic stainless steels intergranular corrosion model proposed and supported by observations of structural changes and corrosion behavior, suggesting methods to reduce susceptibility 03 p0506 A70-13130

Intergranular corrosion mechanisms in ferritic stainless steels observed by electronmicroscopic examination on Cr Fe-base alloys vacuum-melt with C and N 03 p0506 A70-13131

Heat treatment produced semicoherent and incoherent precipitations diminished susceptibility to stress corrosion cracking of aluminum binary and ternary alloys 04 p0708 A70-15370

Aluminum alloys intergranular and stress corrosion, noting electron microscopy application for alloys performance improvement 04 p0710 A70-15680

High temperature oxidation of Ni-Cr alloys and stainless steels in molten salt, observing grain boundary corrosion with electron probe 15 p2757 A70-31875

INTERIOR BALLISTICS

Interior ballistics of high-low propulsion system with fixed volume high pressure combustion chamber coupled to variable volume lower pressure action chamber 03 p0548 A70-14116

Interior ballistics for wide temperature throttling of solid propellant rockets by variable-throat-area nozzle, noting composition effect screening 11 p2103 A70-26154

Internal ballistics equations solution on basis of pressure index law of burning taking into consideration density approximation 15 p2786 A70-31849

Spin effect on internal ballistic of radial burning solid propellant rocket motor spun about longitudinal axis 15 p2791 A70-32794

Internal ballistics of composite propellant charge in first stage of burning 19 p3489 A70-38373

INTERLAYERS

NT MULTILAYER INSULATION

Diffusion welding of dissimilar metals with or without intermediate layers, assessing joint strength factors 03 p0498 A70-14071

Interlayer ionization valley depth influence on F region heights, calculating N/h profiles from ionograms 14 p2571 A70-30229

Energy balance criterion for continuum mechanics analysis of fracture threshold for blistered adhesive elastic layer between elastic material and rigid substrate 19 p3536 A70-37774

Interlayer ionization valley depth influence on F region heights, calculating N/h profiles from ionograms 24 p4331 A70-46304

INTERLOCKING

U LOCKING

INTERMEDIATE FREQUENCIES

IF optimum bandwidth for maximizing output SNR in FM receiver with barrier to noise ratio below discriminator threshold 01 p0051 A70-11119

Ray tracing techniques applied to night sky wave medium frequency propagation, modifying program for absorption and polarization coupling losses 07 p1230 A70-19164

FM/FM telemetry threshold carrier SNR and receiver IF bandwidth optimization through computer program 11 p2014 A70-26272

IF combinator for broadband transhorizonal radio relay transmission improvement by providing optimum SNR 11 p2020 A70-26821

Radio wave field intensity in middle frequency range, determining propagation curves for large distances 14 p2547 A70-30208

Medium wave thin cylindrical dipole antenna arrays design, discussing operating impedance determination 15 p2714 A70-32816

Frequency and stability measurements of IF signals generated between laser far IR radiations and conventional oscillators 17 p3104 A70-35084

Solid state IF or baseband switching elements design for high capacity multichannel microwave systems 23 p4172 A70-44014

Radio wave field intensity in middle frequency range, determining propagation curves for large distances 24 p4316 A70-46283

INTERMEDIATE FREQUENCY AMPLIFIERS

Transistor RF and IF amplifiers designed for 210-ft antenna of Australian National Radio Astronomy Observatory 07 p1243 A70-20350

Wideband microwave transistor IF amplifier for mm wave communication system 14 p2555 A70-30283

Transistorized IF amplifier output matching to long transmission line, deriving formulas for gain and pass-band over wide output impedance range 22 p3995 A70-42520

INTERMETALLICS

Ni-Cb intermetallics phase precipitation during aging of Inconel alloy 718, composition, stability and structure 01 p0116 A70-10093

Martensite structure, discussing intensity anomalies in X ray diffraction pattern of intermetallic Ni-Nb 01 p0121 A70-10900

Al-Ni intermetallic whisker-reinforced Al microstructure and mechanical properties, studying effects of cold rolling 03 p0508 A70-13142

Phase alteration quenching effects in Ni-Mo alloys, discussing high temperature alpha region, isothermal annealing below peritectoid temperature and metastable nickel molybdenide phase 03 p0508 A70-13143

Ni-Nb intermetallic compound precipitation effect on various phase formations in strained samples of Alloy 718 / wrought Ni base alloy/ 03 p0511 A70-13568

Intermetallic precipitates development and mechanical properties of maraging steel as function of composition, tempering time and temperature using electron microscopy 07 p1310 A70-19748

Al-Cr-Zr alloy ingots macrostructural inhomogeneities, studying roles of casting rate and additives in intermetallics primary crystallization 08 p1517 A70-21128

Electrical resistivity of TiNi and TiCo compounds and alloys measured at various temperatures after quenching or annealing 09 p1707 A70-23194

Optical properties of beta prime phase CoAl, CoGa and NiGa as functions of composition and photon energy 10 p1919 A70-23986

Microconstituents effect on wear behavior of high hardness steels on basis of crossed-cylinder testing, discussing intermetallic compounds influence
10 p1895 A70-24853

Mechanism and kinetics of intermetallic layers formation and growth in welded joints of unlike metals
11 p2067 A70-26594

HF electrodeless plasma discharge synthesis of niobium and vanadium intermetallic compounds
11 p2061 A70-26746

Soviet monograph on intermetallic compounds with Laves phases, covering crystallographic and thermodynamic characteristics of Mg-Zn, Mg-Cu and Mg-Ni systems
12 p2252 A70-26885

Superconducting thin films of beta-tungsten structure Nb-Al-Ge compound, discussing high purity sputtering preparation techniques and properties in magnetic fields
12 p2285 A70-27259

Physical metallurgy, discussing metals, intermetallic compounds and polymorphic metals properties, single crystals production, etc
12 p2257 A70-28272

Solid solutions of GaAs with 2B or 6A intermetallic compounds, using metallographic and X ray methods
13 p2469 A70-28856

Phase transformations in TiNi with equiatomic composition, using internal friction, electrical resistivity and dilatometry
13 p2435 A70-29499

Quench hardening and Ni content relationship in Ti-Ni intermetallic compounds, investigating heat treatment effect on mechanical properties
16 p2930 A70-33084

Nb-Sn superconductors multiphase structure with three intermetallic phase, constructing diagram based on phase stability and composition
18 p3299 A70-37221

Magnetic and structural characteristics of ternary intermetallic systems with lanthanides, considering Ln substitution by other rare earth elements
22 p4085 A70-42481

Lanthanide zinc intermetallic compounds magnetic characteristics in 4-300 K range, observing Curie-Weiss behavior
22 p4085 A70-42482

Weak itinerant ferromagnetism theory for Ni-Ga and Ni-Al intermetallics, allowing for molecular field parameter magnetization dependence
22 p4087 A70-43197

Ni-Fe-Cr-Nb alloy, investigating precipitation hardening of Ni3Nb phases by transmission electron microscopy
24 p4357 A70-45226

INTERMITTENCY
Intermittency characteristics associated with fine scale structure and motion of atmosphere from data pertaining to various atmospheric layers
09 p1717 A70-22375

Intermittency role in free turbulent flow and EM wave scattering by hypersonic wakes
11 p1978 A70-26776

Geometrical figure fragmentation produced by intermittent illumination, examining dependence on presentation frequency and temporal factors
20 p3580 A70-39491

Highly accelerated boundary layer turbulence structure, measuring intermittency factor distribution with hot-wire probe
23 p4182 A70-44587

INTERMODULATION
Intermodulation noise performance of FM FDM trunk radio systems in two path fading situations, calculating noise/power ratio and baseband enhancements
09 p1632 A70-22337

Tetrode for single sideband short wave transmitter, discussing design, characteristics and intermodulation distortion reduction
17 p3054 A70-35412

Frequency division multiple access satellite communication system, calculating bandwidth variations effects on intermodulation distortion
21 p3787 A70-41328

Multiple channel VHF testing on ATS 1 and 3, describing transponder intermodulation and compression corrections
21 p3791 A70-41366

Intermodulation distortion reduction in four frequency parametric converter by low impedance path
23 p4169 A70-43785

INTERMOLECULAR FORCES
Well depth determination for weak intermolecular potentials based on dimerization enthalpy measurement of rare gas atoms by mass spectrometry
03 p0527 A70-13299

Transport properties of high temperature gases compared with room temperature differences, considering chemical equilibria, heat conduction and atom-free radical forces
07 p1424 A70-19880

Molecular beam research at low, intermediate and high energies, discussing inelastic processes, intermolecular potentials, etc
07 p1344 A70-20131

Intermolecular potential of atoms and/or molecules determined from scattering cross sections of super-sonic He and/or Ar atomic beams
07 p1344 A70-20132

Atmospheric gases atomic and molecular binary short range repulsive forces, determining interaction potentials from elastic scattering cross sections
07 p1345 A70-20141

Inert gases and nitrogen determined at high temperature, discussing revision of existing functions representing intermolecular energy
08 p1598 A70-21525

Oxygen-kerosene combustion product composition and characteristics in engine thermodynamic design allowing for intermolecular interaction forces
10 p1968 A70-24284

Reduced second virial gas coefficients calculations by modified Lennard-Jones intermolecular potential function
12 p2180 A70-26860

Integral Hellmann-Feynman formula for dissociation energies in H, Li and LiH molecules, discussing transition densities and dissociation energy
12 p2275 A70-27569

Integral Hellman-Feynman formula applied to binding energy of molecular H and LiH, using SCF wavefunctions for atomic states
12 p2276 A70-27570

Real hydrogen driver performance, analyzing intermolecular forces effects under high compression and heat
16 p2998 A70-33889

Cyclopropane-argon mixtures translational and vibrational energies exchange efficiencies analysis based on intermolecular potential
16 p2956 A70-34083

Dilute gases kinetic theory, discussing microscopic explanation of macroscopic properties under intermolecular forces
17 p3072 A70-35533

Fluid intermolecular potential and virial calculation, noting relationships to Boyle and Joule-Thompson inversion temperatures
20 p3671 A70-38988

Intermolecular forces at close approach distances in calculating thermodynamic and transport properties of high temperature dilute gases, using molecular beam methods
23 p4222 A70-44430

INTERNAL COMBUSTION ENGINES

NT DUCTED FAN ENGINES
NT GAS TURBINE ENGINES
NT JET ENGINES
NT RAMJET ENGINES
NT SUPERSONIC COMBUSTION RAMJET ENGINES
NT T-56 ENGINE
NT TURBOFAN ENGINES
NT TURBOJET ENGINES
NT TURBOPROP ENGINES
NT TURBORAMJET ENGINES
NT WANKEL ENGINES

Lubricating oil chemical composition changes influence on combustion engine internal friction, considering surface active Zn, armo-co-iron and Al
01 p0099 A70-10077

Gas mixture internal energy in internal combustion engine cylinder calculated with allowance for thermal discontinuity
06 p1130 A70-17628

Temperature at end of admission process and exhaust gas temperature in cylinder of internal combustion engine using reversible adiabatic hypothesis
06 p1173 A70-17629

Temperature distribution in cylinders of aircraft internal combustion rotary piston engine under air cooling
23 p4234 A70-44742

High speed internal combustion engine mixed flow type liquid cooling system, deriving dynamic thermal characteristics from differential equations solution
24 p4393 A70-45502

INTERNAL ENERGY

Collision induced dissociations of 2000 ev diatomic O, N, CO and NO positive molecular ions as function of reactant ion internal energy
01 p0148 A70-11354

Nonlinear wave propagation in relaxing gas with internal energy characterized by translational and internal temperature, using model equation for piston induced motion
04 p0786 A70-15324

Gas mixture internal energy in internal combustion engine cylinder calculated with allowance for thermal discontinuity
06 p1130 A70-17628

Collective approach to thermodynamics of N- particle electron gas including transverse radiation, calculating internal energy and pressure of modes
08 p1553 A70-21612

Book on energy conversion statics covering state functions, quasi-static processes, internal energy, chemical energy storage and conversion, dynamics and postulates and laws
12 p2165 A70-27670

Jupiter luminosity as indication of internal energy magnitude, comparing limb darkening with predicted brightness distribution
14 p2643 A70-30984

INTERNAL FRICTION

Lubricating oil chemical composition changes influence on combustion engine internal friction, considering surface active Zn, armo-co-iron and Al
01 p0099 A70-10077

High temperature internal friction measurements on miniature torsional pendulum specimens from TD nickel bar, showing damping differences due to microstructural anisotropy
01 p0122 A70-11237

Mixed anisotropic linear elastic solids stability with internal friction due to mechanical interaction, considering asymptotic motion stability
03 p0586 A70-13116

Star rotation and meridional circulation hydrodynamic theory, considering magnetic fields and internal friction
03 p0564 A70-13228

Nb-Mo alloy interstitial oxygen concentration determined by measuring internal friction/Snoek/peak
03 p0512 A70-13763

Internal friction method for studying dislocation, stacking points and strengthening processes in steels and heat resisting austenitic steel behavior at high temperatures
05 p0864 A70-16870

Internal friction and shear modulus of Co under dynamic and steady state conditions, discussing peak at alpha-epsilon transformation
07 p1306 A70-19073

Rotating shaft vibrations on assembly designed to balance rotor in magnetic field, eliminating bearings effect on shaft to determine internal friction
08 p1584 A70-20697

Star rotation and meridional circulation hydrodynamic theory, considering magnetic fields and internal friction
08 p1580 A70-21661

Dopant effect on dislocation mobility in elastically loaded silicon crystal using internal friction and modulus defect measurements
11 p2099 A70-26394

Hydrogen impurities anelastic relaxation effect on internal friction alpha peak in cold worked tantalum and niobium
13 p2435 A70-29350

Zirconium additions effect on Ni internal friction behavior and relaxation spectrum
13 p2435 A70-29498

Phase transformations in TiNi with equiatomic composition, using internal friction, electrical resistivity and dilatometry
13 p2435 A70-29499

Internal friction in hydrogenated Ti-Mn alloys, observing relaxation peak formation under stress induced hydrogen diffusion in beta phase
16 p2930 A70-33082

Hydrogen behavior in Ti and alloys by internal friction measurement, attributing relaxation peaks to stress induced ordering of atoms
17 p3115 A70-34382

Binary titanium-oxygen and titanium-carbon alloys, investigating interstitial pair mechanism for internal friction peak formation
17 p3115 A70-34383

Seismic wave attenuation mechanisms emphasizing partial melting, grain boundary relaxation and high temperature internal friction background
19 p3416 A70-38440

Free vibrating reed apparatus for polymer low temperature internal friction and Young modulus measurements, discussing polystyrene properties
21 p3827 A70-41464

Diluent molecules effect on polymers relaxation behavior at cryogenic temperatures from internal friction measurements, noting loss peaks shift
21 p3844 A70-42138

Internal friction and shear modulus of thin glass fibers of sodium silicate, aluminosodium silicate and nonalkaline aluminoborosilicate
22 p4059 A70-43135

Equations solution for turbine blade flexural vibration, considering internal friction
22 p4117 A70-43363

Impurities and heat treatment effects on W internal friction at high temperatures, considering relaxation processes, recrystallization and microstructure
24 p4357 A70-45227

INTERNAL PRESSURE

Numerical solution of bending stresses in internally pressurized elliptical tubular or ring specimens for testing uniaxial and multiaxial fracture strength
01 p0203 A70-11061

Internal hydrostatic or lateral pressure effect on deformations of infinitely long thin cylindrical isotropic shell subjected to equal concentrated radial loads
03 p0584 A70-12922

Torospherical heads attached to cylinders and under internal pressure as elastic and/or elastic-plastic shells, using finite element
[ASME PAPER 69-WA/PVP-7] 04 p0769 A70-14792

Internal pressure deformed cruciform crack energy and stress intensity factor determined by linear equations
04 p0777 A70-15499

Stress factor-displacement relation in cruciform line crack deformation in elastic medium under arbitrary internal pressure
05 p0926 A70-15976

Steel tube deformation under constant internal pressure and cyclic heating, plotting tangential and axial strain curves as function of cyclic loading
06 p1163 A70-17399

Rheological factors effect on deformation behavior of thin walled spherical shell made of strongly extensible elastically hereditary material and subjected to internal pressure
08 p1587 A70-21168

Collective approach to thermodynamics of N-particle electron gas including transverse radiation, calculating internal energy and pressure of modes
08 p1553 A70-21612

Endurance limit of momentless shells of revolution under uniform internal pressure, deriving differential equations based on aging and creep theories
09 p1779 A70-23096

Cylindrical shell stability under combined torsion and internal pressure, noting yield point effect on critical load, obtaining buckling-internal pressure relationship
09 p1786 A70-23722

Stiffened cylindrical shells under internal pressure numerically analyzed based on C-5A fuselage material parameters
[AIAA PAPER 68-29] 11 p2135 A70-25961

Stresses in cylindrical pressure vessels with heads formed by internal fluid pressure
13 p2509 A70-28532

Slender cylindrical shell loaded by internal pressure analyzed using numerical procedure developed for digital computer
13 p2512 A70-28981

Strength and critical load determination for spherical shells with reinforced hole under internal pressure based on stress-strain state analysis during deformations
15 p2814 A70-31543

Internal pressure deformation of thin cylindrical shells of materials with nonlinear stress-strain relations, considering Al alloy shell and axial strain
15 p2816 A70-32009

Internal pressure maximization for compound cylinders in elastic condition using accelerated direct search technique
16 p2987 A70-32919

Normally intersecting closed cylindrical shells subjected to internal hydrostatic pressure, using Donnell shell theory
16 p2990 A70-33678

Elastic thin walled toroidal shell under internal pressure, investigating large deformation and stress behavior
17 p3184 A70-34910

Circular cylindrical shell with round holes along generatrix subjected to internal pressure, determining stress concentration with aid of computer
18 p3335 A70-36131

Shallow circular cylindrical shell with rigid collar on lateral surface, calculating stress under axial tension and internal pressure loading
19 p3534 A70-37245

Long hollow nonlinearly viscoelastic cylinder in elastic shell, calculating stress and strain under internal pressure
20 p3720 A70-39731

Prestressed loadings on two layer fiberglass-reinforced plastic cylindrical shell under internal pressure
23 p4265 A70-43937

INTERNAL STRESS

U RESIDUAL STRESS

INTERNATIONAL COOPERATION

Legal aspects concerning outer space and boundaries, discussing treaty aspects considered by various international congresses
01 p0220 A70-10333

Noctilucent cloud observation stations and international cooperation in exchanging climatological data concerning annual variations, height distribution and latitude dependence
01 p0072 A70-10579

Intelsat 4 communication system design and international cooperation, considering satellite design, TV and telephone channels capacity, etc
01 p0196 A70-10883

UN General Assembly outer space treaties governing international exploration and use and rescue and return of astronauts and objects
02 p0402 A70-12308

Satellite international system chain consisting of down path, receiving earth station and domestic receiver for Europe, North Africa and Middle East TV distribution
02 p0258 A70-12420

German-French communication satellite project Symphonie for radio, TV, telephone, teletype and data transmission, discussing objectives, organization and technical problems
[DVL-910] 03 p0580 A70-13796

NASA network and Thor Delta type booster to launch Italian satellite to geostationary orbit, evaluating feasibility
03 p0451 A70-13841

Collection of papers on space law with regional viewpoints on peaceful cooperation in outer space
03 p0610 A70-14255

International law framework for outer space, resolutions and recommendations by UN and international bodies and Space Treaty of 27 January 1967
03 p0611 A70-14257

International Law Association and development of legal regime of outer space, discussing treaties
03 p0611 A70-14258

Space activities cooperation of European organizations including CERS/ESRO, CECLES/ELDO and CETS, discussing European Space Conference
03 p0611 A70-14259

Latin American viewpoint on Space Treaty and prior UN Declaration implications, discussing military activity, astronaut legal treatment, liability, information access, etc
03 p0611 A70-14260

Soviet viewpoint of international law regulating space activities, discussing space exploration and exploitation, legal liability, accidents, emergencies, landings, etc
03 p0611 A70-14261

Liability convention requirements for international space law, considering personal injury or property damage caused by space activities of another state
03 p0612 A70-14262

Astronaut rescue and return of objects launched into space, discussing U.S.S.R. and U.S. proposals
03 p0612 A70-14263

Spacecraft registration and legal liability issues, noting UN Treaty assumption of registration
03 p0612 A70-14264

Soviet SS-9 ICBM role in international debates over antiballistic missile, multiple independently targeted reentry vehicles, superhard silos and offensive forces
04 p0760 A70-14501

Mission objectives and technical realization of AZUR research satellite and Symphonie communication satellite
04 p0763 A70-15303

Ground station location, equipment and function for radio communication with German research satellites, noting NASA and ESRO cooperation
04 p0664 A70-15304

Illegal aircraft route diversion by unauthorized persons, discussing air piracy suppression efforts of various international bodies
05 p0960 A70-16539

European role in future INTELSAT Organization operational rules and principles covering proprietary, financial and voting procedures
06 p1184 A70-17579

Legal status of space flights in view of physical effects on atmosphere and near-earth space, discussing international and Polish air traffic statutes
07 p1425 A70-18783

Azur satellite program, describing NASA-German cooperative effort
[DGLR-69-052] 07 p1391 A70-18815

Aircraft noise reduction certifications program by tripartite draft plan
07 p1426 A70-18876

Legal implications of national flags on moon as symbols of national sovereignty, considering spacecraft and lunar colonies legal status by international agreements
07 p1426 A70-18877

International law applicability to national activities regarding exploration and use of space, examining Space Treaty and UN resolutions
07 p1426 A70-18879

Space role in competition between U.S. and U.S.S.R. since August 1957, discussing armament control agreements regarding space
07 p1426 A70-18882

Questions concerning Warsaw convention and supplementary agreements signing, considering membership eligibility and factors for general international laws evolution
07 p1427 A70-18883

International data exchange guide for solar-terrestrial physics, including listing of stations active during International Years of Active Sun
07 p1377 A70-18937

Instrumental space flight internationalization considering manned flight and military obstacles, suggesting scientific and political steps
07 p1427 A70-19097

ICAO Juridical Council criteria for nonnational aircraft registration, discussing international airlines recourse to Article 77 of Chicago Convention
07 p1428 A70-19105

UN treaty based on U.S.-U.S.S.R.-UK agreement banning nuclear arms in space and establishing international law covering space exploration
07 p1428 A70-19106

AEROS satellite A2 launching to investigate aeronomic processes in outer atmospheric layers, discussing scientific research program, mission data, satellite and ground station equipment
[DGLR-69-050] 07 p1393 A70-19149

Peaceful uses of outer space, discussing committee reports and recommendations, direct broadcast satellites, administrative and financial implications, etc
07 p1428 A70-19688

U.S. Civil Aeronautics Board policy in cooperative agreements involving foreign airlines, highlighting significant cases
08 p1600 A70-20578

Management planning for French-British Martel/Missile Antiradar et Television project, emphasizing tasks of government agencies and contractors
08 p1601 A70-21038

World air transport system in 1970s, analyzing industry economic performance, discussing fares, rates, technological developments, passenger and air freight increases, etc
09 p1792 A70-22332

International aircraft engine industry management in Europe, discussing cooperation, corporations, U.S. competition and structural changes
09 p1792 A70-22339

Upper atmosphere research by U.S.S.R. mass spectrometers onboard French rocket probes, discussing design, payloads and equipment tests
09 p1766 A70-22658

Worldwide telephone network optimum interoperation including communication satellites complementation
10 p1834 A70-24328

Civil aviation satellites for aircraft communication, navigation and traffic control, discussing technical, political and administrative problems
10 p1842 A70-24974

Franco-German telecommunication satellite Symphonie mission objectives and system design
[AIAA PAPER 70-406] 11 p1996 A70-25401

Terrestrial interface at SPADE terminals for converting international telephone exchange differences into common signaling format
[AIAA PAPER 70-413] 11 p1997 A70-25407

Initial Defense Communication Satellite Program/augmentation satellite design and mission, on-board communications equipment, control subsystems, American-British cooperation, etc
[AIAA PAPER 70-492] 11 p2121 A70-25449

Satellite video-telephone systems promoting economic growth in developing nations through linkage with developed nations advanced centers
[AIAA PAPER 70-474] 11 p2000 A70-25455

Canada/U.S. scientific sounding rocket program, describing facilities and projects at Churchill Research Range
11 p2032 A70-26292

Italian Sirio project, describing SHF propagation and communication, cosmic ray and confined plasma experiments
11 p2011 A70-26604

European company for providing and operating European application satellite systems (EUROSAT), discussing organization, tasks and financial structure
12 p2335 A70-27469

International safety standards for SST airworthiness
12 p2161 A70-27599

Oceanographic potential of spacecraft, discussing synoptic scanning, International Decade of Ocean Exploration, etc
12 p2225 A70-27746

Article 9 of 1944 Chicago treaty in view of prohibited air navigation area established by Spain around Gibraltar 11 April 1967
13 p2523 A70-28824

European Panavia 100/200 two engine variable wing military aircraft, noting prototype design, use and production sharing
13 p2347 A70-29051

German-French jet aircraft trainers, discussing Alpha Jet TA 501, E 650 Eurotrainer and VF T 291 flight characteristics
13 p2347 A70-29052

Signal decoder for barium USA Germany (BUG) project command reception system, discussing Ba ion cloud propagation and expansion along geomagnetic field
13 p2367 A70-29557

Book on aerospace law covering legal status of space and spacecraft use in scientific research and telecommunications, international cooperation, etc
14 p2667 A70-30375

- International cooperation in military aviation emphasizing cost effectiveness in R and D, production and export prospects
14 p2669 A70-30939
- International airline collaboration in engineering and maintenance for savings in initial and operational costs of aircraft fleets
14 p2669 A70-30940
- International cooperation in global meteorological network, outlining World Weather Watch
14 p2670 A70-31140
- Scientific satellites history, projects, technology, coordination and international collaboration
14 p2655 A70-31146
- Report to COSPAR on ESRO space research /1969/ covering ESRO 1 second flight model, sounding rockets, and sun- and star-pointing rockets development, etc
15 p2829 A70-31705
- Report to COSPAR on space research in Canada, covering Alouette satellites, ISIS I, international cooperation, etc
15 p2829 A70-31708
- Report to COSPAR on Indian space research describing organizational structure, facilities, experiments and international cooperation
15 p2830 A70-31715
- International Aeronautical Federation space records, discussing record classification for suborbital, earth orbital and lunar and planetary missions
15 p2831 A70-32245
- American-German solar probe HELIOS mission parameters for interplanetary and close proximity solar research, discussing spacecraft building and launching
15 p2801 A70-32281
- Outer space exploration and utilization, analyzing 1967 UN treaty provisions from standpoint of war potential inherent in space stations existence
16 p3003 A70-33100
- German-American HELIOS solar probe for solar wind, interplanetary magnetic field and cosmic rays
16 p2987 A70-34343
- Variable sweep high thrust-weight ratio multirole combat aircraft /MRCA/, discussing British- French cooperation, development programs and requirements
17 p3017 A70-34916
- Moon legal status, discussing territorial sovereignty, peaceful uses, UN Resolutions and Space Treaty, rule of occupation, etc
17 p3200 A70-35323
- Space law treaties and UN programs
17 p3200 A70-35324
- Legal problems of space telecommunications, discussing world juridical regime, United Nations work and satellite systems broadcasting
17 p3201 A70-35777
- International norms establishment for direct TV broadcast by satellites
17 p3201 A70-35780
- Legal aspects of telecommunications by satellite systems, discussing international organization, Intel-sat integration and direct broadcasting
17 p3202 A70-35781
- Juridical structure, risks and control of satellite telecommunication ensuring equality of nations
17 p3202 A70-35782
- Liability for damages by space objects, taking into account states and international organizations
17 p3202 A70-35783
- International organizations participation in convention on liability for damage caused by launching of objects into outer space
17 p3202 A70-35784
- Juridical condition of earth orbiting space stations, discussing term definitions in treaty on outer space
17 p3202 A70-35785
- Juridical status and sovereignty of rocket launching and cosmic stations in international law
17 p3202 A70-35786
- Registration procedure for space exploration objects
17 p3202 A70-35788
- Treaty on principles governing activities of states in exploration and use of outer space, appraising various provisions
17 p3173 A70-35792
- Meteorites and celestial products legal status with respect to rights of property
17 p3173 A70-35793
- Lunar and other celestial bodies natural resources, discussing need for international Space Resources Agreement
17 p3203 A70-35794
- Regulations existence and application to exploitation of resources in celestial bodies
17 p3203 A70-35798
- International Civil Aviation Organization /ICAO/ work on bird hazard reduction, including aircraft airworthiness specifications, bird data dissemination, etc
18 p3349 A70-35997
- Earth resources survey satellite programs, examining aspects of international participation
18 p3349 A70-36297
- NASA program for international cooperation in space involving developing and advanced nations, discussing television instruction for India, resource surveys, etc
18 p3349 A70-36514
- European participation in American space program, considering space station, shuttle and tug
19 p3531 A70-37379
- International civil aviation, discussing ICAO functions, airports and terminal facilities problems
19 p3533 A70-37748
- IATA policy on future ATC development, discussing controlled airspace, communications and radar requirements
19 p3555 A70-38630
- IFALPA views on ATC services, emphasizing aircraft approach spacing in North Atlantic airways
19 p3467 A70-38632
- Earth Resources Satellites political background, investigating international implications
20 p3739 A70-39060
- ERTS programs status and prospects from international utility viewpoint
20 p3739 A70-39064
- Earth Resources Technology Satellite program and international participation, taking into account UN involvement in outer space
20 p3741 A70-39796
- Global integrated communications satellite system, discussing International Telecommunication Union regulatory functions, etc
21 p3955 A70-40625
- Monograph on communicating by satellite covering INTELSAT system design, pricing, procurement, broadcasting, international community responsibilities, etc
21 p3955 A70-40739
- Post Apollo space research, discussing Saturn Workshop /Skylab/, Nerva nuclear rocket engine and international cooperation
21 p3956 A70-41496
- British government technological partnership with domestic industry and other countries
21 p3956 A70-41892
- European participation in U.S. space projects, discussing economics, space shuttles and tugs and earth orbital space station
22 p4126 A70-43407
- European avionics role in Post Apollo program, noting space shuttles, space tugs, space stations and modules
22 p3999 A70-43501
- Management organization of European operational application satellite systems, concerning interurban telecommunication and air traffic control
22 p4127 A70-43502
- U.S. aerospace industry participation in European Application Satellites Program
22 p4127 A70-43506
- European-U.S. cooperation in shuttle and space station program, noting experience in unmanned systems
22 p4127 A70-43508
- European cooperation possibilities in future NASA space programs
22 p4127 A70-43510
- Orbital international laboratory and space sciences - Conference, Cloudcroft, New Mexico, September 1969
22 p4107 A70-43626
- Orbital laboratories and international cooperation, discussing national and foreign viewpoints
22 p4128 A70-43631
- International cooperation in space exploration, UN role and benefits for nonspace nations
22 p4128 A70-43632
- European Space Research Organization programs, stressing international cooperation
22 p4128 A70-43633
- Manned orbital laboratories, discussing need for international cooperation
22 p4128 A70-43634
- International space program cooperation, discussing NASA projects, Apollo 11 flight and European and Soviet programs
22 p4129 A70-43655
- International photographic planetary patrol network, discussing filmstrips of Mars and Jupiter using blue, green and red filters
23 p4242 A70-44262
- European space policy decisions regarding continuation of existing programs and participation in U.S. post-Apollo programs
23 p4285 A70-44325
- Orbital space station utilization planning as international laboratory, discussing industry role, experiment program goals, etc
23 p4260 A70-44650
- European space organization as intergovernmental agency developing industry, scientific and technological research, application satellites and boosters
23 p4285 A70-44652
- Space treaty obligations concerning orbital laboratories, discussing legal conflicts and establishment of international organization for protection of common interests
23 p4286 A70-44673
- International earth orbital space laboratory program, discussing objectives, management, stations, shuttles, tugs, tracking, communication, data distribution network, etc
23 p4262 A70-44687
- International Space Research Organization /ISRO/ for space operations, considering political, economic, technical and scientific requirements
23 p4286 A70-44688
- Helios solar probe for automated spacecraft exploration of interplanetary space near sun, considering design, mission planning and U.S.-German cooperation
23 p4245 A70-44689
- Space vehicle for interstellar flight, discussing propulsion concepts, mission implications and international cooperation
23 p4254 A70-45011
- Space systems supporting international air transportation growth, discussing UHF satellite R and D programs on beam antennas
24 p3372 A70-45870
- [SAE PAPER 700760]
International participation in U.S. post-Apollo program involving reusable space transportation system and multipurpose space station
24 p4431 A70-46123
- ### INTERNATIONAL GEOPHYSICAL YEAR
- Earth satellites magnetic survey contributions to World Magnetic Survey project /WMS/, discussing international reference standards and magnetic mapping
01 p0075 A70-10595
- Catalog of solar radio bursts recorded at 208 MHz during IGY and IQSY
08 p1570 A70-20843
- Asian zone solar daily and storm time ionospheric disturbance variations synoptic study during IGY-IGC period
10 p1872 A70-23822
- IGY and IQSY aurora observations, discussing geographic distribution of observations, diurnal variation of aurora frequency, solar activity effects, etc
10 p1884 A70-25261
- Pc-periods dependence on geomagnetic latitude during active sun years, using IGY data
13 p2395 A70-28943
- 5577 A /OI/ airglow emission diurnal variations during IGY by normalization method, observing seasonal effects
14 p2578 A70-31239
- Meridional mean eddy transport of enthalpy in Southern Hemisphere during IGY, comparing results with Northern Hemisphere
20 p3661 A70-39143
- Universal time control of south polar F layer during IGY attributed to low energy electron precipitation, comparing IGY and recent satellite data
21 p3818 A70-41101
- ### INTERNATIONAL LAW
- #### NT SPACE LAW
- International agreement to govern hovercraft use covering application range, registry, rights, owner or user responsibility, leasing and goods transportation
01 p0220 A70-10373
- Juridical measures against air piracy, discussing civil aviation legislation, unlawful acts aboard aircraft and international agreements
01 p0220 A70-10374
- Party autonomy application to standardized international air transport contracts, discussing international treaties, law court judgments and literature
02 p4040 A70-12267
- Illegal in-flight route diversions of aircraft, discussing international juridical means of relief
05 p0960 A70-16535
- Illegal aircraft seizures inspired by political motives, discussing suppression, air traffic volume effects, Tokyo Convention juridical decisions, etc
05 p0960 A70-16537
- Air piracy, maritime law applicability, definition, internal laws and French law
05 p0960 A70-16538
- Montreal agreement of 1966 approved by CAB, considering air carrier liability
07 p1426 A70-18878
- Legal and national justification for limitation in air freight carrier liability taking into consideration Warsaw convention and legal decisions
07 p1426 A70-18880
- Air carriers legal liability, considering case decided in London involving Warsaw convention text
07 p1426 A70-18881
- Questions concerning Warsaw convention and supplementary agreements signing, considering membership eligibility and factors for general international laws evolution
07 p1427 A70-18883
- Inclusive Tour /IT/ Charter definition within framework of commercial air traffic, discussing concepts of scheduled and nonscheduled air services
07 p1427 A70-18885

International air traffic jurisdictional area of German aeronautical law regarding aircraft equipment regulations and residents

07 p1427 A70-18886

ICAO Juridical Council criteria for nonnational aircraft registration, discussing international airlines recourse to Article 77 of Chicago Convention

07 p1428 A70-19105

UN treaty based on U.S.-U.S.S.R.-UK agreement banning nuclear arms in space and establishing international law covering space exploration

07 p1428 A70-19106

Peaceful uses of outer space, discussing committee reports and recommendations, direct broadcast satellites, administrative and financial implications, etc

07 p1428 A70-19688

International legal and political aspects of earth resource surveying by satellite remote sensors, considering U.S. policy

[AIAA PAPER 70-331] 09 p1793 A70-22862

Article 9 of 1944 Chicago treaty in view of prohibited air navigation area established by Spain around Gibraltar 11 April 1967

13 p2523 A70-28824

Soviet book on legal aspects of artificial satellites for meteorology and radio communication purposes

14 p2668 A70-30632

Liability for damages due to supersonic flight sonic booms, discussing pertinent provisions in Dutch and international law

19 p3553 A70-37561

Air freight carrier liabilities in passenger transportation international regulations, noting conflicting interpretations

19 p3553 A70-37562

Book on law relating to activities of man in space covering liability, space communication, international organization, military implications, etc

19 p3553 A70-37676

International Telecommunication Union (ITU) legal recommendations on radio spectrum use, interference and frequency assignment problems

20 p3585 A70-39411

Juridical problems in satellite direct TV broadcasting, discussing regulation proposals submitted to UN and educational applications

24 p4430 A70-45596

INTERNATIONAL PRACTICAL TEMPERATURE

U TEMPERATURE SCALES

INTERNATIONAL QUIET SUN YEAR

Cosmic ray survey measurements during IQSY reduced to common atmospheric depth, determining attenuation coefficients of neutron and muon monitors

01 p0167 A70-10230

Physical processes responsible for conjugate point phenomena involving particles and waves in magnetosphere and IQSY observations

01 p0075 A70-10598

IQSY 27-day recurrence sequence for 1964 solar and terrestrial activity, considering geomagnetic, auroral and ionospheric disturbances correlation with phase

05 p0841 A70-16646

Backscatter observations of F region field-aligned irregularities during IQSY, discussing diurnal variations of echoes

06 p1059 A70-18539

Magnetic activity in Antarctica during IQSY, plotting space-time characteristics of perturbations

07 p1268 A70-19462

Catalog of solar radio bursts recorded at 208 MHz during IGY and IQSY

08 p1570 A70-20843

IGY and IQSY aurora observations, discussing geographic distribution of observations, diurnal variation of aurora frequency, solar activity effects, etc

10 p1884 A70-25261

Geomagnetic short period oscillations occurrence frequency during IQSY, discussing dependence on magnetic activity and time of day

14 p2572 A70-30242

Ionospheric cosmic noise absorption diurnal and seasonal variations at Alma-Ata during IQSY, noting chromospheric flares effects

18 p3306 A70-36089

Magnetic activity in Antarctica during IQSY, plotting space-time characteristics of perturbations

18 p3250 A70-36936

Meteor activity during IQSY by radar observations at 7.6 m wavelength

19 p3514 A70-37654

Whistler density variability correlated with solar activity during IQSY

19 p3462 A70-37924

Wind motions from meteor trails observation during IQSY, tabulating amplitudes and phases of constant, diurnal, semidiurnal and 8-hr components

19 p3526 A70-38788

Cosmic ray beta neutron component barometric coefficients planetary distribution during IQSY, establishing latitude dependence for mountain and sea level equations

20 p3697 A70-39292

Geomagnetic short period oscillations occurrence frequency during IQSY, discussing dependence on magnetic activity and time of day

24 p4332 A70-46317

INTERNATIONAL RELATIONS

NT INTERNATIONAL COOPERATION

International law applications to space, analyzing Space Treaty provisions

12 p2336 A70-27773

Lunar spaceports for military uses from legal viewpoint, considering Space Treaty

12 p2336 A70-27774

INTERNATIONAL SATS FOR IONOSPHERIC STUDY

U ISIS SATELLITES

INTERNATIONAL TRADE

Export market research for military aircraft

19 p3555 A70-38618

Airport planning for air transportation in underdeveloped nations, discussing economic, financial, technical and operational factors

[AIAA PAPER 70-1268] 24 p4323 A70-45926

INTERNUCLEAR PROPERTIES

Heitler-London curves calculation for electron exchange in H-H collisions as function of internuclear distance and velocity

24 p4381 A70-45252

INTERPLANETARY COMMUNICATION

Earth to planet radar signal time delay in general relativity expressed in relativistic spherical polar coordinates of earth and planet

15 p2806 A70-32801

INTERPLANETARY DUST

NT METEOROID DUST CLOUDS

NT ZODIACAL DUST

Libration clouds reality possibility from satellite dust counting experiments

03 p0572 A70-13819

Interplanetary dust measurements near earth compared to theories predicting dust characteristics, discussing concentration, flux, impact rate and solar radiation pressure

04 p0749 A70-14619

F corona heliocentric dust cloud model to account for temperature variations with particle size and optical properties, computing thermal emission

08 p1571 A70-20907

Circumstellar system crushing processes described by integrodifferential equations, deriving particle size distribution of fragments in interplanetary space

21 p3889 A70-41148

INTERPLANETARY FLIGHT

NT GRAND TOURS

High energy propulsion module utilizing F/H fuels for planet flyby, orbiter mission and injection of 24-hr satellites, discussing design and equipment

[JGLR-69-18] 04 p0736 A70-15176

Interplanetary midcourse velocity correction schedules optimization, discussing timing equations modifications, mission simulation and role of earth based radar

09 p1759 A70-22760

Physiology of hibernation and hypothermia, noting potential use for metabolic need reduction during long interplanetary flight

10 p1943 A70-24757

Interstellar flights, discussing human limitations, star systems with habitable planets and possible galactic communities

10 p1943 A70-24759

Evaluation technique for astronautics subsystems in automated spacecraft designed for interplanetary missions, considering operation times, navigation updating and midcourse correction

[AIAA PAPER 69-882] 11 p2079 A70-26118

Orbital laboratories role in planetary manned exploration, discussing flyby missions, flyby/lander modes, periodic orbits, etc

12 p2314 A70-27748

Planetary trajectory handbooks for mission and system analysis covering opportunities for Mercury, outer planets and Mars, contour charts, etc

13 p2486 A70-28525

Manned planetary flight systems engineering, discussing feasibility, objectives, propulsion, transplanet injection via geospace shuttle station, energy requirements for various synodic modes

[AAS PAPER 70-037] 17 p3155 A70-34778

Multiorbit injection earth departure technique for optimal thrust-weight ratio in manned interplanetary missions using NERVA engine

[AAS PAPER 70-039] 17 p3175 A70-34780

Future manned planetary missions with reusable nuclear shuttles, comparing operating modes in terms of propellant requirement, costs, complexity, etc

[AAS PAPER 70-040] 17 p3155 A70-34781

Unmanned flyby missions to Mercury in 1973-1990, discussing scientific objectives and payloads

[AAS PAPER 70-027] 17 p3155 A70-34798

System analysis to determine orbital parameters influence on mission scientific objectives under engineering constraints, using value function

[AIAA PAPER 68-1052] 17 p3172 A70-35648

Orbiting space stations and interplanetary flights, discussing spacecraft design, facilities, Mariner probes, etc

19 p3533 A70-38487

Power loss due to cumulative meteoroid impacts on solar cells during extended planetary missions, investigating hypervelocity particle impacts into glass

[AIAA PAPER 70-1139] 20 p3567 A70-40210

Planetary probes, orbiting space stations and manned spacecraft in interplanetary flights, discussing Mariner, Gemini and Apollo reentry and Venus landing

22 p4109 A70-42313

Interplanetary periodic orbits and flyby dates for multiple earth-Venus swingby missions, describing various iterative solutions for trajectory

[AIAA PAPER 69-931] 23 p4243 A70-44508

Interplanetary mission propellant reduction by using earth-moon-sun gravity field properties, discussing swingby techniques, low energy trajectories, etc

23 p4244 A70-44607

Travel time for trips to Neptune, calculating earth gravitational field escape hyperbola and waiting time before return

23 p4245 A70-44653

INTERPLANETARY GAS

Interplanetary plasma flow simulation around earth magnetosphere and planets not considering initial conditions influence

01 p0172 A70-11488

Compressible gas flow problem in point body gravitational field solved with reference to sun and interstellar gas

01 p0172 A70-11489

Hydrodynamic approximation to interplanetary gas motion influenced by solar flare caused perturbations

01 p0192 A70-11586

Interplanetary plasma inhomogeneity size, shape and spatial orientation and drift velocity and direction determined from radio telescope data

03 p0565 A70-13231

Unsteady state and transit time analysis of geoeffective interplanetary plasma flux observed near earth causing magnetospheric storm of 17-19 April 1965

04 p0683 A70-15736

Magnetic field fluctuations of interplanetary plasma, considering anisotropic temperature instabilities

05 p0915 A70-16750

Gaseous spheres gravitational stability in proper field, considering convection and radial perturbations effects

07 p1383 A70-19408

Integral methods of obtaining electron density profile of planetary ionospheres and interplanetary gases

07 p1388 A70-20160

Inhomogeneities in interplanetary plasma formation due to instability of electron flows moving along interplanetary magnetic field lines of force

08 p1570 A70-20845

Interplanetary density distribution of cold interstellar origin hydrogen dependent on solar EUV flux, considering interaction with solar wind protons

08 p1562 A70-21401

Interplanetary plasma inhomogeneity size, shape and spatial orientation and drift velocity and direction determined from radio telescope data

08 p1580 A70-21664

Type I comet tails orientations dispersion attributed to nonradial plasma waves and discontinuities in interplanetary gas, calculating solar angular momentum loss rate

10 p1947 A70-24987

Antimatter motion in solar system and earth atmosphere, discussing vaporization and annihilation energy in collisions with interplanetary gas atoms

11 p2119 A70-26793

Interplanetary and magnetospheric plasma structures experiments and theory

12 p2298 A70-27060

Unsteady state and transit time analysis of geoeffective interplanetary plasma flux near earth causing magnetospheric storm of 17-19 April 1965

14 p2575 A70-30820

Interplanetary plasma torque due to temperature and pressure anisotropy, considering solar wind angular velocity and sun angular momentum

20 p3712 A70-40423

Neutral interplanetary particle impact ionization of atmosphere, discussing density of neutral interstellar media near solar system

22 p4106 A70-43291

INTERPLANETARY MAGNETIC FIELDS

Interplanetary magnetic field sectoral structure effect on diurnal cosmic ray intensity and geomagnetic field, noting field direction influence

01 p0172 A70-11525

Solar mean magnetic field relation to sector structure of interplanetary magnetic field, discussing Explorer 33 and 35 observations

02 p0371 A70-12206

HEOS-1 satellite development for ESRO to investigate interplanetary magnetic fields, cosmic radiation

- tion, solar wind outside magnetosphere and earth shock wave
02 p0382 A70-12646
- Interplanetary field influence on auroral radio absorption, considering sector structure of solar wind
03 p0476 A70-13915
- Interplanetary magnetic field measurements from Mariner and OGO satellites at various paths, regions and intervals, finding dominant polarity effect dependent on sun latitude
03 p0575 A70-13980
- Geomagnetic tail observations by Pioneer 8 at 500 earth radii, analyzing time-averaged magnetic field data
03 p0575 A70-13983
- Interplanetary magnetic field during solar cycle rise and minimum based on Explorer 33 magnetometer measurements
03 p0575 A70-13999
- Magnetograms by Venera 4 and Mariner 5 compared to determine interplanetary magnetic field nature in Venus proximity
04 p0744 A70-14438
- Galactic cosmic rays scattering by solar wind magnetic field fluctuations, considering energy and momentum transfer
04 p0739 A70-14596
- Interplanetary magnetic field fluctuations stimulated by lunar wake, using Explorer 33 satellite measurements
04 p0753 A70-15122
- Turbulent-plasma electrons ballistic effects on solar wind magnetic field fluctuations in lunar vicinity
04 p0753 A70-15123
- Anomalous Doppler shift interaction between positive ions and right-hand polarized EM waves propagating at small angle to interplanetary magnetic field
05 p0905 A70-15761
- Cosmic ray intensity preceding Forbush effects as function of chromospheric flares solar longitude and solar wind velocity
05 p0903 A70-16730
- Relativistic solar proton propagation fluctuation effects in interplanetary magnetic field during cosmic ray intensity increase
05 p0903 A70-16731
- Cosmic ray angular distribution spectrum and interplanetary magnetic field properties determined from semidiurnal cosmic ray variations data
05 p0903 A70-16732
- Magnetic field fluctuations of interplanetary plasma, considering anisotropic temperature instabilities
05 p0915 A70-16750
- Solar cosmic rays diffusion enclosure in interplanetary space magnetic boundary suggested from balloon, satellite and ground observations of solar flare neutron component
05 p0904 A70-16753
- Pc 2-4 geomagnetic pulsations abrupt disappearance on global scale ascribed to magnetosphere boundary stabilization, noting interplanetary magnetic field role
05 p0843 A70-16766
- Lunar interior electrical conductivity estimated using lunar interaction with solar wind and interplanetary electric and magnetic fields
06 p1153 A70-18544
- Lunar surface magnetometer data interpretation by analysis of moon motion relative to interplanetary magnetic field spatial irregularities, using lunar electrical conductivity models
07 p1378 A70-18974
- Solar flare protons motion in sun radial magnetic field, considering protons interaction with interplanetary field inhomogeneities
07 p1366 A70-19427
- Solar wind velocity anisotropy effect on interplanetary magnetic field inhomogeneity
07 p1366 A70-19443
- Solar wind structural characteristics determination from cosmic ray variations in interplanetary medium, considering interplanetary magnetic field structure and spatial orientation
07 p1372 A70-20337
- Inhomogeneities in interplanetary plasma formation due to instability of electron flows moving along interplanetary magnetic field lines of force
08 p1570 A70-20845
- Lunar limb weak solar wind shock due to conducting crust-interplanetary magnetic field interaction
09 p1764 A70-23485
- Satellite solar wind observations concerning interplanetary magnetic field direction and strength, proton distribution, solar wind velocity, density and direction
10 p1935 A70-25286
- Polar ionospheric current and interplanetary magnetic field directions related from mean diurnal values of solar wind velocity
11 p2044 A70-25551
- Solar wind magnetic field power spectra and plasma velocity, discussing turbulence, viscosity and dissipation
11 p2106 A70-26770
- Interplanetary magnetic field intensity and geomagnetic activity level correlation with 27-day solar activity cycle based on Venera 4 and Mariner 5 data comparison
12 p2310 A70-28263
- Magnetograms by Venera 4 and Mariner 5 compared to determine interplanetary magnetic field nature in Venus proximity
13 p2485 A70-28463
- Monograph on polar aurora with emphasis on solar wind and interplanetary magnetic fields, discussing substorms, particle acceleration in current sheet, etc
13 p2395 A70-28983
- Statistical heliographic latitude dependence of dominant polarity of interplanetary magnetic field, using photospheric synoptic chart
13 p2492 A70-29195
- Pioneer 6-9 low magnetism spacecraft for interplanetary magnetic field observation
13 p2507 A70-30046
- Low and high apogee satellite and rocket magnetometers for space measurements, discussing self oriented fluxgate, proton, quantum cesium and three component types
13 p2415 A70-30047
- Solar wind effect on structure of magnetic field in magnetosphere and interplanetary space, noting interaction with moon
13 p2498 A70-30051
- Interplanetary magnetic field flux relationship to Kp index of magnetic activity
14 p2570 A70-30221
- German-American HELIOS solar probe for solar wind, interplanetary magnetic field and cosmic rays
16 p2987 A70-34343
- Solar flare protons motion in sun radial magnetic field, considering protons interaction with interplanetary field inhomogeneities
18 p3309 A70-36901
- Solar wind velocity anisotropy effect on interplanetary magnetic field inhomogeneity
18 p3309 A70-36917
- Geomagnetic activity relation to large scale variations in interplanetary magnetic field and solar wind deformation velocity, using satellite and space probe observations
19 p3491 A70-37304
- Magnetic field variations and structures in interplanetary space relationship to sun, discussing photospheric field lines random walk transport
19 p3494 A70-37480
- Interplanetary magnetic field during solar particle event of 25 February 1969 from Heos 1 measurements
19 p3495 A70-37500
- Interplanetary magnetic field measurements by Pioneer 8 during 25 February 1969 solar activity, discussing geomagnetic storms, cosmic rays, shock fronts and ionospheric disturbances
19 p3513 A70-37501
- Interplanetary magnetic field large scale structure from cosmic ray intensity secular variations during solar activity cycle
20 p3696 A70-39276
- High energy charged particles equations of motion in quiet interplanetary magnetic field for primary cosmic ray distribution, calculating diurnal and semidiurnal variations
20 p3698 A70-39297
- Interplanetary magnetic field structure, using solar wind model accounting for solar rotation
20 p3704 A70-39474
- Steady state magnetic and electric fields in magnetosheath by linear superposition of field vectors, using axisymmetric velocity function from gas dynamics
21 p3815 A70-41063
- Polar ionospheric current and interplanetary magnetic field directions related from mean diurnal values of solar wind velocity
21 p3819 A70-41301
- Low noise FET amplifier for satellite magnetometer, measuring interplanetary fields
21 p3799 A70-41923
- Helios solar probe magnetic field measurements, discussing magnetometer systems, interplanetary magnetic field implications, shock waves, magnetic storms, etc
21 p3923 A70-42172
- Interplanetary magnetic field directional variation effect on polar caps geomagnetic field, discussing polarity reversals
22 p4022 A70-43285
- Geomagnetic variations origin from satellite space probe data, correlating DP 1 activities to interplanetary magnetic field variations
22 p4022 A70-43286
- Interplanetary magnetic field and plasma structure observed with Mariners magnetometer, noting 27-day deviations from Parker spiral model
23 p4239 A70-43827
- Interplanetary magnetic field inhomogeneities structure from galactic cosmic rays intensity fluctuations observation
23 p4237 A70-44053
- Geomagnetic activity dependence on angle between earth-sun and hourly averaged vectors of interplanetary magnetic field
24 p4405 A70-45523
- Interplanetary magnetic field flux relationship to Kp index of magnetic activity
24 p4331 A70-46296

INTERPLANETARY MEDIUM

- NT INTERPLANETARY DUST
- NT INTERPLANETARY GAS
- NT METEOROID DUST CLOUDS
- NT ZODIACAL DUST
- Quasar 3C 273 scintillation intensity, considering role of interplanetary plasma inhomogeneities
01 p0174 A70-10199
- Low energy proton flux in neighborhood of Moon measured by Luna 12 satellite indicating magnetized plasma region effect on burst
01 p0172 A70-11493
- Mariner 2 measurements of geomagnetic field and interplanetary plasma parameters, analyzing interaction between interplanetary medium and magnetosphere during decreased solar activity
01 p0192 A70-11520
- Pulsar distance and distribution estimation, considering galactic spiral structure and nature of interstellar medium
02 p0371 A70-12201
- Low energy solar proton flux propagation model in interplanetary medium based on satellite data beyond earth magnetosphere
04 p0737 A70-14434
- Radio sources structure observations of Arecibo Ionospheric Observatory, discussing interplanetary scintillations of galaxies and quasars
06 p1138 A70-17216
- Galactic cosmic rays intensity long term modulation, studying roles of solar corona, solar wind and interplanetary electromagnetic field
07 p1369 A70-20075
- Diffraction pattern drift velocity increase with temporal frequency of Fourier components by dispersion analysis of interplanetary scintillation, noting solar wind structure
07 p1388 A70-20076
- Solar wind structural characteristics determination from cosmic ray variations in interplanetary medium, considering interplanetary magnetic field structure and spatial orientation
07 p1372 A70-20337
- Low energy proton distributions in interplanetary medium, correlating intensities with main-phase geomagnetic storm development
08 p1562 A70-21376
- Solar corona and interplanetary plasma structure and dynamics, calculating solar wind velocity as function of distance from sun
08 p1576 A70-21397
- Interplanetary medium kinetic equations to limit ion temperature anisotropies in solar wind, discussing Coulomb collisions and ion-cyclotron instability effects
11 p2105 A70-26561
- Low energy electron flux as interplanetary radiation primary component, considering data from IMP-1 observations
12 p2292 A70-27383
- Interplanetary shock waves layer formation in collisionless medium, using bulk transport parameters for dissipation requirement
12 p2308 A70-27885
- Low energy solar proton flux propagation model in interplanetary medium based on satellite data beyond earth magnetosphere
13 p2475 A70-28459
- Solar cosmic rays interaction with interplanetary shock waves, discussing chromospheric eruptions
13 p2476 A70-28959
- Low energy solar flare electrons scatter-free propagation through interplanetary medium, considering rise, decay and travel times
13 p2477 A70-29194
- Bow shock associated hydromagnetic waves generation in upstream interplanetary medium, constructing model in terms of ion cyclotron resonance
14 p2631 A70-30359
- Atomic hydrogen distribution in upper atmosphere and solar system obtained during spin operation of OGO 5 with Lyman alpha photometer
15 p2798 A70-31655
- Cosmic ray radial gradients and anisotropies, describing behavior in interplanetary medium
15 p2795 A70-32623
- Laboratory experiments applicability to interplanetary plasma physics, describing simulations of solar wind interactions, magnetosphere, collisionless shock waves, etc
17 p3164 A70-35123
- Interplanetary plasma disturbances in Venus proximity from Venera measurements
18 p3312 A70-36172
- Low energy solar and galactic cosmic rays propagation in interplanetary medium observed by Zond and

INTERPLANETARY MONITORING PLATFORM

Venus space probes, discussing shock waves retardation
19 p3493 A70-37475

Interplanetary shock wave of 26 February 1969, discussing association with solar flares
19 p3513 A70-37517

Quiet time intensity increases and long term solar modulation of interplanetary low energy electrons, using IMF observations
19 p3502 A70-38097

Interplanetary cosmic ray positrons energy spectral component with origin different from interstellar mesons decay
19 p3502 A70-38098

Interplanetary medium energetic electrons and isotopes measurement, discussing spectrometer electronics of IMP H and J
21 p3825 A70-41000

Cosmic ray energy loss in interplanetary medium, discussing solar wind effects on low energy particles
21 p3883 A70-42111

Comet Schwassmann-Wachmann 1 brightness variations due to interplanetary shock waves in solar wind
22 p4097 A70-42475

Interplanetary atomic hydrogen density distribution from Lyman alpha scattering calculation, explaining background radiation anisotropy detection by Vela 7 satellite
24 p4403 A70-45392

INTERPLANETARY MONITORING PLATFORM

U IMP

INTERPLANETARY NAVIGATION

Optical approach navigation experiment on 1969 Mariner mission to Mars demonstrating accuracy potential of spacecraft-based measurement
[AIAA PAPER 70-70] 06 p1103 A70-18152

Navigational accuracy of two way Doppler tracking of interplanetary spacecraft during heliocentric and planetary encounter trajectory phases
[AIAA PAPER 69-899] 07 p1331 A70-19727

Onboard navigational requirements for future planetary missions, discussing major subsystems
13 p2448 A70-28701

Deep Space Network (DSN) data accuracy limitations relation with ability to determine orbit of probe, examining improvements after Mariner 2 and trends
13 p2448 A70-28702

Planetary ephemerides accuracy and navigation during interplanetary missions, discussing machine readable ephemerides for outer planets
13 p2448 A70-28703

Spacecraft based data processing stages to perform navigation during outer planet missions
13 p2448 A70-28704

Navigation correction systems for space missions, discussing prelaunch analysis, design and mission operations, hardware, etc
13 p2448 A70-28705

Navigation for planetary orbiter and lander missions, considering orbit insertion, trim corrections and capsule descent for poor planetary gravity field model
13 p2448 A70-28706

Course correction requirements for ballistic grand tours and outer planet missions, considering trajectory disturbances by random nongravitational forces
13 p2448 A70-28707

Navigation instrument geometrical calibration by natural satellites and reference stars during interplanetary flight
[AIAA PAPER 70-1023] 20 p3669 A70-39586

Grand tours navigation system consisting of deep space network radio and onboard TV for future TOPS/Thermoelectric Outer Planet Spacecraft applications
21 p3849 A70-41799

INTERPLANETARY PROPULSION

U INTERPLANETARY SPACECRAFT

R ROCKET ENGINES

INTERPLANETARY SPACE

Interplanetary space investigation by HEOS 1 satellite during maximum solar activity, discussing orbital apogee, mission and technical requirements
01 p0186 A70-11113

Soviet book on physico-technological basis of space research covering near earth and interplanetary environmental factors and effects on spacecraft designs and materials
02 p0360 A70-11693

Cosmic ray protons, He nuclei and electrons solar modulation by betatron deceleration mechanism during interplanetary space passage
02 p0357 A70-12123

Adiabatic invariance of action integral for motion in nonregular fields, explaining charged particles motion through magnetic shock front in interplanetary space
02 p0359 A70-12788

Quiet time primary cosmic ray electron flux and energy spectrum from 10 to 200 Mev in interplanetary space observed byOGO 5 satellite
03 p0553 A70-12902

Large amplitude wave trains in cosmic ray neutron intensity compared with diurnal variations, determining interplanetary space directional distribution from monitor data
03 p0559 A70-13912

Meteoroids average velocity relative to spacecraft determined using sporadic meteor orbital elements data in interplanetary space
04 p0757 A70-15550

Electromagnetic structure of interplanetary space on basis of secondary cosmic ray intensity gradient annual variations as function of earth heliographic latitude
05 p0900 A70-15970

HEOS-A2 project development plan for investigating unexplored interplanetary space in eccentric orbit
05 p0923 A70-16588

Interplanetary plasma flow past earth and planets simulation using kinetic equations
06 p1147 A70-18292

VHF propagation variations relationship to changes in interplanetary plasma associated with interplanetary space sectorial structure rotation
07 p1226 A70-18757

Magnetosphere and interplanetary space diagnostics by micropulsations analysis, discussing geomagnetic cavity boundary, cold plasma density, energetic particles, etc
07 p1264 A70-19191

Solar wind effects on galactic cosmic rays isotropic diffusion and density distribution in interplanetary space in presence of azimuthal asymmetry
07 p1366 A70-19429

Report to COSPAR on Japanese space research including satellite, rocket and balloon observations of ionosphere, magnetosphere, interplanetary space, moon, planets, cosmic rays, etc
15 p2830 A70-31720

Soviet monograph on modulation of cosmic rays in interplanetary space, covering anisotropic diffusion approximation, diffusion equation, Forbush effects energy spectrum, etc
16 p2971 A70-32911

Solar wind effects on galactic cosmic rays isotropic diffusion and density distribution in interplanetary space in presence of azimuthal asymmetry
18 p3309 A70-36903

VHF propagation variations relationship to changes in interplanetary plasma associated with interplanetary space sectorial structure rotation
18 p3229 A70-37101

Solar wind disturbances associated with solar activity observed by spacecraft probing interplanetary space, considering geomagnetic activity classes
19 p3494 A70-37478

Interplanetary plasma observations by Vela satellites in solar wind and plasma sheet of magnetotail during magnetic storm
19 p3410 A70-37490

Proton spectra and time history in interplanetary space during solar flare by satellite observation, investigating particle flux by shock waves
19 p3495 A70-37503

HEOS 1 low energy proton measurements in interplanetary space, discussing particle direction during solar event and anisotropy time history
19 p3495 A70-37505

Solar protons directional and omnidirectional measurements during particle event of 25 February 1969 by Heos 1 spacecraft, indicating particle diffusion in interplanetary space
19 p3496 A70-37506

Large scale electric fields in ionosphere, magnetosphere and interplanetary space, considering further needs for theoretical and observational investigations
22 p4099 A70-42782

Space electric field considered for solar wind plasma drift origin and possible energy source for spacecraft propulsion, estimating intensity on lunar surface
22 p4100 A70-42789

Weak-scattering limit in thin screen model of interplanetary scintillations of radio sources involving solar wind fluctuations at Fresnel scale
22 p4104 A70-42996

Interplanetary plasma electron density inhomogeneities formation explained by instability due to electron stream curvilinearly obtained from spacecraft data
23 p4240 A70-44070

Helios solar probe for automated spacecraft exploration of interplanetary space near sun, considering design, mission planning and U.S.-German cooperation
23 p4245 A70-44689

Lyman alpha radiation scattering intensity during solar radiation period, discussing dependence of interstellar hydrogen density in interplanetary space on solar EUV
23 p4237 A70-44753

INTERPLANETARY SPACECRAFT

NT JUPITER PROBES

NT MARINER SPACE PROBES

NT MARINER 2 SPACE PROBE

NT MARINER 4 SPACE PROBE

NT MARINER 5 SPACE PROBE

NT MARS PROBES

NT PIONEER SPACE PROBES

NT PIONEER 6 SPACE PROBE

NT PIONEER 8 SPACE PROBE

NT PIONEER 9 SPACE PROBE

NT VENERA SATELLITES

NT VENUS PROBES

NT ZOND 3 SPACE PROBE

Advanced reconnaissance electric planetary spacecraft/AREPS/ concept for repeated coverage of Mars or Venus surface, using solar- photovoltaic system
[AIAA PAPER 69-253] 01 p0196 A70-10837

Slow scan TV systems for planetary exploration, discussing sampled vidicon operation, digital encoding, data storage, signal to noise ratio, future design trends, etc
[SMPT PREPRINT 106-3] 02 p0294 A70-11682

Transonic dynamic stability of free flight half angle cones in wind tunnel for high drag planetary entry vehicles, discussing Mars entry trajectories
[AIAA PAPER 69-105] 06 p1154 A70-17164

Electronic packaging and cabling on Capsule System Advanced Development Lander for Mars rough landing
06 p1016 A70-17335

Thermal testing of planetary lander vehicle in vacuum chamber, modeling electronics modules and experiments using resistance heaters
[AIAA PAPER 70-222] 06 p1157 A70-18128

Short duration manned Mars and Venus exploration mission planning with chemical propulsion and Saturn 5 boosters
[AIAA PAPER 70-59] 06 p1147 A70-18238

Navigational accuracy of two way Doppler tracking of interplanetary spacecraft during heliocentric and planetary encounter trajectory phases
[AIAA PAPER 69-899] 07 p1331 A70-19727

NASA future space programs, discussing space shuttle and station, nuclear propulsion, manned Mars landing, unmanned Venus-Mercury probes, etc
09 p1762 A70-23065

Thermoelectric outer planet spacecraft (TOPS) project incorporating adaptable data handling system and self testing and repairing computer with triple redundancy subsystems
11 p1996 A70-25368

Interplanetary space systems, analyzing failure factors to assure reliability
11 p2112 A70-26051

Nuclear pulse propulsion system for manned missions to outer planets of solar system, discussing energy and travel time requirements
11 p2082 A70-26059

Asymmetrical slender planetary entry vehicle roll dynamics, analyzing steady state angular motion
[AIAA PAPER 70-560] 13 p2339 A70-29003

Digital computers for interplanetary spacecraft, comparing centralized and decentralized approaches for implementing onboard functions
[AIAA PAPER 68-840] 14 p2554 A70-30757

Nuclear solid core rocket engine performance for interplanetary orbital launch of spacecraft by multibit injection
[AIAA PAPER 69-535] 14 p2616 A70-30767

Astronomical observations, discussing advantages of human operators on interplanetary spacecraft or Mars
15 p2810 A70-31853

American-German solar probe HELIOS mission parameters for interplanetary and close proximity solar research, discussing spacecraft building and launching
15 p2801 A70-32281

Solar electric spacecraft for interplanetary missions including asteroid belt survey, Jupiter flyby and out-of-elliptic survey
[AIAA PAPER 70-645] 16 p2981 A70-33531

Nuclear orbital launch stages for interplanetary departure, comparing parallel and tandem spacecraft configurations
[AIAA PAPER 70-680] 16 p2950 A70-33580

Instrument size ball bearings lubricated with bonded dry or transfer films in simulated interplanetary spacecraft tests
16 p2923 A70-34166

Manned planetary spacecraft and space stations as ecological systems, considering common features
[AAS PAPER 70-023] 17 p3176 A70-34799

Mariner, explorer, high Data Orbiters, Viking and Rover landers as required systems for unmanned Mars exploration, examining ballistic and lifting entry
[AAS PAPER 70-030] 17 p3156 A70-34805

M-4 SS launch vehicle capabilities and development schedule for low energy interplanetary missions
17 p3168 A70-35253

Slow scan TV systems for planetary exploration, discussing sampled vidicon operation, digital encoding, data storage, signal to noise ratio, future design trends, etc
[SMPT PREPRINT 106-3] 17 p3095 A70-35634

Closed form approximate solution for restricted three body motion of lunar or interplanetary

spacecraft, demonstrating accuracy and flexibility in lunar mission trajectory calculations
[AIAA PAPER 70-1061] 19 p3529 A70-38875

Algorithm for trajectory analysis in closed loop terminal guidance of solar electrically thrusted interplanetary spacecraft
[AIAA PAPER 70-1152] 20 p3670 A70-40203

Solar panel flexibility effect on attitude control of solar electric spacecraft for deep space mission
[AIAA PAPER 70-1140] 20 p3716 A70-40209

Interplanetary solar electric spacecraft performance improvement by mission mode including earth swingby maneuver in solar orbit inclined to ecliptic
[AIAA PAPER 70-1117] 20 p3710 A70-40226

Scientific payloads integration with multimission electric propulsion interplanetary spacecraft, discussing possible contamination effects due to solar electric propulsion system
[AIAA PAPER 70-1141] 21 p3930 A70-41781

Multimission solar electric spacecraft propulsion module design for Asteroid Belt, Jupiter and out-of-ecliptic missions, including thruster failure and power conditioning requirements
[AIAA PAPER 70-1155] 21 p3868 A70-41785

Grand tours navigation system consisting of deep space network radio and onboard TV for future TOPS/Thermoelectric Outer Planet Spacecraft/applications
21 p3849 A70-41799

Venus atmosphere flight vehicle configuration, discussing payload capacity, range, velocity, flight altitude and aerostatic aerodynamic, ground effect and underwater capabilities
23 p4260 A70-44627

Jupiter Orbiting Vehicle for Exploration system for gathering Jupiter atmosphere, magnetic, radiation, gravitation, temperature, topography and interplanetary data
23 p4264 A70-45010

INTERPLANETARY TRAJECTORIES

Interplanetary trajectory selection, discussing transfer orbits, energy considerations, launch window computation, hyperbolic encounters and capture maneuvers
03 p0577 A70-14149

Interplanetary swingby trajectory correcting maneuvers for space vehicles return to earth after planet orbiting, with emphasis on singular points
06 p1142 A70-17877

Ground-based and onboard guidance and navigation systems for outer planet flyby missions concerning direct, Jupiter swingby and Grand Tour trajectories
[AIAA PAPER 70-71] 06 p1104 A70-18194

Earth oblateness effects on lunar and interplanetary trajectories, using algorithm based on orbital elements variations
[AIAA PAPER 70-97] 06 p1146 A70-18203

Interplanetary low thrust orbit transfer optimization by dynamic programming, including gravitational perturbation effects from earth, Mars and Jupiter
14 p2640 A70-30759

Restricted three body interplanetary guidance scheme using midcourse fixed time of arrival velocity correction
14 p2615 A70-30760

Fuel savings by Jupiter moon gravity assisted transfer trajectories from earth, considering initial energy, mass ratio, approach angle, timing and aiming errors
14 p2640 A70-30761

Optimum low thrust ion propelled interplanetary trajectory design using two step Chebyshev method
17 p3167 A70-35232

Interplanetary probes trajectory optimization for minimum energy expenditures, neglecting solar and terrestrial perturbations within earth sphere of influence
17 p3168 A70-35366

Primer vector theory applied to interplanetary trajectory optimization for high thrust chemically propelled spacecraft, considering 1973 Mars opportunity
[AIAA PAPER 70-1039] 19 p3527 A70-38854

Low thrust interplanetary swingby trajectories optimization, considering thrusting and coasting within sphere of influence
[AIAA PAPER 70-1041] 19 p3527 A70-38856

Interplanetary trajectories calculation using constant and/or slowly varying functions for accuracy, noting application to earth-moon spacecraft
[AIAA PAPER 70-1076] 19 p3530 A70-38888

Optimized trajectories and spacecraft for solar-electric missions to asteroids, using chemical booster for injection
[AIAA PAPER 70-1120] 20 p3710 A70-40223

INTERPLANETARY TRANSFER ORBITS

Orbit determination simultaneous optimal strategy and useful information set selection, discussing Mars transfer trajectory
04 p0750 A70-14940

Spacecraft optimal flight from earth orbit to outer planet orbit with ideally controlled engine using differential motion equations
10 p1941 A70-24512

INTERPOLATION

Four dimensional optimal interpolation for maximum wind velocity components, calculating spatiotemporal correlation functions
01 p0135 A70-10205

Table lookup/interpolation function generation for fixed point digital computations, illustrating sine-cosine generator
01 p0047 A70-10459

Interpolation method for predicting and correlating heat transfer in rarefied gases, yielding correct limiting results in free molecular and continuum regimes
[ASME PAPER 69-WA/HT-30] 04 p0782 A70-14808

Integral equations for interpolation process remainder estimation, including convergence of functions interpolation and error analysis
05 p0877 A70-16970

Algorithms based on Newton formula for polynomial interpolation and numerical differentiation
13 p2441 A70-29100

Interpolation method for nonlinear automatic control systems accuracy, discussing numerical integration optimal step and node number selection
22 p4003 A70-42886

Interpolation and smooth curve fitting based on local procedures and piecewise function
24 p4369 A70-45162

Human interpolation accuracy for pointer or index position between two scale graduations
24 p4308 A70-45512

INTERPOLATORS

U REPEATERS

INTERROGATION

Beacon identification-friend-foe/selective-identification-feature code-validation schemes for ATC, deriving expression for cumulative probability of validation on or within N interrogations
10 p1914 A70-24446

Optimal questionnaires characteristics and design algorithms
15 p2705 A70-32450

INTERRUPTION

Interruptions influence in discrete information flow on characteristics of radar tracking system
03 p0446 A70-13198

INTERSECTIONS

Fluid flow at pneumatic network junction, considering junction pressure determination as boundary condition for all transmission lines meeting at junction
[ASME PAPER 69-APM-N] 04 p0627 A70-14862

Geographic coordinates of intersection points determined directly on sphere, noting reduction on ellipsoid and adjustment for surplus intersections
09 p1670 A70-23441

Normally intersecting closed cylindrical shells subjected to internal hydrostatic pressure, using Donnell shell theory
16 p2990 A70-33678

INTERSTELLAR COMMUNICATION

Soviet book on extraterrestrial civilizations and problems of interstellar communication
08 p1457 A70-20766

INTERSTELLAR GAS

Velocity field measurements in NGC 5128 galaxy, discussing relative motion between gas and stars and correspondence of emission and absorption lines
01 p0184 A70-10898

Galactic satellite interpretation for high velocity hydrogen clouds at high latitudes
02 p0363 A70-11780

Cosmic ray primaries and secondaries direct heating of thermal electrons for computation of H I regions electron densities and temperatures
02 p0363 A70-11782

Thermal properties of neutral interstellar gas heated by low energy cosmic rays, noting role of electrons in heating processes
02 p0364 A70-11783

Stimulated emission of RF recombination lines from ionized atoms in H I regions
02 p0372 A70-12251

Ionized matter complex at galactic periphery deduced from neutral hydrogen line and continuous spectrum observations
03 p0564 A70-13222

Galactic bending dynamics, discussing omega and zeta motions coupling of neutral hydrogen in outer region
03 p0570 A70-13553

Molecular and solid hydrogen in dense interstellar clouds suggested from underabundance of neutral atomic hydrogen, discussing grain temperature
04 p0747 A70-14585

L-alpha absorption equivalent width measurements in UV spectra of beta-one, delta and pi Scorpii for interstellar hydrogen densities
04 p0748 A70-14586

Interstellar gas instability, discussing thermal, magnetic and cosmic ray effects
04 p0753 A70-15072

Thermal and dynamical evolution of gas clouds in transparent and opaque stages by comparing rates of cooling, heating, contraction and expansion
05 p0907 A70-16041

Power spectra, modulation indices, frequency distributions and decorrelation frequencies of intensity fluctuations of pulsar radiation consistent with interstellar scintillation theory
05 p0908 A70-16302

NonJeans gravitational instability of stars and interstellar gas in Galaxy due to wave interaction with stars having velocity near wave phase velocity
05 p0917 A70-16906

Density wave theory and Schmidt model applied to Milky Way spiral structure, considering systematic motion of interstellar neutral hydrogen
05 p0918 A70-16928

Pulsars dispersions, setting upper limit to emission measure of dense plasma
05 p0921 A70-16984

Maser-like stimulated OH emission regions observed in interstellar rarefied gas
06 p1148 A70-18391

Dynamic effect of radiation from massive protostar showing formation of transparent zone free of dust about star and gas density decrease until pressure equalization
06 p1148 A70-18400

H I gas and H II regions kinematics, comparing radial velocities near galactic center
06 p1149 A70-18459

Double radiosource W 49 hydrogen line absorption measurements revealing two H I clouds with different radial velocities
06 p1149 A70-18461

Interstellar gas ionization and heating by background X radiation, studying neutral hydrogen density distribution between spiral arms and at galactic peripheries
07 p1383 A70-19401

Interstellar gas clouds collapse using finite difference numerical methods in solving hydrodynamic equations involving gravitation
07 p1390 A70-20288

Interstellar cloud models to investigate heating, cooling and density distribution effects on collapse and to suggest theory of stellar evolution
07 p1390 A70-20292

Stellar formation and explosions in compact gas clouds to explain quasar phenomenon, discussing temporary star concept
08 p1578 A70-21548

Ionized matter complex at galactic periphery deduced from neutral hydrogen line and continuous spectrum observations
08 p1580 A70-21655

Static gravitation field of spherical mass immersed in cosmological gas, using combined model of Einstein and de Sitter static universes and Schwarzschild solutions
09 p1763 A70-23312

Interstellar gas electron number density fluctuations effect on pulsar signals in terms of frequency dependent dispersion, noting long wavelength disturbances
09 p1764 A70-23609

Equivalent widths for rotational lines to detect interstellar hydrogen gas, discussing absorption line
10 p1937 A70-23947

Gas cloud expulsion from galactic nucleus indicated in 21 cm survey of neutral hydrogen
10 p1937 A70-23948

Ionization front interactions in interstellar gas, investigating expanding planar H II region and contact discontinuity in H I region
10 p1937 A70-23975

Interstellar atomic and molecular hydrogen abundance and physical state using rocket observations of Lyman alpha absorption line and ground based observations
10 p1941 A70-24551

H II region properties from non-LTE analysis of alpha, beta, gamma, delta and epsilon radio recombination line data, determining electron temperature and concentrations
10 p1945 A70-24959

Potential flow pertaining to motion of gas surrounding close binary systems generated by orbital motion of stars and matter outflow from stars
10 p1946 A70-24968

Transitions in interstellar OH observed at National Radio Astronomy Observatory
10 p1948 A70-25000

Diffuse galactic radiation and absorbing clouds luminance illuminated by integral stellar radiation in Milky Way
12 p2307 A70-27866

Gas with large radial velocity in radio galaxy NGC 1275, suggesting constitution of separate galaxy
12 p2308 A70-27870

Microwave lines due to hydroxyl radical in interstellar medium, discussing emission from excited OH states
13 p2484 A70-28371

Interstellar hydrogen density around solar system from calibrated Lyman-alpha intensity measurements of Vela 7
13 p2489 A70-28894

Interstellar electron gas distribution and temperature, suggesting cosmic ray heating as main ionization source

13 p2495 A70-29796

Gas injection model in galactic nuclei from evolving stars, producing high temperature, low density, thermally unstable medium

14 p2639 A70-30730

Rotational transition of interstellar formaldehyde in absorption in direction of galactic and extragalactic objects

14 p2641 A70-30878

Stellar associations formation theory including effects of radiation, Rayleigh-Taylor instability and interstellar gas cold regions

15 p2801 A70-32478

Compact ionized hydrogen components inside galactic H II regions of lower electron density, explaining existence and evolution by various models

16 p2980 A70-34308

Disturbances rotational alignment in variable galaxies nuclei, using interstellar gas motions model

17 p3153 A70-34527

Galactic gamma rays from OSO-3 observations attributed to decay of neutral pions produced by cosmic rays interaction with interstellar gas nucleons

17 p3150 A70-34567

Lyman alpha absorption by interstellar neutral hydrogen observed in O and B stars UV spectra

17 p3162 A70-34898

Interstellar Lyman alpha observations with OAO, providing upper limit to neutral hydrogen column density

17 p3162 A70-34899

Nonhydrogen spectral lines in interstellar gas, discussing Ca/Na abundance anomaly

17 p3162 A70-34900

High velocity neutral hydrogen cloud observations, presenting tabulated characteristics and maps

17 p3170 A70-35439

UV absorption lines in H I regions heated by cosmic rays, discussing possible detection by rocket or satellite spectroscopic observations

17 p3152 A70-35748

Interstellar cloud collisions, examining gas and dust particles separation by size

18 p3313 A70-36323

Cosmic X rays interstellar absorption, giving atomic He total photoionization cross section

18 p3308 A70-36899

Interstellar gas thermal instability under cosmic ray heating, investigating perturbations causing transition to dense cool phase in pressure equilibrium with intercloud phase

18 p3309 A70-37003

Interstellar hot low density intercloud medium in H I region, estimating diffuse emission in forbidden lines O I at 6300 Å and N I at 5200 Å

18 p3310 A70-37020

Atomic H electron transition induced by H atom collisional-excitation rates at various thermal energies, explaining anomalous recombination lines in H I regions

18 p3253 A70-37021

Neutral H spiral structure in Milky Way galaxy, discussing map derivation, pattern interpretation, arm characteristics and kinematics

18 p3327 A70-37161

H 2 region and neutral gas spiral structure and radial distribution, using optical observations and radio continuum surveys

18 p3327 A70-37162

Galactic 21 cm line emission motion picture film, discussing contour maps on neutral hydrogen distribution

18 p3327 A70-37163

Milky Way galaxy spiral structure analysis, using neutral H Hat Creek survey with southern observations

18 p3327 A70-37164

Neutral H concentrations far from galactic plane associated with spiral arms

18 p3327 A70-37166

Milky way galactic plane corrugation, discussing maximum hydrogen brightness temperature oscillating in sinusoidal pattern

18 p3328 A70-37167

H I local spiral arm drift curves from radio telescope operation

18 p3328 A70-37171

O type stellar clusters hydrogen line observation revealing associated gas clouds

18 p3328 A70-37172

Interstellar H I gas physical conditions, discussing ionization ratio average values and temperature conditions

18 p3328 A70-37175

H 2 region galactic clusters and exciting stars, reevaluating distances by color magnitude diagrams

18 p3329 A70-37178

Local spiral arm H 2 regions distribution in Cygnus direction, discussing symmetry due to magnetic field

18 p3329 A70-37180

Carina spiral feature progress report covering O and B star distribution, optical and radio H 2 and H I sources and cosmic dust

18 p3330 A70-37185

Neutral hydrogen observations in Sagittarius and Scutum spiral arms, examining circular galactic rotation by density wave theory kinematic models

18 p3331 A70-37197

Galactic spiral arm helical magnetic fields related to interstellar gas flow, using magnetohydrodynamic models

18 p3331 A70-37200

Water vapor and OH spectra overlap, investigating association of galactic OH masers and water emission sources with IR stars

19 p3444 A70-37571

Radio wave emission from dust in H II region by dielectric grain photoelectric charging, rotation through stellar photons and rotating dipoles

19 p3518 A70-38024

H II region radial velocity comparison to galactic spiral structure, using optical and radio investigations

19 p3524 A70-38698

Interstellar molecular H Lyman resonance-absorption bands in far UV spectrum using rocket observation

20 p3701 A70-39002

Thioformaldehyde isotopic species reversible transition in interstellar clouds

20 p3703 A70-39164

Relativistic gas spheres and collisionless star cluster models with large red shifts, showing radial perturbation stability

20 p3703 A70-39175

Double resonator ruby maser for observing transitions of interstellar hydroxyl, noting incorporation in modulation radiometer of astronomical telescope

21 p3835 A70-40641

Soft X ray flux emanation from galactic disk, discussing latitude dependence, interstellar H, maps and discrete sources nature and properties

21 p3878 A70-40707

Cold neutral atomic hydrogen in Taurus dust clouds from 21 cm line dips in radiotelescope observations

21 p3887 A70-41108

Laboratory measurement and low noise search in W3 /OH/ for microwave emission lines in excited rotational level of interstellar OH

21 p3922 A70-41977

Galactic soft X ray and subcosmic ray heating and ionizing of interstellar H I regions

22 p4094 A70-42985

H II regions density-size relationship, using emission measurements and radio data

22 p4109 A70-43746

Interstellar molecules from stellar and galactic evolution viewpoint, emphasizing OH emission spectrum characteristics

23 p4238 A70-43801

Lyman alpha radiation scattering intensity during solar radiation period, discussing dependence of interstellar hydrogen density in interplanetary space on solar EUV

23 p4237 A70-44753

H II region dust grains thermal emission, examining effect on diffuse nebulae

24 p4413 A70-46158

Galactic neutral hydrogen velocity distributions from 21 cm line profiles analysis

24 p4414 A70-46382

INTERSTELLAR MAGNETIC FIELDS

Small amplitude perturbations in interstellar medium, discussing order of magnitude estimates of properties of cosmic rays, thermal gas, dust and magnetic field

03 p0575 A70-14016

Radio emission distribution from supernova remnants and galactic magnetic field

06 p1139 A70-17323

Hydromagnetic self gravitating galactic slab embedded in halo, deriving stability criteria using models of magnetic field

07 p1390 A70-20293

Stellar and nebular magnetic fields formation, considering role of high temperature plasma random charge and current fluctuations

12 p2307 A70-27864

Book on interstellar medium covering gas dynamics, dust, magnetic fields and nonthermal radio emission, cosmic ray diffusion in galaxy, gravitational instability theory, etc

13 p2490 A70-28996

Galactic, stellar and solar magnet fields origin, considering fluid motions role

14 p2641 A70-30876

Physical processes in galactic and extragalactic sources of nonthermal radio emission, assuming pulsars as principal magnetic field and cosmic rays sources

18 p3321 A70-37126

Galactic spiral arm helical magnetic fields related to interstellar gas flow, using magnetohydrodynamic models

18 p3331 A70-37200

Galactic evolution and secular variations of cosmic rays, magnetic fields and turbulence, assuming stellar birth rate dependence on gas density and temperature

21 p3919 A70-41700

Large scale magnetic field and spiral shock pattern of Galaxy, using density-wave theory

22 p4103 A70-42981

Primeval cosmic magnetic fields origin, discussing galactic fields and limits on present intergalactic field

24 p4403 A70-45396

Relativistic gas bulk motion nonrelativistic equations, demonstrating spatially random fluctuations damp suprathermal hydromagnetic perpendicular propagation mode to interstellar magnetic field

24 p4397 A70-45761

INTERSTELLAR MATTER

Solid hydrogen condensation on interstellar grain surfaces at extremely low temperatures related to H atoms density

01 p0183 A70-10896

Interstellar neutral hydrogen flux effects on atmospheric hydrogen density, considering annual and semiannual density variations

01 p0186 A70-11207

PreHayashi phase of stellar evolution, discussing protostellar disks /stellisks/ formation from flattened fragments of collapsed interstellar cloud under turbulent viscosity

01 p0190 A70-11346

Interstellar media under action of supernova or nova, solving Navier-Stokes equations of hydrogen plasma for motion during shock wave formation

03 p0564 A70-13221

Evidence disproving interstellar extinction by diamond crystals

03 p0572 A70-13818

Small amplitude perturbations in interstellar medium, discussing order of magnitude estimates of properties of cosmic rays, thermal gas, dust and magnetic field

03 p0575 A70-14016

Low energy cosmic rays effect on electron density in interstellar medium

04 p0738 A70-14509

Interstellar formaldehyde absorption from radio observations with parametric amplifier

04 p0747 A70-14515

Interstellar propagation effect on spectra and charge ratios due to ionization energy loss and nuclear spallation during traversal of matter

05 p0897 A70-15762

Cepheus light attenuation curve explained by applying polymodal particle size distribution, obtaining interstellar dust density

05 p0918 A70-16915

Color difference method for interstellar extinction laws applied to O stars study

06 p1140 A70-17641

Milky way and interstellar clouds brightness fluctuations statistical analysis by surface photometry, studying dust distribution, cloud absorption and dimensions, star distribution, etc

06 p1149 A70-18463

Faraday rotation in pulsars and in interstellar medium, discussing position angle drift, polarization changes and pulse fine structure

08 p1564 A70-20553

Microwave absorption by rotational transition of interstellar formaldehyde in direction of Sgr B2, Sgr A and W51

08 p1570 A70-20896

Pulsed radio signals time delay due to molecular microwave resonance in earth atmosphere and interstellar medium

08 p1461 A70-20915

Magnetothermal instability and radiative effects on incipient fragmentation of rotating gravitating interstellar fluid forming condensations

08 p1578 A70-21545

Interstellar media under action of supernova or nova, solving Navier-Stokes equations of hydrogen plasma for motion during shock wave formation

08 p1580 A70-21654

Conditions for life in universe, analyzing evolutionary stages of matter to determine steps producing complex organic compounds

09 p1762 A70-23121

Interstellar dust, discussing effective particle size, composition, formation and effects on astronomical observations

09 p1763 A70-23374

X ray scattering from pulsar NP 0532 by interstellar grains

09 p1748 A70-23791

Magnetic funneling model proposed for accretion of matter onto neutron star to study X ray production during motion through interstellar cloud

10 p1931 A70-23902

Line profiles and equivalent widths from Si II, Mg II, Ni II and Fe II spectra of shell star zeta Tauri

10 p1936 A70-23941

Ar-arc-produced dust of iron, carbon, silicon carbide and silica, investigating shapes, sizes, grouping and optical absorption to simulate interstellar grains

10 p1944 A70-24957

- Wisps near Crab Nebula since September 1969 pulsar spin-up, suggesting dynamical changes in neutron star 10 p1947 A70-24994
- Alpha recombination line emission from galactic center detected, discussing possible origins in continuum source or interstellar medium 10 p1947 A70-24995
- X ray scattering by interstellar grains in direction of Crab pulsar and Sco XR-1 10 p1933 A70-25044
- Excess color method for photometric and spectral studies of interstellar absorption in cluster NGC 6913 11 p2116 A70-26585
- Excess color method for studying interstellar absorption around cluster NGC 6823 11 p2116 A70-26586
- Densities and extents of absorbing clouds in open cluster NGC 7086 determined from photometry and spectral classifications of stars 11 p2116 A70-26587
- Diffuse matter distribution in northern region of Milky Way, examining relation with O-BO stars distribution 11 p2116 A70-26588
- IR radiation intensity distribution in solar neighborhood from grain models of dirty ice, graphite and graphite core-dirty ice mantle 11 p2106 A70-26710
- Grains impurities effect on interstellar extinction curve from graphite grain model, discussing dirty ice coatings 13 p2489 A70-28915
- Book on interstellar medium covering gas dynamics, dust, magnetic fields and nonthermal radio emission, cosmic ray diffusion in galaxy, gravitational instability theory, etc 13 p2490 A70-28996
- Stellar light pressure and gravitational force ratios for spherical water, quartz and graphite particles in interstellar space, considering refractive dependence on wavelength 13 p2493 A70-29396
- Light elements detection in interstellar grains by observing halo around X ray source arising from small angle scattering 14 p2631 A70-30539
- Ca atom-graphite grain model for interstellar absorption at 4430 Å, calculating resonant line shift and width as functions of atom-surface distance 14 p2639 A70-30729
- Interstellar grains potential model, discussing plane electromagnetic waves scattering by infinite concentric homogeneous circular cylinders at oblique incidence 14 p2639 A70-30732
- Galactic cosmic ray actions on interstellar medium for origin of Li, Be and boron in stellar atmospheres and solar system 14 p2640 A70-30786
- H II region stellar color anomaly attributed to interstellar extinction 14 p2641 A70-30879
- Faraday rotation in pulsars and in interstellar medium, discussing position angle drift, polarization changes and pulse fine structure 15 p2805 A70-32708
- Angular scattering of interstellar medium resulting in multipath dispersion of pulsar pulses, discussing NP0532 in Crab Nebula 16 p2972 A70-32988
- Cosmic microwaves anomalous absorption by interstellar IR-pumped formaldehyde in dust clouds shock heated layer 17 p3154 A70-34535
- Periodic comet nature, origin and anomalous behavior with space mission planning implications, assuming solar plasma source and solar-interstellar interaction [AAS PAPER 70-029] 17 p3155 A70-34795
- Interstellar silicate absorption in IR spectra, discussing existing observations 17 p3157 A70-34840
- UV interstellar extinction from comparison of epsilon and zeta Persei, noting graphite features 17 p3159 A70-34877
- UV interstellar extinction, examining reddened and unreddened early stars with OAO satellite spectrophotometric scans 17 p3159 A70-34878
- Dielectric models of interstellar grains from calculations for smooth particles of homogeneous materials 17 p3159 A70-34879
- Galactic UV emission attributed to solar radiation scattered by hydrogen atoms, using Mariner 5 measurements 17 p3163 A70-34902
- Lyman alpha radiation from gaseous hydrogen nebula model, taking into account absorption by dust and interstellar neutral hydrogen 17 p3163 A70-34904
- Interstellar dust spatial distribution, indicating galactic spiral structure 18 p3329 A70-37183
- Traversed matter thickness and charge composition for high energy galactic cosmic rays with various propagation modes 19 p3506 A70-38123
- Cosmic rays deuterons abundance calculation from H and He nuclei collisions with interstellar matter 19 p3506 A70-38125
- Interstellar molecular radio frequency lines significance to galactic physics, noting abundance relation to constituent atoms indicating dust catalytic formation 19 p3521 A70-38496
- Cosmic soft X rays scattering by interstellar dust grains, observing source angular size dependence on distance, wavelength and grain properties 20 p3695 A70-39233
- Interstellar silicate absorption bands four color photometric observations in galactic direction, using metal mirror telescope 20 p3713 A70-40431
- Cas A and SN 1572 supernova remnant radio sources X ray spectra, investigating absorption by interstellar medium 21 p3873 A70-40666
- X ray source population type optical observations, discussing interstellar matter and H II regions 21 p3882 A70-41117
- Interstellar spherical dust particles from meteoritic silicates and dirty ice, calculating optical properties and scattering functions 21 p3889 A70-41147
- Circumstellar matter observations between binary star components, considering emission and absorption spectra, velocity and light curve distortion and orbital period changes 21 p3889 A70-41151
- Cosmic X ray extinction and halo by interstellar grains, applying to light elements identification 21 p3883 A70-42200
- Interstellar and intergalactic medium physics, examining H I and H II regions thermal and dynamic states 22 p4098 A70-42578
- Neutral interplanetary particle impact ionization of atmosphere, discussing density of neutral interstellar media near solar system 22 p4106 A70-43291
- Interstellar matter in Scorpius constellation, discussing star counting, gas identification, etc 23 p4254 A70-44901
- Polarized maser emission from interstellar hydroxyl and water related to nonlinear weak magnetoplasma 24 p4381 A70-45258
- Carbon ionization equilibrium in dense interstellar clouds, discussing grains and neutral atoms attenuation effects 24 p4402 A70-45387
- Neutron star or defunct pulsar accretion of interstellar matter, discussing effects on total luminosity and radiation spectrum 24 p4403 A70-45397
- Interstellar dust clouds, discussing graphite, iron and silicate mixture, solid carbon material, starlight extinction and astrophysical processes 24 p4403 A70-45408
- Spallation limits on low energy cosmic and nuclear gamma rays interstellar fluxes, evaluating fast particle effects on interstellar medium 24 p4397 A70-45758
- Hydrogen I region anomalous alpha lines recombination in Orion B spectrum, identifying carbon emitter by measured frequency separation 24 p4410 A70-45773
- INTERSTELLAR MICROWAVE SPECTRA**
- U INTERSTELLAR RADIATION**
- U MICROWAVE SPECTRA**
- INTERSTELLAR RADIATION**
- Diffuse soft X ray photoionization and heating of H I regions compared to cosmic ray heating 02 p0364 A70-11784
- MK stellar spectral types in Monoceros, analyzing spatial distribution and interstellar absorption using slit spectograms 02 p0369 A70-12063
- Galactic interstellar absorption lower limit in selected Area 19 determined from Stellar spectra densities, using Schmidt camera 02 p0370 A70-12073
- Interstellar polarization by graphite-silicate grain mixtures, observing variability in wavelength dependence of polarization for various models 03 p0577 A70-14218
- Power spectra, modulation indices, frequency distributions and decorrelation frequencies of intensity fluctuations of pulsar radiation consistent with interstellar scintillation theory 05 p0908 A70-16302
- Phase variations in polarization parameters of eclipsing binary Z Vul during polarimetric studies for interstellar polarization component 09 p1751 A70-22156
- Elongated neutral-hydrogen emission feature in Sco-Oph region, comparing with interstellar sodium lines for distance from sun 10 p1945 A70-24966
- Interstellar cosmic ray spectra from nonthermal radio background, obtaining electrons and protons modulation by diffusion-convection energy loss theory 14 p2631 A70-30673
- Energy spectrum of primary cosmic ray electrons /negatron and positron/ in interstellar region observed near 1965 solar minimum 19 p3503 A70-38101
- Interstellar electron and positron intensity, observing pion production spectrum from nuclear collisions at machine energies 19 p3504 A70-38111
- INTERSTELLAR SPACE**
- Spacecraft motion parameters and physical characteristics of space determined from statistical analysis of measurement data 01 p0094 A70-11484
- Electron and positron flux steady state in interstellar space relationship to differential energy spectrum exponent in cosmic rays, discussing galactic halo and age 03 p0561 A70-14151
- Thermal stability of graphite core-solid hydrogen mantle grains determined from temperature and evaporation rates calculated for interstellar space 04 p0743 A70-14398
- Gravitational-repulsion forces of interstellar vacuum, investigating relations between magnitudes and red shift of galactic objects and quasars 05 p0920 A70-16968
- Cosmic ray electrons during propagation in interstellar space analyzed for energy spectrum modulation 10 p1816 A70-24633
- Interstellar flights, discussing human limitations, star systems with habitable planets and possible galactic communities 10 p1943 A70-24759
- Solar system and interstellar space exploration phases, manned and unmanned missions, meta and microprobes, propulsion systems, etc 11 p2112 A70-26063
- Spacecraft propulsion systems selection for particular exploration missions including planets, comets and interstellar space 11 p2112 A70-26066
- Cosmic electron detection and measurement techniques, considering presence in solar system, interstellar space and metagalaxy and galactic continuum radio emission 12 p2293 A70-27572
- Cosmic rays intensity frequency spectrum near earth, indicating relativistic electron energy spectra similarity in interstellar space and galactic particles existence 13 p2478 A70-29388
- Molonglo pulsars H line absorption and dispersion in interstellar medium 13 p2495 A70-29788
- Local system interstellar medium thermal electron distribution, synchrotron radiation emissivity, cosmic ray electron flux and spectrum 17 p3152 A70-35583
- Pulsar distance calculation, assuming immersion in uniform average electron density medium 18 p3328 A70-37174
- Galactic low energy cosmic ray positrons and gamma rays, considering production mechanism in interstellar space 19 p3503 A70-38099
- Interstellar cosmic ray electron spectrum flattening below 3 Gev from OGO-5 observations 19 p3504 A70-38106
- Primary cosmic rays energy spectra in interstellar space in relation to sunspot group number 19 p3506 A70-38121
- Cosmic ray nuclei transformation and propagation in interstellar space, considering diffusion equation, cross sections, solar modulation, etc 19 p3509 A70-38145
- Energetic cosmic ray particles transfer through interstellar space based on galactic disk model 19 p3511 A70-38158
- Microwave transitions for molecules in comets and interstellar space 21 p3887 A70-41110
- INTERSTELLAR TRAVEL**
- Interstellar space flight ramjet physical model, describing magnetic field funnel, radiation effects, relativistic effects, etc 02 p0379 A70-12782
- Photon propulsion with constant power in exhaust beam and intragalactic travel in force free space from solving relativistic rocket equations [AIAA PAPER 70-215] 06 p1132 A70-18105
- Soviet book on physics of cosmic propulsion energy covering space vehicle propulsion systems, vehicle-medium interaction, etc 08 p1558 A70-20754
- Minimum time interstellar trajectories for thrust limited rockets by applying Pontryagin maximum principle to relativistic rocket equations of motion 09 p1760 A70-22933

Interstellar transport vehicles design around thermonuclear propulsion plants, discussing weight, mission velocity, acceleration time and fuel costs

11 p2123 A70-26054

Interstellar exploration mission profiles, considering technical constraints, propulsion modes, environmental hazards, spacecraft communications and control, etc

11 p2112 A70-26065

Transstellar space navigation, discussing system concepts, measured observables during flight, instrumentation, etc

15 p2773 A70-32060

Interstellar drag resulting from relativistic rocket elastic collisions with interstellar matter, discussing effects on minimum time acceleration limited relativistic trajectories

17 p3155 A70-34752

Space vehicle for interstellar flight, discussing propulsion concepts, mission implications and international cooperation

23 p4254 A70-45011

INTERSTITIALS

Interstitial atoms ordering effects on low and high temperature phase transformations in alloys with bcc lattice

03 p0505 A70-13102

Nb-Mo alloy interstitial oxygen concentration determined by measuring internal friction / Snoek/ peak

03 p0512 A70-13763

Structure and interstitial impurities effects on Nb modulus of elasticity at normal and high temperatures, noting rolling

05 p0866 A70-17040

Thermal isolation characteristics of interstitial materials in vacuum environment, inserting materials between contacting metal surfaces at various pressures and temperatures

06 p1181 A70-18143

Dislocations and interstitial atoms interactions in Ta, investigating internal friction and deformation resistance and rate dependence on temperature

07 p1309 A70-19637

Interstitial atoms effect on dislocation relaxation and aging of Mo and Nb single crystals

07 p1309 A70-19638

Solid solution softening in bcc Ta-Re alloy system attributed to substitutional-interstitial interaction

07 p1310 A70-19736

Interstitial solutes effect on athermal component of flow stress in alpha titanium

08 p1521 A70-21577

Transition metal alloys electronic effect on solubility of interstitials

08 p1521 A70-21695

Interstitial sinks effect on structure and creep behavior of dispersion-strengthened Cb base alloy

08 p1521 A70-21703

Tensile strain rate and oxygen concentration effects on peaks of niobium hardening zones involving interstitial atoms

12 p2252 A70-27001

Interstitial solid solutions stability in cast molybdenum subjected to heat treatment

12 p2257 A70-28225

Interstitial atoms arrangement in binary alloys with body centered lattice, describing pressure effects by statistical theory

13 p2435 A70-29321

Interstitial Cl molecule formation in NaCl lattice, computing strain field and energetics by energy minimization technique based on point ion lattice model

14 p2544 A70-30352

Stress relaxation of Mo under plastic deformation controlled by diffusion of interstitial atoms and dislocations, determining activation energy

15 p2758 A70-32124

Kinetic simulation of atom rearrangements in order-disorder transformation for point defect movement in Ti alloys, considering vacancies and interstitials properties

17 p3115 A70-34381

Binary titanium-oxygen and titanium-carbon alloys, investigating interstitial pair mechanism for internal friction peak formation

17 p3115 A70-34383

Interstitial impurities effect on mechanical properties of Ti alloys, discussing interaction between solutes and dislocations

17 p3116 A70-34390

Unalloyed alpha titanium mechanical properties, emphasizing grain size and interstitial content effects on strain hardening and deformation dynamics

17 p3116 A70-34391

Yield stress in electron beam-refined Nb-N solid solution at room temperature and specific strain rate range

19 p3454 A70-38813

Ta single crystal inherent lattice and interstitial solution hardening, discussing impurity doping effect on flow stress thermal component

21 p3839 A70-40902

Alpha phase Ti strengthening, investigating interaction between dislocations and interstitial solute atoms

24 p4360 A70-45516

INTERVALS

Microinterval analysis of phased development of human visual color perception in presence of short stimuli

08 p1443 A70-20733

Critical discreteness interval of visual analyzer, investigating dependence on stimulus location, flare brightness and adaptation

08 p1443 A70-20734

Interval of values with stability and convergence for correctors for differential equations

09 p1641 A70-22286

Real cipher places in real function, describing interval analysis method with upper and lower bound indications

18 p3282 A70-36357

Threshold distribution of time intervals between atmospheric contradicting Poisson law

23 p4190 A70-44082

INTERVERTEBRAL DISKS

Radial and tangential stress distribution through annulus fibrosus dependence on material inhomogeneity for human intervertebral disk

15 p2692 A70-32328

INTESTINES

NT RECTUM

Slow waves and spikes in intestinal muscle of cat noting dependence on intracellular iontophoresis of Na

03 p0416 A70-13014

Temporary mitotic activity depression with decrease in aberrant mitoses observed in mice intestinal epithelium cells after exposure to 50 Mev proton doses

03 p0423 A70-13708

Unicellular algae protein diet effects on animal and human enteric microflora composition

09 p1615 A70-22087

Transmural stimulation elicited phasic and tonic contractile responses in circular and longitudinal axes of small intestine under nerve-blocking drugs

09 p1622 A70-23547

Temporary mitotic activity depression with decrease in aberrant mitoses in mice intestinal epithelium cells after exposure to 50 Mev proton doses

11 p1985 A70-25508

Unicellular algae protein diet effects on animal and human enteric microflora composition

15 p2685 A70-32683

Mice intestinal epithelium, investigating high energy protons irradiation effect on cells

23 p4149 A70-45028

INTOXICATION

Altitude effects on Borkenstein Breathalyzer accuracy determined from alveolar ethanol analysis

06 p1000 A70-17303

Alcoholic beverages effect on positional nystagmus and Coriolis acceleration

11 p1993 A70-26520

Gravity effect on positional alcohol nystagmus in man and rabbits, observing threshold value in weightless state

13 p3259 A70-29442

Altitude and alcohol intake effects on blood alcohol concentrations

24 p4306 A70-45329

Alcohol effects on human short term memory, discussing pathological intoxication from flying safety viewpoint

24 p4307 A70-45345

INTRACRANIAL PRESSURE

Respiratory waves formation of intracranial pressure in anesthetized cats and dogs, studying various contributing factors

07 p1213 A70-19792

Intracranial pressure pulse waves formation mechanism mathematical model, estimating role of biomechanical factors

13 p2353 A70-29520

INTRAMOLECULAR STRUCTURES

Intramolecular formation of azo-linkage accompanying N elimination from bis-azide

05 p0810 A70-16052

INTRAOCULAR PRESSURE

Bleached eye pressure blinding at bleaching light termination during wavelength settings, discussing effect on interocular hue shifts

03 p0427 A70-13951

Dogs breathing air or oxygen during slow and rapid decompression, measuring intraocular and cardiovascular pressure changes and retinal responses

09 p1621 A70-23460

Intraocular tension due to muscular fatigue in overheated albino rats, determining Na and K content in eye tissue

14 p2535 A70-30159

INTRAVASCULAR SYSTEM

Dynamic intravascular pressures measured in small vessels of frog lung using micropressure transducer inserted into vessel lumen

19 p3364 A70-38368

INVARIANCE

Radiative transfer in plane parallel atmospheres computed by discrete space techniques based on invariance concept for application to planetary atmospheres

02 p0338 A70-11825

Nonlinear modification of Maxwell equations, discussing conformal invariance and nonsingular solutions to neutral and charged states with zero mass

02 p0339 A70-12067

Lorentz invariance test using bar magnet on torsion fiber, analyzing preferred reference frame in space assuming earth velocity coupled to electron spin through specific term

02 p0341 A70-12849

Poincare invariance compatibility with general relativity, discussing Brandt groupoid, decomposition and local groups

06 p1106 A70-17540

Autonomy and invariance conditions for control systems composed of multivariable components having same number of inputs and outputs

07 p1244 A70-18768

Invariant set existence inside submanifold convex to flow established from vector field properties on submanifold boundary

07 p1324 A70-19198

Invariance and stability of subsets in metric state-time dynamical polysystems

07 p1324 A70-19200

Compton-Getting effect for cosmic ray particles and photons and Lorentz-invariance of distribution functions, discussing thermal background radiation, proton spectra, etc

07 p1369 A70-20071

Linear integral equations solutions using invariant functions

09 p1711 A70-22208

Riemann invariants, discussing method of characteristics in physical and hodograph space applications and multidimensional hyperbolic systems

10 p1865 A70-24103

Invariance conditions and state transition matrix of linear systems

11 p2074 A70-26400

Field equations in conformal theory of gravitation, noting invariance

11 p2084 A70-26552

Turbulent chemical reactions invariance preservation for zero diffusivity

14 p2546 A70-31044

Algebraic aspects of generalized Riemann invariants method of integration of quasi-linear partial differential equations

16 p2944 A70-34329

Lagrangian invariants of inviscid compressible fluid dynamics applied to hydrodynamic equations

17 p3070 A70-35333

First boundary value problem solution for parabolic equation by differential invariant method

17 p3131 A70-35340

Adiabatic invariant of nonlinear periodic wave described by partial differential equations in weakly inhomogeneous medium

18 p3291 A70-36642

Classical invariant characteristic of quantification conditions for flow quantifiers

20 p3671 A70-39122

Invariant automatic control systems - Conference, Kiev, May-June 1966, Volume 2

20 p3601 A70-39826

Invariance conditions for control systems with time varying parameters

20 p3602 A70-39827

Automatic control system components parameter variation effects on invariance conditions

20 p3602 A70-39830

Small parameter effects on absolutely invariant systems under transient perturbation, analyzing gyro stabilizer performance

20 p3603 A70-39831

Automatic control systems with signal recovery, determining invariance conditions, main operators and reproduction errors

20 p3603 A70-39833

Multidimensional automatic control systems polyinvariance, describing compensating cross couplings realization

20 p3603 A70-39834

Complex automatic systems effectiveness synthesis based on invariance principles

20 p3603 A70-39835

Multidimensional control systems synthesized in accord with polyinvariance and coordinating couplings principles

20 p3604 A70-39837

Self adjusting autopilot system based on invariance principle for stabilization against wind gusts

20 p3670 A70-39840

Two dynamic systems synthesis achieving limited influence on each other by coordinates invariance criteria method involving determinant

20 p3604 A70-39841

Invariant systems structural synthesis for automatic control of plant motion, deriving control laws for thrust and angle of attack

20 p3670 A70-39844

Invariance conditions for inertial gyroscopizer with powered stabilization system in presence of dynamic imbalance, noting improvement via compensating loop

20 p3670 A70-39846

Multidimensional control for turbofanjet engine, relating system characteristics to invariance conditions during startup and ascent

20 p3689 A70-39847

Pneumatic actuator control system improvement, using invariance theory to compensate load variability and dynamic response of medium

20 p3564 A70-39848

Invariance conditions in two parameter frequency control unit for electric power generator driven by variable speed motor

20 p3565 A70-39850

Invariance principle in mechanics of deformable continua connecting three dimensional and relativistic space-time formulation

21 p3940 A70-42097

Chronometrically invariant formulation of Petrov gravitational fields algebraic classification at space-time fixed point in general relativity

21 p3851 A70-42239

Deformations with constant strain invariants for elastic bodies under surface traction

22 p4113 A70-42543

Conservation laws in theory of field with group invariance properties, examining infinitesimal transformations method

22 p4075 A70-43400

INVARIANT IMBEDDINGS

Boundary value problems of thin beams theory transformed into initial value problems, using dynamic programming and invariant imbedding

05 p0926 A70-15977

Optimal control problem converted Cauchy problem for obtaining numerical solutions through invariant imbedding

06 p1027 A70-18508

Mixed boundary value potential theory problem numerical solution by integral equation invariant imbedding

06 p1171 A70-18511

Classical eigenvalue problem transformation by invariant imbedding into initial value problem suited for numerical integration, noting applications to columns elastic buckling

12 p2261 A70-27424

Inverse boundary value problems involving elliptic equations solved by Newton method and discrete invariant imbedding

13 p2440 A70-28650

Nonlinear integrodifferential equations of radiative transfer solved by invariant imbedding approach, discussing Rayleigh phase matrix

13 p2451 A70-29130

Invariant imbedding application to solution of partial differential equations by continuous-space discrete-time /CSDT/ method, discussing time dependent heat diffusion

16 p2942 A70-33735

Optimal control problem solution methods, comparing Euler-Lagrange equations, Pontryagin principle, dynamic programming and invariant imbedding

17 p3057 A70-35589

Thermotropic quasi-geostrophic atmospheric model, deriving linear and quadratic integral invariants

19 p3463 A70-38754

INVENTORIES

NT **TIMBER INVENTORY**

VTOL aircraft power plants optimization for future helicopter missions without restrictions of limited off-shelf inventory

17 p3147 A70-34708

INVENTORY CONTROLS

Optimal spare parts inventory determined for stochastically failing components using mathematical model

08 p1501 A70-20603

Equivalent linear programming in integer variables to solve production scheduling for N identical machines, minimizing changeover and inventory costs

10 p1895 A70-24662

Computerized control of aircraft spare parts inventories, using optimization method maximizing aircraft availability and minimizing handling costs

13 p2524 A70-28836

Comparative demand forecasting for military helicopter spare parts, stressing exponential smoothing model

20 p3740 A70-39643

INVERSIONS

NT **CENTRIFUGING STRESS**

NT **POPULATION INVERSION**

NT **TEMPERATURE INVERSIONS**

Trench algorithm for Toeplitz matrix inversion, presenting proof for nonHermitian matrices case

01 p0131 A70-10456

Algebraic method for role of part inversion in fluid structure problems with mixed variables

11 p2135 A70-25979

Multidata and collocation methods compared for numerical Laplace transform inversion

11 p2074 A70-26639

Rational polynomial matrices inversion by automatic computational procedures, considering Gaussian elimination and Faddeev algorithm

22 p4062 A70-42926

INVERTEBRATES

NT **AMOEBAS**

NT **BETTERLES**

NT **CEPHALAPODS**

NT **DROSOPHILA**

NT **INSECTS**

NT **MOLLUSKS**

NT **MOTHS**

NT **PROTOZOA**

NT **SPORES**

Biological tests of fish and invertebrates exposed to Apollo 11 lunar surface material, noting absence of pathological effects

19 p3513 A70-37409

Earth-moon system age and origin from tidal evolution equations, considering growth line counts on living and fossil marine invertebrates

21 p3921 A70-41971

INVERTERS

NT **STATIC INVERTERS**

Discrete diode phase inverter for meter wavelengths providing north-south antenna control of radio telescope by diffraction method

08 p1473 A70-21064

Free-running parallel inverters limitations by critical characteristics of networks, transformers and switching elements

11 p1983 A70-26628

Apollo Command Module inverter experience for post-Apollo spacecraft applications, discussing phase loads and control logic circuits

12 p2165 A70-27693

Reactive filter synthesis for step-voltage output inverter smoothing, using network theory

14 p2559 A70-30373

DC-to-sinusoidal inverter employing PWM waveform, analyzing circuit parameters effect on harmonic content

19 p3358 A70-37854

High power short rise time square wave inverter using power transistors

22 p3965 A70-43336

INVESTIGATION

NT **ACCIDENT INVESTIGATION**

NT **AIRCRAFT ACCIDENT INVESTIGATION**

INVESTMENT CASTING

Monolithic precision castings using photoetched plastic and lost-wax investment techniques

22 p4043 A70-42419

INVESTMENTS

Edwards Report consideration of economic and investment opportunities in civil aviation, discussing denationalizing airways corporations

11 p2153 A70-25859

Investment risks and technical impact on aircraft development, world aviation growth and airline costs

17 p3200 A70-34915

INVISCID FLOW

NT **STAGNATION FLOW**

Inviscid surface pressures calculated on slender wedges and cones at low frequencies and large oscillation amplitudes in hypersonic flow

01 p0003 A70-10854

Boundary layer and singular inviscid stagnation point reacting flow matching, corrections structure and decay and ranking comparison with second order effects in fluid mechanics

01 p0065 A70-11096

Time dependent behavior of separated and unseparated unsteady flow of incompressible viscous and inviscid fluids without heat transfer

01 p0067 A70-11162

Lower bounds of Stekloff and free membrane eigenvalues for sloshing of incompressible inviscid fluid, subject to gravity in rigid tank with free surface

02 p0278 A70-11999

Axisymmetric radiating flow behind paraboloidal shock in ideal inviscid gas hypersonic stream, using differential approximation method for blunt body solution

04 p0669 A70-14937

Inviscid flow problems solution by partial differential equations, considering propagation processes, stratified media, potential, subsonic and three dimensional flows

04 p0672 A70-15170

Fluid mechanical problems with pressure distribution determined by interaction between external supersonic inviscid flow and inner laminar viscous layer

04 p0674 A70-15529

Inviscid Burger turbulence spectral equations for cumulant approximation, obtaining energy spectrum and transfer as initial value problems

05 p0832 A70-16147

Inviscid gas injection through flat plate in supersonic flow, obtaining self similar solution by integrating differential equation for stream function

05 p0791 A70-16963

Lift and vortex drag due to flaps on thin sweptback tapered wings in inviscid incompressible flow, obtaining spanwise loadings

06 p0967 A70-17256

Inviscid hypersonic blunt body flow of hydrogen-oxygen mixtures in shock layer stagnation region

06 p0968 A70-17555

Inviscid flow through staggered airfoil cascades in oscillatory and distorted flow simulating axial flow compressor

[ALAA PAPER 70-131] 06 p0969 A70-18049

Closed form solution of modified inviscid transonic equation embodying character of viscous-transonic equation applied to shockless transonic airfoils

[ALAA PAPER 70-187] 06 p0970 A70-18096

Steady supercritical planar inviscid transonic flows over lifting airfoils, generating unsteady flow by impulsively imposing airfoil boundary condition

[ALAA PAPER 70-47] 06 p0972 A70-18130

Time dependent inviscid gas flow on infinite domain computed by finite difference method

[ALAA PAPER 70-45] 06 p1042 A70-18188

Intensity measurements of molecular beams skimmed from nearly inviscid nitrogen and Ar free jets, interpreting beam attenuation in terms of collisional models

06 p1043 A70-18254

Inviscid hypersonic flow analysis for chemically relaxing air about wedges and pointed circular cones using Dorodnitsyn integral method

[DGLR-69-037] 07 p1188 A70-18986

Asymptotic behavior of inviscid radiating gas flow near stagnation point of blunt body

07 p1188 A70-19315

Circulating flow around elliptical cylinder in inviscid liquid vortex

09 p1659 A70-22435

Shock layer thickness in supersonic inviscid gas flow past blunt bodies, calculating boundary layer near stagnation point

09 p1603 A70-22442

Two dimensional radial flow of inviscid infinitely conducting compressible fluid under influence of magnetic field

09 p1735 A70-22757

Hall effect on MGD flow past axisymmetric body by studying incompressible inviscid flow past body of revolution at zero incidence

09 p1661 A70-23074

Massive blowing from porous cone with embedded shock wave in supersonic flow, assuming inviscid and conical injected flow field

09 p1662 A70-23216

Incompressible inviscid fluid flow behind impeller blades, determining velocity profiles, flow-off angle and stable operation limits

11 p1977 A70-26349

Inviscid incompressible conducting fluid flow past body in aligned magnetic field at low magnetic Reynolds number, discussing small perturbations evolution

11 p2041 A70-26623

Numerical solution for steady supersonic inviscid flow around smooth conical bodies by solving elliptic partial differential equations for conical flow

12 p2155 A70-27202

Inviscid flow theory for ACV high speed peripheral jets, considering component inefficiencies, pressure losses, nozzle geometry, etc

12 p2156 A70-27211

Flow stability of electrically conducting inviscid fluid in coaxial cylindrical annular space under influence of axial magnetic field

12 p2210 A70-27799

Solid particle motions in dusty gas in inviscid hypersonic shock layers of slender wedges and cones and stagnation regions of cylinders and spheres

12 p2156 A70-27827

Viscous and inviscid incompressible fluids motion boundary value problems solutions with aid of kinetic stress functions

13 p2388 A70-29319

Inviscid, incompressible superposed fluids stability in presence of inhomogeneous porous media, noting motion with decaying amplitude

14 p2577 A70-30993

High temperature inviscid flow of ideal radiating gas, analyzing effects of radiation pressure and energy on flow field

14 p2666 A70-30999

Steady state one dimensional nozzle flow of reacting inviscid gas mixtures, giving numerical solution procedure for hydrogen-oxygen reactions

15 p2694 A70-32269

Inviscid film flow by fluid injection through bounding surface, considering porous plate inclination and power law injection rates

16 p2895 A70-34241

- Time dependent solution for inviscid hypersonic flow of chemically reacting gas mixture about blunt bodies
[ALAA PAPER 70-771] 17 p3009 A70-34502
- Hypersonic flow past slender bodies, discussing inviscid flows, outer edge singularity of boundary layer and three dimensional interaction on needle-like bodies
17 p3010 A70-35035
- Lagrangian invariants of inviscid compressible fluid dynamics applied to hydrodynamic equations
17 p3070 A70-35333
- Micropolar fluids turbulent flow, investigating microstress couples, stability, inviscid flow, etc
17 p3071 A70-35435
- Three dimensional inviscid small perturbation compressible flow past lifting axial compressor rotor at subsonic and transonic speeds
18 p3208 A70-36691
- Two dimensional steady inviscid incompressible flow past profiles in parallel flow with nonuniform velocity distribution
19 p3354 A70-38676
- Nonequilibrium processes and body geometry as stagnation point conditions in blunt body inviscid flow
20 p3557 A70-39355
- Energy spectrum function for Gaussian initial velocity field of inviscid turbulence Burger model, using Cameron-Martin-Wiener exact expansion
20 p3609 A70-39653
- Boundary value problems in uniform incompressible inviscid flows past complex profile bodies by R functions method and variational technique
20 p3610 A70-39772
- Nonuniform free stream supersonic flow past aerodynamic decelerators, calculating inviscid flow fields by method of characteristics
[ALAA PAPER 70-1176] 21 p3746 A70-41837
- Acoustic wave propagation in continuum of inviscid compressible heat conducting fluid, determining stability criteria
22 p4073 A70-42571
- Lift determination of slender curved periodically recurring airfoils array in plane potential flow of inviscid incompressible fluid
23 p4133 A70-44158
- Radiative transfer upstream absorption effect on inviscid stagnation region shock layer radiation
23 p4133 A70-44551
- Inviscid rotational supersonic flow near three dimensional stagnation point, examining solutions for compatibility with vortical shock layer boundary conditions
23 p4183 A70-44692
- Time dependent inviscid transonic flow past two dimensional and axisymmetric bodies, presenting numerical procedures including imbedded shock waves as discontinuities
[ALAA PAPER 70-1322] 24 p4288 A70-45943
- Inviscid conducting incompressible fluid steady motion past thin airfoils, presenting crossed and aligned fields and Alfvén motion with Hall effect
24 p4289 A70-46033
- Inviscid hypersonic flow fields past lower compression surface of delta wing calculated by one strip approximation of integral relations method
24 p4289 A70-46245
- INVISIBILITY**
U VISIBILITY
- IODATES**
Ruby laser second harmonics generation in low loss lithium iodide crystal with high conversion efficiency
24 p4355 A70-46085
- IODIDES**
NT SILVER IODIDES
NT SODIUM IODIDES
LiI thermodynamic properties in dimethyl sulfoxide determined by emf method, discussing ionic solution energies
10 p1831 A70-25041
- Iodine concentration effects on epitaxial GaAs p-n junctions growth characteristics
14 p2625 A70-30171
- Optical charge transfer transitions in N-alkyl iodide salts, examining transient absorptions due to flash photolysis
18 p3226 A70-36765
- IODINE**
NT IODINE ISOTOPES
NT IODINE 131
Thyrotropin [TSH] effects on thyroidal iodine metabolism during hypoxia in rats
02 p0231 A70-11703
- Rotational lines in iodine B-X system vibrational bands, calculating Doppler, natural and collisional widths
03 p0527 A70-13298
- Voltage-step method to measure diffusivity of structured region in polar liquid electrolyte solutions, considering iodine near Pt microelectrodes in aliphatic alcohols
03 p0441 A70-14044
- Corrosion shapes from iodine action on metals in methylic medium, discussing morphology dependence on purity, surface state and reaction products diffusion velocity
08 p1518 A70-21241
- Thyroid gland function following radiation injury by measuring plasma protein bound iodine in irradiated rat blood
09 p1621 A70-23150
- Laser action in 5d-6p electron transitions of neutral atomic iodine, measuring electron temperature and density
09 p1699 A70-23517
- Molecular I ground state dissociation energy value, proposing spectroscopic reassignment
12 p2180 A70-26861
- Vibrational energies, rotational constants and internuclear potential of ground state molecular iodine, using reanalyzed spectroscopic data
16 p2954 A70-33056
- Iodine concentrations, temperature gradients and transport ampules etching effects on mass transport rate and crystal growth of MnS-MnSe-iodine system
16 p2960 A70-33088
- Meteorite I-Xe 129, demonstrating cold assembly of unequilibrated chondrite
19 p3519 A70-38036
- Barrier heights for hydrogen-iodine reaction from semiempirical four-electron valence bond calculation
21 p3780 A70-41709
- Rotational quantum numbers from iodine molecule resonance fluorescence measurements during laser excitation using Fabry-Perot interferometer
23 p4202 A70-44938
- IODINE COMPOUNDS**
NT IODATES
NT IODIDES
NT SILVER IODIDES
NT SODIUM IODIDES
Crossed molecular beam study of reactive asymmetry of oriented methyl iodide molecules reacting with Rb, accounting for observations with hard sphere model
07 p1225 A70-20051
- UV absorption cross sections of CO, HCl and ICN, analyzing reactions causing various spectral features
08 p1455 A70-21340
- IODINE ISOTOPES**
NT IODINE 131
I-Xe dating of Abee enstatite chondrite by combined neutron activation and mass spectrometric analysis
05 p0915 A70-16829
- Radioactive dating of meteorites based on high temperature release of iodine-correlated Xe129 and Xe128
10 p1949 A70-25328
- IODINE 131**
Transport ratio for I-131 air to milk concentrations, determining mean value and statistical variation from Project Rover data
19 p3361 A70-38012
- ION ACCELERATORS**
Accumulated plasma density and lifetime measurement of trapped ions between accelerator and periodic magnetic mirror, showing limitation by collisions and charge exchange
03 p0532 A70-13683
- Ion acceleration in spherical and cylindrical plasma layers formed by spherical plasmoid expansion in plasma cylinders
07 p1384 A70-19414
- Plasma ion cyclotron resonance acceleration in nonuniform magnetic field by RF field
07 p1353 A70-20229
- Ion accelerator for doping semiconductors, discussing electronic bombardment of low pressure vapors, electrostatic extraction, focusing and mass spectrometer
09 p1649 A70-23325
- Ions acceleration and motion in corona and solar wind, discussing equation derivation, He abundance, nonMaxwellian distribution functions, minimum flux estimation, etc
17 p3152 A70-35870
- Nonlinear collective ionic acceleration by relativistic electron beam, assuming blob dimensions of plasma wavelength
22 p4077 A70-43471
- ION ATOM INTERACTIONS**
He excitation by low energy He ions giving support for Rosenthal-Foley postcollision-interaction model, testing model predictions
05 p0885 A70-16556
- Energy dependence and threshold behavior of ion Ar lines excited in low-energy He ion-Ar collisions
11 p2087 A70-26402
- Li ion elastic scattering by He, calculating ground state interaction potential
16 p2956 A70-34310
- Atomic hydrogen 2s and 2p excitations by proton and He ion impact, considering ion-multipole interactions effect
21 p3852 A70-40598
- Thermodynamics and statistical physics of dense plasma with particle interaction energy exceeding kinetic energy, discussing three-component model phase equilibrium
23 p4229 A70-45073
- ION BEAMS**
Coaxial ion beams moving in opposite directions in LF magnetic field noting sliding instability development
03 p0530 A70-13061
- Charge exchange and electron loss measurements in steam target exposed to high energy hydrogen ions beam, using equilibrium fractions method
07 p1345 A70-20142
- Plasma beam welding of light metal and heat resistant alloys, discussing weld characteristics, beam I-V characteristics, etc
09 p1690 A70-22077
- Excitation of plasma ion-cyclotron oscillations by ion beam passing through neutral gas along magnetic field, noting radial stabilization
10 p1926 A70-25118
- Helium ion bombardment activated tungsten crystal surface migration using field emission microscopy
11 p2097 A70-25378
- Inhomogeneous ion beam plasma LF instability, showing oscillations amplitude maxima in radial density gradient regions
15 p2780 A70-32193
- Ion beam scattering at turbulent plasma oscillations in glass chamber containing low pressure air
16 p2958 A70-33253
- Low energy ion beam system for studying electron ejection from controlled metal surfaces, describing vacuum, ion source, lens and mass spectrometer components
18 p3261 A70-37086
- SERT 2 measurements for spacecraft and ion beam potential as function of thruster and orbital parameters, using hot wire emissive probes
[ALAA PAPER 70-1127] 20 p3691 A70-40218
- Excitation of plasma ion-cyclotron oscillations by ion beam passing through neutral gas along magnetic field, noting radial stabilization
20 p3685 A70-40511
- Ion beam scattering at turbulent plasma oscillations in glass chamber containing low pressure air
23 p4226 A70-44282
- Cs ion beam space charge and current neutralization by electron capture for partially ionized plasma formation, investigating longitudinal electrostatic wave excitation
24 p4385 A70-45465
- ION CHAMBERS**
U IONIZATION CHAMBERS
- ION CHARGE**
Metallic state basic parameters determined by electron transfer technique, discussing ion charges, electron and hole concentrations current scattering cross sections, etc
13 p2433 A70-28886
- ION CONCENTRATION**
Local contractures in K depolarized amphibian skeletal muscle fibers by intracellular injection or by microperfusion, discussing intracellular Ca ion concentration
02 p0234 A70-11728
- Vertical ion concentration profile in troposphere and stratosphere from ozone distribution satellite measurements using aeronomical reactions
02 p0291 A70-12389
- Release-recovery and dynamic stiffness phenomenon in frog heart muscle at various Ca ion concentrations and temperatures
02 p0241 A70-12771
- Plasmopause observations by ion spectrometer aboard OGO-5 vehicle for early orbits, obtaining O, He and H ion concentration profiles for geomagnetic parameter
06 p1059 A70-18546
- Expansion and deceleration of rocket-released artificial ion cloud in terms of snowplow expansion model and drag deceleration
07 p1271 A70-20159
- Nighttime concentration profiles of O, NO and molecular oxygen ions in ionosphere calculated from daytime values
10 p1874 A70-24428
- Diurnal variations of concentrations of ions and neutral components of NO, O and N in E region from analysis of chemical and photochemical processes
10 p1881 A70-24809
- Mesosphere payload to measure neutral gas density, positive and negative ions concentration and mobility in D region
13 p2393 A70-28682
- Shock wave multiple ionization in hydrogen with impurities, discussing intensity and duration effects on electron temperature profile and ion concentrations
13 p2388 A70-29369
- Electron temperatures and electron and negative ion concentrations in low pressure hydrocarbon flames
14 p2666 A70-31098
- Ion concentrations in premixed propane-air two dimensional laminar nozzle burner flames with seeding, discussing dependence on temperature and equivalence ratio
21 p3772 A70-40880

E region ion composition nighttime variations, examining nitrogen monoxide and O ion nonequilibrium concentrations by ionic-molecular reactions

23 p4189 A70-44074

F 1 region positive nitric oxide and oxygen ions concentrations ratio and conversion rates from rocket data and theoretical formulas

23 p4189 A70-44075

ION CURRENTS

NT ION BEAMS

Collisionless ions trajectories in plasma flowing about cylindrical probe calculated to determine probe ion current, ion density distribution in field and potential distribution

06 p1122 A70-18294

Collisions effects on ion saturation and electron currents in electron retarding region of cylindrical and spherical electrostatic probes, noting applicability over wide range

06 p1123 A70-18303

Current collected by cylindrical Langmuir probe immersed in rarefied collisionless plasma streaming with high velocity

06 p1124 A70-18307

Satellite-borne spectrometer for low energy ion measurement

10 p1874 A70-24314

Electron bombardment ion engine thrust variations, considering effects of electrode misalignment and ion current changes

12 p2291 A70-27808

Surface type airborne electrostatic probes in ambipolar diffusion flux measuring ion saturation current, discussing electrode contamination and temperature and ablation tests

13 p2412 A70-29967

Continuity equation plasma oscillation, discussing ion current waveform flowing from discharge and implications for periodic astrophysical phenomena

14 p2638 A70-30618

Gas kinetic pressure profile and mass density of propagating current sheet in argon pinch discharge, using piezoelectric transducer

14 p2624 A70-31041

Langmuir probe position-dependent ion flow effects on plasma density measurement in low pressure mercury discharge

17 p3083 A70-34995

Spacecraft sheath structure, potential and velocity effects on ion current measurements by traps and mass spectrometers

21 p3816 A70-41087

ION CYCLOTRON RADIATION

Ion-cyclotron oscillations in plasmas, considering plasma waves and oscillation characteristics

03 p0530 A70-13065

Fields and power transfer for electromagnetic waves in hot plasma calculated using Fourier integral and Fourier series methods

05 p0888 A70-16165

Pulsed grid modulation for ion cyclotron resonance spectrometer

07 p1286 A70-19974

Plasma ion cyclotron resonance acceleration in nonuniform magnetic field by RF field

07 p1353 A70-20229

Ion cyclotron whistler in Injun 5 satellite VHF radio noise data

09 p1638 A70-23499

Ion cyclotron resonance spectroscopy technique for determining electrons photodetachment energy from negative ions in gas phase

11 p1995 A70-26001

Collision effect on phenomena associated with ion cyclotron whistler formation, considering ionospheric day time model

13 p2468 A70-29933

Ion-molecule reactions produced in phosphine by ion cyclotron resonance

16 p2855 A70-33061

Ion cyclotron resonance spectroscopy for detecting trapped gaseous ions in analyzer cell, observing ion-molecule reactions

23 p4196 A70-44390

ION DENSITY [CONCENTRATION]

NT IONOSPHERIC ION DENSITY

NT MAGNETOSPHERIC ION DENSITY

NT MAGNETOSPHERIC PROTON DENSITY

NT PROTON DENSITY [CONCENTRATION]

Electron pressure and negative H ion population in late type dwarfs atmospheres by Ca I resonance line observation, noting non-LTE mechanism

01 p0191 A70-11351

Flame positive ion concentration measurements with Langmuir probes with mean free path smaller than probe diameter

02 p0397 A70-12019

Time and altitude induced variations in daytime NO and molecular and atomic oxygen ions

05 p0841 A70-16736

Kinetics of solar wind interaction with moon and planetary bodies using perturbation scheme to obtain ion density distribution on antisolal side

06 p1136 A70-18192

Collisionless ions trajectories in plasma flowing about cylindrical probe calculated to determine probe ion current, ion density distribution in field and potential distribution

06 p1122 A70-18294

Ion resonance instability in nonneutral plasmas, considering ions addition to low density electron cloud with low kinetic energy

07 p1352 A70-19991

Time dependent electrostatic probe theory relating measurements to internal properties of plasma, calculating free stream ion density from collected electric charge

07 p1289 A70-20466

OH, NH and amine radicals concentrations in flame gases from flat ammonia-oxygen-nitrogen flames measured as function of distance from burner surface

09 p1788 A70-22343

Ion density profile across shock in partially ionized gas measured in plasma jet wind tunnel for comparison with Rankine-Hugoniot relation

09 p1662 A70-23235

Spectroscopic technique measuring OH concentrations behind shock waves by measuring absorption of OH lines, using water cooled RF powered lamp

09 p1683 A70-23512

Hydrogen ion flux detected along earth magnetic force lines in Northern Hemisphere midlatitudes, determining flux magnitude

10 p1874 A70-24321

Auroral ion composition and chemistry from rocket-borne mass spectrometer measurements, investigating oxygen density and green line excitation

10 p1874 A70-24431

Flowing afterglow system below 300 K for rate constants of certain gases association with helium third body, investigating oxygen cluster ions formation and reactions

10 p1920 A70-25144

Coupled differential rate equations governing growth and decay of positive and negative ion and electron concentrations in afterglow with ambipolar diffusion and electron attachment

11 p2088 A70-25703

Mass spectrometric analysis of lunar material from soil vaporization products ion component by electron beam

11 p2119 A70-26800

Plasmasphere ion concentration measurements on-board Elektron 2 and 4 satellites, observing dependence on geomagnetic activity

12 p2295 A70-28260

Emissive probes for measuring plasma potentials over different ion density ranges on SERT spacecraft, detailing calibration and mechanical and electronic configurations

13 p2404 A70-28519

Thermal diffusion effects on F 2 region ion densities, deriving diffusion coefficients for partially ionized atomic oxygen plasma

13 p2398 A70-29232

Molecular oxygen positive ion density in upper ionosphere as function of photoionization, ambipolar diffusion velocity and altitude effect

13 p2399 A70-29233

Plasmapause position and density profile from ion concentration measurements by OGO-5, determining reaction to magnetic variations

13 p2482 A70-30074

Concentrations model of metallic atoms and ions in upper atmosphere with deposition from meteors, using diffusion equation

14 p2580 A70-31262

Positive ion composition in Cs plasma as function of normalized pressure

15 p2779 A70-31978

Weak ion concentration in stratosphere and mesosphere measured using accumulated capacity amplifier

18 p3257 A70-36179

Comet Morehouse CO ions lifetime and density from photometric analysis

18 p3313 A70-36324

Ion density and electron temperature variations as function of maximum electric field density in independently excited plasma column striations

19 p3475 A70-37552

Ozone effect on stratospheric electricity based on numerical calculations of ion densities

19 p3413 A70-38005

Anomalous electromagnetic wave absorption in collisionless plasma attributed to instability excitation causing ion density fluctuations

21 p3855 A70-40754

Hydrogen cluster beam discharges, determining transient plasma ion density from Stark broadening measurements of H beta line

23 p4228 A70-44939

ION DISTRIBUTION

Ionospheric molecular ion concentration vertical profile analysis for verifying neutral gas temperature maxima in connection with two ion production maxima

01 p0083 A70-11550

Quasi-linear ion oscillation theory for Maxwellian plasma, considering electron and ion distribution perturbations and energy transfer

02 p0346 A70-12105

Ionized gas height scale changes in polar ionosphere obtained assuming Chapman type ionization distribution

05 p0841 A70-16738

Anisotropic plasma instability in nonlinear stage, studying turbulent relaxation of ion distribution by quasi-linear theory

06 p1119 A70-17501

Electrostatic probe measurements of radial distributions of mean ion density in N and air wakes behind hypervelocity spheres compared with electron microwave measurements

06 p0975 A70-18197

Collisionless ions trajectories in plasma flowing about cylindrical probe calculated to determine probe ion current, ion density distribution in field and potential distribution

06 p1122 A70-18294

Anisotropic angular distribution of electrons and ions emitted from W targets irradiated by ruby laser pulses

08 p1512 A70-21211

Low energy ion spectrum and spatial distribution measurements in auroral zones by Cosmos-261 satellite spectrometer

08 p1492 A70-21798

Plasmapause irregular structure and position indicated by measured distributions of hydrogen and helium thermal positive ions in duskside magnetosphere

13 p2397 A70-29185

Ion effects on VLF propagation in earth-ionosphere waveguide during polar cap absorption events

16 p2859 A70-32933

Langmuir probe position-dependent ion flow effects on plasma density measurement in low pressure mercury discharge

17 p3083 A70-34995

Dynamo role in magnetospheric disturbances and ionospheric inhomogeneities, allowing for charged particle concentration height dependence

23 p4237 A70-44059

Al substituted YIG crystal chemistry by cation distribution determination as function of Al concentration using Mossbauer spectroscopy

24 p4392 A70-46364

ION EMISSION

Foil decarbonization process monitored by mass spectrometry of secondary carbon ion emission

12 p2254 A70-27311

Laser induced ion emission triggering of spark gaps, distinguishing channels due to electrons and ions by high speed shadowgraph technique

13 p2426 A70-28797

Ba II emission lines in solar chromosphere, examining excitation and ionization equilibrium and resonance line intensities by eclipse observations

18 p3317 A70-37010

Thermal release profiles and retention coefficients of injected argon ions for silicates and iron simulating meteoritic materials

19 p3474 A70-38601

Solar equatorial limb brightening of far UV resonance lines of lithium-like N V, O VI, Ne VIII, Mg X and Si XIII ions, interpreting oso-4 data with coronal model

21 p3924 A70-42185

Solar far UV limb brightening of C III, N III, N IV, O III, O IV and Si IV lines in chromospheric-corona transition region, correcting coronal model for spicule effects

21 p3925 A70-42186

Secondary emission detector using linear signal to measure nonrepetitive microsecond ion bursts

23 p4197 A70-44475

Ion source emitter plasma column generated by electron beam injection through gas filled chamber, compensating ion space charge with fast discharge electrons

24 p4385 A70-45451

ION ENGINES

NT CESIUM ENGINES

Chemical engineering problems of resistojets, pulsed plasma, ion bombardment and colloid thrusters

01 p0166 A70-10974

Ion thruster with hollow cathode electron source, discussing operation principles, experimental characteristics, etc

03 p0552 A70-14150

Optimal control for thermionic nuclear reactor space power plant utilizing state variable feedback with limited input simplifying computation

03 p0461 A70-14342

Hot cathode reflex discharges investigated to improve ion generation efficiency in space ion thrusters

03 p0536 A70-14368

Electrostatic charged particle acceleration and ion thruster function in geostationary satellite station-keeping and attitude control, orbital transfer and drag compensation

[ONERA-TP-764]

04 p0735 A70-14934

Optimal outlet velocities of charged particles for spacecraft electrostatic thrusters
[DFVLR-SONDDR-28] 04 p0735 A70-15173

Pulsed plasma and ion microthrusters providing satellite attitude and position control
05 p0896 A70-16119

Cathode emission from hollow cathode controlled by variable magnetic field to ensure proper I-V characteristics for efficient ion generation in thrusters
[AIAA PAPER 70-175] 06 p1131 A70-18032

Experimental data to define idealized thruster discharge model power efficiency limits, computing probabilities for excitation, ionization, propellant escape and wall interception of ions
[AIAA PAPER 70-177] 06 p1131 A70-18034

Optical spectra of discharge chambers of electron bombardment mercury ion thrusters with hollow and oxide cathodes
[AIAA PAPER 70-176] 06 p1132 A70-18157

30 cm diameter mercury bombardment low impulse thruster development for potential space applications, discussing performance and control
[AIAA PAPER 69-238] 07 p1365 A70-19704

Optimal outlet velocities of charged particles for spacecraft electrostatic thrusters
09 p1744 A70-23428

Kaufman thruster with predominant radial field, noting electron mobility across ion extraction screen and advantages of uniform plasma distribution
[AIAA PAPER 69-259] 11 p2102 A70-26120

Space charge sheath electric thruster principles, construction and performance using laboratory test model
[AIAA PAPER 69-282] 11 p2102 A70-26121

Mercury bombardment ion thruster life test in space environment onboard space electric rocket test /SERT/ satellite, describing passive satellite thermal control system design
11 p2127 A70-26606

Electron bombardment ion engine thrust variations, considering effects of electrode misalignment and ion current changes
12 p2291 A70-27808

Causes and magnitudes of thrust misalignment of Kaufman type electron bombardment ion thruster
[AIAA PAPER 69-303] 13 p2473 A70-28506

Ion thrusters and sources in space propulsion, discussing power supply level, efficiency and service lifetime
[ONERA-TP-739] 15 p2787 A70-31808

Discharge chamber plasma processes in electron bombardment ion thrusters, considering factors affecting thruster performance
[AIAA PAPER 69-494] 15 p2791 A70-32501

Submillipound mercury electron bombardment ion thruster efficiency, noting cathode pole piece, baffle position and geometry influence on ion chamber performance
[AIAA PAPER 70-616] 16 p2969 A70-33612

Power conditioning and control system prototype for Mercury spacecraft ion thruster, describing supply subsystems, circuit design, component selection and reliability
[AIAA PAPER 70-649] 16 p2970 A70-33615

Digital computer simulation and analysis of control loops for ion thruster control
[AIAA PAPER 69-239] 17 p3149 A70-35654

High voltage solar arrays for ion engines, discussing spacecraft propulsion, electric generation, insulation integrity, cell degradation and current leakage
[AIAA PAPER 70-1138] 20 p3567 A70-40211

Power conditioning system for Hg ion thruster on SERT 2 spacecraft, considering performance, design, control circuits and arcing
[AIAA PAPER 70-1129] 20 p3568 A70-40216

SERT 2 spacecraft surface contamination by Hg ion thruster effluents, using solar cell sensors
[AIAA PAPER 70-1128] 20 p3690 A70-40217

SERT 2 measurements for spacecraft and ion beam potential as function of thruster and orbital parameters, using hot wire emissive probes
[AIAA PAPER 70-1127] 20 p3691 A70-40218

In-flight thrust measurement methods on SERT 2 ion thrusters, using accelerometer, electrical parameters and orbit change
[AIAA PAPER 70-1126] 20 p3691 A70-40219

SERT 2 spacecraft ion thruster ground tests and flight operation, tabulating performance data
[AIAA PAPER 70-1125] 20 p3691 A70-40220

SERT 2 for testing ion thruster reliability and operational characteristics, discussing design and mission objectives
[AIAA PAPER 70-1124] 20 p3716 A70-40221

Thermionic reactor program for electric propulsion, considering internally fueled flashlight concept
[AIAA PAPER 70-1108] 20 p3568 A70-40235

RF ion source for electrostatic spacecraft propulsion, discussing RIT-10 performance optimization and development
[AIAA PAPER 70-1102] 20 p3692 A70-40236

Kaufman ion thruster providing electric propulsion for satellite spiraling from parking to synchronous orbit
[AIAA PAPER 70-1101] 20 p3692 A70-40237

Electron bombardment Hg thruster with divergent magnetic fields, investigating performance dependence on configuration and propellant utilizations
[AIAA PAPER 70-1092] 20 p3692 A70-40243

Parameters influence on mercury hollow cathode neutralizers for Kaufman ion thruster
[AIAA PAPER 70-1090] 20 p3693 A70-40245

Mercury electron bombardment thruster, measuring effect of geometry and magnetic field inside pole piece region on discharge losses and propulsion efficiency
[AIAA PAPER 70-1088] 20 p3693 A70-40247

Small-orifice hollow cathode discharge properties in electron bombardment ion thrusters, using vaporized mercury propellant
[AIAA PAPER 70-1087] 20 p3693 A70-40248

Thermionic reactor electric propulsion for unmanned outer planets exploration, discussing spacecraft design, launch vehicle, weight factors, etc
[AIAA PAPER 70-1122] 20 p3717 A70-40524

Optimal control of composite spacecraft propulsion system incorporating high thrust-weight ratio chemical engine and low thrust ion engine
21 p3865 A70-40831

Low specific impulse hollow cathode mercury thruster for deep space electric propulsion, using SERT 2 configuration
[AIAA PAPER 70-1099] 21 p3866 A70-40893

Stress tolerant thyristor and transistor switching electronic converter for ion propulsion engine
[AIAA PAPER 70-1157] 21 p3866 A70-40901

Space compatible flight prototype ion engine power conditioning system design for Hg thruster using oxide cathode
21 p3867 A70-41006

Power conditioning requirements and specifications for spacecraft electric propulsion ion thruster
21 p3758 A70-41209

Integrated circuit requirements for space power conditioning equipment for ion thrusters
21 p3797 A70-41211

Solid state switches for operating ion thrusters directly from high voltage solar cells, noting satellite weight saving
21 p3798 A70-41215

Integrated circuits for control and telemetry functions in oxide cathode ion thruster power conditioning system operating from solar panel
21 p3798 A70-41216

Nuclear fusion reactor spacecraft propulsion system using ion rocket with charged deuterium nuclei fuel, emphasizing nuclear plasma confinement problem
21 p3867 A70-41498

Mars and Venus orbiter spacecraft electric propulsion system, discussing Hg electron bombardment ion engine
[AIAA PAPER 70-1154] 21 p3868 A70-41786

Liquid metal /mercury/ cathode thruster system for operation at reduced beam voltages, discussing design and performance
[AIAA PAPER 70-1103] 21 p3868 A70-41788

Thrust vector measuring device using floating suspension system for ion engines, detecting vertical tilt and horizontal drifts of floating platform
[AIAA PAPER 70-1104] 21 p3805 A70-41789

Thermionic reactors for spacecraft auxiliary power and electric propulsion, discussing in-core conversion system and diodes
22 p4071 A70-43191

Jantar 1 automatic ionospheric laboratory flight tests results, investigating Ar ion engine performance
23 p4264 A70-45009

Thermonuclear spacecraft propulsion, comparing X ray pumped gas laser and ion drive systems
24 p4377 A70-46211

ION EXCHANGE MEMBRANE ELECTROLYTES
Polyelectrolyte complexes formed from combined water soluble and negatively charged polyelectrolytes
06 p1005 A70-17513

ION EXCHANGE RESINS
Activated carbons and ion exchange resins bactericidal action as function of silver coating techniques
04 p0641 A70-14574

Peptides removal from Merrifield solid phase by transesterification with anion exchange resin
06 p1003 A70-17154

Carbon dioxide absorption from gas streams by weak base ion exchange resins
18 p3226 A70-36767

ION EXCHANGING
Ion exchange entropy and enthalpy functions calculated from experimental constants and temperature dependence data
06 p1177 A70-17837

Cellulose ion exchanger palladium catalysts preparation and applications in asymmetric hydrogenation reactions
17 p3042 A70-35125

Chloride ion shift of respiration occurring between plasma and erythrocytes as function of carbon dioxide, using rapid filtration method
19 p3364 A70-38366

ION EXTRACTION

Kaufman thruster performance dependence on transmission of ion extraction optics and magnetic field shape
[AIAA PAPER 69-257] 07 p1365 A70-19705

Discharge effects on LF oscillations and ion extraction in hot cathode Penning plasma
13 p2463 A70-29370

Electric field intensity and extension of space charge sheath for ion extraction from nitrogen plasma
14 p2622 A70-30661

Positive ions energy dispersion effused from RF plasma, presenting ion extraction model for plasma sheath system and equivalent circuit
20 p3678 A70-39608

SERT 2 Hg thrust ion extraction, loss, production and energy balance within ionization chamber
[AIAA PAPER 70-1091] 20 p3693 A70-40244

Stationary hydrogen RF plasma, using quadrupole mass analyzer for ion composition and extraction study
22 p4078 A70-42363

Electrostatic potential distribution and ion trajectories in extraction gage design by computer
23 p4198 A70-44873

ION GAGES
U IONIZATION GAGES
ION IMPACT
Secondary electron emission coefficients and energy distributions to investigate interaction between positive ions and Cu/Be dynodes of electron multiplier
07 p1344 A70-20127

Impact ionization effects in electric field domain on stability of current-voltage characteristics of Gunn diodes
11 p2020 A70-26813

Uranium ion impact ejection and electronic excitation of thin foil particles, observing optical spectra of Be, carbon and Al atoms and ions
20 p3674 A70-39135

Atomic hydrogen 2s and 2p excitations by proton and He ion impact, considering ion-multipole interactions effect
21 p3852 A70-40598

Impact ionization effects in electric field domain on stability of current-voltage characteristics of Gunn diodes
24 p4317 A70-45185

Energy loss spectra and collision cross sections for positive ion impact on molecular nitrogen, noting Lyman-Birge-Hopfield system excitation
24 p4381 A70-45599

ION INJECTION
Hydrodynamic stability of high purity insulating incompressible fluid subjected to unipolar ion injection
01 p0151 A70-10669

Critical conditions for hydrodynamic stability of incompressible nonconducting fluids subjected to unipolar injection, establishing variational principle leading to characteristic relation
01 p0152 A70-10672

Plasma injection occurrence as function of temperature in n-InSb subjected to low electric field strengths and fitted with Ohmic contacts
01 p0159 A70-11176

Ion implantation for reducing space charge buildup in thermal oxides on silicon exposed to ionizing radiation
04 p0731 A70-14743

N-type layer formation with ion implanted nitrogen or Sb in p-type alpha-SiC, evaluating electrical characteristics, discussing junction devices formed
04 p0732 A70-15685

Electron clouds injection and containment by magnetic field in toroidal vacuum chamber, studying causes of cloud instability
07 p1353 A70-19994

Semiconductor diamond films electrical conductivity obtained by injecting various ions during isochronal stepwise annealing, studying activation energy values
12 p2286 A70-27479

Hall constant and carrier mobility in semiconductor diamond films doped by boron ion injection, observing temperature dependence of mobility
12 p2287 A70-27480

Ion implantation doping for MOS devices, discussing improved HF performance, integrated circuitry and threshold voltage selection
16 p2872 A70-33054

Plasma injection and confinement in closed quadrupole magnetic trap
22 p4083 A70-43388

ION IRRADIATION
Low energy ions incidence angle effects on secondary electron emission from molybdenum cylinders in low pressure plasma, noting role of Langmuir sheath around target
07 p1355 A70-20356

Laboratory irradiation of rock samples for solar wind flux effects on IR reflectivity of lunar rocks
08 p1579 A70-21565

D-pattern changes of helium ions irradiated polycrystalline Mo and Ni specimens, observing line splitting
09 p1707 A70-23197

Ion-implanted GaAs junction diodes anneal behavior and defect nature 11 p2098 A70-26391

Low resistivity films synthesized on seminsulating GaAs by xenon, krypton, selenium and zinc ions bombardment 12 p2286 A70-27364

Radiation defects in Ge single crystals surface layers caused by low energy bombardment with He ions 12 p2287 A70-27486

B and P ions bombardment techniques for Si doping of multilayered transistor structures 19 p3385 A70-37268

Hybrid ion implanted diffused emitter n-p-n transistor two dimensional doping profiles, considering emitter oxide window edge shape effect 22 p3997 A70-42924

ION MICROSCOPES

He and Ne adsorption and desorption on field ion microscope tip, determining minimum required field strengths of gas films at different temperatures 05 p0891 A70-15975

Optical transformation of field ion micrographs providing orthographic, gnomonic projections and perspective images of hemispheric metal surface 14 p2584 A70-30506

Field-ion microscope image formation, determining periodic surface potential variation effects on high field tunneling 21 p3862 A70-40974

Various Frank loops in quenched and annealed Pt, examining dislocations with field ion microscopy and computer simulated approximations 23 p4230 A70-44758

ION MOTION

F region ion velocity measurements by Thompson scatter probe, deducing neutral winds diurnal and seasonal variations in thermosphere 01 p0078 A70-11214

Rarefied ionospheric plasma flow around rockets and satellites, studying electric field effect on ion motion by kinetic equation and similarity law 04 p0680 A70-15188

Kinetic equation describing dynamics of inhomogeneous cloud of fast electrons and ions trapped in earth magnetic field 07 p1276 A70-20429

Drift dissipative instability of weakly ionized plasma, considering ion motion along magnetic lines in dispersion equation 10 p1923 A70-24407

Ion mobility estimates for air constituents, considering ion-neutral elastic and resonant charge exchange collisions 10 p1919 A70-24427

F 2 field-aligned ion velocity measurement compared with theoretical results, discussing difference at sunspot minimum and daytime ion velocity-plasma loss relation 10 p1881 A70-24815

Radiation emission and transfer in unsteady outer space plasmas, discussing turbulence mechanisms involving electron and ion motion, relativistic and non-relativistic electron beams, etc 12 p2305 A70-27854

Active and passive ion transport mechanisms in excitable animal cell maintaining constant membrane polarization 13 p2352 A70-29351

Plasma sheath boundary as closed Mach surface, demonstrating Bohm criterion application to ion velocity component normal to sheath edge 13 p2464 A70-29465

Spherical ionized cloud movement in ionosphere uniform anisotropic plasma as function of electric field applied to rocket released ion clouds 15 p2726 A70-31867

Ion motion neglecting conditions for radio waves in plasma based on Ohms law uncoupling from momentum transfer 16 p2957 A70-32980

Ions acceleration and motion in corona and solar wind, discussing equation derivation, He abundance, non-Maxwellian distribution functions, minimum flux estimation, etc 17 p3152 A70-35870

Maxwell-Wagner migrational polarization resulting from free ions or electrons drift in dielectrics and semiconductors, considering relaxation time 18 p3298 A70-36595

Supersonic flow of rarefied plasma around plane bodies, allowing for electric field effect on ion motion 19 p3351 A70-37302

Artificial ion clouds motion in magnetosphere, using MHD model 19 p3414 A70-38378

Coupling constant and binary collision expansions for ion motion in plasma line broadening 21 p3855 A70-40722

Satellite-borne sensor for ionospheric ions velocity measurement, describing design and principles of operation 21 p3813 A70-40834

Ionospheric ions drift velocity horizontal and vertical components distribution, using satellite-borne sensor 21 p3813 A70-40835

Rarefied ionospheric plasma flow around rockets and satellites, studying electric field effect on ion motion by kinetic equation and similarity law 21 p3819 A70-41169

Turtle bladders isolated mucosal and serosal fractions histological and physiological properties, discussing ion transport and oxygen consumption 21 p3762 A70-41224

Electron and ion transport in cesium plasma for thermionic and MHD energy converters 21 p3859 A70-41912

Ion and electron ambipolar velocity distribution near plasma sheath boundary in collisional positive column 22 p4080 A70-42542

ION OSCILLATION

U PLASMA OSCILLATIONS

ION PROBES

Response variation and detection efficiency of funnelled channel electron multipliers for low energy protons and Ar ions 06 p1021 A70-17623

Multiple electrode probe characteristics in rarefied plasma flow created by ion source, noting electrode potential role 06 p1064 A70-17886

Molecular ion concentrations, using flat probe collector trap on Cosmos 5 satellite at 200-300 km 07 p1276 A70-20421

Current-voltage relation for ion collection spherical DC probe at high ambient gas pressure 16 p2899 A70-32929

Plasma space potential measurement with heavy ion beam probe using cesium gun and electrostatic energy analyzer 16 p2960 A70-34339

Ion orientation technique based on counterflow sensing in earth upper atmosphere, discussing accuracy 21 p3927 A70-40844

Electrostatic potential distribution and ion trajectories in extraction gage design by computer 23 p4198 A70-44873

ION PRODUCTION RATES

Disturbances effect in Langmuir layer at cathode on ionization rate in arc discharge, estimating ion density and width of nonequilibrium ionization region 01 p0150 A70-10171

Ionospheric molecular ion concentration vertical profile analysis for verifying neutral gas temperature maxima in connection with two ion production maxima 01 p0083 A70-11550

Triggered spark source for multiply charged carbon ions applied to collision cross section measurements 02 p0303 A70-12747

Hot cathode reflex discharges investigated to improve ion generation efficiency in space ion thrusters 03 p0536 A70-14368

Reactor gamma in-pile effects on thermionic diodes simulated in electron accelerator, noting ion production insufficient to support saturation currents 04 p0717 A70-14948

Nitrogen ionization rate increase by admixing neutral molecules of electronically excited nitrogen, noting nitrogen decay controlled by spontaneous radiation and wall collisions 05 p0884 A70-15918

Magnetic disturbance associated with E layer east-west electric current calculated in terms of ionization production and loss 05 p0838 A70-16282

Heavy particle impact ionization in hot gases analyzed for ionization rates relationships 06 p1113 A70-18278

Ion production cross sections determined for alkali atoms and bromine molecules collisions, noting charge transfer 07 p1345 A70-20138

Production rate constants for hydrated positive ions in photoionized nitric oxide-water afterglows 07 p1346 A70-20245

Auroral electron energy distribution and ionization rates characteristics based on satellite and rocket measurements 08 p1487 A70-20642

Molecular cesium ion production by arc discharge in inhomogeneous cesium plasma, describing probable reaction mechanism 08 p1551 A70-20849

Thermal and nonthermal plasmas for ion production, discussing gas pressure, voltage and discharge current effects on electron temperature 09 p1734 A70-22037

Disturbances effect in Langmuir layer at cathode on ionization rate in arc discharge, estimating ion density and width of nonequilibrium ionization region 10 p1925 A70-25017

N and O ions electron impact ionization rates calculated from approximate cross sections 12 p2275 A70-27173

Penumbra and geomagnetic threshold effects on ionospheric electron production by primary cosmic rays 12 p2296 A70-28366

Ionization equilibria and ionization and recombination rates for Fe and Ni ions, discussing dielectronic recombination 14 p2631 A70-30727

F 1 layer formation and ion production rates related to F layer stratification, atomic oxygen, zenith angle and solar activity periods 15 p2730 A70-32086

Energetic ion production by giant pulse lasers measured on Al and Au foil targets 15 p2777 A70-32333

Equatorial F 2 region response during solar eclipse of 7 March 1970, emphasizing ionization production and loss, transport processes and electron temperature 16 p2897 A70-33826

Ionic collision processes in water vapor by high pressure single source mass spectrometry, examining reaction rates as function of primary ion translational energy 16 p2857 A70-34004

Nighttime E region molecular ion production rate estimation, taking into account windshear effect 18 p3245 A70-36022

Ionization rate experimental profiles during maximum solar activity compared with calculations, showing additional source of ionization in E region 19 p3409 A70-37322

Helium plasma ionization rate in positive column with DC discharge, considering gas pressure, electron density, electric field strength and plasma radius 19 p3476 A70-37559

Positive ion and electron production in H atom collisions with atomic and molecular gases, deriving ionization cross sections 20 p3675 A70-39605

Upper atmosphere ammonia release experiments testing hypothetical mechanisms of radicals and ions formation in comets 20 p3708 A70-39962

SERT 2 Hg thrust ion extraction, loss, production and energy balance within ionization chamber [AIAA PAPER 70-1091] 20 p3693 A70-40244

Low voltage arc nonequilibrium ionization rate, taking into account atom-electron collisions 20 p3684 A70-40389

Altitude spectrum of ion formation in interaction of proton flux with atmosphere, using Bragg dissipation function 21 p3878 A70-40846

Plasma sheath boundary in anisotropic plasma taking into account ionization rate, momentum transferring collisions and finite ion temperature 22 p4077 A70-42291

Ionospheric bremsstrahlung X ray flux and ionization rate, considering electron-atom and electron-ion collisions as function of altitude 22 p4095 A70-43293

Ionization rate and electron density height profiles for typical auroral proton energy spectrum, noting radio noise absorption, sporadic E and radio aurora 22 p4024 A70-43307

Ionization rates in auroras detected by atomic oxygen and nitrogen lines 22 p4024 A70-43308

Bremsstrahlung X rays caused by energetic electrons precipitating into upper atmosphere, calculating photoionization rate as function of altitude 22 p4096 A70-43310

E region additional ionization source during solar activity maximum, analyzing ion production function and electron concentration 23 p4190 A70-44077

Autoionization theory application to partial solar photoionization cross sections for production rates of vibrationally excited positive molecular oxygen ions 23 p4222 A70-44785

ION PROPULSION

Solar photoelectric power ion propelled probe of asteroid region, describing design and mission planning [AIAA PAPER 69-1105] 02 p0382 A70-12529

Ion thruster with hollow cathode electron source, discussing operation principles, experimental characteristics, etc 03 p0552 A70-14150

TV data transmitted by Iantars series automatic ionospheric laboratories released by geophysical rockets at 100-400 km, discussing plasma-ion propulsion system performance 04 p0735 A70-14936

Suboptimal stabilization of axially symmetric satellite angular velocity, using ionic propulsion system as control torque 06 p1155 A70-17554

Quasi-steady coaxial MPD arcs characteristics, studying Ar ion velocities, electrostatic ion acceleration mechanism and arc voltage gradient [AIAA PAPER 70-165] 06 p1132 A70-18208

Thrust vectoring of multipaperture Cc electron bombardment ion engines, determining thrust deflection limit by accelerator current rise 11 p2102 A70-26124

- Suboptimal satellite attitude control using ionic microthrusters operating by large modulated amplitude impulses caused by electrostatic deflection of beam 13 p2501 A70-28426
- Switch controlled resonant current pulse modulation for power converters, noting integration with spacecraft ion propulsion engine 14 p2535 A70-31324
- Ion electric propulsion system coupled with small booster for geostationary orbit realization 15 p2790 A70-32276
- Hollow cathode ion thruster and lightweight power conditioner of solar-electric propulsion system for unmanned deep space probes [ALAA PAPER 70-648] 16 p2966 A70-33546
- Optimum low thrust ion propelled interplanetary trajectory design using two step Chebyshev method 17 p3167 A70-35232
- Communication satellites low thrust transfer to synchronous orbit by two-stage operation using hydrogen resistojets and Hg ion motors [ALAA PAPER 70-1116] 20 p3691 A70-40227
- RF ion source for electrostatic spacecraft propulsion, discussing RIT-10 performance optimization and development [ALAA PAPER 70-1102] 20 p3692 A70-40236
- Ion thrust vectoring systems for satellite attitude control and stationkeeping, discussing deflection techniques [ALAA PAPER 70-1150] 21 p3868 A70-41783
- Three axis attitude ion thrust vector control mechanism for solar electric propulsion spacecraft, discussing gimbal and translation actuators, array and cabling [ALAA PAPER 70-1156] 21 p3759 A70-41784
- Low thrust trajectory transfer from low to synchronous orbit, examining hydrogen resistance jet and mercury bombardment ion thruster 22 p4089 A70-42487
- Solar-electric ion propulsion mission analysis and spacecraft designs, discussing thruster, power conditioning, propellant storage and feed, etc 23 p4234 A70-44631
- Ion micropropulsion for geostationary satellites time optimal attitude control 23 p4261 A70-44669
- ION PUMPS**
- Superhigh vacuum pump with orbitron ionizer, describing construction and ionization 16 p2843 A70-33214
- Aerospace coldness and vacuum simulation, discussing uses of cryogenic, titanium sublimation, ion and molecular pumps 19 p3396 A70-37462
- Residual atmosphere analysis and application to ion pumping on Al alloy high pressure chamber of differential vacuum system 19 p3434 A70-37464
- Monovalent cations active transport model in mitochondria, noting membrane potential as driving force and ion pump omission 24 p4304 A70-46230
- ION RECOMBINATION**
- Stimulated emission of RF recombination lines from ionized atoms in H I regions 02 p0372 A70-12251
- Positive ion concentration profiles in lower nighttime midlatitude ionosphere calculated from corpuscular radiation measurements and ion recombination constants 04 p0738 A70-14436
- Neutral gas ionization and ion recombination effect on electrodynamic plasma acceleration in coaxial and flat electrode accelerators 04 p0728 A70-15222
- Dissociative recombination coefficient ratio between O ion and nitrogen oxide ion in ionosphere using rocket data 04 p0683 A70-15743
- Excitation, ionization and recombination rates for charged ions during collisions with electrons in solar corona assuming Maxwellian electron distribution 07 p1384 A70-19409
- Variational model of collisional-radiative recombination of atomic ions in hydrogen and alkali plasmas 09 p1735 A70-22828
- H II region properties from non-LTE analysis of alpha, beta, gamma, delta and epsilon radio recombination line data, determining electron temperature and concentrations 10 p1945 A70-24959
- E and F layer ion chemistry dependence on ion-neutral reactions and dissociative recombination 12 p2223 A70-27220
- Positive ion concentration profiles in lower nighttime midlatitude ionosphere calculated from corpuscular radiation measurements and ion recombination constants 13 p2475 A70-28461
- Laser emission generation on sodium lines, studying pulsed discharge mechanism involving ion recombination in sodium vapor and hydrogen mixture 13 p2425 A70-28600

- Ionization equilibria and ionization and recombination rates for Fe and Ni ions, discussing dielectronic recombination 14 p2631 A70-30727
- Dissociative recombination coefficient ratio between O ion and nitrogen oxide ion in ionosphere using rocket data 14 p2576 A70-30827
- UV oxygen nightglow observation by OGO-4, examining ion-ion neutralization and radiative recombination production mechanisms 20 p3621 A70-39344

ION SCATTERING

- Differential elastic scattering cross section of Ar nozzle beam in nitrogen considered with rainbow effect in determining intermolecular potential well depth 02 p0344 A70-12722
- Magnetic disturbance associated with E layer east-west electric current calculated in terms of ionization production and loss 05 p0838 A70-16282
- Energy distribution of positive Ar ions scattered from thermal diatomic D noting inelastic collisions 07 p1339 A70-20056
- Free-free opacity of stellar interiors by ion correlations applied to red giant degenerate cores 09 p1755 A70-22510
- Cross sections for electron impact excitation of positive helium and hydrogen ions, using non-relativistic Coulomb-Born-Oppenheimer reactance matrices 13 p2455 A70-28988
- Ionized impurity scattering in polar semiconductors by strong electric fields, using energy and momentum conservation equations in electron temperature approximation 13 p2472 A70-30017
- Ion line Stark broadening, considering electron-ion quadrupole excitation and electron resonant scattering 14 p2620 A70-31376
- Ion beam scattering at turbulent plasma oscillations in glass chamber containing low pressure air 16 p2958 A70-33253
- Li ion elastic scattering by He, calculating ground state interaction potential 16 p2956 A70-34310
- Ion beam scattering at turbulent plasma oscillations in glass chamber containing low pressure air 23 p4226 A70-44282

ION SHEATHS

- Extraterrestrial electron density precision measurement using HF impedance probe with guard ring to remove ion sheath effects 10 p1892 A70-25255
- Space charge sheath electric thruster principles, construction and performance using laboratory test model [ALAA PAPER 69-282] 11 p2102 A70-26121
- Cylindrical antenna admittance during immersion in ionospheric plasma, noting influence of ion sheath and plasma anisotropy 13 p2371 A70-29922
- Electron emission effects on ion sheath and probe characteristics in continuum argon plasma 17 p3083 A70-34994
- Slow wave propagation on conducting surface separated from plasma by ion sheath, observing resonances on cylindrical antenna 22 p4082 A70-43238

ION SOURCES

- NT PLASMATRONS**
- Ar X and Ar XIV identification in solar corona and unidentified coronal lines origin, discussing Fe and Ni transitions from metastable levels 03 p0571 A70-13598
- Ionic collision processes in nitrogen and oxygen mixtures in mass spectrometer ion source 04 p0646 A70-14700
- Electrohydrodynamic /EHD/ technique for generating ions from liquid metals by using electrostatic forces to overcome surface tension forces for field emission of ions 06 p1125 A70-18610
- Venusian ionosphere thermal protons and/or deuterons source observed by radio occultation method, suggesting dominance at high altitudes 10 p1938 A70-24068
- Ion thrusters and sources in space propulsion, discussing power supply level, efficiency and service lifetime [ONERA-TP-739] 15 p2787 A70-31808
- Ionspheric spacecraft flight conditions simulation in vacuum chamber, discussing low energy ion sources 15 p2717 A70-31814
- Negative hydrogen ion balance in high intensity plasma source, measuring flux as function of discharge current 15 p2780 A70-32195
- Ionization rate experimental profiles during maximum solar activity compared with calculations, showing additional source of ionization in E region 19 p3409 A70-37322
- Energy distribution of ions transversal to magnetic field in argon plasma source with oscillating electrons,

showing dependence on induction and discharge current 19 p3482 A70-38956

Lower ionosphere electron concentration space-time variations relation to ionization source intensity fluctuations based on rocket observations and ground sounding data 23 p4190 A70-44079

Ion source emitter plasma column generated by electron beam injection through gas filled chamber, compensating ion space charge with fast discharge electrons 24 p4385 A70-45451

ION TEMPERATURE

- Ionspheric measurements of electron density, electron and ion temperature profiles from strength of incoherent radio wave scattering 01 p0082 A70-11530
- Sputtering yield of amorphous and polycrystalline targets bombarded by energetic ions or recoil atoms calculated by integrodifferential equations derived from Boltzmann transport equation 02 p0343 A70-11885
- Ionization and electron temperature dependence on shock wave structure in partially ionized hydrogen plasma allowing for luminescent energy losses 03 p0465 A70-13060
- Radar Thomson backscatter observations of ion temperature and ion-neutral collision frequency used to investigate reversible heating in E region 03 p0477 A70-13988
- Quasi-linear mode coupling in confined hot-ion Penning discharge plasma, discussing externally imposed excitation and internally generated oscillations 05 p0888 A70-16166
- Temperature measurements in magnetic beach of steady state deuterium plasma, confirming ion-cyclotron waves thermalization 05 p0884 A70-16167
- HF drift instabilities of plasma with nonuniform magnetic field, studying anomalous ion heating and resistance in Zeta installations 06 p1119 A70-17502
- Solar wind temperature, using distribution function for solar wind ions in anisotropic Maxwell distribution form 06 p1135 A70-17895
- Waves and differential equations for electromagnetic field in nonuniform magnetized plasma described for all orders in electron and ion temperature 07 p1350 A70-19823
- Aerodynamic coefficients for axisymmetric bodies moving in rarefied plasma, calculating corrections for thermal ion velocities 08 p1432 A70-21089
- Plasma temperatures in magnetosphere, investigating ion energy balance, electron heating and agreement with rocket measurements 08 p1489 A70-21381
- Electron-to-ion temperature ratio determined from ion and plasma line components of radar Thomson scatter signal from ionosphere 08 p1489 A70-21389
- Turbulent diffusion and ion heating in plasmas in presence of current instability 08 p1554 A70-21813
- Stationary collisionless shock waves in hot initial plasma produced by theta pinch discharge, discussing magnetic field, density and electron temperature profiles 10 p1924 A70-24697
- Interplanetary medium kinetic equations to limit ion temperature anisotropies in solar wind, discussing Coulomb collisions and ion-cyclotron instability effects 11 p2105 A70-26561
- Ion temperature gradient along magnetic field lines in outer plasmasphere by thermal diffusion equations compared with electron temperature observations 11 p2047 A70-26568
- Ionspheric electron and ion temperatures information extraction from Doppler broadening of radar returns based on correlation measurement 12 p2183 A70-27163
- Ionspheric electron density, electron and ion temperature profiles measurements, comparing relative merits of radio-rocket ground-based radar and satellite methods 12 p2223 A70-27277
- Drift instability and ion heating by high amplitude magnetosonic wave in plasma waveguide in constant magnetic field 13 p2463 A70-29381
- Ionic temperature difference from Arecibo data indicated in Injun 3 and Alouette 1 sonograms of proton whistlers propagation time, noting Doppler shift role 13 p2372 A70-29928
- Electron and positive ion velocity distributions measurements near earth bow shock by electrostatic analyzer on Vela 4B satellite 13 p2481 A70-30068
- Radial ion temperature distribution in hydrogen arc within axial magnetic field measured spectroscopically by thermal Doppler effect 14 p2621 A70-30657

Ion temperature sensitive end effect in long cylindrical Langmuir probe response in high speed collisionless plasma flow at ionospheric satellite conditions

14 p2577 A70-31038

Electron and ion temperature and electron density relationship in F region during sunspot maximum, using incoherent scatter experiment

14 p2581 A70-31271

Time resolved measurements of ion and electron temperature in pulsed Ar ion laser discharge, observing heating

17 p3108 A70-35907

Hydrogen, He and oxygen ion density, and ion and electron temperatures in upper ionosphere fromOGO 4 observations

18 p3244 A70-36016

Upper atmospheric ions kinetic temperatures based on chromatic broadening of mass spectral lines

18 p3252 A70-36985

Energy levels and spectral broadening of neodymium ions in laser glass from fluorescence and absorption spectra

19 p3445 A70-37760

Ion temperatures and incident intensities in plasmas produced by solid target irradiation with Q switched laser beam

19 p3479 A70-37765

Ion heating during plasma instability due to interaction with electron beam in mirror magnetic trap

20 p3678 A70-39598

Nonlinear resonant heating in magneto-plasma, calculating energy absorption by ions and plasma wave amplitude

20 p3685 A70-40467

Temporal and spatial origin of hot ions in turbulent plasma heating, using particle analysis

21 p3855 A70-40824

F region synoptic electron densities and electron and ion temperatures from Thomson scatter radar data

21 p3816 A70-41065

Midlatitude F region electron and ion temperatures during magnetic storms, examining Thomson scattering, density and time dependence

21 p3817 A70-41094

Ruby giant pulse laser produced plasmas from aluminum and copper surfaces, measuring electron and ion energies by time of flight and retarding potential techniques

21 p3860 A70-41925

Plasma sheath boundary in anisotropic plasma taking into account ionization rate, momentum transferring collisions and finite ion temperature

22 p4077 A70-42291

Constricted arc characteristics in air and nitrogen at various pressures, considering spectral lines radiation transfer and electron, atom and ion temperature difference effects

22 p4079 A70-42369

Ionospheric ion temperature measurements by retarding potential analyzer onOGO-6 satellite

23 p4185 A70-43840

LF plasma waves amplification by beam-plasma interaction, considering electron and ion temperatures effects

24 p4387 A70-45797

Translational temperature measurement of atoms and ions in plasma based on wavelength reduction by X ray spectroscopy

24 p4388 A70-46208

ION TRAPS [INSTRUMENTATION]

Low energy ion spectrum and spatial distribution measurements in auroral zones by Cosmos-261 satellite spectrometer

08 p1492 A70-21798

Elongation characteristics of modulation type charged particle traps and analyzers, discussing ions and electrons trapping

18 p3307 A70-36171

Spacecraft sheath structure, potential and velocity effects on ion current measurements by traps and mass spectrometers

21 p3816 A70-41087

ION-GAS INTERACTIONS

U GAS-ION INTERACTIONS

IONIC COLLISIONS

Ionization instability in low temperature magnetized plasma, analyzing electron concentration perturbation caused by Joule heating during electron-ion collisions

01 p0153 A70-11598

Cross sections determined for formation of secondary positive molecular and atomic hydrogen ions during 1.4-46 kev positive molecular hydrogen passing through hydrogen

02 p0344 A70-12704

Ionization studies in collision dominated high pressure flame plasma using electrostatic probes

03 p0534 A70-14212

Ion collision processes in nitrogen and oxygen mixtures in mass spectrometer ion source

04 p0646 A70-14700

Vibration effects on ion-molecule collision lifetimes and multiple reflections

04 p0723 A70-15638

Lift and drag forces measured on metal surfaces inclined to Ar ion stream above and below earth-satellite speeds in free molecular flow

06 p1111 A70-18269

Collisions effects on ion saturation and electron currents in electron retarding region of cylindrical and spherical electrostatic probes, noting applicability over wide range

06 p1123 A70-18303

Excitation, ionization and recombination rates for charged ions during collisions with electrons in solar corona assuming Maxwellian electron distribution

07 p1384 A70-19409

Electrical conductivity and conductive opacity for relativistic electron gas in presence of ions taking into account ion-ion interaction

09 p1727 A70-22509

Charge exchange cross section of hydrogen position ion-negative ion collisions

09 p1733 A70-23269

Charge exchange probability in proton-hydrogen atom collisions computed with two state atomic orbital expansion

09 p1733 A70-23270

Associative and collisional detachment in H atom and negative ion collisions based on complex adiabatic potential

09 p1733 A70-23431

Ionospheric F and E layers collision frequency estimates, comparing pulse absorption and cosmic radio noise measurements

10 p1880 A70-24804

Ar ions excitations by low energy electron collisions, noting excitation functions and cross sections of lines and levels by optical methods

12 p2278 A70-27501

Diffusion coefficients measurements in velocity space from ion-ion collisions and ion wave microturbulence, supporting theoretical calculations and diffusion equations in plasma

12 p2279 A70-27777

Electron impact excitation cross section of /0,0/ first negative band of nitrogen ion from threshold to 3 keV, using photon counting techniques

12 p2276 A70-27880

Collisional theory of longitudinal wave propagation in partly ionized multitemperature gases

13 p2460 A70-28637

Collision effect on phenomena associated with ion cyclotron whistler formation, considering ionospheric day time model

13 p2468 A70-29933

Charge, hydrogen atom and ion transfer in collisions involving deuterium-labeled methanol- acetaldehyde system and molecular ions

14 p2543 A70-30110

Ion collision processes in water vapor by high pressure single source mass spectrometry, examining reaction rates as function of primary ion translational energy

16 p2857 A70-34004

NO and oxygen ions vibrational excitation due to inelastic scattering from He, calculating scattering angle variation

16 p2955 A70-34010

Inelastic energy losses in oxygen ion beams collisions with neutral molecules, determining vibrational transition probabilities

16 p2955 A70-34011

Collisions effects on ion collection by Langmuir probes, determining plasma density

17 p3139 A70-34494

Total cross sections for production of free electrons in collisions of low energy negative atomic oxygen ions with molecular nitrogen

18 p3292 A70-36188

Ion-polar molecule collision time history plots and computer movies, calculating capture cross sections for mass spectrometry

18 p3292 A70-36561

Ion collision effect in quadrupole mass spectrometer, describing ion energy, total pressure in system and other parameters

19 p3421 A70-37411

Ion-molecule pair relative motion in capture collisions, using computer-made movies

19 p3474 A70-38796

ELF and VLF propagation for perturbed ionosphere models, discussing effects of ion collision frequencies and molecular weights

20 p3585 A70-39454

He/plus/-H/minus/ collisional charge exchange cross sections, using modulated inclined ion beams technique

21 p3852 A70-40599

Collision induced dissociation of nitric oxide and molecular oxygen ions at low kinetic energies, noting internal ionic excitation effects

21 p3773 A70-41398

Mass spectroscopy analysis of neutral and ionic population of plasma in carbon dioxide laser gas mixture, discussing collision processes

21 p3838 A70-42006

Electron impact induced transitions in ions with configurations 3p/q responsible for forbidden lines in gaseous nebulae

22 p4105 A70-43234

LF resonances and potential in plane nonisothermal plasma layer, considering electromagnetic field interaction and ionic collisions

24 p4383 A70-45116

Ion-ion potential for sodium vapor for second virial coefficient as function of temperature at 1200-1700 K

24 p4381 A70-45649

Low energy proton-hydrogen collisions, computing differential cross sections for direct elastic scattering, resonant charge exchange and direct and exchange excitation

24 p4382 A70-46226

IONIC CONDUCTIVITY

U ION CURRENTS

IONIC CRYSTALS

Magnetoresistance effects in impurity conduction mode of n-type GaAs crystals below 6 K, giving electron concentration

07 p1356 A70-19796

Plastic properties of materials to elastic limit of pure metal and ionic solid crystals

12 p2283 A70-27055

Inorganic laser materials containing ionic crystalline structures, including fluorides, oxides, rubies, garnets and oxygen containing complex compounds

16 p2927 A70-33223

Ion magnetic moments in crystallographically nonequivalent lattice regions in ferrites

19 p3484 A70-37622

Sulfur trichloride-Al tetrachloride complex ionic structure from Raman spectra and nuclear quadrupole resonance data

21 p3772 A70-40912

IONIC DIFFUSION

Oxide spinel formation kinetics and reaction mechanisms with emphasis on Ni and Co chromites, discussing cation diffusion

09 p1739 A70-22307

Meteor ionized trails initial expansion and diffusion resulting in dissociation and ionization of air molecules through collision, using electromagnetic wave scattering

09 p1762 A70-23177

Helium ions diffusion perpendicular to magnetic field in He gas, measuring coefficients as function of field strength and for various gas pressures

10 p1925 A70-25108

CaO reaction rate with ZrC in effusion cells as function of reactant ion diffusion through product layer

13 p2362 A70-29496

Slow ions mobility, diffusion and reactions in gases by drift tubes, developing mathematical analysis of drifting ion swarm space-time behavior

20 p3676 A70-40152

Minor ion diffusion coefficients in F 2 region, noting Coulomb collisions role in ion density sensitivity to ionospheric fluxes

22 p4019 A70-43109

Monovalent cations active transport model in mitochondria, noting membrane potential as driving force and ion pump omission

24 p4304 A70-46230

Anions and cations diffusion during oxidation of Ni-V-Ti alloys, using chemical and electron microprobe analyses

24 p4364 A70-46335

IONIC MOBILITY

Cs atomic and molecular ions mobilities and drift velocities in Cs vapor at different pressures in low electric fields

04 p0722 A70-14715

Nitrogen oxide ions mobility in air calculated at high plasma temperatures

12 p2276 A70-27845

Mesosphere payload to measure neutral gas density, positive and negative ions concentration and mobility in D region

13 p2393 A70-28682

Slow ions mobility, diffusion and reactions in gases by drift tubes, developing mathematical analysis of drifting ion swarm space-time behavior

20 p3676 A70-40152

Monovalent cations active transport model in mitochondria, noting membrane potential as driving force and ion pump omission

24 p4304 A70-46230

IONIC PROPELLANTS

U ION ENGINES

IONIC REACTIONS

Negative ion reactions relevant to D region measured in ESSA flowing afterglow system as function of temperature

01 p0070 A70-10406

Ionospheric ion and neutral constituents composition from D region to magnetopause, noting ion-chemical reaction rates

01 p0074 A70-10588

Molecular hydrogen destruction by reaction with carbon dioxide ion in Martian ionosphere, discussing conversion into atomic hydrogen

03 p0575 A70-13997

Ion-neutral reactions in carbon dioxide subjected to electron impact using mass spectrometry

04 p0646 A70-14698

Mass spectrometric determination of proton affinities of simple molecules determined from proton transfer and ion-molecule reactions

05 p0885 A70-17081

Low pressure ionic reactions in gaseous cyclobutane

06 p1004 A70-17328

Kinetic analysis of ion-molecule reactions in Ar-N mixtures with H₂, deuterium and HD using ion ejection mode of ion-cyclotron-resonance spectroscopy

06 p1108 A70-17332

Dissociative charge-transfer reactions of positive He ions with molecular N and O measured in drift tube-mass spectrometer

06 p1109 A70-17490

Reactions determining ion composition in E region, discussing neutral composition variations from day to night and during solar activity cycles

07 p1276 A70-20431

Probability coefficients computation for transitions between energy levels of ion A XIV in solar corona

09 p1761 A70-23060

F region ion-molecule reaction rate constants laboratory measurements, observing reactions energy dependence

10 p1872 A70-23825

Charge transfer reactions of negative ions with oxygen investigated for energy dependence, yielding evidence on oxygen electron affinity

10 p1919 A70-24402

High energy oxygen positive-ion reaction with molecular nitrogen, presenting semiempirical model with assumed crossing of potential energy surfaces

10 p1920 A70-25146

Ionospheric reaction rate coefficients based on electron concentration curves, discussing maximum number and accuracy obtainable

11 p2043 A70-25538

Ion cyclotron resonance spectroscopy technique for determining electrons photodetachment energy from negative ions in gas phase

11 p1995 A70-26001

Reagent translational energy effect on dynamics of ionic and atomic reactions, using nuclear recoil and chemical accelerator methods

11 p1995 A70-26005

Methyl fluoride calculated for ion-molecule reaction rate constants from ion cyclotron resonance spectra

12 p2180 A70-26862

Methanol proton transfer reaction rate energy dependence

12 p2180 A70-26863

Ammonium ions elimination from atmospheric moisture condensates by treatment with metal-exchange resins, discussing volume sorption capacity

13 p2362 A70-29339

Rare gas diatomic ions reactions with molecules and rare gas atoms, measuring rate coefficients and product channels by flowing afterglow technique

15 p2776 A70-31726

Rare gas diatomic and hydride ions reactions with hydrogen, determining rate coefficients and product channels by flowing afterglow technique

15 p2776 A70-31727

Free energy and enthalpy of single ion solvation in water and propylene carbonate, using electrostatic model

15 p2695 A70-32829

Ion-molecule reactions produced in phosphine by ion cyclotron resonance

16 p2855 A70-33061

Ethyl nitrate positive and negative ion-molecule chemistry investigated by ion cyclotron single/double resonance techniques

16 p2855 A70-33090

Thermal energy negative ion-molecule reactions in photoionized NO-water vapor mixtures, determining rate constants by stationary afterglow system

16 p2954 A70-33280

Thermal product distributions and energy dependencies of ion-molecule reactions in allene and propyne, using ion cyclotron resonance

16 p2856 A70-33651

Hydrogen ion-molecule reactions analysis by flowing afterglow technique, noting application to proton affinity measurement

16 p2857 A70-34005

Ethylene and ethylene-acetylene mixtures ion-molecule reaction product distributions calculation using quasi-equilibrium theory of unimolecular reactions

16 p2858 A70-34012

Ion-molecule reactions investigation by resonance principle, discussing ion paths in crossed fields

17 p3081 A70-34574

Tropical UV nightglow, considering oxygen ion-ion neutralization reaction as primary source

18 p3244 A70-36015

Atmospheric ions interaction with rocket exhaust gas water molecules, using sounding rocket mass spectrometric data

18 p3293 A70-36982

Ionospheric Si and SiO ions equilibrium interconversion during Leonid meteor shower

20 p3621 A70-39351

Hydrogen negative ion thermal energy reactions with oxygen, nitric oxide, carbon monoxide and nitrous oxide, determining rate constants

20 p3583 A70-39616

Slow ions mobility, diffusion and reactions in gases by drift tubes, developing mathematical analysis of drifting ion swarm space-time behavior

20 p3676 A70-40152

Ion-molecule reactions in mixtures of hydrogen sulfide with ethylene and acetylene from deuterium labeling studies via ion cyclotron resonance spectroscopy

21 p3773 A70-41200

Ionospheric reaction rate coefficients based on electron concentration curves, discussing maximum number and accuracy obtainable

21 p3819 A70-41288

Moist air expansion through supersonic nozzle, investigating small ions role in water condensation

22 p4011 A70-42774

D region ion chemistry, discussing three body reactions, water cluster ion production, reaction rates and binary collisions

22 p4023 A70-43304

Ionization and loss processes for meteoric elements in lower ionosphere, suggesting hydrates formation role in alkali metal ions depletion

22 p4106 A70-43305

Effective collision cross section for reaction resulting in Cs ions neutralization in thermal Cs plasma calculated from measured ion currents

22 p4082 A70-43374

Ion cyclotron resonance spectroscopy for detecting trapped gaseous ions in analyzer cell, observing ion-molecule reactions

23 p4196 A70-44390

IONIC WAVES

Electron trapping effect on ion-wave instability in plasma, deriving expression for saturation energy spectrum

01 p0152 A70-11361

Auroral radio reflections using two coherent bistatic radio systems, discussing ionoacoustic waves in auroral plasma

05 p0837 A70-16072

Electron plasma wave damping by ion sound wave scattering using Vlasov equation

06 p1125 A70-18638

LF ion-acoustic waves in ionosphere, considering electric and magnetic field variations, instability, etc

07 p1347 A70-19187

Ionic noise during plasma turbulent heating in toroidal facility, discussing oscillation spectrum

07 p1349 A70-19552

Dispersion of ion-acoustic waves in quiescent rare gas discharge plasmas, discussing model simulating ion waves generated by finite sine wave bursts

07 p1352 A70-19990

Ion-acoustic wave oscillations of weak collision plasma in strong electromagnetic field, discussing instability

09 p1736 A70-23198

Ion acoustic wave propagation near sheath at plasma-wall boundary in low pressure argon plasma measured by electron beam probe

10 p1921 A70-23965

Ion-burst excited by pulsed mesh grid in plasma in connection with sheath structure

10 p1922 A70-23989

Type I comet tails orientations dispersion attributed to nonradial plasma waves and discontinuities in interplanetary gas, calculating solar angular momentum loss rate

10 p1947 A70-24987

Diffusion coefficients measurements in velocity space from ion-ion collisions and ion wave microturbulence, supporting theoretical calculations and diffusion equations in plasma

12 p2279 A70-27777

Radiation characteristics of ion acoustic waves from monopole and dipole antennas, observing patterns of longitudinal wave in isotropic plasma

12 p2279 A70-27778

Spherical electroacoustic waves in drifting thermal plasma, describing ion acoustic perturbations

12 p2279 A70-27779

Ionic noise during plasma turbulent heating in toroidal facility, discussing oscillation spectrum

15 p2777 A70-31459

Electron-acoustic, ion-acoustic and electromagnetic plane waves coupling at shock front in two fluid ionized viscous plasma

16 p2958 A70-33282

Collisional effects on second order spatial ion wave echo, evaluating velocity integral

19 p3475 A70-37539

Electrostatic ion waves in uniform magnetic field, calculating phase and group velocities as function of propagation angle for comparison with dispersion measurements

20 p3678 A70-39659

Radio aurora model based on two stream, ion acoustic wave instability, investigating radar backscatter

20 p3623 A70-40465

Current driven ion wave plasma turbulence in collisionless shock, measuring frequency and wave number spectra by shock front light scattering

20 p3685 A70-40497

Phase rate of plasma potential variations in fast ionization waves without electron distribution assumptions

21 p3856 A70-40949

Collisionless shock wave geometry, determining dispersion relation for ion acoustic waves propagating in plasma

21 p3856 A70-41082

Ion sound system one dimensional hydrodynamic equations, examining formation and interaction of nonlinear ion acoustic shock waves

21 p3856 A70-41384

Continuous pseudoacoustic and ion waves excitation and damping in plasma sheath around grid, taking into account transit time effect on ion acceleration

21 p3858 A70-41710

Electron-ion wave interaction due to scattering by electrons, using kinetic wave equation to describe wave-particle interaction

21 p3858 A70-41712

Collisionless nitrogen plasma drift velocity measurement by ion acoustic wave method

21 p3859 A70-41760

Slow and fast ionization waves in inert gas or molecular gas plasma columns, describing striation formation in neon discharge by hydrodynamic equations

22 p4079 A70-42371

Ionization waves excitation and damping in MHD channels, investigating effects on electric conductivity, Hall parameter and electron temperature

22 p4081 A70-42823

Turbulent plasma without external magnetic field, observing low phase velocity ion wave mode

23 p4227 A70-44893

Bunched ion bursts amplitude modulation effects on nonlinear ion acoustic waves in grid plasma system

23 p4229 A70-44989

Ion acoustic wave propagation in collisionless gravity-supported plasma in static magnetic field calculated from linearized Vlasov equation

24 p4382 A70-45109

Electron plasma oscillations excitation by ion-acoustic waves

24 p4386 A70-45607

LF electrostatic ion cyclotron wave energy resonant power absorption in plasma in axially nonuniform magnetic field

24 p4386 A70-45608

IONIZATION

NT ATMOSPHERIC IONIZATION

NT AURORAL IONIZATION

NT AUTOIONIZATION

NT FLAME IONIZATION

NT GAS IONIZATION

NT ION PRODUCTION RATES

NT NONEQUILIBRIUM IONIZATION

NT PHOTOIONIZATION

NT SURFACE IONIZATION

Radar and photographic studies of meteors from Leonid and Perseid showers, presenting velocities, luminance and ionization

01 p0193 A70-11602

Excited terminal states emission in bound exciton-donor materials to determine donor ionization energies, electron effective masses and electron G values

02 p0350 A70-11847

Ionization losses effect on energy spectra of cosmic ray heavy nuclei with Fermi acceleration, using transfer equation

04 p0742 A70-15201

Multichannel ionization calorimeter data readout into electronic computer using short circuit coil magnetic storage

05 p0816 A70-15947

Electromagnetic wave phase characteristics after free space passage through statistical medium with wave disturbance producing density and ionization

05 p0815 A70-16735

Fast electron ionization losses due to multiple scattering with atoms during passage through thin layer, calculating spatial energy distribution function

08 p1547 A70-20989

Ionization front interactions in interstellar gas, investigating expanding planar H II region and contact discontinuity in H I region

10 p1937 A70-23975

Cs atoms excitation and ionization in Cs diode interelectrode space under Knudsen conditions, considering luminescence and electron energy distribution

10 p1926 A70-25116

Field ionization from hydrogen layers adsorbed at 4.2 K on W emitters in sealed-off tubes

12 p2274 A70-26858

Electron-atom collisions, treating elastic and Mott scatterings, Born approximation and ionization

12 p2274 A70-27062

Ionization instability of finite bounded plasma, investigating electrothermal waves in large disturbance domain by numerical simulation

12 p2163 A70-27065

Impurity centers thermal and autoionization and effective capture cross section dependent on free carrier concentration in GaAs under electric field, allowing for plasma shielding

12 p2285 A70-27361

Feedback stabilization and mode coupling of ionization waves in positive column discharges, noting dynamic stabilization of unstable bounded plasma systems

12 p2280 A70-27787

Partially ionized plasma stability with allowance for ionization and recombination processes, discussing ion-acoustic oscillations

15 p2781 A70-32823

Photoresonant cesium plasma ionization, discussing pumping spectra, electron gas, molecular-atomic ion ratio and dynamics

19 p3474 A70-37440

Ionization stability in low temperature magnetized plasma, using physical plasma model and numerical solution

20 p3679 A70-39983

Charged particle collisions, discussing electron impact ionization of positive ions, detachment from negative ions, ion collisions, etc

20 p3676 A70-40154

Welding electron beams metal penetration dependence on ionization phenomena, discussing model based on self focusing

22 p4043 A70-42379

Ionization waves excitation and damping in MHD channels, investigating effects on electric conductivity, Hall parameter and electron temperature

22 p4081 A70-42823

P-n junction conductance at superhigh frequencies in breakdown region with simultaneous tunneling and impact ionization

23 p4232 A70-45064

IONIZATION CHAMBERS

NT BUBBLE CHAMBERS

NT CLOUD CHAMBERS

NT GEIGER COUNTERS

NT PROPORTIONAL COUNTERS

NT SPARK CHAMBERS

Multichannel spectrometer electronic circuitry for ionization colorimeter providing data on low energy particle interactions, emphasizing reliability and accuracy

05 p0846 A70-15948

Wall effect on differential spectral distortions in cylindrical ionization chamber and proportional counter type detectors

05 p0900 A70-15971

Solar proton flare dose rates, discussing tissue-equivalent-ionization-chamber (TEIC) data usefulness in analyzing possible dose received by man behind shielding

06 p1134 A70-17265

Cosmic ray knee interpretation using polar orbiting ionization chambers data from OGO-2/4

15 p2793 A70-31903

Absolute cosmic ray ionization in lower atmosphere, using air-filled ionization chamber

18 p3305 A70-36001

IONIZATION COEFFICIENTS

Ionization spatial growth similarity with Paschen law in air and nitrogen for specific electric field/gas number density values, discussing ionization coefficients

03 p0528 A70-14087

Ionospheric reaction coefficients estimate to correlate equatorial electron density profile and Jaccchia model of neutral atmosphere

04 p0683 A70-15744

Venus-earth carbon dioxide atomic parameters used to determine ionization and optical emission rates in Venus upper atmosphere resulting from solar cosmic rays

05 p0901 A70-16276

Ionization coefficient calculation for preionizers through electron distribution function solution to Boltzmann equation

13 p2468 A70-29962

Ionospheric reaction coefficients estimate to correlate equatorial electron density profile and Jaccchia model of neutral atmosphere

14 p2576 A70-30828

Electron mobility, diffusion, drift velocity and attachment in oxygen, determining Townsend primary ionization coefficient

15 p2776 A70-31969

Dichlorodifluoromethane ionization and attachment coefficients for wide pressure range

22 p4076 A70-42373

IONIZATION COUNTERS

U IONIZATION CHAMBERS

U RADIATION COUNTERS

IONIZATION CROSS SECTIONS

Total cross section for electron impact excitation and ionization in He, CO, nitrogen, oxygen, carbon

dioxide, ethylene and benzene, emphasizing threshold values

01 p0147 A70-10489

Photoelectron energy spectra and partial photoionization cross sections for carbon dioxide determined with spectrometer at monochromatic incident radiation wavelengths

02 p0343 A70-11903

Cross sections determined for formation of secondary positive molecular and atomic hydrogen ions during 1.4-46 kev positive molecular hydrogen passing through hydrogen

02 p0344 A70-12704

Carbon dioxide electron impact cross sections, analyzing discrete excitation, autoionization, direct and dissociative ionization and use to aeronomy

04 p0722 A70-15121

Nitrogen molecule photoabsorption and photoionization cross sections determination, discussing ionization probability variations and radiationless transitions

07 p1347 A70-20358

Note on Bell-Kingston paper on Born total and differential cross sections for proton impact ionization of He

08 p1548 A70-21501

Ionization of rare gases /H and N/ by nitrogen ions, determining cross sections of formation of slow ions and electrons

08 p1549 A70-21801

Elementary processes cross sections in charged states changes during proton-hydrogen molecule interactions

08 p1549 A70-21817

Vacuum UV photons production during ground state neutral argon atomic collisions, measuring relative cross sections energy dependence

09 p1731 A70-22333

Inner-shell ionizations by proton impact calculated for cross section using impulse approximation model, comparing results with Born approximations

09 p1732 A70-22781

Charged particle interaction influence on photoionization cross section of negative hydrogen ion, considering initial state polarization leading to free s wave electron

09 p1732 A70-22826

Lunar daily and monthly tidal variations in horizontal magnetic field and F 2 region maximum electron density and peak ionization height at Puerto Rico

10 p1872 A70-23823

Threshold photoionization cross sections for homonuclear diatomic N molecules calculated from Slater orbitals and Coulomb waves

11 p2086 A70-25833

Radial wave functions and photoionization cross sections for neutral atoms from central potential model based on Slater and Klein-Brueckner approximations

13 p2455 A70-29133

Interlayer ionization valley depth influence on F region heights, calculating N/h/ profiles from ionograms

14 p2571 A70-30229

Electron impact excitation cross sections of oxygen ion first negative bands, considering relationship to oxygen ionization cross section

14 p2620 A70-31363

Primary cosmic ray flux and p-carbon cross sections measurements by satellites showing heavy particle production at high energies

15 p2792 A70-31733

Quiettime cosmic ray ionization altitude dependence over polar regions from measurements by integrating ionization chamber on OGO-2

15 p2793 A70-31902

Effective cross sections for molecular hydrogen and hydrogen positive ion formation in collisions between He, Ne and Ar ions or atoms

16 p2954 A70-33193

Ce atom collision with excited Hg atom, measuring ionization cross section

18 p3292 A70-36154

Cosmic X rays interstellar absorption, giving atomic He total photoionization cross section

18 p3308 A70-36899

Positive ion and electron production in H atom collisions with atomic and molecular gases, deriving ionization cross sections

20 p3675 A70-39605

Electron impact excitation and ionization cross sections, describing various approximation methods

20 p3675 A70-39937

Nitrogen, hydrogen, oxygen and He total ionization cross sections due to electron impact

21 p3852 A70-40597

Ionization cross sections for excited H atom-ground state H atom collisions, using Born approximation

21 p3852 A70-40719

Photoionization cross sections for atoms and ions of carbon, nitrogen, oxygen and neon as function of wavelength for H II regions and planetary nebulae

22 p4104 A70-42997

Autoionization theory application to partial solar photoionization cross sections for production rates of vibrationally excited positive molecular oxygen ions

23 p4222 A70-44785

Energy loss spectra and collision cross sections for positive ion impact on molecular nitrogen, noting Lyman-Birge-Hopfield system excitation

24 p4381 A70-45599

Interlayer ionization valley depth influence on F region heights, calculating N/h/ profiles from ionograms

24 p4331 A70-46304

IONIZATION FREQUENCIES

Statistical electron density distributions and Thomas-Fermi-Dirac screening functions for positive ions with various ionization degrees

04 p0721 A70-14666

Triply ionized oxygen atom spectrum between 500-8000 A, determining energy levels and ionization limit

15 p2777 A70-32428

IONIZATION GAGES

Ionization gage with screened collector, showing limit current in high vacuum equal to X ray radiation component

05 p0847 A70-15997

Ionization gage with reverse biased silicon carbide p-n junction hot electron emitter as source

12 p2231 A70-27263

Orbitron ion gauge experimental designs for low pressure applications

12 p2231 A70-27264

Ionization measurements by OV-3-6 satellite cold cathode ionization gage of Redhead inverted magnetron type in near circular polar orbit

15 p2723 A70-31660

Hot cathode magnetron ionization gauge design, discussing performance and sensitivity

19 p3421 A70-37467

IONIZATION POTENTIALS

Critical impurity concentrations of He-Ne laser quenching determined with mass spectrometer, giving impurities molecular weight and ionization potential for input powers

01 p0110 A70-10491

Interstellar propagation effect on spectra and charge ratios due to ionization energy loss and nuclear spallation during traversal of matter

05 p0897 A70-15762

Plasma behind pressure front of shock wave investigated for ionization mechanism by microwave reflection and transmission, noting electron temperature distribution

05 p0887 A70-16110

Ionization energies and oscillator strengths for Fe XVI, Co XVII and Ni XVIII by frozen core approximation, noting applications to solar corona

06 p1150 A70-18465

Microwave-induced ionization oscillations in resonant plasma column excited by low pressure mercury DC discharge

10 p1922 A70-23988

Plane, cylindrical and spherical blast waves structure with ionization at local thermodynamic equilibrium analyzed using successive approximation to non-similar solution

10 p1967 A70-23991

Satellite-borne spectrometer for low energy ion measurement

10 p1874 A70-24314

Ionization equilibrium of atoms and hydrogen-like ions in nonthermal plasma, transforming into Saha formula for high electron densities

11 p2086 A70-25836

Statistical mechanics of partially ionized hydrogen plasma, deriving Saha equation to calculate ionization degree and potential for various electron densities and temperature

12 p2281 A70-27882

Gas discharge gap preionization by thin preheated tungsten wire ignition without explosion, resulting in plasma turbulence prevention and radiation density increase

13 p2462 A70-28986

Plasma ionization enhancement by laser line radiation matched to specific atomic transitions

13 p2468 A70-29958

Ionization potentials of elemental abundances in lunar rocks compared with earth crust and class I carbonaceous chondrites, showing lunar materials differentiation

15 p2801 A70-32463

Rocket exhaust micro and mm waves attenuation attributed to low ionization potential metal particles in propellants

17 p3196 A70-35215

Ionization losses effect on spectrum of cosmic rays accelerated in solar chromosphere, interstellar space, supernovae, radiogalaxies, etc

18 p3308 A70-36425

Mass spectrometer modified for use with X-Y recorder for accurate and reproducible ionization efficiency curves

18 p3262 A70-37099

Effective dissociation potential measurement for alkali compound seed in MHD generator working fluid

20 p3682 A70-40159

Phase rate of plasma potential variations in fast ionization waves without electron distribution assumptions

21 p3856 A70-40949

Photocurrent multiplication in single crystal n-type epitaxial GaAs due to impact ionization of shallow donors

22 p4087 A70-43218

Limit analysis for ionization potential reduction effect on ionized gas atomic composition, considering temperature and electron density

23 p4220 A70-44435

Surface potential and electron work function of single crystal plane W/110 under zero-field and strong-field conditions

23 p4230 A70-44797

IONIZED GASES

NT STELLAR WINDS

Heat and mass transfer in Couette flow of partially ionized symmetric diatomic gas for chemical equilibrium and chemically frozen flow cases

01 p0060 A70-10290

Particle diffusion distribution function of two component ionized degenerate gas from Boltzmann transport equation, giving tables for various spin and mass ratios

01 p0151 A70-10318

Mach numbers, electron density and temperature in partially ionized frozen equilibrium flows of Ar in hypersonic nozzle

01 p0063 A70-10994

Statistical mechanical method deriving ionization equilibrium and equations of state for low mass stars, considering Coulombic interactions, nonideal effects, etc

01 p0188 A70-11336

Ionized Ar laboratory laser development using Fabry-Perot etalon cavity and amplifying plasma obtained by electric current passage under pressure

02 p0311 A70-11869

Ionized Ne, Ar and Kr first excited p states lifetime and transition probabilities, tabulating energy levels and mixing coefficients

02 p0343 A70-11887

Evolution and entropy of partially ionized collision dominated plasmas interacting with radiation based on statistical analogs of irreversible thermodynamics

02 p0346 A70-11902

Ionized matter complex at galactic periphery deduced from neutral hydrogen line and continuous spectrum observations

03 p0564 A70-13222

Electron density and temperature in ionized gas created by thermal collisions between neutral particles, analyzing chemical ionization and inelastic collisions influence

03 p0532 A70-13631

Phenomena in ionized gases - Conference, Bucharest, September 1969

03 p0534 A70-14359

Ionization study of gas discharge parameters behind shock wave front produced by moving plasma pulse interaction with immovable gas discharge plasma

03 p0535 A70-14361

Maximum plasma decay rate in heterogeneous medium determined from deionization process in rarefied gases

03 p0536 A70-14369

Dissociative recombination coefficients temperature dependence in molecular neon and argon ions measured under equal gas, ion and electron temperature

04 p0722 A70-14668

Stark broadening of ionized helium lines by collective electric fields in theta pinch

04 p0722 A70-14684

Heat transfer in partially ionized argon plasma flowing in water cooled circular tube as function of temperature, Reynolds number and tube entrance diameters

[ASME PAPER 69-WA/HT-54] 04 p0780 A70-14795

Pulsed Ar ion lasers at high currents, measuring plasma parameters, electrical conductivity, electron temperature and density for inversion mechanism

04 p0703 A70-15617

Time and altitude induced variations in daytime NO and molecular and atomic oxygen ions

05 p0841 A70-16736

Ionized gas height scale changes in polar ionosphere obtained assuming Chapman type ionization distribution

05 p0841 A70-16738

Flat plate boundary layer flow of partially ionized gas, measuring charged particle density, electron temperature and plasma potential distributions with Langmuir probe

[AIAA PAPER 70-86] 06 p1041 A70-18174

Operational characteristics, spectroscopy and inversion mechanisms of noble gas ion lasers in light of plasma theories and atomic data

[AIAA PAPER 70-82] 06 p1083 A70-18236

Ionized formations motion direction and velocity in F region from triangular ionospheric sounding

07 p1267 A70-19451

Heat transfer measurement in ionized high temperature gas flows with discharge shock tube and thermal sensors

07 p1283 A70-19663

Shock ionized Ar flow properties estimation using alignment charts

08 p1551 A70-21324

Ionized matter complex at galactic periphery deduced from neutral hydrogen line and continuous spectrum observations

08 p1580 A70-21655

Line strength and radiative lifetimes for Ne II determined from spontaneous emission data obtained from CW neon laser discharge

09 p1730 A70-22070

Ion density profile across shock in partially ionized gas measured in plasma jet wind tunnel for comparison with Rankine-Hugoniot relation

09 p1662 A70-23235

Ar ion laser performance improvement by using beryllia for sealed-off discharge tube

09 p1699 A70-23443

Coupled Boltzmann and rate equations for free electron distribution function and level populations in monatomic partially ionized gas including nonelastic collisions

10 p1918 A70-23958

High electron density plasma generation by ionized gaseous filament explosion, noting plasma frequency effect on spectral brightness

10 p1915 A70-23961

Noncircular ionized gas motions in NGC 253 central region observed in velocity field analysis, indicating outflow from center

10 p1946 A70-24979

Electric field structure at shock wave front propagating in weakly ionized gas under Ramsauer effect

10 p1871 A70-25121

Boltzmann equations for distribution functions of gas, analyzing neutral or ionized components by linearization method

11 p2090 A70-25946

Turbulent ionized wakes Doppler radar scattering spectrum parameters in terms of wake characteristics using double convolution integral

11 p2010 A70-26271

Electrical conductivity of impact-ionized nitrogen across magnetic field, deriving electron collision frequency

11 p2091 A70-26461

Acoustic perturbations in stationary weakly ionized pulsed neon plasma

11 p2096 A70-26842

Laminar boundary layer and heat flux at forward stagnation point of indestructible body in partially ionized air flow calculated as function of enthalpy

12 p2156 A70-27287

Shock ionized xenon electrical conductivity measurement at high temperatures as function of Mach number, noting equilibrium effects

12 p2281 A70-27807

Alternating electric field effect on weakly ionized gases, analyzing electronic temperature and harmonics generation

13 p2458 A70-28560

Finite amplitude stability of plasma column in weakly ionized gases and in semiconductor plasmas in longitudinal magnetic field

13 p2458 A70-28566

Collisional theory of longitudinal wave propagation in partly ionized multitemperature gases

13 p2460 A70-28637

Plasmopause irregular structure and position indicated by measured distributions of hydrogen and helium thermal positive ions in duskside magnetosphere

13 p2397 A70-29185

Time autocorrelation and power spectrum of radar returns from underdense turbulent ionized gas as function of electron density decay

14 p2551 A70-31035

Transport properties of partially ionized argon based on electron velocity distribution function, comparing to Chapman-Enskog calculations

15 p2774 A70-31799

Magnetic field effect on critical flutter speed and frequency of elastic plate in ionized gas flow, deriving dispersion equation

15 p2818 A70-32173

Spherical electrostatic probe in uniform quiescent continuum slightly ionized gas for range of bias potential and radius-Debye length ratio

16 p2912 A70-33863

Turbulence spectrum functions time variations, examining electron density fluctuations in ionized gas

16 p2894 A70-33886

Argon II line transition probabilities, observing UV spectral region, upper energy levels and temperature differences

16 p2956 A70-34251

Continuum theory of spherical electrostatic probes as measuring devices in high density weakly ionized gases

17 p3140 A70-34931

Electrical conductivity of partially ionized gas in magnetic field by Frost mixture rules extension

17 p3141 A70-34985

Single frequency Ar ion laser, discussing power and frequency stability

17 p3105 A70-35095

Heat exchange in dissociating partly ionized gas flow over critical point on permeable surface with injection into laminar boundary layer

17 p3011 A70-35347

Ionized formations motion direction and velocity in F region from triangular ionospheric sounding

18 p3249 A70-36925

Chemical reactions neutralizing electron-ion gas in F region

18 p3255 A70-37044

Ar ion laser gas discharge tube construction, using anodically oxidized directly cooled aluminum segments

19 p3444 A70-37567

Nonuniform one dimensional flow of slightly ionized gas in infinitely segmented MHD generator with imperfect walls

19 p3478 A70-37588

Ionized argon supersonic flow velocity and local electron density by optical methods

19 p3480 A70-38173

Pi sub u states of positive ionized diatomic oxygen by photoelectron spectrometry

19 p3474 A70-38488

Ionic and molecular gas lasers, discussing pumping, transitions, emission, discharge tube dimensions, cooling, pressures, optical elements and applications

19 p3449 A70-38751

Weakly ionized gas subjected to pulsed DC electric field, analyzing transient relaxation of electrons velocity distribution

19 p3482 A70-38899

Intercomponent momentum and energy exchange in weakly ionized gases, examining kinetic theory of subsonic and supersonic transport processes

19 p3482 A70-38945

Particulate matter interaction with ionized gas in external magnetic field and nonequilibrium state, examining free electron density

20 p3677 A70-39324

Electrothermal mode wave propagation in nonequilibrium partially ionized gas, using model with finite ionization

20 p3680 A70-39984

Nonisothermal condensation in ionized vapor as function of energy additions to droplets

20 p3680 A70-39989

Local variables in boundary layer of high temperature ionized gas flowing in magnetic field, using X ray absorption

20 p3613 A70-40344

Electric field structure at shock wave front propagating in weakly ionized gas under Ramsauer effect

20 p3685 A70-40514

Magnetoelectric electromotive force in media of ions and neutral molecules, using Boltzmann transport equation

21 p3855 A70-40909

Limit analysis for ionization potential reduction effect on ionized gas atomic composition, considering temperature and electron density

23 p4220 A70-44435

Partially ionized gas electron-ion recombination rate coefficients calculation methods compared with Ar plasma data

23 p4226 A70-44436

Partially ionized Ar transport properties, computing electron velocity distribution function as perturbation for Lorentzian mixture

23 p4220 A70-44437

Shock wave electrical precursor measurements in weakly ionized gas, describing approximate electrostatic probe theory and high sensitivity gases

23 p4184 A70-44995

Hydrogen I region anomalous alpha lines recombination in Orion B spectrum, identifying carbon emitter by measured frequency separation

24 p4410 A70-45773

Quasi-homogeneous approximation validity for electron velocity distribution function disturbance in gas plasma column ionization waves discharge involving high currents

24 p4386 A70-45794

Echoes with ion sonar waves in ionized gases, considering ion density disturbances under local excitation

24 p4387 A70-45795

Ionized Ar laser developments, considering power output and radiation spectrum

24 p4356 A70-46324

IONIZED PLASMAS

U PLASMAS [PHYSICS]

IONIZERS

Ionizer design for hydrogen atom beam ensuring storage of polarized protons, using electron beam for ionization

09 p1732 A70-22846

Ionization coefficient calculation for preionizers through electron distribution function solution to Boltzmann equation 13 p2468 A70-29962

IONIZING RADIATION

NT ALPHA PARTICLES
NT BETA PARTICLES
NT COSMIC RAY SHOWERS
NT COSMIC RAYS
NT FAR ULTRAVIOLET RADIATION
NT GAMMA RAY BEAMS
NT GAMMA RAYS
NT LYMAN ALPHA RADIATION
NT NEAR ULTRAVIOLET RADIATION
NT PRIMARY COSMIC RAYS
NT SECONDARY COSMIC RAYS
NT SOLAR COSMIC RAYS
NT SOLAR X-RAYS
NT ULTRAVIOLET RADIATION
NT X RAYS

Radiation detectors for ionizing radiation onboard artificial satellites, considering weight and power supply constraints for ionization chamber, GM, proportional and scintillation counters, etc

Probabilities for cell survival after exposure to ionizing radiation obtained by two compartment model 01 p0093 A70-11254

Corpuscular radiation contributions to D layer ionization determined from intensity measurements 01 p0028 A70-11370

Book on photographic action of ionizing radiations in dosimetry and medical, industrial, neutron, auto- and microradiography, emphasizing photographic materials reaction to photons and particles 01 p0172 A70-11490

Free radical antioxidant reactions in lipids from blood, liver, spleen, brain and intestines of rats exposed to ionizing radiation 02 p0337 A70-11696

Dithiols protective effect against ionizing radiation in mice, noting oxygen pressure drop role 03 p0419 A70-13309

Myocardial changes in rabbits after general chronic ionizing irradiation attributed to lower cardiac activity, hypotrophy and dystrophy 03 p0420 A70-13311

Computer modeling of operational amplifier integrated circuit in ionizing radiation environment, using RLC network and voltage transfer curve 03 p0425 A70-13888

Ionizing radiation response of integrated microcircuits with different circuit functions and manufactured by different methods 04 p0658 A70-14740

Ion implantation for reducing space charge buildup in thermal oxides on silicon exposed to ionizing radiation 04 p0658 A70-14741

Chromium doping effect on ionizing radiation damage in MOS field effect transistors 04 p0731 A70-14743

Physical model to study coaxial or triaxial cable systems interaction with ionizing radiation fields, emphasizing effects governing induced signals 04 p0658 A70-14744

Polar cap absorption midday recovery phenomenon analysis in northern and southern polar auroral regions showing increase in ionizing flux rigidity 04 p0658 A70-14746

Soviet monograph on radiobiological effects of ionizing radiation covering physicochemical and functional cellular changes, recovery mechanisms, etc 04 p0682 A70-15729

Ionizing radiation effect on isolated frog retina using ERG recordings noting reduction of b wave 06 p0992 A70-17350

DNA enzymatic breakdown in *Escherichia coli* as function of ionizing radiation and temperature 08 p1444 A70-20739

May 1966 solar eclipse effects on sporadic E layer, including ionizing radiation decrease relation to boundary and blanketing frequencies decrease 08 p1445 A70-20775

Hydrogen peroxide infusion effect on skin remission following exposure to ionizing radiation on rabbit legs 08 p1490 A70-21432

Ionizing radiation effects on tissues of developing cerebellar cortex of rats 09 p1619 A70-22791

Air and solar activity electrical parameters relationship, observing ionizing radiation increase in upper atmosphere during solar activity 09 p1619 A70-22815

Energy deposition in cells by charged particles during ionizing radiation exposure, discussing RBE /relative biological effectiveness/ and dose-effect relation for neutrons 10 p1885 A70-25268

MOS structures and transistors emission-current degradation mechanism at heterojunction under ionizing radiation 11 p1989 A70-26597

12 p2194 A70-27165

Hypothermia and ionizing radiation effects on hamsters influenza immune response 13 p2349 A70-28834

Hereditary UV luminescence of transplanted cancerous and lymphosarcomatous cells in mice and rats after ionizing radiation exposure 13 p2358 A70-29341

Geoactive ionizing radiation emitted by solar flares having metallic spectral lines of various brightness intensities 14 p2630 A70-30219

Polar cap absorption midday recovery phenomenon analysis in northern and southern polar auroral regions showing increase in ionizing flux rigidity 14 p2575 A70-30813

Monograph on ionizing radiation effects on molecular biology of *Escherichia coli*, discussing cellular damage, DNA degradation and synthesis, incorporating radioactivity, mutations, etc 16 p2848 A70-33098

Combined ultrasonic and ionizing radiation effects on electrophoretic mobility of tumor cells from albino mice 17 p3034 A70-35762

MOS structure, measuring ionizing radiation effects on interface barrier energies by internal photoemission techniques 17 p3144 A70-35901

Ionizing radiation effects on endocrine system, studying ACTH metabolism in rats under X ray irradiation 19 p3372 A70-38723

Solar UV radiation contributing to ionization in higher ionospheric layer over Dushanbe during partial solar eclipse of 20 May 1966 19 p3417 A70-38786

Solar spectral intensity distribution and ionizing radiation spatial emission patterns during eclipse, discussing effects on ionosphere 19 p3418 A70-38908

Radicals induced in thymine monohydrate single crystals by ionizing radiation 20 p3583 A70-40455

Industrial radiography, discussing photographic emulsion layers granular structure formation due to ionizing radiation 24 p4337 A70-45714

Gas ionization with Q switched carbon dioxide laser radiation, determining breakdown threshold or minimum power density requirement 24 p4355 A70-46261

Geoactive ionizing radiation emitted by solar flares having metallic spectral lines of various brightness intensities 24 p4398 A70-46294

IONOGRAMS

Ionogram conjugate echoes observed at Singapore longitudes by Alouette 2 topside sounder, attributing sequential occurrence to field-aligned irregularities in magnetosphere 03 p0477 A70-13986

F region ionograms processing with correction for ionization effects between E and F layers 04 p0684 A70-15748

Ionograms for nonmonotonic vertical distribution of electron concentration in ionosphere from rocket and ground sounding 05 p0842 A70-16757

Spread F echoes due to total reflection from large tilted ionized surfaces, using ionograms and airglow observations to study surface geometry 07 p1271 A70-20158

Vertical incidence /V/ F layer ionograms, magnetograms and signal amplitude data obtained during annual eclipse of 23 November 1965 09 p1671 A70-23494

Ionospheric fine structure from signal broadening measurements on ionograms, including scattering region algorithm 11 p2044 A70-25553

Topside ionosphere structure deduced from resonance spikes on ionograms obtained by Alouette 2 satellite and electron density distributions 13 p2395 A70-29091

F 2 critical frequencies from Alouette 2 satellite ionogram data compared with ground-based sounding results 13 p2396 A70-29094

Floating resonance spike on Alouette 2 ionograms after sounder pulse transmission at half upper hybrid frequency, noting harmonic excitation role 13 p2370 A70-29905

Electron density profile calculation method using ionograms on analog-digital computer 14 p2569 A70-30209

F region ionograms processing with correction for ionization effects between E and F layers 14 p2576 A70-30832

Ionospheric electron density profiles between two locations calculated from oblique incidence ionograms, plotting radio path for ground range 15 p2726 A70-31861

Iterative solution for electron density profiles from topside ionograms 16 p2900 A70-32931

Magnetospheric component of entire N/z profile on incomplete ionospheric traces, including invisible part of ionogram 19 p3419 A70-38957

Diffuse plasma resonance sequence observed on Alouette 2 ionograms, showing pattern similar to spread echo 20 p3620 A70-39335

Ionospheric fine structure from signal broadening measurements on ionograms, including scattering region algorithm 21 p3819 A70-41303

Electron density profile calculation method using ionograms on analog-digital computer 24 p4330 A70-46284

IONOSPHERIC

Ionospheric fine structure from signal broadening measurements on ionograms, including scattering region algorithm 21 p3819 A70-41303

Electron density profile calculation method using ionograms on analog-digital computer 24 p4330 A70-46284

Ionospheric probing using pulsed radio waves at oblique incidence, discussing auroral radar, meteor radar, ground backscatter and variable frequency ionospheric techniques 12 p2224 A70-27728

IONOSPHERE

NT D REGION
NT E REGION
NT E-2 LAYER
NT F REGION
NT F 1 REGION
NT F 2 REGION
NT LOWER IONOSPHERE
NT SPORADIC E LAYER

Ionospheric auroral oval, proton aurora and midlatitude trough relationship to magnetospheric structure, trapping outer boundary, storm time belt and plasmopause 01 p0073 A70-10586

Ionosphere atmospheric densities from Explorer 32 drag data including semiannual variations 01 p0077 A70-11206

Cerenkov radiation from electrons in magnetosphere and ionosphere, analyzing radiated power relationship with frequencies and latitudes 01 p0080 A70-11226

Reflection coefficient of electromagnetic wave reflected from thin ionization layer, using frequency dependence of amplitude to estimate ionospheric layer thickness 01 p0083 A70-11532

Electron flux parameters determination from ionograms and reflected signal amplitudes between 120-130 km, considering electron collision frequencies 01 p0084 A70-11551

Ionospheric phenomenon, discussing experimental techniques, physical properties and chemical composition, regular and irregular variations, sporadic E ionization, etc 02 p0289 A70-12071

Hydromagnetic forces effects on tidal period hydrodynamic waves, explaining ionospheric tidal motion behavior 03 p0478 A70-13995

Electron temperature anisotropy in ionospheric plasma for case of ionizing sunlight propagating along geomagnetic field 03 p0479 A70-14376

Intermediate ionospheric layer at high latitudes, discussing relationship to geomagnetic and auroral activity and F region continuity 04 p0678 A70-14974

Steady, ambipolar, low and high speed plasma transport equations developed for terrestrial ionosphere, discussing boundary conditions for supersonic and subsonic flows 04 p0679 A70-15112

Rarefied ionospheric plasma flow around rockets and satellites, studying electric field effect on ion motion by kinetic equation and similarity law 04 p0680 A70-15188

Hydromagnetodynamic equations of two dimensional unsteady geostrophic wind field in turbulent ionosphere 04 p0680 A70-15254

Ionospheric air density profiles revision based on satellite orbits analysis 05 p0839 A70-16287

Correlation function of auroral reflection radio signals with allowance for polar ionospheric scattering and pulse signal transmission and reception 05 p0841 A70-16741

Electron flux-atmosphere interaction solved by numerical integration on computer, discussing auroral ionosphere 05 p0842 A70-16755

Spherical probe impedance in infinite collisional isotropic plasma investigated for ionospheric applications, selecting electron density 06 p1117 A70-17369

RF probe admittance in ionosphere investigated for cold anisotropic and warm isotropic plasma diagnostics 06 p1117 A70-17370

Transequatorial multisite VLF records establishing solar zenith angle for midpoint of sunrise ionospheric 06 p1117 A70-17370

16 p2900 A70-32931

height discontinuity, recomputing magnetic latitude dependent parameters

06 p1054 A70-17590

Laboratory simulation of interactions between ionospheric plasma and diverse spacecraft systems

06 p1029 A70-18067

Satellite wake in ionosphere simulated in cold ion plasma without magnetic field, observing complex far wake structure and peculiar electrostatic probes response

06 p1147 A70-18297

Book on ionospheric physics covering neutral atmosphere, ionospheric measurements, photochemical processes, morphology, phenomena, geomagnetism, storms, etc

07 p1262 A70-18856

Outer ionosphere magnetoionic and MHD waves, combining electromagnetic and plasma kinetic theory with reference to satellite observations

07 p1264 A70-19188

Ionospheric data representation in tabular form for computer storage and processing, noting memory cells reduction

07 p1268 A70-19460

Radio wave sphericity influence on scattering at moving body wake in ionosphere, determining scattering cross section principal maximum

07 p1237 A70-20424

Cold plasma approximation of whistler excitation of lower hybrid resonance at wake of body moving through ionosphere, comparing results with Alouette satellite observations

07 p1276 A70-20425

Earth ionosphere and magnetosphere electrodynamic state as function of neutral gas small scale motions, considering magnetic disturbances and ionospheric discontinuities

07 p1276 A70-20426

Space research in terms of earth environment in space, discussing near-earth spacecraft role in solar, magnetospheric and ionospheric studies

08 p1488 A70-21344

Ionosphere effect on toroidal magnetodynamic waves in idealized representation, analyzing oscillations correlation between adjacent magnetospheric shells

10 p1875 A70-24444

Monograph on ionosphere-satellite interactions, discussing ionosphere layers, plasma sheaths and wakes, electromagnetic wave propagation, spacecraft antennas, etc

10 p1944 A70-24900

Ionospheric fine structure from ionograms, discussing probe and half automatic digital evaluation method

10 p1884 A70-25257

Extraterrestrial electrical and magnetic fields effect on meteorological observations, noting relationship between atmospheric pressure distribution and ionospheric developments

10 p1913 A70-25269

Monograph on ambipolar diffusion and motion instability of satellite produced artificial barium ion clouds in ionosphere and magnetosphere

11 p2048 A70-26825

Very low frequency radio noise in ionosphere, magnetosphere and solar wind, using multiple receivers to measure mathematical relations between direction magnitude and polarization characteristics

12 p2184 A70-27574

Cylindrical electric dipole antenna in magnetoactive ionospheric plasma, noting ion sheath effect on input impedance and active length

13 p2399 A70-29402

Collision effect on phenomena associated with ion cyclotron whistler formation, considering ionospheric day time model

13 p2468 A70-29933

Radiation belt and auroral primary ions, comparing origin possibilities of ionosphere and solar wind

13 p2481 A70-30063

Ionospheric density profiles measurement by accelerometers on SPADES and Cannon Ball 1 satellites, comparing results with prediction from atmospheric model

15 p2724 A70-31866

Report to COSPAR on space research in Bulgaria, considering ionospheric physics, cosmic rays, satellite observations, meteorology and space communications

15 p2829 A70-31704

Ionospheric spacecraft flight conditions simulation in vacuum chamber, discussing low energy ion sources

15 p2717 A70-31814

Spherical ionized cloud movement in ionosphere uniform anisotropic plasma as function of electric field applied to rocket released ion clouds

15 p2726 A70-31867

Soviet collection of papers on ionospheric studies covering F region variations, vertical ground sounding, magnetospheric disturbances, whistlers, satellite experiments, etc

15 p2729 A70-32076

Steady state plasma wind tunnel for flow around ionospheric satellites, studying wakes of cylinders and spheres

16 p2837 A70-33866

Electrostatic near wake model for ionospheric satellites, using low speed fluid dynamic blunt body similarities

[ALAA PAPER 69-674]

16 p2837 A70-33867

Soviet papers on morphology of quiet and perturbed ionosphere covering electromagnetic phenomena, measurements, etc

18 p3245 A70-36084

Book on ionospheric chemistry, covering chemical and photochemical reactions above 60 km and ionization processes

18 p3247 A70-36212

Ionospheric data representation in tabular form for computer storage and processing, noting memory cells reduction

18 p3250 A70-36934

Soviet collection of papers on ionosphere, investigating charged particle diffusion in F region, etc

18 p3253 A70-37026

Striation formation in artificial ion clouds aligned with local geomagnetic fields, considering visual indication of ionospheric electric field transfer along magnetic field

19 p3415 A70-38387

Numerical ionospheric world mapping of plasma frequency, considering height, latitude, longitude and local mean time variations

19 p3380 A70-38403

Plane VLF wave propagation in waveguide formed by earth and inhomogeneous anisotropic ionosphere, determining excitation coefficients and attenuation functions

19 p3381 A70-38568

Solar eclipses and ionosphere - NATO Conference, Lagonissi, Greece, May-June 1969

19 p3417 A70-38901

Laboratory simulation of interactions between ionospheric plasma and diverse spacecraft systems [ALAA PAPER 70-169]

20 p3606 A70-39695

Auroral arcs formation model based on dynamic magnetosphere-ionosphere interaction

21 p3817 A70-41089

Nitrogen photoelectron excitation in dayglow, examining 3371 Å band intensity, energy spectrum and flux in ionosphere

21 p3882 A70-41093

Rarefied ionospheric plasma flow around rockets and satellites, studying electric field effect on ion motion by kinetic equation and similarity law

21 p3819 A70-41169

Large scale electric fields in ionosphere, magnetosphere and interplanetary space, considering further needs for theoretical and observational investigations

22 p4099 A70-42782

Ionospheric electric field origin theory in terms of charge separation due to neutral wind drag

22 p4016 A70-42785

Neutral interplanetary particle impact ionization of atmosphere, discussing density of neutral interstellar media near solar system

22 p4106 A70-43291

Solar flare effects in ionosphere observed at Lindau, collating with heavy geomagnetic storm

23 p4237 A70-44876

European Space Research and Technology Center space science department, examining cosmic ray, ionospheric and surface physics divisions

24 p4323 A70-46356

IONOSPHERE EXPLORER A

U EXPLORER 20 SATELLITE

IONOSPHERIC ABSORPTION

U ELECTROMAGNETIC ABSORPTION

U IONOSPHERIC PROPAGATION

IONOSPHERIC BLACKOUT

U BLACKOUT [PROPAGATION]

IONOSPHERIC COMPOSITION

Ionospheric ion and neutral constituents composition from D region to magnetopause, noting ionospheric chemical reaction rates

01 p0074 A70-10588

Horizontal gradients below satellite orbit effect on reduced and minimum difference in Doppler frequency shifts of coherent radio waves from satellite in inhomogeneous ionosphere

01 p0046 A70-11517

ESRO 4 satellite as ESRO 2 design modification, describing experiments involving topside ionosphere ions, mass spectrometry, auroral particles distribution, solar and trapped particle fluxes

02 p0381 A70-12503

Dynamic model for Martian ionosphere modification by solar wind, assuming negligible Mars magnetic moment and neutral atmosphere

04 p0753 A70-15103

Mass spectrometer design and calibration for ionic composition measurements on ionosphere sounding satellite, noting effects of satellite velocity and attitude

06 p1065 A70-17908

Whistlers role in ionospheric temperature, magnetospheric electron density and ionospheric composition determination

07 p1347 A70-19189

Mariner 4 and 5 and Venera 4 data used for comparing terrestrial planets ionospheres

07 p1386 A70-19488

Simultaneous ionospheric ion and electron measurements by various radiophysical methods, relating results to period of flight of vertical space probe

07 p1237 A70-20428

Reactions determining ion composition in E region, discussing neutral composition variations from day to night and during solar activity cycles

07 p1276 A70-20431

Dye laser tuned to sodium D line used for measuring ionospheric atomic sodium

08 p1492 A70-21757

Ionospheric electron content and distribution determination from Explorer 22 satellite signal amplitude recordings, considering wave propagation and polarization and Faraday effect

09 p1633 A70-22530

Sporadic meteoroid particles in ionospheric spatial density determined from kinetic energy measurements

10 p1940 A70-24322

Nighttime concentration profiles of O, NO and molecular oxygen ions in ionosphere calculated from daytime values

10 p1874 A70-24428

Mapping electric field components perpendicular to magnetic field line in ionosphere at equatorial plane, discussing discrepancy with convection patterns

10 p1875 A70-24437

Diurnal variations of concentrations of ions and neutral components of NO, O and N in E region from analysis of chemical and photochemical processes

10 p1881 A70-24809

Ionospheric fine structure from signal broadening measurements on ionograms, including scattering region algorithm

11 p2044 A70-25553

Upper atmospheric ion and neutral composition from rocketborne mass spectrometry, allowing for rocket velocity and analyzers orientation with respect to velocity vector

14 p2568 A70-30140

E region ion composition from rocket-borne mass spectrometer data

15 p2725 A70-31689

Ionospheric structure characteristics in D, intermediate D-E and E-F 2 regions using deflecting and nondeflecting radiation absorption measurements

15 p2730 A70-32085

Soviet papers on ionospheric studies covering radio, rocket and satellite observations

15 p2730 A70-32088

Mariner 4 and 5 and Venera 4 data used for comparing terrestrial planets ionospheres

15 p2805 A70-32733

Hydrogen, He and oxygen ion density, and ion and electron temperatures in upper ionosphere fromOGO 4 observations

18 p3244 A70-36016

Ion composition and charged particle vertical distribution in F region and protonosphere from satellite and ground based observations

18 p3254 A70-37028

Solar UV radiation contributing to ionization in higher ionospheric layer over Dushanbe during partial solar eclipse of 20 May 1966

19 p3417 A70-38786

Annular solar eclipse of 20 May 1966 effects on ionosphere, discussing regions virtual heights, critical frequency variations, ion production rates, etc

19 p3419 A70-38917

Ionospheric Si and SiO ions equilibrium interconversion during Leonid meteor shower

20 p3621 A70-39351

Soviet book on ionospheric interlayer formations covering electron concentration distribution, E-2 layer occurrence frequency, recombination coefficient, etc

20 p3622 A70-39823

Lower ionospheric structure and electromagnetic resonance phenomena, describing radio equipment for solar activity effects studies

21 p3812 A70-40620

Turbulent mixing effect on vertical distribution of ionosphere atomic and molecular oxygen, using equations of motion and continuity

21 p3813 A70-40907

Ionospheric fine structure from signal broadening measurements on ionograms, including scattering region algorithm

21 p3819 A70-41303

Atmospheric positive ion composition measurements in D region by rocket-borne mass spectrometers, considering water cluster ions formation

22 p4017 A70-42796

Upper atmosphere ionization balance, examining metastable species in E and F regions

22 p4106 A70-43306

Dynamo role in magnetospheric disturbances and ionospheric inhomogeneities, allowing for charged particle concentration height dependence 23 p4237 A70-44059

E region ion composition nighttime variations, examining nitrogen monoxide and O ion nonequilibrium concentrations by ionic-molecular reactions 23 p4189 A70-44074

F 1 region positive nitric oxide and oxygen ions concentrations ratio and conversion rates from rocket data and theoretical formulas 23 p4189 A70-44075

Polar ionosphere ion composition measurement by meteorological rocket-borne RF mass spectrometer 23 p4190 A70-44081

IONOSPHERIC CONDUCTIVITY

Potential created by DC point source in ionosphere at high and medium geomagnetic latitudes, taking into account electrical conductivity anisotropy and altitude variation 01 p0080 A70-11225

Conductivity and permittivity for ion and electron resonance region of ionospheric plasma model calculated in quasi-hydrodynamic approximation 01 p0082 A70-11528

Geomagnetic field directed hydromagnetic waves propagation in lower ionosphere noting inhomogeneous conductivity, Hall effect and lines of forces role 01 p0083 A70-11546

VLF radio monitoring of celestial X ray fluxes from ground for long periods, discussing ionospheric D region conductivity 04 p0739 A70-14521

Computerized numerical integration of nonlinear partial differential equations describing blast wave in ionosphere with finite electric conductivity under uniform magnetic field 12 p2227 A70-28212

Cylindrical antenna admittance during immersion in ionospheric plasma, noting influence of ion sheath and plasma anisotropy 13 p2371 A70-29922

Ionospheric conductivity effects on plasma convective flow in determining magnetospheric electric fields distribution 21 p3816 A70-41084

Satellite-borne loop antenna resistive and reactive impedance measurements in topside ionosphere 22 p4019 A70-43112

IONOSPHERIC CROSS MODULATION

LF waves and irregularities in auroral ionosphere determined by radar measurements, suggesting role of plasma waves cross modulation 07 p1264 A70-19193

Ionospheric D region radio wave probing by cross modulation technique, obtaining electron densities and collision frequencies 12 p2224 A70-27733

Pulsed radio wave interactions with various lower ionosphere models, estimating cross modulation by computer calculation for comparison with measurements 23 p4162 A70-44080

IONOSPHERIC CURRENTS

NT AURORAL ELECTROJETS

NT ELECTROJETS

NT EQUATORIAL ELECTROJET

Rocket and satellite studies of geomagnetic field during IQSY, confirming ionospheric currents responsible for magnetic diurnal variations 01 p0075 A70-10596

Sq data acquisition and analysis, noting automatic standard observatories using nuclear magnetometers and ionospheric current information from instrumented rockets 01 p0075 A70-10597

Polar magnetic disturbances during IQSY characterized by SP field superposed on Sq field generated by ionospheric dynamo 01 p0075 A70-10599

Potential created by DC point source in ionosphere at high and medium geomagnetic latitudes, taking into account electrical conductivity anisotropy and altitude variation 01 p0080 A70-11225

Electrical phenomena in upper atmosphere and solar wind may control geomagnetic disturbances and aurorae 01 p0082 A70-11523

Rocket sounding data on ionospheric currents at mid and low latitudes noting absence in D and above E region 01 p0082 A70-11529

Earth daily rotation effects on magnetosphere electric currents, discussing Pederson currents in dynamo region and E region ionization 02 p0293 A70-12775

F 2 layer electron density changes during geomagnetic storms linked to DS current and electromagnetic disturbances 05 p0838 A70-16280

Magnetic disturbance associated with E layer east-west electric current calculated in terms of ionization production and loss 05 p0838 A70-16282

Tangential solar wind discontinuity observed by Vela 2A satellite, producing ground magnetic disturbances conjunctively with magnetospheric, ground and ionospheric currents 05 p0903 A70-16727

Surface impedance of spherical earth isolated by nonconducting atmosphere from ionospheric currents producing alternating electromagnetic field 05 p0843 A70-16768

Three dimensional model current system with magnetospheric and ionospheric sections connected by currents flowing along geomagnetic field lines proposed for polar magnetic substorms 06 p1059 A70-18535

F 2 small scale inhomogeneities drift relation to current systems of dynamo region, discussing solar activity effects on ionospheric conductivity 07 p1267 A70-19452

Lower ionosphere electric fields and currents vertical profiles above geomagnetic equator under quiet geomagnetic conditions from rocket data 07 p1277 A70-20453

Auroral zone electrojet return current spatial distribution using idealized models for stationary state 08 p1491 A70-21718

Ionospheric current flow past circular inhomogeneous spot with Pedersen and Hall conductivities, calculating earth surface magnetic field by Lipshits-Hankel integral 10 p1873 A70-24309

Ionospheric wind velocity fields calculated from atmospheric dynamo effects taking into account electric field, current density and conductivity tensor 10 p1881 A70-24819

Polar ionospheric current and interplanetary magnetic field directions related from mean diurnal values of solar wind velocity 11 p2044 A70-25551

Vector magnetic field and energetic particle flux profiles, indicating geomagnetically aligned currents associated with visible auroral arc 13 p2397 A70-29197

Horizontal geomagnetic force variations, considering ionospheric wind effects on ions in transition layer 13 p2402 A70-30057

Ba ion cloud motions agreeing with electric field data from balloon measurement in ionosphere and magnetosphere 13 p2402 A70-30079

Ionospheric DC electric fields long period oscillations at high latitudes observed by polar orbiting Injun 5 satellite 13 p2403 A70-30081

Daily variations of geomagnetic field horizontal component at dip equator associated with ionospheric current 14 p2575 A70-30792

Electrostatic discharge at magnetopause by idealized circuit analog, discussing transmission lines and terminal impedances 14 p2579 A70-31247

Ionospheric currents time-space distribution noting rocket data, induction mechanism and geophysical effects 15 p2730 A70-32087

Electric fields in lower ionosphere during solar activity minimum above magnetic equator, using vertical profiles of ionospheric current magnetic fields and electron concentration 18 p3246 A70-36098

F 2 small scale inhomogeneities drift relation to current systems of dynamo region, discussing solar activity effects on ionospheric conductivity 18 p3249 A70-36926

Polarization electric field in drifting ionospheric inhomogeneities, examining role of longitudinal currents 18 p3252 A70-36987

Ionospheric electric current distribution response to horizontal wind induced emf, using lunar tidal wind models 19 p3415 A70-38386

Electron collision frequency profile for energy loss rate in ionospheric G factor for air, considering rotational excitations of molecular oxygen and nitrogen 21 p3812 A70-40618

Polar ionospheric current and interplanetary magnetic field directions related from mean diurnal values of solar wind velocity 21 p3819 A70-41301

Ionospheric current theoretical model and balloon measurement of ionospheric electric field 22 p4017 A70-42795

IONOSPHERIC DISTURBANCES

NT IONOSPHERIC STORMS

NT SUDDEN IONOSPHERIC DISTURBANCES

Internal gravity waves theory to interpret large amplitude oscillations in electron density and temperature and ion temperature and velocity observed in thermosphere 01 p0079 A70-11215

Atmospheric gravity waves in F region, discussing neutral gas-ionization interaction and detection by electron density profile measurements 01 p0079 A70-11216

Ionization variations and correlation coefficients of F 2 critical frequency variations, using airborne ionospheric sounder over Sogra and Kerguelen Island conjugate areas 01 p0080 A70-11224

Ionospheric discontinuities drift velocities from diversity reception data indicating no dependence on solar activity 01 p0083 A70-11531

Hourly N/h/ profiles of F region calculated from monograms by normal integral method during magnetic disturbance, measuring region temperature 01 p0083 A70-11548

Diurnal variations in sporadic E layer and wind in ionosphere during equinox and solstice periods, noting wind shear mechanisms and ambient electron density 01 p0084 A70-11552

Midlatitude ionospheric disturbances accompanied by auroral type radio absorption observed by radio astronomy and probes during 26 May 1967 storm 01 p0084 A70-11555

Data collection for ionospheric disturbances, geomagnetic field, radio wave intensity, cosmic rays and solar activity 02 p0290 A70-12125

F 2 region acoustic waves over Kansas and Nebraska attributed to local storms in troposphere 02 p0290 A70-12158

F region irregularity drift, morphology and generation in magnetosphere, discussing ionospheric structure at different latitudes and solar activity association 02 p0293 A70-12572

VLF radio wave propagation variations occurring in earth-ionosphere waveguide contributing to errors in OMEGA position lines used to obtain worldwide navigational fixes 03 p0523 A70-13614

Traveling ionospheric disturbances from signatures left in columnar electron content records obtained by measuring signal Faraday rotation angle from geostationary satellite 03 p0477 A70-13991

Ionosphere beacon satellites BeB and BeC transits for field alignment of small ionospheric regularities 04 p0678 A70-14975

Ionospheric integral radio absorption measured by radio astronomical A2 method, including anomalous absorption during disturbances 04 p0650 A70-15283

Small scale disturbances and radio wave scattering effects on signal transmission and radiophysical observations in ionosphere 04 p0653 A70-15723

Cosmic ray intensity decreases in relation to geomagnetic and F 2 region disturbances characterized by Forbush decreases from vertical sounding data 05 p0898 A70-15940

IQSY 27-day recurrence sequence for 1964 solar and terrestrial activity, considering geomagnetic, auroral and ionospheric disturbances correlation with plate 05 p0841 A70-16646

Large scale ionospheric inhomogeneities anisotropy, dimensions and drift velocities from simultaneously measured irregular refraction 05 p0841 A70-16739

Radio astronomical observations of shape and drift velocity of focusing ionospheric discontinuities 05 p0841 A70-16740

Radio waves propagation along polar auroras region, obtaining ionospheric parameters for magnetic disturbances based on penetration probability 05 p0842 A70-16744

Oscillations intervals with diminishing period during magnetic storms, noting relationship to midlatitude disturbances in F region 05 p0842 A70-16746

Nighttime F 2 region temperature distribution under geomagnetically calm and disturbed conditions calculated from Alouette 1 satellite data 06 p1057 A70-17887

Temporal and spatial variations and patch velocity of sporadic E layer obtained at Japan ionospheric stations 06 p1057 A70-17906

Backscatter observations of F region field-aligned irregularities during IQSY, discussing diurnal variations of echoes 06 p1059 A70-18539

LF waves and irregularities in ionosphere - Conference, Frascati, Italy, September 1968 07 p1263 A70-19186

Satellite signal scintillation phenomenon morphological study and relationship to ionospheric irregularities 07 p1234 A70-19194

Ionospheric inhomogeneities measured by Explorer 22 radio signals emphasizing satellite scintillation 07 p1265 A70-19195

Charged particle replacement by external plasma particles in ionized inhomogeneities moving in ionosphere, considering magnetic field role 07 p1266 A70-19435

Harmonic analysis of ionospheric electron density oscillation spectra, noting density fluctuations classes due to internal gravity wave propagation and N/h profiles calculation errors

07 p1266 A70-19449

Midlatitude F 2 perturbations from vertical sounding stations data during solar activity minimum, discussing F 2 region critical frequency variation

07 p1266 A70-19450

Ionized formations motion direction and velocity in F region from triangular ionospheric sounding

07 p1267 A70-19451

Electron concentration profiles calculated during vertically moving perturbations to evaluate ionospheric state

07 p1267 A70-19458

Vertically moving disturbance discovered in ionospheric soundings close to magnetic equator, noting correlation with electrodynamic lift

07 p1269 A70-19631

Earth ionosphere and magnetosphere electrodynamic state as function of neutral gas small scale motions, considering magnetic disturbances and ionospheric discontinuities

07 p1276 A70-20426

Perturbed ionospheric regions acting as radio wave focusing lens, discussing frequency, power and pattern selection

07 p1237 A70-20448

Positive and negative correlations in F 2 layer perturbations by network of paired conjugate ionospheric stations at low latitude

07 p1277 A70-20450

Diurnal vertical shifts of constant electron concentration levels in D region, considering effects of chromosphere, nuclear explosions, solar eclipses, etc

08 p1490 A70-21430

Horizontal ionospheric drift rates and traveling wave disturbances, showing differences between winter and summer

09 p1667 A70-22493

Ionospheric irregularities investigated by rocket- and satellite-borne transmitters, obtaining ionization profiles from amplitude, phase and polarization of radio waves

09 p1669 A70-23273

Nighttime D region ionization irregularities deduced from vertically incident VLF radio wave

09 p1671 A70-23663

Ionospheric current flow past circular inhomogeneous spot with Pedersen and Hall conductivities, calculating earth surface magnetic field by Lipshits-Hankel integral

10 p1873 A70-24309

Ionospheric waves positive phases and disturbances related to solar activity variations and cosmic ray modulations

10 p1885 A70-25270

VHF satellite transponders for ranging and position fixing, studying ionospheric and multipath effects [AIAA PAPER 70-489]

11 p1999 A70-25433

F region magnetic disturbances due to low energy solar plasma penetration during proton bursts

11 p2104 A70-25535

Ionospheric magnetic activity effects on cosmic radio noise absorption diurnal and seasonal variations in auroral zone, noting K index and lowest reflection frequency roles

11 p2043 A70-25536

Wind shear caused ionospheric E region irregularities investigated by horizontal plasma density gradients determination

11 p2045 A70-25652

Fluctuations of polarization induced fading periods in short wave transmissions of Soviet earth satellites, showing relation to ionospheric inhomogeneities

11 p2047 A70-26788

Thermonuclear explosion Operation Starfish effect on ionospheric state from recording in central Kazakhstan, studying frequency characteristics

11 p2047 A70-26790

Ionospheric lowest regions and magnetosphere probing based on atmospheric observations, detecting disturbed conditions

12 p2224 A70-27734

Mode-scattering coefficients from ionospheric perturbations for sunrise and sunset propagation paths, comparing results with VLF radio measurements

12 p2189 A70-28053

Hydromagnetic coupling between neutral and ionized atmosphere perturbations, noting role of gravity waves

13 p2397 A70-29191

Auroral currents as source of atmospheric gravity waves and associated traveling ionospheric disturbances

13 p2399 A70-29234

Equatorial electrojet Lorentz coupling to neutral atmosphere as source of long period traveling ionospheric disturbances

13 p2399 A70-29235

One dimensional Alfvén fluctuation spectrum of magnetosphere in toroidal, crimping and twisting modes, using numerical integration

14 p2569 A70-30203

Quasi-periodic influence of traveling disturbances on ionospheric F 2 layer small scale drift discontinuities

14 p2570 A70-30226

Lower ionosphere nonuniformities drift velocity and direction using space diversity reception

14 p2571 A70-30233

Small scale disturbances and radio wave scattering effects on signal transmission and radiophysical observations in ionosphere

14 p2550 A70-30807

Ionospheric and ground level pressure fluctuations correlation from atmospheric models, suggesting ionospheric disturbance measurement from microbarographs on land surface

15 p2769 A70-31446

Lunar tidal diurnal and semidiurnal variations in equatorial sporadic E layer related to H geomagnetic field and sunspot period

15 p2726 A70-31862

Planetary distribution of F region disturbances and related vertical electron concentration using satellite and ground data

15 p2729 A70-32079

Terrestrial magnetosphere dynamics in magnetoionospheric disturbances, analyzing solar wind-geomagnetic field interaction and storm development

15 p2729 A70-32080

Refractive index gradients effect on scattering of radio waves perturbing ionosphere or passing through perturbed region

16 p2863 A70-33259

Ionospheric irregularities properties from San Marco 2 and BE-B satellites recordings, deriving height variation of irregularity size and occurrence

17 p3076 A70-34942

Bounded ionospheric layers gradient instability, discussing perturbation growth and lifetime

17 p3076 A70-34944

Ionospheric plasma disturbances due to moving space vehicle, investigating by electron density measurements in rarefied wake regions using gyro-plasma probe

17 p3142 A70-35763

F2 region disturbance development during magnetic storm, discussing layer height increases

17 p3080 A70-35772

Soviet papers on morphology of quiet and perturbed ionosphere covering electromagnetic phenomena, measurements, etc

18 p3245 A70-36084

Proton flares showing enhancement of ionospheric absorption and complex magnetic disturbances

18 p3306 A70-36087

Charged particle replacement by external plasma particles in ionized inhomogeneities moving in ionosphere, considering magnetic field role

18 p3249 A70-36909

Harmonic analysis of ionospheric electron density oscillation spectra, noting density fluctuations classes due to internal gravity wave propagation and N/h profiles calculation errors

18 p3249 A70-36923

Midlatitude F 2 perturbations from vertical sounding stations data during solar activity minimum, discussing F 2 region critical frequency variation

18 p3249 A70-36924

Ionized formations motion direction and velocity in F region from triangular ionospheric sounding

18 p3249 A70-36925

Electron concentration profiles calculated during vertically moving perturbations for evaluation of ionospheric state

18 p3250 A70-36932

Ionospheric inhomogeneities electrodynamic decay rate, using ellipsoidal model with sharp boundary for irregularity

18 p3252 A70-36986

Electric field strength in earth ionosphere and magnetosphere during irregular motion of fast ions and electrons

19 p3407 A70-37303

Electron concentration disturbances in outer ionosphere and F 2 maximum on daylight side during magnetic storm

19 p3408 A70-37307

F layer absence and nonuniform horizontal electron concentration of nighttime ionosphere at high latitudes, using Alouette 1 sounding

19 p3408 A70-37308

Vertical electron density profile variations during ionospheric perturbations in years of solar activity maximum and minimum

19 p3409 A70-37328

Traveling horizontal ionospheric waves relationship to magnetic storm onset, showing ionization displacement occurrence

19 p3413 A70-38029

Faraday rotation of radio beacon satellite signals during traveling ionospheric disturbances simulated for spaced ground stations

20 p3590 A70-40481

Equatorial F layer irregularity extent from propagation path observations to synchronous satellites

20 p3624 A70-40485

Low latitude F region irregularities from scintillations of beacon satellite signals

20 p3624 A70-40486

Correlation distance of VHF fading from irregularities in equatorial ionosphere, using NASA STADAN in Chile

20 p3590 A70-40487

High scintillation indices associated with vertical spreading of sporadic E layer from minute-by-minute ionograms and signal amplitude recordings from Explorer 22 satellite

20 p3624 A70-40489

High latitude F region irregularity structure during magnetic storm from multistation scintillation observations of ATS 3 transmission

20 p3624 A70-40490

Ionospheric electron density disturbance heights measured via radio signal scintillation from earth satellite, using spaced receiver method

20 p3590 A70-40491

Ionospheric disturbances heights at subauroral latitude from Explorer 22 satellite beacon signals recorded at spaced receivers

20 p3624 A70-40492

Microwave scintillations at sunrise indicating solar point sources at sunspot cycle peak and terrain configuration influence on ionospheric disturbances

20 p3591 A70-40493

Quasi-periodic ionospheric oscillations associated with nuclear explosions, thunderstorms and quiet conditions

21 p3814 A70-40938

Multistation observations of long range field aligned backscatter irregularities in F layer, using ray path calculations

21 p3814 A70-40940

Ionospheric D region irregularities with partially reflected radio wave pulses, using phase path and drift measurements

21 p3814 A70-40941

Low latitude observations of spread F echoes and stationary satellite scintillations, correlating with ionospheric disturbances and geomagnetic activity

21 p3818 A70-41097

F region magnetic disturbances due to low energy solar plasma penetration during proton bursts

21 p3882 A70-41285

Ionospheric magnetic activity effects on cosmic radio noise absorption diurnal and seasonal variations in auroral zone, noting K index and lowest reflection frequency roles

21 p3819 A70-41286

Two echo complex signature in group path vs time records by ionospheric traveling disturbances

21 p3820 A70-42243

Doppler frequency shift of reflected radio waves for ionospheric disturbances, discussing solar flares, geomagnetic variations, etc

21 p3820 A70-42256

F region ionospheric disturbances class and shape from radio amplitude and phase scintillations in satellite transmission to ground stations

23 p4187 A70-43879

Ionosphere seasonal changes from three-point system for observing traveling ionospheric disturbances

23 p4192 A70-44868

Auroral electrojet return current spatial extent from model ionospheric current distribution and geomagnetic variations

23 p4192 A70-44922

Equatorial E region electrojet plasma irregularities, discussing electron density, drift velocity, profile structure, etc

24 p4384 A70-45150

One dimensional Alfvén fluctuation spectrum of magnetosphere in toroidal crimping and twisting modes, using numerical integration

24 p4330 A70-46278

Quasi-periodic influence of traveling disturbances on ionospheric F 2 layer small scale drift discontinuities

24 p4331 A70-46301

Lower ionosphere nonuniformities drift velocity and direction using space diversity reception

24 p4331 A70-46308

IONOSPHERIC DRIFT

Needle-shaped filament artificial ion cloud drift and diffusion in F 1 region plasma in presence of neutral wind and uniform electric field

01 p0070 A70-10401

Synoptic ionospheric observations during IQSY, discussing electron density profiles, absorption, drifts, etc

01 p0073 A70-10584

Seasonal phase changes of semidiurnal tidal wind components in lower ionosphere demonstrated from ionospheric drift measurements

01 p0078 A70-11212

Ionospheric discontinuities drift velocities from diversity reception data indicating no dependence on solar activity

01 p0083 A70-11531

F region irregularity drift, morphology and generation in magnetosphere, discussing ionospheric structure at different latitudes and solar activity association
02 p0293 A70-12572

Electrostatic drift-dissipative plasma instability and nocturnal equatorial spread F irregularities, discussing amplification in collision dominated medium
03 p0477 A70-13990

Electromagnetic drifts and neutral air winds effects on F 2 region derived from electron continuity equation, using Jacchia model atmosphere
04 p0677 A70-14966

Horizontal ionospheric small scale inhomogeneity drift measurements at two closely spaced points, noting agreement with global network stations
04 p0684 A70-15747

Magnetic activity effect on ionospheric drift speeds variation with latitude, observing correlation with electron density
05 p0837 A70-15922

Large scale ionospheric inhomogeneities anisotropy, dimensions and drift velocities from simultaneously measured irregular refraction
05 p0841 A70-16739

Radio astronomical observations of shape and drift velocity of focusing ionospheric discontinuities
05 p0841 A70-16740

VLF propagation between earth and moving dispersive ionosphere, considering medium motion effects in Maxwell-Minkowski equations solutions
06 p1007 A70-17462

Ionization irregularities and drift in sporadic E layer determined using Mitra method for ground based radio reflection
06 p1012 A70-18543

Ionospheric motions and irregularities effects on HF radio propagation using computer simulation involving ray tracing and ionosphere modeling
07 p1264 A70-19192

Horizontal ionospheric drift over Northern Hemisphere during low solar activity, studying spatiotemporal distribution patterns of drift parameters
07 p1266 A70-19438

F 2 small scale inhomogeneities drift relation to current systems of dynamo region, discussing solar activity effects on ionospheric conductivity
07 p1267 A70-19452

Ionospheric irregularities-diffraction patterns relative drifts, verifying point source effect for radio waves reflected from E and sporadic E layers
07 p1236 A70-20162

Horizontal ionospheric drift rates and traveling wave disturbances, showing differences between winter and summer
09 p1667 A70-22493

F region vertical electron drift velocity determined from Thomson scatter observations
09 p1671 A70-23665

Ionospheric irregularities showing dispersive motions from systematic skewness in cross correlation functions for satellite scintillations at spaced receivers
10 p1881 A70-24810

Asymmetric cross correlation functions in D and lower E region drift measurements interpreted in terms of moving screens
10 p1881 A70-24811

Field-aligned plasma velocity dependence on plasma diffusion and wind velocity illustrated with model of night F 2 layer
10 p1881 A70-24814

Scintillation sudden inception in Faraday rotation in Sodankylä and Oulu, noting diurnal north-south frontier movements in polar ionosphere
10 p1884 A70-25262

Ion component drift displacing components from E and F layers ascribed to vertical electric field presence in hydrogen arc
11 p2104 A70-25541

Ionospheric plasma drift vertical and meridional velocity components latitudinal distributions in F 2 region, considering wind effects in upper atmosphere
11 p2045 A70-25931

Three-point simultaneous observations for ionospheric drift characteristics in E and F regions
13 p2396 A70-29097

Finite Larmor radius interchange and LF drift oscillations due to magnetospheric temperature and density gradient stresses in trapped plasma
13 p2401 A70-29936

High altitude meteor winds, investigating atmospheric tides and short term wind oscillations, wind shears and drift nature
14 p2601 A70-30122

Quasi-periodic influence of traveling disturbances on ionospheric F 2 layer small scale drift discontinuities
14 p2570 A70-30226

Lower ionosphere nonuniformities drift velocity and direction using space diversity reception
14 p2571 A70-30233

Neutral winds effect on F region vertical ion drifts derived from continuity equation, noting diurnal and seasonal variations
14 p2574 A70-30738

Correlation apparatus for ionospheric drift measurement by spaced receivers using closed loop of magnetic tape
14 p2550 A70-30741

Lower ionospheric drift motions observed from VHF radio signal, relating to three paths near auroral zone during dark hours
14 p2574 A70-30749

F region horizontal drift velocity height and diurnal variations, using ionograms
14 p2574 A70-30751

Horizontal ionospheric small scale inhomogeneity drift measurements at two closely spaced points, noting agreement with global network stations
14 p2576 A70-30831

Correlated daily variations of ionospheric drift and anisotropy parameters in E and F regions at Thumba, India
15 p2725 A70-31858

Ionospheric drift measurement by 89 antennas array, testing validity of methods using three antennas
17 p3076 A70-34939

Ionospheric vertical base selection for recording discontinuities motion of F region
18 p3246 A70-36085

Ionospheric small scale ionization discontinuities vertical drift effect on diurnal variations of F 2 layer critical frequency
18 p3246 A70-36086

Vertical drift contribution to daytime N/h electron profiles in F 2 region, taking into account ionization-recombination processes and ambipolar diffusion
18 p3247 A70-36292

Horizontal ionospheric drift over Northern Hemisphere during low solar activity, studying spatiotemporal distribution patterns of drift parameters
18 p3249 A70-36912

F 2 small scale inhomogeneities drift relation to current systems of dynamo region, discussing solar activity effects on ionospheric conductivity
18 p3249 A70-36926

Polarization electric field in drifting ionospheric inhomogeneities, examining role of longitudinal currents
18 p3252 A70-36987

Ionospheric drift velocity fluctuations by similar fading method, discussing applicability and errors
19 p3408 A70-37312

Ionospheric movements measurement methods and data interpretation
19 p3415 A70-38415

Satellite-borne sensor for ionospheric ions velocity measurement, describing design and principles of operation
21 p3813 A70-40834

Ionospheric ions drift velocity horizontal and vertical components distribution, using satellite-borne sensor
21 p3813 A70-40835

Anomalous nighttime ionospheric total electron content increases seasonal and solar cycle dependences attributed to ionization sources due to electrodynamic drifts
21 p3815 A70-41061

Ion component drift displacing components from E and F layers ascribed to vertical electric field presence in hydrogen arc
21 p3882 A70-41291

Day and nighttime E and sporadic E layer drifts over low latitude station recorded by spaced receiver technique
22 p4020 A70-43166

Vertical velocity effects on ionospheric horizontal wind magnitude and direction, solving integral equations system by successive approximations
23 p4188 A70-44057

Quasi-periodic influence of traveling disturbances on ionospheric F 2 layer small scale drift discontinuities
24 p4331 A70-46301

Lower ionosphere nonuniformities drift velocity and direction using space diversity reception
24 p4331 A70-46308

IONOSPHERIC ELECTRON DENSITY

Oxygen collisional quenching rate in F region determined by comparing nightglow intensities with intensities calculated from electron density profiles
01 p0070 A70-10403

Synoptic ionospheric observations during IQSY, discussing electron density profiles, absorption, drifts, etc
01 p0073 A70-10584

Lower ionosphere radio wave partial reflection strength relationship to electron density profiles measured by rocket probes
01 p0045 A70-11089

Internal gravity waves theory to interpret large amplitude oscillations in electron density and temperature and ion temperature and velocity observed in thermosphere
01 p0079 A70-11215

Atmospheric gravity waves in F region, discussing neutral gas-ionization interaction and detection by electron density profile measurements
01 p0079 A70-11216

IONOSPHERIC ELECTRON DENSITY

F 1 layer nonlinear ionospheric continuity equation to investigate role of diurnal variations of loss and production processes in electron density midday biteout effect
01 p0079 A70-11221

Ionosphere total electron content diurnal and seasonal variations at midlatitudes, based on data analysis from Explorer 22 in polar orbit
01 p0080 A70-11223

Ionospheric measurements of electron density, electron and ion temperature profiles from strength of incoherent radio wave scattering
01 p0082 A70-11530

Ionospheric slopes and range frequency characteristics obtained from oblique incidence sounding of horizontally nonuniform ionosphere
01 p0083 A70-11534

Hourly N/h profiles of F region calculated from ionograms by normal integral method during magnetic disturbance, measuring region temperature
01 p0083 A70-11548

Molecular reaction rates and ion/electron vertical profile and concentrations in equatorial ionosphere, applying computer simulation to numerical solution of continuity equations
01 p0083 A70-11549

Diurnal variations in sporadic E layer and wind in ionosphere during equinox and solstice periods, noting wind shear mechanisms and ambient electron density
01 p0084 A70-11552

Solar eclipse effects in equatorial F region electron density, noting data analysis method for reexamining existing measurements
02 p0290 A70-12157

Solar activity effect on ionospheric total electron content via Explorer 22 observations, discussing relationship to solar elevation angle
02 p0292 A70-12561

Ionospheric electron concentration irregularities via satellite signal scintillation analysis, using radio wave diffraction theory
02 p0258 A70-12562

Total electron content / fEC , time delay and polarization errors on one way path through ionosphere, discussing measurements and predictions
02 p0293 A70-12568

Ionospheric electron density vertical distribution calculation starting from satellite measurements of total electron content
02 p0293 A70-12575

Geomagnetic activity effect on ionospheric electron content from statistical analysis of data obtained during three year period
02 p0293 A70-12576

Equatorial ionosphere ionization and electron density measurements by San Marco 2 satellite
03 p0475 A70-13830

Electron temperature and density data obtained during Alouette satellite passage over middle latitude red arc, noting influence of intersecting magnetic field lines
03 p0476 A70-13911

Traveling ionospheric disturbances from signatures left in columnar electron content records obtained by measuring signal Faraday rotation angle from geostationary satellite
03 p0477 A70-13991

Winter diurnal behavior of northern high latitude ionospheric electron density using temperature data from Langmuir probes
03 p0478 A70-13993

Uniform stratified layers in equatorial E region determined from Centaur rocket capacitance probe electron density observations, suggesting internal atmospheric gravity waves mechanism
03 p0478 A70-14222

Rocket-borne differential capacity probe measuring electron densities in upper atmosphere, reducing errors caused by temperature and composition variations
04 p0686 A70-14649

[AAS PAPER 69-567] Ion and electron concentrations far field disturbances caused by satellite motion in ionosphere and lower exosphere, deriving plasma drag
04 p0762 A70-14935

Mars and Venus ionospheres from Mariner profiles, discussing radiative equilibrium thermal calculations and F 1 layer hypothesis
04 p0753 A70-15069

Daytime midlatitude ionosphere composition and electron concentration profile measured by synchronized satellites and rocket, investigating discrepancy
04 p0741 A70-15110

Alouette 2 Langmuir probe measurements analyzed for size and amplitude of electron concentration fine structure irregularities in topside ionosphere, discussing F spread
04 p0679 A70-15111

Plasma transport models of polar ionosphere, discussing physical processes involved and effects on electron concentration, ion composition and speeds
04 p0679 A70-15113

Magnetoionic mode coupling in satellite transmissions through ionosphere near transverse region, using electron concentration profiles for night and daytime estimates
04 p0650 A70-15131

Magnetic activity effect on ionospheric drift speeds variation with latitude, observing correlation with electron density
05 p0837 A70-15922

F 2 layer electron density changes during geomagnetic storms linked to DS current and electromagnetic disturbances
05 p0838 A70-16280

Ionospheric electron content, virtual height and profile measured by Faraday effect of satellite radio emissions compared with radar soundings
05 p0839 A70-16288

Upper ionospheric electron density variations at low magnetic activity times observed with Alouette 2 satellite
05 p0901 A70-16307

Plane magnetopause models assuming ionospheric electrons ability to short circuit electric fields, constructing distribution functions by Vlasov theory
05 p0840 A70-16568

Ionospheric horizontal discontinuities of electron density distribution parameters effect on penetration frequency, skip distances and arrival angles
05 p0842 A70-16743

Ionograms for nonmonotonic vertical distribution of electron concentration in ionosphere from rocket and ground sounding
05 p0842 A70-16757

Radio wave absorption coefficient in lower ionosphere related to total radiation absorption and electron concentration profile
05 p0843 A70-16761

D region electron density distribution during night and presunrise period, using full wave integration method for propagation parameters for waves reflected from electron density model
06 p1054 A70-17587

Electron density distributions relation to D region diurnal and seasonal variations in radiowave absorption in terms of transport processes near mesopause
06 p1054 A70-17589

Seasonal variations of maximum electron concentration in stratified E-F region, including E 2 layer recombination coefficient and F layer characteristics probability
06 p1057 A70-17842

Ionospheric vertical electron concentration computer calculations compared to direct measurements data by satellite and rockets over Sofia
06 p1057 A70-17843

Ion and electron density, electron temperature and space potential measured in ion wake formed by Gemini spacecraft using sensors on Agena Target Vehicle
06 p1066 A70-18285

Rocket measurement techniques for electron density profiles in D region, giving results from auroral zone disturbed and midlatitude quiet D region
07 p1263 A70-19152

Reflection coefficient for radio wave pulse reflected from ionosphere with large scale fluctuations in electron density, compared to empirical data for reflecting surface irregularities
07 p1231 A70-19170

Nighttime recombination model of O ion plasma in upper ionosphere, showing temporal behavior and variation of electron concentration
07 p1265 A70-19432

Height scale of loss coefficient in F 2 region under geomagnetic perturbation at midnight based on electron number profiles, estimating thermosphere temperature
07 p1265 A70-19433

Numerical modeling of electron and molecular ion continuity equations describing conditions in lower F region near magnetic equator using analog computer
07 p1265 A70-19434

Harmonic analysis of ionospheric electron density oscillation spectra, noting density fluctuations classes due to internal gravity wave propagation and N/h profiles calculation errors
07 p1266 A70-19449

Sporadic E layer formation by vortical winds, discussing effect on ionospheric electron concentration distribution
07 p1267 A70-19454

Electron concentration profiles calculated during vertically moving perturbations to evaluate ionospheric state
07 p1267 A70-19458

Electron production rate enhancement by solar cosmic rays in lower ionosphere, considering particle distribution and polar cap absorption
07 p1369 A70-20153

Barium ion artificial clouds motions and striations due to cloud-ionosphere coupling, studying electron density variations below cloud in E layer
07 p1271 A70-20155

Closely spaced frequencies method of determining ionospheric electron content from Faraday rotation measurements
07 p1271 A70-20156

Integral methods of obtaining electron density profile of planetary ionospheres and interplanetary gases
07 p1388 A70-20160

Solar corpuscular fluxes directional distribution time dependent changes effect on lower ionospheric electron production rates
07 p1373 A70-20344

Electron production in lower ionosphere by solar cosmic rays, calculating rates by computer as function of nuclear charge number, energy spectrum and height
07 p1373 A70-20348

Ionospheric data of local and integral electron concentration obtained by measuring phase shift of satellite emitted coherent radio waves
07 p1276 A70-20422

Ionospheric electron content and concentration variations analysis based on data of radio waves propagating from satellite, considering Doppler shift and Faraday effect
07 p1237 A70-20427

Simultaneous ionospheric ion and electron measurements by various radiophysical methods, relating results to period of flight of vertical space probe
07 p1237 A70-20428

F region electron and ion concentration vertical distribution, discussing various ionization reactions
07 p1276 A70-20430

Ionospheric electron content estimated from measurements of Faraday rotation of VHF signals from geostationary satellite
08 p1489 A70-21388

Electron, oxygen and NO molecular ions concentrations for E region from computer calculations of diurnal model compared to observations
08 p1490 A70-21391

Diurnal vertical shifts of constant electron concentration levels in D region, considering effects of chromosphere, nuclear explosions, solar eclipses, etc
08 p1490 A70-21430

Venus ionosphere, discussing day and night electron density profiles, carbon dioxide presence, plasma interaction model, etc
09 p1750 A70-22058

Ionospheric electron content and distribution determination from Explorer 22 satellite signal amplitude recordings, considering wave propagation and polarization and Faraday effect
09 p1633 A70-22530

Lunar daily and monthly tidal variations in horizontal magnetic field and F 2 region maximum electron density and peak ionization height at Puerto Rico
10 p1872 A70-23823

Ionospheric electron content diurnal, latitudinal variations and equivalent slab thickness determined from observing satellite signals Faraday fading
10 p1874 A70-24426

Extraterrestrial electron density precision measurement using HF impedance probe with guard ring to remove ion sheath effects
10 p1892 A70-25255

Ionospheric electron content from Doppler data and from Faraday observations of satellite S-66
10 p1884 A70-25256

Ionospheric changes from field intensity and phase data of long distance propagation of long waves, determining electron concentration
10 p1884 A70-25258

Nocturnal E layer electron density profile dependence on solar activity
10 p1885 A70-25265

Polar ionosphere inhomogeneous electron concentration by analyzing satellite signal amplitude fluctuations received by spaced interferometers
11 p2042 A70-25528

Ionospheric reaction rate coefficients based on electron concentration curves, discussing maximum number and accuracy obtainable
11 p2043 A70-25538

Diurnal variation of equatorial ionospheric electron concentration from Schooner observations
11 p2043 A70-25548

Latitudinal ionospheric electron density and temperature variations at 1000 km within and near auroral zone
12 p2222 A70-27186

Ionospheric electron density, electron and ion temperature profiles measurements, comparing relative merits of radio-rocket ground-based radar and satellite methods
12 p2223 A70-27727

Ionospheric D region radio wave probing by cross modulation technique, obtaining electron densities and collision frequencies
12 p2224 A70-27733

Rocket measurement of ionospheric electron density based on radio propagation effects involving Doppler frequency shift, Faraday rotation, wave absorption, etc
12 p2224 A70-27736

E region plasma parameters measurement by in situ probes, considering electron density and temperature
12 p2225 A70-27737

Ionospheric electron content calculations based on satellite measurements of Faraday rotation and phase path length variations
12 p2294 A70-27739

Ionospheric electron content at temperate latitudes during solar cycle increasing phase by radio beacon satellite, discussing diurnal, seasonal and latitudinal variations
12 p2225 A70-27892

Topside ionosphere structural analysis, considering electron density profiles deduced from Alouette 2 satellite data
12 p2226 A70-28062

Ionospheric electron density profiles at various altitudes, using HF impedance probe method
12 p2227 A70-28261

Penumbra and geomagnetic threshold effects on ionospheric electron production by primary cosmic rays
12 p2296 A70-28366

Probe diagnostic techniques for ionospheric electron density and temperature measurement, describing results from P53H firing
13 p2404 A70-28691

Precipitated energetic electrons attenuation and impact ionization in ionosphere, determining vertical energy distribution profile
13 p2476 A70-28722

Ionospheric electrons velocity distribution function in steady state with oscillating electric field imposed in arbitrary direction with respect to magnetic field
13 p2395 A70-28941

Topside ionosphere structure deduced from resonance spikes on ionograms obtained by Alouette 2 satellite and electron density distributions
13 p2395 A70-29091

Low latitude scintillations from satellite transmission scintillations correlation with solar activity spread F, electron content and ionospheric irregularities
13 p2397 A70-29189

Electron density profiles interpretation for quiet daytime D region, noting role of electron-positive ion recombination coefficient
13 p2397 A70-29192

Noise rejection for optimal reception of incoherent binary signals in one beam Rayleigh dispersion radio channel under ionospheric electron density fluctuations
13 p2369 A70-29738

Delayed ionospheric resonance echoes radiated from topside plasma after pulse sequence stimulation by Alouette 2 satellite
13 p2370 A70-29904

Ionospheric electron density measurements with high altitude rocket swept frequency RF impedance probe
13 p2400 A70-29906

Vertical ionospheric electron concentration profiles, horizontal gradients and integral component from Doppler and Faraday signal recording on geophysical rockets, using diversity reception
14 p2569 A70-30205

Subpolar ionosphere electron concentration measurements for both hemispheres during solar activity by Faraday effect signal recordings from satellites
14 p2570 A70-30223

Lower ionosphere electron densities seasonal variations relationship to atmospheric circulation
14 p2574 A70-30742

Ionospheric total electron content measurements by Faraday method and bottom and topside soundings
14 p2580 A70-31258

Hydrogen UV geocorona photoionizing effect on nighttime E region electron density in low and midlatitudes, comparing with ionosonde data
14 p2581 A70-31270

Electron and ion temperature and electron density relationship in F region during sunspot maximum, using incoherent scatter experiment
14 p2581 A70-31271

Ionospheric electron concentration and temperature measurements by cylindrical Langmuir probe on rockets and satellites, emphasizing error sources
15 p2723 A70-31657

D region rocket sounding at geomagnetic equator, measuring electron density, collision frequency, current, temperature, etc
15 p2724 A70-31668

Polar ionospheric electron/ion density measurements by ESRO 1 satellite, observing dependence on Kp index
15 p2724 A70-31669

D region electron concentration and collision frequency in slowly varying plasma, using rocket-borne probe for ground emitted wave detection
15 p2778 A70-31673

Ionospheric electron density profiles between two locations calculated from oblique incidence ionograms, plotting radio path for ground range
15 p2726 A70-31861

Daytime seasonal anomaly in electron density of topside F 2 region near sunspot minimum, using Alouette 1 data

15 p2726 A70-31863

F region electron and ion densities, temperatures and plasma velocities computed for eclipse at Wallops Island on 7 March 1970

15 p2726 A70-31866

Polar peak F layer electron density around magnetic noon related to dayside aurora flux, comparing with soft particle precipitation

15 p2727 A70-31872

Neutral particle and electron density measurements by Explorer 32 proving thermospheric gravity waves association with wave-like structure in F region electron density

15 p2727 A70-31907

Diurnal, seasonal and latitudinal variations of maximum electron concentration in F 2 region, using global network observations

15 p2729 A70-32077

Planetary distribution of F region disturbances and related vertical electron concentration using satellite and ground data

15 p2729 A70-32079

Dynamic spectral characteristics of LF whistler signals for outer ionosphere electron profile determination, using satellite observation

15 p2729 A70-32081

F region electron density profiles interpretation by electron balance equation facilitating comparison of aeronomic and ionospheric data

15 p2731 A70-32091

Prolonged upper ionospheric observations from Sputnik 3, Transit 4A and Explorer 22 signals Faraday fading and phase shifts, showing electron content dependence on solar activity

15 p2731 A70-32093

D region electron density rocket measurements implying recombination coefficient

16 p2896 A70-32939

F region electron content and recombination times during solar eclipse of 7 March 1970, using Faraday rotation technique

16 p2897 A70-33829

Ionospheric electron content measurement during solar eclipse of 7 March 1970, using VHF radio waves from geostationary satellites

16 p2897 A70-33830

Ionospheric electron density during solar eclipse of 7 March 1970, using Faraday rotation measurements of geostationary satellites VHF transmissions

16 p2898 A70-33831

D region electron density variations during solar eclipse of 7 March 1970, using wave interaction technique

16 p2898 A70-33832

F region integrated electron density response during solar eclipse of 7 March 1970, using Faraday rotation of linearly polarized signals from ATS 3

16 p2898 A70-33835

S band occultation experiment for Mariner Mars 1971 orbiters, measuring atmospheric density and ionospheric electron density profiles

16 p2978 A70-34032

Electron density measurements in lower ionosphere by narrow band VLF receiver flown in Tomahawk rocket during quiet daytime

17 p3076 A70-34938

Nighttime E region structure variations observed by Wallops Island rocket flights, obtaining electron density profiles by Langmuir probe during ascent

17 p3076 A70-34941

Ionospheric E layer formation, investigating role of solar X ray control by electron production rate and density calculations

17 p3151 A70-34943

Lower ionosphere electron density and winter anomaly in HF absorption

17 p3077 A70-34948

Time span in total electron content (TEC)/measurements on BE-B and BE-C ionospheric satellites by differential Doppler method, applying chi sub O super 2 test

17 p3077 A70-34986

Winter ionosphere electron density profile from rocket-borne gyro-plasma probe observations

17 p3078 A70-35308

Ionospheric sounding with gyro-plasma probe on Kappa 8-15 rocket, discussing electron density profiles and plasma resonance

17 p3079 A70-35638

Ionospheric VLF radio waves observations via wideband receiver on K-9M-26 rocket, determining electron density profiles

17 p3047 A70-35639

Ionospheric plasma disturbances due to moving space vehicle, investigating by electron density measurements in rarefied wake regions using gyro-plasma probe

17 p3142 A70-35763

Complex impedance measurements for monopole antenna for electron densities in/out of OGO satellite wake in upper ionosphere

17 p3080 A70-35771

Rocket measurements showing removal of electrons above mesopause in summer at high latitude

17 p3081 A70-35775

Electric fields in lower ionosphere during solar activity minimum above magnetic equator, using vertical profiles of ionospheric current magnetic fields and electron concentration

18 p3246 A70-36098

Vertical drift contribution to daytime N/h/ electron profiles in F 2 region, taking into account ionization-recombination processes and ambipolar diffusion

18 p3247 A70-36292

Nighttime recombination model of O ion plasma in upper ionosphere, showing temporal behavior and variation of electron concentration

18 p3249 A70-36906

Height scale of loss coefficient in F 2 region under geomagnetic perturbation at midnight based on electron number profiles, estimating thermosphere temperature

18 p3249 A70-36907

Numerical modeling of electron and molecular ion continuity equations describing conditions in lower F region near magnetic equator using analog computer

18 p3249 A70-36908

Harmonic analysis of ionospheric electron density oscillation spectra, noting density fluctuations classes due to internal gravity wave propagation and N/h/ profiles calculation errors

18 p3249 A70-36923

Sporadic E layer formation by vortical winds, discussing effect on ionospheric electron concentration distribution

18 p3249 A70-36928

Electron concentration profiles calculated during vertically moving perturbations for evaluation of ionospheric state

18 p3250 A70-36932

Ionospheric electric field formation from polarization of electron density inhomogeneities under anisotropic conditions

18 p3252 A70-36988

Electrons and ions diffusion effect on vertical distribution in F region, discussing diurnal variations at various heights

18 p3254 A70-37027

Ionization-recombination parameters based on diurnal variations of electron concentration in F 2 layer maximum, discussing latitudinal variations

18 p3254 A70-37033

Ionization-recombination parameters variation as function of season and solar activity, using diurnal changes of F 2 layer maximum electron concentration

18 p3254 A70-37034

Magnetosphere dynamics relationship with inhomogeneous electron density formation in F region, discussing scattering diurnal variations and intensity in magnetically conjugate points

18 p3255 A70-37035

F layer scattering and earth electromagnetic field short period oscillations, relating electron density with pearl micropulsations amplitude and occurrence

18 p3255 A70-37036

Lower E region electron concentration variations relationship with geomagnetic field disturbances

18 p3255 A70-37037

F 2 layer maximum electron concentration diurnal variations dependence on ionization intensity and dissociative recombination and ion-molecular reactions rate coefficients

18 p3255 A70-37039

Electron concentration disturbances in outer ionosphere and F 2 maximum on daylight side during magnetic storm

19 p3408 A70-37307

F layer absence and nonuniform horizontal electron concentration of nighttime ionosphere at high latitudes, using Alouette 1 sounding

19 p3408 A70-37308

E layer electron concentrations, effective recombination coefficient and ionization sources during solar eclipse, noting soft X radiation intensity

19 p3408 A70-37310

Vertical electron density profile variations during ionospheric perturbations in years of solar activity maximum and minimum

19 p3409 A70-37328

Electron concentration vertical profile in ionosphere as function of altitude of radio wave reflection and group refraction and velocity characteristics

19 p3409 A70-37329

Sporadic ionization occurrences nighttime observation in auroral E region, describing vertical electron concentration profile

19 p3410 A70-37331

Electron density measurements by rocket observation during PCA after solar flare of 25 February 1969, deriving effective loss rates in terms of recombination model

19 p3496 A70-37511

Ionospheric electron density and temperature variation measurements after solar proton event of 25 February 1969, using ESRO 1 satellite

19 p3411 A70-37514

IONOSPHERIC ELECTRON DENSITY

Ionospheric effects in solar eclipse compared with full sun conditions at same elevation angle, emphasizing E, F and D regions ion and electron composition

19 p3418 A70-38902

Ionospheric rocket measurements during solar eclipse of 12 November 1966, observing electron and ion density decrease

19 p3418 A70-38907

D region electron density profiles during solar eclipse from X ray rocket and satellite observations

19 p3419 A70-38913

D region electron densities during 20 May 1966 solar eclipse, using partial reflection and rockets

19 p3419 A70-38914

Ionospheric electron content measurements during 20 May 1966 solar eclipse by Beacon S-66 satellite

19 p3419 A70-38915

E and F region electron density response to incident radiation intensity on upper atmosphere during solar eclipses

19 p3419 A70-38916

Vertical electron concentrations in upper F region during solar eclipses in South Atlantic from satellite observation

19 p3419 A70-38920

Lunar perturbations in horizontal geomagnetic field, F 2 layer thickness and electron density, discussing tidal variations

20 p3617 A70-39141

Stable midlatitude red arc observation by Alouette 2 satellite for electron temperature and density structure measurement, calculating intensity and extent

20 p3620 A70-39333

Seasonally biased electron density enhancements in nighttime response of topside ionosphere to magnetic storms

20 p3621 A70-39342

Solar eclipse effects on equatorial F 2 layer by transient solutions of time dependent continuity equation, calculating electron concentrations

20 p3622 A70-39453

Soviet book on ionospheric interlayer formations covering electron concentration distribution, E-2 layer occurrence frequency, recombination coefficient, etc

20 p3622 A70-39823

Diurnal variations and spatial distribution of total electron content in equatorial ionosphere

20 p3623 A70-40477

Ionospheric electron density response to geomagnetic storms at midlatitudes, noting diurnal variations detected by ATS 3 VHF signals

20 p3623 A70-40479

Total ionospheric electron content nocturnal and latitudinal variations in winter at midlatitudes

20 p3624 A70-40480

Solar activity effects on ionospheric total electron content seasonal variations over Tortosa, using BE-B satellite data

20 p3624 A70-40482

Ionosphere and magnetosphere total electron content from beacon method of measuring difference-differential-doppler (DDD) and Faraday effects via synchronous satellite signal frequencies

20 p3590 A70-40484

Ionospheric electron density disturbance heights measured via radio signal scintillation from earth satellite, using spaced receiver method

20 p3590 A70-40491

D region electron density profiles from high power wave interaction measurements during solar flare, indicating non-X-ray production rate

21 p3879 A70-40942

Geostationary beacon satellite recording of gravity wave influence on ionospheric electron content

21 p3815 A70-40943

Anomalous nighttime ionospheric total electron content increases seasonal and solar cycle dependences attributed to ionization sources due to electrodynamic drifts

21 p3815 A70-41061

Midlatitude F 2 layer electron density structure using theoretical model, accounting for atmospheric physical and chemical processes

21 p3815 A70-41062

F region synoptic electron densities and electron and ion temperatures from Thomson scatter radar data

21 p3816 A70-41065

Ionospheric D region electron production by cosmic X rays, noting Lyman radiation effects

21 p3882 A70-41099

D region electron density profiles, using magnetoionic differential-phase partial-reflection technique

21 p3818 A70-41100

Polar ionosphere inhomogeneous electron concentration by analyzing satellite signal amplitude fluctuations received by spaced interferometers

21 p3819 A70-41278

Ionospheric reaction rate coefficients based on electron concentration curves, discussing maximum number and accuracy obtainable

21 p3819 A70-41288

Diurnal variation of equatorial ionospheric electron concentration from schooner observations

21 p3819 A70-41298

- Nighttime equatorial E region small scale irregularities detected by rocket-borne Langmuir and plasma noise probes, discussing generation mechanism
22 p4018 A70-43108
- F region electron density measurement during magnetic storm by incoherent scatter technique
22 p4019 A70-43157
- Recombination model of diurnal variation of electron density in midlatitude D region, assuming NO ionization by solar Lyman-alpha radiation
22 p4020 A70-43158
- Ionospheric electron content measurement during solar activity cycle, noting temporal and spatial variations
22 p4020 A70-43159
- F region electron content day-to-day changes observation by Early Bird satellite, determining cross correlation with magnetic indices
22 p4020 A70-43161
- Total electron content and equivalent slab thickness statistical data during magnetic disturbances from AT-3 satellite VHF transmission observations
22 p4020 A70-43162
- Lower E region recombination coefficients from electron density and flux measurements in glow aurora by Nike-Apache rocket
22 p4020 A70-43163
- Electron density profiles calculation from model atmosphere, deriving F 2 layer ionization vertical distribution
22 p4023 A70-43303
- Ionospheric electron trough and magnetospheric plasmapause movements from satellite observations, showing statistical correlation with geomagnetic field
23 p4186 A70-43854
- F 2 layer critical frequency and maximum electron concentration statistical characteristics for predicting SW propagation conditions
23 p4188 A70-44056
- E region additional ionization source during solar activity maximum, analyzing ion production function and electron concentration
23 p4190 A70-44077
- E region electron concentration profiles, using ground sounding equipment allowing accurate signal reflection altitude measurements
23 p4190 A70-44078
- Lower ionosphere electron concentration space-time variations related to ionization source intensity fluctuations based on rocket observations and ground sounding data
23 p4190 A70-44079
- Ionospheric electron content measurement from Faraday effect of troposphere on beacon satellite Explorer 22 radio signals
23 p4163 A70-44231
- Electron density measurements in ionosphere along rocket trajectory, using sweep frequency RF impedance probe with guard ring
23 p4192 A70-44877
- Electron density and collision frequency distributions in lower ionosphere, deriving error limits from VLF and LF sounder data
24 p4314 A70-46127
- Vertical ionospheric electron concentration profiles, horizontal gradients and integral component from Doppler and Faraday signal recording on geophysical rockets, using diversity reception
24 p4330 A70-46280
- Subpolar ionosphere electron concentration measurements for both hemispheres during solar activity by Faraday effect signal recordings from satellites
24 p4331 A70-46298
- IONOSPHERIC F-SCATTER PROPAGATION**
Radio wave scattering cross section in wake of body moving in ionosphere, using simplified procedure with asymptotic expressions
11 p2012 A70-26787
- Terrestrial ELF waves F layer nighttime reflections, discussing effects of electron density, geomagnetic field radial component and absorption by ions
13 p2365 A70-29190
- F 2 layer effects on ionospheric short wave scattering lines for operating frequencies above MUF
14 p2547 A70-30231
- Short wave propagation above F2 maximum usable frequency, observing field intensity and SNR seasonal and diurnal variations
18 p3226 A70-36092
- Short wave ionospheric scatter propagation, observing interference and crowding in 16-23 MHz and relationship to F 2 layer maximum usable frequency
18 p3227 A70-36093
- F 2 layer effects on ionospheric short wave scattering lines for operating frequencies above MUF
24 p4316 A70-46306
- IONOSPHERIC HEATING**
Daytime ionospheric electron temperature as function of electron-neutral particle collision reaction and nonlocal heating effect
01 p0170 A70-10407
- Radar Thomson backscatter observations of ion temperature and ion-neutral collision frequency used to investigate reversible heating in E region
03 p0477 A70-13988
- Protonospheric heating by photoelectrons from conjugate ionosphere using Explorer 31 data
08 p1489 A70-21387
- Ionosphere dynamo region thermal input by Joule heating and solar radiation and coupling to various thermostatic modes, observing semidiurnal and semianual effects
11 p2047 A70-26569
- F 2 layer heating by photoelectrons reconsidered in terms of electron inelastic collisions effect on temperature
15 p2727 A70-31870
- F region heating by magnetic storms, discussing electron temperature, ring current conduction and red arcs
21 p3817 A70-41095
- IONOSPHERIC ION DENSITY**
Ionospheric ion and neutral constituents composition from D region to magnetopause, noting ion-chemical reaction rates
01 p0074 A70-10588
- Ionization variations and correlation coefficients of F 2 critical frequency variations, using airborne ionospheric sounder over Sogra and Kerguelen Island conjugate areas
01 p0080 A70-11224
- Hourly N/h/ profiles of F region calculated from nomograms by normal integral method during magnetic disturbance, measuring region temperature
01 p0083 A70-11548
- Molecular reaction rates and ion/electron vertical profile and concentrations in equatorial ionosphere, applying computer simulation to numerical solution of continuity equations
01 p0083 A70-11549
- Ionospheric molecular ion concentration vertical profile analysis for verifying neutral gas temperature maxima in connection with two ion production maxima
01 p0083 A70-11550
- Equatorial ionosphere ionization and electron density measurements by San Marco 2 satellite
03 p0475 A70-13830
- Water vapor ion cluster concentrations in D region, noting discrepancies above mesopause for model atmosphere predictions
03 p0478 A70-13992
- Positive ion concentration profiles in lower nighttime midlatitude ionosphere calculated from corpuscular radiation measurements and ion recombination constants
04 p0738 A70-14436
- Ion and electron concentrations far field disturbances caused by satellite motion in ionosphere and lower exosphere, deriving plasma drag
04 p0762 A70-14935
- Daytime midlatitude ionosphere composition and electron concentration profile measured by synchronized satellites and rocket, investigating discrepancy
04 p0741 A70-15110
- Plasma transport models of polar ionosphere, discussing physical processes involved and effects on electron concentration, ion composition and speeds
04 p0679 A70-15113
- Anomalous ionization variations of F 2 layer at northern geomagnetic pole during winter coincident with decrease in solar plasma density
04 p0682 A70-15726
- Positive correlation between normal ionizations at magnetically conjugate regions in ionospheric F 2 layer from aircraft vertical soundings
04 p0683 A70-15741
- F region ionograms processing with correction for ionization effects between E and F layers
04 p0684 A70-15748
- Ionized gas height scale changes in polar ionosphere obtained assuming Chapman type ionization distribution
05 p0841 A70-16738
- Horizontal electric fields relations to charged particle fluxes in polar auroral ionosphere
05 p0842 A70-16756
- Vertical motion of ionized formations in ionospheric F region related to sporadic E layer
05 p0842 A70-16760
- Ion and electron density, electron temperature and space potential measured in ion wake formed by Gemini spacecraft using sensors on Agena Target Vehicle
06 p1066 A70-18285
- D region positive ion composition measurements by rocket-borne quadrupole mass spectrometer, discussing downleg and upleg data
06 p1137 A70-18537
- Seasonal variation of F 1 region ion composition measured by rocket-borne mass spectrometer, noting altitude dependence of electron and ion temperatures
06 p1059 A70-18540
- Ionization irregularities and drift in sporadic E layer determined using Mitra method for ground based radio reflection
06 p1012 A70-18543
- Diurnal variations of lower F region ion composition and recombination coefficient based on numerical modeling of continuity equations for electrons and molecular species
07 p1265 A70-19431
- 27-day variations in ionization layer created by galactic cosmic rays, discussing association with 27-day cosmic ray and geomagnetic field variations
07 p1373 A70-20345
- Molecular ion concentrations, using flat probe collector trap on Cosmos 5 satellite at 200-300 km
07 p1276 A70-20421
- Simultaneous ionospheric ion and electron measurements by various radiophysical methods, relating results to period of flight of vertical space probe
07 p1237 A70-20428
- F region electron and ion concentration vertical distribution, discussing various ionization reactions
07 p1276 A70-20430
- Electron, oxygen and NO molecular ions concentrations for E region from computer calculations of diurnal model compared to observations
08 p1490 A70-21391
- Venusian ionosphere thermal protons and/or deuterons source observed by radio occultation method, suggesting dominance at high altitudes
10 p1938 A70-24068
- Nighttime concentration profiles of O, NO and molecular oxygen ions in ionosphere calculated from daytime values
10 p1874 A70-24428
- F 2 layer midday ionization level annual variation gradient, noting gradient latitudinal distribution dependence on solar activity level
11 p2042 A70-25532
- F 2 layer midday ionization equatorial anomaly during summer and winter solstices, using calculated mean critical frequencies
11 p2042 A70-25533
- Critical review of Meisel paper on solar X ray source identification using D layer ionization behavior during eclipse
11 p2109 A70-25750
- Temperature and ion effect on refractive index of VLF radio waves in quiet and disturbed ionospheric conditions
11 p2004 A70-25842
- Solar L alpha and X ray emission contribution to lower ionosphere ion production, discussing altitudinal, latitudinal and temporal variations
11 p2106 A70-26789
- Delayed ionization effects in midlatitude nighttime ionosphere after geomagnetic storms, noting time lag vertical distribution
12 p2227 A70-28365
- Positive ion concentration profiles in lower nighttime midlatitude ionosphere calculated from corpuscular radiation measurements and ion recombination constants
13 p2475 A70-28461
- Soviet book on solar short wave radiation effects on ionosphere, covering solar atmosphere and spectra, ionospheric ion concentration vertical distribution, etc
13 p2487 A70-28649
- Upper atmospheric ion and neutral composition from rocketborne mass spectrometry, allowing for rocket velocity and analyzers orientation with respect to velocity vector
14 p2568 A70-30140
- F 1 region ion structure diurnal variations, calculating photoionization rates
14 p2571 A70-30227
- Interlayer ionization valley depth influence on F region heights, calculating N/h/ profiles from ionograms
14 p2571 A70-30229
- Anomalous ionization variations of F 2 layer at northern geomagnetic pole during winter coincident with decrease in solar plasma density
14 p2575 A70-30810
- Positive correlation between normal ionizations at magnetically conjugate regions in ionospheric F 2 layer from aircraft vertical soundings
14 p2575 A70-30825
- F region ionograms processing with correction for ionization effects between E and F layers
14 p2576 A70-30832
- Ionospheric investigation techniques, considering ionization balance, winds and turbulence
14 p2580 A70-31259
- Polar ionospheric electron/ion density measurements by ESRO 1 satellite, observing dependence on Kp index
15 p2724 A70-31669
- E region ion composition from rocket-borne mass spectrometer data
15 p2725 A70-31689
- Terrestrial planetary ionospheres, discussing charged particle density distribution of Mars daytime ionosphere and Venus day and dark sides
15 p2799 A70-31748
- F region electron and ion densities, temperatures and plasma velocities computed for eclipse at Wallops Island on 7 March 1970
15 p2726 A70-31866

F 2 layer afternoon and evening ionization maxima dependence on season, zenith angle and solar activity
15 p2730 A70-32084

Hydrogen, He and oxygen ion density, and ion and electron temperatures in upper ionosphere from OGO 4 observations
18 p3244 A70-36016

Cosmic ray variations during PCA absorption, relating Forbush decreases to lower ionosphere ionization intensity increase
18 p3306 A70-36096

Upper atmospheric ion composition during Orionid meteor shower activity by rocket-borne RF mass spectrometer
18 p3247 A70-36183

Diurnal variations of lower F region ion composition and recombination coefficient based on numerical modeling of continuity equations for electrons and molecular species
18 p3249 A70-36905

Electrons and ions diffusion effect on vertical distribution in F region, discussing diurnal variations at various heights
18 p3254 A70-37027

Ion composition and charged particle vertical distribution in F region and protonosphere from satellite and ground based observations
18 p3254 A70-37028

Indeterminacy interval reduction for ionospheric reaction rate constants by imposing supplementary condition on NO/oxygen molecular ion concentrations ratio
19 p3408 A70-37309

Ionization rate experimental profiles during maximum solar activity compared with calculations, showing additional source of ionization in E region
19 p3409 A70-37322

Nitrogen dioxide and molecular oxygen ions densities in lower ionosphere as function of solar corpuscular radiation
19 p3409 A70-37325

D region positive ion density during solar proton event by Arcas rocket-borne cylindrical electrostatic probe
19 p3411 A70-37512

Simultaneous hydrogen ion composition measurements by upper ionospheric polar orbiting OGO 3 at eccentric orbiting magnetospheric OGO 3 at midlatitude
19 p3520 A70-38377

Ionospheric effects in solar eclipse compared with full sun conditions at same elevation angle, emphasizing E, F and D regions ion and electron composition
19 p3418 A70-38902

Ionospheric rocket measurements during solar eclipse of 12 November 1966, observing electron and ion density decrease
19 p3418 A70-38907

Magnetoionic component of entire N/z profile on incomplete ionospheric traces, including invisible part of ionogram
19 p3419 A70-38957

Positive ionospheric ion species concentration measurements using magnetic deflection mass spectrometer on Explorer 31 satellite
21 p3815 A70-40999

F 2 layer midday ionization level annual variation gradient, noting gradient latitudinal distribution dependence on solar activity level
21 p3819 A70-41282

F 2 layer midday ionization equatorial anomaly during summer and winter solstices, using calculated mean critical frequencies
21 p3819 A70-41283

Minor ion diffusion coefficients in F 2 region, noting Coulomb collisions role in ion density sensitivity to ionospheric fluxes
22 p4019 A70-43109

Ionospheric bremsstrahlung X ray flux and ionization rate, considering electron-atom and electron-ion collisions as function of altitude
22 p4095 A70-43293

Polar cap ionization processes in F region, discussing effects of particle precipitation, solar radiation, electromagnetic field drifts, atmospheric winds and magnetospheric tail distortion
22 p4024 A70-43309

Wind induced modification of E region ionization density profiles, using coupled continuity equations for ion species
23 p4214 A70-44040

Polar ionosphere ion composition measurement by meteorological rocket-borne RF mass spectrometer
23 p4190 A70-44081

F 1 region ion structure diurnal variations, calculating photoionization rates
24 p4331 A70-46302

Interlayer ionization valley depth influence on F region heights, calculating N/h profiles from ionograms
24 p4331 A70-46304

IONOSPHERIC NOISE

NT WHISTLERS
Tabulated values of F 2 mean solar noise indexes predicted by fifteenth degree polynomials
05 p0813 A70-16275

Coulomb collisions effect on electrostatic lower hybrid resonance waves propagation in ionosphere, noting noise bands cut-off shift
10 p1874 A70-24429

Sounding rocket instrumentation for ionospheric VLF radio noise measurement and recording
17 p3090 A70-35398

Ionospheric radio noise measurements with VLF wideband receivers onboard rocket
17 p3046 A70-35399

IONOSPHERIC PROPAGATION

NT IONOSPHERIC F-SCATTER PROPAGATION
VLF wave propagation across sunrise line analysis based on idealized model for earth-ionosphere waveguide
01 p0042 A70-10048

Stratospheric temperature changes connection with winter D region absorption changes
01 p0073 A70-10583

Synoptic ionospheric observations during IQSY, discussing electron density profiles, absorption, drifts, etc
01 p0073 A70-10584

Ionospheric F layer in equatorial, mid and high latitude regions for various major phenomena including anomalies, neutral air winds, photoelectrons, etc
01 p0073 A70-10585

Dual frequency ranging within narrow bandwidth of VHF communications satellite repeater for transmitted signals correction of ionospheric refraction error
01 p0043 A70-10781

Ionospheric reflection coefficients calculations by two full wave theory, using related monoenergetic and collisional frequency profiles and 10-100 kHz frequencies
01 p0076 A70-10870

Lower ionosphere radio wave partial reflection strength relationship to electron density profiles measured by rocket probes
01 p0045 A70-11089

F 1 layer nonlinear ionospheric continuity equation to investigate role of diurnal variations of loss and production processes in electron density midday biteout effect
01 p0079 A70-11221

Book on ionospheric scattering effects on long distance radio communication, considering Arctic ionosphere, scatter propagation, modulation, sporadic E, etc
01 p0046 A70-11305

Radio waves scattering in ionosphere, analyzing dependence on latitude, altitude, azimuth and polarization angle, considering anisotropy due to geomagnetic field
01 p0046 A70-11452

Phase fluctuations measurements of obliquely incident signal reflected from ionosphere performed over distance of 1300 km, showing amplitude dependence
01 p0046 A70-11533

Geomagnetic field directed hydromagnetic waves propagation in lower ionosphere noting inhomogeneous conductivity, Hall effect and lines of forces role
01 p0083 A70-11546

Vertical probe observations of short radio waves propagation through sporadic E at various frequencies and path lengths
01 p0084 A70-11553

Correlation between sunspot number index and solar radio noise index relative to ionospheric propagation, noting computer analysis program and hysteresis effect
02 p0289 A70-12107

Ionospheric absorption associated with sudden stratospheric warmings following geomagnetic disturbances in 1958 and 1963
02 p0290 A70-12159

Electromagnetic pulse duration formed by spectral content in HF bandwidth received after ionospheric reflection
02 p0258 A70-12419

Magnetoionic mode coupling in satellite transmissions through ionosphere near transverse region, showing diurnal variations and error of electron content
02 p0259 A70-12563

Total electron content (TEC), time delay and polarization errors on one way path through ionosphere, discussing measurements and predictions
02 p0293 A70-12568

Dispersive Doppler shift and Faraday rotation second order theory for curved earth-ionosphere geometry, calculating phase path differences
02 p0260 A70-12574

VLF energy propagation using ceramic dielectric model of earth-ionosphere waveguide
02 p0269 A70-12592

Airplane navigation based on VHF ranging between aircraft and geostationary satellite, examining errors by unknown propagation characteristics of signal in ionosphere
02 p0262 A70-12594

Phase distortion and Faraday rotation of wideband radio waves propagating through ionosphere
03 p0449 A70-13584

Solar X-ray bursts observations correlation with sudden phase anomalies measured at long VHF propagation paths in lower ionosphere
03 p0558 A70-13601

VLF radio wave propagation variations occurring in earth-ionosphere waveguide contributing to errors in OMEGA position lines used to obtain worldwide navigational fixes
03 p0523 A70-13614

VLF wave propagation in earth-ionosphere waveguide, comparing ray and waveguide-mode theories
03 p0449 A70-13616

Poynting flux direction for proton whistlers determined from Injun 5 observations, obtaining data on source region and propagation in ionosphere
03 p0477 A70-13987

Traveling ionospheric disturbances from signatures left in columnar electron content records obtained by measuring signal Faraday rotation angle from geostationary satellite
03 p0477 A70-13991

Error correction for previous derivation of radio propagation of wave-hop series for anisotropic ionosphere resulting in improved nighttime field strength accuracy
04 p0649 A70-14967

Nonducted VLF walking trace whistlers and Doppler shifts in fixed frequency transmissions identified on OGO midlatitude spectrographic records
04 p0649 A70-15116

Topside ray trajectories near upper hybrid resonance
04 p0650 A70-15119

Magnetoionic mode coupling in satellite transmissions through ionosphere near transverse region, using electron concentration profiles for night and daytime estimates
04 p0650 A70-15131

Ionospheric propagation experiments to measure radio echo height changes, observing correlation between LF signal reflection and MF transmitter power
04 p0650 A70-15132

Ionospheric integral radio absorption measured by radio astronomical A2 method, including anomalous absorption during disturbances
04 p0650 A70-15283

Signal amplitude and Doppler shift statistical characteristics calculated from sounding data on scattering at lower ionospheric discontinuities
04 p0650 A70-15284

Lower ionospheric cosmic layer state during Forbush decreases from radio absorption observations interpreted on basis of electron production rate analysis
04 p0743 A70-15720

Ionospheric inhomogeneities motion and vertical profile of atomic oxygen concentration associated with solar particle absorption in upper layer
04 p0681 A70-15724

Radio wave scattering increase in moving body wake near caustic in vertically inhomogeneous ionosphere
04 p0653 A70-15725

Radio wave-ionosphere interaction effects on accuracy of radio astronomical observations from earth satellites
04 p0683 A70-15740

Transmission and reflection coefficients of propagating whistler modes for model ionosphere
05 p0837 A70-15880

HF oblique ionospheric soundings over long temperate latitude path, discussing measured angles of elevation and multipath time dispersion
05 p0847 A70-15998

Ionospheric horizontal discontinuities of electron density distribution parameters effect on penetration frequency, skip distances and arrival angles
05 p0842 A70-16743

Radio waves propagation along polar auroras region, obtaining ionospheric parameters for magnetic disturbances based on penetration probability
05 p0842 A70-16744

Seasonal variation in ionospheric radiation absorption related to time variation between sunrise and constant angle attainment of sun
05 p0842 A70-16758

Radio wave absorption coefficient in lower ionosphere related to total radiation absorption and electron concentration profile
05 p0843 A70-16761

Satellite observations of VLF and ELF resonances related to ionospheric plasma singularities
06 p1118 A70-17375

VLF propagation between earth and moving dispersive ionosphere, considering medium motion effects in Maxwell-Minkowski equations solutions
06 p1007 A70-17462

Rate of change of radio ray path length for transionospheric satellite VHF signals determined from Doppler and Faraday effect analyses
06 p1008 A70-17578

Variational ray path calculation method for HF electromagnetic wave in anisotropic inhomogeneous lossless ionospheric plasma

06 p1055 A70-17592

Phase path variation of stable continuous wave transmission reflected from E region during daytime, discussing night time results

06 p1055 A70-17593

Nighttime radio wave absorption in ionosphere during moderate solar activity based on echo observations

06 p1056 A70-17840

Ionospheric absorption at oblique incidence during IQSY, studying seasonal and diurnal variations as solar zenith angle function

06 p1009 A70-17905

Apparent resonance frequencies of earth-ionosphere cavity excited by single dipole source, noting dependence on source-observer separation

06 p1058 A70-18414

VLF noise phenomena observed with satellite electric dipole antennas compared with lower hybrid resonance frequency of ionospheric medium in vicinity

06 p1011 A70-18534

HF signals propagation through auroral curtain investigated for scattering or blanketing effects, discussing ground scatter echo cut-off caused by sporadic E layer

06 p1011 A70-18538

Oblique ionospheric radio wave propagation at frequencies near lowest usable HF - NATO/AGARD Conference, Leicester, England, July 1966

07 p1227 A70-19151

D and lower E region absorption of short waves, studying absorption distribution with height

07 p1263 A70-19153

Ionospheric absorption diurnal and seasonal variations determined from field strength recordings

07 p1263 A70-19154

Pulse amplitudes and delays measured for oblique absorption values during IGY over 1000 km transmission path for correlation with lower ionosphere model

07 p1228 A70-19155

LUF for F layer propagation modes, discussing mode cut-off significance using computer ray tracing program

07 p1229 A70-19159

Polarization and absorption of radio waves in ionosphere using Appleton-Hartree equations, calculating LUF as function of sunspot number

07 p1229 A70-19160

Field strength predictions for expected returns from backscatter ionospheric soundings, predicting ionospheric propagation modes and losses during sunspot minimum

07 p1229 A70-19161

Three dimensional ray tracing computer program in Fortran for determining radio paths in ionosphere

07 p1230 A70-19163

Ionospheric radio transmission field strength calculation for given electron density and collision frequency profiles, considering electron variations along transmission path

07 p1230 A70-19165

Ray tracing in ionospheric HF communications, describing computational method for ray paths and ionospheric absorption

07 p1230 A70-19166

Doppler technique for HF ionospheric radio signal fading, observing frequency spreading during flutter fading conditions in low geomagnetic latitudes

07 p1231 A70-19169

Reflection coefficient for radio wave pulse reflected from ionosphere with large scale fluctuations in electron density, compared to empirical data for reflecting surface irregularities

07 p1231 A70-19170

Ray theory for determining short term and averaged characteristics of nonreciprocal HF ionospheric propagation paths for single magnetoionic waves transmitted between antennas

07 p1231 A70-19171

Oblique measurements in HF on Kiruna-Stockholm path with two fixed frequency pulsed transmitters, comparing results to ionosonde measurements

07 p1232 A70-19175

Ionospheric reflection coefficients from vertical and oblique incidence pulse amplitude data, discussing night conditions effect on Ottawa pulse transmissions

07 p1232 A70-19176

Lowest useful frequency (LUF) prediction on long distance quasi-antipodal circuit, considering E layer blanketing

07 p1232 A70-19178

Effective LUF fade-out and fade-in times seasonal and diurnal variations for oblique ionospheric propagation paths, noting sunspot number effects

07 p1233 A70-19180

Lowest usable frequency (LUF) measurement and prediction through synchronized oblique ionospheric sounding

07 p1233 A70-19181

Oblique incidence HF pulse ionospheric sounding, discussing propagation modes, seasonal and diurnal effects, frequency spectra, etc

07 p1233 A70-19182

Ionospheric HF radio wave propagation, describing oblique backscatter sounding during IQSY

07 p1233 A70-19183

LF waves and irregularities in ionosphere - Conference, Frascati, Italy, September 1968

07 p1263 A70-19186

LF ion-acoustic waves in ionosphere, considering electric and magnetic field variations, instability, etc

07 p1347 A70-19187

Ionospheric motions and irregularities effects on HF radio propagation using computer simulation involving ray tracing and ionosphere modeling

07 p1264 A70-19192

LF waves and irregularities in auroral ionosphere determined by radar measurements, suggesting role of plasma waves cross modulation

07 p1264 A70-19193

Satellite signal scintillation phenomenon morphological study and relationship to ionospheric irregularities

07 p1234 A70-19194

Sunrise effects in lower ionosphere at midlatitude, discussing long wave absorption measurements, summer electron concentration profile and consistency of aeronomic model

07 p1235 A70-19436

Graphic method of calculating radio wave absorption in ionosphere and field strength at reception point with aid of vertical sounding data

07 p1235 A70-19437

Ionospheric radio wave absorption and geomagnetic perturbations correlated with solar activity variations

07 p1267 A70-19457

Ionospheric distortion of linearly FM radio signals used for sounding, considering signal characteristics in distortion equations

07 p1268 A70-19459

Radio wave absorption in Venusian ionosphere, estimating effective collision number

07 p1235 A70-19491

Ionospheric radio wave (auroral) absorption during substorm investigated for longitudinal and latitudinal variations by multistation riometer measurements, inferring electron precipitation characteristics

07 p1269 A70-20030

Ionospheric absorption of hydromagnetic waves propagated normal to magnetic field, comparing daytime to nighttime absorption

[AFCL-70-0133] 07 p1270 A70-20031

Daylight ionospheric scatter propagation and absorption during energetic electron precipitation event in auroral zone using bremsstrahlung observations at balloon altitude

07 p1271 A70-20154

Ionospheric irregularities-diffraction patterns relative drifts, verifying point source effect for radio waves reflected from E and sporadic E layers

07 p1236 A70-20162

Stratosphere-ionosphere coupling, dynamo theory on geomagnetic Sq variation and ionosphere radio wave absorption and reflection

07 p1274 A70-20271

Winter anomaly ionization in lower ionosphere at medium latitudes from radio propagation observations, comparing wave absorption and phase height measurements

07 p1274 A70-20273

Scattering cross sections of radio waves at wake of vertically moving body near reflecting ionospheric layer, noting wave sphericity influence

07 p1237 A70-20423

Electromagnetic field of horizontal LF electric dipole formed by thin ionosphere layer between anisotropic planes

07 p1277 A70-20447

Perturbed ionospheric regions acting as radio wave focusing lens, discussing frequency, power and pattern selection

07 p1237 A70-20448

Recording technique for measuring short period variations of radio signal reflections altitudes from ionosphere applicable to fast ionospheric processes

07 p1277 A70-20454

Scattered field from rough ionospheric irregularities or earth surface for arbitrary polarization of incident wave

08 p1456 A70-20574

Communication channel average binary error and stationary Markov chain state probabilities relationship, using mathematical model and HF ionospheric FSK error sequence measurement

08 p1458 A70-20793

Field strength and interferential structure at different cross sections of inhomogeneous ionospheric channel calculated during bounce mode propagation of radio waves

08 p1461 A70-20969

Electron-to-ion temperature ratio determined from ion and plasma line components of radar Thomson scatter signal from ionosphere

08 p1489 A70-21389

Deviating and nondeviating absorption of radiowaves in ionosphere, deriving vertical distribution of particle collisions in E layer

08 p1490 A70-21431

Earth-ionosphere waveguide propagation variations effects on Omega navigation system position errors

08 p1541 A70-21564

Stationary phase for beam of radio waves propagating in absorbent ionosphere as function of mean directions of real and imaginary parts of wave vector

09 p1665 A70-22049

Ionospheric irregularities investigated by rocket- and satellite-borne transmitters, obtaining ionization profiles from amplitude, phase and polarization of radio waves

09 p1669 A70-23273

Distortion of electromagnetic pulse undergoing total internal reflection in inhomogeneous isotropic plasmas in lower ionosphere

09 p1639 A70-23672

Loran C radio wave field intensity diurnal variations measurements, investigating ionospheric waves characteristics

10 p1832 A70-23921

Coulomb collisions effect on electrostatic lower hybrid resonance waves propagation in ionosphere, noting noise bands cut-off shift

10 p1874 A70-24429

Group velocity and propagation of hydromagnetic waves in ionospheric duct, comparing calculations and measured values

10 p1875 A70-24442

Ionospheric scintillations of lunar radar echo components isolation by CW Doppler shift or coherent pulse time delay techniques

10 p1841 A70-24802

Geometrical light depolarization in randomly inhomogeneous medium, discussing light propagation in turbulent atmosphere and ionospheric radio propagation

10 p1844 A70-25162

Ionospheric changes from field intensity and phase data of long distance propagation of long waves, determining electron concentration

10 p1884 A70-25258

Ionospheric waves positive phases and disturbances related to solar activity variations and cosmic ray modulations

10 p1885 A70-25270

Electromagnetic wave propagation through weakly inhomogeneous plasma layer with frequent electron-molecule collisions, noting applicability to ionosphere

11 p2003 A70-25530

Pulsed radio waves interactions during vertical propagation through perturbed ionosphere using cross modulation theory concepts, considering perturbation waves effects

11 p2003 A70-25531

Radio wave reflection from ionosphere, discussing suppression of magnetoionic component with fluctuating elliptical polarization

11 p2003 A70-25534

Auroral radio wave absorption in ionosphere at longitudinally opposite stations compared for appearance probability and variational properties

11 p2043 A70-25537

Equivalent angles of slope calculations based on rotary oblique probing data for spherical models of earth and ionosphere, deriving minimum equivalent beam path

11 p2043 A70-25539

Polarization regularities of Pc 1 oscillations interpreted from propagation along ionospheric waveguide centered at F 2 layer

11 p2043 A70-25543

Electromagnetic wave propagation in spatially inhomogeneous isotropic ionosphere, determining phase, amplitude, polarization, absorption, arrival angle, etc

11 p2003 A70-25547

Sporadic E formation correlation to geomagnetic activity from ionospheric radio absorption observed at midlatitude and polar zone stations

11 p2044 A70-25554

Temperature and ion effect on refractive index of VLF radio waves in quiet and disturbed ionospheric conditions

11 p2004 A70-25842

Refractive index profiles method for vertically polarized electromagnetic waves in horizontally stratified magneto-plasma extended to anisotropic media, noting relevance to ionospheric propagation

11 p2011 A70-26555

VLF and ELF EM wave propagation in earth-ionosphere cavity during solar flares

12 p2183 A70-27189

D region synoptic ionization changes investigated by radio waves partial reflection from lower ionosphere, relating wave amplitudes to height

12 p2224 A70-27732

Ionospheric absorption measurements by HF and VHF techniques, discussing electron density profiles, collision frequencies, anomalies and aeronomic and ionospheric implications

12 p2224 A70-27735

Rocket measurement of ionospheric electron density based on radio propagation effects involving Dop-

- pler frequency shift, Faraday rotation, wave absorption, etc 12 p2224 A70-27736
- Electromagnetic pulse distortion with Gaussian envelope in longitudinally inhomogeneous anisotropic ionized media to investigate radio wave communication with ionospheric propagation 12 p2189 A70-27962
- Mode-scattering coefficients from ionospheric perturbations for sunrise and sunset propagation paths, comparing results with VLF radio measurements 12 p2189 A70-28053
- Long term ionospheric absorption measurements in Japan from IGY through IQSY using A1 method, discussing annual and diurnal variations correlation with solar activity 12 p2226 A70-28059
- Long term ionospheric absorption measurements in Northern Hemisphere from IGY through IQSY, discussing annual and diurnal variations correlation with solar activity 12 p2226 A70-28060
- Electromagnetic fields features in VLF spectral range for propagation in earth-ionosphere waveguide, discussing effects of ionospheric irregularities 12 p2190 A70-28169
- Seasonal measurements of ionospheric absorption during sunrise in D region at medium sunspot numbers, noting disagreement with rocket observation 13 p2392 A70-28574
- Simultaneous magnetic, photometric and backscatter radio measurement of auroral and ionospheric echoes during geomagnetic storm, confirming electrojet theory 13 p2392 A70-28575
- Wave dispersion in lower exospheric multicompound plasma, investigating mode group velocity frequency dependence at various altitudes 13 p2395 A70-28940
- Wideband FM signals transionospheric propagation, calculating output spectrum, signal to distortion ratios and signal to noise ratios 13 p2367 A70-29588
- Magnetic field measurement of VLF wave propagating in whistler mode in magnetosphere by satellite FR-1 13 p2401 A70-30054
- Lower ionosphere influence on radio reflection from sporadic E layer, determining diurnal variations of D region absorption for various frequencies 14 p2547 A70-30235
- Comparative passband of optimal and fixed frequency systems in ionospheric scatter communications during nighttime 14 p2547 A70-30239
- Scorpio X-1 and Taurus X-1 /Crab/ X ray flux effects on nighttime ionospheric radio transmission, discussing ion production and resulting electron density 14 p2631 A70-30541
- Wave polarization effects on ionospheric HF radio wave transmission and reception in communication and broadcasting networks 14 p2550 A70-30650
- Reflection and conversion coefficients of model ionospheres for VLF and LF radio waves 14 p2573 A70-30735
- VHF wave interference from heavy ion layers in lower ionosphere 14 p2574 A70-30737
- Ionospherically reflected HF radio signal frequency spread measurement involving phase difference crossings counting between antennas 14 p2550 A70-30743
- Earth-ionosphere waveguide electric field strength calculation based on nighttime ionospheric models, comparing results to measurements 14 p2574 A70-30748
- Lower ionospheric cosmic layer state during Forbush decreases from radio absorption observations interpreted on basis of electron production rate analysis 14 p2632 A70-30804
- Ionospheric inhomogeneities motion and vertical profile of atomic oxygen concentration associated with solar particle absorption in upper layer 14 p2575 A70-30808
- Radio wave scattering increase in moving body wake near caustic in vertically inhomogeneous ionosphere 14 p2550 A70-30809
- Radio wave-ionosphere interaction effects on accuracy of radio astronomical observations from earth satellites 14 p2575 A70-30824
- Measurable VLF electromagnetic fluxes from Cerenkov effect in ionosphere produced by artificial electron beams 14 p2579 A70-31249
- WKB method applied to ionospheric equations with strong wave coupling 15 p2725 A70-31857
- Transient excitation of Schumann earth-ionosphere cavity resonances by large ELF atmospherics, using propagation model 15 p2726 A70-31865
- Ionospheric radio wave propagation from rocket and satellite signal transmission using Faraday and Doppler effects, phase delay and refraction measurements 15 p2698 A70-32095
- Ionospheric measurements from observations of incoherently scattered radio waves, describing radar installations specifications 15 p2731 A70-32096
- Radio wave absorption in Venusian ionosphere, estimating effective collision number 15 p2705 A70-32736
- Multimode and dispersive distortion of short quasi-monochromatic pulses in earth-ionosphere VLF channel 16 p2858 A70-32930
- Ion effects on VLF propagation in earth-ionosphere waveguide during polar cap absorption events 16 p2859 A70-32933
- Refractive index gradients effect on scattering of radio waves perturbing ionosphere or passing through perturbed region 16 p2863 A70-33259
- Gravity wave generation during solar eclipse confirmed by satellite observation on Faraday rotation angle of ionospheric VHF transmissions 16 p2898 A70-33836
- Semiautomatic ionospheric absorption recorder, describing components circuitry and operation 16 p2915 A70-34223
- Refractive index equation for Whistler propagation in weakly drifting magnetoplasma 16 p2959 A70-34224
- Transceiving system for recording D region radio signal absorption and reflection, describing component circuitry and operation 16 p2880 A70-34225
- Ionospheric acoustic wave propagation from seismic waves of Kurile Islands earthquake on 11 August 1969 17 p3075 A70-34569
- Winter anomaly of radio wave absorption in midlatitude lower ionosphere in terms of meteorological influences and particle influx enhancements 17 p3076 A70-34936
- Zonal wind component in lower ionosphere observed for gravity waves partial reflections by temperature discontinuities, using least mean square method for reflection coefficient 17 p3077 A70-34946
- VLF and ELF radio wave propagation with mode coupling in inhomogeneous stratified ionosphere 17 p3047 A70-35402
- Electric field component of waves in auroral ionosphere measured by double Langmuir probe field detectors, discussing wave-particle interactions and turbulence 17 p3096 A70-35767
- Ionospheric scatter channel amplitude frequency characteristics recording equipment, discussing design 18 p3256 A70-36090
- Ionospheric scatter communications channel phase frequency characteristics measuring method, considering probability density function 18 p3256 A70-36091
- Receiving antenna for ionospheric scatter lines, calculating input power versus height and energy flux density spreading for position optimization 18 p3230 A70-36094
- Ionospheric radio wave absorption measurements, noting winter anomaly during maximum solar activity year 18 p3227 A70-36101
- Effective reflection height measurement accuracy for pulsed vertical ionospheric sounding, using interference method 18 p3227 A70-36106
- Sunrise effects in lower ionosphere at midlatitude, discussing long wave absorption measurements, summer electron concentration profile and consistency of aeronomic model 18 p3249 A70-36910
- Graphic method of calculating radio wave absorption in ionosphere and field strength at reception point with aid of vertical sounding data 18 p3229 A70-36911
- Ionospheric radio wave absorption and geomagnetic perturbations correlated with solar activity variations 18 p3250 A70-36931
- Ionospheric distortion of linear FM radio signals used for sounding, considering signal characteristics in distortion equations 18 p3250 A70-36933
- Ionospheric refraction during radio wave propagation using space diversity recordings of Faraday and Doppler effects for coherent signals from geophysical rockets 19 p3407 A70-37306
- Group delay times criterion of multibeam propagation of ionospheric radio echoes for communications systems 19 p3375 A70-37332
- Low elevation angle focusing of oblique radio waves after reflection from E and F layers 19 p3379 A70-37965
- Ionospheric absorption of cosmic noise recorded by riometer and corner reflector antenna directed at pole star, noting seasonal variation 19 p3412 A70-37997
- Multiple reflection processes in D and E regions at LF and VLF, using Pitteway full wave method 19 p3413 A70-38001
- Coupling processes in daytime D and E regions at LF and VLF, using thin film optics method for reflection and transmission coefficient matrices 19 p3413 A70-38002
- Intermode coupling processes in nighttime D and E regions, using thin film optical method for propagation phenomena at LF and VLF 19 p3413 A70-38003
- Radio beam trajectory in Fresnel zones of isotropic laminarily inhomogeneous ionosphere, discussing point source field and wave propagation 19 p3381 A70-38569
- Geomagnetic pulsations propagation through horizontally inhomogeneous ionosphere, solving EM wave diffraction problem 19 p3416 A70-38589
- Solar X ray emission during flares from ionospheric absorption measurements, discussing continuous ionograms method 19 p3512 A70-38912
- Lower hybrid resonance frequency propagation ducts in multilayer upper ionosphere, showing association with VLF hiss bands 20 p3584 A70-39331
- Radar for ionospherically propagated ground backscatter sounding, discussing two-aerial aperture synthesis technique and optical spectrum data recording and processing 20 p3585 A70-39393
- ELF and VLF propagation for perturbed ionosphere models, discussing effects of ion collision frequencies and molecular weights 20 p3585 A70-39454
- Ionospheric VLF diurnal transmission loss differences on two long paths, analyzing values for first and second modes 20 p3585 A70-39455
- Whistler mode wave propagation amplitude, polarization and dispersion in lower ionosphere, discussing electric field experiment with Nike-Tomahawk sounding rocket 20 p3622 A70-39456
- Radio waves propagation two dimensional model in earth-ionosphere waveguide across land/sea boundary, solving dual integral equations by Wiener Hopf procedure 20 p3585 A70-39457
- Equatorial F layer irregularity extent from propagation path observations to synchronous satellites 20 p3624 A70-40485
- Long range low loss earth-detached propagation paths in lower ionosphere indicated via OV4-1 satellite experiment on guided ionospheric propagation 20 p3591 A70-40494
- Ionospheric ducting of satellite beacon signals observed on Orbis Cal satellite experiment 20 p3591 A70-40495
- X ray star effects on ionospheric LF radio wave field strength, examining absorption and ionization in D region 21 p3873 A70-40668
- Earth magnetic field effects on midlatitude F 2 layer deviative absorption 21 p3812 A70-40727
- Cosmos 142 satellite measurements VLF radio signals transmitted through ionosphere by ground based stations 21 p3786 A70-40836
- D region water vapor chemistry effects on measurements of radio propagation, ionospheric temperature and seasonal changes 21 p3814 A70-40936
- Low latitude boundary of ionospheric absorption during winter anomaly showing enhancement dependence on solar zenith angle 21 p3815 A70-40944
- Electromagnetic wave propagation through weakly inhomogeneous plasma layer with frequent electron-molecule collisions, noting applicability to ionosphere 21 p3786 A70-41280
- Pulsed radio waves interactions during vertical propagation through perturbed ionosphere using cross modulation theory concepts, considering perturbation waves effects 21 p3786 A70-41281
- Radio wave reflection from ionosphere, discussing suppression of magnetoionic component with fluctuating elliptical polarization 21 p3786 A70-41284
- Auroral radio wave absorption in ionosphere at longitudinally opposite stations compared for appearance probability and variational properties 21 p3819 A70-41287
- Equivalent angles of slope calculations based on rotary oblique probing data for spherical models of earth and ionosphere, deriving minimum equivalent beam path 21 p3819 A70-41289

Polarization regularities of Pc1 oscillations interpreted from propagation along ionospheric waveguide centered at F2 layer

21 p3819 A70-41293

Electromagnetic wave propagation in spatially inhomogeneous isotropic ionosphere, determining phase, amplitude, polarization, absorption, arrival angle, etc

21 p3786 A70-41297

Sporadic E formation correlation to geomagnetic activity from ionospheric radio absorption observed at midlatitude and polar zone stations

21 p3819 A70-41304

Wave polarization effects on ionospheric radio wave transmission and reception

21 p3790 A70-41361

Doppler frequency shift of reflected radio waves for ionospheric disturbances, discussing solar flares, geomagnetic variations, etc

21 p3820 A70-42256

Russian monograph on propagation of LF electromagnetic waves in waveguide formed between earth and ionosphere

22 p3989 A70-42674

ELF and VLF waves in waveguide propagation mode, calculating lower ionosphere effect on attenuation and phase velocity

22 p3989 A70-42960

Radio wave reflection properties in 16-3000 kHz range calculated from D and E region models for comparison with measurement

22 p3989 A70-43164

Daytime ionospheric effect of X ray flare from SCO XR-1, discussing LF radio wave intensity decrease

22 p4095 A70-43165

Magnetosphere radio propagation from ground based measurements for HF, ULF and VLF

22 p4021 A70-43280

Micropulsation Pc-1 phase and polarization comparisons concerning L to R wave coupling in ionosphere

22 p4024 A70-43313

VHF geostationary satellite ranging and range correction systems, calculating second-order ionospheric delay effects on position error

22 p4068 A70-43590

Solar high energy particles penetration into ionospheric heights at equator, analyzing optical flare and solar proton data from ATS-1 and Explorer 34

23 p4235 A70-43816

Ionospheric parametric amplification and frequency mixing due to polarized TEM waves nonlinear interaction with longitudinal electrostatic waves

23 p4185 A70-43838

F2 region anisotropic response to individual internal gravity waves as function of propagation azimuth

23 p4185 A70-43844

D region LF and VLF sky waves opposite phase perturbation behavior

23 p4162 A70-44006

F2 layer critical frequency and maximum electron concentration statistical characteristics for predicting SW propagation conditions

23 p4188 A70-44056

Ionospheric radio wave absorption above polar aurorae during solar activity minimum, discussing diurnal and annual behavior

23 p4162 A70-44058

Lower ionosphere electromagnetic induction effect on geomagnetic field guided MHD wave propagation, considering Hall effect

23 p4189 A70-44072

Geometry and ionosphere effects on radio beacon operation for distress signal monitoring at sea, comparing night performance to daytime

23 p4163 A70-44229

Zi and Ze smallness effect on complex refractive index of ionosphere for VLF propagation

23 p4164 A70-44373

Anomalous multiple reflections from ionosphere showing concave surface focusing

23 p4164 A70-44374

Radar astronomical polarization measurements for lunar echoes by exploiting ionospheric Faraday rotation with linearly polarized antenna

23 p4165 A70-44964

Monthly and annual root-mean-square deviations of ionosphere radio wave absorption

24 p4312 A70-45485

Ionospheric HF Doppler frequency dispersion at low latitudes under various geomagnetic disturbance conditions

24 p4314 A70-46129

Earth-ionosphere cavity ELF electromagnetic pulse propagation from atmospheric source, considering transient field as frequency and time functions

24 p4314 A70-46130

Elevated horizontal and vertical electric dipole VLF fields, discussing ionospheric TE and TM mode coupling, nighttime variations and amplitude fluctuation

24 p4314 A70-46131

Ionospheric wave propagation, using medium model, perturbation theory for vertical variation and computer eigenvalues of matrix system

24 p4314 A70-46132

Lower ionosphere influence on radio reflection from sporadic E layer, determining diurnal variations of D region absorption for various frequencies

24 p4316 A70-46310

Comparative passband of optimal and fixed frequency systems in ionospheric scatter communications during nighttime

24 p4316 A70-46314

IONOSPHERIC REFLECTION U IONOSPHERIC PROPAGATION IONOSPHERIC SOUNDING

Ionospheric slopes and range frequency characteristics obtained from oblique incidence sounding of horizontally nonuniform ionosphere

01 p0083 A70-11534

Wideband HF amplifier development for ionospheric radio sounding, describing various stages

02 p0255 A70-11895

Ionospheric critical frequency recorder development for continuous recording of frequency variations with time

02 p0303 A70-12736

Ionospheric aerodynamics concerning plasma flow and stability, ion motion, radio wave scattering, etc

03 p0479 A70-14386

Rocket-borne differential capacity probe measuring electron densities in upper atmosphere, reducing errors caused by temperature and composition variations

04 p0686 A70-14649

TV data transmitted by Iantars series automatic ionospheric laboratories released by geophysical rockets at 100-400 km, discussing plasma-ion propulsion system performance

04 p0735 A70-14936

Polar lower ionosphere, using radar VLF step frequency sounding to determine reflection phase height at given propagation path

04 p0680 A70-15115

Diurnal fluctuations of quiet F2 region intensity at midlatitude based on vertical probe observations during solar activity minimum

04 p0684 A70-15745

Ionospheric probe for simultaneous measurement of radio signal reflection coefficient and amplitude-frequency characteristics

04 p0684 A70-15746

HF oblique ionospheric soundings over long temperate latitude path, discussing measured angles of elevation and multipath time dispersion

05 p0847 A70-15998

Ionograms for nonmonotonic vertical distribution of electron concentration in ionosphere from rocket and ground sounding

05 p0842 A70-16757

Ionospheric observations of resonance oscillations using satellite-borne radio sounding instruments

06 p1115 A70-17361

Ionospheric resonances observed by swept frequency Alouette topside sounders, discussing plasma nonlinearity

06 p1115 A70-17362

Quadrupole probe for ionospheric plasma resonances involving measurement of mutual impedance between pairs of electrodes

06 p1117 A70-17373

Satellite observations of VLF and ELF resonances related to ionospheric plasma singularities

06 p1118 A70-17375

Ionospheric vertical electron concentration computer calculations compared to direct measurements data by satellite and rockets over Sofia

06 p1057 A70-17843

Mass spectrometer design and calibration for ionic composition measurements on ionosphere sounding satellite, noting effects of satellite velocity and attitude

06 p1065 A70-17908

AEROS satellite A2 launching to investigate aeronomic processes in outer atmospheric layers, discussing scientific research program, mission data, satellite and ground station equipment

07 p1393 A70-19149

Field strength predictions for expected returns from backscatter ionospheric soundings, predicting ionospheric propagation modes and losses during sunspot minimum

07 p1229 A70-19161

Lowest usable frequency (LUF) measurement and prediction through synchronized oblique ionospheric sounding

07 p1233 A70-19181

Oblique incidence HF pulse ionospheric sounding, discussing propagation modes, seasonal and diurnal effects, frequency spectra, etc

07 p1233 A70-19182

Oblique ionospheric pulse sounding records improvement by use of linear FM chirp transmission, discussing time delay resolution, transmitter power and RF interference rejection

07 p1233 A70-19184

Oblique ionospheric sounder automatic data analysis by computer programs, analog to digital conversion, magnetic tape data recording, signal detection, pattern recognition, etc

07 p1234 A70-19185

Ionospheric distortion of linearly FM radio signals used for sounding, considering signal characteristics in distortion equations

07 p1268 A70-19459

Vertically moving disturbance discovered in ionospheric soundings close to magnetic equator, noting correlation with electrodynamic lift

07 p1269 A70-19631

Molecular ion concentrations, using flat probe collector trap on Cosmos 5 satellite at 200-300 km

07 p1276 A70-20421

Ionosphere absolute phase height measurement methods independent of virtual height, using fixed frequency CW emission and pulsed sounding

07 p1276 A70-20432

Positive and negative correlations in F2 layer perturbations by network of paired conjugate ionospheric stations at low latitude

07 p1277 A70-20450

Atmospheric pressure waves generated by high energy disturbance in South Pacific, using ionospheric Doppler signals correlated with ground-level pressure signals

08 p1490 A70-21646

Dye laser tuned to sodium D line used for measuring ionospheric atomic sodium

08 p1492 A70-21757

Ionospheric plasma lower hybrid resonance measurement and excitation via rocket-borne probe

09 p1670 A70-23319

Ionosphere sounding satellite attitude variation dependence on transverse moments of inertia

10 p1949 A70-23918

F region electrons collision frequency from short radio waves amplitude and group path relationship

10 p1876 A70-24535

Ionospheric F and E layers collision frequency estimates, comparing pulse absorption and cosmic radio noise measurements

10 p1880 A70-24804

Ionospheric loss rates from rocket observation during auroral absorption interpreted by two ion model of recombination

10 p1881 A70-24813

Midlatitude sporadic E layer critical frequencies dependence on solar activity using vertical ionospheric sounding data, observing ionization correlation

10 p1882 A70-25197

Equivalent angles of slope calculations based on rotary oblique probing data for spherical models of earth and ionosphere, deriving minimum equivalent beam path

11 p2043 A70-25539

Sporadic E formation correlation to geomagnetic activity from ionospheric radio absorption observed at midlatitude and polar zone stations

11 p2044 A70-25554

Ionospheric electron and ion temperatures information extraction from Doppler broadening of radar returns based on correlation measurement

12 p2183 A70-27163

Intercoms 2 equipment for measurement of positive ion concentration, electron temperature and energy distribution, electron concentration between satellite and ground reception points, etc

12 p2207 A70-27500

Ionospheric electron density, electron and ion temperature profiles measurements, comparing relative merits of radio-rocket ground-based radar and satellite methods

12 p2223 A70-27727

Ionospheric probing using pulsed radio waves at oblique incidence, discussing auroral radar, meteor radar, ground backscatter and variable frequency ionosondes techniques

12 p2224 A70-27728

Ionospheric probing by ground based and satellite-borne vertical incidence sounders

12 p2224 A70-27729

Ionospheric probing using continuous radio waves at oblique incidence, discussing HF Doppler, VHF forward scatter and radio aurorae techniques

12 p2224 A70-27730

Ionospheric probing with LF/VLF/ELF radio waves, discussing measurement techniques and temporal and spatial resolutions

12 p2224 A70-27731

Ionospheric D region radio wave probing by cross modulation technique, obtaining electron densities and collision frequencies

12 p2224 A70-27733

Ionospheric lowest regions and magnetosphere probing based on atmospheric observations, detecting disturbed conditions

12 p2224 A70-27734

Rocket measurement of ionospheric electron density based on radio propagation effects involving Doppler frequency shift, Faraday rotation, wave absorption, etc

12 p2224 A70-27736

E region plasma parameters measurement by in situ probes, considering electron density and temperature

12 p2225 A70-27737

Ionospheric parameters measurements by incoherent RF scattering, discussing current status of theory and observations

12 p2225 A70-27738

Topside ionosphere structural analysis, considering electron density profiles deduced from Alouette 2 satellite data

12 p2226 A70-28062

Topside ionosphere nighttime structure over Japan deduced from Alouette 2 satellite plasma frequency measurements

12 p2226 A70-28063

F 2 region critical frequency from Alouette 2 satellite data compared with ground based measurement

12 p2226 A70-28066

INTA-255 ionospheric sounding rocket, describing vehicle and launcher design, test firings, ground facilities, etc

13 p2504 A70-28686

Topside ionosphere structure deduced from electron density profiles observed by Alouette 2 satellite

13 p2395 A70-29090

Topside ionosphere structure deduced from resonance spikes on ionograms obtained by Alouette 2 satellite and electron density distributions

13 p2395 A70-29091

Proton cyclotron echoes in topside ionograms from Alouette 2 satellite

13 p2396 A70-29092

F 2 critical frequencies from Alouette 2 satellite ionogram data compared with ground-based sounding results

13 p2396 A70-29094

Three-point simultaneous observations for ionospheric drift characteristics in E and F regions

13 p2396 A70-29097

Topside sounder profiles interpretation, discussing ionosphere-protonosphere dynamic coupling

13 p2398 A70-29199

Floating resonance spike on Alouette 2 ionograms after sounder pulse transmission at half upper hybrid frequency, noting harmonic excitation role

13 p2370 A70-29905

Dispersion and group velocity characteristics of topside resonance oblique echoes near plasma frequencies observed by satellite

13 p2467 A70-29909

Collision and motion effect on rocket-borne quadrupole probe transfer impedance near lower hybrid resonance in ionosphere

13 p2371 A70-29919

Polar ionosphere auroral oval position detection by satellite observations of naturally occurring VLF and man-made HF plasma waves

13 p2371 A70-29924

Javelin rocket measurements of ionospheric AC electromagnetic fields, determining amplitude/frequency spectra and dipole antenna performance

13 p2401 A70-29926

Auroral and polar cap ionospheric electric fields and tensor conductivity elements using ion clouds data of Ba release experiment

13 p2402 A70-30080

Ionospheric electric fields variations in ELF-VLF, confirming OV-1 satellite measurements with OGO 6 data

13 p2403 A70-30082

Inclined backscatter sounding of ionosphere in individual channels of multichannel radio link, analyzing data during minimum solar activity

14 p2547 A70-30149

True height of reflection determination for oblique sounding data interpretation, considering method error

14 p2547 A70-30230

Sporadic E layer space diversity reception data from stations 20 km apart, noting horizontal ionization gradient effect

14 p2571 A70-30234

Lower ionosphere radio reflection during solar eclipse of 22 September 1968

14 p2571 A70-30237

Ionospheric electron distribution by true height analysis of oblique incidence HF radio wave sounding data, applying to forward and ground backscatter

14 p2550 A70-30745

Lower ionospheric drift motions observed from VHF radio signal, relating to three paths near auroral zone during dark hours

14 p2574 A70-30749

Solar eclipse of March 1970 observation by sounding rockets, discussing ionospheric and meteorological measurements

14 p2586 A70-30800

Diurnal fluctuations of quiet F 2 region intensity at midlatitude based on vertical probe observations during solar activity minimum

14 p2576 A70-30829

Ionospheric probe for simultaneous measurement of radio signal reflection coefficient and amplitude-frequency characteristics

14 p2576 A70-30830

Ionospheric total electron content measurements by Faraday method and bottom and topside soundings

14 p2580 A70-31258

Ionospheric investigation techniques, considering ionization balance, winds and turbulence

14 p2580 A70-31259

Report to COSPAR on Japanese space research including satellite, rocket and balloon observations of ionosphere, magnetosphere, interplanetary space, moon, planets, cosmic rays, etc

15 p2830 A70-31720

Ground sounding of ionization variations and vertical distribution using model, integral and normal laminar methods

15 p2729 A70-32078

Electric field measurements in ionosphere using satellite and rocket experiments

15 p2729 A70-32082

Soviet papers on ionospheric studies covering radio, rocket and satellite observations

15 p2730 A70-32088

Ionospheric probe designs and measurement errors due to perturbations by satellite carriers

15 p2731 A70-32094

Ionospheric measurements from observations of incoherently scattered radio waves, describing radar installations specifications

15 p2731 A70-32096

Meteorological rocket probing, noting 100 and 170 km range probes in U.S.S.R., thermobaric maps and aerological stations for high altitude aviation

15 p2771 A70-32108

D region electron density rocket measurements implying recombination coefficient

16 p2896 A70-32939

Single pulse ionospheric sounding system for detecting and identifying E region echoes

16 p2859 A70-32940

Time span in total electron content (TEC) measurements on BE-B and BE-C ionospheric satellites by differential Doppler method, applying chi square 2 test

17 p3077 A70-34986

Alouette and ISIS experiments programs and design

17 p3180 A70-35305

Plasma resonance phenomena related to ionospheric plasma parameters using gyroplasma probe on Kappa 8-15 sounding rocket

17 p3077 A70-35307

Ionospheric sounding with gyro-plasma probe on Kappa 8-15 rocket, discussing electron density profiles and plasma resonance

17 p3079 A70-35638

Ionospheric VLF radio waves observations via wideband receiver on K-9M-26 rocket, determining electron density profiles

17 p3047 A70-35639

Rocket measurements showing removal of electrons above mesopause in summer at high latitude

17 p3081 A70-35775

Venus daytime upper ionosphere observations by mariner 5 in terms of ionization sources and sinks, ambipolar diffusion and model atmospheres

18 p3311 A70-36002

Equatorial electrojet measurements by Nike-Apache rockets

18 p3244 A70-36018

Ionospheric vertical base selection for recording discontinuities motion of F region

18 p3246 A70-36085

Ionospheric small scale ionization discontinuities vertical drift effect on diurnal variations of F 2 layer critical frequency

18 p3246 A70-36086

Proton flares showing enhancement of ionospheric absorption and complex magnetic disturbances

18 p3306 A70-36087

F region small scale ionization discontinuities parameters observational data concerning anisotropy, dimensions, velocity and lifetime

18 p3246 A70-36088

Effective reflection height measurement accuracy for pulsed vertical ionospheric sounding, using interference method

18 p3227 A70-36106

Space charge sign distribution sounding in atmosphere by electrode potential difference measurement

18 p3246 A70-36180

Synchronous measurements of reflection coefficient and frequency characteristics of sporadic E layer by ionospheric sounding

18 p3247 A70-36293

Ionospheric distortion of linear FM radio signals used for sounding, considering signal characteristics in distortion equations

18 p3250 A70-36933

Radio wave absorption dependence on ionospheric sounding frequency at vertical incidence, using pulse method

18 p3255 A70-37038

Panoramic vertical sounding method of ionosphere, noting drawbacks

18 p3255 A70-37040

Magnetic tape recorder for panoramic vertical ionospheric sounding data acquisition in digital form

18 p3261 A70-37041

Noise rejection characteristics of ionospheric radiosondes via phase-code modulated signals, noting nonoptimal filter role in power loss

18 p3229 A70-37042

Magnetospheric thermal plasma electron density measurement during solar flare by OGO-5 satellite

19 p3411 A70-37513

Ionospheric observations of solar eclipse of 20 May 1960, using panoramic probe

19 p3419 A70-38918

Ionospheric ionization minimum delay and F region alpha variation during solar eclipse

19 p3419 A70-38919

Satellite wideband transmission of ionosphere data, monitoring amplitude and phase of phase-coherent CW signals from geostationary satellite

20 p3590 A70-40483

Ion orientation technique based on counterflow sensing in earth upper atmosphere, discussing accuracy

21 p3927 A70-40844

Ionospheric transition and ozone correction from D region sunrise auroral rocket flight

21 p3814 A70-40935

Equivalent angles of slope calculations based on rotary oblique probing data for spherical models of earth and ionosphere, deriving minimum equivalent beam path

21 p3819 A70-41289

Sporadic E formation correlation to geomagnetic activity from ionospheric radio absorption observed at midlatitude and polar zone stations

21 p3819 A70-41304

Auroral zone electric field measurements from rocket-borne instruments

22 p4017 A70-42794

Ionospheric current theoretical model and balloon measurement of ionospheric electric field

22 p4017 A70-42795

Nighttime equatorial E region small scale irregularities detected by rocket-borne Langmuir and plasma noise probes, discussing generation mechanism

22 p4018 A70-43108

F region electron density measurement during magnetic storm by incoherent scatter technique

22 p4019 A70-43157

Ionospheric electron content measurement during solar activity cycle, noting temporal and spatial variations

22 p4020 A70-43159

Total electron content and equivalent slab thickness statistical data during magnetic disturbances from AT-3 satellite VHF transmission observations

22 p4020 A70-43162

Day and nighttime E and sporadic E layer drifts over low latitude station recorded by spaced receiver technique

22 p4020 A70-43166

Geostationary satellites for magnetosphere and ionosphere sounding, discussing specific observational capabilities

22 p4024 A70-43397

Ionospheric ion temperature measurements by retarding potential analyzer on OGO-6 satellite

23 p4185 A70-43840

ELF acoustic gravity wave arrival from Apollo launches recorded by Doppler shift ionospheric sounder channelled near mesopause and lower thermosphere

23 p4187 A70-43859

Upper atmosphere optical properties sounding by twilight observation and successive brightness approximation

23 p4187 A70-44047

Ionospheric layers critical frequencies recording, using automatic interplanetary station type probe

23 p4194 A70-44088

Ionospheric electron content measurement from Faraday effect of troposphere on beacon satellite Explorer 22 radio signals

23 p4163 A70-44231

Ionosphere seasonal changes from three-point system for observing traveling ionospheric disturbances

23 p4192 A70-44868

Iantar 1 automatic ionospheric laboratory flight tests results, investigating Ar ion engine performance

23 p4264 A70-45009

Sporadic E layer characteristics from spaced ionogram analysis, discussing layers formation and dissipation and ionization irregularities motions

24 p4328 A70-45352

True height of reflection determination for oblique sounding data interpretation, considering method error

24 p4316 A70-46305

Sporadic E layer space diversity reception data from stations 20 km apart, noting horizontal ionization gradient effect

24 p4331 A70-46309

IONOSPHERIC STORMS

NT SUDDEN IONOSPHERIC DISTURBANCES
Ionospheric storms north-south asymmetry, discussing effects of horizontal and vertical move-

ments of ionization controlled by asymmetric geomagnetic field

06 p1055 A70-17594

Asian zone solar daily and storm time ionospheric disturbance variations synoptic study during IGY-IGC period

10 p1872 A70-23822

Magnetospheric substorms model modification for growth phase inclusion prior to explosive expansion phase

23 p4186 A70-43853

IONOSPHERIC TEMPERATURE

Polar thermosphere temperature measurements from artificial clouds indicating geophysical-associated variations, nocturnal decrease and annual variations

01 p0077 A70-11201

Internal gravity waves theory to interpret large amplitude oscillations in electron density and temperature and ion temperature and velocity observed in thermosphere

01 p0079 A70-11215

Electron gas heating at E region altitudes as function of ionization of atmospheric gases, noting rocket experiments during solar eclipse

01 p0082 A70-11492

Ionospheric molecular ion concentration vertical profile analysis for verifying neutral gas temperature maxima in connection with two ion production maxima

01 p0083 A70-11550

Thermal model for Venus ionosphere, considering photoionization and solar wind influx for possible heat sources

03 p0575 A70-13981

Winter diurnal behavior of northern high latitude ionospheric electron density using temperature data from Langmuir probes

03 p0478 A70-13993

Nighttime F 2 region temperature distribution under geomagnetically calm and disturbed conditions calculated from Alouette 1 satellite data

06 p1057 A70-17887

Whistlers role in ionospheric temperature, magnetospheric electron density and ionospheric composition determination

07 p1347 A70-19189

Nocturnal F layer electron density profile and temperature dependence on solar activity

10 p1885 A70-25266

Temperature, pressure and density extremes between 30 and 80 km, extrapolating estimates to all latitudes

14 p2608 A70-30591

Langmuir probe comparison to electron temperature probe measurements of ionospheric electron temperature during rocket flights

15 p2734 A70-31674

F region electron and ion densities, temperatures and plasma velocities computed for eclipse at Wallops Island on 7 March 1970

15 p2726 A70-31866

F region photoionization rate vs height twin peak profile in presence of temperature maximum, taking into account ionization of atmospheric gases by quasi-monochromatic radiation

18 p3254 A70-37031

Relaxation time for nitrogen molecule vibration temperature in ionosphere due to thermal electron collisions

19 p3409 A70-37324

D region water vapor chemistry effects on measurements of radio propagation, ionospheric temperature and seasonal changes

21 p3814 A70-40936

F region radar and optical temperature measurements, discussing Doppler and backscatter ion temperature

21 p3818 A70-41103

IONOSPHERICS

NT DAWN CHORUS

NT HISS

Ionospheric effects and transmitter characteristics observed on HF standard and time stations, discussing spurious emissions arising from frequency overcrowding

10 p1842 A70-25050

IONS

NT ANIONS

NT CATIONS

NT CESIUM ION

NT DEUTERONS

NT HEAVY IONS

NT HYDROGEN IONS

NT HYDRONIUM IONS

NT MANGANESE IONS

NT METAL IONS

NT MOLECULAR IONS

NT NITROGEN IONS

NT TRITONS

NT TRIVALENT IONS

Ion-neutral coupling in plasma acceleration revealed by velocity disparities determined spectroscopically [AIAA PAPER 70-166]

06 p1133 A70-18219

Light ions acceleration to high energy by pulsed high intensity electron beams

08 p1553 A70-21694

Solar limb brightening of XUV lines of carbon, nitrogen, oxygen and silicon ions in chromospheric-coronal transition region

11 p2108 A70-25740

Electrical conductivity hypothesis based on concept of transition temperature being inversely proportional to ionic mass square root

12 p2282 A70-26880

Ions energy spectra in plasma heated by shock wave, using passive corpuscular diagnostic technique

15 p2781 A70-32821

IP [IMPACT PREDICTION]

U COMPUTERIZED SIMULATION

IQSY [INTERNATIONAL YEAR]

U INTERNATIONAL QUIET SUN YEAR

IRAN

Gravity measurements and adjustments of First Order Gravity Network /FOGN/ in Iran

24 p4332 A70-46409

IRASERS

U INFRARED LASERS

IRIDIUM

Ni alloys with Ir and Rh using X ray diffraction and microscopy, exhibiting continuous solid solutions

09 p1708 A70-23423

Gold and iridium distribution in stony meteorites, discussing metal silicate fractionation process during chondrite formation

13 p2497 A70-29862

Hydrostatic and anisotropic piezoresistance in organometallic crystals, noting iridium and platinum complexes with maximum metal-metal interaction

22 p4086 A70-43021

Fe meteorites with high Ge content, tabulating concentrations of Ni, Ga, Ge and Ir

23 p4241 A70-44259

IRISES [MECHANICAL APERTURES]

Automatic exposure control system for airborne cameras, providing iris and shutter control through taking lens for sudden light changes

05 p0844 A70-15771

Iris coupled YIG tuned filters for 12-4 GHz region, including high field magnets from vanadium permendur

12 p2202 A70-28165

Circular and nearly rectangular irises for resonant cavities in transmission line for microwave band stop filters, discussing design based on merit factor

21 p3792 A70-41992

IRON

NT IRON ISOTOPES

NT IRON 57

Iron group nuclei abundance relative to oxygen determined for solar cosmic ray event of 2 September 1966

01 p0167 A70-10042

Iron behavior in GaAs during crystallization, studying Fe distribution ratio, impurity migration and diffusion coefficient

01 p0156 A70-10219

Photospheric Fe I abundance variation with excitation potential

01 p0175 A70-10239

Cr diffusion coating influence on fatigue life of Fe and steel, discussing residual stress measurement technique

02 p0320 A70-12848

Solar photospheric Fe abundance determined from IR supermultiplet line spectra, considering LTE effects

04 p0749 A70-14597

Fe I line enhancement in flare of 7 August 1958 interpreted as selective excitation effect, discussing similarity to late type dwarf stars observations

04 p0739 A70-14598

Forbidden Fe II lines and AIO band intensities in long period variable stars confirming stratified models of emitting layers

05 p0907 A70-16031

Excitation of ground configuration of Fe XIII for density and temperature range in solar corona, using proton collisions, electron collision strengths, etc

05 p0902 A70-16434

Fe diffusion coefficients measured at various temperatures above 1150 C to calculate homogenization times of Thailand tektite source

05 p0917 A70-16841

Empirical astrophysical damping constants derived for neutral Fe lines using solar spectra, applying constants to abundances and surface gravity determination

05 p0919 A70-16939

Solar core opacity influence on revised photospheric iron abundances, discussing neutrino flux prediction doubling in solar models

05 p0905 A70-16985

Ionization energies and oscillator strengths for Fe XVI, Co XVII and Ni XVIII by frozen core approximation, noting applications to solar corona

06 p1150 A70-18465

Contact resistance measurements used in contaminant removal and metallic adhesion on iron surfaces

07 p1293 A70-18940

Iron ions EPR lines widening in corundum crystals due to lattice defects, estimating mosaic blocks disorientation parameter and point defects density

08 p1556 A70-21122

Oscillator strengths of Fe II lines and solar iron abundance measured by arc burning in Ar with iron chloride admixture

08 p1576 A70-21398

Iron peak nuclei synthesis by charged particles under supernova mechanism conditions predicted by hydrodynamic conditions

09 p1749 A70-21994

Fe abundance in solar photosphere, evaluating various determination methods

09 p1753 A70-22382

Energy levels predicted for various electron orbital configurations in Fe V by Slater parameters

10 p1944 A70-24953

Iron impurity energy level behavior in seminsulating GaAs from determining temperature dependences of Hall coefficient, resistivity, optical absorption and steady spectral photoconductivity

12 p2286 A70-27370

Solar iron-to-hydrogen ratio and oscillator strengths for Fe I lines compared with laboratory measurements of line broadening by neutral atoms

13 p2486 A70-28628

Star eta Arietis spectra analyzed for Fe and V abundance

13 p2487 A70-28715

Ionization equilibria and ionization and recombination rates for Fe and Ni ions, discussing dielectronic recombination

14 p2631 A70-30727

Ionized iron lines observations under coronal conditions, giving halfwidths and kinetic temperatures for forbidden lines Fe X-Fe XV

14 p2651 A70-31377

Antifriction and wear properties of iron fluoride materials and white cast iron under sliding friction in air and vacuum

15 p2743 A70-31637

Pure iron and low carbon steel macroscopic stress measurements, determining correlation between residual stress, fatigue damage and fatigue life

15 p2759 A70-32322

H alpha and Fe I lines, calculating velocity effects on profiles for differentially moving atmosphere

15 p2804 A70-32616

Heat transfer in tungsten-tungsten and Armo Iron-Armo Iron specimens, confirming Bowden-Tabor model of elastoplastic events during cyclic engagement of surfaces

16 p3000 A70-33920

Ti equipment anodizing methods, observing corrosion resistance reduction and embrittlement hydriding due to Fe contamination

17 p3098 A70-34363

Resonance and satellite lines of highly ionized iron in solar spectra, discussing spectrum features during chromospheric flares

17 p3154 A70-34541

Pure Fe and Ta hot hardness using ultrahigh temperature hardness tester

17 p3124 A70-34659

Iron line emission at 1.9 A during solar flares observed by OSO-4 proportional counter spectrometer

17 p3150 A70-34836

Steel and cast iron early stage fatigue failure, using photoelastic coatings

17 p3192 A70-35741

Fe II line behavior in plages near solar limb

17 p3174 A70-35866

Lunar anorthosites Ni-Fe grains from Mare Tranquillitatis, discussing contamination by meteoritic metal, magnetic fractionation and fractional crystallization

19 p3519 A70-38032

Thermal release profiles and retention coefficients of injected argon ions for silicates and iron simulating meteoritic materials

19 p3474 A70-38601

Solar chromospheric Fe abundance, considering f-value effects

19 p3524 A70-38697

Strain component determination for grain boundary sliding influence in creep of alpha iron

20 p3735 A70-40446

Sco X-1 X ray emission data from rocket-borne measurement, indicating Fe K-emission from high ionization states

21 p3873 A70-40667

Clean iron /011/ surfaces, determining sulfur, oxygen and hydrogen sulfide films effects on adhesion behavior

21 p3831 A70-40748

Sodium behavior in young and old late type stars, examining relation to iron abundance in F, G and K dwarf and giant stars

21 p3887 A70-41114

- Solar iron abundance from forbidden Fe II magnetic dipole transition probabilities 21 p3888 A70-41118
- Elemental composition and structure of metallic iron particles in lunar fines compared to meteorites, using neutron activation technique 21 p3774 A70-41556
- Apollo 11 lunar dust hysteresis curves and thermomagnetic curves, discussing metallic Fe abundance, susceptibility, alpha-gamma transition, etc 21 p3918 A70-41676
- Pure Fe and Ta hot hardness tests by ultrahigh temperature tester involving use of electron microscope 21 p3840 A70-41900
- Solar chromosphere elements abundances methods, suggesting Fe differences origin in Fe I and Fe II inconsistencies 21 p3925 A70-42194
- Solar coronal and photospheric iron abundances from absorption forbidden lines, discussing discrepancy with permitted lines 21 p3925 A70-42195
- Forbidden iron emission lines excitation in Seyfert galaxies, discussing various mechanisms 22 p4102 A70-42977
- Electron capture involving iron nuclei in contracting iron stars treated as endothermic nuclear reaction 22 p4104 A70-42992
- Mossbauer effect analysis of Fe impurity atoms in n- and p-type semiconductor compounds with wide and narrow forbidden gaps 24 p4388 A70-45204
- Multiply ionized Fe valence and inner shell transitions from spectrum analysis, noting similarities to solar flares 24 p4401 A70-45315
- IRON ALLOYS**
- NT AUSTENITIC STAINLESS STEELS
- NT BAINITIC STEEL
- NT CARBON STEELS
- NT CHROMIUM STEELS
- NT HIGH STRENGTH STEELS
- NT MARAGING STEELS
- NT MARTENSITIC STAINLESS STEELS
- NT NICKEL STEELS
- NT STAINLESS STEELS
- NT STEELS
- Strain rate, temperature and alloy content effects on plastic flow in binary substitutional alloys of bcc iron 01 p0119 A70-10735
- Ferrite and martensite precipitation hardening in Fe-Ni-Mo alloy, studying dislocation structure and aging kinetics 01 p0123 A70-11243
- FeCo V plastic deformation and fracture, noting temperature and grain size effects on yield and flow stresses, ductile to brittle transition, etc 01 p0123 A70-11244
- Martensite transformation with fcc lattice in Ti alloys containing 5.9 percent Fe as function of cooling rate, using X ray analysis 01 p0124 A70-11590
- Heat and creep resistant Ni- and Fe-base alloys application in gas turbines, superheaters, steam pipes, chemical and petrochemical plants and heat treatment equipment 02 p0319 A70-12711
- Co and Fe base alloys corrosion in Hg tested in reflux capsules and forced flow loops 04 p0710 A70-15631
- Thin film transmission electron microscopy study of precipitation in Fe-Ni-Cr-Mo alloy with added Be and specific thermoelastic properties 05 p0862 A70-16022
- Cracks development in hydrogenated silicon iron, investigating plastic strain relation and brittle rupture propagation 06 p1165 A70-17580
- Ni effect on nitrogen activity in Fe-Ni-N austenite between 600-1200 C using Strohlein analyzer 06 p1088 A70-17612
- Ni-Fe alloys texture formation, studying strong deoxidizers role in secondary recrystallization 06 p1088 A70-17614
- Roll diffusion bonding applicability to Ti, Ni and Fe alloys, discussing fabrication temperatures and tooling [AIME PAPER F-69-3] 07 p1290 A70-18813
- Fe-Cr-Ni alloys for use in high temperature oxidizing environments 07 p1305 A70-18966
- Kirkendall effect in Fe-Ni and Fe-Co systems using measurement of radiotracer and intrinsic diffusion coefficients 07 p1314 A70-20015
- Iron base and nickel base alloys susceptibilities to internal hydrogen and hydrogen environment embrittlements, studying crack initiation inside and at metal surface 08 p1520 A70-21515
- Gamma-gamma prime mismatch effects on stress rupture of Ni and Fe-Ni based alloys with Al and Ti hardeners 08 p1521 A70-21701
- Duplex Fe-Cr-Ni-Ti alloy sigma phase formation mechanism using electron microscope 08 p1525 A70-21958
- Temperature effect on plastic flow in Ti-scavenged Fe, attributing microyielding to edge dislocations motion 08 p1525 A70-21959
- Co-Fe core ability to adjust roll spacing in model rolling mill determined from magnetostriuctive properties 10 p1905 A70-25175
- Fe-Mo-C and Fe-Ti-C alloys microstructure and hardness after rapid cooling from melt, considering phase dispersion and particle size, spacing and shape 11 p2065 A70-25774
- Iron-nickel alloy phase and diffusion relationships, composition gradients and hardness variations involving long time metallic meteorite anneals 12 p2252 A70-26964
- Concentrated Fe-Co alloys, effects of local atomic configurational changes on hyperfine interaction using Mossbauer spectroscopy 12 p2284 A70-27245
- Fe-Cr system and Fe-Cr-Ni liquid alloys studied by Knudsen cell-mass spectrometer combination, deriving phase equilibria from ion current ratios 12 p2255 A70-27602
- Ferritic and martensitic Fe-Ni alloys lattice parameter determined by standard X-ray techniques 12 p2256 A70-27613
- Ni-Fe alloy sheets magnetic shielding effectiveness correlated with DC magnetic properties at various frequencies 12 p2201 A70-28127
- Cu-Fe-Ti ternary system via microscopic, X ray and thermal analyses, measuring microhardness, electrical resistivity and magnetometry 13 p2433 A70-28863
- Titanium effect on iron and steels nitriding at high temperature, obtaining high surface hardness 13 p2423 A70-29773
- Ni-Fe base superalloy notch and rupture properties as function of thermal and chemical changes, using electron microscopy 13 p2437 A70-29829
- Fe-Al and Fe-Si alloys strengthening by pyrolytic graphite fibers 14 p2595 A70-30543
- Hydrogen embrittlement of martensitic Fe-Ni alloys as function of temperature via slow strain rate tensile tests 15 p2755 A70-31559
- Superalloys commercial development, investigating strength, heat resistance and weldability of Fe- and Ni-based alloys [ASM PAPER W70-9.4] 15 p2760 A70-32335
- Martensite-to-austenite reverse transformation in Fe-Ni-Co alloys, using dilatometry and coercive force measurements 15 p2761 A70-32386
- Fe-Ni-P phase diagrams for high temperatures, providing phase equilibria data for Widmanstatten pattern in iron meteorites 15 p2762 A70-32391
- Composition and heat treatment effects on Fe-Ni alloys structure, using micrographic, autoradiographic and potentiokinetic methods 16 p2916 A70-33080
- Convective diffusion and liquid velocity in Co and Fe based alloys corrosion in Hg at high temperature, using reflux capsules and forced flow loops 16 p2933 A70-34207
- High strength ferrous alloys susceptibility to stress corrosion in seawater environment, tension loading single edge notched and fatigue cracked specimens in NaCl solution 17 p3123 A70-34554
- Liquid Fe-Cr-C, Fe-P-C and Fe-Cr-P systems, evaluating interaction coefficients 18 p3272 A70-36032
- Oxygen dilute solutions in liquid Fe-Ni-Co alloys, investigating thermodynamic properties by hydrogen-water vapor equilibrium 18 p3272 A70-36033
- Fe-Co alloys critical points during rapid heating, determining alpha-gamma phase transformations onset from dilatometric curves 18 p3275 A70-36203
- Fe-Ni alloy alpha-gamma phase transformation after heating, noting deformation planes and directions in martensite 18 p3275 A70-36204
- Dilatometric investigation of Fe alloys phase transformations, determining magnetic field effects and Curie temperatures 18 p3276 A70-36206
- Magnetometric, dilatometric, pyrometric and X ray studies of phase transformations in Fe-Ni alloys, considering magnetic characteristics and formation of superstructures 18 p3276 A70-36207
- Fe diffusion in equiatomic Ni-Co alloy, using thin radioactive deposit method with tagged element Fe 59 18 p3277 A70-36440
- Ti and C effects on Fe-Cr-Ni alloys mechanical properties 19 p3449 A70-37271
- Dynamic and static stress effects on martensite formation temperature in Fe-Ni-C alloys 19 p3451 A70-37569
- Phase equilibrium of Fe-rich Fe-Al alloys using single crystal X ray diffraction 19 p3452 A70-37838
- Fe rich Fe-Al alloys single crystals, determining three dimensional order and atomic displacements coefficients by X ray diffuse scattering 19 p3452 A70-37839
- Fe-Ni-C alloys austenite dispersion matrix effects on martensite structural characteristics 20 p3649 A70-39705
- Phase relations in system Ag-Fe-S in 700-1200 C range at various vapor pressures by quenching and differential thermal analysis, observing liquid-immiscibility fields 22 p4053 A70-42732
- Fe-Ni alloy plastic flow behavior during reversible austenite-martensite transformation under constant load 24 p4357 A70-45228
- Bcc Fe base alloys volume diffusion measurements, determining activation energy and frequency factor dependence on solute content 24 p4357 A70-45232
- Crystallography of martensite transformation on /225/ type planes of austenite in Fe-Mn-Cr-C alloy 24 p4358 A70-45237
- Martensite plate substructure in Fe-Mn-Cr-C alloy, using transmission electron microscopy and diffraction study 24 p4358 A70-45238
- Fe-Cr and Fe-Cr-V system miscibility gap, using differential thermal analysis and Mossbauer effect measurements 24 p4362 A70-46190
- Fe-Cr alloy powders obtained with thermodynamic saturation from point sources, determining optimal mixture compositions and parameters 24 p4350 A70-46338
- IRON CHLORIDES**
- Steel surface diffusivity saturation with elements of chlorides, noting role of iron chloride phase in promoting coating uniformity 24 p4350 A70-46332
- IRON COMPOUNDS**
- NT CHROMITES
- NT FERRITES
- NT FERROCHENES
- NT HEMATITE
- NT ILMENITE
- NT IRON CHLORIDES
- NT IRON CYANIDES
- NT IRON OXIDES
- NT MAGNETITE
- NT PYRRHOTITE
- NT SCHREIBERSITE
- NT TROILITE
- Absorption transition fine structure measurements for bulk rare earth garnets single crystals using reflectivity techniques [IEEE PAPER 19.6] 05 p0894 A70-16998
- Alloying elements preventing hot cracking in weld metal by converting iron sulfides into higher melting point sulfides 07 p1293 A70-18979
- Magnon energy theory for temperature dependence of ferrous and magnesium fluorides antiferromagnetic-resonance frequency, sublattice magnetization and magnetic specific heat 09 p1739 A70-22324
- Ferromagnetic cubic sulfide of Fe easy axis by electron diffraction pattern, aligning sulfide particles along magnetic field 13 p2472 A70-29712
- Calcium-bearing iron silicate /pyroxferroite/ from Apollo 11 lunar Tranquility Base samples, discussing petrographic environment, physical and optical properties 21 p3895 A70-41504
- Thermal decomposition of fine-dispersion iron sulfate powders under continuous heating during ferrites manufacture 23 p4205 A70-44041
- IRON CYANIDES**
- Iron cyanide additive for surface stabilization of ZnO irradiated with UV in vacuum 12 p2181 A70-27258
- IRON ISOTOPES**
- NT IRON 57
- Isomer shift, Mossbauer recoil free fraction and nuclear quadrupole splitting for Fe57 in iron fluoride measured for lattice dynamics, fine and hyperfine structure 14 p2626 A70-30484
- IRON METEORITES**
- NT ODESSA METEORITE
- Chondrite-normalized lanthanide pattern of silicate inclusion of Woodbine iron meteorite, showing differences from mesosiderite phase and chondrite 01 p0177 A70-10340

- Naturally and artificially shocked iron meteorites, analyzing microstructure and alterations induced by pressure wave and high temperatures
02 p0377 A70-12506
- Metallographic examination of impact induced deformation textures of Campo del Cielo iron meteorite, analyzing phase homogeneity, microstructures and shock intensity
02 p0377 A70-12511
- Widmanstätten structure in iron meteorites relationship to cooling rate and meteoritic origin
04 p0751 A70-15039
- Chemical compositional evidence of Needles (California) iron meteorite, suggesting distinct fall nature
05 p0912 A70-16465
- X-ray line broadening analysis for lattice damage in kamacite phase of Fe meteorites, evaluating particle size and elastic strain
05 p0915 A70-16828
- Electron microprobe determinations of Si concentrations in metal of iron meteorites, showing weak evidence for Si presence in earth core
05 p0921 A70-17094
- Gibeon meteorite iron strength and ductility tests, discussing fragmentation and relation to parental planet structure
06 p1150 A70-18478
- Half life of Mn53 calculated from measured activity in sample from Fe meteorite and isotopic ratio Mn53/Mn55
07 p1337 A70-19226
- Iron troilite meteorites lead isotopic, Pb and U concentrations, considering fractionation and terrestrial contamination effects
07 p1388 A70-20035
- Magnetic spherules extracted from manganese nodules classified by X ray diffraction and electron microprobe data, suggesting volcanic, stony and iron meteoritic origins
08 p1578 A70-21560
- Ar 37 and Ar 39 isotopes in recently fallen iron-ataxite and stony meteorites, discussing relevance to cosmic ray variations in space
12 p2309 A70-27950
- Iron meteorites electrolytic corrosion using potentiostatic technique, noting roles of Ni content and crystal structure
13 p2432 A70-28697
- Mass distribution of Sikhote Alin meteorite fragmentation, noting similarity to terrestrial rocks
13 p2490 A70-28916
- Weekeroo Station iron meteorite silicate inclusions chemical composition compared to chondrites
13 p2497 A70-29858
- Iron and stony iron meteorite cooling rates and thermal models, showing melting, radioactive heat source redistribution and surface heating effects
13 p2497 A70-29861
- Fe-Ni-P phase diagrams for high temperatures, providing phase equilibria data for Widmanstätten pattern in iron meteorites
15 p2762 A70-32391
- Compressive yield strength of iron meteorites, discussing flow stress, microstructure, grain size, plastic deformation, slip lines, etc
18 p3314 A70-36498
- Silicate inclusions in iron meteorites analyzed by microprobe and classified according to phase assemblages, compositions and textures
20 p3701 A70-38981
- Nitrogen content of Odessa and Canyon Diablo iron meteorites from thermal neutron activation, Kjeldahl distillation and alkali fusion methods
21 p3921 A70-41942
- Fe meteorites with high Ge content, tabulating concentrations of Ni, Ga, Ge and Ir
23 p4241 A70-44259
- Neutron activation determined concentrations of Ni, Ga, Ge and Ir in iron meteorites with silicate inclusions
24 p4401 A70-45376
- Iron meteorites graphite-troilite nodules isomeric alkane composition, using gas chromatography and mass spectrometry
24 p4402 A70-45379
- IRON ORES**
NT HEMATITE
IRON OXIDES
NT CHROMITES
NT HEMATITE
NT ILMENITE
NT MAGNETITE
Wustite partial oxygen pressure measurements using emf in zirconia solid electrolyte
16 p2961 A70-33965
- Mossbauer spectra of Apollo 11 lunar fines and microbreccia, showing iron oxidation, site symmetry and magnetic state
21 p3915 A70-41657
- IRON 57**
Fe 57 contaminant in Ni, studying Mossbauer effect as function of temperature
15 p2784 A70-32023

Fe 57 nuclear hyperfine splittings in clinopyroxenes from lunar igneous rocks, determining temperature dependent cation distribution
21 p3915 A70-41659

IROQUOIS HELICOPTER

U UH-1 HELICOPTER

IRRADIANCE

NT ILLUMINANCE

NT SOLAR CONSTANT

Extraterrestrial solar spectral irradiance at earth mean solar distance within 300 to 2500 nm wavelength region, from NASA CV-990 aircraft research flights
04 p0690 A70-15019

Irradiance factor between perpendicular and arbitrarily positioned plane rectangles calculated by contour and numerical integration
09 p1791 A70-23619

Black body cavity type radiometers for high accuracy measurement of irradiance
15 p2737 A70-32036

Solar spectral irradiance measurements at different altitudes, using multichannel radiometers
22 p4013 A70-42599

IRRADIATION

NT AURORAL IRRADIATION

NT ELECTRON IRRADIATION

NT ION IRRADIATION

NT NEUTRON IRRADIATION

NT PROTON IRRADIATION

NT X RAY IRRADIATION

Radiative heat transfer from longitudinal rectangular conducting fins on plane wall involving mutual irradiation, using iterative method
[ASME PAPER 69-WA/HT-22] 04 p0782 A70-14812

Mice irradiation reactions determination from various metabolism indices including blood sugar level, leucocytes number, proteolytic processes rates, etc
07 p1198 A70-18714

Therapeutic effects of hemopoietic tissue transplantations of bone marrow on irradiated rats, using diffusion chamber for resettlement prevention
13 p2354 A70-29753

Human vision inertia and irradiation algorithm, satisfying Talbot law
18 p3217 A70-36082

Apollo 11 lunar soil irradiation history from solar wind rare gas abundances and cosmic ray spallation products
21 p3908 A70-41590

Terrestrial and chondrites vanadium isotopic ratios indicating irradiation histories difference
24 p4402 A70-45381

IRREGULARITIES

F region irregularity model to include field-aligned columns and sheets and frontal irregularity shapes effect on radio star and satellite scintillations
10 p1841 A70-24805

Nighttime equatorial E region small scale irregularities detected by rocket-borne Langmuir and plasma noise probes, discussing generation mechanism
22 p4018 A70-43108

IRREVERSIBLE PROCESSES

Asymmetric thermoelasticity derived for constitutive equations based on thermodynamics of irreversible processes, formulating variational and reciprocity theorems
01 p0209 A70-11384

Electrical properties thermally induced irreversible changes in CdSb single crystals measured as function of current intensity and flow
03 p0542 A70-13751

MHD equations including energy dissipation terms applied to irreversible processes occurring in fast hydromagnetic shock waves in solar chromosphere
06 p1143 A70-17999

Vlasov equations and irreversibility in plasma physics and stellar dynamics, calculating statistical entropy and relaxation time
08 p1550 A70-20556

Irreversible processes thermodynamics during thermoelastic deformation of solid bodies, deriving thermodynamic potentials, state and coupled heat equations
09 p1777 A70-23077

Irreversible viscosity decrease and thermal stability in polymer-containing lubricating oils under shearing forces effect
09 p1693 A70-23408

Thermodynamics and statistical mechanics taking into account irreversibility, arrow of time and astrophysical schemes
11 p2146 A70-25695

Irreversible yield stress component of aluminum, Armco iron and tantalum with fcc lattice, showing temperature dependence
13 p2436 A70-29500

Vlasov equations and irreversibility in plasma physics and stellar dynamics, calculating statistical entropy and relaxation time
15 p2781 A70-32711

Statistical theory of irreversible transport processes in fluids, considering deviation from equilibrium as stochastic process
17 p3131 A70-35532

Onsager reciprocal relations experimental validity in irreversible processes application to metals, electrokinetics, isothermal diffusion, heat conduction, chemical reactions, etc
17 p3197 A70-35538

Thermodynamic application to strained solids, considering paradoxes, irreversible processes and continuum mechanics
18 p3340 A70-36555

Kinetic equations derivation for correlation functions and time dependent distribution functions of irreversible processes, using projection operators
20 p3672 A70-39588

IRRIGATION

Wheat culture continuous subirrigation for life support system applications in spacecraft, discussing harvest yields
17 p3026 A70-35321

IRRITATION

NT TOXICITY AND SAFETY HAZARD

IRROTATIONAL FLOW

U POTENTIAL FLOW

ISCHEMIA

Pathological manifestations of acute myocardial ischemia without acute myocardial necrosis and myocardial infarction, discussing subjects with chronic occlusive coronary atherosclerosis
04 p0634 A70-15456

Myocardial metabolism in ischemic heart disease using arterial and coronary sinus catheterization
04 p0636 A70-15469

Acute coronary occlusion effects on adjacent unoccluded artery resistance, discussing responsible mechanisms in ischemic heart
04 p0637 A70-15473

Computer program for on-line analysis of exercise ECG considered for improved diagnosis of ischemic heart disease
05 p0805 A70-16105

Acute myocardial ischemic injury and infarction in dogs related to changes in man using oxigraph tracings
06 p0997 A70-18405

Biochemical disturbances during early myocardial ischemia, examining coronary sinus lactate and K levels using electrocardiographic correlation
06 p0997 A70-18406

Ischemic heart disease (IHD) prognosis using abnormal electrocardiographic stress test
10 p1820 A70-24940

Hypercapnia effect on oxygen tension in ischemic myocardium in dogs using polarographic method
24 p4300 A70-45843

ISENTROPIC PROCESSES

Expansion isentropes of TNT/hexogen melts explosion products from measured shock wave parameters in Al, organic glass, foam polystyrene, argon and air
01 p0216 A70-11003

Self similar wave solutions of continuity and momentum equations for two dimensional unsteady isentropic motion of polytropic gas
02 p0278 A70-11998

Isentropic model for time behavior of steady spherical source expanding into arbitrary ambient gas [ALAA PAPER 70-232]
06 p1042 A70-18215

Finite plates impact flow field analysis from isentropic one dimensional flow equations solution through hodograph transformation
09 p1776 A70-22721

Expansion isentropes of TNT/hexogen melts explosion products from measured shock wave parameters in Al, organic glass, foam polystyrene, argon and air
10 p1960 A70-25008

Cylindrical shock wave two dimensional propagation in conducting plasma in magnetic field, assuming isentropic flow along streamline
11 p2091 A70-26174

Steady isentropic weakly perturbed supersonic flows past arbitrary slender tapered wings with subsonic leading edges
16 p2838 A70-33971

Rocket chambers combustion products isentropic expansion effects within nozzle on dissociation degree, assuming shifting and frozen equilibria
16 p2963 A70-34341

Midtropospheric frontogenesis, using three hourly rawinsonde data for isentropic trajectories to describe velocity field in space and time
20 p3664 A70-39374

Perfect gas irrotational isentropic nozzle flow by solving partial differential equations set
21 p3744 A70-41240

Hodography of compressible fluids three dimensional irrotational isentropic flow
21 p3808 A70-41439

Isentropic gas two dimensional unsteady flow through channel contraction, using hydraulic analogy
22 p4012 A70-43438

ISING MODEL

U FERROMAGNETISM

U MATHEMATICAL MODELS

ISIS SATELLITES

NT ALOUETTE 2 SATELLITE

NT ISIS-A

Electromagnetic control system for spin rate and axis orientation of ISIS ionospheric research satellites, describing design parameters
13 p2501 A70-28414

Report to COSPAR on space research in Canada, covering Alouette satellites, ISIS I, international cooperation, etc
15 p2829 A70-31708

Alouette and ISIS experiments programs and design
17 p3180 A70-35305

Soft particle spectrometer in Isis-I satellite using electrostatic deflection for differential energy spectra measurements for electrons and protons
23 p4197 A70-44468

ISIS-A
Canister for protecting DC motors in Isis I antenna unit, noting pressure monitoring device and shaft seal
17 p3100 A70-34753

ISLANDS
NT GREAT BRITAIN
NT GREENLAND
NT JAPAN

ISOBARS (PRESSURE)
Atmospheric circulation indices in Northern Hemisphere on isobaric surfaces, comparing mean diurnal, monthly and climatic values
20 p3662 A70-39180

Arctic and antarctic atmospheric circulation differences, discussing circumpolar vortices and isobaric surfaces altitude changes
22 p4065 A70-43168

ISOBUTANE
U BUTANES

ISOCORIC PROCESSES
Air jets from sonic orifice, investigating three zones of isochor families by visualization and density measurement
17 p3070 A70-35046

Single component fluid behavior in liquid-vapor critical point vicinity, using LF acoustic resonant cavity technique for isochoric measurements
23 p4222 A70-44432

ISOCROMATICS
Photoplastic material thickness change from mechanical and holographic measurements, showing correlation with isochromatics during plastic yielding
15 p2821 A70-32314

Holographic registration of isochromatic and isopachous diffraction patterns of photoelastic birefringent objects, showing stress concentrations
19 p3422 A70-37649

Isochromic change in bleaching of rhodospin, showing additional intermediate without detectable color change
23 p4147 A70-44776

Isoclinic parameter determination from intersection points of secondary isochromatics lines in photoelastic analysis, discussing polariscope theory and imperfect quarter wave plates error effect
23 p4198 A70-44910

ISOCYANATES
Dicyanostilbene formation from phenylethynyl azide and isocyanate
05 p0811 A70-16054

Isomerization of isocyanide into azulene by irradiation and formation from biphenyl isothiocyanate, observing ring expansion and electrophilic carbenoid properties
05 p0811 A70-16055

ISOLATION
NT SOCIAL ISOLATION
Radiation hardened ICs development, discussing problem of dielectric isolation
08 p1468 A70-20627

ISOLATORS
Plastic symmetrical trough waveguides with metalized surfaces for hybrid millimeter-wave integrated circuit systems, discussing ferrite resonant isolator
07 p1243 A70-20151

Gas tube isolator circuit for arcing amplifier in phased arrays, using programmed charge of capacitance bank during interpulse
16 p2879 A70-34072

Shock response of passive nonlinear elastic isolators under pulse excitation with viscous damping
22 p4117 A70-43249

ISOMERIZATION
Isomerization of isocyanide into azulene by irradiation and formation from biphenyl isothiocyanate, observing ring expansion and electrophilic carbenoid properties
05 p0811 A70-16055

Acrolein photoisomerization in lower excited states, determining fluorescence and phosphorescence quantum yields
15 p2694 A70-31730

Heats of combustion and free isomerization energies of exo- and endo-isomers of 2- and 1-methylbicyclo heptane
22 p3982 A70-42680

Light effect on cis-trans-isomerization of cinnamoyl-alpha-chymotrypsin, considering molecular modeling of visual reception
24 p4298 A70-45496

ISOMERS
Hydrocarbon fraction examination of Botryococcus braunii growing in natural environment, discussing unsaturated isomeric hydrocarbons
02 p0249 A70-11679

Mossbauer temperature dependent isomer shift, proposing electron density change at resonant nucleus site by lattice phonons
14 p2626 A70-30483

Isomer shift, Mossbauer recoil free fraction and nuclear quadrupole splitting for Fe57 in iron fluoride measured for lattice dynamics, fine and hyperfine structure
14 p2626 A70-30484

Specific heat and thermodynamic functions of endo- and exo-isomers of 2-methylbicyclo heptane in 12-310 K temperature range
22 p3982 A70-42681

Carbonaceous chondrites isomeric alkanes identification by mass spectrometry and gas chromatography
24 p4402 A70-45378

Iron meteorites graphite-troilite nodules isomeric alkane composition, using gas chromatography and mass spectrometry
24 p4402 A70-45379

ISOMORPHISM
Isomorphous mixed ammonium perchlorate and potassium perchlorate crystals structural homogeneity by X ray diffraction and differential thermal and thermogravimetric analyses
21 p3784 A70-42262

ISOPHOTES
Isophote flattening functions of elliptical galaxies including identification of giant and dwarf galaxies
02 p0377 A70-12449

Solar corona photographs for isophotes during solar eclipse of 22 September 1968 revealing chromospheric flare and prominences
03 p0569 A70-13362

Solar flare H alpha brightness measurement from photograph taken through birefringent filter, deriving flare morphological changes from isophotes
06 p1135 A70-18004

Galactic longitude interval region radio telescope observations, obtaining isophotes of brightness distribution of RF spectral line of neutral H and continuous spectrum
08 p1564 A70-20551

Radio galaxy 3C 371 compact companions, studying luminous isophotes and red shift by long exposure plates with 200 inch telescope
10 p1936 A70-23908

Solar corona photographs for isophotes during solar eclipse of 22 September 1968 revealing chromospheric flare and prominences
11 p2118 A70-26727

Galactic longitude interval region radio telescope observations, obtaining isophotes of brightness distribution of RF spectral line of neutral H and continuous spectrum
15 p2805 A70-32706

Planetary nebula NGC 3242 monochromatic photographs and isophotic contours
24 p4411 A70-45788

ISOPLETHS
U NOMOGRAPHS

ISOSTASY
High temperature effects on evolution of Venus upper lithosphere, considering magnetic differentiation, isostatic adjustments, surface relief, mountain building time and distance scales, etc
02 p0371 A70-12207

De Sitter hydrostatic equations solution possible with help of boundary condition from external potential theory with/without assumed equilibrium in earth interior
04 p0678 A70-15051

Mercury shape estimated with isostatic form of equilibrium controlled by situation near perihelion passage at 3-2 resonance spin rate, discussing solidification thermal effects
05 p0908 A70-16332

Earth deviations from isostatic equilibrium, showing irregularities dependence on distance from surface for various tectonic zones
08 p1487 A70-20715

Lunar maria absolute age from lunar craters rim height changes via isostatic settling and small craters quantity
14 p2649 A70-31213

ISOTHERMAL FLOW
Turbulence intensity and fluctuation rates in isothermal swirling free jets, using constant temperature hot wire anemometer method
01 p0059 A70-10031

Axisymmetric turbulent incompressible and isothermal self preserving jet investigation using linearized constant temperature hot-wire anemometers
01 p0065 A70-11099

System of equations describing isothermal two phase-two component fluid flows with negligible dissipation effects, emphasizing slug flow
02 p0288 A70-12856

Laminar isothermal entrance flows in circular cross section ducts with uniform mass injection at wall from boundary layer equations, discussing molecular weight effects
02 p0288 A70-12859

Dissimilar coaxial axisymmetric jets confined laminar mixing obtained from numerical solution of boundary layer equations, considering binary, isothermal and nonreacting system
04 p0621 A70-15579

Vertically propagating waves in viscous isothermal atmosphere taking into account reflection due to nonlinearities and time dependence
05 p0833 A70-16679

Transition from compressible to incompressible fluid assuming isothermal flows and finite stresses for density at or different from initial value
10 p3954 A70-24008

Two dimensional incompressible isothermal laminar separation of Newtonian fluid in steady flow, obtaining velocity profiles
16 p2892 A70-33635

Variational principle for turbulent shear flow between parallel plates, taking into account isothermal flow and Malkus theory
17 p3073 A70-35595

Karman-Polhausen method applied to unsteady thermal boundary layer on isothermal flat plate
21 p3954 A70-42208

Isothermal steady laminar flow through tube with change in wall temperature, examining velocity profile relationship to temperature profile
22 p4008 A70-42421

MHD laminar isothermal flow in closed cylindrical tube in rotating magnetic field, determining azimuthal velocity distribution
23 p4224 A70-44162

ISOTHERMAL LAYERS
Isothermal sections in Ti-Ni-B, Mo-Ni-B and W-Ni-B at 800 C determined by X ray analysis
06 p1090 A70-17846

Isothermal section determination in Mo-Cr-B at 1000 C using X ray, metallographic analyses and microhardness measurements
06 p1090 A70-17847

Radiant heat transfer predictions between isothermal plates based on diffuse plus specular directional property model
11 p2149 A70-26157

ETA oxides compositions in Hf-Ni-O, Ta-Ni-O and W-Ni-O systems determined by studying 1000 C isothermal sections with X ray diffraction
12 p2255 A70-27607

ISOTHERMAL PROCESSES
Viscoelastic behavior of styrene-butadiene rubber under finite uniaxial and equal biaxial deformations for nonisothermal case
05 p0929 A70-16068

Static and dynamic solutions for isothermal deformation of elastic cylindrical and spherical Cosserat surfaces with holohedral isotropy
05 p0932 A70-16140

Ternary Ti-Al-Mo part phase diagrams constructed from Mo corner to plane titanium aluminide, including isothermal phase diagram for 600 C
05 p0864 A70-16548

Real plasma isotherms using three component /atoms, electrons, positive ions/ model in search for supercooled dense plasma
07 p1349 A70-19651

Isothermal reaction rate determination at given temperature from nonisothermal data illustrated at Knudsen cell vaporizations
07 p1424 A70-19901

Turbulent heat transfer in boundary layer at inlet of porous tube under nonisothermal conditions, studying velocity variations
09 p1787 A70-22169

Nonisothermal loading model of polycrystalline material, investigating tangential stresses in slip direction and plastic deformation using linear strengthening law
09 p1779 A70-23102

Transformation kinetics of Ti alloy under isothermal conditions in solution treatment as function of temperature
10 p1903 A70-24025

Quasi-isothermal heat transfer pipe design and operation
12 p2330 A70-27275

Low carbon Ni steels isothermal transformation characteristics, observing equiaxed ferrite and Widmanstatten and bainitic structures at various temperatures
12 p2256 A70-27615

Isothermal quasi-linear theory of viscoelastic isotropic continuum, considering constitutive equations
13 p2516 A70-29534

Intergalactic medium lukewarm models, considering physical state, cosmic photon spectrum and isothermal and adiabatic expansion
14 p2651 A70-31291

Vibration-rotation band absorbance for nonisothermal gaseous radiation in terms of parameters describing isothermal gas

15 p2825 A70-31816

Maraging nickel steel martensitic transformation temperature reduction after interruption by nonisothermal or isothermal tempering below 460 C

16 p2932 A70-33850

Plane waves superposed on solid during steady state isothermal creep deformation subjected to unidirectional constant initial tensile stress

19 p3537 A70-37791

Nonisothermal condensation in ionized vapor as function of energy additions to droplets

20 p3680 A70-39989

Lorentz lines radiative transfer in nonisothermal gases, developing Landenburg-Reiche analysis for isolated unshifted lines growth curves

21 p3852 A70-40590

Cool flame isothermal theory with oscillatory features accounting for damping time evolution and thermic reaction nature

21 p3942 A70-40886

Superconducting Sn bolometer under isothermal and nonisothermal conditions, measuring noise spectra dependence on displacement current and resistance

22 p4026 A70-42397

Isothermal plasticity thermodynamic foundation, deriving constitutive equations for various deformations

24 p4426 A70-45994

Chromium ions isothermal annealing kinetics in X ray irradiated ruby crystals, using EPR method

24 p4382 A70-46253

ISOTHERMS

Steady temperature field of two dimensional periodic contact surface in vacuum, using conjugate harmonic functions for thermal flux lines, isotherms and thermal resistance

07 p1423 A70-19820

Thunderstorm bottom wind profile model, analyzing flow distribution, isotach, isogon and isotherm characteristics

14 p2607 A70-30584

Physiosorption isotherms for nitrogen on stainless steel at various temperatures and very low pressures

18 p3226 A70-36322

ISOTONICITY

Frog sartorius muscle heat production and work effect measured under isotonic and isometric conditions, using gradient layer calorimetry

02 p0232 A70-11715

ISOTOPE EFFECT

Longitudinal modes competition in He-Ne laser, studying effects of active medium isotopic composition and pressure

08 p1511 A70-20518

Hydrazine decomposition in low pressure flame, investigating isotopic substitution effect on flame speed

14 p2628 A70-31094

Carbon and sulfur concentration and isotopic variations in Apollo 11 fines, breccias and fine-grained basalts

21 p3775 A70-41586

ISOTOPE SEPARATION

Deuterium recovery in Jupiter atmosphere, describing equipment and techniques for hydrogen-helium gathering and processing

11 p2112 A70-26064

Oxygen isotope fractionation and formation temperature of minerals from Apollo 11 rocks, including plagioclase-clinopyroxene-magnetite concordancy diagram

21 p3776 A70-41597

Uranium and Th isotopic composition in Apollo 11 samples compared to earth, using mass and alpha spectrometries

21 p3777 A70-41603

ISOTOPE SHIFT

U ISOTOPE EFFECT

ISOTOPES

NT ALUMINUM ISOTOPES

NT ALUMINUM 26

NT ALUMINUM 27

NT ARGON ISOTOPES

NT BERYLLIUM 9

NT BERYLLIUM 10

NT BORON ISOTOPES

NT CALCIUM ISOTOPES

NT CARBON ISOTOPES

NT CARBON 12

NT CARBON 13

NT CARBON 14

NT CESIUM VAPOR

NT CHROMIUM ISOTOPES

NT COBALT ISOTOPES

NT DEUTERIUM

NT HELIUM ISOTOPES

NT HYDROGEN ISOTOPES

NT IODINE ISOTOPES

NT IODINE 131

NT IRON ISOTOPES

NT IRON 57

NT KRYPTON ISOTOPES

NT KRYPTON 85

NT LEAD ISOTOPES

NT LITHIUM ISOTOPES

NT MAGNESIUM ISOTOPES

NT MANGANESE ISOTOPES

NT NEON ISOTOPES

NT NICKEL ISOTOPES

NT NITROGEN ISOTOPES

NT OXYGEN ISOTOPES

NT OXYGEN 18

NT PLUTONIUM ISOTOPES

NT RADIOACTIVE ISOTOPES

NT RUBIDIUM ISOTOPES

NT RUBIDIUM 86

NT SILICON ISOTOPES

NT SODIUM ISOTOPES

NT SODIUM 22

NT SODIUM 24

NT STRONTIUM ISOTOPES

NT TELLURIUM

NT TELLURIUM ISOTOPES

NT THORIUM ISOTOPES

NT TRITIUM

NT URANIUM ISOTOPES

NT URANIUM 233

NT URANIUM 238

NT VANADIUM ISOTOPES

NT XENON ISOTOPES

NT XENON 129

NT XENON 133

NT ZINC ISOTOPES

Ca-rich basalt achondrites cosmogenic isotopes characteristics, discussing lunar or cosmic origin

01 p0174 A70-10136

Isotopic composition of meteoritic Ti determined in Ivigtut galena, Plainview chondrite, Canyon Diablo troilite and Canyon Diablo metal

03 p0576 A70-14091

Relative rotational lines intensities of carbon dioxide, considering sigma-sigma transitions for abundant isotopes

08 p1549 A70-21575

Preplanetary matter irradiation by solar particles, noting isotopic abundances for evidence of nucleosynthesis induced by proton and alpha bombardment

13 p2486 A70-28619

Thioformaldehyde isotopic species reversible transition in interstellar clouds

20 p3703 A70-39164

Interplanetary medium energetic electrons and isotopes measurement, discussing spectrometer electronics of IMP H and J

21 p3825 A70-41000

Apollo 11 lunar rocks and soil hydrogen, C and Si concentration and isotopic composition

21 p3774 A70-41568

Radiogenic and cosmogenic inert gases and isotopic ratios in Tranquility Base fines indicating solar wind saturation

21 p3775 A70-41581

Apollo 11 lunar fines, breccia and crystalline rocks rare gas data, emphasizing trapped and spallation Ne, Kr and Xe isotopic compositions

21 p3909 A70-41598

Isotopic decay rates, solving time dependent atmospheric turbulent dispersion from steady state measurements

22 p4093 A70-42915

ISOTOPE LABELING

Dibutylryl cyclic adenosine monophosphate stimulation of melatonin and serotonin synthesis from C-14 labeled tryptophan by rat pineals in organ culture

01 p0022 A70-10824

Cr 51 osteotropic properties for osseous system studies, discussing binding to bones, experiments on rats and rabbits, applications for human osseous system diagnosis, etc

01 p0029 A70-11403

Scintiscamera resolving power in radioactivity measurements, discussing mathematical principle of division of radioisotope concentration in biological experiments

01 p0040 A70-11404

Dogs left ventricle areas supplied by coronary arterial branches visualized utilizing scintillation photography and radioactive Xe

03 p0432 A70-12892

Calcium isotopes tracer migration in caged rats in metabolism study

04 p0630 A70-14571

Adhesive joint failure, studying adhesive, cohesive and adherend ruptures by evaporative rate analysis

07 p1292 A70-18931

Electron impact induced fragmentation of androstane using deuterium labeling

08 p1454 A70-20524

Rhesus monkey active bone marrow distribution and volume studied by radioactive tracing techniques

09 p1616 A70-22301

Thymidine tracer distribution in bone marrow chromosomes of rats and mice treated with radioprotectors, noting cell metabolic activity reduction by sulphydryl-type radioprotectors

09 p1619 A70-22818

Cyclohexene oxide mass spectral fragmentation by means of deuterium labeled analogs

09 p1630 A70-23397

German monograph on atmospheric turbulence by Rn 220 as tracer, relating concentration to various meteorological parameters

16 p2946 A70-34080

Acute hypoxia effects on C14-tagged glycine absorption, distribution and discharge in rats organs and tissues

17 p0300 A70-35360

Fe diffusion in equiatomic Ni-Co alloy, using thin radioactive deposit method with tagged element Fe 59

18 p3277 A70-36440

P32 labeled organic phosphate esters in water extracts of soil

20 p3615 A70-38979

Trace elements K, Rb, Sr and Ba distributions and Rb-Sr isotopic relations in Apollo 11 lunar breccia and fine soil samples

21 p3909 A70-41594

ISOTROPIC MEDIA

Transversely isotropic circular cylinder acted upon by transient shearing force at one end, noting forced torsional oscillation using cylindrical coordinates

01 p0200 A70-10550

Thermal stresses in infinite layer of transversely isotropic material due to crack with prescribed normal displacement, deriving temperature distribution

01 p0200 A70-10552

Relativistic formulation of radiation for sources in uniformly moving isotropic dispersionless conducting medium in terms of Green functions

01 p0144 A70-11091

Homogeneous Love-Reissner equations analytical solutions for noncircular pyrolytic graphite cylinders, using asymptotic expansion for transverse materials isotropy

01 p0206 A70-11151

Stressed state of isotropic nonlinear multiply connected media with large deformations, using nonlinear elasticity theory

01 p0212 A70-11446

Curvature and hole spacing effects on stress concentration of isotropic plate weakened by two curvilinear holes, applying small parameter method

01 p0212 A70-11447

Temperature fields and universal motions in homogeneous isotropic thermoelastic body in absence of body forces and external heat supply

02 p3887 A70-12000

Stress-strain state of body of revolution having transversely isotropic elastic properties, using perturbation technique

03 p0591 A70-13441

Finite strain in bending rectangular block into right circular cylindrical shell for transversely isotropic medium along radius vector, using Saint Venant stress-strain relations

03 p0602 A70-14329

Refractive index profile analysis for hypergeometric functions solutions for vertically polarized electromagnetic waves propagating in horizontally stratified isotropic media

04 p0647 A70-14616

Radio wave propagation in linear, isotropic homogeneous medium with irregular boundaries solved by expanding Helmholtz integral

04 p0648 A70-14965

Static deformation fields producible in isotropic homogeneous incompressible elastic body with uniform transverse stretch

05 p0931 A70-16134

Constitutive equations for isotropic elastic and thermoelastic materials with microstructure derived using free energy function, giving uniqueness theorems

05 p0932 A70-16136

Mixed boundary value problems of isotropic elastic half space with ring shaped separation region

05 p0935 A70-16232

Linear isothermal quasi-static theory for homogeneous and isotropic viscoelastic bodies with couple stresses

05 p0938 A70-16425

HF conductivity tensor of isotropic plasma, taking into account particle correlations describing weakly Langmuir turbulent plasma

05 p0889 A70-16532

Bending problem for homogeneous transversely isotropic plate weakened by curvilinear hole

05 p0946 A70-16959

Geometry of limiting surface characterizing strength of isotropic body, discussing material breakdown

05 p0947 A70-16964

Temperature of contact surface between two homogeneous isotropic solid bodies determined by calculating plane heat source of steady three dimensional temperature field

05 p0958 A70-17014

Wave equation for elastic waves in isotropic solid solved in Cartesian and circular cylindrical coordinates for studying microsonic wave guiding structures

06 p1105 A70-17479

Plane light wave diffraction incident upon isotropic dielectric layer traversed by acoustic microwave using guided microwave theory

06 p1105 A70-17484

Limiting stress states analysis in isotropic solids using loading history and replacing nonlinear stress-strain curve by approximating rectilinear polygon

06 p1165 A70-17547

Transient response analysis in isotropic material under thermal galvanomagnetic effects involving interaction electric and thermal conductions in applied magnetic field

[AIAA PAPER 70-17]

06 p1107 A70-18213

Cylindrical antennas immersed in arbitrary homogeneous isotropic media, solving integral equation for current

06 p1074 A70-18607

Frequency equation for harmonic waves propagating in fluid filled circular cylindrical cavity in infinite isotropic solid medium

07 p1253 A70-18846

Isotropic elastic body occupying half plane assuming elasticity coefficients of certain class

07 p1407 A70-19376

Boundary value problems solution for infinite elastic isotropic plane weakened by arbitrarily distributed circular holes based on using series in Taylor functions

07 p1408 A70-19549

Computer procedures for solving temperature stresses in thin infinite isotropic viscoelastic plate with heat transfer

07 p1411 A70-19817

Spectrum of waves emitted from waveguide of two plane dielectric or isotropic plasma layers, solving dispersion equations numerically by computer

08 p1472 A70-20973

Constitutive inequalities for isotropic elastic solids under finite strain generated by introducing concept of conjugate pairs of stress

08 p1590 A70-21351

Split ring load test method for determining shear modulus of isotropic and composite materials

08 p1530 A70-21888

Transversely isotropic body of revolution under combined surface loads and stationary axisymmetric temperature field, obtaining displacement vector and stress tensor in analytic functions

09 p1778 A70-23086

Elastoplastic stressed state of thin walled shells of revolution under repeated loads, assuming isotropic incompressible material

09 p1779 A70-23092

Thermal conductivity of arbitrarily inhomogeneous bodies, considering vectorial field isotropy and temperature gradients dispersion

09 p1789 A70-23103

Point source intensity fluctuations dependence on penetration depth of wave propagating in statistically homogeneous and isotropic media

09 p1636 A70-23133

Reissner-Sagoci transient mixed boundary value problem concerning displacement of infinite half space of isotropic elastic material, deriving surface displacement and reactive torque

09 p1784 A70-23571

Cylindrically isotropic elastic medium statics, deriving general solutions to Lamé equations

09 p1784 A70-23593

Equilibrium equations integration for body in isotropic linear viscoelastic medium with contact-type boundary conditions

10 p1957 A70-24267

Molecular-statistical theory of second-harmonic light generation by isotropic bodies immersed in external AC or DC electric field

10 p1916 A70-24379

Time dependent radiative transfer equation for plane-parallel isotropic scattering medium in first Gaussian approximation

10 p1933 A70-24986

Electromagnetic wave propagation in spatially inhomogeneous isotropic ionosphere, determining phase, amplitude, polarization, absorption, arrival angle, etc

11 p2003 A70-25547

Stress concentration near ellipsoidal cavity in transversely isotropic body using solutions for transversely isotropic ellipsoid of revolution

11 p2129 A70-25564

Equilibrium displacement equations for linear infinitesimal isotropic Cosserat elasticity solved in terms of stress functions

11 p2142 A70-26630

Kane-Mindlin equations and frequency spectra determined for free elastic vibrations in isotropic elastic plate strips

11 p2146 A70-26703

Book on three dimensional problems of linear elasticity of homogeneous and isotropic solids, discussing prismatic bodies, bodies of revolution, notch effect, etc

12 p2326 A70-27669

Radiation characteristics of ion acoustic waves from monopole and dipole antennas, observing patterns of longitudinal wave in isotropic plasma

12 p2279 A70-27778

Simulated isotropic lossless plasma radiating apertures located on nonplanar models, relating results to antenna radiation patterns

12 p2282 A70-27969

Electromagnetic waves emission and propagation in chaotically inhomogeneous media, analyzing mean field and permittivity tensor for isotropic and anisotropic media

12 p2190 A70-28170

Saint Venant principle in linear isotropic viscoelasticity of Toupin estimates for body of arbitrary shape to allow integration by parts

13 p2513 A70-28990

Isotropic elastic three dimensional body steady stressed state under large subcritical triaxial strains described by solving linearized equations

13 p2515 A70-29316

Isothermal quasi-linear theory of viscoelastic isotropic continuum, considering constitutive equations

13 p2516 A70-29534

Diffusely transmitted and reflected radiation fields for planetary isotropically scattering atmosphere bounded by Lambert law reflector

14 p2617 A70-31305

Distant radiation from magnetic line source in moving isotropic plasma, discussing dependence on velocity

15 p2778 A70-31835

Plane electromagnetic waves propagation in isotropic medium in electromagnetic nonequilibrium conditions

15 p2790 A70-32275

Isotropic slab with implanted elastic circular disk, analyzing stress-strain state due to torsional and bending moments

15 p2824 A70-32895

Isotropic composite materials with anisotropic components, determining microconstants for heat conduction, elasticity and thermoelasticity problems

15 p2766 A70-32896

Transversely isotropic elastic plates vibrations without initial specification of field variables spatial dependence on thickness coordinate by two dimensional asymptotic theory

16 p2994 A70-34232

Rigid inclusion effect on stress distribution in isotropic infinite solid with Griffith crack under plane strain

16 p2994 A70-34250

Thermomagnetoelasticity wave equations of heat conduction for thermal and coupled perturbations propagating in isotropic medium at finite velocities

16 p2953 A70-34326

Thermal and thermoelastic constants of macroscopically isotropic composite materials based on self consistent calculations

17 p3194 A70-34555

Transversely isotropic Timoshenko beam statics and dynamics under initial stress and transverse loading

17 p3182 A70-34561

Elastic waves on isotropic and anisotropic surfaces, discussing excitation methods, surface probing, propagation characteristics, etc

17 p3136 A70-34650

Isotropic body screw dislocations, using finite elasticity approach

17 p3190 A70-35453

Parallel edge dislocations in elastically isotropic crystals, discussing climb and glide forces

17 p3126 A70-35454

Isotropic fluid systems in nonequilibrium, investigating thermodynamic characteristics of transport phenomena

17 p3072 A70-35529

Isotropic scattering of radiation from asymmetric spherical source in finite atmosphere

17 p3136 A70-35598

Integral equation for three dimensional Fourier transform applied to isotropic scattering of radiation from point source in finite spheroidal atmosphere

17 p3137 A70-35599

Stationarity of complementary energy in nonlinear elasticity theory, using Piola stress tensor representation for isotropic elastic media

17 p3192 A70-35692

Structural members of isotropic and anisotropic polymers, investigating creep behavior under simple stressed state

17 p3192 A70-35740

Heat transfer across boundary between two stationary fluids, applying elastic wave theory in isotropic media

18 p3345 A70-36118

Linear bending theory of thin homogeneous isotropic plates

18 p3339 A70-36482

Nonuniqueness of collapse load for isotropic frictional material with or without cohesion

19 p3433 A70-37385

Relaxation theory of Rayleigh scattering of light by isotropic continuous medium, deriving spectral densities via fluctuation dissipation theorem

19 p3470 A70-37446

Acceleration wave propagation in materially uniform inhomogeneous isotropic elastic bodies, using tensor analysis

19 p3536 A70-37563

Gyrotropic waveguides parameters computer calculation based on inhomogeneous isotropic region, taking into account discontinuities

19 p3378 A70-37736

Edge dislocation and uniform and radial fissures in elastic isotropic nonhomogeneous bodies under two dimensional deformation

19 p3540 A70-37956

Yield condition and Bauschinger effect in transition conditions for isotropic and orthotropic bodies

19 p3542 A70-38061

Equilibrium equations integration for body in isotropic linear viscoelastic medium with contact-type boundary conditions

19 p3547 A70-38395

Plane wave reflection from stratified isotropic medium using ray tracing in complex space, noting agreement with phase integral method

19 p3380 A70-38404

Antennas impedances in warm isotropic plasma, using hydrodynamic and kinetic /Vlasov/ equations

19 p3380 A70-38406

Skin effect for unsteady radio waves emitted into homogeneous nonmagnetic isotropic half space, calculating electric field

19 p3381 A70-38571

Isotropic finite strain expressions for compressional and shear velocities, noting no discrepancy with ultrasonic and seismic data

20 p3619 A70-39218

Linear relations between stress state and Euler strain rate in isotropic elastic bodies during superposition of small deformation on finite strain

20 p3728 A70-39893

Torsion of composite rectangular cross section beam consisting of isotropic media, using Green function and Fourier expansion

20 p3732 A70-40334

Electromagnetic wave propagation in spatially inhomogeneous isotropic ionosphere, determining phase, amplitude, polarization, absorption, arrival angle, etc

21 p3786 A70-41297

Sommerfeld type radiation conditions for linear homogeneous isotropic elastic materials with microstructure, discussing field equations, displacement and rotation vector and scalar conditions

21 p3936 A70-41417

Elastic wave propagation in isotropic homogeneous bodies, considering free vibrations and propagation velocity

21 p3940 A70-42099

Constitutive equation for homogeneous and isotropic elastic solids

21 p3940 A70-42101

Linear coupled thermoelasticity theory for homogeneous isotropic solid with two temperatures

22 p4123 A70-42540

Plane electromagnetic wave propagation at normal incidence in isotropic lossless plane-stratified inhomogeneous gyration medium, calculating varying profiles from constitutive equations

22 p4073 A70-42640

Isotropic homogeneous elastic cylindrical rods, investigating nonlinear longitudinal dispersive waves corresponding to water wave theory analogs

22 p4115 A70-42952

Spatial problem of elastic spherical transversal isotropic medium solved by reducing Lamé equations

22 p4118 A70-43481

Sound velocity in isotropic nonlinearly elastic continuum with microstructure, showing dispersion coincident with Cosserat constant

22 p4120 A70-43713

Two incompressible isotropic nonlinear elastic solids mixture, investigating entropy production inequality effects

24 p4425 A70-45991

ISOTROPIC TURBULENCE

Isotropic incompressible three dimensional turbulence representation by wave vector scalar functions, discussing maximum functions number determination

02 p0277 A70-11878

Spatial resolution analyses of vorticity meter and hot wire arrays for measuring velocity derivatives in isotropic turbulence

03 p0492 A70-13760

Spectral energy transfer measurements in isotropic grid turbulence to determine validity of dynamical equation

03 p0468 A70-13785

Decaying isotropic turbulence spectrum evolution model, verifying numerical integration of differential equations

04 p0673 A70-15249

Shear-dependent nearly isotropic turbulence energy spectrum theory, considering effects of viscous loss,

shear production and inertial and velocity gradient transfer

04 p0674 A70-15520

Constitutive equations for Reynolds fluxes in large scale transversely isotropic turbulent mixing using gradients of mean quantities

05 p0836 A70-17103

Viscosity superposition principle applied to isotropic turbulence analysis, approximating self similar solution by time factor averaging

07 p1258 A70-19698

Lagrangian tensor formalism for hydrodynamic stretching of material line and surface elements under statistically isotropic incompressible turbulence

07 p1260 A70-19979

Damped isotropic turbulence kinetic and temperature fluctuation energy spectra, neglecting viscosity and molecular heat conduction

08 p1483 A70-20961

Fluid material line growth in grid-generated isotropic turbulent flow measured by tagging lines with hydrogen bubbles

11 p2035 A70-25843

Energy spectrum of homogeneous isotropic incompressible turbulence, discussing eddy relaxation and direct interaction approximation

11 p2040 A70-26541

Incompressible homogeneous isotropic turbulence velocity expanded in Hermite functionals of Gaussian white noise random function advected by fluid

11 p2040 A70-26543

Viscosity coefficient for isotropic turbulence using quasi-self-similar solution

13 p2391 A70-29777

Homogeneous isotropic turbulence velocity field space-time variable correlation functions in fluid flow

15 p2719 A70-31487

Energy dissipation and viscosity effects on isotropic turbulence in extreme short wave region at large Reynolds numbers

18 p3239 A70-36263

Damped isotropic turbulence kinetic and temperature fluctuation energy spectra, neglecting viscosity and molecular heat conduction

20 p3608 A70-39383

High Reynolds number isotropic homogeneous turbulence fine scale structure heuristic model, relating spatial intermittency to vorticity generation

20 p3609 A70-39665

Aerodynamic theory of pressure field induced on lifting surface by isotropic atmospheric turbulence, considering transfer function of Concorde aircraft [ICAS PAPER 70-30]

23 p4138 A70-44104

ISOTROPISM

Isotropic transformation of tensor space, proving theorem for reducing hemitropic function to N invariants of rotations and single vector

24 p4378 A70-45271

ISOTROPY

NT ISOTROPIC MEDIA

Natural vibrational frequencies of trapezoidal, triangular, circular and elliptical isotropic flat plates with different edge conditions tabulated

05 p0936 A70-16319

Two port isotropic antenna excited by independent noise sources for uniform power radiation in all directions and polarizations

06 p1021 A70-17574

Isotropic plate stress-strain state weakened by doubly periodic curvilinear holes using nonlinear theory

07 p1408 A70-19544

Two dimensional continuum of objectivity and isotropy principles applied to study of elastic tridimensional vault

09 p1777 A70-22899

Stress-strain state analysis of transversely isotropic plates with inclusions under bending loads

09 p1782 A70-23298

Transversely isotropic shells stability with respect to subcritical deformation under axial compression using three dimensional linearized equations, determining critical loads

12 p2324 A70-27529

Transversely isotropic hollow spherical shell with elastic filler, analyzing stability

12 p2328 A70-28281

Concentrated force action inside transversely isotropic half space analyzed by mirror image method

13 p2512 A70-28865

Stress distribution in isotropic plates weakened by elliptical holes under bending based on elastic shallow shell theory and small parameter technique

13 p2514 A70-29291

Isotropic plates weakened by circular holes, investigating bending by Ambartsumian plate theory

13 p2515 A70-29509

Pseudoisotropic surfaces in Minkowski space-time with proof of existence, formulating congruencies of normal fiber

13 p2452 A70-29634

Third isotropic point in rectangular beam under bending stresses by Hertzian load, using Stokes-Wilson method and photoelastic comparison

21 p3941 A70-42265

Heat conduction of doubly connected square and triangular isotropic plates with hole, applying small parameter method

23 p4276 A70-44217

ISRAEL

Cretaceous rock paleomagnetism from Israel lava fields, determining original magnetization directions

19 p3413 A70-38034

ITALY

Italian fog distribution charts compiled by Italian Air Force and Istituto Centrale di Statistica compared and criticized

02 p0328 A70-12397

NASA network and Thor Delta type booster to launch Italian satellite to geostationary orbit, evaluating feasibility

03 p0451 A70-13841

Italian space satellite booster programs for launching satellite payloads into low orbit

03 p0609 A70-13846

Italian aviation and space industry development for local and sectional character and participation in European production

10 p1971 A70-24663

Italian Sirio project, describing SHF propagation and communication, cosmic ray and confined plasma experiments

11 p2011 A70-26604

Report to COSPAR on Italian space programs, discussing cosmic ray physics, EM propagation, international research efforts, etc

15 p2830 A70-31717

Italian automated ATC system (ATCAS), discussing subsystem functions, display devices, data acquisition, information distribution, etc

21 p3847 A70-40911

ITERATION

NT ITERATIVE SOLUTION

Boltzmann equation direct numerical integration using successive iterations algorithm

06 p1036 A70-17755

Biharmonic equation numerical solution by finite differences, discussing outer and inner iteration schemes

14 p2599 A70-30647

Computer program for nonlinear differential equations related to nonlinear boundary value problems based on Newtonian iteration process difference analog of linearization method

23 p4212 A70-44338

ITERATIVE SOLUTION

Airfoil cascade blade design by iteration method equating normal velocity distribution about contour with imposed tangential velocity

01 p0001 A70-10263

Successive approximations method for incorrectly posed problems in synthesis of radiating systems, discussing radiation patterns of linear emitter

01 p0044 A70-11036

Integral equation for emissivity inside uniform gray isothermal Lambertian cavity solved using successive approximations

02 p0323 A70-11889

Lubrication problem for centrally pivoted tilting-pad sector thrust bearings with temperature and elasticity effects, noting iterative solution for coupled equations

[ASME PAPER 68-LUB-4]

02 p0307 A70-12166

Thin shells stressed state calculations by iteration, considering suitability for computer adaptation

03 p0592 A70-13442

Iterative computational procedure for generalized quadratic programming problem, formulating convergence theorem

03 p0460 A70-14165

Radiative heat transfer from longitudinal rectangular conducting fins on plane wall involving mutual irradiation, using iterative method

[ASME PAPER 69-WA/HT-22]

04 p0782 A70-14812

Iterative solution to transmission lines termination problems

[ASME PAPER 69-APM-M]

04 p0627 A70-14861

Upper and lower bounds for eigenvalues of lumped parameter straight line torsional system determined by receptance synthesis based on Holzer method

04 p0773 A70-15083

Least squares iterative method for solving simultaneous linear equations having singular coefficient matrix

04 p0714 A70-15450

Three dimensional analysis of nonhomogeneous elastic solids based on finite element method and equilibrium equations, discussing iterative solution

05 p0926 A70-15915

Weinstein approximation and iteration by digital computer for calculating disturbed Fabry-Perot laser resonator modes

06 p1081 A70-17546

Iteration for Boltzmann equation solution for relaxation of gas having solid molecules with time variable and velocity dependent distribution function

06 p1109 A70-17757

Boundary conditions and iterative procedures for plasma sheath problems, using matrix equation to represent differenced Poisson equation

06 p1123 A70-18295

Hybrid patched conic technique as iterative procedure for generating transunar and transearth trajectories emphasizing computing time saving

06 p1152 A70-18495

Iterative solution of nonlinear optimal control delineated for sufficient conditions for convergence

06 p1027 A70-18507

Gyroscopes orientation cross coupling effect on dynamic drift of three axis gyrostabilizer solved by method of successive approximation

07 p1278 A70-18736

Scalar radiative transport equation solved iteratively for microwaves backscattering from turbulent plasma, deriving model for direct and cross polarized cross section

07 p1353 A70-19993

Parameters identification in nonlinear boundary value problems by successive approximations technique, using Lagrange multipliers and Newton-Raphson method

07 p1327 A70-20025

Boundary value problem for self conjugate elliptical fourth order differential equation with variable coefficients, proving convergence of iterative process

07 p1328 A70-20143

Nonlinear difference approximating scheme and iterative method for Stefan problem with several unknown fronts

08 p1534 A70-20851

Radiant heat exchange for rectangular groove represented by integral equations using rapid iteration method

08 p1600 A70-21835

Repetitive electronic differential analyzer with transistorized operational amplifiers for iterated solutions of differential equations

08 p1478 A70-21836

IR absorption spectral curve interpretation using computer program for iterative solution

09 p1726 A70-22138

Eigenvalues and eigenvectors evaluation for real symmetric matrices by iterating simultaneously with trial vectors

09 p1641 A70-22283

Iterative technique for determining zero of differentiable function

09 p1641 A70-22287

Elastoplastic problems incremental solution by iterative method, demonstrating convergence

09 p1771 A70-22394

Boundary problem for displacement equilibrium equations of elastic body using iterative methods, demonstrating convergence of difference equation solution

09 p1771 A70-22467

Artifices to allow computing time reduction in recursive data elaboration for high order differential system

09 p1720 A70-22647

Nonlinear periodic oscillations problem solved by solving nonlinear operator equations, discussing iterative methods based on equations linearization

09 p1728 A70-22668

Space mechanics problem of passing from perigee to radial distance in given time determined by fitting conic to radii, using iteration method

09 p1760 A70-22927

Hybrid patched conic iterative technique for accurate moon-earth (transearth) trajectory generation

09 p1760 A70-22929

Numerical solution of three dimensional equation of elastic body equilibrium in displacements, giving convergence rate of iteration processes

09 p1783 A70-23384

Three stage variable shift iteration algorithm for calculating zeros of polynomial with complex coefficients

09 p1712 A70-23419

Multipoint methods for two point boundary value problems with Banach space self mapped, proving convergence theorems for iterative solutions

09 p1712 A70-23420

Nonlinear operational equation iteration solution error estimation, discussing Banach space nonlinear operator equation

10 p1909 A70-24508

Analytical aerial triangulation iterative solution mathematical convergence parameters tests, considering photogrammetric relations for standard conditions in variable size block

10 p1878 A70-24729

Successive approximations method for incorrectly posed problems in synthesis of radiating systems, discussing radiation patterns of linear emitter

10 p1842 A70-25006

Iterative numerical method for determining optimal mass distribution in complex frameworks, maintaining dynamic response level

10 p1960 A70-25053

Iterative algorithms for numerical solution for time optimal control problems

10 p1856 A70-25232

Nonlinear partial differential operators eigenvalue solution using modified Newton iteration method, noting advantages over perturbation method

11 p2074 A70-26423

Deformation theory for small elastic-plastic strains in orthotropic material and discretization and iterative solution techniques

11 p2144 A70-26684

Nonlinear equations systems iterative solution convergence by extending classical algorithm with optimization process

11 p2074 A70-26850

Book on successive approximation methods in control and oscillation theory covering two point boundary value problems iterative solutions, orbital transfer, etc

12 p2260 A70-26852

Differential equations in two point boundary value problems solved by combining Newton-Raphson iterative method with parameter variation extrapolation

12 p2260 A70-27003

Iteration procedures for boundary value problem of orthotropic rectangular plate under bending loads, discussing convergence of procedures

12 p2325 A70-27552

Iteration solution for three dimensional equations of equilibrium of elastic body in boundary displacements, discussing convergence rate and computer applications

12 p2272 A70-27553

Iterative algorithm for synthesis of discrete minimum time and amplitude controls for linear systems, noting guaranteed convergence

12 p2204 A70-27667

Wide range wind compensated launcher settings for unguided rockets using wind-weighting model and iterative procedure requiring real time computation

13 p2503 A70-28528

Variable mesh multistep predictor-corrector method for iterative solution of ordinary differential equations, considering numerical stability and algorithm efficiency

13 p2440 A70-29087

Computer techniques for rounding error analysis, stability in linear algebra, matrices factorization, Jacobi rotation method and iteration procedures

13 p2443 A70-29768

Algorithm for improving approximate quadratic factor of polynomial with real coefficients using iterative method

14 p2600 A70-31227

Radial Schrodinger equation bound state eigenvalues and properties by iterative method, calculating Coulomb potentials

14 p2600 A70-31360

Iterative solution for electron density profiles from topside ionograms

16 p2900 A70-32931

Generalized iterative inverse algorithm for linear inequalities set involved in pattern recognition and threshold logic requiring decision functions determination

16 p2870 A70-33739

Antenna reflectors of evolution and double curvature optimization by iteration method

16 p2866 A70-34267

Parameter variation effects on iterative identification of linear system by learning method

17 p3130 A70-35299

Multiplying factors role in iterative solution of shock wave structures with large radiation-convection ratios

17 p3075 A70-35888

One dimensional steady gas flow, deriving algorithm for iterative solution of Boltzmann kinetic equation by statistical approach

18 p3241 A70-36285

Boundary value problem for Navier-Stokes equations of viscous incompressible fluid flow, discussing convergence of iterative solution

18 p3241 A70-36290

Iterative determination of time optimal controls, considering dynamic system transition from initial to quiescent state with constraints on control vector

18 p3282 A70-36355

Potential calculation from given source distribution, including direct and iterative methods, error analysis, convergence, computer programs and applications in plasma physics

18 p3284 A70-36790

Iterative Hansen method of general perturbations programmed for digital computer, evaluating major and minor planetary theory

18 p3320 A70-37060

Stochastic approximation iterative algorithms for multivariable plants mathematical models, including steepest descent method

20 p3593 A70-39910

Iterative solutions for systems of nonlinear equations and discretization of elliptic differential equations

21 p3845 A70-40736

Atmospheric temperature and water vapor profiles from iterative solution of radiative transfer equation for comparison with spectral radiance observation from Nimbus satellites

21 p3846 A70-40803

Unsteady flow in rectangular cavity with moving wall, using iterative solution of Navier-Stokes equations

21 p3807 A70-41317

Analytical iteration method extended to critical load of clamped beam with symmetrically variable cross section

21 p3939 A70-41965

Iteration method for calculating self consistent fields in semiconductor surface inversion layers

22 p4085 A70-42745

Nesbet algorithm modified for iterative evaluation of eigenvalues and corresponding eigenvectors for large matrices

22 p4062 A70-42749

Digital differential analyzers one step integration method with iteration procedure truncation to single step

22 p3996 A70-42921

Rayleigh wave scalar electric potential analysis on piezoelectric medium, using iterative techniques for Poisson equation

22 p4074 A70-42967

Iterative linear prediction method for stochastic process with zero mean value and known covariance function

23 p4211 A70-44026

Iterative method based on slender body approximation applied to axisymmetric sonic flow fields, splitting differential equation into coupled parabolic equations

23 p4132 A70-44124

Iterative method for boundary value problems in mathematical physics, showing convergence by heat conduction equation solutions

23 p4276 A70-44218

Torsion in rods with rectangular and trapezoidal cross sections, using functional-analytic iterative method

23 p4268 A70-44241

Linear systems with phase coordinates bounded by given time functions, obtaining optimal control by iterative solution involving Lagrange multipliers

23 p4177 A70-44302

Linear programming problems in optimal control numerical analysis, discussing iterative solution

23 p4177 A70-44303

Time optimal problems involving parabolic equations in heating of rod with piecewise continuous thermophysical characteristics and temperature distribution constraints, deriving iterative solution

23 p4277 A70-44306

Iterative Rayleigh-Ritz method for eigenvalue determination in natural vibration problems

23 p4270 A70-44580

Gradient iterative solution of large algebraic systems arising from finite element discretization, using computer methods

24 p4419 A70-45153

Successive iterative solution for large matrix equations of second kind

24 p4369 A70-45164

Virtual work equations steady state subharmonic solutions by Newton-Raphson method, developing generalized iterative procedure for nonlinear differential equations

24 p4423 A70-45577

ITOS 1

ITOS-1 second generation meteorological satellite launched with Delta N booster, providing direct APT global readout and AVCS TV data recording for playback

23 p4259 A70-44615

IZSAK ELLIPSOID

U ELLIPSOIDS

U GEODESY

J

J-2 ENGINE

Pressure oscillations in LOX pump inducer of J-2 machine, using semianalytical first order model with retarded time mechanism

09 p1693 A70-23257

Saturn 5 S-2 stage propellant feedlines and J-2 engines simulating structural longitudinal oscillation by analog computer

16 p2968 A70-33591

JACKING EQUIPMENT

U JACKS (LIFTS)

JACKS (ELECTRICAL)

U ELECTRIC CONNECTORS

JACKS (LIFTS)

Hydraulic jacks for Boeing 747 support during assembly, discussing operation, console, pressure system and safety features

05 p0798 A70-16422

Hydraulic servomechanism stability and step response, considering unequal oil volume on either side of jack

24 p4292 A70-45159

JACOBI INTEGRAL

Conjugate points for simple integral problems in calculus of variations extended to multiple integral problems, using Jacobi equation

04 p0713 A70-14674

Singularities arising during collisions in restricted n-body problem elimination, discussing Jacobi integral and finite-mass body configuration

04 p0714 A70-15354

JACOBI POLYNOMIALS

U HYPERGEOMETRIC FUNCTIONS

JAGUAR AIRCRAFT

Jaguar flight test instrumentation methods, discussing Anglo-French participation

19 p3356 A70-38534

Airborne magnetic recording flight test instrumentation of Anglo-French Jaguar aircraft

19 p3431 A70-38535

Jaguar flight test data processing system, discussing airborne digital computer

19 p3384 A70-38536

Digital computer magnetic tape recording system for flight tests of Jaguar aircraft, discussing data treatment

19 p3384 A70-38537

JAMMERS

Traveling wave tubes used in electronic countermeasure chain or repeater for deception jammer, discussing design and performance

04 p0653 A70-15658

JAMMING

Pulse position modulation focused TWT for airborne electronic countermeasure broadband jamming, considering output power and thermal design

04 p0653 A70-15656

Automatic meteor station jamming protection using ferrite diode logical elements

19 p3422 A70-37652

JAPAN

Temporal and spatial variations and patch velocity of sporadic E layer obtained at Japan ionospheric stations

06 p1057 A70-17906

Monograph on research by Japanese Institute of Plasma Physics covering theta pinch, plasma heating, flow, diagnostics, etc

07 p1350 A70-19843

Small dispersion whistlers characteristics and propagation at midlatitudes based on observation at Tohokai, Japan

08 p1491 A70-21713

Flying safety and human factors from job dissatisfaction in Japan Air Self Defense Force

08 p1453 A70-21794

Report to COSPAR on Japanese space research including satellite, rocket and balloon observations of ionosphere, magnetosphere, interplanetary space, moon, planets, cosmic rays, etc

15 p2830 A70-31720

JARRING

U MECHANICAL SHOCK

JAVELIN ROCKET VEHICLE

Javelin research rocket payload suspension ensuring limited vibrational accelerations, using viscoelastic materials for damping

04 p0774 A70-15147

Javelin rocket measurements of ionospheric AC electromagnetic fields, determining amplitude/frequency spectra and dipole antenna performance

13 p2401 A70-29926

JEANS THEORY

Dynamic stability of Jeans spheroid and Roches ellipsoid using small perturbations method

09 p1759 A70-22749

Jeans escape rate error for atmospheric H and He attributed to perturbed velocity distribution function, using realistic atom-atom elastic scattering cross sections

13 p2398 A70-29226

JEES

U AUTOMOBILES

JET AIRCRAFT

NT A-7 AIRCRAFT

NT AVRO 707 AIRCRAFT

NT B-52 AIRCRAFT

NT B-70 AIRCRAFT

NT BAC 111 AIRCRAFT

NT BOEING 707 AIRCRAFT

NT BOEING 727 AIRCRAFT

NT BOEING 737 AIRCRAFT

NT BOEING 747 AIRCRAFT

NT BOEING 7207 AIRCRAFT

NT BUCCANEER AIRCRAFT

NT C-5 AIRCRAFT

NT C-9 AIRCRAFT

NT C-135 AIRCRAFT

NT C-141 AIRCRAFT

NT CL-84 AIRCRAFT

NT CONCORDE AIRCRAFT

NT DC 8 AIRCRAFT

NT DC 9 AIRCRAFT

NT DH 121 AIRCRAFT

NT DH 125 AIRCRAFT

NT DO-31 AIRCRAFT

NT F-4 AIRCRAFT

- NT F-5 AIRCRAFT
NT F-8 AIRCRAFT
NT F-28 TRANSPORT AIRCRAFT
NT F-104 AIRCRAFT
NT F-106 AIRCRAFT
NT F-111 AIRCRAFT
NT G-91 AIRCRAFT
NT G-222 AIRCRAFT
NT HFB-320 AIRCRAFT
NT L-1011 AIRCRAFT
NT OV-10 AIRCRAFT
NT SAAB 37 AIRCRAFT
NT T-33 AIRCRAFT
NT TU-134 AIRCRAFT
NT TURBOFAN AIRCRAFT
NT TURBOPROP AIRCRAFT
NT VULCAN AIRCRAFT
NT XV-4 AIRCRAFT
NT XV-5 AIRCRAFT
- Jet aircraft long range flight planning using computer for wind and temperature forecasts, path altitude profile computation and optimization
02 p0403 A70-12841
- Deviation angle optimization for cruising hypersonic jet aircraft, noting effect of rotation losses on design
03 p0406 A70-13019
- Turbojet performance magnitude data represented by components nondimensional characteristic curves
03 p0551 A70-13021
- Flexible pavements for commercial jet planes representative of current and future aircraft
03 p0462 A70-13173
- Rigid and flexible pavements response to jumbo jets load using elastic theory
03 p0462 A70-13175
- Superjets demands on airport fuel handling facilities [SAE PAPER 690559]
03 p0463 A70-13263
- Icing, bird collisions and static charge problems for jet aircraft, discussing protective devices
03 p0413 A70-13792
- Collection of papers on jet transport design covering subsonic zero lift drag rise properties, performance characteristics, supersonic aircraft design, etc.
03 p0414 A70-14018
- Pseudosound field wall pressure correlation obtained to predict response characteristics of aircraft panel mounted along jet wake
05 p0835 A70-16785
- Unstable spiral precursor to jet upset (Mach tucks) in executive jet transports
06 p0987 A70-18248
- Hansa 330 fan jet design for executive and commuter market, discussing forward-swept wing concept and standardized structures and systems
07 p1194 A70-19619
- Lead-acid and vented nickel cadmium batteries compared in redesign of military aircraft battery for cells reduction, low current density, etc.
08 p1440 A70-20712
- Soviet handbook on practical aerodynamics of aircraft with turboreactive engines covering flight stability, aircraft controllability, etc.
08 p1435 A70-20760
- Jet pilot trainee qualification requirements, training process methods and equipment, considering German-French joint trainer aircraft program
08 p1452 A70-21348
- C-5 Galaxy airlifter design, delivery capacity, aerodynamics and flight test program
09 p1609 A70-22020
- Aircraft certification of supersonic and jumbo jet transports assuring acceptable safety level
09 p1610 A70-22948
- Flight simulator for advanced aircraft /FSAA/ featuring six degrees of freedom and 100 ft lateral travel
10 p1858 A70-24205
- Japanese jet aircraft pilots instrument reading and checking procedures during landing operation under contact flight rules
11 p2078 A70-25667
- Small scale and full scale wind tunnel and flight test data correlated for Lear jet aircraft
11 p1981 A70-25906
- Computational methods for multiinput linear control systems applied to designing lateral and longitudinal autopilots for jet transports subject to gust loads
12 p2203 A70-27417
- Jet transport wakes resulting from high engine thrusts considered hazardous to following aircraft, discussing multiple-instrumented runways for measuring visibility
12 p2162 A70-27995
- Gust response calculations compared with flight measurements for two fighter aircraft and jet transport to determine accuracy
12 p2162 A70-28077
- German-French jet aircraft trainers, discussing Alpha Jet TA 501, E 650 Eurotrainer and VF T 291 flight characteristics
13 p2347 A70-29052
- Aircraft turbulence penetration performance numerical rating, applying concept to large subsonic jet transports
13 p2347 A70-29074
- Jet thrust reversers mechanical design limits, objectives and materials
14 p2628 A70-30500
- Passenger survival and evacuation of civil jet transport aircraft after ditching at sea
15 p2676 A70-32223
- Twin jet light transport Corvette airframe, discussing flight characteristics and economical aspects
15 p2676 A70-32793
- Connectors for superjet airliners, discussing butyl rubber grommet, power distribution collector, modular terminal blocks and passenger service connector
16 p2878 A70-33956
- Nonlinear balance mass solutions for tab-aileron flutter free operation of jet trainer for arbitrary store configuration
17 p3185 A70-34923
- High speed civil and commercial transport aircraft, discussing jet-orbital flight
18 p3333 A70-36664
- Air total temperature measurement for jet powered aircraft, discussing subsonic and supersonic wind tunnel data for sensor thermal recovery characteristics
19 p3425 A70-37882
- Military Airlift Command jet aircraft computerized area navigation system operational procedures
19 p3465 A70-38232
- Yak-40 business jet design and flight characteristics
21 p3755 A70-42174
- SN 600 Corvette business jet design and performance
21 p3755 A70-42175
- Short haul jet transport aircraft design, discussing Computer Aid Design, Airline System Simulator and Traffic Demand Predictor computer programs [ICAS PAPER 70-28]
23 p4284 A70-44105
- Superjet airliners wiring connectors for power distribution, signal circuitry and self ejecting push buttons for passenger seats
23 p4174 A70-44545
- Weather modification by jet aircraft contrails, discussing cloud seeding observations in Alaska
24 p4371 A70-45421
- Highlift and blown wing types slow speed STOL aircraft, comparing pilot training requirements with jet airline flying [AIAA PAPER 70-1282]
24 p4292 A70-45971
- JET AIRCRAFT NOISE**
- Jet aircraft flyovers annoyance relationship to physical parameters of sound evaluated, using psychophysical method of constant stimulus differences
01 p0006 A70-11199
- Aerodynamic sound generation by subsonic jet engines noting jet thrust relation to emitted acoustic power
03 p0552 A70-13926
- Aircraft power plant development, discussing thrust, specific weight, speed, jet engine and noise suppression efforts
05 p0896 A70-16346
- Aircraft noise suppression, discussing community aspects of jet and fan noise and physical mechanisms of jet noise
05 p0795 A70-16777
- Engineering methods developed for controlling boundary layer, jet and compressor noise, discussing theoretical formulations usefulness
05 p0896 A70-16778
- Subsonic circular jet noise radiation intensity and directional distribution, based on effects of refraction and Lighthill quadrupole model for aerodynamic noise
05 p0834 A70-16780
- Sound pressure field from stationary and moving jets determined from jet and aircraft trajectory parameters
05 p0834 A70-16781
- Nozzle exit turbulence and excess fuel combustion as low and high speed jet noise source using Lighthill theory
05 p0834 A70-16782
- Aircraft engine fan and compressor noise theory as basis for improved noise prediction
05 p0896 A70-16790
- Jet noise theory application in noise prediction and reduction at source for subsonic and supersonic jets
06 p1038 A70-18066
- Acoustic power output from supersonic jets, considering aerodynamic and acoustic characteristics for supersonic exhaust velocities [AIAA PAPER 70-237]
06 p1132 A70-18115
- Aircraft power plant development, discussing thrust, specific weight speed, jet engine and noise suppression efforts
08 p1558 A70-21029
- Shallow water waves simulation method for studying aerodynamic noise of free jet emitted from nozzle with variable wall roughness
08 p1485 A70-21608
- Jet aircraft engine noise control, discussing noise sources and built-in acoustic absorbers
09 p1743 A70-22759
- Acoustic and gas dynamic characteristics of jet noise muffler using adapters at outlet section of exhaust nozzle
12 p2160 A70-27295
- Jet engines for civil and military aircraft, discussing turbine designs and noise reduction
13 p2474 A70-28546
- In-flight shock cell noise generation by static jets, discussing frequency prediction formula
13 p2474 A70-29078
- Meteorological effects on air and noise pollution at U.S. airports
14 p2530 A70-30610
- Commercial jet aircraft engine noise evaluation, discussing noise reduction and effects on airport neighbors
14 p2630 A70-31335
- Aircraft fan and turbine noise reduction, discussing blade wake interaction, jet mixing and duct acoustic linings
16 p2963 A70-32946
- Sonic boom variation with aircraft geometry, volume, weight, weather and environment conditions, noting effects on structures and people
16 p2840 A70-32947
- Jet engine noise technology evaluation, noting effects on airport neighbor
16 p2971 A70-34262
- Airport operations effects on total environment, considering jet aircraft noise pollution [AIAA PAPER 70-887]
19 p3395 A70-37391
- Jet engine compressor noise analysis, noting inlet swirl role
22 p4090 A70-42725
- Aircraft noise sources, examining compressors with dynamic pressure devices and jets with turbulence investigations [ICAS PAPER 70-22]
23 p4232 A70-44111
- Jet aircraft noise reduction devices directed at turbulence fluctuation noise sources, noting effects on flight characteristics [ICAS PAPER 70-21]
23 p4233 A70-44112
- High bypass model jet noise study, describing test setup and noise measurement results as function of secondary/primary flow velocity ratio
23 p4233 A70-44394
- Intense white pulsed jet engine noise effects on cochlea biocurrents in cats
23 p4157 A70-45076
- Ear protection for persons exposed to various jet aircraft noise environments
24 p4306 A70-45121
- Noise suppression for high-bypass ratio CF6 turbofan engine in DC-10 airplane, considering effect on engine design [SAE PAPER 700804]
24 p4393 A70-45878
- Quiet V/STOL transport aircraft from DC-9-10 modification, discussing flying qualities, propulsion and control system interfaces, configurations, etc [AIAA PAPER 70-1409]
24 p4291 A70-45916
- SST sonic boom noise level reduction by thermal simulation of long body aircraft, considering thermal spike or keel [AIAA PAPER 70-1323]
24 p4291 A70-45942
- JET AIRSTREAMS**
- U JET STREAMS (METEOROLOGY)**
- JET AMPLIFIERS**
- Gas jets collision flowing from parallel wall channels, applying solution to calculating geometrical characteristics or fluid jet amplifiers
01 p0011 A70-11569
- Soviet book on fluidic theory covering jet elements, pneumatic throttles, chambers, communication channels, etc
19 p3357 A70-37469
- Jet-deflection proportional amplifier design and performance, discussing pressure and momentum control, static and dynamic characteristics aspect ratio, geometry effects, etc [ASME PAPER 70-FLCS-17]
22 p3963 A70-42410
- Impact configuration fluidic amplifier, investigating modulation of power jet formed by impacting plane wall jets in bounded region [ASME PAPER 70-FLCS-14]
22 p3963 A70-42413
- JET AUGMENTED WING FLAPS**
- U JET FLAPS**
- U WING FLAPS**
- JET BOUNDARIES**
- Turbulent submerged plasma jet boundaries calculated theoretically and compared with experimental results from dynamic head profiles
03 p0532 A70-13515
- Species concentration, jet structure and diatomic nitrogen rotational temperature measured for diffusive separation of nitrogen-helium mixture free jets, using electron beam
06 p1043 A70-18253
- Multilayered and multiple supersonic jets, deriving dispersion equations for boundaries stability
19 p3354 A70-38663
- Two dimensional peripheral turbulent jet curtain structure, determining curved and impinging jet flow field by pressure and velocity measurements
22 p3957 A70-42277

Aerodynamic forces and torque on airfoil in potential jet from boundary asymptotes position, determining flow characteristics by electrical analogy

24 p4288 A70-45438

Two dimensional incompressible laminar free jet, analyzing higher order viscous interactions with surrounding fluid by matched asymptotic expansions method

[AIAA PAPER 70-1321] 24 p4326 A70-45944

JET CONTROL

Bistable fluidic thrusters and circular sonic control jets interaction with airstream surrounding tactical missile configuration, investigating effect on amplification factors

[AIAA PAPER 70-583] 13 p2391 A70-29887

Reaction jets for control force generation in supersonic environment, analyzing downstream pressure distributions for two dimensional jet interactions

16 p2838 A70-33890

Extratmospheric transport trajectory control by jet assistance

18 p3333 A70-36670

Frequency dependent effects of applied acoustic fields on attached jet flows for Reynolds numbers over curved surfaces

[ASME PAPER 70-FLCS-1] 22 p4008 A70-42430

Aerodynamic characteristics of elliptical airfoils with jet circulation control for VTOL rotors including dual jets and cyclic results

[AIAA PAPER 69-741] 22 p3959 A70-42705

JET DAMPING

U DAMPING

U SPIN REDUCTION

JET DRAGON AIRCRAFT

U HH 125 AIRCRAFT

JET DRIVE

U JET PROPULSION

JET ENGINE FUELS

Turbojet engine controls and control devices design, considering fuel properties and fuel consumption

03 p0552 A70-13806

Fuel requirements for supersonic aircraft, discussing operational conditions and fuel quality problems

03 p0544 A70-14032

Emulsified jet fuels cold flow, combustion and corrosion characteristics in gas turbine combustor compared with JP-4 fuel

[ASME PAPER 69-WA/GT-3] 04 p0732 A70-14892

Emulsified jet fuels combustion characteristics evaluation by laboratory technique, presenting data on emulsifiers and corrosion inhibitors effect

[ASME PAPER 69-WA/GT-2] 04 p0785 A70-14893

Laboratory tests on jet fuels indicating lubricity improvement by corrosion inhibitor addition

[SAE PAPER 690667] 05 p0894 A70-15836

Surface tension plotted against density and temperature of hydrocarbon jet fuels, determining critical temperature

07 p1357 A70-18653

Flame spread rate across surface of liquid fuels, discussing effects of ignition mode, fuel purity and temperature, fuel container dimensions and material

10 p1929 A70-24090

Gelled and emulsified fuels for jet transport aircraft, testing rheological and physical properties regarding fire hazard reduction in crashes

[SAE PAPER 700251] 12 p2160 A70-27430

Resinous compounds content determination in jet fuels using ice cold acetic acid for desorbent to improve accuracy

16 p2961 A70-33203

Field test for microbiological contamination of jet fuel, discussing phosphates detection

18 p3299 A70-36344

Turbojet aircraft engine fuels quality control, considering chemical composition, physical properties and handling problems

18 p3299 A70-36550

Water separation index modified /WSIM/ test for jet fuel surface active materials in relation to filter/separater performance

[SAE PAPER 700279] 18 p3300 A70-36815

Jet fuel system deposits measurement, noting reliability of oxygen combustion and beta ray backscattering techniques

[SAE PAPER 700257] 18 p3214 A70-36824

Jet A kerosene deposit accumulation problem and proposed SST fuel tank design

[SAE PAPER 700256] 18 p3214 A70-36825

Jet fuels ground handling at airfields, describing flow monitors, filters, fueling techniques, etc

22 p4006 A70-43093

Jet engine air pollution in U.S., discussing fuel types, additives and burner design for smoke emission reduction

23 p4233 A70-44200

JET ENGINES

NT DUCTED FAN ENGINES

NT RAMJET ENGINES

NT SUPERSONIC COMBUSTION RAMJET ENGINES

NT T-56 ENGINE

NT TURBOFAN ENGINES

NT TURBOJET ENGINES

NT TURBOPROP ENGINES

NT TURBORAMJET ENGINES

Hybrid boost bearing applied to jet engines thrust bearing life extension and to land turbine equipment for providing high overload capacity

01 p0101 A70-10389

Multifan cross wind jet engine test facility to produce variable wind velocity in various directions

01 p0056 A70-10698

Corrosion induced fatigue damage suppression in jet engine compressor steel components, describing various surface treatment effects

01 p0165 A70-10699

Jet engine noise sources and design of noise suppressors used during airport runway engine tests

02 p0275 A70-12222

Combustion chamber design for engines, considering atomization by rotating disk vs nozzle atomization

03 p0552 A70-14031

Mounted-above-wing jet engine effect on wing pressure distribution and elevator unit, using fluid mechanical model

[DGLR-69-34] 04 p0735 A70-15146

Engine development for 3 and 4 engine large capacity jet aircraft, discussing fan cowl size and weight, installation drag effects, etc

05 p0895 A70-15928

Jet engine risetime effect on spacecraft orientation control system performance, assuming monotonic or extremal thrust mode

06 p1103 A70-17883

Combustion stability in air-liquid fuel zone of jet engine burner with burning rate controlled by droplet vaporization rate controlled mechanism

[WSCI PAPER 69-44] 06 p1178 A70-17980

Chemical composition of scale formation in jet engine injectors for various fuel types tabulated, noting buildup levels in transport aircraft and subsonic jets

07 p1362 A70-18651

Engine performance monitoring system /EPMS/ for aircraft jet onboard operation analysis and failure detection

08 p1558 A70-20668

Jet aircraft engine noise control, discussing noise sources and built-in acoustic absorbers

09 p1743 A70-22759

Airplane dependability on basis of improvements in jet engine, avionics, pilot seat cushions and flight control systems

09 p1611 A70-23453

Soviet book on jet engine construction and operation, discussing turboprop, turbojet, direct flow, gas turbine and bypass engines, thermodynamic cycles, etc

09 p1744 A70-23474

Abradable and abrasive types thermal spray coatings application to jet engine parts

10 p1893 A70-23856

Electrochemical machining for drilling deep holes in alloys and refractory metals used in jet engine hardware

10 p1893 A70-23857

Thrust follower force stability in pod mounted jet engine and nacelle whirl using multiple degrees of freedom model

10 p1930 A70-25070

Low cycle fatigue problems, environmental influence of operational differences on component life, life limits and controls for safe operation of jet engines

[SAE PAPER 700207] 11 p2102 A70-25879

Operating characteristics and performance of business aircraft jet engines compared with piston engine handling

[SAE PAPER 700209] 11 p2102 A70-25880

Tip clearance contactless measurement in jet engine turbine based on radioactive isotopes properties

11 p2055 A70-26446

Fluid mechanics of jet engine turbomachinery, considering supersonic compressor and blade rows flows and airframe propulsion system compatibility

11 p1977 A70-26574

Martensitic stainless steels corrosion damage in jet engine compressors noting effects of temperature, surface condition, time and chloride presence

12 p2252 A70-26963

Jet powered Ultra STOL aircraft engine selection, considering effects of engine size, wing loading, thrust loading, etc

[SAE PAPER 700266] 12 p2161 A70-27435

Maintenance trends for transport aircraft jet engine, considering engine and component pooling, inspection accessibility, monitoring, etc

[SAE PAPER 700316] 12 p2290 A70-27455

Aerojet engine minimum weight design, suggesting use of welding and brazing instead of nut-and-bolt joints in component fabrication

[SAE PAPER 700319] 12 p2243 A70-27457

Protective diffusion coatings for jet engine gas path parts, discussing repair procedures

[SAE PAPER 700332] 12 p2254 A70-27463

Jet engine pollution reduction for airport areas, discussing chemical equilibrium failure in exhaust gases and combustor design

12 p2291 A70-27993

Jet engines for civil and military aircraft, discussing turbine designs and noise reduction

13 p2474 A70-28546

French jet engines, outlining various models built by SNECMA and Turbomeca

13 p2474 A70-29144

Jet engine technology, discussing thrust/weight ratio, compressors, fans, combustors, turbines, materials, manufacturing, maintainability and noise

15 p2787 A70-31698

Non-French jet aircraft engines

15 p2788 A70-32250

Propulsive efficiency definition deficiencies for bypass jet engines

15 p2791 A70-32769

IR optical radiometer for jet engine turbine blade temperature measurement, comparing with junction wire thermocouple

16 p2905 A70-33168

Secondary effect signatures for potential failure detection in jet aircraft engine compressor blades

[ASME PAPER 70-DE-58] 16 p2918 A70-33517

Jet engine combustion chamber design, discussing performance range and geometry

16 p2970 A70-33682

Jet engine noise technology evaluation, noting effects on airport neighbor

16 p2971 A70-34262

Ti alloys use in jet engines design, considering weight, structural stability, useful temperature range, cost, etc

17 p3146 A70-34448

Close-spaced nozzles twin jet configuration, achieving low nozzle and total afterbody drag

[AIAA PAPER 70-934] 17 p3149 A70-35844

High speed and long life bearings and dampers for future jet engines, considering design factors

[SAE PAPER 700318] 18 p3263 A70-36800

Electrochemical machining /ECM/ effects on components surface integrity, discussing jet engine materials

[ASME PAPER 70-GT-111] 18 p3264 A70-36849

Cascade tunnel testing role in designing supersonic compressor rotor blading for lower jet engine weight and fuel consumption

[ASME PAPER 70-GT-79] 18 p3305 A70-36885

Liquid fuel jet engine thrust aftereffect momentum, investigating switching off transient process

19 p3490 A70-37249

Jet engine combustor design and efficiency, discussing heat transfer, cooling and engine materials

20 p3688 A70-39648

Electromagnetic interference in aircraft communication due to jet engine charging, considering various prevention measures

20 p3561 A70-39724

Subsonic jet engine intake duct radar cross section calculation using waveguide model

22 p3992 A70-43584

Aircraft propulsion system test facilities, discussing altitude simulation, large subsonic and supersonic engines and component development

[ICAS PAPER 70-45] 23 p4178 A70-44143

Jet engine air pollution in U.S., discussing fuel types, additives and burner design for smoke emission reduction

23 p4233 A70-44200

German monograph on dynamic control behavior of jet engines covering computation for normal external actions and perturbation effects

23 p4233 A70-44396

Two shaft bypass jet engine analog simulation, determining angular acceleration dependence on angular velocity and fuel consumption

24 p4393 A70-45442

Jet engine combustion chamber pressure loss, flow velocity through flare tube holes and air supply calculation, noting adaptation for computer use

24 p4393 A70-45446

Concorde thrust control by employment of variable area nozzle and reheat system, discussing crew workload

[SAE PAPER 700817] 24 p4394 A70-45900

Jet engine noise propagation near porous surface, predicting anomalous LF dip from direct and reflected waves interference with phase delay

24 p4395 A70-46068

Thrustmeter for direct output reading from jet engines based on stream and total port pressures

24 p4340 A70-46328

Reduced smoke combustion chambers for jet aircraft engines tested in full scale JT8D engine

24 p4396 A70-46387

JET EXHAUST

Wind tunnel tests for engine jet plume effect on boattail pressure drag

[AIAA PAPER 70-132] 06 p1038 A70-18050

Mach disk in underexpanded exhaust plume predicted by dividing flow field into subregions

[AIAA PAPER 70-231] 06 p0974 A70-18176

Particle density of jet plumes exhausting in vacuum calculated for He, Ar and N

06 p1052 A70-18388

- Stable flow distribution of sonic jet exhausting counter to low density supersonic airstream
07 p1189 A70-19982
- Plane rectangular plate in acoustic field of jet engine exhaust, calculating surface stresses
15 p2819 A70-32186
- Fog dissipation on aircraft runways, using aircraft jet engine exhaust heat and mixing properties
17 p1313 A70-35929
- Probability theory of stresses during random vibrations of flat panel in acoustic field of jet engine exhaust
18 p3301 A70-36301

JET FLAMES

U FLAMES
U JET FLOW

JET FLAPS

- Incompressible flow past airfoils with oscillating jet flaps used as rapid lift and momentum generators in aircraft gust load alleviation and mode stabilization
[AIAA PAPER 70-79] 06 p0975 A70-18196
- Airfoil cascade flow deflection angle using linearized jet flap theory
08 p1433 A70-21323
- Numerical solutions of thick cambered jet flap in ground effect for flat plate and diamond shaped airfoil
[AIAA PAPER 69-738] 12 p2155 A70-27199
- Heaving airfoil wakes visualization with jet flap augmented lift, measuring vortex street parameters
13 p2338 A70-28821
- Forward inclined two dimensional circular arc slot nozzle jet flaps at hypersonic speeds, considering amplification and interaction processes
[AIAA PAPER 70-553] 13 p2340 A70-29018
- Increased lift via hinge suction jet flaps on augmentor wings, using thin airfoil model and small disturbance theory
22 p3960 A70-43432
- Free jet stream effect on thin jet-flapped airfoil with fully developed wake, using linear theory
22 p3960 A70-43737
- Jet-ambient air mixing effect on flow characteristics around thin airfoil with jet flap
24 p4288 A70-45439

JET FLIGHT

U JET AIRCRAFT

JET FLOW

- NT AIR JETS
NT PERIPHERAL JET FLOW
NT SUPERSONIC JET FLOW
- Unmixed gases diffusion burning calculations, discussing turbulent flame burning aerodynamics in jet flows
01 p0217 A70-11007
- Axisymmetric turbulent incompressible and isothermal self preserving jet investigation using linearized constant temperature hot-wire anemometers
01 p0065 A70-11099
- Density distributions of electrically charged trace components in axisymmetric jets, considering space charge effect and ambipolar diffusion
01 p0066 A70-11135
- Turbulent and wall jets with wide varieties of geometries and boundary conditions, predicting jet inflow effects on entrainment rate, lift, drag, etc
02 p0288 A70-12840
- Walljet in crossflow, discussing characteristics and pressure field on plate, using flow visualization methods
03 p0465 A70-13004
- Incompressible gas turbulent jet flow characteristics in subsonic wind tunnel, stressing pressure distribution in recirculation region for interpreting heat transfer in separated flows
03 p0593 A70-13495
- Flow parameters of two interacting submerged turbulent jets from rectangular nozzles, determining total pressure profiles of coincident flow
03 p0466 A70-13504
- Laminar capillary jet of viscoelastic fluid, discussing breakup, nonNewtonian jet stability and elastic properties
03 p0468 A70-13782
- Microstructure of turbulent jet in concurrent flow, analyzing wake parameter and measuring profiles of pulsation velocity components and Reynolds shear stresses
03 p0409 A70-13871
- Magnetic field self induction in static fluid-submerged intersecting jet system, calculating required magnetic Reynolds numbers
04 p0726 A70-14541
- Compressible flows with circular sector hodographs, discussing Chaplygin equation for simple wedge flow and theorem on sonic jets
04 p0613 A70-14612
- Boundary layer equations closed form similarity solutions for laminar jet of compressible pseudoplastic fluid, discussing velocity transverse behavior
04 p0671 A70-15053
- Vorticity entrainment effects in zonal jet flows, considering Long asymptotic series, shear enhancement, etc
04 p0715 A70-15519

Acoustic characteristics of high subsonic model cold jet using imaging technique and measurements of energy flux of flow, calculating energy flux from flow-field measurements
[AIAA PAPER 70-234] 06 p1040 A70-18125

Main stream interaction with flame stabilizing jets in combustion chambers and afterburners using gas dynamic models
07 p1419 A70-18754

Second order correction to Glauret wall jet flow around arbitrarily curved surface, discussing initial profiles
07 p1257 A70-19344

Ignition and extinction in opposed jet diffusion flame for flow of compressible fluid with competitive/chain reactions
07 p1422 A70-19578

Solid surface roughness influence on reflection of thermal energy molecular jets, showing shock determined by incidence angle
07 p1343 A70-20121

Local heat transfer coefficients for unsteady conditions in tube determined by gradient method, noting use in reacting flow and jet nozzle protection
08 p1598 A70-21189

Static pressure gradient influence on turbulent shear stresses and energy production in asymmetric wall jet flow
08 p1484 A70-21314

Plane jet velocity profiles determination applied to calculating gain of proportional fluid amplifier
08 p1485 A70-21670

Flow characteristics behind sphere suspended in vertical axisymmetric jet dependent on ratio of specific parameter
09 p1658 A70-22118

Axisymmetric helium jet transition to turbulent flow in air shipstream, measuring temperature and velocity profiles
09 p1660 A70-22439

Vorticity distribution influence on inviscid laminar jet boundary layer instability investigated for large Reynolds numbers, using shear flow and linearized theory
[DFVLR-SONDDR-14] 10 p1868 A70-24163

Flow structure around incurved lateral jet issuing from narrow orifices, determining interaction zone geometry with main current by hot wire technique
10 p1868 A70-24165

Navier-Stokes-Maxwell equations solutions for conducting fluid flow in azimuthal magnetic field, noting jet acceleration near symmetry axis
10 p1924 A70-24574

Monograph on stability of laminar boundary layer separation at free jets and turbulent free jet flames, considering effects of velocity gradients and temperature
11 p2146 A70-25499

Flat plate flowfield for freestream/jet interaction wrap-around on bodies of revolution, using separation shock model and blast wave analogy
11 p1976 A70-26135

Stick-slip problem for motion of free jet at low Reynolds numbers by Wiener-Hopf technique, considering two dimensional Newtonian jet without gravity
11 p2041 A70-26554

Sound radiation from rigid flow spoilers correlated with fluctuating forces, measuring jet-pipe drag and lift components with transducers
11 p2085 A70-26699

Proportional fluid amplifiers noise and instability sources related to geometry and power jet flow, considering noise reduction methods
12 p2164 A70-27071

Coaxially flowing jets axisymmetric turbulent mixing between inner and outer streams
12 p2211 A70-27837

Ideal weightless fluid jet flow past supercavitating plate at incidence using Tulin scheme
12 p2214 A70-28241

Multiple jet flow exhausting into arbitrary crossflow in ground effect, solving continuity and momentum equations for jet path and induced velocity field
13 p2387 A70-29011

Forward inclined two dimensional circular arc slot nozzle jet flaps at hypersonic speeds, considering amplification and interaction processes
[AIAA PAPER 70-553] 13 p2340 A70-29018

Residence times distribution in confined round swirling jet, considering mass conservation of hypothetical tracer substance in combustion efficiency prediction
[WSCI PAPER 70-7] 13 p2522 A70-29609

Jet flow past arc curve approximation using successive conformal mapping on circle and wedge
13 p2391 A70-29746

Jet collisions solutions for impact of pin at obstacle, solid body impact at surface, cylindrical shells longitudinal impact and jets interactions
13 p2453 A70-29771

Discrete sonic jets as boundary layer trips producing turbulent hypersonic flows with negligible intrinsic drag and downstream distortions
13 p2523 A70-29973

Two dimensional jet velocity profile evolution under symmetrical and antisymmetrical perturbations
14 p2567 A70-31200

Jet flow through rectangular orifices in cylindrical wall using conformal mapping for potential, velocity, volume flow rate, viscosity, etc
14 p2567 A70-31359

One flow influence on another at two plane jets interaction zone, applying to proportional fluid amplifier inlet impedance calculation
15 p2720 A70-32020

Vortex streets characteristics determination for plane jet having uniform initial velocity profile
16 p2890 A70-33108

Shear flow perturbations in inviscid incompressible stratified fluid of given density, comparing stability characteristics with jet flow
16 p2895 A70-34243

Interior ideal liquid flow of vertical jet under gravity, using differential equation to relate flow plane to unit half disk
17 p3069 A70-34979

Performance cost functions of on-off limit cycle controllers for reaction jet controlled system
17 p3056 A70-35552

Incompressible laminar boundary layer, vortex and axisymmetric wake/jet flow parabolic equations solution by weighted residuals method, describing use of exponentials
17 p3074 A70-35883

Steam-water jet discharge heat transfer features, examining critical region parameters from nozzle into submerged space with large counterpressure
18 p3345 A70-36117

Axisymmetric ideal incompressible fluid jet outflow from cylindrical vessel with conical bottom, using small parameter technique and conformal mapping
18 p3240 A70-36272

Conducting gas channel and jet flow in electric and magnetic fields, using linearizing equations of motion under assumption of small magnetic Reynolds number
19 p3479 A70-37598

Round laminar jet with swirl, reducing Navier-Stokes equations to ordinary differential equations by similarity transformations
19 p3405 A70-38349

Noise spectra of two dimensional jet flowing from nozzle ejector, using dispersion equation
19 p3354 A70-38662

Freckles origin in unidirectionally solidified castings, noting convective jets role
20 p3646 A70-39102

Direction cosine attitude control logic for spin stabilized axisymmetric spacecraft, using control torques generated by reaction jet system
20 p3669 A70-39679

Radiation field multidimensionality effect on radiating gas jet flow, taking into account radiative energy transfer by differential approximation
20 p3611 A70-39808

Turbulent shear stress correlation with turbulent kinetic energy for wake and circular jet flow conditions
20 p3613 A70-40277

Sound generation by fluctuating subsonic jet flow, considering field directional characteristics and sound pressure variations with Mach number
21 p3850 A70-41422

Jet curtain flow recirculation model based on air-bubble flow visualization technique, determining minimum power for air cushion vehicle
22 p3957 A70-42278

Static and dynamic spring constants of peripheral jet air cushion vehicle in heaving motion, obtaining sinusoidal input response characteristics
22 p3960 A70-42279

Jet flow reattachment to walls of various shapes, measuring undeveloped velocity profiles at nozzle exit
[ASME PAPER 70-FLCS-2] 22 p4008 A70-42429

Large fluid-amplifier-type jets, measuring upstream flow disturbances effects on spreading velocity profiles
[ASME PAPER 70-FLCS-A] 22 p3964 A70-42431

Buoyant hot two dimensional laminar vertical jet in quiescent colder fluid, calculating temperature and velocity distributions by integral method
22 p4010 A70-42639

Irrational incompressible free falling jet, using asymptotic expansion solution for mixed boundary value potential problems
22 p4012 A70-42938

Free jet stream effect on thin jet-flapped airfoil with fully developed wake, using linear theory
22 p3960 A70-43737

Free jet flow axial gradient effects on drag coefficient measurement of slender blunted cones at zero attack angle
23 p4135 A70-44584

Incompressible laminar swirling jet flow, obtaining similarity solution for Navier-Stokes equations
23 p4184 A70-44982

Molecular jet velocity distribution, investigating adiabatic focalization conditions
24 p4351 A70-45370

Two dimensional aperture flow with downstream asymmetric pressure distribution due to jet reattachment to boundary, simulating flows in hydraulic spool valves and fluidic devices

24 p4325 A70-45582

Single stage warm gas directed jet valve for missile attitude control, noting servovalve and auxiliary power unit control applications
[SAE PAPER 700778]

24 p4295 A70-45864

Vortices growth in vortex sheets bounding jets flowing from two dimensional slit and circular orifice observed by computer experiments

24 p4327 A70-46244

Pulsation and turbulence damping in pulsed jet from energy spectra of longitudinal velocity fluctuations

24 p4327 A70-46267

JET FUELS

U JET ENGINE FUELS

JET IMPINGEMENT

Impingement pressure analysis associated with two phase cryogenic propellant venting to space environment

[AIAA PAPER 69-571]

01 p0196 A70-10845

High altitude scale model experiment to evaluate rocket plume impingement effects on Manned Orbital Workshop pressures, heating rates, forces and moments

03 p0579 A70-13646

Propagation of turbulent jet impinging on flat surface at certain incidence angle analyzed for application to V/STOL aircraft, ventilation equipment, etc

03 p0468 A70-13878

Critical load and instability of smooth and mesh surface mechanical systems subjected to impinging fluid jet, noting static buckling and flutter effects
[ASME PAPER 69-WA/APM-10]

04 p0772 A70-14917

Frozen wax measurement of droplet sizes and sprays from impinging injector elements, concerning like and unlike doublets and quintuplets

04 p0786 A70-15416

Rocket nozzle originated oblique shock waves effect on near-field plume impingement flows, heat transfer and pressure distribution

04 p0737 A70-15421

Vorticity effects on drag friction and heat transfer near stagnation point of supersonic jet impinging on obstacle

05 p0833 A70-16290

Acoustic radiation from underexpanded supersonic main jet flow from nozzle impinged upon by annular jet

05 p0835 A70-16784

Heat transfer from impinging gas jets on enclosed concave surface, noting self recirculation currents within cavity

07 p1425 A70-20413

Metal erosion under liquid drop impingement attack, investigating damage from microplastic deformation to surface material removal using wheel and jet apparatus

08 p1519 A70-21354

Axisymmetric swirling jet ejection from semiinfinite tube into free space filled by fluid, solving flow equation by Wiener-Hopf method

09 p1658 A70-22153

Turbulent jet injection from circular opening into unbounded transverse shear flow, determining velocity distribution along axis

09 p1659 A70-22427

Turbulent flow generation by interacting principal stream with transverse jets, obtaining flow domains in test chamber of two dimensional wind tunnel

10 p1870 A70-24785

Flat plate normal to two dimensional impinging air jet, investigating heat /mass/ transfer structure using naphthalene method

11 p1977 A70-26411

Central shock and target displacement of underexpanded supersonic jets with obstacle at nozzle exit, using Toepfer schlieren photographs

12 p2156 A70-27293

Heat transfer increase near stagnation point for turbulent jet impinging on paraffin coated plates used for flow visualization

13 p2521 A70-28866

Three dimensional oblique incidence liquid jet impinging on solid surface, evaluating flow force by applying mass and momentum conservation

13 p2389 A70-29540

Surface heat transfer coefficients under perforated plate of multiple square array round impinging air jets
[ASME PAPER 69-GT-4]

14 p2666 A70-31025

Laminar boundary conditions for heat transfer in gradient flow region for plane turbulent jet impingement on plate normal to flow

15 p2721 A70-32134

Reactive stream separation high speed color photography for impinging streams of nitrogen tetroxide and hydrazine

[AIAA PAPER 70-608]

16 p2998 A70-33605

Plane turbulent impinging jet by iterative finite difference technique, assuming eddy viscosity depen-

dence on energy fluctuations and turbulence length scale

[ASME PAPER 70-FE-27]

16 p2835 A70-33634

Orifice length-to-diameter ratio effect on spray mixture uniformity from unlike impinging jets

17 p3073 A70-35671

Viscosity effect on turbulent supersonic underexpanded jet flow into submerged region

18 p3206 A70-36262

Two dimensional peripheral turbulent jet curtain structure, determining curved and impinging jet flow field by pressure and velocity measurements

22 p3957 A70-42277

Heat transfer from turbulent axisymmetric jet to normal flat wall at critical point with small Reynolds numbers

23 p4181 A70-44321

Two phase plume at various incidence angles on flat plate, determining impinging particle mass flux, forces and damage

23 p4134 A70-44566

JET LIFT

Sound radiation from airfoil in turbulent jet flow, discussing direct correlation of fluctuating lift

01 p0004 A70-11192

Deviation angle optimization for cruising hypersonic jet aircraft, noting effect of rotation losses on design

03 p0406 A70-13019

Exit geometry effects on peripheral jet device lift, considering operating height, curtain thickness, base extension, etc

04 p0619 A70-15388

Jet lift passenger aircraft considered better suited for medium stage routes than rotor/ propeller designs for VTOL transport

08 p1436 A70-21347

Ground simulations data of jet lift V/STOL compared with visual flight results, noting hover, lateral quick start and stop maneuver

18 p3236 A70-35954

Propulsion system impact on military/commercial STOL transport aircraft commonality, taking into account augmented jet flap and externally blown flap powered lift wing concepts

[SAE PAPER 700269]

18 p3214 A70-36819

Lightweight lift jet engine design, testing and performance for V/STOL aircraft

[ASME PAPER 70-GT-32]

18 p3302 A70-36833

Thrust deflector for VTOL aircraft fuselage mounted lift engines designed as isentropic plug nozzle, considering mass flow, pressure forces and Coanda effect

[SAWE PAPER 841]

20 p3563 A70-40379

Wind tunnel wall interference effects for V/STOL aircraft with lift jets, using modified theoretical model for complex jet arrangements

[ICAS PAPER 70-54]

23 p4139 A70-44150

JET MIXING FLOW

Premixed methane-oxygen-nitrogen combustion in conical reactor fed by choked sonic flow jet, analyzing reaction products chromatographically

02 p0397 A70-12030

Fuel injection and mixing and piloted ignition in supersonic flow design principles for scramjet engine, evaluating eddy viscosity model for parallel injection

02 p0354 A70-12047

Time of establishment of steady state mixing in plane and axisymmetrical jets determined, using self similar motions in unsteady state boundary layer and free turbulence

03 p0409 A70-13875

Flow field of jet spoilers downstream from nozzle, accounting for main stream and secondary jet mixing and fuel injection problems during supersonic combustion

03 p0608 A70-14098

Linear spatial stability of two dimensional laminar wake- and jet-like similarity solution of Falkner-Skan equation

04 p0613 A70-14455

Optimum injector design for propellant spray mixing using nonreactive simulants and combustion efficiency model

04 p0737 A70-15419

Dissimilar coaxial axisymmetric jets confined laminar mixing obtained from numerical solution of boundary layer equations, considering binary, isothermal and nonreacting system

04 p0621 A70-15579

Acoustic intensity determined from time, length and velocity scales in mixing region of jet from nozzle with turbulent boundary layers

05 p0834 A70-16779

Water droplets and air supersonic mixing, determining droplets size and optical properties
[AIAA PAPER 70-90]

06 p0975 A70-18199

Unified model for transverse gaseous jet penetration into supersonic stream agreeing with measured flow field properties

[AIAA PAPER 70-93]

06 p0976 A70-18201

Sharp hypersonic flat plates inclined at various angles, obtaining flow field and merged region details

06 p0980 A70-18353

Energy losses due to mixing of primary and secondary flows of jet streams in gas propulsion engine chambers determined by continuum mechanics application

07 p1363 A70-19086

Mixing region and potential cone of two dimensional jet, measuring velocity fluctuations

08 p1485 A70-21587

Velocity and concentration profiles for mixing of two dimensional foreign gas jet injected into parallel air mainstream, emphasizing film cooling applications

10 p1801 A70-24155

Suction force increase resulting from turbulent jet interaction with transverse flow

10 p1868 A70-24166

Turbulent flow downstream from abrupt widening of circular jet, using flow and momentum equations

10 p1870 A70-24782

Injectant stagnation temperature and molecular weight effects in jet interaction flowfield

11 p2036 A70-25989

Cavity pressure and velocities distributions of interfering two dimensional dual jets from parallel slot nozzles

11 p2037 A70-26419

Gaseous injection into supersonic flow, investigating secondary Mach number and injection angle effects on flowfield in supersonic wind tunnel

[AIAA PAPER 70-552]

13 p2339 A70-29017

Bistable fluidic thrusters and circular sonic control jets interaction with airstream surrounding tactical missile configuration, investigating effect on amplification factors

[AIAA PAPER 70-583]

13 p2391 A70-29887

Reynolds momentum and mass transport at velocity half radius of coaxial jet compared to eddy viscosity models

14 p2564 A70-30260

Two phase axisymmetric jet, studying dispersion of pulverized impurity consisting of particles of various sizes

15 p2721 A70-32135

Schlieren optical method for measuring He jet penetration into supersonic flow

15 p2741 A70-32520

Integral model for combustion of metal particle laden jet mixing with subsonic secondary stream in duct, considering air breathing engine design

[AIAA PAPER 70-736]

16 p2964 A70-33490

High velocity gas jet injection into subsonic and supersonic air streams from wall injectors

[AIAA PAPER 70-714]

16 p2834 A70-33538

Two dimensional sonic secondary fluid jet interaction with uniform primary supersonic stream in wind tunnel

[ASME PAPER 70-FE-33]

16 p2835 A70-33638

Combustion effects on mixing of axisymmetric supersonic and turbulent free jets to obtain species concentrations, pitot pressures and temperatures

16 p2998 A70-33860

Retrorocket jet size and structure for scientific instruments soft Mars landing, estimating off- optimum supersonic jet interaction with quiescent atmosphere

17 p3011 A70-35660

Orifice length-to-diameter ratio effect on spray mixture uniformity from unlike impinging jets

17 p3073 A70-35671

Shear stress and velocity profiles in three dimensional mixing layer between grazing perpendicular streams

20 p3608 A70-39356

Asymptotic turbulent boundary layer semiempirical Taylor formula, investigating average motion formed in mixing jet region and surrounding liquid

20 p3611 A70-39809

Potential fluctuations in intersecting plasma jet streams attributed to ion-electron instability, using external probe

20 p3682 A70-40136

Supersonic air flow interaction with transverse gas jet from plate orifice

21 p3749 A70-42222

Computerized integral treatment of turbulent constant pressure mixing of two dimensional gas jet with atmosphere having different temperature and composition

22 p4011 A70-42755

Jet-ambient air mixing effect on flow characteristics around thin airfoil with jet flap

24 p4288 A70-45439

Two dimensional incompressible laminar free jet, analyzing higher order viscous interactions with surrounding fluid by matched asymptotic expansions method

[AIAA PAPER 70-1321]

24 p4326 A70-45944

JET NOISE

U JET AIRCRAFT NOISE

JET NOZZLES

Flow field of jet spoilers downstream from nozzle, accounting for main stream and secondary jet mixing and fuel injection problems during supersonic combustion

03 p0608 A70-14098

- Mean flow and turbulent velocity over noise-producing regions of subsonic jet nozzle with and without delta wings
09 p1610 A70-22239
- External supersonic potential flow effects on turbojet engine ring and needle nozzle performance, considering gas overexpansion operation
10 p1930 A70-24286
- High secondary/primary mass ratio multinozzle jet pump/ejector/operation feasibility
[AIAA PAPER 70-579] 13 p2342 A70-29890
- Cavitation characteristics of jet nozzles, formulating relationship between pressure differential and fluid flow rate
22 p3965 A70-43369
- Turbojet engines noise-suppressing nozzles flow rate and thrust characteristics calculation
22 p4092 A70-43371
- JET PILOTS**
U AIRCRAFT PILOTS
JET PLUMES
U PLUMES
JET PROPULSION
Material flow acceleration in jet propulsion systems, discussing acceleration by gravitational field, thermodynamic nozzle expansion, electrostatic forces and Lorentz force
04 p0671 A70-15090
- Energy losses due to mixing of primary and secondary flows of jet streams in gas propulsion engine chambers determined by continuum mechanics application
07 p1363 A70-19086
- Mass variation laws in light of Tsolkovskii hypothesis, considering particle separation rates and thermal energy losses for actual jet engines
07 p1363 A70-19088
- Ilyushin 62 aircraft geometry, propulsion, structure, onboard equipment and performance
08 p1436 A70-21365
- VTOL aircraft multiple and nonuniform jets aerodynamics, considering induced field and secondary flows
14 p2528 A70-30851
- Hypersonic aircraft technology, discussing long range transport, reusable launch vehicles and propulsion systems
15 p2673 A70-31851
- Optimum adaptation of propulsion gas generators to power jet driven rotors with blown flap control, considering jet engine, fanjet and engine driven compressor
17 p3024 A70-35661
- JET PUMPS**
Jet pump cavitation prediction and elimination using limiting-flow equation based on selected index
[ASME PAPER 69-WA/FE-29] 04 p0666 A70-14773
- High secondary/primary mass ratio multinozzle jet pump/ejector/operation feasibility
[AIAA PAPER 70-579] 13 p2342 A70-29890
- JET STREAMS [METEOROLOGY]**
Equatorial jet stream excitation of longitudinal waves, analyzing plasma beam instability and spectrum of short wave inhomogeneities by quasi-hydrodynamic equations
05 p0842 A70-16759
- Maximum wind velocity regions in tropospheric jet streams under synoptic conditions concerning troughs, ridge sections and cyclonic-anticyclonic curvatures
11 p2075 A70-25919
- Mesoscale waves in jet stream flow within Coriolis force over rotating earth by amplitude functions and phase velocities asymptotic series representation
12 p2265 A70-28334
- Vertical and intensity distributions of wind velocity focuses in tropospheric jet streams
13 p2444 A70-28590
- CAT shear spectra above ground frictional layer in jet stream flight conditions, using aircraft measurements
16 p2946 A70-33825
- Statistical properties of subtropical jet stream maxima over U.S. from Nimbus II IR radiometry
17 p3133 A70-35931
- Scintillation index correlation with mean wind velocity of jet streams
22 p4020 A70-43262
- JET THRUST**
Tangential force applied to column end by jet reaction from nozzle clamped to column end, obtaining critical load and oscillation frequency
02 p0389 A70-12644
- Jet engine risetime effect on spacecraft orientation control system performance, assuming monotonic or extremal thrust mode
06 p1103 A70-17883
- Turbojet engines departure from equilibrium performance during thermal soak transient attributed to heat absorption in turbine and compressor metals, observing thrust loss
09 p1744 A70-23739

- Thrust follower force stability in pod mounted jet engine and nacelle whirl using multiple degrees of freedom model
10 p1930 A70-25070
- Jet assisted orbital spacecraft trajectories equations derivation, considering Kepler trajectories and orbital velocities
15 p2800 A70-32260
- Performance cost functions of on-off limit cycle controllers for reaction jet controlled system
17 p3056 A70-35552
- Direction cosine attitude control logic for spin stabilized axisymmetric spacecraft, using control torques generated by reaction jet system
20 p3669 A70-39679
- Nonlinear adaptive reaction jet attitude control for long life space vehicles, providing optimal performance over bias acceleration disturbances
20 p3716 A70-39680
- Turbojet engines noise-suppressing nozzles flow rate and thrust characteristics calculation
22 p4092 A70-43371
- JET VANES**
Dip brazing aluminum fan vanes used in high bypass turbofan jet engines
10 p1893 A70-23858
- Kuznetsov NK 8-4 bypass turbojet air entry vanes, pressure compressors, gear case, combustion chamber and turbine drives
17 p3147 A70-34629
- JETAVATORS**
U GUIDE VANES
JETTISON SYSTEMS
Compression spring mechanisms for separation of spacecraft and shrouds, summarizing design characteristics
16 p2921 A70-34116
- Reliable collet release mechanism design for separation and ejection of reentry vehicle payload from booster
16 p2922 A70-34118
- Ball-lock-bolt separation mechanism for spacecraft applications requiring low shock, controlled release, nonfragmenting fastener
16 p2922 A70-34119
- JETTISONING**
Apollo service module retrograde motion due to propellants reorientation after reentry jettison predicted by digital simulation
[AIAA PAPER 70-1047] 19 p3534 A70-38862
- JITTER**
U VIBRATION
JOBS
U TASKS
JOINTS [ANATOMY]
NT KNEE [ANATOMY]
Step tracking in normal human subjects, studying muscle system around ankle joint
10 p1824 A70-23898
- Human femur junctions load actions and stresses during walking calculated from measurements
15 p2692 A70-32327
- Human joints boosted lubrication, discussing hyaluronic acid concentration and synovial fluid viscosity during squeeze-film action
24 p4296 A70-45160
- JOINTS [JUNCTIONS]**
NT BUTT JOINTS
NT LAP JOINTS
NT METAL JOINTS
NT SEAMS [JOINTS]
NT SOLDERED JOINTS
NT SPOT WELDS
NT WELDED JOINTS
- Bolted joints inspection using mechanical impedance algorithm method involving bolt head mechanical shock pulse response in adjacent structure
01 p0098 A70-10017
- Bolted and bonded joints design in composite materials loaded in tension, presenting methods for strength prediction, testing and analysis
02 p0306 A70-11952
- Elastic couplings applied as sliding contact-free continuous junction between permanently rotating and fixed parts in rotating coil magnetometer
02 p0298 A70-12214
- Resilience coefficient of intermediate elements of threaded connection related to transverse and axial nut dimensions by least squares method
05 p0856 A70-17012
- Apollo suit features applicable to operational or research program requiring pressure suits, discussing low torque constant volume joints
06 p1002 A70-17704
- Elastic behavior of joint formed by normally intersecting circular cylindrical shells under external bending moment, noting applicability to pipelines and pressure vessels
[ASME PAPER 68-WA/PVP-1] 07 p1400 A70-18710
- Adhesive joint failure, studying adhesive, cohesive and adhering ruptures by evaporative rate analysis
07 p1292 A70-18931

- Green matrices construction for joint shells by method of arbitrary constants variation, considering strained state symmetrical with joint linings
07 p1413 A70-20144
- Fiber composites-Ti alloy adhesive, rivet and combined joints for aircraft applications, noting fiber orientation role in joint tensile strength
08 p1509 A70-21905
- Standing wave ratio frequency dependence in miniature stripline power dividers and ring structure hybrid junction
09 p1652 A70-23653
- Hydraulic loss and secondary circulation of fluid flow in three dimensional bend commercial conduits, discussing relationship to velocity distribution
10 p1871 A70-25094
- Variable sweep wing pivot joint design utilizing double shear tilted spherical journal bearings with Teflon fabric liners
12 p2318 A70-27135
- Axisymmetric postyielded tongue and groove cylindrical joint stress analysis using finite element method
14 p2659 A70-31131
- Wire wrapped, soldered, welded and crimped joints and plug/socket connections in electronic packaging for spacecraft
16 p2879 A70-33958
- Overbraced frame loaded at joints, limiting elastic buckling examinations to geometrically perfect structures
20 p3717 A70-38973
- High temperature endurance strength of temper finished bolt connections under cyclic loads, using programmed fatigue testing machines
20 p3718 A70-39223
- Joint designs, attachment methods and load introduction in composite structures, suggesting adhesive bonding
20 p3730 A70-40041
- Point mass impact on flexibly interconnected rigid bodies with tree structure and spherical joints without dry friction, discussing resulting velocity changes
21 p3849 A70-40552
- Joint strength of three layer fiberglass reinforced plastic panels with bilateral adhesive patches under linear axial force
22 p4115 A70-42812
- Microwave waveguide rotary joint using symmetrical excitation for mode conversion to obviate filters
24 p4318 A70-45221
- Lockseal/flexible joint/ for solid propellant rocket motor thrust vector control, considering construction, operating characteristics and tradeoffs
[SAE PAPER 700777] 24 p4393 A70-45865
- JORDAN FORM**
Controllability and observability of discrete composite systems in tandem with Jordan canonical form representation noting similarity to continuous systems
10 p1856 A70-24873
- Gravitational variable constant in celestial mechanics, considering theories based on vacuum Jordan Lagrangian
18 p3320 A70-37066
- Differential equation systems with Jordan form block-triangular matrix, discussing homeomorphic mapping
23 p4211 A70-44093
- JOSEPHSON JUNCTIONS**
Josephson effect in superconductors emphasizing Josephson junction electrical properties and applications to devices and measuring techniques
03 p0542 A70-14190
- Thermal fluctuations effect on Josephson tunnel contact binding energy and external magnetic field dependence
24 p4388 A70-45203
- JOUKOWSKI TRANSFORMATION**
Pressure distribution in two dimensional incompressible potential flow on Joukowski airfoils with normal upper surface spoilers, emphasizing potential flow theory
[AIAA PAPER 67-737] 12 p2155 A70-27193
- JOULE HEATING**
U OHMIC DISSIPATION
U RESISTANCE HEATING
JOULE-THOMPSON EFFECT
Fluid intermolecular potential and virial calculation, noting relationships to Boyle and Joule-Thompson inversion temperatures
20 p3671 A70-38988
- JOURNAL BEARINGS**
Externally pressurized air journal bearings load capacity, film stiffness, attitude-eccentricity locus and mass flow, studying supply pressure and shaft rotation effects
[ASME PAPER 69-LUB-29] 01 p0100 A70-10380
- Helical journal bearings analysis operated in turbulent regime with incompressible lubricant, determining optimum groove parameters for maximum radial stiffness
01 p0100 A70-10381
- Externally pressurized gas lubricated journal bearings zero load rotating stability, using digital computer
[ASME PAPER 69-LUB-27] 01 p0100 A70-10382

- Externally pressurized journal bearing load tests, comparing load capacity data with analytical values
01 p0103 A70-10559
 - Rigid body dynamics of turborotors in fluid film journal bearings, investigating initial transients effect on motion stability by Runge-Kutta technique
[ASME PAPER 68-LUB-7] 02 p0307 A70-12165
 - Rayleigh step journal bearings, considering pressure distribution, load capacity and attitude angle and optimal film thickness ratio for incompressible fluid lubrication
02 p0307 A70-12167
 - Spiral grooved turbulent screw seal/viscoseal/analysis, combining results of spiral grooved journal bearing study with turbulent fluid film theory
[ASLE FICFS PREPRINT 32] 02 p0308 A70-12169
 - Hydrodynamic journal-thrust bearing system for satellite attitude control flywheel, discussing bearing stability, grease lubricant seal, power consumption, etc
[ASLE PREPRINT 69-LC-22] 02 p0309 A70-12532
 - Augmented small parameter gas film equation for squeeze film journal bearing solved in terms of radial displacement
[ASME PAPER 69-WA/LUB-9] 04 p0697 A70-14766
 - Time transient and step-jump dynamic analyses of gas lubricated bearing, illustrating hybrid journal and Rayleigh-Step thrust bearings
[ASME PAPER 69-WA/LUB-5] 04 p0697 A70-14768
 - Stability characteristics of two degree of freedom gyroscope having hydrodynamic grooved journal rotor bearings, discussing frequency of self excited oscillation
[ASME PAPER 69-LUB-H] 04 p0689 A70-14872
 - Hydrodynamic theory of elastic-viscous liquid lubrication for journal bearings, assuming stress-strain relationship with unequal cross stresses
05 p0855 A70-16509
 - Hydrostatic journal bearing calculation for case of shaft misalignment, deriving linear inhomogeneous equations with symmetrical matrix for pressure
07 p1293 A70-19119
 - Hydrostatic journal bearing dynamic rigidity for compressible and incompressible fluids, describing fluid film elasticity and damping characteristics
07 p1293 A70-19121
 - Load parameters of externally pressurized gas journal bearing with multiple supply holes
09 p1693 A70-22977
 - Hydrostatic oil journal bearings performance with several supply holes and incompressible lubricant, analyzing Reynolds pressure equation by numerical method
10 p1895 A70-24851
 - Externally pressurized porous journal gas bearings with solid sleeve parts for reducing porous media waviness and roughness effects
10 p1896 A70-25097
 - Pressure field equation derivation for hydrodynamic journal bearing in superlaminar regime, using turbulent Couette and screw flow friction correlations
13 p2418 A70-28742
 - Externally pressurized air journal bearing performance prediction, obtaining pressure distribution by numerical solution of Reynolds equation
13 p2418 A70-28743
 - Dynamic instability of multirecess hydrostatic journal bearings at critical shaft rotation velocity
13 p2418 A70-28745
 - Stiffness of multipad externally pressurized journal bearings with incompressible fluid feeding, comparing hydrodynamic and rolling bearings
15 p2745 A70-32445
 - Continuous elastic turboshaft flexible journal bearings, analyzing radial misalignment effects on operation
[ASME PAPER 70-DE-71] 16 p2918 A70-33521
 - Hydrodynamic journal-thrust bearing system for satellite attitude control flywheel, discussing bearing stability, grease lubricant seal, power consumption, etc
17 p3099 A70-34630
 - Pressure distribution in moderately loaded self acting journal bearings with incompressible turbulent film, considering end leakage
17 p3101 A70-35147
 - Load carrying capacity of self acting hydrodynamic journal bearings, considering turbulence and whirling motion in closed form solution
17 p3101 A70-35148
 - Pneumatic instability, capacity and rigidity of thrust and journal gas bearings with external air injection
18 p3264 A70-37072
 - Friction and temperature fields in lubricant film of journal bearings, discussing friction torque and heat dissipation
[ASME PAPER 69-LUB-24] 19 p3434 A70-37601
 - Augmented small parameter gas film equation for squeeze film journal bearing solved in terms of radial displacement
[ASME PAPER 69-WA/LUB-9] 19 p3435 A70-37609
 - Optimum one dimensional journal bearing for maximum load with minimum film thickness, using Pontryagin principle
[ASME PAPER 69-LUB-9] 19 p3435 A70-37614
 - Time transient and step-jump dynamic analyses of gas lubricated bearing, illustrating hybrid journal and Rayleigh-Step thrust bearings
[ASME PAPER 69-WA/LUB-5] 19 p3436 A70-37619
 - Aerostatic journal bearings with double plane admission feeder holes, determining maximum load and stiffness by numerical method
19 p3443 A70-38898
 - Externally pressurized air lubricated journal bearing with multiple supply holes, predicting load carrying capacity, flow requirement and stiffness
20 p3639 A70-40505
 - Rotating shaft system consisting of variable cross sections, disks and journal bearings, calculating unbalance vibration by numerical method
21 p3832 A70-40898
 - Heat generation effects in air hydrostatic journal bearing, including shaft and housing thermal deformation and lubricant viscosity changes
[ASME PAPER 70-LUBS-19] 22 p4044 A70-42442
 - Full and half journal bearings in axial magnetic field, discussing hydromagnetic noncyclic squeeze fluid films
24 p4349 A70-45995
- JOURNALS (SHAFTS)**
U SHAFTS [MACHINE ELEMENTS]
JUDGMENTS
Interindividual differences in judging stimulus similarities, explaining unsatisfactory results obtained by average scalings
19 p3366 A70-38506- Expert judgments validity of human task performance time against empirical measures for use in analytical modeling
24 p4308 A70-45515
- JUNCTION DIODES**
Negative resistance light emitting lateral GaAs diode, analyzing oscillation frequency, I-V characteristics, temperature and magnetic effects
01 p0050 A70-10565- Mo-Si epitaxial planar Schottky barrier diodes, describing reverse I-V characteristics improvement by edge leakage effects elimination
01 p0052 A70-11174
- Cavity resonator linear excitation by Gunn diode, considering external circuit effects on oscillation conditions and GaAs single crystal parameters
03 p0457 A70-13965
- Burst noise in forward biased silicon diodes and transistors, discussing measurements on gate controlled devices
03 p0458 A70-14029
- GaAs microwave diode Gunn oscillator subharmonically injection phase locked at low frequency ratios
03 p0459 A70-14041
- P-n heterojunction diode strain sensor fabricated by vacuum evaporation onto substrate, investigating mechanical input and output impedance characteristics
03 p0495 A70-14192
- N-type layer formation with ion implanted nitrogen or Sb in p-type alpha-SiC, evaluating electrical characteristics, discussing junction devices formed
04 p0732 A70-15685
- Phenomenology theory on conduction and switching behavior of amorphous semiconductor diodes
05 p0891 A70-16021
- Broadband two way switch obtained by p-i-n diodes deposited on alumina substrate
05 p0821 A70-16526
- Self excited microwave mixer and transmitting oscillator using Gunn diode applied to short distance Doppler radar
05 p0822 A70-16678
- Soviet book on microwave devices employing semiconductor diodes design and synthesis covering electric field effects, optimality criteria, tabular data, etc
06 p1019 A70-17536
- GaAs diode amplifiers and switching devices behavior, describing optical coupling between two GaAs lasers
07 p1241 A70-19399
- Seminsulating GaAs doped with Cr, discussing negative resistance segment in current-voltage curves of S diodes
07 p1242 A70-19798
- Gunn diode parallel combinations fabricated for X band with n-type GaAs crystals, discussing output power at CW operation
08 p1477 A70-21296
- Al n-type Si Schottky barrier diode characteristics, discussing I-V, barrier height, temperature dependence, photoemission, LF noise, etc
09 p1644 A70-22210
- X band Gunn oscillators amplitude modulation by pulse signals from another Gunn diode
09 p1646 A70-22707
- Volt-ampere characteristics of metal-semiconductor contacts for Schottky barrier diodes, investigating suppression of minority carriers and frequency response
09 p1741 A70-23352
- Low power semiconductor diode rectifying test apparatus for analysis of fusing and shaping effects on dynamic current-volt and frequency characteristics
09 p1649 A70-23355
- Ion-implanted GaAs junction diodes anneal behavior and defect nature
11 p2098 A70-26391
- Dispersion relation derived for space-charge waves propagating in thick Gunn diode, showing validity limit of one dimensional approach
12 p2194 A70-27164
- Read-diode microwave oscillators performance degradation due to space charge and series resistance, discussing RF power optimization
12 p2194 A70-27167
- Gunn diodes I-V characteristics with as function of carrier concentration/mobility and diode length, noting role of impact ionization in strong electric field
13 p2378 A70-29408
- Nonlinear resistance and reactance type harmonic generator diodes performance with output in millimeter wave decade
14 p2548 A70-30436
- High resistivity Si electron drift velocity measurement by exciting surface barrier diode with subnanosecond superradiant laser pulses
14 p2594 A70-30924
- Gamma radiation effects on GaAs Gunn diodes, measuring Hall effect, low field resistance, output power and FM noise in X band cavity
14 p2558 A70-31322
- High pulse repetition rate digital systems signal processing using Gunn effect diodes
15 p2710 A70-32583
- Lasers and GaAs diode emitters near IR radiation intensity distributions, using IR films and IR display phosphors
15 p2753 A70-32607
- Electron bombardment effect on volt-ampere, voltage-capacitance and pulse characteristics of GaAs point contact pulse diodes
17 p3055 A70-35675
- IV characteristics of high resistivity Ti-doped GaAs single crystals and S-diodes, using Hall constant and conductivity measurements
17 p3144 A70-35709
- GaAs diodes electroluminescence dependence on temperature and injection current
18 p3297 A70-36234
- Negative resistance and conductivity segments in I-V curves of diode structures, taking into account injection junction imperfections
18 p3231 A70-36413
- Close-confinement LPE AlGaAs junction laser properties, examining range of alloy direct bandgap transition
18 p3268 A70-36727
- Pulsed diodes subnanosecond rise time estimation, considering charge carrier lifetime, junction barrier capacitance, signal frequency, etc
20 p3595 A70-38968
- Degenerate p-n diode junction capacitance calculation, taking into account quantum and temperature effects
20 p3596 A70-39117
- Frequency dependence of impedance of p-n diode with short base in presence of large forward current densities
20 p3598 A70-40021
- Motion equation of electron in cylindrical diode subjected to varied voltages
21 p3796 A70-40640
- High energy electron irradiation generated defect centers in GaAs p-n electroluminescent diodes, using capacitance and thermally stimulated current measurements
21 p3863 A70-41914
- Picosecond large amplitude pulse generating GaAs diode with nu-n structure
21 p3800 A70-42116
- Semiconductor junction diode spontaneous emission sources, considering frequency-energy characteristics relationship
22 p4085 A70-42504
- GaAs laser and noncoherent IR emitting diodes fabrication and design, discussing card readers, encoders, alarms, range finders, bomb fuses and night vision systems
22 p4050 A70-43248
- Low noise GaAs Schottky barrier beam lead mixer and chip style diodes, discussing fabrication and performance
22 p3998 A70-43333
- Frequency multipliers with charge controlled junction diode model, predicting operational behavior
22 p3998 A70-43421
- Optimum junction area for maximum microwave output power of silicon IMPATT diodes for X band operation
23 p4167 A70-43775
- Microwave p-i-n diode RLC equivalent circuit parameters experimental determination
23 p4171 A70-43956

Current twisting in double injection ohmic contact long p-n diodes with S-shaped current-voltage curve, showing unstable density at negative resistance segment

23 p4176 A70-45061

Packaged microwave junction diodes in reduced-height waveguide, discussing parasitics and equivalent circuit parameters measurement technique

24 p4318 A70-45220

Variable microwave attenuator using p-n diodes and three-port hybrids built in stripline technique

24 p4318 A70-45222

High efficiency gallium arsenide IR illuminators, comparing dome diodes fabricated from diffused or Si doped solution grown materials

24 p4319 A70-45784

Carrier injection-limited Gunn diode wideband performance, deriving expression for admittance

24 p4319 A70-46081

Pb-Sn-Te junction diodes prepared by Sb diffusion, investigating spontaneous and laserlike emission

24 p4355 A70-46086

JUNCTION TRANSISTORS

Junction gate and MOS field effect transistors thermal noise calculations, using circuit analysis based on equivalent circuits

02 p0258 A70-12424

Field effect transistors with controlled p-n junction and metal-dielectric-semiconductor transistors investigated for radiation effects on physical and electrical properties

04 p0730 A70-14500

Competition mechanism for free carriers in junction isolated transistor collector suggested by current dependence of photocurrent

04 p0657 A70-14732

Transistor circuit design with junction compensation techniques to reduce transient gamma radiation effects

05 p0821 A70-16418

Bipolar n-p-n transistors fabrication to increase driving capabilities of complementary MOS transistors while retaining low power dissipation

05 p0821 A70-16419

Two dimensional numerical analysis of current saturation mechanism for junction field effect transistors with small and large length-to-width ratio values

09 p1740 A70-23110

Germanium p-n-p-m transistor frequency oscillation dependence on emitter current, noting forced air cooling effect

09 p1741 A70-23354

Steady state large signal computer model for junction-gate field effect transistors below pinch-off

11 p2019 A70-26711

MOS structures and transistors emission-current degradation mechanism at heterojunction under ionizing radiation

12 p2194 A70-27165

Neutron irradiation effect on n-channel GaAs junction FET performance, considering transconductance, drain current, pinch-off voltage and cut-off frequency

13 p2376 A70-28932

GaAs-Ge heterojunction transistors with microwave planar geometry, calculating performance for comparison with Ge homojunction transistor

14 p2556 A70-30925

UHF Si p-n-p transistors with low noise and high gain for small signal applications

14 p2557 A70-31161

Junction FET potential field and carrier distribution in channel investigated for current saturation mechanism

15 p2708 A70-31841

Junction and MOSFET transistors thermal noise characteristics at cryogenic temperatures

15 p2710 A70-32585

Large signal junction FET model involving piecewise linear approximation for ECAP circuit analysis program

15 p2711 A70-32596

Alloy junction transistors with emitter larger than collector, analyzing minority carrier distribution in base region and effect on current amplification

15 p2714 A70-32703

Neutron irradiation effect on unijunction transistors and SCRs, developing damage prediction technique

19 p3388 A70-37848

Visual binary state transistor tester for positive and negative logic circuits, illuminating lamp for specific logic states

21 p3801 A70-42244

Hybrid ion implanted diffused emitter n-p-n transistor two dimensional doping profiles, considering emitter oxide window edge shape effect

22 p3997 A70-42924

P- and n-channel MOS transistor instability during superbreakdown voltage application to drain electrode

24 p4319 A70-45811

JUNCTIONS

Cylindrical conical shell junction asymmetric bending, using numerical method and exact solution

15 p2822 A70-32360

Plasma-air junction problem in parallel plate waveguide, obtaining discontinuity admittance expression

22 p3994 A70-42350

JUPITER (PLANET)

Local thermal emission from Jupiter at 5 microns, discussing North Equatorial Belt and atmospheric transparency

01 p0173 A70-10043

Rotation period of Jupiter based on decametric component of radio emission, suggesting anticorrelation with sunspot number for drift observed

01 p0173 A70-10044

Internal powers and effective temperatures of Jupiter and Saturn measured by aircraft mounted telescope, noting restraints on planetary structure and atmosphere models

01 p0173 A70-10045

Atlas of near IR spectra of Venus, Mars, Jupiter and Saturn obtained by Fourier spectroscopy, discussing observational procedures, data recording and processing

01 p0173 A70-10078

Far UV spectroscopy of Jupiter by rocket-borne spectrograph

01 p0179 A70-10528

Giant planets structure, calculating Jupiter and Saturn densities using Russell solar mixture and internal heat from central core radioactivity

01 p0181 A70-10663

Io and Europa mass and density anomalies, indicating asteroid capture by Jupiter as comet origin theory

01 p0182 A70-10671

Jovian decameter radiation polarization during 1966-1967 apparition compared with cyclotron model predictions

02 p0364 A70-11793

Polarization observations of Saturn in UV and visible regions compared with Jupiter data, noting multiple scattering

02 p0368 A70-11818

Jupiter mass determined from observations of Jupiter fourth satellite right ascension and declination differences

02 p0370 A70-12087

Communications of lunar and planetary laboratory, Volume 6, covering Venus atmosphere and photography, Jupiter IR spectrum and Mars multicolor photometry

02 p0377 A70-12553

Jupiter radio telescope observations at cm wavelengths, describing radiation belt emission characteristics and planetary brightness temperature spectrum

03 p0565 A70-13233

Undiscovered satellites of solar system major planets, predicting Jupiter satellites

03 p0569 A70-13360

Jupiter observations /1966-1967/, discussing variations in size and position of polar caps and tropical belts

03 p0574 A70-13887

Circularly polarized synchrotron radiation from distribution of electrically charged particle in magnetic dipole calculated for estimating Jupiter magnetic field

04 p0746 A70-14511

Particle flux and dose rates in Jupiter Van Allen belts based on assumed synchrotron radiation from trapped electrons in dipole magnetic field

04 p0742 A70-15543

Jupiter capture of comets with parabolic orbits taking into account solar gravitational influence

05 p0905 A70-15757

Telescopic circular polarization observations of Jupiter at 9.26 cm related to Jovicentric declination of earth

05 p0906 A70-15896

Photographic photometry of Jupiter belts and zones at reflector Newtonian focus, presenting diagram showing intensity time variation

05 p0914 A70-16650

Circular polarization measurements of Jovian decimeter radiation by 210-ft radio telescope at Goldstone, California

05 p0921 A70-16986

Jovian decametric radiation periodicities analysis refuting evidence of Bigg for new Jovian satellites

06 p1138 A70-17280

Resonance in restricted three body problem applied to asteroidal motion in asteroid-Jupiter-system

06 p1152 A70-18492

Eccentric and inclined motions of satellite of spherical planet in planet centered coordinate system, applying formulas to Jupiter motion

07 p1374 A70-18693

Jupiter conductive molten metallic hydrogen core of moderate temperature suggested from solids melting point temperature dependence on pressure

07 p1390 A70-20238

Figure of gravitating inhomogeneous rotating liquid, applying results to Jupiter and Saturn model construction

08 p1564 A70-20558

Jupiter and Saturn IR reflection spectra observed with Michelson interferometer-spectrometer, eliminating effects of terrestrial atmospheric absorption, solar spectral lines, etc

08 p1570 A70-20895

Orbit analysis of hypothetical comets formed by Jupiter surface eruptions using Lagrange origin hypothesis

08 p1573 A70-21012

Modulation lanes in fine structure of dynamic spectra of Jovian L bursts possibly due to ionosphere or magnetosphere

08 p1576 A70-21394

Fine structure morphology in dynamic spectra of Jupiter decametric radiation determined from spectral recordings

08 p1562 A70-21514

Photometric profiles of Jupiter shadows cast by large natural satellites used as upper atmosphere probes

08 p1579 A70-21571

Jupiter decametric noise storm commencement time defining constant planetary rotation period

08 p1580 A70-21572

Jupiter radio telescope observations at cm wavelengths, describing radiation belt emission characteristics and planetary brightness temperature spectrum

08 p1580 A70-21666

Baseline measurements of Jupiter decametric radiation providing upper size limit to coherent and incoherent sources

09 p1755 A70-22512

Nongravitational effects, systematic residuals and close Jupiter approach problems in motions of comets

09 p1759 A70-22913

Bode law development from dynamical relaxation suggested from comparison of Jupiter, Saturn and Uranus inner satellite systems with planetary system

09 p1765 A70-23796

Jupiter decametric emission modulation by planetary rotation and Io position, suggesting role of magnetic tail diurnal swings

10 p1940 A70-24434

Short period hypothetical orbits distribution formed by flaring on Jovian satellites

11 p2109 A70-25925

Undiscovered satellites of solar system major planets, predicting Jupiter satellites

11 p2118 A70-26725

Jupiter decametric radio bursts observed by tape recording fringe interferometer

13 p2486 A70-28626

Replicating molecules on primordial earth, suggesting chemical evolution on Jupiter via demonstrable alpha-amionitriles synthesis

14 p2536 A70-30364

Fuel savings by Jupiter moon gravity assisted transfer trajectories from earth, considering initial energy, mass ratio, approach angle, timing and aiming errors

14 p2640 A70-30761

Jupiter luminosity as indication of internal energy magnitude, comparing limb darkening with predicted brightness distribution

14 p2643 A70-30984

Twelve year periodicities of Jupiter decametric radiation, noting correlation with Jupiter magnetic field rotation period

14 p2648 A70-31085

Lunar occultation observation of Jupiter by radio telescope, determining one dimensional strip brightness distribution

14 p2648 A70-31086

Jupiter decimeter radiation long term variations from flux density measurements, suggesting correlation with solar activity

14 p2648 A70-31087

Jupiter microwave spectrum from polarimetric observations and previous data

14 p2648 A70-31088

Synchrotron model involving electron trapping in dipolar magnetic field for Jupiter decimeter radiation

14 p2649 A70-31089

Figure of gravitating inhomogeneous rotating liquid, applying results to Jupiter and Saturn model construction

15 p2805 A70-32713

Jovian decimeter radiation, discussing electron drift velocity in dipole field, characteristic time for energy loss and radiation belt dimensions

16 p2980 A70-34192

Trojan asteroids in sun-Jupiter system, determining density near preceding Lagrangian point

17 p3171 A70-35445

Perturbative effects of Jupiter moons on spacecraft flyby and postencounter heliocentric trajectories, noting precision targeting

18 p3316 A70-36680

Jupiter decametric radio emission modulation by Io simulated by DC circuit model

18 p3321 A70-37120

Jovian continuum radiation observation by RAE-1 during lunar occultations

19 p3512 A70-38608

Pioneer-F Jupiter flyby mission planning, considering use of optimum broken plane trajectories to increase launch opportunity and/or payload capability [AIAA PAPER 70-1050] 19 p3528 A70-38865

Jupiter swingbys and multiplanet Jupiter swingby trajectory modes for outer planet missions, comparing in terms of passage conditions [AIAA PAPER 70-1071] 19 p3530 A70-38884

Jupiter RF spectrum in 80 to 10,000 MHz range for dipolar model, noting independent synchrotron component 21 p3891 A70-41185

Jupiter varied color surface area observations /1926-1964/ 22 p4107 A70-43594

Jupiter model thermal profiles, examining metallic core and molecular envelope in convective equilibrium 23 p4241 A70-44251

Jupiter perturbations on short period comets during close approaches, discussing orbital distribution 23 p4241 A70-44252

International photographic planetary patrol network, discussing filmstrips of Mars and Jupiter using blue, green and red filters 23 p4242 A70-44262

Jupiter flux density changes at 2695 MHz correlated with 10.7 cm solar activity, suggesting magnetic anomaly explanation 23 p4246 A70-44751

Jupiter surface drawings and photographs concerning quasi-periodic oscillations of red spot 24 p4411 A70-45800

Albedo and thermal emission of Jovian satellites I-IV at 3 to 12 micron wavelengths 24 p4413 A70-46171

JUPITER ATMOSPHERE

Jupiter and Saturn near IR spectra for relative abundances of atmospheric constituents and distribution with altitude, noting rough solar composition 01 p0179 A70-10526

Structure and composition of clouds of ammonia and water bearing condensates, investigating compositional models of Jupiter atmosphere, considering ammonium hydrosulfide cloud layer 01 p0179 A70-10527

Organic synthesis by electrical discharge in simulated Jovian atmosphere, noting appearance of orange-red cyanogen-ammonia polymer nonvolatile fraction 01 p0179 A70-10529

Spectroscopically active compounds observability in Jupiter atmosphere using solar composition adiabatic equilibrium model 01 p0180 A70-10530

Jovian polar zones enhanced optical transparency causes, discussing thin clouds and difference in molecular optical depth between north and south poles 01 p0180 A70-10531

Blunt and conical body optimum heat shield shapes for Jupiter atmospheric entry, noting shallow flight path [AIAA PAPER 68-1150] 01 p0195 A70-10827

Jupiter chemical composition and atmosphere, considering space probe experiments 01 p0185 A70-11047

Homogeneous scattering model for line formation applied to composition of Jupiter atmosphere 02 p0365 A70-11802

Model construction for structure of planetary atmospheres, particularly Jupiter, discussing gas pressure, density and temperature relationships 02 p0366 A70-11803

Aeronomy of Jovian upper atmosphere at pressures below 25 mb, discussing stratospheric heat sources, thermal emissivity, photochemistry of methane, ammonia, etc 02 p0366 A70-11804

Methane and ammonia absorption bands and possible structure of Jupiter and Saturn cloud layers by spectrophotometric observations 02 p0366 A70-11807

Pressure and line width estimate from high resolution image tube spectra of Jupiter at 11,000 Å 02 p0366 A70-11808

Rotational temperatures and methane abundances in Jovian atmosphere calculated for various Lorentz half widths 02 p0366 A70-11809

Variable distribution of ammonia absorption on Jupiter deduced from IR spectra, indicating scattering in cloud layer 02 p0366 A70-11810

Structure and composition of Jovian atmosphere, discussing hydrogen helium ratio, cloud colors, etc 02 p0367 A70-11811

Venus and Jupiter Aerobee rocket photoelectric UV spectra, determining geometric albedos using reflecting layer and cloud models 02 p0367 A70-11812

Two layer model of Jovian clouds including clear space, showing computed and measured equivalent widths of H quadrupole lines 02 p0367 A70-11813

Jupiter atmosphere temperature and density profiles determined from thermal models based on thermal structure above dense cloud level 02 p0367 A70-11814

Methane photochemistry in Jupiter atmosphere, investigating acetylene, ethylene and ethane photolysis 02 p0367 A70-11815

Absorption of EUV sunlight by Jupiter upper atmosphere, discussing photoelectron energy loss, thermal equilibrium and heating efficiencies 02 p0367 A70-11816

Phase diagrams for binary mixtures at high pressures suggesting layered structures existence in Jupiter and Saturn atmospheres resulting from phase separations in hydrogen-helium mixture 02 p0368 A70-11819

Ammonia spectral lines positions, intensities and half widths under Jovian conditions calculated, including ground state rotation and rotation inversion bands 02 p0368 A70-11820

Ammonia red and green bands measured line positions, strengths and half widths applied to Jupiter atmospheric pressure determination 02 p0368 A70-11821

Collision-narrowed growth curves for interpreting hydrogen quadrupole lines applied to photoelectric observations of Jupiter vibration-rotation bands 02 p0368 A70-11824

Decay times for thermal disturbances near cloud tops in Jupiter atmosphere, discussing hydrogen absorption 02 p0368 A70-11827

Jupiter upper atmosphere cloud bands zonal motion velocities, examining barotropic stability criterion and geostrophic balance hypothesis 02 p0368 A70-11828

Rotation periods of Jovian atmospheric currents showing zonal wind velocity variations with latitude 02 p0369 A70-11829

Ammonia absorption band at 6450 Å in Jovian atmosphere, clarifying controversial absorption time variations 02 p0375 A70-12428

Jovian surface elements spectral and color contrasts from spectrograms obtained between 3200- 4900 Å wavelengths 02 p0375 A70-12429

Jovian atmosphere photometric activity determination, showing time variation and difference in strength between Northern and Southern Hemisphere 02 p0375 A70-12430

Jovian cloud layer light and dark matter albedo determination, applying photographic equidensitometry 02 p0375 A70-12431

Jovian atmosphere convective energy magnitude determination for various atmospheric thicknesses and temperature gradients 02 p0375 A70-12432

IR spectrum of Jupiter with calibrations from laboratory studies of methane and ammonia bands 02 p0378 A70-12559

Cloud layer multiple scattering in Jovian atmosphere, discussing influence on Lorentzian contour of planetary absorption lines 03 p0574 A70-13882

Jupiter observations /1966-1967/, discussing variations in size and position of polar caps and tropical belts 03 p0574 A70-13887

Soviet book on Jupiter atmosphere covering structure, chemical composition, cloud cover, temperature conditions, etc 05 p0910 A70-16412

Methane abundance in Jovian atmosphere deduced from line equivalent widths, obtaining line intensity for J manifolds 05 p0919 A70-16940

Data on Jupiter chemical composition, internal structure and energy sources, discussing Jovian planets origin and role played by gas 07 p1386 A70-19487

Jupiter atmospheric properties on basis of spectrograms analysis 08 p1569 A70-20833

Jupiter geostrophy indicated by circulation, vorticity and Rossby number determined from Great Red Spot observations 08 p1580 A70-21573

Jupiter brightness temperature values and standard deviations from EHF radio telescopic observations 09 p1765 A70-23809

Absorption strengths of j-manifolds in R branch of Jupiter atmosphere methane band, discussing fine structure blending 10 p1919 A70-24473

Predicted Jupiter visual auroras investigated with high sensitivity spectrograph 10 p1947 A70-24993

Jupiter atmospheric composition, gas and dust cloud formation as clues to origin and evolution of solar system 11 p2108 A70-25654

Deuterium recovery in Jupiter atmosphere, describing equipment and techniques for hydrogen-helium gathering and processing 11 p2112 A70-26064

Spectrographic measurements of Jovian Red Spot and Southern Tropical Zone molecular absorption bands related to cloud cover density and depth 12 p2311 A70-28305

Hydrogen abundance in Jupiter atmosphere quadrupole line used in comparing jupiter and solar atmosphere C/H ratios 14 p2650 A70-31221

Data on Jupiter chemical composition, internal structure and energy sources, discussing Jovian planets origin and role played by gas 15 p2805 A70-32732

Jupiter atmosphere ammonia abundance from laboratory curves of growth analysis for ammonia bands 18 p3310 A70-35937

Spectrophotometry of methane and ammonia absorption bands indicating decrease toward Jupiter disk edge 18 p3323 A70-37140

Photolytic model of Jupiter belt excess temperatures and coloration compared to solid ammonia clouds, using IR and visual observations 19 p3513 A70-37410

Steady symmetric flow model for Jupiter cloud banded structure, representing variable concentration of condensing constituents with latitude 19 p3519 A70-38254

Environmental heat shielding for various sized Jupiter atmospheric entry probes [AIAA PAPER 70-1324] 24 p4429 A70-45941

JUPITER PROBES

Ground-based and onboard guidance and navigation systems for outer planet flyby missions concerning direct, Jupiter swingby and Grand Tour trajectories [AIAA PAPER 70-71] 06 p1104 A70-18194

Galilean satellites touring by Jupiter spacecraft, discussing orbit calculation and encounter geometry [AIAA PAPER 70-1070] 19 p3530 A70-38883

Jupiter swingby trajectory analysis for comet flyby and rendezvous missions, discussing approach velocity and payloads [AIAA PAPER 70-1074] 19 p3530 A70-38886

Jupiter Orbiting Vehicle for Exploration system for gathering Jupiter atmosphere, magnetic, radiation, gravitation, temperature, topography and interplanetary data 23 p4264 A70-45010

JUPITER RED SPOT

Jupiter Red Spot observed photographically in 1967-1968, correlating activity in southern component of South Equatorial Belt to spot size 01 p0180 A70-10532

Jupiter Red Spot continuous spectrum intensity distribution and methane/ammonia absorption between 3300-6500 Å 02 p0374 A70-12427

Spectrographic measurements of Jovian Red Spot and Southern Tropical Zone molecular absorption bands related to cloud cover density and depth 12 p2311 A70-28305

Jupiter Red Spot, explaining motion rate in terms of cellular convection in liquid hydrogen-helium layer 15 p2799 A70-31895

Jupiter Red Spot 1968-1969 photographic observations, discussing area darkness, longitude oscillation and acceleration 20 p3708 A70-39963

Jupiter red spot darkness parameter and solar activity as clue to Jupiter-solar relationship 24 p4402 A70-45391

Jupiter surface drawings and photographs concerning quasi-periodic oscillations of red spot 24 p4411 A70-45800

K

K BAND U EXTREMELY HIGH FREQUENCIES K LINES

X ray spectrometer for space science and laboratory research, presenting CrK spectrum and fine structure 01 p0092 A70-11172

K line profiles of Ca II for two component chromosphere, obtaining line source function and optical depth from steady state and radiative transfer equations 05 p0911 A70-16430

Red giants age and mass estimation based on K-line luminosities, noting role of metal abundance 06 p1139 A70-17416

Sunspots narrow and double K lines probable emission by quiescent type prominences 08 p1575 A70-21372

Violet K2 emission in H and K line cores of solar calcium ions using atmospheric model in state of motion 12 p2303 A70-27701

Calcium H and K lines core residual intensities in stars with quiet and active chromosphere, suggesting activity due to thermal gradient 12 p2303 A70-27702

X ray K spectra of Ti-Cr alloy for electron structure in titanium chromide phase region, discussing spectral intensities

13 p2435 A70-29375

Solar Ca II H and K lines formation, discussing double reversal, limb darkening, plage and spot lines and anomalous line ratios

13 p2494 A70-29481

Nitrogen K-L Auger spectrum high energy lines measurement by high resolution electron spectrometer

14 p2620 A70-31301

Fine structure in Ca II K line core, determining reduced high dispersion spectra at solar disk center

15 p2804 A70-32618

Hyades stars between F4 and K5, measuring chromospheric H and K emission lines dependence on bolometric luminosity

17 p3157 A70-34832

Solar chromosphere resonance lines, observing H and K line profiles of Mg ions

17 p3161 A70-34893

Sco X-1 X ray emission data from rocket-borne measurement, indicating Fe K-emission from high ionization states

21 p3873 A70-40667

Spinning cylindrical spicule model with radial and axial gradients in electron number and temperature forming Ca II K line

21 p3879 A70-40955

IR observation of chromospheric Ca II K-line during total eclipse of 7 March 1970

24 p4401 A70-45314

K-MESONS

K-mesons role in high energy cosmic ray muons angular distribution and nuclear interaction

09 p1748 A70-23731

Inertial and gravitational mass equivalence related to observation of anomalous K-meson decay

12 p2272 A70-27391

KA BAND

U EXTREMELY HIGH FREQUENCIES

KALMAN-SCHMIDT FILTERING

Apollo program navigation processing using Kalman optimal linear computer, emphasizing position vector and error matrix and command and lunar landing extrapolation module navigation

03 p0522 A70-13604

Optimum estimation equations as simple averaging extension, considering application to Kalman filtering in integrated space navigation system

03 p0522 A70-13608

Wiener-Hopf equation development and Kalman filter derivation using Leibnitz equation for differentiating integral

04 p0660 A70-15338

Kalman filtering techniques to identify aircraft lateral motion data

08 p1478 A70-20782

Pilot model based on Kalman filtering and optimal control, investigating evaluation for time stationary conditions and sine-wave tracking

10 p1823 A70-23894

Self optimizing Kalman filter for hybrid inertial air navigation systems, noting implementation on airborne digital computer

11 p2078 A70-25682

Kalman filtering applied to moving balloon position and velocity estimates related to upper atmosphere wind measurements by balloon-satellite experiment

11 p2025 A70-26206

Suboptimal nonlinear state estimation from noise corrupted measurements in ballistic trajectory, using simplified extended Kalman filter

11 p2028 A70-26303

Kalman filter modifications for spinning satellite attitude determination in elliptical orbit prior to apogee maneuver, using sun and IR earth sensors

11 p2028 A70-26304

Kalman filtering and differential correction techniques applied to T-33 flight test data for aircraft system parameters identification

11 p1982 A70-26323

Inertial hybrid navigation system optimization, discussing performance curves and numerical filters synthesis and error elimination

13 p2448 A70-28747

Free floating balloon position and velocity determination by satellite, using Kalman filter linear estimation theory

14 p2530 A70-30571

X-22 VTOL aircraft initial parameter, state and covariance matrix estimates by Kalman filter and smoothing algorithms

16 p2885 A70-33329

Recurrence scheme for parameter estimation by quasi-linear equations of motion method and Kalman filtering for nonlinear dynamical systems

16 p2887 A70-33349

Linear sequential Kalman filter for time correlated noise without state augmenting and measurement differencing demanding less computer sizing

16 p2887 A70-33350

Optimal Kalman tracking filter performance estimation for manned maneuvering targets

16 p2949 A70-34057

Recursive estimation and Kalman filtering for space vehicle trajectory tracking, using Doppler shift measurements

16 p2866 A70-34071

Kalman filter set for state vector and observation error variance estimation in discrete-time linear system, using empirical Bayes techniques [ALAA PAPER 70-1058]

19 p3395 A70-38873

Apollo program navigation processing using Kalman optimal linear computer, emphasizing position vector and error matrix and command and lunar landing extrapolation module navigation

21 p3848 A70-41127

Quasi-linearization relationship with Kalman filtering for nonlinear systems parameter estimation in process noise absence

21 p3845 A70-41749

KAMACITE

X-ray line broadening analysis for lattice damage in kamacite phase of Fe meteorites, evaluating particle size and elastic strain

05 p0915 A70-16828

Cliftonite occurrence, internal structure, orientation within kamacite and implications on origin of diamonds in meteorites

05 p0921 A70-17095

KAMAN MILITARY HELICOPTERS

U MILITARY HELICOPTERS

KANSAS

X ray diffraction analysis for composition and structure of meteorites found in Kansas, classifying as hypersthene and bronzite chondrites

05 p0912 A70-16466

KAOLINITE

Photointerpretation applications to kaolin deposit detection, railway tunnel collapse analysis and highway drainage

10 p1873 A70-24075

KAPOETA ACHONDRITE

Kapoeta howardite Xe abundance and isotopic composition for indications of extinct Pu 244 and I 129 decay

24 p4402 A70-45380

KARMAN VORTEX STREET

Karman theory extension to interference between parallel vortex streets, examining geometry of vortex configurations

03 p0406 A70-13274

Karman trail vortices tangential velocity decay measurement by hot film anemometer experiments

09 p1661 A70-22961

Karman vortex shedding phenomenon for flow rate measurement in channel or pipe

14 p2588 A70-31333

Drag estimation for circular cylinders at subcritical Reynolds numbers and subsonic speeds, using Karman vortex street theory for wake

23 p4131 A70-43894

Aeroelastic stability for circular cylindrical structures under periodic Karman vortex excitation

23 p4274 A70-44764

KC-135 AIRCRAFT

U C-135 AIRCRAFT

KELVIN TEMPERATURE SCALE

U TEMPERATURE SCALES

KEPLER LAWS

Optimum orbital transfer of material point subjected to reactive force with minimum mass loss, discussing Kepler motion kinematics

01 p0192 A70-11514

Generalized Keplerian orbits for large cylindrical satellites noting orbit stability

03 p0578 A70-14252

Binary star formation using singular solution of Kepler problem in general theory of relativity

04 p0755 A70-15355

Energy derivation for mechanics and thermodynamics with generalization to systems of more than two dynamic variables, considering transformations and Newton and Kepler laws

12 p2164 A70-27070

Keplerian integrals analogy to integrals of adjoint equations suggested by optimum space navigation trajectories considerations

12 p2261 A70-27834

Computer program for two body problem literal series expansions using Kepler functions with Bessel and Poisson series operation

14 p2638 A70-30702

Satellite path geometry along Keplerian elliptical orbit, taking earth flattening into consideration

18 p3312 A70-36167

Large planets mass determination based on Kepler law and gravitational effects

18 p3318 A70-37045

Resonant satellites geodesy, determining orbit perturbations and gravity constant via mean Kepler elements high speed analysis

24 p4408 A70-45540

KERATINS

Keratinocyte development on epidermal surface of female patient exposed to cosmetic UV irradiation with quartz lamp

01 p0029 A70-11406

KERNEL FUNCTIONS

Time independent kernel integral equations in dynamic contact problems of elasticity and mathematical physics

01 p0146 A70-11571

Quasi-linear stress-strain deviators relations in viscoelastic theory, indicating kernels and functions determinable from creep relaxation loading and deformation tests

02 p0390 A70-12804

Shallow shell theory, discussing equation kernels, reduction of boundary value problems to integral equations, potential theory application and transformation into Fourier series

03 p0589 A70-13338

Monograph on generalized transforms properties and asymptotic behavior, discussing kernel functions, Bessel functions, Laplace transforms, Hankel transforms, etc

03 p0519 A70-13650

Time-varying loads effect on linear elastically hereditary media described by generalized fractional-order exponential functions and Rzhantyn type viscoelastic kernels

05 p0946 A70-16954

Interference kernel discontinuities in integral equations relating amplitude of angle of attack and pressure distribution on T tail harmonically oscillating in subsonic flow

07 p1416 A70-20210

Paired integral equations of elasticity with kernels containing Legendre spherical harmonics, admitting exact solution in quadratures

08 p1544 A70-20960

Orthogonal polynomials in three dimensional contact problems without friction, discussing construction of kernels over finite and seminfinite intervals

08 p1594 A70-21634

Thermoelasticity problem for plane with rectilinear cut with constant temperature at initial moment of time, using approximating kernel of integral equation

10 p1965 A70-25296

Subsonic kernel function applicability limited to surfaces with small inclinations to freestream, considering wing with deflected control surface

12 p2212 A70-28089

Burger turbulence model late decay statistical analysis using kernels of Cameron-Martin-Wiener expansion of random velocity field

13 p2386 A70-28820

Shallow shell theory, discussing equation kernels, reduction of boundary value problems to integral equations, potential theory application and transformation into Fourier series

14 p2657 A70-30716

Linear compressibility assumption incorporated into third order multiple integral representation of nonlinear creep of polyurethane, reducing time independent kernel functions

17 p3186 A70-34972

Paired integral equations of elasticity with kernels containing Legendre spherical harmonics, admitting exact solution in quadratures

20 p3672 A70-39382

Exponential kernel approximation effect on radiative energy transfer in high temperature hydrogen plasma

20 p3684 A70-40278

Radiation shield design and transport calculations, reviewing kernel methods development and relevant computer programs

23 p4217 A70-43811

KEROSENE

Excess air ratio and heat release efficiency in combustion of kerosene mixture determined by volumetric gas analysis

10 p1968 A70-24283

Oxygen-kerosene combustion product composition and characteristics in engine thermodynamic design allowing for intermolecular interaction forces

10 p1968 A70-24284

Jet A kerosene deposit accumulation problem and proposed SST fuel tank design [SAE PAPER 700256]

18 p3214 A70-36825

Oxygen-kerosene fuel combustion products thermodynamic properties, tabulating computed values

21 p3865 A70-41771

KERR CELLS

Picosecond on-off light gate based on Kerr cell design, using optical pulses to induce birefringence in liquids

01 p0111 A70-10571

Electro-optical shutter for optical pumping experiments using Kerr cell controlled by high voltage modulator

07 p1286 A70-19972

Kerr cell-shuttered high speed stigmatic spectrograph for shock tube electron density distribution measurement

09 p1682 A70-23503

KERR EFFECTS

Kerr physical optics formula usefulness for calculation of radar reflectivity of metallic bodies of revolution in terms of electric and magnetic dipoles

02 p0262 A70-12598

Einstein equations solved for steady axisymmetric physical schemes by varying Kerr metric constants, considering electromagnetic field case

22 p4073 A70-42717

KERR ELECTROOPTICAL EFFECT

Pulse propagation inside laser cavity containing amplifying medium and material displaying optical Kerr effect, predicting ultrashort pulses

01 p0113 A70-11177

Collapsing beam transition into self focusing light channel numerically analyzed allowing for Kerr effect saturation, multiphoton absorption and stimulated Raman scattering

04 p0650 A70-15285

Intense light beams self focusing in nonlinear media with quadratic Kerr effect, assuming spherical initial phase front after passing through condensing lens

07 p1296 A70-18720

Photographic still and high speed cameras, using Kerr effect electro-optical shutters with transmission line structure

14 p2589 A70-31404

KERR MAGNETOOPTICAL EFFECT

Magnetic holography, considering Faraday and polar Kerr effect reconstructions and potential as computer storage

22 p3994 A70-43608

KETENES

Bonding scheme of C-O in ketene described by localized orbital technique

08 p1455 A70-20682

Ketene and diazomethane flash photolytic measurement of reaction rates of singlet-triplet methylene deactivation

15 p2694 A70-31729

KETONES

NT ACETONE

Synthesis of 1-oxacyclopent-1-enyl cations from cyclopropyl ketones on heating in strong acids noting rearrangement rates

04 p0646 A70-15088

Computer program to decide structure for aliphatic ketone from low resolution mass spectrum using DENDRAL algorithm

05 p0810 A70-16048

Dialkyl ketone ion in double McLafferty rearrangement, applying ion cyclotron resonance to structural study

08 p1454 A70-20525

Evidence against electron impact induced alkyl shifts in mass spectra of alpha-hydroxy-ketones, showing thermal rearrangements

13 p2363 A70-29803

Electron impact promoted phenyl migration of trans phenylacetalone, considering mass spectrometry and stereochemistry

14 p2544 A70-30189

Oxadiazolone pyrolytic and photolytic fragmentation, noting intramolecular cyclizations and intermediate azomethine nitrene production

17 p3041 A70-34771

KIDNEYS

Acid mucopolysaccharides in distal segments of medullary substance of kidneys of rodents under high ambient temperature, showing stable morphological characteristics

07 p1204 A70-19141

Erythropoiesis inhibitor in blood from rabbit kidney vein during hyperoxia in nitrogen-oxygen atmosphere

14 p2535 A70-30155

Prolonged transverse acceleration effects on rats kidney and posterior hypophysis neurosecretions

20 p3575 A70-40188

Oxidative enzymes histochemistry in nervous system, liver and kidney of rats in immediate and remote periods after 24-hr artificial hypobiosis

21 p3764 A70-41478

Adrenocorticotrophic hormone effect on oxygen tension in rabbit kidney

24 p4301 A70-45845

Structure and function of juxtaglomerular apparatus of kidneys controlling synthesis and secretion of renin

24 p4305 A70-46392

KIMBERLITE

U BIOTITE

KINEMATIC EQUATIONS

Geometrical interpretation of motion of body about fixed point in Hess case based on Kharlamov kinematic equations, using special coordinates system

01 p0144 A70-11428

Laminar boundary layer in incompressible liquid, noting effect of variation of kinematic viscosity and density on stability

03 p0468 A70-13870

Spacecraft orientation control system optimization by plotting controlled motion kinematic models

13 p2501 A70-28417

Poisson kinematic equations solution of symmetric gyrost at in viscous medium for free rotor and constant angular speed, using perturbation technique

23 p4220 A70-44560

KINEMATICS

NT BODY KINEMATICS

Statistical analysis of position angles of Berenice cluster galaxies, estimating mass, expansion, rotation period and age

02 p0376 A70-12448

Noctilucous clouds morphological and kinematic characteristics based on photographs

03 p0476 A70-13885

Nonlinear thin shell theory kinematics generalized in terms of physical strain and surface deformation and geometry

04 p0766 A70-14450

Kinematic characteristics of annular-blank elements extruded by pulsed magnetic fields, noting proportionality to energy stored in capacitor bank

05 p0857 A70-17018

H I gas and H II regions kinematics, comparing radial velocities near galactic center

06 p1149 A70-18459

Cloud base updraft field, three dimensional reflectivity pattern and rain and hailfall pattern for thunderstorms in Alberta, discussing shear

06 p1099 A70-18569

Automatic system of kinematic analysis [ASKA], based on matrix displacement finite element method, applied to structural strains calculations

07 p1417 A70-20362

Proportional navigation law three dimensional vectorial equation analyzed in kinematic conditions, discussing perturbation effects on linearized trajectory

09 p1720 A70-22420

Telemetric systems for moving machine elements tests, discussing seven channel PFM and FM/FM systems

11 p2056 A70-26451

Complex vector parametrization of Lorentz group in relativistic kinematics, discussing Wigner rotation, Lorentz transformation and particles classification during scattering

13 p2453 A70-29722

Viscometric Poiseuille or Couette flow kinematics, considering nonuniform shear rate

14 p2567 A70-31282

Terminal kinematic variables prediction for missile homing, discussing line of sight angle, rate and acceleration

15 p2773 A70-32525

Book on continuum mechanics covering tensor kinematics, energy balance, virtual work, constitutive equations, etc

16 p2987 A70-32914

Kinematics of M 33, M 51 and large Magellanic cloud/LMC/

18 p3326 A70-37157

B stars kinematic parameters determination from radial and tangential velocities

19 p3525 A70-38775

Gravity effects on impact damper performance, investigating dynamic stability and kinematic viability of various steady state motion solutions

20 p3717 A70-38974

Noctilucous cloud kinematics, examining wave structure and lengths, velocities and general motion

20 p3622 A70-39403

Kinematically unsteady aerodynamic coefficients consistent with stiffness and inertia properties of lifting surface in supersonic flow by finite element method

24 p4287 A70-45154

Beltrami flows on spherical surfaces, using scalar equations from kinematic conditions

24 p4326 A70-45990

KINESTHESIA

Head movement effect on accuracy of visual and kinesthetic localization for free and fixed head conditions

05 p0803 A70-16669

KINESTHESIS

U PROPRICEPTION

KINETIC ENERGY

Euler-Poisson equations application to motion of heavy solid body about fixed point to determine kinetic momentum vector relative to fixed reference system

01 p0145 A70-11434

Turbulent mixing and supersonic combustion theories applied to internal flow, comparing various mixers and relating mixing intensity to kinetic energy of turbulence

02 p0399 A70-12045

E layer kinetic energy viscous dissipation and transfer to potential energy by turbulence and irregular winds shear

02 p0327 A70-12292

Dissipation spectrum /viscous dissipation of turbulent kinetic energy as function of wave number magnitude/ data compared and plotted

02 p0327 A70-12294

Kinetic energy of atomic motions for vitreous and crystalline high polymers measured by differential scanning calorimetry and thermal analysis

02 p0253 A70-12522

Momentum-energy complex obtained for nonlocalized fields in variational mechanics, deriving in-

tegral differential identities for Euler equations quadratures

05 p0881 A70-16078

Kinetic, potential and dissipative energies computed in systems of randomly excited coupled oscillators, using Liapunov stability method

05 p0821 A70-16407

Conservation equation for thermal energy in turbulent shear flow, including turbulence kinetic energy equation terms

[WSCIPAPER 69-43]

06 p1179 A70-17983

Solid state laser kinetic regime as function of diffusive and directional motions of active medium excitations

07 p1299 A70-19860

Damped isotropic turbulence kinetic and temperature fluctuation energy spectra, neglecting viscosity and molecular heat conduction

08 p1483 A70-20961

Troposphere-stratosphere kinetic energy transfer during 1967-1968 midwinter warming, comparing calculation by pressure interaction term with direct calculation of vertical velocity fields

08 p1540 A70-21969

General relativistic expressions for angular momentum and rotational kinetic energy of slowly rotating stars

09 p1764 A70-23608

Reagent translational energy effect on dynamics of ionic and atomic reactions, using nuclear recoil and chemical accelerator methods

11 p1995 A70-26005

Scanning Fabry-Perot interferometer for plasma diagnostics, determining kinetic temperatures

12 p2231 A70-27215

General relativistic hydrodynamics near equilibrium, discussing velocity and kinetic energy increase spherically symmetric large masses as function of radius change

12 p2300 A70-27392

Steady state EPR signal I kinetic behavior in wild type Chlamydomonas reinhardtii and in mutant strain AC-206 lacking cytochrome 53

12 p2168 A70-27468

Energy and canonical momentum relationship in relativistic mechanics, discussing particle production and annihilation

13 p2453 A70-29721

Troposphere-stratosphere kinetic energy transfer /1964-1968/, annual variations and vertical flux correlation to circulation pattern

15 p2722 A70-31441

Transverse kinetic energy of electrons at outlet of magnetron-injection gun as function of cathode inclination and magnetic induction

15 p2707 A70-31504

Kinetic energy turbulence spectrum in free atmosphere from rawinsonde and aircraft data

15 p0000 A70-32369

Solar wind observations by Pioneer 6, considering particle density, flux and kinetic energy

16 p2972 A70-32949

Kinetic energy and pressure distribution of three dimensional compressible fluid flow, using invariant transformation of Euler motion equation

16 p2890 A70-33073

Kinetic energy correction factor for nonuniform flow at Vena Contracta, using experimental data and modified Bernoulli equation

16 p2892 A70-33639

Turbulent shear flow velocity and kinetic energy distributions in tunnel

18 p3241 A70-36383

Coordinates for diagonalizing kinetic energy of particle system relative motion, discussing potential energy surface

19 p3373 A70-37841

Atmospheric zonal kinetic energy balance for Northern Hemisphere, assuming frictional destruction due to stresses across horizontal surfaces

20 p3661 A70-39145

Damped isotropic turbulence kinetic and temperature fluctuation energy spectra, neglecting viscosity and molecular heat conduction

20 p3608 A70-39383

Base function selection for energy calculation optimal convergence conditions of frequencies and stresses in turbomachine blades vibrations

20 p3722 A70-39784

Turbulent shear stress correlation with turbulent kinetic energy for wake and circular jet flow conditions

20 p3613 A70-40277

KINETIC EQUATIONS

NT HELMHOLTZ VORTICITY EQUATION

NT HYDRODYNAMIC EQUATIONS

NT KINEMATIC EQUATIONS

Oscillations and decomposition of diatomic gas molecules at high temperatures during atom-molecule collisions, deriving kinetic equations for energy level changes

01 p0148 A70-11630

Electron distribution function for steady homogeneous plasma of arbitrary ionization degree under strong

electric fields, discussing kinetic equations for elastic and nonelectric encounters

02 p0346 A70-12231

Kinetic equation describing variation of distribution function of stellar residual velocities under action of gravitational field, discussing stellar diffusion in velocity field

03 p0564 A70-13227

Boltzmann-type kinetic equation for homogeneous electron plasma in uniform magnetic field, describing relaxation to thermal equilibrium by convergent collision integral

05 p0888 A70-16329

Stratified cloud transport and evolution, solving kinetic equations by numerical method

06 p1053 A70-17210

Numerical methods for solving Boltzmann gas kinetics equation, assessing various methods effectiveness

06 p1036 A70-17752

Spatially homogeneous distribution function describing uniform gas motion derived to permit computer calculations in obtaining numerical solutions to kinetic equation

06 p1036 A70-17753

Kinetic Boltzmann equations for spatially uniform two component gas mixture solved with allowance for relaxation processes, assuming differing temperatures

06 p1109 A70-17754

Interplanetary plasma flow past earth and planets simulation using kinetic equations

06 p1147 A70-18292

Shock wave structure in He-Ar mixture velocity and temperature profiles based on kinetic model equations

06 p1051 A70-18346

Gravitating particles systems equilibrium states, solving kinetic equations for sphere and cylinder in isotropic and anisotropic cases

07 p1389 A70-20207

Kinetic theory equations for completely ionized plasma taking into account Diener method

08 p1550 A70-20615

Kinetic equation describing variation of distribution function of stellar residual velocities under action of gravitational field, discussing stellar diffusion in velocity field

08 p1580 A70-21660

Correlation functions of fluctuations in electrical characteristics of nonequilibrium electron gas during scattering, determining spectral densities and populations by kinetic equation Green function

08 p1554 A70-21806

Kinetic equation for nonlinear interaction of waves, including unstable or damped, using Bogoliubov method

09 p1659 A70-22214

Plasma, Coulomb fields and radiation correlations obtained by relativistic kinetic equations, noting bremsstrahlung, synchrotron, cyclotron radiation, radiative and particle diffusion, etc

09 p1736 A70-23182

Interplanetary medium kinetic equations to limit ion temperature anisotropies in solar wind, discussing Coulomb collisions and ion-cyclotron instability effects

11 p2105 A70-26561

Coupled lasers kinetic operating characteristics, discussing emission power damping

12 p2246 A70-27315

Kinetic equation for electron plasma based on BBGKY hierarchy reducible to set of equations with structure similar to Pines-Schrieffer equations

13 p2458 A70-28561

Vibration spectra, kinetic and dispersion equations of solid spherical particles moving in incompressible weakly viscous liquid

13 p2388 A70-29368

Plasma kinetic equation, expressing interaction term as sum of binary collisions between close and collective interactions among remote particles

14 p2625 A70-31297

Turbulent kinetic energy equation for determining turbulent flow fields applied to free mixing problem of constant density streams

16 p2894 A70-33856

Kinetic equation for rarefied polyatomic gases derived from Liouville equation

17 p3138 A70-35728

Kinetic effects of Barnett equations and slip conditions for continuous dense gas flows at small Knudsen numbers

18 p3239 A70-36256

Luminescence decreases in laser active medium operating in free emission mode, using kinetic equations for integral and spectral level populations

18 p3267 A70-36615

Kinetic equation in strong electric fields, describing current carrier behavior in semiconductors

19 p3483 A70-37293

Kinetic equations derivation for correlation functions and time dependent distribution functions of irreversible processes, using projection operators

20 p3672 A70-39588

Alfven magnetoacoustic waves interaction, deriving kinetic equation for distribution function and relaxation time

20 p3678 A70-39597

Annealing properties of radiation damage in lithium-diffused silicon, formulating kinetic equation to describe processes associated with recovery and instability

20 p3687 A70-40165

Transverse and longitudinal current correlations in fluids from modeled kinetic equations, noting inelastic neutron scattering from liquids

24 p4378 A70-45261

KINETIC FRICTION

NT SLIDING FRICTION

Kinetic friction and friction induced vibration measurements by pin-on-disk tribometer [ASME PAPER 70-LUBS-15]

22 p4044 A70-42446

KINETIC HEATING

NT AERODYNAMIC HEATING

NT SHOCK HEATING

Simulated Concorde kinetic heating system for ground studies of thermal stresses

07 p1250 A70-19744

Radiative heating rates and gas environments effects on ablative material performance from tests at arc image facility

07 p1319 A70-19888

Kinetic temperature estimate for solar corona based on time profile of type 3 bursts

08 p1565 A70-20565

Kinetic temperature estimate for solar corona based on time profile of type 3 bursts

15 p2805 A70-32720

Kinetic heating of spacecraft surfaces, emphasizing materials and fluid circulation cooling devices

18 p3333 A70-36654

KINETIC THEORY

NT CHAPMAN-ENSKOG THEORY

NT MIXING LENGTH FLOW THEORY

NT TRANSPORT THEORY

Enskog method for Boltzmann equation, analyzing asymptotic nature of integral kinetic equation for molecular mean free paths and Laplace probabilities

01 p0068 A70-11568

Molecular rotations and kinetics from spectral features of molecular Raman spectra, using light scattering spectroscopy

02 p0343 A70-12077

Dynamic electric field in solar coronal exosphere on basis of kinetic and hydrodynamic theories, giving estimate of solar wind

02 p0359 A70-12609

Kinetic theory of cracks network formation on LiF crystal surface exposed to plasma jet using high speed camera

04 p0730 A70-14458

Kinetic theory of thermal conduction in collisionless Knudsen gas in arbitrary closed systems with various geometries, establishing similarity law [ASME PAPER 69-WA/HT-20]

04 p0783 A70-14814

Kinetic theory for calculating electron distribution function of weakly ionized plasmas in arbitrarily time dependent electromagnetic fields

05 p0886 A70-15800

Kinetic analysis of ion-molecule reactions in Ar-N mixtures with H, deuterium and HD using ion ejection mode of ion-cyclotron-resonance spectroscopy

06 p1108 A70-17332

Kinetic theory of longitudinal ionic oscillations pertaining to LF plasma oscillations monitored in Ariel 1 satellite wake due to ions trapped in potential trough

06 p1120 A70-17591

Kinetic theory of plasma waves in magnetic field, covering small amplitude waves in infinite homogeneous plasma, limiting cases, etc

06 p1121 A70-17902

Kinetic flow regime in hypersonic flow past flat plate leading edge, using Boltzmann equation [AIAA PAPER 70-181]

06 p0970 A70-18094

Kinetics of solar wind interaction with moon and planetary bodies using perturbation scheme to obtain ion density distribution on antisolar side [AIAA PAPER 70-61]

06 p1136 A70-18192

Kinetic theory applied to free flow in spherical geometry to study collisionless thermal escape of particles from planetary atmospheres

06 p1147 A70-18293

Statistical models in kinetic theory for describing gases ranging from gas with no internal degrees of freedom to multicomponent reacting mixtures

06 p1047 A70-18312

Spatial and temporal relaxation problems approximate solution in kinetic theory, making calculations for Maxwellian molecules and hard spheres

06 p1047 A70-18318

Unsteady nonlinear molecular flow problems concerning plane Couette flow, heat transfer between parallel plates and density discontinuity propagation solved by Monte Carlo method

06 p1113 A70-18321

Kinetic theory treatment of linearized Rayleigh problem using wall boundary condition models

06 p1049 A70-18329

Kinetic theory study of shock wave structure in rotationally relaxing diatomic gases

06 p1050 A70-18339

Kinetic model equation for shock structures in rotationally relaxing gas with internal degrees of freedom

06 p1050 A70-18340

Normal shock wave structure in binary gas mixtures of chemically inert monatomic molecules, using kinetic theory moment method

06 p1051 A70-18343

Kinetic theory of rarefied supersonic flow over finite plate, calculating molecular velocity distribution functions for flowfield

06 p0981 A70-18356

Thermal molecular flow kinetic theory, discussing anisotropic distribution function, thermal transpiration, thermal conduction, entropy production, etc

06 p1113 A70-18369

Superposition of dressed particles in plasma kinetic theory proved by using generalized stochastic equation for conditional probability density for one particle

06 p1124 A70-18500

Kinetic theory of laser emission on direct band-band semiconductor transitions

07 p1299 A70-19853

Kinetic theory equations for completely ionized plasma taking into account Diener method

08 p1550 A70-20615

Diener kinetic theory for charged particles in EM field with Coulomb interactions taking into account transverse plasma waves

08 p1550 A70-20616

Kramer problem in kinetic gas theory and gas dynamics applied to Boltzmann equation, discussing uniqueness theorem [ONERA-TP-776]

08 p1486 A70-21845

Soviet monograph on growth rate of coagulating and condensing aerosol particles, considering kinetic theory

09 p1713 A70-22205

Neutrinos kinetic theory for anisotropic cosmological models

09 p1753 A70-22453

Kinetic model for acid catalyzed Delrin decomposition, testing for Delrin-citric acid system and predicting thermograms with nonlinear regression analysis

09 p1630 A70-22896

Kinetic theory applied to model of interaction between two gas flows colliding at sharp leading edge at different hypersonic speeds

10 p1800 A70-24139

Transition regime of rarefied gas dynamics using kinetic theory of gases, discussing Couette and Poiseuille flow, heat transfer and time dependent problems

10 p1919 A70-24141

Dissipative parameters determination for relativistic gas within kinetic theory framework based on particle interaction model, assuming constant differential effective interaction cross section

10 p1867 A70-24148

Pulsed solid state laser power output stability in terms of kinetic theory noting laser action threshold role

10 p1899 A70-24254

Book on plasma dynamics covering charged particle orbit theory, macroscopic equations, hydromagnetics, hot and cold plasma waves, kinetic theory and plasma radiation

11 p2087 A70-25500

Kinetic theory for fatigue crack propagation using cyclic stress-strain relation in connection with strain hardening characteristics

12 p2322 A70-27208

Kinetic theory of gas composed of identical particles with discrete velocity distribution, using Chapman-Enskog method

12 p2213 A70-28211

Sheath structure of plasma diode using kinetic theory model of plasma-sheath transition

13 p2376 A70-28642

Kinetic theory of cracks network formation on LiF crystal surface exposed to plasma jet using high speed camera

13 p2510 A70-28655

Bipolar moment integral in celestial mechanics formed by product of particle kinetic moments for n body problem order reduction

13 p2494 A70-29399

Many body correlation and conditional probability functions of plasma shield clouds surrounding test particles

14 p2623 A70-31034

Kinetic gas theory mathematical models, analyzing system of N particles in cube

14 p2601 A70-31422

Soviet monograph on gas laws in aviation medicine for reduced oxygen pressure pathology, discussing kinetic theory, temperature effects, solubility, diffusion, etc

15 p2682 A70-31925

Kinetic theory of fatigue crack propagation, discussing stochastic nucleation process and power exponent relation

16 p2992 A70-33968

Generalized Lagrange kinetic potentials, discussing force systems with ideal holonomic constraints
16 p2944 A70-34292

Soviet book on rarefied gas dynamics involving methods and approaches for kinetic description of gas behavior, emphasizing Boltzmann equation
17 p3067 A70-34604

Rarefied gas dynamics at different Knudsen numbers, discussing elements of kinetic theory and analyzing free molecular and slip flows
17 p3070 A70-35037

Dilute gases kinetic theory, discussing microscopic explanation of macroscopic properties under intermolecular forces
17 p3072 A70-35533

Kinetic theory of moderately dense gases, obtaining generalized Boltzmann equation
17 p3072 A70-35534

Thermal diffusion of isotropic, nonisotropic and multicomponent mixtures with monatomic and polyatomic molecules, considering kinetic theory and experimental results
17 p3197 A70-35537

Tonks-Dattner resonances in warm inhomogeneous plasma column, examining kinetic theory for waveform shapes and resonance location
19 p3475 A70-37534

Relativistic kinetic theory of gases, considering phase space quantum statistics, Liouville equation, Boltzmann equation, conservation laws, kinematics, equilibrium distributions, etc
19 p3404 A70-37594

Intercomponent momentum and energy exchange in weakly ionized gases, examining kinetic theory of subsonic and supersonic transport processes
19 p3482 A70-38945

Soviet book on diffusion kinetics in stationary media covering membranes, combustion, flame propagation, hydrodynamics, exothermal reactions, thermodynamics, heat transfer, thermal explosion, insulation, etc
20 p3673 A70-39800

Nitrogen viscosity coefficient at high pressure, describing viscosimeter operation and kinetic theory calculations
20 p3738 A70-40140

Electromagnetic wave propagation in colloidal plasmas analyzed by kinetic approach, obtaining expressions for current density, DC and microwave conductivities, etc
20 p3685 A70-40502

Shock and expansion waves formation by moving piston based on kinetic theory of gases, solving Bhatnagar-Gross-Krook equation by numerical method
21 p3808 A70-41377

Book on electrical probes for plasma diagnostics covering kinetic theory, carrier distribution, current characteristics, plasma resonance, etc
21 p3829 A70-41790

Stochastic kinetic theory for plasma turbulent heating by random fields, predicting acceleration effects
21 p3859 A70-41899

Minimum entropy production in kinetic theory of rarefied gases described by Boltzmann equation
21 p3850 A70-41957

Wind temperature measurement, taking Bernoulli effect and kinetic theory into account
22 p4009 A70-42525

Convolution equation for kinetic theory of EM field excitation in plasma waveguides
23 p4223 A70-43772

Plasma kinetic theory, applying Boltzmann equation, Lorentz gas model and relaxation method
23 p4224 A70-44177

Plasmas kinetic theory, considering crossing from instability to stability, waves decay by collisional damping and emission by bremsstrahlung
23 p4224 A70-44178

Kinetic transport theory for mixed dilute gases consisting of linear rotating diamagnetic molecules in external homogeneous magnetic field
23 p4223 A70-44927

Diabatic steady gas flow vorticity, examining various kinematic and kinetic properties
24 p4328 A70-46365

KINETICS
NT ELECTROKINETICS
NT KINETIC ENERGY
NT NEWTON SECOND LAW
NT NEWTON THEORY
NT REACTION KINETICS
NT VARIABLE MASS SYSTEMS

Kinetic processes in plasma subjected to randomly fluctuating electric field, obtaining chain of single particle distribution functions
07 p1349 A70-19553

Linear kinetic theory for condensation and evaporation at small Knudsen numbers, considering extrapolated temperature jump determination
07 p1422 A70-19656

Kinetic theory of laser emission on band impurity transitions, noting spatial homogeneity effect on laser mode
07 p1299 A70-19852

Mechanical system undergoing internal mass redistribution, showing energy dissipation during motion
08 p1545 A70-21203

Perturbed gyroscopic system consisting of disk hinged by rigid weightless rod, investigating stability condition at axial and equatorial inertia moments
08 p1496 A70-21210

Metallic materials homogeneous and nonhomogeneous corrosion kinetics based on superposition principle of independent partial electrode reactions
09 p1707 A70-23422

Excited gas kinetic state determination from observed spectral profiles during interaction with radiation
10 p1919 A70-24147

Kinetics for two free radical conversion processes in electron irradiated D, L-valine, measuring activation energies by electron spin spectroscopy
14 p2544 A70-30111

Growth kinetics of strengthening phase during aging of Ni-Cr-W-Mo-Al-Ti alloys, considering gamma prime particles at different Al/Ti ratios
14 p1594 A70-30169

Molecular Markov processes application to vibrational relaxation and dissociation, small system kinetics, nucleation and droplet growth, thermalization kinetics and diffusion processes
14 p2619 A70-30615

Kinetic processes in plasma subjected to randomly fluctuating electric field, obtaining chain of single particle distribution functions
15 p2777 A70-31460

Linear kinetic theory for condensation and evaporation at small Knudsen numbers, considering extrapolated temperature jump determination
15 p2828 A70-32693

Soviet papers on kinetics and aerodynamics of fuel combustion processes covering supersonic flow, flame stabilization, fluid atomization, nonequilibrium recombination, etc
20 p3736 A70-39265

Carbon monoxide-nitrogen system vibrational distribution of populations and kinetics in fundamental and harmonic regions, investigating vibroluminescence
21 p3837 A70-41718

KIRCHHOFF LAW
Kirchhoff kinematic analogy applied to solution of gyrostat motion, noting elastic rod deformation under torsion, using Kharlamov equations
01 p0094 A70-11441

KIRCHHOFF LAW OF RADIATION
Optically dense high temperature flame pyrometric diagnostics based on modified Kirchhoff formula
10 p1967 A70-24251

Kirchhoff law validity for freely radiating metallic surfaces, using emissometer to measure hemispherical emittance
16 p2999 A70-33903

KIRCHHOFF-HELMHOLTZ FLOW
U PIPE FLOW

KIRCHHOFF-HUYGENS PRINCIPLE
U DIFFRACTION
U WAVE PROPAGATION

KIRKENDALL EFFECT
Kirkendall effect in Fe-Ni and Fe-Co systems using measurement of radiotracer and intrinsic diffusion coefficients
07 p1314 A70-20015

KITE BALLOONS
U TETHERED BALLOONS

KITS
Civilian survival in emergency situations, discussing basic requirements, environments, vehicles and equipment for survival kits
23 p4153 A70-44495

KLYSTRONS
Frequency shift and FM noise of uncontrolled Gunn effect diode and reflex klystron oscillators
05 p0818 A70-15774

Wobulator measurement of Q factor of microwave resonator cavities using double modulated klystron signal
05 p0822 A70-16528

Optimal electron bunching in two cavity klystron by varying parameters and nonlinear one dimensional approximation
05 p0823 A70-16888

Convection currents calculation in multicavity klystron allowing for space charge forces influence
05 p0823 A70-16889

Klystron amplifier output circuit large signal frequency response, showing dependence on distance between cavities
06 p1021 A70-17672

Klystrons operation at millimeter band, using efficiently bunching drift fields for steady power output at critical wavelength
09 p1651 A70-23636

Millimeter band direct-transit klystrons oscillation and amplification at improved output power obtained by electron bunching in nonuniform drift fields
09 p1651 A70-23637

Electrode curvature effect in radial reflex klystron on processes in electron bunching region
09 p1651 A70-23640

Microwave tubes for high power transmission from space to ground and in deep space communications, discussing klystrons, TWT and crossed field amplifiers
11 p2016 A70-25456

Coupled microwave oscillators interaction, discussing klystron operation regenerative and non-monotonic frequency pulling modes
12 p2196 A70-27847

Radar spectrum control based on two pulse shaping techniques using klystron transmitter
12 p2188 A70-27941

Sum and difference frequency signals generated and propagated by mixing carbon dioxide laser and millimeter wave klystron outputs in GaAs loaded waveguide
12 p2250 A70-28098

Electrostatically focused klystron design, discussing gain, bandwidth, efficiency, noise and reliability
13 p2379 A70-29666

CW traveling wave tubes and klystrons LF output signal fluctuations
14 p2555 A70-30303

Millimeter and submillimeter waves applications, discussing klystron oscillators for spectral purity and coherence
14 p2548 A70-30427

Reflex klystrons operation, efficiency and electronic tuning range, discussing resonators, tuners, voltage and retarding field oscillators, etc
14 p2548 A70-30428

Coulomb force effect on electron beam spatial charge for optimal three resonator transit type klystron, regarding buncher length
15 p2707 A70-31507

Single gap klystron output resonator optimization, showing maximum electronic efficiency during bunched beam excitation
17 p3055 A70-35681

External SHF signal effects on multifrequency spectrum of reflex klystron coupled with long waveguide
17 p3055 A70-35682

Multifrequency oscillator system with reflex klystron loaded by waveguide line, confirming spectrum conversion under action of SHF signal
20 p3598 A70-40299

Polar microwave interferometer using single null path bridge and klystron repeller voltage modulation
22 p4048 A70-42323

Multifrequency autooscillatory systems, comparing reflex klystron with He-Ne laser
22 p3995 A70-42404

Automatic frequency control device for power klystron with two cavities, obtaining stabilization at natural frequency of crystal-containing cavity
22 p3998 A70-43236

Klystron microwave signal generator power stabilization using compact low consumption integrated circuits
23 p4170 A70-43797

Superheterodyne EPR spectrometer microwave bridge using single X band klystron
23 p4170 A70-43798

KNEE [ANATOMY]
Sinusoidal test for measuring knee moment increase required to flex and extend for various conditions of knee angle, angular velocity and steady knee moment
02 p0238 A70-12546

Knee joint walking mechanics, calculating forces transmitted by joint tissue
07 p1205 A70-19246

Muscle function mechanics across knee joint in walking, relating tension to length, velocity and energy absorption
19 p3368 A70-37810

KNOOP HARDNESS
Macroscopic internal stresses in plastics surfaces, discussing stress effect on plastic moulding service life, Knoop hardness test and charts
11 p2132 A70-25597

KNOWLEDGE
NT PARADOXES
NT PHILOSOPHY

KNUDSEN CELLS
U KNUDSEN GAGES

KNUDSEN FLOW
Volumetric flow rate of rare gases, hydrogen and deuterium between parallel plates at various pressures and Knudsen numbers
04 p0665 A70-14414

Kinetic theory of thermal conduction in collisionless Knudsen gas in arbitrary closed systems with various geometries, establishing similarity law
04 p0783 A70-14814

Boltzmann equation at arbitrary Knudsen numbers and kinetics of polyatomic molecule gases
06 p1047 A70-18310

Nonlinear Knudsen layer gas flow using BGK model for Boltzmann equation
06 p1048 A70-18322

Rarefied gas shear flow over infinite plane wall, using Boltzmann-Krook-Welander equation to determine compressibility effect on Knudsen layer
06 p1048 A70-18327

Linear kinetic theory for condensation and evaporation at small Knudsen numbers, considering extrapolated temperature jump determination
07 p1422 A70-19656

Macroscopic properties of thermal molecular flow between coaxial cylinders and concentric spheres, using transpiration theory in Knudsen gas
09 p1788 A70-22906

Near-free molecular flow through orifice measured for velocity distribution dependence on Knudsen number and angular position using time-of-flight technique
10 p1918 A70-23969

Boltzmann equation for Knudsen layer and outer region of weakly rarefied gas flow
15 p2777 A70-32131

Linear kinetic theory for condensation and evaporation at small Knudsen numbers, considering extrapolated temperature jump determination
15 p2828 A70-32693

Rarefied gas dynamics at different Knudsen numbers, discussing elements of kinetic theory and analyzing free molecular and slip flows
17 p3070 A70-35037

Kinetic effects of Barnett equations and slip conditions for continuous dense gas flows at small Knudsen numbers
18 p3239 A70-36256

Knudsen effusion in free molecular flows in supersonic jet during expansion through circular orifice, discussing power and heat transmission
18 p3346 A70-36379

Narrow capillary supermolecular flow density relation to vapor molecule specular reflection, considering Knudsen flow conditions
24 p4381 A70-45491

Plate temperature jump and heat flux in Knudsen layer using Bhatnagar-Gross-Krook model
24 p4429 A70-45997

KNUDSEN GAGES

Knudsen effusion cells high temperature uses, discussing binary alloys phase boundary determination and volume and surface diffusion studies
07 p1424 A70-19900

Isothermal reaction rate determination at given temperature from nonequilibrium data illustrated on Knudsen cell vaporizations
07 p1424 A70-19901

Vapor pressures and dissociation energy of yttrium dicarbide and tetracarbide over extended temperature, measured by Knudsen double focusing spectrometer
16 p2858 A70-34015

KNUDSEN NUMBER

U KNUDSEN FLOW

KOLMOGOROFF THEORY

Kolmogoroff constant determined by Heisenberg turbulence formula and model for transfer of turbulent energy between different wave numbers
06 p1034 A70-17467

Prandtl-Kolmogoroff model of turbulence with inclusion of second order terms for stress and velocity gradient not to vanish coincidentally
08 p1484 A70-21458

Differential Pulse Code Modulation (DPCM)/system with quantizer separating slope overload and granular noise, using Fokker-Planck-Kolmogorov equation
10 p1844 A70-25204

Universal constant measurement methods in Kolmogoroff third hypothesis for high Reynolds number turbulence in wind over open ocean
23 p4184 A70-44980

KRONECKER PRODUCT

U ORTHOGONALITY

KROOK EQUATION

Couette problem for Krook kinetic equation solution, considering shear stress variation at high plate velocities
04 p0672 A70-15228

Plane Couette flow and heat transfer problem numerical solution, using Krook kinetic equation and Maxwell boundary condition
06 p1048 A70-18326

Rarefied gas flow past sphere, using integral iteration method for Krook equation
07 p1187 A70-18675

Rarefied gas flow past sphere, using integral iteration method for Krook equation
15 p2671 A70-31467

Krook gas particle collision model for relaxation from nonequilibrium to equilibrium Boltzmann distribution in spatially uniform gases
17 p3068 A70-34697

Computerized evaluation of Krook kinetic relaxation equation approximating Boltzmann nonlinear integral equation for rarefied gas motion
21 p3851 A70-42201

KRYPTON

NT KRYPTON ISOTOPES

NT KRYPTON 85

Ar-Kr integral collision cross sections based on density measurements of Ar beam passed through liquid nitrogen cooled Kr filled scattering chamber
07 p1344 A70-20135

Specific heat, thermal pressure and molar volume of liquid krypton measured with adiabatic calorimeter, discussing thermal expansion coefficients
14 p2617 A70-31016

KRYPTON ISOTOPES

NT KRYPTON 85

Isotopic composition and contents of xenon and krypton in Pesyanoe meteorite suggesting presence of solar type gas component
04 p0754 A70-15274

Stone meteorites age determination from decay of cosmic ray produced Kr 81 and 78, comparing production rate to He 3 ages
08 p1563 A70-20499

KRYPTON 85

Surface adsorbed and absorbed radioactive Kr 85 gas for displaying surface microdefects in materials
20 p3638 A70-39950

KU BAND

U SUPERHIGH FREQUENCIES

L

L BAND

U ULTRAHIGH FREQUENCIES

L-1011 AIRCRAFT

Design and economic concepts of Lockheed L-1011 wide body trijets, discussing airport and airway congestion alleviation, passenger appeal, etc
04 p0623 A70-15044

Vehicle System Simulator (VSS) test program for L-1011 Tristar encompassing primary and secondary flight controls, avionics, hydraulics and landing gear systems
10 p1861 A70-24917

L-1011 aircraft payload, range, configuration, engine selection, design features, equipment systems, flight characteristics, internal arrangement, maintenance and performance
15 p2673 A70-31947

Boeing 747, L-1011 and DC-10 introduction costs, profits and terminal facilities
19 p3357 A70-38951

L-1011 onboard system for gross weight and center of gravity determination, describing transducers placement, computer design and display panel
20 p3562 A70-40359

L-1011 aircraft optimum minimum noise pod design, describing technology, restraints and system requirements
24 p4393 A70-45877

LABELING (MARKING)

U MARKING

LABORATORIES

NT ENGINE TESTING LABORATORIES

NT ENVIRONMENTAL LABORATORIES

NT LUNAR MOBILE LABORATORIES

NT LUNAR RECEIVING LABORATORY

NT MANNED ORBITAL LABORATORIES

NT MANNED ORBITAL RESEARCH LABORATORIES

NT SPACE LABORATORIES

R and D laboratories quality and performance evaluation techniques, describing Apstein-modified Pelz technique
06 p1185 A70-17603

Laboratory experiments applicability to interplanetary plasma physics, describing simulations of solar wind interactions, magnetosphere, collisionless shock waves, etc
17 p3164 A70-35123

LABORATORY EQUIPMENT

Student development and exercising of electron physics principles by designing, assembling, operating and studying electron and ion devices
01 p0093 A70-11291

Digital systems design laboratory as instructional tool and experimental model for education
02 p0275 A70-12190

Lidar and IR radiometer mobile laboratory for atmospheric optics research, including construction details and support equipment
03 p0463 A70-13677

Vacuum-type thermionic laboratory diode featuring variable electrode spacing, interchangeable electrodes and guard-ring structure
04 p0628 A70-15400

Automatic laboratory or field testing equipment design requirements
13 p2423 A70-29695

Time shared computer system providing real time service to multiple laboratory instrumentation, discussing high speed channel, computer control and data abstracting techniques
13 p2375 A70-29830

Computer merits in test laboratory data acquisition systems
19 p3383 A70-37921

LABYRINTH

NT COCHLEA

NT VESTIBULES

Medicopsychological and labyrinthine exploration of flight crew candidates aeronautical adaptation, using electronystagmographic method of swinging chair
17 p3041 A70-35918

Labyrinthine and sensory information role in driving, discussing car simulator, driver tests with impaired inputs, age factors, etc
22 p3976 A70-43708

LABYRINTHECTOMY

Quantitative characteristics of central compensatory process, investigating nystagmus responses in guinea pigs subjected to bilateral labyrinthectomy
06 p0995 A70-17806

LACTATES

Oxygen uptake increase following sodium L-lactate isomer infusion into anesthetized dogs
02 p0233 A70-11721

Lactate rise diminution in anesthetized paralyzed dogs subjected to hypoxia by gas mixtures before and after beta-adrenergic blockade
02 p0233 A70-11724

Lactate accumulation and anaerobic work threshold in subjects exercised on bicycle ergometer, considering muscle contraction effect on oxygen supply
03 p0431 A70-14293

Blood lactate changes during prolonged exhaustive running at varied intensities and durations
10 p1809 A70-24001

Serum lactate dehydrogenase (LDH) isoenzyme in males before and after muscular exertion, observing change in skeletal muscle and liver fraction
10 p1809 A70-24002

Hypoxia diagnosis based on excess lactate determination as indicator of oxidative metabolism changes
10 p1822 A70-25084

LACTIC ACID

Oxygen consumption, lactic acid production and mechanical performance of anesthetized dog gastrocnemius muscle with increased blood flow
02 p0235 A70-12090

LACTOSE

Chemostat culture method for studying control mechanisms during utilization of glucose/lactose and glucose/L-aspartic acid by populations of Escherichia coli
01 p0021 A70-10787

LAG (DELAY)

U TIME LAG

LAGRANGE COORDINATES

Lagrangian nonenergetic and unconstrained systems introduced in describing Birkhoff classical dynamics, considering space of motions states as connected analytic manifold
10 p1909 A70-24190

Transient flow of viscous incompressible fluids with free surfaces calculated using Lagrangian coordinates
12 p2210 A70-27425

Mechanical-stereomechanical analogy of two index Lagrange equations of second kind
17 p1330 A70-35192

Trojan asteroids in sun-Jupiter system, determining density near preceding Lagrangian point
17 p1371 A70-35445

Gravitational variable constant in celestial mechanics, considering theories based on vacuum Jordan Lagrangian
18 p3320 A70-37066

Plane galactic orbits near spiral field particle resonance, calculating numerically for ring orbits librating near maxima at Lagrangian points
18 p3331 A70-37193

Lagrange time scale of air turbulence from photographic measurements of smoke aerosol particle dispersion in horizontal direction across mean wind
19 p3460 A70-37416

Nonlinear Lagrangians in relativistic cosmology of open oscillating world model
24 p4404 A70-45409

LAGRANGE EQUATIONS OF MOTION

U EULER-LAGRANGE EQUATION

LAGRANGE MULTIPLIERS

Necessary and sufficient conditions for constrained extrema without use of Lagrange multipliers
07 p1325 A70-19335

Indirect methods of trajectory optimization, improving convergence through normalization of state data and Lagrange multipliers
07 p1326 A70-19726

Apportionment optimization of reliability and maintainability by Lagrange multipliers and dynamic programming, discussing maintainability cost model and computerized simulation
09 p1792 A70-22211

Sufficiency conditions and Lagrange multipliers in maxima and minima theory with results restricted to ordinary extremal points, considering constrained optimization
11 p2073 A70-26232

Conforming plate bending solution with third degree polynomial deflection functions in triangular finite elements, using Lagrange multipliers as stress parameters
11 p1243 A70-26642

Coordinate systems generation for optimal trajectories, considering Lagrange multiplier as motion constant 14 p2651 A70-31368

Linear systems with phase coordinates bounded by given time functions, obtaining optimal control by iterative solution involving Lagrange multipliers 23 p4177 A70-44302

LAGRANGE SIMILARITY HYPOTHESIS

Strain rate tensor coincidence in Lagrangian and Eulerian descriptions of turbulence demonstrated for homogeneous flow of incompressible fluid 07 p1252 A70-18672

Semi-Lagrangian formulation of Vlasov equation in two and three dimensional electrostatic problems, investigating tensor determinants and perturbation 08 p1553 A70-21614

Strain rate tensor coincidence in Lagrangian and Eulerian descriptions of turbulence demonstrated for homogeneous flow of incompressible fluid 15 p2718 A70-31464

Generalized Lagrange kinetic potentials, discussing force systems with ideal holonomic constraints 16 p2944 A70-34292

Vibration of combined cylindrical shells via Lagrangian minimization regarding unknown boundary values 21 p3934 A70-40897

Lagrange formulation for deriving energy-conserving numerical approximations for Vlasov plasmas 22 p4080 A70-42750

LAGUERRE FUNCTIONS

Cross coupling relations in Boltzmann equations solution for inhomogeneous plasmas, using spherical harmonics expansion and Laguerre-Sonine polynomials 13 p2464 A70-29539

LAKES

Lake Toba, Sumatra as possible tektite source region based on surrounding welded tuffs composition 21 p3923 A70-41996

LALLEMAND CAMERAS

Shifts method applicability to electronic camera for stellar magnitude photometry, studying instrument limitations and errors 14 p2589 A70-31379

LAMB WAVES

Lamb wave techniques using guided ultrasonic waves for solid cylindrical objects nondestructive testing 01 p0098 A70-10019

Lamb waves behavior applied to defect evaluation in nondestructive tests of solid elongated cylindrical objects 02 p0276 A70-12552

Plane Lamb problem in semiinfinite micropolar elastic body solved by transformation to one-dimensional wave propagation problem in elastic half space 05 p0925 A70-15785

Rayleigh and Lamb waves propagating on solid and hollow elastic cylinders immersed in water, noting correspondence to symmetric and antisymmetric vibrations in shell 05 p0938 A70-16410

LAMBERT LAW

U BOUGUER LAW

LAMBERT SURFACE

Lambert problem solution for moderate timespan arcs by approximation, offering concise formula without iteration 14 p2639 A70-30705

Horizontal Situation Display (HSD) map computer mechanization transforming earth location to X, Y coordinates for Lambert conformal projection [AIAA PAPER 69-987] 22 p4068 A70-42710

LAME FUNCTIONS

Elastic equilibrium of quasi-completely regular rectangular parallelepiped with rigidly clamped lateral faces, obtaining Lamé equations in double Fourier series 04 p0765 A70-14418

Finite difference theory applied to first boundary value problem of elasticity theory for Lamé equation 18 p3280 A70-36158

Spatial problem of elastic spherical transversal isotropic medium solved by reducing Lamé equations 22 p4118 A70-43481

LAME WAVE EQUATIONS

Forced longitudinal oscillations of cylinder with given surface displacements, using Lamé equations 22 p4118 A70-43571

LAMELLA

Lamellae stresses and magnetostriuctive effects on magnetic properties of titanomagnetite and ilmenomagnetite series minerals 15 p2728 A70-31993

Twinned lamella formation in Nb single crystals, examining slip and shear roles in surface tilt formation 15 p2761 A70-32382

Morphology of adult mammalian thoracic and abdominal aortic segments indicating deviation from medial lamellar architecture 24 p4298 A70-45801

LAMINA

U LAYERS

LAMINAR BOUNDARY LAYER

Laminar boundary layer analysis of heat and mass transfer in dispersed two phase flow over heated surface 01 p0214 A70-10293

Flow about blunt wedge with laminar boundary layer at stagnation point and approaching Falkner-Skan flow at infinity, discussing asymptotic behavior 01 p0061 A70-10540

Hypersonic dissociated laminar boundary layers with/without heat transfer calculated by integral method for case of thermodynamic equilibrium 01 p0003 A70-10933

Three dimensional instability of perturbed conducting fluid laminar boundary layer flow on concave walls in transverse magnetic field, analyzing various Hartmann numbers 01 p0152 A70-10934

Thermal conditions and graph-analytic solution of laminar boundary layer combustion of disk rotating in free atmosphere and plate in Couette flow 01 p0218 A70-11017

Diffusion coefficients for laminar multicomponent dissociating boundary layer at surfaces of thermally decomposing protective coatings 01 p0042 A70-11583

Parametric approximation method extended to incompressible laminar boundary layers with surface suction or injection 02 p0277 A70-11857

Laminar and turbulent boundary layer equations with or without wall injection over two dimensional or axisymmetric bodies solved by finite difference techniques 02 p0287 A70-12370

Transient heat transfer in forced convection flow over curved wall with zero Prandtl number, applying to laminar boundary layer with variable free stream velocity 02 p0400 A70-12857

Boundary layer transition from laminar to turbulent in hypersonic wind tunnel, determining Reynolds and Mach number effects [ONERA-TP-737D] 03 p0467 A70-13641

Pressure gradient calculation in three dimensional laminar boundary layer, using method of local similarity 03 p0468 A70-13869

Laminar boundary layer in incompressible liquid, noting effect of variation of kinematic viscosity and density on stability 03 p0468 A70-13870

Asymptotic solutions of paraboloidal boundary layer system for thermally driven convective flows governed by nonlinear Boussinesq equations 03 p0519 A70-14077

Similarity properties of laminar or turbulent boundary layer separation in uniform supersonic flow, discussing wall cooling, pressure evolution, etc 03 p0469 A70-14234

Free convective flows above flat horizontal plate demonstrating laminar boundary layer existence at intermediate Grashof numbers, using semifocusing color schlieren photography 04 p0780 A70-14456

Boundary layer equations for axial laminar and turbulent incompressible flows over slender bodies of revolution solved by finite difference method [ASME PAPER 69-WA/FE-2] 04 p0667 A70-14786

Integral relations and finite difference methods application to problems of boundary layer equations in gas dynamics 04 p0670 A70-14962

Boundary layer along flat plate at zero incidence with homogeneous suction using momentum and kinetic energy integral equations through boundary layer velocity profile 04 p0615 A70-15052

Fluid mechanical problems with pressure distribution determined by interaction between external supersonic inviscid flow and inner laminar viscous layer 04 p0674 A70-15529

Incompressible laminar Falkner-Skan boundary layer suffering sudden acceleration by moving belt, noting boundary layer separation [AIAA PAPER 69-40] 04 p0674 A70-15534

Asymptotic expansion method to analyze laminar boundary layers with zero wall shear, large suction and adverse pressure gradients 04 p0674 A70-15563

Hypersonic laminar separation of slip flow on slender cone with attached compression flares, using surface pressure measurements and Pitot surveys [DFVLR-SONDDR-26] 04 p0620 A70-15577

Heat and mass transfer in reacting laminar boundary layer over porous cylinder with propane injection in wind tunnel experiments 05 p0956 A70-16289

Laminar flow stability along flexible boundary on basis of Orr-Sommerfeld equation 05 p0836 A70-16923

Two dimensional laminar and turbulent boundary layer flow theory covering heat and mass transfer, compressibility, turbulence, roughness, chemical reactions and axial symmetry 06 p1032 A70-17227

Numerical integration of equations of motion of three dimensional laminar compressible boundary layers [DVL-915] 06 p1033 A70-17229

Laminar sublayer resistance to momentum and heat transfer, noting effects of Prandtl number and surface roughness using mathematical model and experiments 06 p1034 A70-17680

Laminar natural convection boundary layer stability over vertical uniform flux surface, measuring disturbance temperature and velocity distributions 06 p1035 A70-17686

Unheated solid starting length effect on skin friction and heat transfer characteristics in incompressible transpired laminar boundary layer on flat plate 06 p1035 A70-17691

Heat and mass transfer across laminar boundary layer around stagnation line of cylinder in crossflow affected by free stream turbulence intensity 06 p1176 A70-17693

Laminar ablation testing under turbulent boundary layer heating conditions, obtaining recession rate and heat of ablation for turbulent ablation of Teflon [AIAA PAPER 70-226] 06 p1179 A70-18071

Integral moment method for interactions between laminar boundary layer and external supersonic flow applied to hypersonic laminar boundary layer near sharp expansion corner [AIAA PAPER 70-186] 06 p1039 A70-18111

Rotation and forward flight effects on separation line of laminar incompressible boundary layer along helicopter blade of airfoil shape [AIAA PAPER 70-49] 06 p0973 A70-18151

Laminar viscous flow on rotating propeller and helicopter rotor blades, studying crossflow and unsteady boundary layer effects, separation, transition, etc [AIAA PAPER 70-50] 06 p0974 A70-18161

Laminar boundary layer on cone at incidence in supersonic flow evaluated by pressure distribution technique, comparing heat transfer, pitot probe measurements, etc [AIAA PAPER 70-48] 06 p0974 A70-18189

Laminar boundary layer in hypersonic flow calculated by integral method, including effects of entropy gradient and induced pressure gradient [ONERA-TP-784] 06 p0984 A70-18468

Laminar boundary layer development on cylindrical body set in motion from state of rest, determining time for boundary layer separation occurrence 07 p1253 A70-18771

Heat transfer on supersonic sweptback wing for case of laminar boundary layer with vortex distribution 07 p1187 A70-18921

Unsteady laminar boundary layers calculation for arbitrary velocity distributions at inner boundary in presence of suction/blowing through porous surface 07 p1254 A70-19080

Nonsimilar laminar boundary layer solutions with negative pressure gradient compared to experimental boundary layer velocity profiles, momentum and displacement thicknesses [AIAA PAPER 69-35] 07 p1256 A70-19312

Laminar boundary layer critical height determination using Rouse stability parameter 07 p1257 A70-19336

Heat exchange in laminar and turbulent boundary layers on plate for arbitrary heat flux distribution allowing for initial unheated plate segment 07 p1423 A70-19657

Integrodifferential equation derived for energy balance in laminar boundary layer of fluid flow, taking into account viscous energy dissipation, radiative energy transfer, etc 07 p1423 A70-19813

Laminar boundary layer equations solution by approximation compared with results from finite difference method 08 p1483 A70-21033

Incompressible laminar boundary layer stability of incompressible fluid for nonparallel oncoming flow, deriving perturbed motion equation 08 p1483 A70-21179

Laminarization parameter magnitude determination for turbulent boundary layer in convergent channel flow 08 p1484 A70-21518

Heat transfer in axially symmetric laminar viscous boundary layer flow due to rotating bodies of revolution, obtaining temperature distribution 08 p1485 A70-21698

Blasius flow stability on deformable surface of membrane using Orr-Sommerfeld equation to calculate amplitude of function for perturbation flow 09 p1658 A70-22182

Heat and mass transfer coefficients in binary laminar boundary layer convection obtained with integral equations and Karman-Pohlhausen method 09 p1787 A70-22264

Thermal conditions and graph-analytic solution of laminar boundary layer combustion of disk rotating in free atmosphere and plate in a Couette flow

09 p1787 A70-22266

Steady laminar gas flow on duct wall boundary layer considering external swirling flow and wall heat transfer

09 p1659 A70-22428

Acoustic pressure sensors positioning on bodies of revolution to determine laminar boundary layer stability loss during ideal liquid flow at nonzero angles of attack

09 p1660 A70-22479

Laminar separation bubble in incompressible flow produced on flat plate by pressure gradients, correlating bursting with Reynolds number and pressure distribution

09 p1660 A70-22770

Laminar boundary layer in adverse pressure gradient calculated for momentum thickness from approximate equation, analyzing error

09 p1660 A70-22832

Stability theory application to laminar boundary layer transition prediction on two dimensional and axisymmetric flows having pressure distributions in incompressible flow

[AIAA PAPER 69-10] 09 p1662 A70-23219

Laminar boundary layer separation noting effect of mass slot suction

09 p1662 A70-23236

Laminar boundary layers behavior in shock tube flows behind primary moving shock wave using perturbation method

09 p1662 A70-23281

Hypersonic laminar boundary layer in strong viscous interaction region on wedge, determining velocity and enthalpy profiles, displacement thickness and induced pressure distributions, etc

09 p1606 A70-23294

Magnetic field effect on free convection in laminar boundary layer formed by laminar flow of viscous conducting fluid along vertical wall

09 p1737 A70-23308

Laminar boundary layer parameters on porous surface in presence of pressure gradient obtained for inner / wall/ and outer regions

09 p1664 A70-23712

Laminar-turbulent boundary layer transition in incompressible fluid under surface roughness action, developing theory by generalizing Taylor hypothesis

09 p1664 A70-23713

Flat plate laminar boundary layer blowoff due to wall injection analyzed by parameter matched asymptotic expansion

10 p1862 A70-23844

Laminar boundary layer with blowing through wedge surface, solving linearized motion equation analytically

10 p1862 A70-23868

Vorticity distribution influence on inviscid laminar jet boundary layer instability investigated for large Reynolds numbers, using shear flow and linearized theory

[DFVLR-SONDDR-14] 10 p1868 A70-24163

Laminar boundary layer flow of incompressible fluid in wake of symmetrical disturbance, deriving higher order approximations and introducing Euler transformation

10 p1802 A70-24420

Unsteady compressible laminar boundary layer flow around flat plate influenced by compressibility as function of Mach number

[ONERA-TP-803] 10 p1869 A70-24543

Laminar boundary layer in symmetry plane of cone of revolution at angle of attack calculated by finite difference method

10 p1802 A70-24706

Laminar boundary layer characteristics in axisymmetric hypersonic nozzle calculated by finite difference method

10 p1804 A70-25187

Nonuniform partitioning of flowfield in three dimensional laminar boundary layer in supersonic conical flow at zero angle of attack, using numerical integration

10 p1804 A70-25192

Monograph on stability of laminar boundary layer separation at free jets and turbulent free jet flames, considering effects of velocity gradients and temperature

11 p2146 A70-25499

Axisymmetric or two dimensional incompressible laminar boundary layer flow field numerical analysis using quasi-linearization and Chebyshev series

11 p2072 A70-25965

Laminar boundary layer behind normal shock wave with vaporization and combustion, obtaining profiles on analog computer

11 p2148 A70-25967

Laminar boundary layer flow with exponential velocity distribution in outer flow described by differential equations, studying slip velocity at wall

11 p2037 A70-26350

Laminar boundary layer equations solved for mass and energy transfer in binary gas mixture, investigating forced and free convection

11 p2151 A70-26558

Simultaneous heat and mass transfer coefficients in laminar free convection boundary layers on horizontal cylinders or vertical axisymmetric bodies

11 p2151 A70-26559

Laminar boundary layer transition to quasi-cellular flow in natural convection above horizontal heated plates and disks

12 p2155 A70-27197

Newtonian fluid laminar boundary layer flow over flat plate with nonNewtonian fluid injection

12 p2209 A70-27212

Laminar boundary layer and heat flux at forward stagnation point of indestructible body in partially ionized air flow calculated as function of enthalpy

12 p2156 A70-27287

Radiation profiles in ablating flat plate air-Teflon laminar boundary layer, discussing visible, UV and IR wavelengths

12 p2211 A70-27803

Interaction of laminar hypersonic boundary layer and supersonic corner expansion wave, discussing upstream influence, transverse pressure gradients and external flow

[AIAA PAPER 69-137] 12 p2211 A70-27826

Similar laminar boundary layer solutions exhibiting separation, pressure gradient and mass transfer

12 p2211 A70-27828

Subsonic, transonic and supersonic laminar boundary layers acceleration and cooling effects, discussing heat transfer and gas enthalpy

12 p2211 A70-27830

Three dimensional laminar boundary layer equations for body of revolution at angle of attack in supersonic gas flow derived for equations

12 p2158 A70-28198

Incompressible two dimensional and axisymmetric oscillating laminar boundary layer flows approximated by momentum integral equation, discussing flow along flat plate

12 p2158 A70-28205

Laminar multicomponent boundary layer for large injection and heat transfer, with particular reference to vehicle entry into planetary atmosphere

12 p2159 A70-28234

Laminar boundary layers in low density supersonic and hypersonic conical and axisymmetric nozzles, treating displacement, transverse curvature, velocity slip and temperature jump

[AIAA PAPER 69-653] 13 p2386 A70-28513

Flow equations for curvilinear boundary layer based on laminar incompressible boundary layer in streamwise corner

13 p2386 A70-28541

Laminar MHD boundary layer equations at nonconducting surface, determining flow core parameters influence on boundary characteristics

13 p2462 A70-28967

Spatial distribution of three dimensional laminar boundary layer transition zone on sharp half angle cone from hypersonic wind tunnel tests

[AIAA PAPER 69-12] 13 p2343 A70-29953

Planview shadowgraph method for observing disturbances generated by spark discharges into laminar boundary layer

13 p2385 A70-29982

Unsteady incompressible laminar boundary layer equations solution after Crocco transformation by implicit finite difference scheme for flow around blunt body

14 p2528 A70-30290

Flow velocity distributions in laminar boundary layer by perturbation methods

14 p2566 A70-30850

Two dimensional incompressible laminar boundary layers asymptotic structure with injection, obtaining velocity profiles

14 p2566 A70-30995

Prandtl number effects on adiabatic wall temperature and pressure gradient at separation point for hypersonic compressible laminar boundary layer

14 p2566 A70-31027

Laminar boundary conditions for heat transfer in gradient flow region for plane turbulent jet impingement on plate normal to flow

15 p2721 A70-32134

Boundary layer equations for laminar flow, drag and heat transfer of gas in circular tube, considering parabolic and uniform entrance velocity profiles

15 p2722 A70-32692

Heat exchange in laminar and turbulent boundary layers on plate for arbitrary heat flux distribution taking into account initial unheated plate segment

15 p2828 A70-32694

Laminar compressible boundary layer similar solutions for axisymmetric blunt body, considering viscosity and density variations

16 p2833 A70-33123

Laminar boundary layer model for viscous losses during transient turbulent liquid flow in tube, assuming slug flow for core

[ASME PAPER 70-FE-8] 16 p2891 A70-33627

Laminar and turbulent boundary layer equations solutions for incompressible/compressible flows about two dimensional and axisymmetric bodies, using finite difference method

[ASME PAPER 70-FE-A] 16 p2892 A70-33641

Laminar compressible flat plate boundary layer dependence on Prandtl number and viscosity-temperature relations

16 p2893 A70-33673

Nonreacting and chemically reacting laminar flows, calculating equilibrium, nonequilibrium and ideal gas laminar boundary and viscous shock layers over hypoboloid

[AIAA PAPER 70-808] 17 p3005 A70-34456

Laminar hypersonic boundary layer interaction with corner expansion wave, presenting numerical solutions to viscous-inviscid equations for small turning angles

[AIAA PAPER 70-807] 17 p3065 A70-34457

Laminar boundary layer transition on sharp cone at zero yaw in supersonic wind tunnels, correlating aerodynamic noise disturbances with transition Reynolds numbers

[AIAA PAPER 70-799] 17 p3006 A70-34462

Fluctuation measurements at wall and across laminar, transitional and turbulent compressible boundary layers on flat plate, using hot film probes

[AIAA PAPER 70-745] 17 p3066 A70-34498

Unsteady laminar boundary layers on infinite porous plate, considering radiative heat transfer and transpiration cooling

17 p3067 A70-34632

Numerical solutions for velocity and concentration profiles to nonsimilar isothermal diffusion laminar boundary layer equations for uniform injection of foreign gas

17 p3069 A70-34824

Incompressible laminar boundary layer, determining thermal conductivity gradient effect on temperature profiles

17 p3070 A70-35045

Incompressible laminar boundary layer along rectangular corner, obtaining similar solutions for velocity distribution

17 p3070 A70-35239

Heat exchange in dissociating partly ionized gas flow over critical point on permeable surface with injection into laminar boundary layer

17 p3011 A70-35347

Laminar free convection boundary layer on vertical heated plate near discontinuity in plate temperature, discussing velocity field

17 p3198 A70-35593

Incompressible laminar boundary layer, vortex and axisymmetric wake/jet flow parabolic equations solution by weighted residuals method, describing use of exponentials

17 p3074 A70-35883

Incompressible laminar boundary layer equations approximate solution by Galerkin-Kantorovich technique

18 p2338 A70-35972

Subsonic and supersonic laminar boundary layers separation near sharp corners, considering curvature and Reynolds number effects

18 p3208 A70-36486

Heat transfer at flat melting surface under forced convection and laminar boundary layer solved by Karman-Pohlhausen method

18 p3347 A70-36502

Heat transfer in plasma flow incident normally on cylinder, examining laminar boundary layers in presence of turbulence

19 p3552 A70-38187

Velocity distribution in boundary layer on thin rotating turbine blade of impeller driven at wind tunnel outlet, solving turbulent and laminar flows momentum equations

19 p3352 A70-38224

Boundary layer oscillatory flow interaction with nonuniformly rotating lamina, calculating velocity distribution and transitional frequencies

19 p3406 A70-38443

Plane symmetrical and axisymmetrical laminar and turbulent free jets, interpreting statistical character of boundary layer profiles

19 p3407 A70-38684

Integrodifferential equation derived for energy balance in laminar boundary layer of fluid flow, taking into account viscous energy dissipation, radiative energy transfer, etc

20 p3736 A70-39261

Divergent channel with porous walls, calculating effect of suction on laminar incompressible boundary layer by Runge-Kutta method

20 p3609 A70-39671

Laminar boundary layer equations on plate with arbitrary catalytic properties in diatomic gas flow undergoing vibrational dissociative relaxation

20 p3611 A70-39802

Laminar boundary layer multidimensional universal equations solution for incompressible liquid using method of characteristics

20 p3611 A70-39804

High velocity gas motion in laminar boundary layer, describing universal motion equations two parameter solution

20 p3611 A70-39805

Compressible viscous fluid steady plane flow in laminar boundary layer on impermeable isothermic surface, describing parametric method of integrating flow equations

20 p3611 A70-39806

Laminar thermal boundary layer at atmospheric pressure adjacent to cooled wall, measuring electron temperature and number density

20 p3737 A70-39990

Laminar viscous effects over blunt cones at hypersonic conditions, taking into account first and second order boundary layer theories

20 p3559 A70-40285

Unsteady incompressible flow in laminar boundary layer with homogeneous suction during longitudinal flow past flat plates, investigating boundary layer stability

20 p3614 A70-40391

Nonstationary compressible laminar boundary layer solutions by parameter-invariant method, obtaining velocity and temperature profiles by partial differential equations numerical integration

21 p3806 A70-40555

Flat plate compressible laminar boundary layer flow with variable fluid properties, using series solution by splitting up flow variables into sets of universal functions

21 p3806 A70-40825

Accelerated self similar compressible laminar boundary layer flows with and without mass transfer, obtaining numerical solutions

21 p3807 A70-41031

Two dimensional compressible laminar MHD boundary layer flow across flat plate with heat transfer, considering continuity, momentum and energy equations

21 p3856 A70-41039

Upstream mass injection effects on downstream heat transfer of supersonic reacting boundary layer

21 p3952 A70-42079

Incompressible laminar boundary layers thermal response behavior in wedge flow, obtaining surface response, temperature fields, heat flux and steady state data

21 p3811 A70-42164

Three dimensional laminar boundary layer equations for film condensation on curved surface in quiescent vapor, investigating flow at stagnation point

21 p3954 A70-42168

Three dimensional laminar and turbulent boundary layers separation criteria

21 p3811 A70-42206

Laminar axisymmetric incompressible boundary layer calculation based on Mangler transformation [ASME PAPER 70-FLCS-13]

22 p4008 A70-42414

Time-mean velocity and skin friction of laminar boundary layer near two dimensional stagnation point with oscillating oncoming flow

22 p4010 A70-42686

Hypersonic viscous interaction between laminar boundary layer growing over flat plate and external flow field extended to curved surfaces

22 p3958 A70-42688

Three dimensional laminar boundary layer equations for body of revolution at angle of attack in supersonic gas flow derived for equations

22 p3960 A70-43323

Laminar to turbulent boundary layer flow transition over flat plate, using space amplified numerical solutions of Orr-Sommerfeld equation

23 p4181 A70-44234

Three dimensional hypersonic laminar boundary layer subdivided into inner and outer regions, obtaining flow description by matching inner and outer solutions

[AIAA PAPER 69-710]

23 p4182 A70-44565

Laminar boundary layer wall shear and velocity profiles by N parameter integral method, using exponentials

23 p4182 A70-44567

Three dimensional laminar boundary layer separation at infinite swept stagnation line with high mass injection rates

23 p4182 A70-44568

Cracked Teflon heat shields ablative behavior for laminar and turbulent boundary layers in supersonic flow, describing heat transfer to substructure

23 p4282 A70-44585

Gas coolant slot injection into hypersonic laminar boundary layer, comparing experimental results to boundary layer equations numerical integration

23 p4282 A70-44694

Laminar boundary layer on uniformly rotating sphere studied by momentum integral method, imposing zero vorticity condition

23 p4184 A70-44981

Three dimensional laminar boundary layer in unsteady incompressible flow, presenting solution by successive approximations method

24 p4325 A70-45594

Unsteady separation criteria for three dimensional laminar boundary layer on finite obstacle

24 p4327 A70-46268

LAMINAR BOUNDARY LAYER SEPARATION

U BOUNDARY LAYER SEPARATION

U LAMINAR BOUNDARY LAYER

LAMINAR FLAMES

U FLAMES

U LAMINAR FLOW

LAMINAR FLOW

NT BLASIUS FLOW

NT HARTMANN FLOW

NT STRATIFIED FLOW

Radiation effect on enthalpy and velocity distributions of laminar compressible planar free jet

01 p0061 A70-10295

Existence theorem used for proof of asymptotic methods in nonlinear stability of laminar flow [ONERA-TP-750]

01 p0061 A70-10298

Inertia forces effect in turbulent and laminar, self acting and infinitely long film bearings, considering compressible and incompressible lubricants

[ASME PAPER 69-LUB-2]

01 p0103 A70-10400

Flow stability criteria in rough pipes, deriving laminar to turbulent flow transition characteristics and drag as function of Reynolds number

01 p0064 A70-10998

Petrov proof of plane Couette and Poiseuille flow stability with respect to infinitesimal disturbances, rejecting validity of proof

01 p0064 A70-11071

Two dimensional plane and axisymmetric free streamline flow problems solved by finite difference methods for supercavitating wedge in potential flows

01 p0065 A70-11127

Unsteady incompressible laminar flow under time dependent body force solved for rectangular and circular conduit and plane and cylindrical Couette flows

01 p0066 A70-11130

Pressure gradient required for self preserving of turbulent jets and wakes with small mean velocity variations compared with free stream velocity

02 p0223 A70-11860

Nonlinear waves in parallel shear flows, discussing laminar flow breakdown due to free stream disturbances

02 p0277 A70-11876

Laminar diffusion flame spread against air stream over solid or liquid fuel bed, noting influence of stoichiometric and thermal properties and data inconsistency

02 p0396 A70-12016

Radiative, conductive and convective combined heat transfer mechanism in nonisothermal atomic hydrogen plasma laminar flow

02 p0400 A70-12660

Laminar isothermal entrance flows in circular cross section ducts with uniform mass injection at wall from boundary layer equations, discussing molecular weight effects

02 p0288 A70-12859

Monograph on laminar flow heat transfer in thermal entrance region of flat and profiled ducts, treating construction and efficiency of plate heat exchangers

03 p0603 A70-12988

Boundary layer approximation for natural convection in flat vertical symmetrically heated channel with stabilized laminar flow for local and mean Nusselt numbers

03 p0605 A70-13395

Laminar-turbulent transition in free axisymmetric viscous incompressible jet from shaped nozzle and long cylindrical tube

03 p0466 A70-13396

Heat transfer under conditions of forced convection from flat plate in laminar flow, considering plate surface temperature arbitrary variation in time

03 p0605 A70-13518

Viscous incompressible laminar two dimensional flows using Navier-Stokes equations, emphasizing near wake and flow around leading edge

[ONERA-TP-757]

03 p0467 A70-13640

Laminar capillary jet of viscoelastic fluid, discussing breakup, nonNewtonian jet stability and elastic properties

03 p0468 A70-13782

Equilibrium model of laminar arc constrictor plasma generator, correlating heat transfer, wall shear stress, friction factor and development length

03 p0533 A70-13952

MHD laminar flow between parallel porous disks for large suction Reynolds number, solving equations of motion with singular perturbation technique

03 p0469 A70-14181

Flow characteristics of compressible fluid in compressor or turbine stage, determining radial distribution of downstream Mach number

03 p0410 A70-14271

Viscous compressible heat conducting laminar perfect gas flow in slender axisymmetric channels with adiabatic walls, using equations of motion

03 p0471 A70-14383

Conducting fluid laminar flow between parallel planes in traveling magnetic field, integrating Maxwell and Navier-Stokes equations

04 p0726 A70-14542

Laminar flow separation, reattachment and transition over downstream step, including visual observations of smoke filaments, velocity fluctuation measurements and velocity profiles

[ASME PAPER 69-WA/FE-5]

04 p0667 A70-14784

Finite difference theory applied to numerical analysis of laminar equilibrium MHD flow in circular tube

[ASME PAPER 69-WA/HT-55]

04 p0727 A70-14794

Instability of viscous laminar plane jet of incompressible fluid, finding minimum critical Reynolds number for various assumptions of parallelism

04 p0670 A70-14990

Laminar and turbulent flows of compressible media in rotating pipes, analyzing velocity distribution, angular velocity and Coriolis effects using Abel equation

04 p0672 A70-15159

Wake behind axisymmetric bluff body in steady laminar flow, noting role of Reynolds number

04 p0619 A70-15392

Supersonic wake flow visualization, obtaining direct photographs of various smoke streamlines [AIAA PAPER 69-346]

04 p0621 A70-15595

Unsteady flow equations for periodic axisymmetric laminar flow of second order fluids in circular cylindrical pipes

05 p0831 A70-15871

Plane Poiseuille flow stability as function of periodic disturbances of finite amplitude in channel axis direction

05 p0832 A70-16018

Periodic perturbations of plane Poiseuille flow, observing neutral curve relationship to disturbance amplitude

05 p0832 A70-16019

Unsteady laminar free convection caused by heating semiinfinite flat vertical plate, obtaining velocity and temperature distributions

05 p0957 A70-16370

Laminar flow in circular pipe with arbitrary axial variation of wall temperature or heat flux, using integral type approximation

05 p0957 A70-16519

Laminar flow stability along flexible boundary on basis of Orr-Sommerfeld equation

05 p0836 A70-16923

Unsteady laminar gas flow near infinite flat plate using Laplace transforms, obtaining closed form solutions for plate velocity and temperature

05 p0836 A70-17106

Steady laminar flow with frictionless central core surrounded by boundary layer in circular curved pipe, discussing friction factor and flowmeter discharge coefficient

05 p0836 A70-17107

Buoyancy effects in laminar forced convection on vertical flat plate, obtaining heat transfer coefficient

06 p1172 A70-17141

Viscoelastic fluid flow through circular tube under time dependent pressure gradient superposed on steady Poiseuille flow

06 p1032 A70-17200

Suddenly started laminar flow in circular tube entrance region, obtaining integral momentum equation for boundary layer thickness, entrance length, velocity profile, etc

06 p1034 A70-17528

Skin friction and heat transfer on flat plate in high velocity laminar motion with mass transfer for any free stream and injected gas combination

06 p1176 A70-17689

Unbranched chain reaction in hydrogen bromide for studying laminar one dimensional flame propagation, determining temperature dependence, velocity and concentrations at fixed time

06 p1177 A70-17797

Laminar steady radial flow of simple fluid of short memory between two parallel disks, demonstrating relation to Newtonian fluid

06 p1037 A70-17915

Laminar flow mixing stability and diffusion flame flow field measurements revealing role of Tollmien-Schlichting waves in enclosed flames vibrations [WSCI PAPER 69-46]

06 p1179 A70-17985

Finite difference solution of time dependent Navier-Stokes equations for two and three dimensional laminar incompressible flow, discussing results for flat plates

[AIAA PAPER 70-46]

06 p1041 A70-18170

Axisymmetric motion of viscous heat conducting gas by constructing indirect analog of Poiseuille gas flow, applying results to slip flow regime

06 p1048 A70-18325

Model for predicting laminar-turbulent transition point in hypersonic wake of two dimensional laminar viscous flow

06 p0985 A70-18499

Plastic lubricants motion in circular pipes, determining drag and cross sectional velocity profile of laminar flows

07 p1290 A70-18652

Nusselt theory of laminar liquid films movement on vertical smooth solid surface, attributing thickness variation to gas movement and surface active agents in liquid

07 p1251 A70-18656

Approximate solution for heat transfer in incompressible fluid laminar flow in circular tube

07 p1253 A70-19060

Laminar flow of compressible gas in axisymmetrical channel in absence of wall insulation using velocity profiles, heat transfer, etc

07 p1253 A70-19062

Heat transfer in Ni wires in laminar air flow from wind tunnel investigation

07 p1420 A70-19064

Viscous fluid flow calculations in fine clearance eccentric annuli allowing for pressure losses in laminar or turbulent flows

07 p1293 A70-19120

Trailing edge region of flat plate in laminar incompressible flow examined for high Reynolds numbers limit using Navier-Stokes reduced equations

07 p1255 A70-19213

Laminar flow forced convection heat transfer in circular pipe entrance region for constant wall temperature and constant wall heat flux

07 p1420 A70-19215

Unsteady boundary layer in compressible fluid laminar flow over accelerating semiinfinite flat plate

07 p1258 A70-19566

Temperature fields and hydrodynamics in laminar flow of vertical liquid layers during free convection

07 p1422 A70-19655

Body surface curvature effect on surrounding laminar flow field, investigating oblate spheroids of various thicknesses

07 p1259 A70-19977

Large axisymmetric disturbances generated in laminar pipe flow by sleeve oscillating at wall, measuring flow with laser-Doppler velocimeter

07 p1286 A70-19995

Turbulent-laminar transition in divergent radial flow between disks, relating velocity fluctuations to Reynolds number

08 p1483 A70-21235

Laminar radial flow between parallel disks, estimating static wall pressure distribution perturbation caused by characteristic time

08 p1484 A70-21237

Suction effect on thin film laminar flow past vertical wall, obtaining approximate solution for small porosity in accelerated region

08 p1484 A70-21309

Very small diameter laminar flow orifice coefficient calculation as function of Reynolds number

08 p1484 A70-21321

Symmetrical laminar distorted velocity profiles between flat parallel plates, analyzing decay using integral method

08 p1433 A70-21325

Thermal boundary layer thickness and Nusselt number approximations for heat transfer in laminar flow along flat plate with power law heat flux distribution

08 p1599 A70-21583

Single fluid theory for plasma laminar flow in field-free region of circular tube, obtaining friction factor and Nusselt number correlations

08 p1552 A70-21585

Unsteady free convection laminar power-law fluid flow past porous vertical wall, studying similarity solution dependence on wall temperature and suction

08 p1486 A70-21765

Laminar-turbulent regions boundary, discussing convective layer form and FM-CW microwave and acoustic radar measurement techniques

09 p1717 A70-22378

Poiseuille and Couette fluid flow with internal rotation in flat channel

09 p1660 A70-22436

Two dimensional Poiseuille flow stability at deformable walls, assuming pressure proportionality to displacement and rate

09 p1660 A70-22533

Sphere motion in laminar flow, postulating absolute velocity as resultant of entrainment and fall velocities and stable position in tube with ascending flow

09 p1663 A70-23309

Plane Poiseuille flow with nonlinear temperature distribution, studying vortex type secondary flow onset due to buoyant forces

[ASME PAPER 69-HT-37]

09 p1790 A70-23555

Boundary layer equations with heat transfer for laminar and turbulent incompressible flows about two dimensional and axisymmetric flows, using finite difference method

[ASME PAPER 69-HT-7]

09 p1663 A70-23560

Laminar viscous flow past semiinfinite flat plate parallel to uniform stream, solving Navier-Stokes equation to determine local skin friction coefficient

09 p1663 A70-23581

Streamwise perturbations in flow downstream of self excited blades cascade calculated by two dimensional theory, discussing periodic circulation shedding

09 p1608 A70-23746

Streamline curvature technique for two dimensional flow equations, deriving optimal damping factor for quasi-orthogonal method to test stability, convergence and accuracy

09 p1609 A70-23749

Nonlinear stability problem posed by Navier-Stokes equations in case of laminar flows stability using semigroups theory

[ONERA-TP-775]

10 p1863 A70-24094

Plane steady flows characteristics of incompressible viscous fluids in rigid walled rectangular channels found asymptotic to Poiseuille and Couette flows

10 p1866 A70-24112

Skin friction near flat plate trailing edge at high Reynolds number by linearizing velocity profile

10 p1801 A70-24159

Steady two dimensional cavity flow past sharp-edged airfoil and blunt nosed obstacle, using linearization hypothesis

10 p1801 A70-24193

Molecular, viscomolecular and laminar gas flows in tubes and porous bodies at low pressures

10 p1869 A70-24287

Navier-Stokes solution to laminar flow past semiinfinite flat plate valid for any Reynolds number, discussing skin friction, displacement thickness, etc

10 p1869 A70-24415

Closed streamline low Mach number compressible fluid flow without temperature restrictions, noting incompressible flow behavior

10 p1869 A70-24547

Laminar flow into channel with symmetrical jets along walls, considering velocity profiles and flow establishment lengths

10 p1870 A70-24790

Viscous compressible fluid steady laminar flow between coaxial cylinders, studying flow characteristics for uniform inner cylinder velocity

10 p1870 A70-24792

Two fluid hydrodynamic model of heat conductivity and viscosity effects on drift laminar flow stability of dense inhomogeneous plasma

10 p1926 A70-25125

Approximate solution for heat transfer in incompressible fluid laminar flow in circular tube

10 p1871 A70-25211

Laminar flow of compressible gas in axisymmetrical channel in absence of wall insulation using velocity profiles, heat transfer, etc

10 p1871 A70-25213

Heat transfer in Ni wires in laminar air flow from wind tunnel investigation

10 p1970 A70-25215

Ultraclean technology to eliminate pollution traces present in laboratories, discussing turbulent flow and horizontal and vertical laminar flow rooms

10 p1828 A70-25240

Numerical techniques and solutions for compressible and incompressible laminar separated flows using time dependent finite difference equations

[AIAA PAPER 68-741]

11 p2035 A70-25972

Newtonian fluid laminar throughflow between coaxial rotating cones, applying solution for flow between disks

11 p2038 A70-26491

Coupled effects of transverse curvature and pseudoplasticity on skin friction characteristics of slender circular cylinder in laminar power law fluids

11 p2038 A70-26493

Turbulent three dimensional Poiseuille channel flow at large Reynolds numbers, investigating eddy shapes and energy balance

11 p2041 A70-26546

Tube relaminarization, predicting turbulent-to-laminar flow transition

12 p2212 A70-28118

Self energized hydrostatic shaft seal operating with incompressible fluid in laminar flow regime, using general lubrication theory

13 p2417 A70-28614

Pressure field equation derivation for hydrodynamic journal bearing in superlaminar regime, using turbulent Couette and screw flow friction correlations

13 p2418 A70-28742

Pressure distributions and heat transfer at wall calculated to investigate supersonic laminar reattachment

13 p2338 A70-28953

Basic flow convergence or divergence effect on steady flow pattern around circular cylinder using fluid motion visualization

13 p2387 A70-29058

Steady diabatic complex lamellar gas flow, obtaining parameters by extending geometric theory of surfaces and curves in fluid flow theory

13 p2387 A70-29122

Laminar near wake flow field of two dimensional adiabatic circular cylinder with surface mass transfer

[AIAA PAPER 69-67]

13 p2343 A70-29951

Viscous shock layer equations of laminar hypersonic flow past blunt body at moderate to high Reynolds numbers

13 p2343 A70-29952

Velocity circulation in laminar motion of fluid in cylindrical tube, assuming equilibrium under dissipative forces

14 p2564 A70-30164

Laminar or turbulent flow in parallel plate channels with combined forced convective and radiative heat transfer, determining gas temperature field and Nusselt numbers

14 p2663 A70-30253

Laminar flow of suspension over flat plate, analyzing particulate velocity and concentration profiles relationships to drag and lift forces

14 p2565 A70-30270

Low Reynolds number laminar flow gas turbine regenerators, investigating manufacturing tolerances effects on heat transfer and flow friction behavior

14 p2629 A70-31022

Viscometric Poiseuille or Couette flow kinematics, considering nonuniform shear rate

14 p2567 A70-31282

Laminar velocity distribution from temperature profiles developed under steady flow through tube, constructing numerical temperature grid

15 p2718 A70-31449

Axial wall conduction effects on steady state laminar flow heat transfer

15 p2825 A70-31815

Laminar natural convective heat transfer along outer surface of vertical cylinder, giving coefficients nondimensionally by approximate formulas

15 p2826 A70-31821

Conducting incompressible fluid laminar flow between rotating disks in transverse magnetic field with source at center

15 p2779 A70-31915

Laminar to turbulent transitions determination in sub/supersonic flows, reviewing methods based on hot-wire anemometer output signal

15 p2720 A70-31918

Laminar to turbulent flow transition observation in laser induced vertical convection, using carbon dioxide-nitrogen laser

15 p2751 A70-31980

Rheological calculation of plate resistance and heat transfer in laminar flow of structurally viscous fluids

15 p2827 A70-32126

Laser velocimeter application to laminar-turbulent flow transition at glass tube centerline

15 p2741 A70-32521

Hydrodynamic internal streamline flow analysis for turboprop inducer blades under cavitating and non-cavitating conditions

[AIAA PAPER 70-629]

16 p2964 A70-33528

Turbulent boundary layer response in flow field downstream of upstanding step change in surface roughness

[ASME PAPER 70-FE-17]

16 p2891 A70-33630

Two dimensional incompressible isothermal laminar separation of Newtonian fluid in steady flow, obtaining velocity profiles

[ASME PAPER 70-FE-29]

16 p2892 A70-33635

Dwell time boundary and mean values for laminar flows through channel and tube reactors, obtaining field representation from streamline network and isochrones

16 p2893 A70-33745

Incompressible ideal fluid plane laminar flows at large Reynolds numbers in region bounded by moving walls with closed concentric streamlines, establishing functional properties

16 p2893 A70-33749

Incompressible free jet characteristics determination from unique differential equation in laminar and turbulent flow regimes by unitary method

16 p2893 A70-33750

Nonreacting and chemically reacting laminar flows, calculating equilibrium, nonequilibrium and ideal gas laminar boundary and viscous shock layers over hyperboloid

[AIAA PAPER 70-808]

17 p3005 A70-34456

Upper pulmonary airways plastic conduit model, measuring laminar and turbulent flow velocity profiles by hot-wire anemometer

17 p3035 A70-34469

Transitional flow separation upstream of compression corner at trailing edge of sharp leading edge flat plate

[AIAA PAPER 70-764]

17 p3007 A70-34487

Laminar incompressible separating and reattaching flows, correlating finite difference solutions with experimentation

[AIAA PAPER 70-763]

17 p3008 A70-34488

Temperature dependent absorption, nonsteady beam propagation and laminar-turbulent transition in laser induced convection column, measuring turbulence onset by fine wire resistance thermometer

[AIAA PAPER 70-800]

17 p3107 A70-35197

Unsteady state Newtonian liquid diffusion in laminar flow in circular tube, using mathematical model

17 p3072 A70-35544

Laminar flow heat transfer in annuli, discussing correlation of local Nusselt numbers

17 p3197 A70-35545

Laminar free convection near two dimensional and axisymmetric nonisothermal bodies, examining surface temperature distribution and heat flux

18 p3345 A70-35999

Airfoil trailing edge stall in laminar flow, investigating circulation around flat plate 18 p3205 A70-36194

Plane stationary supersonic flows with laminar separation zones at large subcritical Reynolds numbers 18 p3206 A70-36257

Laminar gas flow enthalpy determination in stagnation regions based on energy balance equation across separation streamline 18 p3240 A70-36266

Incompressible heavy fluid film stability during flow along inclined plane constituting crystallization front, analyzing linearized equations of perturbed flow 18 p3240 A70-36271

Optical observation of laminar convective flow caused by combined action of concentration and temperature fields 18 p3346 A70-36276

Ablating nose equilibrium shape in laminar hypersonic flow during reentry 18 p3208 A70-36707

Laminar flows with surface injection, calculating thermal boundary layer-porous wall coupling effects [ASME PAPER 70-GT-1] 18 p3243 A70-36860

Laminar incompressible flow in arbitrary cross section entrance region of ducts by numerical technique after transformation to boundary value problem [ASME PAPER 70-GT-91] 18 p3243 A70-36878

Flame propagation velocity of gasoline-air mixture during two stage combustion process in laminar and turbulent flows, discussing combustion products effect 19 p3550 A70-37253

Laminar two dimensional wall jet with small natural disturbances, examining flow stability at various Reynolds numbers 19 p3402 A70-37526

Inertia forces effect in turbulent and laminar, self acting and infinitely long film bearings, considering compressible and incompressible lubricants [ASME PAPER 69-LUB-2] 19 p3435 A70-37613

Lift forces acting on spheres in cylindrical tube laminar flow 19 p3352 A70-37647

Stability of thermal and inertial perturbations superimposed on unstably stratified plane parallel flow with variable vertical shear 19 p3462 A70-37753

Velocity profiles of laminar flow through rectangular duct with moving wall and arbitrary cross section under nonslip boundary condition 19 p3405 A70-38043

Unsteady laminar incompressibles fluid flow in parallel plate channels and circular tubes, solving Navier-Stokes equations for prescribed discharge 19 p3405 A70-38347

Laminar vortex flow interaction with stationary surface, considering flow field, velocity, Reynolds number, etc 19 p3405 A70-38348

Round laminar jet with swirl, reducing Navier-Stokes equations to ordinary differential equations by similarity transformations 19 p3405 A70-38349

Pressure and temperature distribution in constant volume viscous Poiseuille gas flow velocity profile 20 p3608 A70-39121

Laminar incompressible free shear layers by method of weighted residuals for turbulent jets, obtaining velocity profiles for similarity and physical planes 20 p3613 A70-40286

Laminar flow of liquid in duct with zero heat resistance of walls, calculating temperature distribution during radiative convective heating 20 p3613 A70-40297

Laminar fluid flow in pipes of rectangular cross section, determining critical Reynolds numbers and maximum instability locations 20 p3614 A70-40400

Energy dissipation in laminar unsteady incompressible viscous fluid flows, discussing velocity fields, boundaries, tangential motion and entrainment 20 p3614 A70-40402

Laminar convective flow from linear heat source along vertical plate, solving numerically for incompressible fluid by boundary layer approximation 20 p3614 A70-40403

Slightly rarefied and electrically conducting gas, calculating effects of applied magnetic field on steady laminar low speed plane Couette flow 20 p3685 A70-40504

Two fluid hydrodynamic model of heat conductivity and viscosity effects on drift laminar flow stability of dense inhomogeneous plasma 20 p3685 A70-40518

Wall heat transfer for partially ionized argon laminar flow within square channel conducting walls with and without transverse magnetic field 21 p3856 A70-41032

Poiseuille pipe flow instability, considering asymptotic analysis for small wave number disturbances 21 p3807 A70-41241

Unsteady convective heat transfer and hydrodynamics of laminar and turbulent channel flows 21 p3808 A70-41374

Calibration data correlation for constant temperature hot film anemometer for low speed nonisothermal laminar air flow, using modified King law 21 p3828 A70-41475

Eddy currents in Hall generator with conducting side wall, studying velocity and temperature effects for turbulent boundary layer and laminar flows 21 p3859 A70-41733

Viscous laminar parallel flow along cylindrical surfaces, discussing boundaries described by algebraic polynomials 21 p3810 A70-41959

Plane Poiseuille flow in second order Rivlin-Ericksen fluids with small viscoelastic parameters, calculating three dimensional disturbance stability 21 p3810 A70-42030

Constant property unsteady laminar flow thermal entrance problems, using variational formulation in Laplace transformed domain 21 p3954 A70-42169

Two layer gas flows in supersonic axisymmetric nozzles, using method of characteristics 21 p3748 A70-42210

Incompressible Newtonian fluid laminar radial flow between parallel stationary disks, obtaining integral solution for Navier-Stokes equation 22 p4007 A70-42302

Isothermal steady laminar flow through tube with change in wall temperature, examining velocity profile relationship to temperature profile [ASME PAPER 70-HT-C] 22 p4008 A70-42421

Laminar hexane diffusion flame, investigating distribution of final and intermediate combustion products 22 p4123 A70-42522

Buoyant hot two dimensional laminar vertical jet in quiescent colder fluid, calculating temperature and velocity distributions by integral method 22 p4010 A70-42639

Poiseuille-Couette spiral flow stability between concentric rotating cylinders 22 p4010 A70-42691

Laminar geoelectromagnetic field excited by coaxial circular current, determining impedance and magnetic field factors of spherical harmonics 23 p4189 A70-44064

MHD laminar isothermal flow in closed cylindrical tube in rotating magnetic field, determining azimuthal velocity distribution 23 p4224 A70-44162

Heat transfer by laminar forced convection of viscous fluid in noncircular cylindrical channel with internal heat source and varying wall temperature 23 p4276 A70-44236

Incompressible laminar swirling jet flow, obtaining similarity solution for Navier-Stokes equations 23 p4184 A70-44982

Oscillating viscous conducting fluid laminar flow between parallel nonconducting infinite porous flat plates under suction in transverse magnetic field 24 p4383 A70-45146

Incompressible laminar flow in entrance region of rectangular duct allowing direct computation of eigenvalues 24 p4287 A70-45294

Porous tube inlet region, calculating fluid injection effect on laminar flow from integral form boundary layer equations 24 p4326 A70-45782

Local or surface boiling phenomenon under triangular channel laminar flow conditions, investigating heat transfer with and without phase change 24 p4429 A70-46089

Heat flux exchange by natural convection along flat vertical isothermal plate in laminar, transition and turbulent flows, using fluxmeters 24 p4429 A70-46207

LAMINAR FLOW AIRFOILS

Laminar airfoils for Reynolds numbers above 4,000,000, utilizing potential and boundary layer flow theories 01 p0063 A70-10930

LAMINAR FLOW CONTROL

U BOUNDARY LAYER CONTROL

U LAMINAR BOUNDARY LAYER

LAMINAR HEAT TRANSFER

Monograph on laminar flow heat transfer in thermal entrance region of flat and profiled ducts, treating construction and efficiency of plate heat exchangers 03 p0603 A70-12988

Unsteady heat transfer equations for laminar fluid flow in pipe with varying wall temperature 03 p0604 A70-13207

Buoyancy effects in laminar forced convection on vertical flat plate, obtaining heat transfer coefficient 06 p1172 A70-17141

Time dependent pressure fluctuations effect on laminar film pool boiling on vertical flat plate by perturbation method to predict heat transfer 06 p1177 A70-17696

Approximate solution for heat transfer in incompressible fluid laminar flow in circular tube 07 p1253 A70-19060

Laminar flow of compressible gas in axisymmetrical channel in absence of wall insulation using velocity profiles, heat transfer, etc 07 p1253 A70-19062

Heat transfer in Ni wires in laminar air flow from wind tunnel investigation 07 p1420 A70-19064

Solid layer effect on laminar heat transfer and pressure drop in medium surrounding pipe with liquid flows below freezing point, discussing wall temperature effects 08 p1485 A70-21589

Unsteady laminar free convection on heated axially symmetric body under stepwise surface temperature variations and unity Prandtl number 10 p1967 A70-23875

Approximate solution for heat transfer in incompressible fluid laminar flow in circular tube 10 p1871 A70-25211

Laminar flow of compressible gas in axisymmetrical channel in absence of wall insulation using velocity profiles, heat transfer, etc 10 p1871 A70-25213

Heat transfer in Ni wires in laminar air flow from wind tunnel investigation 10 p1970 A70-25215

Turbulent and laminar heat transfer to gases in circular ducts entry region, considering various gas properties 12 p2212 A70-28114

Steady laminar heat transfer in open circuit aligned field MHD flow past flat plate, using parametric differentiation 14 p2664 A70-30272

Low Reynolds number laminar flow gas turbine regenerators, investigating manufacturing tolerances effects on heat transfer and flow friction behavior 14 p2629 A70-31022

Laminar heat transfer to blunted wedge with constant wall temperature, describing energy field in boundary layer by analytic solution 15 p2825 A70-31818

Boundary layer equations for laminar flow, drag and heat transfer of gas in circular tube, considering parabolic and uniform entrance velocity profiles 15 p2722 A70-32692

Laminar flow heat transfer in annuli, discussing correlation of local Nusselt numbers 17 p3197 A70-35545

Laminar heat transfer in circular tube under solar radiation in space 18 p3347 A70-36503

Liquid He 4.2 K in narrow channels with laminar and turbulent flow, measuring boiling heat transfer as function of temperature difference 20 p3735 A70-39155

Laminar heating in hypersonic vehicles interior corners, analyzing helium tunnel heat transfer data for various intersecting wedge corners 20 p3737 A70-39700

Incompressible MHD flow in entrance region of channel with electrically conducting walls, calculating interacted laminar heat transfer by integral method 21 p3856 A70-41038

Heat transfer in laminar channel flow with random velocity variations, using Monte Carlo technique 21 p3949 A70-41312

LAMINAR JETS

U JET FLOW

U LAMINAR FLOW

LAMINAR MIXING

Laminar flow mixing stability and diffusion flame flow field measurements revealing role of Tollmien-Schlichting waves in enclosed flames vibrations [WSCI PAPER 69-46] 06 p1179 A70-17985

Coaxial fluid streams mixing within finite length tube based on dimensional analysis of aerodynamic noise generation, discussing subsonic and supersonic flows within ejector 13 p2474 A70-29080

LAMINAR WAKES

Linear spatial stability of two dimensional laminar wake- and jet-like similarity solution of Falkner-Skan equation 04 p0613 A70-14455

Laminar compressible wake behind thin flat plate at zero angle of attack, solving boundary layer equations in von Mises coordinate plane [ASME PAPER 69-WA/FE-6] 04 p0614 A70-14783

Wake behind axisymmetric bluff body in steady laminar flow, noting role of Reynolds number 04 p0619 A70-15392

Hypersonic near wake, discussing correlations from optical studies, laminar near wake, blunt body and turbulent wake measurements 05 p0790 A70-16120

Laminar hypersonic blunt cone wakes, discussing flow fields and axial static pressure distributions 06 p0968 A70-17553

Finite disturbance effect on laminar incompressible wake behind flat plate determined by interaction between two dimensional fluctuation amplitude and mean flow 08 p1433 A70-21605

Navier-Stokes equations for laminar near wake of blunt based body, obtaining numerical solutions for adiabatic and constant wall temperatures

09 p1605 A70-23176

Series expanding velocity profile in parabolic cylinder functions describing nonlinear evolution of steady laminar incompressible wake from arbitrary initial profile

10 p1802 A70-24418

Laminar near wake of cylinder at free stream Mach 6, using modified Lees-Reeves method

16 p2836 A70-33762

Steady state laminar flow model for near wake of slender body in supersonic flow

17 p3006 A70-34467

Base pressure behind supersonic vehicle, examining Crocco-Lees mixing theory critical point in laminar near wake

21 p3747 A70-42109

Two dimensional laminar near wake of slender body in supersonic flow at high Reynolds number

23 p4135 A70-44693

LAMINATED MATERIALS

U LAMINATES

LAMINATES

Weak interfaces effects in laminates under triaxial tensions at crack tip, analyzing delamination during crack propagation and fracture resistance

01 p0127 A70-10482

Crack propagation mode in laminated steel-Ni composites, analyzing softer layer effect using impact tests and C replica fractographs

01 p0120 A70-10743

Reinforced metals properties and applications including fibers and lamination, notch sensitivity, brittle fracture, failure and heat resistance characteristics

01 p0124 A70-11619

Design allowable curves based on laminate test data for high modulus graphite fiber and resin systems, considering Wagner cantilever beam specimens

02 p0387 A70-11954

Ductile-brittle fracture transition in steel pressure vessels suppressed by utilizing thin laminations

03 p0583 A70-12903

Plane elasticity solution for differential expansion stresses on interface of laminated elastic rectangular strip

03 p0586 A70-13114

Axial and traction loaded boron epoxy laminates tensile and compressive elastic properties and strengths compared from test data including strain gauge measurements

03 p0586 A70-13115

Cylindrical bending in laminated plates displaying bending-extensional coupling approximating behavior of rectangular laminated plates with high length-to-width ratio

03 p0587 A70-13125

Laminate approximation model of randomly oriented fibrous composites estimating stiffness and thermal and expansional strains

03 p0587 A70-13126

Rational design of structurally anisotropic plane multilayer plates with weak binder, suggesting strengthening fibers orientation in internal stresses direction

03 p0516 A70-13379

Thin elastic laminar shells nonlinear physical theory assuming Love-Kirchhoff hypothesis validity, rigidly connected layers and nonlinear mechanical behavior

04 p0765 A70-14419

Matrix analysis of steady state temperature field and heat flux through multilayer, plane, cylindrical or spherical partitions with internal heat sources

04 p0785 A70-14924

Buckling of three layer cylindrical shells under steady creep conditions, deriving axisymmetric deformation

05 p0935 A70-16234

Transient stress waves generated by spatially uniform distribution of transverse forces in laminated medium, using modal analysis

05 p0938 A70-16409

Book on analysis of laminated composite structures covering orthotropic materials stress-strain relations, laminated composite shells, plates, beams and columns

05 p0938 A70-16467

Axial and nonlinear bending performance compared for compression moldings laminated from random glass fiber mat

05 p0870 A70-16577

Bag molding process for molding laminates of reinforced preimpregnated material containing thermosetting resin

05 p0856 A70-16612

Mechanical fastening, adhesive bonding and machining methods for laminated fiberglass reinforced plastic materials

05 p0856 A70-16618

Micro and macromechanics for design and mechanical properties prediction of laminated fibrous composites for airframes and space structures

05 p0941 A70-16619

Guided elastic waves propagation on layered media, considering elastic wave circuitry design for true microminiaturization

06 p1018 A70-17476

Mechanical behavior of cylinders with alternating layers of reinforcing and matrix materials derived from governing equations, including equations of motion

[AIAA PAPER 70-134]

06 p1169 A70-18051

Carbon fabrics and filaments, resin carbonizing and carbon-carbon composites, discussing processing parameters, initial carbonizing resin binder and reinforcement effects on laminate properties

07 p1316 A70-18932

Shallow spherical sandwich shells under concentrated forces, obtaining inhomogeneous equations solution by integral Hankel transforms

07 p1402 A70-19053

Governing equations solution for simply supported laminated anisotropic rectangular plate using Fourier series method

07 p1406 A70-19035

Plane electromagnetic wave reflection from laminar anisotropic medium, analyzing piecewise-constant permittivity tensor as boundary value problem

07 p1235 A70-19448

Air bubble free glass fiber-plastic laminates fabricated by wet-winding method using vacuum, noting void free filament wound pipes

07 p1295 A70-19766

Interlaminar shear strength determination methods taking into account plastics composition, considering polyester and epoxy plastics, glass and graphite fiber reinforcing materials

07 p1410 A70-19767

Transverse stress failure analysis of reinforced extruded plastic laminates taking into account cohesive and adhesive failure

07 p1410 A70-19768

Tensile and compressive stress cycles effect on short term strength of glass fiber plastic laminates

07 p1411 A70-19769

Cycloaliphatic epoxy resins for glass and carbon fiber reinforced plastics and laminates

07 p1318 A70-19773

Fatigue tests to relate boron-epoxy laminate fatigue behavior to thermal preconditioning environments

07 p1320 A70-19960

Isothermal steady state creep extension and flexure of laminated beams with alternating layers, indicating nonlinear stress distribution

07 p1412 A70-19964

Geometrical-mechanical properties in terms of interlaminar shear stress of composite cantilever beams under end load

07 p1412 A70-19965

Three dimensional finite element method for quasi-homogeneous laminate moduli, discussing interlaminar and in-plane shear properties

07 p1321 A70-19966

Thin sheet and laminate bullet hole deformation zone microstructure observation by electron microscopy, considering terminal ballistics approach

07 p1413 A70-20049

Limiting equilibrium of axisymmetric shells consisting of alternating reinforcement layers separated by layers of homogeneous isotropic material

07 p1415 A70-20184

Natural oscillation frequencies of three layer plates with rectangular planar form determined by integrated representations method

08 p1583 A70-20495

Modulus of elasticity of fiber glass reinforced plastic under transverse bending as function of length-to-height ratio in laminates

08 p1526 A70-20532

Test specimen shapes for determining tensile, compressive and edge-wise shear properties of reinforced plastic laminates

08 p1529 A70-21878

Specimen design of laminated angle-ply composite materials for straight-sided axial coupon and long beam flexure tension testing

08 p1530 A70-21885

Test standards for boron epoxy flat laminates, proposing specimen geometries and testing methods

08 p1530 A70-21887

Mechanical testing of metal matrix high modulus B-Al filament composites, using unidirectional and multidirectional reinforcement

08 p1523 A70-21894

Glass fiber reinforced epoxy laminate specimens tests in tension and flexure at various strain rates to determine geometry effect on strength

08 p1532 A70-21898

Fibrous reinforced composites influence in aircraft structural design based on DOD- industry development programs, investigating interlaminar shear

08 p1595 A70-21899

Laminated anisotropic rectangular plates of boron-epoxy composite material, studying shear stability by potential energy and Ritz method

08 p1595 A70-21903

Fiberglass-epoxy laminates mechanical behavior under biaxial loading, describing test equipment and procedures

08 p1532 A70-21904

Stress-strain characteristics of reinforced elastoplastic layer using mathematical model

09 p1769 A70-22183

Fiberglass reinforced plastic laminates shear characteristics determination, giving expressions for shear modulus and tangential stress

09 p1709 A70-22300

Free and forced vibrations of three layer freely suspended plate with allowance for energy dissipation

09 p1772 A70-22468

H guide with laminated dielectric strips separated by air layers, analyzing field distribution and characteristics

09 p1634 A70-22709

Stress concentrations and load transfer around cutouts in fiber reinforced laminates, discussing boron epoxy plates with circular holes

09 p1710 A70-22793

Multilayer orthotropic conical shell cyclic deformation equation obtained in hypergeometric functions

09 p1777 A70-23079

Plastic buckling of eccentrically stiffened circular cylindrical shells with multiple isotropic layers under combined axial and lateral pressure, deriving stability criterion

09 p1780 A70-23213

Radiative heat transfer along adjacent layers of multilayer insulation blanket determined as energy transport mode

09 p1789 A70-23265

Temperature fields and thermal stresses in FN fiberglass reinforced textolite under nonstationary unilateral heating, determining stress as function of time and heating rate

09 p1710 A70-23724

Fiberglass reinforced textolite creep strains as function of stress, temperature and time, noting correlation with theory to 200 C

09 p1710 A70-23725

Energy dissipation in free oscillations of multilayer shells consisting of alternating rigid elastic layers and soft fillers, deriving equations of motion

10 p1956 A70-24249

X ray laminography for nondestructive testing based on synchronous rotation of source, sample and image forming planes

10 p1895 A70-24577

Multilayer plate vibrations calculated with allowance for energy dissipation in material, deriving equations of motion

10 p1965 A70-25297

Temperature and heat flux in plane, cylindrical and spherical multilayer diaphragms with boundary conditions, assuming harmonic temperature variation

10 p1970 A70-25321

Glass epoxy cross ply laminates with brittle or ductile epoxy matrices tensile tested, comparing mechanical performance

11 p2068 A70-25686

Two dimensional photoelastic investigation of crack propagation in fiber-reinforced composites consisting of glass and polyester resin layers

11 p1316 A70-26078

Boundary conditions effect on bending, vibrations and buckling of unsymmetrically laminated rectangular plates

11 p1316 A70-26079

Interlaminar shear stresses analysis for laminated composites under generalized plane stress

11 p1316 A70-26080

Length effect on modulus determination test for thin laminated tube under combined loading using shell theory

11 p2136 A70-26086

Layered electromagnetic absorbers performance analysis by variable metric optimization method, handling functions defined over polyhedral region of real space

11 p2019 A70-26713

Stability analysis of ring-stiffened orthotropic, multilayered shells of revolution under axisymmetric torsionless loads by digital computer

12 p2320 A70-27143

Thermal buckling theory for multilayered stiffened cylindrical shells under various combined loads

12 p2321 A70-27149

Selective optical coatings of alternate Ni and silicon dioxide layers, describing optical and spectral characteristics of black mirror

12 p2272 A70-27307

Stress-strain state of thin revolving shells composed of multiple variable thickness layers, assuming layers deformation free of slipping and separation

12 p2322 A70-27332

Equilibrium equations for thin multilayer shells with variable thickness, assuming simultaneous work without friction under loads

12 p2325 A70-27556

Strain induced in laminated orthotropic fiberglass plastic cylindrical shell by normal concentrated load,

- using equations free from rectilinear normals hypothesis 12 p2328 A70-28279
- Penetration mechanics of multisheet structures based on discrete particle modeling of impact debris [AIAA PAPER 69-371] 13 p2509 A70-28521
- Nonlinear theory describing mechanical behavior of prestressed laminated composites subjected to large deformations 13 p2511 A70-28738
- Laminated glass fiber reinforced cylindrical shell stability resting on hinged supports under axial compression 13 p2514 A70-29285
- Cutting speed, feed parameters and tool tip curvature effects on machined surface roughness of turned fiberglass reinforced epoxy laminates 14 p2590 A70-30873
- Stress wave propagation in solid infinite elastic medium and laminated materials 15 p2823 A70-32784
- Maximum stress distribution in laminar composites, considering loads on boundary of reinforcing layers 15 p2766 A70-32854
- Low cost flame retardant high service temperature glass reinforced electrical grade laminate tested for continuous use 16 p2935 A70-33355
- High service temperature glass reinforced premix compound on Glastic grade electrical laminate, discussing optimum molding and applications 16 p2936 A70-33356
- Epoxy laminating resin evaluation for tooling industry, considering diluent, fillers, thixotropy, hardeners and physical property testing 16 p2936 A70-33360
- Cold forming of thermoset-thermoplastic laminate consisting of reinforced epoxy core sandwiched between thermoplastic face sheets 16 p2916 A70-33362
- Free radical coupling of silyl peroxides in reinforced plastics, laminates and adhesives 16 p2937 A70-33377
- Fluid urethane laminating resin for bonding nylon and glass fabrics, giving physical properties as function of room temperature curing time 16 p2938 A70-33381
- Solvents and chemicals resistant thermosetting resin producing high strength glass reinforced laminates based on polyanhydride crosslinked with monoepoxide 16 p2938 A70-33382
- Polyimide resin as matrix for glass fabric reinforced laminates 16 p2938 A70-33383
- H-guide dielectric losses reduction by use of artificial and laminated dielectric slabs 16 p2875 A70-33401
- Glass reinforced laminates fatigue characteristics, discussing differences from metals due to composites anisotropic structure 16 p2989 A70-33420
- Geometrically nonlinear theory for sandwich type plates symmetrically built of three elastically and thermally anisotropic layers, considering nonuniform temperature field 16 p2990 A70-33744
- Plane strain vibrations of two layered elastic cylinders, analyzing results for lobar mode numbers 2, 3 and 4 16 p2994 A70-34096
- Three dimensional linear small deformation theory of elasticity solution for free vibration of simply supported homogeneous isotropic thick laminated rectangular plates 17 p3181 A70-34522
- Shear coupling effect in cylindrical bending of anisotropic composite laminates 17 p3182 A70-34558
- Anisotropic and laminated cylindrical shells geometric design for reduction of elastic stress gradients to predetermined limit 17 p3182 A70-34559
- Failure prediction for interlaminar shear stress in filament wound rectangular plate 17 p3188 A70-35228
- Plane electromagnetic wave reflection from laminar anisotropic medium, piecewise-constant permittivity tensor as boundary value problem 18 p3229 A70-36922
- Lateral compression of rocks and global shells multilayers, using equations for buckling of single free stratum 18 p3255 A70-37076
- Flexural vibrations of laminated composite plates, maintaining continuity of displacements and surface tractions at intersurfaces between reinforcing layers and composite matrix 19 p3537 A70-37790
- Two-layer slab under aeroheating, solving bondline temperature graphically 20 p3737 A70-39693
- Dynamic theories for wave propagation in laminated and fiber reinforced composites, using dispersion curves for transverse and longitudinal motions 20 p3730 A70-40036
- Prestrained laminated media stability, discussing column buckling, standing waves, natural frequencies, wave propagation, stress-strain relations, motion equations and elastic moduli 20 p3731 A70-40049
- Mechanical behavior of cylinders with alternating layers of reinforcing and matrix materials derived from governing equations, including equations of motion 20 p3732 A70-40267
- Finite deflection discrete element analysis of sandwich plates and cylindrical shells with unbalanced laminated faces 20 p3732 A70-40268
- Numerical solution for multilayer insulation system comprised of infinite parallel metallic films separated by optically thin dielectrics 21 p3947 A70-41054
- Glass plastic composite electrically heated windshields for aircraft, discussing design, fabrication, qualification testing and service experience 21 p3750 A70-41137
- Elastic bending, vibration and buckling of simply supported thick orthotropic rectangular plates and laminates 22 p4116 A70-43205
- Cross ply laminated plates natural frequencies, approximating flexural vibration by classical theory 22 p4119 A70-43679
- Composite laminates under uniform axial strain, determining interlaminar stresses and displacements by finite difference techniques 22 p4060 A70-43684
- Finite element method for bending-extensional coupling in angle-ply laminates deformation behavior 22 p4061 A70-43685
- Temperature distribution and thermal constriction resistance due to steady heat flow in laminated composite 22 p4126 A70-43689
- Stress-strain of thin multilayer isotropic spherical shell under radial load employing shallow shell theory 22 p4120 A70-43716
- Sandwich multilayer structures temperature fields and heat transfer characteristics at high temperature [ICAS PAPER 70-38-BIS] 23 p4276 A70-44136
- Spherical multilayer shell unsteady temperature fields, assuming mixed convective and radiative transfer at inner surface due to hot gas flow 23 p4276 A70-44165
- Thick isotropic rectangular laminates free vibration and buckling, applying three dimensional linear small deformation theory of elasticity 24 p4422 A70-45296
- Holographic nondestructive testing of laminate structures, honeycomb-sandwich panels and rubber-to-metal bonds 24 p4338 A70-45755
- Viscoelastic laminated composite linear anisothermal theory, presenting homogeneous continuum model to describe dynamic characteristics 24 p4368 A70-45992
- X ray and neutron propagation in multilayer film composite, discussing boundary conditions in interferential systems 24 p4380 A70-46095
- Papers on plastics, volume 1 covering materials, design, fabrication, applications, etc 24 p4368 A70-46223
- LAMINATIONS**
- U LAMINATES
- LAMPS**
- U LUMINAIRES
- LAND USE**
- Land use mapping of southwestern U.S. using photographs from Apollo and Gemini missions [AAS PAPER 69-576] 04 p0676 A70-14640
- Remote sensor capability in land use, urban and soil moisture analysis data acquired by NASA Earth Resources Program 04 p0676 A70-14641
- Land and airspace demands in navigation, surveillance and traffic control, discussing application of current techniques 14 p2611 A70-30105
- Land use classification system of photointerpretation from remote sensor imagery 14 p2576 A70-30976
- Multipurpose earth resource satellites design, emphasizing land use factors and data reduction problems 23 p4286 A70-45005
- LANDAU DAMPING**
- Plasma waves and instabilities, detailing linearized Vlasov-Maxwell equations solution appropriate to Landau problem 06 p1118 A70-17378
- Electron plasma wave damping by ion sound wave scattering using Vlasov equation 06 p1125 A70-18638
- Propagation in perturbed magnetically focused electron beams, noting influence of spatially varying drift velocity and damping effect 07 p1239 A70-18867
- Asymptotic method for Vlasov equation formulated for weakly Landau damped monochromatic plasma wave in collisionless electron plasma 07 p1353 A70-20231
- Landau damping and stability of low density crossed field electron beams using analogy with inviscid shear flows 10 p1918 A70-23964
- Landau damping in plasma cyclotron wave interaction by symmetrical counterstreaming double electron beam with uniform magnetic field 13 p2468 A70-29917
- Grid assemblies as electrostatic plasma wave antennas, computing driving point and transimpedances for approximating single pole impedance in heavy Landau damping regime 13 p2371 A70-29918
- Landau and Doppler-shifted cyclotron damping effects on helicon-like and plasma excitations of many-valley semiconductors 13 p2472 A70-30016
- Temporal wave echoes and Landau damping in collisionless plasma using signal averaging and time delay techniques 14 p2622 A70-30687
- Space charge waves in electron beams with velocity distribution, considering dispersion equation and Landau damping 15 p2708 A70-31831
- Electron-neutral collisional damping of longitudinal electron oscillations in weakly ionized plasma, solving linearized Boltzmann-Vlasov equation 21 p3860 A70-42014
- LANDAU FACTOR**
- Surface nucleation critical field for pure superconductors at temperatures outside Landau-Ginzburg region 06 p1125 A70-17218
- Magnetic moment associated with Landau levels in magnetic induction in electron gas and magnetic fields of white dwarfs and neutron stars 09 p1752 A70-22306
- LANDING**
- NT AIRCRAFT LANDING
- NT BLIND LANDING
- NT CRASH LANDING
- NT DITCHING [LANDING]
- NT GLIDE LANDINGS
- NT LUNAR LANDING
- NT MARS LANDING
- NT PLANETARY LANDING
- NT SKID LANDINGS
- NT SOFT LANDING
- NT SPACECRAFT LANDING
- NT VERTICAL LANDING
- NT WATER LANDING
- LANDING AIDS**
- NT AIRPORT BEACONS
- NT AIRPORT LIGHTS
- NT APPROACH INDICATORS
- NT ARRESTING GEAR
- NT AUTOMATIC LANDING CONTROL
- NT INSTRUMENT LANDING SYSTEMS
- NT LANDING INSTRUMENTS
- NT MICROVISION LANDING AID
- NT RUNWAY LIGHTS
- Head-up display for horizon, desired and actual approach paths information to assist pilot during approach, landing and overshoot 02 p0330 A70-11842
- Projected and head-up flight information displays using cathode ray tubes, discussing optical system, lens design and landing aid application 02 p0330 A70-11843
- Aircraft landing measurement system /ALMS/ designed to provide computer analysis of all traffic landing at airport 02 p0331 A70-11964
- Scanning beam radio guidance system for VTOL approach and landing 02 p0336 A70-12766
- Tactical landing approach radar /TALAR/ guidance system for V/STOL aircraft steep angle approach and landing 02 p0336 A70-12767
- ILS systems, considering possible improvements 08 p1541 A70-21021
- Nuclear landing roll aid based on gamma radiation field built along approach line, runway and taxiways 09 p1721 A70-22662
- Sector-TACAN /SETAC/ system suitable for mobile approach and landing aid due to high accuracy and small dimensions 09 p1721 A70-22663
- Holographic dynamic head-up display system for aircraft carrier deck landings in low visibility 12 p2232 A70-27371
- American Airlines-McDonnell Douglas intermetropolitan STOL evaluation tests, noting microwave landing guidance system [SAE PAPER 700336] 12 p2161 A70-27464

Microwave scanning beam landing system providing aircraft radio approach guidance

12 p2269 A70-27918

Pilot landing aids for increasing air traffic, discussing Integrated Communication Navigation Identification

13 p2449 A70-29053

All-weather landing aids, discussing Scan Beam and Multilateration systems including ILS, TACAN, etc

13 p2449 A70-29054

Aircraft vertical channel landing condition autopilot using state variable feedback control techniques

15 p2773 A70-32553

Apollo lunar module alightment system, discussing design, performance and reliability

16 p2985 A70-34122

Millimeter wave radar for high resolution aircraft landing aid, describing experiments to obtain backscatter data from airborne platform

17 p3133 A70-34721

Aircraft perspective display as independent landing monitor based on electronic runway lights, discussing simulator development and flight validation

[AIAA PAPER 70-924] 17 p3064 A70-35835

Precision approach and landing guidance system selection by RTCA committee, discussing aircraft antennas, scan rates, international cooperation, etc

[AIAA PAPER 70-937] 17 p3134 A70-35846

Helicopter radar approach aid for serving oil rigs

19 p3466 A70-38621

Airborne three dimensional area navigation equipment for reducing mid-air collision exposure and for raising landing safety in terminal areas

22 p4066 A70-42296

LANDING GEAR

Cessna single engine aircraft tubular and flat steel landing gear springs, describing quality control through nondestructive testing

01 p0098 A70-10018

Commercial transport aircraft landing gear electrical circuitry dispatch reliability improvement, considering components causing flight delays due to maintenance problems

01 p0006 A70-10703

Concorde aircraft main landing gear reliability, discussing design, corrosion, hydraulic contamination, metallurgy, sealing and tests

02 p0226 A70-12366

Load analysis for aircraft landing gear during touchdown and braking operations

03 p0596 A70-14093

Hydrogen embrittlement of landing gear steels, discussing plating bath program additions for optimum safety conditions

07 p1294 A70-19349

Sailplane design standards concerning retractable undercarriage and trailing-edge flaps revised to achieve better performance

09 p1612 A70-23575

Steerable landing gear system consisting of freely castoring corotating wheel nose gear, tilt-able axle and main gear skids for lifting body spacecraft

[AIAA PAPER 69-790] 13 p2344 A70-28514

Honeycomb shock absorbers, noting landing gear applications

13 p2512 A70-28772

C-5A aircraft six wheel main landing gear bogie pitching control, emphasizing braking torque compensating mechanism design

[AIAA PAPER 70-914] 17 p3020 A70-35826

Large wheel and tire imperfection effects on nosegear parametric shimmy instability, using Mathieu equation

18 p3213 A70-36455

Landing gear weight analytical estimation, discussing ground loads, member cross sectional area, parametric variations, etc

[SAE PAPER 829] 20 p3563 A70-40366

Spacecraft landing gear shock attenuation systems using crushable honeycomb, draw-die tubes and retrorocket skirt jet

23 p4262 A70-44695

LANDING INSTRUMENTS

NT APPROACH INDICATORS

Head-up display for horizon, desired and actual approach paths information to assist pilot during approach, landing and overshoot

02 p0330 A70-11842

V/STOL aircraft ground guidance systems using microwave instruments for approach and landing

[SAE PAPER 700322] 12 p2266 A70-27458

Aircraft instrument landing system replacement requirements in terms of airports, aircraft, approach and landing paths, service classes, etc

12 p2269 A70-27917

Airborne vertical glide path guidance computer for aircraft landing, using barometric altitude and DME data

16 p2871 A70-34053

Low visibility aircraft landing problem concerning pilot instrument and visual cue and federal regulations governing operational approval

[AIAA PAPER 70-936] 17 p3134 A70-35845

SATRAM, multiple trajectory landing system for aircraft position indication within large airspace

18 p3289 A70-36948

Airport capacity and terminal area safety increase by scanning beam instrument landing system, discussing automatic guidance trajectory example

19 p3464 A70-37913

Aircraft onboard radar system with landing monitor perspective display of runway operating independently of ground based electronic equipment

[AIAA PAPER 70-1336] 24 p4373 A70-45932

LANDING LOADS

Optimum damping and stiffness in nonlinear single degree of freedom systems, discussing protection from ground and velocity shock during landing impact

11 p2145 A70-26695

Apollo lunar module structural integrity for lunar landing verified by Monte Carlo dynamic analysis

12 p2312 A70-27114

Unmanned spacecraft landing shock absorption by hybrid pneumatic configuration having hard surfaced footpad with dual pneumatic bag attenuator

12 p2312 A70-27115

Preliminary aircraft wing design for gusts or landing impacts inducing vibrations, inertia effects and dynamic overloads

14 p2655 A70-30177

High impact Ag-Zn cell design for space missions instrument package landing, considering heat sterilization and minimum operational capability

21 p3757 A70-41013

LANDING MODULES

NT LUNAR LANDING MODULES

NT LUNAR MODULE

NT MARS EXCURSION MODULE

Digital computer program /LANDIT/ for predicting structural impact response of axisymmetric landing vehicles consisting of rigid payload and crushable impact limiter system

02 p0380 A70-11945

LANDING SIMULATION

High fidelity simulations for environmental stress evaluations, describing carbon dioxide effects on pilots simulated ground target tracking and reentry vehicle landing

06 p0999 A70-17291

Thermal testing of planetary lander vehicle in vacuum chamber, modeling electronics modules and experiments using resistance heaters

[AIAA PAPER 70-222] 06 p1157 A70-18128

Landing performance of BLEU static cockpit simulator compared with flight data for night conditions in clear and limited visibility

10 p1859 A70-24215

Subsystem weight trade-offs for design optimization of out-of-orbit Mars soft lander, using atmosphere and surface environmental Monte Carlo model

11 p2124 A70-26215

Surveyor spacecraft landing shock absorbers design and performance assessment by digital computer simulation

16 p2922 A70-34123

Aircraft perspective display as independent landing monitor based on electronic runway lights, discussing simulator development and flight validation

[AIAA PAPER 70-924] 17 p3064 A70-35835

TV display simulation of instrument and visual aircraft landing approaches, investigating color, collimation and resolution effects on pilot evaluations

20 p3578 A70-39172

Lunar landing training vehicle using Lunar Module free flight simulator for earth practicing of final descent handling

21 p3750 A70-41193

Pilot heart rate during in-flight simulated ILS approaches in general aviation aircraft

24 p4306 A70-45333

LANDING SITES

NT LUNAR LANDING SITES

Surveyor 7 lunar mission landing site, equipment, operations, etc

05 p0915 A70-16830

Statistical orbit and position determination for Mars orbiters and landers based on Viking 1973 mission requirements, discussing tracking problems

[AIAA PAPER 70-160] 06 p1158 A70-18177

Asteroid vs planet for manned landing site, considering Martian moons mission

11 p2108 A70-25660

Statistical orbit and position determination for Mars orbiters and landers based on Viking 1973 mission requirements, discussing tracking problems

[AIAA PAPER 70-160] 21 p3931 A70-41861

LANDING SPEED

Thrust control unit in Lufthansa Boeing 707 aircraft designed to maintain landing approach speed by adjusting throttle setting and landing flap position

05 p0845 A70-15903

LANDING SYSTEMS

U LANDING AIDS

LANDMARKS

Satellite navigation method for locating Mars landmark or target point for exploration by roving vehicle located as center of coordinate system

11 p2080 A70-26213

LANDSCAPE

U TERRAIN

U TOPOGRAPHY

LANGMUIR PROBES

U ELECTROSTATIC PROBES

LANGUAGE PROGRAMMING

ALGOL Dynamic Display System for debugging and optimizing computer source language program, providing real time portrayal of static and dynamic block structure, etc

02 p0264 A70-12128

Analysis method permitting English speech sound recognition by computer for different speakers

08 p1460 A70-20815

Combined discrete event and continuous systems simulation language, discussing mathematical modeling and various applications

10 p1860 A70-24652

Computer aided on-line test generation for prelaunch checkout, describing interpretive test language for rapid man machine information transfer

[AIAA PAPER 70-384] 10 p1846 A70-24921

Cost effectiveness of higher order language /HOL/ for airborne computers

16 p3003 A70-33428

Natural language a priori description and linguistic algorithms construction, using statistical phrase contraction with Hoffman codes

22 p3993 A70-42492

LANGUAGES

NT ALGOL

NT ENGLISH LANGUAGE

NT FORTRAN

NT MACHINE ORIENTED LANGUAGES

NT ORTHOGRAPHY

NT SENTENCES

NT WORDS [LANGUAGE]

LANTHANIDE SERIES METALS

U RARE EARTH ELEMENTS

LANTHANUM

Sroutium chloride lanthanum ion system with dynamic Jahn-Teller effect, indicating isotropic EPM spectrum resulting from averaging by relaxation

13 p2470 A70-29109

LANTHANUM ALLOYS

Thorium phosphide anti-type microstructure of La-Rh system by X ray diffraction, discussing bcc structure, lattice constants, etc

15 p2695 A70-32549

LANTHANUM COMPOUNDS

NT LANTHANUM OXIDES

Chondrite-normalized lanthanide pattern of silicate inclusion of Woodbine iron meteorite, showing differences from mesosiderite phase and chondrite

01 p0177 A70-10340

Magnetic and structural characteristics of ternary intermetallic systems with lanthanides, considering Ln substitution by other rare earth elements

22 p4085 A70-42481

Perovskite type oxide lanthanum manganese magnetic properties, explaining ferromagnetism by spin Hamiltonian formalism

24 p4389 A70-45601

Magnetic properties of lanthanum calcium manganese, making stoichiometric specimens by controlling oxygen partial pressure

24 p4390 A70-45602

LANTHANUM OXIDES

Partition functions and equilibrium constants for ScO, YO and LaO computed for 1000-8000 K, assuming doublet ground electronic state

10 p1946 A70-24970

LAP JOINTS

Nonuniform stress distribution along side fillet welds and in welded plates of lap joint, discussing tangential stresses and plate width

11 p2058 A70-25598

Solid state butt and lap joint welding of TD-nickel bar, evaluating performance by stress rupture and shear tests

21 p3832 A70-40790

Epoxy and polyurethane adhesives stress-strain behavior in lap joints, examining bond thickness and cryogenic temperature effects

21 p3844 A70-42139

LAPLACE EQUATION

Alternating direction implicit difference schemes for solving Laplace and biharmonic elliptic equations

03 p0518 A70-13026

Green function of region near circle approximation by matrix method, considering Laplace differential equation solution, conjugate harmonic function and conformal transformation

07 p1253 A70-18924

Soviet book on mathematical physics covering equilibrium equations of vibration, thermal conductance and diffusion with emphasis on Laplace equations

08 p1544 A70-20763

Cauchy spatial problem of Laplace equation, obtaining approximate solution based on initial conditions

15 p2767 A70-31584

Numerical solution to Laplace equation in spherical coordinates with axial symmetry, using Dirichlet method to obtain difference equations

15 p2767 A70-31751

Variance reduction technique for hybrid computer generated random walk solutions of partial differential equations, comparing to analytical solution
16 p2942 A70-33731

General potential function in triaxially ellipsoidal coordinates for Laplace equation, examining near earth satellites and Vinti potential
18 p3334 A70-37064

Boundary value problems in potential theory for electrical disk and spherical cap reduced to problems for two dimensional Laplace equation
20 p3657 A70-39446

Doppler effect simplification to classical Laplacian orbit determination, deriving equations in perturbed gravity field for initial point determination
23 p4246 A70-44697

LAPLACE OPERATORS

U LAPLACE TRANSFORMATION

LAPLACE TRANSFORMATION

Summary representations method to determine eigenfrequencies of finite difference Laplace operator for boundary conditions
03 p0518 A70-13079

Laplace transform applied to ordinary differential equations with variable coefficients, obtaining representations of integral and integrodifferential equations
03 p0519 A70-13506

Solar flare cosmic rays confinement to definite solar magnetic field sectors using Laplace transformation
03 p0560 A70-13977

Laplace transform of axial stress resultant in impacting semiinfinite elastic cylindrical membrane as exponential function involving wave propagation speed, applying continued fractions
[ASME PAPER 69-APM-K] 04 p0769 A70-14859

Unsteady temperature field of uniformly thick disk for inhomogeneous boundary conditions and small Fourier numbers solved by Laplace operation
05 p0958 A70-17013

Laplace transform of piecewise continuous function derivative for application to differential equations
06 p1164 A70-17428

Conducting cylindrical shell in constant magnetic field analyzed for magnetoelastic disturbances using Laplace transform
06 p1056 A70-17607

Improper integrals appearing in cross correlation of responses of two single degree of freedom systems to bandwidth limited white noise, deriving Laplace inversion formulas
07 p1236 A70-20067

Temperature distributions in multidimensional transient conduction heat transfer, using variational method and Laplace transformation
09 p1788 A70-22705

Multidata and collocation methods compared for numerical Laplace transform inversion
11 p2074 A70-26639

Variational principles of linear asymmetric elasticity for dynamic problems with initial and boundary conditions, using Laplace transforms
13 p2517 A70-29724

Lossless waveguide propagation analysis as transient problem by means of Laplace transform
14 p2556 A70-30923

Algorithm for inverse Laplace transformation of irrational transfer function via fast Fourier transform
15 p2768 A70-32577

Eigenvalues of transfer matrix and vibrations generation for passive mechanical systems with n degrees of freedom based on Laplace transformation
18 p3337 A70-36225

Inverse Laplace transform of network function with allowance for initial differential equation solution, determining circuit temporal characteristics
19 p3456 A70-37269

Random signal nonlinear transformations using relations between Laplace and Fourier transforms
20 p3583 A70-39123

Laplace and Mellin transforms inversion in one dimensional cascade theory problems, using numerical methods for primary electron and photon spectra
20 p3675 A70-39305

Asymptotic equivalent functions for integral Laplace transformation transition to original in continuous media mechanics
20 p3726 A70-39873

Acoustic propagation from spherical source into surrounding medium, using Laplace transform of function with simple discontinuities
21 p3850 A70-41423

LAPSE RATE

Real gas adiabatic lapse rate applied to Venus atmosphere assumed to consist of pure carbon dioxide
11 p2107 A70-25646

LARGE SCALE INTEGRATION

Digital adaptive-element building blocks in monolithic Si structures for MOS large scale integration, considering serial/parallel multiplier and shift register chips
01 p0047 A70-10458

Large scale integration /LSI/ in electronics, discussing high density microelectronic, memory and logic circuits, fabrication and computer aided design
08 p1468 A70-20468

Polyolithic approach to LSI, studying mechanical, thermal, electric and economic properties of very dense blocks
11 p2021 A70-26829

Computer-aided MOS/LSI four phase logic circuit design, discussing software, design cycles and testing
13 p2380 A70-28375

Integrated logic circuits, considering switching properties and medium and large scale integration
13 p2372 A70-29116

Logic cells for multiple arithmetic functions suitable for LSI
13 p2377 A70-29145

Digital correlator LSI circuits design, layout and mask considerations, diffusion, metallization and dielectric deposition
13 p2378 A70-29551

Reliability assurance of LSI components consisting of complex electronic functions fabricated by semiconductor technology on single chip
15 p2713 A70-32662

Real time variable range digital filter design in suitable form for LSI realization, satisfying reduced dead-band requirement for input interface element
16 p2882 A70-33040

MOS transistor associative memory cell design utilizing LSI technology
16 p2869 A70-33464

LSI circuits in space electronics, discussing packaging, reliability, applications, etc
17 p3053 A70-35274

Multichip hybrid microcircuits design and construction, emphasizing reliability and cost reduction
18 p3232 A70-36759

LSI packaging effects on systems design, discussing physical integration
18 p3232 A70-36761

LSI technology effect on digital circuits and systems designs
19 p3387 A70-37847

Power IC fabrication methods covering monolithic chip, monobrid chips and IC driver with external power transistors
21 p3797 A70-41212

Semiconductor circuits large scale integration for aerospace computers, discussing fabrication and design
21 p3799 A70-41692

LSI 4-bit complementary speed /COS/ MOS parallel processor array
24 p4317 A70-46215

Microminiature solid state LSI imaging system design, construction and performance characteristics
24 p4320 A70-46216

LARMOR PRECESSION

Cyclotron waves absorption study in bounded rarefied plasma having Larmor electron frequency exceeding plasma frequency
10 p1925 A70-25101

Finite Larmor radius interchange and LF drift oscillations due to magnetospheric temperature and density gradient stresses in trapped plasma
13 p2401 A70-29936

LASER ALTIMETERS

Airborne laser profilometer terrain roughness measurement and recording, considering error sources
12 p2244 A70-26938

LASER COMMUNICATION

U OPTICAL COMMUNICATION

LASER HEATING

Electric resistance adjustment of thick and thin film resistors on ceramic substrate, using laser for material evaporation
20 p3640 A70-39416

Microwelding by pulsed ruby laser radiation, discussing characteristics and advantages
20 p3638 A70-40149

Particulate boron levitated electrostatically in air and ignited by pulsed laser to avoid contamination, investigating combustion by high speed photography (SMPT PREPRINT 100)
22 p4032 A70-43034

Plasma generation by pulsed laser heating, investigating ionization effects on temperature
22 p4082 A70-43224

Optical transmission and reflection gratings formed by standing light waves evaporation of thin metallic films in ruby laser cavity
23 p4200 A70-43817

High power pulsed laser fog dispersal, calculating vaporization regimes of droplet interaction with laser radiation
23 p4201 A70-44592

Basalt heating with IR carbon dioxide laser, investigating vapor fractionation for inert atmospheres, very high temperatures and silicon dioxide poor materials
24 p4409 A70-45673

LASER MATERIALS

Absorptivity, transition probability and collision broadening frequency of dimethylether at 3.51 micron

He-Xe laser wavelength, noting pressure dependence, transition lifetime and saturation intensity
21 p3835 A70-40573

Nd-YAIG laser design for sleeve stabilization, discussing flicker problem and rod cladding
21 p3836 A70-40822

Laser characteristics of Nd doped lithium germanate and silicate glasses, discussing spectroscopic properties
21 p3838 A70-42010

Host materials for increasing optically pumped solid state CW laser fundamental mode output power
22 p4048 A70-42333

Inorganic liquid lasers, discussing Nd salts solution preparation and handling methods
23 p4201 A70-44929

LASER MODES

Population inversion induced in middle channel of cascade gas laser, using probability method
01 p10106 A70-10059

Semiconductor laser active element radiation absorbing inhomogeneities effect on l-v characteristics, considering oscillation modes excitation
01 p10106 A70-10095

Ruby ring lasers unidirectional emission obtained by using Faraday rotator with small polarization plane rotation angle
01 p10107 A70-10208

Laser mode selection with slowly opened Q switches, discussing rotating prisms and Faraday rotators types, pulse buildup, far field spatial distribution, etc
01 p10108 A70-10427

Laser mode locking due to saturable absorbers taking into account dispersive property of active material, expanding electric field within cavity
01 p10109 A70-10428

Pulse width and spectrum generated by ring laser mode locked by synchronously modulated absorber as function of modulator waveform curvature and active medium
01 p10109 A70-10430

Frequency sweep /chirp/ and pulse width in externally mode locked laser with host dispersion obtained analytically using circulation pulse method
01 p10111 A70-10572

Unstable laser resonator mode patterns and losses with finite rectangular reflectors of spherical curvature, basing analysis on Cornu spiral
01 p10112 A70-10917

Electrical supply and control of monopulse 6.25 Hz ruby laser for use in optical radar, high speed photography, etc
01 p10114 A70-11270

Soviet book on methods in laser design, Volume 2, covering pumping radiation in active rods, unsteady modes, ruby and Nd glass lasers
02 p0310 A70-11691

Transverse mode controlled hydrogen Stokes laser oscillator optically pumped by pulsed ruby laser
03 p0498 A70-13153

Opposing cavity modes interference effect on passive Q switched ruby laser energy yield
03 p0499 A70-13213

Semiconductor injection laser modes, considering inhomogeneous lasing action levels over p-n junction area
03 p0499 A70-13410

Mode selection in Ar ion laser by plane resonator mirror with hole, plotting output power vs L/R parameters
03 p0500 A70-13458

Frequency spectrum, Q factor and single mode selectivity of two mirror laser resonator with absorbing thin metallic films, showing agreement for Ag and Ni
03 p0500 A70-13459

Electromagnetic field spectrum and spatial distribution in ring laser, considering transverse modes influence
03 p0500 A70-13462

Complex profile aspherical mirrors used in He-Ne gas laser to obtain single mode emission
03 p0500 A70-13465

Low threshold injection lasers in IR and visible spectrum at room temperature employing AlAs-GaAs heterojunctions, noting use for CW mode
03 p0501 A70-13723

Longitudinal and transverse mode locking in laser with passive filter, discussing giant pulse development and duration
03 p0502 A70-13746

He-Ne multimode laser radiation peak as function of pressure in methane-containing absorption cell installed in resonator
03 p0502 A70-13750

Frequency pulling and pulse position modulation of CW GaAs injection lasers by locking signal frequency variation
03 p0502 A70-13815

Power stabilization of single mode monochromatic carbon dioxide laser, using grating in cavity
03 p0503 A70-14076

Laser with nonresonant feedback calculated for single mode and total radiation fields correlation functions from Heisenberg equations

03 p0503 A70-14175

Gain interaction among oscillating modes of gas laser analyzed from rate equations viewpoint

03 p0503 A70-14208

Pico-nanosecond light pulses from mode-locked Nd glass laser with spectral mode selector, noting correspondence between pulse duration and inverse bandwidth

03 p0503 A70-14210

Laser beam broadening in atmospheric propagation from Born approximation and Gaussian model, showing no contribution by second scattered field

04 p0701 A70-14963

Mode patterns and losses for laser resonator with identical tilted spherical rectangular reflectors in stable and unstable configurations

04 p0701 A70-15021

Wavelength selection in Q switched carbon dioxide laser by intracavity gas cell providing selective absorption

04 p0702 A70-15362

He-Ne-Cd II laser operation modes for optimum pressure fill, obtaining red to blue outputs by varying current and/or temperature

04 p0702 A70-15366

Flashlamp pumped coumarin dye laser mode locked by intracavity loss modulation operating in blue region

04 p0703 A70-15622

Photostability of Nd-activated glass elements as function of dopant concentration and laser mode operation

05 p0858 A70-16266

Optical resonator reaction to coupled laser frequency, attributing differences between theory and experiment to errors in mirror reflection efficiency measurement

05 p0859 A70-16354

Frequency reaction of optical resonator to coupled laser in mismatch case, measuring laser and resonator axes displacements

05 p0859 A70-16355

Length shifts measurement with single 2-mode laser by observing beat frequency, obtaining frequency shift proportional to length shifts

05 p0859 A70-16356

Monograph on He-Ne laser beam noise properties and intensity fluctuations during single mode operation

05 p0860 A70-16559

Center dip formation in curve relating output power and frequency of carbon dioxide laser line operating in single mode on single wavelength

05 p0860 A70-16667

Frequency response of 6328 A He-Ne laser interferometer analyzed for multimode oscillations noting plasma diagnostics applications

05 p0861 A70-16989

Continuous passive mode locking of carbon dioxide laser cavity using long optical delay line

06 p1080 A70-17446

Single mode neodymium laser second harmonic radiation self focusing resulting in filamentary fractures in solid dielectrics

06 p1080 A70-17496

Weinstein approximation and iteration by digital computer for calculating disturbed Fabry-Perot laser resonator modes

06 p1081 A70-17546

Photon number per mode for laser with nonresonant feedback for homogeneous and inhomogeneous atomic line broadening

06 p1081 A70-17746

Laser mode interaction characteristics determination using resonator field equation taking into account competition and coupled modes

06 p1081 A70-17765

Ring laser frequency characteristics at two longitudinal modes emphasizing intermodal pulse frequencies

06 p1081 A70-17769

Time characteristics of pulsed calcium fluoride-dysprosium laser in single mode, observing constant emission and peak regime

06 p1082 A70-17808

Optical third harmonic generation in ADP crystals using mode locked and nonmode locked lasers

06 p1082 A70-17943

Two cavity mode locking of He-Ne laser using electro-optic phase modulator

06 p1083 A70-17947

Radiation from nonlinear polarization sideband in Ar lasers, discussing anomalous beat notes and mode locking phenomena

06 p1083 A70-17949

Transverse mode locking for carbon dioxide laser achieved with nonlinear boron chloride absorber, observing emission spatial buildup

06 p1083 A70-18425

Two mode gas laser behavior under external signal action showing mode locking possibility by combination frequencies due to medium nonlinearity

07 p1296 A70-18764

Kinetic theory of laser emission on band impurity transitions, noting spatial homogeneity effect on laser mode

07 p1299 A70-19852

Resonator aberrations and active element imperfections effect on formation of spatial and angular structures of solid state laser modes

07 p1299 A70-19854

Self pulsation in He-Cd laser, noting decreasing number of modes effect on beat frequency stability

07 p1301 A70-20017

Self mode locked pulses with rotating mirror Q switched carbon dioxide laser, attributing pulse shortness to saturation broadening of spectrum

07 p1301 A70-20018

Holograms produced with pulsed argon-ion lasers operating in singly oscillating transverse modes

07 p1287 A70-20088

Coherence improvement of ruby laser emission in free mode using corrective holograms in resonator

07 p1303 A70-20323

Solid state lasers with strongly degenerated modes investigated for induced radiation spectral composition inertial properties

08 p1510 A70-20507

Longitudinal modes competition in He-Ne laser, studying effects of active medium isotopic composition and pressure

08 p1511 A70-20518

Neodymium laser frequency doubling based on nonlinear functional relation between polarization and electric vector in matter

08 p1512 A70-20677

Mode locked laser pulse chopping by interferometrically combined electro-optical frequency shifters

08 p1513 A70-21541

Single mode He-Ne ring laser lock-in threshold and output power relationships to frequency

08 p1514 A70-21692

Spatial and energy characteristics of laser with nonuniform transmittance across resonator mirrors, analyzing transverse modes interaction

08 p1514 A70-21816

He-Ne laser emission in transverse oscillation mode, analyzing spatial and temporal coherence characteristics

09 p1694 A70-22135

Pulse train transition in Nd-YAG and He-Ne lasers mode-locked by intracavity phase modulator

09 p1697 A70-22919

Single mode output power at 6328 A spectral line during He-Ne laser oscillation simultaneously at 6328 A and 3.39 microns

09 p1697 A70-22957

Transverse mode distortions in high gain giant pulse laser oscillators associated with gain saturation effects

09 p1698 A70-23361

Mode coupling and intensity pulsations observed between two 6328 A He-Ne lasers through nonlinear gain characteristics of inverted population

09 p1699 A70-23363

Subnanosecond laser pulses for plasma production obtained via mode selecting uncoated flats inserted in laser cavity

09 p1699 A70-23364

Optical resonators formed by spherical mirrors, deriving mode density-output power relationship by ray analysis

09 p1729 A70-23521

Amplifier properties and oscillator mode structure of multipath carbon dioxide laser

09 p1699 A70-23538

Single-pass multimode carbon dioxide laser amplifier power gain optimization

10 p1897 A70-23815

Ge-Cu IR detector photoconducting characteristics and application to carbon dioxide laser mode pattern measurement

10 p1898 A70-23922

Neodymium glass laser fundamental frequency spatial structure effects on KDP crystal second harmonic generation efficiency, describing optimal system for laser beam shaping

10 p1899 A70-24262

He-Ne laser IR generation in three mirror mismatched resonator, using Fabry-Perot interferometer to study mode and lasing range frequency shift

10 p1900 A70-24265

Circular confocal laser with coupling aperture in mirror for maximum power output in specified mode, calculating field distributions and diffraction losses at reflectors

10 p1900 A70-24941

Axial mode selection and frequency stabilization of Nd-YAG laser by optimally designed crystal quartz etalon

10 p1900 A70-24943

Length shifts measurement with two mode laser, noting frequency shift proportionality to mirror displacement

11 p2062 A70-25632

Divergence measurement of beam emitted by ruby laser in relaxation mode as function of cavity length and excitation voltage

11 p2063 A70-26462

Auto-oscillatory regimes in annular gas laser under coupling due to scattering, considering mode competition

11 p2064 A70-26811

He-Ne lasers mode locking by self beat feedback between cavity modes, achieving nonlinear control by circuit adjustment

12 p2245 A70-27273

Steady state two frequency laser emission threshold and intensity, studying effects of two photon transitions and optical transition probabilities-radiation density relations

12 p2245 A70-27301

Ruby laser with electro-optical Q switching, using polarization element for emission spectrum narrowing to single longitudinal mode

12 p2245 A70-27303

Optical resonator with active medium and lenses, determining caustic surface, radiation characteristics, transverse modes, focusing conditions, etc

12 p2246 A70-27309

Coupled lasers kinetic operating characteristics, discussing emission power damping

12 p2246 A70-27315

Emission spectrum of He-Xe CW laser with nonresonant feedback mode achieved with scattering agent and various mirror schemes

12 p2246 A70-27354

Single mode TW ruby laser with ring resonator, analyzing emission spectral characteristics by Fabry-Perot etalon

12 p2246 A70-27356

Composite resonator for semiconductor laser to increase single mode power generation, determining optimal length of passive part

12 p2247 A70-27484

Brightness distribution in hologram generated image modulated by square of temporal-spatial coherence modulus of laser emitting longitudinal and transverse modes

12 p2233 A70-27503

Local losses distribution effect on intensity and opposing waves generation in ring gas laser analyzed in approximation of noninteracting modes

12 p2248 A70-27510

Interferometric combinations of frequency-shifted mode-locked laser pulses achieved by optical modulation-demodulation methods

12 p2249 A70-27755

Submillimeter range HCN gas laser design and characteristics, noting single mode, linear polarization and output power

12 p2250 A70-28180

Triple passage crystal amplifier of single frequency ruby laser emission, noting radiation structure and coherence

12 p2250 A70-28183

Optical resonator longitudinal modes selection, comparing Michelson interferometer, internal slanted Fabry-Perot interferometer and absorbing film methods

12 p2251 A70-28290

Coherence brightened /superradiance/ laser, discussing conditions for atomic energy single pulse radiation

12 p2251 A70-28369

Three mirror resonator He-Ne laser output spectra, studying frequencies and intensities of generated modes

13 p2424 A70-28595

Two mirror astigmatic resonator mode fields and stability determined by writing Fredholm equation suitable to geometrical optics approximation

13 p2424 A70-28596

Transverse laser modes interaction in traveling and standing wave generators allowing for spatial distribution

13 p2424 A70-28597

Hanle effect in single mode He-Ne laser, observing spontaneous emission on different spectral lines and estimating lifetimes of Ne excited states

13 p2424 A70-28598

Power output dependence on cavity configuration of He-Ne laser in TEM mode operation

13 p2425 A70-28625

CW mode locked lasers picosecond pulse widths and shapes measured, determining harmonics and Fourier expansion

13 p2425 A70-28794

Transparent polymeric materials failure under neodymium-glass laser radiation in free generation mode

13 p2427 A70-29300

Laser cavity modal volume-output power relationship, deriving expression for interaction region

13 p2427 A70-29359

Solid state laser transverse modes maximum dependence on resonator geometrical parameters usable for producing stable kinetic emission mode with narrow spectral line

13 p2428 A70-29410

Giant pulses composed of shorter pulse trains obtained in Q switched carbon dioxide laser with transverse modes

13 p2429 A70-29412

Temporal structure and spectral evolution of Nd laser emission with self locking axial modes, noting gain saturation effects

13 p2430 A70-29776

Continuous operation He-Ne lasers, discussing excitation, structural and optical design, mode selection and performance specifications

14 p2593 A70-30353

Single mode gas laser theory for arbitrary field intensities in terms of ensemble averaged form of density-matrix equations of motion

14 p1594 A70-31361

Opposing mode interaction effect on ring laser unidirectional emission instability, discussing homogeneous and inhomogeneous line broadening

15 p2749 A70-31552

Atomic collision effect on frequency range of opposing traveling wave modes in gas ring laser, using density matrix equation

15 p2749 A70-31553

Luminescent line broadening effect on axial mode selectivity in pulsed neodymium lasers with Fabry-Perot resonator at above-threshold pumping power

15 p2749 A70-31554

Scattering function and image quality in sharp edge holography using single mode laser, analyzing coherent and diffuse light

15 p2733 A70-31556

False signal in scanning interferometer for helium-neon lasers in single and simultaneous TEM modes

15 p2749 A70-31557

CW nonspiking single mode ruby laser operation by end pumping ruby with CW argon ion laser output

15 p2751 A70-31981

Mode controlled Q switched tuneable ruby laser, obtaining frequency scanning by temperature and pressure control

15 p2752 A70-32048

Single mode gas laser with large saturation and dispersion effects, discussing resonator alignment to spectral line frequency

15 p2752 A70-32196

Mirror damage problem with mode locked ruby laser system solved by rough stack mirror fabricated from microscope coverslips

15 p2753 A70-32546

CW argon lasers simultaneous mode selection and phase locking by electro-optic KDDP crystals

15 p2753 A70-32610

Ruby and neodymium glass free running lasers output power modulation relationship to excited modes and active rod position in resonator

15 p2753 A70-32822

Mode locked laser emission intensity correlation measurements by two photon fluorescence (TPF) technique to determine temporal behavior, discussing domain model

16 p2928 A70-33286

Laser mode matching to obscured circular aperture of optical telescope system in terms of antenna gain

16 p2929 A70-33982

Mode locked He-Ne laser nsec pulses propagation along multimode cladged glass fibers

16 p2865 A70-34039

Nd-glass laser operation in giant pulse mode with passive or optomechanical shutter, noting applications

16 p2929 A70-34211

Hydrogen plasma refractive index and absorption constant for laser radiation frequencies as functions of electron temperature and atomic density

16 p2959 A70-34338

High-power Q switched solid state laser radiation intensity measurement methods for multi and single modes

17 p3105 A70-35094

Single frequency Ar ion laser, discussing power and frequency stability

17 p3105 A70-35095

Gas laser phase locking due to loss modulation with double mode spacing

17 p3107 A70-35474

Internally loss modulated multimode ring gas laser, showing pulse peak intensity with detuning for phase locking

17 p3107 A70-35475

He-Cd pulsed laser mode locking at 4416 and 3250 Å using intracavity acoustic loss modulator

18 p3266 A70-36314

Laser mode locking theory, explaining subpicosecond structure and frequency chirp

18 p3266 A70-36315

Nonequidistant structure of axial mode spectrum of ruby laser with plane dielectric mirrors

18 p3266 A70-36418

Luminescence decreases in laser active medium operating in free emission mode, using kinetic equations for integral and spectral level populations

18 p3267 A70-36615

Gain and loss processes in GaAlAs-GaAs heterostructure lasers as functions of current and cavity length

18 p3268 A70-36728

Resonant modes of GaAs junction laser beams with Hermite-Gaussian rectangular symmetry, using stripe geometry with lens-slit combination

18 p3268 A70-36732

Regular relaxation oscillations of ruby laser by moving resonator mirrors

18 p3271 A70-36954

Two mode gas laser behavior under external signal action showing mode locking possibility by combination frequencies due to medium nonlinearity

18 p3271 A70-37108

Monograph on gas laser dynamics, emphasizing single mode intensity measurement as function of cavity loss in He-Ne laser

19 p3446 A70-37978

Gallium aluminum arsenide-GaAs laser diodes properties and applications for CW operation, discussing p-GaAs layer thickness effects

19 p3447 A70-38454

Solid state laser with transverse mode selection to increase brightness, discussing plano-concave resonator

19 p3447 A70-38508

Ultrashort light pulse generation by self mode locking laser, discussing power amplification problems

19 p3448 A70-38509

Single frequency ruby laser with electro-optical Q switching, selecting transverse and longitudinal modes by stepwise voltage application to shutter

19 p3448 A70-38737

Giant pulse neodymium glass laser emission spectrum structure, showing cavity geometry effect on fine structure

20 p3641 A70-39450

Cavity mode mixing effects in internally scanned lasers, considering various geometries and coupling parameters for continuous transverse aperture velocity

21 p3835 A70-40720

Q switched free running mode-locked lasers with cavity mirror consisting of thin glass plates suitable for high power use

21 p3836 A70-40807

YAG-ND laser volume limits condition for high power fundamental mode operation

21 p3836 A70-40808

Mode intensity fluctuations in unlocked multiple mode He-Ne laser related to LF noise

21 p3837 A70-41918

Threshold retinal damage by CW He-Ne lasers due to mode locking

21 p3771 A70-41997

Pulse velocity and mode pulling in inhomogeneously broadened laser with equally spaced modes, noting pulse shape time stability in presence of dispersion

21 p3838 A70-42008

Semiconductor platelet laser stimulated emission visual observation in unwanted reflected modes

21 p3838 A70-42022

Accurate tuning methods for laser mode locking device, using diffracted light measurement and photodiode with LF spectrum analyzer

21 p3838 A70-42047

Host materials for increasing optically pumped solid state CW laser fundamental mode output power

22 p4048 A70-42333

Thin optically pumped pulsed CdSe platelet lasers, detecting mode jumping and tuning effects by time-resolved spectroscopy

22 p4049 A70-42946

He-Ne gas laser, construction, operation and characteristic mode patterns

22 p4049 A70-42959

Frequency modulated gas laser communication system, discussing Raman-Nath effect, Doppler shifting phase grating, monochromatic light, pseudostanding wave, optical heterodyne detector, etc

22 p3989 A70-42966

LF cavity loss modulations of homogeneous four-level CW Nd-YAG laser, including relaxation-oscillation regime

22 p4050 A70-43005

Passive Q switching and mode locking of carbon dioxide laser with saturable absorbers and buffer gases, using electric pulse excitation

22 p4050 A70-43023

Longitudinal, transverse and simultaneous longitudinal-transverse gas laser mode locking

22 p4051 A70-43329

Ruby laser mode excitation, spatial coherence and free emission kinetics investigated by high speed camera scanning

22 p4051 A70-43461

Ruby and Nd glass solid state lasers modes partial self synchronization investigated by spectral time resolution method

22 p4051 A70-43463

Emission spectrum of He-Xe CW laser with non-resonant feedback mode achieved with scattering agent and various mirror schemes

22 p4052 A70-43597

Solid state high energy light detector for pulsed ruby and glass lasers in long pulse mode

22 p4052 A70-43614

Nd-glass mode-locked laser with KDP crystal frequency doubling and pulse selection with Pockels cell

23 p4201 A70-44476

High gain Xe laser effects on longitudinal mode splitting, noting increased frequency of radiation propagation through highly dispersive medium

23 p4201 A70-44918

Reynolds stress measurement, using laser flowmeter with cylindrical lenses and square aperture mask

23 p4202 A70-44945

Axial modes interaction in He-Ne laser with atomic collisions in active medium, computing intensities and emission frequencies

23 p4202 A70-45053

Auto-oscillatory regimes in annular gas laser under coupling due to scattering, considering mode competition

24 p4351 A70-45183

Single mode dye and Nd glass lasers axial mode selection by dye filters, noting radiation spectra and spatial coherence

24 p4352 A70-45462

Laser kinetics based on exothermal chemical reactions for electron transition stimulation, emphasizing single mode operation

24 p4354 A70-45656

Time evolution of instantaneous light intensity mean and variance for Q switched single mode laser near oscillation threshold

24 p4355 A70-46090

Mode locked laser pulses picosecond structure predicted from theoretical model of Gaussian random radiation field with temporal envelope modulation

24 p4355 A70-46263

LASER OUTPUTS

Michelson interferometer with movable mirror using laser beam to measure linear by counting fringes number, discussing design features

01 p0085 A70-10032

Hyperbolic type gas lens design and focusing characteristics for use in laser light beam waveguide

01 p0106 A70-10033

Spectral efficiency of coaxial flash lamp pumping gas laser, noting dependence on geometrical and physical parameters of source and active body

01 p0106 A70-10061

Gas laser beams divergence at various laser power levels vs resonator nonconfocality

01 p0106 A70-10062

Ar ion laser with high discharge current density observed for working level populations by simultaneously measuring power gain and spontaneous emission lines intensity

01 p0106 A70-10063

Output power and gain saturation characteristics for high speed flowing gas molecular lasers, discussing electrically excited fluid mixing carbon dioxide laser

01 p0107 A70-10103

Argon CW lasers stationary thermal self focusing in various absorbing crystals and glasses

01 p0107 A70-10207

Ruby ring lasers unidirectional emission obtained by using Faraday rotator with small polarization plane rotation angle

01 p0107 A70-10208

Optical paths inequality of nonuniform power opposing waves in ring lasers

01 p0107 A70-10209

CW laser perturbation by coupled optical transition at strong pumping with incoherent and coherent perturbing radiation, considering disappearance of laser effect

01 p0108 A70-10231

Difference frequency generation by resonant three photon process during optical mixing in ruby laser medium with simultaneous emission of optical transitions

01 p0108 A70-10350

Optical data display involving laser light deflection by vibrating mirrors actuated by mechanical resonators

01 p0108 A70-10355

Coherent short wave and UV radiation generation using continuous ion gas laser, discussing efficiency, stability and feedback effects

01 p0108 A70-10356

Laser processing applied to optical nondestructive materials tests for surface flaws

01 p0086 A70-10416

Length measuring systems based on Michelson type interferometers, laser sources, fringe counting electronics, ambient air compensation, fringe-inch conversion and digital display

01 p0108 A70-10418

Confocal parameters, spot sizes, waist positions and stability conditions of astigmatic Gaussian beams formed by spherical mirror laser cavity resonators

01 p0108 A70-10426

Gas laser beams short time constant and thermal self defocusing following small spot focusing on thin dye sample

01 p0109 A70-10431

He-Ne gas laser simultaneous oscillation detection based on output power modulation due to variable path length element placed in cavity

01 p0109 A70-10434

Critical impurity concentrations of He-Ne laser quenching determined with mass spectrometer, giving impurities molecular weight and ionization potential for input powers

01 p0110 A70-10491

Superradiant traveling wave laser emission observed with polymethine cyanine dyes pumped by mode locked ruby laser for picosecond duration pulse generation

01 p0110 A70-10564

Frequency locking of flashlamp pumped Rhodamine 6G dye lasers to D lines of Na vapor by Faraday rotation, noting doublet splitting

01 p0110 A70-10568

Threshold laser power density-atom density relation in cesium vapor optical breakdown, suggesting two photon ionization process

01 p0110 A70-10569

Sulfur compound effects on carbon monoxide-nitrogen laser emission stability, obtaining continuous operation independently of tube quality

01 p0111 A70-10660

Raman effect liquid laser power as function of cavity length, using Q switched ruby laser beam focused by cylindrical lens for optical pump

01 p0111 A70-10674

Noise power spectrum characteristics for He-Ne laser as function of discharge characteristics, measuring effect of cold vs hot cathodes

01 p0111 A70-10745

Real time recording and permanent display, using high power energy density focused Ar laser beam for ink transfer

01 p0111 A70-10782

IR CW sum-frequency up-conversion of carbon dioxide laser radiation using phase matched proustite as nonlinear crystal

01 p0111 A70-10786

Laser radiation effects on eye, quantifying light necessary for coagulation for retinal detachment surgery, discussing risks in laser surgery

01 p0037 A70-10859

Gas laser technology, discussing light emission and absorption by gas discharges and basic properties of He-Ne, Ar ion and carbon dioxide lasers

01 p0112 A70-10875

Matrix method applied to achromatic linear phase plates design for polychromatic Ar lasers half wave phase shift

01 p0113 A70-10988

Polarization level dependence of dye lasers emission on angles between direction of forced radiation and pumping laser resonator axis

01 p0113 A70-11037

Laser beam technique applied to thermal shock testing of metal disks, using solid state laser, compared to predicted results

01 p0113 A70-11058

IR radiation absorption from carbon dioxide laser in supersonic gas jet, applying results to nitrogen-carbon dioxide gas dynamic laser action

01 p0148 A70-11123

Optical parametric oscillator pumped by continuously repetitively Q switched Nd:YAG laser output

01 p0113 A70-11171

Pulse propagation inside laser cavity containing amplifying medium and material displaying optical Kerr effect, predicting ultrashort pulses

01 p0113 A70-11177

Atmospheric density profiles based on laser radar return from ruby laser detected by photomultiplier

01 p0079 A70-11220

High output neodymium glass laser with small emission divergence angle using four lamp pumping system

01 p0114 A70-11267

CW laser ranging systems power and signal to power ratio characteristics, finding possible advantages over pulsed systems

01 p0114 A70-11321

He-Ne laser amplifier photon density, bandwidth and gain as functions of inversion and excited Ne atoms density

01 p0114 A70-11357

Ruby laser Q switching by chlorophyll d and derivatives, discussing peak output power

01 p0114 A70-11391

Numerical solutions for laser beams intensity focused by simple lenses with varying primary spherical aberration, demonstrating isophote nonuniformity role in biomedicine

01 p0000 A70-11650

Satellite positions from simultaneous measurement by laser along geocentric arc usable for determining earth mass center position

02 p0253 A70-11752

Thermal resonator effects on YAG-Nd laser rods with dielectric covered ends, using resonant model to study continuous or half wave operation

02 p0311 A70-11850

Ionized Ar laboratory laser development using Fabry-Perot etalon cavity and amplifying plasma obtained by electric current passage under pressure

02 p0311 A70-11869

Semiconductor laser quantum mechanical rate equations derivation to determine temperature and current dependences of light output properties, indicating numerical calculations for GaAs

02 p0311 A70-11884

Focal length-to-aperture ratio for maximizing collection of scattered light at right angles to illuminating laser beam used in Raman spectroscopy

02 p0311 A70-11888

Error probability, signal to noise ratio and average signal level for coherent heterodyne and photon limited laser communication systems, using Poisson distributions

02 p0255 A70-11914

GaAs injection laser operated with external optical resonator for diffraction-limited radiation, considering peak power and quantum efficiency

02 p0311 A70-11920

Kr, Xe and W-iodine lamps efficiencies for pumping Nd-doped YAG compared for use in high continuous power lasers

02 p0311 A70-11922

Spherical detonation waves propagation initiated by laser-induced spark in gaseous explosives, discussing propagation energy regimes

02 p0278 A70-12029

High power pulsed lasers development compared to thermal light sources, discussing applications to nonlinear optics

02 p0312 A70-12070

Local thermodynamic equilibrium conditions in superhigh pressure He plasma produced by laser action, obtaining threshold electric field relationship with gas pressure and temperature

02 p0312 A70-12078

Speckle pattern in image plane of laser illuminated diffuse object, calculating pattern intensity and contrast

02 p0312 A70-12106

Banana self focusing in water of laser beams with nonmonotonic intensity distribution, noting ruby laser experiment

02 p0312 A70-12260

High intensity pulsed laser radiation scattering by free electrons, studying linearly polarized incident radiation

02 p0312 A70-12276

Acoustic transients in mammalian eye induced by normal and Q switched laser pulse absorption

02 p0313 A70-12325

Ruby laser light wavelength temperature dependence measurement using Fabry-Perot etalon

02 p0313 A70-12440

Ruby laser emission wavelength temperature dependence measured spectrographically

02 p0313 A70-12441

Gaussian laser beams diffraction by straight edge bounding opaque plane on basis of Kirchhoff scalar wave theory in Fresnel limit

02 p0313 A70-12456

Partial coherence in spontaneous Raman effect, using He-Ne laser source

02 p0313 A70-12465

Book on ruby laser output power calculation as function of pumping efficiency, considering energy density distribution, absorption, induced emission and excited Cr ions

02 p0314 A70-12692

Photoelectronic measurement of distance from laser beam axis to reference plane, discussing applications to surveying, vibration measurements and atmospheric investigations

02 p0314 A70-12785

Polymethylmethacrylate block breakdown under focused pulsed laser radiation in free emission regime, noting light absorption during crack development

02 p0314 A70-12813

Quasi-classical theory of solid state lasers generation and amplification, describing radiation by Maxwell equations and atoms in external fields by Schroedinger equation

02 p0315 A70-12832

Interferential picture visibility in turbulent atmosphere measured at large path differences with Michelson-Twyman-Green interferometer using He-Ne laser radiation source

03 p0498 A70-12869

Threshold energy value of organic laser emission from coronene in methyl-cyclohexane-isopentane at 100 K

03 p0498 A70-12878

Laser emission action at 4880 Å in plasma discharge from injecting electron beam into Ar at different pressures

03 p0530 A70-13063

Molecular beam laser short term frequency instability found dependent on laser and measuring device noise

03 p0455 A70-13091

Refractive index perturbation from energy absorbed from long pulsed and Q switched Nd doped glass lasers, observing sonic waves generated by Q switched laser

03 p0498 A70-13156

Angular dependence of one dimensional first and second index matching for optical parametric mixing of laser and SRS Stokes beams for tunable laser source

03 p0498 A70-13157

Opposing cavity modes interference effect on passive Q switched ruby laser energy yield

03 p0499 A70-13213

Phonon-photon scattering intensity and line shape used to study laser-excited impurity centers dynamic characteristics in stimulated induction regime

03 p0499 A70-13256

Linearly polarized radiation in Nd-glass laser obtained without energy loss by placing glass plates in resonator at Brewster angle to axis

03 p0499 A70-13257

Vibrational relaxation and optimum population inversion of carbon dioxide molecules under unsteady conditions during pulsed electron excitation, discussing laser output increase

03 p0528 A70-13408

Thermoelastic stresses in diode of pulsed and CW injection lasers, showing energy parameter limitation

03 p0499 A70-13437

Population inversion coefficient as function of optimal impurity concentrations and efficiency of ruby quantum paramagnetic amplifier in 3 cm range

03 p0499 A70-13457

Frequency measurement for HCN laser at 0.357 and 0.311 mm wavelength by mixing signal with backward wave tube harmonics

03 p0500 A70-13464

Complex profile aspherical mirrors used in He-Ne gas laser to obtain single mode emission

03 p0500 A70-13465

Energetic and temporal characteristics of CW and pulse laser radiation measured using instrument with absolute sensor

03 p0500 A70-13480

Ponderomotive meter for laser energy and power measurement, discussing mechanical design and elimination of radiometric and convection disturbances

03 p0500 A70-13481

Population inversion distribution effect on resonator losses of Nd-glass laser, showing threshold limits

03 p0500 A70-13527

Longitudinal magnetic field effect on output power and emission polarization of CW Ar laser employing Brewster windows

03 p0500 A70-13529

Interferogram contrast as spatial frequency function measured for photographic materials used in holography by He-Ne laser

03 p0485 A70-13530

Plastic film precise perforation using carbon dioxide laser and optical tooling permitting double exposure to laser beam

03 p0497 A70-13565

He-Ne laser using K-activated alumina cold cathode and coaxial construction, discussing output, low noise applications, construction and testing

03 p0501 A70-13583

Laser irradiation of RF plasmoid producing electron density increase, discussing resonance sustained RF discharges, mode locking, laser photodetachment, etc [ONERA-TP-751]

03 p0501 A70-13630

Automatic aiming system for laser range finders using directional information carried by light beam transmission [ONERA-TP-761]

03 p0450 A70-13637

Modified Smith-type reflector for long laser cavities using etalon without coatings instead of usual beam splitter, discussing output characteristics

03 p0501 A70-13648

Third harmonic generation detection for strongly absorbing media in reflection with neodymium-glass mode-locked laser, measuring nonlinear susceptibilities of semiconductors and metals

03 p0501 A70-13649

Scattered light photoelastic stress analysis using doubly refracting materials and lasers

03 p0594 A70-13657

Laser transmitter and optical superheterodyne receiver performance tests at 6328 Å, demonstrating aperture size effect and noncoherent operation superiority

03 p0450 A70-13675

Biological hazards of laser radiation, noting eye injuries and cataract from transscleral exposure on rabbits

03 p0434 A70-13679

Laboratory and field laser hazards control, noting beam termination in outdoor environment and optical density marking on protective eyewear

03 p0434 A70-13681

Spectroscopic calibration of laser lines at simultaneous carbon dioxide and nitrous oxide transitions in gas flow, showing abnormal line intensity

03 p0501 A70-13685

Discharge tube rotation effects on ring laser polarization, Q factor and radiation frequency

03 p0501 A70-13744

Power losses in ruby laser with polarized spontaneous luminescence determined as function of laser parameters and light polarization

03 p0502 A70-13747

Bouguer single-scatter theory applicability dependence on angular aperture of receiver and laser beam parameters in water mists

03 p0451 A70-13756

Holographic method for measuring optical instruments transfer function, using laser light source and beams interference

03 p0493 A70-13946

Flash lamp illuminated ruby laser operating with ordinary or extraordinary polarization, measuring gain or absorption

03 p0502 A70-13954

Power stabilization of single mode monochromatic carbon dioxide laser, using grating in cavity

03 p0503 A70-14076

Simple approximations for threshold current, gain and lasing frequency of GaAs injection laser at room temperature

03 p0503 A70-14085

Laser amplifier electromagnetic field in arbitrary quantum mechanical state, deriving complex amplitude distribution function to calculate phase uncertainty

03 p0503 A70-14174

Laser with nonresonant feedback calculated for single mode and total radiation fields correlation functions from Heisenberg equations

03 p0503 A70-14175

Superfluorescence losses in large aperture disk laser systems using Monte Carlo method, determining maximum population inversion from enhanced photon flux density considerations

03 p0503 A70-14209

Pico-nanosecond light pulses from mode-locked Nd glass laser with spectral mode selector, noting correspondence between pulse duration and inverse bandwidth

03 p0503 A70-14210

Laser cavity structure for homogeneous transverse discharge in carbon dioxide-nitrogen-helium mixtures, discussing energy and power increase per unit volume

03 p0503 A70-14357

Light spark and rapid nonlinear effects in focusing powerful light by longitudinal beam

04 p0718 A70-14405

French laser reflectors for lunar telemetry functioning with ruby laser, discussing applications to lunar orbital parameters, continental drift, gravity constant secular variations, etc

04 p0700 A70-14609

Light pulses propagation in nonlinear laser medium, obtaining equations of motion for density matrix

04 p0700 A70-14687

Laser emission intensity fluctuations influence on optical second and higher harmonic production and optical mixing arising from multimode oscillation

04 p0701 A70-14688

UHF self modulation in GaAs laser coupled to external cavity, focusing convergent beam on external mirror

04 p0701 A70-14718

Laser beam broadening in atmospheric propagation from Born approximation and Gaussian model, showing no contribution by second scattered field

04 p0701 A70-14963

Temporal isolation between pulsed orthogonal polarization state laser beams, showing selection dependence on sampling time

04 p0701 A70-15032

Saturable Q switch of cryptocyanine used in ruby laser for pulse sharpening, describing dye sensitivity to solar radiation

04 p0701 A70-15035

Laser communication system for outer space, beam guiding and fiber optical guiding systems

04 p0649 A70-15038

Admixtures effect of chloroform, diethyl ether and acetone vapors on carbon dioxide laser output power

04 p0702 A70-15202

Optical effects in parallel glass fibers irradiated by He-Ne laser beam, studying resonance tunneling and periodic power repumping between fibers

04 p0702 A70-15215

Light signals amplification efficiency, considering double-pass regenerative amplifier

04 p0702 A70-15225

Laser gain investigated for amplifications of short emission pulses in neodymium glass, discussing line broadening nonuniform mechanism

04 p0702 A70-15226

Polarization effects of helium-neon laser emission at 3.39 micron wavelength investigated in longitudinal and transverse magnetic fields

04 p0702 A70-15227

Transient molecular vibrational excitation by picosecond laser pulses found dependent on shape of Stokes pulses in Raman scattering study

04 p0702 A70-15298

He-Ne-Cd II laser operation modes for optimum pressure fill, obtaining red to blue outputs by varying current and/or temperature

04 p0702 A70-15366

Optically trapped filaments in liquid carbon disulfide by side illumination and crossed polarizers using glass laser, noting birefringence and duration time

04 p0703 A70-15619

Saturation induced wave front distortions effect on beam divergence and frequency modulation in laser amplifiers, discussing refractive index changes

04 p0703 A70-15620

Self induced light pulses from GaAs injection lasers in pulse driven diodes at liquid nitrogen temperatures, noting pulse width and frequency

04 p0703 A70-15623

Aminocoumarin derivatives and 2-hydroxyquinoline compounds for flash pumped organic lasers

04 p0703 A70-15624

Laser action observation on IR bands of first positive system of molecular nitrogen using pulsed excitation

04 p0704 A70-15625

Continuous wave chemical laser operation in carbon dioxide pumped by vibrational energy released from DF and HF molecular formation

04 p0704 A70-15686

Power distribution in carbon dioxide laser resonator with external and internal mirror at different power levels

05 p0857 A70-15796

Sonic waves induced by shock of laser produced brass and graphite vapor in air at atmospheric pressure using high speed shadowgraphs

05 p0857 A70-15802

Fusion reactions generation by high power laser beams focused on solid deuterium target

05 p0857 A70-15992

Laser characteristics relevant to microwelding and micromachining, discussing heat conduction based models limitations

05 p0857 A70-15999

Ruby laser giant pulses time stretching and shaping using stimulated Raman scattering in liquid nitrogen cell inserted in laser resonator

05 p0857 A70-16076

Projection display methods using scanned and modulated multicolor laser beams, discussing beam generation, modulation and scanning

05 p0858 A70-16188

High speed photographic study of breakdown, crack formation, thermal explosions and molecular weight of transparent plastic dielectrics under laser beam

05 p0869 A70-16210

Laser pulse registration with pyroelectric detector, noting pyroelectric phenomenon inertia limiting effect on response time

05 p0858 A70-16250

Spectral and lasing characteristics of microwave frequency modulated He-Ne laser operating at 0.63 micron wavelength

05 p0858 A70-16257

Laser beam for measuring particles velocity in two phase air-water jets by heterodyning, describing signal properties

05 p0858 A70-16258

Power output of gas laser pumped by laser contained in single resonator

05 p0858 A70-16259

Gain measurement in He-Ne laser based on small modulation of discharge current

05 p0859 A70-16267

High power giant pulse YAG laser using nonlinear material to achieve complete second harmonic conversion in intracavity experiment

05 p0859 A70-16470

Laser atmospheric backscatter measurements using frequency shifted Raman scatter and Rayleigh components for separating returns due to gaseous and aerosol components

05 p0859 A70-16476

Laser beam modulation by electro-optic devices, investigating modulator characteristics in longitudinal and transverse configurations

05 p0860 A70-16489

Laser radiation coherence origin explainable by mechanism consisting of many photon emission process by many atoms

05 p0883 A70-16500

Transverse Doppler effect of laser beam retroreflected from artificial satellite predicted by special relativity theory, noting transformations

05 p0860 A70-16653

Aperture dissection scheme to reduce transit time of Bragg angle acousto-optical scanning of laser beam

05 p0860 A70-16657

Laser Doppler velocimeter directly measuring detected frequency with passive confocal Fabry-Perot interferometer

05 p0860 A70-16658

Hologram constructed with microwaves with image reconstruction at optical wavelengths using laser

05 p0849 A70-16659

Center dip formation in curve relating output power and frequency of carbon dioxide laser line operating in single mode on single wavelength

05 p0860 A70-16667

Ocean surface roughness time variation effect on incident laser beam, analyzing motion picture data by computer program

05 p0860 A70-16687

Lasers for optical inspection of components and calibration of machine tools

05 p0860 A70-16823

Laser interferometer for earth strain study, measuring Michelson arm length changes by counting fringes in interference pattern

05 p0861 A70-16843

Optical surface degradation during measurements with high power laser, considering atmospheric dust and cleaning solvents

05 p0861 A70-16848

Q spoiled laser bombardment to obtain atomically clean surfaces in vacuum, noting damages

05 p0861 A70-16990

Doppler shift of laser beam reflected from shock wave measuring velocity through optical mixing

05 p0852 A70-16993

Displacement measurement to fractions of micron using laser interferometer

06 p1060 A70-17149

Properties of unstable confocal resonator used with carbon dioxide-nitrogen-helium laser, using geometric models and measurements

06 p1079 A70-17188

Light scattering at 90 deg from laser-induced breakdown plasmas in air, discussing origin

06 p1114 A70-17189

Steady state thermal defocusing of carbon dioxide laser radiation in gases as function of beam power, gas absorption coefficient and pathlength

06 p1079 A70-17190

He-Ne laser emission attenuation coefficient relation to water content of artificial fogs for 0.63, 1.15 and 3.39 microns

06 p1079 A70-17209

Electron transmission diffraction patterns of thin monocrystal films using Ar laser

06 p1080 A70-17444

Chemical laser action in spark excited CS₂-O₂ mixtures, attributing emission to combustion product CO

06 p1080 A70-17445

Carbon dioxide laser beam modulation by molecular Stark effect

06 p1080 A70-17448

Laser produced plasma temperature measurements using method of X rays selective transmissions through different absorbing films

06 p1081 A70-17596

Laser induced alloys erosion under various focusing conditions, determining optimal conditions for spectral studies

06 p1089 A70-17762

Spectral power distribution and ultrashort pulses limiting duration of ruby-neodymium laser with passive shutter

06 p1081 A70-17766

IR laser giant pulses duration and power measured by photomultiplier and lithium metaniobate

06 p1082 A70-17770

Carbon dioxide and monoxide molecules IR emission in laser noting CO contribution to population of higher laser level

06 p1082 A70-17772

Carbon dioxide-nitrogen laser emission absorption in atmospheric surface layer by wings of distant strong lines investigated statistically

06 p1082 A70-17807

Time characteristics of pulsed calcium fluoride-dysprosium laser in single mode, observing constant emission and peak regime

06 p1082 A70-17808

Semiconductor injection laser with large emitting area, discussing light absorption, waveguide channel formation as factors obstructing laser action

06 p1082 A70-17821

Laser harmonic-frequency mixing techniques extended into IR with IR metal-metal point contact diode

06 p1083 A70-17944

Laser induced Raman scattering as diagnostic technique for measuring specie concentrations in gas mixtures

06 p1066 A70-18214

Operational characteristics, spectroscopy and inversion mechanisms of noble gas ion lasers in light of plasma theories and atomic data

06 p1083 A70-18236

Depolarization factor measurements of clear atmospheric air by lidar techniques and laser light scattering

06 p1083 A70-18244

Lasers industrial application to distance and flow rate measurement, automated machining and tunneling, inspection, die hole punching, welding, etc

06 p1078 A70-18431

Earth axis position and displacements measured by earth-moon laser telemetry

06 p1058 A70-18452

Laser radiation increased absorption in opaque solid body attributed to vaporization, analyzing factors determining thermodynamic equilibrium between condensed and gaseous phases

06 p1083 A70-18563

Laser alignment sensors for measurement and control of five degrees of freedom with increased sensitivity, faster recording and remote meter readout

06 p1083 A70-18591

He-Cd laser output improved by transverse magnetic field application

06 p1084 A70-18619

Steels microstructural plastic deformation under pulsed laser irradiation

07 p1303 A70-18712

Laser radiation attenuation coefficient in artificial fog related to water droplet concentration, suggesting single scattering for given optical thickness

07 p1296 A70-18725

Optical system with orthogonal standing waves in liquid used for two dimensional scanning of laser beam in ultrasonic field

07 p1296 A70-18765

Nd glass laser emission spectral width reproducibility as function of flash intervals and pump energy

07 p1297 A70-18869

Hydrogen concentration effect on self sustained detonation wave propagation in hydrogen-carbon monoxide-oxygen mixtures, using Q switched pulsed laser schlieren photography

07 p1420 A70-18918

Laser eye and skin hazard evaluation from view-points of threshold effect levels and worst case assumptions

07 p1219 A70-19224

GaAs laser and laser array applications, discussing pulse generators, laser cooling, laser optics, detectors, etc

07 p1298 A70-19400

Exciton spectrum in semiconductor laser emission, investigating location in Brillouin zone and temperature dependence

07 p1298 A70-19478

Kinetic theory of laser emission on band impurity transitions, noting spatial homogeneity effect on laser mode

07 p1299 A70-19852

Kinetic theory of laser emission on direct band-band semiconductor transitions

07 p1299 A70-19853

Laser pulse power effect on edge absorption of glass filter used for Q switching applications

07 p1299 A70-19855

Transparent semiconductor crystals breakdown under intense ruby laser radiation, noting threshold power correlation with forbidden region and pulse duration

07 p1357 A70-19856

Laser emission photons scattering by semiconductor conduction electrons allowing for electron-phonon interaction

07 p1357 A70-19857

Solid state laser kinetic regime as function of diffusive and directional motions of active medium excitations

07 p1299 A70-19860

Doped semiconductor unsteady stimulated emission, solving kinetic reactions in multimodal approximation

07 p1357 A70-19862

Laser-forced medium anisotropy effects on nonlinear optical frequency mixing and combined forced scattering

07 p1335 A70-19863

Laser beam trajectory equation in scanning ultrasonic cell for nonzero incidence angle, relating input and output beam divergence

07 p1300 A70-19865

Laser emission from organic molecules under neodymium laser harmonics excitation, describing absorption and photochemical inversions effects and emission spectra characteristics

07 p1300 A70-19866

Signal to noise ratios and fluctuation spectrum of photomultiplier illuminated by laser passing through laser amplifier, noting population level effect

07 p1300 A70-19869

Laser amplifier effect on autocorrelation function of laser radiation intensity fluctuations, determining emission coherence time

07 p1300 A70-19870

Emission kinetics variations of ruby laser due to aging attributed to inhomogeneity of active medium developing simultaneously with color centers

07 p1300 A70-19872

End reflectors effects on ruby lasers emission spectra and kinetics

07 p1300 A70-19873

Dynamic pearlite-austenite transformation and melt temperatures measured in laser-irradiated steel, discussing thermal response as function of heating rate

07 p1301 A70-19897

Dye laser stimulation by pumping with pulsed nitrogen laser line to obtain entire visible spectrum

07 p1301 A70-20016

Semiconductor laser signals coupling into thin optical platelet waveguides

07 p1301 A70-20019

Carbon dioxide gas dynamic layer in shock tube facility, measuring shape, time, output energy, beam diameter, etc

07 p1301 A70-20021

Front lit holograms of transient events and live subjects obtained with reflected light pulsed laser system

07 p1287 A70-20087

Detector for focus assessment of laser on target, scanning image by fiber optics

07 p1302 A70-20089

Neodymium-doped glass bars laser amplification efficiency increased by using conical bar and divergent beam

07 p1302 A70-20096

Stress wave propagation in particulate loaded carbonaceous materials induced by homogeneous laser beam

07 p1302 A70-20097

Extrema behavior in nonlinear absorption of organic compounds under high power laser radiation interpreted by triple absorption molecular energy level models

07 p1302 A70-20100

Two photon photoconductivity of CdS crystals stimulated by ruby laser, showing emission self focusing during pumping

07 p1302 A70-20322

Raman effect in liquid nitrogen resonator with light from Q modulated Nd laser pumped into resonator at small angle to axis

07 p1303 A70-20366

Metal cutting by gas jet lasers, discussing single and multimode lasers, carbon dioxide lasers, power and power density requirements, etc

08 p1501 A70-20470

Stokes components generation in presence of stimulated combination radiation in optical cavity, considering interaction between components and effect of material dispersion on interaction

08 p1510 A70-20511

Polarization anisotropy effect of laser cavity on neodymium glass laser output power

08 p1510 A70-20513

Uncontrolled and controlled neodymium glass laser outputs, using ultrasonic traveling wave diffraction modulator

08 p1510 A70-20514

Laser radiation angular distribution determination by self calibrating method based on dividing light beam into spatially similar beams of various intensities

08 p1510 A70-20515

He-Ne single frequency laser output characteristics at various active medium pressures noting emission polarization

08 p1511 A70-20517

He-Ne laser plasma vibrations and radiation power during active medium discharge excitation by DC current, noting characteristic energy hysteresis

08 p1511 A70-20519

Stokes components simultaneous generation in presence of stimulated combination radiation in optical cavity, noting effects of incident monochromatic beam intensity

08 p1511 A70-20520

Optical pumping energy effects on lasing pulse duration during pulse excitation of alcohol solutions of rhodamine 6G

08 p1511 A70-20522

Neodymium-yttrium fluoride crystal laser free and Q switched operating characteristics

08 p1511 A70-20523

Retunable lasers with organic dye dispersive resonators, studying space-angular, spectral and energy emission characteristics

08 p1511 A70-20538

Carbon dioxide laser emission spectrum, considering working mixture emission power and rotational relaxation characteristics

08 p1511 A70-20539

Argon ion laser output powers dependence on discharge tube design and mirror reflection coefficient in emission line

08 p1511 A70-20541

Mechanical shock accelerometer calibration by light frequency Doppler shift measurement using laser interferometer and single sideband carrier insertion circuit

08 p1493 A70-20602

Medical laser systems applications, design criteria, general functions, etc

08 p1450 A70-20819

Laser systems application to automatic or semiautomatic materials processing in metal working and microelectronics, including hole drilling, silicon wafers scribing, etc

08 p1502 A70-20820

Dispersive resonator for near IR frequency control of neodymium-silicate glass laser

08 p1512 A70-20850

Transparent polymethylene methacrylate and polystyrene stressed state effect on failure characteristics under laser beam irradiation

08 p1526 A70-20936

Biological effects of laser radiation on human eye, discussing damage caused by long term exposure to visible, IR and UV wavelengths

08 p1451 A70-21043

Retinal damage thresholds by exposing rhesus monkey and human eyes to laser radiation, testing rabbit eyes for corneal thresholds

08 p1451 A70-21044

USAF permissible human exposure levels for laser irradiation established from monkey retina experiments

08 p1451 A70-21045

Laser radiation protective goggle design, investigating retinal energy density levels and attenuation

08 p1451 A70-21046

Neodymium-glass laser under action of electron beam investigated for population inversion

08 p1512 A70-21204

Gamma radiation effects on emission time, excitation threshold and efficiency of four level Nd glass laser under multimode operation

08 p1512 A70-21209

Neodymium glass laser stimulated by pinch discharge radiation in He and Kr, increasing power, energy and pulse repetition frequency by improved pumping energy coupling

08 p1512 A70-21213

Laser induced vaporization of Bi compounds with group VIa elements, analyzing vapor species, condensed phase and molecular configurations by mass spectroscopy

08 p1455 A70-21338

Vapor composition and condensed phase structure of As and Sb compounds with group VIa elements analyzed by laser mass spectrometer

08 p1455 A70-21339

Holographic technique of coherent light field transformation with desirable phase distribution from laser light beams of arbitrary wavefront characteristics

08 p1497 A70-21410

Electron-positron pair formation in electromagnetic field created by coherent laser light focused into vacuum with ideal lens

08 p1513 A70-21411

Chemical high pressure laser action produced by stimulated phototransition of electrons at contact moment between pair of reacting nonexcited gas molecules

08 p1513 A70-21412

Laser-induced electron emission from metals and insulators in form of evaporated films and single crystals, discussing many-photon photoelectric effects and thermionic emission

08 p1556 A70-21509

Pulsed nitrogen gas laser to obtain continuously tunable dye laser action to 3550 Å with output at 3771 Å in UV

08 p1513 A70-21553

CW GaAs junction laser bistable operation due to saturable absorbing centers in active medium

08 p1513 A70-21598

Laser display systems, discussing mechanical, diffractive and refractive beam deflection techniques, electro-optical polarization devices, holographic displays, etc

08 p1499 A70-21687

Single mode He-Ne ring laser lock-in threshold and output power relationships to frequency

08 p1514 A70-21692

Laser interferometric technique involving use of unstable external resonator to facilitate electron density measurements in presence of transverse plasma density gradients

08 p1499 A70-21693

Power output of sealed carbon dioxide-nitrogen-helium laser as function of gas composition and pressure

08 p1514 A70-21751

Laser radiation absorption in xenon plasma, noting dependence on intensity due to atoms ionization

08 p1554 A70-21803

Statistical characteristics of Q switched He-Ne laser emission gain during transient process from subthreshold to superthreshold value

08 p1514 A70-21814

Unsaturable frequency discriminator influence in semiconductor laser feedback loop on laser emission spectrum

08 p1514 A70-21821

Second harmonic generation and frequency conversion efficiencies for laser beam shaping in nonlinear medium

08 p1514 A70-21984

He-Ne laser investigated for He and Ne population inversion as function of discharge parameters

09 p1694 A70-22006

Line strength and radiative lifetimes for Ne II determined from spontaneous emission data obtained from CW neon laser discharge

09 p1730 A70-22070

Hydrodynamic processes during focusing of monopulse ruby laser emission into water, determining photohydrodynamic coefficient

09 p1694 A70-22111

Organic dyes investigated for amplification characteristics of Raman emission stimulated by Q switched ruby laser

09 p1694 A70-22134

He-Ne laser emission in transverse oscillation mode, analyzing spatial and temporal coherence characteristics

09 p1694 A70-22135

Ruby laser energy threshold dependence on partial shielding of rod by stainless steel tubing

09 p1694 A70-22136

Plasma discharge absorption coefficients measurement using Q switched ruby laser

09 p1694 A70-22139

Single-pulse laser radiation losses dependence on operation time length due to angular dispersion

09 p1694 A70-22140

Plasma discharge studies by holographic interferometry using ruby laser pulse for light source

09 p1674 A70-22171

Laser heating of plasma, motion pattern and shock wave parameters during absorption burst in solid body vapor, using numerical analysis

09 p1695 A70-22181

Nonlinear parameter of two intersecting laser beams in interaction with free electrons plane wave external field coupling

09 p1695 A70-22213

Plasma generation and heating by controlled thermonuclear fusion reactions using pulsed lasers

09 p1734 A70-22249

Collision effects on saturation of He line transition in He-Ne laser, determining power output dependence on cavity tuning and gas pressure

09 p1695 A70-22322

He-Ne and argon lasers for measuring radar scattering cross sections of plane and three dimensional targets

09 p1632 A70-22405

He-Ne laser emission modulation by varying discharge current, studying gas pressure effect and role of ballast resistor

09 p1695 A70-22411

Active element inhomogeneity effects on semiconductor injection lasers emission spectra and radiation intensity distribution

09 p1695 A70-22481

Output energies of Stokes components of stimulated combination scattering excited by pulsed laser

09 p1696 A70-22482

Inert gas glow discharge current change under laser radiation, investigating dependence on discharge region, gas and electrode material and configuration

09 p1696 A70-22484

Microwave in-cavity modulation of helium-neon laser, obtaining frequency dependence of modulation depth

09 p1696 A70-22628

Laser radiation diffuse reflection from rough surfaces, considering surface specularly and reflected waves polarization and spatial structure

09 p1696 A70-22630

Solid state and gas lasers industrial applications in machining and nonmachining areas, discussing limiting factors

09 p1692 A70-22706

Laser beam deflection techniques for directional control of laser beams, noting applications to optical computer memories and active imaging and display devices

09 p1696 A70-22783

Stellar optical spectral power measurement by electronic spectroscopic technique using lasers

09 p1696 A70-22785

Holographic recording of three dimensional rapid events, using Q switched laser pulses with sufficient coherence length for illumination

09 p1676 A70-22786

Laser irradiation effects on mice skin and internal organs, observing inflammatory symptoms, hair follicles destruction and epithelial atrophy

09 p1624 A70-22816

Laser radiation cumulative effects compared to single dose in mice, using hair growth stoppage as test objective

09 p1624 A70-22817

Vitreous transparent solids emission after irradiation by Q switched laser, ascribing luminescence to multiphonic and excitonic phenomenon

09 p1710 A70-22836

Time delay between pulses of discharge current and ionized argon laser power as function of current and discharge pressure

09 p1697 A70-22847

GaAs-Ge platelet laser output, observing absorption edge dynamic Burstein shift

09 p1697 A70-22920

Self stabilization and narrowing of optical pulses from GaAs junction lasers by regenerative feedback of oscillations in injection current

09 p1697 A70-22921

CW water vapor laser line frequency measurements by beating with radiations from HCN laser in metal-on-metal point contact diode

09 p1697 A70-22925

Laser frequency measurement and active and passive stabilization techniques, emphasizing HCN laser phase locking to frequency standard output

09 p1697 A70-22951

Single mode output power at 6328 A spectral line during He-Ne laser oscillation simultaneously at 6328 A and 3.39 microns

09 p1697 A70-22957

Laser measurements of permittivity fluctuations spectrum of turbulent atmosphere, noting proportionality to temperature spectra at optical frequencies

09 p1635 A70-22962

Refractory oxide submillimeter spherical particle preparation by focused emission from carbon dioxide laser

09 p1697 A70-22984

LEPR spectrometer with sample cavity as part of HCN laser for experiments with gases, noting improved sensitivity

09 p1698 A70-22991

He-Ne laser light source for oil damped spiral gauge used as vacuum system pressure nulling device

09 p1698 A70-23000

Pulsed laser beams intensity fluctuations correlation functions dependence on propagation distance in turbulent atmosphere

09 p1636 A70-23135

Axial mode gas laser radiation intensity fluctuations for plane and spherical light waves in turbulent atmosphere

09 p1636 A70-23137

Laser beam intensity fluctuations during propagation through turbulent atmosphere

09 p1637 A70-23142

CRT laser with gallium arsenide crystal excited by electron gun, describing output characteristics

09 p1698 A70-23161

Monopulse ruby lasers for moving object illumination during shadow photography, noting applications to ballistic studies

09 p1698 A70-23173

Laser-produced Al plasmas linear and nonlinear behavior, using framing camera and energy absorption measurements to study outermost ion energy increase and luminous front expansion

09 p1736 A70-23187

He-Ne CW and pulsed lasers operation, design and technology, describing measurement methods for output, beam divergence and radiation spectrum distribution

09 p1698 A70-23303

Injection lasers for multichannel optical communication using composite cavities to improve spectral output

09 p1698 A70-23359

Transverse mode distortions in high gain giant pulse laser oscillators associated with gain saturation effects

09 p1698 A70-23361

Two photon fluorescence and second harmonic generation methods for studying picosecond structure of laser output signals

09 p1699 A70-23362

Electrical narrowband noise model for laser speckle pattern, obtaining image intensity statistical properties

09 p1638 A70-23370

Laser beam with small divergence angle kept in horizontal position by leveling instrument with automatic compensating device, discussing distortion effects on localization

09 p1699 A70-23442

Ar ion laser performance improvement by using beryllia for sealed-off discharge tube

09 p1699 A70-23443

Laser action in 5d-6p electron transitions of neutral atomic iodine, measuring electron temperature and density

09 p1699 A70-23517

Scanning spherical mirror interferometer for carbon dioxide lasers radiation spectrum analysis, discussing instrument errors in mode and wavenumber studies

09 p1683 A70-23519

Fourier spectrum of chopped bivariate normal intensity distribution with coefficients calculated numerically by computer, verifying by chopped laser beam signal analysis

09 p1729 A70-23520

Optical resonators formed by spherical mirrors, deriving mode density-output power relationship by ray analysis

09 p1729 A70-23521

Atmospheric phase jitter for He-Ne locked laser measured by retroreflector for half mile round trip

09 p1699 A70-23539

Population inversion generation through gaseous oxides mixing with nitrogen flow thermally excited

09 p1700 A70-23569

Laser pulse energy ponderomotive meter using mechanical action exerted by light on movable sapphire plate in air at atmospheric pressure

09 p1700 A70-23657

Constant temperature /phase transition/ calorimeter errors in measuring laser energy using ice as working medium

09 p1700 A70-23659

High power CW carbon dioxide laser design and operation for use as heat source in metal fusing, welding and cutting

09 p1897 A70-23816

Upper atmosphere aerosols and cosmic dust properties investigation by laser beam scattering measurements using photoelectron counters for weak signal detection

09 p1898 A70-23818

Apollo 11 lunar laser reflector for earth-moon distance measurement

09 p1898 A70-23847

Relativistic nonlinear coupled longitudinal-transverse propagation of intense laser beams in cold overdense plasma

09 p1921 A70-23968

Ruby monopulse laser emission spectrum wavelength stabilization by frequency tuning of generated radiation using Fabry-Perot interferometer

09 p1898 A70-23970

Thermal lens effect produced by photocurrent in CdS, using focused laser beam to generate photocurrent causing local heating changes of refractivity

09 p1898 A70-23980

Laser beam interaction with metals on basis of energy balance measurements, obtaining time dependent radiation reflectance

09 p1898 A70-23982

Laser radiation conversion into kilovolt X rays using planar heated plasma, discussing electron temperature role

09 p1921 A70-23987

Laser pumped optical parametric oscillators (OPO), considering phase matching, threshold power, transient response, etc

09 p1898 A70-23999

Health hazards of laser operations, considering laser and laser area physical characteristics, operating procedures and controls

09 p1824 A70-24062

Intense laser radiation effect on light absorption, gas breakdown and formation of spark at focus

09 p1899 A70-24154

Strontium fluoride crystals containing trivalent neodymium cations investigated for laser action and radiation characteristics by spectroscopy

09 p1899 A70-24253

Pulsed solid state laser power output stability in terms of kinetic theory noting laser action threshold role

09 p1899 A70-24254

He-Ne laser emission electro-optical modulation by three mirror optical cavity, considering structural and thermal stability and coupled resonators geometry effects

09 p1899 A70-24260

Neodymium/YAG laser emission characteristics, studying spectral selection at various excitation energy levels and output-pumping power relationship

09 p1899 A70-24261

Ruby monopulse laser with narrow emission line, describing two generator system

09 p1899 A70-24264

Portable optical communcator for voice transmission combining pulse position modulation and low power gallium arsenide diode

09 p1840 A70-24530

Laser Doppler velocimeter optics, noting minimal heterodyne alignment needs and stress and vibration stability

09 p1889 A70-24556

Coherent photon responses production in liquids and glasses by superposing trains of giant laser pulses, achieving spatial separation of responses by combining pulse trains

09 p1900 A70-24564

Laser beam ionization of gases, using proportional ionization counter

09 p1890 A70-24588

Turbulent water flow velocity distribution measurement using laser light intensity fluctuation spectroscopy

09 p1869 A70-24600

Circular confocal laser with coupling aperture in mirror for maximum power output in specified mode, calculating field distributions and diffraction losses at reflectors

09 p1900 A70-24941

Carbon dioxide-neon-helium flowing lasers gain characteristics determined by transverse-discharge configuration

09 p1901 A70-24944

He-Ne laser amplifier in axial magnetic field, measuring Faraday rotation and gain for various input signal intensity values

09 p1901 A70-24945

Bouguer single-scatter theory applicability dependence on angular aperture of receiver and laser beam parameters in water mists

09 p1842 A70-25005

Dielectric coatings resistance to laser radiation, measuring rupture threshold of vacuum coatings consisting of zinc sulfide layers

10 p1901 A70-25111

Doppler beat spectrum and modulation depth of He-Ne laser emission with backward beam reflected from moving mirror into resonator

10 p1901 A70-25123

Continuous wave chemical laser operation at 10.6 micron in carbon dioxide pumped by vibrational energy from hydrogen atoms and bromine molecules reaction

10 p1901 A70-25149

Focal plane intensity of focused laser beam passed through turbulent atmospheric layer

10 p1901 A70-25160

Q switched ruby laser light effect on absorption spectra of NaCl crystals

10 p1902 A70-25221

Laser methods for industrial length measurements

11 p2061 A70-25355

Tunable nitrous oxide laser cavity losses and absorption by carbon dioxide determined spectroscopically

11 p2061 A70-25361

Stimulated Mandelstam-Brillouin scattering and fracture of molten quartz and silicate glasses produced by laser giant pulse

11 p2061 A70-25380

Mirror adjustment effect on transverse structure, time dependence and spatial coherence of pulsed UV molecular nitrogen laser emission

11 p2062 A70-25394

Ultrasonic LF modulation of solid state traveling medium lasers radiation intensity attributed to elastic vibrations of rods

11 p2062 A70-25398

Plastic strains at sharp notch roots in Perspex plates using interference patterns formed by gas laser monochromatic light beam for fracture initiation

11 p2131 A70-25594

Corneal thermal response model for carbon dioxide laser radiation, computing temperature rise from power distribution and conducting air-cornea interface

11 p2062 A70-25635

Spatial and amplitude modulators for laser-photographic display system producing real time TV pictures or images

11 p2062 A70-25734

Cyanide gas lasers design for submillimetric region of electromagnetic spectra

11 p2062 A70-25735

He-Ne optical laser CW operation under DC excitation, considering output power, discharge current, total pressure, mixture ratio, etc

11 p2062 A70-25827

Laser-light spatial-domain scanning function for deconvolution of blurred photographs using point-spread and holographic Fourier transform division filter

11 p2050 A70-25832

Temperature instability of electro-optical laser modulators using ADP, KDP and DKDP crystals taking into account phase shift between coherent light beams

11 p2063 A70-25848

Signal amplitude and intensity fluctuations after laser amplification, considering P representation for density operator

11 p2063 A70-25867

CW chemical laser performance using molecular hydrogen diffused into supersonic fluorine atoms streams

11 p2063 A70-26067

Modified laser Michelson interferometer for probing highly transient plasmas occurring behind incident shock waves in shock tubes

11 p2052 A70-26369

Saturation of self induced thermal lens resulting from thermal distortion of carbon dioxide laser radiation in wind

11 p2063 A70-26401

Electro-optical Q switches for generating laser radiation pulses

11 p2064 A70-26809

Statistical properties of random intensity field during coherent laser radiation scattering by moving diffuse surface

11 p2064 A70-26812

Laser field transient properties in switching-on processes, discussing Q switching, detuning switch-off and pump power switch-on

11 p2064 A70-26843

Spatial domain deconvolution by laser scanning of blurred photographs, using holographic Fourier transform division filter and photoelectric integration

12 p2230 A70-26979

Semiquantitative study showing variations in degree of laser beam coherence due to turbulence

12 p2245 A70-26980

Gas heating and ionization by Q switched laser beam, discussing electron collisions, density, etc

12 p2277 A70-27007

Laser light investigations of atoms, molecules and plasmas, considering Raman molecular spectroscopy, acoustic phonons interactions and plasma diagnostics by light scattering

12 p2245 A70-27063

Laser applications of metal machining and micromachining, discussing drilling, cutting, milling, welding, dynamic balancing, automation, etc

[SME PAPER MR-70-715] 12 p2241 A70-27082

Nonlinear optical effects in solids, gases and liquids with light from laser sources, discussing self focusing and absorption of light, transcluciation, harmonics, etc

12 p2245 A70-27277

Ultrasonic effects on synchronization of ruby laser radiation, investigating emission pulse structure and peak sequence

12 p2245 A70-27297

Steady state two frequency laser emission threshold and intensity, studying effects of two photon transitions and optical transition probabilities-radiation density relations

12 p2245 A70-27301

KDP crystal single cut for laser beam frequency conversion and tuning

12 p2245 A70-27302

Optical resonator with active medium and lenses, determining caustic surface, radiation characteristics, transverse modes, focusing conditions, etc

12 p2246 A70-27309

Green light laser using sodium fluorescein pumped by xenon pulse tubes, describing output power spectral characteristics

12 p2246 A70-27316

Electron concentration measurement range expansion in plasma by laser interferometer with optical signal phase modulation

12 p2278 A70-27328

Intense laser radiation effect on electrons interactions with acoustic and optical phonons and ionized impurities in semiconductors

12 p2246 A70-27360

Waveguide optical properties effect on injection GaAs laser threshold lasing and field distribution in near/far zones for various parameters of active region

12 p2246 A70-27365

Ruby laser illuminated Ge recombination radiation intensity measured at room temperature

12 p2286 A70-27369

Gallium arsenide laser with external mirror excited by electron beam, measuring radiation patterns

12 p2247 A70-27482

Composite resonator for semiconductor laser to increase single mode power generation, determining optimal length of passive part

12 p2247 A70-27484

Temperature effects on injection semiconductor lasers optical gain and threshold current using energy spectrum model

12 p2247 A70-27485

Solid state laser with traveling wave during steady state emission, determining pulse shape, duration and amplitude

12 p2247 A70-27497

Holograms formation without reference beam by illuminating transparency with coherent laser light

12 p2233 A70-27505

Transient process statistical characteristics in He-Ne laser operating near excitation threshold with pronounced rise time oscillations of light wave field

12 p2247 A70-27507

Saturation homogeneity ascribed to resonant photon capture in emission of neon laser

12 p2247 A70-27508

Molecular beam carbon dioxide laser Q switching by ethylene as saturating filter, reducing pulse duration by varying ethylene pressure and active mixture composition

12 p2248 A70-27509

Self focusing of ruby laser radiation in CdS single crystal, considering effect on crystal photoconductivity

12 p2248 A70-27540

Ruby crystal surface destruction by laser radiation, studying surface structural and optical properties effect and threshold power dependence on light pulses duration

12 p2248 A70-27541

Intensity and photocounts statistical distribution of harmonic generated in nonlinear crystal by laser and thermal radiation

12 p2248 A70-27547

Amplitude and phase fluctuations in laser with nonlinear absorption due to spontaneous emission, studying lasing instability near hysteresis threshold

12 p2248 A70-27548

Stimulated Mandelstam-Brillouin and entropy backscattering of light pulses, determining intensity and spectral distribution allowing for fluctuations in medium

12 p2248 A70-27550

Carbon monoxide, carbon dioxide and oxygen impurities effects on threshold current and output power of HCN laser

12 p2249 A70-27648

Carbon dioxide laser gain saturation measurements by intracavity Fresnel loss-plate technique, observing dependence on discharge current

12 p2249 A70-27715

Optical processing for measuring frequency spectrum of PM wave induced by turbulent medium in laser beam

12 p2249 A70-27756

Tuned laser radiation to diagnose and enhance local conditions in alkali metal plasma

12 p2281 A70-27793

Phase modulated laser light beam statistical analysis, using Michelson interferometer with piezoelectric crystal driven mirror connected to Gaussian random noise generator

12 p2249 A70-27877

Ruby laser beam used to trigger high voltage spark discharge in vacuum, studying auxiliary photoionization during firing delay or failure

12 p2249 A70-27999

Laser beam intensity distribution determination from measuring Fresnel diffraction pattern at straight edge using photographic plate

12 p2249 A70-28032

Sum and difference frequency signals generated and propagated by mixing carbon dioxide laser and millimeter wave klystron outputs in GaAs loaded waveguide

12 p2250 A70-28098

Laser output energy decreased by microscopic fractures masking effect in neodymium glass laser rod during monopulse operation

12 p2250 A70-28152

Population inversion effect on angular divergence of neodymium glass laser radiation, observing energy independence for refractive index of medium surrounding active rod

12 p2250 A70-28154

Automatic frequency control of single frequency He-Ne laser, tuning cavity length to extremum output power with Lamb dip

12 p2250 A70-28181

Maximum mode selection tuning of scanning interferometer with spherical mirrors applied to He-Ne laser spectrum analysis

12 p2250 A70-28182

Metals purity, gas content and porosity effects on nature and size of material zone affected by laser beam treatment

12 p2250 A70-28219

Upper atmospheric composition by nitrogen molecules radiative transition analysis, using laser resonance backscattering effect

12 p2227 A70-28267

Two-photon transitions effect on two-frequency generation threshold in media with line broadening, considering laser radiation effect on amplification in second channel

12 p2251 A70-28289

Pulsed chemical laser output, considering increase in radiation energy

12 p2251 A70-28292

He-Ne laser optimal mixture component ratio for generating IR radiation at two wavelengths

12 p2251 A70-28293

Ruby and He-Ne laser radiation attenuation found due to scattering by gas molecules and aerosols from atmospheric spectral transparency fine structure studies

12 p2191 A70-28294

Holographic achromatic reconstruction of laser holograms in transmitted white light using zonal plate

12 p2238 A70-28297

Resonant absorption in ruby crystal under combined acoustic and laser pulses, noting use for laser intensity measurements

12 p2251 A70-28331

Plasma properties investigation by laser beam probes, considering direct observation of oscillation mode

13 p2458 A70-28564

Gas laser radiation focusing with spherical mirrors, calculating field distribution and beam path

13 p2424 A70-28592

Anisotropic two phase plates gas laser resonator spectrum, analyzing zero or 90 degree angles between plates

13 p2424 A70-28594

Three mirror resonator He-Ne laser output spectra, studying frequencies and intensities of generated modes

13 p2424 A70-28595

Spontaneous emission modulation, interference beat and level crossings observable in gas laser operating at two output frequencies

13 p2425 A70-28599

Laser emission generation on sodium lines, studying pulsed discharge mechanism involving ion-ion recombination in sodium vapor and hydrogen mixture

13 p2425 A70-28600

Microdefects as centers of disk shaped destructive cracks in polymer dielectrics under laser irradiation

13 p2437 A70-28621

Power output dependence on cavity configuration of He-Ne laser in TEM mode operation

13 p2425 A70-28625

- Macroscopic plasma response to absorption of high intensity laser radiation in one dimensional geometry 13 p2459 A70-28636
- Laser radiation interaction with hot nonuniform plasma, determining thermal and electromagnetic forces for various temperatures and densities 13 p2460 A70-28643
- Far UV emission spectrum of plasma produced by laser beam impact on Al target observed as function of time, determining electron temperature 13 p2460 A70-28729
- Carbon dioxide laser saturated gain constant calculated for low and high electron densities based on thermodynamic approach 13 p2425 A70-28793
- Optical second harmonic generation internal to laser cavity, discussing nonlinearly magnitude for optimum coupling for all power levels 13 p2425 A70-28795
- Laser induced ion emission triggering of spark gaps, distinguishing channels due to electrons and ions by high speed shadowgraph technique 13 p2426 A70-28797
- HCN laser 890 GHz line phase locked to multiplied standard frequency with wide bandwidth loop, narrowing line widths 13 p2426 A70-28798
- High power CO lasers, discussing UV and visible sidelight, gas mixtures, spectral output, gas pressure, etc 13 p2426 A70-28807
- Ar ion lasers investigated for effect of added He on pulse output intensity 13 p2426 A70-28809
- Multiwavelength laser beam propagation with point source transmitters, determining turbulence levels independently 13 p2426 A70-28837
- Laser field structure effect on spectrum of Q switched laser nonmonochromatic emission after amplitude modulation 13 p2426 A70-28872
- Laser beam photography utilization in engineering for optical pointers, interferometers and holographic visualization of surface strain and vibration 13 p2406 A70-28914
- Ruby laser output calculated as function of pumping power, taking into account pumping energy density spatial distribution and laser level depopulation 13 p2427 A70-28985
- Laser with telescopic resonator, examining characteristics at different Fresnel zones and emission losses with geometric optics approximation 13 p2427 A70-29280
- Gas laser active medium nonlinear polarizability calculations with allowance for resonance emission capture effect on atomic velocity and population distributions 13 p2427 A70-29284
- Transparent polymeric materials failure under neodymium-glass laser radiation in free generation mode 13 p2427 A70-29300
- Laser cavity modal volume-output power relationship, deriving expression for interaction region 13 p2427 A70-29359
- Quantum noises in laser systems, deriving kinetic equation for traveling wave generation field density matrix 13 p2428 A70-29360
- Kinetic changes in spectral lines and bands intensity of individual molecular gases and mixtures for carbon dioxide lasers 13 p2428 A70-29361
- Pulsed Ne laser superradiation spectrum fine structure, using Fabry-Perot interferometer 13 p2428 A70-29362
- Homogeneous absorption line and peak power widths relationship in high resolution gas laser with internal absorbing cell 13 p2428 A70-29365
- Focusing lens edge diffraction effect on angular distribution of laser radiation, considering zero mode field distribution 13 p2428 A70-29367
- Steady state laser emission of resonator with two crystals with different optical orientation 13 p2428 A70-29371
- Threshold light flux densities for thin Al film breakdown by laser radiation 13 p2428 A70-29383
- Solid state laser transverse modes maximum dependence on resonator geometrical parameters usable for producing stable kinetic emission mode with narrow spectral line 13 p2428 A70-29410
- Giant pulses composed of shorter pulse trains obtained in Q switched carbon dioxide laser with transverse modes 13 p2429 A70-29412
- Q switched ruby laser pulses nonlinear absorption by partially ionized plasma behind reflected shock wavefront, observing absorptivity dependence on light intensity 13 p2429 A70-29420
- Stimulated emission cut-off characteristics of laser based on crystals with Nd ions under UV irradiation 13 p2429 A70-29505
- He-Ne laser focused beam effect on negative Si diodes base I-V characteristics 13 p2378 A70-29517
- Amplitude and phase modulation of laser beams by tetragonal crystal cuts 13 p2429 A70-29533
- P-type GaAs laser diodes spontaneous emission power temperature dependence, considering radiative recombination mechanism 13 p2378 A70-29545
- IR reflection spectrum of corundum compared for heating by reflecting furnace and laser radiation, discussing phonons statistical distribution 13 p2429 A70-29639
- Crossed field nitrogen laser operation in second positive band to obtain high UV pulse output 13 p2429 A70-29669
- Ruby laser Q switching by chlorophyll thin film, discussing characteristics and mechanics 13 p2429 A70-29670
- Laser acoustooptic quartz modulators inserted inside He-Ne and argon cavities for internal power extraction 13 p2430 A70-29705
- Non Q switched Nd laser light intensity correlation function measurement, using optical gate for producing second harmonic light 13 p2430 A70-29706
- Optical absorption due to imperfections in CdS by sensitive differential technique using laser excitation 13 p2430 A70-29708
- He-Ne laser radiation absorption in dense Li plasma, calculating absorptivity for bremsstrahlung and photoionization 13 p2465 A70-29710
- Strong short coherent light pulses with diffractive divergence generated by ruby lasers in series, showing pulse, emission and far field interferograms 13 p2430 A70-29762
- Repetitively Q switched Nd-YAG laser operated with intercavity second harmonic generator to produce one watt average power 13 p2430 A70-29831
- Electron beam-pumped ZnO laser emission wavelength at various temperatures 13 p2430 A70-29833
- Thermally self induced laser beam phase modulation resulting in far field aberrational rings, describing structure and profile 13 p2431 A70-29834
- Lasing characteristics of Nd glass, measuring efficiency, pump threshold energy and absorption under test conditions instability 13 p2431 A70-29873
- Plasma ionization enhancement by laser line radiation matched to specific atomic transitions [AIAA PAPER 69-47] 13 p2468 A70-29958
- Accident prevention in laser operation emphasizing eye protection 13 p2361 A70-30018
- Laser beams intensity fluctuations dispersions and correlation functions at various distances 14 p2593 A70-30172
- HF and DF continuous chemical lasers output power, obtaining population inversion by deuterium molecules diffusion into F atoms supersonic free jet 14 p2593 A70-30273
- HF and DF continuous chemical lasers vibrational and rotational spectra, comparing lines and relative intensities 14 p2593 A70-30274
- GaAs junction lasers output oscillations, analyzing time dependent equations for low temperatures 14 p2593 A70-30335
- Ultrafast laser-Raman spectroscopy, comparing Scan and No-Scan techniques 14 p2593 A70-30361
- Pulsed molecular and atomic gas laser sources design for submillimeter region 14 p2593 A70-30433
- Millimeter and submillimeter waves generation as difference frequencies of mixed laser beams 14 p2593 A70-30434
- Ultrashort pulse generation by solid state Q switched lasers, discussing spontaneous emission effects, atomic polarization and populations variation 14 p2594 A70-30477
- Nd laser drilling and welding tool for microminature electronic device fabrication 14 p2594 A70-30639
- Plasma production by irradiating solid hydrogen foils with intense pulse ruby laser 14 p2622 A70-30659
- Displacement sensor based on interference fringes counting by laser interferometry 14 p2594 A70-30683
- Image coherence of object by laser illumination through moving diffuser related to diffuser autocorrelation 14 p2588 A70-31208
- Single mode gas laser theory for arbitrary field intensities in terms of ensemble averaged form of density-matrix equations of motion 14 p1594 A70-31361
- CW oscillation in carbon monoxide chemical laser 15 p2748 A70-31432
- Injection semiconductor lasers emission characteristics, discussing gallium arsenide diodes, nonlinear losses in pulsed mode, laser interactions, etc 15 p2749 A70-31453
- Giant pulse generation in ruby laser requiring no introduction of additional modulating elements into resonator 15 p2749 A70-31524
- Semiconductor laser emission at band-band transitions with free carriers participation under quantizing magnetic field, using kinetic equations 15 p2749 A70-31627
- CW injection laser frequency stability, noting injection current influence on lasing frequency 15 p2750 A70-31629
- Short term influences on sealed carbon dioxide laser action and lifetime, using mass spectrometry 15 p2750 A70-31752
- Carbon dioxide-nitrogen and nitrous oxide-nitrogen laser systems, substituting diatomic N 15 for N 14 to investigate radiation intensity 15 p2750 A70-31761
- Vibration modes real time observation of complex surfaces with matt finish using changes in laser speckle 15 p2750 A70-31762
- Gas pressure effects on visible and UV laser action in small argon Z-pinch plasma discharge, using streak photographs 15 p2750 A70-31968
- CW HCN laser driven phase matched traveling wave lithium niobate electro-optic light modulator performance 15 p2750 A70-31976
- Linear power scaling-mass flow relationship in multi-Joule pulsed carbon dioxide-nitrogen-helium laser, noting thermal effects role 15 p2751 A70-31977
- High power CW CO laser operation at room temperature by introducing mercury vapor into discharge 15 p2751 A70-31979
- Laminar to turbulent flow transition observation in laser induced vertical convection, using carbon dioxide-nitrogen laser 15 p2751 A70-31980
- CW nonspiking single mode ruby laser operation by end pumping ruby with CW argon ion laser output 15 p2751 A70-31981
- Optically pumped cadmium phosphide laser, obtaining IR coherent oscillation from Q switched Nd doped YAG laser excitation 15 p2751 A70-31985
- Laser Doppler heterodyning system for velocity measurements without directional ambiguity, employing incident beams of different frequencies through rotating diffraction grating or Bragg cell application 15 p2751 A70-31986
- CW Cd vapor laser oscillation achieved with slotted hollow cathode discharge containing He carrier gas at pressures of several Torr 15 p2751 A70-31988
- Gas flow velocity measurement by coherent detection of scattered laser radiation from small particles suspended in fluid, using Doppler effect 15 p2751 A70-32030
- Laser color TV display acousto-optic deflectors equalization using prisms 15 p2751 A70-32043
- White light laser construction using Ar-Kr laser with suitable mixture and pressure of gases to provide equal output intensities of red, yellow, green and blue 15 p2752 A70-32046
- Laser beam shaping for streak interferometry, obtaining thin beam uniform over filling length 15 p2752 A70-32049
- Temperature dependence of laser emission line self broadened half widths in spectral band of carbon dioxide at constant pressure 15 p2752 A70-32056
- Laser beam scattering by free electrons in terms of classical electrodynamics, discussing radiation damping effects 15 p2752 A70-32451
- Laser beam scattering by free electrons in semiclassical radiation theory, discussing intensity dependent frequency shift 15 p2753 A70-32452
- Glass disk calorimeter for measuring free running and Q switched laser pulses 15 p2742 A70-32545
- Solid state traveling medium laser pulsed emission characteristics and nonlinear intensity distribution 15 p2753 A70-32699
- Ruby and neodymium glass free running lasers output power modulation relationship to excited modes and active rod position in resonator 15 p2753 A70-32822

Bleachable dye filters selection for periodic undamped output power oscillations in laser
15 p2753 A70-32859

Annular lasers energy, polarization, radiation loss and frequency characteristics dependence on phase shift due to anisotropic plate introduction
15 p2753 A70-32860

Backscattered radiation depolarization during illumination of aqueous medium by linearly polarized laser beam
15 p2753 A70-32861

Pulsed carbon dioxide laser production with electron beam pumping, ascertaining beam effect on discharge parameters and output power
15 p2754 A70-32864

Transverse magnetic field effect on CW argon laser operation with linearly polarized radiation
15 p2754 A70-32866

Power density fluctuations in emission peaks of ruby laser determined by splitting beam into two components and using photosensitive element and photomultiplier recording
15 p2754 A70-32874

Peak emission currents from tungsten under ruby laser focused radiation, describing integral emission by heat conduction theory and Richardson equation
15 p2754 A70-32875

Weld brittleness during laser beam welding of Ni-Cu, Ni-Ti and Cu-Ti due to diffusion processes
16 p2916 A70-33052

Spatial vectors determination by two laser measurements and one optical observation of artificial satellite
16 p2926 A70-33118

Laser Doppler velocimeter for measuring turbulence in gas and fluid flows
16 p2926 A70-33140

Laser anemometer for fluid flow measurements, noting sample size restraint, frequency response and velocity range
16 p2926 A70-33141

Laser velocity measuring system (LVMS) for high speed rocket sleds, tracking supersonic sleds through shock front
16 p2926 A70-33142

Laser Doppler-shift velocimeter with self aligning optics, discussing performance parameters
16 p2926 A70-33143

Q switched subnanosecond laser system with increased intensity, using pulse selection technique
16 p2927 A70-33163

Electro-optical sensor night time capabilities with laser illuminator, determining current per unit area from photocathode
16 p2907 A70-33183

Free generation regime of ruby laser studied by electro-optical method of smoothing spatial inversion inhomogeneities
16 p2927 A70-33192

Natural fluctuations sources intensity in annular lasers taking into account field strength dependence
16 p2927 A70-33197

Laser beam anticorrelation after attenuation by two photon amplifier, deriving density matrix in time dependent perturbation theory
16 p2928 A70-33283

Gas laser amplitude, competition, self locking, beat frequency and modes time development, using Kutta-Merson integration method
16 p2928 A70-33284

Mode locked laser emission intensity correlation measurements by two photon fluorescence (TPF) technique to determine temporal behavior, discussing domain model
16 p2928 A70-33286

Laser design for production tool applications, noting use of Nd-YAG and carbon dioxide laser [ASME PAPER 70-DE-1]
16 p2917 A70-33418

Carbon dioxide laser action at 10.6 micrometers at pressures up to atmospheric by transverse electrical discharges
16 p2928 A70-33643

Coaxial gas laser generating high intensity pulses at constant pulse repetition rate, using singly ionized Ar and molecular nitrogen as active media
16 p2928 A70-33698

Raman spectrochemical system design based on laser radiation as parent source, discussing relay optics and photon counting detector system
16 p2913 A70-33979

Holocamera holographic system for wide angle panoramic view, discussing dual laser beam illumination, side and top view diagrams, etc
16 p2913 A70-33984

Laser beam photography by multiple reflections from partially reflecting mirrors
16 p2913 A70-33985

Lasing action and reduced output without beam distortion from misaligned carbon dioxide lasers by DC-Tesla coil pumping
16 p2929 A70-33986

Ruby laser second harmonic radiation generation efficiency, using cylindrical lens beam forming optical system
16 p2929 A70-34212

Giant pulse periodic operation ruby laser with 50 MW power and 10 Hz frequency
16 p2929 A70-34217

Solid state giant pulse laser with small divergence angle, using polymethyl dye solution in nitrobenzene as Q switch
16 p2929 A70-34221

Plasma production by long wavelength lasers applied to controlled thermonuclear reactions [ALAA PAPER 70-779]
17 p3103 A70-34476

Thermal-chemical damage to carbon particles in egg albumin under ruby laser irradiation, using chemical rate equations for protein denaturation
17 p3035 A70-34577

Laser Raman spectroscopy, discussing scattering from vibrational modes in solid and from phonons above optical gap
17 p3081 A70-34599

Hypersonic velocity and turbulence measurements in wind tunnels, using spectral analysis of Doppler shifted laser light
17 p3103 A70-34849

Magnetized plasma electron density measurement by laser self heterodyne
17 p3141 A70-34996

Optical correlator for displacement measurements using laser produced speckle patterns of scattered coherent light
17 p3088 A70-35026

Laser measurements - Conference, Warsaw, September 1968
17 p3103 A70-35080

Optical frequency standards research covering lasers application with superstable emission frequency
17 p3104 A70-35081

Laser energy and power measurement with thermal gradient radiometer
17 p3104 A70-35082

Frequency and stability measurements of IF signals generated between laser far IR radiations and conventional oscillators
17 p3104 A70-35084

Primary wavelength standard established via line produced with wavelength-stabilized laser
17 p3104 A70-35086

Spectral densities of intensity and frequency fluctuations of single frequency He-Ne laser radiation
17 p3105 A70-35092

Atomic spectroscopy of IR laser transitions in gases excited by HF pulsed discharges
17 p3105 A70-35093

Standards for measuring pulsed laser energy, CW laser power and HCN laser frequency
17 p3105 A70-35097

Optical rectification/polarization/ and measurement of Q switched laser energy and time parameters, using crystals and parallel plate capacitor
17 p3105 A70-35098

Laser energy parameters measurement by calorimetric methods based on radiant heating effect
17 p3106 A70-35099

Oscillation frequency retuning and stabilization and loss factor determination in solid state lasers by dispersive resonators
17 p3106 A70-35100

Fluorescence method of determining solid state laser parameters using spontaneous and stimulated emission observations
17 p3106 A70-35101

Solid state laser polarization mechanism, considering isotropic and anisotropic cavities
17 p3106 A70-35103

Crystal and glass lasers activated by Nd ions, examining stimulated emission temperature dependence by high temperature spectroscopy
17 p3106 A70-35105

Meteorological laser radar, discussing basis and techniques determining atmospheric radiation attenuation constant
17 p3045 A70-35106

He-Ne CW laser emission line width measurement, describing apparatus and technique
17 p3106 A70-35108

Submillimeter lasers radiation measurement with n-InSb detectors at liquid He temperature
17 p3107 A70-35109

Ar plasma generation by focused Q switched ruby laser beam, measuring density and temperature by electro-optical spectroscopy
17 p3107 A70-35111

Laser interferometry for accelerometer and dynamic pressure transducer calibration and vibration measurement
17 p3089 A70-35124

Temperature dependent absorption, nonsteady beam propagation and laminar-turbulent transition in laser induced convection column, measuring turbulence onset by fine wire resistance thermometer [ALAA PAPER 70-800]
17 p3107 A70-35197

German monograph on spectral emission behavior of pulsed ruby laser with regard to output intensity
17 p3107 A70-35369

Picosecond pulses in Q switched neodymium glass and ruby lasers, describing pulse measurement with fluorescence
17 p3108 A70-35623

Intensity logarithm fluctuations of focused laser beam propagating in summer daytime atmosphere at 250 and 650 meter path lengths
17 p3048 A70-35685

He-Cd laser discharge, determining population densities and lifetimes for levels of Cd ion excited by He metastables
17 p3108 A70-35903

Channeling and guidance of electrical breakdown streamer via laser induced gas ionization trail
17 p3108 A70-35905

Time resolved measurements of ion and electron temperature in pulsed Ar ion laser discharge, observing heating
17 p3108 A70-35907

Spontaneous megawatt pulsing in ruby laser with output beam reflected back into cavity
17 p3108 A70-35909

Laser oscillation in atomic fluorine from electrically pulsed discharge of fluoride compounds-helium mixtures, identifying as 3p-2P and 3s-2P transitions in fluorine I
17 p3108 A70-35910

Gas laser frequency stabilization using nonlinear effects of magnetic Lamb dip
17 p3109 A70-35911

First luminous lunar echoes obtained by laser telemetry of Pic Du Midi observatory
18 p3310 A70-35948

Laser applications in thermonuclear fusion, analyzing plasma acceleration under laser pulse action
18 p3265 A70-36110

Energy distribution of laser spark spectrum in air, He and Ar, determining transmission coefficients of spark plasmas by self absorption method
18 p3265 A70-36151

Spatial-temporal distribution of laser spark plasma electron density and temperature based on holographic interferometry
18 p3265 A70-36152

MOS devices, investigating laser radiation effects on electrical behavior
18 p3266 A70-36237

Transverse flow CO chemical laser using atomic oxygen reaction with carbon disulfide, comparing output with longitudinal flow devices
18 p3266 A70-36313

Spatial-angular characteristics of Nd doped phosphorus oxychloride liquid lasers, discussing beam divergence effects
18 p3266 A70-36416

Thermal self focusing filaments observation in form of tracks in KDP and ADP crystals damaged by radiation from free emission mode laser
18 p3266 A70-36612

Spectral emission kinetics from neodymium glass laser with rod in translational motion during laser action
18 p3267 A70-36613

Argon and helium breakdown induced by ruby laser 50-picosec pulse at various pressures
18 p3267 A70-36616

Laser emission intensity oscillations during resonator Q sinusoidal variations
18 p3267 A70-36617

Amplitude and phase fluctuations of opposing waves in ring laser with allowance for waves coupling due to backscattering
18 p3267 A70-36618

Gravitational field effect on natural frequencies of rotating ring laser, using general relativity and electromagnetic fields theories in continuous media
18 p3267 A70-36622

Electronmicroscopical structure of laser irradiated Garding-Passy melanoma cell organelles, noting mitochondria damage
18 p3224 A70-36636

CW GaAs junction lasers bistable operation above delay transition temperature based on double acceptor trap theory
18 p3268 A70-36729

Reflectivity effect on external quantum efficiency of Fabry-Perot type GaAs injection lasers
18 p3268 A70-36731

Self induced sustained light pulsations from GaAs injection lasers with tandem double section stripe geometry based on repetitively Q switched model
18 p3269 A70-36735

Semiconductor laser frequency modulation by ultrasonic waves, noting pressure variation effect on sideband resolution
18 p3269 A70-36736

Pulsed GaAs injection lasers second harmonic generation with nonlinear crystal alpha iodic acid phase matched by angular tuning
18 p3269 A70-36737

GaAs lasers with light propagation along curved junctions, discussing threshold current density variation with radius of curvature
18 p3269 A70-36738

- Electron energy effect on output power and beam divergence of electron beam pumped GaAs lasers
18 p3269 A70-36740
- CW multifilament GaAs laser diodes measurement, showing cross correlation between light and current noises
18 p3270 A70-36742
- Q switched laser turn-on nonlinear dynamics, deriving field intensity distribution function
18 p3270 A70-36743
- Nd-YAG Q switched laser using feedback loss control to increase switching speed for digital scanning
18 p3270 A70-36744
- Laser pulse shaping using inducible absorption with Q switched time behavior controlled by nonlinearities within optical resonator
18 p3270 A70-36745
- Carbon dioxide laser producing nearly 100 percent amplitude modulation of output by intracavity polarization modulation technique
18 p3270 A70-36747
- Modulation of carbon dioxide laser with Stark cell internal to cavity, using methyl chloride electrooptical gas
18 p3270 A70-36748
- Variable ratio beam splitter design and operation for lasers, using birefringent optics
18 p3270 A70-36755
- Giant pulses in passively Q switched laser oscillator, calculating time constant of light flux exponential increase
18 p3270 A70-36953
- Laser triggered spark gap /LTSG/ with subnanosecond rise time, describing construction and operating characteristics
18 p3271 A70-37092
- Optical system with orthogonal standing waves in liquid used for two dimensional scanning of laser beam in ultrasonic field
18 p3271 A70-37109
- Coupled fiber lasers maximum energy transfer between passive conductors, determining minimum pulse duration
19 p3443 A70-37286
- Nd glass laser ultrashort light impulse optical rectification, presenting lower harmonics angular dependence
19 p3443 A70-37287
- Coherent light communication system quasi-optical lens line output field examination, using laser assembly to study parasitic, radiative and overall power losses
19 p3443 A70-37288
- CdS crystals luminescence spectrum excitation by UV light of ruby laser, noting excitons and phonons recombination
19 p3444 A70-37368
- Traveling medium solid state lasers radiation intensity modulation by active element motion
19 p3444 A70-37442
- Gas laser radiation depolarization coefficient as function of radiation energy, cavity anisotropy and operating transition type
19 p3444 A70-37445
- Turbulent mixing in supersonic cone near wake, using laser planogram technique for flow visualization
19 p3351 A70-37529
- Laser-produced plasmas production and containment, studying expansion in uniform magnetic field and charge quantity as power density function
19 p3444 A70-37535
- Holographic interferometry of rapid phase objects by two wavelengths from ruby laser and KDP crystal filter, noting application to dense plasmas
19 p3422 A70-37650
- Subnanosecond jitter spark gap obtained with YAG-Nd pulsed laser triggered switching at moderate repetition rates
19 p3444 A70-37666
- Low jitter multiple high voltage spark gaps switching at 50 pps by Q spoiled YAG laser triggering
19 p3444 A70-37667
- Gas lasers intensity expression derived by theory of double resonance spectroscopy, comparing results with He-Ne laser experimental data
19 p3445 A70-37672
- Folded path transversely excited atmospheric pressure carbon dioxide laser using shower or brush discharges, measuring output pulse characteristics
19 p3445 A70-37674
- Organic dye lasers output bandwidth and tunability extension by acidification of solution
19 p3445 A70-37675
- Laser beam alignment system for monitoring dielectric film evaporation
19 p3445 A70-37686
- Plasma lasers, investigating striation oscillations and excess noise phenomena and generation mechanisms
19 p3446 A70-37858
- Dual scatter laser Doppler velocimeter /LDV/ technique, considering system design, performance and experimental verifications
19 p3424 A70-37876
- Optimum laser beam deflection for instrument design, considering tandem, rotary mirror and analog methods
19 p3446 A70-37879
- Pulsed ruby laser holography with coherent light, discussing applications
19 p3425 A70-37886
- Monograph on gas laser dynamics, emphasizing single mode intensity measurement as function of cavity loss in He-Ne laser
19 p3446 A70-37978
- High accuracy length measurement by fringe counting using laser interferometer
19 p3447 A70-38050
- High power neodymium laser with aspherical lenses to focus photon beam for nuclear fusion experiments
19 p3447 A70-38165
- Laser radiation and solid target interaction, calculating temperature and plasma density as function of intensity
19 p3447 A70-38166
- Nuclear fusion realization by focusing from intense beam neodymium glass laser
19 p3447 A70-38167
- Laser beam and matter interaction models for positive energy balance in nuclear fusion, obtaining Lawson criterion
19 p3447 A70-38168
- He-Ne laser beam hazard to human retina
19 p3371 A70-38309
- Strong short coherent light pulses with diffractive divergence generated by ruby lasers in series, showing pulse, emission and far field interferograms
19 p3447 A70-38394
- Laser and electron beam removal of material in manufacturing technology
19 p3447 A70-38451
- Solid state laser with transverse mode selection to increase brightness, discussing plano-concave resonator
19 p3447 A70-38508
- Ultrashort light pulse generation by self mode locking laser, discussing power amplification problems
19 p3448 A70-38509
- Low noise He-Ne laser with capillary elements, measuring current threshold of noise free operation as function of design parameters
19 p3448 A70-38512
- Materials jet-like ejection from metal surfaces under high density laser radiation action, investigating erosion and plasma spectrum
19 p3448 A70-38734
- Transverse magnetic field effect on emission spectrum of He-Ne laser, using scanning interferometer
19 p3448 A70-38735
- Optical emission conversion from solid state lasers into far IR region by nonlinear polarization with difference frequency generation
19 p3448 A70-38741
- Ionic and molecular gas lasers, discussing pumping, transitions, emission, discharge tube dimensions, cooling, pressures, optical elements and applications
19 p3449 A70-38751
- Formaldehyde rotational transition hyperfine components measured by molecular beam maser
20 p3702 A70-39008
- Prototype cloud physics laser nephelometer design and performance, determining droplet concentration and size from scattered light pulse count and amplitudes
20 p3626 A70-39081
- Gratings as laser wavelength-selective end reflectors, noting application to carbon dioxide and dye lasers
20 p3639 A70-39083
- Pulsed argon ion laser output properties from electron temperatures and densities produced by He-Ar gas mixture
20 p3640 A70-39137
- CW second harmonic He-Ne laser light second order intensity correlation function measurements
20 p3640 A70-39153
- He-Xe laser with pure Xe-136 gain cell inside cavity, observing enhanced Lamb dip in power output vs frequency curve
20 p3640 A70-39154
- Laser holography for nondestructive testing of C composite structures, reducing fringe patterns to radial deformation and surface strain for cylinders and cones
20 p3718 A70-39212
- Transparent polymers stress-strain state induced by elastic waves, using model with space and time dependence of laser beam
20 p3654 A70-39248
- Spatial gain variations transverse to discharge in axially flowing carbon dioxide laser amplifier, noting relationship to flow velocity
20 p3640 A70-39391
- He-Ne laser profile-tracing system for contour measurement, suggesting steps for error reduction
20 p3640 A70-39417
- Ring lasers design and performance, measuring angular velocity by interferometry
20 p3641 A70-39418
- Protein solutions and cell cultures changes by ruby and Nd lasers radiation, noting threshold energy
20 p3579 A70-39419
- Laser interferometry with unstable external resonator, determining radial electron density distributions during implosion phase of linear z-pinch discharge in argon
20 p3630 A70-39420
- Laser beam for military weapons applications, investigating energy levels and beam guidance
20 p3641 A70-39421
- Submillimeter gas lasers with low noise and CW operation for far IR spectroscopy, noting emission lines multiplicity
20 p3641 A70-39423
- Transversely excited atmospheric pressure /TEA/ carbon dioxide laser, noting power output and cost
20 p3641 A70-39424
- Ruby laser radiation injury relationship to position and number of energy absorbing pigment particles in iris
20 p3579 A70-39425
- Object visibility limits when illuminated by laser beam with spatial selection method, discussing atmospheric conditions and light source radiation power
20 p3641 A70-39448
- Light He isotope effect on He-Ne laser power output
20 p3641 A70-39737
- Self oscillatory operation of laser with bleachable light filters, solving power balance equations by computer algorithm
20 p3641 A70-39738
- Pulsed composite laser performance with He-Ne active section and neodymium-glass power gain section
20 p3641 A70-39740
- Mirror deformation effect on laser emission angular distribution, estimating output parameters by geometric optics
20 p3642 A70-39741
- Laser beam method sensitivity for spectral emission analysis of nonconducting materials
20 p3642 A70-39743
- Radiation divergence from gas laser resonator with coupling aperture
20 p3642 A70-39752
- Organic laser spectral and energy characteristics, discussing practical operation principles, low generation threshold and harmonic energy
20 p3642 A70-39754
- High radiation intensity neodymium glass laser, describing installation for heating plasmas to high temperatures
20 p3643 A70-39758
- Multidimensional control systems synthesized in accord with polynvariance and coordinating couplings principles
20 p3604 A70-39837
- Ultrasonic LF modulation of solid state traveling medium lasers radiation intensity attributed to elastic vibrations of rods
20 p3643 A70-40092
- Metals purity, gas content and porosity effects on nature and size of material zone affected by laser beam treatment
20 p3643 A70-40094
- Planar thin film optical waveguides for integrated circuits, utilizing information carrying potential of laser light in optical communication
20 p3598 A70-40129
- Plasma nonequilibrium state formation and light absorptivity variation under high power laser pulsed radiation
20 p3684 A70-40387
- Vacuum UV laser action in molecular hydrogen Lyman bands, examining stimulated emission in P branch lines and light pulse duration
20 p3643 A70-40496
- Doppler beat spectrum and modulation depth of He-Ne laser emission with backward beam reflected from moving mirror into resonator
20 p3643 A70-40516
- Thermally induced stress birefringence effect on linearly polarized CW YAG-Nd laser
21 p3834 A70-40566
- Q switching of nitrous oxide laser with Freon 12 and sulfurhexafluoride absorbers, comparing wavelengths with carbon dioxide laser outputs
21 p3834 A70-40567
- Carbon monoxide laser efficiency increase through addition of Xe, noting change in laser output spectral intensity distribution
21 p3835 A70-40572
- Absorptivity, transition probability and collision broadening frequency of dimethylether at 3.51 micron He-Xe laser wavelength, noting pressure dependence, transition lifetime and saturation intensity
21 p3835 A70-40573
- Self focusing schlieren observation in gas breakdown, discussing cubic polarizability of excited atoms in electron cascade due to laser pulses
21 p3835 A70-40594

Carbon dioxide laser pulse shape, duration and power dependence on repetition rate during continuous pumping

21 p3835 A70-40634

Polyethyl methacrylate rupture during omnidirectional compression under laser radiation, showing pressure effect on microdefects and cracks

21 p3841 A70-40644

Electrons optical scale time averaged motion dependence in focused laser beam on light intensity gradient, calculating bremsstrahlung spectrum

21 p3836 A70-40723

Safety factor estimation by nomographic techniques for eye protection against direct viewing of laser beam

21 p3768 A70-40761

Cathode spaces electron concentration, time dependence and axial distribution by laser beams interferometric method, noting accuracy and resolution

21 p3836 A70-40796

Q switched free running mode-locked lasers with cavity mirror consisting of thin glass plates suitable for high power use

21 p3836 A70-40807

YAG-ND laser volume limits condition for high power fundamental mode operation

21 p3836 A70-40808

Laser interferometer system unwanted reflections elimination and intensities control in each arm by linear polarization method

21 p3823 A70-40820

Holography application to marine ecological studies, using laser beam reduction techniques for image recording and reconstruction of large areas and volumes

21 p3823 A70-40821

Optimum tube diameter for maximum radiation output of single and multimode He-Ne lasers

21 p3836 A70-40916

Thermal and birefringent effects on output of continuous Nd-YAG laser rod, using 6328 A probe

21 p3837 A70-41906

Helium and nitrogen role in carbon dioxide laser excitation, discussing optimum gas mixture

21 p3837 A70-41919

Threshold retinal damage by CW He-Ne lasers due to mode locking

21 p3771 A70-41997

Acoustic waves in carbon dioxide at 2-25 torr initial pressures induced by heat from incident carbon dioxide laser pulses

21 p3837 A70-42003

Laser oscillator and amplifier characteristics based on ionic Nd dissolved in aprotic solvents, discussing solution loss

21 p3838 A70-42009

Recombination lifetime /laser/ states in Si doped GaAs light emitting diodes on p-type thin platelets

21 p3838 A70-42016

Isoperibol calorimetry for laser power and energy measurements, discussing boundary value problem for heat flow

21 p3838 A70-42021

Semiconductor platelet laser stimulated emission visual observation in unwanted reflected modes

21 p3838 A70-42022

Single picosecond mode-locked laser pulse selection and multiple pass amplification device, obtaining high energy and signal to noise ratio

21 p3838 A70-42023

Quantum theory of inhomogeneously broadened laser, considering atomic motion-electromagnetic field interactions and detuning effects

22 p4048 A70-42293

High output CW carbon dioxide laser design, using gas pressure variation and fast axial flow

22 p4048 A70-42322

Water cooled carbon monoxide-He-nitrogen-oxygen laser CW output at room temperature

22 p4048 A70-42327

Excited state complexes laser action in coumarin dyes indicated from stimulated fluorescence time dependence

22 p4048 A70-42328

Host materials for increasing optically pumped solid state CW laser fundamental mode output power

22 p4048 A70-42333

Thermal blooming of 10.6 micron laser beam in carbon dioxide absorption cell

22 p4049 A70-42335

Breakdown mechanism in Q switched ruby laser triggered spark gap, noting pulse duration and power peak

22 p4049 A70-42352

Spontaneous emission intensification at 6911 A in potassium to evaluate plasma local conditions, using low pressure arc and Q switched ruby laser

22 p4049 A70-42359

Cadmium sulfide pulsed laser spectrum analysis, discussing laser output stabilization by mode selection and electron beam scanning

22 p4049 A70-42405

Laser heterodyne system for nonsinusoidal vibration measurements, describing calibration and use

22 p4049 A70-42526

Optimal heterodyne receiver for laser signals element-by-element wavefront detection

22 p3987 A70-42558

Laser application to nondestructive testing via holography and hologram interferometry

22 p4028 A70-42587

Thin optically pumped pulsed CdSe platelet lasers, detecting mode jumping and tuning effects by time-resolved spectroscopy

22 p4049 A70-42946

Prism film device coupling laser beam into thin film dielectric light guides, discussing operational theory

22 p4030 A70-42947

Prism film device for high efficiency laser beam coupling into light guiding thin film, deriving operation theory by plane wave analysis

22 p4030 A70-42948

Approximate lasing condition from coupled rate and radiative transfer equations, determining population, energy density and power output

22 p4050 A70-43006

Stereo laser framing camera for miniature surface cracks and perturbations produced in materials by explosively induced shock waves

[SMPT PREPRINT 21]

22 p4035 A70-43052

Acoustic Bragg diffraction for laser light deflection, solving high speed photography and holography motion problems

[SMPT PREPRINT 5]

22 p4035 A70-43055

High speed holographic recording of transient events by single shot ruby and Nd-doped pulsed lasers, applying to shock tubes and wind tunnels

[SMPT PREPRINT 3]

22 p4035 A70-43056

Laser radiation effects on lens lipid content in adult Rana temporaria frogs during cataract development

22 p3978 A70-43139

Wavelength selective carbon dioxide laser using stationary grating to correlate pulses for high J values and line number

22 p4050 A70-43153

Intense laser light pulse longitudinal compression resulting from nonlinear intensity-dependent refractive index

22 p4050 A70-43221

Laser radiation hyper Raman scattering intensity enhancement via resonance processes, using density matrix method

22 p4075 A70-43233

Cuprous chloride /CuCl/ as low-loss electro-optic material modulating 10.6 micron laser radiation

22 p4051 A70-43334

Diffusion effect on carbon dioxide Gaussian laser beam amplification, measuring gain saturation via pinhole method

22 p4051 A70-43335

Compression of laser pulses reflected from periodic and zone plate gratings

22 p3990 A70-43337

High power gas lasers constructed in Poland, describing structural design and operational specifications

22 p4051 A70-43441

Ruby laser mode excitation, spatial coherence and free emission kinetics investigated by high speed camera scanning

22 p4051 A70-43461

Ruby and Nd glass solid state lasers modes partial self synchronization investigated by spectral time resolution method

22 p4051 A70-43463

Threshold parameters of liquid and gaseous helium breakdown caused by ruby laser beam, noting Mandelstam-Brillouin scattering in liquid phase

22 p4051 A70-43465

Two-component optical system for laser radiation collimation, calculating tolerances for fabrication and assembly

22 p4051 A70-43560

Argon laser for long pulse low duty cycle operation, discussing construction and performance

22 p4052 A70-43602

Thermoelectrically cooled GaAlAs injection laser illuminator, discussing optical-electronic interface problems and design and performance characteristics

22 p4052 A70-43603

Material transfer image recording using focused laser beam, discussing experimental setup and test results

22 p4040 A70-43605

Flowing medium turbulent velocity measurement using laser Doppler device

22 p4040 A70-43615

Laser light pulse interaction with solid targets, observing second harmonic generation in induced plasma from time resolved spectra

22 p4084 A70-43673

Thermal energy conversion into coherent laser light, examining various thermodynamic limitations

22 p4076 A70-43674

Ultrasonic light modulation using single crystal lithium niobate transducers in laser communication and information processing systems

22 p3992 A70-43734

Monograph on optimum focusing of laser light with nonideal lenses having spherical aberration

22 p4052 A70-43739

Single frequency gas laser synchronization by small harmonic signal from second laser, deriving frequency shift dependence on power

23 p4200 A70-43929

Optical FM system with laser interferometer and sideband carrier circuit for measuring mechanical shock by Doppler shift

23 p4193 A70-43964

Vibrational relaxation measurements of specific carbon dioxide vibrational-rotational states from tunable carbon dioxide laser beam absorption

23 p4221 A70-44011

Laser induced gas breakdown, considering plasma generation and properties

23 p4225 A70-44185

Laser light scattering in plasma for charged particle correlation function

23 p4225 A70-44187

Laser light polarization and depolarization during backscattering from aqueous suspensions

23 p4215 A70-44271

Live skin tissue electrical parameters changes due to laser radiation, showing coagulative necrosis by histomorphological studies

23 p4150 A70-44313

Laser application to deformation and vibration analysis, discussing optical alignment, contactless measurement and holographic interferometry

23 p4201 A70-44335

Automatic shutter for recording holograms with laser light, controlling exposure time by photoconductor cell

23 p4197 A70-44472

High power pulsed laser fog dispersal, calculating vaporization regimes of droplet interaction with laser radiation

23 p4201 A70-44592

Low threshold laser action of Nd-containing chelate in host media consisting of polymethyl methacrylate and organic liquid

23 p4201 A70-44869

Axial modes interaction in He-Ne laser with atomic collisions in active medium, computing intensities and emission frequencies

23 p4202 A70-45053

Spectroscopic features of mercury laser associated with electron energy levels and spontaneous emission line structure, giving excitation and disruption mechanisms

23 p4202 A70-45054

Quantum noise in narrow-band ring laser, noting mode amplification of weak monochromatic signals

23 p4202 A70-45056

Irradiation influence on emission power of GaAs laser excited by high energy electron beam

23 p4203 A70-45060

Threshold characteristics of injection and electron excitation semiconductor lasers having photoluminescence properties of n-type GaAs single crystals

23 p4203 A70-45065

Spectral and threshold emission from optically pumped semiconductor lasers as function of carrier type and concentration in GaAs single crystals

23 p4203 A70-45069

He-Ne laser with absorbing cell in magnetic field, investigating nonlinear effect in frequency dependence of output power

23 p4203 A70-45070

German monograph on quantum statistics for light propagation in laser-active fluctuating media

24 p4350 A70-45090

Expansion of laser produced plasma into uniform magnetic field, calculating electromagnetic radiation

24 p4382 A70-45108

Electro-optical Q switches for generating laser radiation pulses

24 p4351 A70-45181

Statistical properties of random intensity field during coherent laser radiation scattering by moving diffuse surface

24 p4351 A70-45184

Optical damage center structural defects in transparent dielectrics under high energy ruby laser radiation, noting nontransparent inclusions and dislocation centers

24 p4351 A70-45209

CW laser beam power density distribution monitoring by self calibrating photographic dosimetry technique

24 p4307 A70-45343

Laser sensors as alignment instrument for control and measurement of five degrees of freedom

24 p4351 A70-45383

Beam laser operational efficiency relation to molecule /atom/ interaction in focusing system, explaining lasing power drop at large flow rates

24 p4351 A70-45457

Pulsed ruby laser radiation energy characteristics relation to crystal temperature distribution, thermal deformation and compensating lens focal length

24 p4352 A70-45460

Light scatterers use behind phase object in double exposure holography, determining laser radiation wave front dynamics effect on image quality
24 p4334 A70-45461

Plasma formation from transition metal target under monopulse laser radiation, noting absorbed surface density energy role in onset
24 p4385 A70-45463

CW GaAs semiconductor laser fabrication by liquid epitaxy, noting Ag plating role in output power
24 p4352 A70-45468

Laser operation instability with nonlinear filter, deriving electrons differential velocity distribution functions on inhomogeneous emitter
24 p4352 A70-45469

Optical laser radar for upper atmospheric density and aerosol concentration measurements
24 p4353 A70-45561

Laser light effects on electron beams, considering absence or presence of crystalline optically transparent solid
24 p4353 A70-45564

Laser light scattering by moist air flows with condensed droplets of water vapor
24 p4353 A70-45565

Magnetic field measurement by laser light scattering intensity fine structure determination in plasma
24 p4353 A70-45567

Formation and radiative recombination of free excitonic molecules in CuCl single crystals via Q switched ruby laser excitation
24 p4353 A70-45604

Nd glass laser with smooth emission frequency scanning, giving block diagrams and radiation spectra
24 p4353 A70-45646

Nd laser single picosecond pulse energy, duration and frequency width
24 p4354 A70-45664

SNR of moving diffuser illuminated by laser light, considering image plane and Fresnel field observations
24 p4354 A70-45670

HF chemical laser emission in fluorine-containing organic compounds via arc discharges, noting molecular hydrogen effect on p sub 10 and p sub 21 transitions
24 p4355 A70-46046

Transverse flow deuterium fluoride-carbon dioxide chemical laser for CW output without external energy source
24 p4355 A70-46084

Ruby laser second harmonics generation in low loss lithium iodate crystal with high conversion efficiency
24 p4355 A70-46085

High pressure pulsed Xe laser obtained with transversely excited He-Xe discharge
24 p4355 A70-46087

Nitrogen laser pumped exciplex 4-Methylumbelliferone and rhodamine 6G dye laser amplifier, measuring single pass power gain vs wavelength
24 p4355 A70-46088

Gas ionization with Q switched carbon dioxide laser radiation, determining breakdown threshold or minimum power density requirement
24 p4355 A70-46261

Spectral anomalies due to inhomogeneous optical pumping in masked ruby laser, using mathematical model
24 p4355 A70-46264

Phosphorus and selenium oxychloride based liquid laser transmission loss measurement
24 p4355 A70-46265

Laser gain coefficient increased via organic compounds addition to rhodamine 6G aqueous solution
24 p4356 A70-46273

Ionized Ar laser developments, considering power output and radiation spectrum
24 p4356 A70-46324

Laser Doppler shift theory and applications to vibration and flow velocity field measurements
24 p4340 A70-46351

LASER RADAR
U OPTICAL RADAR
LASER RANGE FINDERS
Laser ranging systems used with retroreflecting satellites in geodetic and geophysical applications
05 p0815 A70-16691

Optimal control of elevation and azimuth of automatic tracking device carrying pulse laser and receiving telescope
06 p1011 A70-18469

Apollo 11 laser ranging retro reflector measurements from McDonald Observatory confirming thermal design analysis performance prediction
06 p1011 A70-18482

Night vision systems with integrated pulse gated viewing and laser ranging, analyzing transmitter and viewer
12 p2236 A70-27902

Apollo lunar laser ranging experiment /LURE/ for range measurements from earth to lunar surface
15 p2750 A70-31675

Laser range finding to satellite equipped with retroreflectors, noting accuracy dependence on signal strength
16 p2925 A70-33021

Reflected ruby, laser pulses from Apollo 11 laser ranging retro-reflector /LRRR/ with telescope, measuring round trip travel time of light
21 p3912 A70-41638

Earth-moon laser distance measurements, examining relationship between Newtonian and relativistic field coordinates
24 p4413 A70-46160

LASER RANGER/TRACKER
Laser ranging and tracking system consisting of mirror tracking pedestal, instrumentation bay and control van featuring manual/automatic tracking capability
16 p2862 A70-33164

Laser ranging and tracking for high velocity targets, discussing SNR considerations, ambiguity resolution, error analysis, measurement centroid and target acquisition
16 p2862 A70-33165

Mathematical-physical parametric model of satellite geodetic laser range accuracy, false alarm and count probabilities, correlating with retroreflector signal strength
16 p2863 A70-33166

Gallium arsenide laser ranging system for helicopters obstacle warning
17 p3103 A70-34720

Mechanical design and mounting technique of Apollo 11 fused silica laser ranging retroreflector array at Tranquility Base
17 p3082 A70-34763

LASERS
NT ARGON LASERS
NT CARBON DIOXIDE LASERS
NT CHEMICAL LASERS
NT GALLIUM ARSENIDE LASERS
NT GAS LASERS
NT INFRARED LASERS
NT INJECTION LASERS
NT LIQUID LASERS
NT ORGANIC LASERS
NT PULSED LASERS
NT Q SWITCHED LASERS
NT RING LASERS
NT RUBY LASERS
NT SEMICONDUCTOR LASERS
NT SOLID STATE LASERS
Book on quantum electronics covering energy levels of materials, matter-radiation interactions and laser theory and applications
01 p0112 A70-10876

Atomic variables elimination technique applied to Markovian laser master equation, resulting in integrodifferential equations for field statistical operator
01 p0112 A70-10884

Laser optoelectronic and spectroscopic methods using fixed gap spherical mirror confocal Fabry-Perot interferometer and multiple beam image tube framing camera
01 p0112 A70-10901

Metal film graded filter fabrication for schlieren photographic system with laser light source and framing camera, using vacuum evaporation
01 p0113 A70-10921

Laser position finding of satellites fitted with corner reflectors, discussing atmospheric attenuation and applications to global triangulation and gravitational field measurements
02 p0256 A70-12083

Laser range finding by mobile missile station compared with geodesic satellite telemetry by ground station
02 p0312 A70-12212

Laser applications for diagnostic and interaction studies, discussing fog removal, droplet shattering, clear air turbulence, reaction rates, spectroscopy, etc.
02 p0314 A70-12780

Steady state inversion coefficient for active substance in quantum paramagnetic amplifier with push-pull pumping determined by nonstationary methods
03 p0455 A70-13088

CW laser light sources for Mach-Zehnder interferometer, obtaining results for carbon dioxide injected through porous bottom wall into air flow
03 p0484 A70-13397

Annotated bibliography of laser eye hazards
03 p0434 A70-13680

Axial geometry deformations of laser resonator due to fabrication errors and misalignment during operation
03 p0502 A70-13748

Tradeoff methodology establishing evaluation criteria for comparing radar and laser systems to meet geodetic satellite altimeter performance requirements
04 p0686 A70-14648

Laser gyro status for major obstacles impeding exploitation, comparing biasing methods
04 p0704 A70-15659

Faraday modulator for polarized laser radiation, eliminating analyzer by oblique magneto-optical active element, converting angular modulation into amplitude modulation
05 p0858 A70-16251

Cylindrical confocal laser resonator with circular coupling aperture in center of mirror calculated for diffraction losses by numerical iteration
06 p1079 A70-17187

Divided photoelectric cell position sensitive detectors in laser alignment systems, obtaining independent signals for displacements in orthogonal directions
06 p1081 A70-17624

Polarization interference filter as laser resonator frequency selector, showing Q factor measurable within spontaneous emission line
06 p1082 A70-17771

Collection of papers on essentials of lasers including submillimeter wave amplifiers, IR masers, interferometer resonant modes, fluorescent solids and coherent light
07 p1297 A70-19025

Book on lasers and holography covering coherence, wave diffraction, zone plates, etc.
07 p1282 A70-19598

Pumping light distribution in rectangular laser rods showing corner maxima and overall nonhomogeneity
07 p1300 A70-19871

Laser characteristics and applications in high temperature research including metal heating, welding, machining, surface particle emission and plasma production
07 p1301 A70-19881

Polarization of laser medium consisting of colliding two level molecules with velocity dependent mean free time
08 p1512 A70-20992

Laser safety programs in biomedical applications, discussing installations, techniques, hazards and protection
08 p1451 A70-21048

Small-scale local flow velocity measurements with laser using differential Doppler method
09 p1694 A70-22125

Laser technology, discussing activation types, applications and commercial development for data processing, voice communication, medical equipment, etc.
09 p1695 A70-22338

Compact unequal-path radial shearing laser interferometer designed for small angular aperture wave front testing
09 p1696 A70-22719

Book on lasers, light amplifiers and oscillators covering optical resonators, optical pumping, pulsed lasers, etc.
09 p1700 A70-23541

Real time wide angle multicolor scanned laser display for visual flight simulators, utilizing flying-spot camera and rotating optical polygons
10 p1857 A70-24203

Stationary regime stability of one dimensional model of optical quantum traveling wave amplifier, determining trapping band of traveling wave laser
10 p1901 A70-25158

Resonant oscillations of passive Fabry-Perot resonator in optically anisotropic medium, using parabolic equations for wave vector amplitudes polarized components
11 p2063 A70-25869

Laser systems for deep space communications, considering high data rates, laser types, systems operation, earth atmosphere effects, hardware reliability, etc.
11 p2005 A70-26036

Resonant nonmonochromatic radiation effects on quantum system, deriving expressions for active medium nonlinear polarization, susceptibility and gain
12 p2245 A70-27304

Laser microplasma formation in focus of two laser beams impinging on crystalline lithium hydride targets
12 p2246 A70-27355

Laser profilometer for airborne ocean wave profile measurement
12 p2249 A70-28003

Book on light and matter covering mathematical laser theory
13 p2429 A70-29574

Composite cylindrical laser rods end region stress and optical pathlength change with thermal expansion or contraction between core and cladding
13 p2429 A70-29703

Operation characteristics of flash, arc, incandescent and explosion type laser pump lamps
13 p2431 A70-29874

DOD laser research and development contracts management
14 p2667 A70-30367

Optically pumped Rb laser theory, taking into account superfine and Zeeman structure of atoms
15 p2749 A70-31521

Optical quantum amplifier frequency characteristics dependence on broad spectral composition amplified signal intensity and resonator parameters
15 p2754 A70-32862

Laser applications in geosciences - Conference, Huntington Beach, California, June-July 1969
16 p2925 A70-33013

Laser Raman scatter process applied to atmospheric probing
16 p2925 A70-33017

Servocontrolled laser strainmeter based on Michelson-Morley interferometer, determining dynamic

characteristics dependence on feedback loop filter type

16 p2925 A70-33022

Laser interferometry strain gage for measuring earth strain, taking into account wavelength stabilization

16 p2925 A70-33023

Laser devices design, emission characteristics, coherent light, etc

16 p2926 A70-33071

Optical system and light source imperfection effects interference image contrast lowering in laser interferometer for length measurements

16 p2928 A70-33292

Laser cavity design with total internal reflection quartz prisms, calculating prism angles tolerances

16 p2915 A70-34219

Glass laser materials characteristics, discussing refractive index thermal coefficient, stress optical coefficients, spontaneous emission, etc

17 p3105 A70-35091

Atomic physics of lasers and active materials, noting multiplet spectra of atoms, molecular spectroscopy, energy level population distribution and amplification

[AIAA PAPER 69-63] 18 p3316 A70-36700

Time dependence of laser rod focal length, measuring thermal lensing effects

18 p3270 A70-36756

Inlet optics modification in Raman laser spectrometer, discussing high pressure gas storage and support plate enlargement

19 p3443 A70-37361

Monochromatic radiation from laser modulated electron beams

19 p3444 A70-37572

Optically bistable crystal applications, discussing photochromaticity, catochromatic tubes, oscilloscopes, computer storage devices and laser systems

19 p3446 A70-37860

Laser aided frequency and amplitude analysis of vacuum test chamber vibration during alignment of orbiting UV spectroheliograph

19 p3396 A70-37877

Ronchi test interferometer for optical quality checking of laser crystals

20 p3627 A70-39094

Laser rod faces parallelism measurement by interferometric method for Brewster or square ended rods

20 p3640 A70-39095

Light focusing glass fiber with variable refractive index using ion exchange process, discussing applications to laser communications and data processing

20 p3671 A70-39129

Power diffraction losses at mirrors of asymmetric confocal laser interferometers with output coupling apertures

20 p3628 A70-39130

Constant false alarm rate bias technique to control avalanche photodiode laser receiver over varying operating conditions of temperature, ambient illumination, etc

20 p3641 A70-39483

Dynamic compensation of thermal pumping, induced deformation of laser active elements via thermal bending of resonator mirrors achieved by coatings

20 p3642 A70-39744

Electron concentration measurement range expansion in plasma by laser interferometer with optical signal phase modulation

21 p3860 A70-42069

Shot, thermal, induced gate and flicker noise in various solid state devices and lasers

21 p3792 A70-42112

Laser and flash X ray shadowgraph techniques in hypervelocity ablation/erosion investigations in hyperballistics range

[SMPTE PREPRINT 28] 22 p4034 A70-43047

Gas velocity measurement by high speed schlieren observation of laser induced breakdown phenomena

[SMPTE PREPRINT 27] 22 p4034 A70-43048

Laser applications in length measurement and holography, describing principles and techniques, modulated laser beams and pulse transit time

23 p4201 A70-43998

Oscillatory flow measurements by directionally sensitive laser velocimeter, discussing concept, design and construction

23 p4197 A70-44473

Rotational quantum numbers from iodine molecule resonance fluorescence measurements during laser excitation using Fabry-Perot interferometer

23 p4202 A70-44938

Industrial laser technology applications, considering high accuracy distance, flow and stress measurements, die hole punching, integrated circuit component welding, etc

24 p4351 A70-45382

Laser measurements in semidynamic space geodesy on DI-D satellite using Mediterranean stations

24 p4352 A70-45541

Lasers biomedical applications based on thermal and ionization effects on biological targets, considering eye surgery, tumor treatment, etc

24 p4308 A70-45568

Lasers for surgical applications, cancerous tissue treatment, ophthalmology and comparison with RF diathermy

24 p4308 A70-45569

Level relaxation constants measurements by three-level laser spectroscopy, using line shape of stimulated shifted resonance scattering in gas

24 p4354 A70-45821

LASV

U F-111 AIRCRAFT

LATCHES

Three dimensional latching dynamics and loads induced during Apollo spacecraft docking, using linear stiffness or flexibility matrices for structural elasticity

[AIAA PAPER 70-21] 06 p1158 A70-18181

Reliable latch diaphragm release mechanism for separation of payload from spacecraft, discussing design, operation and tests

16 p2921 A70-34117

LATENCY

U REACTION TIME

LATERAL CONTROL

Roll control method using recirculating base flow reaction against oriented blades or fins attached to reentry vehicle base to produce rolling moments

01 p0003 A70-10847

Lateral separations using navigation error analysis, showing values for aircraft with or without Dioscours and inertial control under North Atlantic conditions

02 p0336 A70-12607

Lateralization and detection of signals under antiphasic noise masking measured at various SNR levels

06 p1106 A70-17597

Flight maneuver for roll modulated lifting reentry vehicle to reduce deployment dynamic pressure

07 p1394 A70-19724

Kalman filtering techniques to identify aircraft lateral motion data

08 p1478 A70-20782

Root loci construction for differential equations with quadratic free parameters applied to aircraft motion with roll control

11 p2071 A70-25393

Spin-stabilized rockets stage separation dynamics, considering guide shoe-guide rail lateral motion constraint system

13 p2503 A70-28508

Missile roll rate from yawing motion frequencies determined by epicyclic theory

[AIAA PAPER 70-536] 13 p2506 A70-29075

Aircraft optimal roll stabilization control system design using performance index with weighting matrix

14 p2532 A70-31395

Reentry vehicles fluidically controlled hydrazine rocket engine modules for roll rate control

[AIAA PAPER 70-650] 16 p2970 A70-33617

Mariner spacecraft roll control star sensors and trackers design and flight performance

20 p3665 A70-39239

Turbulence effects on lateral directional flying qualities, examining pilot task performance, control workload and compensatory behavior

[AIAA PAPER 70-998] 20 p3560 A70-39533

Rocket course correction by lateral air expulsion /ram air control/, deriving model for performance prediction

[AIAA PAPER 70-90] 20 p3715 A70-39559

Automatic aircraft lateral motion stabilization during flight in perturbed atmosphere by HF invariant systems

20 p3670 A70-39839

UpSTAGE interceptor missile flight control system, discussing command logic to capitalize on lifting body advantages to enhance roll maneuver

21 p3927 A70-40782

Rocket roll control by secondary compressed air injection via slender fins inserted into nozzle convergent

21 p3931 A70-41953

Aircraft rolling motion /eigenmotion/ in flight at small angle of attack following initial disturbance, discussing response to control action

22 p3961 A70-42515

Wheel force and roll moment nonlinearities effect on light STOL aircraft handling qualities during approach

[ICAS PAPER 70-55] 23 p4139 A70-44151

Magnetically stabilized satellites passive roll control, discussing resonance solutions by variational approach

23 p4262 A70-44690

LATERAL OSCILLATION

Lateral vibrations of rigid rotating shaft in viscous fluid using inner and outer expansions method, considering small amplitude vibration and fast rotation

04 p0769 A70-14865

Longitudinal structural vibration and lateral bending response mass and spring coupling in Saturn AS-502 during boost with longitudinal excitation by pogo effect

09 p1766 A70-23239

Spin requirement to limit projectile yawing oscillations in hyperballistic range

12 p2157 A70-27835

Lateral motions of vertical uniform tubular cantilever conveying fluid, considering oscillatory instability at high flow velocities

13 p2511 A70-28741

Numerical method for roots of algebraic equations, computing continuous beam lateral vibrations natural frequencies

14 p2600 A70-31330

Inverted torsion pendulum performance improvement, describing dashpot to dampen lateral vibrations

23 p4202 A70-44950

LATERAL STABILITY

Wing-fuselage interference influence in aircraft dihedral effect, discussing role of velocity direction on wing

03 p0406 A70-13020

Motion equations and dynamic lateral stability of towed glider in steady horizontal flight treated by small perturbations method, including design and handling influence

09 p1611 A70-23063

Poppet valve lateral stability improved by effective seat ratio increase and use of high viscosity fluid

11 p1983 A70-26421

Optimal and suboptimal aircraft lateral directional stability augmentation applying optimal control and model-following techniques

12 p2162 A70-27812

Aircraft lateral and longitudinal motion stability in steady rolling, deriving inertia cross coupled stability criterion

13 p2347 A70-29445

Supersonic aircraft lateral stability and controllability design, discussing directional and weathercock stabilities

15 p2673 A70-31625

Structure of flexural members, analyzing torsional and lateral stability by finite element method and matrix formulation

18 p3339 A70-36494

Lifting reentry flight test vehicle aerodynamic configuration development, emphasizing lateral stability and maneuverability

[ICAS PAPER 70-02] 23 p4257 A70-44118

LATERALITY

U LATERAL STABILITY

LATERALIZATION

U LATERAL CONTROL

LATITUDE

NT GEOMAGNETIC LATITUDE

Icarus radar and optical observations indicating surface smoothness differences between central and higher latitudes, radius size and radar reflectivity

01 p0180 A70-10534

Rotation periods of Jovian atmospheric currents showing zonal wind velocity variations with latitude

02 p0369 A70-11829

Latitude-period relation existence in geomagnetic micropulsations, discussing coupling between components of geomagnetic field fluctuations

05 p0838 A70-16278

Geopotential fields expansion on 500 mb surface for hemisphere in terms of Chebyshev polynomials along meridian and trigonometric polynomials along latitude

07 p1329 A70-19648

Odessa observatory meridian circle pivots wear determined during observations of eclipsing variables

08 p1574 A70-21160

Lunar latitude evaluation investigated for origin of discrepancy between two methods

08 p1577 A70-21494

Longitude and latitude dependence of pc geomagnetic micropulsations related to local time, using analog spectral analysis

09 p1666 A70-22064

Diurnal, seasonal and latitudinal variations of maximum electron concentration in F 2 region, using global network observations

15 p2729 A70-32077

Power spectrum analysis of division errors of graduated circles associated with meridian astronomy

19 p3523 A70-38686

Equations for converting satellite geodetic latitude and altitude into geocentric Cartesian system

20 p3669 A70-39691

Diurnal atmospheric density variations latitude dependence from satellite data

23 p4185 A70-43842

LATITUDE MEASUREMENT

Cosmic ray latitude survey in North America in summer using neutron and muon monitors operating near sea level and on mountains

01 p0167 A70-10226

Cosmic ray latitude survey in Canada using airport sites, noting ground snow effect on neutron monitor counting rate

01 p0167 A70-10227

Earth poles motion influence on latitude, longitude, azimuth and geocentric rectangular coordinates of points determinations on earth surface

03 p0473 A70-13187

Instantaneous latitudes observations during stellar transit at Poltava, describing error correction procedure

08 p1488 A70-21153

Earth free diurnal nutation parameters determination from latitude observations, establishing amplitude and phase time-independent variations

08 p1488 A70-21154

Photoelectric exposure meter for meridian circle readings photographic recording

08 p1496 A70-21159

Latitude observations at Pulkovo, considering star declinations and proper motions

08 p1574 A70-21162

Statistical heliographic latitude dependence of dominant polarity of interplanetary magnetic field, using photospheric synoptic chart

13 p2492 A70-29195

Astronomical navigation on lunar surface with equations for selenographic latitude and longitude

13 p2449 A70-29272

Latitude determination from observations of pairs of bright stars at equal altitudes, using computer ephemeris calculations

14 p2633 A70-30142

LATTICE IMPERFECTIONS

U CRYSTAL DEFECTS

LATTICE PARAMETERS

Shear moduli and lattice parameters effect on screw dislocation equilibrium in bimetallic medium of soft and hard phases

03 p0587 A70-13117

Maraging steels mechanical properties, studying changes in lattice constant and electric resistance to determine Al strengthening effect nature

05 p0865 A70-16872

Neutron irradiation and annealing effects on lattice constants of titanium and chromium carbides analyzed for X ray diffractions

07 p1303 A70-18702

PbTe-based Sn, Se and Ge alloys lattice constant, thermal EMF and resistance, fusibility and microstructure

08 p1555 A70-21117

Gamma-gamma prime mismatch effects on stress rupture of Ni and Fe-Ni based alloys with Al and Ti hardeners

08 p1521 A70-21701

Ferritic and martensitic Fe-Ni alloys lattice parameter determined by standard X-ray techniques

12 p2256 A70-27613

Rhenium alloying effect on room temperature ductility of Cr, Mo and W, measuring lattice parameters by Debye-Scherrer method

12 p2256 A70-27616

Lattice defect influence on EPR spectral and luminescent characteristics of annealed Fe doped gallium arsenide crystals

12 p2288 A70-28330

Phase lattice constants determination by computer method of debyegram line indexing

12 p2258 A70-28350

Atomic planes around crack, noting configuration dependence on law of interplane interaction

13 p2515 A70-29418

Undoped GaAs lattice constants and electrical properties before and after heat treatment

13 p2471 A70-29504

Localized one electron states in perfect crystals of widely separated atoms, using thermal single determinant/Hartree-Fock/ approximation

14 p2626 A70-30488

Lattice planes and interplanar spacings of small vapor deposited gold crystals, using transmission electron microscopy

16 p2961 A70-33644

Ti, Nb and Mo solubility during surface doping in Al melts containing various metals, discussing melt lattice structure effects

18 p3276 A70-36208

Lattice parameter and thermal expansion of AlAs as function of temperature, indicating lattice match at 900 C with GaAs

22 p4086 A70-43004

Addition effects on lattice and electrophysical properties of trititanate prepared by Ba, Pb, Ca and Ti precipitation

22 p4087 A70-43134

Cubic titanium oxycarbide structural characteristics, noting lattice constant dependence on component proportions and mutual solubility during formation

24 p4359 A70-45477

Phase regions and lattice parameters of isothermal section of Mo-Zr-Cr system at 1100 C from microstructural and X ray analyses

24 p4361 A70-45832

Simplex lattice mathematical models of solidus volume for quaternary Nb-W-Ti-Zr system

24 p4361 A70-45833

LATTICE VIBRATIONS

Diamond-like glassy semiconductor compound of cadmium germanium arsenide, determining optical lattice vibrations from IR reflection spectra

01 p0160 A70-11599

Methylamine crystals lattice vibrations IR spectra recordings, making spectral band assignments according to translational and librational motions

07 p1356 A70-18958

Two parameter model for lattice vibrations applicable to diamond structured crystals, calculating phonon dispersion curves from dielectric screening theory

07 p1357 A70-19920

Linear high polymers heat capacity measurements theory emphasizing simple mechanical systems and contribution of lattice vibrations

13 p2438 A70-28997

Chromium lattice vibrational properties based on fourth-nearest-neighbor tensor force model, obtaining agreement with inelastic neutron diffraction data and elastic constants

14 p2626 A70-30480

Methyl-nitroazobenzene-sulphenyl cyanide unit cell dimensions and space group by single crystal oscillation, rotation and Weissenberg X ray diffraction photographs

14 p2581 A70-31300

Phonons and band structure role in metal-insulator phase transition, developing model of electron interactions with lattice vibrations

20 p3686 A70-39149

Solid para hydrogen IR and Raman spectra frequency analysis, examining lattice vibration effects

21 p3853 A70-41721

Boron impurities introduction into InP crystals grown by liquid encapsulation, detecting IR absorption bands due to localized lattice vibration

23 p4231 A70-44891

Al and W specific heat and Al heat of fusion by quasi-adiabatic calorimetry, estimating anharmonic lattice vibrations role via atomic thermodynamic analysis

23 p4208 A70-44931

Monatomic crystal vibrational spectrum, noting quasi-local vibrations near high impurity concentrations

24 p4388 A70-45202

Perovskite crystals phase transitions based on group theory, considering lattice vibration modes as instability source

24 p4389 A70-45206

LATTICES [MATHEMATICS]

NT BOOLEAN FUNCTIONS

Vortex- and Doublet-Lattice methods for calculating aerodynamic lift distributions on surfaces in steady and oscillatory motion at subsonic speeds

13 p2339 A70-29006

LAUE METHOD

Backreflection X ray microbeam camera with arrangement for positioning preselected area to study grain boundary during creep by Laue method

03 p0492 A70-13759

LAUNCH COMPLEXES

U LAUNCHING BASES

LAUNCH TIME

U LAUNCH WINDOWS

LAUNCH VEHICLE CONFIGURATIONS

Launch vehicle selection, utilization and mission planning and analysis in Comsat programs, discussing INTELSAT I-IV

11 p2002 A70-25489

Two stage rocket booster-ram rocket launcher combination compared to single and two stage rockets

11 p2126 A70-26287

Europa 3 satellite carrier system configurations, discussing rocket design, propellant composition, etc

13 p2502 A70-28445

Europa 3D carrier rocket design and operational data, discussing communication satellites

13 p2502 A70-28446

Cost optimal carrier rocket system for European satellite TV, communication, navigation and earth survey networks

13 p2502 A70-28448

European launcher for geostationary orbit/ELGO/ program, describing Europa 3 payload, propulsion unit, propellant transfer, etc

13 p2502 A70-28449

Cost optimal booster stage for European satellite launchers, comparing liquid and solid propellant rockets

13 p2502 A70-28450

Small satellites for scientific technological and operational missions, discussing piggyback launching, command, battery storage, telemetry and attitude control systems

15 p2810 A70-31781

Space shuttle booster configurations, including wing and tail sizes, vehicle balance and engine location

16 p2982 A70-33706

ELDO launch vehicle design, describing high energy upper stages

18 p3333 A70-36300

Europa 2 launcher fourth/perigee/ stage, describing trajectories, propulsion system design and performance, separation systems, etc

19 p3532 A70-37871

ELDO Europa 1 and 2 launchers configurations tendencies, discussing use of liquid propellant boosters, chemical, electrostatic or thermonuclear propulsion system, etc

23 p4263 A70-45002

LAUNCH VEHICLES

NT ATLAS CENTAUR LAUNCH VEHICLE

NT ATLAS LAUNCH VEHICLES

NT BLUE STREAK LAUNCH VEHICLE

NT CENTAUR LAUNCH VEHICLE

NT DELTA LAUNCH VEHICLE

NT DIAMANT LAUNCH VEHICLE

NT ELDORADO LAUNCH VEHICLE

NT EUROPA LAUNCH VEHICLES

NT EUROPA 1 LAUNCH VEHICLE

NT EUROPA 2 LAUNCH VEHICLE

NT EUROPA 3 LAUNCH VEHICLE

NT RECOVERABLE LAUNCH VEHICLES

NT SATURN LAUNCH VEHICLES

NT SATURN 1B LAUNCH VEHICLES

NT SATURN 5 LAUNCH VEHICLES

NT SCOUT LAUNCH VEHICLE

NT THOR DELTA LAUNCH VEHICLE

NT THOR LAUNCH VEHICLES

NT TITAN LAUNCH VEHICLES

NT TITAN 3 LAUNCH VEHICLE

Space station flexibility design based on INT-21 payload capability emphasizing volume and weight factors

[AIAA PAPER 69-1064] 01 p0195 A70-10635

Reusable airbreathing launcher for manned space station ferry operations, considering nozzles, intakes, thrust, acceleration, flight plan, weight analysis, etc

02 p0381 A70-12502

Air force booster growth inventory, noting combination with space-configured upper stages and strap-on solid motors

[SAE PAPER 690713] 05 p0922 A70-15831

Launch vehicles design, propulsion, maneuverability and navigation

05 p0923 A70-16565

Satellite launch vehicle attitude control stability study including fuel sloshing and body bending effects

06 p1155 A70-17320

Launch vehicle control system synthesis based on mode control theory state variable formulations

06 p1156 A70-17958

Launch vehicle minimum cost design emphasizing flight vehicle evolution stages via effect on costs

[AIAA PAPER 70-240] 07 p1396 A70-20378

Air breathing launch vehicle for earth-orbit shuttle assessed in light of hypersonic propulsion and configuration development

[AIAA PAPER 70-269] 07 p1365 A70-20380

Strap-on ferry package for reusable spacecraft and launch vehicles subsonic lift/drag increase

[AIAA PAPER 70-259] 07 p1397 A70-20390

Reusable passenger and cargo shuttle system based on integral launch and reentry vehicle (ILRV), considering propulsion systems, aerodynamic and structural configurations, aerothermal characteristics, etc

08 p1582 A70-20689

Marshall Space Flight Center optical research programs technology base for launch vehicle development support, discussing Apollo Telescope Mount

09 p1657 A70-23518

Launch vehicle automatic checkout methods emphasizing guidance and control equipment performance in real time operations

[AIAA PAPER 70-393] 10 p1952 A70-24912

Launch vehicle first stage cost reduction, considering weight factors, mass production, recoverability, etc

11 p2126 A70-26285

Low cost launch and reentry vehicles, surveying technology and economics of spacecraft

11 p2126 A70-26286

Booster control system reducing maximal wind-induced bending torques, examining booster response to aerodynamic forces

13 p2500 A70-28413

Stochastic processes optimal control theory application to launcher attitude control under wind disturbance

13 p2501 A70-28428

Collection of papers on wind effects on launch vehicles covering aerodynamics, airframes, guidance and control, wind-vehicle interactions, atmospheric turbulence, etc

[AGARDOGRAPH-115] 13 p2504 A70-28751

Wind load aerodynamics effects on launch vehicle flight control systems design

[AGARDOGRAPH-115] 13 p2504 A70-28753

Wind effects on rigid launch vehicle guidance and control system design, using model incorporating structural bending and fuel sloshing

[AGARDOGRAPH-115] 13 p2448 A70-28755

Wind-launch vehicle interaction in flight, using equations of motion for aerodynamic loads

[AGARDOGRAPH-115] 13 p2504 A70-28756

ELGO launcher system with apogee booster for placing payload in geostationary orbit

13 p2505 A70-28768

Single stage reusable launch vehicle/project BETA/ feasibility, considering orbit, payload, reentry, cost, etc

13 p2505 A70-28902

Launch vehicle design, considering tradeoffs between wind effects and analysis time

14 p2653 A70-30589

Hypersonic aircraft technology, discussing long range transport, reusable launch vehicles and propulsion systems

15 p2673 A70-31851

Europa 3 configurations for launching payloads into geostationary orbit using various rocket stage combinations

15 p2789 A70-32254

Scramjets for recoverable booster transporting payloads into earth orbits

15 p2811 A70-32258

Ion electric propulsion system coupled with small booster for geostationary orbit realization

15 p2790 A70-32276

Light weight integrated spin-up launch mechanism for rocket propelled payload

16 p2845 A70-34113

Analytic theory of unsteady separated flow effects on dynamics of heat sink type reentry bodies and elastic launch vehicles

[AIAA PAPER 70-762] M-4 SS launch vehicle capabilities and development schedule for low energy interplanetary missions

17 p3008 A70-34489

Black Arrow launch vehicle for inexpensive and reliable payload injection into low polar orbits

17 p3168 A70-35253

Computerized automatic ground equipment /CAGE/ as intelligence system for checkout and control of launch vehicles and spacecraft

17 p3178 A70-35255

Launch and reentry vehicles pressure transducers, measuring propellant quantity, water systems, fuel, oxidizer, battery compartment and ascent engines, etc

19 p3397 A70-37915

Future spacecraft mission for short period comets rendezvous, considering trajectory requirements and launch vehicle payload capabilities

[AIAA PAPER 70-1072] Launch vehicle injection error sensitivity minimization by trajectory shaping using excess booster capability

19 p3530 A70-38885

Technological and economic problems of reusable aeroballistic and ballistic launch vehicles

19 p3534 A70-38889

Aerodynamic forces on flexible launch vehicles and missiles in supersonic flight based on first order method, solving boundary value problem for surface velocities

20 p3562 A70-40150

Strap-on ferry package for reusable spacecraft and launch vehicles subsonic lift/drag increase

20 p3746 A70-41853

Lunar launch vehicles quality control and reliability, describing management procedures for test facilities, preproduction and purchased materials quality

21 p3931 A70-41867

Launch optimization of artificial satellites for minimizing thermal radiative heat input during low altitude orbit

22 p4126 A70-42384

Launch optimization of artificial satellites for minimizing thermal radiative heat input during low altitude orbit

23 p4264 A70-45047

Launch optimization of artificial satellites for minimizing thermal radiative heat input during low altitude orbit

23 p4264 A70-45047

Launch optimization of artificial satellites for minimizing thermal radiative heat input during low altitude orbit

23 p4264 A70-45047

Launch optimization of artificial satellites for minimizing thermal radiative heat input during low altitude orbit

23 p4264 A70-45047

Launch optimization of artificial satellites for minimizing thermal radiative heat input during low altitude orbit

23 p4264 A70-45047

Launch optimization of artificial satellites for minimizing thermal radiative heat input during low altitude orbit

23 p4264 A70-45047

Launch optimization of artificial satellites for minimizing thermal radiative heat input during low altitude orbit

23 p4264 A70-45047

Launch optimization of artificial satellites for minimizing thermal radiative heat input during low altitude orbit

23 p4264 A70-45047

Launch optimization of artificial satellites for minimizing thermal radiative heat input during low altitude orbit

23 p4264 A70-45047

Launch optimization of artificial satellites for minimizing thermal radiative heat input during low altitude orbit

23 p4264 A70-45047

Launch optimization of artificial satellites for minimizing thermal radiative heat input during low altitude orbit

23 p4264 A70-45047

Kamchatka regions volcanic deposits structural and mechanical characteristics compared with lunar soil characteristics

04 p0744 A70-14440

Lunar dimple /drainage/ craters formation mechanisms, considering analogous earth drainage craters associated with lava tubes

09 p1666 A70-22311

Lunar sinuous rilles formation by fluid flow mechanisms, discussing evidence for lava and rille formation by lava tube collapse

09 p1759 A70-22799

Synthetic silicate liquid viscosity with lunar rock composition compared with volcanic rock on earth

10 p1938 A70-24074

Kamchatka regions volcanic deposits structural and mechanical characteristics compared with lunar soil characteristics

13 p2485 A70-28465

Lunar basalt lava bed formations, examining vacuum and gravity effects during cooling

19 p3517 A70-37988

Cretaceous rock paleomagnetism from Israel lava fields, determining original magnetization directions

19 p3413 A70-38034

Apollo 11 lunar rock lavas and breccias, examining opaque minerals and olivine by reflection microscopy, electron probe and optical absorption measurements

21 p3899 A70-41530

Lava thickness measurement in lunar maria from projecting rim width of partially buried craters

23 p4242 A70-44292

Tycho crater northeast rim scale relief model including lava lakes in outer walls

23 p4253 A70-44881

New Mexico Bandera lava tube systems, noting similarities with lunar surface sinuous rilles

23 p4254 A70-44884

LAVAL NUMBER Gas dynamic functions using critical velocity and Laval number

06 p1033 A70-17237

LAW [JURISPRUDENCE] NT INTERNATIONAL LAW NT LEGAL LIABILITY NT PENALTIES NT SPACE LAW

Victim examination, human factors and forensic problems in flight accident investigations

05 p0807 A70-16497

Aircraft piracy definition by 1958 U.S. Federal Aviation Act, discussing smuggling, escape of prisoners and clandestine airports

05 p0960 A70-16536

U.S. Civil Aeronautics Board policy in cooperative agreements involving foreign airlines, highlighting significant cases

08 p1600 A70-20578

Age discrimination in employment policies of air carriers, discussing legislative measures, hiring practices and retirement rules concerning stewardesses and FAA pilots

12 p2336 A70-27772

Hovercraft operational advantages and legal status

22 p4127 A70-43499

Air passenger legal rights and obligations, discussing contracting states, formalities, hygiene, inoculation and de-insectization

22 p4127 A70-43500

Legal guidance criteria for expert witnesses presentation of technical evidence before jury in products liability litigation

23 p4137 A70-43869

Air hijacking as aviation safety problem, discussing history, prevention and detection methods and equipment, law enforcement, etc

23 p4285 A70-44496

Obstructive lung diseases clinical, radiological and functional diagnosis in legal medicine

24 p4296 A70-45122

LAWS NT CONSERVATION LAWS NT FOURIER LAW NT HOOKES LAW NT KEPLER LAWS NT KIRCHHOFF LAW OF RADIATION NT NEWTON SECOND LAW NT NEWTON-BUSEMANN LAW NT OHMS LAW NT SCALING LAWS NT SIMILITUDE LAW NT STEFAN-BOLTZMANN LAW

LAYERS Stress measurement in discontinuous layered medium subjected to perpendicular load under sliding friction, using photoelastic interferometric models

11 p1231 A70-25587

Boundary value problems of elasticity for layer and strip with arbitrary inhomogeneity along thickness

22 p4120 A70-43712

Stress-strain of thin multilayer isotropic spherical shell under radial load employing shallow shell theory

22 p4120 A70-43716

LC CIRCUITS

Plasma density measurement by LC tank circuit with plasma contained in induction coil, deriving expressions for circuit resistance and resonant frequency

08 p1550 A70-20846

Directional broadband couplers with lumped elements obtained by insertion of LC networks between sum and difference ports of equal hybrids

10 p1848 A70-24221

Air spark gap to switch stored charge in LC circuit, using auxiliary triggering circuit to clamp magnetic flux

23 p4177 A70-44471

LEACHING

Sodiumalumoborosilicate fiber formation and extraction by leaching, obtaining high aluminate content temperature resistant porous fiber and insulation material

24 p4367 A70-45480

LEAD [METAL]

Cosmic ray nuclear interactions under paraffin and lead, using counter controlled multiple cloud chamber

03 p0553 A70-12877

Plastic deformation effects on superconductivity of wire specimens of high purity Pb, In and Tl cold worked at liquid He and annealed

06 p1127 A70-18614

Lead ion effects on single crystal zinc dissolution and electrodeposition in alkaline solutions investigated microscopically

13 p2361 A70-28928

Superconducting lead shell shielding properties in small ambient magnetic fields

13 p2454 A70-30030

Absolute quantum efficiency of phosphor calcium tungstate-lead under monochromatic far UV illumination

15 p2729 A70-32017

Thermal radiation spectrum power of small spherical tin and lead particles

20 p3737 A70-39745

Gas tight lead storage battery with negative plates for oxygen absorption

24 p4295 A70-46352

LEAD [METALS]

NT LEAD ISOTOPES LEAD ALLOYS Metallic superplasticity and superplastic alloys in simple tension, forming tubes and sheets of superplastic Sn-Pb eutectic alloy by pressure forming techniques

16 p2916 A70-32916

Lead alloys as shielding materials in nuclear systems, discussing physical, chemical and metallurgical properties, fabrication and applications

19 p3469 A70-37833

LEAD COMPOUNDS

NT LEAD MOLYBDATES NT LEAD SELENIDES NT LEAD TELLURIDES NT LEAD TITANATES

Literature on IV-VI semiconducting Pb compounds PbTe, PbSe, PbS and PbO, discussing PbTe-SnTe and PbSe-SnSe solid solutions

08 p1555 A70-20584

Lead azide detonation hazards and resulting pressure waves, evaluating protective glove material by dynamic pressure measurements

12 p2289 A70-27665

Lead azide detonation hazards and resulting pressure waves, evaluating protective glove material by dynamic pressure measurements

12 p2289 A70-27665

Lead isotope data from young mantle derived volcanics suggesting mantle evolution and lunar capture

04 p0743 A70-14396

Iron troilite meteorites lead isotopic, Pb and U concentrations, considering fractionation and terrestrial contamination effects

07 p1388 A70-20035

Atmospheric dust natural radioactivity effect on tropospheric Pb 210 mean residence time determination for Pb210 and Ra226 fallout in rain near Moscow

14 p2630 A70-30131

Lead and thallium isotopic compositions of Apollo 11 fines compared with meteorites and earth for lunar surface age determination

21 p3775 A70-41588

Apollo 11 lunar rocks, breccia and fines U, Th and Pb isotopes systematics, considering implications for lunar history

21 p3909 A70-41605

Lead molybdates Acoustooptics materials selection guidelines, estimating lead molybdate figure of merit on basis of chemical composition and density

13 p2469 A70-28796

Lead selenides Epitaxial PbSe films formation mechanism-defect structure relation using moire rotation method, discussing elastic strains, dislocations, boundary formation, etc

01 p0155 A70-10182

PbSe and GeTe cast and pressed samples thermoelectric properties before and after high energy

01 p0155 A70-10182

gamma ray irradiation, using scintillation counter with photomultiplier
01 p0159 A70-10756

LEAD TELLURIDES
Radioisotope thermoelectric generator with lead telluride converter, discussing intact reentry and impact capability, refractory construction and reliability
22 p4072 A70-43196

LEAD TITANATES
Raman spectra of lead titanate, sodium tantalate /potassium tantalate and potassium tantalate/ potassium niobate solid solutions at various temperatures
03 p0542 A70-13824

LEADERSHIP
Pilot leadership qualities as criteria for selection, examining command training
11 p1993 A70-26607

LEADING EDGE SWEEP
Critical flutter behavior of variable geometry aircraft with wing of 70 degree leading edge sweep, noting wing-tail interference
18 p3338 A70-36445

LEADING EDGES
NT SHARP LEADING EDGES
Aerodynamics of conventional aircraft high lift devices, considering effect of leading edge geometry on lift coefficient at stall of plain and flapped airfoils
01 p0001 A70-10046
Wing design optimization for steady and unsteady supersonic flow through computerized simulation and study of leading and trailing edge shape
02 p0223 A70-12208
Supersonic flow separation at antisymmetrical delta wing edges, noting eddy layer and vertical velocity fields effects on aerodynamic characteristics
02 p0224 A70-12625
Viscous incompressible laminar two dimensional flows using Navier-Stokes equations, emphasizing near wake and flow around leading edge
[ONERA TP-757] 03 p0467 A70-13640
Supersonic unsteady gas flow around bodies at low Strouhal numbers, noting angle of attack amplitude and leading edge shock wave
03 p0409 A70-13865
Unsteady state lift and moment action on lattice of profiles moving in incompressible fluid, determining suction originating at leading edges of profiles
03 p0409 A70-13868
Slender wing with blunted leading edge to reduce thermal stresses at supersonic speed studied for aerodynamic characteristics in hypersonic flow
05 p0791 A70-17001
Leading edge phase shift of output pulse from threshold-type pulse shaping circuit determined as function of triggering threshold
06 p1009 A70-17675
Kinetic flow regime in hypersonic flow past flat plate leading edge, using Boltzmann equation
[AIAA PAPER 70-181] 06 p0970 A70-18094
Unsteady airfoil stall in incompressible flow, including pitch rate induced accelerated flow effect on leading edge and trailing edge stall
[AIAA PAPER 70-77] 06 p0976 A70-18237
Hyperthermal leading edge analyzed by examining adjacent relevant mean free paths for collisions, establishing basis for formal expansion of Boltzmann equation
06 p0979 A70-18347
Wall pressure distribution, drag and lift measured on flat plates and wedges at Mach 8 rarefied gas flow for various leading edges
06 p0980 A70-18350
Density field around leading edge of blunted flat plate, using electron beam measurements in low density hypersonic wind tunnel
06 p0980 A70-18351
Hypersonic leading edge problem solved, using merged layer theory to provide link between noncontinuum flow upstream of transition and boundary layer flow downstream
06 p0980 A70-18354
Thunderstorm cold air outflow leading edge structure recorded by NASA meteorological tower at Kennedy Space Center
06 p1100 A70-18575
Supersonic leading edge problem solved by ellipsoidal model using discrete ordinate method compared with BGK model solution
10 p1797 A70-23957
Triangular conical wing with supersonic leading edges analyzed for aerodynamic forces in supersonic flow
10 p1798 A70-24121
Uncooled leading edge effect on cooled-wall hypersonic flat plate boundary layer transition, discussing leading edge bluntness effects
11 p1976 A70-25984
Off-centerline heating on lee surface of supersonic delta wing with separation and vortex initiation at leading edge
11 p1976 A70-25996
Singularities of boundary layer conditions on parabolic cylinder in homogeneous incompressible

viscous flow with leading edge, using Weyl integral equation
12 p2210 A70-27559
Slender wings leading edge vortex flow effect on roll damping at subsonic speeds
[AIAA PAPER 70-540] 13 p2339 A70-29007
Deformable and rigid wings aerodynamic characteristics with subsonic leading and trailing edges, calculating action of gust
15 p2671 A70-31486
Heat transfer and pressure drag of axisymmetric body in hypersonic flow, obtaining minimum energy nose and leading edge shapes by Pontryagin principle
[AIAA PAPER 70-825] 16 p3001 A70-33940
Steady isentropic weakly perturbed supersonic flows past arbitrary slender tapered wings with subsonic leading edges
16 p2838 A70-33971
Yawed two dimensional wedges in hypersonic stream, including leading edge bluntness, viscous interaction and angle of attack effects
[AIAA PAPER 70-783] 17 p3009 A70-34503
Hypersonic flow around delta wings of finite thickness with supersonic leading edges
18 p3206 A70-36260
Flow field about leading edges of tapered wings set at incident angle of attack, using gas dynamic and Monge equations
18 p3207 A70-36376
High angle of attack aerodynamic characteristics of swept wing navy aircraft designs improved via leading edge modifications
[AIAA PAPER 70-904] 19 p3355 A70-37392
Supersonic turbine blade rows design, discussing boundary layer interaction around leading edges and flow around trailing edges
19 p3490 A70-38223
Hypersonic flow pattern past windward side of triangular wing with supersonic leading edges, joining potential and vortex regions behind shock wave
21 p3743 A70-40609
Wall recombination heat transfer in rarefied flow with velocity slip near leading edge
21 p3952 A70-42083
Quasi-conical supersonic wings with curved subsonic leading edges, discussing perturbation potential, boundary conditions, homogeneous flow and gothic and ogee planforms
21 p3747 A70-42108

LEAKAGE
Plastic deformation of wedge shaped model asperities influencing gas leakage between contacting surfaces, discussing critical contact pressure
01 p0060 A70-10267
Mo-Si epitaxial planar Schottky barrier diodes, describing reverse I-V characteristics improvement by edge leakage effects elimination
01 p0052 A70-11174
Leakage in mechanical face seals with hydrodynamic films, noting misaligned seal theories for pumping with cavities and two fluids
[ASLE FICFS PREPRINT 19] 02 p0308 A70-12170
Misalignment and eccentricity effect on face seal, discussing leakage dependence on phase angle
[ASLE FICFS PREPRINT 15A] 02 p0308 A70-12171
Sealing mechanism theory with face seal applications, taking into account load carrying capacity and no leakage pressure gradient
[ASLE FICFS PREPRINT 18] 02 p0308 A70-12172
Lubrication and leakage control mechanics of face seals, considering liquid to vapor boundary within interface
[ASLE FICFS PREPRINT 22] 02 p0308 A70-12173
Load support and leakage from microasperity lubricated face seals, developing hydrodynamic lubricant films
[ASLE FICFS PREPRINT 21] 02 p0308 A70-12174
Noncontacting minimum leakage dynamic seals requiring liquid-vapor interface with leakage tolerance
[ASLE FICFS PREPRINT 40] 02 p0308 A70-12175
Eccentric face seal with tangentially varying film thickness, analyzing leakage flow proportional to eccentricity and surface waviness
[ASLE FICFS PREPRINT 15B] 02 p0308 A70-12176
Long term storage effects on noise, leakage current and thickness of Li drifted Si surface barrier detectors
03 p0482 A70-13023
Allowable leakage guidelines for in-service aircraft hydraulic components, discussing causes and measurements, tabulating rates for static and dynamic seals
05 p0797 A70-15776
Air leakage between contacting surfaces assuming surface irregularities as microscopic truncated cones with ideally plastic or elastic mechanical properties
06 p1031 A70-17133
Surveyor spacecraft vernier propulsion system survival in lunar environment, suggesting temperature resistant seal and valve seat material for fluid loss prevention
06 p1129 A70-17170

Ring seal elements structural parameters influence on fluid leakage at various shaft speeds and fluid pressures
07 p1294 A70-19123
Leak detection methods, analyzing Tesla spark coil, particle counting, vacuum gages and ion pumps, pressure decay, thermal conductivity, etc
08 p1497 A70-21538
Orifice leak test for electronic components hermeticity
13 p2405 A70-28840
Leak detection techniques, describing back pressuring and calibrating methods
15 p2743 A70-32781
Friction and wear effects on leakage path in sliding seal interface
16 p2916 A70-33078
High speed homopolar inductor alternators with minimum leakage reactance, using geometric programming for objective function optimization
16 p2879 A70-34059
Real gas effects in blowdown analysis of leakage through choked nozzle in air flask
17 p3073 A70-35670
Ca ion reversible effects of hydrochloric acid and ammonia water on betacyanin leakage from beetroot sections
19 p3365 A70-38375

LEARNING
NT ASYMPTOTIC METHODS
NT CONDITIONING [LEARNING]
NT ITERATIVE SOLUTION
NT MAZE LEARNING
NT PROBLEM SOLVING
NT THEOREM PROVING
NT TRANSFER OF TRAINING
Retrospective and proactive inhibition in verbal discrimination learning, using paradigms characteristic of paired-associate retention studies
03 p0435 A70-13768
Cats trained for visual form discrimination tested for retention and reversal performance, studying oxygen deprivation influence
04 p0633 A70-15443
Postrest upswing or muscles warm-up in motor skill learning
05 p0803 A70-16671
Steering behavior during learning as function of self generated stimuli by movement compared with stimulus tracking
20 p3580 A70-39674
Bilateral cortical cerebellar hemispheric ablations effect on feline light-dark discrimination learning
21 p3762 A70-41142
Selective stimulus encoding and overlearning in paired associate learning
22 p3971 A70-43401
Neurophysiology of membrane and synaptic mechanisms of prolonged trace changes in neuron activity concerning memory and cellular learning analogs
24 p4305 A70-46393

LEARNING MACHINES
Mathematical models for perception and skilled action in man or machine, noting sensorimotor theory
01 p0034 A70-10498
Human controller in psychology and control engineering, discussing linear and nonlinear modeling of human behavior
05 p0807 A70-16487
Heuristic principles for self organization algorithm of cognitive automation system with active learning strategy
08 p1466 A70-20874
Pattern recognition involving machine extraction of characteristic features and classification based on associated values, discussing design and decision rules for optimal recognition
13 p2373 A70-29577
Learning self learning relationship in image recognition, analyzing resolving function with minimum probability for erroneous recognition
14 p2553 A70-30420
Learning control systems design, deriving general learning algorithms
15 p2705 A70-32448
Control system teaching based on preferred response data, discussing operator determination from purpose control function
15 p2716 A70-32449
Algorithm for implementing learning controller based on subgoal concept applicable to linear stationary system
16 p2868 A70-33312
Learning scheme with probabilistic teacher for unclassified samples, establishing convergence, comparing with linear estimator
17 p3128 A70-34851
Brain-like computer with learning rather than programmable capability, discussing pattern recognition and task performance
18 p3230 A70-36775
Linear reinforcement learning technique for accelerating convergence of successive approximation algorithms
22 p3994 A70-43491

LEARNING THEORY

Collection of papers on theory and applications of learning and pattern recognition systems covering statistics and algorithms, adaptive optimization, stochastic processes, etc

13 p2373 A70-29576
Stochastic reinforcement learning model synthesizing control and pattern recognition systems with learning attributes

13 p2374 A70-29584
Stochastic analog approximation method minimizing criterion functions and for recovering functions from noisy measurements of values in learning systems

13 p2442 A70-29585
Stochastic automata as learning system models in random environments with penalty-nonpenalty expectations, demonstrating convergence

13 p2374 A70-29587
Feedback analysis of learning and performance in hand-yoked, steering and stimulus tracking control of breath-produced visual target

16 p2852 A70-33660
Simultaneous optimal detection and parameter estimation of signals in noise, considering multiple solution, learning and image recognition

18 p3228 A70-36597
Psychological tests for ability to learn association between event and occurrence probability

19 p3363 A70-38319
Statistical pattern recognition and threshold learning in signal detection of noisy binary pulses

21 p3794 A70-41332

LEAST SQUARES METHOD

Least squares method adjusting observation functions in satellite triangulation with correlated observations

01 p0082 A70-11455
Least squares adjustment of observation equations for hybrid systems solved by regarding constraints as observations with zero variances

02 p0289 A70-11798
Aerodynamic derivatives in equations of motion governing aircraft longitudinal short period motion estimated using least squares methods

02 p0224 A70-11866
Earth satellite orbit parameters determination from angle measurements using computer program and least squares estimation technique

03 p0573 A70-13843
Least squares iterative method for solving simultaneous linear equations having singular coefficient matrix

04 p0714 A70-15450
Mathematical and numerical least squares solution of linear equations, using Householder algorithm [JPL-TR-32-1431]

05 p0876 A70-16311
Optimal timing of measurements to minimize dispersion of navigational observation parameters by least squares method applied to Keplerian orbit elements

06 p1103 A70-17878
Least squares method to determine shock thickness at arbitrary Mach number from Boltzmann equation for rigid sphere rarefied gas

06 p1051 A70-18345
Maximum principle least squares (MPLS) nonlinear filter scheme simplified, using digital simulation for stability and tracking performance

11 p2028 A70-26315
Guidance boundary value problem estimation by continuous least mean square (CLMS) method, describing application to generation of velocity required coefficients

11 p2081 A70-26322
Arithmetic mean, least squares method and standard deviation concepts in random error analysis of measurement data

11 p2117 A70-26674
Computerized aircraft navigation utilizing Doppler dead reckoning system and Tacan integration with least square adjustment method

13 p2447 A70-28550
Nonspin stabilized satellite attitude reconstitution using least squares estimate

14 p2654 A70-30775
Linear integral equations for radiative transfer between parallel plates, using least squares method

15 p2826 A70-31822
Iterative weighted nonlinear least squares parameter estimation for human respiratory control system by transfer function modeling, comparing results with visual curve fitting

16 p2851 A70-33322
Nonlinear least squares method reducing Burnett data to compressibility factors and virial coefficients

17 p3136 A70-35594
Mariners 6 and 7 orbits determination by weighted least squares estimation based on common surface features in overlapping TV pictures [AIAA PAPER 70-1066]

19 p3529 A70-38879
Brittle fracture stress statistics for Weibull distribution function parameter determination, comparing linearizing, least squares curve fitting and maximum likelihood techniques

22 p4117 A70-43414

Fitting equations to mixture data by linear least squares method with restraints on compositions, using Scheffe polynomials

22 p4064 A70-43728

Cylindrical heaters in corresponding-states fluids, estimating film boiling heat transfer coefficients by correlation procedure using least squares expression

23 p4279 A70-44361

Suboptimum filter for trajectory estimation from parameters, using modified covariance with least squares formulation in Kalman setting

23 p4177 A70-44601

LEAVES

Diffuse isotropic light interaction with compact corn leaf, using transparent plate model with rough plane-parallel surfaces

02 p0338 A70-11893

Cotton leaf light reflectance and transmittance changes with maturity

12 p2218 A70-26919

Plant leaves discrimination by multispectral reflectance indicated in transmittance measurements via remote sensing from aircraft and spacecraft

12 p2218 A70-26920

Field cotton leaves reflectance and transmittance measurement, predicting linear dimension related to cellular structure

12 p2273 A70-28122

Cotton plant leaves from high saline soil area, observing chlorophyll content on color photographs

14 p2576 A70-30977

Reflectance of single leaves and field plots of cotton, determining Cycocel treatment effects on aerial IR photography

14 p2577 A70-31233

Photoelectric device for recording plant rhythmic leaf movements in space

16 p2849 A70-33998

Ecological potentials in spectral signature analysis, using laboratory leaf and soil spectral reflectance data

17 p3078 A70-35612

Auxin downward transport by gravity in leaves, examining ethylene inhibition

20 p3570 A70-39234

Cotton leaves ammonia induced discoloration spectrophotometric examination, discussing light reflectance, transmittance and absorbance

22 p4014 A70-42771

LECTURES

Lectures on forms in many variables covering Chevalley-Waring and Lang-Nagata theorems for finite and function fields, discrete valuation rings, etc

13 p2441 A70-29454

LEE WAVES

Wave drag in stratified flow lee waves without upstream influence calculated for cylindrical and three dimensional obstacles

03 p0479 A70-14229

Lee wave theory for two dimensional stratified atmospheric models, noting local intense vertical beam into high stratosphere

08 p1540 A70-21972

Earth profile influence on two dimensional nonlinear lee waves in troposphere, discussing Helmholtz perturbation equation and stream function field

11 p2075 A70-25391

Lee wave flow disturbances due to mountains by midtroposphere balloon and aircraft observation, noting flow features nonstationarity

12 p2262 A70-26883

Nonlinear orographic waves in atmosphere, investigating influence of meteorological parameters, temperature jump, incident flow and ridge geometry on flow patterns

12 p2263 A70-27517

Computer plotting of flow patterns and orographic cloud over/in lee wave flow, including rotors, blocking and high level turbulence

12 p2264 A70-27722

Maximum up- and downdrafts altitude, using two dimensional model of lee wave disturbances for post-frontal subsidence modification

16 p2945 A70-32948

Nonlinear orographic waves in atmosphere, investigating influence of meteorological parameters, temperature jump, incident flow and ridge geometry on flow patterns

21 p3846 A70-41165

LEG [ANATOMY]

NT KNEE [ANATOMY]

Speed and accuracy of foot operation of controls tested by circular targets in rows within reach of right foot

02 p0245 A70-12144

Bed rest effects on whole leg venous distensibility, discussing heart rate and leg volume measurements

06 p0999 A70-17288

Orthostatic tolerance in humans increased by lower limb muscles electrostimulation, correlating subjective feelings with heart and pulse rate measurements

09 p1615 A70-22089

Orthostatic tolerance in humans increased by lower limb muscles electrostimulation, correlating subjective feelings with heart and pulse rate measurements

15 p2685 A70-32685

Elastic bounce of body resulting from falling to ground with calf muscles in sustained contraction and without knee bending

21 p3765 A70-42151

Fatigue effects on relationship between oxygen consumption, electromyographic activity and isometric contraction in human leg muscles

21 p3766 A70-42159

Human leg blood flow distribution between deep and superficial veins during alternate treadmill work-rest periods

21 p3767 A70-42160

LEGAL LIABILITY

International law framework for outer space, resolutions and recommendations by UN and international bodies and Space Treaty of 27 January 1967

03 p0611 A70-14257

International Law Association and development of legal regime of outer space, discussing treaties

03 p0611 A70-14258

Latin American viewpoint on Space Treaty and prior UN Declaration implications, discussing military activity, astronaut legal treatment, liability, information access, etc

03 p0611 A70-14260

Liability convention requirements for international space law, considering personal injury or property damage caused by space activities of another state

03 p0612 A70-14262

Spacecraft registration and legal liability issues, noting UN Treaty assumption of registration

03 p0612 A70-14264

Montreal agreement of 1966 approved by CAB, considering air carrier liability

07 p1426 A70-18878

Legal and national justification for limitation in air freight carrier liability taking into consideration Warsaw convention and legal decisions

07 p1426 A70-18880

Air carriers legal liability, considering case decided in London involving Warsaw convention text

07 p1426 A70-18881

Legal aspects of liability for aircraft noise by German laws, discussing property owners obligation to permit flights over properties and admissible claims for compensation

07 p1427 A70-18884

Air cargo damage liability, considering national and international air transportation, delivery schedules, etc

07 p1427 A70-18888

Airfreight carriers secondary services from legal viewpoint

07 p1427 A70-18889

Liability for damage due to space objects, discussing questions before UN juridical subcommittee

12 p2334 A70-26999

Liability for damages by space objects, taking into account states and international organizations

17 p3202 A70-35783

International organizations participation in convention on liability for damage caused by launching of objects into outer space

17 p3202 A70-35784

International juridical discipline of space including moon and other celestial bodies, discussing shortcomings and limitations

18 p3349 A70-36653

Liability for damages due to supersonic flight sonic booms, discussing pertinent provisions in Dutch and international law

19 p3553 A70-37561

Air freight carrier liabilities in passenger transportation international regulations, noting conflicting interpretations

19 p3553 A70-37562

Book on law relating to activities of man in space covering liability, space communication, international organization, military implications, etc

19 p3553 A70-37676

Legal guidance criteria for expert witnesses presentation of technical evidence before jury in products liability litigation

23 p4137 A70-43869

LEGENDE CODE

U COMPUTER PROGRAMMING

U NEUTRON SCATTERING

LEGENDE FUNCTIONS

Coefficients of Legendre polynomial expansion of earth gravitational potential, using Stokes problem solution

03 p0474 A70-13344

Governing equations of plane elasticity to define suitable approximate theories for structural analysis [ASME PAPER 69-WA/APM-22]

04 p0771 A70-14909

Paired integral equations of elasticity with kernels containing Legendre spherical harmonics, admitting exact solution in quadratures

08 p1544 A70-20960

Spherical isotropic shells motion equations solved in terms of associated Legendre functions, considering surface loads and body forces

10 p1953 A70-23876

Arbitrary function expansion into series of Legendre functions by generalizing Weyl-Lebedev-Skalskia integral transform

13 p2441 A70-29312
Coefficients of Legendre polynomial expansion of earth gravitational potential, using Stokes problem solution

14 p2573 A70-30719
Paired integral equations of elasticity with kernels containing Legendre spherical harmonics, admitting exact solution in quadratures

20 p3672 A70-39382

LEGENDRE POLYNOMIALS

U LEGENDRE FUNCTIONS

LEGENDRE TRANSFORMATION

U LEGENDRE FUNCTIONS

LEIDENFROST PHENOMENON

Liquid or solid Leidenfrost film boiling on saturated cryogenic liquid surface, discussing hydrodynamic model similar to propellant spillage accidents

17 p3194 A70-34744

LEM [LUNAR MODULE]

U LUNAR MODULE

LEMMAS

U THEOREMS

LENGTH

Laser methods for industrial length measurements

11 p2061 A70-25355
Length effect on modulus determination test for thin laminated tube under combined loading using shell theory

11 p2136 A70-26086
Thin plates finite length effects on thermal conductivity measurement by impulse method, verifying results with n-type silicon samples

12 p2332 A70-28047

LENNARD-JONES GAS

Reduced second virial gas coefficients calculations by modified Lennard-Jones intermolecular potential function

12 p2180 A70-26860

LENS ANTENNAS

Radiation pattern computation for lens corrected conical scalar horn, comparing patterns and beam-widths with uncorrected horn and waveguide

04 p0656 A70-14721
Radiation patterns widened from plane and circular waveguide ends closed by planoconcave homogeneous dielectric lens

10 p1843 A70-25135
Multiple feed waveguide lens in variable coverage communications antenna for geostationary LES-7 satellite

11 p2016 A70-25461
Antenna pattern and power gain determination from near field measurements on electrically large horn lens, standard gain horn and measuring antenna duplicate

15 p2698 A70-31956
Antenna gain, efficiency, half power bandwidth, sidelobe level and focal length for circularly polarized metallic lens antenna at X band frequencies

16 p2872 A70-32969
Geodesic Luneberg lens Q band antenna design, construction and evaluation, noting point feeding and energy collimation

16 p2876 A70-33408
Lens antennas design for communication satellites, discussing power gain, beam width, sidelobe level, temperature distribution, etc

16 p2982 A70-33772
Lens antennas for performing radiation collimating function through refraction, discussing solid and artificial dielectrics lens design, beam scanning applications, etc

17 p3052 A70-35069
Luneberg lens application to construct multiple beam mechanically despun antenna for spin stabilized satellites, discussing temperature problems

17 p3055 A70-35663

LENS DESIGN

Hyperbolic type gas lens design and focusing characteristics for use in laser light beam waveguide

01 p0106 A70-10033
Microwave holography, discussing zone plate lens design, coherent side-looking radar, large antennas, three dimensional radar display applications

01 p0086 A70-10415
Birefringent lens producing spatially separated multiple images, discussing polarization control, thin crystalline lenses and electro-optic control

01 p0091 A70-10915
Cassegrain telescopes lens corrector systems, critically examining various published articles

02 p0297 A70-11927
Elliptically shaped lenses to eliminate reflection losses by positioning obliquely in optical line

05 p0812 A70-16244
Basic equations governing optical properties of telecentric lens systems for moire analysis, discussing suitability for stress analysis

07 p1248 A70-19238
Objective lens systems with high chromatic aberration correction for visible spectral region

08 p1494 A70-20834

Aerial color photography, considering lens types, exposure, filters, films, etc

08 p1498 A70-21543
Holographic recording of Q switched neodymium laser beam achieved through lens testing on reconstructed beam

09 p1697 A70-22845
TV camera with diffraction limited pinhole lens for visual simulation, solving depth of field and extending field of view without distortion

10 p1887 A70-24217
Big Bear Solar Observatory, discussing site selection, observatory construction and telescope optical system

12 p2205 A70-26864
Multilens quasi-optical transmission lines construction by determining lens profile for optimal conversion of source field into specified field at receiver end

13 p2366 A70-29403
Optical cross correlator with consecutive recording of mutual correlation function, using transparencies on different side of lens

13 p2412 A70-29865
Glancing incidence extreme UV telescopes optical design in solar physics applications, employing surfaces of revolution

15 p2736 A70-32029
Foreground presence for computer generated and painted three dimensional photographic displays using fly eye lenses

16 p2906 A70-33177
Bicylindrical microwave lenses, discussing collimating, virtual line source and point feed scanning lenses design

16 p2876 A70-33405
Allowable transmission bandwidth of lens waveguide with curved axis, considering light beam deflection due to chromatic aberration

17 p3050 A70-34583
Lens antennas for performing radiation collimating function through refraction, discussing solid and artificial dielectrics lens design, beam scanning applications, etc

17 p3052 A70-35069
Spatial signal transmission through open resonator determination based on resonator integral equation, extending to dielectric lens with finite Fresnel diffraction number

18 p3259 A70-36480
Astrophotograph optical center coordinates and camera focal length calculations

18 p3260 A70-36992
Lens systems configuration and aberration, determining suitability for wide angle oculars of Galilean telescopes

19 p3420 A70-37262
Lens with radial symmetry for mm wave scanning antenna

20 p3598 A70-40307
Diffraction theory relationship to ray optics for coherent light propagation through lens systems

21 p3829 A70-41929

LENSES

NT WIDE ANGLE LENSES

NT WIRE GRID LENSES

Fourier transform applied to power spectral distribution determination for two dimensional Fraunhofer holographic data of thin spherical lenses

01 p0090 A70-10907
Circulation gas lens temperature distribution, considering effects of gravity, wall thermal conductivity, glass interlayer, etc

03 p0604 A70-13387
Two loop control system model of human lens accommodative system derived on basis of muscle mechanics, optics and experiments

03 p0439 A70-14275
Ciliary nerve stimulation and lens motion data to identify open-loop plant dynamics of lens accommodation

07 p1216 A70-18858
Thermal lens effect produced by photocurrent in CdS, using focused laser beam to generate photocurrent causing local heating changes of refractivity

10 p1898 A70-23980
Deformed grating frequency multiplication by filtering in Fourier plane of lens, forming moire pattern in image plane by mechanical interference

10 p1890 A70-24592
Lens aberrations compensations in partially coherent image holography

10 p1891 A70-24838
Plasma self Q switching in pulsed far IR lasers, discussing lens effect of plasma electrons delaying laser pulses

11 p2062 A70-25634
Wide angle emitter images transformation into circular by reflecting cone and lens system, describing photographic and photoelectric methods

12 p2237 A70-28157
Focusing lens edge diffraction effect on angular distribution of laser radiation, considering zero mode field distribution

13 p2428 A70-29367

Fourth order aberration in gas lens used as focusing element in light beam waveguide systems

15 p2697 A70-31829
Combined lens-hologram system for strain measurements by moire technique

17 p3087 A70-35024
Coherent light communication system quasi-optical lens line output field examination, using laser assembly to study parasitic, radiative and overall power losses

19 p3443 A70-37288
Large collimator objectives lenses focal lengths measurement in vibrations and temperature gradients

22 p4073 A70-42511
Satellite tracking camera lens-distortion coefficient from comparison of standard stellar and measured X-Y coordinates

22 p4029 A70-42596
Laser radiation effects on lens lipid content in adult Rana temporaria frogs during cataract development

22 p3978 A70-43139
Monograph on optimum focusing of laser light with nonideal lenses having spherical aberration

22 p4052 A70-43739
Pulsed ruby laser radiation energy characteristics relation to crystal temperature distribution, thermal deformation and compensating lens focal length

24 p4352 A70-45460

LEONID METEOROIDS

Radar and photographic studies of meteors from Leonid and Perseid showers, presenting velocities, luminescence and ionization

01 p0193 A70-11602
Leonid meteoroids mass distribution law exponent evaluation based on unstable meteoric radio echo durations integral distribution

03 p0574 A70-13884
Microparticle collection experiments during 1966 Orionid and Leonid meteor showers accomplished by Luster and ALARR /air launched-air recovered rocket/ instruments

08 p1575 A70-21393
Leonid meteor shower radar observation data, analyzing flux rates and particle size distribution

13 p2487 A70-28694
Time-amplitude characteristics and abundance in Leonid meteor shower from azimuthal radar observations

14 p2635 A70-30306
Radio observations of dense briefly visible Leonid meteor shower with fixed pencil beam antenna in coping with wave scattering in trails

15 p2796 A70-31511
Atmospheric turbulence scale and dissipation from 80 to 120 km, using photographic observations of Leonid meteor trails

19 p3515 A70-37663
Leonid meteoroids orbital elements mean values from photographic observations

19 p3526 A70-38776
Spectral energy distribution of meteor trail in Leonid meteor shower from photographic analysis

19 p3526 A70-38779
Ionospheric Si and SiO ions equilibrium interconversion during Leonid meteor shower

20 p3621 A70-39351

LEPTONS

NT ANTINEUTRINOS

Lepton charge and neutrino astrophysics, discussing oscillations role in solar neutrino detection difficulties

07 p1371 A70-20329
Deep inelastic lepton-hadron scattering cross sections universality properties based on Wilson theory

20 p3674 A70-39150
Secondary cosmic ray muon inelasticity in high energy neutrino interactions for deep mine experiments, using lepton current

21 p3845 A70-41139
Neutrino processes in lepton era as primeval fireball relic, discussing coupling constant for muon-electron neutrinos interactions

23 p4253 A70-44849

LES

U LINCOLN EXPERIMENTAL SATELLITES

LESA [LUNAR EXPLORATION SYSTEM]

U LUNAR EXPLORATION SYSTEM FOR APOLLO

LESIONS

NT PULMONARY LESIONS

NN dimethylguanadine for prevention of arterial lesions induced by cholesterol in rabbits

01 p0020 A70-10707
Temporary suppression of cortical associative responses in cats with electrocoagulated thalamic relay nuclei lesions

04 p0632 A70-15220
Time course of changes in rat brain norepinephrine levels after olfactory bulb lesions, discussing autonomic and biological mechanisms

08 p1448 A70-21841
Long bone necrosis in response to reduced atmospheric pressure exposure, comparing lesions with caisson disease

08 p1449 A70-21944

LETTERS [SYMBOLS]

U SYMBOLS

LEUCINE

Refutation of Sylven-Snellman report of catalysis of benzoylarginine beta-naphthylamide and leucine beta-naphthylamide hydrolysis by beef spleen cathepsin B
10 p1812 A70-24534

LEUKOCYTES

NT EOSINOPHILS
NT LYMPHOCYTES

Phagocytic activity and carbohydrate metabolism in peripheral blood neutrophils of men exposed to atmosphere with increased O content, noting neutrophil energy exchange disorder role
03 p0426 A70-13901

Adrenaline effects on rats peripheral blood leukocyte content used for X-irradiation sensitivity estimation
10 p1822 A70-25177

LEVEL [HORIZONTAL]

Two-axis electrolytic bubble level as precision vertical reference and tilt indicator for ballistic missiles inertial navigation systems
[AIAA PAPER 70-949] 20 p3631 A70-39578

LEVEL [QUANTITY]

NT ATOMIC ENERGY LEVELS
NT ELECTRON STATES
NT ENERGY LEVELS
NT GROUND STATE
NT INTERMOLECULAR FORCES
NT MOLECULAR ENERGY LEVELS

LEVELING

Error propagation in rectangular grid leveling networks assuming fixed height of center of mass
11 p2045 A70-25798

LEVITATION

Critical Levitation Loci for floating spheres on cryogenic fluids
17 p3136 A70-34743

High magnetic fields applications, emphasizing metal forming and superconducting rings levitation
19 p3471 A70-37948

LEWIS NUMBERS

Heat transfer coefficient of chemically reacting gas mixture as function of Lewis-Semenov number, discussing nitrogen dioxide decomposition
19 p3550 A70-37251

LIABILITIES

NT LEGAL LIABILITY

LIAPUNOV FUNCTIONS

Nonlocal continuity and correctness of principle for comparing functions with Liapunov vector function, demonstrating continuous dependence of principle on certain parameters
01 p0130 A70-10151

Stability and asymptotic stability criteria for attraction sets in dispersed dynamic systems obtained in terms of Liapunov function
01 p0141 A70-10152

Differential equation comparison with Liapunov vector function, applying Caratheodory condition
01 p0130 A70-10156

Autonomous functional differential equations with finite time lag using Liapunov functionals, discussing stability and instability
01 p0132 A70-11070

Randomly sampled linear systems stability with linear or nonlinear feedback loops, using stochastic Liapunov function method
02 p0272 A70-12727

Liapunov function for automatic control systems, deriving theorem to ensure stability
03 p0460 A70-13434

Liapunov second method extension to dynamical systems stability, illustrating wing torsional divergence and panel supersonic flutter
05 p0941 A70-16564

Liapunov function construction and stability criteria based on linear differential equations containing periodic and aperiodic coefficients and small parameter
05 p0883 A70-16859

Boundary value problems in closed spaces with fine grained Liapunov boundary described by second order elliptic differential operators
05 p0877 A70-16881

Liapunov functions generation by matrix transformation of state-space system vector applicable to linear and nonlinear systems
06 p1023 A70-17544

Liapunov functionals for time delay systems generated by path integrals in state space in terms of convolution equations
06 p1094 A70-17953

Nonlinear control systems stability with stochastic coefficients, applying Liapunov function
06 p1026 A70-17971

Routh theorem and Chetaev method for construction of Liapunov function to investigate steady state motions, obtaining stability conditions
07 p1332 A70-18677

Relay control design for model-tracking system with parameter uncertainties and disturbances using semidefinite Liapunov function
07 p1247 A70-20026

Liapunov vector functions for asymptotically stable omega-periodic solution existence in case of finite dimensional system
08 p1534 A70-21002

Liapunov direct method for synthesizing self adaptive model reference control system with simultaneously used passive /signal/ and active /parameter/ adjustment loops
08 p1480 A70-21018

Extension of Liapunov systems to time lag systems with small periodic parameter
08 p1546 A70-21628

Nonlinear stability theory for applying perturbed equations to dynamical system based on Liapunov stability theorem
09 p1727 A70-22612

Liapunov stability conditions for critical point of ordinary differential equation, determining optimal criterion
09 p1727 A70-22664

Numerical algorithms for solving Liapunov matrix equation in nonlinear stability analysis and optimal systems design
09 p1641 A70-22959

Coupled systems stability and oscillatory behavior analysis using Liapunov theory
10 p1855 A70-24763

Algorithm developed for constructing first approximation system from Cauchy matrix for Liapunov stability problem solution
10 p1917 A70-25302

Triangular system of linear differential equations reducible to block form by Liapunov transformation, deriving indices stability conditions
10 p1911 A70-25303

Asymptotic stability of multivariable autonomous control systems used Liapunov vector function method
11 p2083 A70-25606

Asymptotic stabilization of multivariable dynamic systems, using subsystem decomposition and Liapunov second method
11 p2023 A70-25607

Liapunov functions construction through conversion of differential equation with polynomial nonlinearities into auxiliary exact differential equation using algorithm
12 p2262 A70-28070

Finite time stability of differential equations system using Liapunov functions
13 p2442 A70-29488

Adaptive hydraulic servomechanism control systems synthesis by Liapunov direct method, noting parameter compensation effect on state error reduction
14 p2534 A70-30621

Routh theorem and Chetaev method for construction of Liapunov function to investigate steady state motions, obtaining stability conditions
15 p2774 A70-31469

Floquet-Liapunov theorem matrix representation derivation, improving accuracy of Liapunov classical representation
15 p2774 A70-31643

Rumanian book on flight stability and control covering Liapunov general stability theory, control systems, stability models, etc
15 p2673 A70-31695

Liapunov functions direct generation by state space system vector matrix transformation
15 p2768 A70-32555

Asymptotic motion stability bound for nonholonomic nonlinear electrodynamic systems, using energy metric algorithm for Liapunov functions generation
15 p2768 A70-32556

Digital computer generation of system stability Liapunov functions for ninth order spacecraft attitude control
16 p2867 A70-33043

Criteria for estimating errors in quadratic approximations to asymptotic stability involving Popov condition based on existence of quadratic Liapunov functions
16 p2941 A70-33045

Liapunov functions synthesis for aperiodic linear systems by inspecting traces of state matrix and products
17 p3129 A70-34955

Steady forced regime stability in pulse frequency modulated servosystems, using Liapunov method
18 p3234 A70-36071

Generalized Carleman boundary value problem, discussing analytical function in simply connected region on Liapunov contour
18 p3280 A70-36159

Elastic continuum conducting heat under general loads, investigating stability thermodynamics- Liapunov criterion relations
18 p3337 A70-36336

Gravity stabilized gyrostatt satellite attitude motion stability, using three dimensional diagram and Liapunov functions
18 p3334 A70-37061

Liapunov stability analysis of dynamic systems described by simultaneous ordinary and partial differential equations of motion, applying to satellite spin stabilization
19 p3472 A70-38860

Real matrix stability determination by right half plane eigenvalues, using symmetric solution of Liapunov equation
24 p4370 A70-46098

LIBRARIES

SPIRAL system for free-flowing text information storage and retrieval in machine readable library
02 p0264 A70-12129

Radiation Shielding Information Center computer code library for radiation transport or shielding calculations, listing programs available
07 p1239 A70-20364

LIBRATION

Autonomous two degrees of freedom Hamiltonian system triangular libration points found stable for all mass ratios in circular restricted three body problem
01 p0192 A70-11575

Lunar limb ellipsoid orientation and parameters based on Greenwich meridional measurements of visible lunar diameters, noting use for observation reduction for various librations
03 p0569 A70-13356

Libration clouds reality possibility from satellite dust counting experiments
03 p0572 A70-13819

Libration limits of satellite in Keplerian circular orbit, estimating potential energy of perturbing forces
08 p1582 A70-20967

Lunar photographs on star-calibrated plates for lunar features coordinates or physical libration determination, outlining photographic technique and computer program
09 p1674 A70-22308

Lunar limb ellipsoid orientation and parameters based on Greenwich meridional measurements of visible lunar diameters, noting use for observation reduction for various librations
11 p2118 A70-26721

Librational motion of damped gravity oriented satellite in circular orbit
12 p2313 A70-27201

Computer techniques for determining physical libration of moon in longitude
13 p2488 A70-28765

Lunar rotary motion predetermination for spacecraft landing in mountainous region
15 p2773 A70-32266

Heliostationary spacecraft at L2 point for solar wind observation, describing mission, instrumentation and spacecraft design
17 p3168 A70-35252

Heliostationary spacecraft for solar observation near libration point between sun and earth, discussing attitude stabilization by solar pressure
17 p3178 A70-35254

Triangular libration points stability in elliptic restricted three body problem, determining parametric resonance region
17 p3137 A70-35690

Controlled libration point satellite limit cycle motion, deriving solution in infinite series by harmonic analysis
17 p3181 A70-35752

Planar Tethered Orbiting Interferometer satellite for long wavelength solar and planetary radio astronomy, discussing deployment control and libration damping
18 p3333 A70-36230

Lunar gravitational field effect on sun-earth exterior libration point location, examining placement on line passing through sun and earth-moon barycenter
18 p3320 A70-37059

Gravity gradient attitude control for satellites near lunar far side libration point
19 p3528 A70-38868

Libration limits of satellite in Keplerian circular orbit, estimating potential energy of perturbing forces
20 p3713 A70-39388

Ephemerides for lunar-orbiting observation of dust clouds in earth-moon system libration points L4 and L5 by observer orbiting over lunar equator
22 p4097 A70-42308

Satellites with many flexibly coupled rigid bodies, calculating libration upper bounds for predicting perturbation and stability
23 p4262 A70-44682

LIBRATIONAL MOTION
Moon figure and gravitational field determination based on hydrostatic theory, libration observations, node and perigee motion, lunar satellite trajectories and visible topography
06 p1141 A70-17824

Particle nonlinear motion near equilateral libration points in restricted three body problem
06 p1146 A70-18226

Material particles unrealizability of periodic motion near libration points of triaxial ellipsoid rotating steadily about polar axis
08 p1543 A70-20491

Computer program for generating tables to calculate lunar libration at any epoch

09 p1752 A70-22313

Solar attraction effects on zero-mass body planar motion near triangular earth-moon libration points, obtaining variational equations of motion

09 p1754 A70-22477

Periodic solutions of restricted three body libration point perturbation due to fourth body gravitational and radiative influence using Huang model

09 p1761 A70-23053

Material elasticity effects on librational motion of arbitrary shaped satellite

10 p1950 A70-24177

Newtonian gravitational system of three point masses with oscillatory motion at time t approaching infinity, discussing particles mutual distance

10 p1938 A70-24182

Lunar libration constants determination from Bessel to present, discussing data reduction methods, international cooperation and impact of lunar exploration

13 p2490 A70-28946

Heliometric lunar libration series joined to obtain uniform equation

13 p2490 A70-28949

Soviet book on physical libration constants of moon based on visual and photographic observations of two craters by position angle method

14 p2642 A70-30959

Book on passive gravity gradient libration dampers covering design, flight experience, evaluation criteria, performance monitoring, failure prevention, etc

16 p2983 A70-33954

Torsion wire libration damper for satellite gravity-gradient stabilization at near synchronous altitudes

16 p2985 A70-34134

Plane galactic orbits near spiral field particle resonance, calculating numerically for ring orbits librating near maxima at Lagrangian points

18 p3331 A70-37193

Spacecraft fuel optimal controls for out-of-plane motion about translunar libration point based on phase plane methods

19 p3530 A70-38890

Nonperiodic Transtrojan orbits for various mass parameter values in three body problem, discussing double libration

21 p3888 A70-41144

Optimal moments of inertia of rigid satellite in circular orbit by generalization of Beletskij concept, discussing libration boundaries

23 p4261 A70-44677

Lunar libration amplitude estimation, using stochastic process theory

23 p4247 A70-44771

LIBYAN DESERT

Time-temperature relation necessary to fine Libyan desert glass and remove gas bubbles calculated by viscosity determination at various temperatures

05 p0843 A70-16833

LIDAR

U OPTICAL RADAR

LIE GROUPS

NT SPINOR GROUPS

Perturbation theory based on Lie transforms, reducing Deprit equation to generate general recursion formulas

05 p0908 A70-16336

Birkhoff normalizing canonical transformation built at elliptic type of equilibrium without internal resonance, using Lie transforms

05 p0909 A70-16340

Operational calculus for semisimple complex Lie group

07 p1321 A70-18658

Momentum-energy tensor and angular momentum for hydrodynamic and electrodynamic fields determined in transformations of m -parametric Lie group

10 p1922 A70-24098

Von Zeipel mappings equivalence to Lie transforms shown by order independent method

14 p2639 A70-30706

Artificial satellite theory main problem for small and moderate eccentricities, using perturbation techniques based on Lie transforms for computer programming

18 p3334 A70-37062

LIFE (BIOLOGY)

U LIFE SCIENCES

LIFE (DURABILITY)

NT FATIGUE LIFE

NT HALF LIFE

NT PLASMA LIFETIME

NT SATELLITE LIFETIME

NT SERVICE LIFE

NT STORAGE STABILITY

Dry lubricated instrument-size ball bearings operation in vacuum for long life and quality performance

[ASME PAPER 69-LUB-21] 01 p0101 A70-10386

Load, speed and coating thickness effect on near life of resin bonded solid lubricant, using oscillating motion and low pressure blocks

[ASLE PREPRINT 69-AM-SC-3] 01 p0103 A70-10447

Durability of refractory tubes of small thickness under creep with account of scale factor and unsteady conditions, tabulating experimental and theoretical values

03 p0508 A70-13247

Thermoelectric-couple life tests and efficiency measurements at constant thermal input, noting insulation for limiting parasitic heat losses

[ASME PAPER 69-WA/ENER-14] 04 p0731 A70-14896

NH emission systems radiative lifetimes and SiD and SiH transition probabilities measured, noting effects of radiative cascading

05 p0885 A70-16424

SERT 2 thruster hollow cathode durability tested in bell jar

[AIAA PAPER 69-304] 07 p1364 A70-19703

Mean lives measurement for excited levels in singlet system of neutral He using beam foil technique

07 p1338 A70-19821

Emission kinetics variations of ruby laser due to aging attributed to inhomogeneity of active medium developing simultaneously with color centers

07 p1300 A70-19872

Comet brightness outbursts monochromatic measurements for lifetime of parent gaseous molecules in solar radiation fields

08 p1575 A70-21373

Line strength and radiative lifetimes for Ne II determined from spontaneous emission data obtained from CW neon laser discharge

09 p1730 A70-22070

Solar corpuscular streams effect on meteoric particles behavior in circular orbit around sun, determining lifetime on basis of mass loss due to pulverization

09 p1763 A70-23382

Cramer-Rao efficiencies of best linear invariant estimators, using Weibull distribution in model for survival populations connected with life testing

10 p1910 A70-24604

Aviation equipment and systems operational durability, formulating physical model to construct functions for analysis

12 p2240 A70-27015

Complete sample estimation techniques for reparameterizations of Weibull density function to assign probabilities to components and systems lifetimes

12 p2243 A70-28012

Pulsed CO₂ laser calculating upper level lifetime of carbon dioxide molecule with allowance for gas heating at relaxation

12 p2251 A70-28296

Photon lifetime dependence on hole and electron concentration in GaAs from IR reflection spectra analysis

13 p2470 A70-28882

Safety, microdamages and lifetime of elastic structures under random Poisson pulsed loads

16 p2996 A70-34328

Comet Morehouse CO ions lifetime and density from photometric analysis

18 p3313 A70-36324

Hybrid boost bearing with long life and free starting, stopping and oil system failure characteristics of rolling element bearing

[ASME PAPER 69-LUB-16] 19 p3435 A70-37605

Lifetimes and fine structure of differentially metastable autoionizing states of negative He ion in axial magnetic field, using time of flight techniques

19 p3473 A70-37746

Durability of refractory tubes of small thickness under creep with account of scale factor and unsteady conditions, tabulating experimental and theoretical values

19 p3453 A70-38465

High purity surface-free GaAs epitaxial layer carrier lifetime measurement by optical transmission and excitation technique

22 p4086 A70-43017

Outer zone electrons radial diffusion coefficients and lifetimes determined as functions of magnetic shell parameter, based on satellite measurement following geomagnetic storm

23 p4236 A70-43831

Optimal burn-in testing of repairable equipment, improving reliability by decreasing failure rate with age under operating conditions

23 p4199 A70-43923

LIFE DETECTORS

Bioscience for recovered lunar samples, discussing Surveyor analyses, Lunar Receiving Laboratory methods and life detection using biological markers

01 p0042 A70-11637

Organic compounds detection and identification on Mars surface for living systems existence or evolution

16 p2857 A70-33977

Hydrogen flame ionization detector /HYFID/ for life-derived organic matter in Martian/Lunar soil

19 p3426 A70-37896

Life detection for unmanned planetary exploration from extraterrestrial sample involving growth, gas changes and carbon dioxide fixation

21 p3769 A70-41003

Lunar soil sample preparation and monitoring for viable microorganisms presence

22 p3978 A70-42973

Hydrogen, N, O, Kr methane and carbon dioxide gas chromatographic examination, discussing life detection device for Mars landing

22 p3983 A70-43094

LIFE RAFTS

Physiological research on humans in hypothermia resulting from confinement to life raft on open sea, analyzing thermal conditions, thermoregulation and survival

01 p0013 A70-10233

Three man space escape system, describing emergency situations, parachute descent, life raft design, rescue operations and engineering tests

[AIAA PAPER 68-936] 04 p0763 A70-15403

Physical discomfort and miseries contribution to psychological deterioration during water survival tests on life raft

07 p1218 A70-19009

Emergency equipment for aircraft accidents with dual channel radio beacons installed on life rafts, noting electronically conducted search

07 p1191 A70-19011

LIFE SCIENCES

Chimkurgan reservoir algae life and physicochemical characteristics

09 p1627 A70-23148

Photo-optical processes and optical measuring techniques in research programs at Ames Research Center for aerodynamics, life sciences and space sciences

09 p1657 A70-23501

Microorganisms metabolic activity effects on rocks and minerals, observing solubilization and altered IR absorption in Si-oxygen vibration region during penicillium simplicissimum growth

21 p3761 A70-40712

Bibliographical guide for literature concerning chemical evolution and origin of life

23 p4148 A70-44842

LIFE SUPPORT SYSTEMS

NT CLOSED ECOLOGICAL SYSTEMS

NT EMERGENCY LIFE SUSTAINING SYSTEMS

Langley integrated life support system design, discussing manned test results including system engineering, atmospheric and water chemical analyses and microbial measurements

01 p0038 A70-10973

Life support system model using heart rate to monitor man doing physical work in space suits under simulated space environment

02 p0245 A70-12146

Equations and techniques to analyze transient heat and mass transfer characteristics of packed adsorption beds for spacecraft life support systems

04 p0786 A70-15316

Apollo extravehicular mobility unit /EMU/ system developed from Gemini EVA system with improved thermal control and mobility to support contingency extravehicular transfer in emergency

04 p0645 A70-15665

Water electrolysis module long term operation in providing oxygen for life support systems

05 p0804 A70-15843

Hydrophobic-hydrophilic zero gravity liquid-gas phase separator for Apollo 11 flight life support system

[SAE PAPER 690638] 05 p0804 A70-15844

Regenerative life support system development for multiman crews on extended space missions, considering maintainability, reliability and automation

[SAE PAPER 690637] 05 p0804 A70-15845

Aircraft life support systems and equipment evaluated in Vietnam combat environment, discussing combat ejection conditions, injuries cause and severity, fatalities, etc

05 p0806 A70-16298

Mathematical model of optimal partially closed life support system consisting of man, recycling unit, storage unit and waste disposal outlet

05 p0809 A70-17110

Life support and survival gear design, testing, manufacture, supply and maintenance for combat ejections over rugged enemy terrain, discussing pilot injuries

06 p1002 A70-17706

Physiological training programs and equipment for life support in transports, discussing changes in protective helmet and quick donning harness

06 p1002 A70-17708

Commercial flight crew oxygen system using mask mounted diluter demand regulator

06 p1002 A70-17715

Space stations life support systems for air purification, water reclamation and oxygen recovery

08 p1449 A70-20630

Physicochemical methods of producing formaldehyde for carbohydrate synthesis in life support systems

09 p1623 A70-22080

Life support systems general inspection procedures, personal and survival equipment and accessories

11 p1990 A70-25673

Environmental control of confined spaces and life support systems by Pontryagin maximum principle of optimal control theory, discussing cabins, heat exchanger, etc

11 p1991 A70-26363

Apollo command and service modules environmental control system, discussing redesign of faulty hardware

[SAE PAPER 690618]

12 p2167 A70-27948

Lunar resources classified as rocket fuel, construction and life support materials, discussing implications for manned surface exploration missions

14 p2634 A70-30198

Extraterrestrial resources for space flight maintenance and human life support in space and on extraterrestrial bodies

14 p2634 A70-30199

Physicochemical methods of producing formaldehyde for carbohydrate synthesis in life support systems

15 p2693 A70-32676

Ben Franklin submarine life support systems tested during Gulf Stream Drift Mission, discussing atmosphere control, water, waste and food management

[ASME PAPER 70-DE-60]

16 p2852 A70-33515

Hydrogenomonas vs Chlorella spacecraft life support systems, discussing human requirements and equipment for balanced food supply on long duration space missions

16 p2855 A70-34315

GE-RESO primate life support subsystem design for NASA-ARC biosatellite program

17 p3174 A70-34766

Optimum algae cultivator construction for life support system, using Chlorella culture model

17 p3026 A70-35320

Wheat culture continuous subirrigation for life support system applications in spacecraft, discussing harvest yields

17 p3026 A70-35321

Medicobiological approach to living conditions for sustained residence and human activity during prolonged space flights, describing sealed chamber experiment

19 p3367 A70-37525

Hypoxia warning systems using polarographic sensor and miniaturized electronics for face-mask and cabin installation for aircraft and spacecraft

20 p3579 A70-39429

Portable contingency transfer life support system for crewman of Apollo missions providing oxygen and cooling

20 p3580 A70-39441

Life support systems based on Chlorella-bacterial culture, investigating water exchange and reclamation

20 p3574 A70-40184

Human mass exchange parameters permissible errors for manned space vehicles life support systems design

20 p3581 A70-40200

Environmental control-life support systems (ECLSS) waste methane gas utilization in low thrust resistojet for manned space applications

[AIAA PAPER 70-1131]

20 p3568 A70-40214

Integrated environmental control/life support resistojet systems, surveying NASA programs

[AIAA PAPER 70-1130]

20 p3690 A70-40215

Advanced Integrated Life Support Systems, discussing subsystem requirements and mission parameters

21 p3768 A70-40988

Integrated Life Support System hardware tests, discussing oxygen and water recovery, contaminant control, personal accommodations and failure detection

21 p3833 A70-40989

NASA aircrew oxygen system, describing carbon dioxide control and oxygen generation subsystems

21 p3768 A70-40990

Life support systems oxygen generation mode selection based on mission parameters, including duration, crew size, resupply, vehicle leakage, etc

21 p3768 A70-40991

Life support water electrolysis system design, discussing alkaline or acid electrolyte selection

21 p3768 A70-40993

Spacecraft design to overcome space and launch environment, including environmental protection

23 p4257 A70-44327

Aerospace medicine approach to medical investigator training for aircraft accidents, noting flight surgeon role as life support specialists chief

23 p4152 A70-44454

Continuous flow requirements in aircraft passenger oxygen systems using phased dilution principle, discussing breathing mask efficiencies

23 p4141 A70-44483

Testing laboratory for safety, survival and life support equipment concerning parachutes, aircrew protective helmets and maintenance manuals

23 p4141 A70-44488

Integrated regenerative life support manned tests for space laboratory design and development

23 p4154 A70-44632

Space cabin atmosphere regeneration by unicellular algae photosynthesis, discussing Chlorella cultivation procedures and additional functions in life support systems

23 p4154 A70-44655

Life support systems for biological flight experiments on Biosatellite project and Skylab A mission

23 p4154 A70-44665

Manned space flight regenerative life support systems requirements, considering weight, volume, power, cost effectiveness and integration problems

23 p4156 A70-45023

Closed loop life support system employing algae and bacteria cultures to recycle water in addition to atmospheric regeneration

23 p4156 A70-45024

Biological life support system based on mutual equilibration of human metabolism and technically controlled algae culture, discussing experimental evaluation

23 p4156 A70-45026

Biological life support systems mass exchange processes analysis based on mathematical models, predicting artificial ecological systems stability

23 p4149 A70-45029

Earth-to-orbit space shuttle environmental control and life support system

[AIAA PAPER 70-1253]

24 p4418 A70-45967

Optimal temperature control for confined spaces and life support systems, using mathematical models of environmental control systems

24 p4295 A70-46373

LIFETIME [DURABILITY]

U LIFE [DURABILITY]

LIFT

NT INTERFERENCE LIFT

NT JET LIFT

NT ROTOR LIFT

Canterleaved and doubly supported structures calculated for critical aeroelastic divergence speed resulting from lift and drag

01 p0200 A70-10551

Minimum drag hypersonic delta wing, analyzing shape for given planform, lift, pitching moment and volume using correction for pressure coefficient

01 p0002 A70-10557

Leading edge suction analogy for predicting low speed lift and drag-due-to-lift characteristics of sharp edge delta and related wing planforms

[AIAA PAPER 69-1133]

01 p0002 A70-10607

STOL aircraft configurations optimization including cost effectiveness, considering propulsive lift systems

[AIAA PAPER 69-1131]

01 p0162 A70-10609

Spacecraft horizontal maneuvers in homogeneous gravitational field to achieve soft landing on planetary surface, including optimal liftoff and orbital transfer

01 p0197 A70-11501

Unsteady state lift and moment action on lattice of profiles moving in incompressible fluid, determining suction originating at leading edges of profiles

03 p0409 A70-13868

Vortex separation effects on elliptic bodies lift distribution, analyzing separated flow pattern

04 p0619 A70-15385

Lift effectiveness of slender wings with streamwise root gaps and fences, obtaining lift curve slope variation with fence height

04 p0621 A70-15611

Separated incompressible flow around wing profile, considering calculation of separated potential flow generation with given separation point

06 p0966 A70-17253

Lift and vortex drag due to flaps on thin sweptback tapered wings in inviscid incompressible flow, obtaining spanwise loadings

06 p0967 A70-17256

Lift forces and pressure on vibrating cylinders in plane perpendicular to air flow measured in wind tunnel

06 p0968 A70-17545

Upper surface suction effect on thin plate aerodynamic characteristics, considering relations for lift and pitching moment coefficients

06 p0968 A70-17851

Nonlinear pursuit problem solution taking into account drag and lift in pursuing object equations of motion

07 p1330 A70-18682

Propulsive and lifting motions of pointed profile in ideal incompressible fluid related to alternate vortices emission

08 p1433 A70-21234

Fokker F-28 wing flap, lift dumpers and aileron development, including wind tunnel and flight tests

08 p1438 A70-21864

Shear flow near walls through cascade of untwisted blades, observing variation in lift coefficient across span

11 p1975 A70-25788

Correction factor for finite span effect on unsteady wing lift or moment during sinusoidal gusts or vertical oscillations

12 p2155 A70-27200

Lift and drag characteristics of flexible parawings at subsonic speeds, predicting angle of attack for trailing edge flutter commencement

12 p2157 A70-28079

Rigid wing subsonic and supersonic civil and military aircraft utilizing aerodynamic lift at takeoff and landing

13 p2344 A70-28543

Vortex- and Doublet-Lattice methods for calculating aerodynamic lift distributions on surfaces in steady and oscillatory motion at subsonic speeds

[AIAA PAPER 70-539]

13 p2339 A70-29006

Wing section pressure distributions, lift and drag in transonic mixed flow, considering prediction methods

14 p2529 A70-30866

DC 8 Super 63 aircraft direct lift control flight evaluation

17 p3018 A70-35496

Lifting and side force distributions acting on body in transonic flow

17 p3012 A70-35696

Lift forces acting on spheres in cylindrical tube laminar flow

19 p3352 A70-37647

One dimensional channel flow theory for ram wings, deriving lift and drag laws for comparison with wind tunnel and free flight tests results

[AIAA PAPER 70-971]

20 p3558 A70-39558

Slender wings of low aspect ratio and sharp leading edges, predicting inviscid maximum lift

21 p3743 A70-40585

Flat plate airfoil unsteady lift due to chordwise velocity perturbations, using Horlock frozen gust pattern theory

22 p3957 A70-42303

Short wing lift investigated via lateral fluid jets fired in wind tunnel for various lengths

22 p3958 A70-42614

Optimum pressure distribution and airfoil profiles for maximum lift without separation in incompressible flow determined by second order theory

[AIAA PAPER 69-739]

22 p3959 A70-42704

Vortex induced vibration problems, deriving mathematical model for periodic lift on circular cylinder

22 p3960 A70-43546

Continuous trailing vortex sheet rolling up into two discrete vortices, discussing wing lift limitations

23 p4131 A70-43890

Satellite drag and lift from spatial impulsive surface interaction model

[ICAS PAPER 70-05]

23 p4132 A70-44116

Low speed airfoil two dimensional testing in wind tunnel with slotted wall, examining lift, drag and pitching moments

[ICAS PAPER 70-08]

23 p4132 A70-44119

Lifting quasi-elliptical airfoils with supercritical shock free flow, discussing Nieuwland hodograph theory to compute profile number

[ICAS PAPER 70-15]

23 p4132 A70-44126

Lift determination of slender curved periodically recurring airfoils array in plane potential flow of inviscid incompressible fluid

23 p4133 A70-44158

Hypersonic viscous effects on space shuttle entry trajectory, measuring lift and drag in free flight regime

23 p4258 A70-44526

Aircraft longitudinal motion during takeoff and landing due to loss of lift after boundary layer control system failure

24 p4372 A70-45448

LIFT AUGMENTATION

V/STOL aircraft propellers featuring thrust augmenting air jet slits for increased lift

[DGLR-69-36]

04 p0616 A70-15175

Heaving airfoil wakes visualization with jet flap augmented lift, measuring vortex street parameters

13 p2338 A70-28821

Ground effect for increasing lift during aircraft landing

13 p2345 A70-28973

Plane plate motion in weightless fluid flow with free upper boundary, showing lifting capacity increment by underlying solid surface

13 p2390 A70-29644

High lift airfoils boundary layer separation suppression by blowing, describing wall jets streamwise development prediction methods

[AIAA PAPER 70-872]

17 p3010 A70-34818

Increased lift via hinge suction jet flaps on augmentor wings, using thin airfoil model and small disturbance theory

22 p3960 A70-43432

Wing lift increase by spanwise blowing along upper surface, causing flow reattachment on wing and vortex induced effective aerodynamic camber increase

[ICAS PAPER 70-09]

23 p4132 A70-44120

LIFT COEFFICIENTS

U AERODYNAMIC COEFFICIENTS

U LIFT

LIFT DEVICES

Aerodynamics of conventional aircraft high lift devices, considering effect of leading edge geometry on lift coefficient at stall of plain and flapped airfoils 01 p0001 A70-10046

Research program to improve performance of high lift devices on wings having small sweepback and high aspect ratio 01 p0001 A70-10047

Flight evaluation of direct lift control (DLC) on modified B-52 aircraft, noting controllability improvement during ILS approaches and aerial refueling [SAE PAPER 690406] 03 p0411 A70-12896

Numerical method for attacking-lifting problems of general three dimensional wing executing arbitrary motion in potential flow 03 p0405 A70-12930

Subsonic lifting surface theory including leading edge, discussing singularities in solution of integral equation for determination of aerodynamic properties [AIAA PAPER 69-37] 04 p0619 A70-15387

Aircraft configurations designed for eliminating sonic boom due to lift 05 p0791 A70-16798

High lift devices design and operation problems in short and vertical takeoff 07 p1189 A70-19874

Pneumatically operated lifting mechanism and fluidic control system added to Izod impact testing machine for automatic impact repetition, counting and stopping 11 p2034 A70-26837

Plenum-chamber air-bearing and labyrinth-seal types air cushion lifting mechanisms performance in simulated hovering flight 12 p2162 A70-27981

Lifting surface problem for finite span wing in ground effect using matched asymptotic expansions method 14 p2527 A70-30280

Sears function and lifting surface theory for harmonic gust fields in incompressible flow, modifying function for accurate interpolation of large numbers 14 p2528 A70-30860

Dynamic stability derivatives calculation using steady and oscillatory lifting surface theory with allowance for Bryan limitations 14 p2529 A70-30864

Lightweight lift jet engine design, testing and performance for V/STOL aircraft [ASME PAPER 70-GT-32] 18 p3302 A70-36833

Subsonic high lift cruise wing optimal design using kernel function method of planar lifting surface theory 22 p3959 A70-42709

Aerodynamic theory of pressure lift induced on lifting surface by isotropic atmospheric turbulence, considering transfer function of Concorde aircraft [ICAS PAPER 70-30] 23 p4138 A70-44104

Aerodynamic interferences of lifting surfaces harmonically vibrating in subsonic flow 23 p4136 A70-44765

Kinematically unsteady aerodynamic coefficients consistent with stiffness and inertia properties of lifting surface in supersonic flow by finite element method 24 p4287 A70-45154

LIFT DISTRIBUTION

U FORCE DISTRIBUTION

U LIFT

LIFT DRAG RATIO

Lift-dump system for Hawker Siddeley DH 125, combining aerodynamic drag increase with lift reduction to improve deceleration 02 p0225 A70-12266

Optimal lift-drag ratio of cascades dependence on optimal pitch of cascades calculated for axial flow turbomachinery 02 p0356 A70-12750

Delta wing of given volume and planform with maximum lift-drag ratio in hypersonic flow 04 p0618 A70-15243

Higher order boundary layer effects on zero-lift drag of sphere-cones, investigating transverse curvature, shock vorticity, displacement, slip and temperature jump 06 p1041 A70-18173

Strap-on ferry package for reusable spacecraft and launch vehicles subsonic lift/drag increase [AIAA PAPER 70-259] 07 p1397 A70-20390

Circulation controlled lifting rotor wind tunnel test results concerning factors affecting lift and drag 08 p1432 A70-21039

Wedges calculated for lift-drag ratios at hypersonic speeds to find optimum surface geometry 09 p1606 A70-23282

Ram wing tube ground transportation vehicle, analyzing optimum lift-drag ratio and induced power requirements 11 p1975 A70-25966

Flat-top airfoil determined for lower surface shape to maximize lift drag ratio at hypersonic speeds using calculus of variations 11 p1977 A70-26397

Aerodynamics theory for separated flow effects on helicopter lift-drag capability, taking into account three dimensional flow and blade aeroelasticity 18 p3205 A70-35956

Slender hypersonic airfoil shape optimization for maximum lift to drag ratio for given profile area, chord and free stream conditions 19 p3352 A70-38304

Aerodynamic characteristics of thick sharp edged cropped delta and gothic wings, giving low lift-dependent drag 19 p3353 A70-38615

Atmospheric ascent optimal trajectories for medium to high lift drag ratio space shuttle type rocket vehicles [AIAA PAPER 70-978] 20 p3714 A70-39551

Strap-on ferry package for reusable spacecraft and launch vehicles subsonic lift/drag increase [AIAA PAPER 70-259] 21 p3931 A70-41867

Wave-riders aerodynamics and heat transfer, investigating lift to drag ratios for supersonic and hypersonic vehicles [ICAS PAPER 70-18] 23 p4276 A70-44129

LIFT FANS

Noise radiated from VTOL lifting fan in wing inlet under static inflow conditions, attributing discrete tones to spacing between rotor and stator blades [ASME PAPER 69-WA/GT-6] 04 p0734 A70-14889

Heaving and pitching motion analysis of wave action-induced pressure gradients in captured air bubble /CAB/ ship bubble chamber, discussing fan system design [ASME PAPER 69-WA/AV-6] 04 p0622 A70-14902

Lift fan V/STOL tactical aircraft performance capabilities determination, using digital computer program 07 p1191 A70-18975

Aerodynamic forces and moments effect of VTOL aircraft lift fan configurations on flow past wing 10 p1798 A70-24047

Lift fan propulsion for VTOL passenger aircraft, discussing design, thrust augmentation, optimum element combination, engine-wing integrations and tests [DGLR-70-007] 10 p1929 A70-24049

Low pressure ratio lift fan propulsion system for intercity VTOL transports, considering thrust, safety, noise, weight, components, speed, turbine and transmission [AIAA PAPER 70-670] 16 p2971 A70-33952

LIFT FORCES

U LIFT

LIFTING BODIES

NT LIFTING REENTRY VEHICLES

Aircrew escape/rescue capability /AERCAB/ flying ejection seat design and test programs, noting rotary wing, fixed wing and parawing feasibility 01 p0035 A70-10714

Large-tilt-angle lifting surface theory for V/STOL aircraft based on inclined actuator disk analysis 04 p0619 A70-15377

Subsonic lifting surface theory including leading edge, discussing singularities in solution of integral equation for determination of aerodynamic properties [AIAA PAPER 69-37] 04 p0619 A70-15387

Transonic flow theory, investigating thin three dimensional lifting wings, similarity for lift and drag, plane flow past airfoil, far field and hodograph solutions [D1-82-0878] 05 p0834 A70-16693

Gaussian quadrature integration technique developed for collocation approach for integral equation of steady subsonic lifting surface theory [AIAA PAPER 70-191] 06 p0970 A70-18097

Lifting surface theory for calculation of steady subsonic and supersonic flow over various wing and air-plane configurations, emphasizing finite element load prediction method [AIAA PAPER 70-192] 06 p0971 A70-18114

Steady supercritical planar inviscid transonic flows over lifting airfoils, generating unsteady flow by impulsively imposing airfoil boundary condition [AIAA PAPER 70-47] 06 p0972 A70-18130

Tangent plane method and polar coordinates for lifting surfaces, calculating normal velocity at field point on surface carrying doublet distribution for incompressible flow [AIAA PAPER 70-78] 06 p0975 A70-18195

Wing lifting surface theory for V/STOL aircraft based on inclined actuator disk theory to predict span loading and downwash angle 07 p1190 A70-20408

Perfect fluid sonic flows around weakly lifting three dimensional bodies downstream of shock wave, proving existence of lifting boundary layer 08 p1433 A70-21238

Mathematical model for describing flow in Hele-Shaw cell, predicting attached viscous shear layers in lifting body wake 13 p2338 A70-28818

Load generation on two dimensional thin airfoil by yawed sinusoidal gust in incompressible flow, using lifting surface theory 13 p2344 A70-30025

Lifting surface problem for finite span wing in ground effect using matched asymptotic expansions method 14 p2527 A70-30280

Sears function and lifting surface theory for harmonic gust fields in incompressible flow, modifying function for accurate interpolation of large numbers 14 p2528 A70-30860

Dynamic stability derivatives calculation using steady and oscillatory lifting surface theory with allowance for Bryan limitations 14 p2529 A70-30864

Lifting body pressure and heat transfer measurements at various angles of attack in hypersonic flow [DGLR-70-029] 15 p2828 A70-32841

Nonrolling lifting gliding vehicle hypersonic longitudinal dynamic stability, applying analysis to space shuttles [AIAA PAPER 70-977] 20 p3715 A70-39552

Surface pressure coefficient dependence on specific heat ratio for yawed conical lifting bodies in supersonic streams 21 p3747 A70-41877

ONERA calculations in aeroelasticity including lifting surface optimization, control surface vibration, pressure fields, aircraft transfer functions and panel flutter 23 p4274 A70-44762

Thermal flux surface distribution lifting bodies, discussing aerodynamic efficiency dependence on drag and zero angle of attack Mach number 23 p4136 A70-45019

LIFTING REENTRY VEHICLES

Optimal lift control of hypersonic lifting body during planetary entry, assuming exponential variation of atmospheric density 04 p0620 A70-15532

Reusable lifting entry vehicle flight tests, investigating handling qualities and subsonic-transonic aerodynamics of M2-F2 /M2-F3/, HL-10 and X-24A [SAE PAPER 690662] 05 p0792 A70-15840

Aerodynamic flight characteristics of lifting reentry bodies in subsonic to hypersonic range in wind tunnel tests 06 p1154 A70-17249

Lifting reentry compact body aerodynamic coefficients, comparing calculated and experimental values for subsonic, supersonic and hypersonic flows [DGLR-69-036] 07 p1392 A70-18982

Reusable lifting reentry bodies subsonic and hypersonic aerodynamic characteristics, considering viscosity effects [DGLR-69-038] 07 p1392 A70-18984

Compact reentry flight test body construction featuring extended permissible entry corridor by means of generated lift [DGLR-69-035] 07 p1392 A70-18987

Flight maneuver for roll modulated lifting reentry vehicle to reduce deployment dynamic pressure 07 p1394 A70-19724

Refurbishable ablative thermal protection for reusable lifting reentry vehicles [AIAA PAPER 70-277] 07 p1397 A70-20386

Boride composites with high strength and thermal resistance suitable as nose cap and leading edge materials for reusable lifting reentry systems [AIAA PAPER 70-278] 07 p1315 A70-20387

Abort and staging separation maneuvers of two equal size reusable lifting entry vehicles in wind tunnel tests [AIAA PAPER 70-260] 07 p1397 A70-20389

Adaptive control function technique for lateral stability augmentation system design for manned lifting body entry vehicle 07 p1247 A70-20404

NASA earth-orbit shuttle /EOS/ for achieving routine arrival, conventional landing after orbital flight and reentry 09 p1766 A70-22677

Lifting reentry dynamic stability of flare stabilizers and flap controls 09 p1766 A70-23242

Subsonic glide landing approach guidance for unpowered lifting vehicles, using perturbation feedback and approximation of heading and position coordinates [AIAA PAPER 69-865] 09 p1725 A70-23253

Ground based simulation for hypersonic reusable lifting reentry vehicle design with pilot-in-loop, discussing six degree of freedom simulation [AIAA PAPER 70-385] 10 p1861 A70-24920

Expendable propellant tanks /Tip Tank Concept/ on lifting body reusable booster operations to reduce cost for low earth orbital transport mission 11 p2122 A70-26052

Lifting entry vehicle thermal protection system /TPS/ material performance, analyzing metallic radiator and passive transpiration systems and rigid insulator 11 p2150 A70-26368

Steerable landing gear system consisting of freely casting rotating wheel nose gear, tiltable axle and main gear skids for lifting body spacecraft [AIAA PAPER 69-790] 13 p2344 A70-28514

Temperature rate flight control system /TRFCS/ for lifting reentry vehicles control and guidance 14 p2614 A70-30464

Multibody lifting entry vehicle clusters separation dynamics, describing digital simulation, wind tunnel tests, separation mechanisms, etc

16 p2981 A70-33704

Optimum guidance and control law for lifting reentry bodies, investigating plane descent trajectories for minimum structural heating

16 p2982 A70-33774

Lifting reentry vehicles control surface aerodynamics, considering boundary layer separation, shock interference, unsteady flow, etc

18 p3333 A70-36958

Lifting reentry vehicle two dimensional motion optimization with inequality constraints explicitly containing control by perturbation method

21 p3845 A70-41265

Pressure distribution, force and heat transfer measurements on varied-configurations of lifting reentry vehicles in hypersonic flow

[ICAS PAPER 70-03]

23 p4132 A70-44117

Lifting reentry flight test vehicle aerodynamic configuration development, emphasizing lateral stability and maneuverability

[ICAS PAPER 70-02]

23 p4257 A70-44118

Lifting entry vehicles turbulent boundary layer aerodynamic heating, comparing heat transfer prediction methods

23 p4258 A70-44530

Aeroelastic and aerothermoelastic development of winged interorbital space shuttle concerning panel flutter, stability and nonstationary lifting surface theory

23 p4273 A70-44760

LIFTING ROTORS

Lifting rotor blades flapping response to atmospheric turbulence, discussing time averaging and perturbation schemes

[AIAA PAPER 69-206]

04 p0624 A70-15378

Circulation controlled lifting rotor wind tunnel test results concerning factors affecting lift and drag

08 p1432 A70-21039

Circulation-controlled lifting rotor built and tested on hovering rig, analyzing performance

09 p1611 A70-23284

Bifilar pendulum vibration absorber for counteracting helicopter main motor vibratory forces

10 p1805 A70-24657

Lifting rotor blade motions stability computation using Floquet transition matrix

17 p3009 A70-34726

Helicopter rotor blade stall flutter response prediction based on NACA 0012 airfoil aerodynamic data

17 p3009 A70-34734

Surface pressure and lift measurement on model lifting rotor blade as function of vortex interaction, using flush mounted pressure transducers

17 p3009 A70-34737

Three dimensional inviscid small perturbation compressible flow past lifting axial compressor rotor at subsonic and transonic speeds

18 p3208 A70-36691

Runway test vehicle for lifting rotor performance in simulated forward flight, comparing with wind tunnel tests

19 p3402 A70-38611

LIFTING SURFACES

U LIFT DEVICES

U LIFTING BODIES

U SURFACES

LIGANDS

Shift in nuclear paramagnetic resonance frequency of ligand nuclei in ferromagnets above Neel temperature

10 p1928 A70-24826

LIGHT [VISIBLE RADIATION]

NT AIRGLOW

NT COHERENT LIGHT

NT DAYGLOW

NT GEOCORONAL EMISSIONS

NT LIGHT BEAMS

NT NIGHTGLOW

NT SKY RADIATION

NT SUNLIGHT

NT TWILIGHT LIGHT

NT ZODIACAL GLOW

Tissue protein changes under visible and UV radiation noting denaturation, chemical bonds, protein configurations, clinical disease patterns, etc

01 p0022 A70-10856

Photodynamic damage in biological cells, discussing free radical originators and protective action of thiourea, mono and polyvinylpyrrolidone, cysteine and antibiotics

03 p0419 A70-13306

Thermodynamics of radiation and photosynthesis, discussing Ross-Calvin maximal efficiencies, Duysens method, light and dark conditions and polarized light

03 p0428 A70-14011

Slitless system using interference filter, fixed Fabry-Perot etalon and automatically controlled etalon for recording spectral information for efficient light detection

04 p0685 A70-14523

Beam fluctuations damping in beam waveguide, determining fluctuations cause as random displacement of lenses

04 p0651 A70-15290

Angular distribution measurements of visible and near IR radiation reflected from carbon dioxide cryodeposits formed on liquid nitrogen cooled surface in vacuum

[AIAA PAPER 69-63]

04 p0720 A70-15538

Solar energy converter with shutter, determining light pulse power from solar light intensity and exposure time

07 p1196 A70-19624

Laser focused hologram reconstruction in passing white light

07 p1289 A70-20320

Yearly fluctuations of Seyfert galaxy 3C 120 light curve, discussing effects of ambient temperature

08 p1563 A70-20498

Binocular achromatic and color thresholds of constant and flickering lights determined from background of different brightness

08 p1443 A70-20732

Objective lens systems with high chromatic aberration correction for visible spectral region

08 p1494 A70-20834

Quasi-stellar objects absolute spectral energy distribution, considering electron temperature and photon density

08 p1572 A70-20916

Optical information processing in noncoherent light, considering applicability to simulating antenna radiation patterns using field distribution in aperture obtained by Fourier transformation

08 p1494 A70-20971

Mammalian pineal organ control experiments involving light and sympathetic nerve stimulation

10 p1812 A70-24396

Photon nature, considering light-magnetic flux similarities

11 p2084 A70-26027

Light storage by Venus machine using refractive properties of gas and involving fluid mechanical optics

11 p2114 A70-26575

Light-induced electron paramagnetic resonance signal detected in *Anacystis nidulans*

11 p1989 A70-26847

Holographic achromatic reconstruction of laser holograms in transmitted white light using zonal plate

12 p2238 A70-28297

Wavefront reconstruction by holograms of focused images illuminated by white light, analyzing spatial coherence

13 p2408 A70-29364

UV, visible and IR radiation measurement, discussing spectral distribution, thermopiles, monochromatic radiation and power measurements

13 p2410 A70-29653

Light absorption coefficient of two band superconductor with nonmagnetic impurity, observing electron pairs removal from condensate and transition into excited states

13 p2472 A70-29723

Electron density, characteristic dimensions and vertical density gradient of coronal enhancements in white light, observing elliptical cross section

13 p2479 A70-30004

Atmospheric absorption, scattering and turbulence effect on visible and IR radiation propagation, discussing optical systems performance

14 p2583 A70-30399

Spectropolarimeter for measurements of polarization characteristics of atmospheric radiation in nanometer range

14 p2583 A70-30414

Circadian variation of pituitary-adrenal steroid levels, noting light role

14 p2540 A70-31430

Gas pressure effects on visible and UV laser action in small argon Z-pinch plasma discharge, using streak photographs

15 p2750 A70-31968

Hill reaction color sensitivity in red and blue light during chloroplast disintegration, considering oxygen evolution capacity

15 p2684 A70-32548

Solid state logarithmic radiometer, measuring radiation within narrow portions of optical spectrum

16 p2905 A70-33160

Low light intensities measured using photon counting method, comparing signal to noise ratio with lock-in method

16 p2911 A70-33524

Solid state IR to visible converter, using minority carriers stimulated tunnel injection into wide band gap phosphor

17 p3081 A70-34648

Impulsive loading of structures via light-initiated sprayed explosives

17 p3059 A70-35162

Crab Nebula pulsar NP 0532 optical and X ray synchrotron radiation, explaining ratio of pulsar energy flux to nebula

17 p3152 A70-35747

Star AG Draconis spectrum in visible range by meniscus prismatic camera, deriving energy distribution

18 p3315 A70-36575

Approximate formulas for disperse attenuation and scattering coefficients for water drops in visible and IR spectrum

18 p3260 A70-36973

Nitrogen dioxide continuous visible emission under thermal and recombination excitation, examining spectral characteristics

19 p3374 A70-38267

Light curves bumps properties of Population I cepheids in Magellanic Clouds, Milky Way galaxy and M 31 as function of period

19 p3523 A70-38691

Visible and IR imagery by meteorological satellites measuring surface temperature, atmospheric circulation and state parameters, storm development and tracking, cloud motions, etc

20 p3660 A70-39076

High speed electro-optic spectral scanning in UV, visible and IR regions, using monochromator deflection of dispersed light

20 p3671 A70-39090

Superradiant light /SRL/ converted from electron beam energy by semiconductor targets applied to nanosecond photography

20 p3635 A70-40529

Large sunspot umbra continuum intensity, examining visible spectra

21 p3885 A70-40956

Blue stellar objects emission at 9.5 and 3.5 mm, suggesting quasi-stellar objects with small intrinsic radio luminosity

21 p3922 A70-41993

Fluctuating light pulse packet detection by inertialess photodetector, deriving optimal algorithm

22 p3987 A70-42554

Fluctuating light pulses detection and arrival time estimation for heterodyne reception

22 p3987 A70-42560

Light curve for eclipsing stars with scattering envelopes applied to V444 Cygni binary system

22 p4103 A70-42989

Sources of variability in laboratory carbon arc weathering of light stabilized polyester resin

22 p4059 A70-43080

Hypervelocity impact flash resolved into sub-microsecond continuum radiation pulse succeeded by slow rising long duration light pulse from neutral atomic line emission

23 p4227 A70-44553

[AIAA PAPER 69-364] Light effect on cis-trans-isomerization of cinamoyl-alpha-chymotrypsin, considering molecular modeling of visual reception

24 p4298 A70-45496

Monochromator design for UV and visible wavenumbers linear output, noting application to absorption coefficient measurement

24 p4336 A70-45669

UV Ceti type variable flare stars, observing radio and optical spectral regions for X ray production

24 p4397 A70-45763

Cerenkov light longitudinal distribution from extensive air showers, using near UV receivers

24 p4398 A70-46225

LIGHT ABSORPTION

U ELECTROMAGNETIC ABSORPTION

LIGHT ADAPTATION

Photoperiod variation effects on ambulatory primate *Cebus albifrons* deep body temperature /DBT/, locomotor activity /LMA/ phase relationships and DBT waveform

01 p0011 A70-10035

Light valve projectors and TV cameras, showing disparity between video information generation and large screen real time high brightness image presentation

01 p0088 A70-10811

Melatonin biosynthesis, discussing regulation by light and sympathetic nerves, daily pineal rhythms, estrous rhythms and ovarian hormones

03 p0424 A70-13809

Readaptation times of eyes adapted to darkness using night vision training device in relation to helicopter flight safety conditions

03 p0436 A70-13823

Pupil diameter changes associated with constant change in accommodative stimulus as retinal illuminance varies

03 p0427 A70-13950

Critical discreteness interval of visual analyzer, investigating dependence on stimulus location, flare brightness and adaptation

08 p1443 A70-20734

Visual acuity and light detection after preadaptation to red and orange lights, discussing photopic and scotopic vision

11 p1986 A70-25828

Aircraft pilot and nonpilot night vision adaptation comparison, using Goldman-Weekers adaptometer

17 p3038 A70-35138

Bilateral cortical cerebellar hemispheric ablations effect on feline light-dark discrimination learning
21 p3762 A70-41142

Spatial summation of retinal neurons receptive field centers excitation from single optic tract fibers action potential in light-adapted cats
22 p3971 A70-43403

Spatial aspects of sensitization effect properties compared to background light fields, lowering rod threshold at center by light addition to surrounding annular region
23 p4147 A70-44779

LIGHT AIRCRAFT

NT DH 125 AIRCRAFT
NT F-28 HELICOPTER
NT G-91 AIRCRAFT
NT OH-6 HELICOPTER

German light aircraft construction industry situation and prospects regarding manufacture of gliders, sport-ing and touring aircraft and motor gliders
03 p0413 A70-13791

Forward air control and light attack aircraft survivability design
[SAE PAPER 690707] 05 p0791 A70-15829

Flight deck controls and instrument disposition in business aircraft emphasizing size
06 p1061 A70-17318

Hansa 330 fan jet design for executive and com-muter market, discussing forward-swept wing concept and standardized structures and systems
07 p1194 A70-19619

Light aircraft lateral and longitudinal response to at-mospheric turbulence, presenting equations and charts for design load calculations
[SAE PAPER 700239] 11 p1981 A70-25908

Performance, stability and control improvements of light aircraft, applying computerized parametric analy-sis
[SAE PAPER 700240] 11 p1981 A70-25909

Light general aviation aircraft production cost reduction, considering adhesive bonding, production certification, etc
[SAE PAPER 700242] 11 p1981 A70-25911

Engine design for future small passenger and sports aircraft, discussing piston, shaft turbine, Wankel and bypass engines and synthetic materials application
11 p1981 A70-25949

Falcon 10 simplified airliner-type equipment for operation under Category 2 weather conditions
12 p2167 A70-28028

Light twin engined aircraft airframe fatigue evalua-tion program
[SAE PAPER 700219] 13 p2348 A70-29606

British light aircraft designs, engines and costs, con-sidering business, agricultural, gliding, private, school and club flying
14 p2532 A70-31394

Twin jet light transport Corvette airframe, discussing flight characteristics and economical as-pects
15 p2676 A70-32793

Antenna design for single engine light general avia-tion aircraft weather radar, reviewing attenuation and terrain return problems
16 p2864 A70-33471

Rotary piston engine for powered gliders and light aircraft power source by modifying industrial Wankel engine
17 p3147 A70-34690

Servoactuator for stick force augmentation on light turboprop STOL aircraft at high angles of attack
[AIAA PAPER 70-909] 17 p3019 A70-35821

Four-seat two-engined STOL propeller passenger and sport aircraft design and performance
19 p3355 A70-37371

MBB Bo-209 Monsoon travel, commuter and acrobatics aircraft, discussing configurations, speci-fications, structure and handling characteristics
19 p3355 A70-37388

Air conditioning in piston-powered light general aviation aircraft, comparing vapor cycle and cryogenic systems
19 p3359 A70-38500

Light rigid civil aircraft response to continuous at-mospheric turbulence estimated using two rigid body degrees of freedom method for vertical and lateral gusts
[AIAA PAPER 69-766] 22 p3961 A70-42703

Small airplane unsteady motion downwash angle at low speeds, comparing results from rectilinear steady flights
[ICAS PAPER 70-25] 23 p4138 A70-44108

OV-10A forward air control and light attack aircraft design, specifications and performance
[SAE PAPER 700837] 24 p4290 A70-45883

LIGHT ALLOYS

NT ALUMINUM ALLOYS
NT BERYLLIUM ALLOYS
NT MAGNESIUM ALLOYS

LIGHT AMPLIFIERS

Laser amplifier electromagnetic field in arbitrary quantum mechanical state, deriving complex am-plitude distribution function to calculate phase uncer-tainty
03 p0503 A70-14174

Light signals amplification efficiency, considering double-pass regenerative amplifier
04 p0702 A70-15225

Laser gain investigated for amplifications of shor emission pulses in neodymium glass, discussing line broadening nonuniform mechanism
04 p0702 A70-15226

Injection laser amplifier with emitting and amplifying diodes coupled by planar polyharmonic beam waveguide
04 p0702 A70-15292

Light signals frequency converters and amplifiers applied to detection problems
05 p0813 A70-16264

Laser signal modulation at RF by subjecting emitting atoms of Xe-He laser amplifier to simultane-ous DC and RF magnetic fields
06 p1079 A70-17191

GaAs diode amplifiers and switching devices behavior, describing optical coupling between two GaAs lasers
07 p1241 A70-19399

Signal to noise ratios and fluctuation spectrum of photomultiplier illuminated by laser passing through laser amplifier, noting population level effect
07 p1300 A70-19869

Laser amplifier effect on autocorrelation function of laser radiation intensity fluctuations, determining emission coherence time
07 p1300 A70-19870

Nonresonant multipath carbon dioxide laser ampli-fier small signal gain of 39 dB utilizing White optical reflector design
09 p1699 A70-23365

Amplifier properties and oscillator mode structure of multipath carbon dioxide laser
09 p1699 A70-23538

Book on lasers, light amplifiers and oscillators covering optical resonators, optical pumping, pulsed lasers, etc
09 p1700 A70-23541

Single-pass multimode carbon dioxide laser ampli-fier power gain optimization
10 p1897 A70-23815

He-Ne laser amplifier in axial magnetic field, meas-uring Faraday rotation and gain for various input signal intensity values
10 p1901 A70-24945

Stationary regime stability of one dimensional model of optical quantum traveling wave amplifier, determining trapping band of traveling wave laser
10 p1901 A70-25158

GaAs light amplifier p-n junction gain and output noise determination for wide photon energy ranges, studying input noise levels effects on sensitivity
10 p1928 A70-25167

Signal amplitude and intensity fluctuations after laser amplification, considering P representation for density operator
11 p2063 A70-25867

Triple passage crystal amplifier of single frequency ruby laser emission, noting radiation structure and coherence
12 p2250 A70-28183

Molecular velocity influence of optically active medium in gas dynamic quantum amplifier on monochromatic radiation transport, using corpuscular light model
15 p2721 A70-32356

Optical quantum amplifier frequency characteristics dependence on broad spectral composition amplified signal intensity and resonator parameters
15 p2754 A70-32862

Laser beam anticorrelation after attenuation by two photon amplifier, deriving density matrix in time de-pendent perturbation theory
16 p2928 A70-33283

Three level gas laser amplifier theory, considering quantum mechanical atomic system in interaction with two monochromatic EM waves
19 p3446 A70-37829

Laser pulse amplification by stimulated thermal Rayleigh scattering in absorbing media by transient theory
20 p3640 A70-39113

Pulse light amplification by stimulated thermal Rayleigh scattering measured as function of time, ab-sorption coefficient and interaction length
20 p3640 A70-39114

Spatial gain variations transverse to discharge in ax-ially flowing carbon dioxide laser amplifier, noting relationship to flow velocity
20 p3640 A70-39391

He/Ne laser amplifier and oscillator threshold band-width measurement by double laser device
20 p3643 A70-40126

Single picosecond mode-locked laser pulse selection and multiple pass amplification device, obtaining high energy and signal to noise ratio
21 p3838 A70-42023

Nitrogen laser pumped cyclohex 4-Methylumbel-liferone and rhodamine 6G dye laser amplifier, mea-suring single pass power gain vs wavelength
24 p4355 A70-46088

LIGHT BEAMS

Hyperbolic type gas lens design and focusing characteristics for use in laser light beam waveguide
01 p0106 A70-10033

Confocal parameters, spot sizes, waist positions and stability conditions of astigmatic Gaussian beams formed by spherical mirror laser cavity resonators
01 p0108 A70-10426

Holographic two beam real-time Fizeau inter-ferometer for recording and reconstructing reflected light waves in silvered flat surfaces measurement
01 p0090 A70-10905

Banana self focusing in water of laser beams with nonmonotonic intensity distribution, noting ruby laser experiment
02 p0312 A70-12260

Photoelectronic measurement of distance from laser beam axis to reference plane, discussing applications to surveying, vibration measurements and atmospher-ic investigations
02 p0314 A70-12785

Three dimensional Gaussian light beam propagation in anisotropic inhomogeneous media with dielectric constant decreasing from energy flow direction
03 p0525 A70-13533

Bouguer single-scatter theory applicability depen-dence on angular aperture of receiver and laser beam parameters in water mist
03 p0451 A70-13756

Light spark and rapid nonlinear effects in focusing powerful light by longitudinal beam
04 p0718 A70-14405

Collimated light beam enhanced scattering and anomalous absorption due to decay into plasma waves
04 p0727 A70-14996

Temporal isolation between pulsed orthogonal polarization state laser beams, showing selection de-pendence on sampling time
04 p0701 A70-15032

Collapsing beam transition into self focusing light channel numerically analyzed allowing for Kerr effect saturation, multiphoton absorption and stimulated Raman scattering
04 p0650 A70-15285

Saturation induced wave front distortions effect on beam divergence and frequency modulation in laser amplifiers, discussing refractive index changes
04 p0703 A70-15620

Monograph on He-Ne laser beam noise properties and intensity fluctuations during single mode opera-tion
05 p0860 A70-16559

Optical crossbeam technique for remote sensing of wind speeds, relating light fluctuations to convective wind velocity by space-time correlation methods
05 p0850 A70-16688

Light scattering at 90 deg from laser-induced break-down plasmas in air, discussing origin
06 p1114 A70-17189

Turbine flowmeter with hydraulic bearings opera-tion based on photosensitive recording of light beam interruptions, discussing test results
06 p1065 A70-17911

Successive small birefringences undergone by polarized light ray crossing photoelastic model represented by rotations in equatorial plane on Poin-care sphere
06 p1168 A70-17918

Optical properties of Gabor holograms with pure reference beam, discussing image reconstruction using He-Ne laser
06 p1072 A70-18565

Intense light beams self focusing in nonlinear media with quadratic Kerr effect, assuming spherical initial phase front after passing through condensing lens
07 p1296 A70-18720

Radiation focusing properties of gravitational bodies associated with curving light trajectories analyzed by geometrical and waveguide optics approx-imations
07 p1384 A70-19411

Caustic surface of spherical resonator with external mirrors used to calculate light angular divergence and spectral properties
07 p1299 A70-19859

Laser beam trajectory equation in scanning ul-trasonic cell for nonzero incidence angle, relating input and output beam divergence
07 p1300 A70-19865

Diffuse radiation intensity determination in finite optical thickness atmosphere illuminated by parallel light beams
07 p1389 A70-20204

Laser radiation angular distribution determination by self calibrating method based on dividing light beam into spatially similar beams of various intensities
08 p1510 A70-20515

Birefringence determination from contrast of inter-fering natural light beams
08 p1543 A70-20521

Light beam deflection for three dimensional fixed and time varying visual displays, discussing mechani-cal, acousto-optic, electro-optic, digital and holo-graphic techniques
08 p1449 A70-20673

Light beam intensity variations during propagation in nonlinear medium taking into account combination scattering, solving equations by difference method
08 p1461 A70-20858

Holographic technique of coherent light field transformation with desirable phase distribution from laser light beams of arbitrary wavefront characteristics
08 p1497 A70-21410

Second harmonic generation and frequency conversion efficiencies for laser beam shaping in nonlinear medium
08 p1514 A70-21984

Radiation transfer in semiinfinite medium illuminated by parallel light beams assuming trinomial scattering indicatrix, deriving radiative effects and radiation field
09 p1751 A70-22154

Coherent light beams scanning and propagation direction control by acoustooptical method for laser applications
09 p1695 A70-22315

Laser beam deflection techniques for directional control of laser beams, noting applications to optical computer memories and active imaging and display devices
09 p1696 A70-22783

Pulsed laser beams intensity fluctuations correlation functions dependence on propagation distance in turbulent atmosphere
09 p1636 A70-23135

Relativistic nonlinear coupled longitudinal-transverse propagation of intense laser beams in cold overdense plasma
10 p1921 A70-23968

Einstein theory applied to sample modeling of planetary orbits and light beams touching sun in solar gravitational field
10 p1939 A70-24268

Bouguer single-scatter theory applicability dependence on angular aperture of receiver and laser beam parameters in water mists
10 p1842 A70-25005

Divergence measurement of beam emitted by ruby laser in relaxation mode as function of cavity length and excitation voltage
11 p2063 A70-26462

Semiquantitative study showing variations in degree of laser beam coherence due to turbulence
12 p2245 A70-26980

Laser microplasma formation in focus of two laser beams impinging on crystalline lithium hydride targets
12 p2246 A70-27355

Photoelectric receiver and light beam alignment in gas laser aerial photography, considering directrix rectilinearity verification
12 p2247 A70-27476

Phase modulated laser light beam statistical analysis, using Michelson interferometer with piezoelectric crystal driven mirror connected to Gaussian random noise generator
12 p2249 A70-27877

Laser beam intensity distribution determination from measuring Fresnel diffraction pattern at straight edge using photographic plate
12 p2249 A70-28032

Monochromators dispersion and resolution increased by multiple passage of light through singly dispersive element, comparing optical schemes
12 p2237 A70-28160

Threshold light flux densities for thin Al film breakdown by laser radiation
13 p2428 A70-29383

Fourth order aberration in gas lens used as focusing element in light beam waveguide systems
15 p2697 A70-31829

Solar simulation systems for uniform collimated intense light, noting high intensity lamp development
15 p2717 A70-32034

Pulsed laser alignment using pentaprism-directed continuous laser light beam
15 p2752 A70-32047

Laser beam shaping for streak interferometry, obtaining thin beam uniform over filling length
15 p2752 A70-32049

Laser beam scattering by free electrons in terms of classical electrodynamics, discussing radiation damping effects
15 p2752 A70-32451

Phase modulated holography for inherent noise reduction using thicker recording media, increasing signal beamwidth or beam ratio
16 p2904 A70-33137

Laser beam anticorrelation after attenuation by two photon amplifier, deriving density matrix in time dependent perturbation theory
16 p2928 A70-33283

Laser beam photography by multiple reflections from partially reflecting mirrors
16 p2913 A70-33985

Lasing action and reduced output without beam distortion from misaligned carbon dioxide lasers by DC-Tesla coil pumping
16 p2929 A70-33986

High power Nd-glass solid state laser characteristics measured to improve beam properties
17 p3105 A70-35090

Photodetector frequency response measurement, using beat light signals from mixed single mode He-Ne lasers
17 p3108 A70-35688

Picosecond light pulse measurement by two beam overlap technique using nonlinear photoelectric effect
17 p3097 A70-35912

Electronmicroscopical structure of laser irradiated Garding-Passy melanoma cell organelles, noting mitochondria damage
18 p3224 A70-36636

Resonant modes of GaAs junction laser beams with Hermite-Gaussian rectangular symmetry, using stripe geometry with lens-slit combination
18 p3268 A70-36732

Backscattering of collimated light beam emitted by pulsed point source into opaque medium
19 p3461 A70-37421

Laser beam alignment system for monitoring dielectric film evaporation
19 p3445 A70-37686

Optimum laser beam deflection for instrument design, considering tandem, rotary mirror and analog methods
19 p3446 A70-37879

Nuclear fusion realization by focusing from intense beam neodymium glass laser
19 p3447 A70-38167

He-Ne laser beam hazard to human retina
19 p3371 A70-38309

Einstein theory applied to sample modeling of planetary orbits and light beams touching sun in solar gravitational field
19 p3520 A70-38393

Laser and electron beam removal of material in manufacturing technology
19 p3447 A70-38451

Polarization in inverse Compton effect for arbitrary photon and electron distributions, discussing monochromatic photon beam
19 p3524 A70-38696

Gaseous media absorption coefficient and refractive index in field of two nonmonochromatic radiation streams quasi-resonant with neighboring atoms and molecules transitions
19 p3448 A70-38740

Coherent light beam characteristics with Gaussian radial intensity variation during propagation along optical system axis, determining radius from diffraction theory
20 p3639 A70-39086

Light focusing glass fiber with variable refractive index using ion exchange process, discussing applications to laser communications and data processing
20 p3671 A70-39129

Microwave hologram recording for surface displacement, with laser beam illumination for optical reconstruction of image
20 p3628 A70-39152

Laser beam for military weapons applications, investigating energy levels and beam guidance
20 p3641 A70-39421

Propagation mode conversion of Gaussian light beam due to random fluctuations of turbulent medium, discussing effect of aperture size and fluctuations anisotropy
20 p3585 A70-39451

Turbulence characteristics determination by measuring light beam arrival angle fluctuation using photoelectric recording shadow devices
20 p3634 A70-40401

Electrons optical scale time averaged motion dependence in focused laser beam on light intensity gradient, calculating bremsstrahlung spectrum
21 p3836 A70-40723

Frequency shifted diffraction of monochromatic Gaussian light beam by reflection off ultrasonic surface wave
21 p3850 A70-41907

Total reflectance of composite light diffuser with nonuniform absorption by two beam model, noting application to photochemistry
21 p3829 A70-41936

Single and crossed light beam techniques for optical measurement of fluid turbulence with refractive index fluctuations
22 p4011 A70-42694

Interferometric investigation of rapidly variable frequency dependent phase objects, using ruby laser waves
22 p4034 A70-43049

[SMPTE PREPRINT 26] Intense laser light pulse longitudinal compression resulting from nonlinear intensity-dependent refractive index
22 p4050 A70-43221

Monograph on optimum focusing of laser light with nonideal lenses having spherical aberration
22 p4052 A70-43739

Thermal defocusing and deflection of light beam by lateral wind effect in absorbing media
23 p4200 A70-43950

Plasma diagnostics based on light beam refractivity, considering laser interferometry and holographic methods
23 p4225 A70-44188

Light beam direction variation by crystal deflectors, examining changing internal reflection angle by applied electric field or mechanical stress
23 p4196 A70-44411

Focused image holographic interferometry by double exposure with reconstruction in white light applied to flat rotating subject
23 p4199 A70-45058

Multiple light beam interferences, using complex diagrams for reflection fringe visualization
24 p4381 A70-46096

Interference fringes on gas laser beam reflected by total reflection prism
24 p4356 A70-46272

LIGHT BULBS

U LUMINAIRES

LIGHT COMMUNICATION

U OPTICAL COMMUNICATION

LIGHT DURATION

U FLASH

U PULSE DURATION

LIGHT ELEMENTS

Microprobe analyzer for light elements using electronic optics probe, sample visualization devices and equipment for X photon detection and measurement [ONERA-TP-774]
02 p0275 A70-12210

Mechanical properties of cast light alloys at low temperatures, showing satisfactory plasticity and insensitivity to stress raisers
05 p0864 A70-16868

Light Mg-Li alloys physical and mechanical properties, production and treatment [DFVLR-SONDDR-18]
07 p1306 A70-19234

Light elements detection in interstellar grains by observing halo around X ray source arising from small angle scattering
14 p2631 A70-30539

Cosmic X ray extinction and halo by interstellar grains, applying to light elements identification
21 p3883 A70-42200

Stellar surface and solar system light element abundances, explaining formation by energetic proton flux nucleosynthetic effect
24 p4398 A70-46163

LIGHT EMISSION

NT BIOLUMINESCENCE

NT CHEMILUMINESCENCE

NT ELECTROLUMINESCENCE

NT FLUORESCENCE

NT INCANDESCENCE

NT LUMINESCENCE

NT LUNAR LUMINESCENCE

NT OPTICAL RESONANCE

NT PHOSPHORESCENCE

NT PHOTOLUMINESCENCE

NT SHOCK WAVE LUMINESCENCE

NT THERMOLUMINESCENCE

NT X RAY FLUORESCENCE

Negative resistance light emitting lateral GaAs diode, analyzing oscillation frequency, I-V characteristics, temperature and magnetic effects
01 p0050 A70-10565

Duty factor and contrast in scanned displays, discussing light modulator and emitting displays
01 p0043 A70-10780

Auroral light emission and electron density simultaneous measurements by rocket flights into auroral glow, deriving recombination rates
01 p0171 A70-10872

Light curve and relative dimensions of eclipsing system V338 Herculis, from photoelectric measurements, discussing component stars
01 p0184 A70-10951

Light emission by solids, discussing injection lasers, luminescence semiconductor diodes, group 2 and 6 compounds, etc
01 p0160 A70-11288

Binary system Nova WZ Sge model with nonnegligible secondary component contribution to total light explaining WUMA type light curve
03 p0568 A70-13324

Beta lyrae light curve changes by comparing international program observations with 1958 Lick Observatory results, discussing period, brightness, spectra, etc
03 p0568 A70-13327

Photoconductivity growth and decay curves green edge emission and integral flux in optical flare of cadmium sulfide crystals due to hole trapping process
03 p0540 A70-13503

Relationship between 6300 A monochromatic auroral arc and visible aurora during magnetic storm, determining directional speeds
03 p0478 A70-14000

Supernova light emitted from surrounding gas layer, describing gas density role in type I and type II events
04 p0748 A70-14590

Light emission from collapsing nonrotating gas in general relativity, noting restrictions on range and frequency shift
04 p0719 A70-14702

Lyman alpha auroral emissions observations made with narrow band sky scanning photometer mounted on earth-oriented polar orbiting satellite
04 p0741 A70-15107

Cepheid variable 1 Carinae light curve from photoelectric observations, calculating periodicities from best fitting Fourier series

04 p0759 A70-15708

Visible light emission from nonequilibrium Cs plasma measured for spectral intensity distribution, suggesting excitation mechanism in terms of collision-radiation model

05 p0887 A70-16109

Venus-earth carbon dioxide atomic parameters used to determine ionization and optical emission rates in Venus upper atmosphere resulting from solar cosmic rays

05 p0901 A70-16276

Transient emissions on He I wavelength during breakup phase of auroral events, discussing observational interference by OH bands

05 p0907 A70-16277

Spatial and temporal relations between auroral emission at green line 5577 and cosmic noise absorption studied to determine energy spectra and particles distribution

05 p0907 A70-16281

Light emission and gas phase ignition of homogeneous solid propellants under shock tube conditions [ALAA PAPER 70-120]

06 p1128 A70-18042

UV rocket-borne up-down photometer measuring zenith and nadir intensities for auroral profile studies

06 p1072 A70-18518

Correlation function prediction of rapid brightness variations in quasar based on variable optical emission model including flares

07 p1383 A70-19403

Axicon systems for spectroscopy of light emitted by foil-excited accelerator beams, discussing scattering contribution to spectral line widths

07 p1287 A70-20083

Intensity and altitude profile of H beta light emission and energetic hydrogen fluxes during auroral breakup using rocket soundings

08 p1489 A70-21383

Late stage stellar evolution association with supernovae in terms of gravitational collapse and exploding light emission using evolutionary model

09 p1749 A70-21993

Airglow hydroxyl emissions diurnal variations as function of height, using digital computer for time dependent solution of equations for oxygen-hydrogen atmosphere

10 p1872 A70-23826

Light-emitting integrated circuit semiconductor display devices with inherent memory permitting logic and optical output functions performed on surface

10 p1846 A70-23883

Molecular-statistical theory of second-harmonic light generation by isotropic bodies immersed in external AC or DC electric field

10 p1916 A70-24379

Auroral green line rocket measurements, showing roles of atomic and molecular oxygen dissociative recombinations

10 p1874 A70-24432

Predicted Jupiter visual auroras investigated with high sensitivity spectrograph

10 p1947 A70-24993

Pulsating auroras X ray association with luminosity via balloon-borne X ray detector and ground based image intensifier TV system

13 p2478 A70-29228

Polar auroral hydrogen emission intensity dependence on K index of geomagnetic activity

14 p2569 A70-30213

Electro-optical transducers based on photoconductive cells, phototransistors and microminiature incandescent and solid state light emitters

16 p2904 A70-33144

Simultaneous measurement of optical and X ray emission from Scorpius X-1 and X ray diffuse background, using rocket-borne scintillation counter

17 p3157 A70-34831

Optical frequency standards research covering lasers application with superstable emission frequency

17 p3104 A70-35081

Visible light-emitting p-n junctions formed in AlAs via Zn diffusion into single crystal n-type vapor grown AlAs layers

18 p3297 A70-36316

Auroral physics, discussing visibility, relations to geomagnetism and sunspots spectrum, morphology, optical emissions and particles in magnetosphere

20 p3623 A70-39929

Auroral optical emission measurements, examining oxygen atmospheric and IR bands by rocket sounding

21 p3817 A70-41092

Emission and escape of light from inside spherically symmetric gravitational mass, examining escape cone

21 p3923 A70-42106

Light generation by free electrons interaction with metallic diffraction grating, devising experiments for explaining incompatibility with simple electrostatic image theory

22 p4074 A70-42943

GaAs laser and noncoherent IR emitting diodes fabrication and design, discussing card readers, en-

coders, alarms, range finders, bomb fuses and night vision systems

22 p4050 A70-43248

Mode locked neodymium-glass pulsed laser stimulated picosecond time resolved light emission observation by cross beam technique

24 p4354 A70-45647

Current sheet motion and pulsar radio, optical and X ray emission, investigating finite thickness oscillating interface radiation with independent particle

24 p4397 A70-45760

Polar auroral hydrogen emission intensity dependence on K index of geomagnetic activity

24 p4331 A70-46288

LIGHT INTENSITY

U LUMINOUS INTENSITY

LIGHT MODULATION

NT ULTRASONIC LIGHT MODULATION

Interferometer for compressing linearly FM light pulses and analyzing spectra of picosecond pulses

01 p0111 A70-10670

Duty factor and contrast in scanned displays, discussing light modulator and emitting displays

01 p0043 A70-10780

Light induced modulation of optical absorption of CdS crystals by chopped laser excitation, noting use for fast recombination center detection

02 p0310 A70-11846

Birefringences and phase retardations in lithium niobate crystals for light propagation directions near optical axis, considering electro-optic modulation

02 p0313 A70-12451

Light pulse demodulator using zero crossing technique to eliminate photomultiplier bandwidth and sensitivity limitations

02 p0271 A70-12744

IR light beam modulation in Gunn oscillator near fundamental edge of GaAs, investigating mechanism

03 p0539 A70-13160

UHF self modulation in GaAs laser coupled to external cavity, focusing convergent beam on external mirror

04 p0701 A70-14718

Faraday modulator for polarized laser radiation, eliminating analyzer by oblique magneto-optical active element, converting angular modulation into amplitude modulation

05 p0858 A70-16251

Emission modulation in multifunctional injection laser-photodiode system used as optical memory, pulse generator, multivibrator and trigger

05 p0859 A70-16268

Laser beam modulation by electro-optic devices, investigating modulator characteristics in longitudinal and transverse configurations

05 p0860 A70-16489

Laser signal modulation at RF by subjecting emitting atoms of Xe-He laser amplifier to simultaneous DC and RF magnetic fields

06 p1079 A70-17191

Half octave bandwidth traveling wave X band optical phase modulator, noting multiple interactions of optical and microwave fields in electro-optical crystal

06 p1079 A70-17192

Carbon dioxide laser beam modulation by molecular Stark effect

06 p1080 A70-17448

Microwave in-cavity modulation of helium-neon laser, obtaining frequency dependence of modulation depth

09 p1696 A70-22628

Parametric image transformation during sum frequency generation

09 p1636 A70-23134

He-Ne laser Q factor modulator based on Fabry-Perot interferometer with alternating absorption

10 p1899 A70-24255

He-Ne laser emission electro-optical modulation by three mirror optical cavity, considering structural and thermal stability and coupled resonators geometry effects

10 p1899 A70-24260

Doppler beat spectrum and modulation depth of He-Ne laser emission with backward beam reflected from moving mirror into resonator

10 p1901 A70-25123

Optical modulation using rotating diffraction grating to obtain frequency shifts

11 p2049 A70-25633

Temperature instability of electro-optical laser modulators using ADP, KDP and DKDP crystals taking into account phase shift between coherent light beams

11 p2063 A70-25848

Interferometric combinations of frequency-shifted mode-locked laser pulses achieved by optical modulation-demodulation methods

12 p2249 A70-27755

Phase modulated laser light beam statistical analysis, using Michelson interferometer with piezoelectric crystal driven mirror connected to Gaussian random noise generator

12 p2249 A70-27877

Spontaneous emission modulation, interference beat and level crossings observable in gas laser operating at two output frequencies

13 p2425 A70-28599

Electro-optical light modulators representation by two port matrices, deriving amplitude modulation methods

13 p2427 A70-28924

Amplitude and phase modulation of laser beams by tetragonal crystal cuts

13 p2429 A70-29533

CW HCN laser driven phase matched traveling wave lithium niobate electro-optic light modulator performance

15 p2750 A70-31976

Stabilized platform stellar detector for French probe balloons, using semicircular light modulator

15 p2738 A70-32249

Solid state subnanosecond electro-optic light switch for mode locked laser controller or light shutter

15 p2753 A70-32815

Ruby and neodymium glass free running lasers output power modulation relationship to excited modes and active rod position in resonator

15 p2753 A70-32822

Optical spatial phase modulator array using membrane light modulator for coherent optical processing and character recognition

16 p2904 A70-33147

Light modulation electro-optical device with liquid crystals, determining liquid nematic stability

16 p2907 A70-33181

Traveling wave light modulator with 15 GHz bandwidth using cubic ZnS crystal with anomalous response

16 p2876 A70-33403

Coherent optical computer system driven by membrane light modulator (MLM), describing electro-optical properties and operating characteristics

16 p2871 A70-34055

Modulation method for phase detection in electro-optical light modulator of optical range finder

16 p2914 A70-34213

Gas laser phase locking due to loss modulation with double mode spacing

17 p3107 A70-35474

Real time holographic reconstruction by electro-optic light modulation through crystal

18 p3258 A70-36312

Self phase modulation of stimulated Raman light in carbon disulfide, discussing Stokes and anti-Stokes spectrum regions

18 p3266 A70-36422

Microwave self modulating GaAs diode laser, showing coupled external cavity resonator influence on intrinsic resonance frequency

18 p3269 A70-36733

Carbon dioxide laser producing nearly 100 percent amplitude modulation of output by intracavity polarization modulation technique

18 p3270 A70-36747

Modulation of carbon dioxide laser with Stark cell internal to cavity, using methyl chloride electrooptical gas

18 p3270 A70-36748

Electro-optical SHF modulator characteristics calculation from light wave interaction with traveling wave

19 p3443 A70-37291

Traveling medium solid state lasers radiation intensity modulation by active element motion

19 p3444 A70-37442

Doppler beat spectrum and modulation depth of He-Ne laser emission with backward beam reflected from moving mirror into resonator

20 p3643 A70-40516

Optical communications system for transmission and detection of PCM word pattern at gigahertz rates, discussing optical and electrical modulation

21 p3788 A70-41339

High speed photodetectors for microwave demodulation of light, discussing electrical properties, equivalent circuits and noise factors

21 p3799 A70-41420

Electro-optical modulation lock-in techniques for minimizing statistical fluctuations and eliminating internal noise in sampling of light signals

21 p3827 A70-41462

Light modulator design based on Fabry-Perot interferometer controlled by electro-optical effect

22 p4026 A70-42507

Time average hologram interferometry, calculating light beam modulation effects on fringe loci and localization

22 p4030 A70-42950

Frequency modulated gas laser communication system, discussing Raman-Nath effect, Doppler shifting phase grating, monochromatic light, pseudostanding wave, optical heterodyne detector, etc

22 p3989 A70-42966

Microwave frequency light modulators waveguides, examining optimal cross sections to increase modulator efficiency

23 p4196 A70-44409

LIGHT PRESSURE

U ILLUMINANCE

LIGHT PROBES

U LIGHT BEAMS

LIGHT SCATTERING

Light Raman scattering in semiconductors under constant magnetic field, studying electron-phonon spectrum characteristics

01 p0155 A70-10183

Periodic potential and residual Coulomb interaction effect on inelastic light scattering from electronic excitations in semiconductors, using diagrammatic perturbation theory

01 p0156 A70-10280

Optical data display involving laser light deflection by vibrating mirrors actuated by mechanical resonators

01 p0108 A70-10355

Cirrus clouds signature analysis, discussing light scattering pertinent to lidar equation

01 p0076 A70-10913

Book on scattering of light and other electromagnetic radiation, treating scattering by spheres, cylinders, liquids, Rayleigh-Debye scattering, particle size analysis, etc

02 p0337 A70-11689

Albedo variations for single scattering in atmosphere of arbitrary optical thickness by linearizing transfer equations with perturbation technique

02 p0338 A70-11790

Coherent light scattering disturbance in level-crossing signals of Rb 85 and Rb 87 second excited state by noble gas atoms

02 p0311 A70-11851

Focal length-to-aperture ratio for maximizing collection of scattered light at right angles to illuminating laser beam used in Raman spectroscopy

02 p0311 A70-11888

Holograms of light scattered by clouds of water droplets to determine drop size, noting agreement with Mie theory

02 p0296 A70-11890

Diffuse illumination in holography indicating spread increase dependence on product of phase mean-square value and spatial frequency bandwidth

02 p0296 A70-11891

Light scattering from thermally stable magnesium oxide particles in premixed turbulent flames used for measuring mean and fluctuating temperature values

02 p0398 A70-12039

Water vapor condensation by homogeneous nucleation measured for cluster number using laser light scattering compared with theory in condensing supersonic flow

02 p0279 A70-12048

Molecular rotations and kinetics from spectral features of molecular Raman spectra, using light scattering spectroscopy

02 p0343 A70-12077

High intensity pulsed laser radiation scattering by free electrons, studying linearly polarized incident radiation

02 p0312 A70-12276

Aerosol induced light scattering optical properties in atmospheric boundary layer measured with three photometer setup with He-Ne laser

02 p0328 A70-12437

Brillouin scattering of hypersonic waves produced in liquid medium, using He-Ne laser light source

02 p0313 A70-12471

Three dimensional photoelastic case bonded solid propellant motor model, analyzing stress distribution using scattered light photoelasticity [SESA PAPER 1587]

03 p0583 A70-12885

UV radiation scattering and rocking instrument error source in vertical ozone profile determination with optical ozone probes

03 p0557 A70-13296

Current density and electron concentration fluctuations in semiconductors under electric field, obtaining theory of light scattering at hot electrons

03 p0539 A70-13405

Three dimensional structure determination for weakly scattering semitransparent objects from holographic data, discussing inverse scattering problem and refractive index calculation

03 p0487 A70-13647

Scattered light photoelastic stress analysis using doubly refracting materials and lasers

03 p0594 A70-13657

Bouguer single-scatter theory applicability dependence on angular aperture of receiver and laser beam parameters in water mists

03 p0451 A70-13756

Three dimensional characteristic of light scattered by lunar surface determined for various incidence angles and azimuths from Zond 3 photometric measurements

04 p0744 A70-14441

Illuminating conditions in deep layers of turbid plane-parallel medium for highly elongated scattering characteristic

04 p0745 A70-14497

Laser beam broadening in atmospheric propagation from Born approximation and Gaussian model, showing no contribution by second scattered field

04 p0701 A70-14963

Collimated light beam enhanced scattering and anomalous absorption due to decay into plasma waves

04 p0727 A70-14996

Satellite lines from diffraction grating observed by densitometer tracings of plates connected with optical mixing in stimulated Brillouin scattering

04 p0701 A70-15030

Photocathode internal light scattering effect on photomultiplier time response

05 p0845 A70-15806

Correctness of Meixner assumption of scattered light field singularity near grating edge due to diffraction

05 p0816 A70-16879

Light scattering at 90 deg from laser-induced breakdown plasmas in air, discussing origin

06 p1114 A70-17189

Scattered Lyman alpha radiation intensities measured for mixtures of partially dissociated hydrogen in Ar, measuring quenching cross sections

06 p1053 A70-17327

Laser radiation attenuation coefficient in artificial fog related to water droplet concentration, suggesting single scattering for given optical thickness

07 p1296 A70-18725

Light scattering from free electrons in laboratory plasma, showing frequency spectrum equal to electron density fluctuations

07 p1347 A70-18899

Photon scattering in inhomogeneous medium, deriving expressions for mean number of photons escaping or annihilated in medium

07 p1376 A70-18910

Visibility, atmospheric light scattering coefficient and aerosol mass concentration related by integrating nephelometer measurements

07 p1328 A70-18923

Catalog of lunar features brightness interpreted in terms of photometric function uniformity of lunar surface, considering second order light scattering

07 p1377 A70-18971

Laser emission photons scattering by semiconductor conduction electrons allowing for electron-phonon interaction

07 p1357 A70-19857

Group theory investigation of three photon light scattering tensor for all vibration modes of specific crystal classes

07 p1299 A70-19861

Laser-forced medium anisotropy effects on non-linear optical frequency mixing and combined forced scattering

07 p1335 A70-19863

Light beam intensity variations during propagation in nonlinear medium taking into account combination scattering, solving equations by difference method

08 p1461 A70-20858

Optical to IR conversion in circumstellar dust envelope with spherical symmetry based on optical radiation scattering and absorption by dust

08 p1573 A70-21047

Polarized light electroreflection from GaAs single crystal, noting useful signal linear dependence on electric field

08 p1556 A70-21124

Astronomical sounding balloon to study interplanetary scattered light, discussing actuating and control, structure, onboard and ground electronics

08 p1497 A70-21349

Scattered field amplitude and phase determined from hologram light intensity distribution, noting biological applications

08 p1500 A70-21786

Photon scattering by Ar in vacuum UV measured for cross sections

09 p1730 A70-22071

Radiation transfer in semiinfinite medium illuminated by parallel light beams assuming trinomial scattering indicatrix, deriving radiative effects and radiation field

09 p1751 A70-22154

Radiation transfer in scattering medium with nonuniform density distribution of absorbing matter expressed in terms of photon distribution

09 p1666 A70-22178

Backscattered sun and skylight spectra from sea obtained from low flying aircraft as measure of chlorophyll concentration

09 p1666 A70-22250

Photographic emulsions design for increased water depth penetration during aerial multispectral recording of light absorption and scattering in water masses

09 p1674 A70-22261

Resonance radiation transport in optically thick layer, obtaining conservative light scattering solution

09 p1753 A70-22451

Calibration of shear sensitive cholesteric liquid crystals film, measuring shearing forces and scattering light intensity

09 p1656 A70-22992

Polychromatic nonlinear light scattering in plane parallel layer solved by self consistent optical depths method

09 p1762 A70-23117

Single and clad glass fibers radii and refractive indices measurements on basis of laser light scattering

09 p1699 A70-23444

Upper atmosphere aerosols and cosmic dust properties investigation by laser beam scattering measurements using photoelectron counters for weak signal detection

10 p1898 A70-23818

Granularity spectrum of diffusing screen uniformly illuminated by normally incident coherent light, basing study on long and short distance visual observations

10 p1899 A70-24031

IR light dispersion filters of compressed mixed powdered crystals, discussing optimal preparation procedures, passbands temperature dependence and stability

10 p1915 A70-24256

Plasma magnetic field measurement by scattered light, analyzing electron spectrum modulation with gyration frequency

10 p1916 A70-24401

Polydisperse dielectric system distribution parameters determined from hard monochromatic polarized radiation scatter by artificial aerosols

10 p1916 A70-24500

Power spectrum of light scattered by two level atom driven by monochromatic electric field obtained from atomic dipole moment correlation function

10 p1920 A70-24632

Ozone measurement from satellite by direct beam and scattered light methods employing UV sunlight attenuation

10 p1890 A70-24639

Martian soil surface anomalies observed from polarimetric analysis of light diffused by Hellas region

10 p1943 A70-24708

Bouguer single-scatter theory applicability dependence on angular aperture of receiver and laser beam parameters in water mists

10 p1842 A70-25005

Spectroscopy applied to spontaneous combination scattering of light

10 p1892 A70-25026

Light scattering, turbulent disturbances and absorption by binary oxygen complexes in atmospheric layers

10 p1843 A70-25126

Structural detail in transparent object through holographic measurement of scattered monochromatic light, noting similarity to crystal structure reconstruction in X ray diffraction experiments

11 p2048 A70-25360

Terrestrial clouds near IR light scattering compared to reflectivity of water and ice particles, discussing Mie and multiple scattering

11 p2045 A70-25649

Poincare sphere application to automatic polarization forms measurements and two/three dimensional photoelasticity by scattered light

11 p2142 A70-26633

First order scattering formulae for s- and p-light reflected and transmitted by rough plane surface using perturbation theory

11 p2086 A70-26840

Laser light investigations of atoms, molecules and plasmas, considering Raman molecular spectroscopy, acoustic phonons interactions and plasma diagnostics by light scattering

12 p2245 A70-27063

Reflected light directional diagram effects on scintillating surface luminescence yield, considering scattering function gradient

12 p2231 A70-27310

Honda 1968c comet head light polarization measurements, noting correspondence to scattering on dust particles

12 p2300 A70-27499

Light scattering by atom generalized for multilevel system, showing additional coherent spontaneous scattering and incoherent stimulated combination scattering

12 p2272 A70-27549

Stimulated Mandelstam-Brillouin and entropy backscattering of light pulses, determining intensity and spectral distribution allowing for fluctuations in medium

12 p2248 A70-27550

Upper atmosphere probing based on light scattering from laser radar beam by atmospheric constituents

12 p2185 A70-27740

Cold variable stars intrinsic polarization model proposing light scattering in circumstellar dust shells

12 p2307 A70-27865

Ruby and He-Ne laser radiation attenuation found due to scattering by gas molecules and aerosols from atmospheric spectral transparency fine structure studies

12 p2191 A70-28294

Three dimensional characteristic of light scattered by lunar surface determined for various incidence an-

gles and azimuths from Zond 3 photometric measurements 13 p2485 A70-28466

Small angle light scattering indicatrices in ruby crystals approximated by Gauss type function 13 p2431 A70-29869

Side scattered light effects on atmospheric transmittance measurements, showing influence on total receiver illumination 14 p2603 A70-30411

Light scattering from plasmas with nonMaxwellian electron velocity distribution function 14 p2622 A70-30694

Plane wave ray optical scattering by two spheres for arbitrary angle of incidence and observation, noting importance of first order interaction terms 14 p2551 A70-31157

Autocorrelation of coherence characteristics of polarized components of light scattered at curved rough surface, showing nonadequate Kirchhoff approximation 15 p2749 A70-31555

Scattering function and image quality in sharp edge holography using single mode laser, analyzing coherent and diffuse light 15 p2733 A70-31556

Polarized light scattering angle relationship with Mueller matrix elements for polydisperse systems of irregular randomly oriented particles 15 p2775 A70-32040

Scattered light rosette using three polarized light beams intersecting at surface point to evaluate photoelastic stress data 15 p2739 A70-32320

Laser beam scattering by free electrons in terms of classical electrodynamics, discussing radiation damping effects 15 p2752 A70-32451

Laser beam scattering by free electrons in semiclassical radiation theory, discussing intensity dependent frequency shift 15 p2753 A70-32452

Planetary atmospheric light diffuse reflection and transmission, applying anisotropic scattering theory 15 p2802 A70-32493

Solar stray light, determining spread function, limb profile and aureole at various wavelengths 15 p2795 A70-32625

Light scattering in one dimensional semiinfinite medium with moving boundary, deriving escape and reflection probability expressions 15 p2808 A70-32880

Edson layer theory explaining phase anomaly of inner planets in terms of light scattering by thin layer above Venus cloud cover 16 p2973 A70-33113

Stimulated light scattering by capillary waves on incompressible fluid surface or by Rayleigh waves on surface of isotropic solid body with small opticoelastic moduli 16 p2951 A70-33195

Quantum theory for spontaneous parametric light scattering, determining photon spectral distribution 16 p2951 A70-33196

Atmospheric optical properties stability determination for various optical densities, assuming horizontally homogeneous medium with properties constant during observation 16 p2899 A70-34181

Holographic techniques, investigating ultrasonic fields in transparent media based on light separation by grating into optical moments 16 p2915 A70-34330

Ellipsometry with Poincare sphere representation, describing application to automatic two and three dimensional photoelasticity by scattered light 17 p3086 A70-35014

Optical correlator for displacement measurements using laser produced speckle patterns of scattered coherent light 17 p3088 A70-35026

Remote sensing of plankton and matter in sea by determining spectral changes in scattered light measured with radiometer 17 p3079 A70-35619

Mutual coherence function of light scattered by plasma turbulent electron density fluctuations, taking into account refractive index changes 17 p3137 A70-35722

Quantum mechanical model of stimulated thermal, Brillouin and molecular excitation scattering of light due to absorption 18 p3266 A70-36409

Brightness field spatial structure of solar radiation reflected from earth by Cosmos 149 satellite, discussing homogeneity and isotropy 18 p3247 A70-36629

Unsteady light field spatial moments in turbid medium boundary layer with intense anisotropic scattering during illumination by narrow beam 18 p3285 A70-36631

Backscattering of collimated light beam emitted by pulsed point source into opaque medium 19 p3461 A70-37421

Light propagation in plane parallel layer of scattering medium containing absorbing substance with random density distribution 19 p3461 A70-37422

Light combinatorial scattering by longitudinal photons with frequency near forbidden zone width, calculating Raman scattering cross sections 19 p3444 A70-37444

Relaxation theory of Rayleigh scattering of light by isotropic continuous medium, deriving spectral densities via fluctuation dissipation theorem 19 p3470 A70-37446

Photoelectric and polarimetric observations of comet 1968 c Honda in BV system, noting dust scattering role in emission 19 p3515 A70-37657

Dual scatter laser Doppler velocimeter /LDV/ technique, considering system design, performance and experimental verifications 19 p3424 A70-37876

Maximum secondary principal stress axis and isotropic points determination in scattered light photoelastic analysis, considering bar in uniaxial tension and rectangular beam 19 p3546 A70-38345

Holography, discussing light propagation, basic principles, skew reference wave, diffused illumination interferometry, character recognition, microscopy, high density information storage, etc 19 p3427 A70-38449

Ikeya-Seki /1967n/, Thomas /1968b/ and Honda /1968c/ comet photoelectric spectrum, examining swan bands, continuum and reflected scattered light 20 p3703 A70-39024

Optical properties of system measuring atmospheric transmittance by recording light backscattered from atmospheric layers 20 p3660 A70-39033

Water droplet size measurement by forward light scatter holography, evaluating reconstructed wave front by Fresnel transform 20 p3628 A70-39132

Double holography on phase objects in diffused light using pulsed ruby laser 20 p3630 A70-39499

Hologram line scattering function dependence on light source spatial coherence, presenting quantitative evaluation, theoretical and experimental data 20 p3633 A70-39760

Fuel nozzle sprays mean droplet diameter based on computerized analysis of small angle forward scattered light profile 21 p3806 A70-40805

Photographic emulsions and photosensitive materials for holography, measuring noise spectral power density at high spatial frequencies by scattered light method 21 p3822 A70-40812

Saturn ring photometric properties, discussing multiple scattering and Seeliger principal photometric theory deviation 21 p3885 A70-40932

Refractive index complex part effect on polarization and radiance of reflected and transmitted light for continental haze and nimbostratus cloud models 21 p3847 A70-41724

B-V and U-B colors and B and V polarization calculation in single scattering for slab model reflection nebulae with dielectric or graphite grains 22 p4103 A70-42984

Acoustic Bragg diffraction for laser light deflection, solving high speed photography and holography motion problems [SMPT PREPRINT 5] 22 p4035 A70-43055

Numerical model of light diffraction on plane shock waves at optical phase jump region for shadow and schlieren techniques [SMPT PREPRINT 97] 22 p4035 A70-43058

Laser light pulse interaction with solid targets, observing second harmonic generation in induced plasma from time resolved spectra 22 p4084 A70-43673

Planetary atmospheric light diffuse reflection and transmission, applying anisotropic scattering theory 23 p4240 A70-43915

Laser light scattering in plasma for charged particle correlation function 23 p4225 A70-44187

Light scatterers use behind phase object in double exposure holography, determining laser radiation wave front dynamics effect on image quality 24 p4334 A70-45461

Laser light scattering by moist air flows with condensed droplets of water vapor 24 p4353 A70-45565

Magnetic field measurement by laser light scattering intensity fine structure determination in plasma 24 p4353 A70-45567

LIGHT SCATTERING METERS

Methods and equipments for light dispersion measurements for determining atmospheric refraction in terrestrial angle and electrooptical distance measurements 16 p2911 A70-33523

LIGHT SOURCES

NT ILLUMINATORS

Equilibrium state of high current discharge in low conductivity plasmas, obtaining light sources at low temperatures 01 p0152 A70-10993

Ballistic compressor performance as high intensity pulsed light source, discussing Xe gas heating and laser pumping 02 p0311 A70-11921

High power pulsed lasers development compared to thermal light sources, discussing applications to nonlinear optics 02 p0312 A70-12070

CW laser light sources for Mach-Zehnder interferometer, obtaining results for carbon dioxide injected through porous bottom wall into air flow 03 p0484 A70-13397

Controllable light source for experiments on human pupillary servomechanism 04 p0642 A70-14633

Horizontal disparity and ratio of perceived egocentric distance related in stereoscopic vision during investigation of three point light sources problem 08 p1447 A70-21725

Holographic image reconstruction analysis based on two beam interferometry by spatially incoherent light source, obtaining optical transfer function 08 p1514 A70-21790

Plasma discharge studies by holographic interferometry using ruby laser pulse for light source 09 p1674 A70-22171

Broad spectrum light sources effects on mammalian endocrine apparatus development and function determined in rats 09 p1617 A70-22335

He-Ne laser light source for oil damped spiral gauge used as vacuum system pressure nulling device 09 p1698 A70-23000

Mercury arc injection lamp as radiation source for testing sunlight biological effects 10 p1888 A70-24388

Gas jet bounding of Ar arc column, providing high power/intensity light source 12 p2237 A70-28159

Reflectivity measurement in near IR using black bodies near room temperature for light sources 14 p2588 A70-31210

Light sources design with variable uniform luminance for space exploration cameras calibration [JPL-TR-32-1470] 15 p2737 A70-32037

Amplitude and intensity interference relations from pseudothermal light sources, noting applicability to stellar interferometry 16 p2900 A70-32999

Optical system and light source imperfection effects interference image contrast lowering in laser interferometer for length measurements 16 p2928 A70-33292

Plasma opacity measurements using CW He-Ne and Ar lasers as light sources 17 p3106 A70-35107

Light gathering nonuniformity in cylindrical plastic scintillator, analyzing detector signal amplitudes for various pulsed light source positions 20 p3629 A70-39318

Extreme UV spectroscopy with synchrotron radiation storage ring light sources in 40-400 A range, including thin film photoabsorption measurements 21 p3826 A70-41451

Pulsating light source afterglow increasing high speed film information content, discussing streak image, tearing process and impact stress tests [SMPT PREPRINT 66] 22 p4032 A70-43036

Exploding wire light source modification by immersing in transparent fluid to increase intensity, measuring spectral characteristics [SMPT PREPRINT 64] 22 p4032 A70-43037

Ultrabright nanosecond flash light generation technique, using superradiant light sources for shadowgraph photography in high resolution hypervelocity field [SMPT PREPRINT 74] 22 p4037 A70-43070

Light source spatial coherence measurement, verifying laser heterodyne interferometer theory 24 p4354 A70-45665

Fourier hologram synthesis using laser point source and Wollaston birefringent prism 24 p4336 A70-45667

LIGHT SPEED

Optical and radio pulses from pulsars as test of light speed variation with frequency and photon mass possible existence 02 p0373 A70-12394

Relativity theory and quantum mechanics relation concerning point charge velocity and motion at light speed, deriving elementary particle mass formula 06 p1106 A70-17833

Optimal information selection for determining spacecraft trajectory, considering atmosphere, light speed and series expansion coefficients of planetary gravitational potentials 06 p1142 A70-17891

Light velocity measurement at low cost, describing circuits and experimental results

06 p1067 A70-18399

Tachyons /faster than light particles/ on basis of relativity theory, noting reaction with light speed particles and relation to quantum theory

10 p1916 A70-24385

Nonviscous relativistic fluid energy momentum tensor modification to rule out sound wave propagation velocities above speed of light

13 p2454 A70-29900

Light velocity from frequency and wavelength differences between gas laser lines, using precision long path interferometry

17 p3104 A70-35085

Various light velocities, including controvelocity for describing EM radiation transport

19 p3472 A70-38274

Ne absorption cell and He-Ne gain cell pulse velocities compared with free space light velocity

22 p4048 A70-42329

Faster-than-light particles impossibility in causal loops using nonquantum special relativity framework, considering tachyons

24 p4378 A70-45424

Newton and Einstein gravitation theories applied to light velocity in gravitational field

24 p4379 A70-45487

Light velocity frequency dependence in variable stars gravitational fields suggested from yellow and UV NP 0532 observations

24 p4405 A70-45488

Electro-optical light speed measurements with interference comparator using He-Ne lasers with light modulators

24 p4353 A70-45562

LIGHT TRANSMISSION

NT LIGHT SCATTERING

Metal film graded filter fabrication for schlieren photographic system with laser light source and framing camera, using vacuum evaporation

01 p0113 A70-10921

CRT resolution measurements by double slit method, relating light spot response to slit width

01 p0093 A70-11278

Diffuse isotropic light interaction with compact corn leaf, using transparent plate model with rough plane-parallel surfaces

02 p0338 A70-11893

Resin bonding material suitable for IR detectors noting transmission properties

02 p0321 A70-11926

Visible radiation reflection, transmission and inside intensities of terrestrial clouds calculated by Monte Carlo program utilizing scattering phase function

02 p0326 A70-12286

Birefringences and phase retardations in lithium niobate crystals for light propagation directions near optical axis, considering electro-optic modulation

02 p0313 A70-12451

Optical transmission spectra of polypeptide films showing exciton structure near 1600 A for alpha and polyproline II helices

02 p0345 A70-12723

Optical properties changes of various transmitting materials under simulated micrometeoroid environment, using silicon carbide particles accelerated in shock tube

03 p0523 A70-13027

Three dimensional Gaussian light beam propagation in anisotropic inhomogeneous media with dielectric constant decreasing from energy flow direction

03 p0525 A70-13533

Light pulses propagation in nonlinear laser medium, obtaining equations of motion for density matrix

04 p0700 A70-14687

Phase and amplitude level of plane light wave propagation in medium with randomly discontinuous refractive index, discussing wave phase dependence on dielectric constant

04 p0650 A70-15288

Carbon dioxide-nitrogen laser emission absorption in atmospheric surface layer by wings of distant strong lines investigated statistically

06 p1082 A70-17807

Light inductions and echo intensities in liquids and gases, investigating thermal vibrations, translational Brownian motion, particle collisions and laser diffusion effects

06 p1082 A70-17809

Spectral transparency inversion of aerosol-containing atmosphere

06 p1098 A70-17832

Light refraction in Venusian atmosphere from Venera 4 probe measured data, noting horizontal rays traversing planet along circumference at 8.3 km height

06 p1142 A70-17889

Light pulse propagation in nonlinearly amplifying or absorbing medium, discussing coherent and non-coherent interaction between pulse and medium

07 p1296 A70-18745

Pumping light distribution in rectangular laser rods showing corner maxima and overall nonhomogeneity

07 p1300 A70-19871

Light beam intensity variations during propagation in nonlinear medium taking into account combination scattering, solving equations by difference method

08 p1461 A70-20858

Two photon interaction between ultrashort light pulse and medium, showing pulse propagation through medium without absorption

08 p1514 A70-21820

Supernovae hydrodynamics, discussing early light curves energy requirements and shock wave dynamics in terms of neutrino diffusion

09 p1749 A70-21992

Pulsed laser beams intensity fluctuations correlation functions dependence on propagation distance in turbulent atmosphere

09 p1636 A70-23135

Amplitude measurement of plane light wave propagating in turbulent atmosphere, giving log amplitude dependence on dispersion of logarithm fluctuations

09 p1636 A70-23136

Turbulent medium refractive index fluctuations effect on parameters of focused plane light wave, calculating diffraction patterns center of gravity

09 p1636 A70-23138

Laser beam intensity fluctuations during propagation through turbulent atmosphere

09 p1637 A70-23142

Sensitivity of nondiffuse double exposure holographic interferometry with transparent medium increased via multiple beam passage through medium placed in optical cavity

09 p1682 A70-23360

Magnetophotoelastic model applied to plates bending stress analysis, deriving polarized light propagation equations

09 p1728 A70-23447

Optical transmission technology for aerospace launch operations investigated on wideband communication systems projects involving use of gallium arsenide lasers and diodes

09 p1640 A70-23776

Diffuse light transmission from point sources over horizontal paths in lower atmosphere, discussing effect of range

10 p1912 A70-24424

Electromagnetic radiation frequency shift during passage by sun or earth not caused by electrostatic or magnetic fields

10 p1917 A70-24860

Laser light propagation along strongly inhomogeneous turbulent path, measuring intensity fluctuations dispersion and light amplitude

10 p1844 A70-25161

Geometrical light depolarization in randomly inhomogeneous medium, discussing light propagation in turbulent atmosphere and ionospheric radio propagation

10 p1844 A70-25162

Near IR radiation diurnal variations in corn canopy accounted for by Duntley equations for unidirectionally incident light propagation through diffusing medium

11 p2082 A70-25364

Magneto-optical birefringence anisotropy and light propagation in terbium ferrite garnet in presence of Faraday and Cotton-Mouton effects

11 p2097 A70-25377

Hyperbolic velocity space physical significance based on cosmological model of light propagation associated with uniformly expanding universe

11 p2114 A70-26551

Moire theory applied to direct strain measurement methods based on light diffraction

11 p2058 A70-26835

Monochromatic light propagation in medium with large scale Markov nonuniformities of dielectric constant using parabolic equation approximation

12 p2272 A70-27359

Transmission diffraction grating for astronomical applications constructed holographically with laser light and photoresist films

12 p2234 A70-27589

Light pulse propagation in dispersive nonlinear dielectric analyzed on nonlinear Lorentz model

12 p2274 A70-28216

Multiwavelength laser beam propagation with point source transmitters, determining turbulence levels independently

13 p2426 A70-28837

He-Ne laser beam transmission through atmosphere, investigating intensity, spot size, polarization and power spectrum fluctuations

13 p2427 A70-29103

Light transmission losses in optical resonators partially filled with inhomogeneous dielectric, specifying optimal geometrical parameters

13 p2378 A70-29404

Interferometric measurement of spatial correlation function of optical radiation fields propagating through turbulent atmosphere

13 p2454 A70-29825

Side scattered light effects on atmospheric transmittance measurements, showing influence on total receiver illumination

14 p2603 A70-30411

Venus atmosphere opacity law determination as function of wavelength, comparing interferometric and integrated brightness temperatures with model calculations for various atmospheric compositions

14 p2646 A70-31069

Planetary atmospheric light diffuse reflection and transmission, applying anisotropic scattering theory

15 p2802 A70-32493

Light scattering in one dimensional semiinfinite medium with moving boundary, deriving escape and reflection probability expressions

15 p2808 A70-32880

Coherent light pulses propagation through resonant medium, discussing energy loss

16 p2928 A70-33278

Earth atmosphere transmission coefficients determination by relation between transparency and daytime sky brightness, noting limits of applicability

16 p2899 A70-34180

Earth atmosphere transmission coefficient and optical stability based on solar aureole observation

16 p2899 A70-34186

Atmospheric optical inhomogeneity effect on image quality, investigating deflection angles for spherical light wave passage at various altitudes

16 p2915 A70-34215

Attenuation, refraction and multiple reflection effects on light reflection from shock front at near grazing incidence

16 p2953 A70-34271

Allowable transmission bandwidth of lens waveguide with curved axis, considering light beam deflection due to chromatic aberration

17 p3050 A70-34583

Light propagation-shift relationships in optically pumped atomic vapors, discussing susceptibilities, birefringence, conversion efficiencies, coupling, etc

17 p3103 A70-35000

Intensity logarithm fluctuations of focused laser beam propagating in summer daytime atmosphere at 250 and 650 meter path lengths

17 p3048 A70-35685

Coherent light propagation through turbulent atmosphere observed by applying He-Ne lasers to simultaneous measurements of scintillation effects over homogeneous optical paths

17 p3108 A70-35721

Thick plane fog layers reflection and transmission properties, using emerging light angular distribution for Milne problem

18 p3284 A70-35944

GaAs lasers with light propagation along curved junctions, discussing threshold current density variation with radius of curvature

18 p3269 A70-36738

Contaminated optical surface investigation technique in near UV, visible and near IR range, investigating property changes of systems in transmission and reflection

18 p3292 A70-36786

Atmospheric turbulence effects on light propagation, measuring refractive index variations by high speed temperature sensors

18 p3285 A70-36961

Light propagation in plane parallel layer of scattering medium containing absorbing substance with random density distribution

19 p3461 A70-37422

Coherent light beam characteristics with Gaussian radial intensity variation during propagation along optical system axis, determining radius from diffraction theory

20 p3639 A70-39086

Aircraft navigation light visibility, discussing visual threshold, source intensity, atmospheric transmissivity, color, background luminance, etc

20 p3564 A70-39719

Dynamic compensation of thermal pumping-induced deformation of laser active elements via thermal bending of resonator mirrors achieved by coatings

20 p3642 A70-39744

Short light pulse coherent absorption in homogeneously broadened resonant medium, discussing influence of input pulse area and atomic coherence on propagation properties

21 p3784 A70-40565

Dispersive spectrometer multiplexing light in entrance and exit slit positions compared with Michelson interferometric spectrometers

21 p3823 A70-40848

Light pulse propagation in nonlinearly amplifying or absorbing medium, discussing coherent and non-coherent interaction between pulse and medium

21 p3836 A70-41170

Refractive index complex part effect on polarization and radiance of reflected and transmitted light for continental haze and nimbostratus cloud models

21 p3847 A70-41724

Diffraction theory relationship to ray optics for coherent light propagation through lens systems

21 p3829 A70-41929

Optical communication waveguides with diffused boundaries, calculating modal propagation fields by perturbation theory

21 p3792 A70-42045

Atmospheric communication channel modeling for laser wavelengths, considering point, area, heterodyne and direct detection receivers, nonplanar and infinite plane wave propagations, etc

21 p3793 A70-42179

Fiber optic components quality control by image transmission intensity distribution measurement

22 p4045 A70-42513

Cotton leaves ammonia induced discoloration spectrophotometric examination, discussing light reflectance, transmittance and absorbance

22 p4014 A70-42771

Monochromatic light propagation in medium with large scale Markov nonuniformities of dielectric constant using parabolic equation approximation

22 p4075 A70-43600

Planetary atmospheric light diffuse reflection and transmission, applying anisotropic scattering theory

23 p4240 A70-43915

Delta function approximation in diffuse transmission and reflection of light for phase function with sharp forward peak, using scattering compensation

23 p4214 A70-44034

Signal arrival time variance in optical communication system with high lag photodetectors, examining input, detection and amplification noise

23 p4196 A70-44410

German monograph on quantum statistics for light propagation in laser-active fluctuating media

24 p4350 A70-45090

Optical wave propagation through random atmospheric turbulence, deriving wave equation power series solution for homogeneous random refractive index field

24 p4314 A70-46126

LIGHTHILL GAS MODEL

Subsonic circular jet noise radiation intensity and directional distribution, based on effects of refraction and Lighthill quadrupole model for aerodynamic noise

05 p0834 A70-16780

Hypersonic flow past blunted cylinder at Mach number of infinity, investigating real gas effect using Lighthill ideal dissociating gas model

08 p1431 A70-20646

Equations for unsteady frozen nonequilibrium flow of dissociating and relaxing gas, using Lighthill ideal dissociating diatomic gas for aerothermochemical model

22 p4124 A70-42754

LIGHTHILL METHOD

Surface inhomogeneities effect on sound radiated by nearby turbulence near flexible boundary, using converted Lighthill wave equation to obtain far field radiation

07 p1256 A70-19262

Aerodynamic sound emission from compact eddy region by singular perturbation approach, discussing Lighthill and Ribner theories

11 p1977 A70-26687

LIGHTING

U ILLUMINATING

LIGHTING EQUIPMENT

NT AIRCRAFT LIGHTS

NT AIRPORT LIGHTS

NT ARC LAMPS

NT FLASH LAMPS

NT ILLUMINATORS

NT LUMINAIRES

NT MERCURY LAMPS

NT RUNWAY LIGHTS

NT SEARCHLIGHTS

NT XENON LAMPS

Stroboscope lighting system for microstructural examination of fatigue test sample failure

05 p0845 A70-15882

High speed photographic systems for ballistic studies, describing high intensity lighting systems

20 p3635 A70-40527

LIGHTNING

Thunderstorm lightning discharge formation mechanism, investigating electric charge concentration and motion of free electrons

01 p0134 A70-10169

Transistorized lightning protected VHF ground antenna for air traffic communication providing high operational safety standards

03 p0459 A70-14297

Electromagnetic energy spectra of lightning expressed as function of electric field spectral density of atmospheric

05 p0843 A70-16762

Physical theory of ball lightning based on cooling air spheres models, calculating equilibrium composition, temperature profiles, output radiation and mass density

05 p0843 A70-17102

Spectral amplitude distribution of lightning spherics predicted over VLF-SHF range using theoretical analysis of lightning streamers

07 p1272 A70-20215

Aircraft skin heating by lightning, discussing possibility of exceeding jet fuel vapor ignition temperature

07 p1195 A70-20402

Thunderstorms lightning flashes time distribution recorded visually and on radar screens, discussing statistical variations in sigma

08 p1539 A70-21648

Pulse rate counter for randomly repetitive random processes, noting applications to lightning flash noise bursts in receivers

10 p1848 A70-23996

Lightning protection development programs application to light aircraft plastic components, emphasizing structure and fuel systems designers awareness [SAE PAPER 700220]

11 p1980 A70-25892

Conditions leading to lightning as triggered by Apollo 12 and suggestions for minimizing such hazards

13 p3294 A70-28838

Thunderstorm detection and warning system, measuring vertical potential gradient and changes caused by lightning discharges

14 p2607 A70-30574

Electromagnetic ELF radiation model for multiple return strokes of cloud to ground lightning discharges, considering channel length

15 p2726 A70-31864

Lightning discharge slow tail atmospheric relation to return stroke, using VLF spectra and frequency analysis

15 p2727 A70-31871

Slow tail atmospheric and VLF pulse measurements at close-to-thunderstorm fields, indicating return stroke origin

17 p3046 A70-35395

Nighttime lightning activity observations by orbiting solar satellite OSO-B, determining thunderstorms positions by optical radiation detection

20 p3623 A70-39978

Thunderstorm development processes investigated by aircraft measurements of electrical structure in cumulonimbus clouds, noting lightning probability dependence on turbulence within cloud

22 p4064 A70-42775

Lightning discharge characteristics contributing to electromagnetic background noise at ELF determined from slow tail waveform measurements

22 p4015 A70-42777

Global thunderstorm activity experiment by Ariel 3 satellite, investigating lightning discharge number and noise power

22 p4015 A70-42778

Ball lightning model assuming radiation field within plasma dielectric region resonant at higher than collision frequency

22 p4016 A70-42780

Hot air temperature decay, discussing relaxation process of lightning channel behavior

22 p4016 A70-42781

Computerized simulation of raindrop effects on initiation of cloud-to-ground lightning strokes

24 p4371 A70-45978

LIGHTS

U LUMINAIRES

LIGNIN

Phenolic aldehydes generated from lignin in fossil woods and carbonaceous sediments by oxidative degradation

13 p2361 A70-28911

LIMBS

Solar limb brightening in various ranges, suggesting obtaining temperature distribution during solar eclipse

05 p0911 A70-16436

Limb effect of solar Fraunhofer lines determined by telescope equipped with autocollimated type diffraction spectrograph

05 p0918 A70-16912

LIMBS [ANATOMY]

NT ARM [ANATOMY]

NT FOREARM

NT HAND [ANATOMY]

NT KNEE [ANATOMY]

NT LEG [ANATOMY]

Lower limbs circulation of peripheral vascular diseased patients transcatheterously assessed with ultrasonic flow detector, comparing results with arteriograms

07 p1217 A70-18956

Posthypoxic vasodilation in extremities of anesthetized dogs preserved after carotid and aortic reflexogenic zones exclusion

07 p1204 A70-19139

Weightless astronaut self rotation by limb maneuvers producing pitch and yaw motion

07 p1219 A70-19245

Heterochronism of coordinated cophasal flexor and extensor movements during acrobatic leap in human subjects

12 p2168 A70-27344

LIME

U CALCIUM OXIDES

LIMESTONE

Natural thermoluminescence of limestone within/near Charlevoix meteorite impact structure, discussing impact effects on quartz-rich rocks

18 p3314 A70-36499

LIMITATIONS

U CONSTRAINTS

LIMITER CIRCUITS

NT CLIPPER CIRCUITS

Output autocorrelation properties of ideal limiters driven by binary deterministic signal plus stationary zero-mean Gaussian noise

06 p1013 A70-18625

Narrow band limiter influence on SNR at FM reception output by computer simulation using threshold pulse model

07 p1227 A70-19124

Nonlinear phase distortion measurement in microwave limiters under dynamic conditions using two tone test signal

09 p1647 A70-22714

Nomograms simplifying noise and natural loop bandwidths calculation for phase locked loop receiver, determining limiter suppression factor

10 p1844 A70-25244

Multiple access to communication satellite by limiting repeater, considering model of n signals plus band limited white Gaussian noise in zero memory device

11 p2008 A70-26229

FM limiter-discriminator followed with ideal band-pass filter, deriving output signal to noise ratio

14 p2558 A70-31189

Hard limiting bandpass limiter output signal to noise ratio in PM signal detection calculated using probability density function

14 p2552 A70-31194

Ideal limiter with polyharmonic signal input, calculating output spectral composition by Fourier series expansion

20 p3587 A70-40143

LIMITS

Quasi-brittle materials limit surface, approximating curve in deviator plane by second order curves leading to strength criteria

10 p1965 A70-25292

Plasticity limit theorems applicability extended without geometry change requirement, discussing load elastic buckling and fiber pullout from composite materials

17 p3186 A70-34977

LIMITS [MATHEMATICS]

Limits on signal amplitude, spectrum, derivatives and modulus of variations

03 p0453 A70-14283

Perturbations classes for self adjoint operator limit spectrum preservation

07 p1327 A70-19807

Radio wave propagation equations, applying stationary phase method for finite limits of dimensionless line integral

09 p1638 A70-23662

Limiting distributions of sums of random variables coupled in homogeneous Markov chain with finite number of states

12 p2261 A70-27551

Boundary value problem for Navier-Stokes equations to obtain stationary flows as limits of nonstationary solutions

14 p2600 A70-31347

Limit theorems for sums of multidimensional stochastic step processes, giving necessary and sufficient conditions for convergence to Poisson measures

16 p2942 A70-33700

Displacement bounding principle for finitely deforming rigid plastic structures exhibiting geometric stability, with application to cylindrical shell

17 p1814 A70-34906

Relativistic and nonrelativistic fluid dynamic equations, deriving limiting procedure leading to fluid magnetodynamic Lundquist equations

19 p3478 A70-37590

Safety factor limit analysis for anisotropic nonhomogeneous solids by variational method, exemplifying by four layer rectangular beam

19 p3547 A70-38355

Bounds to direct influence coefficient derived by hybrid stress finite element method

22 p4116 A70-43203

Approximate bounds for differential eigenvalues of self adjoint linear operators in Hilbert space

23 p4211 A70-44245

Limit analysis for ionization potential reduction effect on ionized gas atomic composition, considering temperature and electron density

23 p4220 A70-44435

LINCOLN EXPERIMENTAL SATELLITES

LES-6 satellite solid Teflon pulsed plasma thruster performance, determining energy balance, thrust and circuit parameters

06 p1132 A70-18206

Solar cell degradation by proton damage in synchronous orbit studied on LES-6 satellite [AIAA PAPER 70-600]

11 p2119 A70-25430

Visible light sensors application in LES control system for circular near equatorial orbits [AIAA PAPER 70-477]

11 p2107 A70-25432

LES 5 and 6 feasibility demonstration of satellite communications at VHF/UHF to mobile terminals and as test beds, emphasizing stationkeeping and attitude control [AIAA PAPER 70-494]

11 p2121 A70-25474

Pulsed plasma microthruster propulsion system for synchronous orbit LES 6 satellite [AIAA PAPER 69-298] 13 p2473 A70-28504
RFI measurements at X band on LES-7 prototype pulsed plasma thruster 17 p3149 A70-35669

LINE SHAPE

Lorentz absorption line shape computations in radiation scattered by homogeneous planetary atmosphere compared with results for isotropic scattering by van de Hulst similarity relations 02 p0364 A70-11792

Collision-narrowed growth curves for interpreting hydrogen quadrupole lines applied to photoelectric observations of Jupiter vibration-rotation bands 02 p0368 A70-11824

Giant pulse Q switched lasers generated plasmas, noting VUV spectral line shifts, asymmetries and existence of satellite lines 02 p0345 A70-11894

Stellar spectral lines fine analysis methods compared for curves of growth, line profiles and related contribution curves in model atmospheres for Procyon and sun 02 p0343 A70-11906

O-C diagrams of RR Lyrae variables in M5, considering representation by parabolas or intersecting straight lines 03 p0567 A70-13321

Zeeman-split Fraunhofer line profiles for pure absorption lines determined taking into account solar atmosphere elliptical birefringence 03 p0570 A70-13595

K line profiles of Ca II for two component chromosphere, obtaining line source function and optical depth from steady state and radiative transfer equations 05 p0911 A70-16430

Line profiles in expanding and rotating atmospheres via Monte Carlo techniques, considering noncoherent scattering, atomic levels and atmospheric characteristics 07 p1339 A70-20057

Spectral line shapes determination for radiating atoms immersed in plasma developed without neglecting ion-electron interaction and static-ion assumption 07 p1346 A70-20247

Deuterium Lyman alpha line profiles generated from microwave powered lamp for experimental testing of two layer model characterizing emission line profiles 09 p1730 A70-22066

Generatrix shape determined for body of revolution moving at supersonic speed with minimum wave drag 09 p1603 A70-22434

Excited gas kinetic state determination from observed spectral profiles during interaction with radiation 10 p1919 A70-24147

Ruby monopulse laser with narrow emission line, describing two generator system 10 p1899 A70-24264

Band or line shape effect on radiative transfer in nongray medium between parallel walls, discussing temperature distribution and radiative flux 13 p2521 A70-29136

Non-LTE and LTE line profiles and equivalent widths for transitions in singlet and triplet systems of neutral He in hot stars, explaining anomaly 14 p2641 A70-30884

Stark broadening calculations of H alpha and H gamma hydrogen lineshapes 14 p2620 A70-31303

H alpha and Fe I lines, calculating velocity effects on profiles for differentially moving atmosphere 15 p2804 A70-32616

Spectral line formation in Mars and Venus atmospheres, discussing Lorentz and Doppler broadening 16 p2976 A70-33793

Stellar UV spectral line profiles interpretation, using atmospheric models and line formation theory 17 p3161 A70-34890

Solar potassium resonance line shape and gravitational red shift, using atomic beam technique 17 p3173 A70-35861

Solar C II resonance doublet profiles, discussing possible broadening mechanisms 17 p3174 A70-35862

Hologram line scattering function dependence on light source spatial coherence, presenting quantitative evaluation, theoretical and experimental data 20 p3633 A70-39760

Brillouin effect lines shape dependence on analogous acoustical waves temporal and spatial coherence 21 p3839 A70-42100

LINE SPECTRA

NT BALMER SERIES
NT D LINES
NT ELECTRONIC SPECTRA
NT FRAUNHOFER LINES
NT H ALPHA LINE
NT H BETA LINE
NT H GAMMA LINE
NT H LINES

NT K LINES

NT LYMAN SPECTRA
NT PASCHEN SERIES
NT RYDBERG SERIES
NT TELLURIC LINES

Photospheric Fe I abundance variation with excitation potential 01 p0175 A70-10239

Reply to Swings comments on validity of forbidden SI lines in solar spectrum communicated by Swenson 01 p0175 A70-10240

Solar corona red and green lines during 30 May 1965 total eclipse, discussing indicated radial, turbulent and displacement velocities 01 p0176 A70-10249

X ray line emission from Sco X-1 using Monte Carlo estimates of spectral distribution of scattered photons in terms of Fe line and cosmic abundance 01 p0169 A70-10338

Nova Delphini 1967 emission line spectrum at 8400-9600 A, using diffraction spectrograph attached to astronomical telescope 01 p0182 A70-10675

Galactic water vapor line emission observations indicating short term variability in spectra of several sources 01 p0182 A70-10722

Velocity field measurements in NGC 5128 galaxy, discussing relative motion between gas and stars and correspondence of emission and absorption lines 01 p0184 A70-10898

Antarctic twilight observation by photoelectric scanning spectrometer in search for metallic emission lines in upper atmosphere 01 p0081 A70-11231

Ammonia spectral lines positions, intensities and half widths under Jovian conditions calculated, including ground state rotation and rotation inversion bands 02 p0368 A70-11820

Extreme UV spectral line intensity enhancement during class 3 flare related to abundance of radiating element 02 p0358 A70-12205

Coronal emission lines wide slit photometry systematic error analysis and suggested error elimination by varying observation method 02 p0373 A70-12375

Night airglow emission intensities during IQSY concerning Na, OH and H alpha lines compared with intensities during IGY 02 p0292 A70-12433

Atmospheric oxygen A band individual rotational lines intensities and half widths measurements 02 p0344 A70-12656

Transition probabilities computed for spectral lines due to magnetic quadrupole radiation, discussing deexcitation of excited atoms in solar corona 02 p0359 A70-12706

Satellite lines of forbidden transition in laser-produced He plasma attributed to longitudinal plasma oscillations 02 p0379 A70-12717

Emission lines origin in radio galaxies optical spectra explained by using energy gained from radioactive elements decay 03 p0563 A70-13214

Orbits computation from double lined spectra of eclipsing binaries 31 Men and 9 Cha, emphasizing systemic velocity and mass ratio derivation method 03 p0565 A70-13268

Quasar spectra interpretation, analyzing observational data and absorption lines correspondence to different red shifts 03 p0570 A70-13484

Ar X and Ar XIV identification in solar corona and unidentified coronal lines origin, discussing Fe and Ni transitions from metastable levels 03 p0571 A70-13598

Spectroscopic calibration of laser lines at simultaneous carbon dioxide and nitrous oxide transitions in gas flow, showing abnormal line intensity 03 p0501 A70-13685

Cloud layer multiple scattering in Jovian atmosphere, discussing influence on Lorentzian contour of planetary absorption lines 03 p0574 A70-13882

Peculiar emission object with emissions narrower and with lower ionization lines than cool Wolf-Rayet stars 03 p0574 A70-13933

Xenon sensitized photolysis of carbon dioxide compared with direct photolysis at 1470 A resonance line 03 p0441 A70-14005

Fe I line enhancement in flare of 7 August 1958 interpreted as selective excitation effect, discussing similarity to late type dwarf stars observations 04 p0739 A70-14598

Stark broadening of ionized helium lines by collective electric fields in theta pinch 04 p0722 A70-14684

Satellite lines from diffraction grating observed by densitometer tracings of plates connected with optical mixing in stimulated Brillouin scattering 04 p0701 A70-15030

Statistical model of ozone absorption bands for calculating intensity, rotational line position and transmission functions of complex spectral regions 04 p0680 A70-15252

Axial and rotational velocity profiles of plasma jet from Doppler shift of spectral lines 04 p0729 A70-15612

[DFVLR-SONDDR-27] Solar helium-like ion line intensities, determining electron densities and excitation rate ratios 04 p0758 A70-15696

Line transfer with scattering described by redistribution function numerically solved, using discrete ordinate method 04 p0720 A70-15701

Nickel IV forbidden lines suggested from spectrum study of slow nova RR Telescopii 05 p0905 A70-15758

Excitation temperature functions calculated in rare gases spectrum lines to determine radial plasma temperature distribution 05 p0886 A70-15798

Forbidden Fe II lines and AIO band intensities in long period variable stars confirming stratified models of emitting layers 05 p0907 A70-16031

Length shifts measurement with single 2-mode laser by observing beat frequency, obtaining frequency shift proportional to length shifts 05 p0859 A70-16356

Identification of lines in Mohler photometric atlas of IR solar spectrum wavelengths 05 p0910 A70-16427

Diatomic carbon swan band violet line absence from sunspot suggested in accordance with molecular equilibrium predictions 05 p0911 A70-16433

Flare radiation influence on high photospheric and low chromospheric lines in H alpha, H and K regions 05 p0902 A70-16439

Center dip formation in curve relating output power and frequency of carbon dioxide laser line operating in single mode on single wavelength 05 p0860 A70-16667

Opacity-probability distributions for CO, computing theoretical spectra of line absorption coefficient, discussing effects of temperature and/or turbulent velocity 05 p0919 A70-16938

Empirical astrophysical damping constants derived for neutral Fe lines using solar spectra, applying constants to abundances and surface gravity determination 05 p0919 A70-16939

Neutral Ne emission line in visible solar spectrum during bright events in inner corona, noting 1958 outburst of RS Oph 05 p0920 A70-16944

Sco X-1 line spectra search in X ray spectrum by rocket-borne proportional counters, noting iron line emission 05 p0904 A70-16979

C V lines measured near 1s-2p line of C VI, identifying lines belonging to various transitions 05 p0921 A70-16982

Power spectra of pulsar radiation intensity fluctuations, showing line structure 05 p0921 A70-16983

Dispersion function and measured line profile distortion by rectangular detector slit of order scanning Fabry-Perot spectrometer 06 p1063 A70-17622

Granular and intergranular region solar magnetic field difference detection attempt from line profiles, noting equivalent width increase in ionized Cr line 06 p1142 A70-17989

Solar Cd abundance, using spectrograph and synthetic spectral line computer program 06 p1143 A70-17995

Optical spectra of discharge chambers of electron bombardment mercury ion thrusters with hollow and oxide cathodes 06 p1132 A70-18157

[AIAA PAPER 70-176] Calcium neutral and ionic lines broadening and shift by microfields measured by plasma flame observations 06 p1148 A70-18453

Longitudinal spectral line intensity distributions measured for plasma temperature determination 06 p1074 A70-18601

Doppler shift measurements of axial and rotational velocities in MPD arc, using references from iron arc [AIAA PAPER 69-110] 07 p1364 A70-19324

Pressure-narrowing theory applied to calculating equivalent widths of lines in quadrupole rotation-vibration spectrum of molecular hydrogen 07 p1338 A70-19366

Wave numbers, intensity and half width of lines of vibration-rotation relative to carbon monoxide transition, noting band center displacement dependence on pressure 07 p1338 A70-19380

Absorption lines in quasars spectra indicating line formation close to quasar nucleus 07 p1383 A70-19402

Solar protuberance radiation polarization in Ca I 4227 Å line, discussing depolarization and electron-and photoexcitation

07 p1384 A70-19416

Effective pressure and rotation line intensity in Uranus upper atmosphere obtained from methane band spectrograms, calculating maximum temperature at subsolar point

07 p1385 A70-19423

Predawn enhancement of emission rate of 6300 Å forbidden O I line in nightglow spectrum, discussing onset time

07 p1275 A70-20286

Magnetic field effects on ruby absorption in R-line region

08 p1555 A70-20543

Tunable Q switched pulsed discharge carbon dioxide laser intensity dependence on time delay investigated for various vibrational/rotational lines and gas mixtures

08 p1512 A70-20618

Binary star spectrum analysis establishing seasonal and season-to-season variations in He II emission band intensity and shift toward long wave region

08 p1569 A70-20827

Ti I spectrum oscillator strengths, determining formula for relative-absolute values transition

08 p1569 A70-20832

Brightness distribution of spectroheliograms taken in metal lines reflecting velocity field structure in photosphere

08 p1570 A70-20839

Effective depths of formation of absorption lines in solar atmosphere used for magnetic field recording

08 p1570 A70-20842

Magnesium hydride absorption lines in sunspot spectrograms indicating heavy Mg enhancement in sun relative to earth

08 p1571 A70-20904

Spectral radiometer for observing excited hydrogen radio frequency lines using paramagnetic traveling wave quantum amplifier

08 p1495 A70-21052

Oscillator strengths of Fe II lines and solar iron abundance measured by arc burning in Ar with iron chloride admixture

08 p1576 A70-21398

Anomalous microwave recombination line at 11 cm detected in NGC 2024, Orion A, and IC 1795, discussing peak antenna temperature

08 p1576 A70-21399

Relative rotational lines intensities of carbon dioxide, considering sigma-sigma transitions for abundant isotopes

08 p1549 A70-21575

Line strength and radiative lifetimes for Ne II determined from spontaneous emission data obtained from CW neon laser discharge

09 p1730 A70-22070

Corona green /5303 Å/ and red /6374 Å/ lines during minimum solar activity in 1964, discussing N-S and E-W asymmetries and intensities

09 p1750 A70-22100

Vacuum UV atomic nitrogen and oxygen lines contribution to energy transfer in high density plasma, noting f values and Stark half widths

09 p1730 A70-22229

Collision effects on saturation of He line transition in He-Ne laser, determining power output dependence on cavity tuning and gas pressure

09 p1695 A70-22322

Homogeneous model solar photosphere in strict radiative equilibrium with depth-dependent line blanketing by neutral and ionized metals

09 p1757 A70-22728

Solar equatorial XUV limb brightening for resonance lines of Li-like ions from OSO-4 observations interpreted by coronal model

09 p1757 A70-22732

Ni L alpha X ray emission line shape and position as function of bombarding electron energy, observing differential self absorption in anode

09 p1731 A70-22777

Stark effect He II and H beta on lines observed for transverse and longitudinal fields, using beam-foil light source

09 p1731 A70-22779

Measured and theoretical Stark-broadened line profiles and asymptotic wing approximation of hydrogen Balmer lines at specific electron density and temperature

09 p1732 A70-22782

Doppler effect induced small spectral line shifts measured by modified duochromator in MPD arc jet

09 p1684 A70-23531

Optically variable compact galaxy with broad emission lines similar to Seyfert and N-type galaxies, noting no stellar contribution in continuous spectrum

09 p1765 A70-23808

Predawn enhancement morphology and variations of 6300 Å airglow, discussing solar declination and activity effect

10 p1873 A70-23831

Neutral atomic oxygen auroral and nebular emissions in twilight airglow, suggesting photodissociation of molecules by sunlight

10 p1873 A70-23832

Galactic sources H109 alpha line and continuum surveys, showing thermal continuum spectrum for sources with radio recombination lines

10 p1936 A70-23903

Line profiles and equivalent widths from Si II, Mg II, Ni II and Fe II spectra of shell star zeta Tauri

10 p1936 A70-23941

Auroral green line rocket measurements, showing roles of atomic and molecular oxygen dissociative recombinations

10 p1874 A70-24432

Spectral lines and radial velocities of paired galaxies, noting red shift difference between emission and absorption lines

10 p1946 A70-24978

Gadolinium II solar lines classification from photographic IR observations

10 p1947 A70-24990

Solar limb brightening of XUV lines of carbon, nitrogen, oxygen and silicon ions in chromospheric-coronal transition region

11 p2108 A70-25740

Electron and proton excitation of forbidden transition lines in Ca XV ground configuration determined for coronal densities and temperature

11 p2109 A70-25742

Energy dependence and threshold behavior of ion Ar lines excited in low-energy He ion-Ar collisions

11 p2087 A70-26402

Star 15 Vulpeculae metal lines analyzed by growth curve differential method

11 p2113 A70-26464

Solar photospheric turbulence from observing Ti I line profiles at different center to limb distances, showing anisotropy

11 p2116 A70-26591

Zeeman effect on solar flares metallic lines splitting

11 p2106 A70-26592

Neutral helium line profiles for line-blanketed model atmospheres grid

11 p2117 A70-26660

Nonthermal radiation effects on emission line spectra of Seyfert galaxies and quasars determined from ionization equilibrium of gas envelope

12 p2293 A70-27585

Molecular line identification in sunspot spectrum of CN, diatomic carbon, TiO, MgH, CaH, NiH and water vapor

12 p2302 A70-27590

Computer programs for calculating spectral lines oscillator strength in Coulomb approximation, proposing Fortran program

12 p2192 A70-27595

Solar IR triplet of singly ionized Ca, suggesting limb darkening caused by chromospheric inhomogeneities for source function inequality

12 p2303 A70-27703

Solar rotational line positions due to red band in IR continuum region to resolve blue-violet ambiguity

12 p2303 A70-27704

Magnetically sensitive Fe lines usefulness to solar polarimetry, observing absorption coefficient dependence on temperature variations

12 p2303 A70-27706

Coronal condensation spectra during 4 February 1962 total eclipse, determining abundances, ionization equilibria, electron densities, etc, from Fe and Ca XV lines analysis

12 p2303 A70-27712

Auroral green line decay of atomic oxygen measured photometrically from multiple exposure spectra of meteor wakes

12 p2304 A70-27713

Stellar atmosphere model for multilevel spectral line emission, assuming semiinfinite hydrogen atmosphere with sequence of plane parallel zones

12 p2306 A70-27856

Summertime midnight airglow enhancement of 6300 Å line by sensitive continuum compensating photometer, suggesting F 2 region electron density increase for emission

12 p2225 A70-27895

Energy levels of Th lines computed from weighted averages of interferometrically measured wavelengths data

12 p2277 A70-28119

Forbidden Ne iv lines intensity in high excitation gaseous nebulae based on upper level-j populations

12 p2277 A70-28215

CH molecule line formation mechanism for 4300 Å transition in solar photosphere, noting collisions with hydrogen atoms

12 p2311 A70-28309

Hanle effect in single mode He-Ne laser, observing spontaneous emission on different spectral lines and estimating lifetimes of Ne excited states

13 p2424 A70-28598

Solar iron-to-hydrogen ratio and oscillator strengths for Fe I lines compared with laboratory measurements of line broadening by neutral atoms

13 p2486 A70-28628

Planetary nebula NGC 7027, discussing hydrogen recombination lines

13 p2486 A70-28629

Spectroscopic parameters for attenuation and dispersion caused by 22 GHz water vapor line, using differential microwave refractometer

13 p2393 A70-28784

Stark-broadened neutral atomic line widths and shifts, determining electron densities from H beta profiles and pressure-temperature data

13 p2455 A70-29220

Rossland stellar opacity calculation allowing for photon absorption in spectral lines using non-relativistic dipole approximation

13 p2495 A70-29752

Solar spectral line source function frequency dependence

13 p2496 A70-29842

Photosphere model and magnetic field gradient effects on line contours and magnetographic calibration curves, using nonlinear source function

13 p2496 A70-29845

Forbidden lines of OI, NI, CI, Fe II, Ni II, Si I, Si and Ca II in solar absorption, investigating effects on element abundance and gaps in thermodynamic equilibrium

14 p2637 A70-30339

Atmospheric molecular oxygen photometric absorption spectral bands, calculating growth curves

14 p2572 A70-30403

Water vapor absorption bands in solar IR spectrum, considering earth curvature and atmospheric inhomogeneity and refraction

14 p2572 A70-30404

Arcturus atmosphere Mg abundances from rotational lines noting terrestrial proportions

14 p2637 A70-30540

Heterochromatic spectrophotometry, discussing maxima and integral techniques for line measurement, photoemulsion properties and Eberhard effect

14 p2585 A70-30784

Absorption spectrum of terrestrial atmosphere with sun as source, obtaining formaldehyde line with rotating grid spectrometer

14 p2579 A70-31256

Spectral line formation, assuming frequency redistribution for plane parallel stellar atmosphere containing nonuniform distribution of internal emission sources

14 p2651 A70-31289

Nitrogen K-L Auger spectrum high energy lines measurement by high resolution electron spectrometer

14 p2620 A70-31301

Ionized iron lines observations under coronal conditions, giving halfwidths and kinetic temperatures for forbidden lines Fe X-Fe XV

14 p2651 A70-31377

Temperature influence on luminosity centers and line darkening in synthetic ruby powder with chromium concentration

15 p2782 A70-31558

Rocket engine propellants flame temperature measurement by spectral line intensity comparison method

15 p2786 A70-32270

Solar disk 10830 Å He absorption line, attributing depression at blue wing to triplet

15 p2802 A70-32488

Line formation in solar magnetic fields with allowance for absorption emission and scattering processes, discussing Hanle effect and atomic level polarization

15 p2804 A70-32617

Book on stellar spectra theory covering line absorption coefficient expressions, radiative transfer, line source function, line broadening, etc

16 p2974 A70-33270

Doppler temperature and motion of solar corona from ionized Fe line using Fabry-Perot interferometer

16 p2977 A70-33841

Argon II line transition probabilities, observing UV spectral region, upper energy levels and temperature differences

16 p2956 A70-34251

Diatomic nitrogen ions branch overlapping, discussing rotational line structure in first negative system vibrational bands

16 p2956 A70-34254

Resonance and satellite lines of highly ionized iron in solar spectra, discussing spectrum features during chromospheric flares

17 p3154 A70-34541

Excitation cross sections for Ar I and He I spectral lines in low energy He ion-Ar collisions

17 p3138 A70-34642

Iron line emission at 1.9 Å during solar flares observed by OSO-4 proportional counter spectrometer

17 p3150 A70-34836

Nonhydrogen spectral lines in interstellar gas, discussing Ca/Na abundance anomaly

17 p3162 A70-34900

Optical study of Crab Nebula linear expansion and filamentary proper motions, considering line emission

17 p3164 A70-35113

Solar corona radiation at 1-100 Å for 1-10 million K, using Jordan ionization equilibrium calculations

17 p3151 A70-35582

Lithium-like line spectra in Mg, Al and Si observed with grazing incidence spectrometer and low inductance microfarad spark source

17 p3138 A70-35720

Fe II line behavior in plagues near solar limb

17 p3174 A70-35866

Regular and stochastic oscillations in plasma beam discharge produced by beam instability from observing time dependent variations in spectral line luminescence intensities

18 p3294 A70-36147

Orion nebula core radio recombination line intensities, showing variations in mean electron temperatures and physical conditions

18 p3313 A70-36329

Oxygen absorption coefficients at Lyman alpha line and other transmission windows, verifying dependence on pressure source line width and doublet separation

18 p3293 A70-36753

Solar Ga abundance from spectral synthesis of region around 4172 Å line

18 p3316 A70-36894

Radiative transfer equation for spectral line formed in multidimensional atmosphere, solving for two dimensional atmospheric model

18 p3317 A70-37008

Ba II emission lines in solar chromosphere, examining excitation and ionization equilibrium and resonance line intensities by eclipse observations

18 p3317 A70-37010

Interstellar hot low density intercloud medium in H I region, estimating diffuse emission in forbidden lines O I at 6300 Å and N I at 5200 Å

18 p3310 A70-37020

P Cygni line profiles emission and absorption components rectification procedure, considering errors

18 p3321 A70-37123

Galactic 21 cm line emission motion picture film, discussing contour maps on neutral hydrogen distribution

18 p3327 A70-37163

Raman line coherence degree and polarization rate measurement, applying Wolf matrix

19 p3443 A70-37359

Pulsar AP 2015 21cm line absorption profile, indicating uniform density and temperature neutral H model invalid

19 p3518 A70-38026

Radio polarization of quasars with and without absorption line spectra

19 p3523 A70-38605

Am and Ap stars metallic absorption lines, determining photometrical indices correction

19 p3523 A70-38689

Quasars PHL 5200 and RS 23 spectra absorption lines, examining resonance line transfer of radiation through differentially expanding atmosphere

20 p3701 A70-39006

Non-LTE line blanketed solar model atmospheres with various temperature distributions

20 p3703 A70-39020

Helium II line broadening in high temperature plasma, measuring profile for comparison with theoretical prediction

20 p3677 A70-39115

Transition probabilities of visible and near-IR neon lines, using gas-driven shock tube spectroscopy

20 p3674 A70-39134

Uranium ion impact ejection and electronic excitation of thin foil particles, observing optical spectra of Be, carbon and Al atoms and ions

20 p3674 A70-39135

Coronal data comparison based on 5303 Å line intensities and distribution with respect to position angles

20 p3704 A70-39461

Electric fields influence on emission lines shape of multiply charged ions in coronal plasma, discussing kinetic temperature

20 p3704 A70-39462

Spectral lines self rotation effects on plasma temperature and density measurement in MHD duct boundary layer

20 p3678 A70-39632

RF spectral recombination lines from atomic level transitions, discussing populations, H lines, electron temperature, density and emission and formation

20 p3706 A70-39934

Solar search for neutral rhenium lines using low noise, high resolution photometric tracings of Fraunhofer spectrum

20 p3711 A70-40406

Helium-like resonance, intercombination and forbidden transitions of Ca, Si and S lines during 3b solar flare decay

20 p3700 A70-40420

Lorentz lines radiative transfer in nonisothermal gases, developing Landenberg-Reiche analysis for isolated unshifted lines growth curves

21 p3852 A70-40590

Galactic K series emission at 1-10 keV by low energy cosmic rays and diffuse X rays interaction with H I region heavy ions

21 p3877 A70-40704

Tungsten-helium arc atmospheric contaminants spectral monitoring parameters under welding conditions, using rotating circular wedge to oscillate emission lines across exit slits

21 p3831 A70-40725

Hyades giant stars epsilon and gamma Tau strong line profile analysis, obtaining effective temperatures

21 p3885 A70-40931

Nova Vulpeculae 1968 Number 1 medium dispersion spectra, using radial velocity line identification and line profile reductions

21 p3889 A70-41152

Radiation line transfer in Wolf-Rayet envelopes with rapid radial expansion by escape probability method, including radiation effect from stellar core

21 p3892 A70-41248

Color-color diagram of M92, computing synthetic stellar spectra for line absorption effect

21 p3892 A70-41249

Autoionization spectral lines growth curves analysis, applying to 3s-4p transition in Ar at 466 Å with specified absorption cross section

21 p3781 A70-41931

Electronic transitions in B by beam foil technique for spectral lines in 450-5000 Å range, measuring excited levels mean lives

21 p3781 A70-41932

Laboratory measurement and low noise search in W3 OH/ for microwave emission lines in excited rotational level of interstellar OH

21 p3922 A70-41977

Rossland stellar opacity calculation allowing for photon absorption in spectral lines using non-relativistic dipole approximation

21 p3923 A70-42072

Solar equatorial limb brightening of far UV resonance lines of lithium-like N V, O VI, Ne VIII, Mg X and Si XIII ions, interpreting o-s-o data with coronal model

21 p3924 A70-42185

Constricted arc characteristics in air and nitrogen at various pressures, considering spectral lines radiation transfer and electron, atom and ion temperature difference effects

22 p4079 A70-42369

Beta CMa variable star HD 43818 spectral observations, discussing line profiles and radial velocities

22 p4100 A70-42853

Photospheric metallic line profiles numerical experiment, investigating physical processes causing shape and asymmetry change

22 p4101 A70-42866

Scorpius X-1 X ray line emission, discussing continuum and background counts and cosmic abundance of iron

22 p4094 A70-42931

Planetary nebula NGC 7027 IR line spectra emission, examining S IV and AR III line intensities

22 p4094 A70-42933

Stellar evolution, rotation and atmospheric motion, discussing gravity darkening, spectral lines, angular momentum, braking mechanisms and late stars

22 p4102 A70-42970

Forbidden iron emission lines excitation in Seyfert galaxies, discussing various mechanisms

22 p4102 A70-42977

Alpha hydrogen recombination lines 156, 166, 167 and 168 from galactic center, using radio telescope

22 p4103 A70-42980

Electron impact induced transitions in ions with configurations 3p/q responsible for forbidden lines in gaseous nebulae

22 p4105 A70-43234

Ionization rates in auroras detected by atomic oxygen and nitrogen lines

22 p4024 A70-43308

Spectrum generator with step recovery diode multiplier, discussing line spacing, energy and phase coherence

22 p3990 A70-43485

Auroral spectrophotometer measurements from 1968 NASA airborne expedition, discussing oxygen and nitrogen spectral lines

23 p4186 A70-43855

Solar disk 10830 Å He absorption line, attributing depression at blue wing to triplet

23 p4240 A70-43911

Venus carbon dioxide band, deriving rotational temperatures at various phase angles

23 p4241 A70-44257

Absorption line multiple scattering in thick planetary atmosphere, using successive scattering method for single-scattering phase function based on line profile and equivalent width

23 p4222 A70-44550

Stellar abundance determination, considering rapid uniform rotation effects on equivalent spectral line widths

23 p4250 A70-44811

Solar limb emission spectrum between 300-2803 Å, using Skylark rocket instrumentation

24 p4399 A70-45301

Solar center-limb observations of line brightness and Doppler shift fluctuations for Mg b lines

24 p4399 A70-45302

Li doublet in 21 March 1969 sunspot, examining fine structure caused by self reversal in line core

24 p4400 A70-45309

Solar spectrum O I, obtaining high resolution UV line profiles from rocket-borne spectrograms

24 p4410 A70-45766

G8, IV subdwarf 31 Aql spectrum at 4000-6600 Å, discussing Ba II 4554 Å, G and CN bands and spectral lines

24 p4414 A70-46329

LINEAR ACCELERATORS

Energy spectrum of electrons accelerated in linear plasma betatron close to potential compared to cyclic betatron results

13 p2463 A70-29379

LINEAR AMPLIFIERS

Traveling wave maser with increased linear gain obtained by slow wave structure through asymmetrical positioning of dielectric

06 p1082 A70-17778

LINEAR ARRAYS

NT ENDFIRE ARRAYS

NT YAGI ANTENNAS

Linear arrays computerized design with variable element spacing and excitation amplitude

02 p0269 A70-12596

Optimal linear antenna synthesis, determining current distribution resulting in specified radiation pattern for superdirective antennas

08 p1472 A70-20972

Thin linear antennas in plasma analyzed for radiation characteristics by linearized hydrodynamic theory, showing effect of feed points displacement

09 p1643 A70-22207

Linear antenna array synthesis by variational calculus, minimizing sidelobe level for fixed input powers and field strengths

09 p1644 A70-22404

Electromagnetic wave diffraction on array of plane waveguides, determining scattered field by solving infinite system of algebraic equations

09 p1632 A70-22407

Self focusing antennas directive gain losses reduction for wave with jagged phase front impinging on linear array having passed through inhomogeneous atmosphere

09 p1648 A70-23163

Antenna arrays elements mutual coupling effects on pattern and impedance characteristics

10 p1849 A70-24536

Optimum scattering from linear array of half-wave dipoles at bistatic angle, employing coupled impedance loading network

12 p2198 A70-27958

Superdirective small linear antennas computer aided design using Fourier integral and transform techniques

15 p2711 A70-32601

Optimal perturbation signal waveform linearizing nonlinear transfer characteristic of image sensing receptor array

15 p2705 A70-32725

HF electrical communication based on Kelvin transmission line and Maxwell field theories, noting linear arrays

16 p2860 A70-32951

Linear antennas theory using integral equations for current distributions

17 p3044 A70-35058

Linear phased antenna arrays, calculating influence of interaction between radiating elements on radiation pattern

17 p3048 A70-35686

Acoustic/microwave/ holography for large masses by crossed linear array of microphones, discussing computer simulation of virtual holograms and image reconstruction

21 p3822 A70-40715

Two identical parallel arbitrarily located thin asymmetrical dipole antennas, calculating self and mutual admittances

21 p3800 A70-41945

Linear phased arrays computer aided design, discussing search algorithms in multivariable optimization program

23 p4172 A70-44015

Skew arrays of coupled linear antennas, calculating planar and nonplanar configurations mutual admittance vs rotation angle between dipoles

23 p4166 A70-44969

LINEAR CIRCUITS

Automated modeling and structure optimization of linear dynamic systems and circuits, using hybrid computer techniques and time-domain test data

04 p0654 A70-15452

Linear circuit output waveform calculation without first resolving transfer functions on complex frequency plane, applied to current switching circuit analysis

06 p1018 A70-17460

Corrective open-loop circuit, using delay elements for compensation of transient response in linear circuits with lumped parameters for pulse modulation transmissions

06 p1023 A70-17774

Black box modeling of linear integrated circuits for computer analysis in frequency domain

06 p1026 A70-18416

- On-line computer programs allowing for man machine interactions in linear circuits design 06 p1015 A70-18417
- Linear control circuits transfer function analysis, revising Nyquist criterion 07 p1328 A70-20212
- Four-terminal p-n-p-n small signal semiconductor tetrode amplifier operation principle and linear circuit applications 19 p3390 A70-38305
- Linear IC for RF applications including multistage amplifiers, simulating by actual units 22 p3999 A70-42821
- LINEAR EQUATIONS**
- Solution existence of linear unsteady Boltzmann equation for single space variable in Hilbert space defined by scalar product 01 p0143 A70-10673
- Kharlamov conditions for existence of linear and quadratic invariant relationships between equations of motion of body about fixed point 01 p0145 A70-11435
- Observation process optimization in system described by linear differential equations of motion reducible to optimal control problem 01 p0047 A70-11574
- Linear theory of second grade elastic materials for small deformations, discussing special case of couple stress 02 p0387 A70-11995
- Riccati equation role in solving finite dimensional time invariant transport equations based on equivalent coupled linear equations 02 p0324 A70-12667
- Generalized multiple scales method for solving linear differential equations with variable coefficients applied to Liouville-Green approximation 03 p0518 A70-12994
- Linear regression equations to relate atmospheric precipitable water to surface dew point, sky cover and weather 03 p0520 A70-13163
- Optimal strategies for controlled plant guidance into convex space assuming linear differential equations of motion 03 p0459 A70-13339
- Linear functionals over Sobolev spaces and elliptical boundary value problems generated by theorems on homeomorphisms 03 p0519 A70-13505
- Linearized steady state hydrodynamic equations describing solar wind meridional motions used for studying zonal pressure perturbations 03 p0558 A70-13599
- Existence conditions of conjugate points for non-trivial solution of fourth order differential equation 03 p0519 A70-14079
- Distribution of zeros of solutions of canonical fourth order linear differential equations 04 p0713 A70-14675
- Computational methods of homogeneous ill-conditioned and singular simultaneous linear equations 04 p0714 A70-15096
- Least squares iterative method for solving simultaneous linear equations having singular coefficient matrix 04 p0714 A70-15450
- Solutions existence for differential, integral and integrodifferential equations proved by variational imbedding of nonlocal linear Euler-Lagrange operator functioning as automatic adjoint calculator 05 p0881 A70-16060
- Hori canonical equations solved by eliminating short period terms in general planetary theory, noting reduction to systems of linear differential equations 05 p0907 A70-16160
- Mathematical and numerical least squares solution of linear equations, using Householder algorithm [JPL-TR-32-1431] 05 p0876 A70-16311
- Ordinary linear differential equations of high order and normal form with integrable and bounded coefficients in real and complex planes 05 p0876 A70-16561
- Optimally ordered triangular factorization for solving symmetrical systems of linear matrix equations 05 p0876 A70-16573
- Randomly perturbed linear differential equation involving first derivative of n-vector function of real variable 05 p0878 A70-17096
- Right weak solution of Cauchy problem for first order quasi-linear equation 06 p1093 A70-17531
- Linear Boltzmann equation in bounded domain, studying solutions existence, uniqueness and structure 06 p1047 A70-18317
- Kinetic theory treatment of linearized Rayleigh problem using wall boundary condition models 06 p1049 A70-18329
- Optimal control for distributed parameter systems described by biharmonic linear partial differential equation using dynamic programming 07 p1244 A70-18843
- Optimal control of dynamical systems with transport lag determined using differential-integral equations 07 p1245 A70-19094
- Matrix graph concept to unify signal-flow, flow- and N-graph technique approaches to representation and evaluation of matrices and linear algebraic equations 07 p1238 A70-19676
- Error propagation in linear first order difference equations studied to improve accuracy of derivative recursive computation 07 p1328 A70-20249
- Linear differential controller equations for optimal automatic control system with disturbances 08 p1479 A70-20870
- Mixed problems with linear homogeneous boundary conditions with time-independent coefficients for semihyperbolic equations, discussing constraints 08 p1534 A70-21005
- Cauchy-Dirichlet problem for linear inhomogeneous polycaloric /polyparabolic/ equation with constant coefficients under certain boundary conditions 08 p1597 A70-21006
- Stability of solutions to linear differential equations pair, determining bound conditions having S-property 08 p1534 A70-21100
- Linear integral equations solutions using invariant functions 09 p1711 A70-22208
- Optimal control with time delays in system model described by constant coefficient linear differential-difference equations 09 p1653 A70-22346
- Asymptotic splitting of system of linear differential equations with slowly varying coefficients in cases with characteristic equation having multiple roots 09 p1712 A70-23119
- Solvability of linear problems with minimal smoothness constraints and of mixed problems for quasi-linear hyperbolic equations with coefficients and boundary conditions nonlinearities 09 p1712 A70-23120
- Rarefied gas flow past arbitrary three dimensional body using variational principles based on linearized BGK equation, considering constant and adiabatic wall temperature 09 p1605 A70-23178
- Ill conditioned linear two point boundary value problems solved by Riccati transformation avoiding forward integration 10 p1909 A70-24059
- Monte Carlo method research development concerning techniques for variance reduction, linear equations solutions and use of various random sequences 10 p1910 A70-24844
- Triangular system of linear differential equations reducible to block form by Liapunov transformation, deriving indices stability conditions 10 p1911 A70-25303
- Mixed boundary value problem for linear parabolic equations with discontinuous coefficients, proving solution existence and uniqueness by functional method 10 p1911 A70-25304
- Boundary value problem in parallelepiped constructed for linear partial differential equation with constant coefficients using expansions in Riesz bases 10 p1911 A70-25305
- One-step numerical integration of linear differential equations based on Labotto quadrature, including higher order applications and stability analysis 11 p2071 A70-25840
- Nonlinear dynamic theory describing elastic Cosserat curves plane motion, developing linear displacement equations and dynamic stability concept 11 p2142 A70-26632
- Dispersion relations for linearized Grad equations of three dimensional rarefied gas dynamics, including nonequilibrium pressure term for bulk viscosity 12 p2210 A70-27520
- Linear periodic coefficient differential equations stability analysis by infinite determinate method, considering applications to damped mechanical systems motion and dual spin satellite 12 p2261 A70-27813
- Variational principle in electromagnetics to produce linear algebraic equations with Rayleigh-Ritz procedure for application to dielectrically coated slot antenna 12 p2198 A70-27957
- Asymmetric missile nonlinear angular motion, describing quasi-linear relations for frequencies, damping rates and swerving motion amplitude [AIAA PAPER 70-534] 13 p2506 A70-29002
- Discretized linear theory of arbitrary shell forms 13 p2513 A70-29151
- Periodic solutions to linear differential equations with delay, applying numerical-analytical procedure 13 p2441 A70-29315
- Isothermal quasi-linear theory of viscoelastic isotropic continuum, considering constitutive equations 13 p2516 A70-29534
- Variational principles of linear asymmetric elasticity for dynamic problems with initial and boundary conditions, using Laplace transforms 13 p2517 A70-29724
- Computer techniques for rounding error analysis, stability in linear algebra, matrices factorization, Jacobi rotation method and iteration procedures 13 p2443 A70-29768
- Riccati-like linear functional differential equation with quadratic cost, analyzing feedback control solution existence and uniqueness 14 p2600 A70-31204
- Shock and simple wave interactions, using quasi-linear equations for forward facing wave overtaking forward facing shock 14 p2567 A70-31283
- Linear integral equations for radiative transfer between parallel plates, using least squares method 15 p2826 A70-31822
- Unique solvability of mixed semihyperbolic linear equations of higher order with respect to spatial variables and time 15 p2768 A70-32475
- Solutions behavior of nonlinear system of linear Volterra integral equations, discussing applicability of standard fixed point theorems 16 p2943 A70-34000
- Stochastic approximation for identification of distributed parameter system solutions described by linear partial differential equations 17 p1311 A70-35557
- Power series solutions to linear and nonlinear differential equations in region of asymptotic stability 18 p3279 A70-36155
- Plane electromagnetic waves diffraction by periodic structure of infinite system of parallel strips, reducing problem to solution of linear algebraic equations 18 p3227 A70-36287
- Linear differential equation integration method, using Eulerian technique for error reduction 18 p3282 A70-36358
- Boundary value problem approximation method for large numbers, using projective method applicable to linear integral, integrodifferential and differential equations 18 p3282 A70-36360
- Nonrigorous hyperbolic systems, discussing existence and uniqueness theorems contradiction in linear equations and proof of Cauchy problem 19 p3478 A70-37582
- Linear partial differential equations solvability, deriving necessary conditions for pseudo differential operator 19 p3457 A70-37677
- Uniform asymptotic solutions of second order linear differential equations with arbitrarily many turning points or Stokes lines 19 p3457 A70-37681
- Sufficient conditions for local solvability of linear partial differential equations with operator on complex functions 19 p3457 A70-37682
- Linear equations for wave diffraction in rectangular waveguides with step-shaped inhomogeneities 19 p3378 A70-37730
- Nonlinear integral equations formal solution method, noting relationship to Fredholm solutions of linear integral equations 19 p3458 A70-38063
- Linear homogeneous differential equations nonautonomous systems integration techniques, deriving finite forms of solutions 19 p3460 A70-38938
- Boundary value problems for linear ordinary differential equations with singularities, determining eigenvalues by computer oriented method 20 p3659 A70-40134
- Multidimensional linear differential equations with periodic coefficients, proving analog of Floquet-Liapunov theorem 20 p3659 A70-40170
- Dispersion relations for linearized Grad equations of three dimensional rarefied gas dynamics, including nonequilibrium pressure term for bulk viscosity 21 p3807 A70-41168
- Linear differential equation solution associated with FM signal generation, presenting analytical methods for FM and AM components 22 p4063 A70-43209
- Matrix transformations and minimization of computation algorithms for arbitrary linear equations systems, using direct methods 22 p4063 A70-43479
- Minimal deviation estimates for linear approximations by seminorms for space defined by differential equations 23 p4210 A70-44018
- Non-Chebyshevian moments induced by system of linearly independent functions expanding to seminfinite programs 23 p4211 A70-44243
- Linear algebraic system stability and monotony, investigating plane structures by finite element method 23 p4213 A70-44996

German monograph on Hamilton principle and Hermetian polynomials for solving linear and nonlinear differential equations via computer method
24 p4369 A70-45091

Linear elasticity with constraint couples, establishing existence theorems by variational methods
24 p4420 A70-45267

Algorithm for Chebyshev solution of $n+1$ inconsistent linear equations in n unknowns, using minimax technique
24 p4370 A70-46241

LINEAR FILTERS

Bias-free estimation of linear process in recursive filtering, avoiding numerical inaccuracies introduced by computations with vectors and matrices
02 p0273 A70-12730

Sensitivity analysis of discrete filtering and smoothing algorithms, noting in-track motion of circular orbit satellite and marine inertial navigation [AIAA PAPER 68-824]
03 p0459 A70-12913

Phase lock loop circuit for spacecraft communication noise filtration, describing linear study of first-four-order loops
03 p0448 A70-13537

Differential equations for minimum variance linear filter separating signals from additive correlated noise, using discrete time optimum formulas [AIAA PAPER 69-73]
04 p0663 A70-15586

Sequential filter equations for nonlinear system dynamics and observational model with linear estimator, comparing difference between white and colored noise filter results
11 p2024 A70-26126

Kalman-Bucy filtering for estimating initial conditions and smoothing problems in linear dynamic systems, applicable to rectilinear motion of randomly accelerated spacecraft
12 p2186 A70-27905

Book on stochastic processes and filtering theory covering probability theory, Markov processes, linear and nonlinear filters, etc
13 p2442 A70-29575

Adaptive Kalman filtering with unknown process and measurement noise covariance matrices
16 p2880 A70-32983

Optimal linear filter analysis from singular optimal control viewpoint, considering white and correlated measurement noise
16 p2885 A70-33320

Linear sequential Kalman filter for time correlated noise without state augmenting and measurement differencing demanding less computer sizing
16 p2887 A70-33350

Electron spin-echo device as programmable linear matched filter for PN modulated carrier waveforms detection
16 p2864 A70-33480

Optimal Kalman tracking filter performance estimation for manned maneuvering targets
16 p2949 A70-34057

Digital simulation of linear filter, investigating noise and rounding errors effects on decoding signals from lunar and interplanetary probes
17 p3049 A70-34612

Implementation delay error reduction in discrete Kalman filter, noting application to inertial navigation systems analysis
18 p3236 A70-36712

Linear stochastic continuous feedback system with white noise and control input, investigating combined problem of filtering and optimal control
19 p3393 A70-37850

Optimal synthesis of linear active RC filters with controlled source, using feedforward and feedback weighted signals
20 p3596 A70-39163

Real time kalman filtering of Apollo LM/AGS rendezvous radar data [AIAA PAPER 70-957]
20 p3600 A70-39572

Discrete Kalman-Bucy linear filtering with inaccurate noise covariances, considering optimal and sub-optimal systems, error analysis, probability theory, etc [AIAA PAPER 70-955]
20 p3601 A70-39573

Kalman filter sizing for air-launched tactical missile via covariance sensitivity matrix [AIAA PAPER 70-954]
20 p3601 A70-39574

General linear/Kalman/sequential filter to account for finite correlated white noise without state vector augmentation or measurement differentiation
21 p3828 A70-41735

Quasi-linearization relationship with Kalman filtering for nonlinear systems parameter estimation in process noise absence
21 p3845 A70-41749

Transfer function optimization for linear follow-up frequency filter with controlled resonance, analyzing noise band performance
22 p3985 A70-42402

Kalman filters for data mixing in optimally aided inertial navigation systems
22 p4067 A70-42661

Linear FM radar pulse compression matched filter response calculated by computer evaluation of cross

ambiguity function for design tradeoff between resolution and performance
22 p3992 A70-43589

Suboptimum filter for trajectory estimation from parameters, using modified covariance with least squares formulation in Kalman setting
23 p4177 A70-44601

State-space method of parameter tracking for adaptive control, using Riccati equation and Kalman filtering
23 p4177 A70-44675

LINEAR PREDICTION

Linear statistical forecast accuracy and optimal predictor dimensionality based on multiple regression equation
04 p0715 A70-15251

Adaptive linear estimator for stationary time series, evaluating asymptotic mean square error bound
17 p3128 A70-34852

Nonstationary inhomogeneous random vector fields linear prediction, determining minimum mean square approximation error
20 p3604 A70-39911

Iterative linear prediction method for stochastic process with zero mean value and known covariance function
23 p4211 A70-44026

LINEAR PROGRAMMING

Algorithm for L-shaped linear programs in optimal control problems and stochastic programming, outlining cutting hyperplane
01 p0047 A70-11069

Differential correction procedures, using residuals to obtain celestial body orbital elements by linear programming
04 p0751 A70-14943

Finite element discretization and linear programming methods for shakedown theory in perfect elastoplasticity with associated and nonassociated flow laws
05 p0925 A70-15873

Linear and quadratic programming techniques for large scale continuous time optimal control problems with accurate switching times
07 p1325 A70-19268

Duality theorem for complex quadratic programming over polyhedral cones
07 p1238 A70-19356

Stochastic programming models for flight scheduling within airlift system accounting for cargo uncertainties, using convex programming, linear programming codes, etc
08 p1600 A70-20605

Linear programming for aircraft takeoff and landing schedules for traffic control on airport runway, using simplex technique for proposed algorithm
08 p1540 A70-20872

Narrow throat problems of linear dynamic programming concerning maximum linear functional determination in set of vector functions, giving algorithm for solution
10 p1855 A70-24393

Equivalent linear programming in integer variables to solve production scheduling for N identical machines, minimizing changeover and inventory costs
10 p1895 A70-24662

Penalty function algorithm for linear/nonlinear programming optimization problems subject to equality/inequality constraints, discussing feasibility determination capability
13 p2373 A70-29462

Quasi-linear elliptic boundary value problem approximate solution and error bounds, considering linear programming for computation
14 p2599 A70-30646

Soviet book on numerical methods of Chebyshev approximation covering minimax problems, computer methods, linear programming, etc
19 p3456 A70-37232

Two stage turbine engine parts adjustment optimization in terms of fuel consumption or thrust control by linear programming techniques
19 p3489 A70-37241

Fuel optimal orbital transfer trajectories by linear programming
20 p3711 A70-40337

Book on theory of optimal control and mathematical programming covering linear, nonlinear, quadratic programmings, etc
21 p3845 A70-40891

Discrete decision variable models formulated as linear integer programs, deriving shrinking boundary algorithm for optimization
22 p3994 A70-43497

Radio electronic circuits precision, deriving relationship between frequency response and component variations solvable by linear programming
23 p4171 A70-43958

Linear programming problems in optimal control numerical analysis, discussing iterative solution
23 p4177 A70-44303

LINEAR SYSTEMS

Equivalent linear dynamic systems obtained by analog computers for determining equivalence equa-

tions coefficients and by Chebyshev functional to assess discrepancy
01 p0052 A70-10193

Finite difference scheme for linear second order third boundary value problem in ordinary differential equations
01 p0131 A70-10455

Linear physical chains with Sturm-Liouville characteristic polynomials used for natural frequency determination of coupled harmonic oscillators or electrical analog
01 p0142 A70-10520

Terminal state control systems efficiency from determining permissible range of control parameter variation for steady and unsteady linear dynamic systems
01 p0052 A70-10982

Cauchy problem solution asymptotic behavior for linearized system of rotating compressible fluid at time approaching infinity
01 p0064 A70-11031

Mappings of linear vector spaces induced by transformation matrix applied to linear dynamical systems
01 p0132 A70-11125

Random vibration of interconnected systems, analyzing power flow and energy levels in linear oscillator interacting with environments, using Thevenin-Norton representations
01 p0207 A70-11161

Linear system response to random signal inputs, deriving SNR and noise figure equations using autocorrelation and spectral analysis concepts
02 p0257 A70-12193

Optimal linear controller synthesis with allowance for continuous perturbations effect, describing weighting factors selection
02 p0272 A70-12413

Analytical design of optimum linear multivariable control systems with randomly sampled stationary random signals, evaluating matrix complex convolution integral using Laplace transforms
02 p0272 A70-12610

Singular perturbation problem solution asymptotic expansions applied to linearized theory of elasticity equilibrium problem with stress couples
02 p0389 A70-12685

Randomly sampled linear systems stability with linear or nonlinear feedback loops, using stochastic Liapunov function method
02 p0272 A70-12727

Optimal use of adaptive renewal capability determined for first order time varying linear systems with quadratic performance index by exponential model of component failure
02 p0273 A70-12729

Algorithm for fixed time minimum energy discrete optimal control problems of linear plants with convex constraints imposed on terminal state
02 p0273 A70-12731

Optimal servocontrol via nonquadratic performance index and linear plant dynamics obtainable as nonlinear function of error between controllable states and input vector
02 p0273 A70-12732

Mixed anisotropic linear elastic solids stability with internal friction due to mechanical interaction, considering asymptotic motion stability
03 p0586 A70-13116

Detection efficiency compared for system containing clipper circuit and quasi-optimal linear system for video pulse signal with additive noise background
03 p0446 A70-13201

Control problem of linear system with phase coordinate constraints, discussing solution properties, boundary conditions and function minimization procedure
03 p0460 A70-13340

Unsteady linear automatic control systems transient functions determined by approximation method
03 p0460 A70-13732

Linear separation systems for aerospace applications covering mild detonating fuse and cord flexible linear shaped charge, SUPER ZIP concepts, etc
03 p0546 A70-14103

Structure theorem for time invariant multivariable linear systems proof and formulation for use in controller design and synthesis
03 p0461 A70-14166

Linear system theory in abstract algebraic framework applied to nonlinear machines in automata theory, discussing Ho algorithm, convolution and Kalman module theory
03 p0520 A70-14273

Dual type method solving discrete optimal control problems with linear plants, convex cost and constraint taking into account dynamic structure
03 p0461 A70-14274

Optimal control of multidimensional distributed parameters plants described by linear or nonlinear partial differential equations, considering boundary conditions
04 p0660 A70-14551

Topological analysis of lumped mechanical vibration systems using mathematical induction, considering linear graphs properties

04 p0773 A70-15077

Coefficient matrix-structural method for obtaining transfer function of linear automatic control systems

04 p0662 A70-15277

Automated modeling and structure optimization of linear dynamic systems and circuits, using hybrid computer techniques and time-domain test data

04 p0654 A70-15452

Linear regulator optimal for exponentially time-weighted quadratic performance indices, using cost equivalence concept in infinite terminal time solution

04 p0663 A70-15604

Periodic vibrations of quasi-linear autonomous systems with retardation, deriving sufficient conditions for asymptotic stability

05 p0925 A70-15822

State variable diagram for transfer function of single output/input linear stationary system obtained by parallel, direct and iterative methods

05 p0928 A70-16027

Averaging analysis of oscillations attenuation of relaxing one dimensional linear viscoelastic systems under external force at resonance applied to nonlinear multidimensional systems

05 p0933 A70-16208

Random vibrations of linear system with viscous damping excited by stochastically acting force with monotonically varying frequency, using correlation method

05 p0882 A70-16372

Dynamic strength calculation for linear viscoelastic body and elastic-viscous liquid with retardation and relaxation times spectra respectively

05 p0940 A70-16511

Stochastic differential games with constrained state estimators, involving linear system, quadratic cost functional and white Gaussian noises corrupting output measurements

06 p1024 A70-17954

Adaptive control algorithm for parameter adjustment of unknown dynamic characteristics of linear systems

06 p1025 A70-17956

Optimal control generated by Kalman filter and least mean-squared predictor for linear systems with time delay

06 p1025 A70-17959

Optimal feedback controls design for linear systems relative to time-multiplied performance indices

06 p1025 A70-17960

Separation theorem for nonlinear measurements, discrete-time linear systems and quadratic cost to achieve stochastic control without dynamic programming

06 p1026 A70-17967

Linear optimal stochastic control systems described by covariance matrix correlating errors and estimates of state variables, analyzing instability under parameter variations

[AIAA PAPER 70-36] 06 p1095 A70-18054

Identification algorithm for estimating parameters in constant coefficient linear system independent of prior estimates

[AIAA PAPER 70-34] 06 p1015 A70-18164

Hybrid NASAP program module for direct design of linear dynamic circuits using simple optimization without sophisticated computer programming

06 p1015 A70-18422

Loops and paths in Mason signal flow graph of linear systems using algorithm with remote time shared digital computation

07 p1238 A70-18842

Monograph on functional analysis and time optimal control as application of mathematics

07 p1322 A70-18857

Multivariate linear model and robust estimators of parameters based on rank tests

07 p1323 A70-19027

Suboptimal computational algorithm for terminal control of random linear dynamical system, noting increasing optimality with random variations degeneration to deterministic quantities

07 p1324 A70-19091

Optimal control of linear distributed parameter systems using functional analysis

07 p1245 A70-19096

Control system composed of linear and nonlinear components and distributed parameters, deriving stability criterion for simple crucial case

07 p1246 A70-19539

Digital cross correlator design for impulse response determination in linear systems, noting real time operation without software and storage problems

07 p1236 A70-20068

Motion of second order autonomous quasi-linear system with disturbances, obtaining criterion for recognition of random forced and self oscillations

07 p1247 A70-20180

Quasi-stable linear differential equations systems with nearly periodic coefficients, noting application to

equations with zero real portions of matrix characteristic roots

08 p1533 A70-20492

Optimal feedback control synthesis for linear system with time delay through error criterion minimization

08 p1478 A70-20780

Optimal linear control system with multiple controls, determining stability margins with respect to phase, amplitude, oscillation index and cut-off frequency

08 p1480 A70-21015

Optimal synthesis of linear steady multidimensional systems with common output ensuring minimum rms error in reproducing control action

08 p1480 A70-21497

Existence theorem for linear stochastic systems optimal control described by differential equation with random coefficients, providing rms stabilization

08 p1480 A70-21637

Consistent and inconsistent linear inequalities evaluating speed and efficiency of algorithm for pattern recognition problems

08 p1467 A70-21782

Linear one degree of freedom mechanical system loaded by time dependent force with constraints on loading/unloading rate, studying minimum of dynamic coefficient

09 p1727 A70-22536

Linear high order aircraft and missile control systems design using Horowitz frequency response method

09 p1654 A70-22835

Root-locus approximation technique extended for complex plane analysis of equations with quadratic term in variable parameter for linear multivariable feedback systems

10 p1855 A70-24449

Linear control systems design with restricted number of feedbacks based on optimization criteria concerning responses to initial disturbance

10 p1855 A70-24703

Linear time-varying systems transient responses prediction, using Krylov-Bogoliubov method and parameter plane analysis

10 p1855 A70-24704

Equations of motion, modal vectors and natural frequencies of n-degree of freedom structurally damped linear system determined directly from test data

10 p1961 A70-25058

Undamped natural modes intercoupling resulting from arbitrary linear damping addition to linear dynamic system

10 p1962 A70-25061

Final state vector norm minimizing in linear optimal control, using successive approximation and quadratic programming

10 p1856 A70-25188

Scalar measure of system sensitivity to plant parameter variations applied to design of linear lumped stationary multivariable feedback control systems

10 p1856 A70-25233

Optimal stochastic control investigated for linear systems with driving noise intensity proportional to control input

10 p1856 A70-25234

Optimal feedback control obtained for linear time-varying system with time delay, developing numerical method for solving performance differential equations

10 p1856 A70-25235

Necessary and sufficient conditions for absolute stability of nonstationary nonlinear system, showing equivalency to asymptotic instability in small position equilibrium piecewise linear systems

11 p2021 A70-25337

Linear steady and unsteady systems time optimal control switching points determination by introducing parameterization to reduce number of transcendental equations

11 p2021 A70-25339

Digital simulation of complex dynamic systems using homing missile as example, basing algorithm on l transforms for linear systems

11 p2013 A70-25692

Control theory, Volume 1, covering linear, nonlinear, stochastic, optimal, adaptive and learning systems, sensitivity analysis, etc

11 p2023 A70-25771

Decoupling and pole assignments in linear multivariable control systems using geometric method

11 p2072 A70-26160

Time-invariant linear dynamical systems transfer equivalence leading to algorithm for minimal realizations of transfer function matrices

11 p2072 A70-26161

Linear systems optimal control problems with sensitivity considerations for restriction to linear feedback of output variables

11 p2026 A70-26235

Linear time-varying control process with bounded control amplitudes and rates, deriving conditions for recoverability

11 p2028 A70-26314

Linear networks fault detection and isolation using computerized test procedure and symbolic transfer function generation technique

11 p2029 A70-26337

Invariance conditions and state transition matrix of linear systems

11 p2074 A70-26400

Multidegree of freedom linear vibrating system analysis by dividing differential equation method

11 p2139 A70-26414

Maxima increases without limit in damped linear oscillator response to random wideband excitation interpreted by heuristic explanation

11 p2085 A70-26694

Subdivisional method for linear systems vibration and buckling problems, reducing governing equation to ordinary differential equation with variable coefficients

12 p2320 A70-27145

Computational methods for multiinput linear control systems applied to designing lateral and longitudinal autopilots for jet transports subject to gust loads

12 p2203 A70-27417

Iterative algorithm for synthesis of discrete minimum time and amplitude controls for linear systems, noting guaranteed convergence

12 p2204 A70-27667

Linear time dependent stochastic optimal control with nonquadratic performance indices using function space approach

12 p2204 A70-27668

Book on three dimensional problems of linear elasticity of homogeneous and isotropic solids, discussing prismatic bodies, bodies of revolution, notch effect, etc

12 p2326 A70-27669

Optimal linear band limited time invariant data transmission systems, discussing pulse interference tolerance based on eye parameters as quality criteria

12 p2185 A70-27688

Kalman-Bucy filtering for estimating initial conditions and smoothing problems in linear dynamic systems, applicable to rectilinear motion of randomly accelerated spacecraft

12 p2186 A70-27905

Minimax one step and recursive nonlinear predictors for linear discrete time-invariant first order plant driven by unknown bounded forcing function

12 p2204 A70-28069

Space navigation procedures verification considering vehicle trajectory parameters, noting applicability to linear systems with estimable parameters

13 p2447 A70-28412

Soviet book on theory of oscillations of linear and nonlinear time lag systems

13 p2450 A70-28699

Dynamic linear system simplification and order reduction, showing utilization precautions and validity

13 p2381 A70-28938

Book on linear time varying systems analysis and synthesis covering multivariable systems, operational algebra, controllability, observability, canonical structures, minimal realization, etc

13 p2381 A70-28975

State estimation in linear discrete time systems operating in Markov dependent switching environments, using Bayes theorem for filtering

13 p2381 A70-29062

Gain of optimal filter and predictor, using recursive estimation in discrete linear systems

13 p2381 A70-29063

Optimal constant output feedback gains for linear multivariable systems, noting control vector as time invariant function of output vector

13 p2382 A70-29064

Random reversible failures effect on linear automatic control systems precision treated as randomly varying structure, proposing statistical characteristics calculation

13 p2382 A70-29279

Gradient algorithm for sequential identification of features in dynamic linear systems

13 p2383 A70-29582

Linear distributed system with periodic parameters spectral characteristics based on multidimensional Fourier transforms with drift

13 p2383 A70-29718

Optimal policy for linearly distributed parameter control system, describing sufficient conditions

13 p2384 A70-29899

Discrete time systems, deriving algorithm for testing decomposition property as necessary condition for linearity

13 p2375 A70-29939

Linear control systems identification and synthesis from data containing modulus and phase information as frequency functions

14 p2559 A70-30520

SCAMP I DC statistical circuit analysis program for linear and nonlinear circuits, describing program structure

14 p2560 A70-30664

Dynamical optimal control for infinite dimensional linear systems, examining Balakrishnan solution technique

14 p2562 A70-31201

Recoverability for amplitude and rate bounded optimal control of linear time varying systems

14 p2562 A70-31203

Dynamical systems optimal control approximation without solving differential equations, considering linear systems with quadratic cost functional

14 p2562 A70-31411

Automatic optimal discrete time control for linear distributed parameter systems with quadratic cost function

14 p2562 A70-31412

Soviet book on mathematical theory of linear and nonlinear control systems covering differential and difference equations, calculus variations, etc

15 p2715 A70-32200

Multidimensional linear stationary systems controllability and observability with given transfer matrix

15 p2716 A70-32345

Linear stationary systems observability with stochastic inputs for linearly independent row vectors, determining state vector components mean values

15 p2716 A70-32346

Homomorphic filters, discussing nonlinear filters for generalized linear system

15 p2710 A70-32580

Minimal time closed loop controller design for linear systems with bounded control amplitudes and rates using approximate functional expression

16 p2880 A70-32984

Pursuit-evasion differential games involving two linear dynamic systems with state and control dependent thermal noise

16 p2881 A70-32985

Nonlinear systems stabilization with linear system estimator output state to provide feedback for asymptotic stability of overall system

16 p2881 A70-33033

Stable adaptive control design for linear time-invariant system with same number of inputs as outputs, considering disturbance effect

16 p2881 A70-33035

Control strategy for linear system performance based on synthesis of optimal closed loop controller with both sensitivity and state feedback

16 p2882 A70-33042

Time optimal control for linear distributed parameter system using functional analysis with method of deepest descent

16 p2882 A70-33122

Algorithm for implementing learning controller based on subgoal concept applicable to linear stationary system

16 p2868 A70-33312

Desensitized linear servo model following feedback control systems design using specific optimal control concepts

16 p2884 A70-33315

Linear multivariable feedback control systems design method based on transfer matrix, testing decoupling desirability

16 p2884 A70-33318

Suboptimal nonlinear feedback control synthesis for linear time-invariant system with convex cost functional

16 p2886 A70-33334

Linear continuous vibratory system unknown parameters identification from frequency response data

16 p2988 A70-33337

Linear systems approximate minimum energy controller, suggesting algorithm for mathematical model evaluation

16 p2886 A70-33344

Linear systems simultaneous optimal stochastic control and observation strategies, assuming quadratic observation cost

16 p2886 A70-33346

Linear distributed dynamic system simulation using infinite product expansions for transcendental terms in transfer functions

16 p2942 A70-33348

Quasi-linear hyperbolic systems interactions for rarefaction waves, applying Glimm difference method

16 p2943 A70-33782

Linear second order equation systems decoupling transformation, noting applications to structural feedback, flutter and control systems

16 p2943 A70-33891

Linear dynamic systems under nonconservative and harmonic forces, examining stability conditions

16 p2952 A70-33896

Potential stability theory for linear and nonlinear systems trajectory

16 p2943 A70-34042

Free and forced vibrations of linear systems, dissipative systems with nonlinear friction, aeroelastic vibrations, rotor vibrations, mode locking, random vibrations, etc

16 p3004 A70-34277

Linear system under ergodic random processes, determining optimal dynamic characteristics by approximation of spectral density by Laguerre series

16 p2944 A70-34280

Linear and nonlinear systems natural frequency and stability determination, using theorems for degenerate systems

16 p2944 A70-34284

Linear systems with two degrees of freedom modeled as rigid beam on elastic supports, considering vibration damping

16 p2996 A70-34291

Dynamics of continuously operating linear servosystems stimulated by stochastic signals, using vectorial equation and impulse response matrix

16 p2944 A70-34295

Liapunov functions synthesis for aperiodic linear systems by inspecting traces of state matrix and products

17 p3129 A70-34955

Equilibria stability of linear discrete dynamic systems involving elastic, nonconservative, dissipative and gyroscopic forces, using Liapunov-type energy method

17 p3129 A70-34958

Sufficient condition for asymptotic stability of ergodic coefficient linear stochastic systems

17 p3129 A70-34982

Parameter variation effects on iterative identification of linear system by learning method

17 p3130 A70-35299

Second order incompressible elastic torsion problems reduction to two dimensional classical linear elasticity problem without body force

17 p3189 A70-35434

Linear time invariant plant driven by scalar control, deriving second variation algorithm for minimum fuel problems

17 p3057 A70-35555

Identification-adaptive control algorithm for quadratic cost control of discrete linear systems

17 p3057 A70-35558

Thin elastic shells linear theory, examining three dimensional stress distribution and displacement field

17 p3191 A70-35608

Existence and uniqueness of optimal control for one dimensional linear system with distributed control parameter using input-output integral with quadratic functional

17 p3057 A70-35627

Parametric functions of integral matrices representing linear differential system via continuous coefficients

18 p3279 A70-36156

Graphical stability for linear systems in parameter plane with time delay

18 p3235 A70-36479

Linear control systems stability range with delay time examined by digital computer, discussing critical loop gain

18 p3235 A70-36501

Discrete automatic control theories, including linear, nonlinear, feedback, optimal and adaptive systems and bibliographies

18 p3235 A70-36626

Linear continuous feedback control system with dead time compensated by proportional plus integral controller, considering stability region variations

18 p3236 A70-36943

Linear feedback control system with dead time compensated by proportional integral derivative action controller, evaluating stability by digital computer

18 p3236 A70-36944

Spiral structure gravitational theory, discussing separation between linear and nonlinear effects

18 p3330 A70-37189

Soviet book on vibrations in flight vehicle engines covering linear and nonlinear systems, computer methods, etc

18 p3305 A70-37229

Algorithm for dynamic processes in unsteady linear automatic control system during finite time interval

19 p3470 A70-37256

Soviet book on statistical calculation methods for linear and nonlinear automatic aircraft control systems design, using correlation theory of stochastic processes

19 p3463 A70-37403

Linear stochastic continuous feedback system with white noise and control input, investigating combined problem of filtering and optimal control

19 p3393 A70-37850

Linear time varying systems optimal control through decoupling of boundary value problems

19 p3393 A70-37866

Simultaneous generation of sensitivity functions for linear automatic control system with known characteristic differential equation

19 p3394 A70-37867

Random vibration first threshold crossing probability density function for linear oscillator

19 p3427 A70-38038

Optimal control of processes with lags, including linear analytical regulator problem

19 p3395 A70-38718

Kalman filter set for state vector and observation error variance estimation in discrete time linear system, using empirical Bayes techniques

[AIAA PAPER 70-1058] 19 p3395 A70-38873

Dirichlet problem for elliptic linear system of partial differential equations with constant first order coefficients

20 p3657 A70-39120

Book on optimal control covering optimization, estimation, dynamic and linear control systems, programming, probability and random processes, environmental influence, etc

20 p3600 A70-39124

Variational principles in linear quasi-static theory of inhomogeneous and isotropic viscoelastic solids with microstructure

20 p3718 A70-39229

Anisotropic elastic solids linear dynamic theory, discussing uniqueness theorem, reciprocal identity and far elastodynamic field quiescence

20 p3718 A70-39231

Linear time-invariant system dependent on small parameter epsilon, deriving conditions for bounded-input bounded-state stability

20 p3657 A70-39395

Thor launch vehicles steering filters design using automated method of optimizing large order linear stochastic systems control

20 p3600 A70-39543

Sensitivity optimization for linear optimal control systems design, describing aircraft lateral-directional control case study

20 p3600 A70-39567

Recursive formulas for stability tests and quadratic loss functions evaluation for linear discrete time dynamical systems

20 p3659 A70-40114

Linear feedback control system with quadratic penalty function, deriving lower bound on optimal performance for suboptimality evaluation

20 p3604 A70-40116

Linear multivariable feedback control system, deriving conditions for existence of triangular decoupling transfer function matrices

20 p3605 A70-40118

Optimal terminal control stochastic synthesis for linear systems by Bellman second order nonlinear partial differential equation

21 p3801 A70-40607

Identification adaptive quadratic cost linear system control by mean and covariance correction algorithm

21 p3801 A70-40741

First order linear distributed systems with two point boundary values, obtaining eigenfunction expansion by generalized Fourier method

21 p3846 A70-41949

Structures of linear field theories concerning constitutive equations and operators dual relationship

21 p3851 A70-42098

Noise effect on signal parameter control in linear measurement devices

22 p3984 A70-42394

Dynamical linear thermoelasticity theorem generalization with time dependent conductivities, elasticities and density

22 p4112 A70-42483

Linear dynamic systems stability under various types of forces

22 p4061 A70-42536

Linear elasticity problem approximation by elastic energy expression modification, deriving upper bounds for errors

22 p4113 A70-42537

Linear discrete feedback systems uniqueness, existence and stability under various input-output conditions

22 p4004 A70-43024

Linear distributed parameter systems state estimation from noisy measurements, developing sequential algorithms for prediction, filtering and smoothing

22 p4063 A70-43026

Linear elastomechanical systems natural vibration parameters by harmonic excitation method

22 p4116 A70-43200

Linear control plant identification by solving integral equation obtained from input and output signals

22 p4005 A70-43565

Linear systems with phase coordinates bounded by given time functions, obtaining optimal control by iterative solution involving Lagrange multipliers

23 p4177 A70-44302

Decoupling and pole assignment in linear multivariable control systems, minimizing dynamic compensation

23 p4213 A70-44904

Nonlinear filtering for linear parabolic distributed parameter systems with white noise, considering stochastic boundary value problem

23 p4177 A70-44905

Lightly damped second order linear system mean square response to nonstationary random load excitation

24 p4421 A70-45280

Harmonic oscillations recurrence in linear systems with lumped and distributed parameters, obtaining amplitudes by least squares estimator

24 p4379 A70-45483

Maximum-likelihood decoding in analog form of linear convolutional codes with respect to constraint length by one-step threshold method
24 p4313 A70-46059

Cyclic q-ary codes invariant under linear group substitutions using polynomial method
24 p4313 A70-46062

Necessary and sufficient conditions on coefficients of real nonnegative polynomial π/ω , obtaining algebraic criterion for stability, optimality and passivity of dynamic linear systems
24 p4322 A70-46156

Linear stationary systems rms stability under parametric disturbances by white noise random processes
24 p4427 A70-46379

LINEAR TRANSFORMATIONS

Linear transformation for random-data vector z reduction to smaller dimension vector
04 p0714 A70-15066

Linear transformation of waves in nonuniform magnetoactive plasma by solving wave equation with/without allowance for spatial dispersion
06 p1119 A70-17498

Book on mathematical theory of electromagnetic waves covering vector analysis, reduced wave equation, linear transformations, boundary value problems and radiation patterns
08 p1533 A70-20759

LINEAR VIBRATION

Rectilinear vibration attenuation problem on shop setup, describing adjustable passive and active electromagnetic dampers
14 p2656 A70-30299

Linear, nonlinear and random vibrations - Conference, Poznan, Poland, April 1968
16 p2994 A70-34276

Linear damping theory, discussing simple harmonic motion model extension to transient motion
19 p3472 A70-38041

Harmonically oscillating wing linearized motion in subsonic flow, calculating generalized aerodynamic forces
22 p4105 A70-43118

LINEARITY

Pulsars linear polarization Stokes parameters measured, noting PSR 2045-16 radiation beamed into hollow cone centered on magnetic pole
13 p2487 A70-28631

Microwave radiometric receiver, analyzing video detector saturation effects on linearity
16 p2880 A70-34075

LINEARIZATION

Optimal nonlinear filtering for nonlinear dynamic system subjected to additive white Gaussian noise with corrupted observations, using successive linearization scheme
03 p0461 A70-14340

Boundary layer equations of motion linearized with self similar profiles
04 p0665 A70-14482

Linearized velocity profiles for turbulent free shear layers using transverse shift and longitudinal motion equation
[ASME PAPER 69-WA/APM-28]

04 p0668 A70-14904

Monitor for linearizing nonlinear characteristics of thermistors used for temperature sensors in Apollo Telescope Mount, optimizing circuit values with FORTRAN IV computer program
05 p0851 A70-16692

Nonlinear system theory for optimal linearization in holography, discussing generalized method for photographic emulsion and first order amplitude transmittance
06 p1072 A70-18521

Approximate linearization of nonlinear automatic control systems with two frequency forced oscillations
07 p1243 A70-18687

Quasi-linearization technique in computer program for aircraft parameters identification featuring efficient search for optimal parameters in algebraic or differential equations
08 p1465 A70-20784

Nonlinear transport equations linearization by hodograph and inversion techniques
08 p1597 A70-21125

Proportional navigation law three dimensional vectorial equation analyzed in kinematic conditions, discussing perturbation effects on linearized trajectory
09 p1720 A70-22420

Statistical linearization technique for nonlinear control systems with feedback and zero memory under random input excitation evaluated for output signal characteristics
09 p1654 A70-22960

Quasi-linearization extension to numerical solution of multipoint boundary value problems for ordinary differential equations arising from state constrained optimal control problems
10 p1909 A70-24421

Linearization of elastic forces in vibration system with percussion
10 p1958 A70-24516

Periodic solution existence theorem using harmonic linearization method
11 p2023 A70-25725

Axisymmetric or two dimensional incompressible laminar boundary layer flow field numerical analysis using quasi-linearization and Chebyshev series
11 p2072 A70-25965

Equivalent linearization for random vibration, considering stationary statistics of bilinear hysteretic one degree of freedom oscillator response
14 p2661 A70-31428

Cylindrical shells upper critical loads calculation based on linearization of nonlinear shell theory equations
15 p2818 A70-32181

Linearization error bound analysis in solution of equations of motion of reentry vehicle
16 p2974 A70-33319

Quasi-linearization for VTOL aircraft equations of motion, using spline functions for unknown parameters initial estimation
16 p2942 A70-33328

Nonlinear systems excitation by two harmonic forces, analyzing vibration by linearization of differential equation of motion
16 p2995 A70-34286

Stochastic linearization approximation to solve nonlinear dynamical systems filtering problems in Markovian framework
17 p3056 A70-34953

Quasi-linearization /generalized Newton-Raphson process/ in orbit determination, comparing with differential correction method
17 p3168 A70-35235

Linear representations of symmetry groups and use in discrete automatic control systems
18 p3290 A70-36070

Shallow spherical shell dynamics nonlinear problems solution with algorithm permitting use of straight lines method
18 p3341 A70-36590

Conducting gas channel and jet flow in electric and magnetic fields, using linearizing equations of motion under assumption of small magnetic Reynolds number
19 p3479 A70-37598

Quasi-linearization relationship with Kalman filtering for nonlinear systems parameter estimation in process noise absence
21 p3845 A70-41749

Soviet papers on harmonic linearization method in design of nonlinear automatic control systems
22 p3999 A70-42826

Harmonic linearization method for nonlinear automatic control systems, describing theoretical fundamentals
22 p4000 A70-42827

Harmonic linearization of nonlinear hysteretic elements in automatic control systems
22 p4000 A70-42828

Harmonic linearization method for periodic regimes in nonlinear control systems based on periodic solution sensitivity to higher harmonics and small parameters
22 p4000 A70-42829

Harmonic linearization equations for frequency and amplitude of self oscillations in nonlinear automatic control systems
22 p4001 A70-42832

Harmonic linearization method for periodic regimes in discrete nonlinear automatic control systems performing signal quantization with respect to level or time
22 p4001 A70-42833

Harmonic linearization for nonsearching self adaptive automatic control systems described by nonlinear differential equations
22 p4001 A70-42835

Harmonic linearization method for nonlinear automatic control systems with finite automata, discussing self oscillating modes of operation
22 p4001 A70-42836

Harmonic linearization method application to automatic phase control system with periodic nonlinearities
22 p4002 A70-42840

Harmonic linearization method for automatic control systems having hydraulic or pneumatic actuating device with two nonlinear elements
22 p4002 A70-42841

Nonlinear unsteady thermal conductivity problems linearization based on temperature substitution by integral analogs
22 p4125 A70-43370

Brittle fracture stress statistics for Weibull distribution function parameter determination, comparing linearizing, least squares curve fitting and maximum likelihood techniques
22 p4117 A70-43414

Computer program for nonlinear differential equations related to nonlinear boundary value problems

based on Newtonian iteration process difference analog of linearization method
23 p4212 A70-44338

Monochromator design for UV and visible wavenumbers linear output, noting application to absorption coefficient measurement
24 p4336 A70-45669

LINERS

U LININGS

LINE (GEOMETRY)

Horizontal-vertical illusion and foreshortening of receding horizontal lines during visual observations
02 p0249 A70-12839

Hidden-line determination for computer-drawn polyhedra using edge classification scheme for CRT display applications
09 p1641 A70-22966

Linear and nonlinear parabolic boundary value problems with first boundary conditions solved by method of lines, estimating error
12 p2262 A70-28031

Line tilting aftereffects on central and peripheral vision following spatial coincidence of inspection and test contours
21 p3767 A70-40752

LINE OF FORCE

Magnetic lines of force penetration into magnetosphere accompanied by plasma insertion generating ring current responsible for main phase of magnetic storm
01 p0083 A70-11543

Geomagnetic field directed hydromagnetic waves propagation in lower ionosphere noting inhomogeneous conductivity, Hall effect and lines of force role
01 p0083 A70-11546

Magnetic fields neutral lines length as indicator of solar flare productivity
03 p0561 A70-14001

Geomagnetic field lines inclination effect on hydromagnetic waves propagation in lower ionosphere, using atmospheric model in plane form with integral conductivity tensor
04 p0683 A70-15737

VLF and ULF whistler modes propagating along geomagnetic field-line paths in magnetosphere, studying cyclotron resonance amplification
06 p1118 A70-17379

Geomagnetic field lines coordinates calculation based on coefficients obtained in spherical harmonic analysis
07 p1278 A70-20460

Inhomogeneous elastic half space surface response to moving line loads
08 p1584 A70-20645

Model for magnetic field-line reconnection in conducting incompressible fluid, determining maximum reconnection rate entirely by null point conditions
08 p1553 A70-21615

Hydrogen ion flux detected along earth magnetic force lines in Northern Hemisphere midlatitudes, determining flux magnitude
10 p1874 A70-24321

Mapping electric field components perpendicular to magnetic field line in ionosphere at equatorial plane, discussing discrepancy with convection patterns
10 p1875 A70-24437

Lines of influence of bending moments and cutting force for straight beam using differential equation integration
10 p1959 A70-24777

Ion temperature gradient along magnetic field lines in outer plasmasphere by thermal diffusion equations compared with electron temperature observations
11 p2047 A70-26568

Geomagnetic tail formation, cross section and length and auroral irradiation, discussing observations, models, vacuum magnetic merging and field aligned currents processes
13 p2402 A70-30060

Geomagnetic tail structure and shape from Explorer 33 and Pioneer 8 observation data, examining field lines divergence with distance from earth
13 p2402 A70-30075

Magnetosphere boundary altitude dependence on longitude, considering role of electric current density along geomagnetic lines of force
14 p2570 A70-30217

Geomagnetic field lines inclination effect on hydrodynamic waves propagation in lower ionosphere, using atmospheric model in plane form with integral conductivity tensor
14 p2575 A70-30821

Rod antenna radiation representation by instantaneous pictures of electric field lines, considering wave detachment mechanism
17 p3050 A70-34575

Magnetic field lines reconnection in steady incompressible hydromagnetic two dimensional flow, formulating governing equations with cylindrical polar coordinates
17 p3140 A70-34926

Solstitial solar quiet currents along magnetic lines of force in magnetosphere, discussing ionospheric wind asymmetry effects
17 p3077 A70-34949

Tau-decomposition stability analysis method applied to two degrees of freedom system subjected to retarded follower forces

17 p3176 A70-34957

Equilibria stability of linear discrete dynamic systems involving elastic, nonconservative, dissipative and gyroscopic forces, using Liapunov-type energy method

17 p3129 A70-34958

Syrovatskii mechanism of high energy particle production near neutral line of magnetic field, noting solar flares occurrence conditions

19 p3478 A70-37581

Pc-1 pulsation production by Cerenkov emission of proton beam oscillating along magnetic field line

19 p3417 A70-38590

Thermal plasma model along magnetic field lines outside plasmasphere with sharp density gradient in equatorial plane, using OGO-4 ion composition measurements

21 p3815 A70-41057

Deuterium plasma three dimensional flow in coaxial accelerators, examining magnetic structure of filaments (field lines bundles)

21 p3856 A70-41321

Geomagnetic perturbation effects on conduction along field lines and short period fluctuations associated with plasma turbulence in magnetosphere

23 p4189 A70-44065

Magnetosphere boundary altitude dependence on longitude, considering role of electric current density along geomagnetic lines of force

24 p4331 A70-46292

LING-TEMCO-VOUGHT AIRCRAFT

NT A-7 AIRCRAFT

NT F-8 AIRCRAFT

LING-TEMCO-VOUGHT MILITARY AIRCRAFT

U MILITARY AIRCRAFT

LINGUISTICS

NT MACHINE TRANSLATION

NT SENTENCES

NT WORDS [LANGUAGE]

Natural language a priori description and linguistic algorithms construction, using statistical phrase contraction with Hoffman codes

22 p3993 A70-42492

LINING PROCESSES

Rocket motor combustion chamber lining thickness distribution matching to effusor by designing effusor as multiple nozzle made of circular graphite plate

15 p2790 A70-32271

LININGS

NT ROCKET LININGS

Metal lined glass filament-wound pressure vessel performance at cryogenic temperatures, discussing fibers, resins and liners

06 p1091 A70-17615

Elastomeric liner material for missile launch system design, developing bowed-knotted strut for compression-deflection characteristics

13 p2513 A70-29256

Missile tube liner design with cast polyurethane elastomers, discussing effect of polymer composition and processing on physical properties

13 p2439 A70-29257

Acoustic lining technology and materials for turbofan engine ducts, considering environmental factors and noise spectra

22 p4089 A70-42530

Structural and environmental design criteria for acoustical duct-lining materials in turbofan noise suppression

22 p4089 A70-42531

Duct lining parameters effects on engine inlet and fan discharge noise reduction during fan jet landing

22 p4090 A70-42532

Acoustically treated inlet and fan exhaust duct configurations for JT3D turbofan engine on DC 8 aircraft

22 p4090 A70-42533

LINKAGES

Direct links existence between rabbit temporal cortex neurons and neurons in each division of hippocampus, discussing topographic arrangement and axons quantity

03 p0417 A70-13071

LILOUVILLE EQUATIONS

Final motions of Hamiltonian conservative systems, analyzing Liouville type, homogeneous and similar systems

01 p0146 A70-11561

Local uniqueness and instability theorem for Einstein-Liouville equations using energy inequalities, noting relevance to Cauchy problem

11 p2084 A70-26458

Turbulence theory from Liouville equation for Navier-Stokes velocity field distribution

17 p3073 A70-35629

Kinetic equation for rarefied polyatomic gases derived from Liouville equation

17 p3138 A70-35728

LIPID METABOLISM

Phospholipid metabolism intensity in brains of adrenalectomized and pseudo operated rats under hypoxia

01 p0012 A70-10054

Lipid and carbohydrate behavioral abnormalities in patients with angiographically documented coronary artery disease observed by glucose tolerance tests

01 p0016 A70-10441

LIPIDS

Lung lipid embolization effect in decompression sickness on obese mice, showing no relationship to dysbaric syndrome

01 p0015 A70-10361

Platelet and lipid changes in thrombocytopenic and control rats subjected to bends producing technique in aeroembolism

01 p0015 A70-10364

Gas chromatography study of fatty acids and polar lipids of thermophilic filamentous bacterial masses from hot Yellowstone Park springs

01 p0021 A70-10791

Graft copolymerization and chemiluminescence analysis of lipids complexes in animal and plant tissue homogenates exposed to gamma radiation

03 p0419 A70-13305

Free radical antioxidation reactions in lipids from blood, liver, spleen, brain and intestines of rats exposed to ionizing radiation

03 p0419 A70-13309

Interactions between nutrition, blood coagulation and atherosclerosis by Duguid theory, emphasizing fibrinolysis, thrombosis and alimentary lipids

03 p0431 A70-14280

Plasma lipids and lipoprotein changes following myocardial infarction, discussing rise and normal return times of free fatty acids, cholesterol and beta lipoproteins

04 p0636 A70-15464

Fat embolism and decompression sickness similarities, studying lipid stability changes resulting from liver tissue injury by nitrogen bubbles

07 p1222 A70-19936

Hydration and lipid-protein ionic interaction in stearic acid monolayers during conformation of poly-L-lysine films

19 p3373 A70-37840

LIPOPROTEINS

Plasma lipids and lipoprotein changes following myocardial infarction, discussing rise and normal return times of free fatty acids, cholesterol and beta lipoproteins

04 p0636 A70-15464

Surface active lipoproteins of lung, discussing quantitative determination and labeling on basis of per-bronchial wash-out procedure over trachea

15 p2680 A70-31725

Lipoprotein lipase activation on emulsified triglycerides by specific glycopeptides of human serum lipoproteins

24 p4298 A70-45802

LIPSCHITZ CONDITION

Elastic-plastic torsion of convex cylindrical bars

06 p1165 A70-17534

Nonlinear equations boundary value problem solution by Galerkin method in integrodifferential equations form, determining Lipschitz conditions constant and proving existence and uniqueness

13 p2442 A70-29513

LIQUEFACTION

Nonisothermal condensation in ionized vapor as function of energy additions to droplets

20 p3680 A70-39989

LIQUEFIED GASES

NT LIQUID AMMONIA

NT LIQUID HELIUM

NT LIQUID HYDROGEN

NT LIQUID NITROGEN

NT LIQUID OXYGEN

Temperature limit of efficiency threshold for ground based liquid propane sprayer for supercooled fog dispersal at Orly airport

02 p0324 A70-11872

Liquefied natural gas or liquefied methane as burning propulsion system for SST, examining storage volume, fuel-tank insulation and implosion danger

03 p0543 A70-12998

Specific heat, thermal pressure and molar volume of liquid krypton measured with adiabatic calorimeter, discussing thermal expansion coefficients

14 p2617 A70-31016

LPG use in fuel cells, discussing efficiency, weight and size

18 p3216 A70-36657

LIQUID AMMONIA

Ammonia micropropulsion operation modes and performance for stabilizing synchronous communication satellite, noting advantages over chemical and ion propulsions

11 p2122 A70-25817

Zero gravity liquid ammonia propellant feed system, describing regulator/capillary tube assembly for propellant delivery pressure control

[AIAA PAPER 70-1151] 20 p3690 A70-40204

LIQUID ATOMIZATION

Rocket engines gas/liquid injectors atomization characteristics using molten wax technique, considering drop sizes and gas streams velocity, density and pressure

01 p0161 A70-10326

Ultrasonic atomizer system for liquid fuels combustion

02 p0356 A70-12470

Liquid sheet and jet breakup in supersonic gas stream, characterizing breakup mechanism by gross jet fracture

[AIAA PAPER 70-89] 06 p1039 A70-18109

LIQUID COOLED REACTORS

NT HEAVY WATER REACTORS

NT NRX REACTORS

NT PLUM BROOK REACTOR

Rankine cycle technology concerning high temperature, refractory alloy and liquid metal experience, showing applicability to nuclear Brayton and thermionic power systems

02 p0229 A70-12513

High temperature liquid metal cooled nuclear reactor for military aircraft with long flight endurance and range

22 p4071 A70-43188

LIQUID COOLING

NT FILM COOLING

Contactless asynchronous flowmeter for measuring liquid metal coolant small flow rates, describing design and characteristics

03 p0483 A70-13211

Stable two phase water flow system for transpiration cooling in thermal protection of SST noise suppressor situated in afterburning engine exhaust gas stream

[AIAA PAPER 70-151] 06 p1181 A70-18146

Projection CRT with liquid-cooled phosphor faceplate, showing linear relationship between brightness and beam current

09 p1673 A70-22034

Water cooled space suits automatic control based on physiological changes in astronaut during hard work

09 p1627 A70-23458

Temperature limitation on CRT tube performance in high brightness displays imposed by glass breakage danger, discussing liquid cooling of phosphor substrate

09 p1686 A70-23759

Water cooled metallic diaphragm thermal stability effect on plasmatron electric arc characteristics stabilized by vortex air flow

11 p2093 A70-26736

Al radiator with thin stainless steel tube liner using liquid metal coolant tested for heat rejection system of SNAP-8 Rankine cycle power system

[AIAA PAPER 70-855] 16 p3000 A70-33922

Solar simulators using water cooled 30 kw Xe arc lamps

17 p3060 A70-35248

Ar ion laser gas discharge tube construction, using anodically oxidized directly cooled aluminum segments

19 p3444 A70-37567

Cryogenic pipelines cooldown to operating temperature, calculating cryogen flow rate limits due to thermal stresses in steel and Al flanges

23 p4280 A70-44368

High speed internal combustion engine mixed flow type liquid cooling system, deriving dynamic thermal characteristics from differential equations solution

24 p4393 A70-45502

LIQUID CRYSTALS

Optical reconstruction of microwave holograms recorded by liquid crystal detectors, emphasizing dependence on IR heat bias provided by incandescent bulb

01 p0086 A70-10421

Electric field effects on dielectric properties and molecular arrangements of cholesteric liquid crystals with temperature dependent helical pitch

01 p0160 A70-11352

Honeycomb structure fracture initiation flaw detection method using liquid crystal determination of stress concentration sites, noting absence of external heat source

03 p0515 A70-13121

Optical rotatory power measurement for compensated cholesteric liquid crystal helical structure to observe thermally induced inversion and electric field perturbations

03 p0542 A70-14003

Aircraft visual flight control displays development, considering liquid crystals in alpha numeric data output devices and holograms for three dimensional structures reproduction

05 p0853 A70-17090

Cholesteryl chloride-cholesteryl myristate /CM/ mixture liquid crystal molecular and helical axes orientation from dielectric constant change measurements in magnetic fields

06 p1126 A70-17326

Combining color response in cholesteric liquid crystals generated by trace contaminants applicable to detection of vapors trace amounts

07 p1222 A70-19930

Molecular dipole moments-electric field interaction induction of cholesteric liquid crystal transition to nematic phase

07 p1225 A70-20053

Collection of patent papers on liquid crystals applications including radiation detection, polarizing, thermal imaging, etc

08 p1556 A70-21346

Liquid crystals biaxial smectic C phases tilt and optic axial angles determined from convergent light observations

09 p1738 A70-22271

Room temperature cholesteric liquid crystals retention of information on past electric field excitation by changes in optical transmission properties

09 p1740 A70-22924

Calibration of shear sensitive cholesteric liquid crystals film, measuring shearing forces and scattering light intensity

09 p1656 A70-22992

Liquid crystal of cholesteryl chloride and myristate measured for complex dielectric constant, noting role of molecular rotation modes in dipole relaxation

12 p2180 A70-26859

Acoustographic imaging system (AGIS) using liquid crystal detection screen to provide color display of ultrasonic wave information

12 p2235 A70-27724

Electron paramagnetic resonance of viscous nematic liquid crystal, investigating order as function of temperature

16 p2960 A70-33058

Encapsulated liquid crystal screens for IR laser beam imaging detectors with high thermal sensitivity and real time viewing in bright light

16 p2927 A70-33167

Light modulation electro-optical device with liquid crystals, determining liquid nematic stability

16 p2907 A70-33181

Cutaneous liquid crystal temperature sensors for thermographic patterns of angina pectoris induced by treadmill exercise

19 p3364 A70-38361

Liquid crystal smectic C phase temperature dependent tilt angle, using conoscopic observation and circularly polarized light

21 p3862 A70-41322

Liquid crystals orientational ordering molecular field theory examined by cluster variation method, predicting first order transition

22 p4085 A70-42485

Liquid crystals as solid state organic material with physical properties of liquid, discussing electro-optical properties and applications

22 p4085 A70-42724

LIQUID DROPS

U DROPS (LIQUIDS)

LIQUID DYNAMICS

U FLUID DYNAMICS

U LIQUID FLOW

LIQUID FILLED SHELLS

Pressure waves in accelerated sphere filled with compressible liquid, using convolution integral for pressure distribution on inner surface

01 p0067 A70-11186

Body motions containing cavity filled with viscous fluid under influence of gravity, formulating motion equations for fluid and body

01 p0068 A70-11576

Liquid heating in thin walled porous shells under various boundary conditions, deriving formulas for temperature fields

03 p0604 A70-13208

Natural oscillation frequencies of partially liquid-filled cylindrical shells determined by resonance method

03 p0592 A70-13444

Perturbed motion of solid body with cylindrical cavity partially filled with viscous fluid, using Rabinovich equations

04 p0766 A70-14476

Soviet book on boundary value problems involving motion of ideal fluids in unsteady cavities of various geometries, determining attached fluid masses and oscillation frequencies

04 p0666 A70-14678

Hydrodynamic coefficients of algebraic equations for boundary value problems in disturbed motion of body with rib-reinforced liquid filled cavity

05 p0836 A70-16956

Liquid filled dampers for nutation damping of spacecraft with momentum wheel for attitude stabilization

06 p1154 A70-17163

Dynamic instability of motion of rigid and elastic bodies with liquid filled cavities associated with practical problems of rocket technology

06 p1107 A70-18415

Container fluid viscosity effect on container-obstacle interaction solved in Fourier series form

07 p1252 A70-18676

Frequency equation for harmonic waves propagating in fluid filled circular cylindrical cavity in infinite isotropic solid medium

07 p1253 A70-18846

Human head model for craniocerebral trauma analysis, studying fluid filled spherical shell free vibrations axisymmetric response

07 p1219 A70-19243

Equilibrium of torque-free cylindrical shell vertically positioned and partly filled with liquid, obtaining solution for biaxial stress

07 p1415 A70-20192

Dynamic calculation of oscillating liquid filled elastic cavity on elastic kinematic system under random load, using random signals transmission theory

07 p1416 A70-20194

Soviet book on free, forced and parametric vibrations of thin walled shells containing liquid, gas and continuous elastic medium

08 p1584 A70-20762

Ideal fluid in lightly filled spherical vessel under gravitational force investigated for surface tension effect on vibration frequencies

08 p1482 A70-20853

Elastic body with incompressible fluid filled cavities, studying motion and stability by deriving motion equations starting from principle of least action

08 p1544 A70-20951

Motion of body with cavity completely filled with viscous fluid about center of mass in potential mass-force field, applying small parameter method

08 p1546 A70-21630

Oscillations of highly viscous incompressible fluid in partially filled cavity of body moving about fixed point, solving Navier-Stokes equations by asymptotic method

08 p1485 A70-21632

Nonlinear equations for large fluid oscillations in axisymmetric rotating cavities with radial partitions

09 p1660 A70-22438

Liquid motion dynamic effects in open cylindrical and conical tanks with translational motion

09 p1662 A70-23293

Forced inertial oscillations in rotating processing fluid-filled circular cylinder

09 p1664 A70-23682

Optimization in epiphydrostatics and epiphydrodynamics, discussing liquid in rectangular tank, electro-magneto-epiphydrodynamics and thermal instability

10 p1866 A70-24108

Swirl velocity and cavity stability in rotating container filled radially through porous cylindrical wall at constant and applied pressure

10 p1868 A70-24195

Two dimensional irrotational incompressible fluid motion bounded by flexible stretched and unstretched film, noting hydrodynamic shock for closed film

12 p2213 A70-28238

Motion stability of variable mass solid body with ideal liquid filled cavities about stationary point using Liapunov theorem

13 p2452 A70-29310

Unstable Ekman boundary layer vortex structure analysis by generating similar flow in liquid filled rotating cylinder

14 p2604 A70-30545

Cylindrical propellant tanks dynamic stability and parametric resonance, analyzing axial preload, liquid depth top impedance and ullage pressure by Donnell theory

14 p2657 A70-30764

Elastohydrodynamic monochromatic wave coupling in liquid filled container as model for Alfvén and magnetoacoustic waves transmission in plasma

14 p2625 A70-31356

Container fluid viscosity effect on container-obstacle interaction solved in Fourier series form

15 p2719 A70-31468

Perturbed motion of body with partially filled cylindrical cavity with damping ribs, discussing vibrations boundary value problems of liquid filling

15 p2775 A70-32157

Oscillations of rigidly clamped elastic liquid filled hemispherical shell with gas bubble

18 p3242 A70-36583

Elastic body with incompressible fluid filled cavities, studying motion and stability by deriving motion equations starting from principle of least action

20 p3672 A70-39376

Liquid fuel behavior in right circular cylindrical tank inclined to earth gravitational field, computing fundamental sloshing frequency

20 p3610 A70-39694

Thin walled circular cylindrical steel shells dynamic stability partly filled with liquid and subjected to longitudinal excitation

20 p3723 A70-39852

Perturbed motion linear equations of body rigidly coupled to thin walled elastic shell partially filled with heavy compressible fluid

21 p3806 A70-40602

Sufficient conditions for confined fluids stability, defining critical and modified Rayleigh numbers

21 p3810 A70-41952

Fluid filled elastic spherical shell, calculating free vibration axisymmetric response and fundamental mode

21 p3940 A70-42053

Transient elastic vibrations of air and liquid filled cylindrical shells under radial impact, using shadow-optical cinematography

22 p4031 A70-43030

Flutter of elastic current-carrying shell containing incompressible inviscid nonconducting fluid flow

22 p4117 A70-43383

Artificial liquid satellite orbited to verify tidal theory

23 p4183 A70-44659

Potential liquid flow in pulsating bulb applied to blood flow

23 p4155 A70-44847

LIQUID FLOW

NT WATER FLOW

Turbulence characteristics in liquids measured by hot film anemometry, discussing calibration methods selecting criteria as temperature control, drift influence and relative speed determination

02 p0303 A70-12687

Liquid flow through cylindrical slot of constant and variable thickness, calculating flow variations

06 p1034 A70-17630

Liquid sheet and jet breakup in supersonic gas stream, characterizing breakup mechanism by gross jet fracture

[AIAA PAPER 70-89]

06 p1039 A70-18109

Nusselt theory of laminar liquid films movement on vertical smooth solid surface, attributing thickness variation to gas movement and surface active agents in liquid

07 p1251 A70-18656

Temperature fields and hydrodynamics in laminar flow of vertical liquid layers during free convection

07 p1422 A70-19655

Radiation effect on heat transfer during film boiling in forced convection boundary layer of liquid flow past plate, noting vaporization temperature

07 p1423 A70-19812

Circulating flow around elliptical cylinder in inviscid liquid vortex

09 p1659 A70-22435

Acoustic pressure sensors positioning on bodies of revolution to determine laminar boundary layer stability loss during ideal liquid flow at nonzero angles of attack

09 p1660 A70-22479

Numerical methods of viscous liquid dynamics, considering unsteady flow in simply and multiply connected regions

10 p1866 A70-24110

Small linear disturbance and stability of potential unsteady motion of finite mass of liquid with free boundary

10 p1866 A70-24111

Liquid film steady motion on ablating body surface allowing for radiative heat transfer from interior

12 p2334 A70-28244

Vibration spectra, kinetic and dispersion equations of solid spherical particles moving in incompressible weakly viscous liquid

13 p2388 A70-29368

Permittivity cell and encapsulation for liquids subjected to high pressures and temperature extremes

14 p2533 A70-30502

Unsteady state Newtonian liquid diffusion in laminar flow in circular tube, using mathematical model

17 p3072 A70-35544

Viscous incompressible liquid two dimensional flow around flat plate, discussing visualization techniques and velocity distribution measurement

18 p3239 A70-36218

Radiation effect on heat transfer during film boiling in forced convection boundary layer of liquid flow past plate, noting vaporization temperature

20 p3736 A70-39259

Laminar flow of liquid in duct with zero heat resistance of walls, calculating temperature distribution during radiative convective heating

20 p3613 A70-40297

Cold plate immersed in warm flowing liquid, calculating two dimensional transient and steady state solidification by conformal mapping

21 p3949 A70-41319

Heat transfer in closed partially liquid filled steady state porous systems, testing linear flux force equation validity

21 p3952 A70-42081

Liquid lubricant unsteady motion and pressure distribution during pivot harmonic vibration in hydrodynamic bearing

23 p4200 A70-44163

Gravity waves produced in liquid electric conductor by piston subjected to sinusoidal pulsation, calculating magnetic field effect on amplitude and phase velocity

23 p4225 A70-44208

Mass transfer between sphere and liquid flow at small Reynolds numbers

23 p4276 A70-44219

Potential liquid flow in pulsating bulb applied to blood flow

23 p4155 A70-44847

Flow visualization measuring liquid flow velocity, using flow dichroism

24 p4338 A70-45816

LIQUID HELIUM

Thermodynamic equilibrium of rotating liquid He II on basis of Landau theory, noting stability and dissipative effects

04 p0785 A70-14986

Low temperature thermoelasticity theory for elastic fluids, considering fountain and second sound effects and viscosity anomalies in He II

06 p1164 A70-17442

Liquid helium cryostat for onboard satellite storing designed with allowance for overloads and vibrations during powered flight

08 p1440 A70-21220

Helium low temperature applications to fuel tank pressurization, superconducting magnet cooling and cryopumping of solar space simulators

11 p2083 A70-25620

Heat transport by internal convection through He 2 in two fluid hydrodynamics model noting roles of thermal flux, superfluid component vorticity, normal component turbulence, etc

12 p2329 A70-27022

Liquid He temperature fluctuation effects on cryogenic superconducting bolometer noise spectrum, deriving transfer functions

12 p2237 A70-28156

Jupiter Red Spot, explaining motion rate in terms of cellular convection in liquid hydrogen-helium layer

15 p2799 A70-31895

Microscopic quantum theory of liquid He isotopes emphasizing method of correlated basis functions

16 p2951 A70-32997

Longitudinal and transverse hypersonic mm waves excitation in quartz single crystal at liquid helium temperature

16 p2952 A70-33258

Liquid He surface layer thickness as function of temperature, considering capillary waves effect due to gravity

16 p2952 A70-33288

Energy flow between two superfluid helium baths at different temperatures and separated by thin plate

19 p3471 A70-37648

Liquid He 4.2 K in narrow channels with laminar and turbulent flow, measuring boiling heat transfer as function of temperature difference

20 p3735 A70-39155

Comparative analytic and experimental film boiling heat transfer for horizontal cylinders in helium II [ASME PAPER 70-HT-3]

22 p4122 A70-42441

Threshold parameters of liquid and gaseous helium breakdown caused by ruby laser beam, noting Mandelstam-Brillouin scattering in liquid phase

22 p4051 A70-43465

Longitudinal and transverse hypersonic mm waves excitation in quartz single crystal at liquid helium temperature

23 p4218 A70-44281

Liquid He II, determining correlation of depth effect on film boiling heat transfer with vapor film geometry from motion pictures

23 p4279 A70-44363

Corona discharges from fine W points in liquid He initiated by field ionization or emission, noting anomalous characteristics

23 p4221 A70-44889

Green function theory of evaporation of He 3 atoms from liquid He 3/He 4 mixtures, determining energy distribution

24 p4377 A70-45255

LIQUID HYDROGEN

Far IR spectra of liquid hydrogen at para concentrations, noting absorption coefficient variation consistent with composition

04 p0718 A70-14696

Fluorine injectors for main tank injection of space vehicle liquid hydrogen tank, including study of hypergolicity and reaction product freezing

04 p0736 A70-15406

Liquid and slush hydrogen gravimetric flow calibration system for research in slush generation, slush fluid mechanics and flow instrumentation

06 p1031 A70-18449

Twin spool hydrogen turbopump performance at zero net positive suction pressure (NPSP) saturated fluid in propellant tank, including steady state and simulated transient engine tests

07 p1295 A70-19709

Payload optimization factors for orbital storage of liquid hydrogen, considering payload cost of agitation, tank pressure, pressurant weight, etc

09 p1767 A70-23262

Jupiter Red Spot, explaining motion rate in terms of cellular convection in liquid hydrogen-helium layer

15 p2799 A70-31895

Hydrogen oxygen rocket engine two phase liquid hydrogen pump capability and hydrodynamic design, analyzing constant-quality flow, acoustic effects, compressible flow and cavitation

15 p2791 A70-32511

Thermal conductivity of gaseous and liquid hydrogen with guarded horizontal flat plate calorimeter, investigating temperature and density effects in critical region

16 p2996 A70-33011

Vapor fraction dependence on liquid hydrogen propellant outflow during NERVA operation under stored gas or autogenous pressurization, using computer simulation

[AIAA PAPER 70-677] 16 p2950 A70-33578

Liquid hydrogen axial flow pump inducer, describing suction pressure measurements, fluid conditions and flow rate

[AIAA PAPER 70-627] 16 p2919 A70-33592

Cryogenic single tubes transient cool-down by liquid hydrogen, deriving film boiling heat transfer correlation

[AIAA PAPER 70-660] 16 p2998 A70-33621

Liquid hydrogen balloon inflation system for use at remote locations, discussing characteristics and economy

20 p3607 A70-40086

Pressurized liquid nitrogen and hydrogen dielectrics for cryogenic cables, measuring dissipation factor and voltage breakdown by concentric cylindrical test cell

21 p3851 A70-42125

Quasi-hybrid rocket engines with solid propellant and liquid hydrogen injection, discussing performance in comparison with other propellant systems

22 p4089 A70-42498

Thermodynamic properties, tables and equations of state of liquid para hydrogen from liquid-gas and liquid-solid phase equilibria

23 p4220 A70-44434

LIQUID INJECTION

NT WATER INJECTION

Rocket engines gas/liquid injectors atomization characteristics using molten wax technique, considering drop sizes and gas streams velocity, density and pressure

01 p0161 A70-10326

Combustion and flow characteristics associated with direct injection of liquid hydrocarbons into high speed air stream

[AIAA PAPER 70-88] 06 p1182 A70-18198

Liquid propellant spray injection into high pressure gaseous environment noting geometric, dynamic and thermal characteristics

[AIAA PAPER 70-8] 06 p1182 A70-18211

Interaction shock shape prediction for gaseous and liquid injection in supersonic flow, using solid body and complementary models

09 p1662 A70-23244

Gas turbine engine performance prediction with water-methanol injection, describing analytical method

[SAE PAPER 700208] 11 p2102 A70-25881

Quasi-hybrid rocket engines with solid propellant and liquid hydrogen injection, discussing performance in comparison with other propellant systems

22 p4089 A70-42498

LIQUID LASERS

Raman effect liquid laser power as function of cavity length, using Q switched ruby laser beam focused by cylindrical lens for optical pump

01 p0111 A70-10674

Flash lamp-pumped organic dye scintillator lasers using coaxial Xe-filled lamp, tabulating blue-violet organic liquid lasers characteristics

03 p0499 A70-13161

Inorganic liquid laser materials and use of circulating active medium

08 p1513 A70-21302

Flashlamp-excited organic liquid UV lasers

13 p2427 A70-29141

Mechanically heterogeneous and optically homogeneous solid/liquid mixed laser with active centers contained in Ne bathed in liquid

16 p2926 A70-33109

Spatial-angular characteristics of Nd doped phosphorus oxychloride liquid lasers, discussing beam divergence effects

18 p3266 A70-36416

Low threshold laser action of Nd-containing chelate in host media consisting of polymethyl methacrylate and organic liquid

23 p4201 A70-44869

Inorganic liquid lasers, discussing Nd salts solution preparation and handling methods

23 p4201 A70-44929

Giant pulses by actively and passively Q-switched inorganic neodymium liquid lasers with varying modulation due to mode coupling

23 p4202 A70-44937

Phosphorus and selenium oxychloride based liquid laser transmission loss measurement

24 p4355 A70-46265

Laser gain coefficient increased via organic compounds addition to rhodamine 6G aqueous solution

24 p4356 A70-46273

LIQUID LEVELS

Liquid metal level indicators and resistance type level meters for turbines using alkali metal as working media

14 p2587 A70-31010

Contactless electromagnetic level sensor for liquid metal using eddy currents

14 p2587 A70-31011

LIQUID METALS

NT LIQUID POTASSIUM

NT LIQUID SODIUM

NT MERCURY [METAL]

NT MERCURY VAPOR

Liquid metals contact effect on mechanical strength of T shaped graphite specimens at high temperatures in argon atmosphere

01 p0129 A70-11038

Contactless asynchronous flowmeter for measuring liquid metal coolant small flow rates, describing design and characteristics

03 p0483 A70-13211

Liquid metal MHD, discussing conduction/induction MHD devices, measurement gages and devices for suspending liquid metal by magnetic force

04 p0724 A70-14527

Liquid metal pump design and performance in SNAP 8 Mercury Rankine and Advanced Rankine fluid power systems, including containment materials and corrosion effects

04 p0718 A70-15641

Thermoelectric powers of liquid metals calculated from structure factors, using screened model potential

05 p0892 A70-16313

Refluxing capsule tests of refractory metal alloys-boiling alkali metals corrosion compatibility, noting role of capsule geometry

06 p1087 A70-17510

Hall effect measurements in liquid semiconductors and metals

06 p1127 A70-17919

Liquid metal alloys surface composition and electronic structure roles in electrocatalysis evaluated by studying hydrogen-ion discharge reaction and electrical double layer

06 p1005 A70-18392

Electrohydrodynamic /EHD/ technique for generating ions from liquid metals by using electrostatic forces to overcome surface tension forces for field emission of ions

06 p1125 A70-18610

Rankine cycle two loop Li boiling Ka facility for nuclear turbopump simulation, studying alkali metal corrosion for operation with and without hot traps

07 p1304 A70-18809

Heat pipe structural alloys compatibility with different working fluids using capsule tests at high temperatures, noting corrosion behavior

07 p1304 A70-18812

Liquid metals atomic structure, discussing X ray and neutron diffraction measurements

07 p1338 A70-19575

Molten Al alloys flow rate and behavior in various casting systems, considering gate geometry and casting temperature effects

08 p1505 A70-21133

Heat treatment effects on hardened steels acoustic constants, calculating sound velocity in liquid metals

09 p1692 A70-22643

Oxygen solubility in liquid Mo in presence of volatile oxides, determining equilibrium constant of dissolution reaction

09 p1709 A70-23784

Kinematic viscosity of molten steel containing corundum inclusions as function of temperature

10 p1904 A70-24271

Welding techniques for Nb-stainless steel bimetal tubing for liquid metal containment, determining structural integrity and bond interface condition after thermal cycling

10 p1897 A70-25309

Working body properties effects on one component liquid-metal MHD system efficiency with vapor condensation cycle

12 p2164 A70-27329

Fe-Cr system and Fe-Cr-Ni liquid alloys studied by Knudsen cell-mass spectrometer combination, deriving phase equilibria from ion current ratios

12 p2255 A70-27602

Asynchronous liquid metal MHD generator parameters, assuming constant vertical distribution of working fluid velocity

13 p2349 A70-28968

Liquid metallic particles fragmentation in two phase flow injected into vacuum, noting atomization enhancement by sodium nitrate

13 p2391 A70-29994

Liquid metal level indicators and resistance type level meters for turbines using alkali metal as working media

14 p2587 A70-31010

Contactless electromagnetic level sensor for liquid metal using eddy currents

14 p2587 A70-31011

Liquid metals pump with cylindrical hydraulic coupling for actuating axial wheel, investigating cavitation and pumping effects on performance

14 p2535 A70-31012

Tri- and bipropellants in spacecraft propulsion, discussing liquid and powder metals, hybrids, frozen tripropellants, etc

15 p2789 A70-32253

Al radiator with thin stainless steel tube liner using liquid metal coolant tested for heat rejection system of SNAP-8 Rankine cycle power system
[AIAA PAPER 70-855] 16 p3000 A70-33922

Corrosion by liquid metals - AIME Conference, Philadelphia, October 1969 16 p2932 A70-34201

Refractory metals penetration by liquid alkali metals along grain boundaries and crystallographic planes, considering threshold oxygen concentration 16 p2932 A70-34203

Refractory alloys Li corrosion resistance, examining effects of oxygen contamination during welding 16 p2924 A70-34205

Molten contaminated Li effects on microstructure, tensile strength and stress corrosion of stainless steels and refractory metals 16 p2933 A70-34206

Liquid metal corrosion of heat pipe refractory alloys at high temperatures, noting oxygen role 16 p2933 A70-34208

Liquid Fe-Cr-C, Fe-P-C and Fe-Cr-P systems, evaluating interaction coefficients 18 p3272 A70-36032

Oxygen dilute solutions in liquid Fe-Ni-Co alloys, investigating thermodynamic properties by hydrogen-water vapor equilibrium 18 p3272 A70-36033

Nitrogen solubility calculation in transition metals liquid binary systems, using quasi-chemical model 18 p3273 A70-36045

Ti, Nb and Mo solubility during surface doping in Al melts containing various metals, discussing melt lattice structure effects 18 p3276 A70-36208

Rotating Ti disk in liquid Co flow, investigating titanium carbide dissolution kinetics 20 p3648 A70-39245

Liquid metal MHD conservation cycles, discussing evolution and status of power generation at various temperatures 20 p3563 A70-39325

Liquid metal MHD power conversion system with Cs and Li as working fluids, describing hydraulic, electrical and high temperature tests results 20 p3680 A70-39986

Unmanned nuclear electric propelled spacecraft using reactor with liquid metal MHD power conversion system 20 p3566 A70-40016

Liquid metal hydraulic servoactuation packages for flight control in high temperature environments without coolant systems 21 p3750 A70-40785

Liquid metal heat pipes in magnetic fields of controlled fusion reactors, considering geometry, compound wick structure and vapor flow 21 p3946 A70-41046

Working body properties effects on one component liquid-metal MHD system efficiency with vapor condensation cycle 21 p3760 A70-42070

Liquid metal turbulent jet flow dependence on longitudinal magnetic field, measuring mean velocity profiles at various cross sections 21 p3861 A70-42230

Conduction liquid metal MHD machine channels design with baffles installed to decrease shunting effect of end zones, calculating segments by circuit theory methods 21 p3760 A70-42233

Ti embrittlement by liquid Cd, discussing ductile-brittle transition temperature dependence on strain rate 22 p4054 A70-42738

Nb-Zr alloy and yttria corrosion by high velocity Li flow, discussing material removal depth 22 p4055 A70-43100

High temperature gas turbine blades cooling by liquid Na-K alloy
[ONERA-TP-872] 22 p4125 A70-43458

Al and liquid Al-Mg alloys oxidation at high temperatures, noting Mg content effect 24 p4361 A70-46174

LIQUID NITROGEN
Liquid nitrogen evaporation in PSB foam polystyrene vessels compared with glass vessels for cryogenic application 02 p0305 A70-11875

Solder mechanical contact strength to CdS insulating crystal platelets tested in liquid N, noting Ag epoxy 02 p0319 A70-12738

Sound wave velocity and damping in liquid N measured along saturated vapor line using thermal Brillouin scattering techniques 06 p1105 A70-17491

Liquid nitrogen drops anomalous behavior in film boiling, resolving vaporization time discrepancies 17 p3194 A70-34741

Pressure, subcooling and diameter effects on liquid nitrogen film boiling on thin horizontal wires, using high speed movies 17 p3194 A70-34742

Buoyancy effects on liquid nitrogen film boiling in vertical flow, using resistance heated test apparatus 17 p3195 A70-34745

Liquid nitrogen boil off calorimeter for surface energy measurements, describing construction, calibration and instrument errors 18 p3261 A70-37089

Interfacial instability effect on heat transfer to liquid nitrogen drops undergoing film boiling on flat Al surface, obtaining vaporization rates and times 21 p3948 A70-41203

Pressurized liquid nitrogen and hydrogen dielectrics for cryogenic cables, measuring dissipation factor and voltage breakdown by concentric cylindrical test cell 21 p3851 A70-42125

Forced convection heat transfer to liquid nitrogen near critical point, determining coefficients from given wall temperature and heat flux 23 p4279 A70-44358

Liquid nitrogen drops undergoing film boiling on Al surface, measuring heat transfer coefficient 23 p4279 A70-44360

Liquid nitrogen saturated film boiling from wire at pressures up to critical, discussing liquid-vapor interface configuration 23 p4279 A70-44362

LIQUID OXIDIZERS

Oxygen and fluorine-based liquid fuels and oxidizers development, considering chemical rocket propulsion reaction principles 07 p1361 A70-19917

Materials static tested for compatibility with pure and moisture contaminated chlorine pentafluoride at 160 F and ambient temperatures 09 p1742 A70-23250

Stress corrosion cracking of Ti and Ti-Al-V alloy in liquid dinitrogen tetroxide 15 p2755 A70-31475

LIQUID OXYGEN

Liquid oxygen and water cavitation effects on lead, copper, nickel, iron and zinc 01 p0115 A70-10071

Helium gas shaft seal for spacecraft electrically driven LOX pump, noting advantages of floating carbon face seal type
[ASLE FICFS PREPRINT 24] 02 p0308 A70-12168

Heat transfer and flux density during bubble boiling of liquid oxygen employing simulated weak gravitational fields 03 p0605 A70-13393

Liquid oxygen usage inspection penetrant systems combining nonreactivity with flaw detection sensitivity 08 p1508 A70-21745

Pressure oscillations in LOX pump inducer of J-2 machine, using semianalytical first order model with retarded time mechanism 09 p1693 A70-23257

Fluorinated lubricating oils and greases for use as liquid oxygen compatible lubricants, correlating stability and hydrogen substitution 10 p1907 A70-24064

Centrifugal pumps of various metals for liquid oxygen, describing fire and explosion tests 14 p2617 A70-31020

Pt and Ag surface effects on LOX nucleate boiling heat transfer, considering embedded abrasives relationship to hysteresis 21 p3947 A70-41056

LIQUID PHASES

Wet vapor flow with/without inert diluent, assuming momentum and heat transfer between phases according to Stokes law and Nusselt number of unity 01 p0061 A70-10332

Hydrophobic-hydrophilic zero gravity liquid-gas phase separator for Apollo 11 flight life support system
[SAE PAPER 690638] 05 p0804 A70-15844

Nonequilibrium models describing two phase critical discharge of initially saturated or subcooled liquid through sharp edged and smooth inlet geometries 05 p0956 A70-16162

Supersaturation during droplet-liquid phase formation in clouds estimated from trough formed on curve of distribution function 06 p1097 A70-17796

Thermal control of spacecraft via solid-liquid phase change materials
[AIAA PAPER 70-12] 06 p1092 A70-18137

Liquid nitrogen tetroxide enthalpy measured by indirect heating techniques, obtaining data at supercritical temperatures 06 p1005 A70-18560

Enthalpy of nitrogen tetroxide in liquid phase using direct heating of test substance in calorimeter 07 p1358 A70-19207

Liquid crystals biaxial smectic C phases tilt and optic axial angles determined from convergent light observations 09 p1738 A70-22271

Liquid phase convective heat transfer as rate controlling mechanism for flame propagation, analyzing surface tension driven liquid flow induced by temperature profile 10 p1929 A70-24091

Bismuth oxide resistivity and structural characteristics at high temperature and during transformation from solid to liquid state 10 p1927 A70-24272

Nitrogen tetroxide thermodynamic properties calculation from pressure-volume-temperature equation of state in gas and liquid phases 12 p2332 A70-27975

Liquid crystal smectic C phase temperature dependent tilt angle, using conoscopic observation and circularly polarized light 21 p3862 A70-41322

Liquid and solid phases of substance, calculating thermodynamic properties and vapor pressure logarithm dependence on temperature 22 p4124 A70-42683

Phase analysis for individual multicomponent alloys, discussing chemical composition in case of invariant equilibria and electron beam microprobe 22 p4053 A70-42734

Electric strengths of liquid dielectrics during subjection to Q switched laser pulses, determining threshold currents for breakdown 22 p4051 A70-43338

Cesium high temperature saturated liquid and vapor phase density and critical temperature and pressure 23 p4281 A70-44450

LIQUID POTASSIUM

Solubilities and heats of solutions of Mo, W, V, Ti and Zr in liquid K 04 p0710 A70-15632

Ta oxygen concentration effects on corrosion resistance to NaK in SNAP 8 boilers 16 p2932 A70-34202

Metal corrosion effects in Rankine cycle lithium-bromide potassium test loop simulating working fluids of spacecraft nuclear turbopump propulsion system 16 p2933 A70-34204

Mo, W, V, Ti and Zr solubilities in liquid K 16 p2933 A70-34210

LIQUID PROPELLANT ROCKET ENGINES

NT F-1 ROCKET ENGINE
NT HYDRAZINE ENGINES
NT HYDROGEN OXYGEN ENGINES
NT J-2 ENGINE
Vaporization interaction liquid rocket performance model, discussing performance loss evaluation and test data 01 p0160 A70-10832

Gaseous He bubbles injection into liquid propellant launch vehicle fuel lines to reduce vehicle pogo oscillations by lowering feed system natural frequencies 01 p0196 A70-10851

Nonlinear combustion instabilities in liquid propellant rockets, considering various combustion models and experimental techniques 02 p0351 A70-12007

Three dimensional linear combustion instability in liquid propellant rocket motors using concentrated combustion model, presenting mathematical analysis as boundary value problem 02 p0353 A70-12011

Three dimensional combustion instability in liquid-propellant rocket engines, investigating dependence on design and operating parameters via boundary value problem analysis 03 p0551 A70-13574

Flow distribution inside triangular shaped cavities of variable depth resembling liquid propellant rocket motor baffle cavities, simulating radial and tangential oscillation modes 04 p0674 A70-15566

Liquid rocket technology for chemical engineers, discussing insulating tanks, flexible lines, turbopumps and combustion chamber 05 p0896 A70-16168

Solid propellant motors relative performance as related to intermediate payload missions, considering reusable liquid strap-on stages for post-Saturn payloads 05 p0897 A70-16897

Performance analysis for electrothermal thruster using lithium propellant with supersonic heat addition
[AIAA PAPER 69-286] 06 p1129 A70-17159

Soviet book on guided ballistic missiles design and construction employing liquid and solid propellant engines with emphasis on aerodynamic heating 06 p1155 A70-17410

Liquid propellant rocket nozzle configurations maximum stress and stability limits using computer program for composite ring-stiffened shells of revolution
[AIAA PAPER 70-138] 06 p1014 A70-18053

Liquid rocket motors with concentrated combustion, studying nonlinear longitudinal instabilities with shock waves in combustion chambers 07 p1362 A70-18917

Interagency chemical rocket propulsion group method of treating measurement error for liquid rocket engine performance parameters, using uncertainty model
[AIAA PAPER 69-734] 07 p1365 A70-19723

Liquid rocket engine combustion processes determined by injector design using similarity principles 07 p1362 A70-19919

Soviet book on liquid rocket engines dynamics, emphasizing computational engineering methods and engines automatic control

08 p1558 A70-20757

Turbine pump systems operation in terms of liquid rocket engine combustion stability, noting altitude effects on pressure pulsations

08 p1559 A70-21849

Entropy or material waves effects on HF pressure oscillations in liquid rocket combustor, assuming concentrated combustion zone and zero length nozzle

10 p1929 A70-24088

Valois motor with nitrogen peroxide oxidizer for Diamant B first stage, describing design and assembly problems

10 p1930 A70-24375

Liquid rocket technology for chemical engineers, discussing propellant tanks, lines and valves, tank pressurization, turbopumps and combustion chamber problems

12 p2291 A70-27664

Europa 3 launch vehicle liquid propellant engine design and performance data, discussing West German research in high pressure rocket engines

13 p2473 A70-28447

Cost optimal booster stage for European satellite launchers, comparing liquid and solid propellant rockets

13 p2502 A70-28450

Configurations stress stability liquid propellant rocket nozzle analysis by BOSOR 3 digital program, describing mathematical model construction

13 p2508 A70-28509

Soviet book on dynamics of rockets covering solid and liquid fuel rocket stability, controllability and transfer functions

13 p2505 A70-28799

Turbopump-fed rocket engine for satellite launchers, discussing gas cooling, fuel tank pressurization, etc

13 p2474 A70-29138

Spin detonation of tangential HF vibrations in liquid rocket engine combustion chambers, discussing instability prevention

13 p2474 A70-29422

Soviet book on rocket engine theory covering liquid and solid propellants, combustion physics, nozzle and thrust chamber geometry, etc

14 p2628 A70-30628

Soviet book on liquid propellant rocket motors construction, discussing combustion chambers, frame, ducts, turbopump feed system, etc

15 p2744 A70-31850

Spacecraft propulsion development guidelines concerning rocket engines with storable propellants, rotating solid propulsion systems, cryogenic propellants, etc

15 p2790 A70-32256

Europa 3C light alloy space booster powered by Rolls-Royce engines using kerosene and LOX

15 p2810 A70-32257

Electrothermal thruster with liquid propellant, describing energy dissipation and high specific impulse

15 p2791 A70-32280

Liquid rocket engine combustion analysis, discussing bipropellant spray mass distribution, drop size and velocity, spray evaporation interphase drag and ablative chambers

[AIAA PAPER 70-622]

16 p2997 A70-33527

FLOX methane propellant rocket engines, describing operating conditions, injectors, thrust chambers fabrication and cooling, engine cycles, turbomachinery, etc

[AIAA PAPER 70-718]

16 p2965 A70-33540

Liquid rocket engine injector elements design criteria, using noncircular orifice geometry to predict efficiency

[AIAA PAPER 70-704]

16 p2967 A70-33565

S-IVB liquid rocket engine and propellant feed systems restart shutdown in orbital operations

[AIAA PAPER 70-672]

16 p2967 A70-33574

LF unsteady behavior of liquid propellant rockets from droplets evaporation and combustion rates

[AIAA PAPER 70-620]

16 p2968 A70-33589

Liquid rocket propellant engine exhaust plume flow field, discussing mathematical models for combustion chamber, throat region and nozzle

[AIAA PAPER 70-844]

16 p3001 A70-33927

Throttling venturi valves for thrust modulation of liquid propellant rocket engines, testing pressure recovery, mixture ratio control and gas saturation and boundary layer effects

[AIAA PAPER 70-703]

17 p3146 A70-34510

Pulsed laser holography for liquid rocket combustion studies, describing apparatus and techniques

17 p3092 A70-35477

Liquid propellant rocket engines, investigating fuel injection effect on formation of fuel mixture

18 p3300 A70-36252

Graphites erosion by water and carbon dioxide at high temperatures, using liquid rocket simulator for kinetics study

[AIAA PAPER 70-638]

20 p3736 A70-39587

Reusable rocket engine for space shuttle, discussing propellants, configuration, design, combustion cycle and size

20 p3689 A70-40084

Liquid propellant rocket engines performance and classification based on feed system, discussing heat transfer and thermochemical considerations

21 p3869 A70-42041

Power loss reduction from disk friction and gas leakage through rotor seals of low speed centrifugal pumps in aircraft hydraulic systems and liquid propellant rocket engines

22 p4091 A70-42806

Liquid propellant rocket engine nonisobaric cylindrical combustion chamber parameters from thermodynamic data

22 p4092 A70-43355

European rocket engine technology, discussing liquid rockets, reliability, restart capability, performance, cryogenic engine, components, facilities and U.S. cooperation

22 p4092 A70-43509

Liquid propellant rocket engine combustion instabilities, describing unsteady combustor flow by single nonlinear wave equation with stable and unstable finite amplitude limit cycles

23 p4233 A70-44425

LIQUID ROCKET PROPELLANTS

NT AEROZINE

NT CRYOGENIC ROCKET PROPELLANTS

NT GELLED ROCKET PROPELLANTS

NT HYPERGOLIC ROCKET PROPELLANTS

NT MONOPROPELLANTS

NT SLURRY PROPELLANTS

Gas solubilities investigated for gaseous pressurization of propellants

01 p0160 A70-10840

Ultrasonic atomizer system for liquid fuels combustion

02 p0356 A70-12470

Combustion processes and ignition criteria in shock wave ignition of liquid fuel drop in oxidizing atmosphere

[AIAA PAPER 70-9]

06 p1180 A70-18142

Structural element for discrete element idealization missile and liquid propellant as one composite structure

[AIAA PAPER 70-123]

06 p1042 A70-18182

Liquid propellant spray injection into high pressure gaseous environment noting geometric, dynamic and thermal characteristics

[AIAA PAPER 70-8]

06 p1182 A70-18211

Contaminants formation during pulse mode operation of liquid bipropellant attitude control rocket engine, discussing exhaust plume effects

[AIAA PAPER 69-574]

07 p1394 A70-19708

Numerical analysis of low-g fluid flow and heating problems encountered with liquid propellant storage and supply

[AIAA PAPER 69-567]

07 p1394 A70-19719

ICRPG liquid propellant thrust chamber performance evaluation methodology, reviewing imperfections and limitations

[AIAA PAPER 69-468]

07 p1365 A70-19728

Fuel and oxidizer selection for liquid bipropellant system, considering dependence on vehicle, propulsion system and propellant requirements

07 p1361 A70-19916

Oxygen and fluorine-based liquid fuels and oxidizers development, considering chemical rocket propulsion reaction principles

07 p1361 A70-19917

Laboratory and field tests to evaluate liquid rocket propellant properties for tactical mission

07 p1362 A70-19918

Earth storable liquid propellants combustion products simulation by combustion of gaseous fuel and oxidizer combination, discussing elemental composition and thermodynamic considerations

08 p1557 A70-21622

Analytical model for liquid fluorine no-vent loading operations noting application to flightweight upper stage systems

[AIAA PAPER 69-579]

09 p1662 A70-23251

Satellite attitude and orbit control systems based on electrically heated ammonia or hydrazine

09 p1767 A70-23432

Liquid propulsion studies at CNES

10 p1930 A70-24374

Combustion stability effects of additives on hydrazine/nitrogen tetroxide propellant combination by measuring droplet burning rates

11 p2100 A70-26283

Spin stabilized nonrigid satellite dynamics, considering liquid propellant behavior effect

13 p2499 A70-28401

Ignition delay-reducing catalyst for furfuryl alcohol-fuming nitric acid hypergolic bipropellant

13 p2473 A70-29992

Biphase rockets combustion characteristics, comparing results with propellant vaporization and nonlinear instability models

14 p2665 A70-30950

Space propulsion research with emphasis on tripropellant mixtures, discussing increased combustion pressure, nozzle design, reusable orbital transporter, etc

15 p2789 A70-32252

Tri- and bipropellants in spacecraft propulsion, discussing liquid and powder metals, hybrids, frozen tripropellants, etc

15 p2789 A70-32253

Small rocket engines tailoff impulse and tailoff repeatability, comparing monopropellant hydrazine and storable bipropellant engines impulse data

[AIAA PAPER 70-674]

16 p2967 A70-33576

Structural incompressible liquid element for discrete linear idealization of missile and propellant vibration analysis

16 p2991 A70-33852

Motion perturbation equations for guided space vehicles, allowing for sloshing liquid propellant viscosity effects

18 p3332 A70-36160

Liquid rocket combustion instability due to velocity vector effect, showing importance in longitudinal and transverse modes

20 p3689 A70-40079

Liquid propellant rocket combustion instability, examining droplet vaporization, wake burning and chemical kinetics

20 p3689 A70-40080

Gas velocity and static pressure effects on evaporation rate of moving liquid fuel droplets

21 p3953 A70-42094

Thermodynamic-kinetic analysis of fluorine/lithium/hydrogen tripropellant combustion efficiency, discussing liquid metal atomization, firings, facility and thrust chamber

[AIAA PAPER 68-618]

23 p4232 A70-44512

Discrete element idealization of missile and liquid propellant for vibration analysis, deriving sloshing theory

[SAE PAPER 700847]

24 p4326 A70-45885

Liquid rocket propellants tankage and components long term storage under extreme relative humidity and temperature conditions

[SAE PAPER 700800]

24 p4392 A70-45911

LIQUID ROTATION

U ROTATING LIQUIDS

LIQUID SLOSHING

Lower bounds of Stekloff and free membrane eigenvalues for sloshing of incompressible inviscid fluid, subject to gravity in rigid tank with free surface

02 p0278 A70-11999

Hydroelastic sloshing of liquid in partially filled circular cylinder with rigid or elastic walls, including surface tension effect

04 p0671 A70-15092

Dynamic instability of motion of rigid and elastic bodies with liquid filled cavities associated with practical problems of rocket technology

06 p1107 A70-18415

Simulated low gravity propellant sloshing in spherical, ellipsoidal and cylindrical tanks, discussing Bond number simulation and tank geometry effects

[AIAA PAPER 69-1004]

09 p1657 A70-23255

Liquid motion dynamic effects in open cylindrical and conical tanks with translational motion

09 p1662 A70-23293

Fluid motion in cylindrical tank with arbitrary sector annular cross section subjected to harmonic longitudinal excitation

12 p2211 A70-27818

Spin stabilized nonrigid satellite dynamics, considering liquid propellant behavior effect

13 p2499 A70-28401

Hydroelastic oscillations natural frequencies in incompressible and nonviscous liquid in circular cylinder with free surface, demonstrating wall elasticity effects

13 p2512 A70-28832

Perturbed motion of body with partially filled cylindrical cavity with damping ribs, discussing vibrations boundary value problems of liquid filling

15 p2775 A70-32157

Ideal fluid contained in half space with circular or strip-like aperture, formulating mathematical model to determine sloshing frequencies

18 p3238 A70-36057

Motion perturbation equations for guided space vehicles, allowing for sloshing liquid propellant viscosity effects

18 p3332 A70-36160

Liquid fuel behavior in right circular cylindrical tank inclined to earth gravitational field, computing fundamental sloshing frequency

20 p3610 A70-39694

Viscosity and vessel geometry effects on fluids natural and forced oscillation, taking surface tension into account

20 p3614 A70-40438

Complementary variational principles applied to free oscillations of incompressible fluid in container, using linearized hydrodynamic equations

21 p3807 A70-41323

Free fluid sloshing motion in shallow convex containers, considering isoperimetric problem for planar and axisymmetric vibrations

22 p4009 A70-42534

Principle pressure vector components for liquid in moving V-shaped and U-shaped cross section tanks

23 p4180 A70-44164

Low gravity fuel sloshing in axisymmetric rigid tank, calculating oscillations by modified Galerkin method

24 p4324 A70-45292

Discrete element idealization of missile and liquid propellant for vibration analysis, deriving sloshing theory

[SAE PAPER 700847] 24 p4326 A70-45885

Orbit-to-orbit space shuttle toroidal propellant tank design, construction and testing for outflow and slosh characteristics

[AIAA PAPER 70-1325] 24 p4417 A70-45940

LIQUID SODIUM

Liquid sodium droplets spontaneous ignition and combustion in controlled oxidizing atmosphere, discussing vapor phase diffusion flame, burning rates and evaporation constants

02 p0396 A70-12005

Gravitational effects on heat transfer during evaporation and condensation processes in heat pipe, discussing conditions in Na filled heat pipe

[DGLR-69-44] 04 p0785 A70-15171

Stainless steel corrosion rates in flowing liquid Na from mechanism based on thermodynamic partitioning of oxygen

09 p1706 A70-22942

Gravitational effects on heat transfer during evaporation and condensation processes in heat pipe, discussing conditions in Na filled heat pipe

09 p1789 A70-23427

Ta oxygen concentration effects on corrosion resistance to NaK in SNAP 8 boilers

16 p2932 A70-34202

LIQUID SURFACES

NT MENISCI

Gas chromatography based on sampling gas-vapor phase at liquid surface for determining volatile oxygen containing compounds in biological media

04 p0646 A70-14580

Interaction of infinite shallow draft cylinder oscillating at free surface with train of oblique waves

04 p0618 A70-15321

Gas flow influence on wave characteristics of thin viscous liquid layers pulled by gravity vertical surface compared with water layer experiments

08 p1482 A70-20917

Heat and mass transfer during liquid surface evaporation in vacuum, calculating temperature field on basis of heat balance level

09 p1791 A70-23717

Vortex generation in water tank, discussing velocity distribution on free surface and critical depth of air entrainment for various Reynolds numbers

14 p2567 A70-31275

Liquid or solid Leidenfrost film boiling on saturated cryogenic liquid surface, discussing hydrodynamic model similar to propellant spillage accidents

17 p3194 A70-34744

Equilibrium form shapes of fluid free surface in vessel under gravitational and magnetic field with tension

18 p3240 A70-36269

LIQUID-GAS MIXTURES

NT AEROSOLS

NT FOG

Pressure waves propagation velocity dependence on flow regime in gas-liquid mixtures

01 p0067 A70-11302

Laser beam for measuring particles velocity in two phase air-water jets by heterodyning, describing signal properties

05 p0858 A70-16258

Relation between Fourier harmonics equilibrium distribution and bulk viscosity and second thermal conductivity established in critical regions of liquid-vapor condensation and mixing

05 p0958 A70-16550

Combustion stability in air-liquid fuel zone of jet engine burner with burning rate controlled by droplet vaporization rate controlled mechanism

[WSCI PAPER 69-44] 06 p1178 A70-17980

Gas bubbles formation in supersaturated solutions and body fluids during decompression

07 p1208 A70-19511

Gas bubbles formation in supersaturated solutions and body fluids during decompression

11 p1988 A70-26110

Meniscus curvature correlation to viscosity contrast in capillary during fluid displacement

13 p2390 A70-29633

Thin cylinder longitudinal two phase dispersed flow, examining heat transfer coefficient

18 p3345 A70-36112

Liquid-gas separator design with reduced friction loss for MHD generators using two phase convergent-divergent nozzles

20 p3612 A70-40014

German monograph on flow phenomena in gas containing fluids, covering pressure and ultrasonic induced cavitation in steady and unsteady flow

24 p4324 A70-45098

Shock wave structure calculation in liquids containing gas bubbles, taking into account compression wave steepening by convection

24 p4326 A70-45783

LIQUID-LIQUID INTERFACES

Pressure drop at slender profile performing harmonic vibrations near interface between two media of different density solved by numerical method

07 p1254 A70-19079

Interfacial energy and free energy estimation by quasi-continuum approximation for two component water-organic or organic-organic liquid systems

10 p1915 A70-23843

Heat exchange and temperature distribution between two liquids divided by plate, discussing possible errors

20 p3737 A70-39634

LIQUID-SOLID INTERFACES

Liquid oxygen and water cavitation effects on lead, copper, nickel, iron and zinc

01 p0115 A70-10071

Thin liquid film equilibrium on rotating sphere, determining conditions for detachment as function of angular velocity

01 p0068 A70-11578

Heat and mass transfer in passive transpiration cooling system with two moving boundaries, observing porosities and radius of curvature effects

06 p1176 A70-17692

Unsteady interaction of compressible fluid and flat circular deforming elastic membrane analyzed by coupled computer program method

[AIAA PAPER 70-75] 06 p1039 A70-18082

Solid surface-compressible liquid drop high speed impact damage, discussing contact pressure

06 p1053 A70-18611

Interference between body and porous walls of water tunnels by one dimensional solution for usable length of tunnel

07 p1248 A70-19078

Blood-endothelial surface shear stress in artery inlet, considering asymmetric and radially symmetric plugging effects

07 p1220 A70-19248

Aluminum-base reinforced material synthesis by liquid impregnation, investigating transition layer dependence on holding time and fiber/matrix microhardness

08 p1520 A70-21500

Elastohydrodynamic lubrication of rollers relationship to pressure

09 p1693 A70-22978

Electrical conductance test for composite materials adhesive bond degradation by liquids

11 p2071 A70-26345

Nusselt numbers of nonstationary and stationary heat transfer between metal spheres and liquid flow, showing bulk heat and geometry dependence

12 p2330 A70-27288

Liquid film steady motion on ablating body surface allowing for radiative heat transfer from interior

12 p2334 A70-28244

Cell electrode potential interphasal components, defining problems due to relevant interfacial electrochemistry concepts

14 p2533 A70-30526

High temperature solid-solid reactions and solid-liquid or condensed phase-gas equilibria, using solar furnace

14 p2545 A70-30907

Oxide film and liquid effects on friction coefficient, surface relief and dislocation density along depth related to plastic deformation

15 p2743 A70-31638

Fluid flow damping in flexible liquid filled foams at various frequencies and temperatures

15 p2765 A70-31967

Incompressible flow interaction of perfect irrotational fluid through two blade wheels in relative motion, observing pressure variations at nozzle profile

16 p2836 A70-33755

Wave propagation in infinite elastic plate in contact with inviscid incompressible liquid layer, deriving dispersion relation

16 p2993 A70-34094

Fluid inertia and compressibility effects considered in equations for foil over lubricating film

[ASME PAPER 69-WA/LUB-10] 19 p3435 A70-37615

Polyurethane swelling in liquid media, measuring surface orientation effects during chemical machining on stress strain state

20 p3654 A70-39249

Liquid metal MHD conservation cycles, discussing evolution and status of power generation at various temperatures

20 p3563 A70-39325

Ideal fluid-cylindrical tank elastic bottom coupled forced oscillations, determining hydrodynamic pressure for tank reverse translational motion

20 p3615 A70-40444

Heat transfer mechanism during fluid evaporation in porous wick structure contacting heat pipe surface

21 p3946 A70-41042

Site activation in saturated nucleate boiling tests involving various fluids boiled on transparent oxide coated glass surface, correlating site density data with surface temperature

21 p3948 A70-41202

Nucleation phenomena associated with boiling heat transfer in pure liquids at solid heating surfaces

21 p3948 A70-41205

Freezing and melting of warm water flow at stagnation point over cooled plate for convective condition at solid-liquid interface

21 p3949 A70-41311

Cold plate immersed in warm flowing liquid, calculating two dimensional transient and steady state solidification by conformal mapping

21 p3949 A70-41319

Turbulent heat/mass transfer from solid boundary with shear stress dependent on wall distance for various Schmidt or Prandtl numbers

21 p3953 A70-42088

Surface tension role in microliquid layer formation on solid surface with growing bubble in nucleate boiling, using optical method

21 p3953 A70-42089

Ultrasonic Rayleigh critical angle reflectivity of liquid-solid interface energy, detecting near-surface properties changes

22 p4027 A70-42585

Transient heating by solar radiation of semitransparent solid medium and adjoining fluid, establishing criteria for maximum fluid temperature

22 p4123 A70-42598

Damage data comparison for vibratory cavitation and liquid impact on aluminum alloy, stainless steels and pure nickel

23 p4203 A70-43870

Cellular breakdown in binary Al-Cu alloys in unidirectional solidification, observing small pit stability on solid-liquid interface

24 p4362 A70-46180

Surface temperature distribution of heat generating solid body in contact with parallel viscous fluid flow

24 p4430 A70-46368

LIQUID-VAPOR EQUILIBRIUM

Supersaturated vapor condensation in supersonic nozzles, obtaining flow and droplet growth equations for local equilibrium condition

02 p0279 A70-12049

Liquid nucleation in vapor condensation on wettable, unwettable, smooth, rough and cavitated surfaces, showing positive effect of roughness elements

06 p1177 A70-17838

Vapor-liquid equilibria predictions for multicomponent cryogenic mixtures, applying to correlation selection in critical and low temperature regions

14 p2616 A70-31015

Sound velocity relation with specific heat at constant volume at liquid-gas equilibrium critical point

15 p2826 A70-32022

LIQUID-VAPOR INTERFACES

Two phase flow in cylindrical channel, formulating maximum momentum flow variational principle for laminated adiabatic vapor- and gas-liquid flows

01 p0213 A70-10216

Film-vapor interface shape for thin liquid lubricating film, analyzing two dimensional Newtonian flow including gravity, inertia and surface tension effects

[ASME PAPER 69-LUB-3] 01 p0103 A70-10399

Lubrication and leakage control mechanics of face seals, considering liquid to vapor boundary within interface

[ASLE FICFS PREPRINT 22] 02 p0308 A70-12173

Noncontacting minimum leakage dynamic seals requiring liquid-vapor interface with leakage tolerance

[ASLE FICFS PREPRINT 40] 02 p0308 A70-12175

Two phase liquid-vapor system specific heat increase at temperatures approaching critical point, using nonanalytic vapor pressure equation with data for nitrogen and oxygen

04 p0780 A70-14584

Interaction between surface liquid film and hot gaseous turbulent boundary layer analyzed for hypersonic vehicle surface thermal protection design problems

04 p0669 A70-14927

Melting ablation for two dimensional and axisymmetric blunt bodies with body force, predicting gas-liquid interface temperature for free stream conditions

06 p1176 A70-17690

Heat and mass transfer in passive transpiration cooling system with two moving boundaries, observing porosities and radius of curvature effects

06 p1176 A70-17692

Heat transfer during nucleate boiling, discussing transfer from heated surface to superheated liquid layer and exchange on gas-liquid interface

06 p1176 A70-17695

Entropy fall in superheated liquid related to vapor bubble growth from finite so-called zero radius to critical radius, noting pressure effects

07 p1418 A70-18645

- Phase growth of free vapor bubbles in water, ethanol and isopropanol at uniform superheats under normal and zero gravity 07 p1418 A70-18646
- Empirical method for calculating critical thermal flux density during boiling of underheated liquid-vapor systems 07 p1420 A70-19068
- Taylor instability of vertically accelerated horizontal two dimensional interface between liquid and air solved by method of strained coordinates 09 p1661 A70-23071
- Vapor bubble separation diameter and flow in channel boiling applied to supercooled boiling zone determination 09 p1789 A70-23379
- Empirical method for calculating critical thermal flux density during boiling of underheated liquid-vapor systems 10 p1970 A70-25219
- Microwaves reflection, absorption and thermal emission at smooth air-water interface, tabulating calculated coefficients 12 p2183 A70-27169
- Radiating drop unsteady vaporization or growth for uniformly distributed internal heat sources, discussing gas temperature distribution and diffusion thermal effect 13 p2521 A70-29417
- Shock wave interaction with burning liquid fuel droplets in gaseous oxygen atmosphere, observing wave amplification due to mass combustion rate increase 13 p2522 A70-29424
- Film condensation in tubes, considering liquid-vapor interface, zero gravity and electrostatic field conditions 15 p2828 A70-32541
- Vapor fraction dependence on liquid hydrogen propellant outflow during NERVA operation under stored gas or autogenous pressurization, using computer simulation [AIAA PAPER 70-677] 16 p2950 A70-33578
- Gas-liquid two phase flow dynamics, explaining behavior under normal and oblique shocks 16 p2893 A70-33684
- Film-vapor interface shape for thin liquid lubricating film, analyzing two dimensional Newtonian flow including gravity, inertia and surface tension effects [ASME PAPER 69-LUB-3] 19 p3435 A70-37610
- Turbulent viscoseal with gas-liquid interface, using recirculation loop for gas ingestion reduction [ASLE PREPRINT 70AM 5C-4] 19 p3439 A70-38804
- One dimensional unsteady equilibrium flow stability of relaxing two phase medium consisting of perfect gas and incompressible liquid 20 p3613 A70-40295
- Vapor volume entrained in liquid bulk from boundary layer boiling on vertical plate in low gravity field 21 p3947 A70-41055
- Vapor bubble response to sinusoidal pressure pulsation in water bulk and on metal wall 21 p3949 A70-41309
- Liquid jet breakup in supersonic airstream, using high speed photographic techniques [SMPT PREPRINT 90] 22 p4036 A70-43063
- Liquid droplet breakup by aerodynamic forces, obtaining solutions for fluid flow inside droplet and in coupled liquid-gaseous boundary layer 22 p4012 A70-43741
- Fluorine specific heat derived from measurements on two phase liquid vapor system at constant volume by PVT properties at coexistence 23 p4157 A70-44001
- Liquid nitrogen saturated film boiling from wire at pressures up to critical, discussing liquid-vapor interface configuration 23 p4279 A70-44362
- Liquid He II, determining correlation of depth effect on film boiling heat transfer with vapor film geometry from motion pictures 23 p4279 A70-44363
- Single component fluid behavior in liquid-vapor critical point vicinity, using LF acoustic resonant cavity technique for isochoric measurements 23 p4222 A70-44432
- LIQUIDS**
- NT AEROZINE
- NT CRYOGENIC FLUIDS
- NT CRYOGENIC ROCKET PROPELLANTS
- NT FLOX
- NT GELLED ROCKET PROPELLANTS
- NT HYDRAULIC FLUIDS
- NT HYPERGOLIC ROCKET PROPELLANTS
- NT LIQUEFIED GASES
- NT LIQUID AMMONIA
- NT LIQUID HELIUM
- NT LIQUID HYDROGEN
- NT LIQUID METALS
- NT LIQUID NITROGEN
- NT LIQUID OXIDIZERS
- NT LIQUID OXYGEN
- NT LIQUID POTASSIUM
- NT LIQUID ROCKET PROPELLANTS

- NT LIQUID SODIUM
- NT MERCURY [METAL]
- NT MERCURY VAPOR
- NT MONOPROPELLANTS
- NT ORGANIC LIQUIDS
- NT ROTATING LIQUIDS
- NT SLURRY PROPELLANTS
- Bacterial and viral detection techniques in liquids based on specific property measurement relevant to biological particle, emphasizing industrial processing applications 01 p0013 A70-10127
- Light inductions and echo intensities in liquids and gases, investigating thermal vibrations, translational Brownian motion, particle collisions and laser diffusion effects 06 p1082 A70-17809
- Book on liquid masses ellipsoidal figures of equilibrium extended into coherent mathematical theory, discussing virial equations, potentials of homogeneous and heterogeneous ellipsoids, etc 10 p1917 A70-24701
- Venturi tube optimal design and operation parameters for small liquid quantities dosage 11 p2035 A70-25778
- Bubbles, steady streaming and surface instability in vibrated liquid columns 14 p2663 A70-30255
- Cavitation nuclei in liquids, discussing sources, stability and gas bubble growth [ASME PAPER 70-FE-23] 16 p2891 A70-33632
- Wave propagation from two dimensional expanding load on liquid half space with load fronts decelerating monotonically from initial supersonic speed 17 p3069 A70-34976
- Liquids density measurement from digital data obtained from sample subjected to vibrations 22 p4030 A70-42848
- LIQUIDS**
- Be-Al-Ti system liquidus surfaces and invariant equilibria by chemical, thermal, X ray and microscopic methods, discussing phase diagrams 14 p2595 A70-30839
- Ti-Cu-Ag phase diagrams and liquidus surface structure, using metallographic, thermal and X ray techniques 16 p2931 A70-33221
- LISTS**
- Minimum Equipment List from aircraft manufacturer and airline operations viewpoint [AIAA PAPER 70-900] 17 p3019 A70-35816
- LITERATURE**
- NT DOCUMENTATION
- LITHERGOLIC PROPELLANTS
- U HYBRID PROPELLANTS
- LITHIASIS**
- Renal lithiasis frequency among flight crews during aeronautical activity, noting role of rich food intake 17 p3040 A70-35917
- LITHIUM**
- NT LITHIUM ISOTOPES
- Welding atmosphere purity effects on Li corrosion resistance of refractory metals in space power systems 04 p0709 A70-15627
- Performance analysis for electrothermal thruster using lithium propellant with supersonic heat addition [AIAA PAPER 69-286] 06 p1129 A70-17159
- Rankine cycle two loop Li boiling Ka facility for nuclear turbopump simulation, studying alkali metal corrosion for operation with and without hot traps [AIME PAPER F-69-1] 07 p1304 A70-18809
- Fine structure of excited P states of Li measured for magnetic fields in proton NMR frequency using level crossing and Zeeman effect 07 p1346 A70-20239
- Low field and high field hyperfine structure and lifetimes of excited P states of Li using level crossing spectroscopy 07 p1346 A70-20240
- Lithium-cadmium fluoride battery for aircrew survival beacon radio receivers, considering voltage loss elimination by doping 08 p1439 A70-20708
- Electrochemical cells with lithium anode and nonaqueous electrolyte, discussing research role in designing high specific energy primary batteries 08 p1440 A70-20709
- Steel structure and mechanical properties under preliminary loading at elevated temperature and liquid Li at various exposure times 08 p1515 A70-20935
- High energy density nonaqueous battery with lithium metal anodes, cupric chloride cathodes and organic aprotic solvent electrolyte [AIAA PAPER 70-530] 13 p2349 A70-29038
- Li positive ions in KCl crystals, investigating internal strains effect on paraelectric resonance spectra 14 p2626 A70-30340
- Red twilight emission enhancements origin, concerning atomic lithium release effect in upper atmosphere 14 p2580 A70-31264
- Metal corrosion effects in Rankine cycle lithium-boiling potassium test loop simulating working fluids of spacecraft nuclear turbopump propulsion system 16 p2933 A70-34204

- Refractory alloys Li corrosion resistance, examining effects of oxygen contamination during welding 16 p2924 A70-34205
- Molten contaminated Li effects on microstructure, tensile strength and stress corrosion of stainless steels and refractory metals 16 p2933 A70-34206
- Li ion elastic scattering by He, calculating ground state interaction potential 16 p2956 A70-34310
- Photoelectric conversion efficiency and radiation resistance of Li-doped Si solar cells, showing improved reliability over Li-free cells 17 p3023 A70-35311
- Nb-Zr alloy and yttria corrosion by high velocity Li flow, discussing material removal depth 22 p4055 A70-43100
- Li doublet in 21 March 1969 sunspot, examining fine structure caused by self reversal in line core 24 p4400 A70-45309
- Thermal decomposition of freeze dried Ta and mixed lithium-niobium oxalate, using surface area and electron micrographs 24 p4363 A70-46212
- LITHIUM ALLOYS**
- Electron momentum distributions from Compton profiles of Li-Mg polycrystalline samples, exhibiting discontinuity at free electron value of Fermi momentum 05 p0892 A70-16471
- Light Mg-Li alloys physical and mechanical properties, production and treatment [DFVLR-SONDDR-18] 07 p1306 A70-19234
- Annealing effect on stress-strain curves of overaged and cold-rolled Al-Li alloy, observing yield drop 09 p1708 A70-23727
- LITHIUM CHLORIDES**
- Gallium trichloride and aqueous solution of lithium chloride as solar neutrino detectors 05 p0899 A70-15956
- LITHIUM COMPOUNDS**
- NT LITHIUM CHLORIDES
- NT LITHIUM FLUORIDES
- NT LITHIUM HYDRIDES
- NT LITHIUM HYDROXIDES
- Nonlinear optical properties of lithium niobate single crystals, considering optically induced index inhomogeneity and second harmonic generation 01 p0157 A70-10422
- Thermodynamics of electrochemical cells consisting of Li with lithium chloride or bromide and thallium amalgam with thallium chloride or bromide in propylene carbonate 01 p0042 A70-11107
- Birefringences and phase retardations in lithium niobate crystals for light propagation directions near optical axis, considering electro-optic modulation 02 p0313 A70-12451
- Long range order formation kinetics in lithium ferrite octahedral sublattice after stepwise annealing and quenching in water, using X ray analysis 03 p0537 A70-12867
- Solid and liquid lithium tetrafluoroborate enthalpy relative to 273 K measured at temperatures between 323-873 K, deriving thermodynamic properties 04 p0646 A70-14583
- Thermodynamics of LiBr in anhydrous dimethyl sulfoxide determined at several temperatures using EMF method 06 p1003 A70-17219
- Unsaponifiable, molecular weight acids, alcohols and esters effect on rheological properties of lithium lubricants based on synthetic fatty acids 06 p1076 A70-17800
- LiI thermodynamic properties in dimethyl sulfoxide determined by emf method, discussing ionic solution energies 10 p1831 A70-25041
- Raman spectrum of lithium formate monohydrate single crystal in polarized He-Ne laser light, discussing crystal structure 13 p2425 A70-28714
- NaLi molecular and ionic electronic states, discussing valence formulation, Hartree-Fock calculations, wave functions, excited state potential, etc 15 p2776 A70-31728
- Spinel lithium ferrite magnetic and crystallographic properties, considering effects of Li and oxygen losses, sintering temperature and cooling rate 16 p2961 A70-33272
- Far field diffraction spreading of surface acoustic waves on cut Li-niobate in two directions 23 p4230 A70-44199
- Ruby laser second harmonics generation in low loss lithium iodate crystal with high conversion efficiency 24 p4355 A70-46085
- LITHIUM FLUORIDES**
- Kinetic theory of cracks network formation on LiF crystal surface exposed to plasma jet using high speed camera 04 p0730 A70-14458
- Molecular He and Ar nozzle-type beams scattering from room temperature LiF crystal surfaces, measuring particles flux and speed distributions 06 p1111 A70-18267

LiF prism spectrometer for space applications, discussing vacuum UV transmission and mechanical properties

11 p2049 A70-25629

Kinetic theory of cracks network formation on LiF crystal surface exposed to plasma jet using high speed camera

13 p2510 A70-28655

LITHIUM HYDRIDES

Laser microplasma formation in focus of two laser beams impinging on crystalline lithium hydride targets

12 p2246 A70-27355

LITHIUM HYDROXIDES

Water vapor effect on carbon dioxide reaction with lithium hydroxide in dynamic isothermal system

20 p3582 A70-39227

LITHIUM ISOTOPES

Solar neutrinos detection from recording high energy electrons in reactions, using Li 7, Be 9 and B 11 as detectors

05 p0899 A70-15964

LITHIUM 4

U LITHIUM ISOTOPES

LITHIUM 6

U LITHIUM ISOTOPES

LITHOSPHERE

U EARTH PLANETARY STRUCTURE

LIVER

Nicotinamide adenine dinucleotide (NAD)/deamination and role of nicotinamide hypoxanthine dinucleotide (deamino-NAD) in forming ammonia from amino acids in rats/rabbits brain and liver tissue

01 p0018 A70-10505

Metabolism and biological activity of urea, citrulline, arginosuccinic acid in organism ornithine cycle, discussing role in brain and liver

01 p0019 A70-10513

Blood flow changes in portal vein and hepatic artery of anesthetized cats following intraportal and intrahepatic arterial administration of isoproterenol, epinephrine and norepinephrine

02 p0232 A70-11718

Fructose metabolism in liver and extrahepatic tissues of sea level and high altitude natives, noting lactate and pyruvate accumulation in blood

02 p0233 A70-11722

Postirradiation free radical processes in cellular organelles of rat liver exposed to gamma irradiation detected by graft copolymerization method

03 p0418 A70-13302

Ultraweak luminescence intensity, radiation damage kinetics and spectral properties of cellular organelles of rat liver exposed to gamma radiation

03 p0419 A70-13304

Purification and properties of diphosphopyridine nucleotide-linked glycerol 3-phosphate dehydrogenases from chicken breast muscle and liver

03 p0442 A70-14047

Enzyme beta-hydroxybutyrate dehydrogenase concentration in mitochondria from bovine and sheep liver

03 p0430 A70-14198

Chloride and sulfhydryl activators in glucagon degradation and secretion by purified rat liver dipeptidyl aminopeptidase I/Cathepsin C

04 p0631 A70-14682

Hepatic polysome profiles and tyrosine transaminase activity daily rhythms in rats, studying dietary protein role

06 p0997 A70-18402

Succinic dehydrogenase activity in white rats cerebrum and liver under hypothermia and after warming

07 p1207 A70-19475

Fat embolism and decompression sickness similarities, studying lipid stability changes resulting from liver tissue injury by nitrogen bubbles

07 p1222 A70-19936

Biochemical and histochemical parallels of enzymatic activity in blood, cardiac muscle and liver under hypoxia

08 p1446 A70-21445

Amino acid metabolism time dependent variations, studying tyrosine transaminase rhythm in rat liver

09 p1618 A70-22525

Dietary intake and adrenal cortex effects on diurnal rhythm of hepatic tyrosine transaminase activity and adrenal corticosterone content in rats

09 p1621 A70-23437

Portal vein smooth muscles electrical properties, using double saccharose bridge method

15 p2679 A70-31605

High altitude liver function and blood flow, determining bromsulphophthalein transport maximum and storage capacity and galactose elimination

15 p2683 A70-32531

Albumin and IgG degradation, studying high altitude effect on hepatic function in man

15 p2683 A70-32532

Repeated decelerations effects on mice and rats, noting fibrotic changes in liver

17 p3025 A70-35133

Tyrosine content and utilization in mouse liver, showing daily rhythm in composite metabolism rate

20 p3568 A70-38976

Liver blood flow in dogs during increased oxygen consumption

20 p3577 A70-40448

Oxidative enzymes histochemistry in nervous system, liver and kidney of rats in immediate and remote periods after 24-hr artificial hypobiosis

21 p3764 A70-41478

Oxidative phosphorylation and oxygen intake during circulatory hypoxia in mitochondria of liver and brain in rats subjected to acute ischemia

23 p4145 A70-44315

Oxidative phosphorylation and oxygen consumption during hyperoxia in mitochondria preparations and tissue homogenates from white rat liver

23 p4146 A70-44316

Mammalian tissues metabolic and genetic alteration during weightlessness, relating rats liver regeneration delay to centrifuging intensity following hepatectomy

23 p4146 A70-44617

Heme biosynthesis defect in vitamin E-deficient rats affecting bone marrow synthesis of delta-aminolevulinic acid and liver formation of porphobilinogen

24 p4304 A70-46146

LOAD DISTRIBUTION [FORCES]

Curved cylindrical panel flutter in presence of uniform compressive load, taking into account relationship between actual and ideal shape

01 p0202 A70-10946

Steels tested to evaluate proposed incremental strain theories predicting loads on thin walled cylinders subjected to nonproportionate loading, discussing stress-strain diagram

01 p0202 A70-11057

Clamped skew plates of orthotropic material under transverse load analyzed by stationary potential energy method and compared with isotropic case

01 p0205 A70-11140

Dynamic stability of simply supported column of linear viscoelastic materials under sinusoidal loading

01 p0206 A70-11148

Gas turbine engines vibration characteristics, discussing statistical analysis obtained through condensed vibration overload control program

01 p0166 A70-11420

Materials strength characteristics with respect to breakdown probability parameter by statistical fatigue stability analysis under unsteady loads and various distribution laws

01 p0211 A70-11424

Elastic curve deformation of rod in equilibrium under end loads, using equations analogous to Kharlamov kinematic equations and Chaplygin solution

01 p0094 A70-11440

Thin anisotropic elliptical plate elastic equilibrium weakened by hole and under concentrated loads

01 p0211 A70-11445

Nonlinear equations solvability for elastic cylindrical shells found existing for arbitrary load and clamping conditions

01 p0212 A70-11572

Machine parts fatigue behavior and service life, studying endurance margin under load cycles spectra below initial endurance limit

02 p0383 A70-11657

Aerodynamic load distribution due to wind action on elastic structures, calculating various ratios between wind and critical divergence velocity

02 p0385 A70-11913

Attachment loads and beam bending moments design curves for linear and right angle fittings on honeycomb inserts to determine internal loading

02 p0386 A70-11949

Stress-strain analysis of rectangular plates under concentrated load, noting sealed liquid compressibility effect on deflections and bending moments

02 p0388 A70-12499

Tangential force applied to column end by jet reaction from nozzle clamped to column end, obtaining critical load and oscillation frequency

02 p0389 A70-12644

Thin simply supported circular rigid ideally plastic plate subjected to dynamic transverse load uniformly distributed over central circular region

02 p0389 A70-12668

Rigid plastic body of material insensitive to strain rate under time dependent surface tension and time independent body forces

02 p0391 A70-12816

Service life analysis at randomly varying load - Conference, Muelheim-Ruhr, Germany, April 1969 [DFVLR-SONDDR-4]

02 p0391 A70-12851

Random function theory for determining influence of system oscillation characteristics on load distribution

02 p0324 A70-12852

Shells of revolution having arbitrary stiffness distribution and subjected to arbitrary loads and temperatures

03 p0583 A70-12916

Internal hydrostatic or lateral pressure effect on deformations of infinitely long thin cylindrical isotropic shell subjected to equal concentrated radial loads

03 p0584 A70-12922

LOAD DISTRIBUTION [FORCES]

Incremental strain theories for nonproportionate loading of thin walled cylinders, discussing Tresca flow, von Mises theory and Prandtl-Reuss relations

03 p0480 A70-12953

Case bonded solid propellant rocket motors stresses under transverse body force loading as function of load orientation, case stiffness and support method [SESA PAPER 1502]

03 p0579 A70-12961

Somatic motor unit spikes human biceps during posture holding, obtaining Markov chain and random variable behavior patterns

03 p0416 A70-13011

Cauchy integrals extension to axisymmetric elasticity problems, obtaining numerical results for stressed circularly symmetrical state of hollow cylinder under uniform load

03 p0586 A70-13080

Integral equations for antisymmetric shallow shell stress-strain state with crack, obtaining asymptotic solution in form of power series

03 p0591 A70-13420

Shallow elliptical planform shell under uniformly distributed normal load calculated with 'ritz and Bubnov-Galerkin variational methods

03 p0593 A70-13496

Boundary value problems for orthotropic half plane and infinite orthotropic plane with cuts, considering loads at various points

03 p0593 A70-13497

Circular cylindrical shell stressed state with rectangular opening under compressed torsion, noting opening effect on loads nonuniform distribution

03 p0593 A70-13501

Load analysis for aircraft landing gear during touchdown and braking operations

03 p0596 A70-14093

Linear nonaxisymmetric bending of infinite plate coupled to elastic half space under concentrated loads using double Fourier transforms

04 p0766 A70-14480

Astatic equilibrium loadings in Saint Venant principle for linear elasticity, analyzing physical distinction from self equilibrated loadings to explain smaller long range stresses

04 p0769 A70-14860

Stress analysis of shell loaded at free edge by concentrated forces and moments

04 p0772 A70-14920

Spherical shells axisymmetric equilibrium properties under uniformly distributed external compression

04 p0773 A70-15008

Axisymmetric structures under load and temperature distribution analyzed by matrix displacement method [DGLR-69-62]

04 p0774 A70-15167

Elastoplastic media revised mathematical model with allowance for cumulative damages effect on elastoplastic property under variable loads

04 p0775 A70-15199

Thermoplastic behavior of bodies under variable loads obtainable as function of time variable external temperature field

04 p0775 A70-15200

Swept wings aerodynamic center and span load distributions with respect to quarter-chord line

04 p0619 A70-15393

Spherical caps axisymmetric static and dynamic buckling under load, using axisymmetric nonlinear elastic shell theory approximation and finite difference equations

04 p0778 A70-15587

Stress distribution in long beams with circular annular inclusion under concentrated load solved in series form

05 p0928 A70-16024

Spread criterion and stress distribution near penny shaped crack in elastic solid under axisymmetric body forces distribution

05 p0930 A70-16079

Energy method for analyzing rectangular panels buckling under nonuniform in-plane loading, considering stability under uniform compression

05 p0931 A70-16117

Dynamic response of simply supported rectangular plate under suddenly applied transverse load, comparing solutions of classical and improved plate theories

05 p0933 A70-16174

Stress-strain state of circular orthotropic shells under bending, considering distributed loads applied to shell center

05 p0934 A70-16217

Resistance strain gauge load cell for measuring compressive loads under high hydrostatic pressure, discussing gauge bonding

05 p0848 A70-16377

Load distribution in Christmas tree turbine attachments due to centrifugal force on blades, showing strain diagrams

05 p0939 A70-16488

Lower bound limit analysis of symmetrically loaded thin shells of revolution having arbitrary meridional profiles, demonstrating methods for pressure vessel problems

05 p0944 A70-16815

Shallow spherical shell subjected to arbitrarily located concentrated normal force, discussing boundary effects on resulting stress distribution
05 p0945 A70-16817

Plastic bodies stress-strain state under variable loads generalized to cases of cyclic loads and plasticity
06 p1162 A70-17384

Displacement hybrid finite element models for analyzing shells with distributed loads
06 p1168 A70-17939

Bending stress concentrations in elastic square plate with central hole under uniform load, using finite element solutions of modified Rayleigh-Ritz method
06 p1168 A70-17940

Thin walled cylindrical shell stability with hollow filler under distributed external loads, determining critical loads
07 p1399 A70-18663

Fatigue strength of sintered aluminum powder at room and elevated temperatures, discussing sensitivity to tensile loads misalignment
07 p1304 A70-18840

Critical stresses for plate with circular hole and cracks assuming symmetrical load
07 p1402 A70-19054

Integration by orthogonalizations of envelopes of revolution loaded asymmetrically, introducing boundary conditions and structure discontinuities
07 p1404 A70-19128

Circular cylindrical shells creep buckling under nonuniform external loads, considering thermal effects and initial imperfections
07 p1405 A70-19253

Saint Venant principle in cantilever sandwich beams under two statically equivalent load systems, considering Young moduli effects
07 p1406 A70-19328

Infinite strip with longitudinal crack and under loading, analyzing stress-strain state
08 p1585 A70-20938

Statistical analysis of model parabolic mirror rigidity on multisupported suspension under symmetrically distributed load represented by mirror weight
08 p1586 A70-21057

Elastic paraboloid of revolution under axisymmetrical and nonaxisymmetrical loads, using Bessel functions of real and imaginary arguments with trigonometric functions
08 p1587 A70-21165

Stress-strain state of shells with positive Gaussian curvature under concentrated tangential loads, basing fundamental solution on two dimensional Fourier transform
08 p1587 A70-21169

Finite bending elements for static deflections of annular and circular plates loaded by concentrated forces, calculating free vibrations
08 p1588 A70-21243

Optimal inextensional buckling of uniformly loaded simply supported arches with large opening angle
08 p1589 A70-21310

Circular cylindrical shell supported along generator under arbitrary forces using finite Fourier transform, simplifying results by Euler sum formula
08 p1589 A70-21312

Elastically symmetric thin plate stress-strain state under uniformly distributed load applied to edges
08 p1591 A70-21415

Dugdale crack model extended to include effects of linearly varying tensile loading, noting plastic zone length sensitivity
08 p1593 A70-21512

Elastic equilibrium of semiinfinite two dimensional medium with Griffith crack under axisymmetric load and free and rigidly clamped edges
08 p1594 A70-21771

Metal fatigue by proliferation, diffusion and vanishing of lattice dislocations under varying loadings described by nonlinear inhomogeneous parabolic differential equations
09 p1770 A70-22253

Elastic body equilibrium forms bifurcation solution for uniform strain applied to cylindrical rod and shell under compressive strain
09 p1773 A70-22539

Limit and shakedown loads in creep range investigated on sheet rolled aluminum at room temperature for structural design applications
09 p1775 A70-22591

Fatigue crack probability distributions under oscillatory stationary random loading, basing analysis on crack propagation model
09 p1776 A70-22683

Secondary losses in axial turbine cascades without end clearance noting correlation with blade loading
09 p1743 A70-22980

Transversely isotropic body of revolution under combined surface loads and stationary axisymmetric temperature field, obtaining displacement vector and stress tensor in analytic functions
09 p1778 A70-23086

Nonisothermal loading model of polycrystalline material, investigating tangential stresses in slip

direction and plastic deformation using linear strengthening law
09 p1779 A70-23102

Carrying capacity of shallow shells of revolution, determining buckling stress and limiting equilibrium of shells with varying thickness under transverse load
09 p1781 A70-23288

Elastic ribs reinforced thin cylindrical shells stress-strain state under arbitrary load distribution allowing for rib spacing discreteness
09 p1784 A70-23590

Stress distribution in rib reinforced cylindrical shells under concentrated forces calculated using finite difference scheme
09 p1791 A70-23718

Axial tensile stress effects on stability of cylindrical shell under nonuniform external pressure
09 p1786 A70-23721

Stress distribution in anisotropic disk shaped into wedge loaded at vertex by concentrated moment determined by complex potentials method
10 p1956 A70-24084

Thick-walled toroidal shell under various load distributions, analyzing stress-strain state by networks method using computer program
10 p1957 A70-24250

Axisymmetric elasticity theory problem solution for hollow finite cylinder with symmetrical end loading, employing stress function
11 p2128 A70-25388

Titan 3C boost phase inertia loads on payload estimated for satellite design, using frequency and interface acceleration methods
11 p2120 A70-25446

Aircraft structures fatigue, discussing prediction of response to fatigue environment, load distribution, fatigue life, crack propagation rates and residual strength
11 p2132 A70-25677

Sinusoidal and random loading response of age hardening aluminum alloy determined by fatigue testing
11 p2133 A70-25732

Environment and complex load effects on fatigue life - ASTM Conference, Atlanta, September-October 1968
11 p2137 A70-26088

Spatial correlation effect of unsteady sectional loads in axial direction on average or apparent loads over finite region of circular cylinder immersed in moving fluid
11 p2036 A70-26148

Stresses and displacements determinations in spherical shells under concentrated loads, considering transverse shear deformation effect
11 p2139 A70-26347

Clamped thin circular plate bending under various loadings due to action of rigid square column on center
11 p2139 A70-26404

Fiber reinforced composites under longitudinal shear loading, noting orthotropic nature and shear moduli assuming circular fibers
11 p2141 A70-26489

Monograph on shells of revolution and prismatic shells of arbitrary cross sectional shape with arbitrary load covering partial shells, programs, boundary condition methods, etc
11 p2141 A70-26600

Axisymmetrically loaded shells of revolution with displacement behavior defined by fourth order differential equations, discussing finite difference method suitability for solution
11 p2144 A70-26679

Tension rays and load transfer from compact member via wrinkled membrane determined by variational technique using maximum strain energy
12 p2322 A70-27225

Clamped shallow spherical cap elastic buckling and initial postbuckling behavior under uniformly distributed load over circular region centered at apex
12 p2326 A70-27814

Postwrinkling nonlinear behavior of conical shell of revolution subjected to bending loads
12 p2326 A70-27816

Low aspect ratio wings calculated for roll-damping derivatives, investigating load distribution
12 p2157 A70-27983

Strain induced in laminated orthotropic fiberglass plastic cylindrical shell by normal concentrated load, using equations free from rectilinear normals hypotheses
12 p2328 A70-28279

Critical loads and stability of isotropic cylindrical shells under uniformly distributed longitudinal compression loads based on network method
13 p2514 A70-29287

Transverse bending of isotropic rectangular plate with symmetric crack under uniformly distributed load, considering corrections for stress-strain state near cracks
13 p2516 A70-29516

Creep properties of torsion-tension metal members subjected to nonproportionate loading at high temperatures
14 p2656 A70-30637

Materials durability in presence of stress concentration under biharmonic loading
15 p2813 A70-31527

Axisymmetric nonuniform initial thickness disk under pressure and twisting along interior surface of circular hole using incremental theory of plasticity for deformation analysis
15 p2816 A70-32004

Positive/negative curvature shells local stresses due to concentrated loads and heat sources, deriving approximate solutions
15 p2817 A70-32161

Influence function for thin toroidal shell under uniformly distributed axisymmetric load, determining stresses and displacements in various cross sections
15 p2817 A70-32163

Curvilinear cracks development in flat brittle body under asymmetrical loads using small parameter method
15 p2817 A70-32165

Axisymmetric elastoplastic deformation of compressible plate with arbitrary hardening under uniform load, solving in quadratures
15 p2817 A70-32167

Bifurcation stability in geometrically nonlinear shells of revolution under transverse loads, considering tension and compression deformation
15 p2817 A70-32168

Elastic equilibrium of unbounded body with central hole and concentric cracks under symmetric load
15 p2819 A70-32188

Steel and copper alloys torsion-tension members under nonproportionate loads, predicting creep behavior
15 p2759 A70-32316

Maximum stress distribution in laminar composites, considering loads on boundary of reinforcing layers
15 p2766 A70-32854

Small displacements in noncircular cylindrical shells under various loads
16 p2987 A70-32992

Elastoplastic bending of thin plate under increasing and uniformly distributed loads, defining statically admissible stresses
16 p2988 A70-33107

Membrane stresses on nonspherical domes with axisymmetric loads
16 p2990 A70-33743

Nonlinear dynamic analysis of shells of revolution under symmetric and asymmetric loads, obtaining solutions for shallow cap buckling
16 p2994 A70-34229

Ultrahigh vacuum creep rate measurements with continuously increasing loads on Ta-base alloy, relating creep life with temperature and stress rate
17 p3122 A70-34552

Inelastic analysis of unidirectional composite subjected to transverse normal loading, discussing linear response up to elastic limit and subsequent crack propagation and failure
17 p3182 A70-34557

Transversely isotropic Timoshenko beam statics and dynamics under initial stress and transverse loading
17 p3182 A70-34561

Core flexibility effects on deformation of uniformly loaded clamped parallelogrammic sandwich panels using linear theory
17 p3185 A70-34920

Singular solutions to concentrated loads on shallow shell equations with quadratic middle surface
17 p3186 A70-34968

Solutions for normal and tangential displacements and concentrated forces on shallow cylindrical shells
17 p3186 A70-34969

Normally loaded thin plate displacements, bending moments and stresses determined by hologram interferometry and indirect moire and superposition of grilles
17 p3085 A70-35011

Column end fixity using Euler load and maximum flexibility coefficient for span point lateral load
17 p3188 A70-35226

German monograph on stress and displacement in plane elastic circular rings, disk strips and wedges, considering single load distributions
17 p3189 A70-35370

Curvilinear crack propagation in elastic plane under balanced loads, using singular integral equations
18 p3341 A70-36584

Deflection behavior of uniformly loaded elliptical elastic plates on elastic foundation, using small parameter perturbation technique
18 p3343 A70-36713

Thickness determination of external elastic plates in freely supported three layer structures of uniform strength under perpendicular loads
18 p3343 A70-36717

Stress concentrations in edge-bonded elastic quarter planes with normal and shear loading at boundary
19 p3535 A70-37384

Damped linearly tapered cantilever beam elastically restrained against rotation at wall, analyzing displacement under general initial and distributed load conditions
19 p3539 A70-37802

Edge distribution of transverse reactive forces of rectangular plate with nonuniform flexural rigidity at buckling load

19 p3541 A70-38042

Core-filled thin cylindrical shell under radial ring and band pressure loads, using Boussinesq-Neuber stress function and Flugge shell theory

19 p3543 A70-38247

Clamped spherical shells under concentrated, distributed and ring loadings, analyzing large axisymmetric deflections for prebuckled and postbuckled states

19 p3545 A70-38336

Circular sandwich arc subject to central concentrated load and symmetrically applied edge couple, obtaining shakedown interaction curve

19 p3546 A70-38354

Clamped edge thin flat elliptic plate subject to elliptic paraboloidal loading, determining middle surface deformations for nonlinear large deflections

19 p3547 A70-38359

Machine parts fatigue behavior and service life, studying endurance margin under load cycles spectra below initial endurance limit

19 p3547 A70-38430

Elastic-plastic equilibrium bifurcation in geometrically simple frame model with symmetrically loaded beam, comparing characteristics with Shanley uniformly stressed column model

19 p3549 A70-38671

Elastoplastic deformation of thin circular plates under uniformly distributed transverse loads, using mixed type variational equation

20 p3721 A70-39776

Stress-strain zero moment state of thin walled helicoidal shell under uniformly distributed tensile loads

20 p3721 A70-39778

Concentrated lateral loads effect on elastic stability and moment carrying capacity of circular cylindrical shells in bending

21 p3932 A70-40544

Spacecraft parachute stress analysis, using finite elements with nonlinear elastic properties to obtain shape and load distribution [AIAA PAPER 70-1195]

21 p3753 A70-41821

Load transfer to elastic fiber in infinite elastic matrix, determining fiber force distribution

22 p4113 A70-42539

Stresses and strains concentration around elliptic hole in finite plates subjected to uniform load, using photoelasticity, moire effect and grids

22 p4114 A70-42697

Circular cylindrical shell under longitudinal line load, deriving closed form solution in Fourier series

22 p4118 A70-43547

Elastic plane equilibrium with thin walled flexible rectangular finite inclusion under symmetrical concentrated load, including computer calculated tangential stresses

22 p4118 A70-43569

Natural oscillations of cylindrical shell with elastic filler, using simple load distribution model

22 p4119 A70-43572

Transverse bending of orthotropic glass fiber reinforced plastic plates under uniformly distributed loads

22 p4120 A70-43720

Heavy homogeneous material free elastic rod dynamic stability under distributed scanning load, investigating plane transverse vibrations by differential equations

22 p4121 A70-43722

Optimal load distribution for prestressed rod system, using Chebyshev solution of inequalities

22 p4121 A70-43725

Low disk loading rotors in high speed VTOL aircraft for economical vertical payload lift [ICAS PAPER 70-57]

23 p4139 A70-44153

Spherical shell nonaxisymmetrical deformation under varying loads, relating parameters, Poisson coefficient and complex function

23 p4267 A70-44168

Rigid and elastic rectangular plates vibration under uniformly distributed dynamic load, investigating bending behavior by Galerkin method

23 p4268 A70-44170

Cantilever beam optimal stability under concentrated and uniformly distributed bending loads

23 p4268 A70-44171

Computer program for geometrical nonlinear static and dynamic structural analysis of arbitrarily loaded shells of revolution

23 p4273 A70-44724

Infinite plates and shallow shells stability under doubly periodic surface loadings, using nonlinear analysis

24 p4421 A70-45283

Shallow arch clamped at ends and subjected to uniform lateral load, deriving nonunique equilibrium stability states

24 p4426 A70-46038

Hydraulic load loops with random force signal for aircraft structures endurance testing

20 p3593 A70-39913

LOAD TESTS

Loads effects on refractory alloy fatigue strength and life at high temperatures, describing aircraft turbine blade tests

01 p0115 A70-10069

Loading frequency effects on Duralumin endurance limit in air and in water, noting stress level role

01 p0115 A70-10070

Externally pressurized journal bearing load tests, comparing load capacity data with analytical values

01 p0103 A70-10559

Constant stress creep and recovery behavior experiments of polycarbonate under combined tension and torsion stresses in weakly nonlinear range

01 p0130 A70-11083

Stress rupture strength dependence on specimen geometry /scale effect/ from analyzing metals failure under prolonged loads

02 p0383 A70-11655

Sealing mechanism theory with face seal applications, taking into account load carrying capacity and no leakage pressure gradient [ASLE FICFS PREPRINT 18]

02 p0308 A70-12172

Aircraft structures service life estimation, comparing results of serviceability tests, solo flight tests, programmed random load tests and linear defect buildup hypothesis

02 p0391 A70-12854

Stress-strain state of arbitrarily cracked cylindrical shell under symmetric and asymmetric loading

03 p0594 A70-13736

Stress wave propagation tests in thin walled tubes under combined tension and torsion, discussing predicted and observed strain-time profiles discrepancies

03 p0599 A70-14245

Test rig for load controlled strain fatigue, describing main structure, pin joint bearings and hydraulic specimen clamps

04 p0773 A70-15040

Energy dissipation patterns of metal fatigue failure during static and cyclic loading applied to untreated and heat treated steel samples

06 p1166 A70-17651

Cyclic plastic deformation changes with load increase under uniform stress with normal loading and nonuniform stress with impact loading, considering fatigue limit

06 p1168 A70-17923

Crack formation in resin matrix and effect on fiberglass reinforced composites behavior under loading

07 p1318 A70-19754

Steel strength under prolonged preliminary loading at elevated temperatures

08 p1515 A70-20934

Split ring load test method for determining shear modulus of isotropic and composite materials

08 p1530 A70-21888

Turbine components thermal stress calculations for static and variable loads, considering plastic strain, creep and temperature effects

09 p1775 A70-22592

External respiration, hemodynamics, oxygen transport and consumption in lungs during static load tests

10 p1822 A70-25176

Beam-bending and circular plate testing rigs for creep with constant and variable loading, discussing tests repeatability and accuracy

12 p2207 A70-27618

Materials life estimation under irregular load sequences, discussing computational and graphical method, applications and test and computer equipment

13 p2513 A70-29162

Fracture of failed tensile impact and compression test pieces of hardened SAE 52100 steel, using scanning electron microscope

15 p2745 A70-32443

Crack propagation, fatigue damage and interaction effects in aircraft structures and materials under flight simulation loading

17 p3185 A70-34924

Stainless steel load-strain characteristics and cumulative damage in cyclic fatigue life

18 p3273 A70-36048

MHD slider bearing load carrying capacity in tangential magnetic field, observing optimum profile in step form with riser location and step height ratio

18 p3263 A70-36672

Loading history effect on work of plastic deformation in Ni and Cu pipes, taking into account stress and strain deviators deviation from similarity

18 p3344 A70-36945

Stress rupture strength dependence on specimen geometry /scale effect/ from analyzing metals failure under prolonged loads

19 p3547 A70-38428

Instrument ball bearings running torque prediction at high speed under combined radial and axial loads [ASLE PREPRINT 70AM 3D-3]

19 p3438 A70-38803

Aircraft design fatigue life and cumulation damage problems, discussing information value of programmed load and random tests

20 p3720 A70-39622

Carbon fiber reinforced polymer (CFRP) failure mechanism, discussing nondestructive testing, destructive and cyclic loads

22 p4058 A70-42476

Human tolerance and ventilatory response to inspiratory mechanical loads

23 p4144 A70-43822

Fatigue limits of Ti alloy by Wohler and Locati loading methods

23 p4204 A70-43933

Comparative load capacity of disk models of natural gas blowers of different designs under plastic strain

23 p4232 A70-43941

Aircraft structure fatigue load monitoring, discussing strain gage installation in critical areas [ICAS PAPER 70-31]

23 p4267 A70-44102

LOADING

Dynamic control model of lift helicopters with two cable sling loads using multiple part motion equations [AIAA PAPER 70-929]

17 p3020 A70-35839

LOADING FORCES

U LOADS [FORCES]

LOADING MOMENTS

Structural analysis of rectangular plates simply supported on two edges subjected to free edge uniform moments

03 p0602 A70-14332

Stress analysis of shell loaded at free edge by concentrated forces and moments

04 p0772 A70-14920

Limiting stress states analysis in isotropic solids using loading history and replacing nonlinear stress-strain curve by approximating rectilinear polygon

06 p1165 A70-17547

Compressive stress critical moment induced instability and weakening incorporated in thin walled beam design

11 p2131 A70-25590

Loading conditions measured during aerobatic maneuvers in flight test to determine structural design requirements for aerobatic-type aircraft [SAE PAPER 700222]

11 p1980 A70-25894

Optimal variable shell thickness, describing numerical solution as function of forces, moments and thickness

20 p3725 A70-39865

LOADING OPERATIONS

Onboard cargo load equipment to make aircraft independent of specialized ground equipment

10 p1862 A70-25330

Book on Polish air cargo transport covering transport volumes, aircraft, preparation and loading operations

13 p2524 A70-29453

C-5 aircraft cargo loading system for terminals minimizing ground time

17 p3064 A70-35831

LOADING RATE

Loading frequency effect on carbon steel energy dissipation at large stress amplitudes, deriving strain rate relations

08 p1516 A70-20980

LOADING WAVES

U ELASTIC WAVES

U LOADS [FORCES]

LOADS [FORCES]

NT AERODYNAMIC LOADS

NT AXIAL COMPRESSION LOADS

NT AXIAL LOADS

NT BLAST LOADS

NT COMPRESSION LOADS

NT CYCLIC LOADS

NT DYNAMIC LOADS

NT GUST LOADS

NT IMPACT LOADS

NT LANDING LOADS

NT RANDOM LOADS

NT ROLLING CONTACT LOADS

NT SHOCK LOADS

NT STATIC LOADS

NT THRUST LOADS

NT TRANSIENT LOADS

NT VIBRATORY LOADS

NT WING LOADING

Circular plate nonlinear analysis under load and uniform midplane temperatures, using stationary potential energy principle

01 p0205 A70-11145

Construction of formulas relating stresses and plastic deformations describing inelastic bodies behavior under complex loads

01 p0210 A70-11411

Stiffness matrix derivation for curved beam emphasizing uncoupled normal to plane loads

03 p0584 A70-12949

Carrying capacity and moment of friction calculated for cylindrical MHD bearing for small magnitude of radial clearance

03 p0497 A70-13877

LOAD FACTORS

U LOADS [FORCES]

LOAD TESTING MACHINES

Automatic loading control system for tensile test machine permitting creep and creep-rupture testing

01 p0054 A70-10075

Extrusion forces required for metals and alloys determined by mathematical equations correlating extrusion pressures with process variables, discussing lubrication systems effectiveness
[ASME PAPER 69-WA/LUB-6] 04 p0697 A70-14767

Optimum one dimensional Rayleigh gas slider bearing, calculating step location, pressure and load capacity for range of bearing numbers
[ASME PAPER 69-WA/LUB-1] 04 p0698 A70-14772

Transient processes of strain wave propagation in elastic shells and plates under time varying loads
04 p0773 A70-15010

Load capacity and power loss of spiral groove bearings lubricated by incompressible liquid with temperature-dependent viscosity, using momentum and energy equations
05 p0853 A70-15778

Unloading wave in elastic-plastic half space with rigid unloading for two parameter loads, discussing deformation body model
05 p0925 A70-15825

Fiberglass reinforced rectilinear plastic plates bending under various edge loads, noting shear pliability
05 p0934 A70-16220

Revolving shells local stability developing boundary effect under normal and bending external loads solved by computer program
05 p0935 A70-16237

Structure safety in cumulative damage, considering loading as time dependent stochastic process
05 p0937 A70-16369

Time-varying loads effect on linear elastically hereditary media described by generalized fractional-order exponential functions and Rzhantitsyn type viscoelastic kernels
05 p0946 A70-16954

Plastic deformation of thin flexible axisymmetric shells under load, discussing tensile stresses
07 p1407 A70-19383

Strain gages design and development for small loads
08 p1493 A70-20586

Deformable bodies subjected to given load using method of equivalences
08 p1584 A70-20589

Pairs existence of symmetrical equilibrium forms in nonlinear shallow shell under load applicable to nonshallow shells equilibrium
08 p1591 A70-21416

Bearing capacity increase due to large viscoelastic or normal stress effects in lubricants, obtaining exact results for noncavitating plane slider bearings
08 p1507 A70-21476

Loading effects in measurements involving electrical and nonelectrical systems used in determining gas pressure and fluid flow
09 p1672 A70-22011

Dynamic force measurement methods, considering reaction force and operational compensation
09 p1672 A70-22013

Linear one degree of freedom mechanical system loaded by time dependent force with constraints on loading/unloading rate, studying minimum of dynamic coefficient
09 p1727 A70-22536

Shock absorbing forces for absorber with one degree of freedom optimized for given acceleration during periodic disturbances by variational method
09 p1727 A70-22537

Stress concentrations and load transfer around cutouts in fiber reinforced laminates, discussing boron epoxy plates with circular holes
09 p1710 A70-22793

Load parameters of externally pressurized gas journal bearing with multiple supply holes
09 p1693 A70-22977

Solutions existence for nonlinear partial differential equations describing orthotropic and nonlinear shallow shells under loads and temperature effects
10 p1954 A70-24019

Expansion bellows fatigue strength based on load and displacement measurements performed during low cycle model tests
10 p1965 A70-25299

Stress measurement in discontinuous layered medium subjected to perpendicular load under sliding friction, using photoelastic interferometric methods
11 p2131 A70-25587

Stress level, block size and constant and variable loading sequence effect on fatigue life of Al alloy box beams
11 p2138 A70-26094

Elastic stability of discrete conservative structures under combined loads
11 p2142 A70-26636

Mechanical properties in solids under dynamic incremental shear loading, discussing wave propagation tests on steel, Cu and Al
11 p2143 A70-26669

Airframe structural tests in elevated temperature environment by applied load ratios and room temperature static results
12 p2205 A70-27134

Molding procedure to orient filaments relative to loads for optimizing structural component/compressor blades/of filament reinforced composite
13 p2417 A70-28663

Contact stresses and radial displacements in circular rings with loaded inner and outer boundaries
13 p2515 A70-29506

Electrohydraulic control system dynamics, examining executive component loading at low speeds and nonlinear resistances
13 p2349 A70-29720

Stress distributions in elastomers under different loads, proposing appropriate measuring technique
14 p2655 A70-30178

Tapered cantilever Al plate load characteristics, determining elastic and plastic strain due to regular, reverse and second regular deflection sequence
15 p2821 A70-32307

Human femur junctions load actions and stresses during walking calculated from measurements
15 p2692 A70-32327

Cumulative creep strain and damage based on stress amplitude coefficients, considering continuous single step system of loads
15 p2821 A70-32339

Elastic continuum conducting heat under general loads, investigating stability thermodynamics-Liapunov criterion relations
18 p3337 A70-36336

Gas particle mixtures nozzle flow at high loading ratios
18 p3208 A70-36693

Extrusion forces required for metals and alloys determined by mathematical equations correlating extrusion pressures with process variables, discussing lubrication systems effectiveness
[ASME PAPER 69-WA/LUB-6] 19 p3435 A70-37604

Optimum one dimensional Rayleigh gas slider bearing, calculating step location, pressure and load capacity for range of bearing numbers
[ASME PAPER 69-WA/LUB-1] 19 p3436 A70-37617

Structural design load factors statistical evaluation for element optimal reliability
19 p3550 A70-38850

Overbraced frame loaded at joints, limiting elastic buckling examinations to geometrically perfect structures
20 p3717 A70-38973

Structural fatigue design loads computation for fighter aircraft using multivariable load environment model from oscillograph recorded multichannel aircraft response data
[AIAA PAPER 70-948] 20 p3719 A70-39579

Nonhomogeneous shell theory, considering load carrying surfaces with constitutive equations independent of shell curvature
20 p3719 A70-39619

Oscillation harmonics in rods under loads, giving inequalities to obtain algorithm for determination of overtones
20 p3721 A70-39781

Pneumatic actuator control system improvement, using invariance theory to compensate load variability and dynamic response of medium
20 p3564 A70-39848

Optimal variable shell thickness, describing numerical solution as function of forces, moments and thickness
20 p3725 A70-39865

Joint designs, attachment methods and load introduction in composite structures, suggesting adhesive bonding
20 p3730 A70-40041

Elastic beams optimal design for multipurpose loading, considering compliance and minimum cross section constraints
20 p3733 A70-40382

Elastomechanical system reciprocity relation principles using differential equations for bar with forces in two places
20 p3735 A70-40537

Loads induced by terminal shock boundary layer interaction on cone-cylinder bodies, discussing angle of attack effect
21 p3746 A70-41863

Spiral grooved gas lubricated thrust bearings, calculating self heating induced thermal distortion effects on load capacity
[ASME PAPER 70-LUBS-14] 22 p4044 A70-42447

Hyperelastic bodies stability subject to conservative configuration dependent forces, formulating surface potential for hydrostatic loading
22 p4114 A70-42695

Low friction seal for axial loading piston in triaxial soil testing cells
23 p4199 A70-43873

Minimum weight structural design within given stress limits due to different loads or natural frequency vibrations, using finite element method for structural analysis
23 p4268 A70-44226

Infinite plate perforated with rounded corner square hole under uniform partial loading, examining elasticity with conformal mapping
24 p4427 A70-46367

LOCALIZATION

U POSITION [LOCATION]

LOCATION

U POSITION [LOCATION]

LOCI

Root loci construction for differential equations with quadratic free parameters applied to aircraft motion with roll control
11 p2071 A70-25393

Critical Levitation Loci for floating spheres on cryogenic fluids
17 p3136 A70-34743

Feedback control system characteristic equation generalized root locus following technique using straight line approximation
20 p3659 A70-40121

LOCKHEED AIRCRAFT

NT C-5 AIRCRAFT

NT C-141 AIRCRAFT

NT F-104 AIRCRAFT

NT L-1011 AIRCRAFT

NT T-33 AIRCRAFT

NT XV-4 AIRCRAFT

YF-12A interceptor aircraft development and testing, discussing titanium alloys application, aerodynamics and thermodynamics, escape systems for high speed and altitude tests
18 p3213 A70-36451

LOCKHEED C-5 AIRCRAFT

U C-5 AIRCRAFT

LOCKHEED MILITARY AIRCRAFT

U LOCKHEED AIRCRAFT

U MILITARY AIRCRAFT

LOCKHEED XV-4A AIRCRAFT

U XV-4 AIRCRAFT

LOCKING

Nut and bolt locking, describing cotter pins, lock washers, elastic washers, prestressing, nut with lock nut and self locking nuts
06 p1075 A70-17436

Mechanical methods locking studs, discussing chemical locking based on hardening of resins by polymerization
06 p1076 A70-17437

LOCKS

Supersonic gas jets applicability as vacuum locks for molecular fluxes at thermal velocity in magnetic trap
08 p1549 A70-20509

LOCKS [FASTENERS]

Stress analysis of eyebolts in turbine blades hinged locks based on perforated plate theory with concentrated force, discussing stress distributions
01 p0210 A70-11416

LOCOMOTION

NT ASTRONAUT LOCOMOTION

NT WALKING

Male rats locomotor activity responses to altered photoperiods during exposure to varied-light artificial days
01 p0015 A70-10367

LOG PERIODIC ANTENNAS

Normal mode helical antennas performance in medium and short wave regions, discussing advantage over log periodic antennas and maximum radiation angle achieved by phase shift
02 p0270 A70-12735

Mutual coupling in arrays of log periodic dipole antennas in terms of impedance and admittance matrices
09 p1645 A70-22690

Antenna-duplexer assembly comprising log periodic antennas, power divider and hybrid loop
09 p1649 A70-23324

Log-periodic dipole /LPD/ antennas compressed along transmission-line axis, considering frequency dependent behavior in narrow bands and radiation pattern
12 p2198 A70-27955

Dual mode log periodic spiral DF antenna system, using monopulse to provide azimuth and bearing elevation data
16 p2863 A70-33450

Log periodic antennas, discussing dipole array and planar sheath spiral structures, base current and far field pattern calculations, etc
17 p3052 A70-35073

Log periodic dipole antenna arrays, calculating HF performance and patterns in presence of ground
22 p3997 A70-43176

LOGARITHMIC RECEIVERS

Solid state logarithmic radiometer, measuring radiation within narrow portions of optical spectrum
16 p2905 A70-33160

LOGARITHMS

Quasi-logarithmic readout of conventional binary scaler provided by reduced logic system following generalized equations
05 p0851 A70-16844

Algorithm for Fast Two Dimensional Fourier Transform requiring logarithm additions and multiplication
11 p2073 A70-26250

Image processing and picture enhancement by computer, using fast binary log-antilog conversion
15 p2768 A70-32567

LOGIC

- Attention theory experimental design logic, discussing quantitative theory 19 p3362 A70-38315
- Human memory information structure, discussing pattern recognition, simultaneous attention, problem solving and logic 19 p3363 A70-38322

LOGIC CIRCUITS

- NT THRESHOLD GATES
- MOSFET uses in spacecraft electronic subsystems, describing digital control unit and typical logic circuitry 03 p0456 A70-13534

- Digital network reliability with redundancy to mask logic modules failure for asymmetric failure modes 03 p0454 A70-14022

- Diode transistor microelectronic logic circuit reliability, efficiency and optimization using digital computer 04 p0659 A70-15210

- Angular resolution dependence on bearing ambiguities in radio direction finders based on interference measurement, using digital logic circuits 04 p0659 A70-15335

- Quasi-logarithmic readout of conventional binary scaler provided by reduced logic system following generalized equations 05 p0851 A70-16844

- Digital computers structural and operational address format dependence on number of storage readouts expressible with aid of linear function 05 p0818 A70-17004

- Radiation environments effect on logic circuitry constructed of MOS and bipolar transistors, discussing permanent and transient effects 07 p1242 A70-20149

- Fourth generation systems architecture in microprogramming in terms of control logic, describing inner computer as subroutine processor for controlling interstation communication 08 p1465 A70-20816

- Fluidic logic components for automatic data processing, describing circuits designed to solve specific problems 09 p1612 A70-22771

- Fluidic logic elements for controlling selected cells extinction in hybrid plasma-fluidic display 09 p1738 A70-23758

- Light-emitting integrated circuit semiconductor display devices with inherent memory permitting logic and optical output functions performed on surface 10 p1846 A70-23883

- Book on numerical control covering principles, electromechanical system using digital logic circuits, binary numbers and arithmetic, etc 10 p1854 A70-24023

- Flexible logical elements in integrated circuits with internal connections controllable from outside to realize variety of logical functions 10 p1850 A70-24618

- Digital control systems simulation on analog computer with digital logic, using conventional analog amplifiers and integrators 10 p1860 A70-24655

- Autonomous control system for moving plant based on logic threshold networks and multivariable functional converter 11 p2023 A70-25612

- Test pattern generation algorithm and program for failure detection in asynchronous sequential logic circuits, using combinational method 11 p2024 A70-26205

- T2L logic circuits design and coherent noise immunity 11 p2021 A70-26833

- Solid state proximity switches, sensors, logic and self test circuits for aircraft electrical applications to improve reliability and maintainability over mechanical switches [SAE PAPER 700305] 12 p2195 A70-27449

- Apollo Command Module inverter experience for post-Apollo spacecraft applications, discussing phase loads and control logic circuits 12 p2165 A70-27693

- Computer-aided MOS/LSI four phase logic circuit design, discussing software, design cycles and testing 13 p2380 A70-28375

- Integrated logic circuits, considering switching properties and medium and large scale integration 13 p2372 A70-29116

- Logic cells for multiple arithmetic functions suitable for LSI 13 p2377 A70-29145

- Binary division by logic gates cellular arrays, noting accuracy and operating speed 14 p2556 A70-30517

- Iterative cellular logical array for nonrestoring binary division 14 p2556 A70-30685

- Interference free and frequency stable transistorized multivibrator circuits using High Level Logic /HLL/ units 14 p2561 A70-31163

- Cascade synthesis of multistage logical network with multiple outputs capable of realizing arbitrary logical function from algebraic viewpoint 15 p2715 A70-31840

- Combinational logic cells cellular arrays synthesis, considering truth table and transition matrix 15 p2712 A70-32606

- Logic circuits reliability with series and parallel connected elements during random malfunctions, obtaining failure formulas for trigger 15 p2716 A70-32901

- Scientific satellites pulse height analyzer and associated threshold detection and logic circuitry 16 p2900 A70-33062

- Complex control systems in integrated logic circuits and light laboratory materials production, discussing measurement equipment for quality control 17 p3090 A70-35416

- Microelectronic systems radiation resistance, examining logic IC gates for reactor neutron irradiation 18 p3233 A70-36783

- LSI technology effect on digital circuits and systems designs 19 p3387 A70-37847

- Visual binary state transistor tester for positive and negative logic circuits, illuminating lamp for specific logic states 21 p3801 A70-42244

- Fluid logic sequential circuits with optional input signals, describing synthesis procedure [ASME PAPER 70-FLCS-19] 22 p3963 A70-42408

- Fluid logic circuits with combined feedback input signals, describing synthesis procedure [ASME PAPER 70-FLCS-18] 22 p3963 A70-42409

- Scientific satellites nuclear experiments fast low power drain logic system, using AND and NAND gates, pulse generators, delays and bistables 23 p4143 A70-44299

- Sequential logic circuit synthesis using truth table, minimizing by Quine-McCluskey method 23 p4167 A70-44861

- Hydraulic and pneumatic components for logic circuits of automatic controls, considering amplifiers, interlocked systems and use of fluidics 24 p4293 A70-45618

- High density packaging of micrologic flatpacks using high interconnection method for two-side use of double-sided card in space flight applications 24 p4320 A70-46248

LOGIC DESIGN

- Computerized generation of cost optimal decision logic for malfunction analysis 08 p1470 A70-20659

- Negative radix conversion results applied to logical design of serial converter 09 p1642 A70-22967

- Flexible logical elements in integrated circuits with internal connections controllable from outside to realize variety of logical functions 10 p1850 A70-24618

- Logic cells for multiple arithmetic functions suitable for LSI 13 p2377 A70-29145

- Hybrid computing techniques for solving parabolic and hyperbolic partial differential equations, discussing serial method accuracy and use of parallel logic for integrator control 13 p2373 A70-29461

- State transitions and couplings in reliability of complex systems, using logic algebra suitable for computer 15 p2709 A70-32132

- Digital logic control of chromatographic system for measuring instrumental contributions to band broadening 16 p2855 A70-33120

- Fluid logic systems synthesis by computer aided design programs, proposing referee system [ASME PAPER 70-DE-47] 16 p2844 A70-33510

- Digital logic techniques for pulse modulated radar systems, with application to controlling and timing waveforms for display 17 p3042 A70-34570

- Cellular logic arrays design for nonrestoring binary division, with application to Napierian logarithm generation 17 p3050 A70-34571

- DC transistorized Nor logic gates design based on graphic analytic method permitting influence of circuit parameters variations for reliability improvement 21 p3793 A70-40765

- One dimensional cellular logic arrays fault circumvention by bypass switching out defective cells in cascade 22 p4004 A70-43073

- Digital computer constructed with diodes and transistors logic for evaluating matrix determinants and minors 23 p4166 A70-43955

LOGIC NETWORKS

- U LOGIC CIRCUITS

LOGICAL ELEMENTS

- Semiconductor laser-photodiode system used as optical logic elements for electronic circuits describing storage elements, dynamic trigger and multivibrator 03 p0499 A70-13456

- Frequency selection systems synthesis with digital AND type logical elements, noting basic design relations 04 p0647 A70-14404

- Flexible logical elements in integrated circuits with internal connections controllable from outside to realize variety of logical functions 10 p1850 A70-24618

- Injection lasers as logic elements in optical communication systems with time division multiplexing, examining optimal switching and pulse duration reduction 13 p2428 A70-29406

- Automatic dynamic response system for testing logic and semiconductor devices 13 p2379 A70-29693

- Redundant threshold logic elements synthesis based on von Neumann multiplexing principle for automatic error correction 13 p2376 A70-29940

- Autodiagnosis of logic module failure in complex electronic systems, examining fault simulation methods and Safe system program and apparatus 14 p2561 A70-30669

- Combinational logic cells cellular arrays synthesis, considering truth table and transition matrix 15 p2712 A70-32606

- Component decision logical and temporal arrangement in visual search, defining target by several attribute value combination 19 p3362 A70-38314

- DC transistorized Nor logic gates design based on graphic analytic method permitting influence of circuit parameters variations for reliability improvement 21 p3793 A70-40765

- Scientific satellites nuclear experiments fast low power drain logic system, using AND and NAND gates, pulse generators, delays and bistables 23 p4143 A70-44299

LOGISTICS

- NT LUNAR LOGISTICS

- NT SPACE LOGISTICS

- Integrated logistic support for cost effectiveness of ground communication system 01 p0220 A70-10114

- Project ABLE stabilized platform, discussing logistics support requirement effects on system design and acquisition, reliability, maintainability and costs 02 p0401 A70-11670

- Spares management of large aircraft contract in relationship to total integrated logistics support systems management 02 p0401 A70-11672

- Weapon systems acquisition projects, studying procurement decisions interactions [ASME PAPER 69-WA/MGT-6] 04 p0788 A70-14833

- Integrated logistic support economics considered in selecting support system for generating quantitative data for cost optimization 05 p0959 A70-15846

- Project acquisition based on consideration of logistic effects /ABLE/ for tool measuring logistic consequences of reliability and maintainability 15 p2832 A70-32634

- Avionics maintenance effectiveness logistics, discussing symptom pattern observation technique /SPOT/ for in-flight data 19 p3554 A70-38399

LOH HELICOPTER

- U OH-6 HELICOPTER

LOLA [SIMULATOR]

- U LUNAR ORBIT AND LANDING SIMULATORS

LONG RANGE NAVIGATION

- U LORAN

- U LORAN D

LONG RANGE WEATHER FORECASTING

- U.S. space research and technology applications in aviation, astronomy, weather information, intercontinental communication and space shuttle design 05 p0921 A70-17091

- Nonlinear planetary long range weather forecasting problems analytical solutions, describing quasi-sole-noidal atmospheric motions model 07 p1328 A70-18649

- Numerical weather forecasting for several weeks based on global meteorological satellite network observation 10 p1913 A70-25241

- Global scale atmospheric circulation processes numerical simulation leading to long range weather forecasts for Northern Hemisphere 19 p3462 A70-38753

- Atmospheric global observation for long term weather forecasts, obtaining cloud photographs and radiation data from satellites 21 p3847 A70-42255

LONG TERM EFFECTS

- Heat resistant alloys for gas turbine blades observed for long term heating effects on changes of hardness, tensile, impact and stress-rupture properties and microstructure 01 p0116 A70-10149

Medico-engineering experiment in partially closed ecological system for long term manned space missions

01 p0032 A70-10363

Multipole analysis for earth magnetic field allowing secular variation to be illustrated by time trends in multipole parameters

02 p0288 A70-11742

Secular and short period perturbations calculation of satellite orbital elements under action of solar radiation pressure

02 p0362 A70-11763

Long term memory effects in visual perception of apparent movement, discussing experience prior to tests

02 p0239 A70-12622

Orthotropic cylindrical shell with initial deflection under long term effect of external hydrostatic pressure, solving bending problem

02 p0390 A70-12809

Long term storage effects on noise, leakage current and thickness of Li drifted Si surface barrier detectors

03 p0482 A70-13023

Secular increase in pulsar periods attributed to gravitational emission, velocity effects and galactic escape

03 p0564 A70-13219

Phobos motion observational results compared with Sharpless determination of secular acceleration

04 p0743 A70-14399

Closed life support systems tests, describing effects of long term /one year/ confinement of three human subjects

04 p0641 A70-14565

Pharmacology for long term manned space

04 p0629 A70-14566

Long term behavior of blue photographic luminosity of Seyfert galaxy 3C 120 nucleus, considering similarity to quasar 3C 273B

04 p0748 A70-14589

Secular variation in F region ionization response to sunspot number, noting dominant component as cosine term equal to four sunspot cycles

04 p0678 A70-14972

Water electrolysis module long term operation in providing oxygen for life support systems

05 p0804 A70-15843

Secular variations in small quasar components, discussing compatibility with theory of expanding synchrotron sources

05 p0913 A70-16474

Geomagnetic field secular variations relation to variations of magnetic field of optimum dipoles, noting earth core role

05 p0842 A70-16747

Second order secular perturbations formulas of distant earth satellite motion valid for nearly circular orbits with small inclination to ecliptic plane

06 p1141 A70-17823

Mass loss rates for short period comets from non-gravitational terms in equations of motion, paying particular attention to secular variations

06 p1151 A70-18490

Creep rupture and residual tensile strength tests to evaluate long time properties and structural stability of Inconel 718 alloy, performing phase analysis

07 p1310 A70-19731

Geomagnetic field total vector modulus secular variations from airborne measurements

07 p1278 A70-20461

Tidal friction induced secular changes in earth-moon system near minimum of angular momentum of moon orbit, including temporal changes in moments of inertia

08 p1579 A70-21570

Secular increase in pulsar periods attributed to gravitational emission, velocity effects and galactic escape

08 p1580 A70-21652

Solar radiation variations effect on earth climate, noting atmospheric transparency role in glaciation on thermal regime

08 p1539 A70-21919

Multipole analysis applied to 1965 International Geomagnetic Reference Field, separating secular variation field into drifting and nondrifting components

09 p1666 A70-22065

Central nervous system activity of white rats during hypokinesia, observing organism shifts and long time effects on functions

09 p1615 A70-22093

Major planets secular perturbations represented in trigonometric form using canonical transformations

09 p1751 A70-22176

Climate variations and earth orbital elements secular perturbations, noting solar radiation and celestial mechanics roles

09 p1666 A70-22177

Gas turbine blades design and exploitation processes, discussing long time fatigue strength, static durability and heating effects at elevated temperatures

09 p1772 A70-22469

Secular stability of rotating polytropes in relative equilibrium, isolating bifurcation point by calculating lowest sectorial modes for various sequences

10 p1937 A70-23946

Long time strength and creep rectilinear diagrams constructed for heat resistant alloys to obtain extrapolation values

10 p1903 A70-24239

Test results extrapolation for heat resistant alloys long time strength using exponential relation between time to rupture and value for initial stress decrease

10 p1903 A70-24240

Elongated rotating configuration evolution by gravitational radiation and secular instability using homogeneous figures of Maclaurin and Jacobi

10 p1916 A70-24404

Prolonged hypodynamia effect on human organism, describing organizational and methodological principles for conducting investigations

10 p1813 A70-24667

Prolonged hypodynamia /bed rest/ clinical observations, noting psychological and physical effects

10 p1813 A70-24668

EKG and cardiac rhythm changes during prolonged hypodynamia /bed rest/ with restricted physical activity

10 p1814 A70-24669

Human vascular tonus and hemodynamics during prolonged hypokinesia, observing changes in reaction to cold and reduced vascular tonicity

10 p1814 A70-24670

Prolonged hypodynamia effect on human cardiac cycle phases using poly- and kinetocardiographic data

10 p1814 A70-24672

Prolonged hypodynamia effect on human nutritional habits and protein metabolism, noting decrease in energy requirement and body weight

10 p1814 A70-24675

Geomagnetic field secular variation and cyclic components amplitudes separation by digital filters, observing seasonal and solar activity effects

10 p1880 A70-24808

Minuteman 3 Reentry System real time laboratory aging and surveillance test program to evaluate long-term storage effects on equipment behavior

[ALAA PAPER 70-395]

10 p1952 A70-24910

Ecliptic obliquity secular change rate apparent discrepancy possibly due to earth-moon barycenter motion

10 p1945 A70-24962

Hematologic responses of mice subjected to continuous hypoxia in subatmospheric pressure

11 p1989 A70-26666

Light pressure induced secular effect contributing to planetary satellites and lunar orbits evolution calculated by numerical integration

11 p2118 A70-26777

Earth IR horizon seasonal and longer variations for horizon sensing instruments design

12 p2226 A70-27931

Perturbation function of first order general planetary theory using Hori canonical variables, revealing mixed secular term of determining function

13 p2487 A70-28708

Marrow granulocyte reserve restoration in dogs exposed to chronic gamma radiation, discussing leukocyte reaction to pyrogenic agent

13 p2351 A70-29326

Earth rotation perturbations, analyzing secular polar shift dependence on dimensions, depth and location of seismic event

13 p2400 A70-29604

Decreasing gravitational constant effects on secular earth figure and dimension changes using Clairaut equation

14 p2568 A70-30143

Earth hydromagnetic dynamo spectrum fluctuation related to secular geomagnetic field variations, using unsteady kinematic models

14 p2568 A70-30202

Long term effects model evaluation of meteoritic impact against lunar surface compared with analyses of Lunar Orbiter photographs

14 p2645 A70-31062

Kovpak method for estimating and extrapolating heat resistance characteristics, considering alloy long term strength

15 p2755 A70-31528

Microbial flora in human subjects confined to long term Tektite 1 underwater habitat

15 p2681 A70-31879

Spherical harmonic analysis of geomagnetic secular variation, applying to regional effects

15 p2799 A70-31992

Open faced polyimide-backed strain gage for transducer and/or long term applications, considering drift and zero shifts

15 p2739 A70-32329

Long term storage effects on systems reliability, emphasizing tradeoffs regarding availability, reliability and costs

15 p2712 A70-32637

Central nervous system activity of white rats during hypokinesia, observing organism shifts and long time effects on functions

15 p2685 A70-32689

Secular variations in osculating orbital elements of particle in Saturn ring gravitational field, considering motion in both external and internal space

16 p2973 A70-33226

Biological satellite experiment, considering long term weightlessness effects on metabolism and biological rhythms of medical leech

16 p2854 A70-33993

Unnatural environment behavior of leeches for long term biosatellite experiment, determining temperature, humidity, oxygen pressure, carbon dioxide concentration, calcium hydroxide limits, etc

16 p2854 A70-33994

Long term helium-oxygen atmosphere effects on rats and mice, investigating biochemical and metabolic changes

16 p2849 A70-33996

Long term weightlessness effects on cardiovascular system of rats using miniaturized pump oxygenator

16 p2854 A70-33999

Ti alloy stability after long term creep exposure at various temperatures

17 p3120 A70-34421

Artificial planetary satellites long term orbital evolution under strong perturbations, considering solar and lunar gravitational effects

[AAS PAPER 70-038]

17 p3155 A70-34779

Shooting star shower and solar eclipse frequencies correlation with long term climatic changes

17 p3168 A70-35310

Human operators psychological response to unforeseen information received during routine activity in prolonged solitary isolation

17 p3038 A70-35362

Lunar longitude secular acceleration from occultation observations

17 p3171 A70-35444

Long term effects of ejecting from aircraft, discussing disability incidence after more than ten years

17 p3033 A70-35577

Long term geomagnetic pulsations /PCS/ with sinusoidal waveforms, using IGY data

17 p3080 A70-35642

Secular variations calculation in cosmic ray cutoff rigidities by trajectory tracing process with geomagnetic field models

18 p3306 A70-36023

Solar quadrupole moment effect on secular perturbations of planetary orbital elements

18 p3313 A70-36325

Varying thermoregulatory responses of different rodent species to long term heat and cold

18 p3218 A70-36534

Respiratory activity of internal organs and skeletal muscles in rats exposed to long term heat and cold

18 p3220 A70-36546

Respiratory gas metabolism of liver, heart, brain and muscle tissues in birds exposed to various ambient temperatures for long periods

18 p3220 A70-36547

Respiratory gas metabolism, tissue respiration and enzyme distribution in white rats skeletal muscles following long term cold acclimatization

18 p3220 A70-36548

Astronomically determined latitude longitude and azimuth reduction to common epoch, discussing secular nonperiodic pole motion due to crust drift

18 p3323 A70-37144

Power and exponential time dependences of long term creep strength for wide stress range, assuming linear heat resistance

19 p3449 A70-37340

Plastic deformation in Ni-Cr-Nb alloy precipitation hardened at different long terms of high temperature

19 p3451 A70-37706

Maclaurin spheroid secular stability, examining energy dissipation of gravitational radiation

20 p3702 A70-39017

Spherical harmonic analysis of declination and secular geomagnetic variation

21 p3820 A70-41884

Temperature and long term effects on volatility of perfluoroalkyl ether and polysiloxane greases [ASME PAPER 70-HT-31]

22 p4058 A70-42435

Hemodynamic indices of aged individuals engaging in physical exercises over long period of time

22 p3970 A70-42906

Vacuum-melted and deformed Mo alloys tests, showing long term strength decrease under cyclic heating

22 p4055 A70-43123

High latitude geomagnetic secular variations determination by running 12-month means method, recommending data acquisition free of external sources effect

23 p4190 A70-44087

Long term space flight crew habitation emphasizing food management, station housekeeping, personal hygiene and waste handling

23 p4154 A70-44622

Prolonged REM sleep deprivation effect on gamma-aminobutyric acid concentration in mice
23 p4146 A70-44658

Astronaut biological parameters monitored under prolonged space flight conditions for rescue operations
23 p4146 A70-44678

Orbital elements from secular acceleration in motion assumption, proving Comet Harrington identity with Comet Wolf
23 p4257 A70-45045

Long term storage effects on recalibrated thermistors performance stability, comparing measurements with first calibration data
24 p4333 A70-45136

Earth hydromagnetic dynamo spectrum fluctuation related to secular geomagnetic field variations, using unsteady kinematic models
24 p4330 A70-46277

LONG WAVE RADIATION

Extraterrestrial sources radiation including galactic, solar and magnetospheric radio emissions observed by RAE-I satellite at long wavelengths
[AIAA PAPER 69-1049] 01 p0170 A70-10603

Atmospheric long wave radiation fluxes and energy balance and daytime radiative temperature variations calculated and compared with thermocell measurements
06 p1098 A70-17831

Hypothesis concerning initial spectrum of metric perturbations in Friedman model, discussing long wavelength gravitational waves energy
07 p1383 A70-19406

Sunrise effects in lower ionosphere at midlatitude, discussing long wave absorption measurements, summer electron concentration profile and consistency of aeronomic model
07 p1235 A70-19436

Long wave IR spectrometer with two diffraction gratings for various micron ranges
08 p1493 A70-20544

Microwave propagation along earth-air path, studying tropospheric layer role
08 p1461 A70-20968

Gravity long wave variations correlation with crust and upper mantle geological activity, describing anomaly distribution
08 p1488 A70-21014

Ozone formation in presence of nitrogen oxides and hydrocarbons during long wave UV irradiation, noting energy yield
09 p1629 A70-22328

Long radio wave propagation and effective refraction index in turbulent magnetoplasmas with stochastic density variation
10 p1832 A70-23962

SID effects during recording of long wave transmitter field strength, indicating relation between solar X-ray flares and field anomalies
10 p1932 A70-24485

Long wave transmitter field strength calculation to 1000 km based on optical beam method and ionosphere model to account for radio wave reflection
10 p1840 A70-24495

Vertical profiles of daytime and nighttime long wave radiation fluxes in atmosphere under stratus cloud conditions
12 p2264 A70-27521

Long wave cosmic radio background emission in circumlunar space by Luna 11 and 12 satellites, observing increase in earth magnetosphere tail
12 p2295 A70-28262

IR photography extension into long wave region of spectrum, discussing contact sensitized and electrically controlled semiconductor photographic systems
15 p2734 A70-31632

Background thermal radiation veiling effect on IR photography extension into long wave spectrum
18 p3257 A70-36282

Long wave radiation fluxes calculation in troposphere based on principal radiant heat transfer components separation
18 p3285 A70-36632

Sunrise effects in lower ionosphere at midlatitude, discussing long wave absorption measurements, summer electron concentration profile and consistency of aeronomic model
18 p3249 A70-36910

Ascending long wave radiation brightness from aircraft measurements, observing angular distribution dependence on atmospheric stratification
18 p3287 A70-36970

Long wave outgoing radiation angular distributions based on effective mass and Curtis-Godson methods of accounting for absorption pressure dependence
19 p3461 A70-37634

Slot type oscillations electrodynamic suppression in coaxial magnetrons resonator systems, calculating long wave oscillation frequencies
19 p3387 A70-37738

Ic class variables long wavelength anomalous radiation, discussing emission from circumstellar dust shell
22 p4094 A70-42934

LONGERONS

Band polishing machines slave mechanisms and programmed controllers, describing helicopter longerons finishing process
07 p1291 A70-18829

LONGITUDE

Geopotential fields expansion on 500 mb surface for hemisphere in terms of Chebyshev polynomials along meridian and trigonometric polynomials along latitude
07 p1329 A70-19648

Odessa observatory meridian circle pivots wear determined during observations of eclipsing variables
08 p1574 A70-21160

Longitude and latitude dependence of pc geomagnetic micropulsations related to local time, using analog spectral analysis
09 p1666 A70-22064

Magnetosphere boundary altitude dependence on longitude, considering role of electric current density along geomagnetic lines of force
14 p2570 A70-30217

Power spectrum analysis of division errors of graduated circles associated with meridian astronomy
19 p3523 A70-38686

Magnetosphere boundary altitude dependence on longitude, considering role of electric current density along geomagnetic lines of force
24 p4331 A70-46292

LONGITUDE MEASUREMENT

Earth poles motion influence on latitude, longitude, azimuth and geocentric rectangular coordinates of points determinations on earth surface
03 p0473 A70-13187

Photoelectric exposure meter for meridian circle readings photographic recording
08 p1496 A70-21159

Astronomical navigation on lunar surface with equations for selenographic latitude and longitude
13 p2449 A70-29272

Lunar longitude secular acceleration from occultation observations
17 p3171 A70-35444

LONGITUDINAL CONTROL

Spacecraft longitudinal control during reentry of Lunar Orbiter into atmosphere, analyzing final range prediction, trajectory tracking and accelerometers performance
01 p0197 A70-11497

Hybrid simulation, determining vehicle and performance parameters on longitudinal flying qualities of STOL transport in power approach configuration
[AIAA PAPER 70-387] 10 p1806 A70-24918

Frequency and amplitude during longitudinal control surface pumping by pilots in precise flight path handling for aircraft design
[AIAA PAPER 70-567] 13 p2346 A70-29032

Longitudinal short-period flying qualities as closed-loop pilot-airplane system, noting acceptance values
[AIAA PAPER 70-569] 13 p2346 A70-29034

Optimal fixed-form pilot model computer program for VTOL longitudinal control hover task evaluation
16 p2851 A70-33341

C-5A aircraft six wheel main landing gear bogie pitching control, emphasizing braking torque compensating mechanism design
[AIAA PAPER 70-914] 17 p3020 A70-35826

Pilot/vehicle feedback systems with flight director computer for transport aircraft longitudinal control during landing, discussing design by manual control displays theory
[AIAA PAPER 70-1001] 20 p3560 A70-39530

VTOL aircraft longitudinal motion automatic stabilization in presence of turbulence and internal disturbances, using rotors and jet engines
20 p3561 A70-39838

Fighter aircraft higher order control system dynamics effects on longitudinal handling qualities evaluated by in-flight simulator for role of pilot induced oscillations tendencies
[AIAA PAPER 69-768] 22 p3961 A70-42711

Space shuttle transition trajectory optimization for cruising flight entry, considering longitudinal control, pitchup instability and angle of attack
23 p4244 A70-44623

Aircraft geometry effects on longitudinal flight characteristics calculations, noting wing aspect ratio and horizontal tail changes
24 p4289 A70-45437

LONGITUDINAL STABILITY

Hydrogen-oxygen variable length combustor longitudinal instability, studying hydrogen injection temperature effects on pressure interaction index and pressure sensitive time lag
01 p0214 A70-10324

Gaseous He bubbles injection into liquid propellant launch vehicle fuel lines to reduce vehicle pogo oscillations by lowering feed system natural frequencies
01 p0196 A70-10851

Aerodynamic derivatives in equations of motion governing aircraft longitudinal short period motion estimated using least squares methods
02 p0224 A70-11866

Flexible flight vehicles longitudinal stability with tandem lifting surfaces, studying aerodynamic time delay effects by root locus technique
03 p0408 A70-13802

Kacner method applied to longitudinal vibrations study of nonhomogeneous nonuniform bars, noting applicability to geometrical and elastic properties variations
04 p0779 A70-15702

Liquid rocket motors with concentrated combustion, studying nonlinear longitudinal instabilities with shock waves in combustion chambers
07 p1362 A70-18917

Longitudinal stability of V/STOL aircraft at low speeds, discussing three tilt wings and quad ducted propeller configurations
[AIAA PAPER 69-194] 07 p1195 A70-20410

Transverse oscillation periods of cylinder containing flowing fluid obtained by solving nonlinear partial differential equations describing transverse and longitudinal motion
08 p1592 A70-21480

Longitudinal strength characteristics of filament reinforced composites, discussing bond strength effect on filament fracture
08 p1533 A70-21918

Reinforced cylindrical shells stress-strain state under concentrated longitudinal loads, considering ribs of variable rigidity
09 p1782 A70-23289

Longitudinal distortion reduction in ultrasonic holograms
09 p1689 A70-23805

Static longitudinal stick free and stick fixed aircraft stability equations for several configurations and power effects
[SAE PAPER 700238] 11 p1981 A70-25907

Glider longitudinal stability and control in symmetrical flight positions, determining flight characteristics
12 p2161 A70-27723

Aircraft lateral and longitudinal motion stability in steady rolling, deriving inertia cross coupled stability criterion
13 p2347 A70-29445

Sailplanes flight characteristics concerning longitudinal stability and control position gradient
14 p2531 A70-30634

Parameter identification algorithm for nonlinear equations describing VTOL aircraft longitudinal response
16 p2942 A70-33327

Wings flexural deformability influence on longitudinal stability of glider, using small perturbation theory
17 p3017 A70-35190

Heat pipe performance tests under longitudinal harmonic vibration
17 p3193 A70-35751

Longitudinal dynamics of VTOL aircraft during hover-forward flight transition, using multiple time scale analysis
[AIAA PAPER 69-130] 18 p3213 A70-36681

Nonrolling lifting gliding vehicle hypersonic longitudinal dynamic stability, applying analysis to space shuttles
[AIAA PAPER 70-977] 20 p3715 A70-39552

Aircraft longitudinal motion during takeoff and landing due to loss of lift after boundary layer control system failure
24 p4372 A70-45448

LONGITUDINAL WAVES

LF longitudinal waves propagation in DC gas discharge plasma, obtaining wave dispersion equation for various limiting gases
01 p0149 A70-10162

Longitudinal wave motion in rods, plates and shells based on three dimensional equations and asymptotic expansion
01 p0209 A70-11365

Flexural and longitudinal waves propagation in infinite elastic plate, using solutions to approximate nonlinear equations of plate motion
01 p0213 A70-11634

Asymptotic dynamic theory for elastic cylindrical shells incorporating thickness effects, considering longitudinal wave propagation in infinite length shell
02 p0385 A70-11877

Plane longitudinal elastic monochromatic wave diffraction on stress free circular holes in infinite plate, calculating stresses between holes
03 p0589 A70-13375

Simultaneous equations of longitudinal impact bending, introducing temporal and spatial transformations regarding dispersive wave characteristics in elastic rod
03 p0591 A70-13428

Equatorial jet stream excitation of longitudinal waves, analyzing plasma beam instability and spectrum of short wave inhomogeneities by quasi-hydrodynamic equations
05 p0842 A70-16759

Longitudinal vibration of finite viscoelastic rod with changing boundaries under time-variant force, analyzing impulse response by transform calculus
09 p1777 A70-22833

- Strain and temperature fields interrelation effect on longitudinal wave propagation in viscoelastic cylinder, determining phase velocities and attenuation coefficients 09 p1781 A70-23285
- LF longitudinal waves propagation in DC gas discharge plasma, obtaining wave dispersion equation for various limiting gases 10 p1925 A70-25010
- Narrow band radiation from longitudinal plasma waves nonlinear interactions during solar bursts, comparing flux intensities for Corona single or double shock wave frequencies 10 p1934 A70-25272
- Longitudinal vibrations of circular elastic homogeneous cylinders with end restraints 12 p2321 A70-27152
- Radiation characteristics of ion acoustic waves from monopole and dipole antennas, observing patterns of longitudinal wave in isotropic plasma 12 p2279 A70-27778
- Longitudinal waves propagation in polyethylene bar using Boltzmann-Volterra equation, constructing dynamical stress-strain diagrams by viscous-elastic standard body model 12 p2328 A70-28276
- Longitudinal stress waves propagation in polymeric optically active plastic bars using photoelasticity method 12 p2328 A70-28277
- Collisional theory of longitudinal wave propagation in partly ionized multitemperature gases 13 p2460 A70-28637
- Differential equation for longitudinal vibrations of rod at high temperature, giving asymptotic solution 15 p2814 A70-31589
- Rarefaction wave analytical construction by successive approximation, solving hyperbolic equations for longitudinal vibrations of rods 15 p2815 A70-31644
- Dynamic asymmetric elasticity problems, considering longitudinal and torsional wave propagation in bounded and unbounded micropolar media 15 p2818 A70-32178
- Longitudinal and transverse hypersonic mm waves excitation in quartz single crystal at liquid helium temperature 16 p2952 A70-33258
- Longitudinal wave propagation in variable section bars, solving hyperbolic equation of motion by perturbation method 16 p2993 A70-34088
- Warm homogeneous magnetoplasma longitudinal cyclotron harmonic wave propagation perpendicular to static magnetic field, noting instabilities 17 p3140 A70-34927
- Torsional and longitudinal vibrations of circular cylinders of micropolar elastic solids in terms of Laplace and Helmholtz equations solutions 19 p3537 A70-37789
- Unidirectional composites subjected to free vibration and axial end loading, considering longitudinal stress wave propagation in fiber direction 19 p3540 A70-37954
- Isotropic homogeneous elastic cylindrical rods, investigating nonlinear longitudinal dispersive waves corresponding to water wave theory analogs 22 p4115 A70-42952
- Collision integral model for multicomponent mixture, investigating partially ionized plasma longitudinal vibrations 22 p4083 A70-43382
- Forced longitudinal oscillations of cylinder with given surface displacements, using Lamé equations 22 p4118 A70-43571
- Longitudinal and transverse hypersonic mm waves excitation in quartz single crystal at liquid helium temperature 23 p4218 A70-44281
- Partially ionized viscous plasma longitudinal wave propagation, formulating motion equations for electrons, ions and neutrals from Maxwell and Boltzmann equations 23 p4229 A70-44987
- Finite amplitude longitudinal shock waves in nonlinear hyperelastic materials, deriving solutions for various shock types in accordance with second law of thermodynamics and Lax stability criterion 24 p4420 A70-45265
- Pulsatile flow in circular rigid tube with and without longitudinal vibration, obtaining momentum integral solution 24 p4325 A70-45623
- LOOK ANGLES**
U AZIMUTH
U ELEVATION ANGLE
LOOP ANTENNAS
Parasitic loop counterpoise antenna radiation patterns, considering application to VOR systems 09 p1646 A70-22693
- Input impedances of small vertical and horizontal dipole and loop antennas above conducting ground plane, noting effect of refractive index 12 p2196 A70-27714

- Circular loop antenna with traveling wave current distribution, considering phase change effects on radiation pattern and gain 12 p2198 A70-27965
- Loop antenna current distribution source from radiation pattern synthesis, using Fourier series 15 p2698 A70-31837
- Pulse characteristics received by loop antenna in field of second antenna excited with step functions, calculating radiation characteristics 16 p2871 A70-32961
- Loaded resonant circular loop radiation field patterns table, determining load impedance for antenna design 16 p2872 A70-32971
- Dipole and loop antennas in isotropic compressible plasma under wave incidence, using reciprocity theorem for receiving voltages and maximum powers 16 p2957 A70-32982
- Circular loop antenna for transmission and reception, determining current distribution, admittance and radiation field by integral equation 17 p3051 A70-35061
- Square loop antenna radiation resistance in warm plasma, comparing theoretical results with measured values from Ariel 3 satellite antenna 21 p3796 A70-40562
- Satellite-borne loop antenna resistive and reactive impedance measurements in topside ionosphere 22 p4019 A70-43112
- LOOPS**
NASAP program FORTRAN subroutine LOOPS for loop detection in circuit analysis, discussing automatic instrumentation process for computation time reduction 06 p1015 A70-18421
- Small loop impedance in magnetoplasma determined for magnetic field normal and parallel to loop plane 09 p1738 A70-23671
- LOR [RENDEZVOUS]**
U LUNAR ORBITAL RENDEZVOUS
LORAN
NT LORAN C
NT LORAN D
Reconnaissance uncertainty effect on precision of return to fixed point applied to circular error probable, drms calculations and Loran 04 p0652 A70-15345
- Loran in range-range mode for computing user position based on remote clock synchronization, evaluating accuracy 09 p1719 A70-22192
- Long range navigational aids requirements for airlines, discussing self contained navigation systems capabilities 09 p1722 A70-23028
- Primary long range navigation system for SST, considering operational goals, Doppler radar systems, navigation aids, inertial systems, etc 09 p1722 A70-23029
- Hybrid long range en route navigation system extended to short range route meeting ATC and terrain problems 09 p1722 A70-23032
- Decca, Loran C/D and Omega LF and VLF hyperbolic navigation systems 23 p4215 A70-43865
- LORAN C**
LF wave propagation using Loran C radio navigation system flight performance tests 03 p0523 A70-13615
- Loran and Decca hyperbolic navigation systems 08 p1541 A70-21022
- Loran C radio wave field intensity diurnal variations measurements, investigating ionospheric waves characteristics 10 p1832 A70-23921
- Loran-C and Omega radio navigation systems, discussing hostile environment operation and hardware processing 11 p2081 A70-26507
- Loran C coordinates bias function determination by regression analysis using observed time differences 14 p2615 A70-31195
- Loran C principles, ground station operation and navigation equipment 17 p3135 A70-35881
- LORAN D**
Self contained and ground referenced radio systems combination for tactical air navigation, including Loran D and hybrid Loran/HYLO/ 04 p0716 A70-14628
- LORENTZ CONTRACTION**
Lorentz principle application to general relativity freeing formalism from inconsistencies to derive expressions for Christoffel symbols and Riemann-Christoffel tensor 06 p1105 A70-17537
- LORENTZ FORCE**
Magnetically balanced arcs in supersonic external flows, indicating central core with differential Lorentz forces analogous to Grashof number in free convection phenomena 02 p0347 A70-12233

- Electrically charged earth satellite motion under action of Lorentz force produced by geomagnetic field interaction, relating field trajectories to acceleration 06 p1142 A70-17879
- Infrasonic waves generated by pulsating aurora, using Joule heating and Lorentz force coupling 13 p2399 A70-29236
- LORENTZ GAS**
Electrons velocity distribution function in homogeneous stationary weakly ionized Lorentz plasma in neon, investigating effect on mobility, collision frequency, diffusion and kinetic energy 11 p2089 A70-25871
- Boltzmann equation in circular magnetic field solved by Fourier series and Legendre polynomials, correcting distribution function due to Fourier harmonics 13 p2464 A70-29485
- Electron distribution for transport coefficients in Lorentzian plasma under magnetic field, determining electrical conductivity, thermal diffusion and viscosity 14 p2623 A70-31033
- Lorentz plasma electron velocity distribution with allowance for elastic and inelastic collisions, using Legendre polynomial and spherical harmonic expansions in Boltzmann equation 16 p2945 A70-34337
- Two component fully ionized plasma in HF electric field, demonstrating suppression of runaway electrons in Lorentz plasma 17 p3140 A70-34934
- Lorentz lines radiative transfer in nonisothermal gases, developing Landenberg-Reiche analysis for isolated unshifted lines growth curves 21 p3852 A70-40590
- Plasma kinetic theory, applying Boltzmann equation, Lorentz gas model and relaxation method 23 p4224 A70-44177
- Partially ionized Ar transport properties, computing electron velocity distribution function as perturbation for Lorentzian mixture 23 p4220 A70-44437
- Electron runaway suppression in fully ionized Lorentz plasma by crossed magnetic and electric fields 24 p4382 A70-45105
- LORENTZ TRANSFORMATIONS**
Lorentz invariance test using bar magnet on torsion fiber, analyzing preferred reference frame in space assuming earth velocity coupled to electron spin through specific term 02 p0341 A70-12849
- Compton-Getting effect for cosmic ray particles and photons and Lorentz-invariance of distribution functions, discussing thermal background radiation, proton spectra, etc 07 p1369 A70-20071
- Complex vector parametrization of Lorentz group in relativistic kinematics, discussing Wigner rotation, Lorentz transformation and particles classification during scattering 13 p2453 A70-29722
- Schwarzschild solution singularity elimination using Lorentz transform 20 p3673 A70-39998
- LOS ALAMOS TURRET REACTOR**
U HIGH TEMPERATURE NEUTRON REACTORS
LOSSLESS EQUIPMENT
Lossless waveguide propagation analysis as transient problem by means of Laplace transform 14 p2556 A70-30923
- LOST WAX PROCESS**
U INVESTMENT CASTING
LOUDNESS
Loudness lateralization of acoustic signals in right and left ear during binaural interaction 12 p2174 A70-28357
- LOUDSPEAKERS**
Loudspeaker optimal arrangement for speech intelligibility in aircraft crew compartments, discussing apparent SNR improvement 17 p3039 A70-35564
- Electroacoustic circuits transient behavior, examining loudspeaker effectiveness 24 p4321 A70-45374
- LOVE WAVES**
Rayleigh and Love wave phase velocities for great circle paths from ordinary seismograms of World Wide Standard Seismographic Network (WWSSN)/stations 09 p1672 A70-23702
- Love wave propagation in layers with irregular boundaries, investigating scattered field to determine reflection from triangular notch 13 p2394 A70-28831
- LOW ALTITUDE**
Low altitude satellite system for aircraft navigation, considering cost factors, military applications, traffic control capabilities, etc 12 p2270 A70-27922
- Atmospheric density effect on satellite lifetime and position prediction, utilizing data from Cannon Ball and SPADES low altitude density research satellites 14 p2653 A70-30562

Visual air-to-ground target recognition simulation, comparing predictions from Autonetics Detection Model in low altitude flight 24 p4308 A70-45507

LOW ALTITUDE SUPERSONIC VEHICLES
U F-111 AIRCRAFT

LOW ASPECT RATIO
Flow separation angle and loss coefficient in cascades with small aspect ratio blades under secondary vortex pair expansion over channel 06 p1130 A70-17858

Low aspect ratio wing aerodynamic characteristics in shear flow, noting forces dependence on flow velocity gradients 14 p2529 A70-31274

Low aspect ratio plates flutter analysis for subsonic and supersonic models 16 p2991 A70-33888

Transonic high turning low aspect ratio stator cascades flow field performance prediction, reducing secondary flows by partial slots [ASME PAPER 70-GT-63] 18 p3209 A70-36875

Vibration characteristics of low aspect ratio compressor blades, using thin shell theory and Rayleigh-Ritz method [ASME PAPER 70-GT-94] 18 p3305 A70-36876

Slender wings of low aspect ratio and sharp leading edges, predicting inviscid maximum lift 21 p3743 A70-40585

Low aspect ratio compressor blade cascade performance at blade span center, discussing pressure loss, angle of attack and staggering 22 p3957 A70-42272

LOW ASPECT RATIO WINGS
NT DELTA WINGS
NT TRAPEZOIDAL WINGS

Low aspect ratio wings calculated for roll-damping derivatives, investigating load distribution 12 p2157 A70-27983

Low aspect ratio wings under conditions of creep, calculating stress by method of strains 19 p3534 A70-37244

Low aspect ratio cantilever plate wings supersonic bending torsion flutter speed calculation, using spanwise and chordwise variables and potential energy principle 22 p4112 A70-42276

Aircraft control surface aerodynamic characteristics, considering low aspect ratio wing elevons with variable sweep leading edge as longitudinal and lateral controls [ICAS PAPER 70-26] 23 p4131 A70-44107

LOW COST
Apollo program low cost factors including engineering, management quality, reliability and inspection [AIAA PAPER 70-241] 07 p1429 A70-20377

LOW DENSITY FLOW
Heat transfer from two dimensional hypersonic low density stream to wedges and sharp flat plates at expansion angles of attack 04 p0615 A70-14944

Boundary layer on sharp flat plate in low density flow computed by continuum approach, obtaining parabolic partial differential equation system [DVL-914] 06 p1034 A70-17250

Rotational relaxation times for low density hypersonic nitrogen free jet, comparing measured and predicted impact pressures 06 p1043 A70-18279

Sphere drag measurements in low density hypersonic transition and near free molecular flow 06 p1124 A70-18373

Low density hypersonic flow over slender cone using air and He test gases 07 p1188 A70-19309

Radiation effects on viscous hypersonic low density stagnation flow using two layer model, calculating flow field and heat transfer coefficient 12 p2158 A70-28204

End support cooling in hot-wire anemometry of low density high temperature flows [AIAA PAPER 70-589] 13 p2412 A70-29882

Low density hypersonic flow over finite width flat plate at zero incidence 17 p3007 A70-34473

Mach disk structure in free low density expanding supersonic jet from static pressure probe measurements 17 p3068 A70-34696

Low density gas jet from short circular cylindrical tube, calculating molecular flux radial density variation 22 p4076 A70-43430

Dissociative nonequilibrium hypersonic flow of low density gas mixtures over flat plate in free stream, noting catalytic wall effect on flow field 23 p4135 A70-44604

LOW DENSITY GASES
U RAREFIED GASES

LOW DENSITY MATERIALS
Syntactic foams of high filler content, low density, high compression strength and hydrolytic stability using hollow carbon microspheres in epoxy resin matrix 16 p2936 A70-33365

LOW DENSITY WIND TUNNELS

Flow parameters measured in low density hypersonic nozzle, estimating error of all relevant parameters 06 p1030 A70-18302

Electron beam probe applied to flow visualization in rarefied gas wind tunnels 10 p1860 A70-24549

Vacuum supersonic wind tunnel air continuous dehumidification by using multistage centrifugal blower with/without heat exchanger 12 p2206 A70-27153

Laminar boundary layers in low density supersonic and hypersonic conical and axisymmetric nozzles, treating displacement, transverse curvature, velocity slip and temperature jump [AIAA PAPER 69-653] 13 p2386 A70-28513

Hemisphere model flow field investigations in low density plasma wind tunnel, considering flow regimes of transition and shock formation 15 p2673 A70-32838

LOW FINENESS RATIO

U FINENESS RATIO

LOW FREQUENCIES

NT VERY LOW FREQUENCIES

LF wave propagation using Ioran C radio navigation system flight performance tests 03 p0523 A70-13615

Read theory application to LF operation of avalanche diodes under large signal conditions 04 p0656 A70-14720

Oblique incidence absorption measurements by pulse or CW signal strength observations or LOF data, comparing LUF to LOF 07 p1231 A70-19173

LF waves and irregularities in ionosphere - Conference, Frascati, Italy, September 1968 07 p1263 A70-19186

LF waves and irregularities in auroral ionosphere determined by radar measurements, suggesting role of plasma waves cross modulation 07 p1264 A70-19193

Spaceborne long wavelength radio astronomy, proposing lunar orbit and beyond Pluto observatories to reduce magnetospheric and interplanetary plasma effects 09 p1754 A70-22495

Broadband and highpass LF noise in distant magnetosphere detected by VLF/LF experiment on OGO 1 satellite 12 p2222 A70-27183

Ionospheric probing with LF/VLF/ELF radio waves, discussing measurement techniques and temporal and spatial resolutions 12 p2224 A70-27731

Discharge effects on LF oscillations and ion extraction in hot cathode Penning plasma 13 p2463 A70-29370

LF plane wave scattering from semielliptic groove in conducting ground plane noting validity for arbitrary polarization, incidence, directions and eccentricity 13 p2453 A70-29822

LF signals phase determination during solar eclipse of 22 September 1968, noting frequency shift magnitude 14 p2547 A70-30238

Reflection and conversion coefficients of model ionospheres for VLF and LF radio waves 14 p2573 A70-30735

Incident microwave signal in Tonks-Dattner resonance coupled to discrete LF modes in plasma column 15 p2778 A70-31756

Plane wave incident on oblate spheroid or disk, deriving LF field scattering 18 p3335 A70-35974

LF geomagnetic micropulsations recordings by two component induction magnetometer, relating diurnal frequency and occurrence variations to local K_i index changes 19 p3412 A70-37995

LF cavity loss modulations of homogeneous four-level CW Nd-YAG laser, including relaxation-oscillation regime 22 p4050 A70-43005

Homogeneous helium plasma column LF wave propagation in uniform magnetic field 22 p4082 A70-43216

D region LF and VLF sky waves opposite phase perturbation behavior 23 p4162 A70-44006

Phase and group velocity variations of LF transmission compared against crystal oscillator 23 p4163 A70-44228

LF signals phase determination during solar eclipse of 22 September 1968, noting frequency shift magnitude 24 p4316 A70-46313

LF narrow band-pass amplifiers with distributed RC structures 24 p4321 A70-46397

Discharge effects on LF oscillations and ion extraction in hot cathode Penning plasma 13 p2463 A70-29370

LF plane wave scattering from semielliptic groove in conducting ground plane noting validity for arbitrary polarization, incidence, directions and eccentricity 13 p2453 A70-29822

LF signals phase determination during solar eclipse of 22 September 1968, noting frequency shift magnitude 14 p2547 A70-30238

Reflection and conversion coefficients of model ionospheres for VLF and LF radio waves 14 p2573 A70-30735

Incident microwave signal in Tonks-Dattner resonance coupled to discrete LF modes in plasma column 15 p2778 A70-31756

Plane wave incident on oblate spheroid or disk, deriving LF field scattering 18 p3335 A70-35974

LF geomagnetic micropulsations recordings by two component induction magnetometer, relating diurnal frequency and occurrence variations to local K_i index changes 19 p3412 A70-37995

LF cavity loss modulations of homogeneous four-level CW Nd-YAG laser, including relaxation-oscillation regime 22 p4050 A70-43005

Homogeneous helium plasma column LF wave propagation in uniform magnetic field 22 p4082 A70-43216

D region LF and VLF sky waves opposite phase perturbation behavior 23 p4162 A70-44006

Phase and group velocity variations of LF transmission compared against crystal oscillator 23 p4163 A70-44228

LF signals phase determination during solar eclipse of 22 September 1968, noting frequency shift magnitude 24 p4316 A70-46313

LF narrow band-pass amplifiers with distributed RC structures 24 p4321 A70-46397

LOW GRAVITY

U REDUCED GRAVITY

LOW LATITUDES

U TROPICAL REGIONS

LOW LEVEL TURBULENCE

Atmospheric small scale turbulence observation by Doppler radar, noting role of tracers radial velocity spectrum 09 p1716 A70-22364

LOW MASS

U MASS

LOW MOLECULAR WEIGHTS

Low molecular weight organic semiconductors photoelectron UV emission spectra, studying electron energy distribution and optical ionization, dark bulk conductivity, etc 03 p0541 A70-13728

LOW NOISE

Low noise TWT, discussing dynamic range, gain and phase tracking, environmental performance, life behavior and noise factor interrelations 09 p1644 A70-22233

Low noise nonreciprocal microwave parametric amplifier with up-and-down converter and idlers in cascade 09 p1647 A70-22850

Low noise wideband amplifier design for Intelsat 3 satellite ground stations 16 p2877 A70-33415

Low noise He-Ne laser with capillary elements, measuring current threshold of noise free operation as function of design parameters 19 p3448 A70-38512

Low noise requirements of DC current sources used in circuit design 21 p3797 A70-40854

Low noise GaAs Schottky barrier beam lead mixer and chip style diodes, discussing fabrication and performance 22 p3998 A70-43333

Low noise constant temperature hot-wire anemometer design with second order high-cut filter, determining system stability 23 p4199 A70-45050

LOW PASS FILTERS

Frequency responses bounds of nonnormalized low pass and bandpass filters 05 p0820 A70-16360

Transversal filters with continuously tapped delay lines, emphasizing synthesis of low pass filter and phase shifter 05 p0822 A70-16652

Microstrip oscillator circuit design for operating with high power/efficiency avalanche diodes, describing low pass filter tuning section role 08 p1475 A70-21278

Low pass filter structure of focusing reflectors designed for quasi-optical system, noting energy absorption 08 p1476 A70-21287

Microwave band-stop filters based on ladder network low pass prototypes, comparing performance with bandpass type 14 p2557 A70-31179

Low pass filter synthesis with transfer function having frequency response boost in pass band 15 p2708 A70-31833

Linear time varying low pass filters computer aided design, introducing quadratic performance criterion to calculate steepest descent in function space 15 p2710 A70-32588

Transmitter-antenna matching, using Pi-filter for resonance transformation 19 p3389 A70-38071

Transistorized LF RC filter circuit design for desired frequency response characteristics 23 p4171 A70-43962

Multilevel FSK system with limiter discriminator followed by low pass filter as demodulator, calculating error rates for comparison with other analyses 23 p4161 A70-44003

Directional periodic linear Yagi-Uda arrays application for open low pass or bandpass filters and open resonators 23 p4166 A70-44971

Analog and digital low pass filters for radiometric postdetector filtering 24 p4321 A70-45622

LOW PRESSURE

Low pressure ionic reactions in gaseous cyclobutane 06 p1004 A70-17328

Pressure-time history in spherical shock waves flow field at low ambient pressures recorded with piezoelectric transducers, showing shock strength decrease 06 p1052 A70-18385

Fixed low pressures of nitrogen generated by chemical dissociation in system at equilibrium at constant temperature, applying results to vacuum measurement device calibration 09 p1630 A70-22954

Orbitron ion gauge experimental designs for low pressure applications 12 p2231 A70-27264

Ultravacuum measurement and calibration assembly for pressures down to one picotorr for vacuum gage standards 23 p4143 A70-44871

LOW PRESSURE CHAMBERS

U VACUUM CHAMBERS

LOW SPEED

Electrohydraulic control system dynamics, examining executive component loading at low speeds and nonlinear resistances

13 p2349 A70-29720

Constant temperature linearized hot-wire anemometer for low velocity high turbulence flow

21 p3827 A70-41455

STOL aircraft low speed handling characteristics described via approach and landing profiles, power requirements, wind effects, etc

[AIAA PAPER 70-1332]

24 p4291 A70-45936

LOW SPEED HANDLING

U CONTROLLABILITY

U LOW SPEED

LOW SPEED STABILITY

Longitudinal stability of V/STOL aircraft at low speeds, discussing three tilt wings and quad ducted propeller configurations

[AIAA PAPER 69-194]

07 p1195 A70-20410

Airfoil analysis and synthesis, discussing computer graphics application to low speed shape and improved pressure distribution

08 p1594 A70-21867

Low speed buffet intensity under pressure fluctuations on slender wing aircraft at vortex breakdown, using wind tunnel model

10 p1963 A70-25067

Blunt planetary entry body free fall drop tests determining low speed stability and base pressure characteristics

[AIAA PAPER 70-577]

13 p2342 A70-29892

Small airplane unsteady motion downwash angle at low speeds, comparing results from rectilinear steady flights

[ICAS PAPER 70-25]

23 p4138 A70-44108

LOW SPEED WIND TUNNELS

NT SUBSONIC WIND TUNNELS

Blockage and wall corrections proposed for obtaining uniform results from low speed wind tunnel models

05 p0789 A70-15812

Low speed wind tunnel test results correction program, considering solid, wake blockage, lift, static pressure gradient and wall interference effects

06 p0968 A70-17934

Low speed wind tunnel design and construction for laboratory experiments and research projects, describing test sections

16 p2889 A70-33769

Low speed airfoil two dimensional testing in wind tunnel with slotted wall, examining lift, drag and pitching moments

[ICAS PAPER 70-08]

23 p4132 A70-44119

LOW TEMPERATURE

Mass and radius relations for zero temperature spheres of chemical elements, using equation of state and numerical integration

04 p0749 A70-14599

Chilled emulsion photography for astronomy and spectrography, reducing long exposures with chilled plates

14 p2585 A70-30649

Relaxations from anelastic and dielectric measurements of fused silica and soda-silica glasses at low temperatures ascribed to vibration modes exceeding Debye spectrum

16 p2960 A70-32996

Passive radiative coolers role in utilizing IR detector systems for low temperature spacecraft applications, describing staged radiator design, optimization and tests

[AIAA PAPER 70-854]

16 p2983 A70-33921

Thermocouples and resistance thermometers comparison for low temperature measurements

19 p3432 A70-38703

Pt resistance thermometers for low temperature measurements, discussing structural and mechanical characteristics

19 p3432 A70-38704

Low temperature Ge diode thermometer with computer circuit transforming voltage to temperature readout

21 p3828 A70-41473

LOW TEMPERATURE BRAZING

Ti sandwich structures low temperature brazing with Al alloy, describing fabrication process and mechanical properties

20 p3638 A70-39969

LOW TEMPERATURE ENVIRONMENTS

Temperature measuring devices design for ultrahigh/ultralow temperatures, examining heat effects on gases, liquids and solids

02 p0295 A70-11864

Recombination emission of InSb semiconductor at low temperature during pinch effect with electron gas degeneration, calculating spectral distribution and effective temperature vs current

03 p0539 A70-13406

Thermal conductivity, electrical resistivity, Lorentz ratio and thermopower of aerospace alloys at cryogenic temperatures, considering Inconel, Hastelloy, Ti and Al alloys

03 p0512 A70-13807

Deep freezing of nuclear precession magnetometer elements for improving instrument characteristics accuracy

05 p0851 A70-16769

Testing equipment and methods for metallic materials selection for low temperature applications, characterizing plasticity by yield strength, tensile strength, elongation, etc

05 p0864 A70-16805

Correction factor for free stream Reynolds number errors resulting from low temperature viscosity in He wind tunnels

13 p2385 A70-29985

Electropneumatic actuation systems for rocket engines in extreme environment applications involving high nuclear radiation levels and high and cryogenic temperatures

14 p2535 A70-31343

Titanium monoxide thin film as low temperature getter, measuring activity coefficient and capacity under ultra high vacuum

15 p2783 A70-31844

Charpy impact test evaluation on hot rolled metal plates for low temperature welded structures

15 p2819 A70-32235

Cryobiologic potentialities on earth, investigating life forms physiological response to temperature, cryotolerance mechanisms, etc

16 p2848 A70-33093

Metal bonding at low temperatures, studying atmosphere and metal plating effects

18 p3265 A70-37203

LOW TEMPERATURE PHYSICS

Induction distances, transient pressures and wave propagation rates for detonation waves in cylindrical tube low temperature hydrogen-oxygen mixtures

03 p0607 A70-13919

Semiconductors low temperature photoconductivity fluctuations occurrence during energy relaxation probability by optical phonons

04 p0730 A70-14413

Thermal conductivity and hysteresis measured in cylindrical In foil under magnetic fields at temperatures below 1 K

05 p0891 A70-15792

Low temperature thermoelasticity theory for elastic fluids, considering fountain and second sound effects and viscosity anomalies in He II

06 p1164 A70-17442

Magnetoresistance effects in impurity conduction mode of n-type GaAs crystals below 6 K, giving electron concentration

07 p1356 A70-19796

Helium melting pressure curve to calibrate cerium magnesium nitrate or NMR low temperature thermometers

09 p1728 A70-22999

Amorphous polymers thermal conductivity measured at 0.4-4 K, observing similar temperature dependences

10 p1906 A70-23979

Aluminum alloy deformations and rupture strength under complex stress at low temperatures, observing anisotropy decrease with temperature

10 p1903 A70-24243

Parallel and perpendicular negative magnetoresistance measurements as function of magnetic field in p-type GaAs at 77 K

13 p2471 A70-29374

Specific heat measurements on disordered and ordered phases of Cu-Au alloys at low temperatures

14 p2626 A70-30497

Low temperature terminology at December 1969 Paris conference, discussing temperature scale, superconductivity, liquid He, supercooling, subcooling, cryo and cryogenic

14 p2616 A70-31013

Cryogenics and nuclear physics, discussing particle beam handling magnets, superconducting accelerators, detectors, moderators, low temperature irradiation facilities, etc

14 p2616 A70-31014

Vapor-liquid equilibria predictions for multicomponent cryogenic mixtures, applying to correlation selection in critical and low temperature regions

14 p2616 A70-31015

Thermal and electrical resistances of Na at low temperatures measured by germanium thermometers and galvanometer amplifier

14 p2617 A70-31021

Compressibility factors and virial coefficients for He-N mixture, He and nitrogen at low temperatures and high pressures

18 p3290 A70-36250

Amorphous and partly crystalline polymers low temperature thermal conductivity and heat capacity

21 p3844 A70-42136

Superconductors resonance and oscillation phenomena, discussing particle motion, energy spectrum, magnetic and temperature effects, etc

22 p4088 A70-43476

Specific heat of amorphous polymethyl methacrylate and polystyrene by pulse method below 4 K, comparing Debye and acoustic values

24 p4367 A70-45598

LOW TEMPERATURE TESTS

Critical current density enhancement in Ta-rich Zr alloys in magnetic fields at low temperature after aging

01 p0122 A70-11238

Tensile tests of polycrystalline Nb-H alloys at low temperatures, noting cooling rate effect on ductility in terms of microstructure

01 p0122 A70-11240

Friction and surface damage between clean metal hemispheres and flats at low sliding speeds and 25 K room temperature range

01 p0105 A70-11393

Age hardening characteristics of maraging martensite stainless steels containing Mo and Co subjected to subzero treatment

01 p0125 A70-11641

Calorimetric analysis and hardness test to investigate low temperature aging behavior of maraging stainless steels

01 p0125 A70-11642

Semiconductors low temperature electron energy losses due to inelastic electron scattering at neutral impurity donors shown to exceed scattering losses at phonons

03 p0539 A70-13423

Brittle fracture in neutron irradiated and nonirradiated Mo specimens tested in tension and compression at low temperature

03 p0513 A70-14013

Mechanical properties of cast light alloys at low temperatures, showing satisfactory plasticity and insensitivity to stress raisers

05 p0864 A70-16868

Stress concentration effect on mechanical properties of Ti-Ta alloys at low temperatures, showing insensitivity to notch and suitability for cryogenics

05 p0864 A70-16869

Facility for testing thin walled tubular specimens in stressed state at low temperatures by keeping stresses constant with helical gear

05 p0830 A70-17075

Materials stress rupture strength and elastic constants at liquid hydrogen temperature, describing method and facility

05 p0955 A70-17076

Rat survival rate after prolonged gradually decreased body temperature without motion restraint or kept in fixed position

05 p0804 A70-17115

Low temperature effects on deformability of middle C steel under complex stress state, showing invalid stress-strain relation and deviator similarity

08 p1516 A70-20983

Vinoflex glue for constant strain gauges in low temperature tensometry, showing satisfactory recording at single and multiple loadings

08 p1495 A70-20984

Specimen holder for 300 K/4.2 K resistance ratio measurement

09 p1655 A70-22645

Fracture toughness and deformation kinetics dependence on compositional, microstructural and textural variations of alpha and alpha-beta Ti alloys at low temperatures

09 p1704 A70-22801

Evanohm alloy resistance wire for applications in magnetic field, illustrating percentage change at 4.2 K

09 p1679 A70-22998

Nb-W single crystal low temperature thermally activated deformation, observing slope change in temperature dependence curves of flow stress and strain rate sensitivity

09 p1708 A70-23572

Apiezon N grease thermal conductivity at liquid helium temperatures noting behavior as insulator

12 p2258 A70-27024

Cavity and storage temperature effects on hydrogen maser oscillation in 77-293 K range

13 p2425 A70-28713

Al weldable alloys for cryogenic applications, considering plasticity, brittleness and tensile and yield strengths at low temperatures

14 p2597 A70-30968

Low temperature tensometry application to stress-strain state of turbine disks

15 p2733 A70-31537

Gaseous Al oxide bond bending frequency in Ne and Ar matrices at liquid He temperatures, investigating IR spectrum

15 p2695 A70-32830

Microscopic and macroscopic viewpoints of low temperature brittle fracture, noting Inglis, Griffith and Barenblatt theories

16 p2989 A70-33671

Low temperature effects on Ti alloys welded joints elasticity

17 p3126 A70-35637

Dry friction and wear tests of various materials in vacuum at low temperatures

18 p3263 A70-36471

Cryogenic attachment for cooling and tilting metal samples in electron microscope

18 p3259 A70-36474

Cardioid condenser as radiometer mirror objective in low temperature radiometry, describing optical characteristics 19 p3420 A70-37261

Low temperature creep deformation recorder with liquid He coolant, discussing Al and Pb single crystal tests 19 p3395 A70-37352

Ti alloys low temperature strength and plasticity, noting twinning and additives effects 19 p3450 A70-37457

Friction reducing oxide layer effects on Ti alloys low temperature plastic and mechanical properties 19 p3450 A70-37458

Low temperature electrical resistivities of Al, Ni, Cu, Ti and Fe alloys for different heat treated conditions 19 p3452 A70-37825

Strain measuring apparatus for multiple samples simultaneous compression tests at near absolute zero temperatures 20 p3632 A70-39628

Carbon resistors negative magnetoresistance measurement near absolute zero temperature by helium cryostat, noting anisotropy 20 p3687 A70-40168

Low temperature anharmonicity in thorium dioxide with Co 57 impurities, using Mossbauer effect of Fe 57 21 p3862 A70-40975

Polymers low temperature relaxation behavior, discussing molecular structure, crystallinity, copolymerization, etc 21 p3844 A70-42135

Impurities concentration estimate in metals by low temperature residual resistivity, investigating contact and contactless measurements 22 p4052 A70-42573

Aluminum, duralumin and stainless steel tensile strength tests at cryogenic temperatures 23 p4206 A70-44353

Cryogenic thermocouples of various metal pairs for low temperature measurements, discussing performance tests and calibrations 24 p4378 A70-45385

Vacancies in vanadium carbide /V3C2C8/ crystals with predicted lattice defects at low temperature, considering entropy 24 p4365 A70-46353

LOW THRUST

NT MICROTHRUST

Optimum low thrust ion propelled interplanetary trajectory design using two step Chebyshev method 17 p3167 A70-35232

Communication satellites low thrust transfer to synchronous orbit by two-stage operation using hydrogen resistojets and Hg ion motors [AIAA PAPER 70-1116] 20 p3691 A70-40227

Optimal low thrust transfer between coplanar circular orbits, examining thrust direction and steering as Mayer problem 22 p4097 A70-42489

LOW THRUST PROPULSION

NT ELECTROMAGNETIC PROPULSION

NT ELECTROSTATIC PROPULSION

NT ION PROPULSION

NT MAN OPERATED PROPULSION SYSTEMS

NT PHOTONIC PROPULSION

NT PLASMA PROPULSION

NT SOLAR PROPULSION

Heat exchange unit for low thrust attitude control propulsion system evaporator designed for converting liquid propellants to gas [AICHE PREPRINT 25] 01 p0216 A70-10969

Automated parameter search techniques applied to low thrust mission design, stressing trajectories and mission optimization [AIAA PAPER 69-261] 04 p0736 A70-15404

Tangential thrust, constant acceleration trajectories for close solar probe missions using low thrust electric engines 06 p1137 A70-17177

Heliocentric low thrust spacecraft trajectory analysis using two-variable asymptotic expansion method [AIAA PAPER 70-214] 06 p1145 A70-18064

Low thrust trajectory and performance analysis of solar electric propulsion system for unmanned interplanetary exploration 06 p1145 A70-18081

Analytic Trajectory Optimization Model to develop computational techniques for low thrust mission analysis [AIAA PAPER 70-96] 06 p1159 A70-18230

30 cm diameter mercury bombardment low impulse thruster development for potential space applications, discussing performance and control [AIAA PAPER 69-238] 07 p1365 A70-19704

Optimal acceleration from earth orbit to hyperbolic velocities of low thrust space vehicle, constructing asymptotic expansions near and far from central field 10 p1940 A70-24305

Pulsed plasma microthruster propulsion system for synchronous orbit LES 6 satellite [AIAA PAPER 69-298] 13 p2473 A70-28504

Hollow cathode mercury electron bombardment thruster design, emphasizing low specific impulse operation and discharge chamber improvements 13 p2473 A70-28505

Low thrust mission simulation dependence on hardware definition, discussing power plant characteristics, jet velocity and thruster efficiency 13 p2486 A70-28517

Interplanetary low thrust orbit transfer optimization by dynamic programming, including gravitational perturbation effects from earth, Mars and Jupiter 14 p2640 A70-30759

Low thrust high impulse nuclear and electric space propulsion systems, discussing performance capability for space missions 18 p3290 A70-36566

Three body numerical solutions to low thrust guidance and navigation for outer planet orbiter with nuclear-electric propulsion [AIAA PAPER 70-1040] 19 p3527 A70-38855

Low thrust interplanetary swingby trajectories optimization, considering thrusting and coasting within sphere of influence [AIAA PAPER 70-1041] 19 p3527 A70-38856

Optimal low thrust power plant for spacecraft payload-maneuver tradeoff 21 p3866 A70-40832

Low specific impulse hollow cathode mercury thruster for deep space electric propulsion, using SERT 2 configuration [AIAA PAPER 70-1099] 21 p3866 A70-40893

LOW TURBULENCE

Kinetic equation for nonlinear interaction of waves, including unstable or damped, using Bogoliubov method 09 p1659 A70-22214

Probability densities and distributions, moments and spectra from time derivatives of streamwise velocity fluctuation in curved mixing layer, measuring small scale turbulence structure 20 p3609 A70-39652

LOW VELOCITY

U LOW SPEED

LOW VISIBILITY

Visibility improvement in fog at airports, discussing fog-seeding and warm fog modification operations 01 p0135 A70-11320

Low visibility aircraft landing problem concerning pilot instrument and visual cue and federal regulations governing operational approval [AIAA PAPER 70-936] 17 p3134 A70-35845

Runway low visibility and ceilings frequency and duration at German airports, using 1949-1967 statistical data 19 p3462 A70-37925

Airport fog layers repetition frequency after low visibility periods 22 p4065 A70-43246

LOWER ATMOSPHERE

NT OZONOSPHERE

Book on atmospheric circulation systems structures and physical interpretation, concentrating on lower atmosphere and North America 01 p0069 A70-10126

Upper atmosphere-lower atmosphere interactions, middle atmospheric physics and dynamics and mesospheric seasonal and large scale zonal and meridional behavior 01 p0073 A70-10581

Hydrostatic equation nonequilibrium terms role in single and multicomponent atmospheres, deriving solutions to Boltzmann equation 02 p0328 A70-12386

Primary protons energy estimated from energy ratio with maximum extremal distribution of electron numbers in lower half of atmosphere 03 p0527 A70-13054

Diffusion categories and propagation of radioactive elements in lower atmosphere determined with respect to measured radiation balance, temperature gradient and wind 03 p0521 A70-14290

Atmospheric space charge magnitude and polarity below 50 km based on rocket probes 04 p0675 A70-14437

Lower atmosphere VLF heat turbulence as function of precipitation, indicating atmospheric layers existence for different weather situations 05 p0879 A70-16315

Lower atmospheric photochemistry, discussing tropospheric, stratospheric, mesospheric and polluted atmospheric chemical and photochemical reactions 06 p1058 A70-18485

Short lived cosmic ray produced nuclides as lower atmospheric motion tracers, studying Na 24 characteristics and activity in rain water 07 p1373 A70-20355

Atmospheric variables /velocity, temperature, energy, etc/ spectra in lowest few hundred meters 09 p1714 A70-22352

Wind HF inclination variations in lower atmosphere, considering turbulent kinetic energy dissipation and buoyancy production 09 p1714 A70-22355

Atmospheric momentum and heat flux height variations in surface boundary layer, stressing instrument performance and measurement techniques 09 p1715 A70-22359

Lower atmosphere turbulence under convective conditions, comparing Doppler radar and instrumented aircraft wind speed fluctuation measurements 09 p1716 A70-22367

Stratified atmosphere boundary layer motions, studying turbulence and internal gravity waves characteristics 09 p1716 A70-22369

Diffuse light transmission from point sources over horizontal paths in lower atmosphere, discussing effect of range 10 p1912 A70-24424

Atmospheric space charge magnitude and polarity below 50 km based on rocket probes 13 p2392 A70-28462

Radar meteorology, discussing convection in lower atmosphere and clear air turbulence observations 13 p2443 A70-28475

Lower atmospheric layer temperature and wind vertical distribution effect on wind velocity ratio to geostrophic wind at earth surface 13 p2444 A70-28586

Atmospheric optical thickness from radio telescopic measurements of wave absorption at millimeter wavelengths, showing dependence on lower atmospheric moisture content 14 p2546 A70-30127

Numerical model of diurnal variations of minor neutral constituents in mesosphere and lower atmosphere including molecular and eddy diffusion 15 p2727 A70-31909

Ionospheric E region winds correlations to lower atmosphere meteorological phenomena 17 p3077 A70-34950

Absolute cosmic ray ionization in lower atmosphere, using air-filled ionization chamber 18 p3305 A70-36001

Turbulent energy dissipation in lower atmospheric layer on meteorological mast during various temperature stratifications 18 p3247 A70-36627

Venus lower atmosphere structure and brightness temperature spectrum analysis for composition, temperature and pressure profiles 18 p3323 A70-37139

Lower atmosphere refractive index vertical distribution and fluctuations, using airborne refractometer 20 p3619 A70-39191

Lower atmosphere cosmic ray ionization calculation, using high energy transport code 20 p3699 A70-39348

Gust field in lowest atmospheric layer over homogeneous terrain, deriving statistical models and simulating effects on XV-5 V/STOL aircraft 21 p3750 A70-40784

Clear lower atmosphere meteorological parameters remote sensing for weather forecasting, comparing optical, radio and acoustic radar techniques 21 p3785 A70-40802

Mars lower atmosphere vertical temperature distributions from Mariner 6 and 7 radio occultation data, using improved trajectory estimates 21 p3884 A70-40908

Molecular oxygen density and vibrational distribution in lower atmosphere, observing solar UV radiation absorption by satellite OSO-4 21 p3816 A70-41066

Global atmospheric electrical structure, considering emf from thermally driven tidal motions in lower atmosphere 22 p4016 A70-42783

Lower atmosphere electric field vertical distribution measurement by combined balloon and rocket soundings 22 p4017 A70-42797

Perturbation method with small parameter applied to turbulent transfer equation in lower atmosphere, solving longitudinal diffusion effect on evaporation 22 p4065 A70-42911

Lower atmosphere gravity wave motions due to cooling by solar eclipse shadow 23 p1815 A70-43845

Internal gravity wave shape at temperature inversion in lower atmosphere from high resolution vertically pointing FM/CW radar sounding 23 p4162 A70-44038

Earth atmospheric boundary layer wind velocity, temperature gradients and specific humidity differences, calculating climatic correlations from mathematical circulation model 23 p4214 A70-44264

Monin-Obukhov function and nondimensional transfer coefficients variation, discussing turbulent motion decay in lower atmosphere 24 p4372 A70-46072

LOWER IONOSPHERE
NT D REGION

Lower ionosphere radio wave partial reflection strength relationship to electron density profiles measured by rocket probes

01 p0045 A70-11089

Seasonal phase changes of semidiurnal tidal wind components in lower ionosphere demonstrated from ionospheric drift measurements

01 p0078 A70-11212

Vertical wind observations during lower ionosphere wind measurements by Na release method, discussing gravity effects and standing waves

01 p0078 A70-11213

Geomagnetic field directed hydromagnetic waves propagation in lower ionosphere noting inhomogeneous conductivity, Hall effect and lines of forces role

01 p0083 A70-11546

Solar X-ray bursts observations correlation with sudden phase anomalies measured at long VHF propagation paths in lower ionosphere

03 p0558 A70-13601

Stellar X ray effect on nighttime lower ionosphere wave reflection suggested from VLF propagation data

03 p0562 A70-14224

Positive ion concentration profiles in lower nighttime midlatitude ionosphere calculated from corpuscular radiation measurements and ion recombination constants

04 p0738 A70-14436

Polar lower ionosphere, using radar VLF step frequency sounding to determine reflection phase height at given propagation path

04 p0680 A70-15115

Signal amplitude and Doppler shift statistical characteristics calculated from sounding data on scattering at lower ionospheric discontinuities

04 p0650 A70-15284

Lower ionospheric cosmic layer state during Forbush decreases from radio absorption observations interpreted on basis of electron production rate analysis

04 p0743 A70-15720

Geomagnetic field lines inclination effect on hydromagnetic waves propagation in lower ionosphere, using atmospheric model in plane form with integral conductivity tensor

04 p0683 A70-15737

Radio wave absorption coefficient in lower ionosphere related to total radiation absorption and electron concentration profile

05 p0843 A70-16761

Night lower ionosphere at midlatitudes additional ionization ascribed to solar corpuscular fluxes

06 p1135 A70-17839

Solar particles penetration to lower ionospheric heights at low latitudes indicated from proton flux measurements by Explorer 33 satellite and Calcutta station

07 p1366 A70-18849

Lower ionosphere effects on HF propagation modes observed by pulse system, discussing propagation time, mode structure, transmission loss, etc

07 p1232 A70-19179

Diurnal variations of lower F region ion composition and recombination coefficient based on numerical modeling of continuity equations for electrons and molecular species

07 p1265 A70-19431

Numerical modeling of electron and molecular ion continuity equations describing conditions in lower F region near magnetic equator using analog computer

07 p1265 A70-19434

Sunrise effects in lower ionosphere at midlatitude, discussing long wave absorption measurements, summer electron concentration profile and consistency of aeronomic model

07 p1235 A70-19436

Electron production rate enhancement by solar cosmic rays in lower ionosphere, considering particle distribution and polar cap absorption

07 p1369 A70-20153

Winter anomaly ionization in lower ionosphere at medium latitudes from radio propagation observations, comparing wave absorption and phase height measurements

07 p1274 A70-20273

Solar corpuscular fluxes directional distribution time dependent changes effect on lower ionospheric electron production rates

07 p1373 A70-20344

27-day variations in ionization layer created by galactic cosmic rays, discussing association with 27-day cosmic ray and geomagnetic field variations

07 p1373 A70-20345

Electron production in lower ionosphere by solar cosmic rays, calculating rates by computer as function of nuclear charge number, energy spectrum and height

07 p1373 A70-20348

Lower ionosphere electric fields and currents vertical profiles above geomagnetic equator under quiet geomagnetic conditions from rocket data

07 p1277 A70-20453

Lower ionosphere geomagnetic field local gradients determination by partial reflection method

07 p1277 A70-20455

Cosmic layer in lower ionosphere investigated by 164 kHz frequency absorption at night, discussing solar activity effects

10 p1934 A70-25198

Geomagnetic field upward calculation in lower ionosphere, discussing accurate data acquisition difficulties in Dirichlet problem solution

11 p2043 A70-25544

Solar L alpha and X ray emission contribution to lower ionosphere ion production, discussing altitudinal, latitudinal and temporal variations

11 p2106 A70-26789

Ionospheric lowest regions and magnetosphere probing based on atmospheric observations, detecting disturbed conditions

12 p2224 A70-27734

Forbush effects influence on cosmic layer state in lower ionosphere using long radio waves

12 p2295 A70-28220

Positive ion concentration profiles in lower nighttime midlatitude ionosphere calculated from corpuscular radiation measurements and ion recombination constants

13 p2475 A70-28461

Tidal forces effect on wind system in lower ionosphere, using Navier-Stokes equation for lower layer and Euler equations for upper layer

14 p2571 A70-30232

Lower ionosphere nonuniformities drift velocity and direction using space diversity reception

14 p2571 A70-30233

Lower ionosphere influence on radio reflection from sporadic E layer, determining diurnal variations of D region absorption for various frequencies

14 p2547 A70-30235

Lower ionosphere radio reflection during solar eclipse of 22 September 1968

14 p2571 A70-30237

VHF wave interference from heavy ion layers in lower ionosphere

14 p2574 A70-30737

Lower ionosphere electron densities seasonal variations relationship to atmospheric circulation

14 p2574 A70-30742

Lower ionospheric drift motions observed from VHF radio signal, relating to three paths near auroral zone during dark hours

14 p2574 A70-30749

Lower ionospheric cosmic layer state during Forbush decreases from radio absorption observations interpreted on basis of electron production rate analysis

14 p2632 A70-30804

Geomagnetic field lines inclination effect on hydrodynamic waves propagation in lower ionosphere, using atmospheric model in plane form with integral conductivity tensor

14 p2575 A70-30821

Winter anomaly of radio wave absorption in midlatitude lower ionosphere in terms of meteorological influences and particle influx enhancements

17 p3076 A70-34936

Zonal wind component in lower ionosphere observed for gravity waves partial reflections by temperature discontinuities, using least mean square method for reflection coefficient

17 p3077 A70-34946

Lower ionosphere electron density and winter anomaly in HF absorption

17 p3077 A70-34948

Diurnal variations of lower F region ion composition and recombination coefficient based on numerical modeling of continuity equations for electrons and molecular species

18 p3249 A70-36905

Numerical modeling of electron and molecular ion continuity equations describing conditions in lower F region near magnetic equator using analog computer

18 p3249 A70-36908

Sunrise effects in lower ionosphere at midlatitude, discussing long wave absorption measurements, summer electron concentration profile and consistency of aeronomic model

18 p3249 A70-36910

Nitrogen dioxide and molecular oxygen ions densities in lower ionosphere as function of solar corpuscular radiation

19 p3409 A70-37325

Whistler mode wave propagation amplitude, polarization and dispersion in lower ionosphere, discussing electric field experiment with Nike-Tomahawk sounding rocket

20 p3622 A70-39456

Forbush effects influence on cosmic layer state in lower ionosphere using long radio waves

20 p3700 A70-40095

Long range low loss earth-detached propagation paths in lower ionosphere indicated via OV4-1 satellite experiment on guided ionospheric propagation

20 p3591 A70-40494

Lower ionospheric structure and electromagnetic resonance phenomena, describing radio equipment for solar activity effects studies

21 p3812 A70-40620

Midlatitude stratosphere and lower ionosphere density model, discussing vertical, diurnal and seasonal variations effects on spacecraft trajectories

21 p3813 A70-40830

Geomagnetic field upward calculation in lower ionosphere, discussing accurate data acquisition difficulties in Dirichlet problem solution

21 p3819 A70-41294

ELF and VLF waves in waveguide propagation mode, calculating lower ionosphere effect on attenuation and phase velocity

22 p3989 A70-42960

Ionization and loss processes for meteoric elements in lower ionosphere, suggesting hydrates formation role in alkali metal ions depletion

22 p4106 A70-43305

Lower ionosphere ionization anomalies, discussing sunrise seasonal change effects in VLF-LF propagation, winter radio wave absorption and geomagnetic storm after-effects

22 p4024 A70-43311

Lower ionosphere electron concentration space-time variations relation to ionization source intensity fluctuations based on rocket observations and ground sounding data

23 p4190 A70-44079

Pulsed radio wave interactions with various lower ionosphere models, estimating cross modulation by computer calculation for comparison with measurements

23 p4162 A70-44080

Electron density and collision frequency distributions in lower ionosphere, deriving error limits from VLF and LF sounder data

24 p4314 A70-46127

Tidal forces effect on wind system in lower ionosphere, using Navier-Stokes equation for lower layer and Euler equations for upper layer

24 p4331 A70-46307

Lower ionosphere nonuniformities drift velocity and direction using space diversity reception

24 p4331 A70-46308

Lower ionosphere influence on radio reflection from sporadic E layer, determining diurnal variations of D region absorption for various frequencies

24 p4316 A70-46310

Lower ionosphere radio reflection during solar eclipse of 22 September 1968

24 p4332 A70-46312

LOX [OXYGEN]

U LIQUID OXYGEN

LOX-HYDROGEN ENGINES

U HYDROGEN OXYGEN ENGINES

LRC CIRCUITS

U RLC CIRCUITS

LRV [VEHICLE]

U LUNAR ROVING VEHICLES

LSI

U LARGE SCALE INTEGRATION

LUBRICANT TESTS

Roller bearing endurance dependence on shaft speed, surface finish and elastohydrodynamic lubricants temperature, viscosity and film thickness

[ASME PAPER 69-LUB-18] 01 p0101 A70-10387

Potential lubricants in friction and cup forming tests of stainless steel, Ti- and Ni-base alloys, considering boron nitride, graphitic materials and Mo oxides

02 p0309 A70-12540

Phosphorus compounds inhibition effect on oxidation and wear of graphite lubricants

13 p2437 A70-28854

Lubricating fluids effects on three-body abrasion wear rates, considering roles of viscosity and abrasive type

13 p2419 A70-28896

Materials test fixture design and fabrication for vacuum testing and evaluation of slip rings and brushes, discussing dry film lubrication

16 p2920 A70-33812

LUBRICANTS

NT GAS LUBRICANTS

NT HIGH TEMPERATURE LUBRICANTS

NT LUBRICATING OILS

NT SOLID LUBRICANTS

Film-vapor interface shape for thin liquid lubricating film, analyzing two dimensional Newtonian flow including gravity, inertia and surface tension effects

[ASME PAPER 69-LUB-3] 01 p0103 A70-10399

Inertia forces effect in turbulent and laminar, self acting and infinitely long film bearings, considering compressible and incompressible lubricants

[ASME PAPER 69-LUB-2] 01 p0103 A70-10400

Inertia effect of electrically conducting lubricant on load capacity of hydromagnetic inclined slider bearing under magnetic field

01 p0104 A70-11389

Load support and leakage from microasperity lubricated face seals, developing hydrodynamic lubricant films

[ASLE FICFS PREPRINT 21] 02 p0308 A70-12174

Conducting fluid as MHD lubricant for cylindrical bearings, deriving equations for ideally conducting shaft and bearing and arbitrary Reynolds numbers

04 p0697 A70-14544

Compression test for ductile materials based on Saint Venant principle of plasticity to reduce friction effects on deformation by lubricant pressurization
04 p0776 A70-15373

Load capacity and power loss of spiral groove bearings lubricated by incompressible liquid with temperature-dependent viscosity, using momentum and energy equations
05 p0853 A70-15778

Moisture absorptivity and hydrolytic stability effects on operational parameters of gas turbine engine lubricants
06 p1075 A70-17222

Unspinnable, molecular weight acids, alcohols and esters effect on rheological properties of lithium lubricants based on synthetic fatty acids
06 p1076 A70-17800

Plastic lubricants motion in circular pipes, determining drag and cross sectional velocity profile of laminar flows
07 p1290 A70-18652

Thickening of fluids with tetrafluoroethylene polymer to provide physically and chemically stable grease type lubricants for military applications
07 p1292 A70-18863

Sliding bearings with non-Newtonian lubricants, noting pressure gradient change effect caused by speed fluctuation and material constants
10 p1893 A70-24015

Corrosive wear due to oxygen and/or moisture in air indicated as major failure mode in lubricated gears
10 p1895 A70-24852

Die surface composition effects on lubricant efficiency in metal working judged by friction coefficient and surface damage
13 p2418 A70-28830

Nonaggressive liquid media effect on residual strains and phase transformations initiation and development in polyurethane parts operating in lubricants, discussing wear resistance
13 p2439 A70-29431

SST aircraft fuels and lubricants, discussing fire hazard and pollution minimization
13 p2473 A70-29999

Lubricant ingredients and additives properties effect on surface quality of cold rolled semifinished Al products
14 p2590 A70-30837

Molybdenum disulfide and phenol formaldehyde resin lubricants for hydroextrusion of steel
15 p2743 A70-31639

Lubrication role in aerospace engineering, discussing lubricant and component selection, environmental factors, etc
16 p2923 A70-34155

Friction and temperature fields in lubricant film of journal bearings, discussing friction torque and heat dissipation
[ASME PAPER 69-LUB-24] 19 p3434 A70-37601

Film-vapor interface shape for thin liquid lubricating film, analyzing two dimensional Newtonian flow including gravity, inertia and surface tension effects
[ASME PAPER 69-LUB-3] 19 p3435 A70-37610

Inertia forces effect in turbulent and laminar, self acting and infinitely long film bearings, considering compressible and incompressible lubricants
[ASME PAPER 69-LUB-2] 19 p3435 A70-37613

Liquid lubricant unsteady motion and pressure distribution during pivot harmonic vibration in hydrodynamic bearing
23 p4200 A70-44163

LUBRICATING OILS

Lubricating oil chemical composition changes influence on combustion engine internal friction, considering surface active Zn, armco-iron and Al
01 p0099 A70-10077

Roller bearing endurance dependence on shaft speed, surface finish and elastohydrodynamic lubricants temperature, viscosity and film thickness
[ASME PAPER 69-LUB-18] 01 p0101 A70-10387

Hydrodynamic and elasticity equations for squeeze films between elastic cylinders in normal approach reduced to integral equation
[ASME PAPER 69-LUB-13] 01 p0102 A70-10392

Rigid body dynamics of turborotors in fluid film journal bearings, investigating initial transients effect on motion stability by Runge-Kutta technique
[ASME PAPER 68-LUB-7] 02 p0307 A70-12165

Hydrodynamic theory of elastic-viscous liquid lubrication for journal bearings, assuming stress-strain relationship with unequal cross stresses
05 p0855 A70-16509

Oil vapor lubricated bearing for compensated antenna of spin stabilized spacecraft, discussing service life, power and storage in sintered porous material
[DGLR-69-062] 07 p1391 A70-18775

Liquid and solid lubricants, discussing properties, temperature ranges, costs, environmental effects and outlook
07 p1316 A70-18953

Rheology applied to motor oil viscosity, elastohydrodynamic /EHD/ and extremely thin film lubrication, examining viscosity relationship to film thickness
07 p1293 A70-18954

Ultrasonic testing of hydraulic liquids and aircraft and engine lubricating oils resistance to viscosity decrease, analyzing large molecule compounds disintegration
09 p1693 A70-23405

Lubricating oils viscosity deterioration during sliding motion in machines determined by quantitative evaluation
09 p1693 A70-23407

Irreversible viscosity decrease and thermal stability in polymer-containing lubricating oils under shearing forces effect
09 p1693 A70-23408

Fluorinated lubricating oils and greases for use as liquid oxygen compatible lubricants, correlating stability and hydrogen substitution
10 p1907 A70-24064

Hydrostatic oil journal bearings performance with several supply holes and incompressible lubricant, analyzing Reynolds pressure equation by numerical method
10 p1895 A70-24851

Spectrometric oil analysis program /SOAP/ for engine and transmission components damage detection and preventive maintenance in military aircraft
12 p2240 A70-27017

Synthetic fluids as lubricants, examining physicochemical properties of polyglycols, silicones and esters
[ASME PAPER 70-DE-13] 16 p2917 A70-33421

Aircraft engine failures advanced detection by spectrometric lubricating oil analysis
17 p3061 A70-35481

Rotational stability of heavy horizontal shaft supported on plain lubricated bearings with cavitation in lubricant
19 p3438 A70-38669

Oil seals service life as function of friction horsepower
[ASLE PREPRINT 70AM 5C-1] 19 p3439 A70-38807

Hydraulic fluids and lubrication oils resistance to mechanical shear forces by ultrasonic method based on acoustically induced cavitation effects
20 p3655 A70-39718

LUBRICATION

NT BOUNDARY LUBRICATION

NT SELF LUBRICATION

NT SPACECRAFT LUBRICATION

Elongation and combined shear stresses in incompressible creeping plane flows of viscoelastic lubrication for squeeze-film bearings
[ASME PAPER 69-LUB-22] 01 p0101 A70-10385

Dry lubricated instrument-size ball bearings operation in vacuum for long life and quality performance
[ASME PAPER 69-LUB-21] 01 p0101 A70-10386

Inertia effects in squeeze film between two curved surfaces and in externally pressurized bearing with converging lubricant film
01 p0104 A70-11388

Pressure drops in turbulent flow through circular or plane parallel section pipes, obtaining mean velocity expressions suitable for application to lubrication
02 p0277 A70-11912

Inertia effects on pressure distribution, load capacity and frictional torque in MHD hydrostatic thrust bearing lubrication flow
02 p0307 A70-12162

Lubrication problem for centrally pivoted tilting-pad sector thrust bearings with temperature and elasticity effects, noting iterative solution for coupled equations
[ASME PAPER 68-LUB-4] 02 p0307 A70-12166

Rayleigh step journal bearings, considering pressure distribution, load capacity and attitude angle and optimal film thickness ratio for incompressible fluid lubrication
02 p0307 A70-12167

Newtonian liquid lubricated spiral groove bearing load capacity and power loss dependence on viscosity variations with temperature
[ASLE PREPRINT 69-LC-21] 02 p0309 A70-12533

Calculus of variations used for determining optimum one dimensional MHD slider bearing with bounded control variables
[ASME PAPER 69-WA/LUB-2] 04 p0698 A70-14771

Laboratory tests on jet fuels indicating lubricity improvement by corrosion inhibitor addition
[SAE PAPER 690667] 05 p0894 A70-15836

Tractive behavior in elastohydrodynamic lubrication contact noting role of surface degradation layer
05 p0854 A70-15888

Lip and face seal lubrication used on rotating shafts operating in compartments with fluids under pressure
07 p1293 A70-18955

Elastohydrodynamic lubrication of rollers relationship to pressure
09 p1693 A70-22978

Hydrodynamic lubrication theory two dimensional problem, comparing numerical methods for elliptical nonlinear differential equations
10 p1893 A70-24164

Hydrodynamically lubricated rectangular taper-land bearing pads, analyzing geometry, viscosity, load

capacity, friction and operating temperature conditions
13 p2418 A70-28740

Oil-vapor lubricated ball bearing system for deployable spin-free antenna of spin stabilized spacecraft
13 p2349 A70-28843

Lubrication literature covering rolling bearings, fluid films, seals, automotive, gear and metalworking lubricants, boundary lubrication, friction and wear
13 p2419 A70-29150

Flow dynamic lubrication equation for porous bearings under radial load with undefined axial dimension
15 p2745 A70-32442

Calculus of variations used for determining optimum one dimensional MHD slider bearing with bounded control variables
[ASME PAPER 69-WA/LUB-2] 19 p3436 A70-37620

Pure metals structure effect on friction and lubrication under steady slip in ultrahigh vacuum at low temperatures
19 p3438 A70-38729

Fluid film lubricated, thrust loaded, angular contact ball bearing high speed performance, predicting skidding by isothermal Newtonian behavior in ball to raceway contact
[ASME PAPER 70-LUBS-7] 22 p0405 A70-42452

Ureter fluid mechanical model from lubrication theory viewpoint, discussing waveforms, pressure distribution, etc
23 p4179 A70-43966

Human joints boosted lubrication, discussing hyaluronic acid concentration and synovial fluid viscosity during squeeze-film action
24 p4296 A70-45160

LUBRICATION SYSTEMS

Static and centrifugal filters merits for turbine engine lubrication systems, considering mechanical reliability, efficiency, dirt capacity and maintenance
01 p0164 A70-10686

Extrusion forces required for metals and alloys determined by mathematical equations correlating extrusion pressures with process variables, discussing lubrication systems effectiveness
[ASME PAPER 69-WA/LUB-6] 04 p0697 A70-14767

Sliding wear of bearing Al lubricated with polyphenyl ethers in boundary region tested by pin and cylinder wear machine producing continuous record
05 p0854 A70-15910

Bearing capacity increase due to large viscoelastic or normal stress effects in lubricants, obtaining exact results for noncavitating plane slider bearings
08 p1507 A70-21476

Frictional traction-sliding speed relation in elastohydrodynamic lubrication in Barlow-Lamb model of viscoelastic liquid, discussing oscillatory and continuous shear
09 p1691 A70-22600

Self energized hydrostatic shaft seal operating with incompressible fluid in laminar flow regime, using general lubrication theory
13 p2417 A70-28614

Literature review of sliding electrical contacts in space vehicles, covering heavy aromatic hydrocarbons, molybdenum disulfide and other lubrication materials
16 p2920 A70-33807

Liquid lubricants applications to electrical contacts, discussing hydrodynamic and boundary lubrication, film formation on solid surfaces, etc
16 p2920 A70-33808

Lubrication system components behavior in vacuum environment, investigating evaporation, friction, adhesion, wear, etc
16 p2923 A70-34156

Lubrication system flight performance and laboratory test data for space applications, considering torque motors, slip rings, bearings and gears
16 p2923 A70-34157

Controlled leakage sealing of hydrodynamic bearing lubrication systems for space vehicles in synchronous orbit
16 p2923 A70-34158

Accelerated vacuum testing of ball bearings and slippers at 30-130 F, considering dry lubricated brush/slipping material combinations
17 p3101 A70-34762

Extrusion forces required for metals and alloys determined by mathematical equations correlating extrusion pressures with process variables, discussing lubrication systems effectiveness
[ASME PAPER 69-WA/LUB-6] 19 p3435 A70-37604

Fluid inertia and compressibility effects considered in equations for foil over lubricating film
[ASME PAPER 69-WA/LUB-10] 19 p3435 A70-37615

Parallel circular squeeze film bearing, calculating Newtonian fluid inertia effect on lubrication by perturbation solution
[ASME PAPER 70-LUBS-9] 22 p0405 A70-42451

Lubrication technology for space shuttles, discussing vehicles and airbreathing and rocket engines
22 p0407 A70-43325

LUCITE [TRADEMARK]

U POLYMETHYL METHACRYLATE

LUDEB BANDS

- U PLASTIC DEFORMATION
- U YIELD POINT

LUMBAR REGION

Lumbar vertebrae transverse processes fractures in air crashes, considering factors involved, incidence and pathogenesis

17 p0303 A70-35578

Bioelectric activity changes in rats lumbar neurons, membrane and postsynaptic potential and discharge frequency during and after asphyxiation

22 p3971 A70-43404

LUMINAIRE

- NT AIRCRAFT LIGHTS
- NT AIRPORT LIGHTS
- NT ARC LAMPS
- NT FLASH LAMPS
- NT MERCURY LAMPS
- NT RUNWAY LIGHTS
- NT SEARCHLIGHTS
- NT XENON LAMPS

Kr, Xe and W-iodine lamps efficiencies for pumping Nd-doped YAG compared for use in high continuous power lasers

02 p0311 A70-11922

Electroexplosive devices protection from electrostatic discharge by creation of preferential discharge path, considering use of high intensity neon lamp

03 p0549 A70-14134

Tungsten strip lamps spectral radiance calibration, discussing accuracy requirements for radiation constants, wavelength and black body temperature

13 p2410 A70-29655

Blinking warning lights for air navigation, signaling of obstacles and glider onboard marker lights

16 p2889 A70-34302

Nuclear light bulb and coaxial flow gaseous core nuclear rocket reactors based on energy transfer via thermal radiation

22 p4070 A70-43182

LUMINANCE

Background luminance effect on flash brightness in eyes, measuring increment threshold and luminances required for various brightnesses

01 p0025 A70-11052

Target-field luminance or duration effect on target susceptibility to masking demonstrated in visual backward masking study

01 p0039 A70-11163

Polarization role in radiation scattering by planetary atmosphere, considering luminance variation and Rayleigh scattering

14 p2651 A70-31302

Light sources design with variable uniform luminance for space exploration cameras calibration [JPL-TR-32-1470]

15 p2737 A70-32037

Exposure duration effect on luminance requirements for hue perception and identification

17 p3040 A70-35724

LUMINESCENCE

- NT BIOLUMINESCENCE
- NT CHEMILUMINESCENCE
- NT ELECTROLUMINESCENCE
- NT FLUORESCENCE
- NT LUNAR LUMINESCENCE
- NT OPTICAL RESONANCE
- NT PHOSPHORESCENCE
- NT PHOTOLUMINESCENCE
- NT SHOCK WAVE LUMINESCENCE
- NT THERMOLUMINESCENCE
- NT X RAY FLUORESCENCE

Edge luminescence effect in doped p-GaAs single crystals with various hole concentrations, determining band structure at liquid nitrogen and room temperature

01 p0154 A70-10097

Light emission by solids, discussing injection lasers, luminescence semiconductor diodes, group 2 and 6 compounds, etc

01 p0160 A70-11288

Nitrogen, oxygen and air luminescence spectra excited by fast electrons at low gas pressures in IR spectral region compared with polar auroral spectra

01 p0083 A70-11536

Luminescence quantum yield in neodymium glass, noting independence to stimulating light frequency

01 p0114 A70-11595

Electron-phonon interaction model of temperature dependence of luminescence produced by multiphonon nonradiative transitions in Cr ions of ruby crystal, deriving transition probability

03 p0538 A70-13058

Temperature dependence of luminescence quantum yields and lifetimes in transitions during excitation of ruby crystal atoms

03 p0538 A70-13059

Meteor particles spatial density and energy characteristics on space vehicles, using luminescent sensors coupled with photomultiplier

04 p0744 A70-14445

Enstatite luminescence response for bulk specimens, powders and individual grains, considering selenological implications

05 p0909 A70-16391

Luminescence materials providing primary, secondary and emergency illumination for aircraft safety, discussing application to dials, panels and anticollision measures

06 p0986 A70-17718

Minority carriers lifetime following CdS and ZnTe spontaneous luminescence relaxation after electron beam excitation

07 p1302 A70-20318

Absorption and luminescence in complex molecules and semiconductors, describing particle distribution and Fermi quasi-levels dependence on temperature and excitation intensity

08 p1555 A70-20510

Uranyl ion luminescence and absorption cross section in silicate glass excited by high power light beam, considering Q switching action of ion

08 p1510 A70-20516

Population of P level He excitation in solar prominences in H luminescence regions, noting ionization-recombination mechanism by UV radiation

08 p1564 A70-20555

Vitreous transparent solids emission after irradiation by Q switched laser, ascribing luminescence to multiphonon and excitonic phenomenon

09 p1710 A70-22836

Luminescence and destruction of gaseous boron trichloride by carbon dioxide laser radiation

11 p2064 A70-26818

Luminescing materials remote sensing during daylight by Fraunhofer line depth method with sun as excitation source

12 p2221 A70-26958

Diffuse galactic radiation and absorbing clouds luminescence illuminated by integral stellar radiation in Milky Way

12 p2307 A70-27866

Lattice defect influence on EPR spectral and luminescent characteristics of annealed Fe doped gallium arsenide crystals

12 p2288 A70-28330

Meteor particles spatial density and energy characteristics on space vehicles, using luminescent sensors coupled with photomultiplier

13 p2485 A70-28470

Luminescent line broadening effect on axial mode selectivity in pulsed neodymium lasers with Fabry-Perot resonator at above-threshold pumping power

15 p2749 A70-31554

Artificial B-doped semiconductor diamond crystals resistance temperature dependence, determining conductivity and luminescence spectra

15 p2782 A70-31630

Galactic masses and mass-luminescence ratios from motions data

15 p2801 A70-32480

Population of P level He excitation in solar prominences in H luminescence regions, noting ionization-recombination mechanism by UV radiation

15 p2805 A70-32710

Metal oxides thermal control coatings, investigating mechanisms of interaction between constituents by luminescent technique [AIAA PAPER 70-832]

16 p2940 A70-33936

Defect F centers formation in MgO, discussing optical absorption bands, oscillator strengths, luminescence band, impurity centers, etc [AIAA PAPER 70-828]

16 p2940 A70-33938

Luminescence decreases in laser active medium operating in free emission mode, using kinetic equations for integral and spectral level populations

18 p3267 A70-36615

Emission spectral distribution of atomic nitrogen reaction with carbon tetrachloride for artificial luminescent clouds

18 p3293 A70-36990

CdS crystals luminescence spectrum excitation by UV light of ruby laser, noting excitons and phonons recombination

19 p3444 A70-37368

Apollo 11 lunar fines, rocks and breccias luminescence, electron paramagnetic resonance and optical properties, discussing reflection spectra, heating effects and dipole resonance

21 p3914 A70-41654

Apollo 11 lunar crystalline rock and breccias petrography and luminescent properties, spectral analysis, color, emission bands and shock effects

21 p3918 A70-41678

Carbon monoxide-nitrogen laser luminescent phenomena by electronic spectroscopy

21 p3837 A70-41717

Galactic masses and mass-luminescence ratios from motions data

23 p4240 A70-43905

Solar stimulated terrestrial materials luminescence remote detection by Fraunhofer line depth method using UV grating spectrometer

23 p4199 A70-45007

Luminescence and destruction of gaseous boron trichloride by carbon dioxide laser radiation

24 p4351 A70-45190

LUMINESCENT INTENSITY

U LUMINOUS INTENSITY

LUMINOSITY

Cambridge one mile radio telescope observations of weak sources, extending radio source luminosity function and tabulating, graphing and mapping results

08 p1578 A70-21546

Pulsating auroras X ray association with luminosity via balloon-borne X ray detector and ground based image intensifier TV system

13 p2478 A70-29228

Temperature influence on luminosity centers and line darkening in synthetic ruby powder with chromium concentration

15 p2782 A70-31558

Spacecraft meteoroid protective shield thickness sensitivity relationship to luminous efficiency

15 p2813 A70-32518

Luminous emissions related to Apollo 12 mission observed in Belgium, discussing flight chronology, gas ejection, stage separation, etc

16 p2981 A70-34318

Photometric reduction of meteor luminosity to photovisual /international/ system

19 p3515 A70-37662

Arc luminosity in cathode region of quasi-steady MPD arc jet, using high speed photography and electric and magnetic field probes [AIAA PAPER 70-1094]

20 p3683 A70-40242

LUMINOUS FLUX DENSITY

U LUMINOUS INTENSITY

LUMINOUS INTENSITY

NT ILLUMINATION

NT LUMINANCE

Icarus asteroid rotation period and brightness variation values obtained from photometric observations at Cassegrain reflector focus

01 p0180 A70-10536

Visual observations of bright comets, deriving photometric parameters from comet head total magnitude

01 p0184 A70-10953

Background luminance effect on flash brightness in eyes, measuring increment threshold and luminances required for various brightnesses

01 p0025 A70-11052

Radar and photographic studies of meteors from Leonid and Perseid showers, presenting velocities, luminescence and ionization

01 p0193 A70-11602

Numerical solutions for laser beams intensity focused by simple lenses with varying primary spherical aberration, demonstrating isophote nonuniformity role in biomedicine

01 p0000 A70-11650

Turbulence intensity, light intensity fluctuations and frequency optical measurement in diffusion flames of city gas with air, deriving turbulence spectral functions

02 p0398 A70-12038

Sudden comet brightness changes leading to discovery, tabulating and graphing comet discoveries

02 p0373 A70-12372

High intensity short pulse flash lamps using quartz envelopes and wire electrodes for pumping high energy organic dye lasers

02 p0314 A70-12741

Ultraweak luminescence intensity, radiation damage kinetics and spectral properties of cellular organelles of rat liver exposed to gamma radiation

03 p0419 A70-13304

Beta lyrae light curve changes by comparing international program observations with 1958 Lick Observatory results, discussing period, brightness, spectra, etc

03 p0568 A70-13327

Optical variations of quasars and other radio sources using photographic photometry, emphasizing bright optically violently variable /OVV/ quasars properties

03 p0568 A70-13328

Crab Nebula pulsar light intensity fluctuations on very short time scale, noting negative observations

04 p0747 A70-14545

Long term behavior of blue photographic luminosity of Seyfert galaxy 3C 120 nucleus, considering similarity to quasar 3C 273B

04 p0748 A70-14589

Frequency distribution of apparent visual magnitudes of meteors observed from November 1960 to January 1967

04 p0750 A70-14707

Critique of paper on transverse enhanced bremsstrahlung from supraluminous and subluminal longitudinal waves in isotropic homogeneous plasma

04 p0728 A70-15006

Continuous Chlorella production as function of total illumination in high intensity light system incorporating aerobic fermenter for heterotrophic cells

04 p0645 A70-15454

Monograph on He-Ne laser beam noise properties and intensity fluctuations during single mode operation

05 p0860 A70-16559

Meteor motions at cosmic velocities in real atmosphere studies to determine cause of sudden flares

06 p1140 A70-17735

Cats visual analyzer functional rearrangement mechanisms under prolonged light stimulation, considering evoked potential dependence on pulse duration and intensity

07 p1198 A70-18699

Galactic cluster A 262 luminosity function constructed from integral magnitudes of component galaxies obtained from continuous observations

07 p1376 A70-18904

Barred galaxies colorimetric data to study relative intensities and mean surface brightnesses as function of color

07 p1376 A70-18905

Galactic clusters analyzed for identifying possible relationship between cluster configuration, type of component galaxies and radio emission

07 p1376 A70-18907

Kilston Comet /1966/ total brightness measurements, discussing integral head magnitudes, observational conditions and stars comparative magnitudes

07 p1379 A70-19042

Light intensity and polarization in twilight sky atmosphere at solar depressions

07 p1263 A70-19047

Laser amplifier effect on autocorrelation function of laser radiation intensity fluctuations, determining emission coherence time

07 p1300 A70-19870

Nova Delphini 1967 brightness visual evaluations by amateurs, discussing effect of personal factors and instruments on accuracy

08 p1568 A70-20634

Time requirement determined for visual acuity restoration after illumination with short duration bright light flash

08 p1450 A70-20746

Light sensitivity restoration in humans exposed to bright flashes, studying photonic afferent system braking effect on scotopic system

08 p1450 A70-20747

Fundus oculi in polarized light, investigating light intensity variations and polarization pattern in yellow spot

08 p1444 A70-20748

Light beam intensity variations during propagation in nonlinear medium taking into account combination scattering, solving equations by difference method

08 p1461 A70-20858

Meteor abundance determination by visual observation, calculating sighting probabilities for various magnitudes

08 p1573 A70-20949

Comet brightness outbursts monochromatic measurements for lifetime of parent gaseous molecules in solar radiation fields

08 p1575 A70-21373

Brightness curves for eclipsing binary V448 Cygni indicating gas stream flows in system

08 p1577 A70-21441

Thunderstorms lightning flashes time distribution recorded visually and on radar screens, discussing statistical variations in sigma

08 p1539 A70-21648

OI 6300 A airglow intensity decrease at dawn ascribed to scattered solar radiation

08 p1492 A70-21720

Display devices luminance and luminous efficiency measurement as function of angle

08 p1500 A70-21762

Scattered field amplitude and phase determined from hologram light intensity distribution, noting biological applications

08 p1500 A70-21786

Monocular and interocular threshold luminance changes during flicker stimulation, noting interflash duration effects

08 p1453 A70-21792

Retinal temperature increases produced by intense light absorption described by heat conduction equation

09 p1614 A70-22075

Parametric image transformation during sum frequency generation

09 p1636 A70-23134

Pulsed laser beams intensity fluctuations correlation functions dependence on propagation distance in turbulent atmosphere

09 p1636 A70-23135

Axial mode gas laser radiation intensity fluctuations for plane and spherical light waves in turbulent atmosphere

09 p1636 A70-23137

Laser beam intensity fluctuations during propagation through turbulent atmosphere

09 p1637 A70-23142

Intense light effect on refractive index of potassium niobate crystals

09 p1698 A70-23317

Mode coupling and intensity pulsations observed between two 6328 A He-Ne lasers through nonlinear gain characteristics of inverted population

09 p1699 A70-23363

Compact galaxies, discussing distribution, integral photometry and isophotometry, brightness outbursts, etc

09 p1763 A70-23373

Sodium night airglow analyzed by Chapman mechanism, considering nocturnal intensity seasonal behavior and location in upper atmosphere

10 p1873 A70-23829

Predawn enhancement morphology and variations of 6300 A airglow, discussing solar declination and activity effect

10 p1873 A70-23831

Pulse-biased phototransistor imaging mosaics behavior measurement showing significant photovoltaic mode at high light levels

10 p1846 A70-23880

Hydrogen rich material forming planetary nebula ejected from contracted core of evolved star with 20,000 times solar luminosity

10 p1936 A70-23906

Liverpool airport lighting emphasizing beacons, approach, runway and taxiway high intensity lighting installations

10 p1857 A70-24000

Visual stimuli intensity influence on delay in reaction to second of pair of visual stimuli

10 p1818 A70-24721

Bright rims in North America Nebula, measuring electron temperature to derive profile characteristics

10 p1944 A70-24956

Algol variable RV Ophiuchi photoelectric observation in B and V, representing light curve characteristics by gas stream model

10 p1945 A70-24967

Outer corona brightness and polarization during total solar eclipse from satellite photographs

10 p1947 A70-24988

IR luminosity of galactic nucleus from far IR observations, noting considerations favoring nonthermal model consisting of multiple sources

10 p1947 A70-24996

Focal plane intensity of focused laser beam passed through turbulent atmospheric layer

10 p1901 A70-25160

Laser light propagation along strongly inhomogeneous turbulent path, measuring intensity fluctuations dispersion and light amplitude

10 p1844 A70-25161

Solar outer corona brightness distribution from rocket observation with scanning devices during solar eclipse, estimating error

11 p2107 A70-25397

Ultrasonic LF modulation of solid state traveling medium lasers radiation intensity attributed to elastic vibrations of rods

11 p2062 A70-25398

Hydrogen recombination and hydrogen molecules formation may explain sharp brightness variations in later dwarf stars

11 p2115 A70-26581

VX Cas brightness determination from color plates, giving values in tabular form

11 p2115 A70-26583

Steady state two frequency laser emission threshold and intensity, studying effects of two photon transitions and optical transition probabilities-radiation density relations

12 p2245 A70-27301

Brightness distribution in hologram generated image modulated by square of temporal-spatial coherence modulus of laser emitting longitudinal and transverse modes

12 p2233 A70-27503

Nova Delphini brightness variations, observing absorption lines shift toward violet

12 p2306 A70-27860

Summertime midnight airglow enhancement of 6300 A line by sensitive continuum compensating photometer, suggesting F 2 region electron density increase for emission

12 p2225 A70-27895

Laser beam intensity distribution determination from measuring Fresnel diffraction pattern at straight edge using photographic plate

12 p2249 A70-28032

Psychophysical and evoked potential correlates of changes in stimulus color and intensity compared with minimum subjective flicker conditions

12 p2171 A70-28035

Gas jet bounding of Ar arc column, providing high power/intensity light source

12 p2237 A70-28159

Forbidden Ne iv lines intensity in high excitation gaseous nebulae based on upper level-j populations

12 p2277 A70-28215

Mars border-disk brightness comparison noting atmospheric transparency effects

12 p2311 A70-28303

Resonant absorption in ruby crystal under combined acoustic and laser pulses, noting use for laser intensity measurements

12 p2251 A70-28331

Lunar surface brightness temperatures from IR observations, determining thermal emission directional characteristics to infer surface temperatures from Surveyor data

[AJAA PAPER 69-593]

13 p2486 A70-28501

Radar and optical meteor observations comparison, discussing luminosity function and angular velocity

13 p2490 A70-29042

Visual aurora properties attributed to magnetic storm following solar flare, using multiple channel photometer measurements

13 p2478 A70-29231

Kinetic changes in spectral lines and bands intensity of individual molecular gases and mixtures for carbon dioxide lasers

13 p2428 A70-29361

Absolute magnitudes of first brightest galaxies in rich clusters from luminosity model, allowing for mass variation

13 p2495 A70-29795

Quasars magnitude relation to red shift, discussing scatter in log cz vs m plane correlation with B-V color

13 p2495 A70-29797

Solar magnetic and brightness fields simultaneous measurement by multiimage spectroheliograph

13 p2496 A70-29844

Laser beams intensity fluctuations dispersions and correlation functions at various distances

14 p2593 A70-30172

HF and DF continuous chemical lasers vibrational and rotational spectra, comparing lines and relative intensities

14 p2593 A70-30274

Jupiter luminosity as indication of internal energy magnitude, comparing limb darkening with predicted brightness distribution

14 p2643 A70-30984

Shilts method applicability to electronic camera for stellar magnitude photometry, studying instrument limitations and errors

14 p2589 A70-31379

Night sky visible brightness at minus 19 degrees declination from July 1965-June 1966 in Tsumeb, South West Africa

14 p2581 A70-31390

B, In or Ga doped Si photosensitivity dependence on sample temperature, supply voltage and illumination intensity, determining optimal operating conditions

15 p2782 A70-31631

Chorioretinal damage thresholds spectral dependence of intense light sources, describing temporal, axial and radial temperature distributions

15 p2682 A70-32014

Steady state evoked potentials Fourier analysis from human scalp during psychophysical procedure of heterochromatic flicker photometry, obtaining spectral sensitivity curve

15 p2682 A70-32015

Brightness matching and sensitivity to sinusoidal flicker for various contrasts as function of surround field luminance

15 p2683 A70-32016

Solar simulation systems for uniform collimated intense light, noting high intensity lamp development

15 p2717 A70-32034

Cepheids nonequilibrium continuous emission at maximum brightness, considering phase shift between radiation intensity and stellar contraction

15 p2802 A70-32483

Meteor abundance determination by visual observation, calculating sighting probabilities for various magnitudes

15 p2806 A70-32761

Quasar 3C 298 angular dimensions and 3C 273 scintillating component at 60 MHz based on mean quasi-periods shifts of scintillations

15 p2808 A70-32885

Arp hypothesis regarding radio source ejection from galaxies tested for quasars

15 p2808 A70-32887

Amplitude and intensity interference relations from pseudothermal light sources, noting applicability to stellar interferometry

16 p2900 A70-32999

Electronic zoom for low light level TV sensor employing electrostatic image intensifier coupled optically to SEC camera tube

16 p2903 A70-33128

Low light level TV /LLLTV/ tube, camera and sensor development for military and space applications

16 p2903 A70-33129

Low light level TV systems performance relationship to visual acuity requirements, considering interfering noise characteristics effect on target recognition

16 p2903 A70-33130

Q switched subnanosecond laser system with increased intensity, using pulse selection technique

16 p2927 A70-33163

Spectrophotometric and visual observations of twilight glow from Soyuz 5, comparing vertical monochromatic brightness profiles with calculations for Elterman aerosol model

16 p2896 A70-33218

Nitrogen and air bombardment by relativistic electrons, determining absolute fluorescence intensity of nitrogen molecular ion first negative band

16 p2954 A70-33279

Mode locked laser emission intensity correlation measurements by two photon fluorescence /TPF/ technique to determine temporal behavior, discussing domain model

16 p2928 A70-33286

Low light intensities measured using photon counting method, comparing signal to noise ratio with lock-in method

16 p2911 A70-33524

Comet Alcock flareup on 27-29 May 1969, noting visible rays in coma, dust grains expulsion from nucleus, tail structure, etc

16 p2980 A70-34304

Solar limb intensity distribution in Lyman alpha line, computing LTE departures

17 p3162 A70-34895

Chlorella reproduction rates at steady and variable illumination intensity levels, determining productivity autocorrelation function by statistical analysis

17 p3030 A70-35355

Intensity logarithm fluctuations of focused laser beam propagating in summer daytime atmosphere at 250 and 650 meter path lengths

17 p3048 A70-35685

Spectrophotometric airglow intensity measurements of OH, O 16300, hydrogen H alpha and oxygen Herzberg I bands by airborne laboratory

17 p3080 A70-35769

Regular and stochastic oscillations in plasma beam discharge produced by beam instability from observing time dependent variations in spectral line luminescence intensities

18 p3294 A70-36147

Laser emission intensity oscillations during resonator Q sinusoidal variations

18 p3267 A70-36617

Amplitude and phase fluctuations of opposing waves in ring laser with allowance for waves coupling due to backscattering

18 p3267 A70-36618

Unsteady light field spatial moments in turbid medium boundary layer with intense anisotropic scattering during illumination by narrow beam

18 p3285 A70-36631

Upper atmospheric atomic nitrogen reaction with carbon tetrachloride, estimating radiation intensity and brightness of artificial luminescent cloud

18 p3252 A70-36989

Extragalactic radio source counts analysis, suggesting luminosity evolution as dominating influence

18 p3320 A70-37073

Meteor luminous efficiency and luminosity factor for mass determinations

19 p3515 A70-37661

Gas lasers intensity expression derived by theory of double resonance spectroscopy, comparing results with He-Ne laser experimental data

19 p3445 A70-37672

Prismatic adaptation under scotopic and photopic conditions in subjects, using transfer experiments

19 p3361 A70-38052

Laser radiation and solid target interaction, calculating temperature and plasma density as function of intensity

19 p3447 A70-38166

Nuclear fusion realization by focusing from intense beam neodymium glass laser

19 p3447 A70-38167

Cooled antimony-cesium film photoelectric effect for weak luminous flux, examining electronic camera reciprocity

19 p3427 A70-38175

Luminous intensity profile of optically thick Sr artificial clouds in upper atmosphere, using Monte Carlo calculations

19 p3415 A70-38388

Comet brightness curves asymmetry with respect to perigee attributed to pre- and post-heating

19 p3526 A70-38781

Kylston comet head diameter relation to brightness from photometric observations using north polar sequence stars as reference, noting camera, equipment and exposure times

19 p3526 A70-38784

Orbital elements of photographic meteors brighter than first magnitude, tabulating dates, solar longitudes, corrected radiant, velocities, major axis, etc

19 p3526 A70-38787

Lighting effects on phenylethanolamine-N-methyltransferase (PNMT) activity and adrenal epinephrine content in rats

20 p3568 A70-38982

CW second harmonic He-Ne laser light second order intensity correlation function measurements

20 p3640 A70-39153

Coronal data comparison based on 5303 A line intensities and distribution with respect to position angles

20 p3704 A70-39461

Solar outer corona brightness distribution from rocket observation with scanning devices during solar eclipse, estimating error

20 p3710 A70-40089

Ultrasonic LF modulation of solid state traveling medium lasers radiation intensity attributed to elastic vibrations of rods

20 p3643 A70-40092

Solar equatorial limb brightening at quiet sun from solar disk scanning statistical analysis

20 p3712 A70-40418

Superradiant light (SRL) converted from electron beam energy by semiconductor targets applied to nanosecond photography

20 p3635 A70-40529

Magnitude-color relation for Cygnus X-2 and WX Centauri, indicating opposite correlation to Sco X-1 fluctuations

21 p3873 A70-40672

Electrons optical scale time averaged motion dependence in focused laser beam on light intensity gradient, calculating bremsstrahlung spectrum

21 p3836 A70-40723

Laser interferometer system unwanted reflections elimination and intensities control in each arm by linear polarization method

21 p3823 A70-40820

Large sunspot umbra continuum intensity, examining visible spectra

21 p3885 A70-40956

Sunspot intensity profiles near solar limb, observing center side penumbra photosphere border

21 p3885 A70-40957

Extragalactic radio sources observable and intrinsic properties relationship for distance estimates, considering surface brightness, diameter, luminosity, etc

21 p3889 A70-41145

Earthshine bright parts relationship to average brilliance of sun during total eclipse

21 p3893 A70-41445

Magnesium-sodium nitrate pyrotechnic flare spectral radiant energy comparison with radiative transfer theory data, considering Na resonance continuum formation

21 p3850 A70-41937

Spontaneous emission intensification at 6911 A in potassium to evaluate plasma local conditions, using low pressure arc and Q switched ruby laser

22 p4049 A70-42359

Exploding wire light source modification by immersing in transparent fluid to increase intensity, measuring spectral characteristics

22 p4032 A70-43037

Ultrabright nanosecond flash light generation technique, using superradiant light sources for shadowgraph photography in high resolution hypervelocity field

22 p4037 A70-43070

Light intensity distributions within successive slits imaged by transmission gratings, using theory for spatial moire fringe blurring

23 p4217 A70-43819

Cepheids nonequilibrium continuous emission at maximum brightness, considering phase shift between radiation intensity and stellar contraction

23 p4240 A70-43907

Omicron Ceti (Mira) spectrophotometry before, during and after 1969 maximum, noting TiO bandwidth variations

23 p4242 A70-44294

Molecular oxygen ions 1Ng band and molecular nitrogen 1Pg band relative intensities in normal and type B auroras

23 p4191 A70-44408

Spectrophotometric and visual observations of twilight glow from Soyuz 5, comparing vertical monochromatic brightness profiles with calculations for Elterman aerosol model

24 p4328 A70-45193

Sco XR-1 optical intensity power spectra oscillations searched for in pulsar frequencies and fundamental radial mode vibrations in white dwarfs and neutron stars

24 p4410 A70-45762

Time evolution of instantaneous light intensity mean and variance for Q switched single mode laser near oscillation threshold

24 p3455 A70-46090

Supernovae frequency in Sb and Sc spiral galaxies, considering luminosity class, absolute magnitude and mass of parent galaxy

24 p4413 A70-46164

LUMPING

Current distribution and near field of cylindrical antennas loaded with built-in lumped elements

22 p3998 A70-43422

LUNAR ATMOSPHERES

Lunar atmosphere molecule and atom concentration from isotropic and uniform surface evaporation due to micrometeorite impact

01 p0192 A70-11541

Space research photography role in studying earth and moon atmospheres and surfaces, determining spectral bands for contrast

03 p0483 A70-13168

Gray and colorless features of moon explained as atomic H imported by solar wind replacing lost H by photolytic decomposition of water vapor

05 p0908 A70-16303

Lunar mascons origin explanation in terms of primordial atmosphere and hydrosphere

14 p2646 A70-31065

Lunar atmospheric pressure based on twilight horizon photographic data from Surveyor 7

15 p2803 A70-32500

Lunar atmosphere as source of Ar 40 and other elements in surface materials, discussing implantation by photoionization and subsequent interaction with solar wind fields

17 p3172 A70-35624

Lunar atmospheric pressure based on twilight horizon photographic data from Surveyor 7

23 p4240 A70-43921

LUNAR BASES

Legal implications of national flags on moon as symbols of national sovereignty, considering spacecraft and lunar colonies legal status by international agreements

07 p1426 A70-18877

Lunar vehicles development, emphasizing translunar exploration vehicle (TLEV) for future lunar base

14 p2563 A70-30197

Lunar based radar beacons for nearby spacecraft navigation, noting trajectory determination advantages

14 p2614 A70-30461

Lunar based astronomical research program logistics model taking into account scientific mission, launch vehicle capacities, supply and support requirements, etc

20 p3710 A70-40336

LUNAR CINEMATOGRAPHY

U LUNAR PHOTOGRAPHY

LUNAR COMMUNICATION

Lunar communications systems considering use of satellites, metallic particle belts, rockets, lasers and particle beams

14 p2634 A70-30196

Space vehicle and mission control center telecommunications networks for Apollo lunar landing program, considering NASCOM relay system

17 p3047 A70-35585

LUNAR COMPOSITION

IR reflectance studies of lunar surface composition, showing absorption spectra suggestive of ferrous iron, olivines and orthopyroxenes

01 p0182 A70-10721

Sinus Medii lunar surface material chemical composition from alpha scattering experiment on Surveyor 6

06 p1151 A70-18483

Lunar interior electrical conductivity estimated using lunar interaction with solar wind and interplanetary electric and magnetic fields

06 p1153 A70-18544

Bottom rock structure and composition of young lunar craters compared with Kamchatka volcanic morphological analogs

07 p3385 A70-19424

Lunar science - NASA Conference, Houston, January 1970, covering moon rock composition, magnetic, electrical and physical properties, etc

08 p1565 A70-20587

Lunar surface chemical composition determination by radio astronomy, considering SHF electrical properties of silicate earth rocks

08 p1572 A70-20940

Apollo lunar landing sites geological configuration and composition

09 p1759 A70-22772

Carbon compounds composition and origin in Apollo 11 lunar samples using pyrolytic chromatography and microscopy at elevated temperature

10 p1941 A70-24531

Isotopic ratio anomaly of Re and detection at nanogram level in solar wind using decay curves of Re source from lunar specimen

10 p1932 A70-24532

Solar system objects /earth, moon, planets, meteorites, etc/ chemical composition data and analysis techniques

10 p1942 A70-24609

Lunar and planetary surface chemical composition analysis using neutron inelastic scattering as optimum for unmanned missions

10 p1942 A70-24613

Lunar rocks types determination by mass spectrometry, describing results of terrestrial rocks tests

11 p2119 A70-26799

Lunar surface material composition in terra region from alpha scattering data on Surveyor 7, noting Si Na abundance

13 p2492 A70-29265

Lunar surface terrain types and chemical composition based on Surveyor pictures

14 p2634 A70-30193

Lunar surface thermal emission spectra based on laboratory analysis of rocks and minerals emissivity

14 p2637 A70-30496

Lunar exploration by manned and unmanned space flights, discussing seismology, composition, surface features, etc

15 p2798 A70-31678

Lunar, meteoritic and terrestrial silicate rock chemical individuality based on atomic ratios

15 p2799 A70-31896

Lunar surface chemical composition determination by radio astronomy, considering SHF electrical properties of silicate earth rocks

15 p2805 A70-32752

Sound velocity differences related to composition of lunar and terrestrial rocks

16 p2978 A70-33973

Lunar atmosphere as source of Ar 40 and other elements in surface materials, discussing implantation by photoionization and subsequent interaction with solar wind fields

17 p3172 A70-35624

Apollo 11 lunar rocks mineralogy and petrology, noting anorthosite in powder and breccia

18 p3320 A70-37081

Heavy ions traces in crystals of lunar rocks, discussing applications as detectors

18 p3321 A70-37084

Lunar rock origin based on apollo samples density, impurities and mineral and chemical composition, considering structure and genesis of crust and mantle

19 p3513 A70-37524

Lunar elemental abundances examined by Surveyor project, discussing albedo contrasts, surface rock density, bulk composition, thermal regime and chondritic meteorites

20 p3707 A70-39957

Lunar surface material composition examination by Surveyor 5, discussing formation of surface

20 p3708 A70-39958

Lunar surface spectral reflectivity measured with ground based telescopes for remote mineralogical analysis

20 p3709 A70-39977

Apollo 11 lunar rock and fines chemistry, mineralogy and petrology, discussing composition, igneous rocks, microbreccias, glasses and pyroxene relations

21 p3895 A70-41507

Apollo 11 lunar igneous rocks mineralogical, chemical and petrological features by optical and electron microscopy and X ray spectrometry

21 p3896 A70-41512

Apollo 11 lunar rock mineralogy, examining petrographic and chemical features by light microscopy, electron microprobe microanalysis and detector system

21 p3898 A70-41525

Apollo 11 lunar samples mineralogical and compositional studies concerning lunar origin hypothesis

21 p3899 A70-41534

Lunar sea, mascon and interior composition, discussing crystallization of Apollo 11 Tranquillity samples and synthetic analogs at high pressure

21 p3901 A70-41542

Lunar rock composition difference from meteorites and terrestrial basalts, indicating complexities in solar abundances and initial earth and moon compositions

21 p3906 A70-41567

Apollo 11 lunar material water content and H and C isotope abundance, examining changes in deuterium and O by solar winds

21 p3774 A70-41570

Apollo 11 lunar basalt chemical composition and petrogenesis, using stable isotope dilution method

21 p3907 A70-41573

Rare earth and trace element abundances for Apollo 11 lunar samples by neutron activation, comparing with Bruderheim chondrite and submarine basalts

21 p3907 A70-41578

Apollo 11 lunar samples composition for Na, 22, Al, 26, Th and U, investigating positron activities

21 p3775 A70-41580

Carbon and sulfur concentration and isotopic variations in Apollo 11 fines, breccias and fine-grained basalts

21 p3775 A70-41586

Apollo 11 lunar rock K, Rb, Sr, Ba and rare earth element concentrations, examining relationship to terrestrial and chondritic levels

21 p3776 A70-41600

Halogens, mercury, lithium and osmium concentration measurements in Apollo 11 samples, using neutron and photon activation

21 p3777 A70-41601

Chemical composition and reducing capacity of Apollo 11 igneous rocks, breccia and soil fines, using semimicro X ray fluorescence

21 p3777 A70-41602

Uranium and Th isotopic composition in Apollo 11 samples compared to earth, using mass and alpha spectrometries

21 p3777 A70-41603

Apollo 11 lunar rocks, soil and core samples major, minor and trace elements abundance by radiochemical and instrumental activation analyses

21 p3910 A70-41614

Apollo 11 lunar, terrestrial and meteoritic basalts relationships, examining Ga, Ge, In, Ir and Au concentrations by neutron activation analyses

21 p3778 A70-41617

Apollo 11 lunar fines carbon level, finding largest component carbon monoxide in complex form

21 p3778 A70-41621

Volatilizable C compounds in lunar fines from Mare Tranquillitatis, investigating pyrolysis and acid hydrolysis products by mass spectroscopy and gas chromatography

21 p3779 A70-41628

Lunar carbonaceous, organic and organogenic materials analysis by mass spectroscopy, gas chromatography and various other methods

21 p3780 A70-41633

Mossbauer effect spectrometry application to Apollo 11 lunar rocks composition, using nuclear gamma resonance measurements for nuclide Fe 57

21 p3916 A70-41662

Initial water content on moon implied from hypothetical falling temperature lunar accretion as original earth satellite

22 p4102 A70-42954

Apollo command service module nondispersive X ray detection system for lunar composition map compilation, discussing design and performance

23 p4196 A70-44417

LUNAR CRATERS

NT TYCHO CRATER

Anomalous temperature-time cooling data for surface material of Tycho, Copernicus and Aristarchus craters, suggesting relation to magnetic phase transitions during lunar nights

01 p0183 A70-10825

Meteor explosion theory of origin of lunar craters and round maria, suggesting endogenic origin

01 p0193 A70-11592

Gas volcanic activity, meteoric impact and geological faults as origin of lunar craters, cracks, maria, etc

03 p0563 A70-13169

Far and near side lunar crater chains regularities in distribution and size

03 p0574 A70-13879

Lunar craters origin by study of slowly collapsing fluidized beds

05 p0906 A70-15920

Volcanic and meteoritic processes compared as lunar cratering agency, tabulating terrestrial lopolith and cryptexplosion structures

05 p0913 A70-16553

Apollo 10 and 11 photographs revealing probable igneous intrusions on lunar farside crater

06 p1137 A70-17195

Photometric investigation of lunar crater rays of Tycho, Copernicus, Kepler and Aristarchus compared with terrestrial explosion craters

07 p1377 A70-18972

Bottom rock structure and composition of young lunar craters compared with Kamchatka volcanic morphological analogs

07 p1385 A70-19424

Moon rotational constants determination allowing for crater Moesting A coordinate errors

08 p1574 A70-21156

Lunar origin and history, discussing evolution temperature, large and small craters and association with solar system evolution

08 p1581 A70-21822

Lunar crater meteoritic origin argument based on comparison with earth crater structure

09 p1751 A70-22195

Lunar dimple /drainage/ craters formation mechanisms, considering analogous earth drainage craters associated with lava tubes

09 p1666 A70-22311

Meteor explosion theory of origin of lunar craters and round maria, suggesting endogenic origin

09 p1763 A70-23436

Frequency-size distribution of Martian and lunar craters and oases, suggesting common mode of origin

09 p1765 A70-23810

Lunar cratering and erosion from Orbiter 5 photographs, observing crater densities, highland and maria regions, etc

10 p1942 A70-24643

Temperature distribution in shadowed lunar craters formulated in Fredholm integral equations, showing constant temperature and correction for soil thermal inertia

11 p2112 A70-26155

Lunar gravity correlation with large craters indicated from negative accelerations recorded in Apollo 12 lunar module Doppler radio tracking data

12 p2298 A70-27270

Lunar two cycle interior thermal history influence on maria and crater morphology, noting active and passive phase roles

12 p2311 A70-28302

Micrometeorites impact on lunar surface, using optical reflecting and stereoscan electron microscopes to investigate craters on Apollo 11 samples

13 p2485 A70-28474

Criticism of hypothesis regarding solar flash heating mechanism creating glaze within lunar craterlets at Apollo 11 landing site

13 p2489 A70-28912

Earth shadow enlargement during 13 April 1968 lunar eclipse, discussing craters exit and entry in umbra

13 p2491 A70-29045

Book on stratigraphic view of lunar geology covering lunar craters and terrestrial analogs, remote sensing, material ages, surface interpretations and Apollo mission results

13 p2491 A70-29060

Lunar crater Aristarchus red spot spectrum analysis, determining emission bands

13 p2494 A70-29398

Lunar surface erosion model by small projectiles impact for analytic representation of crater shape change as function of time

14 p2637 A70-30494

Soviet book on physical libration constants of moon based on visual and photographic observations of two craters by position angle method

14 p2642 A70-30959

Long term effects model evaluation of meteoritic impact against lunar surface compared with analyses of Lunar Orbiter photographs

14 p2645 A70-31062

Lunar maria absolute age from lunar crater rim height changes via isostatic settling and small craters quantity

14 p2649 A70-31213

Earth and moon meteor fall probabilities calculation using hyperbolic encounters method and lunar near and far sides crater densities difference interpretation

15 p2798 A70-31658

Lunar dimple craters formation by meteoritic erosion of concentric impact craters

15 p2807 A70-32850

Lunar cratering rates from Apollo flights data on solidation ages for Mare Tranquillitatis

16 p2979 A70-34037

Lunar maria rock thickness estimation, giving depth vs diameter diagrams for craters to show procellarian system thickness

19 p3516 A70-37982

Lunar geomorphological charts of Mare Imbrium southern region, emphasizing crater and maria formations

19 p3516 A70-37983

Small lunar crater structural characteristics and distribution

19 p3517 A70-37989

Lunar crater number and density vs diameter graph, showing rhythmic deviations from mean asymmetrical cosine curve

19 p3517 A70-37990

Lunar craters, walled plains and maria compared with volcanic formations on earth

19 p3517 A70-37991

Lunar maria and constituents characteristic differences in terms of structure, height and distribution of craters across surface, noting temperature anomalies

19 p3518 A70-37993

Lunar crater size and shape characteristics from Surveyor missions, discussing rimless shallow and cup shaped craters

20 p3707 A70-39954

Lunar surface impact cratering, comparing equilibrium size distributions

21 p3919 A70-41701

Small craters number density in southern lunar highlands, supporting Tycho Association cometary impact origin

21 p3920 A70-41882

Lunar crater Plato optical reflectance photoelectric measurements, discussing absorption and luminescent features, radiance factors, phase angles color variations and brightness

21 p3922 A70-41983

Lava thickness measurement in lunar maria from projecting rim width of partially buried craters

23 p4242 A70-44292

Lunar craters size-frequency distributions from photographic analysis, tabulating results

23 p4247 A70-44770

Multiphase volcanic eruptions associated with lunar craters Tycho and Aristarchus

23 p4253 A70-44882

LUNAR CRUST

Alpha particle emissivity measurement of moon by Explorer 35 spacecraft for U 238 abundance in outer crust

01 p0181 A70-10573

Lunar mascons formation by isostatic and volcanic processes, using normal density lunar crust and mantle model

06 p1150 A70-18476

Lunar surface reflectivity determined by measuring reflected cosmic noise, determining dielectric constant and surface material properties

06 p1151 A70-18488

Radio wave reflection coefficient power spectra for three layer lunar surface models consistent with radar spectrum, calculating porous layer thickness

08 p1565 A70-20566

Lunar surface chemical composition determination by radio astronomy, considering SHF electrical properties of silicate earth rocks

08 p1572 A70-20940

Lunar sinuous rilles formation by fluid flow mechanisms, discussing evidence for lava and rille formation by lava tube collapse

09 p1759 A70-22799

Lunar limb weak solar wind shock due to conducting crust-interplanetary magnetic field interaction

09 p1764 A70-23485

- Mascons in lunar maria depressions observed by Lunar Orbiter 5 on basis of two layer model of crust
12 p2299 A70-27281
- Lunar-earth early crust anorthosites comparison, including occurrence sites, physical and chemical properties, etc
13 p2486 A70-28616
- Lunar surface material composition in terra region from alpha scattering data on Surveyor 7, noting Si Na abundance
13 p2492 A70-29265
- Radio wave reflection coefficient power spectra for three layer lunar surface models consistent with radar spectrum, calculating porous layer thickness
15 p2805 A70-32721
- Lunar surface chemical composition determination by radio astronomy, considering SHF electrical properties of silicate earth rocks
15 p2805 A70-32752
- Lunar rock origin based on apollo samples density, impurities and mineral and chemical composition, considering structure and genesis of crust and mantle
19 p3513 A70-37524
- Lunar basalt lava bed formations, examining vacuum and gravity effects during cooling
19 p3517 A70-37988
- Lunar crystalline rock static and dynamic deformation, examining regolith and silicates textures and structures
21 p3897 A70-41515
- LUNAR DUST**
Geocentric orbital elements of lunar particles expelled into space by meteorite impact, using spheres of influence method
03 p0574 A70-13880
- Transient lunar phenomenon (observations and evanescent localized glows) related to dust raised by degassing and electrostatic glow discharges in gas phase
10 p1938 A70-24069
- Lunar rocks and dust from Apollo 11 mission investigated for origin and history of moon and solar system
12 p2310 A70-28049
- Apollo 11 lunar rocks and dust from Tranquility Sea measured for age by Rb-Sr and K-Ar methods
18 p3320 A70-37082
- Apollo 12 rock and dust analyses, discussing modifications to conclusions from Apollo 11 samples with reference to rare gas concentrations
18 p3321 A70-37085
- Lunar fragmental debris layer observations from Surveyor project, examining size, shape, texture, structure, etc
20 p3707 A70-39955
- Lunar fragmental debris physics from Surveyor observations, examining size-frequency distribution
20 p3707 A70-39956
- Lunar surface physical conditions from Surveyor landings, discussing fine cohesive rock powder
20 p3708 A70-39959
- Apollo 11 lunar rocks, breccias, dust and chip mineralogy and petrology, examining composition, texture, grain size and morphologies
21 p3896 A70-41511
- Apollo 11 lunar dust examination by neutron activation analysis, determining spallogenic manganese 53
21 p3908 A70-41579
- Trapped and cosmogenic rare gases from stepwise heated Apollo 11 lunar dust and crystalline rocks, using mass spectrometry
21 p3908 A70-41584
- Apollo 11 lunar dust and microbreccia micropaleontological examination, discussing biological morphology
21 p3778 A70-41620
- Apollo 11 lunar dust and breccia micromorphology and surface characteristics implying weathering processes
21 p3910 A70-41622
- Apollo 11 lunar powder optical and HF electrical properties, discussing reflectivity, polarization, absorption, differential mass spectrum and albedo
21 p3915 A70-41655
- Apollo 11 lunar rock and dust samples thermomagnetic properties, Curie points, magnetization and demagnetization characteristics
21 p3915 A70-41661
- Apollo 11 lunar dust, breccia and igneous rocks, using Mossbauer spectroscopy and petrographic techniques
21 p3916 A70-41664
- Apollo 11 lunar dust hysteresis curves and thermomagnetic curves, discussing metallic Fe abundance, susceptibility, alpha-gamma transition, etc
21 p3918 A70-41676
- Apollo 11 lunar dust small glassy spherules and cylinders examination by interferometry, discussing specular reflection, microcracking, chipping and origin
21 p3919 A70-41682

LUNAR ECHOES**NT LUNAR RADAR ECHOES**

- First luminous lunar echoes obtained by laser telemetry of Pic Du Midi observatory
18 p3310 A70-35948

LUNAR ECLIPSES

- Penumbra visibility of earth on lunar disk related to moon distance during lunar eclipse, discussing moon vanishing
03 p0569 A70-13361
- Penumbra during lunar eclipses analyzed photometrically, considering effects of earth upper atmosphere and lunar luminescence
07 p1377 A70-18973
- Penumbra visibility of earth on lunar disk related to moon distance during lunar eclipse, discussing moon vanishing
11 p2118 A70-26726
- Earth shadow enlargement during 13 April 1968 lunar eclipse, discussing craters exit and entry in umbra
13 p2491 A70-29045
- Atmospheric optical properties at various altitudes, using lunar disk photometric observations at different wavelengths during eclipse
15 p2801 A70-32476
- Peripheral umbra photometric analysis during lunar eclipses based on homogeneous observational material, revealing luminescence excited by solar corpuscular radiation
18 p3319 A70-37055
- Astronomical events observed in 1970 by amateur astronomers, discussing sun and moon eclipses and planets visibility
21 p3886 A70-41074
- Atmospheric optical properties at various altitudes, using lunar disk photometric observation at different wavelengths during eclipse
23 p4239 A70-43901

LUNAR EFFECTS**NT LUNAR GRAVITATIONAL EFFECTS****NT LUNAR TIDES**

- Lunar diurnal variation parameters at Irkutsk determined from IGY data concerning geometric field components
01 p0083 A70-11538
- Lunar daily variation in geophysical data determined by Chapman-Miller method, improving probable error determination method and giving computer program in FORTRAN
09 p1764 A70-23701
- Solar and lunar daily geomagnetic variations, correcting harmonic components calculated values
12 p2303 A70-27673
- Lunar perturbations in horizontal geomagnetic field, F 2 layer thickness and electron density, discussing tidal variations
20 p3617 A70-39141
- Lunar effects on vertical and shape of geoid in universal time
22 p4100 A70-42852
- Thunderstorm frequencies related to lunar phase and declination for ground stations in eastern and central U.S.
22 p4018 A70-42909
- Short period lunar perturbation on satellites by computer program with Fortran statements, considering errors, program output and table driven algebraic processors
24 p4406 A70-45532

LUNAR ENVIRONMENT**NT LUNAR ATMOSPHERES**

- Simulated lunar environmental facility to investigate effects of high risk vacuum, lunar gravity and terrain characteristics and spacesuit encumbrances on astronaut performance
01 p0037 A70-10961
- Turbulent-plasma electrons ballistic effects on solar wind magnetic field fluctuations in lunar vicinity
04 p0753 A70-15123
- Surveyor spacecraft vernier propulsion system survival in lunar environment, suggesting temperature resistant seal and valve seat material for fluid loss prevention
06 p1129 A70-17170
- ALSEP component configuration and deployment environment, describing passive thermal control system for data processing equipment
14 p2651 A70-31340
- Thermal mapping vacuum chamber tests of nuclear fuel capsules for lunar surface experiments, using remote IR radiometric microscope
15 p2718 A70-32800
- Metal-silicate rock friction in ultrahigh vacuum of lunar environment
17 p3101 A70-34760
- Thermal conductivity of particulate basalt as function of density in simulated lunar and Martian environments, noting temperature and pressure effects
18 p3316 A70-36772
- Lunar surface radiative balance and thermal environment measurement by portable meteorological station, considering lunar environment peculiarities for instruments design
19 p3514 A70-37631
- Dipole antenna radiation in compressible anisotropic electron plasma overlying imperfectly conducting half space, solving for lunar environment
19 p3381 A70-38407

- Dipole antenna radiation in compressible anisotropic electron plasma overlying imperfectly conducting half space, evaluating Fourier-Bessel integrals for lunar environment
19 p3381 A70-38408

- Antimatter detection and interaction with matter on moon, discussing radiation from electron-positron annihilation processes
19 p3521 A70-38482

- Lunar postsunset horizon afterglow observed by Surveyor 7, discussing small particle diffraction on surface
20 p3708 A70-39960

- Lunar environment diagnostic features enhancement on IR emission spectra, making moon excellent target for remote sensing
20 p3709 A70-39979

- Apollo 11 drive-tube core samples from Tranquility Base, expressing lunar surface environmental processes
21 p3914 A70-41653

- Hawaiian basalt melted in simulated lunar environment, investigating surface characteristics, internal structure and bearing strength
23 p4254 A70-44883

- Apollo 11 deployed solar cells, investigating degradation of surface properties and thermal control due to lunar module ascent effects
24 p4295 A70-46262

LUNAR EVOLUTION

- Lunar origin theories, considering lunar surface data from Surveyor spacecraft and Lunar Orbiter
01 p0178 A70-10453
- Lunar nature and origin, discussing thermal history, density, composition, surface and evolution hypotheses
01 p0185 A70-11048
- Meteor explosion theory of origin of lunar craters and round maria, suggesting endogenic origin
01 p0193 A70-11592
- Tidal disturbing functions developed with amplitude factor and lag angle expressed as sums of zonal spherical harmonics, discussing lunar formation and orbit evolution
03 p0576 A70-14083
- Pb isotope data from young mantle derived volcanics suggesting mantle evolution and lunar capture
04 p0743 A70-14396
- Moon origin theories emphasizing fission from earth, noting objections to capture theory
04 p0751 A70-15058
- Lunar craters origin by study of slowly collapsing fluidized beds
05 p0906 A70-15920
- Lunar structure and evolution based on satellite measurements of mass distribution, radius moments of inertia, gravity anomalies and topographic irregularities
05 p0920 A70-16945
- Lunar maria hypothetical simultaneous formation by impact, discussing significance of mascons
06 p1138 A70-1727
- Lunar origin and history, discussing evolution temperature, large and small craters and association with solar system evolution
08 p1581 A70-21822
- Lunar internal temperature approximation correcting solution of heat conduction equation for moon thermal histories
09 p1753 A70-22385
- Meteor explosion theory of origin of lunar craters and round maria, suggesting endogenic origin
09 p1763 A70-23436
- Lunar rocks and dust from Apollo 11 mission investigated for origin and history of moon and solar system
12 p2310 A70-28049
- Lunar two cycle interior thermal history influence on maria and crater morphology, noting active and passive phase roles
12 p2311 A70-28302
- Condensed products of vaporized primordial terrestrial material accounting for moon formation, using single stage precipitation earth origin hypothesis
13 p2488 A70-28719
- Ballistic model for lunar regolith evolution based on lunar surface characteristics from Surveyor TV pictures
14 p2644 A70-31053
- Lunar surface optical properties differences for lunar and planetary nature and evolution determination
14 p2645 A70-31063
- Lunar mascons origin explanation in terms of primordial atmosphere and hydrosphere
14 p2646 A70-31065
- Lunar rock origin based on apollo samples density, impurities and mineral and chemical composition, considering structure and genesis of crust and mantle
19 p3513 A70-37524
- Moon origin, surface, exploration, Apollo 11 landing, subsidence/uplift crater formation and Transient Lunar Phenomena
20 p3701 A70-38977

Compositional zoning in pyroxenes from grained Apollo 11 microgabbros, implying supercooled magma origin 21 p3899 A70-41532

Apollo 11 lunar samples mineralogical and compositional studies concerning lunar origin hypothesis 21 p3899 A70-41534

Apollo 11 lunar basalt petrogenesis, examining internal constitution and origin by high pressure 21 p3901 A70-41547

Lunar rock composition difference from meteorites and terrestrial basalts, indicating complexities in solar abundances and initial earth and moon compositions 21 p3906 A70-41567

Rare gas analysis of Apollo 11 lunar soil and breccia for surface layer history 21 p3906 A70-41571

Apollo 11 lunar material trace elements, examining chemical processes during and after formation and meteoritic matter influx rate 21 p3907 A70-41572

Apollo 11 sample elemental abundances, investigating environmental, paragenetic and petrogenetic problems and moon evolution 21 p3907 A70-41575

Apollo 11 lunar material isotopic age determination, discussing rock crystallization, radiogenic dust, lead isotope data and moon origin 21 p3907 A70-41576

Apollo 11 lunar rock K, Rb, Sr, Ba and rare earth element concentrations, examining relationship to terrestrial and chondritic levels 21 p3776 A70-41600

Apollo 11 lunar rock and soil bombardment produced radionuclide patterns, discussing solar flare protons and alphas, age determination and astronomical models 21 p3777 A70-41604

Lunar surface material age and post-crystallization from isotopic investigation of Apollo 11 samples of U-Th-Pb systematics 21 p3909 A70-41608

Apollo 11 lunar, terrestrial and meteoritic basalts relationships, examining Ga, Ge, In, Ir and Au concentrations by neutron activation analyses 21 p3778 A70-41617

Apollo 11 lunar fines carbon compounds, examining chemical state of porphyrins, fatty and amino acids, purines, pyrimidines and carbohydrates, etc 21 p3779 A70-41625

Lunar rocks primordial accretion, examining ablation and transport of solids, liquid and vapor on surfaces 21 p3913 A70-41641

Earth-moon system age and origin from tidal evolution equations, considering growth line counts on living and fossil marine invertebrates 21 p3921 A70-41971

Tidal friction theories relating to earth rotation and lunar evolution 21 p3921 A70-41972

Earth-moon system formation theory, discussing condensation from terrestrial hot extended silicate atmosphere 22 p4098 A70-42548

Apollo 11 data for lunar formation by earth breakup, discussing moon heating phase and correlation with planetary evolution 22 p4098 A70-42549

Lunar origin by capture, discussing moon orbit evolution, thermal history and surface features, earth evolution and tidal interactions 22 p4098 A70-42550

Lunar samples and terrestrial materials isotopic analyses, discussing mineralogical and chemical compositions for lunar origin 22 p4098 A70-42574

Initial water content on moon implied from hypothetical falling temperature lunar accretion as original earth satellite 22 p4102 A70-42954

Lunar formation from ejected terrestrial magma, considering distribution of seas, gravitational anomalies and craters with rays 23 p4247 A70-44772

Lunar formation, investigating accretion rate ratio for earth and moon as function of distance 24 p4409 A70-45674

LUNAR EXPLORATION

Tradeoff criteria between man machine and automated space systems applied to lunar and cosmic ray explorations [AIAA PAPER 69-1045] 01 p0034 A70-10644

Lunar nature and origin, discussing thermal history, density, composition, surface and evolution hypotheses 01 p0185 A70-11048

Existence probability of useful mineral resources on moon, considering physical features and geological formations 03 p0563 A70-13170

Black and white and color Apollo 11 secondary electron conduction TV cameras, discussing characteristics and mission requirements 04 p0688 A70-14692

Surveyor 7 alpha scattering experiment and TV image data revealing lunar surface chemical composition, rocks and fragments, etc 04 p0752 A70-15060

Lunar and planetary exploration costs and technology, discussing role of nuclear propelled passenger vehicles 11 p2082 A70-26061

Dead reckoning navigation of manned lunar roving vehicle (MLRV), describing hardware and coordinate system 12 p2266 A70-27414

Apollo lunar roving vehicles for manned exploration, discussing design proposals 12 p2208 A70-27943

Lunar surface mobility systems designs based on terrestrial transporters or mission requirements consideration, comparing capabilities 13 p2384 A70-28416

Pogo sticks concept for lunar exploration, showing improved performance over lunar surface or flying vehicles 13 p2505 A70-28891

Soviet lunar and interplanetary space missions during 1969 including Venera, Cosmos, Luna and Meteor satellite activities 13 p2505 A70-28901

Applied sciences research and utilization of lunar resources - Conference, New York, October 1968 14 p2633 A70-30192

Solar, nuclear, chemical and thermal energy sources for short and long duration exploration on moon 14 p2634 A70-30195

Lunar communications systems considering use of satellites, metallic particle belts, rockets, lasers and particle beams 14 p2634 A70-30196

Lunar vehicles development, emphasizing translunar exploration vehicle (TLEV) for future lunar base 14 p2563 A70-30197

Lunar resources classified as rocket fuel, construction and life support materials, discussing implications for manned surface exploration missions 14 p2634 A70-30198

Morphological box for extracting chemical elements and compounds from lunar materials for manned operations on moon 14 p2634 A70-30200

Lunar exploration by manned and unmanned space flights, discussing seismology, composition, surface features, etc 15 p2798 A70-31678

Mobile geochemical laboratory for in situ radiation measurement and elemental analyses in lunar exploration 15 p2717 A70-31801

Lunar exploration program based on U.S. antarctic research experience, considering man role, environment, logistics, transportation, economics, etc 15 p2800 A70-32058

Apollo 11 lunar mission results, discussing surface, seismology, laser ranging retroreflector, solar wind and rock samples 15 p2800 A70-32073

Lunar surface exploration vehicle (Lunar Rover) design, analyzing stowage aspects in Lunar Module 16 p2888 A70-33680

Manned lunar orbital research operations capability, systems and scientific objectives [AAS PAPER 70-022] 17 p3156 A70-34800

Moon legal status, discussing territorial sovereignty, peaceful uses, UN Resolutions and Space Treaty, rule of occupation, etc 17 p3200 A70-35323

Legal status of ownership rights of lunar soil samples and objects left on moon by astronauts 17 p3203 A70-35790

Legal aspects concerning lunar matter and product disposal resulting from human cosmic expansion 17 p3203 A70-35795

Caterpillar remote controlled unmanned lunar exploration vehicle, describing construction and scientific missions 18 p3237 A70-36512

Soviet and American lunar exploration by probes, manned surveillance flights and lunar landings, discussing NASA program 18 p3238 A70-37079

Moon origin, surface, exploration, Apollo 11 landing, subsidence/uplift crater formation and Transient Lunar Phenomena 20 p3701 A70-38977

Lunar orbital science, discussing U.S. and Soviet missions, NASA plans and results concerning remote sensing, force field and particle studies 22 p4105 A70-43144

Lunar research via direct exploration, discussing lunar geology, cartography, selenodesy, gravific potential, rotation, etc 23 p4256 A70-45037

Lunar mass and gravitational fields determined from lunar satellite dynamics 24 p4407 A70-45533

Apollo spacecraft pyrotechnic systems and devices functions during lunar exploration mission and in aborts [SAE PAPER 700833] 24 p4416 A70-45888

Book on lunar rocks covering pre-Apollo lunar scientific knowledge, Apollo and future lunar mission planning, lunar mineralogy, petrology and geochemistry, etc 24 p4412 A70-46025

LUNAR EXPLORATION SYSTEM FOR APOLLO

Apollo J mission hardware modification for lunar exploration, describing systems engineering role 21 p3928 A70-40979

LUNAR FAR SIDE

Global exploration of lunar surface by Luna 3 and Zond 3 automatic stations, confirming asymmetric distribution of sea areas on visible and remote hemispheres 01 p0177 A70-10335

Lunar surface far side stereoscopic photography by Apollo 8 mission considered for lunar control 04 p0686 A70-14618

Cartographic tying-in of Zond 3 lunar surface photographs to verify maps of moon far side 05 p0918 A70-16918

Apollo 10 and 11 photographs revealing probable igneous intrusions on lunar farside crater 06 p1137 A70-17195

Lunar surface mapping and far side gravity field probing by satellite photogrammetry 12 p2308 A70-27874

Lunar far side features position from Apollo 8 data, evaluating Apollo navigation system accuracy 12 p2309 A70-27949

Photometric maps of reverse side lunar surface from AIM Zond-3 material 18 p3323 A70-37142

Gravity gradient attitude control for satellites near lunar far side libration point [AIAA PAPER 70-1053] 19 p3528 A70-38868

LUNAR FLIGHT

Translunar Apollo orbit analysis from elementary equations relating to elliptical and hyperbolic orbits in inverse square force field 06 p1148 A70-18397

Lunar orbital science, discussing U.S. and Soviet missions, NASA plans and results concerning remote sensing, force field and particle studies 22 p4105 A70-43144

LUNAR FLYING VEHICLES

Lunar flying vehicle propulsion system optimization, discussing weight, performance, engine life, reliability, etc [AIAA PAPER 70-605] 16 p2969 A70-33602

LUNAR GEOLOGY

Surveyor 5 lunar rock data from Mare Tranquilitatis compared with pyroxene gabbros, indicating gabbro or gabbroic anorthositic classification 01 p0181 A70-10575

Free oscillations and surface wave dispersions from lunar models based on Orbiter data and corresponding pressure region of earth crust 02 p0379 A70-12777

Lunar mascon origin theories, discussing mass transfer by excess pressure generation due to rapid cooling crust and densification by water outgassing 02 p0379 A70-12779

Moon-earth historical relationship, comparing differences in figure and interior with terrestrial planets 03 p0562 A70-12875

Gas volcanic activity, meteoric impact and geological faults as origin of lunar craters, cracks, maria, etc 03 p0563 A70-13169

Existence probability of useful mineral resources on moon, considering physical features and geological formations 03 p0563 A70-13170

Tektites origin, comparing chemical composition with lunar soil from Apollo mission materials 03 p0577 A70-14096

Soviet book on lunar shape and dimensions from astronomical observations, comparing observational and theoretical data 04 p0751 A70-14952

Chemical abundance data of lunar surface rocks, suggesting basaltic achondrites and eucrites origin from moon 06 p1137 A70-17196

Lunar surface samples characteristics correlation with terrestrial igneous rocks /basalts/ and eucrite meteorites based on alpha scattering analysis 07 p1380 A70-19203

Color and black-and-white photomicrographs and photomacrographs of Apollo 11 moon rock sample consisting of spongy gray mass of pumice-like material 07 p1288 A70-20224

Lunar Orientale region structure geological interpretation based on Lunar Orbiter 4 photographs 09 p1751 A70-22196

Lunar dimple /drainage/ craters formation mechanisms, considering analogous earth drainage craters associated with lava tubes 09 p1666 A70-22311

Gaseous species in equilibrium with Apollo 11 holocrystalline rocks during crystallization

09 p1758 A70-22744

Apollo lunar landing sites geological configuration and composition

09 p1759 A70-22772

Physical, chemical, mineralogical and biological analysis of Apollo 12 lunar samples compared to Apollo 11 rocks, discussing landing site geologic setting

10 p1935 A70-23811

Physicomechanical properties of tuff rock based on similarity to lunar surface rock, determining natural density, porosity and compression strength

11 p2119 A70-26798

Lunar rocks types determination by mass spectrometry, describing results of terrestrial rocks tests

11 p2119 A70-26799

Lunar rolling stones anomalous surfaces goniphotometric properties, considering bearing strength as rock density function

12 p2296 A70-26925

Synthetic pyroxenoid stability and crystallography, noting pyroxmangite structure similar to yellow lunar mineral from Mare Tranquillitatis

12 p2226 A70-28022

Book on stratigraphic view of lunar geology covering lunar craters and terrestrial analogs, remote sensing, material ages, surface interpretations and Apollo mission results

13 p2491 A70-29060

Lunar surface fine structure and geological analysis from Ranger 7, 8 and 9 photographs

14 p2644 A70-31052

Ballistic model for lunar regolith evolution based on lunar surface characteristics from Surveyor TV pictures

14 p2644 A70-31053

Mobile geochemical laboratory for in situ radiation measurement and elemental analyses in lunar exploration

15 p2717 A70-31801

Vacuum effect on explosive coupling seismic energy considered in lunar geophysical experiment

16 p2896 A70-33092

Soviet papers on lunar geology problems covering mapping, rocks, maria, lava, craters, etc

19 p3516 A70-37980

Lunar geomorphological map technique, discussing lunar rock formation classifications

19 p3516 A70-37981

Lunar geomorphological charts of Mare Imbrium southern region, emphasizing crater and maria formations

19 p3516 A70-37983

Lunar geomorphological charts of Mare Nubium northern part, considering structural features in equatorial band

19 p3517 A70-37984

Lunar geomorphological charts of Theophilus and Ptolemaeus walled plains, investigating central region tectonics

19 p3517 A70-37985

Lunar geomorphological charts in Archimedes crater and Appenine and Haemus mountain region, examining duration and stages in Mare Imbrium depression development

19 p3517 A70-37986

Lunar basalt lava bed formations, examining vacuum and gravity effects during cooling

19 p3517 A70-37988

Lunar surface mapping and comparison of geological features with earth, considering mass, volume, density, gravity, rotation and energy and matter balance

19 p3518 A70-37994

Soviet collection of lunar geological and morphological maps and relief tracings, showing tectonic features, craters and surface characteristics

19 p3518 A70-38011

Surveyor program results, discussing lunar craters, rock fragments, particle size optical, thermal and radar characteristics and chemical composition

20 p3707 A70-39952

Lunar topographical and geological features examined by Surveyor program

20 p3707 A70-39953

Lunar crater size and shape characteristics from Surveyor missions, discussing rimless shallow and cup shaped craters

20 p3707 A70-39954

Lunar elemental abundances examined by Surveyor project, discussing albedo contrasts, surface rock density, bulk composition, thermal regime and chondritic meteorites

20 p3707 A70-39957

Lunar soil from Apollo 12, identifying chemical composition of orthopyroxene-calcic plagioclase rock fragments for origin

20 p3709 A70-39980

Lunar rock composition difference from meteorites and terrestrial basalts, indicating complexities in solar abundances and initial earth and moon compositions

21 p3906 A70-41567

Lunar carbonaceous, organic and organogenic materials analysis by mass spectroscopy, gas chromatography and various other methods

21 p3780 A70-41633

Tranquility Base regolith origin, examining thickness exposure histories, crater distribution and composition

21 p3918 A70-41677

Apollo 11 lunar samples spectral analysis, discussing Fe and Mn electron paramagnetic resonance and Al 27 nuclear magnetic resonance spectra

21 p3919 A70-41683

Lunar geomorphic features and mass wasting relation, discussing landslides, rockfalls, debris slides, slump and creep play

22 p4102 A70-42972

Crystalline rocks from Mare Tranquillitatis and Oceanus Procellarum, determining K-Ar ages

23 p4238 A70-43803

Apollo 11 and 12 results concerning lunar geology and physical features, discussing impact generated long duration seismic signals and solar wind isotopic composition experiment

23 p4244 A70-44613

Papers on lunar geology covering Tycho northeast rim, multiphase eruptions, basalt melts in simulated lunar environment and lava tubes in New Mexico

23 p4253 A70-44880

Multiphase volcanic eruptions associated with lunar craters Tycho and Aristarchus

23 p4253 A70-44882

Lunar research via direct exploration, discussing lunar geology, cartography, selenodesy, gravific potential, rotation, etc

23 p4256 A70-45037

Apollo 11 lunar fines glassy particles, investigating morphology, optical properties and chemical composition

24 p4403 A70-45401

LUNAR GRAVITATION

Apollo 11 lunar module gravity measurement on lunar surface with pulsed integrating pendulous accelerometer to compute anomaly and radius at landing site

01 p0181 A70-10574

Lunar gravitational field determination from analysis of Lunar Orbiter spacecraft tracking data

03 p0562 A70-12915

Potential determination from gravity disturbances along fixed direction in analysis of residuals of Doppler tracking of Lunar Orbiter satellites for moon gravity field

03 p0577 A70-14177

Gravity anomalies of moon mapped by time differentiation of Doppler-tracked satellite velocities, noting isostatic equilibrium

05 p0915 A70-16827

Lunar structure and evolution based on satellite measurements of mass distribution, radius moments of inertia, gravity anomalies and topographic irregularities

05 p0920 A70-16945

Moon figure and gravitational field determination based on hydrostatic theory, libration observations, node and perigee motion, lunar satellite trajectories and visible topography

06 p1141 A70-17824

Mathematical techniques for selenodesy computer simulation program, solving problems arising from infinite series of spherical harmonics for lunar gravitational potential

06 p1152 A70-18498

Potential and gravity distributions on lunar surface, showing presence of harmonics of all orders

07 p1385 A70-19425

Moon gravity field model derived from long-arc analysis of Lunar Orbiters tracking data, considering lunar mass distribution role

09 p1752 A70-22309

Gravitational field signatures for planetary fine structure analysis, describing lunar orbiter, selenodesy experiment and gravity field and earth gravity field satellite observation

11 p2111 A70-26029

Lunar surface mapping and far side gravity field probing by satellite photogrammetry

12 p2308 A70-27874

Lunar near surface gravity estimation by mass density model for agreement between Doppler tracking data from Lunar Orbiter and trajectory predictions

14 p2645 A70-31064

Mare Orientale positive gravity anomaly

17 p3158 A70-34865

Lunar research via direct exploration, discussing lunar geology, cartography, selenodesy, gravific potential, rotation, etc

23 p4256 A70-45037

Lunar mass and gravitational fields determined from lunar satellite dynamics

24 p4407 A70-45533

LUNAR GRAVITATIONAL EFFECTS

Reduced traction effects on human work performance in weightless and lunar gravity environment

01 p0037 A70-10959

Prototype lunar gravity simulator for studies of reduced gravity effects on human self locomotive capability, using magnetic air bearings and body support system

01 p0037 A70-10960

Satellite motion in lunar orbit by von Zeipel method, considering perturbations due to nonspherical lunar gravity field and earth and solar attraction

10 p1939 A70-24186

Lunar gravity correlation with large craters indicated from negative accelerations recorded in Apollo 12 lunar module Doppler radio tracking data

12 p2298 A70-27270

Lunar gravitational effects on navigation in low altitude lunar orbits using Apollo 12 data

14 p2613 A70-30460

Lunar gravitational field effect on sun-earth exterior libration point location, examining placement on line passing through sun and earth-moon barycenter

18 p3320 A70-37059

Practical stability of highly eccentric orbits quasi-normal to ecliptic, discussing lunar effects on orbital lifetime

23 p4243 A70-44510

Balloon satellite perturbations in orbital period involving air drag, lunar gravity and solar and terrestrial radiation pressures

24 p4414 A70-45358

LUNAR GRAVITY SIMULATOR

Partial gravity simulators at Manned Spacecraft Center for astronaut acquaintance with dynamics of moon walking

21 p3804 A70-41192

LUNAR IONOSPHERE

U LUNAR ATMOSPHERES

LUNAR LANDING

Apollo lunar mission optics concerning liftoff alignment theodolites, spacecraft atmosphere electro-optical sensor, helmet optical coating and laser experiment

04 p0688 A70-14693

Soviet book on piloted flights in near space with lunar landing, discussing flight mechanics of orbital aircraft, launching into space, maneuvering, etc

05 p0923 A70-16554

Emergency ejection from lunar landing training vehicles, describing working sequence and experimental results on astronaut and test pilot

06 p1003 A70-17717

Optimal landing of spacecraft on moon surface from low circular orbit, analyzing rocket thrust, altitude and landing site distance effect on spacecraft mass

06 p1155 A70-17880

Apollo-Saturn Launch Vehicle Targeting Program for Lunar Landing Missions, describing functions of integrated digital computer programs

06 p1145 A70-18093

Apollo 11 premission planning, real time situation and postflight analysis for lunar descent and ascent phases, providing navigation correction capability for Apollo 12

06 p1159 A70-18227

Apollo 11 mission crew observation of operational and scientific phenomena associated with lunar landings, discussing preflight geologic training and briefings

11 p2109 A70-25847

Rough-landing space capsule for omnidirectional touchdown in lunar and Martian missions, tabulating design characteristics and functional capabilities

11 p2123 A70-26053

Space navigation for Apollo 11 mission, emphasizing ground and onboard systems, interfaces with guidance and use in phases of lunar landing

13 p2447 A70-28547

Surveyor spacecraft landing shock absorbers design and performance assessment by digital computer simulation

16 p2922 A70-34123

Apollo docking system for CSM-LM connection and disconnection during lunar landing mission, discussing flight hardware

17 p3175 A70-34768

Apollo lunar landing guidance, navigation and control, discussing inertial and optical measurements, computer, digital autopilots, rendezvous and mid-course navigation

17 p3134 A70-35288

Apollo lunar landing flight control functions, organization, disciplines and activities at Mission Control Center

17 p3134 A70-35292

Legal problems arising from Apollo 11 lunar landing with respect to Space Treaty, discussing lunar soil removal, flag planting, Luna 15 flight, etc

17 p3203 A70-35791

Lunar surface erosion due to Apollo 11 descent engine

18 p3316 A70-36960

Lunar module systems design, describing R and D program and landing mission

21 p3928 A70-40977

Book on decision making in U.S. manned lunar landing commitment covering space policy, technical planning, national interests, Apollo experience, etc

22 p4126 A70-42314

Lunik 16 lunar soft landing technique, discussing automatic and ground controlled mission phases 22 p4110 A70-43210

LUNAR LANDING MODULES

Apollo lunar module descent engine exhaust organic combustion products, estimating ion intensities of various species in all mass spectra 02 p0356 A70-12693

Apollo spacecraft pyrotechnics on lunar landing mission, considering standard initiator, modular cartridges, noninterchangeability of special purpose devices, postmanufacture indexing and data system 03 p0582 A70-14102

Seismic analysis of lunar module impact and missile-earth impact, comparing recorded signal parameters 11 p2118 A70-26748

Apollo lunar module structural integrity for lunar landing verified by Monte Carlo dynamic analysis 12 p2312 A70-27114

Landing point redesignation during Apollo lunar module descent terminal portion, defining information and control system 14 p2613 A70-30454

Apollo 12 navigation for pinpoint lunar landing, correcting errors in downtrack position in guidance computer near powered descent initiation time 14 p2613 A70-30456

Lunar Module landing radar system design, discussing antenna and electronics assembly 16 p2865 A70-33681

Lunar landing training vehicle using Lunar Module free flight simulator for earth practicing of final descent handling 21 p3750 A70-41193

LUNAR LANDING SITES

Apollo 11 lunar module gravity measurement on lunar surface with pulsed integrating pendulous accelerometer to compute anomaly and radius at landing site 01 p0181 A70-10574

Orbiter imagery analysis program for Apollo landing site selection, using photographic interpretive techniques 03 p0571 A70-13660

Photometric reduction of Lunar Orbiter video magnetic tapes for generation of topographic information of proposed Apollo landing sites 03 p0490 A70-13661

Normal albedo of Apollo 11 landing site and intrinsic dispersion in lunar Heiligenschein determined from Apollo and earth based photographic photometry 04 p0747 A70-14549

Relative reflectivity of lunar landing site Apollo 7 compared to site Apollo 2, showing compositional and mineralogical differences 04 p0751 A70-15059

Surveyor 7 highland landing soil mechanical properties and rock diameter similar to previous sites 04 p0752 A70-15063

Apollo lunar landing sites geological configuration and composition 09 p1759 A70-22772

Physical, chemical, mineralogical and biological analysis of Apollo 12 lunar samples compared to Apollo 11 rocks, discussing landing site geologic setting 10 p1935 A70-23811

Selenodetic control system, considering photogrammetric networks, Apollo landing site, topographical maps, lunar photographs, etc 10 p1890 A70-24732

Extraterrestrial photogrammetry role in lunar photographs analysis, considering landing site triangulation and selection, coordinate system improvement, etc 10 p1948 A70-25046

Lunar surface alpha radioactivity at Surveyor 5, 6 and 7 landing sites 11 p2104 A70-25658

Criticism of hypothesis regarding solar flash heating mechanism creating glaze within lunar craterlets at Apollo 11 landing site 13 p2489 A70-28912

Landing point redesignation during Apollo lunar module descent terminal portion, defining information and control system 14 p2613 A70-30454

Apollo 12 navigation for pinpoint lunar landing, correcting errors in downtrack position in guidance computer near powered descent initiation time 14 p2613 A70-30456

Lunar rotary motion predetermination for spacecraft landing in mountainous region 15 p2773 A70-32266

Surveyor spacecraft characteristics and operation, discussing scientific payloads, landing sites, etc 20 p3716 A70-39951

Calcium-bearing iron silicate (pyroxferroite) from Apollo 11 lunar Tranquility Base samples, discussing petrographic environment, physical and optical properties 21 p3895 A70-41504

Tranquility Base lunar soil origin, establishing component nature, size distribution, density, mineralogy, constructional or destructional history 21 p3897 A70-41519

Shock metamorphic granular mafic holocrystalline lithic fragments, microbreccia, glass and anorthosite from Apollo 11 lunar surface material at Tranquility Base 21 p3900 A70-41535

Glass spherule lunar particles and breccia from Apollo 11 site, showing passage through impact generated cloud of hot fragmental material 21 p3901 A70-41541

Tranquility Base regolith origin, examining thickness exposure histories, crater distribution and composition 21 p3918 A70-41677

Apollo 11 and 12 lunar landing sites surface properties from returned rocks chemical, physical and mineralogical analysis 23 p4241 A70-44221

LUNAR LIMB

Lunar limb ellipsoid orientation and parameters based on Greenwich meridional measurements of visible lunar diameters, noting use for observation reduction for various librations 03 p0569 A70-13356

Unipolar induction to calculate moon interior electric field profiles, noting magnetic back pressure as limb shock wave and interaction with solar wind 07 p1377 A70-18970

Lunar limb weak solar wind shock due to conducting crust-interplanetary magnetic field interaction 09 p1764 A70-23485

Lunar limb ellipsoid orientation and parameters based on Greenwich meridional measurements of visible lunar diameters, noting use for observation reduction for various librations 11 p2118 A70-26721

Lunar limb shock wave observed by Explorer 35 satellite defined with respect to solar wind flow direction, discussing formation mechanism 12 p2302 A70-27594

Tropospheric inhomogeneities properties and wind conditions in relation to lunar limb image deformations 16 p2979 A70-34178

Lunar limb tabular position angles accuracy, discussing Watt charts used for star occultation examination 18 p3321 A70-37124

Watts lunar limb correction charts parameters solution, using grazing and total stellar occultations by moon 20 p3705 A70-39478

LUNAR LOGISTICS

Lunar based astronomical research program logistics model taking into account scientific mission, launch vehicle capacities, supply and support requirements, etc 20 p3710 A70-40336

LUNAR LUMINESCENCE

Gray and colorless features of moon explained as atomic H imported by solar wind replacing lost H by photolytic decomposition of water vapor 05 p0908 A70-16303

Catalog of lunar features brightness interpreted in terms of photometric function uniformity of lunar surface, considering second order light scattering 07 p1377 A70-18971

Penumbra during lunar eclipses analyzed photometrically, considering effects of earth upper atmosphere and lunar luminescence 07 p1377 A70-18973

Lunar surface luminescence considered for correlation with tidal forces of earth 09 p1758 A70-22748

Integrated lunar disk wavelength dependence of polarization using photoelectric polarimeter, tabulating results 09 p1759 A70-22910

Transient lunar phenomenon (obscurations and evanescent localized glows) related to dust raised by degassing and electrostatic glow discharges in gas phase 10 p1938 A70-24069

Luminescence of powdered silica and basalt bombarded by atomic hydrogen, relating spectral distributions dependence on ion energy to lunar luminescence 10 p1942 A70-24647

Remote sensing of lunar photometric function at small phase angles by Apollo 8 command service module 12 p2297 A70-26926

Peripheral umbra photometric analysis during lunar eclipses based on homogeneous observational material, revealing luminescence excited by solar corpuscular radiation 18 p3319 A70-37055

Lunar luminescence phenomena, examining gas eruptions from volcanic activity, solar radiation and color 21 p3886 A70-41070

Luminescence efficiencies of Apollo 11 lunar and terrestrial rocks and minerals, using UV excitation 21 p3915 A70-41656

Proton and UV excited luminescence of Apollo 11 Tranquility rocks and fines, indicating solar wind impingement 21 p3917 A70-41672

LUNAR MAGNETIC FIELDS

Magnetic field and plasma variations in lunar wake using Maxwell equations 06 p1153 A70-18636

Unipolar induction to calculate moon interior electric field profiles, noting magnetic back pressure as limb shock wave and interaction with solar wind 07 p1377 A70-18970

Lunar surface magnetometer data interpretation by analysis of moon motion relative to interplanetary magnetic field spatial irregularities, using lunar electrical conductivity models 07 p1378 A70-18974

ALSEP magnetometer mission and environmental requirements and mechanical design 16 p2914 A70-34152

Lunar magnetic monopole charge effects on nearby magnetic field configuration 18 p3316 A70-36898

Earth magnetic field, discussing origin, field absence on planets and moon and MHD theory 19 p3410 A70-37399

Lunar surface local magnetic field measurement, describing Apollo 12 magnetometer 20 p3709 A70-40087

Apollo 11 lunar rock and fines magnetic properties, associating remanent magnetization with lunar magnetic field 21 p3917 A70-41675

LUNAR MAPS

Cartographic tying-in of Zond 3 lunar surface photographs to verify maps of moon far side 05 p0918 A70-16918

Lunar photography interpretation, discussing topographic maps obtained by spacecraft 07 p1284 A70-19779

Extraterrestrial photogrammetry role in lunar photographs analysis, considering landing site triangulation and selection, coordinate system improvement, etc 10 p1948 A70-25046

Selenology by traverse method, discussing equipment and mapping procedure 11 p2111 A70-26043

Polarized and depolarized radar maps of moon, attributing anomalies and average diffuse component of echoes to scattering behavior of surface and subsurface rocks 14 p2645 A70-31060

Hypsometric chart plot of visible lunar hemisphere with consideration of relief, obtaining isohypsies 15 p2803 A70-32494

Lunar surface large scale maps by photogrammetric method requiring triangulation of convergent high resolution Lunar Orbiter photographs by block process 16 p2979 A70-34045

Lunar surface features charting from astrophysical data and direct observation, describing mapping of Sea of Tranquility 18 p3323 A70-37141

Photometric maps of reverse side lunar surface from AIM Zond-3 material 18 p3323 A70-37142

Lunar geomorphological map technique, discussing lunar rock formation classifications 19 p3516 A70-37981

Lunar geomorphological charts of Mare Imbrium southern region, emphasizing crater and maria formations 19 p3516 A70-37983

Lunar geomorphological charts of Mare Nubium northern part, considering structural features in equatorial band 19 p3517 A70-37984

Lunar geomorphological charts of Theophilus and Ptolemaeus walled plains, investigating central region tectonics 19 p3517 A70-37985

Lunar geomorphological charts in Archimedes crater and Apennine and Haemus mountain region, examining duration and stages in Mare Imbrium depression development 19 p3517 A70-37986

Lunar surface mapping and comparison of geological features with earth, considering mass, volume, density, gravity, rotation and energy and matter balance 19 p3518 A70-37994

Soviet collection of lunar geological and morphological maps and relief tracings, showing tectonic features, craters and surface characteristics 19 p3518 A70-38011

Hypsometric chart plot of visible lunar hemisphere with consideration of relief, obtaining isohypsies 23 p4240 A70-43916

LUNAR MARIA

Slopes distribution over finite span on planetary surface excavated by primary impact craters, including typical lunar mare crater densities 01 p0178 A70-10443

Meteor explosion theory of origin of lunar craters and round maria, suggesting endogenic origin

01 p0193 A70-11592

Gas volcanic activity, meteoric impact and geological faults as origin of lunar craters, cracks, maria, etc.

03 p0563 A70-13169

Photoelectric polarimetry of samples of lunar maria, terra, lavas and chemicals for wavelength dependence of polarization, comparing to Mercury, Mars and asteroids

03 p0576 A70-14082

Nonexistence of large mascons at Mare Marginis and Mare Orientale deduced from residual acceleration analysis of Lunar Orbiter Doppler tracking data

04 p0743 A70-14424

Lunar maria hypothetical simultaneous formation by impact, discussing significance of mascons

06 p1138 A70-17279

Satellite impact interpretation of lunar maria surface distribution, discussing lava origins and mascon distribution

09 p1752 A70-22310

Meteor explosion theory of origin of lunar craters and round maria, suggesting endogenic origin

09 p1763 A70-23436

Continental migration role in lunar maria formation, suggesting similarity with geological formation of earth ocean floor

09 p1765 A70-23797

Mascons in lunar maria depressions observed by Lunar Orbiter 5 on basis of two layer model of crust

12 p2299 A70-27281

Lunar two cycle interior thermal history influence on maria and crater morphology, noting active and passive phase roles

12 p2311 A70-28302

Lunar maria absolute age from lunar craters rim height changes via isostatic settling and small craters quantity

14 p2649 A70-31213

Lunar cratering rates from Apollo flights data on solidification ages for Mare Tranquillitatis

16 p2979 A70-34037

Radar reflectivity correlations with lunar surface structure in Mare Imbrium, using delay-Doppler radar maps

17 p3154 A70-34568

Mare Orientale positive gravity anomaly

17 p3158 A70-34865

Lunar regolith depth measurement by Lunar Orbiters 4 and 5 high resolution photographs, discussing thickness relation with sinuous rilles in marial regions

18 p3319 A70-37054

Lunar surface features charting from astrophysical data and direct observation, describing mapping of Sea of Tranquillity

18 p3323 A70-37141

Lunar maria rock thickness estimation, giving depth vs diameter diagrams for craters to show procellarian system thickness

19 p3516 A70-37982

Lunar geomorphological charts of Mare Imbrium southern region, emphasizing crater and maria formations

19 p3516 A70-37983

Lunar geomorphological charts of Mare Nubium northern part, considering structural features in equatorial band

19 p3517 A70-37984

Lunar geomorphological charts in Archimedes crater and Appennine and Haemus mountain region, examining duration and stages in Mare Imbrium depression development

19 p3517 A70-37986

Lunar maria distribution, explaining origin and characteristics by surface brightness

19 p3517 A70-37987

Lunar craters, walled plains and maria compared with volcanic formations on earth

19 p3517 A70-37991

Lunar maria and constituents characteristic differences in terms of structure, height and distribution of craters across surface, noting temperature anomalies

19 p3518 A70-37993

Lunar sea, mascon and interior composition, discussing crystallization of Apollo 11 Tranquillity samples and synthetic analogs at high pressure

21 p3901 A70-41542

Tranquillity Base regolith origin, examining thickness exposure histories, crater distribution and composition

21 p3918 A70-41677

Lunar maria and circular basins interrelations, form, origin and distribution from Lunar Orbiter photographs

23 p4242 A70-44263

Lava thickness measurement in lunar maria from projecting rim width of partially buried craters

23 p4242 A70-44292

LUNAR MOBILE LABORATORIES

Dynamical motion of Lunar Hopping Laboratory in plane change maneuver between ballistic and foot-in-contact phases

13 p2384 A70-28523

Mobile geochemical laboratory for in situ radiation measurement and elemental analyses in lunar exploration

15 p2717 A70-31801

LUNAR MODULE

Apollo spacecraft hardware, command, service and lunar modules, discussing design factors and tests contributing to spacecraft reliability

[AIAA PAPER 69-1095]

01 p0194 A70-10618

Computerized thermal model simulating environment control system, crew and vehicle structure in performance prediction for Apollo lunar module

[SAE PAPER 690621]

05 p0922 A70-15848

Spacecraft telecommunication and tracking systems in Gemini, Mercury and Apollo programs, emphasizing Apollo command and lunar modules equipment and mission ground stations

05 p0813 A70-16326

Lunar module motion during optimal ascent from moon surface into circular orbit of command module, noting descent maneuver similarity

06 p1155 A70-17881

Lunar module rendezvous with command and service module by coelliptic sequence establishing standard lighting and relative position and velocity for final approach

[AIAA PAPER 70-26]

06 p1157 A70-18129

Thermal vacuum simulator for testing manned Lunar Module Test Vehicle, using conformal skin heaters to control heating rates and skin temperature

09 p1656 A70-23241

Apollo lunar module manned testing in thermal vacuum, emphasizing safety aspects of hardware, procedures and training

10 p1859 A70-24389

Apollo lunar module mechanical acceptance tests evaluation based on reported flight anomalies review

[AIAA PAPER 70-401]

10 p1951 A70-24904

Apollo Lunar Module Test Program Management, discussing test requirements optimization, control, planning, etc.

[AIAA PAPER 70-368]

10 p1952 A70-24932

Lunar gravity correlation with large craters indicated from negative accelerations recorded in Apollo 12 lunar module Doppler radio tracking data

12 p2298 A70-27270

Minimum-time thrust vector control law in Apollo lunar module computerized autopilot

13 p2499 A70-28399

Real time Apollo lunar module thermal mission data analysis using computer programs

14 p2653 A70-30774

Mission simulation testing in thermal vacuum environment for Apollo Lunar Module, noting conformal skin heaters

[AIAA PAPER 69-991]

15 p2718 A70-32515

Flight performance of Apollo LM descent-ascent propulsion systems, considering telemetry data, prediction correlation and modifications

[AIAA PAPER 70-673]

16 p2967 A70-33577

Apollo lunar module rendezvous radar redundant gyro system for reliability enhancement, discussing principles and logic

16 p2983 A70-34066

Apollo lunar module alightment system, discussing design, performance and reliability

16 p2985 A70-34122

LM-Apollo rendezvous radar and transponder electronic assemblies packaging and mechanical design

18 p2322 A70-36762

Apollo Lunar Module strapdown Abort Guidance system, correlating performance prediction with flight test results

[AIAA PAPER 70-1028]

20 p3666 A70-39509

Ground based radar tracking data processing method for real time information concerning lunar module /LM/ position and velocity during Apollo 12 flight

[AIAA PAPER 70-1020]

20 p3591 A70-39514

Lunar module digital autopilot design, considering attitude state estimator, reaction control system and thrust vector control

[AIAA PAPER 70-991]

20 p3668 A70-39539

Multiple revolution lunar module reentry problem, analyzing isotropic systems trajectory, reentry environment, thermal response and ablation

[AIAA PAPER 70-989]

20 p3714 A70-39540

Manual attitude control for Lunar Module employing directional stability, coordinated turn and attitude command

20 p3716 A70-39683

Apollo 12 lunar module impact laboratory simulation, investigating possible downrange ballistic effects and cratering process

20 p3709 A70-39976

Lunar and earth surfaces imaging for astronaut training in LEM simulator

20 p3607 A70-40320

Lunar module systems design, describing R and D program and landing mission

21 p3928 A70-40977

Lunar module simulator for Apollo flight training using computers, digital conversion, cockpit replica, infinity-optics display and instructor control

21 p3805 A70-41196

Lunar module rendezvous with command and service module by coelliptic sequence, establishing standard lighting and relative position and velocity for final approach

[AIAA PAPER 70-26]

21 p3931 A70-41860

LUNAR MODULE ASCENT STAGE

Acoustic cavities use in suppressing acoustic modes of combustion instability demonstrated on LM ascent engine

[AIAA PAPER 70-618]

16 p2998 A70-33614

LUNAR OBSERVATORIES

Extrasolar planets photometric observations by telescopic mirror system on moon far side

20 p3710 A70-40131

Lunar based astronomical research program logistics model taking into account scientific mission, launch vehicle capacities, supply and support requirements, etc.

20 p3710 A70-40336

Lunar based vs orbiting astronomical observatories, discussing limitations imposed by geocorona

22 p4108 A70-43630

LUNAR OCCULTATION

NT SOLAR ECLIPSES

Brightness distributions and widths determined from monochromatic radiation intensity at earth during lunar occultation of RF source

05 p0920 A70-16941

Formaldehyde absorption profile in direction of Milky Way center observed using lunar occultation

10 p1936 A70-23905

Radio receiver bandwidth effect on lunar occultation observations

12 p2189 A70-27989

Lunar occultation observation of Jupiter by radio telescope, determining one dimensional strip brightness distribution

14 p2648 A70-31086

S band telemetric signals reception transmitted by Apollo 12 during occultation behind lunar disk, discussing lunar surface reflectivity

15 p2699 A70-32290

Weak radio sources positions, structures and optical identifications from lunar occultation observations, tabulating radio and optical data

17 p3156 A70-34826

Lunar occultation photoelectric measurement covering star angular diameters and diffraction patterns, ephemeris theory, astrometry close double star detection, etc.

17 p3170 A70-35440

High speed photoelectric measurements of lunar occultation using computer and nuclear physics instrumentation

17 p3171 A70-35441

Lunar occultation photoelectric measurements, investigating irregularities of occulted stars

17 p3171 A70-35442

Lunar longitude secular acceleration from occultation observations

17 p3171 A70-35444

Galactic center region lunar occultations in 21 cm neutral hydrogen line

18 p3313 A70-36328

Jovian continuum radiation observation by RAE-1 during lunar occultations

19 p3512 A70-38608

Watts lunar limb correction charts parameters solution, using grazing and total stellar occultations by moon

20 p3705 A70-39478

Pulse counting photoelectric photometer for lunar occultation recording of stars, discussing design, associated equipment and operation principles

22 p4030 A70-42860

Model fitting procedure applied to lunar occultation data and models analysis for point sources, close binaries and resolvable stars

24 p4399 A70-45130

LUNAR ORBIT AND LANDING SIMULATORS

Visual simulation in Lunar Module Mission simulator provided by computer controlled infinity optics system

06 p1031 A70-18603

Lunar landing training vehicle using Lunar Module free flight simulator for earth practicing of final descent handling

21 p3750 A70-41193

Command module simulators for Apollo astronaut training in moon landing, using computer, exterior visual scenes and spacecraft interior replica

21 p3804 A70-41195

Lunar module simulator for Apollo flight training using computers, digital conversion, cockpit replica, infinity-optics display and instructor control

21 p3805 A70-41196

LUNAR ORBITAL RENDEZVOUS

Lunar module rendezvous with command and service module by coelliptic sequence establishing standard lighting and relative position and velocity for final approach
[AIAA PAPER 70-26] 06 p1157 A70-18129
Apollo Guidance Computer operations and functions during lunar orbit rendezvous

13 p2446 A70-28390
Lunar module rendezvous with command and service module by coelliptic sequence, establishing standard lighting and relative position and velocity for final approach
[AIAA PAPER 70-26] 21 p3931 A70-41860

LUNAR ORBITER

Lunar origin theories, considering lunar surface data from Surveyor spacecraft and Lunar Orbiter
01 p0178 A70-10453
Spacecraft longitudinal control during reentry of Lunar Orbiter into atmosphere, analyzing final range prediction, trajectory tracking and accelerometers performance

01 p0197 A70-11497
Lunar gravitational field determination from analysis of Lunar Orbiter spacecraft tracking data

03 p0562 A70-12915
Nonexistence of large mascons at Mare Marginis and Mare Orientale deduced from residual acceleration analysis of Lunar Orbiter Doppler tracking data
04 p0743 A70-14424

Lunar mascon effects on Apollo type spacecraft orbits calculated for minimizing orbital instabilities
07 p1387 A70-19715

Moon gravity field model derived from long-arc analysis of Lunar Orbiters tracking data, considering lunar mass distribution role

09 p1752 A70-22309
Lunar Orbiter spacecraft vibration responses based on mathematical models, comparing results with experiment

12 p2315 A70-27098
Mascons in lunar maria depressions observed by Lunar Orbiter 5 on basis of two layer model of crust

12 p2299 A70-27281
Lunar spaceports for military uses from legal viewpoint, considering Space Treaty

12 p2336 A70-27774
Photographic apparatus for lunar orbiters and Apollo spacecraft, describing lunar surface closeup camera for astronauts, launch photographing, etc

13 p2406 A70-28926
Photographic techniques and optical equipment in orbiter missions for lunar surface photography

13 p2407 A70-29164
Lunar Orbiter Spacecraft Guidance and Control, discussing design and flight results

14 p2613 A70-30455
Lunar surface large scale maps by photogrammetric method requiring triangulation of convergent high resolution Lunar Orbiter photographs by block process

16 p2979 A70-34045
Lunar Orbiter photo subsystem mechanisms, discussing film transport, vacuum and mechanical clamps, focal plane shutter, processor-dryer and optical mechanical scan

16 p2914 A70-34146
Manned lunar orbital research operations capability, systems and scientific objectives

[AAS PAPER 70-022] 17 p3156 A70-34800
Lunar mass and gravitational fields determined from lunar satellite dynamics

24 p4407 A70-45533

LUNAR ORBITS

Reentry trajectories from lunar surface and orbit obtained by computer with allowance for initial data spread

01 p0191 A70-11476
French laser reflectors for lunar telemetry functioning with ruby laser, discussing applications to lunar orbital parameters, continental drift, gravity constant secular variations, etc

04 p0700 A70-14609
Lunar ephemeris, lunar theory constants and coordinate system corrections based on conditional equations formulated by analytical partial derivatives

05 p0908 A70-16334
Apollo lunar orbit irregularities attributed to mascons beneath lunar surface, using short arc perturbation method

[AIAA PAPER 70-163] 06 p1145 A70-18068
Transposition and lunar docking simulation tests for Apollo 9 and subsequent missions using test vehicles equipped with flight type hardware

[AIAA PAPER 70-170] 06 p1030 A70-18209
Lunar periodicity detected from radio aurora data as possible cause of lunar interaction with magnetosphere

07 p1389 A70-20164
Tidal friction induced secular changes in earth-moon system near minimum of angular momentum of moon orbit, including temporal changes in moments of inertia

08 p1579 A70-21570

Satellite motion in lunar orbit by von Zeipel method, considering perturbations due to nonspherical lunar gravity field and earth and solar attraction

10 p1939 A70-24186
Light pressure induced secular effect contributing to planetary satellites and lunar orbits evolution calculated by numerical integration

11 p2118 A70-26777
Navigation for lunar parking orbit with time varying osculating orbital elements, using Apollo 11 Doppler tracking data

14 p2613 A70-30457
Lunar gravitational effects on navigation in low altitude lunar orbits using Apollo 12 data

14 p2613 A70-30460
Synchronous navigation satellite system for ships and aircraft applicable to earth orbital and lunar operations

14 p2614 A70-30463
Translational-rotational motion of axisymmetrical moon in earth gravitational field

15 p2803 A70-32496
Mascon effects on close lunar orbit, using short arc perturbation technique

18 p3314 A70-36518
Transposition and lunar docking simulation tests for Apollo 9 and subsequent missions using test vehicles equipped with flight type hardware

20 p3606 A70-39685
Perturbation of body motion in vicinity of smallest primary according to Huang model of restricted four body problem, discussing near lunar satellite application

21 p3884 A70-40874
Lunar mascon detection in Sinus Aestuum neighborhood by Apollo 8 tracking data analysis

21 p3886 A70-41058
Solar eclipse calculation and prediction, discussing relationship between possible forms and earth-moon orbital configurations

21 p3924 A70-42173
Lunar origin by capture, discussing moon orbit evolution, thermal history and surface features, earth evolution and tidal interactions

22 p4098 A70-42550
Lunar orbital science, discussing U.S. and Soviet missions, NASA plans and results concerning remote sensing, force field and particle studies

22 p4105 A70-43144
Translational-rotational motion of axisymmetrical moon in earth gravitational field

23 p2420 A70-43917
Lunar theory literal solution for average node and perigee movements compared with Delaunay results, using Lie transforms for Hamiltonian function

24 p4399 A70-45141
Solar and terrestrial perturbations on lunar satellite calculated by Brown theory

24 p4407 A70-45534

LUNAR PERTURBATION

U LUNAR EFFECTS

LUNAR PHASES

Thunderstorm frequencies related to lunar phase and declination for ground stations in eastern and central U.S.

22 p4018 A70-42909
Quiet sun and new moon brightness temperature measurements at 3.3 and 5.7 mm wavelengths, giving radiometric maps

23 p4241 A70-44254

LUNAR PHOTOGRAPHS

Visual interpretation of moon and Mars surface photographs taken from satellites, analyzing craters and bumps

04 p0686 A70-14626
Cartographic tying-in of Zond 3 lunar surface photographs to verify maps of moon far side

05 p0918 A70-16918
Apollo 10 and 11 photographs revealing probable igneous intrusions on lunar farside crater

06 p1137 A70-17195
Selenodetic investigations based on lunar photographs with background stars, converting equatorial coordinates to orbital using Cracovian formulas

08 p1564 A70-20560
Selenocentric coordinate system originating at center of mass, determining lunar figure center from photographs with reference stars

08 p1572 A70-20942
Lunar photographs on star-calibrated plates for lunar features coordinates or physical libration determination, outlining photographic technique and computer program

09 p1674 A70-22308
Lunar dimple /drainage/ craters formation mechanisms, considering analogous earth drainage craters associated with lava tubes

09 p1666 A70-22311
Extraterrestrial photogrammetry role in lunar photographs analysis, considering landing site triangulation and selection, coordinate system improvement, etc

10 p1948 A70-25046

Ranger lunar photographic evidence for volcanic hypothesis, considering fracture systems, Caldera analogy, common walls, crater size, etc

12 p2977 A70-26985
Ballistic model for lunar regolith evolution based on lunar surface characteristics from Surveyor TV pictures

14 p2644 A70-31053
Lunar atmospheric pressure based on twilight horizon photographic data from Surveyor 7

15 p2803 A70-32500
Selenodetic investigations based on lunar photographs with background stars, converting equatorial coordinates to orbital using Cracovian formulas

15 p2805 A70-32715
Selenocentric coordinate system originating at center of mass, determining lunar figure center from photographs with reference stars

15 p2806 A70-32754
Mariner 7, 8 and 9 lunar photographs, discussing evidence for internally heated moon

16 p2973 A70-33112
Lunar atmospheric pressure based on twilight horizon photographic data from Surveyor 7

23 p4240 A70-43921

LUNAR PHOTOGRAPHY

Ranger, Surveyor and Lunar Orbiter televised and reconstructed picture quality, suggesting improvements in existing photographic systems

03 p0490 A70-13656
Lunar surface far side stereoscopic photography by Apollo 8 mission considered for lunar control

04 p0686 A70-14618
Multiband photographic system for automatic earth resources aerial sensing and lunar orbital mapping with manual override provisions

[AAS PAPER 69-582] 04 p0687 A70-14657
Surveyor 7 alpha scattering experiment and TV image data revealing lunar surface chemical composition, rocks and fragments, etc

04 p0752 A70-15060
Lunar photography interpretation, discussing topographic maps obtained by spacecraft

07 p1284 A70-19779
Lunar Orientale region structure geological interpretation based on Lunar Orbiter 4 photographs

09 p1751 A70-22196
Photographic apparatus for lunar orbiters and Apollo spacecraft, describing lunar surface closeup camera for astronauts, launch photographing, etc

13 p2406 A70-28926
Photographic techniques and optical equipment in orbiter missions for lunar surface photography

13 p2407 A70-29164
Lunar surface terrain types and chemical composition based on Surveyor pictures

14 p2634 A70-30193
Lunar color differentiation by computer image processing compared to earth based photoelectric photometry

[JPL-TR-32-1472] 16 p2900 A70-33097
Lunar surface large scale maps by photogrammetric method requiring triangulation of convergent high resolution Lunar Orbiter photographs by block process

16 p2979 A70-34045
Planetary and lunar photography at French observatory, discussing Pic du Midi facilities and various photographic emulsions

17 p3082 A70-34676
Surveyor 7 TV system in photon integration mode, analyzing slow scan vidicon storage characteristics and dark current limitations

[SMPT PAPER 105-72] 17 p3095 A70-35635
Lunar volcanic ridges features from interpretation of photographs by telescopes and satellites

19 p3518 A70-37992
Lunar sinuous rilles morphological and distributional observations and implications on theories of origin concerning surface water erosion

19 p3521 A70-38442
Lunar surface spectral reflectivity measured with ground based telescopes for remote mineralogical analysis

20 p3709 A70-39977
Pulsed laser radar tracking and ranging system for monitoring and directing TV camera at astronaut position on lunar surface

22 p3992 A70-43604
Apollo 11 and 12 close-up lunar surface photography, describing specially designed camera

23 p4194 A70-44255
Lunar maria and circular basins interrelations, form, origin and distribution from Lunar Orbiter photographs

23 p4242 A70-44263
Lunar topography from UBVR1 photometry, determining albedos for mountains, dark and light maria and cratered terrae

23 p4247 A70-44769

LUNAR PROBES

NT LUNIK LUNAR PROBES

NT LUNIK 3 LUNAR PROBE

NT LUNIK 12 LUNAR PROBE

NT RANGER LUNAR PROBES

LUNAR PROGRAMS

- NT SURVEYOR LUNAR PROBES
NT SURVEYOR 5 LUNAR PROBE
Cable involving woven multiconductor arrangement and aromatic polyimide insulations to connect thermal moon probe with transmitter for temperature measurements on lunar surface
05 p0798 A70-16034
Celestial methods for lunar navigation, considering terrestrial and selenographic differences
14 p2613 A70-30459
Lunar remote probing by IR and microwave thermal emission and by radar
14 p2644 A70-31056
Saturn 5 launch vehicle targeting methods for lunar missions, solving earth departure variables via iterative process
[ALAA PAPER 70-1052] 19 p3528 A70-38867
- LUNAR PROGRAMS
NT APOLLO PROJECT
NT SURVEYOR PROJECT
Development models for post-Apollo lunar cargo delivery system utilizing Saturn 1B and Centaur stages [DGLR-69-9] 04 p0763 A70-15187
Lunar exploration program based on U.S. antarctic research experience, considering man role, environment, logistics, transportation, economics, etc
15 p2800 A70-32058
- LUNAR RADAR ECHOES
Diffuse component of lunar radar echoes, using model with volume backscattering from within lunar regolith, noting rocks permissivity
05 p0816 A70-16826
Clock synchronization system using lunar radar reflections for Deep Space Network needs, discussing remote clock receiver and antenna
09 p1656 A70-23037
Lunar radar echoes wavelength dependence in terms of backscattering behavior
10 p1841 A70-24644
Ionospheric scintillations of lunar radar echo components isolation by CW Doppler shift or coherent pulse time delay techniques
10 p1841 A70-24802
Lunar surface specific effective radio signal scattering area measured by Luna 9 and 13, describing signal fluctuations
21 p3884 A70-40838
Radar astronomical polarization measurements for lunar echoes by exploiting ionospheric Faraday rotation with linearly polarized antenna
23 p4165 A70-44964
- LUNAR RADIATION
Lunar neutron flux due to cosmic radiation interaction with lunar surface layer, determining angular distribution and energy spectrum
04 p0738 A70-14442
Normal albedo of Apollo 11 landing site and intrinsic dispersion in lunar Heiligenschein determined from Apollo and earth based photographic photometry
04 p0747 A70-14549
Radio emission measurements of moon at 3.2 cm by artificial moon method, calculating radio temperature and phase amplitudes
05 p0918 A70-16919
Book on moon covering motion, earth-moon system, internal structure, hydrostatic equilibrium, thermal history, global form, gravitation, topography, etc
12 p2298 A70-27096
Neutron flux due to cosmic radiation interaction with lunar surface layer, determining angular distribution and energy spectrum
13 p2475 A70-28467
Lunar horizontal and inclined surfaces net radiation and components, discussing surface temperature, thermal emission and absorbed solar radiation
14 p2634 A70-30194
Lunar surface thermal emission spectra, calculating IR emissivities
14 p2637 A70-30495
Lunar remote probing by IR and microwave thermal emission and by radar
14 p2644 A70-31056
Lunar IR radiation measurements for estimating thermophysical properties and small scale surface nature
14 p2645 A70-31057
Balloon-borne midinfrared observations of lunar surface composition from interpreting peak emissivity differences
14 p2645 A70-31058
Lunar surface roughness effects on thermal radiation, using model surface with parallel troughs
14 p2649 A70-31212
Pulverization effects on lunar rocks albedo under full moon conditions for different grain sizes, noting inverse relation to absorption coefficient
14 p2649 A70-31214
Lunar millimeter wavelength thermal radiation measurement noting surface roughness effect on polarization
17 p3171 A70-35559
Moon as standard radio source for eliminating earth atmosphere influence during solar radio radiation measurements
19 p3522 A70-38564

- LUNAR RAYS
Photometric investigation of lunar crater rays of Tycho, Copernicus, Kepler and Aristarchus compared with terrestrial explosion craters
07 p1377 A70-18972
- LUNAR RECEIVING LABORATORY
Bioscience for recovered lunar samples, discussing Surveyor analyses, Lunar Receiving Laboratory methods and life detection using biological markers
01 p0042 A70-11637
Environmental control underground low level radiation counting facility of Lunar Receiving Laboratory for gamma ray spectrometry, including radon adsorption system
05 p0829 A70-16707
Environmental engineering at NASA MSC, surveying Lunar Receiving Laboratory, microbe incinerator, radon adsorption, Apollo Post-Landing Environmental Test Tank and vacuum chamber
10 p1860 A70-24411
Viable organisms in Apollo 11 lunar fines, discussing tests, laboratory and sterile biological barrier system
21 p3911 A70-41634
Apollo 11 rocks natural remanence and induced magnetism by triaxial magnetic gradiometer at Lunar Receiving Laboratory
21 p3914 A70-41650
- LUNAR ROCKS
Physical, chemical, mineralogical and biological analysis of Apollo 12 lunar samples compared to Apollo 11 rocks, discussing landing site geologic setting
10 p1935 A70-23811
Synthetic silicate liquid viscosity with lunar rock composition compared with volcanic rock on earth
10 p1938 A70-24074
Carbon compounds composition and origin in Apollo 11 lunar samples using pyrolytic chromatography and microscopy at elevated temperature
10 p1941 A70-24531
Lunar rolling stones anomalous surfaces goniphotometric properties, considering bearing strength as rock density function
12 p2296 A70-26925
Methane and ethane released from Apollo 11 lunar samples by crushing or acid treatment, suggesting carbides hydrolysis as main source
12 p2304 A70-27719
Lunar rocks and dust from Apollo 11 mission investigated for origin and history of moon and solar system
12 p2310 A70-28049
Rb-Sr internal isochrons of crystalline lunar rocks from Tranquility Sea for moon age estimation
13 p2485 A70-28472
Lunar rocks isotopic composition for Gd and variations due to low energy neutron capture produced by cosmic ray interactions
13 p2485 A70-28473
U and Th abundances correlation in tektites and achondrites based on oxygen isotopic composition of lunar rock specimens
13 p2488 A70-28720
Solar flare proton induced radioactivity in Apollo 11 lunar surface material compared with stony meteorite data, noting cobalt 56 concentration
13 p2489 A70-28910
Anelasticity in lunar seismology, discussing low Q regolith layer model from Apollo 12 LP seismogram
13 p2497 A70-29857
Moon rocks nature and mineralogical constitution, describing methods for age determination
14 p2634 A70-30275
Carbon and sulfur reactions with solar hydrogen atoms in Apollo 11 lunar samples accounting for isotopic composition of fine-grained basaltic rocks
14 p2545 A70-30791
Tektite glass in lunar sample from Apollo 12, discussing chemical composition and possible volcanic origin
14 p2642 A70-30983
Ballistic model for lunar regolith evolution based on lunar surface characteristics from Surveyor TV pictures
14 p2644 A70-31053
Lunar soil and rocks photometric and polarimetric properties from high resolution Surveyor pictures
14 p2644 A70-31054
Polarized and depolarized radar maps of moon, attributing anomalies and average diffuse component of echoes to scattering behavior of surface and subsurface rocks
14 p2645 A70-31060
Pulverization effects on lunar rocks albedo under full moon conditions for different grain sizes, noting inverse relation to absorption coefficient
14 p2649 A70-31214
Apollo 11 lunar mission results, discussing surface, seismology, laser ranging retroreflector, solar wind and rock samples
15 p2800 A70-32073
Ionization potentials of elemental abundances in lunar rocks compared with earth crust and class I carbonaceous chondrites, showing lunar materials differentiation
15 p2801 A70-32463

- Rb-Sr internal isochron ages from Ocean of Storms, discussing analytical results of two texturally and mineralogically distinct crystalline rocks from Apollo 12
16 p2975 A70-33659
Sound velocity differences related to composition of lunar and terrestrial rocks
16 p2978 A70-33973
Apollo 11 lunar rocks mineralogy and petrology, noting anorthosite in powder and breccia
18 p3320 A70-37081
Apollo 11 lunar rocks and dust from Tranquility Sea measured for age by Rb-Sr and K-Ar methods
18 p3320 A70-37082
Mass spectrometric analysis of lunar rocks for rare gases of solar wind, determining relative abundance, isotopic composition, rock age, exposure time, etc
18 p3320 A70-37083
Heavy ions traces in crystals of lunar rocks, discussing applications as detectors
18 p3321 A70-37084
Apollo 12 rock and dust analyses, discussing modifications to conclusions from Apollo 11 samples with reference to rare gas concentrations
18 p3321 A70-37085
Lunar rocks permissivity and density and surface roughness from radio wave scattering data
19 p3512 A70-37276
Lunar rock origin based on apollo samples density, impurities and mineral and chemical composition, considering structure and genesis of crust and mantle
19 p3513 A70-37524
Lunar geomorphological map technique, discussing lunar rock formation classifications
19 p3516 A70-37981
Lunar maria rock thickness estimation, giving depth vs diameter diagrams for craters to show procellarian system thickness
19 p3516 A70-37982
Clinopyroxenes from Apollo 12 rocks studied by X ray diffraction and electron microprobe methods, noting phenocrysts, chemical composition and crystallization
19 p3519 A70-38033
Lunar fragmental debris layer observations from Surveyor project, examining size, shape, texture, structure, etc
20 p3707 A70-39955
Lunar fragmental debris physics from Surveyor observations, examining size-frequency distribution
20 p3707 A70-39956
Lunar soil from Apollo 12, identifying chemical composition of orthopyroxene-calcic plagioclase rock fragments for origin
20 p3709 A70-39980
Lunar rocks almandine-rich garnet chemical composition and crystallography, noting cell edge and refractive index
21 p3883 A70-40711
Apollo 11 mafic crystalline rocks and mineral assemblages, discussing collection, classification and sample environments
21 p3894 A70-41502
Apollo 11 magnesium-rich opaque oxide almalcolite mineral from Tranquility Base noting relation to pseudobrookite series
21 p3895 A70-41503
Calcium-bearing iron silicate (pyroxferroite) from Apollo 11 lunar Tranquility Base samples, discussing petrographic environment, physical and optical properties
21 p3895 A70-41504
Titanian and aluminian chromites and chromian ulvöspinel in Apollo 11 fines, microbreccias and basaltic type igneous rocks
21 p3895 A70-41505
Electron microprobe and petrographic analyses of crystalline rock and separates from apollo 11 lunar soil samples
21 p3895 A70-41506
Apollo 11 lunar rock and fines chemistry, mineralogy and petrology, discussing composition, igneous rocks, microbreccias, glasses and pyroxene relations
21 p3895 A70-41507
Lunar crystalline rock melting at atmospheric pressure under partial oxygen pressure, suggesting crystallization temperature
21 p3895 A70-41508
Trace elements in Apollo 11 lunar glass clinopyroxene, plagioclase and ilmenite, using ion microprobe mass analyzer
21 p3896 A70-41510
Apollo 11 lunar rocks, breccias, dust and chip mineralogy and petrology, examining composition, texture, grain size and morphologies
21 p3896 A70-41511
Apollo 11 lunar igneous rocks mineralogical, chemical and petrological features by optical and electron microscopy and X ray spectrometry
21 p3896 A70-41512
Opaque minerals in Apollo 11 lunar igneous and fragmental rocks, using reflecting microscope and electron microprobe
21 p3896 A70-41513

- Apollo 11 lunar soil volcanic rock samples, mineralogical and petrological description and surface features 21 p3896 A70-41514
- Lunar crystalline rock static and dynamic deformation, examining regolith and silicates textures and structures 21 p3897 A70-41515
- Apollo 11 lunar crystalline rock samples petrology, discussing shock and other metamorphic effects on mineral structure 21 p3897 A70-41516
- Petrology, mineralogy and deformation of Apollo 11 rock samples using microscopic, X ray and electron microprobe methods 21 p3897 A70-41517
- Trace phyllosilicates in Apollo 11 soil sample and rock, using electron microscopy and diffraction studies 21 p3897 A70-41518
- Petrologic analyses of minerals and glass spherules in Apollo 11 lunar rocks, indicating little fractionation and shallow-level differentiation 21 p3897 A70-41521
- Crystallography of euhedral single crystals from lunar troilite indicating hexagonal forms consistent with high temperature NiAs type structure 21 p3898 A70-41522
- Apollo 11 lunar rock pyroxenes, examining band structure and magnetic ordering by high voltage electron microscopy and electron diffraction 21 p3898 A70-41523
- Petrography and shock vaporization origin of Apollo 11 lunar breccias and glasses compared to terrestrial impactites and chondrites 21 p3898 A70-41524
- Apollo 11 lunar rock mineralogy, examining petrographic and chemical features by light microscopy, electron microprobe microanalysis and detector system 21 p3898 A70-41525
- Bulk chemical compositions, mineral and glass analyses, X ray data and physical properties of Apollo 11 lunar fines and rocks 21 p3898 A70-41526
- Apollo 11 lunar rock fluorapatite and trace minerals, examining pressure and oxidizing conditions of formation, grain and crystallization 21 p3898 A70-41527
- Plagioclases, pyroxenes and olivines in lunar soils and rocks, using X ray diffraction and Mossbauer effect 21 p3899 A70-41528
- Lunar breccia and fine sample metal particles, using optical and scanning electron microscopy and electron probe microanalysis 21 p3899 A70-41529
- Apollo 11 lunar rock lavas and breccias, examining opaque minerals and olivine by reflection microscopy, electron probe and optical absorption measurements 21 p3899 A70-41530
- Compositions of lunar fines, crystalline rock and glass spherules, showing high normative anorthite 21 p3899 A70-41531
- Compositional zoning in pyroxenes from grained Apollo 11 microgabbros, implying supercooled magma origin 21 p3899 A70-41532
- Apollo 11 lunar samples mineralogical and compositional studies concerning lunar origin hypothesis 21 p3899 A70-41534
- Shock metamorphic granular mafic holocrystalline lithic fragments, microbreccia, glass and anorthosite from Apollo 11 lunar surface material at Tranquility Base 21 p3900 A70-41535
- Petrology, crystallization and magma origin of lunar clinopyroxene, ilmenite-rich dolerite and microgabbro from Apollo 11 samples 21 p3900 A70-41536
- Fission track uranium distribution studies of Apollo 11 lunar volcanic rocks, using Lexan plastic print method 21 p3900 A70-41537
- Apollo 11 lunar igneous rocks minerals and glassy phases characteristics, using electron probe microanalysis 21 p3900 A70-41538
- Mineralogy and petrology of lunar rock samples indicating meteoritic increments 21 p3900 A70-41539
- Apollo 11 samples compared to stony meteorites and terrestrial basalt, discussing lunar rock formation processes 21 p3900 A70-41540
- Glass spherule lunar particles and breccia from Apollo 11 site, showing passage through impact generated cloud of hot fragmental material 21 p3901 A70-41541
- Shock metamorphism, grain size and mineralogy of lunar surface regolith materials 21 p3901 A70-41543
- Apollo 11 lunar rock clinopyroxene, plagioclase and ilmenite internal substructure, using high voltage transmission electron microscopy 21 p3901 A70-41544
- Mineral chemistry of Apollo 11 igneous rocks, soil and breccia samples, comparing with meteorites 21 p3773 A70-41545
- Apollo 11 lunar rock samples alpha particle activity in polished thin sections, using audioradiography and electron microprobe 21 p3901 A70-41546
- Apollo 11 lunar basalt petrogenesis, examining internal constitution and origin by high pressure 21 p3901 A70-41547
- Lunar petrology of silicate melt inclusions from Apollo 11 rock samples, discussing heating experiments 21 p3902 A70-41548
- Apollo 11 lunar rocks and fines, examining clinopyroxenes augite and pigeonite by single crystal X ray diffraction microprobe optical and electron optical techniques 21 p3902 A70-41549
- Apollo 11 lunar rock and fines shock induced and melting microstructural mineral damage, discussing meteorite bombardment, phases without melting and microbreccia 21 p3902 A70-41550
- Shock metamorphism in lunar microbreccias and loose regolith materials, assuming crater formation by meteorite impacts 21 p3902 A70-41551
- Quantitative optical and electron probe studies of opaque phases in Apollo 11 lunar rocks 21 p3902 A70-41552
- High crystallization temperatures for igneous rocks from Tranquility Base indicated from late formation of sulfide liquid forming complex troilite intergrowths and iron 21 p3902 A70-41553
- Lunar rocks petrography, mineralogy and petrogenesis from Apollo 11 samples 21 p3902 A70-41554
- Apollo 11 lunar rock plagioclases crystallography, obtaining single crystal X ray diffraction patterns by Buerger precession method 21 p3903 A70-41555
- Apollo 11 lunar igneous rock mineralogy and petrology, emphasizing ferrobasalt minerals microanalysis electron probe 21 p3903 A70-41557
- Apollo 11 lunar anorthosites properties and characteristics, discussing grain size, Na content, color, density, chemical composition and geomorphic effects 21 p3903 A70-41559
- Apollo 11 lunar rock trace elements, examining basalt, gabbroic igneous rocks, breccias and fines by DC arc emission spectroscopy 21 p3774 A70-41561
- Apollo 11 lunar rocks and fines cosmic ray produced radioisotopes, considering surface exposure to high energy component flux 21 p3906 A70-41562
- Apollo 11 lunar rocks, breccias and fines age and chemistry, major element, trace element and rare earth abundances, texture, crystallization and meteoritic effects 21 p3906 A70-41563
- Tritium and Ar radioactivities attributable to galactic and solar cosmic ray interactions in Apollo 11 lunar rocks and soil 21 p3906 A70-41564
- Apollo 11 lunar rocks and fines oxygen, Si and Al content determination by neutron activation analysis 21 p3774 A70-41566
- Lunar rock composition difference from meteorites and terrestrial basalts, indicating complexities in solar abundances and initial earth and moon compositions 21 p3906 A70-41567
- Apollo 11 lunar rocks and soil hydrogen, C and Si concentration and isotopic composition 21 p3774 A70-41568
- Apollo 11 lunar material trace elements, examining chemical processes during and after formation and meteoritic matter influx rate 21 p3907 A70-41572
- Apollo 11 lunar basalt chemical composition and petrogenesis, using stable isotope dilution method 21 p3907 A70-41573
- Apollo 11 lunar rocks elemental abundances determination by instrumental activation techniques 21 p3775 A70-41574
- Apollo 11 sample elemental abundances, investigating environmental, paragenetic and petrogenetic problems and moon evolution 21 p3907 A70-41575
- Apollo 11 lunar material isotopic age determination, discussing rock crystallization, radiogenic dust, lead isotope data and moon origin 21 p3907 A70-41576
- Apollo 11 lunar samples composition for Na 22, Al 26, Th and U, investigating positron activities 21 p3775 A70-41580
- Apollo 11 lunar matter rare gas, H and N concentrations and isotopic abundances, discussing solar wind, gas diffusion loss from silicates and spallation component 21 p3908 A70-41583
- Trapped and cosmogenic rare gases from stepwise heated Apollo 11 lunar dust and crystalline rocks, using mass spectrometry 21 p3908 A70-41584
- Apollo 11 lunar rock Rb-Sr isotopic age relationships, discussing magmatic fractionation of Rb relative to Sr in moon primordial material 21 p3908 A70-41585
- Rare gas distribution in grain surfaces of lunar soil, breccias and rocks originating from solar wind, using microhelium probe 21 p3908 A70-41587
- Neutron activation analysis for Re and Os in Apollo 11 volcanic rocks, discussing possible meteoritic contamination of secondary rocks and fines 21 p3775 A70-41589
- Apollo 11 lunar rocks and soil chemical composition, examining major, minor and trace elements 21 p3776 A70-41591
- Carbon and nitrogen abundances in Apollo 11 rocks, basaltic achondrites and terrestrial basalts, using meteorite analytical techniques 21 p3776 A70-41592
- Apollo 11 lunar rock and soil elemental abundances, discussing composition, volatile element depletion, rare earths, basalt and geochemical processes 21 p3909 A70-41593
- Trace elements K, Rb, Sr and Ba distributions and Rb-Sr isotopic relations in Apollo 11 lunar breccia and fine soil samples 21 p3909 A70-41594
- Apollo 11 lunar rock and fines primordial radionuclide abundances and concentration gradients by gamma ray spectrometry at Lunar Receiving Laboratory 21 p3776 A70-41595
- Apollo 11 lunar rocks oxygen isotope ratios, examining relationship to terrestrial basalts 21 p3776 A70-41596
- Oxygen isotope fractionation and formation temperature of minerals from Apollo 11 rocks, including plagioclase-clinopyroxene-magnetite concordancy diagram 21 p3776 A70-41597
- Apollo 11 lunar fines, breccia and crystalline rocks rare gas data, emphasizing trapped and spallation Ne, Kr and Xe isotopic compositions 21 p3909 A70-41598
- Cosmogenic and primordial radionuclides in Apollo 11 lunar soil and rocks, using nondestructive gamma ray spectral measurements 21 p3776 A70-41599
- Apollo 11 lunar rock K, Rb, Sr, Ba and rare earth element concentrations, examining relationship to terrestrial and chondritic levels 21 p3776 A70-41600
- Halogens, mercury, lithium and osmium concentration measurements in Apollo 11 samples, using neutron and photon activation 21 p3777 A70-41601
- Chemical composition and reducing capacity of Apollo 11 igneous rocks, breccia and soil fines, using semimicro X ray fluorescence 21 p3777 A70-41602
- Apollo 11 lunar rock and soil bombardment produced radionuclide patterns, discussing solar flare protons and alphas, age determination and astronomical models 21 p3777 A70-41604
- Apollo 11 lunar rocks, breccia and fines U, Th and Pb isotopes systematics, considering implications for lunar history 21 p3909 A70-41605
- Elemental abundances of Apollo 11 lunar rocks and soils, using activation analysis or mass spectrometric isotope dilution 21 p3909 A70-41606
- Cosmic ray exposure age of lunar surface material by radioactive isotopes Ar 37 and 39 measurement, investigating temperature dependence 21 p3909 A70-41607
- Apollo 11 lunar rocks and minerals oxygen 18-oxygen 16 ratios 21 p3777 A70-41609
- Chemical analysis methods for Apollo 11 lunar rocks, discussing calibration standards, spectral lines and Apollo 12 data 21 p3777 A70-41610
- Chemical analysis for Li, Na, K, Rb, Cs, Ca, Sr and Ba in achondrites and Apollo 11 lunar rocks, breccia and soil samples 21 p3910 A70-41611
- Apollo 11 lunar rocks and soil chemical elements analysis by neutron activation scheme 21 p3777 A70-41612
- Apollo 11 crystalline rocks chemical analysis by argon 40/argon 39 dating techniques 21 p3778 A70-41613

Apollo 11 lunar rocks, soil and core samples major, minor and trace elements abundance by radiochemical and instrumental activation analyses

21 p3910 A70-41614

Apollo 11 fines and rocks major and trace elements data obtained by combined instrumental and neutron activation analysis

21 p3910 A70-41615

Age determination of Apollo 11 samples from isotopic composition measurements by isotope dilution techniques, comparing to terrestrial and meteoritic values

21 p3778 A70-41616

Apollo 11 lunar, terrestrial and meteoritic basalts relationships, examining Ga, Ge, In, Ir and Au concentrations by neutron activation analyses

21 p3778 A70-41617

Apollo 11 lunar surface fine material and rocks cosmogenic radio nuclides Al 26 and Na 22 concentrations determination by gamma ray spectroscopy

21 p3910 A70-41618

Apollo 11 lunar dust and microbreccia micropaleontological examination, discussing biological morphology

21 p3778 A70-41620

Apollo 11 lunar samples organic carbon content analysis by pyrolysis hydrogen flame ionization detection

21 p3779 A70-41624

Volatilizable C compounds in lunar fines from Mare Tranquillitatis, investigating pyrolysis and acid hydrolysis products by mass spectroscopy and gas chromatography

21 p3779 A70-41628

Apollo 11 lunar samples organic compounds analysis by mass spectroscopy, gas and liquid chromatography and nuclear magnetic resonance

21 p3779 A70-41629

Apollo 11 fines and rocks analysis by chromatography, mass spectrometry and light and scanning electron microscopy

21 p3779 A70-41631

Apollo 11 lunar science - Conference, Houston, January 1970, Volume 3, Physical properties

21 p3911 A70-41636

Lunar rocks mineralogy and visible and near IR reflectivity, discussing depression in telescopic curve

21 p3912 A70-41637

Magnetic monopoles electromagnetic search in Apollo 11 rock samples

21 p3912 A70-41639

Micro-breccia, igneous rocks and lunar fines elastic properties at ambient conditions and as function of pressure, discussing near surface mare region models

21 p3913 A70-41640

Lunar rocks primordial accretion, examining ablation and transport of solids, liquid and vapor on surfaces

21 p3913 A70-41641

Apollo 11 rocks IR absorption properties, specific heat and thermal conductivity, discussing heat flow in surface layer

21 p3913 A70-41642

Directional, spectral and total reflectance for Apollo 11 fines and rock chips, observing dependence on illumination angle

21 p3913 A70-41643

Apollo 11 rocks red luminescence and blue thermoluminescence under proton bombardment, discussing energy efficiency

21 p3913 A70-41644

Apollo 11 rocks spectral reflectance and albedo before/after proton irradiation and vitrification, investigating color differences for lunar surface dark and bright areas

21 p3913 A70-41645

Apollo 11 lunar rock and soil mechanical behavior and physical characteristics, discussing color, specific gravity, density, shapes and adhesive and cohesive properties

21 p3913 A70-41646

Nuclear particle tracks in Apollo 11 samples due to galactic cosmic rays and solar flares relationship to dynamic surface processes

21 p3914 A70-41648

Apollo 11 fines, breccias and crystalline rocks thermoluminescence, observing temperature dependence of glow curve peaks

21 p3914 A70-41649

Apollo 11 rocks natural remanence and induced magnetism by triaxial magnetic gradiometer at Lunar Receiving Laboratory

21 p3914 A70-41650

Apollo 11 type C breccia sample remanent magnetism, observing viscous component with several hours time constant

21 p3914 A70-41651

Rock particle tracks of primary cosmic rays, spallation recoil nuclei, nuclear fission and solar wind ions, observing time scale multiple soil orientation

21 p3914 A70-41652

Apollo 11 drive-tube core samples from Tranquility Base, expressing lunar surface environmental processes

21 p3914 A70-41653

Apollo 11 lunar fines, rocks and breccias luminescence, electron paramagnetic resonance and optical properties, discussing reflection spectra, heating effects and dipole resonance

21 p3914 A70-41654

Luminescence efficiencies of Apollo 11 lunar and terrestrial rocks and minerals, using UV excitation

21 p3915 A70-41656

Fe 57 nuclear hyperfine splittings in clinopyroxenes from lunar igneous rocks, determining temperature dependent cation distribution

21 p3915 A70-41659

Apollo 11 lunar rock and dust samples thermomagnetic properties, Curie points, magnetization and demagnetization characteristics

21 p3915 A70-41661

Mossbauer effect spectrometry application to Apollo 11 lunar rocks composition, using nuclear gamma resonance measurements for nuclide Fe 57

21 p3916 A70-41662

Apollo 11 lunar specimen thermal diffusivity, conductivity and inertia in breccias and crystalline igneous rocks measured over wide temperature range

21 p3916 A70-41663

Apollo 11 lunar dust, breccia and igneous rocks, using Mossbauer spectroscopy and petrographic techniques

21 p3916 A70-41664

Thermoluminescence, X ray and stored energy measurements of Apollo 11 samples, comparing surface outputs to interior

21 p3916 A70-41665

Apollo 11 lunar sample elastic wave velocities at high pressures, examining P and S waves, Q value and geophysical implications

21 p3916 A70-41666

Apollo 11 bulk and core tube fines and rock cosmic ray tracks, discussing material history and corpuscular radiation flux and energy spectra near moon

21 p3916 A70-41667

Magnetic properties of Apollo 11 lunar breccia samples, determining natural remanent magnetization and susceptibility via paleomagnetism instruments and methods

21 p3916 A70-41668

Apollo 11 rock and fines magnetic resonance, examining line shapes, temperature dependences and electron spin

21 p3917 A70-41670

Lunar rocks magnetic properties and natural remanent magnetization, examining pyroxene paramagnetism, ferrosilite and ilmenite antiferromagnetism and native iron ferromagnetism

21 p3917 A70-41671

Proton and UV excited luminescence of Apollo 11 Tranquility rocks and fines, indicating solar wind impingement

21 p3917 A70-41672

Fe-group cosmic ray exposure tracks in Apollo 11 lunar rock interior, erosion rate and solar flare paleontology

21 p3917 A70-41673

Apollo 11 sample specific heats at 90-350 K, using adiabatic calorimeter

21 p3917 A70-41674

Apollo 11 lunar rock and fines magnetic properties, associating remanent magnetization with lunar magnetic field

21 p3917 A70-41675

Apollo 11 lunar crystalline rock and breccias petrography and luminescent properties, spectral analysis, color, emission bands and shock effects

21 p3918 A70-41678

Apollo 11 lunar crystalline rock, microbreccia and fines compressibilities at room temperature, loading-unloading and pressure volume curves

21 p3918 A70-41679

Apollo 11 lunar samples spectral analysis, discussing Fe and Mn electron paramagnetic resonance and Al 27 nuclear magnetic resonance spectra

21 p3919 A70-41683

Metallic Fe grains in Apollo 12 igneous rocks, discussing Ni and Co abundances

21 p3920 A70-41881

Lunar samples and terrestrial materials isotopic analyses, discussing mineralogical and chemical compositions for lunar origin

22 p4098 A70-42574

Apollo 11 lunar rock samples examined for clues to moon life

22 p3972 A70-43425

Crystalline rocks from Mare Tranquillitatis and Oceanus Procellarum, determining K-Ar ages

23 p4238 A70-43803

Terrestrial and synthetic lunar igneous rocks thermal conductivities in melting range, discussing thermal gradient

23 p4238 A70-43804

Tektite glass absence in Apollo 12 lunar sample

23 p4238 A70-43806

Apollo 11 ilmenite basalts petrology from regolith samples

23 p4239 A70-43898

Apollo 11 and 12 lunar landing sites surface properties from returned rocks chemical, physical and mineralogical analysis

23 p4241 A70-44221

Book on lunar rocks covering pre-Apollo lunar scientific knowledge, Apollo and future lunar mission planning, lunar mineralogy, petrology and geochemistry, etc

24 p4412 A70-46025

LUNAR ROVING VEHICLES

Optimal traction drive system design for lunar roving vehicle, considering weight, energy consumption, operational flexibility, power supply, motor and power train

11 p2030 A70-25375

Dead reckoning navigation of manned lunar roving vehicle /MLRV/, describing hardware and coordinate system

12 p2266 A70-27414

Apollo lunar roving vehicles for manned exploration, discussing design proposals

12 p2208 A70-27943

Lunar vehicle design, discussing dual power steering, switching and joystick control handle

12 p2208 A70-27944

Bendix design approach for lunar vehicle using operating mockup, noting trend towards lighter machines

12 p2208 A70-27945

Lunar roving vehicle stability and agility design approach by Grumman, using articulated steering and conical wheels

12 p2208 A70-27946

Chrysler lunar vehicle design featuring flexible metal wheels and Ackerman front wheel steering, noting back-to-back seating and centrally mounted control display panel

12 p2208 A70-27947

Pogo sticks concept for lunar exploration, showing improved performance over lunar surface or flying vehicles

13 p2505 A70-28891

Lunar surface exploration vehicle /Lunar Rover/ design, analyzing storage aspects in Lunar Module

16 p2888 A70-33680

Manned lunar roving vehicle /MLRV/ navigation scheme based on dead reckoning concept, discussing instruments effectiveness for vehicle velocity and orientation measurements

19 p3396 A70-37849

LUNAR SATELLITES

NT LUNAR ORBITER

Moon figure and gravitational field determination based on hydrostatic theory, libration observations, node and perigee motion, lunar satellite trajectories and visible topography

06 p1141 A70-17824

Apollo Command and Service Modules for lunar orbital science missions, discussing spacecraft-experiment integration

21 p3928 A70-40978

LUNAR SCATTERING

U DIFFUSE RADIATION

U LUNAR RADAR ECHOES

LUNAR SEISMOGRAPHS

Seismic analysis of lunar module impact and missile-earth impact, comparing recorded signal parameters

11 p2118 A70-26748

Seismic echo produced by jettisoned Apollo 12 S-4B stage impact at lunar surface analyzed by multiscatter scattering theory

12 p2298 A70-27280

Lunar elastic waves anomalous propagation, considering Apollo seismographic records and earth rocks specific dissipation function measurements

13 p2486 A70-28617

Lunar seismogram response behavior in terms of power law model of sedimentary earth rock anelasticity

13 p2497 A70-29856

Anelasticity in lunar seismology, discussing low Q regolith layer model from Apollo 12 LP seismogram

13 p2497 A70-29857

Body waves in lunar models, calculating travel times and amplitudes

14 p2638 A70-30674

Localization of lunar acoustic energy, discussing long reverberation time measured at Apollo 12 site after module explosion

18 p3319 A70-37053

Apollo 11 passive seismic experiment package, discussing design, performance and various received signals

21 p3917 A70-41669

LUNAR SHADOW

Electric field sense and magnitude determination from lunar particle shadows in solar electron fluxes

13 p2492 A70-29196

Moon shadow solar eclipse encounter probability for high altitude satellite in circular earth orbit

15 p2803 A70-32502

Lower atmosphere gravity wave motions due to cooling by solar eclipse shadow

23 p4185 A70-43845

LUNAR SOIL

NT LUNAR DUST

Bioscience for recovered lunar samples, discussing Surveyor analyses, Lunar Receiving Laboratory methods and life detection using biological markers

01 p0042 A70-11637

Photoelectric polarimetry of samples of lunar maria, terra, lavas and chemicals for wavelength dependence of polarization, comparing to Mercury, Mars and asteroids

03 p0576 A70-14082

Kamchatka regions volcanic deposits structural and mechanical characteristics compared with lunar soil characteristics

04 p0744 A70-14440

Lunar neutron flux due to cosmic radiation interaction with lunar surface layer, determining angular distribution and energy spectrum

04 p0738 A70-14442

Lunar regolith and polarized component of earthlight observations by Surveyor 7 TV camera

04 p0752 A70-15061

Surveyor 7 highland landing soil mechanical properties and rock diameter similar to previous sites

04 p0752 A70-15063

Surveyor 7 lunar surface sampler, obtaining soil and rock data

04 p0752 A70-15064

Sinus Medii lunar surface material chemical composition from alpha scattering experiment on Surveyor 6

06 p1151 A70-18483

Thermocouple vacuum gauge joined to Apollo lunar sample return containers (ALSRC), describing two step welding procedure with transition cylinder

08 p1507 A70-21483

Laboratory irradiation of rock samples for solar wind flux effects on IR reflectivity of lunar rocks

08 p1579 A70-21565

Apollo 11 lunar material X ray diffraction and microscope studies, noting chemical composition agreement with Surveyor 7 data

09 p1752 A70-22245

Temperature distribution in shadowed lunar craters formulated in Fredholm integral equations, showing constant temperature and correction for soil thermal inertia

[AIAA PAPER 69-595]

11 p2112 A70-26155

Apollo 13 lunar surface heat flow experiment to measure vertical temperature gradients as function of time and soil thermal conductivity

11 p2118 A70-26747

Mass spectrometric analysis of lunar material from soil vaporization products ion component by electron beam

11 p2119 A70-26800

Kamchatka regions volcanic deposits structural and mechanical characteristics compared with lunar soil characteristics

13 p2485 A70-28465

Neutron flux due to cosmic radiation interaction with lunar surface layer, determining angular distribution and energy spectrum

13 p2475 A70-28467

Lunar soil and rocks photometric and polarimetric properties from high resolution Surveyor pictures

14 p2644 A70-31054

Lunar surface mechanical properties from Surveyor spacecraft interactions with soil /exclusive of surface sampler/

14 p2644 A70-31055

Lunar IR radiation measurements for estimating thermophysical properties and small scale surface nature

14 p2645 A70-31057

Lunar surface optical properties differences for lunar and planetary nature and evolution determination

14 p2645 A70-31063

Lunar mascons origin explanation in terms of primordial atmosphere and hydrosphere

14 p2646 A70-31065

Legal status of ownership rights of lunar soil samples and objects left on moon by astronauts

17 p3203 A70-35790

Lunar soil characteristics, analyzing sample from Apollo 11 mission

18 p3316 A70-36892

Lunar regolith depth measurement by Lunar Orbiters 4 and 5 high resolution photographs, discussing thickness relation with sinuous rilles in maria regions

18 p3319 A70-37054

Physical model of lunar soil prior to Apollo 11 landing, discussing meteoritic shock formation of powdery soil

18 p3320 A70-37080

Apollo 11 and 12 results tabulated for soil packing characteristics, composition and rare gas analysis data

18 p3332 A70-37223

Biological tests of fish and invertebrates exposed to Apollo 11 lunar surface material, noting absence of pathological effects

19 p3513 A70-37409

Hydrogen flame ionization detector /HYFID/ for life-derived organic matter in Martian/Lunar soil

19 p3426 A70-37896

Lunar anorthosites Ni-Fe grains from Mare Tranquillitatis, discussing contamination by meteoritic metal, magnetic fractionation and fractional crystallization

19 p3519 A70-38032

Lunar soil from Apollo 12, identifying chemical composition of orthopyroxene-calcic plagioclase rock fragments for origin

20 p3709 A70-39980

Electron microprobe and petrographic analyses of crystalline rock and separates from Apollo 11 lunar soil samples

21 p3895 A70-41506

Apollo 11 lunar rock and fines chemistry, mineralogy and petrology, discussing composition, igneous rocks, microbreccias, glasses and pyroxene relations

21 p3895 A70-41507

Mineralogy and chemistry of Apollo 11 lunar soil samples, using three-channel electron microprobe analyzer

21 p3896 A70-41509

Apollo 11 lunar soil volcanic rock samples, mineralogical and petrological description and surface features

21 p3896 A70-41514

Trace phyllosilicates in Apollo 11 soil sample and rock, using electron microscopy and diffraction studies

21 p3897 A70-41518

Tranquility Base lunar soil origin, establishing component nature, size distribution, density, mineralogy, constructional or destructional history

21 p3897 A70-41519

Apollo 11 lunar soil and breccia shock metamorphism, examining plastic deformation structures in plagioclase, pyroxene and olivine

21 p3897 A70-41520

Bulk chemical compositions, mineral and glass analyses, X ray data and physical properties of Apollo 11 lunar fines and rocks

21 p3898 A70-41526

Plagioclases, pyroxenes and olivines in lunar soils and rocks, using X ray diffraction and Mossbauer effect

21 p3899 A70-41528

Lunar breccia and fine sample metal particles, using optical and scanning electron microscopy and electron probe microanalysis

21 p3899 A70-41529

Compositions of lunar fines, crystalline rock and glass spherules, showing high normative anorthite

21 p3899 A70-41531

Type 1 carbonaceous chondrites contribution to lunar soil, comparing mineralogical and trace element evidence

21 p3899 A70-41533

Apollo 11 samples compared to stony meteorites and terrestrial basalt, discussing lunar rock formation processes

21 p3900 A70-41540

Mineral chemistry of Apollo 11 igneous rocks, soil and breccia samples, comparing with meteorites

21 p3773 A70-41545

Apollo 11 lunar rocks and fines, examining clinopyroxenes augite and pigeonite by single crystal X ray diffraction microprobe optical and electron optical techniques

21 p3902 A70-41549

Elemental composition and structure of metallic iron particles in lunar fines compared to meteorites, using neutron activation technique

21 p3774 A70-41556

Microprobe analysis of glassy spherules from Apollo 11 lunar regolith, discussing zoning, composition and hypervelocity impact formation

21 p3903 A70-41558

Apollo 11 lunar rocks and fines cosmic ray produced radioisotopes, considering surface exposure to high energy component flux

21 p3906 A70-41562

Apollo 11 lunar rocks, breccias and fines age and chemistry, major element, trace element and rare earth abundances, texture, crystallization and meteoritic effects

21 p3906 A70-41563

Apollo 11 lunar fines trapped noble gas elemental and isotopic abundances, suggesting solar wind origin

21 p3906 A70-41565

Apollo 11 lunar rocks and fines oxygen, Si and Al content determination by neutron activation analysis

21 p3774 A70-41566

Apollo 11 lunar material actinide element abundance and isotopic composition, examining Th, U and transuranium elements by mass spectrometric and radiometric techniques

21 p3774 A70-41569

Apollo 11 lunar material water content and H and C isotope abundance, examining changes in deuterium and O by solar winds

21 p3774 A70-41570

Rare gas analysis of Apollo 11 lunar soil and breccia for surface layer history

21 p3906 A70-41571

Apollo 11 lunar material trace elements, examining chemical processes during and after formation and meteoritic matter influx rate

21 p3907 A70-41572

Apollo 11 fines gas evolution and physical changes via heat treatment, discussing Ar 40 anomaly, lava structure origin and oxidation rate

21 p3907 A70-41577

Radiogenic and cosmogenic inert gases and isotopic ratios in Tranquility Base fines indicating solar wind saturation

21 p3775 A70-41581

Surface correlation of excess Ar 40 in lunar fines from Apollo 11

21 p3908 A70-41582

Apollo 11 lunar matter rare gas, H and N concentrations and isotopic abundances, discussing solar wind, gas diffusion loss from silicates and spallation component

21 p3908 A70-41583

Rare gas distribution in grain surfaces of lunar soil, breccias and rocks originating from solar wind, using microhelium probe

21 p3908 A70-41587

Lead and thallium isotopic compositions of Apollo 11 fines compared with meteorites and earth for lunar surface age determination

21 p3775 A70-41588

Apollo 11 lunar soil irradiation history from solar wind rare gas abundances and cosmic ray spallation products

21 p3908 A70-41590

Apollo 11 lunar rocks and soil chemical composition, examining major, minor and trace elements

21 p3776 A70-41591

Apollo 11 lunar rock and soil elemental abundances, discussing composition, volatile element depletion, rare earths, basalt and geochemical processes

21 p3909 A70-41593

Trace elements K, Rb, Sr and Ba distributions and Rb-Sr isotopic relations in Apollo 11 lunar breccia and fine soil samples

21 p3909 A70-41594

Apollo 11 lunar rock and fines primordial radionuclide abundances and concentration gradients by gamma ray spectrometry at Lunar Receiving Laboratory

21 p3776 A70-41595

Apollo 11 lunar fines, breccia and crystalline rocks rare gas data, emphasizing trapped and spallation Ne, Kr and Xe isotopic compositions

21 p3909 A70-41598

Cosmogenic and primordial radionuclides in Apollo 11 lunar soil and rocks, using nondestructive gamma ray spectral measurements

21 p3776 A70-41599

Halogens, mercury, lithium and osmium concentration measurements in Apollo 11 samples, using neutron and photon activation

21 p3777 A70-41601

Apollo 11 lunar rock and soil bombardment produced radionuclide patterns, discussing solar flare protons and alphas, age determination and astronomical models

21 p3777 A70-41604

Elemental abundances of Apollo 11 lunar rocks and soils, using activation analysis or mass spectrometric isotope dilution

21 p3909 A70-41606

Chemical analysis for Li, Na, K, Rb, Cs, Ca, Sr and Ba in achondrites and Apollo 11 lunar rocks, breccia and soil samples

21 p3910 A70-41611

Apollo 11 lunar rocks and soil chemical elements analysis by neutron activation scheme

21 p3777 A70-41612

Apollo 11 lunar rocks, soil and core samples major, minor and trace elements abundance by radiochemical and instrumental activation analyses

21 p3910 A70-41614

Apollo 11 fines and rocks major and trace elements data obtained by combined instrumental and neutron activation analysis

21 p3910 A70-41615

Apollo 11 lunar, terrestrial and meteoritic basalts relationships, examining Ga, Ge, In, Ir and Au concentrations by neutron activation analyses

21 p3778 A70-41617

Apollo 11 lunar surface fine material and rocks cosmogenic radio nuclides Al 26 and Na 22 concentrations determination by gamma ray spectroscopy

21 p3910 A70-41618

Apollo 11 lunar fines examined for organic compounds via solvent extraction, vacuum crushing, programmed heating and hydrofluoric acid etching

21 p3778 A70-41619

Apollo 11 lunar fines carbon level, finding largest component carbon monoxide in complex form

21 p3778 A70-41621

Amino acids analysis of Apollo 11 lunar fines by hydrolysis of aqueous extracts

21 p3778 A70-41623

Apollo 11 lunar fines carbon compounds, examining chemical state of porphyrins, fatty and amino acids, purines, pyrimidines and carbohydrates, etc
21 p3779 A70-41625

Apollo 11 lunar fines porphyrin-like pigments content demonstrated by fluorescence spectrometry and analytical demetallation, suggesting rocket exhaust source
21 p3910 A70-41626

Lunar fines hydrochloric acid hydrolysates examination by gas-liquid chromatography indicating presence of organosiloxanes
21 p3779 A70-41627

Volatilizable C compounds in lunar fines from Mare Tranquillitatis, investigating pyrolysis and acid hydrolysis products by mass spectroscopy and gas chromatography
21 p3779 A70-41628

Apollo 11 lunar fines chemical analysis for alkanes of 15-30 carbon atom length, obtaining negative results
21 p3779 A70-41630

Apollo 11 fines and rocks analysis by chromatography, mass spectrometry and light and scanning electron microscopy
21 p3779 A70-41631

Apollo 11 lunar fines organic compounds detection and identification by mass spectrometry
21 p3780 A70-41632

Viable organisms in Apollo 11 lunar fines, discussing tests, laboratory and sterile biological barrier system
21 p3911 A70-41634

Organic solvent extracts of Apollo 11 bulk fine sample examined for porphyrins using spectrofluometry
21 p3780 A70-41635

Apollo 11 lunar science - Conference, Houston, January 1970, Volume 3, Physical properties
21 p3911 A70-41636

Micro-breccia, igneous rocks and lunar fines elastic properties at ambient conditions and as function of pressure, discussing near surface mare region models
21 p3913 A70-41640

Apollo 11 lunar rock and soil mechanical behavior and physical characteristics, discussing color, specific gravity, density, shapes and adhesive and cohesive properties
21 p3913 A70-41646

Apollo 11 fines thermal conductivity under vacuum, using line heat source technique
21 p3913 A70-41647

Apollo 11 fines, breccias and crystalline rocks thermoluminescence, observing temperature dependence of glow curve peaks
21 p3914 A70-41649

Apollo 11 lunar fines, rocks and breccias luminescence, electron paramagnetic resonance and optical properties, discussing reflection spectra, heating effects and dipole resonance
21 p3914 A70-41654

Mossbauer spectra of Apollo 11 lunar fines and microbreccia, showing iron oxidation, site symmetry and magnetic state
21 p3915 A70-41657

Time dependent adhesion in ultrahigh vacuum of Apollo 11 lunar soil sample 10065-33, considering microchemical and microphysical properties
21 p3915 A70-41658

Apollo 11 lunar fines, investigating solar radiation effects on optical properties by standing and heating
21 p3915 A70-41660

Apollo 11 bulk and core tube fines and rock cosmic ray tracks, discussing material history and corpuscular radiation flux and energy spectra near moon
21 p3916 A70-41667

Apollo 11 rock and fines magnetic resonance, examining line shapes, temperature dependences and electron spin
21 p3917 A70-41670

Apollo 11 sample specific heats at 90-350 K, using adiabatic calorimeter
21 p3917 A70-41674

Apollo 11 lunar rock and fines magnetic properties, associating remanent magnetization with lunar magnetic field
21 p3917 A70-41675

Apollo 11 lunar crystalline rock, microbreccia and fines compressibilities at room temperature, loading-unloading and pressure volume curves
21 p3918 A70-41679

Apollo 11 lunar breccia and fines magnetic properties, examining remanence, composition, oxidation, volcanic activity and stoichiometry
21 p3918 A70-41680

Apollo 11 lunar fines glass spherules magnetic properties, considering soft and hard ferromagnetic components
21 p3918 A70-41681

Seismic signal by Apollo 12 lunar module impact indicating deep layer of powder by signal propagation
21 p3920 A70-41894

Lunar samples and terrestrial materials isotopic analyses, discussing mineralogical and chemical compositions for lunar origin
22 p4098 A70-42574

Lunar soil sample preparation and monitoring for viable microorganisms presence
22 p3978 A70-42973

Apollo 11 lunar fine thermal conductivity measurement under vacuum conditions and lunar temperature range, using line heat source method
23 p4243 A70-44442

Apollo 11 lunar fines glassy particles, investigating morphology, optical properties and chemical composition
24 p4403 A70-45401

LUNAR SPACECRAFT

NT APOLLO SPACECRAFT

NT LUNAR LANDING MODULES

NT LUNAR MODULE

NT LUNAR ORBITER

NT LUNAR PROBES

NT LUNAR SATELLITES

NT LUNIK LUNAR PROBES

NT LUNIK 3 LUNAR PROBE

NT LUNIK 12 LUNAR PROBE

NT RANGER LUNAR PROBES

NT SURVEYOR LUNAR PROBES

NT SURVEYOR 5 LUNAR PROBE

Lunar launch vehicles quality control and reliability, describing management procedures for test facilities, preproduction and purchased materials quality
22 p4126 A70-42384

LUNAR SURFACE

U LUNAR TOPOGRAPHY

LUNAR SURFACE VEHICLES

NT LUNAR MOBILE LABORATORIES

NT LUNAR ROVING VEHICLES

Lunar surface mobility systems designs based on terrestrial transporters or mission requirements consideration, comparing capabilities
13 p2384 A70-28416

Lunar vehicles development, emphasizing translunar exploration vehicle (TLEV) for future lunar base
14 p2563 A70-30197

Caterpillar remote controlled unmanned lunar exploration vehicle, describing construction and scientific missions
18 p3237 A70-36512

Gyrocompassing for self contained lunar surface vehicles navigation, proposing local vertical determination method
20 p3667 A70-39528

LUNAR TEMPERATURE

Creep behavior of mascons to infer lunar temperatures at depth compared with electrical conductivity data and heat conduction equation
05 p0906 A70-15892

Inhomogeneous model of upper lunar surface layer assuming temperature dependent heat conductivity and capacity, showing agreement with IR measurements
08 p1564 A70-20559

Lunar origin and history, discussing evolution temperature, large and small craters and association with solar system evolution
08 p1581 A70-21822

Lunar internal temperature approximation correcting solution of heat conduction equation for moon thermal histories
09 p1753 A70-22385

Apollo 13 lunar surface heat flow experiment to measure vertical temperature gradients as function of time and soil thermal conductivity
11 p2118 A70-26747

Inhomogeneous model of upper lunar surface layer assuming temperature dependent heat conductivity and capacity, showing agreement with IR measurements
15 p2805 A70-32714

X ray differential drift scans of moon, measuring cold limb brightness temperature and temperature distribution
16 p2974 A70-33646

Lunar rilles temperature distribution analysis, examining contour shape, aspect ratio and solar elevation angles effects
17 p3152 A70-34507

Apollo 11 lunar fine thermal conductivity measurement under vacuum conditions and lunar temperature range, using line heat source method
23 p4243 A70-44442

LUNAR TIDES

Lunar atmospheric tidal wind semidiurnal variations from Hong Kong and Uppsala data, discussing agreement with theory
02 p0325 A70-12217

Tidal disturbing functions developed with amplitude factor and lag angle expressed as sums of zonal spherical harmonics, discussing lunar formation and orbit evolution
03 p0576 A70-14083

Lunar tide in E region phase height from measurements of diurnal phase path change for continuous wave
04 p0678 A70-14973

Lunar tides in midday critical frequency of F 2 layer, determining phase reversal location
04 p0651 A70-15309

Semidiurnal lunar tidal wave influence on clock corrections obtained by observations of stellar meridian passages at four localities
04 p0756 A70-15479

Lunar density gradient, free oscillation and tides study inferring lunar atomic number similarity to Si and earth mantle
05 p0908 A70-16316

Tidal friction induced secular changes in earth-moon system near minimum of angular momentum of moon orbit, including temporal changes in moments of inertia
08 p1579 A70-21570

Lunar daily and monthly tidal variations in horizontal magnetic field and F 2 region maximum electron density and peak ionization height at Puerto Rico
10 p1872 A70-23823

Lunar semidiurnal tidal oscillations of surface pressure in atmosphere, observing constant amplitude with maximum and minimum phase lag variations
11 p2045 A70-25645

Lunar tides relationship with equatorial electrojet currents using daily variations at fixed lunar ages and monthly variations at lunar hours of horizontal magnetic field
11 p2114 A70-26564

Book on thermal and gravitational atmospheric tides covering solar oscillations, lunar air tides, upper air data, ozone radiation absorption, etc
14 p2573 A70-30633

Lunar tide in ionospheric D region absorption near magnetic equator, noting annual variation relationship to sunspots
14 p2574 A70-30747

Lunar tidal diurnal and semidiurnal variations in equatorial sporadic E layer related to H geomagnetic field and sunspot period
15 p2726 A70-31862

Lunar tidal force influence on meteoritic material fission before impact, calculating internal to explain topographical features
18 p3319 A70-37051

Ionospheric electric current distribution response to horizontal wind induced emf, using lunar tidal wind models
19 p3415 A70-38386

Lunar perturbations in horizontal geomagnetic field, F 2 layer thickness and electron density, discussing tidal variations
20 p3617 A70-39141

Lunar tidal components in atmospheric pressure for various observatories, discussing seasonal variations
20 p3661 A70-39142

Earth rotation rate deceleration due to lunar tidal friction taking into account fluctuations from internal processes, discussing moon retreat from earth
21 p3921 A70-41970

Earth-moon system age and origin from tidal evolution equations, considering growth line counts on living and fossil marine invertebrates
21 p3921 A70-41971

Tidal friction theories relating to earth rotation and lunar evolution
21 p3921 A70-41972

Lunar tidal effects on horizontal magnetic field compared at equatorial and midlatitude stations
22 p4021 A70-43279

Hough eigenfunctions of lunar diurnal and semidiurnal atmospheric oscillations using matrix and group methods
24 p4328 A70-45351

LUNAR TOPOGRAPHY

Global exploration of lunar surface by Luna 3 and Zond 3 automatic stations, confirming asymmetric distribution of sea areas on visible and remote hemispheres
01 p0177 A70-10335

Lunar origin theories, considering lunar surface data from Surveyor spacecraft and Lunar Orbiter
01 p0178 A70-10453

Lunar atmosphere molecule and atom concentration from isotropic and uniform surface evaporation due to micrometeorite impact
01 p0192 A70-11541

Space research photography role in studying earth and moon atmospheres and surfaces, determining spectral bands for contrast
03 p0483 A70-13168

Spectral polarization characteristics phase variations used for classifying lunar surface features
03 p0565 A70-13234

Photometric reduction of Lunar Orbiter video magnetic tapes for generation of topographic information of proposed Apollo landing sites
03 p0490 A70-13661

Three dimensional characteristic of light scattered by lunar surface determined for various incidence angles and azimuths from Zond 3 photometric measurements
04 p0744 A70-14441

Lunar surface far side stereoscopic photography by Apollo 8 mission considered for lunar control
04 p0686 A70-14618

Optical facilities of Apollo 11 mission and NASA Manned Spacecraft Center noting Fzadow telescopes, lunar cartography, photometric surface analysis, etc

04 p0687 A70-14690

Soviet book on lunar shape and dimensions from astronomical observations, comparing observational and theoretical data

04 p0751 A70-14952

Surveyor 7 alpha scattering experiment and TV image data revealing lunar surface chemical composition, rocks and fragments, etc

04 p0752 A70-15060

Surveyor 5, 6, 7 missions alpha-scattering experiments, lunar rocks chemical composition compared with earth rocks and chondritic meteorites

04 p0752 A70-15062

Diffuse component of lunar radar echoes, using model with volume backscattering from within lunar regolith, noting rocks permittivity

05 p0816 A70-16826

Gravity anomalies of moon mapped by time differentiation of Doppler-tracked satellite velocities, noting isostatic equilibrium

05 p0915 A70-16827

Surveyor 7 lunar mission landing site, equipment, operations, etc

05 p0915 A70-16830

Cartographic tying-in of Zond 3 lunar surface photographs to verify maps of moon far side

05 p0918 A70-16918

Lunar structure and evolution based on satellite measurements of mass distribution, radius moments of inertia, gravity anomalies and topographic irregularities

05 p0920 A70-16945

Moon figure and gravitational field determination based on hydrostatic theory, libration observations, node and perigee motion, lunar satellite trajectories and visible topography

06 p1141 A70-17824

Catalog of lunar features brightness interpreted in terms of photometric function uniformity of lunar surface, considering second order light scattering

07 p1377 A70-18971

Potential and gravity distributions on lunar surface, showing presence of harmonics of all orders

07 p1385 A70-19425

Lunar photography interpretation, discussing topographic maps obtained by spacecraft

07 p1284 A70-19779

Inhomogeneous model of upper lunar surface layer assuming temperature dependent heat conductivity and capacity, showing agreement with IR measurements

08 p1564 A70-20559

Lunar latitude evaluation investigated for origin of discrepancy between two methods

08 p1577 A70-21494

Spectral polarization characteristics phase variations used for classifying lunar surface features

08 p1580 A70-21667

Lunar Orientale region structure geological interpretation based on Lunar Orbiter 4 photographs

09 p1751 A70-22196

Satellite impact interpretation of lunar maria surface distribution, discussing lava origins and mascon distribution

09 p1752 A70-22310

Soviet book on lunar physics covering exploration, topography, internal structure, etc

09 p1756 A70-22528

Lunar sinuous rilles as volcano-tectonic fracture traces of sites of gas emission

09 p1758 A70-22743

Apollo lunar landing sites geological configuration and composition

09 p1759 A70-22772

Selenodetic control system, considering photogrammetric networks, Apollo landing site, topographical maps, lunar photographs, etc

10 p1890 A70-24732

Lunar sinuous rilles and Mojave desert stream channels similarities, discussing presence of terraces

11 p2108 A70-25701

Random processes correlation functions determined by stochastic differential equations applied to lunar surface statistical characteristics determination

11 p2118 A70-26785

Physicomechanical properties of tuff rock based on similarity to lunar surface rock, determining natural density, porosity and compression strength

11 p2119 A70-26798

Ranger lunar photographic evidence for volcanic hypothesis, considering fracture systems, Caldera analogy, common walls, crater size, etc

12 p2297 A70-26985

Book on moon covering motion, earth-moon system, internal structure, hydrostatic equilibrium, thermal history, global form, gravitation, topography, etc

12 p2298 A70-27096

Lunar surface mapping and far side gravity field probing by satellite photogrammetry

12 p2308 A70-27874

Lunar far side features position from Apollo 8 data, evaluating Apollo navigation system accuracy

12 p2309 A70-27949

Three dimensional characteristic of light scattered by lunar surface determined for various incidence angles and azimuths from Zond 3 photometric measurements

13 p2485 A70-28466

Rb-Sr internal isochrons of crystalline lunar rocks from Tranquility Sea for moon age estimation

13 p2485 A70-28472

Micrometeorites impact on lunar surface, using optical reflecting and stereoscan electron microscopes to investigate craters on Apollo 11 samples

13 p2485 A70-28474

Lunar surface brightness temperatures from IR observations, determining thermal emission directional characteristics to infer surface temperatures from Surveyor data

[AIAA PAPER 69-593] 13 p2486 A70-28501

Proton and electron irradiation producing oxygen vacancies in silicates, minerals and rocks, indicating similar processes in lunar surface materials erosion and transport

13 p2395 A70-28908

Book on stratigraphic view of lunar geology covering lunar craters and terrestrial analogs, remote sensing, material ages, surface interpretations and Apollo mission results

13 p2491 A70-29060

Photographic techniques and optical equipment in orbiter missions for lunar surface photography

13 p2407 A70-29164

Lunar surface material composition in terra region from alpha scattering data on Surveyor 7, noting Si Na abundance

13 p2492 A70-29265

Astronomical navigation on lunar surface with equations for selenographic latitude and longitude

13 p2449 A70-29272

Lunar surface terrain types and chemical composition based on Surveyor pictures

14 p2634 A70-30193

Lunar horizontal and inclined surfaces net radiation and components, discussing surface temperature, thermal emission and absorbed solar radiation

14 p2634 A70-30194

Manned lunar surface navigation requirements emphasizing dead reckoning system

14 p2613 A70-30458

Lunar surface erosion model by small projectiles impact for analytic representation of crater shape change as function of time

14 p2637 A70-30494

Lunar surface thermal emission spectra, calculating IR emissivities

14 p2637 A70-30495

Lunar surface thermal emission spectra based on laboratory analysis of rocks and minerals emissivity

14 p2637 A70-30496

Lunar surface fine structure and geological analysis from Ranger 7, 8 and 9 photographs

14 p2644 A70-31052

Balloon-borne midinfrared observations of lunar surface composition from interpreting peak emissivity differences

14 p2645 A70-31058

Radio astronomical observations of lunar surface material EM properties compared with Surveyor 7 chemical analysis

14 p2645 A70-31059

Topographic variations in lunar surface from bistatic radar observations on Explorer 35

14 p2645 A70-31061

Lunar surface roughness effects on thermal radiation, using model surface with parallel troughs

14 p2649 A70-31212

Apollo lunar laser ranging experiment /LURE/ for range measurements from earth to lunar surface

15 p2750 A70-31675

Lunar exploration by manned and unmanned space flights, discussing seismology, composition, surface features, etc

15 p2798 A70-31678

Apollo 11 lunar mission results, discussing surface, seismology, laser ranging retroreflector, solar wind and rock samples

15 p2800 A70-32073

Lunar rotary motion predetermination for spacecraft landing in mountainous region

15 p2773 A70-32266

Hypsometric chart plot of visible lunar hemisphere with consideration of relief, obtaining isohypsies

15 p2803 A70-32494

Inhomogeneous model of upper lunar surface layer assuming temperature dependent heat conductivity and capacity, showing agreement with IR measurements

15 p2805 A70-32714

Mariner 7, 8 and 9 lunar photographs, discussing evidence for internally heated moon

16 p2973 A70-33112

Lunar surface exploration vehicle /Lunar Rover/ design, analyzing stowage aspects in Lunar Module

16 p2888 A70-33680

Lunar surface large scale maps by photogrammetric method requiring triangulation of convergent high resolution Lunar Orbiter photographs by block process

16 p2979 A70-34045

Lunar rilles temperature distribution analysis, examining contour shape, aspect ratio and solar elevation angles effects

17 p3152 A70-34507

Radar reflectivity correlations with lunar surface structure in Mare Imbrium, using delay-Doppler radar maps

17 p3154 A70-34568

Lunar surface erosion due to Apollo 11 descent engine

18 p3316 A70-36960

Lunar tidal force influence on meteoritic material fission before impact, calculating internal to explain topographical features

18 p3319 A70-37051

Lunar surface features charting from astrophysical data and direct observation, describing mapping of Sea of Tranquility

18 p3323 A70-37141

Moon Surface Basic Points catalogs differences, estimating position dispersion by residuals of transformations

18 p3323 A70-37143

Lunar rocks permissivity and density and surface roughness from radio wave scattering data

19 p3512 A70-37276

Lunar maria distribution, explaining origin and characteristics by surface brightness

19 p3517 A70-37987

Lunar craters, walled plains and maria compared with volcanic formations on earth

19 p3517 A70-37991

Lunar volcanic ridges features from interpretation of photographs by telescopes and satellites

19 p3518 A70-37992

Lunar maria and constituents characteristic differences in terms of structure, height and distribution of craters across surface, noting temperature anomalies

19 p3518 A70-37993

Lunar surface mapping and comparison of geological features with earth, considering mass, volume, density, gravity, rotation and energy and matter balance

19 p3518 A70-37994

Lunar sinuous rilles morphological and distributional observations and implications on theories of origin concerning surface water erosion

19 p3521 A70-38442

Moon origin, surface, exploration, Apollo 11 landing, subsidence/uplift crater formation and Transient Lunar Phenomena

20 p3701 A70-38977

Surveyor program results, discussing lunar craters, rock fragments, particle size optical, thermal and radar characteristics and chemical composition

20 p3707 A70-39952

Lunar topographical and geological features examined by Surveyor program

20 p3707 A70-39953

Lunar surface material composition examination by Surveyor 5, discussing formation of surface

20 p3708 A70-39958

Lunar surface physical conditions from Surveyor landings, discussing fine cohesive rock powder

20 p3708 A70-39959

Lunar postsunset horizon afterglow observed by Surveyor 7, discussing small particle diffraction on surface

20 p3708 A70-39960

Lunar and earth surfaces imaging for astronaut training in LEM simulator

20 p3607 A70-40320

Lunar surface specific effective radio signal scattering area measured by Luna 9 and 13, describing signal fluctuations

21 p3884 A70-40838

Lunar mascon detection in Sinus Aestuum neighborhood by Apollo 8 tracking data analysis

21 p3886 A70-41058

Shock metamorphism, grain size and mineralogy of lunar surface regolith materials

21 p3901 A70-41543

Lunar surface material age and post-crystallization from isotopic investigation of Apollo 11 samples of U-Th-Pb systematics

21 p3909 A70-41608

Lunar rocks mineralogy and visible and near IR reflectivity, discussing depression in telescopic curve

21 p3912 A70-41637

Micro-breccia, igneous rocks and lunar fines elastic properties at ambient conditions and as function of pressure, discussing near surface mare region models

21 p3913 A70-41640

Directional, spectral and total reflectance for Apollo 11 fines and rock chips, observing dependence on illumination angle

21 p3913 A70-41643

- Apollo 11 drive-tube core samples from Tranquility Base, expressing lunar surface environmental processes 21 p3914 A70-41653
- Lunar surface impact cratering, comparing equilibrium size distributions 21 p3919 A70-41701
- Lunar geomorphic features and mass wasting relation, discussing landslides, rockfalls, debris slides, slump and creep play 22 p4102 A70-42972
- Hypsometric chart plot of visible lunar hemisphere with consideration of relief, obtaining isohypes 23 p4240 A70-43916
- Apollo 11 and 12 close-up lunar surface photography, describing specially designed camera 23 p4194 A70-44255
- Lunar maria and circular basins interrelations, form, origin and distribution from Lunar Orbiter photographs 23 p4242 A70-44263
- Apollo 11 and 12 results concerning lunar geology and physical features, discussing impact generated long duration seismic signals and solar wind isotopic composition experiment 23 p4244 A70-44613
- Lunar topography from UBVRI photometry, determining albedos for mountains, dark and light maria and cratered terrae 23 p4247 A70-44769
- Lunar craters size-frequency distributions from photographic analysis, tabulating results 23 p4247 A70-44770
- Lunar surface selenographic reference points tabulation, considering suitability for selenodetic measures 23 p4247 A70-44773
- Tycho crater northeast rim scale relief model including lava lakes in outer walls 23 p4253 A70-44881
- New Mexico Bandera lava tube systems, noting similarities with lunar surface sinuous rilles 23 p4254 A70-44884

LUNAR TRAJECTORIES

- NT CIRCUMLUNAR TRAJECTORIES
- NT EARTH-MOON TRAJECTORIES
- NT MOON-EARTH TRAJECTORIES
- Earth oblateness effects on lunar and interplanetary trajectories, using algorithm based on orbital elements variations 06 p1146 A70-18203
- [AIAA PAPER 70-97] Lunar swingby trajectory analysis with atmospheric reentry, characteristics of geocentric portions of earth-moon and moon-earth transfers 10 p1940 A70-24306
- Computational limitations of midcourse correction velocity for lunar impact trajectories, considering impact miss magnitude correction 11 p2109 A70-25955
- Near parabolic trajectories between moon and cislunar libration point, considering earth perturbative influence 19 p3529 A70-38874
- [AIAA PAPER 70-1059] Closed form approximate solution for restricted three body motion of lunar or interplanetary spacecraft, demonstrating accuracy and flexibility in lunar mission trajectory calculations 19 p3529 A70-38875
- [AIAA PAPER 70-1061]

LUNEBERG LENSES

U RADAR CORNER REFLECTORS

LUNG MORPHOLOGY

- Histopathological evidence for pulmonary emboli in experimental decompression sickness in dogs detected by radioisotopic lung scanning 06 p0991 A70-17295
- Lung alveolar and capillary wall structure in mammals under normal conditions, transverse acceleration and mechanically changed pulmonary circulation 20 p3575 A70-40190
- Obstructive lung diseases clinical, radiological and functional diagnosis in legal medicine 24 p4296 A70-45122
- Air and liquid filled excised lungs P-V hysteresis curves, determining surface tension in situ 24 p4302 A70-46104
- Human lung volume-to-ventilation ratios regional dispersion, using expired nitrogen concentrations analog simulation 24 p4303 A70-46113
- LUNGS
- Lung lipid embolization effect in decompression sickness on obese mice, showing no relationship to dysbaric syndrome 01 p0015 A70-10361
- Respiratory flow rate effect on emptying of lung regions, assessing regional and end-expiratory volumes 03 p0428 A70-14155
- Data analysis of compliance, resistance, inertance and natural frequency of chest-lung system, noting trend with body mass 06 p0993 A70-17521
- Static tensibility and vital capacity of lungs statistically analyzed in relation to sex and age 07 p1210 A70-19524

Oxygen diffusion time into nitrogen in dichotomously branched human lung model calculated by finite difference technique, discussing alveolar plateau 10 p1809 A70-24003

Open circuit gas washout test of lungs under inspiration-expiration transmission symmetry, using Hilbert-Schmidt operators 12 p2175 A70-27021

Human lung closing and subdivision volume relationship to age and body position 12 p2169 A70-27657

Human lung and upper airway pressure drop and fluid flow regime of inspired air 12 p2170 A70-27660

Minute hyperventilation of human lungs causing expiratory suppression of respiration 12 p2173 A70-28315

Nitrogen respiratory elimination by human lung, analyzing expired air by mass spectrometry and volume displacement in closed systems 13 p2351 A70-29325

Gravity dependent lung region emptying sequence effects on alveolar Xe 133 and nitrogen plateaus in pivoted subjects 13 p2356 A70-29944

Stress distribution and pressure distending air spaces in lungs, using mechanical pulmonary elasticity model 13 p2356 A70-29945

Sprometers for ventilation measurement of separate lungs, recording impedance changes during respiratory cycle 14 p2541 A70-30378

Surface active lipoproteids of lung, discussing quantitative determination and labeling on basis of peribronchial wash-out procedure over trachea 15 p2680 A70-31725

Fluid analog for lung tissue response to gravitational acceleration, examining lung density, transpulmonary pressure, expansion, etc 16 p2850 A70-34257

Upper pulmonary airways plastic conduit model, measuring laminar and turbulent flow velocity profiles by hot-wire anemometer 17 p3035 A70-34469

Trans thoracic mutual impedance responses to lung ventilation, discussing spatial and temporal intravariability 17 p3035 A70-34576

Human lung internal surface area automated measurement by computerized image processing techniques, grading emphysema 17 p3035 A70-34578

Lung diffusing capacity for CO in Caucasians native to 3100 m noting membrane diffusing capacity, lung capillary volume and age effects 17 p3031 A70-35427

Topography of pleural surface pressure and vertical gradient of transpulmonary pressure above resting volume in relaxed animals as function of alveolar pressure 21 p3766 A70-42154

Pulmonary blood flow and ventilation distribution during forward acceleration by xenon 133 and lung scanning 24 p4302 A70-46105

Excised perfused dog lungs stratified dead space changes due to transpulmonary pressure and breathing frequency increase, considering pulmonary circulation 24 p4303 A70-46114

Food-water deprivation influence on alveolar surface activity of rat lungs 24 p4303 A70-46115

Recording system errors for measuring pulmonary pressure-volume curves of excised lungs 24 p4309 A70-46122

LUNIK LUNAR PROBES

NT LUNIK 12 LUNAR PROBE

LUNIK LUNAR PROBES

NT LUNIK 3 LUNAR PROBE

NT LUNIK 12 LUNAR PROBE

Lunik 16 lunar soft landing technique, discussing automatic and ground controlled mission phases 22 p4110 A70-43210

Lunik 16 lunar probe recovery technique, using steep angle and high deceleration reentry trajectory for unmanned capsule 23 p4257 A70-44096

Unmanned Luna 16 landing mission, discussing launching and automatic mission control via onboard computer and earth-radioed data 24 p4412 A70-45982

LUNIK 3 LUNAR PROBE

Global exploration of lunar surface by Luna 3 and Zond 3 automatic stations, confirming asymmetric distribution of sea areas on visible and remote hemispheres 01 p0177 A70-10335

LUNIK 12 LUNAR PROBE

Low energy proton flux in neighborhood of Moon measured by Luna 12 satellite indicating magnetized plasma region effect on burst 01 p0172 A70-11493

LYAPUNOV FUNCTIONS

U LYAPUNOV FUNCTIONS

LYMAN ALPHA RADIATION

Solar Lyman alpha line profile and atomic hydrogen vertical distribution measurement method for terrestrial atmosphere in 200-500 km range 01 p0078 A70-11208

High reflectivity mirror construction for H Lyman alpha line using vacuum deposited Al layer coated by magnesium fluoride 02 p0299 A70-12367

D-2 experiments measuring atomic oxygen emission from terrestrial atmosphere and polarization rate and emission intensity from geocoronal hydrogen 03 p0559 A70-13828

L-alpha absorption equivalent width measurements in UV spectra of beta-one, delta and pi Scorpii for interstellar hydrogen densities 04 p0748 A70-14586

Classical path methods for treating Stark spectral line broadening in plasmas illustrated by Lyman alpha line of hydrogen calculations 04 p0726 A70-14670

Lyman alpha auroral emissions observations made with narrow band sky scanning photometer mounted on earth-oriented polar orbiting satellite 04 p0741 A70-15107

Solar Lyman-alpha radiation observed by OGO 4 spacecraft showing short term fluctuations superposed with monthly variation 04 p0741 A70-15128

Lyman alpha transition line in exosphere deuterium line implying enrichment factor ratio to earth surface deuterium 04 p0742 A70-15129

Lyman alpha flux observed by satellite-borne ion chambers during solar flare of 20 March 1966 05 p0902 A70-16442

Scattered Lyman alpha radiation intensities measured for mixtures of partially dissociated hydrogen in Ar, measuring quenching cross sections 06 p1053 A70-17327

X rays from Sco XR-1 compared with galactic cosmic rays and solar Lyman alpha radiation to determine ionospheric ionization causing radio wave attenuation 06 p1134 A70-17443

Geocoronal glow as resonant scattering of solar Lyman-alpha-radiation by H atoms in upper atmosphere 07 p1270 A70-20032

Molecular oxygen concentration determined by absorption spectroscopy of solar hydrogen Lyman alpha line 08 p1490 A70-21390

Deuterium Lyman alpha line profiles generated from microwave powered lamp for experimental testing of two layer model characterizing emission line profiles 09 p1730 A70-22066

Numerical calculation of S matrices for Stark broadening of Lyman-alpha line based on straight line classical path model 09 p1730 A70-22228

Interstellar atomic and molecular hydrogen abundance and physical state using rocket observations of Lyman alpha absorption line and ground based observations 10 p1941 A70-24551

Solar L alpha and X ray emission contribution to lower ionosphere ion production, discussing altitudinal, latitudinal and temporal variations 11 p2106 A70-26789

Lyman alpha intensity and hydrogen concentration at 5 to 19 earth radii determined from OGO 3 spacecraft measurements 12 p2222 A70-27181

Absorption at solar H Lyman alpha line by earth hydrogen atmosphere measured as function of altitude from Aerobee flight spectrograms 12 p2222 A70-27182

Polarized Lyman alpha radiation emitted in electron collisions with atomic and molecular hydrogen and by electric field quenching of metastable atom 13 p2455 A70-29221

Sun Lyman alpha emission line monitoring, describing intensity variations correlation with Zurich number 15 p2798 A70-31654

Photodissociation and fluorescence cross sections for hydrogen by Lyman-alpha photons emission from collisional quenching 16 p2953 A70-33006

Solar radiation intensity at Lyman alpha wavelength and X ray spectrum before and during solar eclipse of 7 March 1970 16 p2972 A70-33827

Solar limb intensity distribution in Lyman alpha line, computing LTE departures 17 p3162 A70-34895

Lyman alpha absorption by interstellar neutral hydrogen observed in O and B stars UV spectra 17 p3162 A70-34898

Interstellar Lyman alpha observations with OAO, providing upper limit to neutral hydrogen column density

17 p3162 A70-34899

Lyman alpha radiation from gaseous hydrogen nebula model, taking into account absorption by dust and interstellar neutral hydrogen

17 p3163 A70-34904

Lyman alpha emission from Comet Bennett observed with photometer on board OGO-5 satellite

17 p3163 A70-35049

Lyman alpha wing resonance broadening opacity effects on solar spectrum in 1500 A to 8000 A range

17 p3169 A70-35383

OGO-4 observations of hydrogen Lyman-alpha airglow surrounding earth, measuring dependence on solar zenith angle

17 p3080 A70-35764

Earth Lyman alpha emission rates as function of atomic hydrogen column density in outer atmosphere, using Mariner 5 measurements

18 p3244 A70-36007

Oxygen absorption coefficients at Lyman alpha line and other transmission windows, verifying dependence on pressure source line width and doublet separation

18 p3293 A70-36753

Near collisions approximation in Stark broadening of hydrogen Lyman alpha line

18 p3296 A70-37227

Lyman alpha geocoronal emission rate as function of altitude at midnight during solar minimum, solving radiative transfer equations

20 p3619 A70-39329

Comet Bennett /1969 i/ spectrograms, discussing linear diameter, trajectory, Lyman alpha emission and hydrogen mass

22 p4097 A70-42468

Lyman alpha sky background measurements by Mariner 6 UV spectrometer

22 p4094 A70-42932

Recombination model of diurnal variation of electron density in midlatitude D region, assuming NO ionization by solar Lyman-alpha radiation

22 p4020 A70-43158

Exospheric neutral hydrogen temperature diurnal variation from satellite resonance filter data, suggesting Lyman alpha source external to geocorona

23 p4186 A70-43852

Solar L alpha absorption in upper atmosphere, using rocket-borne ionization chamber

23 p4191 A70-44270

Lyman alpha radiation scattering intensity during solar radiation period, discussing dependence of interstellar hydrogen density in interplanetary space on solar EUV

23 p4237 A70-44753

Coherent motion effects on brightness of clouds moving above photosphere, describing H alpha Doppler brightening and Lyman alpha Doppler dimming in solar prominences

24 p4400 A70-45313

Interplanetary atomic hydrogen density distribution from Lyman alpha scattering calculation, explaining background radiation anisotropy detection by Vela 7 satellite

24 p4403 A70-45392

LYMAN SPECTRA

Molecular hydrogen Lyman bands radiative transition probabilities, using electronic dipole moment functions

02 p0344 A70-12659

Radiative excitation in planetary and Orion nebulae by solving transfer equations for Lyman line and continuum radiation, using normalized on-the-spot /NOS/ approximation

04 p0758 A70-15700

Lyman-Birge-Hopfield nitrogen bands high resolution emission spectrum, giving energy values of particular states together with corresponding rotational constants and band origins

09 p1730 A70-22067

Solar chromosphere model evaluation using sensitivity of flux emission in Lyman continuum

17 p3170 A70-35386

Interstellar molecular H Lyman resonance-absorption bands in far UV spectrum using rocket observation

20 p3701 A70-39002

Vacuum UV laser action in molecular hydrogen Lyman bands, examining stimulated emission in P branch lines and light pulse duration

20 p3643 A70-40496

LYMPH

NT LYMPHOCYTES

Electrical stimulation of dogs hypothalamus effect on blood and lymph circulation and composition

13 p2352 A70-29354

LYSOGENESIS

LYMPHOCYTES

Local gamma irradiation effect on number of chromosome aberrations in lymphocytes of human blood of oncological patients after hysterectomy

01 p0013 A70-10137

Local stress effect on immunocompetent cells differentiation in guinea pigs lymphatic ganglia, noting increase in number of antibody producing cells

05 p0803 A70-17114

LYOPHILIZATION

U COLLOIDING

LYOPHILS

U COLLOIDS

LYRAE CONSTELLATION

Solar UV radiation reflected from Echo satellites measured and compared with UV fluxes from Lyrae

01 p0095 A70-11614

Photometric results on beta Lyrae from various observatories during 1959 international campaign with data reduced to BV system, showing reddening at primary eclipse

02 p0369 A70-12064

Beta Lyr spectral and brightness characteristics long period variations related to orbital motion perturbations

03 p0564 A70-13229

O-C diagrams of RR Lyrae variables in M5, considering representation by parabolas or intersecting straight lines

03 p0567 A70-13321

Mean magnitudes, colors and amplitudes for RR Lyrae variables in omega Centauri cluster obtained from photometric observations

06 p1148 A70-18455

Beta Lyr spectral and brightness characteristics long period variations related to orbital motion perturbations

08 p1580 A70-21662

Blue-violet and blue minus violet curves for beta Lyrae derived from analyzing photometric materials

12 p2309 A70-27900

LYSINE

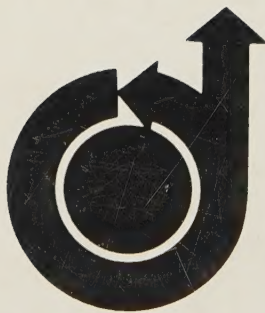
Hydration and lipid-protein ionic interaction in stearic acid monolayers during conformation of poly-L-lysine films

19 p3373 A70-37840

LYSOGENESIS

Lambda prophage induction into lysogens, noting nalidixic acid role in DNA synthesis inhibition

20 p3573 A70-39774



AIAA TECHNICAL INFORMATION SERVICE

750 THIRD AVENUE

NEW YORK, N. Y. 10017